ANGEWANDTE CHEMIE
International Edition in English
Volume 22 · Number 1
January 1983
Pages 1–68

# Molecular Mechanics Calculations in Organic Chemistry[1]: Examples of the Usefulness of this Simple Non-Quantum Mechanical Model

By Eiji Ōsawa* and Hans Musso

Various problems arising in experimental organic chemistry can be clarified by molecular mechanics or force field calculations: molecular dynamics (conformational analysis and internal rotation), the search for the most stable isomer of various polycyclic hydrocarbons, reactivity calculations, including solvolysis of bridgehead substituted systems. Such calculations are shown to be useful in elucidating the mechanism of multistep carbonium ion rearrangements, for predicting the structure and stability of anti-Bredt olefins, and also offer an explanation for the selectivity observed in the hydrogenolysis of strained polycyclic small-ring hydrocarbons, for the identification of long bonds and electronic effects, for the analysis of late transition states, and for the product distribution in complex reactions.

## 1. Introduction

The utility of computers in organic chemistry can no longer be disputed, even by conservative chemists. A new field called computer chemistry has been established with its own conferences and journals. Here we would like only to direct attention to this development; on the one hand purely theoretical calculations as well as their heuristic applications[2] and, on the other, those involving computer assisted synthesis[3] and drug design[4].

There are three main categories of theoretical calculations: *ab initio*, and semiempirical molecular orbital (MO) methods[5], as well as empirical force field calculations[6], also called molecular mechanics (MM). Although pure theory can hardly gain from the results of MM calculations, use of this method is becoming more and more popular and its prospects are recognized as highly promising[7–9]. In fact, this is the method of choice for calculating and optimizing structures and energies of molecules containing anywhere from ten to several hundred atoms—the programs are readily accessible from the Quantum Chemistry Program Exchange (QCPE)[10]—and this size of molecule is of considerable current interest to chemists.

[*] Prof. Dr. E. Ōsawa
Department of Chemistry, Faculty of Science, Hokkaido University
Sapporo 060 (Japan)
Prof. Dr. H. Musso
Institut für Organische Chemie der Universität
Richard-Willstätter-Allee 2, D-7500 Karlsruhe 1 (Germany)

## 2. The Force Field Method

The steric energy ($E_{st}$) and geometrical parameters, such as distances between atoms and bond angles of molecules, can be represented as the sum of terms arising from all stretching ($E_r$) and bending ($E_\theta$) vibrations and torsions ($E_\phi$), as well as from all nonbonding interactions between atoms ($E_d$) [Fig. 1 and eq.(a)].

$$E_{st} = E_r + E_\theta + E_\phi + E_d\,(+ E_{r\phi}\ etc.) \qquad (a)$$

Valence angles down to 90°, which improve the results in strained polycycles like norbornane or cyclobutane derivatives, are taken into consideration by additional terms like the cross term $E_{r\phi}$.

 © Verlag Chemie GmbH, 6940 Weinheim, 1983 0570-0833/83/0101-0001 $ 02.50/0 

Up-to-date accounts of the origin and development of force field methods have been covered in excellent review articles[7-9]. *Engler's* force field (1973)[11] as well as that of *Allinger* (1971)[12] are stored together in program BIGSTRN, and have been used successfully by *Mislow et al.*[13], *Rüchardt et al.*[14,15], *DeTar et al.*[16], *White et al.*[17], *Müller et al.*[18], *Harris et al.*[19], and *Lenoir et al.*[20] among others.

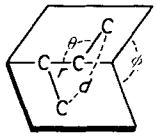
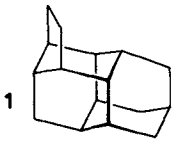


Fig. 1. Intramolecular coordinates used in MM-calculations: r = bond length, θ = bond angle, d = distance between nonbonded atoms, φ = torsion angle.

The most recent steps of refinement hardly influence the results for hydrocarbons. Despite its simplicity with only four terms[21], *Engler's* force field is so well balanced in C/C, C/H, and H/H interactions between nonbonded atoms that it reproduced all observed C—C bond lengths of $C_s$-ethanodiamantane **1**[23,24] with a standard deviation of 0.7 pm, a value as accurate as that obtained by *Altona's* force field known to be excellent for calculation of structures[7f]. Bond angles are reproduced in general within ±1—2° and energy values within ±2 kcal/mol[25]. If similar structures are compared, the mean error decreases further since they, in part, compensate each other.



**1**

The improvement of force fields at the present time causes changes only after the decimal point[26], and this is of course important for calculating the energies of different conformations of simple molecules. The data in Table 1 indicate how *Engler's* force field may be evaluated in this respect. The hydrogen in this force field is now recognized as somewhat too "hard" and the carbon too "soft"[27]; this leads to an opening of the valence angles in molecules with bulky substituents[28]. A further disadvantage of the program BIGSTRN is its low efficiency in the search for the energy minimum[29].

Table 1. Energy differences $\Delta E$ between the *anti*- and *gauche*-conformations of simple alkanes.

| Compound | $\Delta E_{exp}$ [kcal/mol] | | $\Delta E_{calc}$ [kcal/mol] | |
|---|---|---|---|---|
| | *Verma* [a] | *Engler* [11] | *Allinger* [12] | *Boyd* [b] |
| *n*-Butane | 0.966±0.054 | 0.93 | 0.67 | 0.68 |
| 2-Methylbutane | 0.809±0.050 | 0.78 | 0.44 | 0.59 |
| 2,3-Dimethylbutane | 0.054±0.030 | −0.03 | 0.08 | 0.20 |

[a] A. L. Verma, W. F. Murphy, H. J. Bernstein, *J. Chem. Phys. 60* (1974) 1540. [b] S. Chang, D. McNally, S. Shary-Tehrany, M. J. Hickey, R. H. Boyd, *J. Am. Chem. Soc. 92* (1970) 3109.

Currently, users are shifting to the more sophisticated second-generation force fields such as MM2[10a,22], MUB-2[27b] or recent versions of the consistent force field[10d,30].

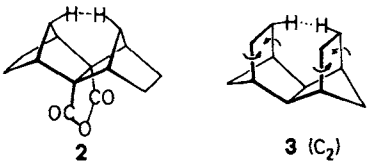
## 3. Conformational Analysis

### 3.1. The *gauche* H—H-Interaction

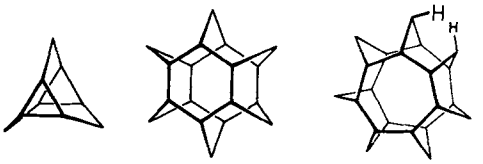
The somewhat daring proposal by *Wertz* and *Allinger*[31] that nonbonded repulsions between vicinal hydrogen atoms play a dominant role in destabilizing the *gauche* form of *n*-butane aroused considerable attention. Careful examination by at least three other force fields MUB-2[27], *Boyd's*[32] and *Engler's*[33] unanimously indicated that the classical explanation involving repulsion between the methyl groups is more important than the *gauche*-hydrogen interaction. This indicates that the H—H interactions in MMI are too hard.

### 3.2. Very Short C—H···H—C Contacts

All the existing force fields treat hydrogen atoms as being somewhat too rigid at very short H/H contacts (distance < 190 pm) between nonbonded C—H groups[34,35]. The lowest value (168 pm) found in a tetracyclododecane derivative **2**[36] has not quite been obtained by MM-calculations. Recently, applying the consistent force field in a number of related compounds, *e.g.* **3**, *Ermer* has shown that skew twisting of the molecule can occur and that the shift to short wavelength of the C—H vibrational frequencies are correctly reproduced[37].



**2** **3** ($C_2$)



**4** **5** **6**

Table 2. C—H···H—C contacts (distances *d* and interaction energies $E_E$), enthalpies of formation ($\Delta H_f$), and strain energies (*SE*) in the asterane-series calculated using the Engler force field[11].

| Asterane | *d* [Å] | $E_E$ [kcal/mol] | $\Delta H_f^\circ$ [kcal/mol] | *SE* [kcal/mol] |
|---|---|---|---|---|
| Diasterane | 1.978 | 2.48 | 64.52 | 93.68 |
| Triasterane **4** | 3.169 | −0.04 | 94.05 | 122.40 |
| Tetraasterane | 2.441 (2.40) [a] | 0.28 | 20.35 | 58.15 |
| Pentaasterane | 2.070 | 1.68 | −0.71 | 46.54 |
| Hexaasterane **5** | 1.903 | 3.37 | 58.70 | 115.40 |
| Heptaasterane **6** | 1.835 | 4.43 | 165.52 | 231.67 |
| Octaasterane | 1.829 | 4.54 | 291.48 | 367.08 |
| Nonaasterane | 1.86 | 4.06 | 423.13 | 508.18 |
| Decaasterane | 1.96 | −0.03 | 550.23 | 644.73 |

[a] X-ray structure analysis: J. Chesick, J. D. Dunitz, U. von Gizycki, H. Musso, *Chem. Ber. 106* (1973) 150.

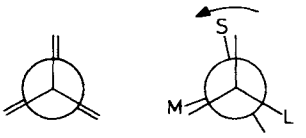
This problem also appears in the asterane series (Table 2). For hexaasterane **5** *Engler's* force field still furnishes linear C—H···H—C contacts of distance 190 pm and completely planar six-membered rings. However, in heptaasterane **6** the C—H···H—C repulsion (distance = 183 pm) causes twisting of the cyclohexane boat conformations and puckering of the seven-membered rings. It still remains an experimental challenge to present evidence which indicates above which ring-size asteranes in fact become distorted.

### 3.3. Internal Rotations

Most structures have been reproduced by MM-calculations very well[38], but this occurs only for the conformation at the energy minimum. An important question is how accurately transition states and energy barriers $E_{rot}$ for the rotation of mobile parts of the molecule can be calculated by these methods. *Allinger's* force field MM2[22] includes torsional contributions by means of a cosine function of the type $K_t/2\cdot(1\pm\cos(n\omega))$ not only for the usual third power ($n=3$) but also for the square and linear terms ($n=1, 2$); hence it looks favored for dealing with this type of problem. Rotational barriers calculated by MM2 are smaller than the observed values, and the discrepancy increases with the steric hindrance around the rotating bond (cf. also Table 3)[39,40]. The biggest problem is the uncertainty in the experimental barriers of *n*-butane, for which no reliable results have been reported from *ab initio* calculations[41].

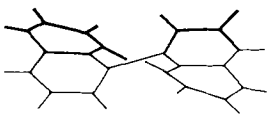
The simplest way of improving the situation using MM2 would be to increase the third-order torsional force constant for the C—C—C—C system so as to reproduce the observed high barriers in congested molecules, since the difference between the observed and calculated barriers (Table 3) seems to be proportional to the number of eclipsing C—C—C—C units. However, *Allinger et al.* express some reservation towards such a straightforward remedy[41]. We continue to warn the users of the MM2 force field to keep in mind that the calculated barriers of open chain systems may be underestimated[42].

In the course of MM studies of internal rotation, firstly by *Mislow et al.*[43], it was noticed that a transition state in which all three bonds are simultaneously eclipsed, as shown in the Newman projection **7**, never occurs but that the smallest substituent S passes the threshold first, while larger substituents follow as in **8**. The conformers having nonalternating Newman projections are generally difficult to identify experimentally, but can be detected by simulation of the internal rotation process using the MM technique[40]. Highly congested ethane derivatives, like tetra-*tert*-butylethane **9**, exist in such a nonalternating conformation, even at the energy minimum[14,43,44].




**7** ($E_3$) **8** ($F_2BF_2$)

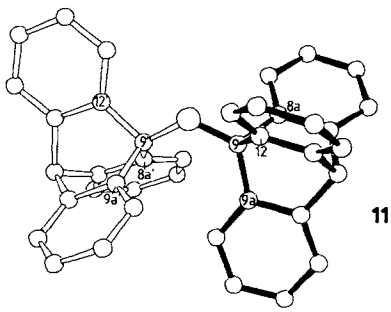
$[(CH_3)_3C]_2CH-CH[C(CH_3)_3]_2$ **9**



**10**

The racemization of the 1,1'-binaphthyl **10** provides another example illustrating that MM-calculations have indicated an initially unexpected reaction course. The experimental barrier of about 22 kcal/mol is reproduced correctly only if the axis of chirality is broken and both H···H interactions are treated consecutively in the calculation. With a rigid axis and simultaneous flipping, *Allinger's* force field[31] yields 35 kcal/mol[45].

The dynamic "gear effect" makes very low barriers of rotations possible even for molecules with bulky substituents: for ditriptycylmethane **11** a rotational barrier of only 1.0 kcal/mol is calculated[46a]; of course, the barrier in the tetramethyl derivative is much higher: a vulue of 14.2 kcal/mol has been found experimentally, whereas the calculated value is 16.5 kcal/mol[46b].



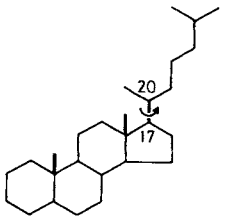

**11**

There was some controversy over restricted rotation around $C_{17}$—$C_{20}$ bond of the steroid systems, *e.g.* cholestane **12**. The failure to freeze this rotation in a *tert*-butyl derivative **13** appeared to suggest a low barrier for **12** also. However, the corrected MM-barrier of **12** is 12 kcal/mol, which can be frozen at low temperatures. The unexpectedly high barrier calculated for **12** relative to that for **13** (8.5 kcal/mol) is the result of a secondary effect arising from β-branching in **12**[40].

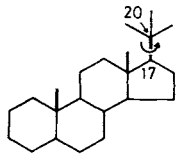
Table 3. Observed and calculated rotation barriers $E_{rot}$ for the central C—C bond of hydrocarbons.

| Compound | | $E_{rot}$ [kcal/mol] exp. [a] | calc. [b] |
|---|---|---|---|
| *n*-Butane | *anti-gauche* | 3.4, 3.6 [c] | 3.35 [c], 3.56 [d] |
| | *anti-anti* | 5.9–6.1 [c] | 4.76, 5.99 [d], |
| 2,3-Dimethylbutane | *anti-gauche* | 4.3 | 6.13 [e] |
| 2,2,3-Trimethylbutane | | 6.9, 7.0 | 3.1 |
| 2,2,3,3-Tetramethylbutane | | 9.6–10.0 | 4.1 |
| 2,2,4,4,5,5,7,7-Octamethyloctane | | 13.8 | 5.3 |
| | | | 7.8 |

[a] See [40], unless otherwise stated. [b] Using the MM2 force field. Taken from [40], unless otherwise stated. [c] From [41]. [d] *ab initio* STO-3G calculation using MM2-optimized geometry [41]. [e] *ab initio* 4-31G calculations using optimized geometry obtained from application of a gradient method in each SCF cycle; C. Taime, E. Osawa, submitted for publication.



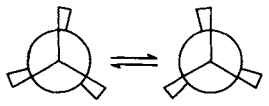

**12**, $\Delta H^{\ddagger}_{calc.}$ = 12 kcal/mol



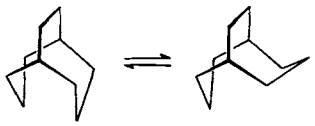

**13**, $\Delta H^{\ddagger}_{calc.}$ = 8.5 kcal/mol

### 3.4. Dynamics in "Rigid Systems"

The well-known twist motion in bicycles, such as bicyclo[2.2.2]octane **14**, was established experimentally after it had first been predicted from MM calculations[47]. At least two equivalent bonds have to be rotated simultaneously in such rigid polycycles. Energy potential profiles have been calculated for bicyclo[3.3.1]nonane **15** and tricyclo[6.4.0.0$^{4,9}$]dodecane **16**. As seen in Figure 2, the curves of **15** and **16** are not as smooth around the minimum as that of **14**. In spite of the 3-H···7-H repulsion in **15**, the



**14**



**17**

3-H···9-H interaction favors the double-chair conformation without twisting. In **16** there are two such interactions, 2-H···6-H and 3-H···11-H, and the molecule is twisted by 5—7° to avoid this strain, as confirmed by X-ray structural analysis of a derivative[48]. Similarly MM-calculations indicate that in bicyclo[3.3.2]decane **17** the chair-boat conformation predominates[49].

By simple modification of the MM2 program we can simultaneously rotate as many bonds as we please[49–51]. Using this technique we have examined conformational mobility in polycyclic molecules having ethano bridges, *e.g.* tricyclo[4.2.2.2$^{2,5}$]dodecane **18**, tetracyclo[6.2.1.1$^{3,6}$.0$^{2,7}$]dodecane **3**, and perhydrotriquinacene **19**. All of these compounds possess twisted conformations in the ground state[52], but the energy barriers calculated for interconversions between the twist forms are so low that there is no possibility of detecting the process by dynamic NMR. This prediction has been confirmed experimentally for **18**[53] and **19**[54].

**18** ($D_{2h}$)





**19** ($C_3$)

*Ermer's* calculation predicts that all C—H bonds of dodecahedrane are fully exclipsed in the ground state energy minimum[55], and exactly this was recently found by X-ray structural analysis of the dimethyl derivative[56].

## 4. Search for the Most Stable Isomers

The success achieved in adamantane chemistry[57] prompted us to seek the most stable isomer of other $C_nH_m$ polycycles. For all tri-, tetra- and pentacycles with $C_8$ to $C_{14}$ frameworks we now know all the most stable isomers, the "stabilomers" of each family[58]. The strategy is illustrated below for pentacycloundecane. Firstly all the 15358 isomeric pentacycloundecanes are produced by the structure generating programs JAL-30XA and CISGEN; all structures having quaternary C-atoms are then eliminated, because these must be highly strained. Visual inspection of about 500 structures left on the TV screen reveals only one

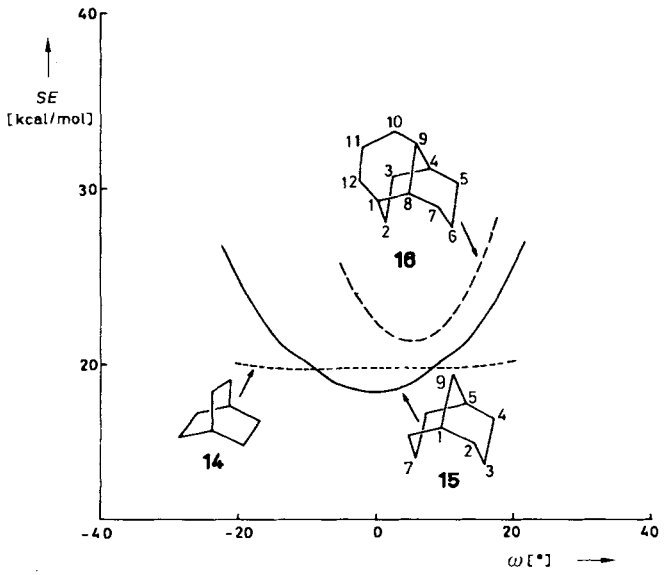



Fig. 2. Strain energies (*SE*) of bicyclo[2.2.2]octane **14**, bicyclo[3.2.1]nonane **15** and tricyclo[6.4.0.0$^{4,9}$]dodecane **16** [49] as a function of torsion angle $\omega$.

Table 4. Enthalpies of formation ($\Delta H_f^0$) and strain energies (*SE*) of optimized structures of some low-energy pentacycloundecanes, calculated using the Engler force field.

| | $\Delta H_f^0$ [kcal/mol] | *SE* [kcal/mol] |
|---|---|---|
| **20** | 9.38 | 42.05 |
| | 18.82 | 51.49 |
| | 19.62 | 52.29 |
| | 23.88 | 56.55 |
| | 32.46 | 65.13 |
| | 30.80 | 63.47 |

structure **20**, that has neither three- nor four-membered rings. To be on the safe side, calculations using MM-methods were performed on five isomers with one cyclobutane unit. Table 4 shows $D_3$-trishomocubane **20** to be far and away the most stable. Thermodynamic isomerization of appropriate precursors with $AlBr_3$ gives a single product (86% yield, Fig. 3)[59], whose structure was later confirmed by X-ray diffraction[60]. Since the number of possible isomers increases exponentially with the size of the molecules,

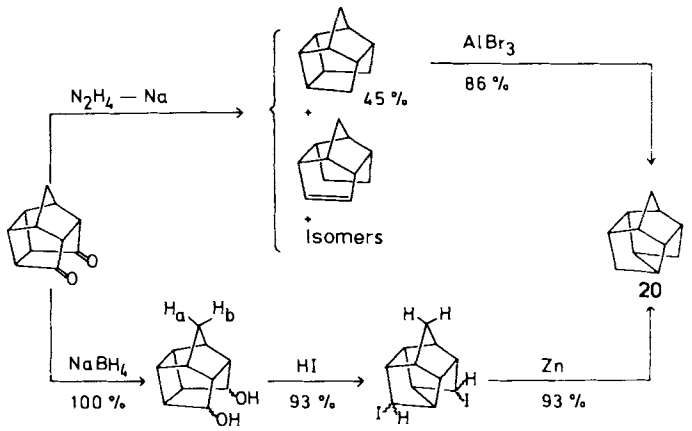



Fig. 3. Synthetic routes to $D_3$-trishomocubane **20**.

such an approach becomes more difficult with increasing number of C-atoms. Furthermore, a number of local minima having almost the same energy may exist on the energy hypersurface of the products[58]. For example, the thermodynamic rearrangement of the heptacyclic $C_{16}$-hydrocarbon **21** yields two novel cage compounds **22** and **23**, but calculations indicate that both should be less stable than bisnortriamantane **24**[24] (Fig. 4).

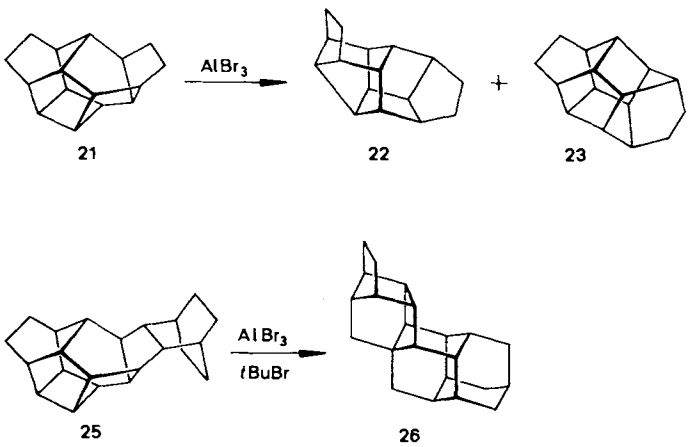
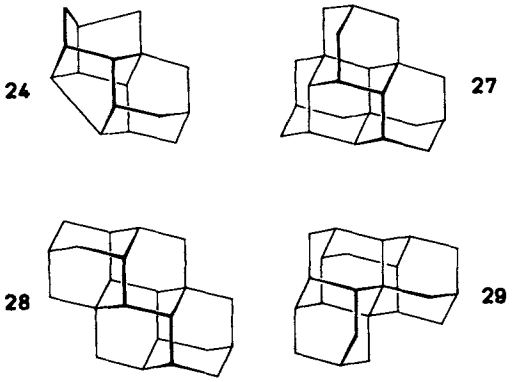



Fig. 4. Examples of rearrangements which do not lead to the most stable isomer under conditions of thermodynamic control.

Another notable example of such local minima is the isolation of bastardane **26** in the rearrangement of the nonacyclic $C_{22}$-precursor **25**, instead of the expected tetramantanes **27**—**29**[24,61,62].




## 5. Reactivity Problems

In order to gain insight into chemical reactions from calculations it is necessary to probe the multidimensional potential surface near the transition state region as precisely as possible for troughs, corresponding to stable products, and defiles in which the molecule can be transformed from a labile state into a stable product[63]. In this respect, MM techniques are perfectly suited if the energy is calculated point by point for fixed geometrical parameters.

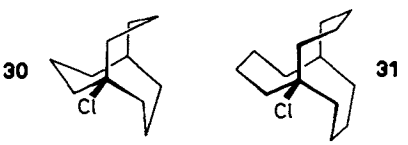
### 5.1. Solvolysis

With the strong preference of carbenium ions to adopt a planar configuration of the ligands attached to the C atom it is possible to estimate the difference in strain ($\Delta_{st}$) between the strain energy (SE) of the cation and that of the hydrocarbon (HC) [eq. (b)].

$$\Delta_{st} = SE_{cation} - SE_{HC} \quad \text{(b)}$$

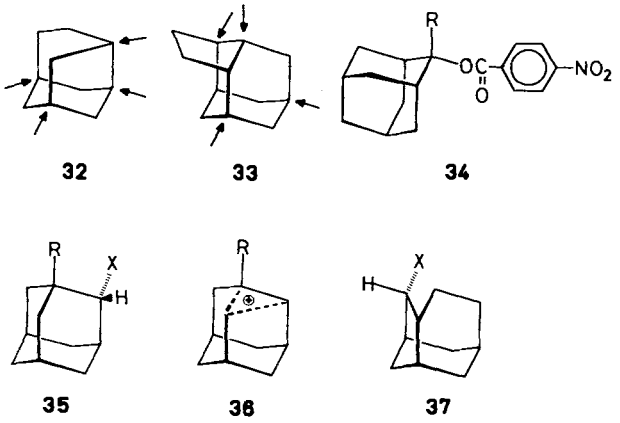
$$\log k = \alpha \cdot \Delta_{st} + b \quad \text{(c)}$$

The logarithm of the rate constant $k$ is proportional to $\Delta_{st}$ [eq. (c)], and rates varying over a range of more than $10^{18}$ have been found to conform to equations of type (b) and (c)[64]. The 1-manxyl cation is calculated to have a negative $\Delta_{st}$ value due to the presence of three medium-sized rings in the molecule. In the next higher homolog the $\Delta_{st}$ value should be more negative. 1-Chloromanxane **30** indeed solvolyzes $10^4$ times faster than t-butyl chloride, and the unknown homolog **31** is predicted to be $10^9$ times more reactive ($\Delta_{st} = -21$ kcal/mol)[65].




This method also proved to be capable of explaining the different reactivity in carbenium ion reactions at the bridgehead positions marked with an arrow in protoadamantane **32**[66] or ethanoadamantane **33**[67]. This theory explains the increase in solvolysis rates of adamantane derivatives **34**[68,69] and **35**[70,71] with variation of R(H, $CH_3$, $C_2H_5$, $i$-$C_3H_7$, $t$-$C_4H_9$) neither in terms of anchimeric nor solvation assistance, but predominantly by steric effects[71];

nonclassical ions, such as **36** are not involved[70]. *Smith* and *Harris*[72] have shown the Engler II force field to be useful for explaining the solvolytic behavior of protoadamantane derivatives **37**.




**32** **33** **34**

**35** **36** **37**

Table 5. Parameters used in the force fields for carbenium ions [a].

| | | *Schleyer/ Gleicher* [b] | *Engler*-I [c] | *Engler*-II [d] |
|---|---|---|---|---|
| *Stretching vibration* | | | | |
| C⊕—H | $r_0$ [Å] | — | 1.084 | 1.084 |
| | $k$ [mdyn/Å] | — | 7.40 | 7.40 |
| C⊕—C | $r_0$ [Å] | 1.480 | 1.480 | 1.480 |
| | $k$ [mdyn/Å] | 7.17 | 7.40 | 7.40 |
| *Angle deformation* | | | | |
| C—C⊕—H | $\theta_0$ [°] | — | 120 | 120 |
| | $k$ [mdyn/Å] | — | 2.00 | 2.28 |
| C—C⊕—C | $\theta_0$ [°] | 120 | 120 | 120 |
| | $k$ [mdyn/Å] | 2.30 | 2.40 | 2.28 |
| C⊕—C—H | $\theta_0$ [°] | 108.7 | 109.2 | 109.5 |
| | $k$ [mdyn/Å] | 0.396 | 0.40 | 0.57 |
| C⊕—C—C | $\theta_0$ [°] | 109.5 | 110.0 | 109.5 |
| | $k$ [mdyn/Å] | 0.565 | 0.57 | 0.57 |
| *Torsion* $V_3$ | | | | |
| C⊕—C—C—H | | — | 0.70 | 0.70 |
| C⊕—C—C—C | | — | 0.45 | 0.70 |
| C—C⊕—C—H | | — | 0.0 | 0.70 |
| C—C⊕—C—C | | — | 0.0 | 0.70 |
| C—C—C⊕—H | | — | 0.0 | 0.70 |
| H—C—C⊕—H | | — | 0.0 | 0.70 |
| *Nonbonding interaction* | | | | |
| H···C⊕ | $d$ [Å] | | 3.35 | 3.35 |
| | $10^{-4}\,\varepsilon$ [°] | | 3.0 | 3.0 |
| | $\alpha$ [°] [e] | | 12.0 | 12.0 |
| C···C⊕ | $d$ [Å] | | 3.85 | 3.85 |
| | $10^{-4}\,\varepsilon$ [°] | | 9.5 | 9.5 |
| | $\alpha$ [°] [e] | | 12.0 | 12.0 |
| C⊕ *flattening* | | | 5.5 | 80.0 |

[a] J. B. Collins, P. von R. Schleyer, unpublished results. We thank the authors for supplying us with their results. Symbols: $r$ = equilibrium distance; $k$ = force constant; $\theta$ = equilibrium bond angle; $V_3$ = torsion constant in the equation $E^{\circ}_{(\phi)} = 0.5\ V_3\ (1 + \cos 3\phi)$ [$10^{-11}$ erg]; $d$ = distance between nonbonding atoms; $\varepsilon$ = well depth; $\alpha$ = steepness parameter [$10^{-11}$ erg] in the modified Buckingham equation [11]. [b] G. J. Gleicher, P. von R. Schleyer, *J. Am. Chem. Soc. 89* (1967) 582. [c] Used in [65, 69]. [d] Used in program BIGSTRN [10b]. [e] The same as the hydrocarbons.

### 5.2. Mechanism of Multistep Carbenium Ion Rearrangements

The Engler I cation force field (Table 5) has been used to elucidate the reaction path along which adamantane is formed from perhydrodicyclopentadiene **38**. The strategy is to calculate the enthalpies of formation of all the carbenium ions resulting from every 1,2-alkyl shift of an intermediate and then to look for the reaction path of lowest energy leading from intermediate **38** to **39** (Fig. 5).

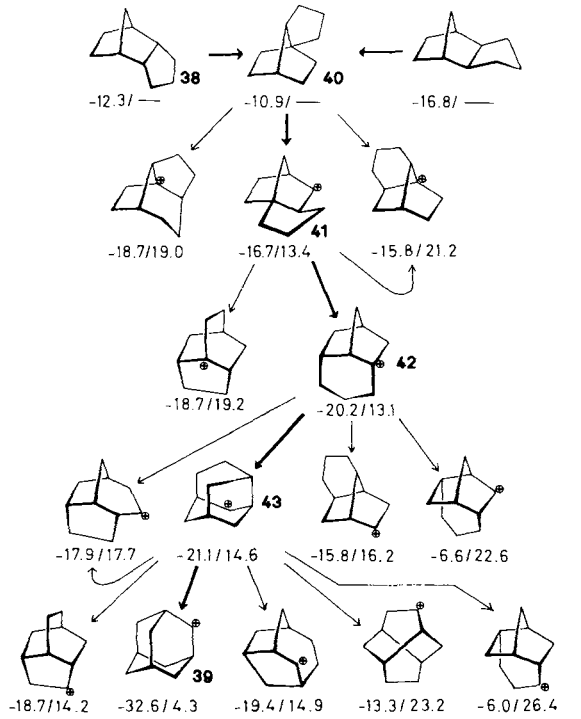
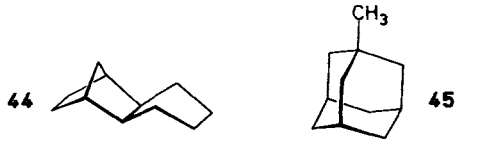



Fig. 5. The most probable pathway for the rearrangement of *endo*-perhydrodicyclopentadiene **38** to adamantane. Enthalpies of formation and activation energies [kcal/mol], calculated using the Engler force field (Table 5), are given below the structural formulas.

The first shift of an alkyl substituent **38** → **40** must be rate determining since it has never been possible to detect any intermediates. Starting from **41**, however, first **42** and then **43** have been established as intermediates[73,74].

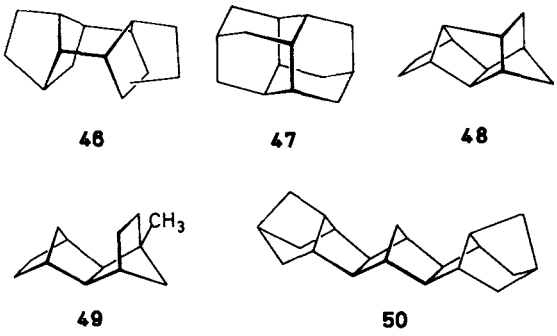
The same result is found when instead of the stability of the cations that of the neutral hydrocarbons is compared. In this way, calculations have been carried out on all 69 tricycloundecanes and from the order of enthalpies of formation it has been shown that the rearrangement of the tricycloundecane **44** to form methyladamantane **45** proceeds on an energy surface with several shallow minima around the deep energy hole of the product **45**; several pathways seem to be possible. About two dozen intermediates could be detected. The most reasonable route involves eight intermediates, six of which have in fact been isolated[75].




**44** **45**

This method has also proved useful for determining the stabilomers of tetracycloundecanes[76], -dodecanes[67,77], -tri- and -tetradecanes[78], as well as of pentacyclotetradecanes[79]. Only five 1,2-alkyl shifts are needed in the rearrangement of tetrahydrobinor S **46** into diamantane **47**:

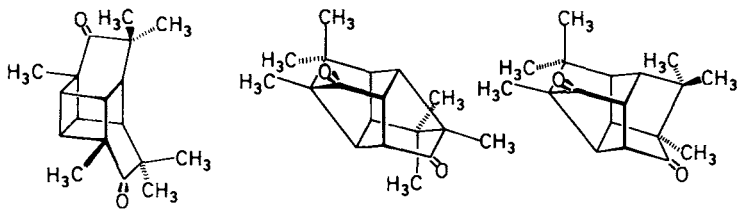
Correspondingly, the yield (80%) is very high[80,81]. Recently, a general program for describing such isomerizations was presented which confirmed the most favorable path from **46** to **47**[82], and proved to be useful in such complicated systems as **21**→**22**+**23**[24] and heptacyclooctadecane→triamantane[83].



**46** **47** **48** **49** **50**

There are polycyclic hydrocarbons, however, built up from norbornane units like **48**[67,77], **49**[78], and **50**[84], which only undergo degenerate interconversions, and from which no single interesting product could be isolated. MM calculations indicate that in these molecules the routes leading to the stabilomers are blocked by exceedingly strained intermediates.

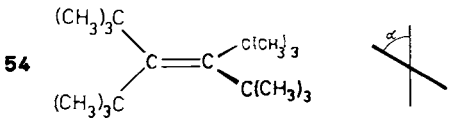
The acid catalyzed isomerization of the polycyclic ketone **51** to give **52**[85] provides another example where MM calculations give a plausible explanation why the energetically favored isomer **53** is not formed, and that no favorable pathway for the establisment of an equilibrium exists between **52** and **53**[86].



**51** **52** **53**

### 5.3. Bredt's Rule

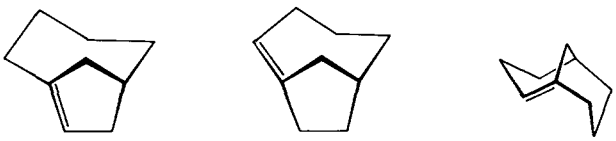
In recent years considerable effort has been invested in the synthesis of "anti-Bredt olefins"—bicyclic bridgehead olefins which contradict Bredt's rule; attempts have also been made to prepare distorted olefins, such as tetra *t*-butyl ethylene **54** in which, due to steric hindrance, a planar arrangement of all the substituents is not possible. Several



**54**

revisions of Bredt's rule have been proposed but none of them have survived. The failure of previous theories can be attributed to their inability to separate the strain of the double bond from the residual strain associated with the carbon skeleton.

*Burkert* pointed out in 1977 that a bridgehead olefin with the double bond in the smaller ring can be more stable than the isomer with the double bond in the larger ring *e.g.* **55** is more stable than **56**[87]. Experimental enthalpies of hydrogenation measured recently by *Roth* and *Lennartz*[88] come very close to the calculated values as shown in Table 6 for **55**, **56** and **57**.



**55** **56** **57**

Table 6. Experimental and calculated heats of hydrogenation of the bicyclo [4.2.1]nonenes **55** and **56**, as well as of bicyclo [3.3.1]non-1(2)-ene **57**.

| | Heat of hydrogenation [kcal/mol] | | |
|---|---|---|---|
| | **55** | **56** | **57** |
| exp. [88] | 36.3 | 42.0 | 37.9 |
| calc. [87, 89] | 39.0 | 54.1 | 47.3 |
| calc. [90] | 35.2 | 40.2 | 39.1 |

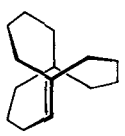
*Ermer*[89] has estimated the energy of deformation for double bonds ($V_{oop}$) in many nonplanar compounds. He came to the conclusion that $V_{oop} < 15$ kcal/mol represents the limit for the criterion "stable at room temperature". *Schleyer et al.*[90a] defined olefinic strain (*OS*) as the difference between the total strain energy of the bridgehead olefin *SE*(olefin) and that of the saturated hydrocarbon *SE*(HC), each being in its most stable conformation [eq. (d)].

$$OS = SE(\text{olefin}) - SE(\text{HC}) \qquad \text{(d)}$$

The *OS* values have been calculated with the Allinger MMI-force field[10e,12] for approximately 80 compounds. Comparison with the chemical stability leads to the following rule:

> Compounds with $OS \leqslant 17$ kcal/mol can be isolated, those with $OS = 17-21$ kcal/mol can be detected, possibly at very low temperatures, and those with $OS \geqslant 21$ kcal/mol are unstable and not directly detectable.

In this respect the extremely unstable (*E*)-bicyclo[3.3.1]non-1-ene[90b] ($OS = 44.2$ kcal/mol) should be mentioned; the (*Z*)-isomer **57** (concerning the cyclohexane ring) has been isolated. These rules have had no exception to date. Bicyclo[4.4.4]tetradec-1-ene **58** even has a negative



**58**

*OS* value (−14 kcal/mol), and should, therefore, be a particularly stable anti-Bredt olefin[90a]. The first member of this type of hyperstable bridgehead olefin, bicyclo[4.4.2]dodec-1-ene, was recently synthesized by *de Meijere et al.*[101a].

What we can do to make unstable bridgehead olefins isolable? *Ermer*[89] suggests first using bulky substituents in

close proximity to the strained double bond, an old trick, but his second proposal is quite interesting and new: installation of a second bridge in order to relieve the strain at the double bond ($V_{oop}$ or *OS*) and hence to increase the strain in the remaining molecular framework.

Calculations have been made on twisted olefins of type **54** by *Ermer* and *Lifson*[91]. In spite of numerous attempts, **54** has still not been detected; according to calculations this has an twist angle $\alpha$ of 82°[91]. With a modified twist potential ($V_{oop}$=23 kcal/mol) an angle of 43° is obtained[9]; *Lenoir et al.*[92] and *Simonetta et al.*[93] predict this angle to be 45°. It is time to solve this descrepancy experimentally.

### 5.4. Hydrogenolysis of Strained Hydrocarbons

Normal C—C bonds do not undergo catalytic hydrogenation on Pd, Pt or Ni catalysts at atmospheric pressure and room temperature. Principally, cyclopropane but also cyclobutane derivatives can be opened hydrogenolytically relatively easily because of the high angle strain. In particular, when small rings are incorporated into a strained cage structure they are rapidly hydrogenated under mild conditions. Although there are often several possibilities for which bond is opened first, there are cases in which specifically one product is formed, *e.g.* in the hydrogenation of cubane **59**[94], basketane **60**[95,96], snoutane **61**[96,97], deltacyclane **62**[96-98] (Fig. 6) or barettane **64**[101b].




However, there are other examples, such as triasterane **4**[99] and homocubane **63**[100] (Fig. 6), as well as diademane **65**[101c] and others[101d] in which several of the possible products are formed. Whether only one or several products are formed depends on the following factors: In the small ring compound the longest and most strained bond is

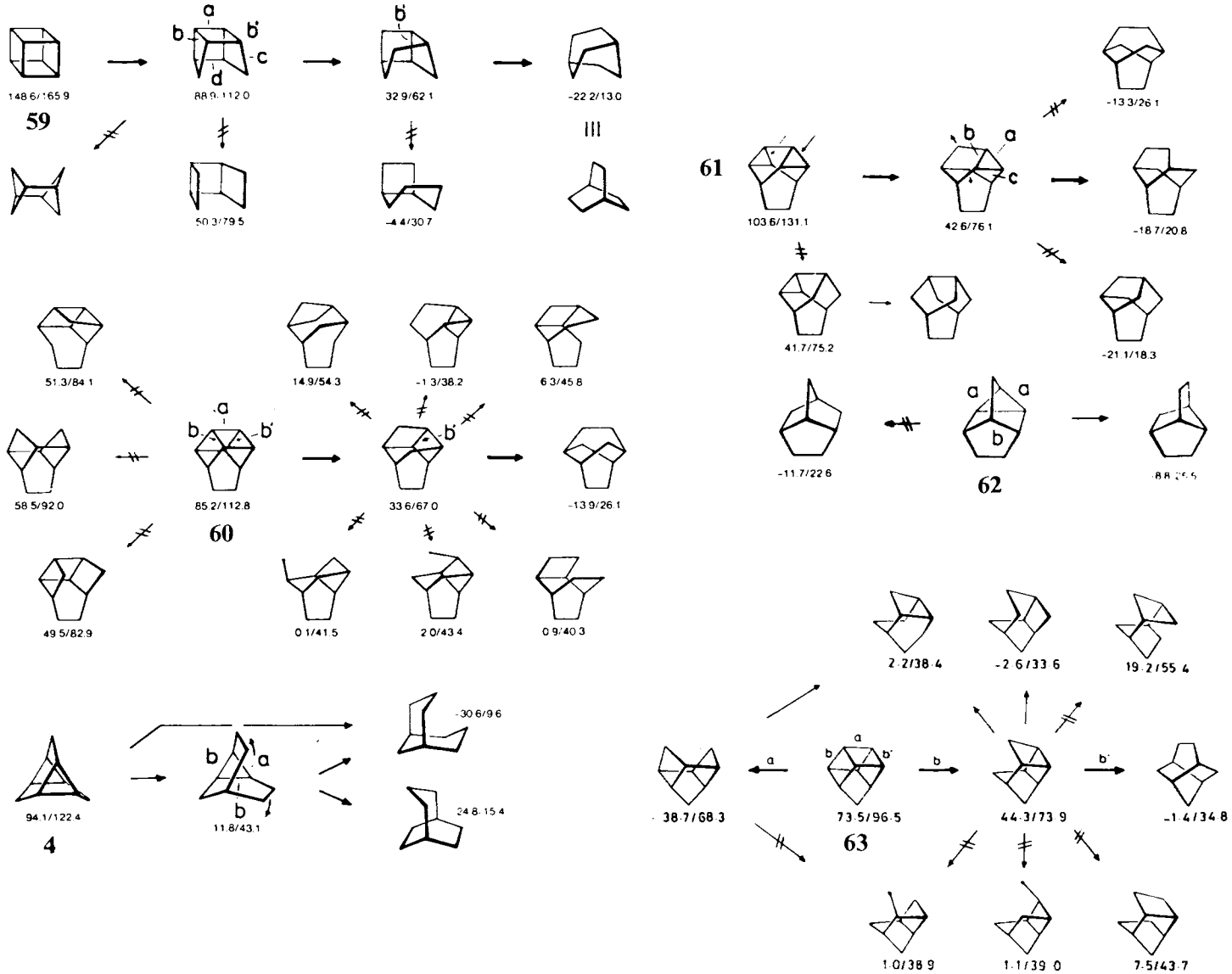



Fig. 6. Catalytic hydrogenation of strained cage hydrocarbons: cubane **59**, basketane **60**, snoutane **61**, deltacyclane **62**, triasterane **4**, and homocubane **63**. The enthalpies of formation and strain energies [kcal/mol] given below the compounds were calculated using the Engler force field [11].

opened first. On the other hand cleavage of the bond which gives most relief of strain during hydrogenolysis should be preferred. If both factors coincide, the reaction gives a specific product. If however, the bonds in the small ring differ by too little or the energy differences of two routes differ by less than 10 kcal/mol, two or more products may be formed. MM calculations are particularly suitable for explaining these correlations: not only the difference in total strain energies between the educt and all the products is given with high accuracy but also the bond lengths and angles (with the separate energy contributions for each bond). In the hydrogenation of the dihydrosnoutane ester **66** (Fig. 7), only bond *a* is opened. That the calculation correctly reproduces the bond length order has been confirmed by X-ray structural analysis[97].

**66**

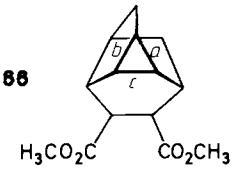



Fig. 7. Bond lengths Å in dimethyl dihydrosnoutanedicarboxylate; calc. $a = 1.538$, $b = 1.515$, $c = 1.530$; found $a = 1.516$, $b = 1.505$, $c = 1.507$.

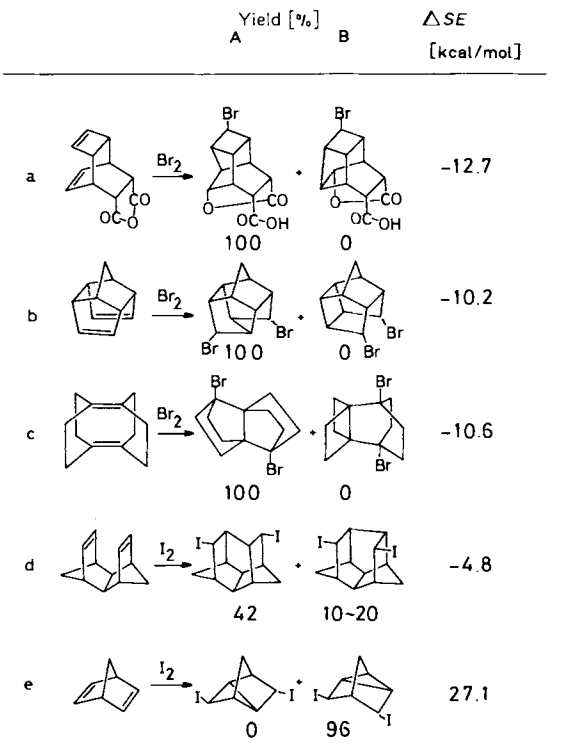



Fig. 8. Formation of C—C bridges in the electrophilic addition of halogens to compounds having double bonds facing each other; the difference in strain energy determines whether the "crossed" or "parallel" product is formed. Calculated using the Engler force field for (a), (b), (d), and (e) [102], as well as using the MM2 force field for (c) [103].

### 5.5. Late Transition States

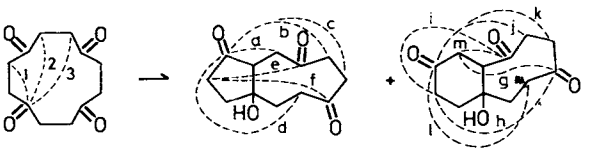
Although hydrogenations are not reversible and the products are not in equilibrium on the catalyst, the products are often formed according to their thermodynamic stabilities. The transition states resemble the product, and hence occur "late" on the reaction coordinate. The same principle is valid for electrophilic additions to parallel double bonds.

In reactions a—c and e, respectively, (Fig. 8) the "cross" (A) or "parallel" products (B) are formed exclusively, since the observed products are calculated to be stable by more than 10 kcal/mol than the others. Except for example d, where the difference in strain $\Delta SE = SE(A) - SE(B)$ is only −4.8 kcal/mol, both products can be detected[104, 105].

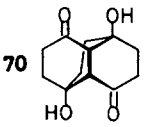
### 5.6. Product Distribution

One of the best applications of the MM method is undoubtedly the calculation of the composition of equilibrium mixtures. Even for closely related structures the relative energies and amount of products should be calculable with high degree of confidence, *e.g.* the adamantoid structures in Table 7[106–108].

Of the many recent examples[7, 8] only one is presented here in detail. The acid-catalyzed cyclization of cyclododecatetraone **67** proceeds *via* the bicyclo compound **69** to give the dioldione **70** as the sole product[48]. A completely different product was initially expected, at least in low yield. In view of numerous possibilities for intramolecular aldol-type condensations, shown in formulas **68** and **69** by dotted lines, MM calculation of enthalpies of formation of all the possible tricyclic products clearly demonstrate that **70** is stable by more than 16 kcal/mol than the other isomers. This energy difference explains why only **70** was isolated as the main product.




**67** **68** **69**




**70**

## 6. Electronic Effects and Long Bonds

When C—C bonds are stretched by bulky groups, *e.g.* in highly substituted ethane derivatives, these bonds are always reproduced well by MM calculations[14]; one of the most recent examples is the central C—C bond in pentaphenylethane which has been calculated to lie in the range 1.58—1.60 Å compared to the observed value of 1.61 Å[118].

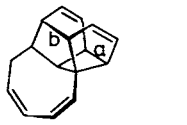
MM methods were unable to reproduce the long bonds correctly in compounds like **71**—**74** (Table 8); some other electronic effect must, therefore, be operating. *Mislow et al.* suggested the "through-bond" coupling of π-orbitals to explain this disagreement, *e.g.* in lepidopterene **74** X-ray

Table 7. Calculated and experimental equilibrium parameters for the isomerization of some adamantanoid systems [a].

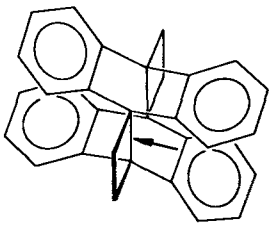
| Isomerization | | $G$ (298) [kcal/mol] | $H$ [b] [kcal/mol] | $S$ [cal/mol·K] | Ref. |
|---|---|---|---|---|---|
| 2-Methyl- ⇌ 1-Methyladamantane | exp. | −2.47 ± 0.19 | −2.6 ± 0.11 | −3.0 ± 0.3 | [106] |
| | calc. | −2.52 | −1.9 | −2.1 | |
| 1-Methyl- ⇌ 4-Methyldiamantane | exp. | −1.88 [c] | −2.14 ± 0.2 | −1.19 ± 0.3 | [107] |
| | calc. | −2.12 [c] | −2.2 | −2.18 | |
| 1,1′-Bi- ⇌ 2,2′-Biadamantane | exp. | −0.51 ± 0.21 | −0.33 ± 0.12 | 5.4 ± 0.3 | [108] |
| | calc. | −0.48 | −0.34 | 5.3 | |

[a] Using the Engler force field [10b, 11]. [b] Corrected for the differences in substitution type. [c] 433 K.

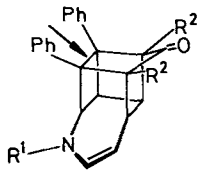
structural analysis gives a value of 1.64 Å, whereas calculation yields 1.57 Å. The bond in question is surrounded by four parallel π-orbitals[110]. Recently it was found, that such elongation of a σ-bond is most effective if this bond is mechanically strained by the molecular framework as in **71**, **72** and **73**[111].



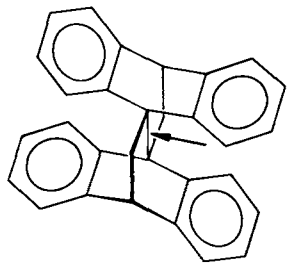

**71**



**72**




**73**, $R^1 = CO_2C_2H_5$, $R^2 = CO_2CH_3$



**74**

Table 8. Long bonds (indicated by an arrow or a/b in the formulas) in cyclobutanes arising from "through-bond" interaction with vicinal π-systems.

| Comp. | | C—C Bond lengths [Å] Exp. [a] | Calc. | Ref. |
|---|---|---|---|---|
| **71** | a | 1.617 ± 0.003 | 1.551 [b] | [109] |
| | b [c] | 1.578 ± 0.003 | 1.547 [b] | |
| **72** | | 1.77 ± 0.01 | 1.574 [b] | [110] |
| **73** | | 1.657 ± 0.005 [d] | 1.565 [e] | [111] |
| | | | 1.643 [f] | |

[a] From X-ray structure analysis. [b] MM2. [c] This is not the cyclobutane bond, but is rather a bond given for purposes of comparison in order to indicate the lengthening of a non-strained bond by π-coupling. [d] $R^1 = COOC_2H_5$, $R^2 = COOCH_3$. [e] MMPI, $R^1 = C_{sp^2}$—H, $R^2 = COOCH_3$. [f] MNDO, $R^1 = CHO$, $R^2 = H$.

## 7. Prospects

The increasingly ready access to fast computers will stimulate the application of all theoretical methods. The superiority of MM methods will still persist for medium to large molecules: In the meantime convincing evidence on larger molecules has accumulated, where the high precision of MM calculations has been confirmed by X-ray structural analysis. In order to optimize computer time there is a need for a data base of accurate structural information for the gas phase. Since most of these data have been obtained from X-ray diffraction results on crystals[112], it is now time to establish a basis set independent of crystal lattice and packing effects[113].

Force fields for hydrocarbons are very accurate indeed, but developments in the future will still be directed to continuously improving these. Much more important is the introduction of parameters for heteroatoms like oxygen[114], nitrogen, silicon[115], halogens[116], and sulfur, as well as force fields for functional groups[7] like ethers, carbonyl and azo groups[117]. In consequence, the programs as well as the computer times will become larger. In future we shall have to put effort into simplifying the problems to be handled by MM-methods to analogs of the simplest hydrocarbon structures possible.

*Professor Paul von R. Schleyer has contributed with many helpful discussions. We would like to thank the Alexander von Humboldt-Foundation (Bonn) and Kureha Chemical Industries AG for financial support of our own research in this field described here. Computer time has been provided by the Rechenzentrum der Universität Karlsruhe, and by both the Hokkaido University and the Institute for Molecular Sciences.*

Received: April 6, 1982 [A 434 IE]
German version: *Angew. Chem. 95* (1983) 1

[1] Application of Potential Energy Calculations to Organic Chemistry, Part 15 from Hokkaido. - Part 14: E. Osawa, *J. Comput. Chem., 3* (1982) 400; Part 13: [8].

[2] J. G. Nourse, R. E. Carhart, D. H. Smith, C. Djerassi, *J. Am. Chem. Soc. 101* (1979) 1216; T. H. Varkony, D. H. Smith, C. Djerassi, *Tetrahedron 34* (1978) 841.

[3] W. T. Wipke, W. J. Howe: *Computer Assisted Organic Synthesis, ACS Symp. Ser. No. 61*, Washington D.C. 1977. H. Bruns, *Naturwissenschaften 66* (1979) 197; M. Bersohn, A. Esack, *Chem. Rev. 76* (1979) 269; E. J. Corey, A. P. Johnson, A. K. Lang, *J. Org. Chem. 45* (1980) 2051; E. J. Corey, N. F. Feiner, *ibid. 45* (1980) 757, 765; T. D. Salatin, W. L. Jorgensen, *ibid. 45* (1980) 2043; K. K. Agarwal, D. L. Larsen, H. L. Gelernter, *Comput. Chem. 2* (1978) 75; P. E. Blower, Jr., H. W. Whitlock, Jr., *J. Am. Chem. Soc. 98* (1976) 1499.

[4] E. C. Olson, R. E. Christoffersen: *Computer-Assisted Drug Design, ACS Symp. Ser. No. 12, American Chemical Society, Washington D. C. 1979.*

[5] T. A. Halgren, D. A. Kleier, J. H. Hall, Jr., L. D. Brown, W. N. Lipscomb, *J. Am. Chem. Soc. 100* (1978) 6595; M. J. S. Dewar, G. P. Ford, *ibid. 101* (1979) 5558; K. Jug, *Theor. Chim. Acta 54* (1980) 263; J. Bargon: *Computational Methods in Chemistry*, Plenum Press, New York 1980.

[6] Also termed empirical force field calculations. The expression molecular mechanics was coined by L. S. Bartell (*J. Chem. Educ. 45* (1968)

754) and has, in the meantime, become popular; see *e.g.*:D. B. Boyd, K. B. Lipkowitz, *J. Chem. Educ. 59* (1982) 269 and P. Cox, *ibid. 59* (1982) 275.
[7] Summaries: N. L. Allinger, *Adv. Phys. Org. Chem. 13* (1976) 1; M. B. Hursthouse, G. P. Moss, K. D. Sales, *Annu. Rep. Prog. Chem. Sect. B 75* (1978) 23; A. I. Kitaigorodsky, *Chem. Soc. Rev. 7* (1978) 133; S. R. Niketic, K. Rasmussen: *The Consistent Force Field*, Springer, Berlin 1977; O. Ermer, *Struct. Bonding (Berlin) 27* (1976) 161; C. Altona, D. H. Faber, *Top. Curr. Chem. 45* (1974) 1.
[8] E. Osawa, H. Musso, *Top. Stereochem. 13* (1982) 117.
[9] O. Ermer: *Aspekte von Kraftfeldrechnungen*, Wolfgang Baur Verlag, München 1981; D. F. DeTar, *Comput. Chem. 1* (1977) 139.
[10] The following MM programs can be obtained from the Quantum Chemistry Program Exchange, Chemistry Building 204, Indiana University, Bloomington, Indiana 47401, USA: a) MM2, No. 395, N. L. Allinger, Y. H. Yuh. This is the latest version of *Allinger's* force field, and contains numerous heteroatom parameters; b) BIGSTRN, No. 348, J. D. Andose, E. M. Engler, J. B. Collins, J. P. Hummel, K. Mislow, P. von R. Schleyer containing *Engler's* and *Allinger's* 1971 force fields cf. also [29]; c) CONFI, No. 334, S. Sharafi-Ozeri, K. A. Kuszkat. Simple force field, suitable for aromatic hydrocarbons; d) MCA/QCFF/PI, No. 325/247, E. Huler, R. Sharon, A. Warshell. Combination of a quantum mechanical extension of the consistent force field and a molecular crystal packing analysis; e) MMI/MMPI, No. 318, N. L. Allinger, Y. H. Yuh. *Allinger's* 1973 force field with an extension to conjugated π-electron systems (using a VESCF-MO method).
[11] E. M. Engler, J. D. Andose, P. von R. Schleyer, *J. Am. Chem. Soc. 95* (1973) 8005.
[12] N. L. Allinger, M. T. Tribble, M. A. Miller, D. H. Wertz, *J. Am. Chem. Soc. 93* (1971) 1637.
[13] K. Mislow, *Acc. Chem. Res. 9* (1976) 26; K. Mislow, D. A. Dougherty, W. D. Hounshell, *Bull. Soc. Chim. Belg. 87* (1978) 555.
[14] C. Rüchardt, H.-D. Beckhaus, *Angew. Chem. 92* (1980) 417; *Angew. Chem. Int. Ed. Engl. 19* (1980) 429.
[15] H.-D. Beckhaus, K. J. McCullough, H. Fritz, C. Rüchardt, B. Kitschke, H. J. Lindner, D. A. Dougherty, K. Mislow, *Chem. Ber. 113* (1980) 1869.
[16] D. F. DeTar, N. P. Luthra, *J. Am. Chem. Soc. 102* (1980) 4505.
[17] D. N. J. White, M. J. Bovill, *J. Chem. Soc. Perkin Trans. II 1977*, 1610.
[18] J. C. Perlberger, P. Müller, *J. Am. Chem. Soc. 99* (1977) 6316.
[19] J. M. Harris, S. G. Shafer, M. R. Smith, S. P. McManus, *Tetrahedron Lett. 1979*, 2089.
[20] D. Lenoir, *Nachr. Chem. Tech. Lab. 27* (1979) 762.
[21] The original Engler force field did not contain subtleties such as cross-terms for stretch and deformation vibrations, particularly for three- and four-membered rings, or extra terms having lower powers of the torsion potential, as are contained in the MM2 force field [22].
[22] N. L. Allinger, *J. Am. Chem. Soc. 99* (1977) 8127.
[23] S. T. Rao, M. Sundaralingam, *Acta Crystallogr. B 28* (1972) 694.
[24] E. Osawa, A. Furusaki, N. Hashiba, T. Matsumoto, V. Singh, Y. Tahara, E. Wiskott, M. Farcasiu, T. Iizuka, N. Tanaka, T. Kan, P. von R. Schleyer, *J. Org. Chem. 45* (1980) 2985.
[25] T. Clark, T. McO. Knox, H. Madele, M. A. McKervey, J. J. Rooney, *J. Am. Chem. Soc. 97* (1975) 3835.
[26] D. N. J. White, M. J. Bovill, *J. Chem. Soc. Perkin Trans. II 1977*, 1610.
[27] a) D. N. J. White, M. J. Bovill, *J. Mol. Struct. 33* (1976) 273; b) S. Fitzwater, L. S. Bartell, *J. Am. Chem. Soc. 98* (1976) 5107.
[28] Cf. in this respect: O. Ermer, C. D. Bödecker, *Chem. Ber. 114* (1981) 653.
[29] These aspects have been improved in the recently revised version BIGSTRN-2 (QCPE No. 410).
[30] A. T. Hagler, P. S. Stern, R. Sharon, J. M. Becker, F. Naider, *J. Am. Chem. Soc. 101* (1979) 6842; A. T. Hagler, S. Lifson, P. Dauber, *ibid. 101* (1979) 5122.
[31] D. H. Wertz, N. L. Allinger, *Tetrahedron 30* (1974) 1579.
[32] R. H. Boyd, *J. Am. Chem. Soc. 97* (1975) 5353.
[33] E. Osawa, J. B. Collins, P. von R. Schleyer, *Tetrahedron 33* (1977) 2667.
[34] See Tables 3–5 in [8].
[35] 1.84 Å: W. Wagemann, K. Müller, E. Vogel, T. Pilati, M. Simonetta, *Angew. Chem. 89* (1977) 176; *Angew. Chem. Int. Ed. Engl. 16* (1977) 170.
[36] P. D. Bartlett, A. J. Blakeney, M. Kimura, W. H. Watson, *J. Am. Chem. Soc. 102* (1980) 1383.
[37] O. Ermer, *Angew. Chem. 89* (1977) 833; *Angew. Chem. Int. Ed. Engl. 16* (1977) 798.
[38] D. A. Dougherty, K. Mislow, *J. Am. Chem. Soc. 101* (1979) 1401.
[39] A. Gavezzotti, L. S. Bartell, *J. Am. Chem. Soc. 101* (1979) 5142.
[40] E. Osawa, H. Shirahama, T. Matsumoto, *J. Am. Chem. Soc. 101* (1979) 4824.
[41] N. L. Allinger, S. Profeta, Jr., *J. Comput. Chem. 1* (1980) 181.
[42] The energy barriers for rotations in ring systems are excellently reproduced by MM calculations; see *e.g.* [8] and F. A. L. Anet, J. Krane, *Isr. J. Chem. 20* (1980) 72.
[43] W. D. Hounshell, D. A. Dougherty, K. Mislow, *J. Am. Chem. Soc. 100* (1978) 3149.
[44] H.-D. Beckhaus, G. Hellmann, C. Rüchardt, *Chem. Ber. 111* (1978) 72.
[45] R. E. Carter, T. Liljefors, *Tetrahedron 32* (1976) 2915; T. Liljefors, R. E. Carter, *ibid. 34* (1978) 1611.
[46] a) W. D. Hounshell, C. A. Johnson, A. Guenzi, F. Cozzi, K. Mislow, *Proc. Natl. Acad. Sci. USA 77* (1980) 6961; F. Cozzi, A. Guenzi, C. A. Johnson, K. Mislow, W. D. Hounshell, J. F. Blount, *J. Am. Chem. Soc. 103* (1981) 957; Y. Kawada, H. Iwamura, *J. Org. Chem. 45* (1980) 2587; *Tetrahedron Lett. 22* (1981) 1533; *J. Am. Chem. Soc. 103* (1981) 958; b) C. A. Johnson, A. Guenzi, K. Mislow, *J. Am. Chem. Soc. 103* (1981) 6240.
[47] E. M. Engler, L. Chang, P. von R. Schleyer, *Tetrahedron Lett. 1972*, 2525.
[48] H.-G. Fritz, H. Henke, H. Musso, *Chem. Ber. 107* (1974) 3164.
[49] E. Osawa, K. Aigami, Y. Inamoto, *J. Chem. Soc. Perkin Trans. II 1979*, 172.
[50] U. Burkert, N. L. Allinger, *J. Comput. Chem. 3* (1982) 40.
[51] E. Osawa, *J. Comput. Chem. 3* (1982) 400.
[52] E. Osawa, *J. Am. Chem. Soc. 101* (1979) 5523.
[53] L. A. Paquette, C. W. Doecke, C. Klein, *J. Am. Chem. Soc. 101* (1979) 7599.
[54] I. T. Jacobson, personal communication.
[55] O. Ermer, *Angew. Chem. 89* (1977) 431; *Angew. Chem. Int. Ed. Engl. 16* (1977) 411.
[56] L. A. Paquette, D. W. Balogh, R. Usha, D. Kountz, G. G. Christoph, *Science 211* (1981) 575; L. A. Paquette, D. W. Balogh, *J. Am. Chem. Soc. 104* (1982) 774; G. G. Christoph, P. Engel, R. Usha, D. W. Balogh, L. A. Paquette, *ibid. 104* (1982) 784. No X-ray data are as yet available for dodecahedrane, which in the meantime has also been synthesized: R. J. Ternansky, D. W. Balogh, L. A. Paquette, *J. Am. Chem. Soc. 104* (1982) 4503; *Chem. Eng. News. 60*, Aug. 16, 1982, p. 25.
[57] R. C. Fort, Jr.: *Adamantane: The Chemistry of Diamond Molecules*, Marcel Dekker, New York 1976.
[58] S. A. Godleski, P. von R. Schleyer, E. Osawa, W. T. Wipke, *Prog. Phys. Org. Chem. 13* (1981) 63.
[59] S. A. Godleski, P. von R. Schleyer, E. Osawa, G. J. Kent, *J. Chem. Soc. Chem. Commun. 1974*, 976; G. J. Kent, S. A. Godleski, E. Osawa, P. von R. Schleyer, *J. Org. Chem. 42* (1977) 3852.
[60] A. P. Marchand, T.-C. Chou, J. D. Ekstrand, D. van der Helm, *J. Org. Chem. 41* (1976) 1438.
[61] P. von R. Schleyer, E. Osawa, M. G. B. Drew, *J. Am. Chem. Soc. 90* (1968) 5034.
[62] M. A. McKervey, *Tetrahedron 36* (1980) 971.
[63] K. Müller, *Angew. Chem. 92* (1980) 1; *Angew. Chem. Int. Ed. Engl. 19* (1980) 1.
[64] R. C. Bingham, P. von R. Schleyer, *J. Am. Chem. Soc. 93* (1971) 3189.
[65] W. Parker, R. L. Tranter, C. I. F. Watt, L. W. K. Chang, P. von R. Schleyer, *J. Am. Chem. Soc. 96* (1974) 7121.
[66] A. Karim, M. A. McKervey, E. M. Engler, P. von R. Schleyer, *Tetrahedron Lett. 1971*, 3887.
[67] E. Osawa, E. M. Engler, S. A. Godleski, Y. Inamoto, G. J. Kent, M. Kausch, P. von R. Schleyer, *J. Org. Chem. 45* (1980) 984.
[68] J. L. Fry, E. M. Engler, P. von R. Schleyer, *J. Am. Chem. Soc. 94* (1972) 4628.
[69] J. S. Lomas, P. K. Luong, J.-E. Dubois, *J. Am. Chem. Soc. 99* (1977) 5478.
[70] D. Lenoir, D. J. Raber, P. von R. Schleyer, *J. Am. Chem. Soc. 96* (1974) 2149.
[71] D. Fărcaşiu, *J. Org. Chem. 43* (1978) 3878.
[72] M. R. Smith, J. M. Harris, *J. Org. Chem. 43* (1978) 3588.
[73] E. M. Engler, M. Fărcaşiu, A. Sevin, J. M. Cense, P. von R. Schleyer, *J. Am. Chem. Soc. 95* (1973) 5769.
[74] For futher examples of the use of the force field involving cations in the rearrangements of hydrocarbons see: N. Takaishi, Y. Inamoto, K. Aigami, Y. Fujikura, E. Osawa, M. Kawanisi, T. Katsushima, *J. Org. Chem. 42* (1977) 2041.
[75] E. Osawa, K. Aigami, N. Takaishi, Y. Inamoto, Y. Fujikura, Z. Majerski, P. von R. Schleyer, E. M. Engler, M. Fărcaşiu, *J. Am. Chem. Soc. 99* (1977) 5361.
[76] S. A. Godleski, P. von R. Schleyer, E. Osawa, Y. Inamoto, Y. Fujikura, *J. Org. Chem. 41* (1976) 2596.
[77] D. Fărcaşiu, E. Wiskott, E. Osawa, W. Thielecke, E. M. Engler, J. Slutsky, P. von R. Schleyer, *J. Am. Chem. Soc. 96* (1974) 4669.
[78] E. Osawa, Y. Tahara, A. Togashi, T. Iizuka, N. Tanaka, T. Kan, D. Fărcaşiu, G. J. Kent, E. M. Engler, P. von R. Schleyer, *J. Org. Chem. 47* (1982) 1923.
[79] T. M. Gund, P. von R. Schleyer, P. H. Gund, W. T. Wipke, *J. Am. Chem. Soc. 97* (1975) 743.

[80] T. M. Gund, W. Thielecke, P. von R. Schleyer, *Org. Synth. 53* (1973) 30.
[81] A novel diamantane synthesis with 89% yield has been described: F. Turecek, V. Hanus, P. Sedmera, H. Antropiusova, K. Mach, *Coll. Czech. Chem. Commun. 46* (1981) 1474.
[82] N. Tanaka, T. Kan, T. Iizuka, *J. Chem. Inf. Comput. Sci. 3* (1979) 162.
[83] T. Iizuka, personal communication.
[84] P. Engel, W. Nowacki, J. Slutsky, P. Grubmüller, P. von R. Schleyer, *Chem. Ber. 111* (1979) 3566.
[85] K. Hirao, M. Taniguchi, O. Yonemitsu, J. L. Flippen, B. Witkop, *J. Am. Chem. Soc. 101* (1979) 408.
[86] E. Osawa, K. Aigami, Y. Inamoto, *J. Chem. Soc. Perkin Trans. II 1979,* 181.
[87] U. Burkert, *Chem. Ber. 110* (1977) 773.
[88] a) H. W. Lennartz, Dissertation, Universität Bochum 1979; b) W. R. Roth, H. W. Lennartz, unpublished results.
[89] O. Ermer, *Z. Naturforsch. B 32* (1977) 837.
[90] a) D. J. Martella, M. Jones, W. F. Maier, P. von R. Schleyer, *J. Am. Chem. Soc. 101* (1979) 7634; W. F. Maier, P. von R. Schleyer, *ibid. 103* (1981) 1891; b) J. R. Wiseman, J. E. Kipp, *J. Am. Chem. Soc. 104* (1982) 4688
[91] O. Ermer, S. Lifson, *Tetrahedron 20* (1974) 2425.
[92] D. Lenoir, H. Dauner, R. M. Frank, *Chem. Ber. 113* (1980) 2642.
[93] G. Favini, M. Simonetta, R. Todeschini, *J. Comput. Chem. 2* (1981) 149.
[94] R. Stober, H. Musso, *Angew. Chem. 89* (1977) 430; *Angew. Chem. Int. Ed. Engl. 16* (1977) 415.
[95] N. A Sasaki, R. Zunker, H. Musso, *Chem. Ber. 106* (1973) 2996; E. Osawa, P. von R. Schleyer, L. W. K. Chang, V. V. Kane, *Tetrahedron Lett. 1974,* 4189.
[96] H. Musso, *Chem. Ber. 108* (1975) 337.
[97] B. Deppisch, H. Guth, H. Musso, E. Osawa, *Chem. Ber. 109* (1976) 2956.
[98] I. Schneider, H. Musso, unpublished results; P. von R. Schleyer, E. Wiscott, *Tetrahedron Lett. 1967,* 2845.
[99] U. Biethan, U. Cuntze, H. Musso, *Chem. Ber. 110* (1977) 3649.
[100] K. J. Toyne, *J. Chem. Soc. Perkin Trans. 1 1976,* 1346; I. Schneider, K. J. Toyne, H. Musso, E. Osawa, unpublished results.
[101] a) H. Kukuk, E. Proksch, A. de Meijere, *Angew. Chem. 94* (1982) 304; *Angew. Chem. Int. Ed. Engl. 21* (1982) 306; *Angew. Chem. Suppl. 1982,* 696; b) D. Bosse, A. de Meijere, *Chem. Ber. 111* (1978) 2223; c) D. Kaufmann, O. Schallner, L.-U. Meyer, H.-K. Fick, A. de Meijere, *Chem. Ber.*, in press; A. de Meijere, *Angew. Chem. 91* (1979) 867; *Angew. Chem. Int. Ed. Engl. 18* (1979) 809.
[102] E. Osawa, K. Aigami, Y. Inamoto, *Tetrahedron 34* (1978) 509.
[103] Note on reaction c) in Fig. 7, experiment: K. B. Wiberg, M. G. Matturro, R. D. Adams, *J. Chem. Soc. Chem. Commun. 1981,* 878; calculation: enthalpy of formation/strain energy (kcal/mol)=2.43/51.47 for "crossed" and 13.23/62.07 for "parallel" products, as calculated using MM2.
[104] W. Burns, M. A. McKervey, J. J. Rooney, N. G. Samman, J. Collins, P. von R. Schleyer, E. Osawa, *J. Chem. Soc. Chem. Commun. 1977,* 95.
[105] E. Osawa, K. Aigami, Y. Inamoto, *J. Org. Chem. 42* (1977) 2621; T. Katsushima, R. Yamaguchi, M. Kawanisi, E. Osawa, *Bull. Chem. Soc. Jpn. 53* (1980) 3313.
[106] E. M. Engler, K. R. Blanchard, P. von R. Schleyer, *J. Chem. Soc. Chem. Commun. 1972,* 1210.
[107] R. Hamilton, D. E. Johnston, M. A. McKervey, J. J. Rooney, *J. Chem. Soc. Chem. Commun. 1972,* 1209.
[108] J. Slutsky, E. M. Engler, P. von R. Schleyer, *J. Chem. Soc. Chem. Commun. 1973,* 685.
[109] E. Osawa, H. Henke, G. Schröder, *Tetrahedron Lett. 1976,* 847.
[110] D. A. Dougherty, H. B. Schlegel, K. Mislow, *Tetrahedron 34* (1978) 1441; D. A. Dougherty, W. D. Hunshell, H. B. Schegel, R. A. Bell, K. Mislow, *Tetrahedron Lett. 1976,* 3479.
[111] K. Harano, T. Ban, M. Yasuda, E. Osawa, K. Kanematsu, *J. Am. Chem. Soc. 103* (1981) 2310.
[112] S. R. Wilson, J. C. Huffman, *J. Org. Chem. 45* (1980) 560; F. H. Allen, *J. Chem. Inf. Comput. Sci. 20* (1980) 68.
[113] A compilation of data for very small molecules: Carnegie-Mellon Quantum Chemistry Archive (R. A. Whiteside, J. S. Binkley, R. Krishnan, D. J. DeFrees, H. B. Schlegel, J. A. Pople), Department of Chemistry, Carnegie-Mellon University, Pittsburgh, Pennsylvania 15213, USA.
[114] N. L. Allinger, D. Y. Chang, *J. Am. Chem. Soc. 98* (1976) 6798; U. Burkert, *Tetrahedron 33* (1977) 2237.
[115] J. P. Hummel, J. Stackhouse, K. Mislow, *Tetrahedron 33* (1977) 1925. Z. Smith, A. Almenningen, E. Hengge, D. Kovar *J. Am. Chem. Soc. 104* (1982) 4362.
[116] A. Y. Meyer, J. Chem. Soc. Perkin. Trans. II, *1982,* 1199.
[117] M. Schmittel, A. Schulz, Ch. Rüchardt, E. Hädicke, *Chem. Ber. 114* (1981) 3533, and literature cited therein.
[118] G. Bernardinelli, R. Gerdil, *Helv. Chim. Acta. 64* (1981) 1365, 1371.

# Synthetic Gene Fragments in Genetic Engineering— The Renaissance of Chemistry in Molecular Biology**

**By Julian E. Davies* and Hans Günter Gassen**

Chemistry and biology paved the way for a new scientific discipline, molecular genetics. The breathtaking progress in deciphering the genetic machinery of a living being within the last 20 years may be attributed mainly to the experimental skill and ingenuity of molecular biologists. Chemists lost interest in the investigation of biological problems. The advances in genetic engineering exemplify the new demands chemists are confronted with in contemporary science. Following a short introduction on the genetics of bacteria, the article deals with the molecular basis of gene cloning, which is subdivided into *in vitro* recombination of nucleic acids and *in vivo* transformation of cells. Next, the criteria for the selection of passenger DNA, vectors, and host cells are discussed. Recombination and transformation are easy-to-learn experimental techniques, whereas the search for the positive clone requires detailed knowledge of microbiology and the ability to handle of a battery of modern biochemical techniques. Finally, the automated chemical synthesis of gene fragments serves to demonstrate that chemistry is starting to make its comeback into molecular biology.

## 1. Introduction[***]

In the last 100 years synthetic chemistry has produced about 6 million different compounds, which are either reproductions of natural substances or are chemicals which previously did not exist on earth. The synthetic world built up by organic chemists within such a short time period deserves recognition.

A bacterium such as *Escherichia coli* reproduces in 20 minutes under optimal growth conditions. In other words a complete new living being is assembled within a third of an hour. Table 1 lists the main components that must be synthesized during this period of time. If we focus our attention on only two classes of biomolecules, deoxyribonucleic acid (DNA) and the proteins, the synthetic ingenuity of a living cell is clearly demonstrated. The length of the *E. coli* genome is about 1–2 μm, and its molecular weight is $2.4 \times 10^9$. Its DNA contains approximately $4 \times 10^6$ nucleotide pairs, consisting of four different bases, which are linked in an identical manner by the phosphate-ribose backbone. The sequence of the nucleotide pairs has to be an exact replica of the parental genome. Even one incorrectly placed base pair may be lethal for the cell.

Furthermore, *E. coli* must produce about 3500 different proteins within 20 minutes. The larger ones, such as the fatty acid synthetase complex, have a molecular weight of *ca.* $3 \times 10^6$ and contain about 25000 amino acids, which are determined by the nucleotide sequence of the DNA. All proteins must adopt a unique tertiary structure in order to fulfill their function within the bacterium. Cells not only have the capacity to produce these compounds (Table 1), but the amounts of each individual substance produced are strictly regulated according to an exact time plan.

Table 1. Molecular compounds of an *E. coli* bacterium. *E. coli* can be grown in a medium containing only glucose as carbon and energy source. The rest of the culture medium consists of inorganic salts; oxygen is introduced by intensive aeration.

| Compounds | Percentage of total weight | Approximate number of molecular species |
|---|---|---|
| Water | 70 | 1 |
| Proteins | 15 | 3500 |
| DNA | 1 | 1 |
| RNA | 6 | 1000 |
| Polysaccharides | 3 | 50 |
| Lipids | 2 | 20 |
| Intermediates [a] | 2 | 500 |
| Inorganic ions | 1 | 12 |

[a] Intermediates are compounds such as coenzymes or dicarboxylic acids.

Compared with the synthetic capacity of a simple microorganism, today's synthetic organic chemistry is still in the Stone Age. However, one should appreciate the fact that bacteria had *ca.* $3.5 \times 10^9$ years to optimize their synthetic procedures.

In the future, organic chemists may adapt their strategies to use biological pathways in order to avoid high temperatures and pressures and the production of toxic waste substances. Chemists have to learn to use substrate-specific, high turnover-number catalysts such as enzymes and highly reactive, but specific, substrates such as coenzymes. There is still a long way to go, but some encouraging improvements have been made in the synthesis of stereospecific compounds. As a temporary solution to synthetic problems one may alter the synthetic capacity of a living cell by manipulating its genetic program; this process is called genetic engineering.

[*] Prof. Dr. J. E. Davies
Biogen S. A.
Route de Troinex 3, CH-1227 Carouge/Genève (Switzerland)
Prof. Dr. H. G. Gassen
Institut für Organische Chemie und Biochemie
der Technischen Hochschule
Petersenstrasse 22, D-6100 Darmstadt (Germany)

[**] Based on an introductory lecture delivered by J. E. Davies at the EMBO-Workshop "Prospects of Automation in Gene Synthesis" March 27, 1982 in Darmstadt (see also [100]).

[***] A glossary of genetic terms can be found in *Science 209* (1980) 1435, Lehninger: *Principles of Biochemistry*, Worth Publishers, New York 1982, p. 969, and R. C. King: *A Dictionary of Genetics*. Oxford University Press, New York 1974.

In the following article we use the recent progress in genetic engineering to demonstrate the decline and the advance, as well as the prospects of chemistry in modern biology.

## 2. Both Chemistry and Biology Contributed to Molecular Biology

The deciphering of the genetic apparatus of a living cell actually started with the chemistry of nucleic acids, when in 1859 *Friedrich Miescher* isolated nucleic acids[1]. Only six years later *Gregor Mendel* reported on his experiments with hybrid plants at the Naturforschende Verein in Brünn, and so the genetic approach started[2]. Over the next 50 years many chemists such as *Alfred Kossel, Emil Fischer,* and *Wilhelm Traube* concentrated on the chemistry of nucleic acid components, particularly the bases[3]. Around 1930 *Levene et al.* obtained deoxynucleosides by the enzymatic degradation of DNA and identified deoxyribose as a constituent of DNA[4]. By 1950 the field of nucleic acid chemistry was beginning to enter the stage of maturity. Major contributions came from *Todd, Fox* and *Griffith,* and from *Chargaff*[5]; the linkage and the linearity of the nucleic acid strand were determined. Finally *Watson* and *Crick* formulated the concept of a right-handed double helix, in which the complementary base pairs form the interior of the helix, whereas the ribose-phosphodiester chain is directed outwards (see Fig. 2)[6, 7]. The diameter of the helix is constant, since one base pair always consists of a small pyrimidine and a large purine base. The base pairs are stabilized by formation of two or three hydrogen bonds. Molecular biologists usually specify the molecular weight of DNA in terms of base pairs (bp) or kilo base pairs (kbp). More correctly these comprise a nucleotide pair, *i.e.* G : C or A : U, with a molecular weight of 660 and a "DNA length" of 0.34 nm. Since the manipulation of DNA almost always involves the nucleotide pairs, which only differ in their heterocyclic bases, the term base pair will be used here.

In the meantime numerous scientific techniques have become available for studies of nucleic acid chemistry[8]: paper and ion exchange chromatography, UV absorption spectroscopy, electrophoresis, sedimentation analysis, light scattering, viscosimetric studies, electron microscopy, X-ray diffraction techniques, and the use of radioactive isotopes. The application of each novel technique opened a new vista in nucleic acid chemistry. Soon nucleic acid chemistry became the cornerstone of the rapidly developing field of molecular biology.

The significance of nucleic acid chemistry is related to the role of nucleic acids as genetic material in the living cell. However, despite the work of *Miescher* and many others it took roughly 80 years before *Avery, MacLeod,* and *McCarthy* demonstrated the relationship between DNA and genetics in 1944. They showed that DNA was the bacterial transforming factor, the carrier of hereditary information[9]. This function of the "nuclein" had been postulated previously by *Hartwig* and *Fol* when they examined the function and role of chromosomes. Their experiments led *Hartwig* to state "I believe that I have at least made it highly probable that "nuclein" is the substance that is responsible not only for fertilization but also for the transmission of hereditary characteristics"[10, 11].

Neither the ingenious and prophetic view of *Hartwig* nor the cause and effect experiment of *Avery* convinced the entire scientific community to accept the role of DNA as the hereditary material. Not until the classic experiment of *Hershey* and *Chase* in *1953,* in which the genetic substance of a bacteriophage was clearly shown to be the $^{32}P$-labeled DNA and not $^{35}S$-labeled protein, was the biological role of DNA ultimately accepted[12]. It was then that chemistry and genetics really came together to give us what we now know as molecular genetics or molecular biology.

Since then, the advances in nucleic acid chemistry and molecular genetics have been breathtaking. To name but a few: the mode of DNA replication, the establishment of the genetic code and the role of mRNA, tRNA, and ribosomes in protein synthesis and, last but not least, the chemical synthesis of genes such as tyrosine tRNA and interferon[13].

However, without wishing to be disrespectful to chemists, chemistry then became subordinate to biology, mainly because chemists lost interest in biological problems: a physicist, and not an organic chemist, worked out one of the methods of DNA sequencing. The majority of chemists were not sufficiently interested in DNA chemistry to want to find out how to develop methods for the specific cleavage of phosphodiester bonds in DNA[14]. *Walter Gilbert* sharded the Nobel prize for this development, and DNA sequencing became one of the essential prerequisites of genetic engineering[15].

## 3. The Genetics of a Bacterial Cell

What follows is a short outline of the genetic machinery of a cell which helps to explain the basis of genetic engineering[16]. We will restrict ourselves mainly to prokaryotic organisms since the basic genetic principles are similar in both prokaryotes and eukaryotes. In particular, we will concentrate mainly on one species of bacteria, *Escherichia coli,* which was discovered by the German microbiologist *Escherich.* It is an organism whose major habitat is the lower part of the intestine of warm blooded animals. Things have changed a little bit since then. Nowadays the natural habitat of *E. coli* is a molecular biology laboratory! This small bacterium (1 μm × 2 μm) has played a tremendous role in the development of molecular biology in the research laboratory.

The DNA-encoded protein synthesizing machinery of *E. coli* is shown in Figure 1. Nearly all of the genetic information is stored in a large circular DNA molecule (the genome or the chromosome) which contains about 3500 genes programming protein and RNA syntheses. One unit of information on the DNA is called an operon[17]. It consist of a regulatory region, operator and promoter, and one or more structural genes. A structural gene is a small segment of DNA containing the information for the synthesis of an RNA or a protein (Fig. 2). Frequently the enzymes required for a synthetic pathway, such as the four enzymes

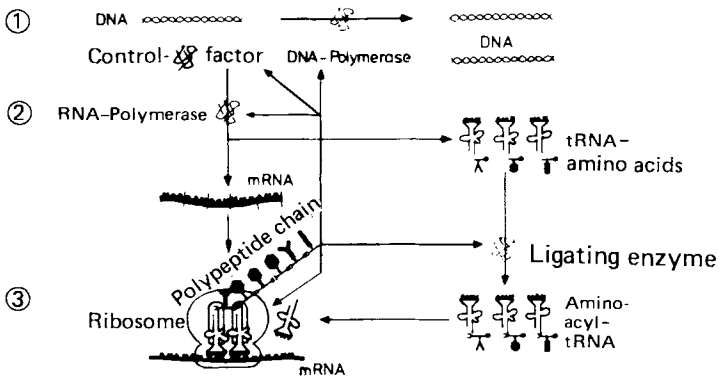



Fig. 1. Flow of information from deoxyribonucleic acid (DNA) to polypeptide chains. The figure shows a highly simplified scheme for the DNA encoded, ribosome-dependent synthesis of proteins in three steps: replication ①, transcription ②, and translation ③. During replication the DNA is doubled with the aid of DNA polymerase and many other enzymes and factors. In transcription the DNA is copied into three types of single stranded RNAs; the messenger (mRNA) as the matrix of genetic information, the ribosomal RNA (rRNA) as building blocks for ribosomes and the transfer RNA (tRNA) as carrier molecules for the amino acids. These are attached to the tRNAs with the aid of aminoacyl synthetases. Ribosomes translate the mRNA using aminoacyl-tRNAs as substrates into the genetically determined sequence of a protein.

involved in the synthesis of tryptophane, are located together on one operon to permit a coordinated regulation of the amounts of catalysts[18]. The promotor is the binding site for the DNA-dependent RNA polymerase, whereas

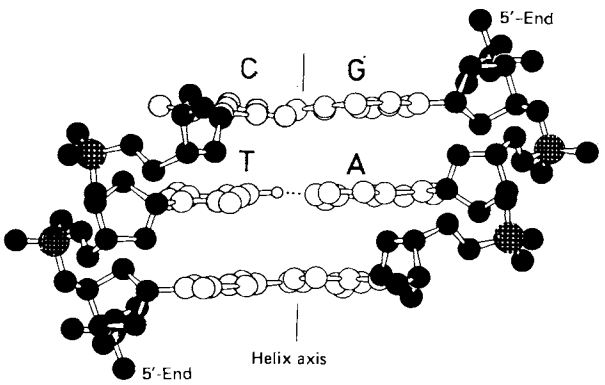



Fig. 2. Three base pair segment of DNA. The (3'→5' and 5'→3') ribose-phosphate chains are shown as solid circles and the P atoms are hatched. The heterocyclic bases adenine, cytosine, guanine, and thymine are almost at right angles to the axis of the helix. A and T, as well as G and C each form a base pair stabilized by two and three hydrogen bonds, respectively.

the operator represents the "on-off" switch for a single- or multi-structural gene (Fig. 3). If a repressor protein binds to the operator, the subsequent genes of an operon are switched off. The repressor can only be displaced from the DNA by a specific inducer—*e.g.* a metabolite. The mRNA is copied as an exact base-complementary replica from the structural part of the operon from one of the two DNA strands, the codogenic strand. As a "short-living" single strand ribonucleic acid, the mRNA delivers the program which in a translation step is deciphered by the ribosomes and transformed into an amino acid sequence, a protein[19]. The amount of protein can also be regulated in the transla-

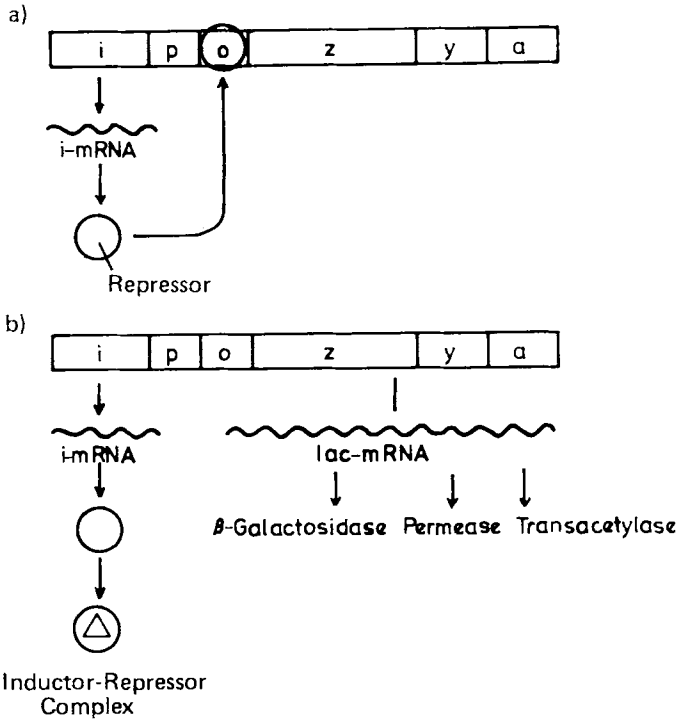



Fig. 3. The diagram shows the organization of the lactose operon (lac operon). The expression of the three enzymes β-galactosidase, permease, and transacetylase, which are necessary for the breakdown of lactose, is controlled by the regulative part of the operon. The promoter region (P), about 40 bp long, represents the binding site for the DNA-dependent RNA polymerase (transcribing enzyme). The operator (O) is the master switch for gene expression. The repressor protein, the product of the distant "i" gene, shuts off transcription. In lac operon the operator consists of 28 bp. The inductor, *e.g.* allolactose, inactivates the repressor. a) A repressor is synthesized which blocks the operator and hence prevents transcription of the structural genes (z, y, a). b) The repressor is deactivated by an inducer by forming an inductor-repressor complex; synthesis of the three enzymes proceeds normally.

tion step. At the 5'-end, the mRNA has a binding site for ribosomes, termed the Shine-Dalgarno sequence[20]. The affinity of this sequence for ribosomes is decisive in determining how often a particular mRNA is used as a program for protein synthesis. In eukaryotes, replication, *i.e.* the copying of the DNA before cell division, and transcription, proceed in the cell nucleus. The synthesis of mRNA is considerably more involved[21].

In 1944 it was discovered that *E. coli* enjoyed the benefit of sexual intercourse[22]; subsequently, sexual transfer mechanisms of bacteria were studied in some detail and in the late 1950's it was found that *E. coli* contained DNA elements that are independent of the central chromosome and that are capable of autonomous replication and expression[23,24]. The discovery of the fertility factor F (sex factor) as an independent autonomous piece of DNA was a crucial event with respect to what we now talk about as gene technology.

Although bacterial cells can exchange parts of their genetic material, unlike eukaryotic cells they do not form true zygotes. In the mating process (conjugation) DNA is transferred from the male bacteria or donor cell to the female bacteria or recipient cell. Male bacteria contain the sex factor, and are termed $F^+$. This small circular DNA, representing 2% of the total genetic material of *E. coli*, de-

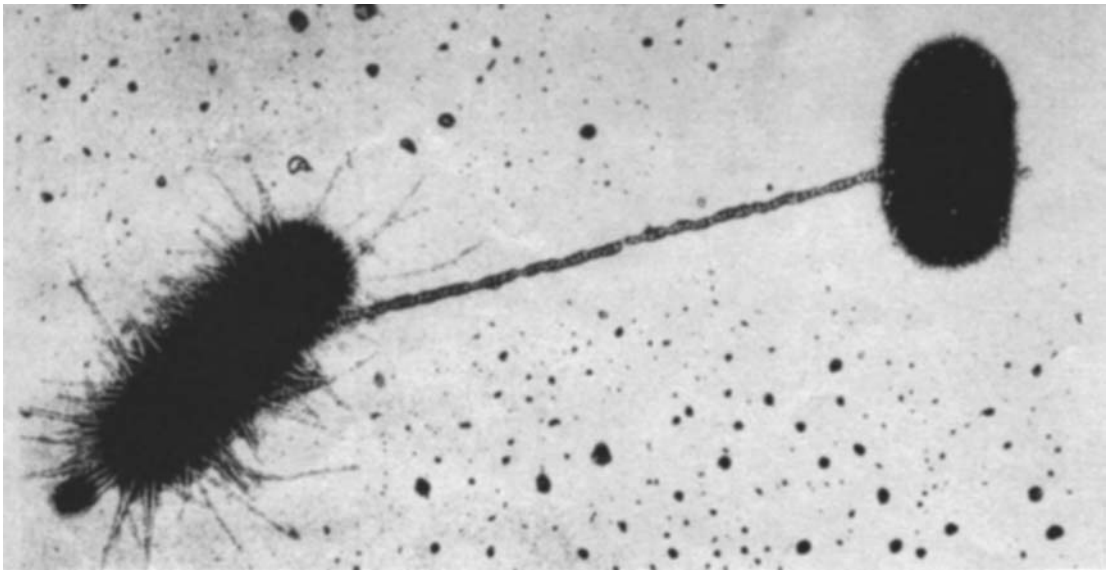


Fig. 4. Conjugation of bacteria. During this process a bridge is formed between the $F^+$ and the $F^-$ bacterium (donor and acceptor, resp.). By a reaction called conjugation DNA can be transferred from donor to acceptor.

termines the sex of a bacterium. A similar DNA molecule, the so-called Hfr-factor (high frequency of recombination) follows integration of the F factor into the chromosome and allows the transfer of the entire chromosome from one cell to the other (Fig. 4).

Shortly after the discovery of sex factors came the finding that bacteria may contain resistance transfer factors (R-factors), which are similar small circular DNA molecules containing the genetic determinants which make bacteria resistant to antibiotics or colicin[25]. These R-factors were first discovered in *Shigella dysenteriae* during an outbreak of dysentery in Japan in 1959. Shigella strains isolated from patients undergoing chemotherapy were found to be simultaneously resistant to four drugs: streptomycin, chloramphenicol, tetracycline, and sulfonamides[26]. When cells of a multiply-resistant strain were mixed with a sensitive strain, multiple resistance was found to be transferred at high frequency to the sensitive recipient. Later it was discovered that all four resistance genes were located on a circular DNA, called a self-transferable plasmid. This demonstrated two important facts, namely that extrachromosomal DNA elements encode proteins and that they can be exchanged between cells[27].

Another equally important event was the discovery of the bacteriophage λ by *Lederberg et al.* in 1951[28]. This phage (49 kbp) may exist as either circular or linear double

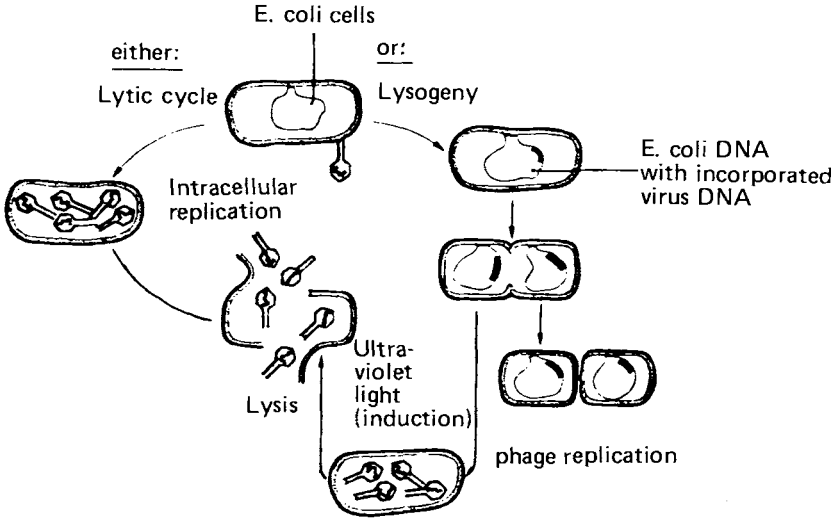



Fig. 5. Lytic and lysogenic life cycle of the bacteriophage λ using *E. coli* as host cell. In the transition from lysogeny to virulence, λ-phages are able to transfer parts of the bacterial genome to other bacteria. Viruses of the λ-phage type are temperate phages, which after infection can either become virulent or remain temperate. The λ-DNA incorporated into the host DNA is termed prophage: cells having prophages in their genome are termed lysogenic bacteria. λ-Phages insert their gene specifically between the lactose and biotin genes (taken from P. Knippers: *Molekulare Genetik*, Thieme, Stuttgart 1981 with the kind permission of the author and publisher).

stranded DNA. In cells the phage DNA is incorporated into the genome of the host, the lysogenic pathway, and thus will replicate together with the bacterial genome. On induction, *e.g.* by UV irradiation, the phage DNA is released and replicates autonomously in a similar manner to a plasmid. After completion of the synthesis of DNA and envelope proteins to generate mature progeny, the phage will finally kill (lyse) its host. During the transition between lysogenic and lytic life cycles the phage may often carry along a piece of the bacterial genome. Genetic material may be transferred from one bacterium to another by phages in a process called transduction (Fig. 5)[29]. The phage λ inserts its DNA into a specific position of the host genome, whereas phages such as P22 insert nonspecifically.

The bacteriophage λ provided scientists working with *E. coli* with an excellent opportunity to carry out genetic manipulations. Over a period of some 15 years, when no *in vitro* recombination was possible, phage λ was used for *in vivo* recombination of genetic material; it provided a mechanism for the specific interbacterial transfer of genetic material. The ability to integrate into the host's chromosome, the ability to inactivate host genes by insertion, and to pick-up genes by directed transduction have been important aspects in the development of gene cloning.

Table 2. Molecular weight *MW* and contour length *l* of some organisms.

| Organism | *MW* [kbp] [a] | *l* [μm] |
|---|---|---|
| Polyoma or SV 40 virus | 5.1 | 1.8 |
| Phage-λ | 48.6 | 17 |
| *E. coli* | 4000 | 1360 |
| Yeast | 13500 | 4600 |
| *Drosophila* [b] | 165000 | 56000 |
| Human | 2900000 | 990000 |
| Plasmid pBR322 | 4.361 | 1.4 |

[a] 1 kbp ≙ 1000 × 660 Da = 660000 Da. 1 kbp represent $2.5 \times 10^{-4}$ of the E. coli genome, however, only $3.4 \times 10^{-7}$ of the human genome. *MW* and *l* of the human genome summarizes all 23 chromosomes and only represents a estimated number. [b] [b] *Drosophila* = fruit fly.

If we compare the molecular weight of the bacterial chromosome with that of F-factors, plasmids, and phages then these represent an insignificant part of the total cellular DNA (Table 2). However, these small molecules are highly significant in terms of the genotype and phenotype of the cell and for biotechnology and genetic engineering. Table 3 summarizes the methods we possess at present that enable the transfer of DNA between the cells of various microorganisms to be accomplished and also enable exchange between plasmid and genome and the converse (Fig. 6). These methods have been refined quite recently and a number of them are applicable to a wide variety of microorganisms other than *E. coli*. The important thing to realize is that we are now able to manipulate the program which guides the synthetic capacity of a cell.

Table 3. Methods used to exchange genetic material between cells.

| Method | Principle |
|---|---|
| Transformation | Introduction of exogenous DNA into a cell, causing it to aquire a new phenotype |
| Transduction | Transfer of genetic material from one cell to another by means of a viral vector |
| Transfection | Infection of cells with isolated viral DNA |
| Conjugation | The process by which DNA is transferred from an $F^+$ to an $F^-$ bacterium |
| Cell fusion | Integration of cell nuclei |

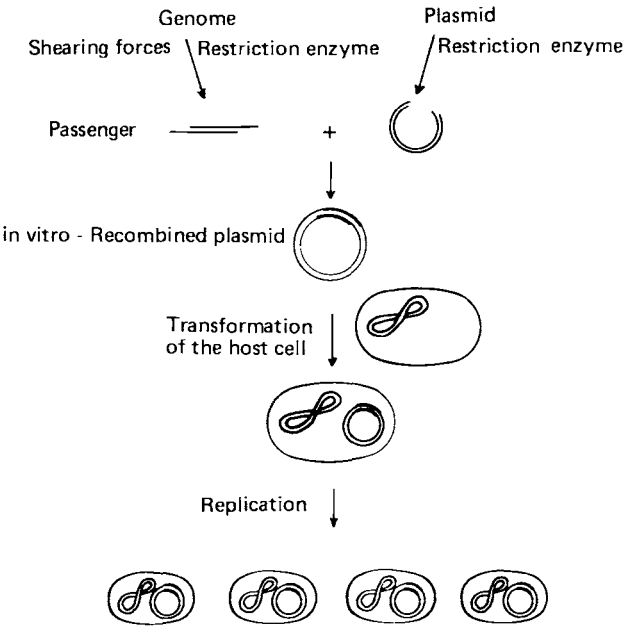



Fig. 6. Insertion of a passenger DNA into a vector. The plasmid can either be linearized by only one restriction endonuclease cut, or a stuffer fragment can be removed by two cuts. By the use of this procedure the size of the vector remains the same when the passenger is inserted.

The small circular DNAs such as F- and R-factors and phages have been used in many ingenious experiments for the manipulation of cellular DNA. They have enabled us to learn a considerable amount about gene structure, gene regulation, and gene expression. However, genetic engineering is not something molecular biologists have dreamed up. This kind of gene exchange between genomes and microorganisms has been taking place for a long time in nature using a variety of methods, often by-passing the guidelines required for *in vitro* recombinant DNA research in laboratories.

## 4. Principles of Genetic Engineering

The fascination of genetic engineering lies in the possibility of purifying and self-propagating a substance by transforming and cloning cells, *e.g.* bacteria[30-37]. By means of genetic engineering, it is possible to uniformly isolate mg quantities of a fragment present in a solution containing one fmol of a DNA fragment as 0.01‰ of a population, a mixture which appears to be completely hopeless to the chemist.

The "reprogramming" of life can therefore be considered as a novel branch of chemistry, which makes possible the self-reproduction of substances. In somewhat simplified terms genetic engineering can be divided into the following steps: 1) Isolation or synthesis of a gene or of a

DNA fragment; 2) Insertion of the fragment into a vector, usually a plasmid; 3) Channeling the vector into a cell, which accepts it as an additional piece of information; 4) Autonomous replication or integration into the host genome; 5) Expression of the foreign gene by the host machinery and hence synthesis of the corresponding RNA and proteins. In order to simplify matters in what follows we classify the first two steps as *in vitro* recombination, and all the others as *in vivo* transformation.

Finally the transformed cells must be reproduced at the expense of the native cells; for this purpose certain growth conditions are necessary, which enable only the transformed cells to replicate by division. When a colony or a clone has formed in a Petri plate, it is isolated in a second Petri plate in such a way that each contains approximately 50 colonies. In a subsequent screening test each clone must be checked whether it contains the desired DNA fragment or the protein as gene product. Frequently 20000 colonies have to be examined before a positive clone is found. A 1 mL liquid culture is first inoculated with this clone and an approximately 10 mL culture with the transformed bacterium is obtained by stepwise scale-up. Decisive in cloning is the screening step, the method of finding the correct positive clone as quickly as possible from 20000 colonies, followed by its selective reproduction.

Taken together, recombination and transformation are often loosely referred to as "cloning". However, cloning is really the process of cell reproduction starting from one original cell; in consequence, the cells produced (clones) contain only cells which are genotypically and phenotypically identical. Cloning diploid eukaryotes is more complex.

First of all let us consider a simple experiment. We remove a definite gene from the central genome, insert it into a plasmid, and reintroduce the modified plasmid into the cell. What advantage does this procedure offer? The *E. coli* chromosome contains $4 \times 10^6$ bp, and the average number of base pairs for one gene is 1150. Thus the central genome contains 3500 genes and one particular gene represents about 0.3% of the total genome. A plasmid contains on average $10^4$ bp. A gene incorporated into a plasmid may represent *ca.* 10% of the genome of the plasmid. Furthermore one can insert genes in tandem duplications on a plasmid, *i.e.* the plasmid may contain up to 10 copies of a single gene under the control of one regulatory unit. With so-called high-copy number plasmids the number per cell may be even further increased. If cells are treated with the antibiotic chloramphenicol, then the replication of the central chromosome is inhibited whereas the so-called Col-E1 plasmids (plasmids carrying the colicin production gene) replicate normally. The cell may turn into a sack full of plasmids with 100—200 plasmids per cell.

All the experimental tricks serve only one goal: to turn a microorganism into a factory for the preferential production of one particular gene (DNA segment) or protein in mg quantities from 1 L cultures.

## 5. The *in vitro* Recombination of Nucleic Acids

Reactions carried out on DNA outside the cell may be summarized as "cutting and splicing" procedures. The cutting of DNA serves two purposes: by cutting the large source genome into fragments of about 10—20 kbp one obtains an overlapping collection that contains all genes. This fragmentation can either be carried out by physical means (the 2 nm × 1.2 mm DNA thread is very sensitive to shearing forces) or by enzymatic hydrolysis with so-called restriction endonucleases (Table 4)[38-40]. These are DNA nucleases which recognize specific four, five, or six base pair sequences, which in double strand DNA have a twofold sequence symmetry (palindromes). They cut the DNA double strand leaving either flush (double stranded ends) or staggered ends (single stranded ends of two, three, or four nucleotides) (Table 4). With a four base pair specificity, a mean fragment length of 256 bp ($4^4$) is obtained, whilst with 6 bp the mean fragment size goes up to 4096 ($4^6$) bp. The perfect manipulation of *ca.* 200 currently known restriction endonucleases for the preparation of DNA fragments of surveyable chain length is a basic requirement for successful genetic engineering (Fig. 7).

Table 4. Origin, sequence type [a], recognition sequence, and average number of recognition sequences of a vector for prokaryotes, pBR322, and for eukaryotes, SV 40, for some of the approximately 200 known restriction endonucleases (restriction enzymes); approximately 50 of the enzymes are commercially available.

| Restriction endonuclease | Origin | Recognition sequenze | Sequence type [a] | Number of recognitions pBR322 | SV 40 |
|---|---|---|---|---|---|
| *Eco*RI | *Escherichia coli* RY13 | GAATCC | II | 1 | 1 |
| *Hind*III | *Haemophilus influenzae* | AAGCTT | II | 1 | 6 |
| *Hpa*II | *Haemophilus parainfluenza* | CCGG | II | 26 | 1 |
| *Pst*I | *Providencia stuartii* | CTGCAG | II | 1 | 2 |
| *Hae*III | *Haemophilus aegyptius* | GGCC | I | 22 | 19 |
| *Hpa*I | *Haemophilus parainfluenzae* | GTTAAC | I | | 4 |

[a] Sequence type I, *e.g.*

*Hae*III —GG|CC— ⇒ —GG + CC— double stranded
—CC|GG— —CC GG— (blunt) ends

Sequence type II, *e.g.*

*Eco*RI —G|AA TTC— ⇒ —G + AATTC— single stranded
—CTT AA|G— —CTTAA G— (sticky) ends

Such DNA fragments containing a gene or portions of a gene are called the passenger DNA. In order to function as a gene within a cell the "passenger" has to be spliced *in vitro* to a plasmid or to a phage DNA; usually phages and plasmids are used to transport the passenger DNA into the cell. The DNA molecule which is used to carry the passenger DNA into the cell is called a vector. Since both vectors are circular DNA molecules, either the plasmid is linearized by one endonuclease cut or alternatively a part of the plasmid DNA is removed by two cuts. In the first procedure one obtains an insertion vector and in the second method a replacement vector (stuffer fragment). The latter is cut by an enzyme having two targets, one on each side of the designated sequence to be removed, and replaced by the foreign passenger. Passenger DNA, plasmid, and other

vector DNA fragments can be separated and purified like other macromolecules by reversed phase chromatography (RPC-5), high pressure liquid chromatography (HPLC) or by polyacrylamide gel electrophoresis (PAGE)[41-43].

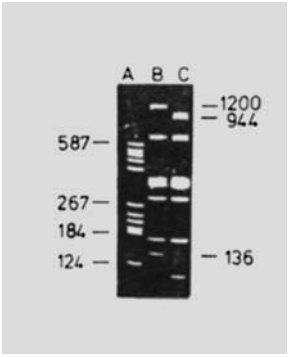



Fig. 7. The formation of a restriction map between vector and passenger is always the prerequisite for a recombination. The DNA fragment is digested by a number of restriction endonucleases of different specificity. The DNA segments obtained are separated by acrylamide gel electrophoresis according to their molecular weight. The individual bands are recognized by their red fluorescence after staining with ethidium bromide. From this type of data a restriction map of the DNA can be assembled, which is absolutely necessary for every recombination experiment. The figure shows the hydrolysis products obtained by digestion of a plasmid and separated by gel electrophoresis. Lane A shows the *Hae* III hydrolysis products of pBR322 as molecular weight standard. The numbers give the molecular weight in bp; Lanes B and C: digestion of pWH233 and pVH51, respectively, by the restriction enzyme *Hinf* I.

For the *in vitro* recombination of DNA, vector, and passenger by splicing, principally two enzymes are required; the oligonucleotide kinase[44] and DNA ligase[45]. DNA ligase is used to form the phosphodiester bonds between the 3'-OH group of one fragment (acceptor) and the 5'-phos-

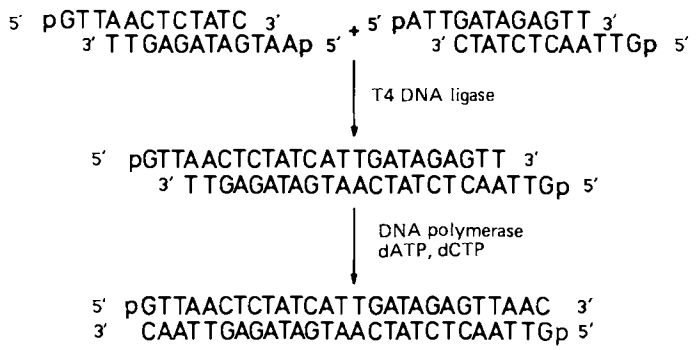



Fig. 8. Mechanism of ligation of two DNA fragments with DNA ligase. Free 5'-hydroxides must first be phosphorylated with ATP and oligonucleotide ligase. The single stranded ends may be furnished with the complementary bases by DNA polymerase.

phate group of the second (donor) (Fig. 8). Radiolabeling of DNA fragments is usually carried out using polynucleotide kinase and [$^{32}$P]ATP as cosubstrate, a procedure which phosphorylates the 5'-OH groups of DNA. With the aid of this technique *ca.* one fmol quantities of oligonucleotide can be detected by autoradiography. The usual enzyme repertoire used in genetic engineering is summarized in Table 5[44,45].

All *in vitro* recombinations follow the simple equation: passenger DNA + vector DNA = recombinant DNA. If a restriction endonuclease of the type *Eco*RI is used for the

Table 5. A selection of enzymes which are used in the *in vitro* recombination of nucleic acids.

| Enzyme | Function |
|---|---|
| Restriction endonucleases (EC 3.1.23) | Sequence-specific hydrolysis of DNA |
| Polynucleotide kinase (EC 2.7.1.78) | 5'Phosphorylation of DNA and RNA, radiolabeling with [$^{32}$P]Phosphate |
| DNA-ligase (EC 6.5.1.1) | Joins DNA from either sticky- or blunt-ended DNA fragments |
| DNA-polymerase (EC 2.7.7.7) | Polymerizes deoxynucleotide triphosphates, requires a single-stranded DNA as a matrix, but a double-stranded origin of replication |
| Terminal deoxynucleotidyl transferase | Tails the 3'ends of DNA or RNA with tracts of homooligonucleotides |
| Reverse transcriptase | Synthesizes DNA from a RNA template |
| S1 nuclease | Hydrolyzes single-stranded DNA (loop DNA) |
| Deoxyribonuclease (EC 3.1.21.1) | Hydrolyzes DNA non specifically |
| Ribonuclease A (EC 3.1.27.5) | Hydrolyzes RNA after (3'→5') pyrimidine nucleotides |
| Alkaline phosphatase (EC 3.1.3.1) | Dephosphorylates RNA and DNA at 5' and 3' ends |

cutting step, both for the isolation of the passenger DNA from the bacterial genome and for the linearization of the vector, then in both fragments we obtain identical four-nucleotide protruding single stranded ends. The single stranded ends of the passenger DNA and the vector are complementary to one another. This allows the formation of an overlapping precomplex between vector and passen-

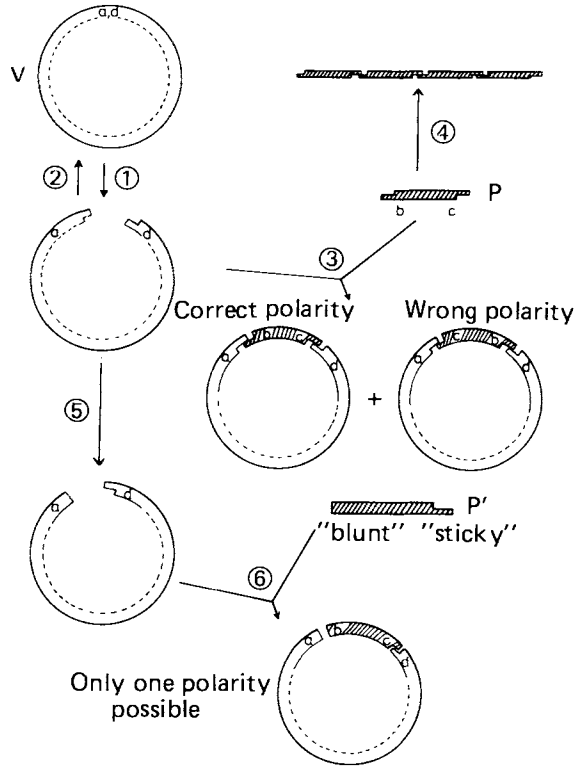



Fig. 9. Pitfalls occurring during recombination of DNA fragments. ① Linearization of a plasmid by a restriction enzyme. ② Recyclization of the linearized plasmid with a linear ligase. ③ Recombination of the vector V and the passenger P; the products, depending on whether they are provided with "suitable" ends or not, can exhibit the correct or incorrect polarity. ④ The passenger P can also oligomerize. ⑤ The linearized vector V contains a "blunt end" since it is cut by a second recombination enzyme. ⑥ Recombination of the vector thus obtained with a suitable passenger P', hence only one product with the correct polarity can be formed.

ger which is stabilized by the formation of hydrogen bonds between four base pairs. The formation of this intermediate facilitates the next step, the covalent joining of the two diester bridges between the DNA fragments. This type of splicing or ligation is termed "sticky-end" ligation. The coupling of DNA fragments with double strands requires higher DNA-ligase concentrations, and this is termed "blunt-end" ligation (Fig. 9).

The recombination of DNA fragments *in vitro* is in general a fairly simple process, but may be complicated by three problems: the passenger can be incorporated into an insertion vector in two different orientations only one of which is required, the passenger DNA tends to oligomerize because of the overlapping "sticky ends", and the vector may recyclize preferentially. Successful recombination is easily monitored by hydrolyzing the recombinant DNA with the restriction enzyme used for construction. The fragments obtained (vector and passenger) are separated and identified by polyacrylamide electrophoresis from their molecular weight (Fig. 7). The correct orientation (polarity) of the passenger within the vector can be identified only by its proper biochemical function. The insertion is unambiguous with respect to the polarity if the vector at one site is cut smoothly and at the second site staggered. An analogously treated passenger can then be inserted only in one direction (Fig. 9, ⑥).

## 6. The *in vivo* Transformation of Cells

In the next step we have to introduce the recombinant DNA in a linear or circular form into the bacterial cell. This is not an easy problem since the cell wall and the cell membrane represent sturdy barriers against macromolecules. The simplest way to introduce a naked DNA into a microorganism is by transformation. The rate of incorporation, however, is very low and only one out of $10^6$ cells may take up a foreign DNA molecule[46a]. When *E. coli* are treated with 10 mM $CaCl_2$ solution, the cell membrane and cell wall become more penetrable (leaky), and the transformation rate is increased by a factor of 1000. Cells treated in this way are called competent cells[46b]. Bacteriophages such as λ or P22 exercise an efficient method of injecting their DNA into the bacterial cell, a procedure called transduction. Mimicking this procedure, the phage genome and passenger, which in the case of λ can be as large as 20—30 kbp, is packaged into the protein head of a λ phage[47]. The phage functions as a transport vehicle that injects the recombinant DNA into the host cell very efficiently. Since this method only functions if the passenger and vector DNA are approximately the size of λ-DNA (49 bp), the procedure can also be used simultaneously to size-select the passenger DNA.

Once inside the cell the foreign linear DNA is either joined head-to-tail to form a circular DNA molecule, a plasmid, or as a lytic phage it may be integrated into the recipient cell genome. If a plasmid contains a so-called "origin of replication", a nucleotide sequence which is recognized by the host DNA polymerase, then the plasmid is replicated with the same efficiency as the host genome[48]. It is segregated into progeny when the cell divides, and hence the number of plasmids in the daughter cell remains constant.

With Col E1 plasmids the number of plasmid copies can, however, be increased if the replication of the bacterial genome is inhibited by a protein synthesis inhibitor such as chloramphenicol. Under these circumstances cells may contain greater than 200 plasmid molecules. If, in addition, the passenger DNA has been inserted in tandem duplications into the plasmid, with an upper limit of 6—10 copies then there may be more than 2000 identical copies of one gene in a bacterial cell[49].

In the next stage of gene expression, the transcription process, mRNA has to be copied from genes encoded on a plasmid. This requires that "upstream" (in the 5′ direction) of the structural gene the regulatory signals for transcription are in the correct positions. These are promoter sequences which act as binding sites for the DNA-dependent RNA polymerase, while another sequence, the operator, binds the repressor protein and acts as a means of regulating the rate of transcription of a gene. Regulation by the repressor is an all or none effect; with the repressor present the gene is not transcribed. When the repressor is removed by an inducer or a metabolite from the medium, then the gene is free for transcription. The affinity of the promoter for the polymerase regulates the rate of transcription of the structural gene and thus the number of mRNA copies made from one gene[50]. Viral genes often contain high efficiency promoters, which guarantee that the viral genes are transcribed at the expense of the host's genes[51].

For most gene transfer experiments one selects a plasmid which already contains a well characterized promoter, for example the lactose promoter[52, 53]. The operator sequence can be partially deleted so that the lac-repressor can no longer bind to the operator. An intact operator can switch the synthesis of a protein on or off. In the case of the lactose operon, the repressor protein is encoded on a distant gene called the i-gene (Fig. 3).

The transcribed mRNA contains a specific sequence, the ribosomal binding site about 10—20 nucleotides upstream of the initiation codon AUG. This binding site shows a high affinity for ribosomes when it contains the Shine-Dalgarno sequence, a spacer of seven nucleotides and the initiator binding codon AUG. The start signal AUG which decodes methionine and the succeeding elongation codons, each of which is a trinucleotide, correspond to the number of amino acids in a protein. The termination codons UAA, UGA, and UAG do not decode an amino acid but function as stop signals to promote the release of the protein chain from the translation machinery[19].

Only when the recombinant plasmid or phage contains these regulatory elements in correct juxtaposition with the inserted passenger gene, is a protein made from the recombinant DNA inside the cell.

## 7. Selecting the Vector

The choice of vector is influenced by many factors including the type of passenger DNA being inserted, the type of restriction endonuclease used, whether or not ex-

pression of the insert is required, and the nature of the host. Commonly used vectors are mostly small plasmids or bacteriophages that have a number of useful restriction endonuclease sites (genetic markers) and a means of identifying bacteria that carry a recombinant DNA molecule (Table 6)[54–56]. Viral vectors have the advantage that they infect cells highly efficiently and reproduce rapidly.

Table 6. Survey of the main types of vectors.

| Vector | Advantages |
|---|---|
| Phage λ, specific insertion | Can incorporate passenger DNA up to 20–30 kbp; high transformation rate |
| Phage P22, unspecific insertion | |
| Plasmids | Low molecular weight, ideal for reconstruction, insertion of genes and promotors: exist multiply in cells and can be amplified [a] |
| Cosmids [b] | DNA can be packaged in the phage λ head |
| Eukaryotic viruses such as SV40 | Infect and transform mammalian cells, can be reconstructed into a "broad host range vector; from *E. coli* the human cells. |

[a] Plasmids can only be amplified if they contain a replication starting point derived from colicine producers. [b] Cosmids are plasmids which contain the cos region of phage λ.

Figure 10 shows everyone's favorite plasmid pBR322 (where p stands for plasmid, BR are the initials of the constructor and the digits represent the less successful predecessors)[57]. Here it may serve to demonstrate the essential features of a good cloning vector. It contains an origin of replication (Or), exists in multiple copies in the cell (20–50), has two antibiotic resistance genes ($Tc^r$ and $Ap^r$) and scattered restriction endonuclease digestion sites. One antibiotic resistance gene may be used to search for bacteria containing the plasmid (a selective marker); an antibiotic such as penicillin or tetracycline is often added to the growth medium to maintain the vector in the cell. By means of this selective pressure, only microorganisms which contain the antibiotic resistance plasmid will survive. The second antibiotic gene used for insertional inactivation, the passenger DNA, is inserted into the gene causing its inactivation. Cells resistant to the drug become sensitive when the plasmid contains the passenger-insert in the middle of the gene (inactivation). Thus the antibiotic resistance genes on a vector can serve two purposes: we can test for the presence of the plasmid in the cell and for insertion of passenger into the plasmid by antibiotic sensitivity/resistance tests (Fig. 11)[58].

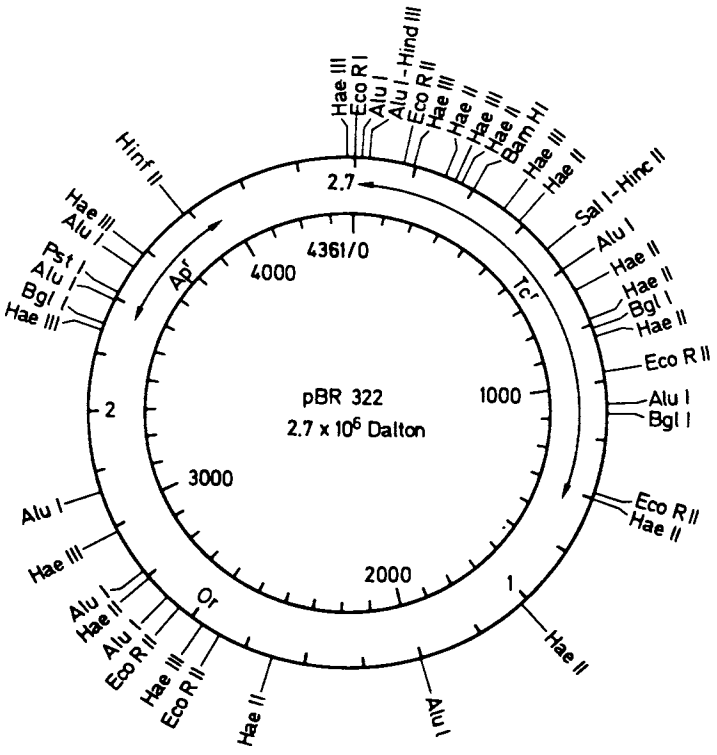



Fig. 10. Restriction map of the plasmid pBR322. The inner circle lists the number of base pairs. In the interspace between the circles we find the origin of replication (Or) and the two antibiotic resistant genes directed to ampicillin ($Ap^r$) and tetracycline ($Tc^r$). The positions at which the various restriction endonucleases cut are indicated on the outer circle.

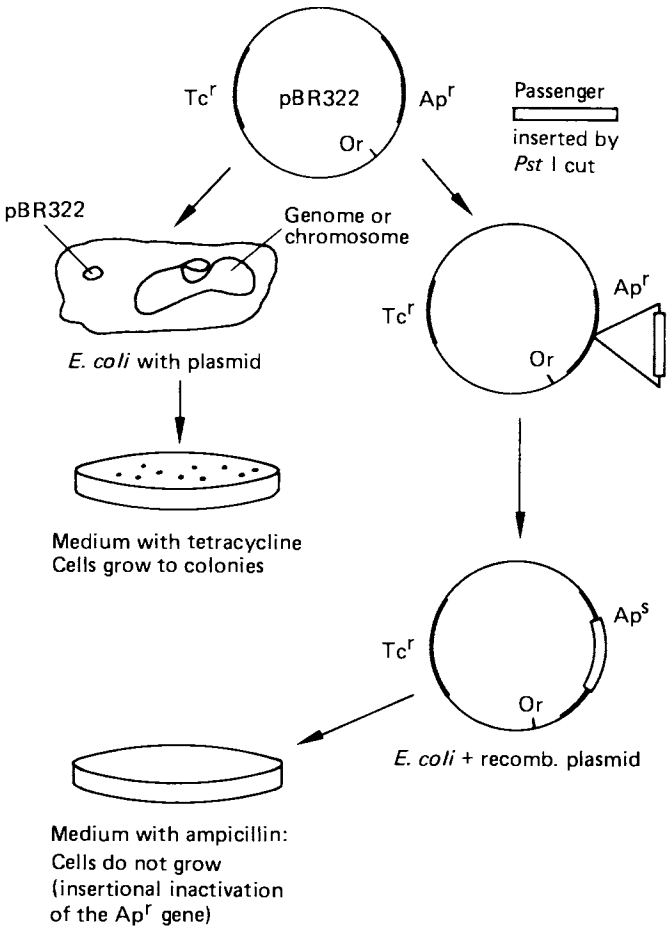



Fig. 11. Function of the two antibiotic resistance genes for selection and screening. Only cells which contain the $Tc^r$ gene can multiply on a tetracycline-containing medium. Following a Pst I cut the passenger is inserted into the $Ap^r$ gene, causing its inactivation. As a consequence cells become sensitive against ampicillin (insertional inactivation).

Plasmids or phages can be altered almost at will by insertions and deletions of foreign DNA fragments. Recombinations are aimed at the inclusion of effective promoters, the introduction of genetic markers, the construction of shuttle vectors, which can exist in different cells such as *E. coli* and yeast, and at reducing the biological hazards (Table 7)[59,60]. Many of the good vectors are patented now-a-days and can be obtained from commercial sources[59–61].

Table 7. Example of a host cell (χ 1776) suited for recombination experiments with plasmids using *E. coli*-plasmids in which a biological hazard may be suspected [a].

| Genotypic modification [b] | Effect |
|---|---|
| dap D8 | Dependence of diaminopimelinic acid in medium |
| min A1 | May form minicells |
| min B2 | |
| sup E42 | Suppression of amber mutants |
| nal A25 | Resistance against nalidixic acid |
| Δ29 (bio H-asd) | Deletion results in dependence of diaminopimelic acid and threonine |
| hsd R2 | Inactive restriction systems, favors transformation |
| F⁻ | Host cell without F factor |

[a] The safety standards are regulated in different ways in every country. Usually there are biological and laboratory safeguards, which have the character of either recommendations or rules. Charon 4A is a modified λ-phage which is often used for the manipulating of human DNA (gene libraries). It contains amber mutations in the gene for phage maturation, for the synthesis of the envelope proteins, and the lysis proteins of the host. Charon 4A can therefore be used to clone eukaryotic DNA. [b] Mutations are selected such that the phages can no longer self replicate *i.e.* it can only exist in the laboratory as part of the bacterium *E. coli* 1776 (biological safety level B2).

## 8. The Choice of the Passenger DNA

The choice of the passenger is of course determined by the research aim. A gene can be isolated preparatively in order to determine the DNA sequence, to delete an operator, to study the cell differentiation process, to transfer a gene from the genome into a plasmid, to cause overproduction of a protein, to produce a gene for a prenatal diagnosis, or to produce human proteins in bacteria[61]. Passenger DNA may be isolated directly by fragmentation of the genome, it can be made as a complementary copy from purified mRNA using reverse transcriptase, or it can be synthesized chemically. Finally it is purified by cloning and produced in preparative amounts.

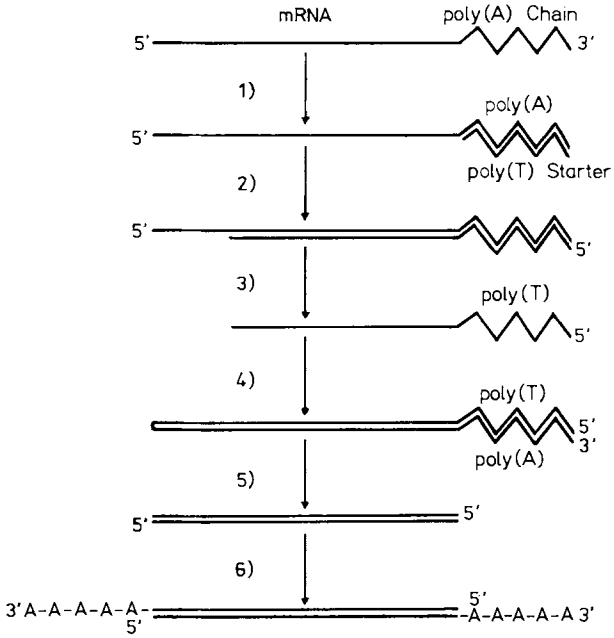



Fig. 12. Six-step synthesis of a double-stranded, complementary DNA (cDNA) using an mRNA as a template. Eukaryotic mRNA can be isolated by affinity chromatography on poly(dT)cellulose, since the mRNA contains a poly(A) segment at the 3'-end. The individual steps are: 1) Affinity chromatography on poly(dT). 2) Synthesis of the complementary strand with the reverse transcriptase and the four deoxynucleoside triphosphates. 3) Hydrolysis of the mRNA matrix strand with ribonuclease A digestion, addition of DNA polymerase I and dNTPs. 4) Duplication of the DNA strand with DNA polymerase. 5) Cleavage of hairpin and removal of tails by specific S1-nucleases. 6) Elongation of double-stranded DNA at the 3'-end by terminal transferase and ATP to form poly (A) tails. The vector is tailed by oligo(dT) tails to allow sticky end ligation of passenger and vector.

In order to establish a gene library, the genome must first be dissected into fragments of approximately 20 kbp size. Each fragment is inserted into a plasmid and the vector is channeled into the bacterium. A collection of all the possible genes in a genome is called a gene library. A collection of recombinant phages is obtained with all genes of a genome in the form of inserts into the phage DNA (Fig. 10). Such libraries exist for *E. coli,* rat, mouse, human, and many other organisms[62, 63].

In eukaryotic genomes the situation is more complex than in prokaryotes, since the structural genes are discontinuous in sequence. They are made up of translated regions (exons) and untranslated regions (introns) and the primary transcription product is processed to give the functional mRNA coding sequence[64]. To obtain a library of the coding regions of the DNA, the entire population of mRNA molecules is re-transcribed by means of the reverse transcriptase into a set of complementary or copy DNAs. Consequently such a collection of structural genes is called a cDNA library. The main steps of these methods are shown in Figures 12 and 13[65].

## 9. The Choice of the Host Cells

For most laboratory experiments *E. coli* is used, since the genetics of this microorganism are well understood and an ever increasing number of useful mutants is available. *E. coli* can be grown conveniently in a simple apparatus, and from a 1 L culture one may obtain 50 g wet weight of cells within 24 h. Laboratory strains of *E. coli* are not pathogens. However, as a producer of protein for industry *E. coli* may have some limitations, especially since as a gram negative bacterium it does not excrete proteins into the medium. Since considerable experience already exists on the large scale cultivation of yeasts, attempts are now being made to construct plasmids which express their passenger genes in yeast. *Bacillus subtilis,* a gram-positive bacterium exports many proteins into the medium. Unfortunately this organism has a number of disadvantages in that less is known about the organism, and there appears to be problems with the plasmid stability[66].

In gene transfer experiments with eukaryotic cells several types of passenger can be used. Simian virus 40 (SV40) is often used as a vector and the recipient cells are usually embryonic cells, such as baby hamster kidney (BHK) or Chinese hamster ovary (CHO)[67–69].

At the moment we don't have perfect vectors and we don't have perfect hosts.

## 10. The Search for the Correct Clone

To understand the problems in recombinant DNA research one has to realize the following: approximately one

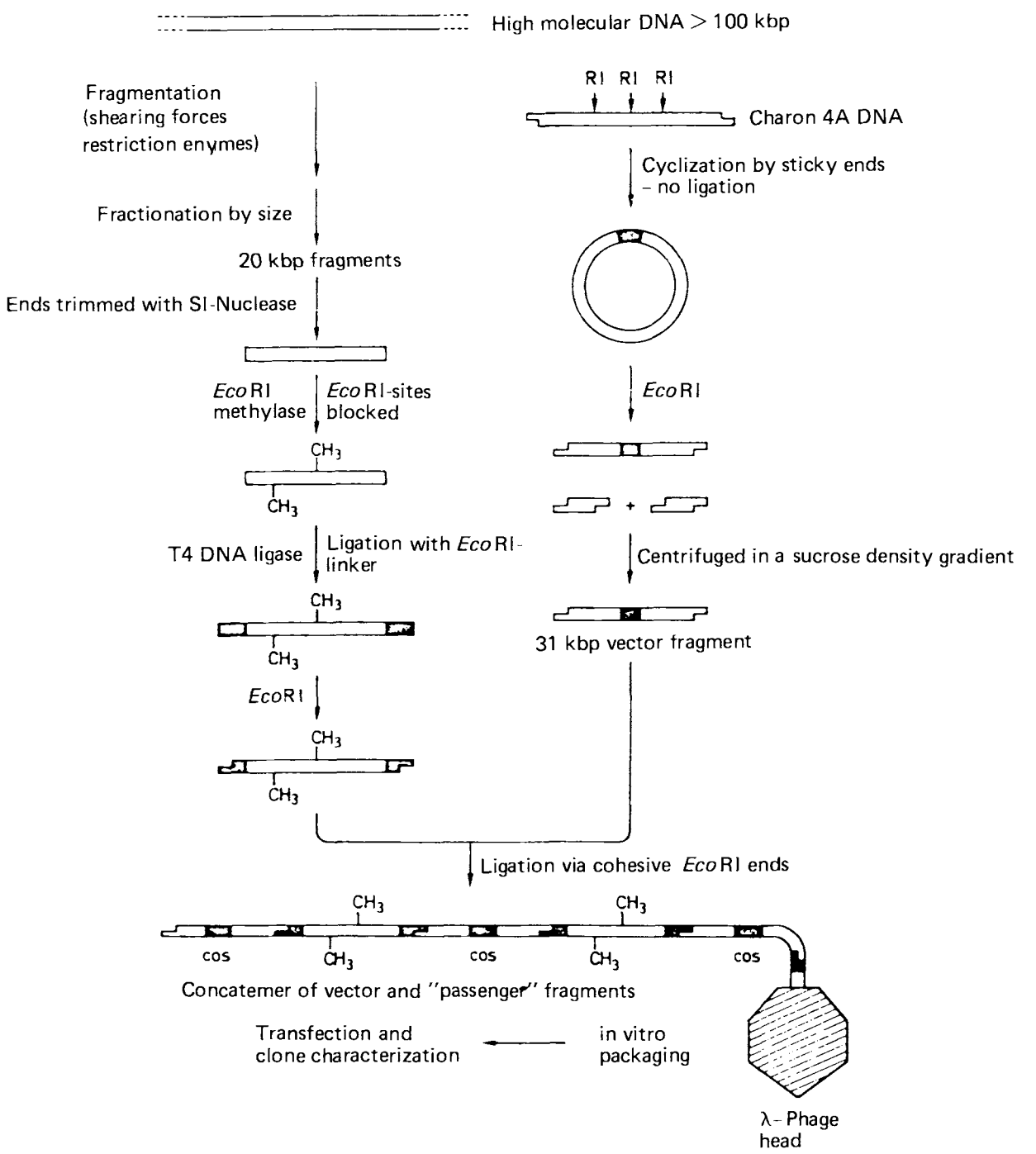



Fig. 13. Strategy for the production of a gene library from Drosophila-DNA after *Maniatis et al.* (*Cell 15* (1978) 687). With kind permission of the author and publisher (taken from R. Knippers: *Molecular Genetik*, Thieme, Stuttgart 1981). If one prepares a DNA library from an eukaryontic organism, then a number of additional tricks have to be used: The foreign DNA is cleaved into large fragments and is ligated to a modified phage vector called Charon 4A (Table 6). This vector contains the cos loci which allow vector plus passenger to be packaged into a phage's head. At first a concatemer is formed which is threaded into the phage's head. The DNA is split at the cos site to fragments 38—53 kbp long. Thus Charon 4A (31 kbp) can harbor 22 kbp of passenger DNA. If the long passenger fragments contain troublesome internal restriction sites they can be blocked by methylation (restriction). After adding *Eco*RI linkers (Fig. 22A) by blunt end ligation, *Eco*RI sticky ends are produced, which allow the oligomerization of the vector into a concatemer.

cell in 1000 takes up the recombinant DNA. Of these only one in 1000 may contain the passenger DNA correctly inserted in the vector. Only then can the cognate protein be made from the inserted gene. Bacteria have the advantage that they divide every 20 min and that $2^{72} = 4{\cdot}7 \times 10^{21}$ cells are produced in less than one day. Ideally these should be identical copies of the parental cell; however, bacterial cells have a relatively high frequency of mutation and may lose or exchange plasmids, and inserted foreign genes may be deleted by *in vivo* cutting and splicing. Therefore, the genetic stability of a recombinant strain is of critical importance[66].

The presence of recombinants can be assayed by antibiotic resistance or sensitivity. Plasmid-containing cells are

resistant to one drug. If the passenger is correctly inserted into the second antibiotic resistant gene then the cells become sensitive to a second drug *e.g.* tetracycline (insertional inactivation) (Fig. 11). This negative test has to be supplemented by a positive assay for the correct insertion of the passenger into the vector. In one very elegant system an enzyme is used which consists of two domains. Cells and plasmids are constructed such that the α-domain of β-galactosidase is located on the plasmid and the β-domain on the central genome[70]. If cells contain the native plasmid then the active enzyme is formed and (5-bromo-4-chloro-3-indolyl)-β-D-galactoside is hydrolyzed to the indole derivative, which in turn is oxidized in air to yield an indigo dye *i.e.* a cell clone with intact plasmid appears blue on the Petri plate. Insertion of a passenger into the plasmid does not result in formation of β-galactosidase and the colonies on an agar plate remain white, since no α-subunit of the enzyme can be synthesized. Thus positive clones (white colonies) can be selected from a background of blue colonies. Another test is based on the hybridization of the passenger with radioactive DNA or RNA directly on a nitrocellulose filter (colony hybridization). Using a radioactively labeled single strand DNA, which is base complemented to the passenger, one can investigate whether a double strand is formed between the test DNA and passenger *i.e.* whether both nucleic acids hybridize[71,72]. An obvious method, and the most informative one, is to assay the bacterial colony for direct expression of the plasmid-encoded protein. Since in the initial stages of cloning only minute amounts of passenger-encoded proteins are made by the host cells it is often difficult to identify the expression of the plasmid-encoded protein. When the enzymatic activity of the protein is to be examined, one needs a mutant host cell which is defective with respect to production of similar enzymatic activity. Plasmid and host cells first build a complementary system, which is capable of producing the enzyme (complementation test).

The enzymatic test has to be sufficiently sensitive to detect a pmol of protein and fast enough that one can test more than 1000 bacterial colonies per day. A more general approach is the use of a radioimmunoassay with radioactive antibodies directed against the protein in question[73]. Newer additions to the analysis of gene expression are the so-called mini- and maxicells. Both have in common the fact that the expression of the host genome can be eliminated, so that only plasmid-encoded proteins are produced[74]. The minicell strains, derivatives of *E. coli* K12, divide in such a way that a minicell without the host chromosome is produced on cell division. However, they maintain the plasmid and the protein synthesizing apparatus necessary for gene expression. With [$^{35}$S] labeled methionine the plasmid-encoded radioactive proteins are synthesized and can easily be analyzed by polyacrylamide gel electrophoresis. In maxicell strains the genome is inactivated by a dose of UV irradiation which destroys the genome but leaves the plasmid intact[75].

In addition to *in vivo* systems for gene expression there are several cell-free protein synthesizing procedures using wheat germ, *E. coli* extracts, reticulocyte lysates and others[76-78]. They show the advantage that linear DNA (in the case of *E. coli*) and mRNA can be translated. The efficiency of these systems is low since the nucleic acid templates are rapidly degraded by cellular nucleases and the endogenous RNA concentration is high. However, appropriate labeling conditions in combination with precipitation with antisera can be used to identify the required product. Furthermore one can inject the DNA directly into the nucleus of a frog oocyte or an embryo cell[79,80].

The vector containing the passenger is then isolated in preparative amounts and the position of the passenger within the plasmid is verified by mapping with restriction endonucleases. Finally, the passenger including flanking DNA regions is sequenced by either the *Maxam* and *Gilbert* or the *Sanger* procedure[81-83]. DNA sequence and gene expression represent the final proof for a successful cloning experiment.

## 11. Processing the Polypeptide Chains

Up to now we have discussed protein synthesis in very simplified terms; a nucleotide sequence of either DNA or RNA is translated into an amino acid sequence of a protein. However, in reality the process is much more complex, particularly in the metabolism of higher organisms. The newly made polypeptide chain often does not attain its final biologically active conformation until it has been subjected to processing or covalent modification. Such changes are called posttranslational modifications[84,85]. Proteins may be modified by glycosidation, phosphorylation, disulfide bond formation, and a whole battery of other substituents: another group of proteins is translated as so-called preproproteins. Insulin from bovine pancreas is translated, *e.g.* by ribosomes, as preproinsulin and has 104 amino acids[86]. The pre- or signal-sequence, which consists of 23 amino acids, directs the ribosomes to the endoplasmic reticulum and causes this protein to be channeled into the interior of the reticulum. Subsequently, the signal sequence is cleaved. Proinsulin, the inactive precursor of insulin contains 81 amino acids. Only after removal of the middle C-peptide does the active enzyme, with 51 amino acids, result. In general, signal sequences channel peptides into the endoplasmic reticulum, or in bacteria into the periplasmic space or the culture medium.

In order to understand the processing and the activation of a protein it is necessary to elucidate the chemical principles of the protein synthesizing machinery of a cell[19], and to understand the chemistry of membranes[87,88], as well as the effect of chemical modifications of individual amino acids on the tertiary structure of proteins[89]. There are many fascinating questions in molecular biology, but until recently chemists were not interested in tackling them.

## 12. Models are to Molecular Biology what Mechanisms are to Chemistry

Figure 1 shows our present understanding of DNA encoded, ribosome-dependent protein synthesis. Over the details little is understood at present. This is especially true for the function of regulatory sequences for mRNA production and translation, for the selection of the cognate tRNA, for the conversion of GTP-stored energy into mRNA movement, and so on.

Even more limited is our understanding of the structure and function of membranes or of the cytoskeleton of cells: there are plasma membranes, nuclear membranes, and the membranes of organelles such as the inner mitochondrial membrane. They all have specific functions in substrate transport, as binding sites for multienzyme complexes, in the production of ATP from proton gradients, and in the generation of electric potentials. We know much about the protein and phospholipid composition of membranes and a variety of models describing membrane function exist. Beautiful names such "fluid mosaic model" most convincingly demonstrate our lack of chemical knowledge[90].

Why is one protein transported through the plasma membrane into the periplasmic space whereas another stays in the cytoplasm? This is an important question for the large scale production of proteins by microorganisms[91,92]. We know that excreted proteins contain signal sequences of approximately 30 amino acids in length, that hydrophobic amino acids are clustered in one part of the signal sequence, and that the occurrence of a proline in a defined position is often of critical importance for the function of signal sequences. But why is a protein, a macromolecule, excreted through the membrane? At present these problems seem to be of no interest to organic chemists. It may be easy to elucidate the configuration of a steroid by X-ray crystallography, but it still takes a battery of techniques and considerable imagination to elucidate the chemistry of membranes.

## 13. Chemical Synthesis of Gene Fragments on Supports: Synthesis Using Syringes and Serum Caps

The synthesis of nucleic acids in the laboratory started about thirty years ago. Early synthetic efforts concentrated on the search for suitable protective groups for the bases and the ribose moiety and selection of the proper condensing agents for phosphodiester bond formation. The phosphodiester approach used at that time enabled, albeit with some effort, the preparation of short oligonucleotides containing 10—20 nucleotides[93]. Using the enzymes oligonucleotide kinase and DNA ligase, which had just been discovered by biochemists, these oligonucleotides were assembled into longer DNA fragments. The synthesis of the structural gene for tyrosine tRNA, a DNA segment containing 200 bp, by *Khorana et al.* highlighted many years of continuous efforts in nucleic acid synthesis[94]. However, in comparing effort and achievement it became clear that chemical gene synthesis was unlikely to become a standard laboratory method. This was due to the low yields in the condensation step, the long reaction times, and especially the time-consuming purification of intermediates. However, the real handicap in DNA synthesis was that DNA could not be sequenced at that time. Thus *Khorana et al.* had to synthesize a tRNA gene since he could deduce the DNA sequence from the known primary structure of a ribonucleic acid, tyrosine tRNA.

With the discovery of genetic engineering techniques for the cutting and handling of DNA fragments of biological interest in combination with the fast and easy sequencing methods for DNA, the situation changed dramatically. However, most experts in the field concentrated on the isolation of gene fragments from natural sources by genetic methods.

It was the chemical synthesis of the structural gene for the human leukocyte interferon, a DNA fragment with 517 bp, which convincingly demonstrated the tremendous progress chemical oligonucleotide synthesis had made (Fig. 14)[95].

This outstanding success in gene fragment synthesis was mainly due to the switch from the phosphodiester ap-

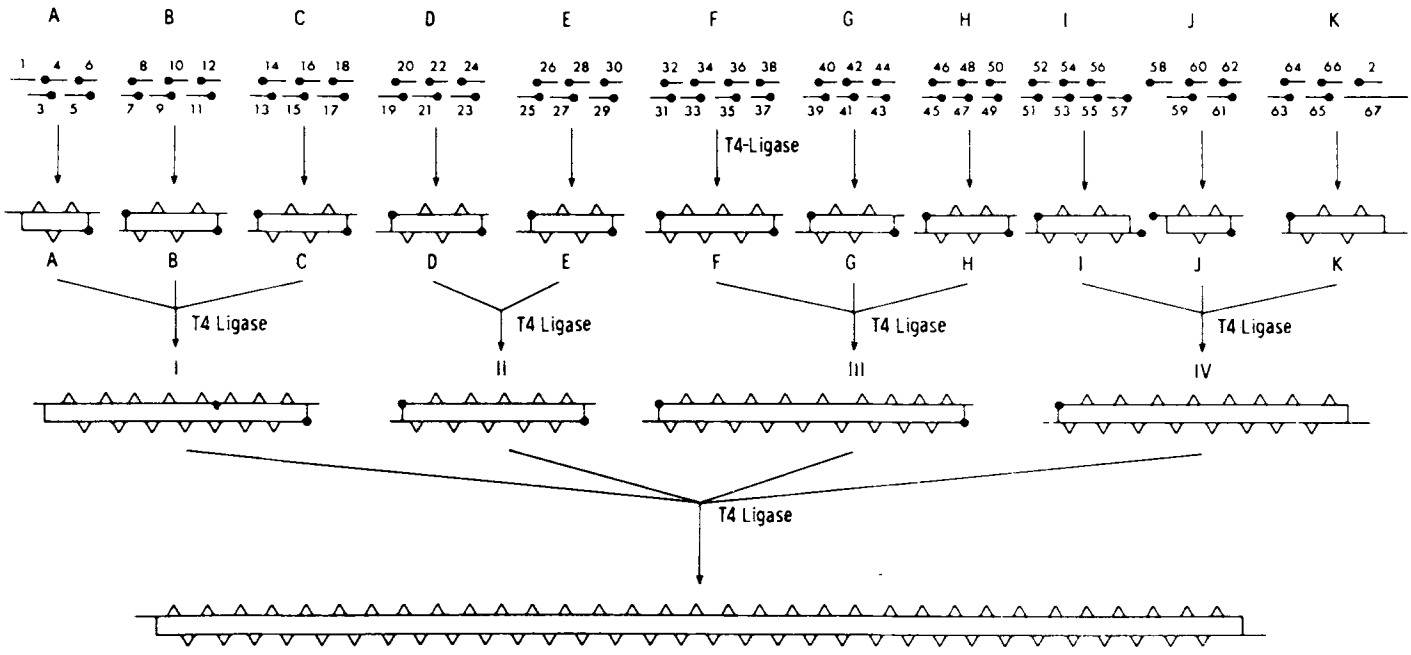



Fig. 14. Synthetic strategy for the preparation of the human leucocyte interferon gene. 67 Oligonucleotide of chain lengths 10—20 were prepared by the phosphotriester approach. By means of T4 DNA ligase they were spliced to yield the structural gene for interferon. Although the product, a 517 bp fragment, only exhibits a low degree of purity, the interferon gene could be enriched by cloning and be isolated.

proach to the triester methodology (Fig. 15) and to the Merrifield-analogous polymer synthesis on supports[96,97]. In addition there were other reasons why developments in this field speeded up tremendously, above all instrumental developments in preparative separation methods, such as HPLC and polyacrylamide gel electrophoresis.

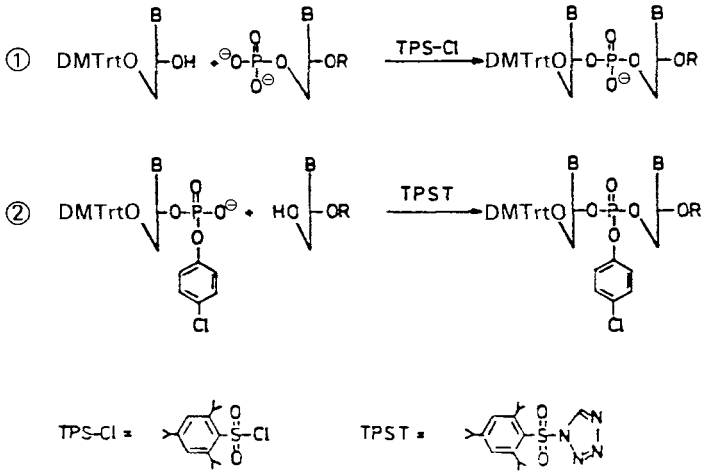



Fig. 15. Chemical principles of the phosphodiester ① and the phosphotriester methods ②. The essential difference between the two methods is that, because of the absence of charge, the triesters are no longer polar and are hence readily soluble in nonpolar solvents. DMTrt = dimethoxytrityl.

In 1970, using a mechanized "peptide synthesizer", *Merrifield* and *Gutte* made the enzyme ribonuclease A on a polymer carrier. For a protein consisting of 124 amino acids they had to employ 369 reactions, representing 11391 mechanical operations[98]. In the nucleic acid field the coupling of nucleotides on synthetic supports was not efficient enough and the product yields were extremely low[99].

There were two basic reasons for their failures: firstly the supports chosen were not appropriate for the chemical reactions used in DNA synthesis, and secondly the chemical reactions were insufficient in terms of their selectivity and yields to meet the extra demands of a stepwise polycondensation. The classical phosphodiester approach to DNA synthesis proved to be ill-suited since the charged, and thus highly polar, nucleotide diesters are barely soluble in organic solvents and are incompatible with the hydrophobic properties of the solid support. Completely anhydrous conditions and nonpolar solvents, however, are a *conditio sine qua non* for fast and quantitative condensation reactions.

In the phosphotriester approach, as pioneered by *Letsinger et al.* and perfected by *Itakura et al.* and *Gait et al.*, the growing oligonucleotide chains contain uncharged, fully protected phosphates. They are found to be compatible in solvation properties with a variety of polymer supports such as polyamides, polystyrenes and silica[100].

The triester approach can be subdivided; the monomer coupling technique is used as a cost-effective method for the synthesis of oligonucleotides containing up to 20 bases. The method of choice at present is the charged compound coupling reagent method[101-103]. The protected monomers are used as the triethylammonium salts of the phosphodiesters, which are readily soluble in pyridine: 1-(mesitylenesulfonyl) 3-nitrotriazole (MSNT) is used as a condensing agent. With these reagents coupling times are about 45 min at 45 °C and the yields are greater than 95% per coupling (Fig. 16).

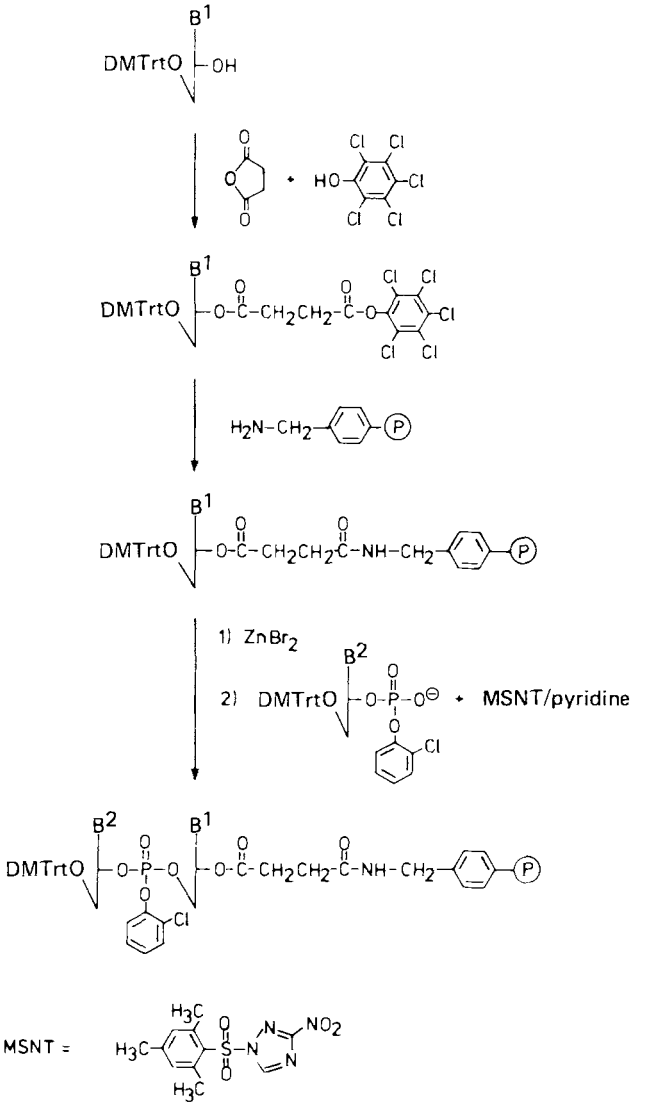
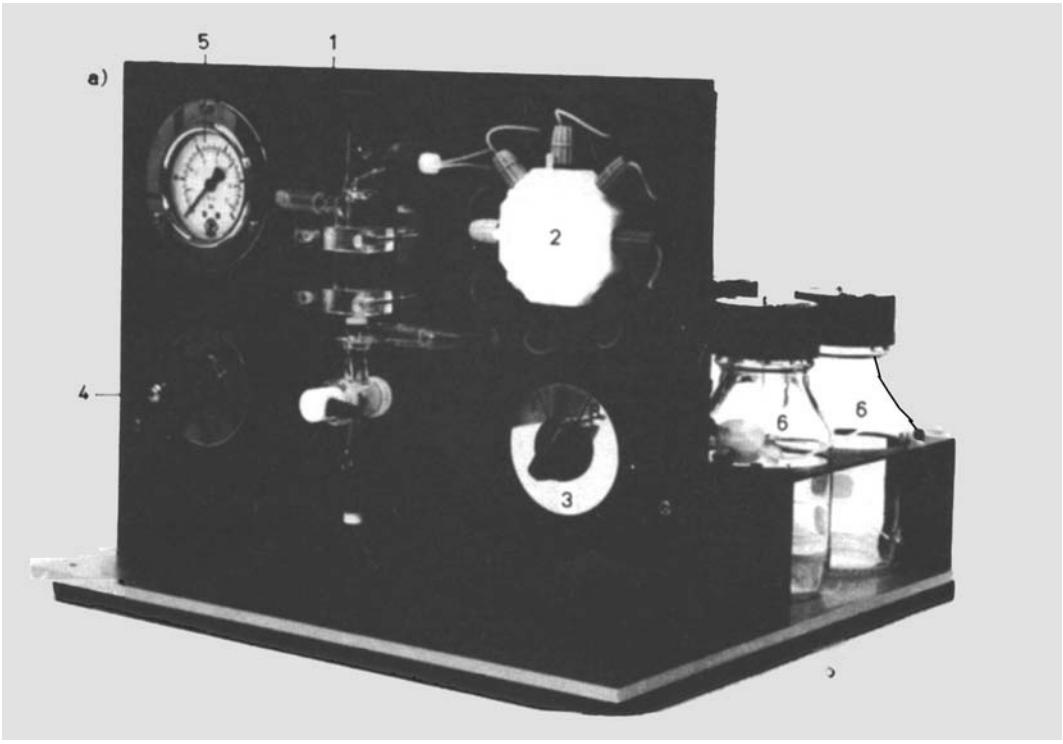



Fig. 16. Functionalization of a polystyrene support with a protected nucleoside, and synthesis of a dinucleotide. The 5'-dimethoxytrityl group of the first nucleoside is removed by $ZnBr_2$. Subsequently, the condensation step follows using the charged-compound coupling method with 1-(mesitylenesulfonyl)-3-nitrotriazole (MSNT) as condensing agent. DMTrt = dimethoxytrityl.

If one wishes to prepare oligonucleotides containing more than 20 bases it is wise to proceed *via* the block-coupling method. This method is identical to the procedure described previously but uses dimers or trimers as coupling compounds and by this means DNA containing up to 40 bases can be prepared. Both types of polymer support syntheses are easily accomplished using a bench-type DNA synthesizer or a fully automated machine as depicted in Figure 17[104].

In recent years a chemically more elegant route for internucleotide bond formation has been developed by *Caruthers et al.*, and is referred to as the "phosphite method"[105,106]. It overcomes the problem of negative charge by first preparing the dinucleotide phosphite ester which in a second step is oxidized by iodine to a phosphate bond.



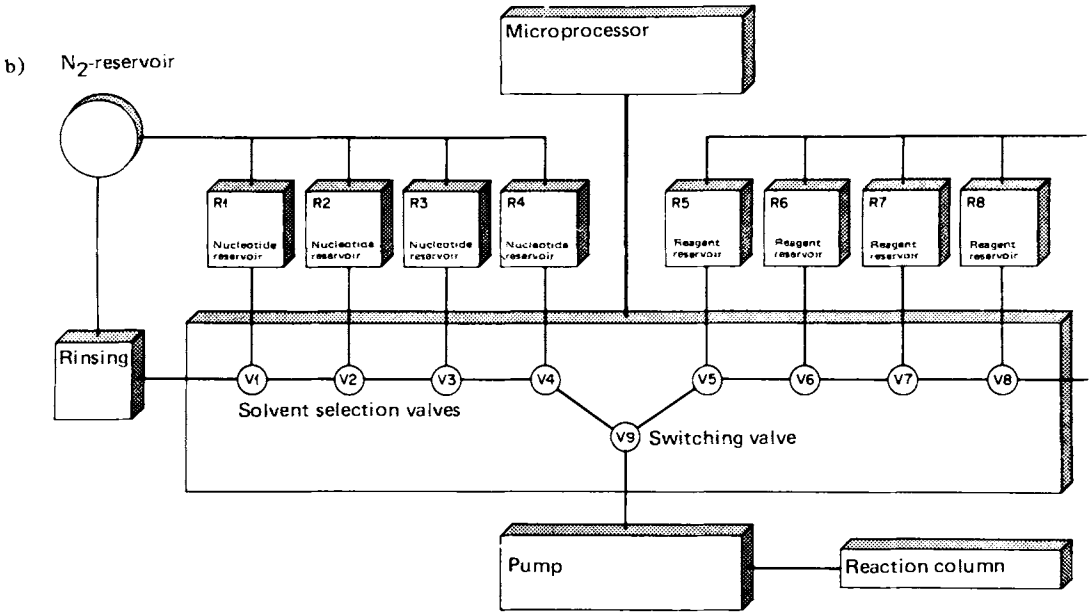




Fig. 17. a) Semiautomatic "DNA synthesizer": 1) reaction column, 2) eight-way valve, 3) three-way valve, 4) pressure control, 5) manometer, 6) reagent bottles. Photo by courtesy of Firma Labor Service, Darmstadt. b) Schematic diagram of a microprocessor-controlled, automated gene fragment synthesizer. Courtesy of *R. M. Cook*, Biosearch, San Raffael, CA, USA.

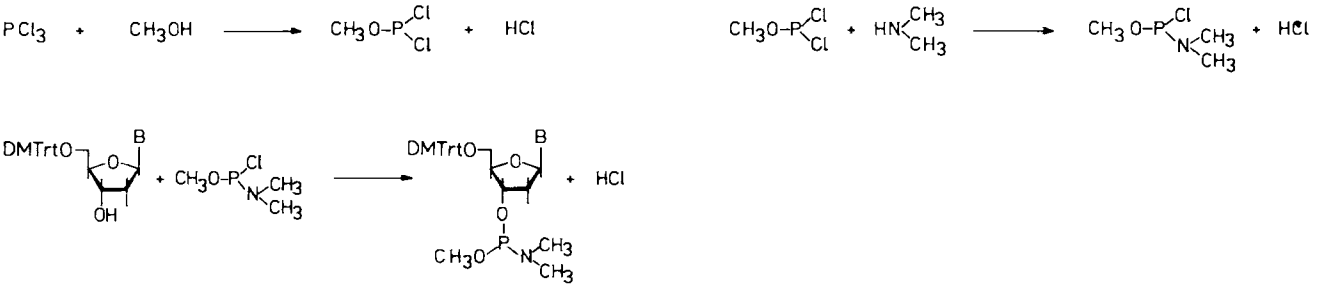



Fig. 18. Scheme for the synthesis of the deoxynucleoside phosphoramidites. DMTrt = dimethoxytrityl, B = thymine or the protected bases $N^6$-benzoyladenine, $N^4$-benzoylcytosine, $N^2$-isobutyrylguanine.

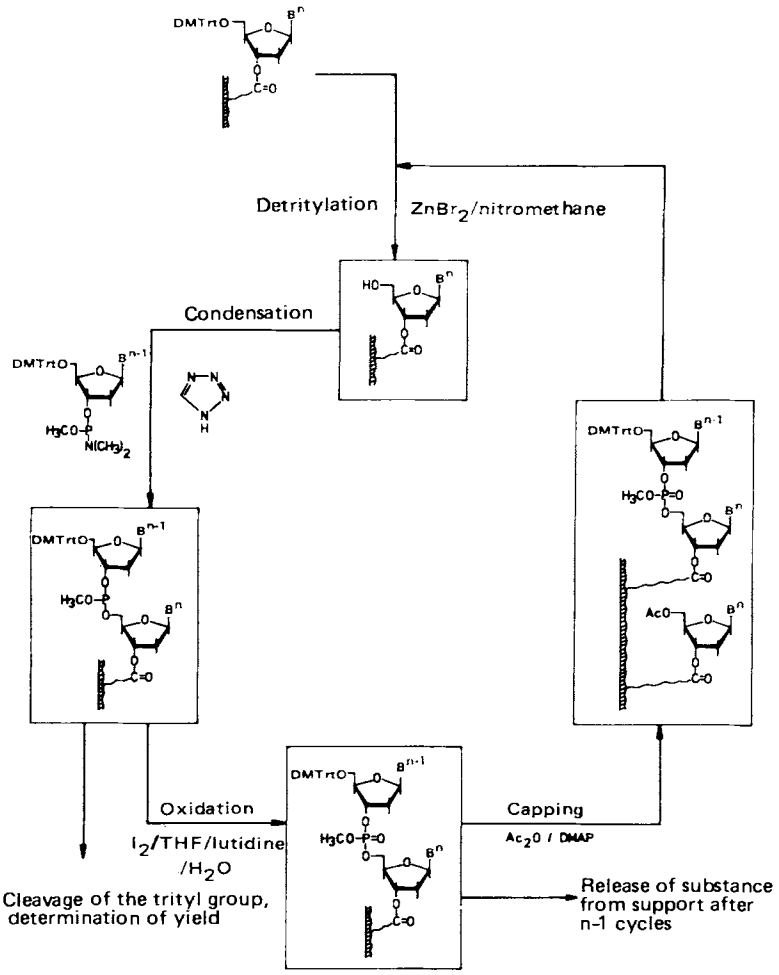



Fig. 19. Synthesis of DNA fragments on a polymer support by the phosphite method.

The preparation of the deoxynucleoside phosphoroamidites from the protected nucleosides and chloro(*N,N*-dimethylamino)methoxyphosphane is a simple and convenient method (Fig. 18)[107]. However, synthesis of the trisubstituted phosphane from trichlorophosphane is very tricky since it is spontaneously pyrophoric when it comes into contact with water. The phosphorylating agent must be highly purified by triple distillation and its purity checked by $^{31}$P-NMR spectroscopy; only when this is fulfilled does the condensation reaction proceed in high yield. With these highly reactive intermediates, called "reaction bombs" by *van Boom et al.*, a new type of synthetic chemistry started in the nucleic acid field[108]. Its tools are the syringe, the serum cap, absolute exclusion of moisture, and ultrapure reagents. Its rewards are coupling times of 5 min at room temperature and yields in the range of 90% (Fig. 19)[100].

Even with 90% yield in each reaction cycle polymer synthesis comes out of phase after about 10 cycles. Therefore, both methods use a capping step: unreacted oligonucleotide chains are blocked by acetylation of the 5′-hydroxyl groups. After completion of the synthesis the protective groups have to be removed and the oligonucleotide is split off the support. Total recovery of oligomer with 20 members is usually 5–10% relative to the nucleoside-activated support (Fig. 20)[109]. The "correct oligonucleotide" can be selected by the bacterium even from a crude mixture of

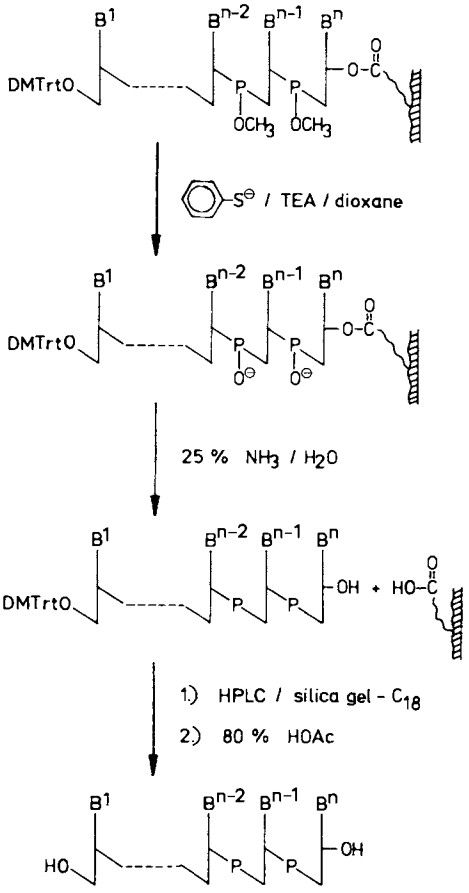



Fig. 20. Individual steps in the release of the oligonucleotide from the solid support and the removal of the protective groups. TEA = triethylamine; silica gel-$C_{18}$ = reversed phase material with $C_{18}$ alkyl residues. The trityl group is removed after an initial separation of the oligonucleotide by reversed phase chromatography with $C_{18}$-silica gel. This allows the separation of the desired oligonucleotide from incomplete and thus trityl-lacking oligonucleotides. Finally the oligonucleotide is purified by HPLC ion exchange chromatography.

oligonucleotides and the DNA sequence reproduced at will by cloning.

For the conventional purification of the nucleotides mainly three techniques are used: 1) reversed phase chromatography and size exclusion chromatography, 2) high pressure liquid chromatography with reversed phase or ion-exchange columns, 3) polyacrylamide gel electrophoresis (Fig. 21). The oligonucleotide bands may be visualized by UV-shadowing using an "intensifier screen" or by autoradiography if the oligonucleotide had been previously labeled with [$^{32}$P]phosphate. Following purification, the sequence of the oligonucleotide has to be confirmed by analysis. This may be done by the *Maxam* and *Gilbert* procedure, as adapted for oligonucleotides, or by two dimensional fingerprinting (wandering spot method)[100].

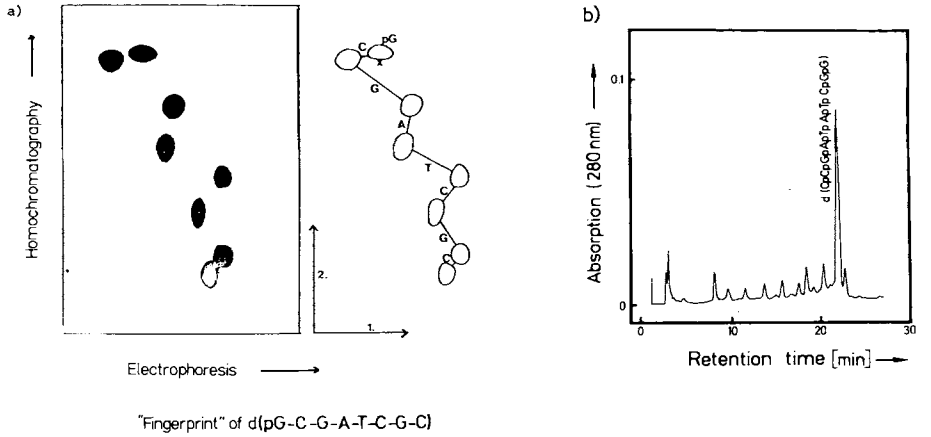



Fig. 21. Sequence determination of chemically synthesized oligonucleotides. a) Two-dimensional separation of oligonucleotides by the "wandering spot" method after limited hydrolysis of snake venom phosphodiesterase (*A. R. Frank, H. Blöcker* in [100], p. 225). b) Separation of a decamer by HPLC using a 4.6 mm × 250 mm ion exchange column (*L. W. McLaughlin, J. V. Krusche* in [100], p. 177).

Obviously the synthesis of the interferon gene by chemical fragment synthesis followed by enzymatic assembly has been a good advertisement for chemical gene synthesis. However, gene synthesis is not a major goal of nucleic acid chemists. The isolation of complete genes is accomplished more easily by cutting plasmids or genomes with a variety of restriction endonucleases. However, it is very difficult to cut out a 20 bp fragment, even from a plasmid, since two convenient restriction sites are usually not very close and the recovery, 20 bp out of $10^4$ bp, is low.

Thus, gene isolation and fragment synthesis are two complementary techniques. Small fragments are needed as linkers and adapters for the introduction of new restriction sites into a plasmid (Fig. 22). They are used to introduce high-affinity promotors or operators into the regulatory unit of the gene. They serve to partially double strand a single stranded DNA either for sequence analysis or for the preparation of copy DNA[110] and are the ideal affinity probes for the isolation of a defined mRNA from the cytoplasm of prokaryotes and eukaryotes[111]. Synthetic methods enable the insertion of unusual nucleotides, such as 5-methyldeoxycytidine, into the regulatory part of a gene and the study of their influence on cell differentiation. Unexplored as yet is chemical mutagenesis[112]. By introducing a small synthetic DNA fragment into a defined position on a genome we can produce proteins which are altered in a chosen amino acid. Using this method we can then study the influence of one amino acid change on the active center of an enzyme and on its catalytic properties. Besides the biological applications, we can now isolate mg-amounts of genes and study the chemical details of protein-nucleic acid interaction.

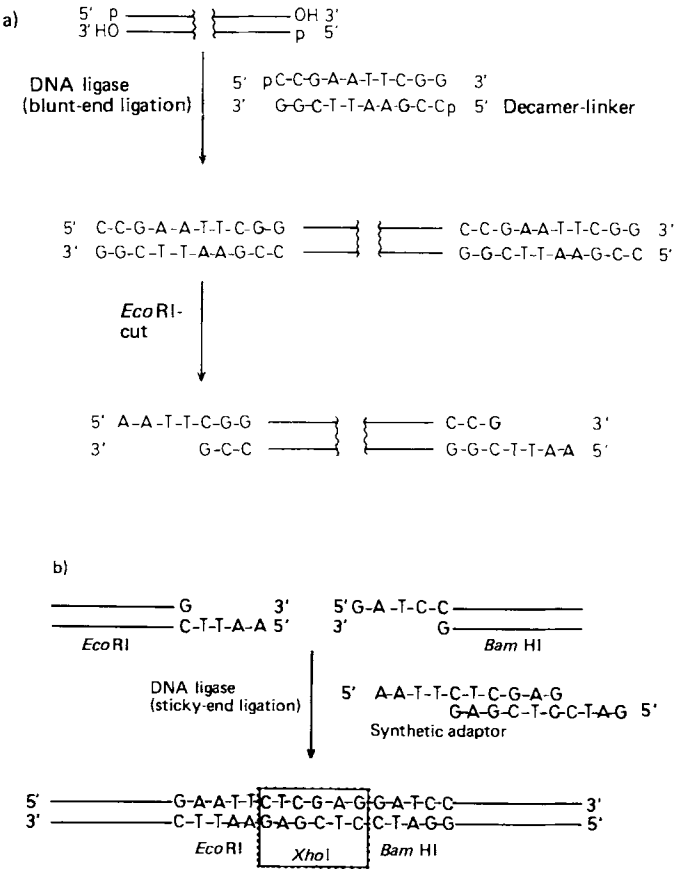



Fig. 22. a) Construction of single strands by "blunt-end" ligation of chemically prepared linker and adaptor with a subsequent *Eco*RI step. Such a fragment can be incorporated into an *Eco*RI linearized plasmid pBR322. b) Use of a synthetic adaptor to create a new restriction site within a DNA fragment (*Xho*I = C↓TCGAG).

## 14. The Future Role of Chemistry in Molecular Biology

In the last 20 years the advances in molecular biology have been dominated by geneticists. But now it seems that chemists are making a comeback. Chemists have learned to isolate, to sequence, and to synthesize genetic material. Of course genetics is only one aspect in the wide field of molecular biology. However, there is some hope that chemists will turn to protein conformation, to cell walls and membranes, and eventually to cell differentiation and information storage. The tackling of the chemistry of the living being requires, besides a good knowledge of chemistry, an open mind, some imagination, and the willingness to accept and to learn.

*The financial support of the Fonds der Chemischen Industrie and the Otto-Röhm-Stiftung to one of us (HGG) is gratefully acknowledged. We are grateful to Mrs. E. Rönnfeldt for her expert help in preparing the manuscript.*

Received: September 23, 1982 [A 438 IE]
German version: *Angew. Chem. 95* (1983) 26

[1] F. Miescher, *Hoppe-Seyler's Med. Chem. Unters. 1871,* 441.
[2] C. Correns, *Ber. Dtsch. Bot. Ges. 18* (1900) 158.
[3] P. O. P. Ts'o in P. O. P. Ts'O: *Basic Principles in Nucleic Acid Chemistry,* Academic Press, New York 1974, p. 2ff.
[4] P. A. Levene, L. A. Mikeska, T. Mori, *J. Biol. Chem. 85* (1930) 785.
[5] E. Chargaff, J. H. Davidson: *The Nucleic Acids, Vol. I–III,* Academic Press, New York 1955.
[6] J. D. Watson, F. H. C. Crick, *Nature 171* (1953) 737.
[7] R. Olby: *The Path to the Double Helix,* University of Washington Press, Seattle WA, 1974.
[8] V. A. Bloomfield, D. M. Crothers, I. Tinoco, Jr.: *Physical Chemistry of Nucleic Acids,* Harper and Row, Bussum 1974.
[9] O. T. Avery, C. M. MacLeod, M. McCarty, *J. Exp. Med. 79* (1944) 137.
[10] O. Hartwig, *Morphol. Jahrb. 1875,* 1.
[11] H. Fol, *Mem. Soc. Phys. Geneve 1879,* 26.
[12] A. D. Hershey, M. Chase, *J. Gen. Physiol. 36* (1953) 39.
[13] J. D. Watson: *Molecular Biology of the Gene,* W. A. Benjamin, Menlo Park, CA 1970.
[14] A. M. Maxam, W. Gilbert, *Proc. Natl. Acad. Sci. USA 74* (1977) 560.
[15] a) W. Gilbert, *Angew. Chem. 93* (1981) 1037; b) F. Sanger, *ibid. 93* (1981) 937.
[16] R. Knippers: *Molekulare Genetik,* Thieme, Stuttgart 1981.
[17] F. Jacob, J. Monod, *J. Mol. Biol. 3* (1961) 318.
[18] C. Janofsky in R. H. Hagnes, P. C. Hanawald: *The Molecular Basis of Life,* Freeman, San Francisco 1968, p. 224ff.
[19] H. G. Gassen, *Angew. Chem. 94* (1982) 15; *Angew. Chem. Int. Ed. Engl. 21* (1982) 23.
[20] J. Shine, L. Dalgarno, *Proc. Natl. Acad. Sci. USA 71* (1974) 1342.
[21] P. Kourilsky, P. Chambon, *Trends Biochem. Sci. 3* (1978) 244.
[22] R. Y. Stanier, E. A. Adelbery, J. L. Ingraham: *The Microbial World,* 4th edit., Prentice-Hall, London 1976.
[23] A. J. Bukhari, J. A. Shapiro, S. L. Adhya: *DNA: Insertion Elements, Plasmids and Episomes,* Cold Spring Harbor Laboratory, Cold Spring Harbor, NJ 1977.
[24] N. Willets, R. Skurray, *Annu. Rev. Genet. 14* (1980) 41.
[25] R. C. Clowes, *Sci. Am. 228* (1973) No. 4, p. 18.
[26] R. Watanabe, *Bacteriol. Rev. 27* (1963) 87.
[27] R. P. Novick, *Sci. Am. 243* (1980) No. 6, p. 102.
[28] N. D. Zinder, J. Lederberg, *J. Bacteriol. 64* (1952) 679.
[29] a) A. D. Hershey: *The Bacteriophage Lambda,* Cold Spring Harbor Laboratory, Cold Spring Harbor, NJ 1971; b) H. A. Nash, *Annu. Rev. Genet. 15* (1981) 143.
[30] J. Abelson, E. Butz: *Science 209* (1980) 1317.
[31] W. Gilbert, L. Villa-Komaroff, *Sci. Am. 242* (1980) 74.
[32] J. K. Setlow, A. Hollaender: *Genetic Engineering, Principles and Methods,* Plenum Press, New York 1979.
[33] P. Berg, *Angew. Chem. 93* (1981) 885.
[34] K. E. Davies, *Hum. Genet. 58* (1981) 351.
[35] A. E. H. Emery, *Lancet II 1981,* 1406.
[36] R. Wu, *Methods Enzymol. 68* (1979) 1.
[37] Industrial Microbiology in *Sci. Am. 245* (1981) No. 3, p. 42ff.
[38] R. Yuan, *Annu. Rev. Biochem. 50* (1981) 285.
[39] W. Arber, *Mannheimer Forum 81/82,* Boehringer Mannheim 1982, p. 9ff.
[40] H. Smith, *Science 205* (1979) 455.
[41] W. Hillen, R. D. Klein, R. D. Wells, *Biochemistry 20* (1981) 3748.
[42] R. Blaich: *Analytische Elektrophorese-Verfahren,* Thieme, Stuttgart 1978.
[43] T. G. Cooper: *Biochemische Arbeitsmethoden,* de Gruyter, Berlin 1981.
[44] C. C. Richardson, *Proc. Natl. Acad. Sci. USA 54* (1965) 158.
[45] B. Weis, A. J. Sablon, T. R.Live, G. C. Fareed, C. C. Richardson, *J. Biol. Chem. 242* (1968) 4543.
[46] a) S. H. Goodgal, R. M. Harriot, *J. Gen. Physiol. 44* (1961) 1201; b) S. N. Cohen, A. C. V. Chang, L. Hsu, *Proc. Natl. Acad. Sci. USA 61* (1972) 2110.
[47] J. Collins, B. Hon, *Proc. Natl. Acad. Sci. USA 75* (1978) 4242.
[48] P. Starlinger, *Annu. Rev. Genet. 11* (1977) 103.
[49] J. K. Davies, P. Reeves, *J. Bacteriol. 123* (1975) 96.
[50] A. Travers, *Nature 263* (1976) 641.
[51] R. Losick, M. Chamberlin: *RNA Polymerase,* Cold Spring Harbor Laboratory, Cold Spring Harbor. NJ 1976.
[52] W. S. Reznikoff, J. N. Abelson in J. H. Miller, W. S. Reznikoff: *The Operon,* Cold Spring Harbor Laboratory, Cold Spring Harbor, NJ 1978, p. 221ff.
[53] R. Dickson, J. Abelson, W. Barnes, W. Reznikoff, *Science 187* (1975) 27.
[54] S. N. Cohen, *Nature 263* (1976) 731.
[55] D. B. Clewell, *Microbiol. Rev. 45* (1981) 409.
[56] a) P. Broda: *Plasmids,* W. H. Freeman, San Francisco 1979; b) D. R. Helinski, *Crit. Rev. Biochem.* (1979) 83.
[57] J. G. Sutcliffe, *Cold Spring Harbor Symp. Quant. Biol. 43* (1979) 77.
[58] F. W. Stahl: *Genetic Recombination,* W. H. Freeman, San Francisco 1979.
[59] E. L. Korvak, *Gene 15* (1981) 1.
[60] Bundesministerium für Forschung und Technologie (BMFT): *Richtlinien zum Schutz vor Gefahren durch in vitro neukombinierte Nukleinsäuren,* 3rd edition, BMFT-Bundesanzeiger, Bundesanzeiger-Verlagsgesellschaft, Köln 1980.
[61] W. Klingmüller, *Naturwissenschaften 66* (1979) 182.
[62] T. Maniatis, R. C. Hardison, E. Lacy, J. Laver, C. O'Connell, D. Quon, G. K. Sim, A. Efstratiadis, *Cell 15* (1978) 687.
[63] W. B. Anderson, E. G. Diacumakos, *Sci. Am. 245* (1981) 106.
[64] J. Abelson, *Annu. Rev. Biochem. 48* (1979) 1035.
[65] R. Wu, C. P. Bahl, S. A. Narang, *Prog. Nucleic Acid. Res. Mol. Biol. 21* (1978) 101.
[66] W. J. Whelan, S. Black: *From Genetic Experimentation to Biotechnology,* Wiley, Chichester 1982.
[67] R. C. Mulligan, B. H. Howard, P. Berg, *Nature 277* (1979) 108.
[68] J. T. Elder, R. A. Spritz, *Annu. Rev. Genet. 15* (1981) 295.
[69] P. Berg, *Biosci. Rep. 1* (1981) 269.
[70] U. Rüther, M. Koenen, M. Otto, B. Müller-Hill, *Nucleic Acids Res. 9* (1981) 4087.
[71] M. Grünstein, D. S. Hogness, *Proc. Natl. Acad. Sci. USA 72* (1975) 3961.
[72] E. M. Southern, *J. Mol. Biol. 98* (1975) 503.
[73] L. Grossman, K. Moldave, *Methods Enzymol. 65* (1980) 705.
[74] H. Hofmann, M. E. Frank, *J. Bacteriol. 86* (1963) 1075.
[75] Maxicell-System: A. Sanchor, A. M. Hack, D. D. Rupp, *J. Bacteriol. 137* (1979) 692.
[76] A. Marcus, D. Efron, D. P. Weeks, *Methods Enzymol. 30* (1974) 49.
[77] H. R. B. Pilham, R. J. Jackson, *Eur. J. Biochem. 6* (1976) 247.
[78] H. Schmitt, I. Gozes, U. Z. Littauer, *Brain Res. 121* (1977) 327.
[79] J. D. Richter, N. C. Jones, L. D. Smith, *Proc. Natl. Acad. Sci. USA 79* (1982) 3789.
[80] A. Gräsmann, M. Gräsmann, C. Müller, *Methods Enzymol. 65* (1980) 816.
[81] W. Gilbert, *Biosci. Rep. 1* (1981) 353.
[82] A. M. Maxam, W. Gilbert, *Methods Enzymol. 65* (1980) 499.
[83] F. Sanger, *Biosci. Rep. 1* (1981) 3.
[84] G. Blobel, P. Walter, G. N. Chang, B. M. Goldmann, A. H. Erickson, U. R. Lingappa, *Symp. Soc. Exp. Biol. 33* (1979) 9.
[85] J. E. Rothman, H. F. Lodish, *Nature 269* (1977) 775.
[86] M. P. Czech, *Annu. Rev. Biochem. 46* (1977) 359.
[87] R. Harrison, G. G. Lunt: *Biological Membranes, Their Structure and Function,* Halsted, New York 1980.
[88] R. A. Capaldi, *Sci. Am. 230* (1974) No. 3, p. 26.
[89] H. D. Jakubke, H. Jeschkeit: *Aminosäuren, Peptide, Proteine,* Verlag Chemie, Weinheim 1982.
[90] S. J. Singer, G. L. Nickolson, *Science 1975* (1972) 720.
[91] R. Talmadge, H. Brosius, W. Gilbert, *Nature 294* (1981) 176.
[92] K. Neugebauer, R. Sprengel, H. Schaller, *Nucleic Acids Res. 9* (1981) 2577.
[93] H. Kössel, H. Seliger, *Prog. Chem. Org. Nat. Prod. 32* (1975) 297.
[94] H. G. Khorana, *Science 203* (1979) 614.

[95] M. D. Edg, A. R. Greene, G. R. Heathcliffe, P. A. Meacock, W. Schuch, D. B. Scanlon, T. C. Atkinson, C. R. Newton, A. F. Markham, *Nature 292* (1981) 756.
[96] R. L. Letsinger, M. J. Kornet, *J. Am. Chem. Soc. 85* (1963) 4045.
[97] R. B. Merrifield, *J. Am. Chem. Soc. 85* (1963) 2149.
[98] R. B. Merrifield, B. Gutte, *J. Biol. Chem. 246* (1971) 1922.
[99] K. Itakura, *Trends Biochem. Sci. 5* (1980) 114.
[100] H. G. Gassen, A. Lang: *Chemical and Enzymatic Synthesis of Gene Fragments: A Laboratory Manual*, Verlag Chemie, Weinheim 1982.
[101] K. Migoshi, K. Itakura, *Nucleic Acids Res. Symp. Ser. 7* (1980) 281.
[102] M. J. Gait, M. Singh, R. C. Sheppard, M. D. Edge, A. R. Greene, G. R. Heathcliffe, T. C. Atkinson, C. R. Newton, A. F. Markham, *Nucleic Acids Res. 8* (1980) 1081.
[103] M. J. Gait, H. W. D. Matthes, M. Singh, B. S. Sproat, R. C. Titmas: *Synthesis of Oligodeoxynucleotides by a Continuous Flow Phosphotriester Method on a Kieselgur/Polyamide Support* in [100], p. 1.
[104] R. M. Cook, D. Hudson, E. Mayran, J. Ott: *Principles of Automated Gene Fragment Synthesis* in [100], p. 111.
[105] S. L. Beaucage, M. H. Caruthers, *Tetrahedron Lett. 22* (1981) 1859.
[106] M. D. Matteucci, M. H. Caruthers, *J. Am. Chem. Soc. 103* (1981) 3185.
[107] M. H. Caruthers: *Chemical Synthesis of Oligonucleotides Using the Phosphite Triester Intermediates* in [100], p. 71.
[108] G. van der Marel, C. A. A. van Boeckel, G. Wille, J. H. van Boom, *Tetrahedron Lett. 1981*, 3887.
[109] H. Seliger, S. Klein, Ch. K. Narang, B. Seemann-Preising, J. Eiband, H. Hauel: *Solid-Phase Synthesis of Oligonucleotides Using the Phosphite Method* in [100], p. 81.
[110] M. T. Pardue, J. G. Gall, *Methods Cell Biol. 10* (1975) 1.
[111] A. P. Bird, *J. Mol. Biol. 118* (1978) 49.
[112] H. Weber, T. Taniguchi, W. Müller, F. Meyer, C. Weissmann, *Cold Spring Harbor Symp. Quant. Biol. 43* (1978) 669.

# Organometallic Compounds of Titanium and Zirconium as Selective Nucleophilic Reagents in Organic Synthesis[1]

**New synthetic methods (37)**

**By Beat Weidmann and Dieter Seebach***

The addition of carbanionic organometallic compounds (usually RLi or RMgX) to a carbonyl group—a key step in numerous syntheses—is not always straightforward. Depending on the substrate, various complications and problems may arise, but in many cases these can be remedied by addition of $(RO)_3TiCl$, $(RO)_3ZrCl$ or $(R_2N)_3TiX$ to the classic lithium and Grignard reagents. This usually leads to formation of stable organo-titanium and -zirconium compounds which react highly selectively with carbonyl groups. For example, $CH_3Ti(OiPr)_3$ reacts five orders of magnitude faster with benzaldehyde than with acetophenone at room temperature; reagents of the type $RTi(OiPr)_3$ add smoothly to nitro-, iodo-, or cyano-subsituted benzaldehyde, and the reactions may be performed in chlorinated solvents or acetonitrile; the zirconium analogues have particularly low basicity and add in high yield to α- and β-tetralones or to substrates containing a nitroaldol group; the inclusion of chiral OR* groups gives enantioselective reagents (up to 90% *ee*); allylic $(RO_3)Ti$-derivatives react only at the more highly substituted carbon atom and, in addition, react diastereoselectively (up to 98% *ds*) with unsymmetrical ketones. Finally, titanium reagents have also been found to effect novel transformations such as direct geminal dialkylation ($C{=}O \rightarrow CMe_2$) and alkylative amination [$C{=}O \rightarrow CR(NR'_2)$]. The modification and fine-tuning ("taming") of carbonyl reactivity obtainable by use of the new reagents is not dearly bought; starting materials are the cheap and harmless "titanates", "zirconates" and the corresponding tetrachlorides.

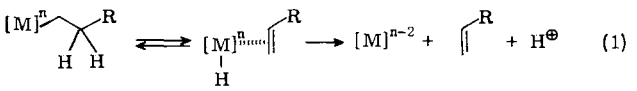
## 1. Introduction—The Problem

If one considers the development of so-called new synthetic methods, one can hardly avoid the impression that the elements of the periodic table have been "grazed" without consideration of price, toxicity, or availability, and without knowledge of alternative methods already developed. On the other hand, it is clear that there is a multitude of presently awkward synthetic transformations for which—on pure statistical grounds—a solution lies hidden somewhere in the periodic table. In the area of organometallic reagents, those in which the organic part has nucleophilic, carbanionic reactivity occupy a central position. After the work of *Frankland*[2] on organozinc compounds (the first known organometallic compounds) in the middle of the nineteenth century, it was *Grignard* who in 1900 first recognized the seminal importance of organomagnesium compounds for synthetic chemistry[3]. Since then, the Grignard reagents named after him, together with compounds of the other main-group metals such as lithium[4], boron[5], aluminum[6], zinc[7], and cadmium[8], have become an indispensable tool in the hands of the preparative organic chemist. Unfortunately, however, the high reactivity of these classic organometallic compounds is often coupled

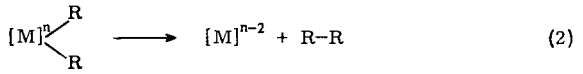
[*] Prof. Dr. D. Seebach, Dr. B. Weidmann
Laboratorium für Organische Chemie der
Eidgenössischen Technischen Hochschule
ETH-Zentrum, Universitätstrasse 16, CH-8092 Zürich (Switzerland)

with disadvantages, which may ultimately lead to a lack of selectivity[9]: a) the nucleophilic reagent may only be stable below a certain temperature; b) other carbonyl groups in the substrate must be protected; many other functional groups (*e.g.* CN, $NO_2$, I) may not be present; c) instead of addition, deprotonation (enolate formation) may take place; d) instead of the desired 1,2-addition, 1,4-addition may occur (or *vice versa*); e) allylic nucleophilic reagents can react with or without allylic double bond shifts ($S_E$ *vs.* $S_{E'}$); f) two diastereomeric products may be unselectively formed; g) nucleophilic organometallic reagents of this type can only be modified with difficulty such that they react enantioselectively. Variation of the metal is a classical possibility for the solution of such selectivity problems, but this has often led to the use of toxic metals (cadmium compounds[10] and copper derivatives[11,12]).

It is not surprising that the use of transition metals to modify *carbanion reactivity* was at first not considered. Indeed, for a long time, the only isolable complexes with carbon-transition metal σ bonds ($\eta^1$-complexes)[13] were copper(I) compounds with $d^{10}$-configuration of the metal and the corresponding Pt- and Au-derivatives. The reason for this is that so-called β-H-abstraction [reaction (1), reductive elimination] is much faster with alkyl-transition metal compounds than with the equivalent main-group metal compounds. In addition, oxidative dimerization of two organic residues (with concomitant reduction of the metal) occurs at a transition metal center much more readily [reaction (2)][14]. These two processes may, in fact, be of considerable significance when deliberately employed on a laboratory or an industrial scale[15,16]; they have, however,



(1)



(2)

hindered for a long time the introduction of alkyl-transition metal compounds as carbanionic reagents in synthesis. After the reason for the instability was recognized, inorganic chemists succeeded in isolating an immense number of complexes on keeping to the following "rules"[17]:

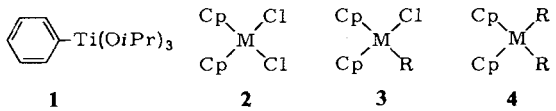
a) Use of alkyl groups which either have no hydrogen atom on the β-carbon, or, for steric reasons, cannot form a stable double bond. Typical examples are: methyl, benzyl, neopentyl, trimethylsilylmethyl, phenyl, and 1-norbornyl.
b) Complexation of the metal with strongly coordinating ligands until the stable noble gas configuration is reached (18 electron rule); steric hindrance of β-abstraction is often an added advantage.
c) Use of metals in low oxidation states which cannot easily be further reduced.
d) Synthesis of compounds in which the equilibrium for β-abstraction [Eqn. (1)] lies on the side of the alkyl compound, and which are thus accessible by hydrometalation.

Complexes which owe their stability to having alkyl groups without β-hydrogen atoms [Rule (a)] are of interest to the inorganic chemist for the investigation of the structural and thermodynamical properties of the transition metal-carbon bond. Even should a preparative method emerge from these investigations, however, the restriction to such systems would be a severe limitation. Thus it is the possibilities mentioned under b), c), and d) which are of consequence in the search for sufficiently stable organo-transition metal reagents for organic synthesis.

## 2. Properties of Organo-titanium and -zirconium Compounds without Cyclopentadienyl Ligands—Aim and Limits of the Review

In 1952, *Herman* and *Nelson*[18] described phenyltitanium isopropoxide as the first compound with a carbon-titanium σ bond[19] (Scheme 1). Two further discoveries at the same time stimulated the development of organotitanium chemistry: the synthesis of ferrocene by *Kealy* and *Pauson*[20], and the observation by *Ziegler et al.*[21] that titanium compounds in mixtures with alkylaluminum compounds are extremely active catalysts for the polymerization of olefins.

After elucidation of the structure of ferrocene[22–24], cyclopentadienyl-titanium and -zirconium halides **2** were some of the first compounds to be prepared by the action of cyclopentadienylmagnesium halides on transition metal salts, and from which the σ-derivatives of type **3** and **4**, which have until recently dominated the picture in organic synthesis, are derived[25]. As a result of the work of *Herman* and *Nelson*[18], complexes of the general type **5** have been systematically synthesized mostly for the purpose (as with the Cp-derivatives) of investigating the catalytic effect on olefin polymerization. The chloro derivatives **5**, X = Cl, proved to be rather unstable expect in the absence of easily-abstractable β-ligands, and the stability decreased markedly with increasing degree of alkylation. On the



**1** **2** **3** **4**

M = Ti, Zr

$R_nMX_{4-n}$

**5** M = Ti, Zr; X = Cl, Br, OR', $NR'_2$; n = 1–4

Scheme 1. Various types of organo-titanium and -zirconium compounds with π-ligands (**2**—**4**) and σ-ligands (**1**, **3**, **5**) attached to the metal center. Cp = cyclopentadienyl.

other hand, the alkoxy and, especially the dialkylamino complexes **5**, X = OR' or $NR'_2$, showed a thermal stability which was sometimes fully comparable with that of the Cp-derivatives[26].

The alkoxy and aryloxy derivatives **5**, X = OR', n = 1 were chosen for the first investigations in our group on the use of organo-titanium and -zirconium compounds for the following reasons:

a) There were structural[27] and thermodynamic[28] indications that alkoxy groups do not only form a σ-bond with titanium, but also act as strong π-donors, *i.e.* as 4-electron ligands. This should make an important contribution to the stability of such complexes.

b) There were some indications that compounds of this type can add to carbonyl groups (Gilman-test[29] with *Michler*'s ketone).

c) Titanates—compounds of the type $Ti(OR)_4$—which serve as starting materials for the complexes $R'Ti(OR)_3$ are industrially available and therefore cheap. When purchasing 50 kg batches, 1 kg $Ti(OiPr)_4$ presently costs *ca.* \$ 5.00, 1 kg $Zr(OBu)_4$ *ca.* \$ 10.00.

d) In contrast to compounds of most other heavy metals, hardly any toxic effects of $Ti(OR)_4$ and $Zr(OR)_4$ are known[30], not least because—unlike the Cp-derivatives—they are very rapidly hydrolyzed by water and the resulting oxide-hydrates cannot be reabsorbed.

In the present article, we will concentrate on the applications of the organometallic reagents derived from $Ti(OR)_4$, $Ti(NR_2)_4$ and $Zr(OR)_4$ which do not contain Cp-ligands or additional metals. Some other new, general applications of Ti- and Zr-derivatives will be mentioned in Section 9. No experimental details will be given here because a further article on the subject is currently in preparation, in which the preparative aspect will be given prominence (—with many "recipes"!)[31].

## 3. Preparation of $(R'O)_3TiR$, $(R'O)_3ZrR$, and $(R'_2N)_3TiR$ Compounds in Solution—Metal Exchange from Li- and Mg-Derivatives

Tetraalkoxy- and tetraaryloxy-titanium and -zirconium compounds, the so-called titanates and zirconates are, in general, available by reaction of the corresponding tetrahalides with alcohols. On a laboratory scale, the exchange

$$Ti(OR)_4 \xrightarrow[-\,ROH]{+\,R'OH} Ti(OR')_4 \quad (3)$$

$$ClTi(OR)_3 \xrightarrow[-\,ROH]{+\,R'OH} ClTi(OR')_3 \quad (4)$$

$$TiCl_4 \xrightarrow{LiNR_2} Ti(NR_2)_4 \xrightarrow{tBuOH} Ti(OtBu)_4 \quad (5)$$

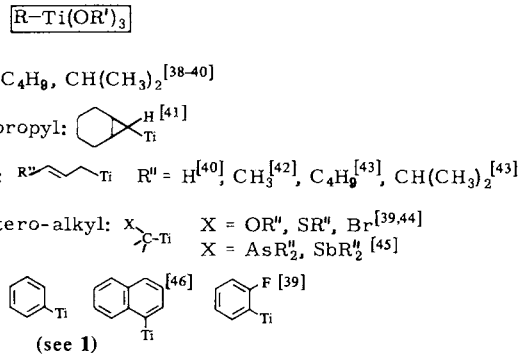
$$3\ M(OR)_4 + MCl_4 \longrightarrow 4\ ClM(OR)_3 \quad (6)$$

$$3\ Ti(NR_2)_4 + TiBr_4 \longrightarrow 4\ BrTi(NR_2)_3 \quad (7)$$

$$\left.\begin{array}{l} RLi + ClM(OR')_3 \xrightarrow{-\,LiCl} \\ RMgX + ClM(OR')_3 \xrightarrow{-\,MgXCl} \end{array}\right\} \rightarrow R\text{–}M(OR')_3 \quad (8)$$

$$RLi + XTi(NR'_2)_3 \xrightarrow[-\,LiX]{} R\text{–}Ti(NR'_2)_3 \quad (9)$$

reaction (3) has proved simpler and more flexible. The low boiling alcohols ROH are distilled out of the equilibrium mixture; conditions which also succeed for the trialkoxy-chloro compounds, [Reaction (4)][32a]. Titanium tetra-*tert*-butoxide is prepared by alcoholysis of the tetramino compounds according to reaction (5)[32b]. Trialkoxy-, triaryloxy-, and tris(dialkylamino)-titanium halides and the corresponding $(RO)_3Zr$ halides are best prepared according to reactions (6) and (7)[33,34]. Treatment of the so-obtained monohalides with lithium or Grignard derivatives, the classical nucleophilic σ-organometallic compounds, leads quite generally—and in the case of titanium more rapidly than in the case of zirconium—to the expected organometallic reagents [see Reactions (8) and (9)][26]. Dialkylzinc[35], dialkylcadmium[35], tetraalkyllead[36], and alkylaluminum[37] derivatives have also been described as materials for the alkylation of titanium compounds. The more stable organotitanium compounds which are protected against β-H-abstraction can be isolated without difficulty. Thus, $MeTi(OiPr)_3$ can be obtained as a bright yellow oil which distills without decomposition at 50 °C/0.001 torr and which can be kept unchanged in the refrigerator under argon for at least a month. $PhTi(OiPr)_3$ **1** is precipitated as colorless crystals by cooling a hexane solution, and appears to be even stabler than the methyl derivative when similarly stored. Other organotitanium compounds of this general type are also stable, at least in solution. A list is given in Scheme 2. The reagents with R = butyl, 1,3-di-




Scheme 2. Different types of R—$Ti(OR')_3$ derivatives prepared by addition of organo-lithium or -magnesium compounds in ether or tetrahydrofuran (THF) to $ClTi(OR')_3$ in the same solvents [38—46]. *o*-Fluorophenyltitanium triisopropoxide is isolable in crystalline form at room temperature, whilst the Li- and Mg-derivatives eliminate fluoride above −50 °C [47].

thian-2-yl, and *o*-fluorophenyl are stable enough for reaction at temperatures of up to +25 °C. The suspected α- or β-eliminations do not compete with the desired reactions. Because of the lesser carbanion character of the organic residue attached to titanium, the α-sulfur substituted titanium compounds and the *o*-fluorophenyl derivatives for example are significantly more stable than the Li- and Mg-analogues (see legend to Scheme 2).

## 4. Reactions of Organotitanium Triisopropoxides—Superselectivity of the Additions to Carbonyl Groups

An introduction to the reactivity and selectivity of these compounds for comparison with the corresponding Li- and Grignard-reagents is provided by a study of $MeTi(OiPr)_3$, which can easily be prepared on a large scale and free from metal halides according to reaction (8).

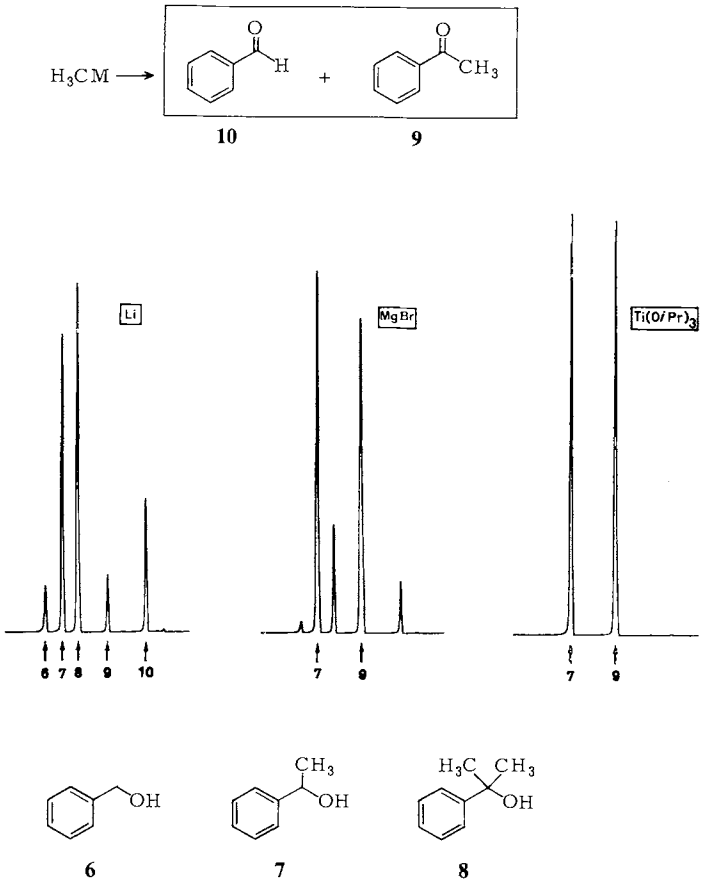



Fig. 1. Comparison of the 1:1:1 reactions of methylmetal derivatives with benzaldehyde and acetophenone in ether at room temperature. The titanium reagent distinguishes perfectly between aldehyde and ketone! (The reactions with $CH_3Li$ and $CH_3MgBr$ are further complicated by the occurrence of aldol reactions between the carbonyl compounds.)

Treatment of a 1:1 mixture of benzaldehyde and acetophenone in ether with 1 equivalent of $MeTi(OCHMe_2)_3$ at room temperature gives a product mixture for which the gas chromatographic analysis is shown in Figure 1[38]. As one sees, there is a difference between the results for methyl-lithium and -magnesium bromide on the one hand, and for the methyltitanium reagent on the other "like day and night". It can be roughly estimated from these experiments that the difference $\Delta\Delta G^{\neq}$ for the addition of methyllithium to benzaldehyde and to acetophenone is less than 1 kcal/mol (see Fig. 2)[48]. By way of contrast, aldehydes react with methyltitanium triisopropoxide at $-50$ to $-20\,^{\circ}C$, whereas ketones require room temperature for reaction. We estimate that the $\Delta\Delta G^{\neq}$ value for the competition reactions shown in Figures 1 and 2 is *ca.* 7 kcal/mol, which corresponds to a ratio of reaction rates of $10^5:1$ at room temperature. As can be seen from the results of further competition experiments (Table 1), all the organotitanium compounds tested by us are able to distinguish between aldehyde and ketone to a similarly high degree. Addition of the R group from $RTi(OiPr)_3$ to esters, thiolesters, nitriles, and nitro groups was not observed and, in addition, no reaction occurred with alkyl halides, aryl halides, and epoxides. Some examples of reactions with substrates having functionality additional to the aldehyde group[39,49,50] are shown in Scheme 3.

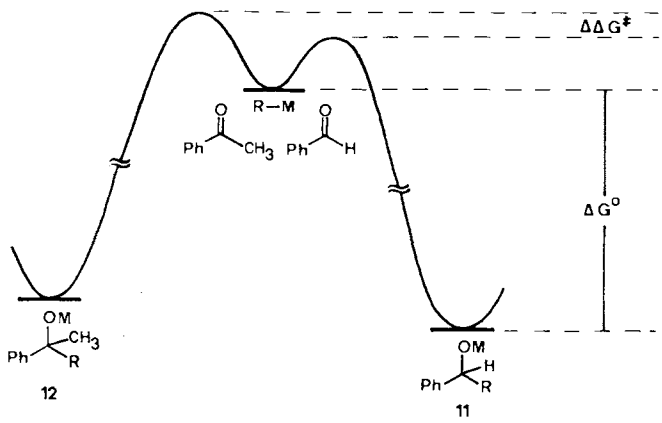
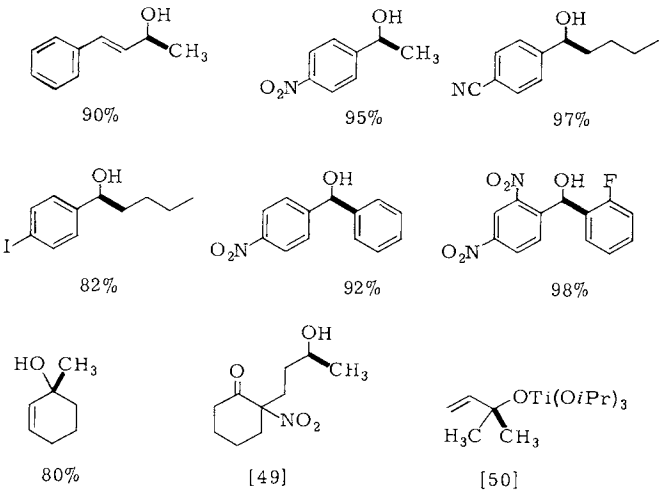



Fig. 2. Selectivity of organolithium and organotitanium reagents in reactions with a 1:1 mixture of benzaldehyde and acetophenone: Reaction energy profile. $\Delta G^0 > 40$ kcal/mol.

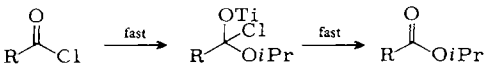
Table 1. Selectivity of organo-lithium and -titanium reagents in reactions with a 1:1 mixture of benzaldehyde and acetophone: Examples.

| R— in R—Li and R—$Ti(OiPr)_3$ | Li-reagent $T$ [°C] | 11/12 | Ti-reagent $T$ [°C] | 11/12 |
|---|---|---|---|---|
| $H_3C$— | 20 | 40/60 | 20 | >98/2 |
| $H_5C_6$— | 0 | 40/60 | 0 | >98/2 |
|  | | — | −95→RT | >98/2 |
|  | | — | −80→RT | >98/2 |
|  | −80 | 33/67 | −80→RT | >95/5 |
| $H_5C_6SCH_2^-$ | −50 | 67/33 | 20 | >98/2 |
|  | −70 | 67/33 | 20 | >98/2 |
|  | | — | −95→RT | >98/2 |

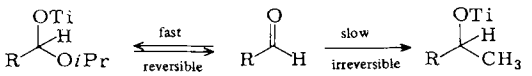



Scheme 3. Products from the reactions of organotitanium triisopropoxides $RTi(OiPr)_3$ with functionalized carbonyl compounds [39]. The bonds made during the reaction are drawn with thick lines. The percentages given refer to isolated yields of $^1H$-NMR spectroscopically pure compounds.

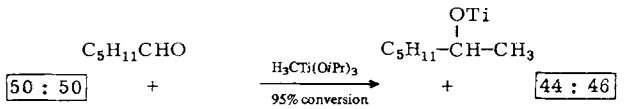
Organic esters are transesterified at room temperature to the corresponding isopropyl esters[38] (cf. also Section 9). Similarly, acid chlorides react at lower temperature to give isopropyl esters and not the expected methyl ketones! This surprising effect may be explained if in both cases the isopropoxy group is transferred faster than the methyl group to the carbonyl center [see Reactions (10) and (11)]. Elimination of chloride in the case of the acid chloride then gives the ester, whereas in the case of the aldehyde, the reversibility of the initial transfer allows ultimate reaction with the methyl group.




(10)



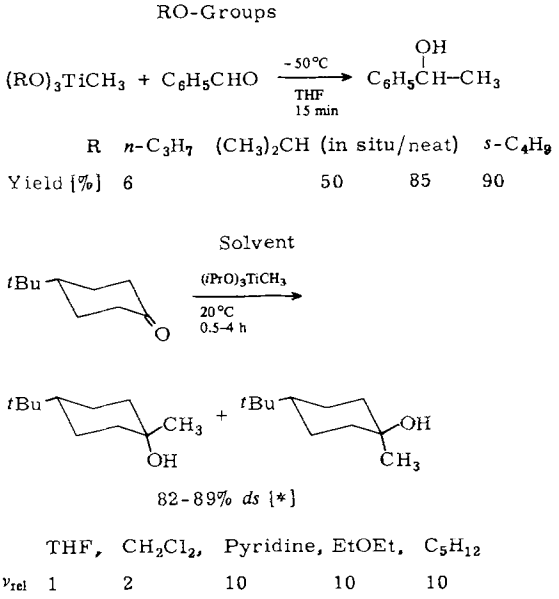

(11)




(12)

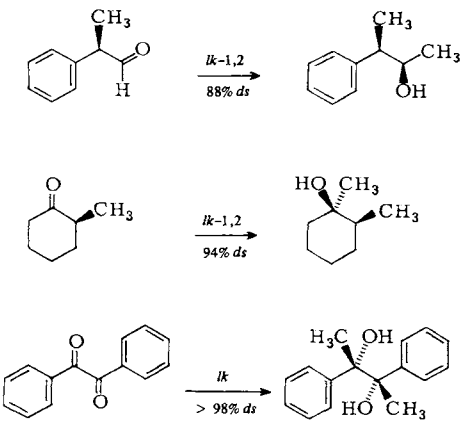
The methyltitanium reagent also cleanly distinguishes between two aldehydes having different degrees of steric hindrance[51] [see Reaction (12)].

By varying the RO-groups attached to the reagent, it can be shown that there is a clear tendency for bulky groups R to increase the reactivity (see Scheme 4 and cf. Section 7). This unexpected result appears plausible when one considers the structural properties of the titanium alkoxides[53]: The X-ray structure analysis of $Ti(OEt)_4$[52] shows that in the crystalline state the compound is present as a tetramer (Fig. 3), so that every metal atom has an octahedral surrounding of oxygen atoms. Cryoscopic molecular weight determinations also show titanium tetra(*n*-alkoxides) to exist as tetramers in concentrated solutions. In more dilute solutions they exist as trimeric aggregates[53]. If, however, the alkyl chain is branched, as in isopropyl and *tert*-butyl titanates, the solutions can be shown to contain monomeric species[53], as for $MeTi(OiPr)_3$ itself[54]. The steric hindrance at the metal center, which hinders aggregate formation, leads therefore to a more reactive (because monomeric) reagent.




Scheme 4. Dependence of the rate of the addition of methyltitanium trialkoxides to aldehydes and ketones on the RO groups (yield, top) and on the solvent (relative rate, bottom) [39].

The reactions are only slightly influenced by solvent, as exemplified in Scheme 4 by the addition of $MeTi(OiPr)_3$ to *tert*-butylcyclohexanone. The diastereoselectivity (% *ds*)[55] of the equatorial attack on this ketone is hardly dependent on solvent[39]. It is worth noting that solvents such as dichloromethane, pyridine, and acetonitrile, which would all react with lithium or Grignard reagents, can be used without difficulty[39]. Further examples of highly diastereoselective carbonyl additions of $CH_3Ti(OiPr)_3$ with 1,2- (see Scheme 5), 1,3-, and 1,4-induction are known[56].




Scheme 5. Further diastereoselective additions of $CH_3Ti(OiPr)_3$ to carbonyl groups [40, 56] (cf. also Scheme 4). The relative topicities of the reactions are specified with the *lk,ul*-nomenclature [57].

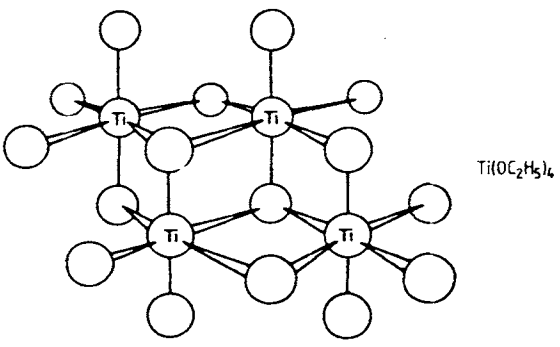
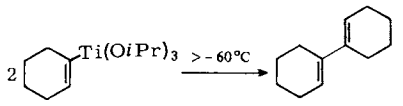



Fig. 3. Crystal structure of titanium tetraethoxide. The ethyl groups have been omitted [52].

[*] *ds* is the abbreviation for diastereoselectivity: 82—88% *ds* signifies that 82—88% of one diastereomer and 18—12% of the other are formed.

## 5. Organozirconium Tributoxides—High Carbonylophilicity, Low Basicity

In the reactions of the organotitanium reagents mentioned up to now, the organic group has shown marked nucleophilic, carbanionic reactivity instead of acting as a base. Thus, $RTi(OR')_3$ compounds behave like especially nucleophilic main group metal derivatives with R-metal σ-bonds, this being the case even when R is an allylic ligand (see Section 6). However, in certain cases, the here undesired transition metal character of titanium becomes apparent, which limits the application of reactions of this type. For example, it is not possible to add *vinyl*titanium reagents to carbonyl compounds: On heating a solution of 1-cyclohexenyltitanium triisopropoxide in the presence of benzaldehyde, one observes an oxidative coupling according to reaction (13) with reduction of the metal[58].

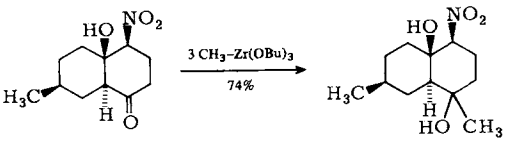



(13)

It is also impossible to add *tert*-alkyltitanium compounds: Addition of benzaldehyde to the mostly black solutions derived from chlorotrialkoxytitanium and *tert*-butyllithium gives, besides unreacted benzaldehyde, only benzyl alcohol and the pinacol formed from benzaldehyde, which indicates the presence of reduced titanium compounds[59]. The β-H-elimination (reductive elimination) obviously takes place more rapidly than addition to the carbonyl group in this case.

These limitations led to the investigation of the analogous zirconium compounds, as it was expected that zirconium, an element from the *second* transition metal period, would be less easily reduced. Up to now, investigations[60] have been centered almost exclusively[56] on the most easily available organozirconium tributoxides, for which the following common features and differences in comparison with titanium have come to light:

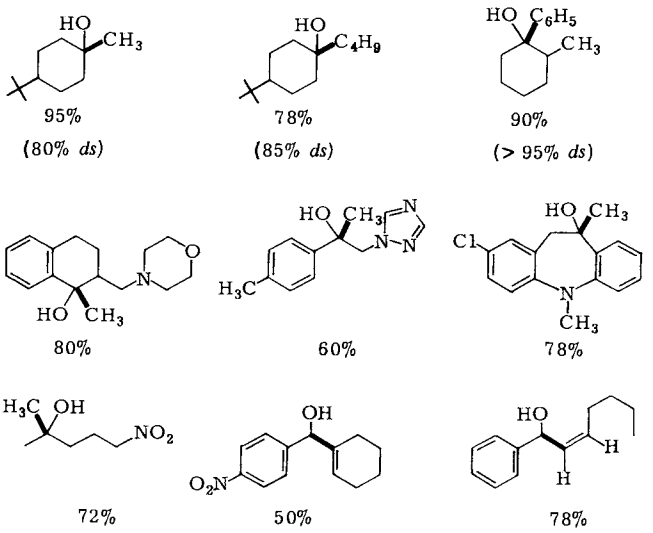
a) Similar preference for aldehyde- as for ketone-carbonyl groups.
b) Similar behavior to the organotitanium derivatives with respect to diastereoselectivity and compatability with other functional groups; see the list of examples in Scheme 6 and the "shop-window" reaction (14).




(14)

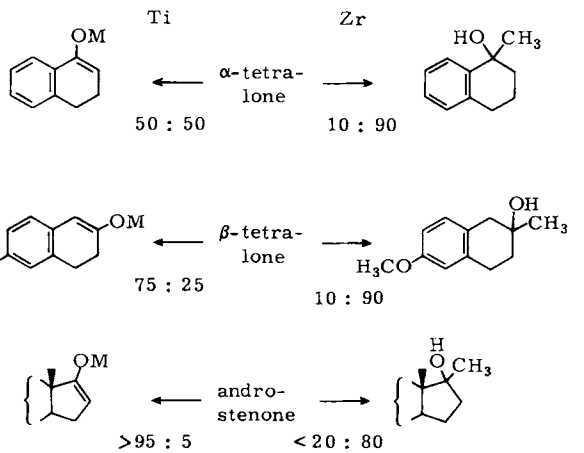
*one* Diastereomer

c) Although organotitanium derivatives are certainly much less basic than lithium or Grignard reagents, their *C*-nucleophilicity is not high enough with respect to the carbonyl group of easily enolizable ketones. As emerges from Schemes 6 and 7, the zirconium compounds show a marked affinity for the carbonyl group of these substrates.—The low basicity of the organozirconium compounds is the most useful aspect of these reagents from a preparative point of view.
d) In contrast to the titanium analogues, vinylzirconium compounds are stable for a short time at room temperature and may be added to aldehydes and ketones; see examples in Scheme 6 (bottom).




Scheme 6. Alcohols by reaction of organozirconium tributoxides with carbonyl compounds [60]. The newly made bonds are drawn with thick lines. The adducts obtained from three particularly easily enolizable aryl ketones verify the high nucleophilicity and low basicity of the organozirconium compounds, while the three adducts from substituted cyclohexanones and the reaction product from the *cis*-hexenyl derivative display their diastereoselectivity and configurative stability respectively.

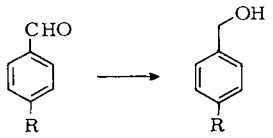
e) α-Branched alkyl groups attached to titanium lead to difficulties: The isopropyl group may be added to *ca.* 60% extent to aldehydes, whilst the *tert*-butyl group only acts as a reducing agent on the metal. In contrast to this, the corresponding zirconium reagents transfer even the *tert*-butyl group to carbonyl compounds to a large extent[60].
f) For reactions of certain organozirconium reagents (as for example butyl-, vinyl-, and *tert*-butyl-zirconium al-




Scheme 7. Comparison of the reactions of methyltitanium and methylzirconium trialkoxides with easily enolizable ketones. The ratios of enolate formation to addition for methyltitanium triisopropoxide are shown on the left; those for methylzirconium tributoxide are shown on the right.

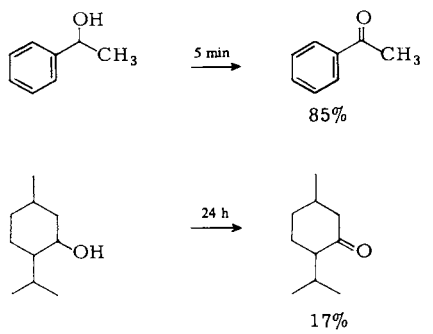
koxides) reduction of the carbonyl compound is observed as well as the desired addition (Table 2). Since

Table 2. Reaction times of the zirconium tetraalkoxide-catalyzed Meerwein-Ponndorf-Verley reduction as a function of the *p*-substituents of benzaldehydes (10 mol-% $Zr(OiPr)_4$, isopropyl alcohol, room temperature).



| R | *t* [h] | Yield [%] |
|---|---|---|
| $NO_2$ | 8 | ≈100 |
| C≡N | 24 | >90 |
| Cl | 24 | >90 |
| H | 24 | ≈60 |
| $OCH_3$ | 24 | ≈10 |
| $N(CH_3)_2$ | 24 | <1 |

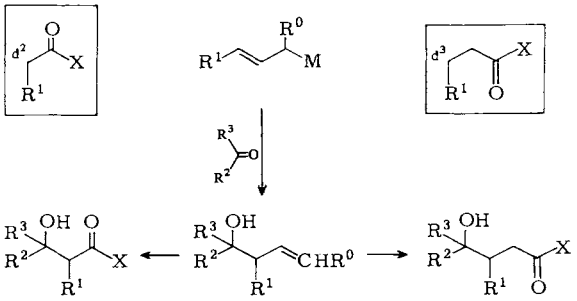
this reduction occurs also with zirconium tetraalkoxides, it must be due to a Meerwein-Ponndorf-Verley reaction rather than β-H-abstraction [see Reaction (1)]. Indeed, *Meerwein* himself showed the effectiveness of zirconium tetralkoxides for this reaction, as well as that of the more conventional aluminum alkoxides[61]. Scheme 8 shows how zirconium tetraalkoxides represent interesting alternatives to aluminum alkoxides[63] with regard to reaction conditions, catalytic effectiveness, and selectivity, particularly also for the analogous Oppenauer oxidation[62].




Scheme 8. Oppenauer oxidation of two alcohols with chloral (in each case 1:1.2, 5 mol-% $Zr(OiPr)_4$, room temperature); note the dramatically different rates of the two reactions.

## 6. Allylic Organotitanium Compounds—Amazing Diastereoselectivity of the Addition to Ketones

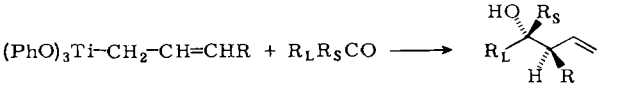
Nucleophilic allylmetal derivatives are synthetically equivalent to enolates ($d^2$-reactivity) or $d^3$-reagents[9] (see Scheme 9). If their reactions are diastereoselective, they lead to configuratively pure, branched-chain homoallylic alcohols and thus to β- or γ-hydroxy-carbonyl compounds. They are therefore important for the stereoselective synthesis of open-chain or macrocyclic natural products. Since a review article on this subject has recently appeared in this journal[64], it is only necessary here to deal briefly with the significance of allylic organotitanium derivatives, laying particular stress on the newest results which have not yet appeared in the literature.

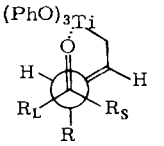


Scheme 9. The nucleophilic allylation reagent seen as corresponding to a $d^2$- or a $d^3$-synthon depending on the nature of $R^0$ and way the primary adduct from the addition to aldehydes or ketones is further transformed. In the first case, it serves for the synthesis of aldols. To be preparatively useful, allylic metal derivatives must react regioselectively at the $R^0$- *or* $R^1$-substituted C-atom and diastereoselectively to give *l*- *or u*-isomers.

Reagents of this type, which are derived from hydrocarbons, are most easily prepared from $ClTi(OR)_3$ and allyl-Grignard reagents according to reaction (8)[42,43]. Of those RO-groups tested up to now, the phenoxy group has proved most useful. For a large number of examples, it has been established that the relative topicity *lk* for the joining of the two trigonal centers is preferred (Table 3)[42,43,57]. High diastereoselectivity (*ds*[55]) is observed even with ketones, which is surprising considering the necessarily smaller difference in steric requirements of the groups $R_L$ and $R_S$. Thus, the reagents distinguish equally well between phenyl ($R_L$) and H ($R_S$) as between phenyl ($R_L$) and

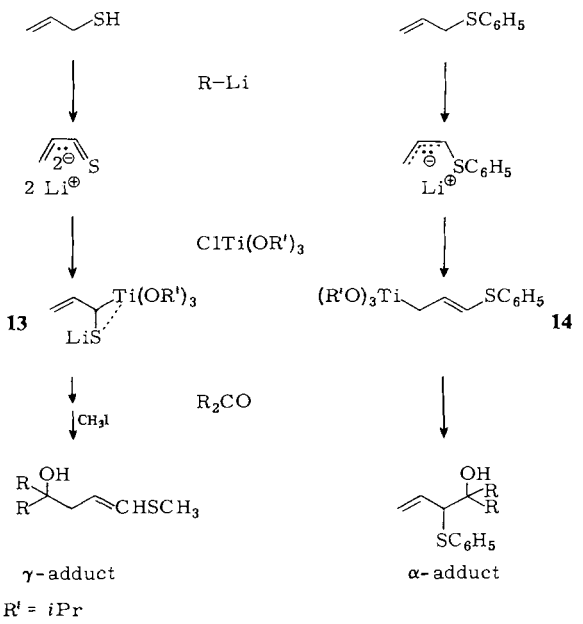
Table 3. Diastereoselectivity (*ds*) for the addition of 2-alkenyltitanium triphenoxide to aldehydes and ketones. Up to now, 28 examples are known [42, 43, 57]. Only for ketones with a small difference in sizes between $R_L$ and $R_S$ (*e.g.* cyclohexyl/ethyl) is the selectivity insufficient for preparative purposes (<70%). The highest induction is observed with aliphatic aldehydes. Other alkoxy or aryloxy groups on titanium (*e.g.* isopropoxy, 2,4,6-trimethylphenoxy) give lower selectivity than the phenoxy group, which has the further advantage that the acidic phenol formed on work-up may be easily removed.—It is also worth noting, that the selectivity increases on going from R = methyl to R = butyl and R = isopropyl, *i.e.* as the group R of the allyl residue attached to Ti gets larger.
*lk* (if priority $R_L > R_S$)



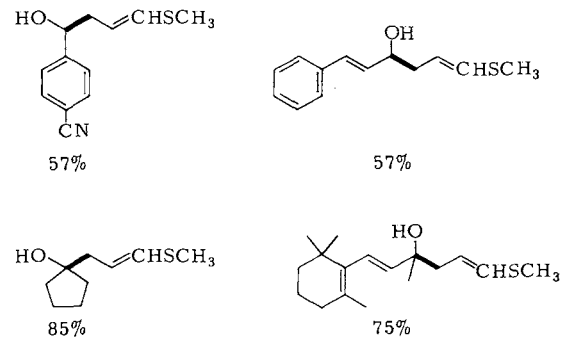


| $R_L$ | $R_S$ | % *ds* with R = $CH_3$ | $C_4H_9$ | $CH(CH_3)_2$ |
|---|---|---|---|---|
| Ph | H | 85 | 93 | 98 |
| Ph | $CH_3$ | 88 | 87 | 87 |
| Ph | C≡C—$CH_3$ | 72 | 77 | 77 |
| *t*Bu | H | >98 | | |
| *t*Bu | $CH_3$ | >98 | | |
| *t*Bu | Ph | 96 | | |

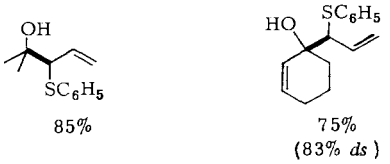
methyl ($R_S$) or *tert*-butyl ($R_L$) and phenyl ($R_S$). To our knowledge, no other examples of such highly diastereoselective addition to ketones are known[65].



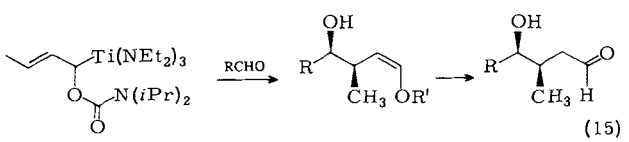

Example with **13**:




Example with **14**:




Scheme 10. Titanation of sulfur-substituted allyllithium compounds, which themselves show unsatisfactory α/γ-selectivity. The dilithiated thioacrolein reacts with one equivalent of titanium chlorotriisopropoxide to give the reagent **13** which adds completely (>98%) γ-selectively to aldehydes and ketones (altogether 18 examples). In contrast, the titanated allylphenyl sulfide, reagent **14**, is fully α-selective (examples, bottom right). The structures given for **13** and **14** are based on the assumption that the allyl groups in this type of titanium derivative are $\eta^1$-ligands and react at the unmetalated C-atom (cf. Newmann projection in Table 3) [42, 43, 66].

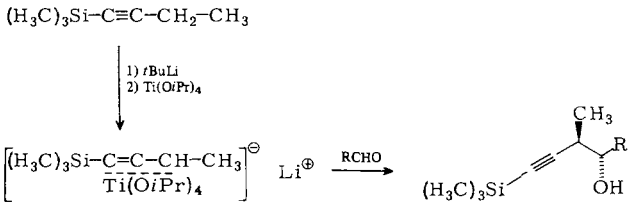



(15)

Hetero-substituted allyltitanium derivatives also show high regioselectivity [see Scheme 10 and Reaction (15)].

The sulfur-substituted allyl anion derivatives 2-propene-1-thiol and allyl(phenyl) sulfide have, up to now, only been reacted with a maximum of 90% α- or γ-selectivity[67,68]. After treatment with titanium chlorotriisopropoxide, however, the selectivity achieved is so high that the "wrong" isomer cannot be detected by $^1$H-NMR spectroscopy[69].— In the case of the metalated allylurethane [Reaction (15)], the derivatives were compared with Li, Al(*i*Bu)$_2$ and Ti(NEt$_2$)$_3$, and titanium again performed best; it gave almost exclusively the *Z*-enol-urethanes with relative topicity *lk*. These latter compounds may be hydrolyzed to diastereomerically pure β-methyl-γ-hydroxyaldehydes[66,70].

An example of a regio- and diastereo-selective propargylation[71] using an anionic titanium complex is shown in Scheme 11.

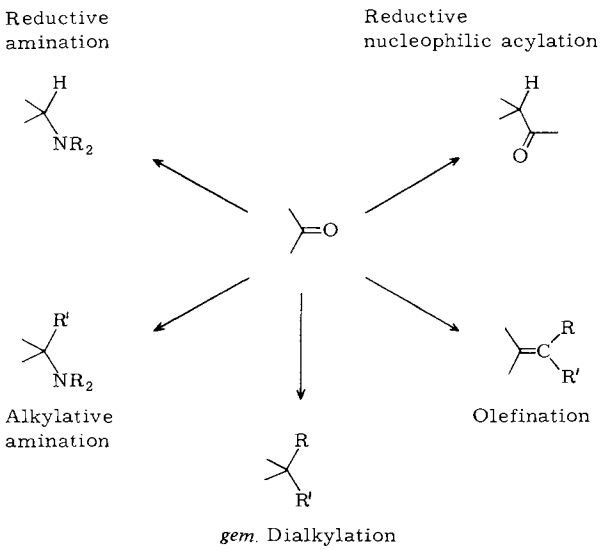



Scheme 11. Diastereoselective synthesis of alkynols by reaction of lithiated allenyl derivatives with aldehydes in the presence of Ti(O*i*Pr)$_4$ [71].—By mixing solutions of MeLi and Ti(O*i*Pr)$_4$ a reagent is formed which behaves neither as methyllithium nor, however, as MeTi(O*i*Pr)$_3$. Acetophenone is extensively enolized[72]. A complex is also formed with Ti(NEt$_2$)$_4$ which does not behave like MeTi(NEt$_2$)$_3$ [72].—Possibly in all three cases ate-complexes of the type (RTiX$_4$)Li are present.

As may also be inferred from the summary of an article concerned with the addition of crotylmetal compounds to aldehydes[64], one can see that the (RO)$_3$Ti-allyl derivatives described here are in general the reagents of choice for stereoselective CC bond formation with relative topicity *lk*. This also applies even when the allyl groups are more highly substituted than with a methyl group (→crotyl), and especially for additions to unsymmetrical ketones.

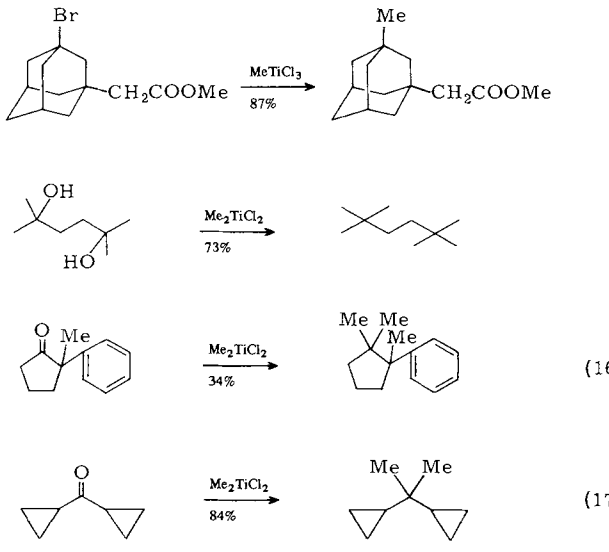
## 7. Geminal Dialkylation and Amination/Alkylation of Carbonyl Compounds—The Dramatic Influence of the Ligands X in RTiX$_3$ and R$_2$TiX$_2$

There exists a group of transformations through which the oxygen of carbonyl derivatives is replaced by other atoms (see Scheme 12). Reagents which perform such reactions in *one* step are particularly useful, *e.g.* Na[B(CN)H$_3$] and an amine (reductive amination)[73], 2-lithio-2-trimethylsilyl-1,3-dithianes and ketene-thioacetal hydrolysis (reductive nucleophilic acylation)[74], or olefination by the Wittig-Horner or Peterson[75] methods. For geminal dialkylation, practically[76] only multi-step methods are known up to now. This is true also of the geminal amination/alkylation reaction reminiscent of the Mannich reaction and the Strecker amino-acid synthesis. The latter two transformations can be realized in one step with organotitanium reagents if, instead of the (RO)$_3$Ti-derivatives, those bearing halide or amino ligands, or having more than one carbon substituent are used.



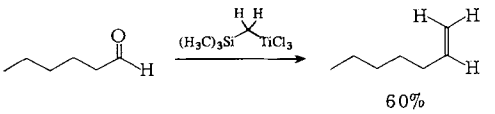

Scheme 12. Examples of the replacement of the oxygen in the C=O group by other atoms. One step reactions of this type represent particularly useful synthetic transformations.

While the organotitanium triisopropoxides mentioned up to now are inert with respect to aliphatic and aromatic halides, the alkyltitanium halides obviously retain enough Lewis acidity of $TiCl_4$ and thus react with typical $S_N1$ active alkylating agents[77,78]. However, since no carbon-chain rearrangement occurs, even in particularly favorable cases, the reaction is certainly not of the $S_N1$ type (see examples in Scheme 13; cf. the *tert*-alkylation of silyl enol ethers catalyzed by $TiCl_4$[79]). Dimethyltitanium dichloride also effects a direct geminal dimethylation of ketones[78] [see Reactions (16) and (17) in Scheme 13].



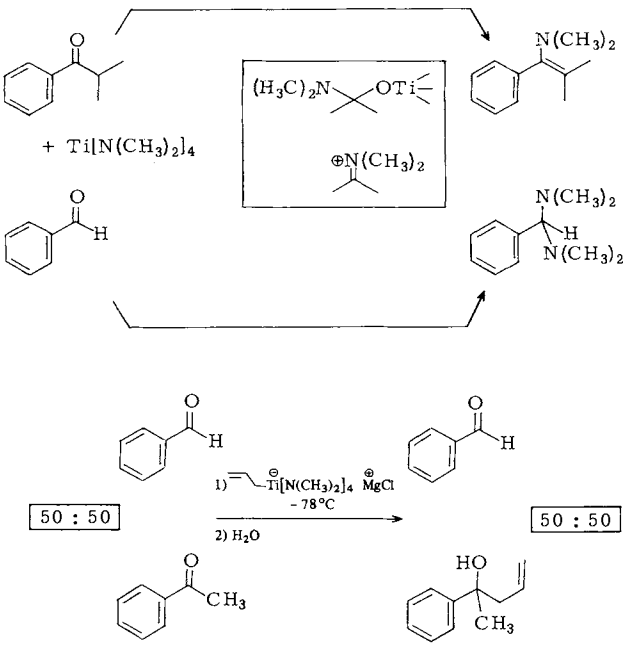

Scheme 13. CC bond formation of the Wurtz type. Replacement of tertiary hydroxy groups with methyl and one-step geminal dimethylation of ketones (without rearrangement of the carbon framework!). Such reactions do not occur when the substrates shown here are treated with $MeTi(OiPr)_3$ [77, 78]. The role of the titanium in the geminal dimethylation is not yet clear: $Me_2TiCl_2$ is prepared from $ZnMe_2$ or reacted in presence of $ZnCl_2$-catalyst [78]. Up to now, no examples of direct geminal dialkylation with alkyl groups other than methyl are known.

The titanium-modified Peterson reagent in reaction (18) demonstrates once more the "tuning" possible for organometallic reagents by which exactly that reactivity desired for the planned applications is obtained: While the lithium or the magnesium derivative reacts similarly with aldehydes *and* ketones[75], the titanium reagent trimethylsilylmethyltitanium trichloride reacts selectively with aldehydes[80]. The corresponding trialkoxides do not react under the same conditions[41].



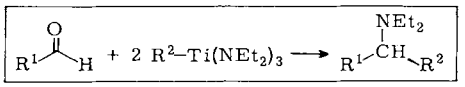

(18)

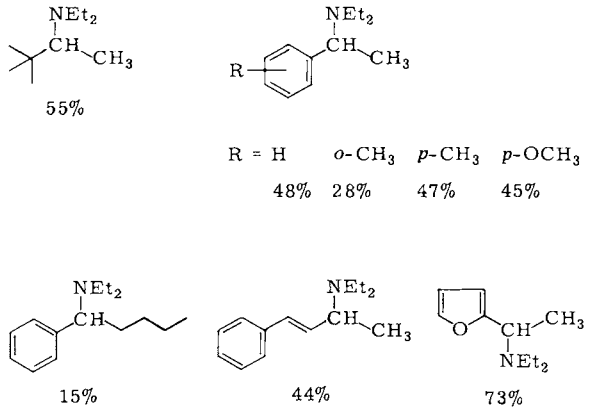
From the most reactive to the most stable $RTiX_3$ derivatives! Because of the donor properties and steric hindrance of the amino groups, the alkyltitanium tris(dialkylamides) show the least tendency to undergo reductive elimination. They can indeed be isolated—sometimes by sublimation at temperatures of over 100 °C[34]. The affinity for oxygen ligands is particularly high in the case of aminotitanium compounds. The known reactions of titanium tetrakis(dialkylamides) with enolizable and non-enolizable carbonyl compounds are shown in Scheme 14. We have found that the easily obtainable methyltitaniumtris(diethylamide) [Reaction (9)] reacts with non-enolizable aldehydes with cleavage of the oxygen function and transfer of both the methyl *and* a dialkylamino group to the carbonyl C-atom




Scheme 14. *First and second conversion:* Reactions of an enolizable and of a non-enolizable carbonyl compound with titanium tetrakis(dimethylamide) to give the enamine and aminal, respectively. The oxygen atom is removed from the organic substrate [81] (cf. also the Weingarten method [82] for the preparation of enamines [34] from ketone or aldehyde + $TiCl_4$ + excess $R_2NH$). *Third reaction:* Reaction of the allyl ate-complex with a 1 : 1 mixture of aldehyde and ketone affords the adduct of the *ketone* with >99% selectivity. Apparently, formation of the titanated hemi-aminal of the aldehyde is preferred, which is stable at low temperature and serves as protecting group, so that the allyl group is transferred to the ketone. "Ketone selectivity" based on the same principle has also been observed with $Ti(NEt_2)_4/CH_3Li$ (see also Scheme 11 [72] and the examples in the review [124]).

(see Scheme 15). All the attempts made so far to elucidate the reaction mechanism show that it is the diethylamino group rather than the methyl group which is first transferred. This behavior of $CH_3Ti(NEt_2)_3$ is reminiscent of the reaction of $CH_3Ti(OiPr)_3$ with acid chlorides [Reaction (10)]. In that case also we were forced to conclude that the hetero-ligand (O*i*Pr) is transferred faster to the carbonyl C-atom than the carbon nucleophile ($CH_3$). For allylic titanium tris(diethylamides) derivatives[51,66,70] the picture is obviously reversed: the allyl group is faster [see *e.g.* Reaction (15)]. The scope and limitations of geminal amination/alkylation are at present under study[72].



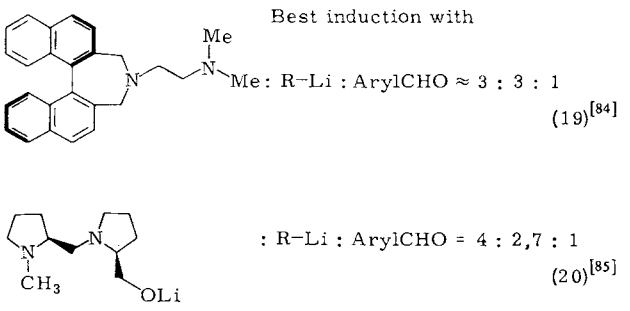


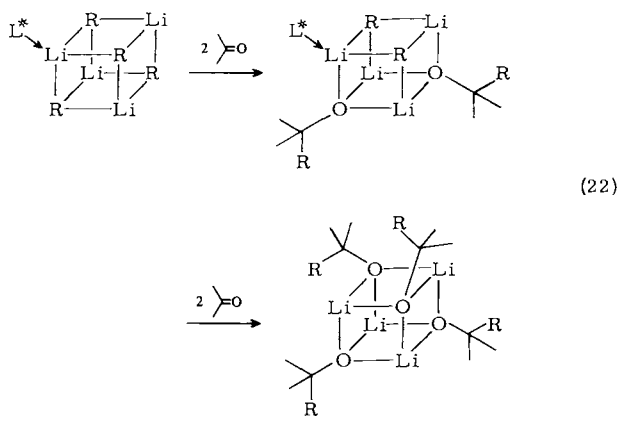

Scheme 15. Geminal diethylamination/alkylation of non-enolizable aldehydes with methyl- and butyltitaniumtris(diethylamide). The mechanism probably involves transfer of an alkyl group to the C-atom of the methyleneammonium ion $R^1CH{=}\overset{\oplus}{N}Et_2$.

## 8. Enantioselective Addition of Chiral Organotitanium Reagents RTi(OR*)$_3$ to Aldehydes— There are Two Sides to Every Carbonyl Group

Many attempts have been made to render the carbanionic, nucleophilic organo-lithium and -magnesium reagents enantioselective by addition of chiral auxiliaries ("enantioface differentiation"). As the examples in Scheme 16 show, it is extremely difficult to know how to go about rationally developing reagents for distinguishing the enantiotopic faces of an electrophilic substrate in this way.

Certain properties of the organotitanium reagents already described may facilitate a rational approach to the designing of enantioselective reagents for addition to carbonyl compounds: (1) Whilst the auxiliaries for organolithium reagents can only bind to the metal center *via* their hetero atoms with relatively weak coordinate forces, for the titanium reagents *charged* hetero atoms can be used[90]. This means that Coulomb forces will, especially in organic media, hinder the dissociation of ligands of this type from the metal. (It is obviously important for the effectiveness of a chiral ligand shell that it should remain intact during

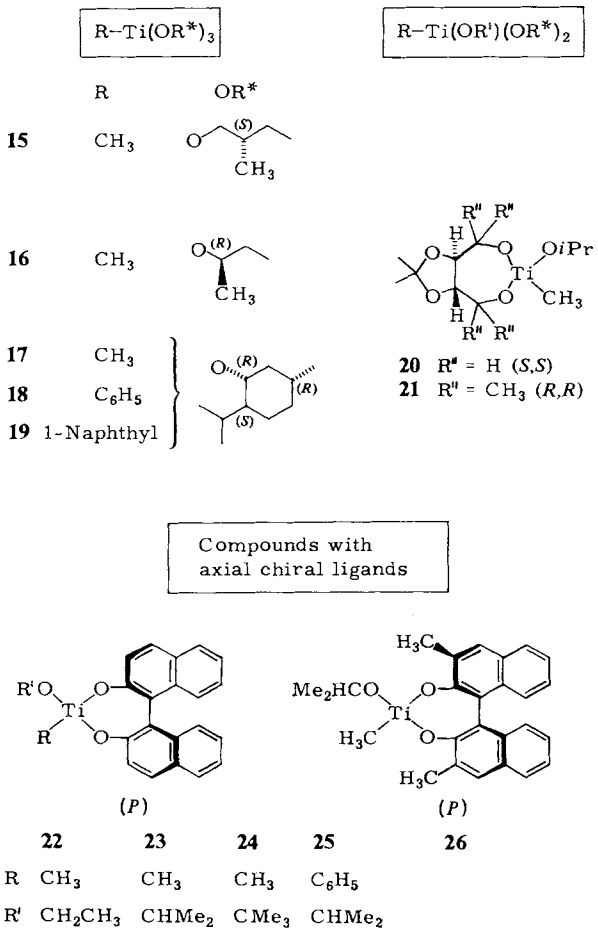



Scheme 16. Asymmetric induction for RLi-addition to aldehydes under the influence of chiral ligands, solvents, alkoxides, and amides [83–86]. "Recipes" (19)—(21) have been successfully applied, in which only a part of the reagent reacts. The reason for this is probably that the chiral modified lithium compounds occur as aggregates and the intermediate products as mixed aggregates [Reaction (22)] [87–89]. Thus, the effective reagent, and therefore the degree of asymmetric induction, is different at the beginning and at the end of the reaction!

the build up of steric strain when the "wrong" face of a carbonyl group is approached.) (2) In many cases, it can be expected that *mononuclear* titanium complexes will occur (cf. discussion in Section 4), for which a study of the interaction between chiral reagent and substrate is much easier. (3) Not least, the great structural resemblence to modified lithium aluminum hydrides should be pointed out. The extensive work already carried out in this area[91,92] may serve as a guide for the choice of suitable ligands.

The modification of the organotitanium derivative with chiral ligands is simple. The alcohol or phenol is treated with titanium chloride triisopropoxide and isopropanol is distilled off [Reaction (4)]. The so-obtained chlorotitanium derivative with chiral OR* groups is converted *in situ* into the chiral reagents **15—26** shown in Scheme 17 by treatment with the desired organo-lithium or -magnesium compound. Some of the results already obtained for the enantioselective additions to aldehydes and to one ketone are collected in Table 4[46].




Scheme 17. Chiral organotitanium reagents **15**—**26** from amyl alcohol of fermentation, (*R*)-2-butanol, (*R,S,R*)-menthol, two tartaric acid derivatives [93, 94], and two binaphthol derivatives [95-97].

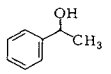
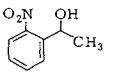
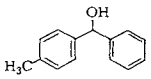
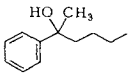
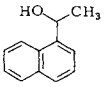
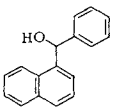
It is not surprising that the derivatives of simple alcohols (with the exception of menthol) effect only a small asymmetric induction, since the alkoxy groups may freely rotate, allowing the adoption of many different conformations. This rotation is frozen in the complexes with bidentate ligands, and this may be the main reason for the greater effectiveness of these systems. Whilst only insoluble, polynuclear complexes were obtained on attempting to form the tartaric acid derivative **20**, **21** has proved to be an effective reagent, which, since it is derived from tartaric acid, has the advantage of being easily obtainable in both enantiomeric forms[94,98,99].

The marked influence of the third alkoxy group in the axially chiral binaphthol derivatives **22**—**26** makes the geometry shown in Figure 4 appear plausible. The high enantioselectivity for the addition of the phenyltitanium reagent **25** to *p*-tolualdehyde is worth noting, as the best examples previously have been limited to the transfer of alkyl groups[99].

As may also be seen from Table 4, the reagents show a strong substrate dependence. Thus it is, for example, better to add methyl to naphthaldehyde than the alternative naphthyl (with **19**) to acetaldehyde.

Enantiomeric excesses (*ee*) of up to nearly 90%, without optimization, have been obtained for reaction partners which either cannot be reacted with chiral modified or-

Table 4. Some examples of the enantioselective addition of the reagents **15**–**26** to aldehydes and to a ketone (valerophenone). As expected (see also Scheme 3) the reactions are "carbonyl selective", and the entire alkyl equivalent is probably transferred with constant enantioselectivity (in contrast to the examples in Scheme 16).

| Product | Reagent | Config. | *ee* [%] |
|---|---|---|---|
|  | **15** | *S* | 8 |
| | **16** | *S* | 12 |
| | **17** | *S* | 23 |
| | **21** | *R* | 39 |
| | **22** | *S* | 28 |
| | **23** | *S* | 59 |
| | **24** | *S* | 66 |
| | **26** | *S* | 54 |
|  | **17** | *S* | 76 |
|  | **18** | *R* | 29 |
| | **25** | *S* | 88 |
|  | **23** | | 40 |
|  | **17** | *S* | 58 |
| | **21** | *R* | 50 |
| | **23** | *S* | 46 |
| | **26** | *S* | 40 |
| | **19** | *R* | 5 |
|  | **25** | | >80 |

ganolithium compounds, or else do not react nearly so well[99,100]. It appears to us to be just a matter of time before the most broadly applicable OR* group combination, reaction conditions and substrates for these enantioselective additions are found.

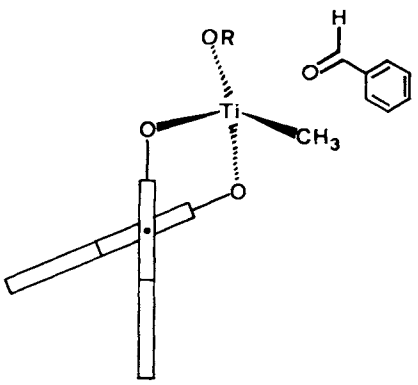
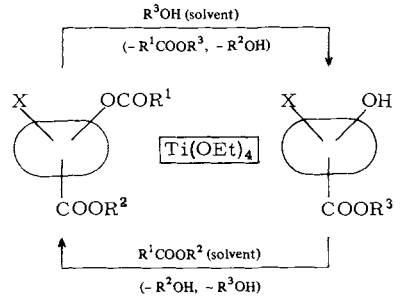


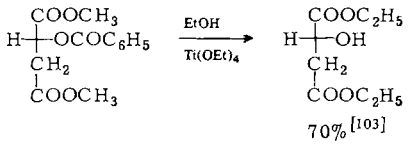

Fig. 4. Geometry of the approach of the titanium reagents **22**—**26** on the *Si* face of benzaldehyde; relative topicity *lk*.

## 9. Other New Applications of Titanium and Zirconium Derivatives in Organic Synthesis—Titanium with its Finger in Every Pie!

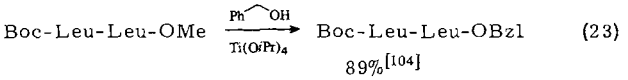
Derivatives of these metals are not just important as components of the Ziegler-Natta catalysts for use in indus-

try. They also play a key role in many other important processes. Thus, they have been employed in many investigations of nitrogen fixation[101]; they are used to effect olefin metathesis[102], and they serve as catalysts for esterification and transesterification on a laboratory as well as an industrial scale (see Scheme 18).

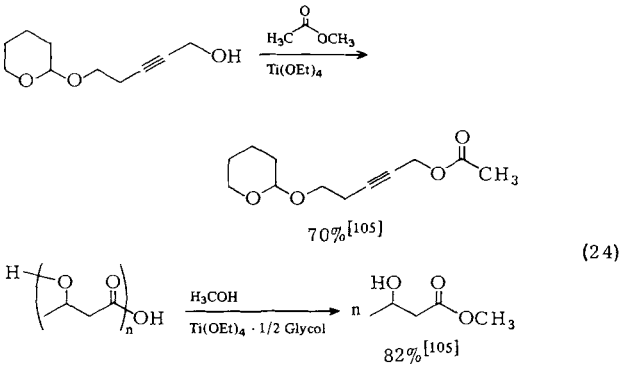



70%[103]




89%[104] (23)



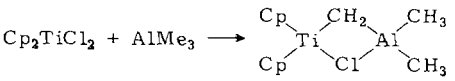

70%[105]

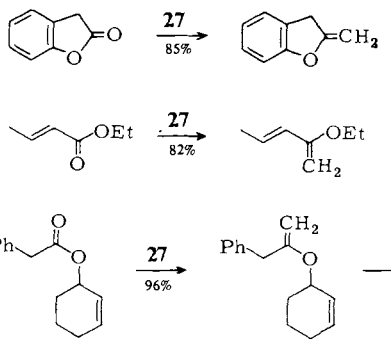
82%[105] (24)

Scheme 18. Titanium catalyzed transesterification [104–106] of acid- and/or base-sensitive substrates. The general scheme at the top shows that, depending on the medium, OH-groups may be esterified, and OCOR-groups saponified or transesterified. The method was first described in the patent literature nearly 3 decades ago, but, until recently, it has been practically unknown in research laboratories, particularly in the universities [103], despite its unique advantages. The examples shown, demonstrate that β-OR-substituted esters neither racemize nor are converted into α,β-unsaturated esters during the reaction. The selectivity of the method can be seen from reactions (23) and (24): amides of carbonic acids—and therefore peptide bonds—remain unaffected, as do acetals and the CC triple bond. Boc esters are only slowly transesterified [104, 106], whereas methyl and ethyl esters react much faster. Many applications of this method in the area of protecting-group chemistry are doubtless still to be discovered.

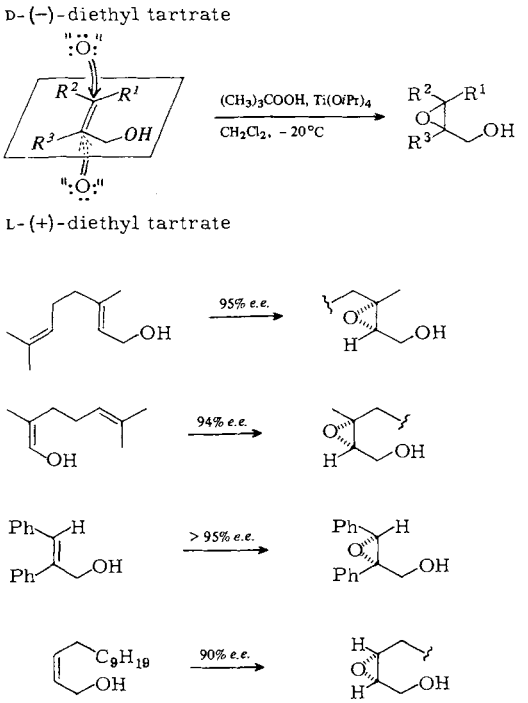
During the last decade, countless synthetic methods have been discovered and developed which make use of the special properties of titanium and zirconium derivatives. Review articles dealing with several of these applications have appeared in the literature: The hydrozirconation of olefins[25, 107], the use of $TiCl_4$ as a Lewis acid for reactions of silyl enol-ethers[79, 108], and the coupling of carbonyl compounds and olefins with low-valent titanium[108, 109]. In the modification of enolates for diastereo- and enantio-selective aldol reactions it has been found that $Cp_2ZrCl$- and $(iPrO)_3Ti$-enolates react with *ul*-additions, independent of the enolate configuration[110–112]; the *ul* addition of titanium enehydrazinates of aldehydes to aldehydes to give aldol-like products has also been recently reported[125].

Two very different processes involving the use of titanium compounds, one stoichiometric, one catalytic, have recently excited attention: The olefination of esters[113, 114] with the Tebbe reagent **27**[115] (Scheme 19), and the highly




Scheme 19. Methylenation of esters and lactones with the Tebbe reagent **27** according to *Evans, Grubbs et al.* [113]. As reaction (25) shows, this method makes possible a novel application of the Claisen rearrangement.




Scheme 20. Titanium-catalyzed enantioselective epoxidation according to *Sharpless et al.* [116]. Regardless of the substrate structure, particularly of the degree of substitution and the configuration of the olefinic double bond of the allylic alcohol, attack is always at one enantiotopic face, with ≥95% selectivity (→ ≥90% *ee* in the product)! The method has been applied in the preparation of key compounds for the synthesis of methymycin, erythromycin, disparlure, leucotriene C-1 [117], leucotriene A, C, D, and E [118], as well as in the total synthesis of (+)-disparlure and of salt marsh caterpillar moth pheromone [119]. Carbohydrates have also been synthesized by a new sequence depending upon the method [120, 121].

enantioselective epoxidation of allyl alcohols with $Ti(OiPr)_4/tBuOOH$/diethyl tartrate[116] (Scheme 20). It is beyond the scope of this article to attempt to estimate the importance of these applications of Ti- and Zr-reagents. They are mentioned here only to demonstrate the variety of chemistry Ti and Zr display to interest the synthetic organic chemist.

## 10. Final Remarks and Outlook

The development of synthetic methods has reached a stage in which it has become more important to find more and more selective conditions for performing known reactions than to discover entirely new reaction types. Realization of this goal will fulfill the synthetic chemists dream of having reagents which attack polyfunctional substrates completely specifically, at only *one* center, without the necessity of recourse to protecting group techniques. Thus, the present article describes only three new reaction types: direct geminal dimethylation, geminal amination/alkylation of aldehydes and ketones and the olefination of esters and lactones to give enol ethers; the stress lies on carrying out old reaction types "made to measure". Non-toxic titanium and zirconium derivatives can discriminate almost perfectly between the polar C=X groups of aldehydes, ketones, esters, amides, carbon dioxide, nitriles and nitro compounds. The differences in reaction rates with different functional groups are sometimes so high, that selectivities are achieved reminiscent of those obtained in enzyme reactions of natural substrates. On the other hand, the tartaric acid/titanate-catalyzed enantioselective epoxidation of allylic alcohols is actually superior to typical enzymatic transformations in that it proceeds with >95% enantioselectivity almost independent of the substrate structure.

The possibilities for further applications of the novel nucleophilic reagents discovered so far, as well as entirely new discoveries in this area are equally exciting. Thus, it is imaginable that these reagents will become available directly from alkyl halides or olefins avoiding the intermediacy of lithium and magnesium derivatives. A catalytic variation might also be possible!

We are convinced that further selective processes of this type, based on transition metals, will soon be discovered. Thus, for the forseeable future, organic synthesis will not lose its potential to surprise and hence its attractiveness.

The following sentence from *Karl Ziegler* from the year 1965[123] has once more become true: "... the organometallic compounds, that is to say the products of a type of symbiosis between the two main branches of chemistry, which finally led to success".

*The results from our laboratory mentioned here have naturally come about through team work. We wish to thank P. Booth, E. Hungerbühler, R. Lehmann, R. Naef, C. D. Maycock, A. Olivero, A. Planta, M. Schiess, P. Schnurrenberger, T. Weber, L. Widler, M. Yoshifuhi and M. F. Züger for their enthusiasm and their work, for varying lengths of time, in the area of Ti- and Zr-derivatives. We are also grateful to the firm of Dynamit-Nobel AG, Troisdorf for generous supplies of titanates and zirconates. We thank Sandoz AG, Basel for their continuing financial support of our group. Finally, we are indebted to Miss S. Sigrist, Mrs. D. Westen and to Mrs. H. Zass for preparing the manuscript and to Dr. K. Lawson for translating it from German into English.*

Received: October 20, 1982 [A 437 IE]
German version: *Angew. Chem. 95* (1983) 12

[1] Taken in part from the Dissertation of B. Weidmann, ETH Zürich (1982), Diss. No. 7203.
[2] E. Frankland, *J. Chem. Soc. 2* (1849) 263; *Justus Liebigs Ann. Chem. 71* (1849) 171, 213.
[3] a) V. Grignard, *C. R. Acad. Sci. 130* (1900) 1322; *Chem. Zbl. 1900*, II 33; b) see also K. Nützel in Houben-Weyl-Müller: *Methoden der organischen Chemie, Vol. XIII/2a*, 4th Edit., Thieme, Stuttgart 1973, p. 50.
[4] B. J. Wakefield: *Organolithium Compounds*, Pergamon Press, Oxford 1974.
[5] H. C. Brown: *Organic Synthesis via Boranes*, Wiley, New York 1975; *Angew. Chem. 92* (1980) 675.
[6] T. Mole, E. A. Jeffery: *Organoaluminium Compounds*, Elsevier, Amsterdam 1972.
[7] N. I. Sheverdina, K. A. Kocheshkov: *The Organic Compounds of Zinc and Cadmium*, North-Holland, Amsterdam 1967.
[8] K. Nützel, „*Cadmiumorganische Verbindungen*" in [3b], p. 859.
[9] D. Seebach, *Angew. Chem. 91* (1979) 259; *Angew. Chem. Int. Ed. Engl. 18* (1979) 239.
[10] J. Cason, *Chem. Rev. 40* (1947) 15.
[11] M. S. Kharasch, D. O. Tawney, *J. Am. Chem. Soc. 63* (1941) 2308.
[12] G. H. Posner: *An Introduction to Synthesis Using Organocopper Reagents*, Wiley, New York 1980; J. F. Normant, A. Alexakis, *Synthesis 1981*, 841.
[13] W. Jehn: *Chronologische Übersicht zur Entwicklung der metallorganischen Chemie*, Universitätsbibliothek Jena 1980.
[14] M. S. Kharasch, J. K. Hambling, T. P. Rudy, *J. Org. Chem. 24* (1959) 303, and references cited therein.
[15] J. P. Collman, L. S. Hegedus: *Principles and Applications of Organo-Transition Metal Chemistry*, University Science Books, Mill Valley 1980.
[16] C. K. Rofer-de Poorter, *Chem. Rev. 81* (1981) 447; W. A. Herrmann, *Angew. Chem. 94* (1982) 118; *Angew. Chem. Int. Ed. Engl. 21* (1982) 117.
[17] G. E. Coates, M. L. H. Green, K. Wade: *Organometallic Compounds*, 3rd. Edit., Vol. 2, Chapman and Hall, London 1968.
[18] D. F. Herman, W. K. Nelson, *J. Am. Chem. Soc. 74* (1952) 2693.
[19] P. C. Waites, R. S. P. Coutss, H. Weigold: *Organometallic Chemistry of Titanium, Zirconium, and Hafnium*, Academic Press, New York 1974.
[20] T. J. Kealy, P. J. Pauson, *Nature 168* (1951) 1039.
[21] K. Ziegler, E. Holzkamp, W. Breil, H. Martin, *Angew. Chem. 67* (1955) 426.
[22] G. Wilkinson, M. Rosenblum, M. C. Whiting, R. B. Woodward, *J. Am. Chem. Soc. 74* (1952) 2125.
[23] E. O. Fischer, W. Pfab, *Z. Naturforsch. B 7* (1952) 378.
[24] J. D. Dunitz, L. E. Orgel, *Nature 171* (1953) 121; *J. Chem. Phys. 23* (1955) 954.
[25] J. Schwarz, J. A. Labinger, *Angew. Chem. 88* (1976) 402; *Angew. Chem. Int. Ed. Engl. 15* (1976) 333.
[26] For the most complete compilation of organotitanium compounds at the moment see: U. Thewalt in: *Gmelin Handbuch der Anorganischen Chemie Vol. 40, Parts 1 and 2*, 8th Edit., Springer, Berlin 1977 and 1980.
[27] J. C. Huffman, K. G. Moloy, J. A. Marsella, K. G. Caulton, *J. Am. Chem. Soc. 102* (1980) 3009.
[28] J. A. Marsella, K. G. Moloy, K. G. Caulton, *J. Organomet. Chem. 201* (1980) 389.
[29] H. Gilman, F. Schulze, *J. Am. Chem. Soc. 47* (1925) 2002.
[30] Which is not to say that titanium compounds are biologically totally inactive. The cytostatic properties of $Cp_2TiCl_2$ have recently been investigated: H. Köpf, P. Köpf-Maier, *Nachr. Chem. Tech. Lab. 29* (1981) 154, and references cited therein. Growth regulating effects of titanium complexes seen to have been established: F. Sagi, I. Pais, H. Sagi, *Tagungsber. Akad. Landwirtschaftswiss. DDR Berlin 179* (1980) 103; E. Farkas, A. Richnovszky, I. Pais, *Acta Agron. Acad. Sci. Hung. 30* (1981) 371.
[31] D. Seebach et al. in R. Scheffold: *Modern Synthetic Methods 1983*, Wiley, New York and Salle/Sauerländer, Aarau 1983, in press.
[32] a) O. V. Nogina, R. Kh. Freidlina, A. N. Nesmeyanov, *Izv. Akad. Nauk SSSR, Otd. Khim. Nauk 1952*, 74; *Chem. Abstr. 47* (1953) 1583; b) M. Thomas, *Can. J. Chem. 39* (1961) 1386.
[33] C. Dijkgraaf, J. P. G. Rousseau, *Spectrochim. Acta A 24* (1968) 1213.
[34] H. Bürger, H. J. Neese, *Z. Anorg. Allg. Chem. 370* (1969) 275.
[35] J. G. Dillard, *Inorg. Chem. 8* (1969) 2148; K.-W. Thiele, P. Zdunneck, D. Baumgart, *Z. Anorg. Allg. Chem. 378* (1970) 62; C. Beermann, DBP 1089382 (1960).

[36] C. E. H. Bawn, J. Gladstone, *Proc. Chem. Soc. (London) 1959*, 227; B. J. Hewitt, A. K. Holliday, R. J. Puddephatt, *J. Chem. Soc. Dalton Trans. 1973*, 801.

[37] C. Beermann, H. Bestian, *Angew. Chem. 71* (1959) 618; D. Behar, H. Feilchenfeld, *J. Organomet. Chem. 4* (1965) 278; J. F. Hanlan, J. D. McCowan, *Can. J. Chem. 50* (1972) 747; C. Blandy, M. T. Sadani, D. Gervais, *Synth. React. Inorg. Met.-Org. Chem. 8* (1978) 381.

[38] B. Weidmann, D. Seebach, *Helv. Chim. Acta 63* (1980) 2451.

[39] B. Weidmann, L. Widler, A. G. Olivero, C. D. Maycock, D. Seebach, *Helv. Chim. Acta 64* (1981) 357.

[40] M. T. Reetz, R. Steinbach, J. Westermann, R. Peter, *Angew. Chem. 92* (1980) 1044; *Angew. Chem. Int. Ed. Engl. 19* (1980) 1011.

[41] C. D. Maycock, unpublished results, ETH 1981.

[42] L. Widler, D. Seebach, *Helv. Chim. Acta 65* (1982) 1085.

[43] L. Widler, D. Seebach, *Helv. Chim. Acta 65* (1982) 1972.

[44] P. Booth, Diplomarbeit, ETH 1981.

[45] T. Kauffmann, E. Antfang, B. Ennen, N. Klas, *Tetrahedron Lett. 23* (1982) 2301.

[46] A. G. Olivero, B. Weidmann, D. Seebach, *Helv. Chim. Acta 64* (1981) 2485.

[47] H. Gilman, T. S. Soddy, *J. Org. Chem. 22* (1957) 1715.

[48] Previously unpublished findings of Z. Brich (Sandoz AG, Basel) and A. Hidber (ETH Zürich) have enabled the determination of the following thermodynamic data for the addition of butyllithium to benzaldehyde in THF at $-80\,^{\circ}C$: $\Delta G^{0}$ *ca.* $-45$ kcal/mol; $E_a$ *ca.* 12 kcal/mol.

[49] K. Kostova, A. Lorenzi-Riatsch, Y. Nakashita, M. Hesse, *Helv. Chim. Acta 65* (1982) 249.

[50] C. Blandy, D. Gervais, *Inorg. Chim. Acta 62* (1981) 79.

[51] M. Reetz, *Chem. Ind. (London) 1981*, 541.

[52] J. A. Ibers, *Nature 197* (1963) 686.

[53] D. C. Bradley, R. C. Mehrotra, D. P. Gaur: *Metalalkoxides*, Academic Press, London 1978, and references cited therein.

[54] K. Kühnlein, K. Clauss, *Makromol. Chem. 155* (1972) 145.

[55] D. Seebach, R. Naef, *Helv. Chim. Acta 64* (1981) 2704.

[56] M. T. Reetz, R. Steinbach, J. Westermann, R. Urz, B. Wenderoth, R. Peter, *Angew. Chem. 94* (1982) 133; *Angew. Chem. Int. Ed. Engl. 21* (1982) 135.

[57] D. Seebach, V. Prelog, *Angew. Chem. 94* (1982) 696; *Angew. Chem. Int. Ed. Engl. 21* (1982) 654.

[58] G. M. Whitesides, C. P. Casey, J. K. Krieger, *J. Am. Chem. Soc. 93* (1971) 1379.

[59] T. Mukaiyama, T. Sato, J. Hanna, *Chem. Lett. 19* (1973) 1041 (For application of low-valent Ti-compounds in organic synthesis see Section 9).

[60] B. Weidmann, C. D. Maycock, D. Seebach, *Helv. Chim. Acta 64* (1981) 1552.

[61] H. Meerwein, B. V. Bock, B. Kirschnick, W. Lenz, A. Migge, *J. Prakt. Chem. N. F. 147* (1936) 211; see also A. L. Wilds, *Org. React. 2* (1944) 178.

[62] C. Djerassi, *Org. React. 6* (1951) 207.

[63] A. Planta, Diplomarbeit, ETH Zürich 1982.

[64] R. W. Hoffmann, *Angew. Chem. 94* (1982) 569; *Angew. Chem. Int. Ed. Engl. 21* (1982) 555.

[65] High stereoselectivity has also been observed in single cases for the addition of the magnesium enolates derived from α-sulfinyl esters to ketones; Review article: G. Solladié, *Synthesis 1981*, 185.

[66] R. Hanko, D. Hoppe, *Angew. Chem. 94* (1982) 378; *Angew. Chem. Int. Ed. Engl. 21* (1982) 372; *Angew. Chem. Suppl. 1982*, 939.

[67] K.-H. Geiss, B. Seuring, R. Pieter, D. Seebach, *Angew. Chem. 86* (1974) 484; *Angew. Chem. Int. Ed. Engl. 13* (1974) 479; P. Pohmakotr, K.-H. Geiss, D. Seebach, *Chem. Ber. 112* (1979) 1420; see also D. A. Evans, G. C. Andrews, *Acc. Chem. Res. 7* (1974) 147.

[68] B. W. Erickson, Ph. D. Thesis, Harvard University, Cambridge 1970.

[69] L. Widler, unpublished results, ETH Zürich 1981; T. Weber, Diplomarbeit, ETH Zürich 1982.

[70] D. Hoppe, F. Lichtenberg, *Angew. Chem. 94* (1982) 378; *Angew. Chem. Int. Ed. Engl. 21* (1982) 372.

[71] M. Ishiguro, N. Ikeda, H. Yamamoto, *J. Org. Chem. 47* (1982) 2225.

[72] M. Schiess, unpublished results, ETH Zürich 1982.

[73] C. F. Lane, *Synthesis 1975*, 135; R. O. Hutchins, N. R. Natale, *Org. Prep. Proced. Int. 11* (1979) 201.

[74] Review article: B. T. Gröbel, D. Seebach, *Synthesis 1977*, 357.

[75] D. J. Peterson, *Organomet. Chem. Rev. A 7* (1972) 295; A. Krief, *Tetrahedron 36* (1980) 2531.

[76] A geminal dimethylation of carbonyl compounds using a large excess of trimethylaluminum under pyrolytic conditions is already known: A. Meisters, T. Mole, *Aust. J. Chem. 27* (1974) 1665.

[77] M. T. Reetz, J. Westermann, R. Steinbach, *Angew. Chem. 92* (1980) 931, 933; *Angew. Chem. Int. Ed. Engl. 19* (1980) 900, 901; M. T. Reetz, B. Wenderoth, R. Peter, R. Steinbach, J. Westermann, *J. Chem. Soc. Chem. Commun. 1980*, 1202; M. T. Reetz, R. Steinbach, B. Wenderoth, *Synth. Commun. 11* (1981) 261.

[78] M. T. Reetz, J. Westermann, R. Steinbach, *J. Chem. Soc. Chem. Commun. 1981*, 237.

[79] M. T. Reetz, *Angew. Chem. 94* (1982) 97; *Angew. Chem. Int. Ed. Engl. 21* (1982) 96.

[80] T. Kauffmann, R. König, C. Pahde, A. Tannert, *Tetrahedron Lett. 22* (1981) 5031.

[81] H. Weingarten, W. A. White, *J. Org. Chem. 31* (1966) 4041; for a detailed review of the tetrakis(dialkylamino)compounds of titanium, see H. Bürger, H.-J. Neese, *Chimia 24* (1970) 209.

[82] W. A. White, H. Weingarten, *J. Org. Chem. 32* (1967) 213.

[83] a) D. Seebach, H.-O. Kalinowski, B. Bastani, G. Crass, H. Daum, H. Dörr, N. P. DuPreez, V. Ehrig, W. Langer, C. Nüssler, H.-A. Oei, M. Schmidt, *Helv. Chim. Acta 60* (1977) 301; b) D. Seebach, W. Langer, *ibid. 62* (1979) 1701; W. Langer, D. Seebach, *ibid. 62* (1979) 1710; c) D. Seebach, G. Crass, E. M. Wilka, D. Hilvert, E. Brunner, *ibid. 62* (1979) 2695.

[84] J. P. Mazaleyrat, D. J. Cram, *J. Am. Chem. Soc. 103* (1981) 4585.

[85] T. Mukaiyama, K. Soai, T. Sato, H. Shimizu, K. Suzuki, *J. Am. Chem. Soc. 101* (1979) 1455.

[86] T. Mukhophadhyay, R. Amstutz, J. Hansen, G. Simson, unpublished results, ETH Zürich 1982.

[87] R. Amstutz, W. B. Schweizer, D. Seebach, J. D. Dunitz, *Helv. Chim. Acta 64* (1981) 2617; D. Seebach, R. Amstutz, J. D. Dunitz, *ibid. 64* (1981) 2622.

[88] W. Köster, D. Thomas, E. Weiss, *J. Organomet. Chem. 160* (1979) 1.

[89] R. Hässig, J. Gabriel, unpublished results, ETH Zürich 1982.

[90] A low (3.6% *ee*) enantioselectivity has been achieved by complexation of $MeTiCl_3$ with/sparteine: M. T. Reetz, J. Westermann, *Synth. Commun. 11* (1981) 647. Reactions of $MeTi(O\mathit{i}Pr)_3$ with benzaldehyde in presence of the chiral reagents 2,3-dimethoxy-*N,N,N',N'*-tetramethyl-1,4-butanediamine (DDB) [83b] and 4,5-bis(dimethylaminomethyl)-*N,N,N',N'*-tetramethyl-3,6-dioxa-1,8-octanediamine (DEB) [83c] do not show measurable enatioselectivity: M. Yoshifuji, unpublished results, ETH Zürich 1980.

[91] M. Schmidt, R. Amstutz, G. Crass, D. Seebach, *Chem. Ber. 113* (1980) 1691, and references cited therein.; D. Seebach, H. Daum, *ibid. 107* (1974) 1748, and references cited therein.

[92] R. S. Brinkmeyer, V. M. Kapoor, *J. Am. Chem. Soc. 99* (1977) 8339; R. Noyori, *Pure Appl. Chem. 53* (1981) 2315; T. Mukaiyama, *Tetrahedron 37* (1981) 4111, and references cited therein.

[93] Ligand of **20**: M. Carmack, C. J. Kelley, *J. Org. Chem. 33* (1968) 2171; P. W. Feit, *J. Med. Chem. 7* (1964) 14.

[94] The diol for **21** is prepared by reaction of diethyl tartrate acetonide (diethyl 2,2-dimethyl-1,3-dioxolane-4,5-dicarboxylate) with MeLi: R. Lehmann, Diplomarbeit, ETH Zürich 1982.

[95] Binaphthol ligand of **22–25** according to: E. P. Kyba, G. W. Gokel, F. de Jong, K. Koga, L. R. Sousa, M. G. Siegel, L. Kaplan, G. Dotsevi, G. D. Y. Sogah, D. J. Cram, *J. Org. Chem. 42* (1977) 4173.

[96] **22** and **24** prepared from $ClTi(OEt)_3$ and $ClTi(O\mathit{t}Bu)_3$, respectively, and the corresponding diol.

[97] The ligand for **26** is obtained by oxidative dimerization of 3-hydroxy-2-naphthoic acid with $FeCl_3$ and subsequent reduction of the resulting diacid (resolved by use of L-leucine methyl ester) with $LiAlH_4$ followed by Pd/C [94]; see also R. C. Helgeson, J. M. Timko, P. Moreau, S. C. Peacock, J. M. Mayer, D. Cram, *J. Am. Chem. Soc. 96* (1974) 6763.

[98] D. Seebach, E. Hungerbühler in R. Scheffold: *Modern Synthetic Methods 1980*, Salle/Sauerländer, Aarau 1980.

[99] K. Tomioka, K. Koya, *Kagaku No Ryoiki 34* (1980) 762.

[100] For general reviews dealing with enantioselective reactions see *e.g.* J. W. ApSimon, R. P. Seguin, *Tetrahedron 35* (1979) 2797; D. Valentine, Jr., J. W. Scott, *Synthesis 1978*, 329.

[101] J. Chatt, G. L. M. daCâmara Pina, R. L. Richards: *New Trends in the Chemistry of Nitrogen Fixation*, Academic Press, New York 1981.

[102] E. Thorn-Csányi, *Nachr. Chem. Tech. Lab. 29* (1981) 700, and references cited therein.

[103] D. Seebach, E. Hungerbühler, R. Naef, P. Schnurrenberger, B. Weidmann, M. F. Züger, *Synthesis 1982*, 138.

[104] H. Rehwinkel, W. Steglich, *Synthesis 1982*, 826.

[105] P. Schnurrenberger, M. F. Züger, D. Seebach, *Helv. Chim. Acta 65* (1982) 1197; D. Seebach, M. F. Züger, *Helv. Chim. Acta 65* (1982) 495.

[106] M. F. Züger, unpublished results, ETH Zürich 1981.

[107] Compare also the carbometalation with Ti/Zr-derivatives: E. I. Negishi, *Pure Appl. Chem. 53* (1981) 2333.

[108] T. Mukaiyama, *Angew. Chem. 89* (1977) 858; *Angew. Chem. Int. Ed. Engl. 16* (1977) 817; see also J. Fleming, *Chem. Soc. Rev. 10* (1981) 83; T. H. Chan, J. Fleming, *Synthesis 1979*, 761.

[109] See also J. E. McMurry, *Acc. Chem. Res. 7* (1974) 281; E. J. Corey, R. L. Danheiser, S. Chandrasekaran, *J. Org. Chem. 41* (1976) 260; B. P. Mundy, R. Srinivasa, Y. Kim, T. Dolph, *ibid. 47* (1982) 1657.

[110] D. A. Evans, L. R. McGee, *Tetrahedron Lett. 21* (1980) 3975; Y. Yamamoto, K. Maruyama, *ibid. 21* (1980) 4607.

[111] M. T. Reetz, R. Peter, *Tetrahedron Lett. 22* (1981) 4691.

[112] J. Schartz, Y. Hayasi, *Tetrahedron Lett. 21* (1980) 1497.

[113] S. H. Pine, R. Zahler, D. A. Evans, R. H. Grubbs, *J. Am. Chem. Soc. 102* (1980) 3270.

[114] J. W. S. Stevenson, T. A. Bryson, *Tetrahedron Lett. 23* (1982) 3143.
[115] F. N. Tebbe, G. W. Parshall, G. S. Reddy, *J. Am. Chem. Soc. 100* (1978) 3611.
[116] T. Katsuke, K. B. Sharpless, *J. Am. Chem. Soc. 102* (1980) 5974.
[117] B. E. Rossiter, T. Katsuki, K. B. Sharpless, *J. Am. Chem. Soc. 103* (1981) 464.
[118] E. J. Corey, S. I. Hashimoto, A. E. Barton, *J. Am. Chem. Soc. 103* (1981) 721.
[119] K. Mori, T. Ebata, *Tetrahedron Lett. 22* (1981) 4281.
[120] T. Katsuki, A. W. M. Lee, P. Ma, V. S. Martin, S. Masamune, K. B. Sharpless, D. Tuddenham, F. J. Walker, *J. Org. Chem. 47* (1982) 1373; P. Ma, V. S. Martin, S. Masamune, K. B. Sharpless, S. M. Viti, *ibid. 47* (1982) 1378; A. W. M. Lee, V. S. Martin, S. Masamune, K. B. Sharpless, F. J. Walker, *J. Am. Chem. Soc. 104* (1982) 3515.
[121] W. R. Roush, R. J. Brown, *J. Org. Chem. 47* (1982) 1371.
[122] K. B. Sharpless, C. H. Behrens, T. Katsuki, A. W. M. Lee, V. S. Martin, M. Takatani, S. M. Viti, F. J. Walker, S. S. Woodard, *Pure Appl. Chem.*, in press.
[123] K. Ziegler, *Naturwiss. Rundsch. 18* (1965) 1.
[124] M. T. Reetz, *Topics, in Curr. Chem. 106* (1982) 1.
[125] M. T. Reetz, R. Steinbach, K. Kesseler, *Angew. Chem. 94* (1982) 872; *Angew. Chem. Int. Ed. Engl. 21* (1982) 864; *Angew. Che. Suppl. 1982*, 1899.

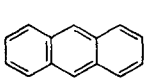
# COMMUNICATIONS

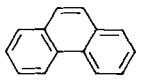
**When submitting manuscripts, authors of articles which are intended for publication as "Communications" are requested to conform to the guidelines reproduced at the beginning of each issue following the list of contents.**

## Unusual NMR Phenomena of Anthracene and Phenanthrene Dianions – Thermal Stimulation of Triplet States in Antiaromatic Systems

By *Abraham Minsky, Amatzya Y. Meyer,* and *Mordecai Rabinovitz**

Many aromatic polycyclic benzenoid hydrocarbons undergo a facile reduction process with electropositive metals to yield the corresponding dianions. The $^1$H-NMR spectra of some of these doubly charged species exhibit characteristic high-field chemical shifts, which reflect the existence of an enhanced antiaromatic-paratropic ring current[1–3]. We report here some unusual NMR phenomena which occur in the metal reduction of anthracene **1** and phenanthrene **2** under various conditions.


**1**


**2**

Anthracene **1** was reduced by adding lithium metal to a THF solution of the hydrocarbon[1,2]. The blue-green solution of the dianion exhibited a well resolved high-field $^1$H-NMR spectrum consisting of an AA'BB' multiplet and a singlet. Over the range $-60\,^\circ$C to $+40\,^\circ$C the $^1$H-NMR spectrum remained unchanged. No change could be detected in the $^{13}$C-NMR spectrum, which is identical with that already reported[1].

[*] Prof. M. Rabinovitz, Prof. A. Y. Meyer, A. Minsky
Department of Organic Chemistry,
The Hebrew University of Jerusalem
Jerusalem 91904 (Israel)

A different and rather unexpected situation occurs when sodium is used as reducing agent. The $^1$H-NMR spectrum of $\mathbf{1}^{2\ominus}2\,Na^{\oplus}$ is strongly temperature dependent. At $+40\,^\circ$C the blue solution of the dianion exhibits no signals, whereas at $+20\,^\circ$C three very broad signals at $\delta \approx 3.85$ (2,3,6,7-H), 2.90 (1,4,5,8-H), and 1.65 (9,10-H) are detected. As the temperature was gradually decreased, the signals became markedly sharper. However, even at $-60\,^\circ$C the fine structure expected from an AA'BB' system was not observable. The change in line width of the absorptions was reversible, *i.e.* lowering the temperature produced line sharpening. We could not obtain the $^{13}$C-NMR spectrum of $\mathbf{1}^{2\ominus}2\,Na^{\oplus}$ at room temperature, and even at $-30\,^\circ$C the signal/noise ratio was poor.

The same experiment was conducted in a solution of THF and dimethoxyethane (DME) (95:5). At $+20\,^\circ$C the $^1$H-NMR signals were much sharper than those exhibited in pure THF at the same temperature. Already at $0\,^\circ$C, the signals at $\delta = 3.9$ and 2.9 exhibited fine structure, and at $-30\,^\circ$C the spectrum revealed a well resolved AA'BB' multiplet along with a narrow singlet at $\delta = 1.64$. At this temperature the $^{13}$C-NMR signals were similar to those exhibited by $\mathbf{1}^{2\ominus}2\,Li^{\oplus}$. As with pure THF, the changes in the NMR spectrum as a function of temperature were completely reversible.

When the reduction was carried out with potassium at $-80\,^\circ$C in THF, a $^1$H-NMR spectrum could not be recorded for the dianion, even at $-20\,^\circ$C. At lower temperatures very broad absorptions at $\delta = 3.8$, 2.9 and 1.6 were found.

Reduction of phenanthrene **2** with sodium in THF to the corresponding dianion did not afford NMR signals over the temperature range $-80\,^\circ$C to $+40\,^\circ$C. However, reduction with lithium resulted in very broad, high-field $^1$H-NMR signals at $-30\,^\circ$C. Decreasing the temperature further to $-80\,^\circ$C caused line sharpening, but a highly resolved spectrum could not be recorded. Conducting the experiment in THF/DME (95:5) caused further sharpening. The chemical shifts were similar to those already reported [$\delta = 0.5$ (1,8-H), 2.7 (2,7-H), 1.6 (3,6-H), 0.7 (4,5-H), $-1.9$ (9,10-H)][3]. A clear reversibility of the NMR line shapes as a function of temperature was observed.

All these phenomena are strongly related to factors which dominate the ion solvation equilibrium[4]—highly solvated ion pairs exhibit sharp well-resolved NMR signals, whereas contact pairing results in dramatic line

 © *Verlag Chemie GmbH, 6940 Weinheim, 1983* *0570-0833/83/0101-0045 $ 02.50/0* 

broadening. Several interpretations are possible, of which the most plausible is based on theoretical considerations which assign a relatively narrow LUMO-HOMO energy gap to antiaromatic species. We presume that the anthracene and phenanthrene dianions are thermally excited triplet state systems in equilibrium with the singlet ground state. At elevated temperatures the excited triplet is highly populated and this results in total disappearance or significant broadening of the NMR signals. Decreasing the temperature causes a relaxation to the singlet ground state as indicated by the observation of NMR signals. This interpretation is consistent with the results of ESR measurements carried out on $\mathbf{1}^{2\ominus}2Na^{\oplus}$ and $\mathbf{2}^{2\ominus}2Na^{\oplus}$. The ESR spectra of the frozen THF solutions (−130 °C) of $\mathbf{1}^{2\ominus}2Na^{\oplus}$ and $\mathbf{2}^{2\ominus}2Na^{\oplus}$ reveal a broad signal centered at 3200 G, along with a sharp signal at 1590 and 1595 G, respectively. The low-field signals are assigned to the $\Delta m_s = 2$ transition, a feature highly characteristic of a triplet state[5].

The presumed singlet-triplet equilibria are not simple thermal processes but are strongly related to factors which dominate the solution equilibria, *i.e.* nature of the counterion and the solvent[4].

Received: April 28, 1982;
revised: November 15, 1982 [Z 28 IE]
German version: *Angew. Chem. 95* (1983) 45

[1] K. Müllen, *Helv. Chim. Acta 59* (1976) 1357.
[2] R. G. Lawler, C. V. Ristagno, *J. Am. Chem. Soc. 91* (1976) 1534.
[3] K. Müllen, *Helv. Chim. Acta 61* (1978) 1296.
[4] O. H. O'Brien, C. R. Russel, A. J. Hart, *J. Am. Chem. Soc. 101* (1979) 633.
[5] J. E. Wertz, J. R. Bolton: *ESR-Elementary Theory and Practical Applications*, McGraw-Hill, New York 1972, pp. 223–246.

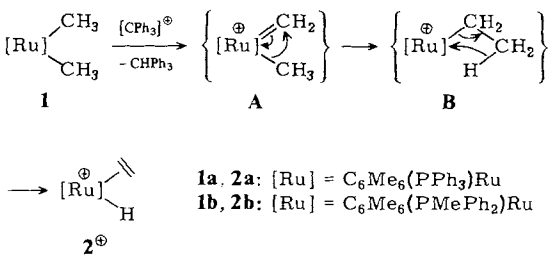
## A Model Reaction of an Elementary Step in the Fischer-Tropsch Synthesis: $[C_6Me_6RuH(C_2H_4)PR_3]^+$ from $C_6Me_6Ru(CH_3)_2PR_3$

By *Heidrun Kletzin, Helmut Werner*, Orhan Serhadli,* and *Manfred L. Ziegler*

Studies of the mechanism of the heterogeneous Fischer-Tropsch synthesis have established that the chain-forming step, *i.e.* the coupling of C—C bonds on the surface of the catalyst proceeds *via* successive insertion of methylene groups into the metal-alkyl bonds[1a]. Following a β-H elimination, α-olefins are formed as the initial products of the F.T. synthesis.

Model studies, which are based on reactions *in solution* (*i.e.* in a homogeneous phase), have mainly been directed towards the hydrogenation of CO ligands and the insertion of methylene or alkylidene groups into metal-alkyl bonds[1b]. *Maitlis et al.* showed that thermolysis of the dinuclear complex *cis*-$[C_5Me_5RhCH_3]_2(\mu\text{-}CH_2)_2$ produces, apart from methane, mainly ethylene and propene, which can be explained by single and double $CH_2$-insertion, respectively, into a Rh—$CH_3$ bond[1c]. The *in situ* synthesis of a mononuclear $W(CH_2)CH_3$ complex was achieved by *Cooper et al.*[1d], who allowed the $PF_6$ salt of the paramagnetic cation $[(C_5H_5)_2W(CH_3)_2]^+$ to react with 3-diphenylmethylene-6-triphenylmethyl-1,4-cyclohexadiene (as source of the trityl radical), and isolated the ethylene(hydrido) complex $[(C_5H_5)_2WH(C_2H_4)]^+$ as the major product. In addition to the methyl(methylene) complex $[(C_5H_5)_2W(CH_2)CH_3]^+$, a further intermediate $[(C_5H_5)_2WC_2H_5]^+$ was also postulated.

We have now found that an analogous reaction sequence probably occurs after elimination of a *hydride* ion from a *neutral* (diamagnetic) dimethylmetal compound. Dropwise addition of a solution of $[CPh_3]PF_6$ in $CH_2Cl_2$ to a solution of $C_6Me_6Ru(CH_3)_2PPh_3$[2] **1a** in $CH_2Cl_2$ at −78 °C, and subsequent warming to room temperature, leads, after addition of ether, to formation of a colorless, rather air-stable solid. The yield after recrystallization from $CH_2Cl_2/Et_2O$ is 71%. Elemental analysis and spectroscopic data[3a] confirm the composition $[C_6Me_6RuH(C_2H_4)PPh_3]PF_6$ **2a**. The analogous reaction of $C_6Me_6Ru(CH_3)_2PMePh_2$ **1b** with $[CPh_3]PF_6$ in the molar ratio 1:1 affords $[C_6Me_6RuH(C_2H_4)PMePh_2]PF_6$ **2b**[3a] in 56% yield. We presume that the trityl cation attacks an $RuCH_3$ group of **1** and eliminates a hydride ion. The initially formed cationic methyl(methylene) complex **A** undergoes $CH_2$-insertion (or $CH_3$-migration) to give the isomeric coordinatively unsaturated ethyl compound **B**, from which the product **2** is formed by hydride shift from the β-C atom to the metal. That the solvent is *not* involved in the formation of **2a** or **2b** is proved by the synthesis of pure $RuH(C_2H_4)$ cations in $CD_2Cl_2$.




The $CH_2$-insertion, which mechanistically presumably corresponds to CO-insertion[4a], should proceed very rapidly according to MO calculations[4b]. Apart from our findings and those of *Cooper et al.*, the results of *Thorn* and *Tulip*[4c] are also consistent with this. They found that *mer*-$IrBr_2(C_2H_5)(PMe_3)_3$ is formed from *mer*-$IrBr(CH_3)CH_2OCH_3(PMe_3)_3$ and $BrCH_2OCH_3$, probably also *via* a cationic $Ir(CH_2)CH_3$ intermediate, which spontaneously rearranges to the isomeric $IrC_2H_5$ compound.

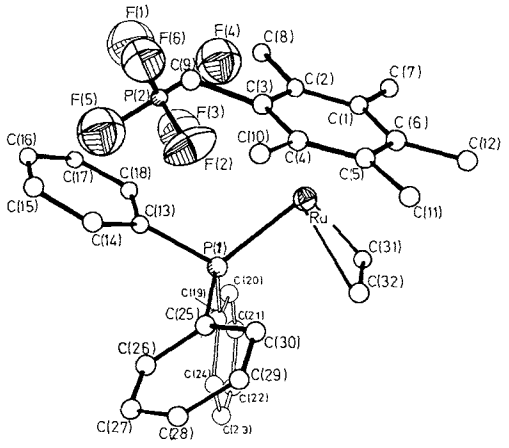



Fig. 1. Structure of **2a** in the crystal. Selected bond lengths [pm]: Ru—P(1) 229.7(2), Ru—C(31) 216.8(10), Ru—C(32) 219.4(9), C(31)—C(32) 141.1(13).

[*] Prof. Dr. H. Werner, H. Kletzin
Institut für Anorganische Chemie der Universität
Am Hubland, D-8700 Würzburg (Germany)
Prof. Dr. M. L. Ziegler, O. Serhadli
Anorganisch-chemisches Institut der Universität
Im Neuenheimer Feld 270, D-6900 Heidelberg 1 (Germany)

 © Verlag Chemie GmbH, 6940 Weinheim, 1983 0570-0833/83/0101-0046 $ 02.50/0 

The structure of **2a** has been established by X-ray crystal structure analysis[3b]. Although the position of the hydride ligand cannot be given precisely, the bond angle of 90.2° between P(1), Ru, and the midpoint of C(31)—C(32) confirms the octahedral coordination around ruthenium. Since the $^1$H-NMR spectrum does not change between −80 and +35 °C ([D$_6$]acetone), it seems certain that the ethylene(hydrido)cations **2**$^{\oplus}$ are configurationally stable in solution, and that the equilibrium with the ethyl tautomers—in contrast to the structurally analogous complexes $[C_5H_5RhH(C_2H_4)PR_3]^+$ (R = Me, *i*Pr)[5]—is almost completely shifted to the side of $[C_6Me_6RuH(C_2H_4)PR_3]^+$.

Received: August 13, 1982 [Z 132 IE]
German version: *Angew. Chem. 95* (1983) 49

[1] a) R. C. Brady III, R. Pettit, *J. Am. Chem. Soc. 102* (1980) 6181; b) W. A. Herrmann, *Angew. Chem. 94* (1982) 118; *Angew. Chem. Int. Ed. Engl. 21* (1982) 117; c) K. Isobe, D. G. Andrews, B. E. Mann, P. M. Maitlis, *J. Chem. Soc. Chem. Commun. 1981*, 809; d) J. C. Hayes, G. D. N. Pearson, N. J. Cooper, *J. Am. Chem. Soc. 103* (1981) 4648.

[2] H. Werner, H. Kletzin, *J. Organomet. Chem. 228* (1982) 289.

[3] a) **2a**: IR [ν(RuH), cm$^{-1}$]: 2050 (Nujol). $^1$H-NMR [100 MHz, 25 °C, $CD_3NO_2$, int. TMS]: δ($C_6H_5$) 7.26—7.56 (m), δ($C_6Me_6$) 1.96 (d, $J_{PH}$ = 0.6 Hz), δ($C_2H_4$) 1.45—1.76 (m), δ(RuH) −10.52 (d, $J_{PH}$ = 35.0 Hz).—**2b**: IR [ν(RuH), cm$^{-1}$]: 2025 (Nujol). $^1$H-NMR [100 MHz, 25 °C, $CD_3NO_2$, int. TMS]: δ($C_6H_5$) 7.32—7.73 (m), δ($C_6Me_6$) 2.16 (d, $J_{PH}$ = 0.7 Hz), δ($PCH_3$) 1.93 (d, $J_{PH}$ = 10.0 Hz), δ($C_2H_4$) 1.40—1.72 (m), δ(RuH) −10.54 (d, $J_{PH}$ = 36.0 Hz); b) rhombic (from $CH_2Cl_2$), space group Pcam ($D_{2h}^{11}$), $Z$ = 4; $a$ = 1886.0(2), $b$ = 1816.4(3), $c$ = 883.3(3) pm; AED; $2° \le 2\theta \le 30°$; 3966 independent reflections with $I > 3.0\sigma(I)$; $R_{iso}$ = 0.090; $R_{aniso}$ = 0.044. Further details on the crystal structure determination can be obtained from the Fachinformationszentrum Energie-Physik-Mathematik, D-7514 Eggenstein-Leopoldshafen by quoting the depository number CSD 50284, the name of the author, and the journal citation.

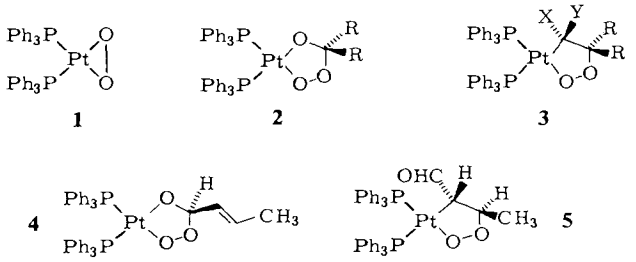
[4] a) F. Calderazzo, *Angew. Chem. 89* (1977) 305; *Angew. Chem. Int. Ed. Engl. 16* (1977) 299; H. Brunner, H. Vogt, *ibid. 93* (1981) 409; *20* (1981) 405; b) H. Berke, R. Hoffmann, *J. Am. Chem. Soc. 100* (1978) 7224; c) D. L. Thorn, T. H. Tulip, *ibid. 103* (1981) 5984.

[5] H. Werner, R. Feser, *J. Organomet. Chem. 232* (1982) 351.

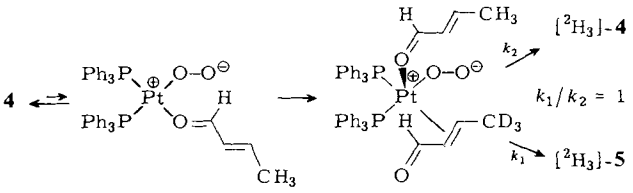
## Kinetic and Thermodynamic Control in the Reaction of $(Ph_3P)_2PtO_2$ with (*E*)-2-Butenal

By *Michael J. Broadhurst, John M. Brown**, and *Robert A. John*

$(Ph_3P)_2PtO_2$ **1** reacts with aldehydes and ketones to form stable adducts **2**[2]. In a small number of cases, electrophilic olefins react with **1** to form related cycloadducts of structure **3** *via* formal Michael addition of a ring-opened platinum peroxide[4]. We report that (*E*)-2-butenal reacts with **1** to form both types of complex sequentially and define the mechanism of their interconversion.

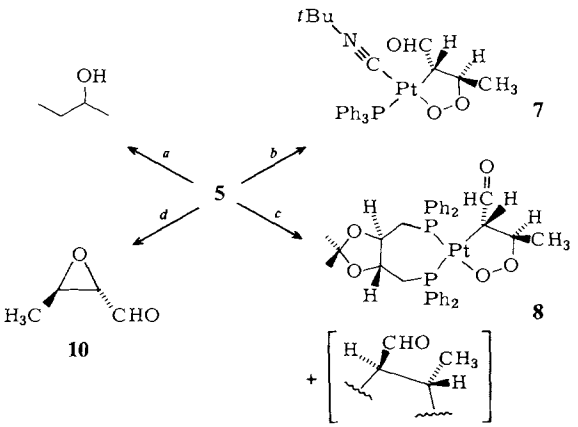


Reaction of excess (*E*)-2-butenal with complex **1** in $CH_2Cl_2$ for a few hours at ambient temperature leads to formation of adduct **4** (m.p. = 130 °C, decomp.), which can be isolated and purified. Redissolution of **4** in $CH_2Cl_2$ in the presence of excess (*E*)-2-butenal causes formation of its isomer **5** (m.p. = 145 °C, decomp.) in quantitative yield after several days at 35 °C. The mechanism of this transformation was established using [4-$^2$H]$_3$-(*E*)-2-butenal[8] and monitoring the reaction by $^1$H- or $^2$H-NMR spectroscopy. Only a pathway requiring displacement of bound (*E*)-2-butenal by deuterated material without reversion to complex **1** is consistent with the relative levels of deuteriated and protiated material at different stages of rearrangement; intramolecular reaction is ruled out. The preferred mechanism is shown in Scheme 1.



Scheme 1. Mechanism for the rearrangement of **4** into [$^2$H$_3$]-**4** and [$^2$H$_3$]-**5**.

The reaction product **5** undergoes a range of ligand displacement reactions (Scheme 2). One $PPh_3$ moiety is displaced by *t*-BuNC with high regioselectivity, and both moieties by chelating bisphosphanes, such as DIOP. Reduction of **5** with $NaBH_4$ led to 2-butanol as the only organic product, whereas **4** gave only (*E*)-2-buten-1-ol under similar conditions. Notably, the reaction of **5** in $CD_2Cl_2$ gave oxirane **10** as the main (90%) organic product (93% stereoselectivity) together with $(PPh_3)_2Pt(CF_3CO_2)_2$. The reaction course is unaffected by a 5 mol excess of $PPh_3$, implying that reaction occurs within the coordination sphere rather than by release of (*E*)-2-butenal and $H_2O_2$[10], followed by epoxidation. The sequence constitutes a formal stoichiometric epoxidation by molecular oxygen[11] and is of considerable relevance to catalytic studies.



Scheme 2. Reactions of **5**. *a:* $NaBH_4$, $CH_3OH$; *b:* *t*-BuNC, $CH_2Cl_2$; *c:* *P,P'*-[2,2-dimethyl-1,3-dioxolane-4,5-bis(methylene)]bis(diphenylphosphane) (DIOP), $CH_2Cl_2$; *d:* $CF_3CO_2H$, $CD_2Cl_2$ or $C_6D_6$.

Received: August 18, 1982 [Z 134 IE]
German version: *Angew. Chem. 95* (1983) 57
The complete manuscript of this communication appears in: *Angew. Chem. Suppl. 1983*, 1-9

[*] Dr. John M. Brown, Dr. Robert A. John
Dyson Perrins Laboratory
South Parks Road, Oxford OX1 3QY (U.K.)
Dr. Michael J. Broadhurst
Roche Products P.L.c.
Welwyn Garden City, Herts AL7 3AY (U.K.)

[2] Y. Tatsuno, S. Otsuka, *J. Am. Chem. Soc. 103* (1981) 5832; R. Ugo, G. M. Zanderighi, A. Fusi, D. Carreri, *ibid. 102* (1980) 3745.

[4] R. A. Sheldon, J. A. Van Doorn, *J. Organometal. Chem.* **94** (1975) 115.

[8] Following the procedure described for 4-hydroxy-2-hexenal *via* 1,3-bis(methylthio)allyllithium, employing $[^2H]_3$methylmethanesulphonate as electrophile; B. W. Erickson, *Organic Syntheses 54* (1974) 19.
[10] A. Sen, J. Halpern, *J. Am. Chem. Soc. 99* (1977) 8337; G. Wilke, H. Schott, P. Heimbach, *Angew. Chem. 79* (1967) 62; *Angew. Chem. Int. Ed. Engl. 6* (1967) 92.
[11] Cf. A. Heumann, F. Chauvet, B. Waegell, *Tetrahedron Lett. 23* (1982) 2767.

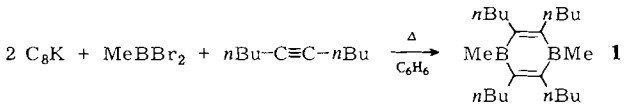
## Synthesis of Borirenes and Diboretenes — a Novel Class of 2π-Aromatic Compounds

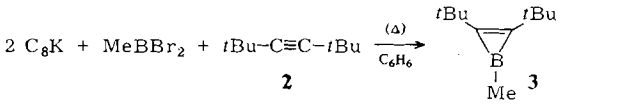
By *Sies M. van der Kerk*, Peter H. M. Budzelaar, Anca van der Kerk-van Hoof, Gerrit J. M. van der Kerk,* and *Paul von Ragué Schleyer*

Despite the fact that theoretical considerations[1] indicate that borirenes should be stabilized to a considerable extent by aromaticity, attempts at their synthesis have thus far met with little success.

From the reaction of di-*n*-alkylacetylenes with the methylboranediyl-generating system $2C_8K/MeBBr_2$[2,3] no borirenes can be isolated; 1,4-dibora-2,5-cyclohexadiene derivatives **1**, their formal dimers, are found instead. It was felt that, if borirenes are instrumental in the formation of dimers, there might be a better chance of trapping them by using an acetylene with bulky substituents as a substrate. Thus, the dimerization to a dimeric derivative might be sterically hindered.

Reactions were carried out between the graphite intercalation compound $C_8K$, $MeBBr_2$, and 2,2,5,5-tetramethyl-3-hexyne (di-*tert*-butylacetylene) **2**[4] in benzene, both under reflux and at room temperature. After work-up, GC/MS investigation of the distillate fractions showed that **1** had not been formed; instead, both reactions produced 2,3-di-*tert*-butyl-1-methylborirene **3**. It is suggestive for the stability of this borirene that in the mass spectrum of **3** the borirene-ring stays intact throughout the fragmentation of the molecule[5a].

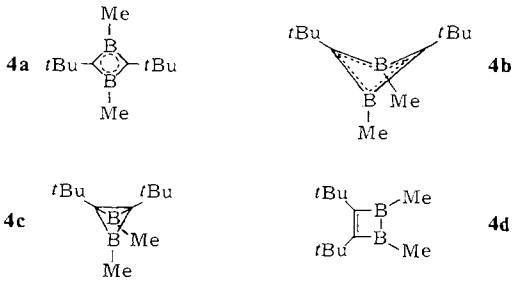




+ $tBu_2C_2(BMe)_2$ **4**

In both reactions, but especially in the one carried out at room temperature, a compound of composition $t\text{-}Bu_2C_2(BMe)_2$ **4**[5b], the product of the reaction of two methylboranediyl units with one molecule of di-*tert*-butylacetylene was also formed.

**3** and **4** appear to have similar properties. They are colorless, extremely air- and moisture-sensitive liquids; their boiling points are close to that of di-*tert*-butylacetylene and they could not be separated by distillation. The NMR data[5c] were determined using mixtures and represent the results of preliminary experiments.



Several structures are possible for compound **4**: two 1,3-diboretenes (**4a** and **4b** of symmetries $D_{2h}$ and $C_{2v}$, respectively), a diborabicyclobutane **4c**, and a 1,2-diboretene **4d**. In the mass spectrum of **4** an additional fragment is found with half the molecular mass (rel. intensity 34%). We assign this to the fragment $[t\text{-BuCBMe}]^+$, originating from cleavage of the four-membered ring in a 1,3-diboretene (**4a** or **4b**). Fragmentation of the four-membered ring of the 1,2-diboretene **4d** is not expected to proceed *via* CC bond cleavage. Rather, cleavage of the B—C bonds should occur to produce fragments $[t\text{-}Bu_2C_2]^+$ and/or $[Me_2B_2]^+$ (or $[MeB]^+$), which are not found.

Our assignment of the 1,3-diboretene structure **4a** or **4b** in preference to the alternative 1,2-diboretene structure is supported by the results of extensive calculations on the possible isomers of the compound $(CH)_2(BH)_2$[1]. Further, it has been predicted[1] that of the 1,3-diboretenes the compound with $C_{2v}$ (puckered) symmetry (**4b**) should be the most stable.

The borirene derivative **3** appears to be thermally quite stable, in view of the fact that in the course of one of its syntheses a reflux period (in benzene) of 24 h was involved. This is borne out by the calculated resonance energy of $(CH)_2(BH)$, which is 70—75% of that of its carbocation analogue[1].

Received: August 25, 1982 [Z 140 IE]
revised: November 2, 1982
German version: *Angew. Chem. 95* (1983) 61

[*] Dr. S. M. van der Kerk, Drs. P. H. M. Budzelaar, A. van der Kerk-van Hoof, Prof. Dr. G. J. M. van der Kerk
Organisch Chemisch Laboratorium, Rijksuniversiteit van Utrecht
Croesestraat 79, NL-3522 AD Utrecht (Netherlands)
Prof. Dr. P. von R. Schleyer (Guest Professor, 1982 in Utrecht)
Institut für Organische Chemie, Universität Erlangen-Nürnberg
Henkestrasse 42, D-8520 Erlangen (Germany)

[1] K. Krogh-Jespersen, D. Cremer, J. D. Dill, J. A. Pople, P. von R. Schleyer, *J. Am. Chem. Soc. 103* (1981) 2589.
[2] S. M. van der Kerk, A. L. M. van Eekeren, G. J. M. van der Kerk, *J. Organometal. Chem. 190* (1980) C8.
[3] S. M. van der Kerk, G. J. M. van der Kerk, *J. Organometal. Chem. 190* (1980) C11.
[4] We wish to thank Prof. L. Brandsma for kindly supplying a sample of di-*tert*-butylacetylene.
[5] a) Main fragmentation scheme of **3**: *m/z* 164 ($M^+$, 64%), 149 ($[M-CH_3]^+$, 63), 107 ($[M-C_4H_9]^+$, 100), 93 ($[149-C_4H_8]^+$, 22), 77 ($[93-CH_4]^+$, 7), 65 ($[107-C_3H_6]^+$, 75), 51 ($[93-C_3H_6]^+$, 17), 41 ($[CH_3)_2B]^+$, 52) (fragmentation of the ring). b) Main fragmentation scheme of **4**: *m/z* 190 ($M^+$, 4%), 175 ($[M-CH_3]^+$, 77), 148 ($[M-C_3H_6]^+$, 11), 133 ($[M-C_4H_9]^+$ and/or $[148-CH_3]^+$, 84), 119 ($[175-C_4H_8]^+$, 39), 117 ($[133-CH_4]^+$, 47), 105 ($[133-C_2H_4]^+$, 13), 91 ($[117-BCH_3]^+$, 23), 77 ($[119-C_3H_6]^+$, 12), 65 ($[91-C_2H_2]^+$, 51), 41 ($[(CH_3)_2B]^+$, 100); 95 (see text, 34%). c) $^1$H-NMR ($C_6H_6$, TMS internal standard): *t*-Bu: $\delta = 1.30$ (**2**), 1.31 (**3**), 1.28 (**4**); MeB: 0.97 (**3** and **4**, broad). $^{13}$C-NMR ($[D_8]$toluene, both at ambient temperature and at −60 °C, broadband decoupled, TMS internal standard): $CH_3$: $\delta = 32.5$ (**3**), 30.9 (**4**); $CMe_3$: 34.1 and 35.0 (**3** and **4**); $BCH_3$: 16.3 br. (**3** and **4**, only observable at −60 °C). At −60 °C broad signals were seen to arise in the aromatic region ($\delta = 127$–133). It was not possible to lower the temperature sufficiently for these signals to sharpen. We assign these resonances to the ring carbon atoms of both **3** and **4**.

 © Verlag Chemie GmbH, 6940 Weinheim, 1983 0570-0833/83/0101-0048 $ 02.50/0 

## [2+2]-Cycloadditions of Allyl Cations**

By *Herbert Klein, Gerhard Freyberger,* and *Herbert Mayr**

Allyl cations are versatile building blocks for the construction of carbocycles. *Hoffmann* has reported the syntheses of six- and seven-membered ring systems *via* [2+4]- and [3+4]-cycloadditions of allyl cations to 1,3-dienes[1]. We previously found that [3+2]-cycloadditions of allyl cations to alkenes provide an easy access to cyclopentenes[2a], and now report [2+2]-cycloadditions of allyl cations to afford cyclobutane derivatives.

When a mixture of 4-chloro-2-methyl-2-pentene **1** and 2,3-dimethyl-2-butene **2** is treated with zinc chloride-ether at −78 °C, the cyclobutane **3**[3a] is obtained in 72% yield[2]. Similarly, 4-chloro-2,4-dimethyl-2-pentene **4** and 1-ethoxy-2-methyl-1-propene **5** give 80% **6**[3b]. In both cases only one (probably the sterically favored *trans*) isomer is detected by NMR spectroscopy. No linear intermediates were detected. Lewis acid catalyzed rearrangements of **3** and **6** to give thermodynamically more stable five-membered rings, which would have to proceed *via* secondary carbenium ions, were not observed. Treatment of **3** with zinc chloride-ether at 20 °C yields a complex mixture of products, which contains 2-chloro-2,3-dimethylbutane; its formation can be rationalized by [2+2]-cycloreversion of the cyclobutylcarbinyl cation and addition of HCl to **2**.

**1** $(CH_3)_2C{=}CH{-}CH(CH_3)Cl$

\+

**2** $(CH_3)_2C{=}C(CH_3)_2$

$\xrightarrow{ZnCl_2}$ **3**

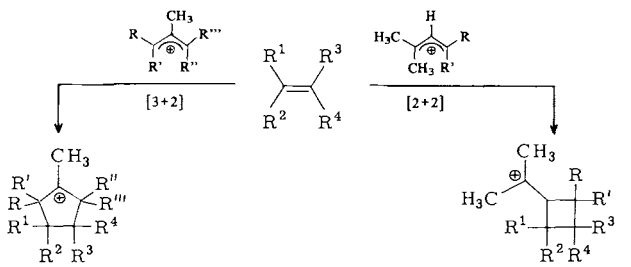
**4** $(CH_3)_2C{=}CH{-}C(CH_3)_2Cl$

\+

**5** $(CH_3)_2C{=}CHOC_2H_5$

$\xrightarrow{ZnCl_2}$ **6**

2-Alkyl substituted allyl cations and alkenes undergo [3+2]-cycloadditions with formation of tertiary cyclopentyl cations[2a]. We have now obtained four-membered rings by reaction of alkenes with 1,1-dialkylated, 2-unsubstituted allyl cations. Here [2+2]-cycloadditions are preferred since they give tertiary carbenium ions, whereas the corresponding [3+2]-cycloadditions would afford secondary carbenium ions.




[*] Priv.-Doz. Dr. H. Mayr, H. Klein, G. Freyberger
Institut für Organische Chemie der Universität Erlangen-Nürnberg
Henkestrasse 42, D-8520 Erlangen (Germany)

[**] This work was supported by the Deutsche Forschungsgemeinschaft and the Fonds der Chemischen Industrie.

However, not all 1,1-dialkylated, 2-unsubstituted allylic systems react to form four-membered rings: under identical conditions reaction of 1-chloro-3-methyl-2-butene with isobutene, 2-methyl-2-butene, and 2,3-dimethyl-2-butene yields exclusively linear addition products[2b]. According to molecular mechanics calculations[4], these acyclic adducts are more stable than the isomeric cyclobutane derivatives. On the other hand, the heat of formation of **3** is calculated[4] to be 3.8 kcal/mol more negative than that of the isomeric 6-chloro-2,4,5,5,6-pentamethyl-2-heptene; *gauche*-interactions destabilize the linear isomer to a greater extent than the cyclic system (*gem*-dialkyl effect[5]). Since steric effects should be similar in the corresponding carbenium ions, the different behavior of **1** and 1-chloro-3-methyl-2-butene in addition reactions with tetramethylethylene **2** can be rationalized.

[2+2]-Cycloadditions of this type can be expected if they are electronically favored over [3+2]-cycloadditions and if steric effects destabilize the linear adducts relative to the four-membered rings.

Received: September 22, 1982;
revised: October 27, 1982 [Z 154 IE]
German version: *Angew. Chem. 95* (1983) 62

[1] H. M. R. Hoffmann, *Angew. Chem. 85* (1973) 877; *Angew. Chem. Int. Ed. Engl. 12* (1973) 819; H. M. R. Hoffmann, H. Vathke-Ernst, *Chem. Ber. 114* (1981) 2208.

[2] For experimental details see a) H. Klein, H. Mayr, *Angew. Chem. 93* (1981) 1069; *Angew. Chem. Int. Ed. Engl. 20* (1981) 1027; b) H. Klein, A. Erbe, H. Mayr, *ibid. 94* (1982) 63 and *21* (1982) 82; *Angew. Chem. Suppl. 1982,* 105.

[3] a) 3-(1-Chloro-1-methylethyl)-1,1,2,2,4-pentamethylcyclobutane **3**: $^1$H-NMR (100 MHz, $CCl_4$): $\delta$ = 0.81, 0.88, 0.96, 1.08 (4 s; 15 H, 1-$CH_3$, 2-$CH_3$, the two middle signals are overlapped by the d of 4-$CH_3$), 1.50 (s; 6 H, $(CH_3)_2CCl$), 1.82–2.14 (m; 2 H, 3-H, 4-H); $^{13}$C-NMR (25 MHz, $CDCl_3$): $\delta$ = 13.71, 19.44, 20.63, 22.75, 25.54, 32.18, 32.64 (7 q), 38.65 (s), 39.10 (d), 42.86 (s), 60.33 (d), 72.93 (s); b) 3-(1-chloro-1-methylethyl)-4-ethoxy-1,1,2,2-tetramethylcyclobutane **6**: $^1$H-NMR (60 MHz, $CCl_4$): $\delta$ = 0.98 (s; $CH_3$), 1.00 (s; 2 $CH_3$ and right branch of the O—$CH_2CH_3$ triplet), 1.13 (s, $CH_3$), 1.15 (t, $J$ = 7 Hz; $OCH_2CH_3$), 1.57 (s; $C(CH_3)_2Cl$), 2.06 (d, $J$ = 10 Hz; 3-H), 3.46 (q, $J$ = 7 Hz; $OCH_2$—$CH_3$), 3.59 (d, $J$ = 10 Hz; 4-H); $^{13}$C-NMR: $\delta$ = 15.59, 18.93, 21.23, 23.60, 25.84, 32.67, 32.91 (7 q), 37.40, 42.50 (2 s), 59.30 (d), 65.73 (t), 71.71 (s), 81.42 (d).

[4] N. L. Allinger, Y. Yuh, *MM2 Molecular Mechanics, Program No. 395 QCPE,* Indiana University, Bloomington 1980; N. L. Allinger, *J. Am. Chem. Soc. 99* (1977) 8127.

[5] N. L. Allinger, V. Zalkow, *J. Org. Chem. 25* (1960) 701; B. Capon, S. P. McManus: *Neighboring Group Participation, Vol. 1,* Plenum Press, New York 1976, p. 58 ff.

## NMR Studies of Yeasts Grown on Substrates at "Zero" Level Radioactivity

By *Ricardo Basosi, Claudio Rossi, Enzo Tiezzi**, and *Gianni Valensin*

The cultivation of different protein-rich microorganisms which utilize hydrocarbons (petrochemicals) as sources of carbon and energy has been frequently suggested[3]. The nutritional and biological value as well as the level of toxic substances have still to be studied; the effect induced by a prolonged alimentation on substrates which have less than the natural level of $^{14}$C radioactivity has also still to be investigated.

Since many correlations have been found between the NMR parameters of water and the physiological or pathological states of cells, as well as the conformations of cell constituents[8, 10–12], we have used water relaxation studies

[*] Prof. Dr. E. Tiezzi, R. Basosi, C. Rossi, G. Valensin
Institute of General Chemistry, University of Siena
Pian dei Mantellini 44, I-64100 Siena (Italy)

to investigate rapidly growing populations. The yeasts selected (*Saccharomyces cerevisiae* ATCC 9763, *Candida utilis* CBS 621 and *Saccharomycopsis lipolytica*) can be easily grown on ethanol, glucose and *n*-paraffin substrates. We used an ethanol substrate having various $^{14}C$ levels to ascertain whether a biological effect is apparent after many generations. Moreover the use of ethanol yields a cell biomass having a chemical composition quite similar to that obtained with a glucose substrate.

Cell samples were centrifuged, washed three times, and suspended in distilled water. NMR samples were prepared by adding 0.7 mL $D_2O$ (99.75%) to 0.3 mL of the cellular suspension. The $^1H$ spin-lattice relaxation time ($T_1$) was measured on a Bruker WH-90 NMR spectrometer using the ($\pi$-$\tau$-$\pi/2$) pulse sequence[10, 12]. The relaxation data obtained from *Candida utilis* and *Saccharomyces cerevisiae* with ethanol having various $^{14}C$ levels are shown in Table 1. A concentration of $2 \times 10^8$ cells per mL was used in each case. The error in this value is relatively large (*ca.* 20%). However, the dependence of $T_1$ on cell concentration[3], is not sufficient to account for the observed changes in $T_1$, suggesting a dependence on the level of radioactivity of the substrate, especially in the case of *Candida utilis*. Compared with cells grown on substrates having the "minimum" natural radioactivity, those cultivated on the same substrate without radioactivity give rise to shortening of $T_1$ whereas, in contrast, those grown on the substrate enriched by radioactivity give rise to longer $T_1$ values. A similar trend was shown by measurements on cultures at lower growth levels and also on lyophilized samples, but the effects were much less marked.

Table 1. Spin lattice relaxation times of water protons in *Saccharomyces cerevisiae* ATCC 9763 and *Candida utilis* CBS 621 grown on ethanol at different levels of radioactivity [a].

| Source of ethanol | Radioactivity [disintegrations per min/g] | $T_1$ [s] *Candida utilis* | *Saccharomyces cerevisiae* |
|---|---|---|---|
| Petrochemical | 0.2 | $1.7 \pm 0.1$ | $1.7 \pm 0.2$ |
| Fermentation | 19.0 | $3.6 \pm 0.2$ | $2.9 \pm 0.3$ |
| $^{14}C$ enriched | 6740.0 | $5.3 \pm 0.3$ | $3.9 \pm 0.2$ |

[a] Samples contained $(2 \pm 0.4) \times 10^8$ cells/mL.

Table 2 shows the spin-lattice relaxation data obtained from *Saccharomycopsis lipolitica* cultivated on different carbon and energy sources. The longest $T_1$ value was found for yeast cultivated on a glucose substrate, a "natural" substrate, while the cultures grown on *n*-paraffins displayed relatively shorter $T_1$ values. Similar results were obtained from lyophilized samples of *Candida boidinii* grown on both "natural" (glucose and xylose) and synthetic (methanol and ethanol) substrates[11].

Table 2. Spin-lattice relaxation times of water protons in *Saccharomycopsis lipolytica* grown on different substrates [a].

| Substrate | $T_1$ [s] |
|---|---|
| Glucose | $4.6 \pm 0.3$ |
| $C_{15}H_{32}$ | $3.1 \pm 0.2$ |
| $C_{16}H_{34}$ | $3.7 \pm 0.2$ |
| $C_{15}H_{32} + C_{16}H_{34}$ (1 : 1) | $3.4 \pm 0.3$ |

[a] Samples contained $(2 \pm 0.4) \times 10^8$ cells/mL.

The results reported here, together with those obtained on *Candida boidinii*[5] grown on different substrates, can be interpreted by assuming that the level of radioactivity of the substrate causes a biological effect that is detectable by measurement of the cell-water $T_1$. To our knowledge, this is the first time that "zero level" radioactivity is reported to affect cell behavior. Previously, NMR studies of cell water, besides other techniques, have been used to show biological damage resulting from radioactive sources[12]. Since ESR signals were not detected and the samples were carefully deoxygenated, paramagnetic impurities cannot account for the results. On the contrary, conformational modifications of cell constituents and changes in water content and in the molecular complexity of the sample have been alternatively used to explain the NMR behavior of cell water[8, 10, 12]. As a consequence, the observed change in $T_1$ could reflect any one of these phenomena or any combination of them. However, high levels of radiation are expected to cause cellular damage liberating interstitial water, so that a change in the water content seems the most proper explanation for the water $T_1$ behavior. It is important to underline that this effect becomes detectable only in populations after many generations.

Received: November 13, 1981 [Z 408 IE]
revised: October 22, 1982
German version: *Angew. Chem. 95* (1983) 55
The complete manuscript of this communication appears in: *Angew. Chem. Suppl. 1983*, 57-62

[3] J. H. Litchfield, *Adv. Appl. Microbiol. 22* (1977) 267.
[8] G. Valensin, N. Niccolai, *Chem. Phys. Letters 79* (1981) 47.
[10] P. E. Valensin, M. L. Bianchi Bandinelli, M. L. Di Cairano, G. Valensin, E. Gaggelli, E. Tiezzi, *Biophys. Chem. 14* (1981) 357 and references cited therein.
[11] R. Basosi, E. Gaggelli, E. Tiezzi, G. Valensin, *Proc. XX Amperé Congr. 20* (1978) 537.
[12] R. M. De Vré, *Prog. Biophys. Mol. Bio. 35* (1979) 109.

## C-Scrambling in the *tert*-Butyl Cation**

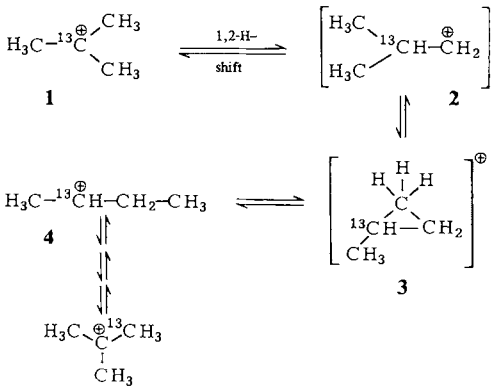
By *G. K. Surya Prakash, Altaf Husain,* and *George A. Olah**

The ease of hydrogen scrambling in secondary and tertiary carbocations in superacid media is well documented[1]. *Saunders* and *Rosenfeld* have shown[2, 3] that *tert*-pentyl and 1-methylcyclopentyl cations in $SbF_5/SO_2ClF$ solutions undergo methyl- and methylene-hydrogen scrambling at 110—140 °C, rendering all C and H atoms equivalent on the NMR time scale. The activation energy $E_A$ for this process was found[2, 3] to be *ca.* 18—19 kcal/mol for both systems. The scrambling was shown to occur *via* secondary cations and protonated cyclopropane intermediates rather than free primary cations.

A similar process is expected to occur in the *tert*-butyl cation. *Saunders et al.* mention[2a] an attempt to observe such a scrambling in the hexadeutero-*tert*-butyl cation at 100 °C, but were unable to observe any H/D exchange. We now wish to report that scrambling does occur in the *tert*-butyl cation **1**, but that the rate of exchange is too slow to be observed by NMR line-broadening experiments.

[*] Prof. Dr. G. A. Olah, Dr. G. K. Surya Prakash, Dr. A. Husain
Hydrocarbon Research Institute and Department of Chemistry
University of Southern California
Los Angeles, CA. 90089 (USA)

[**] Stable Carbocations, Part 237. This work was supported by the National Institutes of Health. *G. A. Olah* thanks the Alexander-von-Humboldt Stiftung for a Senior US Scientist Award.—Part 236, see G. A. Olah, A. L. Berrier, L. D. Field, G. K. S. Prakash, *J. Am. Chem. Soc. 104* (1982) 1349.



The cation **1** (60% $^{13}C$ enriched at the cationic center) was prepared from the correspondingly labeled *tert*-butyl chloride in $FSO_3H/SbF_5/SO_2ClF$ solution at −78 °C. A sample was sealed in a 10 mm NMR tube and heated to 70 °C in an oil bath. The $^{13}C$-NMR spectrum of the ion was recorded intermittently at room temperature (Fig. 1). $^{13}C$-scrambling is negligible at room temperature, but is essentially complete in 20 h at 70 °C. Even at 100 °C the rate of scrambling is too slow to be observed by NMR line-broadening, and hence it was not possible to determine any activation parameters for the process. A lower limit of $E_A \approx 30$ kcal/mol[4a] can be estimated for the scrambling process, which should correspond to the energy difference between the *tert*-butyl and isobutyl cations. A similar lower limit of 28 kcal/mol was estimated by *Saunders* and *Hagen*[2b] from the absence of hydrogen scrambling in the hexadeuterio-*tert*-butyl cation.

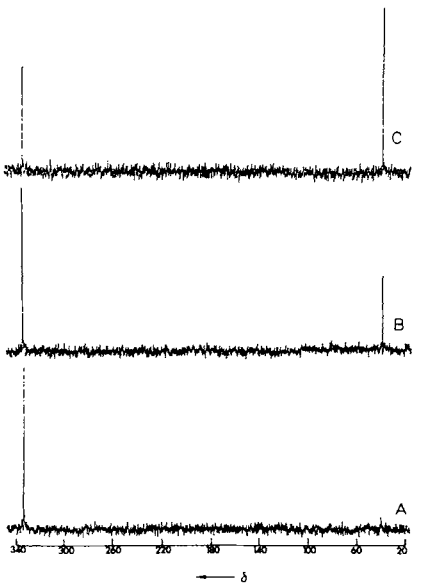



Fig. 1. $^1H$-decoupled $^{13}C$-NMR spectrum (20 MHz) of **1** in $FSO_3H/SbF_5/SO_2ClF$ at room temperature. A: immediately after preparation, B: after 2.5 h at 70 °C, C: after 9.5 h at 70 °C.

The most likely mechanism[4b] for the scrambling process is rearrangement *via* the primary isobutyl cation **2** involving the delocalized protonated methylcyclopropane intermediate (or transition state) **3** to the *sec*-butyl cation **4**. The *sec*-butyl cation scrambles all hydrogens and carbons and reverts back to the *tert*-butyl cation through the well documented pathway[1]. Furthermore, it was shown by *Brouwer*[5] that [1-$^{13}C$]-*n*-butane isomerized in HF/$SbF_5$/pentane solution at 2 °C to [2-$^{13}C$]-*n*-butane without giving isobutane. Under the reaction conditions, however, the protonated methylcyclopropane intermediate (or transition state) is quenched by the hydride-donor *n*-pentane before rearranging to an incipient primary cation leading to isobutane.

Received: August 13, 1981;
revised: October 21, 1982 [Z 409 IE]
German version: *Angew. Chem. 95* (1983) 51

[1] a) M. Saunders, P. Vogel, E. L. Hagen, J. Rosenfield, *Acc. Chem. Res. 6* (1973) 53; b) M. Saunders, J. Chandrasekhar, P. von R. Schleyer in P. De Mayo: *Rearrangements in Ground and Excited States, Vol. 1*, Academic Press, New York 1980, Chapter 1.
[2] a) M. Saunders, J. Rosenfield, *J. Am. Chem. Soc. 91* (1969) 7756; b) M. Saunders, E. L. Hagen, *J. Am. Chem. Soc. 90* (1968) 2436.
[3] a) D. M. Brouwer, E. L. Mackor, *Proc. Chem. Soc. 1964*, 147; b) D. M. Brouwer, *Recl. Trav. Chim. Pays-Bas 87* (1968) 210.
[4] a) G. J. Karabatsos, F. M. Vane, *J. Am. Chem. Soc. 85* (1963) 729; b) We believe that the scrambling occurs through a monomolecular pathway since no hydrogen-deuterium exchange was observed in deuterated superacids. No deprotonation of the *tert*-butyl cation to isobutylene leading to a dimer or oligomer occurs under the reaction conditions.
[5] D. M. Brouwer, *Trav. Chim. Pays-Bas Recl. 87* (1968) 1435.

## Generation of the Tetraphenylcyclobutadiene Radical Cation by Ionizing Gas-Phase Decarbonylation**

By *Wolfgang Blum, Harry Kurreck, Wilhelm J. Richter, Helmut Schwarz**, and *Helga Thies*

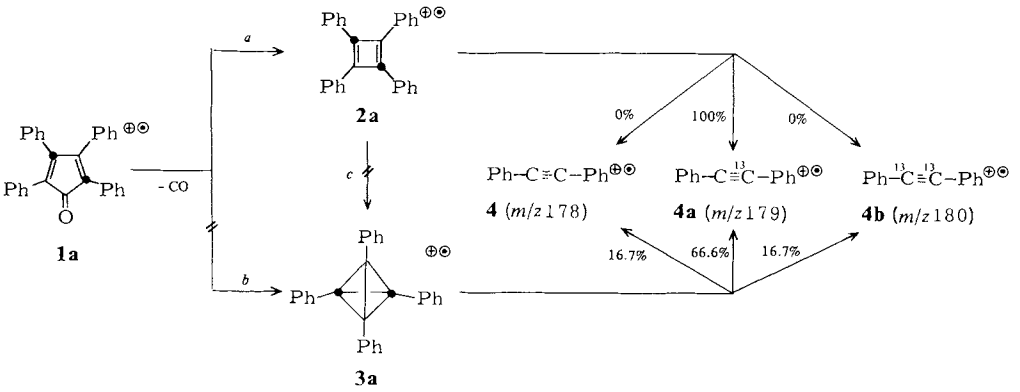
*Dedicated to Professor Hans-Werner Wanzlick on the occasion of his 65th birthday*

Oxidation of tetra-*tert*-butylcyclobutadiene and -tetrahedrane with $AlCl_3/CH_2Cl_2$ and *t*-$C_4H_9^{\oplus}$, respectively, leads to formation of radical cations[1a], whose ESR and collisional activation spectra are identical. MNDO analysis[1a] of the valence isomerization, tetrahedrane ⇌ cyclobutadiene indicates for the sterically non-hindered tetramethyl system that the tetramethyltetrahedrane radical cation possesses no local minimum on the potential energy hypersurface; it spontaneously isomerizes to the tetramethylcyclobutadiene radical cation[1c]. From this it was concluded that a flattening to the cyclobutadiene system also occurs with the radical cation of the sterically more restricted tetra-*tert*-butyltetrahedrane.

We now report on an independent method of generating the previously unknown tetraphenylcyclobutadiene radical cation **2**. In the decarbonylation of 2,3,4,5-tetraphenyl-2,4-cyclopentadienone **1** ($M^{\oplus\odot}$ = 45% rel. int.) by electron impact ionization (70 eV), a signal is, *inter alia*, observed at *m/z* 356 (35%). The collisional activation mass spectrum[2] using MS/MS conditions[3] with ions of *m/z* 356, mass-selected by a triple quadruple instrument, only contains a single signal at *m/z* 178, which can be assigned to the diphenylacetylene radical cation **4**.

[*] Prof. Dr. H. Schwarz, H. Thies
Institut für Organische Chemie der Technischen Universität
Strasse des 17. Juni 135, D-1000 Berlin 12 (Germany)
Prof. Dr. H. Kurreck
Institut für Organische Chemie der Freien Universität
Takustrasse 3, D-1000 Berlin 33 (Germany)
Dr. W. J. Richter, W. Blum
Ciba-Geigy AG, CH-4002 Basel (Switzerland)

[**] This work was supported by the Fonds der Chemischen Industrie and the Deutsche Forschungsgemeinschaft. We thank Dr. W. Kieslich for supplying a sample of **1a**.




Scheme 1. ● = $^{13}C$.

When the experiment was carried out using the [2,4-$^{13}C_2$]-labeled isotopomer **1a** the following results were obtained: as expected, *m/z* 356 is quantitatively shifted to *m/z* 358, and its MS/MS spectrum contains only a single signal at *m/z* 179 (≙ **4a**) after isotopic correction[4]. The following conclusion can be drawn from this: Decarbonylation of **1** by electron impact ionization leads to an intermediate, which must be a derivative of ionized cyclobutadiene **2**. Generation of a tetraphenyltetrahedrane radical cation **3**, whose existence was postulated previously[5], is completely inconsistent with the data obtained for **1a**. If the tetrahedrane intermediate **3a** were really involved or a carbon scrambling of the $C_4$ moiety in the $[M-CO]^{\oplus\odot}$ ion obtained from **1a** were to occur, then the distribution pattern shown in Scheme 1 should be observed in the formation of the ionized diphenylacetylene isotopomers (**4**, **4a**, and **4b**). This does not occur. The results are only compatible with route *a* and certainly exclude route *b* and isomerization *c*.

Received: September 21, 1982 [Z 153 IE]
German version: *Angew. Chem. 95* (1983) 59

[1] a) H. Bock, B. Roth, G. Maier, *Angew. Chem. 92* (1980) 213; *Angew. Chem. Int. Ed. Engl. 19* (1980) 209; b) R. Wolfschütz, H. Schwarz, unpublished results; c) For the photo induced generation of the tetramethylcyclobutadiene radical cation see: Q. B. Broxterman, H. Hogeveen, D. M. Kok, *Tetrahedron Lett. 22* (1981) 173.
[2] K. Levsen, H. Schwarz, *Angew. Chem. 88* (1976) 589; *Angew. Chem. Int. Ed. Engl. 15* (1976) 509.
[3] H. Schwarz, *Nachr. Chem. Tech. Lab. 29* (1981) 687.
[4] A weak signal at *m/z* 180 (6%) can be attributed to incomplete [$^{13}C_2$]-labeling of **1a**. 38% of **1** is present as the [$^{13}C_1$]-isotopomer, and the natural [$^{13}C$]-abundance in the $[M-CO]^{\oplus\odot}$ ion of this species gives rise to the formation of *m/z* 180. A signal at *m/z* 178 is not observed in the MS/MS spectrum of *m/z* 358.
[5] M. M. Bursey, T. A. Elwood, *Org. Mass Spectrom. 1* (1968) 531.

## Novel One-Step Synthesis of Oxocyclopentanecarboxylates by Electrochemical Reduction of Cinnamic Acid Esters

By *Ikuzo Nishiguchi** and *Tsuneaki Hirashima*

The electrochemical reduction of α,β-unsaturated esters in aqueous solution usually gives the corresponding hydrodimers, *i.e.* adipic acid derivatives, as the main products[1c,2]. We have now found that oxocyclopentanecarboxylates **2** are formed in moderate to good yields by electrochemical reduction of cinnamate derivatives **1**. A remarkable solvent effect was observed in this dimerization. For example, exclusively **2a** was obtained in 74–76% yield (Table 2[4]) from **1a** in acetonitrile or dimethylformamide (DMF), whereas electrochemical reduction of **1a** in methanol gave dimethyl 3,4-diphenyladipate **3a** as the sole product[3] in 75% yield.

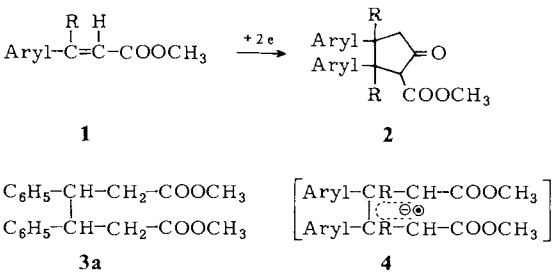



Table 2. Electrochemical reduction of **1a–1h** to **2a–2h** [a].

| | Ar | R | Yield [%] [b] | M.p. [°C] |
|---|---|---|---|---|
| **a** | $C_6H_5$ | H | 76 | 126–127 |
| **b** | $C_6H_5$ | $CH_3$ | 67 | 83–87 |
| **c** | $C_6H_5$ | $C_2H_5$ | 63 | 75–80 |
| **d** | $C_6H_5$ | $C_6H_5$ | 78 | 131–133 |
| **e** | $C_5H_4N$ [c] | H | 62 | 101–104 |
| **f** | *p*-$CH_3OC_6H_4$ | H | 52 | 121–123 |
| **g** | *p*-$CH_3C_6H_4$ | H | 64 | 115–116 |
| **h** | *p*-$ClC_6H_4$ | H | 75 | 134–135 |

[a] Cell, which is fitted with a stirring device, consists of a ceramic diaphragm, Cu cathode, Pt anode, DMF as solvent, tetraethylammonium *p*-toluenesulfonate as supporting electrolyte, at 10–15 °C, cathode potential −1.9 to −2.2 V *vs.* SCE, 4.0 F/mol. [b] Isolated yield. [c] 2-Pyridyl.

Information on the reaction pathway was obtained by electrochemically reducing **1h** and **3a** (molar ratio 1:1) under similar conditions as in Table 2. As a result, exclusively the dimeric cyclization product **2h** was formed in 74% yield, and **3a** was recovered quantitatively: **2a** was not detected. This result clearly shows that the reaction proceeds *via* a dimeric anionic intermediate such as **4**[5], which yields the cyclization product **2** or the simple hydrodimer **3** depending upon the proton-donating ability of the solvent: this also excludes the possibility of Dieckmann condensation of **3** to **2** under the reaction conditions.

Received: March 9, 1981 [Z 406 IE]
revised: October 22, 1982
German version: *Angew. Chem. 95* (1983) 61
The complete manuscript of this communication appears in: *Angew. Chem. Suppl. 1983*, 70–74

[*] Dr. I. Nishiguchi, Dr. T. Hirashima
Osaka Municipal Technical Research Institute
1-6-50 Morinomiya, Jyoto-ku, Osaka 536 (Japan)

[1] c) N. L. Weinberg: Technique of Electroorganic Synthesis, Part II, Wiley, New York 1974, pp. 87–136, and references cited therein.
[2] M. M. Baizer, J. M. Anderson, *J. Electrochem. Soc. 111* (1964) 223.

[3] a) E. L. Totton, R. C. Freeman, T. L. Yarboro, *J. Org. Chem. 26* (1961) 343; b) J. P. Petrovich, M. M. Baizer, M. R. Ort, *J. Electrochem. Soc. 116* (1969) 749.
[4] All the products were isolated and identified by spectroscopic and/or elemental analyses.
[5] M. M. Baizer, J. P. Petrovich, D. A. Tyssee, *J. Electrochem. Soc. 117* (1970) 173.

## Incorporation of Mercury into Graphite *via* K/Hg Intercalation Compounds**

By *Mordecai Rabinovitz**, *Henry Selig*, and *Jaacov Levy*

The intercalation of metals and salts into the graphite lattice markedly changes the chemical properties and behavior of the intercalated species[1,2]. For example, the reaction of potassium intercalated in graphite with $H_2$ is very fast, even at room temperature, whereas metallic potassium reacts very sluggishly with $H_2$ below 200 °C[3]. We report here the preparation of a series of novel Hg/graphite compounds, which should be interesting electrode materials or reagents. Until now, intercalation compounds of Hg/graphite have only been prepared in the form of ternary compounds with alkali metals[4]. The synthesis of binary compounds, or even nonstoichiometric mixtures of graphite/Hg has hitherto been unsuccessful.

The reaction of $C_8K$ with an equivalent amount of Hg yields $C_8KHg$[4]; it has also been reported that graphite and KHg afford $C_4KHg$. We report that the reaction of $C_8K$ with varying amounts of Hg allows the preparation of a series of compounds, of general formula $C_8KHg_x$. $C_8K$ was prepared by evaporating the stoichiometric amount of potassium over graphite, under an inert gas atmosphere at 200 °C. The potassium intercalate so formed was allowed to cool to room temperature and the calculated amount of mercury was added. The mixture was heated to 80 °C for 10 min, and then cooled to room temperature. When the $C_8KHg_x$ was hydrolyzed with a protic solvent, $C_8Hg_y$ was obtained together with metallic Hg.

$$C_8KHg_x + ROH \rightarrow C_8Hg_y + Hg_{(x-y)} + KOR + 0.5\,H_2 \qquad (a)$$

The formation of $C_4KHg$[4] has previously seen assumed to occur in two stages: firstly, the potassium intercalates with graphite to form $C_8K$, which then reacts with Hg to form $C_4KHg$, in which the Hg atoms form layers between two layers of K atoms. However, although we started with $C_8K$, we failed to obtain $C_4KHg$; instead, the X-ray spectrum was identical with that reported for $C_8KHg$[4] ($D = 10.15$ Å). This is plausible if one takes into account that $C_4KHg$ is unstable in the presence of KHg, and disproportionates to $C_8K$, $C_8KHg$ and Hg. In all the reactions of $C_8K$ with Hg, even in presence of a large excess of Hg, blue $C_8KHg$ was always formed, which then reacts further.

Investigation of the relationship between the initial amount of Hg present and the amount retained in the graphite after hydrolysis gave the following results: Molar ratios of K : Hg from 1 : 1 to 1 : 22.5 resulted in complete reaction of mercury with $C_8K$, and formation of a gray-metallic powder. The results shown in Figure 1 indicate a retention curve that asymptotically approaches 0.120 mol Hg; this corresponds to a stoichiometric formula of $C_8Hg_6$. All the $C_8KHg_x$ ($x \neq 1$) and $C_8Hg_y$ compounds obtained strongly absorb X-ray radiation. This could indicate that Hg atoms are situated randomly between the carbon layers.

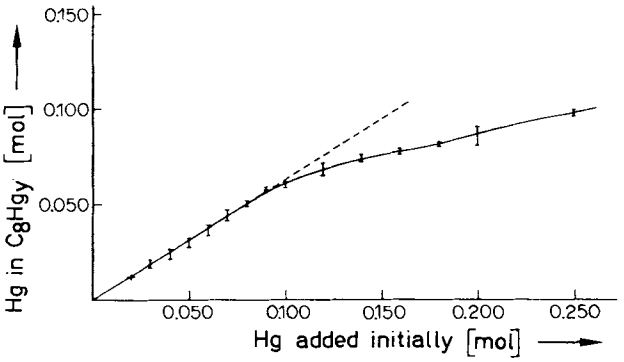



Fig. 1. Plot of amount of Hg in $C_8Hg_y$ after hydrolysis of $C_8KHg_x$ against the amount of Hg originally present.

Thermogravimetric analyses (TGA) of $C_8Hg_y$ indicate that the Hg is lost completely at 400 °C. This suggested that the Hg is intercalated as $Hg^0$. The residual material after TGA exhibits the interlayer spacing of pure graphite.

Received: August 10, 1981 [Z 410 IE]
revised: October 28, 1982
German version: *Angew. Chem. 95* (1982) 45

[1] A. McKillop, D. W. Young, *Synthesis 1979*, 401, 481.
[2] H. Selig, L. Ebert, *Adv. Inorg. Chem. Radiochem. 23* (1980) 281.
[3] H. Remy, *Treatise on Inorganic Chemistry, Vol. 1*, Elsevier, New York, 1956, p. 156ff.
[4] P. Lagrange, M. El Makrini, D. Guerard, A. Herold, *Synth. Metals 2* (1980) 19, 197.

## 1-Alkynylamines by Electrophilic Amination

By *Gernot Boche**, *Michael Bernheim*, and *Manfred Niessner*

The direct synthesis of 1-alkynylamines, *e.g.* **3**, from 1-alkynes should be possible by electrophilic amination of the readily accessible acetylides **1** with **2**.

$$\underset{\mathbf{1}}{R{-}C{\equiv}C{-}M} \xrightarrow[2]{X{-}N(CH_3)_2} \underset{\mathbf{3}}{R{-}C{\equiv}C{-}N(CH_3)_2}$$

M = metal(derivative); X = anionic leaving group

Actually, the first directed synthesis of 1-alkynylamines was carried out according to this scheme in 1960[1]; however, the yields were so unsatisfactory (1.7%) that alternative synthetic routes had to be developed[2].

$$\underset{}{C_6H_5{-}C{\equiv}C{-}M} \xrightarrow{X{-}N(CH_3)_2} \underset{\mathbf{3a}}{C_6H_5{-}C{\equiv}C{-}N(CH_3)_2}$$

**1a-Li**: M = Li **2α**: X = $CH_3SO_3$
**1a-MgBr**: M = MgBr **2β**: X = $(C_6H_5)_2PO_2$

[*] Prof. M. Rabinovitz, Prof. H. Selig, J. Levy
Department of Organic Chemistry,
The Hebrew University of Jerusalem
Jerusalem 91904 (Israel)

[**] This work was supported by the Israel Commision for Basic Research of the Israel Academy of Science and Humanities.

[*] Prof. Dr. G. Boche, Dr. M. Bernheim, M. Niessner
Fachbereich Chemie der Universität
Hans-Meerwein-Strasse, D-3550 Marburg (Germany)

We were able to confirm the earlier observation[1] by allowing **1a-Li** and **1a-MgBr** to react with **2**[4e]: **1a-Li** afforded no **3a** and **1a-MgBr** only traces thereof.

In contrast to this the 1-alkynylcuprates **4**[6,7], which could be prepared from lithium acetylides **1-Li** *via* routes A, B, or C, could be aminated electrophilically.

Route A: $2\,R{-}C{\equiv}C{-}Li + R{-}C{\equiv}C{-}Cu \rightarrow (R{-}C{\equiv}C)_3CuLi_2$ **4**
Route B: $3\,R{-}C{\equiv}C{-}Li + CuCN \rightarrow$ **4** $+ LiCN$
Route C: $3\,R{-}C{\equiv}C{-}Li + CuBr{\cdot}S(CH_3)_2 \rightarrow$ **4** $+ (CH_3)_2S + LiBr$

Even the use of an excess of **2α** or **2β** resulted in amination of only two of the three acetylene groups of **4**; the remaining one precipitates as copper acetylide and hence can, in principle, be reisolated [see equation (1) and routes A–C].

**4a–h** + 2 **2α (β)** → 2 **3a–h** + R–C≡C–Cu + 2 LiX (1)

The results are summarized in Table 1; yields are relative to two acetylene moieties which can be aminated.

Table 1. Reaction of 1-alkynylcuprates **4a–h**, prepared *via* routes A, B, or C, with **2α** or **2β** in ether to give 1-alkynylamines **3a–h**. The products **3a**, **f**, **g** are described; **3b**, **c**, **d**, **e**, **h** were characterized by $^1$H-NMR and mass spectroscopy, as well as by C,H,N-analysis; **2α** can give acetylene coupling products in ≈20% yield.

| | 1-Alkynylcuprate R | Route | Amination reagent | 1-Alkynylamine | Yield [%] |
|---|---|---|---|---|---|
| **4a** | $C_6H_5$ | A | **2α** | **3a** | 52 [a] |
| | | A | **2α** | | 83 [b, c] |
| | | B | **2α** | | 26 [a] |
| | | C | **2β** | | 70 [b] |
| **4b** | *n*-$C_3H_7$ | A | **2α** | **3b** | 69 [b, d] |
| | | A | **2β** | | 72 [b, d] |
| | | C | **2β** | | 87 [b, d] |
| **4c** | *n*-$C_4H_9$ | A | **2α** | **3c** | 60 [a] |
| | | A | **2β** | | 67 [a] |
| | | B | **2β** | | 78 [a] |
| | | C | **2β** | | 66 [a] |
| **4d** | *n*-$C_6H_{13}$ | A | **2β** | **3d** | 67 [b] |
| | | B | **2β** | | 82 [a] |
| **4e** | Cyclohexyl | B | **2β** | **3e** | 44 [a] |
| | | C | **2β** | | 75 [b] |
| **4f** | *tert*-$C_4H_9$ | B | **2β** | **3f** | 71 [b] |
| | | C | **2β** | | 60 [a] |
| **4g** | $(CH_3)_3Si$ | C | **2β** | **3g** | 45 [a, e] |
| | | C | **2β** | | 67 [a] |
| **4h** | $C_6H_5S$ | B | **2β** | **3h** | 17 [b] |
| | | C | **2β** | | 45 [a] |

[a] Isolated **3**. [b] Yield determined by $^1$H-NMR spectroscopy from the crude product. [c] Isolated as dimethyl phenylacetamide. [d] Complete removal of the diethyl ether is associated with reduction in yield. [e] CuBr instead of $CuBr{\cdot}S(CH_3)_2$.

By this means acetylenes can be converted directly into 1-alkynylamines **3** *via* lithium compounds **1** and cuprates **4**.

Received: August 9, 1982,
revised: September 27, 1982 [Z 129 IE]
German version: *Angew. Chem. 95* (1983) 48
The complete version of this manuscript appears in:
*Angew. Chem. Suppl. 1983*, 34–38

[1] V. Wolf, F. Kowitz, *Justus Liebigs Ann. Chem. 638* (1960) 33, allowed the Grignard compound of phenylacetylene to react with diethylchloroamine to afford *N,N*-diethylphenylethynylamine.

[2] a) H. G. Viehe, M. Reinstein, *Angew. Chem. 76* (1964) 537; *Angew. Chem. Int. Ed. Engl. 3* (1964) 506; b) J. Ficini, C. Barbara, *Bull. Soc. Chim. Fr. 1964*, 871; c) *ibid. 1965*, 2787; d) R. Buijle, A. Halleux, H. G. Viehe, *Angew. Chem. 78* (1966) 593; *Angew. Chem. Int. Ed. Engl. 5* (1966) 584; f) H. G. Viehe: "Ynamines" in: *Chemistry of Acetylenes*, Marcel Dekker, New York 1969, p. 861–912.

[4] For recent results on the electrophilic amination of "carbanions" see *e.g.* G. Boche, F. Bosold, M. Niessner, *Tetrahedron Lett. 23* (1982) 3255.

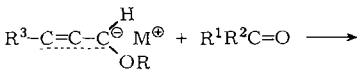
[6] The formula of **4**, $(R{-}C{\equiv}C)_3CuLi_2$, only represents the stoichiometric composition.

[7] a) G. H. Posner, *Org. React. 19* (1972) 1; b) *ibid. 22* (1975) 253; c) G. M. Whitesides, W. F. Fischer, J. San Filippo, R. W. Bashe, H. O. House, *J. Am. Chem. Soc. 91* (1969) 4871; d) E. J. Corey, D. Floyd, B. H. Lipshutz, *J. Org. Chem. 43* (1978) 3418.

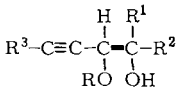
## Regio- and Diastereoselective Synthesis of (4-Hydroxy-3-methyl-1,2-alkadienyl)carbamates from α-Titanated 2-Butynylcarbamates and Aldehydes**

By *Dieter Hoppe** and *Charlotte Riemenschneider*

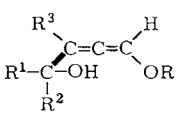
Metalated 2-alkynyl ethers **1** react with carbonyl compounds **2** to give α-adducts of the type **3**[1]. Apart from a few exceptions[1c–d], no isomeric allenes **4** are formed as has also been reported for the tetrahydropyranyl (thp) derivatives **1a–1c**[1b].



**1** **2**



**3**

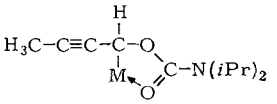


**4**

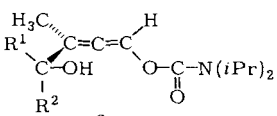
**1a-c**, R = thp, $R^3 = CH_3$,
M = Li, ZnBr, $Ti(OiPr)_3$

We have now found a method of reversing the regioselectivity. The 2-butynylcarbamate **5** is rapidly lithiated to **6**[2] (*n*BuLi, diethyl ether, 15 min at −78 °C); **6** adds aldehydes and ketones **2** to afford the title compounds **8** (besides **9**) in >80% regioselectivity; **8c** is formed as a diastereomeric mixture (Table 1).

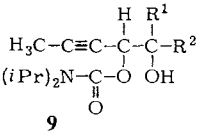
Lithium-metal exchange in **6** (1.1 equiv. $Ti(OiPr)_4$[1b], 10 min at −78 °C) affords the titanium reagent[3] **7**, which forms isomer-free γ-adducts **8c–e** with aldehydes **2c–e**[4]; in each case only one diastereomer is detectable. Diastereoselective allene syntheses of this type—by combination of a centro- and an axial-prochiral moiety—were, to our knowledge, previously unknown[5].



**5**, M = H
**6**, M = Li
**7**, M = $Ti(OiPr)_3$



**8**



**9**

[*] Prof. Dr. D. Hoppe, C. Riemenschneider
Institut für Organische Chemie der Universität
Tammannstrasse 2, D-3400 Göttingen (Germany)

[**] Metalated Nitrogen Derivatives of Carbonic Acids in Organic Synthesis, Part 24. This work was supported by the Fonds der Chemischen Industrie.—Part 23: D. Hoppe, A. Brönneke, *Synthesis 1982*, 1045.

Table 1. Synthesized allenes **8**.

| Educt | $R^1$ | $R^2$ | Product [a] | Yield **8**+**9** [%] | **8** : **9** [b] | Diastereomeric Ratio [b] |
|---|---|---|---|---|---|---|
| **6**, **2a** | $CH_3$ | $CH_3$ | **8a**, **9a** | 76 | >95 : <5 | — |
| **6**, **2b** | $-(CH_2)_4-$ | | **8b**, **9b** | 63 | 82 : 18 | — |
| **6**, **2c** | $(CH_3)_2CH$ | H | **8c**, **9c** | 75 | 87 : 13 | 53 : 47 |
| **7**, **2c** | $(CH_3)_2CH$ | H | **8c** [d, c] | 87 | >95 : <5 | >95 : <5 |
| **7**, **2d** | $CH_3$ | H | **8d** [c] | 89 | >95 : <5 | >95 : <5 |
| **7**, **2e** | $(CH_3)_3C$ | H | **8e** [c] | 59 | >95 : <5 | >95 : <5 |

[a] **8** or **8**-acetate is analytically pure. [b] Determined by $^1$H-NMR spectroscopy on the crude product. [c] The *l*-[3b](*R*R**)configuration has not been confirmed; it is suggested in view of the less hindered transition state (Fig. 1). [d] **8c**, IR (film): 1975 (C=C=C), 1710 $cm^{-1}$ (C=O); $^1$H-NMR ($CDCl_3$, TMS): $\delta = 7.36$ (dq, each $^5J = 2.0$ Hz, 1-H), 1.84 (d, $^5J_{1,3'} = 2.0$ Hz, 3-$CH_3$), 3.84 (dd, $^3J_{4,5} = 6.0$ Hz, $^5J_{1,4} = 2.0$ Hz, 4-H), 0.94, 1.04 (each d, $J = 7.0$ Hz, each 5-$CH_3$).

We presume that—by analogy to metalated allylcarbamates[2, 3c]—the cation $M^{\oplus}$ is fixed by the carbamoyloxy group in the α-position, hence leading to stabilization of the propargylic forms **6** and **7**; these react preferentially *via* propargyl-allenyl inversion[1a] (Fig. 1).

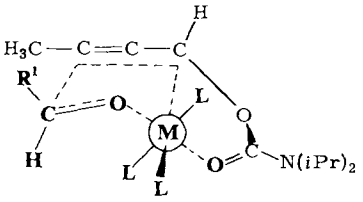
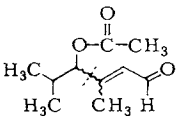
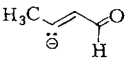


Fig. 1. Transition state of the reaction of **7** with **2c**—**e**; $ML_3 = Ti(OiPr)_3$.

Hydrolysis of the acetate of **8c** ($CH_3OH$, $CH_3SO_3H$, 1 mol-% $Hg(OAc)_2$; $H_2O$) leads to the enal **10** ($E/Z \approx 9:1$;



**10**



**11**

30% yield after chromatographic purification), which rapidly decomposes. Thus **6** and **7** are potentially useful as synthetic equivalents for the β-formylvinyl anion **11**.

Received: September 3, 1982,
revised: October 15, 1982 [Z 143 IE]
German version: *Angew. Chem. 95* (1983) 64

[1] a) Review: J.-L. Moreau in S. Patai: *The Chemistry of Ketenes, Allenes, and Related Compounds*, Wiley, New York 1980, p. 363–414; b) M. Ishiguro, N. Ikeda, H. Yamamoto, *J. Org. Chem. 47* (1982) 2225, and literature cited therein. c) R. Mantione, Y. Leroux, H. Normant, *C. R. Acad. Sci. C270* (1970) 1808; d) P. Pappalardo, E. Ehlinger, P. Magnus, *Tetrahedron Lett. 23* (1982) 309.

[2] D. Hoppe, R. Hanko, A. Brönneke, F. Lichtenberg, *Angew. Chem. 93* (1981) 1106; *Angew. Chem. Int. Ed. Engl. 20* (1981) 1024.

[3] Synthetic uses of titanium reagents: a) M. T. Reetz, *Top. Curr. Chem. 106* (1982) 1; b) B. Weidmann, D. Seebach, *Angew. Chem. 95* (1983) 12; *Angew. Chem. Int. Ed. Engl. 22* (1983) 31; c) R. Hanko, D. Hoppe, *Angew. Chem. 94* (1982) 378; *Angew. Chem. Int. Ed. Engl. 21* (1982) 372, and references cited therein.

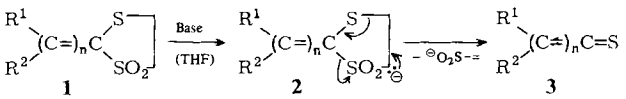
[4] *General procedure, titanium variant:* 11.0 mmol of a 1.5 N solution of *n*BuLi in hexane is injected into a *ca.* 0.5 M solution of **5** (10.0 mmol) in diethyl ether under $N_2$ at a temperature below −70 °C, followed 15 min later by $Ti(OiPr)_4$ (11.0 mmol). After a further 10 min, **2** (11.0 mmol) is injected into the mixture, which is stirred at −78 °C for 1.5 h (**2d**) or 7 h (**2c** and **2e**). The mixture is allowed to warm up to 0 °C and is poured onto a mixture of 20 mL 2 N hydrochloric acid, 30 mL ether, and 20 g ice. The usual work-up and chromatographic purification (silica gel; ether/petroleum ether) affords **8**.

[5] Reviews: W. Runge in [1a], p. 99; H. Hopf in [1a], p. 779.—Prof. Hopf, Braunschweig and Dr. Runge, Heidelberg, are thanked for helpful suggestions.

## A Novel Route to Thiocarbonyl Compounds**

By *Ernst Schaumann**, *Ulrich Wriede*, and *Gerd Rühter*

For the conversion of a carbonyl into a thiocarbonyl group the recommended reagents either usually have to be refluxed with the substrate or require strongly acidic media, and hence often fail in the preparation of labile thiones[1]. We report on a novel route to thiocarbonyl compounds **3**, in which the carbonyl function is initially protected as the dithiolane *S,S*-dioxide **1**[4] and is released by treatment with base[5]. The method is characterized by its mild reaction conditions and, on the whole, by good yields, and appears to be very generally applicable (Table 1).

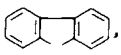


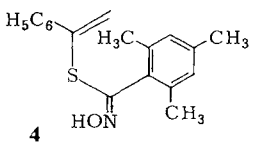
**1** **2** **3**

**a**, $R^1 = R^2 = C_6H_5$, n = 0;

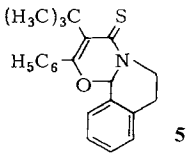
**b**, $R^1 + R^2 =$  , n = 0;

**c**, $R^1 = C_6H_5$, $R^2 = CH_3$, n = 0;
**d**, $R^1 = C(CH_3)_3$, $R^2 = COC_6H_5$, n = 1;
**e**, $R^1 = C(CH_3)_3$, $R^2 = CN$, n = 1;

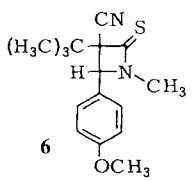
**f**, $R^1 + R^2 =$  , n = 1



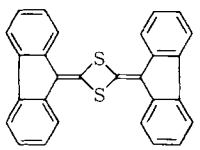
**4**



**5**



**6**



**7**

Table 1. Reaction conditions and yields of thiocarbonyl compounds **3** or their secondary products. Reactions performed in tetrahydrofuran (THF). LDA = lithium diisopropylamide. HMPT = hexamethylphosphoric triamide.

| Educt | Base | *T* [°C] | Product ([%] Yield) | M.p. [°C] |
|---|---|---|---|---|
| **1a** | $KOC(CH_3)_3$ | 0 | **3a** (82) | 50–51 |
| **1b** | LDA/HMPT | 0 | **3b** (47) | 119 |
| **1c** | LDA/HMPT | −78 | **4** (71) | 119–120 |
| **1d** | $KOC(CH_3)_3$ | −78 | **5** (97) | 170–171 (decomp.) |
| **1e** | $KOC(CH_3)_3$ | −78 | **6** (43) | 123–124 |
| **1f** | $KOC(CH_3)_3$ | −78 | **7** (98) | >350 |

[*] Prof. Dr. E. Schaumann, U. Wriede, G. Rühter
Institut für Organische Chemie und Biochemie der Universität
Martin-Luther-King-Platz 6, D-2000 Hamburg 13 (Germany)

[**] This work was supported by the Fonds der Chemischen Industrie.

The stable thioketones **3a**, **b** can be isolated. The less stable thioacetophenone **3c** is trapped by mesitonitrile oxide as the addition product **4**. The labile thioketenes **3d**, **e** are converted *in situ* by azomethines into the Diels-Alder adduct **5** and the β-thiolactam **6** as [2+2]-cycloadduct, respectively. In the absence of scavenger the thioketene dimer **7** is obtained from **1f**.

Received: September 16, 1982;
revised: November 2, 1982 [Z 148 IE]
German version: *Angew. Chem. 95* (1983) 52
The complete version of this manuscript appears in:
*Angew. Chem. Suppl. 1983*, 63-69

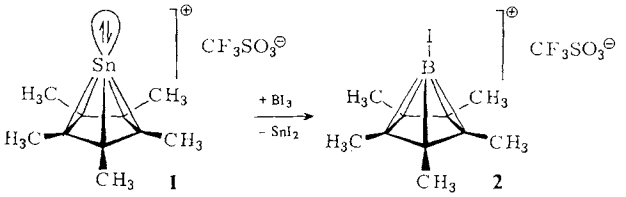
[1] F. Duus in D. H. R. Barton, W. D. Ollis: *Comprehensive Organic Chemistry, Vol. 3*, Pergamon Press, Oxford 1979, p. 373.
[4] H. B. Henbest, S. A. Khan, *Chem. Commun. 1968*, 1036; D. Arndt in Houben-Weyl-Müller: *Methoden der Organischen Chemie*, 4th edit., *Vol. IV/1b*, Thieme, Stuttgart 1975, p. 647.
[5] In a similar manner formaldehyde can be liberated from 1,3-oxathiolane *S,S*-dioxide: K. Schank, R. Wilmes, G. Ferdinand, *Int. J. Sulfur Chem. 8* (1973) 397.

## Exchange of the Apical Tin Atom in the *nido*-Cluster $(CH_3)_5C_5Sn^+$

By *Franz Kohl* and *Peter Jutzi**

Nucleophiles attack the pentagonal-pyramidal cluster $(CH_3)_5C_5Sn^+$ [1] at the apical Sn atom, resulting in a weakening of the $\eta^5$-cyclopentadienyl-tin bond and formation of the adducts $[(CH_3)_5C_5Sn{\leftarrow}Nu]^+$ (*e.g.* with Nu = pyridine[2a], 2,2′-bipyridyl[2b]). From preliminary investigations with electrophiles it follows that these do not attack at the lone pair of electrons of the Sn atom but at the pentagonal base of the cluster. We report here on a reaction which leads *via* cyclopentadienyl-transfer to exchange of the apical atom in the *nido*-cluster.

On reaction of ($\eta^5$-pentamethylcyclopentadienyl)tin trifluoromethanesulfonate **1** with boron triiodide[3] in dichloromethane, precipitation of yellow tin(II) iodide was observed; the product remaining in solution was spectroscopically (NMR, MS) identified as ($\eta^5$-pentamethylcyclopentadienyl)iodoboron trifluoromethanesulfonate **2**[4].




Mechanistically, this reaction can be explained in terms of an electrophilic attack at the cyclopentadienyl ring, as also was observed for the formation of $(CH_3)_5C_5H$ or $(CH_3)_6C_5$ on protonation (with $CF_3SO_3H$) or alkylation (with $CF_3SO_3CH_3$) of **1**[5]. However, the halide transfer is accompanied by a complex reaction sequence, which finally results in exchange of the apical component in the *nido*-complex. This novel type of reaction provides general access to a variety of other cyclopentadienyl-element compounds with *nido*-cluster structure.

Received: August 20, 1982 [Z 136 IE]
German version: *Angew. Chem. 95* (1983) 55

[*] Prof. Dr. P. Jutzi, Dr. F. Kohl
Fakultät für Chemie der Universität
Postfach 8640, D-4800 Bielefeld 1 (Germany)

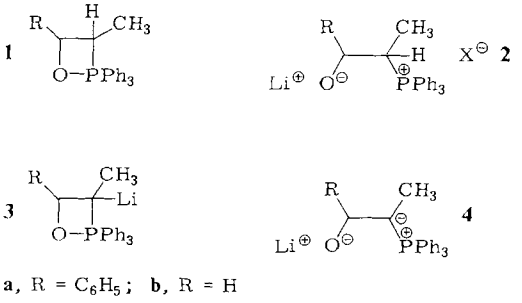
[1] P. Jutzi, F. Kohl, C. Krüger, *Angew. Chem. 91* (1979) 81; *Angew. Chem. Int. Ed. Engl. 18* (1979) 59; P. Jutzi, F. Kohl, P. Hofmann, C. Krüger, Yi-Hung Tsay, *Chem. Ber. 113* (1980) 757.
[2] a) P. Jutzi, F. Kohl, C. Krüger, G. Wolmershäuser, P. Hofmann, P. Stauffert, *Angew. Chem. 94* (1982) 66; *Angew. Chem. Int. Ed. Engl. 21* (1982) 70; *Angew. Chem. Suppl. 1982*, 25; b) F. Kohl, P. Jutzi, E. Schlüter, unpublished.
[3] Experimental: A solution of **1** (2.50 g, 6.20 mmol) in $CH_2Cl_2$ (25 mL) is added dropwise to a solution of freshly sublimed $BI_3$ (2.49 g, 6.36 mmol) in $CH_2Cl_2$ (125 mL). A yellow precipitate separates out, while the solution turns bright red in color. Repeated filtration and evaporation of the solution affords a slurry of red crystals from which the readily volatile components are removed by evaporation and condensation using a cold finger (0.15 torr, 80 °C). Recrystallization of the residue from 2 mL $CH_2Cl_2$ furnishes 0.40 g (15%) of **2**.
[4] P. Jutzi, A. Seufert, *Angew. Chem. 89* (1977) 339; *Angew. Chem. Int. Ed. Engl. 16* (1977) 330; *Chem. Ber. 112* (1979) 2481.
[5] F. Kohl, P. Jutzi, unpublished results.

## Some Cautions in the Interpretation of Oxidoylide Reactions based on $^{31}$P-NMR Data

By *Edwin Vedejs* and *G. P. Meier*

Synthetically useful species described as β-oxidotylodes ("betaine ylides", type **4**) are formed when alkyllithiums are added to the low temperature Wittig intermediates formed from aldehydes and LiX-containing alkylidenetriphenylphosphoranes[1]. Under these conditions, oxaphosphetanes such as **1** (+LiX) exist to some extent in equilibrium with ionic betaine-LiX adducts **2**[2a], and the deprotonation process can be understood as a typical base-phosphonium salt reaction.

Recently deprotonation of **1** by alkyllithium reagents in the absence of lithium halides has been described[3a,b]. In *salt-free* Wittig reactions, betaines or other ionic species have not been observed by direct methods[2], and hence the mechanism of oxidoylide formation in these examples is unclear. Our own experiments with salt-free **1** contradict some of the published results[3a,b].




**a**, R = $C_6H_5$; **b**, R = H

Homogeneous solutions of **1a** prepared from salt-free ethylidenetriphenylphosphorane in tetrahydrofuran (THF) do not undergo significant deprotonation with *n*-$C_4H_9Li$ or *sec*-$C_4H_9Li$ at −78 °C in contrast to the literature[3a]. Although a red color appears immediately, the $^{31}$P-NMR spectrum shows only traces of new complex signals in the $P^{IV}$ region. A strong, sharp signal of unreacted **1a**[2a] is observed and remains unchanged over 1.5 h at −80±2 °C in THF in presence of *sec*-$C_4H_9Li$. Neither the signal at $\delta = -54$ previously assigned to a metalated oxaphosphe-

[*] Prof. Dr. E. Vedejs, G. P. Meier
McElvain Laboratory of Organic Chemistry
Department of Chemistry, University of Wisconsin
Madison, Wisconsin 53706 (USA)

[**] This work was supported in part by the National Science Foundation (GD 43891X).

tane **3**[3a] nor that at $\delta = +12$ attributed to the oxidoylide **4**[3a] was detected. Upon warming the sample to $-30\,^{\circ}C$, the oxaphosphetane signal gradually disappears over *ca.* 45 min (0.1 to 0.3 M solution), and within a few minutes at $-78\,^{\circ}C$ if 1 equivalent of anhydrous LiBr is added to the solution. New $^{31}P$ signals are observed in the range $\delta = 2$—$10$[2c] but these are extremely complex, and suggest the presence of numerous $P^{IV}$ species (aggregates?). In contrast, alkylidenetriphenylphosphoranes give characteristic symmetrical multiplets (aryl H decoupled) or sharp singlets (H noise decoupled)[2a]. We assume that our results differ in part from those previously reported[3a], because the earlier studies used nondecoupled $^{31}P$ spectra[3a] which tend to obscure differences in chemical shift and lineshape information.

*Salt-free* **1b** does react with *sec*-$C_4H_9Li$ at $-78\,^{\circ}C$ to afford **4b** (0.3 M, THF, 20 min). No evidence for **3b** was observed, and the $^{31}P$-NMR signals are again extremely complex ($\delta = 0$—$15$, no distinct maximum). Lithium ion catalysis of oxaphosphetane ring-opening (**1b** → **2b**, X unknown) cannot be ruled out, and **1b** may be more reactive than **1a** for simple steric reasons.

The formation of ylides *synthetically equivalent* to **4a** and **4b** in these experiments is not disputed. However, idealized structures of type **4** should be regarded only as convenient abbreviations for the far more complex species actually present in solution. Both "**4a**" and "**4b**" react with benzaldehyde at $-78\,^{\circ}C$ to give $^{31}P$-NMR signals in the $P^{IV}$ region[4], but assignment of oxaphosphetane structures is only tentative due to poor resolution. In principle, two oxaphosphetane positional isomers can be formed in each case. There is no evidence to show whether or not such positional isomers can interconvert in the absence of lithium halides[3b,5], and the mechanistic details of the oxidoylide condensation step remain essentially unknown[6].

Received: June 19, 1981 [Z 81 IE]
German version: *Angew. Chem. 92* (1982) 53

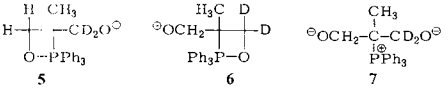
[1] M. Schlosser, K. F. Christmann, *Angew. Chem. 78* (1966) 115; *Angew. Chem. Int. Ed. Engl. 5* (1966) 126; E. J. Corey, H. Yamamoto, *J. Am. Chem. Soc. 92* (1970) 226; M. Schlosser, K. F. Christmann, A. Piskala, *Chem. Ber. 103* (1970) 2814; M. Schlosser, D. Coffinet, *Synthesis 1971*, 380; *ibid. 1975*, 575.

[2] a) E. Vedejs, G. P. Meier, K. A. J. Snoble, *J. Am. Chem. Soc. 102* (1981) 2823; b) E. Vedejs, K. A. J. Snoble, *ibid. 95* (1973) 5778; c) 40.5 MHz, 85% $H_3PO_4$ ext., Varian-XL-100-FT system; for measuring technique see [2a].

[3] a) M. Schlosser, A. Piskala, C. Tarchini, H. B. Tuong, *Chimia 29* (1975) 341; b) M. Schlosser, H. B. Tuong, *Angew. Chem. 91* (1979) 675; *Angew. Chem. Int. Ed. Engl. 18* (1979) 633; c) G. Wittig, H. Eggers, P. Duffner, *Justus Liebigs Ann. Chem. 619* (1958) 10; M. Schlosser, K. F. Christmann, *ibid. 708* (1967) 1; d) M. Schlosser, personal communication (with typical NMR spectra).

[4] **4a** + PhCHO; $\delta = -56$ (width at half-height, 1 ppm at $-78\,^{\circ}C$), disappears on warming to $20\,^{\circ}C$; unassigned minor signals at $\delta = -49$ and $-55$ which do not disappear; some **1a** is regenerated ($\delta = -63$ width 0.2 ppm). — **4b** + PhCHO: $\delta = -51$ (width at half-height 0.3 ppm) no multiplicity resolvable using aryl H decoupling.

[5] In [3b] the reaction of **4b** with $CD_2O$ is not unequivocally interpreted. The formation of $CD_2{=}C(CH_3)CH_2OH + CH_2{=}C(CH_3)CD_2OH$ does not prove that oxaphosphetanes **5** and **6** interconvert *unless* the authors can rule out the initial formation of betaine **7** in the condensation step between **4b** and $CD_2O$. Their argument is valid if the condensation step maintains an intact oxaphosphetane.



**5** **6** **7**

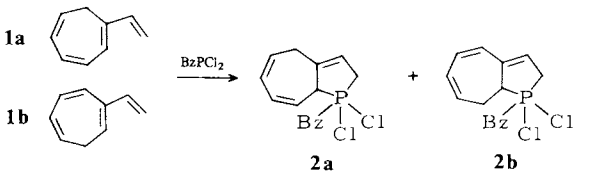
[6] We retract footnote 12 in [2b], since it assumes an oxidoylide structure which is unrealistic in light of the $^{31}P$-NMR evidence. Recent evidence shows that high oxidoylide regioselectivity does not require a cycloaddition mechanism: E. J. Corey, P. Ulrick, and A. Venkateswarlu, *Tetrahedron Lett. 1977*, 3231.

## 2-Benzyl-1-Phosphaazulene

By *Gottfried Märkl** and *Ernst Seidl*

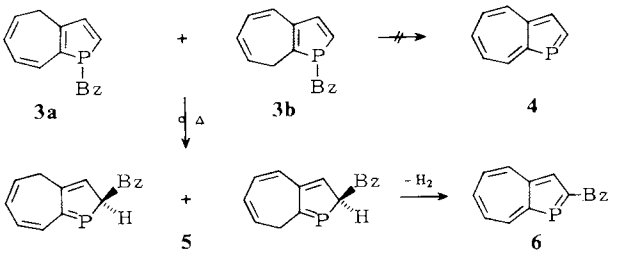
In contrast to the azaazulenes, azulenes in which one methine group is replaced by trivalent phosphorus of coordination number 2—phosphaazulenes—are unknown.

We report the synthesis of the first member of this novel class of compounds. The mixture of 1-vinyl- and 2-vinyl-1,3,5-cycloheptatriene **1a**/**1b** (40/60), prepared according to the method described by *Dran et al.*[3], reacts with benzyldichlorophosphane in the presence of Cu stearate *via* McCormack cyclization[4] (reaction time *ca.* 4 weeks) to afford the isomeric 1-benzyl-1,1-dichlorotetrahydro-1$\lambda^5$-phosphaazulenes **2a**/**2b**, which firstly precipitate as a greasy mass and then as colorless crystals from the solution of the educts in petroleum ether (b.p. = 50—70 °C).



Bz = $C_6H_5CH_2$

The benzyldichlorophosphoranes **2** can be hydrolyzed to the phosphane oxides; direct dehydrochlorination of **2** with α-picoline in dichloromethane/petroleum ether[5] furnishes the 1-benzyldihydro-1-phosphaazulenes **3a** and **3b** (b.p. ≈ 125 °C/$10^{-2}$ torr).



Contrary to what was expected by analogy to the thermolyses of 1-benzyl-1,2- and -1,4-dihydrophosphorines to give $\lambda^3$-phosphorines, the 1-phosphaazulene **4** is not formed from **3** by elimination of toluene. After **3** had been heated in diphenyl ether or xylene for ≈ 20 min at 300 °C, chromatography on silica gel (eluent: petroleum ether/benzene) and purification by distillation at 120—125 °C/$10^{-2}$ torr afforded a blue-green oil, which from the spectroscopic data surprisingly proved to be 2-benzyl-1-phosphaazulene **6**.

**6** must be formed from **3** *via* a 1,5-shift of the benzyl moiety to give **5**, followed by aromatization with concomitant elimination of hydrogen.

The $^1H$-NMR spectrum (250 MHz, $CDCl_3$) of **6**, displays signals for the ring protons $H^3$; $H^4$, $H^6$, and $H^8$ at $\delta = 7.82$, 8.18, 7.57, and 8.79, respectively, and for $H^5$, $H^7$, and the phenyl protons at $\delta = 7.06$—$7.39$ (m).

The mass spectrum of **6** confirms the empirical formula. The fragmentation scheme is determined from the elimination of phosphorus-containing fragments and from the decomposition to 2-benzyl-$\lambda^3$-phosphorine.

[*] Prof. Dr. G. Märkl, E. Seidl
Institut für Organische Chemie der Universität
Universitätsstrasse 31, D-8400 Regensburg (Germany)

 © *Verlag Chemie GmbH, 6940 Weinheim, 1983* *0570-0833/83/0101-0057 $ 02.50/0* 

The UV spectrum of **6** proves its azulene structure. Whereas aza substitution of azulene in the 1-position produces a hypsochromic shift of the longest wavelength absorption maximum by *ca.* 120 nm, the position of longest wavelength absorption maximum of **6** (700 nm) is practically identical with that of azulene (697 nm) but is shifted bathochromically by *ca.* 23 nm relative to that of 2-benzylazulene[10] (677 nm) [**6**, (*n*-hexane): $\lambda_{max}(\varepsilon)=788$ sh (93); 756 sh (116); 700 (270); 684 (270); 640 (286); 588 sh (179); 400 (4110); 380 (5240); 364 (3260); 322 (40700); 310 (38000); 246 (17200)].

Received: July 16, 1982;
revised: November 8, 1982 [Z 95 IE]
German version: *Angew. Chem. 95* (1983) 58
The complete manuscript of the communication appears in:
*Angew. Chem. Suppl. 1982*, 75-83

CAS Registry numbers:
**3a**, 83998-96-3; **3b**, 83998-97-4; **6**, 83998-95-2

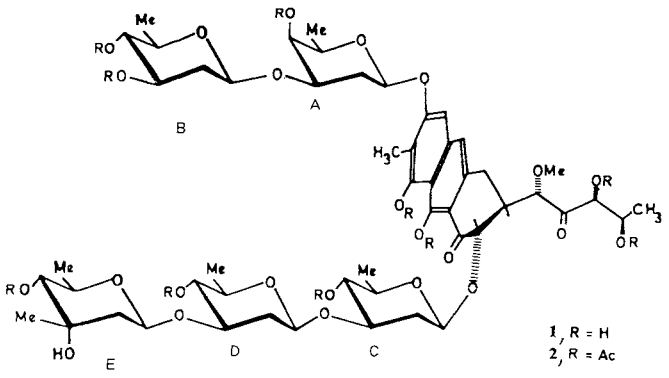
[3] R. B. Dran, B. T. Le Révérend Decock, *C. R. Acad. Sci. C270* (1970) 1036.
[4] W. B. McCormack, US-Pat. 2671077 (1954); *Chem. Abstr. 48* (1954) 6737.
[5] A. Breque, F. Mathey, P. Savignac, *Synthesis 1981*, 983, and literature cited therein.
[10] J. F. Tilney-Bassett, W. A. Waters, *J. Chem. Soc. 1959*, 3123.

## Synthesis and Structure of the Disaccharide Fragment B-A of Mithramycin**

By *Joachim Thiem** and *Günther Schneider*

*Dedicated to Professor Hermann Schildknecht on the occasion of his 60th birthday*

Because of its cytostatic properties the aureolic acid mithramycin **1** is used in considerable amounts for the clinical treatment of solid tumors. After the structure of its aglycone chromomycinone and the five monosaccharide components had been identified[1a] we could present spectroscopic evidence and decisively revise older conceptions concerning the linkages of the building units[1b]. However, the type of interglycosidic bonding between the terminal 2,6-dideoxy-D-*arabino* component B and the 2,6-dideoxy-D-*lyxo* sugar A remained uncertain. We could now finally elucidate the structure of mithramycin **1** by synthesis of the disaccharide fragment B-A and spectroscopic comparison with the natural product.




[*] Prof. Dr. J. Thiem, G. Schneider
Institut für Organische Chemie und Biochemie der Universität
Martin-Luther-King-Platz 6, D-2000 Hamburg 13 (Germany)

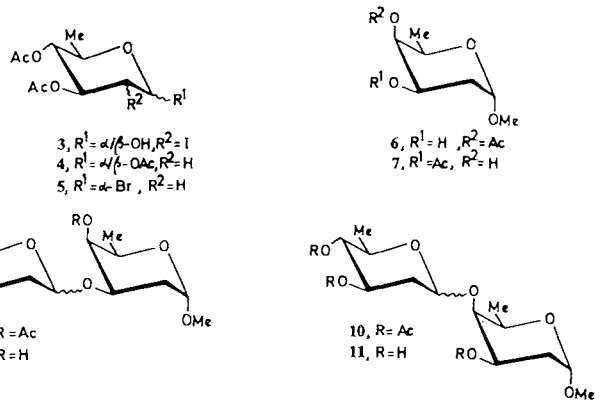
[**] This work was supported by the Deutsche Forschungsgemeinschaft and the Fonds der Chemischen Industrie.

For the preparation of a reactive D-*arabino* building unit B, D-glucal is converted into the diacetate of 6-deoxy-6-iodo-D-glucal[2a], which is catalytically hydrogenated ($Pd(OH)_2/C$) to 3,4-di-*O*-acetyl-D-quinoval[2b]. Treatment of this with *N*-iodosuccinimide and water in acetonitrile affords the mixture of the β-D-*gluco*-/α-D-*manno*-2-iododiacetates **3** (89%). Renewed reduction together with reacetylation leads to formation of the anomeric 1,3,4-tri-*O*-acetyl-2,6-dideoxy-D-*arabino*-hexopyranoses **4** (55%, α:β = 4:3), which can be cleanly converted in anhydrous benzene with bromo(trimethyl)silane (3.5 h, 20 °C) into the pure 3,4-di-*O*-acetyl-2,6-dideoxy-α-D-*arabino*-hexopyranosyl bromide **5** (88%; for the preparation of the L-compound cf. [3a,b]). The 2,6-dideoxy-D-*lyxo*-monoacetates **6** and **7**[3c] were considered to be most suitable as precursors for the reducing saccharide A[3c].

The preparation of the interglycosidic α- and β-linked disaccharides was accomplished by condensation of the aglycone components **6** and **7** with the glycosyl bromide **5**, whereby the use of toluene/nitromethane (2:1) as solvent and reaction at −45 °C for 1 h in presence of *sym*-collidine, 4 Å molecular sieves and silver trifluoromethanesulfonate, followed by very slow heating to room temperature has proven to be most convenient. After work-up, the mixture of the anomeric disaccharides was separated by twofold HPLC on silica gel (toluene/acetone (7:1) and ethyl acetate/*n*-hexane (1:2)).

In this way, reaction of **5** with **6** furnished the α(1→3)- and β(1→3)-disaccharides **8α** and **8β**, respectively, in 56% yield (**8α** : **8β** = 2:1). On deacetylation with 1.5% methanolic sodium hydroxide, the α(1→3)-disaccharide of type B-A **8α**[4a] yielded the deblocked disaccharide **9α**[4b]; likewise, **8β**[4c] furnished the derivative **9β**[4d].

Correspondingly, it is possible to synthesize the isomeric α(1→4) and β(1→4) disaccharides **10α** and **10β** in 54% yield (**10α** : **10β** = 2:1) from **5** and **7**. Zemplén transesterification of the crystalline **10α**[4e] yields the unblocked compound **11α**[4f], while **10β**[4g] affords **11β**[4h].




In our spectroscopic investigations[1b] of mithramycin **1**[5] no differentiation could be made between interglycosidic β(1→3) and β(1→4) linkages in the B-A fragment of **1**, so the unprotected β(1→3) and β(1→4) disaccharide derivatives **9β** and **11β** were to be used for comparison. Unexpectedly, no assignment was possible by comparison of the $^1$H-NMR data. **1** was therefore converted into its decaacetate **2**, whose spectroscopic data for the decisive B-A part were compared with those of the tetradeoxydisaccharide triacetates **8β** and **10β**.

In the $^1$H-NMR spectrum of **2**[4i], 3A-H is observed at higher field ($\delta = 3.92$) and 4A-H at lower field ($\delta = 5.13$). In

the spectrum of the β(1→4) linked disaccharide peracetate **10β**, however, 3-H appears at lower field ($\delta = 5.18$) and 4-H at higher field ($\delta = 3.87$), *i.e.* an acetyl group is located on C-3 in the *lyxo* building unit, and the interglycosidic bond is different from that in the B-A part of **2**. In contrast, in the β(1→3) linked, acetylated derivative **8β** 3-H ($\delta = 4.16$) and 4-H ($\delta = 5.21$) show only slight deviations in the chemical shifts compared to those of the B-A fragment of **2**. Hence, in mithramycin **1** there is a β(1→3) linkage between the D-*arabino*-(B) and the D-*lyxo*-building unit (A).

Received: July 20, 1982 [Z 99 IE]
revised: November 2, 1982
German version: *Angew. Chem. 95* (1983) 54

[1] a) G. P. Bakhaeva, Yu. A. Berlin, E. F. Boldyreva, O. A. Chupronova, M. N. Kolosov, V. S. Soifer, T. E. Vasiljeva, I. V. Yartseva, *Tetrahedron Lett. 1968*, 3595; b) J. Thiem, B. Meyer, *Tetrahedron 37* (1981) 551.

[2] a) G. Descotes, J.-C. Martin, Tachi-Dung, *Carbohydr. Res. 62* (1968) 61; b) F. Micheel, *Ber. Dtsch. Chem. Ges. 63* (1930) 347.

[3] a) H. S. Khadem, D. S. Swartz, J. K. Nelson, L. A. Berry, *Carbohydr. Res. 58* (1977) 230; b) M. Gerken, Universität Hamburg, 1980; c) J. Thiem, B. Meyer, *Chem. Ber. 113* (1980) 3058.

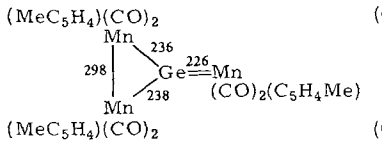
[4] a) M.p. 157 °C, $[\alpha]_D^{20}$ 175 (ethyl acetate); $^1$H-NMR ($C_6D_6$, 400 MHz): 1-H $\delta = 4.57$ dd, 1'-H, 5.19 dd; $J(1,2a) = 3.5$, $J(1,2e) = 1.0$, $J(1',2a') = 3.3$, $J(1',2e') = 1.2$ Hz; b) 72%, m.p. 140 °C, $[\alpha]_D^{20}$ 200 (acetone); c) syrup, $[\alpha]_D^{20}$ 19 (ethyl acetate); $^1$H-NMR ($CDCl_3$, 400 MHz): 1-H $\delta = 4.84$ dd, 3-H 4.16 ddd, 4-H 5.21 dd, 1'-H 4.62 dd; $J(1,2a) = 3.4$, $J(1,2e) = 1.2$, $J(2a,3) = 12.0$, $J(2e,3) = 5.1$, $J(3,4) = 3.1$, $J(4,5) = 1.0$, $J(1',2a') = 9.7$, $J(1',2e') = 2.0$ Hz; d) syrup, $[\alpha]_D^{20}$ 38 (acetone); $^1$H-NMR ([D$_6$]-acetone, 270 MHz): 1-H $\delta = 4.70$ dd, 1'-H 4.72 dd; $J(1,2a) = 3.5$, $J(1,2e) = 1.2$, $J(1',2a') = 9.7$, $J(1',2e') = 2.0$ Hz; e) m.p. 145 °C, $[\alpha]_D^{20}$ 169 (ethyl acetate); $^1$H-NMR ($CDCl_3$, 400 MHz): 1-H $\delta = 4.82$ dd, 1'-H 4.95 dd; $J(1,2a) = 3.2$, $J(1,2e) = 1.1$, $J(1',2a') = 3.3$, $J(1',2e') = 1.1$ Hz; f) m.p. 134 °C, $[\alpha]_D^{20}$ 64 (acetone); g) m.p. 92 °C, $[\alpha]_D^{20}$ 72 (ethyl acetate); $^1$H-NMR ($CDCl_3$, 400 MHz): 1-H $\delta = 4.84$ dd, 3-H 5.18 ddd, 4-H 3.87 dd, 1'-H 4.55 dd; $J(1,2a) = 3.2$, $J(1,2e) = 1.1$, $J(2a,3) = 12.2$, $J(2e,3) = 5.0$, $J(3,4) = 2.8$, $J(4,5) = 1.2$, $J(1',2a') = 9.7$, $J(1',2e') = 2.0$ Hz; h) syrup, $[\alpha]_D^{20}$ 37 (acetone); $^1$H-NMR ([D$_6$]-acetone, 270 MHz): 1-H $\delta = 4.67$ dd, 1'-H 4.82 dd; $J(1,2a) = 3.4$, $J(1,2e) = 1.0$, $J(1',2a') = 9.7$, $J(1',2e') = 2.0$ Hz; i) $^1$H-NMR ($CDCl_3$, 400 MHz): 3A-H $\delta = 3.92$ ddd, 4A-H 5.13 dd; $J(2aA,3A) = 12.1$, $J(2eA,3A) = 4.6$, $J(3A,4A) = 3.2$, $J(4A,5A) = 0.9$ Hz.

[5] We thank Dr. H. Krisch, Pfizer GmbH (Karlsruhe), for supplying the mithramycin.

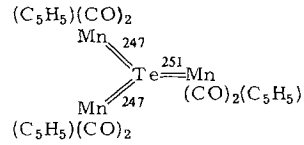
## Tellurium as Six-Electron Donor–Synthesis and Structure of $\mu_3$-Te[Mn(CO)$_2$($\eta^5$-C$_5$H$_5$)]$_3$**

By *Max Herberhold**, *Dietmar Reiner*, and *Dietmar Neugebauer*

Formally, the bridging of coordinatively unsaturated transition metal complex fragments by substituent-free main group elements–with participation of all the valence electrons of the bridge-atom–can lead to formation of multiple bonds. Thus, two Cr≡S triple bonds are formulated for the almost linear CrSCr bridge in S[Cr(CO)$_2$($\eta^5$-C$_5$H$_5$)]$_2$ **1**[1], and two Mn=Ge double bonds for the linear MnGeMn bridge in Ge[Mn(CO)$_2$($\eta^5$-C$_5$H$_4$Me)]$_2$ **2**[2]; in the almost planar $\mu_3$-GeMn$_3$ skeleton of the "homologous" complex **3**, the four-electron donor germanium participates in formation of one Mn=Ge double bond and two Mn—Ge single bonds[2]. We now report here on the novel tellurium complex **4**, which according to an X-ray structure analysis has an almost planar $\mu_3$-TeMn$_3$ skeleton. It can therefore be assumed that the central Te atom in **4** functions as six-electron donor and forms a star-shaped arrangement of three Mn=Te double bonds to the [Mn(CO)$_2$($\eta^5$-C$_5$H$_5$)] fragments, in each of which two electrons are missing for completion of the noble gas configuration.




**3** [2]




**4**

The compound **4** is formed on reaction of $TeH_2$, generated *in situ* from $Al_2Te_3$/HCl, with a solution of the THF-stabilized complex fragment [Mn(CO)$_2$($\eta^5$-C$_5$H$_5$)], which is obtained by photolysis of tricarbonyl(cyclopentadienyl)manganese in tetrahydrofuran (THF); as by-product the complex Te$_2$[Mn(CO)$_2$($\eta^5$-C$_5$H$_5$)]$_3$ **5** could also be isolated (yields 47% **4** and 0.8% **5**). To our knowledge these are the first complexes of a metal of the 7th subgroup with substituent-free tellurium.

The IR and NMR spectra of **4** and **5** are almost identical (Table 2). In the mass spectrum of **5** the signal of the molecular ion could not be observed.

Table 2. Spectroscopic data of the complexes **4** and **5**.

| | Te[Mn(CO)$_2$(C$_5$H$_5$)]$_3$ **4** | Te$_2$[Mn(CO)$_2$(C$_5$H$_5$)]$_3$ **5** |
|---|---|---|
| IR: $\nu$(CO) [cm$^{-1}$] in ether solution | 1998 m, 1992 m (sh), 1940 s, 1928 vs, 1909 m, 1886 w | 1994 s, 1982 m (sh), 1935 vs, 1919 vs, 1901 s, 1886 m (sh) |
| $^1$H-NMR: $\delta$(C$_5$H$_5$) in [D$_6$]acetone, 25 °C | 5.23 (s) | 5.23 (s) |
| $^{13}$C-NMR: $\delta$(C$_5$H$_5$), $\delta$(CO) in [D$_6$]acetone, −80 °C | 87.8 (s), 232.0 (s) | |
| MS: *m/z* | 658 [*M*]$^+$ | 658 [*M* − Te]$^+$<br>612 [*M* − Mn(CO)$_2$(C$_5$H$_5$)]$^+$ |

The crystal structure analysis of **4** (Fig. 1) shows an isosceles triangular (to a first approximation equilateral) arrangement of the three manganese atoms. The central tellurium atom lies only 3.4(1) pm above the center of the Mn$_3$ plane. The bond lengths and angles in the [Mn(CO)$_2$($\eta^5$-C$_5$H$_5$)] moieties show no special features; manganese-manganese interactions can be ruled out.

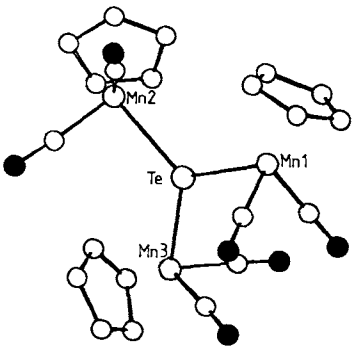



Fig. 1. Molecular structure of **4** in the crystal (black, monoclinic, space group $P2_1/c$, $Z = 4$).

[*] Prof. Dr. M. Herberhold, Dr. D. Reiner
Laboratorium für Anorganische Chemie der Universität
Postfach 3008, D-8580 Bayreuth (Germany)
Dr. D. Neugebauer
Anorganisch-chemisches Institut der Technischen Universität München
Lichtenbergstrasse 4, D-8046 Garching (Germany)

[**] This work was supported by the Deutsche Forschungsgemeinschaft and the Fonds der Chemischen Industrie.

Although no data for MnTe bond lengths are available for comparison, assumption of formal Mn=Te double bonds for the $\mu_3$-$TeMn_3$ skeleton of the diamagnetic complex **4** according to the noble gas rule seems plausible. The sum of the covalent single-bond radii[3] of tellurium (137 pm) and manganese (117 pm) is greater than the observed MnTe distances (average value 248.5 pm).

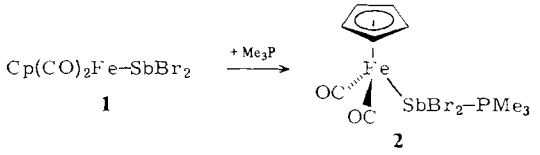
Received: August 6, 1982 [Z 128 IE]
German version: *Angew. Chem. 95* (1983) 46
The complete manuscript of this communication appears in:
*Angew. Chem. Suppl. 1983*, 10-22

[1] T. J. Greenhough, B. W. S. Kolthammer, P. Legzdins, J. Trotter, *Inorg. Chem. 18* (1979) 3543.
[2] W. Gäde, E. Weiss, *J. Organomet. Chem. 213* (1981) 451.
[3] Cf. L. Pauling: *Die Natur der chemischen Bindung*, 3rd Edit., Verlag Chemie, Weinheim 1968/1976, p. 244–245; The Nature of the Chemical Bond, 3rd Edit., Cornell University Press, Ithaca, NY 1960.

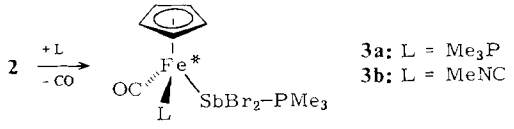
## Transition-Metal Substituted Stibanes as Acceptors: $Cp(CO)(L)Fe—SbBr_2 \cdot PMe_3$ (L = CO, $Me_3P$, MeNC)—1:1-Ferriostibane-Trimethylphosphane Complexes[1]

By *Hans-Achim Kaul, Dieter Greissinger, Wolfgang Malisch*, Heinz-Peter Klein*, and *Ulf Thewalt***

One of the CO ligands in the ferriostibane $Cp(CO)_2Fe—SbMe_2$ can be readily substituted by tertiary phosphanes to form an asymmetric metal center[2]. In contrast, we have now found that the reaction of the bromine derivative $Cp(CO)_2Fe—SbBr_2$[3] with $Me_3P$ in benzene leads to addition of the phosphane to the trivalent antimony atom to afford complex **2**, exclusively[4]. A straightforward CO/$Me_3P$ exchange at the metal only takes place in presence of a large excess of phosphane and at higher temperatures (60 °C), without elimination of the Sb-bonded donor. The corresponding exchange with MeNC already proceeds at temperatures above 40 °C.




**1** **2**




The novel complexes, **2**, **3a**, and **3b** have to be described as adducts of trimethylphosphane and the Lewis acid $Cp(CO)(L)Fe—SbBr_2$. Coordination of $Me_3P$ to antimony is confirmed by the high field $^{31}P$-NMR signals [$\delta = -42.3$ (**2**), $-53.1$ (**3a**), $-43.2$ (**3b**)] and by the low-frequency shift of the $\nu CO_{as}$ and $\nu CO_s$ bands of **1** by 20 and 60 $cm^{-1}$, respectively[3].

[*] Prof. Dr. W. Malisch, Dr. H. A. Kaul, D. Greissinger
Institut für Anorganische Chemie der Universität
Am Hubland, D-8700 Würzburg (Germany)
Prof. Dr. U. Thewalt, H. P. Klein
Sektion für Röntgen- und Elektronenbeugung der Universität
Oberer Eselsberg, D-7900 Ulm (Germany)

[**] X-ray structure analysis.

In contrast to the "metal-free" Lewis acids $SbX_3$ (X = Cl, Br)[7, 10], the metal-stibanes do not form complexes with more than one neutral donor[7], and, moreover, their monoadducts are thermally less stable. This applies in particular to **2**, which upon heating completely releases the phosphane.

**3a**, which like **2** and **3b** can be assigned to the $X_3Sb(L)L'$ type of compound (L = ligand, L' = lone pair of electrons), has the molecular structure shown in Fig. 1 with approximately pseudo-trigonal bipyramidal coordination of the Sb atom. In accordance with the electronegativity rule, the two bromine atoms occupy the apical, and the lone-pair of electrons, the transition-metal moiety, as well as the trimethylphosphane the equatorial positions.

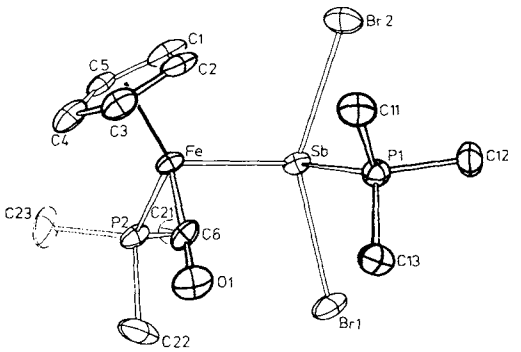



Fig. 1. Structure of **3a** in the crystal. Most important bond lengths [Å] and angles [°]: Sb—Fe 2.551(2), Sb—P(1) 2.596(4), Sb—Br(1) 2.807(2), Sb—Br(2) 2.903(2), Br—Sb—Br 149.1(1), Fe—Sb—P(1) 104.6(1), Fe—Sb—Br(1) 103.8(1), Fe—Sb—Br(2) 103.9(1), Br(1)—Sb—P(1) 82.8(1), Br(2)—Sb—P(1) 77.3(1). Further details on the crystal structure investigation can be obtained from the Fachinformationszentrum Energie-Physik-Mathematik, D-7514 Eggenstein-Leopoldshafen, by quoting the depository number CSD 50303, the name of the author, and complete citation of the journal.

The considerable contraction of the Br(1)—Sb—Br(2) angle to 149.1° is mainly caused by the large steric demand of the cyclopentadienyl or trimethylphosphane ligand immediately adjacent to the bromine atoms. Despite this large steric influence of the transition-metal moiety on the $SbBr_2PMe_3$ part of the molecule, the Fe—Sb—P(1) angle is reduced from the ideal value of 120° to 104° which indicates that the lone-pair, known to have the greatest spatial requirement, occupies the equatorial position.

Of particular note are the Sb—P single bond character [bond length 2.596 Å, sum of covalent radii 2.46 Å] as well as the Sb—Br bond lengths of 2.807 and 2.903 Å, respectively, which are unusually long, even taking into account the normal bond lengthening to axial ligands in TBP structures.

The reason for this finding could be the preferential acceptance of the high electron density at the Sb atom, originating from the electron-rich ligands $Cp(CO)(Me_3P)Fe$ and $Me_3P$, by the halogen atoms.

The trimethylphosphane adducts **2**, **3a**, and **3b** provide the first evidence that trivalent compounds of group 5B elements with σ-bonded transition-metal ligands are able to function not only as excellent electron donors but also as acceptors.

Received: August 16, 1982 [Z 133 IE]
German version: *Angew. Chem. 95* (1983) 56
The complete manuscript of this communication appears in:
*Angew. Chem. Suppl. 1983*, 47-56

[1] Lecture delivered at the Chemiedozententagung 1982, Kaiserslautern.—This work was supported by the Deutsche Forschungsgemeinschaft and the Fonds der Chemischen Industrie. Hoechst AG, Werk Knapsack is

thanked for the gift of chemicals.—Transition-Metal Substituted Phosphanes, Arsanes, and Stibanes, Part 32.—Part 31: W. Malisch, H.-A. Kaul, E. Groß, U. Thewalt, *Angew. Chem. 94* (1982) 554; *Angew. Chem. Int. Ed. Engl. 21* (1982) 549; *Angew. Chem. Suppl. 1982*, 1281–1288.

[2] H. A. Kaul, D. Greissinger, M. Luksza, W. Malisch, *J. Organomet. Chem. 228* (1982) C 29.

[3] P. Panster, W. Malisch, *Chem. Ber. 109* (1976) 692.

[4] $Cp(CO)_3Mo—SbBr_2$, whose CO ligands are more readily exchangeable, also yields an adduct $Cp(CO)_3Mo—SbBr_2—PMe_3$ (m.p. = 124 °C, $\delta^{31}P = 4.33$) with $Me_3P$ under these conditions.

[7] R. R. Holmes, E. F. Bertaut, *J. Am. Chem. Soc. 80* (1958) 2980, 2983.

[10] E. Hough, D. G. Nicholson, *J. Chem. Soc. Dalton Trans. 1981*, 2083.

## Ring-Opening by [3,3]-Diphospha Cope-Rearrangement**

By *Rolf Appel**, *Johannes Hünerbein*, and *Falk Knoch*

In the reaction of succinic dichloride with phenylbis(trimethylsilyl)phosphane **1** a phospha Cope-rearrangement found to take place was with cleavage of the central CC bond[1]. This observation encouraged us to extend our investigations to cyclic 1,2-dicarboxylic acid chlorides. A corresponding reaction course should, *e.g.*, afford the ten-membered ring system **3** on reaction of *trans*-cyclohexane-1,2-dicarboxylic acid chloride **2** with **1**.

Indeed, it was found that **3** could be isolated in good yields on performing this reaction. We assume that the initial condensation is followed by a migration of the silyl groups with formation of the phospha-alkene, which is likewise unstable and is rapidly converted even at low temperature into 1,2-diphenyl-3,10-bis(trimethylsiloxy)-1,2-diphospha-3,9-cyclodecadiene **3** by sigmatropic shift with concomitant opening of the CC bond.

Consistent with this structure, in the methanolysis of **3** the suberic acid dimethyl ester **5** with $C_8$ unit instead of a

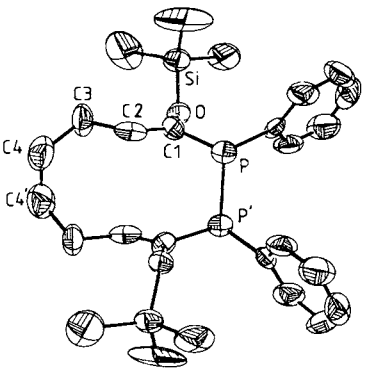
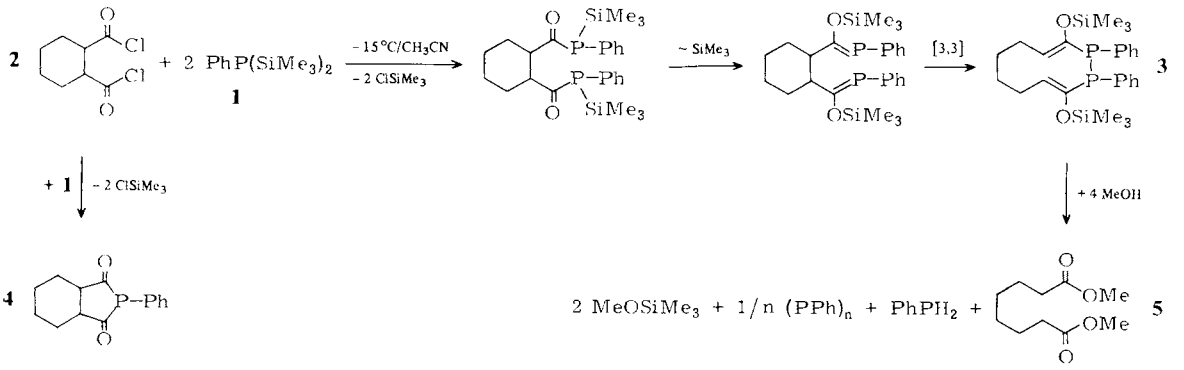



Fig. 1. Structure of **3** in the crystal [3]. Important bond lengths [pm] and angles [°]: Si—O 164.1(8), O—C1 133.5(14), C1—C2 135.2(15), C2—C3 154.2(18), C3—C4 154.5(24), C4—C4′ 155.1(25), C1—P 182.0(10), P—P′ 225.4(5); Si—O—C1 127.5(6), O—C1—P 123.7(7), O—C1—C2 123.4(9), C2—C1—P 112.7(9), C3—C2—C1 125.3(8), C4—C3—C2 112.2(10), C4′—C4—C3 113.5(14), C1—P—P′ 96.6(3).

cyclohexane skeleton, could be isolated in 82% yield along with silylmethyl ethers, phenylcyclophosphanes and phenylphosphane. The fragment 1,2-diphenylphosphane expected to be initially formed in the methanolysis (24 hours boiling) could not be detected, since it disproportionates under such drastic reaction conditions.

Received: September 9, 1982 [Z 146 IE]
supplemented: November 10, 1982
German version: *Angew. Chem. 95* (1983) 63




In addition to **3**, varying amounts of 8-phenyl-8-phosphabicyclo[4.3.0]nonane-7,9-dione **4** are also formed depending on the reaction temperature and solvent[4]. **3** (m.p. 112–116 °C) and **4** (m.p. 75–77 °C) were unequivocally identified by elemental analysis, molecular weight determinations (MS and cryoscopic), and by $^{31}P\{^1H\}$-, $^{13}C\{^1H\}$- and $^1H$-NMR findings[2]. The X-ray structure analysis reveals *E*-configuration at both double bonds and *S*-configuration at the phosphorus atoms (Fig. 1)[3,4].

CAS Registry numbers:
**1**, 24103-44-4; **2**, 36909-95-2; **3**, 84041-44-1; **4**, 84041-45-2

[*] Prof. Dr. R. Appel, J. Hünerbein, F. Knoch
Anorganisch-chemisches Institut der Universität
Gerhard-Domagk-Str. 1, D-5300 Bonn (Germany)

[**] Lower Coordinated Phosphorus Compounds, Part 19. This work was supported by the Deutsche Forschungsgemeinschaft and the Minister für Wissenschaft und Forschung des Landes Nordrhein-Westfalen.—Part 18: R. Appel, F. Knoch, B. Laubach, R. Sievers, *Chem. Ber.*, in press.

[1] R. Appel, V. Barth, M. Halstenberg, *Chem. Ber. 115* (1982) 1617.

[2] $^{31}P\{^1H\}$-NMR ($CDCl_3$, $H_3PO_4$ ext.): **3**: $\delta = -9.3$ (s), **4**: $\delta = -17.0$ (s); $^{13}C\{^1H\}$-NMR ($CDCl_3$, TMS int., selected data): **3**: $\delta = 149.3$ (pt, $J' = 12.9$ Hz, C-1), 128.1 (pt, $J' = 24.6$ Hz, C-2); **4**: $\delta = 222.9$ (m, CO).

[3] Further details of the crystallographic investigation of **3** can be obtained on request from the Fachinformationzentrum Energie Physik Mathematik, D-7514 Eggenstein-Leopoldshafen, by quoting the depository number CSD 50276, the name of the author and the name of the journal.

[4] *Experimental:* A solution of **2** (15.5 g, 0.074 mol) in acetonitrile (250 mL) is added dropwise within 4 h to a stirred and cooled (−15 °C) solution of **1** (9.3 g, 0.148 mol) in acetonitrile (30 mL). The solvent is removed from the reaction mixture and the precipitated products **3** and **4** are recovered by filtration. On washing with *n*-pentane, **4** dissolves and analytically pure **3** remains. Work-up is repeated, since also some **3** is dissolved along with **4**. Yield of **3**: 27.8 g (75%); **4**: 3.6 g (20%).

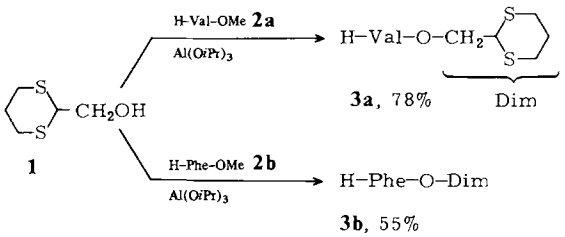
## 1,3-Dithian-2-yl Methyl Ester as Two-Step Protecting Group for the Carboxy Function in Peptide Synthesis**

By *Horst Kunz** and *Herbert Waldmann*

The synthesis of sensitive peptides, especially glycopeptides, requires the use of protecting groups which can be removed under very mild conditions[1]. We have now extended the two-step amino-protecting principle of the 1,3-dithian-2-yl-methoxycarbonyl (Dmoc) group[2], in modified form, to the protection of the carboxy function.

Neither acid-catalyzed esterification nor the chlorosulfite method[3] can be applied to the preparation of amino acid 1,3-dithian-2-yl-methyl(Dim)esters **3** because of insufficient stability of the dithiane methanol **1** towards strong acids.

In contrast, transesterification of the amino acid methyl esters **2** with **1** in presence of aluminum isopropoxide[3] yields the desired amino acid Dim esters **3** directly[4].




Because of their stability towards moderate acids and bases, the Dim esters **3** (characterized as the hydrochlorides by $^1$H-NMR spectroscopy and elemental analysis) can be coupled with Z- and Boc-amino acids using the mixed-anhydride method or ethyl-2-ethoxy-1,2-dihydro-1-quinolinecarboxylate (EEDQ)[5], to give protected dipeptide Dim-esters **4**.

Boc-Ala-OH + H-Val-O-Dim $\xrightarrow{\text{EEDQ}}$ Boc-Ala-Val-O-Dim
**3a** **4a**, 95%

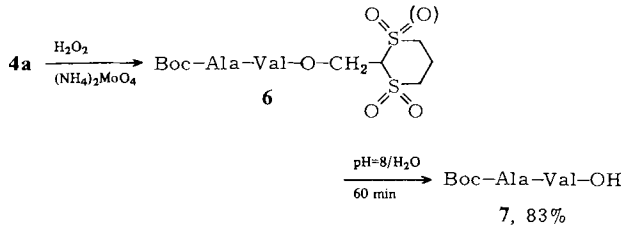
Z-Ala-OH + H-Phe-O-Dim $\xrightarrow[\text{NEt}_3]{\text{Cl—COOEt}}$ Z-Ala-Phe-O-Dim
**3b** **4b**, 75%

Like the Dmoc derivatives[2], the Dim esters are also stable towards trifluoroacetic acid or hydrogen chloride in dichloromethane or ether at room temperature; thus, the Boc group of the dipeptide ester **4a** can easily and selectively

**4a** $\xrightarrow[20\,^\circ\text{C}/60\text{ min}]{\text{HCl/Ether}}$ H-Ala-Val-O-Dim **5**, $\approx$100%

be removed from the dipeptide. In order to deblock the carboxy function from the triethylamine-stable Dim esters **4** the dithiane group is oxidized to the sulfoxide-sulfone or disulfone form **6** by hydrogen peroxide/ammonium molybdate.

**6** is so labile towards bases that complete deblocking of the C-terminal can be carried out even at pH 8 and room temperature in a E1cB reaction.




Thus, the Dim esters provide an effective protection of the carboxy group in syntheses, especially in peptide synthesis, being stable to acids and moderate bases, and easily removable after oxidation. The method cannot be used, however, when oxidizable groups are present in the molecule, *e.g.* in cystein, methionine and tryptophan derivatives.

Received: August 5, 1982 [Z 123 IE]
revised: September 9, 1982
German version: *Angew. Chem. 95* (1983) 47

CAS Registry numbers:
**1**, 37721-88-3; **2a**, 4070-48-8; **2b**, 2577-90-4; **3a**, 84010-53-7; **3b**, 84010-54-8; **4a**, 84010-55-9; **4b**, 84010-56-0; **6**, 84010-57-1; **7**, 60209-59-8; Boc-Ala-OH, 15761-38-3; Z-Ala-OH, 1142-20-7

[1] H. Kunz, M. Buchholz, *Angew. Chem. 93* (1981) 917; *Angew. Chem. Int. Ed. Engl. 20* (1981) 894.
[2] a) R. Barthels, H. Kunz, *Angew. Chem. 94* (1982) 302; *Angew. Chem. Int. Ed. Engl. 21* (1982) 292; b) H. Kunz, R. Barthels, *Chem. Ber. 115* (1982) 833.
[3] M. Brenner, W. Huber, *Helv. Chim. Acta 36* (1953) 1109.
[4] *L*-Valine-1,3-dithian-2-yl methyl ester hydrochloride (**3a** · HCl): A mixture of **1** (0.015 mol), aluminum isopropoxide (60 mg), and **2a** (0.01 mol) is heated under reflux for 4 h at 75 °C/12 torr. Excess **2a** is distilled off under high vacuum. The residue is taken up in ether and treated with anhydrous HCl/ether. The precipitated **3a** · HCl is reprecipitated from acetone/ether. Yield 2.25 g (75%), m.p. 180 °C, $[\alpha]_D^{22} = +3.3$ ($c = 1$, MeOH).
[5] B. Belleau, G. Malek, *J. Am. Chem. Soc. 90* (1968) 1651.

## *O*-Glycopeptide Synthesis using 9-Fluorenylmethoxycarbonyl (Fmoc)-Protected Synthetic Units**

By *Petra Schultheiss-Reimann* and *Horst Kunz**

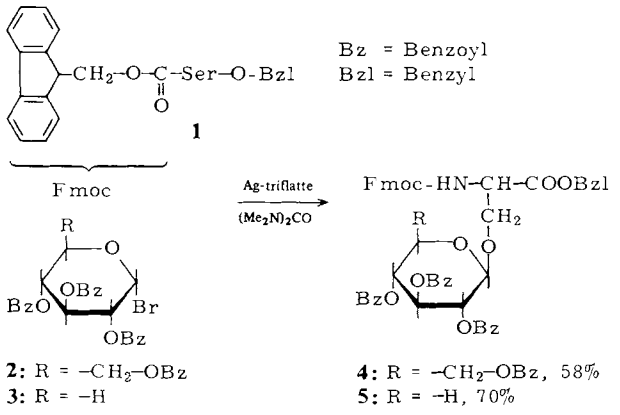
The *O*-glycosidic bonds of serine and threonine glycopeptides—characteristic substructures of many connective tissue-, serum- and membrane-glycoproteins—are somewhat sensitive towards acids and bases[3]. Whereas serine esters protected at the *N*-terminal with the base-labile 2-triphenylphosphonioethoxycarbonyl (Peoc) group[5] cannot be directly glycosylated, the coupling of the 9-fluorenylmethoxycarbonyl-(Fmoc[8]-)serine benzyl ester **1** with 2,3,4,6-tetra-*O*-benzoyl-α-D-glucopyranosyl bromide **2** can be readily accomplished in presence of silver trifluoromethanesulfonate/tetramethylurea[7a] to give the completely protected β-glucosylserine derivative **4** in good yields. The β-configuration of **4** is confirmed by its $^1$H- and $^{13}$C-NMR spectra. The analogous reaction of **1** with tri-*O*-benzoylxylopyranosyl bromide **3** affords the glycosylated serine derivative **5**.

[*] Prof. Dr. H. Kunz, H. Waldmann
Institut für Organische Chemie der Universität
Johann-Joachim-Becher-Weg 18—20, D-6500 Mainz (Germany)

[**] This work was supported by the Deutsche Forschungsgemeinschaft and the Fonds der Chemischen Industrie.—H. W. thanks the Adolf-Todt-Stiftung for a grant.

[*] Prof. Dr. H. Kunz, P. Schultheiss-Reimann
Institut für Organische Chemie der Universität
Johann-Joachim-Becher-Weg 18—20, D-6500 Mainz (Germany)

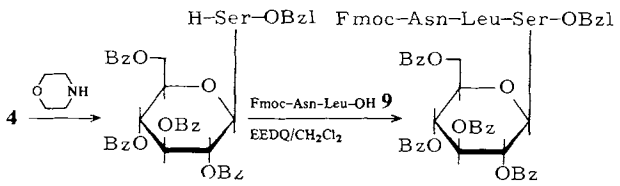
[**] This work was supported by the Deutsche Forschungsgemeinschaft and the Fonds der Chemischen Industrie.




**2**: R = $-CH_2-OBz$
**3**: R = $-H$

**4**: R = $-CH_2-OBz$, 58%
**5**: R = $-H$, 70%

The value of the Fmoc group[8] in glycopeptide synthesis is demonstrated by the highly selective deblocking of **4** using morpholine, to give **6** in essentially quantitative yield.

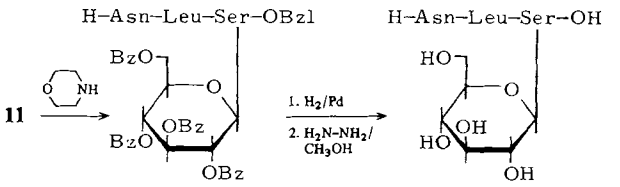



**6**, 97%
**11**, 81%

Neither aminolysis of the ester groups nor β-elimination of the glyconic moiety[3] is observed. The composition and structure of **6** are confirmed by $^1$H-NMR spectroscopy.

The free amino group of **6** can be coupled with Fmoc amino acids as well as with Fmoc dipeptide **9** in presence of ethyl-2-ethoxy-1,2-dihydro-1-quinolinecarboxylate (EEDQ)[11]. The protected glycotripeptide **11** so obtained in good yield will serve in our investigations as model substance for *O*→*N* transglycosylations.

The amino protecting group can be selectively removed in high yield with morpholine from both the Fmoc glycodipeptide ester, which is formed by condensation of **6** with Fmoc-leucine, and from fully protected glycotripeptide **11**.




**13**, 83%
**15**, 62%

After hydrogenolysis of the benzyl group in **13**, the benzoyl groups can be removed so smoothly with hydrazine hydrate in methanol at room temperature that the sensitive *O*-glycosidic bond is wholly preserved. The structure of the free glucotripeptide **15** is confirmed by NMR.

Thus, the Fmoc group is a valuable tool for directed *N*-terminal chain elongation of sensitive *O*-glycopeptides, whereby the carboxy group of the glycopeptides remains reversibly protected as benzyl ester.

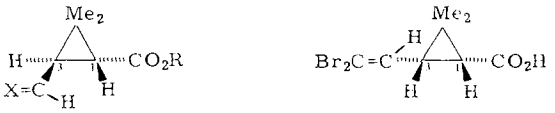
Received: September 16, 1982 [Z 147 IE]
supplemented: November 10, 1982
German version: *Angew. Chem. 95* (1983) 64
The complete manuscript of this communication appears in: *Angew. Chem. Suppl. 1983*, 39-46

[3] A. E. Lützow, J. R. Vercellotti, *J. Chem. Soc. C1967*, 1750.
[5] a) H. Kunz, H. Kauth, *Angew. Chem. 93* (1981) 918; *Angew. Chem. Int. Ed. Engl. 20* (1981) 895; b) *Liebigs Ann. Chem.*, in press.
[7] a) S. Hanessian, J. Banoub, *Carbohydr. Res. 52* (1977) 26.
[8] L. A. Carpino, N. Y. Han, *J. Org. Chem. 37* (1972) 3404.
[11] B. Belleau, G. Malek, *J. Am. Chem. Soc. 90* (1968) 1651.

## Diastereo- and Enantioselective Synthesis of (1*R*,3*R*)-Caronaldehyde Acid Methyl Ester and (1*R*,3*R*)-Chrysanthemic Acid Methyl Ester from (*R*)-Glycerinaldehyde Acetonide**

By *Johann Mulzer** and *Michael Kappert*

Certain esters of the (1*R*,3*R*)-chrysanthemic acid **1** and its *cis*-dibromovinyl analogue **2**, which are generally known as pyrethroids, have found widespread application as insecticides[1]. Remarkably, their physiological activity is closely associated with the (1*R*)-configuration; the (1*S*)-enantiomers of **1** and **2** are many times less effective[1]. For this reason suitable routes to optically active **1** and **2** are being intensively investigated. The (1*R*,3*R*)-caronaldehyde acid methyl ester **3** plays a key role in many of these syntheses[2]. We report here on a rational synthesis of optically pure **3** and the conversion of this intermediate into (1*R*,3*R*)-chrysanthemic acid methyl ester **4**.



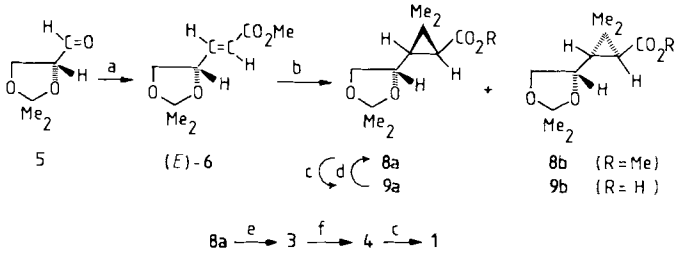
**1**, X = $CMe_2$, R = H
**3**, X = O, R = Me
**4**, X = $CMe_2$, R = Me

**2**

As shown in Scheme 1, (*R*)-glycerinaldehyde acetonide **5** can be converted without separation of diastereomers with 86% *ee* into **3** (total yield 55% in 5 steps) and **4** (39% in **6** steps). Optically pure **3** and **4** are obtained by hydrolysis of the mixed cyclopropanecarboxylates **8a/b** to the corresponding acids **9a/b**, from which pure **9a** can be isolated by crystallization and then reesterified to **8a**. Further reaction according to Scheme 1 affords **3** (total yield 36%) and **4** (24%) with >99% *ee*. Remarkably, the enantioselectivity of the cyclopropanation increases considerably if the corresponding methyl ester is employed in place of (*E*)-**6**. The diastereomeric ratio at the stage of **8** in this case rises to >98:2; alkaline hydrolysis furnishes diastereomerically pure **9a** in quantitative yield. In this way, **5** is converted into optically pure **4** in 35% total yield without any separation of isomers. Esters other than **8** can also be prepared from **9a** *via* the acid chloride, which opens an entry to a variety of optically pure pyrethroids. This finding is not trivial, as the hydrolysis of **4** to **1** causes 23% racemization, even under mild conditions (5% KOH, MeOH, 22 °C, 14 h).

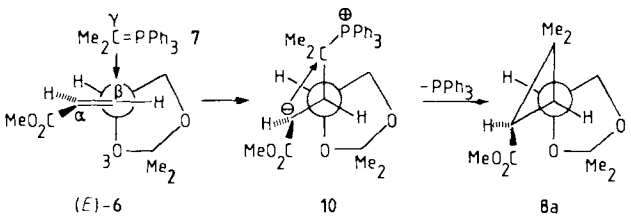
[*] Dr. J. Mulzer, M. Kappert
Institut für Organische Chemie der Universität
Karlstrasse 23, D-8000 München 2 (Germany)
Present address:
Institut für Organische Chemie der Universität
Universitätsstrasse 1, D-4000 Düsseldorf (Germany)
[**] This work was supported by the Deutsche Forschungsgemeinschaft, the Fonds der Chemischen Industrie, and BASF Ludwigshafen.

The key step of our reaction sequence is the enantio- and diastereoselective cyclopropanation of the acrylate derivative (*E*)-**6** with isopropylidene-triphenylphosphane **7**[6]. A rationalization of the high stereoselection in favor of the (1*R*)-isomer is presented in Scheme 2. The assump-



Scheme 1. a: NaH, $MeO_2CCH_2P(O)(OEt)_2$, dimethoxyethane, 22 °C, 1 h, 95%.—b: $Me_2C{=}PPh_3$ **7**, tetrahydrofuran (THF), −78 °C, 1 h, 10 °C, 2 h, 60%.—c: 5% KOH in MeOH, 22 °C, 24 h, quant.—d: $CH_2N_2$, ether, 22 °C, 5 min, quant.—e: $NaIO_4$, 2N $H_2SO_4$/THF, 22 °C, 24 h, 95%.—f: **7**, THF, −30 °C, 1 h, 64%.

tion of a transoid conformation in *E*-(**6**) seems plausible; **7** attacks $C_\beta$ *anti* to O-3—which could be explained in terms of an electrostatic repulsion between $C_\gamma$ and O-3. The zwitterion **10** cyclizes to give **8a** with retention of configuration. Formally (*E*)-**6** thus corresponds to a chiral fumaraldehyde ester-equivalent, in which attack at the C=C bond shows a significant degree of diastereo face control.



Scheme 2.

In order to prepare optically pure compounds the crucial question always is: Can the enantioselective synthesis (defined as "asymmetric induction under the influence of optically active centers, which on further reaction are either eliminated or are converted into achiral centers") compete with other methods such as resolution, isolation from natural sources, or chiral-pool synthesis (defined as "synthesis of an optically active target compounds from an optically active natural product, so that at least one chiral center of the starting material either remains unchanged or is transformed in a stereochemically unambiguous way")? For **1**, **3**, and **4** sufficient data are available[1] to permit a conclusive answer, at least for this particular case: The enantioselective synthesis—whether according to our variant or that of other authors[17]—affords chemical and optical yields comparable to those obtained by optical resolution, whereas the "chiral pool" syntheses starting from 3-carene, pantolactone or α-pinene, clearly appear to be inferior. Although such a comparison is not quite conclusive—one would have to repeat all the reported syntheses under optimized conditions—the results obtained so far emphasize the efficiency of the enantioselective approach.

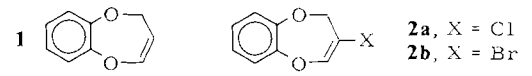
Received: September 21, 1982 [Z 151 IE]
revised: October 25, 1982
German version: *Angew. Chem. 95* (1982) 60
The complete manuscript of this communication appears in *Angew. Chem. Suppl. 1983*, 23-33

[1] Review: D. Arlt, M. Jautelat, R. Lantzsch, *Angew. Chem. 93* (1981) 719; *Angew. Chem. Int. Ed. Engl. 20* (1981) 703.
[2] J. Martel, DOS 1935386 (1970), Roussel-Uclaf.
[6] A. Krief, DOS 2615160 (1976), Roussel-Uclaf; M. J. Devos, L. Hevesi, P. Bayet, A. Krief, *Tetrahedron Lett. 1976*, 3911.
[17] a) T. Aratani, Y. Yoneyoshi, T. Nagase, *Tetrahedron Lett. 1977*, 2599; b) M. Franck-Neumann, D. Martina, M. P. Heitz, *ibid. 23* (1982) 3493.

## 2*H*-1,5-Benzodioxepin and 3-Halo Derivatives

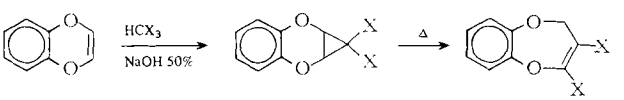
By *Gérald Guillaumet, Gérard Coudert**, and *Bernard Loubinoux*

Up to the present, very few benzodioxepin derivatives have been isolated[1]; thus, 2*H*-1,5-benzodioxepin **1** and its 3-halo derivatives **2a** and **2b** were hitherto unknown. These compounds should offer a simple means of preparing 2,3-disubstituted 1,5-benzodioxepins and 3,4-dihydro-1,5-2*H*-benzodioxepins.



**2a**, X = Cl
**2b**, X = Br

We have now prepared the *gem*-dihalocyclopropane derivatives **4a**[3] and **4b** in 95% yields from the readily accessible 1,4-benzodioxine **3**[2] by carbene-addition under "liquid-liquid" phase-transfer catalysis conditions.



**4a**, X = Cl
**4b**, X = Br

**5a**, X = Cl
**5b**, X = Br

**4a** and **4b** are heated at 185 °C for 5 h and 170 °C for 25 min, respectively[4]. The compounds **5a** and **5b** thus obtained are not isolated but immediately reduced to **2** and **1**, respectively[5] (Table 1).

Table 1. Some data for the synthesis of **1** as well as **2a** and **2b**. (THF = tetrahydrofuran, HMPT = hexamethylphosphoric triamide).

| Substrate | Reagent | Solvent [d] | *t* [h] | *T* [°C] | Product | Yield [%] [e] |
|---|---|---|---|---|---|---|
| **5a** | $LiAlH_4$ [a] | Ether | 0.5 | 25 | **2a** [5b] | 85 |
| **5a** | $LiAlH_4$ [b] | THF | 16 | 40 | **1** [5a] | 70 |
| **5b** | $NaBH_3CN$ [c] | HMPT | 22 | 25 | **2b** [5c] | 55 |
| **5b** | $LiAlH_4$ [a] | THF | 40 | 25 | **1** [5a] | 70 |

[a] $LiAlH_4$ : **5** = 2 : 1. [b] $LiAlH_4$ : **5a** = 4 : 1. [c] $NaBH_3CN$ : **5b** = 8 : 1. [d] 5 mL per mmol of substrate. [e] Yield referred to **4a** and **4b**.

Received: November 17, 1980 [Z 407 IE]
revised: October 19, 1982
German version: *Angew. Chem. 95* (1983) 50

CAS Registry numbers:
**1**, 265-19-0; **2a**, 83968-11-0; **2b**, 83968-12-1; **3**, 255-37-8; **4a**, 65041-40-9; **4b**, 83968-08-5; **5a**, 83968-09-6; **5b**, 83968-10-9; $HCCl_3$, 67-66-3; $HCBr_3$, 75-25-2

[*] Dr. G. Coudert, Dr. G. Guillaumet, Dr. B. Loubinoux
Université de Nancy I—Faculté des Sciences—B. P. n° 239
F-54506 Vandœuvre-les-Nancy Cédex (France)

[1] a) W. Schroth, W. Kaufmann, *Z. Chem. 17* (1977) 331; b) A. W. Archer, P. A. Claret, D. F. Hayman, *J. Chem. Soc. B 1971*, 1232.
[2] G. Coudert, G. Guillaumet, B. Loubinoux, *Tetrahedron Lett. 1978*, 1059.
[3] W. Schroth, W. Kaufmann, *Z. Chem. 18* (1978) 15.
[4] a) R. Barlet, Y. Vo-Quang, *Bull. Soc. Chim. Fr. 1969*, 3729; b) C. W. Jefford, U. Burger, F. Delay, *Helv. Chim. Acta 56* (1973) 1083.
[5] a) **1**: oil; $^1$H-NMR ($CCl_4$): $\delta = 6.93$ (s, 4H), 6.40 (dt, 1H), 5.0—4.6 (m, 1H), 4.46 (dd, 2H); IR: $\nu$(C=C) = 1670 cm$^{-1}$; b) **2a**: Fp = 35 °C; $^1$H-NMR ($CCl_4$): $\delta = 7.00$ (s, 4H), 6.76 (t, 1H), 5.55 (d, 2H); IR: $\nu$(C=C) = 1665 cm$^{-1}$; c) **2b**: m.p. = 37 °C; $^1$H-NMR ($CCl_4$): $\delta = 6.98$ (s, 4H), 6.80 (t, 1H), 4.60 (d, 2H); IR: $\nu$(C=C) = 1655 cm$^{-1}$.

## Strong Distortion of the Tetrahedral Geometry in a Spirosilicate: Molecular Structure of Bis(tetramethylethylenedioxy)silane

By *Dietmar Schomburg**

Silicon compounds usually have a tetracoordinated Si atom and exhibit only slight deviations from tetrahedral geometry. Evidence of planar tetracoordinated silicon in bis(*o*-phenylenedioxy)silane has been reported by *Meyer* and *Nagorsen*[1a]. Using a semiempirical MO method (MNDO) a considerably smaller energy difference between tetrahedral and planar structures of silicon compounds is calculated than for the corresponding carbon compounds: nevertheless, in the silicic acid ester mentioned, the tetrahedral structure is 32.9 kcal/mol lower in energy[1b]. It was presumed that further stabilization of the planar structure should occur by pseudooctahedral coordination *via* silicon-electron donor interaction[1].

The only proof for the existence of compounds having planar coordinated silicon would be a total structure analysis. For bis(ethylenedioxy)silane, MNDO calculations indicated a similar energy difference between tetrahedral and planar structures as for the unsaturated compound (34.4 kcal/mol)[1c]. The X-ray structure analysis of its permethylated derivative, therefore, appeared attractive.

The title compound, prepared using a method described by *Frye*[2], crystallizes in the space group C2/c[3] with $Z = 4$. The molecule displays crystallographic $C_2$ symmetry, in which the axis of symmetry passes through the silicon atom and the center of the C—C bonds of the rings (Fig. 1).

The bonding geometry at the silicon atom is distorted tetrahedrally. However, the angle of 88.3° between the planes through O(1), Si, O(1)′ and O(2), Si, O(2)′ shows that no significant planarization has occurred. The strong distortion arises from the incorporation of the Si atom into the five-membered rings. The endocyclic OSiO angles are *ca.* 11° smaller than the tetrahedral angle, and the OCC angles of the rings are also markedly smaller. Whereas the Si—O bond lengths do not deviate significantly from comparable values[4a], the C—O distances are conspicuously long (cf. the mean value 1.476 Å, *e.g.*, with 1.427 Å in $CH_3OH$[4b]). The five-membered rings exhibit a twist conformation, in which the ring carbon atoms are displaced 0.30—0.31 Å away from the plane formed by Si and its neighboring atoms.

The strong distortion of the bonds at silicon and carbon is probably the reason for the stability of the compounds of *penta*coordinated silicon, in which the silicon atom forms the center of a spiro[4.4]octane system[5].

[*] Dr. D. Schomburg
Lehrstuhl B für Anorganische Chemie der Technischen Universität
Pockelsstrasse 4, D-3300 Braunschweig (Germany)

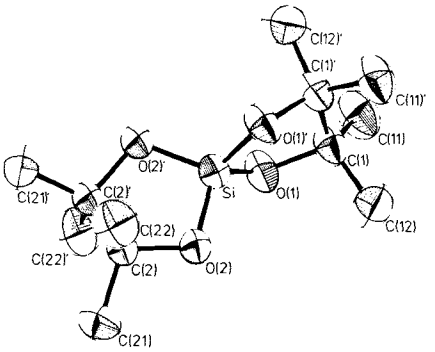



Fig. 1. Structure of bis(tetramethylethylenedioxy)silane in the crystal.

| | Ring I | Ring II |
|---|---|---|
| Bond lengths [Å] | | |
| Si—O | 1.622(3) | 1.628(3) |
| O—C | 1.477(5) | 1.475(5) |
| C—C | 1.544(10) | 1.567(10) |
| C—$C_{Me}$ | 1.524(6), 1.539(8) | 1.517(7), 1.548(8) |
| Bond angles [°] | | |
| C—O—Si | 109.1(2) | 109.4(3) |
| O—C—C | 103.7(4) | 104.1(4) |
| O—C—$C_{Me}$ | 105.7(4), 108.0(4) | 105.9(4), 108.0(4) |
| $C_{Me}$—C—$C_{Me}$ | 112.3(4) | 113.0(4) |
| O—Si—O(endocycl.) | 98.3(2) | 98.8(2) |
| O—Si—O(exocycl.) | 114.1(2), 116.3(2) | |

Received: August 10, 1981,
revised: October 25, 1982 [Z 411 IE]
German version: *Angew. Chem. 95* (1982) 52

CAS Registry numbers:
Bis(tetramethylethylenedioxy)silane, 837-00-3

[1] a) H. Meyer, G. Nagorsen, *Angew. Chem. 91* (1979) 587; *Angew. Chem. Int. Ed. Engl. 18* (1979) 551; cf. also J. D. Dunitz, *ibid. 92* (1980) 1070; *19* (1980) 1033; G. Nagorsen, H. Meyer, *ibid. 92* (1980) 1071; *19* (1980) 1034; b) E. U. Würthwein, P. v. R. Schleyer, *ibid. 91* (1979) 588; *18* (1979) 553; c) M. J. S. Dewar, W. Thiel, *J. Am. Chem. Soc. 99* (1977) 4899, 4907.
[2] C. L. Frye, *J. Org. Chem. 34* (1969) 2496.
[3] Crystals obtained by sublimation; $a = 15.353(10)$, $b = 10.695(2)$, $c = 11.825(6)$ Å, $\beta = 130.33(3)°$, $\rho_{calc.} = 1.168$ g/cm$^3$; 774 reflections ($Mo_{K\alpha}$, $3° \leq 2\theta \leq 50°$), $R = 0.058$.
[4] a) Cf., *e.g.*, Si—O 1.64(3) in $Si(OCH_3)_4$: M. Yokoi, Y. Ueda, *J. Chem. Phys. 18* (1950) 1414; b) P. Venkateswarlu, W. Gordy, *ibid. 23* (1955) 1200.
[5] C. L. Frye, *J. Am. Chem. Soc. 92* (1970) 1205; D. Schomburg, *Z. Naturforsch. B 37* (1982) 195.

## Trifluoromethanesulfonates of α-Hydroxycarboxylates—Educts for the Racemization—Free Synthesis of *N*-Substituted α-Amino Acids

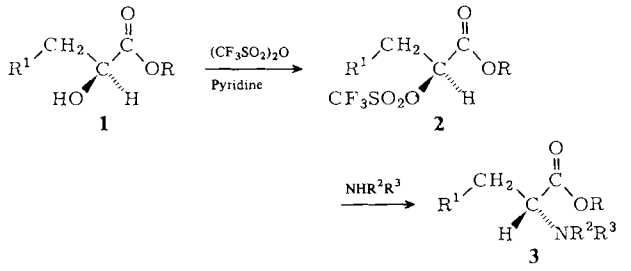
By *Franz Effenberger**, *Ulrike Burkard*, and *Joachim Willfahrt*

Many *N*-substituted α-amino acids exhibit high biological activity[1]. They can be prepared by substitution at the $NH_2$ group of the respective amino acid; this synthetic procedure is limited, though, by the reactivity of the alkylating or arylating agent as well as by the possibility of

[*] Prof. Dr. F. Effenberger, U. Burkard, Dr. J. Willfahrt
Institut für Organische Chemie der Universität
Pfaffenwaldring 55, D-7000 Stuttgart 80 (Germany)

 © *Verlag Chemie GmbH, 6940 Weinheim, 1983* *0570-0833/83/0101-0065 $ 02.50/0* 

either elimination or multiple reactions. Alternatively, the desired amino function can be introduced directly by nucleophilic substitution of appropriate α-substituted carboxylic acid derivatives. Especially with α-halo carboxylates, however, this reaction is accompanied by extensive racemization; with α-methanesulfonyloxy and α-toluenesulfonyloxy carboxylic acid derivatives, both racemization and elimination products are formed, *inter alia,* owing to the drastic conditions required[1a,2].




1 2 3

α-Trifluoromethanesulfonyloxy carboxylates **2** are obtained in high yield from α-hydroxy carboxylates **1** and trifluoromethanesulfonic acid anhydride/pyridine[3]. The trifluoromethanesulfonates **2** are fairly stable and can be kept for months at 0—10 °C. Even with weakly nucleophilic amines, however, they are smoothly converted, with Walden inversion, into the corresponding α-amino carboxylates **3**; the compounds **3** are isolated in excellent yield by distillation or filtration through a silica gel column (Table 1).

Comparison of the relative reactivity of various α-substituted ethyl propionates towards benzylamine in refluxing dichloromethane reveals a strong dependence on the nature of the leaving group, not quite expected for $S_N2$ reactions[4]. **2c** is converted quantitatively into **3f** within 20 min; for α-bromo, α-methanesulfonyloxy, α-toluenesulfonyloxy and α-chloro ethyl propionate, on the other hand, conversion to **3f** is only 40, 10, 5, and < 1%, respectively, after 22 h.

The high reactivity of the trifluoromethanesulfonates 2 proves especially advantageous for the synthesis of phenylalaninic and aspartic acid derivatives since in this case poorer leaving groups (*e.g.* $Br^{\ominus}$, $CH_3SO_3^{\ominus}$) strongly favor elimination. The unequivocal stereochemistry of the substitution reaction has been confirmed by reaction of **2** with optically active amines; the diastereomeric amino carboxylates **3** can be differentiated by capillary GLC.

Table 1. *N*-Substituted α-aminocarboxylic esters **3** from **2** and amines in dichloromethane at room temperature [5]. In the reaction scheme, *S*-configuration is given for **2**, and *R*-configuration for **3**.

| Educts | | | | | Products | Yield |
|---|---|---|---|---|---|---|
| **2** | R | $R^1$ | $R^2$ | $R^3$ | **3** | [%] |
| (*S*)-**2a** | Me | Ph | $PhCH_2$ | H | (*R*)-**3a** | 92 |
| | | | Ph | H | (*R*)-**3b** | 93 |
| | | | $-(CH_2)_4-CH(Et)-$ [b] | | (2*R*,2′*R*)-**3c** | 83 |
| (*S*)-**2b** | Et | $EtCO_2$ | $PhCH_2$ | H | (*R*)-**3d** | 93 [c] |
| | | | Ph | H | (*R*)-**3e** | 94 |
| (*S*)-**2c** | Et | H | $PhCH_2$ | H | (*R*)-**3f** | 85 |
| | | | $-(CH_2)_4-$ | | (*R*)-**3g** | 84 |
| | | | $2,6-(CH_3)_2C_6H_3$ | H | (*R*)-**3h** | 92 |
| | | | Ph | Me | (*R*)-**3i** | 75 |
| | | | Ph–CH(Me)– [a] | H | (2*R*,1′*S*)-**3j** | 76 |
| | | | Ph–CH(Me)– [b] | H | (2*R*,1′*R*)-**3k** | 78 |
| | | | $EtCO_2$–CH(Me)– [a] | H | (2*R*,2′*S*)-**3l** | 81 |
| (*R*)-**2c** | | | $EtCO_2$–CH(Me)– [a] | H | (2*S*,2′*S*)-**3m** | 93 |

[a] *S*-form. [b] *R*-form. [c] Addition at −65 °C.

Both *R*- and *S*-α-amino carboxylates can be prepared by the synthetic procedure described here; subsequent hydrolysis of the esters to the corresponding *N*-substituted α-amino carboxylic acids proceeds without detectable racemization.

Received: August 19, 1982 [Z 135 IE]
revised: November 16, 1982
German version: *Angew. Chem. 95* (1983) 50

[1] a) R. M. Scott, G. D. Armitage, DOS 2650434 (3. Nov. 1976), Shell Int. Res. Maatschappij B.V.; *Chem. Abstr. 87* (1977) 67990n; b) J. D. Kemp, *Biochem. Biophys. Res. Commun. 74* (1977) 862.
[2] A. J. Speziale, E. G. Jaworski, *J. Org. Chem. 25* (1960) 728.
[3] a) C. D. Beard, K. Baum, V. Grakauskas, *J. Org. Chem. 38* (1973) 3673; b) K. Shiosaki, G. Fels, H. Rapoport, *ibid. 46* (1981) 3230.
[4] R. D. Howells, J. D. McCown, *Chem. Rev. 77* (1977) 69.
[5] *Procedure:* (*R*)-**3f**: A solution of (*S*)-**2c** (1.75 g, 7 mmol) in $CH_2Cl_2$ (25 mL) is added dropwise within 5 min at room temperature to a stirred solution of benzylamine (1.50 g, 14 mmol) in $CH_2Cl_2$ (25 mL), and stirring continued for 30 min at room temperature. The reaction mixture is filtered, the solution washed with water, dried over $Na_2SO_4$, concentrated, and the residue (1.36 g) distilled *in vacuo*. Yield 1.24 g (85%) (*R*)-**3f**, b.p. 73 °C/5 × $10^{-3}$ torr.

# BOOK REVIEWS

**Organic Trace Analysis by Liquid Chromatography. By** *J. F. Lawrence.* Academic Press, New York 1981. xii, 288 pp., bound, $ 34.00.

The identification and determination of traces in a great variety of matrixes are gaining importance and therefore call for suitable analytical methods. Capillary gas chromatography and thin-layer chromatography have proved to be particularly useful for separation, but the many possibilities offered by high-pressure liquid chromatography (HPLC) have not yet been fully utilized in this field. It is therefore useful to demonstrate the possibilities and to specify the limitations of this new method in trace analysis.

The ten chapters in this book have the following headings (with the number of pages given in parentheses after each title): General Considerations in Developing a Trace Analytical Technique Employing Liquid Chromatography (17), Pumping Systems (13), Sampling Technique and Injection Ports (12), Chromatographic Columns and Packing Materials (7), Detectors (52), Chromatography Theory (30), Chemical Derivatization (46), Sample extraction and Cleanup (34), Approach to Method Development and Routine Analysis (10), and Applications (41).

About half of the book is thus devoted to general aspects of HPLC and to description of the apparatus used. It is regrettable that the individual components of the HPLC ap-

paratus are not assessed for their applications in trace analysis.

Chapter 6 deals with the theory of chromatography, which the reader will presumably study in other works written by competent authors and giving all the important relationships, such as the dependence of band broadening on the linear velocity, so that wrong conclusions, which can have particularly serious consequences in trace analysis, can be avoided.

In Chapter 7 the author has taken great pains to collect the possible chemical reactions and especially those that are carried out before the separation to improve the sensitivity of detection; no fewer than 335 references are mentioned in this chapter. It would have been desirable to include a critical account of the problems associated with this method (*i.e.* pre-column derivatization) in the determination of traces in complex matrixes.

Chapter 8 deals with the methods of sample preparation and contains 67 references. Chapter 9 discusses in general terms the very important subject of how to choose the right chromatographic system. However, in the case of phase systems, we only find here a brief account of chromatography on silica gel and on materials used in reversed-phase chromatography. No mention is made of ways to utilize specific selectivities, *e.g.* by column switching.

Chapter 10 gives a selection of clinical and biological applications as well as of ones from the fields of environmental protection and food analysis, and these examples give a good idea of the use of HPLC in trace analysis.

The overall impression is that this book is really an introduction to HPLC. There is a large number of useful references, but one misses an evaluation of the methods and apparatus for specific applications.

*F. Eisenbeiss* [NB 572 IE]

**Analytiker-Taschenbuch.** Vol. 2. Edited by *R. Bock, W. Fresenius, H. Günzler, W. Huber,* and *G. Tölg.* Springer-Verlag, Berlin 1981. viii, 351 pp., bound, DM 78.00.

It is a pleasure to find that, as expected, the contents of this second volume match those of the first volume[*] published in this "Taschenbuch" series in 1980. The material is again divided into four parts, namely Theory, Methods, Applications, and Miscellaneous data, and within this framework 16 authors working at universities and in industry offer a wealth of information to the analytical chemist.

*J. F. Cordes* (BASF Ludwigshafen and the University of Mannheim) gives a comprehensive survey of *practical quantities and units and the SI system.* The author covers the history of legislation in this field and the work of the ISO, IUPAC, and DIN committees that has led to the current method of dimensioning in analytical chemistry. This will help analytical chemists in the official and commercial sectors.

*H. Bartels* (Ciba-Geigy, Basel) deals with the difficult topic of *automation* of chemical analysis and gives an account of instrumentation in (automated) analysis, together with useful fundamentals that can greatly help in rationalizing laboratory work. It would perhaps have been helpful to distinguish more clearly between mechanization, instrumentation, and automation.

*H. Specker* (University of Bochum) reflects his wide experience in an account of the *extraction of metal halides from aqueous media,* a powerful method for separating cations.

The first contribution in the section on analytical methods, by *W. Brümmer* (E. Merck, Darmstadt), deals with *affinity chromatography.* This is a special form of adsorption chromatography that is particularly useful for biological substances. This excellent chapter is also full of useful information for analytical chemists who do not work in the field of biochemistry.

*C. Wydler* (University of Basel) demonstrates the power of purely physical methods in his contribution on *electron spin resonance of organic radicals in solution.* This chapter constitutes a very useful aid for analysis and the interpretation of ESR spectra, especially by including a list of coupling constants in tabular form.

*H. Englhardt* and *G. M. Ahr* (University of Saarbrücken) call their contribution *HPLC—rapid liquid chromatography.* The treatment of the broad field of high-pressure liquid chromatography is certainly very good, but more information about the separation systems used in the next chapter, possibly in tabular form, would be appreciated.

*G. Schwedt* discusses *gas-chromatographic separation and determination methods in inorganic trace analysis* and gives the principles of derivatization, together with tables of the most important information about the volatile compounds to be prepared, the detectors to be used, the sensitivity limits, and practical applications.

The next chaper is by *R. Klockenkämper* (Institute of Spectrochemistry and Applied Spectroscopy, Dortmund), who also wrote *X-ray spectral analysis in combination with scanning electron microscopy* in Part 1. The new contribution, on *wavelength dispersion spectrometry,* gives useful numerical values, performance figures, and a comparison between wavelength-dispersion and energy-dispersion spectrometers.

Two chapters deal with the electrochemical aspects of analytical chemistry: *New titrations with electrochemical end-point indication* by *E. Schumacher* and *F. Umland* (University of Münster) and *Differential pulse polarography, pulse voltammetry, and pulse inverse voltammetry* by *H. W. Nürnberg* (Jülich Nuclear Research Center). Both authors are highly competent and give an excellent account of the present-day knowledge of ion-selective electrodes.

The part devoted to applications begins with an account of the *chemical detection of organic functional groups* by *W. Huber* (BASF Ludwigshafen). This chapter represents a welcome revival of *chemical* processes and includes very useful tables.

*Methods for the determination of elements in natural waters* by *G. Schwedt* (University of Göttingen) is a short but good survey of the analytical schemes and the methods of determination involved. *Indicators and their characteristics* by *V. Schmidt* and *W. D. Mayer* (Merck, Darmstadt) is a longer account and one that is fundamental to classical analysis. It gives the IUPAC names and the properties of the indicators for aqueous and non-aqueous systems, with a number of tables. *C. E. von der Smissen* (Drägerwerk, Lübeck) deals with filter-type respirators, a highly topical subject. This is an outstanding account of the present-day situation in the domain of work safety and environmental protection.

The last part of the book begins with the *relative atomic weights of the elements* and continues with *threshold limit values* at working premises (with some important tabulated material) and *intoxication-information and treatment cen-*

[*] Cf. *Angew. Chem. 94* (1982) 325; *Angew. Chem. Int. Ed. Engl. 21* (1982) 896.

*ters with a 24-hour service* (in the Federal Republic of Germany), together with addresses of *organizations in the field of analytical chemistry in the German-speaking countries.*

All in all, this book can be highly recommended for all chemists and for responsible authorities in industry and in universities.

*Hanns Malissa* [NB 573 IE]

**Recent Books**

**The following books have been received by the editor. Detailed reviews will not be published in all cases because of the limited space available under this heading in the journal. All the publications listed are available through W & P Buchversand für Wissenschaft und Praxis, Boschstrasse 12, D-6940 Weinheim (Federal Republic of Germany). Tel. (06201) 602653 (606-0), Telex 465516 vchwh d, Telefax (06201) 602328.**

**Structure and Bonding. Vol. 52: Structures versus Special Properties.** Edited by M. J. Clarke, J. B. Goodenough, J. A. Ibers, C. K. Jørgensen, J. B. Neilands, D. Reinen, R. Weiss, and R. J. P. Williams. Springer-Verlag, Berlin 1982. 202 pp., bound, DM 108.00.—ISBN 3-540-11781-4

**Die chemische Literatur. Ihre Erschließung und Benutzung.** By M. Mücke. Verlag Chemie, Weinheim 1982. xi, 271 pp., bound, DM 58.00.—ISBN 3-527-25983-X

**Anthracycline Antibiotics.** Edited by H. S. El Khadem. Academic Press, New York 1982. xii, 285 pp., bound, $ 25.00.—ISBN 0-12-238040-1

**Advances in Experimental Medicine and Biology. Vol. 152: New Vistas in Glycolipid Research.** Edited by A. Makita, S. Handa, T. Taketomi, and Y. Nagai. Plenum Press, New York 1982. xiii, 490 pp., bound, $ 62.50.—ISBN 0-306-41108-3

**Experimental Methods in Photochemistry and Photophysics. Part 1 and 2.** Von *J. F. Rabek.* John Wiley, Chichester 1982. xvii, pp. 1–592/xviii, pp. 593–1098, bound, £ 89.95.—ISBN 0-471-90028-X/0-471-90030.3, both volumes together 0-471-10090-0

**Biological Magnetic Resonance. Vol. 4.** Edited by *L. J. Berliner and J. Reuben.* Plenum Press, New York 1982. xx, 340 pp., bound, $ 42.50.—ISBN 0-306-40968-2

**Thermal Analysis. Vol. 1 and 2. Edited by** *B. Miller.* John Wiley, Chichester 1982. xxxii, pp. 1–792/xxxii, pp. 793–1530, bound £ 40.00.—ISBN 0-471-26244-7/0-471-26245-5, both volumes together 0-471-26243-9

**Annual Reports in Organic Synthesis 1981.** Edited by *L. G. Wade Jr.* and *M. J. O'Donnell.* Academic Press, New York 1982. xiii, 498 pp., bound $ 26.00.—ISBN 0-12-040812-0

**Russisch für Chemiker.** *Several authors.* VEB Verlag Enzyklopädie Leipzig 1982. 284 pp., bound, *ca.* DM 16.00.—Best.-Nr.: 577205 5

**The production and Application of Fluorescent Brightening Agents.** By *M. Zahradnik.* John Wiley, Chichester 1982. 147 pp., bound, £ 12.50.—ISBN 0-471-10125-7

**The elements of Polymer Science and Engineering. An Introductory Text for Engineers and Chemists.** By *A. Rudin.* Academic Press, New York 1982. xv, 485 pp., bound, $ 29.95.—ISBN 0-12-601680

**Free Radicals and Cancer.** Edited by *R. A. Floyd.* Marcel Dekker, Basel 1982. xii, 541 pp., bound, SFr. 198.00.—ISBN 0-8247-1551-9

**Chemical and Biological Generation of Excited States.** Edited by *W. Adam* and *G. Cilento.* Academic Press, New York, 1982. xi, 388 pp., bound, $ 59.50.–ISBN 0-12-044080-6

**Anorganische Chemie.** 3rd, completely revised edition. By *V. Gutmann* and E. Hengge. Verlag Chemie, Weinheim 1982. xii, 438 pp., stitched, DM 78.00.—ISBN 3-527-25943-0

**Electron Distributions and the Chemical Bond.** Edited by *P. Coppens* and *M. B. Hall.* Plenum Publishing Corporation, New York 1982. ix, 479 pp., bound, $ 55.00.—ISBN 0-306-4100-1

**Advances in X-Ray Spectroscopy.** Edited by *C. Bonnelle* and *C. Mande.* Pergamon Press, New York 1982. xiv, 466 pp., bound, $ 80.00.—ISBN 0-08-025266-4

*Registered names, trademarks, etc. used in this journal, even without specific indication thereof, are not to be considered unprotected by law.*

© Verlag Chemie GmbH, D-6940 Weinheim, 1983. – Printed in the Federal Republic of Germany by Zechnersche Buchdruckerei, Speyer/Rhein.

All rights reserved (including those of translation into foreign languages). No part of this issue may be be reproduced in any form – by photoprint, microfilm, or any other means – nor transmitted or translated into a machine language without written permission from the publishers. Only single copies of contributions, or parts thereof, may be reproduced for personal use. Copies reproduced and used other than for private purposes in an industrial or commercial undertaking are subject to copyright and, in such cases, a copyright fee must be paid to the VG WORT, Abteilung Wissenschaft, Goethestr. 49, 8000 München 2, from whom conditions of payment can be obtained on request.

**Valid for users in the USA:** The appearance of the code at the bottom of the first page of an article in this journal (serial) indicates the copyright owner's consent that copies of the article may be made for personal or internal use, or for the personal or internal use of specific clients. This consent is given on the condition, however, that the copier pay the stated per-copy fee through the Copyright Clearance Center, Inc., for copying beyond that permitted by Sections 107 or 108 of the U.S. Copyright Law. This consent does not extend to other kinds of copying, such as copying for general distribution, for advertising or promotional purposes, for creating new collective works, or for resale. For copying from back volumes of this journal see 'Permissions to Photo-Copy: Publisher's Fee List' of the CCC.

**Editorial office:** Pappelallee 3, D-6940 Weinheim, Federal Republic of Germany, Telephone (06201) 602-1, Telex 465516 vchwh d, Telefax (06201) 602328.

**Editors:** *P. Gölitz, I. G. Neil, O. Smrekar, A. Stimson.*

**Publishers:** Verlag Chemie GmbH. (Managing Directors: *Dr. Helmut Grünewald* and *Hans Dirk Köhler*), Pappelallee 3, D-6940 Weinheim, Federal Republic of Germany.
Correspondence concerning advertisements should be addressed to Verlag Chemie GmbH. (Advertising Manager *R. J. Roth*), Pappelallee 3, P.O. Box 1260/1280, D-6940 Weinheim, Federal Republic of Germany, Telephone Weinheim (06201) 602-1, Telex 465516 vchwh d, Telefax (06201) 602328.

ANGEWANDTE CHEMIE
International Edition in English
Volume 22 · Number 2
February 1983
Pages 69–170

# On the Description of Complex Inorganic Crystal Structures

By Sten Andersson*

*Dedicated to Professor Harald Schäfer on the occasion of his 70th birthday*

To describe a structure is to describe chemistry. A description of structure should be simple yet also open up ways for an understanding of complex structures and their properties. Such interrelationships are gained on inspection and discussion of structures in models of interpenetrating partial structures and on application of symmetry operations to whole structures. Transition regions between interpenetrating partial structures can be approximated to periodic minimal surfaces. Chemical reactions, *e.g.* in ion-exchange, in heterogeneous catalysis, or in molecular separations in complicated zeolites will take place on these minimal surfaces.

## 1. Introduction

To describe a structure is to describe chemistry—and what is chemistry? Whether a substance is a solid, a liquid or a gas, we split it or decompose it into its component parts, *i.e.* building blocks, phases, polyions, molecules, atoms, electrons *etc.* to find out what it is made of. The analysis may be carried out by means of simple chemical methods, diffraction methods or quantum physical methods, and when it is complete we try to put the components of the substance together again to see if we can synthesize what we have just analyzed. When we think we have found out something about a structure and about the effective forces that hold the atoms of a substance together, we try to predict what happens with different combinations of these substances under various conditions of, *e.g.*, temperature and pressure.

Solid substances are almost always crystalline and have structures which are periodic, but the larger the repeat unit the more difficult it becomes to describe the structure. Really large complex structures are beyond comprehension and we cannot explain why they exist. With an appropriate description, however, we may sometimes be led to think that we understand a structure, understand how it is formed, and how to explain its properties.

Recently, on the occasion of *Wilhelm Klemm*'s 85th birthday, a series of review articles appeared in this journal in which *von Schnering, Simon, Hoppe* and *Bronger* outline their methods for the description of crystal structures[1–4]. It is immediately apparent that these descriptions stem from the same school—each of these authors were at Münster at the same time for a number of years—and that they are also strongly influenced by the chemistry of cluster compounds, in its infancy at that time and pioneered by *Harald Schäfer*. Another concept for the description of structures, the concept of "nested polyhedra" was developed by *Parthé* to simplify the description of complex cubic structures[5]. There are, of course, many ways in which to describe a structure, and I doubt whether we can say at this stage that any one is better than another.

Nevertheless, what we expect from a structure description is undisputed:

[*] Prof. Dr. S. Andersson
Oorganisk Kemi 2, Kemicentrum
Box 740, S-22007 Lund (Sweden)

 © Verlag Chemie GmbH, 6940 Weinheim, 1983 0570-0833/83/0202-0069 $ 02.50/0 

1. It should be simple, and should show as many relationships as possible to other structures.
2. It should facilitate the explanation of diffusion and reaction mechanisms.
3. It should be useful in explaining physical properties like conductivity, hardness, *etc.*
4. It should help us to interpret high-resolution electron microscopic lattice images—this often means trying to understand the defect structure of a crystal.

The first statement means, among other things, that a structure description should provide us with many ideas and associations. The description should thus allow us to apply Birkhoff's equation for the aesthetic measure[6]:

$$M = \frac{O}{C}$$

where O may contain elements of the associations (of order) and ideas, and C is the complexity, which in a polygon, for example, is measured by the number of sides. In simple terms this means a structure description should be "beautiful". (When solving the large block structures of various niobium oxides, *Wadsley* and I used to have two criteria for the proposed models: The chemical formula, and the *beauty*[7].) We are reminded of an old definition for beauty—as "that which gives us the greatest number of ideas in the shortest space ot time" (*Hemsterhuis*).

## 2. Simple Structures

The principal idea is that a complex structure is built up of much simpler structures[28]. What are much simpler structures and how can they be combined to give a complex structure? This is what we shall deal with in this article.

Before we outline our methods for the description of complex structures, we shall first describe simple structures. Such structures are, *e.g.*, hexagonal close packing (hcp) of the atoms, cubic close packing (ccp), body centered cubic (bcc), hexagonal primitive (hp), cubic primitive (cp), or just simply primitive packing of lower symmetry (Fig. 1).

Two simple and identical structures can interpenetrate to give a new structure, as shown in Figure 1. Examples are NaCl, diamond, and $Mg_3Cr_2Al_{18}$. Three simple and identical structures can also interpenetrate to give a new structure.

This can be vividly demonstrated using the concept of rod packing[8]: The alloy $Cr_3Si$ has the so-called A15 structure, in which infinite Cr-chains with short metal-metal distances run in three perpendicular directions. One explains *via* this peculiarity the existence of many superconductors with this type of structure, *e.g.* $Nb_3Sn$ and $Nb_3Ge$. These chains with short metal-metal distances are represented by rods (arranged with quadratic mesh) which interpenetrate to form the simple, cubic A15 structure (Fig. 1).

Four simple and identical structures can also interpenetrate—to form the garnet structure $[Ca_3Al_2(SiO_4)_3]$ shown in Figure 2. In this case, we have hexagonal meshes of rods

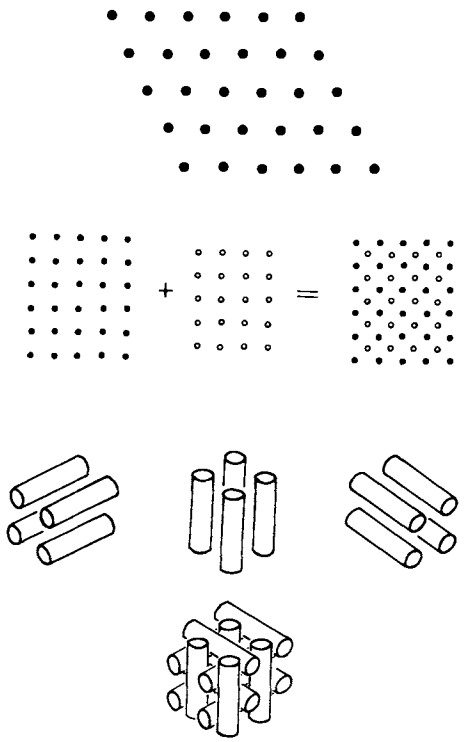


Fig. 1. Top: A simple structure.—Center: Two simple structures interpenetrate.—Bottom: Three simple structures interpenetrate to form the $Cr_3Si$ structure (A15-type).

in each simple structure, where each rod consists of face-sharing octahedra (filled) and trigonal prisms (empty) and all the oxygens are used to form the rods. Tetrahedra and twisted cubes (for the larger cations) are created between the rods by the oxygen atoms of adjacent rods. This structure is also taken up by alloys like $Th_4Bi$, in which all the Th atoms are in the oxygen positions of the garnet structure, and the Bi atoms are in the interstices formed by the Th rods (the large cation position in the garnet structure).

Two simple and different structures can interpenetrate to form a structure. One example is $ReO_3$, shown in Figure 3, another is NiAs, in which the hcp structure of As atoms interpenetrate a hp structure of Ni atoms. In $Cr_3Si$ the silicon structure (bcc) interpenetrates the chromium rod struc-

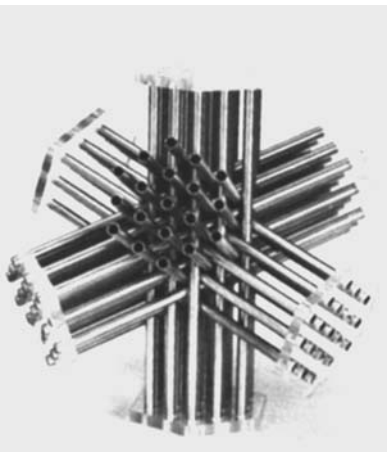


Fig. 2. Four simple structures interpenetrate to form the garnet structure.

ture, which itself consists of three identical interpenetrating structures. In $W_3Fe_3C$ the octahedral structure of tungsten atoms interpenetrates the tetrahedral structure of the iron atoms (Fig. 5) and the carbon atoms in the tungsten octahedra form a third structure, which is the same as that of the zinc atoms in $MgZn_2$, and the oxygen atoms in cristobalite (idealized).

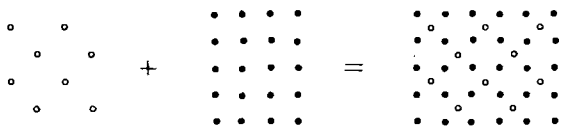


Fig. 3. Two different structures interpenetrate.

Of course, many more examples could be given. Between these simple structures there exist many relationships which we will leave undefined at this stage. Suffice it to say that from one simple structure many other simple structures are easily obtained by small shifts of atoms in various directions. Good examples of these topological operations are found, for example, in *Bärnighausen*'s work[9].

## 3. Complex Structures

"Most isometries are familiar in everyday life. When you walk straight forward you are undergoing a translation. When you turn a corner it is a rotation; when you ascend a spiral staircase, a twist (screw). The transformation that interchanges yourself and your image in an ordinary mirror is a reflection, and it is easy to see how you could combine this with a rotary reflection or a glide reflection, respectively" (from *Coexter*'s Introduction to Geometry). By using a point instead of "you", we describe the symmetry operations that give rise to the 230 space groups. By using *building blocks* of atoms, which may be parts of simple structures, we analogously describe the symmetry operations that give the complex structures. The symmetry operations that describe the space groups leave all distances and angles unchanged, and similarily the building blocks are left unchanged during a transformation.

We thus assume that complex structures can be described as parts of simple, or simpler structures. We shall demonstrate this with a number of examples.

## 4. Parallel Translation

Figure 4 shows how a simple structure (Fig. 1) may be repeated by a single parallel translation to build up a more complex structure. This operation, called crystallographic shear, or slip, produces two interesting new features in the structure: In the shear planes there are triangles of atoms, in which each of the three participating atoms is now pentacoordinated, and the sheared complex structure is more dense than the simple structure. Two examples of formal shear structures are those of compounds $Nb_3O_7F$ and

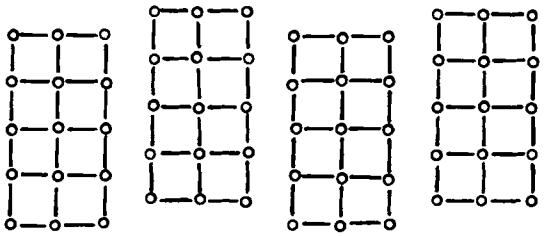


Fig. 4. Shear by parallel shifts.

R–$Nb_2O_5$ (Fig. 5). In both cases the simple parent structure type is $ReO_3$.

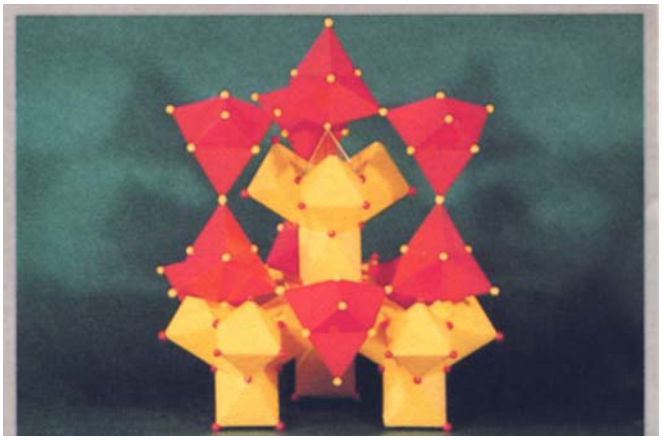
The structure of $TiNb_2O_7$ (Fig. 5) contains columns of the $ReO_3$ structure ($3 \times 3$ octahedra in size) stretching infinitely in the direction perpendicular to the plane of the picture. The structure is formally derived from double translations of the parent $ReO_3$ structure, or equally well from a single translation of the $Nb_3O_7F$ structure. Figure 5 shows the structure of $NaNb_{13}O_{33}$, which also is derived from a double translation of the parent $ReO_3$ structure or a single translation of the $Nb_3O_7F$ structure.

Two different column sizes of the same $ReO_3$ parent structure type, occurring in the same crystal in an ordered way, are found in the structure of $W_4Nb_{26}O_{77}$[7]. This important compound was first prepared by *Gruehn* in *Schäfer*'s laboratory in Münster. $W_4Nb_{26}O_{77}$ could easily be described as composed of alternate slabs of the oxides $WNb_{12}O_{33}$ and $W_3Nb_{14}O_{44}$, and is called an intergrowth or hybrid compound, the first example of its kind (Fig. 6).

A variation in composition of a compound due to random variations of column or slab size were predicted earlier by *David Wadsley* in Melbourne. He, together with *Sanders* and *Allpress*, were also the first to use the now so well known lattice imaging technique in a classical study on various niobium oxides[10]. I shall always remember my feelings of joy upon receiving his enthusiastic letters, always accompanied by many lattice images of these oxides with random shear planes. After his untimely death we named these faults, now also known to be so common in minerals, metals and alloys, Wadsley defects, in honour of the man who proposed and predicted their occurrence so many years before they were actually discovered. *Schäfer* realized at an early date the importance of *Wadsley*'s pioneering work on oxides, which he wholeheartedly supported.

Nowadays, microscopes are far more better and it is possible to achieve atomic resolution almost routinely. A study by *Bovin et al.* on crystals of $NaNb_{13}O_{33}$ clearly demonstrates this[11]. Columns, sized $3 \times 5$ octahedra and similar in structure to those of $TiNb_2O_7$ (cf. Fig. 5, bottom left), are intergrown with the normal column of the $NaNb_{13}O_{33}$ structure (Fig. 7). Thus, it is vividly clear how the crystal is able to accomodate variations in the sodium content.

It is obvious that for these transition metal oxides structure description is now a well established procedure, with full theoretical and experimental support from computer calculations and high resolution electron microscopy. The structures of many, many more oxides can be developed



$CuAl_2$. If the translation operation is continued as shown in Figure 8, larger columns of $Cr_3Si$ can build into the structure of $Mo_3CoSi$, which can also be derived from the $CuAl_2$ structure.

Complete experimental support for this structure description is obtained from *Stenberg*'s lattice images of $Mo_3CoSi$ (Fig. 9)[13]. Furthermore, we note that the short metal-metal distances, typical for $Cr_3Si$ in three dimensions, are restricted to two dimensions for the single translation structures, and to one dimension for double shear structures.

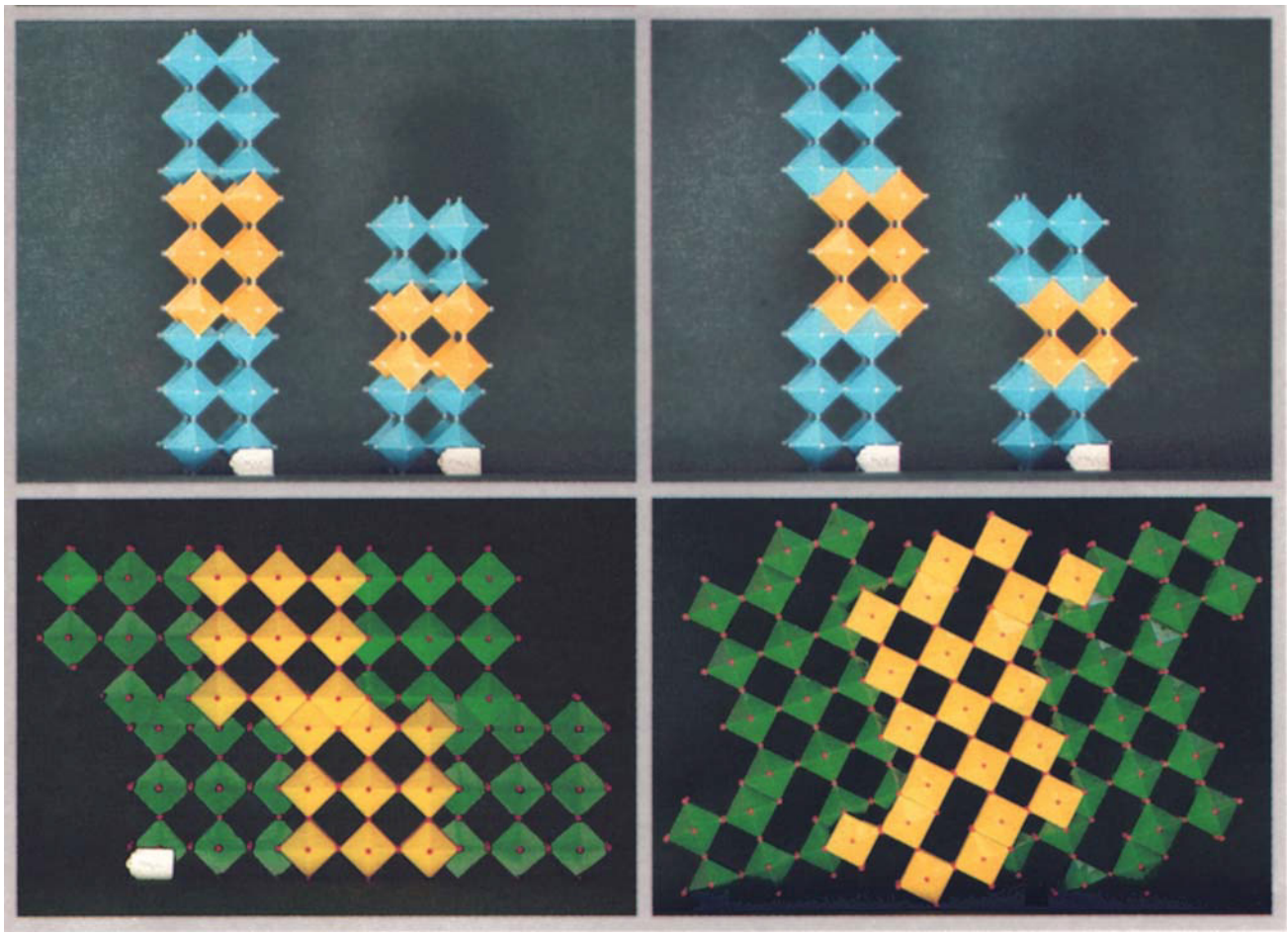


Fig. 5. Top: Structure of $W_3Fe_3C$. The structure of the tungsten atoms (red spheres), with carbon in the center of the (yellow) octahedra interpenetrate the tetrahedral iron structure (yellow spheres).—Center: The structures of $Nb_3O_7F$ (left) and R-$Nb_2O_5$ (right) shown in two different projections.—Bottom: The structures of $TiNb_2O_7$ (left) and $NaNb_{13}O_{33}$ (right).

by simple parallel translation. For further detailed information on this subject the reader is referred to the literature[12].

In Section 2 we described the $Cr_3Si$ structure as a rod structure, but here we can describe it in a slightly different way, as shown in Figure 8. The shaded regions consist of five irregular tetrahedra—an arrangement which *Schubert* calls a "Tetraederstern". In Figure 8 we have applied single and double translation (shear) to the structure and obtained two very important structure types, $Zr_4Al_3$ and

## 5. Parallel Reflection

Figure 10 illustrates twinning of a hcp structure. This simple parallel reflection is called "chemical twinning", or also "unit cell twinning"[14a]. New polyhedra are created in the twin plane by this operation, in this case trigonal prisms. The first example is cementite, $Fe_3C$ (see Fig. 10 and 11). The hcp slabs are four iron atoms wide, and the trigonal prisms in the twin planes contain carbon atoms. If the slabs are alternately 4 and 3 iron atoms wide, we obtain

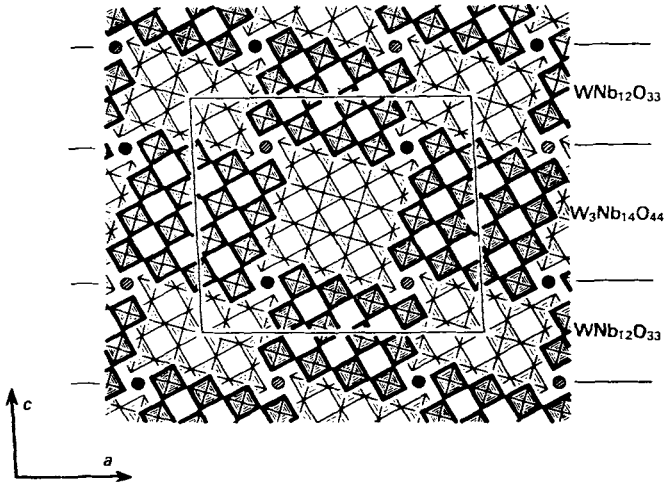



Fig. 6. Structure of the intergrowth or hybrid compound of $W_4Nb_{26}O_{77}$ formed by the components $W_3Nb_{14}O_{44}$ and $WNb_{12}O_{33}$.

the structure of $Fe_5C_2$, which is of the $Pd_5B_2$ type. Variation of stoichiometry can easily be achieved by varying the block size (Fig. 11), and this has recently been verified experimentally by electron microscopy[14b]. There are many

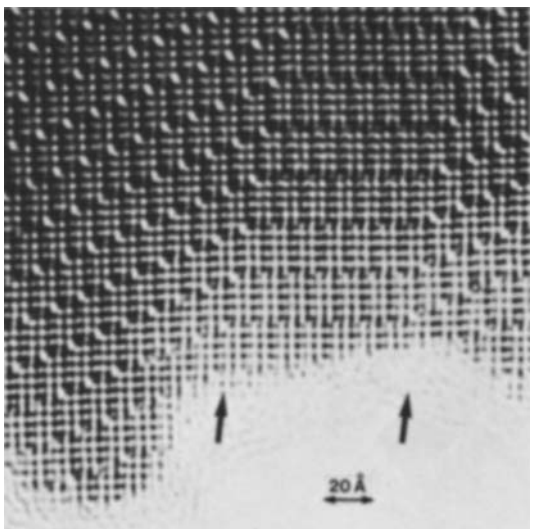



Fig. 7. Lattice image of a defect in a crystal of $NaNb_{13}O_{33}$. The intergrowth of the $NaNb_{13}O_{33}$ structure with a $TiNb_2O_7$-type structure is easily discernible (region between the arrows) [11].

compounds with the $Fe_3C$ structure, of which we shall mention only three here, namely $SbCl_3$, $BiCl_3$, and, as a special case, $XeO_3$. Likewise, ccp nets may be twinned, and this operation also produces trigonal prisms in the twin planes. The structures of $Re_3B$, $CaTi_2O_4$ and lillianite ($Pb_3Bi_2S_6$) are typical examples (Fig. 11). *Parthé*[15] has pointed out that unit-cell twinning is also observed in mixed hcp and ccp structures, for example in $Sc_3Co$ and one modification of TbNi.

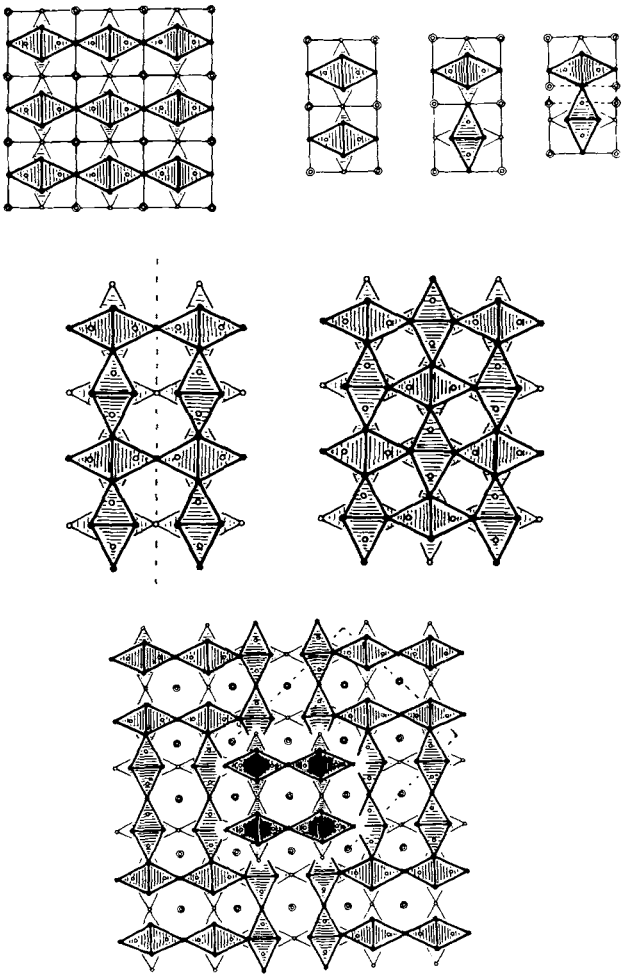


Fig. 8. Top: Structure of $Cr_3Si$ (A15-type) (left) and single steps of the shear operation (right) (cf. text).—Center left: $Zr_4Al_3$ structure (idealized) is formed from the $Cr_3Si$ structure by a vertical shear of each second slab followed by a connection of the tetrahedra-stars. Center right: Structure of $CuAl_2$ formed by an additional shear operation of the same type along the broken line in $Zr_4Al_3$. (In both cases the central atoms are omitted.)—Bottom: The structure of $Mo_3CoSi$ generated by the same shear operation but only of each second slab of $Cr_3Si$.

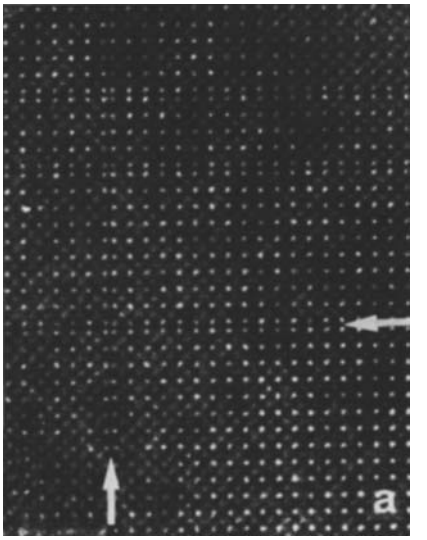



Fig. 9. High resolution lattice image of $Mo_3CoSi$. The light dots are the center of mass of the hexagonal antiprisms, the weaker dots correspond to the square antiprisms. The intersection of the arrows is the $Cr_3Si$ structure.

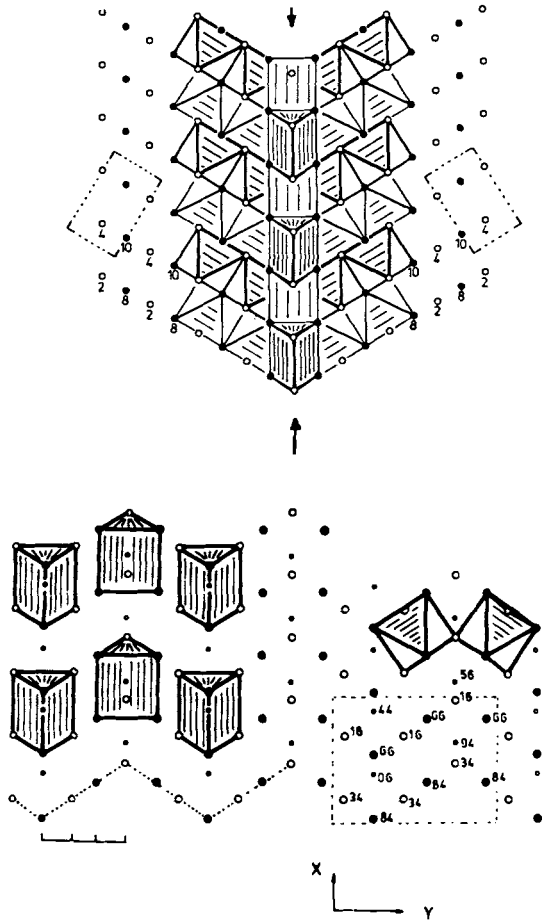


Fig. 10. Top: Twinning in hcp. Heights are in units of 1/12th. Trigonal prisms in the twin planes are shown, as are also some octahedra.—Bottom: The structure of $Fe_3C$ formed by four atom layer slabs (as indicated on the bottom left).

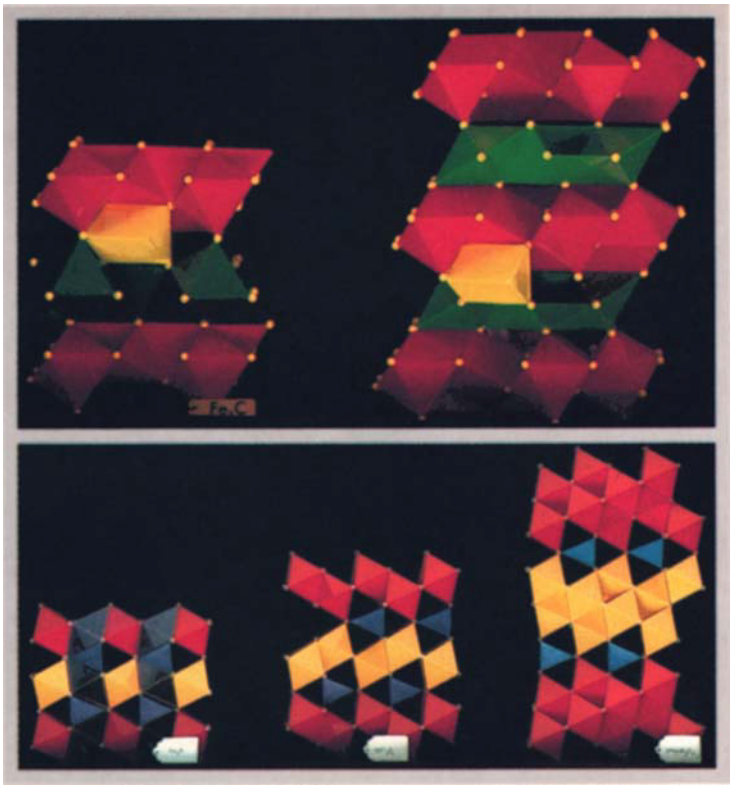


Fig. 11. Top: Structures of $Fe_3C$ and $Fe_5C_2$. Carbon atoms fill the yellow trigonal prisms, between the green and red hcp slabs of the Fe atoms (yellow spheres). Note that the green slabs in $Fe_5C_2$ (right) are not as wide as those in $Fe_3C$ (left).—Bottom: The structure of $Re_3B$, $CaTi_2O_4$ and lillianite (trigonal prisms = blue polyhedra).

Unit-cell twinning of a primitive cubic structure is also possible. One example is the structure of $Ru_4Si_3$ shown in Figure 12 as twinned RuSi (CsCl type), but here the reflection is combined with a translation. $Rh_5Ge_3$ ($Ru_5Si_3$ is isostructural) follows the same scheme, but the slab size is only five atoms wide (Fig. 12), whereas in $Ru_4Si_3$ it is eight atoms wide. Naturally, one expects a crystal to have faults which correspond to various distances between the twin planes. The presence of faults was confirmed in some early electron microscopic studies on $Ru_4Si_3$ crystals, but since no really high resolution was available, we had to make a histogram analysis of the fringes in the one-dimensional lattice images[16]. Figure 13 shows the various *c*-axis lengths found, corresponding to the different RuSi block sizes in the $Ru_4Si_3$ crystal.

## 6. Complex Parallel Intergrowth

The extremely important alloy structure type $W_6Fe_7$ (μ-phase) is best described as an intergrowth of slabs of two structure types, namely those of $Zr_4Al_3$ and $MgCu_2$ (Fig. 14). This suggests that disorder may exist, since the two different slabs can vary in size and orientation; this has in

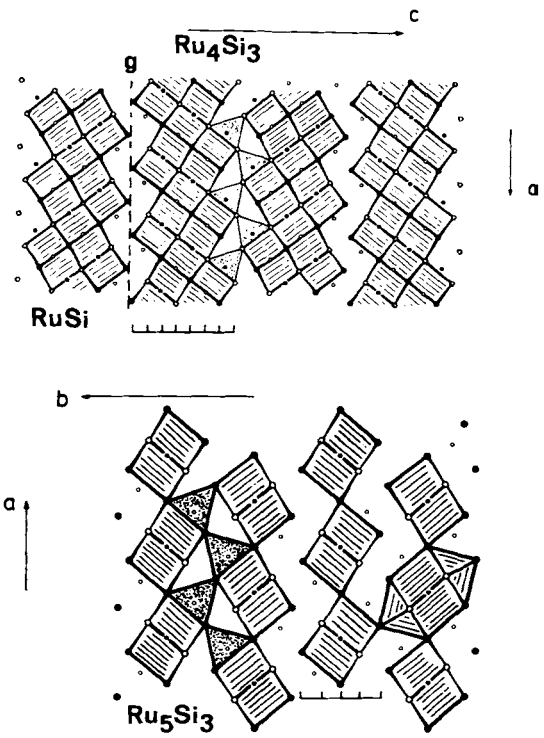



Fig. 12. Top: Structure of $Ru_4Si_3$ formed by RuSi (eight atomic layers).—Bottom: The structure of $Ru_5Si_3$ ($Rh_5Ge_3$) generated by RuSi-slabs (five atomic layers).

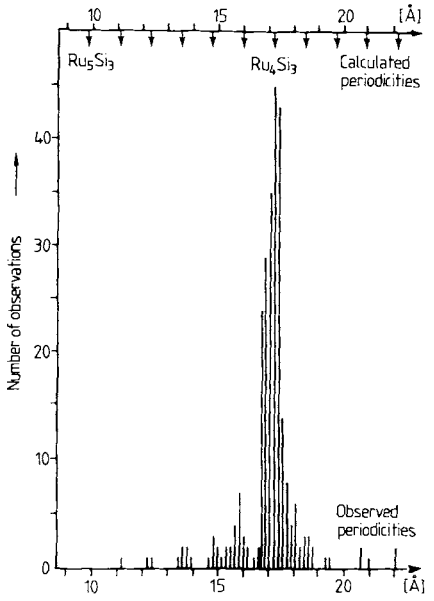



Fig. 13. Frequency distribution of the *c*-axis lengths found in five different crystals of $Ru_4Si_3$.

fact been confirmed by electron diffraction[17]. One of the reasons we include the so-called μ-phase structure here is that it can be sheared and twinned, and thus lends itself for the description of at least three more structures.

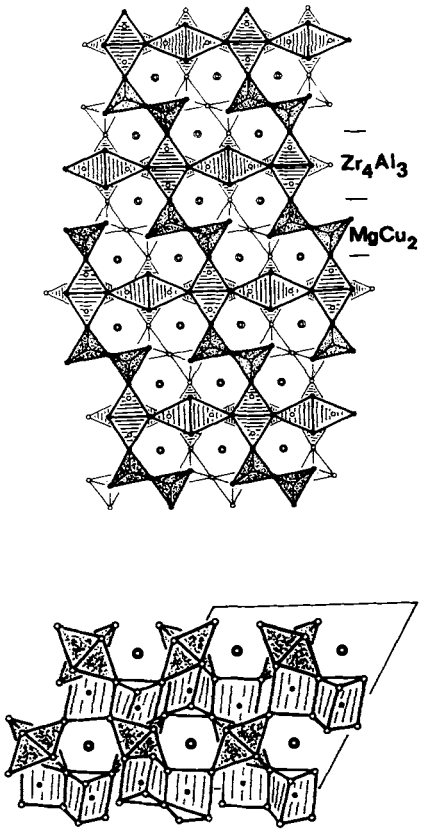



Fig. 14. Top: Structure of $W_6Fe_7$ composed of $Zr_4Al_3$ and $MgCu_2$ slabs.—Bottom: Structure of $Ta_6S$ composed of $Zr_4Al_3$ and $Fe_5C_2$ slabs.

Another spectacular example of intergrowth is found in the crystal structure of $Ta_6S$ (Fig. 14). Slabs of the $Zr_4Al_3$ type are intergrown with slabs of the $Fe_5C_2$ type and thus form the $Ta_6S$ structure. The tantalum atoms occupy the Fe, Zr and Al positions, and the sulfur atoms lie in the trigonal prisms (at the positions of the carbon atoms in $Fe_5C_2$).

## 7. Parallel Translation and Reflection in Combination

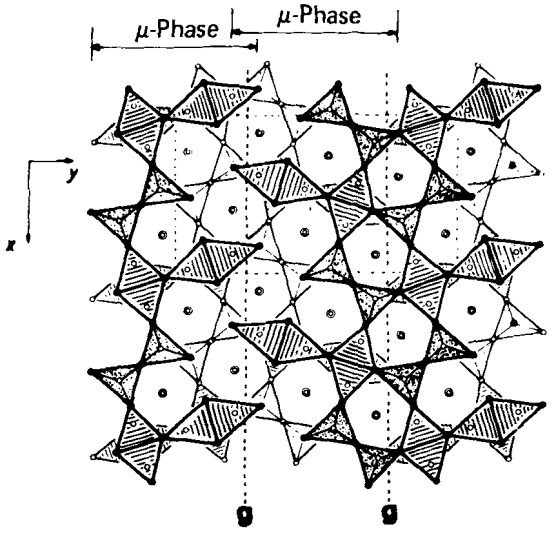
We have already given one example of this very common combined operation for describing structures in Section 5. Another example is the M-phase ($Nb_{48}Ni_{39}Al_{13}$) structure, which is accurately derived by twinning and shear of the μ-phase structure (Fig. 15). If the μ-phase slabs are extended in size a hypothetical structure is obtained, and with thinner slabs we get the $FeSiW_2$ structure shown in Figure 15. If the operation is continued by an additional shear, the melilith ($Ca_2MgSi_2O_7$) structure is obtained. Excellent experimental support for this description is again obtained from *Stenberg*'s electron microscopic investigations. Figure 16 shows part of a crystal of the M-phase containing large parts of the μ-phase, sheared and twinned as in the M-phase structure[18].

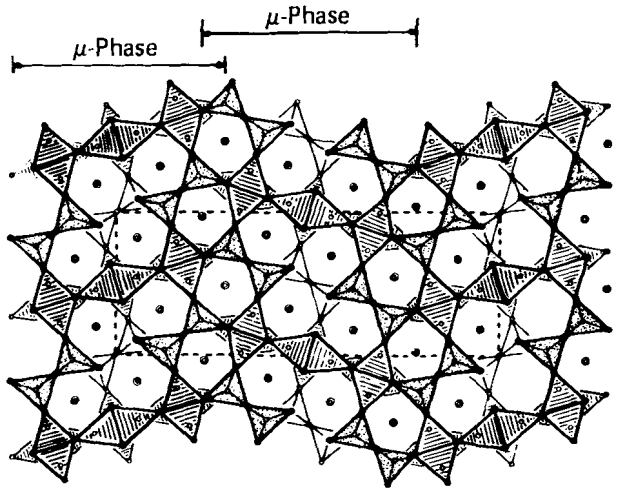
## 8. Cyclic Operations: Translation and Reflection

A simple example of this is shown in Figure 17, where the tetragonal bronze structure is generated by a cyclic twin operation from the $ReO_3$ structure. A large part of the bronze structure is recognizable in the center; the central octahedron is formed partly by the cyclic operation and then merely completed. In addition, the $BaNb_2O_6$ structure is formed in the twin planes. Naturally, this offers a geometrical model for the formation of the compound by nucleation. Repetition to a larger crystal may then occur if it is energetically possible, *e.g.* if the right ions are present under the right conditions of temperature and pressure.

The structure of $W_5Si_3$ is a further example for this operation: The simple construction of a fourling of the $Cr_3Si$ structure (Fig. 17) enables the demarcation of a column of $W_5Si_3$, whose structure is commonly described with square antiprisms, octahedra, and hexagonal antiprisms. Here also the structure in the center was completed by the insertion of an individual atom.

The $Zr_4Al_3$ structure is obtained by a shear (or translation) operation in the $Cr_3Si$ structure. If a $Zr_4Al_3$ column, similar to the $Cr_3Si$ column above, is used again for a fourling construction we obtain the $Ta_2S$ structure, as shown in Figure 17. *Bursill* and *Hyde* have shown that the tetragonal bronze structure can also be derived by a rotation of one-dimensional columns of the $ReO_3$ structure[19]. A similar transformation mechanism has also been proposed by us for the formation of the $Ni_3P$ and $W_5Si_3$ structures from that of $Cr_3Si$[20].



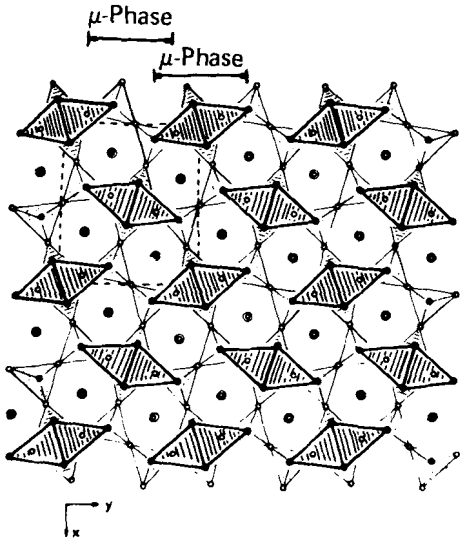




Fig. 15. Top: The M-phase structure. The glide planes (g) transform the intergrowing slabs of the μ-phase into each other.—Center: A hypothetical structure with thicker slabs of the μ-phase.—Bottom: The $FeSiW_2$ structure composed of thinner μ-phase slabs.

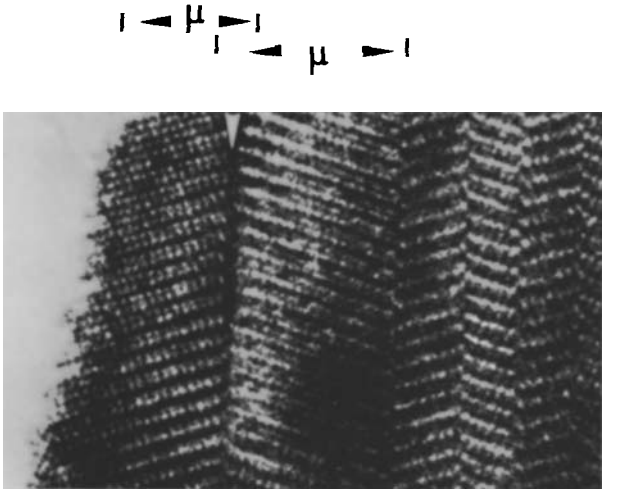


Fig. 16. High resolution lattice image of an M-phase crystal, with large regions of the μ-phase. (One glide plane is indicated by an arrow.)

## 9. Cyclic Intergrowth

Cyclic intergrowth has recently been used by us[21] to describe several structures; here we shall only mention a few cases. Figure 18 shows a simple model for this operation and clearly demonstrates how the important σ-phase (FeCr) structure is very accurately derived by intergrowing $Cr_3Si$ and $Zr_4Al_3$. This provides an alternative but simple and attractive description of the σ-phase, previously described with Kagomé nets.

*Simon* has described the suboxides of the alkali metals discovered by him as cluster compounds with the structural units $Rb_9O_2$ or $Cs_{11}O_3$, respectively[22]. An alternative description is possible for the suboxide $Cs_7O_3$ by a cyclic intergrowth of an hcp structure and the $Zr_4Al_3$ structure (Fig. 18). In the center of this cyclic intergrowth we note a cluster of three face sharing octahedra, namely the $Cs_{11}O_3$ unit, which represents the basis of the $Cs_7O_3$ structure (shown inside the heavy line).

## 10. Complex Applications

The validity and accuracy of this general method for the description of structures has been demonstrated experimentally with high resolution electron microscopy for some groups of compounds. We have shown earlier[23] that some complex alloy structures and even some so-called giant cubic structures could be very accurately described with these methods. Examples are γ-brass, $Rh_7Mg_{44}$, and $Cu_4Cd_3$.

Another unusually complex structure is found in the silicate paulingite $[K_2(Ca,Ba)_{1.3}(Si,Al)_{12}O_{24}\cdot 14H_2O]$, which has a cubic unit cell containing about 2500 atoms[24]. The methods discussed here led to an alternative description of this structure[25], which differs considerably from the one given by *Samson et al.* A reflection operation as initial step

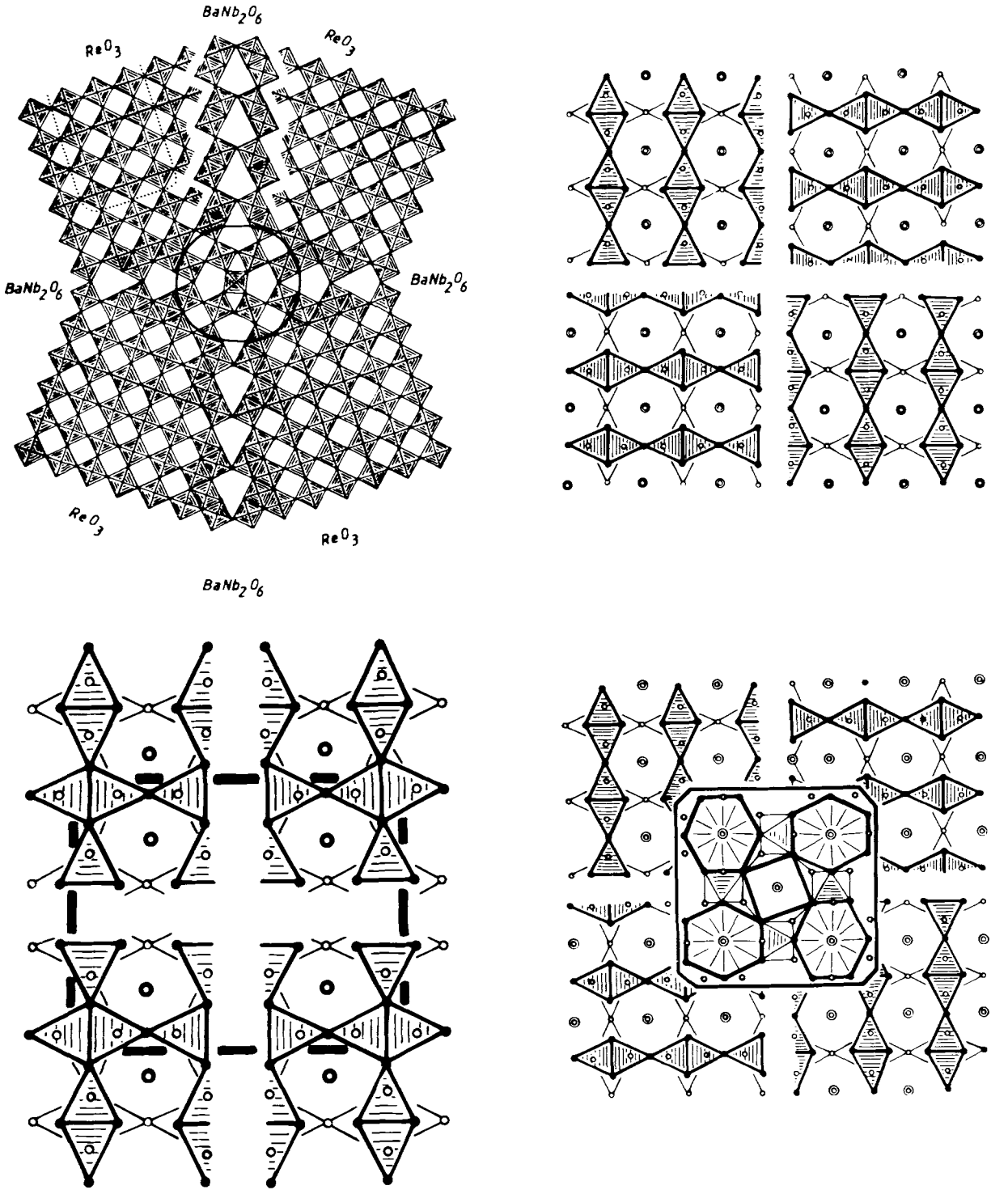



Fig. 17. Top left: A fourling of perovskite (or $ReO_3$) generated by two perpendicular reflections, to give the tetragonal bronze structure in the center (framed). The main structural units of $BaNb_2O_6$ (partially isolated in the upper part) are formed along the twin planes.—Top right: Fourling of the $Cr_3Si$ structure (formed by fourfold rotation) generates the $W_5Si_3$ structure.—Bottom right: Fourling of the $Cr_3Si$ structure with the region of the $W_5Si_3$ structure in the center (framed).—Bottom left: Fourling construction of the $Zr_4Al_3$ structure to give the $Ta_2S$ structure (framed with bold lines).

converted the very simple structure of cristobalite ($SiO_2$) into the gismondine structure ($CaAl_2Si_2O_8 \cdot 4H_2O$)[26]. A fourling of this structure (Fig. 19) formed by two orthogonal reflections generates the structure of merlionite ($K_5Ca_2Al_9Si_{23}O_{64} \cdot 24H_2O$) in the center. This mode of operation also leads to the structure of phillipsite ($KCaAl_3Si_5O_{16} \cdot 6H_2O$) from two pieces of gismondine in the mirror plane region. If a whole packet of atoms is now taken from the center of this fourling construction (only Si atoms are shown in Fig. 20) and put together in three-dimensional space by a translation operation, the paulingite structure is obtained (Fig. 20). The coordinates of all atoms of the paulingite structure, as calculated from the gismondine structure, agree exactly with the data of a crystal

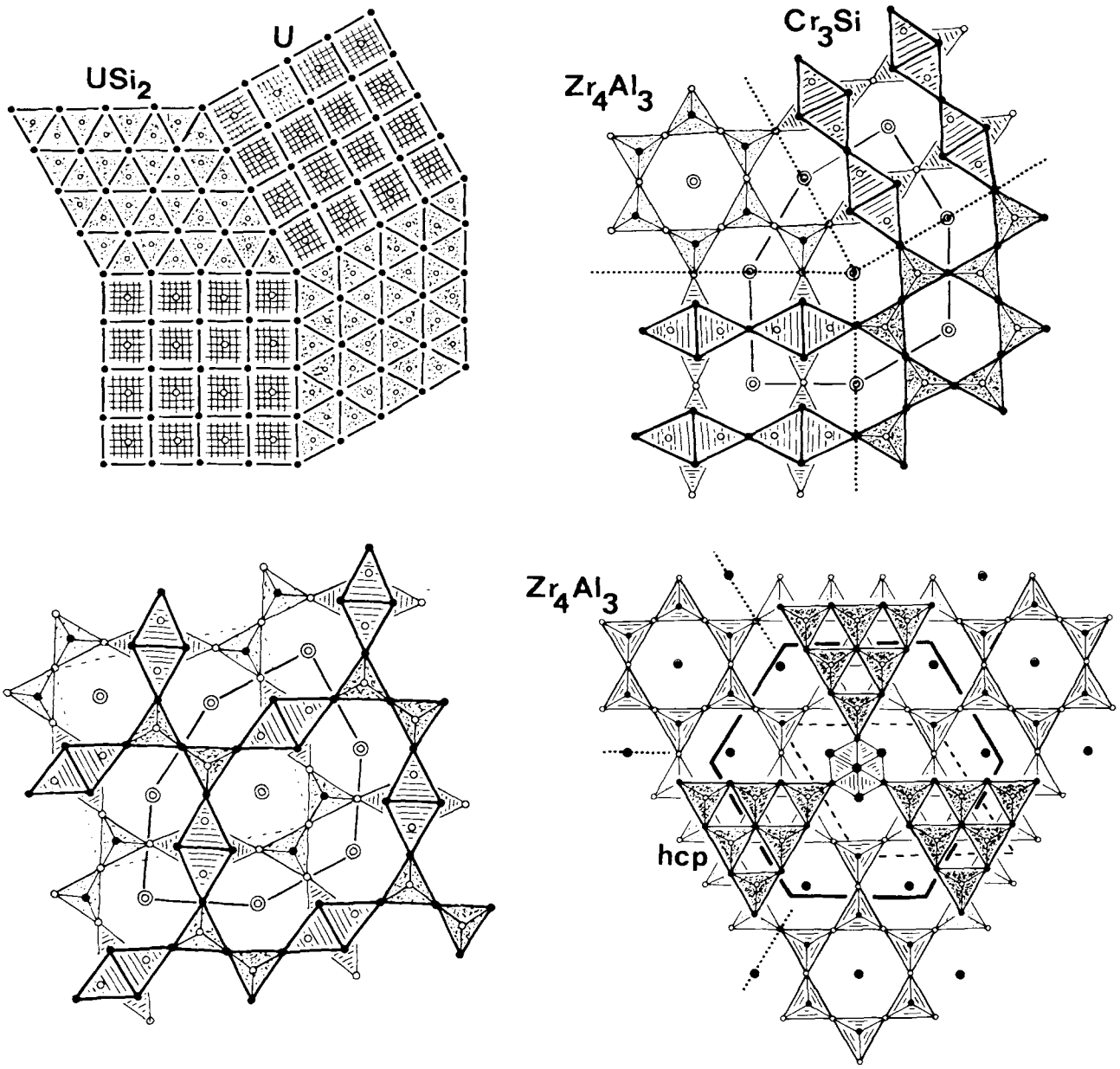



Fig. 18. Top left: Cyclic intergrowth of two simple structures.—Top right: Cyclic intergrowth of the $Zr_4Al_3$ (view along the hexagonal $c$-axis) and $Cr_3Si$ structures to give the σ-phase structure (framed in the center).—Bottom left: The complete σ-phase. The same region as in upper right has been framed in the center.—Bottom right: Cyclic intergrowth of the hcp and $Zr_4Al_3$ structures to give the $Cs_7O_3$ structure (indicated by a bold line). In the center the $Cs_{11}O_3$ cluster is formed (only Cs-atoms). The unit cell is indicated by broken lines.

structure analysis by *Samson et al.*, which again confirms the validity and accuracy of our description[25].

Our method for the description of these large cubic structures can, of course, be used to *solve* unknown complex structures as well. The systematic tracing of relationships to much simpler structures in the reciprocal lattice of a complex structure provides a direct method for structure determination. It was with this in mind that *Fälth* and I undertook the structure determination of a very large cubic structure, that of zeolite N with a lattice constant $a = 36.9$ Å, and about 3500 atoms in the unit cell[27]. Crystals of this zeolite were grown by *Fälth* using a method developed by him for silicates. In the Patterson function we quickly found a simple relationship to the sodalite structure $[Na_4(AlSiO_4)_3Cl]$, and by taking out exactly half of all the atoms from this structure, the remainder could be fitted to the space group of zeolite N, namely Fd3. This accounts for half the number of tetrahedra in the structure shown in Figure 20, and it was clear from this development that a second partial structure still had to be inserted in the sodalite skeleton in order to construct the complete structure of zeolite N. By trial and error we found that this missing part is a fragment of the zeolite K5 structure (Fig. 20). This part was taken in a similar way from the zeolite K5 structure as described for the sodalite fragment, namely with the criterion to fulfill the symmetry of the space group of zeolite N. Both structures, sodalite and K5 thus interpenetrate into the complete skeleton of zeolite N (Fig. 20)[27]—a formidable and elegant example of a structure, generated

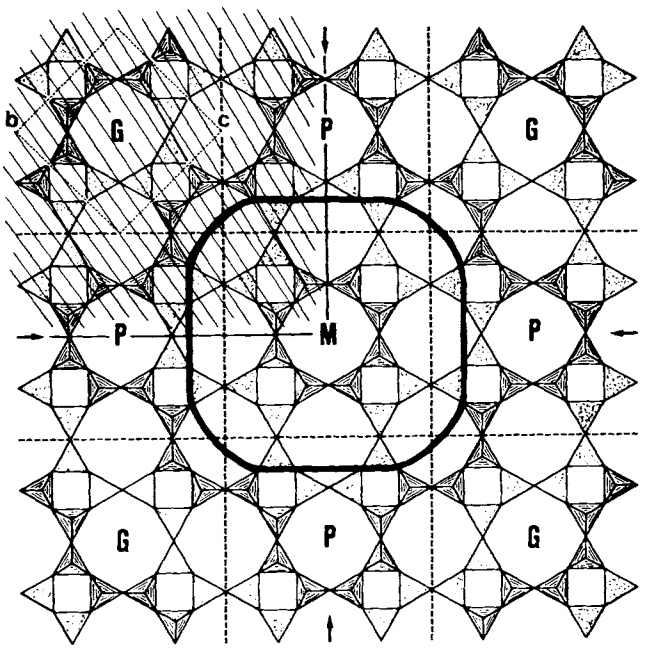



Fig. 19. Fourling of gismondine G (hatched region) and merlionite M in the center. In the region of the mirror planes (indicated by arrows) phillipsite P is formed by two parts of G.

by different interpenetrating complex point systems, which are operated as a whole by symmetry[28].

## 11. Periodic Minimal Surfaces

Some of these interpenetrating structures are hard to describe and understand but if we persist then some new and exciting developments emerge. Consider first:

a) $Cu_4Cd_3$, a pyrochlore-like structure with mainly Cd atoms which interpenetrates a complex Laves phase structure, of mainly Cu atoms.
b) Zeolite N, a sodalite structure which interpenetrates a zeolite K5 structure.
c) $W_3Fe_3C$, a tungsten octahedral structure which interpenetrates a tetrahedral structure of iron atoms (Fig. 5).
d) $Cr_2Mg_3Al_{18}$, where two identical structures interpenetrate.

If we study especially that part of the $Cu_4Cd_3$ structure which is built up of Friauf polyhedra intergrown in a manner typical for Laves phases, then we can recognize that a very smooth surface, close to the interface between the two interpenetrating structures, covers as well as separates the two parts (pyrochlore and Laves phase) in three dimensions. We propose that this interface is *an infinite periodic minimal surface.*

The Schwarz periodic minimal surfaces have been systematically described by *Schoen*[29]. One of the most spectacular is the so called Neovius surface[30]. According to *Hilbert*, it has the diamond symmetry and also contains the famous "monkey saddle"[31] (cf. Fig. 21).

*Scriven*[32] has suggested that a minimal surface might play a role in fluid or liquid crystals and that the structures differ on each side. Other crystallographical applications for these surfaces have been suggested by *Mackay*[33]. Actual use of the concept has been found for a cubic liquid-crystalline phase by *Larsson, Fontell* and *Krog*[34], and *Fontell*[35]. Truncated octahedra are one type of polyhedra that fill space and if half these are taken out of space-filling packing in a primitive way, the cubic liquid structure is obtained. In this case the truncated octahedra share only square faces, and the structure, which corresponds to Schwarz's primitive periodic minimal surface, is the one found by *Larsson, Fontell,* and *Krog.* On the other hand, if half of the polyhedra are removed from the space-filling packing of truncated octahedra in such a way that the remaining polyhedra share hexagonal faces, a cubic face centered structure is obtained (diamond symmetry), which represents half of the Si,Al structure of zeolite N (Fig. 20).

It is clear that the interface between, *e.g.*, the interpenetrating W and Fe structures in $W_3Fe_3C$, the interpenetrating Laves and pyrochlore-like structures in $Cu_4Cd_3$, and the interpenetrating sodalite and ZK 5 structures in zeolite N can all be approximated to a *periodic minimal surface,* as shown in Figure 21 for the tetrahedral part of $Fe_3W_3C$. This is the first periodic minimal surface of *Schwarz*; it has diamond symmetry. We can now continue this description by saying that the skeleton atoms in the Linde A and K 5 zeolites also form a minimal surface[33], like the one found by *Fontell et al.* in their liquid crystals. Faujasite (zeolite X and Y), which belongs to the same family as the zeolite N, as well as the pyrochlore structures may also be treated similarly. Finally, the hexagonal tunnel structures and the hexagonal bronze structures are also topologically related to *Schoen*'s H, or H-T structures[36].

A useful concept in the description of structures has been the close packing of spheres in a plane. Intuitively however, we feel that atoms of different sizes, like Fe and W, Cd and Cu, will pack more efficiently on a curved surface than on a plane. It is obvious therefore, that on these periodic minimal surfaces, atoms will pack with non-Euclidian geometry, and that reactions like ion-exchange, heterogeneous catalysis or molecular separations occur on these minimal surfaces.

A logical step leads us to three or even four interpenetrating structures, as in $Cr_3Si$ or garnet. Do such minimal surfaces exist in these cases? Can a minimal surface divide space into three or even more interpenetrating subvolumes? This I do not know.

## 12. Concluding Remarks

In this article a number of structures have been described by geometrical methods, which we consider are exact and general, and from which we can obtain some understanding of defect structures and of how transformations and diffusion occur.

Formerly it used to be almost impossible for us to imagine how a complex crystal is formed, but now there is a glimmer of hope. If we assume that Nature treads well

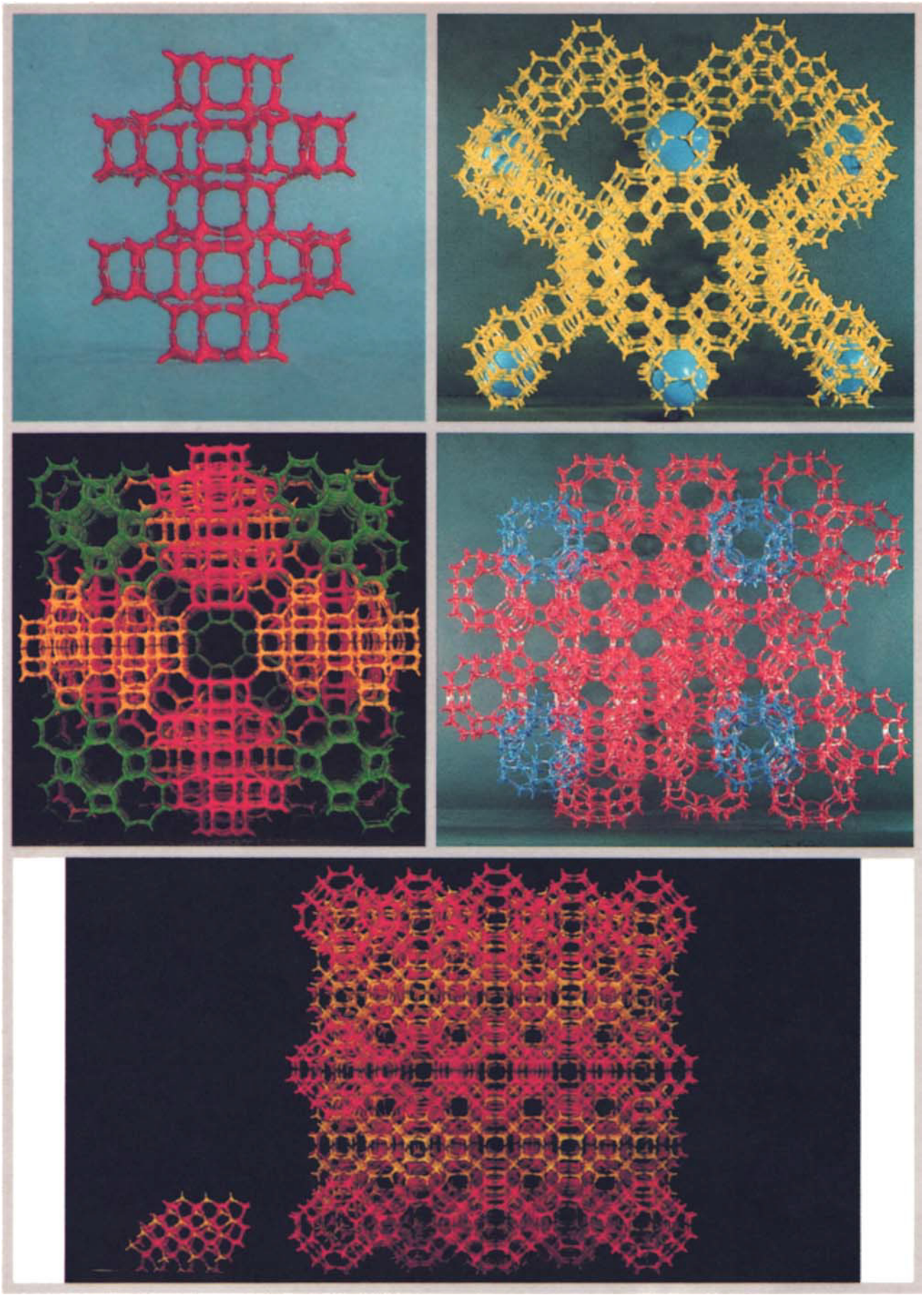
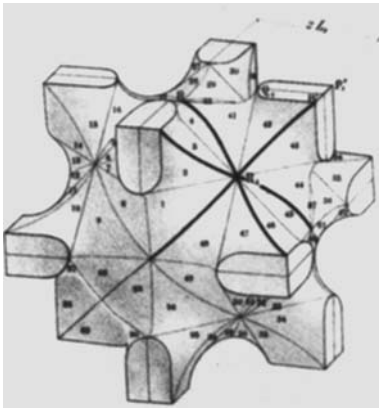
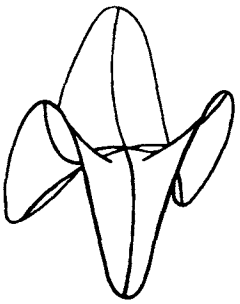


Fig. 20. Top left: A model of a packet of atoms (only silicon atoms are shown) taken out from the fourling center in Fig. 19.—Center left: The paulingite structure.—Top right: The sodalite part of the zeolite N structure. Blue spheres mark the unit cell.—Center right: The ZK5 part of the zeolite N structure. The blue units (identical with red) mark the unit cell. Bottom: The complete structure of zeolite N. A model of quartz in the left corner has been included for the purpose of comparison.

known paths, *e.g.* she builds parts of simple structures first, and then uses the classical symmetry operations, or periodic minimal surfaces, to build complex structures, we begin to feel a sense of excitement at understanding something of the phenomenon.





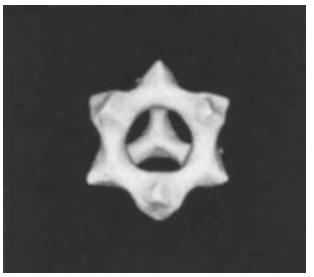


Fig. 21. Top: The *Neovius* minimal surface. The saddle lines of Hilbert's monkey saddle are indicated.—Bottom right: A monkey saddle after Hilbert which builds the surface on which we believe ion exchange, catalysis and molecular sieve reactions occur in structures of, *e.g.*, the faujasite type.—Bottom left: The D minimal surface as formed in the region between the interpenetrating structures of the $W_3Fe_3C$ structure (cf. Fig. 5).

Can we explain why complex structures exist? The achievement of an energy minimum is the plausible but not very helpful answer. The energy minimum is necessary, but is it enough?

It is clear that the transformations discussed above seem to be invariant, or nearly so, and since Nature aspires to attain maximum symmetry we suggest that she prefers complex structures to coexisting phases. We notice that complex structures like $Cu_4Cd_3$ are better packed than the metals, which means that the minimal surface in the interface region contains atoms with very efficient packing. It is here, in the interface region that the five-membered ring or icosahedral packing occurs in the structure.

Having worked on the methods for the description of structures, and having had a very straightforward application in the solution of the giant structure of zeolite N, we are unable to resist making a more human and exultant conclusion: We feel we can at least challenge Nature and solve whatever she is able to repeat.

*This work was supported by the Swedish Natural Science Research Council. I thank Prof. H. G. von Schnering, Dr. W. Hönle (Stuttgart) and Dr. F. J. Lincoln (Western Australia) for a critical reading of the manuscript.*

Received: September 27, 1982 [A 443 IE]
German version: *Angew. Chem. 95* (1982) 67

[1] H. G. von Schnering, *Angew. Chem. 93* (1981) 44; *Angew. Chem. Int. Ed. Engl. 20* (1981) 33.
[2] A. Simon, *Angew. Chem. 93* (1981) 23; *Angew. Chem. Int. Ed. Engl. 20* (1981) 1.
[3] R. Hoppe, *Angew. Chem. 93* (1981) 64; *Angew. Chem. Int. Ed. Engl. 20* (1981) 63.
[4] W. Bronger, *Angew. Chem. 93* (1981) 12; *Angew. Chem. Int. Ed. Engl. 20* (1981) 52.
[5] B. Chabot, K. Cenzual, E. Parthé, *Acta Crystallogr. A 37* (1981) 6.
[6] G. D. Birkhoff: *Aesthetic Measure*, Harvard University Press, Cambridge MA, USA, 1933.
[7] S. Andersson, W. G. Mumme, A. D. Wadsley, *Acta Crystallogr. 21* (1966) 803.
[8] M. O'Keeffe, S. Andersson, *Acta Crystallogr. A 33* (1977) 914.
[9] H. Bärnighausen, *Match (Commun. Math. Chem.) 9* (1980) 139.
[10] J. G. Allpress, J. V. Sanders, A. D. Wadsley, *Acta Crystallogr. B 25* (1969) 1165.
[11] J. O. Bovin, L. Douxing, L. Stenberg, H. Annehed, *Proc. 10th Int. Congr. Electron Microscopy*, Hamburg *1981*, 55.
[12] R. Gruehn, W. Mertin, *Angew. Chem. 92* (1980) 531; *Angew. Chem. Int. Ed. Engl. 19* (1980) 505.
[13] L. Stenberg, *Acta Crystallogr. A 35* (1979) 387.
[14] a) S. Andersson, B. G. Hyde, *J. Solid State Chem. 9* (1974) 92; b) J. M. Thomas, *Ultramicroscopy 8* (1982) 13.
[15] E. Parthé, *Acta Crystallogr. B 32* (1976) 2813.
[16] S. Andersson, C. Leygraf, T. Johnsson, *J. Solid State Chem. 14* (1975) 78.
[17] L. Stenberg, *J. Solid State Chem. 28* (1979) no. 3.
[18] L. Stenberg, *Chem. Scr. 14* (1978/79) 219.
[19] L. A. Bursill, B. G. Hyde, *Nature (London) Phys. Sci. 240* (1972) 122.
[20] S. Andersson, *J. Solid State Chem. 23* (1978) 191.
[21] S. Andersson, L. Stenberg, *Z. Kristallogr. 158* (1982) 133.
[22] A. Simon, *Z. Anorg. Allg. Chem. 422* (1976) 208.
[23] S. Andersson in M. O'Keeffe: *Structure and Bonding in Crystals, Vol. II*, Academic Press, New York 1981, p. 233.
[24] E. K. Gordon, S. Samson, W. B. Kamb, *Science 154* (1966) 1004.
[25] S. Andersson, L. Fälth, *Z. Kristallogr.*, in press.
[26] S. Hansen, L. Fälth, S. Andersson, *J. Solid State Chem. 39* (1981) 137.
[27] L. Fälth, S. Andersson, *Z. Kristallogr.*, in press.
[28] S. Andersson, B. G. Hyde, *Z. Kristallogr. 158* (1982) 119.
[29] A. Schoen, *NASA Tech. Note D-5541* (1970) 1-98: Infinite Periodic Minimal Surfaces without Self-Intersections.
[30] E. R. Neovius: *Bestimmung zweier speziellen periodischen Minimalflächen*, J. C. Frenckel, Helsingfors 1883.
[31] D. Hilbert, S. Cohn-Vossen: *Geometry and the Imagination*, Chelsea, New York 1952.
[32] L. E. Scriven, *Nature (London) 263* (1976) 123.
[33] a) A. L. MacKay, *Izvj. Jugosl. Centr. Krist. (Zagreb) 10* (1975) 15; b) *IUC* Copenhagen, August 1979.
[34] K. Larsson, K. Fontell, N. Krog, *Chem. Phys. Lipids 27* (1980) 321.
[35] K. Fontell, *Mol. Cryst. Liq. Cryst. 63* (1981) 59.
[36] S. Andersson, L. Fälth, unpublished.

# Preparation of Solid-State Compounds by Chemical Transport—Interpretation and Control Using the Cooperative Transport Model**

**By Reginald Gruehn* and Hans-Jürgen Schweizer**

*Dedicated to Professor Harald Schäfer on the occasion of his 70th birthday*

The demand of solid-state chemists for a method capable of producing interesting solids in a reproducible way is not easily fulfilled. It is well-known that data published on the synthesis of new compounds are often irreproducible after some time—even within the same research group. Some progress has been made by the development of the chemical transport method, which for relatively straightforward cases also allows predictions to be made about suitable experimental conditions. But for complicated phase relationships, and compounds of only slightly differing composition and stability, the experimental conditions could hardly be predicted. Here we present a more advanced transport model, which allows the prior determination of favorable experimental conditions for the preparation of various solids even in complicated systems, based on thermodynamic data. The usefulness of the method is shown using as examples complex systems of binary and ternary metal oxides.

## 1. Introduction

The synthesis of inorganic solids is often associated with considerable problems for the chemist, be it that high-melting substances are difficult to induce to react or that they exhibit a particular sensitivity towards moisture, oxygen, or special impurities, which complicate their manipulation. Among the oldest methods of solid-state synthesis is the reaction of a mixture of components at elevated temperatures[1], a technique which is still widely used, *e.g.* for the preparation of high-melting ceramic materials. The completeness of the reaction sought, *i.e.* the establishment of a state of equilibrium ("equilibration") demands especially high temperatures because of small diffusion coefficients and relatively large diffusion distances (grain size!). Besides a limited choice of temperature no other experimental parameters are available for a direct thermodynamic control of this relatively "crude" preparative method, because the reaction paths are mostly unknown. However, when a solvent phase is present the synthetic methods become comprehensible and more variable; even without detailed calculations they generally give useful information for a directed synthesis based on simple thermodynamic models[2]. Products yielded in this way are mostly crystalline and sometimes even form as large single crystals.

A variety of possibilities is opened up if we use the gas phase as solvent for solids. We are indebted to *Harald Schäfer* for the first detailed description of this field; in his monograph[3] he presented a generally useful concept for the wide-ranging application of "chemical transport reactions", as he called them (cf. Section 2.1). In the laboratory, transport experiments in sealed ampoules are especially useful and we shall discuss this method in particular. For many classes of compounds *Schäfer*[3] showed that chemical transport has clear advantages compared to other preparative methods[2]:

1) Promotion of the reaction ("mineralizer" effect of the transport gas) by increasing the mobility of the building elements of the reactants.
2) Avoidance of formation of impeding coatings; removal of the reaction product or of impurities due to differential migration in the temperature gradient leads to purifying effects.
3) Relatively low reaction temperatures allow both the preparation of compounds which are only stable at moderate temperatures and the formation of "metastable" phases.
4) Formation of well-formed crystalline samples (Fig. 1) and single crystals in suitable sizes for X-ray investigations ($\leq 1$ mm), without special precautions.
5) The extensive reversibility of the heterogeneous reaction facilitates the determination of reproducibile procedures for the synthesis of a substance.
6) The use of suitable equilibrium gas-phases allows the preparation of single-phase compounds with homogeneity ranges.

Furthermore, observations from preparative experiments, *e.g.* whether a reaction actually occurs or not, can give qualitative indications of unknown gaseous species (gas complexes), of kinetic inhibitions of heterogeneous reactions in the condensed phase, and of the thermodynamic parameters of the synthesis. The reaction process in complicated systems, however, can only be comprehended by a complete thermodynamic analysis with the inclusion of all relevant constituents[10]. The aim of this progress report is, therefore, to provide an introduction to the thermodynamic description of steady transport states in systems with closely neighboring phases and to present the various

[*] Prof. Dr. R. Gruehn, H.-J. Schweizer
Institut für Anorganische und Analytische Chemie der Universität
Heinrich-Buff-Ring 58, D-6300 Giessen (Germany)

[**] The model was developed in the dissertation presented by H.-J. Schweizer (Universität Giessen 1983).

 © Verlag Chemie GmbH, 6940 Weinheim, 1983 0570-0833/83/0202-0082 $ 02.50/0 

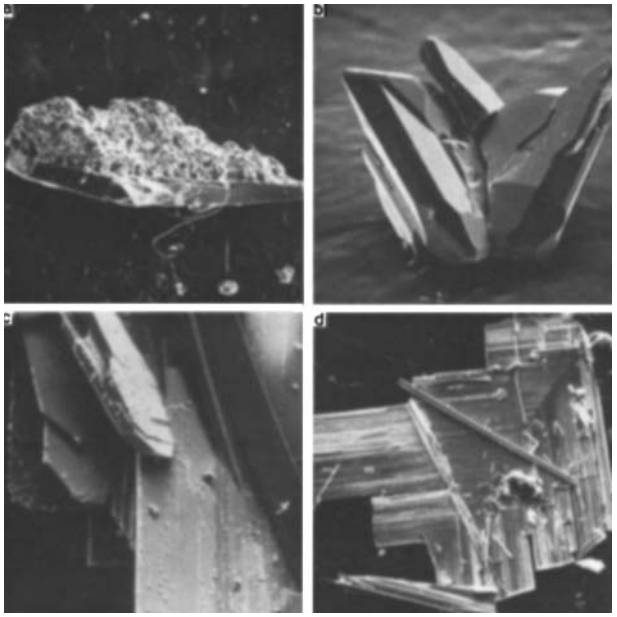


Fig. 1. Crystal growth by chemical transport (scanning electron microscope photographs). a) Cristobalite (top) as a product of recrystallization of quartz glass (ampoule wall, below); effect of $NbCl_5$; 1100 °C; enlargement × 36. b) $Ti_6O_{11}$ as an example of a Magnéli phase [4]; deposited in the less hot zone from the gas phase at 920 °C; transport agent: HCl [5]; enlargement × 155. c) $LaNb_3O_9$ (metastable) as an example of a novel structural type [6]; the same as b), but at 980 °C; transport agent: $Cl_2$ [7]; enlargement × 115. d) $Nb_{12}O_{29}$ (orthorhombic), because of its "block structure" especially well suited for high resolution transmission electron microscopy (TEM) [8, 9]; the same as b), but at 1000 °C; transport agent: $Nb_3O_7Cl(NbCl_5)$; enlargement × 66.

possibilities offered by our transport model as exemplified by several transport systems which have been studied experimentally (cf. also [11–16]).

## 2. Recent Developments

### 2.1. Fundamentals

The prerequisite for chemical transport is a reversible reaction of solid A, to be transported, with a transport agent B, which under the experimental conditions is gaseous [eq. (1)]. Only gaseous products should be formed:

$$a\,A_s + b\,B_g \rightleftharpoons c\,C_g(+ d\,D_g \ldots) \qquad (1)$$

If a closed tube (transport ampoule), which can be thought of as being divided into two subvolumes I and II (Fig. 2), contains a solid phase A which has different chemical potentials in I and II, migration of A is expected to occur in the direction of the potential drop. For a temperature gradient between the subvolumes (the lower temperature is usually termed $T_t$[3]) the sign of the enthalpy of reaction $\Delta_R H$ is decisive for determining the direction of migration. For an endothermic transport reaction the solubility of A in the gas phase increases with temperature. Therefore, A is transported from $T_2$ to the less hot zone at $T_1$ (subvolume I). The solubility can be determined from the equilibrium pressures at $T_1$ and $T_2$, *e.g.* by means of the transport equation [eq. (1)] or by using a system of independent reaction equilibria ($K_p$ method, cf. Section 3.1).

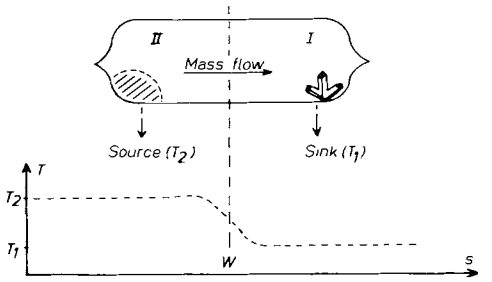



Fig. 2. The principle of chemical transport in a closed tube (transport ampoule) illustrated by an endothermic transport reaction. Due to the different temperatures, the tube can be considered as being divided into two equilibrium volumes (subvolumes I, II) by a hypothetical wall (W). The resulting mass flow of the deposit [*e.g.* A in eq. (1)] is obtained by addition of the gas flows of B (I ⟶ II) as well as C and D (II ⟶ I).

The calculation of the transport rate $n$(A) (cf. Table 1) follows a model which, after establishment of equilibrium in I and II, assumes a steady-state gas flow between the subvolumes due to diffusion (if necessary superposed by a flow due to a change in the number of moles in the transport reaction) after reaching the equilibrium state[3]. The resulting *steady-state* is characterized by the fact that the flows of the source elements (source→sink) correspond to the composition of the precipitated solid. For the calculation of equilibria and transport rates it must generally be assumed that no kinetic inhibitions, *e.g.* of the heterogeneous reaction, occur.

Table 1. Transport of niobium oxides from $SiO_2/NbO_x$-sources ($100/2 \times 10^{-3}$ mol); transport agent $NbCl_5$ ($1.25 \times 10^{-4}$ mol); tube volume ≈ 14 cm³ (∅ = 1.5 cm), $\Sigma P = 3$ atm; deposition temperature = 1300 K; $(T_2 - T_1) = 100$ K.

| Source ($T_2$)<br>Equilibrium phases | Sink ($T_1$)<br>Transported phases[a] | Reduced transport rate ($n_r \times 10^4$)[b]<br>Calculated | <br>Observed |
|---|---|---|---|
| $SiO_2/Nb_{12}O_{29}$ | $Nb_{12}O_{29}$ | 2 | 1 |
| $SiO_2/Nb_{12}O_{29}/NbO_{2.024}$ | $Nb_{12}O_{29}$ | 1 | 2 |
| $SiO_2/NbO_{2+\Delta x_2}$ | $NbO_{2+\Delta x_1}$[c] | 3 | 2 |
| $SiO_2/NbO_2/NbO$ | $NbO_2$ | 5 | 4[d] |
| $SiO_2/NbO$ | NbO | 0.2 | < 0.1[e] |

[a] The model calculation yields the phases at $T_1$ under the assumption that deposition of $SiO_2$ at $T_1$ is inhibited. These phases are also obtained in the experiment. [b] Reduced transport rate $n_r = \Delta P/\Sigma P$; transport rate according to *Schäfer* [3]: $n(A) = \frac{c}{a} \cdot \frac{\Delta P}{\Sigma P} \cdot \frac{T^{0.8} q}{d} \times 1.8 \times 10^{-4}$ [mol h$^{-1}$] (with $T = \frac{T_1 + T_2}{2}$[K]; $q$[cm²] = diameter of the diffusion distance with length $d$ [cm]; a, c = stoichiometry coefficients [eq. (1)]). [c] $\Delta x_2 < \Delta x_1$ ($\Delta x_2 < \varepsilon \Rightarrow \Delta x_1 \leq 0.024$ [68], $\Delta x_2 > \varepsilon \Rightarrow$ transport of $Nb_{12}O_{29}$; for all cases with $\varepsilon = 0.01$, see text). [d] Deposition of α- or β-$NbO_2$ (cf. Section 4.5). [e] The minimal endothermic transport of NbO was also observed by *Schaum* [62] ($\Sigma P \approx 5$ atm, $T_2 = 1400$ K, $\Delta T = 200$ K).

### 2.2. Additional Preparative Possibilities

New transport agents which are optimally adjusted thermodynamically to the reacting solids are of great interest. The investigation of *gaseous halide complexes*, chiefly by *Schäfer*[17-19], has led to considerable advances here.

Highly volatile (monomeric or dimeric) trihalides ($AlX_3$, $GeX_3$, $FeX_3$...) are particularly suitable complexing agents. If the mobility of the metal component M of the solid in a transport system is considerably limited by the low saturation pressures of the halides $MX_n$, the resulting "labile" halide complexes, whose formation and dissociation proceed without kinetic inhibition, make the metal halide $MX_n$ available in high concentrations. By means of this method [transport agent $Al_2Cl_6$; eq. (2)] many metal halides can be transported and thus obtained as single crystals at relatively low temperatures. (400 °C→350 °C[18]).

$$MCl_{2,s} + Al_2Cl_{6,g} \rightleftharpoons MAl_2Cl_{8,g} \qquad \Delta_R H > 0 \qquad (2)$$

M = Mg, Ca, Cr, Mn, Fe, Co, Ni, Cu, Pd, Pt[18]

By analogy, transport agents and complexing agents (halides, hydrogen halides) can be combined for the chemical transport of metals, oxides and chalcogenides[17].

For the growth of *single crystals*, *e.g.* for X-ray structure analysis, the transport method is especially useful when purely thermal processes, such as sublimation or flux techniques, fail for thermodynamic reasons. Thus larger crystals of only slightly thermally stable anhydrous sulfates were obtained, especially those of the transition metals ($Mn^{II}$, $Fe^{II}$, $Fe^{III}$, Co, Ni, Cu, Zn, Cd, Hg, as well as Pb), deposition occurring in the less hot zone (transport agents $Cl_2$, HCl, $HgCl_2$)[20-22]. Another example which shows the advantage of a decrease of the reaction temperature is the chemical transport of fluorides ($AlF_3$, $FeF_3$, $TiF_3$[23], $ScF_3$[24]) with $SiCl_4$.

Preparatively and structurally interesting *metastable* compounds usually remain inaccessible at high reaction temperatures (solid-state reaction). Their formation, however, is considerably supported by low deposition temperatures, imbalanced states (*e.g.* for small $\Sigma P$), or by additives ("impurities"). The competing solid phases differ only slightly in their energy contents, so that nucleation and nuclear growth increase in importance[2,25]. Examples of polymorphism are the various modifications of $Nb_2O_5$[26], $TiO_2$, as well as chalcogenides (ZnS, $NbS_2$)[25]. Metastable compounds have also become accessible in the systems La/Nb/O/Cl[7], Fe/Nb/O/Cl[27], and $NbO_2/NbCl_5$[28]. Even a slight difference in the composition of the metastable solid relative to that of a more stable phase can be taken advantage of. In these cases states of deposition and/or formation with minimal free energy (Gibbs' energy) can be realized[28,29] by choice of suitable gas phase compositions (cf. Section 4.5).

The remarkable physical and chemical properties of *nonstoichiometric* compounds make them a favorite subject for preparative investigations[30-35]. The preparation of nonstoichiometric metal oxides or sulphides by chemical transport in a complex system with a close sequence of phases, generally only leads to reproducible results if the thermodynamics of reactions of the neighboring phases and the transport agent are known. Even small changes in the experimental conditions (temperature gradient, amounts of transport agent, volume of the ampoule) can lead to deposition of heterogeneous solid phases or to other phases of the system (*e.g.* the system Ti/O/HCl[16]; Section 4.2). By choosing suitable starting materials and by fixing the free variables of the transport system (thermodynamic calculation!) it is possible, however, to set up steady transport states which permit continuous crystal growth of the desired phase[28].

Solids with homogeneity ranges show particularly impressively the dependence of the composition of the deposited phase on the composition of the solid in the source subvolume, which in turn depends on the increase or decrease in concentration of elements due to the transport process. These problems were treated in exemplary fashion by *Krabbes et al.*[36] for the transport of $FeS_x$ with $I_2$ ($1 < x \leq 1.15$).

### 2.3. Progress in the Thermodynamic Description

In systems with several closely neighboring phases the calculation of the chemical transport of the *outer phases* ("border phases", cf. Fig. 3) can still be carried out straightforwardly[3] if the formation of solid neighboring phases is excluded by the choice of an appropriate transport agent (TA). Model calculations for "inner phases" are difficult since, due to their limited range of stability (Fig. 3), these phases are easily converted under the experimental conditions into heterogeneous mixtures.

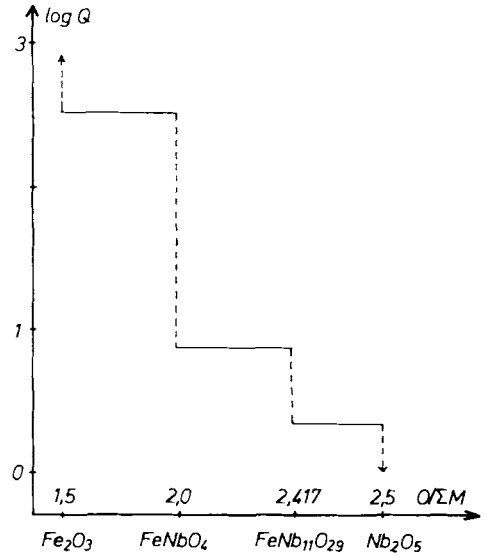



Fig. 3. Isotherm diagram ($T = 1400$ K) for the system $Fe_2O_3/Nb_2O_5/Cl_2$ [27]; ------ = single phase, ——— = two-phase regions; outer phases (border phases): $Fe_2O_3$; $Nb_2O_5$; inner phases: $FeNbO_4$; $FeNb_{11}O_{29}$; O/ΣM is not plotted to scale; $Q = P(FeCl_3)/P(NbOCl_3)$ is defined by the exchange reaction [*e.g.* eq. (4)].

For ternary oxide systems having two binary border phases and one ternary (inner) phase, qualitative rules were first discussed by *Emmenegger*[37]. If the stability of the ternary oxide is comparatively large compared with that of the binary oxides [$\Delta_B G°$(ternary) $\ll \Sigma \Delta_B G°$(binary)], its chemical transport can be treated mathematically

like that of binary oxides ($NiFe_2O_4/HCl$[38]). The composition of the equilibrium gas phase over a homogeneous ternary solid phase of sufficient stability is then variable over a wide range (Fig. 3), so that it can actually be adjusted to a composition which corresponds to the stoichiometry of a transport reaction or a complex system of equations. In consequence, the ternary solid phase remains undecomposed and can be transported as a single phase. However, for the majority of the systems investigated (*e.g.*[7, 16, 27, 28, 39–43]), because of its poor stability the ternary phase becomes heterogeneous in the reaction with the transport gas.

*Wehmeyer*[39] and *Schäfer*[25, 43] treated in detail the possibilities of preserving a homogeneous ternary solid phase during transport experiments. Basically, all statements of *Schäfer*'s transport model depend strictly on the existence of the same condensed phase in both source *and* sink. The partial decomposition of a ternary compound leading to formation of one of the neighboring phases must therefore be prevented by adjusting the experimental conditions, such as temperature, amount of transport agent, or by shifting the equilibrium by adding a gas-phase constituent as well as, if necessary, by the use of another transport agent[43]. The thermodynamic basis for this concept is the equation for the free energy $\Delta_R G$ of the transport reactions of the participating binary border phases:

$$\Delta_R G = \Delta_R G^0 + RT \ln \prod_i P_i^k \qquad (3)$$

The $\Delta_R G$ values indicate whether the ternary compound under consideration remains stable ($\Delta_R G < 0$) (calculated from a suitable set of equations) in presence of its gas phase ($P_i$; $i = 1, \ldots$), or whether decomposition ($\Delta_R G > 0$) is to be expected. If, however, a constituent of the gas phase is added to the transport gas for the stabilization or formation of a single-phase solid, the establishment of a steady-state mass flow between source and sink must be redefined (see below), since the stoichiometry of the gas phase is no longer equivalent in the two subvolumes I and II. In the description of the transport of stable binary compounds ("border phases") it is usually assumed that the gas flow has reached a steady state.

The variable stoichiometry of the gas phase in the transport system causes an additional degree of freedom[27, 44]. Besides the difficulty of suitably fixing this degree of freedom with respect to the starting composition, it is also increasingly more problematic (with increasing number of simultaneous transport reactions) to use $\Delta P_i$ (Table 1) as a measure of the transport effect. We must, therefore, differentiate more strongly between the determination of the transport rate $n$(A) and the equilibrium calculation. This is achieved, in general, by using the concept of solubility $\lambda$ of the solid phase (cf. Fig. 4)[45–47]. *Schäfer* determined $\lambda$ from the ratio of the number of moles of the solid dissolved in the gas phase to the amount of solvent. The transport rate $n$(A) is calculated using the solubility difference $\Delta\lambda(A) = \lambda(T_2) - \lambda(T_1)$ of the solid phase A in source ($T_2$) and sink ($T_1$) (cf. [47]).

Since reaction of the starting phase with the transport gas frequently leads to formation of heterogeneous materials, two-phase material is used to start the reaction. The

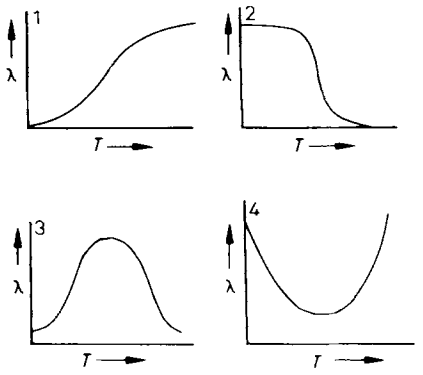



Fig. 4. Solubility $\lambda$ of the solid in the gas phase as a function of temperature ($\Sigma P$ = const.) after *Schäfer*[18]; 1) endothermic, 2) exothermic transport reaction [eq. (1)]; 3) solubility maximum, 4) solubility minimum obtained by combining endothermic and exothermic processes.

composition of the transporting gas phase can, therefore, be adjusted precisely, even in systems with closely neighboring phases (buffer effect of the solid phases), such that constant conditions for the growth of single crystals are established. The isothermal source-equilibria can be described approximately by suitable exchange reactions (after *Gruehn*[40, 48] and *Brunner*[27]), which determine the coexistence of two neighboring phases in multicomponent systems, *e.g.* in the system $Fe_2O_3/Nb_2O_5$[27] (Fig. 3):

$$FeNb_{11}O_{29,s} + NbOCl_{3,g} \rightleftharpoons FeCl_{3,g} + 6\,Nb_2O_{5,s} \qquad (4)$$

$$Q = \frac{P(FeCl_3)}{P(NbOCl_3)}$$

The characteristic composition of the equilibrium gas phase above the heterogeneous solid materials, as well as its width of variation with respect to the range of stability of a single phase compound can be clearly represented by the ratio $Q$ of the partial pressures of the reacting gases ($FeCl_3$, $NbOCl_3$) in an isotherm diagram (Fig. 3). If, however, the solid phases have a range of homogeneity, the situation becomes much more complicated (cf. [50]).

Firstly *Schäfer*[51] and then *Gruehn et al.* tried to derive criteria for the transport of well-defined phases from heterogeneous starting materials using *intersections of the isotherms* of both equilibrium spaces ($T_1$, $T_2$; Fig. 5). The $Q$ values obtained by this graphical method for the deposition subvolume (sink; $T_1$) correspond to a composition of a "metastable" gas phase at $T_1$ ($[Q(T_1)]_*$). The correlated position of equilibrium $Q(T_1)$, has to be determined accurately. This can lead to substantial deviations from the graphically determined phase relations in the sink ($T_1$; Fig. 5).

By considering only diffusion in the absence of laminar flow, *Brunner*[27] successfully used the condition of steady-state transport for the calculation of the previously unknown equilibrium value $Q(T_1)$ for the deposition of iron(III) niobates using $Cl_2$ as transport agent (cf. Section 4.1.2). Independently of this, *Oppermann et al.*[33, 44] discussed a transport model, which allows both gas diffusion and laminar flow of the total gas mass because of changes in the number of moles in the heterogeneous reaction in sink and source. This method also requires information on the nature and number of solid equilibrium phases in at

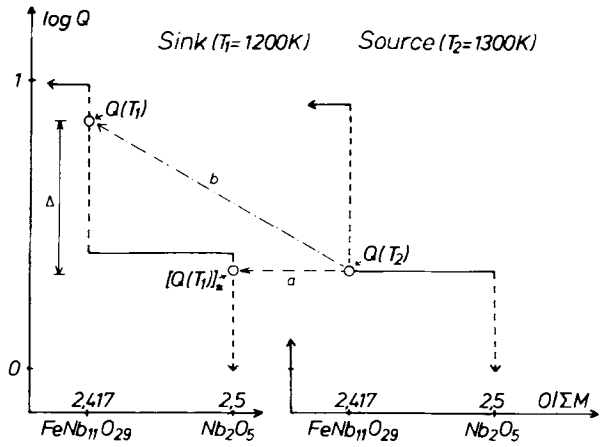



Fig. 5. Isotherms ($T_1$; $T_2$) for the subsystem $FeNb_{11}O_{29}/Nb_2O_5$ [27]. With heterogeneous material at $T_2$ [eq. (4)] the intersecting arrow *a* leads to a metastable gas phase at $T_1$: the arrow *b* indicates the position of equilibrium calculated for $T_1$; for further details see legend to Fig. 3. In the system $AlNb_{11}O_{29}/Nb_2O_5$ [49] the arrow *a*, however, leads to the $AlNb_{11}O_{29}$ region.

least one subvolume; the composition of equilibrium phases in the other subvolume is then determined iteratively using a suitable system of equations, taking into account the conditions of steady-state transport.

## 3. Extended Transport Model for Experiments with Heterogeneous Source Materials

### 3.1. Isothermal Calculation of Equilibria

For the description of chemical transport the result of an isothermal calculation on the position of equilibrium at $T_1$ and $T_2$ is, in general, required. This calculation includes all gaseous and solid constituents *b* which participate in the transport, and which can be formed from the various components *k* of the chemical system under consideration. It should be noted that the number of components *k* is not necessarily identical to the number of elements in the particular system (cf. c).

In general, the equilibria are determined using a system of linearly independent reaction equations, *i.e.* using the equilibrium constant method ($K_p$ method)[41,43,52-54] (*e.g.* computer program GEPA[55]). The use of the $K_p$ method is associated with several assumptions:

a) The nature and number of equilibrium phases *p* must be known, but not necessarily be identical to the phase relations in the initial state;
b) the determination of "stoichiometric" degrees of freedom $f_s$ of the gas phase is dependent on the distribution of elements in the initial and equilibrium states (newly formed phases!);
c) the number of linearly independent reaction equations e is determined by an at first "unknown" number of components k ($e = b - k$).

Whereas the successful establishment of a suitable system of equations [cf. c)] is mainly dependent on experience in using this method, the requirements a) and b) are a matter of principle, since they consider the *problems in relating* experimental to calculated equilibrium states. Especially in systems with closely neighboring phases, the determination of the nature and number of solid equilibrium phases is (in the case of the $K_p$ method) only possible *experimentally, e.g.* using a series of experiments with variable amounts of transport agent. An impedement here is that thermodynamically stable phases might not be formed due to (unknown) kinetic reasons. In addition to this [in systems with several degrees of freedom ($f > 2$)], constraints (*e.g.* pressure equation) on the determination of the "stoichiometric" degrees of freedom of the gas phase with respect to the initial experimental state have to be located.

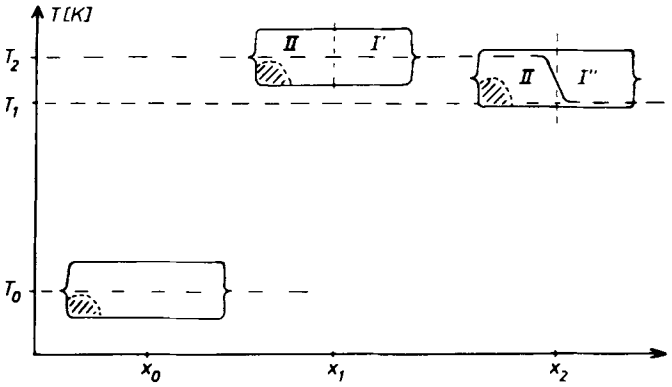



Fig. 6. Model experiment for an endothermic transport process. For the division into subvolumes I and II see legend to Fig. 2: $x_0$, start of experiment at $T_0 = 298$ K; $x_1$, isothermal initial state at $T_2$; $x_2$, metastable initial state (for $T_1$).

Mass-equivalent changes of initial states ($x_0$ in Fig. 6) to afford corresponding equilibrium states ($x_1$) can be unequivocally calculated for closed systems using the free energy function ($\Sigma P, T = \text{const.}$), considering both *mass balances* and the ability of all the solid phases to exchange (Gibbs' phase rule). The numbers of moles $n_i$ and partial pressures $P_i$ of all constituents in the equilibrium phases as a function of the quantitative initial composition $n_i^0$ can be calculated by means of the program EPCBN[56-59], which uses the free energy minimum, *i.e. the G(min) method.* The basic mass balance of the elements in the closed system is to be strictly maintained in each phase of the iterative determination of $G$(min).

On fixing $\Sigma P$ and $T$, the values of the system variables p and $f_s$ are clearly limited by the number of components k of the system ($p + f_s \leq k$). With k equations for mass balances, which are fixed using the initial numbers of moles of the participating elements (≙the experimental initial state $x_0$), all "stoichiometric" degrees of freedom of the gas phase ($f_s \leq k - 1$) can be determined. Due to this property of mass balance, the criterion $G$(min) ($T, \Sigma P = \text{const.}$) allows the determination of the solid equilibrium phases (according to the phase rule) independently of the nature and number of the initial phases.

### 3.2. Thermodynamic Treatment of the Complete Model Experiment

In the simplest case the interpretation of the reaction process in chemical transport experiments is based on the assumption that the reaction of a *single phase* starting ma-

terial (border phase) with a given transport agent leads to an equilibrium gas-phase composition corresponding to the stoichiometry of the transport equation [eq. (1)]. For reversible heterogeneous reactions this also holds for the deposition side, so that the resulting partial pressure differences $\Delta P_i$ of relevant gas particles between source and sink behave like the stoichiometry coefficients (c,d...) in the transport equation. The flow of the source elements thus corresponds to the composition of the initial phase; the conditions of steady-state transport are, therefore, fulfilled.

In all other complicated cases (see *e.g.* Section 2.3), especially if *two-phase* materials are present in *one* of the subvolumes, the above assumption about the relationship between $\Delta P_i$ and the stoichiometry coefficients (c,d...) in the gas phase of the subvolumes no longer applies. For the calculation of the position of equilibrium in the subvolume with fewer phases an additional variable of the gas phase [*e.g.* $Q(T_1)$] must be fixed by considering the conditions of steady-state transport (Section 2.1).

According to Section 3.1 the unequivocal calculation of isothermal equilibria using the $G$(min) method is based on information about the initial states. Statements about the nature of initial state in the deposition subvolume (the subvolume with fewer phases) can be deduced from the course of a model experiment (Fig. 6).

I') is then brought to temperature $T_1$ ($x_2$). In the "metastable" initial state ($x_2$) the composition of the gas phase at $T_1$ in the sink (I'') is identical to that of the equilibrium gas phase at $T_2$ (source). In the model experiment solid precipitates from the supersaturated mother gas phase by establishment of a stable equilibrium state at $T_1$.

For closed systems the previously outlined isothermal change of state can be unambiguously calculated using the free energy function (program EPCBN) (Fig. 7). The determination of the position of equilibrium in the sink (I) by means of the number of moles in the equilibrium gas phase in the source (II) allows the determination of the resulting steady-state mass exchange (diffusion and laminar flow) according to *Schäfer*'s[47] model of solubility. The basis of this method is the conservation of mass for the isothermal, isobaric equilibration in the deposition volume, which is consistent with the steady-state flow of the elements of the solid between the subsystems (cf. Section 2.1 and [58–60]). The *cooperative transport model* describes this steady transport state by coupling the two subvolumes *via* identical mass balances of the gas phase of the source and the resulting equilibrium gas phases at $T_1$, as shown in Figure 7. In this model a special preference is assigned to the labile equilibria in the deposition volume for the establishment of steady transport states. The model, therefore, does not depend on the nature and number of phases in the source

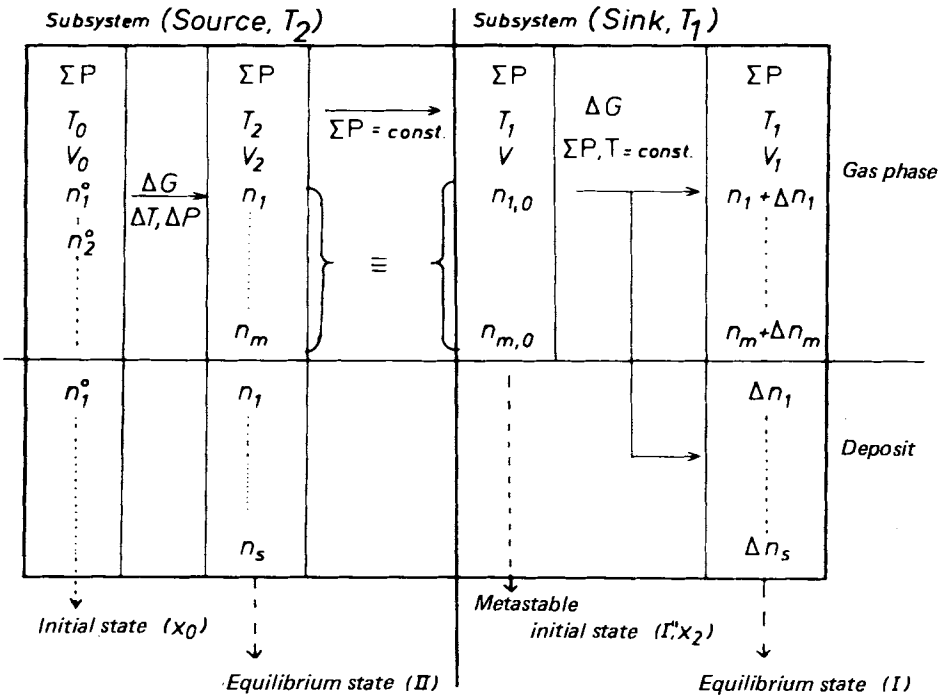



Fig. 7. Scheme of the thermodynamic calculation on the basis of the model experiment (Fig. 6). The equilibration in the individual subvolumes is considered; furthermore the identity of the material of the metastable initial state in the sink and the equilibrium gas phase of the source is taken into consideration.

*Model experiment:* In the first step ($x_1$) the complete transport system is heated from the initial conditions ($x_0$) to temperature $T_2$; one half of the transport ampoule (sink subvolume (II). Also that solid phase is deposited which shows a minimum in the free energy of deposition with respect to subvolume I.

### 3.3. Aids in Interpretating the Thermodynamic Results

*Isotherm diagrams* ($\log Q$ *vs.* composition, cf. Section 2.3, Figs. 3 and 5) are well suited for a clear presentation of stability relationships based on thermodynamic data. Beyond this, these isotherms can also be used for graphical interpretation of the thermodynamics of transport reactions. Statements about experiments with the following questions are possible:

1) Predictions about stability or decomposition of single phase solids in the presence of a transport agent by comparison of the value of $\log Q$, derived from a suitable transport equation, with the form of the $\log Q$-isotherms of the system ($T$, $\Sigma P$ = const.).
2) Approximate determination of equilibrium temperatures for the conversion of a single phase starting solid into a two-phase equilibrium source material (cf. Section 4.2).
3) Transport behavior of heterogeneous source materials.
4) Comparison of different transport agents. A prerequisite for the continuous deposition of single phase material is the suitable choice of thermodynamic parameters ($T$, $Q$, and $\Sigma P$) as well as a mass flow of sufficiently high intensity between source and sink [$n$(A)]. The $Q(T_1)$ value of the sink and the deposition rate $n$(A) are, therefore, suited for an evaluation of different transport agents, if these quantities are normalized to equivalent thermodynamic conditions (amount of solvent, $T$, $\Sigma P$, $\Delta T$).

## 4. Use of the Cooperative Transport Model for the Interpretation of Experimental Results

### 4.1. Preparation of Single-Phase Substances from Heterogeneous Source Materials

#### *4.1.1. Binary Solids—The Chemical Transport of Niobium Oxides; Transport Agent $NbCl_5$*

*Fundamentals:* The preparation of the niobium oxides NbO and $NbO_2$ in pure, coarsely crystalline form was first described by *Schäfer* and *Huesker*[51]. *Gruehn* was able to prepare pure $NbO_x$-phases (especially $Nb_{12}O_{29}$) in gram amounts by chemical transport with $NbCl_5$; a general transport reaction [eq. (5)] for the migration of the niobium oxides ($NbO_x$-phases) to the less hot zone is formulated thus[48]:

$$NbO_{x,s} + (4-x)\,NbCl_{5,g} \rightleftharpoons x\,NbOCl_{3,g} + (5-2x)\,NbCl_{4,g} \qquad (5)$$

*Schaum*[62] combined this reaction with an oxidation step and used it to interpret the transport of $NbO_2$ by $HgCl_2$. Independently of this *Ritschel et al.*[41] discussed the transport of niobium oxides by gaseous $NbCl_5$, $NbOCl_3$, and $NbCl_4$ in the system $NbO_2/Nb_{12}O_{29}/TeCl_4$. Further experimental details for the systems Nb/O/transport agent can be found in [63–65]. Our transport experiments were performed in sealed quartz glass ampoules with the usual dimensions as described in [29] (cf. also Table 2). The assignment and determination of the number of phases were carried out by X-ray analysis (Guinier method, quartz monochromator, $Cu_{K\alpha_1}$ radiation).

Table 2. Transport experiments in quartz ampoules with $NbO/NbO_2$-source materials; $NbCl_5$ as transport agent; $T_2 = 1472$ K, $T_2 - T_1 = 100$ K; ampoule dimensions: $\varnothing = 1.55$ cm, $l = 9$–$11$ cm.

| No. | Initial composition at $T_2$ (source) | | | | | $V$ | $t$ | Residue[a] | Deposit ($T_1$) precipitated | | $\Sigma P$ |
|---|---|---|---|---|---|---|---|---|---|---|---|
| | $NbO_{2.5}$ | Nb | O/Nb | $NbCl_5$ | $CO_2$ | [cm³] | [h] | at $T_2$ (source) | in the sink | | |
| | [mmol] | | | [mmol] | | | | | Phase (n) | [mg] | [atm] |
| 1 | 4.913 | 2.953 | 1.56 | 0.482 | — | 18.9 | 24 | NbO, α-$NbO_2$, β-$NbO_2$ | α-$NbO_2$ | 40 | 5.5 |
| 2 | 4.761 | 1.203 | 2.0 | 0.499 | — | 19.8 | 30 | α-$NbO_2$ | α-$NbO_2$ | 60 | 5.1 |
| 3 | 2.002 | 2.163 | 1.20 | 0.245 | — | 18.3 | 32 | β-$NbO_2$, NbO | α-$NbO_2$, β-$NbO_2$ | 30 | 2.9 |
| 4 | 7.126 | 2.771 | 1.80 | 0.460 | 0.823 | 18.5 | 36 | α-$NbO_2$ | α-$NbO_2$ | 68 | 10.3 |
| 5 | 4.409 | 2.703 | 1.55 | 0.248 | — | 18.9 | 46 | β-$NbO_2$, (NbO) | α-$NbO_2$, β-$NbO_2$ | ≈ 40 | 2.8 |
| 6 | 2.647 | 2.867 | 1.20 | 0.439 | 0.844 | 18.9 | 60 | β-$NbO_2$, NbO | β-$NbO_2$ | ≈ 100 | 10.3 |
| 7 | 3.858 | 3.028 | 1.40 | 0.483 | 0.844 | 18.9 | 75 | β-$NbO_2$, NbO | β-$NbO_2$ | 63 | 10.3 |
| 8 | 4.761 | 1.203 | 2.00 | 0.499 | — | 19.4 | 89 | β-$NbO_2$, (NbO) | β-$NbO_2$ | 180 | 5.4 |
| 9 | 7.750 | 3.139 | 1.79 | 0.098 | — | 18.9 | 144 | β-$NbO_2$, NbO | β-$NbO_2$ | 16 | 1.1 |

[a] (NbO) indicates small amounts of NbO.

According to *Scholz*[61], crystal growth procedures with constant gradients can be described using *energy term diagrams* (Fig. 14), since the crystallization process is determined by the exchange of energy between the energy state of the source material and that of the growing crystal. Here, this procedure is modified on the basis of our chemical transport model, in as far as we do not consider the free energy of isolated solid phases but of heterogeneous equilibrium states (gas + solid phases). This view point is outlined schematically for the chemical transport of β-$NbO_2$ (cf. Section 4.5).

*Thermodynamic Calculations:* Because of reliable thermodynamic data, transport experiments using niobium oxides of the subsystem $NbO/Nb_{12}O_{29}$ and the transport agent $NbCl_5$ are well suited for a complete thermodynamic analysis using the cooperative transport model (cf. [28,66]). As the calculation shows, the transport agent firstly reacts with the starting material by exchange equilibria irrespec-

tive of whether it is single-phase or two-phase. Starting from $NbO_2/NbCl_5$

$$3\,NbO_{2,s} + 3\,NbCl_{5,g} \rightleftarrows 5\,NbOCl_{3,g} + NbO_s \quad (6)$$

a minor amount of the neighboring phase containing less oxygen is first produced. Due to the respective $O_2$-partial pressure the coexisting phases ($NbO_x/NbO_z$; $x<z$) are decisive for the composition of the gas phase. When $SiO_2$ from the quartz glass wall is considered as the third solid phase this leads to the four-component system Si/Nb/O/Cl with two degrees of freedom, so that the equilibrium pressures of the gaseous species $NbOCl_3$, $NbCl_5$, $NbCl_4$, $SiCl_4$, $SiCl_2$, $Cl_2$, and $O_2$ can be calculated after $\Sigma P$ and $T$ have been fixed. Figure 8 shows isotherms of the various gaseous species of coexisting niobium oxide pairs over the range $0<O/Nb<2.417$; the formation of $Nb_5Si_3$[67] on the side of lower O/Nb ratio has not been included.

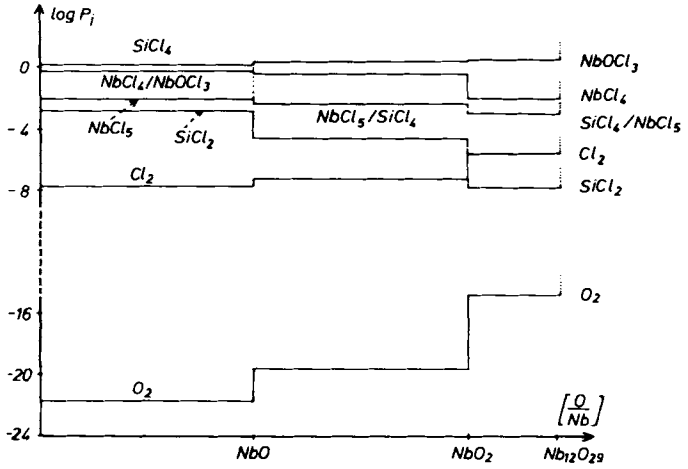



Fig. 8. Isotherms of equilibrium partial pressures [atm] over the heterogeneous source materials $SiO_2/NbO_x/NbO_z$ ($x<z$); addition of $NbCl_5$ (Table 1); calculated for $T=1400$ K and $\Sigma P=3$ atm.

As the O/Nb ratio of the starting material increases, the pressure of $NbOCl_3$ approaches the total pressure at temperatures above 1300 K, whereas the $Nb^{IV}$ fraction of the gas phase [$P(NbCl_4)$] decreases considerably. This characterizes the ability of the transport agent $NbCl_5$ to dissolve preferentially the oxygen-richer phase of a niobium oxide pair because of the considerable thermodynamic stability of the resulting gaseous $NbOCl_3$, which increases with the temperature.

In addition to the isotherms of Figure 8 the relationship between partial pressures of relevant gaseous species at constant $\Sigma P$ and temperature is shown in Figure 9 for the *equilibrium system* $NbO/NbO_2/SiO_2$. As seen in Figure 8 the oxygen partial pressure is so small [$P(O_2)_{1400\,K}=0.24\times10^{-19}$ atm] that only bound oxygen (as $NbOCl_3$) can migrate. The steep rise in the degree of oxidation of the gas phase with increasing temperature is caused by formation of $NbOCl_3$ as the main component instead of $NbCl_4$. Thus, the ratio $O/Nb^{IV}$ of the gas phase at 1150 K corresponds to $NbO_2$, whereas at 1500 K $O/Nb^{IV}=14.7$ is found. A direct connection between the composition of gas phase and that of the source material to be transported ($NbO_2$) can always be formulated in a transport equation but for complex systems with heterogeneous source materials it can only be realized for special values of $T$ and $\Sigma P$ (*e.g.* 1150 K and 3 atm).

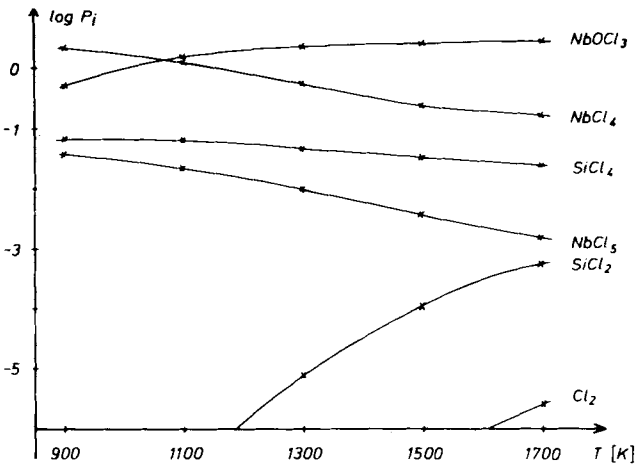



Fig. 9. Temperature dependence of the equilibrium partial pressures [atm] in the system $SiO_2/NbO/NbO_2/NbCl_5$ for $\Sigma P=3$ atm (cf. Table 1).

As we know (Section 2.3) predictions about the nature of the deposited phase(s) by means of isothermal approaches are only reliable to a limited extent for heterogeneous source materials. Using the cooperative transport model the deposition behavior in the system $NbO/Nb_{12}O_{29}$ for different source materials can be calculated for well-defined conditions [$n^0(NbCl_5)$; $\Delta T$; $V$; $\Sigma P$; $T_1$; kinetic inhibition of $SiO_2$-deposition] and then compared with the experimental data (Table 1).

*Interpretation of the Experiments:* In the *transport experiments* the ratio O/Nb of the starting material was varied over the range NbO to $Nb_{12}O_{29}$ using the corresponding $Nb/Nb_2O_5$ mixtures. The amount of $NbCl_5$ employed was such that the $NbOCl_3$ partial pressure at the experimental temperatures ($T_2=1473$ K, $T_2-T_1=100$ K) never exceeded 6 atm. In reference experiments, $CO_2$ was added to produce sufficiently stable deposition conditions *via* the increased buffer effect of the resulting $CO/CO_2$ equilibria (Table 2).

As shown by the *thermodynamic calculation*, niobium oxide is transported by the endothermic flow $I$ of the source elements with
$I(Nb)=I(NbOCl_3)+I(NbCl_4)-I(NbCl_5)$ and
$I(O)=I(NbOCl_3)$. For the steady-state the transport equation [eq. (5)] can be confirmed by means of the solubility differences $\Delta\lambda$ of corresponding gaseous species, which describe the mass exchange between the subsystems, but *not* their complex equilibrium composition (Fig. 9).

Experiments and calculations show in accordance (Tables 1 and 2) that in heterogeneous mixtures of $NbO_{2.024}/Nb_{12}O_{29}$ or of $NbO/NbO_2$ only the respective oxygen-richer niobium oxide migrates as a single phase to the less hot zone (but see Section 4.3). If O/Nb is close to the *upper* phase boundary ($O/Nb>2.01$), transport of $Nb_{12}O_{29}$ primarily occurs followed by a (separate) deposi-

tion of $\alpha$-$NbO_2$ in the hotter part of the zone at $T_1$. The transport of single phase $\alpha$-$NbO_2$ is only possible for source materials having compositions within the homogeneity range ($2.0 \leq O/Nb \leq 2.024$; $T = 1573\,K$[68]) and up to a calculated upper limit $O/Nb < 2.01$; cf. Table 1). The composition of single phase samples of $NbO_2$ was checked using a special microanalytical method[69,70].

At the *lower* phase boundary the transport behavior is extremely sensitive to changes in the O/Nb-ratio of the solid equilibrium phases in the source [$\Delta(O/Nb) < 0.01$]. For $O/Nb \approx 2.0$ it is observed that either single phase $\alpha$- or $\beta$-$NbO_2$, or a mixture of the two, is deposited in the less hot zone. $\alpha$-$NbO_2$ is formed preferentially when the source materials are slightly oxidized by additional $NbOCl_3$ (*e.g.* from $NbCl_5/H_2O$; $NbCl_5/O_2$; especially in experiments with higher total pressure) or by a perturbation in the establishment of isothermal equilibrium between the surface and the interior of a sample (cf. Section 4.4).

The preparation of pure $\beta$-$NbO_2$ single crystals was for the first time successful using source materials with equilibrium composition $O/Nb < 2.0$. Thermodynamic optimization of experiments using $NbCl_5$ as transport agent leads to the following experimental parameters: starting material; $Nb/Nb_2O_5$ (source, $T_2$) with $O/Nb \approx 1.5$; $P(NbOCl_3)_{1500\,K} \leq 2\,atm$, $T_1 = 1400\,K$, $\Delta T = T_2 - T_1 = 100\,K$, duration of experiment $> 70\,h$[29]. If $HgCl_2$[62] or $TeCl_4$[28,41] is chosen as *transport agent*, extensive oxidation of the source materials, which depends on the redox potential of the transport agent, is observed. In order to compare these transport agents with $NbCl_5$, solid equilibrium phases in the source subvolume must be generated (by addition of NbO), which at a given temperature lead to identical $P(O_2)$-values in the respective gas phases. The partial pressures calculated for the heterogeneous equilibrium $NbO/NbO_2/SiO_2/HgCl_2$ (Fig. 10) correspond to those in the system with $TeCl_4$ and thus show that the contribution of gaseous oxides, oxide chlorides, and chlorides of Hg or Te does not exceed the transport barrier $\Delta P_i/\Sigma P = 10^{-5}$. As with the transport agent $NbCl_5$, the niobium oxides migrate *via* the gaseous species $NbOCl_3$, $NbCl_5$, and $NbCl_4$ into the lower temperature zone. The observed sequence of phases with $HgCl_2$ as transport agent is consistent with the results of experiments and model calculations (Table 1) for transport processes starting from heterogeneous source materials with $NbCl_5$ (cf. [66]).

#### 4.1.2. *Ternary Solids—The Chemical Transport of Niobates; Transport Agent $Cl_2$*[27,48,49]

At temperatures $\approx 1300\,K$ the following compounds are formed preferentially in the stable systems $M_2O_3/Nb_2O_5$ (M = Fe, Al): $M_2O_3$, $MNbO_4$, $MNb_{11}O_{29}$, and the high-temperature modification of niobium(V) pentoxide H-$Nb_2O_5$[27,49,71–75] (for further phases, such as $MNb_{24}O_{62}$ cf. [75]). The ternary oxides $MNb_{11}O_{29}$ and $MNbO_4$ can be obtained by heating mixtures of $M_2O_3$ and $Nb_2O_5$, and in well crystallized form[27,48,49] by transport methods.

*$MNb_{11}O_{29}$:* Starting from a heterogeneous mixture of H-$Nb_2O_5/FeNb_{11}O_{29}$[27] or H-$Nb_2O_5/AlNb_{11}O_{29}$[49] with $Cl_2$ as the transport agent, in the Fe/Nb/O-system $FeNb_{11}O_{29}$ is transported to the less hot zone, whereas in the Al/Nb/O-system H-$Nb_2O_5$ is transported. The *opposite* result, however, would be expected (with respect to the deposited phases) if we were to examine the intersection of isotherms (arrow a in Fig. 5).

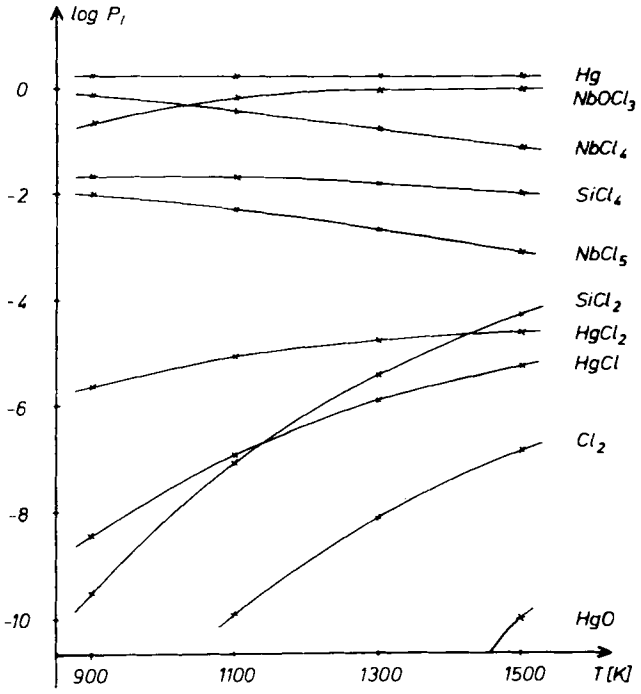



Fig. 10. Temperature dependence of the equilibrium partial pressures [atm] in the system $SiO_2/NbO/NbO_2/HgCl_2$ for $\Sigma P = 3$ atm [66].

Using the cooperative transport model both the different depositional behavior and the discrepancy with the assertions from the isotherms can be explained. The difference is due to a change in the $Q(T_2)$-values on transporting the source gas phase to the sink volume [$\Delta = \log Q(T_1) - \log Q(T_2)$]: This change has a different sign in the two systems. Whereas in the model of the system Fe/Nb/O/Cl an increase in the $Q(T_1)$-value (arrow *b* in Fig. 5) in the direction of the stability region of the phase $FeNb_{11}O_{29}$ leads to formation of the latter, in the system Al/Nb/O/Cl formation of a heterogeneous deposit consisting of $AlNb_{11}O_{29}$ and H-$Nb_2O_5$ could be expected because of a lower $Q(T_1)$-value. Since the solubility $\lambda$ of Al (cf. Section 2.3) in both subvolumes differs only marginally [$\Delta\lambda(T_2 - T_1) \approx 10^{-6}$], only the transport of $Nb_2O_5$ is observed (which is faster by a factor of $10^3$) and not the expected simultaneous transport of both solid phases.

### 4.2. Dependence of the Nature of Transported Phase on Experimental Parameters

Conflicting statements about the chemical transport in binary and ternary systems with closely neighboring phases are often due to insufficient consideration of the complex connections between the variables of the transport system and the nature of deposited phase[31,76,77]. For given solid materials (SM) [$n^0$(SM); O/$\Sigma$M] and defined

ampoule dimensions, the parameters $T$, $\Delta T$ and $n^0$ (nature/amount of transport agent) occur as variable experimental quantities.

In systems with a narrow succession of phases the *temperature gradient* $\Delta T = T_2 - T_1$ [at a constant average transport temperature $(T_1 + T_2)/2$] is of special importance for the phase relationships on the deposition side. Whereas the connection between the temperature gradient $\Delta T$ and transport rate has frequently and extensively been investigated, only few authors have looked at the importance of $\Delta T$ for the *composition* of the precipitated material[31,36,37] Here, we consider the chemical transport of Magnéli phases $Ti_nO_{2n-1}$[4] in this connection (transport agent: HCl or $NH_4Cl$[5,78,79]).

Model calculations by *Seiwert*[5] show that the starting phase $Ti_nO_{2n-1}$ is first oxidized by HCl to a heterogeneous mixture of $Ti_nO_{2n-1}$ and $Ti_{n+1}O_{2n+1}$; the equilibrium gas phase consists mainly of HCl, $H_2$, $TiCl_4$, $TiCl_3$, and $H_2O$ (Fig. 11). The subsequent transport of the oxygen-richer phase (*e.g.* $Ti_5O_9$) can be represented to a first approximation by the following mass equation [eq. (7)][5]:

$$Ti_5O_{9,s} + 362\,TiCl_{4,g} + 183\,H_{2,g} \rightleftharpoons 366\,TiCl_{3,g} + TiCl_{2,g} + 9\,H_2O_g + 348\,HCl_g \qquad (7)$$

After calculation of the position of equilibrium in the two subvolumes the deposition regions of single, homogeneous $TiO_x$ phases were determined as a function of $\Delta T$. For small temperature gradients $\Delta T \triangleq 50$ K, the oxygen-richer phase is always transported from the heterogeneous source material to the subvolume of temperature $T_1$. If larger temperature gradients are chosen, phases with higher O/Ti-ratios are obtained; for $\Delta T = 370$ K only $TiO_2$ is transported (cf. Fig. 11). Diagrams of this kind make it possible to optimize the deposition condition at $T_1$ for each $TiO_x$-phase

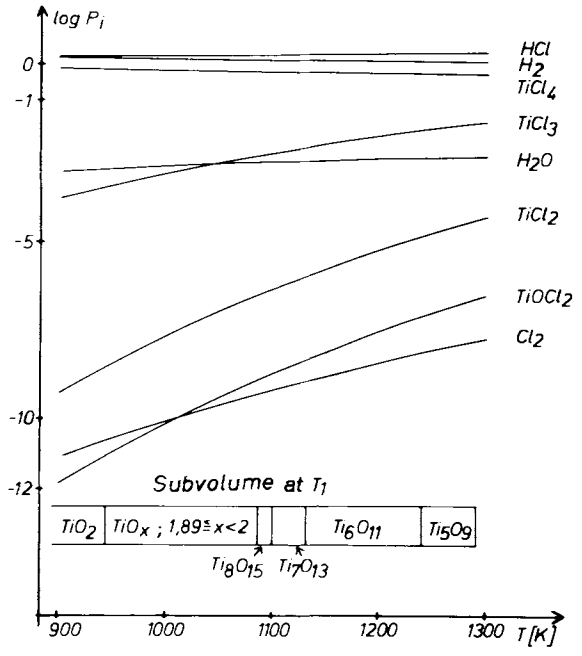



Fig. 11. Temperature dependence of the equilibrium partial pressures [atm] in the system $TiO_x$/HCl for $\Sigma P = 4$ atm and $n^0(HCl) = 1.34 \times 10^{-3}$ mol [5]. For $Ti_4O_7 + Ti_5O_9$ as heterogeneous source materials at $T_2 = 1300$ K the $TiO_x$-phase which occurs at $900 < T_1 < 1300$ K is given.

by a variation of $\Delta T$ (O/Ti in the source material at $T_2$, $n^0$ of the transport agent, and $T_2$ are given).

The formation of a heterogeneous solid (phases I and II) from the homogeneous starting phase I, depending on the nature and amount of the transport agent, is often observed at quite different temperatures ($T_l$; $T_u$, Fig. 12). Since the resulting phase relationships in the source (1, 2 in Fig. 12) can lead to different transport results, a comparison of similar, but complex transport systems without

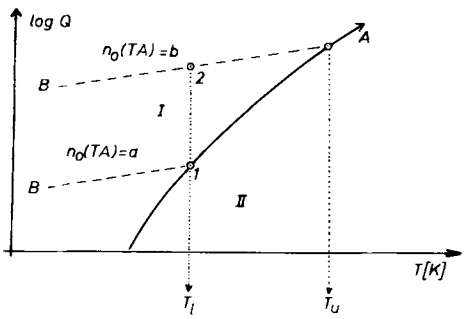



Fig. 12. Temperature dependence of $\log Q$-values for a transport reaction (B) of the solid phase I for two different amounts of transport agent $a < n_0$ (transport agent) $< b$ ($\Sigma P$ = const.) as well as for an exchange equilibrium A; the coexistence line A separates the regions of stability of solids I and II; with $T = T_1$, because of the different amounts of transport agent, *e.g.* the deposit at 1 is heterogeneous whereas at 2 it is homogeneous; for increasing amounts of transport agent the homogeneous/heterogeneous transition is shifted to higher temperatures (TA = transport agent).

consideration of free variables is only possible to a limited extent. Examples are the investigations by *Bald et al.*[80,81] of the transport of anhydrous metal sulfates and their oxide sulfates with various transport agents ($Cl_2$, $HgCl_2$, $I_2$). Experiments with $CuSO_4$ as starting material show the influence of the individual transport agents. With $Cl_2$ as transport agent, single phase $CuSO_4$ is deposited at $T_1$, and pure $CuSO_4$ remains as solid phase in the source volume. With $HgCl_2$, $CuSO_4$ also is transported to $T_1$, whereas $Cu_2OSO_4$ occurs in addition to $CuSO_4$ at $T_2$. The formation of different phases at $T_2$ is attributed to the different chlorinating power of $Cl_2$ and $HgCl_2$, since under the given experimental conditions ($T$, $V$ = const.) the resulting $P(SO_3)$ ($\triangleq Q$-value in Fig. 12) is higher for the transport system with $Cl_2$ ($\Rightarrow CuSO_4$) than with $HgCl_2$ ($\Rightarrow CuSO_4/Cu_2OSO_4$)[81]. The choice of a different transport agent has the same effect as varying the amount of transport agent (Fig. 12).

### 4.3. Influence of Impurities on the Position of Equilibrium

The interior of the ampoule can be contaminated by attack of the vessel material by the reactants as well as by release of impurities from the vessel itself. The example of the *transport of NbO* into the hotter zone (system $NbO/NbO_2/NbCl_5$) shows the influence of $SiO_2$ of the container material as well as of smaller amounts of $H_2O$ (from the quartz wall of the transport ampoules)[14,82,83] on the deposition of this oxide.

*Experimental Procedure* (cf.[29]): Mixtures of $NbO/NbO_2$ or $Nb/Nb_2O_5$ (O/Nb = 1.95) and $Nb_3O_7Cl$ (< 0.4 mmol)

were introduced into the cooler end ($T_1$) of the transport tube (vol. $\approx 4$ cm$^3$). In the "natural" temperature gradient of a silite tube furnace ($100 \leq \Delta T \leq 200$ K) NbO is deposited in the form of single regular NbO-crystallites or of shining golden NbO linings at $T_2$ (*ca.* 22 mg NbO in 6 d). Simultaneously $SiO_2$ (cristobalite layer) migrates to the less hot side ($T_1$).

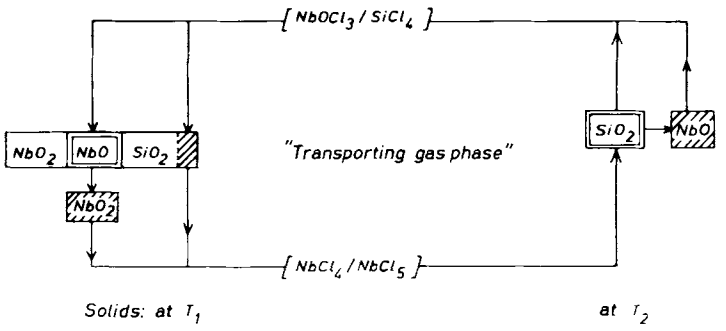



Fig. 13. Influence of the quartz wall on the position of equilibrium, illustrated by the partial chemical transport of NbO to the hotter zone. Solids which react in the exchange equilibrium [eq. (8)] with the gas phase are framed twice; ▨ resulting, □ starting materials.

*Discussion:* Under conditions of extensive exclusion of $H_2O$, migration of NbO to the hotter zone as a consequence of an opposing $NbOCl_3$-flow is related to the existence of an oxygen donor at $T_2$ (Fig. 13). Thus, we observe here the (more special) case of "partial" chemical transport[3], for which the flow of only *one* source element is needed (represented by the reduced transport rate $n_r$, cf. Table 1). If migration of Nb is attributed to the flow of $NbCl_4$, the observed transport rate for NbO [$n_r(\text{obs.}) \leq 2 \times 10^{-4}$] is substantially below the calculated value [$n_r(\text{calc.}) = 5 \times 10^{-3}$]. The lower observed value can be rationalized on the basis of the calculated minimal flow of $NbCl_5$ [$\Delta P(NbCl_5)/\Sigma P \approx 4 \times 10^{-4}$]. If we assume that mainly $NbCl_5$ serves as solvent for the oxygen donor $SiO_2$ at $T_2$, then $\Delta P(NbCl_5)$ limits the deposition of NbO *via* the exchange equilibrium [eq. (8)].

$$2\,SiO_{2,s} + 3\,NbCl_{4,g} + NbCl_{5,g} \rightleftarrows 2\,SiCl_{4,g} + 3\,NbOCl_{3,g} + NbO_{s} \quad (8)$$

The presence of small amounts of $H_2O$ ($< 10^{-5}$ mol, *e.g.* from the container wall[14]) does not change the situation markedly.

If additional $H_2O$ is introduced into the system [$n^0(H_2O) \geq 4 \times 10^{-5}$ mol], NbO can migrate into the hotter zone according to a simpler transport reaction [eq. (9)].

$$NbO_s + 3\,HCl_g \rightleftarrows NbOCl_{3,g} + 1.5\,H_2 \quad (9)$$

A complete calculation for the system containing water yields $n_r(\text{calc}) = 2 \times 10^{-4}$ (for the transport of NbO with HCl from $NH_4Cl$ cf. also [65]). Deposition of $SiO_2$ at $T_1$ is not expected in this case.

The chemical *transport of $TiO_x$-phases* with $TeCl_4$ or $HgCl_2$[16] provides another example of the importance of $H_2O$ for the transport of metal oxides. If $H_2O$ is completely excluded from the system, practically no transport of the *Magnéli phases* takes place[4], since the transport agents used partially oxidize the $TiO_x$ source material, but do not provide sufficiently high partial pressures of gaseous oxides or oxide chlorides for the O-flow; hence, the gas phase remains essentially "oxygen-free". If $H_2O$ [$n^0(H_2O) > 3 \times 10^{-5}$ mol] is present in addition to $TeCl_4$ or $HgCl_2$, the observed transport effect can be attributed to the function of HCl as transport agent (Section 4.2)[5, 16].

### 4.4. Kinetic Influences

The explanations of the chemical transport of binary and ternary solids presented here are strictly based on the calculated thermodynamic models. The reliability of the interpretation of the experimental results thus depends, on one hand, on the accuracy of the thermodynamic data, and on the other to what extent the nature and degree of kinetic inhibitions in the reaction process can be neglected.

In the system $NbO_2/NbCl_5$ (cf. Section 4.1.1), the kinetics of the *equilibration in the source material* determine the nature of the transported phase. At the beginning of the experiment several simultaneous processes have to be distinguished in the source volume:

1) Redox reactions on the surface of the starting material with a variable gas phase.
2) Equilibration between the surface and the interior of the sample.
3) Superposition of isothermal equilibrations [from 1) and 2)] by selective transport of elements of the solid.

The deviations of the O/Nb-value on the surface of the sample from the desired equilibrium value for the overall source material cause the duration of the experiment to influence the result; after reaching an equilibrium state ($> 50$ h) only β-$NbO_2$ is transported (Table 2). Deposition of α-$NbO_2$ can almost completely be suppressed by an isothermal equilibration which precedes the steady-state, as well as by a reduction of the deposition rate ($\Sigma P < 2$ atm).

The importance of the establishment of equilibrium *in the heterogeneous deposits of the sink* was shown by *Schmidt et al.*[15] for the transport of Ge (1123 → 1023 K) in the presence of high initial concentrations of the transport agent $H_2O$. Deposition of an additional solid ($GeO_2$), which appears in minimal amount at the start of the experiment, leads to a drastic change of the transport rate of Ge. Measurement of the experimental transport rate as a function of time (the ampoule is suspended as on a beam-balance) indicates that a sudden drop occurs after a certain time (166 mg/d ⟶ 50 mg/d), followed by a region of constant transport rate for the remainder of the experiment. Model calculations as well as further experiments led to the following explanation: over a short period of time deposition of Ge together with that of hexagonal $GeO_2$ occurs until steady-state transport of Ge is reached. The change of the transport rate with time is based on the transformation (hexagonal ⟶ tetragonal) of $GeO_2$ into its stable modification, which is promoted by extremely small amounts of alkali ("mineralizer"). The change in modification of $GeO_2$ at $T_1$ leads to a substantial shift of the position of equilibrium in this transport system.

### 4.5. Preparation of Metastable Solids

The observed influence of the duration of an experiment on the nature of the deposited phase (Section 4.4) in the system $NbO/NbO_2/NbCl_5$ (Table 2) suggests that the initially formed $\alpha$-$NbO_2$ is not stable with respect to the equilibrium gas phase formed later, and is, therefore, gradually converted into $\beta$-$NbO_2$. This view is supported by observations made during isothermal studies of mixtures of $\alpha$-$NbO_2/NbO$ in the presence of $NbCl_5$. Here, $\alpha$-$NbO_2$ crystals are completely or partially dissolved, whereas newly formed $\beta$-$NbO_2$ grows on the $\alpha$-$NbO_2$ crystals already present.

Although both modifications differ only slightly in composition and thermodynamic stability, the conversion of the $\alpha$- into the $\beta$-form is caused by a slight gain in stability of the subsystem ($\approx 1$ kcal/mol). That solid phase is formed ($\beta$-$NbO_2$), whose formation causes a smaller decrease in concentration for gas particles with low free energy ($NbOCl_3$) [eq. 10]. This "gas phase effect" is strongly dependent on the composition of the $\beta$-$NbO_2$ phase formed and vanishes for strictly stoichiometric $\beta$-$NbO_2$ (O/Nb = 2.00).

$$2.01\,\alpha\text{-}NbO_{2,s} + 0.03\,NbCl_{4,g} \rightleftharpoons 0.04\,NbOCl_{3,g} + 2\beta\text{-}NbO_{1.99,s} \quad (10)$$

The situation can be schematically presented in a "modified" energy term diagram[61] (cf. Fig. 14 and Section 3.3). The $\Delta G^*$ state sketched represents a "metastable" initial state of the sink (Fig. 14), which is caused by transfer of the gas phase of the source volume to the deposition zone ($T_1$). The difference between this $\Delta G^*$ state and the free energy of the source volume ($\Delta G_{source}$) determines the extent of the precipitation of the competing phases $\alpha$-$NbO_2$ and $\beta$-$NbO_2$; the phase actually deposited (here $\beta$-$NbO_2$), however, is determined by the smallest free energy of deposition ($\Delta_R G = \Delta G_{sink} - \Delta G_{source}$) in the system. If the corresponding deposition is kinetically inhibited, the tendency for deposition to occur is shifted to increasing $\Delta_R G$ values.

The simple thermodynamic relationships[28] between $\Delta_R G$-values of competing phases and the corresponding

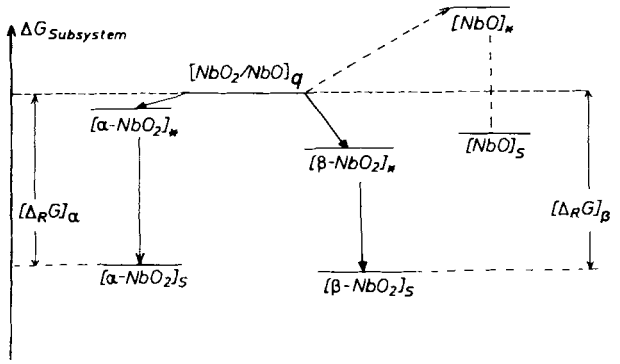



Fig. 14. Energy term diagram for the formation of metastable $\beta$-$NbO_2$. The value of the free energy of deposition ($\Delta_R G$) determines the nature of the transported phase and the transport path leading from the heterogeneous equilibrium substance of the source (index: *q*) *via* a metastable initial state (*) to the lowest-energy deposition level(s). At the given high temperature ($T > 1300$ K and $\Delta T = 100$ K) transport of NbO is impossible because of its energy-rich $\Delta G^*$ state.

gas phase effect allow an approximate interpretation of the deposition behavior of such metastable solids, whose composition differs only slightly from that of a more stable phase.

The thermodynamic calculation used [*G* (min) method] is also suited for the determination of "metastable" intermediate states of a subsystem, such as occur upon transition from the initial state to the steady-state equilibrium. This was confirmed by *Schmidt et al.* for the system $GeO_2/H_2$[11,12].

## 5. Perspectives

The cooperative transport model is based on the thermodynamics of *reversible* equilibria, as well as on the assumption of a *steady-state* mass flow of the elements of the solid between source and sink, which is limited by the choice of appropriate equilibrium states in the subsystems of a transport ampoule. By measuring the deposition process as a function of time using a continuous balance method[15] (cf. Section 4.4) it can be shown, also for individual sections during the experiment, that the transport is a steady-state process.

Perturbation of the position of thermodynamic equilibrium in source and sink caused by heat and mass flows in the transport system have to be taken into account, just as in the kinetic inhibition of heterogeneous reactions.

However, some extensively investigated examples indicate that, aside from thermodynamic equilibrium states, solids can be transported in a steady-state manner as shown by *Vepřek et al.* in experiments on nonisothermal plasmas[84,85]. Industrial applications of this method, *e.g.* the preparation of thin films or the nitridization of metals[86], have already gained some importance. Solids in otherwise inaccessible states can also be obtained, *e.g.* a novel "amorphous" form of elemental phosphorus having unexpected properties[87].

More information on the thermodynamic data of ternary compounds is desirable. Whereas well characterized data for many binary substances are at hand for others, especially ternary solids, we are restricted to estimated values for enthalpies of formation so that the calculation of the transport behavior becomes uncertain. Further measurements are urgently needed.

Experimental details of systems with well characterized thermodynamic data (*e.g.* $GeO_2/H_2$)[12] indicate that for a larger difference in the binary diffusion coefficients "induced" gas flows occur, which lead to a shift of the position of equilibrium in the transport system. For a description of this situation, where the assumption of identical mass balances (Section 3.2)[60] must be abandoned, a "dynamic" model based on the thermodynamics of irreversible processes would have to be developed.

The cooperative transport model allows extensive analysis of the complicated phase relationships in systems with several components, if the restrictions mentioned (kinetic inhibition, steady-state imbalances, reliability of thermodynamic data, average diffusion coefficients) are taken into account: directed syntheses therefore become possible. Use of this model for solid state synthesis could help make novel compounds accessible, especially if they are

only obtainable *via* chemical transport (*e.g.* the "bronze" $Ge_{0.25}WO_3$[88]) or if the required crystalline arrangement can only be reached in this way (*e.g.* for $Ti_7Cl_{16}$[89]). Special techniques, such as the pendulum method[3] or transport in alternating temperature gradients[88] have already been developed for growing single crystals with especially low defect concentrations and defined physical properties (garnets[39], $Fe_2O_3$[90]). On the basis of the currently available experimental data it should also be possible to further optimize technical procedures. For flowing systems *Spear et al.* were able to calculate the deposition conditions for the formation of epitaxial films ($SiO_2$[91], $TiB_2$[93], $Nb_3Ge$[94]) from gas mixtures using the $G$(min) method.

Model calculations based on the free energy function principally allow investigation of the experimental effect of variable thermodynamic parameters ($\Sigma P$, $T$, $P_i$) on structural properties, such as symmetry changes in series of solid solutions[28] or on the concentration and type of defects, *e.g.* in block structures[8]. The possibility of gaining new insight into chemical processes by means of qualitative transport experiments, which was realized fairly early[3], has so far not been fully exploited. Simple thermodynamic considerations have stimulated further investigations and applications, such as the chemical transport of W[10], which led to construction of the halide lamp, or give indications on the existence of new gaseous compounds, such as polysulfides in the system $TaS_2/S_2$[95], the gaseous species causing the migration of $SiO_2$ with $H_2O$[96], or the oxide gas complexes in the system $GeO_2/WO_2$[97]. Even a qualitative understanding of these phenomena requires an appropriate transport model because of the increasing complexity of the chemical systems investigated. Thermodynamic calculations using this model yield a set of parameters which are related to the experiments. On this basis the apparent abundance of seemingly contradictary experimental results can be ordered, interpreted, and compared.

*The transport method was developed by Schäfer over a period of two decades. This article was only made possible by his contributions and the basis which he laid. One of us (R. G.) thanks his mentor for many stimulating discussions which reached far beyond the scope of this review article. We also thank the co-workers L. Bald, H. Brunner, H. Hibst, Th. Kohlmann, V. Plies, W. Redlich, E. Schaum, G. Schmidt, F.-J. Seiwert, M. Spiess, and J. Sturm for their efforts. The Deutsche Forschungsgemeinschaft and the Fonds der Chemie are thanked for financial support.*

Received: October 28, 1982 [A 440 IE]
German version: *Angew. Chem. 95* (1983) 80
Translated by: Dr. W. J. Westermann, Mannheim

[1] Hk. Müller-Buschbaum, *Angew. Chem. 93* (1981) 1; *Angew. Chem. Int. Ed. Engl. 20* (1981) 22.
[2] H. Schäfer, *Angew. Chem. 83* (1971) 35; *Angew. Chem. Int. Ed. Engl. 10* (1971) 43.
[3] H. Schäfer: *Chemische Transportreaktionen*, Verlag Chemie, Weinheim 1962.
[4] S. Andersson, B. Collen, U. Kuylenstierna, A. Magnéli, *Acta Chem. Scand. 11* (1957) 1641.
[5] F. J. Seiwert, Diplomarbeit, Universität Gießen 1981.
[6] J. Sturm, R. Gruehn, *Naturwissenschaften 62* (1975) 296.
[7] J. Sturm, Dissertation, Universität Gießen 1976.
[8] R. Gruehn, W. Mertin, *Angew. Chem. 92* (1980) 531; *Angew. Chem. Int. Ed. Engl. 19* (1980) 505.
[9] B. Meyer, R. Gruehn, *Comments Inorg. Chem. 1* (1982) 361.
[10] H. Schäfer, *J. Cryst. Growth 9* (1971) 17.
[11] G. Schmidt, R. Gruehn, *Z. Anorg. Allg. Chem. 478* (1981) 75.
[12] G. Schmidt, R. Gruehn, *Z. Anorg. Allg. Chem. 478* (1981) 111.
[13] G. Schmidt, R. Gruehn, *J. Cryst. Growth 55* (1981) 599.
[14] G. Schmidt, R. Gruehn, *J. Cryst. Growth 57* (1982) 585.
[15] G. Schmidt, R. Gruehn, *J. Cryst. Growth 58* (1982) 623.
[16] F. J. Seiwert, R. Gruehn, *Z. Anorg. Allg. Chem.*, in press.
[17] H. Schäfer, *Angew. Chem. 88* (1976) 775; *Angew. Chem. Int. Ed. Engl. 15* (1976) 713.
[18] H. Schäfer, *Z. Chem. 19* (1979) 362.
[19] H. Schäfer: Vorträge N 306, Rheinisch-Westfälische Akademie der Wissenschaften, Düsseldorf 1981.
[20] M. Spieß, Dissertation, Universität Gießen 1978.
[21] R. Gruehn, M. Spieß, Jahrestagung der GDCh-Fachgruppe „Festkörperchemie", Gießen 1978.
[22] L. Bald, R. Gruehn, *Z. Kristallogr. 156* (1981) 9.
[23] C. Bonnamy, J. C. Launay, M. Pouchard, *Rev. Chim. Miner. 15* (1978) 178.
[24] W. Redlich, Th. Petzel, Rev. Chim. Miner., in press.
[25] H. Schäfer, *Nat. Bur. Stand. (US) Spec. Publ. 364, Solid State Chem.* (1972) 413.
[26] H. Hibst, R. Gruehn, *Z. Anorg. Allg. Chem. 440* (1978) 137.
[27] H. Brunner, Dissertation, Universität Gießen 1975.
[28] H.-J. Schweizer, Dissertation, Universität Gießen 1983.
[29] H.-J. Schweizer, R. Gruehn, *Z. Naturforsch. B37* (1982) 1361.
[30] Y. Bando, K. Nagasawa, Y. Kato, T. Takada, *Jpn. J. Appl. Phys. 8* (1969) 1267.
[31] J. Mercier, S. Lakkis, *J. Cryst. Growth 20* (1973) 195.
[32] P. Gibart, *J. Cryst. Growth 18* (1973) 129.
[33] H. Oppermann, M. Ritschel, *Krist. Tech. 10* (1975) 485.
[34] G. Krabbes, H. Oppermann, *Z. Anorg. Allg. Chem. 450* (1979) 27.
[35] J. Mercier, *J. Cryst. Growth 56* (1982) 235.
[36] G. Krabbes, H. Oppermann, E. Wolf, *Z. Anorg. Allg. Chem. 416* (1975) 65.
[37] F. Emmenegger, *J. Cryst. Growth 3/4* (1968) 135.
[38] P. Kleinert, *Z. Anorg. Allg. Chem. 389* (1972) 129.
[39] F. H. Wehmeyer, *J. Cryst. Growth 6* (1970) 341.
[40] Symposium on crystallization by chemical transport reactions, Berlin 1967.
[41] M. Ritschel, H. Oppermann, *Krist. Tech. 13* (1978) 1035.
[42] P. Kleinert, J. Kirchhof, *Z. Anorg. Allg. Chem. 429* (1977) 147.
[43] H. Schäfer, M. Trenkel, *Z. Naturforsch. B33* (1978) 1318.
[44] G. Krabbes, H. Oppermann, E. Wolf, *Z. Anorg. Allg. Chem. 450* (1979) 21.
[45] R. F. Lever, *J. Chem. Phys. 37* (1962) 1078.
[46] R. R. Fergusson, T. Gabor, *J. Elektrochem. Soc. 111* (1964) 585.
[47] H. Schäfer, *Z. Anorg. Allg. Chem. 400* (1973) 242.
[48] R. Gruehn, Habilitationsschrift, Universität Münster 1968.
[49] J. Sturm, Diplomarbeit, Universität Gießen 1972.
[50] G. Krabbes, H. Oppermann, *Krist. Tech. 12* (1977) 929.
[51] H. Schäfer, M. Huesker, *Z. Anorg. Allg. Chem. 317* (1962) 321.
[52] S. R. Brinkley, *J. Chem. Phys. 15* (1947) 107.
[53] M. M. Faktor, I. Garret: *Growth of Crystals from the Vapor*, Chapman and Hall, London 1974.
[54] K. Klosse, *J. Solid State Chem. 15* (1975) 105.
[55] J. Obermann, Rechenprogramm GEPA, Universität Gießen 1977.
[56] G. Eriksson, *Acta Chem. Scand. 25* (1971) 2651.
[57] B. I. Noläng, The Computer Program EPCBN, Institute of Chemistry, University of Uppsala 1978.
[58] M. W. Richardson, *Acta Univ. Nova Acta Regiae Soc. Sci. Ups. Ser. VC 464* (1978).
[59] B. I. Noläng, M. W. Richardson, *J. Cryst. Growth 34* (1976) 198.
[60] B. I. Noläng, M. W. Richardson, *J. Cryst. Growth 42* (1977) 90.
[61] H. Scholz, *Solid State Commun. 19* (1976) 429.
[62] E. Schaum, Diplomarbeit, Universität Gießen 1974.
[63] H. Kodama, M. Goto, *J. Cryst. Growth 29* (1975) 77.
[64] H. Kodama, M. Goto, *J. Cryst. Grwoth 29* (1975) 222.
[65] H. Komatsu, H. Kodama, *J. Cryst. Growth 36* (1976) 121.
[66] H.-J. Schweizer, R. Gruehn, unpublished results.
[67] H. Schäfer, W. Fuhr, *J. Less-Common Met. 8* (1965) 375.
[68] H. Schäfer, D. Bergner, R. Gruehn, *Z. Anorg. Allg. Chem. 365* (1969) 31.
[69] R. Gruehn, *Z. Anal. Chem. 221* (1966) 146.
[70] H. Hibst, Dissertation, Universität Gießen 1977.
[71] V. K. Trunov, L. M. Kovba, Z. Ya. Polshchikova, *Russ. J. Inorg. Chem. 13* (1968) 786.
[72] H. Schröcke, *Beitr. Mineral. Petrogr. 7* (1960) 166.
[73] J. Graham, M. R. Thorner, *Am. Mineral. 59* (1974) 1026.
[74] M. Harder, Hk. Müller-Buschbaum, *Z. Anorg. Allg. Chem. 459* (1979) 99.

[75] R. Norin, *Acta Chem. Scand. 23* (1969) 1210.
[76] T. Sakata, K. Sakata, G. Höfer, T. Horiuchi, *J. Cryst. Growth 12* (1972) 88.
[77] P. Kleinert, J. Kirchhof, *Z. Anorg. Allg. Chem. 429* (1977) 137.
[78] Z. Hauptmann, D. Schmidt, Sk. Banerjee, *Czech. J. Phys. B15* (1965) 64.
[79] F.-J. Seiwert, R. Gruehn, *Z. Anorg. Allg. Chem.*, in press.
[80] L. Bald, planned Dissertation, Universität Gießen.
[81] L. Bald, M. Spiess, R. Gruehn, T. Kohlmann, *Z. Anorg. Allg. Chem.*, in press.
[82] S.-H. Hong, *Acta Chem. Scand. A 36* (1982) 207.
[83] H. Schäfer, T. Grofe, M. Trenkel, *J. Solid State Chem. 8* (1973) 14.
[84] S. Vepřek, C. Brendel, H. Schäfer, *J. Cryst. Growth* **9** (1971) 266.
[85] S. Vepřek, *Chimia 34* (1980) 489.
[86] S. Vepřek, M. Venugopalan: *Plasma Chemistry, Vol. 1-3*. Springer-Verlag, Berlin 1980.
[87] S. Vepřek, *Pure Appl. Chem. 48* (1976) 163.
[88] V. Plies, unpublished results cf. V. Plies, W. Redlich, R. Gruehn, *Z. Anorg. Allg. Chem.*, in press.
[89] H. Schäfer, R. Laumanns, *Z. Anorg. Allg. Chem. 474* (1981) 149.
[90] H. Scholz, *Philips Tech. Rundsch. 28* (1967) 220.
[91] G. Eriksson, E. Rosen, *Scand. J. Metall. 2* (1973) 95.
[92] K. E. Spear, M. S. Wang, *Solid State Technol. 23* (1980) 63.
[93] K. E. Spear, *Pure Appl. Chem. 57* (1982) 1297.
[94] C. F. Wan, K. E. Spear: *Proc. 8 Int. Conf. on CVD*, The Electrochemical Society, Princeton 1981.
[95] H. Schäfer, *Z. Anorg. Allg. Chem. 471* (1980) 21.
[96] G. Heurung, personal communication.
[97] V. Plies, *Z. Anorg. Allg. Chem. 484* (1982) 165.

# Intermetallic Compounds and the Use of Atomic Radii in Their Description

**By Arndt Simon***

*Dedicated to Professor Harald Schäfer on the occasion of his 70th birthday*

Metallic radii, which are obtained from atomic distances in the pure elements, are generally used for the calculation of distances in intermetallic compounds. However, the procedure for using such radii depends on the individual structural type: a) For high coordination numbers and only slightly differing distances between atoms of the same kind and different atoms, all distances in a structure are proportional to the sum of radii, weighted according to the composition. Such a "Vegard" relationship for ordered compounds is obeyed by intermetallic compounds with topological close packings, but strictly only if the various kinds of distances are correlated *via* symmetry relationships. For compounds with low coordination numbers the simple sum of radii holds for atoms participating in the shortest bond (*e.g.* in ionic crystals).—b) The number of neighbors determines the size of each atom. It can be shown that the bond strength-bond length concept, developed for valence compounds, and often dealt with in the literature over the last ten years, is also applicable for alloys. On this basis a formalism is developed which uniformly describes the size of the atoms as a function of the coordination number for both the limiting cases of multiple bonds in molecules and for close packed atomic arrangements in alloys.

## 1. Introduction

Ever since it has been possible to determine atomic distances in molecules and crystals experimentally, efforts have also been made to draw conclusions from such distances about the nature of the chemical bonding. A wealth of empirical data has been collected, from which tables of atomic, ionic, covalent and van-der-Waals radii have been drawn up, and which are fitted to the actual case with the aid of various formulas. The nature of the fit (or better: the fitability) is then used as an indication for bonding criteria such as covalent and ionic bonding, bond order, and coordination number. However, if not enough details about the sample are known, statements about bonding can be wrong.

Let us assume that one is asked to take an X-ray photograph of a sample, whose composition according to conventional chemical analysis practically corresponds to that of cesium and that he actually finds the simple diagram of a face centered cubic (fcc) lattice in which the Cs–Cs distance is only 450 pm as compared to 530 pm in Cs metal. He will be surprised to have found a modification which normally requires more than 20000 bar to produce. Finally, he will have thoughts about the bonds in question, since shorter distances are usually associated with stronger bonds. Hopefully he will find out in time that the sample is, in fact, CsH.

This example is, of course, entirely misleading. As a rule, the chemist will know the composition of the substance whose structure he is to determine by X-ray analy-

[*] Prof. Dr. A. Simon
Max-Planck-Institut für Festkörperforschung
Heisenbergstrasse 1, D-7000 Stuttgart 80 (Germany)

sis. Furthermore, CsH is one of those tricky solids, presenting difficulties which normally do not arise with most molecules.

Nevertheless, this is a good example to illustrate the fact that we tend to draw conclusions about the bonding in a crystal in an indirect way, namely from interatomic distances, bond angles, atomic volumes *etc.*, and tend further to correlate bond lengths with bond orders. Recently determined electronic deformation densities[1] for binuclear transition metal complexes indeed show the huge problems associated with such a correlation, even in relatively simple systems.

The above mentioned interatomic distance arises in a matrix of other atoms and for a discussion of the bonding in solids as well as in individual molecules it is important to know the geometrical strain of the matrix or, to put it in other words, to have a knowledge of the influences of the packing and linkage of all atoms. "Intermetallic phases", those compounds between metals, on which comparatively few studies have been carried out in modern inorganic chemistry, serve as suitable models for investigating this problem, for there are many compounds whose existence is due to an optimal packing of atoms without any participation of strong chemical bonds. What sizes have the atoms in these compounds? Are they describable as rigid or as deformable spheres? In which way do they and the distances between them change when, in addition to the effects of geometrical strain of the packing, strong chemical bonds are formed? Finally, is it true that bond valence concepts fail[2] when one attempts to extend their application beyond classical valence compounds to intermetallic compounds with their often unusual compositions, which do not obey conventional valence rules.

## 2. Starting Points

A well trodden path in the (empirical) attempt at understanding a crystal structure is the search for general criteria for specific atomic arrangements (*e.g.* characteristic radius ratios or space filling in rigid sphere models) and then to check how far the range of existence of real compounds reflects the effectiveness of such criteria. We cannot recount the many authors who have persued studies in this direction. Only *Pearson*'s method[3,4] will be briefly outlined.

### 2.1. Near Neighbor Diagrams (n.n.d.) according to *Pearson*

The atoms M and N in a compound $MN_n$ are treated as deformable spheres, each of which are characterized by radii $r'_M$ and $r'_N$, respectively[*]. In a crystal, the distances $d_{MM}$, $d_{NN}$ and $d_{MN}$ exist. These distances are designated as strain free, when they correspond to a contact of atoms, without deformation of one or the other atom. Hence, for strain free MM contacts we have $d_{MM}=2r'_M$, and accordingly $d_{NN}=2r'_N$, and $d_{MN}=r'_M+r'_N$ for strain free NN and MN contacts. If we choose the formula $(2r'_M-d_{MM})/2r'_N$ as a representation of the strain parameter, then the conditions for strain freeness for the different kinds of distances are describable as linear functions of the radius ratio $r'_M/r'_N$. This procedure will now be outlined using the ZnS (zinc blende)-type structure as example.

As can be seen in Figure 1, the structure of ZnS consists of two face centered cubic (fcc) lattices which are shifted with respect to each other by one fourth of the space diagonal. The shortest interatomic distances are $d_{MM}=d_{NN}=a\sqrt{2}/2$ and $d_{MN}=a\sqrt{3}/4$. From these, one obtains the linear equations for strain freeness of the various atomic distances:

$$\text{MM:}\quad \frac{2r'_M-d_{MM}}{2r'_N}=0$$

$$\text{NN:}\quad \frac{2r'_M-d_{MM}}{2r'_N}=\frac{r'_M}{r'_N}-1$$

$$\text{MN:}\quad \frac{2r'_M-d_{MM}}{2r'_N}=\left(1-\sqrt{\frac{2}{3}}\right)\frac{r'_M}{r'_N}-\sqrt{\frac{2}{3}}$$

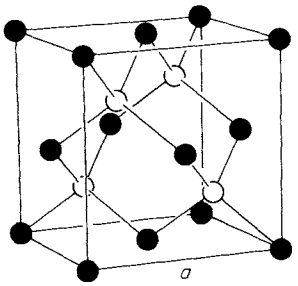



Fig. 1. Unit cell of ZnS ($a$ = lattice constant).

The straight lines shown in Figure 2 represent the geometrical "frame" of the zinc blende structure. Each compound with the ZnS structure is shown as a point in the n.n.d. *via* the experimentally determined distance $d_{MM,exp.}$ and the tabulated radii $r_M$ and $r_N$[*] of the participating elements. As can be seen from Figure 2, all points concentrate around the line of strain-free MN contacts. The conclusion, that the ZnS-type obviously "lives" from MN contacts, corresponds to the usual view of the ZnS structure as a structure with strong bonds between M and N atoms.

One obtains a completely different result—at first sight—for typical intermetallic phases like the so-called Laves phases (Fig. 3). The distribution of points for the existing compounds neglects the straight lines which stand for the strain freeness of the different interatomic distances. We rather get the impression that no preferred contacts in Laves phases exist but that a well balanced adaption is reached by a deformation of all atoms. This result again reflects the usual view that these alloy-like phases lack a preference for bonds between special kinds of atoms and that the only important condition is the formation of a

[*] The notation $r'$ indicates that the radii employed have been fitted to the coordination number. The method of fitting is described in [4], p. 146 and 150 (cf. Section 3.5). The value for close packed spheres is designated as $r$.

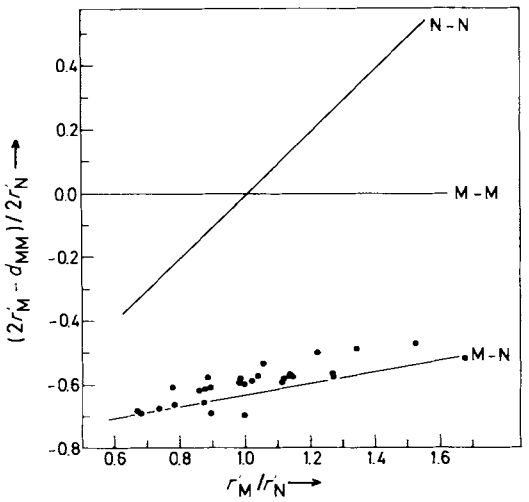



Fig. 2. Near neighbor diagram (n.n.d.) for the ZnS type [4]. The lines correspond to strain freeness of the indicated atomic contacts. The dots characterize real compounds, whose radii have been converted to coordination number 4 (cf. footnote [*] on p. 96).

topologically dense packing. Laves phases represent an ideal system to check the matrix effect, *i.e.* the effect of packing on the origin of individual atomic distances.

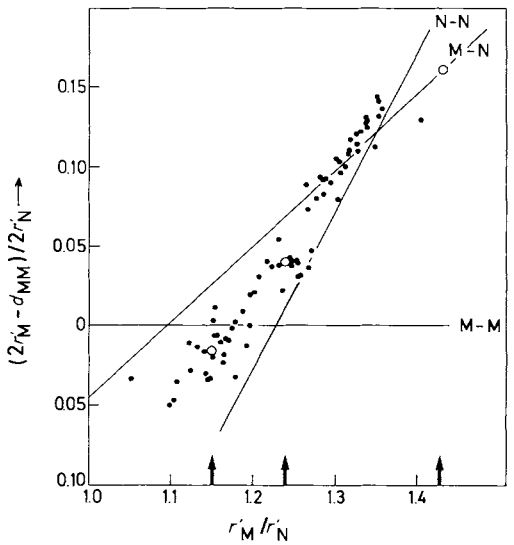



Fig. 3. Near neighbor diagram (n.n.d.) for Laves phases crystallizing in the $MgZn_2$ type. The construction of lines is based on ideal parameters (cf. Section 2.2). The positions of $CsNa_2$ ($r_M/r_N = 1.43$), $KNa_2$ (1.24) and $CsK_2$ (1.15) are especially emphasized.

## 2.2. Laves Phases

Laves phases are intermetallic phases of composition $MN_2$ whose structures are closely related (cf. [4]). In the cubic $MgCu_2$-type (Fig. 4), there is an arrangement of M atoms as in the diamond structure. Each M atom is surrounded by 12 N and 4 M atoms (conventional coordination number cn = 16) and each N atom has both 6 nearest M and 6 nearest N atoms (cn = 12). $MgZn_2$ is a hexagonal stacking variant and $MgNi_2$ shows alternating hexagonal and cubic stacking of the same typical structural units. The interatomic distances for the cubic $MgCu_2$-type are $d_{MM} = a\sqrt{3}/4$, $d_{NN} = a\sqrt{2}/4$ and $d_{MN} = a\sqrt{11/4}/4$. On the premises of ideal positional parameters and $c/a$ ratios, coordination numbers and the relations between corresponding distances are equal in all Laves phases. Starting from the observed distance ratio $d_{MM}/d_{NN} = \sqrt{3/2}$, *Laves* defined the "ideal" radius ratio $r_M/r_N = 1.225$ for a model of rigid spheres. For this "ideal" ratio the M and N atoms just touch each other (according to *Pearson:* strain freeness of the MM and NN contacts). According to *Laves,* phases are found predominantly around this ideal value[5–7]. Should, however, the radius ratio for two metals differ considerably from this value, strong chemical bonds usually stabilize the structure. As a tentative direct proof of this view *Laves* used the compound $KNa_2$[8]: Strong chemical bonds between the atoms are missing and therefore the only reason for the existence of this compound is the closeness of the radius ratio $r_K/r_{Na} = 1.24$ to the ideal value.

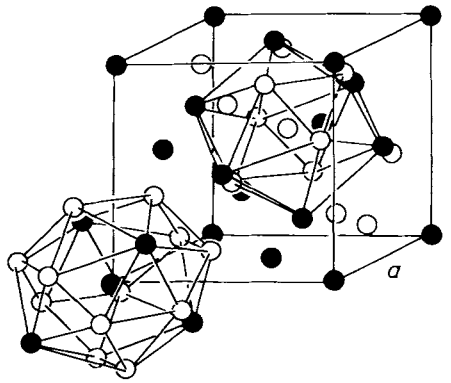



Fig. 4. Unit cell of the $MgCu_2$ structure with coordination polyhedra for Mg and Cu atoms [4]. The full circles represent Mg atoms.

This "proof" became invalid with the preparation and structural characterization of $CsK_2$[9] and $CsNa_2$[10]. Especially the value $r_{Cs}/r_{Na} = 1.43$ for $CsNa_2$ differs greatly from the "ideal", but still the compound cannot balance the geometrically implied destabilization by the formation of strong bonds, as is the case with *e.g.* $KPb_2$, because of the much larger difference in electronegativity in the latter case.

From Figure 3 we can see that none of the phases lie on the point of intersection of the straight lines for strain-free MM and NN contacts (ideal radius ratio); instead, an accumulation around the point of intersection of the straight lines for strain-free NN and MN contacts is observed. The deviation from the horizontal line for strain-free MM contacts is especially notable; the distances $d_{CsCs} = 487$ and 557 pm in $CsNa_2$ and $CsK_2$, respectively[*], are in one case smaller, in the other case larger than the distance in elemental cesium (532 pm). One could be tempted to explain

[*] The lattice constants [8–10] were extrapolated to room temperature on the basis of thermal expansion coefficients, which have been determined by X-rays, for alkali metals and binary mixed crystals [11]: $a = 790.0$, $c = 1312.6$ pm ($CsNa_2$), $a = 749.1$, $c = 1229$ pm ($KNa_2$) and $a = 912.1$, $c = 1484.6$ pm ($CsK_2$).

this shortening of $d_{CsCs}$ in $CsNa_2$ as a strengthening of the Cs–Cs bonds with regard to the element; it can be shown however, that this shortening is due to the matrix in which the Cs atom is embedded.

The influence of the matrix is even more pronounced in the case of $K_7Cs_6$[9], in the structure of which $Cs_2$ pairs with a still shorter distance $d_{CsCs}=469$ pm, are observed. The contraction of about 12% compared to elemental cesium almost reaches that in CsH, which was discussed in Section 1. It could be shown however[12–14], that these distances in $K_7Cs_6$, too, have nothing to do with strong Cs–Cs bonds, but follow almost entirely from the packing of atoms. At this point there is a direct connection to the discussion of bonding between metal atoms in binuclear transition metal complexes which are "forced" into a bridged frame of ligands (cf. Section 1).

The points for $CsNa_2$, $KNa_2$ and $CsK_2$ in the n.n.d. can be linked by a straight line whose analysis leads to an interesting result: the interatomic distances in the three compounds follow the relation $d=F(r_M+2r_N)$. This means that each distance is determined, on the one hand, by the sum of the radii weighted according to the composition, and, on the other, by a factor which accomodates the special geometry. For the shortest distances $d_{MM}$, $d_{MN}$ and $d_{NN}$ the factors are $F_{MM}=0.740$, $F_{MN}=0.708$ and $F_{NN}=0.604$[9]. Obviously the three compounds only obey the geometrical restraints which are the same to all of them in this particular type of structure, for an adjustment of interatomic distances. The straight line for these compounds simply describes the matrix effects, since the chemical bonding is very similar to that in the pure alkali metals.

It is not the size of a *single* atom alone which determines the distances to its neighbors, rather the community of *all* atoms is responsible for *all* distances. A truly democratic principle!

To prevent a misunderstanding: the atoms certainly search an optimal arrangement. Thus the geometrical restraints of the particular structure type could be better described as a condition on the part of the atoms for the formation of a suitable structure. In this context one should mention the interesting result of pseudopotential calculations[12–14] for the binary alkali metal systems. The effective interatomic pair potentials follow from the balance of repulsive interactions of the ionic cores and attractive band-structure contributions (ion-electron-ion interactions). Figure 5 shows that the interatomic distances in the Laves phase $CsK_2$ more or less follow the pair potential functions for a mixture of this composition. The formation of the $MgZn_2$ structure thus corresponds to an accumulation of as many atoms as possible of the correct kind around each atom, approximately at the minimum of the respective pair potential. For $KNa_2$ and $CsK_2$ the observed and calculated[14] lattice constants and positional parameters are in good agreement. It should be mentioned, however, that the existence of $CsNa_2$ cannot be verified by these calculations.

Figure 6 shows that the majority of all Laves phases follow quite closley the straight line which is typical for $CsNa_2$, $KNa_2$ and $CsK_2$. But, especially for those compounds marked by crosses, one observes considerable and systematic deviations. In these compounds the differences

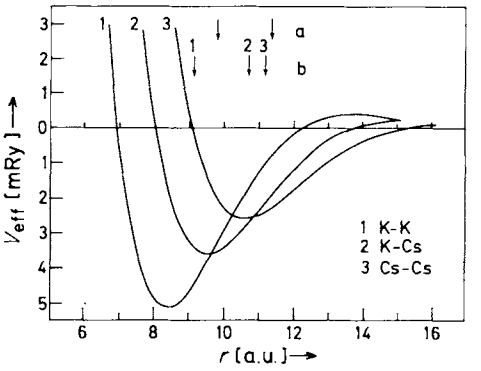



Fig. 5. Effective interatomic pair potentials for an alloy $KCs_{0.5}$ [12, 13]. The arrows indicate atomic distances in the mixed crystal (a) and in the Laves phase $CsK_2$ (b) (cf. text).

in electronegativity are $\Delta\chi > 1$, *i.e.* to a first approximation heteropolar bonds lead to a shortening of distances and to changes in the relative atomic sizes, which manifest themselves in excessively large values for the strain parameters. Here, an interesting way is indicated to distinguish between influences due to the packing (described by the straight line) and those due to chemical bonds (deviations from the straight line). At the same time, however, these deviations which can be easily explained by additional effects, make it quite clear that it is not very meaningful to start an analysis of packing effects in a particular structure type on the basis of *all* known representatives. One should, at first, rather concentrate on the behavior of compounds where these additional effects are likely to be missing.

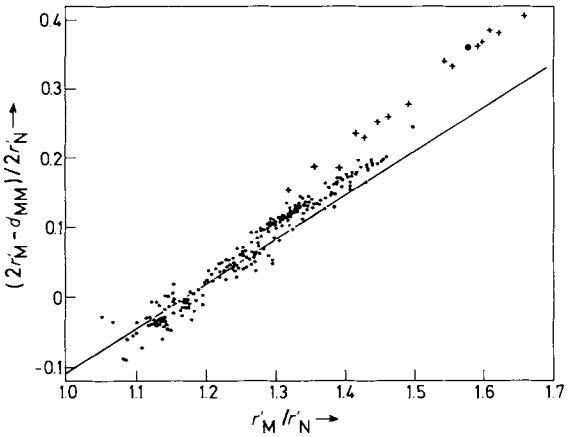



Fig. 6. Strain parameters for all cubic and hexagonal Laves phases [4]. The line drawn includes the points for $CsNa_2$, $KNa_2$ and $CsK_2$. For compounds indicated by crosses the components have electronegativity differences $\Delta\chi > 1.0$.

### 2.3. Vegard's Rule

*Vegard*[15] noticed, on examining mixed crystals of different potassium and ammonium salts, that the lattice constants of a mixed crystal vary linearly with its composition. According to Vegard's rule the averaged shortest atomic distance in mixed crystals of composition $MN_2$ therefore is $d_0=(1/3)(d_M+2d_N)$, where $d_M$ and $d_N$ are the shortest atomic distances in the pure elements M and N. If the structure of the mixed crystal can be regarded as a close

packing, then the averaged shortest atomic distance can be calculated with $d_0 = 2/3(r_M + 2r_N)$ using the tabulated atomic radii for coordination number 12. For other atomic arrangements, *e.g.* in mixed crystals of body centered cubic (bcc) metals, the radii have to be converted to the coordination number in question *via* a factor f, after which Vegard's rule takes the following form:

$$d_0 = \frac{2}{n+1}(r'_M + n r'_N) = \frac{2f}{n+1}(r_M + n r_N) \quad (1)$$

The relation for the ordered Laves phases of the alkali metals corresponds closely to a Vegard relation for disordered phases. But, whereas in the mixed crystal with only *one* factor F = 0.667 only *one* shortest distance is allowed despite different atomic sizes, the different factors F in the ordered phases permit a certain "easing" of the individual interatomic contacts. In the Laves phases of the alkali metals the distances between the larger M atoms are greater by 1.225 than those between the small N atoms. The identical treatment of all atoms is the reason for the non-existence of mixed crystals when the lattice constants of the pure compounds differ by more than 15%. Contrary to this, Figure 6 shows extensive realization of a linear relation of the kind of Vegard's rule within a much larger span of radius ratios for the (ordered) Laves phases.

A complete understanding of Vegard's rule for mixed crystals does not exist to date. In fact there are so many deviations from this rule that most papers deal with explanations for observed deviations rather than with the rule itself. A review[16] of the many models explaining deviations of real systems from the rule indicates that quantitative predictions are only possible to a limited extent. Perhaps we can learn more about the rule from ordered phases, because in these cases the atomic sizes can differ to a much larger extent and because one problem does not exist, namely the general assumption of a completely statistical distribution of atoms in the mixed crystal, an assumption which usually cannot be proven.

As an alternative to the rule of distance additivity, *Biltz*[17] formulated the rule of volume additivity, following the works of *Niggli*[18] as well as of *Fajans* and *Grimm*[19]. Today, this is sometimes curiously called Zen's rule[20]. *Biltz* came to this result by evaluating extensive experimental findings, and he showed in this book that the rules of radii additivity as well as of volume additivity are approximations which may be valid for certain families of substances as well as within one family.

Both relationships are shown graphically in Figure 7 for the Laves phases formed only by alkali metals, for which substantial deviations from a volume additivity are observed. The volumina can be calculated more accurately from the atomic radii weighted according to stoichiometry. The volume contraction of the compounds with respect to the elements results from the higher packing density of atoms of different sizes.

In the following we shall not try to give another proof for Vegard's rule by means of ordered compounds, but look for a way to a quantitative understanding of the empirically found relationship followed so accurately by the alkali metal compounds and to investigate its validity and limits for other classes of compounds.

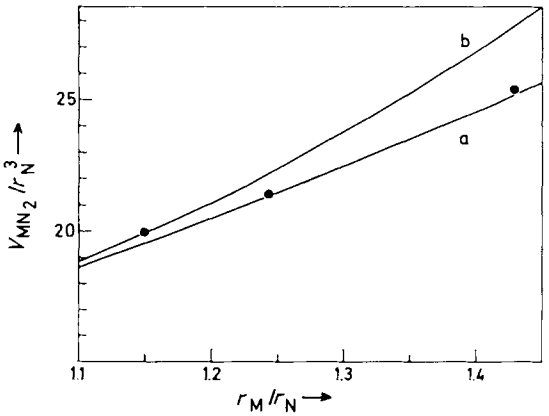



Fig. 7. Reduced volumina of Laves phases $CsK_2$, $KNa_2$, $CsNa_2$ (cf. footnote [*] on p. 97). Tabulated atomic radii [21] were used; the volumina are in each case for one formula unit. The curves represent the limits (a) sum of radii [in analogy to Vegard's rule $V = (2 \times 0.74/\sqrt{3})^3 (r_M + 2r_N)^3$] and (b) sum of volumina [$V = 4\sqrt{2}(r_M^3 + 2r_N^3)$].

The concept of calculating interatomic distances *via* radii which are weighted according to the composition is not new. *Shoemaker* and *Shoemaker*[22] used this approach to analyze Frank-Kasper phases[23,24], whose structures are composed of close packed tetrahedra. *Villars et al.*[25] proceed in the same way, when they try to predict new intermetallic compounds. Obviously *Pauling*[26] was the first to come up with this idea, after *Geller*[27] had doubted the validity of the "resonating valence bond theory" for A15 compounds (β-W or $SiCr_3$ type), which he described with a special set of linearly weighted atomic radii. *Pauling* could show that the conventional atomic radii changed only up to 5% and when weighted 1 : 3 according to the composition gave a much better agreement with experiment than *Geller*'s special radii. The answer from *Geller*[28] was followed by a reply from *Pauling*[29] where he strengthened his arguments by means of the $AuCu_3$ type compounds. The last act of the play is worth quoting[30]: "The writer believes that his position regarding the various aspects of the β-W type structure has been made abundantly clear in his two papers (Geller, 1956, 1957) and, therefore, that there is no point in his further discussing this most recent paper (Pauling, 1957)".

## 3. Searching

The obvious and essential difference between covalent or salt-like structures on the one hand and alloys on the other is a correspondence of shortest interatomic distances to the simple sum of radii in the former case, but to a weighted sum of radii, according to the composition, for the latter compounds. Near neighbor diagrams can be used to investigate which relationship actually holds, because each way of weighting corresponds to a line. Furthermore, this form of presentation has been chosen here, because a wealth of data about known compounds has already been classified and graphically represented in the published diagrams[4].

### 3.1. Stoichiometric and Geometric Relationships

The analysis shall at first be restricted to alloys of composition $MN_n$, which follow a Vegard law for ordered phases (cf. Section 2.3) and will only later be treated in general. A linear relationship between atomic sizes - given by their radii - and the atomic distances in a structure is represented by a straight line in the n.n.d., which is derived from the expression $d_{MM} = F_{MM}(r'_M + n r'_N)$ with $F_{MM} = 2 - 2\alpha$:

$$\frac{2r'_M - d_{MM}}{2r'_N} = \alpha \frac{r'_M}{r'_N} - n(1-\alpha) \qquad (2)$$

Equations (1) and (2) lead to

$$\alpha = 1 - \frac{d_{MM}}{d_0(n+1)} \qquad (3)$$

The result for alloys[31] is shown schematically in Figure 8. For each value of n there exists a fan of straight lines, whose origin in the n.n.d. lies at $-n/-n$. Within a group of compounds of equal composition $MN_n$ (n = const.) the different structure types can be distinguished by different slopes $\alpha$ for the respective straight lines, which thus represent "leading lines" for the different types.

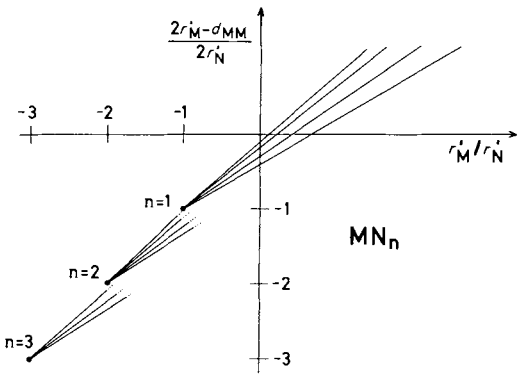



Fig. 8. The representation of structure families for alloy phases with constant composition $MN_n$ (n = const.) corresponds, according to eq. (2), to a fan of lines with origin $(-n/-n)$ in the n.n.d. [31].

All quantities in equation (3) are defined by composition and crystal structure. For the ZnS type presented in Section 2.1, *e.g.*, $n = 1$, $d_{MM} = a\sqrt{2}/2$ and $d_0 = d_{MN} = a\sqrt{3}/4$. The line constructed for the ZnS type using eqs. (2) and (3) is identical to the line for strain-free MN contacts. Above all, however, those alloys are described correctly by eq. (3), whose structures are not dominated by the condition of strain freeness for MN contacts, as shall be shown in the following. An example for this is the $AuCu_3$ family.

### 3.2. The $AuCu_3$ Structure

Atoms in a face centered cubic (fcc) lattice have 12 equidistant neighbors. If face centers and corners of the unit cell are occupied by different atoms M and N, we obtain the simple $AuCu_3$ type which is formed by many intermetallic compounds. Since both kinds of atoms are still surrounded as in close packing, we can use the unchanged tabulated metallic radii[21] for a calculation of strain parameters and radius ratios. Thus complications due to erroneous adaptations of radii to coordination numbers do not exist.

The interatomic distances are $d_{MM} = a$ and $d_{MN} = d_{NN} = a/\sqrt{2}$; with $d_0 = d_{MN} = d_{NN}$, we obtain a value for the slope of $\alpha = 0.6465$. The result is identical to the statement that the contact distances between atoms in cubic close packed mixed crystals and in the likewise cubic close packed compound $AuCu_3$ follow the simple Vegard's rule $[d_0 = (2/4)(r_M + 3r_N)]$.

As shown in Figure 9, the calculated line for the $AuCu_3$ type is a good description of the various representatives of this type in the n.n.d. and it is thus almost a "backbone"

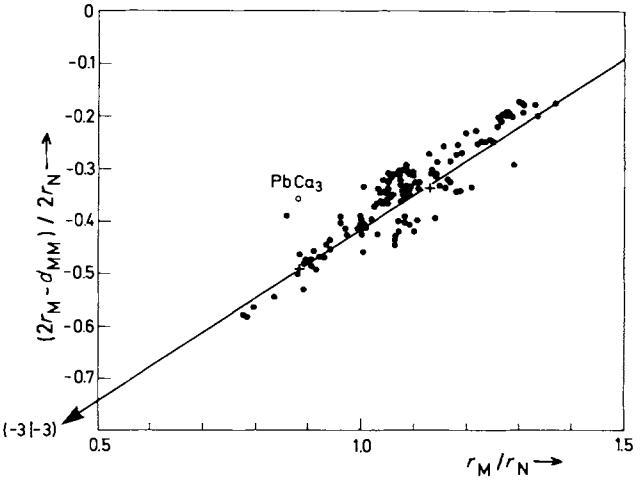



Fig. 9. Distribution of compounds of the $AuCu_3$ type [32, 33] in the near neighbor diagram. The line includes the point with coordinates $(-3/-3)$ and has a slope $\alpha = 0.6465$. The phases $AuCu_3$ and $CuAu_3$ are indicated by crosses. As example for deviations due to large differences in electronegativity of the participating elements, $PbCa_3$ is emphasized.

for the family. The pair $AuCu_3$ and $CuAu_3$ is especially emphasized. The calculated lattice constants agree well with the experimental values [$a_{0,exp.} = 395.3$, $a_{0,calc.} = 396.2$ pm for $CuAu_3$ (mixed crystal) and $a_{0,exp.} = 374.8$, $a_{0,calc.} = 373.0$ pm for $AuCu_3$]. Considerable deviations from the expected positions are found, not unexpectedly, for those phases which are formed from metals with large differences in electronegativity, like $LiAu_3$ or $PbCa_3$ (cf. discussion for Fig. 6).

### 3.3. Structure Fields for Compounds MN

Alloy-like and salt-like compounds of composition MN should group around straight lines in the n.n.d. whose slopes vary depending on the structure, but which have the same point of intersection $(-1/-1)$ because of their identical atomic ratio and, for salts, because of the simple radii additivity. A few structure types of this composition MN are given in Figure 10. The dots representing the many individual phases were taken from *Pearson*[4]. The radius values $r'$ are fitted to the different coordination numbers (cf. footnote on p. 96). The calculated leading lines, using eqs. (2) and (3) with $d_0 = d_{MN}$, correspond to the lines constructed by *Pearson* for strain free MN contacts.

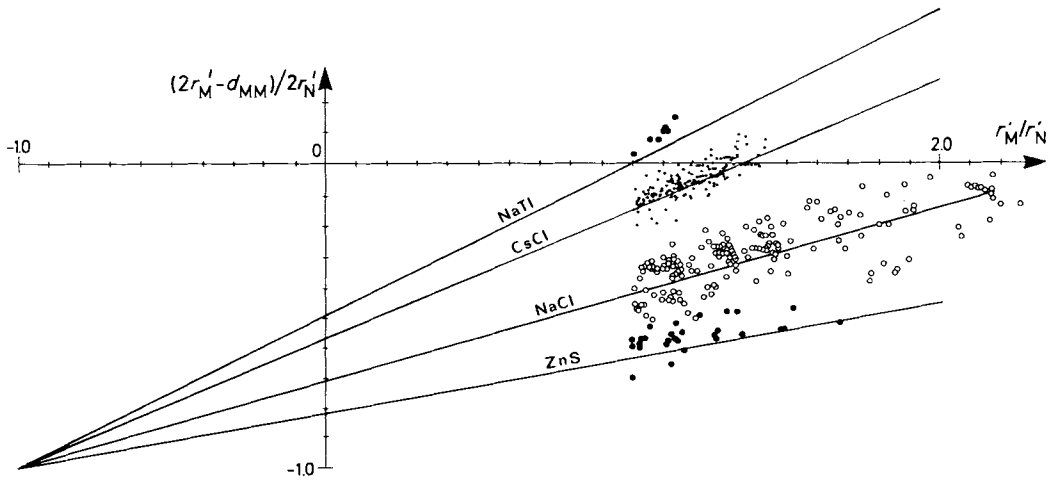



Fig. 10. Representation of compounds belonging to the NaTl, CsCl, NaCl and ZnS types in the near neighbor diagram. The distribution of compounds was taken from the individual diagrams [4] and takes into account the respective coordination numbers (cf. footnote [*] on p. 96). The compounds group around a line, constructed using eqs. (2) and (3), which corresponds to the line of strain free MN contacts.

The accumulation of all phases around the respective straight lines for strain free MN contacts does not necessarily lead to the conclusion that bonds between M and N atoms are decisive for the structure (cf. Section 2.1), but this concentration is a consequence of the composition MN and the condition that atoms of the same kind are always at least as far apart as atoms of different kinds. Conclusions about the chemical bonding in this type should not be drawn from the fact that the compounds follow the lines for strain free MN contacts, but rather from their deviation from the proper line which is specific for the structure and stoichiometry. These deviations can appear as a distribution of points for individual compounds, but they can also show as a systematic deviation of all compounds, as in the case of the NaTl type.

This last mentioned NaTl type is especially interesting. The deviations of the compounds of this type from the "structure specific line" are easily understandable. LiZn, LiCd, LiAl, LiGa, LiIn, NaIn and NaTl are binary representatives of this type. As can be seen from Figure 11, M and N atoms each form diamond structures which are shifted with respect to each other by $a/2$. *Zintl*[34] explained this as due to the simultaneous existence of strong heteropolar and homopolar bonds. We can write $Na^+Tl^-$ for NaTl; the $Tl^-$ ions which are isoelectronic to the elements of the 4th main group form a covalently bonded framework with diamond structure whose vacancies are filled with the cations. This simple explanation of the structure is confirmed by the results of perturbation calculations[35], which show that electron density is transferred from the Na atoms to the regions between the Tl atoms. In this interpretation strong chemical bonds are responsible for the volume contraction, and thus for the resulting position of all Zintl phases above the straight line in Figure 10. It is interesting to note that all compounds follow the condition of strain free NN contacts[4] which corresponds to the above mentioned description of chemical bonding in Zintl phases. Nevertheless, one should recall the close relationship of these phases to typical alloy systems like the brasses, which are formed at other valence concentrations (*Hume-Rothery*[36]).

The special feature of the NaTl structure as compared to other MN types is the fact that the shortest MM, NN and MN distances are identical. Thus, the various distances all correspond to $d_0$, contrary to *e.g.* ZnS. With this equality of all different kinds of distances the NaTl type becomes an "ordered mixed crystal" of composition MN (cf. Section 2.3). Therefore, it is not astonishing that the field of existence for this type is very small (Fig. 10) and does not substantially exceed the value $r_M/r_N = 1.15$. An arrangement of atoms as in the CsCl type, which is found in a large number of intermetallic phases[32] (*e.g.* $CsAu = Cs^+Au^-$, but also LaMg), is obviously not quite so sensitive in its span of tolerable radius ratios.

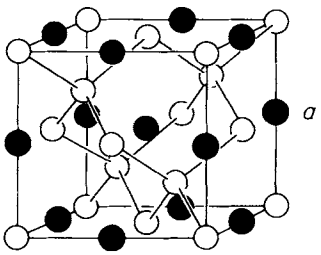



Fig. 11. Unit cell of the NaTl structure. The diamond-like thallium partial structure (empty circles) is emphasized.

Another consequence of this equality of $d_{MM}$, $d_{MN}$ and $d_{NN}$ in the NaTl type is the fact that the value $\alpha$ for the slope of the line reaches a maximum for MN types in this case. For arbitrary compositions the slope of the lines cannot take higher values than $\alpha = 1$. Knowing the upper limit of the fan of lines for MN types, we immediately search for the lower limit. For three-dimensionally linked structures the ZnS type constitutes this lower limit. But even smaller values for $\alpha$ are possible when the three-dimensional linkage is broken down into units of lower dimensionality. For the structure of BN a value $\alpha = 1 - \sqrt{3}/2 = 0.134$ is calculated. Under the premises that van-der-Waals contacts represent the shortest possible distances for crystals with diatomic molecules one even obtains values $\alpha \leq 0$

(*e.g.* for CO). But, since intra- and intermolecular distances are not strictly correlated, well-defined straight lines no longer exist in these cases.

### 3.4. Elements as "Limits" of MN Structures

The structure types shown in Figure 10 were chosen because the simple sum of radii and the weighted sum, according to composition, are identical and because for all these types elements exist, which can be regarded as limits of the various structure types. It can be seen from Figure 12, that both the NaTl and the CsCl type result in a bcc lattice when M and N are equal. This lattice therefore appears on both lines. The cubic primitive lattice of α-polonium is the limit for the NaCl structure, whereas the diamond structure is the equiatomic extreme for the ZnS type.

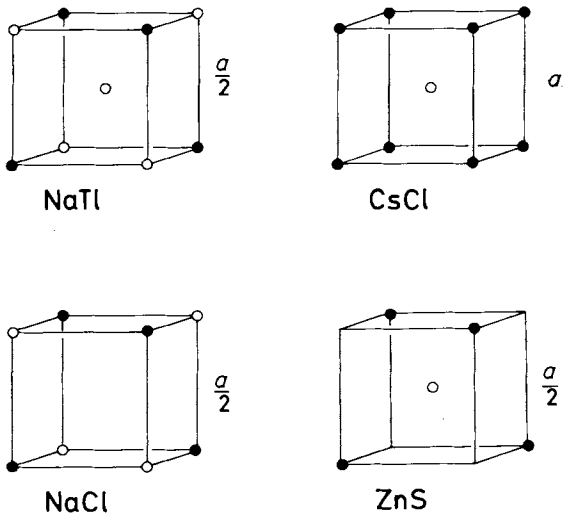



Fig. 12. Arrangements of neighboring atoms in the NaTl, CsCl, NaCl, and ZnS types. For identical atoms the NaTl and CsCl types degenerate to the bcc lattice, the NaCl type to a cubic primitive lattice and the ZnS type yields the diamond structure.

In the elements, $r_M$ is equal to $r_N$ and there are no heteropolar contributions to the bonding. These structures can therefore be used for calibrating the lines calculated according to eqs. (2) and (3), and for the generalization from the individual structure specific $r'$-values to the tabulated metallic radii. How do the shortest atomic distances, which for elements are equal to twice the radius, change as a function of the coordination number?

Table 1 contains a comparison of experimentally determined atomic distances and calculated distances for the elements mentioned here, using the tabulated metallic radii[21]. Since the actual coordination numbers are not taken into account, considerable deviations obviously occur between observed and calculated values. It is however notable, that the ratio of these values remains nearly constant for the bcc metals, although the largest given distance is more than twice the shortest distance. For the other elements variations in the ratio of up to *e.g.* 8% are observed, as in the case of grey tin compared to diamond. If one queries the reason for this disagreement, a (superficial) explanation is easily found, but a more comprehensive treatment has far-reaching consequences.

Table 1. Comparison of experimentally determined atomic distances in some elements [37] with the sum of metallic radii according to [21].

| Structure type | Element | $d_{exp.}$ [pm] | $2r$ [pm] [21] | $d_{exp.}/2r$ |
|---|---|---|---|---|
| Body centered cubic lattice | α-Fe | 248.2 | 255.4 | 0.972 |
| | W | 274.1 | 281.6 | 0.973 |
| | Li | 303.9 | 312.4 | 0.973 |
| | K | 462.8 | 475.2 | 0.974 |
| | Cs | 531.8 | 546.2 | 0.974 |
| Primitive cubic lattice | P(6) | 238 | 256 | 0.930 |
| | α-Po | 336.6 | 352 | 0.956 |
| Diamond | C | 154.5 | 183.2 | 0.843 |
| | Si | 235.2 | 263.8 | 0.892 |
| | Ge | 245.0 | 273.8 | 0.895 |
| | α-Sn | 281.0 | 309.0 | 0.909 |

### 3.5. Metallic Radii

Distances between atoms in an element are simple to measure with high precision. As such they are, however, little help in predicting interactomic distances in chemical compounds. In a uniform procedure, reference values from the individual values, *e.g.* "atomic radii", have to be extracted and various functions can be used for this purpose. Since these radii are combined for the description of distances in compounds, it is meaningful to use just one normalizing function for all values.

The disagreements in the values given in Table 1 are due to the fact that the metallic radii, which are used today by many chemists, crystallographers, metallurgists and physicists[21], have been obtained from the atomic distances in elements by using different functions. Only the function used for the determination of the individual radii is suitable for conversion of the value based on cn = 12 to arbitrary coordination numbers. Therefore only the radii measured as half the atomic distance in fcc element lattices need no further discussion. The radii determined from hcp lattices, however, already include various assumptions: In which way is the *effective* coordination number taken into consideration in these cases as a function of the $c/a$ ratio? Fortunately, there are some bcc elements which also crystallize in a fcc lattice and thus present an empirical function for the conversion of all other bcc metals. But: the user of the tables must not apply any other correction function for the radii concerned. Especially problematical are all radii of non-metallic and semi-metallic elements, because they have been extrapolated from structures with small coordination numbers, which often cannot be described with classical integer values. This extrapolation is carried out according to the procedure described by *Pauling*[38], and the function used is of a substantially different form than the above mentioned function. Table 1 indicates the size of the error which occurs if we treat *Pauling*'s radii for the fourth group elements in analogy to the radii for the bcc metals.

We could of course use those metallic radii which were obtained by *Pauling*[38] himself with the aid of only one function. This however presupposes that the experimental data available at present are correctly described by this function.

## 4. Finding

The preceding discussion leads to a question of central importance in chemistry which has often been dealt with, not only in the early days but also to a large extent in recent years. It arises from the wish to make predictions about bond lengths or ionic distances in a compound with the aid of normalized distances and a suitable function. This function should be as simple as possible and the distances derived should have the same accuracy as those found by experiment.

Ionic radii usually refer to cn = 6 (NaCl structure) as normalized state, metallic radii to cn = 12. The calculation of interatomic distances in a compound by means of a simple or in some way weighted sum of radii presupposes that the radius $r_i$ of the i-th atom in a structure is fitted to the environment with the aid of a function $f_i$:

$$r_i' = f_i r_i \tag{4}$$

Chemists concerned with bond lengths in molecules are probably more used to single bonds as the normalized state, a reference state which has also become customary in the discussion of complicated solid state structures. Since, however, "coordination number" and "bond strength" are closely related and one could be exchanged for the other, the different reference states actually only correspond to a shifting of the origin.

Before finding a suitable function f, two problems have to be solved:

1) Which color has the chameleon "coordination number"[39]?
2) Does it have the same color as the branch named "chemical bond", to which it clings?

### 4.1. Coordination Number

From the point of view of the bond length-bond strength concept[40], atoms form strong bonds to some, but not necessarily all neighboring atoms. The distribution of bonding electrons (or charges) of an atom (or ion) over its neighbors is reflected in the individual bond lengths to the various atoms of the coordination sphere. "The number of bonds is called the coordination number"[40]. But what is the coordination number of the atom, surrounded by 12 neighbors, in a noble gas crystal, according to this definition; is it vanishingly small, or do the atomic distances obey completely different laws on changing the coordination number? This question is justified, because the intermetallic phases which are treated here neither represent van-der-Waals crystals nor ionic crystals, so that "coordination number" could again mean something else.

The coordination number is in fact a description of the environment of an atom reduced to one single number. The arbitrary act lies in the choice of which atoms are included in the environment. One criterion could be, that the neighboring atoms should touch the central sphere. Then the $I^-$ ion in LiI[39] would have the coordination number 18; but we could get used to that. Problems arise at a different point: For a structure type as a whole this procedure does not allow statements to be made about characteristic coordination numbers, because these are in each case functions of the radius ratios (which radii?) of the particular compounds.

Usually structures are described using the centers of gravity of the various atoms. If one adheres to this description, to such an extent that the thus "unsubstantial" atoms become indistinguishable, the coordination numbers are independent of the individual representatives of a particular structure type. Different pathways are then open. They lead to values of effective coordination numbers (ecn), which not only take nearest neighbors into account, but also, albeit with less weight, more distant atoms. The effective coordination number can be related to the valency v of the central atom and to the mean bond strength $\bar{s}$ of all individual bonds:

$$v = ecn \cdot \bar{s} \tag{5}$$

The "vectorial" path consists of the construction of perpendicular faces in the middle of all lines connecting the center with the centers of surrounding atoms[23] and counting the faces of the resulting polyhedron (Wigner-Seitz-cell, Voronoi polyhedron). The counting is accomplished with various weighting schemes depending on a) the sizes of the various faces of the polyhedron[39,41], or b) the volume of each pyramid, formed by face and center[41], or c) the solid angle at the top of each pyramid[42,43].

On the "scalar" path, only the *distances* to a given central atom are used for a determination of its coordination number. It has been suggested[44], that one should search for the largest gap in the spectrum of distances, to count all distances up to this value with a weighting of $1/d_j$ and to forget all others. However, the determination of a "largest gap" sometimes asks for a good eye, and is left to anyone's discretion. The procedure will be more unbiased, if the search for the gap and the task of forgetting is left to a rapidly converging function, such as ECoN (effective coordination number) proposed by *Hoppe*[*]: The individual contributions of all neighbors to the coordination number are summed together and each contribution $ECoN_j$ quickly becomes vanishingly small with increasing atomic distance $d_j$ according to $ECoN_j = \exp[1-(d_j/\bar{d})^6]$. The reference distance $\bar{d}$ corresponds to a "mean fictive" atomic or ionic size[45,46], which is determined beforehand from the structure.

[*] According to [45, 46] the mean fictive ionic or atomic diameters $\bar{d}$ for each independent ion (atom) are calculated first (as radii: MEFIR or MEFAR = Mean Fictive Ionic (Atomic) Radius).
The empirical probability density function, simplified for the special case of atoms of equal size

$$ECoN(h\rightarrow i) = \sum_{i}\sum_{j=1}^{\infty} n(h\rightarrow i)\cdot\exp\left[1-\left(\frac{d(h\rightarrow i)_j}{\bar{d}(h\rightarrow i)}\right)^6\right]$$

leads to the "effective coordination number" ECoN, by referring all distances to the fictive size $\bar{d}_{M,N}$ of ions and atoms respectively (n = frequency of a specific distance).

Superficially, the function ECoN only fulfills the duty of forgetting the atoms at large distances. Its importance, however, is far-reaching; for it can be shown[47] that each term of the sum $ECoN_j$ corresponds to *Pauling*'s bond strength-bond length relationship in merely a modified form. The result fulfills the generally formulated criteria[41] for obtaining coordination numbers, *i.e.* ECoN represents an approximation which is equivalent to the "vectorial" path. Its utility depends on the accuracy of the approximation.

The thought of using the fictive atomic size $2 \cdot$"MEFAR" $= \bar{d}$, which was employed for the ECoN calculation, to determine f in eq. (4) immediately springs to mind. The idea is promising, since the distances in the bcc lattice $d_0/\bar{d} = 0.976$ are in good agreement with the values tabulated in Table 1. But one may not rejoice: Despite the even smaller ratio expected for the diamond structure, a value of 1.000 is calculated. The result of the conventional coordination number ECoN = cn = 4 is payed for with a loss of information, how to handle the radii for this result. Therefore we choose another procedure.

### 4.2. Bond Length-Bond Strength Concepts

Since the time of *Goldschmidt*'s work[48] we have known that the atomic distances in ionic crystals increase with increasing coordination number. An interpretation of this was soon found[49]: Ionic distances result from the balance of Coulomb attraction and Born repulsion. For a change of the coordination number the repulsion term is essentially proportional to the number of ion contacts, *i.e.* proportional to cn, whereas the attraction term changes only slightly—proportional to the ratio of Madelung factors A[50]:

$$d = d_0 (A_0 \cdot cn / A \cdot cn_0)^{1/a-1} \qquad (6)$$

To a first approximation ($A_0 \simeq A$), it is the change of the coordination number which determines the atomic or ionic size. The reason is the rapid increase of the repulsion which determines the Born exponent *a*. If the coordination numbers cn in (6) are replaced by the effective coordination numbers ecn and these in turn by valency and bond strengths (cf. (5)), this formal step leads to a relationship between distances *d* and bond strengths s, which, with the approximation $A \simeq A_0$ for small differences in coordination number (N = a − 1),

$$s = s_0 (d/d_0)^{-N} \qquad (7)$$

represents the fundamental principle of a great number of papers, associated with the names *Donnay, Allmann, Brown* and *Shannon*[2,40,51-62], who made important progress in representing atomic distances in crystal structures.

With eq. (7) the approach has essentially changed: Now, the attraction, the bonding between atoms, and not the repulsion seems to be in the foreground. The step to the empirical description of the relationship between bond order and bond length of covalent bonds by *Pauling*[38] is thus only marginal.

The lengths of the CC single, double and triple bonds follow the well-known relation (*Pauling*[38]):

$$d = d(1) - F \lg s. \qquad (8)$$

For integral bond orders (= bond strengths) s = 1, 2, 3 we have the factor $F = 71$ pm; $d(1)$ represents the single bond distance. *Pauling* assumed that partial bonds ($s \leq 1$), *e.g.* in metals, can also be described by the same expression, but with $F = 60$ pm.

*Pauling*'s relation is based on the plausible idea that the bond strength of each individual bond decreases when the available valence electrons of an atom are distributed over increasingly more bonds to neighboring atoms (ecn > 1). The elongation of interatomic distances on going from a bcc lattice (ecn < 12) to a close packed structure thus becomes easily understandable.

If variations of the factor *F* in eq. (8) are also allowed outside the given range, this equation also describes ionic distances with satisfying precision[59]. Obviously we can use all equations (6), (7) and (8) to describe the dependence of atomic sizes or radii on the coordination number, although the equations were developed for various bonding types, and seemingly different forces lead to the change in atomic size. A closer comparison of the three relationships, however, reveals a significant variance: In equations (6) and (7) the difference in atomic distance with altered coordination number (or bond strength) is proportional to the atomic size. Contrary to this, the change in distance should be constant using equation (8), independent of the atomic size[*].

The transition of some elements from the bcc lattice to close packed structures allows a crucial test of the relationships. Figure 13 clearly shows that the increase in distance associated with this transition is largely proportional to the atomic size[63]. It is obviously independent of the valence

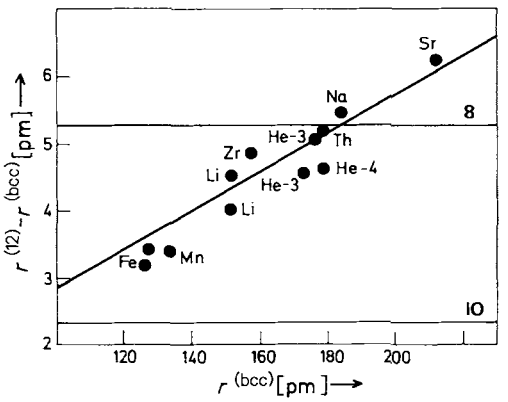



Fig. 13. Decrease of the atomic radius on transition of a close packing into the body centered cubic (bcc) lattice for metals (and helium), which crystallize in both arrangements [63]. The corrections calculated according to *Pauling* [eq. (8)] (drawn for coordination numbers 8 and 10) are independent of the atomic size.

[*] One could argue at first that the atomic size enters the conversion *via* the valency (v), *i.e.* few binding electrons are equivalent to a large atomic diameter. We can easily convince ourselves that v remains unconsidered:
$d^{(ecn)} = d(1) - 60 \times \lg(v/ecn)$ and
$d^{(12)} = d(1) - 60 \times \lg(v/12)$, *i.e.*
$d^{(12)} - d^{(ecn)} = 60 \times \lg(12/ecn)$

electron concentration of the element, and, on the average, corresponds to the line which represents the condition of equal volumina for both modifications. The factor for a conversion of distances from one modification into the other, derived from the line representing the condition $\Delta V = 0$, is once again f = 0.972.

To force atoms with large differences in atomic size into a uniform description, equation (8) is simplified one step too far. If the equation is changed slightly to fulfill the condition of proportionality

$$d = d(1)(1 - A \ln s), \tag{9}$$

it can be shown that A is not constant, but can be represented as a function of the valency of an element: $A \simeq (B + \ln v)^{-1}$.

Starting from the single-bond distances[64] $d_{C-C} = 154.5$ pm (diamond), $d_{N-N} = 146$ pm ($H_4N_2$) and $d_{O-O} = 146.7$ pm ($H_2O_2$), we get the following double and triple bonds when B = 3.6: $d_{C=C} = 133.0$ pm (exp. 133.4), $d_{C\equiv C} = 120.4$ pm (exp. 120.4), $d_{N=N} = 124.4$ pm (exp. 122.4), $d_{N\equiv N} = 111.9$ pm (exp. 109.4), $d_{O=O} = 123.0$ pm (exp. 121.1). The calculated values using eq. (9) correspond slightly better to the experimental distances than the values calculated with the aid of eq. (8). Apart from this, eq. (9) describes the transition from close packed arrangements to the bcc lattice correctly (cf. Section 4.3) and can also be applied to calculate interatomic distances in alloys, *e.g.* in Laves phases (cf. Section 6.2).

Equation (9) demonstrates that the prelogarithmic factor $F$ in (8) must show considerable variations as a function of $d(1)$ and the valency v, and also as a function of the value chosen for B (cf. Section 7). For element-oxygen bonds, values between $75 \leq F \leq 110$ pm are quoted in the literature[56]. In fact, $F$ follows the values for $d(1)$ and v quite closely and, as expected, becomes a maximum for the monovalent cations. A direct comparison of calculated distances using eq. (9) and recent values for element-halogen and element-chalcogen bonds[40] is, however, only possible to a limited extent, because for the latter bonds also the reference distances for a bond strength s = 1 deviate from *Pauling*'s values. Another, more important reason for the difficulty in comparing calculated and observed distances directly, is the fact that the dependence of the bond distance is based on only *one* bond strength (*e.g.* that of the cation). In principle, this procedure is in agreement with *Pauling*'s[65] valence sum rule. Generally speaking, differences in dependence of bond distance on bond strength hold for the cation (or Lewis acid) and anion (or Lewis base) according to eq. (9). These differences are hidden in the averaged values. A further incrementation of distances yielding radii for the atoms therefore seems sensible and desirable, also within the framework of modern bond strength-bond length concepts[40, 51–62].

### 4.3. Coordination Number and Atomic Radius

The discussion has shown that many ways exist for determining the effective coordination number of an atom in a crystal structure. The following step, the adjustment of the atomic size to a special coordination number, can be made in different ways, starting from the tabulated radii $r$ for close packed spheres.

Somewhat "heterogeneous", but numerically simple, is the following procedure. Eq. (9), calibrated with reference to carbon-carbon multiple bonds, yields, together with eq. (5), the simple expression:

$$f = r^{(ecn)}/r = 0.59 + 0.38 \lg(ecn) \tag{10}$$

Using this expression one obtains, *e.g.*, f = 0.973 for the bcc lattice in very good agreement with the experiment, if a value of ecn ≃ 10.2 is used, which is obtained *via* the polyhedron-procedure[43]. The "scalar" path *via* ECoN provides a simpler alternative for the polyhedron-procedure. In connection with eq. (5), however, we already mentioned the problems arising with ECoN, which are associated with the relativity of the function. If ECoN is "stripped" to its essentials and all distances $d_j$ of an atom to its neighbors are referred to the shortest distance $d_{i0}$, one obtains for each atom the relationship (ecn ≃ ECoN'):

$$ECoN'_i = \sum_{j=0}^{\infty} \exp\left[1 - \left(\frac{d_{ij}}{d_{i0}}\right)^5\right]. \tag{11}$$

The exponent 5 is chosen in such a way that the atomic sizes in the bcc lattices are correctly represented in connection with eq. (10). The system of equations (10), (11) describes the following examples of selected intermetallic phases with sufficient accuracy. The procedure is convenient, since it is adequate, due to the rapid convergence of function (11), to include only those distances which exceed the respective shortest distance by less than 50%. Yet the "heterogeneous" procedure is unsatisfactory because of the different character of the individual steps. Moreover, the weakness of this procedure becomes evident for small coordination numbers, in which case function (11) suppresses second-nearest neighbors too much (cf. Section 7). The heterogeneous procedure is therefore only an indication of the indivisibility of chemistry.

The "homogeneous" way uses the same function to determine the effective coordination number ecn as well as to calculate atomic sizes as a function of coordination numbers. With the bond strength-bond length relationship (7) both steps can easily be carried out. With this relationship the effective coordination number ecn* is first calculated, and then the radius adaption *via* f* to this coordination number.

The valency v of an atom i corresponds to the sum of all bonds of this atom:

$$v_i = \sum_j s_{ij} = \sum (d_{ij}/d(1)_i)^{-N} = ecn^*_i (d_{i0}/d(1)_i)^{-N}$$

The single bond distance $d(1)$ corresponds to the value s = 1 (as is indicated by the name). The effective coordination number $ecn^*_i$ indicates how many atoms at a distance $d_{i0}$ saturate the valency of the central atom in place of the quasi-infinite number of atoms with distances $d_{ij}$ in the whole lattice.

$$ecn^*_i = \sum_{j=0}^{\infty} (d_{ij}/d_{i0})^{-N} \tag{12}$$

The second step follows immediately:

$$f^* = r^{ecn^*}/r = (ecn^*/\text{“12”})^{1/N} \quad (13)$$

Writing "12" for the coordination number in a close packed structure indicates the price which has to be payed for the transparency of this procedure. With N = 6, *i.e.* a value which is used for the exponent in many halide and oxide systems[40] one obtains ecn* = 14.45 in the close packed structure instead of the conventional and familiar value 12, and even with N = 8, ecn* = 12.79 is still increased. If the effective coordination number is regarded as a measure of the interactions of an atom with its total surroundings, however, this increase is sensible[41].

A disadvantage of function (12) compared to function (11) is the rather slow convergence. The calculations for the following examples were therefore carried out with N = 8 and summations up to a distance ratio $d_j/d_0 = \sqrt{3}$. The value ecn* = 12.67 obtained for close packing, which has to replace "12" in eq. (13), leads to an error of only 0.1% in f as compared to the complete lattice sum.

## 5. Result

The description of a crystal structure by means of atomic distances only, leads to a loss of information about directions. Tortuous paths, using effective coordination numbers for the atoms, can partially compensate this loss of information. Whereas each single value, taken for itself, does not mean anything, the combination of all values contains a hidden statement about the total arrangement. The entire structure can be described as sum of the individual atoms, each of which are adjusted to the entirety. For a structure with atoms of equal size, the atomic size is identical to the respective shortest distance $d_{i0}$ to its neighboring atoms. If we assume that this statement is, on average, also valid for atoms of different size, we get the following expression, with $z$ being the number of atoms in the unit cell:

$$\sum_{i=1}^{z} 2f_i r_i/d_{i0} = z \quad (14)$$

In this expression each sum contains the individually shortest distance $d_{i0}$ for the i-th atom. One can easily show that the relation (14) is freed from this "relativity" by expressing each f, by the two equations (12) and (13), *i.e.* the result becomes independent of the chosen reference distance ($\sqrt[8]{12.67}/2 = 0.6868$).

$$\sum_{i=1}^{z} \left( \sum_{j=0}^{\infty} d_{ij}^{-8} \right)^{1/8} r_i = 0.6868 z \quad (15)$$

If the distances $d_j$ for a cubic crystal are given by fractions of the lattice constant (*e.g.* $z = 1$ in the primitive cell, $d_0 = a\sqrt{3}/2$, (8×), $d_1 = a$ (6×), $d_2 = a\sqrt{2}$ (12×), ... for the bcc lattice) one directly obtains the lattice constant $a$ as a function of the metallic radii. If $d_j$ refers to $d_{MM}$ (cf. Section 2.1) one obtains this kind of distance as a function of the metallic radii and it becomes possible to calculate the slope α of the Vegard line in the n.n.d., already corrected for the coordination numbers.

For a summation in equations (14) and (15) over all atoms $z$ of the unit cell, both equations represent generalizations of (1) and refer to mixed crystals as well as ordered alloys. In these systems an almost identical weighting is given to *all* atoms for the formation of *all* interatomic distances. This expression, however, cannot be generally valid, but only holds in those cases where the spectrum of distances in a compound contains only slightly differing values for all the various kinds of distances. This asks for high coordination numbers, which are typical for the topologically close packed alloy structures. On the other hand, structures with relatively low coordination numbers, occurring in most compounds with strong covalent or ionic bonds, are dominated by the shortest bonds. Thus if the distance $d_0$ in a structure is of the kind $d_{MN}$, and this distance is shorter than $d_{NN}$ and $d_{MM}$, the summation in eqs. (14) and (15) can be terminated at i = 2 in the simplest case, if the terms of the sum are arranged according to increasing $d_{i0}$. In this case the well-known relationship with simple radii additivity is valid, $d_0 = f_M r_M + f_N r_N$, independent of the composition. The result signifies strain free MN contacts[4] and can be represented as a straight line in the n.n.d. which intersects the line calculated for a weighting according to the composition at $r_M/r_N \simeq 1$, has a smaller slope α′ than this line, and almost includes the point (−1/−1).

If the shortest distance occurs between atoms of the same kind (*e.g.* $d_0 = d_{NN}$), usually belonging to the majority component, these distances can, but not necessarily must, dominate all others. In this case, all distances follow $d_0 = 2f_N r_N$ and the structure field is described by the line with slope α″ = 1.

Summary: A structure type is characterized in the n.n.d. by a "leading line", which corresponds to a Vegard behavior and which is obtained by weighting the radii according to the composition. This line passes the field of compounds crystallizing in this type close to $r_M/r_N = 1$. To what extent the compounds follow this "leading line" over a wide range depends on the spectrum of distances in the given structure type. A small value for the slope α of the leading line corresponds to a large difference in distances

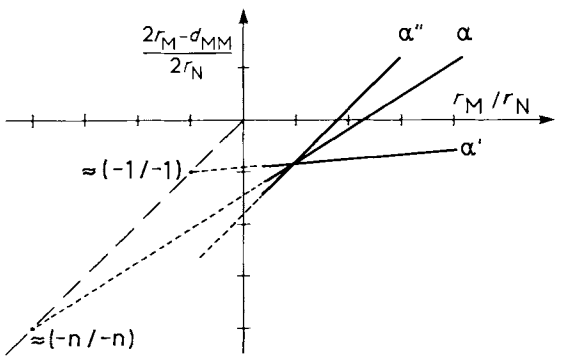



Fig. 14. Schematic representation of the distribution of phases in the n.n.d. The line with slope α resulting from a weighting of radii according to the composition forms a "leading line". In the case of shortest distances $d_{MN}$, the compounds follow the line for a simple sum of radii (α′); if the distances $d_{NN}$ are the shortest ones, they alone can determine the dimension of the compound (α″). The resulting near neighbor diagrams are constructed with the radii for close packing.

of the various kinds and to small coordination numbers in the structure, so that the compounds follow the condition of simple radii additivity for the distances $d_{MN}$ ($\alpha'$). If the shortest distance is $d_{NN}$, the slope of the corresponding line is $\alpha''=1$ and thus at its maximum.

The result is shown schematically in Figure 14.

## 6. Examples

The heading "Democracy and Individuality" was rejected. Table 2 contains the results of calculations for structure types explained in the following.

### 6.1. Elements

At this point only the radii of those elements are discussed which have been dealt with in Section 3.4. Table 3 gives a comparison of atomic radii for the bcc metals at NTP. The correction function of *Teatum, Gschneidner,* and *Waber*[21] corresponds closely to the function used in this work. The values agree to within 0.7 pm; overall, the newly calculated radii are somewhat larger than the published values. The relevance of the radii calculated using eqs. (12) and (13) for the elements of the fourth main group still has to be tested (cf. Section 7). After all, both modifications of tin can be described quite satisfactory within the same formalism using only *one* radius value. In the structure of (metallic) white tin (β-Sn) each atom is surrounded by the following neighbors: $4\times302.2$, $2\times318.2$, $4\times376.8$, $8\times442.0$, $4\times476.4$ and $4\times493.1$ pm. According to eq. (12) the atoms in β-Sn have the effective coordination number ecn* = 6.575. With this value one obtains (eq. (13)) the shortest distance $d_0=298$ pm; with eqs. (10) and (11) one obtains $d_0=299$ pm.

### 6.2. Once Again Laves Phases

In a thorough analysis of all well-characterized Laves phases *Pearson*[66,67] shows that these structure families are very inhomogeneous with respect to the compounds belonging to them. For the $MgCu_2$ type the distribution of points in the n.n.d. (Fig. 6) can be separated into several groups. The lattice constants of compounds belonging to one of the various groups (*e.g.* lanthanoids (Ln)/platinum metals; Ln/Mn, Ln/Al) can be represented with high precision by linear functions of the atomic radii with up to 4 fitted parameters. The chemistry—packing and chemical bonding—of this class of compounds lies hidden in 9 equations with 23 free parameters for the $MgCu_2$ type and 20 equations with altogether 56 parameters for the $MgZn_2$ type[68]. The approach in earlier attempts to come to the simplest possible and most uniform description for the entire family at the expense of accuracy in an individual

Table 2. Data and linear equations for the representation of some structure types in the near neighbor diagram [4] ($x=r_M/r_N$; $y=(2r_M-d_{MM})/2r_N$; α, α', α'' cf. Section 5). The calculations were carried out using equations (10), (11) or (15). Distances in pm.

| Structure typ | Neighbors considered in the calculation | Linear equations |
|---|---|---|
| NaTl | M: 4 M($a\sqrt{3}/4$), 4 N($a\sqrt{3}/4$), 6 N($a/2$), 12 M($a\sqrt{2}/2$)<br>N: as for M | (15) α: $y=0.5138x-0.4862$<br>α'': $y=x-0.9725$ |
| CsCl | M: 8 N($a\sqrt{3}/2$), 6 M($a$), 12 M($a\sqrt{2}$)<br>N: as for M | (15) α: $y=0.4386x-0.5615$ |
| NaCl | M: 6 N($a/2$), 12 M($a\sqrt{2}/2$), 8 N($a\sqrt{3}/2$)<br>N: as for M | (15) α: $y=0.3453x-0.6548$ |
| ZnS | M: 4 N($a\sqrt{3}/4$), 12 M($a\sqrt{2}/2$)<br>N: as for M | (15) α: $y=0.2880x-0.7120$ |
| $MgCu_2$ | M: 12 N($a\sqrt{11/4}/4$), 4 M($a\sqrt{3}/4$)<br>N: 6 N($a\sqrt{2}/4$), 6 M($a\sqrt{11/4}/4$) | (15) α: $y=0.6450x-0.7670$ |
| $CaF_2$ | M: 8 N($a\sqrt{3}/4$), 12 M($a\sqrt{2}/2$)<br>N: 4 M($a\sqrt{3}/4$), 6 N($a/2$), 12 N($a\sqrt{2}/2$) | (10),(11) α: $y=0.4912x-0.9687$<br>α': $y=0.2368x-0.7265$ |
| $AuCu_3$ | M: 12 N($a\sqrt{2}/2$)<br>N: 4 M($a\sqrt{2}/2$), 8 N($a\sqrt{2}/2$) | (10),(11) α: $y=0.6465x-1.0608$ |
| $SiCr_3$ | M: 12 N($a\sqrt{5}/4$), 8 M($a\sqrt{3}/2$), 12 N($a\sqrt{13}/4$)<br>N: 2 N($a/2$), 4 M($a\sqrt{13}/4$), 8 N($a\sqrt{3/8}$) | (15) α: $y=0.6134x-1.1637$<br>α': $y=0.2267x-0.7758$ |
| $AsNa_3$ | M: 3 N(294.3), 2 N(299.7), 6 N(330.5)<br>$N_1$: 3 M(294.3), 6 N(330.5), 6 N(420.1), 2 N(450.0)<br>$N_2$: M(299.7), N(300.6), 3 N(330.1), 3 M(330.5), 3 N(330.5), 3 N(420.1) | (10),(11) α: $y=0.6062x-1.1816$<br>α': $y=0.1907x-0.7801$ |
| $BaCd_{11}$ | M: 8 N(373), 2 N(387), 8 N(387), 4 N(418)<br>$N_1$: 4 N(316), 8 N(324), 2 M(387)<br>$N_2$: 4 N(292), 4 N(294), 2 N(316), 2 M(418)<br>$N_3$: N(292), N(294), N(296), 2 N(300), N(303), N(306), 2 N(324), N(328), M(373), M(378) | (15) α: $y=0.8536x-1.8569$<br>α'': $y=x-2.0220$ |
| $BaHg_{11}$ | M: 9 N(362.5), 5 N(372.8), 8 N(391.8)<br>$N_1$: 12 N(305.0), 24 N(523.3)<br>$N_2$: 3 N(297.1), 3 N(297.3), 3 N(368.5), 3 M(391.8), 3 N(420.2)<br>$N_3$: 2 N(297.1), 2 N(297.3), 4 N(304.9), 2 M(362.5), N(420.2), 4 N(467.7), 4 N(473.5), 2 N(488.6)<br>$N_4$: 5 N(305.0), 4 N(309.9), 2 N(368.5), M(372.8), 2 N(431.3), 4 N(473.5), 2 N(488.5) | (15) α: $y=0.8380x-1.9595$ |

Table 3. Comparison of tabulated [21] and calculated metallic radii using Eq. (15) and the measured lattice constants for (A) metals, crystallizing in a bcc lattice at NTP [37] and (B) fourth main group elements crystallizing in the diamond structure [37]. The value for C was calculated using Eq. (10) (cf. Section 7).

| | Element | $a$ [pm] | $r$ according to [21] | $r$ according to (15) |
|---|---|---|---|---|
| (A) | α-Fe | 286.6 | 127.4 | 127.6 |
| | Cr | 288.5 | 128.2 | 128.5 |
| | V | 302.6 | 134.6 | 134.7 |
| | Mo | 314.7 | 140.0 | 140.1 |
| | W | 316.5 | 140.8 | 140.9 |
| | Ta | 330.6 | 146.7 | 147.2 |
| | Nb | 330.7 | 146.8 | 147.2 |
| | Li | 350.9 | 156.2 | 156.2 |
| | Na | 429.1 | 191.1 | 191.1 |
| | Ba | 502.5 | 224.3 | 223.8 |
| | K | 534.4 | 237.6 | 237.9 |
| | Rb | 570.3 | 254.6 | 253.9 |
| | Cs | 614.1 | 273.1 | 273.4 |
| (B) | C | 356.7 | 91.6 | 94.2 |
| | Si | 543.1 | 131.9 | 134.8 |
| | Ge | 565.7 | 136.9 | 140.4 |
| | α-Sn | 648.9 | (4) 154.5<br>(2) 162.3 | 161.1 |

case[69], is deliberately ignored here in order to reach the high accuracy of the single case.

Our result is given in Figure 15, which represents the calculated specific line for the $MgCu_2$ and $MgZn_2$ types (ideal $c/a$-ratio) together with the positions for some compounds between aluminum and the lanthanoids. The latter have been chosen to show the influence of weak, but additional chemical interactions.

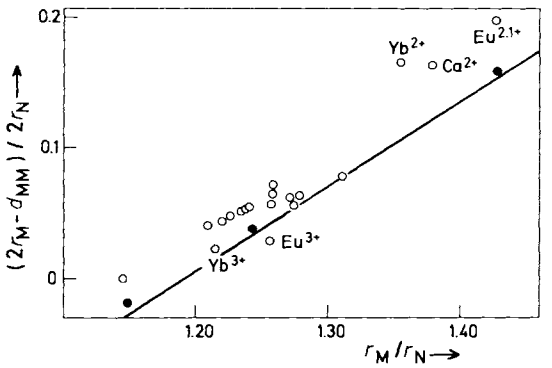



Fig. 15. Representation of compounds $CsK_2$, $KNa_2$, $CsNa_2$ (full circles), $ScAl_2$, $YAl_2$, $LnAl_2$ and $CaAl_2$ (empty circles) *vs* the structure-specific line in the n.n.d. for Laves phases, calculated using eq. (15). Under the premise of different "metallic valencies" for the lanthanoid atom, different positions for one and the same compound result, as is emphasized for $EuAl_2$ and $YbAl_2$.

The distribution of values for the lanthanoid compounds is in part due to the fact that the number of electrons which are donated to the conduction band for the various lanthanoid systems is not exactly known. The value of the radius for the calculation of both strain parameter and radius ratio is therefore undetermined. Do we have to choose the value of "metallic valency" $\simeq 2$ (194 pm) or 3 (174 pm) for $YbAl_2$? For this reason the compounds of Ce, Eu and Yb are not included in the detailed analysis[66].

The example of the phase $CaAl_2$ shown additionally in Figure 15 reveals that the valence difference does not only influence the geometrical construction, but leads to chemical consequences which determine its position in the diagram. $EuAl_2$ shows the same deviation from the line as $CaAl_2$, if the value 2.1 is used for the "metallic valency". It must be concluded that Eu is in the same valence state in this compound as in the element. The position of $YbAl_2$ with respect to the specific line, however, indicates that it is better described with a valency 3 (which differs from that in the element) or with a state somewhere between 2 and 3, if we consider its position with respect to the other lanthanoid phases. In fact, *Iandelli*[70] had already been able to show by magnetic measurements for the compound that the ytterbium is present in a temperature dependent "mixed valence state", whose $Yb^{3+}$ fraction at room temperature amounts to approx. 17%.

The problems discussed above do not occur with the Laves phases of alkali metals. Using eq. (15) one calculates a value of $\alpha = 0.65$ for the slope of the specific line, which is in good agreement with the experimentally found slope ($\alpha = 0.63$[9]) for $KNa_2$, $CsNa_2$, and $CsK_2$. This result verifies the assumption that the interatomic distances in these compounds correspond almost exclusively to an optimization of the packing (cf. Section 2.2). The calculated interatomic distances show such a good agreement with the experimental values (Table 4) that the assumption of ideal positional parameters, on which the determination of experimental values is based, is strongly supported.

Table 4. Comparison of experimental (cf. footnote [*] on p. 97) and calculated interatomic distances [pm] using (15) or (10), (11) for $KNa_2$, $CsNa_2$ and $CsK_2$ [8-10]. The experimental values were obtained with the positional parameters $z(M) = 1/6$ and $x(N) = 5/6$.

| | $KNa_2$ | (15) | (10), (11) | $CsNa_2$ | (15) | (10), (11) | $CsK_2$ | (15) | (10), (11) |
|---|---|---|---|---|---|---|---|---|---|
| $d_{MM}$ | 461 | 462 | 462 | 487 | 487 | 488 | 557 | 558 | 559 |
| $d_{MN}$ | 441 | 442 | 443 | 465 | 466 | 467 | 534 | 535 | 535 |
| $d_{NN}$ | 376 | 377 | 377 | 397 | 398 | 398 | 456 | 456 | 456 |

### 6.3. The $SiCr_3$ Type

Some representatives of this structure type comprising 70 phases like $SnNb_3$ and $GeNb_3$, which is usually incorrectly called the A15, β-W or, correctly, $SiCr_3$ type, have gained great importance as superconductors having the highest known critical temperatures. The structure is shown in Figure 16; as essential feature the chains of transition metals should be emphasized. These are arranged perpendicularly to each other. Many papers associate the structural aspect of superconductivity with these chains.

Even after the already mentioned dispute[26-30] (cf. Section 2.3), several attempts were made to describe the geometrical conditions of A15 phases with special atomic radii[71,72]. Can the dispute between *Geller* and *Pauling* be decided?

The atomic separations within the chains ($d_{NN} = a/2$) are the shortest in the $SiCr_3$ type, but the (more frequent) distances $d_{MN} = a\sqrt{5}/4$ are only larger by 12%. We can expect that both kinds of contacts—as in the $AuCu_3$ family—determine the structure. Figure 17 shows the result of calculations for A15 phases. The distribution of the compounds

in the n.n.d. could be taken directly from a recent paper[73] on this class of compounds. The line shown with slope $\alpha$ corresponds to a weighting of radii according to the composition. The additional line with slope $\alpha'$, which represents the condition of a simple sum of radii for M and N atoms, as proposed by *Geller*, only yields a good description of the structure field close to the radius-ratio $r_M/r_N = 1$. *Pauling* had the better position in the dispute[26-30]. Obviously the description of atomic distances with the aid of radii summations weighted according to the composition is the best approximation for A15 phases over its whole range of existence. The deviations for large values of the radius-ratio, however, indicate that the chemical bonds between the transition metal atoms give rise to smaller lattice dimensions than would be expected just from an analysis of the packing.

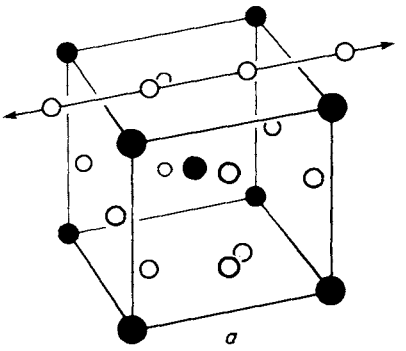



Fig. 16. Unit cell of the (A15, β-W) $SiCr_3$ structure. The chain formed by the transition metals (empty circles) is emphasized.

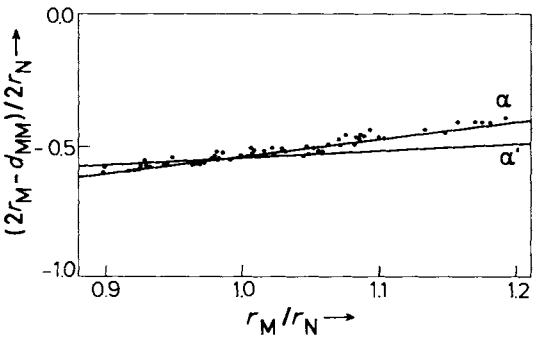



Fig. 17. Distribution of representatives of the $SiCr_3$ type in the near neighbor diagram [73]. The line with slope α corresponds to the radius-lattice constant relation as given by *Pauling* [26]; it is almost identical to the line calculated using eq. (15). A simple sum of radii ($d_{MN} \sim r_M + r_N$) corresponds to the line with slope α'.

*Pauling*[26] used the equation $a = 0.8944(r_M + 3r_N)$ for calculating the lattice constants of A15 compounds; according to equation (15) we find the expression $a = 0.8929(r_M + 3.01 r_N)$.

If one looks at a former representation of A15 phases in the n.n.d.[3,4], deviations to increasingly smaller strain parameters become evident, when the radius-ratio falls below 0.8. Interestingly, the positions of compounds in this range can be described quite well by the line given in Table 2 corresponding to dominating NN contacts (slope $\alpha'' = 1$). This result bears the fascinating aspect that a structure type contains general restrictions which are of different importance for various combinations of elements with respect to a critical radius-ratio. Conclusions of this kind, however, cannot be drawn unambiguously from[3,4], since the compounds with a radius-ratio smaller than 0.8 are β-W ($W_3O$) and $Cr_3O$. What is their real composition and what size has the oxygen atom?

### 6.4. $BaCd_{11}$ and $BaHg_{11}$, "Contaminated Metals"

For a composition $MN_2$ or $MN_3$ one might ask why M and N atoms should influence the formation of all interatomic distances $d_{MM}$ to the same extent. For a compound $MN_{11}$ this is quite obvious: The M atoms are so far apart that distances $d_{MM}$ must be mainly influenced by the size of the N atoms. The question is rather whether there is any chance for the M atoms to have a correcting influence at all?

$BaCd_{11}$ and some other compounds of this type have a complicated tetragonal structure[74], in which the M atoms are surrounded by 22 N atoms and the N atoms by 14, 12 and 12 M and N atoms as nearest neighbors. The coordination polyhedra are characterized by a fan of closely separated distances for the central atoms.

The same holds for the $BaHg_{11}$ type. In the cubic structure[75] 20 N atoms are arranged around the M atom, whereas the four crystallographically different N atoms are each surrounded by 12 N, 3 M and 9 N, 2 M and 8 N, and 1 M and 11 N atoms.

Both structures have been chosen for a comparison, firstly because they fulfill the condition $n \gg 1$, and secondly because the combination of previously reported n.n.d.'s[4] yields distinctly separate fields for both structure types, in which the respective compounds concentrate. Figure 18 shows that the lines which have been calculated according to eqs. (12) and (13) using the positional parameters for $BaCd_{11}$ and $BaHg_{11}$ (cf. Table 2) describe both classes of compounds quite well. In particular, the difference between the two lines is a very good indication of the relative position of the structure fields with respect to each other. For both families, deviations from the respective Vegard line are observed, which can be associated with the simplified calculation of the lines, since for the determination of the effective coordination number only those atoms are considered which belong to the "classical" coordination polyhedra. It is however notable that the rapidly converging function (11) in combination with (10) leads to a result which is identical within the accuracy of drawing. This means that the too large values for the strain parameter in these compounds, which were determined experimentally, are obviously due to chemical effects, which were also discussed for the Laves phases: All compounds contain alkaline earth or rare earth metals, *i.e.* especially electropositive elements besides Zn, Cd and Hg. The formation of heteropolar bonds causes a contraction of the structure with an increase of the strain parameter.

Especially notable are the deviations for the $BaCd_{11}$ structure. The compounds are much better described by the line with slope $\alpha''$ (dominating NN contacts). The same

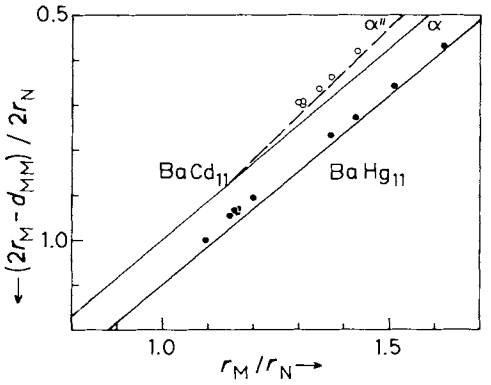



Fig. 18. Near neighbor diagrams for the representatives of the $BaCd_{11}$ and $BaHg_{11}$ types [32]. The interatomic distances in $BaHg_{11}$ follow the sum of radii, weighted according to the composition (slope $\alpha$); in contrast, the distances in $BaCd_{11}$ are almost exclusively determined by the size of the N atoms (slope $\alpha''$).

result, namely "participation in the decision" of the minority component in the case of $BaHg_{11}$, but a "dictatorship" of the majority component in $BaCd_{11}$, was obtained by *Pearson*[76]. He offers an explanation for the difference: If the N atoms which surround the M atom have variable positional parameters, the difference in size of various M atoms is "neutralized" by the immediate environment ($BaCd_{11}$); if however the surrounding N atoms occupy special positions ($BaHg_{11}$), this difference in size is transferred to the entire lattice. Thus, an additional restraint for the validity of Vegard's rule for ordered compounds exists. Besides a suitable spectrum of distances it is the symmetry of the structure which has to be considered, at least for large values of n.

### 6.5. $AsNa_3$ as an Example for Strong Heteropolar Bonds

The $AsNa_3$ type is found for 20 different compounds which are predominantly ionic. Besides the compounds of alkali metals with elements of the 5th main group, which are all insulators or semiconductors, typical intermetallic compounds like $HgMg_3$ and $PtMg_3$ also crystallize in this structure type[32]. Starting from the structure of wurtzite, the hexagonal analogue of zinc blende, the $AsNa_3$ structure results from a filling of all tetrahedral sites with N atoms and introduction of more N atoms, which form chains parallel to the *c*-axis. M atoms are surrounded by 11 N atoms, the N atoms by 3 or 4 M atoms. That the actual environment is only inadequately described with theses statements is seen in Table 2. Here the almost identical effective coordination number is notable despite very different geometrical arrangements around the N atoms.

In contrast to the other structures discussed so far in Section 6, the shortest distance $d_o$ (=294.3 pm) in the crystal structure of $AsNa_3$ is of the kind $d_{MN}$. The next longer distance also belongs to this kind. According to Section 5, we should expect that all other distances are dominated by the shortest ones. The assumption is correct. *Pearson* has already shown that the compounds of the $AsNa_3$ type follow the line of strain free MN contacts very closely. The line constructed with a simple sum of radii describes the structure field of the $AsNa_3$ type very accurately (Fig. 19). This line intersects the "leading line" for Vegard behavior at $r_M/r_N = 0.92$; the latter intersects only one end of the structure field for the $AsNa_3$ representatives. Most compounds crystallizing in this type have strongly reduced strain parameters as compared to the calculated line with slope $\alpha'$. As in the preceding example this is to be expected, since the strong heteropolar bonds in the $AsNa_3$ structure lead to a contraction of the lattice which is not incorporated in the radii employed.

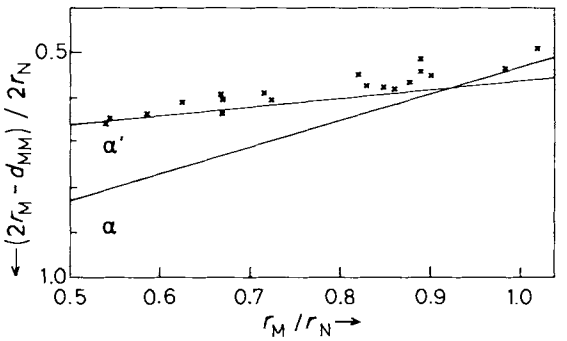



Fig. 19. Distribution of compounds of the $AsNa_3$ type [32] in the near neighbor diagram. The lines were calculated using eqs. (10) and (11) ($\alpha$ and $\alpha'$). With strain parameters as given by *Pearson* [4] the compounds follow the line with slope $\alpha'$ even closer. His values, however, do not refer to the shortest MM-distances.

### 6.6. The $CaF_2$ Type; Link between Intermetallic Phases and Ionic Crystals

When the empty tetrahedral sites in the ZnS structure (Fig. 1) are occupied by N atoms, the well-known fluorite structure results. The M atom is surrounded by a cube of N atoms each of which in turn is surrounded by a tetrahedron of M atoms. Counting the conventional way yields cn=8 for each M atom and cn=4 for each N atom. But what is sauce for the bcc lattice is sauce for the fluorite. Each N atom only has 4 M atoms as neighbors, but the 6 N atoms belonging to the closer environment are only 15% further apart, so that, *e.g.*, with eq. (11) an effective coordination number ECoN′=6.09 results. One might accept this value, at least for intermetallic compounds with atoms of nearly equal radii (cf. [39]).

Numerous compounds crystallize in the $CaF_2$-type structure (or its anti-type). The fluorides and chalcogenides of main group metals are colorless, and thus already indicate the kind of chemical bonding. But also typical intermetallic compounds with metallic properties like $AuIn_2$ or $PtSn_2$ occur with this structure.

Figure 20 summarizes the results of calculations for this structure type. The compounds in which both components are metals, gather, when characterized by the respective metallic radii, in a narrow interval around the intersection of lines with slope $\alpha$ (radii weighted according to the composition) and $\alpha'$ (simple sum of radii). It cannot be decided, to which condition the compounds pay tribute: they unify both conditions $d_{MN} \approx r_M + r_N$ and $d_{MN} \approx r_M + 2r_N$. For typical salt-like compounds, however, the expected simple sum of radii holds for the $d_{MN}$ distances. The positions for fluorides and oxides are considerably spread out,

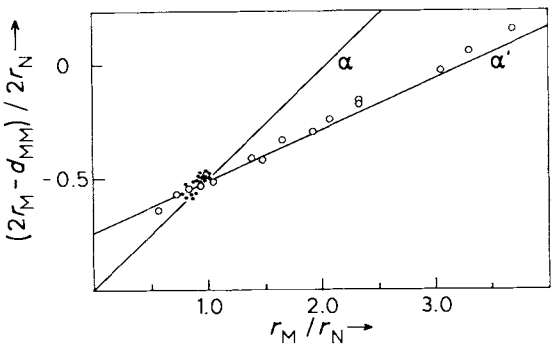



Fig. 20. Distribution of some compounds with $CaF_2$ structure in the near neighbor diagram. The positions of compounds formed by metallic components (dots) were calculated with atomic radii. The positions for the salt-like oxides, calculated with ionic radii, follow the condition of a simple sum of radii [*].

but this is understandable: Using the metallic radii for sodium and (extrapolated) oxygen, a position for $ONa_2$ in the diagram can be calculated, but this position is not very close to reality. It is much more realistic to assume a complete electron transfer to the (fluorine) or oxygen atom and then to describe the atoms by their ionic radii[*]. As can be seen, the worlds of intermetallic phases and ionic crystals are close neighbors.

## 7. Concluding Remarks

According to Section 4.2 the ratio of the distances of nearest neighbors in metals with close packing on the one hand and a bcc lattice on the other follows the same law as the ratio of the distances of carbon atoms in diamond and in a molecule with carbon-carbon double bonds. Even a noble gas crystal obeys this law up to a certain extent, although in this case concepts like valency or bond strength do not allow a description of the effective forces.

Helium crystallizes in a bcc lattice as well as with cubic close packing or hexagonal close packing[37]. The observed changes in the distances between the atoms at the phase transition largely correspond to those which are found for metals (Fig. 13). The changes are correctly described by eqs. (10) and (13), which do not explicitly contain a valency dependence.

The van-der-Waals interactions between noble gas atoms are described to a good approximation by a Lennard-Jones potential; the lattice constants of the solids can be calculated quite accurately with the potential determined for the gas phase[78]. With this potential a distance between nearest neighbors in the bcc lattice results at the energy minimum, which indeed is shortened by a factor of 0.978 as compared to the close packed structure[**]. But any hope that noble gases might provide a law as to how distances are related to coordination numbers, soon disappears. Due to the rapid increase in the repulsion potential, which is not opposed by strong bonding forces, the noble gas atoms reject any additional deformation; for the primitive cubic lattice (α-Po) almost the same value of f is calculated as for the bcc arrangement. An extrapolation to small coordination numbers is impossible with this type of bonding. Since the interaction potential of a noble gas does not help any further, perhaps the criterion of constant volumina, inspite of changing coordination number, might be of help. But little reflection on this point is necessary: The diamond structure corresponds to a bcc lattice, which is only half occupied. The waste of space is impossibly compensated by a compression of the atoms. As Figure 21 is intended to show, the truth is somewhere between the individual extremes of (a) rigid spheres, which do not allow any adjustment to a given structure and (b) non-rigid spheres, which compensate for the reduced space filling at low coordination numbers by correspondingly smaller atomic sizes. Helium is close to one extreme: Only for almost close packed structures do the weak van-der-Waals bonds affect the atomic size in the same way as strong chemical bonds. The elements C, N and O are close to the other extreme: Over a wide range of coordination numbers the connecting line $f = 0.59 + 0.38 \lg(ecn)$ [equation (10)] is almost identical to the condition of constant volumina.

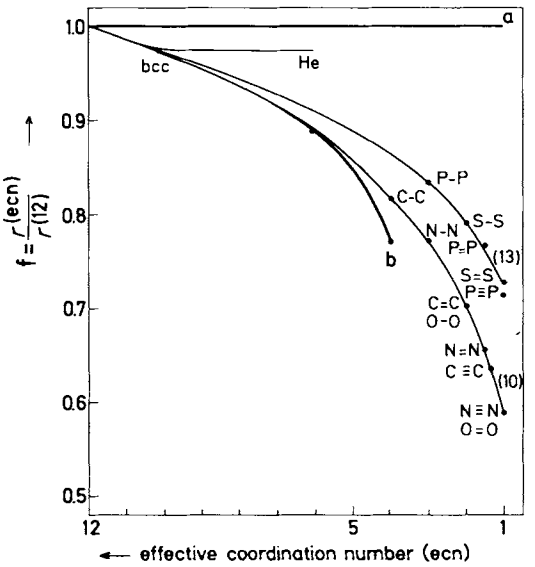



Fig. 21. Atomic sizes as function of the effective coordination number. The limits are given by (a) the model of rigid spheres, and (b) the model of constant volumina for isotropic changes of the sizes of the atoms in the bcc-lattice, the primitive lattice of α-Po and in the diamond structure. The multiple bonds of C, N and O are well represented by relation (10); for the elements P and S [79, 80] the relative changes in bond lengths are smaller and better represented by eq. (13) with N = 8. The He crystal is described by a Lennard-Jones potential [**].

Some explanations are required in order to gain a better understanding of Figure 21. With 3-dimensional structures (bcc, α-Po, diamond type) the effective coordination number is normalized to ecn = 12 for close packed structures. Taking N = 8 for, *e.g.*, the diamond structure, we get the

[*] *Pauling*'s radii [38] were used. To allow for a comparison with lines calculated for metallic radii, the ionic radii tabulated for cn = 6 were converted to the close packing with the aid of eq. (10). *Shannon*'s radii [77] lead to an almost identical result, provided one starts from the values for cn = 6; only the values for Li-compounds yield strain parameters too large.

[**] A summation of all Lennard-Jones potentials over all atom pairs yields the bonding energy $U \sim \sum \left(\frac{\sigma}{p_{ij} d}\right)^{12} - \sum \left(\frac{\sigma}{p_{ij} d}\right)^{6}$ of the noble gas crystal; the partial sums for the fcc lattice have values $(\sum p_{ij}^{-12})_{fcc} = 12.13$ and $(\sum p_{ij}^{-6})_{fcc} = 14.15$. For the bcc lattices one obtains $(\sum p_{ij}^{-12})_{bcc} = 9.15$ and $(\sum p_{ij}^{-6})_{bcc} = 12.25$. The ratio of equilibrium distances follows *via* $dU/dd = 0$ as $d_0^{(bcc)} = 0.978\, d_0^{(fcc)}$.

value ecn* = 4.24 according to eq. (12) and thus ecn = 12 × (4.24/12.67) = 4.02. The result is almost identical to ECoN′ = 4.00. Good agreement is also found for α-Po and the bcc lattice; therefore, the calculated curves (using eqs. (10) and (13)) can be compared for the same values of the effective coordination number. The calculation of coordination numbers for single and double bonds was simplified by considering only nearest neighbors. For example, at a coordination number 3, phosphorus[79,80] forms 3 single bonds (221 pm); in the $P_2$ molecule each P atom has the coordination number 1 and forms a triple bond to its neighboring atoms (189.4 pm). For the double bond (203.4 pm) an effective coordination number 1.57 is calculated using eq. (12) with single bond and double bond distances, instead of the value 1.5 according to eq. (5). The curve (13) quite accurately represents the relative change of distances (= change of size) for the elements P and S in single and multiple bonds. The larger differentiation of distances in C, N and O is represented by the curve calculated using eq. (10)[*]. The disagreement observed for the atomic radii of the fourth group elements (Table 1) is due to representation of the elements by different curves. This is also the basic reason why the additive correction of distances (radii) according to eq. (8) works rather satisfactory *via* an error compensation.

Equilibrium distances between atoms are the result of a balance between attractive and repulsive interactions. From this point of view not only the formal similarity of the descriptions for various bond types like covalent, ionic, metallic and van-der-Waals bonds can be rationalized, but also the fact that not all atoms have the same capability. The rapid increase of repulsive forces limits the mutual approach of atoms. The relationship (10), which is calibrated to the shortest bonds in chemistry, obviously represents the maximum possible approach. The relative change of distances in C, N and O as function of the coordination number is much larger than for the elements P and S, which have a fully occupied Ne shell.

In Section 3.5 the problems arising from the application of different correction functions was mentioned for the derivation and use of atomic radii. From Figure 21 it becomes clear, that even for the simplest case of an atom surrounded by identical atoms, the atomic size cannot be described as a function of the environment by only one expression for all elements. However, whereas according to [21] the radii are treated with different correction functions depending on the coordination number, Figure 21 indicates that different functions are necessary for different atoms (or more precisely for atoms with different cores). On the average, the system of equations (12) and (13) used here yields satisfactory results with N = 8 for the intermetallic compounds under discussion. A more sophisticated procedure, however, must permit variations of the exponent N[*]. There is hope in arriving at a consistent system of metallic radii which is a prerequisite for discussion of additional chemical interactions that reach beyond packing effects (*e.g.* interactions due to different electronegativities).

The attentive reader will have noticed that the aim and center of interest have changed during the writing of this review. At first the question of how the relative amounts of elements in an intermetallic compound determine the atomic distances, was in the foreground. Our discussion has shown that in close packed arrangements with high coordination numbers, as in alloys, *all* atoms together determine *all* distances, at least when the different kinds of distances are correlated *via* the symmetry. If only few neighbors saturate the valency of an atom (low coordination number) the shortest distances in the structure are only determined by the size of the atoms forming these bonds. The shortest distances then dominate all others, provided there is a correlation.

At a later state of the work another aspect increasingly became dominant, namely, that concepts and formal descriptions of bonds in molecules could be used almost unchanged with intermetallic systems, although seemingly unbridgeable contrasts exist. One side follows a valency principle and obeys clear-cut stoichiometric rules. The other side, according to current views, exists outside the border line of a valency concept and thus does not follow the rules, as they are familiar to every chemist, on the composition of compounds. Nevertheless, Figure 21 demonstrates or recalls that both sides are not in principle different but represent uniformly describable limits of the same phenomenon, namely the chemical bond.

*I thank H.-G. von Schnering and V. Heine as well as my co-workers for many helpful discussions and also W. J. Westerhaus for the careful translation of the text. Generous support of this work by the Fonds der Chemischen Industrie is gratefully acknowledged.*

Received: October 29, 1982 [A 441 IE]
German version: *Angew. Chem. 95* (1982) 94
Translated by Dr. W. J. Westerhaus, Stuttgart

[*] Problems with ECoN′ for small coordination numbers have already been mentioned in conjunction with eq. (11): The carbon atom linked to other C atoms *via* a single and triple bond, would have the coordination number ECoN′ = 1.08 (instead of 1.33 according to eq. (5)). If an exponential representation according to eqs. (12) and (13) using N ≈ 4.3 is chosen for the elements C, N and O, a good agreement between bond lengths and the corresponding coordination numbers is reached in the "homogeneous" way, as in the case of P and S.

[1] R. Goddard, C. Krüger in P. Coppens, M. Hall: *Electron Distribution and the Chemical Bond*, Plenum Press, London 1982, p. 297.
[2] I. D. Brown, *Chem. Soc. Rev. 7* (1978) 359.
[3] W. B. Pearson, *Acta Crystallogr. B 24* (1968) 1415.
[4] W. B. Pearson: *The Crystal Chemistry and Physics of Metals and Alloys*, Wiley-Interscience, New York 1972.
[5] F. Laves, H. Witte, *Metallwirtsch. Metallwiss. Metalltech. 14* (1935) 645.
[6] F. Laves "Crystal Structure and Atomic Size" in: *Theory of Alloy Phases*, American Society for Metals, Cleveland, OH 1956, p. 124.
[7] R. L. Berry, F. B. Raynor, *Acta Crystallogr. 6* (1953) 178.
[8] F. Laves, H. J. Wallbaum, *Z. Anorg. Allg. Chem. 250* (1942) 110.
[9] A. Simon, W. Brämer, B. Hillenkötter, H.-J. Kullmann, *Z. Anorg. Allg. Chem. 419* (1976) 253.
[10] A. Simon, G. Ebbinghaus, *Z. Naturforsch. B29* (1974) 616.
[11] A. Simon, H.-J. Kullmann, unpublished.
[12] J. Hafner, *Phys. Rev. B15* (1977) 617.
[13] J. Hafner, *Phys. Rev. B19* (1979) 5094.
[14] J. Hafner, *Phys. Rev. B21* (1980) 406.
[15] L. Vegard, *Z. Phys. 5* (1921) 17.
[16] K. A. Gschneidner, G. H. Vineyard, *J. Appl. Phys. 33* (1962) 3444.
[17] W. Biltz: *Raumchemie der festen Stoffe*, Voss-Verlag, Leipzig 1934.
[18] P. Niggli, *Z. Kristallogr. 56* (1921) 17.
[19] K. Fajans, H. G. Grimm, *Z. Phys. 2* (1920) 299.
[20] E-an Zen, *Am. Mineral. 41* (1956) 523.
[21] E. Teatum, K. Gschneidner, J. Waber, *LA-2345*, U. S. Dept. Commerce, Washington DC 1960; cited in [4].

[22] C. B. Shoemaker, D. P. Shoemaker "Structural Properties of some σ-Phase related Phases" in B. C. Giessen: *Developments in the Structural Chemistry of Alloy Phases*, Plenum Press, London 1969, p. 107.
[23] F. C. Frank, J. S. Kasper, *Acta Crystallogr. 11* (1958) 184.
[24] F. C. Frank, J. S. Kasper, *Acta Crystallogr. 12* (1959) 483.
[25] P. Villars, K. Girgis, F. Hulliger, *J. Solid State Chem. 42* (1982) 89.
[26] L. Pauling, *Acta Crystallogr. 10* (1957) 374.
[27] S. Geller, *Acta Crystallogr. 9* (1956) 885.
[28] S. Geller, *Acta Crystallogr. 10* (1957) 380.
[29] L. Pauling, *Acta Crystallogr. 10* (1957) 685.
[30] S. Geller, *Acta Crystallogr. 10* (1957) 687.
[31] A. Simon, *Proc. 3rd Eur. Crystallogr. Meet.*, Zürich 1976, p. 335.
[32] W. B. Pearson in G. V. Raynar: *Handbook of Lattice Spacings and Structures of Metals and Alloys*, Vol. 1 and 2, Pergamon Press, Oxford 1958 and 1967.
[33] J. D. H. Donnay, H. M. Ondik: *Crystal Data, Determinative Tables*, 3rd Ed., Vol. II, U. S. Dept. Commerce, Natl. Bur. Stand., Comm. Powder Diffr. Stand., Washington DC 1973.
[34] E. Zintl, W. Dullenkopf, *Z. Phys. Chem. B16* (1932) 183.
[35] E. Inglesfield, *J. Phys. C4* (1971) 1603.
[36] W. Hume-Rothery, *J. Inst. Met. 35* (1926) 309.
[37] J. Donohue: *The Structures of the Elements*, Wiley, New York 1974.
[38] L. Pauling: *Die Natur der chemischen Bindung*, 3rd Ed., Verlag Chemie, Weinheim 1976; *The Nature of the Chemical Bond*, 3rd Ed., Cornell University Press, Ithaca NY 1960.
[39] R. Hoppe, *Angew. Chem. 82* (1970) 7; *Angew. Chem. Int. Ed. Engl. 9* (1970) 25.
[40] I. D. Brown: *The Bond-Valence Method, Structure and Bonding in Crystals*, Vol. II, Academic Press, New York 1981, p. 1.
[41] F. L. Carter, *Acta Crystallogr. B34* (1978) 2962.
[42] A. L. Mackay, *Acta Crystallogr. A30* (1974) 440.
[43] M. O'Keeffe, *Acta Crystallogr. A35* (1979) 772.
[44] G. O. Brunner, *Acta Crystallogr. A33* (1977) 226.
[45] R. Hoppe, *Z. Kristallogr. 150* (1979) 23.
[46] R. Hoppe, G. Meyer, *Z. Metallkd. 71* (1980) 347.
[47] H. G. von Schnering, supplement to [45].
[48] V. W. Goldschmidt, *Skr. Nor. Vidensk. Akad. Oslo 2* (1926); *8* (1927).
[49] W. H. Zachariasen, *Z. Kristallogr. 80* (1931) 137.
[50] D. H. Templeton, *J. Chem. Phys. 21* (1953) 2097.
[51] G. Donnay, R. Allmann, *Acta Crystallogr. A28* (1972) 108.
[52] Yu. A. Pyatenko, *Kristallografiya 17* (1972) 773.
[53] W. H. Baur, *Am. Mineral. 57* (1972) 709.
[54] I. D. Brown, R. D. Shannon, *Acta Crystallogr. A29* (1973) 266.
[55] G. Donnay, J. D. H. Donnay, *Acta Crystallogr. B29* (1973) 1417.
[56] R. Allmann, *Monatsh. Chem. 106* (1975) 779.
[57] I. D. Brown, Kang Kun Wu, *Acta Crystallogr. B32* (1976) 1957.
[58] W. H. Zachariasen, *J. Less-Common Met. 62* (1978) 1.
[59] W. H. Zachariasen, R. A. Pennemann, *J. Less-Common Met. 69* (1980) 369.
[60] W. H. Baur: *Structure and Bonding in Crystals*, Vol. II, Academic Press, New York 1981, p. 31.
[61] R. D. Shannon in [60], p. 53.
[62] O. Slupecki, I. D. Brown, *Acta Crystallogr. B38 (1982) 1078.*
[63] J. Donohue, *J. Am. Chem. Soc. 85* (1963) 1238.
[64] A. F. Wells: *Structural Inorganic Chemistry*, 4th Ed., Clarendon Press, Oxford 1975.
[65] L. Pauling, *J. Am. Chem. Soc. 51* (1929) 1010.
[66] W. B. Pearson, *Acta Crystallogr. B37* (1981) 1174.
[67] W. B. Pearson, *Acta Crystallogr. B37* (1981) 1183.
[68] W. B. Pearson, *J. Less-Common Met. 76* (1980) 255.
[69] A. R. Edwards, *Metall. Trans. 3* (1972) 1365.
[70] A. Iandelli, *Z. Anorg. Allg. Chem. 330* (1964) 221.
[71] C. R. Johnson, D. H. Douglas, *J. Low Temp. Phys. 14* (1974) 565.
[72] Y. Tarutani, M. Kudo, *J. Less-Common Met. 55* (1977) 221.
[73] R. M. Waterstrat, *J. Solid State Chem. 37* (1981) 370.
[74] M. J. Sandersen, N. C. Baenziger, *Acta Crystallogr. 6* (1953) 627.
[75] G. Peyronel, *Gazz. Chim. Ital. 82* (1952) 679.
[76] W. B. Pearson, *Z. Kristallogr. 152* (1980) 23.
[77] R. D. Shannon, *Acta Crystallogr. A32* (1976) 751.
[78] C. Kittel: *Einführung in die Festkörperphysik*, Oldenbourg-Verlag, München 1973, p. 141.
[79] *Tables of Interatomic Distances and Configuration in Molecules and Ions, Suppl.*, Spec. Publ. No. 18, The Chemical Society, London 1965.
[80] M. Yoshifuji, I. Shima, N. Inamoto, *J. Am. Chem. Soc. 103* (1981) 4587.

# Thio- and Seleno-Compounds of Main Group Elements—Novel Inorganic Oligomers and Polymers

**By Bernt Krebs***

*Dedicated to Professor Harald Schäfer on the occasion of his 70th birthday*

During the last decade modern preparative and structural methods have led to novel and often unexpected oligomeric and polymeric main group element-sulfur compounds having remarkable bonding and structural properties and reactivities. Examples of important new developments in this area are: the discovery of boron sulfides $B_8S_{16}$ and $(BS_2)_n$ and of ion-conducting air-stable thioborates with tetrahedrally coordinated boron; the successful use of boron sulfides in organic and inorganic syntheses; the preparation of different homologous series of molecular polynuclear thio- and selenoanions of Ga, In, Si, Ge and Sn, and of new polynuclear sulfide- and selenide-halides of Si and Ge as interesting reagents for inorganic and organic reactions; the synthesis of argyrodite($Ag_8GeS_6$)-like phases with remarkable solid-state properties; and the characterization of the S–H···S type hydrogen bridge in thiocarbonic acid and thiophosphinic acids, which is of importance for an understanding of certain interactions in sulfur-containing biomolecules.

## 1. Introduction

Compounds of sulfur with other main group elements are remarkable for their extraordinarily variable bonding characteristics, which extend from ionic sulfides of the alkali and alkaline earth metals to sulfur compounds of boron, aluminum and silicon, which are highly sensitive to hydrolysis, to the polymeric sulfides of germanium, tin, arsenic and antimony, which are able to form thioanions, to molecular sulfides of carbon and phosphorus, and to molecular compounds with nitrogen or halogens, where, in

[*] Prof. Dr. B. Krebs
Anorganisch-Chemisches Institut der Universität
Corrensstrasse 36, D-4400 Münster (Germany)

contrast to all the other types of compounds mentioned, sulfur is the electropositive reaction partner. It is obvious that these variations in bond properties lead to a wide range of chemical and physical characteristics as well as to a variety of practical applications. Comprehensive reports and reviews have recently appeared in the literature concerning several sectors of this rather heterogenous chemistry, *e.g.* the large and highly topical area of sulfur-nitrogen compounds[1,3], other aspects of non-metal sulfur compounds[2,3] or carbon-sulfur compounds[4].

The following progress report summarizes some important new developments in the chemistry and structural chemistry of sulfur compounds of semimetals and metals of the 3rd to 5th main groups. This sector of chemistry, which has progressed considerably over the last few years, is of special interest because of its relation to both molecular chemistry as well as solid-state chemistry.

## 2. Boron Sulfides and Boron Selenides

### 2.1. Synthetic Methods

Although the first investigations on boron-sulfur compounds were already reported by *Berzelius*[5] and *Wöhler*[6] ("Dreifachschwefelbor") early in the last century, so far remarkably little is known about binary and ternary sulfides and selenides of boron. The reason for this undoubtedly stems from the fact that boron chalcogenides are extraordinarily sensitive towards exchange reactions with oxygen and towards hydrolysis (at least in the case of trigonally coordinated boron) and that the amorphous boron previously used as starting material was not pure, thus making the preparation of pure compounds difficult.

In the synthesis of binary phases from the elements, or of ternary phases from sulfides of the components by fusion reactions in evacuated ampoules at elevated temperatures, it is necessary to employ special techniques because of the high aggressivity of B–S and B–Se-systems towards most container materials. In uncoated quartz glass ampoules, for example, $B_2S_3$ reacts quantitatively at temperatures above about 400 °C according to

$$2\,B_2S_3 + 3\,SiO_2 \longrightarrow 2\,B_2O_3 + 3\,SiS_2$$

with complete S/O exchange; similar reactions occur with ternary thioborates. For clean syntheses the following have proven most effective: a) coatings on the inner walls of quartz glass ampoules with glassy carbon, prepared by thermal decomposition of acetone-vapor, b) closed graphite crucibles or open corundum finger crucibles in evacuated quartz ampoules (possibly with a temperature gradient in the reaction vessel), and c) closed tantalum crucibles in which the reactions can be performed under a protective gas atmosphere. Boron nitride can also be used as a crucible material[7,8].

Of the solid boron sulfides $B_2S_5$[7,9], $BS_2$[10–13], $B_2S_3$[9,14–21], BS[22,23] and $B_{12}S$[24,25] mentioned in the literature, only the existence of $B_2S_3$ has so far been proven as a unique phase (cf. also [22,23]), although only a few reliable spectroscopic, thermodynamic and structural data are available, even for this compound[18,23]. In a similar way this is also true for $B_2Se_3$[26–31], which can be obtained from the elements at 850 °C. The formation of $B_2S_5$, which was reported to occur as a solid phase by reaction of amorphous boron with excess sulfur at 590 °C[7,9], could not be reproduced in subsequent investigations[11,32,33]. Solid $BS_2$ is postulated from the thermal analysis of the system B/S with high sulfur contents[11,23], while BS is claimed to develop in two modifications at a pressure of 60 kbar and 1400–1500 °C[23,34]. On heating boron and sulfur rapidly to 1600–1700 °C, a boron-rich phase $B_{12}S$ was obtained, which, considering the bonding in icosahedral structures, is probably better formulated as $B_{12}SB$[24,25].

Considerable progress has been made over the last few years through the structural characterization of $B_2S_3$ and the preparation of new oligomeric and polymeric sulfides and selenides of the composition $BS_2$ and $BSe_2$, which will be dealt with subsequently.

### 2.2. $B_2S_3$

$B_2S_3$ is a colorless glassy solid and is extremely sensitive to hydrolysis. It is prepared, *e.g.*, by a) reaction of boron with sulfur or $H_2S$ in an inert gas atmosphere, b) reaction of boron with metal sulfides (*e.g.* FeS, ZnS, $Al_2S_3$), c) conversion of metal borides (*e.g.* $MgB_6$, $FeB_2$) with sulfur or $H_2S$, d) thermal decomposition of cycloborothianes (*e.g.* $H_3B_3S_6$, $B_3S_3Br_3$), or e) by thermolysis of metal thioborates, in all cases at elevated temperatures of about 400–900 °C[9,14–21,23].

No suitable procedures were hitherto available for purifying the reaction products, so that in many earlier preparations considerable amounts of impurities (at least 5%) have to be assumed. With this aspect in mind, the thermal decomposition of molecular compounds, which can be purified more easily, is the method of choice for the synthesis of pure samples[9,21]. This is exemplified by the decomposition of the trimeric cyclic metathioboric acid $H_3B_3S_6$[35–38] according to

$$3\,BBr_3 + 6\,H_2S \xrightarrow[CS_2,\,C_6H_6]{40-80\,^\circ C} H_3B_3S_6 + 9\,HBr$$

$$2\,H_3B_3S_6 \xrightarrow{100-200\,^\circ C} 3\,H_2S + 3\,B_2S_3$$

However, with the precautions mentioned, pure preparations can also be obtained from the elements.

Like the homologous compounds $B_2O_3$ and $B_2Se_3$, $B_2S_3$ also shows a distinct tendency towards formation of glassy phases. Crystalline samples are more difficult to obtain, *e.g.*, by vacuum distillation of glassy $B_2S_3$ at 550–600 °C[19], by reaction of boron with FeS under He at 700–730 °C[16,17] and as a product of the thermolysis of $H_3B_3S_6$[9,21]. Single crystals suitable for X-ray structure analysis could only be obtained by controlled thermal decomposition of heavy metal thioborates, *e.g.* according to

$$2\,Ag_3B_5S_9 \underset{650\,^\circ C}{\overset{750\,^\circ C}{\rightleftharpoons}} 3\,Ag_2S + 5\,B_2S_3$$

$$Pb_2B_2S_5 \underset{800\,^\circ C}{\overset{850\,^\circ C}{\rightleftharpoons}} 2\,PbS + B_2S_3$$

employing reversible formation-dissociation equilibria of the ternary phases[8,39–42].

The structure of $B_2S_3$ was first determined in 1977 using these (twinned) crystals. The compound is monoclinic[40,41,43] and forms a remarkable layer structure. It consists of planar six-membered $B_3S_3$ and four-membered $B_2S_2$ rings which are coupled *via* S bridges to form planar two-dimensional polymeric layers (Fig. 1). Within the

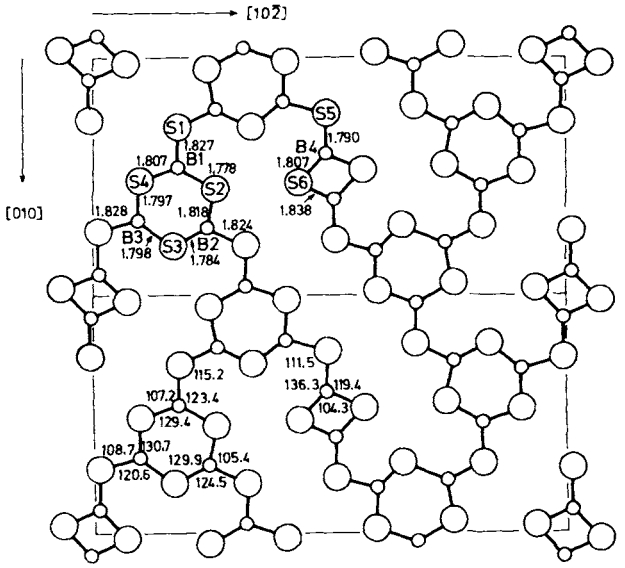



Fig. 1. Layer structure of $B_2S_3$ (two unit cells) with bond lengths [Å] and bond angles [°].

layers, zigzag chains of six-membered rings run parallel to *b*; each six-membered ring is connected to a six-membered ring of a neighboring chain by way of a four-membered ring (located at a center of inversion). All boron atoms have trigonal-planar coordination. Whereas the structure and bonding of the $B_3S_3$ ring correspond to those found for trimeric metathioboric acid $H_3B_3S_6$ and its alkali metal salts[8,38,40,44], the 1,3,2,4-dithiadiboretane ring is highly interesting because the four-membered ring structures in $[BSN(C_2H_5)_2]_2$[45] and in $(BSSH)_2$ and $(BSSC_2H_5)_2$[35-37] could hitherto not be characterized. The very short transannular B...B- (2.237 Å) and S...S distances (2.878 Å) in the strained four-membered ring are remarkable; the mean B–S bond length in the ring (1.823 Å) is slightly larger than the mean value over all B–S bonds of the structure (1.808 Å).

Apart from the trigonal-planar coordination of the boron atoms, the $B_2S_3$ structure has no common features with the three-dimensionally polymeric $B_2O_3$ crystal structure[46,47]. In $B_2O_3$-I, chains of corner-linked planar $BO_3$-triangles running in three different directions are conneted *via* further corners to form a three-dimensional polymer (Fig. 2).

The comparison of the $B_2S_3$ and $B_2O_3$ structures with the recently discovered structure of the metastable high-pressure modification $B_2O_3$-II of much higher density[48,49] (Fig. 3) is particularly instructive. $B_2O_3$-II can be prepared at 65 kbar/1100 °C; it contains tetrahedrally coordinated boron, and its kinetic stability is shown by its insolubility in concentrated acids. From experience in the successful synthesis of thioborates with tetrahedrally coordinated

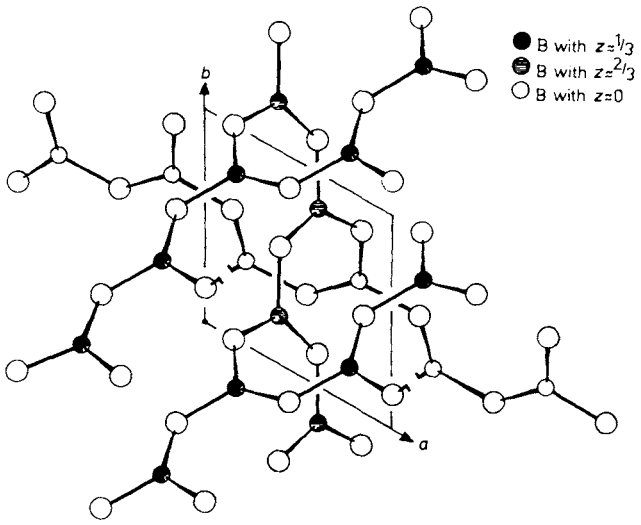



Fig. 2. Crystal structure of $B_2O_3$-I (normal pressure modification [46, 47].

boron ($Ag_6B_{10}S_{18}$, $Pb_4B_4S_{10}$[8,40,42,50]; cf. Section 3) it cannot be ruled out that a similar high pressure form of $B_2S_3$ may exist.

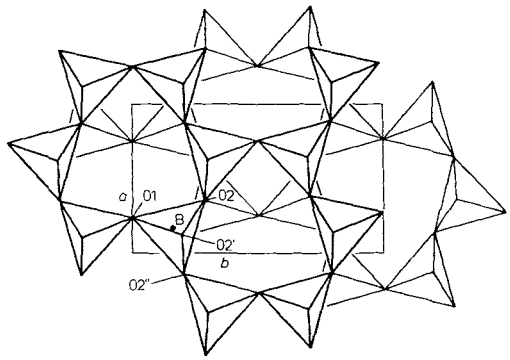



Fig. 3. Structure of the high pressure modification $B_2O_3$-*II* [48].

In spite of the difficulties in its handling, $B_2S_3$ has recently proved to be a valuable starting material for the preparation of new boron compounds as well as an effective sulfurizing agent in organic and inorganic syntheses under mild conditions employing its high reactivity towards proton-containing reagents. Thus, it reacts with alcohols, thiols, amines and carboxylic acids with evolution of $H_2S$ to give $B(OR)_3$, $B(SR)_3$, $B(NHR)_3$, $(BNR_2S)_3$, and $B(OCOR)_3$, respectively[51-57]; acyl complexes such as $(C_5H_5)Fe(CO)_2COR$ and $(CO)_5MCOR$ (M = Mn, Re) react to give dithiocarboxylate complexes $(C_5H_5)Fe(CO)S_2CR$ and $(CO)_4MS_2CR$[57]; $WCl_6$, $NbCl_5$, $TaCl_5$ and $MoCl_5$ are sulfurized to form $WSCl_4$, $NbSCl_3$, $TaSCl_3$, and $MoSCl_3$, respectively[58]. Using $B_2S_3$ as sulfurizing agent for the vanadyl group, the V=S unit in thiovanadyl complexes[59] was obtained for the first time.

### 2.3. $B_6S_{16}$, an "Inorganic Porphin"

A novel and unexpected molecular boron sulfide as well as another crystalline product, both of them having the composition B : S = 1 : 2, were obtained by us on reacting

the elements or $B_2S_3$ and sulfur in a closed system with a temperature gradient[32,33,60,61].

Crystalline colorless $B_8S_{16}$ is formed, *e.g.*, within a narrow zone in the cooler part of the reaction tube, if a $B_2S_3$/S mixture (1 : 1.5) is heated quickly to about 300 °C at $10^{-4}$ bar in a closed protected quartz glass tube in a two-zone furnace with a sharp temperature profile (300/100 °C). Under inert gas, the compound, which is highly sensitive to hydrolysis, melts under normal pressure at 115 °C with decomposition. The crystals consist of discrete, exactly planar $B_8S_{16}$ molecules, the macrocyclic porphin-like arrangement of which contains four 1,2,4,3,5-trithiadiborolane rings joined over sulfur bridges[62] (Fig. 4). Within the limits of error, the molecule has $D_{4h}$-symmetry. The mean bond length (1.811 Å) corresponds to that in $B_2S_3$ (1.808 Å[40,41]) and also indicates strong (n-p)π interaction, in agreement with the planarity of the molecule and the results of the MO-calculations.

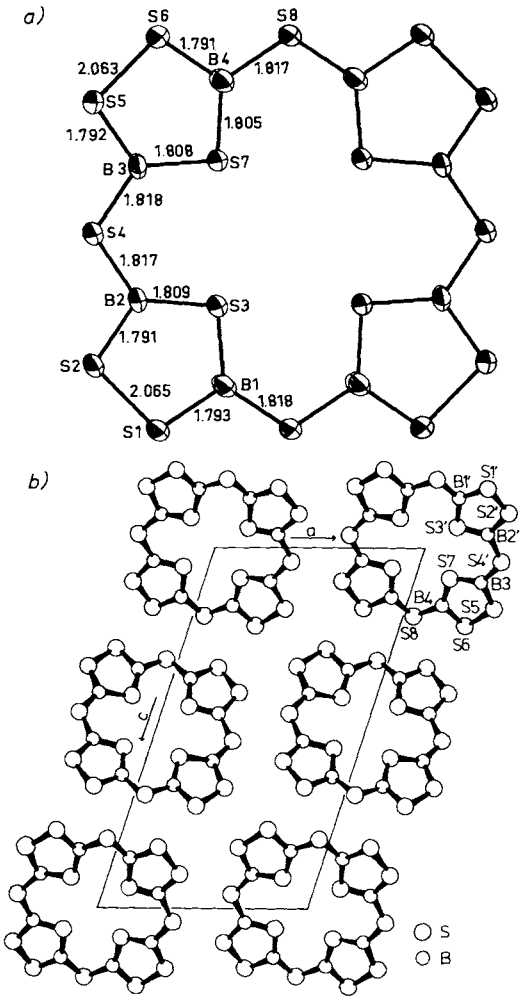



Fig. 4. a) $B_8S_{16}$ molecule with bond lengths [Å] and bond angles [°]. b) Packing of the molecule in the crystal structure.

The significant difference in the two types of B–S bond lengths within the five-membered rings (1.789 and 1.822 Å) corresponds well with the trend of the calculated π-bond orders for trithiadiborolanes[63] and for $B_8S_{16}$[64,65] (Fig. 6). The similarity of the structural characteristics to those of dimethyl- and dichloro-1,2,4,3,5-trithiadiborolane in the gas phase[66,67] shows remarkable constancy of the bonding in the stable five-membered ring, being independent of the substituents. This constancy is also indicated by very similar vibrational spectra (Fig. 5).

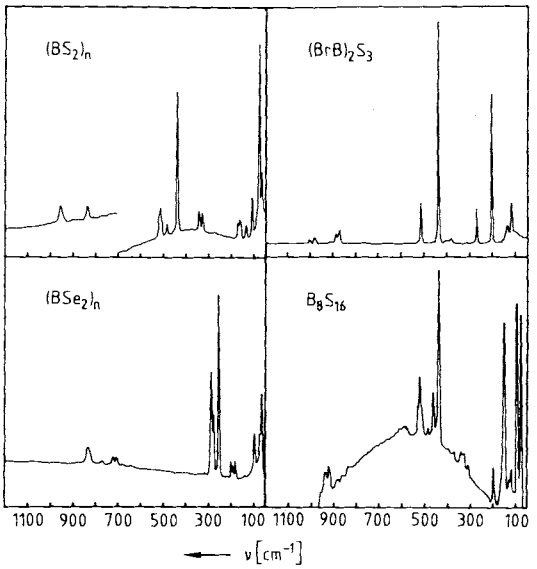



Fig. 5. Raman spectra of 3,5-dibromo-1,2,4,3,5-trithiadiborolane, of $B_8S_{16}$, and of crystalline $(BS_2)_n$ and $(BSe_2)_n$.

The comparison of the bond properties of $B_8S_{16}$ with those of the topologically analogous porphin system is of theoretical and preparative interest with respect to the potential use of the $B_8S_{16}$ macrocycle as a quadridentate ligand in metal complexes. The geometry of the planar molecule (transannular S···S distance about 4.60 Å, cf. Fig. 4) enables a planar coordination of the quadridentate system. Complex formation is observed especially with $d^8$- and $d^9$-transition metals ($Ni^{2+}$, $Pt^{2+}$, $Cu^{2+}$). Indeed, the cyclization of the trithiadiborolanes is favored by these metals. However, the preparative chemistry of $B_8S_{16}$ is complicated by its poor solubility in non-polar solvents and its marked instability towards polar ones. Some quantitative evidence on the bonding is obtained from results of Hückel-MO-calculations on the 32π-electron system of $B_8S_{16}$ as compared to the 26 and 28π-electron systems of porphin and of the porphin dianion[64,65] (Fig. 6).

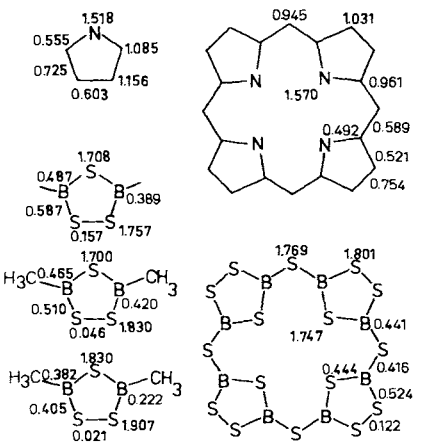



Fig. 6. π Charge densities and π bond orders in $B_8S_{16}$ determined from simple Hückel MO calculations as compared with the $B_2S_3$ ring, with pyrrole, and with porphin [64]. In addition (lower left), values from CNDO/2 and CNDO/S MO calculations for the $(H_3CB)_2S_3$ system are given [63, 65].

In analogy to the simple $(RB)_2S_3$ system there is considerable $\pi$ bonding in $B_8S_{16}$ with remarkable similarities of the relative distribution compared to that in porphin. The difference in HOMO-LUMO energies ($\pi$-$\pi^*$ transition energy) is only slightly dependent on the semiempirical heteroatom parameters and is, in accordance with electronic spectra, large compared to porphin. The "electron-rich" $B_8S_{16}$ system with more strongly antibonding MO's being occupied has, as expected, a lower delocalization energy and a lower topological resonance energy as compared to porphin. A considerable influence on the size of the HOMO-LUMO gap is observed by inclusion of the 3d-AO's of sulfur in the base set and by the choice of the semiempirical parameters for these functions[65] (Fig. 7). The calculations for $B_8S_{16}$ and for a hypothetical $[CuB_8S_{16}]^{2+}$ complex show qualitatively that $B_8S_{16}$ is a less effective complex ligand as compared to porphin, but that the stabilities of possible transition metal chelates should be comparable to those of macrocyclic thioether complexes.

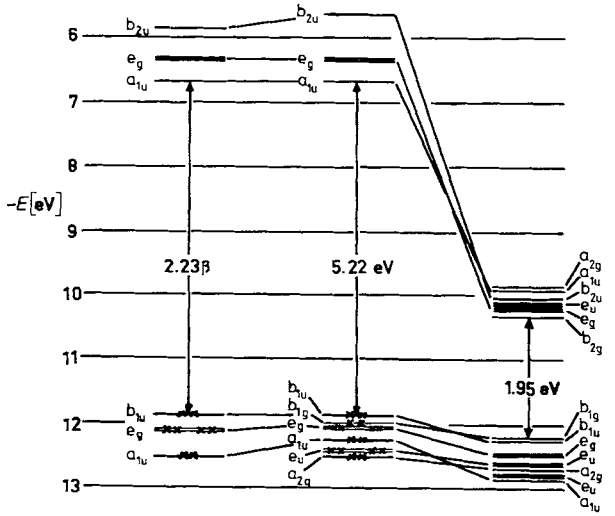
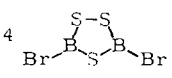



Fig. 7. Energy diagram of $B_8S_{16}$ in the region of the HOMO-LUMO gap (indicated by arrows). Left: simple Hückel calculations; center: extended Hückel calculation without d-AO's of sulfur; right: with d-AO's [65].

Another promising route for the synthesis of $B_8S_{16}$ has been found in the formation of the macrocycle from the components by thiolysis of the halogen-substituted trithiadiborolanes[68-71]. In this way the reaction of 3,5-dibromo-1,2,4,3,5-trithiadiborolane with $H_2S$, with dry $Na_2S$, or with $H_2CS_3$ as $H_2S$-generating agent[72] according to




$$+ 4\ SC(SH)_2 \longrightarrow B_8S_{16} + 4\ CS_2 + 8\ HBr$$

yields the porphin-like $B_8S_{16}$, together with polymeric $(B_2S_4)_n$ chains consisting of S-linked five-membered $B_2S_3$-rings[32,33,60,61,73].

### 2.4. $(BS_2)_n$ and $(BSe_2)_n$

In a slightly modified reaction of $B_2S_3$ with sulfur (cf. Section 2.3), fixing the temperature of deposition at 120–250 °C, surprisingly a new phase is formed, which has been identified by X-ray structure analysis as one-dimensionally polymeric $(BS_2)_n$[32,33,61] (Fig. 8). Similarly to $B_8S_{16}$, this compound consists of trithiadiborolane rings linked by

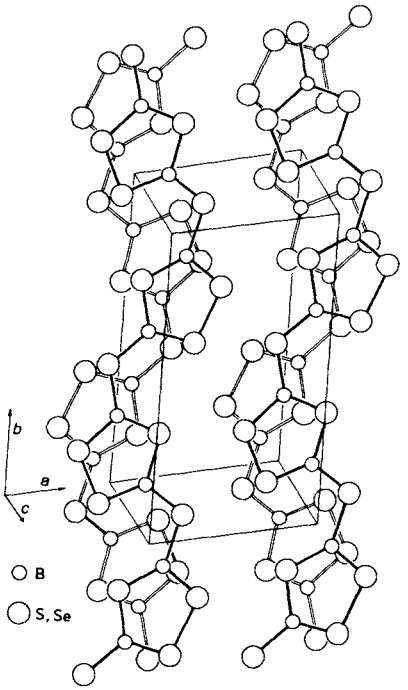



Fig. 8. Crystal structure of $(BS_2)_n$ and $(BSe_2)_n$.

sulfur atoms. The chains are exactly planar. As shown in Figure 9 the bonding is very similar to that in $B_8S_{16}$. The S···S distance between neighboring $B_2S_3$ rings is remarkably short, indicating weak bonding interaction which stabilizes the configuration of the chains. In the isotypic $(BSe_2)_n$, which was prepared in much the same way and which is the first boron selenide to have been structurally

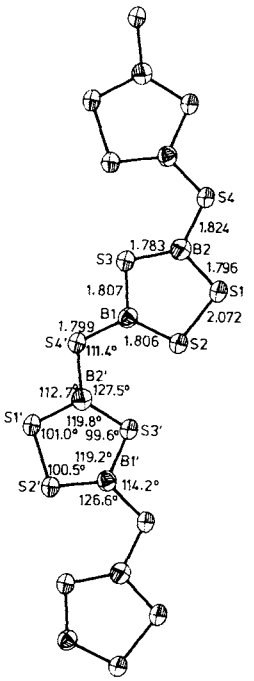
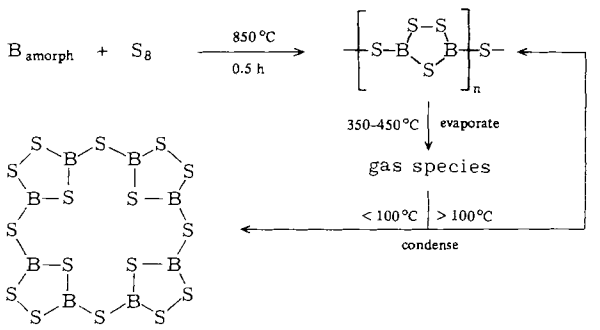



Fig. 9. $(BS_2)_n$-chain with bond lengths [Å] and bond angles [°]. The distance S2...S3' is 3.167 Å.

characterized[32,33,61], the corresponding Se···Se distance is 3.295 Å (B–Se bond lengths 1.90–1.98 Å, Se–Se distance in the ring 2.347 Å).

In a simplified way the synthesis of $B_8S_{16}$ and $(BS_2)_n$ (and analogously of $(BSe_2)_n$) is possible as a concerted reaction according to the following scheme:




$(BSe_2)_n$ can be transported chemically with $I_2$ in a temperature gradient from 300 to 200 °C[32,74].

### 2.5. Mass Spectra and $^{11}$B-NMR Spectra

The mass spectra of the boron sulfides and selenides show remarkable differences[14–18,32,33,75,76]. For stoichiometric $B_2S_3$ as well as for sulfur-rich samples a great number (*ca.* 30) of different fragments between $B_2S_3^+$ and $B_{10}S_{17}^+$ are found at temperatures of 300–650 °C for which $(B_2S_3)_n^+$ and $(BS_2)_n^+$ must be considered parent ions. The volatility of the sulfide (which is polymeric as solid $B_2S_3$) and the relative intensity of the molecular ion $B_8S_{16}^+$ and of its fragments increase considerably with an excess of sulfur over the composition $B_2S_3$ in the solid sample. This finding, which could not be explained previously, is well in accordance with the stability of the cyclic $B_8S_{16}$ molecule.

In the mass spectrum of $B_2Se_3$ and more selenium-rich samples up to $BSe_2$, however, essentially only $BSe^+$, $BSe_2^+$, $B_2Se_2^+$, $B_3Se_2^+$, $BSe_3^+$, $B_2Se_3^+$, and $B_3Se_3^+$ are observed[33,74,76]. This points to a porphin-like $B_8Se_{16}$ molecule being unstable in contrast to the polymeric $(BSe_2)_n$ chain.

Important results regarding the structure of glassy boron chalcogenide systems were recently obtained from $^{11}$B-broad line-NMR experiments[77] (cf. also [78–83]). In this method, which is very well suited for the investigation of noncrystalline boron compounds, the line-shape of the NMR signals is primarily determined by the interaction of the $^{11}$B nuclear quadrupole moment with the electrical field gradient generated by chemical bonding, and so reflects the state of hybridization of the boron atoms. With regular tetrahedral coordination, the spectrum shows a sharp line not influenced by quadrupole effects, whereas, $sp^2$ hybridization results in 2nd order quadrupole splitting (Fig. 10).

In the course of the study[77–79] the bond formation of boron with sulfur and selenium was monitored NMR-spectroscopically. The investigations confirm the existence in the glass of the binary compounds $B_2S_3$, $BS_2$ and $BSe_2$, which can be prepared in almost quantitative yield, and whose NMR signals indicate that the boron atoms are trigonally planar coordinated. The compounds $B_4S$, BS, $B_2S_5$, $B_4Se$ and $B_2Se_3$ (!) published in the literature *(vide supra)* could not be detected. According to the NMR data about one third of the S atoms in $B_2S_3$ can be substituted by Se without losing the homogeneity of the phase. A sample "$B_2Se_3$" disproportionates into $BSe_2$ and an amorphous boron-rich subselenide, whose B : Se ratio depends on the reaction conditions. Compound formation between boron and tellurium (with the exception of possible boron-rich tellurides) could not be observed.

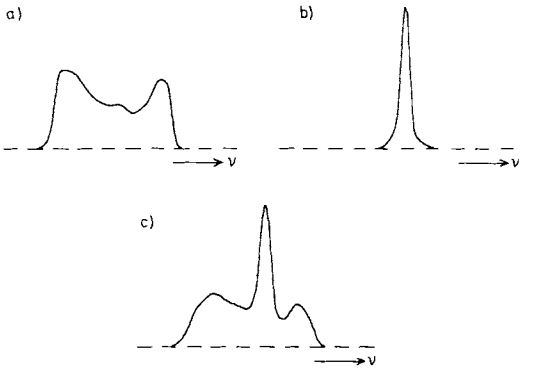



Fig. 10. $^{11}$B-NMR broad line spectra (integrated line form) of (a) trigonally planar and (b) tetrahedrally coordinated boron-sulfur compounds. (c): Spectrum of a $B_2S_3/Tl_2S$ mixture in a 10 : 1 molar ratio (superposition of signals for trigonally planar and tetrahedrally coordinated boron).

The exact value of the quadrupole-coupling constants of $sp^2$-hybridized boron compounds is influenced by the extent of the (n-p)π bonding by which excess electron density is transferred from the non-bonding electron pairs of the substituents into the free p-orbital of the boron atom. The symmetry of the electronic environment of the $^{11}$B core is increased with concomitant lowering of the quadrupole-coupling constant. The data for the boron chalcogenides investigated (cf. Fig. 11) indicate significantly more π-bonding in $BS_2$ and $BSe_2$ than in $B_2S_3$. This demonstrates the increased donor-effect of the disulfide bridge (B–S–S–B) as opposed to the sulfide bridge (B–S–B), and agrees with the trends derived from the CNDO- and simple Hückel-calculations on trithiadiborolanes and $B_8S_{16}$ (cf. Fig. 4 and 6).

The quantitative interpretation of the $^{11}$B quadrupole coupling constants of $B_2O_3$ and $B_2S_3$ indicates significantly smaller double bonding character in the B–S bonds than in the B–O bonds. From the analysis of the $^{11}$B line shape the next-neighbor-structure in glassy $B_2S_3$ is definitely more uniform than in the $B_2O_3$ glass, owing to different connecting principles of the trigonal planar units. In spite of this, added network modifiers seem to have an almost identical influence in both glasses. As in analogous oxide systems[84], tetrahedrally coordinated boron is produced by the additional chalcogen also in $B_2S_3/Tl_2S$ glasses (Fig. 10). Above 33.3 mol-% $Tl_2S$ the concentration of these units decreases again; parallel to this the sudden change of the $^{205}$Tl-resonance parameters indicates the formation of a new configuration with trigonal $sp^2$-hybridized boron atoms as well as much more covalent Tl–S bonds. However, the glassy structure accepts these species only in low

concentration; above 57 mol-% $Tl_2S$, separation of a crystalline phase of the probable composition $Tl_3BS_3$ is observed.

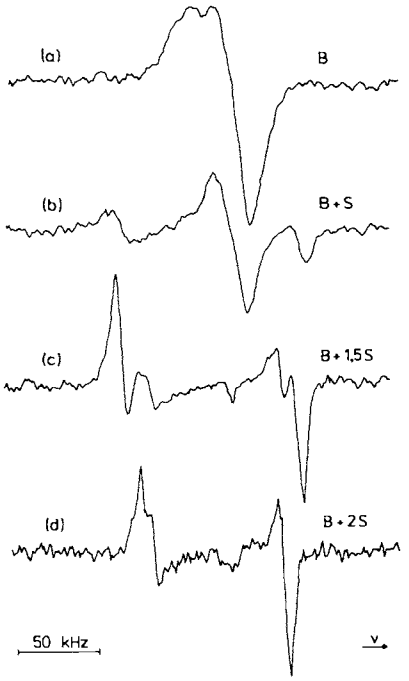



Fig. 11. $^{11}$B-NMR-study of compound formation in the boron-sulfur system (measuring frequency 7.06 MHz). The first derivatives of the frequencies are recorded. Besides elementary (amorphous) boron in (b) the signals of $B_2S_3$ appear, which reach their maximum in (c). In (c) weak signals of $BS_2$ with smaller quadrupole splitting are already present, which occur in the spectrum (d) with maximum intensity.

## 3. Thioborates

As in the case of binary boron chalcogenides there are a number of references in the literature on ternary phases, which, however, are incomplete and partly contradictory. Information about the structure and bonding have been obtained only recently. Generally, high temperature reactions of the solid elements or the binary sulfides in closed systems are employed as preparative methods. As reaction products (frequently insufficiently characterized) alkali, alkaline earth and heavy-metal salts $M^{I}BS_2$[44,85–90], $M^{II}(BS_2)_2$[91,92], $M^{I}_4B_2S_5$[86,90], $M^{II}_2B_2S_5$[39,50,92,93], $M^{I}_3BS_3$[86,89], $M^{I}_8B_2S_7$[86,90], $M^{I}_5BS_4$[94] and $M^{I}_4B_6S_{11}$[89] are described, as well as "perthioborates" $M^{I}_2B_2S_5$[95] and $M^{I}BS_3$[89,95] and the sulfur-deficient phases CuBS and AgBS[87,96].

Sulfur can also be introduced by $H_2S$ (*e.g.* according to $3K_2S+6B+9H_2S \rightarrow 2K_3B_3S_6+9H_2$)[22]. Interesting methods of preparation employ tetrahydroborates and sulfur. Without solvents, metathioborates $MBS_2$ (M = Li, Na, K) are formed at 200–300 °C[97,98], while hydrothioborates $Li[BH_3SH]$ and $Li[B_3S_2H_6]$ are discussed as reaction products in solution[97], as is also a $BH_2S_3^-$ ion, which is supposed to be in equilibrium with a cyclic $H_2B(S_3)_2BH_2^{2-}$[99].

Successful structure analyses of some of these phases and of some new compounds led to progress in an understanding of the structural and bonding principles in question. The thioborates $M^{I}BS_2$ are derivatives of the trimeric cyclic metathioboric acid $H_3B_3S_6$ (cf. Section 2.2), which can be obtained, *inter alia*, by reaction of $BBr_3$ with $H_2S$ in $CS_2$ or $C_6H_6$ solution[36,100], and, like the acid, they therefore resemble the corresponding oxo-compounds $H_3B_3O_6$ and $M^{I}_3B_3O_6$. The crystal structures of $H_3B_3S_6$[38], $Na_3B_3S_6$ and $K_3B_3S_6$[8,40], in accordance with the vibrational spectra[8,44], show exactly planar six-membered ring molecules. $Na_3B_3S_6$ and $K_3B_3S_6$ are isotypic and crystallize rhombohedrally (space group $R\bar{3}$, $a=9.080$ (9.390) Å, $\alpha=112.70$ (111.46)°[8,40,42]). As shown in Figure 12, the terminal B–S bonds of the anions are significantly shortened compared to those in the acid ( and to all bonds of $B_2S_3$), indicating here remarkably higher $\pi$-bond orders.

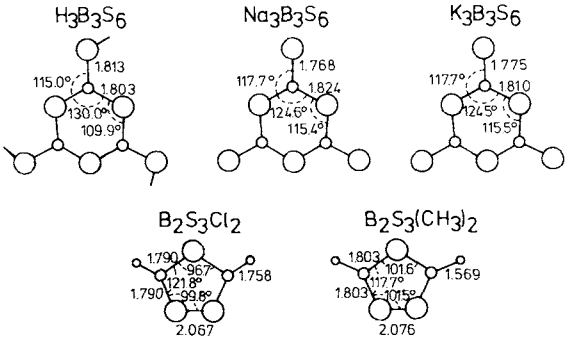



Fig. 12. Molecular geometry of metathioboric acid $H_3B_3S_6$ as compared to the $B_3S_6^{3-}$ ions in $Na_3B_3S_6$ and $K_3B_3S_6$.

The unusual and surprising coordination number 4 of boron towards sulfur is observed in the two heavy metal thioborates $Pb_2B_2S_5$[8,40,50] and in the new $Ag_3B_5S_9$[8,40,42], which does not belong to any known formula type. In both compounds, tetrahedral $BS_4$-groups are linked to larger units *via* corners, in the case of the black $Pb_2B_2S_5$ to quasi-isolated tetrameric adamantane-like $B_4S_{10}^{8-}$ anions (Fig. 13). The stability of the highly negatively charged ion, which is isostructural and iso-valence-electronic to $P_4O_{10}$, $P_4S_{10}$ and $Ge_4S_{10}^{4-}$, is remarkable; however, it must be assumed that this high formal charge is reduced by stabilizing covalent bond contributions to the $Pb^{2+}$ cations.

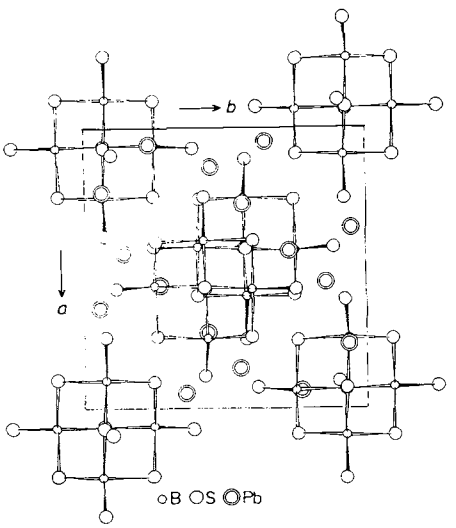



Fig. 13. Adamantane-like $B_4S_{10}^{8-}$ anions in the structure of $Pb_2B_2S_5$.

In the dark-red $Ag_3B_5S_9$, ten $BS_4$ tetrahedra form rigid $B_{10}S_{20}$ "super-tetrahedra" which may be regarded as fragments of the diamond (zinc blende) structure. The super-tetrahedral $B_{10}S_{20}$ units are linked over all four corners into a layer-like framework with the stoichiometric composition of $B_{10}S_{16}S_{4/2}^{6-} = B_{10}S_{18}^{6-}$ (Fig. 14). According to the model of significant π-bonding in trigonally planar coordinated boron compounds, the B–S bond lengths in the tetrahedra, with mean values of 1.927(14) Å in $Pb_2B_2S_5$[8,40] and 1.915(5) Å in $Ag_3B_5S_9$[8,40], are considerably longer than the values in the region of 1.79–1.81 Å for planar $BS_3$-groups[101].

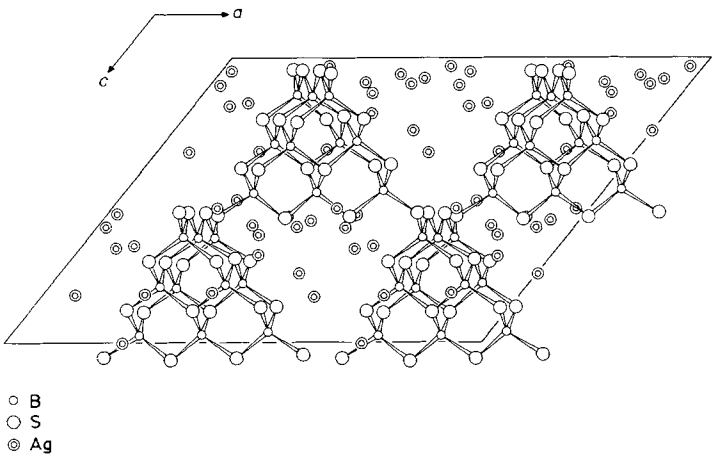



Fig. 14. $Ag^+$ ion-conducting $Ag_3B_5S_9$: Section of the structure with corner linked $B_{10}S_{20}$ "supertetrahedra" and partially occupied silver positions.

There is special chemical interest in the absolute stability of both compounds with regard to hydrolysis and oxidation as opposed to all planar coordinated BS compounds; the electronically rather saturated boron in the $BS_4$ polyhedra is effectively shielded against nucleophilic attack. This stability, which in this case is enhanced by the heavy metal coordination of sulfur, can also be expected in other boron compounds tetrahedrally coordinated by sulfur. $Ag_3B_5S_9$ is of special interest because it is a $Ag^+$ ionic conductor already at room temperature. In the crystal structure[102] the 6 $Ag^+$ ions of the asymmetric unit are distributed over 18 partially occupied sites with occupancy factors ranging from 0.10 to 0.84 and with coordination numbers of 2, 3 and 4, so that there are favorable conditions for mobility of the $Ag^+$ ions[8,42,209].

So far, there is no model in thioanion chemistry for the structure of the first "perthioborate" $TlBS_3$[103], which is obtained in crystalline form from a 1:2:5 mixture of $Tl_2S$, B and S at 800 °C with subsequent annealing at 170/350 °C[89,103]. The polymeric chain-shaped $(BS_3^-)_n$ anion consists of corner-sharing, practically undistorted $BS_4$ tetrahedra ($d_{BS} = 1.927$ Å); two corners of each tetrahedron are part of $S_2$ groups ($d_{SS} = 2.09$ Å) which form additional bridges to neighboring tetrahedra (Fig. 15). The molecular structure can also be described as a poly-spirocyclic system of non-planar B–S–S–B–S five-membered rings with boron atoms as bridgehead centers (Fig. 16).

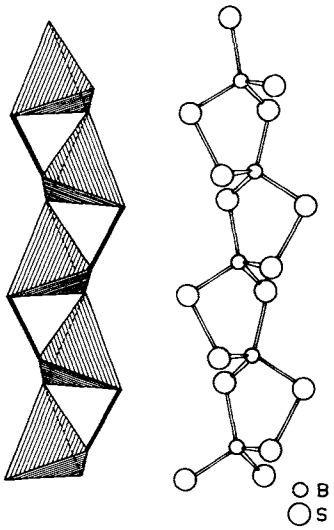



Fig. 15. $(BS_3^-)_n$ chain in the crystal structure of $TlBS_3$ (cf. also Fig. 26) in two different representations. The structure of this novel perthioanion may be considered as an addition product of $(BS_2)_n$ (Fig. 9) and $S_2^{2-}$ ions.

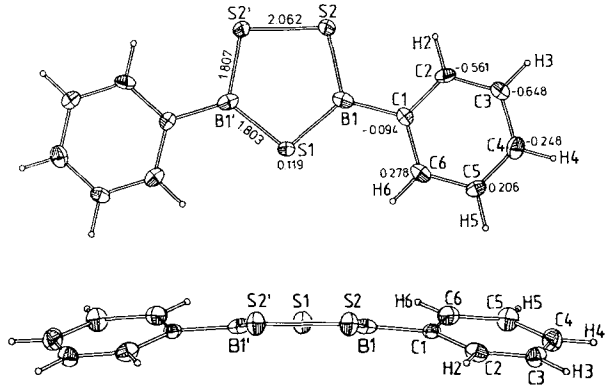



Fig. 16. Non-planarity of the 3,5-diphenyl-1,2,4,3,5-trithiadiborolane molecule. The $B_2S_3$ ring has envelope configuration. The plane of the phenyl ring is tilted by 21.0° with respect to the B1S2S2'B1' plane, and by 18.8° with respect to the B1S1S2C1 plane. The $BS_2C$ triangle is exactly planar. Bond lengths in Å. The numbers in the right part of the upper figure give the distances of the atoms from the B1S2S2'B1' plane.

The relation to the $(BS_2)_n$ and $(BSe_2)_n$ chain-structures (Fig. 8 and 9) is remarkable: $(BS_3^-)_n$ can be formed in a simple way according to

$$(BS_2)_n + \frac{n}{2} S_2^{2-} \longrightarrow (BS_3^-)_n$$

by nucleophilic addition of the $S_2^{2-}$ ions to the boron atoms with accompanying $sp^2 \rightarrow sp^3$ extension of the coordination and formation of new (non-planar) $B_2S_3$ rings. Interesting relationships also exist between the $(BS_3^-)_n$ configuration and the different $(GeS_3^{2-})_n$ and $(SnS_3^{2-})_n$ chain structures (Fig. 26).

## 4. Remarks on the BS Bonds

The concept that significant π bonding through the interaction of p electrons of sulfur with the $p_z$ orbital of $sp^2$-hybridized boron is present in trigonal-planar sulfur compounds like in BF, BO and BN compounds, has been con-

troversial for some time[104-106]. Arguments against π bonding are, *e.g.*, spectroscopically determined stretching force constants of 2.5 to 2.85 N/cm for $(CH_3S)_3B$, $(CH_3)_2S-SH$, $(CH_3)_2B-SCH_3$ and $(CH_3)_2B-S-B(CH_3)_2$[106], which are not larger than the estimated single bond value[107] (see Table 1). Besides the reactive properties of many BS compounds (*e.g.* of thioboranes or of planar cyclic trithiadiborolanes[108,109]), ionization energies from mass spectra[110], PE spectra of the thioboranes $(CH_3S)_nB(CH_3)_{3-n}$[109] and of sulfur-containing five-membered ring heterocycles[111], the mentioned CNDO/2 and CNDO/S-MO calculations on trithiadiborolanes[63,64] as well as *ab initio* calculations on $H_2B-SH$[112] support the presence of significant (n-p)π bonding contributions.

Another argument for an effective π overlap is the exact planarity (within the limits of error) of the $sp^2$-$BS_3$, $BS_2R$ and the $BSR_2$ systems (*e.g.* [38,40]) structurally characterized so far. In this context the non-planarity of $B_2S_3(C_6H_5)_2$, as a further derivative of the trithiadiborolane series, is all the more surprising[113] (Fig. 16). Only the $BS_2C$ unit is strictly planar, while the $C_6H_5$ rings are twisted around the BC bond. This indicates reduced BC π bonding; (n-p)π overlap in the S1B1S2 fragment, using suitable hybridized orbitals of sulfur, is, however, possible.

With values of *ca.* 1.78—1.82 Å (mean value 1.80 Å) for trigonally coordinated and *ca.* 1.92—1.94 Å (mean value 1.93 Å) for tetrahedrally coordinated boron, the B—S bond lengths are remarkably constant in all compounds examined so far[23], while the difference in the two values is considerably greater than in the homologous systems $BCl_3$ (1.76 Å) and $BCl_4^-$ (1.84 Å). This, together with the experimental B—C single bond lengths of 1.55 Å in $B_2S_3(C_6H_5)_2$[113] (Fig. 16) and of 1.58 Å in trimethylborane[114] suggests single bond covalent radii of 0.93 Å for tetrahedrally coordinated boron as well as 0.85 Å for trigonal-planar boron[115]. These values (cf. [23]) correspond better to the new experimental data than the *Pauling* values[116] of 0.88 and 0.81 Å.

## 5. Thiogallates and Thioindates—New Synthetical Methods and New Structural Principles

Ternary chalcogenides of gallium and indium are usually prepared by high-temperature melt or solid-state reactions (*e.g.* [117-122]), since in polar solvents solvolysis was to be expected. By nucleophilic degradation of $Ga_2S_3$ and $In_2S_3$ in concentrated aqueous sulfide solutions, however, molecular thiogallates and thioindates as well as analogous seleno compounds have recently been synthesized[123-127] (see also [128]). Over a wide concentration range, $Ga_4S_{10}^{8-}$, $Ga_4Se_{10}^{8-}$, $In_4S_{10}^{8-}$ and $In_4Se_{10}^{8-}$ are the predominant species which can be isolated, in the form of strongly hydrated, colorless alkali metal salts (*e.g.* $Na_8In_4S_{10}\cdot 14H_2O$, $K_8Ga_4S_{10}\cdot 14H_2O$)[123-127]. X-ray structural analyses of these phases show that the anions, like $B_4S_{10}^{8-}$ in $Pb_2B_2S_5$, are adamantane-like and have almost ideal $T_d$ symmetry (Fig. 17). Their thermal and solvolytic stability is remarkable.

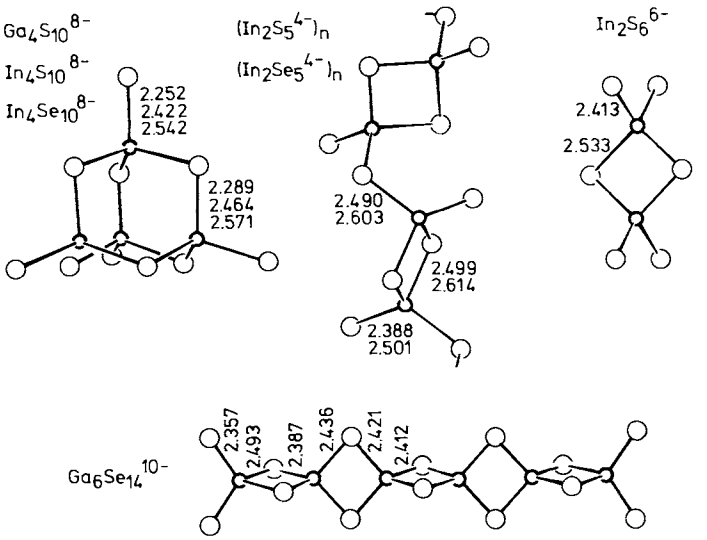



Fig. 17. Adamantane-like $Ga_4S_{10}^{8-}$, $Ga_4Se_{10}^{8-}$, $In_4S_{10}^{8-}$ and $In_4Se_{10}^{8-}$ from aqueous solution, as well as $(In_2S_5^{4-})_n$, $(In_2Se_5^{4-})_n$, $In_2S_6^{6-}$ and $Ga_6Se_{14}^{10-}$ prepared by high-temperature methods, with bond lengths [Å].

Anhydrous thioindates and thiogallates of the alkali metals and their seleno analogues known so far have the composition $MInS_2$, $MGaS_2$, $MInSe_2$ and $MGaSe_2$ (M = Li, Na, K, Rb, Cs), and have been investigated in earlier systematic structural work[117,118] and in connection with high-pressure transformations[119]. According to these investigations $NaInS_2$ and $NaInSe_2$[117] as well as the high-pressure modification $KInS_2$-III[119] belong to the α-$NaFeO_2$-type with octahedral coordination of In; the high-pressure forms $KInS_2$-II and $RbInS_2$-II are isotypic with TlSe ($InS_4$ tetrahedra)[119], whereas the structural principle of the important stable form of the K, Rb and Cs compounds was hitherto unknown, owing to extensive disorder and twinning problems. Recently, the structural principle could be solved in $KInSe_2$[129,130]: The compound does not form the predicted $KFeS_2$-type chain structure (which is realized in $CsGaS_2$[120]) but shows a layer structure in which adamantane-like $In_4S_{10}$ groups are linked two-dimensionally *via* corners. K is in trigonal-prismatic coordination (Fig. 18). This type of structure corresponds to that of $TlGaSe_2$, which was structurally characterized in 1978[131] and which, as a semiconductor, is of some importance for opto-electronic applications[132].

Other novel thioindates and selenogallates could be obtained by unconventional reactions of rubidium with indium monosulfide or of cesium with gallium monosele-

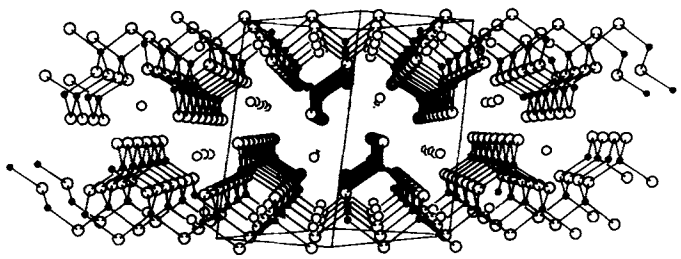


Fig. 18. $KInSe_2$ and $TlGaSe_2$ structures: layers of corner-linked adamantane-like $In_4Se_{10}(Ga_4Se_{10})$ groups.

nide. In the first case $Rb_4In_2S_5$ and $Rb_6In_2S_6$[133] are formed which contain dimeric $In_2S_6$ units of two edge-sharing $InS_4$ tetrahedra. In $Rb_4In_2S_5$, as well as in the similar $Rb_6In_2Se_5$[129], these units are linked to form polymeric $(In_2S_5^{4-})_n$ and $(In_2Se_5^{4-})_n$ chains by corner-sharing; in $Rb_6In_2S_6$ they exist as isolated $In_2S_6^{6-}$ ions (Fig. 17). In the case of the Ga/Se/Cs reaction the 19 Å-long, edge-coupled, unusual $Ga_4Se_{14}^{10-}$ ion is obtained in the compound $Cs_{10}Ga_4Se_{14}$[134], which was also characterized by X-ray structural analysis (Fig. 17).

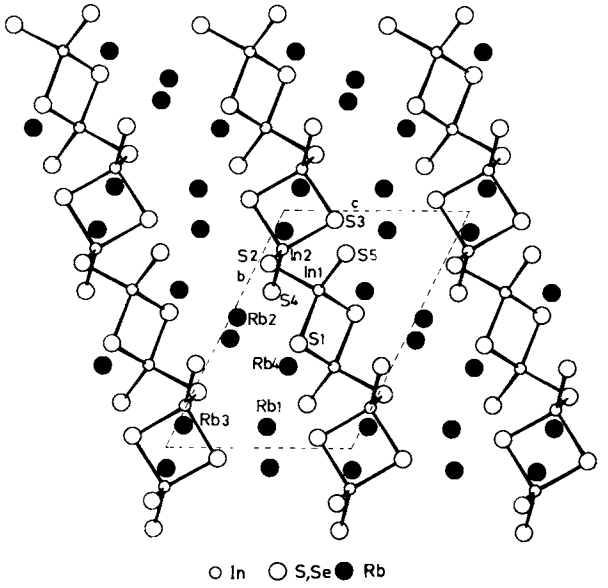



Fig. 19. $(In_2S_5^{4-})_n$ and $(In_2Se_5^{4-})_n$ chain structure in the unit cell of $Rb_4In_2S_5$ [133] and $Rb_4In_2Se_5$.

A selenogallate $Na_2Ga_2Se_3$ with Ga–Ga bonds (2.40 Å) can be synthesized from a 2:2:3 mixture of the elements at 990 °C; the structure contains, in a distorted $NaCrS_2$-type, layers of linked $Ga_2Se_6$ groups with staggered conformation[135].

## 6. Thiosilicates, Thiogermanates, and Thiostannates

Particularly impressive developments have been taking place over the last decade in this area of thioanion chemistry. Preparative work in solution at normal temperature and also in the area of high-temperature melt and solid-state reactions in conjunction with modern methods of X-ray structure analysis and of Raman spectroscopy has enabled a system of monomeric, oligomeric and polymeric thioanions to be developed. In spite of essentially different principles of formation and structure, and of different chemical properties (see below), some features of this new class of compounds are reminiscent of the diversity of the corresponding oxygen compounds, particulary the silicates.

A systematic survey, in particular of the solid state and structural aspects of ternary sulfides of silicon, germanium and tin[136] has recently been published[137] which summarizes the important literature up to 1976, so that in this review our account of some recent remarkable developments in this field will concentrate mainly on the molecular aspects.

### 6.1. Polynuclear Thio- and Selenoanions from Condensation Reactions

Every student of chemistry who, in his practical inorganic training, has learned the qualitative analytical separation procedures for cations by means of precipitation of the sulfides, is familiar with the formation of thioanions of tetravalent tin, of arsenic, and of antimony. In textbooks these are correctly formulated as $SnS_4^{4-}$ or $SnS_3^{2-}$ and as $AsS_3^{3-}$, $SbS_3^{3-}$, $AsO_xS_{4-x}^{3-}$ or $SbO_xS_{4-x}^{3-}$; however, up to 1970 no further information about the chemistry of these monomeric tetrahedral ions had been published. On critical examination it could not be understood why thionanions should not be able to enter into similar condensation reactions in solution as the corresponding oxoanions. Indeed, in the case of thiogermanates and thiostannates a series of new polythioanions can be successfully prepared by conventional nucleophilic degradation of the polymeric sulfides $GeS_2$ and $SnS_2$ with aqueous alkaline sulfide solutions. For the isolation of pure phases an exact control of the pH value and the concentration ratio of the individual reaction components is necessary. Like the thioanions of the neighboring elements of the 3rd and 5th main groups, the thioanions are colorless and, as alkali metal and alkaline earth salts, are readily soluble in water. So far, the following thiogermanates and thiostannates have been generated in solution, isolated as crystalline phases, and have been structurally completely characterized:

- monomeric species $GeS_4^{4-}$ and $SnS_4^{4-}$ as well as corresponding selenoanions $GeSe_4^{4-}$ and $SnSe_4^{4-}$, which are present as undistorted tetrahedral (hydrated) ions in solution and in the crystalline salts[138–141] (Fig. 20);

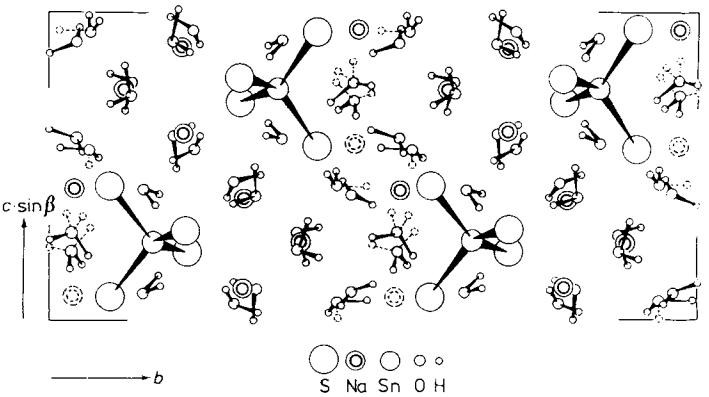



Fig. 20. Structure of $Na_4SnS_4 \cdot 14\,H_2O$. The $Na^+$ ions are coordinated octahedrally by $H_2O$ molecules; the thioanions and $H_2O$ molecules are linked by OH···S hydrogen bridges. Part of the Na-$H_2O$ system is disordered in the crystal [138].

- dimeric species $Ge_2S_7^{6-}$, $Ge_2Se_7^{6-}$, $Sn_2S_7^{6-}$ and $Sn_2Se_7^{6-}$, composed of two corner-sharing tetrahedra, the structures of which correspond to familiar oxoanions such as $Si_2O_7^{6-}$, $P_2O_7^{4-}$, $S_2O_7^{2-}$ or $Cr_2O_7^{2-}$ and represent the first step of the tetrahedral condensation reactions[142];
- a new type of dimeric species $Ge_2S_6^{4-}$, $Ge_2Se_6^{4-}$, $Sn_2S_6^{4}$ and $Sn_2Se_6^{4-}$, consisting of two edge-sharing tetrahedra[143–145];

- polymeric species $(GeS_3^{2-})_n$ and $(SnS_3^{2-})_n$, formed by corner-sharing tetrahedral chains which are produced by crystallization from solutions with similar intermediate pH values (Fig. 25) and which are isomeric with $Ge_2S_6^{4-}$ and $Sn_2S_6^{4-}$[146];
- tetrameric adamantane-like species of the composition $Ge_4S_{10}^{4-}$, $Ge_4Se_{10}^{4-}$, $Sn_4S_{10}^{4-}$ and $Sn_4Se_{10}^{4-}$, which are produced as the predominant condensation products in solutions of lower pH-values (depending on the system, between pH = 7 and pH = 3), *i.e.* at higher degrees of protonization of the thioanions and sulfide anions taking part in the condensation reactions[147-149] (Fig. 21);

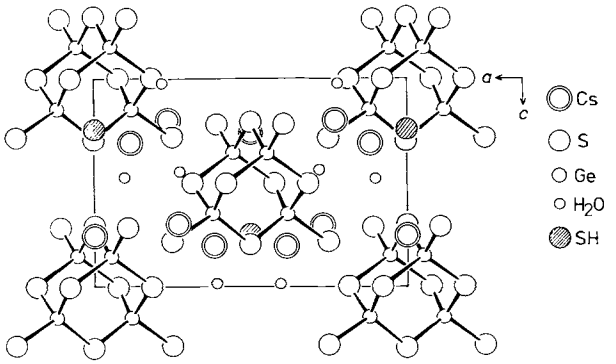



Fig. 21. Adamantane-like $Ge_4S_{10}^{4-}$ ions in the crystal structure of $Cs_4Ge_4S_{10} \cdot CsSH \cdot 4H_2O$.

- $Ge_8S_{19}^{6-}$, which is formed from two adamantane-like species by condensation over one corner[150, 151] (Fig. 22);

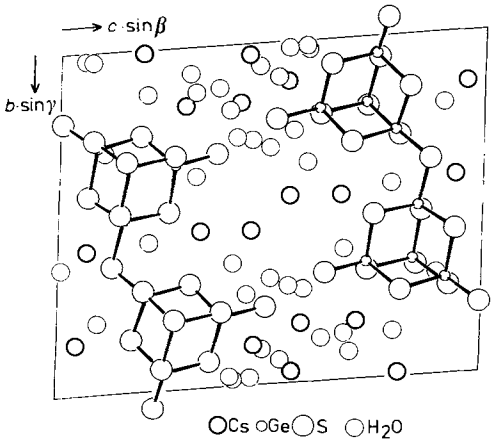



Fig. 22. $Ge_8S_{19}^{6-}$ ions in $Cs_6Ge_8S_{19} \cdot 12H_2O$.

- in the case of tin, at pH = 3 a novel macro-polyanion of the composition $Sn_{10}O_4S_{20}^{8-}$ having unusual structural properties[151, 152] (Fig. 23).

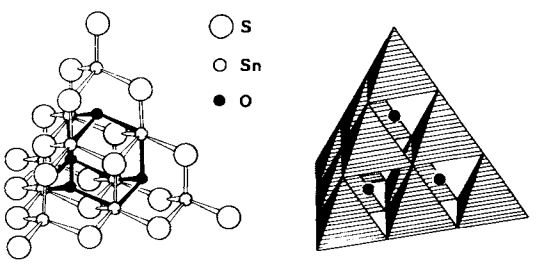



Fig. 23. $Sn_{10}O_4S_{20}^{8-}$, the largest known molecular main group thioanion. The oxygen atoms are bonded to only three of the four neighboring Sn atoms [152].

All the types of ions mentioned are listed in Figure 24. Figure 25 schematically presents the stability ranges of thiogermanates in aqueous solution. Generally it can be recognized that in comparison to the condensation reactions of oxoanions, *e.g.* of silicates and germanates, the pH ranges for comparative degrees of condensation are shifted to lower values in the case of sulfur compounds due to their markedly higher acidity.

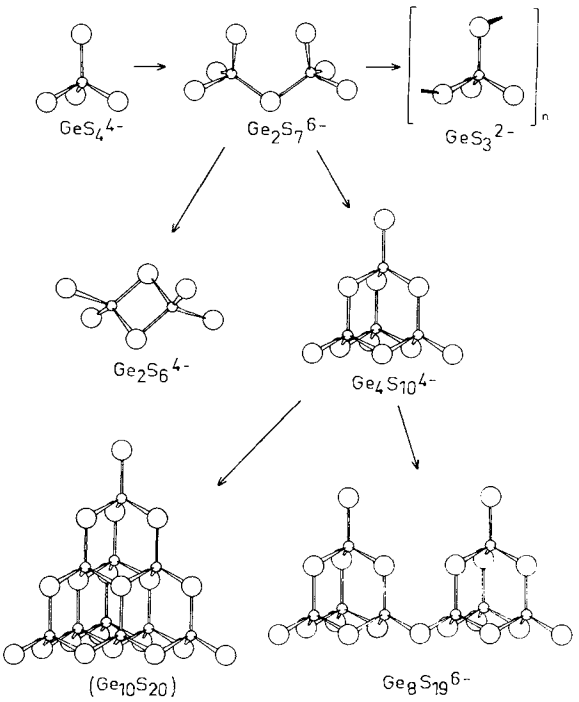



Fig. 24. Condensation paths of thioanions in aqueous solutions, shown for the thiogermanates. The $X_{10}Y_{20}$ "supertetrahedron" at the lower left has not yet been prepared in the case of germanium; it is realized in $Sn_{10}O_4S_{20}^{8-}$ with inserted oxygen atoms (Fig. 23), and in the corner-linked polymeric anion $(B_{10}S_{18}^{6-})_n$ of $Ag_3B_5S_9$ (Fig. 14).

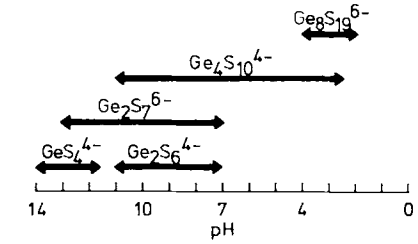



Fig. 25. Ranges of existence of oligomeric thiogermanate anions in aqueous solution.

Like the dimeric and tetrameric ions the simple tetrahedral species produced in solution (Fig. 20) have features in common with several water-free phases, which were prepared by solid-state reactions[137] and correspond to the tetrahedral structural units in the phases $M_4^IM'S_4$, $M_2^{II}M'S_4$ and $M_4^{III}(M'S_4)_3$ (with $M^I$ = Na, Tl, Cu; $M^{II}$ = Mg, Ca, Sr, Ba, Pb, Mn, Fe, Eu; $M^{III}$ = rare earth metal; M' = Si, Ge, Sn) or in chalcopyrite-type phases like $Cu_2M^{II}GeS_4$ or $Cu_2M^{II}SnS_4$ (cf. [137]).

The edge-sharing of the tetrahedra in $Ge_2S_6^{4-}$ and related species, just as in the similar $In_2S_6^{6-}$ and $In_2Se_6^{6-}$ ions and in formally analogous thio-compounds of the

transition metals such as $Fe_2S_6^{6-}$[153], shows a general structural principle which appears to be typical for certain sulfur and selenium compounds, whereas it is realized only in exceptional cases in oxygen compounds[154]. Important examples illustrating this are the structures of $SiS_2$ and of $SiSe_2$ (edge-sharing tetrahedral chains[155, 156]) in contrast to the different modifications of $SiO_2$[157], and, furthermore, the silicon sulfide halides $(SiSCl_2)_2$ and $(SiSBr_2)_2$ (cf. Section 7) and unusual edge-sharing of tetrahedra in the high-temperature modifications of $GeS_2$ and $GeSe_2$[160]. $Ge_2S_6^{6-}$ and its related ions may formally be considered to be dimeric fragments of the polymeric $SiS_2$ chain structure. The "metathiostannate" $SnS_3^{2-}$ of the earlier literature is thus identified by structural analysis as a hexathiodistannate $Sn_2S_6^{4-}$.

The structural principle of the $(GeS_3^{2-})_n$ and $(SnS_3^{2-})_n$ chains, *e.g.* in $K_2SnS_3 \cdot 2H_2O$[146], corresponds to the "Zweiereinfachketten" in silicate chemistry[161] and is also realized in the water-free phases $PbGeS_3$[162] and $Na_2GeS_3$[163] in cation-dependent variants, as well as in a modified form in the novel $TlBS_3$ phase[103] (Fig. 26).

The adamantane-like $Si_4S_{10}^{4-}$ and analogous $Si_4Se_{10}^{4-}$ cannot be prepared in solution due to the sensitivity of the Si–S bond towards solvolysis, but it is a product of high-temperature reactions, *e.g.* as $Na_4Si_4S_{10}$[164]. Water-free thio- and selenogermanates (*e.g.* $Na_4Ge_4S_{10}$[165], $Ba_2Ge_4S_{10}$[164], $Tl_4Ge_4S_{10}$[166], $Tl_4Ge_4Se_{10}$[167]) can be prepared in the same way from high-temperature solid-state and melt reactions, in contrast to the crystalline phases from solution (for example $Cs_4Ge_4S_{10} \cdot 3H_2O$[148] and $Na_4Ge_4S_{10} \cdot 17H_2O$[151]). The adamantane-like thiogermanic acid $H_4Ge_4S_{10} = Ge_4S_6(SH)_4$ can be obtained in dimethylformamide as monomeric solvated molecules which, however, tend to polymerize if its isolation in the solid state is attempted[149].

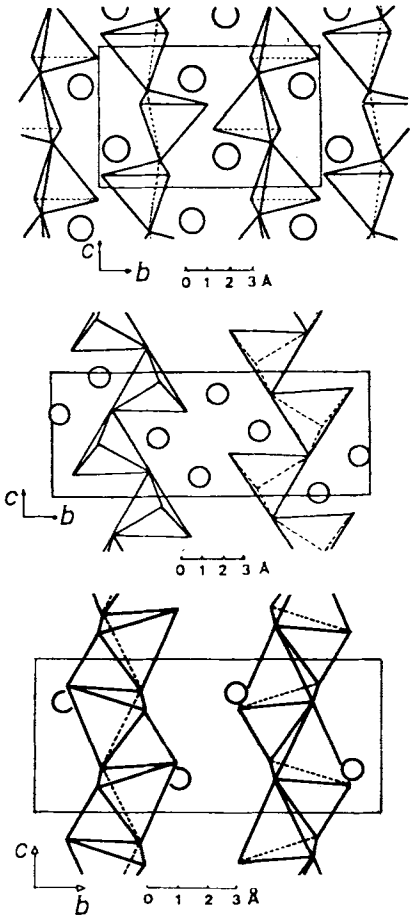



Fig. 26. Different configurations of the $(GeS_3^{2-})_n$ chains of tetrahedra and cation distribution in $PbGeS_3$ [162] and $Na_2GeS_3$ [163] as compared to the disulfide-bridged similar $(BS_3^{3-})_n$ chain in $TlBS_3$. All three structures have "Zweiereinfachketten" [161].

The tetrameric thioanions of silicon, germanium and tin complete a remarkable series of isoelectronic species of the elements of the 5th–3rd main groups which extends from the neutral molecules $P_4O_{10}$ and $P_4S_{10}$ to the ions $M_4^{IV}S_{10}^{4-}$ and $M_4^{IV}Se_{10}^{4-}$ ($M^{IV}$ = Se, Ge, Sn) and to the aforementioned highly charged ions $M_4^{III}S_{10}^{8-}$ and $M_4^{III}Se_{10}^{8-}$ ($M^{III}$ = B, Ga, In). Table 1 presents some bonding parameters of this class of compounds, which show typical common bonding characteristics of main group element chalcogenoanions (cf. Fig. 17).

Table 1. Structural and bond data of isoelectronic oxides, sulfides, thio- and selenoanions with adamantane-like structures as compared to simple tetrahedral anions. Bond lengths in Å, force constants in N/cm.

| | Bond lengths | | | Force constants | | | |
|---|---|---|---|---|---|---|---|
| | $d_{M-S(O)}$ | | | $f_{M-S(O)}$ | | | |
| | terminal | bridge | $d_1$ | terminal | bridge | $f_1$ | Ref. |
| $P_4O_{10}$ | 1.43 | 1.60 | 1.71 | 11.2 | 5.38 | 4.00 | [169] |
| $P_4S_{10}$ | 1.96 | 2.09 | 2.12 | 3.01 | 2.61 | 2.37 | [169] |
| $Si_4S_{10}^{4-}$ | 2.04 | 2.15 | 2.16 | | | 2.21 | [137, 164] |
| $Ge_4S_{10}^{4-}$ | 2.12 | 2.24 | 2.23 | 2.17 | 2.10 | 2.13 | [137, 148, 149, 169] |
| $Ge_4Se_{10}^{4-}$ | 2.26 | 2.37 | 2.36 | | | 1.91 | [167, 170] |
| $B_4S_{10}^{8-}$ | 1.92 | 1.92 | 1.91 | | | 2.67 | [8, 40, 50] |
| $Ga_4S_{10}^{8-}$ | 2.25 | 2.29 | 2.26 | 1.95 | 1.89 | 2.07 | [125–127] |
| $Ga_4Se_{10}^{8-}$ | 2.38 | 2.41 | 2.39 | | | 1.85 | [125, 126] |
| $In_4S_{10}^{8-}$ | 2.42 | 2.46 | 2.46 | 1.59 | 1.53 | 1.67 | [125–127] |
| $In_4Se_{10}^{8-}$ | 2.54 | 2.57 | 2.59 | | | 1.50 | [125, 126] |
| $PS_4^{3-}$ | 2.06 | | 2.12 | 2.64 | | 2.37 | [169] |
| $AsS_4^{3-}$ | 2.22 | | 2.22 | 2.26 | | 2.20 | [169] |
| $AsSe_4^{3-}$ | 2.32 | | 2.35 | 1.95 | | 1.97 | [33] |
| $SbS_4^{3-}$ | 2.35 | | 2.43 | 2.13 | | 1.74 | [169] |
| $SiS_4^{4-}$ | 2.12 | | 2.16 | 2.32 | | 2.21 | [137, 171–174] |
| $GeS_4^{4-}$ | 2.21 | | 2.23 | 2.12 | | 2.13 | [137, 139, 169] |
| $GeSe_4^{4-}$ | 2.35 | | 2.36 | 1.90 | | 1.90 | [140] |
| $SnS_4^{4-}$ | 2.39 | | 2.42 | 1.71 | | 1.75 | [137–139, 169] |
| $SnSe_4^{4-}$ | 2.52 | | 2.55 | 1.59 | | 1.53 | [141] |

The rounded bond lengths given are partly mean values of several compounds.
$d_1$: sum of the covalent single bond radii, corrected according to *Schomaker-Stevenson* = "single bond distance".
$f_1$: force constant to be expected for a single bond, estimated according to *Siebert* [107].
$f_{M-S(O)}$: stretching force constant from normal-coordinate analysis.

It becomes quite clear, *e.g.*, that the ions of the 4th main group, in accordance to their simple valence structures, contain essentially single bonds. However, π-bonding is also quite weak in $P_4S_{10}$ and thio- and selenoanions of the 5th main group elements. This is in complete contrast to the corresponding oxo compounds and to the strongly π-bonded thio- and seleno-compounds of the transition metals, *e.g.* of $V^V$, $Mo^{VI}$, $W^{VI}$, and $Re^{VII}$[168]. There is, howev-

er, a typical shortening of the terminal bonds to the negatively charged, stronger (n-d)π-donor S and Se atoms compared to the bridge bonds. This effect increases with decreasing number of terminal S or Se atoms per central atom. In the adamantane-like ions of boron, gallium, and indium there are four additional negative charges localized on the central cage. The total bond orders being significantly lower, there is practically no recognizable tendency for π-strengthening of terminal bonds.

Valuable analytical information for the spectroscopic identification of the adamantane-like cages is the symmetric vibration $\nu_2(A_1)$, which is very strong in the Raman spectrum, and which is characteristic for each species (cf. Table 2).

Table 2. Wave numbers of the symmetric stretching vibrations $\nu_2(A_1)$ of adamantane-like oxo- and thio-compounds.

| | $\nu_2$ [cm$^{-1}$] | Ref. |
|---|---|---|
| $P_4S_{10}$ | 406 | [169] |
| $As_4O_6$ | 381 | [169] |
| $Sb_4O_6$ | 256 | [169] |
| $Na_4Si_4S_{10}$ | 375 | [164] |
| $Si_4S_6(SC_6H_5)_2(SHNC_5H_5)_2$ | 374 | [185] |
| $Si_4S_6Br_4$ | 366 | [185] |
| $Ge_4S_{10}^{4-}$ (aqueous solution) | 348 | [169] |
| $Ba_2Ge_4S_{10}$ | 360 | [164] |
| $Na_4Ge_4S_{10}\cdot 17H_2O$ | 348 | [150] |
| $Cs_4Ge_4S_{10}\cdot 3H_2O$ | 340 | [169] |
| $Ge_4S_6(C_6H_5)_4$ | 355 | [169] |
| $Ge_4S_6Br_4$ | 363 | [221] |
| $Ge_4S_6I_4$ | 359 | [221] |
| $Ge_4Se_6I_4$ | 207 | [184] |
| $Na_4Ge_4Se_{10}\cdot xH_2O$ | 207 | [170] |
| $Ga_4S_{10}^{8-}$ (aqueous solution) | 313 | [125] |
| $K_8Ga_4S_{10}\cdot 16H_2O$ | 311 | [127] |
| $In_4S_{10}^{8-}$ (aqueous solution) | 302 | [125] |
| $K_8In_4S_{10}\cdot 16H_2O$ | 297 | [127] |

As shown in Figures 22 and 24, the $Ge_4S_{10}$ units in $Ge_8S_{19}^{6-}$ are linked in a parallel fashion so that the ion as a whole, like $Ge_4S_{10}^{4-}$, represents a section of the zinc blende structure. The ion is formed upon acidification of aqueous thiogermanate solutions to pH = 2.5, and it is the largest anion to be isolated prior to precipitation of polymeric $GeS_2$ on slightly stronger acidification.

### 6.2. Thio-oxoanions of Germanium and Tin

In $Sn_{10}O_4S_{20}^{8-}$, ten parallel corner-sharing $SnS_4$ tetrahedra are polymerized to a $Sn_{10}S_{20}$ "supertetrahedron" in the same way as in the $B_{10}S_{20}$ units of $Ag_3B_5S_9$ (Fig. 14); four additional O atoms, inserted in tetrahedral voids, complete the coordination of six of the ten Sn atoms to give distorted $SnS_4O_2$ octahedra[152]. So far, this is the only thio-oxostannate which is stable as a molecular ion in aqueous solution, and it can be isolated as hydrated alkali salts (*e.g.* $Cs_8Sn_{10}O_4S_{20}\cdot 13H_2O$[152], $Na_8Sn_{10}O_4S_{20}\cdot 32H_2O$[150]) (Fig. 27).

Novel thio-oxogermanates can also be obtained from aqueous solution. The anions $GeS_2(OH)_2^{2-}$ and $GeS_3OH^{3-}$[175,176] (Fig. 28), formed from stoichiometric sulfide-hydroxide mixtures, are protonated at the oxygen atoms. The remarkably low acidity of the oxygen functions

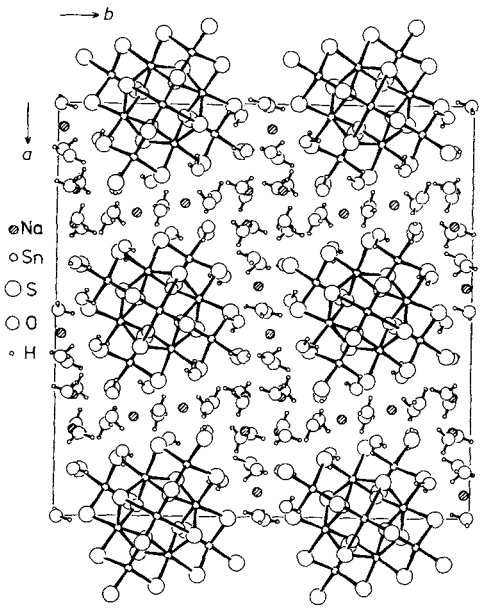



Fig. 27. Arrangement of the $Sn_{10}O_4S_{20}^{8-}$ ions in the $Na_8Sn_{10}O_4S_{20}\cdot 32H_2O$ structure, which is stabilized by an extensive OH···S hydrogen bridge system between the hydrated cations $[Na(OH_2)_6]^+$ and the thioanions.

distinguishes these ions from the thiophosphates $PS_xO_{4-x}^{3-}$ and thioarsenates $AsS_xO_{4-x}^{3-}$, in which the mesomeric stabilization of the $PO_{4-x}$ and $AsO_{4-x}$ fragments favors deprotonization. More highly condensed thiooxogermanates also ought to be obtainable from solution. High-temperature solid-state reaction of BaS, ZnO and $GeS_2$ furnished $S_3GeOGeS_3^{6-}$ as a $Ge_2S_7^{6-}$-type thiooxo anion in the phase $Ba_2ZnGe_2S_6O$, which, however, is associated through $ZnS_4$ tetrahedra[177].

Most of the alkali metal thiogermanates and thiostannates and the analogous seleno-compounds isolated from solutions crystallize strongly hydrated with typical compositions of $Na_4SnS_4\cdot 14H_2O$[138], $Na_4SnSe_4\cdot 16H_2O$[141],

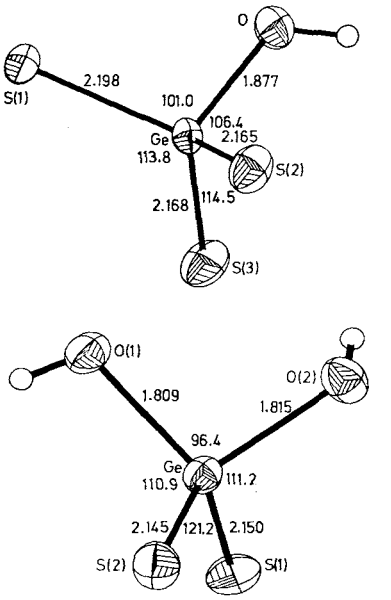



Fig. 28. $GeS_3OH^{3-}$ ion in the structure of $Na_3GeS_3OH\cdot 8H_2O$ and $GeS_2(OH)_2^{2-}$ ion in solid $Na_2GeS_2(OH)_2\cdot 5H_2O$ with bond lengths [Å] and bond angles [°] [174].

$Na_4Ge_2S_6 \cdot 14H_2O$[144], $K_2SnS_3 \cdot 2H_2O$[146], $Cs_4Ge_4S_{10} \cdot 3H_2O$[148], $Cs_6Ge_8S_{19} \cdot 12H_2O$[150], $Na_2GeS_2(OH)_2 \cdot 5H_2O$[176], $Na_3GeS_3OH \cdot 8H_2O$[175] *etc.* All these compounds contain extensive and structurally well characterized O–H···S and O–H···Se hydrogen-bridge systems between the hydrated cations (*e.g.* octahedral $Na(OH_2)_6^+$ groups) and the thio- or seleno-anions, so that they represent important model systems for this hydrogen-bridge type. In this respect Schlippe's salt $Na_3SbS_4 \cdot 9H_2O$, which is related to the phases under discussion, is especially well characterized[178–180].

### 6.3. Thio- and Seleno-compounds with Si–Si and Ge–Ge Bonds

Some thio-compounds with Si–Si and Ge–Ge bonds which have only recently been synthesized are of special chemical interest. $(S_3Ge-GeS_3)^{6-}$ and $(Se_3Ge-GeSe_3)^{6-}$ are formed by nucleophilic decomposition of glass-like $Ge_2S_3$ and $Ge_2Se_3$, respectively, with methanolic $Na_2S$[181, 182]. Their molecular structure can be deduced from the similarity of the vibrational spectra with those of $Si_2Cl_6$ and of $P_2S_6^{4-}$ (Fig. 29). In the same way, novel mixed thio- and seleno-bromogermanates $GeS_3Br^{3-}$ and $GeSe_3Br^{3-}$ can be identified by vibrational spectroscopy as products of the cleavage of the Ge–Ge bonds in $Ge_2S_6^{6-}$ and $Ge_2Se_6^{6-}$ with $Br_2$[183].

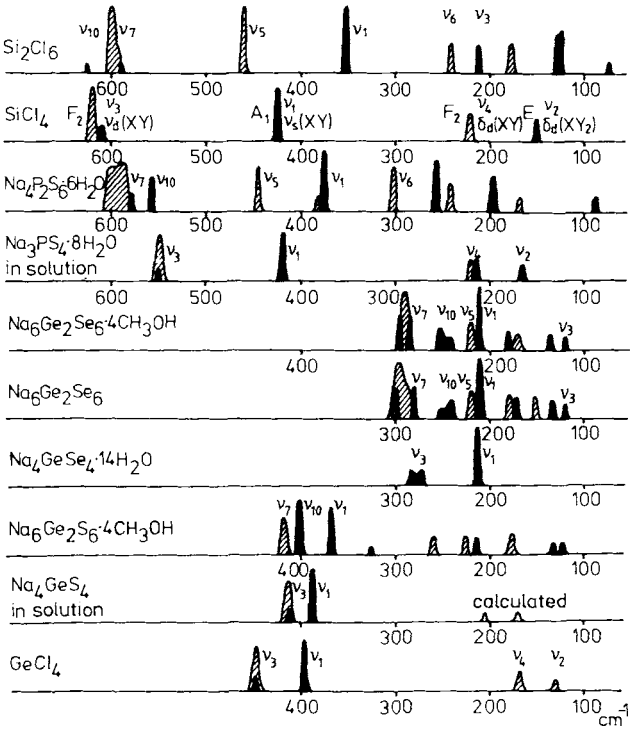
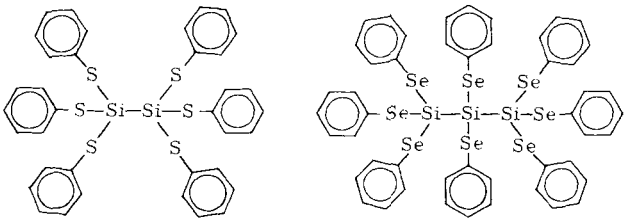



Fig. 29. Survey of the infrared bands (hatched) and Raman bands (solid) of different thio- and seleno-compounds with related compounds for comparison [181].

Novel air- and moisture-stable disilane and trisilane derivatives $Si_2(SR)_6$ **1** (Fig. 30), $Si_3(SR)_8$, and $Si_3(SeR)_8$ **2** are interesting products of the amine-catalyzed thiolysis of halogenosilanes[184, 185], *e.g.* according to




$$Si_3Br_8 + 8C_6H_5SeH + 8N(C_2H_5)_3 \xrightarrow[-20\,^\circ C]{\text{toluene}} Si_3(SeC_6H_5)_8 + 8(C_2H_5)_3NHBr$$

**2**

They can serve as important reagents for the synthesis of new Si-S and Si-Se compounds by cleavage with $Br_2$.

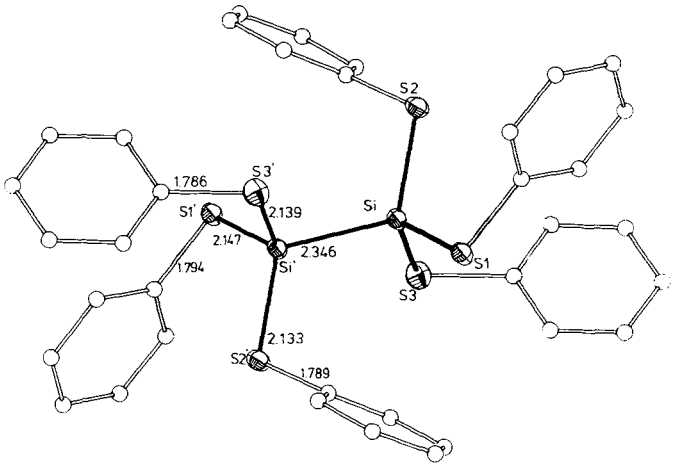



Fig. 30. Molecular structure of $Si_2(SC_6H_5)_6$ 1 with bond lengths [Å].

### 6.4. Higher Coordination Numbers in Thiostannates

In the thio- and seleno-compounds dealt with in this article, coordination numbers higher than four are found only in the case of In and Sn, where the compounds, with the exception of $Sn_{10}O_4S_{20}^{8-}$[151, 152], are solid-state materials which are prepared by high-temperature methods. $Na_4Sn_3S_8$[186] (Fig. 31) and $Tl_2Sn_2S_5$[187] contain five-coordinated $Sn^{IV}$ in a trigonal bipyramidal surrounding (axial and equatorial bond lengths: 2.59 and 2.43 Å, respectively).

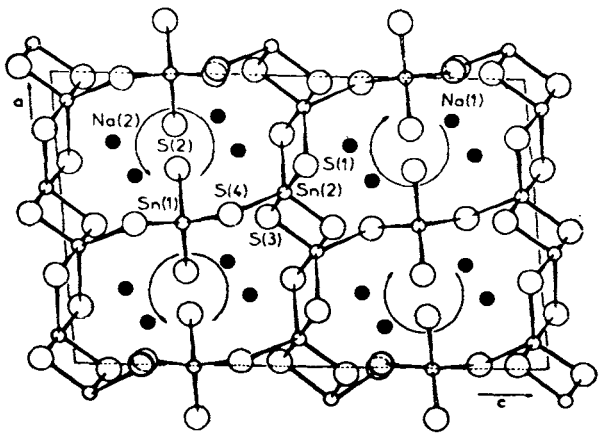



Fig. 31. Five-coordinated tin in $Na_4Sn_3S_8$: The trigonal bipyramids about Sn(2) form chains in the *ab* plane which are linked to helices parallel to b *via* the $SnS_4$ tetrahedra about Sn(1) [186].

Octahedrally coordinated Sn is observed in LT-$Na_2SnS_3$[188] (NaCl-type), in $Sn_2S_3$[189] and $PbSnS_3$[190] ($NH_4CdCl_3$-type), and in $La_2SnS_5$[191] (Sn–S 2.56 Å). Systematic $^{119}$Sn-Mössbauer investigations of thio- and selenostannates[192, 193] confirm the structural findings. In the case of $Na_4Sn_3S_8$, *e.g.*, two doublets are observed for the $SnS_5$ and the distorted tetrahedral $SnS_4$ polyhedra, with isomer shifts of 1.19 and 1.30 mm/s relative to $BaSnO_3$ and with quadrupole splittings of 0.54 and 1.40 mm/s[193].

### 6.5. Argyrodites—Example of a Class of Silver Ion Conductors

The mineral argyrodite $Ag_8GeS_6$, as a thiogermanate, is the prototype of an increasing number of sulfide materials which are of current interest because of their structural and physical properties[174, 194–203]. Argyrodite and the related phases $Ag_8MX_6$ with M = Si, Ge, Sn and X = S, Se, Te[196] form a cubic, face-centered, highly symmetrical structure at elevated temperatures. On cooling, they pass through one or several phase changes with stepwise lowering of the symmetry. Depending on the modification they have different electronic and/or ionic conductivities, which are (as in the case, *e.g.*, of AgI) especially large in the highly symmetrical high-temperature (γ-) modifications. Several argyrodite-related phases with tri- or pentavalent central atoms such as $Ag_9GaS_6$[204, 205], $Ag_7PS_6$, $Ag_7AsS_6$[206, 207], and the corresponding selenium compounds show similar electric properties.

An insight into the bonding and ion-conducting properties of argyrodites became possible through the first successful structural analyses of argyrodite-like phases, initially of $Cd_4GeS_6$[208] and $Cd_4SiS_6$[172], and later of the first "genuine" argyrodites α-$Ag_8SiS_6$[174] (Fig. 32), α-$Ag_8GeS_6$[197], γ-$Ag_8GeTe_6$[199], β-$Ag_8GeSe_6$[200], and related phases such as $Cu_6PS_5Br$[203] and $Ag_7GeS_5I$[201].

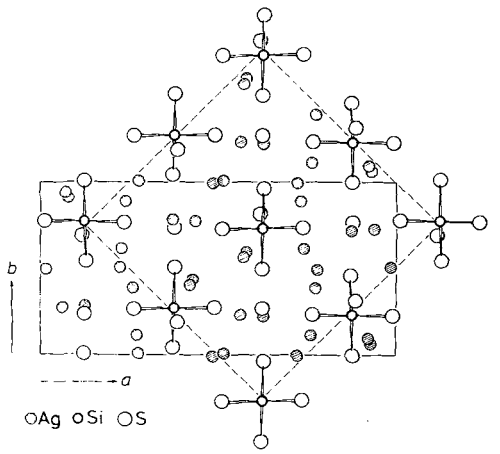



Fig. 32. α-$Ag_8SiS_6$: Example of an argyrodite structure with ordered cation distribution (low-temperature modification) [147]. The compound can be regarded as a "double salt" $Ag_8(SiS_4)S_2$ with $SiS_4^{4-}$ and $S^{2-}$ anions. The relation to the cubic high-temperature form (pseudo-cubic superstructure) is indicated. α-$Ag_8GeS_6$, the genuine argyrodite, is isotypic with α-$Ag_8SiS_6$.

As the structures show, they differ essentially in varying degrees of order in the cation lattice, while the characteristic anionic partial structure, in principle, remains intact. The arrangement of the chalcogenide ions can be described as a system of interpenetrating 12-icosahedra and 16-polyhedra (Frank-Kasper and Friauf polyhedra) (cf. *e.g.* [199, 201, 203]) in which each atom of one polyhedron centers another polyhedron (Fig. 33).

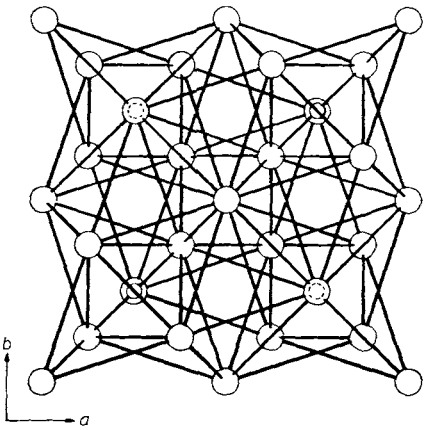



Fig. 33. Framework structure of the Te atoms in the cubic, $Ag^+$-conducting argyrodite phase γ-$Ag_8GeTe_6$ [199]. Ge (small circles) fills, in an ordered manner, 4 of the 136 tetrahedral voids of the unit cell and the 32 $Ag^+$ ions of the cell are distributed statistically over 116 other voids.

This icosahedral structure forms a system of face-sharing tetrahedral voids in which or between which the $Ag^+$ ions of the HT modifications are distributed more or less statistically with coordination numbers, 2, 3, or 4. Both factors—kind of anion packing and the low occupancy in the Ag sites—give optimal conditions for $Ag^+$ conductivity (the same is true for $Cu^+$-containing phases; cf. Fig. 34 and ref. [209]). With regard to these concepts, it appears

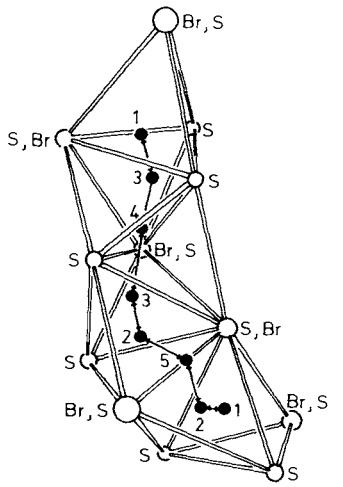



Fig. 34. Possible diffusion path of the $Cu^+$ ions in the $Cu^+$ ion-conducting argyrodite-analogous icosahedral structure of $Cu_6PS_5Br$ [203].

plausible that no ionic conductivity will be observed in the ordered low-temperature modifications. An ordered distribution is observed in the more silicon-rich argyrodite derivative $Ag_{10}Si_3S_{11}$, where, remarkably, two different thiosilicate groups are present[173] (Fig. 35).

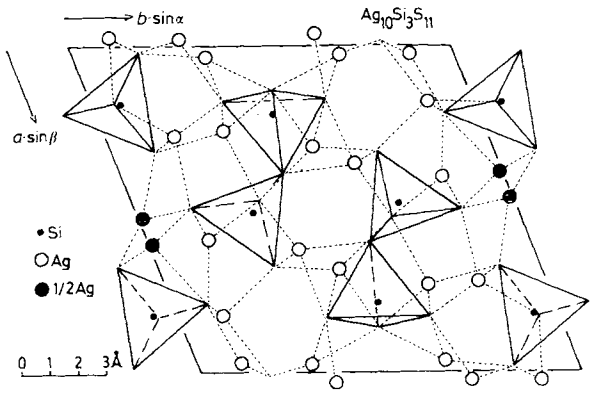



Fig. 35. $Ag_{10}Si_3S_{11}$: Argyrodite-related thiosilicate with two different anionic groups $SiS_4^{4-}$ and $Si_2S_7^{6-}$. The $Ag^+$ ions are essentially ordered.

## 7. Sulfide and Selenide Halides of Silicon and Germanium

The molecular sulfide halides $(SiSX_2)_2$, with X = F, Cl, Br, are of preparative interest as reagents for the synthesis of different SiS compounds. They are obtainable by reaction of $SiX_4$ with $H_2S$[210–213] (cf. also [214]). Their 2,2,4,4-tetrahalo-1,3,2,4-dithiadisiletane structure (Fig. 36) is analogous to $Ge_2S_6^{4-}$ and to dimeric thiophosgene $(CSCl_2)_2$[215]. It was initially derived spectroscopically[216], and has now been confirmed by X-ray structural analysis of $(SiSCl_2)_2$ and $(SiSBr_2)_2$[184, 185, 217, 218].

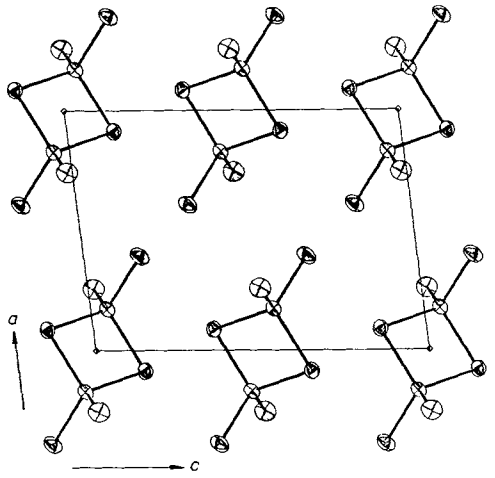
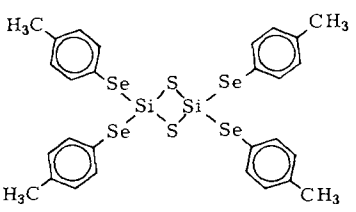



Fig. 36. $(SiSCl_2)_2$: Molecular and crystal structure. $(SiSF_2)_2$ and $(SiSBr_2)_2$ are similar.

Reactions with thiolates or their selenium analogues lead, *e.g.*, to substitution without cleavage of the central $Si_2S_2$ ring. Thus, by reaction of $(SiSBr_2)_2$ with selenols in pyridine/$CS_2$, novel mixed Si–S–Se compounds such as **3** can be synthesized[184, 185, 217].




**3**

A new class of adamantane-like silicon sulfide halides is produced by dismutation of $(SiSCl_2)_2$ or $(SiSBr_2)_2$ according to

$$3(SiSX_2)_2 \longrightarrow 2SiX_4 + Si_4S_6X_4 \quad (X = Cl, Br)^{[184, 185, 217]}$$

According to $^{29}Si$-NMR investigations[219] at least one additional species is present in the reaction mixture besides $(SiSBr_2)_2$ ($\delta = -47.1$), $SiBr_4$, and $Si_4S_6Br_4$ ($\delta = -27.1$), which might be a further member of a homologous series $Si_nS_{2n-2}X_4$ (X = Cl, Br) which was mentioned earlier[210].

The extraordinary stability of the adamantane cage is also demonstrated by the recently synthesized first sulfide halides and selenide halides of germanium: $Ge_4S_6Br_4$ and $Ge_4S_6I_4$ (Fig. 37)[220, 221] are synthesized from $GeBr_4$ or $GeI_4$ and $H_2S$ in $CS_2/AlBr_3$ or $CS_2/AlI_3$ as molecular solids stable to hydrolysis, which can serve as reagents for the introduction of the $Ge_4S_6$ cage. $Ge_4Se_6I_4$ ($d_{Ge-Se}$ = 2.353(2), $d_{Ge-I}$ = 2.507(2) Å) is isotypic with $Ge_4S_6I_4$ and can be isolated in crystalline form by $CS_2$-extraction from glasses of the composition $Ge_2Se_3I_2$, which are prepared from the elements[184, 185, 218] (cf. also [222]). It is useful for syntheses in a similar way to $Ge_4S_6Br_4$.

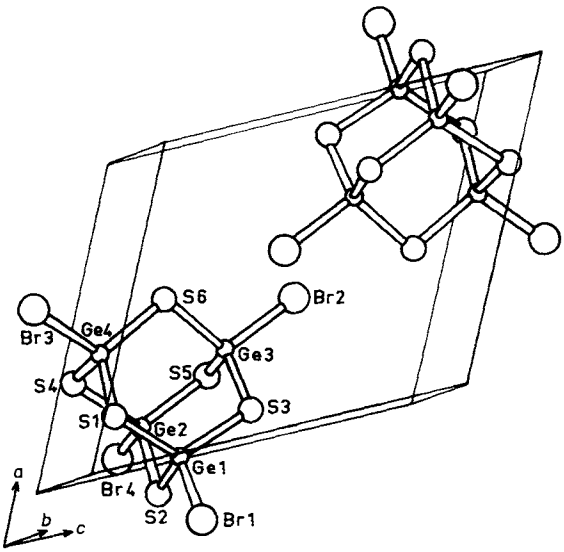
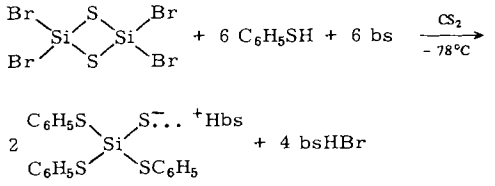



Fig. 37. Arrangement of molecules in the triclinic unit cell of the adamantane-like $Ge_4S_6Br_4$ [221]; $Si_4S_6Br_4$ ($d_{Si-S}$ 2.125, $d_{Si-Br}$ 2.181 Å) is isotypic with $Ge_4S_6Br_4$.

## 8. Organosubstituted Thiosilicates—A New Class of Compounds

It is possible by reaction of the chalcogenide halides of Si and Ge in non-polar solvents to synthesize a number of novel organosubstituted thiosilicates, which can be used as potential ligands in transition metal complexes. Nucleophilic attack of $Si_2S_2Br_4$ by thiolate and cleavage of the ring according to




(bs = pyridine, quinoline etc.)

affords the $(C_6H_5{-}S)_3SiS^-$ monoanion, the structure of which is shown in Figure 38[184,185].

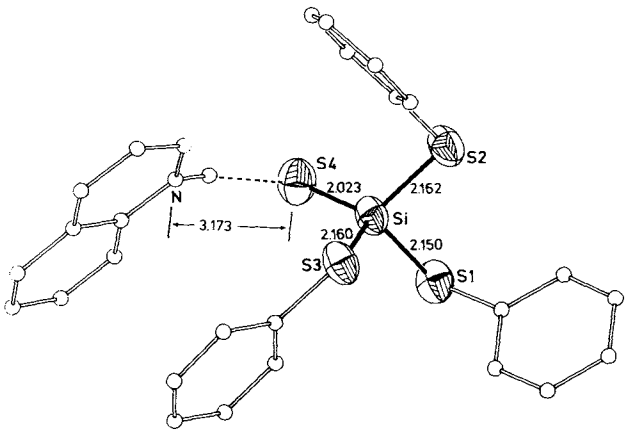



Fig. 38. Molecular structure of pyridinium-tris(phenylthio)silanethiolate $Si(SC_6H_5)_3SHNC_5H_5$ (bond lengths in Å). The Si–S(thiolate) bond is exceptionally short.

If the adamantane-like $Si_4S_6Br_4$ is employed, addition of $H_2S$ yields the tetrameric organothiosilicate dianion, which is isolated as an ion pair with the base (Fig. 39)[184,185] according to

$$Si_4S_6Br_4 + 6\,bs + 2\,C_6H_5{-}SH + 2\,H_2S \xrightarrow[-20\,^\circ C]{CS_2} Si_4S_6(SC_6H_5)_2(S^- \cdots {}^+Hbs)_2 + 4\,bsHBr.$$

In both types of ions the Si – S bond lengths of 2.02 – 2.04 Å are the shortest observed so far. As in $Si_4S_{10}^{4-}$ (2.04 Å[164]), this indicates unusually strong π-bonding.

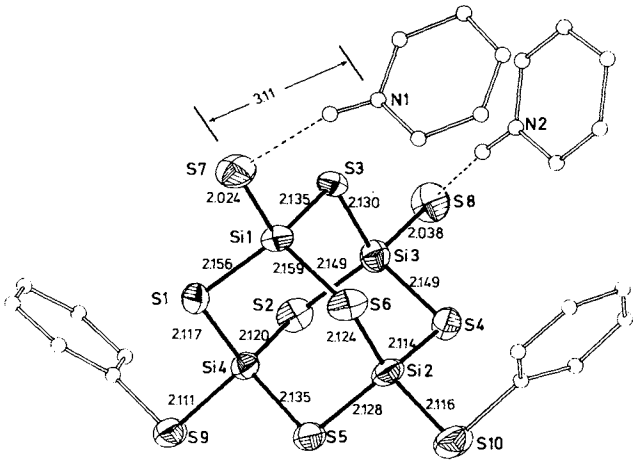



Fig. 39. An organothiosilicate dianion: Molecular structure of dipyridinium-bis(phenylthio)-2,4,6,8,9,10-hexathia-1,3,5,7-tetrasilaadamantanedithiolate $Si_4S_6(SC_6H_5)_2(SHNC_5H_5)_2$ (bond lengths in Å).

## 9. Thioanions of Main Group Elements as Ligands in Metal Complexes

Thioanions of the main group elements have a lesser tendency to function as ligands in transition metal complexes than corresponding transition metal thioanions such as $MoS_4^{2-}$ and $WS_4^{2-}$[168]. Although they are electron pair donors, there is no stabilizing electron-delocalization over energetically low π-orbitals as in the strongly π-bonded transition metal thioanions. Whereas the strongly π-bonded planar trithiocarbonate ion $CS_3^{2-}$ forms several stable complexes, *e.g.* with $Cr^{3+}$, $Co^{3+}$, $Ni^{2+}$, $Cu^+$, $Zn^{2+}$, $Cd^{2+}$, $Pd^{2+}$ and $Pt^{2+}$[223], so far little is known about tetrahedral thioanions of Si, Ge and Sn as complex ligands. $Cs_2NiGe_4S_{10}$ is formed as an amorphous yellow-brown polymeric complex according to[149,224]

$$Cs_4Ge_4S_{10} \xrightarrow[EtOH/HAc/H_2O]{NiAc_2} Cs_2NiGe_4S_{10}$$

The electron spectrum indicates octahedral coordination of nickel with mono- or bi-dentate ligation. Organosubstituted complexes are prepared according to

$$(R_2GeS)_3 \xrightarrow{Na_2S} R_2Ge(S^-)_2 \xrightarrow[EtOH/HAc/H_2O]{NiAc_2} \left[R_2Ge(S)_2Ni(S)_2GeR_2\right]^{2-}$$

R = $C_2H_5$, $C_6H_5$

and precipitated with large organic cations[149,224]; very little is known about their properties.

Also in the 5th main group, there are only few examples of complexes with pure thioanions $MS_4^{3-}$ (M = P, As, Sb) as ligands. Such are the polymeric mixed-ligand complexes $[Ni_3en_6(AsS_4)_2]$ and $[Ni_3phen_5(AsS_4)_2]$[225] as well as $[Ni_3en_6(PS_4)_2]$, $[Ni_3en_6(SbS_4)_2]$ and $[Coen_2AsS_4]$ with octahedral coordination of the transition metals[226].

## 10. S–H···S Hydrogen Bridge Bonds in Thioacids

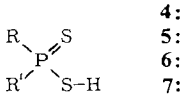
Some thioacids of the main group elements, especially trithiocarbonic acid $H_2CS_3$ and a number of substituted dithiophosphinic acids RR'P(S)SH, have proved to be important model systems for the characterization of the hitherto largely unknown S–H···S-type hydrogen bridge bond.

Hydrogen bridges between sulfur as donor and acceptor are generally quite weak. The bond enthalpies of S–H···S bridges are smaller by a factor of ten compared to those of hydrogen bridges of the homologous oxygen[227]. Reasons for this are the low polarity of the S–H group and the comparatively diffuse character of the acceptor electron pair.

Detailed knowledge about S–H···S bridge bonds and their structural activity is important because of the occurrence of sulfur in numerous biologically active compounds and their influence on equilibrium configurations, redox potentials, and reactivities[228].

S–H···S hydrogen bridges can be inferred from the frequencies of the S–H stretching vibrations. The greatest shifts from the frequency of the free SH group was found in the derivatives of the dithiophosphoric and dithiophosphinic acids[229–231]. Being *ca.* 200 $cm^{-1}$ they are greater by a factor of ten than the shifts in monofunctional mercaptans[232,233]. Similarly large shifts of the S–H vibrations as in the thioacids of phosphorus could be observed only in trithiocarbonic acid[234]; effects due to S–H···S association in dithiocarbonic acids[235] and in dithiotropolone[236] are only about half as great. The first quantitative struc-

tural data on S–H···S hydrogen bridges were obtained by X-ray structural analyses of disubstituted dithiophosphinic acids **4**–**8**.



**4**: R, R' = phenyl
**5**: R, R' = 3,5-dimethylphenyl
**6**: R, R' = *p*-tolyl
**7**: R = ethyl, R' = phenyl
**8**: R, R' = 3,4-dimethylphenyl

Here the strongest S–H···S bridge bonds known so far have bond enthalpies of about 12 kJ mol$^{-1}$[237] and S···S distances between 3.75 and 3.84 Å[231,238,239]. The limiting S···S distance calculated for pure van der Waals contacts of a linear S–H···S configuration (4.35 Å) is longer by *ca.* 0.5–0.6 Å. Predictions about the existence of extremely strong symmetrical S–H···S bridges with bonding enthalpies of about 15 kcal mol$^{-1}$ and S···S bridge distances of *ca.* 3.49 Å in the system $H_2S/SH^{\ominus}$, as were published in the literature on the basis of *ab initio* calculations[240], could not be confirmed by experiment. In the compound $[(CH_3)_3(C_7H_7)N][SH]\cdot 2H_2S$, prepared in liquid $H_2S$[241], the observed S···S distances are of the same magnitude as in the dithiophosphinic acids, thus ruling out symmetrical bridges.

Further information on S–H···S hydrogen bridge bonding has been obtained from crystal structure analyses of two modifications of trithiocarbonic acid[241,242] and dithiotropolone[243]. In the substituted dithiophosphinic acids the individual molecules are associated through almost linear S–H···S hydrogen bridges to form either centrosymmetric cyclic dimers (in **6**, **7** and **8**) or helically twisted chains (in **4** and **5**), with the thiophosphoryl group functioning as acceptor also in the chain associates. Its polar character favors considerably the extent of the S–H···S associations. In contrast to the dimeric carboxylic acids with their planar arrangement of the bridge atoms, the planes of the associated P(S)S groups in **6**, **7** and **8** are separated from each other by *ca.* 3.5 Å. The H atoms are twisted about the P–S bonds out of the P(S)S-planes in such a way that almost linear S–H···S bridges result. A similar arrangement of the P, S and H atoms can be observed in the chain-like associate of **5**. Within the spiral-shaped chains of **4** all atoms of the P(S)SH group are in one plane, with the H atoms in a *trans* position to the S atom of the thiophosphoryl-group. Figures 40, 41 and 42 show the three principles of association as exemplified by **7**, **5** and **4**. Structural and spectroscopic data on these systems are listed in Table 3.

Table 3. Distances [Å] and angles [°] as well as spectroscopic data [cm$^{-1}$] for the S–H···S hydrogen bridges in substituted dithiophosphinic acids. The $\Delta\nu$ values refer to $\nu_{S-H}=2570$ cm$^{-1}$ for the dilute solutions of the monomeric acids in $CCl_4$.

| | $d$(S···S) | ∢P–S···S | ∢P=S···S | ∢S–H···S | $\nu_{S-H}$ | $\Delta\nu_{S-H}$ |
|---|---|---|---|---|---|---|
| **4** [a] | 3.790 | 98.9 | 96.7 | 170 | | |
| **4** | 3.837 | 99.4 | 97.4 | 166 | 2340 | 230 |
| **5** | 3.763 | 89.0 | 115.1 | 159 | 2350 | 220 |
| **6** | 3.746 | 98.0 | 115.6 | 173 | 2325 | 245 |
| **7** | 3.810 | 88.9 | 109.6 | 168 | 2380 | 190 |
| **8** | 3.832 | 107.9 | 115.9 | 163 | 2400 | 170 |

[a] At −133 °C.

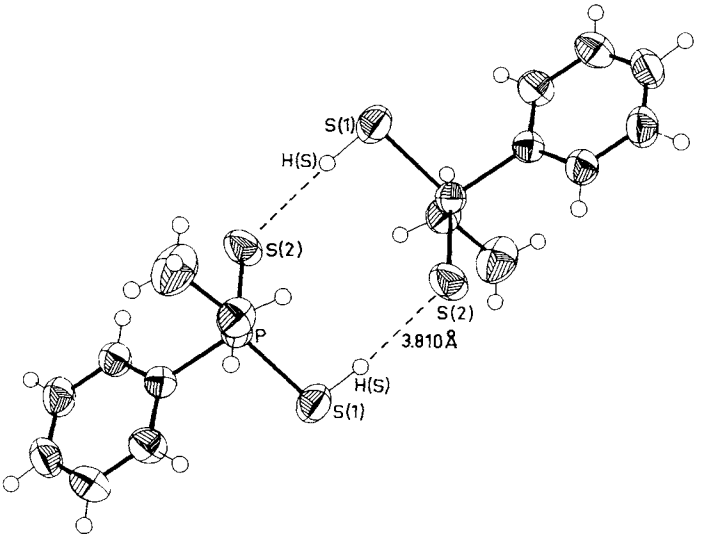



Fig. 40. $(C_6H_5)(C_2H_5)P(S)SH$ **7**: Cyclic dimers by association through S–H···S hydrogen bridges.

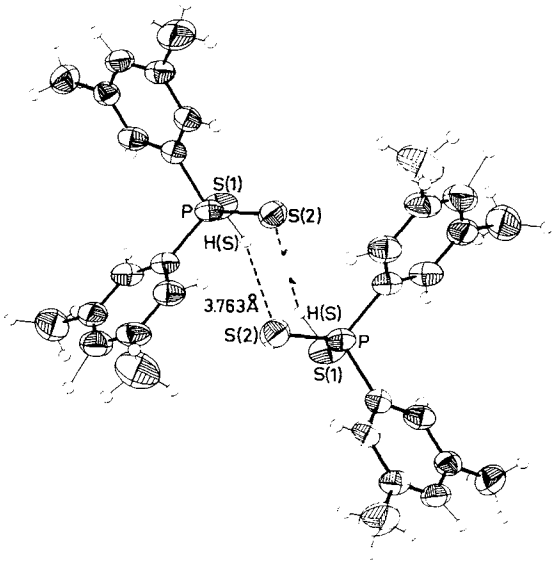



Fig. 41. $(C_8H_9)_2P(S)SH$ **5**: Projection of a molecular chain produced by association through S–H···S hydrogen bridges.

With the exception of **4**, an essentially linear relation results between S···S bridge distances and the S-H frequency shifts, as is also true for weak O–H···O hydrogen bridges[244]. This correlation implies a uniform electronic hydrogen-acceptor system ($sp^2$-hybridized free electron pairs) for the S–H···S bridges in **5**–**8**; in **4** the acceptor functions are p-electron pairs, which are perpendicular to the planes of $sp^2$-hybrid orbitals of the thiophosphoryl S atoms.

In the two modifications of trithiocarbonic acid there are also intermolecular S–H···S bridges, which, according to low-temperature structure analyses, are in part distinctly nonlinear. Unlike α-$H_2$-$CS_3$, in which all H-acceptor functions are thiocarbonyl groups, bridges occur between the SH groups in β-$H_2CS_3$. The S···S distances of the S–H···S bridges vary between 3.80 and 3.97 Å.

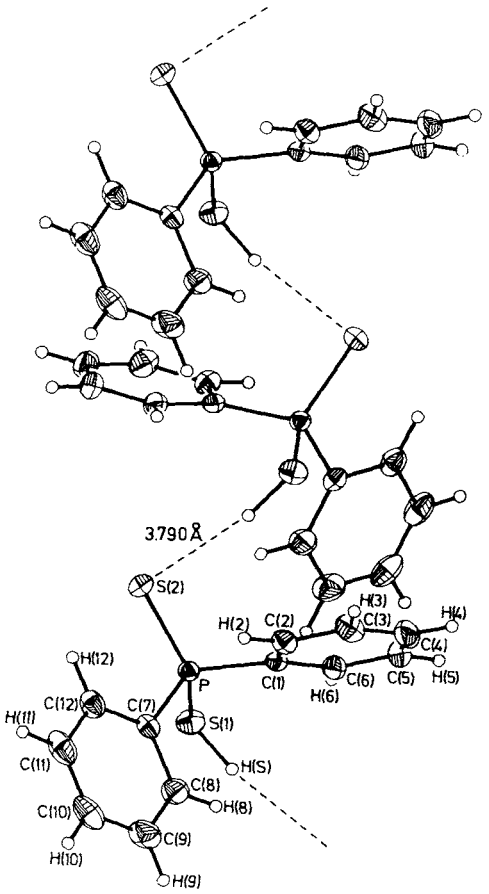



Fig. 42. $(C_6H_5)_2P(S)SH$ 4: Chain of molecules formed through S–H···S hydrogen bridges (−133 °C).

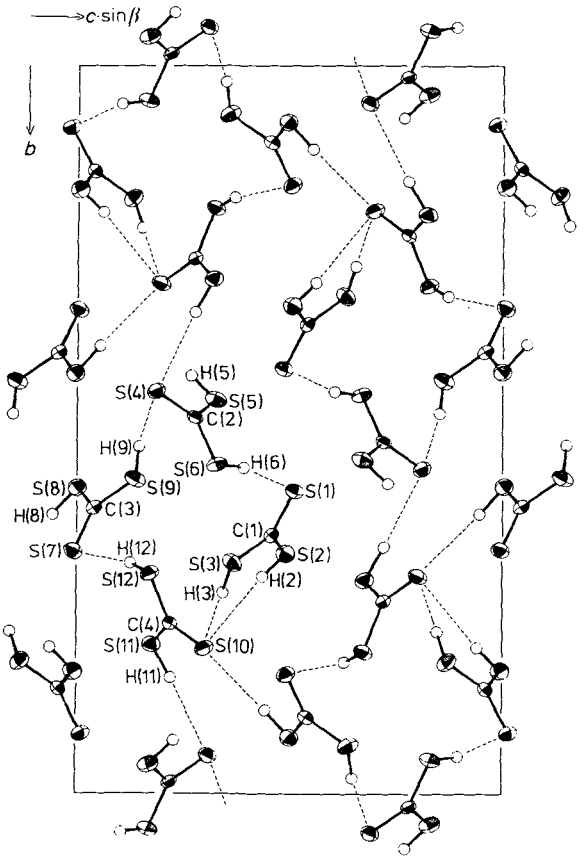



Fig. 43. α-$H_2CS_3$: Projection of the unit cell with S–H···S hydrogen bridges (−133 °C).

In both modifications the $H_2CS_3$ molecules are planar. Whereas the conformation of the molecules in β-$H_2CS_3$ is uniform with idealized symmetry $C_s$, in α-$H_2CS_3$ there are three molecules with symmetry $C_s$ together with one molecule with $C_{2v}$ symmetry and neighboring H-atoms. Figure 43 shows a projection of the unit cell of α-$H_2CS_3$, in which the hydrogen bridges and the different conformations can be recognized. In dithiotropolone (Fig. 44) intramolecular S–H···S bridge bonds were detected for the first time. This type of bridge cannot be linear because of the geometrical constraints of the molecule. The S–H···S bridge bond angle is 133° with a S···S separation of 3.12 Å and a H···S distance of 2.08 Å.

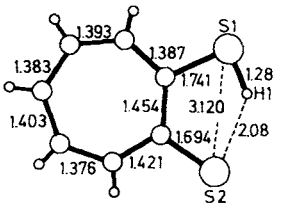



Fig. 44. Dithiotropolone: Molecular structure with intramolecular S–H···S hydrogen bond (−133 °C).

## 11. Final Remarks and Outlook

The chemistry and structural chemistry of the thio-compounds of 5th main group elements, which will be the subject of a later review, is quite extensive and has also progressed considerably during recent years, especially in the field of solid-state chemistry of the thioarsenates(III) and thioantimonates(III). While the chemistry of the thio- and selenoarsenates(V) and their antimony analogues is still restricted to the simple tetrahedral ions $AsO_xS_{4-x}^{3-}$ and $SbO_xS_{4-x}^{3-}$, a greater number of differently condensed polynuclear thiocompounds with the oxidation state +3 could be characterized[245]. Some interesting novel thiophosphates have been reported recently. Besides $(S_3P{-}PS_3)^{4-}$[246,247] and a number of its derivatives, $P_2S_8^{2-}$[248] with a six-membered $PS_2PS_2$ ring and $P_4S_8^{4-}$[249] with a central planar $P_4$ ring have been synthesized.

Remarkable new developments in the less extensive field of thio-compounds of the chalcogens are the synthesis and structural description of some thiotellurates(IV) with $TeS_3^{2-}$ anions[250,251] and the first synthesis of a dithiosulfate $SO_2S_2^{2-}$ stabilized by coordination to Mo in the complex $[(S_2)OMoS_2MoO(S_2SO_2)]^{2-}$[252].

What kind of developments are to be expected? The results reviewed here on the synthesis, structural chemistry, bonding, and reactivity of novel sulfur and selenium compounds of the 3rd–5th main group elements show the following trends, opening new paths in this field of inorganic chemistry:

New classes of attractive polynuclear and polymeric inorganic compounds can be prepared by consistent use of the ability of the trigonal-planar (B), tetrahedral (Ga, In, Si, Ge, Sn) or pyramidal (As, Sb) monomeric building blocks to undergo condensation and to polymerize to polynuclear units. In this borderline field between molecular and solid-

state chemistry the possibilities of the synthetic methods are variable, since reactions in polar and nonpolar solvents can be used successfully besides conventional solid-state methods of synthesis. Here, further efforts will have to concentrate on the mechanisms of formation and on the equilibria in solution which have to be known for new successful syntheses. A second important field to be investigated is the preparation of new mixed polynuclear thio-oxo compounds which can serve as a basis for more "silicate-like" products with intermediate chemical and physical properties. The chalcogenides and chalcogenoanions can be used as valuable starting materials for many other inorganic and organic syntheses, as is shown by the successful use of the boron sulfides in organic synthetic reactions or the potential of $B_8S_{16}$ or thiogermanates as ligands in transition metal complexes. Further intensive research work is also necessary in this field in the future.

Polynuclear chalcogenide halides can be employed for the preparation of novel organosilicon sulfur compounds and of the corresponding germanium analogues. The potential of the reactions presented here is still far from being exhausted. In this field, *e.g.*, novel organosubstituted thioanions can be employed for the synthesis of Si and Ge sulfur compounds not obtainable with known starting materials, which can produce new Si–S–R and Ge–S–R compounds for practical applications.

The ion-conducting and other electrical properties of the $Ag^+$ and $Cu^+$ thio-compounds which have been exemplified here by $Ag_3B_5S_9$ and the argyrodites, will be a field of further very active chemical and physical research in the near future.

The structural results referred to in this review have made important contributions to the problem of bonding in main group thio- and seleno-anions, and especially to the question of the existence of $\pi$-contributions in the boron-sulfur and boron-selenium bonds as well towards an understanding of the novel S–H···S hydrogen bond type. However, also in this field many questions remain open and will have to be answered by further research.

*I sincerely thank my co-workers, past and present, who have contributed to the work cited in this article, for their active and enthusiastic cooperation over many years. I am also indebted to Dr. G. Henkel and to Dr. H. Eckert for valuable discussions. Continuous support of our research by the Minister für Wissenschaft und Forschung des Landes Nordrhein-Westfalen, by the Deutsche Forschungsgemeinschaft, and the Fonds der Chemischen Industrie is gratefully acknowledged.*

Received: October 18, 1982 [A 444 IE]
German version: *Angew. Chem. 95* (1983) 113

[1] O. Glemser, R. Mews, *Adv. Inorg. Chem. Radiochem. 14* (1972) 333; R. Mews, *ibid. 19* (1976) 185; M. M. Labes, P. Love, L. F. Nichols, *Chem. Rev. 79* (1979) 1; H. W. Roesky, *Adv. Inorg. Chem. Radiochem. 22* (1979) 239; T. Chivers, R. T. Oakley, *Top. Curr. Chem. 102* (1982) 117.

[2] a) F. Seel, *Adv. Inorg. Chem. Radiochem. 16* (1974) 297; B. Meyer, *ibid. 18* (1976) 287; b) J. Fenner, A. Rabenau, G. Trageser, *ibid. 23* (1980) 329; c) R. Steudel, R. Laitinen, *Top. Curr. Chem. 102* (1982) 177; R. Steudel, *ibid. 102* (1982) 149.

[3] A. Senning: *Sulfur in Organic and Inorganic Chemistry*, Vol. 4, Marcel Dekker, New York 1982.

[4] G. Gattow, W. Behrendt "Carbon Sulfides and Their Inorganic and Complex Chemistry" in A. Senning: *Topics in Sulfur Chemistry*, Vol. 2, Thieme, Stuttgart 1977.

[5] J. J. Berzelius, *Ann. Phys. Chem. 2* (1824) 113.

[6] H. Sainte-Clair Deville, F. Wöhler, *Liebigs Ann. Chem. 105* (1858) 67.

[7] F. Chopin, Dissertation, Université de Bordeaux 1966.

[8] H. Diercks, Dissertation, Universität Kiel 1975.

[9] P. Hagenmuller, F. Chopin, *C. R. Acad. Sci. 255* (1962) 2259.

[10] A. Sommer, P. N. Walsh, D. White, *J. Chem. Phys. 33* (1960) 296.

[11] Z. S. Medvedeva, V. A. Boryakova, Ya. Kh. Grinberg, E. G. Zhukov, *Zh. Neorg. Khim. 13* (1968) 1440.

[12] Ya. Kh. Grinberg, E. G. Zhukov, V. A. Koryazhkin, Z. S. Medvedeva, *Zh. Neorg. Khim. 14* (1969) 2583.

[13] Ya. Kh. Grinberg, E. G. Zhukov, V. A. Koryazhkin, *Dokl. Akad. Nauk SSSR 1970*, 589.

[14] F. T. Greene, P. W. Gilles, *J. Am. Chem. Soc. 84* (1962) 3598.

[15] F. T. Greene, P. W. Gilles, *J. Am. Chem. Soc. 86* (1964) 3964.

[16] H.-Y. Chen, P. W. Gilles, *J. Am. Chem. Soc. 92* (1970) 2309.

[17] H.-Y. Chen, B. Conard, P. W. Gilles, *Inorg. Chem. 9* (1970) 1776.

[18] H.-Y. Chen, P. W. Gilles, *J. Phys. Chem. 76* (1973) 2035.

[19] E. G. Zhukov, Ya. Kh. Grinberg, *Izv. Akad. Nauk SSSR Neorg. Mater. 5* (1969) 1646.

[20] Electron diffraction investigations on the $B_2S_3$ molecule in the gas phase: P. A. Akishin, V. P. Spiridonov, *Dokl. Akad. Nauk SSSR 129* (1959) 1317.

[21] D. Thomas, G. Tridot, *C. R. Acad. Sci. 259* (1964) 3559.

[22] E. L. Muetterties: *The Chemistry of Boron and its Compounds*, Wiley, New York 1967, p. 647 and references cited therein.

[23] Gmelin Handbuch der Anorganischen Chemie, Supplement to 8th edit., Vol. 19, Borverbindungen Part 3, p. 6ff., Springer-Verlag, Berlin 1975; and references cited therein.

[24] V. I. Matkovich, *J. Am. Chem. Soc. 83* (1961) 1804.

[25] J. L. Hoard, R. E. Hughes in E. L. Muetterties: *The Chemistry of Boron and its Compounds*, Wiley, New York 1967, p. 25.

[26] W. E. Hutchinson, H. A. Eick, *Inorg. Chem. 1* (1962) 434.

[27] J. Cueilleron, R. Hillel, *Bull. Soc. Chim. Fr. 1967*, 2973.

[28] J. Cueilleron, R. Hillel, *Bull. Soc. Chim. Fr. 1968*, 3635.

[29] V. A. Boryakova, Ya. Kh. Grinberg, E. G. Zhukov, V. A. Koryazhkin, Z. S. Medvedeva, *Izv. Akad. Nauk SSSR Neorg. Mater. 5* (1969) 477.

[30] R. Hillel, J. Cueilleron, *Bull. Soc. Chim. Fr. 1972*, 98.

[31] Cf. [23], p. 75ff.

[32] H.-U. Hürter, Dissertation, Universität Münster 1981.

[33] B. Krebs, H.-U. Hürter, W. Hamann, unpublished results.

[34] D. C. Carlson, Thesis, Brigham Young University, Salt Lake City 1966; *Diss. Abstr. 27* (1967) 2664.

[35] A. Stock, O. Poppenberg, *Ber. Dtsch. Chem. Ges. 34* (1901) 399.

[36] E. Wiberg, W. Sturm, *Angew. Chem. 67* (1955) 483.

[37] E. Wiberg, W. Sturm, *Z. Naturforsch. B8* (1953) 530.

[38] W. Schwarz, H. D. Hausen, H. Hess, J. Mandt, W. Schmelzer, B. Krebs, *Acta Crystallogr. B29* (1973) 2029; cf. also $(BSBr)_3$: W. Schwarz, H. D. Hausen, H. Hess, *Z. Naturforsch. B29* (1974) 596.

[39] P. Hagenmuller, F. Chopin, R. Castagna, *C. R. Acad. Sci. C262* (1966) 418.

[40] B. Krebs, H. Diercks, *Acta Crystallogr. A31* (1975) S66.

[41] H. Diercks, B. Krebs, *Angew. Chem. 89* (1977) 327; *Angew. Chem. Int. Ed. Engl. 16* (1977) 313.

[42] B. Krebs, H. Diercks, unpublished results.

[43] Crystallographic data: monoclinic, $P2_1/c$, $a=4.039$, $b=10.722$, $c=18.620$ Å, $\beta=96.23°$, $Z=8$.

[44] F. Chopin, G. Turrell, *J. Mol. Struct. 3* (1969) 57.

[45] J. A. Forstner, E. L. Muetterties, *Inorg. Chem. 5* (1966) 164.

[46] G. E. Gurr, P. W. Montgomery, C. D. Knutson, B. T. Gorres, *Acta Crystallogr. B26* (1970) 906.

[47] S. L. Strong, R. Kaplow, *Acta Crystallogr. B24* (1968) 1032.

[48] C. T. Prewitt, R. D. Shannon, *Acta Crystallogr. B24* (1968) 869.

[49] Crystallographic data: $B_2O_3$-I (normal-pressure modification): trigonal, space group $P3_1$, $a_H=4.3358$, $c_H=8.340$ Å [46, 47]; $B_2O_3$-II: orthorhombic, space group $Ccm2_1$, $a=4.613$, $b=7.803$, $c=4.129$ Å [48].

[50] A. Hardy, *Bull. Soc. Fr. Mineral. Cristallogr. 91* (1968) 111.

[51] J. M. Lalancette, *Can. J. Chem. 42* (1964) 2356.

[52] J. Brault, J. M. Lalancette, *Can. J. Chem. 42* (1964) 2903.

[53] S. Jerumanis, J. M. Lalancette, *Can. J. Chem. 42* (1964) 1928; B. J. Yager, W. L. Wootan, *ibid. 56* (1978) 1043.

[54] S. Jerumanis, J. M. Lalancette, *J. Org. Chem. 31* (1966) 1531.

[55] J. M. Lalancette, F. Bessette, J. M. Cliche, *Can. J. Chem. 44* (1966) 1577.

[56] F. M. Dean, J. Goodchild, A. W. Hill, *J. Chem. Soc. C1969*, 2192.

[57] L. Busetto, A. Palazzi, E. Foresti Serantoni, L. Riva Di Sanseverino, *J. Organomet. Chem. 129* (1977) C55.

[58] A. O. Baghlaf, A. Thompson, *J. Less-Common Met. 53* (1977) 291.

[59] K. P. Callahan, P. J. Durand, *Inorg. Chem. 19* (1980) 3211.

[60] B. Krebs, H.-U. Hürter, *Angew. Chem. 92* (1980) 479; *Angew. Chem. Int. Ed. Engl. 19* (1980) 481.

[61] B. Krebs, H.-U. Hürter, *Acta Crystallogr. A 37* (1981) C 163.
[62] Crystallographic data: monoclinic, space group $P2_1/c$, $a = 12.158$, $b = 4.089$, $c = 21.961$ Å, $\beta = 107.65°$, $Z = 2B_8S_{16}$ [60]. In Fig. 1 of l.c. [60] the values 1.789 and 1.822 Å must be interchanged.
[63] O. Gropen, P. Vassbotn, *Acta Chem. Scand. 27* (1973) 3079.
[64] B. M. Gimarc, N. Trinajstić, *Inorg. Chem. 21* (1982) 21.
[65] B. M. Gimarc, J.-K. Zhu, *Inorg. Chem.*, in press.
[66] H. M. Seip, R. Seip, W. Siebert, *Acta Chem. Scand. 27* (1973) 15.
[67] A. Almenningen, H. M. Seip, P. Vassbotn, *Acta Chem. Scand. 27* (1973) 21.
[68] M. Schmidt, W. Siebert, *Angew. Chem. 76* (1964) 687; *Angew. Chem. Int. Ed. Engl. 3* (1964) 637.
[69] M. Schmidt, W. Siebert, *Z. Anorg. Allg. Chem. 345* (1966) 87.
[70] M. Schmidt, W. Siebert, *Angew. Chem. 78* (1966) 607; *Angew. Chem. Int. Ed. Engl. 5* (1966) 597; M. Schmidt, F. R. Rittig, W. Siebert, *Z. Naturforsch. B 25* (1970) 1344.
[71] M. Schmidt, W. Siebert, *Chem. Ber. 102* (1969) 2752 and references cited therein.
[72] B. Krebs, G. Gattow, *Z. Anorg. Allg. Chem. 338* (1965) 225.
[73] Under mild conditions this condensation reaction of $(XB)_2S_3$ with $SC(SH)_2$ can be used for the preparation of new boron-carbon-sulfur compounds [32].
[74] M. Binnewies, W. Hamann, B. Krebs, unpublished results.
[75] J. G. Edwards, P. W. Gilles, *Adv. Chem. Ser. 72* (1968) 211.
[76] R. C. Melucci, P. G. Wahlbeck, *Inorg. Chem. 9* (1970) 1095.
[77] H. Eckert, H.-U. Hürter, W. Müller-Warmuth, B. Krebs, *J. Noncryst. Solids*, in preparation.
[78] H. Eckert, Dissertation, Universität Münster 1982.
[79] W. Müller-Warmuth, H. Eckert, *Phys. Rep.*, in press.
[80] V. I. Svergun, Ya. Kh. Grinberg, V. M. Kusnets, T. A. Babushkina, *Izv. Akad. Nauk SSSR Ser. Khim. 1970*, 1448.
[81] J. R. Hendrickson, S. G. Bishop, *Solid State Commun. 17* (1975) 301.
[82] M. Rubinstein, *Phys. Rev. B 14* (1976) 2778.
[83] H. Nöth, B. Wrackmeyer: *Nuclear Magnetic Resonance Spectroscopy of Boron Compounds*, Springer-Verlag, Berlin 1978, p. 26ff.
[84] J. F. Baugher, P. J. Bray, *Phys. Chem. Glasses 10* (1969) 77.
[85] J. Kamsu Kom, J. Flahaut, L. Domange, *C. R. Acad. Sci. 257* (1963) 3919.
[86] P. Hagenmuller, F. Chopin, *C. R. Acad. Sci. 256* (1963) 5578.
[87] J. Kamsu Kom, *Ann. Chim. Paris 9* (1964) 179.
[88] F. Chopin, A. Hardy, *C. R. Acad. Sci. 261* (1965) 142.
[89] F. Chopin, A. Richard, B. Castagna, *C. R. Acad. Sci. C 269* (1969) 921.
[90] V. V. Kirilenko, *Izv. Akad. Nauk SSSR Neorg. Mater. 14* (1978) 1992.
[91] D. Thomas, G. Tridot, *C. R. Acad. Sci. 258* (1964) 2587.
[92] F. Chopin, B. Capdepuy, *Bull. Soc. Chim. Fr. 1970*, 505.
[93] J. C. Rosso, *C. R. Acad. Sci. C 267* (1968) 1609.
[94] D. Thomas, *C. R. Acad. Sci. C 265* (1967) 1325.
[95] F. Chopin, P. Hagenmuller, *Bull. Soc. Chim. Fr. 1965*, 3031.
[96] J. Flahaut, L. Domange, J. Kamsu Kom, *C. R. Acad. Sci. 254* (1962) 299.
[97] H. Nöth, G. Mikulaschek, *Z. Anorg. Allg. Chem. 311* (1961) 241.
[98] Z. K. Sterlyadkina, O. N. Kryukova, V. I. Mikheeva, *Zh. Neorg. Khim. 10* (1965) 583.
[99] J. M. Lalancette, A. Frêche, R. Monteux, *Can. J. Chem. 46* (1968) 2754.
[100] E. Wiberg, W. Sturm, *Z. Naturforsch. B 8* (1953) 529, 530.
[101] A direct relation of the interatomic distances to $\sigma$ and $\pi$ bond strength, however, cannot be obtained without difficulties, and it must take into account that (a) the B–S bonds in the $BS_4$ tetraedra have charge-dependent $\sigma$ bond orders $< 1$ and that (b) the $\sigma$ bond lengths depend on the hybridization of the central atom.
[102] $Ag_3B_5S_9$: monoclinic, C2/c, $a = 21.663$, $b = 21.639$, $c = 16.572$ Å, $\beta = 129.40°$.
[103] B. Krebs, W. Hamann, unpublished results.
[104] J. Goubeau, *Angew. Chem. 78* (1966) 565; *Angew. Chem. Int. Ed. Engl. 5* (1966) 567.
[105] H. J. Becher, *Z. Anorg. Allg. Chem. 271* (1953) 243.
[106] H. Vahrenkamp, *J. Organomet. Chem. 28* (1971) 181.
[107] H. Siebert: *Anwendungen der Schwingungsspektroskopie in der Anorganischen Chemie*, Springer-Verlag, Berlin 1966.
[108] W. Siebert, E. Gast, M. Schmidt, *J. Organomet. Chem. 23* (1970) 329.
[109] J. Kroner, D. Nölle, H. Nöth, *Z. Naturforsch. B 28* (1973) 416.
[110] M. F. Lappert, M. R. Litzow, J. B. Pedley, P. N. K. Riley, T. R. Spalting, A. Tweedale, *J. Chem. Soc. A 1970*, 2320.
[111] J. Kroner, D. Nölle, H. Nöth, W. Winterstein, *Chem. Ber. 108* (1975) 3807.
[112] O. Gropen, E. W. Nilssen, H. M. Seip, *J. Mol. Struct. 23* (1974) 289.
[113] B. Krebs, M. Wienkenhöver, unpublished results.
[114] L. S. Bartell, B. L. Carroll, *J. Chem. Phys. 42* (1965) 3076.
[115] Values used for the calculations: $r_{Cl}$ 0.99, $r_S$ 1.04, $r_{C(sp^3)}$ 0.77, $r_{C(sp^2)}$ 0.74 Å; Schomaker-Stevenson corrections 0.04 Å for B–C and B–S, 0.08 Å for B–Cl.
[116] L. Pauling: *The Nature of the Chemical Bond*, 3rd Ed., Cornell University Press, Ithaca, NY 1960; *Die Natur der chemischen Bindung*, 3rd Ed., Verlag Chemie, Weinheim 1976.
[117] R. Hoppe, W. Lidecke, F. C. Frorath, *Z. Anorg. Allg. Chem. 309* (1961) 49.
[118] H. Schubert, R. Hoppe, *Z. Naturforsch. B 25* (1970) 886.
[119] K.-J. Range, G. Mahlberg, *Z. Naturforsch. B 30* (1975) 81.
[120] D. Schmitz, W. Bronger, *Z. Naturforsch. B 30* (1975) 491.
[121] J. Weis, H. Schäfer, G. Schön, *Z. Naturforsch. B 31* (1976) 1336.
[122] B. N. Ivanov-Emin, Ya. I. Rabovik, *J. Gen. Chem. USSR 17* (1947) 1247.
[123] B. Krebs, H.-J. Wallstab, D. Voelker, *6th Eur. Crystallogr. Meet.*, Barcelona 1980, *Abstr.*, p. 96.
[124] B. Krebs, H.-U. Hürter, D. Voelker, H.-J. Wallstab, *Z. Kristallogr. 154* (1980) 63.
[125] B. Krebs, D. Voelker, K.-O. Stiller, *Inorg. Chim. Acta 65* (1982) L 101.
[126] B. Krebs, D. Voelker, K.-O. Stiller, unpublished results.
[127] D. Voelker, Dissertation, Universität Münster 1983.
[128] F. Ensslin, B. Ziemeck, L. DeSchaepdryver, *Z. Anorg. Allg. Chem. 254* (1947) 309.
[129] B. Krebs, K.-O. Stiller, unpublished results.
[130] $KInSe_2$ is monoclinic, space group C2/c with $a = 11.423$, $b = 11.428$, $c = 15.621$ Å, $\beta = 100.51°$, $Z = 16$. Also $TlGaSe_2$, which has erroneously been described as having space group Cc [131], has this space group.
[131] D. Müller, H. Hahn, *Z. Anorg. Allg. Chem. 438* (1978) 258.
[132] W. Henkel, H. D. Hochheimer, C. Carlone, A. Werner, S. Ves, H. G. von Schnering, *Phys. Rev. B 26* (1982) 3211.
[133] H.-J. Deiseroth, *Z. Naturforsch. B 35* (1980) 953.
[134] H.-J. Deiseroth, H. Fu-Son, *Angew. Chem. 93* (1981) 1011; *Angew. Chem. Int. Ed. Engl. 20* (1981) 962.
[135] J. Weis, H. Schäfer, *Z. Naturforsch. B 31* (1976) 1341.
[136] A remark concerning nomenclature: The term "thio salt" with "thioanions" *vs.* the term "ternary sulfide" for a solid phase $A_xB_yS_z$ is preferable in those cases where discrete (also polymeric) $B_yS_z$ structural units can be recognized; criteria for this are significantly stronger (and more covalent) B–S bonds relative to weaker A···S bonds (with more ionic character). Example: $Na_6Sn_2S_7$ is a sodium thiostannate, $ZnAl_2S_4$ is rather a zinc aluminum sulfide, the bond character of Zn–S and Al–S being not very different.
[137] J. Olivier-Fourcade, J. C. Jumas, M. Ribes, E. Philippot, M. Maurin, *J. Solid State Chem. 23* (1978) 155, and references cited therein.
[138] W. Schiwy, S. Pohl, B. Krebs, *Z. Anorg. Allg. Chem. 402* (1973) 77.
[139] S. Pohl, W. Schiwy, N. Weinstock, B. Krebs, *Z. Naturforsch. B 28* (1973) 565.
[140] B. Krebs, H.-J. Jacobsen, *Z. Anorg. Allg. Chem. 421* (1976) 97.
[141] B. Krebs, H.-U. Hürter, *Z. Anorg. Allg. Chem. 462* (1980) 143.
[142] B. Krebs, W. Schiwy, *Z. Anorg. Allg. Chem. 398* (1973) 63.
[143] B. Krebs, S. Pohl, W. Schiwy, *Angew. Chem. 82* (1970) 884; *Angew. Chem. Int. Ed. Engl. 9* (1970) 897.
[144] B. Krebs, S. Pohl, W. Schiwy, *Z. Anorg. Allg. Chem. 393* (1972) 241.
[145] B. Krebs, H. Müller, *Z. Anorg. Allg. Chem.*, in press.
[146] W. Schiwy, C. Blutau, D. Gäthje, B. Krebs, *Z. Anorg. Allg. Chem. 412* (1975) 1.
[147] B. Krebs, S. Pohl, *Z. Naturforsch. B 26* (1971) 853.
[148] S. Pohl, B. Krebs, *Z. Anorg. Allg. Chem. 424* (1976) 265.
[149] S. Pohl, Dissertation, Universität Kiel 1974.
[150] H.-J. Wallstab, B. Krebs, unpublished results.
[151] H.-J. Wallstab, Dissertation, Universität Bielefeld 1979.
[152] W. Schiwy, B. Krebs, *Angew. Chem. 87* (1975) 451; *Angew. Chem. Int. Ed. Engl. 14* (1975) 261.
[153] P. Müller, W. Bronger, *Z. Naturforsch. B 34* (1979) 1264.
[154] H. Rieck, R. Hoppe, *Z. Anorg. Allg. Chem. 408* (1974) 151.
[155] J. Peters, B. Krebs, *Acta Crystallogr. B 38* (1982) 1270, and references cited therein.
[156] A. Weiss, A. Weiss, *Z. Naturforsch. B 7* (1952) 483; R. Hillel, J. Cueilleron, *Bull. Soc. Chim. Fr. 1971*, 394.
[157] A fibrous modification of $SiO_2$ which can be prepared at 1200–1400 °C from SiO, is however known [158]. $SiS_2$ has a high-pressure form with quartz structure [159].
[158] A. Weiss, A. Weiss, *Z. Anorg. Allg. Chem. 276* (1954) 95.
[159] C. T. Prewitt, H. S. Young, *Science 149* (1965) 535.
[160] G. Dittmar, H. Schäfer, *Acta Crystallogr. B 31* (1975) 2060; *B 32* (1976) 2726, and references cited therein.
[161] F. Liebau, *Naturwissenschaften 49* (1962) 481.
[162] M. Ribes, J. Olivier-Fourcade, E. Philippot, M. Maurin, *Acta Crystallogr. B 30* (1974) 1391.
[163] J. Olivier-Fourcade, E. Philippot, M. Ribes, M. Maurin, *Rev. Chim. Miner. 9* (1972) 757.
[164] M. Ribes, J. Olivier-Fourcade, E. Philippot, M. Maurin, *J. Solid State Chem. 8* (1973) 195.
[165] E. Philippot, M. Ribes, O. Lindqvist, *Rev. Chim. Miner. 8* (1971) 477.
[166] G. Eulenberger, *Acta Crystallogr. B 32* (1976) 3059.
[167] G. Eulenberger, *Z. Naturforsch. B 36* (1981) 521.

[168] A. Müller, E. Diemann, R. Jostes, H. Bögge, *Angew. Chem. 93* (1981) 957; *Angew. Chem. Int. Ed. Engl. 20* (1981) 934.
[169] A. Müller, B. N. Cyvin, S. J. Cyvin, S. Pohl, B. Krebs, *Spectrochim. Acta A 32* (1976) 67, and references cited therein.
[170] B. Krebs, H. Müller, unpublished results.
[171] M. Neyrand, M. Ribes, E. Philippot, M. Maurin, *Rev. Chim. Miner. 12* (1975) 406.
[172] B. Krebs, J. Mandt, *Z. Anorg. Allg. Chem. 388* (1972) 193.
[173] J. Mandt, B. Krebs, *Z. Anorg. Allg. Chem. 420* (1976) 31.
[174] B. Krebs, J. Mandt, *Z. Naturforsch. B 32* (1977) 373.
[175] B. Krebs, H.-J. Wallstab, *Inorg. Chim. Acta 54* (1981) L123.
[176] B. Krebs, H.-J. Wallstab, *Z. Naturforsch. B 36* (1981) 1400.
[177] C. L. Teske, *Z. Naturforsch. B 35* (1980) 672.
[178] K. Mereiter, A. Preisinger, H. Guth, *Acta Crystallogr. B 35* (1979) 19.
[179] K. Mereiter, A. Preisinger, H. Guth, G. Heger, K. Hiebl, W. Mikenda, *Z. Kristallogr. 150* (1979) 215.
[180] W. Mikenda, A. Preisinger, *Spectrochim. Acta A 36* (1980) 365; W. Mikenda, H. Steidl, A. Preisinger, *J. Raman Spectrosc. 12* (1982) 217.
[181] A. Feltz, G. Pfaff, *Z. Anorg. Allg. Chem. 442* (1978) 41, and references cited therein.
[182] Analogous anions $(Te_3M-MTe_3)^{6-}$ with M = Si, Ge, Sn are known: G. Dittmar, *Angew. Chem. 89* (1977) 566; *Angew. Chem. Int. Ed. Engl. 16* (1977) 554; *Z. Anorg. Allg. Chem. 453* (1978) 68; *Acta Crystallogr. B 34* (1978) 2390.
[183] A. Feltz, G. Pfaff, *Z. Anorg. Allg. Chem. 467* (1980) 211.
[184] J. Peters, Dissertation, Universität Münster 1982.
[185] J. Peters, B. Krebs, unpublished results.
[186] J. C. Jumas, E. Philippot, M. Maurin, *J. Solid State Chem. 14* (1975) 152.
[187] G. Eulenberger, *Z. Naturforsch. B 36* (1981) 687.
[188] W. Mark, O. Lindqvist, J. C. Jumas, E. Philippot, *Acta Crystallogr. B 30* (1974) 2620.
[189] D. Mootz, H. Puhl, *Acta Crystallogr. B 23* (1967) 471; R. Kniep, D. Mootz, U. Severin, H. Wunderlich, *Acta Crystallogr. B 38* (1982) 2022.
[190] J. C. Jumas, M. Ribes, E. Philippot, M. Maurin, *C. R. Acad. Sci. C 275* (1972) 269.
[191] S. Jaulmes, *Acta Crystallogr. B 30* (1974) 2283.
[192] S. Ichiba, M. Katada, H. Negita, *J. Inorg. Nucl. Chem. 37* (1975) 2249.
[193] R. Greatrex, N. N. Greenwood, M. Ribes, *J. Chem. Soc. Dalton Trans. 1976*, 500, and references cited therein.
[194] H. Hahn, H. Schulze, L. Sechser, *Naturwissenschaften 52* (1965) 451.
[195] O. Gorochov, J. Flahaut, *C. R. Acad. Sci. C 264* (1967) 2153.
[196] O. Gorochov, *Bull. Soc. Chim. Fr. 1968*, 2263.
[197] G. Eulenberger, *Monatsh. Chem. 108* (1977) 901.
[198] J. von Unterrichter, K.-J. Range, *Z. Naturforsch. B 33* (1978) 866.
[199] N. Rysanek, P. Laruelle, A. Katty, *Acta Crystallogr. B 32* (1976) 692; S. Geller, *Z. Kristallogr. 149* (1979) 31.
[200] D. Carré, R. Ollitrault-Fichet, J. Flahaut, *Acta Crystallogr. B 36* (1980) 245.
[201] A. Nagel, K.-J. Range, *Z. Naturforsch. B 34* (1979) 360.
[202] W. F. Kuhs, R. Nitsche, K. Scheunemann, *Mater. Res. Bull. 11* (1976) 1115.
[203] W. F. Kuhs, R. Nitsche, K. Scheunemann, *Acta Crystallogr. B 34* (1978) 64, and references cited therein.
[204] J. P. Deloume, M. Roubin, *C. R. Acad. Sci. C 283* (1976) 747.
[205] G. Brandt, V. Krämer, *Mater. Res. Bull. 11* (1976) 1381.
[206] W. F. Kuhs, M. Schulte-Kellinghaus, V. Krämer, R. Nitsche, *Z. Naturforsch. B 32* (1977) 1100.
[207] P. Toffoli, P. Khodadad, *C. R. Acad. Sci. C 286* (1978) 349.
[208] K. Susa, H. Steinfink, *Inorg. Chem. 10* (1971) 1754.
[209] K. Funke, *Prog. Solid State Chem. 11* (1976) 345; S. Geller: *Solid Electrolytes (Top. Appl. Phys.*, Vol. 21), Springer-Verlag, Berlin 1977; S. Geller, *Acc. Chem. Res. 11* (1978) 87; G. H. Mahan, W. L. Roth: *Superionic Conductors*, Plenum Press, New York 1976; P. Vashishta, J. N. Mundy, G. K. Shenoy: *Fast Ion Transport in Solids*, North Holland, New York 1979.
[210] A. Haas, *Angew. Chem. 77* (1965) 1066; *Angew. Chem. Int. Ed. Engl. 4* (1965) 1014, and references cited therein.
[211] V. Gutmann, P. Heilmayer, K. Utvary, *Monatsh. Chem. 92* (1961) 942.
[212] D. J. Panckhurst, C. W. Wilkins, P. W. Craighead, *J. Chem. Soc. 1955*, 3395.
[213] M. Blix, *Ber. Dtsch. Chem. Ges. 36* (1903) 4218.
[214] M. Weidenbruch, G. Röttig, *Inorg. Nucl. Chem. Lett. 13* (1977) 85.
[215] B. Krebs, H. Beyer, *Z. Anorg. Allg. Chem. 365* (1969) 199.
[216] J. Goubeau, W. D. Hiersemann, *Z. Anorg. Allg. Chem. 290* (1957) 292.
[217] A. Weiss, A. Weiss, Colloquium der Sektion Anorg. Chem., IUPAC, Münster 1954; Verlag Chemie, Weinheim 1955, p. 41 (cf. [210]).
[218] J. Peters, J. Mandt, M. Meyring, B. Krebs, *Z. Kristallogr. 156* (1981) 90.
[219] H. Marsmann, J. Peters, B. Krebs, unpublished results.
[220] S. Pohl, *Angew. Chem. 88* (1976) 162; *Angew. Chem. Int. Ed. Engl. 15* (1976) 162.
[221] S. Pohl, U. Seyer, B. Krebs, *Z. Naturforsch. B 36* (1981) 1432.
[222] S. A. Dembovskii, N. P. Popova, *Izv. Akad. Nauk SSSR Neorg. Mater. 6* (1970) 138; further references in [2b].
[223] References, cf. [4], p. 161 ff.
[224] S. Pohl, B. Krebs, unpublished results.
[225] I. Gergen, R. Micu-Semeniuc, I. Haiduc, *Synth. React. Inorg. Met.-Org. Chem. 7* (1977) 183.
[226] M. C. Chakravorti, H.-J. Korte, P. Werle, A. Müller, B. Krebs, unpublished results.
[227] S. Singh, C. N. R. Rao, *J. Phys. Chem. 71* (1967) 1074.
[228] P. C. Jocelyn: *Biochemistry of the SH Group*, Academic Press, New York 1972.
[229] A. Menefee, D. Alford, C. B. Scott, *J. Chem. Phys. 25* (1956) 370.
[230] G. Allen, R. O. Colclough, *J. Chem. Soc. 1957*, 3912.
[231] G. Henkel, Dissertation, Universität Bielefeld 1976.
[232] J. G. David, H. E. Hallam, *Spectrochim. Acta 21* (1965) 841.
[233] G. Geiseler, H. Seidel, J. Fruwert, *Spectrochim. Acta A 29* (1973) 1385.
[234] B. Krebs, G. Gattow, *Z. Anorg. Allg. Chem. 340* (1965) 294.
[235] R. Mecke, H. Spiesecke, *Chem. Ber. 89* (1956) 1110.
[236] C. E. Forbes, R. H. Holm, *J. Am. Chem. Soc. 92* (1970) 2297.
[237] R. R. Shagidullin, I. P. Lipatova, L. I. Vachugova, R. A. Cherkasov, F. Kh. Khairutdinova, *Izv. Akad. Nauk SSSR Ser. Khim. 1972*, 847.
[238] G. Henkel, B. Krebs, S. A. Mason, *4th Eur. Crystallogr. Meet.*, Oxford 1977, *Abstr.*, p. 381.
[239] B. Krebs, G. Henkel, *Z. Anorg. Allg. Chem. 475* (1981) 143.
[240] J. R. Sabin, *J. Chem. Phys. 54* (1971) 4675.
[241] G. Henkel, B. Krebs, *Z. Kristallogr. 149* (1979) 98.
[242] B. Krebs, G. Henkel, H.-J. Dinglinger, G. Stehmeier, *Z. Kristallogr. 153* (1980) 285.
[243] W. Stücker, Diplomarbeit, Universität Münster 1982.
[244] A. Novak, *Struct. Bonding (Berlin) 18* (1974) 177, and references cited therein.
[245] H. Schäfer with G. Dittmar, B. Eisenmann, G. Cordier, K. Volk, H. A. Graf et al., Publications in *Z. Naturforsch. B* and *Z. Anorg. Allg. Chem.* (1975–1982).
[246] H. Falius, *Z. Anorg. Allg. Chem. 356* (1968) 189.
[247] W. Klingen, G. Eulenberger, H. Hahn, *Naturwissenschaften 55* (1968) 229.
[248] P. C. Minshall, G. M. Sheldrick, *Acta Crystallogr. B 34* (1978) 1378.
[249] H. Falius, W. Krause, W. S. Sheldrick, *Angew. Chem. 93* (1981) 121; *Angew. Chem. Int. Ed. Engl. 20* (1981) 103.
[250] H. Gerl, B. Eisenmann, P. Roth, H. Schäfer, *Z. Anorg. Allg. Chem. 407* (1974) 135.
[251] G. Dittmar, H. Schäfer, *Z. Anorg. Allg. Chem. 439* (1978) 212.
[252] A. Müller, U. Reinsch-Vogell, E. Krickemeyer, H. Bögge, *Angew. Chem. 94* (1982) 784; *Angew. Chem. Int. Ed. Engl. 21* (1982) 790.

# Catalysis by Molecular Metal Clusters

**By Earl L. Muetterties* and Michael J. Krause**

*Dedicated to Professor Harald Schäfer on the occasion of his 70th birthday*

Molecular metal clusters form a very large and diverse family. They present the opportunity of modeling the intermediates involved in surface mediated catalytic reactions, of providing a source of very reactive mononuclear metal fragments, and of effecting catalytic cycles in which the cluster remains intact. The last mentioned aspect is the subject of this review article. The state-of-the-art of cluster catalysis is critically analyzed. The possibilities offered by molecular metal catalysts of performing catalytic reactions at multimetal atom sites are also discussed.

## 1. Introduction

Catalysis of inorganic and organic reactions by metal atoms is a well-established area of scientific and technological investigation. Metal atom catalysts[1a] or potential catalysts may be classified[1b,c] as follows:

1) Surfaces of metals, alloys, metal oxides, sulfides, and halides.

2) Metal atoms dispersed in a low temperature matrix or immobilized on a support.

3) Small metal clusters (without ligands)—sufficiently small to be distinguished from metals.

4) Molecular mononuclear metal complexes.

5) Molecular polynuclear metal complexes

Classes 1)[2] and 4)[3] have been studied extensively and have been the subjects of reviews and monographs. Although classes 2) and 3) are of great theoretical interest, experimental studies of "naked" metal atoms or "naked" clusters have been limited since even at very low temperatures they form larger aggregates. Generally, these potential catalysts must be immobilized on a support to prevent aggregation, but even then there is evidence that the metal atoms are mobile under very mild conditions. This class of supported catalysts is now a broad area of intensive study[4]. A comparitave study of these classes of metal catalysts should provide important insights, but more detailed investigations are required. It should then be possible to delineate the electronic and structural factors that significantly change the catalytic activity as the nuclearity of the metal framework increases. This review article presents a critical analysis of the state-of-the-art of molecular cluster catalysis with emphasis on reaction mechanisms.

Molecular metal clusters[**] present catalysis research with at least three major opportunities. The first is that they can serve as models of chemisorbed molecules or molecular fragments on surfaces of metals or metal oxides and sulfides, *etc.*[4–8]. Structure and stereochemistry can be determined readily and precisely for molecular species like clusters, but cannot be established precisely for chemisorbed species apart from simple cases such as CO and NO. Comparison of the spectroscopic data of clusters with those of chemisorbed species can provide information on the structure of the latter[9]. The use of clusters as models of surfaces has been analyzed in substantial detail[7,8] and will not be reviewed here. Secondly, molecular clusters enable the generation of reactive mononuclear fragments[13,14] of high catalytic activity by thermally or photochemically initiated scission of all metal-metal bonds in the cluster. For example, $Fe_3(CO)_{12}$ reacts thermally with alkenes at 80 °C to form [Fe(CO)$_4$(alkene)] complexes which are catalytic intermediates in alkene isomerization[14a]; $[Ru_3(CO)_9\{P(C_6H_5)_3\}_3]$ is partially or fully fragmented by photolysis to give species that initiate alkene isomerization[15]. The third opportunity, and the one addressed in this article, is catalysis by clusters. In this analysis, special emphasis is given to mechanistic features. Also considered are potentially unique reactions catalyzed by molecular metal clusters in which more than one metal atom site participates in the transformation ("multimetal atom site reactions"). The review is not comprehensive.

Molecular metal clusters comprise an extremely diverse family in which the *formal* oxidation state of the metal atoms may vary from +3 to 0 or even have slightly negative values[15,16a]. Potentially, clusters with metal atoms of high oxidation state can mimic metal oxide or metal sulfide catalysts and those of low metal atom oxidation state can mimic metallic catalysts. Few studies have been reported for the former class of clusters but a number of exploratory studies have been described for clusters in which the metal atoms have a low or zero oxidation state, and we will focus on such clusters in this article.

One interesting feature offered by metal clusters is the possibility of performing unique catalytic reactions. Specific possibilities are unusual stereoselectivity or chemosel-

[*] Prof. E. L. Muetterties, M. J. Krause
Department of Chemistry, University of California
Berkeley, CA 94720 (USA)

[**] Some scientists classify clusters as those metal complexes with three or more metal atoms mutually bonded to each other; however, it is more common today, and semantically correct, to refer to dinuclear metal complexes with a metal-metal bond as clusters and this classification will be used here.

 © *Verlag Chemie GmbH, 6940 Weinheim, 1983* *0570-0833/83/0202-0135 $ 02.50/0* 

ectivity due to participation of more than one metal atom in key steps of the catalytic cycle[6]. Another is cluster catalysis of reactions that either cannot be effected or are very difficult to effect at single metal atom centers. Examples are the hydrogenation of the triple bonds in CO, $N_2$, $CN^-$, RCN, and RNC. All of these species can be catalytically hydrogenated on metal oxide or metal surfaces or catalytically reduced by the nitrogenase enzymes, but none has been catalytically hydrogenated *with facility* by molecular metal catalysts in solution[6].

Metal clusters have an extremely broad chemistry, and many aspects of this relate directly to metal cluster catalysis. An illustrative list of important related studies is the relation between large metal clusters and metal particles[16a], the use of support-bound clusters for catalysis[4, 16b], cluster-mediated organic chemistry[11], ligand mobility in clusters[16c], changes in cluster shape due to variations in the electron count[16d], modes of cluster activation[16e], activation of $H_2$ by clusters[16f], "unsaturated" clusters[16g], substrate binding and modification over triangular cluster faces[16h], the binding of acetylene on clusters[16i], the variety of reactions offered by mixed metal clusters[16j], the possibility of cluster chirality[16k], mechanistic studies of metal-metal bond reactivity[16l], and the stepwise reactions of C atoms[16m], CO[16n], and RCN molecules[16o] bound to several metal atoms of a cluster. All this work forms the basis for the following discussion of the catalytic reactions and their possible mechanisms in the presence of transition metal clusters.

## 2. Carbonylmetal Clusters

Carbonylmetal clusters constitute the largest group of clusters in which the metal atom has a low oxidation state. These include dinuclear and trinuclear clusters, those with tetrahedral $M_4$ and octahedral $M_6$ cores, and the largest cluster which has 38 platinum atoms with a $Pt_{38}$ core of $O_h$ cubeoctahedral symmetry[15, 16a]. No carbonylmetal clusters appear to possess high catalytic activity and most of the reported reactions with these "catalysts" required relatively high temperatures. Nevertheless, these clusters exhibit a stoichiometric chemistry that provides insight *vis-a-vis* intermediates in reactions catalyzed by metal surfaces[7, 8].

Metal-metal and metal-carbonyl bond energies appear to be comparable in most carbonylmetal clusters[7, 8, 17], but their magnitudes are small compared to those of bonds between elements of the first and second rows. Hence, catalytic or stoichiometric carbonylmetal cluster reactions may involve scission of one or all metal-metal bonds. The trend in metal-metal bond energies is that for a given group they increase in going from 3d to 4d to 5d metals; this trend holds both for clusters and for bulk metals. Clusters based on 3d metals therefore exhibit a proclivity for fragmentation, whereas those based on 5d metals like osmium and iridium show a marked resistance to metal-metal bond scission. For example, $Fe_3(CO)_{12}$ reacts with alkenes at 80 °C[14a] to form $[(\eta^2\text{-alkene})Fe(CO)_4]$[18] complexes, which can initiate catalytic isomerization of olefins. In contrast, $Os_3(CO)_{12}$ does not even react with alkenes at moderate temperatures, and at higher temperatures the reaction proceeds by scission of an Os—CO bond, not an Os—Os bond, to give $[H_2Os_3(CO)_9]$ clusters with vinylidene and with acetylene groups[19]. Furthermore, carbonyl clusters based on 3d metals can be used as sources of $LM(CO)_x$ fragments under relatively mild reaction conditions for the synthesis of heteronuclear carbonylmetal clusters. Some syntheses of heteronuclear carbonylmetal clusters by fragmentation reactions are illustrated [Eqs. (a) and (b)][20, 21].

$$2(\mu_3\text{-RC})Co_3(CO)_9 + [(\eta^5\text{-}C_5H_5)Fe(CO)_2]_2 \xrightarrow{h\nu} 2[(\mu_3\text{-RC})Co_2(CO)_6Fe(\eta^5\text{-}C_5H_5)(CO)] + Co_2(CO)_8 \quad (a)$$

$$2(\mu_3\text{-RC})Co_3(CO)_9 + [(\eta^5\text{-}C_5H_5)NiCO]_2 \longrightarrow 2[(\mu_3\text{-RC})Co_2(CO)_6Ni(\eta^5\text{-}C_5H_5)] + Co_2(CO)_8 \quad (b)$$

In contrast, thermal synthesis of heteronuclear metal clusters using clusters consisting of 4d or 5d metals requires rather severe conditions [Eq. (c)][22].

$$Ru_3(CO)_{12} + Os_3(CO)_{12} \xrightarrow[90\ h]{175\ °C} Ru_2Os(CO)_{12} + RuOs_2(CO)_{12} \quad (c)$$

Metal-metal bond scission can be an important reaction step in cluster reactions such as ligand substitution, a specific class of reactions that often represents key steps within a catalytic cycle. For ligand substitution in mononuclear metal complexes, a mechanistic distinction can be made between dissociative (comprising a preequilibrium step in which an intermediate of lower coordination number is formed by scission of a metal-ligand bond), associative (involving an intermediate of higher coordination number) and interchange (no detectable intermediate). The number of possible reaction mechanisms for clusters is higher because metal-metal bond cleavage may occur along the reaction pathway. For example, two reaction mechanisms have been proposed for the thermal reaction of $Mn_2(CO)_{10}$ and of $Re_2(CO)_{10}$ with phosphanes ($PR_3$) to give $M_2(CO)_9PR_3$ and $M_2(CO)_8(PR_3)_2$[23]: either scission of the metal-metal bond [Eq. (d)] or M—CO bond scission [Eq. (e)].

$$M_2(CO)_{10} \rightleftharpoons 2\,M(CO)_5 \xrightarrow{PR_3} \text{products} \quad (d)$$

$$M_2(CO)_{10} \rightleftharpoons CO + M_2(CO)_9 \xrightarrow{PR_3} \text{products} \quad (e)$$

Metal-metal bond scission does not occur despite the high temperatures of 120—160 °C. Double labeling studies[24, 25] with $^{185}Re_2(CO)_{10}$ and $^{187}Re_2(CO)_{10}$ as well as with $Mn_2(^{12}CO)_{10}$ and $Mn_2(^{13}CO)_{10}$ have established that Eq. (e) prevails for both manganese and rhenium.

In the ligand substitution reactions of $Co_2(CO)_8$[23] there is a greater diversity in reaction mechanism and products. With relatively poor electron donors like $As(C_6H_5)_3$ or

bulky phosphanes, $Co_2(CO)_8$ probably reacts *via* initial cleavage of the Co–CO bond to yield $Co_2(CO)_7L$ and $Co_2(CO)_6L_2$ species. In contrast, less bulky trialkylphosphanes form $[Co(CO)_3PR_3]^+[Co(CO)_4]^-$ products with obvious Co–Co bond scission at some step along the reaction pathway.

Mechanistic studies of ligand substitution reactions of trinuclear and tetranuclear carbonylmetal clusters, *e.g.* $Ru_3(CO)_{12}$, $Co_4(CO)_{12}$, and $Ir_4(CO)_{12}$, are currently being performed[23]. With the exceptions of $Fe_3(CO)_{12}$ and possibly $Ru_3(CO)_{12}$, complete fragmentation into mononuclear products is not a facile process. Definitive characterization of the mechanism of ligand substitution has not been achieved to date. Some of the substitutions may proceed *via* M–CO predissociation and others by M–M bond dissociation. If only one M–M bond is cleaved, this kind of mechanism cannot be distinguished by metal atom labeling (as described for $Re_2(CO)_{10}$ and $Mn_2(CO)_{10}$) from M–CO bond scission.

Also critical to a basic understanding of potential cluster catalytic reactions are mechanistic studies of oxidative additions, since these are steps in catalytic cycles involving, for example, hydrogenation. An example of an oxidative addition involving mononuclear metal complexes is addition of hydrogen [Eq. (f); a specific example from cluster chemistry is shown in Eq. (g)].

$$H_2 + ML_x \rightleftharpoons H_2ML_x \quad (f)$$

$$H_2 + Os_3(CO)_{12} \rightleftharpoons H_2Os_3(CO)_{10} + 2CO \quad (g)$$

Mechanistic studies of oxidative additions have not been reported for carbonylmetal clusters.

## 3. Reaction Mechanisms

Because metal clusters can fragment, especially at high temperatures, characterization of catalytic cycles, even those in which the cluster precursor preserves its nuclearity throughout the cycle, is difficult. Even quantitative recovery of the precursor after many catalytic cycles establishes nothing about the nuclearity of the catalytically active intermediates. Kinetic data alone rarely provide substantive insights into details of the catalytic cycles and cannot be used to "prove" catalysis by clusters. Spectroscopic monitoring of the catalytic reaction can be helpful, but there are many possible pitfalls in the interpretation of such data: detectable species may not be intermediates; intermediates may be so short-lived as to escape spectroscopic detection; a reaction system may be so complex, irrespective of whether the catalytic precursor[1a] is mononuclear or polynuclear, that detectable species present under catalytic conditions may have a large range of nuclearity—a potpourri of possible catalytically active intermediates. An important question in "cluster catalysis" applies also to mononuclear precursors: are the intermediates mononuclear or polynuclear in character? Nevertheless, under ideal conditions, it is possible to detect catalytic intermediates by spectroscopic techniques or even to isolate them by studying the reactions as a function of temperature, especially for those reactions that are fast at or near room temperature.

The problem of molecular features of catalytic reaction cycles is complex and generally requires chemical, kinetic, spectroscopic, and labeling studies for insight. There is no precise protocol for experimental definition of cluster catalysis. Each spezific system must be considered on its own merits using the experimental data that can be obtained. The challenge here is great and the answers are feasible for some, although not all systems, given the techniques now practicable.

In the following sections, implicated catalytic reactions are discussed first in terms of an illustration of scope and catalytic systems for which some mechanistic data are available. Most of these discussions are limited to"zero-valent" metal clusters, namely the carbonyl clusters and a closely related group of alkyl isocyanide compounds. Finally "reactive" metal clusters, particulary coordinately unsaturated metal clusters, are considered.

## 4. Multiplicity and Variety of Metal Cluster Catalyzed Reactions

The scope of catalytic reactions initiated by metal clusters is given in Table 1. It should, however, be particularly borne in mind that this listing is not comprehensive and that no presumption about the nuclearity of the actual intermediates should be made in any of the reactions listed. Also, we call attention to recent general reviews of cluster catalysis[42].

Table 1. Metal Cluster catalyzed Reactions.

| Reaction | References |
|---|---|
| alkene isomerization | [14b, 26, 27] |
| reduction of CO and of ketones | [28] |
| alkene hydrogeneration | [26, 27] |
| hydroformylation of alkenes | [27, 29, 30, 41] |
| ketone hydrogenation | [31] |
| Fischer-Tropsch-synthesis | [32] |
| hydrogenation of alkyl cyanides and -isocyanides | [33, 34] |
| synthesis of methanol from CO and $H_2$ | [35, 36] |
| synthesis of polyols from CO and $H_2$ | [36] |
| hydrogenation of nitrobenzene to aniline | [27, 30, 38] |
| hydrogenation of amides | [37] |
| alkyne hydrogenation | [27] |
| alkyne cyclization to arenes | [40] |
| aminomethylation [a] | [41] |
| hydroxymethylation [b] | [41] |
| water gas shift reaction | [39] |

[a] $RCH{=}CH_2 + 3CO + H_2O + HNR'_2 \longrightarrow RCH_2CH_2CH_2NR'_2 + 2CO_2$

[b] $RCH{=}CH_2 + 3CO + 2H_2O \longrightarrow RCH_2CH_2CH_2OH + 2CO_2$ or $RCH(CH_3)CH_2OH + 2CO_2$

## 5. Hydrogenation of Alkenes, Ketones, and Carboxylic Acids, and Isomerization of Alkenes

The coordinatively unsaturated cluster $[(\mu\text{-}H)_2Os_3(CO)_{10}]$ reacts with two equivalents of ethylene to form ethane and $[(\mu\text{-}H)Os_3(\mu\text{-}CH{=}CH_2)(CO)_{10}]$[26]. Analogous reactions occur with other terminal alkenes with rates which are sensitive to electronic and steric properties of the alkene; rates decrease along series vinyl acetate >

ethylene > propylene or isobutylene[26]. With the dihydrido complex as catalyst, hydrogen and alkene are converted into alkane and, depending upon the olefin, into isomerized alkene. For example, hydrogen and 1-hexene were slowly converted into hexane and a mixture of 2- and 3-hexene (alkane : alkene ratio 31 : 69) at 50 °C and *ca.* 3.4 atm[26]. The formation of the internal hexenes indicates the reversibility of the alkene coordination and the alkyl-forming insertion reaction. Accumulation of 2- and 3-hexenes is consistent with the observation that $[(\mu\text{-H})_2Os_3(CO)_{10}]$ does not react with internal alkenes such as cyclooctene. With functionally substituted alkenes, intermediate hydrido(alkyl) clusters were isolated and characterized from reaction with $(\mu\text{-H})_2Os_3(CO)_{10}$. These species react with hydrogen to form the alkane and the initial cluster $[(\mu\text{-H})_2Os_3(CO)_{10}]$. All these results provide substantial support for the proposed mechanism of the catalytic reaction cycle (Scheme 1)[26]. Only two of the intermediates in the cycle have not been detected either directly in the catalytic reaction or by independent synthesis. One of these is the alkene complex $[H(\mu\text{-H})Os_3(\eta^2\text{-alkene})(CO)_{10}]$ **2**, which should not occur in high concentration, and the other is either $Os_3(CO)_{10}$ **4** or $[Os_3(CO)_{10}(\eta^2\text{-alkene})]$. It should be noted in this catalytic cycle, based on a coordinately unsaturated cluster precursor, that CO ligand dissociation is not an integral feature. The experimental data indicate that the cluster is intact throughout the catalytic cycle, and this is consistent with the relatively high Os–Os bond energy.

Only a few catalytic reactions have been reported involving clusters in which the formal oxidation state of the metal atoms is high. One such cluster $[Ru_3(\mu_3\text{-O})(\mu\text{-OCOCH}_3)_6(OH_2)_3]^+(OCOCH_3)^-$ has been used in the hydrogenation of alkenes and alkynes. This complex, in which the ruthenium atoms have the +3 oxidation state, is not strictly a cluster because the Ru–Ru distances are probably > 3 Å. Catalysis of reactions involving alkene hydrogenation proceeds at *ca.* 80 °C and 1 atm in dimethylformamide (DMF). Surprisingly, the reactivity of the unsaturated molecules decreases along the series: cyclic alkene > internal alkene > terminal alkene > terminal alkyne. Kinetic studies[43] established a rate equation with a first-order dependence on the concentrations of alkene, hydrogen, and ruthenium cluster. The first reaction steps for this system[43] are shown in Eqs. (h) and (i).

$$[Ru_3(\mu_3\text{-O})(\mu\text{-OCOCH}_3)_6(OH_2)_3]^+(OCOCH_3)^- + (DMF) \longrightarrow [Ru_3(\mu_3\text{-O})(\mu\text{-OCOCH}_3)_6(DMF)_x]^+(OCOCH_3)^- + 3\,H_2O \quad (h)$$

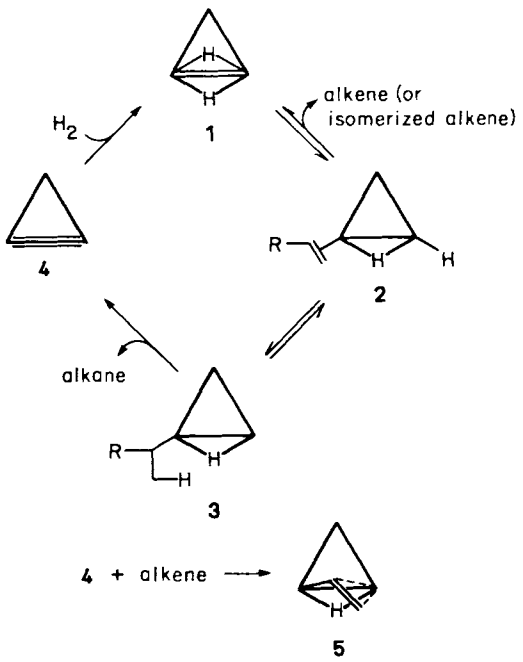
$$[Ru_3(\mu_3\text{-O})(\mu\text{-OCOCH}_3)_6(DMF)_x]^+(OCOCH_3)^- + H_2 \longrightarrow [HRu_3(\mu_3\text{-O})(\mu\text{-OCOCH}_3)_5(DMF)_x]^+(OCOCH_3)^- + CH_3COOH \quad (i)$$

The hydrido cluster, which could be characterized, is a catalyst for the isomerization of alkenes in the absence of hydrogen. It has been postulated that the hydrido complex adds to alkenes and that this alkene complex then undergoes a reversible insertion reaction to form the alkyl analog of the hydrido complex. The final two steps in the proposed cycle are addition of $H_2$ and elimination of alkane to reform the hydrido cluster. However, more important for the hydrogenation is another cycle involving reductive elimination of acetic acid from the hydrido cluster [Eq. (j)].

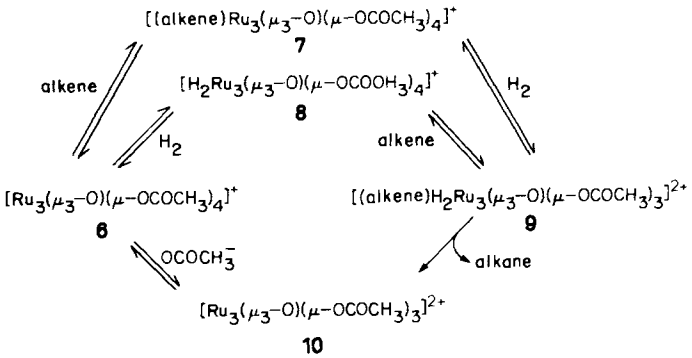
$$[HRu_3(\mu_3\text{-O})(\mu\text{-OCOCH}_3)_5(DMF)_x]^+(OCOCH_3)^- \longrightarrow CH_3COOH + \underset{\mathbf{6}}{[Ru_3(\mu_3\text{-O})(\mu\text{-OCOCH}_3)_4(DMF)_x]^+(OCOCH_3)^-} \quad (j)$$

The reduced cluster, **6**, is not fully characterized but has been postulated to provide entry to the major catalytic cycle by reaction with $H_2$ or the alkene. The steps[43] postulated in the cycle are shown in Scheme 2.

The activation of hydrogen by **6** (Scheme 2) is postulated to be heterolytic with only one ruthenium atom in-




Scheme 1. The catalytic cycle, proposed by *Keister* and *Shapley* [26] for alkene hydrogenation initiated by the $[(\mu\text{-H})_2Os_3(CO)_{10}]$ cluster. The $Os_3$ core is represented by a triangle; each osmium atom has three terminal CO ligands, which are not depicted. Multiple lines in the triangles imply metal-metal bond orders approaching two and three in intermediates **1** and **4**. Species **1**, **2**, and **5** are reasonably well defined; **3** and **4** have only been postulated. Intermediate **4**, $Os_3(CO)_{10}$, could also be $[Os_3(CO)_{10}(\eta^2\text{-alkene})]$.




Scheme 2. Depicted here is the postulated [43] major catalytic reaction cycle for alkene hydrogenation by the catalyst precursor $[Ru_3(\mu_3\text{-O})(\mu\text{-OCOCH}_3)_6(OH_2)_3]^+(OCOCH_3)^-$ in dimethylformamide. The reduced cluster, **6**, is formed in several steps from the precursor *via* solvation by the amide [Eq. (h)] and the steps shown in Eq. (i) and (j). Omitted from the formulas in the cycle are dimethylformamide molecules and the acetate counter ion; in the conversion of **7** and **8**, respectively, into **9** an acetato ligand is cleaved and this is also not shown. The conversion of **10** into **6** is assumed to be irreversible. If it were reversible, complex **6** might provide entry to the cycle and would not be a catalytic intermediate [43].

volved in this step and in the complexation of the alkene. Although all experimental results for the catalytic cycle are fully consistent with the proposed mechanistic features, neither the character of the intermediates beyond **6** nor the number of ruthenium atoms involved in the $H_2$ addition step have been definitively established. It should be noted that in this cluster-based catalytic cycle, dissociation of an acetate ion is an integral step.

Catalytic hydrogenation of ketones to alcohols by $[(\mu\text{-H})_4Ru_4(CO)_{12}]$ occurs at 100 °C and 100 atm[44a]. The rate of hydrogenation appears to be first order with respect to cluster, ketone, and hydrogen partial pressure as indicated from a series of experiments involving cyclohexanone in tetrahydrofuran[44a]. In this reaction, the ruthenium cluster is recovered unchanged. No catalytic cycle has been proposed for this system. The data do not preclude the possibility of cluster fragmentation within the catalytic cycle. A qualitative indication of the mechanism was provided by the hydrogenation of $(CD_3)_2CO$ to give $CD_3CH(OH)CD_3$ as the sole product: in the reduction sequence the ketone is not present in the enol form and must be bound through the carbonyl oxygen atom.

Phosphane derivatives of $[H_4Ru_4(CO)_{12}]$ are catalyst precursors for the hydrogenation of aliphatic carboxylic acids and anhydrides at 130 atm and 20 °C[44b]. In one of the systems, IR studies showed the presence of carbonylruthenium carboxylates. $[Ru(CO)_2(OCOCH_3)\{P(n\text{-}C_4H_9)_3\}]_2$, which was isolated from the $\{H_4Ru_4(CO)_8[P(n\text{-}C_4H_9)_3]_4\}$ system, was independently shown to be a catalyst precursor.

In contrast to the hydrogenation of ketones catalyzed by $[(\mu\text{-H})_4Ru_4(CO)_{12}]$, the analogous reaction with $Rh_4(CO)_{12}$ clearly involves cluster fragmentation. For this system *Heil* and *Marko*[45] found that the reaction order is proportional to one-sixth of the concentration of $Rh_4(CO)_{12}$.

A number of clusters initiate isomerization of alkenes. As mentioned previously, $Fe_3(CO)_{12}$ is one such species, but in this case the key catalytic intermediates[14] are monomeric, *i.e.* $[(\eta^2\text{-alkene})Fe(CO)_x]$ complexes. As mentioned above isomerization of alkenes by clusters is initiated by $[(\mu\text{-H})_2Os_3(CO)_{10}]$[26] and $[HRu_3(\mu\text{-O})(\mu\text{-OCOCH}_3)_5(DMF)_x]^+(OCOCH_3)^-$[43]. $[(\mu\text{-H})_4Ru_4(CO)_{12}]$ as well as its phosphite and phosphane derivatives are also catalysts for the isomerization of alkenes[46]. For the isomerization of 1-pentene at 70 °C, the initial rate is proportional to the ruthenium cluster concentration and the cluster is unchanged in the course of the catalytic cycle[46]. The nature of the catalytic intermediates has not been established and no catalytic cycle was postulated, although a CO ligand dissociation step and allylmetal intermediates were implicated for the catalytic cycle.

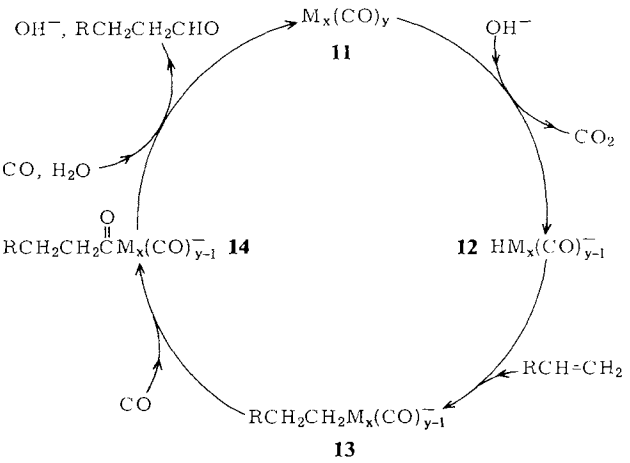
## 6. Hydroformylation of Alkenes

In hydroformylation, alkenes react with CO and either $H_2$ or $H_2O$ to form aldehydes [Eqs. (k) and (l)]

$$RCH{=}CH_2 + CO + H_2 \longrightarrow RCH_2CH_2CHO \quad (k)$$

$$RCH{=}CH_2 + 2\,CO + H_2O \longrightarrow RCH_2CH_2CHO + CO_2 \quad (l)$$

Various clusters such as $Rh_6(CO)_{16}$[29,47], $[H_4Ru_4(CO)_{12}]$[47], $Os_3(CO)_{12}$[47], $[H_2Os_3(CO)_{10}]$[47], $[H_4Os(CO)_{12}]$[47], $Ir_4(CO)_{12}$[47], $[Pt_3(CO)_6]_5^{2-}$[47], $Ru_3(CO)_{12}$[29,47], $[Co_4(CO)_8(\mu_2\text{-CO})_2(\mu_4\text{-PC}_6H_5)_2]$[27], and $[Co_2(CO)_8M(\eta^5\text{-}C_5H_5)(\mu_3\text{-CCH}_3)]$ (M = Mo, W)[27] are catalyst precursors for one or both of these reactions. Reaction (l) requires the presence hydroxide ion. Typically, the cluster reacts with an $OH^-$ ion to form an anionic hydrido cluster which reacts further as shown in Scheme 3[29]. For example, hydroformylation with $[(\mu\text{-H})_4Ru_4(CO)_{12}]$ as the catalyst precursor appears to generate a $[H_3Ru_4(CO)_{12}]^-$ intermediate. The acyl derivatives that model the acyl intermediate **14** shown in Scheme 3 have been characterized for other clusters[48].




Scheme 3. Hypothetical mechanism for the hydroformylation of alkenes catalyzed by clusters.

The reaction in Eq. (k) is also catalyzed by clusters. It has been proposed that $[Co_4(CO)_8(\mu_2\text{-CO})_2(\mu_4\text{-PC}_6H_5)_2]$ retains its framework throughout the catalytic cycle[27], and that the intermediates in the cycle model are those typically proposed for hydroformylation reactions, *i.e.* those catalyzed by mononuclear metal complexes[49]. No experimental data to support this hypothesis were presented.

Catalytic hydroformylation reactions do not require multimetal atom site catalysis although unique selectivities might be achieved with cluster catalysts, *e.g.* a selectivity to branched or to linear products.

## 7. Hydrogenation of Aromatic Nitro Compounds

Nitrobenzene has been catalytically hydrogenated to aniline using cluster catalyst precursors. For example, *Pettit et al.*[38,50] used water, CO, and a base with a diverse group of clusters as catalyst precursors. Some of the more active of these were $Rh_6(CO)_{16}$, $Os_3(CO)_{12}$, $[H_4Os_4(CO)_{12}]$, $Ru_3(CO)_{12}$, and $Ir_4(CO)_{12}$. All of these catalyze the water-gas shift reaction (see Section 9), but the rates are lower than for the hydrogenation of nitrobenzene to aniline[38,50]. Hence, an intermediate hydrido cluster must transfer hydride ion directly to nitrobenzene. Anions such as $[HRu_3(CO)_{11}]^-$ are probably important intermediates for the ruthenium system (see Section 8). Nitrobenzene has

also been converted into aniline by hydrogen using $[(\eta^5\text{-}C_5H_5)Fe(\mu_3\text{-}CO)]_4$ as the catalyst precursor[27], which was recovered unchanged at the end of the catalytic reaction. It was shown that a mononuclear fragment $[(\eta^5\text{-}C_5H_5)Fe(CO)_2H]$, does not catalyze this hydrogenation reaction.

To date, mechanistic studies have not been reported for the hydrogenation of nitrobenzene initiated by clusters. Even though some or all of these systems *may* have only cluster intermediates in the catalytic cycle, cluster intermediates, *per se*, are not necessary conditions for this type of catalytic reaction. Hydrogenation of aromatic nitro compounds probably does not involve multimetal atom site catalysis.

## 8. Alkyl Group Exchange and H/D Exchange in Amines

Using cluster reactions *Laine et al.*[51–53] have attempted to model the basic steps in the hydrodenitrogenation reaction, *i.e.* the removal of nitrogen as ammonia from aromatic nitrogen compounds. Basic to the hydrodenitrogenation reaction is cleavage of C–N bonds. *Shvo* and *Laine*[52] found that $Ru_3(CO)_{12}$, $Os_3(CO)_{12}$ and $Ir_4(CO)_{12}$ catalyze the fast exchange of alkyl groups in tertiary amines in the presence of water (presence is essential) at 125–150 °C. The observed rates exceed those for palladium-black catalyzed reactions which require temperatures of 200 °C. Postulated intermediates are "iminium" ($R_2C{=}NR_2^+$) cluster complexes and aldehyde-*s*-amine cluster complexes. The latter are postulated to form by hydrolysis of the iminium derivatives. No definitive mechanistic information is available for these very interesting alkyl group exchange reactions initiated by clusters.

These same clusters also catalyze H/D exchange in tertiary amines; here very unusual stereoselectivities occur which can serve as a model for reactions catalyzed by Pd-black[51,53]. The reaction mechanism proposed appears plausible, although no kinetic or spectroscopic studies have been presented: it involves iminium clusters *(vide supra)*, amino substituted ethylidyne clusters with $(\mu_3\text{-}R_2NCH_2C)M_3$-frameworks, and $(\eta^2\text{-}R_2NCH_2CHR)M_3$ clusters as intermediates. Formally, these three types of intermediate have analogs in cluster chemistry[7] and there are specific analogs for the postulated iminium derivatives[54]. Only for the ruthenium system, could a post-catalytic reaction species be isolated, the imino derivative $[HRu_3(\mu\text{-}\eta^2\text{-}CH_3C{=}NC_2H_5)(CO)_9]$. The relevance of this cluster to the proposed catalytic cycle was not established but it could represent a local energy minimum, off the catalytic cycle for the proposed minimum intermediate. For the mechanism it was postulated that multimetal atom sites are involved. The unusual stereoselectivity of the H/D exchange reactions may be unique to multisite catalyses.

Relevant also to the hydrodenitrogenation reactions, are the hydrogenation studies of *Fish et al.*[55], who established that $[H_4Ru_4(CO)_{12}]$ is an effective catalyst precursor for the hydrogenation of such arenes at 180 °C. The cluster was recovered unchanged from these reactions. No mechanistic studies have been completed yet.

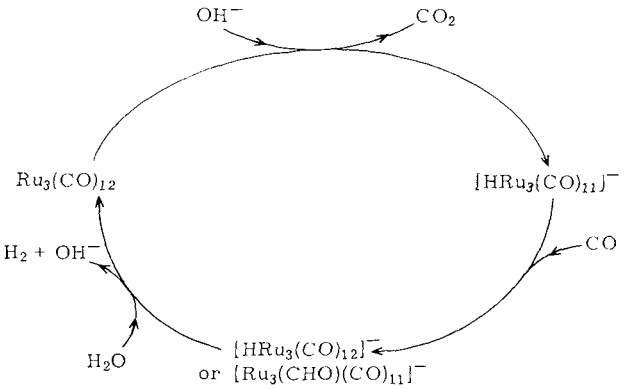
## 9. Water-Gas Shift Reaction

In the water-gas shift reaction, which is of substantial technological importance, water is reduced by carbon monoxide to give $H_2$ [Eq. (m)].

$$H_2O + CO \rightleftharpoons H_2 + CO_2 \qquad (m)$$

The first reports of catalysis of the water-gas shift reaction by molecular metal complexes in the solution state included the observation[39,56] that $Ru_3(CO)_{12}$ in ethoxymethanol in presence of KOH effected, at a low rate, catalysis of the shift reaction at *ca.* 100 °C. Studies with labeled solvent established that $H_2O$ was the source of $H_2$. A catalytic cycle can also be effected with $[H_4Ru_4(CO)_{12}]$ as initiator. Tetranuclear carbonylruthenium species have been proposed[57] as the major catalytic intermediates in this system; however, recent studies[58] indicate that trinuclear Ru clusters are the major intermediates, especially under flow reaction conditions. According to Eq. (n) the hydrido cluster anion $[HRu_3(CO)_{11}]^-$ is formed and this reacts with $H_2O$ and CO to produce $Ru_3(CO)_{12} + H_2$; the deutero cluster produces HD. Thus, the net effect is a transfer of hydride ion, ultimately to a water molecule, thereby forming $H_2$ and regenerating $OH^-$ ion. One of the proposed[58] catalytic cycles is shown in Scheme 4. For a discussion of $[H_4Ru_4(CO)_{12}]$ transformations in the catalytic system, the reader is directed to the article by *Bricker, Nagel,* and *Shore*[58].

$$Ru_3(CO)_{12} + OH^- \longrightarrow HRu_3(CO)_{11}^- + CO_2 \qquad (n)$$




Scheme 4. Proposed mechanism for the $Ru_3(CO)_{12}$-catalyzed water-gas shift reaction [58].

Many other clusters[59], *e.g.* $Ir_4(CO)_{12}$, $Os_3(CO)_{12}$, $Rh_6(CO)_{16}$, and $[Pt_{15}(CO)_{30}]^{2-}$, initiate catalysis of the water-gas shift reaction, as also do many simple mononuclear metal complexes[56]. There is nothing magical about clusters for this specific catalytic reaction. Multi-atom sites are not a requirement[56] for any of the catalytic reaction steps—the only requirement is that a good hydride transfer species be readily generated.

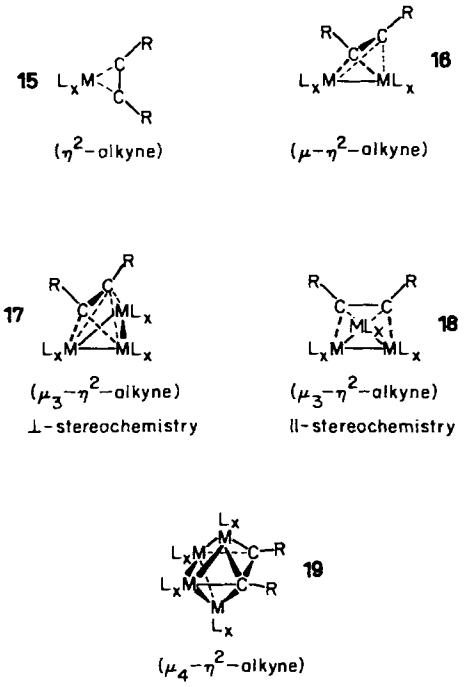
Some clusters that initiate the water-gas shift reaction also form species that can catalyze hydroformylation and hydrogenation reactions. Combination of these reactions

then allows the use of CO + $H_2O$ as the source of the hydrogen reactant (see Sections 6 and 7).

## 10. Alkyne Hydrogenation Reactions

Alkyne hydrogenation may yield an alkene or an alkane as initial product, according to whether the hydrogenation product dissociates from the metal center(s) of the catalytic intermediate. If the product is an alkene, *cis*- or *trans*-isomers or both may be formed. In those systems in which the metal complex catalyst intermediate is mononuclear a *cis*-isomer is invariably formed. Because of possible chemoselectivity and stereoselectivity a study of an alkyne hydrogenation can be more mechanistically informative than that of alkene hydrogenation[60]. A number of dinuclear or polynuclear metal complexes have been reported to catalyze alkyne hydrogenation[60-69]. Some have been studied mechanistically and the salient features are described here.

Alkynes bind to a single metal atom to form ($\eta^2$-alkyne)metal bonds; the alkyne ligand can function formally as a two-electron up to a four-electron donor. Scheme 5 shows the various ways in which alkynes can bond to metal atoms in clusters.




Scheme 5. Five modes (**15**—**19**) of binding of alkynes to metal atoms of clusters. Specific examples of the bridging modes are [$\mu$-$\eta^2$-alkyne)$Co_2(CO)_6$], [($\mu_3$-$\eta^2$-alkyne)$Fe_3(CO)_{10}$]($\perp$-stereochemistry), [($\mu_3$-$\eta^2$-alkyne)$Os_3(CO)_{10}$] (||-stereochemistry), and [($\mu_4$-$\eta^2$-alkyne)$Co_4(CO)_{10}$].

Studies of a variety of dinuclear ($\mu$-$\eta^2$-alkyne)$M_2L_x$ complexes have shown that some are initiators for alkyne hydrogenations and some have been shown to be true cluster catalysts[60-69]. The coordinatively unsaturated nickel(0) complex [{($\eta^4$-1,5-cyclooctadiene)Ni}$_2$($\mu$-$\eta^2$-$C_2Ph_2$)] is an effective initiator of alkyne hydrogenation and gives rise to *cis*-alkenes; alkyne trimerization is a competing catalytic reaction[61,63]. All the data for this $d^8$-metal system suggest that the catalyst intermediate for the alkyne hydrogenation is the dinuclear complex. Nevertheless, the dimer also reacts with alkyne to form a mononuclear species [Eq. (o)], which has been isolated[61] and crystallographically defined[64].

[{($\eta^4$-1,5-cyclooctadiene)Ni}$_2$($\mu$-$\eta^2$-alkyne)] + alkyne
$\rightleftharpoons$ 2[($\eta^4$-1,5-cyclooctadiene)Ni($\eta^2$-alkyne)] (o)

This mononuclear complex is probably the active catalyst for the competing alkyne trimerization reaction but it does not react with hydrogen to give alkenes.

A true cluster catalytic cycle was established for alkyne hydrogenation by [{($\eta^5$-$C_5H_5$)Mo(CO)$_2$}$_2$($\mu$-$\eta^2$-alkyne)][65]. Here, alkynes such as 2-butyne, 3-hexyne, $C_2H_2$ and $C_2D_2$ give *cis*-alkenes. No fragmentation of the cluster under catalytic reaction conditions was detected: using a mixture of [($\eta^5$-$C_5H_5$)Mo(CO)$_2$]$_2$($\mu$-$\eta^2$-alkene) and [($\eta^5$-$CH_3C_5H_4$)Mo(CO)$_2$]$_2$($\mu$-$\eta^2$-alkene), no cross-labeled dimer in the recovered catalyst was detected by mass spectrometry. Studies[65] of the rate of alkyne exchange, CO ($^{13}$CO) exchange, and inhibition of the catalytic reaction by CO strongly implicated CO-dissociation from the saturated dimer as the first step in the catalytic cycle. In the terminal steps of the catalytic cycle, the *cis*-alkene is eliminated and the dimer [($\eta^5$-$C_5H_5$)Mo(CO)$_2$]$_2$ is formed, which reacts rapidly with acetylene to reform the initial ($\mu$-$\eta^2$-alkyne) complex.

Under relatively severe conditions, the tetranuclear cluster [($\eta^5$-$C_5H_5$)Fe($\mu_3$-CO)]$_4$ is reported[27] to catalyze hydrogenation of alkynes (as well as of activated olefins and nitrobenzene). At 7—70 atm $H_2$ and 130—140 °C, the turnover rate for 1-pentyne conversion to largely 1-pentene is *ca.* 15 $min^{-1}$. The cluster was recovered unchanged from the reactions. Also, it was demonstrated that [($\eta^5$-$C_5H_5$)Fe(CO)$_2$H], a possible cluster fragmentation product, was not a catalyst for alkyne hydrogenation. The data, although not inconsistent with cluster catalysis, are insufficient to establish molecular character of the catalytic cycle.

In the small group of zerovalent metal clusters in which all ligands are alkyl isocyanides,

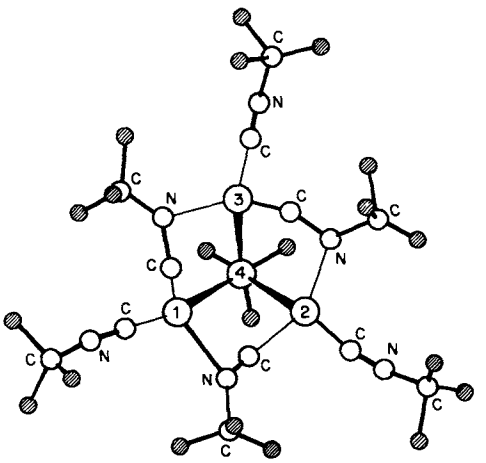



Fig. 1. Structure of the coordinately unsaturated cluster, [$Ni_4$[$\mu$-$\eta^2$-CNC$(CH_3)_3$]$_3$[CNC$(CH_3)_3$]$_4$], in the crystal [40]. The nickel atoms form an irregular $C_{3v}$ tetrahedron with one enlarged face (Ni1Ni2Ni3). Each nickel atom is terminally bonded to one isocyanide ligand through the carbon atom only (the CNC unit of the isocyanide terminally bound to Ni4 is eclipsed by the Ni4 atom in this projection). The remaining three isocyanide ligands bridge the long tetrahedral edges (Ni—C—N—Ni bonding).

$[Ni_4\{\mu\text{-}\eta^2\text{-}CNC(CH_3)_3\}_3\{CNC(CH_3)_3\}_4]$ (Fig. 1) initiates alkyne hydrogenation at 20 °C that largely yields *cis*-alkenes[66]. This cluster and the derivative alkyne complexes discussed below do not react with alkenes nor do they effect alkene hydrogenation. Thus, the cluster chemoselectivity in the catalytic reactions is easy to explain.

The $Ni_4$-cluster reacts with diarylalkynes[67-69] to form $[Ni_4(\mu_3\text{-}\eta^2\text{-alkyne})_3\{CNC(CH_3)_3\}_4]$ (Fig. 2) and $[(\eta^2\text{-alkyne})Ni\{CNC(CH_3)_3\}_2]$. The tetranuclear alkyne-nickel cluster is the catalytic precursor in alkyne hydrogenation and is the nickel species recovered from the reaction mixtures[67-69]. Hydrogenation rates are first order with respect to alkyne cluster concentration. The data, however, do not definitively establish that fragmentation of the cluster does not occur in one or more steps of the cycle.

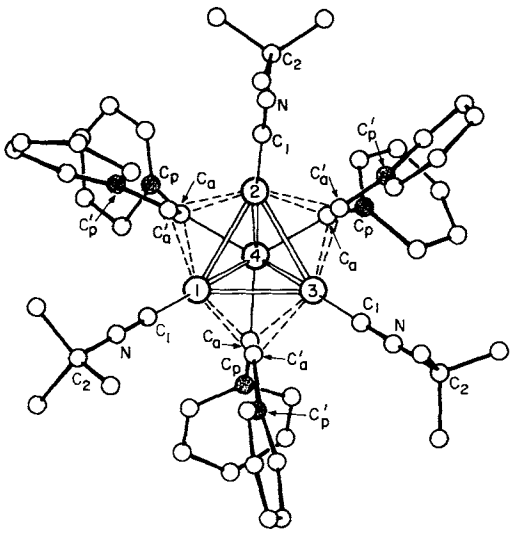
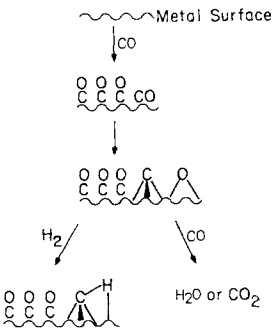



Fig. 2. Structure of $[Ni_4(\mu\text{-}\eta^2\text{-}C_6H_5C{\equiv}CC_6H_5)_3\{CNC(CH_3)_3\}_4]$ in the crystal [67], viewed normal to the triangular base along the (idealized) threefold axis. Ni atoms are represented by large open circles, and C and N atoms by small open circles. Ni4 is the unique apical nickel atom which lies on the pseudo-threefold axis. C atoms $C_a$ and $C'_a$ represent the acetylenic C atoms. $C_a$ is bonded to two basal Ni atoms and to Ni4; $C'_a$ is bonded to only two basal Ni atoms.

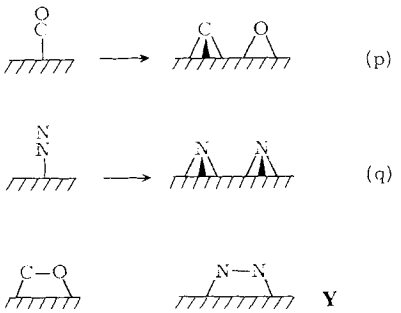
## 11. Hydrogenation of CO, $CN^-$, RCN, RNC, and $N_2$

In the preceding section, mechanistic features of the hydrogenation of alkynes by cluster precursors were discussed. Generally, this catalytic cycle is very easy to maintain with mononuclear metal complexes, clusters, or on metal surfaces. Multisite metal atom catalysis is not a requirement of this type of reaction. In sharp contrast, it is relatively difficult to effect hydrogenation of the triple bonds in molecules or ions like CO, $CN^-$, alkyl cyanides, alkyl isocyanides, and $N_2$. Typically, the catalysts of choice for these hydrogenations are solid-state materials, *e.g.* metals, alloys, metal oxides, and metal carbides, although some molecular compounds have been reported to be catalysts. Conditions are generally quite severe: temperatures of 200–300 °C and elevated pressures are necessary for reasonable reaction rates in the hydrogenation of CO or $N_2$. It is extremely difficult to gather incisive mechanistic data for such high temperature reactions in which transient reaction intermediates occur. Most studied has been the hydrogenation of CO to give hydrocarbons (the methanation reaction and Fischer-Tropsch synthesis) and of $N_2$ to give ammonia. For solid-state metallic or metal carbide catalysts, a dominant first step appears to be dissociative chemisorption of CO to form surface-bound carbon and oxygen atoms[70] and of $N_2$ to give surface-bound nitrogen atoms[71]. Scheme 6 shows a model for the metal-surface catalyzed hydrogenation of CO to give hydrocarbons. In the next section the reduction of $N_2$, RNC, RCN and $CN^-$ by nitrogenase is discussed. These reactions may involve participation of multimetal atom sites in the reduction steps.




Scheme 6. The first step of a possible mechanism for the Fischer-Tropsch synthesis.

The triple bonds of CO or $N_2$ are not cleaved at a single metal site of mononuclear metal complexes. An early postulate[6] in cluster catalysis was that hydrogenations, such as those of CO and $N_2$, which proceeded with difficulty might be more facile than with mononuclear metal catalyst precursors, since multimetal atom site reactions are possible and, in particular, these could achieve the formal analog of dissociative chemisorption of CO and $N_2$ on metal surfaces. The reactions described in Scheme 6 and Eqs. (p) and (q) proceed through intermediates or transition states of type **X** and **Y**, respectively.




Models of the intermediate or transition state for the CO case may be found in a number of metal clusters in which both the oxygen and the carbon atoms are bound to metal atoms. The first well-characterized species of this group was $[HFe_4(\mu\text{-}\eta^2\text{-}CO)(CO)_{12}]^-$ (Fig. 3)[72]. In addition, it has been shown that carbonylmetal clusters are converted into carbidometal clusters under a variety of conditions, and are thus formally models for the overall process

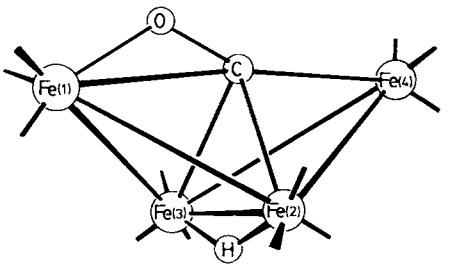



Fig. 3. Structure of the $Fe_4$-core of the cluster ion $[HFe_4(\mu\text{-}\eta^2\text{-}CO)(CO)_{12}]^-$[72]. The iron atoms have a butterfly structure and a hydrido ligand bridges the basal edge. Each iron atom has three terminal CO ligands which are indicated only by line projections. Unique is the bridging CO ligand in which both the oxygen and the carbon atoms are bonded to the Fe-framework atoms. The C-O bond order in this bridging ligand is substantially reduced, as evidenced by the relatively long C–O bond distance of 1.26 Å (typical cluster carbonyl C–O distances are *ca.* 1.1 to 1.14 Å for CO ligands that are bound only through the carbon atom).

of dissociative chemisorption of CO on metal surfaces. Using labeling experiments and NMR studies, ***Bradley et al.***[73, 16m] have demonstrated in an iron and a ruthenium system that the carbido C atom is derived from a CO molecule [Eqs. (r) and (s)]

$$Fe(^{13}CO)_5 \xrightarrow{Mn(CO)_5^-} [Fe_6{}^{13}C(^{13}CO)_{16}]^{2-} \quad (r)$$

$$Ru_3(^{13}CO)_{12} \xrightarrow{Mn(CO)_5^-} [Ru_6{}^{13}C(^{13}CO)_{16}]^{2-} \quad (s)$$

Also *Tachikawa et al.*[75] have shown that carbido clusters in which the carbido C-atom has a coordination number of four can react with hydrogen to form C–H bonds [Eq. (t)].

$$[Fe_4(\mu_4\text{-}C)(CO)_{12}]^{2-} \xrightarrow{Ag^+} [Fe_4(\mu_4\text{-}C)(CO)_{12}] \xrightarrow{H_2} [HFe_4(\mu\text{-}\eta^2\text{-}CH)(CO)_{12}] \quad (t)$$

The existence of a cluster model of the transition state for the dissociative chemisorption of CO and the stoichiometric cluster reactions that simulate the CO dissociation and the hydrogenation of the carbido C atom suggests that cluster catalyzed hydrogenation of CO might be feasible. In principle, this concept could be extended to $N_2$, $CN^-$, RCN, and RNC. Actually, there are clusters in which cyanides and isocyanides are bonded to metal atoms through both the carbon and nitrogen atoms, as well as stoichiometric cluster reactions[160, 76] that hydrogenate these triple bonds. No metal clusters have yet been described with $N_2$ or $CN^-$ bound to metal atoms through both atoms.

Although cluster precursors have been reported for the catalytic conversion of CO into hydrocarbons, it is not known whether the catalytic intermediates are actually clusters. A major problem in mechanistic studies of such systems is that the reaction conditions are relatively severe and all or most intermediates are transient. Also, under conditions of high temperature and high CO pressures most carbonylmetal clusters enter into facile equilibria[77, 78] with carbonylmetal complexes whose nuclearity may range between one and 12 to 15. It is extremely difficult to accurately assess the molecular features of the catalytic cycle or cycles.

One of the most noteable examples of carbonylmetal catalyzed CO-$H_2$ reactions is the hydrogenation of CO to ethylene glycol using soluble anionic carbonylrhodium compounds[36, 77, 79]. At CO pressures of *ca.* 1000 atm and temperatures of 200 to 290 °C, ethylene glycol is produced relatively selectively; methanol and other polyalcohols are the major byproducts. A detailed FT-IR study[77] of these reaction systems as a function of temperature (50–220 °C) and CO pressure (500–1000 atm) showed that below 180 °C the predominant species present in solution are $[Rh(CO)_4]^-$ and $[Rh_5(CO)_{15}]^-$. Above 180 °C, clusters of higher nuclearity, such as $[H_nRh_{13}(CO)_{24}]^{5-n}$, and possibly $[Rh_{14}(CO)_{25}]^{4-}$, $[Rh_{15}(CO)_{28}]^{3-}$, and $[Rh_{12}(CO)_{30}]^{2-}$ are favored. These results are consistent with the fact that Rh–Rh bond energies generally are lower than Rh–CO bond energies. Despite these very elegant spectroscopic studies, the carbonylrhodium system is too complex to allow realistic characterization of the reaction mechanism in the catalytic cycle. The catalytic cycle or cycles in this system may be based solely on mononuclear metal species, solely on cluster intermediates, or both.

Solutions of carbonylmetal clusters, *e.g.* $Os_3(CO)_{12}$ or $Ir_4(CO)_{12}$, react with $H_2$ and CO under very mild conditions (150–180 °C, 1–2 atm CO) to produce $CH_4$ and other hydrocarbons, but the rates are so low that it is unclear whether the reactions are truly catalytic[80, 81]. Another problem in cluster-initiated CO hydrogenation is encountered with the less robust $Ru_3(CO)_{12}$ cluster. Initial studies suggested that this cluster catalyzed the conversion of CO and $H_2$ into hydrocarbons at 250–300 °C and 1–200 atm[82]. However, a later study established that ruthenium metal, generated by thermal decomposition of $Ru_3(CO)_{12}$, was the actual catalyst[35, 83]. Also, at *ca.* 250 °C and 1300 atm it was shown that $Ru_3(CO)_{12}$ and other ruthenium mononuclear and cluster complexes initiated catalytic conversion of CO and $H_2$ into methanol[35, 83]. Kinetic and spectroscopic studies for this reaction at 25 °C indicated that the catalysis is propagated by $Ru(CO)_5$, rather than by a cluster[35, 83]. However, the data were insufficient to establish a reaction mechanism.

Other reports of cluster-initiated catalysis of CO-hydrogenation involve $Ir_4(CO)_{12}$[84, 85] in a NaCl-$AlCl_3$ melt at 160 °C and 1 atm (formation of methane, ethane, propane, and higher branched alkanes), $[Os_2(CO)_6Br_4]$[86] in solution in $BBr_3$ at 180 °C and 1–2 atm (formation of alkanes as well as methyl, ethyl, propyl and butyl bromides), and $[Os_2(CO)_6Cl_4]$[86] in solution in $BCl_3$ at 110 °C and 1–2 atm (formation of hydrocarbons only). In the first system, the $Ir_4(CO)_{12}$ catalyst precursor was converted into a carbonyliridium species that was not charaterized, and in the last two systems the carbonylosmium halides were recovered unchanged. It was proposed that Ir-CO-Al and Os-CO-B interactions facilitated the hydrogenation reaction, but no catalyst intermediates were characterized and the nuclearity of the catalytic intermediates was not established. In these three systems, the $AlCl_3$ or $BBr_3$ "solvents" were consumed because the oxygen atoms of the CO molecules which are converted into hydrocarbons or alkyl halides are eventually bound to aluminum or boron.

It is improbable that any CO hydrogenation reaction initiated by a carbonylmetal cluster will provide definitive

mechanistic insight. Possibly a metal cluster which does not contain CO ligands and one that does not strongly bind CO will be found that will catalyze CO hydrogenation at temperatures low enough that the intermediates will be sufficiently long lived to allow spectroscopic characterization.

Cluster-initiated catalytic hydrogenation of $N_2$ or $CN^-$ has not been reported, but appears to be possible. Catalytic hydrogenation[34] of acetonitrile and of alkyl isocyanides can be realized using the coordinately unsaturated cluster $[Ni_4\{\mu\text{-}\eta^2\text{-}CNC(CH_3)_3\}_3\{CNC(CH_3)_3\}_4]$. With $Ni[CNC(CH_3)_3]_4$ as the isocyanide source and temperatures of 90 °C, hydrogenation of the isocyanide proceeds with high selectivity to give $(CH_3)_3CNHCH_3$ with only small amounts of the cleavage product $(CH_3)_3CNH_2$. The tetranuclear nickel cluster also catalyzes the hydrogenation of acetonitrile to ethylamine at 90 °C but at a very low rate[34]. Neither $Ni(CNR)_3$ nor $Ni(CNR)_4$ are catalyst precursors for this type of hydrogenation. The mechanism of the cluster-initiated reaction is not known, but possibly the $Ni_4(CNR)_7$ cluster or a $Ni_4(CNR)_6$ species derived from it is an active intermediate. Certainly, the bond order of the isocyanide group is substantially reduced in the $\mu\text{-}\eta^2$ binding established for the parent $Ni_4(CNR)_7$ (Fig. 1).

*Yoshida, Okano,* and *Otsuka*[33] have reported that $[HRh\{P(iC_3H_7)_3\}_3]$ and $[H_2Rh_2(\mu\text{-}N_2)\{P(cyclohexyl)_3\}_4]$ catalyze the hydrogenation (20 °C, 1 atm) of nitriles to give primary amines. The mechanism of this intriguing catalytic reaction was not established but since it proceeds under quite mild conditions, it may be amenable to low temperature NMR studies.

## 12. Biological Reaction Cycles Based on Molecular Metal Clusters

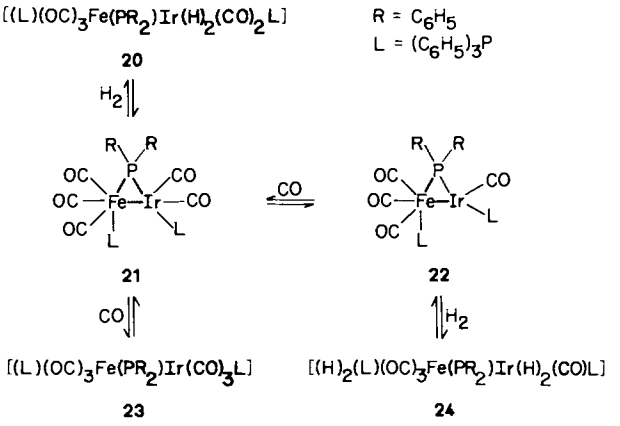
Electron transfer is the prime function of the nonheme iron proteins, the ferredoxins. These $Fe_4$-clusters have a cubane-like structure with alternating iron and sulfur atoms at the vertices and with iron-iron distances that range from 2.7 to 2.8 Å. The $Fe_4S_4$ core is bonded to the protein through an Fe-S bond (Fe from the cluster, S from protein cysteine).

Biological fixation of nitrogen may proceed through multimetal (iron and molybdenum) sites of the nitrogenase enzymes but the nature of $N_2$ binding and the activation steps have not been established for any of the enzymes. The enzymes can also reduce the triple bonds in the cyanide ion, alkyl cyanides, alkyl isocyanides, and acetylenes. Recent reviews provide critical accounts of the state of the art of modeling the active sites[87] and of the biological studies[88].

## 13. Coordinately Unsaturated Clusters

An efficient catalyst precursor patently should provide easy entry to an intermediate in the catalytic cycle or be a real intermediate. The majority of isolable metal clusters are coordinately saturated with all low lying molecular orbitals filled, and have a relatively large energy gap between the HOMO and LUMO. For many of these clusters entry into a catalytic cycle requires scission of a metal-ligand or a metal-metal bond. In carbonyl clusters, the dissociation energy for loss of the first CO molecule varies widely. One way to lower this energy is to initially replace one or more CO ligands in the cluster with weak-field ligands, such as acetonitrile. The paradigm would be a carbonyl cluster in which a carbonyl ligand on every metal atom has been replaced with a weak-field ligand. We have attempted to synthesize such clusters but have not been able to obtain the ideal case. For example, successive replacement of CO by acetonitrile by photoexcitation of $[Fe_3(\mu_3\text{-}PC_6H_5)_2(CO)_9]$ yielded $[Fe_3(\mu_3\text{-}PC_6H_5)_2(CO)_7(NCCH_3)_2]$. Unfortunately, both acetonitrile ligands were on the same iron atom and the cluster was not notably active as a catalyst precursor[89]. In $Os_3(CO)_{12}$, two CO ligands on different osmium centers have been replaced by acetonitrile, but a tris(acetonitrile) derivative has not been reported[90]. To date, no catalytic process has been reported for $[M_x(CO)_y(L)_z]$, where L is a weak-field ligand. Nevertheless, this basic strategy for generating reactive cluster catalysts is sound and should be successful, especially for the $[M(CO)_x(L)]_y$ class of clusters.

Another tack exploits the relatively weak metal-metal bonds in clusters, particularly those between 3d metals, which upon scission provide vacant coordination sites at two (or more) neighboring metal atoms. In order to inhibit complete dissociation of the cluster into mononuclear molecular fragments, O, S, RP, and $R_2P$ ligating atoms or groups are employed. This strategy has been pursued by a number of groups, including those of *Adams*[76d], *Geoffroy*[91], and *Vahrenkamp*[92]. One system designed by *Geoffroy et al.*[91] is based on a dinuclear $Fe^0\text{–}Ir^I$ complex in which a long Fe-Ir separation is supported by a bridging $P(C_6H_5)_2$ ligand, and both metal sites are coordnatively saturated. Ligand dissociation and association, as well as ox-




Scheme 7. Outlined here is the chemistry of a coordinately unsaturated iron-iridium complex. The structure of **21** has been determined by X-ray crystallography [91]. The FePIr angle is 81.62(7)°, which is thus considerably compressed from the regular tetrahedral angle for tetracoordinate $P^{III}$; the Fe–Ir distance is 2.960(1) Å, a value substantially larger than the sum of the metallic radii. A bonding interaction was proposed and was characterized as a Fe ⟶ Ir donor-acceptor bond following an earlier proposal by *Vahrenkamp* for analogous complexes. Addition of CO and of $H_2$ to the iridium center is proposed to proceed through Fe-Ir bond scission to form **23** and **20**, respectively. Loss of CO from **21** generates **22**; this complex adds $H_2$ to both metal centers to give **24**. The tetrahydrido complex **24** is shown here without a direct Fe–Ir bond, although in the original publication a two-center two-electron Fe–Ir bond was proposed [91].

idative addition reactions are outlined in Scheme 7. Such approaches to coordinately unsaturated clusters should yield clusters which are catalytically active, but none has been reported to date.

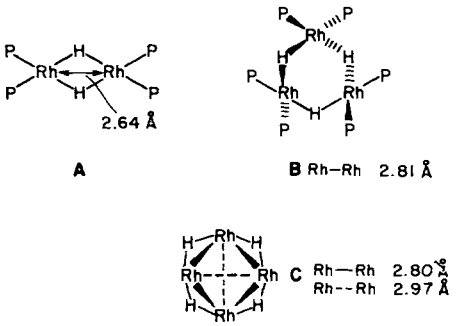
A focal point of our research interest has been coordinately unsaturated metal clusters in which every metal atom has a vacant coordination site[93-103]. In this type of cluster, ready advantage can be taken of the possible unique features of multi-site catalytic reactions. Presently, this potentially large family of unsaturated clusters is limited to the platinum clusters synthesized by *Gregson et al.*[105,106] and to rhodium clusters of the general formula $[(\mu\text{-H})RhL_2]_x$ $(x=2-4)$[93-104]. In the Rh clusters each rhodium atom is planar four-coordinate ($H_2ML_2$) and in addition has an "open" coordination site. To date, the clusters in Scheme 8 have been characterized; their structures are shown in Scheme 9. The platinum clusters[105,106] include triangular $[H_2PtP(tC_4H_9)_3]_3$, trigonal bipyramidal $[H_8Pt_5\{PC_6H_5(tC_4H_9)_2\}_5]$, tetrahedral $[H_2Pt_4\{P(tC_4H_9)_3\}_4]$ and $[H_8Pt_4\{PC_6H_5(iC_3H_7)_2\}_4]$ with two relatively long Pt–Pt bonds. The last compound is formally related to **28**[103]. These clusters should prove interesting as catalysts.

$[(\mu\text{-H})RhL_2]_2$ **25a**, L = $P(OiC_3H_7)_3$[94,96,98]; **25b**, L = $P[N(CH_3)_2]_3$[102]

$[(\mu\text{-H})RhL_2]_3$ **26a**, L = $P(OCH_3)_3$[93,97,98]; **26b**, L = $P(OC_2H_5)_3$[98]

**27**[104] $\left[(\mu\text{-H})Rh\left(\begin{array}{c}CH_3O\\CH_3O\end{array}\!\!>\!P\!-\!CH_2\!-\!CH_2\!-\!P\!<\!\begin{array}{c}OCH_3\\OCH_3\end{array}\right)\right]_4$ $[(\mu\text{-H})Rh(\eta^4\text{-1,5-cyclooctadiene})]_4$ **28**[103]

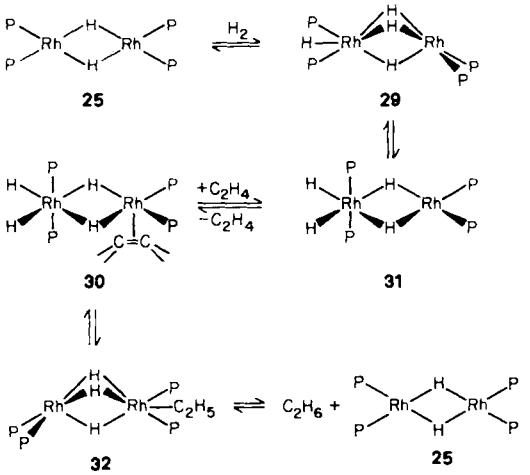
Scheme 8.




Scheme 9. The dinuclear $[(\mu\text{-H})RhL_2]$ complexes have a coplanar array of P, Rh, and H atoms. Each Rh atom has a coplanar four-coordinate form (A). The $Rh_2H_2$ bonding is best described in terms of two closed four-center two-electron molecular orbitals (of $a_{1g}$ and of $b_{2u}$ symmetry). Precise structural details for the dimer **25a** were afforded by X-ray and neutron crystallographic studies [94–96]. An analogous set [93, 96] of crystallographic studies on the trimer **26a** established square-planar stereochemistry for each Rh atom (B). Because each Rh–Rh interaction comprises only one Rh–H–Rh three-center two-electron bond, the Rh–Rh distance is longer, and this trinuclear cluster is more susceptible to fragmentation than the dimers. An X-ray crystallographic study [103] of the tetramer **28** established a $D_{2d}$ tetrahedral array of Rh atoms with two long Rh–Rh distances (C). One description of the tetramer is that it consists of a puckered ring of $H_2Rh$(diene) units with three-center two-electron Rh–H–Rh bonds are in the trimer.

All the $[(\mu\text{-H})Rh(PY_3)_2]_x$ clusters are highly reactive, a feature that complicates their manipulation in the laboratory but that facilitates the study of their catalytic reactions[98]. These reactions proceed at room temperature or below and involve many long-lived intermediates, which can be detected spectroscopically or even isolated at very low temperatures.

The dinuclear and trinuclear clusters **25a** and **26a**, respectively, are effective initiators of the catalytic hydrogenation of alkenes and alkynes. Mechanistic discussion of these catalytic cycles is limited here to those initiated by the dimer **25**, because these are relatively simple (Scheme 10)[98]. For terminal olefins the reaction rate is limited by hydrogen diffusion rates at 25 °C. The reaction is initiated by addition of hydrogen, not by addition of alkene. Hydrogen addition is fast, converting the brown-black dimer **25** into the green hydrogen adduct $[H_4Rh_2\{P(OiC_3H_7)_3\}_4]$ **29**, which reacts immediately with alkene to give alkane and the dimer **25**. At very low temperatures (*ca.* −120 °C) the hydrogen adduct forms an olefin complex **30** which at *ca.* −85 °C forms the dimer **25** and alkane.




Scheme 10. Mechanism of the hydrogenation of alkenes by **25a**. The first step, addition of hydrogen, is fast and reversible and is well characterized. The structure of the primary hydrogen adduct **29** in solution has only been determined spectroscopically. The excited state of the complex **31** was implicated by dynamic $^1$H-NMR spectroscopy and is supported by an X-ray crystallographic study [102] of the tetrahydrido complex of $[(\mu\text{-H})Rh\{P[N(CH_3)_2]_3\}_2]_2$. Low temperature NMR studies provided evidence for the next step of olefin addition to the active hydrogen adduct **31**, in which a four-coordinate $Rh^I$ occurs. The olefin complex is probably converted in two steps into alkane and educt complex **25**, *via* the intermediate **32** (not detected).

The dimer **25a** also catalyzes the hydrogenation of alkynes, although at a rate which lies an order of magnitude lower than that of alkanes[98,101]; in presence of a mixture of hydrogen, internal alkenes, and alkynes the alkyne is hydrogenated first to give the corresponding alkene. The alkene produced has solely the *trans*-configuration; an extraordinarily result, since all other reported molecular and solid-state systems produce *cis*-alkenes as the first-formed product.

Internal alkynes react with the dimer **25a** to form initially an intermediate with a bridging alkyne intermediate that can be intermediate spectroscopically detected by NMR at *ca.* −80 °C. Above −80 °C, an insertion reac-

tion occurs whereby a derivative with a bridging vinyl group, **34**, is formed. This intermediate, stable in the absence of $H_2$ or excess alkyne, has been crystallographically defined for the molecules derived from 2-butyne and di-*p*-tolylacetylene (Fig. 4). The significant feature of this inter-

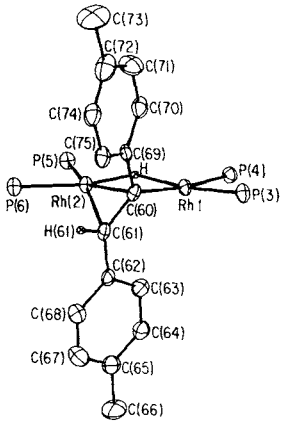
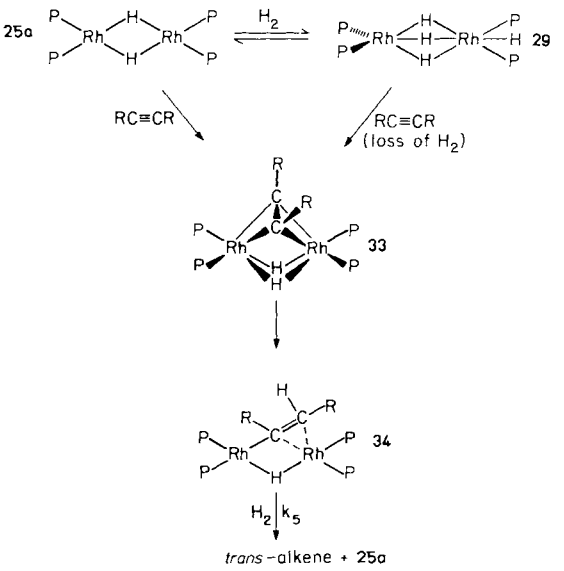



Fig. 4. Structure of the bridging vinyl complex **34** (Scheme 11) derived from di-*p*-tolylacetylene and **25a** [101]. Not depicted here are the hydrogen atoms associated with the *p*-tolyl groups, and the isopropoxy groups bonded to the P atoms. Notable features are the near coplanar array of the four P atoms, the two Rh atoms, and the bridging H atom, as well as the *trans*-arrangement of the *p*-tolyl substituents of the bridging vinyl group.

mediate is the *trans*-stereochemistry of the vinyl ligand, a fact that fully accounts for the stereoselective feature of the catalytic cycle. The next step, which is rate determining, is addition of hydrogen to the vinyl derivative and the final step is presumably migration of a hydrogen atom to the vinyl group to give the alkene and **25a**. Scheme 11 shows the catalytic cycle[101].




Scheme 11. Mechanism of the hydrogenation internal alkynes catalyzed by **25a**. Every intermediate has been detected by low temperature NMR spectroscopy, and the vinyl derivative characterized by X-ray crystallography (see Fig. 4) [101].

The dimer-mediated catalytic cycle is short-lived because alkyne addition competes with hydrogen addition to the vinyl intermediate is. This process leads to formation of a monomeric species

$[RHC{=}\overline{CRCR{=}CR{-}Rh\{P(OiC_3H_7)_3\}_2}]$ which is also an alkyne hydrogenation catalyst but one that produces *cis*-alkenes[101].

Coordinately unsaturated molecular metal clusters offer several advantages. They are extremely reactive and the intermediates in the catalytic cycles are amenable to characterization. Also, they escape fragmentation, not because the metal atom framework is necessarily so stable but because molecules can be incorporated and hydrogen oxidatively added without the necessity of metal-ligand or metal-metal bond scission. Nevertheless, strong-field ligands like CO or phosphites react rapidly, even at low temperatures, to produce relatively inert mononuclear metal complexes[98,99]. Thus, none of these clusters are effective catalysts for hydrogenation of CO. Finally, the alkyne hydrogenation demonstrates that catalytic reactions can be initiated by clusters wherein more than one metal atom site takes part in the catalytic cycle.

## 14. Prospects

Ever since the potential of molecular metal cluster catalysts began to be discussed, recurrent questions to reported claims of cluster catalysis have been: "Is it really a cluster catalyzed cycle?", "How do you know that monomeric species are not the active catalytic intermediates?", "Is the real catalyst metal particles formed by decomposition of the cluster?". All such questions are relevant to any catalytic cycle ostensibly effected in solution, irrespective of whether the catalyst precursor is monomeric or polynuclear. But none of these questions addresses itself directly to the basic issues in cluster catalysis. Cluster catalysts will only gain significance if they catalyze reactions that are unfeasible with monomeric metal complexes or that are stereoselectively or chemoselectively distinct from those initiated by such complexes. To date, only one unique cluster catalyzed reaction has been discovered: the selective hydrogenation of internal alkynes to *trans*-alkenes by the dinuclear complex **25a** (Section 13). Presumably other catalytic reactions of this type will be uncovered through studies of reactive clusters in which all or most metal atoms have either vacant coordination sites or an easily exchangeable ligand. Critical here are exploratory synthetic studies directed at such clusters.

Also critically needed is a more detailed understanding of basic types of cluster reactions such as ligand substitution, oxidative addition, reductive elimination, insertion, and redox reactions. This understanding is essential for the logical design of clusters that can function as true cluster catalysts and that may initiate unique types of catalytic reactions.

Investigations of the reaction mechanisms of catalytic cycles initiated by very reactive metal clusters should prove valuable in enlarging the base of understanding in cluster chemistry and for the design of new cluster catalyts. The possibility of incisive and informative mechanistic data generally will be higher for catalytic reactions that can be effected at low temperatures. The probability of relatively high concentration catalytic intermediates will be far higher for these systems than those that require high

temperatures. Finally, we note the inevitability of the unexpected and suggest that there should be more exploratory catalytic studies of *all* classes of metal clusters.

*The work described here which was carried out in the authors' laboratory was supported by the National Science Foundation. We are indebted to Mr. O. R. Krause for a search of patent literature, to Dr. R. M. Laine for information concerning unpublished data, and to E. J. Wucherer, R. M. Wexler, M. Kulzick, and R. T. Price for critical comments.*

Received: November 8, 1982 [A 442 IE]
German version: *Angew. Chem. 95* (1983) 135

[1] a) The catalyst introduced into a reaction system is more accurately described as the catalyst precursor because the active catalytic species may be formed under the reaction conditions. b) Catalysts are conventional classified as homogenous or heterogenous. However, is general classification is at best misleading in that even interfacial catalytic reactions can be homogenous because they occur largely in a single phase, although it may be predimonantly two dimensional. c) This classification obviates the need for imprecise and inelegant descriptions like "heterogenezing of a homogenous catalyst". *e.g.* anchoring or immobilizing a molecular catalyst to a unit support does not alter the nature of the catalysis. The effect of supporting the molecular species may however, inhibit reactions that normally would occur with the same species in solution, although metal atoms are mobile to varying degress on such surfaces. This mobility is sensitive to the nature of the gaseous reactants: CO has a marked tendency to "mobilize" metal atoms.

[2] B. C. Gates, J. R. Kratzer, G. C. A. Schuitt: *Chemistry of Catalytic Processes*, McGraw-Hill, New York 1979.

[3] G. W. Parshall: *Homogeneous Catalysis*, John Wiley, New York 1980.

[4] R. Psaro, R. Ugo, G. M. Zanderighi, B. Besson, A. K. Smith, J. M. Basset, *J. Organomet. Chem. 213* (1981) 215, and references cited therein. Lit.

[5] a) R. L. Burwell, *Chem. Eng. News 44* (1966) No. 34, p. 56; b) R. Ugo, *Catal. Rev. Sci. Eng. 11* (1975) 225.

[6] E. L. Muetterties, *Bull. Soc. Chim. Belg. 84* (1975) 959; *ibid. 85* (1976) 451.

[7] E. L. Muetterties, T. N. Rhodin, E. Band, C. F. Brucker, W. R. Pretzer, *Chem. Rev. 79* (1979) 91.

[8] E. L. Muetterties, R. M. Wexler, *Surv. Prog. Chem.*, in press.

[9] In the characterization of chemisorbed acetylene and hydrogen on Pt(111) the results of IR studies indicated [10] that 1) the surface species was ethylidyne ($CH_3C$) and 2) that the α-carbon atom was over a three-fold surface site and symmetrically bonded to three platinum atoms (the CC-bond vector is normal to the $Pt_3$-plane). The paradigm for this species in cluster chemistry is $[(\mu_3\text{-}CH_3C)Co_3(CO)_9]$ [11]. A comparative vibrational spectroscopic analysis of this cluster with the data for acetylene/hydrogen chemisorbed on Pt confirmed the ethylidyne hypothesis [12].

[10] L. L. Kesmodel, L. H. DuBois, G. A. Somorjai, *J. Chem. Phys. 70* (1979) 2180.

[11] D. Seyferth, *Adv. Organomet. Chem. 14* (1976) 98.

[12] M. H. Howard, S. F. A. Kettle, I. A. Oxton, D. B. Powell, N. Sheppard, P. Skinner, *J. Chem. Soc. Faraday Trans. II 77* (1981) 397.

[13] E. L. Muetterties, B. A. Sosinsky, K. I. Zamaraev, *J. Am. Chem. Soc. 97* (1975) 5299.

[14] a) C. P. Casey, C. R. Cyr, *J. Am. Chem. Soc. 95* (1973) 2248; b) J. L. Graff, R. D. Sanner, M. S. Wrighton, *ibid. 101* (1979) 273.

[15] E. L. Muetterties, *Chem. Eng. News 60* (1982) No. 35, p. 28.

[16] a) P. Chini, *J. Organomet. Chem. 200* (1980) 37; b) R. Whyman in B. F. G. Johnson: *Transition Metal Clusters*, Wiley, New York 1980, p. 545; c) B. F. G. Johnson in [16b], p. 471; d) K. Wade in [16b], p. 193; e) B. F. G. Johnson, J. Lewis, D. Pippard, *J. Organomet. Chem. 160* (1978) 263; f) A. P. Humphries, H. D. Kaesz, *Prog. Inorg. Chem. 25* (1979) 145; g) B. F. G. Johnson, J. Lewis, *Adv. Inorg. Chem. Radiochem. 24* (1981) 225; h) A. J. Deeming in [16b], p. 391; i) W. Hübel in I. Wender, P. Pino: *Organic Synthesis via Metal Carbonyls, Vol. 1*, Wiley, New York 1968, chap. 2; j) W. C. Gladfelter, G. L. Geoffroy, *Adv. Organomet. Chem. 18* (1980) 207; k) F. Richter, H. Vahrenkamp, *Chem. Ber. 115* (1982) 3224, 3243; l) A. J. Poë, M. V. Twigg, *Inorg. Chem. 13* (1974) 2982; m) J. S. Bradley, *Phil. Trans. R. Soc. London*, in press; n) E. M. Holt, K. H. Whitmire, D. F. Shriver, *J. Organomet. Chem. 213* (1981) 125; o) M. A. Andrews, H. D. Kaesz, *J. Am. Chem. Soc. 101* (1979) 7238; M. A. Andrews, G. van Buskirk, C. B. Knobler, H. D. Kaesz, *ibid. 101* (1979) 7245; M. A. Andrews, H. D. Kaesz, *ibid. 101* (1979) 7255; M. A. Andrews, C. B. Knobler, H. D. Kaesz, *ibid. 101* (1979) 7260.

[17] J. A. Connor, *Top. Curr. Chem. 71* (1977) 71.

[18] $\eta^x$ and $\mu_x$ indicate the number of ligand atoms bonded to the metal atom and how many metal atoms are bonded to one ligand, respectively: $\mu$ without an index signifies that the ligand bridges two metal atoms.

[19] A. J. Deeming, S. Hasso, M. Underhill, A. J. Carty, B. F. G. Johnson, W. G. Jackson, J. Lewis, T. W. Matheson, *J. Chem. Soc. Chem. Commun. 1974*, 807.

[20] F. Richter, H. Beurich, H. Vahrenkamp, *J. Organomet. Chem. 166* (1979) C 5.

[21] a) H. Beurich, R. Blumhofer, H. Vahrenkamp, *Chem. Ber. 115* (1982) 2409; b) H. Beurich, H. Vahrenkamp, *ibid. 115* (1982) 2385.

[22] B. F. G. Johnson, R. D. Johnson, J. Lewis, F. G. Williams, P. A. Kitty, *Chem. Commun. 1968*, 861.

[23] For a recent review of mechanistic features of metal cluster reactions see E. L. Muetterties, R. R. Burch, A. M. Stolzenberg, *Annu. Rev. Phys. Chem. 33* (1982) 89.

[24] A. M. Stolzenberg, E. L. Muetterties, *J. Am. Chem. Soc.*, in press.

[25] N. J. Coville, A. M. Stolzenberg, E. L. Muetterties, *J. Am. Chem. Soc.*, in press.

[26] J. B. Keister, J. R. Shapley, *J. Am. Chem. Soc. 98* (1976) 1056.

[27] a) C. U. Pittman, Jr., R. Ryan, W. D. Wilson, G. Wileman, M. Absi-Halabi, the Division of Petroleum Chemistry, Am. Chem. Soc. Meet., San Francisco, August 24, 1980, p. 714; b) C. U. Pittman, Jr., R. C. Ryan, J. McGee, J. P. O'Connor, *J. Organomet. Chem. 178* (1979) C 43.

[28] G. D. Mercer, J. S. Shu, T. B. Rauchfuss, D. M. Roundhill, *J. Am. Chem. Soc. 97* (1975) 1967.

[29] R. M. Laine, *J. Am. Chem. Soc. 100* (1978) 645; *Ann. N. Y. Acad. Sci. 133* (1980) 124.

[30] F. L'Eplattenier, P. Matthys, F. Calderazzo, *Inorg. Chem. 9* (1970) 342.

[31] M. Biachi, U. Matteoli, G. Menchi, P. Frediani, S. Pratesi, F. Pacenti, *J. Organomet. Chem. 198* (1980) 73.

[32] M. G. Thomas, B. F. Beier, E. L. Muetterties, *J. Am. Chem. Soc. 98* (1976) 1296.

[33] T. Yoshida, T. Okano, S. Otsuka, *J. Chem. Soc. Chem. Commun. 1979*, 870.

[34] E. Band, W. R. Pretzer, M. G. Thomas, E. L. Muetterties, *J. Am. Chem. Soc. 99* (1977) 7380.

[35] J. S. Bradley, *J. Am. Chem. Soc. 101* (1979) 7419.

[36] W. Walker, J. B. Cropley, US-Pat. 3940432 (1976), Union Carbide; E. S. Brown, US-Pat. 3974259 (1976), Union Carbide; J. L. Vidal, Z. C. Mester, W. Walker, US-Pat. 4115428 (1978), Union Carbide.

[37] R. M. Laine, B. R. Cho, R. B. Wilson, Jr., *J. C; Molecules 1* (1983), in press.

[38] K. Cann, T. Cole, W. Slegeir, R. Pettit, *J. Am. Chem. Soc. 100* (1978) 3969.

[39] R. M. Laine, R. G. Rinker, P. C. Ford, *J. Am. Chem. Soc. 99* (1977) 252.

[40] V. W. Day, R. O. Day, J. S. Kristoff, F. J. Hirsekorn, E. L. Muetterties, *J. Am. Chem. Soc. 97* (1975) 2571.

[41] R. M. Laine, *J. Org. Chem. 45* (1980) 3370.

[42] a) R. M. Laine, *J. Mol. Catal. 14* (1982) 137; b) A. K. Smith, J. M. Basset, *ibid. 2* (1977) 229.

[43] S. A. Fouda, G. L. Rempel, *Inorg. Chem. 18* (1979) 1.

[44] a) P. Frediani, U. Matteoli, M. Bianchi, F. Piacenti, G. Menchi, *J. Organomet. Chem. 150* (1978) 273; b) M. Bianchi, G. Menchi, F. Francalanci, P. Piacenti, U. Matteoli, P. Frediani, C. Botteghi, *ibid. 188* (1980) 109.

[45] B. Heil, L. Marko, *Acta Chim. Acad. Sci. Hung. 55* (1968) 107.

[46] a) G. A. Vaglio, M. Valle, *Inorg. Chim. Acta 30* (1978) 161; b) M. Valle, D. Osella, G. A. Vaglio, *ibid. 20* (1976) 213.

[47] H. Kang, C. H. Mauldin, T. Cole, W. Slegeir, K. Cann, R. Pettit, *J. Am. Chem. Soc. 99* (1977) 8323.

[48] P. Chini, S. Martinengo, G. Garaschelli, *J. Chem. Soc. Chem. Commun. 1972*, 709.

[49] Review: R. L. Pruett, *Adv. Organomet. Chem. 17* (1979) 1.

[50] T. Cole, R. Ramage, K. Cann, R. Pettit, *J. Am. Chem. Soc. 102* (1980) 6184.

[51] R. M. Laine, D. W. Thomas, L. W. Cary, S. E. Buttrill, *J. Am. Chem. Soc. 100* (1978) 6527.

[52] Y. Shvo, R. M. Laine, *J. Chem. Soc. Chem. Commun. 1980*, 753.

[53] Y. Shvo, D. W. Thomas, R. M. Laine, *J. Am. Chem. Soc. 103* (1981) 2461.

[54] C. C. Yin, A. J. Deeming, *J. Organomet. Chem. 133* (1977) 123.

[55] R. H. Fish, A. D. Thormodsen, G. A. Cremer, *J. Am. Chem. Soc. 104* (1982) 5234.

[56] C.-H. Cheng, D. E. Henriksen, R. Eisenberg, *J. Am. Chem. Soc. 99* (1977) 2791.

[57] C. Ungermann, V. Landis, S. A. Moya, H. Cohen, H. Walker, R. G. Pearson, R. G. Rinker, P. Ford, *J. Am. Chem. Soc. 101* (1979) 5922; P. Ford, *Acc. Chem. Res. 14* (1981) 31.
[58] J. C. Bricker, C. C. Nagel, S. G. Shore, *J. Am. Chem. Soc. 104* (1982) 1444.
[59] H. Kang, C. H. Mauldin, T. Cole, W. Slegeir, K. Cann, R. Pettit, *J. Am. Chem. Soc. 99* (1977) 8323.
[60] E. L. Muetterties, *Inorg. Chim. Acta 50* (1981) 1.
[61] E. L. Muetterties, W. R. Pretzer, M. G. Thomas, B. F. Beier, D. L. Thorn, V. W. Day, A. B. Anderson, *J. Am. Chem. Soc. 100* (1978) 2090.
[62] S. Slater, E. L. Muetterties, *Inorg. Chem. 20* (1981) 1604.
[63] V. W. Day, S. S. Abdel-Meguid, S. Dabestini, M. G. Thomas, W. R. Pretzer, E. L. Muetterties, *J. Am. Chem. Soc. 98* (1976) 8289.
[64] V. W. Day, D. L. Thorn, E. L. Muetterties, unpublished results.
[65] S. Slater, E. L. Muetterties, *Inorg. Chem. 19* (1980) 3337.
[66] V. W. Day, R. O. Day, J. S. Kristoff, E. L. Muetterties, *J. Am. Chem. Soc. 97* (1975) 2571.
[67] M. G. Thomas, E. L. Muetterties, R. O. Day, V. W. Day, *J. Am. Chem. Soc. 98* (1976) 4645.
[68] M. G. Thomas, W. R. Pretzer, B. F. Beier, F. J. Hirsekorn, E. L. Muetterties, *J. Am. Chem. Soc. 99* (1977) 743.
[69] E. L. Muetterties, E. Band, A. Kokorin, W. R. Pretzer, M. G. Thomas, *Inorg. Chem. 19* (1980) 1552.
[70] A. T. Bell, *Catal. Rev. Sci. Eng. 23* (1981) 203.
[71] M. Boudart, *Catal. Rev. Sci. Eng. 23* (1981) 1.
[72] M. Manassero, M. Sansoni, G. Longoni, *J. Chem. Soc. Chem. Commun. 1976*, 919.
[73] J. S. Bradley, G. B. Ansell, E. W. Hill, *J. Organomet. Chem. 184* (1980) C33.
[74] M. Tachikawa, E. L. Muetterties, *J. Am. Chem. Soc. 102* (1980) 4541.
[75] a) M. Beno, J. M. Williams, M. Tachikawa, E. L. Muetterties, *J. Am. Chem. Soc. 102* (1980) 4542; b) *ibid. 103* (1981) 1485.
[76] a) R. D. Adams, N. M. Golembeski, *J. Am. Chem. Soc. 101* (1979) 2579; b) R. D. Adams, *Acc. Chem. Res.*, in press.
[77] J. L. Vidal, W. E. Walker, *Inorg. Chem. 19* (1980) 896.
[78] J. N. Nicholls, D. H. Farrar, P. F. Jackson, B. F. G. Johnson, J. Lewis, *J. Chem. Soc. Dalton Trans. 1982*, 1395.
[79] R. L. Pruett, W. W. Walker, US-Pat. 3833634 (1974), 3957857 (1976), Union Carbide.
[80] M. G. Thomas, B. F. Beier, E. L. Muetterties, *J. Am. Chem. Soc. 98* (1976) 1296.
[81] R. A. Schunn, G. C. Demitras, H. W. Choi, E. L. Muetterties, *Inorg. Chem. 20* (1981) 4023.
[82] C. Masters, J. A. Van Doorn, DOS 2644185 (1975), Shell Ltd.
[83] J. S. Bradley in M. Tsutsui: *Fundamental Research in Homogeneous Catalysis, Vol. 3*, Plenum, New York 1979, p. 165.
[84] G. C. Demitras, E. L. Muetterties, *J. Am. Chem. Soc. 99* (1977) 2796.
[85] H.-K. Wang, H. W. Choi, E. L. Muetterties, *Inorg. Chem. 20* (1981) 2661.
[86] H. W. Choi, E. L. Muetterties, *Inorg. Chem. 20* (1981) 2664.
[87] R. H. Holm, *Chem. Soc. Rev. 10* (1981) 455.
[88] W. E. Newton, W. H. Orme-Johnson: *Nitrogen Fixation, Vol. I, II*, University Park Press, Baltimore, MD 1980.
[89] J. Kouba, E. L. Muetterties, V. W. Day, unpublished results.
[90] B. F. G. Johnson, J. Lewis, W. J. H. Nelson, J. Pruga, P. R. Raithby, M. Schröder, K. H. Whitmire, *J. Chem. Soc. Chem. Commun. 1982*, 610.
[91] M. J. Buen, M. R. Duttern, G. L. Geoffroy, G. C. Novtak, D. A. Roberts, P. M. Schulman, G. R. Steinmetz, *Organometallics 1* (1982) 84.
[92] H. Vahrenkamp, D. Wolter, *Organometallics 1* (1982) 874.
[93] V. W. Day, M. F. Fredrich, G. S. Reddy, A. J. Sivak, W. R. Pretzer, E. L. Muetterties, *J. Am. Chem. Soc. 99* (1977) 8091.
[94] R. K. Brown, J. M. Williams, M. F. Fredrich, V. W. Day, A. J. Sivak, E. L. Muetterties, *Proc. Natl. Acad. Sci. USA 76* (1979) 2099.
[95] E. L. Muetterties, A. J. Sivak, R. K. Brown, J. W. Williams, M. F. Fredrich, V. W. Day in M. Tsutsui: *Fundamental Research in Homogeneous Catalysis, Vol. 3*, Plenum, New York 1979, p. 487.
[96] R. G. Teller, J. M. Williams, T. F. Koetzle, R. R. Burch, R. M. Gavin, E. L. Muetterties, *Inorg. Chem. 20* (1981) 1806.
[97] R. K. Brown, J. M. Williams, A. J. Sivak, E. L. Muetterties, *Inorg. Chem. 19* (1980) 370.
[98] A. J. Sivak, E. L. Muetterties, *J. Am. Chem. Soc. 101* (1979) 4878.
[99] R. R. Burch, E. L. Muetterties, A. J. Schultz, E. G. Gebert, J. M. Williams, *J. Am. Chem. Soc. 103* (1981) 5517.
[100] R. R. Burch, E. L. Muetterties, V. W. Day, *Organometallics 1* (1982) 188.
[101] a) R. R. Burch, E. L. Muetterties, R. G. Teller, J. M. Williams, *J. Am. Chem. Soc. 104* (1982) 4257; b) R. R. Burch, A. J. Shusterman, E. L. Muetterties, R. G. Teller, J. M. Williams, *ibid.*, in press.
[102] E. B. Meier, R. R. Burch, E. L. Muetterties, V. W. Day, *J. Am. Chem. Soc. 104* (1982) 2661.
[103] M. Kulzick, R. T. Price, E. L. Muetterties, V. W. Day, *Organometallics 1* (1982) 1256.
[104] M. D. Fryzuk, *Organometallics 1* (1982) 408.
[105] P. W. Frost, J. A. K. Howard, J. L. Spencer, D. G. Turner, D. Gregson, *J. Chem. Soc. Chem. Commun. 1981*, 1104.
[106] D. Gregson, J. A. K. Howard, M. Murray, J. L. Spencer, *J. Chem. Soc. Chem. Commun. 1981*, 716.

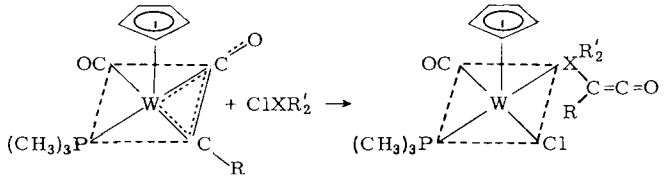
**When submitting manuscripts, authors of articles which are intended for publication as "Communications" are requested to conform to the guidelines reproduced at the beginning of each issue following the list of contents.**

## Generation and Stabilization of Phosphanyl- and Arsanylketenes within the Coordination Sphere of Tungsten[1]**

By *Fritz Roland Kreissl**, *Mathias Wolfgruber*, *Werner Sieber*, and *Helmut Guido Alt*

Ketenes of the general formula RR'C=C=O, in which R and/or R' are bonded to the terminal ketene C atom *via* an element of group IVb (Si, Ge, Sn), VIb (O, S), or VIIb (F, Cl, Br) have been synthesized in great variety and thoroughly characterized[2]. Analogues with elements of group Vb are only known, for example, for a few phthalimidoketenes[9]: in contrast phosphoranylideneketenes $R_3P{=}C{=}C{=}O$[11] and their metal complexes are viewed as ylides. We have now succeeded for the first time in synthesizing phosphorus- and arsenic-substituted ketenes within the coordination sphere of a transition metal and stabilizing them as ligands.

The cleavage of the ketene function from the $\eta^2$-ketenide complexes $[\eta^5\text{-}C_5H_5(CO)\{P(CH_3)_3\}W(\eta^2\text{-}C(R)CO]$[14] by compounds containing halides, such as dichloromethane or thionyl chloride[1], has already proved itself as a method for the preparation of novel ketene derivatives. By analogy, reactions with halogenated phosphanes and arsanes should open up a preparative route to phosphanyl- and arsanylketenes, respectively. Reaction of chloro(dimethyl)phosphane with carbonyl($\eta^5$-cyclopentadienyl)($\eta^2$-4-methylphenylketenyl)(trimethylphosphane)tungsten **1a**, as well as of chloro(diphenyl)arsane with carbonyl($\eta^5$-cyclopentadienyl)($\eta^2$-methylketenyl)(trimethylphosphane)tungsten **1b** in dichloromethane at room temperature leads in high yield to the phosphanyl-, and arsanylketene complexes **2a** and **2b**, respectively.

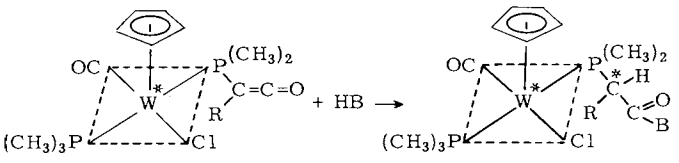



**1a, b** **2a, b**

**a**: $R = C_6H_4{-}CH_3{-}$ (4), $XR'_2 = P(CH_3)_2$
**b**: $R = CH_3$, $XR'_2 = As(C_6H_5)_2$

The result that despite variation of R, X, and R' similar ketene complexes are formed, leads one to expect a larger range of application of this synthesis.

At *ca.* −78 °C conversion of **1a** into **2a** proceeds *via* an isolable intermediate with a WCP three-membered ring[16]. The expected release of the ketene ligand from the metal could not be observed. The ketene structure of **2a** was also confirmed by addition of methanol and dimethylamine.




**2a** **3, 4**

**3**: $B = OCH_3$; **4**: $B = N(CH_3)_2$

Addition of a proton to the prochiral C atom generates a second chiral center in the molecule, and in consequence **3** and **4** are obtained as diastereomeric mixtures. This manifests itself principally in the $^1$H-NMR spectra, which each exhibit a double set of signals, apart from the signals of the $PCH_3$-protons. In the $^{31}P\{^1H\}$-NMR spectra two doublets for the $P(CH_3)_2$ groups occur in each case.

The diamagnetic complexes **2a–4** are isolated as orange colored solids, which are soluble in dichloromethane, ether, and pentane, the compositions and structures of which were confirmed by elemental analysis, IR, $^1$H-, $^{31}$P-, $^{13}$C-NMR, and mass spectroscopy. The IR spectra of **2a** and **2b** exhibit a characteristically very sharp absorption at 2100 $cm^{-1}$, and in the $^{13}C\{^1H\}$-NMR spectrum signals in the typical chemical shift region of ketene C atoms [$CD_2Cl_2$, −20 °C; **2a**: $\delta = 184.8$ ($J(^{31}P\text{-}^{13}C) = 21.5$ Hz), 39.2 (39.6); **2b**: $\delta = 185.0$, 20.4]. In addition to the molecular ion the mass spectra (EI, 70 eV) of **2**, **3**, and **4** exhibit a fragmentation at *m/z* 388, which arises by cleavage of the intact ketene, ester, and amide ligands, respectively. This suggests the possibility of a preparative route to free phosphanyl- and arsanylketenes.

Received: September 27, 1982,
revised: December 10, 1982 [Z 157 IE]
German version: *Angew. Chem. 95* (1983) 159
The complete manuscript of this communication appears in: *Angew. Chem. Suppl. 1983*, 148–155

[*] Priv.-Doz. Dr. F. R. Kreissl, M. Wolfgruber, W. Sieber
Anorganisch-chemisches Institut
der Technischen Universität München
Lichtenbergstrasse 4, D-8046 Garching (Germany)
Priv.-Doz. Dr. H. G. Alt
Laboratorien für Anorganische Chemie der Universität
Universitätsstrasse 4, D-8580 Bayreuth (Germany)

[**] This work was supported by the Deutsche Forschungsgemeinschaft and the Fonds der Chemischen Industrie. Prof. Dr. E. O. Fischer is particularly thanked for the valuable means provided by the institute and Herr M. Barth and Fräulein U. Graf for the elemental analysis.

[1] Part 11 of the series "Transition-Metal Ketene Compounds", Part 10: F. R. Kreissl, W. Sieber, M. Wolfgruber, *Z. Naturforsch. 37B* (1982) 1485.
[2] S. Patai: *The Chemistry of Ketenes, Allenes and Related Compounds, Part 1* and *2*, Wiley, Chichester 1980.
[9] S. Winter, H. Pracejus, *Chem. Ber. 99* (1966) 151.
[11] H. J. Bestmann, *Angew. Chem. 89* (1977) 361; *Angew. Chem. Int. Ed. Engl. 16* (1977) 349.
[14] W. Uedelhoven, K. Eberl, F. R. Kreissl, *Chem. Ber. 112* (1979) 3376.
[16] M. Wolfgruber, F. R. Kreissl, unpublished results.

 © *Verlag Chemie GmbH, 6940 Weinheim, 1983* *0570-0833/83/0202-0149 $ 02.50/0* 

# The First $^{13}$C-ENDOR Investigation of an Organic Triradical in the Quartet State; Synthesis of a Triply $^{13}$C-Labeled Trisgalvinol**

By *Klemens Schubert, Burkhard Kirste,* and *Harry Kurreck**

$^1$H-ENDOR (Electron Nuclear Double Resonance) spectroscopy has hitherto been used successfully for the investigation of organic multi-spin systems with weak electron-interaction up to a tetraradical in the quintet state[2], whereas $^{13}$C-ENDOR studies, besides those on doublet molecules, have been restricted to diradicals in the triplet state[3]. We report here on the synthesis of the triply $^{13}$C-labeled trisgalvinol **5**, which serves as key compound for the generation of mono-, di-, and triradicals. The Scheme opposite outlines the synthesis of labeled trimesic acid ester **4** from 97% enriched $Ba^{13}CO_3$ and the conversion of **4** into **5**.

Figure 1 shows the ESR and ENDOR spectra of the mono-, di- and triradicals accessible from **5** by alkaline $K_3[Fe(CN)_6]$-oxidation. The $^1$H- and $^{13}$C-ENDOR signals for all oxidation steps can be detected. The triradical gives

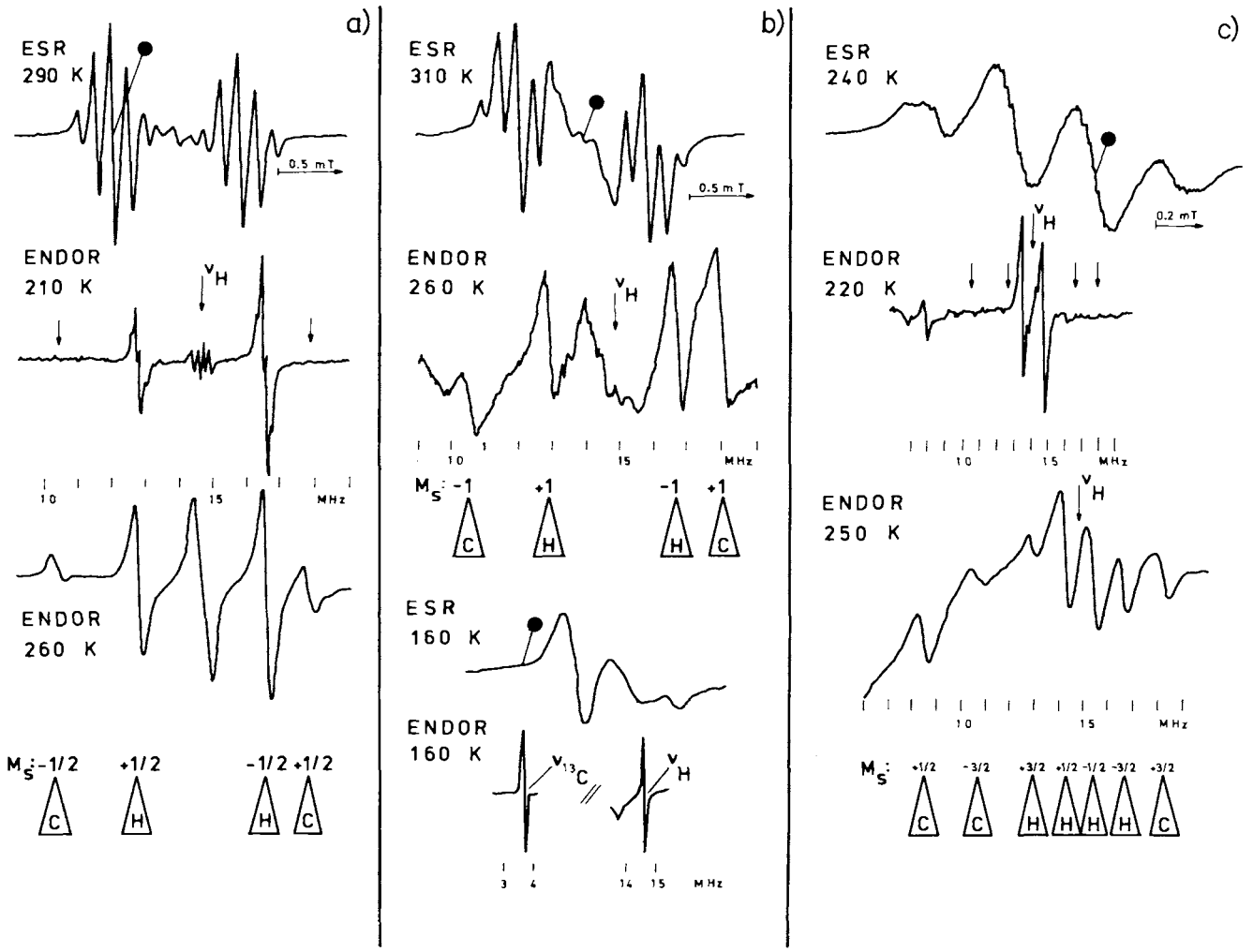



Fig. 1. ESR and ENDOR spectra of **5** in various oxidation states (in toluene). The arrows indicate the calculated resonance positions of signals which appear only at higher temperatures and RF power levels. The bold points indicate the ESR positions chosen for the ENDOR measurements. The RF power levels (P) are naturally cavity-dependent and thus only relative values. They can be converted approximately into field strengths in a rotating frame, $B_{rot}$ [mT] $\simeq 0.07\sqrt{P}$[W]. In our spectrometer configuration the RF power is not constant over the frequency range used. a) Doublet: ESR: $MW_{290K} = 2$ mW; ENDOR: $MW_{210K} = 50$ mW, $RF_{210K} = 25$ W (14 MHz), $MW_{260K} = 50$ mW, $RF_{260K} = 110$ W (15 MHz). b) Triplet: ESR: $MW_{310K} = 2$ mW; ENDOR: $MW_{260K} = 200$ mW, $RF_{160K} = 110$ W (15 MHz), ESR: $MW_{160K} = 6.3$ mW, ENDOR: $MW_{160K} = 200$ mW, $RF_{160K} = 110$ W ($\nu_H$), $RF_{160K} = 330$ W ($\nu_{^{13}C}$). At 160 K the toluene solidifies vitreously. c) Quartet: ESR: $MW_{240K} = 2$ mW, ENDOR: $MW_{220K} = 20$ mW, $RF_{220K} = 55$ W (14 MHz), $MW_{250K} = 200$ mW, $RF_{250K} = 120$ W (15 MHz).

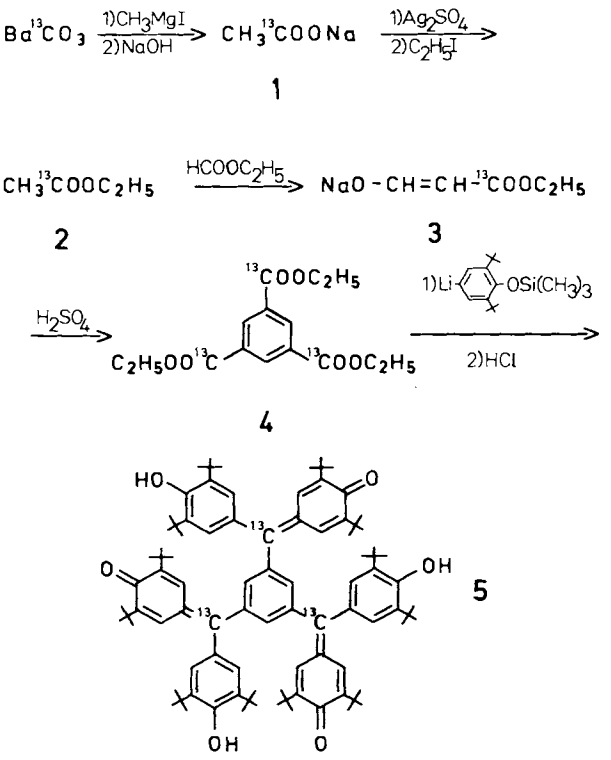
[*] Prof. Dr. H. Kurreck, Dr. K. Schubert
Institut für Organische Chemie der Freien Universität
Takustr. 3, D-1000 Berlin 33 (Germany)
Dr. B. Kirste
Present address: Department of Chemistry,
University of Massachusetts
Boston, MA 02125 (USA)

[**] Delivered in part in a lecture at the Gordon Research Conference "Radical Ions" 1980.—This work was supported by the Fonds der Chemischen Industrie and the Deutsche Forschungsgemeinschaft.

rise to *two* pairs of ENDOR lines for each set of equivalent nuclei, *i.e.* the 12 equivalent *m*-protons and the three equivalent $^{13}$C-nuclei, originating from NMR transitions in the $\pm 1/2$ and $\pm 3/2$ $M_S$ states. This corresponds to the ENDOR resonance condition $\nu_{ENDOR} = |\nu_N - M_S a^S|$, provided $|J| \gg |a|$.

The experimental results of the investigation of the organic multi-spin systems reveal the superiority of ENDOR spectroscopy over conventional ESR. In addition to

 © Verlag Chemie GmbH, 6940 Weinheim, 1983 0570-0833/83/0202-0150 $ 02.50/0 



markedly better resolution and the possibility of selecting the desired species in a mixture by suitable positioning of the external magnetic field, the ENDOR experiment shows *unequivocally* that both the $^1$H- as well as the $^{13}$C-ENDOR signals have to be assigned to diradicals in the triplet state or to triradicals in the quartet state. For the quartet state ($S=3/2$), $|J| \gg |a|$, $a^q_{^{13}C} = -9.4$ MHz and $a^q_{H_m} = +1.2$ MHz holds in the case of small dipolar coupling ($D=22$ MHz).

Received: September 22, 1982 [Z 155 IE]
revised: November 22, 1982
German version: *Angew. Chem. 95* (1982) 149
The complete manuscript of this communication appears in: *Angew. Chem. Suppl. 1983*, 128–139

[2] a) B. Kirste, W. Harrer, H. Kurreck, *Angew. Chem. 93* (1981) 912; *Angew. Chem. Int. Ed. Engl. 20* (1981) 873. b) B. Kirste, H. van Willigen, H. Kurreck, K. Möbius, M. Plato, R. Biehl, *J. Am. Chem. Soc. 100* (1978) 7505, and references cited therein.—$^1$H-ENDOR experiments could recently also be carried out on dicarbene-like systems in the quintet state (single crystals of partially polymerized diacetylene); W. Hartl, Thesis, Universität Bayreuth 1981.

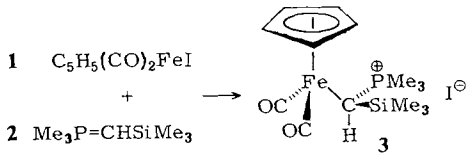
[3] B. Kirste, H. Kurreck, W. Lubitz, K. Schubert, *J. Am. Chem. Soc. 100* (1978) 2292; B. Kirste, H. Kurreck, K. Schubert, *Tetrahedron Lett. 1978*, 777.

## Metal-Induced Carbonylation of a Phosphane-Stabilized "Carbyne Ligand": Conversion of a Phosphorus Ylide-Carbonylmetal Adduct into an $\eta^1$-Ketenyl Complex[1]

By *Siegfried Voran* and *Wolfgang Malisch**

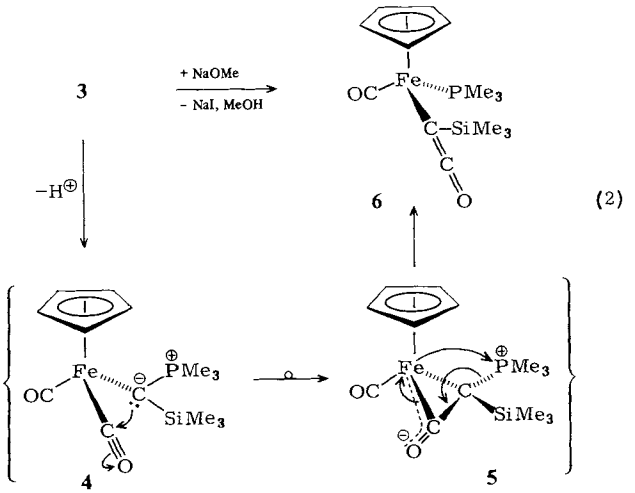
Trialkyl(alkylidene)phosphoranes react with metal-coordinated carbon monoxide *via* addition at the carbon and transylidation[2]. For the $R_3\overset{\oplus}{P}-CH=C(\overset{\ominus}{O})-$ moiety formed by this process at the metal a strong $\pi$-interaction between ylide- and acyl-carbon has been proved, making the carbon monoxide a component of an enolate group[2]. We have now investigated whether carbonyl ligand and ylidic system can be also connected, when the latter is generated directly at the metal center.

The cationic ylide complex **3**, obtainable from the iron iodide **1** and the silylated phosphorus ylide **2**, provides a suitable precursor for the synthesis of a model substance, since silyl substituents usually favor the formation of carbanionic centers.



(1)

Although **3** is inert towards transylidation with **2** or $Me_3P=CH_2$ it can be smoothly deprotonated with sodium methoxide. However, instead of the corresponding neutral complex **4**, its isomer **6** is obtained, containing an $\eta^1$-bonded ketenyl-ligand, which formally derives from the insertion of the carbyne $C(SiMe_3)$ into an Fe–CO bond. **6** forms deep-red crystals (m.p. 65 °C), is very readily soluble in pentane and cyclohexane, and is briefly stable towards air [IR(pentane): $\nu CO_{ketene}$ 2025 (s), $\nu CO$ 1938 (s) $cm^{-1}$].

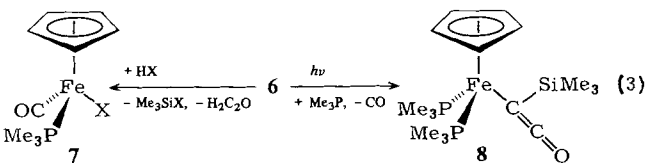


(2)

The plausible rearrangement **4** → **5** → **6** represents a novel type of reaction for metal-ylides[5a,b].

The attempt to perform an $Me_3Si/H$ exchange on **6** with HCl (or $HOSO_2CF_3$) leads to degradation of the metal-ketenyl arrangement with formation of **7**, $Me_3SiCl$ and ketene, which polymerizes under the reaction conditions.

**6** can be converted photochemically in the presence of trimethylphosphane into **8**, which like **6**, shows, neither in boiling benzene nor in acetonitrile, $\eta^2$-coordination with ligand elimination which is characteristic for ketenyl complexes of molybdenum and tungsten[5b].



(3)

X = Cl, $OSO_2CF_3$

[*] Prof. Dr. W. Malisch, S. Voran
Institut für Anorganische Chemie der Universität
Am Hubland, D-8700 Würzburg (Germany)

The intramolecular carbonylation of a carbyne-metal fragment outlined in Scheme (2) is in our opinion of significance in connection with the homogeneously and heterogeneously catalyzed reduction of CO with $H_2$[7a,b], even though there is so far evidence in only one case for the existence of M≡CR units as primary essential species for the carbon-carbon coupling in the Fischer-Tropsch synthesis[7c]. The ketenyl derivatives synthesized from such species by CO addition possibly occur, *inter alia*, as intermediates during formation of oxygen-containing organic compounds. Moreover, reaction (2) shows that the CR part of a metal-bonded ylide moiety $R_3P{=}C-$ is synthetically available and behaves like a carbyne ligand[8].

Received: September 28, 1982 [Z 159 IE]
revised: November 8, 1982
German version: *Angew. Chem. 95* (1983) 151
The complete manuscript of this communication appears in:
*Angew. Chem. Suppl. 1982*, 114–119

[1] Reaction of metal-coordinated carbon monoxide with ylides, Part 9. This work was supported by the Deutsche Forschungsgemeinschaft, the Fonds der Chemischen Industrie, and Hoechst AG, Werk Knapsack.—Part 8: H. Blau, W. Malisch, *J. Organomet. Chem. 235* (1982) C 1.

[2] H. Blau, W. Malisch, *Angew. Chem. 92* (1980) 1063; *Angew. Chem. Int. Ed. Engl. 19* (1980) 1020; H. Blau, W. Malisch, S. Voran, K. Blank, C. Krüger, *J. Organomet. Chem. 202* (1980) C33; S. Voran, H. Blau, W. Malisch, U. Schubert, *ibid. 232* (1982) C33; W. Malisch, H. Blau, U. Schubert, *Chem. Ber.*, in press.

[5] a) F. R. Kreissl, D. Stückler, E. W. Meineke, *Chem. Ber. 110* (1977) 3040; b) F. R. Kreissl, K. Eberl, W. Uedelhoven, *Chem. Ber. 110* (1977) 3782; *112* (1979) 3376.

[7] a) C. K. Rofer-De Poorter, *Chem. Rev. 81* (1981) 447; b) W. A. Herrmann, *Angew. Chem. 94* (1982) 118; *Angew. Chem. Int. Ed. Engl. 21* (1982) 117; c) R. W. Joyner, *J. Catal. 50* (1977) 176.

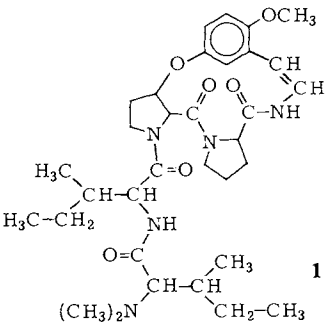
[8] M. R. Churchill, H. J. Wasserman, S. J. Holmes, R. R. Schrock, *Organometallics 1* (1982) 766.

## Total Synthesis of Mucronin B**

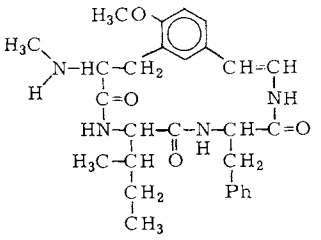
By *Ulrich Schmidt** and *Ute Schanbacher*

Over the last twenty years approximately 80 peptide alkaloids have been isolated and clarified[1]. They complex alkaline metal ions and function as ionophores in plants. In the majority of cases they are active against gram-positive bacteria and fungi. Some inhibit the transfer of energy in chloroplasts.

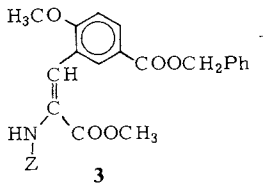
Recently we reported the first total synthesis of a 13-membered peptide alkaloid—of ziziphin A **1**[2a] - and we now describe the first total synthesis of a peptide alkaloid—of mucronin B **2α**[3]—having a 15-membered ring system. As characteristic structural unit it contains a benzene ring with a 12-membered "handle" over the *m*-position. In contrast to the 12- and 13-membered peptide alkaloids, which are derived biogenetically from tyrosine and contain a β-phenoxy amino acid in the ring, in the 15-membered compounds the handle is not linked to the benzene ring *via* a phenol ether function but *via* a C–C bond. The biogenesis of these compounds presumably starts from a *m*-phenylenedialanine.



**1**

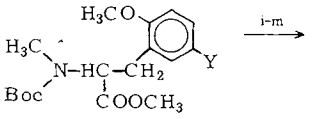


**2α**



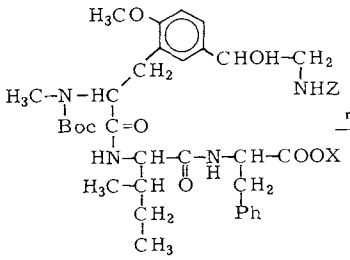
**3**

a-h →



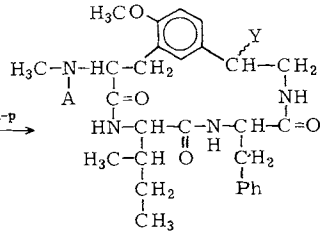
**4:** Y = COOH
**5:** Y = CO–$CH_2$–$COOCH_2Ph$
**6:** Y = CHOH–$CH_2$–NHZ

i-m →



**7:** X = $CH_3$
**8:** X = H
**9:** X = $C_6F_5$

n-p →



**10α + 10β:** Y = OH, A = Boc
**11α + 11β:** Y = $OCOCH_3$, A = Boc
**12α + 12β:** Y = SePh, A = H
**α:** *SSS* [4]
**β:** *RSS* [4]

q → **2α** + **2β** → **2α**

**3** → **6** : 50%
**6** → **9** : 65%
**9** → **11α** + **11β** : 60%
**11α** + **11β** → **2α** + **2β** : 40%

a: $CH_3I$, $K_2CO_3$, DMF, RT, 3 d; b: $H_2$/Pd, $CH_3OH$, RT, 3 bar, 5 h; c: $O(COOtBu)_2$, Dioxane/$H_2O$, $NaHCO_3$, 10 h; d: Carbonyldiimidazole, THF, RT, 0.5 h; e: $Mg(OOC{-}CH_2{-}COOCH_2Ph)_2$, THF, 50 °C, 5 h; f: $NaNO_2$, $CH_3COOH/H_2O$ (2:1), 0 °C, 2 h; g: $H_2$/Pd, $CH_3COOH$, RT, 9 h; h: $ClCOOCH_2Ph$, Dioxane/$H_2O$, $NaHCO_3$, 0 °C, 10 h; i: NaOH, $H_2O$/Dioxane, RT, 4 h; k: Dicyclohexylcarbodiimide (DCCD), (*S,S*)-H-Ile-Phe-$OCH_3$, $CH_2Cl_2$, 0 °C, 10 h; l: NaOH, $H_2O$/Dioxane, RT, 4 h; m: DCCD, $C_6F_5OH$, $CH_2Cl_2$, 0 °C, 10 h; n: $H_2$/Pd, Dioxane, 95 °C, 5 h; o: $Ac_2O$, Pyridine, RT, 20 h; p: 10 $CF_3COOH$, 1.2 PhSeH, 50 °C, 20 h; q: 3 $NaIO_4$, THF/$CH_3OH/H_2O$ (1:2:1), RT, 0.5 h.—Z = $PhCH_2OCO$, Boc = *t*BuOCO.

The dehydroamino acid **3** serves as starting material for the synthesis of mucronin[2b]. After *N*-methylation, hydrogenation, and introduction of the Boc group to afford **4**, the carboxy group was transformed into the aminoethanol size chain (**4** → **5** → **6**). Hydrolysis of **6** to give the amino acid and coupling with Ile-Phe-$OCH_3$ led to the tripeptide **7**, which was converted into the pentafluorophenyl ester **9**, the educt for the ring closure. Cyclization proceeded by "catalytic hydrogenation under high-dilution conditions"[2c]. The high yields (85%) of ring compounds **10α** and **10β**[4] provide further evidence for the superiority of this ring-closure method, compared to conventional methods, for the synthesis of 12- to 15-membered cyclopep-

[*] Prof. Dr. U. Schmidt, U. Schanbacher
Institut für Organische Chemie der Universität
Pfaffenwaldring 55, D-7000 Stuttgart 80 (Germany)

[**] Synthesis of Peptide Alkaloids, Part 8; Amino Acids and Peptides, Part 40. This work was supported by the Fonds der Chemischen Industrie, BASF AG, and the Deutsche Forschungsgemeinschaft. Dr. W. Rozdzinski is thanked for numerous mass spectra and Prof. Dr. K.-D. Jany for the determinations of *allo*-isoleucine. Degussa AG is thanked for a generous gift of amino acids and noble metal catalysts.—Part 7: *Liebigs Ann. Chem.*, in press; Part 39: *Angew. Chem.*, in press.

tides[5]. The acetate mixture **11α + 11β** was purified by treatment with trifluoroacetic acid/selenophenol to afford the mixture of diastereomeric phenyl selenides **12α + 12β**. Oxidative elimination ($NaIO_4$) to exclusively the (*Z*)-olefin yielded mucronin **2α** and the diastereomeric isomucronin **2β**, which were completely separated by chromatography. MS, NMR, and optical rotation measurements of the synthetic mucronin were identical with those of the natural product.

Received: September 27, 1982;
revised: October 29, 1982 [Z 158 IE]
German version: *Angew. Chem. 95* (1983) 150

[1] Review: R. Tschesche, E. K. Kaussmann in R. H. Manske: *The Alkaloids, Vol. 15*, Academic Press, New York 1975.

[2] a) U. Schmidt, A. Lieberknecht, H. Bökens, H. Griesser, *Angew. Chem. 93* (1981) 1121; *Angew. Chem. Int. Ed. Engl. 20* (1981) 1026; b) U. Schmidt, A. Lieberknecht, U. Schanbacher, Th. Beuttler, J. Wild, *ibid. 94* (1982) 797; *21* (1982) 770; *Angew. Chem. Suppl. 1982*, 1682; example **6d**; c) U. Schmidt, A. Lieberknecht, H. Griesser, J. Talbiersky, *Angew. Chem. 93* (1981) 271; *Angew. Chem. Int. Ed. Engl. 20* (1981) 280; *J. Org. Chem. 47* (1982) 3261.

[3] H.-W. Fehlhaber, J. Uhlendorf, S. T. David, R. Tschesche, *Liebigs Ann. Chem. 759* (1972) 195.

[4] In compounds **8–10** a mixture of four diastereomers is present in each case. The spatial arrangement at the benzyl site and at the Ile side-chain is not, however, considered in the designation.

[5] J. C. Lagarias, R. A. Houghten, H. Rapoport, *J. Am. Chem. Soc. 100* (1978) 8202; D. Goff, J. C. Lagarias, W. C. Shih, M. P. Klein, H. Rapoport, *J. Org. Chem. 45* (1980) 4813; F. Rocchiccioli, F. X. Jarreau, M. Pais, *Tetrahedron 34* (1978) 2917.

## Reversible Opening of a Thioketene-Iron Cluster Containing a $\mu_2$-$C_2$,$\mu_2$-*S*-Thiocarbonyl Group[1]

By *Henning Umland, Frank Edelmann, Detlev Wormsbächer,* and *Ulrich Behrens**

In previously known metal complexes the thiocarbonyl group of thioketones, thioketenes, and carbon disulfide functions mostly as a two-electron donor. X-ray crystallographic analysis of the thioketene-iron cluster **2** has established for the first time a C=S group which provides six electrons for the metal-ligand bonding. In addition, **2** exhibits a further special structural feature: a dipolar molecule with positive charge on C2 (metal-stabilized carbenium ion) and the negative charge delocalized over the tetrahedral $Fe_2CS$ cluster framework (cf. formula **2a** and Fig. 1). Rotation about the C1-C2 axis is not observed up to 100 °C (stabilization of the carbenium ion by hyperconjugation). [**2a**: $^1$H-NMR (270 MHz, [$D_8$]-toluene, 95 °C): $\delta = 0.91$ (s, $2CH_3$), 1.04 (s, $2CH_3$), 1.17 (m, $CH_2$), 1.30 (m, $2CH_2$); $^{13}$C-NMR (22.63 MHz, $CDCl_3$, 30 °C): $\delta = 118.7$ (C1), 219.3 (C2), 44.6, 45.8 (C3, C7), 38.5, 39.1 (C4, C6). 16.8 (C5), 32.4, 34.4 (C8, C11), 211.1 (CO)].

The most characteristic property of the hexacarbonyl compound **2a** is its smooth reaction with triphenylphosphane at room temperature to afford the half-opened cluster **8a**; the dinuclear iron complex reacts analogously with trialkylphosphanes and phosphites. The structure of **8a** was determined by X-ray crystallography[4].

Photochemically induced scission of CO from **8a** leads to the closed cluster **2b**. By further addition of phosphane and renewed elimination of CO this reaction cycle can be repeated to form the disubstituted compound **2c**. All CO-eliminations are reversible. The stepwise exchange of CO by $PPh_3$ in **2** stabilizes the carbenium ion markedly [$^{13}$C-NMR: $\delta = 219.3$ (**2a**), 210.4 (**2b**), 183.7 (**2c**)].

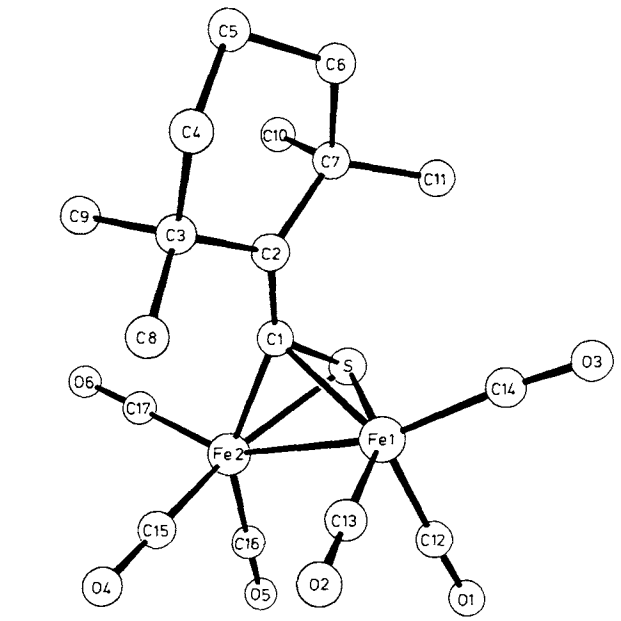
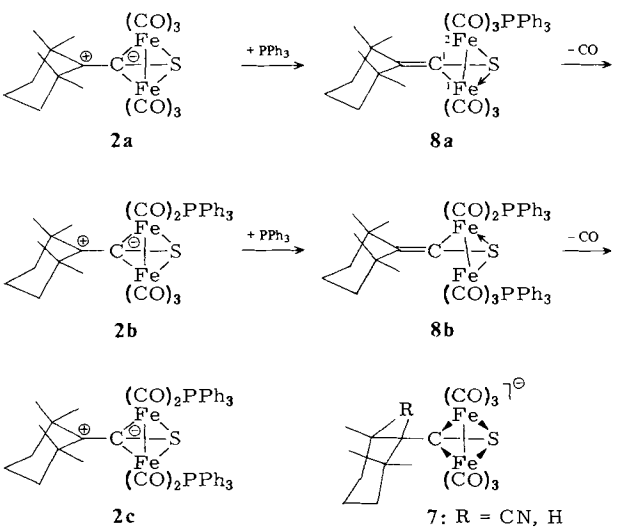



Fig. 1. Structure of the thioketene complex **2a** in the crystal. $R = 0.045$. Selected bond lengths [pm] and angles [°]: C1–Fe1 206.4(9), C1–Fe2 193.8(10), C1–S 173.3(10), Fe1–S 222.9(3), Fe2–S 222.0(3), Fe1–Fe2 251.8(2), C1–C2 136.1(14); C2–C1–Fe1 113.4(7), C2–C1–Fe2 155.2(8), C2–C1–S 129.8(8), C3–C2–C1 118.7(9), C7–C2–C1 121.7(9), C7–C2–C3 118.3(9) [5].




In contrast to phosphanes, anions such as $CN^-$ or $H^-$ (from $BH_4^-$) add to **2a** to afford the negatively charged complexes **7**, with retention of the closed tetrahedral cluster.

Received: September 30, 1982;
revised: November 12, 1982 [Z 161 IE]
German version: *Angew. Chem. 95* (1983) 148
The complete manuscript of this communication appears in: *Angew. Chem. Suppl. 1983*, 156–168

[*] Priv.-Doz. Dr. U. Behrens, H. Umland, F. Edelmann, D. Wormsbächer
Institut für Anorganische und Angewandte Chemie der Universität
Martin-Luther-King-Platz 6, D-2000 Hamburg 13 (Germany)

[1] Transition Metal-Thioketene Complexes, Part 4. This work was supported by the Deutsche Forschungsgemeinschaft.—Part 3: D. Wormsbächer, F. Edelmann, U. Behrens, *Chem. Ber. 115* (1982) 1332.

[4] D. Wormsbächer, Dissertation, Universität Hamburg 1982.—Selected atomic distances in **8a**: C1–Fe1 198.6(8), C1···Fe2 310.7(8), C1–S

 © *Verlag Chemie GmbH, 6940 Weinheim, 1983* *0570-0833/83/0202-0153 $ 02.50/0* 

173.5(8), Fe1–S 218.2(2), Fe2–S 227.9(2), Fe1–Fe2 267.5(1), C=C1 134.0(12) pm.

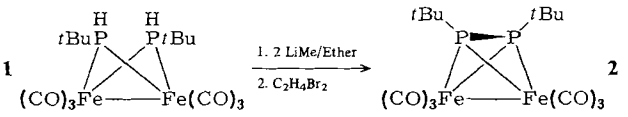
[5] Details of the crystal structure investigation can be obtained from the Fachinformationszentrum Energie Physik Mathematik, D-7514 Eggenstein-Leopoldshafen by quoting the depository number CSD 50259, the name of the author and the citation of the journal.

## A Diphosphene as Tetrahedrane Building Block: Synthesis of $[Fe_2(CO)_6(P_2tBu_2)]$**

By *Heinrich Vahrenkamp** and *Doris Wolters*

Diorganodiphosphenes $R_2P_2$ are stable in the free form only when bearing very bulky substituents R[1]. To our knowledge, unlike the analogous compounds $Ph_2As_2$ and $Ph_2Sb_2$, they were previously unknown in the form of complex ligands[2][***]. We have now succeeded in carrying out a directed synthesis of an $R_2P_2$ species (R = *t*Bu) in the ligand sphere of a complex.

The doubly *t*BuPH-bridged dinuclear complex **1**[3] was deprotonated with MeLi (ether, 0 °C); *in situ* oxidation of the intermediate with 1,2-dibromoethane (ether, 0 °C→RT), evaporation to dryness, dissolution in *n*-hexane, and chromatography on silica gel, (*n*-hexane/benzene, 10:1) furnished the complex **2** (red crystals, m.p. 120 °C (decomp.) 11% yield).




Complex **2** was identified by elemental analysis and spectra: IR ($C_6H_{12}$): $\nu = 2053$ (m), 2015 (s), 1988 (vs), 1968 (s), 1958 (m) $cm^{-1}$; NMR ($CDCl_3$): $\delta = 1.52$, $J = 22.0$ Hz, EI-MS: $m/z$ 456 ($M^+$). A crystal structure analysis revealed the molecular geometry given in Figure 1[4].

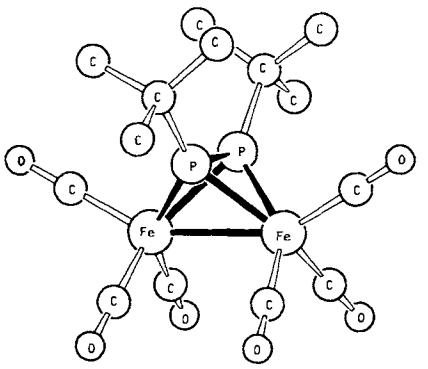



Fig. 1. Structure of $[Fe_2(CO)_6(P_2tBu_2)]$ **2** in the crystal [4]. Bond lengths: Fe-Fe 274.0(1), P-P 205.9(3), Fe-P 221.2–223.2(2) pm.

[*] Prof. Dr. H. Vahrenkamp, D. Wolters
Institut für Anorganische und Analytische Chemie der Universität
Albertstr. 21, D-7800 Freiburg (Germany)

[**] This work was supported by the Fonds der Chemischen Industrie and the Rechenzentrum der Universität Freiburg. We thank Dr. *K. Steinbach*, Marburg, for recording the mass spectrum.

[***] Note added in proof (January 10, 1983): A mononuclear complex of $P_2(SiMe_3)_2$ has recently been described: B. Deppisch, H. Schäfer, *Z. Anorg. Allg. Chem. 490* (1982) 129.

The tetrahedrane molecule **2** is isoelectronic and structurally related to the $R_2N_2$- and $S_2$-analogues[5]. However, whereas the N–N bond in $[Fe_2(CO)_6(N_2Me_2)]$ and the S–S bond in $[Fe_2(CO)_6S_2]$ are about the same length as a normal N–N or S–S single bond, the P–P bond in **2**, with a length of *ca.* 206 pm, is markedly shorter than a P–P single bond in oligophosphanes; it is almost the same length as the P–P bond in the diphosphene $P_2(C_6H_2tBu_3)_2$ (203 pm)[1]. Hence, the classification of the ligand $P_2tBu_2$ in **2** as diphosphene appears justified.

To achieve an 18-electron balance for each iron atom, the diphosphene must function as a 6-electron ligand (one π-electron pair and two n-electron pairs). According to *Hoffmann*'s isolobal relationship[6] $[(CO)_3FE^{\ominus} \rightarrow \delta \leftarrow CH$ and $RP^{\oplus} \rightarrow \delta \leftarrow CH]$ the complex **2** can be regarded as a derivative of the tetrahedrane $(CH)_4$.

Received: September 30, 1982 [Z 163 IE]
German version: *Angew. Chem. 95* (1983) 152

[1] M. Yoshifuji, I. Shima, N. Inamoto, K. Hirotsu, T. Higuchi, *J. Am. Chem. Soc. 103* (1981) 4587; however, see also A. H. Cowley, J. E. Kilduff, T. H. Newman, M. Pakulski, *ibid. 104* (1982) 5820; C. Couret, J. Escudié, J. Satgé, *Tetrahedron Lett. 23* (1982) 4941; E. Niecke, R. Rüger, *Angew. Chem. 95* (1983) 154; *Angew. Chem. Int. Ed. Engl. 22* (1983) 155.

[2] M. Jacob, E. Weiss, *J. Organomet. Chem. 153* (1978) 31; G. Huttner, U. Weber, B. Sigwarth, O. Scheidsteger, *Angew. Chem. 94* (1982) 210; *Angew. Chem. Int. Ed. Engl. 21* (1982) 215; *Angew. Chem. Suppl. 1982*, 411.

[3] P. M. Treichel, W. K. Dean, W. M. Douglas, *Inorg. Chem. 11* (1972) 1609.

[4] Monoclinic; $P2_1/n$; $a = 1543.5(2)$, $b = 1543.1(2)$, $c = 853.9(1)$ pm; $\beta = 91.34(1)°$; $Z = 4$; 3336 reflections, $R$ (anisotropic, without H-atoms) = 0.051. Further details about the crystal structure investigation can be obtained on request from the Fachinformationszentrum Energie Physik Mathematik, D-7514 Eggenstein Leopoldshafen, quoting the depository number CSD 50242, the name of the authors and full citation of the journal.

[5] Cf. B. K. Teo, M. B. Hall, R. F. Fenske, L. F. Dahl, *Inorg. Chem. 14* (1975) 3103.

[6] R. Hoffmann, *Angew. Chem. 94* (1982) 725; *Angew. Chem. Int. Ed. Engl. 21* (1982) 711 (Nobel lecture).

## Photochemical Four-Electron Redox Reaction of Hexaazidoplatinate(IV)**

By *Arnd Vogler** and *Joachim Hlavatsch*

In many transition-metal complexes intramolecular photoredox reactions occur, in which an electron is transfered from a ligand to the metal (one photon-one electron redox reaction). In contrast, only a few photo-induced two-electron transfer reactions are known. Reactions of this type are meeting with increasing interest in connection with photosynthesis or in the photochemical cleavage of water[1]. Reductive eliminations are particularly straightforward intramolecular two-electron redox reactions of metal complexes. Here, two ligands are oxidatively cleaved off and the metal is reduced by two units by the electrons from the ligands. Some reactions of this type have also been observed to occur photochemically[2] (one photon—two electron redox reaction). We now report on two consecutive reductive photoeliminations (two photon—four electron redox reaction). By this means $Pt^{IV}$ is reduced to $Pt^0$ *via* $Pt^{II}$, whereas in total four ligands are oxidatively cleaved off.

[*] Prof. Dr. A. Vogler, J. Hlavatsch
Institut für Anorganische Chemie der Universität
Universitätsstrasse 31, D-8400 Regensburg 2 (Germany)

[**] This work was supported by the Deutsche Forschungsgemeinschaft and by the Fonds der Chemischen Industrie.

The complex ion $[Pt(N_3)_6]^{2-}$, first synthesized and characterized by *Beck et al.*[3], has a charge-transfer band ($N_3 \rightarrow Pt$) at $\lambda_{max} = 308$ nm ($\varepsilon = 37\,154$)[3]. Irradiation of a solution of $[Pt(N_3)_6]^{2-}$ in $CH_2Cl_2$ with light of wavelength $\lambda = 314$ nm led to photolysis of the complex ion. Over the complete absorption region of the ion between 590 and 285 nm[4] the extinction decreased by the same ratio at all wavelengths. Simultaneously, bubbles of nitrogen were evolved from the solution. From this observation we conclude that photolysis according to

$$[Pt^{IV}(N_3)_6]^{2-} \longrightarrow [Pt^{II}(N_3)_4]^{2-} + 3\,N_2$$

occurs. The decrease in extinction is accounted for by the considerably smaller absorption of the primary photolysis product $[Pt(N_3)_4]^{2-}$ over the entire absorption range relative to that of $[Pt(N_3)_6]^{2-}$[3]. Upon complete absorption of light ($A \geq 2$) by $[Pt(N_3)_6]^{2-}$ the photolysis proceeds with zero order. Irradiation with light of wavelength $\lambda = 314$ nm gives a quantum yield $\Phi = 0.27$.

If irradiation is further continued the solution becomes black due to precipitation of colloidal platinum. As a consequence this caused an increase in extinction which became larger with decreasing wavelength, such as is expected for light scattering by the colloidal particles. Simultaneously, evolution of bubbles of nitrogen continued. Moreover, azide was released, which could be quantitatively determined by spectrophotometry of its $Fe^{III}$ complex[2a]. These observations are consistent with the following secondary photolysis.

$$[Pt^{II}(N_3)_4]^{2-} \longrightarrow Pt^0 + 3\,N_2 + 2\,N_3^-$$

The same result was also obtained by direct photolysis of $[Pt^{II}(N_3)_4]^{2-}$[3] in a separate experiment. The quantum yield for the photolysis of $[Pt(N_3)_4]^{2-}$ is $\Phi = 0.17$ at an excitation wavelength of $\lambda = 314$ nm.

Formation of colloidal platinum during the photolysis of $[Pt(N_3)_6]^{2-}$ and of $[Pt(N_3)_4]^{2-}$ is also interesting in connection with heterogeneous catalysis by platinum metal. It is known that the catalytic activity increases as the size of the colloidal particles decreases[1]. Photolysis of azidoplatinate complexes could lead to better control of the particle size.

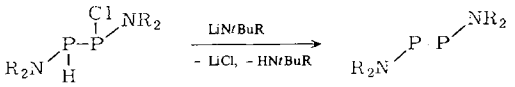
Received: September 30, 1982;
revised: December 10, 1982 [Z 165 IE]
German version: *Angew. Chem. 95* (1983) 153

[1] M. Grätzel, *Acc. Chem. Res. 14* (1981) 376.
[2] a) A. Vogler, A. Kern, B. Fusseder, J. Hüttermann, *Z. Naturforsch. B 33* (1978) 1352; b) A. Vogler, R. E. Wright, H. Kunkely, *Angew. Chem. 92* (1980) 745; *Angew. Chem. Int. Ed. Engl. 19* (1980) 717; c) A. Vogler, H. Kunkely, *J. Am. Chem. Soc. 103* (1981) 6222.
[3] W. Beck, W. P. Fehlhammer, P. Pöllmann, E. Schuierer, K. Feldl, *Chem. Ber. 100* (1967) 2335.
[4] $[Pt(N_3)_6]^{2-}$ was studied as its $[As(C_6H_5)_4]^+$ salt. The cation exhibits intense self-absorption below 285 nm.

## Tetrakis(trimethylsilyl)diaminodiphosphene**

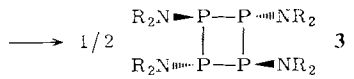
By *Edgar Niecke** and *Reinhold Rüger*

The synthesis of the first stable diphosphene has recently been reported[1]. We have now found that base-induced "HCl"-elimination from the diphosphene **1**[2] affords entry to a novel, further example of this interesting class of compounds with phosphorus-phosphorus (p-p)π bonding.

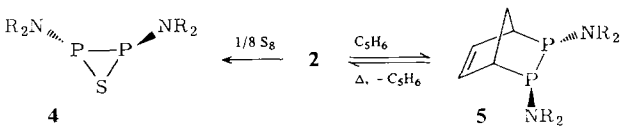



**1** R = $SiMe_3$ **2**

The pyrophoric diaminodiphosphene **2** is a ruby-red liquid at room temperature. In solution, the compound is stable for several days; without solvent it dimerizes within hours to the cyclotetraphosphane **3**[3a,b], which can be isolated as a crystalline, colorless, almost inert solid.




The synthetic potential of **2** has already been demonstrated by its reactions with sulfur or cyclopentadiene, which lead to cycloaddition products—the thiadiphosphirane **4**[3a,c] and the 2,3-diphosphanorbornene **5**, respectively, each of which forms only one isomer. According to the NMR data[4] only the *trans*-form of **5** is formed.




**4** **5**

No cycloreversion takes place in the case of **4**, at least up to 150 °C, whereas **5** already decomposes above 40 °C into its components, and it can thus serve as a storable source of the diphosphene.

The composition and structure of the tetrasilylated diaminodiphosphene **2** and its reaction products **3**—**5** are confirmed by elemental analysis, mass spectra (**2**—**4**), and NMR data[4]. Noteworthy is the extremely large downfield shift of the $^{31}P$-NMR signal of $\delta = 572$ in the case of **2** (30% in $CD_2Cl_2$, $H_3PO_4$ ext.)[5]. The $^1H$-, $^{13}C\{^1H\}$- and $^{29}Si\{^1H\}$-NMR spectra (30%, in $CD_2Cl_2$, TMS int.) show the groups of signals with pseudo-triplet structure that are to be expected for free rotation about the P–N bond: $\delta(^1H) = 0.32$ (1.2 Hz), $\delta(^{13}C) = 3.4$ (8.4 Hz), $\delta(^{29}Si) = 7.1$ (2.8 Hz).

Received: October 14, 1982 [Z 175 IE]
revised: November 23, 1982
German version: *Angew. Chem. 95* (1983) 154

[*] Prof. Dr. E. Niecke, Dr. R. Rüger
Fakultät für Chemie der Universität
Postfach 8640, D-4800 Bielefeld 1 (Germany)

[**] This work was supported by the Deutsche Forschungsgemeinschaft and the Fonds der Chemischen Industrie.

[1] M. Yoshifuji, I. Shima, N. Inamoto, K. Hirotsu, T. Higuchi, *J. Am. Chem. Soc. 103* (1981) 4587; B. Cetinkaya, P. B. Hitchcock, M. F. Lappert, A. J. Thorne, H. Goldwhite, *J. Chem. Soc. Chem. Commun. 1982*, 691; G. Bertrand, C. Couret, J. Escudie, S. Majid, J. P. Majoral, *Tetrahedron Lett. 23* (1982) 3567.
[2] E. Niecke, R. Rüger, *Z. Naturforsch. B 37* (1982) 1593.
[3] The stereochemistry of **2**, **3**, and **4** cannot be derived unequivocally from the NMR data; structural investigations on similar compounds indicate that **2**, **3**, and **4** might also contain *trans*-oriented amino groups.—b) **3** has already been identified as a decomposition product of tetraphosphabicyclobutane, $P_4(NR_2)_2$: E. Niecke, R. Rüger, B. Krebs, *Angew. Chem. 94* (1982) 553; *Angew. Chem. Int. Ed. Engl. 21* (1982) 544.—c) The synthesis of a thiadiphosphirane by cyclocondensation has been reported: M. Baudler, H. Suchomel, G. Fürstenberg, U. Schings, *ibid. 93* (1981) 1087 and 20 (1981) 1044.

[4] **2**: MS (70 eV) $m/z$ 382 ($M^+$, 4%), 73 (R, 100%). **3**: decomp. 230 (5) °C; $m/z$ 764 ($M^+$, 6%), 73 (R, 100%); $\delta(^{31}P)=63.8$, $\delta(^{13}C)=5.1$, $\delta(^{29}Si)=9.5$. **4**: b.p. = 105–108 °C/0.1 torr; $m/z$ 414 ($M^+$, 9%), 73 (R, 100%); $\delta(^{31}P)=-21.9$, $\delta(^{13}C)=4.6$ ($|J_{CP}+J_{CP'}|=11.6$ Hz), $\delta(^{29}Si)=9.2$ ($|J_{SiP}+J_{SiP'}|=6.5$ Hz). **5**: decomp. 40–45 °C; $\delta(^{31}P)=57.4$, 64.2 ($J_{PP}=330.2$ Hz), $\delta(^{13}C)=5.7$ ($|J_{CP_A}+J_{CP_B}|=13.0$ Hz), 39.2 (22.5 Hz), 47.2 (51.3 Hz), 54.3 (43.6 Hz), 128.3 (12.2 Hz), 134.8 (12.3 Hz), $\delta^{29}Si=6.8$, 7.8 ($|J_{SiP_A}+J_{SiP_B}|=12.2$, 12.4 Hz).

[5] The phosphorus nucleus with $\delta=561$ is similarly strongly deshielded in the diaminodiphosphene $(Me_2tBuSi)_2N-P=P-N(SitBuMe_2)_2$: E. Niecke, R. Rüger, M. Lysek, S. Pohl, W. Schoeller, unpublished. Even stronger deshielding has been found in the dialkyldiphosphene $(Me_3Si)_3C-P=P-C(SiMe_3)_3$: A. H. Cowley, J. E. Kilduff, T. H. Newmann, M. Pakulski, *J. Am. Chem. Soc. 104* (1982) 5820; C. Couret, J. Escudié, J. Stagé, *Tetrahedron Lett. 23* (1982) 4941.

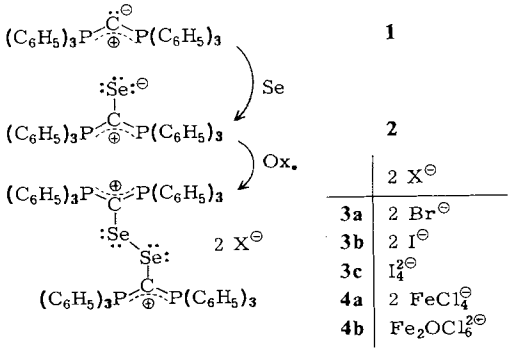
[6] *Experimental:* A solution of **1** (20.9 g, 0.05 mol) and $LiNtBuSiMe_3$ (7.5 g, 0.05 mol) in diethyl ether (150 mL) was stirred for 5 h at room temperature, whereupon the solution turned deep-red. After removal of precipitated LiCl by filtration and of most of the solvent and $HNtBuSiMe_3$ by evaporation, the resulting residue was fractionated by short-path distillation. The diphosphene 2 distilling over at 84–87 °C/0.1 torr was collected in an ice-cooled receiver. Yield 8.6 g (45%). The residue contained essentially **3**, which was isolated by recrystallization from petroleum ether (100–140 °C) as a pure crystalline solid, which is practically inert towards water.

## Oxidative Coupling of the Selenolate Functions in $(C_6H_5)_3PC(Se)P(C_6H_5)_3$: Crystal Structure of $[[(C_6H_5)_3P]_2CSe]_2^{2\oplus}Fe_2OCl_6^{2\ominus}\cdot 4CH_2Cl_2$ Containing a Linear Fe–O–Fe Axis

By *Hubert Schmidbaur**, *Christian E. Zybill*, and *Dietmar Neugebauer*

Redox systems with thiolate/disulfide or selenolate/diselenide pairs are currently of widespread interest. We recently discovered that addition of chalcogen atoms to hexaphenylcarbodiphosphorane **1** under mild conditions furnishes novel thiolate/selenolate zwitterions **2**, in which the cationic component is formed from a carbodiphosphorane moiety[4]. The thiolate-analogous behavior of these compounds suggested the possibility of an oxidative coupling to give products containing disulfide or diselenide bridges. Preliminary redox-potential measurements indeed demonstrated[5] that, *e.g.*, **2** can be oxidized electrochemically already at a potential of *ca.* −0.36 V.

The use of chemical oxidizing agents on a preparative scale in an inert solvent allowed the isolation of crystalline products which contain the diselenide dication corresponding to **2**. Thus, elemental bromine or iodine yield the halides or polyhalides **3a–c**, respectively. The constitution of the anion in the salt **3c** is still uncertain, though spectroscopic investigations (FIR and Raman data) indicate the presence of the dianion $I_4^{2\ominus}$ [6].




| | 2 X⊖ |
|---|---|
| **3a** | 2 $Br^{\ominus}$ |
| **3b** | 2 $I^{\ominus}$ |
| **3c** | $I_4^{2\ominus}$ |
| **4a** | 2 $FeCl_4^{\ominus}$ |
| **4b** | $Fe_2OCl_6^{2\ominus}$ |

[*] Prof. Dr. H. Schmidbaur, Ch. E. Zybill, Dr. D. Neugebauer
Anorganisch-chemisches Institut der Technischen Universität München
Lichtenbergstr. 4, D-8046 Garching (Germany)

With four equivalents of anhydrous $FeCl_3$ in dichloromethane the tetrachloroferrate(III) **4a** was obtained along with two parts of $FeCl_2$. However, on working with solvents not previously dried or on addition of stoichiometric amounts of water, the μ-oxo-hexachlorodiferrate(III) **4b** was generated, which precipitates as red-brown triclinic crystals.

X-ray diffraction analysis of **4b** (still containing 4 molecules of $CH_2Cl_2$) confirmed the structure of the dication (Fig. 1) and of the dianion (Fig. 2).

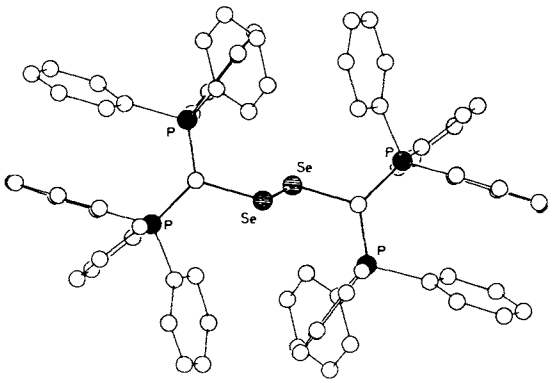



Fig. 1. Structure of the cation in $[[(C_6H_5)_3P]_2CSe]_2^{2\oplus}Fe_2OCl_6^{2\ominus}\cdot 4CH_2Cl_2$.

Interestingly, the structural details of **1** as determined repeatedly by X-ray diffraction[3] show remarkably little alteration on conversion of **1** into the selenide **2**[4] and on subsequent oxidation to **3**, **4**. The ylidic C atoms in **4b** are planar configurated, as in **2** ($P_2CSe$). The Se–Se bond, which contains a crystallographic center of symmetry, is not unusual at $d(SeSe)=249.2(2)$ pm.

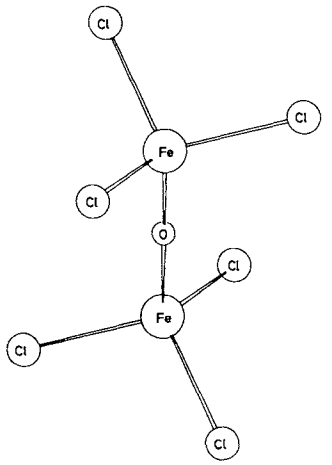



Fig. 2. Structure of the anion in $[[(C_6H_5)_3P]_2CSe]_2^{2\oplus}Fe_2OCl_6^{2\ominus}\cdot 4CH_2Cl_2$.

The $Fe_2OCl_6^{2\ominus}$ anion is also centrosymmetric in the crystal lattice (Fig. 2). The IR absorption $\nu_{as}$(FeOFe) is found at 832 $cm^{-1}$, $\nu$(FeCl) at 378 and 321 $cm^{-1}$. Associated with this symmetry are a staggered arrangement of the 2×3 chlorine atoms and also the linearity of the Fe–O–Fe axis. This linear geometry is novel for the $Fe_2OCl_6^{2\ominus}$ anion as well as for all other known compounds with $Fe^{III}-O-Fe^{III}$ bridging which show strongly bent oxo linkages[8]. The magnetic behavior of such complexes and

 © Verlag Chemie GmbH, 6940 Weinheim, 1983 0570-0833/83/0202-0156 $ 02.50/0 

other aspects of their structure are currently under investigation.

Received: October 19, 1982 [Z 181 IE]
revised: November 10, 1982
German version: *Angew. Chem. 95* (1983) 161
The complete manuscript of this communication appears in: *Angew. Chem. Suppl. 1983*, 169—183

CAS Registry numbers:
**2**, 82813-08-9; **3a**, 84369-05-1; **3b**, 84369-06-2; **3c**, 84369-07-3; **4a**, 84369-03-9; **4b**, 84369-04-0.

[3] Cf. H. Schmidbaur, G. Hasslberger, U. Deschler, U. Schubert, C. Kappenstein, A. Frank, *Angew. Chem. 91* (1979) 437; *Angew. Chem. Int. Ed. Engl. 18* (1979) 408, and references cited therein.
[4] H. Schmidbaur, Ch. E. Zybill, D. Neugebauer, *Angew. Chem. 94* (1982) 321; *Angew. Chem. Int. Ed. Engl. 21* (1982) 310; *Angew. Chem. Suppl. 1982*, 590—605.
[5] We thank Mr. R. Bruchhaus, Technische Universität München, for these measurements.
[6] K.-F. Tebbe, *Z. Anorg. Allg. Chem. 489*, 93 (1982), reports a broad absorption at 143—152 $cm^{-1}$ in the IR spectrum of $[Cu(NH_3)_4]I_4$.
[8] K. S. Murray, *Coord. Chem. Rev. 12* (1974) 1; M. G. B. Drew, V. McKee, S. M. Nelson, *J. Chem. Soc. Dalton Trans. 1978*, 80.

## Some Substituent Effects in the Photocycloaddition of Dihalomaleiimides to Uracils**

By *Géza Szilágyi* and *Heinrich Wamhoff**

*Dedicated to Professor Alexander Schönberg on the occasion of his 90th Birthday*

As model reactions in photochemotherapy[1] we have studied the photoreactions of the 1,3-dimethyluracils **1a—e** and of 1,3-dimethyl-6-azauracil **6** with dibromo-*N*-methylmaleiimide **2** and with the phenyl-substituted dichloro-*N*-phenylmaleiimides **7a—c**, very few reports on which have so far appeared in the literature[3,4]. Of particular interest in such reactions are the substituent effects and the tendency for cycloaddition (→ **3a—d**, **4b**, **8a**, **b**) and photosubstitution (→ **5a**, **c**, **9a—c**) to take place.

Long-wavelength UV-irradiation (Hg high-pressure lamp HPK 125 W, $\lambda > 313$ nm) of 10 mmol **1a—e** with equimolar amounts of **2** in acetone (200 mL solvent and sensitizer) yielded, aside from the *cis,anti,cis*- and *cis,syn,cis*-[2+2]-cycloadducts **3a—d** and **4b**, the photosubstitution products **5a**, **c**.

According to Table 1, the steric effect is the controlling factor for the direction and stereochemistry of the fusion in the reaction of **1a—c** and **2**. In comparison to the reaction of **1a** and **2**[4] the preparative yields of cycloadducts

Table 1. Preparative yields of **3a—d**, **4b**, and **5a**, **c**.

| Educt | $R^1$ | $R^2$ | Products; Yield [%] | | | | | |
|---|---|---|---|---|---|---|---|---|
| **1a** | H | H | **3a** | 41 | — | | **5a**[1] | 1 [a] |
| | | | | | | | **5a**[2] | 7 [b] |
| **1b** | $CH_3$ | H | **3b** | 8 | **4b** | 3 | — | |
| **1c** | H | $CH_3$ | **3c** | 1 | — | | **5c** | 29 [c] |
| **1d** | $CH_3$ | $CH_3$ | **3d** | 7 | — | | — | |
| **1e** | $NO_2$ | H | — | | — | | — | |

[a] **5a**[1]: $R^3$ = Br. [b] **5a**[2]: $R^3$ = 1,3-dimethyl-5-uracilyl. [c] **5c**: $R^3$ = Br.

**3b**, **d** are lower in the case of the 5-methyl- **1b** and 5,6-dimethyluracils **1d**, even though no alternative 5-substitution is possible. The introduction of the bulky and electron-withdrawing 5-nitro residue prevents any photoreaction[9]. On the other hand, reaction of the sterically hindered 6-methyluracil **1c** with **2** leads to only traces of the cycloadduct **3c**, together with exclusively the 5-substitution product **5c**. These findings are in agreement with observations on the influence of the substituents on C-5 and C-6 on the uracil photodimerization[10].

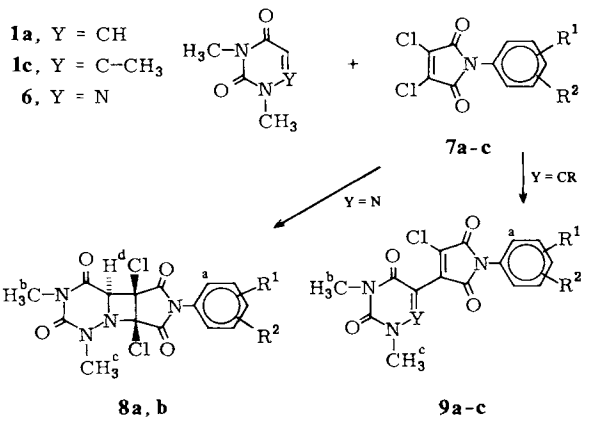
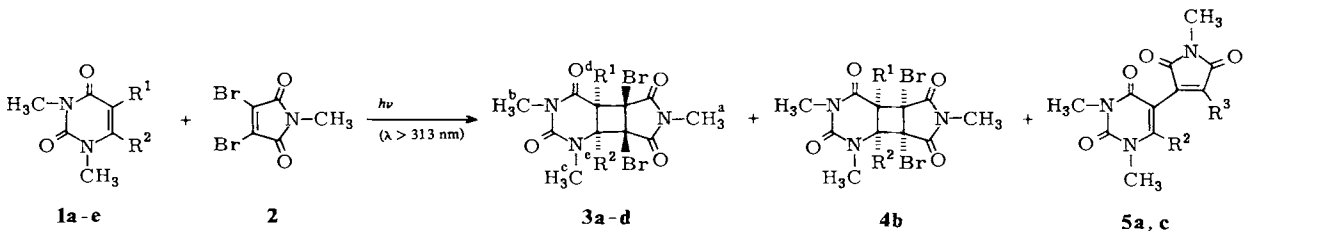



Table 2. Preparative yields of **8a**, **b** and **9a—c**.

| Educts | | $R^1$ | $R^2$ | Products; Yield [%] | | | |
|---|---|---|---|---|---|---|---|
| **1a** | **7a** | 3-Cl | 5-Cl | — | | **9a** | 31 |
| **1c** | **7a** | 3-Cl | 5-Cl | — | | **9b** | 13 |
| **6** | **7a** | 3-Cl | 5-Cl | **8a** | 62 | — | |
| **1a** | **7b** | 4-$CO_2$Et | H | — | | **9c** | 6 |
| **6** | **7b** | 4-$CO_2$Et | H | **8b** | 47 | — | |
| **1a/6** | **7c** | 4-$CH_3$ | H | — | | — | |




[*] Prof. Dr. H. Wamhoff, Dr. G. Szilágyi [***]
Institut für Organische Chemie und Biochemie der Universität Gerhard-Domagk-Strasse 1, D-5300 Bonn 1 (Germany)
[**] Photochemistry of Heterocycles, Part 11. This work was supported by the Minister für Wissenschaft und Forschung des Landes Nordrhein-Westfalen and the Fonds der Chemischen Industrie.—Part 10: [1].
[***] Alexander-von-Humboldt Fellow 1979/80.

*N*-substitution of the dichloromaleiimides **7a—c** also plays a significant role (see Table 2). On irradiation, **2** is known to react with **6** and **1a** exclusively with cycloaddition[1,4]. The photoreaction of **7a**, **b** with **1a**, **c**, on the other hand, leads merely to substitution products, electron withdrawing substituents on the aryl group (**7a**, **b**)

markedly promoting the tendency to substitution; donors (**7c**) lead to the opposite effect. **7a, b** undergo smooth [2+2]-cycloaddition on reaction with the 6-azauracil **6**. The stereochemistry of the coupling of **3a—d** and **8a, b** follows from the $^1$H-NMR data; **3a**[4] analogously shows *cis,anti,cis* stereochemistry. **1b** and **2** yield, aside from **3b**, the isomer **4b** with *cis,syn,cis* stereochemistry; the signal of the $C-CH_3$ protons is correspondingly diamagnetically shifted by the vicinity of the imide-C=O (**3b**: $\delta = 1.67$; **4b**: $\delta = 1.40$).

Received: March 7, 1980 [Z 412 IE]
revised: March 5, 1982
German version: *Angew. Chem. 95* (1983) 156
The complete manuscript of this communication appears in *Angew. Chem. Suppl. 1983*, 120—127

CAS Registry numbers:
**1a**, 874-14-6; **1b**, 4401-71-2; **1c**, 13509-52-9; **1d**, 59264-09-4; **1e**, 41613-26-7; **2**, 3005-27-4; **3a**, 52695-22-4; **3b**, 84174-91-4; **3c**, 84174-92-5; **3d**, 84174-93-6; **4d**, 84236-34-0; **5a**, ($R^3$ = Bu) 52695-23-5; **5b**, ($R^3$ = 1,3-dimethyluracil-5-yl), 52724-81-9; **5c**, 84174-94-7; **6**, 15677-10-8; **7a**, 84174-90-3; **7b**, 65833-17-2; **7c**, 29244-55-1; **8a**, 84174-95-8; **8b**, 84174-96-9; **9a**, 84174-97-0; **9b**, 84174-98-1; **9c**, 84174-99-2.

[1] G. Szilágyi, H. Wamhoff, *Angew. Chem. 92* (1980) 1066; *Angew. Chem. Int. Ed. Engl. 19* (1980) 1026.
[3] A. Wexler, R. J. Balchunis, J. S. Swenton, *J. Chem. Soc. Chem. Commun. 1975*, 601; A. Wexler, J. S. Swenton, *J. Am. Chem. Soc. 98* (1976) 1602.
[4] G. Szilágyi, H. Wamhoff, P. Sohár, *Chem. Ber. 107* (1974) 1265.
[9] The photoreaction of 5- or 6-halogenated or 5,6-dihalogenated uracil derivatives with **2** will be reported elsewhere.
[10] Cf. G. J. Fischer, H. E. Johns in S. Y. Wang: *Photochemistry and Photobiology of Nucleic Acids, Vol. 1, Chemistry*, p. 255, Academic Press, New York 1976.

## Synthesis of the Thionitrosylrhenium Dication $[Re(CO)_5(NS)]^{2+}$; Reactions and Structure of the Thiazylfluoride Complex $[Re(CO)_5(NSF)]^+$

By *Rüdiger Mews** and *Chao-shiuan Liu*

Several different routes exist to thionitrosyl complexes[1]. We have found that thiazylfluoride complexes, which can be readily prepared from the corresponding $SO_2$ derivatives, are suitable precursors for the preparation of the thionitrosyl ligand in complexes.

$$[Re(CO)_5(SO_2)]^+AsF_6^- + NSF \xrightarrow[-30\,^\circ C]{SO_2} [Re(CO)_5(NSF)]^+AsF_6^- + SO_2$$
**1**

As in free NSF[3], a fluoride ion can be removed by fluoro-Lewis acids, *e.g.*

$$\mathbf{1} + AsF_5 \xrightarrow[-30\,^\circ C]{SO_2} [Re(CO)_5NS]^{2+}(AsF_6^-)_2$$
**2**

[*] Prof. Dr. R. Mews
Institut für Anorganische Chemie der Universität
Tammannstrasse 4, D-3400 Göttingen (Germany)
Prof. Dr. C. S. Liu
Department of Chemistry, National Tsing Hua University
Hsinchu, Taiwan (Republic of China)

[**] This work was supported financially by the Land Niedersachsen and by the Fonds der Chemischen Industrie.

leading, in quantitative yield, to the hexafluoroarsenate of the pentacarbonyl(thionitrosyl)rhenium dication[2b]. The novel compound **2** was identified by elemental analysis and IR spectroscopy. As expected, the CO stretching frequencies in the dication [$A_1$ 2219 (m), B 2191 (w), E 2157 (s), $A_1$ 2073 $cm^{-1}$ (m)] are shifted very strongly to higher wavenumbers; due to the doubly positive charge and the "soft" thionitrosyl ligand (good $\pi$ acceptor), backbonding from the central atom to the CO ligands should only be very weak, and the CO bonds correspondingly strong. Compared to **1**, the MCO deformation and MC stretching frequencies [546 (m), 524 (m), 491 (w), 318 $cm^{-1}$ (m)] are shifted to lower wave numbers. The SN stretching frequency is observed at 1371 $cm^{-1}$, and hence lies approximately 80 $cm^{-1}$ higher than in all previously known thionitrosyl complexes[1].

The hexafluoroantimonate **3** corresponding to **2** could be obtained in low yield from $Re(CO)_5Br$ and $NS^+SbF_6^-$.

$$NS^+SbF_6^- + Re(CO)_5Br \longrightarrow [Re(CO)_5NS]^{2+}(SbF_6^-)_2 + \cdots$$
**3**

Received: July 20, 1980;
revised: September 23, 1981 [Z 414 IE]
German version: *Angew. Chem. 95* (1983) 156

CAS Registry numbers:
**1**, 84303-51-5; **2**, 84303-53-7; **3**, 84303-54-8; $[Re(CO)_5(SO_5]^+AsF_6^-$, 55853-08-2; $Re(CO)_5Br$, 14220-21-4.

[1] Review: M. Herberhold, *Nachr. Chem. Tech. Lab. 29* (1981) 369, and literature cited therein; cf. also K. K. Pandey, U. C. Agarwala, *Inorg. Chem. 20* (1981) 1308.
[2] a) NSF (0.297 g, 4.56 mmol) and 10 mL $SO_2$ (solvent) were condensed onto $[Re(CO)_5SO_2]^+AsF_6^-$ [4] (2.64 g, 4.56 mmol) at −196 °C, the clear solution stirred for 1 h at −30 °C, and the volatile components removed by oil vacuum pump at this temperature. Analytically pure, orange-red crystals of **1** (decomp. 115 °C) remain. $^{19}$F-NMR: $\delta(SF) = 219.7$, $\delta(AsF) -100.0$, $J(AsF) = 930$ Hz. IR: 2179 m, 2146 vs, br ($\nu_{CO}$); 1390 vw ($\nu_{SN}$); 647 m ($\nu_{SF}$); 585 s, 450 w, 341 w ($\delta_{Re-C-O}$, $\nu_{Re-C}$); 702 vs, 678 vw, 400 s $cm^{-1}$ ($\nu_{As-F}$). Raman (in $SO_2$): 1396 s ($\nu_{SN}$).—b) A solution of **1** (0.9259 g, 1.596 mmol) and $AsF_5$ (0.293 g, 1.666 mmol) in 10 mL $SO_2$ is stirred for 1 h at −30 °C. After removal of the volatile products, **2** remains in quantitative yield as a red solid which is insoluble in $SO_2$, decomp. 130 °C; c) **3** IR: $\nu_{CO}$ 2218 (m) ($A_1$), 2191 (w) (B), 2152 (s) (E), 2067 (m) ($A_1$); $\delta_{MCO}$, $\nu_{MC}$ 545 (m), 524 (m), 491 (w), 320 (w); $\nu_{SN}$ 1366 (m) $cm^{-1}$.
[3] O. Glemser, W. Koch, *Angew. Chem. 83* (1971) 145; *Angew. Chem. Int. Ed. Engl. 10* (1971) 127; *An. Asoc. Quim. Argentina 59* (1971) 143.
[4] R. Mews, *Angew. Chem. 87* (1975) 667; *Angew. Chem. Int. Ed. Engl. 14* (1975) 640.

## Chromatographic Resolution of Cyclic Organic Compounds on a Λ-Tris(1,10-phenanthroline)ruthenium(II) Montmorillonite Column

By *Akihiko Yamagishi** and *Ryuichiro Ohnishi*

A number of methods have been developed for the resolution of optically active organic molecules[1]. We describe here the first example of the use of an absorbent consisting of clay modified by an optically active metal complex.

The column (length 3 cm, outer diameter 1.2 cm) was filled with sodium montmorillonite, whose cation-exchange sites were replaced to 67% with Λ-Ru(phen)$_3^{2+}$ (Λ ≙ *R*-enantiomer) ions[2]. About 100 mg of the enantiomeric mixture to be separated was loaded onto the column

[*] Dr. Akihiko Yamagishi
Department of Chemistry, Faculty of Science
Hokkaido University, Sapporo 060 (Japan)
Dr. Ryuichiro Ohnishi
Research Institute for Catalysis
Hokkaido University, Sapporo 060 (Japan)

and eluted with water (0.02 mL $min^{-1}$). The concentration and degree of resolution of the enantiomers were measured by UV absorption and ORD spectroscopy ($\lambda = 210$–700 nm).

The first group of compounds studied were acyclic (±)-α-amino acids, such as alanine, serine, threonine, asparagine, and lysine. The total amount of every amino acid loaded was recovered within the first 4 mL eluted. No optical activity was detected in the eluates (error limit 0.01° $cm^{-1}$, $\lambda = 210$—700 nm), *i.e.* these compounds were not resolved to a measurable extent. When (±)-proline was eluted, however, the eluates exhibited an ORD spectrum. Amino acid analysis of the eluates indicated that they only contained proline as a solute. Accordingly, neither decomposition of proline nor replacement of the ligand in the rhodium complex occurred during elution. The molecular rotation at 250 nm ($[m]_{250}$) varied with the elution volume from an initial negative value (−33°) to a final positive value (+34°). Since $[m]_{250}$ for (*S*)-proline is −880°, it is concluded that (*S*)-proline was eluted first with 3.8% followed by (*R*)-proline with 3.9% enantiomeric purity. These values were improved to 14 and 16%, respectively, when the fractions for $V = 0$—3 mL and 3—7 mL were chromatographed again.

Table 1. Resolution on a Λ-Ru(phen)$_3^{2+}$ montmorillonite column [a].

| Compound | $[m]_\lambda$ [b] *ee* [%] [c] | $\lambda$ [nm] | Configuration |
|---|---|---|---|
| proline | −33 (+34) [3.8 (3.9)] | 250 | *S*(*R*) |
| 5-oxoproline | +390 (−1000) [12 (30)] | 230 | *R*(*S*) |
| 5-methyl-2-pyrrolidinone | +250 (−560) [19 (43)] | 230 | *S*(*R*) |
| γ-valerolactone | +20 (−39) [5 (29)] | 250 | *R*(*S*) |
| 2-piperidinecarboxylic acid | −11 (+54) [6.8 (33)] | 300 | *S*(*R*) |
| 4-thiazolinecarboxylic acid | −20 (+98) [2.3 (12)] | 300 | *S*(*R*) |

[a] Eluent: water. [b] Rotation values of the first and the last fractions are shown without and in parenthesis, respectively. [c] Values in the square brackets show the corresponding enantiomeric excess (*ee*).

This success, together with the failure to resolve acyclic α-amino acids, led us to attempt the resolution of other kinds of *cyclic* organic compounds. Five of these (Table 1) were successfully resolved, but five others (xylose, 2-methylpiperidine, 2-ethylpiperidine, 3-piperidinecarboxylic acid, and α-acetyl butyrolactone) were not.

The present findings indicate that clay-metal chelate adducts are highly promising absorbents for the chromatographic resolution of enantiomeric mixtures of organic compounds. In addition, the systems are interesting as models for the propagation of chirality in nature during chemical evolution. Indeed, clay modified by optically active metal complexes could lead to the resolution of amino acids.

Received: September 7, 1982; revised: November 19, 1982 [Z 144 IE]
German version: *Angew. Chem. 95* (1983) 158
The complete manuscript of this communication appears in: *Angew. Chem. Suppl. 1983*, 140–147

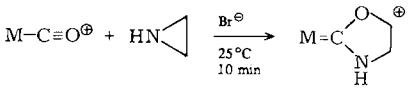
CAS Registry numbers:
Λ-Ru(phen)$_3^{2+}$, 24162-09-2; (±)-Proline, 609-36-9; *S*-Proline, 147-85-3; *R*-Proline, 344-25-2; (±)-5-Oxoproline, 149-87-1; *R*-5-Oxoproline, 4042-36-8; *S*-5-Oxoproline, 98-79-3; (±)-5-Methyl-2-pyrrolidinone, 62182-32-5; *S*-5-Methyl-2-pyrrolidinone, 1558-60-7; *R*-5-Methyl-2-pyrrolidinone, 21395-93-7; (±)-γ-Valerolactone, 57129-69-8; *R*-γ-Valerolactone, 58917-25-2; *S*-γ-Valerolactone, 19041-15-7; (±)-2-piperidinecarboxylic acid, 4043-87-2; *S*-2-piperidinecarboxylic acid, 3105-95-1; *R*-2-piperidinecarboxylic acid, 1723-00-8; (±)-4-thiazolidinecarboxylic acid, 19291-02-2; *S*-4-thiazolidinecarboxylic acid, 45521-09-3; *R*-4-thiazolidinecarboxylic acid, 34592-47-7; montmorillonite, 1318-93-0.

[1] P. E. Hare, E. Gil-Av, *Science 204* (1979) 1226; V. A. Davankov, Yu. A. Zolotarev, A. A. Kurganov, *J. Liq. Chromatogr. 2* (1979) 1191; G. Blaschke, *Angew. Chem. 92* (1980) 14; *Angew. Chem. Int. Ed. Engl. 19* (1980) 13; V. Schurig, R. Weber, *J. Chromatogr. 217* (1981) 51.
[2] A. Yamagishi, R. Ohnishi, M. Soma, *Chem. Lett. 1982*, 85; A. Yamagishi, R. Ohnishi, *J. Chromatogr. 245* (1982) 213; *Inorg. Chem. 21* (1982) 4233.

## Expansion of Three-Membered Heterocycles to Five-Membered Cyclic Carbenes—Novel Reactions of Aziridine, Oxirane, and Thiirane with CO and CS Ligands in Iron, Ruthenium, and Manganese Complexes**

By *Mono M. Singh* and *Robert J. Angelici**

Aziridine **1**, oxirane **2**, and thiirane **3** react with carbonylmetal complexes and undergo ring opening; initial reaction is at the metal centers[3, 4b]. So far, however, there have been no reports of direct reactions of CO or CS ligands with **1**, **2**, or **3**. We describe here some novel reactions of **1**, **2**, and **3** with these ligands in certain carbonylmetal compounds, yielding cyclic carbenes as the end products. Thus, reaction of **1** with the metal complexes **4a**—**d** and the ammonium bromide $Br(CH_2)_2NH_3^+Br^-$ (molar ratio 1:1:1) in $CH_3CN$ affords the cyclic amino(oxy)carbenes **5a**—**d**.

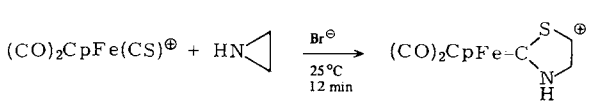



**4a-d** **1** **5a-d**

**a**, M = CpFe(CO)$_2$; **b**, M = CpMn(CO)(NO); **c**, M = CpRu(CO)$_2$; **d**, M = CpFe(CO)(PPh$_3$); anions: $PF_6^-$

**5a**—**d** are obtained as crystalline hexafluorophosphates in 98%[7], 87%[7], 87%, and 70% yields, respectively, by extraction of the vacuum-dried residue with $CH_2Cl_2$ and precipitation with ether at −20 °C. Several other halides, such as $Br(CH_2)_3NH_3^+Br^-$, NaBr, $(nBu)_4N^+Br^-$, $Et_3NH^+Br^-$ and $(nBu)_4N^+I^-$ were also observed to catalyze the reaction of **1** with **4a**. **5a** is still obtained in 80% yield on decreasing the concentration of the $Br(CH_2)_2NH_3^+Br^-$ tenfold.

Similarly, reaction of **1** with the carbonyl(thiocarbonyl)-complex **6** in THF in the presence of $Br^-$ furnishes the cyclic amino(thio)carbene **7** in 83% yield.

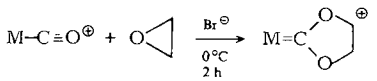



**6** **1** **7**

[*] Prof. Dr. R. J. Angelici, Dr. M. M. Singh
Department of Chemistry and Ames Laboratory U. S., DOE
Iowa State University, Ames, IA 50011 (USA)

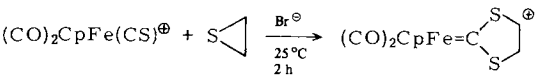
[**] Ames Laboratory is operated for the U. S. Department of Energy by Iowa State University under Contract No. W-7405-Eng-82. This research was supported by the Office of Basic Energy Sciences, Chemical Sciences Division.

Reaction of **2** in excess with **4a—d** in the presence of $Br^-$ in $Br(CH_2)_2OH$ as solvent leads to formation of the cyclic dioxycarbenes **10a—d** in 81%[7], 80%, 73%, and 81% yields, respectively. High yields (>70%) of **10a**, **10b**, and **10d** are also obtained when $Br(CH_2)_3OH$ is used instead of $Br(CH_2)_2OH$.



**4a-d** **2** **10a-d**

Unlike **1** and **2**, **3** does not react with **4a—d** to form the oxy(thio)carbene. However, it does form the dithiocarbene **13**[10] on reaction with **6** in presence of NaBr.



**6** **3** **13**

All the cyclic carbene compounds have been fully characterized as $PF_6^-$ salts by elemental analysis, and IR and $^1H$- and $^{13}C$-NMR spectral data. The formation of carbene ligands has been conclusively proven by the $^{13}C$-NMR signals of the carbene carbon atoms [($CD_3CN$), **5a—d**: $\delta = 220.24, 228.56, 206.28, 234.20$; **10a—d**: $\delta = 242.51, 253.43, 227.08, 254.00$; **7**: $\delta = 234.36$; **13**: $\delta = 295.40$].

Received: October 4, 1982 [Z 166 IE]
revised: November 19, 1982
German version: *Angew. Chem. 95* (1983) 160
The complete manuscript of this communication appears in:
*Angew. Chem. Suppl. 1983*, 184-192

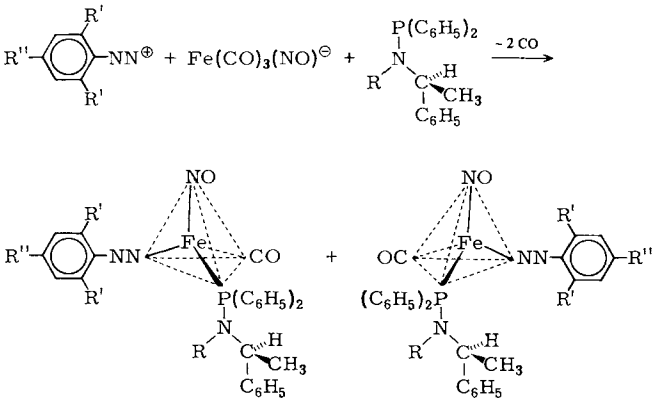
[3] W. P. Giering, M. Rosenblum, J. Tancrede, *J. Am. Chem. Soc. 94* (1972) 7170.
[4] b) W. Danzer, W. P. Fehlhammer, A. T. Liu, G. Thiel, W. Beck, *Chem. Ber. 115* (1982) 1682, and references cited therein.
[7] H. Motschi, R. J. Angelici, *Organometallics 1* (1982) 343.
[10] F. B. McCormick, R. J. Angelici, *Inorg. Chem. 20* (1980) 1111.

## Optically Active Iron Complexes with Tetrahedral Structure

By *Henri Brunner** and *Wolfgang Miehling*

Most of the previously documented optically active organometallic compounds of the transition elements have an (arene)$ML^1L^2L^3$-type structure[1]. These complexes are designated as pseudotetrahedral, because the central metal is bound to four ligands, and consequently only the isomeric "image" and "mirror image" tetrahedral structures are possible. The geometry of these compounds is, however, octahedral with the 6 π-arene ligand, frequently benzene or cyclopentadienyl, occupying three *cis*-positions of the octahedron. This is born out, in particular, by the angles between the ligands $L^1$, $L^2$ and $L^3$ to the metal atom, which are always approximately 90°[2]. Optically active organometallic compounds of elements of the transition series with actual tetrahedral structure are, as yet, unknown.

A plausible strategy for the synthesis of such compounds would be the use of $Fe(CO)_2(NO)_2$ as starting material, a member of the pseudo-$Ni(CO)_4$ series in the sense of the nitrosyl-shift principle[3]. Replacement of a CO group in $Fe(CO)_2(NO)_2$ by another two-electron ligand, *e.g.* a phosphane, and of an NO group by another three-electron ligand, *e.g.* an aryldiazenyl group, would result in the Fe atom in the compounds $Fe(CO)(NO)(NNR)PR_3$ being a center of chirality. On using a pure phosphane enantiomer, *e.g.* one of the aminophosphanes (*S*)-$PPh_2\{N(R)CHMePh\}$[5] of Scheme 1, each complex is formed in the form of two diastereomers **a** and **b**, which differ only in the configuration at the Fe atom.



| R | R'=R''=H | R'=H, R''=$CH_3$ | R'=R''=$CH_3$ | R'=R''=$C_6H_5$ |
|---|---|---|---|---|
| H | **1a, b** | **2a, b** | | |
| $CH_3$ | **3a, b** | **4a, b** | **5a, b** | **6a, b** |
| $CH_2C_6H_5$ | | | **7a, b** | |

Scheme 1

The anion $Fe(CO)_3(NO)^-$ reacts with diazonium ions $arylNN^+$ in acetone at −78 °C to give the complex $Fe(CO)_2(NO)(NNaryl)$, which is unstable at room temperature[6]. However, if one equivalent of aminophosphane is added at −78 °C, further exchange of CO takes place with formation of the complexes **1—7** (Scheme 1), which can be isolated in 40—65% yield after warming to room temperature: **1** and **2** as readily decomposable red oils, **3—7** as stable reddish-brown powders.

The IR spectra of the complexes **1—7** in pentane solution each show sharp, very intense bands for $\nu_{CO}$ (1975—1980), $\nu_{NO}$ (1730—1735) and $\nu_{NN}$ (1662—1682 $cm^{-1}$). The diastereomers **a** and **b** of complexes **3**, **4**, and **6** do not differ in their $^1H$-NMR spectra. In the case of compounds **3** and **4** substituted in the *p*-position or without substituents on the diazoaryl moiety this is not surprising, but is, however, for the complex **6** which has phenyl substituents on the *o*-position. Only the compounds **5** and **7**, substituted by methyl in the *o*-positions, showed different chemical shifts in the *o*-$CH_3$ signals [$\delta = 2.22$ (**7a**) and 2.28 (**7b**), $C_6D_6$], the $C^*CH_3$, and the $NCH_3$ signals, from which the diastereomeric ratio **a** : **b** can be determined.

None of the diastereomers of complexes **3—7** can be enriched by fractional crystallization. In contrast, the diastereomeric pairs of **4**, **5**, and **7** can be separated by preparative liquid chromatography on Merck-Lobar B-columns.

[*] Prof. Dr. H. Brunner, W. Miehling
Institut für Anorganische Chemie der Universität
Universitätsstrasse 31, D-8400 Regensburg (Germany)

[**] Optically Active Transition Metal Complexes, Part 82. This work was supported by the Deutsche Forschungsgemeinschaft, the Fonds der Chemischen Industrie, and BASF AG, Ludwigshafen.—Part 81: I. Bernal, W. H. Ries, H. Brunner, D. K. Rastogi, *Inorg. Chem.*, in press.

For this purpose, 200—300 mg of each of the complexes in petroleum/ether 5:1 were chromatographed on a two-column system[5]. In all three cases the $(+)_{436}$-diastereomer **a** was eluted more rapidly then the $(-)_{436}$-diastereomer **b**.

In the case of complex **7** a distinct partition into two zones is achieved after passage through three columns, corresponding to a complete separation of **7a** and **7b**. In contrast, in the case of complexes **4** and **5** a broad zone is formed after passage through four columns in which **a** is enriched in the fronts and **b** in the tails. As shown by the CD spectra, the front and tail fractions can be obtained in high optical purity by cutting out the central part of the zone.

Of all the compounds investigated the diastereomers of **7** are the easiest to separate and to detect by $^1$H-NMR spectroscopy. Therefore, **7a** was chosen for investigation of the configurational stability at the Fe atom. No epimerization occurs up to 50 °C in $C_6D_6$ solution in a sealed $^1$H-NMR tube, with or without addition of free *N*-benzylaminophosphane (*S*)-$PPh_2$\{N(Bz)CHMePh\}; at about 55 °C the epimerization **7a** $\rightleftarrows$ **7b** takes place within a few hours. However, the fact that the change of configuration at the Fe atom is accompanied by side reactions *e.g.* formation of $Fe(NO)_2[PPh_2\{N(Bz)CHMePh\}]_2$ prevents kinetic measurements.

Received: October 15, 1982 [Z 176 IE]
German version: *Angew. Chem. 95* (1983) 162
The complete manuscript of this communication appears in:
*Angew. Chem. Suppl. 1983*, 84—91

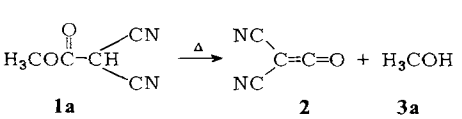
[1] H. Brunner, *Adv. Organomet. Chem. 18* (1980) 151.
[2] G. M. Reisner, I. Bernal, H. Brunner, M. Muschiol, *Inorg. Chem. 17* (1978) 783.
[3] F. Seel, *Z. Anorg. Allg. Chem. 249* (1942) 308.
[5] H. Brunner, J. Doppelberger, *Chem. Ber. 111* (1978) 673.
[6] W. E. Carrol, F. J. Lalor, *J. Organomet. Chem. 54* (1973) C 37; W. E. Carrol, F. A. Deeney, F. J. Lalor, *ibid. 198* (1980) 189.

## Dicyanoketene: Flash Vacuum Thermolysis of Alkyl Dicyanoacetates**

By *James E. Gano**, *Roy H. Jacobson*, and *Richard H. Wettach*

A need to know the spectral data of dicyanoketene[2], **2**, prompted a search for a direct and unambiguous synthesis of this compound[3]. Although precedent suggested (a) dehydration of dicyanoacetic acid with phosphorus(v) oxide, (b) pyrolysis of metal enolates of alkyl dicyanoacetates, and (c) pyrolysis of alkyl dicyanoacetates would all produce dicyanoketene, [4] only route (c) proved successful.

Methyl dicyanoacetate **1a**[5], which slowly became yellow upon storage at room temperature, was purified by vacuum sublimation.




**1a** **2** **3a**

[*] Prof. Dr. J. E. Gano, R. H. Jacobson, Dr. R. H. Wettach
Department of Chemistry, Bowman-Oddy Laboratories
University of Toledo, Toledo, OH 43606 (USA)

[**] Financial support of this work by the Research Corporation and The University of Toledo Faculty Research Award and Fellowship program, and the technical assistance of L. Cooley, J. Werstler, and W. Opdycke are gratefully acknowledged.

For generation of **2**, **1a** was sublimed into an oven, which was directly attached to a mass spectrometer operating at a low (≈9 eV) ionizing voltage[6]. At an oven temperature of 500 °C the peak characteristic of **1a** (*m/z* 59, $CO_2CH_3$) was almost entirely replaced by peaks clearly characterized by dicyanoketene (*m/z* 92 and 64, $(NC)_2C$) and methanol (*m/z* 32 and 31)[3b].

When the products of pyrolysis of **1a** were codeposited with argon directly on a CsI window cooled to 12 K, infrared bands appeared assignable to residual **1a** and methanol. Dicyanoketene appeared at 2251 (w), 2246 (m), 2175 (vs), 1081 (w), and 571 (m) $cm^{-1}$[6]. When the argon was omitted during the deposition, the thin film (Fig. 2) showed broader bands for residual **1a**, methanol ($\nu$ = 1130 (w), 1030 (m, broad) $cm^{-1}$) and dicyanoketene ($\nu$ = 2230 (w), 2175 (vs), 1090 (vw) and 580 (w) $cm^{-1}$).

Clearly, dicyanoketene is an extremely reactive intermediate. Upon slowly warming the thin film devoid of argon, the dicyanoketene absorptions (Fig. 2) started disappearing near 60 K as the methanol absorption also disappeared (probably by sublimation) and new bands appeared ($\nu$ = 2295 (s), 2090 (s), 1125 (m) and 745 (w) $cm^{-1}$)[9]. Dicyanoketene has been reported elsewhere to react below 100 K[2].

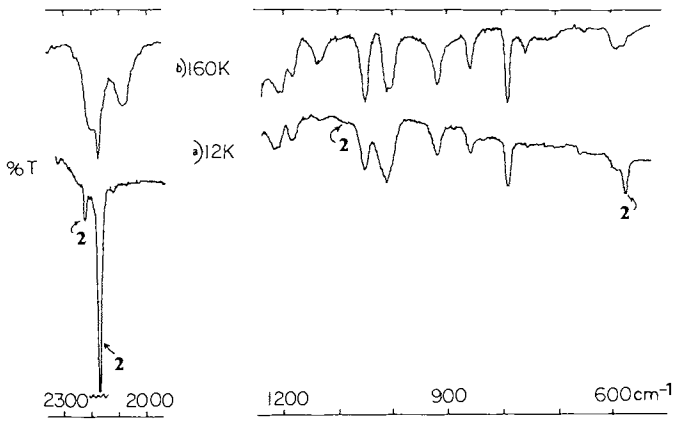



Fig. 2. IR spectrum (CsI window) of the oven effluent, which contains dicyanoketene **2**, on pyrolysis of **1a**. (a) Window temperature 12 K, (b) window temperature 160 K.

Received: August 26, 1981 [Z 413 IE]
revised: November 24, 1982
German version: *Angew. Chem. 95* (1983) 155
The complete manuscript of this communication appears in:
*Angew. Chem. Suppl. 1983*, 193-197

CAS Registry numbers:
Methyl dicyanoacetate, 2040-70-2; dicyanoketene, 4361-47-1

[2] Dicyanoketene appears to be an intermediate in the low-temperature photolysis of 1,3-dioxolane-2-methylenedicarbonitrile; *J. E. Gano et al.*, Nouv. J. Chim., in press.
[3] During the tenure of this work, an alternate route to dicyanoketene, requiring multiple steps to obtain a rather unstable precursor, was reported: a) R. Neidlein, E. Bernhard, *Angew. Chem. 90* (1978) 395; *Angew. Chem. Int. Ed. Engl. 17* (1978) 369; b) A. Hotzel, R. Neidlein, R. Schultz, A. Schweig, *ibid. 92* (1980) 751 and *19* (1980) 739; c) W. H. Gilligan, M. J. Kamlet, *Tetrahedron Lett. 1978*, 1675.
[4] a) D. C. England, C. G. Krespan, *J. Am. Chem. Soc. 88* (1966) 5582; b) D. F. Sullivan, R. P. Woodbury, M. W. Rathke, *J. Org. Chem. 42* (1977) 2038; c) T. J. Jorwski, S. Kwiatowski, *Rocz. Chem. 44* (1970) 691.
[5] a) F. Arndt, H. Scholz, E. Frobel, *Justus Liebigs Ann. Chem. 521* (1935) 95; b) some new spectral data of **1a**: $^1$H-NMR ($CDCl_3$): $\delta$ = 4.72 (1 H), 3.99 (3 H); $^{13}$C-NMR ($CDCl_3$): $\delta$ = 157.8 (C=O), 107.8 (CN), 55.9 ($CH_3$, $J_{C,H}$ = 150 Hz), 29.3 (CH, $J_{C,H}$ = 129 Hz).
[6] The oven was fitted with a quartz tube (I.D. 0.8 cm, length ≈15 cm), which was lightly packed over one third its length with quartz wool. The

orifice led directly into the ionization chamber of a mass spectrometer (Nuclide 12—90 G). Peak positions in argon are accurate to $\pm 1.5$ $cm^{-1}$.

[9] Attempts to identify this product have so far proved unsuccessful. Clearly **2** does not simply react with methanol to give the ester **1a** nor does it undergo [2+2]-cycloaddition to form a β-lactone or 1,3-diketone. Tetracyanoallene is a very attractive possibility.

## FT-FIR Spectroscopy of Ligand-Free Metal Clusters; Matrix Effects on the Molecular Geometry of Trichromium, $Cr_3$**

By *Geoffrey A. Ozin**, *Mark D. Baker*, *Steven A. Mitchell*, and *Douglas F. McIntosh*

We report here the first infrared spectroscopic data for a ligand-free triatomic metal cluster, $Cr_3$, immobilized in solid Ar or Xe matrices. In freshly deposited Cr/Ar and Cr/Xe condensates, prepared under conditions which are conducive to the co-isolation of Cr atoms, and $Cr_2$ and $Cr_3$ species, but not higher clusters[11] (Cr : noble gas = $1/10^3$ to $1/10^4$ at 12 K), Cr–Cr stretching and deformational modes were observed in the IR spectrum between 350 and 95 $cm^{-1}$. The FIR spectra at various Cr : Ar ratios and thermal annealing conditions are shown as examples in Figure 2 (Table 1 in the Supplement contains the assignments of the bands to the vibrational modes of the various $Cr_3$ clusters).

Our results indicate that the preferred structure of $Cr_3$ for a particular choice of experimental parameters is influenced by whether it is produced during the agglomeration stage of the film deposition process or from diffusion controlled nucleation reactions induced by thermal annealing of the condensate. Thus, in freshly deposited Xe matrices at 12 K, $Cr_3$ shows a single broad band centered around 210 $cm^{-1}$, which can be ascribed to the single IR-active E′ vibrational mode of the $D_{3h}$ equilateral triangular form. In Ar matrices, on the other hand, this same $Cr_3$ species is observed centered around 215 $cm^{-1}$ only after annealing to 40 K (Fig. 1). Annealing the Xe matrices containing the $D_{3h}$ form of $Cr_3$ to 25—75 K, however, generates $Cr_3$ with angles between 60—90° and those with *ca.* 120°. In Ar matrices, larger angle $Cr_3$ molecules tend to be preferred in freshly deposited as well as in films annealed at 25 K. Between 25 and 40 K these $Cr_3$ clusters are transformed into the thermally favored 60—80° small angle structures.

A normal coordinate calculation for $Cr_3$ as a function of angle (60—180°) proved to be particularly valuable for assigning the isomeric and isotopic contributions to the FT-FIR bands: these establish that the contribution to the band width from $Cr_3$ isotopomers lies in the range 8—10 $cm^{-1}$ for $\nu_1$ and $\nu_3$ stretching modes, and in the range 2—8 $cm^{-1}$ for the $\nu_2$ deformation mode. Furthermore, for the $D_{3h}$ isomer of $Cr_3$ the position of the bands and their shape are virtually identical in Ar and Xe, indicating that phonon and/or vibronic coupling contributions to the band widths are comparable, although not necessarily negligible, in these matrices. The origin of the pronounced band widths in the FIR absorptions of $Cr_3$ in Ar matrices under low dispersion conditions (Fig. 2A) can, therefore, be understood in terms of contributions from isotopomers, phonon and/or vibronic coupling, inhomogeneous effects, as well as from a distribution of structural isomers (angles vary between 100 and 150° in quench-condensed films, and collapse to 60—80° on annealing at 40 K). In contrast, conditions of high dispersion of $Cr_3$ in Ar tend to favor narrower band widths and better resolved FIR spectra (Fig. 2C), which permit a clearer identification of individual $Cr_3$

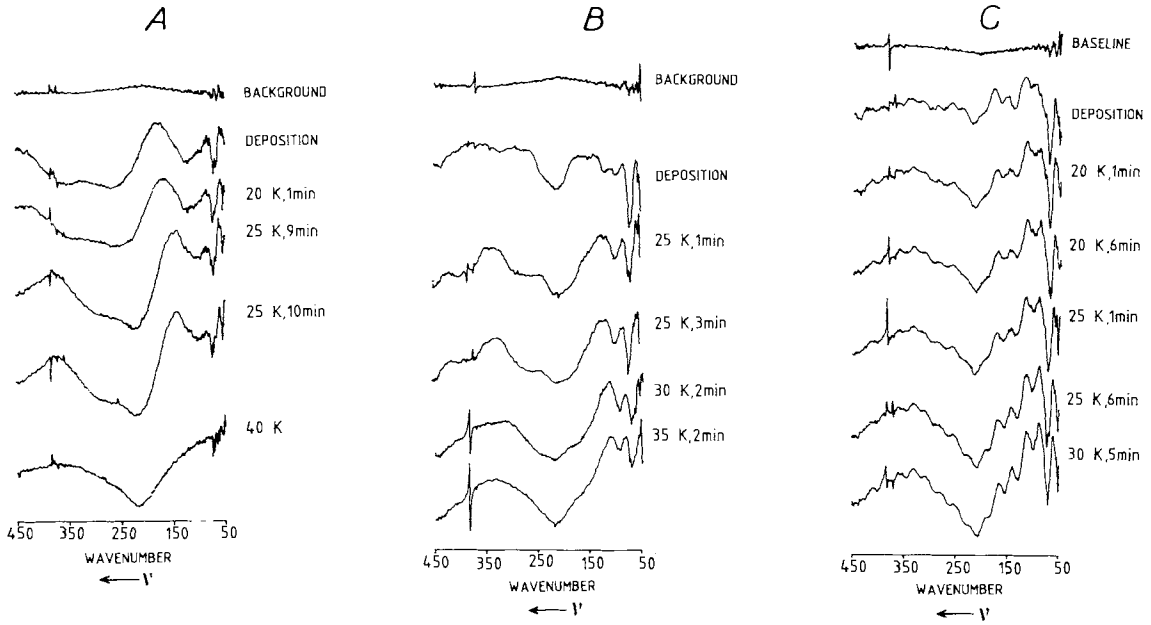



Fig. 2. FT-FIR spectra of Cr/Ar matrices for Cr : Ar ratios of *ca.* $1:10^3$ (A), *ca.* $2.5:10^4$ (B), *ca.* $1:10^4$ (C) deposited at 12 K and annealed at the temperatures indicated. Peak to peak noise at 200 $cm^{-1}$ = 0.5%.

[*] Prof. G. A. Ozin, Dr. M. D. Baker, Dr. D. F. McIntosh
Lash Miller Chemical Laboratories, University of Toronto
80 St. George St., Toronto, Ontario, M5S 1A1 (Canada)
Dr. S. A. Mitchell
Chemistry Division, National Research Council of Canada
Sussex Drive, Ottawa (Canada)

[**] The generous financial assistance of the Natural Sciences and Engineering Research Council of Canada's Operating, Major Equipment and Strategic Energy Programmes and the Connaught Fund of the University of Toronto is gratefully acknowledged. *S. A. M.* expresses his gratitude to NSERC and Noranda for graduate scholarships throughout the duration of his Ph. D. research. The expert design and technical assistance of *K. Molnar* and *W. Panning* proved to be invaluable.

clusters (angles from 60° to at least 130°). Under conditions of high dilution the $Cr_3$ isomers with larger angles (100—130°) appear to be favored on deposition at 12 K, whereas the smaller angle forms (60—90°) seem to be preferred in films annealed at 40 K.

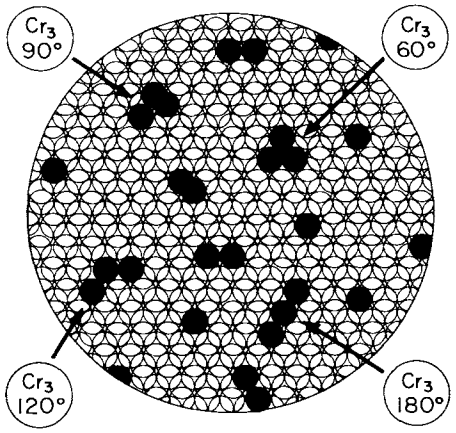



Fig. 4. Possible structures (schematic) of $Cr_3$ clusters in Ar or Xe matrices.

In summary, this study demonstrates for the first time that FT-FIR spectroscopy is a viable and useful technique for probing the vibrational and structural properties, and interaction with the support for "ligand-free" metal clusters. The FIR cluster data provide a valuable adjunct to the complimentary information from Raman, resonance Raman, and resonance fluorescence spectroscopic studies[7-9]. $Cr_3$ immobilized in Ar and Xe matrices at different metal concentrations and thermal conditions can occur in a range of molecular geometries ranging from equilateral triangular to that of almost linear (Fig. 4). It is evident that the $Cr_3$ cluster must have a rather shallow potential energy surface[16], and that variation of the experimental conditions can produce extremely subtle perturbations which profoundly influence the cluster geometry. The results underscore that even a "weak" interaction between a support and a molecular metal cluster can markedly influence the electronic, vibrational, and geometrical properties of such a supported metal cluster[17].

Received: October 5, 1982 [Z 168 IE]
German version: *Angew. Chem. 95* (1982) 157
The complete manuscript of this communication appears in: *Angew. Chem. Suppl. 1983*, 92-113

[7] W. Schulze, H. U. Becker, R. Minkwitz, K. Manzel, *Chem. Phys. Lett. 55* (1978) 59; W. Krasser, U. Kettler, P. S. Bechthold, *ibid. 86* (1982) 223.
[8] M. Moskovits, D. P. DiLella, *J. Chem. Phys. 72* (1980) 2267.
[9] K. Manzel, W. Schulze, F. W. Froben, *Chem. Phys. Lett. 82* (1981) 557; K. Manzel, U. Engelhardt, H. Abe, W. Schulze, F. W. Froben, *ibid. 77* (1981) 514; V. E. Bondybey, J. H. English, *J. Chem. Phys. 73* (1980) 42; F. Ahmed, E. R. Nixon, *ibid. 75* (1981) 110; V. E. Bondybey, G. P. Schwartz, J. E. Griffiths, *J. Mol. Spectrosc. 89* (1981) 328; D. D. Stranz, R. K. Khanna, *J. Chem. Phys. 74* (1981) 2116.
[11] G. A. Ozin, W. Klotzbücher, *J. Mol. Catal. 3* (1977/78) 195; *Inorg. Chem. 18* (1979) 2101; *J. Am. Chem. Soc. 100* (1978) 2262.
[16] H. Basch, *J. Am. Chem. Soc. 103* (1981) 4657.
[17] V. E. Bondybey, L. E. Brus, *Adv. Chem. Phys. 36* (1980) 269; G. A. Ozin, S. A. Mitchell in M. H. Chisholm: *Chemistry Towards the 21st Century, ACS Symp. Ser.*, in press; G. A. Ozin, F. Hugues, D. F. McIntosh in G. Stucky: *Intrazeolitic Chemistry, ACS Symp. Ser.*, in press, and literature cited therein.

## Novel Synthesis of Acetylenes

By *Hans-Jürgen Bestmann**, *Kamlesh Kumar*, and *Wolfgang Schaper*

Phosphorus ylides **1** can be acylated with acid chlorides **2** in a reaction involving transylidation. The products obtained are the phosphonium salts **4** together with the acyl ylides **3**[1,2], the best yields of which are obtained if, as we have found out in the meantime, the reaction is carried out with **1** prepared from the corresponding salts **4** and sodium bis(trimethylsilyl)amide[1b]. Thermolysis of **3**[3] only leads to pure acetylenes **7** when $R^1$ and $R^2$ are aryl groups or when $R^2$ is an ester group[4]. This also holds true for the reaction of **3** with $PCl_5$ or Vilsmeier reagents and subsequent cleavage of the resulting β-chlorovinylphosphonium salts with bases[5]. The methodology described in this communication now enables directed conversion of the acyl ylides **3** into the acetylenes **7**.

Reaction of the ylides **3** with trifluoromethanesulfonic anhydride **5** furnishes the triflates **6**. Subsequent treatment of the salts **6** with sodium amalgam in tetrahydrofuran leads to formation of the acetylenes **7** along with triphenylphosphane **8** and sodium triflate **9** (for examples cf. Table 1).

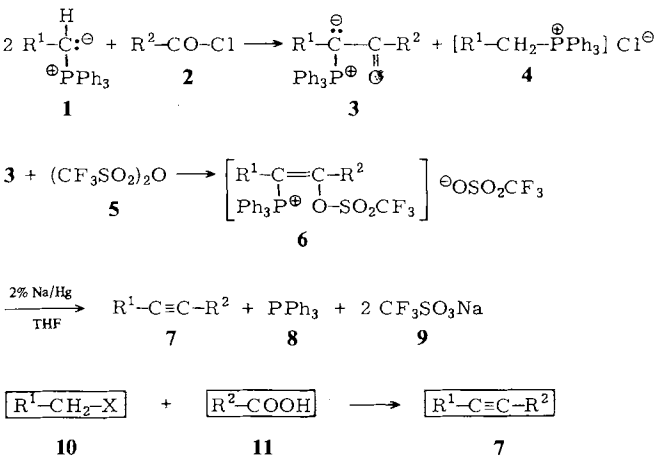


Table 1. Yields and melting or boiling points of products **3**, **6**, and **7**.

| $R^1$ | $R^2$ | **3** Yield [%] | **3** M.p. [°C] | **6** [a] Yield [%] | **6** [a] M.p. [°C] | **7** [b] Yield [%] | **7** [b] B.p. [c] [°C/torr] |
|---|---|---|---|---|---|---|---|
| Me | Ph | 84 | 171 | 90 | 132 | 80 | 72—77/17 |
| *n*Bu | *n*Bu | 75 | 107 | 81 | 140 | 45 | 110—115/60 |
| *n*Bu | *n*Pent | 83 | 125 | 93 | 135 | 47 | 97-102/40 |
| *n*Bu | *n*Hex | 76 | 101 | 87 | 141 | 52 | 100—105/16 |
| *n*Bu | Ph | 94 | 176 | 83 | 111 | 79 | 120—125/15 |

[a] **5** (30 mmol) is added dropwise at 0—5 °C to a solution of **3** (30 mmol) in benzene (75 mL) and the mixture stirred for 2 h at room temperature. After removal of solvent, the residue is dissolved in a little $CH_2Cl_2$ and reprecipitated with ether.—[b] A solution of **6** (7 mmol) in THF (35 mL) is added at −20 °C to a 2% sodium amalgam, prepared from 0.81 g (35 mmol) sodium and 36.00 g mercury and covered with a layer of THF (5 mL), and the mixture stirred for 17 h at +5 °C. After separation from the mercury, the solvent is distilled over a Vigreux column and the residue distilled twice in a Kugelrohr. [c] Bath temperature during Kugelrohr distillation.

The use of this method with alkyl halides or tosylates **10** (X = halogen, OTos) and carboxylic acids **11** as starting

[*] Prof. Dr. H. J. Bestmann, Dr. K. Kumar, Dr. W. Schaper
Institut für Organische Chemie der Universität Erlangen-Nürnberg
Henkestrasse 42, D-8520 Erlangen (Germany)

materials enables the synthesis of the acetylenes **7** with the triple bond in a specific position. Triphenylphosphane **8** can be recovered, and the anhydride **5** can be regenerated from the sodium salt **9**.

Received: October 7, 1982 [Z 171 IE]
revised: November 16, 1982
German version: *Angew. Chem. 95* (1983) 154

CAS Registry numbers:
**1** ($R^1$ = Me), 1754-88-7; **1** ($R^1$ = *n*Bu), 29541-98-8; **2** ($R^2$ = Ph), 98-88-4; **2** ($R^2$ = *n*Bu), 638-29-9; **2** ($R^2$ = *n*Pent), 142-61-0; **2** ($R^2$ = *n*Hex), 2528-61-2; **3** ($R^1$ = Me, $R^2$ = Ph), 1450-07-3; **3** ($R^1$ = $R^2$ = *n*Bu), 84393-96-4; **3** ($R^1$ = *n*Bu, $R^2$ = *n*Pent), 84393-97-5; **3** ($R^1$ = *n*Bu, $R^2$ = *n*Hex), 84370-12-7; **3** ($R^1$ = *n*Bu, $R^2$ = Ph), 84370-13-8; **6** ($R^1$ = Me, $R^2$ = Ph), 84370-15-0; **6** ($R^1$ = $R^2$ = *n*Bu), 84370-17-2; **6** ($R^1$ = *n*Bu, $R^2$ = *n*Pent), 84370-19-4; **6** ($R^1$ = *n*Bu, $R^2$ = *n*Hex), 84370-21-8; **6** ($R^1$ = *n*Bu, $R^2$ = Ph), 84370-23-0; **7** ($R^1$ = Me, $R^2$ = Ph), 673-32-5; **7** ($R^1$ = $R^2$ = *n*Bu), 1942-46-7; **7** ($R^1$ = *n*Bu, $R^2$ = *n*Pent), 2294-72-6; **7** ($R^1$ = *n*Bu, $R^2$ = *n*Hex), 19780-12-2; **7** ($R^1$ = *n*Bu, $R^2$ = Ph), 1129-65-3.

[1] a) H. J. Bestmann, B. Arnason, *Chem. Ber. 95* (1962) 1513; b) cf. H. J. Bestmann, O. Vostrowsky, W. Stransky, *ibid. 109* (1976) 1694.
[2] H. J. Bestmann, *Angew. Chem. 77* (1965) 609, 651; *Angew. Chem. Int. Ed. Engl. 4* (1965) 583, 645.
[3] S. T. D. Gough, S. Trippett, *J. Chem. Soc. 1962*, 2333; G. Märkl, *Chem. Ber. 94* (1961) 3005.
[4] H. J. Bestmann, F. Seng, T. Brosche, K. Kumar, unpublished results.
[5] G. Märkl, *Angew. Chem. 74* (1962) 217; *Angew. Chem. Int. Ed. Engl. 1* (1962) 160.

# BOOK REVIEWS

**Protein-Protein-Interactions.** Edited by *C. Frieden* and *L. W. Nichol,* John Wiley & Sons, New York 1981, 403 pp., bound, £ 36.95.

The publication of this book is timely, because interactions of proteins with themselves, with other macromolecules and with small ligands have proved to be of great significance for operation and control of biochemical processes. Moreover, in the last two decades, important advances have been made in the experimental and theoretical clarification of interacting macromolecular systems. Eleven authors with international reputation have contributed to this book, which summarizes the most important recent developments made in this field, covering the literature up to 1979/80.

In the opening chapter, *L. W. Nichol* gives a short general introduction (28 pages), defining the basic thermodynamic and kinetic properties of protein systems. Starting with the behavior of a non-interacting protein in solution, self-interacting protein systems, mixed two-component systems, and multicomponent heterogeneous systems are treated.

In the second chapter, a detailed account of structural and energetic aspects of protein-protein interactions is given by *L. J. Banaszak, J. J. Birktoft* and *C. D. Barry*. The treatment is well balanced giving equal consideration to each of these aspects. Thus, the authors devote about 50 pages to structure, symmetry and conformation, and 35 pages to interatomic forces and calculations of conformations. The wide range and the depth of the critical exposition of experimental and theoretical approaches to structure determination and prediction makes this chapter, which is the longest of the book, one of its highlights. The strategy is typical for crystallographers, namely to focus mainly on X-ray crystallographic studies while neglecting solution studies. The treatment of the hierarchical levels of protein structure is up-to-date including a description in terms of super-secondary structures, domains, lobes and symmetrical and non-symmetrical assemblies *etc.* In an Appendix, energy minimization, empirical structure predictions, Monte Carlo calculations *etc.* are considered with regard to environmental effects, molecular dynamics and protein folding.

*D. J. Winzor* gives an excellent survey (40 pages) of the present state of the art in the theory and application of mass migration methods, such as sedimentation velocity, gel chromatography, electrophoresis, activity transport *etc.* Reversibly self-associating systems, as well as association-dissociation equilibria of heterogeneous systems are dealt with. Reactions which are considered are not limited to protein-protein-interactions, but also include protein-ligand interactions in a wider sense. Thus, monomer-oligomer equilibria that may result from exclusive or preferential binding of substrates or (allosteric) effectors to monomers or oligomers are discussed. These processes are of importance for enzyme regulation, gene expression, hormone action, immune response, *etc.*

An introduction to boundary analysis is given in a separate chapter by *D. J. Cox* and *R. S. Dale*. Instead of considering all available simulation methods (Bethune-Kegeles, Cann-Goad, Dishon-Weiss-Yphantis, *etc.*), the authors treat only the "distorted grid simulation" *(Cox)* and the "finite element simulation" *(Claverie)* since these are considered as particularly effective methods. *P. D. Jeffrey* deals with classical "equilibrium methods" for the characterization of interacting mixtures of macromolecules in solution in terms of stoichiometry and equilibrium constants. He does so in an admirably concise manner, starting with a unified formal description of thermodynamically non-ideal homogeneous and heterogeneous multicomponent systems. Within this framework, protein-protein-interactions may be interpreted on the basis of second (or higher) virial coefficients making use of the "Adams-Fujita approach".

*G. G. Hammes* describes fluorescence methods. After giving basic definitions, fluorescence polarization and resonance energy transfer are treated. The latter is the "pièce de résistance" of *Hammes'* contribution. He provides a knowledgeable and helpful introduction to the use of energy transfer in the study of protein-protein interactions. The usefulness of this approach is exemplified by work with antibodies and by Hammes' own work with chloroplast coupling factor. Finally, the use of energy transfer for distance measurements between molecules on cell surfaces is introduced, an aspect which is presently receiving a lot of attention.

*C. Frieden* deals with the kinetics of associating-dissociating enzyme systems. This author has made important contributions to the field of kinetics of allosteric enzymes

and has developed the concept of the "hysteretic" enzyme. Introducing his topic, he makes the point that a careful comparison of kinetic with binding data may help to distinguish certain kinds of enzyme regulation but that a comparison is only valid when enzyme substrates and enzyme-substrate complexes are at equilibrium. *Frieden*'s critical treatment of activity as a function of enzyme concentration is masterly and should be read by every kineticist interested in control of enzyme activity. It rests firmly on the author's own studies. Computer programs were developed for the evaluation of kinetic data using a numerical integration for solving differential equations. The importance of rate measurements for the attainment of monomer-polymer equilibria is emphasized, and suitable methods for the correlation of molecular weight and activity of an enzyme are discussed. Interactions of enzymes with other proteins (with and without enzymic function) and with cellular structures (*e.g.* membranes, cytoskeleton and nucleic acids) are considered, and the model character of immobilized enzymes and coupled enzyme reaction chains is emphasized. In view of the physiological importance of association-dissociation reactions of enzymes, which drastically alter the kinetic and regulatory behavior of enzymes when monomer and polymer exhibit different kinetic properties, *Frieden*'s contribution should encourage all enzymologists concerned with rate controlling enzymic processes to purchase this book.

In Chapter 9, *L. W. Nichol* and *D. J. Winzor* deal with ligand binding. Although the thorough theoretical treatment provides a sound basis for practical applications with useful hints for the experimenter, on a whole, this chapter does not turn out as well as the others. Most of the important aspects of ligand binding considered in this chapter have already been dealt with in detail elsewhere, and, unfortunately, the treatment of some specific problems does not meet up with the present state of the art.

In contrast, the chapter contributed by *S. N. Timasheff* on self-assembly of long rodlike structures exemplifies what makes this book attractive and worthwile. A single system, namely the polymerization of tubulin, which *Timasheff* and his colleagues have investigated in detail, is used to develop lucid theories on the linear and nucleated polymerization of proteins based on *Osawa*'s theory of the helical polymerization of actin. Especially valuable are *Timasheff*'s remarks on current methodology: Drawing from a wealth of his own experience he outlines not only the merits but also the limitations of light-scattering, viscosity and centrifugation methods which are widely used for the analysis of polymerizing proteins.

This book has not been written for graduate students. Rather, it is directed at the researcher engaged in the physical study of interacting proteins and enzymes. For this group of biochemists enzymologists and molecular biologists the book is of great use and fills a need. As a Matter of fact, it will be difficult to find another recent publication which is of so much practical value. Theory, practical application of methods and critical evaluation of data are treated in depth, so that the reader rarely needs to consult original papers. However, the book is by no means perfect: There is inevitably some redundancy and overlap, and in some cases the treatment is too detailed, reflecting more the enthusiasm of the authors rather than the needs of the user. Moreover, certain aspects, for example elementary step kinetics, have been neglected. But despite these criticisms, we can recommend this book without reservations to everybody who has to deal with protein-protein interactions in his research. Thus, the number of potential users should be large, for who does not need to come to terms with a quantitative treatment of protein-protein interactions, which are of such fundamental importance for an understanding of structure, function and regulation of proteins and enzymes *in vitro* and in the living cell.

*Rainer Jaenicke* and *Ernst J. M. Helmreich* [NB 578 IE]

**Recent Books**

**The following books have been received by the editor. Detailed reviews will not be published in all cases because of the limited space available under this heading in the journal. All the publications listed are available through W & P Buchversand für Wissenschaft und Praxis, Boschstrasse 12, D-6940 Weinheim (Federal Republic of Germany). Tel. (06201) 602653 (606-0), Telex 465516 vchwh d, Telefax (06201) 602328.**

**Progress in Analytical Atomic Spectroscopy. Volume 4.** Edited by *C. L. Chakrabarti*. Pergamon Press, New York 1982. v, 456 pp., bound, $ 106.00.—ISBN 0-08-029659-9

**Material Behavior and Physical Chemistry in Liquid Metal Systems.** Edited by *H. U. Borgstedt*. Plenum Press, New York 1982. xiv, 548 pp., bound, $ 69.50.—ISBN 0-306-40917-9

**Wissenschaft, Staat, Mäzene** (Veröffentlichung des Deutschen Historischen Instituts London). By *P. Alter*. Klett-Cotta, Stuttgart 1982. 327 pp., bound, DM 96.00.—ISBN 3-608-91070-0

**Progress in Medicinal Chemistry. Vol. 19.** Edited by *G. P. Ellis* and *G. B. West*. Elsevier Biomedical Press BV, Amsterdam 1982. viii, 345 pp., bound, HFl. 220.00.—ISBN 0-444-80415-3 (Series number 0-7204-7400-0)

**The Chemistry of Organophosphorus Pesticides.** By *C. Fest* and *K.-J. Schmidt*. Springer-Verlag, Berlin 1982. x, 360 pp., bound, DM 164.00.—ISBN 3-540-11303-7

**Advanced Sugar Chemistry.** By *R. S. Shallenberger*. Ellis Horwood Ltd. Chichester 1982. xxi, 323 pp., bound, £ 31.50.—ISBN 0-85312-541-4

**NATO Advanced Study Institutes Series. Series C: Mathematical and Physical Sciences. The Biological Chemistry of Iron.** Edited by *H. B. Dunford, D. Dolphin, K. N. Raymond,* and *L. Siecker*. D. Reidel Publishing Company Dordrecht 1982. xiii, 517 pp., bound, HFl. 145.00.—ISBN 90-277-1444-4

**Progress in Nuclear Magnetic Resonance Spectroscopy. Vol. 14.** Edited by *J. W. Emsley, J. Feeney,* and *L. H. Sutcliffe*. Pergamon Press, Oxford 1982. v, 325 pp., bound.—ISBN 0-08-029698-X

**Jahrbuch für den Praktiker aus der Öl-, Fett-, Seifen- und Waschmittel-, Körperpflegemittel-, Wachs- und sonstigen chem.-techn. Industrie einschließlich Aerosole.** Edited by *B. Ziolkowsky*. Verlag für chemische Industrie H. Ziolkowsky KG, Augsburg 1983. 536 pp.—ISBN 3-87846-110-0

**Unfallanalyse '80.** By W. Abt. Issued by the Hauptverband der gewerblichen Berufsgenossenschaften e. V., Bonn 1982. 256 pp., Paperback.

**Progress in Solid State Chemistry. Vol. 13.** Edited by *G. M. Rosenblatt* and W. L. Worrell. Pergamon Press, Oxford 1982. vi, 386 pp., bound, $ 112.00.— ISBN 0-08-029712-9

**Optical Engineering Series, Vol. 1: Electron and Ion Microscopy and Microanalysis. Principles and Applications.** By *L. E. Murr*. Marcel Dekker, Basel 1982. xiv, 793 pp., bound SFr. 185.00.—ISBN 0-8247-1553-5

**Pergamon Series on Environmental Science, Vol. 6: Inorganic Chemistry and the Earth. Chemical Resources. Their Extraction, Use and Environmental Impact.** By *J. E. Fergusson*. Pergamon Press, Oxford 1982. ix, 400 pp., Paperback, £ 9.95.—ISBN 0-08-023994-3

**Pergamon Series in Analytical Chemistry, Vol. 5: Applied Complexometry.** By *R. Pribil*. Pergamon Press, Oxford 1982. xv, 410 pp., bound, £ 55.00.— ISBN 0-08-026277-5

**Organic Chemistry Series, Vol 2: Organotransition Metal Chemistry: Applications to Organic Synthesis.** By *S. G. Davies*. Pergamon Press, Oxford 1982. xv, 411 pp., bound, *ca.* £ 60.00.— ISBN 0-08-026202-3

**Polyether Antibiotics. Naturally Occurring Acid Ionophores. Volume 1: Biology.** Edited by *J. W. Westley*. Marcel Dekker, Basel 1982. xvii, 465 pp., bound SFr. 185.— ISBN 0-8247-1655-8

*Registered names, trademarks, etc. used in this journal, even without specific indication thereof, are not to be considered unprotected by law.*

© Verlag Chemie GmbH, D-6940 Weinheim, 1983. - Printed in the Federal Republic of Germany by Zechnersche Buchdruckerei, Speyer/Rhein.

All rights reserved (including those of translation into foreign languages). No part of this issue may be be reproduced in any form - by photoprint, microfilm, or any other means - nor transmitted or translated into a machine language without written permission from the publishers. Only single copies of contributions, or parts thereof, may be reproduced for personal use. Copies reproduced and used other than for private purposes in an industrial or commercial undertaking are subject to copyright and, in such cases, a copyright fee must be paid to the VG WORT, Abteilung Wissenschaft, Goethestr. 49, 8000 München 2, from whom conditions of payment can be obtained on request.

**Valid for users in the USA:** The appearance of the code at the bottom of the first page of an article in this journal (serial) indicates the copyright owner's consent that copies of the article may be made for personal or internal use, or for the personal or internal use of specific clients. This consent is given on the condition, however, that the copier pay the stated per-copy fee through the Copyright Clearance Center, Inc., for copying beyond that permitted by Sections 107 or 108 of the U.S. Copyright Law. This consent does not extend to other kinds of copying, such as copying for general distribution, for advertising or promotional purposes, for creating new collective works, or for resale. For copying from back volumes of this journal see 'Permissions to Photo-Copy: Publisher's Fee List' of the CCC.

**Editorial office:** Pappelallee 3, D-6940 Weinheim, Federal Republic of Germany, Telephone (06201) 602-1, Telex 465516 vchwh d, Telefax (06201) 602328.

**Editors:** *P. Gölitz, I. G. Neil, O. Smrekar, A. Stimson.*

**Publishers:** Verlag Chemie GmbH. (Managing Directors: *Dr. Helmut Grünewald* and *Hans Dirk Köhler*), Pappelallee 3, D-6940 Weinheim, Federal Republic of Germany.
Correspondence concerning advertisements should be addressed to Verlag Chemie GmbH. (Advertising Manager *R. J. Roth*), Pappelallee 3, P.O. Box 1260/1280, D-6940 Weinheim, Federal Republic of Germany, Telephone Weinheim (06201) 602-1, Telex 465516 vchwh d, Telefax (06201) 602328.

ANGEWANDTE CHEMIE
International Edition in English
Volume 22 · Number 3
March 1983
Pages 171–258

# The Versatile Chemistry of 1,4-Diazines: Organic, Inorganic and Biochemical Aspects

By Wolfgang Kaim*

In chemical research attention is increasingly being focussed on composite "complex" systems with special properties and functions. As components of such systems 1,4-diazines are steadily gaining in popularity. Here, 1,4-diazines means pyrazine and its derivatives as well as compounds with partial pyrazine structure; examples are quinoxaline, phenazine, pteridine, flavin and their derivatives. All these compounds are characterized by a low lying unoccupied π-molecular orbital and by the ability to act as bridging ligand. Due to these two properties 1,4-diazines, and especially their parent compound pyrazine, possess a characteristic reactivity. 1,4-Diazines may be employed to study inter- and intramolecular electron transfer in organic, inorganic and biochemical reactions. In the redox system of 1,4-diazines the paramagnetic 7π-electron intermediate exhibits exceptional stability, whereas the 1,4-dihydro-1,4-diazines with 8π-electrons in a six-membered ring are not generally accessible due to their potential antiaromaticity and their large excess of π electrons. Its inherent bifunctionality and the low lying unoccupied molecular orbital permit pyrazine to form coordination polymers having unusual electrical and magnetic properties. Finally, the phenomena observed for pyrazines may be used in the interpretation of the reactivity of naturally occurring 1,4-diazines, such as flavins and bioluminescent natural products.

*"Wer nur (an)organische Chemie versteht, versteht auch die nicht recht"*[**].

*(After G. C. Lichtenberg, 1742–1799)*

## 1. Introduction

The ring system of pyrazine **1** forms the common structural unit of 1,4-diazines. The reactions of 1,4-diazines may be described either in terms of "conventional" chemistry, generally corresponding to that of other aromatic heterocycles[1], or in terms of a reactivity characteristic of only this particular system.



**1**

The aim of the present review is to illustrate this special reactivity with the aid of selected examples, to discuss possible model interpretations thereof, and to indicate some potential applications. Organic as well as inorganic and biochemical results are discussed, giving an indication of the versatility of this system.

[*] Dr. Wolfgang Kaim
Institut für Anorganische Chemie der Universität
Niederurseler Hang, D-6000 Frankfurt/Main 50 (Germany)

[**] "He who only understands (in)organic chemistry does not completely understand that either".

 © Verlag Chemie GmbH, 6940 Weinheim, 1983 0570-0833/83/0303-0171 $ 02.50/0 

## 2. Premises

The replacement of two opposite CH-groups in benzene by nitrogen atoms has the following consequences: The degeneracy of the π-frontier orbitals is removed (Fig. 1); the $B_{3g}$ orbital, which is not influenced by the 1,4-perturbation, becomes the only highest occupied π-orbital. The lowest unoccupied molecular orbital (LUMO) is now $B_{1u}$, whose energy is lowered by the CH→N exchange.

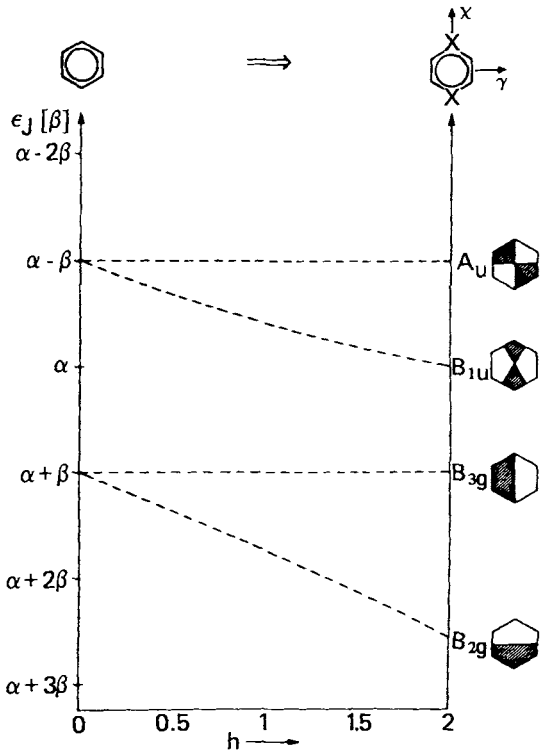



Fig. 1. The frontier orbitals of pyrazine as text book case [2a]: According to the Hückel model, perturbation of the benzene π-system by CH→N exchange in positions 1 and 4 may be represented by an enlargement of the Coulomb integral $\alpha_N = \alpha_C + h \cdot \beta$ (X = N). The relation $\alpha_N > \alpha_C$ (positive $h$) corresponds to the larger effective nuclear charge or the greater "electronegativity" of the nitrogen atom. The molecular orbitals $B_{1u}$ and $B_{2g}$ are energetically lowered, while orbitals $A_u$ and $B_{3g}$ remain unaltered by the 1,4-perturbation (nodal plane through 1 and 4). In pyrazine **1** $B_{2g}$ and $B_{3g}$ are occupied, $h_N \approx 0.5$ [2b]. The same correlation diagram may be used for planar 1,4-dihydropyrazine **9**, in which case $B_{1u}$ is also occupied ($h_N \simeq 1.0$ [3]—1.5 [2b]). The sequence of π-orbitals given by the HMO model is confirmed by quantitative calculations for pyrazine [4] and 1,4-dihydropyrazine [5].

This model is supported by the reactivity of pyrazine. Compared to benzene, **1** is an electron-deficient molecule and already takes up an electron in the gas phase[6] as well as in solution[7,8]. Accordingly, the organic chemistry of pyrazine is characterized by easy nucleophilic attack[1] (IP = ionization potential[9], EA = electron affinity[6]).

$$\mathbf{1}^{+} \xleftarrow[\text{IP} \approx 9.5\ \text{eV}]{-e} \mathbf{1} \xrightarrow[\text{EA} \approx 0.4\ \text{eV}]{+e} \mathbf{1}^{-}$$

On the other hand, the oxidation of pyrazine is not an energetically favored process; the ionization potential of **1** is somewhat higher than that of benzene (IP = 9.25 eV)[9]. In the condensed phase the pyrazine radical cation may only be formed by radiolytic methods and is rather unstable[10]. UV, ESR[10] and photoelectron spectroscopic studies[9] show that in the first ionization step an electron is lost from a σ-orbital.

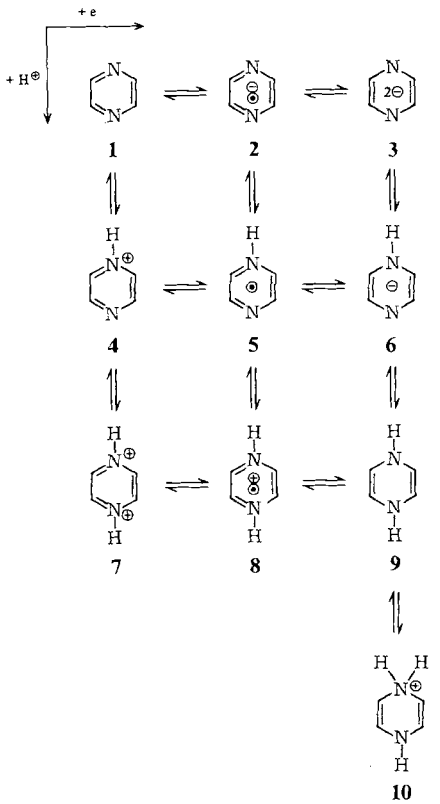
Because of the introduction of two nitrogen atoms pyrazine contains two unshared electron pairs arranged orthogonally to the π-system.



In the HMO approximation σ- and π-systems are separable[2], but the N-electron pairs influence each other because of through bond and through space interactions[9]. Since the electron pairs are oriented in opposite directions, pyrazine **1** is a bifunctional, bridging ligand which does not form chelates (μ-pyrazine). In fact, **1** and related 1,4-diazines form both monomeric 1:2 adducts (Sections 3 and 4) and polymeric coordination compounds (Section 5) with numerous electrophiles.

## 3. Coordination of $H^{\oplus}$: The Pyrazine/1,4-Dihydropyrazine Redox System

The simplest electrophilic coordination partner of pyrazine is the proton. The combination of stepwise protonation with a two step redox reaction results in a scheme characteristic of Weitz redox systems[11] (Scheme 1).




Scheme 1. The pyrazine/1,4-dihydropyrazine redox system.

According to *Hünig et al.*[11], Weitz redox systems differ from quinonoid[12] and other systems through the incorporation of coordination atoms *into* the ring and through the aromaticity of the *oxidized* forms. Several species from Scheme 1 are known:

The protonated pyrazines **4** and **7** have been detected in strong acids[13, 14]; the low basicity of pyrazine in the first step ($pK_a = 0.6$) and especially in the second step ($pK_a = -6$)[14] is remarkable. For comparison: the acidity constant of the pyridinium ion is 5.2[15].

The reduction of pyrazine in aprotic media leads first, in a reversible step, to the radical anion **2**[7]; reduction to the dianion **3** cannot be observed electrochemically[16]. From the potential difference $E(2/3) - E(1/2) > 0.82$ V[16] the formation constant $k_{SEM}$[11] of the radical anion **2** may be estimated to be $k_{SEM} > 10^{15}$, an exceptionally high value[11].

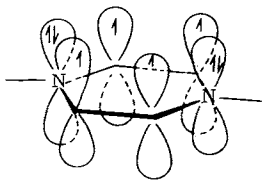
$$k_{SEM} = \frac{[2]^2}{[1][3]} = 10^{(\Delta E/0.059\,V)}$$

Protonation changes the redox potentials since the formation of the radical intermediates **5**[17] and **8**[17, 18] is then increasingly favorable. In strongly acidic aqueous solution two separate reduction steps have been detected: The stable radical cation **8** is formed first; further electron uptake, however, does not lead to the neutral 1,4-dihydropyrazine **9** but, after addition of a further proton, to the 1,4-dihydropyrazinium ion **10**[19].

$$\mathbf{1} \xrightarrow[+e]{+2H^{\oplus}} \mathbf{8} \xrightarrow[+e]{+H^{\oplus}} \mathbf{10}$$

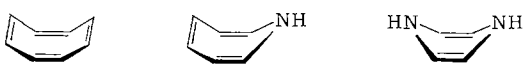
$E_{1/2} = -0.09 \times pH - 0.308$ [V] (*vs.* SCE)[19b]

Compound **9** is of especial interest: Whereas in the quinonoid redox system[12] the reduced neutral form is an aromatic hydroquinone, in the Weitz redox system (Scheme 1) the analogous stage is represented by the potentially "antiaromatic"[20] 1,4-dihydropyrazine[5, 21–24]. The antiaromaticity of **9** and also of **3** and **6** would arise as a result of the cyclic conjugation of a total of 8 (4n)π-electrons[20], including the unshared electron pairs of the two nitrogen atoms.



It should be noted that heteroconjugation gives rise to a smaller antiaromatic destabilization than expected for an isoconjugated system[25]. For **9** an antiaromatic destabilization of 12 kJ/mol has been calculated[5].

The cyclic conjugation of all 8π-electrons is bound by steric requirements. In the boat conformation the six-membered ring **9** does not tolerate such large single bond torsional angles $\theta$ as the related 8π-electron systems cyclooctatetraene **11**[26] ($\theta = 56°$[27]) and 1*H*-azepine **12**[28] ($\theta \simeq 60°$ and 30°[29]), but enforces a closer to planar structure[23].



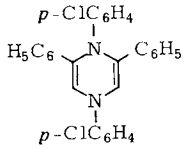
**11** **12** **9**

However, due to the different positions of the *N*-substituents conformational isomerism is possible[23, 30, 31] (angle $\varphi$).



**9**

The extent of cyclic 8π-electron delocalization in **9** depends on the shape of the boat conformation. A geometry-optimized MNDO calculation was carried out[32] in order to obtain a quantitative estimate of the structural effects involved in the redox system **7/8/9**. The results are presented in Figure 2 and Table 1, where they have been compared with structural parameters of the stable derivative **13**.



**13**

Table 1. Calculated (**7**, **8**, **9**) [30] and experimental (**13**) [31] structures of pyrazine derivatives. According to a geometry-optimized MNDO calculation, an increasing localization of the C-C double bond is observed in the redox system **7/8/9**. This corresponds to decreasing aromatic delocalization. For **7** and **8** the conformation of minimum energy is found to be planar; for **9** two conformations of minimum energy are obtained [32]. In agreement with calculations for 1-substituted 1,4-cyclohexadienes [34], diaxial arrangement of the N—H bonds does not produce a conformation of minimum energy, due to the repulsion between the hydrogen atoms in the ring and the larger substituent (in this case the N electron pair). The structural X-ray analysis [31] of a 1,2,4,6-tetraaryl-1,4-dihydropyrazine **13** shows the more marked boat conformation and the bending into an axial conformation as the result of steric hindrance. Hence, cyclic 8π-electron conjugation becomes impossible: The compound is stable [33]. (Atomic distances $d_{XY}$ in pm, $\theta$: torsional angle CCNCC.)

| Cpd. | $d_{CC}$ | $d_{CN}$ | $d_{NH}$ | $\theta$ [°] | Structure |
|---|---|---|---|---|---|
| **7** | 143 | 137 | 103 | 0 | planar |
| **8** | 139 | 139 | 101 | 0 | planar |
| *e,a*-**9** | 136 | 143 | 101 | 0.8 | Fig. 2 Ⓐ |
| *e,e*-**9** | 135 | 143 | 101 | 8.3 | Fig. 2 Ⓑ |
| **13** | 133 | 144<br>141 | — | 27.2<br>37.3 | Fig. 2 Ⓒ |

It can be seen that for **9** all conformations of minimum energy deviate only slightly from the planar ring structure.

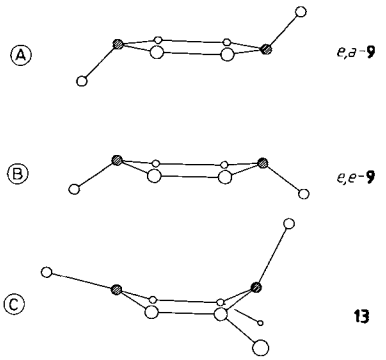
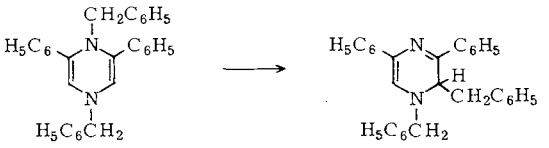


Fig. 2. Computer-drawn conformations of the 1,4-dihydropyrazines *e,a*-**9**, *e,e*-**9** and **13** (Table 1) [32]. Nitrogen atoms are striped; for reasons of clarity *C*-protons are omitted and the phenyl substituent in **13** [33] is represented by a single carbon atom.

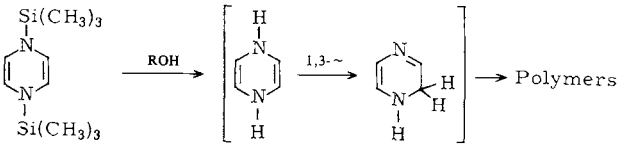
A further interesting aspect of 1,4-dihydropyrazine **9** is its isosteric relationship with benzene. In the HMO approximation[2], *i.e.* assuming the molecule to be planar with a cyclic delocalized π-system, not only **1** but also **9** may be described by the correlation diagram in Figure 1. This is accomplished simply by filling the lowest unoccupied molecular orbital of pyrazine **1** with two electrons and by adding a correction to the Coulomb integral parameter $h_N$ (Fig. 1). In 1961 *Streitwieser*[3] already predicted that the molecule **9** would contain an occupied antibonding MO; thus compound **9** should be very electron-rich and should endeavor to give up at least one electron. This is no doubt one reason for the ready formation and unusual stability of the radical intermediates with 7π-electrons (cf. Table 2).

Attempts to prepare 1,4-dihydropyrazine **9** in the condensed phase have been unsuccessful. Electrolytic reduction of strongly acidic aqueous solutions of pyrazine leads to **8**, but not to **9**. Instead, one obtains the further protonated and therefore *no longer* cyclically conjugated compound **10**, which decomposes with opening of the heterocyclic ring[19]. Another possible reaction for **9** is the 1,3-hydrogen shift observed in numerous derivatives, *e.g.* **14**[22,36-39], and in the related 1*H*-azepine **12**[28].



**14** **15**

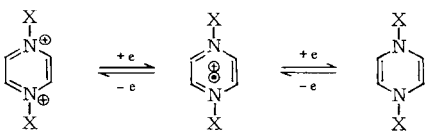
Both unsubstituted 1,2-dihydropyrazine **16** and the 1,4-isomer **9**[1] have yet to be prepared; thus, attempts to hydrolyze 1,4-bis(trimethylsilyl)-1,4-dihydropyrazine **17** failed to give any low molecular weight products[40,41].




**17** **9** **16**

## 4. Monomeric *N*-Coordination Compounds of Pyrazine

Pyrazine **1** and its reduction products **2** and **3**, in addition to coordinating with protons, also coordinate with numerous other organic and inorganic electrophiles. In the following sections the influence of various electrophiles X on the properties of the components of the redox system (Scheme 2) will be discussed. Some characteristic spectroscopic parameters have been compiled in Tables 4 and 5 (Sections 4.2 and 4.6).

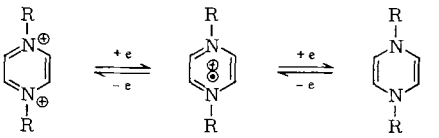



**A** **B** **C**

Scheme 2. The pyrazine dication/1,4-dihydropyrazine redox system.

### 4.1. Pyrazines according to Scheme 2, with X = R (R = Alkyl, Aryl)

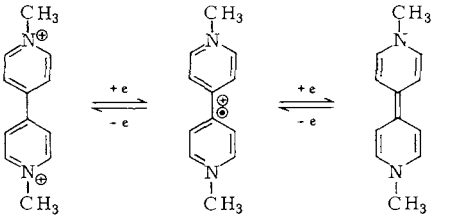
Due to the low basicity of pyrazine, the use of conventional alkylating agents only leads to formation of the monoquaternary salts; oxonium salts are required for production of diquaternary species **18A**[42]. These may thus be readily prepared and, in certain solvents, be examined spectroscopically (cf. Table 4). However, even when stored carefully they are unstable[16,42]; discoloration occurs, accompanied by the formation of free radicals[16]. When these compounds are dissolved in alcohols[42,43] or in water[16], one obtains persistent, concentrated solutions of the radical intermediate **18B**. The mechanism of radical formation is still unclear[42] (but cf. Scheme 3).




**18A** **18B** **18C**

R = $C_2H_5$: $\lambda_{SEM}$ = 350 nm; $k_{SEM}$ = $10^{13}$

The unusual stability of the radical cation **18B** is reminiscent of the behavior of the paraquat or methyl viologen radical cation **19B**[11,44] (see Section 6.2). A comparison of the redox systems **18**, R = $C_2H_5$, and **19** reveals a higher oxidation potential, larger formation constant and shorter wavelength light absorption for the pyrazinium radical intermediate[11,16].




**19A** **19B** **19C**

$\lambda_{SEM}$ = 600 nm; $k_{SEM}$ = $10^7$

According to the HMO model the easy reducibility of the diquaternary species **18A**, in comparison to the neutral compound **1**, is related to the increase in the Coulomb integral at the nitrogen atoms[2b]. Thereby the energy of the lowest unoccupied molecular orbital is lowered (Fig. 1), so facilitating electron acceptance by the system.

In the case of *C*-unsubstituted systems **18** the 1,4-dihydropyrazine stage **18C** could not be isolated. The chemistry of some stable, but highly substituted 1,4-dialkyl- and 1,4-diaryl-1,4-dihydropyrazines has been reviewed by *Schmidt*[23]. *All* such derivatives contain bulky substituents in the 2,6-positions (**13**, **14**). The reason for the stability of these molecules may be seen in Table 1 and Figure 2: Steric repulsion between the vicinal substituents in the 1, 2, and 6 positions prevents conjugation of the free electron pair on N-1 with the rest of the π-system. Thus, an antiaromatic destabilization with corresponding chemical (Table 3) and spectroscopic consequences (cf. Table 4) is no longer possible. In all other cases the system tries to avoid

the unfavorable 8 π-electron situation (Table 3), sometimes by the formation of other isomers (1,2- and 2,5-dihydropyrazines)[45]. As examples, the syntheses of radical cations of the type **18B** may be cited.

Thus the most stable oxidation state of the 1,4-dialkyl- and 1,4-diarylpyrazine system **18** is neither the oxidized nor the reduced form, but the paramagnetic intermediate (Table 2). This is confirmed by further examples of electron transfer reactions[46,47] (cf. Scheme 3):

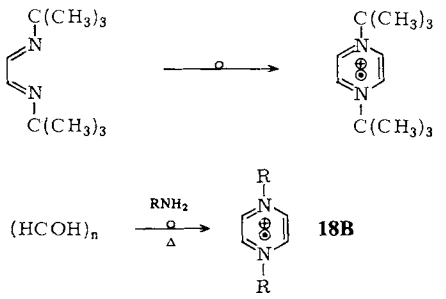


Table 2. Molecular strategies for generating the cyclic 7 π-electron-configuration in 1,4-diazine radical intermediates.

- Electron addition in the gas phase [6] (positive electron affinity)
- Electron uptake in solution [7, 8, 19]
- (Photo-)Reduction of pyrazinium ions [17, 18b] and pyrazine dications [16, 42, 43]
- Reduction by SET reaction [a] with alkyl- and arylmetal compounds as well as metal hydrides [62, 69–72]
- Reduction by metal ions [136, 140]
- Oxidation of 1,4-dihydropyrazines by $O_2$ [22a, d, 35, 88]
- Oxidation and dehydrogenation of 1,2,3,4-tetrahydropyrazines [24c]
- Oxidation and ring expansion [185]
- Ring closure and SET reaction [46, 47, 67]

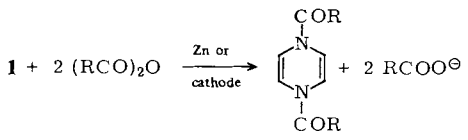
[a] SET = *S*ingle *E*lectron *T*ransfer).

Table 3. Molecular strategies to avoid the cyclic 8 π-electron configuration in 1,4-dihydro-1,4-diazines

- Reoxidation to the pyrazine [21, 69]
- One-electron oxidation to the radical cation (cf. Table 2)
- Addition of electrophiles ($H^{\oplus}$, $R^{\oplus}$) to the nitrogen atom [19, 181]
- Addition of $H_2$ [21, 22d, 24a, 163], $H_2O$ [53] or RSH [22d] to the double bond
- Retro-Diels-Alder reaction [21]
- 1,3-Hydrogen shift [22b–e, 36–38]
- Formation of unexpected isomers [35, 39, 45]
- Stabilization by conformative reasons [23, 35] and by *C*- [88] or *N*-acceptor substituents [24b, 48, 49, 51]

### 4.2. Pyrazines according to Scheme 2, with X = COR (R = H, Alkyl, Aryl, OR', $NR'_2$)

Due to the π-acceptor function of the carbonyl group, *N*-acylation of the redox system (Scheme 2) causes a stabilization of the reduced form **C**. Accordingly, *N*-acyl-1,4-dihydropyrazines are known[21,48] (cf. Section 7.3); however,



**20C**

R = H, $CH_3$, $C(CH_3)_3$, $C_6H_5$, $N(CH_3)_2$ [49], $OC_2H_5$ [51]

parent compounds of the type **20C** have only recently been described by *Gottlieb* and *Pfleiderer*[49].

Compounds **20C** do not possess any unusual properties; they are colorless, stable in air, and their $^1$H-NMR spectra do not reveal the paratropic[50] characteristics expected for a cyclic conjugated 4n π-system (Table 4).

Table 4. Chemical shifts δ of the ring protons in pyrazines and 1,4-dihydropyrazines. The outer ring protons of "aromatic" pyrazine derivatives with 6 π-electrons show the expected downfield shift (diatropic [50] behavior). Most 1,4-dihydropyrazines are stabilized by steric or electronic modification and do not demonstrate paratropic [50] characteristics. However, a clear upfield shift is detected in unsubstituted *N*-silyl derivatives **17** (and **29**), indicating the presence of cyclic 8 π-electron conjugation [24].

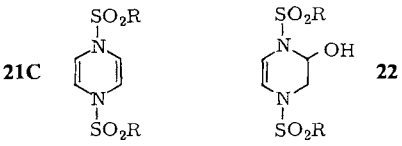
| Compound | Type | Solvent | δ | Ref. |
|---|---|---|---|---|
| *Pyrazines:* | | | | |
| $[1(C_2H_5)_2]^{2\oplus}\ 2BF_4^{\ominus}$ | **18A** | $CF_3COOH$ | 9.86 | [42] |
| $[1(H)_2]^{2\oplus}\ SO_4^{2\ominus}$ | **7** | $H_2SO_4$ | 9.37 | [13] |
| $[1(AlMe_3)_2]$ | **26A** | $CDCl_3$ | 8.89 | [69] |
| **1** | | $CDCl_3$ | 8.63 | [1] |
| *1,4-Dihydropyrazines:* | | | | |
| $[1(COMe)_2]$ | **20C** | $C_2D_2Cl_4$ | 6.19 [a] | [49] |
| $[1(CONMe_2)_2]$ | **20C** | $CDCl_3$ | 5.86 | [49] |
| **14** | | $CDCl_3$ | 5.57 | [22d] |
| $[1(PSMe_2)_2]$ | **35** | $CDCl_3$ | 5.48 | [69] |
| **34** | | $CDCl_3$ | 5.46 | [24a, c] |
| $[1\,SiMe_3)_2]$ | **17** | $CDCl_3$ | 4.64 | [24, 77] |

[a] Average value for *cis*/*trans*-isomers.

The corresponding derivatives of urea (1,4-dihydro-1,4-pyrazinedicarboxamides)[49] and urethanes (1,4-dihydro-1,4-pyrazinedicarboxylates)[51] may be prepared by electrochemical methods.

### 4.3. Pyrazines according to Scheme 2, with X = $SO_2R$ (R = Aryl)

Earlier reports[52] concerning a 1,4-bis(phenylsulfonyl)-1,4-dihydropyrazine **21C**, R = $C_6H_5$, have been refuted by more recent work[53].

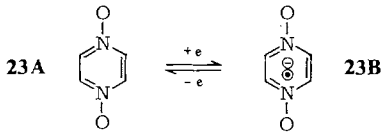


However, due to the acceptor function of the $SO_2R$-group compounds **21C** would be expected to be stable. Evidence for the presence of **21C**, R = *p*-$CH_3C_6H_4$, was found in experiments by *Eisner* and *Williams*[53], who isolated **22** as a product of hydrolysis.

### 4.4. Pyrazines according to Scheme 2, with X = $O^{\ominus}$

1,4-Pyrazine dioxide **23A** is a weaker base than pyrazine[54]. Because of the acceptor effect of the coordinated oxygen atoms **23A** is more readily reduced than **1**, forming a stable radical *anion* **23B**, whose ESR spectrum indi-

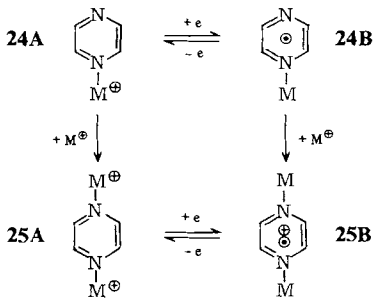
cates that the unpaired electron is delocalized towards the oxygens[55] (cf. Table 5).




The free electron pairs on the oxygen atoms cause **23A** to be a bifunctional ligand for electrophiles, particularly for metal ions[56].

### 4.5. Pyrazines according to Scheme 2, with X = M (M = Alkali Metal)

As a weak base pyrazine does not form very stable complexes **24A** and **25A** with alkali metal cations[57]. However, upon its formation by alkali metal, the radical anion **2** coordinates very readily with the corresponding $Li^{\oplus}$, $Na^{\oplus}$ or $K^{\oplus}$ ions. As a result one obtains paramagnetic ion pairs **24B**[58] or "triple ions" **25B**[59].



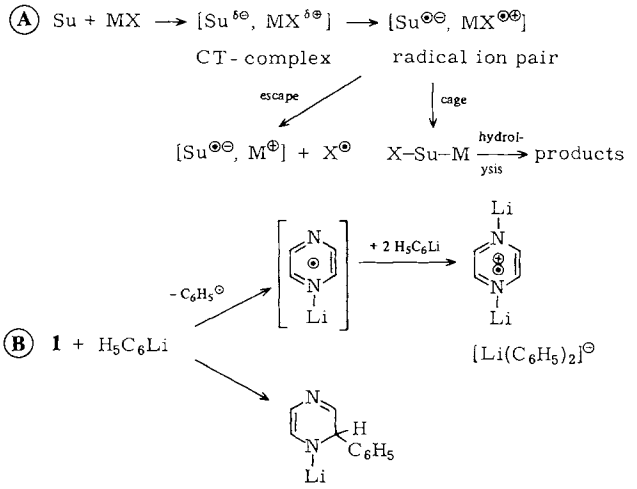

In the 1 : 1 adducts **24B** the metal cation is not fixed to pyrazine at one coordination site, exchange processes take place in the range of the ESR time scale of approx. $10^{-7}$ s[58,60]. 1 : 2 Radical complexes **25B** (triple ions) are formed at low temperatures[61] and especially after addition of soluble alkali metal salts[59].

These triple ions are also formed in the reaction of pyrazine with organometallic reducing agents in coordinating solvents[62,63].

$$\mathbf{1} \xrightarrow[LiAlH_4]{LiR} \mathbf{25B},\ M = Li$$

Such reactions, in which radicals are formed from two diamagnetic compounds, occur *via* an intermolecular electron exchange. They may be taken as an indication of a *s*ingle *e*lectron *t*ransfer (SET) mechanism[64] (Scheme 3, Fig. 3). In the reaction of pyrazine with electron transfer reagents the formation of diamagnetic products is as expected[65] (Scheme 3Ⓑ); however, the presence of polymeric byproducts is characteristic for SET reactions of N-heterocycles[65,66].

Alkali metal/pyrazine radical complexes have also been detected in the reaction of ethylenediamines with *n*-butyllithium[67]. This provides further proof of the tendency to form the 7 π-electron intermediate (cf. Table 2).




Scheme 3. Ⓐ Intermolecular single electron transfer (SET) mechanism for the reduction of a substrate Su by an organometallic compound MX (X = H, R; M = metal ion or metal fragment). The reaction between donor (MX) and acceptor (Su) leads, *via* a charge transfer complex, to formation of a radical ion pair, which may undergo two possible reactions in the solvent cage. Migration of the particle to be transferred X *within* the cage (cage reaction) leads to formation of a diamagnetic metal complex, whose hydrolysis gives the desired reaction product. On the other hand, dissociation of a free radical $X^{\odot}$ out of the solvent cage (escape reaction) gives a paramagnetic complex, which if sufficiently stable may be observed. The effectiveness of the SET reaction and the ratio of cage to escape products depend on numerous external factors, such as temperature, solvent and irradiation.—Ⓑ In the reaction of pyrazine with phenyllithium one observes the following: A diamagnetic reaction product, the expected 1,2-dihydropyrazine addition product, may be detected at low temperatures [65a]. However, as suggested by the NMR line widths [65a], radicals are formed in the solution. According to the ESR spectrum (Fig. 3) triple ions of type **25B** are produced with excess phenyllithium [62].

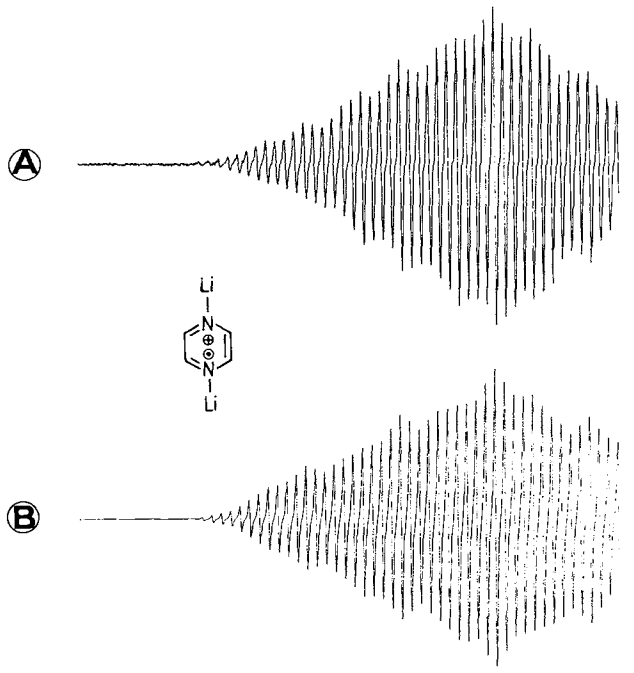
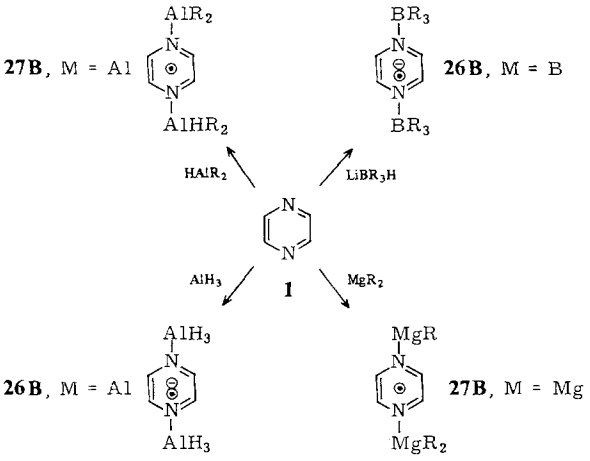



Fig. 3. In the reaction of pyrazine with excess phenyllithium in tetrahydrofuran a stable radical is formed, whose high resolution ESR spectrum (low field region) is shown in Ⓐ. Its graphic reproduction by computer-controlled spectrum synthesis Ⓑ was carried out with the coupling constants given in Table 5 and a line width of 0.013 mT. The radical formed is the triple ion [59, 62] [$Li^{\oplus}$, $1^{\ominus}$, $Li^{\oplus}$] of type **25B** (cf. Scheme 3).

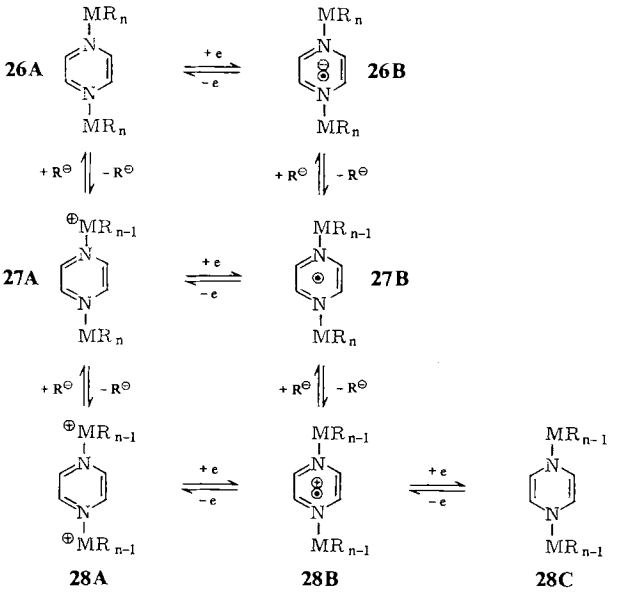
### 4.6. Pyrazines according to Scheme 2, with $X = {}^{(\ominus)}MR_n$ (M = Main Group Metal; R = H, Alkyl, Aryl)

Electron-deficient organometallic compounds $MR_n$ form 1:2 adducts **26A** with pyrazine, *e.g.*, complexes with $B(C_2H_5)_3$[68], $Al(CH_3)_3$[69] and $Zn(C_6H_5)_2$[69] (Table 4). Due to π-backbonding into the LUMO of ligand **1** (see Section 4.7), the electronic spectra of some of these complexes exhibit charge transfer bands at long wavelengths[69]. For very electron-rich organometallic compounds and metal hydrides, such as LiR[62], $MgR_2$[70], $AlR_2H$[71], $AlH_3$[72], $BH_3$[69] and $LiBR_3H$[69], a complete electron exchange replaces the charge transfer and one observes stable radical complexes, formed by SET mechanisms (cf. Scheme 3).




The composition of these radical complexes varies due to the low basicity of pyrazine and also of the pyrazine radical anion[62,72]: **2** may coordinate with two molecules (to give **26B**), two cations (to give **28B**), or with one neutral molecule and one cation (to give **27B**). Complexes of the last type have very complicated ESR spectra[69,71] and undergo intramolecular exchange processes[70a].

In SET reactions of complex organometallic compounds ($LiAlH_4$[62], $LiBR_3H$[69]) several reaction pathways are possible, and, according to the position of the coordination equilibrium, one observes different radicals and their products. This radical product selectivity[72] should also furnish clues to the selectivity of the "cage" reaction (Scheme 3), which leads to diamagnetic compounds.




Organometallic halides, such as $R_3SiCl$, $R_2BCl$ and $R_2AlCl$, also form complexes with pyrazine[69]. Formally, these compounds correspond to quaternary salts such as **18A**. They can generally be dehalogenated by reduction with an alkali metal, so giving a positively charged radical complex **28B**. Such species may also be prepared by alkali metal reduction of pyrazine/organometal complexes[70,73,74], due to the electrolytic dissociation of metal alkyls in coordinating solvents[75].

$$2\,MR_n \rightleftharpoons [MR_{n-1}]^{\oplus} + [MR_{n+1}]^{\ominus}$$

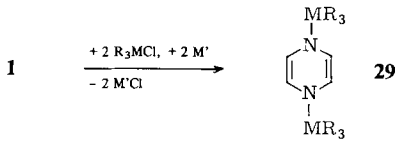
By varying the Coulomb integral $\alpha_N$[76], the results of electron spin resonance investigations on the radical complexes **28B** (Table 5) may again be interpreted in terms of the HMO model[2]. The ESR coupling constant $a_H$ and thus the distribution of the unpaired electron correlate with the squares of the Hückel coefficients in the singly occupied molecular orbital $B_{1u}$ (Fig. 4).

Table 5. ESR coupling constants $a_x$ [μT] of pyrazine π-radical ions. The sequence in which the coupling constants of the ring protons $a_H$ increase shows the influence of charge, polarization (Fig. 4) and delocalization of the *N*-coordinated species.

| Compound | Type | Solvent [a] | $a^{1}_{H}$ | $a^{14}_{N}$ | $a_X$ (X) | Ref. |
|---|---|---|---|---|---|---|
| $[1(O)_2]^{\ominus}$ | **23B** | DMF | 137 | 949 | — | [55] |
| $[1(W(CO)_5)_2]^{\ominus}$ | **38B** | THF | 254 | 823 | 286 ($^{183}$W) | [93] |
| $[1(BEt_3)_2]^{\ominus}$ | **26B** | THF | 255 | 802 | 255 ($^{11}$B) | [74] |
| $[1]^{\ominus}$ | **2** | THF | 264 | 718 | — | [8] |
| $[1(Li)_2]^{\oplus}$ | **25B** | THF | 273 | 685 | 70 ($^{7}$Li) | [62] |
| $[1(MgPh)_2]^{\oplus}$ | **28B** | THF | 285 | 677 | 37 ($^{25}$Mg) | [70] |
| $[1(AlH_3)_2]^{\ominus}$ | **26B** | THF | 285 | 693 | 285 ($^{27}$Al)<br>197 ($^{1}$H, Al) | [76] |
| $[1(C_2H_5)_2]^{\oplus}$ | **18B** | $H_2O$ | 290 | 850 | 540 ($^{1}$H, $CH_2$)<br>23 ($^{1}$H, $CH_3$) | [16] |
| $[1(SiR_3)_2]^{\oplus}$ | **32** | $CH_2Cl_2$ | 313 | 664 | 279 ($^{29}$Si) | [87] |
| $[1(H)_2]^{\oplus}$ | **8** | THF | 316 | 745 | 805 ($^{1}$H, N) | [18, 73] |

[a] DMF = dimethylformamide, THF = tetrahydrofuran.

The $R_3SiCl$ and $R_3GeCl$ adducts of pyrazine may readily be completely dehalogenated, giving 1,4-dihydropyrazines **29**[24,40,77] (type **28C**; **29**, $MR_3 = SiMe_3 \equiv$ **17**).




M' = Li, Na, K
$MR_3$ = $Si(CH_3)_3$ (≙ **17**),
$SiH(CH_3)_2$, $Si(tC_4H_9)(CH_3)_2$, $Si[Si(CH_3)_3]_3$, $Ge(CH_3)_3$

Although compounds **29** are quite stable thermally, other properties, such as their color and ready inflammability in air, are indications of the antiaromatic character expected for a "true" 1,4-dihydropyrazine system. From the special properties of the silicon-nitrogen bond[78] it is

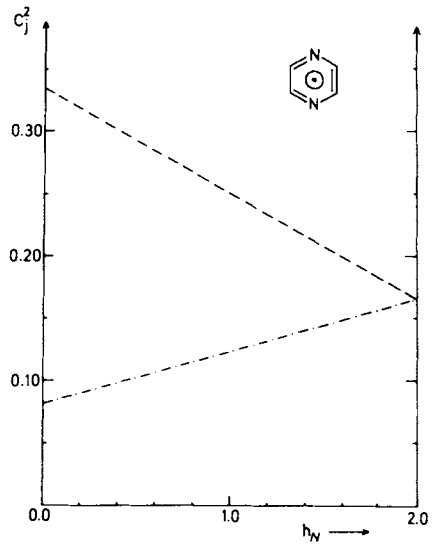
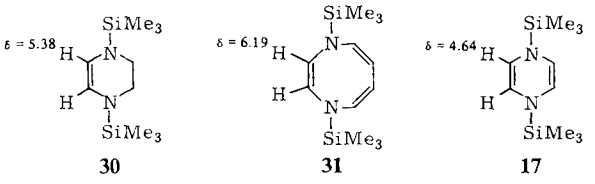



Fig. 4. In planar π-radicals the ESR coupling constants of α-*C* protons are proportional to the squares of the Hückel coefficients of the singly occupied molecular orbital [2c]. For the pyrazine $B_{1u}$ orbital (Fig. 1) the squares of the coefficients in the 1,4- (----) and 2,3,5,6-positions (-·-·) are linearly dependent on the perturbation parameter $h_N$; $c_N^2 = 1/3 - 1/12h_N$ and $c_C^2 = 1/12 + 1/24h_N$ [63]. The coupling constant $a_H$ (Table 5) should increase with growing $h_N$ (increasing N "electronegativity").

clear that **17** does not undergo a 1,3 shift Si–N→Si–C as readily as the NR derivatives (bond order Si–N > 1). Furthermore, due to the widening of angles at the nitrogen atom[78,79] considerable conjugation between olefinic π-electrons and the free N-electron pairs takes place. Therefore, compounds **29** serve as excellent models[24,41] for the hypothetical planar 1,4-dihydropyrazine **9**.

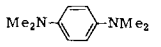
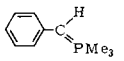
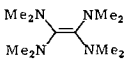
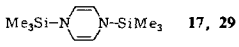
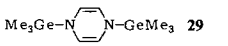
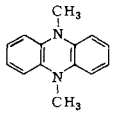
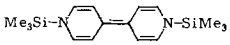
Comparison with non-conjugated **30** and a reference compound containing 10 π-electrons **31**[80] clearly demonstrates an upfield shift for the ring protons in the $^1$H-NMR spectrum of the 8 π-electron compound **17**. This shift confirms the "antiaromatic" character of the 1,4-dihydropyrazine system[5] (Scheme 4).




Scheme 4. The $^1$H-NMR spectrum shows the presence of cyclically conjugated π-electrons. In aromatic compounds with 4n+2 π-electrons the outer proton signals are shifted downfield (diamagnetic ring current), whereas in the antiaromatic case (4n π-electrons) the opposite effect, *i.e.* upfield shift, is to be expected (paratropism [50]). Compared with the non-conjugated compound **30**, the 10 π-electron system **31** [80] shows a downfield shift, while the 8 π-electron compound **17** has an almost equally large upfield shift of its *N,N'*-bis(trimethylsilyl)endiamine protons [24c].

With a first vertical ionization energy of 6.16 eV[24] (adiabatically: 5.7 eV) **17** belongs to the electron-richest main group element compounds (Table 6). Moreover, for the red trimethylgermyl derivative $IE_1^v = 5.87$ eV has been determined[24b] (cf. $IE_1$(Na) = 5.1 eV).

Table 6. First vertical ionization energies $IE_{1,2}^v$ [eV] of electron-rich main group element compounds.

| Compound | Type | $IE_1^v$ [eV] | $IE_2^v$ [eV] | Ref. |
|---|---|---|---|---|
|  TTF | | 6.83 | 8.69 | [81] |
|  TMPD | | 6.75 | 8.35 | [82] |
|  | | 6.19 | 8.32 | [83] |
|  | | 5.95 | 7.5 | [84] |
|  | **17, 29** | 6.16 | 9.5 | [24b] |
|  | **29** | 5.87 | 9.15 | [24b] |
|  | **68** | 6.57 | 8.00 | [85] |
|  | **80** | 6.50 | 8.35 | [24c] |

Using Koopman's theorem the remaining π-ionizations also allow an excellent correlation with the expected orbital sequence given in Figure 1 (Fig. 5).

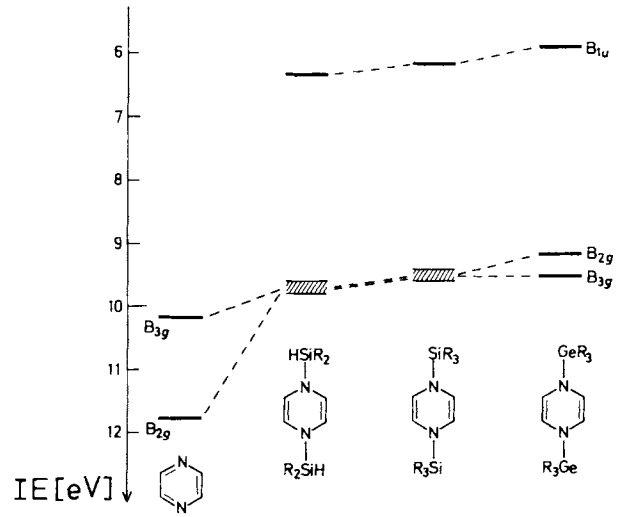
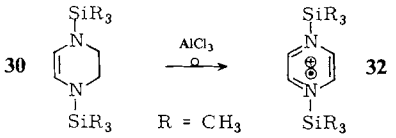


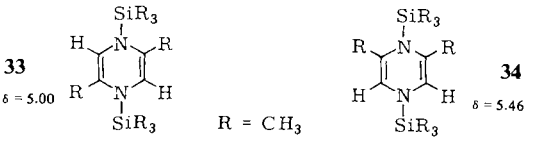

Fig. 5. Using Koopman's theorem $IE_n = -\varepsilon_{SCF}^j$ ionization energies *IE*, determined by photoelectron spectroscopy, may be correlated with orbital energies $\varepsilon^j$ (Fig. 1). A comparison of π-ionizations of pyrazine **1** [9] and three 1,4-dihydropyrazines [24b] shows that the ionization assigned to the $B_{3g}$ orbital remains constant at approx. 10 eV (nodal plane through positions 1 and 4). On the other hand, organometallic substitution in the 1,4 position lowers the ionization energies of the π-molecular orbitals with large Hückel coefficients $c_N$. This not only affects the bonding orbital $B_{2g}$ but also the antibonding orbital $B_{1u}$, which in 1,4-dihydropyrazines is occupied. A lowering of the ionization energies occurs in the sequence of *N*-substituents $HSiR_2$, $SiR_3$, $GeR_3$, since the $\pi_S$ and $\pi_S^*$ orbitals have comparable Hückel coefficients [2].

The spectroscopic properties of compounds **29** (≙ **28C**) are in agreement with their chemical reactivity, especially their sensitivity towards oxidation[40,77]. The controlled oxidation of **28C** with $AlCl_3$[86] leads to the paramagnetic intermediate **28B**[87]. The radical **32** is also formed in the reaction of the tetrahydropyrazine **30** with $AlCl_3$ in dichloromethane. This is a further example of the strong tendency to form the 7 π-electron intermediate (Table 2).

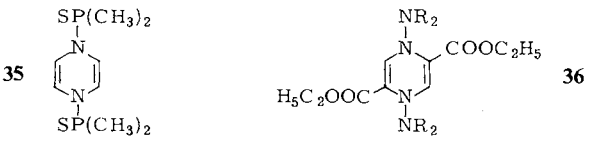



The thermal stability of *N*-trialkylsilyl-1,4-dihydropyrazines permits one to study substituent effects in greater detail. The, at first sight surprising, results of NMR, UV and photoelectron spectroscopic studies[24] showed that the compounds become *less* electron-rich with increasing *C*-methyl substitution. Such behavior contradicts the "normal" (+I)-substituent effect of an alkyl group[86]. However, the results may be interpreted in the light of the discussion on the conformation of 1,4-dihydropyrazines[24] (Table 1, Fig. 2):

Increasing *C*-methylation leads to increasing steric interaction with the bulky $R_3Si$-groups and thus a larger deviation from the planar conformation of the ring and of the *N*-substituents. The impairment of the cyclic 8 π-electron conjugation is not compensated by the donating effect of the methyl groups. In agreement with this model and with Figure 2, the effect observed[24] for dimethyl derivatives of **17** was found to be smallest in the 2,5-isomer **33** (no vicinal arrangement of substituents) and largest in the 2,6-isomer **34**.



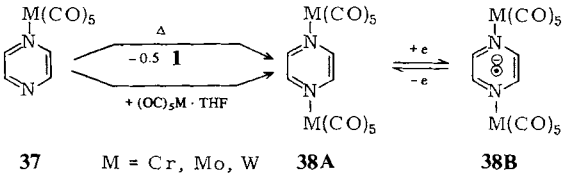

Obviously the 1,4-dihydro-1,4-diazine system is characterized by considerable structural flexibility, which is caused by the unfavorable presence of 8 π-electrons. In the following sections the consequences of this flexibility on the possible structures of reduced phenazines (Section 6.1) and on the redox behavior of flavoenzymes (Section 7.1) will be demonstrated.




The derivatives **35**[69] and **36**[88] are related to the organoelement-substituted 1,4-dihydropyrazines **29**. The stability of **35** is due to the π-acceptor effect of the thiophosphinyl group[89], while **36** is stabilized by the ester substituents attached to the heterocyclic ring. As in the case of many other 1,4-dihydro-1,4-diazines (Table 2), compound **36** is already oxidized to the radical cation by atmospheric oxygen[88].

### 4.7. Pyrazines according to Scheme 2, with $X = {}^{\ominus}M(CO)_5$ (M = Cr, Mo, W)

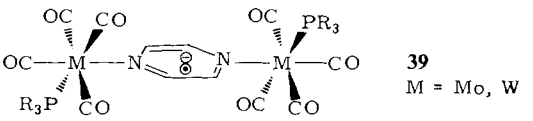
Binuclear bis(pentacarbonylmetal) complexes **38A** are formed from the mononuclear derivatives **37** by a thermal solid state reaction[90] or upon addition of $THF \cdot M(CO)_5$[91].



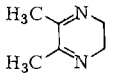

Compounds **38A** are colored and, as has been demonstrated for the tungsten complex[92], give rise to two charge transfer bands in the region between 450 and 600 nm which may be differentiated in Resonance Raman experiments. *Both* electronic transitions occur from occupied metal-centered orbitals to the lowest unoccupied molecular orbital $B_{1u}$ of pyrazine. This is named a *m*etal-to-*l*igand *c*harge *t*ransfer (MLCT)[92].

The addition of one electron to **38A** occurs reversibly at reduction potentials markedly raised by the coordination[91]. However, stable radical anions **38B** (M = Mo, W) have only been obtained by *in-situ* complex formation[93]. The ESR data (cf. Table 5) confirm the predominantly ligand-like character of the singly occupied molecular orbital in **38B**. The stability and spin distribution of radicals **18B** and **38B** are in agreement with *Hoffmann*'s concept of an isolobal relationship between $R^{\oplus}$ and $M(CO)_5$[94].

Substitution reactions may be carried out with radical complexes **38B**; with phosphanes, bis[tetracarbonyl(phosphane)metal] complexes **39** are formed[69].

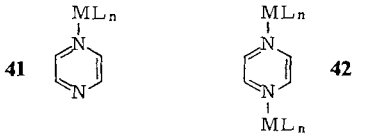



Besides pyrazine itself[90,91,95-99], 2,3-dihydropyrazines such as **40** are also suitable complexing ligands for carbonylmetal species[101] because of their 1,4-diazabutadiene structure[100]. However, the coordination modes of these compounds are not yet certain[101].




### 4.8. Pyrazines according to Scheme 2, with $X = ML_n$ (M = Transition Metal, L = Ligand)

Pyrazine forms numerous monomeric 1:1 (**41**) and 1:2 complexes (**42**) with transition metal compounds.

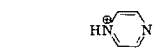
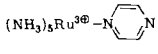
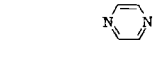
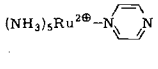
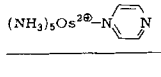


Not only inorganic ions and molecules, such as $Ni^{2\oplus}(aq)$[102], $[IrCl_5]^{n\ominus}$[103], $Re_3Cl_9$[104] or $OsO_4$[105], but also coordinatively unsaturated organometallic fragments, *e.g.* $Fe(CO)_4$[97], $Rh(CO)_2Cl$[98], $[Rh(PR_3)_2(CO)]^{\oplus}$[99], $ZrR_4$[106], $Yb(C_5H_5)_3$[107a], $U(C_5H_5)_3$[107b], $Pt(C_2H_4)Cl_2$[108], may form coordination compounds with pyrazine. Except for the effects of differing basicities[97,99,104], many of these compounds are comparable to the corresponding pyridine complexes. However, some of these coordination compounds are of special interest for the following reasons: Electron-rich $d^6$ metal fragments such as $L_nFe^{II}$ or $L_nRu^{II}$ can undergo a charge transfer interaction with the π-system of electron-deficient pyrazine. One indication of this interaction is the appearance of intense MLCT bands in the visible region.

In binuclear complexes an interaction between both coordinated metal fragments is possible. The distance between two coordinated metal atoms in μ-pyrazine complexes is *ca.* 600—800 pm, and the question of whether, to which extent, and in which manner an electron interaction between the two coordinated species takes place *via* the ligand is of considerable interest, especially in relation to electron transfer in biological systems[109]. In pyrazine there is not only the π-system with a low lying LUMO (Fig. 1) but also the σ-system including the two *N*-electron pairs[110] available for electron transfer propagation. According to recent theoretical investigations[111] it seems likely that in pyrazine *both* transfer mechanisms can play a role.

*1:1 Complexes:* Similarly to the pentacarbonyls $M(CO)_5$[112], the low spin $d^6$ species of divalent iron[113–115], ruthenium[116] and osmium[117] may backbond into the LUMO of pyrazine. This backbonding results in the appearance of intense MLCT bands in the visible region of the spectrum[113–117] and in accompanying photochemical processes[118], in a reduction of the metal-pyrazine distance[119], and in a drastic increase of the basicity of the second nitrogen atom in the ligand (Table 7). In such cases binuclear complexes **42** are formed without difficulty[120,121].

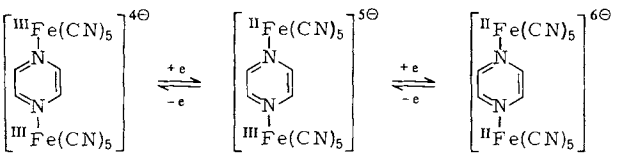
Table 7. Acidity constants $pK_a$ of pyrazine and pyrazinium ions. Coordinated $(NH_3)_5Ru^{II}$ and $(NH_3)_5Os^{II}$ metal fragments can π-backbond into the lowest unoccupied ligand orbital and thus cause an exceptional increase in basicity of the free nitrogen atom.

| Compound (conjugated base) | Type | $pK_a$ | Ref. |
|---|---|---|---|
|  | 4 | −6 | [14] |
|  | 41 | −0.8 | [116] |
|  | 1 | +0.6 | [14] |
|  | 41 | +2.5 | [116] |
|  | 41 | +7.4 | [117] |

*1:2 Complexes:* If the *N*-coordinated ions and not, as described in Sections 4.1 to 4.7, the pyrazine is the redox-active or spin-carrying species, then for binuclear complexes new phenomena appear:

a) The electrochemistry of these complexes is generally characterized by several reversible redox steps, in which first of all the coordinated metal ions take up or lose electrons[122].
b) Mixed valence compounds which contain the same metal fragment, at least formally, in different oxidation states are especially interesting. The ground states of such systems may be unsymmetrical (localized valences) or symmetrical (delocalized valences)[123].
c) If two different metal ions are coordinated to the same ligand, then the mechanism and rate of a possible electron transfer *via* the ligand are of predominant interest (inner-sphere electron transfer)[124].
d) The coordination of two paramagnetic ions may lead to a molecular magnetic exchange interaction ("superexchange") between the two centers; the spins may couple giving either a ferromagnetic or an antiferromagnetic type of interaction[125].

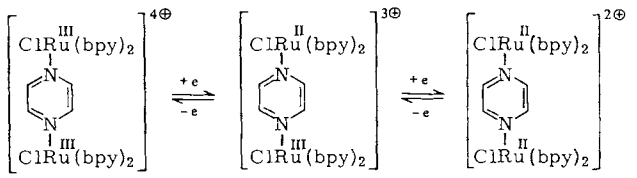
Re a): Due to the coordination of two redox-active metal fragments to pyrazine, the binuclear complex establishes a multistep redox system. If the interaction between the coordinated ions is small the two potentials are similar[122]. Examples are the systems **43** and **44**[121,126].



**43A** **43B** **43C**

$\lambda_{IT}$ = 1200 nm; $k_{SEM} \approx 50$

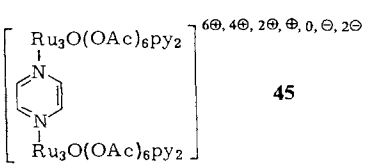
From the two potentials of a two-step system one may again calculate a stability constant $k_{SEM}$ for the intermediate. In this way the mixed-valence ions **43B** and **44B** are found to be relatively stable towards disproportionation (IT = intervalence transfer).



**44A** **44B** **44C**

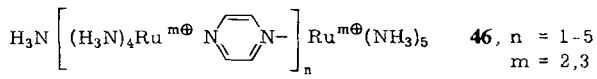
$\lambda_{IT}$ = 1300 nm; $k_{SEM}$ = 100

The number of accessible separate oxidation states increases further upon coordination of cluster compounds[127b] which store electrons[127a] (**45**) or upon con-



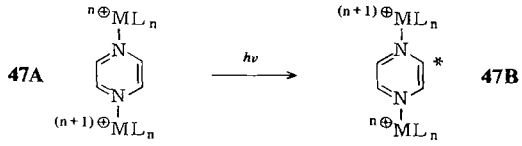
**45**

struction of multiple bridges with μ-pyrazine (**46**)[128]. These compounds are interesting intermediates on the way to the formation of coordination polymers (Section 5); the crowding of discrete energy levels marks the beginning of an energy band behavior[127b].



**46**, n = 1-5, m = 2,3

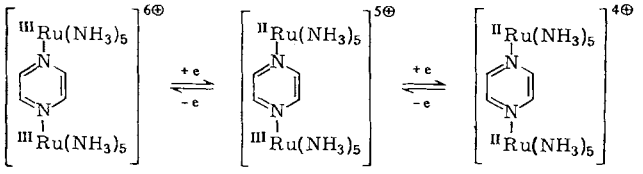
Re b): According to the classification of *Robin* and *Day*[123] mixed-valence compounds of the type **43B** or **44B** may occur as localized, unsymmetrical or as delocalized, symmetrical species. In the first case, if there is only a weak interaction between the coordinated ions of different valence, one would expect a long wavelength absorption in the electronic spectrum, due to an IT or MMCT process (cf. Fig. 6) (MMCT = metal-to-metal charge transfer).



**47A** **47B**

Due to the Franck-Condon principle the electronic transition from **47A** to **47B** occurs considerably faster than the change in geometry accompanying movement of nuclei. For only small differences in coordination geometry (*e.g.* $Fe^{II}/Fe^{III}$ or $Ru^{II}/Ru^{III}$[119]) the amount of energy $E_0$ (Fig. 6) required for this process is very small, and the corresponding absorption often takes place in the near infrared[129]. The rate constant of intramolecular electron transfer in **44B** has been calculated to be *ca.* $10^{-8}\ s^{-1}$[130].

Originally a localized structure, *i.e.* $Ru^{II}/Ru^{III}$ instead of $Ru^{II\,1/2}/Ru^{II\,1/2}$, was also assumed for the "Creutz-Taube" complex **48B**[120], which is related to **44B**.



**48A** **48B** **48C**

$\lambda_{\text{"IT"}} = 1570$ nm; $k_{SEM} = 4 \times 10^6$

However, certain data, such as the large formation constant and the position and symmetry of the long-wavelength absorption band[131], were not compatible with this description. In the meantime the lengthy, controversial discussion[132] surrounding the nature of this ion appears to have been settled[119] by recent theoretical[133] and experimetal results: **48B** is a borderline case with a very small barrier to delocalization appearing between the localized forms (Fig. 6). The absorption in the IR could then be assigned to a "normal" $^2A_{1g} \rightarrow {}^2A_{2u}$ transition[134]. The height of the delocalization barrier $E_t$ does not only depend on the distance between the metal ions[135] but also on the degree of electronic interaction between the metal fragments and the bridging ligand ("resonance energy" $E_r$, Fig. 6)[119].

The pentaammineruthenium ions in **48B** experience quite a considerable interaction *via* the electron system of pyrazine, while in the related mixed-valence complex **44B** this interaction is distinctly smaller. In this case pyrazine obviously has to compete with 2,2'-bipyridyl, which is also easily reduced[7], for the metal charge available for back-bonding. This is further confirmation of the importance of low-lying π*-molecular orbitals for intramolecular electron transfer[120].

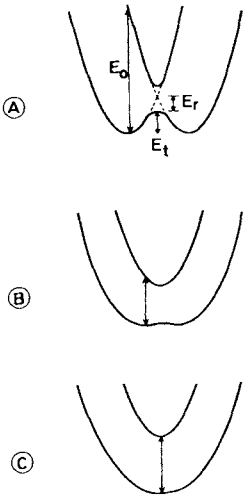
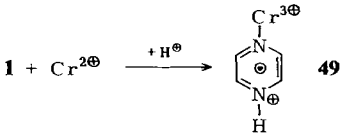


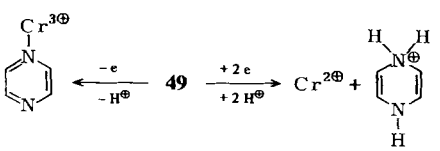

Fig. 6. Thermal and light-induced intramolecular electron transfer reactions in a binuclear mixed-valence complex may be described by potential curves along one configuration coordinate. Ⓐ In the case of localized valences with a small exchange interaction across the bridging ligand, a thermally surmountable energy barrier $E_t$ exists between the two equivalent states. The "resonance energy" $E_r$ is a measure of the exchange interaction occurring *via* the ligand. The optical transition ($E_0$) corresponds to an IT or an MMCT process (cf. **47A** → **47B**). Ⓑ Growing interaction between the localized valences *via* the bridging ligand leads to an increase in resonance energy and a decrease in the thermal barrier, until in case Ⓒ a symmetrical species of "delocalized" valence is formed [119, 123, 129].

Re c): The low-lying LUMO of pyrazine is not only useful for the study of charge transfer interactions but also for investigations into complete electron exchange in the ground state. A striking example is the reaction of **1** with $Cr^{2\oplus}$ to give **49**, which leads to coordination of the metal, electron transfer to the ligand, and to the addition of a proton onto the reduced ligand[136].



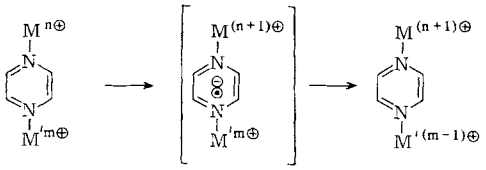
**1** + $Cr^{2\oplus}$ → **49**

The electrochemistry of complex **49** is also informative[137], since it reveals two well-known aspects of the pyrazine system, namely the stability of cation **10** (*i.e.*, the instability of 1,4-dihydropyrazine **9**), and the low basicity of the oxidized compound **1** (Section 3).



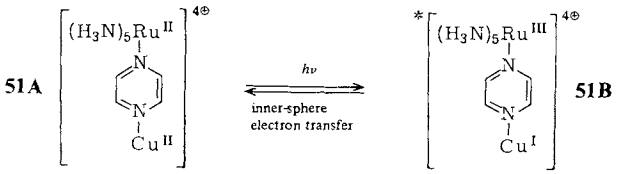
**50** **10**

The coordination of two different redox-active metal ions to pyrazine permits one to carry out kinetic studies on the ligand-bridged (inner-sphere) electron transfer between the metal centers[124]. In the radical ion mechanism of inner-sphere electron transfer the bridging ligand—an ion or molecule—has to take up the electron for a certain time[138]. The pyrazine molecule is obviously capable of carrying out this function.

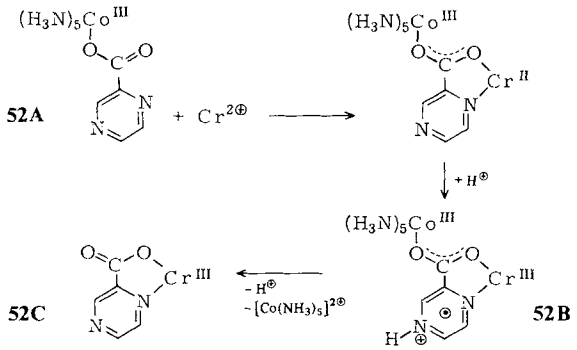


Two instructive examples of the use of the pyrazine system are provided by the complexes **51A** and **52A**.

Complex **51A** has the MLCT band in the visible region, which is typical of such $Ru^{II}$ compounds. If electron transfer to **51B** is induced by flash photolysis, this absorption band fades ("electron transfer photochromism"). The kinetics of the regeneration of **51A** indicate the presence of a unimolecular electron transfer relaxation[139].

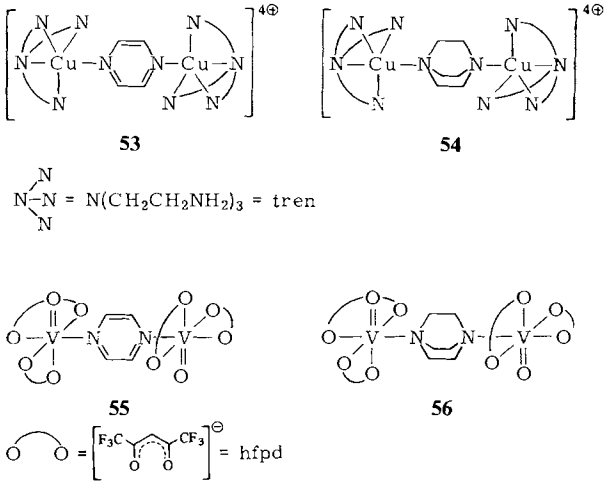



The reduction of the $Co^{III}$-pyrazinecarboxylate complex **52A** by $Cr^{2\oplus}$ was expected to occur *via* an inner-sphere radical ion mechanism. Kinetic measurements and pulse radiolysis studies have confirmed the existence of the postulated intermediate **52B** (cf. **49**)[140].




Re d): In monomeric pyrazine complexes magnetic interactions between coordinated metal ions have seldom been observed[134]. However, studies on complexes **53**—**56**[141] have shed light on the mechanism of such exchange interactions.

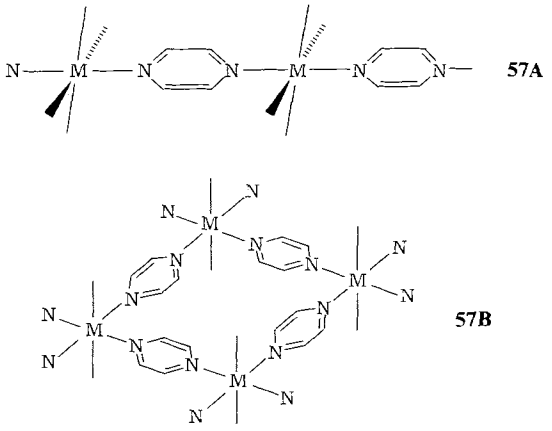
For pyrazine, mechanisms involving not only its π- but also its σ-system have been discussed[111], whereas the likewise bifunctional ligand 1,4-diazabicyclo[2.2.2]octane (DABCO) only has a σ-system available[110]. An antiferromagnetic spin-spin interaction has been observed only in



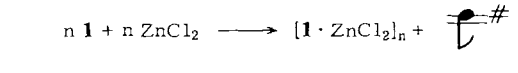

those $Cu^{II}$ and $V^{IV}$ complexes in which pyrazine acts as bridging ligand[141] (cf. Table 8). These findings demonstrate that the participation of the pyrazine π-system is necessary for the formation of a magnetic interaction. In the following section further evidence for this effect will be provided by a comparison of polymeric $Cu^{II}$-pyrazine complexes.

## 5. Coordination Polymers containing Pyrazines

The series of compounds **46** demonstrates how coordination oligomers and polymers may be produced by coordination of the bridging ligand μ-pyrazine with polyfunctional metals. In fact such complexes have long been known[142]. Depending on the coordination properties of the metal they may exist as chain (**57A**) or sheet polymers (**57B**).




Metal salts especially[142–144], but also quadruply bonded metal dimers[145] and metalloporphyrins[146] are suitable multiply unsaturated coordination partners. Incidentally, the formation of the polymeric adduct **1** · $ZnCl_2$ is accompanied by an acoustic emission[144].



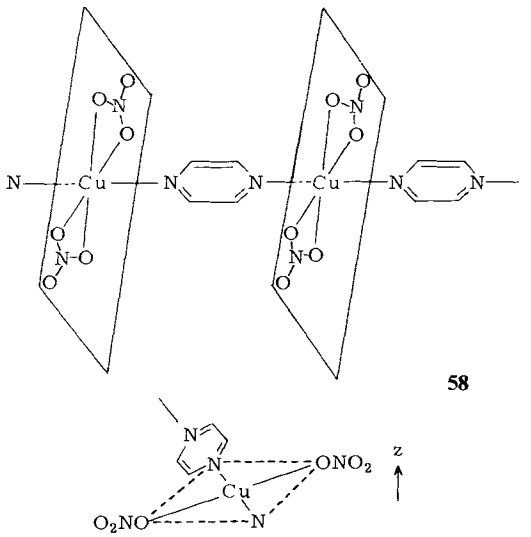
In polymeric complexes of anisotropic structure, electrical[147] and magnetic[148] properties are of interest. The following discussion concentrates on the magnetic exchange phenomena in $Cu^{II}$-μ-pyrazine complexes (Table 8).

Table 8. Magnetic exchange parameters $J$ [$cm^{-1}$] of pyrazine-bridged $V^{IV}$ and $Cu^{II}$ complexes of low dimensionality Positive and negative signs indicate ferro- and antiferromagnetic exchange behavior, respectively.

| Complex | Dimensionality | $J$ | Ref. |
|---|---|---|---|
| **55** | "Dimer" | −19 | [141] |
| **53** | "Dimer" | − 3.2 | [141] |
| **58** | 1 D | − 3.7 | [151] |
| **60** | 2 D | − 5.3 | [153] |
| **61** | 1 D | − 0.1 [a] | [154] |
| **62** | 1 D | + 1.3 | [156] |

[a] Inter-dimer exchange.

$[Cu(NO_3)_2 \cdot 1]_n$ **58** has been the subject of numerous investigations[149–151]. It is a linear coordination polymer in which the nitrate ions lie in a plane perpendicular to the Cu-pyrazine chain[150]. The substance behaves as a one-dimensional Heisenberg antiferromagnet (Table 8). In an elegant study employing various 1,4-diazines *Richardson* and *Hatfield*[151] were able to show that the variation of the antiferromagnetic coupling correlates neither with the σ-basicity nor with steric factors but with the energy of the $\pi \rightarrow \pi^*$ transition. This result already indicates the presence of an exchange mechanism involving the pyrazine π-system. It is interesting that this is confirmed by the structure of complex **58**, since the $CuN_2O_2$ unit forms an angle of $\gamma = 48°$ with the pyrazine plane, thus permitting sufficient overlap between the spin-bearing $d_{z^2}$ metal orbital and the π-system of the ligand[150,151].

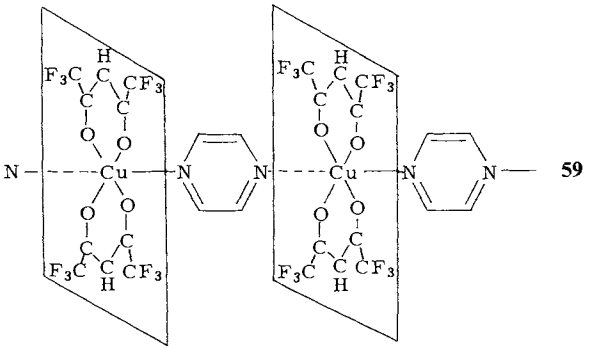


**58**



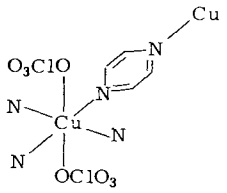
In $[Cu(hfpd)_2 \cdot 1]_n$ **59**, with two bidentate hexafluoropentanedionate ligands hfpd, an overlap of the spin-carrying orbital with the pyrazine π-system is not possible due to the coordination geometry at the metal. Accordingly, *no* magnetic exchange interaction is observed[152].

The use of the very weak base $ClO_4^{\ominus}$ as anion for $Cu^{II}$ in $[Cu(ClO_4)_2 \cdot (1)]_n$ **60** permits four pyrazine molecules to coordinate to the metal, so forming a two dimensional



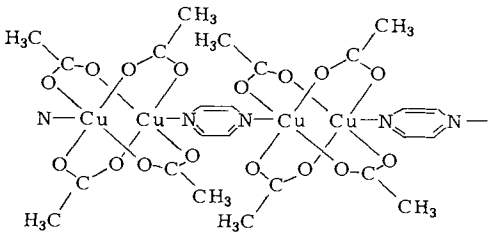
**59**

sheet polymer of type **57B**. In **60** the angle lying between the laminar plane and the plane of the pyrazine molecules is 66°, so that an interaction between the spin-carrying $Cu^{II}$ orbitals and the pyrazine π-system is possible, and a two dimensional, antiferromagnetic exchange interaction may be observed[153] (Table 8).



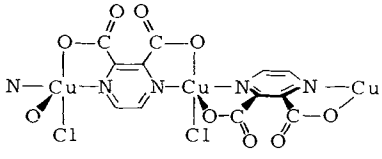
**60**

For $[Cu_2(OAc)_4 \cdot 1]_n$ **61** there are two possible magnetic exchange interactions: the "direct" interaction between neighboring copper atoms in the dimer $Cu_2(OAc)_4$ and inter-dimer exchange *via* the pyrazine bridges. Measurements of ESR line widths indicate that the latter process also takes place[154] (Table 8).



**61**

Pyrazinecarboxylates are anionic, bidentate bridging ligands with good complexing properties[155]. Reaction of $CuCl_2$ with 2,3-pyrazinedicarboxylic acid furnishes $[Cu(pzdc) \cdot HCl]_n$ **62**, whose structure has been shown by X-ray analysis to be a polymeric chain with alternating orthogonal heterocyclic bridges[156].

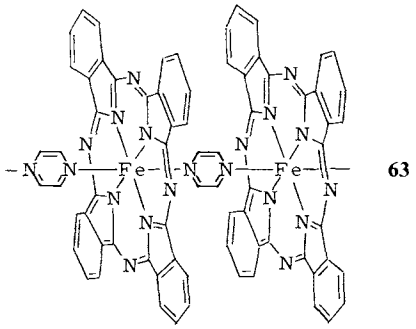


**62**

In contrast to previously characterized pyrazine coordination polymers, compound **62** exhibits one dimensional *ferro*magnetic behavior (Table 8), which had previously only been observed for complexes with a bridging *atom*. A requirement for ferromagnetic behavior is that the spin-

carrying orbitals be orthogonal[157]. Hence, this result provides fresh evidence for the π-transfer mechanism of magnetic exchange with pyrazine bridging ligands. Still in doubt is the extent to which occupied and/or unoccupied π-orbitals take part in the exchange mechanism[151]; theoretical studies leave both options open[111].

The low dimensionality of polymeric pyrazine-metal complexes and thus the potential availability of "polymeric π-systems" have prompted investigations into the conductivity of such substances. In general, theoretical[147] expectations have not been fulfilled. Studies on pyrazine[158,159] and 2,5-pyrazinedicarboxylate complexes[160] have shown no marked rise in conductivity due to their polymeric structures. However, *Schneider* and *Hanack*[161] recently described a system, in which a $10^6$-fold increase in conductivity was observed on going from a monomeric 1:2 adduct to the polymeric complex **63**:



**63**

## 6. Modification of Pyrazines

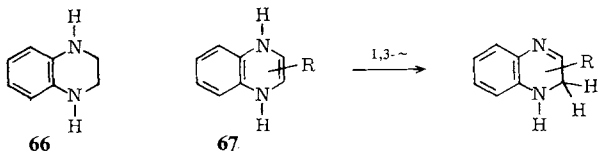
### 6.1. Annelation of Benzene Rings

The 1,4-diazines quinoxaline **64** and phenazine **65** differ from pyrazine **1** in that their π-frontier orbitals are closer together and in that *N*-coordination of sterically bulky groups is more difficult due to *peri* interactions[93].



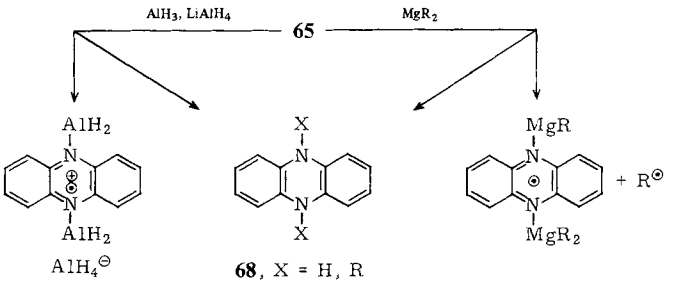
**64** **65**

However, **64** and **65** would be expected to demonstrate the same reactivity as pyrazine, although in modified form. For example, they take up electrons even more readily than pyrazine[7], and stable radical intermediates are known[162]. The 1,4-dihydro compounds also become more stable. The 1,2,3,4-tetrahydro derivative **66**[163,164] is formed by reduction of quinoxaline **64**, while substituted 1,4-dihydroquinoxalines **67** play a role as intermediates in color-bleach photography processes[37b].




**66** **67**

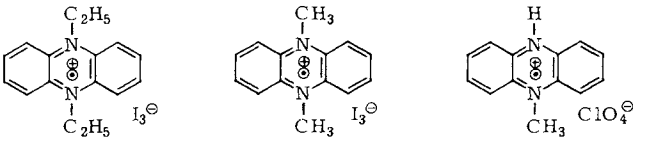
The dihydrophenazines **68** are stable, well-known compounds[165] which are formed by reduction of **65**[166] by an SET mechanism[69].




$AlH_4^{\ominus}$ **68**, X = H, R

Due to the low-lying LUMO of **65**, compounds **68** are not as electron-rich as their monocyclic analogs[24b,c,85] (Table 6). However, the greater stability of compounds **68** promotes their use as electron transfer reagents.

The radical salts **69**—**71** already exhibit a variety of different conformations[167,168], as would be expected from Section 4.6. The dihydro compounds **68** tend to form π-

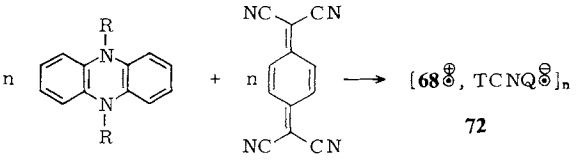


**69** **70** **71**

Planar Boat Twist

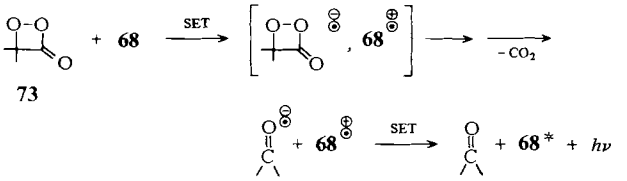
complexes. Deeply colored donor-acceptor complexes (**65**, **68**) of the quinhydrone type[165,166] are already obtained during preparation of the dihydro compounds.

The much investigated molecular π-complexes between reduced phenazines and the acceptor TCNQ also exhibit a large variety of structures, *e.g.*, columnar structures containing mixed or separated stacks of molecules[169]. Such donor-acceptor complexes of low dimensionality are of interest because of their potentially high conductivities ("organic metals")[170].



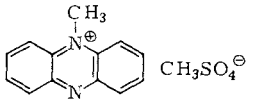
**68** TCNQ **72**

1,4-Dihydrophenazines **68** are also widely used as electron donors in photochemical investigations[171]. In connection with the reactivity of naturally occurring 1,4-dihydro-1,4-diazines (Section 7), it should be noted that reduced phenazines are employed as electron transfer activators in the chemiluminescence of dioxetanones (α-peroxylactones) **73**[172].

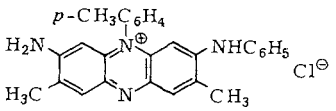



**73**

The stability of its redox states, its "physiological" redox potential and the presence of a free coordination site have led to the widespread use of *N*-methylphenazinium methyl sulfate **74** as electron acceptor in biochemical investigations[173]. Closely related to **74** are phenazine dyes such as Perkin's mauveine **75**[174].

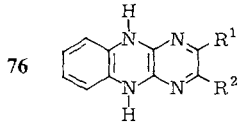


**74**

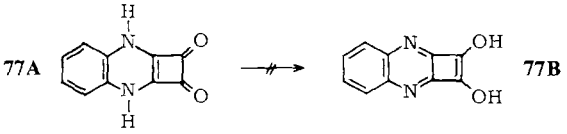


**75**

Stable 1,4-dihydro-1,4-diazines are also known in other fused ring systems[175,176]. The squaric acid amide **77A**[176] possesses a remarkable stability, since here the formation of a more strongly antiaromatic cyclobutadiene system **77B** is avoided.



**76**

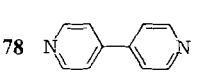


**77A** **77B**

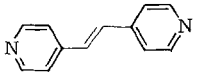
### 6.2. Separated N-Atoms

4,4'-Bipyridyl **78** and (*E*)-1,2-di-4-pyridylethene **79** are closely related to the 1,4-diazines.

Other than in quinoxaline **64** and phenazine **65**, *N*-coordination in these compounds is as sterically unhindered as in pyrazine, so that even *N,N'*-coordination compounds with large metal fragments may be formed[135,177].

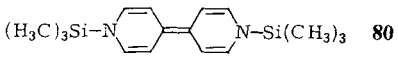


**78**



**79**

*Hünig et al.* have studied the redox system of *N,N'*-disubstituted 4,4'-bipyridyls in detail[11], and in many cases the observed phenomena are comparable to the results for pyrazine. Due to the presence of a low-lying LUMO 1,1'-dihydro compounds such as **80** are not quite as electron-rich as the corresponding reduced pyrazines (Table 6).

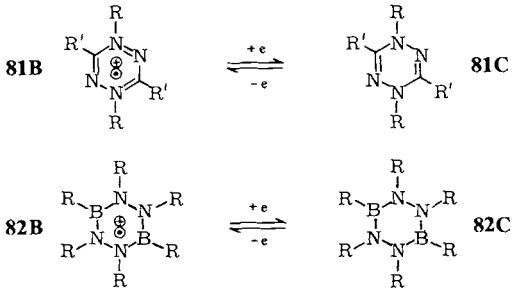


**80**

The position and reversibility of the first redox potential of the diquaternary compound **19A** (methyl viologen, paraquat) and the intense blue color of the radical cation **19B** have led to the widespread use of this redox pair as electron transfer reagent. Examples of its application are found in bio-electrochemistry[178], in photochemical systems for the conversion of solar energy[179], and in plant protection[180].

### 6.3. Substitution in the Ring

1,4-Dihydro-1,2,4,5-tetrazines (CH→N) **81** and 1,2,4,5-tetraaza-3,6-diboracyclohexanes (C=C→N–B) **82** are isoelectronic with 1,4-dihydropyrazines. Both **81C** (R = $CH_3$, R' = H)[181] and **82C** (R = $CH_3$[182a], twist conformation[182b]) are, in fact, electron-rich compounds (*IP*(**82C**) = 6.83 eV[183]) and form stable radical cations **81B**[184] and **82B**[185].

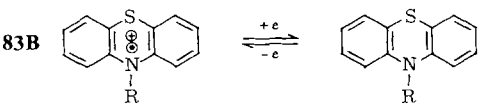


**81B** **81C**



**82B** **82C**

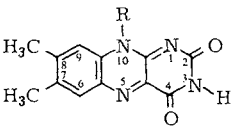
The replacement NR→S in 1,4-dihydropyrazines leads to 4*H*-1,4-thiazines. These compounds should also still be quite electron-rich. The pharmacologically important phenothiazines **83C** are characterized by a tendency, which may be of physiological significance, to form stable radical cations **83B**[186].



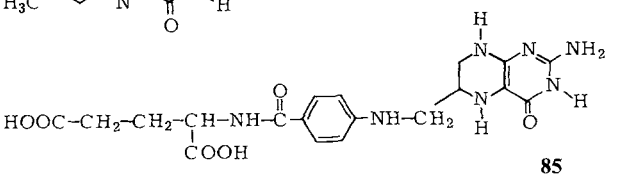
**83B** **83C**

## 7. 1,4-Diazines in Biochemistry

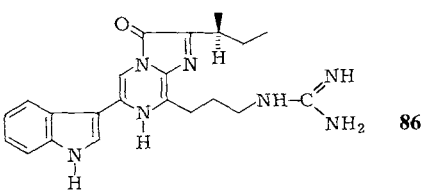
Several important groups of naturally occurring compounds contain the 1,4-diazine structure. Some typical examples are riboflavin (vitamin $B_2$) **84** (R = ribityl), tetrahydrofolic acid **85**, quinoxaline antibiotics of the Streptomyces type[187] and luciferins from marine organisms **86**[188].



**84**



**85**



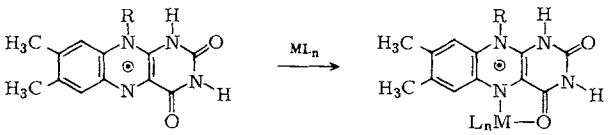
**86**

The specific reactivity of 1,4-diazines described in Sections 2–6 plays a role in the chemistry of flavoenzymes in particular. In view of the comprehensive reviews of this

field by *Hemmerich et al.*[189-191], *Bruice*[192] and *Walsh*[193], in the present article an attempt will be made to relate this reactivity to that observed for the parent system.

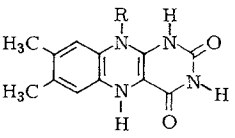
### 7.1. Flavoenzymes

Flavoenzymes fulfill a series of important functions in biochemical redox processes. Among other things they act as dehydrogenases, as one- *and* two-electron transfer reagents, and as activators of molecular oxygen[191-193]. The redox-active group of the flavocoenzymes FMN and FAD[189-193] is the tricyclic isoalloxazine system **84**, which contains the 1,4-diazine structure in its central ring. Due to the presence of the 2,4-pyrimidinedione ring the redox and coordination chemistry of **84** is more complicated than that of the simpler 1,4-diazines. Although it also constitutes a two step redox system in which electrophiles may coordinate, this coordination takes place at N-5 and N-1[190]. The coordination of metals to N-5 is favored by the chelate effect of O-4; the paramagnetic intermediate **87**, in particular, readily forms such complexes[194-198].




**87**

The fully reduced, N-10-substituted form, 1,5-dihydroisoalloxazine **88**, contains the 1,4-dihydropyrazine structure in its central ring, which determines the reactivity of this compound[191].



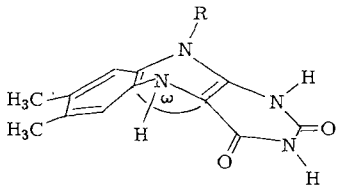

**88**

The following characteristics of the flavin system are related to its 1,4-diazine substructure:

a) The presence of a two step redox system in flavins implies that stable radical intermediates exist (cf. **87**). Stable "semiquinones" of flavins were first isolated in 1937[199] and have since been characterized by numerous further studies, especially by ESR spectroscopy[189]. Recently, high resolution ESR/ENDOR studies have finally established that the unpaired electron in the flavin radical cation is mainly localized in the central ring[200].

The stability of the radical corresponds to the electron transfer reactivity of the flavin system[31,191]. Similarly to pyrazines (Scheme 3), flavins react as one electron acceptors with carbanions[192]. "Perturbed" flavins such as the 5-deaza derivatives, which do not contain the 1,4-diazine structure, do not exhibit SET reactivity nor do they form any stable radicals[191]. However, by altering their coordination to the apoprotein, flavocoenzymes may switch from one to two electron transfer and thus act as mediators, for example, between NAD⊕/NADH (2e) and iron-sulfur proteins (1e) in biological redox chains[183].

b) During redox reactions the structure of the tricyclic system **84** alters in a characteristic way. The molecular geometry of oxidized isoalloxazines (**84**) is planar[201], whereas that of the reduced species (**88**) is the nonplanar boat or "butterfly" conformation[191,202]. This change in geometry is in agreement with the structures of minimum energy of the pyrazine system (Fig. 2, Table 1).




c) The electrochemical potentials of flavoenzyme redox systems vary over a range of 0.6 V and obviously depend on the type of apoprotein present[30,193]. The apoprotein can force the flexible (see Section 4.6) 1,5-dihydro system to adopt a certain conformation. Moreover, the affinities of the single flavin redox stages to the apoprotein (σ-coordination) differ markedly[193].

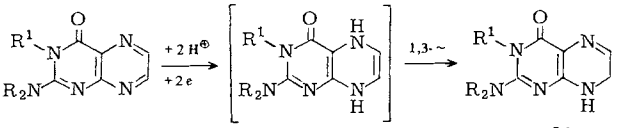
d) During their redox reactions flavoenzymes may act as dehydrogenases because they have at least one coordination site free for electrophiles ($H^{\oplus}$ or $R^{\oplus}$)[191-193]. Furthermore, flavins are suitable electron transfer substrates for transition metals[198].

e) Due to the one-electron reactivity of 1,5-dihydroflavins **88** (formation of paramagnetic oxidation products) their reaction with $^3O_2$ is not spin forbidden. Thus flavins are the only oxygen-activating enzymes which do not have to contain paramagnetic transition metal ions. According to recently published results[203] the activation of $^3O_2$ probably occurs *via* a radical ion pair [**87**, $O_2^{\ominus}$] (SET, see Scheme 3) and with formation of flavin peroxide adducts. Such peroxide species also play a role in bacterial bioluminescence, in which 1,5-dihydroflavins, $^3O_2^{\ominus}$, an aldehyde and the enzyme luciferase are essential components[204] (see Section 7.3).

Further similarities between the chemistry of simple 1,4-diazines and the reactivity of flavins may be found in the field of photochemistry[205] and in the tendency to form π-complexes[206].

### 7.2. Pteridines

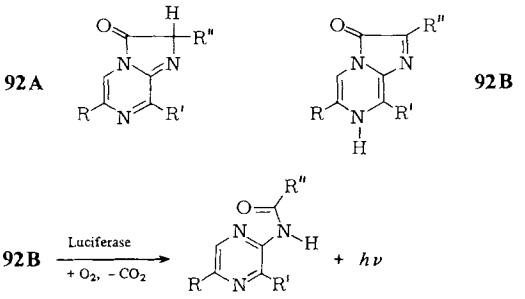
The 1,4-diazine reactivity observed for the isoalloxazine system **84** is also found in modified form for the pteridines **89**, *e.g.*, in the formation of stable radicals[207]. Similarly to quinoxaline **64**[37], complete reduction of pteridines leads *via* a 1,3-hydrogen shift to 7,8-dihydro derivatives **91** and not to antiaromatic isomers **90**[38].




**89** **90** **91**

### 7.3. Imidazo[1,2-*a*]pyrazine-3-ones

Numerous marine organisms exhibit the phenomenon of bioluminescence[188,208]. In many cases the substrates[188] for the ring opening in presence of luciferase[209], which leads to light emission, have been found to be imidazo[1,2-*a*]pyrazine-3-ones **92** (cf. **86**). These may occur as 2*H*-(**92A**) or as 7*H*-tautomers (**92B**)[209,210].




Spectroscopic studies of the model compound **92**, R, R′ = H, R″ = $CH_3$, have established that **92B** is the favored tautomer[210]. The luciferase reaction then corresponds to an aromatization of the (formally) antiaromatic 1,4-dihydropyrazine system. Hence, as in the chemiluminescence during dihydrophenazine- and dihydroflavin-catalyzed decomposition of dioxetanones **73**, the involvement of the electron-rich system **92B** in an electron transfer interaction constituting the first step of oxygen activation should be considered.

## 8. Summary and Outlook

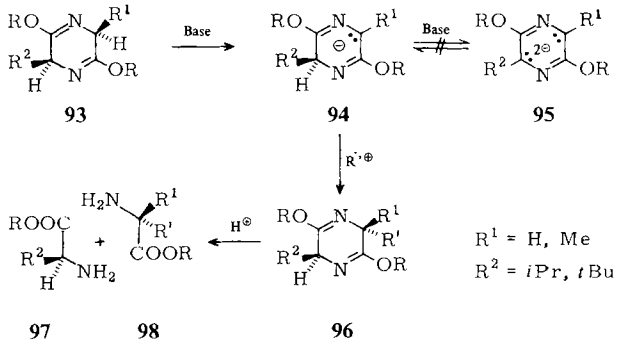
In the preceding sections the special reactivity of 1,4-diazines has been illustrated by examples from several different branches of chemistry.

The redox system of 1,4-diazines is characterized by the exceptional stability of the paramagnetic intermediate. In *N,N′*-dialkylated pyrazines the cyclic 7 π-electron configuration even becomes the favored and only stable oxidation state. Thus one finds one-electron reactivity to be characteristic of 1,4-diazine chemistry, which in this sense is similar to that of inorganic transition metal ions. Consider, for example, SET mechanisms, $^3O_2$ activation, conducting radical ion complexes, and electron transfer chemiluminescence.

The completely reduced state with 8 π-electrons in a six-membered ring exhibits a large excess of electrons. Furthermore, certain 1,4-dihydropyrazines clearly exhibit antiaromatic behavior. There exist numerous, effective (Scheme 5) methods to avoid this unfavorable electronic situation (Table 3), one significant consequence being the large structural flexibility of 1,4-dihydro-1,4-diazines.

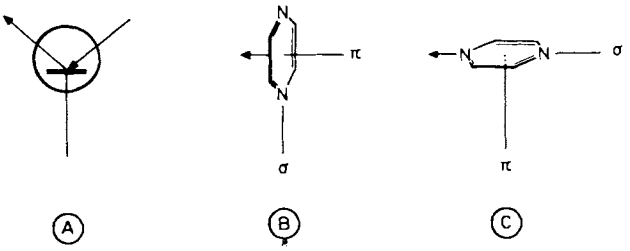
The 1,4-diazine system is also an instructive example of how σ-coordination and π-redox reactivity may influence one another (Scheme 6).

Such interrelated reactivities have model character for more complex chemical and biochemical processes. In the enzymatic and non-enzymatic fixation of molecular nitrogen, for example, one observes the cooperation between the



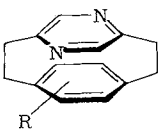

Scheme 5. The reluctance of pyrazines to form the antiaromatic 8 π-electron system (Table 3) is of synthetic value [211]: 3,6-Bis(alkoxy)-2,5-dihydropyrazines **93**, produced from optically active cyclic dipeptides by a Meerwein alkylation, react with strong bases to form the monoanions **94**. Further metalation to the pyrazine dianion **95** (8 π-electrons!), with an accompanying loss of optical information, does not take place. Instead, diastereo-selective alkylation of **94**, followed by hydrolysis of **96** leads to very good yields of almost pure enantiomers of α-amino acid esters **97** and **98**.

σ-coordination through an electrophile and the uptake of electrons ("reduction") by the π-system[213], as in the present case[212]. Such an interdependence between σ- and π-reactivities also exists for the biochemically important metalloporphyrins[214].




Scheme 6. Pyrazine as a "molecular device", in analogy to the transistor Ⓐ: *N*-Coordination governs the redox potential and the π-electron distribution Ⓑ (Table 5, Fig. 4), in return, the *N*-basicity may be modified by uptake of electrons or merely by π-backbonding into the lowest unoccupied molecular orbital Ⓒ (Table 7).

Although pyrazine itself does not tend to form π-complexes[215], its introduction into a cyclophane system **99**[216] leads to the presence of a detectable intramolecular charge transfer interaction.



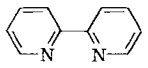
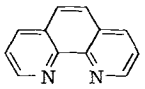

**99**

This is yet another case in which the π-interaction may be greatly influenced by σ-coordination (protonation) at the nitrogen atom. Due to the lowering of the pyrazine LUMO (Fig. 1), increasing solvent acidity causes a considerable bathochromic shift of the charge transfer band in **99**[216].

Similarly to the classical complexing agents 2,2′-bipyridyl **100** and 1,10-phenanthroline **101**, pyrazine is an easily reduced σ-ligand[7].

However, in contrast to **100** and **101** pyrazine is a linearly bridging and not a chelating ligand. This bridging

function permits the formation of binuclear complexes and coordination polymers, and in many cases the π-system of the ligand is of great importance for the propagation of electronic exchange interactions.

**100**   **101**

A report on heterocyclic systems with 8 π-electrons from 1975 ends with the following paragraph[23]: "Some of these systems are excellent models for biologically relevant systems. Further model studies should help us to answer questions of electron-transfer properties and proclivity to radical formation, as well as those concerning the influence of ligands and conformations on redox properties, to mention just a few". The present article not only presents answers to these questions but shows that the study of 1,4-diazines has opened up new perspectives.

As demonstrated by the examples of typical 1,4-diazine reactivity, these compounds have become increasingly attractive molecular building blocks of more complex systems. Two main objectives of future research on 1,4-diazine chemistry are:

Further stable or metastable derivatives of pyrazine are required for comparison with theoretical predictions, which are easily available. The most attractive of these compounds is certainly the unsubstituted 1,4-dihydropyrazine **9**. Another topic of current interest lies in the field of low dimensional materials with interesting magnetic and electrical properties[217]; recent experiments with 1,4-diazine components have been quite promising[156, 161, 169].

*A review covering several branches of chemistry would scarcely be possible without personal experience in various fields and at different universities. I therefore would like to express my sincere thanks to Prof. E. Daltrozzo, Prof. H. Bock and Prof. F. A. Cotton. My own research work referred to in this article has been supported in many ways by Prof. Bock. I also owe thanks to my co-workers on these projects, U. Lechner-Knoblauch and B. Roth, and to Professors A. Alberti, A. Hudson, S. Hünig, K. N. Raymond and H. Taube for kindly providing preprints of their work. Generous support by the Fonds der Chemischen Industrie, by the Deutsche Forschungsgemeinschaft, and by the Karl Winnacker-Stiftung is gratefully acknowledged.*

Received: November 3, 1982 [A 445 IE]
German version: *Angew. Chem. 95* (1983) 201
Translated by Dr. *C. Dyllick-Benzinger*, Mutterstadt

[1] G. B. Barlin: *The Chemistry of Heterocyclic Compounds, Vol. 41, The Pyrazines*, Wiley, Chichester 1982; G. W. H. Cheeseman, E. S. G. Werstiuk, *Adv. Heterocycl. Chem. 14* (1972) 99.
[2] E. Heilbronner, H. Bock: The HMO-Model and its Application, Vol. 1, Wiley, New York 1976, a) p. 191 and 233, b) p. 180, c) p. 308.
[3] A. Streitwieser, Jr.: *Molecular Orbital Theory for Organic Chemists*, Wiley, New York 1961.
[4] M. Hackmeyer, J. L. Whitten, *J. Chem. Phys. 54* (1971) 3739.
[5] N. Trinajstic, *J. Mol. Struct. 8* (1971) 236.
[6] Estimation of electron affinity: I. Nenner, G. J. Schulz, *J. Chem. Phys. 62* (1975) 1747.
[7] B. J. Tabner, J. R. Yandle, *J. Chem. Soc. A 1968*, 381; K. B. Wiberg, T. P. Lewis, *J. Am. Chem. Soc. 92* (1970) 7154.
[8] A. Carrington, J. dos Santos-Veiga, *Mol. Phys. 5* (1962) 21; W. Lubitz, T. Nyrönen, *J. Magn. Reson. 41* (1980) 17.
[9] R. Gleiter, E. Heilbronner, V. Hornung, *Helv. Chim. Acta 55* (1972) 255; cf. also P. Bischof, R. Gleiter, P. Hoffmann, *J. Chem. Soc. Chem. Commun. 1974*, 767.
[10] T. Kato, T. Shida, *J. Am. Chem. Soc. 101* (1979) 6869.
[11] S. Hünig, H. Berneth, *Top. Curr. Chem. 92* (1980) 1; cf. also K. Deuchert, S. Hünig, *Angew. Chem. 90* (1978) 927; *Angew. Chem. Int. Ed. Engl. 17* (1978) 875.
[12] Cf. P. Rys, H. Zollinger: *Leitfaden der Farbstoffchemie*, Verlag Chemie, Weinheim 1976, 2nd edit., p. 44.
[13] H. Kamei, *J. Phys. Chem. 69* (1965) 2791.
[14] A. S. Chia, R. F. Trimble, *J. Phys. Chem. 65* (1961) 863; P. J. Brignell, C. D. Johnson, A. R. Katritzky, N. Shakir, H. O. Tarhan, G. Walker, *J. Chem. Soc. B 1967*, 2396; Proton affinities in the gas phase: J. E. DelBene, *J. Am. Chem. Soc. 99* (1977) 3617; M. Meot-Ner, *ibid. 101* (1979) 2396.
[15] D. D. Perrin: *Dissociation Constants of Organic Bases in Aqueous Solution*, Butterworths, London 1965.
[16] W. Kaim, U. Lechner-Knoblauch, unpublished.
[17] H. Zeldes, R. Livingston, *Mol. Phys. 27* (1974) 261; D. V. Bent, E. Hayon, P. N. Moorthy, *J. Am. Chem. Soc. 97* (1975) 5065; A. Castellano, J. P. Catteau, A. Lablache-Combier, *J. Chem. Soc. 1972*, 1207.
[18] a) J. R. Bolton, A. Carrington, J. dos Santos Veiga, *Mol. Phys. 5* (1962) 465; B. L. Barton, G. K. Fraenkel, *J. Chem. Phys. 41* (1964) 1455; R. W. Fessenden, P. Neta, *Chem. Phys. Lett. 18* (1973) 14; b) L. Grossi, F. Minisci, G. F. Pedulli, *J. Chem. Soc. Perkin 2 1977*, 948.
[19] a) L. N. Klatt, R. L. Rouseff, *J. Am. Chem. Soc. 94* (1972) 7295; b) J. Swartz, F. C. Anson, *J. Electroanal. Chem. 114* (1980) 117.
[20] R. Breslow, *Angew. Chem. 80* (1968) 573; *Angew. Chem. Int. Ed. Engl. 7* (1968) 565; cf. also S. Masamune, *Tetrahedron 36* (1980) 343.
[21] S. J. Chen, F. W. Fowler, *J. Org. Chem. 36* (1971) 4025.
[22] a) J. W. Lown, M. H. Akhtar, *J. Chem. Soc. Chem. Commun. 1972*, 829; b) *ibid. 1973*, 511; c) *J. Chem. Soc. Perkin Trans. 1 1973*, 683; d) J. W. Lown, M. H. Akhtar, R. S. McDaniel, *J. Org. Chem. 39* (1974) 1998; e) J. W. Lown, M. H. Akhtar, *Tetrahedron Lett. 1974*, 179.
[23] R. R. Schmidt, *Angew. Chem. 87* (1975) 603; *Angew. Chem. Int. Ed. Engl. 14* (1975) 581.
[24] a) W. Kaim, *Angew. Chem. 93* (1981) 620; *Angew. Chem. Int. Ed. Engl. 20* (1981) 599; b) *ibid. 93* (1981) 621 and (1981) 600; c) *J. Am. Chem. Soc. 105* (1983) in press.
[25] B. A. Hess, L. J. Schaad, C. W. Holyoke, Jr., *Tetrahedron 28* (1972) 3657.
[26] N. Z. Huang, F. Sondheimer, *Acc. Chem. Res. 15* (1982) 96.
[27] Cf. J. Bordner, R. G. Parker, R. H. Stanford, *Acta Crystallogr. B 28* (1972) 1069.
[28] E. Vogel, H. J. Altenbach, J. M. Drossard, H. Schmickler, H. Stegelmeier, *Angew. Chem. 92* (1980) 1053; *Angew. Chem. Int. Ed. Engl. 19* (1980) 1016.
[29] Structural data for 1*H*-azepine derivatives: H. J. Lindner, B. von Gross, *Chem. Ber. 105* (1972) 434.
[30] Cf. the discussion on reduced flavins: L. Tauscher, S. Ghisla, P. Hemmerich, *Helv. Chim. Acta 56* (1973) 630.
[31] T. C. Bruice, Y. Yano, *J. Am. Chem. Soc. 97* (1975) 5263.
[32] B. Roth, W. Kaim, unpublished.
[33] J. J. Stezowski, *Cryst. Struct. Commun. 4* (1975) 21.
[34] D. J. Raber, L. E. Hardee, P. W. Rabideau, K. B. Lipkowitz, *J. Am. Chem. Soc. 104* (1982) 2843; cf. also K. B. Lipkowitz, P. W. Rabideau, D. J. Raber, L. E. Hardee, P. von R. Schleyer, A. S. Kos, R. A. Kahn, *J. Org. Chem. 47* (1982) 1002.
[35] R. R. Schmidt, M. Dimmler, P. Hemmerich, *Chem. Ber. 109* (1976) 2395.
[36] J. Armand, P. Bassinet, K. Chekir, J. Pinson, P. Souchay, *C. R. Acad. Sci. Ser. C 275* (1972) 279; J. Armand, K. Chekir, J. Pinson, *Can. J. Chem. 52* (1974) 3971.
[37] a) M. Schellenberg, *Helv. Chim. Acta 53* (1970) 1151; b) M. Schellenberg, H. P. Schlunke, *Chem. Unserer Zeit 10* (1976) 131; c) J. Pinson, J. Armand, *Collect. Czech. Chem. Commun. 36* (1971) 585.
[38] H. Braun, W. Pfleiderer, *Liebigs Ann. Chem. 1973*, 1082.
[39] J. R. Williams, J. J. Cossey, M. Adler, *J. Org. Chem. 37* (1972) 2963.
[40] Preparation of 17 from 1 with $Hg(SiMe_3)_2$: H. P. Becker, W. P. Neumann, *J. Organomet. Chem. 37* (1972) 57.
[41] W. Kaim, unpublished.
[42] T. J. Curphey, K. S. Prasad, *J. Org. Chem. 37* (1972) 2259.
[43] M. K. Ahn, C. S. Johnson, Jr., *J. Chem. Phys. 50* (1969) 632.
[44] Cf. the summary in: A. J. Bard, A. Ledwith, H. J. Shine, *Adv. Phys. Org. Chem. 13* (1976) 155.
[45] H. Alper, J. E. Prickett, S. Wollowitz, *J. Am. Chem. Soc. 99* (1977) 4330.
[46] K. D. Franz, Dissertation, Universität Frankfurt 1975; A. Alberti, A. Hudson, in press.
[47] T. Hayashi, M. Namiki, *Agric. Biol. Chem. 45* (1981) 933.
[48] T. H. Kappe, K. Burdeska, E. Ziegler, *Monatsh. Chem. 97* (1966) 77.

[49] R. Gottlieb, W. Pfleiderer, *Liebigs Ann. Chem. 1981,* 1451; G. Kollmannsberger, R. Gottlieb, W. Pfleiderer, *Ber. Bunsenges. Phys. Chem. 85* (1981) 1148.

[50] P. J. Garatt: *Aromaticity,* McGraw-Hill, Maidenhead 1971; F. Sondheimer, *Acc. Chem. Res. 5* (1972) 81; cf. also J. A. Pople, K. G. Untch, *J. Am. Chem. Soc. 88* (1966) 4811; J. F. Labarre, F. Crasnier, *Fortschr. Chem. Forsch. 24* (1971) 33.

[51] D. Michelet, Fr. Pat.-Anm. 2444030; *Chem. Abstr. 94* (1981) 164821k.

[52] W. Marckwald, A. Ellinger, *Chem. Ber. 26* (1893) 98.

[53] U. Eisner, A. J. Williams, *J. Chem. Soc. Chem. Commun. 1979,* 606.

[54] C. J. Popp, G. D. Garlough, *J. Inorg. Nucl. Chem. 43* (1981) 501.

[55] T. Kubota, K. Nishikida, H. Miyazaki, K. Iwatani, Y. Oishi, *J. Am. Chem. Soc. 90* (1968) 5080.

[56] Cf. D. E. Chasan, L. L. Pytlewski, C. Owens, N. M. Karayannis, *J. Inorg. Nucl. Chem. 41* (1979) 13, and references cited therein.

[57] C. J. Marzzacco, *J. Phys. Chem. 79* (1975) 1706.

[58] N. M. Atherton, A. E. Goggins, *Trans. Faraday Soc. 62* (1966) 1702.

[59] S. A. Al-Baldawi, T. E. Gough, *Can. J. Chem. 48* (1970) 2798.

[60] Cf. G. F. Pedulli, A. Alberti, *Chem. Phys. Lett. 48* (1977) 72.

[61] C. Gooijer, W. Oosterbeek, N. H. Velthorst, C. MacLean, *Org. Magn. Reson. 6* (1974) 448.

[62] W. Kaim, *Angew. Chem. 94* (1982) 150; *Angew. Chem. Int. Ed. Engl. 21* (1982) 141; *Angew. Chem. Suppl. 1982,* 298.

[63] W. Kaim, unpublished.

[64] G. A. Russell, E. G. Janzen, E. T. Strom, *J. Am. Chem. Soc. 86* (1964) 1807; J. K. Kochi: *Organometallic Mechanisms and Catalysis,* Academic Press, New York 1978; E. C. Ashby, *Pure Appl. Chem. 52* (1980) 545; *Chem. Eng. News 59* (1981) No. 15, p. 26 and No. 30, p. 38; M. Chanon, M. L. Tobe, *Angew. Chem. 94* (1982) 27; *Angew. Chem. Int. Ed. Engl. 21* (1982) 1.

[65] a) R. E. van der Stoel, H. C. van der Plas, *Recl. Trav. Chim. Pays-Bas 97* (1978) 116; b) W. Kurtz, *Chem. Ber. 108* (1975) 3415.

[66] Cf. G. E. Coates, S. I. E. Green, *J. Chem. Soc. 1962,* 3340; W. Kaim, *J. Am. Chem. Soc. 104* (1982) 3833.

[67] J. H. Wotiz, R. D. Kloepfer, P. M. Barelski, C. C. Hinckley, D. F. Koster, *J. Org. Chem. 37* (1972) 1758.

[68] H. Nöth, B. Wrackmeyer, *Chem. Ber. 107* (1974) 3070.

[69] W. Kaim, unpublished.

[70] a) W. Kaim, *Angew. Chem. 94* (1982) 150; *Angew. Chem. Int. Ed. Engl. 21* (1982) 140; *Angew. Chem. Suppl. 1982,* 289; b) *Z. Naturforsch. B 36* (1981) 1110.

[71] W. Kaim, *Z. Naturforsch. B 37* (1982) 783.

[72] W. Kaim, unpublished.

[73] W. Kaim, *J. Organomet. Chem. 215* (1981) 337.

[74] W. Kaim, *Z. Naturforsch. B 36* (1981) 677. In the case of the boron radical a molecular complex $[\mathbf{1}(BEt_3)_2]^{\cdot-}$ is formed.

[75] W. Strohmeier, K. Hümpfer, *Z. Elektrochem., Ber. Bunsenges. Phys. Chem. 60* (1956) 396; *61* (1957) 1010.

[76] Cf. W. Kaim, *Chem. Ber. 114* (1981) 3789 (2,2'-bipyridyl complexes); *J. Organomet. Chem. 241* (1983) 157 (4,4'-bipyridyl complexes).

[77] R. A. Sulzbach, A. F. M. Iqbal, *Angew. Chem. 83* (1971) 145; *Angew. Chem. Int. Ed. Engl. 10* (1971) 127.

[78] E. A. V. Ebsworth in A. G. MacDiarmid: *Organometallic Compounds of the Group IV Elements, Vol. 1,* Part 1, p. 1, Marcel Dekker, New York 1968.

[79] Cf. C. Glidewell, D. W. H. Rankin, A. G. Robiette, G. M. Sheldrick, *J. Mol. Struct. 4* (1969) 215; *J. Chem. Soc. A 1970,* 318.

[80] H. J. Altenbach, H. Stegelmeier, M. Wilhelm, B. Voss, J. Lex, E. Vogel, *Angew. Chem. 91* (1979) 1028; *Angew. Chem. Int. Ed. Engl. 18* (1979) 962.

[81] R. Gleiter, M. Kobayashi, J. Spanget-Larsen, J. P. Ferraris, A. N. Bloch, K. Bechgaard, D. O. Cowan, *Ber. Bunsenges. Phys. Chem. 79* (1975) 1218.

[82] W. Kaim, H. Bock, *J. Am. Chem. Soc. 100* (1978) 6504; *Chem. Ber. 111* (1978) 3843.

[83] K. A. Ostoja-Starzewski, H. Bock, *J. Am. Chem. Soc. 98* (1976) 8486.

[84] B. Cetinkaya, G. K. King, S. S. Krishnamurthy, M. F. Lappert, J. B. Pedley, *J. Chem. Soc. Chem. Commun. 1971,* 1370.

[85] H. J. Haink, J. R. Huber, *Chem. Ber. 108* (1975) 1118.

[86] H. Bock, W. Kaim, *Acc. Chem. Res. 15* (1982) 9.

[87] W. Kaim, *Angew. Chem. 92* (1980) 940; *Angew. Chem. Int. Ed. Engl. 19* (1980) 911.

[88] O. S. Wolfbeis, *Synthesis 1977,* 136.

[89] W. Kaim, P. Hänel, U. Lechner-Knoblauch, H. Bock, *Chem. Ber. 115* (1982) 1265.

[90] H. Daamen, H. van der Poel, D. J. Stufkens, A. Oskam, *Thermochim. Acta 34* (1978) 69.

[91] K. H. Pannell, R. Iglesias, *Inorg. Chim. Acta 33* (1979) L161.

[92] H. Daamen, D. J. Stufkens, A. Oskam, *Inorg. Chim. Acta 39* (1980) 75.

[93] W. Kaim, *Inorg. Chim. Acta 53* (1981) L151; *Chem. Ber. 115* (1982) 910.

[94] R. Hoffmann, *Angew. Chem. 94* (1982) 725; *Angew. Chem. Int. Ed. Engl. 21* (1982) 711.

[95] R. Ernhoffer, R. E. Shepherd, *J. Chem. Soc. Chem. Commun. 1978,* 859.

[96] M. Herberhold, M. Süss-Fink, *Z. Naturforsch. B 31* (1976) 1489.

[97] F. A. Cotton, J. M. Troup, *J. Am. Chem. Soc. 96* (1974) 3438.

[98] A. L. Balch, R. D. Cooper, *J. Organomet. Chem. 169* (1979) 97.

[99] G. K. N. Reddy, B. R. Ramesh, *J. Organomet. Chem. 87* (1975) 347.

[100] G. van Koten, K. Vrieze, *Recl. Trav. Chim. Pays-Bas 100* (1981) 129.

[101] H. tom Dieck, I. W. Renk, H. P. Brehm, *Z. Anorg. Allg. Chem. 379* (1970) 169.

[102] J. M. Malin, R. E. Shepherd, *J. Inorg. Nucl. Chem. 34* (1972) 3203.

[103] F. Lareze, *C. R. Acad. Sci. Ser. C 282* (1976) 737.

[104] D. G. Tisley, R. A. Walton, *Inorg. Chem. 12* (1973) 373.

[105] M. J. Cleare, P. C. Hydes, W. P. Griffith, M. J. Wright, *J. Chem. Soc. Dalton Trans. 1977,* 941.

[106] J. F. Clarke, G. W. A. Fowles, D. A. Rice, *J. Organomet. Chem. 74* (1974) 417.

[107] E. C. Baker, K. N. Raymond, *Inorg. Chem. 16* (1977) 2710; C. W. Eigenbrot, Jr., K. N. Raymond, *Polyhedron 1* (1982) 417.

[108] F. Benayache, J. Jullien, D. Solgadi, *J. Chem. Res. (S) 1981,* 159.

[109] G. R. Moore, R. J. P. Williams, *Coord. Chem. Rev. 18* (1976) 125.

[110] P. J. Hay, J. C. Thibeault, R. Hoffmann, *J. Am. Chem. Soc. 97* (1975) 4884.

[111] S. Larsson, *J. Am. Chem. Soc. 103* (1981) 4034.

[112] H. Daamen, A. Oskam, *Inorg. Chim. Acta 26* (1973) 81.

[113] H. E. Toma, J. M. Malin, *Inorg. Chem. 12* (1973) 1039.

[114] A. Vogler, H. Kunkely, *Inorg. Chim. Acta 44* (1980) L211.

[115] J. H. Fuhrhop, M. Baccouche, M. Bünzel, *Angew. Chem. 92* (1980) 320; *Angew. Chem. Int. Ed. Engl. 19* (1980) 318.

[116] P. Ford, De F. P. Rudd, R. Gaunder, H. Taube, *J. Am. Chem. Soc. 90* (1968) 1187.

[117] J. Sen, H. Taube, *Acta Chem. Scand. A 33* (1979) 125; R. H. Magnuson, P. A. Lay, H. Taube, in press.

[118] J. M. Malin, B. S. Brunschwig, G. M. Brown, K. S. Kwan, *Inorg. Chem. 20* (1981) 1438, and references cited therein.

[119] M. E. Gress, C. Creutz, C. O. Quicksall, *Inorg. Chem. 20* (1981) 1522.

[120] C. Creutz, H. Taube, *J. Am. Chem. Soc. 95* (1973) 1086.

[121] F. Felix, U. Hauser, H. Siegenthaler, F. Wenk, A. Ludi, *Inorg. Chim. Acta 15* (1975) L7; F. Felix, A. Ludi, *Inorg. Chem. 17* (1978) 1782; cf. also G. Calzaferri, F. Felix, *Helv. Chim. Acta 60* (1972) 730.

[122] T. J. Meyer, *Adv. Chem. Ser. 150* (1976) 73.

[123] M. B. Robin, P. Day, *Adv. Inorg. Radiochem. 10* (1967) 247.

[124] H. Taube, E. S. Gould, *Acc. Chem. Res. 2* (1969) 321; A. Haim, *ibid. 8* (1975) 264; H. Taube, *Ber. Bunsenges. Phys. Chem. 76* (1972) 964; K. Wieghardt, *Chem. Unserer Zeit 13* (1979) 118.

[125] C. J. O'Connor, *Prog. Inorg. Chem. 29* (1982) 203.

[126] R. W. Callahan, F. R. Keene, T. J. Meyer, D. J. Salmon, *J. Am. Chem. Soc. 99* (1977) 1064.

[127] a) F. A. Cotton, J. G. Norman, *Inorg. Chim. Acta 6* (1972) 411; J. A. Baumann, D. J. Salmon, S. T. Wilson, T. J. Meyer, W. E. Hatfield, *Inorg. Chem. 17* (1978) 3342; b) S. T. Wilson, R. F. Bondurant, T. J. Meyer, D. J. Salmon, *J. Am. Chem. Soc. 97* (1975) 2285; J. A. Baumann, D. J. Salmon, S. T. Wilson, T. J. Meyer, *Inorg. Chem. 18* (1979) 2472; J. A. Baumann, S. T. Wilson, D. J. Salmon, P. L. Hodd, T. J. Meyer, *J. Am. Chem. Soc. 101* (1979) 2916.

[128] A. von Kameke, G. M. Tom, H. Taube, *Inorg. Chem. 17* (1978) 1790.

[129] N. S. Hush, *Prog. Inorg. Chem. 8* (1967) 391; T. J. Meyer, *Acc. Chem. Res. 11* (1978) 94; N. Sutin, *ibid. 15* (1982) 275.

[130] T. J. Meyer, *Chem. Phys. Lett. 64* (1979) 417.

[131] C. Creutz, H. Taube, *J. Am. Chem. Soc. 91* (1969) 3988; cf. also the summary in: M. Tanner, A. Ludi, *Inorg. Chem. 20* (1981) 2348.

[132] Cf. the indroduction in: P. H. Citrin, A. P. Ginsberg, *J. Am. Chem. Soc. 103* (1981) 3673.

[133] S. B. Piepho, E. R. Krausz, P. N. Schatz, *J. Am. Chem. Soc. 100* (1978) 3805.

[134] N. S. Hush, A. Edgar, J. K. Beattie, *Chem. Phys. Lett. 69* (1980) 128.

[135] M. J. Powers, T. J. Meyer, *J. Am. Chem. Soc. 102* (1980) 1289.

[136] T. G. Dunne, J. K. Hurst, *Inorg. Chem. 19* (1981) 1152.

[137] J. Swartz, F. C. Anson, *Inorg. Chem. 20* (1981) 2250.

[138] H. Taube: *Electron Transfer Reactions of Complex Ions in Solution,* Academic Press, New York 1970.

[139] V. A. Durante, P. C. Ford, *J. Am. Chem. Soc. 97* (1975) 6898.

[140] H. Spiecker, K. Wieghardt, *Inorg. Chem. 16* (1977) 1290; K. Wieghardt, H. Cohen, D. Meyerstein, *Angew. Chem. 90* (1978) 632; *Angew. Chem. Int. Ed. Engl. 17* (1978) 608.

[141] M. S. Haddad, D. N. Hendrickson, J. P. Cannady, R. S. Drago, D. S. Bieksza, *J. Am. Chem. Soc. 101* (1979) 898.

[142] Cf. A. B. P. Lever, J. Lewis, R. S. Nyholm, *Nature* 189 (1961) 58; H. D. Stidham, J. A. Chandler, *J. Inorg. Nucl. Chem. 27* (1965) 397; R. G. Vranka, E. L. Amma, *Inorg. Chem. 5* (1966) 1020; K. Brodersen, N. Hacke, G. Liehr, *Z. Anorg. Allg. Chem. 409* (1974) 1.

[143] 2,5-Pentanedionate-complexes: S. Ambe, F. Ambe, *J. Inorg. Nucl.*

*Chem. 35* (1973) 1109; M. S. Ansari, N. Ahmad, *ibid. 37* (1975) 2099; J. B. Hodgson, G. C. Percy, D. A. Thornton, *Transition Met. Chem. 3* (1978) 302.
[144] J. A. C. van Ooijen, E. van Tooren, J. Reedijk, *J. Am. Chem. Soc. 100* (1978) 5569.
[145] F. A. Cotton, T. R. Felthouse, *Inorg. Chem. 19* (1980) 328; D. A. Edwards, G. Uden, W. S. Mialki, R. A. Walton, *Inorg. Chim. Acta 40* (1980) 25.
[146] T. M. Cotton, R. P. Van Duyne, *J. Am. Chem. Soc. 103* (1981) 6020.
[147] F. F. Seelig, *Z. Naturforsch. A 34* (1979) 986.
[148] M. Inoue, M. Kubo, *Coord. Chem. Rev. 21* (1976) 1.
[149] Cf. H. Kuramoto, M. Inoue, S. Emori, S. Sugiyama, *Inorg. Chim. Acta 32* (1979) 209; P. D. W. Boyd, S. Mitra, *Inorg. Chem. 19* (1980) 3547.
[150] A. Santoro, A. D. Mighell, C. W. Reimann, *Acta Crystallogr. B 26* (1970) 979.
[151] H. W. Richardson, W. E. Hatfield, *J. Am. Chem. Soc. 98* (1976) 835.
[152] H. W. Richardson, J. R. Wasson, W. E. Hatfield, *Inorg. Chem. 16* (1977) 484.
[153] J. Darriet, M. S. Haddad, E. N. Duesler, D. N. Hendrickson, *Inorg. Chem. 18* (1979) 2679.
[154] J. S. Valentine, A. J. Silverstein, Z. G. Soos, *J. Am. Chem. Soc. 96* (1974) 97.
[155] Cf. A. L. Magri, A. D. Magri, F. Balestrieri, E. Cordarelli, G. D'Ascenzo, A. Panzarelli, *Thermochim. Acta 48* (1981) 253, and references cited therein.
[156] C. J. O'Connor, C. L. Klein, R. J. Majeste, T. M. Trefonas, *Inorg. Chem. 21* (1982) 64; cf. also C. Klein, R. J. Majeste, L. !. Trefonas, C. J. O'Connor, *ibid. 21* (1982) 1891.
[157] A. P. Ginsberg, *Inorg. Chim. Acta Rev. 5* (1971) 45; Y. Journaux, O. Kahn, H. Coudanne, *Angew. Chem. 94* (1982) 647; *Angew. Chem. Int. Ed. Engl. 21* (1982) 624.
[158] A. Teuerstein, B. A. Feit, G. Navon, *J. Inorg. Nucl. Chem. 36* (1974) 1055.
[159] F. Kubel, J. Strähle, *Z. Naturforsch. B 36* (1981) 441.
[160] S. B. Brown, M. J. S. Dewar, *Inorg. Chim. Acta 34* (1979) 221.
[161] O. Schneider, M. Hanack, *Angew. Chem. 92* (1980) 391; *Angew. Chem. Int. Ed. Engl. 19* (1980) 392.
[162] Cf. the literature in P. Hanson, *Adv. Heterocycl. Chem. 25* (1979) 205.
[163] Y. Kikugawa, K. Saito, S. Yamada, *Synthesis 1978,* 447.
[164] J. M. Cosmao, N. Collignon, G. Queguiner, *J. Heterocycl. Chem. 16* (1979) 973; J. Armand, K. Chekir, J. Pinson, *ibid. 17* (1980) 1237.
[165] H. McIlwain, *J. Chem. Soc. 1937,* 1704.
[166] L. Birkofer, A. Birkofer, *Chem. Ber. 85* (1952) 286; F. Bohlmann, *ibid. 85* (1952) 390; cf. also D. K. Root, R. O. Pendarvis, W. H. Smith, *J. Org. Chem. 43* (1978) 778.
[167] B. Morosin, *Acta Crystallogr. B 34* (1978) 1905.
[168] H. J. Keller, W. Moroni, D. Nöthe, M. Scherz, J. Weiss, *Z. Naturforsch. B 33* (1978) 838.
[169] Z. G. Soos, H. J. Keller, W. Moroni, D. Nöthe, *J. Am. Chem. Soc. 99* (1977) 5040; I. Goldberg, U. Shmueli, *Acta Crystallogr. B 29* (1973) 421; H. Endres, H. J. Keller, W. Moroni, D. Nöthe, *ibid. B 36* (1980) 1435.
[170] J. H. Perlstein, *Angew. Chem. 89* (1977) 534; *Angew. Chem. Int. Ed. Engl. 16* (1977) 519.
[171] V. S. F. Chew, J. R. Bolton, G. R. Brown, G. Porter, *J. Phys. Chem. 84* (1980) 1903, 1909.
[172] S. P. Schmidt, G. B. Schuster, *J. Am. Chem. Soc. 102* (1980) 306; *Adv. Phys. Org. Chem. 18* (1982) 187.
[173] Cf. *e.g.*, K. Ishizu, H. H. Dearman, M. T. Huang, J. R. White, *Biochemistry 8* (1969) 1238.
[174] Cf. [12], p. 117ff.
[175] J. Armand, L. Boulares, K. Chekir, C. Bellec, *Can. J. Chem. 59* (1981) 3237.
[176] S. Hünig, H. Pütter, *Chem. Ber. 110* (1977) 2524.
[177] Cf. *e.g.*, J. E. Sutton, H. Taube, *Inorg. Chem. 20* (1981) 3125.
[178] H. L. Landrum, R. T. Salmon, F. M. Hawkridge, *J. Am. Chem. Soc. 99* (1977) 3154; W. J. Albery, M. J. Eddowes, H. A. O. Hill, A. R. Hillman, *ibid. 103* (1981) 3904; H. Simon, H. Günther, J. Bader, W. Tischer, *Angew. Chem. 93* (1981) 897; *Angew. Chem. Int. Ed. Engl. 20* (1981) 861; cf. also J. J. Grimaldi, S. Boileau, J. M. Lehn, *Nature 265* (1977) 229.
[179] Cf. M. Grätzel, *Acc. Chem. Res. 14* (1981) 376; H. D. Abruna, A. J. Bard, *J. Am. Chem. Soc. 103* (1981) 6898; M. S. Tunuli, J. H. Fendler, *ibid. 103* (1981) 2507; D. C. Bookbinder, M. S. Wrighton, *ibid. 102* (1980) 5123; E. Baumgartner, J. H. Fuhrhop, *Angew. Chem. 92* (1980) 564; *Angew. Chem. Int. Ed. Engl. 19* (1980) 556.
[180] L. A. Summers: *The Bipyridinium Herbicides,* Academic Press, New York 1980.
[181] H. Kohn, R. A. Olofson, *J. Org. Chem. 37* (1972) 3504.
[182] a) D. Nölle, H. Nöth, *Chem. Ber. 111* (1978) 469; b) J. C. Huffman, H. Fussstetter, H. Nöth, *Z. Naturforsch. B 31* (1976) 289.
[183] J. Kroner, D. Nölle, H. Nöth, W. Winterstein, *Z. Naturforsch. B 29* (1974) 476.
[184] F. Gerson, W. Skorianetz, *Helv. Chim. Acta 52* (1969) 169; W. M. Tolles, W. R. McBride, W. E. Thun, *J. Am. Chem. Soc. 91* (1969) 2443.
[185] H. Nöth, W. Winterstein, W. Kaim, H. Bock, *Chem. Ber. 112* (1979) 2494; cf. also H. Bock, W. Kaim, H. Nöth, A. Semkow, *J. Am. Chem. Soc. 102* (1980) 4421.
[186] Cf. H. M. Swartz, J. R. Bolton, D. C. Borg: *Biological Applications of Electron Spin Resonance,* Wiley, New York 1972; p. 318ff.
[187] E. Hyde, J. R. Kalman, D. H. Williams, D. G. Reid, R. K. Olsen, *J. Chem. Soc. Perkin Trans. 1 1982,* 1041, and references cited therein.
[188] F. McCapra, R. Hart, *Nature 286* (1980) 660.
[189] V. Massey, P. Hemmerich, *Enzymes 12* (1976) 191.
[190] P. Hemmerich, C. Veeger, H. C. S. Wood, *Angew. Chem. 77* (1965) 699; *Angew. Chem. Int. Ed. Engl. 4* (1965) 671.
[191] P. Hemmerich, V. Massey, H. Michel, C. Schug, *Struct. Bonding (Berlin) 48* (1982) 93.
[192] T. C. Bruice, *Acc. Chem. Res. 13* (1980) 256.
[193] C. Walsh, *Acc. Chem. Res. 13* (1980) 148.
[194] P. Hemmerich, *Helv. Chim. Acta 47* (1964) 464.
[195] F. Müller, A. Ehrenberg, L. Eriksson in: *Magnetic Resonance in Biological Systems,* Pergamon Press, Oxford 1967.
[196] D. T. Sawyer, R. L. McCreery, *Inorg. Chem. 11* (1972) 779.
[197] M. J. Clarke, M. G. Dowling, *Inorg. Chem. 20* (1981) 3506.
[198] A. N. Singh, E. Gelerinter, E. S. Gould, *Inorg. Chem. 21* (1982) 1232; A. N. Singh, V. S. Srinivasan, E. S. Gould, *ibid. 21* (1982) 1236.
[199] R. Kuhn, R. Ströbele, *Chem. Ber. 70* (1937) 753.
[200] M. Bock, W. Lubitz, H. Kurreck, H. Fenner, R. Grauert, *J. Am. Chem. Soc. 103* (1981) 5567, and references cited therein.
[201] M. Wang, C. J. Fritchie, Jr., *Acta Crystallogr. B 29* (1973) 2040.
[202] R. Norrestam, M. von Glehn, *Acta Crystallogr. B 28* (1972) 434.
[203] G. Eberlein, T. C. Bruice, *J. Am. Chem. Soc. 104* (1982) 1449.
[204] J. W. Hastings, K. H. Nealson, *Annu. Rev. Microbiol. 31* (1977) 549.
[205] P. E. Heelis, *Chem. Soc. Rev. 11* (1982) 15.
[206] A. Abramowitz, V. Massey, *J. Biol. Chem. 251* (1976) 5321.
[207] A. Ehrenberg, P. Hemmerich, F. Müller, W. Pfleiderer, *Eur. J. Biochem. 16* (1970) 584; on the importance of reduced pterins cf. M. Viscontini, *Fortschr. Chem. Forsch. 9* (1968) 605.
[208] W. Adam, *Chem. Unserer Zeit 7* (1973) 182.
[209] F. McCapra, *Acc. Chem. Res. 9* (1976) 201.
[210] T. Goto, M. Isobe, Y. Kishi, S. Inoue, S. Sugiura, *Tetrahedron 31* (1975) 939.
[211] U. Schöllkopf, W. Hartwig, U. Groth, *Angew. Chem. 91* (1979) 922; *Angew. Chem. Int. Ed. Engl. 18* (1979) 863; U. Schöllkopf, W. Hartwig, U. Groth, K. O. Westphalen, *Liebigs Ann. Chem. 1981,* 696; U. Schöllkopf, U. Groth, C. Deng, *Angew. Chem. 93* (1981) 793; *Angew. Chem. Int. Ed. Engl. 20* (1981) 798.
[212] The reactivity of the 1,4-diazines resembles that of molecular nitrogen in many ways; cf. I. M. Treitel, M. T. Flood, R. E. Marsh, H. B. Gray, *J. Am. Chem. Soc. 91* (1969) 6512; R. H. Magnuson, H. Taube, *ibid. 94* (1972) 7213; N. Wiberg, *Angew. Chem. 83* (1971) 379; *Angew. Chem. Int. Ed. Engl. 10* (1971) 374.
[213] J. Chatt, J. R. Dilworth, R. L. Richards, *Chem. Rev. 78* (1978) 589; cf. also T. Yamabe, K. Hori, K. Fukui, *Inorg. Chem. 21* (1982) 2816.
[214] J. H. Fuhrhop, *Angew. Chem. 86* (1974) 363; *Angew. Chem. Int. Ed. Engl. 13* (1974) 321.
[215] Cf., however, CT complexes of 2,3,5,6-pyrazine tetracarbonitrile: S. Fukuzumi, J. K. Kochi, *J. Org. Chem. 46* (1981) 4116.
[216] H. A. Staab, W. K. Appel, *Liebigs Ann. Chem. 1981,* 1065.
[217] Cf. the search for stabilized radical ions for conducting polymers: G. Wegner, *Angew. Chem. 93* (1981) 352; *Angew. Chem. Int. Ed. Engl. 20* (1981) 361.

# Dye Diffusion Systems in Color Photography

**By Christian C. Van de Sande***

*In memoriam Otto Bayer*

Dye diffusion instant color photography has been a commercial success ever since its introduction in 1963. No doubt this is partly due to the spectacular nature of this innovation, and for the same reason it has never really rid itself of its gadget image. Moreover, the picture quality was inferior to that of traditional color photography. Photographic materials are now available whose image quality approaches that of the traditional color print. It is not well known that chemistry, and organic chemistry in particular, is the cornerstone of these new photographic products. Insights from this field have spurred creativity, not only in the fields of dye and polymer chemistry, but above all in the search for more efficient and, hopefully better, dye diffusion transfer systems. The result of all these efforts is a finely tuned microscale chemical factory which continues to open rewarding perspectives for the photographic industry.

## 1. Introduction

Dye diffusion transfer systems are becoming increasingly important in color photography. To a large extent this is due to the success of their most popular application, instant color photography. But recently, other interesting applications for both the amateur and professional photographer have been introduced which make it possible to obtain copies of colored originals within a few minutes, without a complicated processing sequence. The chemistry behind such materials is relatively unknown outside the community of photographic scientists. A previous, less-detailed review[1b], although published in a reference work on photography of outstanding quality, remained relatively unnoticed (cf. [1c]). The present review is intended to bring some of the chemistry involved in dye transfer systems to the attention of a much broader readership.

With conventional photographic materials the final image is located in the layer which initially contained the light-sensitive silver halide (Fig. 1, left). In black and white pictures it is composed of metallic silver, and in color images of dye particles. In diffusion transfer materials the image is created in a layer which is not the initial light-sensitive layer (Fig. 1, right). During development, active components migrate from the light-sensitive layer to a receiving layer where the image particles are formed. The recorded image is, therefore, transferred by diffusion.

A black and white image is produced when the mobile components are soluble silver salts which are converted into metallic silver on silver nuclei present in the receiving layer. Such systems will not be dealt with here and the reader is referred to the literature for more information[2,3]. We will rather concern ourselves with those diffusion transfer systems which produce a dye image. The discussion of these systems will be limited to the organic chemistry of imagewise or anti-imagewise diffusion of components which give rise to a dye image in the receiving layer.

[*] Dr. C. C. Van de Sande
R & D Laboratories
Agfa-Gevaert NV
Septestraat 27, B-2510 Mortsel (Belgium)

Due to limitations of space the chemistry of the dyes and polymers involved in diffusion transfer color photography can only be touched upon (see [4]).

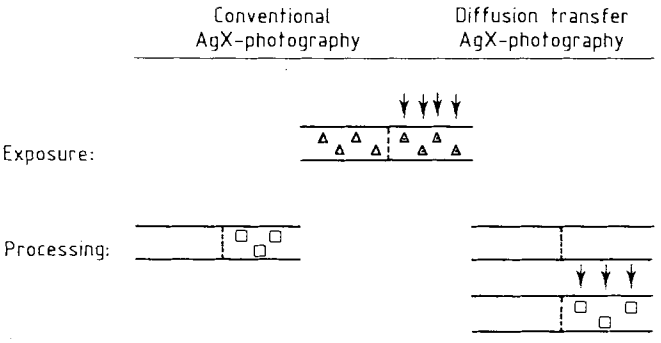



Fig. 1. Comparison between conventional and diffusion transfer systems. Characteristic for the latter is diffusion of active components from the initially light-sensitive layer to a remote layer (image build-up occurs by deposition of these components). The fate of the silver halide in the initially light-sensitive layer of a diffusion transfer material depends on several factors, but is irrelevant here. △: Non-exposed silver halide; ▲: exposed silver halide; □: image.

## 2. Basics

To produce colored images the mobile active components of a diffusion transfer system must lead to formation of dyes in the receiving layer. Irrespective of the composition of these components—dyes, dye precursors, or dye-forming reagents which react in the receiving layer—to obtain a transferred image their diffusion must be correlated with the exposure of the sensitive layer from which they originate. For photography this leaves us with two alternatives:

- *imagewise diffusion: i.e.* proportional to the amount of silver halide developed;
- *anti-imagewise diffusion: i.e.* as a negative function of the amount of silver halide developed.

A colored image can be obtained by either means.

The subtractive color system[5] for photographic registration of colored objects makes use of superposition of three silver halide containing layers (Fig. 2), which are sensitive to the blue (B), the green (G), and red regions (R) of the spectrum. An active component, which produces the complementary color of the spectral region to which the layer is sensitized, is associated with each layer: yellow for the B layer, magenta for the G layer, and cyan (blue-green) for the R layer.

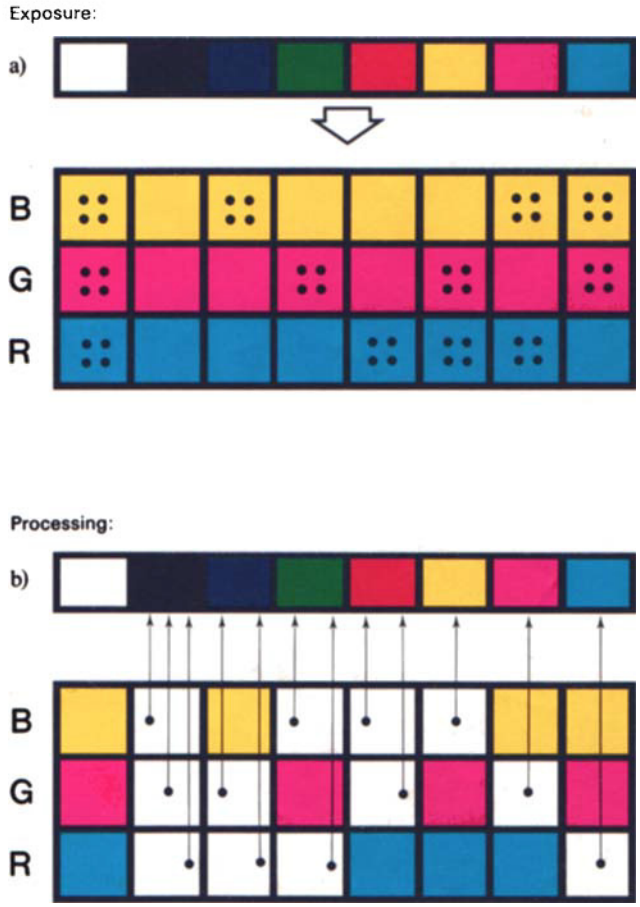



Fig. 2. Anti-imagewise diffusion yields correct (*i.e.* positive) images. Dye release then occurs as a negative function of the exposure dose of the layer in which the dye or the dye-precursor is incorporated. For a blue original, for example, dye release occurs from the green-sensitive G-layer (magenta dye) and from the red-sensitive R-layer (cyan dye). Since magenta is white minus green and cyan is white minus red, superposition of these two dyes in the receiving layer yields a blue image. a) Object; :: exposed silver halide. b) Image receiving layer; ⊷ diffusible components.

Let us assume that we have found a way to obtain anti-imagewise diffusion and that a blue object has been recorded (Fig. 2). A latent image is thus produced in the blue-sensitive layer (B). Processing leads to diffusion of components from the G and R layers, resulting either in formation or deposition of magenta and cyan dyes in the receiving layer. The combination of these two dyes yields a blue image of the blue original. A similar procedure applies to all other colors and hues (see Fig. 2), from which it can be deduced that anti-imagewise diffusion yields correct or positive transfer images: systems which cause anti-imagewise diffusion are therefore referred to as positive-working. Conversely, imagewise diffusion yields complementary or negative transfer images: such systems are referred to as negative-working. These points only apply to normal, negative-working silver halide containing layers (as in Fig. 2), which upon development produce metallic silver in amounts directly proportional to the exposure dose. In some cases, however, it can be arranged that upon development the silver halide layers produce metallic silver as a negative function of exposure dose[6]. Imagewise diffusion is then required to obtain a positive transferred image. Throughout this article normal silver halide is assumed, unless otherwise stated.

Knowing that imagewise or anti-imagewise diffusion can lead to a useful image, one is faced with the problem of its practical realization. Clearly, the mobility of the active ingredients is modified as a function of the exposure dose of the silver halide in their immediate neighborhood, and this leaves two alternatives:

- The active components are initially mobile in alkaline media and become immobilized during processing or
- they are initially immobile and are mobilized during processing.

There is a way to achieve such exposure-controlled mobility changes: the exposure dose can be chemically translated into "amount of reducible silver halide", "amount of developer used", and hence "redox equivalents". This is the key to the solution: *molecules whose mobility can be redox-controlled are needed.*

Nearly thirty years have elapsed since the first patent describing the practical realization of this problem was filed by Polaroid[7]. In the meantime, virtually all important photographic companies have spent a considerable amount of effort in devising and optimizing systems involving this principle. Four important categories can be distinguished:

- redox-controlled solubility changes;
- systems based on chromogenic coupling reactions known from color photography;
- redox-controlled cleavage reactions;
- reactions with silver ions.

These methods will be discussed in the following four sections. A separate section will treat some less important systems.

## 3. Redox-Controlled Solubility Changes

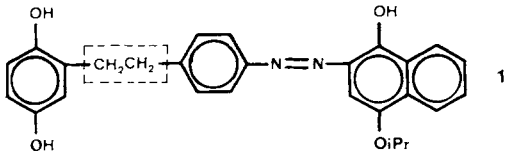
### 3.1. The Dye-Developer System

The dye-developer system is the most important system based on redox-controlled solubility changes. Conceived by *Rogers* at Polaroid Corporation[7], it provided the basis for the Polaroid instant color film, which was introduced in 1963, and is still employed in today's Polaroid color films. The "active components" in this system are *dye-developer molecules.*

Dev–Link–Dye

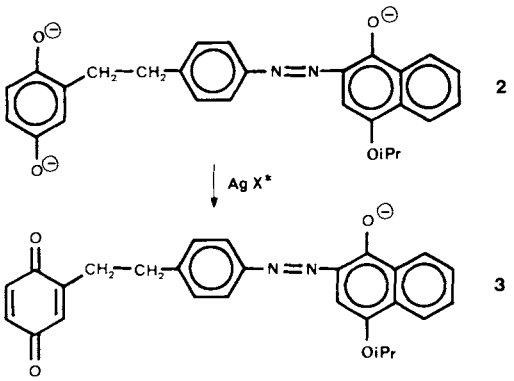
As the name suggests these molecules contain a developer moiety *Dev* (*e.g.* a hydroquinone or *p*-aminophenol unit)

as well as a dye (or dye precursor) moiety. Both fragments are linked by an insulating group (*Link*), whose main function is to electronically insulate the *Dye* and *Dev* portions: redox changes in the *Dev* moiety are then unable to affect the chromophore of the *Dye* moiety directly. An additional requirement for this *Link* is that it should be hydrolytically stable under the development conditions and for the duration of the development process (order of magnitude: minutes). **1** is an example of an early dye-developer molecule: the ethylene group effectively links the hydroquinone fragment to the magenta azonaphthol dye. More recent developments in dye-developer chemistry have primarily focused on achieving better light stability, and have resulted in the introduction of premetallized (*i.e.* metal-ion complexed) dyes in the Polacolor 2 material (1975). More details on this topic can be found in[4].




1

The dye-developer molecules are present in the material as a very fine emulsion in a gelatine binder which may also contain the light-sensitive silver halide. Alternatively, the silver halide may be incorporated into an adjacent layer. In the alkaline medium of the development phase these molecules ionize, dissolve, and consequently become diffusible. In exposed areas these ionized dye-developer molecules (*e.g.* **2**) are oxidized (Scheme 1) to form immobile quinones (*e.g.* **3**)[8], as a result of development of the exposed silver halide (AgX*) (Scheme 1).



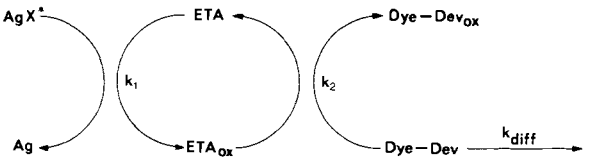

2

3

Scheme 1. Oxidation of the dye-developer molecule **2** to **3**.

If no oxidation takes place (as in unexposed areas) the ionized dye-developers (*e.g.* **2**) migrate to the receiver layer (or sheet) where they are mordanted. The system leads to anti-imagewise diffusion and yields a positive transferred image if normal silver halide layers are used (see Section 2).

Although the dye-developer molecules could principally act as developers for exposed silver halide (by definition!) this function has been assumed by a conventional auxiliary developer molecule (*e.g. p*-tolylhydroquinone) for reasons which will become clear after an analysis of the kinetics of the system. Scheme 2 gives a schematic representation of the reactions which take place in the exposed areas. The *electron transfer agent* (ETA) is the auxiliary developer which reduces exposed silver halide at a rate $k_1$, whereby it is converted into its oxidized form $ETA_{ox}$. This in turn then oxidizes (rate $k_2$) the dye-developer molecules: this oxidation reaction regenerates ETA, which consequently serves no other purpose than to pump electrons from dye-developer molecules to exposed silver halide.




Scheme 2. Redox reactions in the dye-developer system (exposed areas). ETA (*E*lectron *T*ransfer *A*gent) assists in the development. The insulating group "*Link*" has been omitted.

To function properly this system must meet several requirements. Firstly the redox potentials of the systems involved must be such that the processes described by Scheme 2 produce a sufficiently negative free energy change in the system. This amounts to the requirement

$$E^0(\text{Dye–Dev}) < E^0(\text{ETA}) < E^0(\text{Ag/AgX*}) \qquad \text{(a)}$$

which limits the choice of dye-developer as well as that of ETA.

Considering the system from a point of view of kinetics, it is clear that good differentiation between exposed and non-exposed areas will only be achieved if the rates $k_2$ and $k_{diff}$ comply with the following inequality:

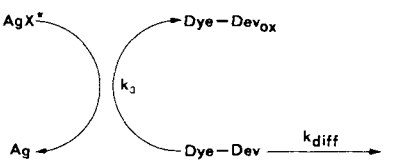
$$k_2 \gg k_{diff} \qquad \text{(b)}$$

If this is not fulfilled, *i.e.* if diffusion of dye-developer effectively competes with its oxidation, unwanted transfer of dye will occur in exposed areas leading to color fog. The interaction rate $k_2$ is a composite of the diffusion rate $k'_{diff}$ of $ETA_{ox}$ and the actual redox interaction rate, and therefore complies with the relation

$$k'_{diff} > k_2 \qquad \text{(c)}$$

Combination of inequalities (b) and (c) indicates that in a practical system the diffusion rate of $ETA_{ox}$ must exceed that of dye-developer. This is achieved by the selection of small and compact ETA molecules (*e.g. p*-tolylhydroquinone or 1-phenyl-3-pyrazolidinone (phenidone)).

One may ask why an ETA is necessary. If it were to be omitted (see Scheme 3), development (rate $k_3$) of exposed silver halide would consist of a composite of actual redox




Scheme 3. Simplified but impractical dye-developer system.

reaction and diffusion of dye-developer to the grains. Inequality (d) would then hold, *i.e.* migration of dye-developer molecules to the receiving layer would compete strongly with their oxidation, leading to formation of color fog.

$$k_3 < k_{diff} \qquad (d)$$

Although the mechanism outlined in Scheme 2 provided the foundation for the Polaroid instant material, a multitude of problems had to be solved before it became a commercial reality (see [3],[4]). Figure 3 gives an idea of the complexity of an integral film of Polaroid design.

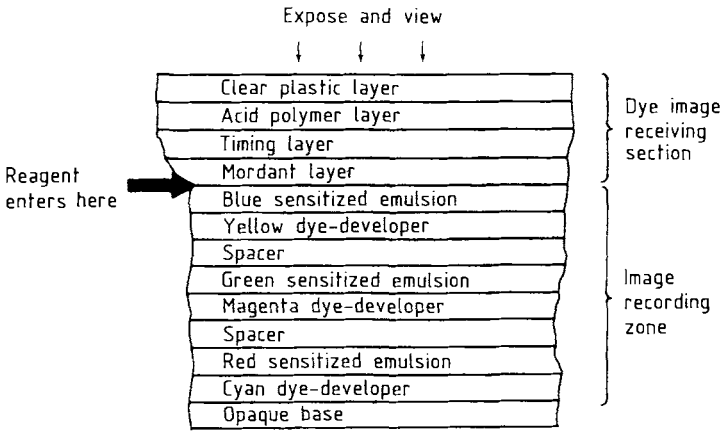



Fig. 3. Schematic section through an integral film unit of Polaroid design (see text).

After exposure, such a film unit is ejected from the camera through a pair of rollers which rupture a container located at the edge of the unit holding the processing solution. This "solution" is a viscous paste containing alkali, water, titanium dioxide, and opacifying dyes which protect the image recording zone and allow formation of the image in daylight. A dye-developer layer is located below each sensitive layer: this arrangement is necessary because the dye-developers absorb in the same spectral region to which the associated silver halide layers are sensitized. Inclusion of the dye-developers in the AgX layers would have caused severe reduction in photographic sensitivity, even if their absorption were shifted to shorter wavelengths by conversion into alkali-labile derivatives (*"shifted dye-developers"*[9]). The image-receiving section contains a mordant layer to capture the transferred dyes, an acid layer to neutralize the excess of alkali present in the processing liquid, and a timing layer to monitor the time of neutralization.

A disadvantage inherent to the dye-developer system is that the diffusing or mordanted dye-developer molecules are still redox active and may, therefore, be oxidized by $ETA_{ox}$ on their way through other image recording layers of (see Fig. 3), or undergo aerial oxidation in the mordant layer. These lead to improper color rendition and formation of yellow fog, respectively.

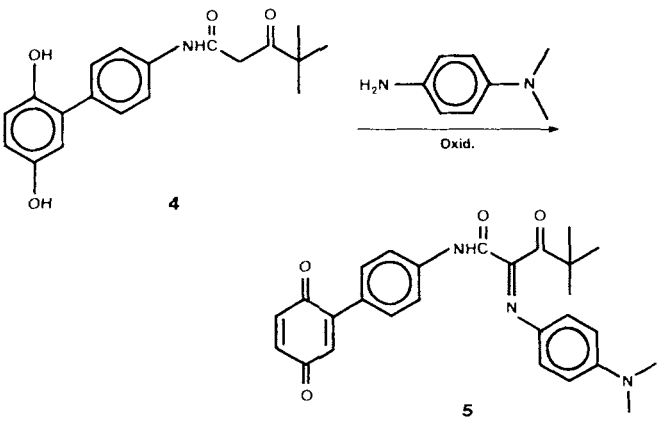
Oxidation by $ETA_{ox}$ can be limited to some extent by accurate control of the development in, and the diffusion from, the three light-sensitive layers: only when development of the blue-sensitized layer and all redox reactions therein have ceased does development start in the green-sensitized layer *etc.* Precisely these two imperfections in the Polaroid dye-developer system have stimulated a search for other dye-transfer systems (see Sections 4–7).

### 3.2. Coupler Developers

An alternative to shifted dye-developers are the so-called *coupler developers*[10,11]. These are virtually colorless molecules (*e.g.* **4** in Scheme 4) of the type

Dev–Link–Coup

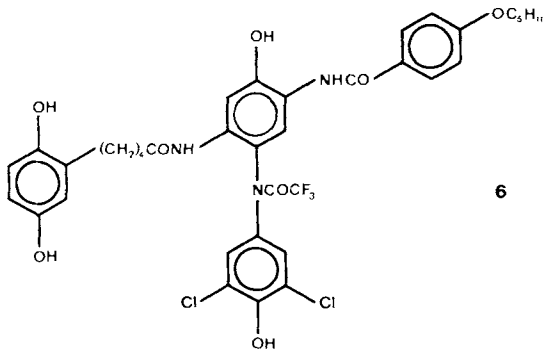
where *Dev* and *Link* have the same meaning as before and *Coup* represents a chromogenic coupler group. Such coupler residues are known from conventional color photography[12]. Like dye-developers, coupler-developer molecules are immobilized by oxidation as a function of exposure dose. Residual coupler-developer migrates to the receiving layer where it is mordanted. Color formation can then occur in two ways (Scheme 4). 1) The receiving layer




Scheme 4. Immobilization of coupler-developers **4** in exposed areas leading to formation of **5**.

is separated from the photosensitive unit, and is subsequently immersed in a color developer solution followed by an oxidizing solution[10]. 2) Alternatively an oxidant can be incorporated into the receiving layer and a color developing agent elsewhere in the material[11]. Chromogenic coupling then takes place in the mordant layer without separation or additional processing steps.

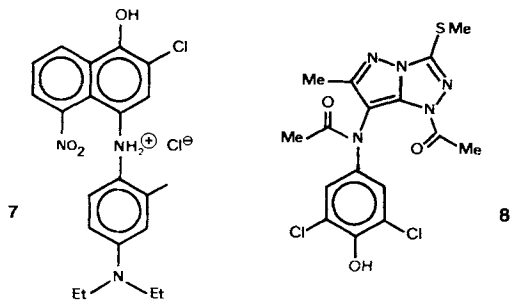
Closely related to coupler developers are the so-called *oxichromic developers*[13]. These are developers containing stabilized (*i.e.* protected) reduced azomethine or indophenol structures (*e.g.* **6**). Since these molecules are colorless, they can be incorporated directly into the sensitive emulsion layers. Differentiation between exposed and non-exposed areas occurs as for dye-developers. Dye formation results by deblocking (*e.g.* alkaline cleavage of the trifluoroacetyl group in **6**) and aerial oxidation or, better, interaction with oxidants incorporated into the receiving layer. Organic peroxides[14], iodosyl compounds[15], and nitroxide radicals[16] have been proposed in this respect.



6

### 3.3. Leuco Dyes

In some instances leuco dyes can be used as a very special kind of oxichromic dye-developer in which developer and reduced dye form the same structural moiety[17–19]. They must be able to reduce exposed silver halide, the leuco dye must be sufficiently mobile in the alkaline medium, and the oxidized leuco dye must be immobile in the alkaline medium. Imagewise immobilization as a function of exposure dose and migration of residual leuco dyes to an oxidizing mordant layer produce a positive image. A particularly interesting category are the leuco-indoaniline or leuco-azomethine dyes[20] and their derivatives (*e.g.* 7, 8)[21]. Since the free leuco dyes are too sensitive to aerial oxidation, hydrochlorides or acylated derivatives are used.



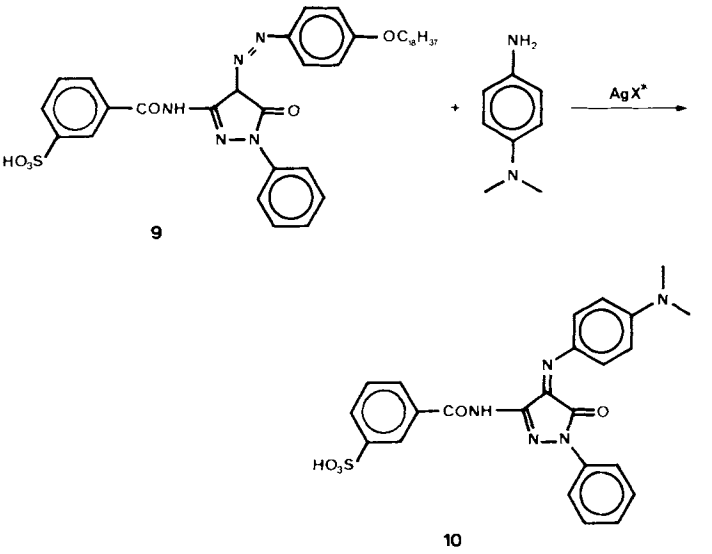
7 8

## 4. Systems Based on Chromogenic Coupling Reactions

Considerable effort has been directed at modifying oxidative coupling reactions known from color photography[12] to meet the requirements of diffusion transfer photography. Crucial is that the coupling reaction results in formation of a mobile dye or that a mobile dye becomes immobilized. Although much activity has been invested in optimizing the systems described in Sections 4.1—4.6 no commercially viable material is available. For the systems discussed in Sections 4.1—4.3 and 4.5, this is almost certainly due to staining of the receiving layer(s) by aerial oxidation of excess color developer.

### 4.1. The "Diffusible Dye Release" System

There are two straightforward methods[22–24] of exploiting classical chromogenic coupling reactions[12] for diffusion transfer photography.

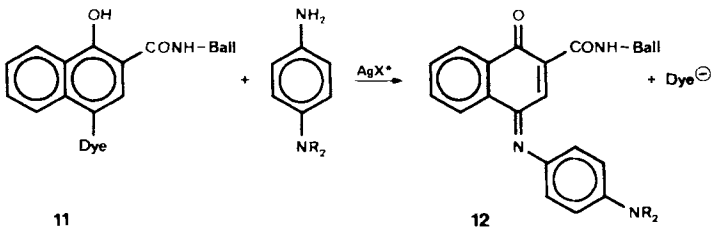


9 10

Scheme 5. Formation of diffusible dye **10** by release of a ballast group (*i.e.* diffusion impeding) from the coupling position of a coupler molecule **9**.

Couplers, such as compound **9** (Scheme 5), which contain an immobilizing ballast group in the coupling position, are initially non-diffusing but release this ballast group upon coupling. A diffusible dye (here the magenta dye **10**) is thereby generated and contains one or more solubilizing groups (*e.g.* $SO_3H$) which assist in achieving the required diffusion rate.

Alternatively, diffusible dye-releasing couplers[25] can be used. Such couplers are immobilized by the presence of a ballast group (Ball) in any except the coupling position (see **11** in Scheme 6).

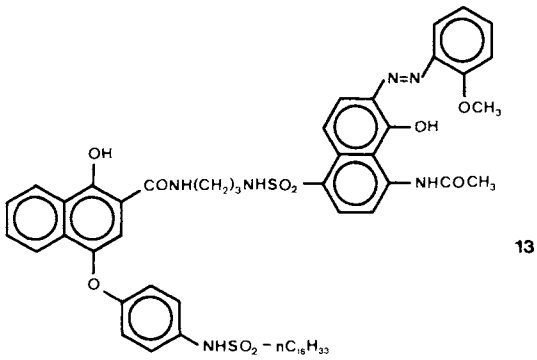


11 12

Scheme 6. Diffusible dye release from a coupler molecule **11** (with a ballast group) containing a dye moiety in its coupling position.

Additionally, they are substituted at the site of coupling by a solubilized dye residue. Upon reaction with oxidized color developer, these *DDR* (diffusible dye release) couplers[25] release the diffusible dye. The other coupling product having a ballast group is colored (cyan in the case of **12**), but this is of no significance since it remains in the original layer.

Couplers of these two types cause imagewise dye-diffusion and, therefore, require positive-working light-sensitive layers (see Section 2)[6] if a positive transferred image is required. However, couplers containing a ballast group at the coupling position and a dye residue at another position (*e.g.* **13**) allow the use of normal negative-working silver halide layers if the retained image is used instead of the transferred dye image[26].



13

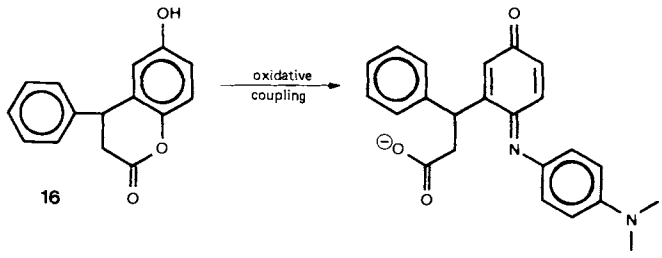
Chromogenic coupling of species such as **13** leaves only colorless ballast groups in the light-sensitive layer because the indoaniline dye produced migrates to the receiving layer. Since the degree of coupling is proportional to exposure, an anti-imagewise distribution of retained coupler results and if the incorporated dyes are complementary to the sensitivity of the silver halide layer, a positive retained image remains (cf. Fig. 2).

The kinetics of the system can be tuned to the photographic specifications to a limited extent by varying the kinetics of the coupling reaction; this can be achieved *via* structural changes in either the coupler residue or the color developer itself. An interesting third alternative is to interpose a *timing group* (as shown in Scheme 7) between a diffusible dye and the coupling position of a DDR coupler. Upon coupling with oxidized color developer the combination of timing group and dye is released. The timing group temporarily slows down migration of the dye to the receiving layer since subsequent intramolecular reaction in the timing group is required to obtain a diffusible dye: this provides a means of correctly timing dye release. Both the cyclization reaction[27] (as in **14**) and quinonemethide formation[28] (as in **15**) are useful timing mechanisms.

A disadvantage of DDR couplers which contain a releasable dye is their light absorption with concomitant loss of photographic speed when they are incorporated into a sensitive layer. "Shifted dyes" as well as oxichromic dyes (acylated leuco-dyes)[13b] are, once again, possible solutions.

### 4.2. Chromogenic Formation of a Solubilizing Group

A variant of the compounds dealt with in Section 4.1 are two-equivalent couplers, such as **16**[12], in which the leaving group is a sulfonic or carboxylic acid precursor and which is bonded to the mainframe of the coupler molecule *via* a ring (Scheme 8)[29].

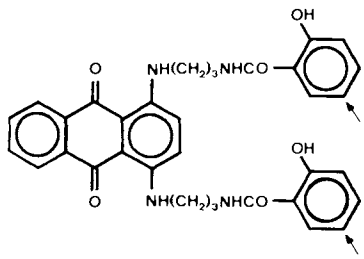


16

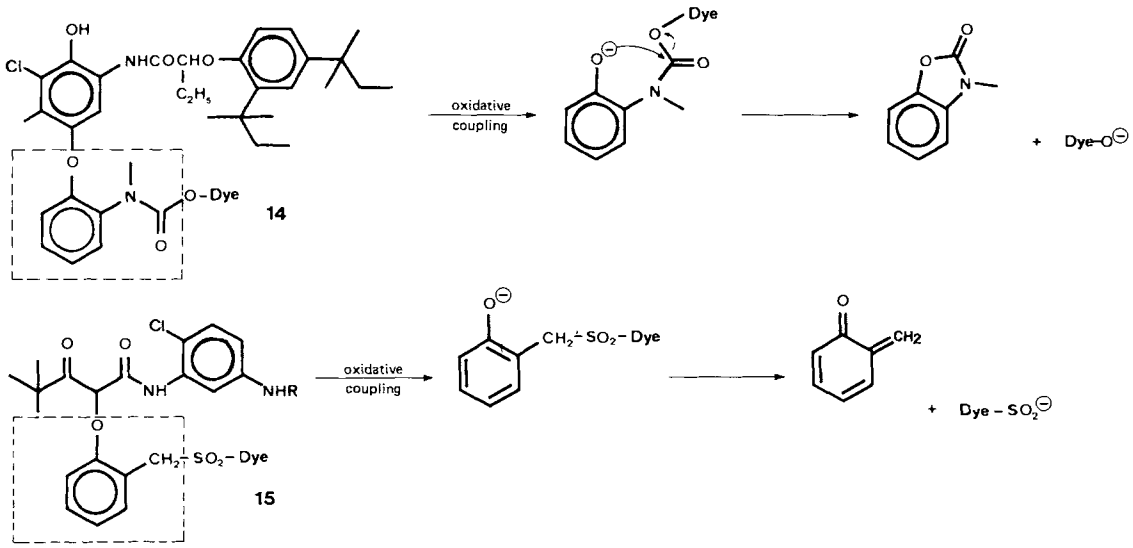
Upon coupling with oxidized color developer a solubilizing group is generated. Since a ballast group is absent it is doubtful whether this system provides enough differentiation of mobility.

### 4.3. Coupling Dyes

Dyes can not only be made diffusible by means of the classical coupling reaction but also non-diffusing[30,31]. This is achieved using dyes, such as **17**, which contain one or more coupling sites (indicated by arrows) for the oxid-



17

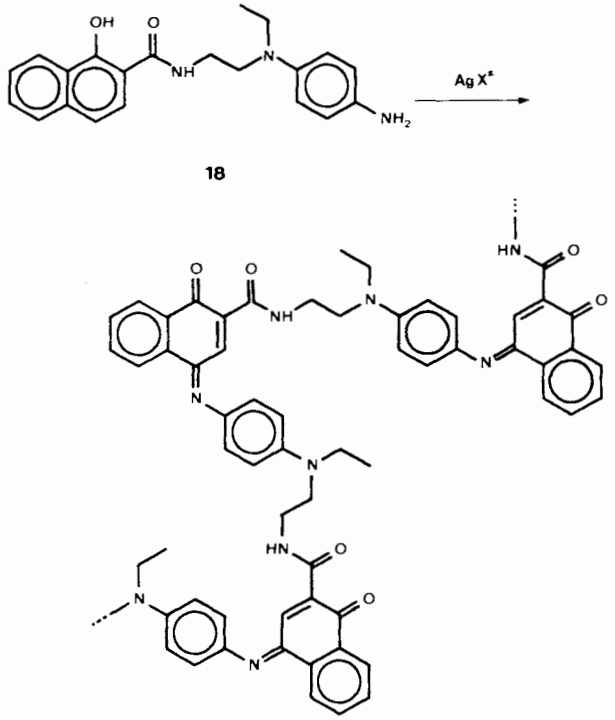


Scheme 7. Two-stage dye release from the couplers **14** and **15** by use of timing groups (framed).

ized color developer. Oxidative coupling removes solubilizing groups (phenolic hydroxyls in **17**) and increases the bulk of the molecule, hence hindering diffusion. In contrast to the systems discussed in Section 4.1 and 4.2, this is a positive-working system (anti-imagewise diffusion).

### 4.4. Auto-Coupling Developers

Upon oxidation, molecules such as **18**, which contain both a coupler and a color developer moiety, are able to couple intermolecularly to form polymers (Scheme 9)[32]. When they are incorporated into a sensitive layer auto-coupling developers are immobilized in exposed areas.

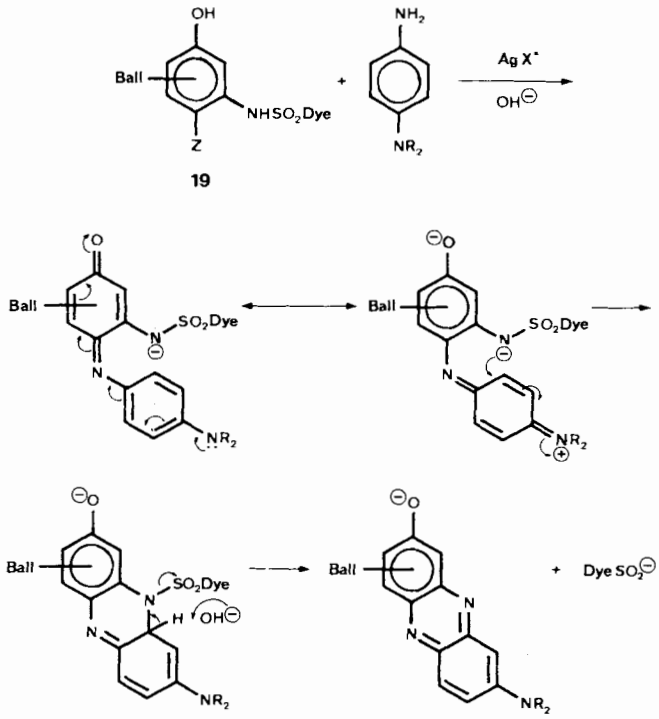



Scheme 9. Oxidation of the auto-coupling developer **18** leading to a polymeric coupling product.

Unreacted auto-coupler (predominantly in unexposed areas) diffuses into the receiving layer, where an oxidant causes the immobilization and the dye-forming coupling reaction. Because of the anti-imagewise diffusion, this is a positive-working transfer system.

### 4.5. The Azine System

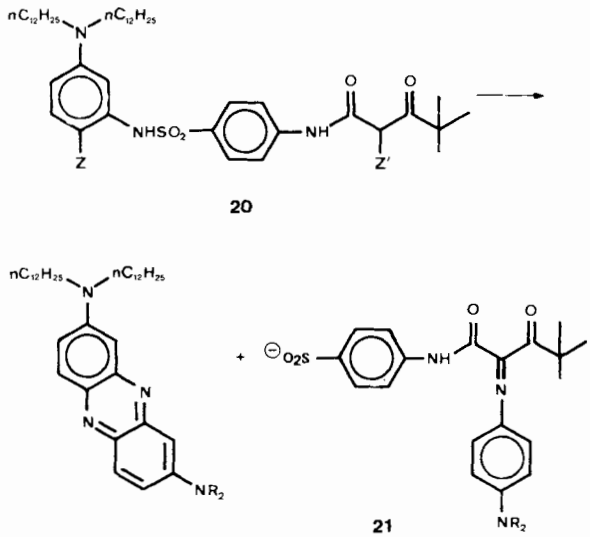
*m*-Sulfonamido-substituted phenols (*e.g.* **19**, Scheme 10) or anilines, as well as their naphthalenic analogs, are known to cyclize to azine dyes following oxidative coupling with color developers[33]. This reaction can be used for diffusion transfer purposes (Scheme 10) if the *m*-sulfonamido substituent contains a dye moiety and if the coupler contains a ballast group (*i.e.* an immobilizing group)[34,35]. The substituent Z can be hydrogen or any group[12] which can be replaced by oxidized color developers (halide, alkoxy, arylthio, *etc.*). According to Scheme 10,




Scheme 10. Release of dye from *m*-sulfonamido substituted phenols **19** by means of chromogenic coupling and subsequent cyclization.

sulfinate solubilized dyes are released in the cyclization step.

Instead of a dye, a solubilized coupler residue (*e.g.* from **20**, Scheme 11) can be released[36]. Formation of the actual diffusible dye (*e.g.* **21**) requires a second oxidative coupling reaction.

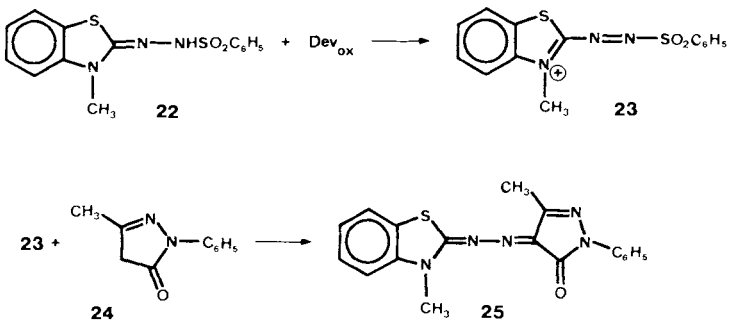



Scheme 11. Formation of azomethine (or indophenol or indoaniline) dye and its release by phenazine formation.

Both versions of azine-forming couplers are characterized by imagewise dye diffusion: the systems are therefore negative-working. An additional disadvantage of the coupler releasing version is that between four (Scheme 11, Z, Z' ≠ H) and eight equivalents (Z = Z' = H) of silver halide are required.

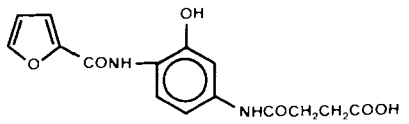
### 4.6. The Sulfonyl Hydrazone System

Because they can react with phenolic or activated methylene couplers (*e.g.* **24**) known from traditional color photography[12] (Scheme 12) sulfonyl hydrazones, especially those derived from cyclic amidines (*e.g.* **22**, Scheme 12), have been extensively studied by *Hünig et al.*[37]. Colored products (*e.g.* **25**) are formed and the reaction can be used as the basis for an alternative color photographic chemistry (in contrast to that of Fischer[12]).

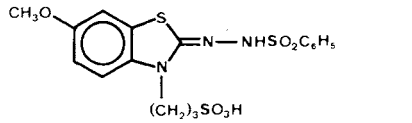


Scheme 12. Oxidative coupling of the sulfonyl hydrazone **22** with the coupler **24**, which contains an active methylene group, to yield the colored product **25**.

The coupling reaction is suited for diffusion transfer if both the coupler (*e.g.* **26**) and the sulfonyl hydrazone (*e.g.* **27**) present in the emulsion layer are diffusible in alkaline media[38]. In non-exposed areas both coupler and sulfonyl



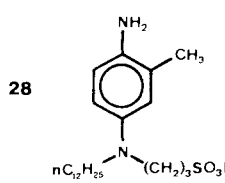
**26**



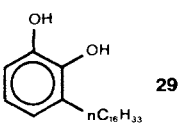
**27**

hydrazone diffuse to a receiving layer which contains an oxidant. This instigates coupling between these two components to produce a dye, which is subsequently mordanted. In exposed areas either of the two mobile components can be immobilized, depending on the nature of the bulk developer. If an *N,N*-dialkyl-*p*-phenylenediamine containing a ballast group is used (*e.g.* **28**), oxidative coupling with its oxidation product immobilizes the coupler. If, however, a pyrocatechol is used (*e.g.* **29**) diffusion of sulfonyl hydrazone is hindered by oxidative coupling.

Due to the ballast group neither **28** nor **29** are active developers for exposed silver halide. Hence, a small amount



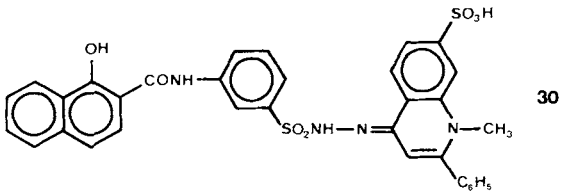
**28**



**29**

of a very mobile developer, *e.g.* 1-phenyl-3-pyrazolidone, is used as an electron transfer agent (ETA) between the bulk developer, containing ballast group, and exposed silver halide[39]: in exposed areas ETA is oxidized to $ETA_{ox}$ which oxidizes the bulk developer to regenerate ETA (cf. Scheme 2). The system produces anti-imagewise dye formation in the receiving layer and is therefore positive working.

Good color rendition requires that three coupler/sulfonyl hydrazone pairs be used (each associated with one of the sensitive layers), which have one partner (coupler or sulfonyl hydrazone) in common. Otherwise, unwanted mixed couplings could occur in the receiving layer. Hence, four color-forming components are incorporated into the material. This number can be reduced[38] to three if both coupler and sulfonyl hydrazone are combined into diffusi-



**30**

ble molecules such as **30**. The three molecules must either contain the same coupler or the same sulfonyl hydrazone.

## 5. Redox-Controlled Cleavages

Dye-developer and related systems have the disadvantage that the diffusing molecules can undergo unwanted oxidations on their way through other light-recording layers and, once mordanted, are sensitive to aerial oxidation (cf. Section 3.1). On the other hand, use of systems containing color developers results in formation of stains from their aerial oxidation. Both for these practical reasons, as well to avoid patent infringement, other systems have been sought by virtually all companies active in color photography. Among the alternatives, the most important group is based on redox-controlled cleavage reactions[40]; with the exception of the Polaroid system all other commercial dye-transfer systems belong to this category.

Ball-Redox-Link-Dye

1. Ball-Ox-Link-Dye ⟶ Ball-Ox + Link-Dye

2. Ball-Red-Link-Dye ⟶ Ball-Red + Link-Dye

Fig. 4. There are two classes of DRR systems: 1) oxidatively cleavable, 2) reductively cleavable systems. See text for additional information.

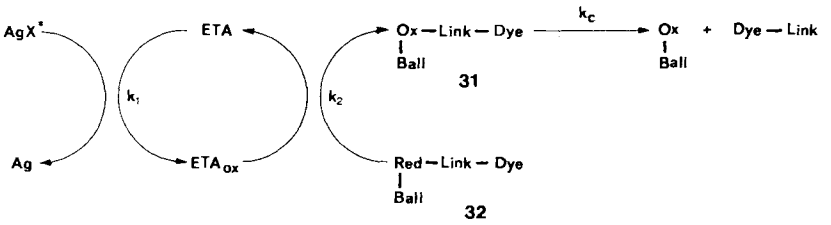
The active molecules in a dye-releasing redox system contain (see Fig. 4) a redox moiety *Redox*, linked to a dye or dye precursor moiety, and carry a ballast group *Ball*, which renders the whole molecule non-diffusing. Characteristic for the *Link* between *Redox* and *Dye* (or dye pre-

cursor) is that under the conditions of development it is labile in only one redox state and stable in all others. Hence, release of dye is redox-controlled and can be correlated with the exposure dose of sensitive silver halide *via* the development process. For photographic applications two subgroups in the *DRR* family[40] are considered:

- Systems releasing dyes or dye precursors in their oxidized state (type 1 in Fig. 4);
- Systems releasing dyes or dye precursors in their reduced state (type 2 in Fig. 4).

### 5.1. Dye Release in the Oxidized State

All systems based on oxidative cleavage reactions make use of compounds with ballast groups of the type represented by **32** (Scheme 13): their redox system is in its reduced state. The ballast group is necessary to immobilize these molecules, but as a result they are unable to reduce silver halide directly. A mobile developer, which acts as an electron transfer agent (ETA) between **32** and exposed silver halide, is therefore required. Scheme 13 shows all the reactions involved in exposed areas. In non-exposed areas no interaction occurs, and consequently no dye transfer takes place. In exposed areas ETA develops exposed silver halide (AgX*) and is itself oxidized to $ETA_{ox}$. The latter oxidizes **32** to **31**, regenerating ETA, and finally **31** decomposes releasing the dye. The other product of this cleavage, the redox moiety or "carrier" with the ballast group, is immobile and remains in the layer. Diffusion of the dye is imagewise, and all systems based on oxidative cleavage are negative-working.




Scheme 13. Generalized reaction scheme for oxidatively cleavable DRR systems.

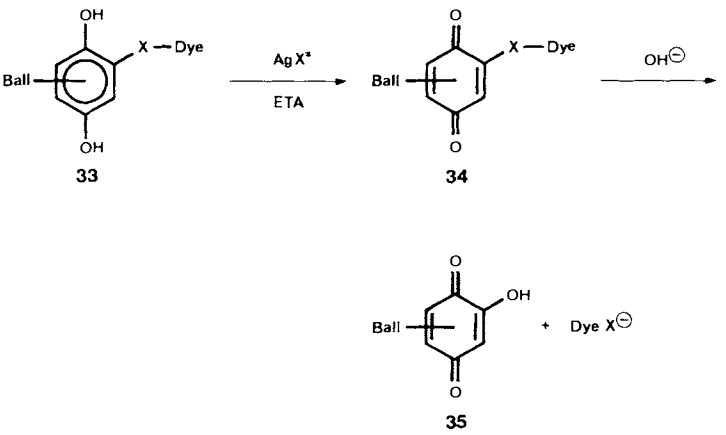
The redox potentials of the participating redox systems must satisfy the condition:

$$E^0(\text{Redox}) < E^0(\text{ETA}) < E^0(\text{Ag/AgX*}) \qquad \text{(e)}$$

Moreover, the cleavage reactions and the diffusion of the released mobile dyes must be sufficiently fast in order to obtain satisfactory photographic performance. Build-up of $ETA_{ox}$ is undesired since side-reactions can then occur and hence the situation $k_1 \gg k_2$ is to be avoided.

#### 5.1.1. Addition-Elimination Reactions in Benzoquinones

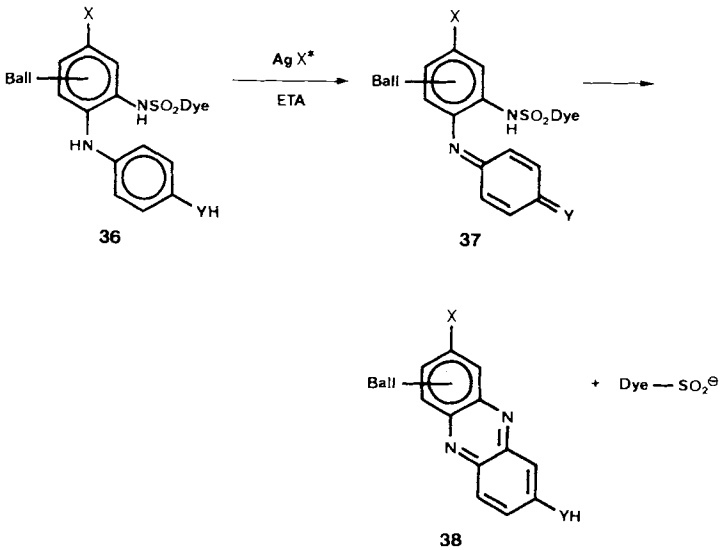
Hydroquinone derivatives **33** with ballast groups are inactive developers. In combination with a diffusible developer—which functions as an electron transfer agent—they undergo imagewise oxidation to yield *p*-benzoquinones **34** (Scheme 14). In the alkaline development medium these undergo an addition-elimination sequence[41] and thereby release diffusible dyes[42,43].




Scheme 14. Dye release *via* addition-elimination reactions at substituted *p*-benzoquinones, such as **34**. X = O, S, $SO_2$.

#### 5.1.2. Cyclization to Azines

Anilinophenol (or anilinoaniline) derivatives **36** having ballast groups[35,44] undergo imagewise oxidation with oxidized developer (Scheme 15).



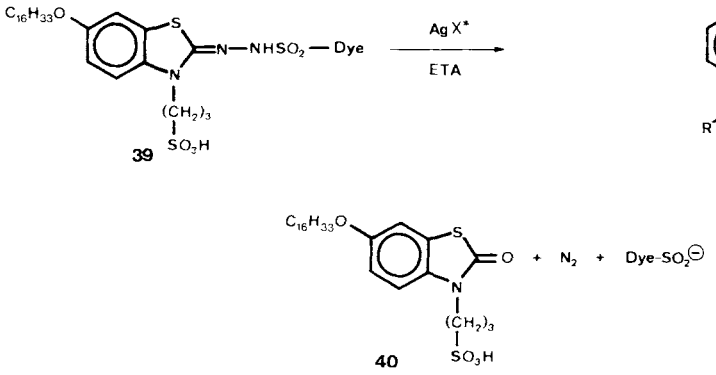

Scheme 15. Dye release by oxidation and subsequent cyclization of appropriately substituted diphenylamines **36**. X = H, OH, $NH_2$; Y = O, NH.

The product **37**, which resembles the coupling product of *m*-sulfonamidophenols (see Scheme 10), undergoes a dye-releasing ring closure to give a phenazine **38** with ballast groups *via* the same mechanism described in Scheme 10. Sulphinate solubilized dyes are released.

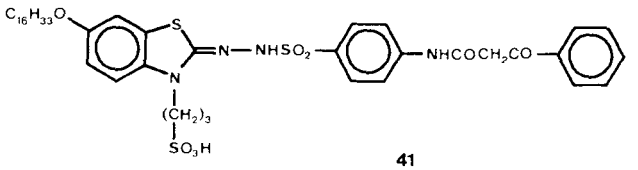
### 5.1.3. Cleavage of Sulfonyl Hydrazones

Oxidation of sulfonyl hydrazones leads to azosulfones, which are cleaved by nucleophiles[37]. Several methods have been elaborated of adapting this chemistry to diffusion transfer conditions. Sulfonyl hydrazones, such as *e.g.* **39**, with ballast groups are oxidized by oxidized ETA in exposed areas to yield an azosulfone, which undergoes alkaline cleavage to afford a diffusible sulfinate-solubilized dye (Scheme 16)[39,45,46].

Compounds like **41** are also useful in combination with color developers[47]. Instead of a dye they contain a releasable coupler moiety, which, subsequent to oxidative cleavage, can diffuse and produce a dye *via* a classical coupling reaction.



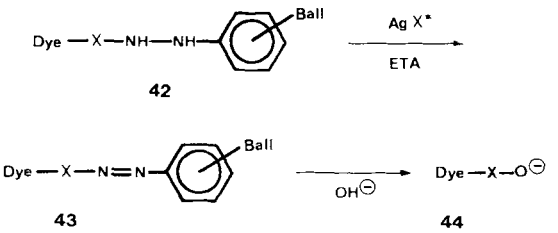

Scheme 16. Dye release by oxidative cleavage of sulfonyl hydrazones **39**.




It is also possible to interchange ballast and dye (or coupler) moieties in **39** or **41**.

### 5.1.4. Cleavage of Hydrazides

Closely related to the sulfonyl hydrazones **39** and **41** are hydrazides[48], such as **42**, which undergo oxidation by oxidized developer to yield acylazo or sulfonylazo compounds **43** (Scheme 17).

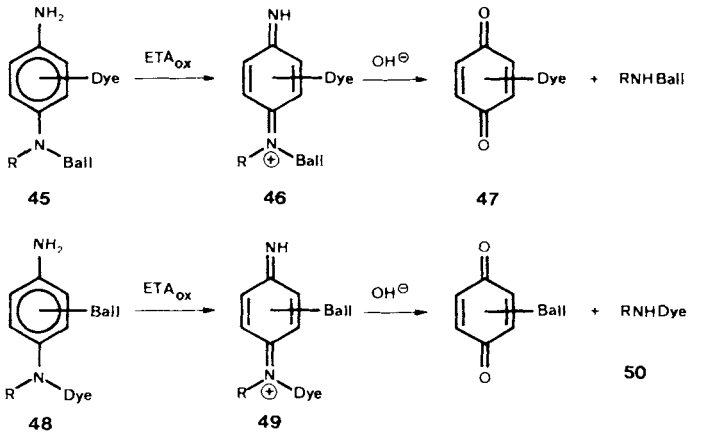



Scheme 17. Oxidative cleavage of acyl or sulfonyl hydrazides. X = CO, $SO_2$.

These[49] undergo alkaline hydrolysis to release diffusible dyes **44**.

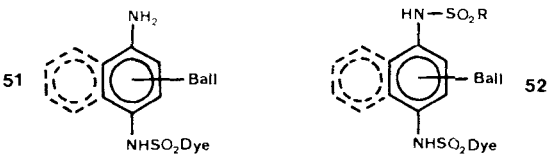
### 5.1.5. Hydrolysis of Quinone Imines

A well-known side reaction of color development is the deamination of oxidized *p*-phenylenediamines by alkaline hydrolysis[50]. On the basis of this reaction[51], two types of compounds (**45** and **48**) can be used for dye transfer as illustrated in Scheme 18. In **45** and **48** the relative positions of ballast group and dye differ, but both produce quinone imines **46** and **49**, which undergo hydrolytic cleavage to give the ballast-free and, hence, more mobile dyes **47** and **50**, respectively. With regard to the behavior of dye-developers (see Section 3.1), compounds **48** are preferred.




Scheme 18. Dye release by deamination of oxidized *p*-phenylenediamines **46** and **49**.

The *p*-sulfonamides **51**[52,53] and **52** are also suitable[54,55].

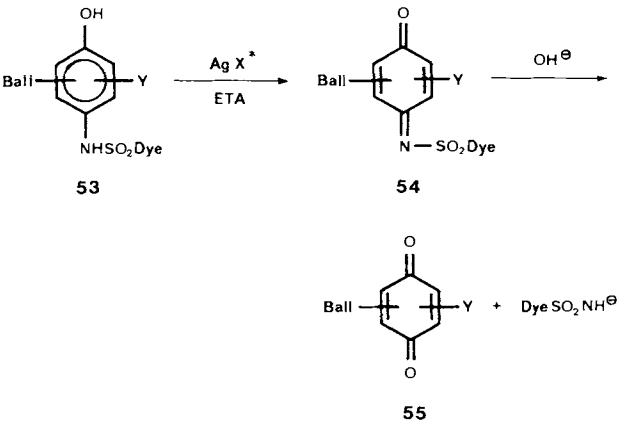



### 5.1.6. 4-Sulfonamido-Substituted Phenols and Naphthols

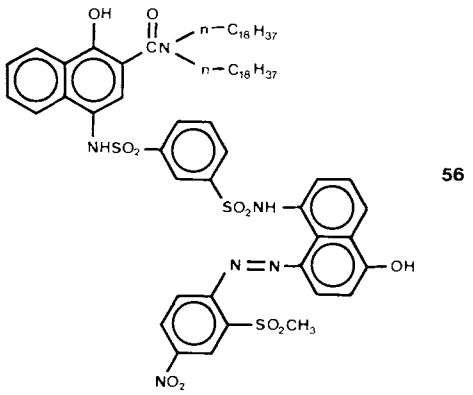
Closely related to the deamination of oxidized color developers, discussed in the previous section, is the alkaline hydrolysis of *N*-sulfonyl quinonemonoimides **54**[52,53,56]. These species result from the imagewise oxidation of *p*-sulfonamido-substituted phenols **53** having ballast groups, and release sulfamoyl-solubilized dyes (Scheme 19).

The substituent Y in **53** *e.g.* can also be an annelated benzene ring. From the naphthalene derivative **56** a cyan dye can be released. Examples of variations of the system are 4-sulfonamido-substituted phenols[57,58] having four additional substituents, tetrahydronaphthalene derivatives[59], and 4-sulfonamido-substituted naphthols having ballast groups in the 7-position[60].

The chemistry of *p*-sulfonamido-substituted naphthols has been successfully used in the Eastman-Kodak integral image transfer material[61] (Fig. 5).




Scheme 19. Dye release by oxidation of 4-sulfonamido substituted phenols **53** (or naphthols) and subsequent hydrolysis of the resulting *p*-quinone imine derivatives **54**.




**56**

Its construction differs substantially from that of the Polaroid material shown in Figure 3, particularly with respect to the arrangement of the light-sensitive layers relative to the image receiving section. This has to do with the fact that with the Eastman-Kodak film exposure and viewing occur from opposite sides. With the Polaroid film, the exposure and viewing directions are the same.

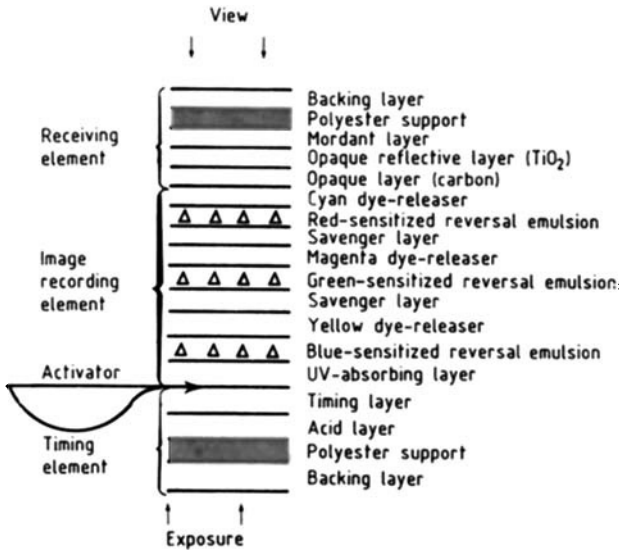



Fig. 5. Schematic structure of a Kodak integral film unit (see text for additional information).

Another innovation is the presence of the two scavenger-layers for oxidized developer. Their use is illustrated in Figure 6. In an exposed area of the green-sensitized layer, development of the latent image produces $ETA_{ox}$, which can either diffuse to the layer in which the magenta dye is released or to the layer in which the yellow dye is released. The latter is unwanted, and the purpose of the scavenger layer is to block diffusion of $ETA_{ox}$ in the wrong direction by means of a *scavenger*. This is a non-diffusing reducing substance which reconverts $ETA_{ox}$ into ETA.

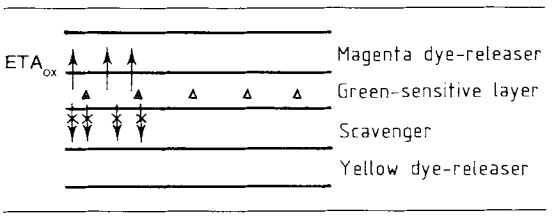
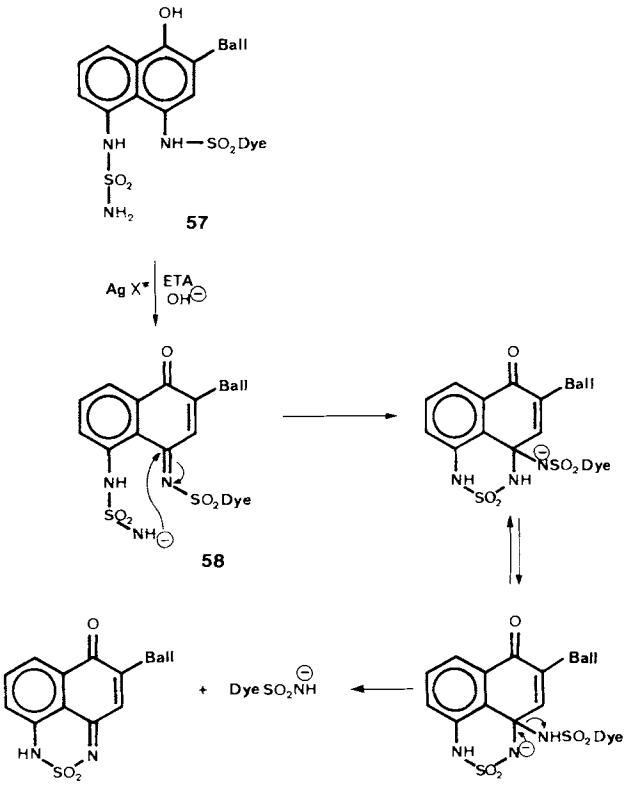



Fig. 6. Function of a scavenger layer. It blocks unwanted migration of oxidized electron transfer agent ($ETA_{ox}$) by reconverting it into ETA (see text for details).

The opaque layers in the receiving element (Fig. 5) protect the image-recording element from daylight once the unit is ejected from the camera. Daylight protection from the other side is provided by components in the activator fluid.

As described in Section 5.1 a rapid cleavage reaction is required (rate $k_c$ in Scheme 13). Structural variations, such as those cited above, are however of limited effect. A more efficient modification is the introduction of a nucleophilic substituent at a *peri*-position to the sulfonamido function[61] as *e.g.* in **57** (Scheme 20). Neighboring group parti-

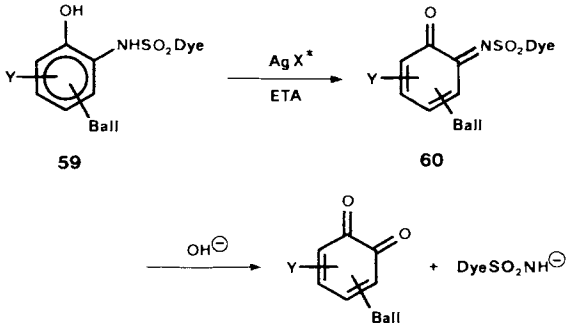



Scheme 20. Faster and less pH-dependent dye release in the 4-sulfonamidonaphthol system by neighboring group participation.

cipation in **58** should lead to much faster monomolecular release of dye, which should also be considerably less pH-dependent than its the bimolecular analog[62].

### 5.1.7. 2-Sulfonamido-Substituted Phenols and Naphthols

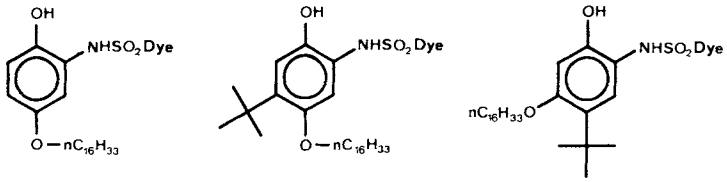
2-Sulfonamido-substituted phenols or naphthols undergo imagewise oxidative cleavage[63–67], presumably *via* a mechanism (Scheme 21) analogous to that outlined for their 4-isomers (Scheme 19).




59 60 61

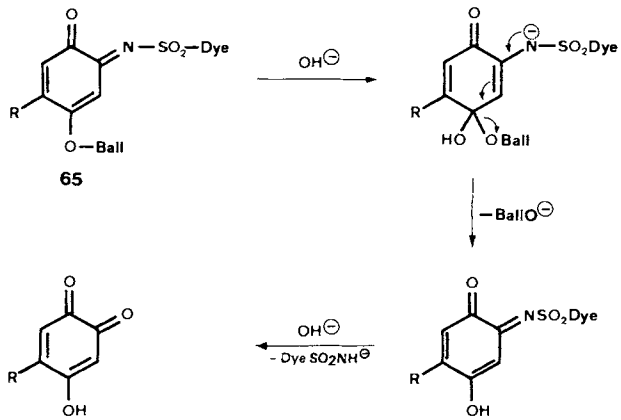
Scheme 21. Dye release by oxidation of 2-sulfonamido-substituted phenols **59** and subsequent hydrolysis of the resulting *o*-quinone imine derivatives **60**.

The topic has been extensively investigated in the Fuji laboratories[64–67], and several structural variations, *e.g.* compounds **62**—**64**, have been proposed. The 2-sulfonamido system has found commercial application in the recently launched Fuji instant photographic material.




62 63 64

Dye release may not always involve direct hydrolysis of the sulfonylimino group in **60**[68]. In compounds of type **65**




65

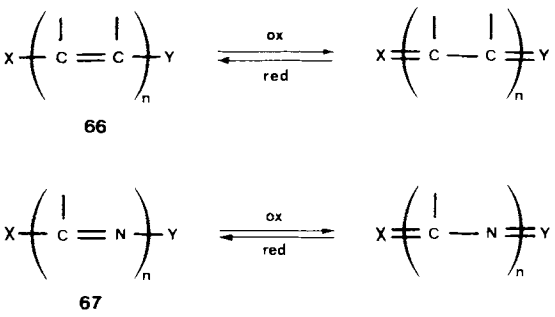
Scheme 22. Stepwise hydrolysis of some substituted *o*-quinone imine derivatives **65** (cf. Scheme 21).

the hydroxide ions initially attack the alkoxy- rather than the imino-substituted C atom (Scheme 22). The ballast group is removed *via* an addition-elimination reaction, followed by subsequent hydrolysis of the imino group.

Faster and less pH-dependent dye release can be achieved by neighboring group participation of nucleophilic substituents in the *o*-position to the sulfonamido group[61], by analogy to the effect of *peri*-substituents in 4-sulfonamido substituted 1-naphthols (see Section 5.1.6).

### 5.1.8. Other Sulfonamido Systems

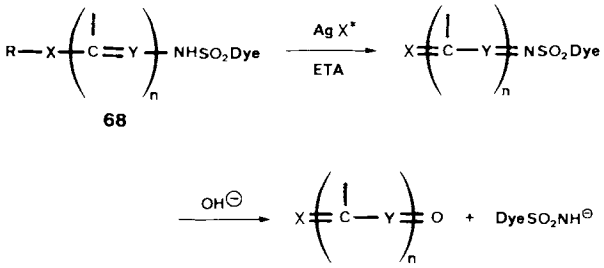
According to the Kendall-Pelz rule[69,70], compounds containing the substructure **66** or **67** (see Scheme 23) are




66 67

Scheme 23. The Kendall-Pelz rule predicts which compounds are potential silver halide developers. X, Y = OH, O-Acyl, $NR_2$, NHR; R = H, alkyl, acyl.

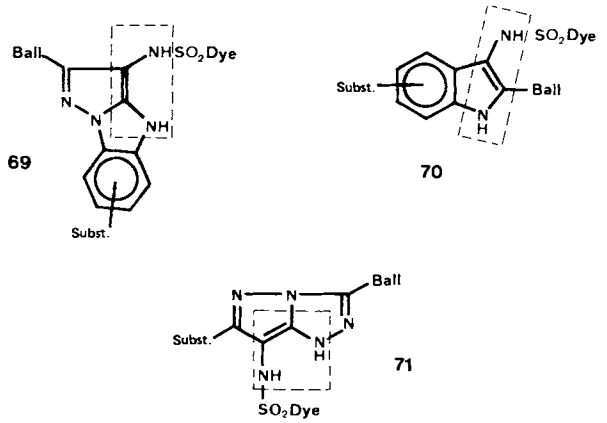
potential developers for silver halide. The sulfonamido-substituted phenols in Sections 5.1.6 and 5.1.7 follow this rule (X = OH, Y = $NHSO_2$-Dye, n = 2 or n = 1). The Kendall-Pelz rule, therefore, predicts that all molecules containing the moiety **68** could be potentially useful DRR compounds (see Scheme 24). The realization of this fact




68

Scheme 24. Generalization of the sulfonamidophenol system on the basis of the Kendall-Pelz rule. X = O, NH; Y = CR', N; R = H, acyl.

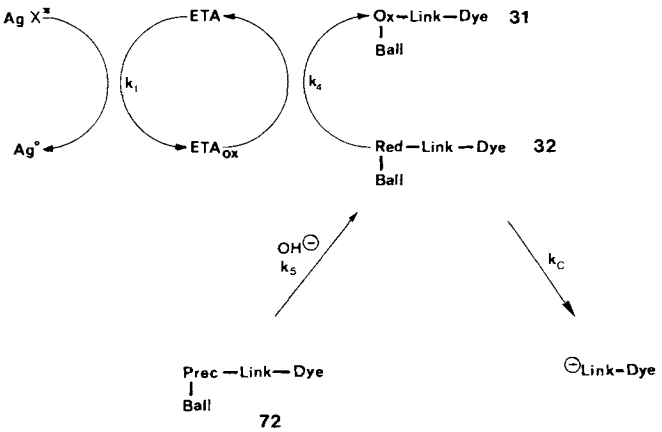
prompted Agfa-Gevaert to develop systems based on sulfonamido-substituted pyrazolo[2,3-*a*]benzimidazoles **69**[71] and indoles **70**[72–75]. Proposals from other sources involve *e.g.* 5-hydroxypyrazoles[76], ketones[77], and pyrazolo[3,2-*c*][1,2,4]triazoles **71**[78] with sulfonamido substituents in the 4-, α-, and 7-position, respectively (for a review of other possibilities see [79]).




### 5.2. Dye Release in the Reduced State

In contrast to the situation for oxidatively cleavable DRR systems (see Section 5.1) there is no single general scheme applicable to reductively cleavable DRR systems. This is because for some cases the reduced inactive DRR compounds can be incorporated into the photographic material and activated by contact with alkali. The inactive form can contain either an undissociated version of the redox system (Prec) or an alkali-labile derivative.

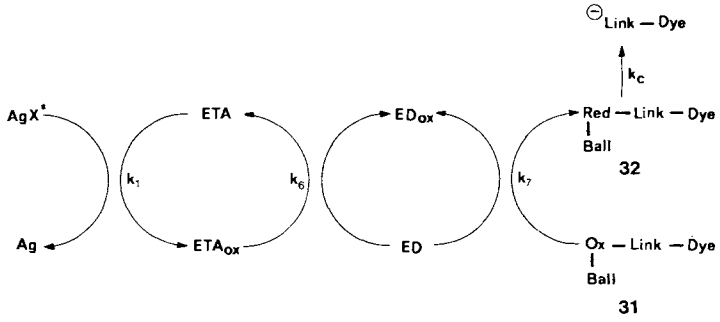
Scheme 25 applies to such inactivated DRR molecules. For this operating mode the acronym *IHO*[80] has been coined. Here again the electron transfer agent (ETA) is necessary because of the presence of ballast groups in the DRR compounds (see Section 5.1). In non-exposed areas the alkaline medium converts the inactive precursor **72** into **32** by dissociation or deblocking (rate $k_5$); subsequent cleavage (rate $k_c$) releases diffusible dye. In exposed areas the cleavage reaction competes with oxidation (rate $k_4$) of **32** by $ETA_{ox}$ to the stable oxidized counterpart **31**.




Scheme 25. Generalized reaction scheme for reductively cleavable DRR systems operating in the IHO mode [80].

If $k_4 \gg k_c$ oxidation effectively immobilizes dye, and good differentiation of exposed and non-exposed areas is achieved. This condition is not easily fulfilled, since in most IHO systems $k_c$ is very large *(vide infra)*. The use of protected derivatives rather than the undissociated parent redox system in **72** can alleviate the problem to some extent, since it allows an increase in the concentration of $ETA_{ox}$ by slowing down (relative to the unprotected analogue) conversion of **72** into **32**. As a consequence, the reaction **32** → **31** becomes more competitive. With large values of $k_c$, the competing cleavage reaction in exposed areas is always a nuisance.

The only way to overcome this is to use the *IHR* mode of operation (Scheme 26)[81]. In contrast to the IHO mode, a fourth redox pair $ED/ED_{ox}$[82] is required. It concerns




Scheme 26. Generalized reaction scheme for reductively cleaving DRR systems operating in the IHR mode [81].

ballast group-substituted reducing agents capable of reducing **31** to **32**, as well as $ETA_{ox}$ to ETA. In exposed areas, development of the latent image causes imagewise formation of $ETA_{ox}$, which oxidizes the electron donor ED to $ED_{ox}$, thereby removing the electron donor necessary for reduction of **31**. In unexposed areas ED is not attacked (no $ETA_{ox}$) and reduces **31** to **32**, thus causing release of dye. Several prerequisites must be fulfilled to achieve satisfactory performance. The redox potentials should correspond to inequality (f). The first and third inequalities

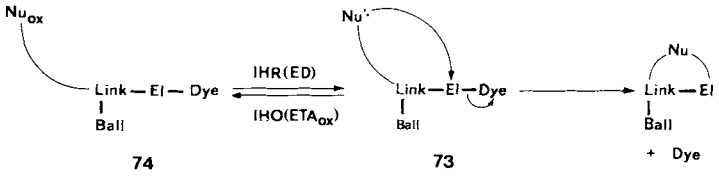
$$E^0(\mathrm{ED}) < E^0((\mathbf{31})/(\mathbf{32})) < E^0(\mathrm{ETA}) < E^0(\mathrm{Ag/AgX^*}) \qquad \text{(f)}$$

follow from the above description of the course of the reaction. The second ensures that ETA does not reduce **31** directly (in competition with ED) which would otherwise occur because of its high mobility (in contrast to ED substituted with ballast groups). From the kinetic point of view the condition $k_6 \gg k_7$ must be met in order to consume the electron donor in exposed areas. Both redox reactions are diffusion controlled and consequently the condition is fulfilled by using an electron donor with ballast groups and a very mobile $ETA_{ox}$. Also, $k_1 > k_6$ must be avoided, since this would lead to build up of $ETA_{ox}$.

Finally, the preceding discussions indicate that reductively cleavable DRR systems are positive working (see Section 2), irrespective of their operating mode. This is a great advantage over oxidatively cleavable systems, since it permits use of normal, negative-working silver halide layers!

#### 5.2.1. *Cleavage by Cyclization*

For an important group of reductively cleavable DRR systems dye is released by cyclization[83–86]. Both IHO and IHR modes are possible.




Scheme 27. Reductive dye release by cyclization reactions.

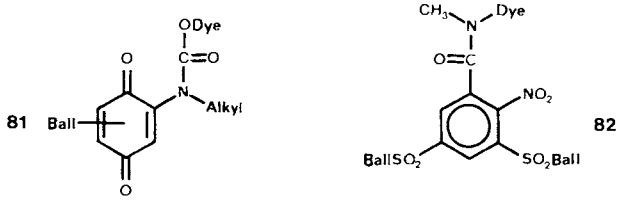
In the IHO mode[87] the ballast group-substituted active molecules **73** (see Scheme 27) contain an oxidizable nucleophilic group *Nu* (or a *Nu*-precursor) as well as an electrophilic group *El* bearing the fragment (*e.g.* a dye) to be released. Intramolecular attack of *Nu* on *El* yields the free fragment, *i.e.* in this case the dye. Oxidation of *Nu* to $Nu_{ox}$ (by $ETA_{ox}$) makes cyclization impossible. In an alternative application, the substituents are exchanged: cleavage of the ballast group then releases the rest of the molecule.

Two patent applications have been made for *IND* systems[87] by Eastman Kodak: one is based on *N*-(2,5-dihydroxyphenyl)urethanes **75**[73] and the other on benzisoxazolones **78**[84] (see Scheme 28). The system **75**→**76**→**77** makes use of the extremely high rate of cyclization ($k_{obs} > 2\,sec^{-1}$!) of *N*-(2-hydroxyphenyl)carbamates[88] in alkaline media, and provides the possibility of oxidative inactivation of the phenolic function by incorporation into a hydroquinone group.

**78**→**79**→**80** is an example of a system in which the redox system (a hydroxylamine anion, see **79**) is protected (see discussion of Scheme 25) as an alkali-labile derivative (benzisoxazole **78**). Here use is made of rapid cyclization[89] of 2-(hydroxylamino)benzamides to benzisoxazoles (*e.g.* **80**). Oxidation of **79** by $ETA_{ox}$ converts the hydroxylamine anion into a nitryl radical, which is unable to act as a nucleophile.

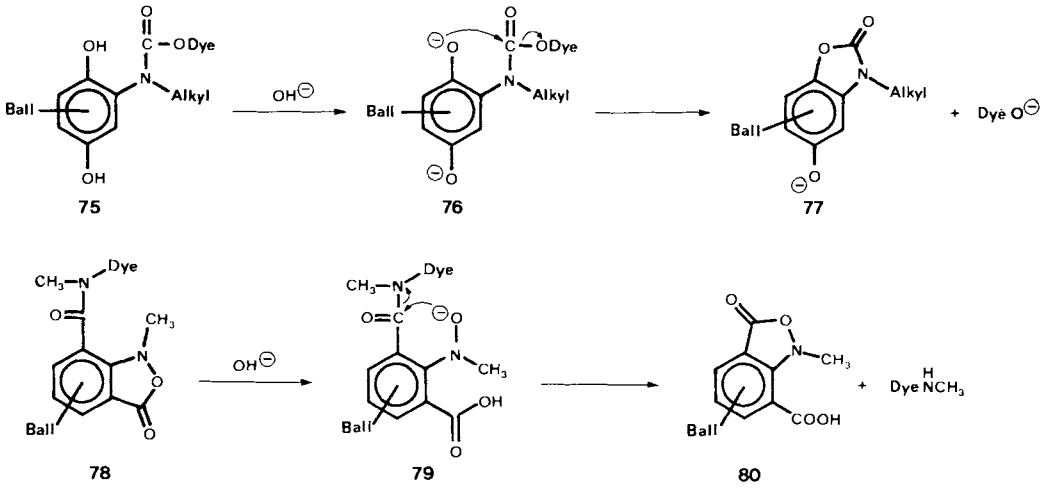
In the IHR mode[90] compounds **74** are used containing an oxidized nucleophilic group $Nu_{ox}$ (Scheme 27), which by electron acceptance (*i.e.* reduction by ED, see Scheme 26) is converted into the active nucleophile *Nu* (in **73**): this initiates cyclization and concomitant dye release.

Both of the IHO mode cyclizing systems have an IHR mode counterpart containing the oxidized redox function. Compounds **81** correspond to **75**, whereas the nitro group in **82** is the oxidized precursor of the hydroxylamine function in **79**. Because of their electron withdrawing effect the two sulfonyl substituents, reduce the electron density at the nitro function in **82** and make it amenable to reduction by practical ED compounds (instead of *e.g.* by $H_2$ or $NaBH_4$[89]).



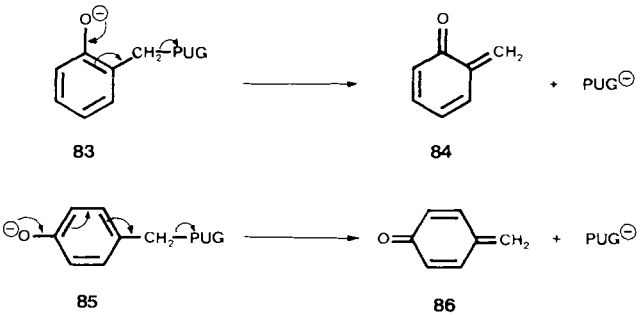

### 5.2.2. *Quinonemethide Formation*

2- and 4-Hydroxybenzyl derivatives of photographic reagents have been described as their alkali-labile precursors[91,92]. The release of the photographically useful groups (PUG in Scheme 29) is caused by formation of the quinonemethides[93] **84** and **86**.



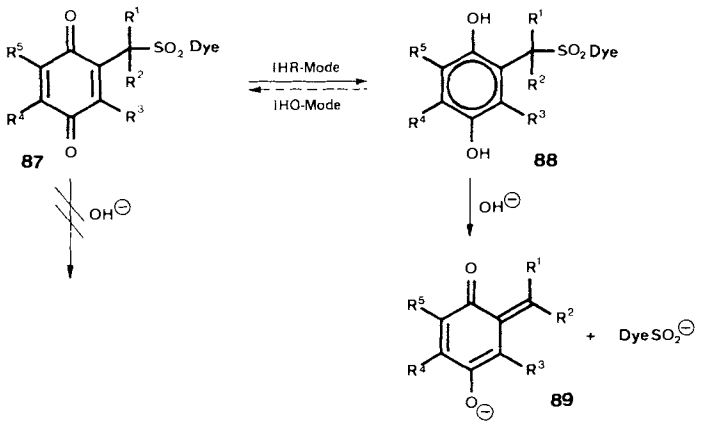

Scheme 28. Examples of cyclization-based DRR systems operating in the IHO mode (IND systems [87]).

Kinetic data[94,95] suggest that some hydroxybenzyl sulfones could react sufficiently fast at high pH-values to be




Scheme 29. Release of photographically useful groups, PUG (*e.g.* dyes) by quinonemethide formation.

of practical use for diffusion transfer purposes. As discussed in Section 2, this requires that the reactions shown in Scheme 29 should be redox-controlled, and this is readily achieved by incorporation of the phenolic function into a hydroquinone (or catechol) unit. This is the basis of the Agfa-Gevaert quinonemethide system (Scheme 30).




Scheme 30. Use of redox-controlled formation of quinonemethides, such as **89**, for anti-imagewise dye release (see text for additional explanations).

In the IHO mode[80] the hydroquinones **88** are incorporated into the material[96,97]. One of the substituents $R^1$–$R^5$ acts as a ballast group, which makes **88** non-diffusing. In exposed areas, oxidation of **88** to **87** by $ETA_{ox}$ (cf. also Scheme 25) blocks cleavage, whereas in non-exposed areas quinonemethide **89** and diffusible dye are formed.

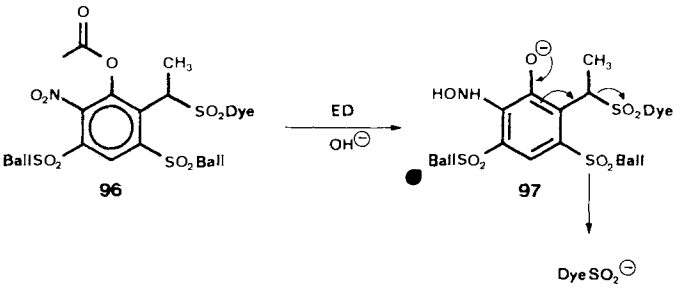
In the IHR mode[81] the quinones **87** are incorporated into the material[98,99]; in this case their use (see Scheme 26) necessitates the introduction of an electron donor (ED). In exposed areas this ED is oxidized by $ETA_{ox}$, and is no longer available for reduction of **87**. In unexposed areas **87** is reduced to **88** by unspent ED and undergoes alkali-induced dye release.

In this context mention should be made of an earlier system based on dye releasing hydroquinone derivatives of type **90** having a quaternary ammonium group bonded to an α-methylene group[100].

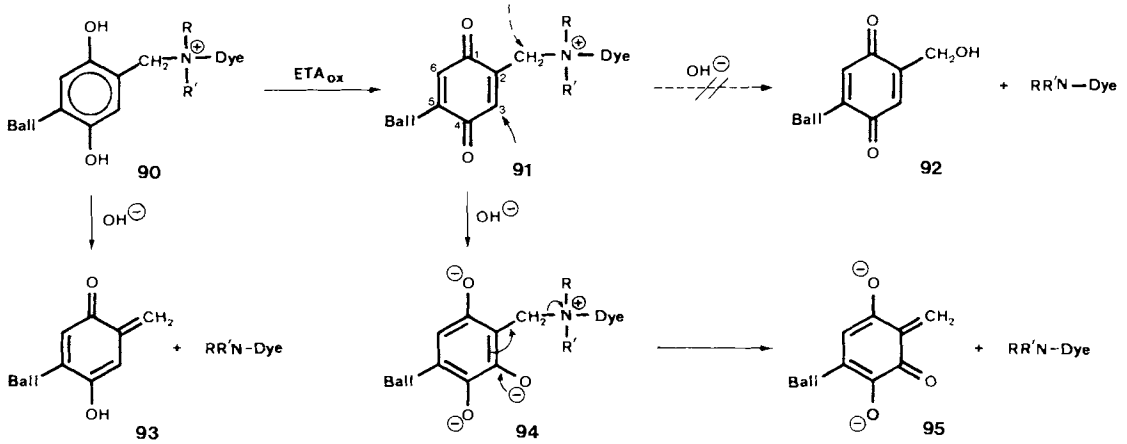
The system produces imagewise dye release (**90**→**91**→**92**, Scheme 31) assuming that hydrolysis ($S_N2$ type!) of **90** is sufficiently slower than that of **91** to differentiate between exposed and non-exposed areas. This rationale does not hold. In our opinion the strong inductive attraction which the positively charged nitrogen atom exerts on the enone CC double bond must be considered. As a result C-3 in **91** becomes a very strong electrophilic center[101], much stronger than C-5 and C-6, and, hence, becomes the preferential site of attack. Hydroxide addition to **91** followed by enolization leads to **94**, in which the normal quinonemethide mechanism operates to release the dye.

It could be asked why the direct formation of **93** from **90** does not compete with the longer route **90**→**91**→**94**→**95**. The higher electron density in **94** with respect to doubly ionized **90** makes reaction **94**→**95** faster than **90**→**93**. Since oxidation of **90** with $ETA_{ox}$ is extremely fast, one is, therefore, forced to conclude that the conversion **91**→**94** is also faster than cleavage of **90** to **93**. In view of the reactivity of C-3 in **91**, this is not entirely surprising. In any case, in the IHO mode[100] the competition between reactions **90**→**93** and **90**→**95** in exposed areas precludes good differentiation between exposed and non-exposed areas. On the other hand, the IHR mode is unpractical because the reactivity of **91** makes it impossible to incorporate into a gelatine layer.

For the system in Scheme 30 the sulfonyl group does not strongly activate the enone CC double bond. Hence, the—here unwanted—side reaction of the type **91**→**94** is strongly retarded and quinonemethide formation




Scheme 32. Quinonemethide formation is blocked by a deactivating nitro group; reductive deblocking in alkaline medium releases dye.



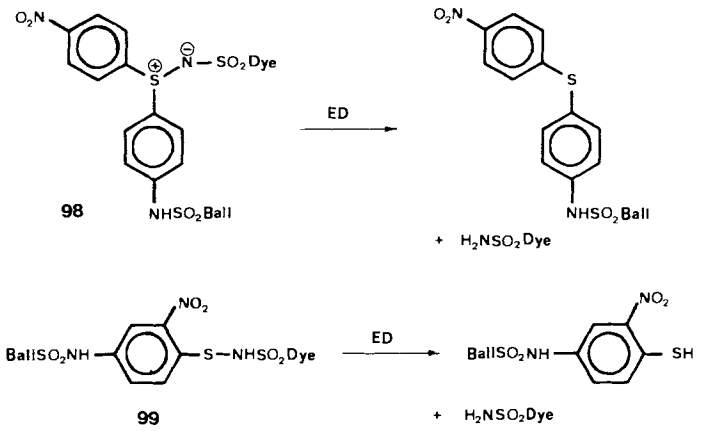

Scheme 31. How is the dye released from **90**?

**88**→**89** dominates. A substituent at C-3[97–99] helps to differentiate between exposed and non-exposed areas.

Another application of quinonemethide chemistry makes use of the deactivating effect of a nitro group (Scheme 32)[102]. Only after reduction of the nitro group in **96** by unspent ED (*i.e.* in non-exposed areas) and subsequent hydrolysis of the acetyl group is dye release (in **97**) possible. The system is a hybrid of the nitro-*BEND*[90] (*e.g.* compound **82**) and the quinonemethide systems (Scheme 29).

### 5.2.3. *Sulfilimines and Sulfenylsulfonamides*

Characteristic for the systems discussed in Sections 5.2.1 and 5.2.2 is that the redox system and the bond to be cleaved are separate chemical entities which can interact if the redox system is in its reduced state. Other potentially useful systems[103] are conceivable in which the redox system and the bond to be cleaved form a unit: here "true reductive-cleavage" is necessary to bring about dye release. So far, only sulfilimines (*e.g.* **98**) and sulfenylsulfonamides (*e.g.* **99**) have been claimed for this class[104]. These compounds can undergo reductive S–N bond cleavage[105, 106], which can be used (see Scheme 33) in an IHR-type system (see Scheme 26).



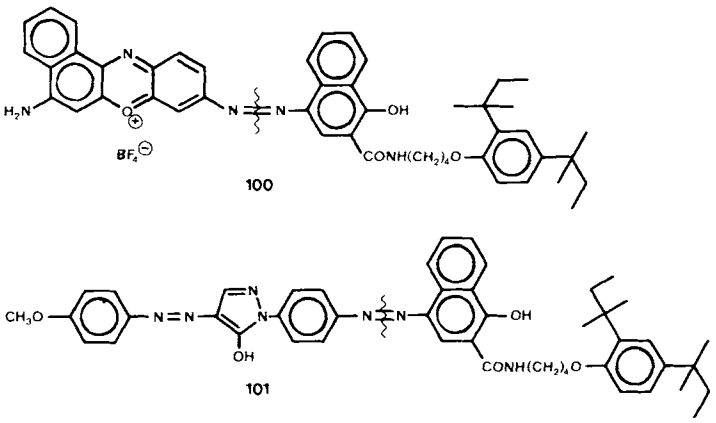

Scheme 33. Direct reductive cleavage of sulfilimines **98** and sulfenylsulfonamides **99**.

### 5.2.4. *Dye-Bleach Chemistry*

All dye-transfer systems discussed so far operate in the alkaline development medium. The *silver dye-bleach process*[107], however, functions in strong acid and can also be adapted to diffusion transfer[108–110]. The basic reaction involved is the reductive cleavage of an azo bond in acidic media.

$$\text{Dye–N=N–Ball} + 4\,H^{\oplus} \longrightarrow \text{Dye–NH}_2 + \text{Ball–NH}_2 \qquad \text{(g)}$$

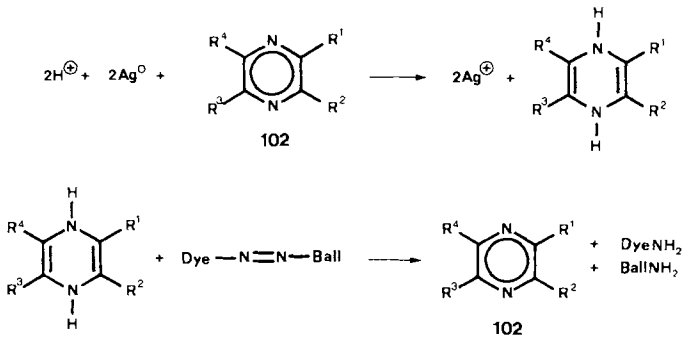
Examples of *bleach-type dye releasers* are **100** and **101**. Upon reduction, the indicated azo compounds are cleaved and an oxazine and azopyrazolone dye, respectively, are released. Also useful are phenazine, thiazine, acridine, pyrylium, rhodamine[108], as well as anthraquinone dyes[109].




In a first mode of operation, exposure is followed by treatment with an acidic solution of a *Dymodev* compound[111]. In non-exposed areas unspent *Dymodev* "*dy*e *mo*difiying and *dev*eloping" compound reduces the azo bond, resulting in release of dye and its diffusion. In exposed areas the *Dymodev* compound is consumed in developing the silver halide and is not available for dye release. Anti-imagewise dye transfer occurs, *i.e.* the system is positive working.

Alternatively, the material is first subjected to conventional black and white development: a silver image results. Subsequently the azo bond is reduced in a dye-bleach bath[112] (see Scheme 34); **102** is an example of a dye-bleach catalyst. Dye diffusion occurs imagewise and a negative-transferred image results.

The dye-bleach procedures outlined here are not limited to azo compounds: hydrazide, azoxy, imino, and α-amino carbonyl functions can also be used[109].




Scheme 34. Two-stage dye diffusion based on dye bleach chemistry. After a black and white development step producing metallic silver, the material is exposed to an acidic solution of a dye-bleach catalyst **102**. The catalyst is reduced by $Ag^0$ and in turn subsequently reduces the azo bond, thereby releasing dye and regenerating **102**.

## 6. Reaction with Silver Ions

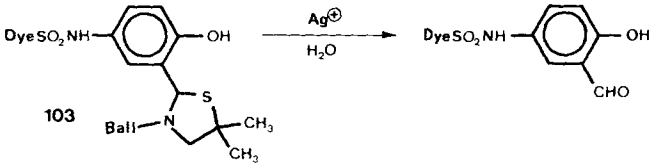
In the previously discussed systems redox-controlled mobility changes are achieved by incorporation of a redox system into a dye or dye precursor. Another possibility is to use dyes or dye precursors which contain no active redox system (under the conditions of development), but are able to react with free silver ions. In presence of complexing agents for $Ag^+$, the development step should yield an anti-imagewise distribution of silver ion complex and free

silver ions, and thus induce an anti-imagewise interaction with dye precursor. Patent applications have been made for both complexation and argentolysis.

### 6.1. Argentolytic Reactions

Thioaminals[113,114] have been patented which undergo argentolysis to form their ketone or aldehyde precursors. In a first application[113] mobile ketones or aldehydes are released which migrate to a receiving layer and condense with an active methylene compound to yield a dye (anti-imagewise, positive-working system). Useful methylene compounds include α-cyanoacetanilides, 1,3-dimethylthiobarbituric acid, and malonitrile. Alternately, both carbonyl and methylene compounds capable of diffusing can be liberated anti-imagewise. This version is required for multicolor material.

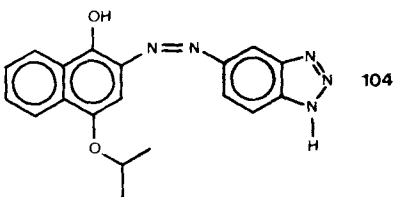
Far more attractive is the second application[114] involving compounds such as **103**, which contain the partial structures –S–C–N– or –S–C–N= (or vinylogs thereof) and release a diffusible dye by argentolysis (see Scheme 35). A similar result is obtained with thiol esters of the type Ball–S–CO–Dye[115].




Scheme 35. Argentolytic cleavage of (cyclic) thioaminals.

### 6.2. Complexation

Heterocycles, such as benzotriazoles and thiazolethiols, form strong complexes with $Ag^+$ ions which are insoluble in aqueous media. In consequence, dye molecules such as **104** which contain such moities are immobilized anti-imagewise upon development[116].



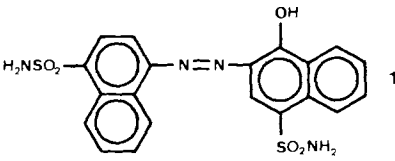

104

Dye diffusion occurs imagewise and yields a negative transferred image. The same result can also be achieved by incorporating the silver salts of such heterocyclic dyes into a material[117]. In exposed areas the metallic silver produced during development strongly catalyzes dissociation of these salts and reduction of the $Ag^+$ ions thus liberated.

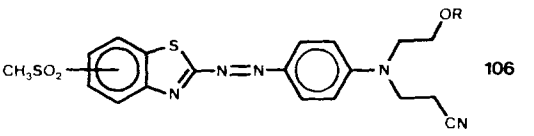
## 7. Other Systems

### 7.1. pH-Controlled Diffusion

Dyes can be used[118] which are only diffusible in alkaline media (*e.g.* **105**). The developer fluid contains the stoichiometric amount of alkali required for the reduction of the silver halide present. As a result, all the alkali is consumed in fully exposed areas, and no dye-diffusion can occur. In non-exposed areas unspent alkali converts the dyes into ions which migrate to a receiving layer (positive-working system). In another modification[119] dyes can be used which are non-diffusing in alkaline medium: for example,




105

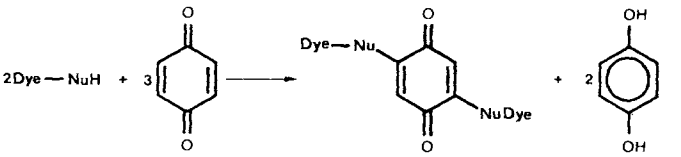



106

**106** first becomes mobile following protonation. Since development of exposed silver halide causes a decrease in pH, imagewise dye migration could be achieved (negative-working system).

### 7.2. Immobilization by Addition Reactions

p-Benzoquinones add nucleophiles such as amines or electron-rich alkenes (*e.g.* enamines)[41]. This property can be used[120] to immobilize dyes if the latter contain a sufficiently nucleophilic function (*Nu*), which can add to the *p*-benzoquinone generated in exposed areas when a hydroquinone is used as developer (Scheme 36). Since *p*-benzoquinone has four reactive centers, more than one addition occurs and the mobility of the dye is drastically reduced.



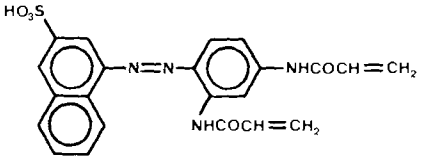

Scheme 36. Dye immobilization by addition to *p*-benzoquinone. Since the adducts are more electron-rich than hydroquinone, they are oxidized to quinones.

Due to steric effects probably only two molecules add, presumably at C-2 and C-5[41]. Introduction of two nucleophilic groups into the dye molecule leads to polymerization. Since immobilization occurs imagewise, a positive-working system is involved.

Not only dyes, but any dye-forming component can be similarly immobilized to yield an anti-imagewise distribution of this component in a receiving layer. It only requires that this layer also contains a reactant with which the component can react to form a dye. A system of this type is based on the addition of enamines to *p*-benzoquinones[121].

### 7.3. Immobilization by Polymerization

Dye molecules, such as **107**, which contain polymerizable functions can be oxidatively immobilized if the oxidation product of the silver halide developer is an active initiator for polymerization[122]. Suitable developers are acylhydrazides or sulfonylhydrazides, as well as hydroxylamines.




**107**

## 8. Concluding Remarks

The present review article illustrates how vast the field of dye diffusion photography is, particularly for organic chemists. Organic chemistry is, in fact, the source of all the systems discussed. Quite likely this trend will continue, since new ideas and mechanisms are constantly appearing: the source is certainly not drying out. This is fortunate, since only a few of the systems proposed and studied have found commercial application. Although all systems described here fulfill the basic requirement of exposure-modulated diffusion, most of them apparently have not met the exacting photographic requirements, even after extensive optimization. We will undoubtedly witness the discovery of new mechanisms for dye diffusion transfer in the near future[123]. Rewarding perspectives continue to be opened, particularly with regard to image quality. In view of growing competition from constantly improving electronic imaging systems, this is gratifying.

*I am indebted to Dr. J. Jaeken for introducing me to the field of dye diffusion transfer, to Dr. W. Janssens for the many valuable discussions, and to the entire staff of the Chemistry Department for their continuing assistance.*

Received: November 4, 1982 [A 446 IE]
German version: *Angew. Chem. 95* (1983) 165

[1] a) T. H. James: *The Theory of the Photographic Process*, 4th Edition, Macmillan, New York 1977; b) K. J. Fleckenstein: „Image Transfer Processes", in [1a], pp. 366–372; c) S. Fujita, „Organic Compounds for Instant Photography", *Yuki Gosei Kagaku Kyokai Shi 39* (4) (1981) 331; this article (in Japanese) partly deals with dye diffusion systems.

[2] A. Rott, E. Weyde: *Photographic Silver Halide Diffusion Processes*, Focal Press, London 1972.

[3] E. H. Land, H. G. Rogers, V. K. Walworth in J. Sturge: *Neblette's Handbook of Photography and Reprography*, 7th Edition, Van Nostrand-Reinhold, Princeton 1977, Chap. 12.

[4] a) K. Venkataraman: *The Chemistry of Synthetic Dyes*, Academic Press, New York; b) A good discussion of the complexity of research on diffusion transfer dyes is found in: S. M. Bloom, M. Green, M. Idelson, M. S. Simon: „The Dye Developer in the Polaroid Photographic Process", in [4a], Vol. 8, Chap. 8, 1978, pp. 331–387.

[5] For a discussion of additive and substractive color systems in photography as well as the chemistry of color development see J. Bailey, L. A. Williams in [4a], Vol. 6, 1971, Chap. 6, pp. 342–346.

[6] See R. E. Bacon: „Latent Image Effects Leading to Reversal or Desensitization", in [1a], Chap. 7, pp. 182–193.

[7] H. Rogers, US-Pat. 2983606 (1961; filed 9. 3. 1954).

[8] According to E. Land, *Photogr. J. 114* (1974) 338, semiquinone radical anions are the primary oxidation products.

[9] A selection of "shifted dye-developer" patents: a) E. Idelson, H. Rogers, US-Pat. 3336287 (1967); b) S. Dershowitz, R. B. Woodward, US-Pat. 3230085 (1966) and 3329670 (1967); c) R. F. W. Cieciuch, M. S. Simon, US-Pat. 3826801 (1970) and 3579334 (1971).

[10] N. Kunieda, M. Fujiwara, A. Miyamoto, T. Kobayashi, Jap. Pat. 80-07578 (1980); *Chem. Abstr. 93* (1980) 195469k.

[11] Y. Yoshida, DOS 2334035 (1974).

[12] For a good review of the chemistry of color photography see [5] as well as: L. J. Fleckenstein, "Color Forming Agents", in [1a], Chap. 12, pp. 353–362.

[13] a) G. J. Lestina, W. M. Bush, US-Pat. 3880658 (1975); b) G. J. Lestina, W. M. Bush, US-Pat. 3935262 (1976) and 3935263 (1976).

[14] I. F. Salminen, S. J. Ciurca, Jr., *Res. Discl. 124* (1974) 34; Eastman Kodak, Fr. Demande 2232776 (1975).

[15] S. J. Ciurca, Jr., *Res. Discl. 120* (1974) 67; US-Pat. 3928043 (1975).

[16] J. C.-M. Chang, A. P. Marr, S. J. Ciurca, Jr., *Res. Discl. 128* (1974) 31.

[17] R. S. Corley, M. Green, US-Pat. 2992105 (1961).

[18] L. R. Cohler, M. S. Simon, US-Pat. 2892710 (1959).

[19] H. G. Rogers, US-Pat. 3065074 (1962).

[20] H. G. Rogers, US-Pat. 2909430 (1959).

[21] J. Bailey, W. Landon, M. V. Mijovic, P. J. Hillson, Br. Pat. Appl. 2061537 (1981).

[22] K. E. Whitmore, P. M. Mader, Br. Pat. Appl. 840731 (1960); Can. Pat. 602607 (1960); US-Pat. 3227550 (1966).

[23] C. R. Barr, US-Pat. T900029 (1972).

[24] C. R. Barr, W. M. Bush, L. J. Thomas, H. E. Cole, Br. Pat. Appl. 1330524 (1973).

[25] The acronym *DDR* (diffusible dye releasing) has been coined for any system that releases a mobile dye as a result of a coupling reaction, whether conventional or unconventional.

[26] F. Bredoux, M. Compère, G. Gehin, Fr. Demande 2414745 (1979).

[27] P. T. Lau, US-Pat. 4248962 (1981).

[28] R. Sato, Y. Hotta, K. Matsuura, Br. Pat. Appl. 2072363 (1981).

[29] F. Viro, M. C. Mourning, US-Pat. 4036643 (1977).

[30] H. G. Rogers, US-Pat. 2774668 (1956).

[31] Ilford Ltd., Br. Pat. Appl. 1157505 und 1157506 (1966).

[32] M. S. Simon, US-Pat. 3711546 (1973).

[33] W. A. Schmidt, V. Tulagin, J. A. Sprung, R. C. Gunther, R. F. Coles, D. E. Sargent, *Ind. Eng. Chem. 45* (1953) 1726, and literature cited therein.

[34] S. M. Bloom, H. G. Rogers, US-Pat. 3443940 (1969).

[35] S. M. Bloom, US-Pat. 3751406 (1973).

[36] J. Figueras, M. H. Stern, US-Pat. 3734726 (1973).

[37] S. Hünig, *Angew. Chem. 80* (1968) 343; *Angew. Chem. Int. Ed. Engl. 7* (1968) 335.

[38] W. Janssens, G. Lemahieu, Belg. Pat. 781026 (1972).

[39] H. Vetter, J. Danhauser, K. Kabitzke, P. Marx, A. Melzer, W. Pelz, W. Püschel, Br. Pat. Appl. 1309133 (1973).

[40] The acronym *DRR* (Dye Releasing Redox) has been coined for such systems. The compounds used in DRR systems are also often referred to as RDR compounds (Redox Dye Releasing).

[41] a) Houben-Weyl: *Methoden der organischen Chemie*, 4th edit., Thieme, Stuttgart; b) for an excellent compilation of *p*-benzoquinone chemistry see H. Ulrich, R. Richter in [41a], vol. VII/3a, 1977.

[42] A. Anderson, K. Lum, US-Pat. 3725062 (1973).

[43] T. Gompf, K. Lum, US-Pat. 3698897 (1972).

[44] S. M. Bloom, R. Stephens, US-Pat. 3443939 (1969).

[45] W. Püschel, J. Danhauser, K. Kabitzke, P. Marx, A. Melzer, K.-W. Schranz, H. Vetter, W. Pelz, DOS 1930215 (1970).

[46] W. Püschel, H. Vetter, H. Odenwälder, DOS 2228361 (1973).

[47] W. Janssens, M. Peters, A. Melzer, DOS 2317134 (1974).

[48] G. J. Lestina, C. A. Bishop, R. J. Tuite, D. S. Daniel, *Res. Discl. 128* (1974) 22.

[49] See R. Pütter in: [41a], vol. X/3, 1977, pp. 551–626.

[50] J. R. Thirtle in: [1a], Chap. 12, pp. 343–344.

[51] K. E. Whitmore, P. M. Mader, Can. Pat. 602607 (1960).

[52] L. Fleckenstein, J. Figueras, Fr. Demande 2154443 (1972); Br. Pat. 1405662 (1975); US-Pat. 4076529 (1978).

[53] L. Fleckenstein, US-Pat. 3928312 (1975).

[54] A. Melzer, P. Marx, W. Püschel, DOS 2406664 (1975).

[55] A. Melzer, M. Peters, W. Püschel, M. Becker, DOS 2534424 (1977).

[56] J. M. Fernandes, M. D. McCreary, R. E. Ross, J. T. Staples, US-Pat. 4135929 (1979); *Res. Discl. 177* (1979) 45.

[57] P. D. Collet, C. F. Claude, T. E. Gompf, DOS 2916582 (1979).

[58] C. F. Gerbal, P. Collet, T. E. Gompf, R. L. Orvis, *Res. Discl. 180* (1979) 183.

[59] H. Ideguchi, J. Takahashi, M. Uemura, S. Aoki, N. Kunieda, Jap. Pat. 7850736 (1978).

[60] C. Fritsch, Fr. Demande 2424568 (1979); *Res. Discl. 174* (1978) 52.

[61] W. T. Hanson, Jr., *Photogr. Sci. Eng. 20* (1976) 155.

[62] K. Koyama, S. Fujita, Br. Pat. Appl. 2081466 (1982).

[63] L. J. Fleckenstein, Fr. Demande 2284140 (1976); *Res. Discl. 130* (1975) 37.

[64] K. Koyama, Y. Maekawa, M. Miyakawa, US-Pat. 4055428 (1977).

[65] K. Koyama, Jap. Pat. 56-016130 (1981).
[66] K. Koyama, Jap. Pat. 56-012642 (1981).
[67] Sh. Fujita, K. Koyama, Y. Inagaki, K. Waki, DOS 3027291 (1981).
[68] Sh. Fujita, *J. Chem. Soc. Chem. Commun. 1981*, 425.
[69] W. E. Lee, E. R. Brown in [1a], Chap. 11, p. 299.
[70] W. Pelz, *Angew. Chem. 66* (1954) 231.
[71] H. Vetter, W. Püschel, A. Melzer, M. Peters, DOS 2505248 (1976).
[72] H. Vetter, W. Püschel, R. Otto, DOS 2620088 (1977).
[73] H. Vetter, P. Marx, DOS 2645656 (1978).
[74] W. Liebe, K. Lohmer, P. Marx, W. Pelz, M. Peters, W. Verburg, DOS 2647480 (1978).
[75] J. Jaeken, A. Verhecken, H. Vetter, P. Marx, DOS 2811720 (1979).
[76] *Res. Discl. 156* (1977) 32.
[77] H. Deguchi, J. Takahashi, N. Kunieda, DOS 2729820 (1978).
[78] E. T. Holmes, J. P. Pepe, *Res. Discl. 174* (1978) 64.
[79] M. M. Kestner, P. T. S. Lau, R. E. Ross, W. C. Farley, M. M. Staples, *Res. Discl. 151* (1976) 68.
[80] „*I*nhibited *H*ydrolysis by *O*xidation". This is an unfortunate choice as the actual cleavage reaction is not a hydrolysis!
[81] „*I*ncreased *H*ydrolysis by *R*eduction". Equally unfortunate choice for the same reason as *IHO* [80].
[82] ED means Electron Donor.
[83] D. L. Fields, R. P. Henzel, P. T. S. Lau, R. A. Chasman, DOS 2543902 (1976); *Res. Discl. 144* (1976) 43.
[84] J. C. Hinshaw, P. B. Condit, US-Pat. 4199354 und 4199355 (1980); *Res. Discl. 144* (1976) 65.
[85] R. A. Chasman, R. P. Dunlap, J. C. Hinshaw, US-Pat. 4139379 (1979).
[86] J. C. Hinshaw, R. P. Henzel, US-Pat. 4278750 (1981).
[87] The acronym *IND* ("*I*ntramolecular *N*ucleophilic *D*isplacement") is often used [83, 84] for reductively cyclizing *DRR* systems operating in the *IHO* mode.
[88] J. E. Hutchins, T. H. Fife, *J. Am. Chem. Soc. 95* (1973) 2282.
[89] T. Cohen, W. F. Gray, *J. Org. Chem. 37* (1972) 741.
[90] The acronym *BEND* ("*B*allasted *E*lectron accepting *N*ucleophilic *D*isplacement") is used [85, 86] for reductively cyclizing *DRR*-systems operating in the *IHR* mode.
[91] L. D. Taylor, J. M. Grasshoff, M. Pluhar, *J. Org. Chem. 43* (1978) 1197.
[92] J. M. Grasshof, L. D. Taylor, US-Pat. 3698898, 3674478, 3685991 (1972), and 3932480 (1976).
[93] For a good review of quinonemethide chemistry see P. Grünanger in [41a], Vol. VII/3b, 1979, pp. 395–521.
[94] J. Velek, B. Koutek, O. Schmidt, L. Pavlickova and M. Soucek, *Collect. Czech. Chem. Commun. 41* (1976) 1419.
[95] B. Koutek, L. Pavlickova, J. Velek, V. Beranek, M. Soucek, *Collect. Czech. Chem. Commun. 41* (1976) 2607.
[96] E. Meier, W. Lässig, DOS 2654213 (1977) and 2823159 (1979).
[97] H. H. Credner, K. Küffner, W. Lässig, E. Meier, DOS 2854946 (1980).
[98] W. Janssens, Eur. Pat. Appl. 04399 (1979).
[99] C. C. Van de Sande, W. Janssens, W. Lässig, E. Meier, Eur. Pat. Appl. 38092 (1981).
[100] R. Becker, J. Ford, D. Fields, D. Reynolds, US-Pat. 3728113 (1973).
[101] Similar observations have been made for acyl-substituted *p*-benzoquinones; see V. M. Ruiz, R. Tapia, J. Valderrama, J. C. Vega, *J. Heterocycl. Chem. 18* (1981) 1161 and previous papers from this group. See also [41] for a discussion of the reactivity of *p*-benzoquinones bearing strongly electron withdrawing groups.
[102] G. Renner, E. Wolff, DOS 3014669 (1981).
[103] The acronym *CR* ("*C*leavage by *R*eduction") has beeb used [104].
[104] H. H. Credner, W. Lässig, K. Schranz, DOS 3008588 (1981).
[105] T. L. Gilchrist, C. J. Moody, *Chem. Rev. 77* (1977) 409.
[106] J. Drabowicz, P. Lyzwa, M. Mikolajczyk, *Synthesis 1981*, 890.
[107] J. R. Thirtle: "Silver Dye Bleach Process", in [1a], pp. 363–366.
[108] R. Kitzing, B. R. D. Whitear, W. E. Long, D. L. R. Reeves, G. P. Wood, DOS 2907435 and 2907437 (1979).
[109] L. F. A. Mason, R. Kitzing, B. R. D. Whitear, W. E. Long, G. P. Wood, D. L. R. Reeves, DOS 2907440 (1979).
[110] W. E. Long, DOS 2907436 (1980); Br. Pat. Appl. 2043282 (1980).
[111] This is a "*Dye Mod*ifying and *Dev*eveloping" compound *i.e.* a substance capable of reducing the azo bond in the dye-releaser and of developing exposed silver halide. Most frequently used are reduced 1,4-diazines *e.g.* reduced pyrazines, quinoxalines *etc.*
[112] An acidic (pH < 3) solution of a dye bleach catalyst, most frequently of 1,4-diazine type [107].
[113] L. Locatell, Jr., F. A. Meneghini, H. G. Rogers, US-Pat. 3719488 (1973).
[114] R. F. W. Cieciuch, R. R. Luhowy, F. A. Meneghini, H. G. Rogers, US-Pat. 3719489 (1973), 4060417 (1977) and 4098783 (1978).
[115] H. G. Rogers, Br. Pat. Appl. 1243046 (1971).
[116] H. G. Rogers, US-Pat. 3443941 (1969).
[117] C. Holstead, M. J. Simons, Br. Pat. Appl. 1590956 (1981); *Res. Discl. 169* (1978) 54.
[118] E. H. Land, Br. Pat. Appl. 860234 (1961).
[119] J. W. Meyer, *Res. Discl. 148* (1976) 63.
[120] G. Gehin, P. Gautier, M. Compère, Fr. Demande 2287711 (1976).
[121] S. M. Bloom, US-Pat. 3537851 and 3537852 (1970).
[122] W. Pelz, E. Günther, H. D. Meissner, Belg. Pat. 719339 (1969).
[123] See *e.g.* Van Poucke, C. C. Van de Sande, A. Verhecken, Br. Pat. Appl. 82-07583 (16. 3. 1982). See also: S. H. Ikeuchi, M. Kanbe, T. Takahashi, H. Ryuichiro, S. Sugiraka, M. Miuzkura, DOS 3150804 (1982).

# Symmetry Breaking and Non-Born-Oppenheimer Effects in Radical Cations

By Horst Köppel, Lorenz S. Cederbaum*, Wolfgang Domcke, and Sason S. Shaik

The various electronic states in which molecules can exist are often considered to be independent. In this article we turn our attention to the limitations of this assumption, namely the interaction between different electronic states through the nuclear motion. This interaction can have several important consequences, two of which are discussed in some detail. One is a distortion of the molecular framework, leading to a lowering of the symmetry of a molecule in excited or ionic states compared to the neutral ground state. General aspects of this symmetry lowering are outlined and interpreted with the aid of typical examples. The other consequence considered is the ability of the nuclei to "jump" between different molecular potential energy surfaces (non-Born-Oppenheimer effects). The nature of this behavior is analyzed and it is argued that the "jumping" can be very fast and efficient, dominating completely the nuclear motion. To exemplify our general ideas we refer to the photoelectron spectra of ethylene and related compounds and demonstrate that they are governed by strong non-Born-Oppenheimer effects. It emerges that the Franck-Condon principle fails in the analysis of their vibronic structure.

## 1. Introduction

A knowledge of molecular structure is of primary importance in chemistry. Besides the intrinsic interest in the structure as such, it contains essential information on bonding properties, chemical reactivity *etc.* and has therefore been the subject of numerous investigations. Almost equally important is the phenomenon that most molecules *change* their shape when going from the neutral ground state to electronically excited or ionized states. Often this amounts to a decrease in the molecular symmetry. For example, many linear molecules, such as $CO_2$[1a], $CS_2$[1b], HCN[1c] or $C_2H_2$[1d] are known to become bent upon electron excitation[1e] or electron attachment[1f]. Symmetrical $XY_2$ molecules can acquire unequal bond lengths ($SO_2$[2a], $NO_2$[2b], $ClO_2$[2c]), planar molecules may become nonplanar ($H_2CO$[3a], HCOF[3b], $Cl_2CS$[3a]). Among many other examples we mention asymmetric ring distortions in benzene[4a] and in *p*-benzoquinone[4b], and a twisting around the central C=C bond in ethylene[5a], stilbene[5b] and thioindigo[5c]. Clearly, the phenomenon of symmetry lowering or symmetry breaking in electronically excited states is so widespread that it deserves special attention and calls for an explanation.

In the following article we present and discuss a mechanism that enables one to *understand* the observation of symmetry breaking in electronically excited or ionic states. To be sure, the amount of the distortion can, in principle, always be determined by calculating the potential surface (the potential energy of the molecular system) point by point, either by ab initio or by semiempirical techniques. What we have in mind here, however, is rather to *explain* the experimental findings in simple terms, to relate the distortion to a few elementary molecular parameters and to rationalize the trends observed in chemically related compounds.

The mechanism we wish to describe is commonly termed "vibronic coupling" in the literature. It deals with the *interaction of two (or more) energetically close-lying electronic states of a molecule through the nuclear motion.* This leads to a joint *vib*rational and elec*tronic* motion in the molecule and can account also for other interesting observations (see below). Distortions of the nuclear framework are described in this approach in terms of a mutual repulsion of the potential energy surfaces of the interacting states. Under certain well defined conditions this leads to a double minimum structure of the lower surface which just corresponds to a lower symmetry of the respective state compared to the neutral ground state.

Vibronic coupling is a well established subject in optical spectroscopy and there is a wealth of literature available on the subject[7, 8]. As already mentioned, the explanation of symmetry lowering[4] and related "anomalous" potential curves[8l, q] is only one aspect of the mechanism. It can account also for many other features of the vibrational structure of electronic bands which are not understood within the picture of independent electronic states. For example, one often observes[8e, p] vibronic bands which are symmetry forbidden according to the usual selection rules for electric dipole transitions[7d]. This is rationalized in terms of a "borrowing" of intensity from another electronic state[7b]. Closely related is the loss of mirror symmetry[8n] between an absorption and the corresponding emission band[7d]. Finally, what appears to us most interesting, is the observation that the high energy electronic bands often exhibit a much more diffuse (large molecules) or erratic (small molecules) fine structure than the low energy bands[8d, g]. In this case regular vibrational progressions are completely absent and *the nuclear motion no longer takes place on a single potential energy surface*[8d] (non-Born-Oppenheimer

[*] Prof. Dr. L. S. Cederbaum, Dr. H. Köppel, Prof. Dr. W. Domcke
Theoretische Chemie, Institut für Physikalische Chemie der Universität
Im Neuenheimer Feld 253, D-6900 Heidelberg 1 (Germany)
Dr. S. S. Shaik
Department of Chemistry, Ben Gurion University
P.O.B. 653, Beer-Sheva 84120 (Israel)

 © Verlag Chemie GmbH, 6940 Weinheim, 1983 0570-0833/83/0303-0210 $ 02.50/0 

or nonadiabatic effects). It appears that these latter effects might occur even more often than the aforementioned effect of symmetry breaking. They have been identified in a large number of aromatic and heteroaromatic molecules[8d-s]. In this connection, benzene[4a], pyrazine[8m] and naphthalene[8g] have been particularly well studied. A quite different class of molecules is provided by the mixed-valence compounds[8t] and by molecular dimers[8a-c]. However, despite considerable effort a quantitative analysis of the data has so far mostly proven impossible. Even for a molecule as small as $NO_2$, after decades of work the clarification of the interactions remains an outstanding challenge to experimentalists and theoreticians[8u].

It is not the purpose of this article to review all these developments in the field in detail. Rather, we wish to focus on a particular area where considerable progress has been made over the past few years, namely the field of molecular ions[9] (especially radical cations). Such a limitation is justified, not only because of the increasing interest in molecular ions themselves[6], but for several other reasons. Firstly, a rather accurate theoretical description of the vibronic coupling effects in ions has proven possible, allowing for a detailed understanding of the nuclear motion in the interacting electronic states[9]. This was realized through concentrating on rather small systems where accurate (ab initio) computational schemes are available. The results can also help towards an understanding of larger chemical systems. Secondly, an interpretation of the effects is usually simpler in the case of ions than in the case of excited states of the neutral species, since the interaction between the ionic *states* can be reduced to an interaction between molecular *orbitals*. For excited states of the neutral molecule a description in terms of orbitals and orbital interactions is generally only a poor approximation and often completely impossible[10]. For ions, the orbital picture allows for an attractive visualization of the effects and for the use of simple qualitative (semiempirical) schemes to estimate their magnitude. Finally, from the experimental point of view, for ionization spectra there exist neither the dipole selection rules nor the emission process ("inverse" to the ionization) which are pertinent to the absorption spectra[11]. Hence, increased importance attaches to the aforementioned diffuseness of the bands, since this is now the dominating dynamic effect (*i.e.* involving the nuclear motion) of the vibronic coupling. Besides the effect of symmetry lowering, the nonadiabatic nature of the nuclear motion will therefore be the second cornerstone of this article. Anticipating our findings, the nonadiabatic effects turn out to be surprisingly strong, due to the intimate interplay of several modes participating in the vibronic coupling.

Nonadiabatic transitions between different potential energy surfaces are important not only in spectroscopy but also in many other chemical processes. Often, for example, fragmentation of a molecule occurs even if a bound electronic state is populated initially (predissociation[7d]). Typical *photoreactions* proceed *via* light-excitation of the reactants and subsequent formation of the product molecules in the ground state. Conversely, in chemiluminescent reactions the products are formed in excited states under thermal conditions, *i.e.* starting with ground state reactants[7u]. All these observations are rationalized in terms of nonadiabatic transitions between the different potential energy surfaces. However, the discussion is usually only qualitative and only takes a single nuclear coordinate into consideration. The present work should contribute to an understanding of nonadiabatic nuclear motion—and especially the influence of *several* nuclear degrees of freedom—in more detail than was possible before. Thus, it could be an important step to a more quantitative calculation of the corresponding chemical reaction rates.

We might emphasize at this juncture that our concept is of course *not* restricted to molecular ions. Only in our applications shall we refer to the case of ionization or, more precisely, to the vibrational structure of photoelectron bands[11]. To have something specific in mind we will use the photoelectron spectra of the hydrocarbons

$$H_2C{=}(C{=})_nCH_2 \quad \mathbf{1} \quad (n = 0\text{–}3)$$

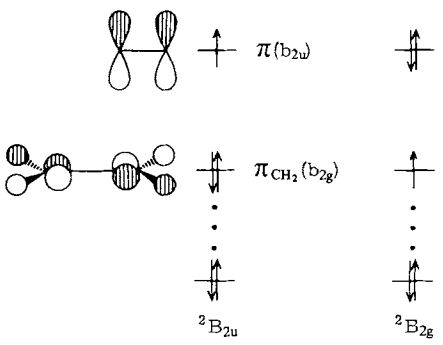
and some related compounds as examples. First of all, let us mention the photoelectron spectrum of butatriene (**1**, n = 2). This spectrum exhibits three low energy bands, of which the central one could not be assigned to any of the high binding molecular orbitals, and was termed "*the mystery band*"[12]. No such band was observed in the spectrum of the tetramethyl and tetra-*tert*-butyl derivatives of butatriene[12a]. Interestingly, the complex band structure for butatriene broadly resembles that for allene[13a] (**1**, n = 1) and for pentatetraene[13c] (**1**, n = 3), which was attributed to a Jahn-Teller instability[13b]. Even in the simplest member of the series, ethylene (**1**, n = 0), the first photoelectron band corresponding to the π molecular orbital is quite complex, and shows a strong excitation of the torsional mode[14]. On the other hand, in substituted ethylenes like fluoroethylene, the first band is accompanied mainly by a normal progression of the C=C stretching mode[15]. What we have here is a family of compounds whose members exhibit a different degree of vibronic coupling, depending on the number of double bonds and the number and type of substituents. The spectra of these compounds indicate that the *vibronic coupling always involves the torsional mode together with at least one stretching mode*. Thus, the vibronic coupling that we are going to describe involves many active modes, all of which contribute simultaneously to the spectral and geometrical features of the ion.

For the exposition of our general ideas we will begin with the smallest member of the family—the ethylene molecule. We will first attempt to gain an insight into the determinants affecting the structure of its positive ion, and then develop simple rules for understanding the structure—spectrum relationship. The chemical significance of the mechanism shall then be explored by studying the structural and spectral features of the higher homologues of ethylene and of some of their derivatives.

## 2. The Vibronic Coupling Model and the Adiabatic Potential Energy Surfaces

The two lowest electronic states of the ethylene cation arise by removal of an electron from either of the two high lying ground state-occupied molecular orbitals, $\pi(b_{2u})$ and

$\pi_{CH_2}(b_{2g})$. These are the $^2B_{2u}$ and the $^2B_{2g}$ states, respectively, in $D_{2h}$ symmetry, each of which we describe by a single configuration:




(1)

Why do we restrict ourselves to these two ionic states? Simply because they are close in energy and the ionic ground state is well separated from the other ionic configurations, in the valence region[9b].

Consider now a torsion of the terminal $CH_2$ groups around the central C=C bond. When the twisting is effected, the two orbitals acquire the same symmetry and hence can have non-vanishing overlap. Since both orbitals involve similar atomic wave functions at the C atoms (2p type functions perpendicular to the C=C double bond) this overlap may become quite large. As a result, the electronic Hamiltonian operator of the molecule will have a substantial nondiagonal element between the two configurations (1). The true ionic states, defined as eigenvectors of the Hamiltonian, are therefore a mixture of these configurations.

To investigate the consequences of this mixing we formulate now a suitable model Hamiltonian $\mathscr{H}$. As we are dealing with two electronic states, we represent the Hamiltonian as a $2\times 2$ matrix

$$\mathscr{H} = \begin{pmatrix} H_{11} & H_{12} \\ H_{21} & H_{22} \end{pmatrix} \tag{2a}$$

where the element $H_{11}(H_{22})$ is the energy of the pure configuration $^2B_{2u}$ ($^2B_{2g}$) and the nondiagonal element $H_{12}$ is responsible for the mixing that occurs upon twisting[16]. The elements $H_{ij}$ (i, j = 1, 2) are functions of the nuclear coordinates. In what follows we use the normal coordinates of the neutral molecule[17]. For the moment we include only the torsion or twisting coordinate $Q_u$ and the C=C stretching coordinate $Q_g$ ($Q_g = Q_u = 0$ represents the equilibrium geometry of the ground state of the neutral molecule). In the vicinity of the equilibrium geometry of the neutral molecule the matrix elements $H_{ij}$ (i, j = 1, 2) can be approximated by the following simple expressions:

$$H_{ii} = \frac{\omega_g}{2} Q_g^2 + \frac{\omega_u}{2} Q_u^2 + E_i + \kappa_i Q_g \quad (i = 1, 2)$$
$$H_{12} = \lambda Q_u = H_{21} \tag{2b}$$

Here the first two terms in $H_{11}$ and $H_{22}$ describe the harmonic potential energy surface of the neutral molecule in its electronic ground state; $\omega_g$ und $\omega_u$ are the vibrational frequencies of the C=C stretching- and torsional-modes, respectively. The other terms account for the changes in the potential energy that occur upon ionization. $E_i$ (i = 1, 2) denotes the energy of either of the ionic states at $Q_g = Q_u = 0$, measured with respect to the neutral species. The terms $\kappa_i Q_g$ (i = 1, 2) and $\lambda Q_u$ are responsible for the change in shape of the potential curves on going from the neutral molecule to the ion. The parameters $\kappa_i$ and $\lambda$ are the so-called coupling constants[9, 18].

In order to find out which modes should be taken into account in the Hamiltonian we take recourse to symmetry considerations. Elementary selection rules tell us that the mode $Q_u$ must have the symmetry of the product of the electronic states in order to produce a mixing. In the case of the ethylene cation, we have

$$B_{2u} \times B_{2g} = A_u \tag{3}$$

and $A_u$ is just the symmetry of the torsional mode. The mode $Q_g$, on the other hand, can be any of the totally symmetric modes and, in principle, all of these modes should be retained. It is only for the purpose of illustration that we confine ourselves here to the C=C stretching mode.

What are the meaning and chemical implications of the above Hamiltonian? To develop a qualitative feeling we will examine now the adiabatic potential energy surfaces, *i.e.* the energies of the true ionic states, which follow from eq. (2).

Let us start by ignoring the totally symmetric mode. The adiabatic potentials $V_1$ and $V_2$ are the eigenvalues of the $2\times 2$ matrix $\mathscr{H}$. A simple calculation gives

$$V_1 = \frac{\omega_u}{2} Q_u^2 + \frac{1}{2}\left[E_1 + E_2 - \sqrt{(E_1 - E_2)^2 + 4\lambda^2 Q_u^2}\right] \tag{4a}$$

$$V_2 = \frac{\omega_u}{2} Q_u^2 + \frac{1}{2}\left[E_1 + E_2 + \sqrt{(E_1 - E_2)^2 + 4\lambda^2 Q_u^2}\right] \tag{4b}$$

They are drawn in Figure 1c for parameters representing ethylene. The lower of the two curves, representing the ionic ground state, exhibits a double minimum, *i.e.* two

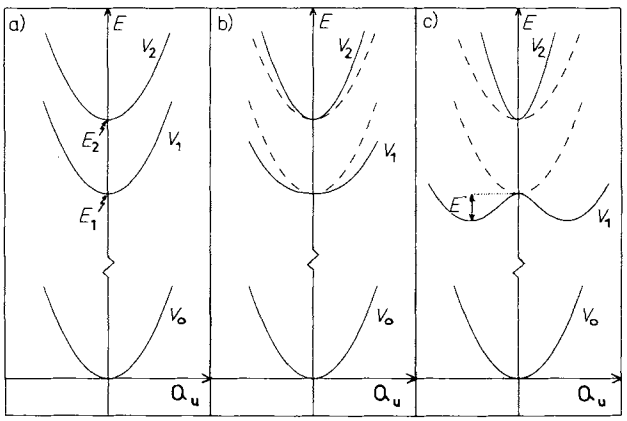



Fig. 1. Diabatic (dashed lines) and adiabatic (full lines) torsional potential curves for the two lowest cationic states of ethylene ($V_1$ and $V_2$ according to eq. (4), schematic). In each case the potential curve $V_0$ of the neutral state is also shown, assuming the same frequency $\omega_u$ for all the states. $E_1$ and $E_2$ are the vertical ionization potentials. Vibronic coupling is shown only for the ionic states.—a) A case of zero coupling $\lambda = 0$.—b) The limit of weak vibronic coupling.—c) A case of a strong vibronic coupling; $E^*$ is the barrier for becoming planar.

symmetric minima at nonzero values of the torsional coordinate $Q_u$ and a maximum at the planar geometry $Q_u = 0$. This means that the ionic ground state is nonplanar, with a torsional angle at equilibrium given by the minima of the lower surface $V_1$.

The appearance of the nonplanar equilibrium geometry might seem surprising at first sight. Let us therefore try to interpret it on a more qualitative level, in terms of orbitals and orbital interactions. There are two basically different contributions to the ionic potential energies. One is the repulsive diagonal term, $1/2\omega_u Q_u^2$, which expresses the reluctance of the *pure* configurations ($^2B_{2g}$ and $^2B_{2u}$) to distort. This just reflects the behavior of the $\pi$ orbital which is occupied by 1 electron in the $^2B_{2u}$ state and by 2 electrons in the $^2B_{2g}$ state and whose energy increases upon twisting (in the same way the presence of two electrons in the $\pi$ orbital makes the neutral molecule planar). Secondly, the effect of orbital mixing must be taken into account. In the $^2B_{2u}$ ground state it involves three electrons, two of which occupy the $\pi_{CH_2}$ orbital which is stabilized by the interaction, and one occupies the $\pi$ orbital which is destabilized by the interaction (cf. Fig. 2a). The net result is roughly the stabilization of one electron[19a]. If this gain in binding energy is sufficiently large (as in ethylene), it overcomes the previously discussed energy rise inherent in the twisting of the $\pi$ orbital. Consequently, the potential of the ground state cation exhibits a double minimum, leading to a nonplanar structure. Unlike the ground state, the upper cationic state which originates from the planar $^2B_{2g}$ state, remains planar, since now the net result of distortion is the destabilization of one electron (Fig. 2b).

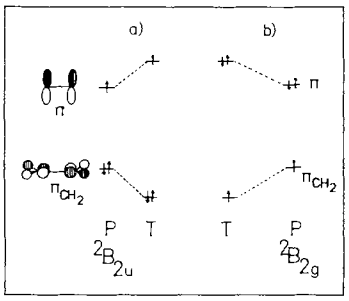



Fig. 2. The $\pi$-$\pi_{CH_2}$ orbital interaction upon distortion of the $CH_2$-terminal groups in the ethylene cation from planarity at some angle $0° < \alpha < 90°$. P denotes planar and T twisted conformation.—a) The ground state of the cation.—b) First excited state of the cation.—Note the difference of the orbital population in the two states. The energy changes shown are due only to the orbital interaction.

We can gain more insight into the reasons behind the distortion of the ground state cation away from planarity, if we consider the bonding characteristics of the cation. The doubly occupied lower orbital of the twisted cation is now $\pi_{CH_2}$ mixed with some of the $\pi$ orbital which is C=C bonding. Thus, there is a net gain of C=C bonding upon distortion in the ground state of the cation (Fig. 2a). Exactly the opposite situation obtains in the upper cationic state. Here there are two electrons in the $\pi$ orbital which combines with it some of the C=C antibonding $\pi_{CH_2}$ orbital. The net result is a weakening of the C=C bonding upon distortion and, therefore, the preferred geometry of the upper cationic state remains planar (Fig. 2b).

The importance of this orbital interaction for the stabilization of a nonplanar structure of the radical cation and the Rydberg state of ethylene was noted quite some time ago by *Mulliken*[19b,c], who gave this interaction the name "isovalent hyperconjugation", meaning the delocalization of electrons from a pure p or $\pi$ orbital to a pseudo $\pi$ orbital ($\pi_{CH_2}$). The result of this delocalization is a strengthening of the C=C bonding, which was described by *Mulliken* in terms of additional resonance structures which contain a full $\pi$ bond[19b].

We have now managed to relate the predictions of the vibronic coupling model for ethylene to simple molecular orbital considerations. We see from this example that vibronic coupling is a mechanism that leads to a lowering of the symmetry of cations as compared to the neutral molecules. This effect is of course not limited to ethylene. It governs the behavior of the whole family of ethylene derivatives and facilitates an understanding of the different trends observed in this group of chemically related compounds[9a-d] (cf. Section 4). It is neither limited to the above type of symmetry lowering (planar-to-twisted) nor to the case of ionization. In a completely analogous way, the mechanism is effective in the case of radical anions and electronically excited states of the neutral molecules[7,8]. It is responsible also for quite different distortions[4], such as nonlinearity of linear molecules in excited or ionic states[9e], unequal bond lengths in symmetric triatomic molecules[20] or Jahn-Teller type distortions in non-degenerate electronic states[9g]. In principle, most of the examples mentioned in the introduction, as well as many other similar cases, are candidates for the vibronic coupling mechanism. This concept is therefore considered as a powerful tool that can explain why many molecules are less symmetric in excited or ionic states than in the neutral ground state.

One of the important aspects of the vibronic coupling model is that it enables one to predict the geometries of cations, anions and molecules in excited electronic states using only symmetry arguments and simple molecular orbital concepts. Knowing the symmetries of the molecular orbitals, it is easily found from a selection rule such as eq. (3) which non-totally symmetric mode can operate in a particular example. This determines the type of distortion that is possible. Furthermore, there are simple qualitative criteria which allow one to estimate the strength of the distortion. As an illustration, let us consider the barrier height $E^*$ by which the unsymmetric (nonplanar) structure is energetically stabilized. It is given by eq. (4)

$$E^* = \begin{cases} \dfrac{\omega_u}{8\lambda^2}\left[\dfrac{2\lambda^2}{\omega_u} - |E_2 - E_1|\right]^2 ; & \dfrac{2\lambda^2}{\omega_u} > |E_2 - E_1| \\ 0 ; & \dfrac{2\lambda^2}{\omega_u} < |E_2 - E_1| \end{cases} \quad (5)$$

The ratio between the barrier height $E^*$ and the energy gap $|E_2 - E_1|$ thus depends only on the following dimensionless combination x of parameters

$$x = \frac{2\lambda^2}{\omega_u |E_2 - E_1|} \quad (6)$$

as depicted in Figure 3.

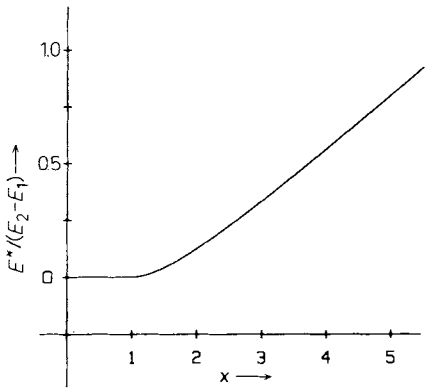



Fig. 3. The dependence of the barrier height $E^*$ on the dimensionless quantity x according to equations (5)—(6). $E^*$ represents the amount by which the unsymmetric configuration is stabilized energetically. For values of x smaller than unity no distortion occurs, *i.e.* $E^*=0$. In the opposite limit ($x \gg 1$) there is an approximately linear dependence of the barrier height on x.

This quantity and hence the barrier height become large with increasing vibronic coupling constant $\lambda$ and decreasing energy gap $|E_2-E_1|$. The strength of the distortion therefore depends on the balance between these two opposing factors. If the ratio x is smaller than unity the double minimum in the lower surface $V_1$ vanishes and the vibronic coupling is reflected only in the difference in curvature of the two potential curves: The upper curve $V_2$ is steeper near the minimum than that of the molecular ground state $V_0$, whereas the lower curve $V_1$ is relatively flat[8l,q] (cf. Fig. 1b). This is plausible, since in the limiting case of no coupling ($x=0$) both potential curves must exhibit identical shapes, the minima occurring at the symmetric configuration $Q_u=0$ (Fig. 1a).

To decide whether the coupling leads to a distortion in a particular molecule one must therefore calculate the coupling constant $\lambda$ and energy gap $|E_2-E_1|$ and check whether the ratio x is larger than unity. The frequency $\omega_u$ can be taken from experiment. We have already indicated above for ethylene how the constant $\lambda$ can be related to the mixing of orbitals that occurs upon the appropriate deformation. More quantitatively it is given by either of the following equivalent expressions[21]

$$\lambda = (E_2-E_1)\int \pi^*(r)\,\partial/\partial Q_u\,\pi_{CH_2}(r)\,d^3r \tag{7a}$$

$$\lambda = \frac{1}{\sqrt{8}}\left[\partial^2(V_1(Q)-V_2(Q))^2/\partial Q_u^2\right]^{1/2} \tag{7b}$$

(the integration in eq. (7a) is over the electronic coordinates, and both expressions are to be evaluated at the equilibrium geometry of the neutral molecule). Similarly, also the energy gap can be approximated on the orbital level. In the case of ionization it roughly equals the energy difference of the mixing orbitals (Koopmans' theorem[22]). Thus, simple estimates and well known chemical approximation schemes can be used to apply the vibronic coupling concept to a particular case of interest.

We have now ascertained the relation between vibronic coupling and symmetry lowering in excited or ionic states, taking the ethylene cation as an example. We have, however, neglected so far the totally symmetric mode that appears in our Hamiltonian, eq. (2). To establish the impact of the latter mode on the vibronic coupling, we note that from eq. (2) the energy gap $E_2-E_1$ of the interacting states has to be replaced now by the following function of the additional coordinate $Q_g$

$$\Delta E = E_2-E_1+(\kappa_2-\kappa_1)Q_g \tag{8}$$

Therefore (cf. discussion to eqs. (5)—(6)), the barrier height $E^*$ and the shape of the torsional potential depend on this coordinate. In other words, the totally symmetric stretching modulates the energy gap and, hence, the coupling strength.

The importance of the modulating or tuning effect according to eq. (8) depends on the difference of $\kappa_1$ and $\kappa_2$. These constants are defined as the derivatives of the potential curves with respect to $Q_g$ at the equilibrium geometry of the neutral molecule (indicated below by a subscript "0"). In order to estimate these derivatives for ethylene we again use Koopmans' theorem[22] and inspect the negative derivatives of the corresponding orbitals which partake in the coupling

$$\kappa_i = -\left(\frac{\partial\varepsilon_i}{\partial Q_g}\right)_0; \quad \varepsilon_i = \text{orbital energy} \tag{9}$$

From the nodal properties of the two orbitals, it is obvious that $\kappa_1<0$, since the $\pi(b_{2u})$ orbital is C=C bonding, whereas $\kappa_2>0$, since the $\pi_{CH_2}(b_{2g})$ orbital is antibonding in the same region. This is shown in Figure 4a along with a plot of the potential curves as a function of the stretching coordinate $Q_g$ in Figure 4b.

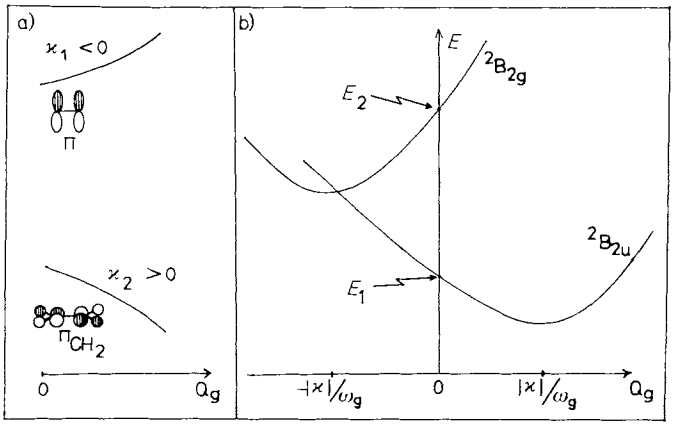



Fig. 4. a) The behavior of the $\pi(b_{2u})$ and $\pi_{CH_2}(b_{2g})$ molecular orbitals upon C=C stretching. The coupling constants $\kappa_1$ and $\kappa_2$ behave as the negative values of the corresponding slopes.—b) The $^2B_{2u}$ and $^2B_{2g}$ diabatic potentials along the stretching coordinate, $Q_g$, assuming $|\kappa_1|=|\kappa_2|=|\kappa|$. Note the modulation of their energy gap as $Q_g$ is varied.

One can see that as a result of the opposite signs of $\kappa_1$ and $\kappa_2$, the totally symmetric mode can modulate the energy gap of the two states. For positive $Q_g$, *i.e.* as the C=C bond is stretched beyond its value in the neutral molecule, the gap $\Delta E$ widens. On the other hand, for negative values of $Q_g$, *i.e.* when the C=C bond is shortened, the energy gap becomes smaller. Eventually, at some negative value of $Q_g$ the two states coincide and then reverse their order.

This tuning of the energy gap will affect the magnitude of the coupling of the two states upon twisting. This is illustrated in Figure 5, where we have plotted the torsional potentials at different values of $Q_g$.

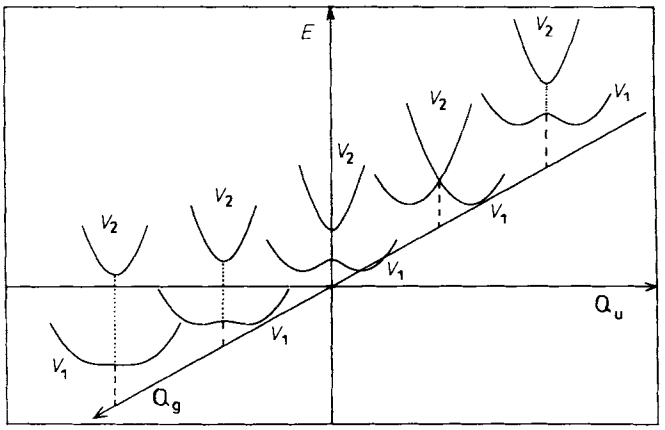



Fig. 5. A plot of the torsional potentials $V_1$ and $V_2$ of the two lower ionic states at different $Q_g$ values. Note how the depth of the minima varies as $Q_g$ changes. This indicates the tuning up or down of the vibronic coupling.

It can be seen that towards positive values of $Q_g$, as the gap widens, the barrier to planarity decreases (cf. eq. (5)) and eventually it vanishes completely. According to our calculations[9b] the absolute minimum of the lower potential surface of $C_2H_4^+$ occurs at positive $Q_g$. Indeed, it is quite obvious from Figure 4 that at the optimum value of $Q_g$ for the radical cation the energy gap is larger than at $Q_g = 0$, which will lead to a decrease of the coupling. In general, whenever the modulating effect of the stretching mode is strong, *i.e.* the signs of $\kappa_1$ and $\kappa_2$ differ, this will lead to a quenching of the distortion. When the signs of $\kappa_1$ and $\kappa_2$ are equal, the totally symmetric mode can lead either to a quenching or an enhancement of the distortion.

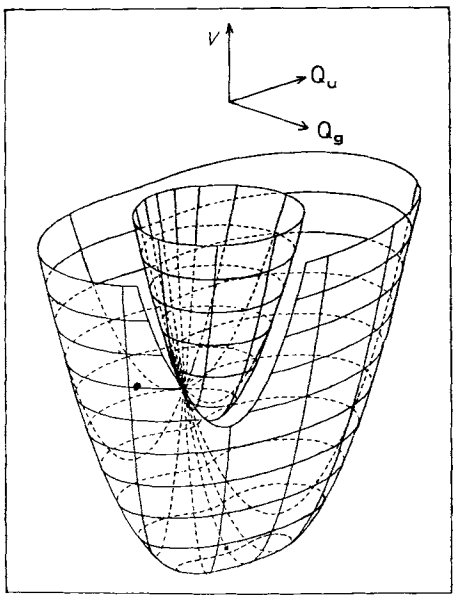



Fig. 6. A plot of the adiabatic potential surfaces $V_1$ and $V_2$ of the lower ionic states as functions of the C=C stretching coordinate $Q_g$ and the torsional coordinate $Q_u$. The surfaces are represented by a system of cuts in coordinate space and by equipotential lines. The cuts originate from the geometry of intersection where the surfaces touch each other ($Q_g = -3.3$, $Q_u = 0$). At the bottom of the lower surface the double minimum nature of the torsional potential is discernible. Vibrational motion on the upper surface can practically always reach the point of intersection and, hence, interconvert to the lower surface.

Going in the opposite direction—for negative values of $Q_g$—the two potentials approach each other and the barrier of the lower surface increases in accord with increasing coupling of the two states. At some negative value of $Q_g$ both surfaces coincide for $Q_u = 0$ (planar geometry). This degeneracy is lifted in first order when the system moves in an arbitrary direction away from the geometry of intersection. That is, the upper surface rests on the lower one like a cone on the apex of another cone. This is termed a conical intersection[23]. Figure 6 shows the potential surfaces of the two cationic states as a function of the twist and the C=C stretching coordinates. They exhibit a conical intersection on the negative $Q_g$ axis at $Q_g = -3.3$; $Q_u = 0$.

The conical intersection is most important for the behavior of the nuclear motion, since in its vicinity the nuclei can easily jump between the different surfaces[9d], leading to what are known as nonadiabatic effects. These will be discussed in more detail in the next section.

## 3. The Photoelectron Spectrum and the Nonadiabatic Effects

So far we have considered only the static aspects of the vibronic coupling mechanism, namely the adiabatic potential energy surfaces and the corresponding geometries of the ionic states. In the static calculations the nuclear kinetic energy operator $T_N$ and, hence, the nuclear motion on the potential surfaces is ignored. In this section we turn to the problem of the nuclear motion on these surfaces. Such a study is important for at least two reasons. Firstly, it is a prerequisite for comparing the predictions of the vibronic coupling with experiment. In optical spectroscopy the vibrational structure of the electronic bands contains information on the geometry changes that occur during the electronic transition. In the case of vibronic coupling this allows one to deduce the extent of the distortion from the excitation strength of the appropriate nontotally symmetric mode in the experimental spectrum. To this end, however, the problem of nuclear motion must be resolved. Secondly, a study of the nuclear motion is interesting in itself because it furnishes information about the significance of the "jump" between the different surfaces. These nonadiabatic effects are usually considered negligible in chemical processes. We shall see that in the presence of conical intersections (cf. Fig. 6) they can be extremely fast and efficient. This poses the question whether they are not of more importance in chemical phenomena than is usually believed.

Let us again consider ethylene as an example. Figure 7 shows the experimental recording of the first band of the photoelectron (PE) spectrum of this simplest alkene. The band represents the removal of an electron from the outermost occupied orbital of the $H_2C{=}CH_2$ molecule, and its fine structure reflects the vibrational motion in the corresponding ionic state (ground state).

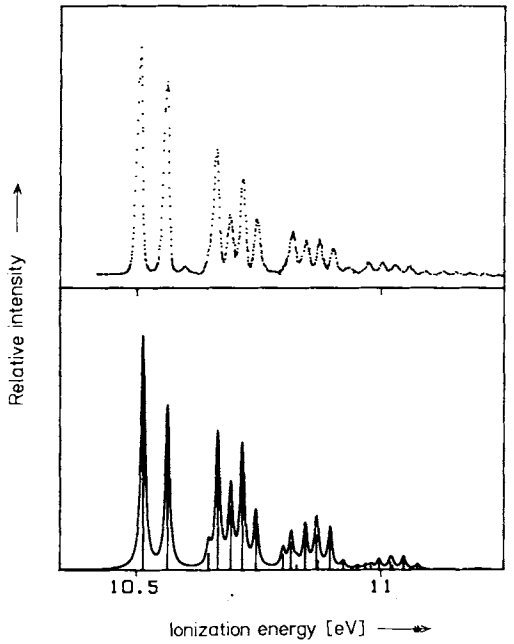


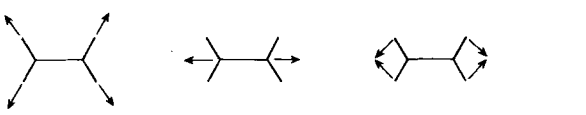

Fig. 7. The first band in the photoelectron spectrum of ethylene. Top: the experimental recording [14f]. A supersonic molecular beam has been used to achieve high resolution. The curve represents the number of counts of photoelectrons as a function of their kinetic energy. The ionization energy is obtained by subtracting the kinetic energy from the energy of the incident photon (here 21.1 eV). Bottom: the calculated spectrum is given by the vertical lines (for the values of the parameters used cf. Table 1). To compare with experiment they are subsequently broadened to give Lorentzians of suitable width (here 0.01 eV). The sum of these Lorentzians is drawn above the lines as a continuous envelope and reproduces the observations accurately.

Three progressions of vibrational modes can be distinguished. They have been attributed[14] to the C=C stretching mode $\nu_2$, the C–H bending mode $\nu_3$, and the torsional mode $\nu_4$. However, the determination of the equilibrium geometry of $C_2H_4^+$ from these data has not been attempted[14].

We now try to reproduce the observations by means of the vibronic coupling mechanism. To this end we have to include the nuclear kinetic energy $T_N$,

$$\hat{\mathscr{H}} = \mathscr{H} + \begin{pmatrix} T_N & 0 \\ 0 & T_N \end{pmatrix} \tag{10}$$

and solve for the exact quantum mechanical eigenstates of the Hamiltonian $\hat{\mathscr{H}}$. The computation of the spectrum is then straightforward[9]. Before presenting the result, two remarks are appropriate. Firstly, as is evident from the experimental spectrum in Figure 7, we should include all three totally symmetric modes (**2**—**4**) of ethylene, not just the C=C stretching mode (**3**).



$\omega_1 = 0.3915$ $\omega_2 = 0.2054$ $\omega_3 = 0.1710$ eV

**2** **3** **4**

Secondly, numerical values are needed for the energies and coupling constants which enter into our Hamiltonian. In our case we choose a so-called Green's function calculation[24], which is known to yield accurate ionization potentials and, hence, also coupling constants[9]. Since the spectrum turns out to depend sensitively on these parameters, some of them are subsequently slightly readjusted to improve the agreement with the observations. The final result of the calculation is included in Figure 7, the values of the parameters are collected in Table 1.

Table 1. Energies, coupling constants and frequencies used in the calculation of the first photoelectron band of ethylene (Fig. 7). For the second band (Fig. 8) slightly different values of the totally symmetric frequencies have been employed [9f]. All quantities are in eV.

| | $^2B_{2u}$ | $^2B_{2g}$ | $\omega$ |
|---|---|---|---|
| $E$ | 10.750 | 12.650 | – |
| $\kappa(\nu_1)$ | 0.025 | −0.362 | 0.360 |
| $\kappa(\nu_2)$ | −0.178 | 0.249 | 0.155 |
| $\kappa(\nu_3)$ | 0.155 | 0.107 | 0.180 |
| $\lambda$ | 0.404 | | 0.110 |

The calculated and experimental spectra agree in all essential details. This is conclusive evidence that the vibronic coupling concept indeed applies to the lowest states of the ethylene cation and that we have arrived at an accurate description of the potential energy surfaces of these states[25]. According to the calculation the three lines following the transition to the zero vibrational level represent (in the order of increasing energy) excitation of the torsional, C=C stretching, and C–H bending modes. The appearance of the C=C stretching mode is attributed to the elongation of the C=C bond that occurs upon ionization of the $\pi$ electron (1.41 Å as against 1.33 Å in the neutral molecule). In the same way the excitation of the torsional mode reflects the distortion of the ion from planarity: using the parameter values of Table 1 and searching for the energetic minimum of the full four-dimensional potential surface we get[9b] a torsional angle of $\approx 25°$ for the equilibrium geometry of $C_2H_4^+$. The optimized barrier to planarity turns out to be $\approx 0.03$ eV.

The quality of the calculated spectrum leaves no doubt about the nonplanarity of the ethylene cation[25]. It should be mentioned that also the ab initio (Green's function) data predicts $C_2H_4^+$ to be nonplanar, although the torsional angle turns out to be too small[9b]. The question of the nonplanarity of $C_2H_4^+$ has been examined before by pointwise calculations of the torsional potential curves. Whereas ab initio results have been controversial, most semiempirical calculations yielded a nonplanar cation[26]. In the present work we have settled this question[27] and have also specified the mechanism leading to the nonplanarity of $C_2H_4^+$.

In the discussion of the photoelectron band we have tacitly assumed the Franck-Condon principle[28] to be applicable. This is not justified a priori. In the calculated spectrum also the effects of jumping between different surfaces are included, which the Franck-Condon principle neglects. One can, however, recalculate the spectrum and enforce the nuclei to stay on a given surface throughout, *i.e.* neglect the nonadiabatic effects[9d]. If one does this for the first PE band of ethylene, one gets virtually the same result as before. This shows that nonadiabatic effects are negligible and the vibrational motion proceeds solely on the lower of the two surfaces, corresponding to the ionic ground state.

The reason for this behavior can be visualized from Figure 6. Upon ejecting an electron from the $\pi(b_{2u})$ orbital the ion is left (speaking classically) on the lower surface at the equilibrium geometry of the neutral species, $Q_g = Q_u = 0$. At this point its internal energy is well below the minimum energy of the upper potential surface. Therefore the nuclei will not jump from the lower to the upper surface *simply because their energy content is insufficient to reach the latter!*

The situation changes, of course, if we consider the vibrational motion which starts on the upper potential surface. This occurs upon ionization out of the $\pi_{CH_2}(b_{2g})$ molecular orbital. Indeed, the second photoelectron band looks completely different from the first band. We show it in Figure 8 together with the result of the exact calculation and the Franck-Condon calculation[9f].

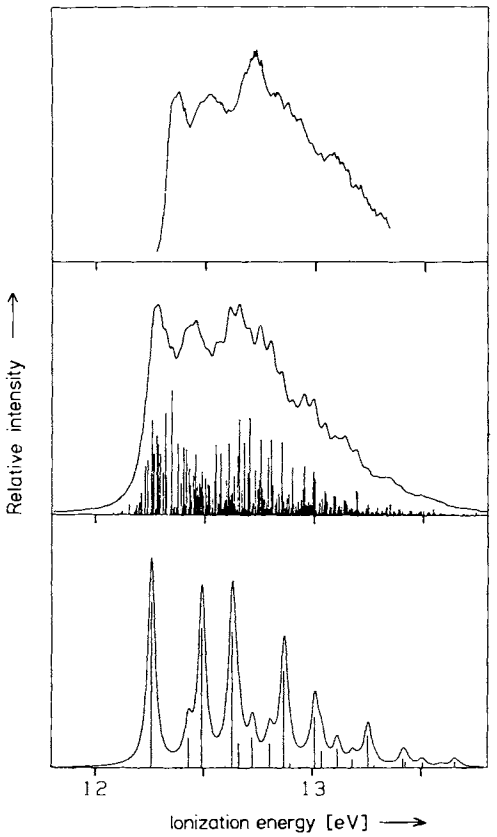



Fig. 8. The second band in the photoelectron spectrum of ethylene. Top: The experimental recording [11a]. Center: The spectrum according to the full vibronic coupling calculation. A line width of 0.04 eV has been used corresponding to the lower experimental resolution (for more details see Fig. 7). Bottom: The Franck-Condon spectrum. Whereas the exact calculation reproduces the observations quite well, the Franck-Condon spectrum bears no resemblance to experiment. Therefore the vibrational motion is not even approximately confined to the upper potential energy surface.

In the exact calculation we use the same Hamiltonian as before. In the Franck-Condon calculation we apply the Franck-Condon principle to the upper potential energy surface of the vibronic coupling model. The exact calculation reproduces the experiment quite well: The envelope exhibits three broad humps and different slopes of the low and high energy wings of the band, just like the experimental spectrum. Therefore the vibronic coupling mechanism is seen to govern also the first excited ionic state. Surprisingly *the Franck-Condon spectrum fails completely to reproduce the observations*. The comparison with the exact calculation reveals striking nonadiabatic effects, not only with regard to the intensity distribution but also with regard to the *number* of spectral lines (the exact spectrum consists of more than 1000 individual lines!). Moreover, the nonadiabatic effects extend over the entire energy range of the band including the lowest vibrational levels of the $^2B_{2g}$ state. This gives direct evidence that the *nuclear motion is not even approximately confined to the upper potential energy surface.*

Another way of looking at the phenomenon is to follow the time evolution of the nuclear motion. In Figure 9 we have plotted the probability that the nuclei are on the upper surface as a function of the time $t$ that has elapsed since the ionization out of the $\pi_{CH_2}$ orbital. Since this ionization process transfers the molecule to the upper potential surface, the probability is unity at $t = 0$. If the vibronic coupling were to vanish ($\lambda = 0$), the nuclei would stay on the upper surface and the probability would remain unity throughout.

We see from Figure 9 that because of the vibronic coupling the *confinement to the upper surface lasts only for the extremely short time of $10^{-14}$ s, i.e. about a period of vibration.* After that time the probability fluctuates around a constant value which is considerably smaller than unity. It is roughly given (within our model) by the relative density of vibrational levels of both surfaces. In other words, after an initial rapid decay the nuclei move essentially freely between both surfaces with a relative occupation probability determined only by statistical factors.

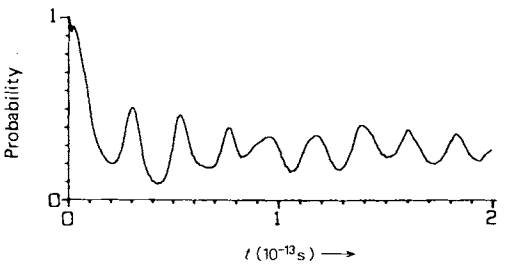



Fig. 9. The probability of the $C_2H_4^+$ nuclei residing on the upper potential energy surface as a function of the time that has elapsed since the ionization out of the $\pi_{CH_2}$ orbital. The confinement to the upper surface lasts only $\approx 10^{-14}$ s. After that time the nuclei interconvert freely between both surfaces. This behavior accounts in a natural way for the strong nonadiabatic effects in the photoelectron spectrum (Fig. 8).

Typically, nonadiabatic (or nonradiative) decay times determined experimentally range from $\approx 10^{-6}$—$10^{-10}$ seconds[7p,q]. The present value is more than four orders of magnitude smaller. It just represents the strong nonadiabatic effects found before in the spectrum in a different manner. The ultrafast nonadiabatic decay makes it plausible that the Franck-Condon principle fails completely in the calculation of the spectrum.

A closer examination reveals that the strong nonadiabatic effects are intimately connected with the existence of several modes[29]. If only a single mode (torsion) is retained they vanish almost completely: In this case the Franck-Condon spectrum becomes virtually exact and the probability of population of the upper surface (Fig. 9) remains

practically unity. The additional totally symmetric modes bring the potential energy surfaces close together and thus enhance the probability that the nuclei jump between the different surfaces. At the extreme situation, when a conical intersection exists and is accessible energetically (as in the ethylene cation), the nuclei interconvert freely between the surfaces and the nuclear motion behaves completely nonadiabatically.

It now becomes clear why the adiabatic approximation has proven so successful in the assignment of highly resolved electronic spectra of diatomic molecules[8v]. Most of the previous work on the vibronic coupling problem in polyatomic molecules has also been confined to a single vibrational mode and, consequently, only moderate nonadiabatic effects have been reported. In contrast, in all the polyatomic molecules we have analyzed to date we find that several modes participate in the coupling and lead to strong nonadiabatic effects for the upper electronic state. Furthermore, many conical intersections are meanwhile becoming known from ab-initio calculations[30], which illustrates that they are a common phenomenon, even in small polyatomic molecules. This holds all the more for larger systems of chemical interest.

The importance of the nonadiabatic effects in radical cations is also indicated by the generally diffuse photoelectron spectra of polyatomic molecules[11]. The present mechanism can explain this diffuseness through the demolition of the vibrational progressions that occurs and the high density of vibronic lines. Further evidence comes from the absence of detectable emission in most organic radical cations[31] (including the ethylene cation[31c]). This suggests rapid radiationless decay with decay times $< 10^{-12}$ s. We have seen above that the present mechanism (conical intersections) leads to decay times of $\approx 10^{-14}$ s. Thus it constitutes a prototype of rapid radiationless decay that *explains* the ultrashort decay times and makes the frequent absence of detectable emission understandable.

To summarize, Sections 2 and 3 provide an overview of the basic impact which the vibronic coupling exerts on the structural features of molecules as well as on the behavior of the nuclear motion. It appears remarkable that a *single* mechanism can explain such different classes of phenomena as distortions of the molecular shape, excitation of nontotally symmetric modes (in the low energy electronic band), diffuseness of the high energy band, and the absence of detectable emission.

## 4. Vibronic Coupling in Alkenes, Allenes and Cumulenes

The general ideas have been illustrated above by referring to the ethylene cation. It is interesting now to inquire about the trends occurring in a series of chemically related compounds. In this way we can gain more insight into the chemical significance of the vibronic coupling mechanism.

### 4.1. Substituted Ethylenes

Let us start by considering the effect of chemical substitution in ethylene. Clearly, the substituent can exert its electronic influence either through the value of $\lambda$ or of $E_2 - E_1$. The variation of $\lambda$ (eq. 7) can be predicted if one describes the molecular orbitals as a linear combination of atomic orbitals. Retaining only the terms belonging to the carbon atoms, one obtains an expression with integrals over atomic orbitals multiplied by products of the atomic orbital coefficients in the $\pi$ and $\pi_{CH_2}$ molecular orbitals. Since substitution tends to "dilute" the atomic orbital coefficients on the carbon atoms[32], one expects that, generally, $\lambda$ will become smaller upon substitution.

The other factor is $E_2 - E_1$, *i.e.* the difference between the vertical ionization potentials. As we discussed before in reference to Figure 2, this quantity can be related to the energy gap of the two orbitals, $\pi$ and $\pi_{CH_2}$ (eq. 2). Thus we must inquire about substituent effects on the energy levels of these orbitals. Notable among the substituents is fluorine. What it usually does is to leave the energy of the $\pi$ orbital largely unaffected, but to decrease the energy of the $\pi_{CH_2}$ orbital through its inductive effect[32]. Perfluorination just accentuates this effect, and it is commonly known among photoelectron spectroscopists as the "perfluoro effect"[33]. In order to understand this effect, we should see how one reconstructs the $\pi$ and $\pi_{CH_2}$ orbitals of ethylene. Figure 10a shows the reconstruction of these orbitals by interacting the orbitals of two $CH_2$ fragments.

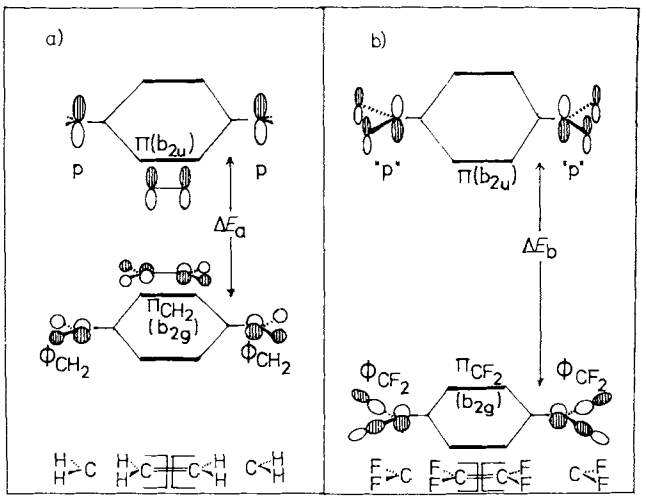



Fig. 10. Interaction diagram which describes the reconstruction of the $\pi$ and $\pi_{CX_2}$ molecular orbitals (X = H, F) of ethylene and tetrafluoroethylene, from the appropriate fragment orbitals of two $CX_2$ (X = H, F) units. The fragments are indicated by brackets in the molecular formulas.—a) The interaction diagram for ethylene, $C_2H_4$. The fragment orbitals are p and $\phi_{CH_2}$. $\Delta E_a$ is the resulting energy gap of the $\pi$ and $\pi_{CH_2}$ molecular orbitals.—b) The interaction diagram for $C_2F_4$. The fragment orbitals are "p" and $\phi_{CF_2}$. Note that $\varepsilon(\text{"p"}) \approx \varepsilon(p)$ and $\varepsilon(\phi_{CF_2}) < \varepsilon(\phi_{CH_2})$. The resulting $\pi$-$\pi_{CF_2}$ energy gap is $\Delta E_b$. Note that $\Delta E_b > \Delta E_a$ because of the large energy gap of the fragment orbitals "p" and $\phi_{CF_2}$.

The $\pi$ orbital results from the in-phase combination of two pure carbon p orbitals, whereas $\pi_{CH_2}$ results from the out-of-phase combination of the two fragment orbitals which are C–H bonding (*i.e.* $\phi_{CH_2}$) and, hence, low lying. Thus, the intrinsic large energy difference between the fragment orbitals p and $\phi_{CH_2}$ leads to a relatively large energy gap for the molecular orbitals (see Table 1).

Let us replace the hydrogens by fluorines. Now, we have two $CF_2$ fragments. Each fragment has a "p" orbital which

arises from the antibonding combination of the fluorine p orbitals with the carbon p orbital. As a result of this antibonding character, the "p" orbital has a higher energy than the pure p orbital of carbon. This effect is counterbalanced, however, by the above mentioned inductive effect of fluorine. Therefore the resulting $\pi$ orbital of $C_2F_4$, which is the in-phase combination of the two fragment "p" orbitals will have a similar energy as the $\pi$ orbital of $C_2H_4$.

The other orbital in question is the $\pi_{CF_2}$ orbital. This orbital arises from the out-of-phase combination of the $\phi_{CF_2}$ orbitals. There are several orbitals of this type, all of which are lower lying than the analogous $\phi_{CH_2}$ fragment orbital, but in Figure 10b we show only one $\phi_{CF_2}$ orbital per fragment. This fragment orbital is considerably lower in energy than the $\phi_{CH_2}$ orbital because it is essentially a C–F bonding orbital. The resulting $\pi_{CF_2}$ orbital is therefore, likewise more energetically favorable than the $\pi_{CH_2}$ orbital (compare Fig. 10a with 10b). Consequently, the $\pi$-$\pi_{CF_2}$ energy gap is much larger than the corresponding $\pi$-$\pi_{CH_2}$ gap. Once again, what sets up the final gap, is the energy difference of the two fragment orbitals. This becomes larger upon fluorine substitution and, hence, it will lead to a larger value of the energy gap.

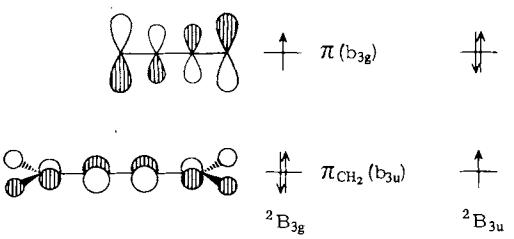
How this difference affects the vibronic coupling and the structure of the ground state ion is quite obvious from our discussion with reference to Figure 2. Since the nonplanarity of the cation is dependent upon the magnitude of the interaction of the two molecular orbitals $\pi$ and $\pi_{CX_2}$ (X = H, F), then replacement of H by F will lead to a considerably weaker interaction. Thus, the fluorinated cation will behave as expected for cases of weak coupling, and will most likely remain planar. The weakening effect will obviously depend on the degree of substitution and will become more pronounced as the number of fluorine atoms increases. This weakening of the vibronic coupling will leave its marks on the PE spectrum. This is indeed the impression one gets from the first bands (corresponding to the $\pi$ ionization) in the photoelectron spectra of vinyl fluoride and the difluoroethylenes[34], which show a normal progression in the C=C stretching mode. However, some high resolution PE results will be needed in order to evaluate the magnitude of the vibronic coupling in this family of compounds.

What is the situation with substituents other than F? Our experience with substituent effects[32] shows that most usual chemical substituents which are electron donors, like $CH_3$, OR, $NR_2$ *etc.*, will raise the energy of the $\pi$ orbital considerably and will change the $\pi_{CH_2}$ type orbital to a lesser extent. On the other hand, electron acceptors, like CN or COH, will lower both orbitals but will affect more the $\pi_{CH_2}$ type orbital[32]. The conclusion is that within the family of substituted ethylenes, the electronic factors $\lambda$ and $E_2 - E_1$ will favor strong vibronic coupling effects mostly in the unsubstituted parent ion $C_2H_4^+$.

Until now we have neglected effects of steric congestion[35]. It has been claimed[26] that in the case of tetramethyl substitution the distortion from planarity is larger than in ethylene itself, mainly because of the effects of steric hindrance of the methyl groups. This should hold all the more for isopropyl or other bulkier substituents[26]. In the vibronic coupling model the effects of steric hindrance are contained in the torsional frequency $\omega_u$. Indeed, when comparing ethylene and the tetramethyl derivative and correcting for the different masses, the torsional frequency is smaller by a factor $\approx 1.6$ in the latter molecule[36]. This favors a larger vibronic coupling in the derivative. The energy gap of the interacting states is taken as 2.4 eV (difference of the two lowest ionization potentials[37]). Neglecting totally symmetric modes and taking $\lambda$ from ethylene, one finds with eq. (5) for the energy barrier to planarity a value of 0.18 eV and a torsional angle of 42° at equilibrium. This compares favorably with the previously reported values of 0.22 eV and 40°, respectively[26,38]. It is therefore to be expected, that steric congestion will generally lead to an increase of the vibronic coupling strength.

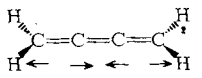
### 4.2. The Butatriene Radical Cation

The principles which govern the spectrum of butatriene and the geometry of its ion are almost the same as were described for ethylene. The two adjacent ionic states arise by ionization from the $\pi(b_{3g})$ and $\pi_{CH_2}(b_{3u})$ molecular orbitals.




(11)

Inspecting these MOs, one notices that the nodal properties across the terminal bonds are exactly the same as those across the C=C bond of ethylene. Consequently, the linear coupling constants for the totally symmetric mode **5**, $\kappa_1$ and $\kappa_2$, will have different signs, and the two states $^2B_{3g}$ and $^2B_{3u}$ will behave much the same as the two corresponding ionic states of ethylene (Fig. 2 and 4). In addition, the two states are coupled *via* an $A_u$ type motion



**5**

which consists in an opposite torsion of the two $CH_2$ termini. This can result in a cation which is nonplanar and which has a short central C=C bond. Therefore, the butatriene problem is not much different from the ethylene problem in its essential features. Considering that $\lambda$ is expected to be smaller than in the case of ethylene owing to the dilution of the AO coefficients (cf. Section 4.1), one asks oneself why the photoelectron spectrum of butatriene is upset by the bothersome "mystery band"[12], whereas that of ethylene is not? The answer to this question can be found in the much smaller energy gap in the case of butatriene. In fact, both our Hartree-Fock and Green's function computations[9a] predict that the difference between the vertical ionization potentials is much smaller than that in ethylene (*e.g.*, 0.72 eV in $C_4H_4$ *vs* 2.4 eV in $C_2H_4$ using Green's function values). This means that the vibronic coupling effects are stronger in the butatriene case.

The ab initio calculations also show that among the four totally symmetric vibrations it is indeed only the mode **5** that has to be considered. Once again, slight adjustment of the parameters (the values are given in Table 2) furnishes the theoretical spectrum, which is depicted in Figure 11 along with the experimental recording.

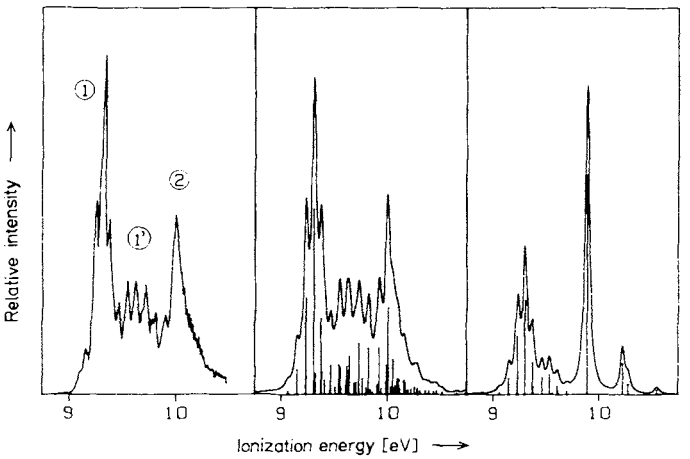



Fig. 11. The first band system in the photoelectron spectrum of butatriene. Left: The experimental recording [12a]. The bands ① and ② have been attributed to ionization out of the outermost occupied orbitals of butatriene. Band ①' was termed a "mystery band" [12a]. Center: The spectrum according to the full vibronic coupling calculation. For the values of the parameters cf. Table 2 (line width 0.04 eV). Right: The Franck-Condon spectrum. The Franck-Condon calculation is realistic only for low vibrational energies and fails completely for the high energy part of the band system. The mystery band is clearly seen to be a nonadiabatic effect.

There is almost perfect agreement between theory and experiment. Therefore, the vibronic coupling mechanism accurately describes the nuclear motion also in the butatriene radical cation. To reveal the origin of the "mystery band" we have recalculated the spectrum according to the Franck-Condon principle, *i.e.* discarded the possibility that the nuclei jump between the individual potential energy surfaces. The result is included in Figure 11. By comparing the exact calculation and the Franck-Condon calculation one can see that for low energies the vibrational motion is indeed confined to a single potential energy surface (that of the ionic ground state). This is just the energy range where vibrational progressions are still discernible in the exact spectrum. On the other hand, for energies at and above the center of the band system the exact line structure is highly erratic and completely different from the FC line structure. Note that the conical intersection of the two potential energy surfaces occurs at an energy of $\approx 9.7$ eV. In other words, *as soon as the upper potential surface becomes energetically accessible the vibrational motion can no longer be attributed to either of the ionic states but is determined by the joint nuclear motion on both potential energy surfaces.* This is the same behavior as observed in the ethylene cation. The main difference between both examples is the smaller energy gap in the present case, which leads to the overlapping of the bands and the formation of the mystery band.

Using the parameters of Table 2, one finds that the geometry of the cation is nonplanar with $\alpha = 46°$. This is in complete contrast to the predictions of ab-initio computations (STO-3G), which predict a planar geometry[12a]. Once again, the reason for the failure of the STO-3G calculation may be the underestimation of the effect owing to a much too large an energy gap[27].

Table 2. Energies, coupling constants and frequencies used in the calculation of the photoelectron spectrum of butatriene (Fig. 11). All quantities are in eV.

| | $^2B_{3g}$ | $^2B_{3u}$ | $\omega$ |
|---|---|---|---|
| $E$ | 9.450 | 9.850 | – |
| $\kappa$ | −0.212 | 0.255 | 0.258 |
| $\lambda$ | 0.318 | | 0.091 |

Before we proceed any further, we must make sure that we understand all the qualitative features behind the results. Especially interesting is the energy gap factor. Why is it smaller for butatriene than for ethylene? This can be rationalized if one uses an interaction diagram to reconstruct the $\pi$ and $\pi_{CH_2}$ orbitals of the two systems. Such a diagram for ethylene has been shown before in Figure 10a. We have concluded then that the intrinsic larger energy difference between the fragment orbitals, $\phi_{CH_2}$ and p, sets the value of $E_2 - E_1$, leaving it large. The situation in butatriene is quite different and the $\pi(b_{3g})$ and $\pi_{CH_2}(b_{3u})$ orbitals remain close in energy since they originate from fragment orbitals of about *equal* energies. This is illustrated in Figure 12, where we have reconstructed the $\pi$ and $\pi_{CH_2}$ molecular orbitals of butatriene by the union of two different fragments, in a way which best demonstrates the effect.

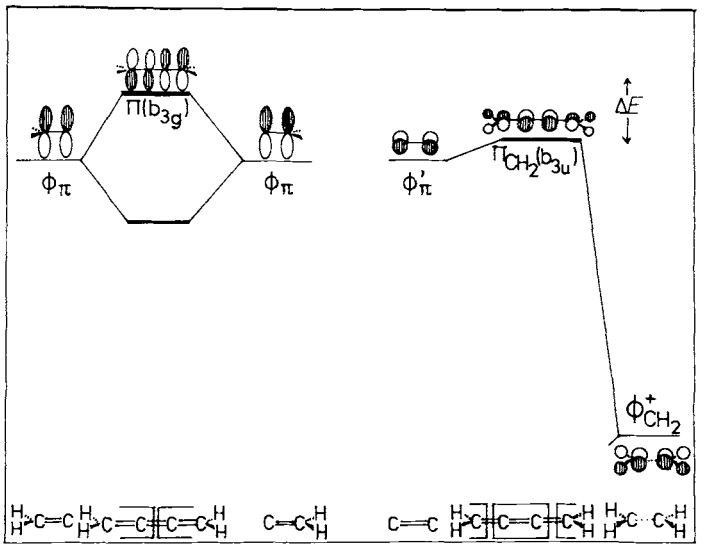



Fig. 12. Interaction diagram which describes the reconstruction of the $\pi$ and $\pi_{CH_2}$ molecular orbitals of butatriene from fragment orbitals. $\pi$ arises from the out-of-phase combination of the two out-of-plane $\pi$ type orbitals ($\phi_\pi$) of the terminal $C{=}CH_2$ fragments. The $\pi_{CH_2}$ orbital arises from the union of the in-plane-$\pi$ type orbital ($\phi'_\pi$) of the central C=C fragment with the positive combination ($\phi^+_{CH_2}$) of the in-plane orbitals of the two terminal $CH_2$ fragments. The fragments are indicated by frames and brackets in the molecular formulas.

Thus the $\pi(b_{3g})$ orbital, in the left hand part of Figure 12, results from the union of two degenerate out-of-plane $\pi$-type orbitals each belonging to a $C{=}CH_2$ fragment, and labeled as $\phi_\pi$. The $\pi_{CH_2}(b_{3u})$ orbital, on the other hand, is re-

constructed from the union of a $\pi$-type fragment orbital ($\phi'_\pi$) of the central C=C unit, with a low lying $\phi^+_{CH_2}$ orbital, which is the in-phase combination of two $\phi_{CH_2}$ orbitals belonging to the fragment $H_2C\ldots CH_2$. Thus, the two molecular orbitals $\pi(b_{3g})$ and $\pi_{CH_2}(b_{3u})$ originate from fragment orbitals $\phi_\pi$ and $\phi'_\pi$, which are roughly degenerate and the result is that the molecular orbitals $\pi$ and $\pi_{CH_2}$ remain close in energy, being separated by a very small energy gap.

The interaction diagram in Figure 12 will help us understand why derivatives like tetramethyl-, tetra-*tert*-butyl- and tetrafluoro-butatriene[12] do not exhibit the "mystery band". A partial reason may be the prospective decrease of the coupling constant $\lambda$ upon chemical substitution, which we have discussed before. But this certainly cannot be the full story, in view of the striking differences in the spectra[12]. Therefore, we must look again at the energy gap factor, $E_2-E_1$.

The line of reasoning is very similar to the one used for discussing substituent effects on the energy gap in the case of ethylene. Let us go back to Figure 12 and consider the case of a donor substituent such as in the tetramethyl derivative. As a result of replacing H by $CH_3$, the energy of $\phi_\pi$, the $\pi$ type orbital of the fragment $C{=}C(CH_3)_2$, will increase, whereas $\phi'_\pi$, the $\pi$-type orbital of the central C=C fragment, will not be affected by the terminal substitution. This energy gap between the fragment orbitals $\phi_\pi$ and $\phi'_\pi$ will now be reflected in $E_2-E_1$, which will increase.

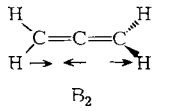
Replacing H by F will similarly increase the $\phi_\pi-\phi'_\pi$ energy gap and, in addition, $\phi^+_{CF_2}$ will be much lower than $\phi^+_{CH_2}$, so that the resulting gap will be even larger than in the case of methyl substitution. This is indeed reflected in the experimental spectrum, and the measured values of $E_2-E_1$ for the tetramethyl, tetra-*tert*-butyl and tetrafluoro derivatives respectively are 1.22 eV[12a], 1.17 eV[12a], and 2.65 eV[12b], all much larger than that for the parent unsubstituted compound.

Once again, we encounter the same trend. In a family of compounds generated by substitution of the same cumulene, the vibronic coupling effects are weakened by chemical substitution. This will be reflected both in the PE bands and in the degree of geometric distortion of the ground state cation (note that the effects of steric hindrance will be less pronounced than in ethylene due to the larger separation of the terminal C atoms). The substituted cations will distort away from the geometry of the neutral molecule *less than* the unsubstituted cation, and their PE bands will appear *less complex*.

### 4.3. The Jahn-Teller Effect in Allene and Pentatetraene

Allene and pentatetraene form a group where the lowest cationic state is doubly degenerate ($^2$E). The vibronic coupling effect in this group is known as the Jahn-Teller effect[7i]. It consists of a coupling by two vibrational modes: the torsional mode, $B_1$, describing the twisting of the $CH_2$ termini about the C=C=C axis, and a stretching mode, but a non-totally symmetric one, $B_2$ (**6**).

A symmetry analysis of the Hamiltonian reveals that it is almost identical to eq. (2) except that certain parameters



**6**

coincide[9c]. As a consequence, the conical interesection of the adiabatic potential surfaces is now right in the center of the Franck-Condon zone or, equivalently, of the PE band. Thus, strong nonadiabatic effects will always be present in the spectrum. This is confirmed by calculation[9c] (cf. Fig. 13), which gives regular progressions (torsional mode) only for low energies and an erratic line structure for high energies. The behavior is very similar to that of the butatriene molecule.

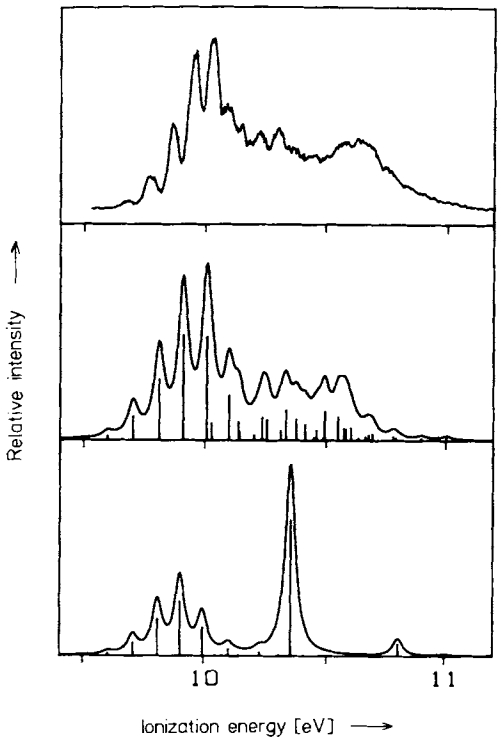



Fig. 13. The first band in the photoelectron spectrum of allene representing ionization out of a degenerate orbital (symmetry e). Top: The experimental recording [13a]. Center: The spectrum according to the full vibronic coupling (Jahn-Teller) calculation [9c]. Bottom: the Franck-Condon spectrum. As in the butatriene molecule the Franck-Condon calculation fails completely for the high energy part of the band. For low energies vibrational (torsional) progressions are still discovered in the exact calculation. The similarity between both examples shows that Jahn-Teller type effects are not limited to degenerate states but occur likewise in case of near-degeneracy (strong vibronic coupling).

With regard to the cationic structure, only either the $B_1$ or the $B_2$ coordinate can change in the Jahn-Teller case. For both allene and pentatetraene this is found to be the torsional angle[9c], with values of 51.6° and 38° at equilibrium, respectively. Clearly, the behavior is uniform throughout the "cumulene series".

The close analogy between the Jahn-Teller effect and the vibronic coupling in the other members of the cumulene series deserves some attention. The impact of the Jahn-Teller effect on symmetry breaking and nonadiabaticity of the nuclear motion is well recognized in the literature. We see from the present comparison that these "Jahn-Teller type" phenomena likewise occur if the electronic states are

nondegenerate but sufficiently close in energy. Therefore the vibronic coupling mechanism can be considered as a generalization of the Jahn-Teller effect to nondegenerate electronic states. In other words all the phenomena pertinent to the Jahn-Teller effect are not *restricted to highly symmetrical molecules with degenerate electronic states but will occur also in many others which are less symmetric and possess only nondegenerate states.*

The effect of substituents in the odd-carbon members is also similar to that in the even-carbon members. Substitution will generally remove the degeneracy of the $^2$E cationic state and will create a nonvanishing energy gap. Therefore, it is expected to reduce the magnitude of the vibronic coupling, much the same as it does in the derivatives of other "cumulenes".

### 4.4. Substituent Effects in the "Cumulene Family"—an Overview

We have now achieved to some extent an overview of the structure of the ground state cations of "cumulenes" and of the shape of the bands in their PE spectra. The picture which has emerged is quite appealing and deserves special attention.

The extent of the vibronic coupling effects is determined mainly by the energy gap of two uppermost occupied orbitals of the neutral molecule. When this gap is small, the cation distorts away from the neutral geometry, and the photoelectron spectrum in this energy region will be upset by nonadiabatic effects. When this energy gap is large, the distortion of the cation is smaller and so are the nonadiabatic effects in the first PE band.

Since we now know the pattern of substituent effects on the energy gap, we can map the vibronic coupling effects in all the cumulenes in two "dimensions". The first is the "dimension" of the number of carbon atoms. As we vary the number of carbon atoms the energy gap oscillates: it is nonzero for all the even-carbon members, and it vanishes for all the odd-carbon members. As the number of carbon atoms increases, the oscillations become tempered and converge to zero. This convergence is quite fast, since already for butatriene the gap is $\approx 0.5$ eV.

Let us consider first the even-carbon members. In this subset, ethylene has the largest energy gap ($\approx 1.9$ eV), and this decreases as the even number of carbon atoms increases. Thus, within this subset, vibronic coupling effects increase along the series, as we indeed witnessed on comparing the results of ethylene and butatriene. Both exhibit strong nonadiabatic effects, but the cation of the latter exhibits a larger distortion from planarity ($\alpha = 46°$ *vs* $25°$).

In the second subset, that of the odd-carbon members, the energy gap is zero throughout the series, and, hence, the vibronic coupling effects are always strong. The distortion of the cation away from the geometry of the neutral molecule now depends on the balance of two opposing trends. The torsional frequency, $\omega$, which determines the energy rise inherent in the twisting, decreases as the number of carbons increases. The second factor, $\lambda$, also decreases in the same direction owing to the dilution of the atomic orbital coefficients in the increasingly delocalized molecular orbitals. Our best fit calculations show that the values of $\omega$ for allene and pentatraene are 0.107 eV and 0.08 eV, respectively, whereas, the respective values of $\lambda$ are 0.24 eV and 0.21 eV. These values indicate that the effect on $\lambda$ will be less pronounced, and that the variation in $\omega$ will dominate the distortion in the odd-carbon members. This is confirmed on comparing the degree of distortion away from the geometry of the neutral molecule ($\alpha = 90°$), in the radical cations of allene ($\alpha = 51.6°$) and of pentatetraene ($\alpha = 38°$).

The second "dimension" is the "dimension" of chemical substitution. In the subset of even-carbon members, increasing degree of substitution causes an increase of the energy gap and, hence, it often leads to a decrease in the vibronic coupling effects. In the subset of odd-carbon members, mono- and di-substitutions on one terminus increasingly remove the degeneracy of the $^2$E state of the cation and lead to a decrease of the vibronic coupling. A higher degree of substitution achieves exactly the opposite effect, and the tetrasubstituted derivative has again a degenerate $^2$E ionic state.

## 5. Outlook

We have described in this article a mechanism (vibronic coupling) which allows one to gain an insight into two quite different chemical phenomena: the lowering of the molecular symmetry in ionic or excited states and the nonadiabatic behavior of the nuclear motion, *i.e.* the ability of the nuclei to jump between different potential energy surfaces. Such a unified description appears to us to be very attractive from a conceptual point of view. Of course, the value of the approach rests on its ability to describe the behavior of actual molecules. This has been demonstrated here for the series of "cumulene" cations. In all cases the fine structure of the photoelectron spectra could be accurately reproduced, from which information on the structure of the cation in the ground state could be derived.

What could the future perspectives look like? Detailed applications of the type shown above have been limited to comparatively small polyatomic molecules. This was motivated by the availability of accurate computational methods and well resolved experimental spectra for these systems, both essentials for a detailed verification of the mechanism. Often, however, one is interested in larger molecules and focuses on qualitative trends rather than on extensive calculations. The present results should provide a sound basis from which one can also proceed to understand larger systems of chemical interest. For instance, the quantities appearing in the Hamiltonian can be approximated on the orbital level and the standard semiempirical schemes can be used[4] to calculate them. Often, still simpler reasoning should be successful, for example, for comparing chemically similar compounds. In this way, the present approach can also be extended to larger molecules and reveal information about their interactions.

With regard to the nuclear motion, we have witnessed surprisingly strong nonadiabatic effects, *i.e.* an extremely efficient "jumping" of the nuclei between different potential energy surfaces. This is intimately connected to conical intersections of these surfaces, which in turn owe their existence to the interplay of several vibrational modes. *The*

*importance of the multi-mode effects for the nuclear motion can hardly be overestimated.* They should be even more pronounced for larger molecules with more internal degrees of freedom. Many absorption spectra of aromatic molecules exhibit indeed an erratic or diffuse fine structure, which was attributed to nonadiabatic effects[8d-s]. It is suggested that these be analyzed in terms of a multi-mode vibronic coupling mechanism as above.

More generally, the strong nonadiabatic effects are expected to be of some relevance also for non-spectroscopic applications, such as the theory of radiationless transitions or of chemical reactions. An important class of radiationless transitions involves a jump between different potential energy surfaces, thereby quenching the observed fluorescence intensity. If the transition proceeds within $< 10^{-12}$ s, no fluorescence is expected. Indeed, fluorescence is not observed in the majority of organic radical cations[31] studied to date. The same applies for higher excited states of a given multiplicity in neutral molecules (Kasha's rule[39]). Conical intersections of potential energy surfaces and the associated nuclear dynamics can in a natural way account for these observations and it is expected that this mechanism will indeed be found to operate in a large class of molecules and ions.

With regard to chemical reactions, these involve geometry changes along more than a single molecular mode. The question arises whether one can interpret chemical reactivity in terms of a many-mode vibronic coupling mechanism[7r-t,40]. To be sure, in most treatments of the problem a reaction coordinate is introduced which is taken as a sort of average trajectory of the nuclear motion on the potential energy surfaces. However, the present investigation shows that near an intersection of potential surfaces the nuclear motions can in no sensible way be decoupled any more. Thus, it lends serious doubt to the idea of a "reaction coordinate" when conical intersections of potential surfaces are involved. Conical intersections of potential energy surfaces may play an important role in many photochemical processes. It should be remembered that this type of chemical reaction always consists in (at least) one nonadiabatic transition between different potential energy surfaces[7u]. The present findings suggest that the multidimensionality of the nuclear motions be taken into consideration in order to gain a better insight into photochemical reaction dynamics.

*This work was financially supported by the Deutsche Forschungsgemeinschaft, the Fonds der Chemischen Industrie, and the Deutscher Akademischer Austausch-Dienst (S. S. S.).*

Received: February 16, 1981 [A 447 IE]
revised: July 9, 1982
German version: *Angew. Chem. 95* (1983) 221

[1] a) W. B. England, W. C. Ermler, *J. Chem. Phys. 70* (1979) 1711; b) B. Kleman, *Can. J. Phys. 41* (1963) 2034; c) G. M. Schwenzer, S. V. O'Neil, H. F. Schaefer III, C. P. Baskin, C. F. Bender, *J. Chem. Phys. 60* (1974) 2787; d) O. Nomura, S. Iwata, *ibid. 74* (1981) 6830; e) J. W. Rabalais, J. M. McDonald, V. Scherr, S. P. McGlynn, *Chem. Rev. 71* (1971) 73; f) W. B. England, *Chem. Phys. Lett. 78* (1981) 607.

[2] a) A. R. Hoy, J. C. D. Brand, *Mol. Phys. 36* (1978) 1409; b) C. F. Jackels, E. R. Davidson, *J. Chem. Phys. 64* (1976) 2908; c) Y. Hamada, A. J. Merer, S. Michelsen, S. A. Rice, *J. Mol. Spectrosc. 86* (1981) 499.

[3] a) J. B. Coon, N. W. Naugle, R. D. McKenzie, *J. Mol. Spectrosc. 20* (1966) 107; b) G. Fischer, Y. Sorek, *ibid. 74* (1979) 136.

[4] a) J. H. van der Waals, A. M. D. Berhuis, M. S. de Groot, *Mol. Phys. 13* (1967) 301; G. C. Nieman, *J. Chem. Phys. 50* (1969) 1674; b) M. F. Merienne-Lafore, H. P. Trommsdorff, *ibid. 64* (1976) 3791.

[5] a) A. H. Merer, R. S. Mulliken, *Chem. Rev. 69* (1969) 639; b) G. Olbrich, *Ber. Bunsenges. Phys. Chem. 86* (1982) 209; c) E. A. Gastilovich, K. V. Tskhai, D. N. Strigorin, *Opt. Spectrosc. 41* (1976) 332.

[6] P. Ausloos: *Kinetics of Ion-Molecule Reactions*, Plenum Press, New York 1979; M. T. Bowers: *Gas Phase Ion Chemistry*, Vol. *I* und *II*. Academic Press, New York 1979.

[7] The following list is necessarily incomplete. Here we select some papers from a systematic point of view, whereas in ref. [8] we classifiy others with regard to the examples studied by the authors. - General investigations: a) G. Herzberg, E. Teller, *Z. Phys. Chem. B 21* (1933) 410; b) A. C. Albrecht, *J. Chem. Phys. 33* (1960) 156, 169; c) H. C. Longuet-Higgins, *Adv. Spectrosc. 2* (1961) 249; d) G. Herzberg: *Molecular Spectra and Molecular Structure, III. Electronic Spectra and Electronic Structure of Polyatomic Molecules*, Van Nostrand, Princeton, NJ 1967. - Jahn-Teller- and Renner-Teller-Effects: e) Cf. [7c, d]; f) W. Moffit, A. D. Liehr, *Phys. Rev. 106* (1957) 1195; g) H. C. Longuet-Higgins, U. Öpik, M. H. L. Pryce, R. A. Sack, *Proc. R. Soc. London A 244* (1958) 1; h) C. Jungen, A. J. Merer, *Mol. Phys. 40* (1980) 1; i) Review in R. Englman: *The Jahn-Teller Effect*, Wiley, London 1973. - Pseudo-Jahn-Teller-Effect: j) R. L. Fulton, M. Gouterman, *J. Chem. Phys. 35* (1961) 1059; *41* (1964) 2280; k) R. L. Fulton, *ibid. 56* (1972) 1210; l) M. H. Perrin, M. Gouterman, *ibid. 46* (1967) 1019; m) M. Garcia Sucré, G. Geny, R. Lefebvre, *ibid. 49* (1968) 458; n) W. Henneker, A. P. Penner, W. Siebrand, M. Z. Zgierski, *ibid. 69* (1978) 1884; o) A. R. Gregory, R. Silbey, *ibid. 65* (1976) 4141 and references cited therein. - Radiationless decay: p) K. F. Freed, *Top. Appl. Phys. 15* (1976) 23; q) P. Avouris, W. M. Gelbart, M. A. El-Sayed, *Chem. Rev. 77* (1977) 793. - Chemical reactions: r) R. F. W. Bader, *Can. J. Chem. 40* (1962) 1164; s) L. Salem, *Chem. Phys. Lett. 3* (1966) 99; t) R. G. Pearson, *Acc. Chem. Res. 4* (1971) 152; u) N. J. Turro: *Modern Molecular Photochemistry*, Benjamin, Menlo Park 1978.

[8] Spectroscopic applications of vibronic coupling. - Dimeric molecules: a) A. Witkowski, W. Moffit, *J. Chem. Phys. 33* (1960) 872; b) E. Chandross, J. Ferguson, E. G. McRae, *ibid. 45* (1966) 3547, 3554, 3564; c) M. Pawlikowski, M. Z. Zgierski, *ibid. 76* (1982) 4789. - Arenes: d) R. M. Hochstrasser, C. Marzzacco, *ibid. 49* (1968) 971; e) M. H. Perrin, M. Gouterman, C. L. Perrin, *ibid. 50* (1969) 4137; f) Cf. [4a]; g) J. Wessel, D. S. McClure, *Mol. Cryst. Liq. Cryst. 58* (1980) 121; h) M. Z. Zgierski, *Chem. Phys. Lett. 47* (1977) 499; *69* (1980) 608; i) W. D. Hobey, *J. Chem. Phys. 43* (1965) 2187. - N-Heterocycles: j) Cf. [8d]; k) E. C. Lim, R. Li, Y. H. Li, *J. Chem. Phys. 50* (1969) 4925; l) P. J. Chappell, I. G. Ross, *Chem. Phys. Lett. 43* (1976) 440; m) D. B. McDonald, S. A. Rice, *J. Chem. Phys. 74* (1981) 4893; n) J. Brickmann, *Ber. Bunsenges. Phys. Chem. 80* (1976) 917; o) J. D. Webb, K. M. Swift, E. R. Bernstein, *J. Chem. Phys. 73* (1980) 4891; p) G. Fischer, G. J. Small, *ibid. 56* (1972) 5934; q) K. K. Innes, *ibid. 76* (1982) 2100. - Aromatic aldehydes and ketones: r) Cf. [8d, k]; s) I. Özkan, L. Goodman, *Chem. Rev. 79* (1979) 275 and references cited therein. - Mixed valence compounds: t) S. B. Piepho, E. R. Krausz, P. N. Schatz, *J. Am. Chem. Soc. 100* (1978) 2996. - $NO_2$: u) Review in D. K. Hsu, D. L. Monts, R. N. Zare: *Spectral Atlas for Nitrogen Dioxide*, Academic Press, New York 1978. - Diatomic molecules: v) G. Herzberg: *Molecular Spectra and Molecular Structure, I. Spectra of Diatomic Molecules*, Van Nostrand, New York 1950; w) A. Lofthus, P. H. Krupenie, *J. Phys. Chem. Ref. Data 6* (1977) 113; x) R. Gallusser, K. Dressler, *J. Chem. Phys. 76* (1982) 4311.

[9] a) L. S. Cederbaum, W. Domcke, H. Köppel, W. von Niessen, *Chem. Phys. 26* (1977) 169; b) H. Köppel, W. Domcke, L. S. Cederbaum, W. von Niessen, *J. Chem. Phys. 69* (1978) 4252; c) L. S. Cederbaum, W. Domcke, H. Köppel, *Chem. Phys. 33* (1978) 319; d) W. Domcke, H. Köppel, L. S. Cederbaum, *Mol. Phys. 43* (1981) 851; e) H. Köppel, L. S. Cederbaum, W. Domcke, W. von Niessen, *Chem. Phys. 37* (1979) 303; f) H. Köppel, L. S. Cederbaum, W. Domcke, *J. Chem. Phys. 77* (1982) 2014; g) E. Haller, H. Köppel, L. S. Cederbaum, W. von Niessen, G. Bieri, *ibid.*, in press.

[10] Quite generally, the independent electron model represents a better approximation for (low energy) ionic states than for excited states of the neutral molecule (Koopmans' theorem [22]). In addition, the interacting excited states of neutral species often differ in the quantum number of more than a single electron. Since the vibronic coupling operator is effectively a one electron operator [7k, 8e] the interaction vanishes within the single particle picture and occurs only by virtue of electron correlation effects. In the case of ions, the interacting states usually differ by the quantum number of a single electron and the vibronic coupling exists on the single particle level of approximation. This also appears to be the reason why the vibronic coupling effects are often stronger in ions than in the neutral molecules.

[11] Summaries and many examples can be found in: a) D. W. Turner, C. Baker, A. D. Baker, and C. R. Brundle: *Molecular Photoelectron Spectroscopy*, Wiley-Interscience, New York, 1970; b) J. H. D. Eland: *Photoelectron Spectroscopy*, Butterworths, London, 1974; c) W. C. Price, *Advan. At. Mol. Phys. 10* (1974) 131; d) E. Heilbronner, "Organic Chemical

Photoelectron Spectroscopy", in A. R. West: *Molecular Spectroscopy*, Heyden, London 1977. - For an excellent review on the relation between molecular orbitals and photoelectron bands, see: e) H. Bock, *Angew. Chem. 89* (1977) 631; *Angew. Chem. Int. Ed. Engl. 16* (1977) 613.

[12] a) F. Brogli, E. Heilbronner, E. Kloster-Jensen, A. Schmelzer, A. S. Manocha, J. A. Pople, *Chem. Phys. 4* (1974) 107; b) H. Basch, G. Bieri, E. Heilbronner, T. B. Jones, *Helv. Chim. Acta 61* (1978) 46.

[13] a) C. Baker, D. W. Turner, *Chem. Commun. 1969*, 480; b) E. Haselbach, *Chem. Phys. Lett. 7* (1970) 428; c) G. Bieri, J. D. Dill, E. Heilbronner, J. P. Maier, J. L. Ripoll, *Helv. Chim. Acta 60* (1977) 629.

[14] A. D. Baker, C. Baker, C. R. Brundle, D. W. Turner, *Int. J. Mass Spectrom. Ion Phys. 1* (1968) 285; C. R. Brundle, M. B. Robin, H. Basch, M. Pinsky, A. Bond, *J. Am. Chem. Soc. 92* (1970) 3863; G. R. Branton, D. C. Frost, T. Makita, C. A. McDowell, I. A. Stenhouse, *J. Chem. Phys. 52* (1970) 802; C. R. Brundle, D. B. Brown, *Spectroschim. Acta A 27* (1971) 2491; R. Stockbauer, M. G. Inghram, *J. Electron Spectrosc. 7* (1975) 492; J. E. Pollard, D. J. Trevor, Y. T. Lee, D. A. Shirley, *Rev. Sci. Instrum. 52* (1981) 1837.

[15] Cf. [11a], p. 245ff.

[16] Electronic states such as the pure configurations (1) which diagonalize the electronic part of the molecular Hamiltonian only for a specific nuclear geometry are called diabatic states. For an illustrative discussion, see reference [7c].

[17] Normal coordinates are derived from regular coordinates by a standard transformation cf. E. B. Wilson, J. C. Decius and P. C. Cross: *Molecular Vibrations*, McGraw-Hill, New York, 1955). In the present work we use dimensionless normal coordinates which are obtained from the normal coordinates by multiplication by $(\omega/\hbar)^{1/2}$. In the one-dimensional case the dimensionless normal coordinates are related to regular coordinates by $(\mu\omega/\hbar)^{1/2}$, where $\mu$ is the reduced mass of the atoms performing the motion and $\omega$ is the frequency.

[18] In the original formulation in [9a, b] the normal coordinates are replaced by boson operators b and $b^+$, with $Q=(b+b^+)/\sqrt{2}$. When comparing with the previous work all values of the coupling constants must therefore be divided by the factor $\sqrt{2}$.

[19] a) F. Bernardi, W. Cherry, S. Shaik, N. D. Epiotis, *J. Am. Chem. Soc. 100* (1978) 1352; N. D. Epiotis, R. L. Yates, S. Shaik, W. Cherry, F. Bernardi, *Top. Curr. Chem. 70* (1977) Chapter 1; b) R. S. Mulliken, *Tetrahedron 5* (1959) 253; c) A. J. Merer, R. S. Mulliken, *Chem. Rev. 69* (1969) 639.

[20] For example in $O_2^+$: H. Köppel, unpublished.

[21] The first form, eq. (7a), allows estimation of the coupling constant in a simple way from the overlap of the $\pi$ orbital with the slightly rotated $\pi_{CH_2}$ orbital. The second form, eq. (7b), is advantageous for numerical computations since only energies and no wave functions are needed.

[22] According to Koopmans' theorem, the ionization potentials are given up to first order in the electron interaction by the negative values of the orbital energies from which the ionization occurs (cf. T. Koopmans, *Physica 1* (1933) 104).

[23] H. C. Longuet-Higgins, *Proc. R. Soc. London A 344* (1975) 147.

[24] L. S. Cederbaum, W. Domcke, *Adv. Chem. Phys. 36* (1977) 205.

[25] Throughout the computations, the spectrum of $C_2D_4$ was calculated along with the experimental spectrum; the results compare favorably with the observations.

[26] Cf. D. J. Bellville, N. L. Bauld, *J. Am. Chem. Soc. 104* (1982) 294, and references cited therein.

[27] One might wonder why extensive ab initio calculations came short of reproducing the nonplanarity of the cation. We believe one reason has to do with the variational treatment, during which the energy of the lower cationic state $^2B_{2u}$ is minimized and, simultaneously, the energy of the higher state $^2B_{2g}$ becomes much too high. Since the geometry of the cation depends on the coupling of these two states, then the ab initio treatment would tend to underestimate their mixing, leading to a planar cation.

[28] The Franck-Condon principle is the common tool in optical spectroscopy to assign the vibrational structure of electronic bands [7d]. It requires that the nuclear motion proceeds on a single potential energy surface before and after the electronic transition. The relative vibrational intensities are approximated by the squared overlaps of the vibrational wave functions of these surfaces. See reference [7d] for more details and many examples.

[29] H. Köppel, *Chem. Phys.*, in press.

[30] Cf. *e.g.* [2b] and E. R. Davidson, *J. Am. Chem. Soc. 99* (1977) 397; G. G. Balint-Kurti, R. N. Yardley, *Chem. Phys. Lett. 36* (1975) 342; C. F. Jackels, *J. Chem. Phys. 72* (1980) 4873; M. Descouter-Lecomte, C. Galloy, J. C. Lorquet, M. Vaz Pirez, *ibid. 71* (1979) 3661.

[31] a) J. P. Maier, *Angew. Chem. 93* (1981) 649; *Angew. Chem. Int. Ed. Engl. 20* (1981) 638; b) *Acc. Chem. Res. 15* (1982) 18; c) J. P. Maier, O. Marthaler, G. Bieri, *Chem. Phys. 44* (1979) 131; d) M. Allan, E. Kloster-Jensen, J. P. Maier, *J. Chem. Soc. Faraday Trans. II 73* (1977) 1406.

[32] For a discussion of substituent effects cf. N. D. Epiotis, R. L. Yates, S. Shaik, W. Cherry, F. Bernardi, *Top. Curr. Chem. 70* (1977). See also the energy level correlations in [11a], p. 244ff and 261ff.

[33] M. B. Robin: *Higher Excited States of Polyatomic Molecules*, Academic Press, New York 1974; J. H. D. Eland: *Photoelectron Spectroscopy*, Butterworth, London 1974; C. R. Brundle, M. B. Robin, N. A. Kuebler, H. Basch, *J. Am. Chem. Soc.* **94** (1972) 1466; M. B. Robin, N. A. Kuebler, C. R. Brundle in D. A. Shirley: *Electron Spectroscopy*, North Holland, Amsterdam 1972, p. 357; cf. also [11d].

[34] J. A. Sell, A. Kuppermann, *J. Chem. Phys. 71* (1979) 4703.

[35] a) D. A. Demeo, M. A. El-Sayed, *J. Chem. Phys. 52* (1970) 2622; b) P. Masclet, D. Grosjean, G. Mouvier, J. Dubois, *J. Electron Spectrosc. 2* (1973) 225; c) P. D. Mollere, K. N. Houk, D. S. Bomse, T. H. Morton, *J. Am. Chem. Soc. 98* (1976) 4732; d) F. Gerson, J. Lopez, A. Krebs, W. Rüger, *Angew. Chem. 93* (1981) 106; *Angew. Chem. Int. Ed. Engl. 20* (1981) 95.

[36] D. W. Scott, H. L. Finke, J. P. McCullough, M. E. Gross, J. F. Messerly, R. E. Pennington, G. Waddington, *J. Am. Chem. Soc. 77* (1955) 4993.

[37] D. M. Mintz, A. Kuppermann, *J. Chem. Phys. 71* (1979) 3499.

[38] The experimental spectrum [35c] does not allow for a final answer to the problem, since the spectrometer resolution was too small to resolve a torsional progression with a spacing of only $\approx 165\ cm^{-1}$.

[39] M. Kasha, *Discuss. Faraday Soc. 9* (1950) 14.

[40] For initial attempts along similar lines see: S. S. Shaik, "The role of geometric distortions along the reaction coordinate. Transition State Structure in $S_N2$ reactions", unpublished.

# Linear Control of Temperature with Time—A New Approach to Reaction Kinetics

By Erhard Koch*

The temperature dependence of the rate of chemical reactions has been known for a long time; very often it is characterized by the Arrhenius plot. However, kinetic methods that take this phenomenon into account in *one* measurement in a planned manner have been applied to reactions in solution only in isolated examples—with the exception of the temperature jump method developed by *Eigen et al.* for fast reactions, based on a stepped temperature program. A mathematical analysis, however, reveals to the chemist that from the point of view of information theory the course of the reaction rate *versus* time under conditions of constantly increasing temperature is the measured signal which should lead to the most effective understanding of the reaction mechanism. Analysis of the measured peaks, which may overlap, allows the characterization of reactions either in the solid state or in solution by "mechanistic coordinates", which extend the concept of reaction order. Their behavior allows further experiments to be planned, enabling elementary steps to be eliminated. Each reacting system can be characterized kinetically by one series of experiments using different starting concentrations for each reactant and, additionally, using different heating rates. The experimental verification of these considerations can be seen in *ca.* 1400 DTA and UV experiments for *ca.* 120 different systems. Furthermore, the example of the oscillating Belousov-Zhabotinsky reaction shows that "fast" reactions frequently may also be recognized. A test for proposed reaction mechanisms is provided by integration programs which allow immediate comparison between experimental and theoretical signal curves.

## 1. Introduction

For several years the field of reaction kinetics has been undergoing far-reaching changes[1]. This branch of research—supported by mathematics—aims at providing an understanding of the mechanisms of complex chemical reactions. Recently, bifurcation theory, stability analysis, reaction kinetics at low temperatures, self-organization of reaction mechanisms[2], and nonlinear irreversible thermodynamics have provided novel contributions. In addition, the development and miniaturization of computers have improved the mathematical tools decisively: now, simulation of processes in proposed networks[3,8]—in futurology this is even used to construct global models[4]—can also be considered as an efficient new tool for the chemist, since analytical solutions are no longer required[5,6]. Nowadays processes involving some hundred elementary steps can be computed in advance[7].

In order to take full advantage of these possibilities in chemical kinetics we require the development of new experimental methods which allow systematic solution of the central problem of "inverse reaction kinetics"[8], *i.e.* the determination of the underlying reaction mechanism and the activation data for all elementary steps from an experimental signal curve.

Alternatives to currently preferred isothermic kinetic methods are techniques using temperature programs[9-15], termed "thermoanalytical methods"[10,16,17]. These are superior to the isothermal techniques in many respects, especially for the economical description of processes in natural or artificial surroundings, since they provide data on a reaction over the complete range of temperature using only *one* experiment. For a *linear* increase of temperature with time, the reaction mechanism may be displayed in a "mechanistic diagram"[3,18-21]. The verification of this concept, even for complicated mechanisms having fast partial steps, appears to be a promising method of solving the problem of inverse reaction kinetics.

Thermoanalytical methods are usually used for heterogeneous reactions in the solid state, but less frequently for the homogeneous organic reactions in solution discussed here; with solids, mechanisms based on topochemical considerations occur. The efficiency of these methods was shown by their application to exotic problems, such as the pyrolysis of lunar samples or the study of the thermostability of atomic waste dumps. This article, therefore, also discusses the application of the theory of mechanistic coordinates to heterogeneous kinetic models[21,24], and thereby reveals astonishing kinetic selectivity.

## 2. Signals and Measurement Methods

A suitable measure for the progress of a reaction is its rate $v$. An unknown chemical reaction can be more effectively interpreted by considering the *derivative* instead of the *integrated conversion* curves[11,25-31].

If in a system with $p$ elementary processes the temporal change $y$ of a quantity $x$ is followed, it is found for many measurement methods that

$$y(t) = \frac{dx}{dt} = \sum_{i=1}^{p} y_i(t) = \sum_{i=1}^{p} \lambda_i \cdot v_i(t) = \sum_{i=1}^{p} \lambda_i k_i \cdot \pi_i \qquad (1)$$

[*] Dr. Erhard Koch
Max-Planck-Institut für Strahlenchemie
Stiftstrasse 34—36, D-4330 Mülheim a. d. Ruhr 1 (Germany)

 © *Verlag Chemie GmbH, 6940 Weinheim, 1983* *0570-0833/83/0303-0225 $ 02.50/0* 

The quantities $\lambda_i$ are indication parameters containing the complete change of the property $x_i$ ($=x_{\infty i}-x_{0i}$) in the partial step i for the selected method. Thus, in a volumetric measurement $\lambda_i$ is the number of moles of evolved gas; in the measurement of UV extinction $\lambda_i$ is the product of layer thickness and extinction coefficient. The $\lambda_i$'s may depend on temperature (*e.g.* reaction enthalpies in calorimetric and extinction coefficients in spectroscopic methods). They are *exactly* constant only for methods based upon the change of numbers of moles (*e.g.* gas volumetry, mass spectroscopy, thermogravimetry[32]).

The products $k_i \pi_i$ are the mass-action terms for the elementary processes i, and characterize the internal kinetic processes. It applies

1. To an unimolecular step A $\longrightarrow$ products: $\pi_i=[A]_i$
2. To a bimolecular step A + B $\longrightarrow$ products: $\pi_i=[A]_i \cdot [B]_i$

The time-dependences of the concentrations (terms $\pi_i$) can be found by integration of the basic set of differential equations. The graphic representation of the course of the reaction for each reaction path consists in the *isothermic case* of a monotonically decreasing curve (Fig. 1). The maximum height of the signal *i.e.* the initial value of the reaction rate cannot be exactly determined experimentally, since in first-order reactions the system must be heated to the reaction temperature, whereas in a bimolecular reaction the second reactant has to be added. The adjustment of temperatures and of the concentrations thus leads to time delays and to errors in the temperature. Further, the *final part* of the isothermal curve, indispensable for formal kinetic reasons, cannot often be used because of long reaction times, especially for second-order reactions.

Measurements in which the temperature is increased in a *defined way* are much more suitable than isothermal measurements: If only the temperature coefficient differs significantly from unity, a bell-shaped reaction signal is shown, which has a defined beginning given by the first deviation from the base line and corresponds to the lowest characteristic initial temperature (cf. Section 3.1). Furthermore, both the maximum and final temperatures contain a considerable amount of information; the final temperature is reached much faster than in isothermal experiments because of the monotonically increasing rate constants (Fig. 1). These temperatures, and the width and asymmetry of this signal characterize kinetic properties.

Under conditions of *programmed temperature increase* eq. (1) is valid without limitations if the dependence of the $\lambda_i$'s on temperature is considered. The rate coefficient $k_i$ is given approximately by the Arrhenius equation

$$k_i = k_{\infty i} \exp(-E_i/RT) \tag{2}$$

## 3. Nonisothermal Reaction Kinetics of Elementary Processes

In developing analytical relationships for *temperature-programmed* runs of chemical reactions it is found that a *linear increase of the temperature of the system with time* leads to especially useful criteria for the reaction analysis by mathematical expressions. Because of linear superposition of the individual signals [eq. (1)] complex processes can be described comparatively readily thus simplifying the precalculations and analyses performed by computer.

### 3.1. Specific Time and Specific Temperature Differences

The advantages of a linear increase of temperature with time can be shown by some striking empirical rules found for *elementary first-order signal curves*.

Under homogeneous conditions the temperature program $T=T_0+mt$ affords the following derivative conversion curve when the Arrhenius equation (2) applies:

$$v(t)=k(T)[A]=k_\infty [A]_0 \exp\left[-\varepsilon/t - k_\infty \int_0^t \exp(-\varepsilon/\xi)\,d\xi\right] \tag{3}$$

$$\varepsilon = \frac{E}{m \cdot R} = \text{relative activation energy}$$

$m$ = heating rate

The term $\exp(-\varepsilon/t)$ describes the initial slow growth of the signal curve, determined by the increasing rate coefficient $k(t)$. The integral term is decisive for the later decay because of consumption of reactant A.

The lower limit of the time integral in eq. (3) corresponds to a temperature of absolute zero. The integral can be split into two partial integrals (limits $0/t_0$ and $t_0/t$, see Section 3.2) by introducing the time $t_0$ for the start of the signal; compared to the second integral, the first can be neglected. In the following discussion, the time $t$ refers to the time if the measurement were to have started at absolute zero.

No explicit analytical expression exists for the time integral[34–37]. However, introducing an unknown time function $u(t)$

$$\int_0^t k(t)\,dt = u(t)k(t) \tag{4}$$

and using an approximate solution for $\int k(t)\,dt$, arrived at by series expansion of the so-called exponential integral, and neglecting all terms higher than the second[37–39], gives:

$$\int_0^t k(t)\,dt = \frac{RT^2}{m \cdot E} k(t) = \frac{t^2}{\varepsilon} k(t) \tag{5}$$

Comparison of eq. (4) with eq. (5) and introduction of $T$ from eq. (2) gives

$$u(t) \approx \frac{RT^2}{m \cdot E} = \frac{t^2}{\varepsilon} = \frac{E}{Rm(\ln k_\infty - \ln k(t))^2} \tag{6}$$

At the maximum of the curve, the product of $u(t)$ and $k(t)$ is unity, since the term in brackets in the derivation of eq. (3) disappears

$$\begin{aligned} dv/dt &= [A]_0 \left(\frac{\varepsilon}{t^2} - k\right) k \exp(-uk) \\ &= [A]_0 \left(\frac{1}{u} - k\right) k \exp(-uk) \end{aligned} \tag{7}$$

By including the approximation equation (6), which is exact for high frequency factors $k_\infty$, $u(t)$ at the maximum ($=u_m$) may be iteratively computed from the activation parameters and the heating rate:

$$u_m = \frac{E}{R m (\ln k_\infty + \ln u_m)^2} \tag{8}$$

where $u_m$ has the dimension of time. Since this parameter allows the computation of all interesting signal features we term it the "specific time". In eq. (8) the product of $u_m$ and the heating rate $m$ is specific for each reaction ("specific temperature difference"). It depends only on activation parameters; the term $\ln u_m$ in eq. (8) functions only as a correction term.

The significance of the *specific time* may be compared with that of the *half-time* in isothermal kinetics (Fig. 1): In an isothermal rate law the product $k \cdot t$ in the exponential term determines the course with time; for the nonisothermal case it is substituted by the product $u \cdot k$. The role of the independent variable "time" is formally assumed by the rate "constant", which now becomes a time-dependent variable.

Compared with the enormous variations in $k$, the factor $u$ is nearly constant; with a linear heating rate it is more characteristic of the reaction than an isothermal rate constant, since it comprises the complete range of the experiment. Along with the initial temperature and the peak temperature it unequivocally describes all the characteristics of the signal of an elementary reaction.

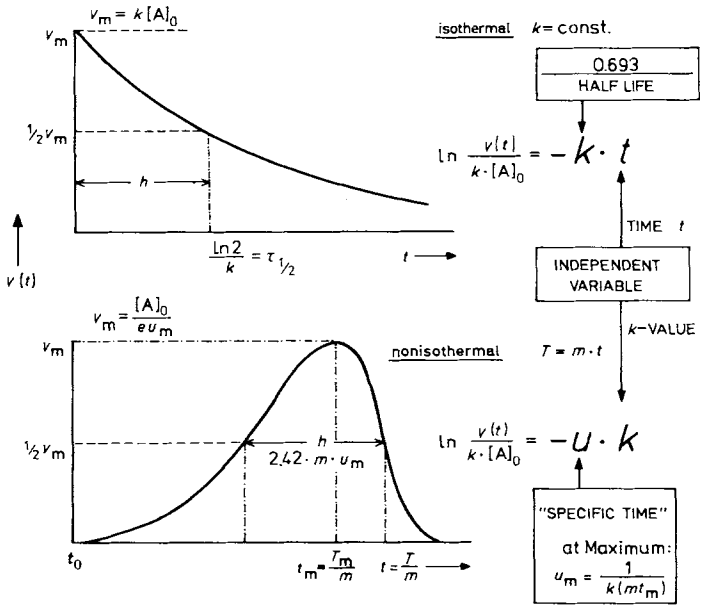



Fig. 1. First-order isothermal and nonisothermal rate laws and their corresponding rate signals.

### 3.2. Onset and Height of a Signal

The height of a peak follows directly from eq. (3) and eq. (5) with $k_m = 1/u_m$

$$v_m = [A]_0/e u_m \quad (e = 2.71828\ldots) \tag{9}$$

The initial time $t_0$ and temperature $T_0$ of the observed signal follow from the first observed deviation from the base line (threshold $\chi = v(t_0)/v_m = 0.5\%$)[37] from

$$k(t_0) = k_\infty \exp(-\varepsilon/t_0) = k_\infty \exp(-E/RT_0) = \chi/e u_m \tag{10}$$

### 3.3. Half-Width, Peak-Width, and *M* Index

The importance of the half-width for the determination of the mechanism follows from the introduction of a temperature difference $\Delta T$ in the Arrhenius equation:

$$\Delta T = T_2 - T_1 = \frac{E \cdot \ln(k_2/k_1)}{R(\ln k_\infty - \ln k_1)(\ln k_\infty - \ln k_2)} = \frac{E \cdot \ln(k_2/k_1)^2}{R(\ln k_\infty - \ln \hat{k})^2} \tag{11}$$

where $k_1$ and $k_2$ are the rate coefficients for $T_1$ and $T_2$ and, according to the mean value law, $\hat{k}$ lies between $k_1$ and $k_2$. For all striking temperature differences $\Delta T$ (such as half-width $h$, signal-width, distance between the two points of inflection) and *linear increase of temperature*, the quotient $k_2/k_1$ becomes almost independent of the activation parameters of the elementary reaction under consideration[37,40]. Hence, assuming $\Delta T = h$ the ratio

$$M = \frac{E}{h(\lg k_\infty - \lg \hat{k})^2} = \frac{R}{\lg^2 e \ln(k_2/k_1)} = \frac{m u_m R}{h(\lg e)^2} \tag{12}$$

which we term "*reaction type index*"[20,37,41] also becomes invariant. If $\hat{k}$ is viewed as the reciprocal specific time $u_m$ defined by eq. (8), then all typical differences of temperature and time become proportional to this quantity:

$$\Delta T = m \Delta t = m \ln(k_2/k_1) \cdot u_m \tag{13}$$

### 3.4. Reactions of n-th Order

The term "reaction of n-th order" is considered here as a process, whose reaction rate may be formally supposed to be proportional to the power n of only *one* concentration ($-\mathrm{d}[A]/\mathrm{d}t = k \cdot [A]^n$). This definition is more restricted than usual. Its existence is based on the possibility of substituting all other variable concentrations of the rate law by a *single one*.

It will be shown here that only this *scheme of order* based on a mathematical formalism enables a satisfactory discussion and classification of the kinetic phenomena. The factor of proportionality $\ln(k_2/k_1)$ follows from computer simulations[44] for a reaction of n-th order (unit concentration of the reactants) as

$$\ln(k_2/k_1) \approx 2.25 \times n^{0.52} = \begin{matrix} 2.25 \pm 0.04 & \text{(first-order)} \\ 3.23 \pm 0.14 & \text{(second-order)} \end{matrix} \tag{14}$$

The complete signal width is given by

$$n = 1: \ \ln \frac{k_2}{k_1} = 2.9 - \ln \chi \tag{15}$$

$$n \neq 1: \ \ln \frac{k_2}{k_1} = n \ln \frac{n}{n+1} + (n-1) \ln [A]_0 - n \ln \chi \tag{16}$$

During registration of the "bell signal" and with $\chi = 0.5\%$, the rate coefficient for a first-order elementary process always increases by three, however, for a second-order process by as much as five orders of magnitude[37]. An additional value typical for the reaction order[20] is the "shape index" which characterizes the asymmetry of the peaks. It was introduced by *Kissinger*[9,42,43] some thirty years ago. For $n > 1$ Kissinger's formula shows increasing deviations from reality. We, therefore, developed a general empirical relationship (for $0.6 < n < 10$) by computer simulation. For $n = 1$ and $n = 2$ it has also been successfully verified experimentally[44].

$$S = \frac{n^2(1.21 + 0.21n)}{n^2 + 1.59} (\approx 0.63n^2 \text{ for } n < 1)^{[43]} \quad (17)$$

The shape index $S$ and the reaction type index $M$ have proved to be especially valuable in characterizing complex processes. We therefore term these quantities "mechanistic coordinates".

## 4. Signals of Complex Processes

### 4.1. Series of Reactions

By reaction mechanism we mean the combination of all the elementary steps involved in the conversion of the educt (or educts) into the final product(s). When considering the most simple "mechanisms" of a system that contains only *two elementary processes* of first-order (EP1; index 1) we have to discuss four elementary types

1. Reactions with *consecutive* coupling (consecutive reactions F11). The second reaction can only occur after the first.
2. Reactions with *concurring* coupling (concurrent reactions P11). Both reactions proceed from the same educt(s), and each individual reaction reduces the rate of the other.
3. Reactions with *reversible* coupling (opposing reactions G11). The educt can be re-formed from the product.
4. *Uncoupled* reactions (independent reactions U11). Two different reactions step from two different educts (or pairs of educts), possibly yielding the same product.

If reactions of second-order (index 2) or of the bimolecular AB type (index $\bar{2}$) are also taken into consideration, *concurring consecutive* reactions (F1a, F2a, F$\bar{2}$a), in which the final product reacts again with the educt, and *autocatalytic* reactions (1a), in which product makes the reaction possible by acting as bimolecular, but unchanged reactant, ensue as special cases.

### 4.2. Nonisothermal Classification Criteria

The bell shape of the signals described yields a number of classification criteria for complex reactions (Table 1).

Table 1. Criteria for the interpretation of derivative signals of complex processes. The indication parameters $\lambda_i$ of the continuing processes [eq. (1)] must have the same sign. EP1 = elementary process of 1st order, P22 = two parallel processes of 2nd order, etc. (cf. Table 6).

| No. | Quantity | Behavior/Interpretation | | | Remarks |
|---|---|---|---|---|---|
| Whole curve | | | | | |
| 1 | Number of peaks | is smaller than or equal to the number of elementary steps; is equal to the number of slower successive steps | | | Competing processes show only one peak |
| Isolated Signals [19, 45] | | | | | |
| 2 | Sign of the signal | Change of sign | ⇒ | Opposing reactions with $\vec{E} > \vec{E}$ | Peak pairs |
| | | | | *Corresponding processes?* | |
| 3 | Initial temperature $T_0$ of a peak (relative to $\chi$, eq. [10]) for sinking initial concentration of the reaction-determining reactant | remains constant | ⇒ | type: EP1 or P11 | Only when cross-terms or catalytic processes are absent: $T_0$ characterizes the reaction which forms the basis of the peak; $\theta_m$ characterizes |
| | | converges to a limiting value | ⇒ | type: P12 | |
| | | increases without limit | ⇒ | type: EP2 or P22 | |
| | | | | *Previous processes?* | the kinetic flux at this point of the reaction scheme, *i.e.* previous reactions! |
| 4 | Relative signal height $\bar{\theta}_m$ for sinking initial concentration of the reaction-determining reactant | remains constant | ⇒ | no or unbranchend reaction sequence or branches of type | |
| | | converges to a limiting value | ⇒ | continues by unimolecular steps of type P12 branches | |
| | | disappears | ⇒ | continues by at least *one* bimolecular step of P12 branching | |
| Overlapping signals | | | | | |
| 5 | Shape index $S$ [a] | constant = $S_1$ or $S_2$ | ⇒ | EP1/2 (if also $M = M_{1(2)}$) | Only for linear temperature increase: $M$ from eq. (12) [11, 13, 33, 46], cf. Table 6 and [20]. |
| 6 | Reaction type index $M$ [a] | constant = $M_1$ or $M_2$ | ⇒ | EP1/2 (if also $S = S_{1(2)}$) | |

[a] To be extrapolated to absent thermal feedback [44,48]; $M_1 = 0.0019$, $M_2 = 0.0013$ kJ/mol/K; $S_1 = 0.58$, $S_2 = 1.15$.

*Isolated peaks* are specifiable kinetically by the dependence of the initial temperature on concentration (see eq. (10). The relative signal height gives information on possible branching reactions (cf. Fig. 1).

### 4.3. The Mechanistic Diagram

In order to characterize more distinctly a single, possibly overlapped peak, a "mechanistic diagram", obtained by plotting the reaction index $M$ versus the shape index $S$, may be used. All mechanistic points corresponding to a reaction of n-th order should, because of the validity of equations (12), (14), and (17), lie on a universal decreasing curve[47]. The simplest complex reactions, which consist of the fundamental mechanisms of the P, F, G, and U type, respectively, show typical regions that include the source points for elementary processes of first and second order[3, 19, 20].

The "mechanistic coordinates" $M$ and $S$ appear to be equivalent for the kinetic diagnosis, however, they yield different kinds of information. This follows from the different methods used for their determination. The $S$ factor may be extracted directly from the derivative conversion curves[43], whereas the computation of the $M$ index requires a reference reaction. A plausible method of relating $M$ to the activation parameters of the initiating reaction[19, 20, 45, 49] leads to errors at the onset of the signal curve because of the noise level. If gross activation data are used to determine $M$ then the optimizing criteria become more important as the reaction increases in complexity. Depending on the definition of the reference reaction, different patterns of the "mechanistic regions" relative to the $M$ axis follow (cf. Fig. 9a/b).

## 5. Evaluation of Differential Curves

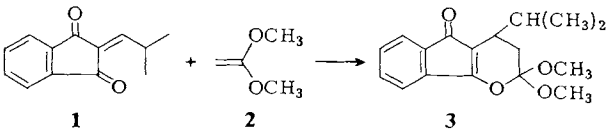
### 5.1. Conversion Curves of Elementary Processes

The rate coefficient for the rate law of a reaction of n-th order is given by

$$k(T)=k(m\cdot t)=\frac{v(t)}{\left(\int_0^\infty v\,\mathrm{d}t-\int_0^t v\,\mathrm{d}t\right)^n} \qquad (18)$$

The temperature dependence of $k$ yields the order n and the activation parameters. Since for elementary processes in homogeneous kinetics n is only 1 or 2, and less usually 3 (collision reactions of neutral molecules in the gase phase), it was not optimized. A noninteger value of n may formally characterize a complex process, but is irrelevant for mechanistic considerations. For n = 1 and n = 2 (or a reaction A + B → products; AB type[47, 50]) it may be tested which of these proposals affords the best approximation. For this purpose the complete curve (net data) as well as the first 25% of the curve (initial data, cf. Section 7.2) were used.

The method of evaluation may be tested directly *e.g.* by temperature-programmed UV reaction photometry at a fixed wavelength[51–54]. In order to evaluate equipment specifically developed for this purpose[55], we used a reaction that had been previously studied isothermally[56], the 1,4-addition of isobutylideneindanedione **1** to 1,1-dimethoxyethene **2**, which was performed pseudo-unimolecularly in presence of a large excess of **2**.




**1** **2** **3**

The computer calculation[50, 55] using eq. (18) affords a satisfactory Arrhenius plot ($r = 0.9956$) for the recorded curve of the extinction change at 392 nm, corresponding to an activation energy of 41.8 kJ/mol and an $A$ factor of $4.05 \times 10^{-5}$ $M^{-1}$ $s^{-1}$: isothermal reaction spectroscopy in toluene gave 40.9 and $3.23 \times 10^4$, respectively, and in acetonitrile 44.9 and $3.03 \times 10^7$, respectively[56]. Since the polarity of ether lies between that of toluene and of acetonitrile, our new result may be considered reasonable. With DTA we found that increasing the concentration of **1** by a factor of 1000 gave values of 53.2 kJ/mol and $4.28 \times 10^7$ $M^{-1}$ $s^{-1}$.

Hitherto, eq. (18) has been applied to thermoanalytic data from solid samples (thermogravimetry, differential scanning calorimetry). Under these conditions local variations in the temperatures or in the concentrations frequently cause difficulties[57, 58].

### 5.2. Kinetic Measurements by Differential Thermal Analysis

To experimentally verify the relationships and rules found for nonisothermal conditions[13, 48, 60, 107] we have usually preferred a special form of differential thermal analysis (DTA)[61, 62], which can also be used as a thermokinetic method[59]. The signal, the temperature difference $\theta(t)$ between sample and a reference material, can be viewed as a delayed differential conversion curve with delayed decay. Eq. (1) can be applied directly only in the limiting case of an infinitely high cell constant $c$, under which conditions no measurable temperature difference occurs[44]. Generally, for equipment with uniform temperature distribution eq. (19) applies

$$\frac{\mathrm{d}\theta}{\mathrm{d}t}=\frac{V}{c\cdot C_p}\sum_{i=1}^{P}\frac{\mathrm{d}q_i}{\mathrm{d}t}-c\,\theta(t)=\frac{V}{c\cdot C_p}\sum_{i=1}^{P}\Delta H_i v_i(t)-c\,\theta(t) \qquad (19)$$

$V$ is the volume of the sample and $C_p$ its heat capacity.

The total heat flow $\dot{Q}=\sum\dot{q}_i$ generated by the reaction can, according to eq. (1), be represented as the sum of the products of the reaction rates $v(t)$ and the enthalpies $\Delta H$ in the individual branches of the reaction scheme[33, 40, 41].

DTA is often used uncritically in studies of the solid state[13, 57, 63] where it is assumed that the measured signal[43, 64, 69, 70] $\theta(t)$ and reaction rate according to eq. (1) are synchronous. This is generally inadmissible and can only yield the approximately correct kinetic data in individual cases by compensation of opposing errors, *e.g.* inhomogeneities in temperature[65, 66]. In the solid state or in nonstirred solutions the spatially complex interrelations of reaction and transport processes preclude an exact and

straightforward evaluation. For our studies we therefore developed an *apparatus for DTA studies of solutions,* in which a stirring device guarantees satisfactory validity of eq. (19)[48,59,60,67]. Assuming different cell constants $c$ and various maximum differences in temperature, our model computations have led to several empirical approximation equations, which can even be worked out on a simple pocket calculator. Thus, the typical mechanistic coordinates of a reaction [cf. eqs. (11) and (12)] can be expressed in terms of the ideal values of the reaction rate curve which corresponds to a DTA curve with infinitely high $c$ and, hence, to a vanishing temperature difference[44,47].

A DTA plot can be evaluated by comparison with a theoretical curve, by use of reaction rates computed by means of eq. (19) or, more easily, using an equation reported by *Botchardt* and *Daniels*[68] that gives $k(t)$ directly[69,70].

Using our DTA equipment we have studied many processes that proceed practically *via* one elementary step, and have always observed good agreement with activation parameters determined isothermally[69-71]. Furthermore, the experimental signal curves could be readily reproduced from these values by numerical integration.

### 5.3. Conversion Curves of Complex Processes

The large number of kinetic phenomena from isothermal reaction kinetics are further increased by the influence of one controlling parameter, the heating rate; such a variety can only be made fully comprehensible and rendered useful for reaction analysis using a computer[3,11,13,41,44,46,47]. We use three different types of computer programs (cf. Fig. 2)[19,40,70]:

1. Evaluation programs which accept and calculate the various kinds of data from the experimental curves under the assumption of an elementary step. The results are optimized activation parameters and related kinetic data such as the mechanistic coordinates.
2. Simulation programs which, starting from a kinetic model or from data predetermined by an evaluation program, calculate a theoretical signal curve, and compare this with experimental curves.
3. Search programs which extract data for the given combination of reactants (systems) and for given ranges of the selected parameters from an experimental library. From the tabulated series produced, any input and/or results' parameters can be mutually compared and displayed graphically.

#### 5.3.1. *Pre-evaluation Assumpting an Elementary Process*

The experimental curves should first be evaluated assuming an *elementary* step, because calculation of the reaction type index $M$ requires the activation data of a reference reaction. If one is dealing with an elementary reaction, then the real activation data are produced. For a complex process indications of how to split the curve into elementary signals are provided[20] (cf. Section 6.3). The behavior of the mechanistic coordinates strongly limits the possible types of reactions (cf. Section 4.3).

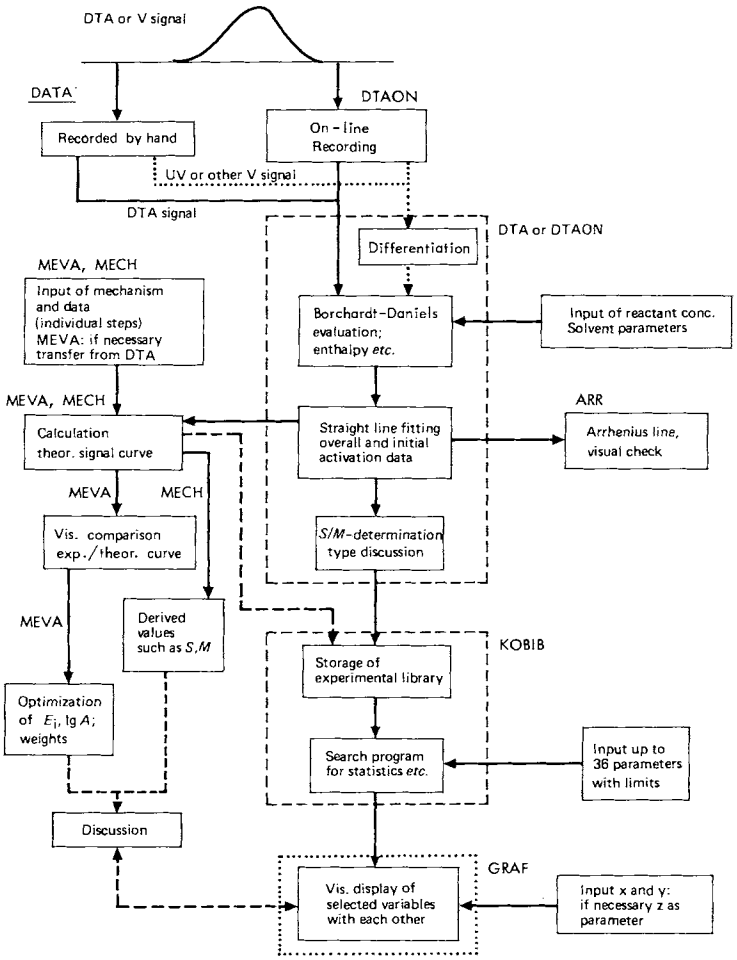



Fig. 2. Scheme for data processing and data compilation.

#### 5.3.2. *Isolated Signals*

When a number of *isolated* peaks is present, which only overlap at a particular range of reactant concentrations, the kinetic criteria 1–4 of Table 1 in combination with the systematic selection of reaction partners are often sufficient to ascertain the overall mechanism. For example, in the decomposition of triphenyl phosphite-ozonide **4** in presence of triphenyl phosphite above 190 K[72,73], up to seven elementary processes can be involved. Figure 3 shows that completely different signal curves with up to four peaks can be obtained simply by changing the $(PhO)_3PO_3$ : $(PhO)_3P$ component ratio. The phosphite itself acts as a scavenger for the ozonide (reaction 1 in Fig. 3). A change in its concentration causes a shift of the peaks of bimolecular processes along the temperature axis, whereas unimolecular peaks such as the actual decomposition reaction (reaction 2; γ peak) remain unchanged in position.

As in isothermal kinetics, the influence of the starting concentrations of the reactant(s) forms the basis for the determination of the reaction mechanism.

#### 5.3.3. *Overlapping Signals*

The detailed investigation is based on the position and trends of the $S/M$ points[18,20,74] and is facilitated by comparative numerical integration.

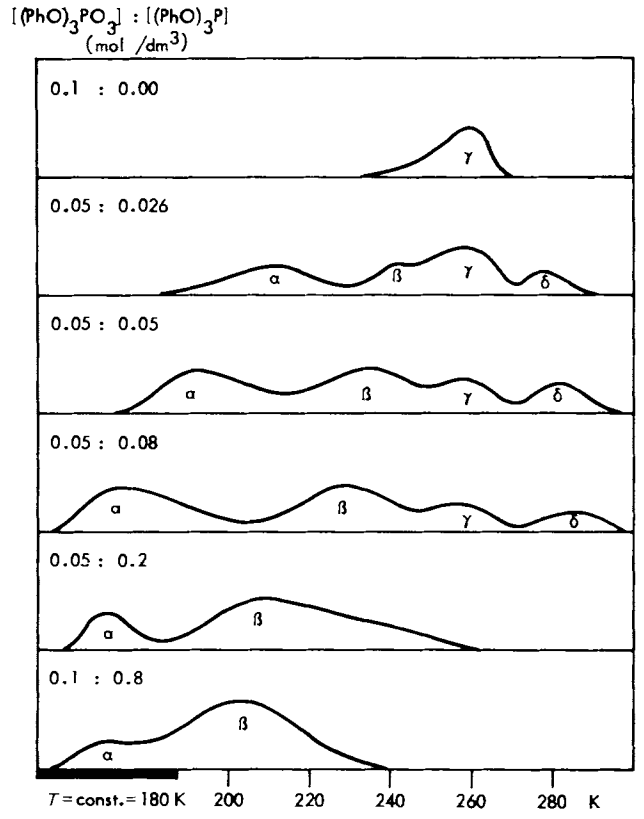


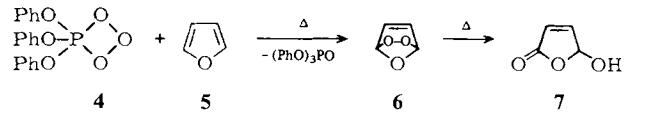

Fig. 3. DTA curves for the decomposition of triphenyl phosphite-ozonide (≙ $PO_3$) in presence of increasing amounts of triphenyl phosphite (≙ P)

Reactions:

| | | | |
|---|---|---|---|
| 1 | $P + PO_3 \longrightarrow PO_2 + PO$ | | (α-peak) |
| 2 | $PO_3 \longrightarrow PO + O_2$ | | (γ-peak) |
| 3 | $2\,PO_2 \longrightarrow PO_3 + PO$ | } | (β-peak) |
| 4 | $2\,PO_2 \longrightarrow (PO_2)_2$ | } | |
| 5 | $P + PO_2 \longrightarrow 2\,PO$ | } | |
| 6 | $(PO_2)_2 \longrightarrow 2\,PO + O_2$ | | (δ-peak) |

Computer programs which calculate the kinetic measurement curve directly from a given model allow the comparison of the proposed mechanistic model of a reaction with the real process—a procedure which was not available to classical chemistry. However, the possibilities offered by such programs[5,7,45,75] should not be overestimated. Even if one finds a suitable model for a complicated process, for example with 20 reaction steps, this still requires 60 different parameters, *i.e.* 20 activation energies, 20 frequency factors, and 20 (in some cases even more) indication parameters. Some of these parameters may be calculated from others and it may often be possible to use literature data for some of the steps. Nevertheless the remaining variation possibilities are so large that, despite progress in computer techniques, the problem of finding the appropriate reaction mechanism and the optimum values of *all the parameters* only by comparative numerical integration does not appear to have been solved for such large numbers of individual processes. On the other hand, the value of a model is only apparent when a large number of curves having different boundary conditions can be exactly reproduced, because only then have the calculated kinetic parameters sufficient significance.

Figure 4 shows the computer printout for a relatively easily understandable case with experimental (bar chart) and theoretical best fit curves (solid line) for the formation and subsequent decomposition of the ozonide-like peroxide **6**. If furan **5** is allowed to react directly with triphenyl phosphite-ozonide **4**, whose decomposition above 240 K is thought to involve singlet oxygen[71,73], then DTA curves are produced, whose simulation can be performed with the help of data given in Figure 4. Hence, in this case two consecutive processes are involved, resulting in two overlapping peaks: these correspond to the oxidation and the isomerization of the oxidation product[74,76].




4 5 6 7

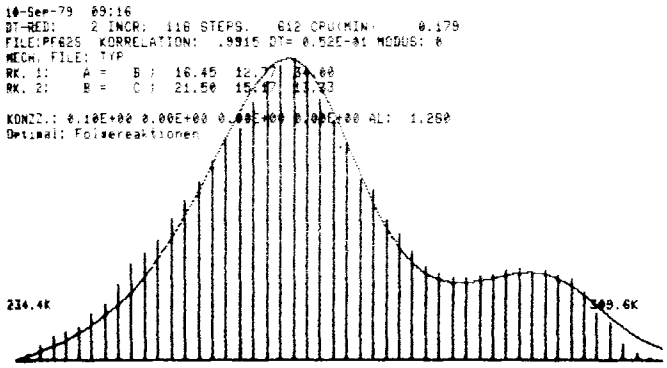



Fig. 4. Thermal formation and isomerization of epidioxidihydrofuran **6**.

Table 2 shows the data for reactions of different complexities which have been similarly determined. For those elementary processes which have been individually investigated, the activation parameters have been confirmed using the Borchardt-Daniels equation[41,70,72,74,76].

### 5.3.4. *Reactions with Fast Consecutive Steps*

The kinetics of *successive reactions* where the second step is much faster than the first are determined only by the initiating reaction. Although this may appear to be trivial, in this particular case computer simulation may often involve unacceptably long computation times.

Such problems always arise when the rate constants of the corresponding individual steps differ from one another by large orders of magnitude ("stiff" systems). Such systems are quite common in chemical kinetics, and in the last few years special application programs have been developed[5–7,75,77].

For nonisothermal simulation of successive reactions of this type, in which the second reaction continuously slows down, a transition range is observed in which the signal is split into two peaks. In particular, this splitting is of major importance for the investigation of *intermediates* which are the prerequisite for the *existence of consecutive steps*. By application of integration programs developed by *Gear*[77] to reaction systems where the second step is much faster than the first, it was found that the gross index ($M_g$) as well as initial index ($M_0$) can still show differences from the elementary values. Whereas the $S$ value shows the limiting value $S_1$ (Table 3), a variation of $\geq 5\%$ in $M$ must be considered as significant; often the $M$ value enters this toler-

Table 2. Simulation of experimental DTA curves of some complex processes between 140 and 400 K. $r$ = correlation coefficient; $E$ and $\Delta H$ in kJ/mol; $k_\infty$ in $s^{-1}$.

| Reactants | [Solvent] | Intermediates | Final products/ remarks | Type | Step | $E$ | $\lg k_\infty$ | $-\Delta H$ | $r$ |
|---|---|---|---|---|---|---|---|---|---|
| 2,5-Epidioxy-2,5-dimethyl-dihydrofuran (=A) 1:1 | Triphenyl-phosphane (=A) [Tetrahydrofuran] | — | 1,4-Diketo compounds parallel decomposition [18] | P12 | 2A→B | 58.8 | 9.03 | 330.6 | 0.9953 |
| | | | | | A→C | 37.7 | 4.95 | 450.7 | |
| (+)-Limone (excess) (=A) | $(PhO)_3PO_3$ $[CH_2Cl_2]$ | Peroxide (=B) | Various decomposition products [74] | P1a | A→B | 39.4 | 7.65 | 1044.6 | 0.9976 |
| | | | | | A+B→C | 58.5 | 9.43 | 835.3 | |
| Ozone (=A) | [Diisopropyl ether] | Trioxide (=B) Peroxides | Dimethyl ether, Ethyl methyl ether, Methyl isobutyrate [18] | F11 | A→B | 63.0 | 11.37 | 1.47 | 0.9943 |
| | | | | | B→C | 84.0 | 14.59 | 5.02 | |
| Furan (=A) | Bromine (=B) $[CH_2Cl_2/Ethanol\ (9:1)]$ | Dibromide (=C) | Tetrabromide | F$\bar{2}$1 | A+B→C | 40.2 | 6.19 | 46.9 | 0.9950 |
| | | | | | C→D | 58.6 | 9.34 | 21.8 | |
| 2,5-Epidioxy-2-chlormethyl-dihydrofuran (=A) | Methanol (=B) [Tetrahydrofuran] | Hydroperoxide (=C) | Dicarbonyl compound [18, 74] | F$\bar{2}$1 | A+B→C | 61.1 | 16.96 | 49.9 | 0.9953 |
| | | | | | C→D | 100.1 | 14.07 | 239.2 | |
| Acetone (=A) | Benzaldehyde (=B) [Methanol] | Aldol (=C) | Dehydration product | F$\bar{2}$1 | A+B→C | 95.4 | 11.72 | 23.9 | 0.9905 |
| | | | | | C→D | 122.7 | 15.42 | 26.8 | |

Table 3. Splitting of signals of successive reactions. Data for the first reaction: $E_1 = 62.5$ kJ/mol, $k_{\infty 1} = 1.67 \times 10^{10}\ s^{-1}$.

| Mechanism | $\lg k_{\infty 2} = 6.18$ | | | Deviations in % | | $\lg k_{\infty 2} = 14.18$ | | | Deviations in % | |
|---|---|---|---|---|---|---|---|---|---|---|
| | $E_2$ | $(k_2/k_1)_m$ | $S$ | $M_0$ | $M_B$ | $E_2$ | $(k_2/k_1)_m$ | $S$ | $M_0$ | $M_B$ |
| A→B→C F11 | 41.7 | 2.01 | +5 | + 4.5 | +0.5 | 75.0 | 26.2 | −2 | −13 | −11 |
| | 37.5 | 14.6 | +2 | −17 | −5 | 70.9 | 190 | 0 | − 7 | − 7 |
| | 33.3 | 106 | 0 | −14 | −3 | 66.7 | 1340 | −2 | − 3 | − 3 |
| | 29.2 | 769 | 0 | − 2 | 0 | 62.5 | $10^4$ | −5 | − 1 | − 1 |
| $A \rightarrow B \xrightarrow{+B} C$ $F_2$ | 29.2 | 769 | +2 | −28 | −6 | 58.4 | $7.3 \times 10^4$ | 0 | −24 | − 4 |
| | 25.0 | 5600 | 0 | −24 | −3 | 54.2 | $5.2\ 10^5$ | 0 | −10 | − 2 |
| | 20.8 | $1.1 \times 10^5$ | 0 | −12 | −3 | 50.2 | $3.8\ 10^6$ | 0 | − 4 | − 1 |
| | 16.7 | $2.9\ 10^6$ | +1 | − 5 | −1 | 45.8 | $2.7 \times 10^7$ | +1 | −.1 | − 1 |

ance range only when $k_2 > 10^4 k_1$. Consequently, by careful nonisothermal investigation of apparently elementary processes it is possible to obtain information about intermediates.

### 5.3.5. *Reactions with Kinetic Feedback*

The concept of the *initial reaction* of a complex process becomes problematic either if *reversible processes* lead back to the educt or if *chemical feedback systems*[23] are involved so that the educt reacts again with the product(s). Typical examples for this are oscillating reactions which can be interpreted using nonlinear *differential equation systems* and which exhibit close relationships to the thermodynamics of systems in far-from-equilibrium states and to biochemistry[23, 40, 78].

At present, the best known reaction of this type is the oscillating oxidation of malonic acid (MA) by bromate which is catalyzed by Ce salts or ferroin in presence of bromide (Belousov-Zhabotinsky reaction). *Field* and *Noyes*[79] have developed a simple model ("Oregonator") which reproduces almost quantitatively the main kinetic properties of this system, especially the oscillations:

Tentative assignment [79]

| | | |
|---|---|---|
| A + Y = X | (M1) | Formation of $HBrO_2$ from $HBrO_3^-$ and $Br^-$ |
| X + Y = P | (M2) | Termination reaction $HBrO_2$ and $Br^-$ |
| B + X = 2X + Z | (M3) | Formation of $Ce^{IV}/HBrO_2$ from $BrO_3^-$ and $HBrO_2$ |
| 2X = Q | (M4) | Disproportionation of $HBrO_2$ |
| Z = fY | (M5) | Re-formation of $Br^-$ and $Ce^{III}$ |

Net reaction fA + 2B = fP + Q
A = B = $[BrO^-]$; Y = $[Br^-]$; X = $[HBrO_2]$; Z = $[Ce^{IV}]$;
Q, P = final products = HCOOH, CO, dibromo-MA, monobromo-MA
f = number of $Br^-$ formed from two $Ce^{IV}$ ions.

This reaction (cf. [84]), many details of which have not yet been completely investigated, served as a model for the further development of nonisothermal kinetic methods[78].

Stable oscillations occur only when the system is open, *i.e.* when the reserves of bromate are maintained constant.

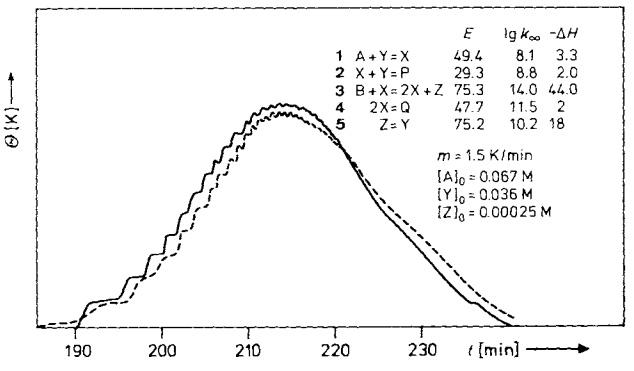



Fig. 5. Oscillating DTA curves for the Belousov-Zhabotinsky reaction: —— experimental; --- theoretical.

If, however, the reaction is carried out in a closed system, for example as in a DTA experiment, only damped oscillations occur (Fig. 5). They are mainly caused by the strongly exothermic (M3) process. For this a overall activation energy of 67 kJ/Mol has been discussed[80].

The oscillative fine structure is caused by the energy changes in the limiting cycle which is based on the variations in the maximum concentration of the $Ce^{IV}$-salt in one pass. Their visible detection in the DTA apparatus requires a much higher concentration than with UV spectroscopic or potentiometric measurements ($\approx 10^{-2}$ M instead of $\approx 10^{-4}$ M). The frequency, amplitude, and temperature position of the calorimetric oscillations are reproducible, and can be closely simulated assuming that the "Oregonator" mechanism applies (Fig. 5) when the parameters are adjusted for each experiment[78,81].

Study of the unstructured DTA signal curve provides insight into the kinetics of essential steps responsible for the consumption of bromate. In this case lower concentrations of catalyst can be used to enable comparison of the results of the isothermal experiments with those reported in the literature.

Almost half of the curves from 50 experiments with $Ce^{III}$ chloride or ferroin as catalyst could be described by simple bimolecular reactions[47,50] despite changed heating rates, bromate, and catalyst concentrations (Table 4). In contrast, a large part of the rest can be described by the following three-step mechanism[78,82,83].

| | | |
|---|---|---|
| A + B = C | (S1) | bimolecular initiation |
| A + C = 2C + D | (S2) | autocatalytic step |
| D = B + E | (S3) | regeneration of bromide |

By limiting the number of steps to three the termination reactions (M2) and (M4) are neglected, which requires the assumption of widely differing reaction enthalpies (up to 1:50, cf. Table 4). This is an indication that the three apparently elementary steps (S1)–(S3) have to be considered only as the *representative rate-determining reactions* for the more extensive part mechanisms[78,84]. A systematic analysis of fast consecutive steps should make use of the results discussed in Sections 5.3.4 and 6.2; in the meantime 24 elementary steps for this reaction have been discussed[84]. A possible solution at present would be to extend the preliminary approximate nonisothermal model by using the results obtained on the subsystems ($Br^- + BrO_3^-$, $Ce^{4+}$ + malonic acid *etc.*)[3]. It will be shown later in detail that a nonisothermal investigation offers many starting points for recognising the kinetic part-structures of a reaction mechanism.

Table 4. Kinetic data and enthalpies of the oscillating Belousov-Zhabotinsky reaction for the three-step mechanism from DTA curves (cf. text).

Unit of time: min; $[KBr]_0 = 0.053$ M
Universal activation energies: $E_1 = 49.3$, $E_2 = 79.7$, $E_3 = 41.8$ kJ/mol

11 Experiments with ferroin as catalyst
$[KBrO_3]_0 = 0.04$, 0.06, 0.075 or 0.10 M (0.10 in 5 cases); Heating rates: 0.6–1.6 K/min; correlation coefficient: $0.970 \pm 0.036$

| Step | $\lg k_\infty$ | $k_{298}$ | $-\Delta H$ (kJ/mol) |
|---|---|---|---|
| 1 | $7.59 \pm 0.34$ | 0.097 | 8–130 |
| 2 | $13.43 \pm 0.61$ | 0.33 | 6– 80 |
| 3 | $5.17 \pm 0.38$ | 0.008 | 15–197 |

7 Experiments with $CeCl_3 \cdot 6H_2O$ as catalyst; $[KBrO_3]_0 = 0.06$, 0.10, 0.12 or 0.14 M;
Heating rates: 0.5–1.5 K/min; correlation coefficient: $0.964 \pm 0.044$

| Step | $\lg k_\infty$ | $k_{298}$ | $-\Delta H$ (kJ/mol) |
|---|---|---|---|
| 1 | $7.57 \pm 0.43$ | 0.092 | 4– 15 |
| 2 | $12.93 \pm 0.39$ | 0.105 | 42–133 |
| 3 | $5.18 \pm 0.32$ | 0.008 | 72–238 |

## 6. Summary of Phenomena in Homogenous Kinetics

Using the search programs mentioned in Section 5.3 it is possible to test all the currently stored data, presently comprising *ca.* 1400 measurements on about 120 different systems (Table 5), under various aspects. In this respect, it is not only possible to search the complete data for representative samples but also to consider series of experiments determined by the type of reactant and/or by definite ranges of some 40 parameters specifying the conditions or results.

Table 5. Systems studied under nonisothermal conditions.

| |
|---|
| Unimolecular reactions |
| Decomposition of diazonium salts, triphenyl phosphite-ozonides, epidioxides, hydroperoxides, and pentazoles |
| Pseudo-unimolecular reactions |
| Addition of solvents to unstable peroxides |
| Scavenging reactions of unstable olefins with dienes |
| Oxidation of dienes |
| Quasi-elementary bimolecular reactions |
| Diels-Alder reactions |
| Reduction and scavenging reactions of peroxides and ozonides |
| Thermal oxidation reactions |
| Reaction of CH-active compounds with ozone |
| Reactions involving the formation of peroxides and trioxides |
| Bromination of peroxides |
| Benzoylation of alcohols |
| Complex reactions |
| Decomposition of sulphoxides [88], sulfides, boranes, phenylthiatriazole |
| Reactions of trioxides |
| Decomposition of peroxides, ozonides or their scavenging reactions |
| Reactions of $Fe(CO)_4$- and $Ni^0$ phosphite complexes |
| Reactions with hydrazine, diazomethane, $HN_3$, and their photoproducts |
| Catalyzed oscillative oxidations with bromate |
| Uncatalyzed oscillative oxidation of arenes with bromate [106] |
| Autocatalyzed oxidation of malonic acid with $KMnO_4$ |
| Reaction of iodate with hydrogen peroxide, also in presence of $MnSO_4$ |

When one considers the components which are present in less than stoichiometric proportions then the following reaction types appear in the proportions indicated.

1. First-order reactions (unimolecular; area 1 Fig. 9; 12%)
2. Second-order reactions (bimolecular; for different reactants, molecular proportions 1 : 1, area 2; 4%)
3. Bimolecular reactions, reactants in nonequimolar proportions (areas A and 2 after correction; 27%)
4. Complex reactions with rate law of n-th order ($n \neq 1$, $n \neq 2$; 7%)
5. Other complex reactions (areas Ø, B–H; 50%)

The given percentages should only be seen as approximate, because the results depend upon the limits which define the elementary areas (3% of the $S$ or $M$ value) and also partly upon the selection of the problem to be investigated.

### 6.1. Relationships for Elementary Processes

A *first-order reaction* which is often used for test purposes is the decomposition of benzenediazonium sulfate, formed by diazotization of aniline in acidic media at 273 K (Fig. 6a–d)[60,85]. Figure 6a shows the mechanistic points $S/M$ for all the experiments which have been carried out in the aniline concentration range $<0.5$ M and for $0.1 < m < 5$ K/min. The sensitivity of this particular method is shown by the fact that only under optimum experimental conditions (such as excess of nitrite) do the resulting $S/M$ points lie near the *first-order source point*. In addition to the reaction type, the total activation energies of approximately first-order reactions are independent of the heating rate (Fig. 6b).

If thermal feedback is not too large then the maximum recorded temperature difference of the DTA curve is proportional to the concentration of the reactants[19]; here this is the concentration of aniline used for the reaction (Fig. 6c) because diazotization proceeds practically quantitatively.

The initial temperature $T_0$ of the DTA curve and the relative signal height $(\theta_m/[A]_0)$ turn out, as expected, to be independent of the initial concentration. On the other hand $T_0$ of a *rate curve* increases monotonically *with the heating rate* because of the temperature dependence of the initial rate coefficient [eq. (10)]:

$$T_0 = m t_0 \approx \frac{E}{R(\ln k_\infty - \ln k_0)} = \frac{E}{R\{\ln k_\infty + (1 - \ln\chi) + \ln(u_m m) - \ln m\}} \quad (20)$$

For the peak temperature $T_m$, the same relationship holds, but without the term $(1 - \ln\chi)$ in the denominator. The specific temperature difference $(u_m m)$ is practically independent of the heating rate, and for the decomposition reaction it is *ca.* 7.8 K. For the DTA curves rather complicated, but formally similar expressions for the typical temperatures are found[19]. In spite of this it is possible to satisfactorily describe the observed influence of heating rate on DTA by adjusting the sensitivity limit $\chi$ in eq. (20), (Fig. 6d).

Pure *second-order signal curves* are only rarely observed. Usually the results do not exactly obey the strict nonisothermal criteria of a bimolecular reaction of the type EP2, thereby indicating side reactions[47,50]. Indeed, it follows from the law of mass action that the requirements for the quantitative course of a bimolecular reaction with a 1 : 1 ratio of the components are highly unfavorable. In this case possible competitive reactions of first order would be most highly favored.

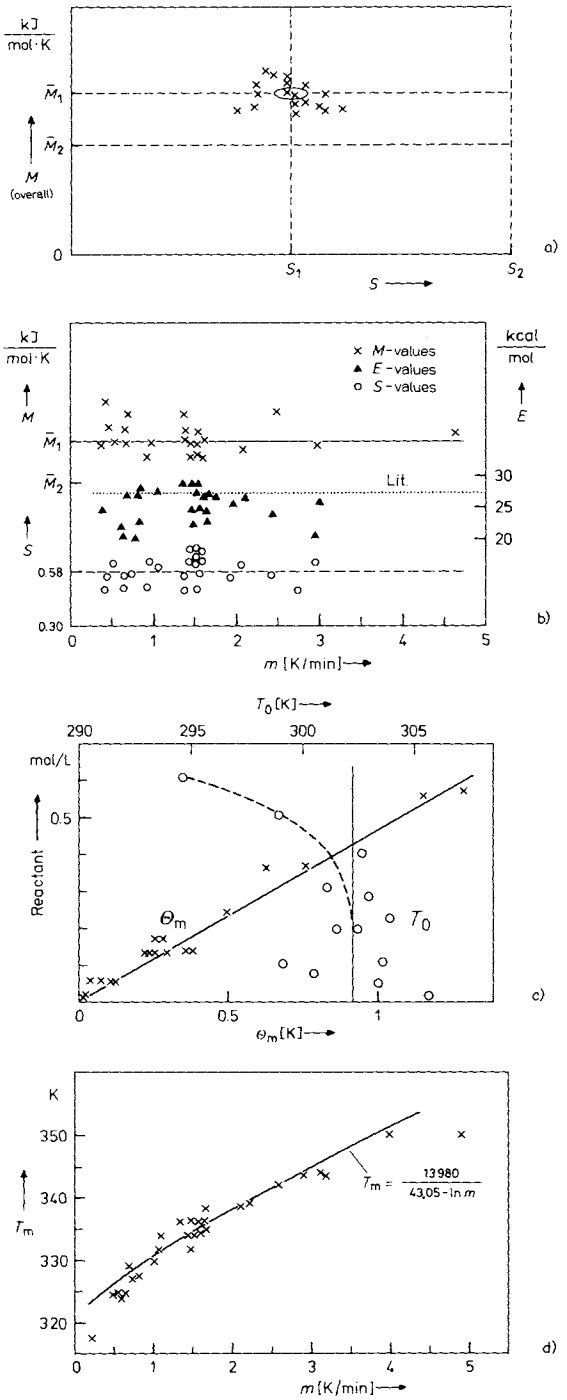



Fig. 6. Various correlations for the decomposition of benzenediazonium sulfate in dilute sulfuric acid: a) Mechanistic coordinates ($M$ and $S$); b) $M$-index, shape index $S$ and activation energy $E$ *vs.* heating rate $m$; c) relative signal height $\Theta_m/c_0$ and initial temperature $T_0$ *vs.* concentration $c_0$; d) Peak temperature $T_m$ *vs.* heating rate $m$.

The quantitative relationships are similar to those of elementary signal curves of first order. However, for some values the initial concentration is involved, *e.g.* for the half-width and the mechanistic coordinates (see also Fig. 8a; cf. [37,47]). An increase in concentration produces a similar effect to that of raising the $A$ factor, and the characteristic temperatures are shifted to lower values.

### 6.2. Bimolecular Processes

A preliminary kinetic investigation of *bimolecular processes* is of use in optimizing organic preparative procedures, since the observation that kinetically complex relationships are involved is only an expression of the fact that the main product cannot be prepared in 100% yield. The results of reactions with nonequivalent concentrations are especially interesting (AB-type)[47,50], because particularly in low-temperature reactions poor solubility may often prevent the use of large excess of one component. The mechanistic coordinates of experiments with two reactants of different concentrations (Fig. 8b/c) belong mainly in area C or A, and only rarely in E or others. On the other hand, use of coordinates corrected for a 1:1 ratio leads to a grouping near the horizontal line $M=\bar{M}_2=0.013$ kJ/mol/K. Since only a small fraction of experiments show the corrected $S$ value of 1.15 corresponding to a reaction of second order, the major proportion of these reactions must be complex. This is also shown by the values found for overall $A$ factors which lie above the realistic limit ($\lg A=17$), particularly when $M$ differs markedly from $\bar{M}_2$.

At very high initial concentrations, large thermal feedback caused by the heat of reaction is to be expected. This can lead to difficulties in interpretation because the solution shows inhomogeneities; in extreme cases an explosion may occur. For this reason the correlation coefficients of the optimized Arrhenius straight lines decline with large peak heights (Fig. 7).

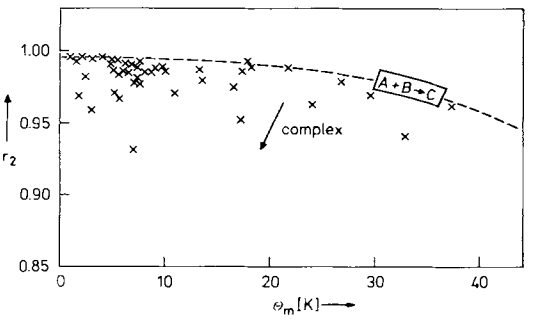



Fig. 7. Correlation coefficient for the expected bimolecular processes as a function of the DTA peak heights $\Theta_m$.

### 6.3. Complex Processes

It is possible to describe complex reactions by interpreting the signal curves by two parameters depending differently on the reaction order. This opens a route to answering questions on apparent elementary reactions and, hence to those involving the rate-determining step (cf. Sections 5.3.4/5).

Figure 8 shows the results of about 50 different experiments with initial temperatures of 200 to 260 K. For the selection of the correct reference reaction, the concentration of *one reactant* or the concentrations of *two reactants* were considered. Only a small fraction of the experiments having *expected unimolecularity* (Fig. 8a) actually correspond to an overall unimolecular reaction. Only for these cases are the overall activation parameters representative of *one* reaction. In most of the other cases, only the $M$ index conforms to the expected type EP1 ($M\approx 0.019$), whereas the remainder fall predominantly into the area of autocatalytic reactions or concurring successive reactions ($M>\bar{M}_1=0.019$)[20,21,45]. The number of points near the curve for reactions of n-th order are low[40] (cf. Fig. 9a/b).

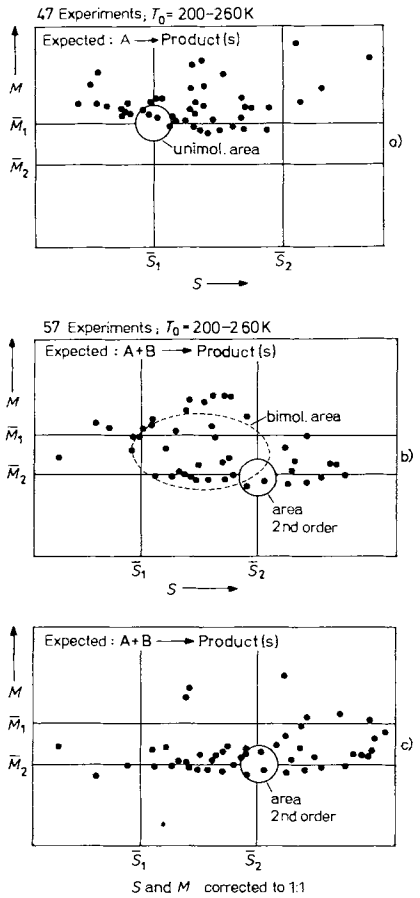



Fig. 8. Overall $M/S$ characteristics of various types of reactions: a) expected unimolecularity, b) expected bimolecularity c) as b), but after readjustment to a 1:1 molar ratio.

The results for the examples of *expected bimolecularity* are similar. The $M$ index shows the expected concentration in the A area and near the horizontal line $M=\bar{M}_2=0.013$ kJ/mol/K (Fig. 8b). After recalculation on the basis of a 1:1 molecular ratio ($[A]_0=[B]_0$) this preference becomes even greater (Fig. 8c). Even after recalculation, the $S$ factor seldom corresponds to that of a reaction of 2nd order. Most of the experimental results are located in the area $S>S_1$; $\bar{M}_2<M<\bar{M}_1$. Reactions with $M<\bar{M}_2$ or those which are of pure n-th order are rare.

If instead of the overall $M$ indices, the initial $M$ indices are taken as the basis, then a shift in the opposite direction takes place; for *experiments expected to be unimolecular*, the $M$ values of cases, which "do not fit" decline from $\bar{M}_1$, in part, to $M_2$. In contrast, for experiments *expected to be bimolecular* they rise from $\bar{M}_2$ to considerably more than $M_1$. The initial $M$ values appear to be even more specific than the overall values; until now, their wide application has been difficult because of the observed scattering which can be up to $\pm 10\%$. Even in experiments under practically similar conditions, differences in the complexity can hardly be completely ruled out. The variations can therefore often be explained by the kinetic effect of amplified variations in the starting conditions, and this is typical for the reaction mechanisms involved. Large kinetic amplification effects are shown, for example, by mechanisms having *feedback reactions* when a "triggering" of an otherwise inhibited reaction can suddenly take place by a minimal change in the initial conditions[23, 86]. Such phenomena are shown by the variances of the different parameters which for the Belousov-Zhabotinsky-reaction have been determined by a series of experiments in which the concentrations of the reactants or the heating rates were varied[81, 83, 87].

What reaction types in the mechanistic diagram now lead to satisfactory straight lines in the Arrhenius plot? Experience shows that even after correction to a 1 : 1 molecular ratio an "elementary" $M$ or S does not result, and an exact straight line is not obtained, *i.e.* formally the kinetics of such reactions have to be defined by at least two elementary processes. If one picks out only those cases *which are expected to be unimolecular* with $S \approx S_1$, then it is indicated that only with $M \approx \bar{M}_1 = 0.019 \pm 12\%$ is the expected high correlation coefficient of more than 0.99 obtained. As soon as $M$ diverges markedly from $\bar{M}_1$, the linear conformity becomes poorer; on the other hand, when $M \approx \bar{M}_1$ the shape index can vary widely around $S_1 = 0.56$ (by $\pm 20\%$) without leading to unsatisfactory fitting of the straight lines. In experiments on reactions *expected to be bimolecular* the upper limit for allowed $M$ values when $S \approx S_2$ lies about 20% above $\bar{M}_2$.

A linear relationship between $\ln k$ and $1/T$ is, therefore, with the exception of the precluded temperature dependence of the frequency factor, not a sufficient experimental criterion for the presence of an elementary process. For example, a bimolecular autocatalytic process (area 1a in Fig. 9a; A + B = 2 B) would produce a point lying above the elementary point 2 for smaller concentrations of B. Assuming an elementary process of 2nd order, the interpretation would give an Arrhenius straight line with good correlation ($r > 0.994$), but with unrealistically high activation parameters, since the signal for such a process would be too narrow.

The kinetic analysis of a reaction system may be carried out more selectively by investigating the *influence of the initial concentration* of one of the reactants on the parameters obtained according to Section 5.3.1 (Table 6). For many parameters, computer simulations show, depending upon the mechanism, concentration/parameter correlations with one or more *sections with a constant or an asymptote*. We were able to confirm this by means of concentration series for 20 different systems[3, 107]. A parameter should be *especially selective* in determining a reaction mechanism when it shows *a maximum number of such constant sections*, since each of these would be ascribed to a *rate-determining step* of the reaction mechanism.

Table 6. Concentration dependence of nonisothermal parameters and reaction mechanism. EP = Elementary process; Pxx = Concurring processes of the same order; Gxy = Elementary process of second-order etc. The valuation numbers represent the contribution of constant sections (cf. text).

| Parameter | Valuation | Behavior and interpretation of the concentration dependence $f(c_0)$ |
|---|---|---|
| Peak temperature $T_m$ | 0.67 | Similar to the initial temperature; for processes inhibited by feedback, however, increases for small concentrations |
| Initial activation energy $E_0$ | 0.70 | Characterizes the initial reaction: constant ⇒ EP, Gxx, Gxy or Pxx; decreasing ⇒ simple autocatalytic process; step(s) ⇒ Pxy |
| Overall activation energy $E$ | 0.71 | Describes optimal overall reaction. Can be determined more accurately then $E_0$; almost equivalent information on mechanism |
| Special index $I_{mech}$ [18, 37] | 0.76 | $I_{mech} = 1 \Rightarrow$ formal overall reaction of n-th order |
| Relative signal height $\theta_m/c_0$ | 0.80 | Typical for orders of previous branches: Pxy or EP, Pxx or no pre-reaction at all (see Table 1) |
| Initial temperature $T_0$ | 0.81 | Characterizes the classification of the reaction type: constant ⇒ EP1, P11; decreasing ⇒ EP2 or P22; step(s) ⇒ Pxy; rising ⇒ inhibition. In overlapping peaks the initial reaction is characterized. |
| Overall frequency factor $k_\infty$ | 0.81 | $k_\infty(c_0)$ is to be interpreted similarly $E(c_0)$; $> 10^{16} \Rightarrow$ complex reaction |
| Initial reaction type index $M_0$ | 0.84 | Constant ⇒ EP or special mechanism types; Variant ⇒ steps or asymptotes can in some cases represent EPs |
| Shape index $S$ | 0.92 | Areas of elementary steps as for $M_0$ or $M$ but trend curves of different type $S = f(c_0)$. The curve $M_0 = f(S)$ is typical for mechanism. |
| Overall reaction type index $M$ | 0.94 | Like $M_0$ but the functions $M = f(S)$ are shifted or different |

A statistical analysis of our results under this aspect showed that of all the quantities shown in Table 6, the reaction-type indices and the shape indices have the most constant sections[107]. The "mechanistic coordinates", therefore, have to be considered as the fundamental parameters. Even for two-reaction models they show an elementary limiting behavior characteristic of the reaction mechanism for very high or low concentrations or heating rates[19,20,40].

## 7. Heterogeneous Mechanisms in the Mechanistic Diagram

### 7.1. Problems in the Kinetic Analysis of Solid-State Reactions

The advantages of performing measurements with increasing temperature also apply to solid-state reactions[89,90], even when the behavior of species produced photo- or radiochemically at very low temperature is investigated[48]. In this way DTA curves with a number of peaks can be recorded subsequent to irradiation of hydrazoic acid at 20 K in methanol. These correspond to reactions of thermally produced products, such as nitrenes and H atoms[105].

However, the quantitative analysis of such signals is difficult because for *solid-state reactions* the kinetic conditions can hardly be compared with those of homogeneous kinetics[21,89,90]. In place of concentration, a formal conversion parameter $x$ (fractional conversion), which changes from 0 to 1 in course of the reaction, has been introduced.

$$x = \frac{[A_i]_0 - [A_i]}{[A_i]_0} \tag{21}$$

On the whole, one does not use additive terms such as in eq. (1)[24,63,89-100] in these complex processes, rather, only *one* rate constant is assumed so that consecutive or parallel reactions have to be interpreted for a *number of sections*[24,89,90,95-100]. *Sestak et al.*[24] have suggested a general rate law which covers most of the known heterogeneous mechanisms (Table 7).

$$\frac{dx}{dt} = k x^m (1-x)^n [-\ln(1-x)]^p \tag{22}$$

For $m = p = 0$, $n \neq 0$ eq. (22) is transformed to the rate law of n-th order; cases where $m > 0$, $n = 0$, $p = 0$ (power law) and $m = 0$, $n = 0$, $p > 0$ correspond to a strong autocatalytic character in the homogenous kinetics.

The difficulties encountered in interpretating kinetic data (inhomogenities in temperature and concentration, restriction to only one reaction coefficient) mentioned at the beginning of this section are further augmented by others[25,95,101]. The significance of "activation energy" in the solid-state is a difficult problem[24,25,57,102]. In homogenous kinetics, the Arrhenius equation is explained by the statistical distribution of energy over the reactant molecules present. But in the solid state a molecule, because of its lack of translational energy, cannot receive the surplus energy from its nearest neighbor. Many solid-state reactions, however, can only be explained with the aid of relatively high activation energies so that this quantity must have another significance.

A second problem is concerned with the relationship between the reactants present and the reaction rate, which in homogenous kinetics is always present because of the law of mass action. However, in most of the mechanisms detailed in Table 7, the relationship between fractional conversion and the reaction rate is based on topochemical models. For example, for surface reactions (types R1, R2, R3) it is difficult to imagine how the reaction rate should be dependent on the fraction of unreacted molecules which are far removed from the surface. Here, the previously frequently applied rate laws should rather be de-

Table 7. The most important rate laws for reactions in the solid state.

| Logogramm | m | n [Gl. (22)] | p | Name/Remarks | |
|---|---|---|---|---|---|
| Mechanisms controlled by phase boundary | | | | | |
| R1 | 0 | 0 | 0 | Polanyi-Wigner: | one-dimensional movement of the phase boundary |
| R2 | -0 | 1/2 | 0 | | two-dimensional movement of the phase boundary |
| R3 | 0 | 2/3 | 0 | Hume-Colvin: | three-dimensional movement of the phase boundary (Contracting sphere mechanism) |
| Mechanisms controlled by diffusion | | | | | |
| D1 | −1 | 0 | 0 | Parabolic law: | one-dimensional diffusion |
| D2 | 0 | 0 | −2 | | two-dimensional diffusion |
| D3 | 0 | 1/3 | −1 | Jander: | three-dimensional diffusion |
| Mechanisms controlled by nucleation growth | | | | | |
| NP1/2 etc. | ≤1 | 0 | 0 | Nucleation power law: m = 1/4, 1/3, 1/2, 1 | |
| A2 | 0 | 1 | 1/2 | Avrami: | two-dimensional growth of phase boundary |
| A3 | 0 | 1 | 2/3 | Avrami-Erofe'ev: | three-dimensional growth of phase boundary |
| NPT | 1 | 1 | 0 | Prout-Tompkins-Mechanisms | |
| N2H | 0 | 1 | 0.63 | Heterogeneous bimolecular reaction | |
| Seed formation/linear growth of nuclei | | | | | |
| NLX | ≪−1 | 0 | 0 | Explosive reactions/branchings | |
| NLZ | >1 | <1 | 0 | Later stages during growth | |
| NLD | m | n | 0 | Growth of spherical particles in diffusion-controlled region | |

rived from geometrical concepts than from the point of view of a molecule which is activated to react.

The *significance of the frequency factor* in solid-state reactions is even more difficult, and a number of concepts have already been developed (cf. [24, 102]).

Despite all of these problems in interpretation it is apparent (especially in thermogravimetric measurements) that many solid-state reactions can be satisfactorily described by means of eq. (22), even though the coefficients m, n, and p are relatively poorly defined: in most cases it is, therefore, not possible to specify a definite reaction mechanism[21, 96, 97, 103].

### 7.2. Selection of Reference Reaction and Theoretical Studies

In the theory of homogenous kinetics, reactions of either 1st or 2nd order could be used as a reference for the reaction type index. For a formal initial reaction of n-th order, the initial activation energy calculated from the initial part of the differential conversion curve is practically independent of the order of the reaction; in eq. (18), the partial integral is then small compared to the total integral so that introduction of the conversion variable $x$ gives

$$k(t) = \frac{\dot{x}(t)}{\left(1 - \int_{t_0}^{t} \dot{x}\,dt\right)^n} \quad \lim_{t \to t_0} = \dot{x}(t) \tag{23}$$

Efforts should now be made to achieve an A factor which is independent of the initial concentrations of the reactants. The *reaction of 1st order* is, therefore, the most suitable reference for comparison of homogenous and heterogenous reactions in an extended mechanistic diagram[3].

By generation and re-evaluation of conversion curves with different assumed activation parameters it is easy to determine the mechanistic parameters for all the mechanisms in Table 7; $M$ can then be related to

- activation data *selected* for model curves (theoretical $M$-indices)[20] (not shown here)
- activation parameters evaluated from eq. (18) or from the DTA-programs based on the Borchardt-Daniels equation *from the initial range* assuming 1st order (initial $M$, Fig. 9a)
- activation parameters *from the whole curve* (overall $M$, Fig. 9b)

The resulting mechanistic diagrams differ only in the ordinates. Since the *theoretical M* indices are of little practical value, we compare here only the "re-evaluated" initial and overall values. For comparison, some of the homogeneous kinetic areas[3] are also shown. While these are always clustered around the elementary points of first or second order and extend to areas H and B (high $S$- and low $M$-values), most of the heterogeneous mechanisms are found in the area Ø (small $S$, large $M$) and near the $S/M$ curve for n-th order. The surface-controlled mechanisms (R) can, in part, be easily confused with those controlled by diffusion (D), *i.e.* D1 with R1 or D3 with R2[97, 98, 103]. Similarly, the Avrami equations (A) lead to initial diagram functions

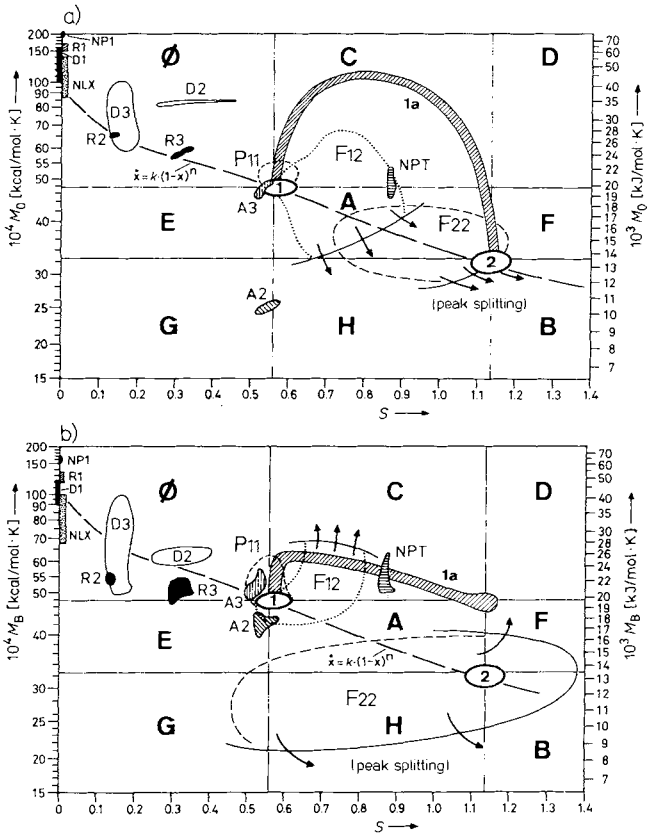



Fig. 9. Mechanistic diagram with the most important heterogeneous and some homogenous reaction mechanisms [3, 20] (cf. Section 4.1 and Table 7; heating rates 1.5–5 K/min; $A$ factors $10^6$–$10^{14}$ $s^{-1}$): a) with initial $M$ values; b) with overall $M$ values.

which differ only slightly from a first-order reaction. In contrast, Prout-Tompkins kinetics (NPT) and the nucleation-growth mechanisms (NP) can be easily identified.

The thermal decomposition of nickel oxalate is a relatively attractive system for which the Prout-Tompkins mechanism (m = 1, n = 1, p = 0 in Table 7) has been definitely established by thermogravimetric and isothermal measurements[104]. If theoretical curves are generated from the given kinetic data ($E = 100.5$ kJ/mol, $k_\infty = 1.4 \times 10^{10}$ $s^{-1}$) and the mechanistic coordinates calculated assuming that a first-order reaction prevails throughout, then for initial $M$ and a chosen heating rate of 5 K/min a point within the theoretically determined Prout-Tompkins area is produced (Fig. 9a).

This kind of characterization of heterogeneous reactions which can be described by eq. (22) should even enable identification of the mechanisms of reactions having very similar conversion curves. Thus, the kinetics of diffusion and phase controlled mechanisms have been compared with one another thermogravimetrically by *Criado* and *Morales*[103], with the result that types R1 and D1 or R3 and D3 in Table 7 cannot be differentiated. But Figure 9 shows that R3 and D3 have distinctly different mechanistic coordinates. For the decomposition of $CaCO_3$ under discussion here, the coordinates $S = 0.142$ and $M_0 = 0.0485$ are found for the D3 mechanism (three-dimensional diffusion), whereas for the R3 mechanism (three-dimensional movement of the phase interface) the values $S = 0.318$, and

$M_0 = 0.02406$ are found. Because the $M$ value gives a better fit, R3 is the more probable mechanism.

However, such a detailed selection of the reaction mechanism as in homogeneous kinetics does not appear to be possible, because the criterion of the *concentration dependence of phenomena,* which is important for practical reaction kinetics, can be applied only with difficulty (*e.g.* dilution of the sample with inert material after pulverization). Furthermore, because during the course of the reaction the mechanism often changes and, therefore, the introduction of several rate constants is essential, it is only in rare cases that the whole experimental curve can be described by additive combinations like eq. (1) or even by eq. (22).

## 8. Outlook

Analysis of reactions using linear control of temperature with time, which first led to success in the investigation of the chemistry of compounds available only by low temperature photosynthesis[48], appears theoretically to be a widely applicable kinetic method. It is especially suited for the clarification of reaction mechanisms over a wide temperature range. DTA experiments, some UV measurements, and thermogravimetric results from the literature served to check the models produced by computer programs. Our results confirm that "slow" chemical reactions in solution are mostly complex, but according to the new concept they can be classified kinetically over a wide temperature range. For elementary reactions the same activation parameters were found as by isothermal measurements[69-71], and many complicated reactions could be split into elementary processes. UV measurements appear to be a promising additional tool for the future, since kinetic studies using selected wavelengths can concentrate on part structures of the participating species[55].

By means of these possibilities it is often feasible with this new concept to discover the reaction mechanism and calculate the parameters underlying its individual steps. The best proof of a proposed model is provided by the definitive reproduction of random experimental signal curves using univariant data for all elementary steps.

Often, *fast successive* steps are also indicated by nonisothermal measurements. Occasionally a variation in the $M$ value is shown directly; if they compete with other steps they either influence the indication parameters [cf. eq. (1)] of the previous slow reactions or, after branching, the $A$ factors of the slow successive steps[21]. Even fast initial processes ($k_{298}$ up to *ca.* $10^{11}$ $s^{-1}$) with activation energies of 10–20 kJ/mol, which until now could be evaluated only using relaxation and pulse techniques, can be followed directly by low temperature measurements in suitable solvents—if necessary using very high heating rates[9, 13, 28].

Hence, using simulation methods, such areas as diffusion kinetics, photochemical kinetics, or the kinetics of oscillating reactions can now, in part, be investigated. It is, therefore, worthwhile to follow the path of nonisothermal reaction analysis outlined here in order to investigate and classify the kinetic phenomena in chemistry more effectively than was previously possible.

*I wish to express my thanks to the co-authors of my publications cited here, to my co-workers Messers. B. Stilkerieg, G. Lindner, and Mrs. C. Mummerz, and also to the computer section of the Max-Planck-Institut für Kohlenforschung, especially to Mr. K. Boll and Mr. H.-D. Schmitz. Valuable suggestions in the preparation of this manuscript were made by Prof. Dr. O. E. Polansky, Dr. H. Hermann, and Dr. P. Potzinger. These are gratefully acknowledged.*

Received: May 4, 1981;
revised: October 18, 1982 [A 439 IE]
German version: *Angew. Chem. 95* (1983) 185

[1] M. Eigen, R. Winkler: *Das Spiel - Naturgesetze steuern den Zufall,* Piper, München 1975.
[2] H. Kuhn, J. Waser, *Angew. Chem. 93* (1981) 495; *Angew. Chem. Int. Ed. Engl. 20* (1981) 500.
[3] E. Koch, *Thermochim. Acta 56* (1982) 1.
[4] M. Mesarovic, E. Pestel: *Menschheit am Wendepunkt,* Deutsche Verlags-Anstalt, Stuttgart 1974; *Multilevel Computer Model of World Development Model.* Extract of the Proceedings Laxenburg (Austria) 29. 4.–3. 5. 1974, I IASA-SP-74-06.
[5] D. Edelson, *J. Chem. Educ. 52* (1975) 642.
[6] R. M. Noyes, *J. Phys. Chem. 81* (1977) 2315.
[7] M. B. Carver, A. W. Boyd, *Int. J. Chem. Kinet. 11* (1979) 1097.
[8] K. H. Ebert, P. Deuflhard, W. Jäger: *Modelling of Chemical Reaction Systems,* Springer Series in Chemical Physics *18* (1981) 216–225.
[9] H. Jüntgen, K. H. van Heek, *Fortschr. Chem. Forsch. 13* (1970) 601.
[10] P. D. Garn: *Thermoanalytical Methods of Investigation,* Academic Press, New York 1965.
[11] J. H. Flynn, L. A. Wall, *J. Res. Natl. Bur. Stand. A 70* (1966) 487.
[12] B. Carroll, E. P. Manche, *Thermochim. Acta 3* (1972) 449.
[13] E. Koch: *Non-Isothermal Reaction Analysis,* Academic Press, New York 1977.
[14] A. G. Merzhanov, V. V. Barzykin, A. S. Shteinberg, V. T. Gonthovskaya, *Thermochim. Acta 21* (1977) 301.
[15] R. Chen, *J. Mater. Sci. 11* (1976) 1521.
[16] G. Lombardi (Secretary ICTA): *For better Thermal Analysis,* Istituto di Mineralogica e Petrografie dell'Universita di Roma 1978.
[17] R. C. Mackenzie, *Talanta 16* (1969) 1229; *J. Therm. Anal. 4* (1972) 343; *Thermochim. Acta 8* (1975) 197; *28* (1979) 1.
[18] E. Koch, *J. Therm. Anal. 6* (1974) 483.
[19] Cf. [13], p. 280–292.
[20] E. Koch, *Angew. Chem. 85* (1973) 381; *Angew. Chem. Int. Ed. Engl. 12* (1973) 381.
[21] Cf. [13], pp. 160–171.
[22] R. M. Noyes, *Ber. Bunsenges. Phys. Chem. 84* (1980) 295; A. M. Zhabotinsky, *ibid. 84* (1980) 303; P. Gray, *ibid. 84* (1980) 309; E. Wicke, P. Kummann, W. Keil, J. Schieffer, *ibid. 84* (1980) 315; E. D. Gilles, *ibid. 84* (1980) 323; U. F. Franck, *ibid. 84* (1980) 334; P. Müller, *ibid. 84* (1980) 341; B. Hess, A. Boiteux, *ibid. 84* (1980) 346; F. Schlögl, *ibid. 84* (1980) 351; cf. also *ibid. 84* (1980) 358–418.
[23] U. F. Franck, *Angew. Chem. 90* (1978) 1; *Angew. Chem. Int. Ed. Engl. 17* (1978) 1.
[24] J. Stestak, G. Berggren, *Thermochim. Acta 3* (1971) 1.
[25] P. D. Garn, *J. Therm. Anal. 10* (1976) 99.
[26] T. Ozawa, *J. Therm. Anal. 2* (1970) 301.
[27] M. Selvaratnam, P. D. Garn, *J. Am. Ceram. Soc. 59* (1976) 376.
[28] J. H. Flynn, L. A. Wall, *J. Res. Natl. Bur. Stand. A 70* (1966) 2060.
[29] J. H. Sharp, S. A. Wentworth, *Anal. Chem. 41* (1969) 2060.
[30] E. S. Freeman, B. Carroll, *J. Phys. Chem. 62* (1958) 394.
[31] F. Skvara, J. Sestak, V. Sestak'ova, *Therm. Anal. Int. Conf. (4th) Budapest 1* (1975) 105.
[32] A. W. Coats, J. P. Redfern, *Analyst (London) 88* (1963) 906.
[33] Cf. [13], pp. 401–410.
[34] J. Sestak, *Talanta 13* (1966) 567; *Thermochim. Acta 3* (1971) 150.
[35] G. Gyulai, E. J. Greenhow, *Thermochim. Acta 6* (1973) 239.
[36] A. van Tets, *Thermochim. Acta 17* (1976) 372.
[37] Cf. [13], pp. 90–117, 124–125.
[38] E. Madelung: *Die mathematischen Hilfsmittel des Physikers,* 6th edition Springer, Berlin 1957, p. 56, 62, 123.
[39] G. Gyluai, E. J. Greenhow, *Thermochim. Acta 5* (1972) 481.
[40] E. Koch, Plenar lecture on the occasion of the award of the Netzsch-GEFTA-Prize in Rapperswiler, April 20, 1979; in E. Marti, H. R. Oswald, H. G. Wiedemann: *Angewandte chemische Thermodynamik und Thermoanalytik,* Birkhäuser, Basel 1980, pp. 141–147.
[41] E. Koch, *Chem. Ing. Tech. 44* (1972) 111.
[42] H. Anderson, D. Haberland, E. Witte, *Z. Chem. 18* (1978) 153.
[43] H. E. Kissinger, *Anal. Chem. 29* (1957) 1702.
[44] E. Koch, B. Stilkerieg, *Thermochim. Acta 17* (1976) 1.

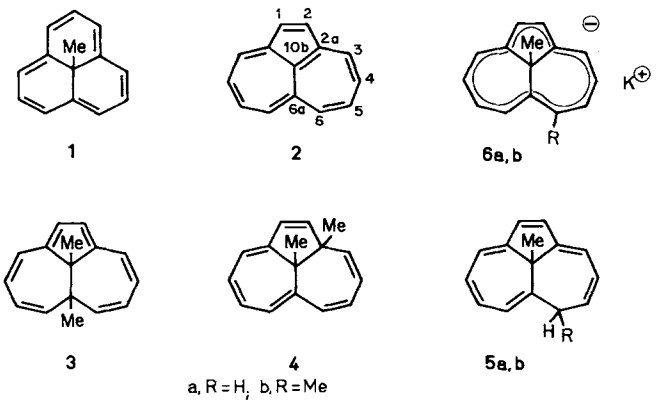
[45] Cf. [13], pp. 133–135, 252–268.
[46] J. H. Flynn, *Thermochim. Acta 37* (1980) 225.
[47] E. Koch, B. Stilkerieg, *Thermochim. Acta 27* (1978) 69.
[48] E. Koch, *Angew. Chem. 82* (1970) 306; *Angew. Chem. Int. Ed. Engl. 9* (1970) 288.
[49] K. H. Ebert, H. J. Ederer, G. Isbarn, *Angew. Chem. 92* (1980) 331; *Angew. Chem. Int. Ed. Engl. 19* (1980) 333.
[50] E. Koch, B. Stilkerieg, *J. Therm. Anal. 17* (1979) 395.
[51] B. Meyer: *Low Temperature Spectroscopy*, American Elsevier, New York 1971; R. Huisgen, *Angew. Chem. 82* (1970) 783; *Angew. Chem. Int. Ed. Engl. 9* (1970) 751.
[52] H. E. Hallam, *Annu. Rep. Prog. Chem. 67* (1970) 117; *Phys. Bl. 28* (1972) 555.
[53] H. E. Hallam: *Vibrational Spectroscopy of Trapped Species*, Wiley, New York 1973.
[54] H. Mauser, *Z. Naturforsch. B 23* (1968) 1021, 1030.
[55] E. Koch, B. Stilkerieg in E. Marti, H. R. Oswald, H. G. Wiedemann: *Angewandte chemische Thermodynamik und Thermoanalytik*, Birkhäuser, Basel 1980, pp. 210–215.
[56] J. Bitter, J. Leitich, H. Partale, O. E. Polansky, W. Riemer, U. Ritter-Thomas, B. Schlamann, B. Stilkerieg, *Chem. Ber. 113* (1980) 1020.
[57] J. Sharp in [61], *Vol. 2*, pp. 47–77.
[58] Cf. [13], pp. 196–197, 201–203, 209.
[59] F. Becker, *Chem. Ing. Tech. 40* (1968) 933.
[60] E. Koch, *Chem. Ing. Tech. 37* (1965) 1004.
[61] R. C. Mackenzie: *Differential Thermal Analysis, Vol. 1* „Fundamental Aspects" (1970), *Vol. 2* „Applications" (1972), Academic Press, New York.
[62] D. Schultze: *Differentialthermoanalyse*, Verlag Chemie, Weinheim 1969; M. I. Pope, M. D. Judd: *Differential Thermal Analysis*, Heyden, London 1977.
[63] L. Battezati, A. Lucci, G. Riontino, *Thermochim. Acta 23* (1978) 213.
[64] G. O. Piloyan, I. D. Ryabchikov, O. S. Novikova, *Nature (London) 212* (1966) 1229.
[65] P. D. Garn, *Thermochim. Acta 28* (1979) 185.
[66] P. K. Gallagher, D. W. Johnson Jr., *Thermochim. Acta 6* (1973) 67.
[67] W. Hemminger, G. Höhne: *Grundlagen der Kalorimetrie*, Verlag Chemie, Weinheim 1979.
[68] H. J. Borchardt, F. Daniels, *J. Am. Chem. Soc. 79* (1957) 41.
[69] E. Koch, B. Stilkerieg, L. Carlsen, *Thermochim. Acta 33* (1979) 387.
[70] E. Koch, B. Stilkerieg, L. Carlsen, *Ber. Bunsenges. Phys. Chem. 83* (1979) 1238.
[71] Cf. [13], pp. 340–400.
[72] Cf. [13], pp. 332–333, 340–374.
[73] R. W. Murray, M. L. Kaplan, *J. Am. Chem. Soc. 90* (1968) 537; *91* (1969) 5358.
[74] E. Koch, *Anal. Chem. 45* (1973) 2120.
[75] D. D. Warner, *J. Phys. Chem. 81* (1977) 2329.
[76] E. Koch, *Tetrahedron 26* (1970) 3503.
[77] C. W. Gear: *Numerical Initial Value Problems in Ordinary Differential Equations*, Prentice Hall, Englewood Cliffs 1971. – Prof. R. J. Field is thanked for providing a modern version of one of Gear's programs.
[78] E. Koch, B. Stilkerieg, *Thermochim. Acta 29* (1979) 205.
[79] R. J. Field, R. M. Noyes, *J. Chem. Phys. 60* (1974) 1877.
[80] E. Körös, *Nature (London) 251* (1974) 703.
[81] E. Koch, B. Stilkerieg, *Therm. Anal. Int. Conf. (6th) Bayreuth 1* (1980) 75.
[82] A. Skrabal, S. R. Weberitsch, *Monatsh. Chem. 36* (1915) 211.
[83] R. J. Field, E. Körös, R. M. Noyes, *J. Am. Chem. Soc. 94* (1972) 8649.
[84] D. Edelson, R. M. Noyes, R. J. Field, *Int. J. Chem. Kinet. 11* (1979) 155.
[85] R. C. Reed, L. Weber, B. S. Gottfried, *Ind. Eng. Chem. Fundam. 4* (1965) 38.
[86] R. J. Field, R. M. Noyes, *Symp. Faraday Soc. 9* (1974) 21.
[87] E. Koch, B. Stilkerieg, unpublished results.
[88] L. Carlsen, A. Holm, E. Koch, B. Stilkerieg, *Acta Chem. Scand. B 31* (1977) 679.
[89] D. A. Young: *Decomposition of Solids*, Pergamon Press, Oxford 1966.
[90] J. M. Criado, *Thermochim. Acta 28* (1979) 307.
[91] J. H. Sharp, G. W. Brindley, B. N. N. Achar, *J. Am. Ceram. Soc. 49* (1966) 379.
[92] L. F. Jones, D. Dollimore, T. Nicklin, *Thermochim. Acta 13* (1975) 240.
[93] K. Heide, W. Höland, *Thermochim. Acta 13* (1975) 365.
[94] S. Boy, K. Böhme, *Thermochim. Acta 20* (1977) 195.
[95] P. D. Garn, *J. Therm. Anal. 13* (1977) 581; Dupont-Award-Address on ICTA 5th Int. Conf., Kyoto 1977.
[96] P. D. Garn, *Thermochim. Acta 5* (1973) 485.
[97] P. S. Nolan, H. E. Lemay Jr., *Thermochim. Acta 6* (1973) 179.
[98] P. D. Garn, *J. Therm. Anal. 7* (1975) 475.
[99] D. Dollimore, P. F. Rodgers, *Thermochim. Acta 30* (1979) 273; D. Dollimore, G. R. Heat, B. W. Krupay, *ibid. 24* (1978) 293.
[100] R. R. Baker, *Thermochim. Acta 28* (1979) 45.
[101] P. D. Garn, personal communication.
[102] H. F. Cordes, *J. Phys. Chem. 72* (1968) 2185.
[103] J. M. Criado, J. Morales, *Thermochim. Acta 19* (1977) 305.
[104] J. M. Criado, F. Gonzales, J. Morales, *Thermochim. Acta 12* (1975) 337.
[105] E. Koch, unpublished results.
[106] E. Körös, E. Koch, unpublished results.
[107] E. Koch, *Thermochim. Acta 49* (1981) 25.

When submitting manuscripts, authors of articles which are intended for publication as "Communications" are requested to conform to the guidelines reproduced at the beginning of each issue following the list of contents.

## Direct Synthesis of a [13]Annulenide Ion**

By *Bernd C. Becker, Gerd Neumann, Hans Schmickler,* and *Klaus Müllen**

The failure of all attempts to obtain the long elusive 9b-methylphenalene **1** from ionic phenalene precursors[2] underscores the difficulty of initiating reaction at the angular centers of *peri*-annelated polycyclic π-systems. We now wish to report the synthesis of an analogue of **1** with 14π-perimeter (**6a**) by reductive alkylation of aceheptylene **2**.




The directed conversion of anions of an unsaturated compound by kinetically controlled addition of electrophiles[1] requires knowledge of the charge distribution in such anions. Thus, for the preparation of an analogue of **1**, a *peri*-annelated tricycle is required whose anions have a high π-charge density at the central quaternary C atom. According to MO models[3] this requirement is fulfilled in the aceheptylene **2**, first synthesized by *Hafner*[4]; the selection of **2** is experimentally supported by the NMR spectra of the diamagnetic dianion $\mathbf{2}^{2-}$ (dilithium salt)[6]: On reduction of **2** the carbon atom C-10b experiences by far the greatest charge-induced shielding, recognizable by the extreme upfield shift of the $^{13}$C-NMR signal [$\Delta\delta_C = -61.2$].

Methylation of $\mathbf{2}^{2-}/2Li^+$ [tetrahydrofuran (THF), dimethyl sulfate, −20 °C] furnishes a mixture of the three dimethyl adducts **3**, **4** and **5b**, which are separable by column chromatography and subsequent preparative gas-chromatography, and whose structures have been elucidated NMR spectroscopically. A notable feature of all derivatives is that a methyl group is incorporated at the inner position 10b. An independent chemical proof for the structure of the orange-yellow **5b** was provided by deprotonation (THF, potassium hydride, room temperature) to the bridged 13-center 14π-system **6b** [$^1$H-NMR (90 MHz, [D$_8$]THF): $\delta = 8.1-6.8$ (ring protons); 3.15 ($CH_3$ on C-6); −3.90 ($CH_3$ on C-10b)].

This synthetic strategy is impaired by the fact that three different adducts are formed, only one of which is suitable for the production of monocyclic conjugated π-structures. If, however, the reductive methylation of **2** is carried out with dimethyl sulfate in liquid ammonia at −78 °C, only the monomethyl derivative **5a** is formed (58% after chromatographic purification on silica gel). **5a** is also formed in small yields on addition of methyllithium to **2**, followed by hydrolytic work-up.

The structure of **5a** (especially the position of the newly formed methylene group), which is of importance regarding knowledge of the hydromethylation and secondary reactions of **5a**, has been elucidated by assignment of all the resonances in the complex $^1$H-NMR-spectrum [$^1$H-NMR (300 MHz, $CDCl_3$): $\delta = 6.22$, 6.08 (H-1, H-2); 5.66 (H-3); 6.11 (H-4); 6.07 (H-5), 3.79, 2.81 (H-6, H-6'); 5.65 (H-7); 5.75 (H-8); 6.01 (H-9); 5.88 (H-10); 1.41 ($CH_3$)].

Deprotonation of **5a** affords the salt **6a** [green solution; $^1$H-NMR (300 MHz, [D$_8$]THF): $\delta = 7.69$ (H-1); 8.11, 8.16 (H-3 and H-6); 6.96, 7.09 (H-4 and H-5); −3.75 ($CH_3$); $^{13}$C-NMR (75 MHz, [D$_8$]THF): $\delta = 144.1$ (C-2a); 119.2 (C-6a); 120.1, 118.9, 111.7, 110.9, 108.6 (C-1, C-3 to C-6); 43.4 (C-10b); 20.5 ($CH_3$)]. Characteristic for the 14π-perimeter system **6a** are the extreme upfield resonance of the "inner" methyl protons and—despite excess charge—the pronounced deshielding of the ring protons. Both observations support the expected diatropism of the cyclopentadienyl homologue **6a**, the first salt of a [13]annulenide ion.

Both the temperature as well as the choice of electrophile influence the course of the trapping reaction of $\mathbf{2}^{2-}$: When the reaction is carried out in boiling ammonia the yields are poorer, and on methylation with methyl chloride or methyl bromide increasing amounts of reoxidized educt **2** are obtained because the C-halogen bond is reductively cleaved. Under the conditions of the Birch reduction ($NH_3$, liq.; Li, 2eq.; −78 °C; methanol as source of protons), three dihydro derivatives are formed[4], in which, according to the spectroscopic data, an azulene fragment is preserved in each case. A rapid H-shift in the primary adduct is plausible under the reaction conditions.

The systems **5a** and **6a**, which are readily accessible by reductive methylation, appear suitable for further modification of the ring skeleton.

Received: September 21, 1982 [Z 152 IE]
German version: *Angew. Chem.* 95 (1983) 238
The complete manuscript of this communication appears in: *Angew. Chem. Suppl. 1983*, 282–287

[*] Prof. Dr. K. Müllen, Dr. B. C. Becker, G. Neumann, Dr. H. Schmickler
Institut für Organische Chemie der Universität
Greinstr. 4, D-5000 Köln 41 (Germany)

[**] Reductive Transformations, Part 3. This work was supported by the Deutsche Forschungsgemeinschaft and the Fonds der Chemischen Industrie.—Part 2: [1].

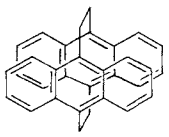
[1] W. Huber, W. Irmen, J. Lex, K. Müllen, *Tetrahedron Lett. 23* (1982) 3889.

[2] K. Grohmann, lecture at the "4th Int. Symp. on the Chemistry of Novel Aromatic Compounds", Jerusalem 1981.
[3] P. Bischof, R. Gleiter, K. Hafner, M. Kobayashi, J. Spanget-Larsen, *Ber. Bunsenges. Phys. Chem. 80* (1976) 532; S. L. Wallace, J. Michl, *Isr. J. Chem. 20* (1980) 253.
[4] K. Hafner, *Pure Appl. Chem. 28* (1971) 153.
[6] K. Hafner, K. Müllen, M. Rabinovitz, unpublished results.

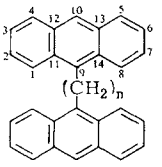
## Successive Electron Transfers in Molecules with Two Electrophoric Groups: Novel Singlet, Doublet, and Triplet States**

By *Walter Huber, Heinz Unterberg,* and *Klaus Müllen**

Successive electron transfers to molecules containing two or more electroactive groups can lead to ionic products having completely different structures, whose characteristic features are the charge distribution and the spin multiplicity. Such reactions play an important role in biological processes[1]. For our studies in this sector we used as model compounds the anthracenophane **1** and the 1,n-di-9-anthrylalkanes **2**—**4**, in which the electronic interaction of two anthracene moieties should differ drastically on steric grounds.



**1**



**2**, n = 2
**3**, n = 3
**4**, n = 4

We have succeeded in generating for the first time the dianion of **1**[2] as well as the complete series of radical monoanions, dianions, radical trianions and tetraanions of **2**—**4**[3] and in characterizing them by NMR and/or ESR spectroscopy. (For chemical proof of structure and Table of spectroscopic data see Supplement.)

The ESR spectra of the radical anions $\mathbf{2}^{\cdot-}$—$\mathbf{4}^{\cdot-}$ ($K^+$, dimethoxyethane (DME)/hexamethylphosphoric triamide (HMPT) 2:1) consistently show five sets of coupling constants for each four equivalent hydrogen atoms and one set for two equivalent hydrogen atoms. This finding confirms that the spin density is distributed over both electrophores in the time scale of the experiment. Furthermore, the $^1$H-coupling constants can be assigned in such a way that they correlate surprisingly well with the corresponding values in $\mathbf{1}^{\cdot-}$. Thus, independently of the length of the polymethylene chain, $\mathbf{2}^{\cdot-}$—$\mathbf{4}^{\cdot-}$ behave analogously to the anthracenophane $\mathbf{1}^{\cdot-}$ (with enforced proximity of the anthracene fragments)[6].

The dianions $\mathbf{1}^{2-}$ and $\mathbf{2}^{2-}$ ($2K^+$ or $2Li^+$) give highly resolved $^1$H- and $^{13}$C-NMR spectra, thus indicating the existence of singlet states [$\mathbf{1}^{2-}/2K^+$: $^1$H-NMR (300 MHz, [D$_8$]tetrahydrofuran (THF), −30 °C): $\delta = 5.11$ (H-1, H-4, H-5, H-8), 5.55 (H-2, H-3, H-6, H-7), 1.84 ($CH_2$); $^{13}$C-NMR (75 MHz, [D$_8$]THF, −30 °C): $\delta = 116.2$, 117.2 (C-1—C-4, C-5—C-8), 112.6 (C-9, C-10), 141.9 (C-11—C-14), 23.2 ($CH_2$); $\mathbf{2}^{2-}/2K^+$: $^1$H-NMR: $\delta = 7.33$ (H-1, H-8), 6.55 (H-2, H-7), 6.04 (H-3, H-6), 6.55 (H-4, H-5), 5.07 (H-10), 4.17 ($CH_2$); $^{13}$C-NMR: $\delta = 122.5$, 125.7, 124.4, 111.2 (C-1—C-4, C-5—C-8), 120.7 (C-9), 85.2 (C-10), 144.7, 139.4 (C-11—C-14), 76.4 ($CH_2$)]. From the inherent symmetry shown by the spectra it follows that the excess charge, as in the radical anions, is distributed over both anthracene rings.

The charge distribution and the spin multiplicity of $\mathbf{2}^{\cdot-}$ and $\mathbf{2}^{2-}$, however, critically depend on the experimental conditions: The observation of seven different ESR coupling constants for $\mathbf{2}^{\cdot-}$ (6 × 2 H, 1 × 1 H) in a solvent-counterion system [$K^+$, 2-methyltetrahydrofuran (MTHF)], which enables an intimate interaction between anion and cation, must be ascribed to localization of the spin density in one anthracene moiety. A triplet diradical (zero field parameter $D = 8.4$ mT) can be detected ESR spectroscopically for $\mathbf{2}^{2-}/2K^+$ in a glass (MTHF or HMPT, −170 °C).

All attempts to characterize $\mathbf{3}^{2-}$ and $\mathbf{4}^{2-}$ ($2K^+$, [D$_8$]THF) by well resolved $^1$H-NMR spectra have so far failed. However, also here, triplet states can be detected ESR spectroscopically [$2K^+$, MTHF or HMPT (glass), −140 °C to −170 °C; $D = 5.5$ and 3.5 mT, respectively].

The transition to the corresponding radical trianions and tetraanions produces novel bonding features. According to the ESR coupling constants the spin density in $\mathbf{2}^{3\cdot-}$—$\mathbf{4}^{3\cdot-}$ remains localized in an electroactive moiety in each case, even in solvents with effective cation solvation. Also significant is that the coupling constants in $\mathbf{2}^{3\cdot-}$—$\mathbf{4}^{3\cdot-}$ deviate only slightly ($\Delta a_H \leq 0.04$ mT) from those in $\mathbf{2}^{\cdot-}$—$\mathbf{4}^{\cdot-}$ (MTHF, localization of the spin density) and, to a good approximation, are twice as large as the values measured for $\mathbf{2}^{\cdot-}$—$\mathbf{4}^{\cdot-}$ in DME/HMPT (delocalization of the spin density).

The NMR spectroscopic properties of the tetraanions $\mathbf{2}^{4-}$—$\mathbf{4}^{4-}$ correspond to those of the anthracene dianion and 9-methylanthracene dianion. $\mathbf{2}^{4-}$—$\mathbf{4}^{4-}$ are thus made up of two essentially independent dianion fragments.

For the anions derived from **2**, "*anti*" or "*syn*" conformations are plausible, with different interaction of the redox centers. The analogy of the (symmetric) spin density distribution in $\mathbf{1}^{\cdot-}$ and $\mathbf{2}^{\cdot-}$ and the π-charge distribution in the singlet dianions $\mathbf{1}^{2-}$ and $\mathbf{2}^{2-}$ can best be explained in terms of a preferred dianthrylethane conformation with eclipsed or partially eclipsed π-moieties. This hypothesis does not apply in the case of the triplet state of $\mathbf{2}^{2-}$ (or of $\mathbf{3}^{2-}$ and $\mathbf{4}^{2-}$): The mean distance of the unpaired electrons in triplet $\mathbf{2}^{2-}$ estimated from the zero-field parameter $D$ is 6.9 Å ($\mathbf{3}^{2-}$: 8.0 Å, $\mathbf{4}^{2-}$: 9.3 Å), a value which is more consistent with an *anti*(*s-trans*) arrangement of the electrophores.

Received: October 8, 1982 [Z 172 IE]
German version: *Angew. Chem. 95* (1983) 239
The complete manuscript of this communication appears in: *Angew. Chem. Suppl. 1983*, 288—298

[*] Prof. Dr. K. Müllen, H. Unterberg
Institut für Organische Chemie der Universität
Greinstr. 4, D-5000 Köln 41 (Germany)
Dr. W. Huber
Physikalisch-chemisches Institut der Universität
Klingelbergstr. 80, CH-4056 Basel (Switzerland)

[**] This work was supported by the Deutsche Forschungsgemeinschaft, the Swiss National Science Foundation, and the Fonds der Chemischen Industrie.

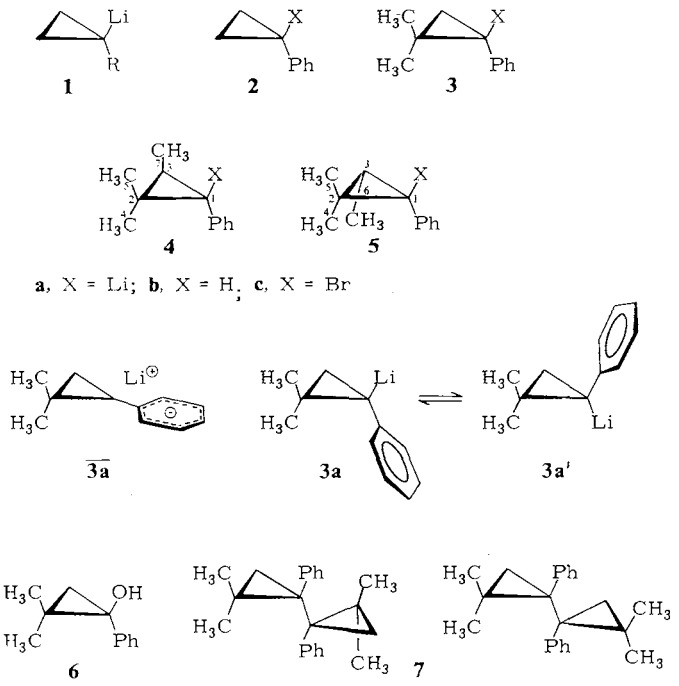
[1] J. S. Lindsey, D. C. Mauzerall, *J. Am. Chem. Soc. 104* (1982) 4498.
[2] J. H. Golden, *J. Chem. Soc. 1961*, 3741.
[3] E. de Barry Barnett, M. A. Matthews, *Chem. Ber. 59* (1926) 768; M. Daney, G. F. R. Lapouyade, H. Bouas-Laurent, Fr. Demande 2314165 (1977).
[6] F. Gerson, W. B. Martin, Jr., C. Wyder, *J. Am. Chem. Soc. 98* (1976) 1318.

## 1-Lithio-1-phenylcyclopropanes—Structure and Dynamics**

By *Detlef Hoell, Christoph Schnieders,* and *Klaus Müllen**

Lithiocyclopropanes **1** are ideal model systems for configuratively stable carbanions[1–3]. Their properties can be changed drastically by variation of the substituents R. We report here on the structure and dynamics of the 1-lithio-1-phenylcyclopropanes **2a—5a** and the stereochemistry of the metalation reaction. Compounds **2a—5a** could have covalent or, as in benzyllithium, partial ionic structures; depending on the relative energy of **3a** and $\overline{\mathbf{3a}}$ an inversion of configuration should also be detectable.

For the preparation of **3a—5a**, the reaction of the bromides **3c—5c** with lithium at low temperatures proves to be superior to the alternative method of metalation of **3b—5b** with *n*-butyllithium/potassium *tert*-butoxide[5].







The structure of the lithiated compounds could be proven chemically by protonation, by oxidation with oxygen, and by oxidative coupling with $Cu^{II}$ salts; thus, **3a** furnished respectively the hydrocarbon **3b**, the alcohol **6**, and the bicyclopropyl system **7** (as a mixture of the *meso*- and (+)/(−)-forms). Insight into the relevant bonding situation is provided by the following NMR-spectroscopic findings (see Table 1): 1) The low-temperature $^1$H- and $^{13}$C-NMR spectra of **3a** (< −60 °C) indicate non-equivalence of the geminal methyl groups, which is consistent only with fixation of the metal on one side of the plane of the three-membered ring. 2) The upfield shift of the $^1$H-NMR and $^{13}$C-NMR phenyl signals of **3a** compared to those of **3b** (higher charge density in the phenyl moiety of **3a** than in that of **3b**). 3) The downfield shift of the $^{13}$C-NMR signal of C-1 on going from **3b** to **3a** (as opposed to an upfield shift of the corresponding signal on lithiation of the parent cyclopropane system), which is indicative of an increased $sp^2$ character of the carbanionic C-atom in **3a**.

Also characteristic for the structure of **3a** are the dynamic properties. Above −45 °C the two $^1$H-NMR signals of the methyl groups in **3a** broaden and finally coincide, as is to be expected on the NMR time scale for a rapid conversion **3a** ⇌ **3a'**. The activation barrier of this process, with $\Delta G^{\neq}$ (4 °C) = 56 ± 2 kJ mol$^{-1}$ ($\Delta S^{\neq} = -137$ JK$^{-1}$ mol$^{-1}$), is distinctly smaller than that estimated for the corresponding transformation in the case of lithiocyclopropane.

All findings can be explained in terms of the contribution of an ionic borderline structure to the ground state of the (predominating) covalent lithiocyclopropane **3a**; however, the participation of temperature-dependent ion-pair equilibria cannot be ruled out. The assumption that the inversion of configuration in **3a** proceeds *via* a transition state with stronger ionic character is supported by the fact that solvents with stronger (weaker) cation solvating properties accelerate (decelerate) the conversion. The inversion barrier is higher at lower substrate concentrations. This and the stronger negative activation entropy point to the participation of aggregate structures.

Table 1. $^1$H- and $^{13}$C-NMR chemical shifts [a] of **3a—5a** and **3a—3c**.

| | | | | | *$^1$H-NMR* | | | | |
|---|---|---|---|---|---|---|---|---|---|
| | 3-H | 4-H | 5-H | 6(7)-H | *o*-H | *m*-H | *p*-H | | |
| **3a** | 0.17<br>0.53 | 0.80 | 1.04 | — | 6.35<br>6.46 | 6.57 | 6.00 | | |
| **4a** | 0.24 | 0.79 | 0.99 | 1.05 | 6.40 | 6.58 | 6.00 | | |
| **5a** | [b] | 0.8 [b, c] | 1.24 | 0.9 [b, c] | 6.24 | 6.6 [b] | 5.84 | | |
| | | | | | *$^{13}$C-NMR* | | | | |
| | C-1 | C-2 | C-3 | C-4 | C-5 | *o*-C | *m*-C | *p*-C | *ipso*-C |
| **3a** | 46.5 | 19.2 | (29.5, | 32.1, | 25 [b]) [c] | 123.0<br>124.1 | 126.7<br>127.9 | 112.2 | 163.9 |
| **3b** | 29.8 | 18.9 | 18.3 | (20.3, | 27.4) [c] | 127.3 | 128.4 | 125.5 | 140.2 |
| **3c** | 46.2 | 23.4 | 27.9 | (23.2, | 26.1) [c] | 129.2 [c] | 128.2 [c] | 127.5 [c] | 142.4 |

[a] The spectra of **3a—5a** were measured in [D$_8$]THF at −80 °C [300 MHz ($^1$H-NMR) and 75 MHz ($^{13}$C-NMR)], the spectra of **3b** and **3c** in $CHCl_3$ at room temperature (20 MHz). [b] Partially superposed signals make it difficult to determine the chemical shifts exactly. [c] The assignment of the signals is not confirmed experimentally.

The hindrance to rotation of the phenyl moiety due to partial double bond character of the C-1-C-phenyl bond leads to pairwise splitting of the signals of the *ortho* and *meta* phenyl protons in the $^1$H-NMR spectrum of **3a** below −10 °C. The characteristic preference of a conforma-

[*] Prof. Dr. K. Müllen, D. Hoell, C. Schnieders
Institut für Organische Chemie der Universität
Greinstr. 4, D-5000 Köln 41 (Germany)

[**] This work was supported by the Fonds der Chemischen Industrie. We thank Prof. Dr. G. Boche, Universität Marburg, for helpful discussions and for communication of unpublished results.

tion with non-bisecting arrangement of cyclopropane and phenyl ring for the lithio system is supported by the equivalence of the *ortho*- and *meta*-phenyl protons in **2a**.

The inversion of configuration implicates an enantiomeric conversion in the case of **3a**, but a diasteromeric conversion in the case of **4a**. Investigation of compounds of type **4** should provide information about the stereochemical course of the metalation and quenching reactions. We have prepared **4c** in diastereomerically pure form. The metalation of pure **4c**, however, like that of a 1:1 mixture of **4c** and **5c**, leads to a 5:1 mixture of the lithio derivatives **4a** and **5a**. Presumably the configurationally labile cycloproplyl radicals occur as intermediates[23], from which the thermodynamically more stable product is formed. Depending on the temperature of the trapping reaction the following mixtures are obtained on protonation: 25 °C, **4b** : **5b** ≈ 1.3 : 1; −78 °C, **4b** : **5b** ≈ 2 : 1. Obviously, the diastereomeric ratio of the organolithio systems cannot be determined correctly by this reaction.

Received: October 8, 1982 [Z 173 IE]
German version: *Angew. Chem. 95* (1983) 240
The complete manuscript of this communication appears in: *Angew. Chem. Suppl. 1983*, 299–306

[1] M. P. Periasamy, H. M. Walborsky, *J. Am. Chem. Soc. 99* (1977) 2631, and references cited therein.
[2] G. Köbrich, D. Merkel, K. Imkampe, *Chem. Ber. 106* (1973) 2017.
[3] J. W. Henderson, *Chem. Soc. Rev. 2* (1973) 397.
[5] M. Schlosser, P. Schneider, *Helv. Chim. Acta 63* (1980) 2404.
[23] G. Boche, D. R. Schneider, H. Wintermayr, *J. Am. Chem. Soc. 102* (1980) 5697; G. Boche, D. R. Schneider, *Tetrahedron Lett. 1978*, 2327.

## Carbonyl Olefinations with Organomolybdenum Compounds**

By *Thomas Kauffmann**, *Beate Ennen*, *Jörg Sander*, and *Raphael Wieschollek*

Molybdenum(V) chlorides appear to react in a surprising way with $CH_3Li$ (molar ratio 1:2) in THF to give methylene-Mo complexes: In a systematic, comparative study[1c] of the carbanionoid reactivity induced by d- and f-metals we found four molybdenum compounds which react with aldehydes and ketones with carbonyl olefination. We ascribe these reagents, hitherto prepared only in the form of brown solutions, the structures **1**, **2b**, **3b**, and **4b**. They each possibly exist—as formulated in **1**—in equilibrium with a dimer. The most easily accessible reagent **1** is formed when $MoCl_5$ is allowed to react with 2 moles of $CH_3Li$ in THF/ether (≈8:2) at −70 °C and the mixture warmed to 20 °C. Approximately 1 mole of $CH_4$ (found, 0.85 mole) is liberated.

$$MoCl_5 \xrightarrow[-\,CH_4\ -\,2\,LiCl]{+\,2\,CH_3Li} \underset{\mathbf{1}}{Cl_3Mo{=}CH_2} \rightleftharpoons 1/2\ Cl_3Mo\begin{matrix}CH_2\\ \\ CH_2\end{matrix}MoCl_3$$

This reaction is reminiscent of a previously described synthesis of alkylidene-metal compounds (M = Nb, Ta), the mechanism of which is still unclear:

$$(Me_3C{-}CH_2)_3MCl_2 + 2\,LiCH_2{-}CMe_3 \longrightarrow (Me_3C{-}CH_2)_3M{=}CH{-}CMe_3 + CMe_4 + 2\,LiCl$$

The reagents **2b**, **4b** and **3b** were prepared analogously to **1** by reaction of $CH_3Li$ with the previously documented compounds **2a**[5] and **4a**[6] or with the hitherto unknown compound **3a** (1 mol **4a** + 1 mol NaOEt) in solution (molar ratio 2:1, 3:1 and 2:1, respectively).

**2a** $Cl_3Mo(THF)_2 \longrightarrow$ **2b**

**3a** $(EtO)_3MoCl_2 \longrightarrow (EtO)_3Mo{=}CH_2$ **3b**

**4a** $(EtO)_2MoCl_3 \longrightarrow$ **4b**

Table 1. Reaction of molybdenum reagents with carbonyl compounds in THF/ether (≈8:2) at −70 °C and subsequent warming to +20 °C in 15 h followed by hydrolysis with water. Yields determined gas-chromatographically.

| Reagent | Substrate | Molar Ratio Reagent/ Substrate | Yield [%] of Olefin of Type **5** | Recovery of Carbonyl Compound [%] |
|---|---|---|---|---|
| **1** [a] | Heptanal | 2:1 | 65 | 25 |
| | Benzaldehyde | 2:1 | 65 | 30 |
| | *p*-Methoxy-benzaldehyde | 2:1 | 84 | 3 |
| | Acetophenone | 2:1 | 53 | 41 |
| **2b** | *p*-Methoxy-benzaldehyde | 2:1 | 93 | 0 |
| | Acetophenone | 2:1 | 49 | 39 |
| | Benzophenone | 2:1 | 2 | 80 |
| **3b** | Heptanal | 2:1 | 67 | 0 |
| | Benzaldehyde | 1:1 | 25 | 72 |
| | Benzaldehyde | 2:1 | 45 | 41 |
| | Benzaldehyde | 3:1 | 70 | 19 |
| | *p*-Methoxy-benzaldehyde | 2:1 | 31 | 48 |
| | Acetophenone | 3:1 | 2 | 94 |
| **4b** [a] | Heptanal | 1:1 | 32 | 50 |
| | Hexanal | 1:1 | 44 | 45 |
| | Benzaldehyde | 1:1 | 24 | 51 |
| | *p*-Methoxy-benzaldehyde | 2:1 | 4 | 72 |
| | Acetophenone | 3:1 | 2 | 91 |

[a] No reaction with benzophenone.

For the carbonyl olefination the reagents were generated by addition of $CH_3Li$ to the respective molybdenum(V) chloride at −70 °C. After addition of the carbonyl compound the mixture was stirred for 1–2 h and then slowly warmed to 20 °C. From Table 1 it follows, *inter alia* (reactions with *p*-methoxybenzaldehyde and acetophenone), that the reactivity increases along the series **4b** < **3b** < **1** ≈ **2b**.

$$\underset{\mathbf{1}}{Cl_3Mo{=}CH_2} + O{=}CRR' \xrightarrow[-\,70\text{–}20\,^\circ C]{THF} Cl_3Mo{-}\underset{\displaystyle O-CRR'}{\underset{|}{CH_2}} \longrightarrow \underset{\mathbf{5}}{CH_2{=}CRR'} + \underset{\mathbf{2a}}{Cl_3Mo(THF)_2}$$

[*] Prof. Dr. T. Kaufmann, B. Ennen, J. Sander, R. Wieschollek
Organisch-chemisches Institut der Universität
Orléans-Ring 23, D-4400 Münster (Germany)

[**] Transition Metal-Activated Organic Compounds, Part 13. This work was supported by the Deutsche Forschungsgemeinschaft (Ka 144/35-2) and the Fonds der Chemischen Industrie.—Part 12: [1c].

 © Verlag Chemie GmbH, 6940 Weinheim, 1983 0570-0833/83/0303-0244 $ 02.50/0 

In competition experiments with heptanal/diethyl ketone (1:1) it could be shown that **1**, **3b** and **4b** olefinate aldehyde groups without the keto groups being attacked.

Presumably the carbonyl olefinations proceed as formulated for **1**[7]. The postulated product **2a**, however, has so far evaded detection.

Received: July 26, 1982 [Z 105 IE]
revised: December 27, 1982
German version: *Angew. Chem. 95* (1983) 237
The complete version of this communication appears in: *Angew. Chem. Suppl. 1983*, 222—227

[1] c) T. Kauffmann, E. Antfang, B. Ennen, N. Klas, *Tetrahedron Lett 23* (1982) 2301.
[4] R. R. Schrock, J. D. Fellmann, *J. Am. Chem. Soc. 100* (1978) 3359.
[5] C. A. McAuliffe, A. Werfali, W. E. Hill, D. M. A. Minahan, *Inorg. Chim. Acta 60* (1982) 87.
[6] D. C. Bradley, R. K. Multani, W. Wardlaw, *J. Chem. Soc. 1958*, 4647.
[7] Analogous formulation of carbonyl olefination with an alkylidene-Ta complex: R. R. Schrock, *J. Am. Chem. Soc. 98* (1976) 5399.

## $[Mo\{N_2C(S)SC_2H_5\}\{NH_2NC(S)SC_2H_5\}\{(CH_3)_2NCS_2\}_2]$ – A Sulfur-Rich Haptacoordinated Diazenidohydrazido(1–)molybdenum Complex**

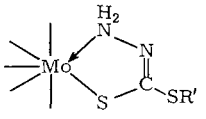
By *Rainer Mattes** and *Heinz Scholand*

*Dedicated to Professor Harald Schäfer on the occasion of his 70th birthday*

Hydrazido(2–) and diazenido complexes of molybdenum are presumably intermediates in the reduction of coordinated dinitrogen; they can be prepared *inter alia* by allowing oxomolybdenum compounds to react with disubstituted or monosubstituted hydrazines[1a]. Although a plausible mechanism for the reaction leading to hydrazido(2–) complexes was recently postulated[1b], the course of the reaction to the diazenido complexes is still largely unexplained (postulated intermediates are hydrazido(1–) complexes, M-NHNHR, which can be oxidized by atmospheric oxygen[1]). We have now obtained "mixed" diazenidohydrazido complexes of composition

$[Mo\{N_2C(S)SR'\}\{NH_2NC(S)SR'\}\{R_2NCS_2\}_2]$

($R=CH_3$, $C_2H_5$ and $R'=CH_3$, $C_2H_5$; **1**: $R=CH_3$, $R'=C_2H_5$) by allowing $MoO_2(R_2NCS)_2$ ($R_2NCS_2=N,N$-dialkyldithiocarbamate) to react with alkyldithiocarbazates $NH_2NHC(S)SR'$[2]. In these complexes the hydrazido(1–) ligand is not monodentate (–NHNHR) but is bonded as an *N,S* chelate[3]:




Further oxidation to the bis(diazenido) complex was not observed. The novel compounds are diamagnetic and molybdenum has the formal oxidation state +IV. The 18 electron rule is fulfilled; diazenido and hydrazido ligands function as 3e donors. $NH_2$ stretching vibrations occur at 3180 and 3140 $cm^{-1}$ in the IR spectrum (KBr) of **1**; we assign the sharp bands of intermediate intensity at 1577 $cm^{-1}$ to $\nu(N=N)$, and the very intense, broad bands at 1540—1520 $cm^{-1}$ to the $\nu(C=N)$ vibration. The $^1H$-NMR spectrum ($CDCl_3$) exhibits a singlet at $\delta=7.16$ for the $NH_2$ protons, in addition to multiplets for the $NCH_3$, $CH_2$ (2 quartets), and $CCH_3$ groups.

X-ray structure analysis of **1** (cf. Fig. 1) indicated that the central molybdenum atom has a distorted pentagonal-bipyramidal coordination. The chelate ring of the hydrazido(1–) ligand lies in the equatorial plane, together with three of the four sulfur atoms of the two $Me_2NCS_2$ ligands; the remaining sulfur atom and the diazenido ligand occupy the two apices of the coordination polyhedron. The Mo-diazenido group is almost linear (Mo-N1-N2: 178(1)°); the distances Mo-N1 (177(1) pm) and N1-N2 (121(1) pm) suggest multiple bonding and considerable electron delocalization; the distance N2-C is 136(1) pm and the angle N1-N2-C 120(1)°. The framework atoms of the diazenido ligand and those of the hydrazido ligand lie in a plane. The N–N distance in the chelate ring of the latter is 145(1) pm, the C–N distance of 123(1) pm corresponds to the formulation as a double bond, and the Mo–N distance (amino group) of 225.0(8) to a normal coordinative bond[4]. The Mo–S distances in the equatorial plane vary between 246.4(4) and 252.6(4) pm; $Mo-S_{ax}$ is longer (256.2(4) pm) due to the *trans*-effect of N1.

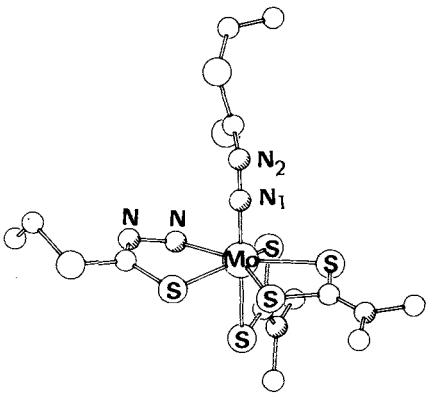



Fig. 1. Molecular structure of complex **1** in the crystal. Space group Pbca, $a=1509.2$, $b=2217.4$, $c=1424.7$ pm, $Z=8$; 3076 reflections with $F>4\sigma(F)$, 253 parameters, $R=0.075$, $R_w=0.085$. Further details on the crystal structure investigation can be obtained from the Fachinformationszentrum Energie Physik Mathematik, D-7514 Eggenstein-Leopoldshafen by quoting the depository number CDS 50315, the names of the authors, and the journal citation.

Our structural investigation indicates that different substituents on N2 decisively influence the bonding relationship in the diazenido group and, hence, the reactivity of the nitrogen atoms. Thus, the Mo-N1 and N1-N2 distances in the diazenido complex $[Mo\{Me_2NCS_2\}_3\{N_2C(O)OEt\}]$ with the electronegative ethoxycarbonyl substituent are 173.2(5) and 127.4(7) pm, respectively[5].

Received: October 15, 1982 [Z 178 IE]
German version: *Angew. Chem. 95* (1983) 246

[*] Prof. Dr. R. Mattes, H. Scholand
Anorganisch-chemisches Institut der Universität
Corrensstrasse 36, D-4400 Münster (Germany)

[**] This work was supported by the Minister für Wissenschaft und Forschung des Landes Nordrhein-Westfalen.

[1] a) M. W. Bishop, G. Butler, J. Chatt, J. R. Dilworth, G. J. Leigh, *J. Chem. Soc. Dalton Trans. 1979*, 1843; b) P. L. Dahlstrom, J. R. Dilworth, P. Shulman, J. Zubieta, *Inorg. Chem. 21* (1982) 933.
[2] Procedure for synthesis of **1**: A suspension of $MoO_2(Me_2NCS_2)_2$ (3.25 mmol) and $NH_2NHC(S)SEt$ (16 mmol) in 60 mL methanol is stirred for 4

d at room temperature under an inert gas atmosphee. The color of the reaction mixture changes from yellow to red-brown. The crude product is filtered off and recrystallized from $CH_3OH/CH_2Cl_2$; yield ca. 51%.


[3] Cf. H. Weber, R. Mattes, *Chem. Ber. 113* (1980) 2833 and literature cited therein.

[4] B. Spivack, Z. Dorti, *Coord. Chem. Rev. 17* (1975) 99.

[5] G. Butler, J. Chatt, W. Hussain, G. J. Leigh, *Inorg. Chim. Acta 30* (1978) L 287.


## Allyl(hydrido)platinum(II)-Catalyzed Partial Hydrogenation of Dienes


By *Roberta Bertani, Giovanni Carturan*,* and *Alberto Scrivanti*


We previously observed that $[(\eta^3\text{-}C_3H_5)Pt(L)H]$ **2** is stable in toluene between $-80$ and $-30\,^\circ C$, but decomposes with evolution of propene above $-20\,^\circ C$[3]. This represents the collapse of the 14-electron $Pt^0$ intermediate **3**, the occurrence of which has been demonstrated by variable temperature NMR spectroscopy.



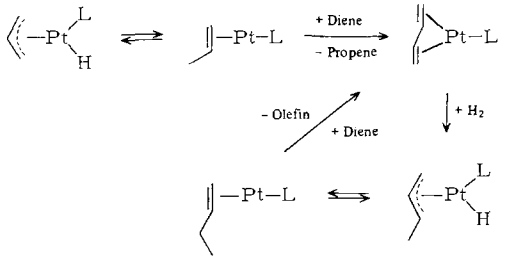
**a**, L = $P(C_6H_{11})_3$; **b**, L = $PtBu_3$

The $^1$H-NMR spectrum of "**2b**" at $-32\,^\circ C$ clearly indicates the presence of the isomer **3b** ($\delta = 5.86$, $H^a$, $J_{H^a-CH_3} = 6.3$ Hz; 4.93, $H^b$, $J_{H^b-H^c} = 10.2$, $J_{H^b-Pt} = 83$ Hz; 5.03, $H^c$, $J_{H^a-H^c} = 15.3$, $J_{H^c-Pt} = 103$ Hz). Equilibrium **2b** $\rightleftharpoons$ **3b** (70:30) is slowly established at this temperature; at $-81\,^\circ C$ only **2b** is detected. A leading example of this type of equilibrium was reported some years ago for the complex $[(\eta^3\text{-}C_3H_5)Ni(PF_3)(H)]$[6]; other cases refer to $d^6$ organometallic complexes[7].

The hydrido complexes **2** are low temperature catalysts for the selective partial hydrogenation of conjugated diolefins to monoolefins (butadiene→1-butene; isopropene→2-methyl-1-butene; 2,3-dimethylbutadiene→2,3-dimethyl-1-butene). The course of these reactions at $-78\,^\circ C$ under conditions of constant $H_2$ pressure was studied by gas chromatography. After addition of diene, immediate and quantitative evolution of propene occurs; this also happens in the absence of $H_2$, whereas in the absence of diene the $Pt^{II}$ complex **2** does not react with $H_2$ at low temperature. Kinetic profiles of diene concentration as a function of time are linear up to 95% substrate consumption; the reaction is, therefore, pseudo-zeroth order. All reactions display *ca.* 100% selectivity; *i.e.* the monoolefins are not further hydrogenated.

The kinetic data (see table in Supplement) indicate a linear dependence of $k_{obs}$ on $H_2$ pressure; this suggests that $H_2$ activation should be the rate determining step. The reduction in catalytic activity upon increasing the temperature may, therefore, be related to the reduction in the concentration of dissolved $H_2$. These arguments suggest the simplified catalytic mechanism shown in Scheme 1.

It is noteworthy that the selectivity of the process arises from the occurrence of the equilibrium **2** $\rightleftharpoons$ **3** and from the fact that $H_2$ activation must be attributed to diene-$Pt^0$ intermediates. Apart from other possible speculations on alternative or parallel steps, the proposed scheme is consistent with the chemistry of $\eta^3$-allyl(hydrido)transition-metal derivatives[9] and strongly coordinatively unsaturated complexes[10].



Scheme 1.


[*] Prof. Dr. G. Carturan, Dr. R. Bertani, Dr. A. Scrivanti
Centro Chimica Metallorganica CNR
via Marzolo 9, Padova (Italy)



Received: October 15, 1982 [Z 177 IE]
revised: December 20, 1983
German version: *Angew. Chem. 95* (1983) 241
The complete version of this communication appears in: *Angew. Chem. Suppl. 1983*, 228-233



[3] G. Carturan, A. Scrivanti, F. Morandini, *Angew. Chem. 93* (1981) 103; *Angew. Chem. Int. Ed. Engl. 20* (1981) 112.

[6] H. Bönnemann, *Angew. Chem. 82* (1970) 699; *Angew. Chem. Int. Ed. Engl. 9* (1970) 736.

[7] a) F. Nixon, B. J. Wilkins, *J. Organomet. Chem. 80* (1974) 129; b) J. W. Byrne, H. U. Blaser, J. A. Osborn, *J. Am. Chem. Soc. 97* (1975) 3871; c) T. H. Tulip, J. A. Ibers, *ibid. 101* (1979) 4201.

[9] E. L. Muetterties, J. R. Bleeke, *Acc. Chem. Res. 12* (1979) 324.

[10] N. M. Boag, M. Green, J. L. Spencer, F. G. A. Stone, *J. Chem. Soc. Dalton Trans. 1980*, 1200; see also references in [7] and E. O. Sherman, P. R. Schreiner, *J. Chem. Soc. Chem. Commun. 1978*, 223.


## Unexpected Ring-Opening of Benzocyclobutenes upon Reaction with Lithium in Tetrahydrofuran

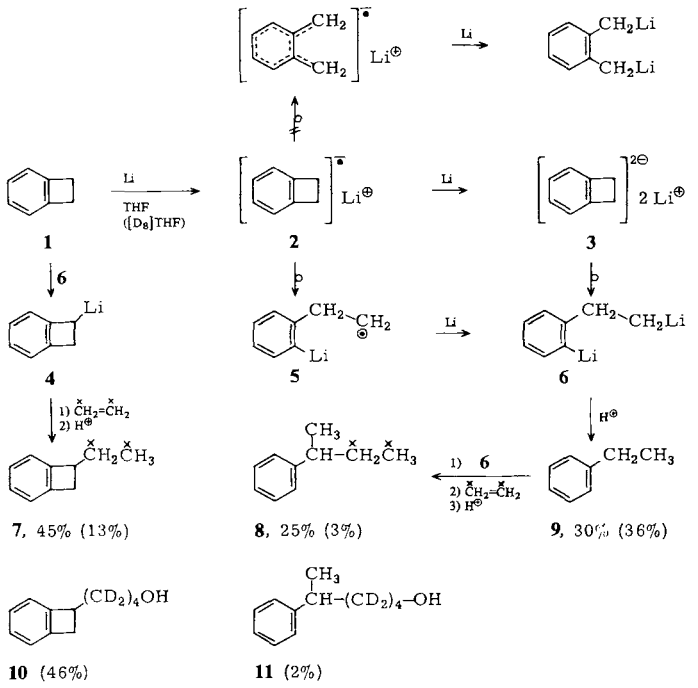

By *Adalbert Maercker*, Willi Berkulin,* and *Peter Schiess*


Although the conrotatory ring-opening of the benzocyclobutene radical anion is thermally allowed, previously reported results were revoked shortly after their publication[1].

We have found a completely different reaction path—scission of a $C_{aryl}-CH_2$ bond—in the reaction of benzocyclobutene (1,2-dihydrocyclobutabenzene)[**] **1**[2] with lithium powder in tetrahydrofuran (THF). The expected *o*-xylene was not detected, even in trace amounts. Instead, after hydrolysis ethylbenzene **9** and its subsequent product **8**, which may have been formed *via* the dilithio compound **6**, was obtained (Scheme 1; the relative yields were determined by gas chromatography: after four weeks at room temperature conversion was only 20%). Due to the long reaction time **6** metalates some of the educt **1** and the product **9** at the benzyl position. Solvent is cleaved to form ethylene, which readily adds to benzyllithium compounds[3]; the ethylene adducts **7** and **8** are formed in this


[*] Prof. Dr. A. Maercker, W. Berkulin
Institut für Organische Chemie der Universität
Adolf-Reichwein-Strasse, D-5900 Siegen 21 (Germany)
Prof. Dr. P. Schiess
Institut für Organische Chemie der Universität
St.-Johanns-Ring 19, CH-4056 Basel (Switzerland)

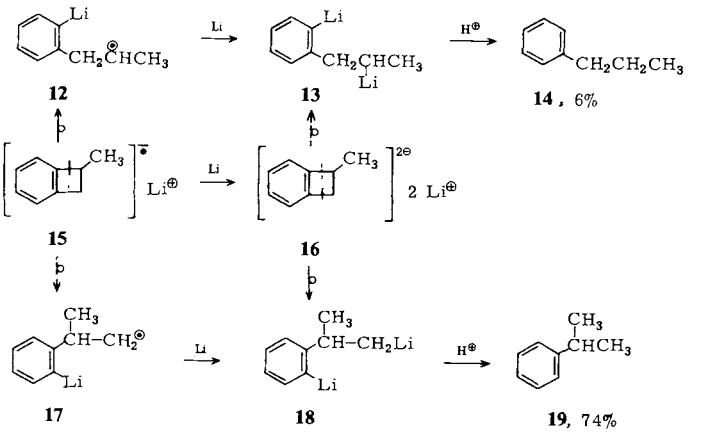

[**] According to IUPAC rules, benzocyclobutenes are termed 1,2-dihydrocyclobutabenzenes.



Scheme 1.

way. That the ethyl group in these compounds actually originates from THF could be established by use of perdeuteriotetrahydrofuran ([$D_8$]THF; relative yields in parenthesis, conversion after 4 weeks: 6%). Carbon atoms marked with an asterisk bear in this case two deuterium atoms.

However, due to the isotope effect protophilic decomposition of the solvent takes place considerably more slowly[4], and hence its nucleophilic cleavage to alcohols **10** and **11** becomes more important.



Scheme 2.

In principal, ring opening of the benzocyclobutene **1** can not only occur at the stage of radical anion **2**, but also at that of the dianion **3**. To clarify this we allowed α-methylbenzocyclobutene[5] to react with lithium powder in THF (Scheme 2). After a week the conversion was 10%. Formation of cumene **19** and *n*-propylbenzene **14** in the ratio of *ca.* 12:1 suggests dianion **16** as intermediate, which should preferentially react further *via* the primary alkyllithium compound **18**. Ring-opening at the stage of the radical anion **15** should result in formation of *n*-propylbenzene **14** as the major product *via* the secondary radical **12**. Additionally, the corresponding ethylene adducts are also obtained. Reaction of a mixture of α-methylbenzocyclobutene and **1** indicates that the latter is cleaved approximately twice as rapidly. The rates of separate runs, however, are not comparable, since the yields are markedly dependent on the nature of the lithium powder and on the mixing procedure.

Received: October 15, 1982 [Z 179 IE]
German version: *Angew. Chem. 95* (1983) 248

[1] N. L. Bauld, F. Farr, *J. Am. Chem. Soc. 91* (1969) 2788; N. L. Bauld, F. Farr, G. R. Stevenson, *Tetrahedron Lett. 1970*, 625; cf. also N. L. Bauld, J. Cessac, C.-S. Chang, F. R. Farr, R. Holloway, *J. Am. Chem. Soc. 98* (1976) 4561.
[2] P. Schiess, M. Heitzmann, *Helv. Chim. Acta 61* (1978) 844; P. Schiess, M. Heitzmann, S. Rutschmann, R. Stäheli, *Tetrahedron Lett. 1978*, 4569.
[3] A. Maercker, J. Troesch, *J. Organomet. Chem. 102* (1975) C1.
[4] A. Maercker, W. Theysohn, *Justus Liebigs Ann. Chem. 747* (1971) 70.
[5] P. Schiess, S. Rutschmann, V. V. Toan, *Tetrahedron Lett. 23* (1982) 3665, 3669. IUPAC nomenclature: 1-methyl-1,2-dihydrocyclobutabenzene.

## Synthesis and Structure of $\mu_2$-Oxobis[chloro(tetra-*p*-tolylporphyrinato)molybdenum(IV)]: A Complex with Central $Mo^{IV}-O-Mo^{IV}$ Unit

By *Jocelyne Colin, Bernard Chevrier, André De Cian,* and *Raymond Weiss**

The oxo chemistry of molybdenum(V) is dominated by binuclear μ-oxo complexes. Recently, the synthesis and structure of two mixed valence ($Mo^{IV}-O-Mo^{V}$) μ-oxo complexes were also reported[1]. In contrast, so far no molybdenum(IV) μ-oxo derivative has been structurally characterized. We have now isolated and characterized such a complex [Cl(TTP)Mo−O−Mo(TTP)Cl)], TTP=*meso*-tetra(*p*-tolyl)porphyrinate(2−), and examined its remarkable magnetic behavior.

Reaction of the dichloro complex $MoCl_2$ (TTP)[2] with an excess of *N*-phenylhydroxylamine in presence of small amounts of pyridine in toluene as solvent leads to rapid formation of a finely crystalline, air-sensitive red solid, which was identified by an X-ray structural study as a binuclear μ-oxo species. In the IR spectrum of this novel complex, a medium-strength band appears at 730 $cm^{-1}$ which we tentatively assign to the μ-oxo ligand. The corresponding bands in $Mo_2O_3$(TPP) and $Mo_2O_3$(OEP) appear at 615 and 630 $cm^{-1}$, respectively[3] (TPP = tetraphenylporphyrinato, OEP = octaethylporphyrinato anions), while in the case of the $Mo^{V}/Mo^{IV}$ mixed valence complex, $[Mo_2O(S_2CNEt_2)_6]BF_4$, this band is observed at 655 $cm^{-1}$[1]. An intense band appears at 280 $cm^{-1}$, which we ascribe to the Mo−Cl stretching vibration[2]. The UV/VIS spectrum shows four absorptions: $\lambda_{max}(\lg\varepsilon) = 5.90$ (3.50), 5.54 (4.11), 508 (3.88), and 430 nm (5.35).

Surprisingly, the magnetic susceptibility follows the Curie law between 4.2 and 293 K. The magnetic moment ($\mu_{eff} = 2.82\ \mu_B$ per Mo atom) is consistent with a high spin $d^2$ configuration with no magnetic exchange interactions between the two metal centers through the μ-oxo bridge.

[*] Prof. R. Weiss, Dr. J. Colin, Dr. B. Chevrier, Dr. A. De Cian
Laboratoire de Cristallochimie et de Chimie Structurale (E.R.A. 08)
Université Louis Pasteuer
4, rue Blaise Pascal, F-67060 Strasbourg Cedex (France)

 © *Verlag Chemie GmbH, 6940 Weinheim, 1983* *0570-0833/83/0303-0247 $ 02.50/0* 

Similarly, no such magnetic couplings occur in $Mo_2O_3(TPP)$ and $Mo_2O_3(OEP)$[3].

Suitable single crystals of the dichloromethane solvate $[Mo(TTP)Cl]_2O \cdot 2CH_2Cl_2$ were obtained from a $CH_2Cl_2$/ether mixture under anaerobic conditions. The result of the X-ray structural analysis[4] (cf. Fig. 1) shows quite clearly that gross structural features are similar to those observed in the other known μ-oxo metalloporphyrins[5a].

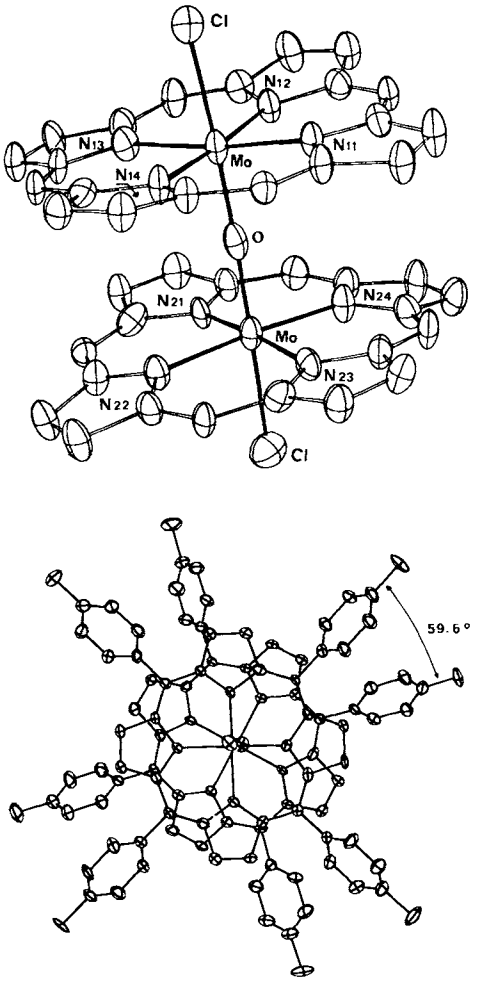



Fig. 1. Structure of the binuclear complex $[Mo^{IV}Cl(TTP)_2]O$ in the crystal (above: without tolyl groups; below: viewed along the MoOMo axis).

The two Mo atoms are displaced 0.08 Å from the $N_4$-plane of their TTP ligands in the direction of the bridging oxo atom; the distance between the best planes (24-atoms) of the chelate rings is 4.007 Å. As in the other known TPP and TTP complexes with $-O-$[5a], $-N=$[5b], and $=C=$[5c] bridges, the proximity of the two rings leads to a staggered conformation (torsion angle 59.6°) and to small dihedral angles between the substituent rings at the periphery and the porphyrin rings (50–62°). Moreover, both porphyrin rings are significantly nonplanar (quasi $D_{2d}$ ruffling). The mean values of the most important distances are: Mo–N 2.080(6)±0.019 Å, Mo–O 1.851(6)±0.006 Å, Mo–Cl 2.407(3)±0.007 Å; the MoOMo angle is 177.5(3)°.

The pathway by which the Mo–O–Mo linkage is formed is still unclear. The reaction of *N*-substituted hydroxylamines with FeCl(TPP) leads under the same experimental conditions to mononuclear nitroso complexes [Fe(py)(RNO)(TTP)][6].

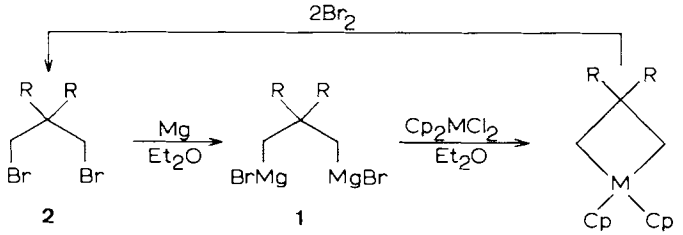
Received: October 19, 1982 [Z 180 IE]
revised: January 19, 1983
German version: *Angew. Chem. 95* (1983) 252

[1] J. A. Broomhead, M. Sterns, C. G. Young, *J. Chem. Soc. Chem. Commun. 1981*, 1262, and references cited therein.
[2] T. Diebold, B. Chevrier, R. Weiss, *Angew. Chem. 89* (1977) 819; *Angew. Chem. Int. Ed. Engl. 16* (1977) 788; *Inorg. Chem. 18* (1979) 1193.
[3] J. W. Buchler, K. Rohbock, *Inorg. Nucl. Chem. Lett. 8* (1972) 1073.
[4] Monoclinic, space group C2/c, $a=29.233(8)$, $b=16.872(6)$, $c=37.980(10)$ Å, $\beta=108.88(8)°$, $\rho_{calc}=1.339$ gcm$^{-3}$, $Z=8$; 6319 reflections ($I>3\sigma(I)$, $2\theta<114°$), $R_1=0.069$, $R_2=0.095$. Further details of the structure determination can be obtained on request from the Fachinformationszentrum Energie Physik Mathematik, D-75514 Eggenstein-Leopoldshafen, by quoting the depository number CSD 50343, the name of the author and full citation of the journal.
[5] a) B. C. Schardt, F. J. Hollander, C. L. Hill, *J. Am. Chem. Soc. 104* (1982) 3964; J. F. Johnson, W. R. Scheidt, *Inorg. Chem. 17* (1978) 1280, and references cited therein; b) W. R. Scheidt, D. A. Summerville, I. A. Cohen, *J. Am. Chem. Soc. 98* (1976) 6623; c) V. L. Coedken, M. R. Deakin, L. A. Bottomley, *J. Chem. Soc. Chem. Commun. 1982*, 607.
[6] D. Mansuy, P. Battioni, J. C. Chottard, M. Lange, *J. Am. Chem. Soc. 99* (1977) 6441.

## Zircona- and Hafnacyclobutenes—A New Route to Metallacyclobutanes

By *Johannes W. F. L. Seetz, Gerrit Schat, Otto S. Akkerman,* and *Friedrich Bickelhaupt**

Transiton-metal cyclobutanes have recently been the subject of intensive study. We report here the first general method for their preparation: the reaction of 1,3-dimagnesioalkanes with metal dihalides. The prerequisite for this long-known synthetic principle is the recently developed facile synthesis of 1,3-bis(bromomagnesio)propane **1a** from 1,3-dibromopropane **2a**[15a] and of its 2,2-dimethyl derivative **1b** from **2b**[15b]. The effectiveness of the new method is demonstrated using the example of the metallacyclobutanes of group IVB metals.




**a** : R = H ; **b** : R = Me ; Cp = Cyclopentadienyl

Reaction of **1b** with dichlorodicyclopentadienyltitanium, -zirconium or -hafnium yields the metallacyclobutanes **3b**, **4b**, and **5b**, respectively, which were characterized by elemental analysis (**4b**, **5b**), reaction with bromine to afford **2b**, as well as by their spectra. The high-field shift of the $^{13}$C-NMR signal of the quaternary carbon atom in the 2,2-dimethyl derivatives is particularly characteristic; this is caused by a shielding effect of the $Cp_2M$ frag-

[*] Prof. Dr. F. Bickelhaupt, Dr. O. S. Akkerman, Drs. J. W. F. L. Seetz, G. Schat
Vakgroep Organische Chemie, Vrije Universiteit
De Boelelaan 1083, 1081 HV Amsterdam (Netherlands)

 © Verlag Chemie GmbH, 6940 Weinheim, 1983 0570-0833/83/0303-0248 $ 02.50/0 

ment, which is only possible in a four-membered ring (Table 1).

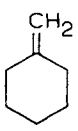
Table 1. NMR data of **3b**, **4b**, and **5b** [a].

| | $^1$H-NMR δ-values [b] | | | $^{13}$C-NMR δ-values ($^1J_{CH}$ [Hz]) | | | |
|---|---|---|---|---|---|---|---|
| | $CH_3$ | $CH_2$ | $C_5H_5$ | $CH_3$ | $CH_2$ | $C_2H_5$ | C(β) |
| **3b** | 1.01 | 2.46 | 5.43 | 38.1, q (124) | 83.4, t (137) | 110.8, d (172) | 5.4, s — |
| **4b** | 1.19 | 1.87 | 5.57 | 40,2, q/m (125) | 66.4, t (133) | 109.2, d/m (171) | 7.4, s — |
| **5b** | 1.28 | 1.81 | 5.53 | 39.7, q (124) | 71.7, t (130) | 108.9, d (173) | 7.4, s — |

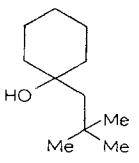
[a] Bruker WM 250 spectrometer; in [$D_8$]toluene at −30 °C. [b] All signals are singlets.

Analogous attempts to prepare **3a** and **4a** provided only indirect evidence for formation of the metallacyclobutanes in low yield: treatment of the reaction mixture with bromine yields **2a** (< 1 to 5%) and larger amounts of 1,2,3-tribromopropane, which indicates the presence of an allylmetal compound formed by β-hydrogen scission.

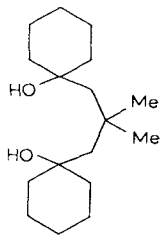
In accord with calculations[9], the stability of the metallacyclobutanes increases from titanium to hafnium: the half-lives of the 2,2-dimethyl derivatives are *ca.* 1—2 h (**3b**), 3 h (**4b**), and 9 d (**5b**). Noteworthy is the fact that **4a**, **4b**, and **5b** have not been described previously; presumably they are not accessible using the route[1] described for titanacyclobutanes.




**6**




**8**




**9**

**3b**, **4b**, and **5b** exhibit surprising differences in chemical behavior: upon reaction with cyclohexanone (diethyl ether, 0 °C) only **6** is formed from **3b**; from **4b**, besides traces of **6**, the major products **8** and **9** (ratio 45:55) are formed, and from **5b** only **8** is obtained. We presume that **3b** fragments to a metal-carbene complex (and isobutene)[18], which reacts with cyclohexanone to afford **6** *via* a Wittig-type reaction. In contrast, with **4b** and **5b** normal addition of the alkylmetal compound to the carbonyl group occurs; the difference in reaction behavior of **4b** and **5b** requires further clarification.

Received: October 25, 1982; revised December 2, 1982 [Z 185 IE]
German version: *Angew. Chem. 95* (1983) 242
The complete manuscript of this communication appears in: *Angew. Chem. Suppl. 1983*, 234—242

[1] T. R. Howard, J. B. Lee, R. H. Grubbs, *J. Am. Chem. Soc. 102* (1980) 6876; J. B. Lee, G. J. Gadja, W. P. Schaefer, T. R. Howard, T. Ikariya, D. A. Straus, R. H. Grubbs, *ibid. 103* (1981) 7358.

[9] A. K. Rappé, W. A. Goddard III, *J. Am. Chem. Soc. 104* (1982) 297, 448, and references cited therein.

[15] a) J. W. F. L. Seetz, F. A. Hartog, H. P. Böhm, C. Blomberg, O. S. Akkerman, F. Bickelhaupt, *Tetrahedron Lett. 23* (1982) 1497; b) J. W. F. L. Seetz, G. Schat, O. S. Akkerman, F. Bickelhaupt, *J. Am. Chem. Soc. 104* (1982) 6848.

[18] R. H. Grubbs et al., cited in *Chem. Eng. News 60* (1982) No. 16, p. 34.

## Synthesis and Structure of $[AsPh_4][Ru_6H(\mu\text{-}O{=}CNMe_2)_2(\mu\text{-}CO)_4(CO)_{14}]\cdot Me_2C{=}O$; A Cyclic Hydrido-Hexametallic Anion**

By *Neil M. Boag, Carolyn B. Knobler,* and *Herbert D. Kaesz**

We were interested in examining single crystals containing the triruthenium anion $[Ru_3(\mu\text{-}O{=}CNMe_2)(\mu\text{-}CO)_3(CO)_7]^-$, which we obtained quantitatively as the hexamethylguanidium salt, **1a**, by treating $Ru_3(CO)_{12}$ with $C(NMe_2)_4$[1]. Since crystals of **1a** proved unsuitable for X-ray study we prepared the potassium salt, **1b**, by deprotonation of the neutral precursor **2**.

$$[Ru_3(\mu\text{-}H,\mu\text{-}O{=}CNMe_2)(CO)_{10}] + KOH/MeOH \xrightarrow[25\,^\circ C,\ 3\ h]{THF/CO\ (1\ atm)} K[Ru_3(\mu\text{-}O{=}CNMe_2)(CO)_{10}] \quad (1)$$

**2** → **1b**

The salt, **1b**, is a convenient starting material for metathetic reactions. For its synthesis, however, the conditions cited in reaction (1) must be strictly adhered to, since degradation of **2**, probably by attack of $OH^-$ at the carbon of coordinated CO, competes with the desired deprotonation. Rapid addition of base gives rise to a dark microcrystalline contaminant, which proved to be the tetraphenylarsonium salt of the title compound, **3**. We were able to obtain **3** in 45% yield by simply adding the base to a refluxing THF solution of **2** in the *absence* of carbon monoxide and then adding $AsPh_4Cl$.

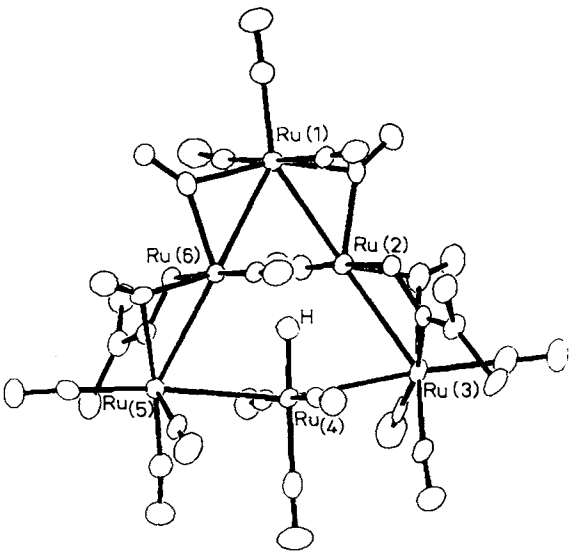



Fig. 1. ORTEP projection of the hexanuclear anion of the title compound **3** in the crystal.

The crystal structure of **3** (Fig. 1) was determined from data collected at −156 °C. The metal framework of the anion is a puckered six-membered ring consisting of two intersecting planes: Ru2, Ru4, and Ru6 define one plane, while Ru1, Ru3, and Ru5 define the second. The two

[*] Prof. Dr. H. D. Kaesz, Dr. N. M. Boag, Dr. C. B. Knobler
Department of Chemistry and Biochemistry, University of California
Los Angeles, CA 90024 (USA)

[**] This work was supported by U. S. National Science Foundation (H. D. K.) and a NATO-SERC Fellowship (N. M. B.).

planes intersect at the line defined by Ru4 and Ru1. An H atom is located on this line *inside* the metal ring at a separation of 1.50(11) Å from Ru4 and at an average distance of 2.07 Å from Ru2 and Ru6.

A six-membered metal ring, containing no transannular linkages, achieves a closed-shell configuration with 96 ($6 \times 16$) valence electrons. A recently reported planar hexametallic cluster, $Os_6(CO)_{17}[P(OMe)_3]_4$[2], contains 90 valence electrons, and attains a closed shell with a fully-formed internal triangle and three metal-metal bonds in the range 2.834—2.848 Å. By contrast, the title anion contains 92 valence electrons, six of which are derived from the two bridging $O{=}CN(Me)_2$ groups; *two* cross-ring metal-metal bonds are required to attain a closed valence-shell. Rather long separations, approximately 0.3 Å longer than Ru—H—Ru separations previously observed for other compounds of this type, are found for the central triangle (Ru2—Ru6 3.242(2), Ru4—Ru2 3.226(2), and Ru4—Ru6 3.213(2) Å). This appears to be a compromise between the requirements of a closed valence-shell and forces opposing the closed approach along any two edges of the central triangle.

Received: October 25, 1982;
revised: December 16, 1982 [Z 186 IE]
German version: *Angew. Chem. 95* (1983) 243
The complete manuscript of this communication appears in:
*Angew. Chem. Suppl. 1983*, 198—209

[1] A. Mayr, Y. C. Lin, N. M. Boag, H. D. Kaesz, *Inorg. Chem. 21* (1982) 1704.
[2] R. J. Goudsmith, B. F. G. Johnson, J. Lewis, P. R. Raithby, K. H. Whitmire, *J. Chem. Soc. Chem. Commun. 1982*, 640.

## Synthesis and Structure of Metallocene Cations of the Vb Elements Arsenic and Antimony

By *Peter Jutzi*, Thomas Wippermann, Carl Krüger,* and *Hans-Jürgen Kraus*

The existence of cationic $\eta^5$-cyclopentadienyl complexes of the type $(R_5C_5)_2M^+$ (M = Vb element), isoelectronic with the IVb-metallocenes $(R_5C_5)_2M$ (M = Ge,Sn,Pb), has been suggested on the basis of NMR spectroscopic findings[1] as well as theoretical considerations[1b]. We have now been able to isolate the first such "metallocenium" ions as tetrafluoroborates and, in one case, to determine the crystal structure.

On reaction of bis(pentamethylcyclopentadienyl)fluoroarsane or -stibane[2] with boron trifluoride or boron trifluoride-diethyl ether, respectively, in hexane at −20 °C, abstraction of fluoride takes place with concomitant formation of the corresponding bis(pentamethylcyclopentadienyl)element cation.

$$(Me_5C_5)_2MF + BF_3 \rightarrow (Me_5C_5)_2M^+BF_4^-$$
$$\mathbf{1}: M = As,\ \mathbf{2}: M = Sb$$

The salts **1** and **2** are very sparingly soluble in hexane but readily dissolve in polar and aprotic solvents; they crystallize from dichloromethane as yellow or orange crystals, whose identity is confirmed by analytical and spectroscopic data.

The NMR spectra[3] of **1** and **2** indicate the existence of dynamic structures in solution, whereas an X-ray structure analysis carried out on **1**[4] shows that the cyclopentadienyl ligands are not ideally *pentahapto*-bonded to the central atom in the cation; rather a distortion in the sense of a *di*- and *trihapto*-coordination is observed (cf., in Fig. 1, the respective bond lengths and the tilting of five methyl groups away from the ring plane (C6: 12°, C7: 3.8°, C10: 3.2°, C17: 9.7°, C18: 10.3°)). Such a deviation from the ideal *pentahapto*-structure had already been indicated in the case of decamethylstannocene[5]. As expected, the two cyclopentadienyl rings in **1** are not coplanar, the angle between them is 36.5°.

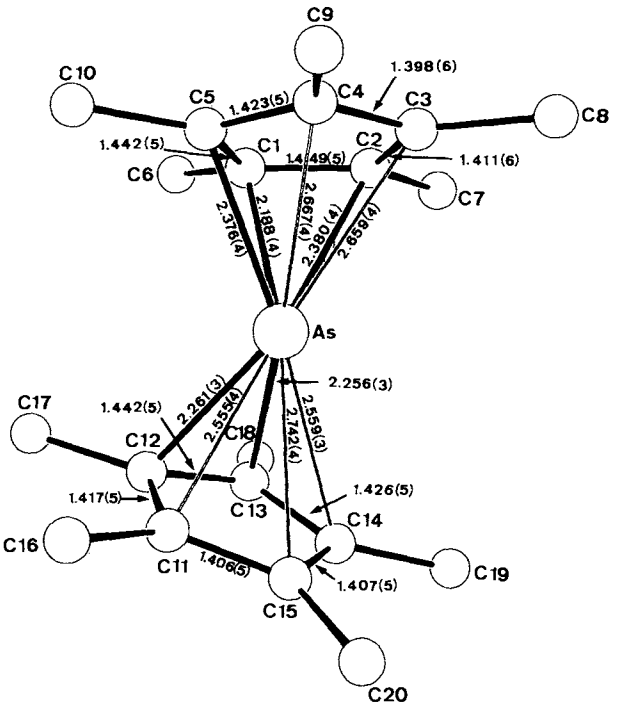



Fig. 1. Structure of the cation of **1** in the crystal.

For the stability of such cations the choice of the anion is decisive: species with $AlCl_4^-$, $BCl_4^-$ or $SbCl_6^-$ as counterions defy isolation.

Received: October 25, 1982 [Z 187 IE]
German version: *Angew. Chem. 95* (1982) 244

[*] Prof. Dr. P. Jutzi, T. Wippermann
Fakultät für Chemie der Universität
Postfach 8640, D-4800 Bielefeld 1 (Germany)
Dr. C. Krüger, Dr. H.-J. Kraus
Max-Planck-Institut für Kohlenforschung
Lembkestrasse 5, D-4330 Mülheim-Ruhr 1 (Germany)

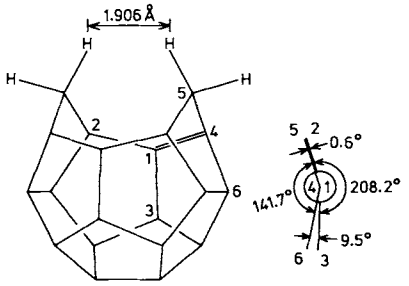
[1] a) P. Jutzi, F. Kohl, H. Saleske, A. Sufert, *IX. Int. Conf. Organomet. Chem.*, Dijon 1979, *Abstr.* A 38; b) S. G. Baxter, A. H. Cowley, S. K. Mehrotra, *J. Am. Chem. Soc. 103* (1981) 5572; S. G. Baxter, A. H. Cowley, J. G. Lasch, M. Lattman, W. P. Sharum, C. A. Stewert, *ibid. 104* (1982) 4064.
[2] P. Jutzi, T. Wippermann, unpublished results.
[3] **1**: $^1$H-NMR ($CDCl_3$, TMS int.): $\delta(CH_3) = 2.20$ (s); $^{13}$C-NMR ($CDCl_3$, TMS int.): $\delta(CH_3) = 9.8$ (s), $\delta$(C-ring) = 129.8 (s); $^{11}$B-NMR ($CDCl_3$, $BF_3 \cdot Et_2O$ ext.): $\delta(BF_4^-) = -0.6$; $^{19}$F-NMR ($CDCl_3$, $C_6F_6$ int.): $\delta(BF_4^-) = 9$ (s).—**2**: $^1$H-NMR: $\delta(CH_3) = 2.22$ (s); $^{13}$C-NMR: $\delta(CH_3) = 10.5$ (s), $\delta$(C-ring) = 127.4 (s); $^{11}$B-NMR: $\delta(BF_4^-) = -0.9$ (s); $^{19}$F-NMR: $\delta(BF_4^-) = 12$ (s).
[4] Structural data: $P2_1/n$, $a = 13.1946(7)$, $b = 12.4792(6)$, $c = 13.1980(9)$ Å, $\beta = 104.349(4)°$, $V = 2105.4$ Å$^3$, $\varrho_{calc} = 1.365$ g cm$^{-3}$, $Z = 4$; reflections: 4314, 3636 observed ($I > 2\sigma(I)$), refined parameters: $R = 0.047$, $R_W = 0.067$, Further details of the crystal structure investigation can be obtained on request from the Fachinformationszentrum Energie Physik Mathematik, D 7514 Eggenstein-Leopoldshafen, quoting the despository number CSD 50293, the name of the author, and full citation of the journal.
[5] P. Jutzi, F. Kohl, P. Hofmann, C. Krüger, Yi-Hung Tsay, *Chem. Ber. 113* (1980), 757.

## Cautionary Example of Incorrect Structural Assignment Due to Crystallographic Disorder**

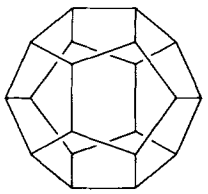
By *Otto Ermer**

In the course of crystal structure analyses, disorder phenomena often prove to be perturbations of unclear origin, which lead to unreliable structural parameters or, in the extreme case, can even prevent the derivation of a qualitatively correct structural model. As a spectacular example, the crystal structure analysis of the secododecahedrene **1**[1] at room temperature is reported here. The present study was stimulated by our interest in non-planar double bonds[2a]. According to empirical calculations using our force field[2b], **1** has marked pyramidal distortions at the $C_{sp^2}$ atoms (out-of-plane bending; cf. the calculated double bond torsion angles in the formula diagram). Furthermore, its short calculated H···H distance of 1.906 Å is noteworthy.

Crystals of **1** were optically isotropic and gave X-ray photographs with Laue symmetry m3 ($T_h$), corresponding to a cubic crystal system. An all-face centered lattice and the space groups F23 or Fm3 followed from the systematic extinctions. The cell constant $a = 10.895(5)$ Å was measured on a four-circle diffractometer. There are four $C_{20}H_{20}$ formula units per unit cell resulting in a plausible density $\rho_{calc} = 1.337$ g cm$^{-3}$ (due to lack of material a macroscopic density measurement was not performed). For an ordered structure, these crystallographic data impose molecular symmetry T or $T_h$. Clearly, this condition cannot be met by the unsymmetrical secododecahedrene **1**, and hence a disordered structure must be concluded: the high crystallographic symmetries apply only for a molecular structure *averaged* over time and/or space.




1



2

An ordered crystal structure would in the present case be possible if it were assumed that the crystals examined did not consist of the secododecahedrene **1** but of the highly symmetrical dodecahedrane **2**[1]. Gaseous **2** has $I_h$ symmetry[2a,3], whose highest possible crystallographically allowed subgroup is $T_h$. Originally, we had indeed assumed an ordered structure and, based on simple structural-chemical and geometrical criteria, constructed a dodecahedrane crystal structure model in the centrosymmetric space group Fm3. Subsequently, this model was optimally fitted by least-squares to a set of 68 reflection intensities measured on a diffractometer at room temperature ($Mo_{K\alpha}$ radiation; $\sin\theta/\lambda < 0.48$ Å$^{-1}$). The final $R$ value was 0.048 ($R_w = 0.051$; $w = 1/\sigma^2(F_o)$; C refined anisotropically, H isotropically)[4]. It should be noted that in later test calculations direct methods also produced appropriate dodecahedrane structure models. The very plausible results of the refinement are shown in Figure 1 and correspond entirely to expectations for the crystal structure of an almost spherical hydrocarbon: highly symmetrical space group, high crystallographic molecular symmetry, (cubic) closest packing, relatively high thermal motion in the crystal and, hence, somewhat shortened CC bond lengths[4].

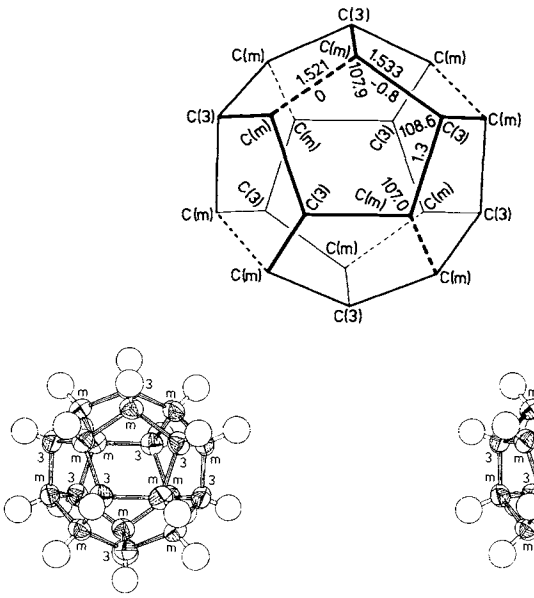



Fig. 1. Geometry (above; estimated standard deviations for distances, angles, and torsion angles, formally *ca.* 0.004 Å and 0.3°, respectively) and thermal motion (below; 10% ellipsoids) of the dodecahedrane model refined on the room temperature intensities of the secododecahedrene **1**. The C atoms on the threefold axes are designated by C(3) and those on the mirror planes by C(m). The C(m)–C(m) bonds are dashed in the top drawing in order to illustrate the $T_h$ symmetry[4].

The crystallographic identification of the material studied as dodecahedrane raised doubts based on the chemistry of the substance[5]. Therefore, a $^1$H-NMR spectrum was recorded of a fragment of the crystal which had been used for the X-ray intensity measurements. This spectrum showed unequivocally that the crystal consisted of the secododecahedrene **1**, as originally presumed[5]. Accordingly, the crystal structure of **1** at room temperature is disordered in such a way that it can be described well by an ordered structural model of **2**. Probably the still rather spherical secododecahedrene **1** adopts 30 statistically distributed preferred orientations in the crystal, in each of which the line interconnecting the methylene C atoms is parallel to a dodecahedral edge. A structure averaged over these orientations differs only slightly from that of dodecahedrane **2**.

The present experiences may serve as a cautionary example that a satisfactory $R$ value and even physically highly plausible structural results do not always safeguard against incorrect assignments in crystal structure analyses.


[*] Priv.-Doz. Dr. O. Ermer
Abteilung für Chemie der Universität
Postfach 102148, D-4630 Bochum 1 (Germany)



[**] This work was supported by the Fonds der Chemischen Industrie and the Deutsche Forschungsgemeinschaft.



Received: October 28, 1982 [Z 189 IE]
German version: *Angew. Chem. 95* (1983) 251


CAS registry numbers:
5,2,1,6,3,4-[2,3]Butanediyl[1,4]-diylidenedipentaleno[2,1,6-*cde*: 2′,1′,6′-*gha*]pentalene, 53129-39-8.

[1] R. J. Ternansky, D. W. Balogh, L. A. Paquette, *J. Am. Chem. Soc. 104* (1982) 4503. Prof. L. A. Paquette, Columbus, is thanked for crystals of **1**.

[2] a) O. Ermer: *Aspekte von Kraftfeldrechnungen*, Wolfgang Baur Verlag, München 1981; b) O. Ermer, S. Lifson, *J. Am. Chem. Soc. 95* (1973) 4121.

[3] O. Ermer, *Angew. Chem. 89* (1977) 431; *Angew. Chem. Int. Ed. Engl. 16* (1977) 411.

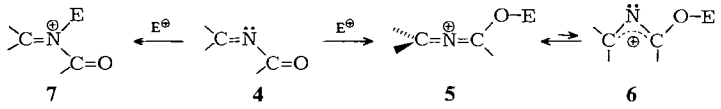
[4] The refined parameters of the dodecahedrane model (symmetrie $T_h$) fitted to the intensity data of the secododecahedrene **1** are for the C atom on a threefold axis C(3): $x=y=z=0.1131(2)$; $U_{11}=U_{22}=U_{33}=0.145(2)$, $U_{12}=U_{13}=U_{23}=-0.017(2)$ Å$^2$, for the C atom on a mirror plane C(m): $x=0.1848(3)$, $y=0$, $z=0.0698(3)$; $U_{11}=0.119(3)$, $U_{22}=0.173(4)$, $U_{33}=0.150(3)$, $U_{12}=U_{23}=0$, $U_{13}=-0.020(2)$ Å$^2$. The corresponding results for H(3) are: $x=y=z=0.155(3)$; $U_{iso}=0.20(2)$ Å$^2$, for H(m): $x=0.267(5)$, $y=0$, $z=0.090(4)$; $U_{iso}=0.22(2)$ Å$^2$. Deviations from $I_h$ symmetry of this (averaged) structure are small, as would be expected for the relatively rigid dodecahedrane molecule [1, 2a, 3]. Further details on the crystal structure investigation can be obtained from the Fachinformationszentrum Energie, Physik, Mathematik, D-7514 Eggenstein-Leopoldshafen, by quoting the depository number CSD 50312, the name of the author, and the journal citation.

[5] L. A. Paquette, personal communication.

## Reactions of *N*-Methylenecarboxamides with Electrophiles: 1-Alkoxy-2-azaallenium Salts and *N*-Acyl(methylene)ammonium Salts**

By *Ernst-Ulrich Würthwein*, Rainer Kupfer,* and *Claus Kaliba*

Like the simpler amides, *N*-methylenecarboxamides **4**[4] are ambident nucleophiles which can be attacked by electrophiles at oxygen or at nitrogen. Alkylation at the oxygen atom is expected to yield 1-alkoxy-2-azaallenium salts **5** or 1-alkoxy-2-azaallyl cations **6**; attack at the nitrogen atom should lead to *N*-acyl(methylene)ammonium salts **7**[5].



**7** **4** **5** **6**

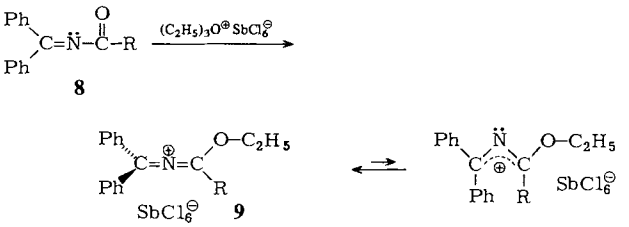
The *N*-methylenecarboxamides **8a, b** were synthesized by acylation of diphenylmethaneimine. These were then alkylated with oxonium salts or protonated with strong acids. All products are stable, hygroscopic, crystalline solids, which can be purified and fully characterized (Table 1). According to their $^{13}$C-NMR-spectra, the alkylation products **9a, b** have 1-ethoxy-2-azaallenium structures of type **5**. This structural assignment is supported, in particular by the $^{13}$C-chemical shifts of the methylene groups (**9b**: $\delta=73.32$; ether-region). Both phenyl groups give rise to only four signals, even at low temperatures (*e.g.* **9a**: $-70$ °C, $CDCl_3$, 25.15 MHz), which is consistent with the formulated allene-type structure ($C_s$ symmetry). Strong IR absorptions at 1695 and 1700 cm$^{-1}$, respectively, are ascribed to C=N=C– heteroallene stretching vibrations[7].

The *N*-acylated methyleneammonium salt **11**, which is isomeric to **9b**, was synthesized from *N*-diphenylmethylene(ethyl)amine and *p*-methylbenzoylium hexachloroantimonate. The $^{13}$C-chemical shift of its methylene group ($\delta=55.33$) is typical for an *N*-ethyl(methylene)ammonium salt. The two phenyl groups give rise to eight signals, in accordance with the planar $C_s$-structure **11**. These spectroscopic data indirectly support the favored alkylation of *N*-methylenecarboxamides at the oxygen atom.

Table 1. Physical data and yields for the compounds **9**, **10**, and **11**.

| Cpd. | IR $\nu$ [cm$^{-1}$] | $^{13}$C-NMR [$\delta$ values] [c] C=N– | –N–C–O– | $-CH_2-$ | M.p. [°C] | Yield [%] |
|---|---|---|---|---|---|---|
| **8a** | 1640, 1690 [a] | 164.11 | 184.83 | — | 43.5—44 | 71 |
| **8b** | 1620, 1650 [b] | 167.41 | 179.19 | — | 153.5—154.5 | 63 |
| **9a** | 1585, 1700 [b] | 168.33/173.31 [d] | | 71.65 | 97—102 (dec.) | 66 |
| **9b** | 1585, 1695 [b] | 169.67/176.22 [d] | | 73.32 | 158—159.5 (dec.) | 45 |
| **10a** | 1580, 1758 [b] | 189.68 | 170.00 | — | 113—117 (dec.) | 70 |
| | | 188.20 | 169.81 [e] | — | | |
| **10b** | 1600, 1735 [b] | 190.44 | 166.63 | — | 109—114 (dec.) | 63 |
| **11** | 1585, 1725 [b] | 188.92 | 171.36 | 55.33 | 126—129 (dec.) | 64 |

[a] In $CHCl_3$. [b] In Nujol. [c] 25.15 MHz, 25 °C, solvent: $CDCl_3$ (**8a, b, 9a**); $CD_3NO_2$ (**9b, 10a, b, 11**). [d] Assignment uncertain. [e] Solvent: $SO_2$, $-70$ °C, $CF_3SO_3H$-excess.

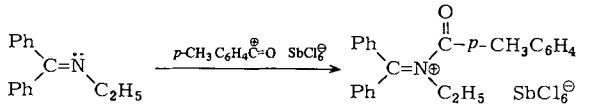


**8**

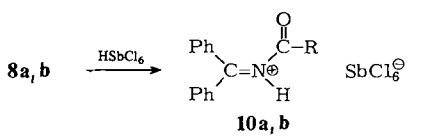
**9**

**a**, R = $CH_3$ **b**, R = *p*-$CH_3C_6H_4$

The $^{13}$C-NMR data of the protonated derivatives **10a, b** are very similar to the data of **11**, but they differ significantly from those of the *O*-alkylated compounds **9a, b**. In particular, the low temperature $^{13}$C-NMR spectra (liquid $SO_2$, excess of trifluoromethanesulfonic acid) indicate the favored nitrogen protonation: the C=N-signal is found at $\delta=189.99$, the C=O signal at $\delta=170.00$; eight signals for the two phenyl groups and the IR-absorptions (at 1758 and 1735 cm$^{-1}$, respectively) provide further evidence for attack at the nitrogen atom (c.f. also[8]).



**11**



**10a, b**

Quantum mechanical calculations (*ab initio*, 3—21G[9]) support the experimental results. A twisted cisoid conformation (dihedral angle C=N–C=O: 25.4°) is predicted as

[*] Dr. E.-U. Würthwein, R. Kupfer, C. Kaliba
Institut für Organische Chemie der Universität Erlangen-Nürnberg
Henkestrasse 42, D-8520 Erlangen (Germany)

[**] This work was supported by the Deutsche Forschungsgemeinschaft and the Fonds der Chemischen Industrie.

the most favorable structure for the unsubstituted *N*-methyleneformamide; the *s-cis*-conformer is 0.11 kcal/mol, the *s-trans* conformer 2.90 kcal/mol higher in energy.

Both according to experiment as well as to calculation, the protonation of formamide takes place preferentially at the oxygen atom. *N*-methylenecarboxamides, on the other hand, are predicted by the calculations to be attacked at the nitrogen atom. Oxygen protonation is less favorable by 7.00 kcal/mol. 1-Hydroxy-2-azaallyl cations are much higher in energy (19.6 kcal/mol for the *endo*-isomer) than the linear allenium ions.

Calculations on the structure of the 1-hydroxy-2-azaallenium ion reveal its unusual dynamic properties. An energy of only 4 kcal/mol is necessary to convert the linear allene-like form into a 150°-bent structure; the methylene groups remain twisted during this motion. Favorable compromises in the overlap between the π-electron systems and the lone pairs on nitrogen and oxygen are responsible for the unusual molecular flexibility predicted for these ions by the calculations.

Received: October 28, 1983 [Z 190 IE]
revised: December 20, 1982
German version: *Angew. Chem. 95* (1983) 247
The complete manuscript of this communication appears in:
*Angew. Chem. Suppl. 1983*, 264–270

[4] M. C. Lasne, J.-L. Ripoll, A. Thuillier, *J. Chem. Res. (S) 1982*, 214.
[5] *N*-Acyl(methylene)ammonium salts as amidoalkylation reagents: *e.g.* H. E. Zaugg, *Synthesis 1970*, 49; as isolated salt: *e.g.* T. Cohen, J. Lipowitz, *J. Am. Chem. Soc. 86* (1964) 2514.
[7] E.-U. Würthwein, *Angew. Chem. 93* (1981) 110; *Angew. Chem. Int. Ed. 20* (1981) 99, and unpublished results.
[8] Evidence of *N*-protonation from $^1$H-$^1$H-NMR coupling constants: G. R. Krow, C. Pyun, C. Leitz, J. Marakowski, *J. Org. Chem. 39* (1974) 2449.
[9] J. S. Binkley, J. A. Pople, W. J. Hehre, *J. Am. Chem. So.c 102* (1980) 939.

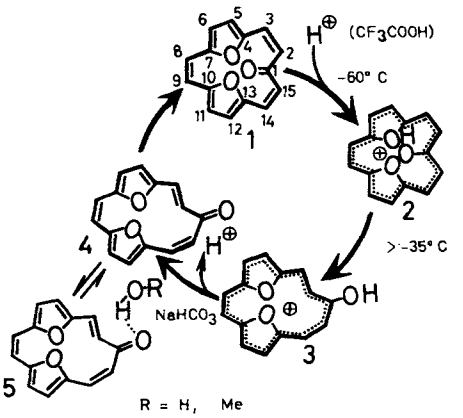
## Straightforward Preparation and Stabilization of 2-*trans*-4,7 : 10,13-Diepoxy[15]annulenone

By *Haru Ogawa**, *Tadashi Inoue*, *Taiji Imoto*, *Izumi Miyamoto*, *Hidefumi Kato*, and *Yōichi Taniguchi*

Although the 2-*trans*-[15]annulenone **4** with two oxygen bridges has been prepared[1], its fugitive existence has precluded further studies. We now report a [15]annulenone–hydroxy[15]annulenylium ion cycle, from which **4** could be isolated as predominant isomer. It was also found that the ground state of **4** could be stabilized by $H_2O$ to form a 14π-annulenylioolate **5**, R = H (Scheme 1).

The *cis*-annulenylium ion **2** was formed by dissolving **1** in $CF_3COOD + CD_2Cl_2$ (1 : 5) at −60 °C [$^1$H-NMR: AB system centered at $\delta = 8.61$ and 8.99 ($J_{cis} = 9.77$ Hz), 4H, H-2, H-3, H-14, and H-15; singlet at $\delta = 9.06$, 6H, H-5, H-6, H-8, H-9, H-11, and H-12].

On warming the solution the $^1$H-NMR spectrum changed dramatically to give nine outer proton resonances ($\delta = 8.85 - 10.30$) and one inner proton resonance ($\delta = -3.68$, $J_{trans} = 14.6$ Hz), indicating that the *cis-trans* equilibrium **2** ⇌ **3** shifts considerably towards **3** (**3** : **2** ≈ 12 : 1). Addition of saturated $NaHCO_3$ solution to **3**, which could be regenerated at 25 °C in $CF_3COOD$, followed by chromatographic separation ($CH_2Cl_2$, $Al_2O_3$, activity III) gave pure **4**. **4** proved to be diatropic; the outer protons absorb in the region $\delta = 6.82 - 8.18$ (9H) and the inner proton at $\delta = 4.54$ ($J_{trans} = 16$ Hz, in $CDCl_3$, 27 °C).




Scheme 1. The [15]annulenone–hydroxy[15]annulenylium ion cycle.

The chemical shift of the inner proton is highly temperature- and solvent-dependent. In $D_3COD$ progressive high-field shifts occur on cooling [$\delta = 2.51$ (0 °C), 1.85 (−25 °C), and 0.57 (−55 °C)]. Such large shifts were also observed at 25 °C on increasing the $D_2O$ content [$\delta = 3.02$ ($D_3COD$ : $D_2O$ = 100 : 0), 2.60 (100 : 16), 1.31 (100 : 40), 0.87 (100 : 56)]. These observations indicate that the dipolar stretched form **5** is formed by H-bonding to stabilize the *trans* geometry.

Kinetic measurements of the isomerization **4** → **1** (UV spectroscopy) confirmed these results. As expected, the rates of isomerization, which could be best approximated by eq. (1), became slower in aqueous solvents indicating that $k_{H^+}$ in $CH_3OH$ is *ca.* 3 times greater than $k_{H^+}$ in 25% aqueous $CH_3OH$, and that $k_{H^+}$ (in acetone)/$k_{H^+}$ (in 25% aqueous MeOH) is at least several thousand.

$$\text{rate} = (k_{H^+}[H^+] + k_{therm})[\mathbf{4}] \quad (1)$$

A significant feature of the annulenone cycle is the fact that a series of cooperative conformational changes could occur in succession to drive it by a protonation-deprotonation sequence. Interestingly, similar transformations occur in bacteriorhodopsin[6]. Thus, the cycle could provide the first example of a "closed" cycle[5], whose rates and equilibria can be investigated as a model of a biological cycle using conventional kinetics and thermodynamics[5].

Received: May 27, 1981 [Z 415 IE]
revised: January 10, 1983
German version: *Angew. Chem. 95* (1983) 244
The complete version of this communication appears in:
*Angew. Chem. Suppl. 1983*, 243–253

CAS Registry numbers:
**1**, 36216-07-6; **2**, 74651-55-1; **3**, 74651-57-3; **4**, 36216-08-7.

[*] Prof. Dr. H. Ogawa, T. Inoue, Prof. Dr. T. Imoto
Faculty of Pharmaceutical Sciences, Kyushu University 62
Maidashi, Fukuoka 812 (Japan)
I. Miyamoto, Dr. H. Kato, Prof. Dr. Y. Taniguchi
Department of General Chemistry, National Kurume Technical College
Komorino, Kurume 830 (Japan)

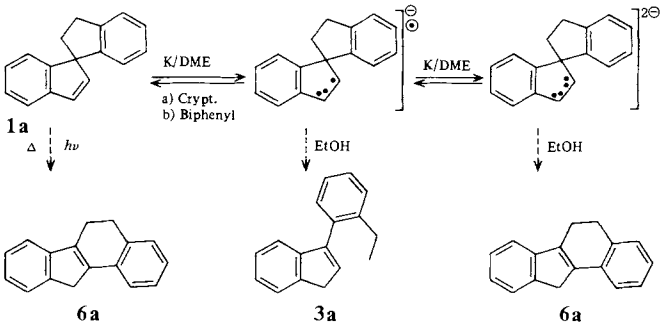
[1] H. Ogawa, N. Shimojo, H. Kato, H. Saikachi, *Tetrahedron 30* (1974) 1033.
[5] T. L. Hill: *Free Energy Transduction in Biology*, Academic Press, New York 1977, p. 213.
[6] D. Oesterhelt, *Angew. Chem. 88* (1976) 16; *Angew. Chem. Int. Ed. Engl. 15* (1976) 17; W. Stoekenius, R. H. Rozier, R. A. Bogomolni, *Biochim. Biophys. Acta 505* (1978) 215.

## Can Radicals Participate in Pericyclic Reactions? Model Reactions for Electron-Transfer Induced Valence Isomerization of 1-Arylindenes**

By *Herbert Kiesele**

Theoretical predictions state that pericyclic radical reactions should be forbidden, since they violate the principles of conservation of orbital- and of spin-symmetry[5]. Nevertheless, more and more examples for electron-transfer (ET) induced valence isomerizations have been reported, which, according to the concordant opinion of the authors, proceed *via* radical anions and are to be considered as pericyclic reactions[7]. This contradictory situation invites a more thorough study of ET induced valence isomerizations.

As a first example we selected the sigmatropic [1,5] shift in 1-arylindenes, which can be induced oxidatively (anodically), thermally, photochemically, and reductively (cathodically), and hence enable comparison of different oxidation states and electron configurations (Scheme 1).




Scheme 1. Thermal, photochemical, and ET induced reactions of 2',3'-dihydro-1,1'-spirobiindene **1a**. DME = 1,2-dimethoxyethane; Crpt. = [2.2.2]cryptand.

Preparative, electrochemical, and spectroscopic studies on a series of indene derivatives indicated that the reductive aryl shift proceeds exclusively *via* diamagnetic *dianions*, whose formation is favored thermodynamically by preceeding ion pair equilibria.

When the generation of dianions is prevented by complexing the counter ions with a macrocyclic ligand or by addition of an appropriate redox reagent (Scheme 1), relatively persistent radical anions[12] are obtained at low temperatures, which undergo dimerization and fragmentation at room temperature (cf. Supplement). The different reactions of the individual oxidation states (and electron configurations) are outlined in Scheme 1 using the dihydrospirobiindene **1a** as example; Table 1 shows how the product distribution changes with the reaction conditions.

The "alternating" tendency of neutral molecules[14], radical anions, and dianions to rearrange, confirms the "Yamaguchi rules", which allow linear transition states (fragmentation) for open-shell species but forbid cyclic ones.

According to our most recent observations, the ET induced ring-opening of cyclobuta[1]phenanthrene can proceed not only *via* a radical anion, but als *via* a dianion. The radical ring-opening, however, only occurs if ion pairs can form[21]. This result provides further confirmation for the efficiency of orbital- and spin-symmetry barriers in pericyclic radical reactions. But this example also shows that the barriers can be circumvented by ion pairing.

Table 1. Alkali metal reduction of **1a** in DME at room temperature.

| Reaction conditions [a] | Fragmentation [b] **3a** | Rearrangement [b] **6a** |
|---|---|---|
| K | 20 | 80 |
| K/[2.2.2]cryptand | 100 | — |
| K/biphenyl | 100 | — |

[a] Fused glass apparatus; the reaction mixture was quenched with oxygen-free EtOH/AcOH. [b] Relative yields [%]; for isolated yields and side products, see Supplement.

Received: February 28, 1980;
revised: December 21, 1982 [Z 417 IE]
German version: *Angew. Chem. 95* (1982) 253
The complete manuscript of this communication appears in:
*Angew. Chem. Suppl. 1983*, 210–221

[5] L. Salem: *Electrons in Chemical Reactions: First Principles*, Wiley, New York 1982, p. 96 and 189.
[7] L. L. Miller, R. F. Boyer, *J. Am. Chem. Soc. 93* (1971) 646.
[12] H. Kiesele, *Chem. Ber. 111* (1978) 1908.
[14] H. Kiesele, *Tetrahedron Lett. 22* (1981) 1097.
[21] H. Kiesele, Euchem Conf. Pericyclic Reactions, Ferrara 1982.

## The Structure of Tris(diphenylthiophosphinoyl)methanide, a Mesomerically Stabilized Carbanion**

By *Samuel O. Grim**, *Richard D. Gilardi*, and *Samuel A. Sangokoca*

The carbanion $[\{(C_6H_5)_2P(S)\}_3C]^-$, **1**, is a novel and versatile ligand which reacts by metathesis with metal halides to form cage complexes in which it behaves as singly negatively charged, tridentate, six-electron donor[1]. The anion **1** is prepared by proton abstraction[1a] from the neutral parent compound, $[(C_6H_5)_2P(S)]_3CH$, **2**, which was first reported by *Issleib et al.*[2]. It is also similar to the analogue $[\{(CH_3)_2P(S)\}_3C]^-$, **3**, which was recently reported by *Karsch*[3]. **1** and **3** are presumably mesomerically stabilized[3] by partial delocalization of the electronic charge of the central carbon through phosphorus onto the sulfur atoms. Maximum delocalization occurs if the anionic carbon has planar geometry.

The X-ray crystallographic structure of **1**, isolated as the stable tetra-*n*-butylammonium salt, has now been solved (cf. Fig. 1) and is the first such molecular structure to be determined. The salient features of the structure are as follows: First, the geometry about the central carbon is planar, with a mean P–C–P bond angle of 119.9°, although there is considerable deviation from the mean. The carbon is displaced only 6.8 pm from the plane of the three phosphorus atoms. Secondly, two of the sulfurs lie on one side

[*] Priv.-Doz. Dr. H. Kiesele
Fakultär für Chemie der Universität
Postfach 5560, D-7750 Konstanz 1 (Germany)

[**] This work was supported by the Deutsche Forschungsgemeinschaft and the Fonds der Chemischen Industrie.

[*] Prof. S. O. Grim, S. A. Sangokoya
Department of Chemistry, University of Maryland
College Park, MD 20742 (USA)
Dr. R. D. Gilardi
Naval Research Laboratory
Washington, DC 20375 (USA)

[**] Polydentate Ligands Containing Phosphorus, Part 10.—Part 9: [1a].

of this plane, while the third sulfur lies on the opposite side. This arrangement is similar to that of the stable conformation[4] of **2** and is expected for steric reasons, although NMR data[1a] indicate that there is no restricted rotation about the phosphorus central-carbon bonds in **1**,

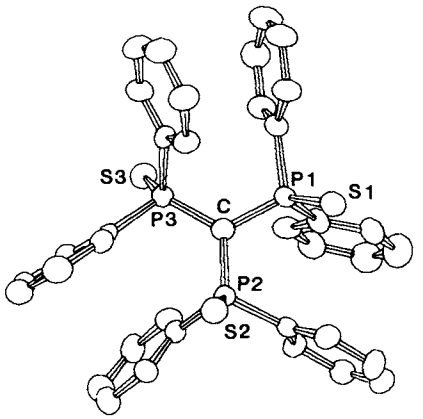



Fig. 1. Structure of **1** as the $n$-$Bu_4N^+$ salt, which crystallizes along with one acetone molecule. Space group $P2_1$, $a=1189.4$, $b=1933.1$, $c=1259.9$ pm, $\beta=111.42°$, $Z=2$; 3644 reflections, $R=0.070$. Most important bond lengths [pm] and angles [°]: P1-S1, 197.4; P2-S2, 197.2; P3-S3, 198.1; P1-C, 176.7; P2-C, 177.4; P3-C, 174.6; P1-C-P2, 116.0; P2-C-P3, 122.0; P2-C-P3, 121.6.

even at temperatures as low as 178 K. Thirdly, as expected for a mesomerically stabilized compound of this type, the P–S bond order decreases and the P–C (central) bond order increases in going from the neutral parent compound **2** to the anion **1**. This is indeed the case and is reflected by P–S bond lengths, which are greater in **1** (mean, 197.6 pm) than in **2** (mean, 194.4 pm)[4] and by the P–C (central) bond lengths, which are shorter in **1** (mean, 176. 2 pm) than in **2** (mean, 188.3 pm)[4]. The structure bears a striking resemblance to the structure of the mesomerically-stabilized dication, $[(CH_3)_3P]_3C]^{2+}$, **4**, which has a planar geometry at the central carbon and which has one unique and two stereochemically equivalent phosphonium groups[5a]. The P–C (central) bond length (175 pm) in **4** is similar to that in **1** (176.2 pm) but both are longer than in ylides such as $Ph_3P{=}CH_2$ (166.1 pm)[5b] and $Ph_3P{=}C{=}PPh_3$ (162.4 pm)[5c].

Received: July 2, 1982 [Z 81 IE]
revised: January 5, 1983
German version: *Angew. Chem. 95* (1983) 237
The complete manuscript of this communication appears in: *Angew. Chem. Suppl. 1983*, 271–281

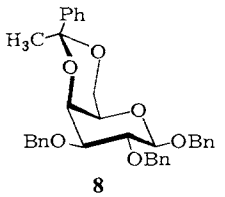
CAS Registry number:
**1**·$Bu_4N^+$, 84507-40-4.

[1] a) S. O. Grim, S. A. Sangokoya, I. J. Colquhoun, W. McFarlane, *J. Chem. Soc. Chem. Commun. 1982*, 930; b) S. O. Grim, P. H. Smith, L. C. Satek, I. J. Colquhoun, W. McFarlane, *Polyhedron 1* (1982) 137; S. O. Grim, P. H. Smith, S. Nittolo, H. L. Ammon, L. C. Satek, S. A. Sangokoya, R. J. Khanna, I. J. Colquhoun, W. McFarlane, J. R. Holden, unpublished.
[2] K. Issleib, H. P. Abicht, *J. Prakt. Chem. 312* (1970) 456.
[3] H. H. Karsch, *Chem. Ber. 115* (1982) 818.
[4] I. J. Colquhoun, W. McFarlane, J.-M. Bassett, S. O. Grim, *J. Chem. Soc. Dalton Trans. 1981*, 1645.
[5] a) B. Zimmer-Gasser, D. Neugebauer, U. Schubert, H. H. Karsch, Z. Naturforsch. B **34** (1979) 1267; b) J. C. J. Bart, *Angew. Chem. 80* (1968) 697; *Angew. Chem. Int. Ed. Engl. 7* (1968) 730; c) A. T. Vincent, P. J. Wheatley, *J. Chem. Soc. Chem. Commun. 1971*, 582.

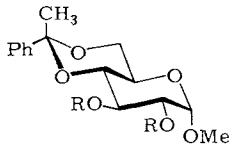
## Formation, Structure, and Synthetic Use of Gluco- and Galactopyranoside Acetophenone Acetals with 1,3-Dioxane Rings

By *András Lipták** and *Péter Fügedi*

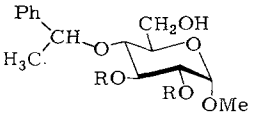
There are only two examples in the literature concerning the preparation of 4,6-*O*-α-methylbenzylidene-hexopyranosides[1]. In both cases principally one of the diastereomeric acetals was formed, and an equatorial phenyl group proposed for these derivatives by analogy with the corresponding benzylidene derivatives[2].



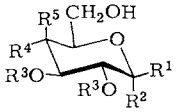
**8**



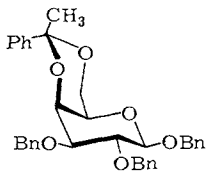
**5**, R = H; **6**, R = Me; **7**, R = Bn



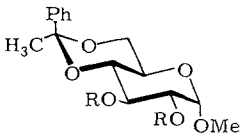
**13**, R = Me; **14**, R = Bn



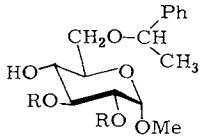
**1**, $R^1 = R^3 = R^5 = H$; $R^2 = OMe$; $R^4 = OH$
**2**, $R^1 = R^5 = H$; $R^2 = OMe$; $R^3 = Me$; $R^4 = OH$
**3**, $R^1 = R^5 = H$; $R^2 = OMe$; $R^3 = Bn$; $R^4 = OH$
**4**, $R^2 = R^4 = H$; $R^1 = OBn$; $R^3 = Bn$; $R^5 = OH$



**12**
Bn = $PhCH_2$



**9**, R = H; **10**, R = Me, **11**, R = Bn



**15**, R = Me; **16**, R = Bn

[*] Dr. A. Lipták, Dr. P. Fügedi
Institute of Biochemistry, Kossuth L. University
P.O.B. 55, H-4010 Debrecen (Hungary)

 © *Verlag Chemie GmbH, 6940 Weinheim, 1983* *0570-0833/83/0303-0255 $ 02.50/0* 

Reinvestigation of the acetal exchange reaction (dimethylformamide, *p*-toluenesulfonic acid, room temperature) between acetophenone dimethyl acetal and glucopyranoside derivatives **1**—**3** revealed formation of both isomeric acetals, whereby the products of kinetic control (**5**—**7**), isolable in yields of 20—30%, were readily converted into the thermodynamically favored isomers **9**—**11**. Under equilibrium conditions the latter accumulate exclusively and can be isolated nearly quantitatively. The galactopyranoside derivative **4** reacted similarly to give **8** and **12**.

The configurations of the acetal carbons were assigned from $^1H$ and $^{13}C$ chemical shifts of the C-2′ substituents; these data are highly diagnostic in 2,2-disubstituted 1,3-dioxanes. For an axial methyl group the $^1H$-NMR signals are observed at lower[3] and the corresponding $^{13}C$-NMR signals at higher field[4] than in the equatorial isomer. In the present case the products of kinetic control (**5**—**8**) (Table 1) surprisingly proved to be the (*R*)-isomers with axial methyl groups, whereas the products of the thermodynamic control (**9**—**12**) were the (*S*)-isomers with axial phenyl groups.

Table 1. Selected data for compounds **5**—**16**.

| Compound | M.p. [°C] | $[\alpha]_D$ [a] | $^1H$-NMR [b] | $^{13}C$-NMR [c] |
|---|---|---|---|---|
| **5** | 107—109 | + 29 [d] | 1.68 [e] | 20.9 [e] |
| **6** | 95—96 | + 64 | 1.72 | 21.8 |
| **7** | 112—113 | − 57 | 1.73 | 22.1 |
| **8** | 85 | − 71 | 1.69 | 22.1 |
| **9** | 168—170 | +209 [d] | 1.43 [e] | 31.8 [e] |
| **10** | syrup | +154 | 1.55 | 31.9 |
| **11** | syrup | +106 | 1.55 | 32.0 |
| **12** | 118 | + 21 | 1.65 | 32.3 |
| **13** | syrup | +192 | 1.52 | |
| **14** | syrup | +126 | 1.44 | |
| **15** | syrup | +140 | 1.46 | |
| **16** | syrup | + 33 | 1.43 | |

[a] In chloroform. [b] C—$CH_3$, in $CDCl_3$, TMS internal standard, δ values. [c] C—$CH_3$, in $CDCl_3$. [d] In pyridine, *δ* values. [e] In [$D_6$]dimethyl sulfoxide.

This result is in marked contrast to earlier conceptions of carbohydrate acetals of this type, but agrees well with the finding of *Eliel* et al.[3] that in a 2-methyl-2-phenyl-1,3-dioxane derivative the axial phenyl isomer is more stable by 2.55 kcal/mol. This can be explained by the fact that in the "perpendicular" rotamer an axial phenyl group can avoid unfavorable interactions with other H atoms[3].

Hydrogenolytic ring-cleavage of the diasteromeric α-methylbenzylidene acetals with $LiAlH_4$—$AlCl_3$[6] exhibited a high degree of regio- and stereoselectivity. The (*R*)-isomers gave only the 4-*O*-(α-methylbenzyl)derivates **13** and **14**, whereas the (*S*)-isomers afforded the 6-*O*-(α-methylbenzyl) derivatives **15** and **16**. In both cases only one of the two possible diastereomeric ethers was formed; the configurations of the new chirality centers are being investigated. The regioselectivity is reminiscent of the results obtained in the reduction of the five-membered *exo*- and *endo*-benzylidene acetals of carbohydrates[6].

Because compounds **10** and **11** are the only products of acetalization in equilibrium, and their hydrogenolysis with $LiAlH_4$—$AlCl_3$ results in 6-ethers, a new route is opened for the preparation of glucopyranosides selectively unprotected at position 4.

Received: March 18, 1982 [Z 416 IE]
revised: December 28, 1982
German version: *Angew. Chem. 95* (1983) 245
The complete version of this communication appears in:
*Angew. Chem. Suppl. 1983*, 254—263

[1] M. E. Evans, F. W. Parrish, L. Long, *Carbohydr. Res. 3* (1967) 453; B. C. Lipshutz, M. C. Morey, *J. Org. Chem. 46* (1981) 2419.
[2] N. Baggett, J. M. Duxbury, A. B. Foster, J. M. Webber, *Carbohydr. Res. 1* (1965) 22.
[3] W. F. Bailey, H. Connon, E. L. Eliel, K. B. Wiberg, *J. Am. Chem. Soc. 100* (1978) 2202, and references cited therein.
[4] P. J. Garegg, B. Lindberg, I. Kvarnström, *Carbohydr. Res. 77* (1979) 71.
[6] A. Lipták, P. Fügedi, P. Nánási, *Carbohydr. Res. 51* (1976) C19, and references cited therein.

# BOOK REVIEWS

**Properties of Ligands and Solutions.** By *J. N. Murrell* and *E. A. Boucher*. John Wiley & Sons, Chichester 1982. x, 288 pp., bound, £ 8.90.

This book is an excellent introduction to the fundamentals of the science of liquids, its 13 chapters giving a brief but clear account of virtually all topics of interest to chemists, biologists, physical chemists, and other scientists.

Chapter 1 is a short introduction and Chapter 2 deals with intermolecular forces. Chapter 3 outlines the modern theories and models of liquids, including the latest developments in statistical thermodynamics and computer simulations. The thermodynamic properties of pure liquids are discussed in Chapter 4, and liquid crystals (though rather briefly) in Chapter 5. The topics dealt with in Chapters 6 and 7 are respectively: mixtures of non-electrolytes, and the phase behavior of multicomponent systems. Chapter 8 is devoted to polar liquids and Chapter 9 to aqueous electrolyte solutions. The authors discuss chemical equilibria in solution in Chapter 10 and polymer solutions and their special characteristics in Chapter 11. Chapter 12 deals with the problems of liquid boundary layers and adsorption phenomena and Chapter 13 gives an account of colloidal systems.

The book is not limited to general and standard cases but often gives direct applications of particularly interesting systems. For example, Section 8.5 discusses the structural model of water that has emerged from the various investigations. Wherever possible, the statistical and thermodynamic models are explained as far as is necessary for understanding the principles.

Although the aim of the book is to give an introduction, which in fact it does, it presupposes some background knowledge in various areas: from thermodynamics, the basic relationships, from statistical mechanics only the Max-

well-Boltzmann distribution law and the partition function, and from quantum mechanics a few fundamental concepts of the theory of chemical bonding.

The sequence of the topics is almost invariably from the easier to the more difficult (for example, non-electrolytes are discussed before electrolytes and colloids), because the material was originally used for a course of lectures at the University of Sussex. The book is most suitable for accompanying such a course of lectures for scientists, but it can also be recommended to interested students for self-study. The very good style and makeup of the book justify its price.

*Rüdiger N. Lichtenthaler* [NB 577 IE]

**Macrocyclic Polyether Syntheses.** By *G. W. Gokel* and *S. H. Korzeniowski*. Springer-Verlag, Berlin 1982. xviii, 410 pp., bound, DM 238.00.

The chemistry of macrocyclic polyethers (crown ethers) and of their hetero-analogues has shown a meteoric rise in its 15 years of history, which is also reflected in the number of crown compounds synthesized so far. This number is so large that often even experts cannot decide whether a certain macrocyclic compound exists or whether a given structural element has already been used as a component of a crown compound. However, this book settles the matter, for it lists 2369 compounds with their structural formulas in 86 tables, giving their ring size, melting point, and the yields of the various ligands. This number far surpasses any given in previous monographs on crown ethers. When it comes to the methods of synthesis, however, the book gives only the essentials in a brief account at the beginning of each of Chapters 3—8, the rest being left to the 750 references listed (it would have been useful to include a separate index for the methods).

On the other hand, the whole of Chapter 2 is devoted to the "Template Effect", a device useful for raising the yield of simple crown ethers but playing only a subordinate role in the synthesis of more complex ligand systems. Space could therefore have been saved here and utilized to discuss some more general synthetic strategies.

The first chapter (Introduction and General Principles) describes how the various types of crown compounds are built up and deals at length with their nomenclature. The oxirane oligomerization (Section 1.4) would have fitted in better in Chapter 2 ("template catalysis"), while the account of polyazamacrocyclic compounds (Section 1.5) could have been better treated in Section 1.3.2 ("Aza-crowns"), so as not to violate the definitions established earlier.

The bulk of the information is contained in Chapters 3—8, in which the material is divided as follows: Chapter 3: Syntheses of Oxygen Macrocycles (simple crown ethers and crown ethers with aromatic residues, both with up to 81 members in the ring, together with lariat ethers and polytopic ligand systems). Chapter 4: Syntheses of Aza-crowns (including heteroaromatic and chromoionophores, but not the large field of ligands with a porphine structure and Schiff base-type ligands complexing with transition-metal ions). Chapter 5: Crown Esters and Macrocyclic Polyether Lactones. This chapter also covers thioesters, many crown ether amides, and urea derivatives, so that it would have been more accurate to use the word "lactams" instead of "lactones" in the heading. Chapter 6: Miscellaneous Macrocycles (*e.g.* with heteroatoms other than oxygen or nitrogen, also acetal-type and polymer-bound crown compounds). Chapter 7: Open-chained Equivalents of Crown Ethers (linear and branched podands with up to 88 atoms in the chain and with special donor end groups; also octopus molecules and synthetic ionophores). Chapter 8: Cryptands and Related Polycyclic Systems (including lipophilic and large-lumen bicyclic and oligocyclic compounds with N and C bridgehead atoms, as well as polymer-fixed cryptands and spherands).

The backbone of these chapters is formed by the extensive tables, which are most clearly laid out and graphically well presented. Captions and footnotes are added to clarify difficult points. Perhaps the order of chapters 7 and 8 could have been reversed to take the polycyclic compounds before the open-chain ones.

Readers interest in an inventory of all the known crown compounds or in an encyclopedia of the usual methods of synthesizing neutral ligands are advised to acquire this book. However, one should not expect anything on the complexing characteristics of the ligands, because the book does not even touch on this subject. The reader interested in this must turn to the many previous studies, to which this book constitutes a welcome addition that will often save a laborious literature search. The reader will soon realize its value as an inventory of the structural components and other structural details of crown ethers when using it as a starting point for new syntheses. The book should therefore be bought by all libraries, even though its very high price might at first be discouraging.

*Edwin Weber* [NB 575 IE]

**Recent Books**

**The following books have been received by the editor. Detailed reviews will not be published in all cases because of the limited space available under this heading in the journal. All the publications listed are available through W & P Buchversand für Wissenschaft und Praxis, Boschstrasse 12, D-6940 Weinheim (Federal Republic of Germany). Tel. (06201) 60 26 53 (606-0), Telex 465 516 vchwh d, Telefax (06201) 60 23 28.**

**Forschung in der Bundesrepublik Deutschland. Beispiele, Kritik, Vorschläge.** A *Deutsche Forschungsgemeinschaft publication*. Verlag Chemie, Weinheim 1983. xvi, 975 pp., bound, DM 92.00.—ISBN 3-527-27001-9

**Clinical Cellular Immunology. Molecular and Therapeutic Reviews.** Edited by *A. A. Luderer* and *H. H. Weetall*. Humana Press, Clifton, NJ 1982. xviii, 391 pp., bound, $ 59.50 (in USA $ 49.50).—ISBN 0-89603-011-3

**Advances in Heterocyclic Chemistry. Vol. 31.** Edited by *A. R. Katritzky*. Academic Press, New York 1982. ix, 350 pp., bound, $ 68.00.—ISBN 0-12-020631-5

**Chemistry and Physics of Carbon. Vol. 18.** Edited by *P. A. Thrower*. Marcel Dekker, Basel 1982. xii, 185 pp., bound, SFr. 135.00.—ISBN 0-8247-1740-6

**Electrical Properties of Polymers.** Edited by *D. A. Seanor.* Academic Press, New York 1982. xii, 379 pp., bound, $ 52.00.—ISBN 0-12-633680-6

**Atomspektrometrische Spurenanalytik. Lectures delivered at the Colloquium "Spurenanalytik mit Atomspektroskopie" in Konstanz (April 1981).** Edited by *B. Welz.* Verlag Chemie, Weinheim 1982. xvi, 564 pp., bound, DM 148.00.—ISBN 3-527-26027-7

**Chemistry and Biology of β-Lactam Antibiotics.** Edited by *R. B. Morin* and *M. Gorman.* Academic Press, New York 1982. Vol. 1: Penicillins and Cephalosporins. xxxix, 553 pp., bound, $ 73.00.—ISBN 0-12-506301-6; Vol. 2: Nontraditional β-Lactam Antibiotics. xiv, 408 pp., bound, $ 64.00.—ISBN 0-12-506302-4

**Chemie der Räucherung.** By *L. Tóth.* A Deutsche Forschungsgemeinschaft publication. Verlag Chemie, Weinheim 1982. xi, 331 pp., bound, DM 68.00.—ISBN 3-527-27501-0

**The Substance Abuse Problems.** By *Sidney Cohen.* The Haworth Press, New York 1981. xiii, 392 pp., Paperback, $ 19.95.—ISBN 0-917724-22-4

**Structure and Activity of Natural Peptides.** Edited by *W. Voelter* and *G. Weitzel.* Walter de Gruyter & Co., Berlin 1981. xii, 634 pp., bound, DM 150.00.—ISBN 3-11-008264-0

**Chemistry of Peptides and Proteins. Vol. 1: Proceedings of the Third USSR-FRG Symposium.** Edited by *W. Voelter, E. Wünsch, Y. Ovchinnikov,* and *V. Ivanov.* Walter de Gruyter & Co., Berlin 1982. xiii, 554 pp., bound, DM 196.00.—ISBN 3-11-008604-2

**Developments in Ionic Polymers—1.** Edited by *A. D. Wilson* and *H. J. Prosser.* Applied Science Publishers, Barking, Essex 1983. ix, 336 pp., bound, £ 34.00.—ISBN 0-85334-159-1

**Biophysics of Water.** Edited by *F. Franks* and *S. Mathias.* John Wiley & Sons, Chichester 1982. xxv, 400 pp., bound, £ 29.95.—ISBN 0-471-10229-6

**Ösophaguschirurgie. Achalasie, Strukturen, Benigne Tumoren, Divertikel, Perforationen.** Edited by *R. Häring.* edition medizin, Weinheim 1982. xxi, 338 pp., stitched, DM 78.00.—ISBN 3-527-15077-3

**Ultraschall-Atlas. Internistische Ultraschalldiagnostik mit schnellen B-Bild-Geräten.** By *H.* und *A. Weiss.* edition medizin, Weinheim 1983. xiv, 423 pp., bound, DM 112.00.—ISBN 3-527-15068-4

**Industrial Crystallization. The State of the Art.** 2nd newly revised edition. By *J. Nývtlt.* Verlag Chemie, Weinheim 1982. vi, 180 pp., bound, DM 62.00. ISBN 3-527-26065-X

**Advances in Inorganic Chemistry and Radiochemistry. Vol. 25.** Edited by *H. J. Emeléus* and *A. G. Sharpe.* Academic Press, New York 1982. vii, 355 pp., bound, $ 56.00.—ISBN 0-12-023625-7

**Hochdisperse Metalle.** By *W. Romanowski* and *S. Engels.* Verlag Chemie, Weinheim 1982. 171 pp., bound, DM 65.00.—ISBN 3-527-25982-1

**Gaschromatographische Retentionsindices toxikologisch relevanter Verbindungen.** *Mitteilung I der Kommission für klinisch-toxikologische Analytik der Deutschen Forschungsgemeinschaft.* Verlag Chemie, Weinheim 1982. 48 pp., stitched, DM 20.00.—ISBN 3-527-27303-4

**Atome und Moleküle als Bausteine der Materie.** By *H. Preuss.* Verlag Salle + Sauerländer. Frankfurt 1982. x, 298 pp., bound, DM 48.00.—ISBN 3-7941-5695-6

**Texte zur Chemie und Chemietechnik. Moderne Regressionsanalyse. Mit Anwendungsbeispielen aus Biologie, Chemie und Medizin.** By *H. Mager.* Verlag Salle + Sauerländer. Frankfurt am Main 1982. x, 342 pp., bound, DM 128.00.—ISBN 3-7941-2242-9

---

**Corrigendum**

The following correction should be made to the communication entitled "Electron Density Distribution on the Bonds of the Bridged Bicyclo[1.1.0]butane System 1,5-Dimethyltricyclo[2.1.0.$0^{2,5}$]pentan-3-one" by Hermann Irngartinger and Annette Goldmann, *Angew. Chem. Int. Ed. Engl. 21* (1982) 775:

Footnote 1b) on p. 776, right-hand column, line 7 should read, b) H. Irngartinger, A. Goldmann, R. Schappert, P. Garner, P. Dowd, *J. Chem. Coc. Chem. Commun. 1981,* 455.

*Registered names, trademarks, etc. used in this journal, even without specific indication thereof, are not to be considered unprotected by law.*

© Verlag Chemie GmbH, D-6940 Weinheim, 1983. - Printed in the Federal Republic of Germany by Zechnersche Buchdruckerei, Speyer/Rhein.

All rights reserved (including those of translation into foreign languages). No part of this issue may be be reproduced in any form - by photoprint, microfilm, or any other means - nor transmitted or translated into a machine language without written permission from the publishers. Only single copies of contributions, or parts thereof, may be reproduced for personal use. Copies reproduced and used other than for private purposes in an industrial or commercial undertaking are subject to copyright and, in such cases, a copyright fee must be paid to the VG WORT, Abteilung Wissenschaft, Goethestr. 49, 8000 München 2, from whom conditions of payment can be obtained on request.

**Valid for users in the USA:** The appearance of the code at the bottom of the first page of an article in this journal (serial) indicates the copyright owner's consent that copies of the article may be made for personal or internal use, or for the personal or internal use of specific clients. This consent is given on the condition, however, that the copier pay the stated per-copy fee through the Copyright Clearance Center, Inc., for copying beyond that permitted by Sections 107 or 108 of the U.S. Copyright Law. This consent does not extend to other kinds of copying, such as copying for general distribution, for advertising or promotional purposes, for creating new collective works, or for resale. For copying from back volumes of this journal see 'Permissions to Photo-Copy: Publisher's Fee List' of the CCC.

**Editorial office:** Pappelallee 3, D-6940 Weinheim, Federal Republic of Germany, Telephone (06201) 602-1, Telex 465516 vchwh d, Telefax (06201) 602328.

**Editors:** *P. Gölitz, I. G. Neil, O. Smrekar, A. Stimson.*

**Publishers:** Verlag Chemie GmbH. (Managing Directors: *Prof. Dr. Helmut Grünewald* and *Hans Dirk Köhler*), Pappelallee 3, D-6940 Weinheim, Federal Republic of Germany.
Correspondence concerning advertisements should be addressed to Verlag Chemie GmbH. (Advertising Manager *R. J. Roth*), Pappelallee 3, P.O. Box 1260/1280, D-6940 Weinheim, Federal Republic of Germany, Telephone Weinheim (06201) 602-1, Telex 465516 vchwh d, Telefax (06201) 602328.

ANGEWANDTE CHEMIE
International Edition in English
Volume 22 · Number 4
April 1983
Pages 259–336

# Magic-Angle-Spinning NMR (MAS-NMR) Spectroscopy and the Structure of Zeolites

By Colin A. Fyfe, John M. Thomas*, Jacek Klinowski, and Gian C. Gobbi

After outlining the chemical features and properties which make zeolites such an important group of catalysts and sorbents, the article explains how high-resolution solid-state NMR with magic-angle spinning reveals numerous new insights into their structure. $^{29}$Si-MAS-NMR readily and quantitatively identifies five distinct $Si(OAl)_n(OSi)_{4-n}$ structural groups in zeolitic frameworks ($n=0,1,\ldots 4$), corresponding to the first tetrahedral coordination shell of a silicon atom. Many catalytic and other chemical properties of zeolites are governed by the short-range Si, Al order, the nature of which is greatly clarified by $^{29}$Si-MAS-NMR. It is shown that, as expected from Pauling's electroneutrality principle and Loewenstein's rule, both in zeolite X and in zeolite A (with $Si/Al=1.00$) there are no $-Al-O-Al-$ linkages. In zeolite A and zeolite X with $Si/Al=1.00$ there is strict alternation of Si and Al on the tetrahedral sites. Ordering models for Si/Al ratios up to 5.00 (in zeolite Y) may also be evaluated by a combination of MAS-NMR experiments and computational procedures. $^{29}$Si-MAS-NMR spectra reveal the presence of numerous crystallographically distinct $Si(OSi)_4$ sites in silicalite/ZSM-5, suggesting that the correct space group for these related porosilicates is not Pnma. $^{27}$Al-MAS-NMR clearly distinguishes tetrahedrally and octahedrally coordinated aluminum, proving that, contrary to earlier claims, Al in silicalite is tetrahedrally substituted within the framework. In combination, $^{29}$Si- and $^{27}$Al-MAS-NMR is a powerful tool for monitoring the course of solid-state processes (such as ultrastabilization of synthetic faujasites) and of gas-solid reactions (dealumination of zeolites with silicon tetrachloride vapor at elevated temperatures). They also permit the quantitative determination of *framework* Si/Al ratios in the region $1.00<Si/Al<10\,000$. Since most elements in the periodic table may be accommodated within zeolite structures, either as part of the exchangeable cations or as building units of the anionic framework, there is immense scope for investigation by MAS-NMR and its variants (cross-polarization, multiple pulse and variable-angle spinning) of bulk, surface and chemical properties. Some of the directions in which future research in zeolite science may proceed are adumbrated.

[*] Prof. J. M. Thomas, Dr. J. Klinowski
Department of Physical Chemistry, University of Cambridge
Lensfield Road, Cambridge CB2 1EP (England)
Prof. C. A. Fyfe, G. C. Gobbi
Guelph-Waterloo Centre for Graduate Work in Chemistry
Department of Chemistry, University of Guelph
Guelph, Ontario N1G 2W1 (Canada)

## 1. Introduction

Zeolites are microporous, crystalline aluminosilicates of general formula $M_{x/n}[(AlO_2)_x(SiO_2)_y]\cdot m\,H_2O$. They may be regarded as open structures of silica, $SiO_2$, in which aluminum has been substituted in a fraction $x/(x+y)$ of the te-

 © Verlag Chemie GmbH, 6940 Weinheim, 1983 0570-0833/83/0404-0259 $ 02.50/0 

trahedral sites. The net negative charge of the aluminosilicate framework is neutralized by exchangeable cations, M, of valence n; and the void space, which may be more than 50% of the crystal volume, is occupied by m molecules of water per unit cell. Depending upon the particular structure of the zeolite, the porosity may consist of one-, two- or three-dimensional networks of interconnected channels and cavities of molecular dimensions (Fig. 1). If the zeolitic water is removed, many other molecular entities may be accommodated in the intracrystalline cavities including $CO_2$, $NH_3$, hydrocarbons, alkanols and a wide range of other organic and inorganic species.

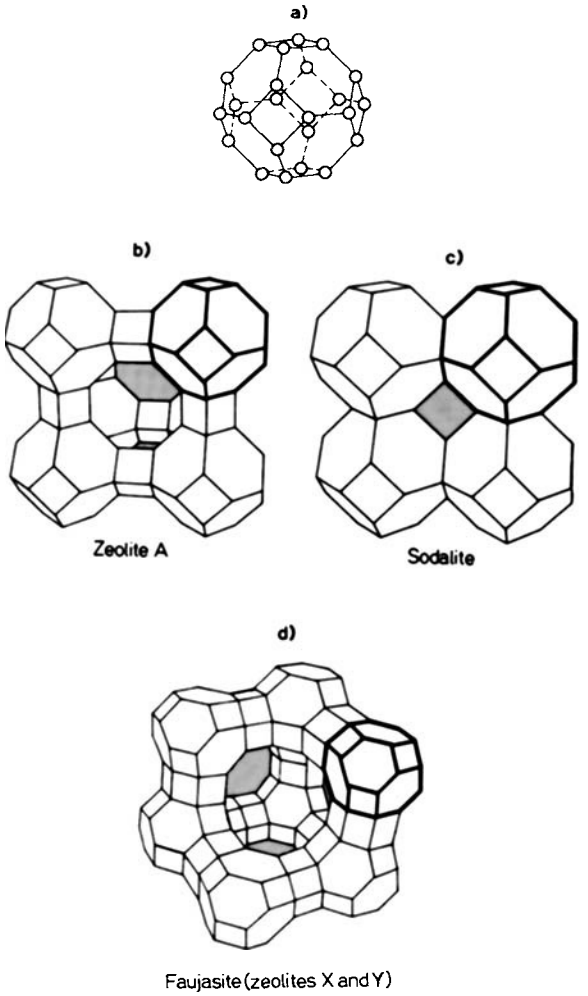
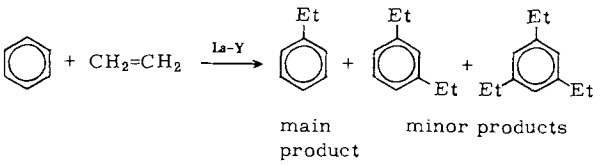



Fig. 1. a) The truncated octahedron building block (also termed "cuboctahedron", "sodalite cage" or "β-cage"). Tetrahedral atoms (denoted as o) are located at the corners of polygons with oxygen atoms (not shown) approximately half-way between them.—b) The structure of zeolite A formed by linking the sodalite cages through double four-membered rings.—c) The sodalite structure formed by direct face-sharing of four-membered rings in the neighboring sodalite cages.—d) The faujasite structure formed by linking the sodalite cages through double six-membered rings.—Non-framework cations are not shown.

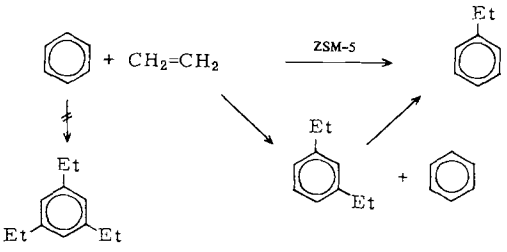
There are, at present, 37 identified types of zeolitic minerals and well over 100 synthetic zeolites. The unit cell stoichiometry of the idealized, naturally occurring zeolite faujasite is $Na_{56}[(AlO_2)_{56}(SiO_2)_{136}]\cdot 250\,H_2O$, and that of the closely related synthetic zeolite, known as Linde A, is $\{Na_{12}[(AlO_2)_{12}(SiO_2)_{12}]\cdot 27\,H_2O\}_8$. Some other elements, notably Be, Mg, B, Ga, Ge and P can take the place of Si and Al in the zeolitic framework: there have been claims that many other elements, including transition metals, may enter the framework substitutionally. The term "porotectosilicate" has been suggested[1] as a general description of porous zeolite-like materials.

## 2. Zeolites as Sorbents and Catalysts with Shape-Selectivity

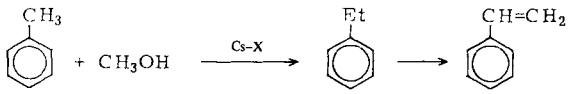
The remarkable sorptive properties of zeolites have long been recognized, as has their ion-exchange capacity[2–6]. They are capable of ionic and molecular sieving, the size and shape of the admitted species being determined by the dimensions of the aperture openings in the zeolite. The ease with which they undergo ion exchange is utilized commercially in water softening, in the treatment of brackish water, in the recovery of precious metals (as complex cations), and in the removal of radioactive species from solution[7,8]. By appropriate adjustment of their cation composition, certain zeolites may be "tuned" further to serve as efficient gas separation agents (separating, for example, methane from ethane or oxygen from nitrogen). But, most importantly, zeolites, particularly those with relatively high Si/Al ratios and rich in free protons, exhibit impressive activity and selectivity as catalysts for the cracking, hydrocracking and isomerization of hydrocarbons[8–11]. Indeed, in these functions, faujasitic zeolites are amongst the most widely used of all commercial catalysts: they far surpass the performance of their silica-alumina gel predecessors, and possess the useful property of being sufficiently thermally stable to withstand regeneration at high temperatures[12]. Faujasitic zeolites are the premier components in fluidized cracking catalysts for the petroleum industries. Two examples will serve to illustrate the additional catalytic potential of zeolites: the ethylation of benzene over $La^{3+}$-exchanged zeolite Y (a synthetic faujasite) occurs at 200 °C with close to 100 percent selectivity[13]; likewise, the conversion of toluene by methanol to ethylbenzene (and thence to styrene) over a $Cs^+$-exchanged zeolite X is also very efficient[13b] (cf. Scheme 1).



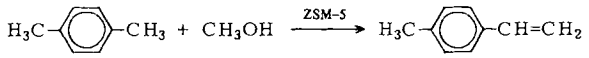

a) Ethylation of benzene on La-Y




b) Ethylation of benzene on ZSM-5




c) Ethylation of toluene on Cs-X




d) Synthesis of *p*-methylstyrene on ZSM-5

Scheme 1.

In the early 1970's a new class of porotectosilicates was discovered[14, 15a]. Members of the highly siliceous ZSM series (for *Z*eolite *S*ocony[15b] *M*obil) possess optimal pore diameters (*ca.* 5.5 Å, see Fig. 2) and attractive catalytic properties including the ability to synthesize gasoline from methanol as well as ethylbenzene from ethylene and benzene in a manner which could well supplant the traditional Friedel-Crafts procedure[16] (Scheme 1). The particular member that catalyzes these reactions is ZSM-5, the unit cell formula of which is $H_x[(AlO_2)_x(SiO_2)_{96-x}]\cdot 16\,H_2O$, with $x<27$ and typically about 3. A crystalline microporous solid called silicalite is very closely similar in framework to ZSM-5[17]. Silicalite is organophilic and hydrophobic and removes from water by preferential adsorption, alkanols, certain alkanes and some other organic entities. In the patent describing the preparation and properties of silicalite it is claimed that this porotectosilicate contains no constitutional aluminum. We show later that $^{27}$Al-MAS-NMR indicates otherwise (cf. Section 6).

An important attribute of both ZSM-5 and silicalite, and of many other zeolites, as was first recognized by *Weisz et al.*[14b, 18], is their shape selectivity. Because of the dimensions and the geometry of the channels only certain reactants may, for example, enter and diffuse through crystals of ZSM-5. Likewise, shape restrictions are imposed upon the transition states accessible to the catalytic reactions that take place in the intracrystalline regions and upon the products that may diffuse out from within the catalyst particle.

Early work on the sorptive properties of zeolites, notably on the mineral chabazite, was summarized by *McBain* more than 50 years ago[3]. Subsequent work on structure, syntheses and properties has been comprehensively reviewed in texts by *Barrer*[4], the founder of the modern study of zeolites, and by *Breck*[5], who along with *Milton* and other collaborators at the Union Carbide Corp. also made extensive contributions to the subject. Other reviews dealing with catalytic performance[6, 7-11], structure[19-21] and general chemical properties[22] are available.

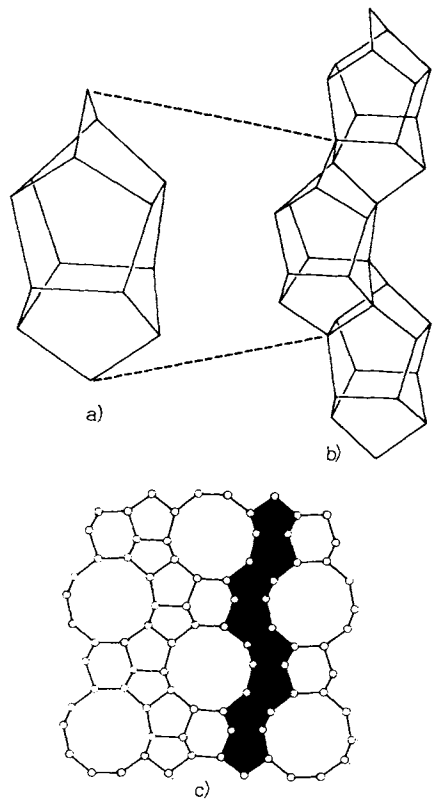



Fig. 2. a) The "pentasil unit", the building block of ZSM-5/silicalite and ZSM-11.—b) Pentasil units are linked into chains, one of which is shown in the *c* direction.—c) In the structure of ZSM-5/silicalite the chains are interlinked to form a three-dimensional framework in which there are ten-membered ring openings (≈ 5.5 Å in diameter) running along the [010] direction. In this portion of the *ac* structural projection, O denotes a tetrahedral site.

## 3. Structural Considerations

Whereas the overall framework structure of most zeolites can be satisfactorily determined by conventional X-ray methods, the detailed Si, Al ordering within the tetrahedral framework itself—a factor of great importance since it governs the catalytic performance and the myriad other properties of zeolites—cannot, in general, be readily extracted from X-ray crystallography. This arises partly because of the similar scattering powers of Si and Al, but also because it is very difficult to obtain single crystals of sufficient quality and dimension. This is especially true for synthetic zeolites which are usually obtained as fine powders: In some cases they may consist of intergrowths of closely similar structural types. Different approaches adopted to tackle this problem, mainly with faujasitic zeolites, have included: (i) X-ray powder diffractometry involving careful measurement of lattice parameters as a function of aluminum content[23]; measurement (from X-ray single-crystal data) of bond lengths and bond angles[20, 24] and the determination of cation positions which are necessarily correlated with the location of anionic Al centers in the framework[25]; (ii) theoretical studies involving electrostatic and statistical calculations[26-28]; (iii) measurements of the change of zeolitic acidity on successive extraction of aluminum from the framework[29]; (iv) examination of the kinetics of crystallization[30]; (v) a combined diffraction-*cum*-adsorption approach used particularly effectively by *Kokotailo et al.*[21b] for the study of porotectosilicates; and (vi) use of refined infrared absorption measurements, which are often revealing in identifying the location of the loosely bound protons (*i.e.*, the "active sites") in zeolitic catalysts[31, 32].

Apart from the last-named, and the single crystal X-ray procedure, all these methods are indirect and most are of

limited applicability. Significant progress has, however, recently been made in the structural elucidation of zeolites because *three* powerful new techniques have been introduced to supplement the rather incomplete information provided by X-ray diffraction and other methods:

*High-resolution electron microscopy* (HREM), which, in favorable circumstances, is capable of determining the structural characteristics of solids in real space[33-38], has brought to light a hitherto unknown tunnel structure. It has also characterized several quasi-crystalline zeolites[34-41] and, in conjunction with optical diffractometry, has elucidated[42] the nature of the intergrowths that may form between ZSM-5 and its closely related analogue, ZSM-11.

*Rietveld neutron diffraction (powder) profile analysis* has achieved a degree of structural refinement for zeolite Linde A which rivals that obtained by X-ray single-crystal methods[43,44] so far as Al, Si ordering and cation position are concerned. The Rietveld neutron diffraction approach to crystal structure determination is a promising and effective new technique, the great merit of which is that it is applicable to polycrystalline materials in general. Provided long-range order may be assumed and some preliminary model structure is known in broad outline, refinement of the observed and calculated line-profiles (intensity of scattering *versus* $2\theta$) permits the structure to be fully determined. In the case of zeolites, dehydrated samples have to be used because of the strong scattering of neutrons by water. Rietveld X-ray powder profile analyses are now quite widely developed[44b] for the structural determination of (ordered) powdered materials in general, and are already in use for the characterization of hydrated zeolites.

*High-resolution solid-state NMR with magic-angle spinning (MAS-NMR),* which is the sole technique upon which we shall concentrate in this account, since it has, to date, had the greatest single impact in the structural elucidation of zeolites in terms of the Si/Al distribution. When, as is described below, the zeolitic samples are spun rapidly at the magic angle of 54°44′ to the magnetic field (magic-angle spinning = MAS), the NMR spectra comparable to those displayed by species in solution are obtained. The spectra, in turn, enable us to establish the immediate chemical environment of the tetrahedrally coordinated Si "centers" and readily to distinguish tetrahedral from octahedral Al, the latter being often produced when zeolitic catalysts are subjected to various chemical treatments. Many other important structural issues have now been resolved by $^{29}$Si- and $^{27}$Al-MAS-NMR and some hitherto unanswerable questions have been greatly clarified (see Table 1).

Table 1. A summary of the information obtainable from the application of $^{29}$Si- and $^{27}$Al-MAS-NMR to the study of zeolites.

1. Identifies five distinct structural groups $Si(OAl)_n(OSi)_{4-n}$ ($n = 0, 1, \ldots 4$).
2. Confirms exact alternation of Al and Si among tetrahedral sites in zeolite A and zeolite X, when Si/Al = 1.00.
3. Monitors the course of solid-state (or gas-solid) reactions.
4. Quantitatively determines framework Si/Al ratios (for Si/Al ≈ 1.0 to > 1000).
5. Resolves numerous crystallographically distinct $Si(OSi)_4$ sites in silicalite (ZSM-5).
6. Readily distinguishes tetrahedral from octahedral Al.
7. Proves that Al in silicalite is tetrahedrally substituted within framework.
8. Elucidates nature of short-range Si, Al order.

## 4. High-Resolution Solid-State MAS-NMR Spectroscopy as Applied to Zeolites

### 4.1. Principles

In the last decade, techniques and equipment have been developed which yield NMR spectra of moderate resolution from solid samples. These have been described in detail elsewhere[45] and are only briefly reviewed here with especial emphasis on the aspects relevant to the study of zeolites.

The NMR spectra of abundant nuclei such as $^1$H in the solid state are dominated by the direct dipole-dipole interactions between the nuclei resulting in characteristic, broad, featureless absorptions ("wide-line" NMR). These interactions are orders of magnitude larger than the chemical shift and spin-spin couplings, the observation of which in solution, where the dipolar interactions average to zero, has made high-resolution NMR the most widely used technique for the structural elucidation of soluble chemical species. Although, in principle, it is possible to remove the dipolar interactions in the case of abundant nuclei, the finite efficiency of the experiment coupled with the small range of proton chemical shifts greatly limit the use of solid-state NMR of abundant nuclei.

However, in the case of "dilute" nuclei, where there is a low concentration of magnetically-active spins of the nucleus of interest in the sample, it has been demonstrated[46-48] that it is possible to obtain spectra of moderate resolution for a whole range of nuclei in the solid state. The total magnetic interaction, $H_{tot}$, appropriate for a dilute "spin 1/2" nucleus such as $^{13}$C in the presence of an abundant one such as $^1$H is given by:

$$H_{tot} = H_{ZEEMAN} + H_{^1H\text{-}^{13}C(DIPOLAR)} + H_{^{13}C\text{-}^{13}C(DIPOLAR)} + H_{^{13}C(CSA)} \quad (1)$$

The $^1$H-$^{13}$C dipolar interactions (the second term on the RHS of equation (1)) involve different nuclear species and can be removed by a powerful dipolar decoupling field applied at the proton resonance frequency. The $^{13}$C-$^{13}$C dipolar term involves interactions between nuclei of the same spin; but because of the dilution of $^{13}$C in the sample caused by the low (1.1%) natural abundance of $^{13}$C, this term is negligible. The only remaining line broadening contribution is the chemical shift anisotropy, $H_{^{13}C(CSA)}$, which results from the different chemical shieldings of nuclei caused by their different orientations to the magnetic field. In solution, the random motion of the molecules produces an average (isotropic) value of this shielding; but in the solid a broad envelope characteristic of the chemical environment of the nucleus results. This remaining interaction may be averaged to the isotropic chemical shift value, producing a "high-resolution" spectrum, by mechanical spinning of the sample about an axis inclined at the so-called "magic angle" of 54°44′ to the magnetic field vector, as first described by *Andrew et al.*[49] and *Lowe*[50]. Spinning frequency must be comparable to the frequency spread of the signal.

We see how this "magic angle" arises by examining the equation for the Hamiltonian describing the chemical shift anisotropy as modified by sample spinning.

$$H_{CSA} = (3\cos^2\theta - 1)(\text{other terms}) + (3/2\sin^2\theta)\sigma_i I_z B_0 \qquad (2)$$

where $\theta$ is the angle subtended by the axis of spinning with respect to the direction of the magnetic field, $B_0$, and $\sigma_i$ and $I_z$ are respectively, the isotropic chemical shielding and the spin angular momentum. When $\theta = 54°44'$, the prefactor to the first term becomes zero, leaving only the second term, the value of which is now $\sigma_i I_z B_0$, which, in turn, yields the isotropic chemical shift. Spinning at frequencies less than the frequency spread of the shift anisotropy pattern yields a spectrum consisting of a central peak at the isotropic chemical shift value of the same line width as before but flanked by a series of "spinning sidebands" separated by the spinning frequency and with intensities that approximate the profile of the shift anisotropy pattern.

A combination of high-power decoupling and magic-angle spinning (MAS) produces a spectrum of moderate resolution, the signals of which occur at the isotropic (average) shift values similar to those in solution. In addition, the intensity of the signals arising from the dilute nuclei in the system may be substantially enhanced from the magnetization of the abundant nuclei (usually protons) in the sample by use of the "cross-polarization" (CP) pulse sequence introduced by *Pines, Gibby,* and *Waugh*[51]. It should, however, be noted that this technique does not affect the widths of the signals and therefore the *resolution* of the experiment and that the resulting enhancements may be quite different for chemically different nuclei producing spectra which may not normally be quantitatively reliable. The first combined CP/MAS experiment was reported by *Schaefer* and *Stejskal*[52], and in recent years there have been numerous applications of these techniques to a variety of chemical systems in the solid state[45-48].

So far as zeolites are concerned two important points may be made:

1. Although the above discussion has been presented in terms of $^{13}C$, the experiment is equally applicable to a whole range of nuclei, *e.g.*, $^{29}Si$, $^{57}Fe$, $^{113}Cd$, $^{119}Sn$, $^{207}Pb$. Further, it is not necessary that the "dilution" criterion be satisfied by way of low isotopic abundance of the magnetically active nucleus; spectra may be obtained from 100% abundant nuclei such as $^{31}P$ or $^{27}Al$ as long as the term corresponding to the third one in equation (1) is small. This may be attained by physical dilution, which is relatively easy for almost all nuclei except $^{1}H$ which, in addition to being of common occurrence, has the highest magnetic moment and largest dipolar intensities of all nuclei. Thus MAS-NMR spectra may, for example, be obtained for every nucleus in a typical zeolitic system ($^{23}Na$, $^{29}Si$, $^{27}Al$, $^{17}O$, *etc.*).
2. Usually there are no $^{1}H$ nuclei covalently bonded to the framework of zeolites (this applies to many other inor-

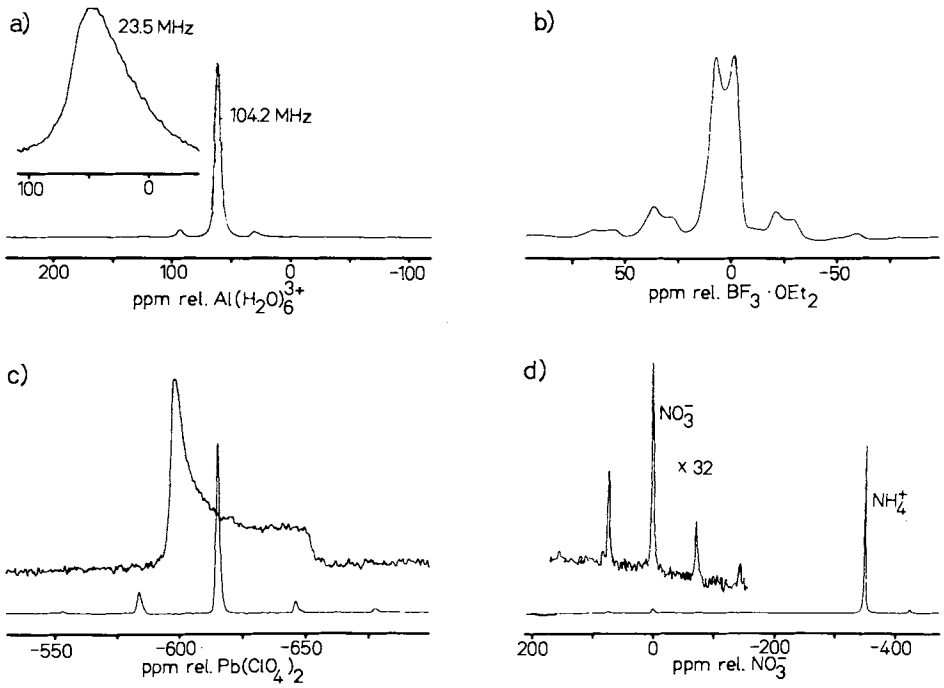



Fig. 3. Solid-state magic-angle-spinning NMR spectra: a) $^{27}Al$ spectra of zeolite Y at 23.5 MHz (7771 scans, 25 Hz line broadening, 0.1 s relaxation delay) and at 104.2 MHz (2656 scans, no line broadening, 0.1 s relaxation delay). Note the spectral improvement at higher field.—b) $^{11}B$ spectrum of Corning 7070 glass at 128.4 MHz (13775 scans, 25 Hz line broadening, no relaxation delay). Note the characteristic pattern of the residual quadrupolar interaction.—c) $^{207}Pb$ spectra of $Pb(NO_3)_2$ at 83.4 MHz. The powder pattern (420 scans, 20 Hz line broadening, 2 s relaxation delay) is shown above the spinning spectrum (230 scans, 20 Hz line broadening, 2 s relaxation delay).—d) $^{15}N$ spectrum of $^{15}NH_4{}^{15}NO_3$ at 40.5 MHz (2978 scans, 40 Hz line broadening, 1 s relaxation delay). The $NO_3^-$ portion of the spectrum, magnified 32 times, is also shown. The small absorptions in the spectra are due to spinning sidebands (see text).

ganic solids). This means that the term corresponding to the second one in equation (1) vanishes. High-power decoupling is rendered unnecessary and cross-polarization not possible, thus reducing the experiment to one of simple MAS of the sample, which can easily be carried out using a conventional high-resolution NMR spectrometer available to most chemists, as indicated in Figure 3 for a variety of systems. Further, there are advantages in performing the experiment at as high a magnetic field strength as possible. For nuclei with spin half ($I=1/2$) such as $^{29}Si$, there is a very substantial gain in resolution due, at least in part, to the superior field homogeneity and stability of superconducting solenoid magnets. With quadrupolar nuclei of non-integral spins (of which $^{27}Al$ with $I=5/2$ is particularly important in the present context), the $(m=1/2)\leftrightarrow(m=-1/2)$ transition which is observed is independent of the quadrupolar interaction to first order as illustrated in Figure 4; but it is affected by second order quadrupolar effects. These vary inversely with the magnetic field and the best spectra will, therefore, be obtained at the highest available field strength (Figure 3a). In our own work we have used[53] a high-resolution Bruker WH-400 narrow-bore spectrometer with a home-built MAS broad-banded probe fitted with a standard Andrew-Beams[54] spinning assembly capable of observing $^{29}Si$ (80 MHz), $^{27}Al$ (104 MHz) and $^{11}B$ (128 MHz) directly, and additional nuclei with modification. The spectra shown in the present account are thus easily obtainable using simple techniques and widely available equipment.

The first application of these techniques to the investigation of zeolites was made by *Lippmaa* and *Engelhardt*[55], who, in a pioneering paper[56], showed clearly that up to five peaks could be observed for $^{29}Si$-spectra of various zeolites (cf. Fig. 5), corresponding to the five possible Si environments: $Si(OAl)_4$; $Si(OAl)_3(OSi)$; $Si(OAl)_2(OSi)_2$; $Si(OAl)(OSi)_3$ and $Si(OSi)_4$. Further, and most importantly, they showed that characteristic ranges of these isotropic shifts could be assigned as shown in Figure 6 and used for further investigations of zeolite structures in terms of the microenvironments of the nuclei. Further investigations[57-75] have expanded the range of nuclei studied and the techniques used (cf. Sections 4.2-8); it is to be noted that the

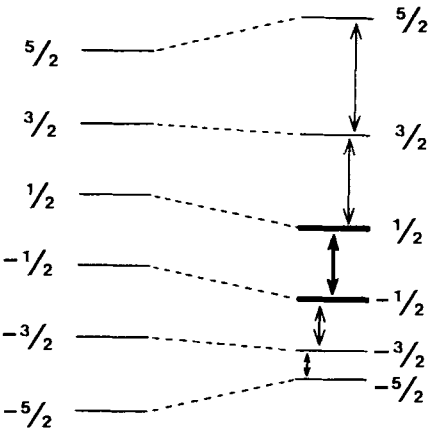



Fig. 4. Energy level diagram for a spin 5/2 nucleus showing the effect of the first-order quadrupolar interaction on the Zeeman energy levels. The $(m=1/2)\leftrightarrow(m=-1/2)$ transition (shown in bold lines) is independent of the quadrupolar interaction to first order but is subject to second-order quadrupolar effects (see text).

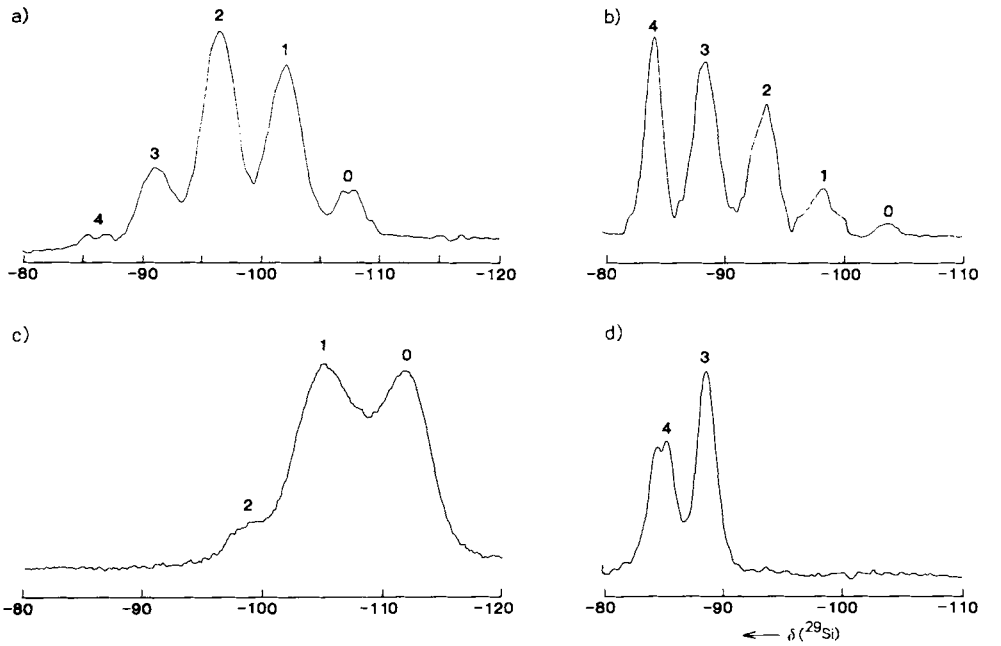



Fig. 5. $^{29}Si$-MAS-NMR spectra at 79.80 MHz of four zeolites. Numbers above peaks are the n in Si(n Al), the five possible environments of an Si atom (cf. Fig. 6): a) gmelinite; b) analcite; c) mordenite; d) zeolite Z.

assignment of the $^{29}$Si-coordination remains, as before, central to the application of the technique.

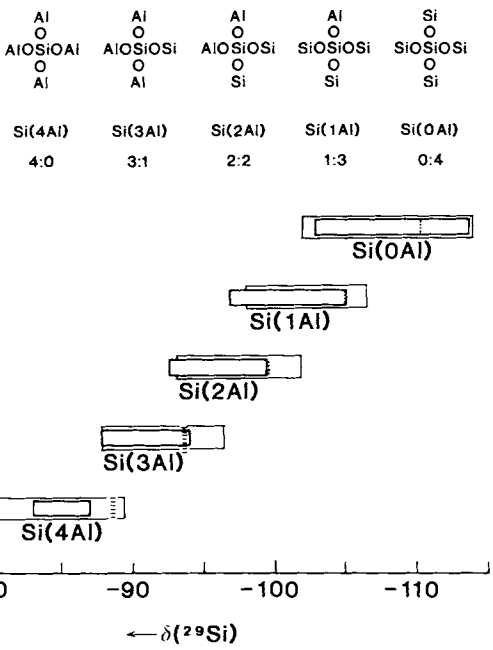



Fig. 6. The five possible local environments of a silicon atom together with their characteristic chemical shift ranges. The chemical shifts of the five resonances of zeolite ZK-4 are shown in broken vertical lines. The inner boxes represent the $^{29}$Si shift ranges suggested in the earlier literature (refs. [56a] and [59]). The outer boxes represent the recently extended $^{29}$Si shift ranges (taken from refs. [56b] and [74b]).

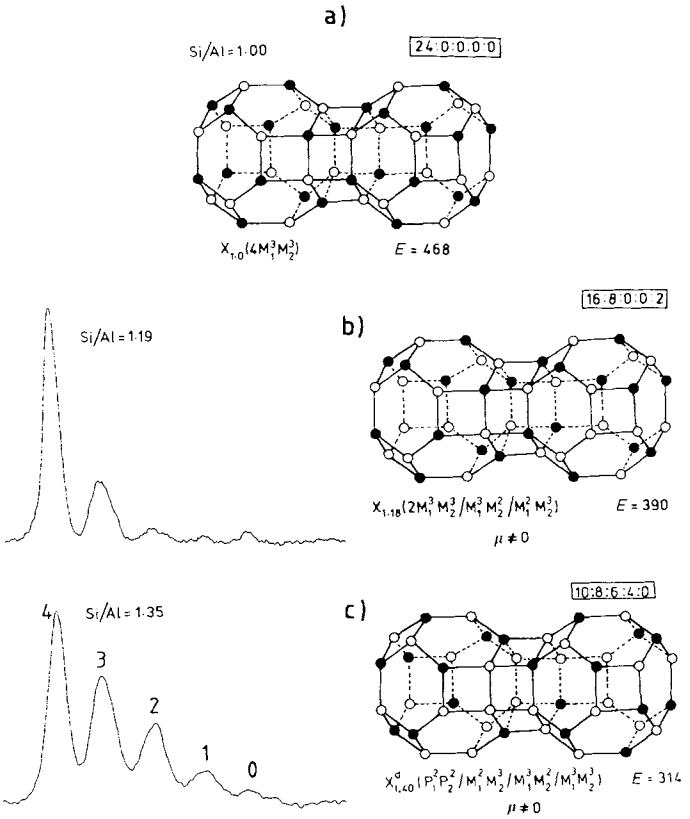



Fig. 7. a) The Si,Al ordering scheme in a hypothetical zeolite X (synthetic faujasite) with Si/Al = 1.00. Tetrahedrally-bound Si and Al atoms are denoted by ○ and ●, respectively. The ratio of the populations of the basic Si(nAl) building units, Si(4Al):Si(3Al):Si(2Al):Si(1Al):Si(0Al) corresponding to the scheme is given in the upper right-hand corner. The type of linking of the sodalite cages, using notation developed in [74a] is given below the structure. $E$ is the calculated electrostatic energy for the double cage in units of $(qe)^2/a$.—b) and c) In the left-hand column are given high-resolution $^{29}$Si-MAS-NMR spectra of two zeolites NaX of the compositions indicated (determined from the spectra using eq. (3)). Numbers above NMR peaks refer to the n in Si(nAl). In the right-hand column are the corresponding most probable structures based on electrostatic and other considerations (see text) for the nearest "ideal" Si/Al ratio. $\mu \neq 0$ denotes net dipole moment in double sodalite cage; the meaning of other symbols as in (a).

## 4.2. Determination of Zeolite Composition by $^{29}$Si-MAS-NMR Spectroscopy — Si,Al Ordering in Zeolites X and Y

The $^{29}$Si-MAS-NMR spectrum of zeolite X when Si/Al = 1.0 consists of one peak corresponding to $Si(OAl)_4$ (also written for simplicity Si(4Al)). *It therefore follows that there is strict ordering* within the aluminosilicate framework, the Al and Si alternating as tenants of the tetrahedral sites. In other words, Loewenstein's rule[76], which states that two Al atoms cannot be adjacent on tetrahedral sites, is obeyed. As the Si/Al ratio progressively increases, all five peaks, corresponding to $Si(OSi)_{4-n}(OAl)_n$ with n equal to 0, 1, ... 4, appear until, at the higher values of the ratio, typically Si/Al > 2.0, the Si(4Al) peak disappears and the Si(nAl) peaks, with n small, grow in relative intensity as expected from the gradual build-up of the more siliceous faujasite (Fig. 7). By convention Si/Al ratios between 1.0 and 1.5 are designated zeolite X; beyond that ratio faujasitic zeolites are designated zeolite Y.

The fact that there is strict alternation of Al and Si amongst the tetrahedral sites when Si/Al = 1.0, prompts us to enquire whether, as the Si/Al ratio increases, the charge-deficient ions ($Al^{3+}$) adopt ordering schemes according to some readily comprehensible principles. For example, Loewenstein's rule may still be obeyed. $^{29}$Si-MAS-NMR permits us to demonstrate that this is indeed the case in zeolites X and Y. If the immediate neighborhood of every Al tetrahedral site is $Al(OSi)_4$ (*i.e.*, Al(4Si)) then each Si–O–Al– linkage in a Si(nAl) structural unit incorporates 1/4Al atom. It follows[60, 71, 74], therefore, that the Si/Al ratio in the tetrahedral aluminosilicate framework is given by

$$(Si/Al)_{NMR} = \sum_{n=0}^{4} I_{Si(nAl)} \; / \; \sum_{n=0}^{4} 0.25\, n\, I_{Si(nAl)} \qquad (3)$$

We note, in passing, that this equation is valid for all zeolites irrespective of structural type, and represents a powerful new quantitative method of determining *framework* Si/Al ratios, provided no Al–O–Al linkages are present.

In a series of ten zeolites X and Y of different composition, synthesized under conditions that excluded coprecipitation of extra-framework aluminosilicate, it has been found[74] that the Si/Al ratios determined by X-ray fluorescence and by MAS-NMR (see Table 2) are in very good agreement. Loewenstein's rule clearly holds, at least on the spatially-averaged basis—it is not inconceivable that there may be a few local infractions where Al–O–Al linkages are formed as kinetically stabilized structural defects. *Mel-*

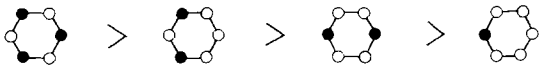
*chior et al.*[65] reached the same conclusion when they demonstrated that, for a series of faujasitic zeolites, the observed intensities of Si(nAl) signals conformed to a 1/R (where R = Si/Al) dependence rather than to a 1/(R+1) dependence, which would imply a truly random (non-Loewensteinian) distribution of aluminum atoms in the tetrahedral sub-lattice.

Table 2. Comparison between $^{29}$Si-MAS-NMR and X-ray fluorescence (XRF) as methods of determining Si/Al ratios of zeolites X and Y (see text and eq. (3)).

| Sample No. | Si/Al Ratio by XRF [a] | | Si/Al Ratio by $^{29}$Si-MAS-NMR [b] |
|---|---|---|---|
| 1 | 1.19 | Zeolites X | 1.14 |
| 2 | 1.35 | | 1.39 |
| 3 | 1.59 | Zeolites Y | 1.57 |
| 4 | 1.67 | | 1.71 |
| 5 | 1.87 | | 1.85 |
| 6 | 2.00 | | 1.98 |
| 7 | 2.35 | | 2.46 |
| 8 | 2.56 | | 2.69 |
| 9 | 2.61 [c] | | 2.56 |
| 10 | 2.75 | | 2.69 |

[a] The fluorescence measurements were kindly carried out by Dr. *A. E. Comyns* and his colleagues (Laporte Industries), who also supplied us with the samples. [b] The normalized intensities of individual $^{29}$Si-peaks are given in the original paper [74]. Sample 1, for example, had the following peak intensities: Si(4Al), 64.0; Si(3Al), 26.5; Si(2Al), 6.2; Si(1Al), 1.4; and Si(0Al), 1.9 with $\Sigma I_{Si(nAl)} = 100$. Using equation (3), the framework Si/Al ratio is computed to be 1.14. [c] Composition of this sample determined by energy-dispersive X-ray analysis using analytical electron microscopy.

We may proceed to calculate average populations of the five configurations Si(nAl) (n = 0, 1, ... 4), which is tantamount to computing the relative intensities of the $^{29}$Si-MAS-NMR signals, $I_{Si(nAl)}$, in all zeolite structures that comply with Loewenstein's rule, but in which the Si,Al ordering is otherwise random. Since each Al in the framework must be surrounded by four Si atoms, the probability of the occurrence of an Si–O–Al linkage is p (= 1/R). The probability of occurrence of Si–O–Si, the only other type of permitted linkage, is (1 – p). The probabilities of the five possible configurations are thus given by the binomial formula as: $p^4$ for Si(4Al), $4(1-p)p^3$ for Si(3Al), $6(1-p)^2p^2$ for Si(2Al), $4(1-p)^3p$ for Si(1Al), and $(1-p)^4$ for Si(0Al). A comparison of the observed $I_{Si(nAl)}$ intensities with those computed on the basis of the constrained (by Loewenstein's rule) random model reveals rather poor agreement at low values of the Si/Al ratio, but somewhat better agreement as the ratio increases. There are clearly some other factors, besides those of avoidance of Al on adjacent tetrahedral sites, governing the distribution of the aluminum atoms in the framework. We have analyzed[74a] these additional factors elsewhere, and taken into account the fact that there are other independent items of information which suggest that there is some tendency for Si,Al ordering, beyond that associated with Loewensteinian behavior. The first item is the report that there are discontinuities[23,77a] in the plot of the (cubic) unit cell dimension versus Si/Al ratio. The second is that there are different electrostatic repulsion energies for various occupancies of individual six-membered rings in the faujasite structure:



Sequences of decreasing electrostatic repulsion energy for complete sodalite cages, as well as for preferred occupancies of "double-six" prisms may also be constructed.

A viable method of determining possible preferred Si,Al ordering schemes by means of $^{29}$Si-MAS-NMR spectroscopy can now be described. From the experimentally (NMR) determined ratio of the populations of Si(nAl) units for each specific (Si/Al) ratio in the zeolite X and Y family, bearing in mind the above-mentioned restrictions and the need to comply with cubic crystal symmetry ($a_0 = 24.7$ Å), a series of likely ordering schemes is constructed. Approximate estimates of energies of electrostatic interactions ($Al^{3+} \cdots Al^{3+}$ repulsions) are expressed in units of $(qe)^2/a$, where $qe$ is the effective charge placed on an Al site and $a$ is the T–O–T distance. For most Si/Al ratios more than one ordering scheme is compatible with the Si(nAl) intensities determined by $^{29}$Si-MAS-NMR. The choice between the competing ordering schemes is finally made on the basis of three criteria:

1. goodness of fit of experimental and model-generated Si(nAl) intensities;
2. compliance with cubic symmetry and unit cell repeat;
3. minimal electrostatic repulsion within the aluminosilicate framework.

It is worth emphasizing that MAS-NMR yields spatially and temporally averaged information, that the sharpness of the spectral peaks reflects the degree of crystallinity but does not connote long range order, that the total peak intensities may enable the space-group to be ascertained (cf. Section 6), that, apart from zeolites yielding single-peak $^{29}$Si-spectra, MAS-NMR cannot *directly* determine structure (and, therefore, the Si, Al ordering schemes).

The most likely ordering for the compositions corresponding to the spectra on the left-hand side of Figure 7 are given on the right of that figure. Attempts have been made to interpret observed $^{29}$Si-MAS-NMR intensities for a family of faujasites in terms of what may be designated a "constrained random" basis for Si, Al ordering, the constraint being obedience to Loewenstein's rule. While our earlier data, obtained at lower field[58], lent some credence to this view, our data at higher field[74a] do not support it. It has to be admitted, however, that, as the Si/Al ratio increases beyond 2.4 the constrained random model is not altogether unrealistic.

It may legitimately be argued that the procedures for estimating electrostatic energy are oversimplified; and that the zeolite structures and thus Al,Si ordering adopted within them are not at thermodynamic equilibrium. Taken all in all, however, we believe that the present approach offers considerable insight, not otherwise attainable, into the precise population of, and distribution within, the aluminosilicate framework of zeolites. A similar approach could, with profit, be applied to many other recalcitrant structural problems involving inorganic solids, both crystalline and amorphous. As discussed elsewhere, this approach does

offer support for the view that a discontinuity in the unit-cell parameter should occur at a well-defined Si/Al ratio. It transpires that the repulsion energy per number of Al ions in the unit cell changes abruptly at a Si/Al ratio of close to 2.0. The approach also throws some light on the effect of second-nearest (tetrahedral) neighbors on chemical shifts.

### 4.3. Determination of Zeolitic Composition by $^{27}$Al-MAS-NMR Spectroscopy

As discussed in the previous section, the Si/Al ratio of any zeolite can be derived from $^{29}$Si-MAS-NMR spectra provided that Loewenstein's rule is obeyed. However, as the silicon content of the material increases, the determination of composition by this method becomes progressively less reliable and fails for the porotectosilicates encompassing silicalite and ZSM-5 where the intensity of Si(n Al) signals cannot be reliably measured (not even when n = 1). In these circumstances $^{27}$Al-MAS-NMR can be used to estimate the composition. First, it is to be noted that the technique can readily and quantitatively distinguish between tetrahedrally and octahedrally coordinated aluminum (cf. Fig. 8). Again, the areas of the two peaks are directly proportional to the amounts of aluminum in each coordination. Furthermore, the 100 per cent isotopic abundance of $^{27}$Al and its relatively short spin-lattice relaxation times (the nucleus is quadrupolar) makes $^{27}$Al-MAS-NMR especially sensitive. By adding to the sample increments of materials containing known amounts of octahedrally or tetrahedrally coordinated Al and repeating the $^{27}$Al-MAS-NMR experiment, one may[69] measure accurately the Si/Al ratio even in very siliceous materials, such as silicalite, where this ratio can exceed 1000 (cf. Section 6). Si/Al ratios in excess of 10000 may be estimated in this way.

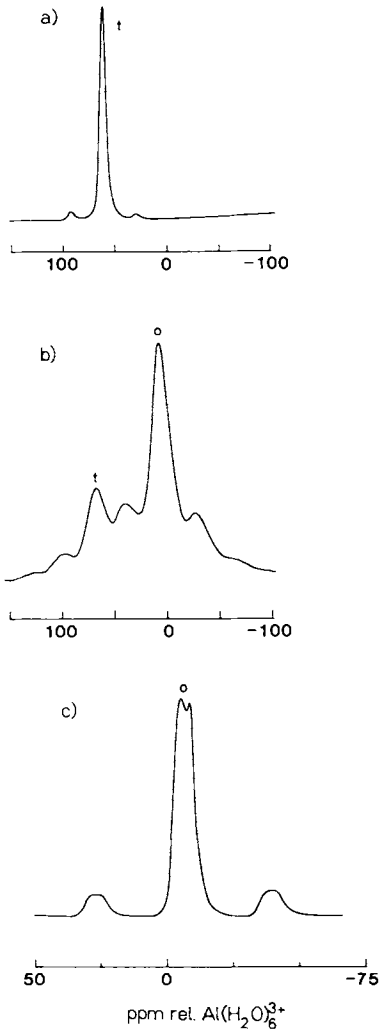



Fig. 8. $^{27}$Al-MAS-NMR spectra at 104.22 MHz: a) The spectrum of zeolite NaY showing a single resonance due to tetrahedral coordination of framework aluminum. — b) Alumina, $\gamma$-$Al_2O_3$, showing both tetrahedral (t) and octahedral (o) coordination of Al. — c) The mineral beryl showing only octahedral coordination of Al.

Extensive measurements of $^{29}$Si spectra of aluminosilicates indicate that tetrahedral aluminum tends to favor situations where a central aluminum is surrounded, *via* oxygen bridges, by four silicons, *i.e.* Al(4Si). Crystallographically non-equivalent tetrahedral Al atoms have, however, been resolved in silicalite[69], and in zeolite omega[73c]. $^{27}$Al-MAS-NMR is not, in general, as powerful as $^{29}$Si-MAS-NMR in determining the ordering within the zeolitic aluminosilicate framework. Because of the relative insensitivity of the $^{27}$Al-MAS-NMR chemical shift to the occupants of the second and further coordination shells, a rather broad $^{27}$Al single peak is usually observed. On the basis of our recent measurements[74b] on gallosilicate zeolites the same appears to be true of $^{71}$Ga-MAS-NMR.

## 5. Modifying the Zeolitic Framework by Chemical Means

Faujasitic solids have been the subject of numerous studies, the objective of which was to remove the Al from, or to modify its distribution within, the tetrahedral sub-lattice while at the same time retaining the original topology and crystallinity of the parent open structure[78]. Acid-leaching and use of reagents such as EDTA, gaseous $Cl_2$, or acetyl acetone have been used for this purpose, but none of these reagents is as effective as two others which we shall describe in this section. One of these involves[64,79,80] dealumination using $SiCl_4$; the other entails heat treatment of the ammonium-exchanged zeolite where ammonium ions have replaced the sodium ions originally present. This latter process is currently preferred, commercially, for effecting "ultrastabilization", a term used to describe the production of extremely effective cracking and hydrocracking zeolitic catalysts that possess high thermal stability. $^{29}$Si- and $^{27}$Al-MAS-NMR can be used to monitor, for the first time, the subtle changes that accompany these processes[66,67,70,72].

### 5.1. Dealumination of Faujasitic Zeolites by $SiCl_4$

After recognizing the success with which the aluminum may be removed, as volatile $AlCl_3$, from alumina when reacted at red heat with $SiCl_4$—a reaction described well over a hundred years ago[79c,d]—*Beyer* and *Belenykaja*[79a] recently demonstrated that zeolite Y can be dealuminated in like fashion *without collapse of the crystal structure.* We have ourselves confirmed that this is an effective means of

converting zeolite Y to faujasitic silica, since the final Si/Al ratio may be *ca.* 100. X-ray powder diffraction, infrared spectroscopy[79b] and high-resolution electron microscopy[64,80], all show that there is no significant difference in the pore system following extensive dealumination by $SiCl_4$. The overall reaction may be written:

$$Na_x[(AlO_2)_x(SiO_2)_y] + SiCl_4 \longrightarrow Na_{x-1}[(AlO_2)_{x-1}(SiO_2)_{y+1}] + AlCl_3 + NaCl$$

However, it can be seen from the $^{27}$Al-MAS-NMR spectrum (Fig. 9a–c) that, as well as the diminished peak corresponding to residual tetrahedral Al (*i.e.*, $Al(OSi)_4$ groups) and the emergent octahedral Al, which is occluded by the framework, there is an additional peak indicative of tetrahedral Al arising from $Na^+(AlCl_4)^-$ ion pairs also occluded in the zeolite. Upon washing this dealuminated zeolite with water, the $Na^+(AlCl_4)^-$ is largely removed or converted to the hydrated ion $[Al(H_2O)_6]^{3+}$ which may then function, in place of the original $[Na(H_2O)_n]^+$, as the neutralizing "exchangeable" cation. (It is significant that from Figure 9c we can deduce that the amount of octahedral $[Al(H_2O)_6]^{3+}$ is *ca.* a third of the residual tetrahedral aluminum as required for charge balance.)

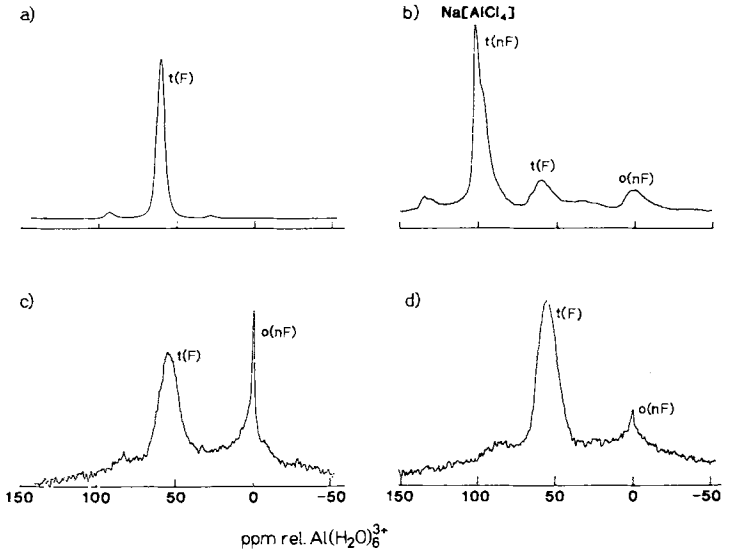



Fig. 9. Dealumination of zeolite NaY using $SiCl_4$ vapor studied by $^{27}$Al-MAS-NMR spectroscopy at 104.22 MHz: a) Parent NaY zeolite; b) dealuminated material before washing; c) after washing with dilute acid; d) after repeated washing. Note that the aluminum jettisoned from the zeolitic framework is first of all bound tetrahedrally (as $Na^+AlCl_4^-$, see text), but after washing adopts octahedral coordination. t(F) = tetrahedral (framework), t(nF) = tetrahedral (non-framework), o(nF) = octahedral (non-framework).

The $^{29}$Si-MAS-NMR spectrum shown in Figure 10b also refers to a Na–Y sample dealuminated by $SiCl_4$. The single peak in this spectrum arises from Si(0Al), *i.e.* from Si(4Si) groupings: essentially all other groupings have been eliminated in the course of dealumination. The chemical shift of this peak ($\delta = -107.0$) is very close to that found in quartz[56]. The sharpness of the peak further signifies the high degree of homogeneity and crystallinity of the faujasitic silica produced by this process.

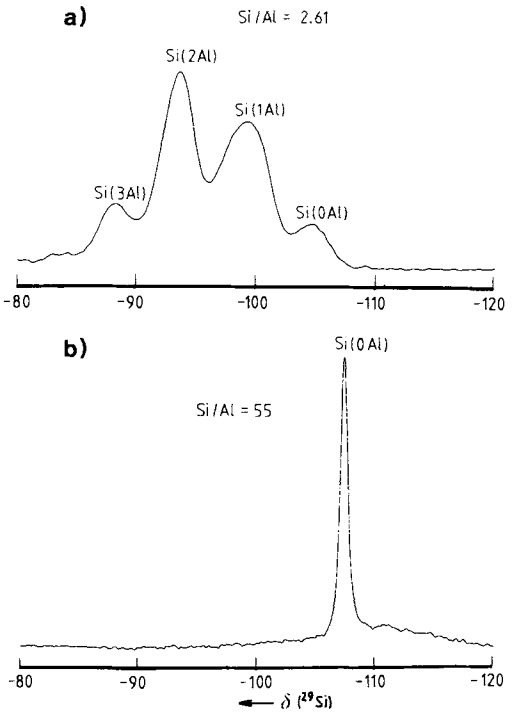



Fig. 10. Dealumination of zeolite NaY using $SiCl_4$ vapor studied by $^{29}$Si-MAS-NMR spectroscopy at 79.80 MHz: a) Parent material; b) after "complete" dealumination (corresponding to the $^{27}$Al-MAS-NMR spectrum in Fig. 9d).

Wet chemical analysis of the global Si/Al ratio of this sample yielded a value of 55. But since Al has been removed from the tetrahedral sites and some of it retained, ultimately as neutralizing octahedrally coordinated $[Al(H_2O)_6]^{3+}$, the true framework Si/Al ratio is significantly greater than 55. It is possible to determine the amount of extra-framework Al directly from the absolute intensity of the $^{27}$Al spectrum as previously indicated, and the method constitutes one of the few reliable sensitive techniques for measuring the amount of Al *not* substitutionally incorporated into a zeolite framework.

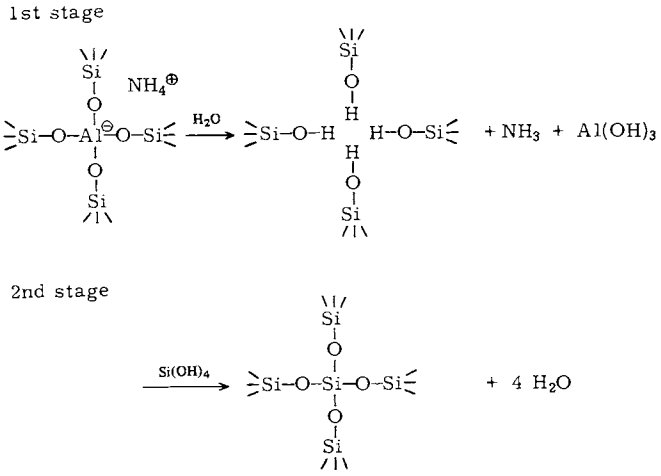
MAS-NMR has recently enabled us to show[81] that mordenite, another industrially important zeolite, can also be dealuminated by $SiCl_4$, and so also may zeolite omega[73c]. It is clear that this method of dealumination is potentially widely applicable to other zeolites as well as to clays, gels, amorphous and crystalline silica-aluminas. It is of great commercial interest that the $^{29}$Si-MAS-NMR spectrum of dealuminated ZSM-5 approaches that of silicalite[81b,c]. It has been claimed[79b,82] that elimination of framework aluminum may be effected by other volatile reagents including $PCl_3$, $TiCl_4$ and $CrO_2Cl_2$.

### 5.2. Charting the Course of Ultrastabilization of Zeolites

Faujasitic zeolites are good cracking catalysts, but in their "as-prepared" condition they are too acidic and insufficiently thermally stable to be useful as hydrocracking catalysts[10]. However, the process of ultrastabilization[83,84], which entails hydrothermal treatment of the ammonium-exchanged form of synthetic faujasite, $NH_4^+$–Y,

under well-defined conditions, results in the production of a $H^+$–Y zeolite possessing desirable thermal stability and high internal surface area, which is admirably suited for hydrocracking reactions. Ever since ultrastabilization was first discovered, there has been much speculation[78b–d] as to what, precisely, was occurring at the atomic scale inside the zeolite. That aluminum was being removed from the framework and ammonia eliminated from the $NH_4^+$ ions was obvious, but what reorganization occurred within the framework? (cf. Scheme 2). Thanks to MAS-NMR this question can now be partly answered.

In a series of four samples subjected[67] to different types of hydrothermal treatment $^{29}$Si-MAS-NMR clearly shows how Al is removed from the framework, and how the resulting vacancies in the framework are subsequently reoccupied (see Scheme 2) by silicons from other parts of the crystalline sample (Fig. 11). The $^{27}$Al-MAS-NMR spectra for the same four samples show[67] directly how the occluded octahedrally-bound Al builds up at the expense of the tetrahedrally-bound variety. Hydrothermal dealumination studies, using $^{29}$Si-MAS-NMR have also been carried out by *Engelhardt et al.*[60,70] and by *Maxwell et al.*[66]. The




Scheme 2.

use of cross-polarization MAS-NMR by the first-named group makes possible the detection of "surface" Si atoms to which are attached one or two hydroxyl groups, as the cross-polarization technique discriminates in favor of these

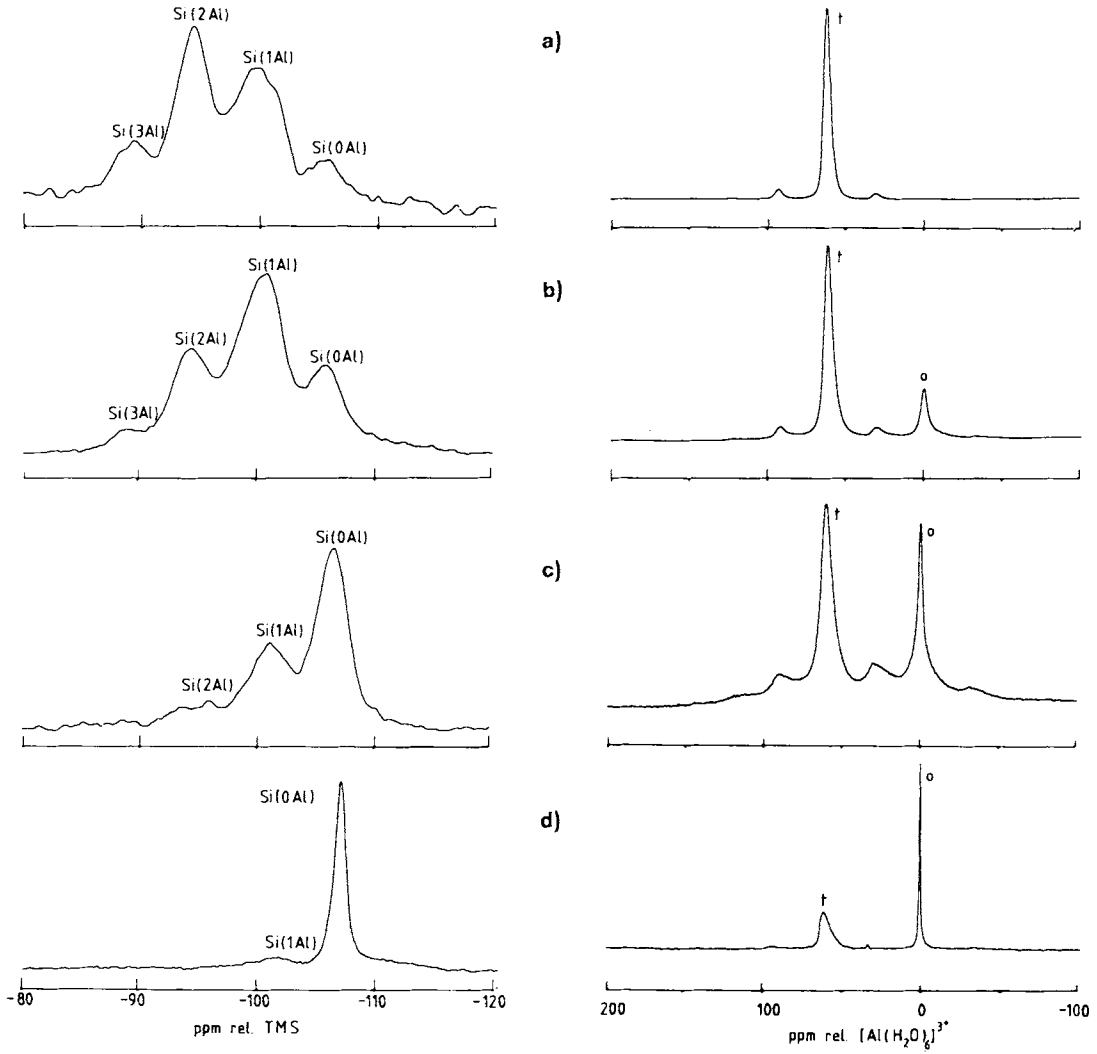



Fig. 11. High-resolution $^{29}$Si- (79.80 MHz) and $^{27}$Al-MAS-NMR studies (104.22 MHz) of the ultrastabilization of zeolite Y: a) Parent $NH_4$-Na-Y zeolite; b) after calcining in air for 1 h at 400 °C; c) after heating to 700 °C for 1 h in the presence of steam; d) after repeated ion exchange, heating and prolonged leaching with nitric acid. t = tetrahedral, o = octahedral.

atoms due to their proximity to the "abundant" $^1H$ spins in the system. These resonances may then be identified in the "normal" spectrum and an estimate made of their concentration (the CP spectra are not quantitatively reliable for this purpose). It would appear that, apart from situations where the Si/Al ratio is large, the concentration of such groups is relatively small, given the number of Al atoms removed. This, in turn, suggests that a process of "healing" takes place subsequent to dealumination (cf. second stage of Scheme 2).

## 6. Resolving Crystallographically Distinct Tetrahedral Sites in Silicalite and ZSM-5

The framework structure of the new, thermally stable, crystalline porous silica called silicalite is topologically closely similar if not identical to that of the shape-selective catalyst ZSM-5 (cf. Fig. 2). It has been claimed[17a,85] that silicalite has no aluminum in the framework and, hence, no exchangeable cations, and that such aluminum as may be adventitiously present in silicalite is in the form of $Al_2O_3$. It could therefore be argued that, strictly speaking, silicalite is not a zeolite. We have recently shown[69] by MAS-NMR that:

- the aluminum in silicalite is readily detectable by $^{27}Al$-MAS-NMR;
- all the aluminum is tetrahedrally coordinated to oxygen;
- there are at least two distinct types of tetrahedral framework sites occupied by the aluminum;
- the Si/Al ratio can be easily estimated;
- several crystallographically distinct sites for silicon in the lattice may be directly detected.

Figure 12a shows the $^{29}Si$-MAS-NMR spectrum of silicalite. The chemical shift range of all the peaks is characteristic of $Si(OSi)_4$ groupings in highly siliceous materials. The observed multiplicity arises from the crystallographically non-equivalent tetrahedral environments of the $Si(OSi)_4$ sites. The spectrum may be simulated by a minimum of nine Gaussian signals, the intensities (peak areas) of which are approximately in the ratio 1 : 3 : 2 : 3 : 10 : 1 : 1 : 2 : 1 (see Fig. 12b). Using the intensities of the well-resolved lowest- and highest-field signals as base units (generating functions) of one, the total intensity of the peaks in the Si(4Si) multiplet is found to be approximately 24. This result suggests that the space group of silicalite is one which contains 24 non-equivalent sites in the structural repeat unit. In particular, it signifies that $Pn2_1$ or $P2_1/n$ are more likely space groups for silicalite than Pnma, which has only 12 distinct sites. To date, the detailed structure and space group of ZSM-5 and silicalite do not seem to have been satisfactorily resolved by single-crystal X-ray methods, and the MAS-NMR results emphasize that view. These results further suggest that other space-groups, possibly $P2_12_12_1$, could be more appropriate than the currently favored (on X-ray grounds) Pnma.

The $^{27}Al$-MAS-NMR spectrum of silicalite (Fig. 13) shows an absorption centered at $\delta = 55.6$, clearly characteristic of tetrahedral coordination. The peak shows fine structure arising from at least two components, indicating

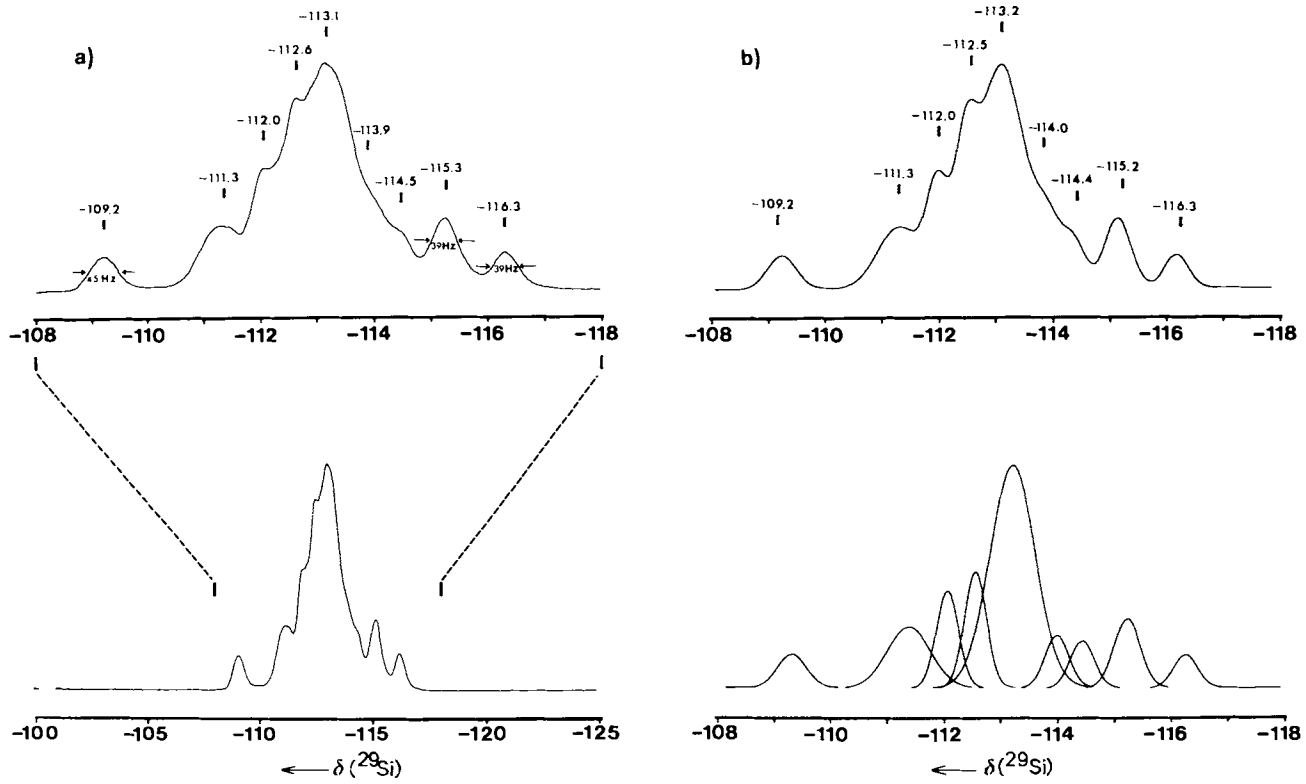



Fig. 12. a) High-resolution $^{29}Si$-MAS-NMR spectrum of silicalite at 79.80 MHz. 6550 free induction decays were accumulated; repetition time 5 s.—b) The spectrum given in (a) can be computer-simulated using the minimum number of nine Gaussian-shaped peaks, shown individually below the simulated spectrum. The areas of the peaks are from left to right, in the ratio 0.98 : 2.70 : 2.19 : 2.63 : 10.35 : 1.30 : 1.61 : 1.87 : 0.82 (see text).

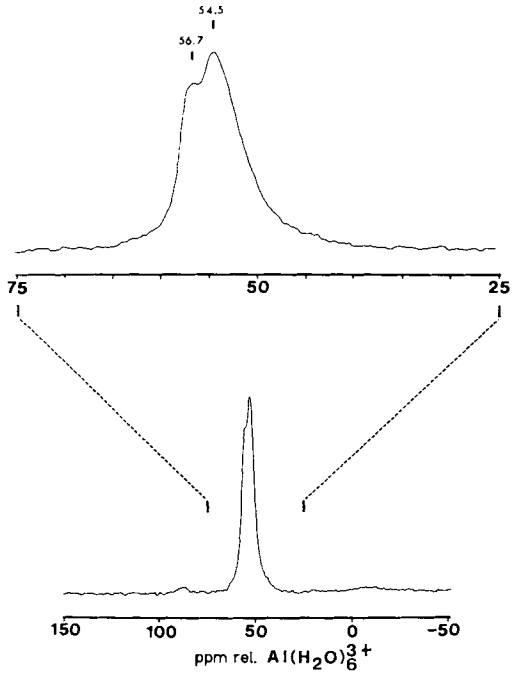



Fig. 13. High-resolution $^{27}$Al-MAS-NMR spectrum of silicalite at 104.22 MHz. 176214 free induction decays were accumulated; repetition time 0.1 s. Note the absence of octahedrally coordinated aluminum in the sample.

the presence of crystallographically non-equivalent sites for tetrahedral aluminum. The amount of aluminum present is very small, but it is clear that all of it is tetrahedrally-bound and constitutional, and not present as occluded $Al_2O_3$ impurity, since the various forms of $Al_2O_3$ which we have investigated for comparison show an intense MAS-NMR peak at $\delta = 9 \pm 1$ (signifying predominantly octahedrally-bound Al) and, in some forms, a relatively small peak at $\delta = 72 \pm 3$ arising from tetrahedral coordination. (These are the kind of spectral features to be expected, for example, from $\gamma$-$Al_2O_3$.) Furthermore, a peak at $\delta = -106$ corresponding to Si(1Al) may be observed in $^{29}$Si-MAS-NMR spectra of a commercial grade silicalite recorded under conditions of high gain. A quantitative determination of aluminum concentration in the sample of high purity silicalite was carried out by adding a known amount of reference compound containing octahedrally-coordinated Al and comparing the intensities of the two signals. This gave a Si/Al ratio $\geq 1000$.

## 7. The Structure of Zeolite A

X-ray structural investigations of hydrated and dehydrated single crystals of Na-exchanged zeolite A yield results which indicate[86,87] that the symmetry of the structure is cubic, space group Fm3c, and that, in particular, there is strict alternation of the Si and Al amongst the tetrahedral sub-lattice. This is equivalent to a so-called 4:0 ordering scheme: each Si or Al is surrounded tetrahedrally *via* an oxygen bridge by four Al or Si; and it indicates that Loewenstein's rule[76], defined earlier, is obeyed (Fig. 14a). One of the most remarkable results of the early $^{29}$Si-MAS-NMR work on zeolites was the observation[55,56] that, in the spectrum of Linde A, there is a single sharp resonance centred at $\delta = -89.0 \pm 1$. This result was confirmed by ourselves[57,88a] and others[65,89]. On the basis of the chemical shift ranges found by *Lippmaa, Engelhardt et al.*[56] (see Fig. 6), this result pointed to a 3:1 rather than 4:0 ordering, *i.e.*, to ordering in which each Si atom is linked tetrahedrally *via* an oxygen bridge to *three* Al atoms and *one other* Si atom and *vice versa*, so that, in view of the inevitable occurrence of Al–O–Al bonds with this ordering scheme, Loewenstein's rule appeared to be systematically violated. *Lippmaa* and *Engelhardt*'s original conclusion that 3:1 ordering exists in zeolite A was drawn because the resonance at $\delta = -89.0 \pm 1$ in zeolite A coincides almost exactly with the position of the 3:1 peak in faujasitic zeolites.

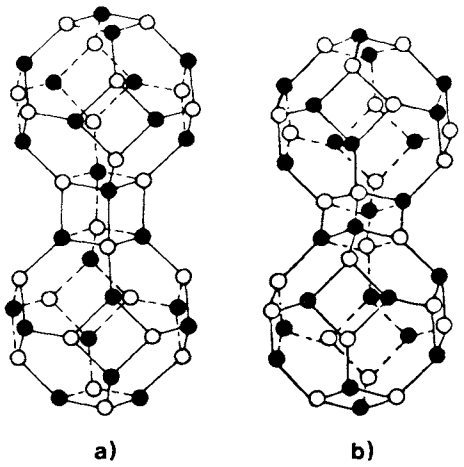



Fig. 14. a) The original model for the structure of zeolite A: Two sodalite cages (cubooctahedra) are linked through double four-membered rings. At the vertices of the cubooctahedra Si (○) and Al (●) atoms alternate such that 4:0 coordination results, *i.e.* each Si is surrounded tetrahedrally by four Al atoms, *via* oxygen bridges, which are not shown for simplicity. This double unit of cubooctahedra repeats itself three-dimensionally resulting in a cubic (Fm3c) space group. Exchangeable cations are not shown.—b) An alternative model in which cubooctahedra are slightly distorted (not shown) and again repeat themselves three-dimensionally, yielding a rhombohedral space group $R\bar{3}$. The ordering scheme within the aluminosilicate framework is such that each Si atom is surrounded by three Al atoms and one Si atom, and each Al atom by three Si atoms and one Al atom (3:1 coordination). Al–O–Al bridges are an integral feature of the structure. In this model, there are centers of inversion at the mid-points of the double four-membered rings. Notwithstanding earlier interpretations, $^{29}$Si-MAS-NMR supports the 4:0 ordering scheme (see text).

*Bursill et al.*[88a], accepted the validity of this conclusion and set about a detailed re-examination of the foundations upon which the 4:0 model of the structure of zeolite A was based. They had discovered[89b] that dehydrated Na-A exhibited a slight but unmistakable rhombohedral distortion and that, therefore, the space-group assignment Fm3c, which had been used for the structural refinement for the 4:0 structure, was not valid. Furthermore, many of their electron diffraction patterns appeared[88a] to be irreconcilable with the 4:0 ordering scheme. They therefore concluded that Al–O–Al linkages were probably responsible for the rhombohedral distortion, and were able to show how a cubic structure (space group Pn3n) for zeolite A could be assembled from rhombohedral units. They also found[88b] that encouraging structural refinement of their

neutron diffraction data could be obtained in space group $R\bar{3}$. All this, as well as the fact that some measured X-ray reflections of dehydrated Na-A are incompatible[86-88] with the Fm3c space-group, led *Bursill et al.*[88] to propose a new model for the structure of zeolite A (see Fig. 14b).

This new model was, however, soon scrutinized in the light of yet more recent discovery. First, *Rayment* and *Thomas*[90] showed, by X-ray powder diffractometry, that the crystal symmetry of Na-A is a function of the degree of hydration and of temperature, the rhombohedral form being favored only when the samples are desiccated and at low temperature. In the hydrated condition the structure is cubic. Secondly, using neutron diffraction, *Cheetham et al.*[43,44a] found that the rhombohedral distortion, present in Na-A, is vanishingly small in dehydrated Tl-A (using the *same* sample but with the $Na^+$ largely replaced by $Tl^+$), and in dehydrated Ag-A, and that Fm3c was a more appropriate (through not entirely satisfactory) space group than Pn3n to interpret their powder diffraction data. Then, independent $^{29}$Si-MAS-NMR experiments by *Thomas et al.*[71] and by *Melchior et al.*[75] on zeolite ZK-4, which has the same aluminosilicate framework as zeolite A but a Si/Al ratio greater than unity[91], pointed strongly in favor of the 4:0 rather than the 3:1 scheme, so that the structural model shown in Figure 14a was reaffirmed[44] for zeolite A. It has recently come to light[91b] that cancrinite, which, like zeolite A, was also thought to violate Loewenstein's rule, probably does not do so. $^{29}$Si-MAS-NMR results on cancrinite samples of different Si/Al ratios point to 4:0 ordering when Si/Al = 1.0.

In view of the fact that $^{29}$Si-MAS-NMR had first of all raised doubts about the authenticity of the accepted structural model of zeolite A, and that the very same technique (applied to ZK-4) had later vindicated the model, we shall here summarize the essential features of the MAS-NMR study of ZK-4. This study has also led to extension of the chemical shift ranges for the various tetrahedral functional groupings in zeolites generally (Fig. 6).

The fact that zeolite A exhibits only one sharp $^{29}$Si-resonance itself signifies that Si,Al ordering is pronounced, just as with zeolite X discussed earlier. But does this peak imply a 3:1 or 4:0 arrangement? By taking zeolite ZK-4, with Si/Al ratios substantially in excess of unity, the $^{29}$Si-MAS-NMR spectrum must exhibit several resonances corresponding to $Si(OAl)_n(OSi)_{4-n}$, as with zeolites X and Y (see Fig. 7). One of the peaks in the spectrum of ZK-4 should therefore correspond to the peak in the spectrum of zeolite A. (It has already been established that, *for a given aluminosilicate structure*, $^{29}$Si-chemical shifts of $Si(OAl)_4$ and $Si(OAl)_3(OSi)$ peaks are only marginally affected by variation of the Si/Al ratio.) Thus, assignment of the signal in the spectrum of zeolite A is in principle possible by matching it with one of the peaks in the spectrum of ZK-4, even though the ordering pattern of the latter is different from that of zeolite A. Moreover, by determining the Si/Al ratio independently (using analytical electron microscopy) one may further test[71] whether the resonance at $\delta = -89$ is attributable to 3:1 or to 4:0 by comparing the $(Si/Al)_{NMR}$ ratio, calculated using equation (3) with that obtained by electron microscopy using X-ray emission intensities, $(Si/Al)_{XRE}$.

The $^{29}$Si-MAS-NMR spectrum of ZK-4 does indeed contain several peaks (Fig. 15); and good agreement between $(Si/Al)_{NMR}$ and $(Si/Al)_{XRE}$ ratios are obtained if the resonance at $\delta = -89 \pm 1.0$ is assigned to $Si(OAl)_4$ rather than to $Si(OAl)_3(OSi)$. It will be recalled that, in zeolites X and Y (synthetic faujasites) the $Si(OAl)_4$ resonance lies between $\delta = -83.7$ and $-84.1$. We believe that the relatively large difference between these two $Si(OAl)_4$ resonances stems from the occurrence of considerable strain in the zeolite A (ZK-4) framework. The strained double four-membered rings, which give rise to T–O–T angles close to 180°, affect the value of the chemical shift at which the $^{29}$Si-nucleus resonates. Just as with silicalite, which also has T–O–T angles close to 180°, the resonances for a given functional grouping are shifted to more negative values. The strong influence that structural strain and, hence, unusual T–O–T angles may exert upon $^{29}$Si chemical shifts is well illustrated in the recent work of *Jarman*[91c] on sodalites. This fact can, of course, be turned to advantage in structure determinations.

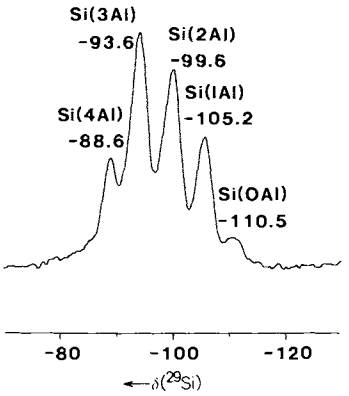



Fig. 15. $^{29}$Si-MAS-NMR spectrum at 79.8 MHz of zeolite ZK-4 showing five peaks, at the chemical shift values indicated, corresponding to the silicon environments shown in the figure.

Two broader issues are raised by the results obtained with ZK-4. First, now that the original 4:0 model for Si,Al ordering is reinforced, it is relevant to enquire more deeply into the interpretation of the neutron diffraction and electron diffraction data[88] on zeolite A; second, a revised tabulation of $^{29}$Si-chemical shifts is called for in the case of the zeolites. So far as the first of these two points is concerned, excellent agreement has been obtained[43,44] between the T–O bond distances determined by Rietveld analysis of neutron powder data on the one hand and by single crystal X-ray analysis on the other. The electron diffraction data that implied the occurrence of three-fold superlattices in zeolite A when the crystals were viewed along the ⟨110⟩ axes can be interpreted[92] in terms of the facile twinning of zeolite A on {111} planes. (Such twins are readily revealed in scanning electron microscopic studies.) The second point has prompted us to construct a revised tabulation (Fig. 6) which indicates how much the ranges of resonances previously published have to be extended. This information can now be used to help identify the individual groupings present within strained structures, including possibly amorphous or quasicrystalline aluminosilicates.

## 8. Future Prospects

With the application of multinuclear MAS-NMR spectroscopy many other currently intractable structural problems in zeolite chemistry are likely to be resolved. It is especially noteworthy that many zeolitic structures can be synthesized with the framework made up of atoms all of which have NMR-active nuclei: Si, Al, O, Be, B, Ga, Ge, P, *etc.* Whereas it is unlikely that the richness of information retrievable from $^{29}$Si-MAS-NMR, and to a lesser degree $^{27}$Al-MAS-NMR, will be matched with nuclei of all these elements, it is nevertheless significant that an environmental probe exists for each atomic constituent of the framework structure. Moreover, the majority of the exchangeable cations in zeolites have NMR-active nuclei: Fe, Rh, Ag, Cd, Tm, Yb, Pt, Hg, Tl, Pb (all possessing spin 1/2), and Na, Mg, K, Ca, Sc, Ti, V, Cr, Mn, Co, Cu, Zn, Ga, Rb, Sr, Cs, Ba, La (all quadrupolar). Some of these elements are also capable of being incorporated into the framework structure.

In the case of quadrupolar nuclei of non-integral spin such as $^{27}$Al, improved spectral resolution may be obtained by spinning at angles other than 54°44′ *if quadrupolar effects are the dominant interaction*[45,93]. In the present context, successful application of this technique has been made in the $^{27}$Al-spectra of cordierite crystallizing from its vitreous precursor and of various minerals where the quadrupolar effects are much larger than those in zeolites[94]. Stereochemical issues alone are likely to be clarified by use of MAS-NMR techniques for the appropriate nucleus. In addition, many of the guest species or reactants accommodated within the cavities and tunnels of a zeolite, or bound to its active centers, possess amenable NMR nuclei, $^{13}$C, $^{1}$H, $^{2}$H, $^{14}$N, $^{15}$N and $^{31}$P especially. The prospects of resolving some hitherto inaccessible aspects of zeolite structural chemistry are therefore good, especially when it is recognized that previous $^{13}$C-NMR studies of rather mobile organic guests in aluminosilicate hosts have already produced useful information. Two studies of relevance in this connection are those of *Derouane et al.*[95] who, in a simulated *in situ* study, followed the conversion of methanol, in contact with ZSM-5, to gasoline and our own[96] on sheet silicate intercalates where the concentration of intercalated isomers (*e.g.* xylene and ethylbenzene) or the interlamellar tautomeric equilibrium of acetylacetone could each be quantitatively determined. Using $^{1}$H-MAS-NMR it proved[97] possible to obtain two very sharp peaks, in the ratio of 6 : 4, from relatively immobile *p*-xylene intercalated within a synthetic hectorite. Combined $^{1}$H- and $^{2}$H-MAS-NMR as well as $^{13}$C-MAS-NMR, with or without cross polarization of the kind already carried out to determine the nature and location of organic bases in ZSM-5 zeolites[98] and uncalcined silicalite[99] are already viable techniques. The use of benign probes, such as $N_2$, Xe or Kr, which are ideally suited for testing the range of different environments within the zeolites is also feasible by MAS-NMR.

The particular advantage that CP/MAS affords in discriminating surface species has already been seen in the studies of untreated and derivatized silicas and silica gels[100] and of ultrastabilized zeolites[70]. In this way it has been possible to identify such groups as $Si(OH)_1$, $Si(OH)_2$, and $Si(OH)_3$ at silica or zeolite internal surfaces. By introducing organic derivatives (deuterated if appropriate[101] and containing, for example, $^{13}$C, $^{31}$P, or $^{19}$F) to the internal or external surfaces of aluminosilicates, a great deal more is likely to be learnt about the catalytic properties and specific acid sites of these materials from the relevant MAS-NMR studies. The structures of a variety of the new, technically important, ceramics[94,102] that can be formed by heat-treatment of various cation-exchanged zeolitic precursors, are eminently amenable to multinuclear MAS-NMR studies. The detailed mechanism of zeolite dealumination (in which the groups $Si(OAl)_4$, $Si(OAl)_3(OSi)$, *etc.* are eroded at different rates by exposure to $SiCl_4$ vapor), or of the exchange of oxygen between the framework and its environment under mild conditions can now be investigated directly. Our preliminary measurements[99] using $^{17}$O-MAS-NMR reveal that the oxygens in the linked $SiO_4^{4-}$ and $AlO_4^{5-}$ zeolite tetrahedra are much more labile than was formerly suspected.

*We acknowledge support from the Universities of Cambridge and Guelph and from B. P. Research Centre, Sunbury. C. A. F. was the recipient of financial aid from the Natural Sciences and Engineering Council of Canada. We are grateful for the cooperation of numerous colleagues (listed in the references). The NMR spectra were obtained at the South-Western Ontario High-Field NMR Facility, Manager, Dr. R. E. Lenkinski.*

Received: July 23, 1982 [A 450 IE]
German version: *Angew. Chem. 95* (1983) 257

[1] a) The term porotectosilicates has been proposed by *Barrer* to encompass that class of siliceous crystalline materials which includes both zeolites and solids that resemble zeolites in crystal structure but which may not be capable of ion exchange. Tectosilicates are characterized by the fact that the $SiO_4$ tetrahedra are linked at all corners to form three-dimensional arrays. The recent discovery of new families of crystalline microporous borophosphates [1b], $BPO_4$, and aluminophosphates [1c], $AlPO_4$, which possess structures reminiscent of, if not identical to, those of many zeolites but which are partly- or non-siliceous, suggests that a new term is needed to encompass these materials. We suggest "porotectophosphates", which could encompass elements other than Al in the structure, as such a generic name; b) J. Haber et al., Faraday Society Discussion, Nottingham, September 1981, p. 346; c) S. T. Wilson, B. M. Lok, C. A. Messina, T. R. Cannan, E. M. Flanigen, *J. Am. Chem. Soc. 104* (1982) 1146.

[2] M. G. Evans, *Proc. R. Soc. London A134* (1939) 96.

[3] J. W. McBain: *The Sorption of Gases and Vapours by Solids*, Routledge, London 1932, Chapter 5.

[4] R. M. Barrer: *Zeolites and Clay Minerals as Sorbents and Molecular Sieves*, Academic Press, London 1978; *The Hydrothermal Chemistry of Zeolites*, Academic Press, London 1982.

[5] D. W. Breck: *Zeolite Molecular Sieves*, Wiley, New York 1974.

[6] "Zeolite Chemistry and Catalysis", *ACS Monogr. 171* (1976).

[7] "Molecular Sieves - II", *ACS Symp. Ser. 40* (1977).

[8] D. E. W. Vaughan in [22a], p. 294.

[9] D. Naccache, Y. Ben Taarit, *Pure Appl. Chem. 52* (1980) 2175; K. Topchieva in G. K. Boreskov, Kh. M. Minachev: *Applications of Zeolites in Catalysis*, Mir, Moscow 1980.

[10] J. S. Magee, J. J. Blazek in [6], p. 615; P. A. Jacobs: *Carboniogenic Activity of Zeolites*, Elsevier, Amsterdam 1977.

[11] S. M. Csiscery in [6], p. 680; J. A. Rabo in B. Imelik et al.: *Catalysis by Zeolites*, Elsevier, Amsterdam 1980, p. 437; M. L. Poutsma in [6], p. 437.

[12] C. J. Plank, E. J. Rosinski, W. P. Hawthorne, *Ind. Eng. Chem. Prod. Res. Div. 3* (1964) 165; J. Turkevich, *Catal. Rev. 1* (1967) 1; P. B. Venuto, P. S. Landis, *Adv. Catal. 18* (1968) 259; H. Heinemann, *Catal. Rev. 23* (1981) 315.

[13] a) T. Yashima, N. Yokoi, N. Hara, *Bull. Jpn. Pet. Inst. 13* (1971) 215; b) M. L. Unland, G. E. Barker in W. R. Moser: *Catalysis of Organic Reactions*, Dekker, New York 1981, p. 51.

[14] a) R. J. Argauer, G. R. Landolt, US-Pat. 3702886 (1972); b) P. B. Weisz, V. J. Frilette, R. W. Maatman, E. G. Mower, *J. Catal. 1* (1962) 307; c) C. D. Chang, A. J. Silvestri, *ibid. 47* (1977) 249.

[15] a) S. L. Meisel, J. P. McCullough, C. H. Lechthaler, P. B. Weisz, *Chemtech 6* (1976) 86; b) Acronym for *S*tandard *O*il Company of *N*ew *Y*ork; and the Mobil Company was called Socony Mobil.

[16] F. G. Dwyer in W. R. Moser: *Catalysis of Organic Reactions*, Dekker, New York 1981, p. 39.

[17] a) E. M. Flanigen, J. M. Bennett, R. W. Grose, J. P. Cohen, R. L. Patton, R. M. Kirchner, J. V. Smith, *Nature (London) 271* (1978) 512; b) G. T. Kokotailo, S. L. Lawton, D. H. Olson, W. M. Meier, *ibid. 272* (1978) 437.

[18] P. B. Weisz, *Chemtech 3* (1973) 498; *Proc. 7th Int. Congr. Catal., Tokyo 1980*, P1; P. B. Weisz, V. J. Frilette, *J. Phys. Chem. 64* (1960) 382.

[19] W. H. Taylor, *Proc. R. Soc. London A 145* (1934) 80; W. L. Bragg, *Nature (London) 125* (1930) 510; W. L. Bragg, C. F. Claringbull: *Crystal Structure of Minerals*, Bell, London 1965; L. Pauling: *The Nature of the Chemical Bond*, 3rd Ed., Cornell University Press, Ithaca, NY 1960; *Die Natur der chemischen Bindung*, 3rd Ed., Verlag Chemie, Weinheim 1976.

[20] J. V. Smith in [6], Chapter 1.

[21] a) W. M. Meier, *Z. Kristallogr. 113* (1960) 430; W. M. Meier, H. Villiger, *ibid. 129* (1969) 411; W. M. Meier, D. H. Olson: *Atlas of Zeolite Structure Types*, Int. Zeolite Assoc., Juris Druck, Zürich 1978; b) G. T. Kokotailo, J. L. Schlenker, *Adv. X-Ray Anal. 24* (1981) 49.

[22] a) "The Properties and Applications of Zeolites", *Spec. Publ. Chem. Soc. London 33* (1980); b) *Proc. 5th Int. Conf. Zeolites, Naples 1980*, Heyden, London 1980.

[23] E. Dempsey, G. H. Kühl, D. H. Olson, *J. Phys. Chem. 73* (1969) 387.

[24] G. E. Brown, G. V. Gibbs, P. H. Ribbe, *Am. Mineral. 54* (1969) 1044.

[25] D. H. Olson, *J. Phys. Chem. 74* (1970) 2758.

[26] E. Dempsey in R. M. Barrer: *Molecular Sieves*. Soc. Chem. Ind., London 1968, p. 293.

[27] E. Dempsey, *J. Phys. Chem. 73* (1969) 3660.

[28] R. J. Mikovsky, J. F. Marshall, *J. Catal. 44* (1976) 170; *49* (1977) 120; *58* (1979) 489.

[29] R. Beaumont, D. Barthomeuf, *J. Catal. 27* (1972) 45.

[30] H. Kacirek, H. Lechert, *J. Phys. Chem. 80* (1976) 1291.

[31] E. M. Flanigen in [6], p. 80.

[32] J. W. Ward in [6], p. 118.

[33] J. M. Thomas, *Ultramicroscopy 8* (1982) 13; J. M. Thomas, D. A. Jefferson, *Endeavour, New Ser. 2* (1978) 127; J. M. Thomas, *New Sci. 88* (1980) 580; J. M. Thomas, S. Ramdas, G. R. Millward, *ibid. 96* (1982) 435; J. M. Thomas, D. A. Jefferson, E. S. Crawford, D. J. Smith, *Chem. Scr. 14* (1978–79) 167; J. M. Thomas, D. A. Jefferson, G. R. Millward, *J. Microsc. Spectrosc. Electron. 7* (1982) 315.

[34] J. M. Thomas, G. R. Millward, L. A. Bursill, *Philos. Trans. R. Soc. London A 300* (1981) 43.

[35] L. A. Bursill, E. A. Lodge, J. M. Thomas, *Nature (London) 286* (1980) 111.

[36] L. A. Bursill, J. M. Thomas, K. J. Rao, *Nature (London) 289* (1980) 157.

[37] J. M. Thomas, G. R. Millward, S. Ramdas, L. A. Bursill, M. Audier, *Faraday Discuss. Chem. Soc. 72* (1981) 346.

[38] J. M. Thomas, M. Audier, J. Klinowski, *J. Chem. Soc. Chem. Commun. 1981*, 1221.

[39] J. M. Thomas, L. A. Bursill, *Angew. Chem. 92* (1980) 755; *Angew. Chem. Int. Ed. Engl. 19* (1980) 745.

[40] L. A. Bursill, L. G. Mallinson, S. R. Elliott, J. M. Thomas, *J. Phys. Chem. 85* (1981) 3004.

[41] L. A. Bursill, J. M. Thomas, *J. Phys. Chem. 85* (1981) 3007.

[42] G. R. Millward, J. M. Thomas, *J. Chem. Soc. Chem. Commun. 1982*, 1380; J. M. Thomas, G. R. Millward, S. Ramdas, M. Barlow, *J. Chem. Soc. Faraday Trans II* (1983), in press.

[43] A. K. Cheetham, M. M. Eddy, D. A. Jefferson, J. M. Thomas, *Nature (London) 299* (1982) 24.

[44] a) A. K. Cheetham, C. A. Fyfe, J. V. Smith, J. M. Thomas, *J. Chem. Soc. Chem. Commun. 1982*, 823; b) R. A. Young, P. E. Mackie, *Mater. Res. Bull. 15* (1980) 17; c) A. K. Cheetham, M. M. Eddy, J. M. Thomas, J. Klinowski, *J. Chem. Soc. Chem. Commun. 1983*, 23.

[45] E. R. Andrew, *Int. Rev. Phys. Chem. 1* (1981) 195; M. Mehring "High Resolution NMR Spectroscoy in Solids" in P. Diehl, E. Fluck, R. Kosfeld: *NMR Basic Principles and Progress, Vol. II* Springer-Verlag, New York 1976.

[46] R. G. Griffin, *Anal. Chem. 49* (1977) 951A; R. K. Harris, K. J. Packer, *Eur. Spectrosc. News 21* (1978) 37; F. P. Miknis, V. J. Bartuska, G. E. Maciel, *Am. Lab.* (Nov. 1979) 19; C. S. Yannoni, *Acc. Chem. Res. 15* (1982) 201; J. R. Lyerla, C. S. Yannoni, C. A. Fyfe, *ibid. 15* (1982) 208; R. Wasylishen, C. A. Fyfe, *Annu. Rev. NMR Spectrosc.*, in press.

[47] J. Schaefer, E. O. Stejskal, *Top. Carbon-13 NMR Spectrosc. 3* (1979) 283; W. W. Fleming, C. A. Fyfe, R. D. Kendrick, J. R. Lyerla, H. Vanni, C. S. Yannoni in "Polymer Characterization by ESR and NMR", *ACS Symp. Ser. 142* (1980) 193; J. R. Lyerla, *Contemp. Top. Polym. Sci. 3* (1979) 143.

[48] J. Schaefer, E. O. Stejskal, M. D. Sefcik, R. A. McKay, *Philos. Trans. R. Soc. London A 299* (1981) 475; A. N. Garroway, D. L. Van der Hart, W. L. Earl, *ibid. A 299* (1981) 609; G. E. Balimann, C. J. Broombridge, R. K. Harris, K. J. Packer, B. J. Say, S. F. Tanner, *ibid. A 299* (1981) 643; S. J. Opella, J. G. Hexem, M. H. Frey, T. A. Cross, *ibid. A 299* (1981) 665.

[49] E. R. Andrew, A. Bradbury, R. G. Eades, *Nature (London) 182* (1958) 1659.

[50] I. J. Lowe, *Phys. Rev. Lett. 2* (1959) 285.

[51] A. Pines, M. G. Gibby, J. S. Waugh, *Chem. Phys. Lett. 15* (1972) 273.

[52] J. Schaefer, E. O. Stejskal, *J. Am. Chem. Soc. 98* (1976) 1031.

[53] C. A. Fyfe, G. C. Gobbi, J. S. Hartman, R. E. Lenkinski, J. H. O'Brien, E. R. Beange, M. A. R. Smith, *J. Magn. Reson. 47* (1982) 168.

[54] E. R. Andrew, *Prog. Nucl. Magn. Reson. Spectrosc 8* (1971) 1; J. W. Beams, *J. Appl. Phys. 8* (1937) 795.

[55] G. Engelhardt, D. Kunath, A. Samoson, M. Tarmak, M. Mägi, E. Lippmaa, Workshop on Adsorption of Hydrocarbons in Zeolites, Berlin-Adlershof, November 19–22, 1979.

[56] E. Lippmaa, M. Mägi, A. Samoson, G. Engelhardt, A.-R. Grimmer, *J. Am. Chem. Soc. 102* (1980) 4889; G. Engelhardt, M. Mägi, E. Lippma, *Abstr. 2nd Workshop Zeolites, Eberswalde 1982*, Vol. 2, p. 1.

[57] J. M. Thomas, J. Klinowski, C. A. Fyfe, J. S. Hartman, L. A. Bursill, *J. Chem. Soc. Chem. Commun. 1981*, 678.

[58] S. Ramdas, J. M. Thomas, J. Klinowski, C. A. Fyfe, J. S. Hartman, *Nature (London) 292* (1981) 228.

[59] J. Klinowski, J. M. Thomas, C. A. Fyfe, J. S. Hartman, *J. Phys. Chem. 85* (1981) 2590.

[60] G. Engelhardt, U. Lohse, E. Lippmaa, M. Tarmak, M. Mägi, *Z. Anorg. Allg. Chem. 482* (1981) 49.

[61] E. Lippmaa, M. Mägi, A. Samoson, M. Tarmak, G. Engelhardt, *J. Am. Chem. Soc. 103* (1981) 4992.

[62] C. A. Fyfe, G. C. Gobbi, J. S. Hartman, J. Klinowski, J. M. Thomas, *J. Phys. Chem. 86* (1982) 1247.

[63] G. Engelhardt, E. Lippmaa, M. Mägi, *J. Chem. Soc. Chem. Commun. 1981*, 712.

[64] J. Klinowski, J. M. Thomas, M. Audier, S. Vasudevan, C. A. Fyfe, J. S. Hartman, *J. Chem. Soc. Chem. Commun. 1981*, 570.

[65] M. T. Melchior, D. E. W. Vaughan, A. J. Jacobson, *J. Am. Chem. Soc. 104* (1982) 4859.

[66] I. E. Maxwell, W. A. van Erp, G. R. Hays, T. Couperus, R. Huis, A. D. H. Clague, *J. Chem. Soc. Chem. Commun. 1982*, 523.

[67] J. Klinowski, J. M. Thomas, C. A. Fyfe, G. C. Gobbi, *Nature (London) 296* (1982) 533.

[68] D. Freude, H.-J. Behrens, *Cryst. Res. Tech. 16* (1981) K36; D. Müller, W. Gessner, H.-J. Behrens, G. Scheler, *Chem. Phys. Lett. 79* (1981) 59.

[69] C. A. Fyfe, G. C. Gobbi, J. Klinowski, J. M. Thomas, S. Ramdas, *Nature (London) 296* (1982) 530.

[70] G. Engelhardt, U. Lohse, A. Samoson, M. Mägi, M. Tarmak, E. Lippmaa, *Zeolites 2* (1982) 59.

[71] J. M. Thomas, C. A. Fyfe, S. Ramdas, J. Klinowski, G. C. Gobbi, *J. Phys. Chem. 86* (1982) 3061; J. Klinowski, J. M. Thomas, S. Ramdas, C. A. Fyfe, G. C. Gabbi, *Abstr. 2nd Workshop Zeolites, Eberswalde 1982*, Vol. 2, supplement.

[72] J. Klinowski, J. M. Thomas, C. A. Fyfe, G. C. Gobbi, J. S. Hartman, *Inorg. Chem. 22* (1983) 63.

[73] a) J. M. Thomas, S. Ramdas, G. R. Millward, J. Klinowski, M. Audier, J. Gonzalez-Calbet, C. A. Fyfe, *J. Solid State Chem. 45* (1982) 368; b) J. M. Thomas, J. Gonzalez-Calbet, C. A. Fyfe, G. C. Gobbi, M. F. Nicol, *Geophys. Res. Lett. 10* (1983) 91; c) J. Klinowski, M. W. Anderson, J. M. Thomas, *J. Chem. Soc. Chem. Commun. 1983*, in press.

[74] a) J. Klinowski, S. Ramdas, J. M. Thomas, C. A. Fyfe, J. S. Hartman, *J. Chem. Soc. Faraday Trans. II 78* (1982) 1025; b) J. M. Thomas, J. Klinowski, C. A. Fyfe, G. C. Gobbi, S. Ramdas, M. W. Anderson, in "Intrazeolite Chemistry", *ACS*, in press.

[75] M. T. Melchior, D. E. W. Vaughan, A. J. Jacobson, R. H. Jarman, *Nature (London)*, in press.

[76] W. Loewenstein, *Am. Mineral. 39* (1954) 92.

[77] a) G. H. Kühl, *J. Inorg. Nucl. Chem. 33* (1971) 3261; b) A. W. Peters, *J. Phys. Chem. 87* (1983), in press; c) R. J. Mikovsky, *Zeolites 3* (1983), in press.

[78] a) R. M. Barrer, R. G. Jenkins, G. Peeters in [7], p. 258; b) D. W. Breck, G. W. Skeels in [7], p. 271; c) G. W. Skeels, W. H. Flank, *Abstr. Div. Petrol. Chem. ACS Meeeting, Las Vegas 1981*, 519; d) J. Schertzer, *J. Catal. 54* (1978) 285.

[79] a) H. K. Beyer, I. Belenykaja in B. Imelik et al.: *Catalysis by Zeolites*, Elsevier, Amsterdam 1980, p. 203; b) M. W. Anderson, Certificate of Postgraduate Studies Thesis, University of Cambridge, June 1982; c) M. Daubrée, *C. R. Acad. Sci. 34* (1854) 135; d) L. Troost, P. Hautefeuille, *ibid. 75* (1872) 1819.

[80] J. M. Thomas, M. Audier, J. Gonzalez-Calbet, J. Klinowski, S. Ramdas, C. A. Fyfe, G. C. Gobbi, *Abstr. Div. Petrol. Chem. ACS Meeting, Las Vegas 1981*, 531.

[81] a) J. Klinowski, J. M. Thomas, M. W. Anderson, C. A. Fyfe, G. C. Gobbi, *Zeolites 3* (1983) 5; b) J. M. Thomas, J. Klinowski, M. W. Anderson, M. Barlow, unpublished; c) C. A. Fyfe, G. C. Gobbi, unpublished.
[82] C. D. Chang, US-Pat. 4273753 (1981).
[83] C. V. McDaniel, P. K. Maher in R. M. Barrer: *Molecular Sieves* Soc. Chem. Ind., London 1968, p. 186.
[84] C. V. McDaniel, P. K. Maher in [6], p. 285.
[85] R. W. Grose, E. M. Flanigen, US-Pat. 4061724 (1977).
[86] V. Gramlich, W. M. Meier, *Z. Kristallogr. 133* (1971) 134.
[87] J. J. Pluth, J. V. Smith, *J. Phys. Chem. 83* (1969) 741.
[88] a) L. A. Bursill, E. A. Lodge, J. M. Thomas, A. K. Cheetham, *J. Phys. Chem. 85* (1981) 2409; b) L. A. Bursill, E. A. Lodge, J. M. Thomas, *Nature (London) 291* (1981) 265.
[89] J. B. Nagy, J.-P. Gilson, E. G. Derouane, *J. Chem. Soc. Chem. Commun 1981*, 1129.
[90] T. Rayment, J. M. Thomas, *Zeolites 3* (1983) 2.
[91] a) G. T. Kerr, *Inorg. Chem. 5* (1966) 1537; b) D. E. W. Vaughan, A. J. Jacobson, unpublished; c) R. H. Jarman, unpublished.
[92] G. R. Millward, J. M. Thomas, S. Ramdas, M. Barlow, *Proc. 6th Int. Conf. Zeolites, Reno 1983*, in press.
[93] E. Oldfield, S. Schramm, M. D. Meadows, K. A. Smith, R. A. Kinsey, J. Ackerman, *J. Am. Chem. Soc. 104* (1982) 919.
[94] C. A. Fyfe, G. C. Gobbi, J. Klinowski, A. Putnis, J. M. Thomas, *J. Chem. Soc. Chem. Commun. 1983*, in press.
[95] E. G. Derouane, J. B. Nagy, P. Dejaifve, J. H. C. van Hoof, B. P. Spekman, J. C. Vedrine, C. Naccache, *J. Catal. 53* (1978) 40.
[96] C. A. Fyfe, J. M. Thomas, J. R. Lyerla, *Angew. Chem. 93* (1981) 104; *Angew. Chem. Int. Ed. Engl. 20* (1981) 96.
[97] C. A. Fyfe, J. M. Thomas, unpublished.
[98] G. Boxhoorn, R. A. van Santen, W. A. van Erp, G. R. Hays, R. Huis, A. D. H. Clague, *J. Chem. Soc. Chem. Commun. 1982*, 264; G. R. Hays, A. D. H. Clague, R. Huis, G. van der Velden, *Appl. Surf. Sci. 10* (1982) 247; J. B. Nagy, Z. Gabelica, E. G. Derouane, *Zeolites 3* (1983) 43.
[99] G. C. Gobbi, C. A. Fyfe, J. Klinowski, M. Barlow, J. M. Thomas, unpublished.
[100] a) G. E. Maciel, D. W. Sindorf, *J. Am. Chem. Soc. 102* (1980) 7607; b) S. J. Mann, R. J. P. Williams, G. C. Gobbi, C. A. Fyfe, G. W. Kennedy, *J. Chem. Soc. Chem. Commun. 1983*, in press.
[101] D. Freude, T. Fröhlich, H. Pfeiffer, G. Scheeler, *Abstr. 2nd Workshop Zeolites, Eberswalde 1982*, Vol. 2, p. 9; V. Bosáček, D. Freude, T. Fröhlich, H. Pfeiffer, H. Schmiedel, *J. Coll. Interface Sci. 85* (1982) 502.
[102] a) D. W. Breck in [22a], p. 391; b) J. M. Thomas, J. Klinowski, P. A. Wright, R. Roy, *Angew. Chem. 95* (1983) and *Angew. Chem. Int. Ed. Engl. 22* (1983), in press.

# Structure and Evolution of the "*Atmungsferment*" Cytochrome c Oxidase

**By Bernhard Kadenbach***

*In memory of the 100th anniversary of Otto Warburg's birth*

Approximately 50 years ago, *Otto Warburg* received the Nobel Prize for his fundamental work on the "*Atmungsferment*". But not until the end of the fifties was it possible to isolate this complicated membrane enzyme, which is necessary for respiration and energy production in most living organisms on earth. Since then, intensive research has been performed to elucidate the mechanism of reduction of oxygen to water and the coupled translocation of protons across the membrane which is involved in ATP synthesis. Until now the results have been unsatisfactory because the four catalytic heavy-metal redox centers are bound to proteins, the structures of which have begun to be studied only recently. In the course of this research, it was discovered that cytochrome c oxidase from bacteria contains only two or three, whereas the enzyme complex from animals contains thirteen different protein components. The present article analyzes the possible functions of the various protein subunits and, using the example of cytochrome c oxidase, shows that biochemical evolution proceeds in such a way as to increase regulatory capacity.

## 1. Historical Survey

The catalytic role of iron in cellular respiration was proven first by *Otto Warburg* in 1924. He found that this process involved a change in the valence of the metal ion: $Fe^{3+}$ is reduced by an organic substance to $Fe^{2+}$ and oxidized by molecular oxygen to $Fe^{3+}$[1]. In 1926, *Warburg* discovered that hydrocyanic acid and carbon monoxide inhibit respiration, and that the inhibition by CO could be reversed by the action of light. This enabled him to determine the action spectrum of the respiratory enzyme, and this agreed well with that of other iron porphyrins, such as hemoglobin and the cytochromes described by *Keilin* in 1925[2]. *Warburg*'s "*Atmungsferment*", however, adsorbs at longer wavelengths and results, in contrast to the known red hemins, in the green color of the hemin component[3]. In 1931 *Otto Warburg* received the Novel Prize for Medicine and Physiology for this work.

The action spectrum, measured by *Warburg* with intact yeast cells[3], corresponds well with the difference spectrum of isolated green cytochrome c oxidase[4].

A dispute arose between *Warburg* and *Keilin* over the question whether the cytochromes a, b and c[2], first observed in 1886 by *McMunn* using a manual spectroscope and denoted histo- or myohematins[5,6], and rediscovered by *Keilin* in 1925, are directly involved in the oxidation of respiratory substrates by molecular oxygen[7]. The controversy was ended in 1939 by *Keilin*'s discovery that cytochrome a was made up of two components: one of these, de-

[*] Prof. Dr. B. Kadenbach
Fachbereich Chemie der Universität
Hans-Meerwein-Strasse, 3550 Marburg (Germany)

noted cytochrome $a_3$ or cytochrome oxidase, reacts with CO and HCN and has the same spectrum as *Warburg*'s "*sauerstoffübertragendes Ferment*"[8,9].

After isolation methods for cytochrome c oxidase were developed in the fifties, the molecular properties of the enzyme could be investigated in detail. They have been described in a series of excellent review articles[10–26].

## 2. The Function of Cytochrome c Oxidase

Cytochrome c oxidase (EC 1.9.3.1, also termed cytochrome oxidase or cytochrome $aa_3$) represents the oxygen-activating enzyme of cellular respiration and is present in almost all eukaryotic cells, where it is located in the inner membrane of mitochondria. In several aerobic bacteria cytochrome c oxidase is also found, where, however, it is located in the plasma membrane.

Cytochrome c oxidase, the terminal enzyme of the respiratory chain, transfers four electrons from cytochrome c to molecular oxygen, leading to the formation of water without producing toxic intermediates, such as $H_2O_2$ or the superoxide radical $O_2^-$. The four reducing equivalents originate from the respiratory substrates, which transfer hydrogen equivalents mainly *via* the coenzyme NADH to the respiratory chain. In the respiratory chain, which consists of flavoproteins, non-heme iron proteins, ubiquinone and cytochromes[27], the redox energy of the reducing equivalents is diminished stepwise from one component to the next, whereby the energy released is used at three sites (NADH-dehydrogenase complex, cytochrome $bc_1$ complex, and cytochrome c oxidase) for the synthesis of ATP (Fig. 1).

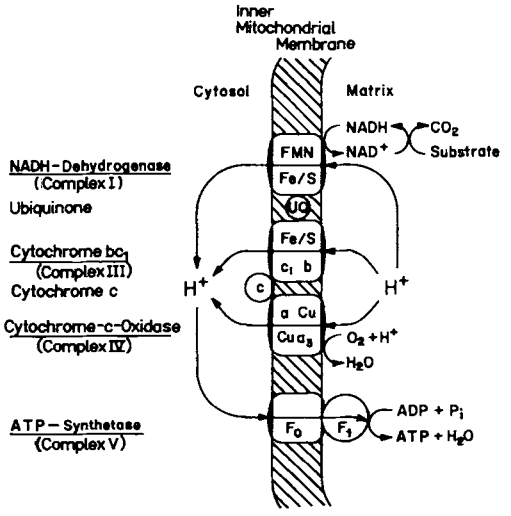



Fig. 1. Schematic representation of the respiratory chain of mitochondria. The respiratory chain is made up of several multiprotein complexes I–V, which are freely mobile in the lipid phase of the inner membrane. Hydrogen and electron transfer between the complexes occurs *via* the lipid ubiquinone (UQ) and *via* cytochrome c (c), a soluble protein that is bound from the outside to the membrane complexes; these processes are coupled at three sites with a proton translocation from the matrix into the cytosol. The succinate dehydrogenase complex (complex II) does not translocate protons and is omitted from the figure. The proton gradient is used by the ATP-synthetase for the formation of ATP from ADP and inorganic phosphate ($P_i$).

According to *Mitchell*'s "chemiosmotic hypothesis", the "energy-rich intermediate" of this reaction is represented by a proton gradient across the membrane, the "protonmotive force" ($\Delta P$), which is made up of an electrical ($\Delta\Psi$) and a concentration potential ($\Delta p$H) [eq. (a)][28].

$$\Delta P = \Delta\Psi - \frac{RT}{F}\Delta p\mathrm{H}\,; \quad \left(\Delta p = \frac{\mu \mathrm{H}^+}{F}\right) \tag{a}$$

Many results prove that this proton gradient represents the "energy-rich intermediate" of oxidative phosphorylation, the most important process of energy production in all aerobic cells which was searched for over a period of almost two decades. The membrane bound ATP synthetase complex uses this proton gradient to synthesize ATP from ADP and inorganic phosphate ($P_i$)[27].

Cytochrome c oxidase, the third energy conserving component of the respiratory chain, is composed of several polypeptides ("subunits"), two heme a groups, two copper ions, as well as bound phospholipids (cardiolipin essentially[29–31]). The two heme a groups, although chemically identical, can be distinguished by spectroscopy: in the $Fe^{II}$ form cytochrome $a_3$ binds $O_2$ and CO, and in the $Fe^{III}$ form HCN, $HN_3$, and $H_2S$; cytochrome a, in contrast, does not bind these components, as previously shown by *Keilin* and *Hartree*[8]. This points to a different environment or to different complexing ligands for the two heme a groups. Indeed, both heme a groups are localized in different polypeptides of the enzyme complex (polypeptides I and II)[32], although ESR spectroscopic studies indicate only a distance of 10—14 Å between them[33]. In addition, both copper ions are localized within polypeptide II, which indicates that the four redox centers of the enzyme are in close proximity to each other. This seems to be essential for the mechanism of oxygen reduction, where $4e^-$ from the four redox centers are rapidly transferred to $O_2$ (2nd order rate constant at room temperature: $10^{-8}$ M$^{-1}$ s$^{-1}$[35]). Using a number of physical methods (low temperature absorption spectroscopy, ESR, CD, and MCD spectroscopy, X-ray diffraction, EXAFS, ENDOR, magnetic susceptibility measurements, Mössbauer and resonance Raman spectroscopy) the mechanisms of electron transport from cytochrome c to $O_2$, as well as the structural environment of the four redox centers, were examined. Figure 2 shows a simplified scheme of current conceptions[26,36,37].

The Y-shaped, three-dimensional structure of the cytochrome c oxidase complex could be determined by electron microscopic studies of two-dimensional crystals[38,39]. Both upper ends of the "Y" protrude into the matrix, and the lower end into the cytosol. Whereas the binding site for $O_2$ is uncertain[21,40], the protons required for the formation of water according to equation (b)

$$O_2 + 4e^- + 4H^{\oplus} \longrightarrow 2H_2O \tag{b}$$

originate from the matrix[40]. This involves the transfer of four charge equivalents across the membrane.

From equation (b), the formation of a proton gradient through cytochrome c oxidase is not apparent. *Mitchell* neither postulated this in his hypothesis[28], nor did he find it in any of his experimental studies[41]. *Wikström et al.*, in contrast, were able to establish using intact mito-

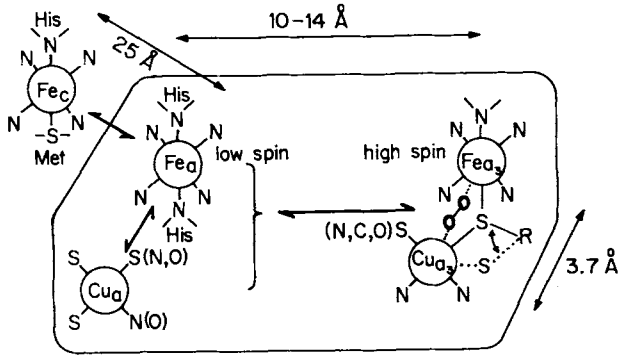



Fig. 2. The active center of cytochrome c oxidase (schematic). At the four redox centers of the enzyme the N-atoms of the porphyrin systems are indicated by one bond, that of histidine (5th and 6th ligands of iron) by three bonds. The exact nature of the four ligands at the copper atoms is not yet known. In some cases the identity of the atom through which the ligand is attached to Cu is still not clear (other possibilities are shown in parenthesis). The four redox centers are reduced successively by reduced cytochrome c ($Fe_c$) *via* cytochrome a ($Fe_a$). The 6th coordination site of cytochrome $a_3$ ($Fe_{a3}$) in the oxidized state ($Fe_{a3}^{3+}/Cu_{a3}^{2+}$) is occupied by sulfur, which forms a bridge between Fe and Cu. After reduction of both redox centers, the sulfur arm opens up and $O_2$ is bound between $Fe_{a3}$ and $Cu_{a3}$, whereby a peroxide intermediate is formed ($Fe_{a3}^{3+}-O^- - O^- - Cu_{a3}^{2+}$, "compound B"). Thereafter two electrons are transferred almost immediately from $Fe_a + Cu_a$ to the peroxide intermediate. It is not yet known when and from what source the four protons for the formation of water originate.

chondria[42–44], as well as with isolated cytochrome c oxidase which had been reconstituted in liposomes[45], proton pump activity from the matrix to the cytosol or across the membrane, respectively. The measured $H^+/e^-$ stoichiometry was *ca.* 1. Other authors corroborated the same results, although the measured $H^+/e^-$ stoichiometry was always $< 1$[40,46].

The functional unit of cytochrome c oxidase is a dimer of the complex which contains four heme a groups and four copper ions. This follows from electron microscopic studies of two-dimensional crystals[39] and from sedimentation analysis on the isolated enzyme dissolved in detergent[47,48]. Also, the complete inhibition of enzyme activity after covalently binding only 0.5 mol azidoarylcytochrome c per mol cytochrome $aa_3$[49] points to a dimer complex as the functional unit. The monomeric enzyme could certainly transfer electrons from cytochrome c to $O_2$ but the proton pump activity seems to occur only through the dimeric enzyme complex, as put forward in the "reciprocating site model" of *Wikström et al.*[26].

## 3. Polypeptide Composition of Animal Cytochrome c Oxidase

The many subunits of animal cytochrome c oxidase are associated so strongly in the enzyme complex through noncovalent bonds that they are not even separated during dissolution of the membrane by detergents such as Triton X-100 or Na-cholate (the first step in isolating the enzyme). *Hackenbrock et al.* have shown that the cytochrome c oxidase complex is not firmly associated with the other enzyme complexes of the respiratory chain within the "two-dimensional liquid" of the biological membrane: specific antibodies lead to aggregation of the enzyme complex[52]; enlargement of the membrane surface area by fusion with protein-free liposomes leads to dilution of the enzyme complex in the membrane, which is visible by electron microscopy, and is accompanied by a reduction of the rate of electron transport, *via* the respiratory chain, from NADH to $O_2$[53]. The mobility of the enzyme complex in the membrane is also evident from the change in dichroism after photolysis of the cytochrome c oxidase-CO complex with a linear polarized laser flash. The observed relaxation time of several 100 μs indicates that the enzyme complex rotates around an axis perpendicular to the membrane[54]. ESR measurements on spin-labeled cytochrome c oxidase reconstituted in liposomes yielded a rotation of the enzyme complex with a correlation time of 40[55] or 34 μs at 4 °C[56].

The close association of several polypeptides to give a complex of defined spatial structure points to a specific function for the various subunits. It was, therefore, of great interest to find out which and how many polypeptides constitute the enzyme complex. This proved to be an especially difficult problem, particularly because the term "subunit" was interpretated differently. We define all polypeptides that are firmly associated within the complex as subunits, irrespective of these could have a catalytic or regulatory function.

The two most important methods for analyzing the polypeptide composition of the cytochrome c oxidase complex are: 1) Separation of the subunits (either dissociated in 2% Na-dodecylsulfate (SDS) or in 10–70% acetic acid solution) by gel filtration, based on their different molecular weights, and identification of the isolated proteins by *N*-terminal amino acid determination or sequence analysis. Using this method two research groups have identified twelve[57] or eleven[58] different proteins, from which six or seven were found to occur in stoichiometric and five in substoichiometric amounts. 2) Separation of the SDS-dissociated subunits by SDS-gel electrophoresis, also based on different molecular weights. With this most commonly used separation system[59,60], animal cytochrome c oxidase is usually separated into only seven polypeptide bands. By analogy to the most carefully investigated enzyme from yeast, where also seven subunits were identified[61,62], it was generally assumed that the animal enzyme also consists of seven subunits[16,17,19,20,22,26,50,53,55,61,63–75], although often more than seven polypeptide bands were found[55,68,69,71,73,76–79].

By further improving the SDS-gel electrophoretic separation system, we were able to separate highly purified animal cytochrome c oxidase into thirteen different polypeptide bands (Fig. 3)[24,80], representing intrinsic components of the enzyme complex as shown by various results: the isolated enzyme from different organs (liver, kidney, heart) of different mammals and from chicken always exhibited thirteen different polypeptide bands[81–83]; all polypeptides had a different amino acid composition[84], occurred in stoichiometric amounts[81], and all of them could be immunoprecipitated from a Triton X-100 extract of total rat liver mitochondria with a specific antiserum against polypeptide IV[84]. Specific antibodies for the isolated polypeptides I, II, III, IV, Vab, VIa, VIbc, VIIabc, and VIII reacted only with the corresponding polypeptides, whereby proteolytic artifacts were eliminated[86]. The com-

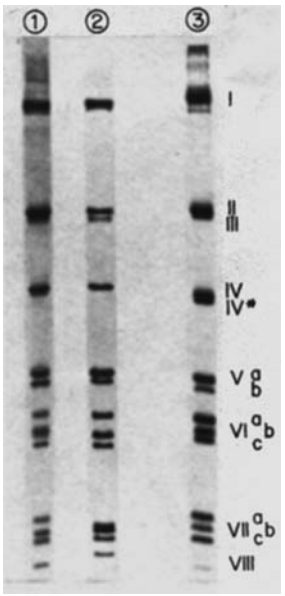



Fig. 3. Polypeptide composition of animal cytochrome c oxidase, which was isolated from mitochondria of porcine heart ①, bovine heart ②, and rat liver ③ according to the procedure in [81]. After high-performance SDS-gel electrophoresis [80], the protein bands were stained using Coomassie blue R 250.

plete amino acid sequences of twelve polypeptides of the bovine heart enzyme all differ from one another[85].

## 4. Polypeptide Composition of Cytochrome c Oxidase from Species in Different Developmental Stages

In studying the biosynthesis of the enzyme, the polypeptide composition of cytochrome c oxidase from *Neurospora crassa* and from yeast was carefully analyzed, and eight[87,88] and seven[61,62] different subunits, respectively, identified. An interesting observation made was that the three largest polypeptides (I, II, and III) are coded by mitochondrial DNA and synthesized in the mitochondria, whereas all other polypeptides are coded on nuclear DNA and synthesized in the cytoplasm[63,89], as demonstrated schematically in Figure 4. Also in animal cytochrome c oxidase the large polypeptides I—III are synthesized in the mitochondria, and the other polypeptides in the cytoplasm[90–94]. The information for the directed transport of the polypeptides synthesized in the cytoplasm into the mitochondria is contained in additional amino acid sequences of 2000—6000 dalton ("signal peptides"), which are cleaved proteolytically during or after transport through the mitochondrial membrane[95–99].

Recently, cytochrome c oxidase was also isolated from bacteria and the surprising observation was made that this enzyme contains only two [100–103] or three[104,105] subunits. Nevertheless, the isolated enzyme is functionally active. After reconstitution of the two-subunit enzyme from *Paracoccus denitrificans* in liposomes, an electron transport-dependent proton translocation was found with a stoichiometry of $0.6\,H^+/e^-$[106]. The ability of the enzyme from *P. denitrificans* to actively pump protons has not yet been explained, since the corresponding proton translocating polypeptide III of the eukaryotic enzyme (cf. Section 5) is absent.

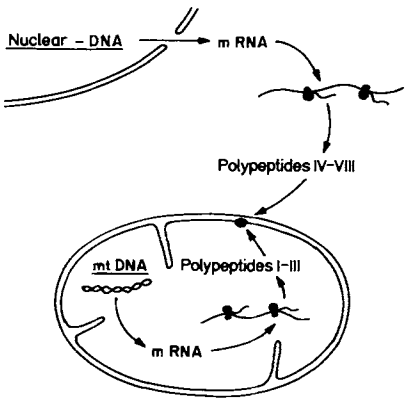



Fig. 4. Coordinated biosynthesis of cytochrome c oxidase in mitochondria and in the cytoplasm. The information for polypeptides I—III is coded on mitochondrial DNA (mtDNA) and, after transcription into mRNA, the proteins are synthesized on mitochondrial ribosomes. The polypeptides are then anchored on the inner membrane. The polypeptides IV—VIII are coded on nuclear DNA. They are synthesized on cytoplasmic ribosomes. The transport of the precursor proteins to the inner mitochondrial membrane occurs with the help of additional signal sequences which are cleaved off during passage through the membrane. The mechanism of assembly of the intact enzyme complex (binding of two heme a and two copper ions) is not known.

The polypeptides of cytochrome c oxidase from prokaryotes are related to the mitochondrial-synthesized polypeptides of the yeast enzyme: An antiserum against polypeptide II from *P. denitrificans* reacted with polypeptide II of the yeast enzyme and *vice versa*[25]. The amino acid sequences of the polypeptides I, II, and III from higher animals are also related to the corresponding polypeptides from yeast, as shown by comparison of the yeast, bovine, and human mitochondrial DNA sequences[107–112]. Between polypeptide II from yeast and bovine, a sequence homology of 49% was found, and between bovine and human 72%[111].

## 5. Mitochondrial-Synthesized Polypeptides I-III—Carriers of Catalytic Activity

The findings described in Sections 3 and 4 suggest that only the polypeptides I-III synthesized in the mitochondria are required for the catalytic function of the animal enzyme. This assumption was supported by the localization of both heme a groups in equal amounts in polypeptides I and II, as well as of both copper ions in polypeptide II[32]. The localization of the copper ions in polypeptide II also follows from its amino acid sequence which is very similar to those of the copper-binding proteins azurin and plastocyanin[113]. Polypeptide II also contains the binding site for cytochrome c, which binds through the same lysines of a defined surface area (Lys-8, -13, -72, -87) to the electron acceptor (cytochrome $aa_3$), as well as to the electron donor (cytochrome $bc_1$)[114–116]. From kinetic data two binding sites for cytochrome c, a high-affinity and a low-affinity site, were defined at the oxidase[114,117]. The high-affinity binding site is located at polypeptide II, as was shown by cross-linking of cytochrome c with the reagent 3,3′-dithiobis(succinimidopropionate)[118] and with the

photoreactive azido-3-nitrophenylcytochrome c (modified at Lys-13)[49,67,119]. Low-affinity bound cytochrome c, modified at Lys-13 or Lys-22, reacts only with phospholipids[49].

Polypeptide III seems to contain the proton channel of the oxidase: as in ATP-synthetase[120], *N,N'*-dicyclohexylcarbodiimide inhibits proton translocation in reconstituted cytochrome c oxidase vesicles[121] with concomitant partial inhibition of respiratory activity and specific covalent binding to polypeptide III[122,123]. Thus all known functional activities of cytochrome c oxidase (electron transport from cytochrome c to $O_2$ and proton translocation) can be attributed to the three polypeptides I—III synthesized in the mitochondria. We therefore refer to them as *catalytic subunits*. Although no definite function for the ten polypeptides synthesized in the cytoplasm which are firmly associated with polypeptides I—III is yet known, the following findings indicate a "regulatory" or "modifying" function, mediated by conformative interaction with the catalytic subunits I—III.

## 6. Tissue-Specific Isoenzymes of Animal Cytochrome c Oxidase

By comparing the polypeptide pattern obtained by SDS-gel electrophoretic separation of cytochrome c oxidase from the liver and heart of the same animal, we found different molecular weights for the polypeptides VIa, VIIa, and VIII synthesized in the cytoplasm[82,83]. The different bands were eluted from the acrylamide gel, and the *N*-terminal amino acid sequences determined[124,125]. As seen in Table 1, the *N*-terminal sequences of polypeptides VIa, VIIa, and VIII from bovine liver and heart are different but still very similar. In contrast, the twelve *N*-terminal amino acids of polypeptides IV and Va from the bovine liver and heart enzymes are identical. Two conclusions can, therefore, be drawn: 1) For each of the polypeptides VIa, VIIa, and VIII there exist two different genes in the bovine genome; 2) the corresponding genes for the different polypeptides from liver and heart originate from a common precursor gene and developed independently of each other in the course of evolution.

Table 1. Comparison of the *N*-terminal amino acid sequences of some polypeptides of cytochrome c oxidase from bovine heart and liver. The polypeptides of the bovine heart enzyme were isolated by gel chromatography, those from bovine liver from the gel bands after SDS-gel electrophoresis [124, 125].

| Polypeptide | Tissue | *N*-Terminal amino acid sequence |
|---|---|---|
| IV | heart | $H_2N$-Ala-His-Gly-Ser-Val-Val-Lys-Ser-Glu-Asp-Tyr-Ala |
| | liver | $H_2N$-Ala-His-Gly-Ser-Val-Val-Lys-Ser-Glu-Asp-Tyr-Ala |
| Va | heart | $H_2N$-Ser-His-Gly-Ser-His-Glu-Thr-Asp-Glu-Glu-Phe-Asp |
| | liver | $H_2N$-Ser-His-Gly-Ser-His-Glu-Thr-Asp-Glu-Glu-Phe-Asp |
| VIa | heart | $H_2N$-Ala-Ser-Ala-Ala-Lys-Gly-Asp-His-Gly-Gly-Thr- |
| | liver | $H_2N$-*Ser*-Ser-*Gly*-Ala-*His*-Gly-*Glu*-*Glu*-Gly-*Ser-Ala*- |
| VIIa | heart | $H_2N$-Phe-Glu-Asp-Arg-Val-Val- |
| | liver | $H_2N$-Phe-Glu-Asn-*Lys*-Val-Ala-(Phe) |
| VIII | heart | $H_2N$-Ile-Thr-Ala-Lys-Pro-Ala- |
| | liver | $H_2N$-Ile-*His-Ser*- Lys- Pro-*Pro*-(Phe) |

In order to study the immunological relationship of cytochrome c oxidase polypeptides from different organs and species, the method of immunodetection after protein transfer onto nitrocellulose ("western blot") was used. The polypeptides, separated on an acrylamide gel, were transferred electrophoretically onto nitrocellulose and incubated with a specific antiserum. Polypeptides which reacted with the antibody were visualized with fluorescein-labeled protein A, which binds specifically to immunoglobulins. We found large differences in the immunological reactivity of the tissue-specific polypeptide VIa from different tissues of the rat (liver, heart, skeletal muscle) with an antiserum against rat liver cytochrome c oxidase. The reactivity of the tissue-unspecific polypeptides I—V from the same organs of different species (*e.g.* rat and blackbird) with the antiserum was, however, very similar[86]. We conclude that the time elapsed since tissue-specific polypeptides of the same species evolved separately must be considerably greater than that elapsed since mammals and birds developed separately.

## 7. Cytoplasmical-Synthesized Polypeptides IV-VIII— Modulators of Catalytic Activity

The different amino acid sequences of the polypeptides VIa, VIIa, and VIII in liver and heart have an influence on the catalytic activity of the cytochrome c oxidase: Compared to the enzyme from bovine heart, that from bovine liver exhibited a higher initial rate $V_{max}$ and different $K_m$-values for the high-affinity, as well as for the low-affinity binding sites for cytochrome c. These differences were measured on intact membranes, on membranes dissolved in deoxycholate, and also on the isolated enzymes[126].

The physiological meaning of these differences could be based on the different composition of the enzyme in liver and heart mitochondria. In the outer membrane of liver mitochondria a NADH-cytochrome $b_5$ reductase was found which oxidizes extramitochondrial NADH[127-129].

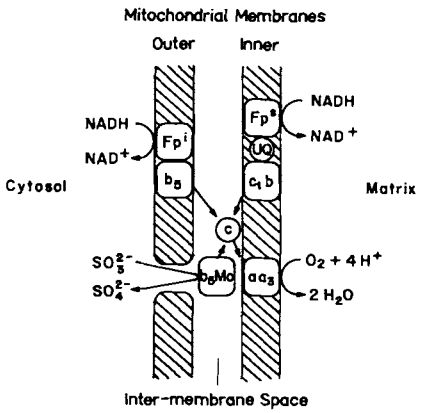



Fig. 5. Schematic representation of the electron transport pathways in liver mitochondria *via* cytochrome c to cytochrome c oxidase. Cytochrome c ©, a small water-soluble protein, is located in the intermembrane space and transfers electrons in all mitochondria from the cytochrome $bc_1$ complex to cytochrome c oxidase ($aa_3$). In liver mitochondria electrons can also be transferred from the rotenone-insensitive NADH-dehydrogenase of the outer membrane ($Fp^i$) *via* cytochrome $b_5$ ($b_5$), and from the sulfite oxidase ($b_5$Mo), located in the intermembrane space, *via* cytochrome c to cytochrome c oxidase. $Fp^s$: rotenone-sensitive NADH-dehydrogenase; UQ: ubiquinone.

In the intermembrane space of liver mitochondria, a soluble sulfite oxidase was found that contains molybdenum and a $b_5$-type heme as prosthetic groups, and which oxidizes sulfite to sulfate[130-133]. The sulfite oxidase represents the terminal step of sulfur metabolism in higher animals and can account for approximately 20% of the oxygen consumption of the liver (maximal rate of sulfite oxidation in perfused rat liver at 30 °C: 1.2 μmol/g wet weight/min[132], compared with an $O_2$ consumption of *in vivo* rat liver of *ca.* 3 μmol/g wet weight/min[134]). The sulfite oxidase and the NADH-cytochrome $b_5$ reductase in liver mitochondria transfer electrons *via* cytochrome c to the oxidase as well as the cytochrome $bc_1$ complex of the respiratory chain (Fig. 5). Liver mitochondria appear to be adapted to these additional electron donors: the ratio of cytochrome c + cytochrome $c_1$ to cytochrome $aa_3$ is greater than that of *e.g.* heart mitochondria (Table 2). The different catalytic activity of liver and heart cytochrome c oxidase[126] could be explained by the differences in the electron transport pathways.

Table 2. The ratio of the amounts [nmol/mg mitochondrial protein] of cytochrome $c+c_1$ to cytochrome $aa_3$ is different in liver and heart mitochondria.

| Tissue | $c+c_1$ | $aa_3$ | $(c+c_1)/aa_3$ | Ref. |
|---|---|---|---|---|
| bovine liver | 0.23 | 0.08 | 2.9 | [126] |
| bovine heart | 0.47 | 0.68 | 0.69 | [126] |
| rat liver | 0.38 | 0.27 | 1.4 | [135] |
| rat heart | 0.83 | 0.98 | 0.85 | [135] |
| chicken liver | 0.44 | 0.36 | 1.2 | [135] |
| chicken heart | 0.49 | 0.63 | 0.78 | [135] |

Upon incubating isolated cytochrome c oxidase from bovine heart with trypsin, polypeptides VIa, b, and c are completely, and polypeptide I *ca.* 50% cleaved, whereas the other polypeptides are not changed[83]. Simultaneously, the affinity of the enzyme to cytochrome c is reduced by 50% and $V_{max}$ increased (Fig. 6). This result points to a modifying influence of the polypeptides VIa, VIb, and/or VIc on the catalytic activity of the enzyme.

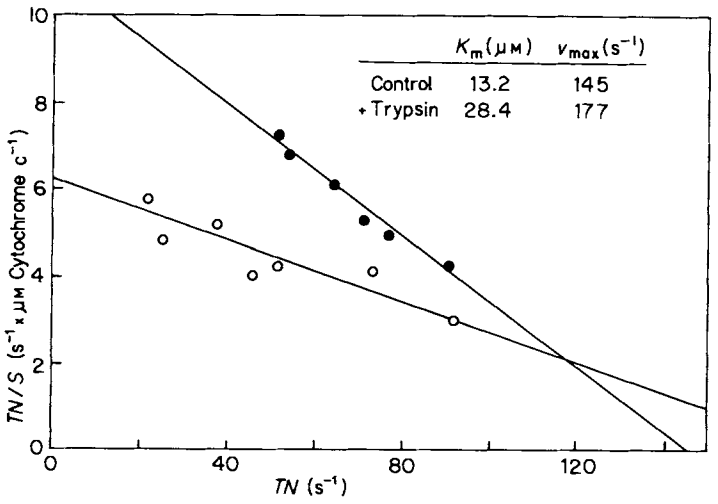



Fig. 6. Effect of trypsin on the kinetic properties of cytochrome c oxidase. Cytochrome c oxidase isolated from bovine heart (2 mg/mL) was dissolved in 2% solution of Na-cholate containing 20 mg/mL asolectin and 50 mM Na-phosphate at pH 7.6, and incubated for 30 min at 23 °C in the presence and absence of 0.02 mg/mL DPCC-trypsin. The enzyme activity was measured photometrically with 2—20 μM reduced cytochrome c [135]. In the reciprocal representation according to *Eadie-Hofstee*, the molecular activities (*TN*) are given in mol cytochrome c × $s^{-1}$ per mol cytochrome c oxidase. *S*: concentration of cytochrome c. • control, o+ tripsin.

Isolated cytochrome c oxidase from rat liver was incubated with the cleavable cross-linking reagent 3,3'-dimethyldithiobis(propionimidate). The reaction products were analyzed by two-dimensional SDS-gel electrophoresis in the absence and presence of β-mercaptoethanol, which cleaves the adducts again. The polypeptides VIa and VIb were only cross-linked with polypeptides II and Va, and polypeptide VIc only with polypeptide II[136]. This indicates that polypeptides VIa, VIb, and VIc are located in the close proximity of polypeptide II, which contains the binding site for cytochrome c. This assumption is corroborated by findings of *Bisson* and *Montecucco*, who cross-linked the cytochrome c—cytochrome c oxidase complex and found not only adducts between cytochrome c and polypeptide II but also between cytochrome c and polypeptides VIa, b, and/or c[137].

These results indicate a "regulatory" or "modifying" effect of the cytoplasmical-synthesized polypeptides. At present, their physiological meaning can now only be presumed: The respiratory rate, normally controlled by the supply of ADP ("respiratory control")[138], could be additionally regulated in a tissue-specific way by the type of substrate available (intramitochondrial NADH, sulfite, extramitochondrial NADH). Some polypeptides could function as substrate-specific receptors that modify the activity *via* a conformational change. The coupling of respiration and proton translocation could be variable[24] and regulated by tissue-specific polypeptides, which may, for example, represent receptors for cellular effectors (cAMP, cGMP, $Ca^{2+}$, $P_i$, thyroid hormones *etc.*). By partially "uncoupling" electron and proton transport, more heat would be produced, and thus a tissue-specific regulation of thermogenesis would be conceivable.

## 8. The Evolution of Cytochrome c Oxidase

Comparison of cytochrome c oxidase from mammals with that from prokaryotes reveals an astonishing structural and functional similarity that has remained unchanged during the course of more than two billion years of independent evolution: 1) Both enzymes react with animal cytochrome c, although at different rates[25, 100]. 2) The active center of both enzymes contains two heme a and two copper ions[25]. 3) In both cases electron transport from cytochrome c to $O_2$ is coupled with an active proton translocation across the membrane[40, 45, 46, 106]. This uniformity of respiration in most aerobic organisms was already recognized by *Otto Warburg*, who wrote in 1928[139]: "Entsprechend gibt es in der Natur nicht nur 1 Atmungsferment, aber der Mechanismus der Atmung in einem bestimmten Fall ist, wie der Mechanismus des Sauerstofftransports, ein bestimmter und einheitlich. Wie zum Transport des Sauerstoffs, so benutzt die Natur zur Verbrennung durch Sauerstoff *vorwiegend einen* Mechanismus. Denn das Atmungsferment in Hefezellen und Chorion, in Leber-

zellen und Blutplättchen, in Leukozyten und Seeigeleiern verhält sich im Prinzip gleich"[*].

In spite of this, with increasing differentiation and specialization of cells we find a growing complexity of the enzyme, which is reflected in its increasing number of "subunits". While the same function ($O_2$-reduction and proton translocation) in the prokaryotic enzyme is carried out by two or three polypeptides, in unicellular eukaryotic organisms seven or eight polypeptides are involved in the enzyme complex. The differentiation to multicellular organisms, composed of specific organs, is connected with a further increase in the polypeptide number (in mammals up to thirteen), as well as with a multiplication and independent evolution of tissue-specific polypeptides in the same organism (Fig. 7).

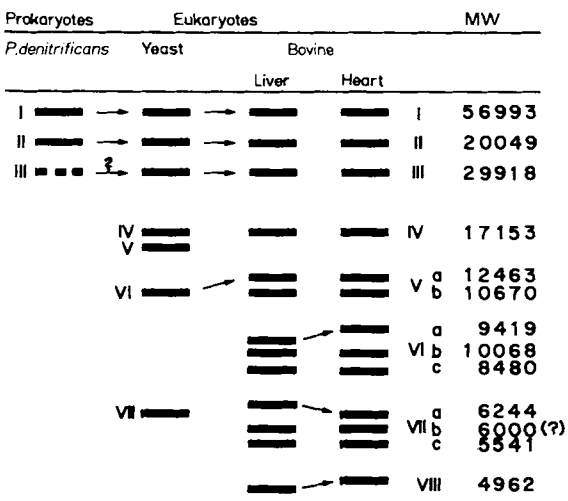



Fig. 7. Evolution of the cytochrome c oxidase complex. The bands represent individual polypeptides that correspond to the bands of SDS-gel electrophoresis. MW is the relative molecular mass of the bovine heart polypeptides [85] calculated either from the DNA-sequence (I, III) or from the amino acid sequence. The arrows indicate evolutionary relationships. The relationship of the other bands between bovine liver and heart has established yet not been. The homology of polypeptide VI from yeast with V from bovine heart was demonstrated [142].

If we consider the mitochondrial-synthesized polypeptides I—III as catalytic and the cytoplasmic synthesized as regulatory or modifying subunits of the enzyme complex, the evolution of cytochrome c oxidase is reflected by an increase in regulatory capacity. Here a general principle of the evolution of biological systems becomes evident: The basic principles of energy and substrate metabolism (respiration, glycolysis), as well as the storage and expression of information (DNA-replication, protein synthesis) have remained unchanged during the course of evolution in all living organisms. The regulation of the various steps, however, has changed and has led to extremely complicated mechanisms in highly differentiated organisms (*e.g.* regulation of glycogen synthesis and degradation[140, 141]).

[*] "Correspondingly, in nature not only is there 1 *Atmungsferment*, but the mechanism of respiration in a particular case is, as the mechanism of transport of oxygen, specific and uniform. Just as in the transport of oxygen, nature uses *predominantly one* mechanism for combustion by oxygen. Because, in principle, the *Atmungsferment* in yeast cells and chorion, in leukocytes and sea urchin eggs behave the same".

## 9. Outlook

Since the discovery of the *Atmungsferment* by *Otto Warburg* in the twenties, our knowledge about this enzyme has grown enormously. But with every new finding the number of unanswered questions increased. At present, intensive research is being carried out to determine the structure of the active center and the mechanism of $O_2$-reduction. Here, a detailed interpretation can be expected in the near future. Far more difficult appears to be the investigation of the coupling of electron transport and proton translocation in the cytochrome c oxidase complex. So far, the mechanism of the directed proton transport cannot be explained for any of the proton translocating membrane enzymes, although for one enzyme (bacteriorhodopsin) the amino acid sequence and the three-dimensional structure are known. Of particular interest is the occurrence of isoenzymes of cytochrome c oxidase in different organs of higher animals which differ in their catalytic and structural properties as well. The differences presented in this progress report point to a complex regulation of the enzyme. Intensive research on the structural differences of the polypeptides as well as on the functional meaning of the various subunits is necessary to provide an understanding of the adaptation of respiration and the associated ATP synthesis to the specific requirements of the different tissues of higher organisms.

*I would like to thank Prof. R. Thauer for his helpful criticism, Mrs. Roller-Müller for typing the manuscript, the Deutsche Forschungsgemeinschaft (SFB 103, A2) for grants, and the Fonds der Chemischen Industrie for a generous donation.*

Received: October 20, 1982;
revised: January 24, 1983 [A 449 IE]
German version: *Angew. Chem. 95* (1983) 273

[1] O. Warburg, *Biochem. Z. 152* (1924) 479.
[2] D. Keilin, *Proc. R. Soc. London Ser B 98* (1925) 312.
[3] O. Warburg, *Angew. Chem. 45* (1932) 1.
[4] T. Yonetani, *J. Biol. Chem. 235* (1960) 845.
[5] C. A. McMunn, *Philos. Trans. R. Soc. London Ser. B 177* (1886) 267.
[6] C. A. McMunn, *J. Physiol. London 8* (1887) 57.
[7] O. Warburg, *Biochem. Z. 207* (1929) 494.
[8] D. Keilin, E. F. Hartree, *Proc. R. Soc. London Ser. B 127* (1939) 167.
[9] J. Keilin: *The History of Cell Respiration and Cytochromes*. Cambridge University Press, Cambridge 1966.
[10] E. C. Slater, B. V. Van Gelder, K. Minneart in T. E. King, H. S. Mason, M. Morrison: *Oxidases and Related Redox Systems*. Wiley, New York 1965, p. 667.
[11] M. R. Lemberg, *Physiol. Rev. 49* (1969) 48.
[12] R. Lemberg, J. Barrett: *Cytochromes*. Academic Press, New York 1973, S. 17.
[13] B. G. Malmström, *Q. Rev. Biophys. 6* (1973) 389.
[14] P. Nicholls, B. Chance in D. Hayashi: *Molecular Mechanism of Oxygen Activation*. Academic Press, New York 1974, p. 479.
[15] M. Florkin in M. Florkin, E. H. Stotz: *Comprehensive Biochemistry, Vol. 31*. Elsevier, Amsterdam 1975, p. 187.
[16] W. S. Caughey, W. J. Wallace, J. A. Volpe, S. Yoshikawa in P. D. Boyer: *The Enzymes*, 3rd edit., *Vol. 13C*. Academic Press, New York, 1976, p. 299.
[17] R. A. Capaldi, M. Briggs in A. Martonosi: *The Enzymes of Biological Membranes, Vol. 4*. Wiley, New York, 1976, p. 87.
[18] M. K. F. Wikström, H. J. Harmon, W. J. Ingledew, B. Chance, *FEBS Lett. 65* (1976) 259.
[19] M. Erecinska, D. F. Wilson, *Arch. Biochem. Biophys. 188* (1978) 1.
[20] B. G. Malmström, *Biochim. Biophys. Acta 549* (1979) 281.
[21] M. Wikström, K. Krab, *Biochem. Biophys. Acta 549* (1979) 177.
[22] A. Azzi, R. P. Casey, *Mol. Cell. Biochem. 28* (1979) 169.

[23] A. Azzi, *Biochim. Biophys. Acta 594* (1980) 231.
[24] B. Kadenbach, P. Merle, *FEBS Lett. 135* (1981) 1.
[25] B. Ludwig, *Biochim. Biophys. Acta 594* (1980) 177.
[26] M. Wikström, K. Krab, M. Saraste: *Cytochrome Oxidase, A Synthesis*, Academic Press, London 1981.
[27] G. von Jagow, W. D. Engel, *Angew. Chem. 92* (1980) 684; *Angew. Chem. Int. Ed. Engl. 19* (1980) 659.
[28] P. Mitchell, *Biol. Rev. 41* (1966) 445.
[29] N. C. Robinson, F. Strey, L. Talbert, *Biochemistry 19* (1980) 3656.
[30] M. Frey, D. E. Green, *Biochem. Biophys. Res. Commun. 93* (1980) 1238.
[31] N. C. Robinson, *Biochemistry 21* (1982) 184.
[32] D. B. Winter, W. J. Bruyninckx, F. G. Foulke, N. P. Grinich, H. S. Mason, *J. Biol. Chem. 255* (1980) 11408.
[33] T. Ohnishi, R. LoBrutto, J. C. Salerno, R. C. Bruckner, T. G. Frey, *J. Biol. Chem. 257* (1982) 14821.
[34] See discussion in [26], p. 34–38.
[35] C. Greenwood, Q. H. Gibson, *J. Biol. Chem. 242* (1967) 1782.
[36] L. Powers, B. Chance, Y. Ching, P. Angiolillo, *Biophys. J. 34* (1982) 465.
[37] M. Brunori, M. T. Wilson, *Trends Biochem. Sci. 1982*, 295.
[38] R. Henderson, R. A. Capaldi, J. S. Leigh, *J. Mol. Biol. 112* (1977) 631.
[39] S. D. Fuller, R. A. Capaldi, R. Henderson, *J. Mol. Biol. 134* (1979) 305.
[40] E. Sigel, E. Carafoli, *Eur. J. Biochem. 111* (1980) 299.
[41] J. Moyle, P. Mitchell, *FEBS Lett. 88* (1978) 268.
[42] M. Wikström, K. Krab, *FEBS Lett. 91* (1978) 8.
[43] M. Wikström, *Nature 266* (1977) 271.
[44] M. Wikström, H. T. Saari, *Biochim. Biophys. Acta 462* (1977) 347.
[45] K. Krab, M. Wikström, *Biochim. Biophys. Acata 504* (1978) 200.
[46] R. P. Casey, J. B. Chappel, A. Azzi, *Biochem. J. 182* (1979) 149.
[47] R. A. Capaldi, M. Briggs in A. Martonosi: *The Enzymes of Biological Membranes*. Wiley, London 1976, p. 87.
[48] N. C. Robinson, R. A. Capaldi, *Biochemistry 16* (1977) 375.
[49] R. Bisson, B. Jacobs, R. A. Capaldi, *Biochemistry 19* (1980) 4173.
[50] M. T. Wilson, W. Lalla-Maharajh, V. M. Darley-Usmar, J. Bonaventura, C. Bonaventura, M. Brunori, *J. Biol. Chem. 255* (1980) 2722.
[51] V. M. Darley-Usmar, N. Alizai, A. I. Al-Ayash, G. D. Jones, A. Sharpe, M. T. Wilson, *Comp. Biochem. Physiol. B68* (1981) 445.
[52] M. Höchli, C. R. Hackenbrock, *Proc. Natl. Acad. Sci. USA 76* (1979) 1236.
[53] H. Schneider, J. J. Lemasters, M. Höchli, C. R. Hackenbrock, *Proc. Natl. Acad. Sci. USA 77* (1980) 442.
[54] S. Kawato, E. Sigel, E. Carafoli, K. J. Cherry, *J. Biol. Chem. 255* (1980) 5508.
[55] M. S. Swanson, A. T. Quintanilha, D. D. Thomas, *J. Biol. Chem. 255* (1980) 7494.
[56] B. H. Ariano, A. Azzi, *Biochem. Biophys. Res. Commun. 93* (1980) 478.
[57] G. Buse, G. J. Steffens, *Hoppe Seyler's Z. Physiol. Chem. 359* (1978) 1005.
[58] F. E. A. M. Verheul, J. C. P. Boonman, J. W. Draijer, A. O. Muijsers, D. Borden, G. E. Tarr, E. Margoliash, *Biochem. Biophys. Acta 548* (1979) 397.
[59] U. K. Laemmli, *Nature 227* (1970) 680.
[60] N. W. Downer, N. C. Robinson, R. A. Capaldi, *Biochemistry 15* (1976) 230.
[61] M. S. Rubin, A. Tzagoloff, *J. Biol. Chem. 248* (1973) 4269.
[62] R. Poyton, G. Schatz, *J. Biol. Chem. 250* (1975) 752.
[63] G. Schatz, T. L. Mason, *Annu. Rev. Biochem. 43* (1974) 51.
[64] C.-A. Yu, L. Yu, *Biochim. Biophys. Acta 495* (1977) 248.
[65] S. H. P. Chan, R. P. Tracy, *Eur. J. Biochem. 89* (1978) 595.
[66] L. Höchli, C. R. Hackenbrock, *Biochemistry 17* (1978) 3712.
[67] R. Bisson, A. Azzi, H. Gutweniger, R. Colonna, C. Montecucco, A. Zanotti, *J. Biol. Chem. 253* (1978) 1874.
[68] T. G. Frey, S. H. P. Chan, G. Schatz, *J. Biol. Chem. 253* (1978) 4389.
[69] B. Ludwig, N. W. Downer, R. A. Capaldi, *Biochemistry 18* (1979) 1401.
[70] T. Nagasawa, H. Nagasawa-Fujimori, P. C. Heinrich, *Eur. J. Biochem. 94* (1979) 31.
[71] J. F. Hare, E. Ching, G. Atardi, *Biochemistry 19* (1980) 2033.
[72] M. Swanson, L. Packer, *Arch. Biochem. Biophys. 204* (1980) 30.
[73] M. Frey, D. E. Green, *J. Bioenerg. Biomembr. 13* (1981) 61.
[74] J. Kolarov, A. Wielburski, I. Mendel-Hartwig, B. D. Nelson, *Biochim. Biophys. Acta 652* (1981) 334.
[75] Y.-H. Wei, T. E. King, *J. Biol. Chem. 256* (1981) 10999.
[76] J. R. Bucher, R. Penniall, *FEBS Lett. 60* (1975) 180.
[77] E. Hundt, B. Kadenbach, *Hoppe Seyler's Z. Physiol. Chem. 358* (1977) 1309.
[78] C. Bonaventura, J. Bonaventura, M. Brunori, M. Wilson, *FEBS Lett. 85* (1978) 30.
[79] R. D. Poyton, E. McKemmie, C. George-Nascimento, *J. Biol. Chem. 253* (1978) 6303.
[80] B. Kadenbach, J. Jarausch, R. Hartmann, P. Merle, *Anal. Biochem.*, in press.
[81] P. Merle, B. Kadenbach, *Eur. J. Biochem. 105* (1980) 499.
[82] P. Merle, B. Kadenbach, *Hoppe Seyler's Z. Physiol. Chem. 361* (1980) 1257.
[83] B. Kadenbach, U. Büge, J. Jarausch, P. Merle in F. Palmieri, E. Quagliariello, N. Siliprandi, E. C. Slater: *Vectorial Reactions in Electron and Ion Transport in Mitochondria and Bacteria*. Elsevier/North-Holland Biomedical Press, Amsterdam 1981, p. 11.
[84] P. Merle, J. Jarausch, M. Trapp, R. Scherka, B. Kadenbach, *Biochim. Biophys. Acta 669* (1981) 222.
[85] G. Buse, G. C. M. Steffens, G. J. Steffens, L. Meinecke, R. Biewald, M. Erdweg, *Eur. Bioenerg. Conf. Rep. 2* (1982) 163.
[86] J. Jarausch, B. Kadenbach, *Hoppe Seyler's Z. Physiol. Chem. 363* (1982) 1133.
[87] W. Sebald, W. Machleidt, J. Otto, *Eur. J. Biochem. 38* (1973) 311.
[88] S. Werner, *Eur. J. Biochem. 79* (1977) 103.
[89] H. Weiss, A. J. Schwab, S. Werner in A. Tzagoloff: *Membrane Biogenesis*. Plenum, London 1975, p. 125.
[90] G. Koch, *J. Biol. Chem. 251* (1976) 6097.
[91] R. W. Yatscoff, K. G. Freeman, W. J. Vail, *FEBS Lett. 81* (1977) 7.
[92] J. D. Bernstein, J. R. Bucher, R. Penniall, *J. Bioenerg. Biomembr. 10* (1978) 59.
[93] E. Hundt, M. Trapp, B. Kadenbach, *FEBS Lett. 115* (1980) 95.
[94] J. Kolarov, S. Kuzela, A. Wielbruski, B. D. Nelson, *FEBS Lett. 126* (1981) 61.
[95] A. S. Lewin, I. Gregor, T. L. Mason, N. Nelson, G. Schatz, *Proc. Natl. Acad. Sci. USA. 77* (1980) 3998.
[96] K. Mihara, G. Blobel, *Proc. Natl. Acad. Sci., USA 77* (1980) 4160.
[97] E. Schmelzer, P. C. Heinrich, *J. Biol. Chem. 255* (1980) 7503.
[98] S. Parimoo, G. Padmanaban, *Biochem. Biophys. Res. Commun. 95* (1980) 1673.
[99] E. Schmelzer, W. Northemann, B. Kadenbach, P. C. Heinrich, *Eur. J. Biochem. 127* (1982) 177.
[100] B. Ludwig, G. Schatz, *Proc. Natl. Acad. Sci. USA 77* (1980) 196.
[101] T. Amanaka, K. Fujii, Y. Kanuta, *J. Biochem. 86* (1979) 821.
[102] T. Yamanaka, k. Fujii, *Biochim. Biophys. Acta 591* (1980) 53.
[103] J. A. Fee, M. G. Choc, K. L. Findling, R. Lorence, T. Yoshida, *Proc. Natl. Acad. Sci. USA 77* (1980) 141.
[104] R. B. Gennis, R. P. Casey, A. Azzi, B. Ludwig, *Eur. J. Biochem. 125* (1982) 189.
[105] A. Azzi, K. Bill, R. Bolli, C. Broger, R. P. Casey, M. Corbley, *Eur. Bioenerg. Conf. Rep. 2* (1982) 125.
[106] M. Solioz, E. Carafoli, B. Ludwig, *J. Biol. Chem. 257* (1982) 1579.
[107] G. Coruzzi, A. Tzagoloff, *J. Biol. Chem. 254* (1979) 9324.
[108] T. D. Fox, *Proc. Natl. Acad. Sci. USA 76* (1979) 6534.
[109] B. E. Thalenfeld, A. Tzagoloff, *J. Biol. Chem. 255* (1980) 6173.
[110] S. G. Bonitz, G. Coruzzi, B. E. Thalenfeld, A. Tzagoloff, G. Macino, *J. Biol. Chem. 255* (1980) 11927.
[111] S. Anderson, A. T. Bankier, B. G. Barrell, M. H. L. de Bruijn, A. R. Coulson, J. Drouin, I. C. Eperon, D. P. Nierlich, B. A. Roe, F. Sanger, P. H. Schreier, A. J. H. Smith, R. Staden, I. G. Young, *Nature 290* (1981) 457.
[112] S. Anderson, M. H. L. de Bruijn, A. R. Coulson, I. C. Eperon, F. Sanger, I. G. Young, *J. Mol. Biol. 156* (1982) 683.
[113] G. Steffens, G. Buse, *Hoppe Seyler's Z. Physiol. Chem. 360* (1979) 613.
[114] S. Ferguson-Miller, D. L. Brautigan, E. Margoliash, *J. Biol. Chem. 253* (1978) 149.
[115] H. T. Smith, N. Standenmayer, F. Millet, *Biochemistry 16* (1977) 4971.
[116] R. Rieder, H. R. Bosshard, *J. Biol. Chem. 255* (1980) 4732.
[117] S. Ferguson-Miller, D. L. Brautigan, E. Margoliash, *J. Biol. Chem. 251* (1976) 1104.
[118] M. M. Briggs, R. A. Capaldi, *Biochem. Biophys. Res. Commun. 80* (1978) 553.
[119] R. Bisson, H. Gutweniger, C. Montecucco, R. Colonna, A. Zanotti, A. Azzi, *FEBS Lett. 81* (1977) 147.
[120] R. B. Beechy, A. M. Roberton, T. Holloway, I. G. Knight, *Biochemistry 6* (1969) 3867.
[121] R. P. Casey, M. Thelen, A. Azzi, *Biochem. Biophys. Res. Commun. 87* (1979) 1044.
[122] R. P. Casey, M. Thelen, A. Azzi, *J. Biol. Chem. 255* (1980) 3994.
[123] L. J. Prochaska, R. Bisson, R. A. Capaldi, G. C. M. Steffens, G. Buse, *Biochim. Biophys. Acta 637* (1981) 360.
[124] B. Kadenbach, R. Hartmann, R. Glanville, G. Buse, *FEBS Lett. 138* (1982) 236.
[125] G. Buse, B. Kadenbach, unpublished results.
[126] P. Merle, B. Kadenbach, *Eur. J. Biochem. 125* (1982) 239.
[127] P. Bernardi, G. F. Azzone, *J. Biol. Chem. 256* (1981) 7187.
[128] A. A. Jasaitis, Z. J. Krivickiene, *Eur. Bioenerg. Conf. Rep. 1* (1980) 111.
[129] P. Bernardi, G. F. Azzone, *Biochim. Biophys. Acta 679* (1982) 19.

[130] M. Heimberg, J. Fridovich, P. Handler, *J. Biol. Chem. 204* (1953) 913.
[131] J. L. Johnson, K. V. Rajagopalan, *J. Biol. Chem. 252* (1977) 2017.
[132] N. Oshino, B. Chance, *Arch. Biochem. Biophys. 170* (1975) 514.
[133] S. H. Speck, W. H. Koppenol, j. D. Dethmers, N. Osheroff, E. Margoliash, K. V. Rajagopaan, *J. Biol. Chem. 256* (1981) 7394.
[134] M. Sato, M. Shichiri, N. Hayashi, T. Kamada, H. Abe, B. Hagihara in T. E. King, J. Orii, B. Chance, K. Okunuki: *Cytochrome Oxidase*. Elsevier/North-Holland Biomedical Press, Amsterdam 1979, p. 319.
[135] J. N. Williams, *Biochim. Biphys. Acta 162* (1968) 175.
[136] J. Jarausch, B. Kadenbach, unpublished results.
[137] R. Bisson, C. Montecucco, *FEBS Lett. 150* (1982) 49.
[138] W. E. Jacobus, R. W. Moreadith, K. M. Vandegaer, *J. Biol. Chem. 257* (1982) 2397.
[139] O. Warburg, *Biochem. Z. 201* (1928) 486.
[140] P. B. Chock, S. G. Rhee, E. R. Stadtman, *Annu. Rev. Biochem. 49* (1980) 813.
[141] R. J. Fletterick, N. B. Madsen, *Annu. Rev. Biochem. 49* (1980) 31.
[142] I. Gregor, A. Tsugita, *J. Biol. Chem. 257* (1982) 13081.

# Proximity Effects in Organic Chemistry—The Photoelectron Spectroscopic Investigation of Non-Bonding and Transannular Interactions**

**By Hans-Dieter Martin* and Bernhard Mayer**

Classical structural formulas often convey the impression *only those* relationships between the atoms are of importance which hold a molecule together as symbolized by the chemical bonds. However, many interactions between atoms or groups of atoms are not adequately denoted in this manner. Nevertheless, their existence can have important consequences for *ground state energies* (*cis*-difluoroethylene is more stable than *trans*-difluoroethylene), *conformations* (the *syn* form of methyl vinyl ether is more stable than the *anti* form), *reactivities* (an *endo* cyclopropane ring in 7-*anti*-norbornyl derivatives accelerates solvolysis by a factor of $10^{14}$), *UV spectra* ("superposition" of the π-systems of acridine and purine—bonded through a four-membered chain—results in hypochromism), *CD spectra* (the inherently symmetrical but dissymmetrically perturbed chromophore of 2-deuterionorbornadiene allows the observation of three transitions in the near UV), and *ESR spectra* (the long-range coupling with H-4 in the bridgehead bicyclo[2.1.1]hex-1-yl radical equals 22.5 G). Since orbital interactions are involved in most intramolecular effects of this kind, *photoelectron spectroscopy* has proven an informative and valuable extension to other methods.

## 1. Introduction

### 1.1. Substituent Effects

The empirical knowledge that functional groups profoundly determine the reactivity of organic compounds led to the formulation of the concept of substituent effects. These can be broadly divided into three categories: polar or electrostatic effects, as well as conjugational and steric effects[1]. The discussion of the polar effects and their subdivision into inductive and field components (through-bonds and through-space, respectively) fills an important and voluminous part of the literature[2] but for our purposes is less decisive. Classical π-conjugation and π-delocalization may or may not occur within groups or chromophores which interact with each other in a non-bonding manner. Steric effects (steric hindrance) are generally associated with non-bonding compression and repulsion; in principle they can, however, be either repulsive or attractive[3].

Because the effects treated in this review do not, by definition, concern the relationships between neighboring atoms, these will be treated only with regard to a possible relay action. Orbital interactions between neighboring atoms have already been reviewed[4–7]. A summary of important 1,2-interactions is shown in Figure 1.

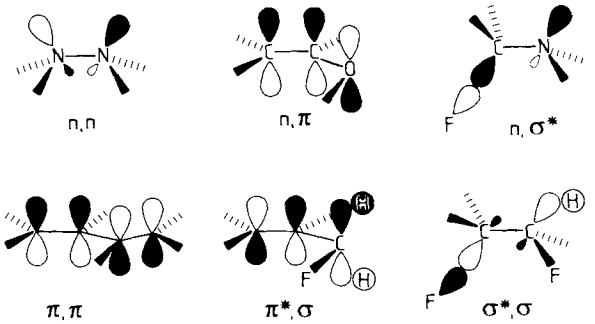



Fig. 1. 1,2-Interactions [4—6] between orbitals on neighboring atoms. The relaying action of these vicinal 1,2-contacts is of importance for longer range effects: n = localized lone pair of electrons; π = p-orbital in a π-system; σ = localized two-center σ-orbital [8]. The nomenclature is as in [4—6]. n,n: hydrazine; n,π: enol ethers; n,σ*: fluoromethylamine; π,π: 1,3-dienes; π*,σ: 3-fluoropropene; σ*,σ: 1,2-difluoroethane.

[*] Prof. Dr. H.-D. Martin, B. Mayer
Institut für Organische Chemie I der Universität
Universitätsstraße 1, D-4000 Düsseldorf (Germany)

[**] Because the term neighboring group participation is reserved for "through space" interactions between substituent and reaction center [19], all interactions between non-neighboring groups or orbitals (distance ≥ 1,3) are designated as proximity effects in this article, irrespective of whether they are "through space" or "through bond" in nature.

### 1.2. Classification

The classification of non-bonding interactions ($\geq 1,3$) used here is shown in Figure 2. Topology rather than the nature of the interaction is decisive in this classification, *e.g.* the question is one of the extent to which two electron pairs in a 1,4-relationship "feel" each other[9a].

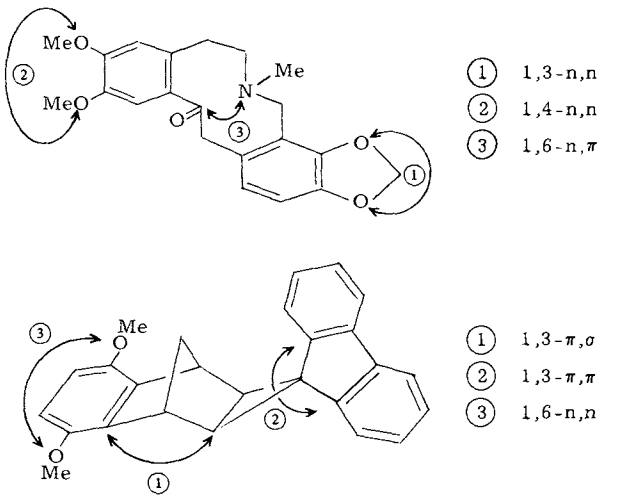
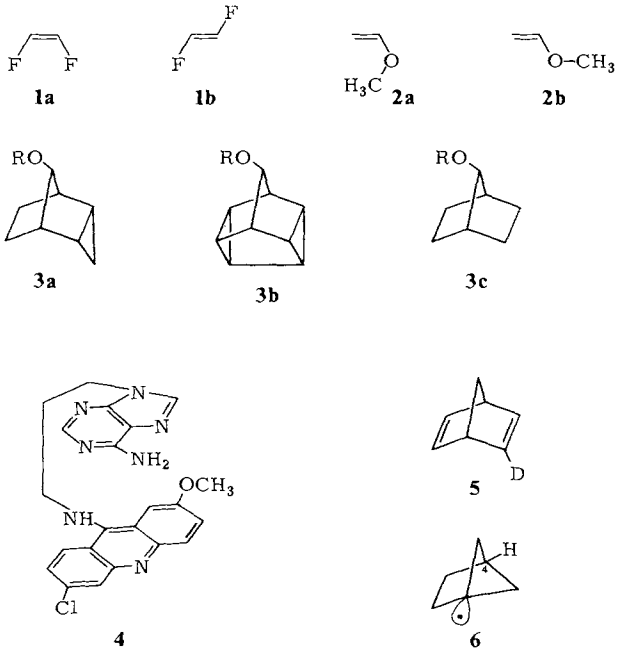



Fig. 2. Classification of non-bonding interactions used in this article. The examples, *i.e.* the alkaloid cryptopine and the spirocyclic fluorene, contain several groups or chromophores relevant to transannular interactions and show interesting neighboring group participation effects [8b].

### 1.3. Examples

The importance of non-bonding interactions as well as their influence on ground and excited states, transition states, and the relationship with PE spectroscopy is illustrated by the following examples.




#### *1.3.1. Ground State Energies*

*cis*-1,2-Difluoroethylene **1a** is $1080 \pm 120$ cal/mol more stable than the *trans*-isomer **1b**. Different explanations have been given[5, 10–15] for this *cis-effect* (see also Chap. V, 13 in [5]). The following results are derived from *ab initio* calculations[13], also taking polarization functions and correlation energies[10] into account: with a sufficiently large basis set the Hartree-Fock approximation predicts that **1a** is more stable than **1b**; also, the *steric attraction* of the F atoms in **1a** cannot be neglected (Fig. 3a). Hence, nonbonding interactions of this kind could also be detectable by PE spectroscopy.

#### *1.3.2. Conformations*

The *syn*-form **2a** is more stable than the *anti*-form **2b**. A plausible reason may be found in the attractive 1,4-$\pi,\sigma$-interaction (Fig. 3b). This has consequences for the PE spectrum[4].

#### *1.3.3. Reactivities*

That **3a** and **3b** are several orders of magnitude more reactive than **3c** can be ascribed to the stereoelectronically favored participation of the three-membered ring leading to formation of a homoaromatic transition state[16] (Fig. 3c). This $\pi$-type $\sigma$-participation ($\pi\sigma$[17a]) can also be detected by means of the $\rho^+$ values of arylated derivatives having increased electron demand[17–19] (Fig. 3d). Photoelectron spectroscopy ought to be able to detect such delocalization of electrons in three-membered rings, even (or especially) in cases where the reaction has not progressed so far that nuclear displacements have occurred and a bridged homoaromatic ion has been formed.

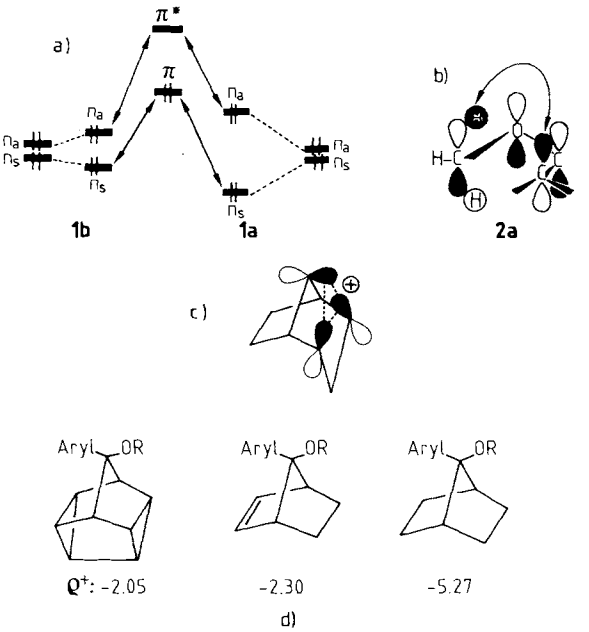



Fig. 3. a) $\pi$-Orbital interactions in **1a** and **1b**. The larger splitting $n_a/n_s$ in **1a** has the consequence that, *inter alia*, the two-electron interaction, $\Delta E_{\pi^* n_a} = 2(H_{\pi^* n_a} - SE_{n_a})^2/(E_{n_a} - E_{\pi^*})$, is more important in **1a** than in **1b** [5, 13] ($H$ = Interaction parameter, $S$ = Overlap integral). The symmetry elements are: $\sigma$ in **1a**, $C_2$ in **1b**. b) Attractive 1,4-$\sigma,\pi$-interaction in **2a** [4, 5]. c) Homoaromatic ion in the solvolysis of **3a**. d) "Tool of increasing electron demand" with $\rho^+$ values indicating $\pi\sigma$- or $\pi$-participation [17a]. The $\rho^+$ values were derived using species with Aryl = *p*-$CH_3OC_6H_4$, $C_6H_5$, *p*-$CF_3C_6H_4$, 3,5-$(CF_3)_2C_6H_3$; R = *p*-$O_2NC_6H_4CO$.

### 1.3.4. UV and CD Spectra

These spectra may exhibit effects (batho- and hypsochromic shifts; hyper- and hypochromic effects) indicative of interactions between two non-conjugated (*i.e.* non-neighboring) chromophores in a molecule. The reason may be found in a non-zero direct overlap of non-neighboring atomic orbitals, or in the transmission properties of other suitable orbitals (electron delocalization). However, it should be borne in mind that a delocalization of the excitation energy is possible even with a vanishing overlap (exciton delocalization)[20–25]. The molecules **4** and **5** represent typical examples of this. The contribution made by PE spectroscopy in the interpretation of unusual UV phenomena in homoconjugated π-systems will be illustrated using the example of norbornadiene **7** (Fig. 4). The locally ex-

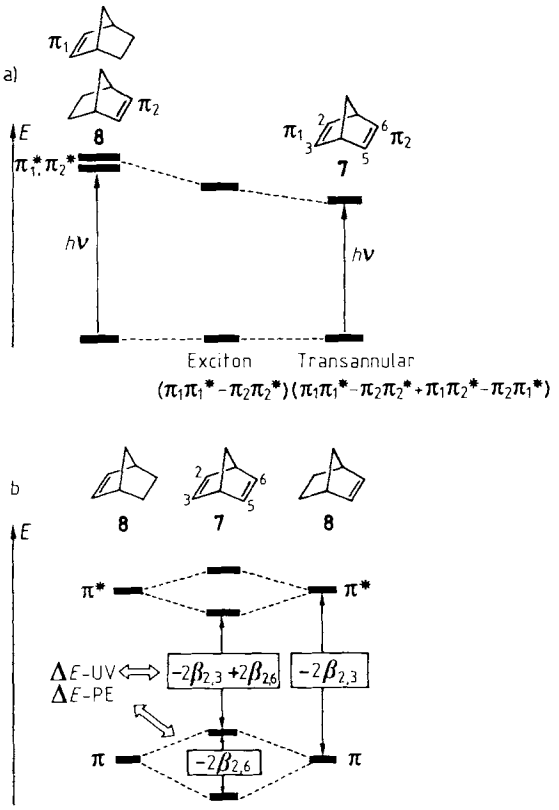



Fig. 4. Relationship between transannular π-overlap and UV properties in **7** [20—22]. a) Model with exciton and charge-resonance states. b) Simple LCAO model with UV and PE spectroscopic energy differences.

cited configurations of one of the two double bonds of **7** mix with each other and lead to a first excited minus-exciton state ($^1Ex^-$), which is in reasonable agreement with experiment[20, 21]. If the transannular overlap of the π-orbitals $\pi_1$ and $\pi_2$ is also taken into account, as expressed by the resonance integral $\beta_{2,6}$, the exciton state will also interact with the minus charge-resonance state ($^1CR^-$) in which a $\pi_1$ electron has been excited into the $\pi_2^*$ orbital. This latter interaction is given by $2\beta_{2,6}$[21]. Of course, the value of the transannular $\beta_{2,6}$ is significantly smaller than that of the vicinal resonance integral $\beta_{2,3}$; the following approximate relationship holds: $\beta_{2,6} \approx 0.3\beta_{2,3}$[26] (Fig. 4a). The influence of the transannular resonance integral $\beta_{2,6}$ on the UV spectrum of **7** is even more evident in the LCAO model[21, 22] (Fig. 4b): the HOMO-LUMO difference in **7** is $\Delta E = -2\beta_{2,3} + 2\beta_{2,6}$, *i.e.* in this model norbornadiene **7** should absorb at approximately $2\beta_{2,6}$ longer wavelength than norbornene **8**. The difference between the occupied MO's of **7** also amounts to $2\beta_{2,6}$. Such differences are measurable by PE spectroscopy.

### 1.3.5. ESR Spectra

Long-range interactions and spin density distributions in radicals have been thoroughly investigated[27]. The mechanism of these interactions can also be analyzed by means of the paramagnetic NMR contact shift[28]. The coupling constant $a_M$ with nucleus M can be resolved into spin delocalization $a_d$ and spin polarization $a_{sp}$ components[27a, b], whose magnitudes and signs are often decidedly dependent on stereochemistry. Furthermore, spin delocalization may also be discussed in terms of through-space and through-bond interactions which may mutually influence each other. Figure 5 illustrates the interpretation of the $a_{H4}$ values in bicyclo[2.2.1]hex-1-yl **6** and bicyclo[2.2.2]oct-1-yl **9** as a combination of through-bond and through-space terms[27c]. Orbital interactions of this type should be measurable using PE spectroscopy, *e.g.* in the diamine 1,4-diazabicyclo[2.2.2]octane **10**.

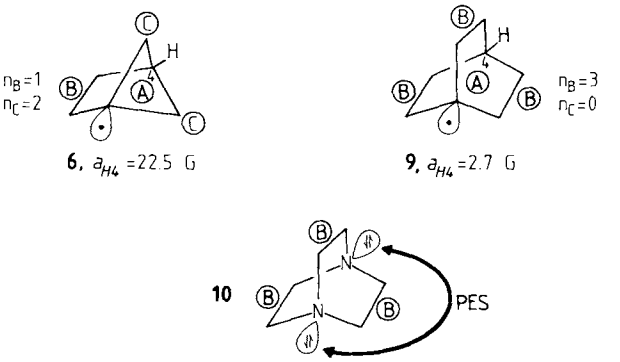



Fig. 5. Spin delocalization in bridgehead radicals [27c, f].
$a_{H4} = (A - n_B B + n_C C)^2$
A: "through space"; B: "through 3 bonds"; C: "through 2 bonds".
The coupling routes A and C amplify each other in **6**. Routes A and B compensate each other in **9**. The analogous interaction between the electron lone-pairs of both N atoms in **10** can be measured by PE spectroscopy [218].

## 2. Nomenclature and Terminology

The following is a description of some concepts which are important in proximity effects. They are not, however, always used in a consistent manner.

*Homoconjugation:* This denotes the through-space interaction between π-bonds that are separated from each other by formal isolators, such as $(CH_2)_x$. The concept was derived from observations made on the cholesteryl system and the cyclobutenyl cation[29]. Compounds **4** and **7** represent further examples of homoconjugation.

*Transannular Conjugation:* This has been used to describe homoconjugation involving π-overlap only[30]. It is only one extreme of the more general phenomenon of homoconjugation.

*Homoaromaticity:* Homoaromatics are cyclic $(4n+2)$ π-systems interrupted in one or more places by saturated centers, but whose geometry is such that overlap of the p orbitals is maintained across the formally isolating gap[29c-e]. Classical examples of homo-, bishomo-, and trishomoaromatics are found in the chemistry of carbocations. Homoconjugative interactions in neutral closed-shell systems seem, with possibly only a few exceptions[31d], to lead to destabilization[31a]. This homoaromatic conjugation also plays no role in mono- or bicyclic anions[31b,c]. Only in cations is the energy difference between the low-lying LUMO and a HOMO of the proper symmetry sufficiently small. The same holds for bicycloarenes[32].

*Hyperconjugation:* This expression, coined by *Mulliken*[33], describes the overlap of suitably oriented σ-bonds ($CH_3$, $CH_2$, C–C) with π-systems (*e.g.* the π*,σ interaction shown in Fig. 1). Hyperconjugation is important in stabilizing conformations of ions[34,35], and hence also in PE spectroscopy.

*Homohyperconjugation:* Whereas hyperconjugation can be comprehended as a β- or a 1,2-vicinal effect (Fig. 1), homohyperconjugation describes the corresponding γ- or 1,3-through-space effect[36a]. Experimental evidence has been obtained from ESR[28a,36b,c], PES[37a,b], and electron transmission spectroscopic studies[38].

*Through-Space and Through-Bond Interactions:* These involve homoconjugative and multiple hyperconjugative interactions, respectively[9].

*Spiro-, Lati-, and Longicyclic Conjugation:* These terms characterize topologies formed by union of two or three polyene ribbons[32]. The interaction between the π units in these polycycles is composed of homo- and hyperconjugation.

*Subjacent Orbital Control:* This is an electronic factor which favors symmetry-forbidden concerted reactions[39a]. For example, the pericyclic transition state of the suprafacial 1,3-sigmatropic shift can be electronically stabilized by participation of the $\psi_1(S)$ allyl orbital.

*Superjacent Orbital Control:* n-Orbitals are repulsively destabilized by vicinal adjacent lower-lying C–H σ-orbitals

$$E_{\text{repuls}} \approx 2 \cdot S^2 (E_n + E_\sigma) - 4 S H_{n\sigma}$$

higher-lying C–X σ*-orbitals (X = Cl, OR, *etc.*) stabilize attractively[39b]

$$E_{\text{attract}} \approx 2 (H_{n\sigma^*} - S \cdot E_n)^2 / (E_n - E_{\sigma^*})$$

$S$ = overlap integral, $H$ = interaction parameter

This results in a preference for conformations in which the n- and σ*-orbitals are nearly eclipsed. The *anomeric effect* may be rationalized in this manner[40].

*σ-Conjugation:* This concept was developed to describe the 1,2-vicinal conjugation of a vacant p-orbital with a σ-bond without bridging[18,41]. This is a special case of hyperconjugation. The cyclopropylmethyl cation is a particularly interesting and problematic example: a change in the bond lengths leads to stabilization over and above normal hyperconjugation[19,42].

*σ,π-Conjugation and Vertical Stabilization:* Polarizable σ-bonds stabilize neighboring cationic centers without leading to a change in bond lengths and bond angles[43]. This, too, is a case of hyperconjugation for which the more fitting description "vertical stabilization" is used. Since these interactions are important in all Franck-Condon processes, they will also be of importance in PE spectroscopy.

π-Conjugation: The classical $p_\pi p_\pi$-conjugation in the allyl cation, for example, is the result of allylic overlap of a vacant cationic p-orbital with a double bond[18].

*n-, σ-, π-, and π,σ-Participation:* Reactive centers can be stabilized in a non-vertical manner by homoconjugated n- or π-orbitals or by appropriate σ-bonds. Bridging and/or rearrangement may result[17-19,41]. *Neighboring group participation* can be defined by the nature of the electrons involved, that of the participating group, and the size of the ring formed in the transition state, *e.g.* n-$NH_2$-5-participation[19].

*Perpendicular Conjugation:* This is a type of homoconjugation in which the participating p- or π-orbitals form a more or less perpendicular structure. This kind of conjugation is realized in some polycycles or propellanes[44].

*Non-Bonding Interactions:* Attractive dispersion forces, repulsion between electron shells, and electrostatic interactions can occur between non-bonded atoms. Non-bonding interactions (potential: $V_{nbi}$) play a significant role in aliphatic compounds, alicycles, and biopolymers[3,45-49]. The following heading describes a different type of non-bonding attraction.

*Steric Attraction:* The stabilizing two-electron interaction

$$\Delta E = 2 (H_{ij} - S_{ij} \cdot E_i)^2 / (E_i - E_j)$$

can also occur between atoms not bonded directly with each other provided the wave functions are of appropriate phase[5,50].

*Supraannular Effect:* Axial electron-withdrawing substituents in the 4-position in cyclohexenes purportedly interact electronically with the π-bond. It is doubtful whether such an effect exists[51].

*cis-Effect:* This term covers the higher stability of many *cis*-disubstituted ethylenes compared with their *trans*-isomers (see Section 1.3.1)[5,10-15].

*Circumannular Conjugation:* This describes the interaction between oppositely situated π-centers across an interposed $CH_2$ group, and is especially evident in four-membered rings. It is a hyperconjugative effect which is distinct from the direct transannular homoconjugation[52a-d].

*The Frangomeric Effect:* This refers to an increase in reactivity due to synchronous fragmentation[52e].

*Nonequivalent Orbital Extension:* π-Orbitals can rehybridize and distort unsymmetrically under the influence of neighboring σ-orbitals, for example. The geometry of the molecule is altered by the tilting of the π-orbitals[52f].

*π-Electron Steric Effect:* This effect describes the axial-equatorial equilibrium in 1-methoxy-3-(methylene)cyclohexane as a result of dipole-dipole and orbital interactions[52g].

## 3. Method

Reviews on photoelectron spectroscopy at various levels[53-60] as well as monographs for further study[61-66] are available. The uninitiated reader is advised to study the following references in the sequence given: [56, 58, 59]→[53, 54]→[62, 63].

### 3.1. Vertical Ionization

Photoelectron spectroscopy allows the experimental determination of vertical ionization energies $IE_v$, more rarely adiabatic ionization potentials. In vertical ionization occuring on a time scale of *ca.* $10^{-15}$ s, the internuclear distances remain unchanged during the transition and the process can be represented by a vertical line in a plot of the potential energy against nuclear separation. The vertical ionization energy is of importance in the discussion of proximity effects for two reasons. Firstly, it allows a determination of orbital energies using Koopmans' approximation (see Section 3.2). Secondly, chemists are normally interested in interactions concerning the neutral non-ionized ground state. Hence, if one wishes to obtain information on the neutral ground state from the radical cation, it is sensible to examine a radical cation in which the geometric parameters such as internuclear distances and bond angles have remained constant. This is the "vertical ion". The vertical ionization potential $IE_v$ corresponds to the distance between the potential curves for the molecule and the ion at the nuclear configuration $R$ at which the lower curve exhibits its minimum. The value of $IE_v$ is usually determined from the maximum $E_{max}$ of the PE band. This is, however, not entirely correct: it is better to take the centroid $E_{cg}$ of the band[62,67]. Thus, for example, $E_{max}$ of the second band of $N_2$ lies at 16.91 eV, whereas $E_{cg}$ is 17.02 eV[67].

In connection with proximity effects, the value of $IE_v$ is of importance as a measure of *vertical stabilization* (cf. Section 2)[19,43]. According to *Traylor et al.*, a substituent stabilizes a developing positive center vertically if the geometry remains invariant upon approaching the transition state. Otherwise, the stabilization is said to be non-vertical. Thus σ,π-hyperconjugation is a vertical stabilization; however, bridging is a non-vertical stabilization. Therefore, if substituent effects on rates of reaction are found to correlate with the ionization energies $IE_v$ (or with the frequencies of charge-transfer bands), this is a clear indication of vertical stabilization in the transition state[68]. Tetraazatricyclo[4.4.1.1$^{4,9}$]dodecane **11** offers an instructive example of the difference between vertical and non-vertical radical ions (Fig. 6)[69]. If the PE spectrum of **11** ($D_{2d}$ symmetry) is analyzed in terms of vertical ionization in the gas phase, the orbital structure obtained is that of a $D_{2d}$ ion of the same geometry. The unpaired electron in this ion occupies a $b_2$-HOMO. However, if the $D_{2d}$ ion is generated in solution, it undergoes distortion to a $C_{2v}$ ion, which has roughly the same energy, but is more strongly solvated because of the presence of a transannular three-electron σ-bond between the two N atoms. This equilibrating $C_{2v}$ ion $\mathbf{12}^{\oplus}$ can be detected by ESR spectroscopy (Fig. 6). Only the "vertical" $D_{2d}$ ion can give information on the proper-

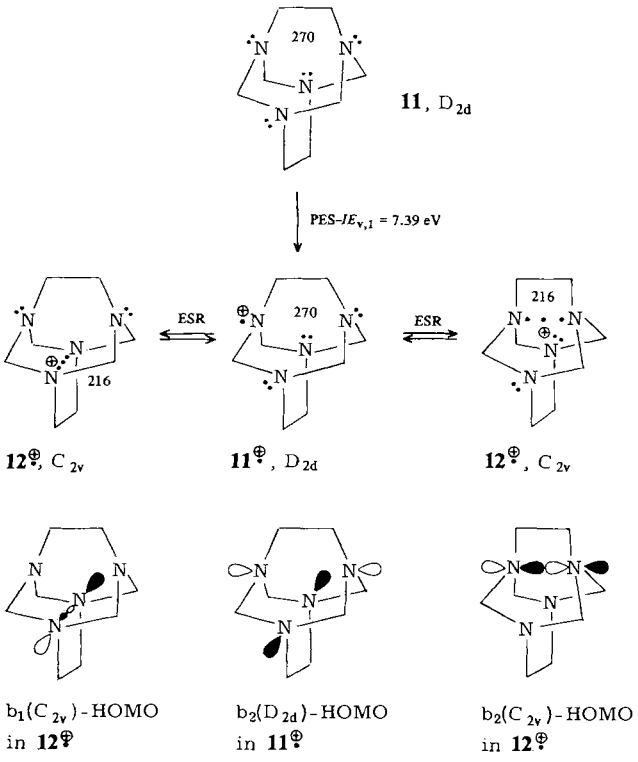
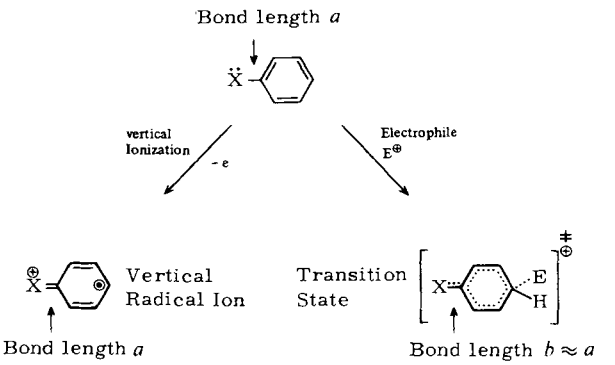



Fig. 6. Vertical and non-vertical ionization of **11**. NN distances (MINDO/3) in pm [69]. PE ionization gives $\mathbf{11}^{\oplus}$, $D_{2d}$; $\mathbf{12}^{\oplus}$, $C_{2v}$, is more stable in the condensed phase.

ties of the ground state ($D_{2d}$ symmetry) of **11**, *e.g.* the magnitude of the transannular overlap. Vertical ionization energies can also yield information on how substituents influence the reactivity of a particular system. That the vertical $b_1$ ionization energies of substituted benzenes $C_6H_5X$ correlate with the substituent constants σ indicates that at least a sizable part of the stabilization of the transition state by the substituent is of a vertical nature; accordingly, no significant geometrical change should occur[43,70].




### 3.2. Use of Koopmans' Theorem

According to Koopmans' theorem[71], the negative SCF orbital energies, $-\varepsilon_k^{SCF}$, for a closed shell molecule equal—to a first approximation—the vertical ionization energies:

$$-\varepsilon_k^{SCF} = IE_{v,k}$$

In this approximation the ionic state is described in terms of the molecular orbitals pertaining to the ground state. Both electron correlation and electron reorganization are neglected. The reliability of the approximation is usually due to cancellation, to a certain extent, of the two effects. The assignment of orbital energies to the ionization energies is a prerequisite for the use of PE spectroscopy to study neighboring group effects and requires, therefore, that Koopmans' theorem be valid. This approximation can be used for the valence electrons in connection with conformational analysis. No difficulties are expected, even in the case of highly localized orbitals capable of reorganization, as long as the nature of the orbital is not influenced by a conformational change[4]. In order to be of use in the study of proximity effects, the relevant orbitals must have so-called Koopmans' defects of the same sign and magnitude. The Koopmans' defect $\Delta K$ is defined as the difference between the *ab initio* Hartree-Fock orbital energy $\varepsilon_k^{ai}$ and the experimentally determined vertical ionization energy $IE_{v,k}$[71c]:

$$\Delta K(k) = -(\varepsilon_k^{ai} + IE_{v,k})$$

Koopmans' defects concern both π- and σ-orbitals, as is clearly seen from $F_2$ and $N_2$; in both cases the theorem is invalid. These two molecules are excellent candidates to provide an explanation for the defects by means of symmetry arguments. If, for example, in $F_2$ only the three highest occupied orbitals, $1\pi_g$, $3\sigma_g$, and $1\pi_u$, together with the LUMO, $3\sigma_u$, are considered, $\Delta K$ is described by the following dominant term[71d]:

$$\Delta K_i = [V_{ijkl}^2 + V_{ijlk}^2 + (V_{ijkl} - V_{ijlk})^2]/(\varepsilon_i + \varepsilon_j - \varepsilon_k - \varepsilon_l)$$

Here, i denotes the orbital to be ionized ($1\pi_g$, $3\sigma_g$, or $1\pi_u$), j the unoccupied orbital $3\sigma_u$, and k and l the other two occupied levels. $V_{ijkl}$ symbolizes $\langle\varphi_i(1)\varphi_j(2)|r_{12}^{-1}|\varphi_k(1)\varphi_l(2)\rangle$, and $\varepsilon$ denotes the orbital energy. The magnitude of the integral $V_{ijkl}$, which can be estimated using relatively simple symmetry arguments, determines $\Delta K$. The Koopmans' defects of the occupied orbitals in $F_2$ are shown in Figure 7. Although Koopmans' theorem may be expected to be valid

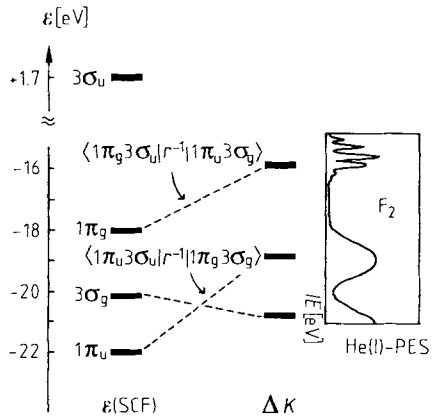



Fig. 7. Invalidity of Koopmans' theorem for $F_2$ [71c, d]. $\varepsilon$(SCF): *ab initio* orbital energy, $\Delta K$: Koopmans' defect. The important contributing integrals are indicated for the large defects from $1\pi_g$ and $1\pi_u$.

for the range of valence electron energies of interest here[71h], exceptions are known. These include formamide[66, 71h, i], acrolein[66, 71l–n], and nitrosomethane[71o–p] (Fig. 8). It is instructive, therefore, to examine the Koopmans' defects of valence electrons in some groups relevant to proximity effects: *cis*-1,2-difluoroethylene, **1a**, glyoxal, **13**, diazene, **14**, cyclopropane, **15**, norbornadiene, **7**, formamide, acrolein, and nitrosomethane. Proximity effects occur in some of these examples: 1,4-n,n-interactions are operative in **1a** and **13** and 1,3-π,π-interactions occur in **7**. Three-membered rings and azo groups are interesting partners for neighboring group effects. Figure 8 illustrates calculated and measured ionization energies, as well as the

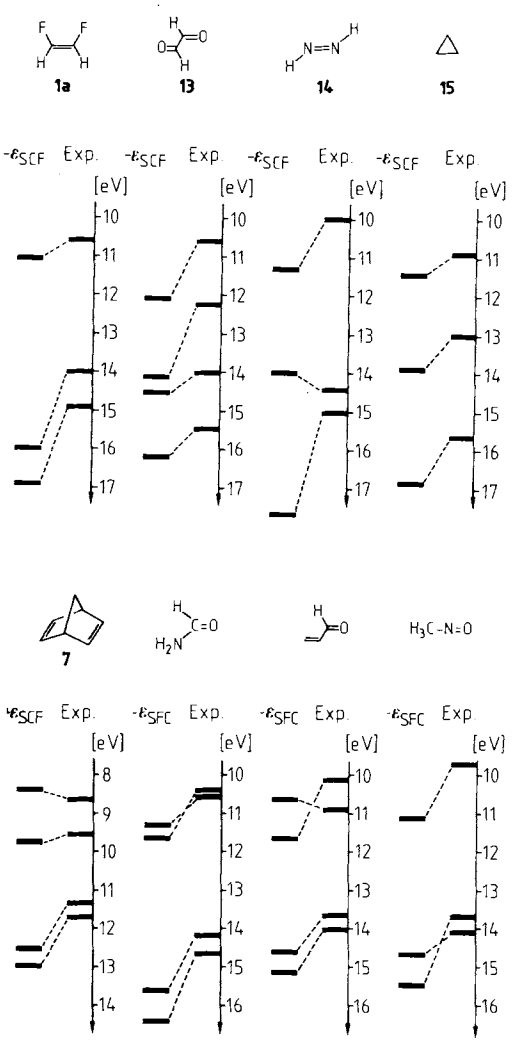



Fig. 8. Koopmans' defects for valence electrons: **1a** [71j], **13** [72a], **14** [72b], **15** [71c], **7** [72c], formamide [66, 71h, i], acrolein [71l–n], and nitrosomethane [71o, p]. As a rule, Koopmans' approximation may be assumed to be valid for molecules of this type in this energy range. Exceptions: formamide, acrolein, and nitrosomethane.

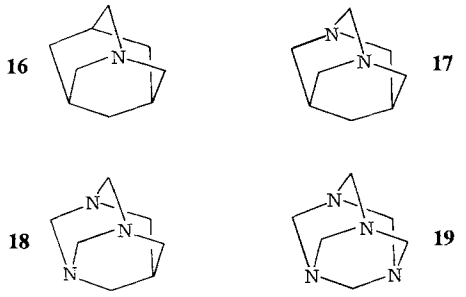
corresponding Koopmans' defects. Despite often sizable $\Delta K$ values, the sequence is usually maintained: a crossover is rarely observed for molecules of this type in this energy range. Rule of thumb[71k, o]: if in linear or planar molecules a low-lying π(σ) virtual orbital and a π(σ) occupied valence orbital exist, significant corrections to the valence ionization energies of σ(π) orbitals may be expected.

## 4. Interactions of the X,X-Type

### 4.1. n,n-Interactions

#### *4.1.1. 1,3-n,n-Interactions*

For geometrical reasons, 1,3-n,n-interactions may be expected in the azaadamantanes **17**—**19**.




The analysis will start with the monoamine **16**, in which the ionization energy of the nitrogen lone pair $IE_{1,v}=7.95$ eV[73,74]. In **17**, two effects caused by the second nitrogen atom need to be considered: a) the inductive or polar effect, which is associated with the electronegativity, and b) direct overlap of n-orbitals.

The inductive effect causes a *stabilization* of the average

$$\overline{IE_v(n)}=\frac{1}{m}\sum IE_{v,i}(n)=A_n$$

similar to that in azaarenes[77]. This can be interpreted as a stabilization of the n-basis orbital energies:

$$\Delta\overline{IE_v(n)}=\Delta A_n=\frac{1}{m-1}[A_n(\text{poly(m)azaadamantane})-A_n(\text{mono-azaadamantane})]$$

(m=2, 3, 4)

From the ionization energies $IE_v(n)$ the following values of $\Delta A_n$ are obtained for compounds **16**—**19**, respectively: 0.32, 0.37, and 0.47 eV. This inductive influence of n(N)-orbitals, which is in general possible for all polar groups, can be quantitatively correlated with the inductive substituent constants. The quinuclidine moiety has been the subject of detailed studies which show that the ionization energies are altered over a distance of three σ-bonds (or through space in the interior of the cage) by substituents in position 4 (Fig. 9)[78].

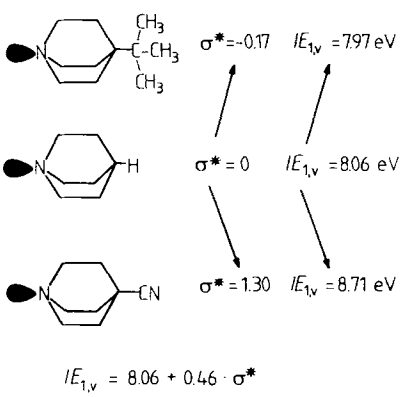



Fig. 9. Ionization energy as a function of inductive substituent constants using quinuclidine as an example [78].

Further analysis requires either the introduction of an interaction parameter $H_{nn}=\langle n_1|H|n_2\rangle$, obtainable either theoretically or from experimental data, or by direct evaluation of empirical $H_{nn}$ values from the observed spectrum (Fig. 10). It should be noted that the value of

$$H_{nn}=\langle n_1|H|n_2\rangle=1/2(IE_{v,1}(\mathbf{17})-IE_{v,2}(\mathbf{17}))=-0.52\,\text{eV}$$

obtained in this manner may, in principle, be a composite of several effects, even if only the direct overlap was taken into account in Figure 10.

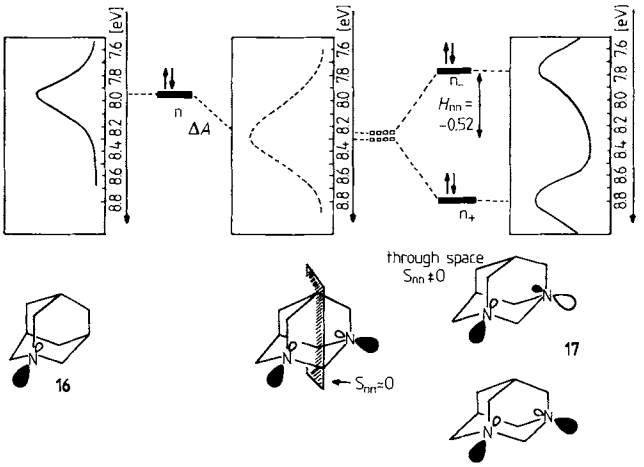



Fig. 10. 1,3-n,n-Homoconjugation in **17** as a consequence of inductive stabilization $\Delta A$ and direct overlap ($S_{nn}\neq 0$) [73—76]. The fictive spectrum in the center is for $S_{nn}=0$ and without through-bond coupling.

For the triazaadamantane **18** ($C_{3v}$ symmetry) two bands separated by $3\times 0.52=1.56$ eV are expected using this value of $H_{nn}$; furthermore, the intensity of the first band should be about twice that of the second. This expectation is confirmed by the PE spectrum of a methyl derivative[73] for which a separation of 1.8 eV was found, in surprisingly

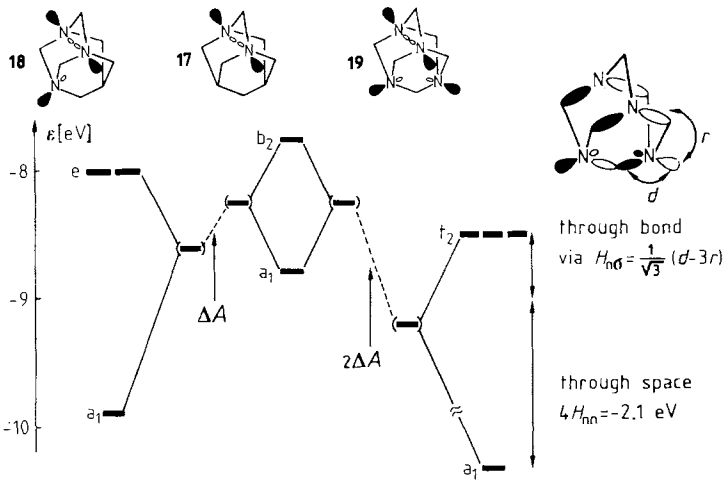



Fig. 11. 1,3-n,n-Interactions in di-, tri-, and tetraazaadamantanes **17**—**19** [73—76]. The energies correspond to experimental ionization energies. Levels in parenthesis represent estimated basis energies of the n-electrons. $\Delta A$: inductive effect. Through-bond coupling is described using equivalent orbitals (EO) [76, 79].

good agreement with the prediction (Fig. 11). Finally, the last member of this series, the tetraazaadamantane **19**, is interesting because of its high symmetry ($T_d$). Using the same value of $H_{nn}$ as for **18**, two bands with relative intensities of *ca.* 3 : 1, separated by $4H_{nn} \approx 2.1$ eV are predicted (Fig. 11). The observed band separation of at least 3.6 eV indicates the occurrence of additional interactions and, at the same time, illustrates the limits of the naive treatment. One effect ignored so far is the through-bond[9] interaction between n(N)-orbitals and interposed σ-bonds. It is, therefore, indicated in Figure 11 how such mixing with σ-levels of the same symmetry can lead to an increased $t_2$-$a_1$ separation.

### *4.1.2. 1,4-n,n-Interactions*

In Section 1.3.1 it was shown that non-bonding interactions in **1** might also be observable in the PE spectrum. Corresponding predictions for the orbital energies of **1a** and **1b** have been made[80]. Somewhat surprisingly, however, the spectra of **1a** and **1b** are extraordinarily similar and can hardly be distinguished within the limits of experimental error[71j]. The similarity is reproduced both by HAM/3 and GF calculations. Nevertheless, *ab initio* calculations[10,80] confirm that steric attraction may be expected as a result of charge transfer from the $n_a$- to π*-orbital: a positive F,F-π overlap population is computed[79]. Considerable 1,4-through bond couplings between the n-levels and the interposed π- or σ-orbitals associated with the C—C bond are found. Difluoro- and dibromoolefins show an interesting difference (Fig. 12): whereas in **1a** mixing with the C—C σ-bond leads to the sequence $a_1$ above $b_2$, in *cis*-dibromoethylene **20a** direct homoconjugation dominates with the result that the level ordering is now $b_2$ above $a_1$[81]. This through-space coupling disappears in the *trans*-isomer **20b**: the two levels ($a_g$, $b_u$) are now degenerate.

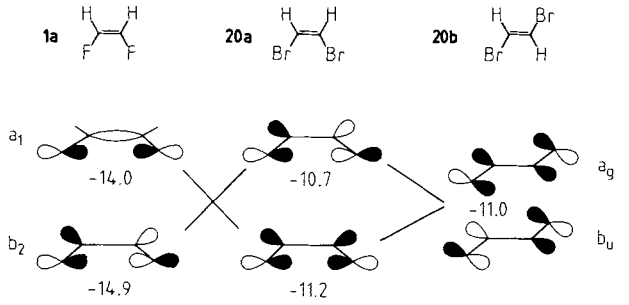
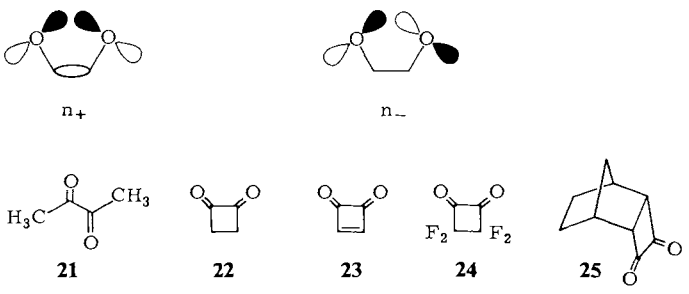



Fig. 12. Interplay between 1,4-n,n-through-bond coupling and direct 1,4-n,n-homoconjugation in difluoro- and dibromoethylene [71j, 81]. Energies in eV.

1,4-n,n-Interaction in α-dicarbonyl compounds is of particular importance, since it is closely associated with their color[20-22,82-93]. This is exemplified by the four-membered ring α-diketones **22**—**25**[85-91] (Table 1). A splitting $\Delta n \approx 2.2 \pm 0.3$ eV is found for all the diketones **21**—**25**, which can be considered as a measure of comparable 1,4-n,n through-bond coupling. Accordingly, other reasons must be found for the drastic color differences between these compounds: in **23** destabilization of $\pi^*_{CO}$ by $\pi_{CC}$[89], in **24** a larger inductive lowering of $\pi^*_{CO}$ than of $n_+$[90,91,99],




and in **25** a raising of the $n_+$ level by the inductive effect of the alkyl group[88].

Table 1. 1,4-n,n-Coupling in α-diketones. Different $n_+ \pi^*_+$ transition energies are found in spite of comparable n,n-interactions. This is due to several different effects.

| | **21** | **22** | **23** | **24** | **25** |
|---|---|---|---|---|---|
| $IE(n_+)$ [eV] | 9.55 | 9.61 | 9.79 | 10.45 | 8.85 |
| $IE(n_-)$ [eV] | 11.46 | 11.71 | 11.87 | 13.04 | 10.90 |
| Δn | 1.91 | 2.10 | 2.08 | 2.59 | 2.05 |
| $\lambda_m(\varepsilon) n_+ \pi^*_+$ [nm] | 417(9) | 487(53) | 340(20) | 645(17) | 533(91) |
| Color | yellow | yellow | colorless | blue | red |
| Ref. | [84] | [85, 86] | [86, 89] | [90, 91, 99] | [88] |

### *4.1.3. 1,5-n,n-Interactions*

1,3-Diketones and their tautomeric enols exist in equilibrium, which is markedly influenced by the solvent. The PE spectrum of 2-methyl-1,3-cyclopentanedione **26** is shown schematically in Figure 13[94]. The two tautomers

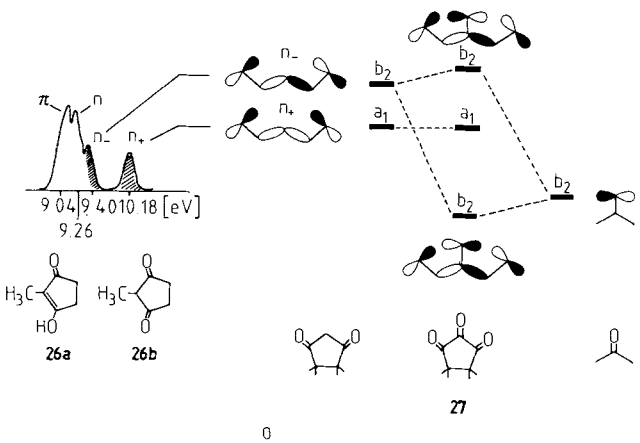



Fig. 13. Keto-enol equilibrium and PES of **26**. Hatched bands belong to **26b** [94]. The orbital sequence $n_- > n_+$ is confirmed by comparison with **27** [95].

give rise to four bands; the enol form dominates, and its two highest occupied MO's (π,n) have almost identical energies. The observation of two n-*IE*'s for the diketone is of interest: this arises from a 1,5-n,n coupling over the four σ-bonds[83,91]. The orbital sequence, $n_- > n_+$, could be elucidated by comparison with the tricarbonyl compound **27**[95].

*Peri*-substituted naphthalenes are examples of molecules with intramolecular steric hindrance resulting in exceptional properties. 1,8-Bis(dimethylamino)naphthalene, **28**, ("proton sponge") has a $pK_a$ value of 12.34 and is thus

more basic than normal aliphatic amines. This can be ascribed to a lowering of the strain energy on protonation. The PE spectrum of **28** demonstrates that an n,n-repulsion between the somewhat twisted amino groups is also present (cf. Fig. 14)[96]. The larger $n_-/n_+$ splitting in **28** relative to that in **29** is remarkable, as is the fact that not only direct homoconjugation but also through-bond interaction with lower lying naphthalene σ-orbitals of appropriate symmetry are responsible for this splitting.

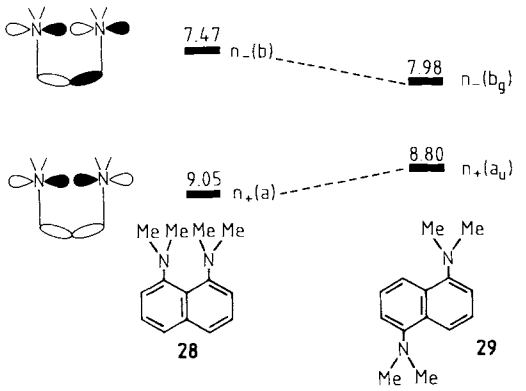



Fig. 14. Simplified representation of 1,5-n,n-repulsions in **28** and **29**. In reality the system is twisted and a clean σ-π separation cannot be expected [96] ($C_2$ conformation in **28**. The large splitting in **28** is the combined result of homo- and hyperconjugation which separate in the same direction.

### 4.1.4. 1,6-n,n-Interactions

The PE spectrum of *p*-benzoquinone **30** has been the subject of considerable discussion[82,97]. The first four ionization energies of **30** are ascribed to two n- and two π-orbitals. Depending on the assignment, a value of at least 0.07 eV and at most 1.01 eV is obtained for the 1,6-n,n-coupling. If the first two bands are described as $n_-(b_{3g})$ and $n_+(b_{2u})$, respectively[97a,c] a n,n-splitting of 0.30 eV is obtained, whose absolute value compares well with that found for the three diketones **31**—**33**[97d,98,99]; however, the sign of the splitting remains uncertain (*i.e.*, $n_+ > n_-$ or $n_- > n_+$, Fig. 15). It is, in principle, possible that a purely electronic model with its associated orbital sequence fails to give an adequate description of *p*-benzoquinone, and that vibronic coupling between the states may have to be taken into account because of the small splitting between the ion states (PE bands). In addition, the geometry of **30** is not sufficiently well defined to allow sophisticated and costly calculations[97e].

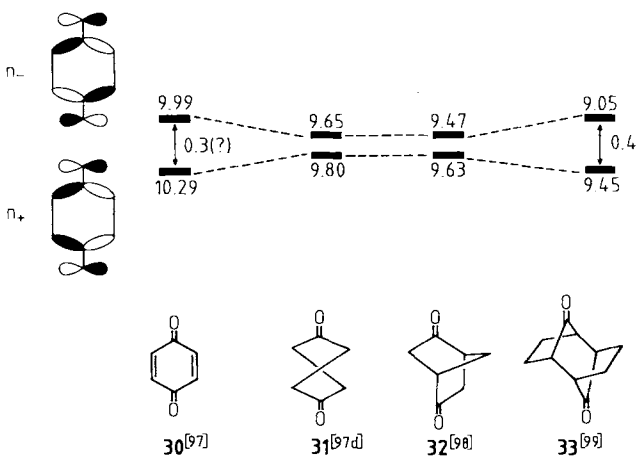
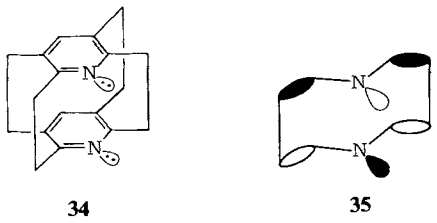



Fig. 15. 1,6-n,n-Interaction in γ-diketones. The size of the splitting in **30** and the sequences for **31**—**33** are uncertain. For fundamental difficulties in interpreting the PE spectrum of **30**, see text.

An entirely different topology for the 1,6-n,n coupling occurs in the diaza-phane **34**[100]. Its order of magnitude is 0.8 eV. The very small overlap integral $\langle n_1/n_2\rangle \approx 0.01$ signals the dominance of a through-bond mechanism, possibly occurring *via* **35**.




### 4.1.5. 1,7-n,n-Interactions

Bicyclo[3.3.0]octane-3,7-dione with $\Delta n = 0.33$ eV is the only δ-diketone to be described so far[91]. However, the tetraketone **36** was recently synthesized, and its dicarbonyl chromophore was found to exhibit an exceptionally large transannular $n_+/n_+$-coupling of 0.7 eV[87]. Since this interaction is also found in **37**, it is clearly a through-bond phenomenon. The cyclohexane σ-orbital of $b_2$-symmetry proves to be an effective transmitter. Although the $\pi_{CC}$-bond in **36** possesses the proper symmetry, it behaves as an effective insulator. The sensitivity of such σ-conjugations toward changes in the topology is shown by the bishomoadamantanetetraone **38**, in which the α-dicarbonyl groups are also separated by four σ-bonds, but whose topology is fundamentally different. No $n_+/n_+$-splitting greater 0.15 eV is observed in **38**. The σ-framework in adamantane does not possess any effective orbitals that could enable a clear discrimination between $1/\sqrt{2}(n_+ + n'_+)$ and $1/\sqrt{2}(n_+ - n'_+)$ (Fig. 16).

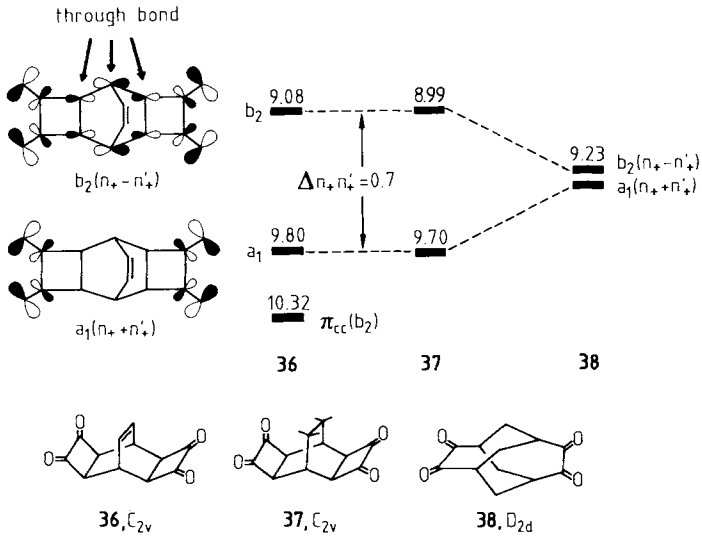



Fig. 16. Sizable 1,7-n,n-coupling *via* σ-bonds in **36** and **37**, as well as negligible n,n-conjugation in **38** [87] (experimental *IE*'s in eV). The calculated splitting, $\Delta n_+ n'_+ = 0.75$ eV (STO-3G), agrees well with the experimental value.

## 4.2. π,π-Interactions

### *4.2.1. 1,3-π,π-Interactions*

Since 1960 norbornadiene **7** has been a key compound for the study of transannular interactions[26]. The transannular conjugation of the two π-bonds is evident from the chemical[101], photochemical[102], and UV spectroscopic[20,103] properties. Norbornadienes have been proposed as reservoirs for storage of solar energy[102b,c]. Only limited information is obtainable from the UV spectrum; however, clearer results are provided by photoelectron spectroscopy[104], electron impact spectroscopy[105], circular dichroism[25a], and electron transmission spectroscopy[106]. Such studies have not only allowed an experimental determination of the theoretically predicted orbital energy differences (Fig. 17), but also, using **39** and **40** as reference compounds, of the sequence in **7**. This relies on the fact that in **40** the exocyclic π-bond must necessarily have $b_1$ symmetry; in **39** this orbital mixes only with the highest lying π-orbital of **7**, thereby defining the symmetry of the latter as $b_1$.

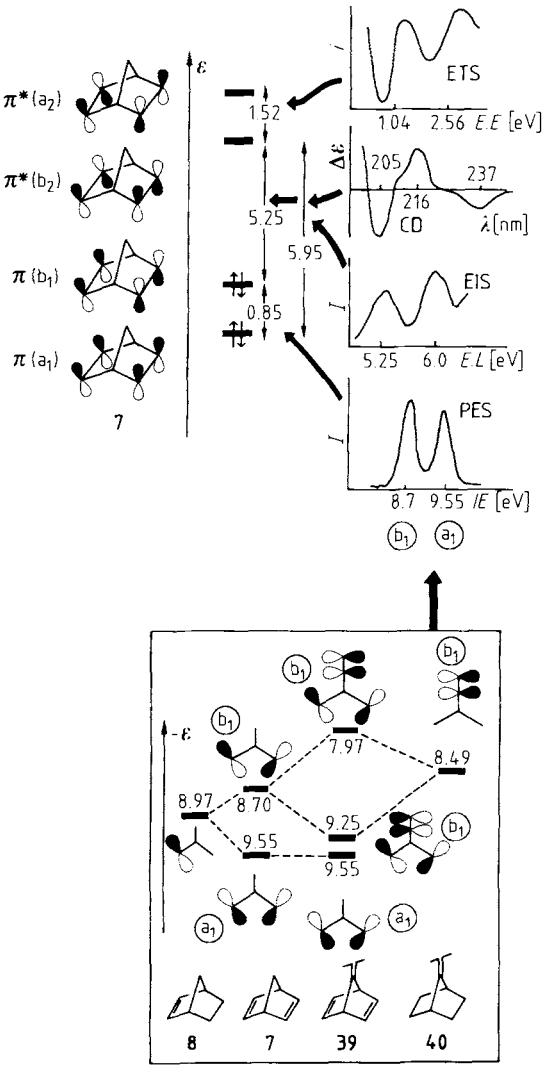



Fig. 17. Orbital energy differences in norbornadiene **7** obtained by different methods. PES: photoelectron spectroscopy [104]; EIS: electron impact spectroscopy (*E.L.* = energy loss) [105]; CD: circular dichroism [25a]; ETS: electron transmission spectroscopy (*E.E.* = electron energy) [106]; (I = intensity, i = current). Energies in eV. The orbital sequence $b_1 > a_1$ in **7** can be established with the aid of compounds **39** and **40**: only the higher orbital in **7** mixes with the exocyclic π-orbital $b_1$, the energy of which is known from the spectrum of **40** [104a].

The experimental spectrum is reproduced exactly by *ab initio* calculations which take reorganization and correlation effects (see Section 3.2) into account. The calculations also provide an independent confirmation of the assignment made on the basis of **39**, and at the same time demonstrate the validity of Koopmans' theorem in **7** (see Fig. 8)[72c]. Apart from thes direct homoconjugative 1,3-π,π-interactions in **7**, π,σ-hyperconjugations should also be considered. The fact that in 7,7-difluoronorbornadiene both the $a_1$ and the $b_1$ π-orbitals are stabilized by the F-effect, even although the latter orbital has a node at the bridge bond, demonstrates a σ-contribution[107]. The relay action becomes evident by determining which σ-orbitals ("precanonical") combine linearly with the π-orbitals to give the canonical orbitals. Figure 18 shows the two relevant relay

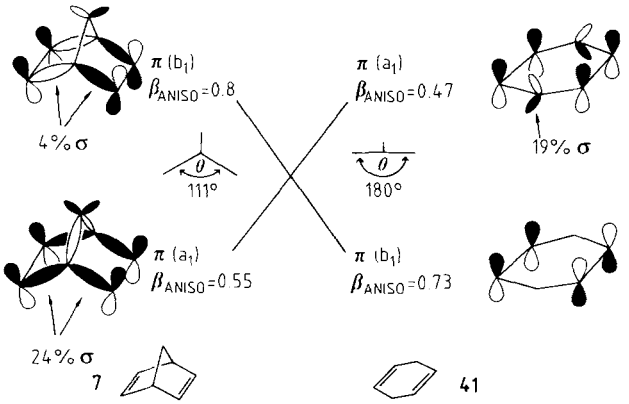


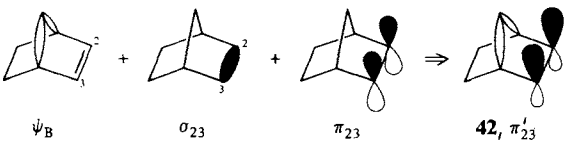

Fig. 18. Through-bond interactions in **7** and **41** within the concept of relaying σ-orbitals, and their dependence on the dihedral angle θ. Note that in **7** ($\theta = 111°$), not only $\pi(a_1)$, but *also* $\pi(b_1)$ experiences σ-coupling. In 1,4-cyclohexadiene **41**, in contrast, only $\pi(a_1)$ can mix with a precanonical $\sigma(a_1)$ for symmetry reasons. Consequently, the orbital sequence changes from $b_1 > a_1$ to $a_1 > b_1$ [9, 107–109]. This assignment is supported by the anisotropy parameter $\beta_{ANISO}$ [112]; the value of β is higher for the antisymmetric than for the symmetric orbital.

orbitals, $\sigma(a_1)$ and $\sigma(b_1)$, as determined by SPINDO-calculations, together with their percent contribution to the π-orbitals. An important trend becomes apparent: as the dihedral angle flattens to 180°, $\pi(b_1)$ can no longer participate in σ-coupling for symmetry reasons, and, as a consequence, the orbital sequence is reversed ($a_1 > b_1$)[9, 107–109]. Chemical consequences of 1,3-π,π-homoconjugation in **7** and of hyperconjugation in **8** include a) the ready photocyclization to quadricyclane following excitation $\pi(b_1) \rightarrow \pi^*(b_2)$[102], b) homo-Diels-Alder reaction under the polarizing influence of a dienophile[110], and c) *exo*-stereoselectivity resulting from non-equivalent orbital distorsion of the inclined and now hybridized π-orbitals[52f,111].

The *exo*-hybridization was explained using perturbation theory

$$\pi'_{23} = \pi_{23} + a \cdot \sigma_{23} + b \cdot \psi_b (a > 0,\ b < 0)$$

as shown in **42**. However, calculations indicate that the out-of-plane bending angle of the C–H bond in **7** amounts to only 2.3°[52f].




1,3-π,π-Homoconjugation plays a fundamental role in homoaromatic systems (see Section 2). The interesting question whether homoaromatic stabilization and/or interaction between the π-orbitals occurs in the neutral homoconjugated 1,4,7-cyclononatriene **43** can be unambiguously answered[113]: neither bond lengths and bond angles nor enthalpies of hydrogenation give any indication of a ground state stabilization. On the other hand, the PE spectrum of **43** shows an appreciable splitting between the π(e) and π(a$_1$) levels[113a,249,268] (Fig. 19). The interaction

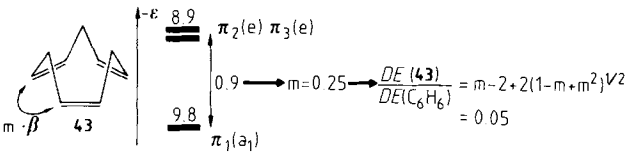
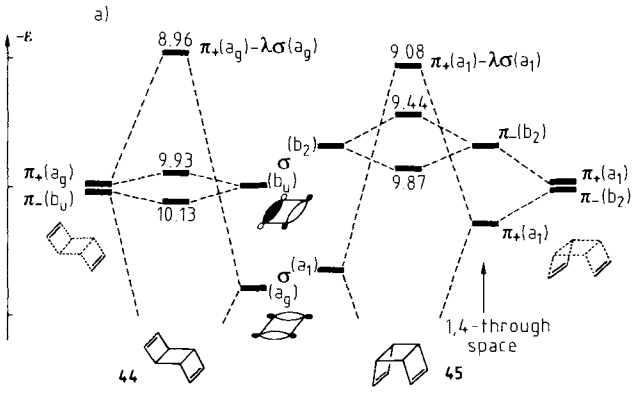



Fig. 19. Homoconjugation and homoaromaticity in **43**. A value $m = 0.25$ is calculated from the splitting, $\pi(e) - \pi(a_1) = 0.90$ eV, using $\beta = -2.4$ eV. Consequently, $DE(\mathbf{43}) = 0.05 \times DE$(benzene) [113a].

can be described by the resonance integral $\beta' = m \cdot \beta = 0.25\beta$, where $\beta$ represents the resonance integral of, *e.g.* butadiene ($\beta = -2.4$ eV). This gives a value of $\beta' = -0.60$ eV. A comparison of the delocalization energies ($DE$) in benzene and in **43** indicates why this appreciable 1,3-homoconjugation does not lead to ground state stabilization. For $m = 0.25$, the ratio $DE(\mathbf{43})/DE$(benzene) has the value 0.05, *i.e.* $DE(\mathbf{43}) \approx 1.8$ kcal/mol (in benzene, $DE \approx 36$ kcal/mol). This value is much too small to be detectable in view of the steric and conformational strain of the σ-framework in **43**[113a].

### 4.2.2. 1,4-π,π-Interactions

In analogy with the situation described in Section 4.1.2, 1,4-π,π-interactions are strongly dependent on topology. The *anti*-dimer **44** and *syn*-dimer **45** of cyclobutadiene provide instructive examples (Fig. 20). Although a change from pure through-bond coupling in **44** to mixed interaction in **45** is already evident from the form of the PE spectrum, the exact orbital sequences in these two compounds are a matter of dispute[107,114]. The interpretation given in Figure 20 extends the sequence given in [114a] inasmuch as it also considers mixing between the $\pi_-$-combination and a corresponding σ-orbital; this is similar to the situation in norbornadiene. According to HAM/3-calculations, and in contrast to previous conceptions, the extent of this mixing is not negligible (Fig. 20b). This analysis resolves some inconsistencies: the second and third levels in **45** are approximately first-order linear combinations of $\pi_-(b_2)$ and $\sigma(b_2)$, in which the relative π- and σ-contributions are markedly dependent on the geometry! The main consequence of the different topologies is that $\Delta E(\pi_+ - \pi_-) \approx 1$ eV in **44** and $\Delta E(\pi_+ - \pi_-) \approx 0.4$ eV in **45**.



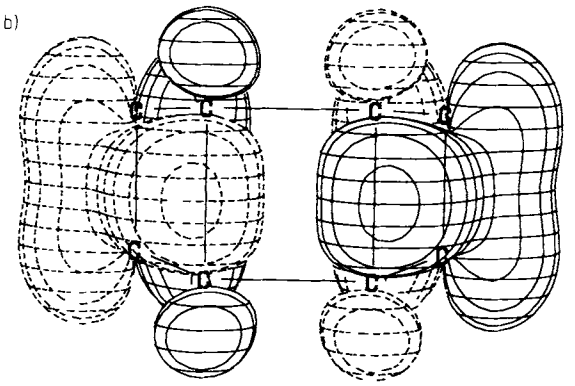




Fig. 20. a) 1,4-π,π-Interactions in **44** and **45** [114]. Qualitative interpretation according to the HAM model. The basis π-energies [114e] correspond to an inductively destabilized ethylenic π-bond. Different $\sigma(b_u, b_2)$ basis energies are obtained for **44** and **45** [114a]. The through-space homoconjugation amounts to *ca.* 0.6 eV. The sequences in **44** and **45** are in good agreement with the results of HAM/3 [114i] and MNDO calculations [114f] but are sensitive to the geometry. There is significant mixing of $\pi_-$ with $\sigma(b_u, b_2)$. Small changes in the geometry (MMI *versus* MMII calculations) result in differing π- and σ-contributions to the second and third orbitals in **44** and **45**. b) Second highest occupied orbital, $\pi_-(b_2) - \sigma(b_2)$ of **45** according to HAM/3 [114i] ($\varepsilon_{calc.} = -9.74$ eV; $\varepsilon_{exp.} = -9.44$ eV).

Whereas in **45** the π-orbitals overlap in a σ-manner, an interesting case of a pure 1,4-p,p-homoconjugation of the π-type is observed in **46**. However, the effect reveals itself only in the second lowest unoccupied orbital ($\pi_2^*$), and not in the occupied orbital ($\pi_2$)[115]. Consequently, electron transmission spectroscopy rather than its pendant, PE spectroscopy, is applicable. One suggestion for this is that the wave functions of anions are appreciably more diffuse and hence more sensitive to long-range effects than those of the neutral molecules or cations (Fig. 21).

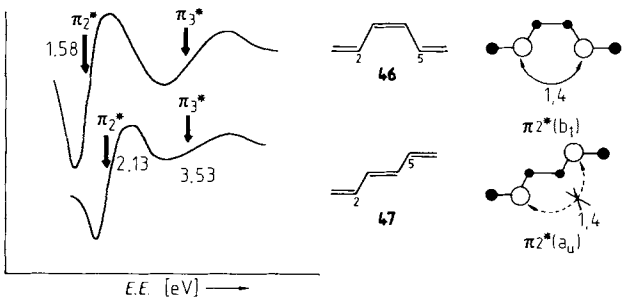



Fig. 21. 1,4-π,π-Interaction between C-2 and C-5 in **46**, measured from the electron transmission spectra of **46** and **47** [115] (*E.E.* = electron energy, *i* = current).

#### 4.2.3. 1,5-$\pi,\pi$-Interactions

The laticyclically conjugated dienyl cation **48** is of fundamental interest to an understanding of the factors which determine the chemical reactivities of dienols **49**[32,116]. Further information on long-range $\pi,\pi$-couplings in these systems may be expected from PE spectroscopic studies of the dienes **50**—**52** with isodrine and aldrine frameworks.




**48** **49**

However, the problem is complicated by the fact that the through-space and through-bond interactions do not operate in opposing directions as in **45**; rather, they are additive[9].

This leads to sizable splittings. The participating effects can, however, be partly separated[117,396] by analysis of the three topologies **50**—**52**. In **50** the symmetry-allowed $\pi$-combinations can *only* mix with $\sigma$-orbitals of the same symmetry (orbital interaction through four bonds, OIT-4-B[117d,e]). In **51** the 1,5-homoconjugation (through space) produces an additive effect[117a]. The two $\pi$-bonds in **52** are no longer symmetry-equivalent, so that the through-bond interaction deviates from that found in **50** and **51**[117] (Fig. 22).

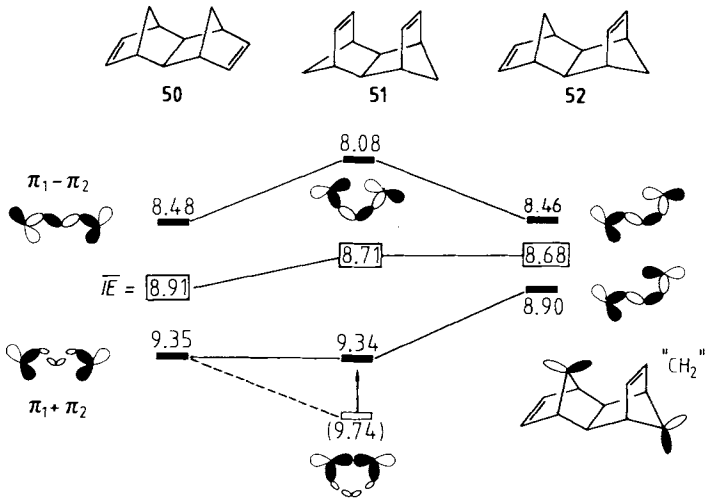



Fig. 22. Orbital interactions through four bonds (OIT-4-B) and 1,5-homoconjugation in **50**—**52** [117]. In **50**, $\pi_1-\pi_2$ is more highly destabilized by the $\sigma$-skeleton than $\pi_1+\pi_2$ (so-called depression effect) [117d, e]. Homoconjugation in **51** acts in concurrence; however, $IE_2$(**51**) is not found to be *ca.* 9.7 eV: rather, $IE_2$(**51**)$\approx IE_2$(**50**). The $\pi_1+\pi_2$ combination is more highly destabilized than in **50**, as also seen from the position of $\overline{IE}=(IE_1+IE_2)/2$ and from the band shape [117a]. This homoconjugation disappears again in **52**: the two non-symmetry-equivalent $\pi$-orbitals are closer together [117a]. Also the "$CH_2$" group has been proposed as a relaying $\sigma$-orbital in **52** [117f].

It is noteworthy that the mean $(IE_1+IE_2)/2$ for **50** is lower than for **51** and **52**. If only homoconjugation were of importance when going from **50** to **51**, one should expect $IE_2\approx 9.74$ eV. The decrease in $IE_2$ to 9.34 eV and that of the mean value to 8.71 eV can be interpreted in terms of an increased through-bond coupling with $\pi_1+\pi_2$. The band shape supports this interpretation: in **50** the second PE band is sharp and narrow, whereas in **51** it is just as broad as the first[117a,d]. This increased $\sigma$-coupling is maintained in **52**, as seen from the mean value, $\overline{IE}$; however, 1,5-homoconjugation is absent. As a result, $\pi_1-\pi_2$ is stabilized, and $\pi_1+\pi_2$ is destabilized by the same amount. It is also interesting to note that the $\sigma$-"$CH_2$"-orbital has been proposed to be responsible for the relay action in **52**; this is what one would intuitively expect because of the transannular strain[117f].

#### 4.2.4. 1,3-$\pi_{AB},\pi_{AB}$-Interactions

Homo- and hyperconjugation between bonds other than CC multiple bonds can only be adequately analyzed by PE spectroscopy if their ionization energies differ significantly from those of the $\sigma$-electrons. However, for $>C=O$, $-N=N-$, and other groups this is often not the case. More favorable situations occur if the number of $\sigma$-orbitals is kept small, or if the A=B bond is easily ionized. This is observed in malononitrile **53**[118] and tetramethyl-1,3-cyclobutanedithione **54**[119]. There is a surprising range of

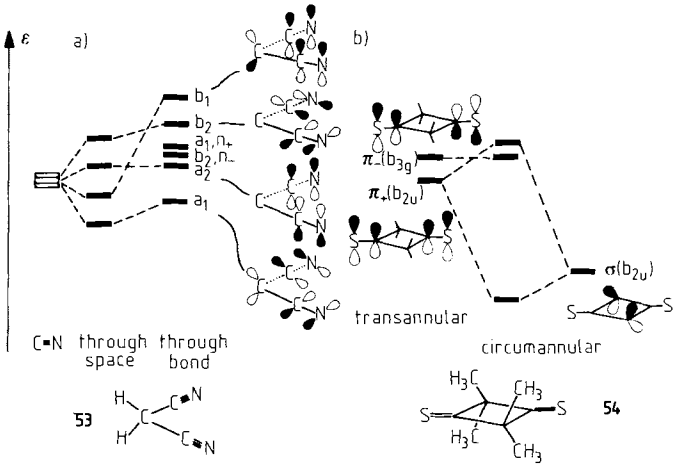



Fig. 23. a) 1,3-$\pi_{CN},\pi_{CN}$- and b) 1,3-$\pi_{CS},\pi_{CS}$-interactions in **53** [118, 310] and **54** [119]. The $\sigma$-contributions to $\pi(b_2)$ are omitted in a). The n-orbitals are not shown; their treatment would belong in Section 4.1.3.

possible interactions in **53**: $p_\pi p_\pi$ and $p_\sigma p_\sigma$ interactions represent 1,3-homoconjugations, $\pi$-$CH_2$-$\pi$ and $\sigma$-$CH_2$-$\sigma$ interactions are hyperconjugative, and the n,n-interaction is a through-bond coupling over four bonds (OIT-4-B). The resulting orbital sequence is given in Figure 23a. In **54** the $\pi$-orbitals are just discernable from the $\sigma$-levels and are split by 0.5 eV. However, in this case 1,3-circumannular hyperconjugation is more dominant than transannular 1,3-homoconjugation (Fig. 23b). This through-bond coupling between diagonal $\pi$-bonds in cyclobutane rings has been extensively studied in 1,3-dimethylenecyclobutane[52b] and trimethylenecyclobutane[52a] (cf. Section 2). It is also important for the interpretation of the UV spectrum of tetramethyl-1,3-cyclobutanedione[52c].

### 4.3. Arene, Arene-Interactions

The interactions between two nonannelated arenes or heteroarenes are fundamental, not only to an understand-

ing of the coupling between weakly interacting chromophores, their electron or energy delocalization[20,21], but also to the related thermodynamic preference for complex formation. The coplanar intercalation of heteroarenes such as proflavine, ethidium bromide, or quinacrine in the stacking of nucleic acid bases in DNA causes a hypochromic effect[20,23,24,120]. This hypochromism may be interpreted as a result of delocalization of the excitation energy. The effect is observable also in compounds like **4** in the "stacked" conformation[24]. It has been shown that the direct overlap of π-systems can also lead to hypochromism[23,121]. Effects of this type will be described below.

#### *4.3.1. 1,3-Arene, Arene-Interactions*

The topology of triptycene makes this system ideal for transannular homo- and hyperconjugation[122]. The effects will be similar to those in barrelene (bicyclo[2.2.2]octatriene)[123]. Furthermore, delocalization of energy upon electronic excitation of a benzene moiety may be expected. The ESR spectrum of tribenzotriptycene **55** shows interesting temperature dependence[124]. At 20 K the spectrum is very similar to that of naphthalene. At 77 K the two outer doublets disappear. This can be explained in terms of a thermally-activated transfer of excitation energy between the naphthalene moieties, *i.e.*, the excitation energy of a naphthalene unit is localized at low temperatures, at higher temperatures it delocalizes and the ESR signals are exchange-broadened (Fig. 24a). Electron delocalization is measurable in the PE spectrum of triptycene **56** (Fig. 24b).

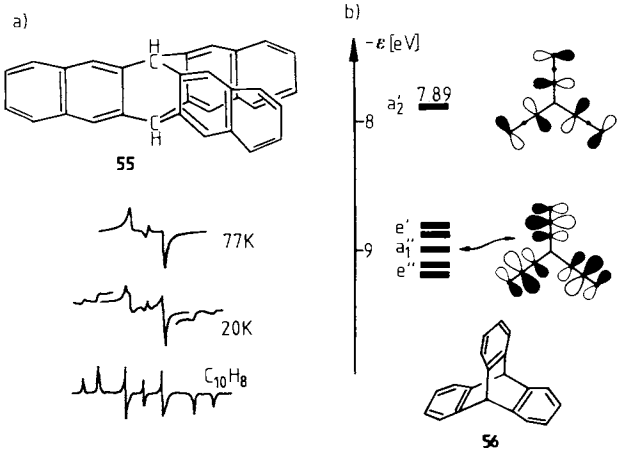



Fig. 24. a) Temperature-dependent ESR spectrum of **55** at 77 K with delocalization of excitation energy, and at 20 K with localized energy. ESR spectrum of naphthalene at 77 K is also shown [124]. b) Ionization energies of **56** assigned using a simple ZDO model [125]. 1,3-Homoconjugation causes a destabilization of $a_2'$ to 7.89 eV.

Here, the $a_2'$-level is more strongly destabilized than $a_1''$ by transannular 1,3-homoconjugation. The total electron delocalization (through-space and through-bond) is satisfactorily described by the ZDO model using an empirical interaction parameter

$$\beta_{ij} = \langle p_i | H | p_j \rangle = -0.55 \text{ eV}$$

for the 1,3-homoconjugation between the atomic orbitals[125].

#### *4.3.2. 1,4-Arene, Arene-Interactions*

[2.2]Paracyclophanes have been intensely studied because of their non-planar benzene rings, anomalous bond lengths and bond angles, and transannular π,π-interactions[126,127,131,317–320,367,409]. Significant 1,4-interactions can be expected because of the short intramolecular distance (270 pm) between the bridged carbon atoms in the two benzene rings of **57**. If 1,4-homoconjugation dominates in **57**, two PE bands would be expected to move toward lower ionization energies: these two bands would correspond to the antibonding combinations $\pi(b_{2g})$ and $\pi(b_{3g})$. Actually, three ionization energies were discernible in the first PE band[127]. A plausible reason is hyperconjugative destabilization of $\pi(b_{3u})$ (Fig. 25).

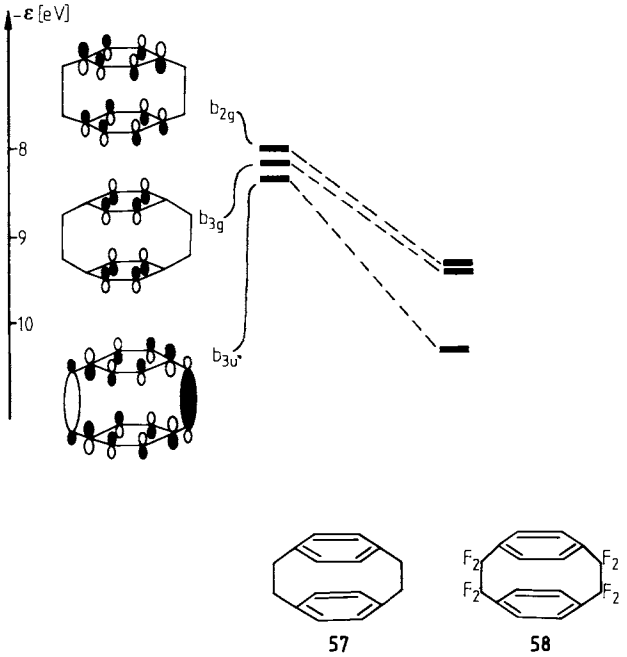



Fig. 25. 1,4-Homoconjugation and 1,4-through-bond interactions in **57** and **58**. In **57** destabilization results in similar ionization energies for $\pi(b_{2g})$, $\pi(b_{3g})$, and $\pi(b_{3u})$. In **58** hyperconjugation is suppressed by fluorine substitution, and $\pi(b_{3u})$ is lowered more than $\pi(b_{2g})$ and $\pi(b_{3g})$ [127].

Confirmation of this conclusion is provided by the PE spectrum of octafluoroparacyclophane **58**. Replacement of arene methyl groups by trifluoromethyl groups results in stabilization of the π-orbitals by about 0.5 eV; corresponding σ-orbitals may be stabilized by an even larger amount (the "fluoro effect"[128]). For this reason, less effective hyperconjugation and through-bond interaction may be expected in **58**. Consequently, $\pi(b_{3u})$ separates from the other π-orbitals and moves toward higher ionization energies. Just this is seen in the spectrum of **58** (Fig. 25). Thus, hyperconjugation with σ-bonds may to a large extent be "annulled" by perfluorination. Homoconjugation, described by the parameter $\tau = \langle p_i | H | p_j \rangle$, is found to be dependent on the intramolecular distance $D$ in a series of cyclophanes[127b]

$$\tau = 3.9 - 0.013 \times D.$$

### 4.3.3. 1,5-Arene, Arene-Interactions

The effective interaction, $(IE_{1,v} - IE_{2,v})/2$, in the isodrine parent compound **51** is $-0.63$ eV (see Fig. 22). If in this compound the two double bonds are replaced by benzene rings, a correspondingly large splitting of the benzenoid levels is expected. The geometry of **59** has been determined by X-ray structure analysis[129]. The benzene-benzene repulsion leads to the transannular distances $d_1 = 304$ and $d_2 = 382$ pm (Fig. 26).

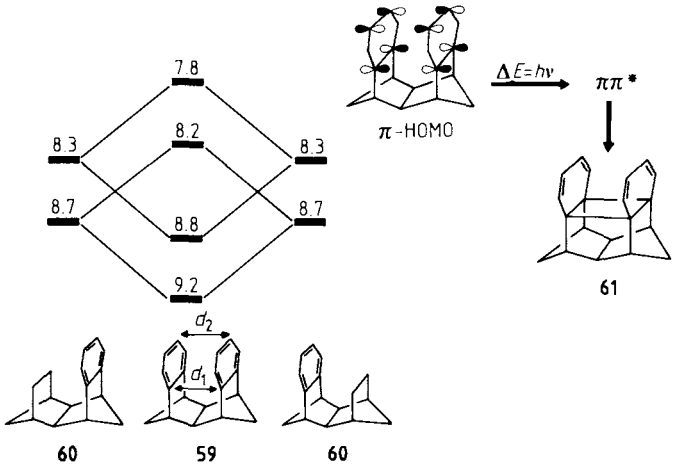



Fig. 26. 1,5-Homoconjugation in **59**. An average value ($\beta_{Av} = -0.5$ eV) is assumed for the nonequal transannular resonance integrals. The numbers given are experimental ionization energies. Photochemical excitation of an electron from the $d_1$-antibonding π(HOMO) to a π*-orbital leads to bond formation, giving **61** [129].

For this reason, the resonance integrals $\beta$ between the corresponding atomic orbitals of the two benzene rings will not be equal: the larger is related to the distance $d_1$ and a smaller to $d_2$. To a first approximation it is reasonable to use an average resonance integral $\beta_{av}$ for all benzenoid carbon atoms. By analogy to **56** and **57** a value $\beta_{av} = -0.5$ eV is plausible. In this way the first four orbital energies of **59** are well reproduced using the ionization energies of **60** (Fig. 26). Thus, the HOMO in **59** exhibits an appreciable degree of antibonding character between the two centers separated by the distance $d_1$. A bond across $d_1$ may be formed by photo-excitation of an electron from the HOMO level. Indeed, **61** is formed upon photolysis[129]. In conclusion, photo-induced processes in olefins such as **51**, arenes such as **59**, and azo-compounds with isodrine structure[159] follow a scheme largely determined by orbital sequences.

### 4.3.4. 1,6-Arene, Arene-Interactions

The molecular geometry and reactivity of the [2.2]metacyclophanes[130] make these compounds just as interesting as the *para*-isomers. The two molecular halves of **62** form a step-like system in which the benzene rings are deformed into boat-like conformations (Fig. 27). The transannular distance between the opposing benzenoid carbon atoms C-8 and C-16 is 268 pm. The reactivity of **62** is determined by this transannular interaction. Two principal electrophilic substitution routes (*a* and *b*) have been discussed.

In any event, the electrophile (or other reagent) may induce transannular ring closure. Since the π(HOMO) of **62** is an important factor in such a substitution reaction, the reactivity may be predicted from the position and electron density of this orbital. Four "arene" bands, the first two of which are very close in energy, are found in the PE spectrum of **62** (Fig. 27). The small energy separation has prevented a definitive ordering of $IE_{1,v}$ and $IE_{2,v}$[131]: $\pi(a_u)$ is dominated by a destabilizing 1,4-through-bond interaction, whereas 1,6-homoconjugation dominates in $\pi(b_u)$. The removal of an electron from $\pi(b_u)$ diminishes 8,16-antibonding and thus favors transannular ring closure. The reactivity observed on photo-excitation or interaction with an

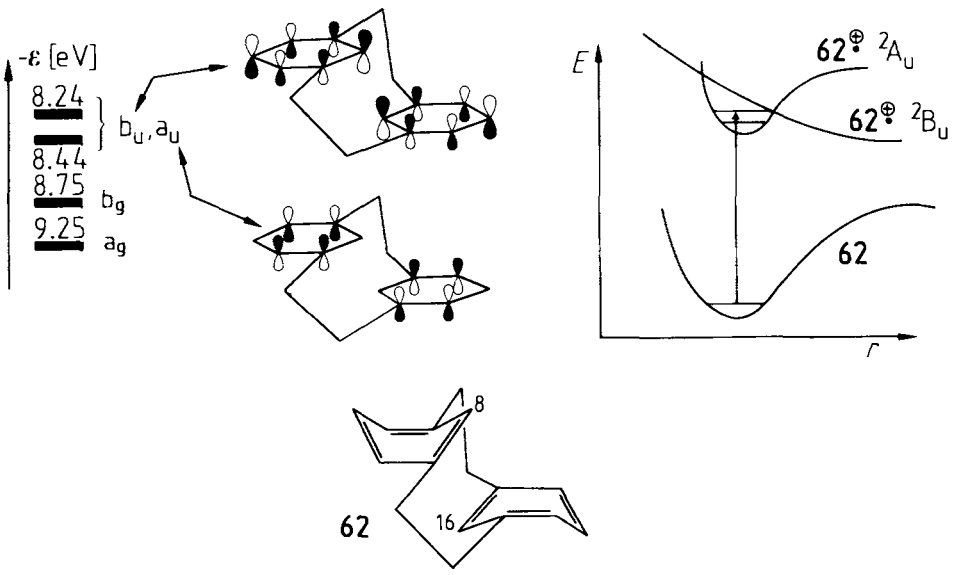
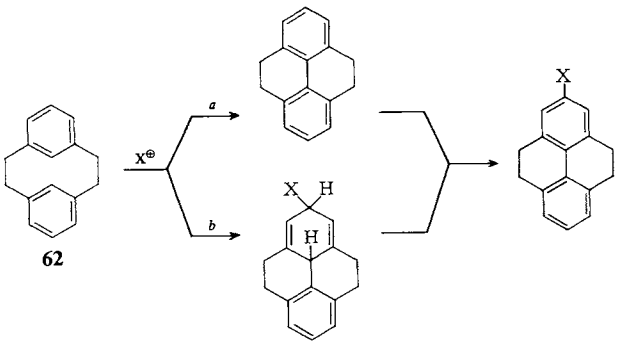



Fig. 27. PE spectrum and interaction in **62** [131]: $\pi(b_u)$ is predominately destabilized by a 1,6-homoconjugative interaction, and $\pi(a_u)$ by a 1,4-through bond interaction. The crossing of the $^2A_u$ and $^2B_u$ states is shown in the energy diagram, which makes both of these accessible [131b].




electrophile is in accord with this scheme. Clearly, the 8,16-overlap measured in the vertical radical cation **62**$^{\oplus}$ is also present in the ground state, where it exerts a destablizing effect. This has consequences for the molecular geometry and the heat of formation. Even if $\pi(b_u)$ should be assigned to $IE_{2,v}$ rather than $IE_{1,v}$, the decisive function of $\pi(b_u)$ is maintained because the potential curves for the radical ions cross due to the small energy difference between $\pi(b_u)$ and $\pi(a_u)$ (Fig. 27).

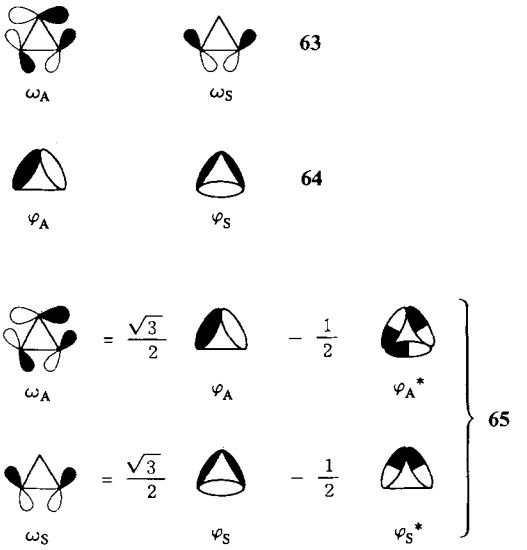
### 4.4. σ,σ-Interactions

Energies and symmetries of valence MO's in linear and branched hydrocarbons are subjects of long-standing interest; moreover, σ-bonds play a fundamental role in organic reactivity. Nevertheless, relatively little information on this subject is obtainable from PE spectra. This is due to a large conformational flexibility and a lack of vibrational fine structure which often lead to broad, unresolved, and difficult-to-analyze PE bands ("σ-mountains"). It is understandable, therefore, that highly symmetrical rigid molecules having high energy σ-orbitals have been particularly well studied[336]. Examples are neopentane[76], adamantane[76], cyclopropane[65,66], cyclobutane[79,132], quadricyclane[133], and cubane[134]. Besides *ab initio* and semiempirical SCF calculations, localized CC- and CH-orbitals are used advantageously in the interpretation of σ-effects[76,79,117b-d,134,135].

#### *4.4.1. 1,3-σ,σ-Interactions*

The two highest occupied MO's of cyclopropane **15** are degenerate; their ionization energies are $IE_{v,1} = 10.60$ eV and $IE_{v,2} = 11.30$ eV (Jahn-Teller splitting)[65,66]. These orbitals are the most important for interaction with other groups or chromophores, and can be represented by the Walsh and Förster-Coulson-Moffit models **63** and **64**, respectively[79,136].

It should be noted that the two models become equivalent only after inclusion of antibonding orbitals[79,136]. This is easily seen from the relevant transformation (**65**) and it should be borne in mind in the discussion of PE spectra. The dispirotricyclic compound **66** provides an interesting example of 1,3-σ,σ-interaction[137]. In this article the following basis orbitals *suffice* for the interpretation of the PE spectrum and interactions in dispiro[2.1.2.1]octane **66**: $\omega_A$, $\omega_S$, and $\pi_{CH_2}$. The basis energies and interaction parameters shown in Figure 28 lead to a satisfactory agreement




with the observed spectrum and, above all, the mechanism of σ,σ-interaction becomes apparent: it is dominated by a circumannular 1,3-through bond coupling *via* hyperconjugation of $\omega_A$ with $\pi_{CH_2}$, together with direct transannular 1,3-homoconjugation.

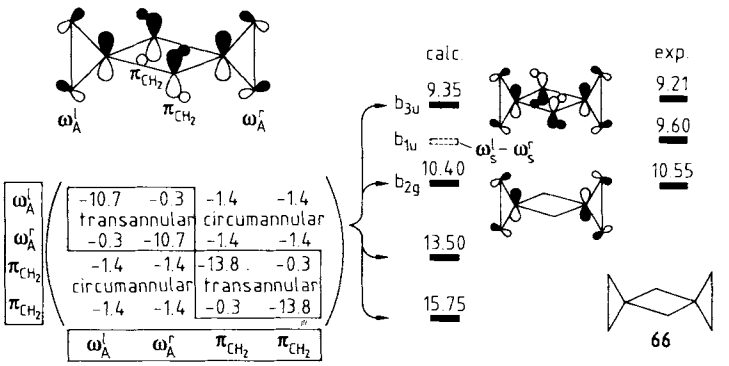



Fig. 28. 1,3-σ,σ-Homoconjugation (transannular) and 1,3-through bond interaction (circumannular) in **66** [137]. The basis orbitals are $\omega_A$ and $\pi_{CH_2}$. Note that, for symmetry reasons, $\omega_S$ cannot interact with $\omega_A$ or $\pi_{CH_2}$. The calculated orbital energies are obtained by diagonalization of the matrix. Calculated and experimental energies are given in eV.

#### *4.4.2. 1,4-σ,σ- and 1,5-σ,σ-Interactions*

The heat of formation of *syn*-tricyclo[4.2.0.0$^{2,5}$]octane **67** is 5.8 kcal/mol higher than that of the *anti*-isomer **68**[138]. This strain energy is in part reflected in structural data[139], and caused by transannular H,H-repulsion. According to *ab initio* calculations[114b], the MO's which make the larger contribution to the CH-bonds in **67** and **68** have different energies: the transannular repulsion in **67** leads to a destabilization by *ca.* 1 eV (Fig. 29). It is noteworthy that this difference is also predicted by HAM/3 calculations ($IE_{8,v}(\mathbf{68})^{HAM} = 12.48$ eV; $IE_{7,v}(\mathbf{67})^{HAM} = 12.01$ eV). Furthermore, the $b_g$(CH)-orbital in **68**, which presumably corresponds to an ionization energy of 12.5 eV, is destabilized in **67** and gives rise to a band at 11.9 eV in the PE spectrum[140].

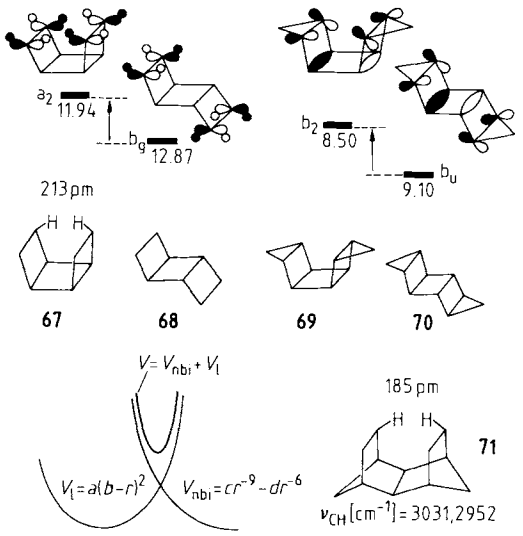



Fig. 29. Transannular non-bonding 1,4- and 1,5-σ(CH),σ(CH) interactions. The orbital energies [eV] of **67** and **68** are from *ab initio* calculations [114b], those of **69** and **70** from the PE spectra [114e]. The effect of transannular strain on CH stretching vibrations is shown in **71**. The frequency increase is interpreted in terms of the increase in curvature arising from a superposition of the two curves, $V_{nbi}$ (non-bonding interaction) and $V_l$ (bond stretching) [47].

Cyclopropanation of the outer CC-bonds in **67** and **68** to **69** and **70**, respectively, causes a shift of the σ-bonds of high p-character in a direction suitable for PE analysis. In **69** the $\sigma(b_2)$-orbital is destabilized by direct, transannular homoconjugation. This decreases the ionization energy by 0.6 eV relative to the $\sigma(b_u)$-level of **70**[114e] (Fig. 29). Strong non-bonding interactions between opposite CH-bonds prevail in the *endo,endo*-tetracyclododecane **71**[47]. Here, the PE spectrum shows ionization energies of 9.50, 9.90, 10.20, and 11.10 eV, resulting from destabilizing effects of the kind described for **67**[117a, 140]. The higher strain energy of the *endo,endo*- relative to that of the *exo,exo*- and *exo,endo*-isomers is reflected in a higher heat of formation (cf. the dienes **50** and **52**, respectively)[141]. Vibrational frequencies constitute important indices of non-bonding repulsion; they have been thoroughly studied in the case of **71**[47, 142]. The frequency is found to increase as a result of the summation of the potentials for bond stretching and nonbonding H,H-interaction ($V = V_{nbi} + V_l$), *i.e.*, tantamount to an increased curvature of the potential curve (Fig. 29).

## 5. Interactions of the X,Y-Type

An analysis is usually more complicated when unequal rather than symmetry-equivalent groups or chromophores interact. The reason is clear: the interaction gives rise to second-order shifts, $\delta\varepsilon$, which in spite of significant resonance integrals are often too small, since the energy difference between the basis orbitals is too large. This is impressively illustrated by an example[113a]: using a typical interaction parameter $\langle\phi_1|H|\phi_2\rangle = -0.33$ eV and an energy difference $\Delta E = 1.6$ eV, one obtains $\delta\varepsilon = (0.33)^2/1.6 = 0.07$ eV!

### 5.1. n,π-Interactions

#### 5.1.1. 1,3-n,π-Interactions

Homoallylic and bishomoallylic conjugations between n(N) and π(CC), as in **72** and **73**, have been thoroughly studied[28, 143]. The difference between the two couplings is due to the low symmetry of **72**; n(N) mixes both with π(CC) and with π*(CC). In contrast, in **73** with $C_S$-symmetry, the interaction between n(N) and π*(CC) is symmetry forbidden (Fig. 30).

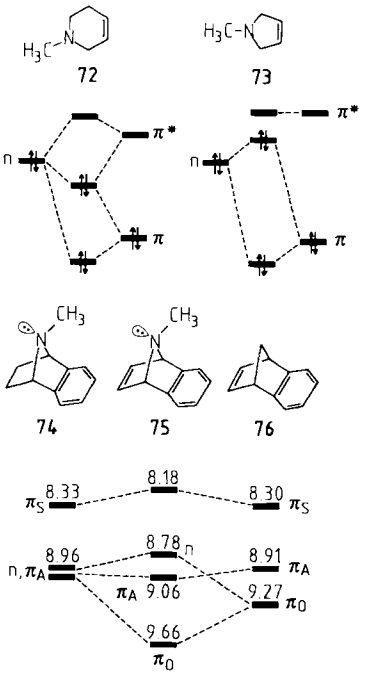
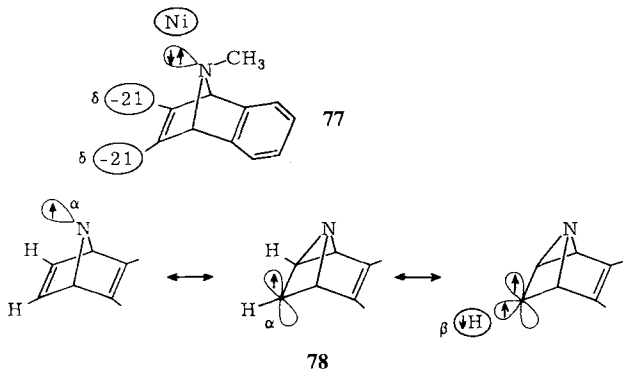



Fig. 30. Difference between homoallylic and bishomoallylic interactions in **72** and **73**. 1,3-n,π-Interaction in **75**: $\pi_S$ and $\pi_A$ are the benzene orbitals, $\pi_0$ the norbornene-type π-orbital and n the N lone-pair *syn* to the isolated double bond in **75**. These are short-hand notations; the 9.66 eV orbital in **75** is more correctly described as $\pi_0 + \lambda\pi_s + \mu \cdot n$ [143b, f].

Homoallylic systems like **72** are not only destabilized by repulsive n,π-4e-interactions, but also stabilized by attractive n,π*-2e-mixing. Since the latter is absent in bishomoallylic systems such as **73**, the analysis of the PE spectra should be more straightforward. The azabenzonorbornadiene **75** is a good example[143b, f]. If the HOMO is assigned to $\pi_S$(aromatic) rather than to n(N)[143f], the destabilizing influence of $\pi_O + \lambda\pi_S$ on n(N) is clearly seen in the correlation between **74**, **75**, and **76** (Fig. 30).

Supplementing these PE studies, the spin delocalization in **74** and **75** has also been investigated[28, 147]. To this end the paramagnetic contact shifts induced by bis(pentanedionato)nickel are measured. The contact shift $\delta$ (which can be positive or negative) is proportional to the hyperfine coupling constant $a$, and hence to the spin density of the unpaired electron at the proton. In this manner the transmission of the electron spin and the nature of the underlying mechanism can be ascertained. Large negative shifts ($\delta = -21$) and hence spin densities are found for the vinylic protons in **75** (see **77**)[28a]. Of the various possible mechanisms of spin transmission (*i.e.* spin polarization, homoconjugation, and homohyperconjugation), only direct delocalization into the π-system, compatible with the symmetries of the n- and $\pi_O$-orbitals involved, would ap-

pear to account for the transfer of β-spin to the protons (see **78**)[28a]. Interestingly, this overlap is also noticeable in the PE spectrum (Fig. 30).




### 5.1.2. 1,4-n,π-Interactions

The relative basicities of the azaadamantanes **16**, **79**, and **80** indicate a marked influence of the methylene or carbonyl groups[144a]. Since the same sequence is found in the gas phase and in solution, it is tempting to try to correlate this with the ionization energy ($H_2O$: p$K_b$ (**16**) 2.96, p$K_b$ (**79**) 4.16, and p$K_b$ (**80**) 5.43). Surprisingly, however, **79** rather than **16** has the lowest ionization energy in this series: $IE_{1,v}(\mathbf{79}) < IE_{1,v}(\mathbf{16}) < IE_{1,v}(\mathbf{80})$. The reason for this is a combination of through-bond couplings and inductive effects. A comparison of the orbital energies of **16**, **79**, and **81** reveals a striking increase in the energy differences: $IE_2(\mathbf{79}) - IE_1(\mathbf{79}) > IE_1(\mathbf{81}) - IE_1(\mathbf{16})$. σ-Couplings and, to a smaller extent, inductive effects may be responsible. The stabilization of the π-orbital in **79** is reminiscent of the "depression effect" in **50** (Fig. 22); this causes the stable π+π-combination to be of lower energy than the π-orbital in the monoolefin[117d,e]. The σ-delocalization of the nitrogen lone-pair in **79** reveals itself not only in a loss of vibrational fine structure in the corresponding PE band, but also in a decreased basicity (despite a smaller $IE_{1,v}$!) In contrast, the energy of the nitrogen lone-pair orbital in **80** is lowered by 0.27 eV ($IE_{1,v}(\mathbf{80}) = 8.21$ eV). Undoubtedly, this is due to the inductive effect of the carbonyl group. Usually, one does not distinguish between σ-inductive and field effect contributions to the inductive stabilization of ion states in PE spectroscopy[2]. It appears, however, that in many cases the field effect dominates or at least contributes to the stabilization[78, 145]. In **80** the stabilization of n(N) by CO can also be understood in these terms[144]. The electrostatic stabilization of $IE$(n) by the dipolar carbonyl group leads to a value of 0.33 eV in good agreement with that observed, $\Delta IE = 0.27$ eV (Fig. 31). This is also the reason for the reduced basicity *vis-a-vis* **79**.

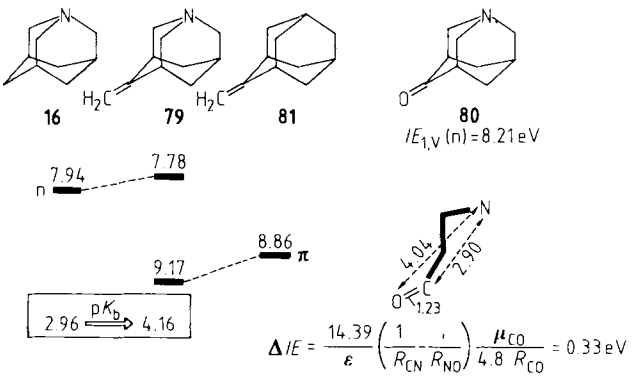



Fig. 31. 1,4-n,π-Through-bond interaction in **79** and relation to basicity. Stabilization of the N lone pair from 7.94 to 8.21 eV caused by an inductive 1,4-field effect. Energies in eV; distances in Å. $\mu_{CO} = 2.8$ D; $\varepsilon = 2$ [144a]. $R$ = distance.

### 5.1.3. 1,5-n,π-Interactions

The inverse Diels-Alder reaction between cyclobutenes **82** and tetrazines is markedly influenced by substituents on the bridge of the norbornene moiety[146]. Donors, *e.g.* $OCH_3$, increase the rate of reaction; acceptors, *e.g.* COR, slow it down. Direct 1,5-n,π-homoconjugation destabilizes the cyclobutene π-orbital, thereby increasing the frontier orbital interaction with the tetrazine.

Such 1,5-homoconjugative interactions are measurable by PE spectroscopy. In the bridgehead amine **83**, whose N atom is pyramidalized on the inside and is weakly basic,

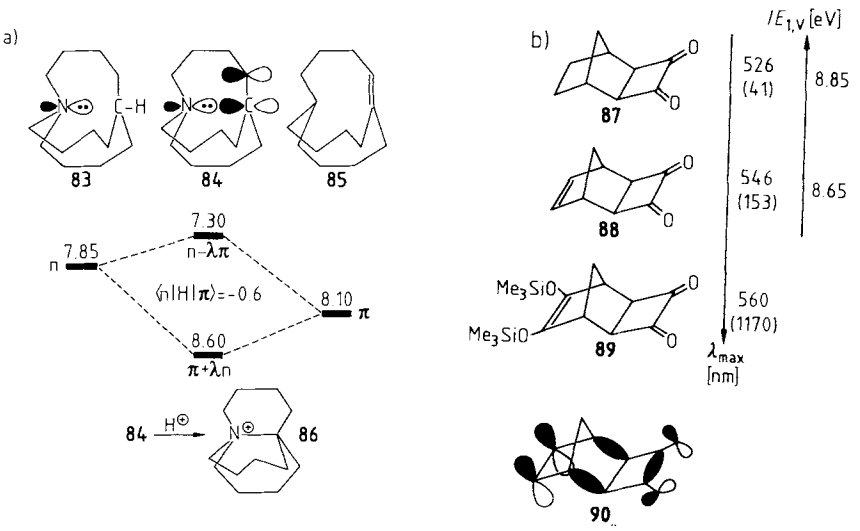
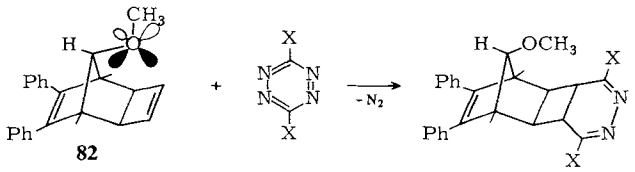



Fig. 32. a) 1,5-n,π-Homoconjugation in **84** [147]. Energies in eV. b) 1,5-n,π-Through-bond interaction (**90**) in the diketones **88** and **89**. UV(cyclohexane): $\lambda_{max}$ [nm] ($\varepsilon$). **87** is orange, **88** red, and **89** violet [88, 89].



82

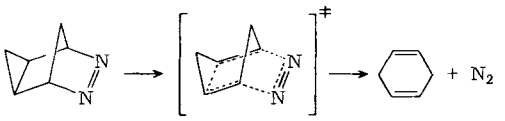
X = 2-Pyridyl

the N lone-pair ionizes at $IE_{1,v} = 7.85$ eV[147]. The introduction of a bridgehead double bond in compound **84** leads to a dramatic splitting of the orbital energies *via* 1,5-through-space conjugation (basis π-energy in **85**, −8.1 eV). The measured interaction parameter, $H_{n\pi} = \langle n|H|\pi\rangle = -0.64$ eV, is comparable with those in phanes (Section 4.3.2) and isodrines (Section 4.2.3). The chemical properties of **84** are a direct consequence of this homoconjugation. **84** is extremely easily oxidized and undergoes C-protonation to give **86**. It behaves as a homoconjugated enamine (Fig. 32a).

A σ-coupled 1,5-n,π-interaction is observed in the unsaturated diketones **88** and **89**. Both absorb at considerably longer wavelengths than the saturated analog **87**; indeed, **89** is violet[88,89]! The ionization energies of **87** and **88** indicate that the color change is due to increased $n_+$-HOMO energies: the double bond causes a decrease of 0.20 eV in the ionization energy ($IE_1$); the effect in **89** is expected to be even larger. The coupling mechanism is indicated in **90** (Fig. 32b). Not only a bathochromic shift but also a hyperchromic effect is observed.

### 5.2. 1,3-n,σ-Interactions

The thermal and photochemical decompositions of azo-compounds have been intensely investigated because of the important role they play in the formation and study of free radicals[148]. The azo-compound **91** is unstable due to the *exo*-cyclopropane ring which participates in a symmetry-allowed pericyclic transition state.



91 41

The thermal lability of cyclopropanated azo-compounds of this type is markedly dependent on the dihedral angle between the diazanorbornane skeleton and the cyclopropane ring[148,149]. Thus, the kinetic stability increases from **91** to **93**[149], the prismane derivative **93** being strikingly stable (Fig. 33). The angle $\Theta$ is the most obvious structural variable in this series, and it is reasonable to conclude that a decrease in $\Theta$ leads to increased stability. This is readily understood by considering that in the transition state involved in the decomposition of **91** one of the cyclopropane bonds must be partly broken and overlaps efficiently with the CN-bonds as the nitrogen molecule departs. This overlap in the transition state should be described well by the orbital interaction between the three-membered ring and the C−N=N−C group which occurs in the ground state or in the vertical radical cation. Because of the molecular $C_S$-symmetry and the requirement of efficient overlap, only the symmetric orbitals $\omega_S$ (in **63**) and $\varphi_S$ (in **64**),

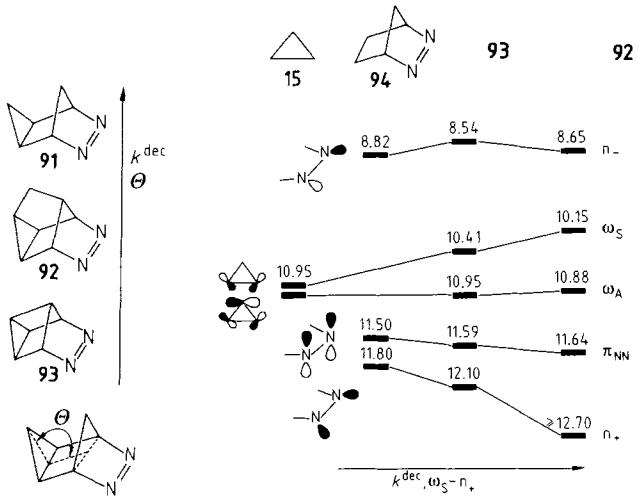



Fig. 33. Relative kinetic thermal stability of azo-compounds **91**—**93**: $k^{dec}$ is the relative first-order rate constant for thermal elimination of $N_2$. Correlation of ionization energies [eV] for **15**, **92**, **93**, and **94**. $k_{dec}$ and $\Theta$ increase in the series **93** < **92** < **91**. The orbital energy difference ($\omega_s - n_+$) increases in the series **93** < **92** [149].

together with the $n_+$- and π(NN)-levels can be involved. The instabilities and the orbital energy differences $\omega_S - n_+$ have the same sense, *i.e.*, the better the overlap between the cyclopropane ring and the C−N=N−C fragment, the lower is the activation energy for the thermal decomposition. The thermal stability of **93** is seen even in its photochemical reactivity[102a]: there is still an activation energy of *ca.* 6 kcal/mol for $N_2$ extrusion in the excited $S_1$ state. At lower temperatures this may not be available, and in consequence **93** isomerizes to diazacyclooctatetraene instead.

### 5.3. π,σ-Interactions

#### *5.3.1. 1,3-π,$\sigma_{CC}$-Interactions*

Increases in the rate of solvolysis due to favorably oriented cyclopropane rings are among the most remarkable neighboring group effects[16-19]. The relative rates measured for the compounds **3a**, **3b**, and **3c** are approximately $10^{14} : 10^{12} : 1$. The extraordinarily strong π,σ-participation is indicated in particular by the degenerate rearrangement of **3b** and by a comparison of $\rho^+$-values ("tool of increasing electron demand", Fig. 3d)[17,18,150]. The ion **95**, which exists in super-acid solution, has $C_{3v}$-symmetry[151]. Since the vertical ionization energy (Section 3.1) is an indicator of possible stabilization of ions possessing the same geometry as the ground state, PE spectroscopy ought to be able to give information on the $C_{2v}$-radical cation **96**. The intramolecular interactions from the cyclopropane rings and the *exo*-methylene double bond are recognizable in the PE spectrum of **97** (Fig. 34)[152]. The dominant 1,3-π,σ-homoconjugation is evident. In correlating the orbital energies of **97**, **98**, and **99** it must be considered that the introduction of the *exo*-methylene double bond results in a small inductive stabilization of the σ- or π-orbitals present (cf. Section 4.1.1). A value of −0.15 eV for this inductive effect can be determined from the PE spectrum of 5-methylene-2-norbornene[153]. Thus, 1,3-π,σ-homoconjugation with a resonance integral $\beta = -0.33$ eV gives information not only about the extent of the interaction in **97**, but also

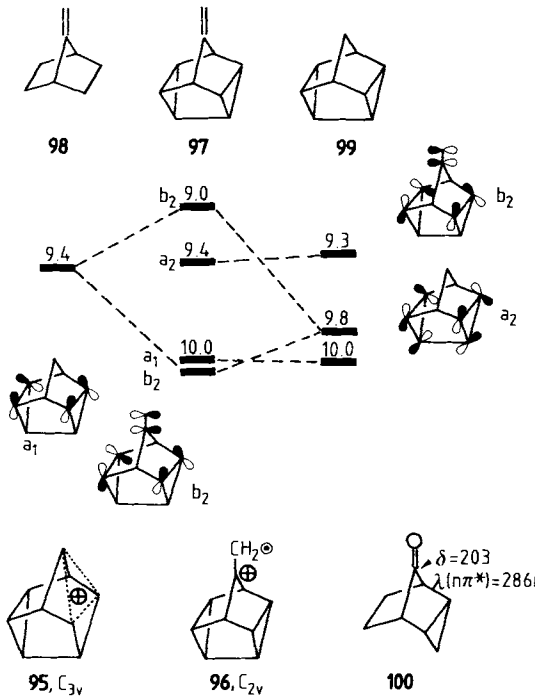



Fig. 34. Cation **95** ($C_{3v}$ symmetry) observed in solution [151], and vertical radical cation **96** ($C_{2v}$ symmetry) generated by photoionization of **97** [152]; 1,3-π,σ-homoconjugation in **97**. Energies in eV. The basis energies in **99** are 0.15 eV more stable than the observed ionization energies due to the inductive effect of the exocyclic double bond. Homoconjugation in ketone **100** is evidenced by $^{13}$C-NMR shifts and nπ*-excitation energies [155].

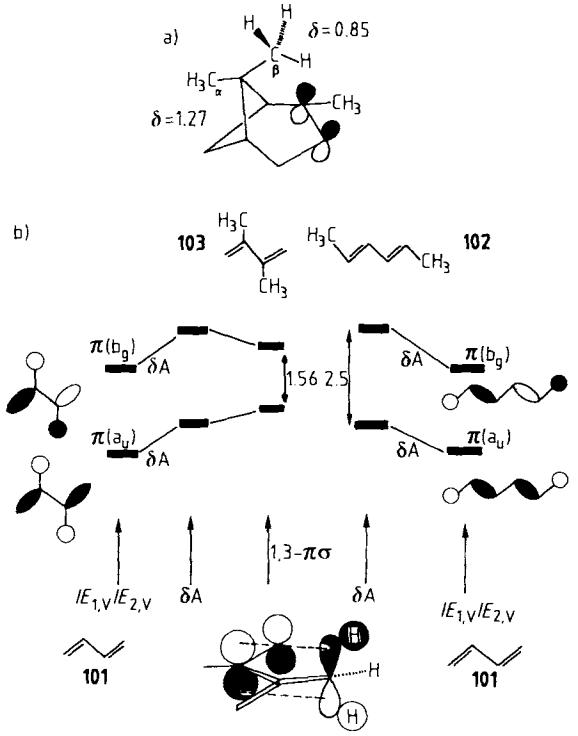



Fig. 35. π,σ-Effects. a) Shielding of the double bond in α-pinene due to magnetic anisotropy [156]. b) 1,3-π,σ-Orbital interaction in **103** using ionization energies of **101** as starting point. δ*A* is the inductive effect of the methyl groups. $CH_3$-π-overlap leads to a smaller splitting, $\pi(b_g)-\pi(a_u)$, for **103**, but not for **102** [37a].

on the orbital sequence in **99**. One can make the following statement on the influence of the solvolysis rate: if only the vertical stabilization of the radical ion **96** were important, acceleration of the solvolysis rate by perhaps $10^4$ by the cyclopropane rings could be expected[154]. The observed value of $10^{12}$ strongly indicates the importance of non-vertical π,σ-participation with homoaromatic stabilization of the ion **95**[152a]. Further information on homoconjugation with *endo*-three-membered rings can be obtained from $^{13}$C-NMR chemical shifts and nπ*-excitation energies of the ketones **100**[155].

### 5.3.2. 1,3- and 1,4-π,$\sigma_{CH}$-Interactions

Important shielding effects in $^1$H-NMR spectroscopy are linked to interactions between π-orbitals and CH-bonds *via* magnetic anisotropy[156]. For example, the protons of the β-$CH_3$ group facing the π-bond in α-pinene appear at $\delta=0.85$, and the α-$CH_3$ protons at $\delta=1.27$ (Fig. 35a). The π,$\sigma_{CH}$-interactions observable by PE or electron transmission spectroscopy are of a fundamentally different nature. Using a simple LCBO model, the PE spectrum of butadiene **101** can be described in terms of a direct interaction between the two occupied π-orbitals; the resonance integral $B_{ab}=\langle\pi_a|H|\pi_b\rangle=-1.21$ eV signifies a strong conjugation[37a]. Substitution at positions 1 and 4 by methyl groups has hardly any influence on the value of $B_{ab}$ ($B_{ab}$(**102**) $=-1.25$ eV). On the other hand, methyl groups in positions 2 and 3 clearly cause a smaller splitting: $B_{ab}$(**103**) $=-0.78$ eV (Fig. 35b). This surprising result can be understood using the pseudo-π orbitals of the methyl groups. The π-levels of **101** are inductively destabilized by $\delta_A$ by the methyl groups. In **103** a further effect occurs: the through-space conjugation between the pseudo-π-$CH_2$ and $\pi_a$- or $\pi_b$-orbitals. This homoconjugation has a stabilizing effect on the higher orbital, a destabilizing effect on the lower, and thus results in a smaller overall splitting[37a].

The existence of such a through-space effect is also indicated by measurements of electron affinities (*i.e.* π*-orbital energies)[38]. A significantly larger $\pi_3^*$-$\pi_4^*$ gap for **104** than for **102** is found by transmission spectroscopy (Fig. 36). In the simplest case, the π-orbitals of the methyl-substituted dienes are described by the linear combination, $\pi^*-\pi(CH_3)$. Therefore, 1,4-π,σ-homoconjugation stabilizes $\pi_3^*$(**104**) and destabilizes $\pi_4^*$(**104**) relative to the energies of the orbitals $\pi_3^*$(**102**) and $\pi_4^*$(**102**). As already mentioned in connection with **46** (Fig. 21) the diffuse character of anion states manifests itself in far-reaching through-

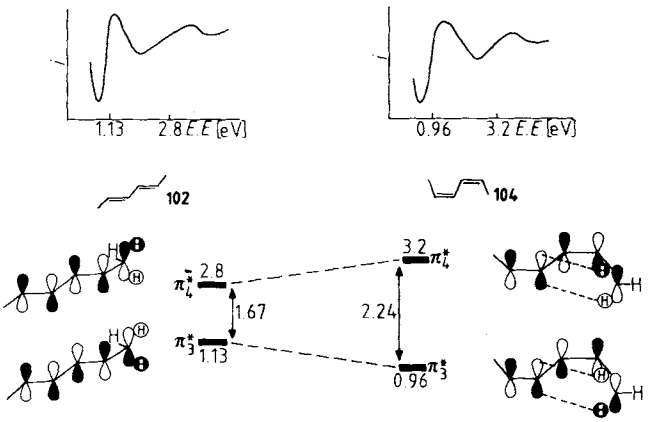
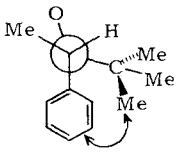



Fig. 36. Electron transmission spectra of **102** and **104** [38]. The pseudo-π-orbitals are shown for only one of the methyl groups. 1,4-π,σ-Homoconjugation in **104** stabilizes $\pi_3^*$ and destabilizes $\pi_4^*$ (*E.E.* = electron energy, i = current).

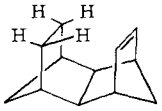
space effects, more so than for neutral molecules or cations; this also applies to **104**.

### 5.3.3. *1,5-π,σ- and 1,5-Arene,σ-Interactions*

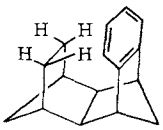
An attractive interaction between methyl groups and arenes has been deduced from NMR and X-ray analysis of benzyl *tert*-butyl sulfoxides and *e.g.* in the α-methyl derivative is largely responsible for the stabilization of conformation **105**[157].



**105**



**106**



**60**

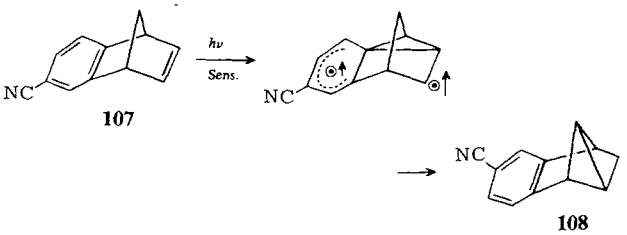
Only a few PE spectroscopic investigations of arene, σ-interactions have been reported. The strikingly low value of 8.60 eV for $IE_{1,v}$(**106**)[158] relative to that of 8.97 eV for norbornene **8** can be ascribed to the transannular strain between the ethano bridge and the π-bond. The calculated H($CH_2$)–H(C=C) distance is 229 pm[47]. It can be concluded that a similar relationship exists between the $CH_2$ group and the arene in **60**. Here, the first two ionization energies ($IE_{1,v}$ and $IE_{2,v}$ = 8.30 and 8.70 eV, respectively[129]) are markedly reduced compared to those in benzonorbornene ($IE_{1,v}$ = 8.45 and $IE_{2,v}$ = 8.95 eV[125b]). This transannular influence on π-orbitals is satisfactorily reproduced by semiempirical calculations (CNDO/2, INDO, and MNDO)[159].

## 5.4. 1,3-Arene, π-Interactions

The triplet sensitized photochemical di-π-methane rearrangement of benzonorbornadiene is remarkably regioselective[160]. Both donors and acceptors in *ortho*-position favor *ortho*-ring closure, whereas acceptors in the *meta*-position effect *para*-bridging (**107** → **108**).

The orbital sequences of **107** and the parent compound **76**, determined both by PE spectroscopy and STO-3G calculations, provide the key to an explanation[160, 161, 358, 373].

In **76** the symmetrical benzene π-orbital ($\pi_S$) is destabilized, not only by the alkyl substituents, but also by 1,3-homoconjugation with the symmetrical olefinic π-orbital ($\pi_O$): $\pi_S - \lambda\pi_O$ becomes the HOMO, $\pi_O + \lambda\pi_S$ appears at $IE_{3,v}$, and $\pi_A$ is assigned to the second measured ionization energy $IE_{2,v}$ because for symmetry reasons this orbital cannot participate in transannular overlapping (Fig. 37). The −I and −M effects of the *meta*-nitrile function in **107** result in a drastic lowering of the orbital energies. Furthermore, the cyano group effects a polarization of the benzene orbitals. The LUMO ($\pi_4$) allows formation of the lowest triplet configuration, $\pi_3\pi_4$. The preferred transannular ring closure is immediately predictable from the magnitudes of the coefficients: it occurs in the position *para* to the nitrile function. The photochemical reactivity of donor substituted benzonorbornadienes can be interpreted in an analogous manner.




**107** **108**

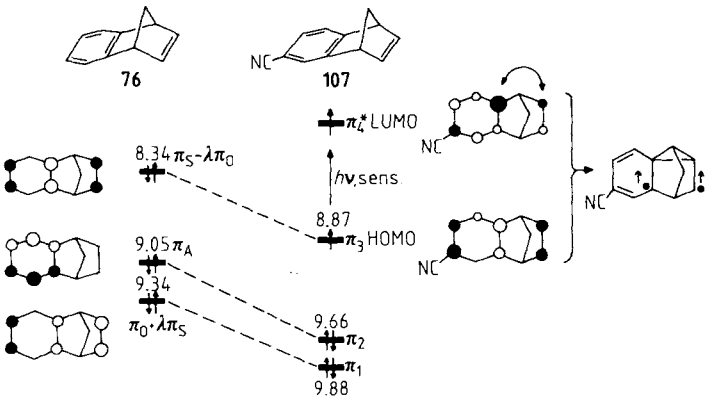
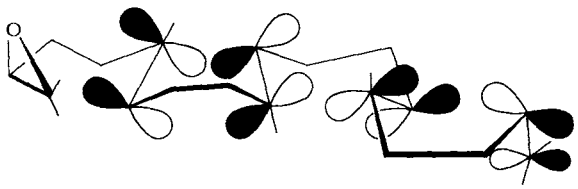



Fig. 37. 1,3-Homoconjugation in **107** and **76**: $\pi_3$ is antibonding, $\pi_4$ bonding with respect to transannular bond formation. Hence, triplet sensitized excitation generating the $\pi_3^1\pi_4^1$ configuration increases transannular bonding, especially in the position *para* to the nitrile group in **107** [160, 161].

## 6. Summary and Outlook

In this article is has been attempted to illustrate how PE spectroscopy may be used to analyze non-bonding orbital or electrostatic interactions between n-, π-, and σ-systems. In this respect, PE spectroscopy is a valuable complement to other methods used in the investigation of proximity effects, *i.e.* methods employing magnetic, electronic, vibrational, kinetic, or ground state measurements. Apart from purely spectroscopic and chemical questions, specific interactions in bioorganic chemistry[162] and molecular pharmacology[163] will become important areas of inquiry in the future. Phenomena such as drug-receptor interaction, orbital steering, and steric compression may be studied using suitable model substances. As an example, the biochemical key reaction in the stereospecific synthesis of steroids is the cyclization of squalene epoxide by the enzyme squalene oxide cyclase. The enzyme serves to fix the carbon skeleton in a conformation conducive to transannular orbital overlap:




Undoubtedly, this is one of the most remarkable and fascinating cases of homoconjugation, and it will be an exciting task to analyze this process using models of proper stereochemistry, applying the methods described in the present article.

Necessarily, only a limited selection of examples could be treated here. For this reason, the appendix gives references to further work where similar interactions are described.

## Appendix

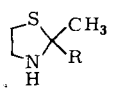
### 1,3-n,n-Interactions (Section 4.1.1; cf. also 11[69])



[165-170]



[166,167,169,171]



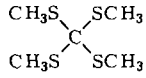
[172]



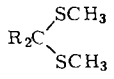
[167,173,180]



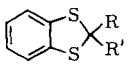
[174]



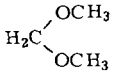
[169,174]



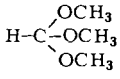
[170,173,175]



[164,176]



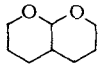
[177]



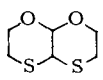
[178]



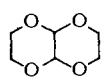
[179]



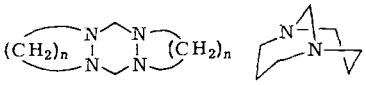
[180]



[180]



[181]



[34,182]



[73]



[167,183,380]



[184,185]



[77b,186-189]



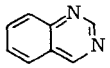
[77b]



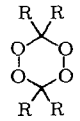
[77b]



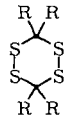
[191]



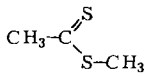
[77a,190,191]



[266]



[379]



[195]



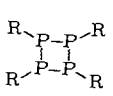
[71j,81]



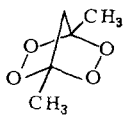
[193,194, 383-385]



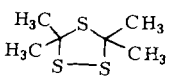
[196]



[384]

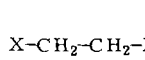


[192]



[388,415]

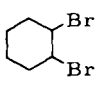
### 1,4-n,n-Interactions (Section 4.1.2; cf. also 10[69,79,218–220])



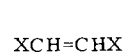
[197-200,400,404]



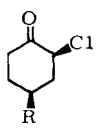
[198,201]



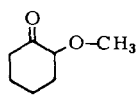
[201,202]



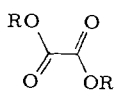
[71j,81,203-206, 360]



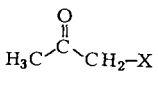
[208]



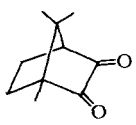
[209]



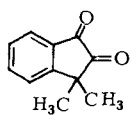
[72a,84b,97d, 210-212]



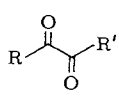
[213]



[97d,341]



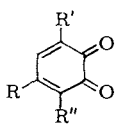
[92]



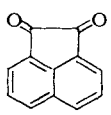
[91,92,214]



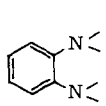
[86,93]



[86]



[215]



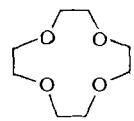
[220]



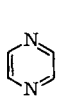
[73,179,216,380, 382]



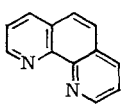
[217,382]



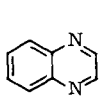
[376]



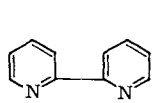
[77b,187,223]



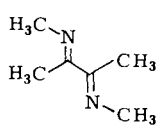
[221]



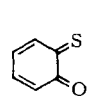
[77a,189-191,399]



[222]



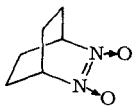
[224]



[225]



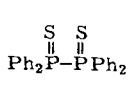
[226]



[227]



[228]

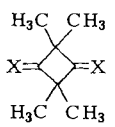


[229]

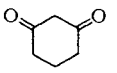


[242]

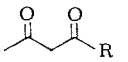
**1,5-n,n-Interactions (Section 4.1.3)**



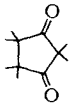
[97d,119,381,382]



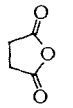
[94,91]



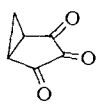
[84b,230,231]



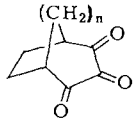
[95a]



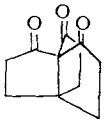
[233,234]



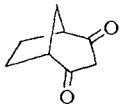
[378]



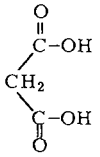
[95]



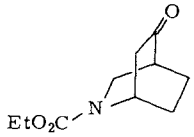
[232]



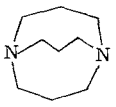
[95a]



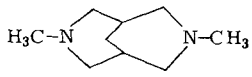
[236,211]



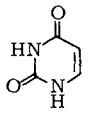
[237]



[147b]



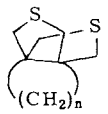
[235]



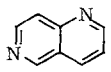
[238]



[240]



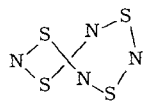
[239,382]



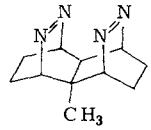
[189,190]



[228]

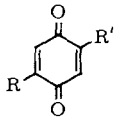


[377]

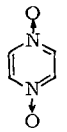


[375]

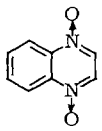
**1,6-n,n-Interactions (Section 4.1.4)**



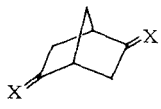
[241,97,91]



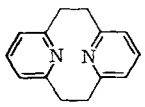
[242]



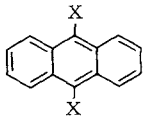
[243]



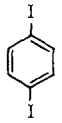
[98]



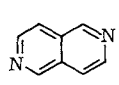
[245]



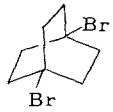
[246]



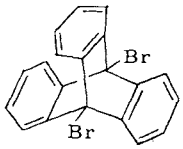
[228]



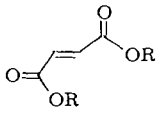
[190]



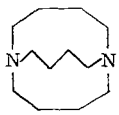
[412]



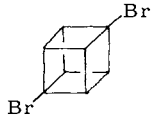
[125a]



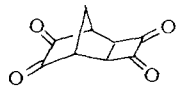
[207]



[147b]

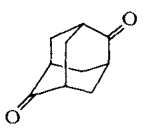


[412]

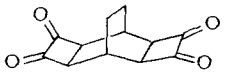


[417]

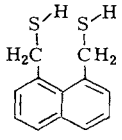
**1,7-n,n-Interactions (Section 4.1.5)**



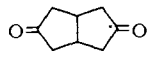
[247]



[417]

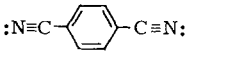


[416]



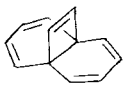
[91]

**1,8-n,n-Interactions**



[314,315]

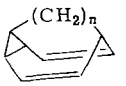
## 1,3-π,π-Interactions (Section 4.2.1)



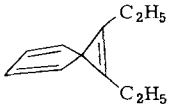
[271]



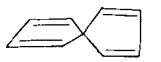
[113a]



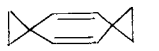

[272,284]



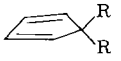

[273]



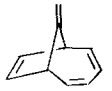
[274-276,366,390]



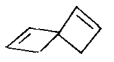
[277,278]



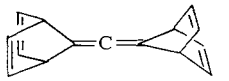

[279-281]



[283]



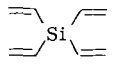
[284]




[282]



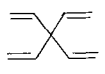

[285]



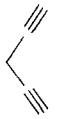

[286,287]



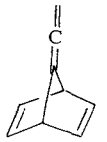
[249,288]



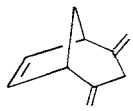
[289]



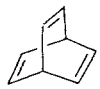
[290]



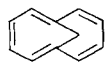

[265]



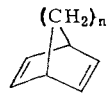
[362]



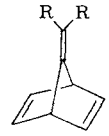
[123,284]



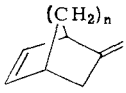
[291,361,31d]



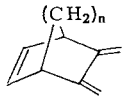

[72c,104,107-109, 112,248-250,389]



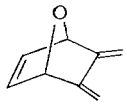

[104,152b] 263-265]



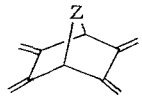

[252,153]



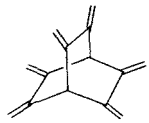

[252,253]




[253]




[254]



[255]



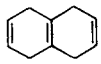
[52b]



[52a]



[52a]



[104,251]



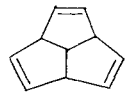
[256-261]



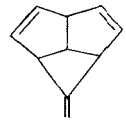
[262]



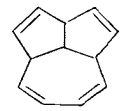
[267]



[268]



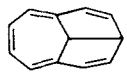
[269,393]



[270]



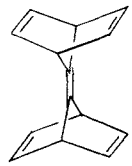

[113b]



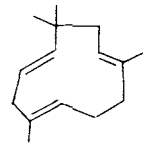
[292,359]



[262,284]

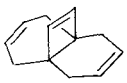


[294]



[293]

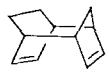
## 1,4-π,π-Interactions (Section 4.2.2)



[271,295]



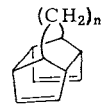
[274]



[296]



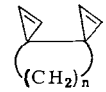
[114h,401]



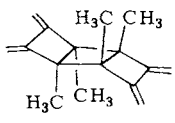

[114g]



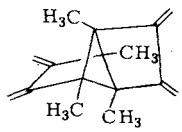
[365,297]




[298,299]




[300]




[300]



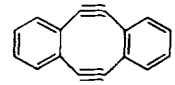
[363]



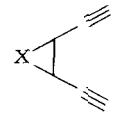
[267]



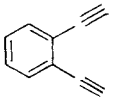
[301]



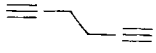
[402]



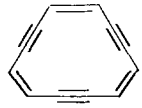

[290]



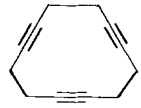
[290]



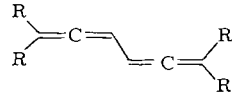
[290,302]



[402]



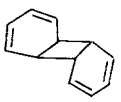
[407]



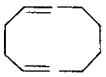

[302,303]



[405]



[305]



[306]



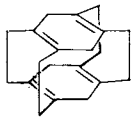
[398]



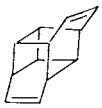
[288]



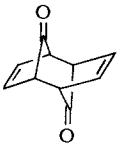
[307]



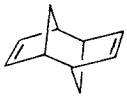
[127b]



[364]



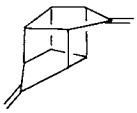
[99]



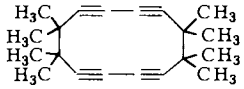
[406]



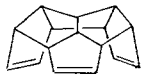
[410]



[99]

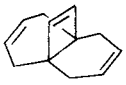



[408]

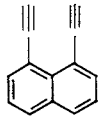


[403]

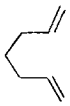
**1,5-π,π-Interactions (Section 4.2.3)**



[271]



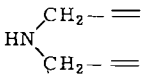
[308]



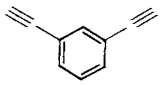
[288]



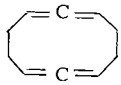
[306]



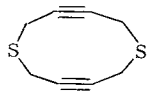

[309]



[290]

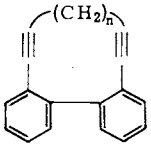



[304]




[301]

**1,6-π,π-Interactions**

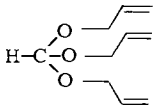



[308]



[288]

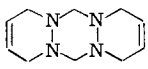
**1,7-π,π-Interactions**



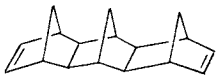

[178]



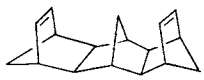
[288]



[182]



[117e,352]

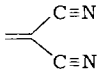


[352]

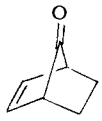
**1,3-$\pi_{AB}$,$\pi_{AB}$-Interactions (Section 4.2.4)**



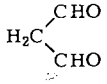

[118]




[310,311]

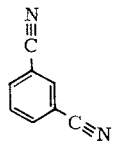



[371,372]

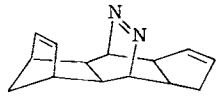



[313]

**1,5-$\pi_{AB}$,$\pi_{AB}$-Interactions**

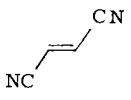



[314,315]

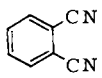



[159]

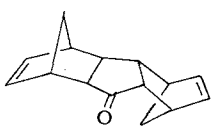
**1,4-$\pi_{AB}$,$\pi_{AB}$-Interactions**




[118,312,310]

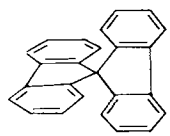



[314,315]



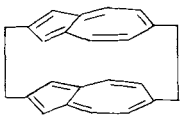

[368]

**1,3-Arene,Arene-Interactions (Section 4.3.1)**

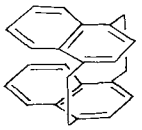


[275,316]

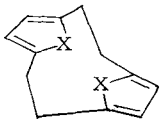
**1,4-Arene,Arene-Interactions (Section 4.3.2)**



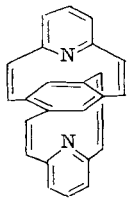
[321]



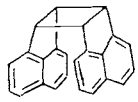
[322,409]




[244]

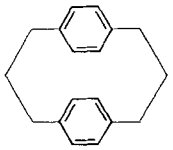



[374]



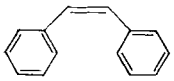
[395]

**1,5-Arene,Arene-Interactions (Section 4.3.3)**



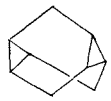
[127b,322]

**1,6-Arene,Arene-Interactions (Section 4.3.4)**

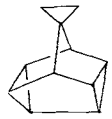


[207]

**1,3-σ,σ-Interactions (Section 4.4.1)**



[323]

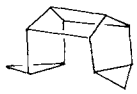


[152]

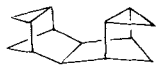
**1,4-σ,σ- and 1,5-σ,σ-Interactions (Section 4.4.2)**



[278]

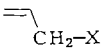


[297]

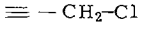


[324]

**1,3-n,π-Interactions (Section 5.1.1)**




[325-329]



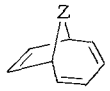

[330]




[331]




[143b,332,333, 386,387,391]



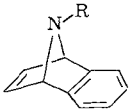

[334,335,394]



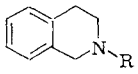

[391]



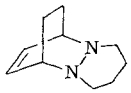

[332]



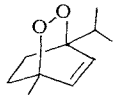

[143]



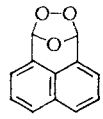

[143]




[392]

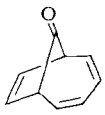



[397]

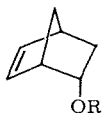



[192]

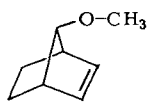
**1,4-n,π-Interactions (Section 5.1.2)**



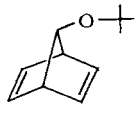

[337]



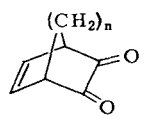

[338]



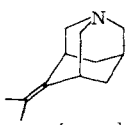

[338-340]



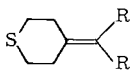

[111,340]



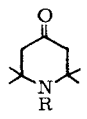

[341,414]




[144a]



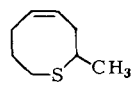

[144b]



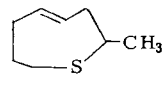

[411]




[71m]

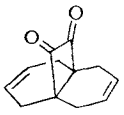



[413]

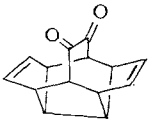



[413]

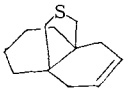
**1,5-n,π-Interactions (Section 5.1.3)**



[295]

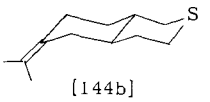


[342]



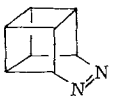
[343,382]

**1,6-n,π-Interactions**

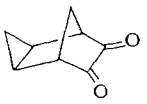


[144b]

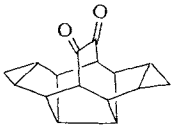
**n,σ-Interactions (Section 5.2)**



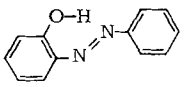
[149b]



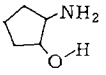
[341]



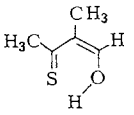
[342]



[344]

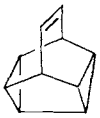


[345]

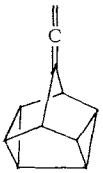


[369]

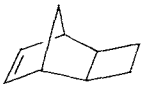
**π,σ-Interactions (Section 5.3)**



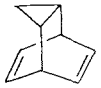
[346]



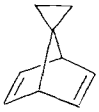
[152c]



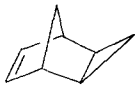
[114h]



[349]



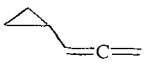
[264]



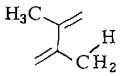
[347]



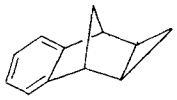
[348]



[350,351]



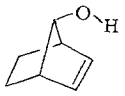
[37]



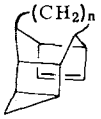
[347]



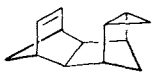
[297]



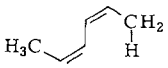
[339,370]



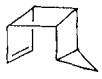
[114g]



[158]



[38]

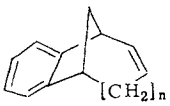


[114e]

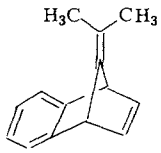


[114h]

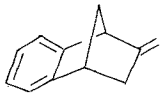
**Arene,π-Interactions (Section 5.4)**



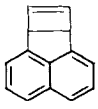
[373]



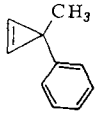
[143b,161,353,356]



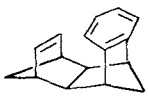
[357]



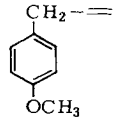
[354]



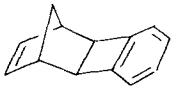
[355]



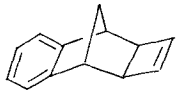
[129]



[154]



[357]



[373]

*We are indebted to Professor H. Prinzbach, who aroused our interest in proximity effects, and to Professor E. Heilbronner, who pointed out how such interactions can be analyzed by PE spectroscopy. Our thanks are due to Professors R. Gleiter and P. Rademacher for numerous discussions and measurements. Our own synthetic and spectroscopic work would not have been possible without the enthusiastic efforts of our co-workers, whose names are found in the references. This work enjoyed generous financial support from the Deutsche Forschungsgemeinschaft, the Fonds der Chemischen Industrie, and BASF AG.*

Received: December 23, 1982 [A 448 IE]
German version: *Angew. Chem. 95* (1983) 281
Translated by: Dr. Edeline Wentrup-Byrne, Marburg

[1] J. Shorter: *Correlation Analysis in Organic Chemistry,* Clarendon Press, Oxfort 1973, p. 5.
[2] a) C. A. Grob, A. Kaiser, T. Schweizer, *Helv. Chim. Acta 60* (1977) 391; b) R. D. Topsom, *J. Am. Chem. Soc. 103* (1981) 39; c) O. Exner, P. Fiedler, *Collect. Czech. Chem. Commun. 45* (1980) 1251; d) W. F. Reynolds, *J. Chem. Soc. Perkin Trans. 2, 1980,* 985; e) R. B. Davidson, C. R. Williams, *J. Am. Chem. Soc. 100* (1978) 2017.
[3] a) L. S. Bartell, *J. Chem. Educ. 45* (1968) 754; b) M. Charton, *J. Am. Chem. Soc. 91* (1969) 615; *101* (1979) 7356.
[4] M. Klessinger, P. Rademacher, *Angew. Chem. 91* (1979) 885; *Angew. Chem. Int. Ed. Engl. 18* (1979) 826.
[5] N. D. Epiotis, W. R. Cherry, S. Shaik, R. L. Yates, F. Bernardi, *Top. Curr. Chem. 70* (1977) 1.
[6] T. K. Brunck, F. Weinhold, *J. Am. Chem. Soc. 101* (1979) 1700.
[7] a) F. A. Van-Catledge, *J. Am. Chem. Soc. 96* (1974) 5693; b) S. Wolfe, *Acc. Chem. Res. 5* (1972) 102.
[8] a) For localized two-center bonds see: W. Kutzelnigg: *Einführung in die theoretische Chemie,* Band 2, Verlag Chemie, Weinheim 1978, p. 199; b) N. Filipescu, *J. Lumin. 1* (1970) 489; c) A. G. Cook: *Enamines,* Marcell Dekker, New York 1969, p. 272.
[9] a) R. Hoffmann, *Acc. Chem. Res. 4* (1971) 1; b). R. Gleiter, *Angew. Chem. 86* (1974) 770; *Angew. Chem. Int. Ed. Engl. 13* (1974) 696; c) T. K. Brunck, F. Weinhold, *J. Am. Chem. Soc. 98* (1976) 4392.
[10] a) J. S. Binkley, J. A. Pople, *Chem. Phys. Lett. 45* (1977) 197; b) S. R. Gandhi, M. A. Benzel, C. E. Dykstra, T. Fukunaga, *J. Phys. Chem. 86* (1982) 3121.
[11] a) A. Skancke, J. E. Boggs, *J. Am. Chem. Soc. 101* (1979) 4063; b) D. Cremer, *ibid. 103* (1981) 3633.
[12] M. H. Whangbo, D. J. Mitchell, S. Wolfe, *J. Am. Chem. Soc. 100* (1978) 3698.
[13] a) N. D. Epiotis, S. Sarkanen, D. Bjorkquist, L. Bjorkquist, R. L. Yates, *J. Am. Chem. Soc. 96* (1974) 4075; b) N. D. Epiotis, *ibid. 95* (1973) 3087; c) F. Bernardi, A. Bottoni, N. D. Epiotis, M. Guerra, *ibid. 100* (1978) 6018.
[14] R. C. Bingham, *J. Am. Chem. Soc. 98* (1976) 535.
[15] C. H. Yoder, *J. Chem. Educ. 54* (1977) 402.
[16] J. Haywood-Farmer, *Chem. Rev. 74* (1974) 315.
[17] a) H. C. Brown, M. Ravindranathan, *J. Am. Chem. Soc. 99* (1977) 299; b) R. M. Coates, E. R. Fretz, *ibid. 99* (1977) 297.
[18] H. C. Brown (comments by P. von R. Schleyer): *The Nonclassical Ion Problem,* Plenum Press, New York 1977.
[19] B. Capon, S. P. McManus: *Neighboring Group Participation,* Plenum Press, New York 1976.
[20] J. N. Murrell: *Elektronenspektren organischer Moleküle,* Bibliographisches Institut, Mannheim 1967.
[21] H. Suzuki: *Electron Absorption Spectra and Geometry of Organic Molecules,* Academic Press, New York 1967.
[22] H. H. Jaffé, M. Orchin: *Theory and Applications of Ultraviolett Spectroscopy,* Wiley, New York 1964.
[23] J. Ladik: *Quantenbiochemie für Chemiker und Biologen,* Enke, Stuttgart 1972.
[24] a) J. Bolte, C. Demuynck, M. F. Lhomme, J. Lhomme, J. Barbet, B. P. Roques, *J. Am. Chem. Soc. 104* (1982) 760; b) N. J. Leonhard, *Acc. Chem. Res 12* (1979) 423.
[25] a) D. A. Lightner, J. K. Gawronski, T. D. Bouman, *J. Am. Chem. Soc. 102* (1980) 5749; b) A. Moscowitz, K. Mislow, M. A. W. Glass, C. Djerassi, *ibid. 84* (1962) 1945.
[26] C. F. Wilcox, S. Winstein, W. G. McMillan, *J. Am. Chem. Soc. 82* (1960) 5450.
[27] a) F. W. King, *Chem. Rev. 76* (1976) 157; b) Y. Ellinger, R. Subra, G. Berthier, *J. Am. Chem. Soc. 100* (1978) 4961; c) T. Kawamura, M. Matsunaga, T. Yonezawa, *ibid. 100* (1978) 92; d) M. Ohsaku, A. Imamura, K. Hirao, T. Kawamura, *Tetrahedron 35* (1979) 701; e) R. L. Blankespoor, D. Gollehon, *J. Org. Chem. 42* (1977) 63; f) P. J. Krusic, T. A. Rettig, P. von R. Schleyer, *J. Am. Chem. Soc. 94* (1972) 995.
[28] a) G. R. Underwood, H. S. Friedman, *J. Am. Chem. Soc. 99* (1977) 27; b) I. Morishima, K. Yoshikawa, K. Okada, *ibid. 98* (1976) 3787.
[29] a) D. E. Applequist, J. D. Roberts, *J. Am. Chem. Soc. 78* (1956) 4012; b) M. Simonetta, S. Winstein, *ibid. 76* (1954) 18; c) S. Winstein in: *Aromaticity,* Spec. Publ. No. 21, The Chemical Society, London 1967, p. 6; d) S. Winstein, J. Sonnenberg, *J. Am. Chem. Soc. 83* (1961) 3244; e) L. A. Paquette, *Angew. Chem. 90* (1978) 114; *Angew. Chem. Int. Ed. Engl. 17* (1978) 106.
[30] a) L. N. Ferguson, J. C. Nnadi, *J. Chem. Educ. 42* (1965) 529; b) L. N. Ferguson: *Organic Molecular Structure,* Willard Grant Press, Boston 1975, p. 350.
[31] a) K. N. Houk, R. W. Gandour, R. W. Strozier, N. G. Rondan, L. A. Paquette, *J. Am. Chem. Soc. 101* (1979) 6797; b) J. B. Grutzner, W. L. Jorgensen, *ibid. 103* (1981) 1372; c) E. Kaufmann, H. Mayr, J. Chandrasekhar, P. von R. Schleyer, *ibid. 103* (1981) 1375; d) H. J. Dewey, H. Deger, W. Frölich, B. Dick, K. A. Klingensmith, G. Hohlneicher, E. Vogel, J. Michl, *ibid. 102* (1980) 6412.
[32] M. J. Goldstein, R. Hoffmann, *J. Am. Chem. Soc. 93* (1971) 6193.
[33] a) R. S. Mulliken, C. A. Rieke, W. G. Brown, *J. Am. Chem. Soc. 63* (1941) 41; b) A. Streitwieser: *Molecular Orbital Theory,* Wiley, New York 1961, p. 131.
[34] a) R. Hoffmann, L. Radom, J. A. Pople, P. von R. Schleyer, W. J. Hehre, L. Salem, *J. Am. Chem. Soc. 94* (1972) 6221; b) Y. Apeloig, P. von R. Schleyer, J. A. Pople, *ibid. 99* (1977) 5901.
[35] a) W. L. Jorgensen, L. Salem: *Orbitale organischer Moleküle,* Verlag Chemie, Weinheim 1974, p. 28ff.; b) W. J. Hehre, *Acc. Chem. Res. 8* (1975) 369.
[36] a) D. E. Sunko, S. Hiršl-Starčević, S. K. Pollack, W. J. Hehre, *J. Am. Chem. Soc. 101* (1979) 6163; b) H. Regenstein, A. Berndt, *Angew. Chem. 86* (1974) 132; *Angew. Chem. Int. Ed. Engl. 13* (1974) 145; c) G. A. Russel, G. W. Holland, K.-Y. Chang, *J. Am. Chem. Soc. 89* (1967) 6629.
[37] a) M. Beez, G. Bieri, H. Bock, E. Heilbronner, *Helv. Chim. Acta 56* (1973) 1028; b) R. A. Wielesek, T. Koenig, *Tetrahedron Lett. 1974,* 2429.
[38] S. W. Staley, J. C. Giordan, J. H. Moore, *J. Am. Chem. Soc. 103* (1981) 3638.
[39] a) J. A. Berson, L. Salem, *J. Am. Chem. Soc. 94* (1972) 8917; b) S. David, O. Eisenstein, W. J. Hehre, L. Salem, R. Hoffmann, *ibid. 95* (1973) 3806.
[40] W. A. Szarek, D. Horton: *Anomeric Effect,* American Chemical Society, Washington, DC 1979.
[41] H. C. Brown, E. N. Peters, M. Ravindranathan, *J. Am. Chem. Soc. 99* (1977) 505.
[42] See P. von R. Schleyer in [18], p. 79f.
[43] T. G. Traylor, W. Hanstein, H. J. Berwin, N. A. Clinton, R. S. Brown, *J. Am. Chem. Soc. 93* (1971) 5715.
[44] a) L. A. Paquette, R. E. Wingard, J. M. Photis, *J. Am. Chem. Soc. 96* (1974) 5801; b) P. Bischof, R. Gleiter, R. Haider, *ibid. 100* (1978) 1036.
[45] J. D. Dunitz, H. B. Bürgi, *Int. Rev. Sci. Phys. Chem. Ser. 2, 11* (1976) 81.
[46] R. E. Rosenfield, R. Parthasarathy, J. D. Dunitz, *J. Am. Chem. Soc. 99* (1977) 4860.
[47] O. Ermer: *Aspekte von Kraftfeldrechnungen,* Wolfgang Baur Verlag, München 1981.
[48] G. E. Schulz, R. H. Schirmer: *Principles of Protein Structure,* Springer, New York 1979.
[49] L. Salem, *J. Chem. Phys. 37* (1962) 2100.
[50] R. Hoffmann, C. C. Levin, R. A. Moss, *J. Am. Chem. Soc. 95* (1973) 629.
[51] B. P. Mundy, T. R. Schwartz, *J. Org. Chem. 47* (1982) 576.
[52] a) H. D. Martin, M. Eckert-Maksić, B. Mayer, *Angew. Chem. 92* (1980) 833; *Angew. Chem. Int. Ed. Engl. 19* (1980) 807; b) P. Hemmersbach, M. Klessinger, P. Bruckmann, *J. Am. Chem. Soc. 100* (1978) 6344; c) R. Spafford, J. Baiardo, J. Wrobel, M. Vala, *ibid. 98* (1976) 5217, 5225; d) M. Simonetta, S. Carra, *Tetrahedron Lett. 1965,* 913; e) C. A. Grob, *Angew. Chem. 81* (1969) 543; *Angew. Chem. Int. Ed. Engl. 8* (1969) 535; W. Fischer, C. A. Grob, *Helv. Chim. Acta 61* (1978) 1588; f) S. Inagaki, H. Fujimoto, K. Fukui, *J. Am. Chem. Soc. 98* (1976) 4054; R. Huisgen, P. H. J. Ooms, M. Mingin, N. L. Allinger, *ibid. 102* (1980) 3951; G. Wipff, K. Morokuma, *Tetrahedron Lett. 21* (1980) 4445; E. M. Burgess, C. L. Liotta, *J. Org. Chem. 46* (1981) 1703; J. Spanget-Larsen, R. Gleiter, *Tetrahedron Lett. 23* (1982) 927, 2435; S. Ito, A. Kakehi, *Bull. Chem. Soc. Jpn. 55* (1982) 1869; g) J. B. Lambert, K. M. Taba, *J. Am. Chem. Soc. 103* (1981) 5828.
[53] a) H. Bock, B. G. Ramsey, *Angew. Chem. 85* (1973) 773; *Angew. Chem. Int. Ed. Engl. 12* (1973) 734; b) H. Bock, *ibid. 89* (1977) 631 *16* (1977) 613.
[54] H. Bock, P. D. Mollère, *J. Chem. Educ. 51* (1974) 506.

[55] A. D. Baker, *Acc. Chem. Res. 3* (1970) 17.
[56] N. Knöpfel, T. Olbricht, A. Schweig, *Chem. Unserer Zeit 5* (1971) 65.
[57] S. D. Worley, *Chem. Rev. 71* (1971) 295.
[58] D. W. Turner, *Chem. Br. 4* (1968) 435.
[59] E. Heilbronner, H. Bock: *Das HMO-Modell und seine Anwendung*, 2nd Ed., Verlag Chemie, Weinheim 1978, p. 393.
[60] E. Heilbronner, J. P. Maier: „Some Aspects of Organic Photoelectron Spectroscopy", in [61], p. 205.
[61] C. R. Brundle, A. D. Baker: *Electron Spectroscopy: Theory, Techniques and Applications*, Vol. 1, Academic Press, London 1977.
[62] J. H. D. Eland: *Photoelectron Spectroscopy*, Butterworths, London 1974.
[63] J. W. Rabalais: *Principles of Ultraviolet Photoelectron Spectroscopy*, Wiley, New York 1977.
[64] T. A. Carlson: *Photoelectron and Auger Spectroscopy*, Plenum Press, New York 1975.
[65] D. W. Turner, C. Baker, A. D. Baker, C. R. Brundle: *Molecular Photoelectron Spectroscopy*, Wiley-Interscience, London 1970.
[66] K. Kimura, S. Katsumata, Y. Achiba, T. Yamazaki, S. Iwata: *Handbook of He1 Photoelectron Spectra of Fundamental Organic Molecules*, Halsted Press, New York 1981.
[67] W. H. E. Schwarz, *J. Electron Spectrosc. Relat. Phenom. 6* (1975) 377.
[68] J. M. Jerkunica, T. G. Traylor, *J. Am. Chem. Soc. 93* (1971) 6278.
[69] S. F. Nelsen, E. Haselbach, R. Gschwind, U. Klemm, S. Lanyova, *J. Am. Chem. Soc. 100* (1978) 4367; S. F. Nelsen, J. M. Buschek, *ibid. 96* (1974) 6424.
[70] M. Thompson, P. A. Hewitt, D. S. Wooliscroft in D. Briggs: *Handbook of X-Ray and UV Photoelectron Spectroscopy*, Heyden, London 1977, p. 348.
[71] a) T. Koopmans, *Physica 1* (1933) 104; b) W. G. Richards, *Int. J. Mass Spectrom. Ion Phys. 2* (1969) 419; c) B. Kellerer, L. S. Cederbaum, G. Hohlneicher, *J. Electron Spectrosc. Relat. Phenom. 3* (1974) 107; d) L. S. Cederbaum, *Chem. Phys. Lett. 25* (1974) 562; e) W. von Niessen, G. H. F. Diercksen, L. S. Cederbaum, *J. Chem. Phys. 67* (1977) 4124; f) M. Jungen, *Helv. Chim. Acta 61* (1978) 864; g) F. Brogli, P. A. Clark, E. Heilbronner, M. Neuenschwander, *Angew. Chem. 85* (1973) 414; *Angew. Chem. Int. Ed. Engl. 12* (1973) 422; h) G. Kluge, M. Scholz, *Int. J. Quantum Chem. 20* (1981) 669; i) W. von Niessen, *Chem. Phys. 45* (1980) 47; j) G. Bieri, W. von Niessen, L. Asbrink, A. Svensson, *Chem. Phys. 60* (1981) 61; k) W. von Niessen, G. H. F. Diercksen, L. S. Cederbaum, *J. Am. Chem. Soc. 100* (1978) 6347; l) G. Granozzi, D. Ajo, I. Fragala, *J. Electron Spectrosc. Relat. Phenom. 18* (1980) 267; m) G. Hentrich, E. Gunkel, M. Klessinger, *J. Mol. Struct. 21* (1974) 231; n) W. von Niessen, G. Bieri, L. Asbrink, *J. Electron Spectrosc. Relat. Phenom. 21* (1980) 175; o) D. P. Chong, F. G. Herring, D. McWilliams, *ibid. 7* (1975) 445; p) N. P. Ernsting, J. Pfab, J. C. Green, J. Römelt, *J. Chem. Soc. Faraday Trans. 2, 1980*, 844.
[72] a) W. von Niessen, *J. Am. Chem. Soc. 99* (1977) 7151; b) W. von Niessen, W. Domcke, L. S. Cederbaum, W. P. Kraemer, *J. Chem. Phys. 67* (1977) 44; c) W. von Niessen, G. H. F. Diercksen, *J. Electron Spectrosc. Relat. Phenom. 16* (1979) 351.
[73] S. F. Nelsen, J. M. Buschek, *J. Am. Chem. Soc. 96* (1974) 7930.
[74] R. Gleiter, M. Kobayashi, J. Kuthan, *Tetrahedron 32* (1976) 2775.
[75] T. Sasaki, S. Eguchi, T. Kiriyama, Y. Sakito, H. Kato, *J. Chem. Soc. Chem. Commun. 1974*, 725.
[76] W. Schmidt, *Tetrahedron 29* (1973) 2129; J. N. Murrell, W. Schmidt, *J. Chem. Soc. Faraday Trans. 2, 1972*, 1709.
[77] a) F. Brogli, E. Heilbronner, T. Kobayashi, *Helv. Chim. Acta 55* (1972) 274; b) R. Gleiter, E. Heilbronner, V. Hornung, *ibid. 55* (1972) 255.
[78] a) G. Bieri, E. Heilbronner, *Helv. Chim. Acta 57* (1974) 546; b) C. A. Grob, M. G. Schlageter, *ibid. 59* (1976) 264; c) H. W. Gibson, *Can. J. Chem. 55* (1977) 2637.
[79] M. Klessinger: *Elektronenstruktur Organischer Moleküle*, Verlag Chemie, Weinheim 1982, p. 278.
[80] N. D. Epiotis, S. Shaik, J. R. Larson, F. Bernardi, *Tetrahedron 33* (1977) 3275.
[81] K. Wittel, H. Bock, *Chem. Ber. 107* (1974) 317.
[82] J. R. Swenson, R. Hoffmann, *Helv. Chim. Acta 53* (1970) 2331.
[83] W. Hug, J. Kuhn, K. J. Seibold, H. Labhart, G. Wagnière, *Helv. Chim. Acta 54* (1971) 1451.
[84] a) J. L. Meeks, H. J. Maria, P. Brint, S. P. McGlynn, *Chem. Rev. 75* (1975) 603; b) S. P. McGlynn, J. L. Meeks, *J. Electron. Spectrosc. Relat. Phenom. 6* (1975) 269; c) U. C. Singh, P. K. Basu, C. N. R. Rao, *J. Mol. Struct. 87* (1982) 125.
[85] H. G. Heine, *Chem. Ber. 104* (1971) 2869.
[86] P. Schang, R. Gleiter, A. Rieker, *Ber. Bunsenges. Phys. Chem. 82* (1978) 629.
[87] H. D. Martin, B. Albert, H. J. Schiwek, *Tetrahedron Lett. 1979*, 2347.
[88] H. D. Martin, H. J. Schiwek, J. Spanget-Larsen, R. Gleiter, *Chem. Ber. 111* (1978) 2557.
[89] H. D. Martin, A. Oftring, R. Iden, E. Schwichtenberg, H. J. Schiwek, *Tetrahedron Lett. 23* (1982) 841.
[90] D. C. England, *J. Am. Chem. Soc. 83* (1961) 2205.
[91] D. Dougherty, P. Brint, S. P. McGlynn, *J. Am. Chem. Soc. 100* (1978) 5597.
[92] J. F. Arnett, G. Newkome, W. L. Mattice, S. P. McGlynn, *J. Am. Chem. Soc. 96* (1974) 4385.
[93] R. Gleiter, P. Schang, G. Seitz, *Chem. Phys. Lett. 55* (1978) 144.
[94] K. N. Houk, L. P. Davis, G. R. Newkome, R. E. Duke, R. V. Nauman, *J. Am. Chem. Soc. 95* (1973) 8364.
[95] a) R. Gleiter, P. Hofmann, P. Schang, A. Sieber, *Tetrahedron 36* (1980) 655; b) P. Bischof, R. Gleiter, P. Hofmann, *Helv. Chim. Acta 58* (1975) 2130; c) J. Kroner, W. Strack, *Angew. Chem. 84* (1972) 210; *Angew. Chem. Int. Ed. Engl. 11* (1972) 220.
[96] J. P. Maier, *Helv. Chim. Acta 57* (1974) 994.
[97] a) L. Asbrink, G. Bieri, C. Fridh, E. Lindholm, D. P. Chong, *Chem. Phys. 43* (1979) 189; b) P. Jacques, J. Faure, O. Chalvet, H. H. Jaffé, *J. Phys. Chem. 85* (1981) 473; c) D. Dougherty, S. P. McGlynn, *J. Am. Chem. Soc. 99* (1977) 3234; d) D. O. Cowan, R. Gleiter, J. A. Hashmall, E. Heilbronner, V. Hornung, *Angew. Chem. 83* (1971) 405; *Angew. Chem. Int. Ed. Engl. 10* (1971) 401; e) W. von Niessen, personal communication.
[98] D. C. Frost, N. P. C. Westwood, N. H. Werstink, *Can. J. Chem. 58* (1980) 1659.
[99] H. D. Martin, P. Pföhler, unpublished results.
[100] Y. Zongh-zhi, E. Heilbronner, H. C. Kang, V. Boekelheide, *Helv. Chim. Acta 64* (1981) 2029.
[101] J. A. Berson in P. de Mayo: *Molecular Rearrangements*, Vol. 1, Interscience, New York 1963, p. 198.
[102] a) N. J. Turro: *Modern Molecular Photochemistry*, The Benjamin/Cummings Publishing Co., Menlo Park 1978, p. 428; b) K. Maruyama, K. Terada, Y. Yamamoto, *Chem. Lett. 1981*, 839; c) H. D. Scharf, J. Fleischhauer, H. Leismann, I. Ressler, W. Schleker, R. Weitz, *Angew. Chem. 91* (1979) 696; *Angew. Chem. Int. Ed. Engl. 18* (1979) 652.
[103] M. B. Robin, N. A. Kuebler, *J. Chem. Phys. 44* (1966) 2664.
[104] a) E. Heilbronner, H. D. Martin, *Helv. Chim. Acta 55* (1972) 1490; b) P. Bischof, J. A. Hashmall, E. Heilbronner, V. Hornung, *ibid. 52* (1969) 1745.
[105] a) R. P. Frueholz, W. M. Flicker, O. A. Mosher, A. Kuppermann, *J. Chem. Phys. 70* (1979) 1986; b) J. P. Doering, R. McDiarmid, *ibid. 75* (1981) 87, 2687.
[106] K. D. Jordan, P. D. Burrow, *Acc. Chem. Res. 11* (1978) 341.
[107] E. Heilbronner, A. Schmelzer, *Helv. Chim. Acta 58* (1975) 936.
[108] E. Heilbronner, *Isr. J. Chem. 10* (1972) 143.
[109] M. J. Goldstein, S. Natowsky, E. Heilbronner, V. Hornung, *Helv. Chim. Acta 56* (1973) 294.
[110] H. Fujimoto, S. Inagaki, *J. Am. Chem. Soc. 99* (1977) 7424; H. Fujimoto, S. Uemura, H. Miyoshi, *Tetrahedron 37* (1981) 55.
[111] P. H. Mazzocchi, B. Stahly, J. Dodd, N. G. Rondan, L. N. Domelsmith, M. D. Roozeboom, P. Caramella, K. N. Houk, *J. Am. Chem. Soc. 102* (1980) 6482.
[112] M. H. Kibel, M. K. Livett, G. L. Nyberg, *J. Electron Spectrosc. Relat. Phenom. 14* (1978) 155.
[113] a) P. Bischof, R. Gleiter, E. Heilbronner, *Helv. Chim. Acta 53* (1970) 1425; b) M. H. Palmer, J. D. Nisbet, *J. Mol. Struct. 67* (1980) 65.
[114] a) R. Gleiter, E. Heilbronner, M. Hekman, H. D. Martin, *Chem. Ber. 106* (1973) 28; b) J. M. Lehn, G. Wipff, personal communication; G. Wipff, Thèse, Universität Straßburg 1974; c) N. Bodor, B. H. Chen, S. D. Worley, *J. Electron. Spectrosc. Relat. Phenom. 4* (1974) 65; d) H. Iwamura, H. Kihara, K. Morio, T. L. Kunii, *Bull. Chem. Soc. Jpn. 46* (1973) 3248; e) J. Spanget-Larsen, R. Gleiter, L. A. Paquette, M. J. Carmody, C. R. Degenhardt, *Theor. Chim. Acta 50* (1978) 145; f) H. J. Chiang, S. D. Worley, *J. Electron Spectrosc. Relat. Phenom. 21* (1980) 121; g) G. Sedelmeier, H. Prinzbach, H. D. Martin, *Chimia 33* (1979) 329; h) H. D. Martin, S. Kagabu, R. Schwesinger, *Chem. Ber. 107* (1974) 3130; i) H. D. Martin, B. Mayer, unpublished results.
[115] P. D. Burrow, K. D. Jordan, *J. Am. Chem. Soc. 104* (1982) 5247.
[116] E. L. Allred, G. D. Lyon, G. Stroebel, *J. Am. Chem. Soc. 101* (1979) 3415.
[117] a) H. D. Martin, R. Schwesinger, *Chem. Ber. 107* (1974) 3143; b) J. W. Verhoeven, P. Pasman, *Tetrahedron 37* (1981) 943; c) J. W. Verhoeven, *Recl. Trav. Chim. Bays-Pas 99* (1980) 369; d) M. N. Paddon-Row, H. K. Patney, R. S. Brown, K. N. Houk, *J. Am. Chem. Soc. 103* (1981) 5575; e) M. N. Paddon-Row, *Acc. Chem. Res. 15* (1982) 245; f) M. C. Böhm, *J. Mol. Struct. 87* (1982) 335.
[118] a) H. Stafast, H. Bock, *Z. Naturforsch. B 28* (1973) 746; b) H. Bock, E. Haselbach, E. Maier, H. Stafast, *Helv. Chim. Acta 59* (1976) 1035.
[119] a) P. K. Basu, U. C. Singh, K. N. Tantry, V. Ramamurthy, C. N. R. Rao, *Theochem. 1* (1981) 237; b) J. M. Behan, R. A. W. Johnstone, J. J. Worman, T. P. Fehlner, *J. Mol. Struct. 40* (1977) 151; c) R. D. Gordon, S. E. Gransden, R. Marion, *J. Mol. Spectrosc. 81* (1980) 340.
[120] a) A. J. Hopfinger: *Intermolecular Interactions and Biomolecular Organization*, Wiley, New York 1977, p. 171; b) R. Rein in B. Pullman: *Intermolecular Interactions: From Diatomics to Biopolymers*, Wiley, New York 1978, p. 307.
[121] J. Ladik, K. Sundaram, *J. Mol. Spectrosc. 29* (1969) 146.

[122] P. D. Bartlett, E. S. Lewis, *J. Am. Chem. Soc. 72* (1950) 1005.
[123] E. Haselbach, E. Heilbronner, G. Schröder, *Helv. Chim. Acta 54* (1971) 153.
[124] S. P. McGlynn, T. A. Zumi, M. Kinoshita: *Molecular Spectroscopy of the Triplet State*, Prentice Hall, Englewood Cliffs, NJ 1969, p. 378.
[125] a) H. D. Martin, B. Mayer, R. Gleiter, W. Schäfer, F. Vögtle, *Chem. Ber.*, in press; b) E. Haselbach, L. Neuhaus, R. P. Johnson, K. N. Houk, M. N. Paddon-Row, *Helv. Chim. Acta 65* (1982) 1743.
[126] a) F. Vögtle, P. Neumann, *Top. Curr. Chem. 48* (1974) 67; b) F. Vögtle, G. Hohner, *ibid. 74* (1978) 1; c) H. Vogler, *Theor. Chim. Acta 60* (1981) 65; d) H. A. Staab, V. Schwendemann, *Angew. Chem. 90* (1978) 805; *Angew. Chem. Int. Ed. Engl. 17* (1978) 756; e) H. A. Staab, U. Zapf, *ibid. 90* (1978) 807 *17* (1978) 757.
[127] a) E. Heilbronner, J. P. Maier, *Helv. Chim. Acta 57* (1974) 151; b) B. Kovač, M. Mohraz, E. Heilbronner, V. Boekelheide, H. Hopf, *J. Am. Chem. Soc. 102* (1980) 4314.
[128] C. R. Brundle, M. B. Robin, N. A. Kuebler, H. Basch, *J. Am. Chem. Soc. 94* (1972) 1451.
[129] H. Prinzbach, G. Sedelmeier, C. Krüger, R. Goddard, H. D. Martin, R. Gleiter, *Angew. Chem. 90* (1978) 297; *Angew. Chem. Int. Ed. Engl. 17* (1978) 271.
[130] F. Vögtle, P. Neumann, *Angew. Chem. 84* (1972) 75; *Angew. Chem. Int. Ed. Engl. 11* (1972) 73.
[131] a) R. Boschi, W. Schmidt, *Angew. Chem. 85* (1973) 408; *Angew. Chem. Int. Ed. Engl. 12* (1973) 402; b) T. Koenig, M. Tuttle, R. A. Wielesek, *Tetrahedron Lett. 1974*, 2537.
[132] P. Bischof, E. Haselbach, E. Heilbronner, *Angew. Chem. 82* (1970) 952; *Angew. Chem. Int. Ed. Engl. 9* (1970) 953.
[133] H. D. Martin, C. Heller, E. Haselbach, Z. Lanyjova, *Helv. Chim. Acta 57* (1974) 465.
[134] P. Bischof, P. E. Eaton, R. Gleiter, E. Heilbronner, T. B. Jones, H. Musso, A. Schmelzer, R. Stober, *Helv. Chim. Acta 61* (1978) 547.
[135] a) R. Daudel, C. Sandorfy: *Semiempirical Wave-Mechanical Calculations on Polyatomic Molecules*, Yale University Press, New Haven 1971; b) O. Sinanoglu, K. W. Wiberg: *Sigma Molecular Orbital Theory*, Yale University Press, New Haven 1970.
[136] E. Honegger, E. Heilbronner, A. Schmelzer, W. Jian-Qi, *Isr. J. Chem. 22* (1982) 3.
[137] P. Hemmersbach, M. Klessinger, *Tetrahedron 36* (1980) 1337.
[138] a) H. D. Martin, E. Eisenmann, M. Kunze, V. Bonačič-Koutecký, *Chem. Ber. 113* (1980) 1153; b) R. Walsh, H. D. Martin, M. Kunze, A. Oftring, H. D. Beckhaus, *J. Chem. Soc. Perkin Trans. 2, 1981*, 1076.
[139] B. Andersen, L. Fernholt, *Acta Chem. Scand. 24* (1970) 445.
[140] H. D. Martin, B. Mayer, unpublished results.
[141] W. V. Steele, *J. Chem. Thermodyn. 1980*, 187.
[142] A. T. Hagler, P. S. Stern, S. Lifson, S. Ariel, *J. Am. Chem. Soc. 101* (1979) 813.
[143] a) K. Yoshikawa, A. Matsui, I. Morishima, *J. Chem. Soc. Perkin Trans. 2, 1977*, 1057; b) I. Morishima, K. Yoshikawa, M. Hashimoto, K. Bekki, *J. Am. Chem. Soc. 97* (1975) 4283; c) G. R. Underwood, H. S. Friedman, *ibid. 96* (1974) 4989; d) I. Morishima, K. Yoshikawa, *ibid. 97* (1975) 2950; e) K. Yoshikawa, K. Bekki, M. Karatsu, K. Toyoda, T. Kamio, I. Morishima, *ibid. 98* (1976) 3272; f) J. B. Grutzner, *ibid. 98* (1976) 6385.
[144] a) C. W. Worrell, J. W. Verhoeven, W. N. Speckamp, *Tetrahedron 30* (1974) 3525; b) R. Sarneel, C. W. Worrell, P. Pasman, J. W. Verhoeven, G. F. Mes, *ibid. 36* (1980) 3241.
[145] J. Kroner, W. Kosbahn, W. Runge, *Ber. Bunsenges. Phys. Chem. 81* (1977) 826.
[146] a) M. N. Paddon-Row, *Tetrahedron Lett. 1972*, 1409; b) M. N. Paddon-Row, H. K. Patney, R. N. Warrener, *J. Org. Chem. 44* (1979) 3908.
[147] a) R. W. Alder, R. J. Arrowsmith, C. S. J. Boothby, E. Heilbronner, Y. Zhong-zhi, *J. Chem. Soc. Chem. Commun. 1982*, 940; b) R. W. Alder, R. J. Arrowsmith, A. Casson, R. B. Sessions, E. Heilbronner, B. Kovač, H. Huber, M. Taagepera, *J. Am. Chem. Soc. 103* (1981) 6137.
[148] P. S. Engel, *Chem. Rev. 80* (1980) 99.
[149] a) H. Schmidt, A. Schweig, B. M. Trost, H. B. Neubold, P. H. Scudder, *J. Am. Chem. Soc. 96* (1974) 622; b) R. J. Boyd, J. C. G. Bünzli, J. P. Snyder, *ibid. 98* (1976) 2398; c) E. L. Allred, A. L. Johnson, *ibid. 93* (1971) 1300.
[150] In this context the discussion by H. C. Brown and P. von R. Schleyer in [18], p. 272–281 is of particular interest.
[151] R. M. Coates, E. R. Fretz, *J. Am. Chem. Soc. 97* (1975) 2538.
[152] a) H. D. Martin, C. Heller, R. Haider, R. W. Hoffmann, J. Becherer, H. R. Kurz, *Chem. Ber. 110* (1977) 3010; b) R. W. Hoffmann, H. R. Kurz, J. Becherer, H. D. Martin, *ibid. 111* (1978) 1275; c) P. Bischof, M. Böhm, R. Gleiter, R. A. Snow, C. W. Doecke, L. A. Paquette, *J. Org. Chem. 43* (1978) 2387.
[153] S. A. Cowling, R. A. W. Johnstone, A. A. Gorman, P. G. Smith, *J. Chem. Soc. Chem. Commun. 1973*, 627.
[154] D. F. Eaton, T. G. Traylor, *J. Am. Chem. Soc. 96* (1974) 7109.
[155] R. Bicker, H. Kessler, A. Steigel, G. Zimmermann, *Chem. Ber. 111* (1978) 3215.
[156] F. A. Bovey: *Nuclear Magnetic Resonance Spectroscopy*, Academic Press, New York 1969, p. 72.
[157] Y. Kodama, K. Nishihata, M. Nishio, N. Nakagawa, *Tetrahedron Lett. 1977*, 2105.
[158] H. Prinzbach, G. Sedelmeier, H. D. Martin, *Angew. Chem. 89* (1977) 111; *Angew. Chem. Int. Ed. Engl. 16* (1977) 103.
[159] B. Albert, W. Berning, C. Burschka, S. Hünig, H. D. Martin, F. Proksch, *Chem. Ber. 114* (1981) 423.
[160] C. Santiago, E. J. McAlduff, K. N. Houk, R. A. Snow, L. A. Paquette, *J. Am. Chem. Soc. 100* (1978) 6149.
[161] E. Haselbach, M. Rossi, *Helv. Chim. Acta 59* (1976) 278.
[162] a) H. Dugas, C. Penney: *Bioorganic Chemistry*, Springer, New York 1981; b) J. H. Fuhrhop: *Bio-organische Chemie*, Thieme, Stuttgart 1982; c) J. Rétey, J. A. Robinson: *Stereospecificity in Organic Chemistry and Enzymology*, Verlag Chemie, Weinheim 1982.
[163] a) W. C. Holland, R. L. Klein, A. Briggs: *Molekulare Pharmakologie*, Thieme, Stuttgart 1967; b) A. Korolkovas: *Grundlagen der molekularen Pharmakologie*, Thieme, Stuttgart 1974; c) W. G. Richards: *Quantum Pharmacology*, Butterworths, London 1977.
[164] J. Spanget-Larsen, R. Gleiter, M. Kobayashi, M. E. Engler, P. Shu, D. O. Cowan, *J. Am. Chem. Soc. 99* (1977) 2855.
[165] C. Guimon, G. Pfister-Guillouzo, *J. Electron Spectrosc. Relat. Phenom. 7* (1975) 191.
[166] K. Wittel, E. E. Astrup, H. Bock, G. Graeffe, H. Julsen, *Z. Naturforsch. B 30* (1975) 862.
[167] D. A. Sweigart, D. W. Turner, *J. Am. Chem. Soc. 94* (1972) 5592.
[168] A. J. Berlinsky, J. F. Carolan, L. Weiler, *Can. J. Chem. 52* (1974) 3373.
[169] A. D. Baker, M. A. Brisk, T. J. Venanzi, Y. S. Kwon, S. Sadka, *Tetrahedron Lett. 1976*, 3415.
[170] F. Bernardi, G. Distefano, A. Modelli, D. Pietropaolo, *J. Organomet. Chem. 128* (1977) 331.
[171] A. D. Bain, D. C. Frost, *Can. J. Chem. 51* (1973) 1245.
[172] C. Guimon, G. Pfister-Guillouzo, J. L. Larice, *J. Chim. Phys. Phys.-Chim. Biol. 74* (1977) 1097.
[173] H. Bock, G. Wagner, *Angew. Chem. 84* (1972) 119; *Angew. Chem. Int. Ed. Engl. 11* (1972) 150.
[174] M. Kobayashi, R. Gleiter, D. L. Coffen, H. Bock, W. Schulz, U. Stein, *Tetrahedron 33* (1977) 433.
[175] C. Guimon, M. F. Guimon, G. Pfister-Guillouzo, *Tetrahedron Lett. 1975*, 1413.
[176] C. Guimon, G. Pfister-Guillouzo, M. Arbelot, *J. Mol. Struct. 30* (1976) 339.
[177] F. S. Joergensen, *J. Chem. Res. (S) 1981*, 212.
[178] T. H. Gan, J. B. Peel, G. D. Willett, *Chem. Phys. Lett. 51* (1977) 464.
[179] T. Kobayashi, S. Nagakura, *Bull. Chem. Soc. Jpn. 46* (1973) 1558.
[180] F. S. Joergensen, L. Norksov-Lauritsen, *Tetrahedron Lett. 23* (1982) 5221.
[181] F. S. Joergensen, L. Norksov-Lauritsen, R. B. Jensen, G. Schroll, *Tetrahedron 37* (1981) 3671.
[182] P. Rademacher, H. Breier, R. Poppek, *Chem. Ber. 112* (1979) 853.
[183] C. Fridh, L. Asbrink, B. O. Jonsson, E. Lindholm, *Int. J. Mass Spectrom. Ion Phys. 8* (1972) 85.
[184] G. Salmona, R. Faure, E. J. Vincent, C. Guimon, G. Pfister-Guillouzo, *J. Mol. Struct. 48* (1978) 205.
[185] M. H. Palmer, H. Findlay, R. G. Egdell, *J. Mol. Struct. 40* (1977) 191.
[186] L. Asbrink, C. Fridh, B. O. Jonsson, E. Lindholm, *Int. J. Mass Spectrom. Ion Phys. 8* (1972) 215.
[187] R. J. Suffolk, *J. Electron. Spectrosc. Relat. Phenom. 3* (1974) 53.
[188] M. Ohsaku, A. Imamura, K. Hirao, *Bull. Chem. Soc. Jpn. 51* (1978) 3443.
[189] J. Spanget-Larsen, *J. Electron Spectrosc. Relat. Phenom. 3* (1974) 369.
[190] D. M. W. van den Ham, D. van der Meer, *Chem. Phys. Lett. 12* (1972) 447.
[191] D. M. W. van den Ham, D. van der Meer, *J. Electron Spectrosc. Relat. Phenom. 2* (1973) 247.
[192] M. Kunze, H. D. Martin, B. Mayer, unpublished results.
[193] C. R. Brundle, M. B. Robin, H. Basch, *J. Chem. Phys. 53* (1970) 2196.
[194] S. Katsumata, K. Kimura, *Bull. Chem. Soc. Jpn. 46* (1973) 1342.
[195] A. Flamini, E. Semperini, G. Condorelli, *Chem. Phys. Lett. 32* (1975) 365.
[196] K. Wittel, A. Haas, H. Bock, *Chem. Ber. 105* (1972) 3865.
[197] F. T. Chau, C. A. McDowell, *J. Electron Spectrosc. Relat. Phenom. 6* (1975) 365.
[198] Y. Gaunelle, C. Menard, J. M. Pechine, D. Solgadi, F. Menes, R. Botter, *J. Electron Spectrosc. Relat. Phenom. 7* (1975) 247.
[199] T. H. Gan, J. B. Peel, G. D. Willett, *J. Mol. Struct. 44* (1978) 211.
[200] Y. Hoppillard, D. Solgadi, *Tetrahedron 36* (1980) 377.
[201] R. Botter, F. Menes, Y. Gounelle, J. M. Pechine, J. M. Solgadi, *Int. J. Mass Spectrom. Ion Phys. 12* (1973) 188.
[202] F. T. Chau, C. A. McDowell, *J. Mol. Struct. 34* (1976) 93.
[203] R. F. Lake, H. Thompson, *Proc. R. Soc. London Ser. A 315* (1970) 323.
[204] R. Manne, *J. Electron Spectrosc. Relat. Phenom. 3* (1974) 327.

[205] H. Bock, K. Wittel, *J. Chem. Soc. Chem. Commun. 1972,* 602.
[206] J. Neville, K. Ross, V. Tomlinson, *Int. J. Mass Spectrom. Ion Phys. 4* (1970) 51.
[207] T. Kobayashi, K. Yokota, S. Nagakura, *Bull. Chem. Soc. Jpn. 48* (1975) 412.
[208] M. Loudet, M. Grimaud, F. Metras, G. Pfister-Guillouzo, *J. Mol. Struct. 35* (1976) 213.
[209] R. S. Brown, *Can. J. Chem. 54* (1976) 3203.
[210] J. L. Meeks, J. F. Arnett, D. Larson, S. P. McGlynn, *Chem. Phys. Lett. 30* (1975) 190.
[211] S. Chattopadhyay, J. L. Meeks, G. L. Findley, S. P. McGlynn, *J. Phys. Chem. 85* (1981) 968.
[212] S. P. McGlynn, J. L. Meeks, *J. Electron Spectrosc. Relat. Phenom. 8* (1976) 85.
[213] V. Y. Young, K. L. Cheng, *J. Chem. Phys. 65* (1976) 3187.
[214] J. Kelder, H. Cerfontain, B. R. Higginson, D. R. Lloyd, *Tetrahedron Lett. 1974,* 739.
[215] A. Bigotto, V. Gallasso, G. Disteffano, A. Modelli, *J. Chem. Soc. Perkin Trans. 2, 1979,* 1502.
[216] D. Gonbeau, M. Loudet, G. Pfister-Guillouzo, *Tetrahedron 36* (1980) 381.
[217] R. Gleiter, M. Kobayashi, N. S. Zefirov, V. A. Palyulin, *Dokl. Akad. Nauk SSSR 235* (1977) 347.
[218] E. Heilbronner, K. A. Muszkat, *J. Am. Chem. Soc. 92* (1970) 3818.
[219] P. Bischof, J. A. Hashmall, E. Heilbronner, V. Hornung, *Tetrahedron Lett. 1969,* 4025.
[220] S. F. Nelsen, L. A. Greezo, W. C. Hollinsed, *J. Org. Chem. 46* (1980) 283.
[221] N. S. Hush, A. S. Cheung, P. R. Hilton, *J. Electron Spectrosc. Relat. Phenom. 7* (1975) 385.
[222] L. Klasinc, J. Novak, J. Rieger, M. Scholz, *Monatsh. Chem. 112* (1981) 697.
[223] C. Fridh, L. Asbrink, B. O. Jonsson, E. Lindholm, *Int. J. Mass Spectrom. Ion Phys. 8* (1972) 101.
[224] H. T. Dieck, K. D. Franz, W. Majunke, *Z. Naturforsch. B 30* (1975) 922.
[225] R. Schulz, A. Schweig, *Angew. Chem. 93* (1981) 603; *Angew. Chem. Int. Ed. Engl. 20* (1981) 570.
[226] K. E. Gilbert, *J. Org. Chem. 42* (1977) 609.
[227] J. C. Buenzli, H. Olsen, J. P. Snyder, *J. Org. Chem. 42* (1977) 614.
[228] T. Cvitaš, H. Güsten, L. Klasinc, *J. Chem. Soc. Perkin Trans. 2, 1977,* 962.
[229] M. V. Andreocci, C. Furlani, L. Alagna, C. Cauletti, *Congr. Naz. Chim. Inorg. [Atti], 13th 1980,* 223.
[230] G. W. Mines, H. Thompson, *Proc. R. Soc. London Ser. A 342* (1975) 327.
[231] A. Schweig, H. Vermeer, U. Weidner, *Chem. Phys. Lett. 26* (1974) 229.
[232] T. Prange, J. Drouin, F. Leyendecker, J. M. Conia, *J. Chem. Soc. Chem. Commun. 1977,* 430.
[233] M. Almemark, J. E. Baeckvall, C. Moberg, B. Akermark, L. Asbrink, B. Roos, *Tetrahedron 30* (1974) 2503.
[234] S. H. Gerson, S. D. Worley, N. Bodor, J. J. Kaminski, T. W. Flechtner, *J. Electron Spectrosc. Relat. Phenom. 13* (1978) 421.
[235] P. Livant, K. A. Roberts, M. D. Eggers, S. D. Worley, *Tetrahedron 37* (1981) 1853.
[236] D. Ajo, E. Ciliberto, I. Fragala, G. Granozzi, *J. Mol. Struct. 62* (1980) 189.
[237] F. Carnovale, T.-H. Gan, J. B. Peel, A. B. Holmes, *J. Chem. Soc. Perkin Trans. 2, 1981,* 991.
[238] T. J. O'Donnell, P. R. LeBreton, J. D. Petke, L. L. Shipman, *J. Phys. Chem. 84* (1980) 1975.
[239] M. Kobayashi, R. Gleiter, Z. Naturforsch. B 33 (1978) 1057.
[240] R. Gleiter, N. S. Zefirov, V. A. Palyulin, K. A. Potekhin, E. N. Kurkutova, Y. T. Struchkov, M. Y. Antipin, *Zh. Org. Khim. 14* (1978) 1630.
[241] T. Kobayashi, *J. Electron Spectrosc. Relat. Phenom. 7* (1975) 349.
[242] J. P. Maier, J. F. Muller, T. Kubota, *Helv. Chim. Acta 58* (1975) 1634.
[243] J. P. Maier, J. F. Muller, T. Kubota, *Helv. Chim. Acta 58* (1975) 1641.
[244] F. Bernardi, A. Bottoni, F. P. Colonna, G. Distefano, U. Folli, P. Vivarelli, *Z. Naturforsch. A 33* (1978) 959.
[245] F. Bernardi, F. P. Colonna, P. Dembech, G. Distefano, P. Vivarelli, *Chem. Phys. Lett. 36* (1975) 539.
[246] D. G. Streets, T. A. Williams, *J. Electron Spectrosc. Relat. Phenom. 3* (1974) 71.
[247] S. D. Worley, G. D. Mateescu, C. W. McFarland, R. C. Fort, Jr., C. F. Sheley, *J. Am. Chem. Soc. 95* (1973) 7580.
[248] D. A. Demeo, A. J. Yencha, *J. Chem. Phys. 53* (1970) 4536.
[249] D. A. Demeo, M. A. El-Sayed, *J. Chem. Phys. 52* (1970) 2622.
[250] M. H. Palmer, R. H. Findlay, *Chem. Phys. Lett. 15* (1972) 416.
[251] E. Heilbronner, F. Brogli, E. Vogel, *J. Electron Spectrosc. Relat. Phenom. 9* (1976) 227.
[252] P. Asmus, M. Klessinger, *Tetrahedron 30* (1974) 2477.
[253] H. U. Pfeffer, M. Klessinger, G. Erker, W. R. Roth, *Chem. Ber. 108* (1975) 2923.
[254] M. Moharz, C. Batich, E. Heilbronner, P. Vogel, P.-A. Carrupt, *Recl. Trav. Chim. Pays-Bas 98* (1979) 361.
[255] M. Mohraz, J.-Q. Wang, E. Heilbronner, P. Vogel, O. Pilet, *Helv. Chim. Acta 63* (1980) 568.
[256] J. P. Delwich, M. T. Praet, *J. Electron Spectrosc. Relat. Phenom. 7* (1975) 317.
[257] D. Bougeard, B. Schrader, P. Bleckmann, T. Plesser, *Liebigs Ann. Chem. 1974,* 137.
[258] F. Marschner, H. Juds, H. Goetz, *Tetrahedron Lett. 1973,* 3983.
[259] G. Bieri, F. Burger, E. Heilbronner, J. P. Maier, *Helv. Chim. Acta 60* (1977) 2213.
[260] G. Bieri, E. Heilbronner, T. Kobayashi, A. Schmelzer, M. J. Goldstein, R. S. Leight, M. Lipton, *Helv. Chim. Acta 59* (1976) 2657.
[261] G. Bieri, E. Heilbronner, M. J. Goldstein, R. S. Leight, M. S. Lipton, *Tetrahedron Lett. 1975,* 581.
[262] P. Bischof, R. Gleiter, E. Heilbronner, V. Hornung, G. Schroeder, *Helv. Chim. Acta 53* (1970) 1645.
[263] R. W. Hoffmann, R. Schüttler, W. Schäfer, A. Schweig, *Angew. Chem. 84* (1972) 533; *Angew. Chem. Int. Ed. Engl. 11* (1972) 512.
[264] F. Brogli, E. Heilbronner, J. Ipaktschi, *Helv. Chim. Acta 55* (1972) 2447.
[265] R. W. Hoffmann, A. Riemann, H. D. Martin, B. Mayer, unpublished results.
[266] P. Rademacher, W. Elling, *Liebigs Ann. Chem. 1979,* 1473.
[267] C. Batich, P. Bischof, E. Heilbronner, *J. Electron Spectrosc. Relat. Phenom. 1* (1973) 333.
[268] J. C. Bünzli, D. C. Frost, L. Weiler, *Tetrahedron Lett. 1973,* 1159.
[269] L. N. Domelsmith, K. N. Houk, C. R. Degenhardt, L. A. Paquette, *J. Am. Chem. Soc. 100* (1978) 100.
[270] P. Bischof, D. Bosse, R. Gleiter, M. J. Kukla, A. de Meijere, L. A. Paquette, *Chem. Ber. 108* (1975) 1218.
[271] R. Gleiter, E. Heilbronner, L. A. Paquette, G. L. Thompson, R. E. Wingard, Jr., *Tetrahedron 29* (1973) 565.
[272] R. Askani, R. Gleiter, E. Heilbronner, V. Hornung, H. Musso, *Tetrahedron Lett. 1971,* 4461.
[273] P. Bischof, R. Gleiter, H. Dürr, B. Ruge, P. Herbst, *Chem. Ber. 109* (1976) 1412.
[274] P. Bischof, R. Gleiter, R. Haider, *Angew. Chem. 89* (1977) 122; *Angew. Chem. Int. Ed. Engl. 16* (1977) 110.
[275] A. Schweig, U. Weidner, D. Hellwinkel, W. Krapp, *Angew. Chem. 85* (1973) 360; *Angew. Chem. Int. Ed. Engl. 12* (1973) 310.
[276] C. Batich, E. Heilbronner, E. Rommel, M. F. Semmelhack, J. S. Foos, *J. Am. Chem. Soc. 96* (1974) 7662.
[277] Y. Harrada, K. Ohno, K. Seki, H. Inokuchi, *Chem. Lett. 1974,* 1081.
[278] P. Asmus, M. Klessinger, L. U. Meyer, A. de Meijere, *Tetrahedron Lett. 1975,* 381.
[279] S. Cradock, R. H. Findlay, M. H. Palmer, *J. Chem. Soc. Dalton Trans. 1974,* 1650.
[280] R. Gleiter, E. Heilbronner, A. de Meijere, *Helv. Chim. Acta 54* (1971) 1029.
[281] P. Bischof, R. Gleiter, A. de Meijere, L. U. Meyer, *Helv. Chim. Acta 57* (1974) 1519.
[282] B. Kovač, E. Heilbronner, H. Prinzbach, K. Weidmann, *Helv. Chim. Acta 62* (1979) 2841.
[283] M. T. Reetz, R. W. Hoffmann, W. Schäfer, A. Schweig, *Angew. Chem. 85* (1973) 45; *Angew. Chem. Int. Ed. Engl. 12* (1973) 81.
[284] N. Bodor, M. J. S. Dewar, S. D. Worley, *J. Am. Chem. Soc. 92* (1970) 19.
[285] C. Müller, A. Schweig, *Tetrahedron 29* (1973) 3973.
[286] U. Weidner, A. Schweig, *J. Organomet. Chem. 37* (1972) C29.
[287] U. Weidner, A. Schweig, *Angew. Chem. 84* (1972) 550; *Angew. Chem. Int. Ed. Engl. 11* (1972) 537.
[288] J. C. Bünzli, A. J. Burak, D. C. Frost, *Tetrahedron 29* (1973) 3735.
[289] A. Schweig, U. Weidner, J. G. Berger, W. Grahn, *Tetrahedron Lett. 1973,* 557.
[290] F. Brogli, E. Heilbronner, J. Wirz, E. Kloster-Jensen, R. G. Bergmann, K. P. C. Vollhardt, A. J. Ashe, *Helv. Chim. Acta 58* (1975) 2620.
[291] R. Boschi, W. Schmidt, J. C. Gfeller, *Tetrahedron Lett. 1972,* 4107.
[292] G. P. Ceasar, J. Green, L. A. Paquette, R. E. Wingard, *Tetrahedron Lett. 1973,* 1721.
[293] B. Albert, H. D. Martin, B. Mayer, unpublished results.
[294] H. Prinzbach, C. Heller, H. D. Martin, unpublished results.
[295] D. Dougherty, J. J. Bloomfield, G. R. Newkome, J. F. Arnett, S. P. McGlynn, *J. Phys. Chem. 80* (1976) 2212.
[296] G. Klein, L. A. Paquette, C. W. Doecke, *J. Am. Chem. Soc. 100* (1978) 1596.
[297] J. Spanget-Larsen, R. Gleiter, G. Klein, C. W. Doecke, L. A. Paquette, *Chem. Ber. 113* (1980) 2120.
[298] A. Greenberg, J. F. Liebmann, *J. Am. Chem. Soc. 103* (1981) 44.
[299] J. Spanget-Larsen, C. de Korswagen, M. Eckert-Maksič, R. Gleiter, *Helv. Chim. Acta 65* (1982) 968.

[300] W. T. Borden, S. D. Young, D. C. Frost, N. P. C. Westwood, W. L. Joergensen, *J. Org. Chem. 44* (1979) 737.
[301] G. Bieri, E. Heilbronner, E. Kloster-Jensen, A. Schmelzer, J. Wirz, *Helv. Chim. Adta 57* (1974) 1265.
[302] P. Bischof, R. Gleiter, H. Hopf, F. T. Lenich, *J. Am. Chem. Soc. 97* (1975) 5467.
[303] F. Brogli, J. K. Crandall, E. Heilbronner, E. Kloster-Jensen, S. A. Sojka, *J. Electron Spectrosc. Relat. Phenom. 2* (1973) 455.
[304] M. C. Böhm, R. Gleiter, *Chem. Ber. 111* (1978) 3516.
[305] R. Gleiter, K. Gubernator, W. Grimme, *J. Org. Chem. 46* (1981) 1247.
[306] P. Bischof, E. Heilbronner, *Helv. Chim. Acta 53* (1970) 1677.
[307] P. Bischof, R. Gleiter, K. Gubernator, R. Haider, H. Musso, W. Schwarz, W. Trautmann, H. Hopf, *Chem. Ber. 114* (1981) 994.
[308] R. Gleiter, W. Schäfer, M. Eckert-Maksič, *Chem. Ber. 114* (1981) 2309.
[309] J. B. Peel, G. D. Willet, *Chem. Phys. Lett. 38* (1976) 479.
[310] H. Bock, H. Stafast, *Tetrahedron 32* (1976) 855.
[311] I. Ikemoto, K. Samizo, T. Fujikawa, K. Ishii, T. Ohta, H. Kuroda, *Chem. Lett. 1974,* 785.
[312] H. Bock, H. Stafast, *Chem. Ber. 105* (1972) 1158.
[313] C. Nishijima, H. Nakayama, T. Kabayashi, K. Yokota, *Chem. Lett. 1975,* 5.
[314] B. J. M. Neijzen, C. A. DeLange, *J. Electron Spectrosc. Relat. Phenom. 14* (1978) 187.
[315] M. H. Palmer, W. Moyes, M. Spiers, *J. Mol. Struct. 62* (1980) 165.
[316] A. Schweig, U. Weidner, R. K. Hill, D. A. Cullison, *J. Am. Chem. Soc. 95* (1973) 5426.
[317] J. P. Colpa, K. H. Hauser, D. Schweitzer, *Chem. Phys. 29* (1978) 187.
[318] T. Koenig, M. Tuttle, *J. Org. Chem. 39* (1974) 1307.
[319] D. Schweitzer, K. H. Hausser, M. W. Haenel, *Chem. Phys. 29* (1978) 181.
[320] V. Boekelheide, W. Schmidt, *Chem. Phys. Lett. 17* (1972) 410.
[321] B. Kovač, M. Mohraz, E. Heilbronner, S. Ito, Y. Fukazawa, P. M. Keehn, *J. Electron Spectrosc. Relat. Phenom. 22* (1981) 327.
[322] B. Kovač, M. Allan, E. Heilbronner, *Helv. Chim. Acta 64* (1981) 430.
[323] E. Haselbach, E. Heilbronner, H. Musso, A. Schmelzer, *Helv. Chim. Acta 55* (1972) 302.
[324] G. Sedelmeier, Disseration, Universität Freiburg 1979.
[325] C. W. Worell, *J. Electron Spectrosc. Relat. Phenom. 3* (1974) 359.
[326] J. B. Peel, G. D. Willet, *Aust. J. Chem. 30* (1977) 2571.
[327] P. C. Burgers, C. W. Worrell, M. P. Groenewege, *Spectrosc. Lett. 13* (1980) 381.
[328] W. Schaefer, A. Schweig, *J. Chem. Soc. Chem. Commun. 1972,* 824.
[329] W. Schaefer, A. Schweig, *Tetrahedron Lett. 1972,* 5205.
[330] R. Botter, Y. Gounelle, Y. Henry, J. Jullien, F. Menes, D. Solgadi, *J. Electron Spectrosc. Relat. Phenom. 10* (1977) 393.
[331] E. J. McAlduff, P. Caramella, K. H. Nouk, *J. Am. Chem. Soc. 100* (1978) 105.
[332] A. D. Bain, J. C. Bünzli, D. C. Frost, L. Weiler, *J. Am. Chem. Soc. 95* (1973) 291.
[333] H. Schmidt, A. Schweig, *Chem. Ber. 107* (1974) 725.
[334] C. Müller, A. Schweig, A. G. Anastassiou, J. C. Wetzel, *Tetrahedon 30* (1974) 4089.
[335] H. Schmidt, A. Schweig, A. G. Anastassiou, J. C. Wetzel, *Tetrahedron 32* (1976) 2239.
[336] R. Gleiter, *Top. Curr. Chem. 86* (1979) 196.
[337] W. Schaefer, H. Schmidt, A. Schweig, R. W. Hoffmann, H. Kurz, *Tetrahedron Lett. 1974,* 1953.
[338] B. J. M. Neijzen, R. F. Schmitz, G. W. Klumpp, C. A. DeLange, *Tetrahedron 31* (1975) 873.
[339] R. S. Brown, *Can. J. Chem. 54* (1976) 3206.
[340] K. B. Astin, K. Mackenzie, *J. Chem. Soc. Perkin Trans. 2, 1975,* 1004.
[341] R. Gleiter, R. Bartetzko, P. Hoffmann, H. D. Scharf, *Angew. Chem. 89* (1977) 414; *Angew. Chem. Int. Ed. Engl. 16* (1977) 400.
[342] R. Bartetzko, R. Gleiter, J. L. Muthard, L. A. Paquette, *J. Am. Chem. Soc. 100* (1978) 5589.
[343] M. C. Böhm, R. Gleiter, *Tetrahedron 35* (1979) 675.
[344] S. Millefiori, A. Millefiori, *Can. J. Chem. 59* (1981) 821.
[345] R. S. Brown, *Can. J. Chem. 54* (1976) 642.
[346] H. D. Martin, C. Heller, J. Werp, *Chem. Ber. 107* (1974) 1393.
[347] P. Bischof, E. Heilbronner, H. Prinzbach, H. D. Martin, *Helv. Chim. Acta 54* (1971) 1072.
[348] R. Gleiter, P. Bischof, W. E. Volz, L. A. Paquette, *J. Am. Chem. Soc. 99* (1977) 8.
[349] P. Bruckmann, M. Klessinger, *Angew. Chem. 84* (1972) 543; *Angew. Chem. Int. Ed. Engl. 11* (1972) 524.
[350] D. J. Pasto, T. P. Fehlner, M. E. Schwartz, H. F. Baney, *J. Am. Chem. Soc. 98* (1976) 530.
[351] M. J. S. Dewar, G. J. Fonken, T. B. Jones, D. E. Minter, *J. Chem. Soc. Perkin Trans. 2, 1976,* 764.
[352] P. E. Schipper, M. N. Paddon-Row, *Aust. J. Chem. 35* (1982) 1755.
[353] L. A. Paquette, F. Bellamy, G. J. Wells, M. C. Böhm, R. Gleiter, *J. Am. Chem. Soc. 103* (1981) 7122.
[354] R. Gleiter, R. Haider, I. Murata, R. M. Pagni, *J. Chem. Res. S 1979,* 72.
[355] V. V. Plemenkov, Kh. Z. Giniyatov, Ya. Ya. Villem, N. V. Villem, L. S. Surmina, I. G. Bolesov, *Dokl. Akad. Nauk SSSR 254* (1980) 456.
[356] L. A. Paquette, L. W. Hertel, R. Gleiter, M. C. Böhm, M. A. Beno, G. G. Christoph, *J. Am. Chem. Soc. 103* (1981) 7106.
[357] F. Scully, T. Nylund, F. Palensky, H. Morrison, *J. Am. Chem. Soc. 100* (1978) 7352.
[358] L. A. Paquette, A. Y. Ku, C. Santiago, M. D. Rozeboom, K. N. Houk, *J. Am. Chem. Soc. 101* (1979) 5972.
[359] L. A. Paquette, C. C. Liao, R. L. Burson, R. E. Wingard, Jr., C. N. Shih, J. Fayos, J. Clardy, *J. Am. Chem. Soc. 99* (1977) 6935.
[360] J.-P. Stadelmann, J. Vogt, *Int. J. Mass Spectrom. Ion Phys. 35* (1980) 83.
[361] C. Batich, E. Heilbronner, E. Vogel, *Helv. Chim. Acta 57* (1974) 2288.
[362] H. D. Martin, C. Heller, B. Mayer, H. D. Beckhaus, *Chem. Ber. 113* (1980) 2589.
[363] H. D. Martin, M. Kunze, H. D. Beckhaus, R. Walsh, R. Gleiter, *Tetrahedron Lett. 1979,* 3069.
[364] H. D. Martin, P. Pföhler, *Angew. Chem. 90* (1978) 901; *Angew. Chem. Int. Ed. Engl. 17* (1978) 847.
[365] W. Schmidt, B. T. Wilkins, *Tetrahedron 28* (1972) 5649.
[366] H. Dürr, R. Gleiter, *Angew. Chem. 90* (1978) 591; *Angew. Chem. Int. Ed. Engl. 17* (1978) 559.
[367] Y. Zhong-zhi, E. Heilbronner, S. Eltamany, H. Hopf, B. Kovač, *Helv. Chim. Acta 64* (1981) 1991.
[368] M. D. Brown, J. Hudec, J. M. Mellor, *Chem. Commun. 1971,* 1640.
[369] F. S. Joergensen, L. Carlsen, F. Duus, *J. Am. Chem. Soc. 103* (1981) 1350.
[370] R. S. Brown, R. W. Marcinko, *J. Am. Chem. Soc. 99* (1977) 6500.
[371] D. Chadwick, D. C. Frost, L. Weiler, *J. Am. Chem. Soc. 93* (1971) 4962.
[372] L. Weiler, D. Chadwick, D. C. Frost, *J. Am. Chem. Soc. 93* (1971) 4320.
[373] L. N. Domelsmith, P. D. Mollere, K. N. Houk, R. C. Hahn, R. P. Johnson, *J. Am. Chem. Soc. 100* (1978) 2959.
[374] I. D. Reingold, W. Schmidt, V. Boekelheide, *J. Am. Chem. Soc. 101* (1979) 2121.
[375] H. Prinzbach, G. Fischer, G. Rihs, G. Sedelmeier, E. Heilbronner, Z. Yang, *Tetrahedron Lett. 23* (1982) 1251.
[376] M. Kajitani, A. Sugimori, N. Sato, K. Seki, H. Inokuchi, Y. Harada, *Bull. Chem. Soc. Jpn. 52* (1979) 2199.
[377] R. H. Findley, M. H. Palmer, A. J. Downs, R. G. Egdell, R. Evans, *Inorg. Chem. 19* (1980) 1307.
[378] E. Beck, P. Hofmann, S. Sieber, *Tetrahedron Lett. 22* (1981) 4683.
[379] M. F. Guimon, C. Guimon, F. Metras, G. Pfister-Guillouzo, *J. Am. Chem. Soc. 98* (1976) 2078.
[380] J. Daintith, J. P. Maier, D. A. Sweigart, D. W. Turner in: D. A. Shirley: *Electron Spectroscopy,* North-Holland, Amsterdam 1972, p. 289.
[381] J. J. Worman, E. A. Schmidt, E. S. Olson, W. P. Jensen, R. D. Schultz, *Spectrochim. Acta A 32* (1976) 1415.
[382] R. Gleiter, J. Spanget-Larsen, *Top. Curr. Chem. 86* (1979) 139.
[383] A. W. Potts, H. J. Lempka, D. G. Streets, W. C. Price, *Phil. Trans. R. Soc. London Ser. A 268* (1970) 59.
[384] A. H. Cowley, M. J. S. Dewar, M. Lattman, J. L. Mills, M. McKee, *J. Am. Chem. Soc. 100* (1978) 3349.
[385] F. T. Chau, C. A. McDowell, *J. Electron Spectrosc. Relat. Phenom. 6* (1975) 357.
[386] A. Schweig, U. Weidner, G. Manuel, *Angew. Chem. 84* (1972) 899; *Angew. Chem. Int. Ed. Engl. 11* (1972) 837.
[387] I. Bertoti, S. Cradock, E. A. V. Ebsworth, R. A. Whiteford, *J. Chem. Soc. Dalton Trans. 1976,* 937.
[388] M. F. Guimon, C. Guimon, G. Pfister-Guillouzo, *Tetrahedron Lett. 1975,* 441.
[389] R. Hoffmann, E. Heilbronner, R. Gleiter, *J. Am. Chem. Soc. 92* (1970) 706.
[390] C. Batich, E. Heilbronner, M. F. Semmelhack, *Helv. Chim. Acta 56* (1973) 2110.
[391] M. Bloch, E. Heilbronner, T. B. Jones, J. L. Ripoll, *Heterocycles 11* (1978) 443.
[392] S. F. Nelsen, W. C. Hollinsed, L. A. Grezzo, W. P. Parmelee, *J. Am. Chem. Soc. 101* (1979) 7347.
[393] L. A. Paquette, H. C. Berk, C. R. Degenhardt, G. D. Ewing, *J. Am. Chem. Soc. 99* (1977) 4764.
[394] H. Schmidt, A. Schweig, A. G. Anastassiou, H. Yamamoto, *J. Chem. Soc. Chem. Commun. 1974,* 218.
[395] K. Gubernator, R. Gleiter, *Chem. Ber. 115* (1982) 3811.
[396] V. Balaji, K. D. Jordan, P. D. Burrow, M. N. Paddon-Row, H. K. Patney, *J. Am. Chem. Soc. 104* (1982) 6849.
[397] a) R. S. Brown, *Can. J. Chem. 54* (1976) 805; *53* (1975) 3439; b) R. Gleiter, P. Schang, W. Adam, H. Eggelte, I. Erden, A. J. Bloodworth, *J. Electron Spectrosc. Relat. Phenom. 19* (1980) 223.

[398] a) S. W. Staley, M. D. Bjorke, J. C. Giordan, M. R. McMillan, J. H. Moore, *J. Am. Chem. Soc. 103* (1981) 7057; b) J. Giordan, M. R. McMillan, J. H. Moore, S. W. Staley, *ibid. 102* (1980) 4870.
[399] H. J. Dewey, R. D. Miller, J. Michl, *J. Am. Chem. Soc. 104* (1982) 5298.
[400] R. Carnovale, T. H. Gan, J. B. Peel, *J. Electron Spectrosc. Relat. Phenom. 16* (1979) 87.
[401] F. Brogli, W. Eberbach, E. Haselbach, E. Heilbronner, V. Hornung, D. M. Lemal, *Helv. Chim. Acta 56* (1973) 1933.
[402] J. Wirz, *Helv. Chim. Acta 59* (1976) 1647.
[403] G. G. Christoph, J. L. Muthard, L. A. Paquette, M. C. Böhm, R. Gleiter, *J. Am. Chem. Soc. 100* (1978) 7782.
[404] T. H. Gan, J. B. Peel, G. D. Willett, *J. Chem. Soc. Faraday Trans. 2, 1977*, 965.
[405] K. W. Shen, N. A. Kuebler, *Tetrahedron Lett. 1973*, 2145.
[406] W. Grimme, L. Schumachers, R. Gleiter, K. Gubernator, *Angew. Chem. 93* (1981) 98; *Angew. Chem. Int. Ed. Engl. 20* (1981) 113.
[407] K. N. Houk, R. W. Strozier, C. Santiago, R. W. Gandour, K. P. C. Vollhardt, *J. Am. Chem. Soc. 101* (1979) 5183.
[408] C. Santiago, K. N. Houk, G. J. DeCicco, L. T. Scott, *J. Am. Chem. Soc. 100* (1978) 692.
[409] B. Kovač, M. Allan, E. Heilbronner, J. P. Maier, R. Gleiter, M. W. Haenel, P. M. Keehn, J. A. Reiss, *J. Electron Spectrosc. Relat. Phenom. 19* (1980) 167.
[410] L. A. Paquette, C. W. Doecke, G. Klein, *J. Am. Chem. Soc. 101* (1979) 7599.
[411] N. Bodor, J. J. Kaminski, S. D. Worley, R. J. Coltan, T. H. Lee, J. W. Rabalais, *J. Pharm. Sci. 63* (1974) 1387.
[412] E. Heilbronner, E. Honegger, N. Heß, H. D. Martin, B. Mayer, T. Urbanek, unpublished results.
[413] H. D. Martin, B. Mayer, A. Fava, unpublished results.
[414] D. Dougherty, R. L. Blankespoor, S. P. McGlynn, *J. Electron Spectrosc. Relat. Phenom. 16* (1979) 245.
[415] M. F. Guimon, C. Guimon, F. Metras, G. Pfister-Guillouzo, *Can. J. Chem. 54* (1976) 146.
[416] H. G. Guttenberg, H. J. Bestmann, F. L. Dickert, F. S. Joergensen, J. P. Snyder, *J. Am. Chem. Soc. 103* (1981) 159.
[417] H. D. Martin, B. Mayer, A. Oftring, unpublished results.

# COMMUNICATIONS

**When submitting manuscripts, authors of articles which are intended for publication as "Communications" are requested to conform to the guidelines reproduced at the beginning of each issue following the list of contents.**

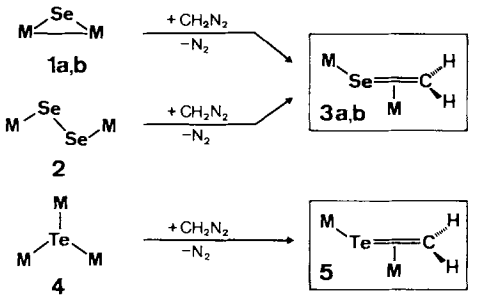
## Seleno- and Telluroformaldehyde as Bridging Ligands in Organometallic Complexes**

By *Wolfgang A. Herrmann**, *Josef Weichmann*, *Ricardo Serrano*, *Klaus Blechschmitt*, *Heike Pfisterer*, and *Manfred L. Ziegler*

*Dedicated to Professor Hermann Schildknecht on the occasion of his 60th birthday*

Originating from the work of *Roper et al.*, the organometallic chemistry of formaldehyde has opened new perspectives in the field of metal-catalyzed hydrogenation of carbon monoxide[5]. Among the heavier congeners of the series $CH_2=X$ (X = S, Se, Te), only thioformaldehyde has unambiguously been characterized in the free state by spectroscopic means[6] and also stabilized by complexation[9]. By way of contrast, only tentative spectroscopic evidence is available for selenoformaldehyde. Finally, neither the character of a reactive intermediate was demonstrated for telluroformaldehyde nor has any organometallic derivative of this species been reported up to the present. Using a novel synthetic strategy, namely addition of methylene to bonds between main group elements and transition metals, we have now succeeded in synthesizing the first organometallic complexes of seleno- and telluroformaldehyde, in which these species function as bridging ligands[***].

The precursor compounds **1**, **2**, **4**[11-13] used in this work have been synthesized by reacting the metallic modifications of selenium and tellurium with the tetrahydrofuran complexes of composition $(\eta^5\text{-}C_5R_5)Mn(CO)_2THF$ (R = H, $CH_3$). The $\mu_2$-selenium and $\mu_3$-tellurium complexes thus obtained react rapidly and quantitatively at −70 °C with




M = $(\eta^5\text{-}C_5Me_5)Mn(CO)_2$ (**1b**,**3b**)
$(\eta^5\text{-}C_5H_5)Mn(CO)_2$ (**1a**,**2**,**3a**,**4**,**5**)

Scheme 1.

diazomethane with concomitant elimination of dinitrogen to give deep blue, air-stable, crystalline products having the general formula $(\eta^5\text{-}C_5R_5)_2Mn_2(CO)_4(X{=}CH_2)$ (**3a**, **3b**, **5**).

[*] Prof. Dr. W. A. Herrmann, J. Weichmann, Dr. R. Serrano
Institut für Anorganische Chemie der Universität
Niederurseler Hang, D-6000 Frankfurt am Main 50 (Germany)
Prof. Dr. M. L. Ziegler, K. Blechschmitt, H. Pfisterer
Anorganisch-chemisches Institut der Universität
Im Neuenheimer Feld 270, D-6900 Heidelberg 1 (Germany)

[**] Transition Metal Methylene Complexes, Part 41. This work was supported by the Deutsche Forschungsgemeinschaft, the Fonds der Chemischen Industrie, and the Spanish Ministry of Education (Fellowship *R. S.*).—Part 40: W. A. Herrmann, Ch. Bauer, M. L. Ziegler, H. Pfisterer, *J. Organomet. Chem. 243* (1983) C 54.

[***] Note added in proof (March 13, 1983): This method has also been successful in the preparation of the analogous thioformaldehyde derivative [M. Herberhold, W. Ehrenreich, W. Bühlmeyer, *Angew. Chem. 95* (1983) 332; *Angew. Chem. Int. Ed. Engl. 22* (1983) 315]. Other synthetic routes to thio-, seleno- and telluroformaldehyde complexes are reported by W. Paul, H. Werner, *ibid. 95* (1983) 333 and *22* (1983) 316, and by C. E. L. Headford, W. R. Roper, *J. Organomet. Chem.*, in press. - The synthetic strategy described in the present paper has successfully been used for the synthesis of the first germylidene complex, $(\mu_3\eta^2\text{-}GeCH_2)[(\eta^5\text{-}C_5H_5)Mn(CO)_2]_3$ (W. A. Herrmann, F. Weichmann, unpublished results).

 © Verlag Chemie GmbH, 6940 Weinheim, 1983 0570-0833/83/0404-0314 $ 02.50/0 

The structural features of the novel dinuclear complexes (Scheme 1) have been established by IR-, $^1$H-NMR, $^{13}$C-NMR and mass spectroscopy. Aside from spectroscopic characterization, the structure of **3a** has been examined by single-crystal X-ray diffraction techniques (Fig. 1). The

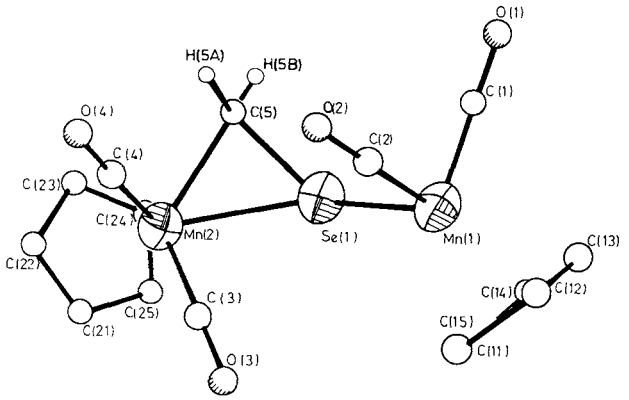
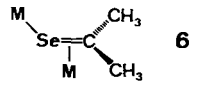



Fig. 1. Crystal structure of the novel $\mu_2,\eta^2$-selenoformaldehyde complex **3a**. Monoclinic, space group $C_{2h}^5$-$P2_1/n$; $a = 1561.6(6)$, $b = 1315.2(5)$, $c = 1599.9(4)$ pm; $\beta = 103.95(3)°$, $Z = 4$; 2599 reflections, $R_w = 0.039$. For details of the crystal structure investigation see *Angew. Chem. Suppl. 1983*, 363–395.

| Bond Lengths [pm] | | Bond Angles [°] | |
|---|---|---|---|
| Se(1)–Mn(1) | 237.1(2) | Se(1)–C(5)–Mn(2) | 76.7(4) |
| Se(1)–Mn(2) | 248.8(2) | Se(1)–Mn(2)–C(5) | 48.0(3) |
| Se(1)–C(5) | 190.0(11) | Mn(2)–Se(1)–Mn(1) | 121.5(1) |
| Mn(2)–C(5) | 210.4(12) | C(5)–Se(1)–Mn(1) | 112.2(3) |
| | | Mn(2)–Se(1)–C(5) | 55.4(4) |

molecule **3a** consists of two $(\eta^5$-$C_5H_5)Mn(CO)_2$-fragments that are connected with each other by means of the bridging chalcogen atom Se(1). A metal-to-metal bond is clearly not present in the molecule ($d$(Mn–Mn) > 380 pm). Since each organometallic fragment is missing two electrons to conform to the EAN rule, a formal Mn(1)=Se(1) double bond is to be postulated; the relatively short interatomic distance of 237.1(2) pm also lends support to this view. The bond length between Se(1) and C(5) is indicative of a single bond (190.0(11) pm). The same argument holds for the Mn(2)–C(5) distance, which is even longer (210.4(12) pm) than the corresponding bond length in the dimetallacyclopropane-type methylene complexes of composition $\mu$-$CH_2[(\eta^5$-$C_5H_4R)Mn(CO)_2]_2$ (R = H, $CH_3$)[16]. The question as to whether the cyclic geometry corresponds to an olefin-type $\pi$-complexation of the selenoformaldehyde ligand to the metal center Mn(2) or if this structure is more consistent with the requirements of a $\mu$-methylene derivative of a manganese-selenium framework, Mn–$CH_2$–Se, is open to further debate. The bonding theory of dimetallacyclopropanes favors the description of the present compound as a $\mu_2,\eta^2$-selenoformaldehyde complex, and the striking high field shift of the $CH_2$-signal in the $^{13}$C-NMR spectra of **3a**, **b** also supports this view[16].

The general applicability of our new synthetic method is exemplified by the stepwise construction of a related selenoketone ligand. Thus, compound **6** has cleanly been obtained by the reaction of 2-diazopropane and the organometallic precursor **1b**. This reaction also follows the very same methodology: the isopropylidene moiety is released,




**6**

M=$(\eta^5$-$C_5Me_5)Mn(CO)_2$

with $N_2$-elimination, from the diazo precursor and is transferred to one of the manganese-selenium bonds of **1b**. The structure of the resulting selenoketone complex **6** has been established by complete elemental analysis and spectroscopy.


Received: January 14, 1983 [Z 244 IE]
German version: *Angew. Chem. 95* (1983) 331
The complete version of this communication appears in: *Angew. Chem. Suppl. 1983*, 363–395

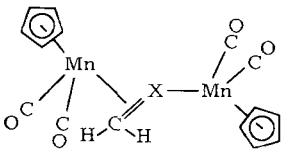


[5] Review: W. A. Herrmann, *Angew. Chem. 94* (1982) 118; *Angew. Chem. Int. Ed. Engl. 21* (1982) 117.
[6] B. Solouki, P. Rosmus, H. Bock, *J. Am. Chem. Soc. 98* (1976) 6054.
[9] T. J. Collins, W. R. Roper, *J. Chem. Soc. Chem. Commun. 1977*, 901.
[11] W. A. Herrmann, Ch. Bauer, J. Weichmann, *J. Organomet. Chem. 243* (1983) C21.
[12] M. Herberhold, D. Reiner, B. Zimmer-Gasser, U. Schubert, *Z. Naturforsch. B35* (1980) 1281.
[13] M. Herberhold, D. Reiner, D. Neugebauer, *Angew. Chem. 95* (1983) 46; *Angew. Chem. Int. Ed. Engl. 22* (1983) 59; *Angew. Chem. Suppl. 1983*, 10–22.
[16] W. A. Herrmann, *Adv. Organomet. Chem. 20* (1982) 159.


## A Binuclear Complex with a Thioformaldehyde Bridge**


By *Max Herberhold**, *Wolfgang Ehrenreich*, and *Wolfgang Bühlmeyer*


According to a method developed by *Herrmann et al.*[1], selenium- and tellurium-bridged transition metal complexes such as $[\eta^5$-$C_5H_5)Mn(CO)_2]_2Se_n$ (n = 1, 2)[2a] and $[(\eta^5$-$C_5H_5)Mn(CO)_2]_3Te$[2b] are converted by diazomethane into new compounds which contain seleno- and telluroformaldehyde, respectively, as $\mu_2,\eta^2$-bridging ligand (**2**, **3**). We report here on the analogous thioformaldehyde complex **1**, which extends the series and enables comparisons to be made.




**1**, X = S
**2**, X = Se
**3**, X = Te

**1** was first obtained in 1981 in low yield (50 mg, 2.4%) from a reaction of the tetrahydrofuran-stabilized complex fragment $[(\eta^5$-$C_5M_5)Mn(CO)_2]$ with $K_2SN_2$[2c] when we extracted the residue of the reaction mixture with $CH_2Cl_2$. A more efficient synthesis of **1** makes use of $CH_2N_2$ as a source of methylene[1]; it is not necessary[3] to isolate the intermediate sulfur complexes $[(\eta^5$-$C_5H_5)Mn(CO)_2]_2S_n$ (n = 1, 2)[2a].

The composition of the blue, diamagnetic binuclear complex **1** emerges from its elemental analysis and mass spectrum; its structure can be derived from the IR and NMR spectra and their similarity with those of the selenoformaldehyde complex **2** studied by X-ray analysis (Table 1).

In the $^1$H-NMR spectrum of **1** the two methylene protons of the thioformaldehyde bridge are observed as a AB system; a surprisingly large difference between the two $\delta$ values is found in polar solvents. The AB system of the methylene protons is shifted to lower fields and $^2J$(H,H)


[*] Prof. Dr. M. Herberhold, W. Ehrenreich, W. Bühlmeyer
Laboratorium für Anorganische Chemie der Universität
Postfach 3008, D-8580 Bayreuth (Germany)



[**] This work was supported by the Deutsche Forschungsgemeinschaft and the Fonds der Chemischen Industrie.

Table 1. Spectroscopic data of the complexes $[(\eta^5\text{-}C_5H_5)Mn(CO)_2]_2(CH_2X)$ **1**—**3**.

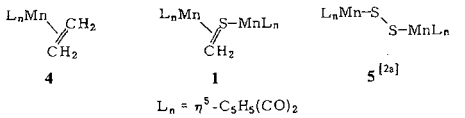
| | X = S (**1**) | X = Se (**2**) [1] | X = Te (**3**) [1] |
|---|---|---|---|
| IR: $\nu$ (CO) [$cm^{-1}$] | 2001 s, 1951 s<br>1933 s, 1878 s<br>(in $CCl_4$) | 2000 vs, 1955 s<br>1934 vs, 1882 s<br>(in $CCl_4$) | 2000 m, 1950 s,<br>1937 vs, 1892 s<br>(in *n*-hexane) |
| $^1$H-NMR (in $C_6D_6$): | | | |
| $\delta(C_5H_5)$ (2 × 5 H) | 4.39 (s), 3.74 (s) | 4.34 (s), 3.71 (s) | 4.29 (s), 3.79 (s) |
| $\delta(CH_2)$ (2 × 1 H) | 3.82 (d), 3.66 (d) [a] | 4.88 (d), 4.66 (d) | 5.96 (d), 6.02 (d) |
| $^2J$(H,H) | 1.1 Hz | 1.5 Hz | 3.7 Hz |
| $^{13}$C-NMR (in $C_6D_6$): | | | |
| $\delta(C_5H_5)$ | 86.81, 83.70 | 87.07, 83.37 | |
| $\delta(CH_2)$ | 54.57 | 56.74 | |

[a] Solvent dependence of the chemical shifts observed for the methylene protons: In [$D_8$]toluene 3.74, 3.54 (Δ 0.20 ppm); in $CD_2Cl_2$ 4.36, 3.58 (Δ 0.78 ppm); in [$D_6$]acetone 4.46, 3.43 (Δ 1.03 ppm).

increases from 1.1 to 3.7 Hz in the order X = S, Se, Te (**1**—**3**).

The thioformaldehyde complex **1** represents the connecting link between the ethylene complex **4**[4] and the disulfur complex **5**[2a]; it combines the structural elements of both a π-bonded hetero-olefin ligand and a sulfur bridge. The mononuclear complex $[(\eta^5\text{-}C_5H_5)Mn(CO)_2(CH_2S)]$ is observed as a fragment ion in the mass spectrum. A comparison of **1**, **4** and **5** facilitates the assignment of the $^1$H- and $^{13}$C-NMR cyclopentadienyl signals to the two different $[(\eta^5\text{-}C_5H_5)Mn(CO)_2]$ moieties of **1** (Table 2).

Table 2. Spectroscopic data of the complexes **1**, **4** and **5**.




**4** **1** **5**[2a]

$L_n = \eta^5\text{-}C_5H_5(CO)_2$

| | | | |
|---|---|---|---|
| IR [a] | | | |
| $\nu$(CO) [$cm^{-1}$] | 1969 s, 1908 s | 1999 s, 1949 s<br>1930, 1875 s | 1999 m, 1958 vs<br>1940 s |
| $^1$H-NMR [b] | | | |
| $\delta(C_5H_5)$ | 4.55 | 4.99, 4.58 | 5.32 |
| $\delta(CH_2)$ | 2.26 | 4.46 and 3.43 | — |
| $^{13}$C-NMR [b] | | | |
| $\delta(C_5H_5)$ | 84.8 | 88.8, 84.2 | 91.0 |
| $\delta(CH_2)$ | 37.0 | 54.3 | — |

[a] In diethyl ether. [b] In [$D_6$]acetone.

Monomeric thioformaldehyde is unstable under normal conditions; the small number of its transition metal compounds known so far comprises either mononuclear complexes containing $CH_2$=S as a hetero-olefin ligand[5a–c] or trinuclear complexes containing a $CH_2S$ bridge[5d]. **1** is the first binuclear complex of thioformaldehyde.

Received: February 9, 1983 [Z 275 IE]
German version: *Angew. Chem. 95* (1983) 332

[1] W. A. Herrmann, J. Weichmann, R. Serrano, K. Blechschmitt, H. Pfisterer, M. L. Ziegler, *Angew. Chem. 95* (1983) 331; *Angew. Chem. Int. Ed. Engl.* **22** (1983) 314; *Angew. Chem. Suppl. 1983*, 363–395.

[2] a) M. Herberhold, D. Reiner, B. Zimmer-Gasser, U. Schubert, *Z. Naturforsch. B35* (1980) 1281; b) M. Herberhold, D. Reiner, D. Neugebauer, *Angew. Chem. 95* (1983) 46; *Angew. Chem. Int. Ed. Engl. 22* (1983) 59; *Angew. Chem. Suppl. 1983*, 10—22; c) M. Herberhold, W. Ehrenreich, *ibid. 94* (1982) 637 and *21* (1982) 633, and *1982*, 1346—1352, respectively.

[3] Procedure: A solution of 408 mg (2 mmol) $C_5H_5Mn(CO)_3$ in 300 mL THF is photolyzed and—after addition of 640 mg (20 mmol) sulfur—stirred for 12 h at 0 °C. The dark-green solution of the sulfur complexes $[(C_5H_5)Mn(CO)_2]_2S_n$ (n = 1, 2) is brought to dryness; the residue is taken up in diethyl ether and combined with an etheral solution of *ca.* 50 mmol diazomethane at −78 °C. The mixture is slowly warmed to 0 °C (evolution of $N_2$) and stirred for 2 h. The solvent is removed, and the crude product **1** is purified by column chromatography (silicagel, −30 °C, exclusion of light). Using pentane/$CH_2Cl_2$ (5:1), small amounts of $C_5H_5Mn(CO)_3$ (yellow), $[(C_5H_5)Mn(CO)_2]_2CH_2$ (red-brown) and $[(C_5H_5)Mn(CO)_2]_2S_n$ (n = 1, 2; green) are washed out, and **1** is subsequently eluted as a deep-blue zone with pentane/$CH_2Cl_2$ (1:1). Crystallization from pentane/$CH_2Cl_2$ at −30 °C. Blue-black crystals which are air-stable for short periods, dec. 90 °C; the solutions are light-sensitive. Yields 250 mg (63%).

[4] H. P. Kögler, E. O. Fischer, *Z. Naturforsch. B15* (1960) 676; E. O. Fischer, M. Herberhold, *Experientia Suppl. IX* (1964) 259.

[5] a) $Os(CO)_2(PPh_3)_2(CH_2S)$: T. J. Collins, W. R. Roper, *J. Chem. Soc. Chem. Commun. 1977*, 901; *J. Organomet. Chem. 159* (1978) 73; b) $(C_5H_5)Re(NO)(PPh_3)(CH_2S)$: F. B. McCormick, J. A. Gladysz, ACS Meeting, Kansas City, Sept. 1982; c) cf. W. Paul, H. Werner, *Angew. Chem. 95* (1983) 333; *Angew. Chem. Int. Ed. Engl. 22* (1983) 316; d) $Os_3(CO)_n(PMe_2Ph)S(CH_2S)$ (n = 8,9): R. D. Adams, N. M. Golembeski, J. P. Selegue, *J. Am. Chem. Soc. 101* (1979) 5863, *ibid. 103* (1981), 546.

## Synthesis of $[(\eta^5\text{-}C_5H_5)Rh(PMe_3)(\eta^2\text{-}CH_2E)]$ with E = S, Se, Te: Thio-, Seleno-, and Telluroformaldehyde as Ligands in Mononuclear Rhodium Complexes**

By *Wilfried Paul* and *Helmut Werner**

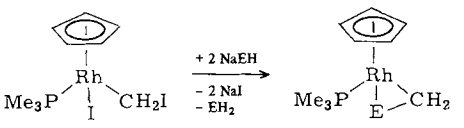
The first example of a mononuclear thioformaldehyde complex, $[(CO)_2Os(PPh_3)_2(\eta^2\text{-}CH_2S)]$ **1**, was described by *Roper et al.*[1]. Corresponding transition-metal compounds with seleno- or telluroformaldehyde as ligands were, to the best of our knowledge, unknown[***]. During studies with carbenoid-metal complexes it was found[2] that rhodium complex **2** reacts with neutral as well as anionic nucleophiles by cleavage of the $CH_2$—I bond. Thus, with $PPh_3$ and $SMe_2$ salts of the cations $[(C_5H_5)Rh(CH_2L)(PMe_3)I]^+$ (L = $PPh_3$, $SMe_2$) are formed, whereas with NaOMe the neutral compound $[(C_5H_5)Rh(CH_2OMe)(PMe_3)I]$ is obtained[2]. Surprisingly, with NaOH in the presence of a phase-transfer catalyst isomerization of **2** occurs to give $[(C_5H_5)Rh(CH_2PMe_3)I_2]$[4].

Using NaSH, NaSeH or NaTeH as substrates in the reaction with **2** (tetrahydrofuran, 25 °C, molar ratio **2** : NaEH ≈ 1 : 10), we have now succeeded in preparing complexes **3**—**5** in good yield (E = S: 48%; E = Se: 72%; E = Te: 24%). The composition of the crystalline, slightly air-sensitive compounds (**3**: pale yellow, **4**: red-violet, **5**: dark green) has been confirmed by elemental analysis and mass spectra.

[*] Prof. Dr. H. Werner, W. Paul
Institut für Anorganische Chemie der Universität
Am Hubland, D-8700 Würzburg (Germany)

[**] This work was supported by the Deutsche Forschungsgemeinschaft, the Fonds der Chemischen Industrie, and through gifts of chemicals by BASF AG and DEGUSSA.

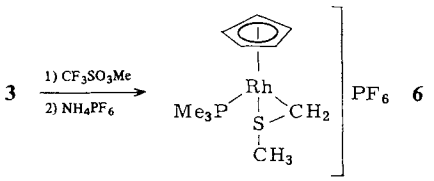
[***] Note added in proof (11. 3. 1983): In the meantime, the synthesis of osmium complexes of selenoformaldehyde and telluroformaldehyde from formaldehyde precursors has been achieved: C. E. L. Headford, W. R. Roper, *J. Organomet. Chem. 244* (1983) C 53. The formation of dinuclear complexes with $CH_2Se$ and $CH_2Te$ as ligands is described by W. A. Herrmann *et al.*, *Angew. Chem. 95* (1983) 331; *Angew. Chem. Int. Ed. Engl. 22* (1983) 314; *Angew. Chem. Suppl. 1983*, 363-395.



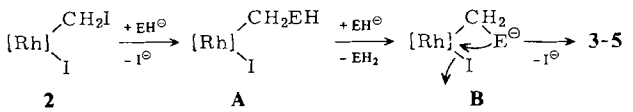
**2** **3**, E = S; **4**, E = Se; **5**, E = Te

We assume that in the new chalcogenoformaldehyde complexes **3**—**5** a rigid RhCE three-membered ring is present, *i.e.* the $CH_2E$ ligands are not coordinated like ethene (at least not at room temperature). Consequently, the molecules should be chiral and thus show *two* signals for the diastereotopic $CH_2E$-protons in the $^1$H-NMR spectrum. [**3**: $\delta(CH_2)$ 3.19 ddd, $J(HH)=2.0$, $J(RhH)=1.2$, $J(PH)=3.3$ Hz; 4.49 ddd, $J(HH)=2.0$, $J(RhH)=2.0$, $J(PH)=0.5$ Hz. **4**: $\delta(CH_2)$ 4.26 ddd, $J(HH)=1.2$, $J(RhH)=0.8$, $J(PH)=8.3$ Hz; 5.31 ddd, $J(HH)=1.2$, $J(RhH)=2.2$, $J(PH)=0.6$ Hz. **5**: $\delta(CH_2)$ 5.50 ddd, $J(HH)=0.6$, $J(RhH)=0.6$, $J(PH)=10.2$ Hz; 6.63 ddd, $J(HH)=0.6$, $J(RhH)=2.0$, $J(PH)=0.6$ Hz]. In the $^1$H-NMR spectrum of the *achiral* compound **1** only *one* signal for the $CH_2S$-protons is observed[1].

Complex **3** reacts smoothly with methyl trifluormethanesulfonate to form the corresponding S-methylated cation, which is isolated as the $PF_6$ salt **6**. The yellow solid is highly soluble in acetone or $CH_2Cl_2$. Complex **1** also reacts with $CF_3SO_3Me$ in an analogous manner[1].



In the straightforward synthesis of complexes **3**—**5**, which at least for E = S and Se leads to good yields, the species $CH_2E$, which are very unstable in the monomeric form (cf. [7,8]), are generated and trapped in the coordination sphere of a transition-metal. Presumably, initial nucleophilic substitution on **2** affords intermediate **A**. Following deprotonation of **A**, the more nucleophilic chalcogen atom of **B** displaces the iodide bonded to rhodium.



**2** **A** **B**

[Rh] = $(C_5H_5)Rh(PMe_3)$

Received: February 9, 1982 [Z 276 IE]
German version: *Angew. Chem. 95* (1983) 333
The complete version of this communication appears in:
*Angew. Chem. Suppl. 1983*, 396-404

[1] T. J. Collins, W. R. Roper, *J. Chem. Soc. Chem. Commun. 1977*, 901; *J. Organomet. Chem. 159* (1978) 73.
[2] H. Werner, R. Feser, W. Paul, L. Hofmann, *J. Organomet. Chem. 219* (1981) C29.
[4] W. Paul, Diplomarbeit, Universität Würzburg 1981.
[7] a) D. L. Klayman, W. H. H. Günther: *Organic Selenium Compounds: Their Chemistry and Biology*, Wiley, New York 1973, Chap. VII and XI; b) Pyrolysis experiments point to the existence of monomeric selenoformaldehyde in the gas phase: H. Bock, S. Aygen, unpublished results; S. Aygen, Dissertation, Universität Frankfurt/Main 1982.
[8] F. O. Rice, A. L. Glasebrook, *J. Am. Chem. Soc. 56* (1934) 2381; T. G. Pearson, R. H. Purcell, G. S. Saigh, *J. Chem. Soc. 1938*, 409.

## Equilibria in the Formation of $A_4B_3$ Molecules**

By *Roger Blachnik** and *Ulrike Wickel*

Molecules of type $A_4B_3$ (Fig. 1) having the compositions $P_xAs_{4-x}S_3$ and $P_4S_xSe_{3-x}$ (x = 1, 2, 3 and 1, 2, respectively) have hitherto only been detected in mixed crystals[5,6] formed from melts of the pure components.

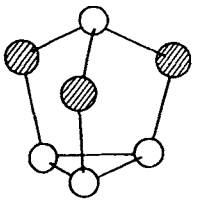


Fig. 1. Structure of $A_4B_3$ type molecules. ○ = P, As; ◎ = S, Se.

We have now been able to isolate such species in pure form by high performance liquid chromatography on an RP-18 column (solvent $CS_2$, eluent methanol/water). *Steudel et al.* had already separated $S_{8-x}Se_x$ mixtures in a similar way by HPLC. The concentrations of the individual species in the mixtures could previously only be determined approximately from mass spectra. Assuming that the extinction coefficients of the molecules in the series $P_xAs_{4-x}S_3$ and $P_4S_xSe_{3-x}$ change linearly with x we were able to plot the concentration curves presented in Figure 2 using data obtained from HPLC measurements.

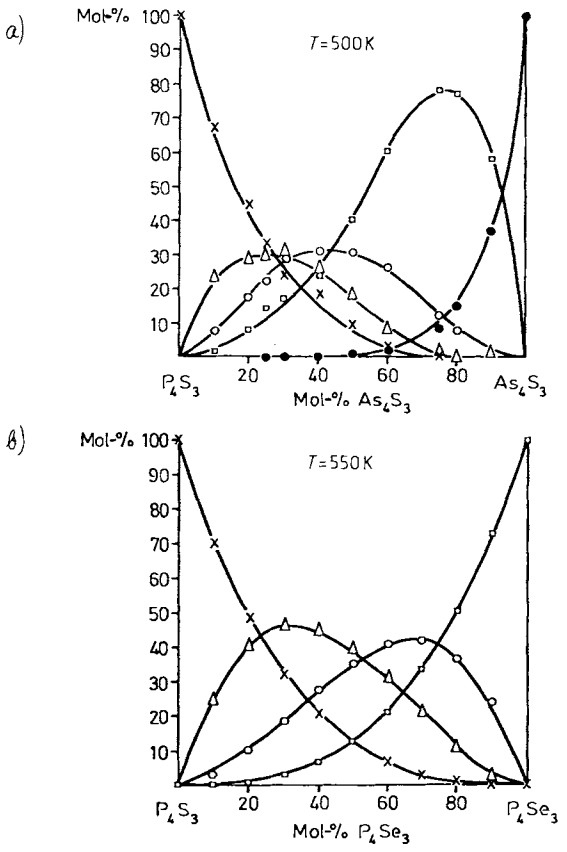



Fig. 2. a) Concentration curves in the system $P_4S_3/As_4S_3$ for $P_4S_3$ (×), $P_3AsS_3$ (△), $P_2As_2S_3$ (○), $PAs_3S_3$ (□), $As_4S_3$ (●).—b) Concentration curves in the system $P_4S_3/P_4Se_3$ for $P_4S_3$ (×), $P_4S_2Se$ (△), $P_4SSe_2$ (○), $P_4Se_3$ (□).

[*] Prof. Dr. R. Blachnik, U. Wickel
Anorganische Chemie, Fachbereich 8 der Universität—Gesamthochschule
Postfach 1012 40, D-5900 Siegen (Germany)

[**] This work was supported by the Fonds der Chemischen Industrie.

The results illustrate the influence of the bond energies on the formation of various species. In the system $P_4S_3/P_4Se_3$ the number of phosphorus-chalcogen bonds is not altered by the "mixed" molecules that are formed; the reaction is thus entropy-controlled, and therefore the distribution of the products is statistical and temperature-independent. The bond energy of a PS bond is higher than that of an AsS bond; therefore, for the reaction

$$P_4S_3 + 3\,As_4S_3 \longrightarrow 4\,PAs_3S_3$$
(6 P–S bonds) (12 P–S bonds)

there is a considerable gain in energy. Hence, in mixtures of $P_4S_3$ and $As_4S_3$ the formation of the molecule $PAs_3S_3$ with an apical phosphorus atom is preferred (cf. Fig. 1). The concentration of this species decreases with increasing temperature.

Novel molecules of type $A_4B_3$ can be obtained in pure form *via* separation of the molecular mixtures. All the compounds form plastic phases at elevated temperatures. Aside from the possibility of preparing derivatives of these molecules, a way is now also open for studying the transformation into the plastic phase as a function of the molecular structure. The $A_4B_3$ systems also exemplify how the formation of the same molecular structure can be controlled either by the entropy or by the enthalpy.

Received: October 4, 1982;revised: February 4, 1983 [Z 167 IE]
German version: *Angew. Chem. 95* (1983) 313
The complete manuscript of this communication appears in: *Angew. Chem. Suppl. 1983*, 405–410

CAS Registry numbers:
$P_4S_3$, 1314-85-8; $As_4S_3$, 12512-13-9; $P_4Se_3$, 1314-86-9; $As_3Ps_3$, 80585-65-5; $As_2P_2S_3$, 54321-45-8; $AsP_3S_3$, 85135-63-3; $P_4S_2Se$, 85135-64-4; $P_4SSe_2$, 85135-65-5.

[5] R. Blachnik, A. Hoppe, U. Rabe, U. Wickel, *Z. Naturforsch. B36* (1981) 1493.
[6] R. Blachnik, U. Wickel, *Z. Naturforsch. B37* (1982) 1507.
[7] R. Steudel, R. Laitinen, *Top. Curr. Chem. 102* (1982) 177.

## $[Co_3\{\mu_3\text{-}S\}\{o\text{-}(SCH_2)_2C_6H_4\}_3]^{2-}$: The First Trinuclear Cobalt Cluster with Tetrahedral $CoS_4$-Coordination**

By *Gerald Henkel**, *Wolfgang Tremel*, and *Bernt Krebs*

Increasing interest has recently been focussed on compounds of cobalt with sulfur and sulfur-containing ligands, chiefly because a comparison of isostructural polynuclear Co–S- and Fe–S-complexes is expected to enable important conclusions to be drawn about the bonding in such species.

The only Co-complex known to have tetrahedral S-coordination, in which short metal-metal distances have been found, is $[Co_8S_6(SC_6H_5)_8]^{4-}$[7]. The analogous iron complex $[Fe_8S_6(SC_6H_5)_8]^{4-}$, however, which is considered as parent compound of a $[(RS)_nMoFe_7S_6(SR)_7]^{z-}$ cluster (with $n=1$, 2 or 3) recently postulated as a model for the active site of nitrogenase[7,8], has so far not been detected.

During investigations of the $FeCl_2/X/Y$ system ($X=RS^-$, $S^{2-}$, 1,1-dithiolate; $Y$=1,4-dithiolate), which led, *inter alia*, to a direct synthesis of the $Fe^{II}$ cluster $[Fe_3S(SRS)_3]^{2-}$ [SRS = *o*-xylene-α,α′-dithiolate ($S_2$-*o*-xyl) (**1**) or durene-α,α′-dithiolate ($S_2$-dur) (**2**)][11], we have also synthesized the title compound $[Co_3S(S_2\text{-}o\text{-}xyl)_3]^{2-}$ **3**. Complexes **1** and **2** claim interest as possible model compounds for the [3-Fe] centers of some ferredoxins[14]. **3** is obtained analogously to **1** or **2** by treatment of the precipitate initially formed in the reaction of $CoCl_2/Na_2S_2$-*o*-xyl with $S^{2-}$ in methanol and, by precipitation with $(CH_3)_4NCl$, can be isolated as $[(CH_3)_4N]_2[Co_3S(S_2\text{-}o\text{-}xyl)_3]\cdot 2CH_3OH$ **4**. The salt **4** crystallizes in the monoclinic space group $P2_1/c$, $a=1341.6(4)$, $b=1956.9(6)$, $c=1629.8(4)$ pm, $\beta=90.60(2)°$, $Z=4$ at $T=140$ K. The structure was determined from single crystal diffractometer data ($R_1=0.031$, $R_2=0.034$). In Figure 1, the $Co_3S_7$ skeleton of the anion **3** is accentuated by vibration ellipsoids.

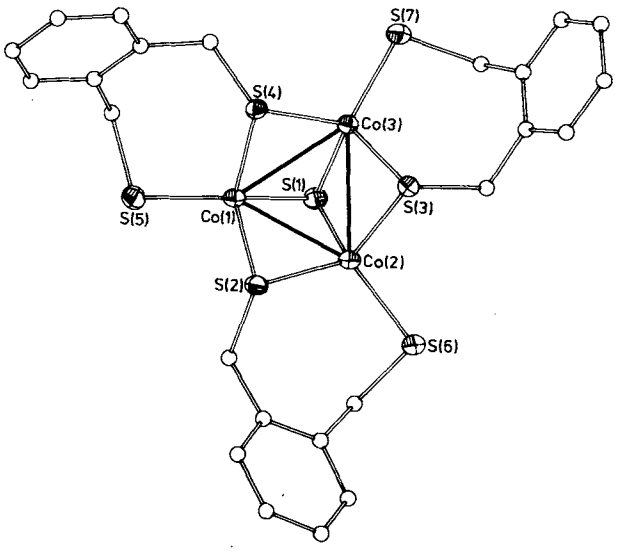



Fig. 1. Structure of the anionic cluster **3** with vibration ellipsoids of the Co and S atoms (140 K, 50% probability), Selected bond lengths [pm] (σ: 0.1 pm): Co(1)–Co(2) 271.5, Co(1)–Co(3) 282.5, Co(2)–Co(3) 280.0, Co(1)–S(1) 226.4, Co(2)–S(1) 226.6, Co(3)–S(1) 229.5, Co(1)–S(2) 228.1, Co(2)–S(2) 229.7, Co(1)–S(4) 232.7, Co(2)–S(3) 231.6, Co(3)–S(4) 231.5, Co(3)–S(3) 231.0, Co(1)–S(5) 223.8, Co(2)–S(6) 222.6, Co(3)–S(7) 224.6; S–Co–S angles [°] (σ: 0.03°): Co(1) 102.38 to 119.19, Co(2) 103.56 to 117.46, Co(3) 99.90 to 119.78. Further details of the crystal structure investigation can be obtained on request from the Fachinformationszentrum Energie Physik Mathematik, D-7514 Eggenstein-Leopoldshafen, quoting the depository number CSD 50378, the name of the author, and full citation of the journal.

In comparison to **2**, with $C_{3v}$ symmetry of the metal-sulfur skeleton, **3** contains only one mirror plane; besides two rather longer metal-metal distances one short bond length [Co(1)–Co(2) 271.5(1) pm] is observed[15]. These distortions are obviously determined electronically, since the central $Co_3S_7$ moiety in **3** contains three valence electrons more than the isostructural $Fe_3S_7$ moiety in **2**. The CoS bonds of the $(\mu_3\text{-}S)Co_3$ pyramids are of different lengths. Also the bond lengths in the Co(1)–S(2)–Co(2) bridge are on average *ca.* 3 pm shorter than the other $(\mu_2\text{-}S)Co$ bonds. Since the average CoS bond lengths for Co(1) and Co(2) in **3** (227.8 and 227.6 pm, respectively), are significantly shorter than for Co(3) (229.2 pm), Co(1) and Co(2) should be electronically equivalent, but different from Co(3), which is also in accordance with the short metal-metal distance.

The UV/VIS spectrum of a solution of **3** in $CH_3CN$ shows a broad band (center *ca.* 1480 nm) with shoulders at 1520 and 1415 nm [$^4A_2 \rightarrow {}^4T_1(F)(\nu_2)$] as well as the broad flank of a LMCT band increasing steeply below 800 nm ($\lambda_{max}=406$ nm), which superposes the d-d band in the VIS region [$^4T_2 \rightarrow {}^4T_1(P)(\nu_3)$] of the tetrahedrally S-coordinated

[*] Dr. G. Henkel, W. Tremel, Prof. Dr. B. Krebs
Anorganisch-chemisches Institut der Universität
Corrensstr. 36, D-4400 Münster (Germany)

[**] This work was supported by the Fonds der Chemischen Industrie.

cobalt. The $\nu_3$ band, split into three components, is still noticeable by shoulders at 761, 692 and 570 nm. Spectroscopic investigations show that **3** is less sensitive to oxidation than the analogous iron compounds **1** and **2**. Reaction of **3** with a large excess of thiophenolate leads to degradation of the cluster.

Received: October 25, 1982;
revised: November 25, 1982 [Z 188 IE]
German version: *Angew. Chem. 95* (1983) 314
The complete version of this communication appears in:
*Angew. Chem. Suppl. 1983*, 307–322

CAS Registry number:
**4**, 84836-09-9

[7] G. Christou, K. S. Hagen, R. H. Holm, *J. Am. Chem. Soc. 104* (1982) 1744.
[8] G. Henkel, H. Strasdeit, B. Krebs, *Angew. Chem. 94* (1982) 204; *Angew. Chem. Int. Ed. Engl. 21* (1982) 201; *Angew. Chem. Suppl. 1982*, 489.
[11] G. Henkel, W. Tremel, B. Krebs, *Angew. Chem. 95* (1983) and *Angew. Chem. Int. Ed. Engl. 22* (1983), in press.
[14] G. Henkel, W. Tremel, B. Krebs, *Angew. Chem. 93* (1981) 1072; *Angew. Chem. Int. Ed. Engl. 20* (1981) 1033.
[15] The metal-metal distances in trinuclear Co complexes, which aside from bridging S-atoms also contain carbonyl or cyclopentadienyl ligands, are in some cases substantially shorter than in **3**; cf., *e.g.*, A. B. Rives, Y. Xiao-Zeng, R. F. Fenske, *Inorg. Chem. 21* (1982) 2286.

## $[Fe_2\{o\text{-}(SCH_2)_2C_6H_4\}_2\{SC_6H_5\}_2]^{2-}$ and $[Fe_2\{o\text{-}(SCH_2)_2C_6H_4\}_3]^{2-}$: Binuclear Thiolatoiron(II) Anions with Tetrahedral $FeS_4$-Coordination**

By *Gerald Henkel**, *Wolfgang Tremel*, and *Bernt Krebs*

Polynuclear $Fe^{II}$-thiolate complexes whose molecular skeletons consist of sulfur polyhedra sharing edges are hardly known. To this class of complexes belong the anion $[Fe_3S(S_2\text{-dur})_3]^{2-}$ **1**[1] ($S_2$-dur = durene-α,α'-dithiolate), an interesting species because of the similarity of its coordination unit and the [3-Fe]-center of *Desulfovibrio gigas* (Dg Fd II)[2], as well as $[Fe_2(SEt)_6]^{2-}$ **2**[4] and $[Fe_2(S_2\text{-dur})_2(S_2CNMe_2)_2]^{2-}$ **3**[5]. During investigations on the system $FeCl_2/X/Y$ [X = *o*-xylene-α,α'-dithiolate ($S_2$-*o*-xyl) or $S_2$-dur; Y = $RS^-$, $RSe^-$, $S^{2-}$, $Se^{2-}$ or 1,1-dithiolate] we have isolated two novel anions $[Fe_2(S_2\text{-}o\text{-xyl})_2(SPh)_2]^{2-}$ **4** and $[Fe_2(S_2\text{-}o\text{-xyl})_3]^{2-}$ **5**[11] as $[Me_4N]_2[Fe_2(S_2\text{-}o\text{-xyl})_2(SPh)_2]\cdot 1/3\,MeCN\cdot 2/3\,THF$ **6** and $[Me_4N]_2[Fe_2(S_2\text{-}o\text{-xyl})_3]\cdot 5\,MeOH$ **7**, respectively. Both **4** and **5** are potential models for the active centers of the reduced form of desulforedoxin, a [2 Fe]-protein without labile sulfur from *Desulfovibrio gigas*[15]. In addition, we have found a direct synthetic route for the trinuclear cluster $[Fe_3S(S_2\text{-}o\text{-xyl})_3]^{2-}$ **8**, which has a structure similar to that of **1**.

Reaction of $FeCl_2$ with equimolar amounts of $Na_2S_2$-*o*-xyl in methanol affords a dark brown precipitate having the composition $FeS_2$-*o*-xyl. On addition of thiophenolate the binuclear anion **4** is formed; in an analogous way addition of selenophenolate furnishes the anion $[Fe_2(S_2\text{-}o\text{-xyl})_2(SePh)_2]^{2-}$. Treatment of the precipitate with $K_2S$ or Na/NaHS in methanol affords the trinuclear anion **8**, while treatment with $K_2Se$ furnishes the analogous product $[Fe_3Se(S_2\text{-}o\text{-xyl})_3]^{2-}$. On reaction with $NaS_2P(p\text{-tol})_2$, **5** was obtained as unexpected secondary component of a product mixture in which also **8** could be detected.

The salt **6** crystallizes from acetonitrile/tetrahydrofuran/ether in space group $R\bar{3}$ of the trigonal system, the salt

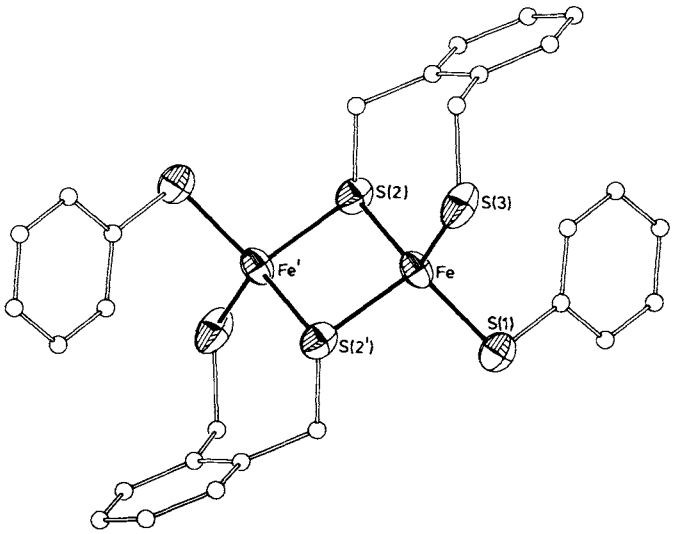



Fig. 1. Structure of the anion **4** in the crystal of **6**, with vibration ellipsoids of the Fe and S atoms (140 K, 50% probability). Selected bond lengths [pm] (σ: 0.1 pm): Fe–Fe' 297.7, Fe–S(1) 230.3, Fe–S(2) 236.8, Fe–S(2') 236.3, Fe–S(3) 230.3; SFeS angles [°] (σ: 0.05°): 102.03 (S(2)-Fe-S(2')) to 115.80 (S(1)–Fe–S(3)).

**7** from methanol in space group $P2_1/n$ of the monoclinic system. The $Fe_2S_6$ frameworks of their complex anions consist of $FeS_4$ tetrahedra, whose edge-to-edge linking leads to short metal-metal distances (297.7(1) pm in **4**, 287.9(1) pm in **5**).

The central $Fe_2S_2$ ring in **4** is exactly planar. The $Fe_2S_6$ framework has $D_{2h}$ symmetry; a comparable framework (Fe–Fe 297.8 pm) is found in the complex **2**, which contains exclusively monofunctional SR ligands.

In the anion **5** with $C_{2v}$ symmetry of the $Fe_2S_6$ framework, the surprising structural characteristic is a handle-like $S_2$-*o*-xyl bridge spanning the $Fe_2S_2$ ring, leading to generation of a nine-membered heterocycle in the polycyclic system. Thus, **5** derives from **4** by replacement of the monothiolate ligands by a dithiolate group bound to two

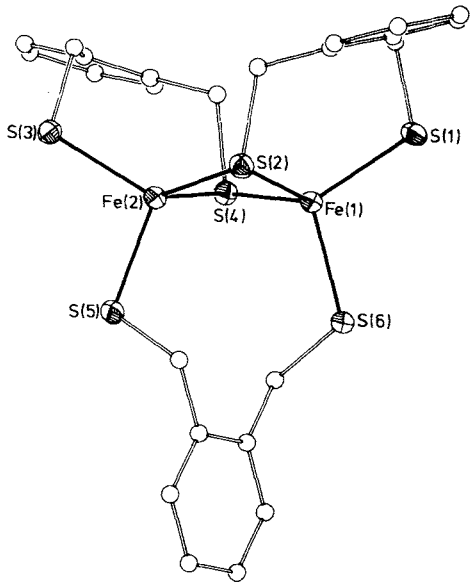



Fig. 2. Structure of the anion **5** in the crystal of **7**, with vibration ellipsoids of the Fe and S atoms (140 K, 50% probability). Selected bond lengths [pm] (σ: 0.1 pm): Fe(1)–Fe(2) 287.9, Fe(1)–S(1) 230.6, Fe(1)–S(2) 236.6, Fe(1)–S(4) 235.1, Fe(1)–S(6) 231.4, Fe(2)–S(2) 236.1, Fe(2)–S(3) 229.1, Fe(2)–S(4) 236.9, Fe(2)–S(5) 231.1; SFeS angles [°] (σ: 0.04°): 102.11 (S(2)-Fe(1)-S(4)) to 119.31 (S(2)-Fe(2)-S(3)).—Further details of the crystal structure investigations are available on request from the Fachinformationszentrum Energie Physik Mathematik, D-7514 Eggenstein-Leopoldshafen quoting the number CSD 50397, the name of the author, and complete citation of the journal.

[*] Dr. G. Henkel, W. Tremel, Prof. Dr. B. Krebs
Anorganisch-chemisches Institut der Universität
Corrensstr. 36, D-4400 Münster (Germany)

[**] This work was supported by the Fonds der Chemischen Industrie.

Fe atoms. Due to the short S...S distance in the "handle" the central $Fe_2S_2$ ring in **5** is no longer planar but folded along the S...S vector; the mean S...S distance in the two equivalent dithiolate ligands is 393.1 pm, and is thus 32.2 pm shorter than the distance in the ligand with non-bridging S atoms (425.3(1) pm). The metal-metal distance of 287.9(1) pm in **5** is *ca.* 10 pm shorter than in **4**; this could be due to steric effects.

The complexes **1**, **2**, **4** and **5** differ from the adamantane analogues $[Fe_4(SPh)_{10}]^{2-}$[10] in the coupling of the $FeS_4$ tetrahedra. In the case of corner-linkage, Fe–Fe distances of *ca.* 393 pm are achieved, while edge-linkage leads to shorter distances and thus stronger metal-metal interactions in FeS clusters.

The electronic spectrum of **4** (in MeCN) shows no bands in the VIS region ($\lambda > 400$ nm), while absorption increases strongly in the UV region through charge-transfer transitions. The spectrum of **5** (in dimethylformamide) shows a characteristic band at 360 nm. In the spectrum of **8**, a characteristic band is found at 345 nm which is suitable for identification.

Received: November 11, 1982;
revised: January 18, 1983 [Z 200 IE]
German version: *Angew. Chem. 95* (1983) 317
The complete version of this communication appears in:
*Angew. Chem. Suppl. 1983*, 323–346

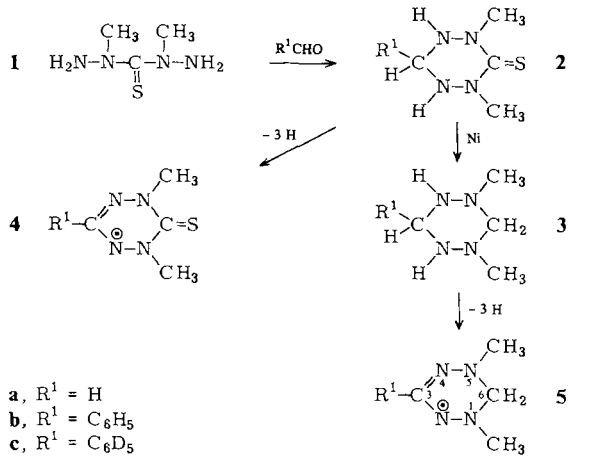
[1] G. Henkel, W. Tremel, B. Krebs, *Angew. Chem. 93* (1981) 1072; *Angew. Chem. Int. Ed. Engl. 20* (1981) 1033.
[2] M. R. Antonio, B. A. Averill, I. Moura, J. J. G. Moura, W. H. Orme-Johnson, B.-K. Teo, A. V. Xavier, *J. Biol. Chem. 257* (1982) 6646.
[4] K. S. Hagen, R. H. Holm, *J. Am. Chem. Soc. 104* (1982) 5496.
[5] G. Henkel, W. Tremel, U. Kuhlmann, B. Krebs, *XXI. Int. Conf. Coord. Chem., Toulouse 1980, Abstr.* 351.
[10] K. S. Hagen, J. M. Berg, R. H. Holm, *Inorg. Chim. Acta 45* (1980) L17.
[11] A compound $[Et_4N]_2[Fe_2(S_2\text{-}o\text{-}xyl)_3]$ has already been prepared *via* an alternative route and been characterized on the basis of its electronic spectrum and cyclovoltammogram (R. W. Lane, J. A. Ibers, R. B. Frankel, R. H. Holm, *Proc. Natl. Acad. Sci. USA 72* (1975) 2868). It follows from a footnote in [4] that the anion in this compound and the anion **5** are isomers.
[15] I. Moura, B. H. Huynh, R. P. Hausinger, J. Le Gall, A. V. Xavier, E. Münck, *J. Biol. Chem. 255* (1980) 2493.

## 1,5-Dimethylverdazyls, Hydrazidinyl Radicals with Pyramidal 1,5-Nitrogen Atoms**

By *Franz A. Neugebauer** and *Rolf Siegel*

The reaction of 2,4-dimethylthiocarbonohydrazide **1** with aldehydes in the molar ratio 1:1 yields as the major product colorless 1,4,5,6-tetrahydro-1,2,4,5-tetrazine-3(2*H*)-thiones **2**, some of which undergo desulfurization with Raney nickel, with retention of the hexahydro-1,2,4,5-tetrazine framework, to give **3**. The constitution of these compounds is assigned from the $^1$H-NMR spectra.

By dehydrogenation of **2** (*e.g.* with $FeCl_3$ in formic acid) we obtained the monomeric 6-thioxoverdazyl radicals **4**. **4a** crystallizes from dichloromethane to form dark red crystals; ESR spectrum (toluene, 220 K): $a(N_{2,4}) = 0.637$, $a(N_{1,5}) = 0.545$, $a(H_{CH_3}) = 0.545$ (6H), $a(H_{CH}) = 0.053$ mT, $\langle g \rangle = 2.0037$. **4b** forms violet needles; ESR (benzene, 293 K): $a(N_{2,4}) = 0.635$, $a(N_{1,5}) = 0.540$, $a(H_{CH_3}) = 0.540$ (6H) mT, $\langle g \rangle = 2.0037$. The crystals can be stored unchanged for several months at $-10$ °C; however, at room temperature **4a** and **4b** start to decompose after *ca.* one day.




Dehydrogenation of **3**, *e.g.* with tetrakis(4-methylphenyl)hydrazine in toluene, results in formation of violet (**3a**) or green (**3b**) paramagnetic solutions. However, the generated 1,5-dimethylverdazyls (**5**) contained therein, which apparently also do not dimerize, have thus far eluded isolation. Comparison of the ESR spectra [(toluene, 293 K); **5a**: $a(N_{1,5}) = 1.155$, $a(N_{2,4}) = 0.616$, $a(H_{CH_3}) = 0.396$ (6H), $a(H_{CH}) = 0.109$, $a(H_{CH_2}) = 0.035$ mT, $\langle g \rangle = 2.0037$; **5c**: $a(N_{1,5}) = 1.123$, $a(N_{2,4}) = 0.611$, $a(H_{CH_3}) = 0.408$ (6H) mT, $\langle g \rangle = 2.0037$] with those of previously known verdazyl types[4] reveals the following differences (cf. also Fig. 1):

- $a(N_{1,5})$ is considerably larger (factor 2)
- $a(H_{CH_3})$ proves to be markedly smaller (factor 0.6),
- the ESR spectra are temperature dependent: because $a(N_{1,5})$ increases with decreasing temperature ($\approx 10\%/100$ K, Fig. 1).

The anomalously large $a(N_{1,5})$ coupling constant (increased s character of the spin-bearing orbital of those atoms) and its pronounced negative temperature coefficient indicate that the 1,5-nitrogen atoms have a nonplanar equilibrium geometry, *i.e.* are pyramidal. The smaller $a(H_{CH_3})$ coupling constant is also consistent with a pyramidal arrangement of the substituents, since the angle between the axis of the spin-bearing orbital and the *N*-methyl bond becomes greater than 90°[5].

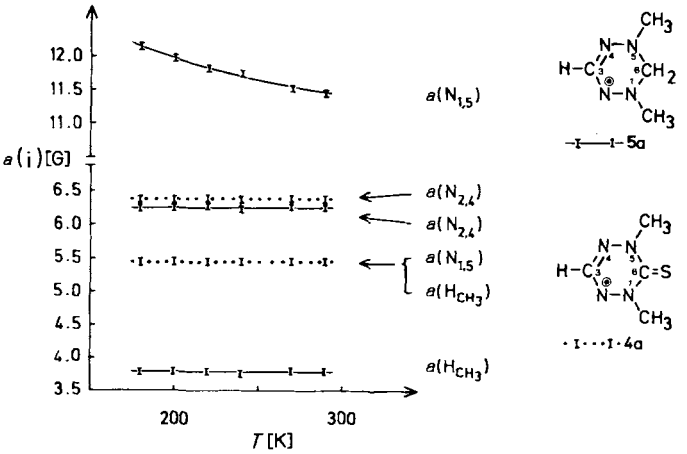



Fig. 1. Temperature dependence of the dominating coupling constants of **4a** and **5a** in cyclopropane (1G = 0.1 mT).

[*] Prof. Dr. F. A. Neugebauer, Dr. R. Siegel
Max-Planck-Institut für Medizinische Forschung
Abteilung Organische Chemie
Jahnstrasse 29, D-6900 Heidelberg (Germany)

[**] Verdazyls, Part 31.—Part 30: F. A. Neugebauer, H. Fischer, *J. Chem. Soc. Perkin Trans. 2* (1981) 896.

1,5-Dimethylverdazyls, **5**, are apparently the first hydrazyl derivatives[6] in which a nonplanar substituent arrangement at the tricoordinate nitrogen has been detected experimentally. This nonplanarity is largely cancelled, not only by aryl substituents ($CH_3 \rightarrow C_6H_5$) but also by electron acceptor bridges [$>CH_2 \rightarrow >C=S$ (**4**); $>CH_2 \rightarrow >C=O$][4].

Received: December 8, 1982;
revised: January 26, 1983 [Z 218 IE]
German version: *Angew. Chem. 95* (1983) 329
The complete manuscript of this communication appears in:
*Angew. Chem. Suppl. 1983*, 457-462

[4] F. A. Neugebauer, *Angew. Chem. 85* (1973) 485; *Angew. Chem. Int. Ed. Engl. 12* (1973) 455; F. A. Neugebauer, H. Fischer, *ibid. 92* (1980) 766; *19* (1980) 724; *Z. Naturforsch. B 35* (1980) 250.

[5] Corresponding C-centered radicals, *e.g.* $CH_3\dot{C}F_2$: K. S. Chen, J. K. Kochi, *J. Am. Chem. Soc. 96* (1974) 794.

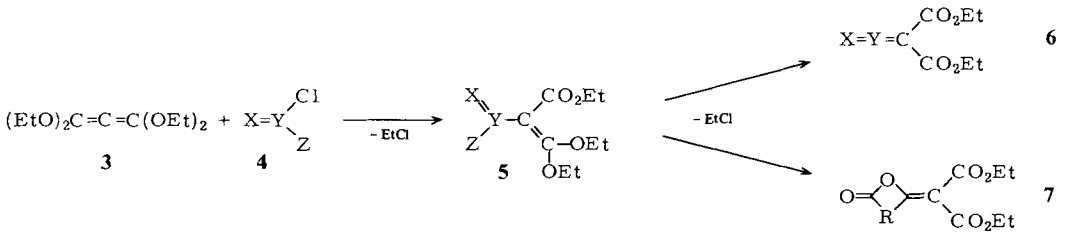
[6] For nonplanar bicyclic hydrazine radical cations see S. F. Nelsen, G. R. Weisman, P. J. Hintz, D. Olp, M. R. Fahey, *J. Chem. Soc. 96* (1974) 2916.

## Tetraethoxyallene: Equivalent of the Fictive Malonic Ester Dianion—A Versatile Synthetic Building Block**

By *Rolf W. Saalfrank** and *Walter Rost*

Donor/acceptor-substituted allenes are ambiphilic, and react at the central atom (C-2) with both nucleophiles and electrophiles[1]. Correspondingly, it is predicted that 1,3-donor/donor-substituted allenes have dinucleophilic properties.

We have now employed tetraethoxyallene **3**[2,5] (Table 1) as an equivalent for the fictive malonic ester dianion. As expected, **3** reacts with phosgene **4A** or thiophosgene **4B** (Z = good leaving group) with elimination of two moles of ethyl chloride (per mol **3**) to give bis(ethoxycarbonyl)ketene **6A** (Table 1) and bis(ethoxycarbonyl)thioketene **6B**, *via* the non-isolable intermediates **5A** and **5B**, respectively. **6B** spontaneously dimerizes to 1,3-dithietane-2,4-diylidenebis(malonic acid diethyl ester).




| 4-6 | A | B | C | D |
|---|---|---|---|---|
| X | O | S | $C(CN)_2$ | O |
| Y | C | C | C | C |
| Z | Cl | Cl | Cl | Cl–C(=O)–R– |

| 4D/5D/7 | a | b | c | d |
|---|---|---|---|---|
| R | $(CH_2)_2$ | $(CH_2)_3$ | $(CH_2)_4$ |  |

Attempts to prepare the allene **6C** with the "phosgene-equivalent" dichloromethylenemalononitrile **4C**[8] failed. In this case cleavage of the second mole of ethyl chloride does not take place and one can isolate the ethyl 3-chloro-4,4-dicyano-2-(diethoxymethylene)-3-butenoate **5C** (Table 1).

Table 1 (in part). Data for the compounds **3**, **6A**, and **5C**.

**3**: B.p. = 82 °C/0.05 torr; IR (film): 1905 $cm^{-1}$ (C=C=C); $^1$H-NMR (60 MHz, $CDCl_3$): $\delta$ = 1.32 (t, 12H, $CH_3$), 3.80 (q, 8H, $OCH_2$); $^{13}$C-NMR (25.15 MHz, $CDCl_3$): $\delta$ = 13.89 ($4CH_3$), 63.70 ($4CH_2$), 115.15 (=C), 148.12 (2 =$C(O)_2$)

**6A**: B.p. = 81 °C/0.1 torr; IR (film): 2142 $cm^{-1}$ (=C=O); $^1$H-NMR: $\delta$ = 1.30 (t, 6H, $CH_3$), 4.28 (q, 4H, $OCH_2$); $^{13}$C-NMR: $\delta$ = 14.35 (2 $CH_3$), 48.26 (=C), 61.34 (2 $CH_2$), 161.05 (O–C=O), 184.59 (C=O)

**5C**: B.p. = 125 °C/0.05 torr; IR (film): 2220 $cm^{-1}$ (CN), 1700 $cm^{-1}$ (C=O); $^1$H-NMR: $\delta$ = 1.32 (t, 3H, $CH_3$), 1.45 (t, 6H, 2 coinciding $CH_3$), 4.23 (q, 2H, $OCH_2$), 4.43 (q, 4H, 2 coinciding $OCH_2$)

If, as in compounds **4Da–d**, Z is not a leaving group, then reaction with **3** with elimination of ethyl chloride initially furnishes the intermediates **5Da–d**, which subsequently undergo intramolecular ring closure and renewed loss of ethyl chloride, with formation of the lactones **7a–d**[10]. As exemplified by the synthesis of diethyl 1,3-dihydro-3-oxo-2-isobenzofuranylidenemalonate **7d**, 2,3-annelated 4-alkylidene-2-buten-4-olides should be generally accessible *via* analogous reactions.

Received: November 26, 1982;
revised: January 24, 1983 [Z 211 IE]
German version: *Angew. Chem. 95* (1983) 328
The complete version of this communication appears in:
*Angew. Chem. Suppl. 1983*, 451–456

[1] R. W. Saalfrank, W. Paul, H. Liebenow, *Angew. Chem. 92* (1980) 740; *Angew. Chem. Int. Ed. Engl. 19* (1980) 713.

[2] Tetraethoxyallene **3** is prepared from tetraethoxyethylene using the procedure given for tetramethoxyallene.

[5] For the PE spectrum of **3** cf. R. Gleiter, R. W. Saalfrank, W. Paul, D. O. Cowan, M. Eckert-Maksić, *Chem. Ber. 116* (1983) in press.

[8] For the analogy of the structural elements $O/C(CN)_2$ cf. K. Wallenfels, K. Friedrich, J. Rieser, W. Ertel, H. K. Thieme, *Angew. Chem. 88* (1976) 311; *Angew. Chem. Int. Ed. Engl. 15* (1976) 261; L. M. Doane, A. J. Fatiadi, *ibid. 94* (1982) 649 and *21* (1982) 635.

[10] Regarding 4-ylidenebutenolides cf. R. W. Saalfrank, P. Schierling, *Chem. Ber. 116* (1983), in press.

[*] Prof. Dr. R. W. Saalfrank, W. Rost
Institut für Organische Chemie der Universität Erlangen-Nürnberg
Henkestrasse 42, D-8520 Erlangen (Germany)

[**] 1,3-Donor-donor substituted allenes in synthetic chemistry, Part 1 (Part of a Diplomarbeit by W. R. (1982)). This work was supported by the Fonds der Chemischen Industrie.

## Extremely Long-Range $^2$H Isotope Effects on the Chemical Shifts in the $^{13}$C-NMR Spectra of Compounds with Conjugated Double Bonds**

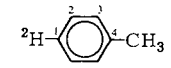
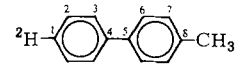
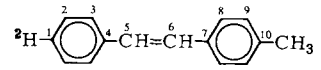
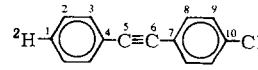
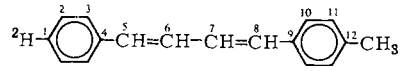
By *Stefan Berger** and *Hermann Künzer*

$^2$H isotope effects on the $^{13}$C chemical shifts of organic compounds have recently been intensively studied[1]. In

[*] Priv.-Doz. Dr. S. Berger, H. Künzer
Fachbereich Chemie der Universität
Hans-Meerwein-Strasse, D-3550 Marburg (Germany)

[**] This work was supported by the Deutsche Forschungsgemeinschaft (Be 631/6) and the Fonds der Chemischen Industrie.

Table 1. $^2H$ Isotope effects on the $^{13}C$ chemical shifts of compounds **1**—**5**.

| Compound | C atoms; $\Delta\delta$-values [ppb] [a] | | | | | | | | | | | | |
|---|---|---|---|---|---|---|---|---|---|---|---|---|---|
| | 1 | 2 | 3 | 4 | 5 | 6 | 7 | 8 | 9 | 10 | 11 | 12 | Me |
| **1**  | 276 | 110 | 11 | 7 | | | | | | | | | −3 |
| **2**  | 277 | 109 | 8 | 0 | −10 | 0 | 0 | 6 | | | | | 0 |
| **3**  | 278 | 110 | 7 | 0 | − 9 | 10 | −2 | 0 | 0 | 3 | | | 0 |
| **4**  | 275 | 109 | 4 | 0 | − 8 | 15 | 0 | 0 | 0 | 2 | | | 0 |
| **5**  | 279 | 110 | 6 | 0 | − 9 | 10 | 0 | 7 | 0 | 0 | 0 | 2 | 0 |

[a] Positive sign indicates a shift to high field of the signals of the deuterated compound relative to those of non-deuterated. Spectra were recorded in [$^2H_6$]acetone at 100.6 MHz using a Bruker WH-400 spectrometer; in each case *ca.* 2 : 1 mixtures of deuterated and non-deuterated compounds were used. The spectral width was limited to a minimum in order to collect a large number of data points and hence achieve a high precision. Assignment of the signals follows by standard methods and for difficult cases was verified using the 2D-INADEQUATE technique. Errors amount to 0.5 ppb.

addition to the isotopic perturbation of equilibria[2] there is considerable interest on the influence of deuterium on π-systems[3]. Under discussion are the mechanisms of interaction which have been invoked to clarify the isotope shifts[4]. According to the Born-Oppenheimer approximation, a deuterium substituted molecule has the same electronic properties as an unsubstituted one; all differences in the NMR data should therefore originate from different zero point vibrations. This model predicts positive signs for most isotope effects, *i.e.* a shift to high field. Some authors presume an "isotope-induced" inductive effect, whereas others correlate long-range isotope effects with the reduced capacity of deuterium to undergo hyperconjugation, although strictly speaking this is a violation of the Born-Oppenheimer approximation[5].

We have prepared the compounds **1**—**5** (Table 1), which allow the observation of the $^2H$ isotope effects on the $^{13}C$ chemical shifts of conjugated C=C bonds arranged in long chains. As shown in Table 1, extremely long-range deuterium effects (over 12 bonds in **5**) occur together with a change of sign of the isotope effect at certain sites.

The ethene bridge in **3**, the ethyne bridge in **4**, and the butadiene bridge in **5** are polarized as if the deuterium were a "real" substituent with different electronic properties than hydrogen. Here, hyperconjugation cannot be the reason, since $^2H$ is bonded directly to an aryl moiety. The results question the general validity of the so far discussed mechanism of NMR isotope effects.

Received: November 3, 1982 [Z 194 IE]
German version: *Angew. Chem. 95* (1983) 321

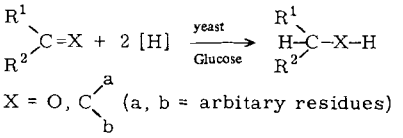
[1] P. E. Hansen, *Annu. Rep. NMR Spectrosc.*, in press.
[2] G. Maier, H. O. Kalinowski, K. Euler, *Angew. Chem. 94* (1982) 706; *Angew. Chem. Int. Ed. Engl. 21* (1982) 693.
[3] S. Berger, H. Künzer, *Tetrahedron*, in press.
[4] a) E. A. Halevi, M. Nussim, A. Ron, *J. Chem. Soc. 1963*, 866; b) E. A. Halevi, *Prog. Phys. Org. Chem. 1* (1963) 109; c) C. J. Jameson, *Bull. Magn. Res. 3* (1981) 3.
[5] a) J. R. Wesener, H. Günther, *Tetrahedron Lett. 23* (1982) 2845; b) L. Ernst, S. Eltamany, H. Hopf, *J. Am. Chem. Soc. 104* (1982) 299.

## Electromicrobial Reduction Using Yeasts**

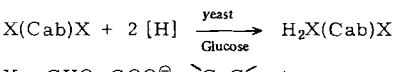
By *Helmut Günther, Cornelia Frank, Hans-Jürgen Schuetz, Johann Bader,* and *Helmut Simon**

Aerobic and facultative aerobic microorganisms, particularly yeasts, have been used for decades to obtain chiral compounds by stereospecific reduction of substituted unsaturated compounds[1]. In this connection, two types of reaction are distinguished [eqs. (a) and (b)].

We have previously indicated the principal disadvantages of such methods[4,5]. In the anaerobic mode using yeast and glucose as electron donor, per mol of NADH 1 mol acetaldehyde is formed, which is then preferentially reduced consuming NADH; in the aerobic mode a considerable amount of the NADH formed as intermediate is reoxidized in the respiration chain. The desired reaction therefore always occurs as a side reaction.




(a)




(b)

[*] Prof. Dr. H. Simon, Dr. H. Günther, C. Frank, Dr. H.-J. Schuetz, J. Bader
Lehrstuhl für Organische Chemie und Biochemie
der Technischen Universität München
Lichtenbergstrasse 4, D-8046 Garching (Germany)

[**] This work was supported by the Deutsche Forschungsgemeinschaft (Sonderforschungsbereich 145) and the Fonds der Chemischen Industrie.

 © *Verlag Chemie GmbH, 6940 Weinheim, 1983* *0570-0833/83/0404-0322 $ 02.50/0* 

We report here on the possibility of stereospecifically reducing compounds with yeasts *(Saccharomyces cerevisiae, Candida utilis, Kluyveromyces fragilis, inter alia)*, which are supplied electrons from continuously electrochemically reduced methylviologen ($MV^{+}$). An example is the formation of (*R*)-1,2-propanediol from hydroxyacetone by *S. cerevisiae* in the presence and absence of additional NAD.

In the absence of NAD the propanediol is formed only slowly; with glucose as electron donor, the propanediol is produced just as slowly with or without NAD. Addition of catalytic amounts of NAD results in relatively rapid formation of propanediol. Using two methods we were able to show that the NADH is actually formed by the yeast. 1) The formation of NADH from NAD, catalyzed by crude extract of yeast, and the corresponding decrease in concentration of $MV^{+}$ can be observed photometrically. 2) Figure 3 shows that current flows in an electrochemical cell containing intact yeast cells and $MV^{+}$ upon addition of NAD. After the cell has taken up a charge corresponding to the amount of NAD, only NADH and no NAD could be detected in solution. Addition of hydroxyacetone results in an increase in the current to a level somewhat above that resulting from the formation of NADH. These results suggest that reactions (c)—(e) occur in the electrochemical cell in the presence of yeast.

$$2\,MV^{\oplus\ominus} + 2\,e \longrightarrow 2\,MV^{+} \qquad (c)$$

$$2\,MV^{+} + H^{\oplus} + NAD^{\oplus} \xrightarrow{\text{yeast}} NADH + 2\,MV^{\oplus\oplus} \qquad (d)$$

$$H^{\oplus} + NADH + CH_3COCH_2OH \xrightarrow{\text{yeast}} NAD^{\oplus} + CH_3CHOHCH_2OH \qquad (e)$$

Total:

$$CH_3COCH_2OH + 2\,H^{\oplus} + 2\,e \longrightarrow CH_3CHOHCH_2OH \qquad (f)$$

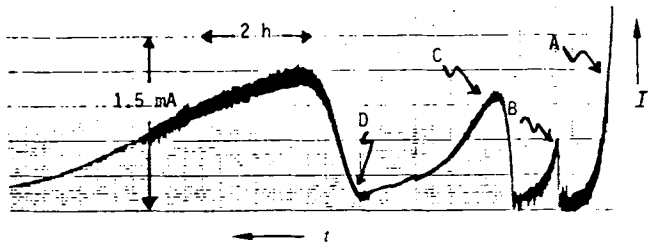



Fig. 3. Current as a function of time for the electromicrobial reduction of hydroxyacetone in an electrochemical cell. A: Reduction of $MV^{\oplus\oplus}$ (4 mM), B: Addition of *S. cerevisiae*; C: Addition of NAD (1.5 mM); D: Addition of hydroxyacetone (5 mM). The increase in the current after addition of yeast presumably involves the reduction of traces of oxygen and endogenic electron acceptors of the yeast.

To date we have obtained rates of formation of *ca.* 0.4 μmol NADH per min and 20 mg yeast (dry weight). This corresponds to a current of 1.3 mA. In the reduction of hydroxyacetone the rate of formation of NADH is rate determining; hence, after addition of hydroxyacetone the current is not larger than in presence of NAD alone (Fig. 3).

The (*R*)-1,2-propanediol thus obtained showed an optical rotation of $[\alpha]_D^{25}$ +20.1° ($H_2O$; $c = 8$). This is close to the highest value ($[\alpha]_D^{25}$ +20.76°) reported in the literature[6].

Compared to cofermentations, the electrochemical reduction by yeast has the following advantages: 1) After addition of catalytic amounts of NAD the reductions are much faster; this arises because the rate-determining step for the formation of NADH is not the glycolysis. This is regulated by the concentration of ATP and is presumably difficult to influence. Introduction of the ratio product/(biocatalyst × time) as a figure of merit gives a value approximately ten times greater for our method than for a bioreduction of hydroxyacetone described in *Organic Synthesis*[7]. Since the products have to be separated from considerably less biocatalyst, and other metabolic products of the biocatalyst are also not formed, they are considerably easier to isolate. 2) A reduction and its rate can be continuously monitored by measuring the current. 3) Reactions between substrate and/or product and reactive intermediates of glycolysis cannot occur.

The catalysis of the reduction of NAD by *intact* yeast cells is surprising. Apparently, NAD can enter the cells and leave again as NADH. So far it is not known which enzymes catalyze reaction (d).

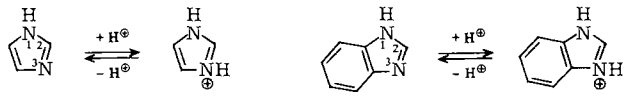
Received: November 22, 1982 [Z 207 IE]
German version: *Angew. Chem. 95* (1983) 325

[1] K. Kieslich: *Microbial Transformations*, Thieme, Stuttgart 1976.
[4] H. Simon, H. Günther, J. Bader, W. Tischer, *Angew. Chem. 93* (1981) 897; *Angew. Chem. Int. Ed. Engl. 20* (1981) 861.
[5] H. Simon, H. Günther, "Biomimetic Chemistry" in Z. Yoshida, N. Ise: *Studies in Organic Chemistry*, Kodansha, Vol. XIII, Tokyo, and Elsevier, Amsterdam.
[6] E. Baer, H. O. L. Fischer, *J. Am. Chem. Soc. 70* (1948) 609.
[7] P. A. Levene, A. Walti, *Org. Synth. 10* (1930) 84.

## The Relative Basicities of Imidazole and Benzimidazole

By *Javier Catalan**, *José Elguero*, *Robert Flammang*, and *André Maquestiau*

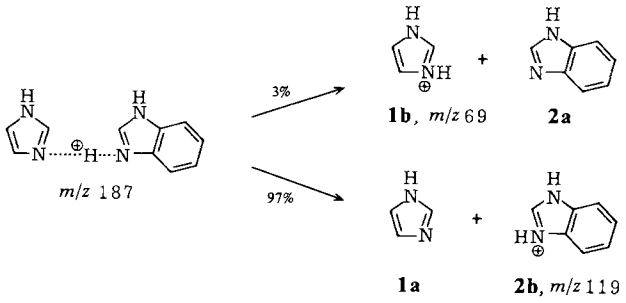
Values in the literature show that imidazole **1a** is more basic than benzimidazole **2a** by *ca.* 1.5 $pK_a$ units. However, theoretical results strongly suggest that in the gas phase the intrinsic basicity of **1a** should be lower than that of **2a**.




**1a** **1b** **2a** **2b**

Three criteria have been used to discuss the proton affinities of these 1,3-diazoles: 1) The calculated value of the energy change ($\Delta E = -7.1$ kcal/mol) for the isodesmic reaction **1b** + **2a** → **1a** + **2b** is comparable with experimental values on the effects of benzoannelation determined on other systems[15]. 2) The charge density on H-3 is smaller in **1b** (0.811) than in **2b** (0.823), indicating that **2b** should be the weaker acid[20]. 3) The charge density on N-3 in **1a** (5.239) is smaller than that in **2a** (5.266), indicating that **2a** should be more basic[21].

[*] Dr. J. Catalan
Departamento de Química Física y Química Cuántica
Facultad de Ciencias, C-XIV, Universidad Autónoma de Madrid
Cantoblanco, Madrid-34 (Spain)
Dr. J. Elguero
Instituto de Química Médica, CSIC
Juan de la Cierva 3, Madrid-6 (Spain)
Dr. R. Flammang, Prof. Dr. A. Maquestiau
Laboratoire de Chimie Organique, Université de l'Etat à Mons
19 Avenue Maistriau, B-7000 Mons (Belgium)




To verify this prediction the relative proton affinities of **1a** and **2a** have been determined by mass spectrometry using *Cooks*' method[23]. The MIKE (mass analyzed ion kinetic energy) spectrum of the benzimidazole-imidazole protonated adduct (*m/z* 187) showed formation of protonated benzimidazole **2b** (*m/z* 119) to be 40 times greater than that of protonated imidazole **1b** (*m/z* 69). As expected[23], the interaction of the adduct with a collision gas (CID/MIKE) somewhat increases the relative abundance of protonated imidazole (**2b** : **1b** = 13). Both experiments show unambiguously that benzimidazole **2a** is more basic than imidazole **1a**. From the experimental proton affinity of imidazole (223.3 kcal/mol)[16], the calculated $\Delta E$ value for the isodesmic reaction **1b** + **2a** → **1a** + **2b**, and the experimental results for the annelation effect (*ca.* −6 kcal/mol)[15] the proton affinity for benzimidazole ought to lie in the range 228–230 kcal/mol.

A plausible explanation for the inversion of basicity in **1a** and **2a** on going from the gas phase to aqueous solution takes into account hydrogen bonding between the solvent and both neutral and protonated species. But the main reason is a polarizability effect[29] due to the annelated benzene ring. It disappears in water by dispersion of the positive charge through the hydrogen bonds.

INDO calculations (optimized geometries) give energies and charge densities in accord with the experimental results.

Received: November 22, 1982;
revised: February 8, 1983 [Z 206 IE]
German version: *Angew. Chem. 95* (1983) 323
The complete manuscript of this communication appears in:
*Angew. Chem. Suppl.* 1983, 411–418

[15] M. Meot-Ner (Mautner), *J. Am. Chem. Soc. 101* (1979) 2396.
[16] D. H. Aue, personal communication at the EUCHEM Conf. Ionic Chem.: Gaseous *vs.* Solvated Ions, Lido di Ostia (Roma), September 1982.
[20] J. Catalan, A. Macias, *J. Chem. Soc. Perkin Trans. 2 1979*, 1632; W. J. Hehre, M. Taagepera, R. W. Taft, R. D. Topsom, *J. Am. Chem. Soc. 103* (1981) 1344 and references cited therein.
[21] J. Catalan, O. Mo, P. Perez, M. Yañez, *J. Am. Chem. Soc. 101* (1979) 6520.
[23] S. A. McLuckey, D. Cameron, R. G. Cooks, *J. Am. Chem. Soc. 103* (1981) 1313.
[29] J. J. Brauman, J. M. Riveros, L. K. Blair, *J. Am. Chem. Soc. 93* (1971) 3914; J. F. Wolf, J. L. M. Abboud, R. W. Taft, *J. Org. Chem. 42* (1977) 3316 and references cited therein.

## A Novel Lead-Oxygen Structural Group: $Pb_8O_4^{8+}$

By *Hans-Lothar Keller**

Like the thallium compound $TlPb_8O_4Br_9$ **1**[11], the tetragonally crystallizing $Pb_9O_4Br_{10}$ **2** also contains remarkable and novel $Pb_8O_4$-groups in the crystal structure (Fig. 1).

[*] Dr. H.-L. Keller
Institut für Anorganische Chemie der Universität
Olshausenstr. 40, Haus N13a, D-2300 Kiel (Germany)

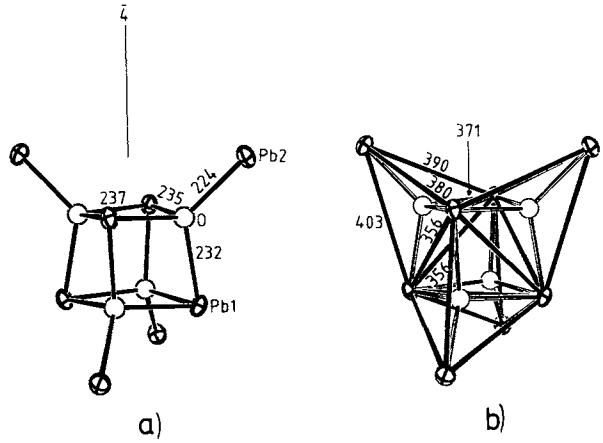



Fig. 1. The $Pb_8O_4$ group in $TlPb_8O_4Br_9$ **1** [1]: a) without, and b) with emphasis of the $Pb_4$-tetrahedra centered by O atoms (distances in pm).

Nucleus of this structural unit is a $Pb_4O_4$-cube with point symmetry $\bar{4}$, reminiscent of the "cubane" units in $[Pb_4(OH)_4](ClO_4)_4 \cdot 2H_2O$[7] and $Sn_{21}Cl_{16}(OH)_{14}O_6$[8]. However, unlike in the latter two compounds, in **1** and **2** there is a further lead atom above each corner of the cube occupied by oxygen atoms. This lead atom is located on the extrapolated diagonal of the cube. The oxygen atoms are thus tetrahedrally surrounded by lead atoms. Four of these $OPb_4$-tetrahedra are each coupled to one another *via* three edges and thus build the $Pb_8O_4$-unit, which can be regarded as an isolated polynuclear metallo-complex[9]. The charges of the outer Pb-ions are compensated by Br-ions, whereby the whole $Pb_8O_4$-group is enveloped (Fig. 2). Two of these lead-oxygen units separated by a bromide ion matrix are present in each unit cell.

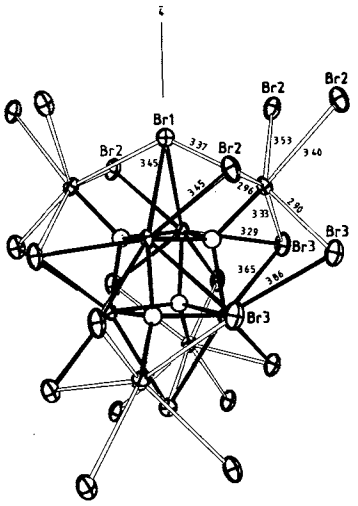



Fig. 2. The $Pb_8O_4$ group with bromide-ion environment in $TlPb_8O_4Br_9$ [1].

In **1** and **2**, slightly distorted tetragonal prisms formed from bromine atoms are stacked one on top of the other parallel to the fourfold symmetry axes in the unit cell. In **1**, every next but one prism is centered with thallium atoms; the prisms in between are unoccupied and elongated along [001] compared to the occupied prisms (Fig. 3a). Interatomic distances between thallium and bromine correspond to those in TlBr[10]. In **2**, the tetragonal prisms are considerably more elongated and compressed than in **1**;

 © *Verlag Chemie GmbH, 6940 Weinheim, 1983* *0570-0833/83/0404-0324 $ 02.50/0* 

the elongated prisms accomodate bromine atoms, the compressed neighboring prisms lead atoms (Fig. 3b).

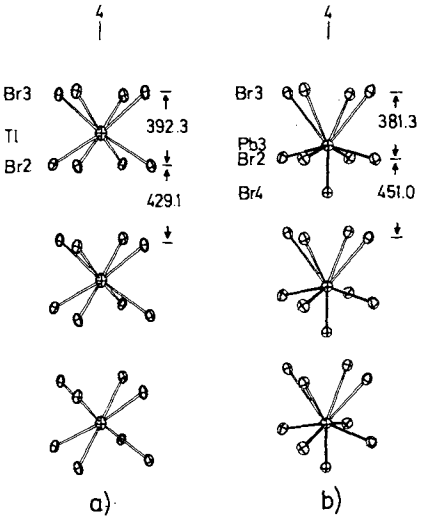



Fig. 3. The sequence of tetragonal prisms formed from Br-ions parallel to [001] in: a) $TlPb_8O_4Br_9$, and b) $Pb_9O_4Br_{10}$. The five nearest Br neighbors of Pb3 are emphasized by filled connecting lines. Further details of the crystal structure determination can be obtained on request from the Fachinformationszentrum Energy Physik Mathematik, D-7514 Eggenstein-Leopoldshafen by quoting the number CSD 50365, the name of the author, and full citation of the journal.

The latter atoms are shifted from the center in the direction of the square basal plane, leading to a short Pb–Br-distance of 257.7 pm. To a first approximation each such Pb-ion shows a one-sided fivefold environment of bromine (Fig. 3b, filled connecting lines to Br2 and Br4). This at first sight unusual environment might be explained in terms of the effect of the lone pair electrons (on Pb3) if these are oriented in the opposite direction of the short Pb–Br-distance. For the lead atom in question, in contrast to the other, pseudotetrahedrally coordinated lead atoms, there results in the primary neighborhood a pseudooctahedral environment. This suggests comparison with a $BiCl_5^{2-}$ group in the bismuth subchloride $Bi_{24}Cl_{28}$[11].

Received: November 22, 1982;
revised: January 21, 1983 [Z 208 IE]
German version: *Angew. Chem. 95* (1983) 318
The complete version of this communication appears in:
*Angew. Chem. Suppl. 1983*, 427–444

[1] H.-L. Keller, *Z. Anorg. Allg. Chem. 491* (1982) 191.
[7] S. H. Hong, A. Olin, *Acta Chem. Scand. A 28* (1974) 233.
[8] H. G. von Schnering, R. Nesper, H. Pelshenke, *Z. Naturforsch. B 36* (1981) 1551.
[9] G. Bergerhoff, *Angew. Chem. 76* (1964) 697; *Angew. Chem. Int. Ed. Engl. 3* (1964) 686.
[10] A. Smakula, J. Kalnajs, *Nuovo Cimento 6, Suppl. No 1* (1957) 214.
[11] A. Hershaft, J. D. Corbett, *Inorg. Chem. 2* (1963) 979.

## Isotope Effects in the Low-Pressure, High-Pressure, and Thin-Layer Chromatography of the Lanthanoids

By *Alfons Hufnagel* and *Hermann Specker**

During experiments on the HPLC separation of the lanthanoids we were able to detect an isotope effect in the case of the isotopes samarium-154 and samarium-144[1]. The total separation factor G, as defined by *Heumann*[2], was 1.06. The detection was accomplished mass spectroscopically. In continuation of these experiments we have now investigated the lanthanoids cerium and europium. Both elements have proven to be especially suitable for such studies regarding their natural isotopic composition and their subsequent determination by neutron activation analysis. Table 1 lists the physical properties of the isotopes used for the measurement of the isotopic enrichment.

Table 1. Physical properties of the isotopes employed. $T_{1/2}$ = halflife, $E$ = γ-energy, $P$ = emission probability (absolute intensity).

| Stable nuclide | Abundance [%] | Active nuclide | $T_{1/2}$ | $E$ [keV] | $P$ [%] |
|---|---|---|---|---|---|
| $^{140}Ce$ | 88.48 | $^{141}Ce$ | 32.5 d | 145.45 | 47 |
| $^{142}Ce$ | 11.07 | $^{143}Ce$ | 33 h | 293.3 | 43.3 |
| $^{151}Eu$ | 47.8 | $^{152}Eu$ | 12.7 y | 344.3 | 27 |
| $^{153}Eu$ | 52.2 | $^{154}Eu$ | 8.5 y | 123.1 | 40.46 |

In the first series of experiments, $Ce(NO_3)_3$ was subjected to multiple repurification and then chromatographed on two low-pressure columns coupled in cascade [Lobar, Merck, size A (240-10), Li Chroprep Si 60 (40–64 μm)]. 50 μL of a 1 M $Ce^{3+}$-solution (≙ 7 mg $Ce^{3+}$) in methanol/$HNO_3$ (3 : 1) was introduced onto the column *via* a three-way tap. Elution was carried out with a mixture of diisopropyl ether/tetrahydrofuran/$HNO_3$ (65%) in the ratio 100 : 20 : 5. The consistently reproducible retention time for cerium was 187 min, the peak width 39 min. After fractionation of the cerium peak into three twelve-minute fractions the respective "head" and the "tail" fractions were very carefully worked-up and then irradiated (neutron flux $10^{14}$ n $cm^{-2}$ $s^{-1}$). The absolute content of cerium in each of the fractions was not measured; for measurement of the isotope effect according to the aforementioned definition of the total separation factor G, we calculated the quotients of the net count rates of the characteristic γ-emission lines of the isotopes Ce-143 to Ce-141 in the "head" fraction and in the "tail" fraction. From ten single measurements an enrichment of the heavier isotope was found in the "head" fraction of the cerium peak with a mean total separation factor of 0.65 : 0.59 = 1.102 at the 99.9% confidence level.

In the case of HPLC- and TLC-enrichment we used previously activated cerium and europium samples as starting material. The eluent used in the HPLC separation [HPLC "Constametric" pump, Knauer columns (250 × 4.6 mm), silica gel 60 Li Chrosorb, particle size 7 μm, pore size 60 Å] was diisopropyl ether/tetrahydrofuran/$HNO_3$ (100 : 35 : 4), the amount of sample 150 μg $Ce^{3+}$ and 0.38 μg $Eu^{3+}$, respectively. The monitoring was carried out with a continuous flow NaI(Tl) scintillator. On the basis of the chromatograms obtained, five 1-minute fractions were collected in each case and the individual fractions measured γ-spectroscopically. For the cerium isotopes a total separation factor of 1.085 was obtained; this result was also measured at the 99.9% confidence level, from 18 measurements. The corresponding factor in the case of europium amounted to 1.03, at the same confidence level. According to our investigations so far, the different average total separation factors measured for the elements cerium and europium are not in the first instance the result of different fractionation but rather of different retention times. We

[*] Prof. Dr. H. Specker, Dr. A. Hufnagel
Lehrstuhl Anorganische Chemie I der Universität
Postfach 102138, D-4630 Bochum 1 (Germany)

are at present investigating the step heights in our sample carrier-eluent systems, so as to enable calculation of the element separation factors.

So far, TLC has proven to be the most efficient chromatographic method for the separation of the lanthanoids[3] [Merck plates, silanized silica gel (0.25 mm), size 20 × 20 cm, without fluorescence indicator]. We therefore resorted to TLC for the enrichment of the europium isotopes. The zones in conventional chromatography cannot, of course, be reproducibly defined as "head" and "tail" zones and so separated. It is known, however, that the zones can be concentrated by constricting the flow of eluent[4]. In this way the zones could indeed be separated into "head", "tail" and "middle" zones. Diisopropyl ether/tetrahydrofuran/$HNO_3$ (100:50:5) was used as eluent. In the case of the isotopes europium-154:europium-152 we obtained a total separation factor of 1.06 from 21 single measurements on the "head" and "tail" zones. The corresponding depletion in the "tail" zones was also confirmed from 23 single measurements at the 99.9% significance level. To our knowledge an isotope effect has hitherto never been detected in inorganic TLC. In the case of the isotope effects so far detected, an enrichment of the heavier isotopes in the "head" fraction or "head" zone was found in all cases during column and thin-layer chromatography, respectively. This is consistent with the chromatographic methodologies developed by us for the separation of lanthanoids using the same eluent system.

Received: November 19, 1982 [Z 205 IE]
German version: *Angew. Chem. 95* (1983) 327

CAS Registry numbers:
$^{140}$Ce, 14191-73-2; $^{142}$Ce, 14119-20-1; $^{151}$Eu, 14378-48-4; $^{153}$Eu, 13982-02-0; $^{141}$Ce, 13967-74-3; $^{143}$Ce, 14119-19-8; $^{152}$Eu, 14683-23-9; $^{154}$Eu, 15585-10-1; *diiso*propyl ether, 108-20-3; tetrahydrofuran, 109-99-9

[1] H. Specker, W. Weuster, *Fresenius Z. Anal. Chem. 302* (1980) 205.
[2] K. G. Heumann, *Z. Naturforsch. B 27* (1972) 492.
[3] K. Jung, H. Specker, *Fresenius Z. Anal. Chem. 300* (1980) 15.
[4] E. Stahl: *Dünnschichtchromatographie*, 2nd edition, Springer, Berlin 1967.

## Capping of Metal Atom Triangles in Clusters by $R_3PAu$ Moieties**

By *Eckehart Roland, Klaus Fischer,* and *Heinrich Vahrenkamp**

The growth of metallic microcrystallites or metal-rich clusters requires the incorporation of the monometal species at energetically favored face positions. Sporadic examples suggest that the additional species is bonded preferentially over triangles or quadrangles of metal atoms[1]. The recently[2] discovered exchange of hydride ligands for $R_3PAu$ moieties in clusters offers a method of studying these types of growth reactions systematically. Previously, a $R_3PAu$ moiety could be incorporated as a $\mu_2$-bridge across two metal atoms[3] or as a $\mu_3$-bridge across three metal atoms[2,4]. We have now found that incorporation of two $R_3PAu$ moieties leads to a repetition of the $\mu_3$-bridging principle.

Deprotonation of $H_2Fe_3(CO)_9S$ or $H_2Ru_2Co_2(CO)_{12}$ by KH in tetrahydrofuran (THF) leads to dianions which react smoothly with $Ph_3PAuCl$ to give the pentanuclear cluster **1** (47%, black crystals, m.p. = 150 °C) or the hexanuclear cluster **2** (38%, black crystals, m.p. = 133 °C). **1** and **2** were identified by crystal structure analysis (see Figs. 1 and 2, as well as Table 1).

$(Ph_3PAu)_2Fe_3(CO)_9S$ **1**

$(Ph_3PAu)_2Ru_2Co_2(CO)_{12}$ **2**

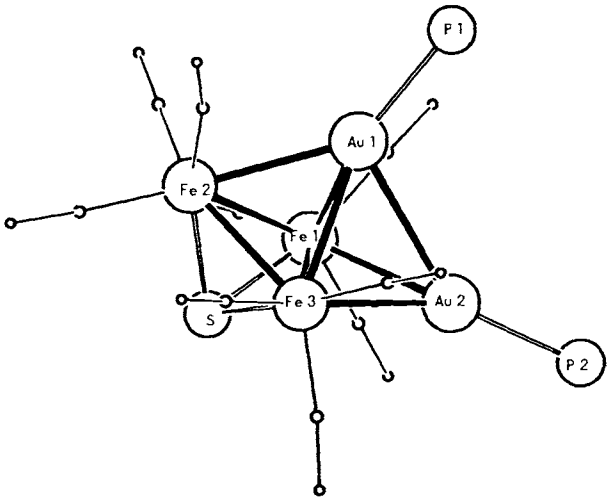



Fig. 1. Molecular framework of **1** in the crystal (small circles represent CO ligands; phenyl groups are not shown).

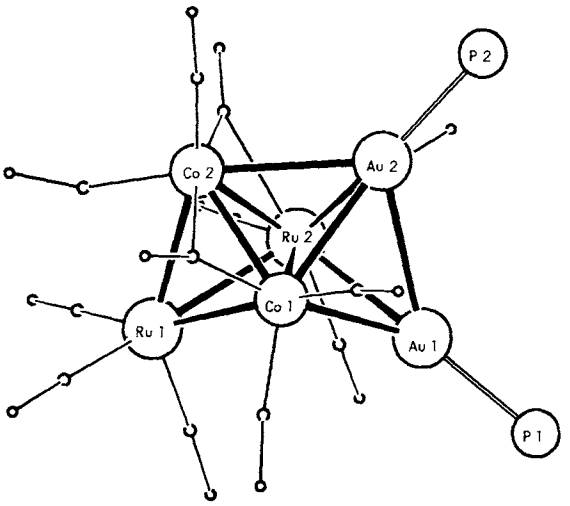



Fig. 2. Molecular framework of **2** in the crystal (small circles represent CO ligands; phenyl groups are not shown).

The stepwise growth of the clusters is apparent from their structures. One of the two gold atoms is located over a triangular face of the starting material, and the other over a triangular face formed by addition of the first gold atom. Of the metal-metal bonds, the inner (Fe1-Fe3 and Co1-Ru2, respectively) are extraordinarily long. This indicates a tendency of these bonds to rupture; the simultaneous formation of the Au2-S and Ru1-Au1 bonds, respectively, would lead to an octahedral cluster framework. By analogy, the growth of polymetal species can be comprehended as a sequence of $\mu_3$-cappings and reorganizations. Recently described triply gold-bridged ruthenium clusters[11] exhibit the same structural principle, whereas the carbido cluster $[CFe_4(CO)_{12}(AuPR_3)_2]$[12], obtained in a

[*] Prof. Dr. H. Vahrenkamp, E. Roland, K. Fischer
Institut für Anorganische und Analytische Chemie der Universität
Albertstrasse 21, D-7800 Freiburg (Germany)

[**] Basic Cluster Reactions, Part 4. This work was supported by Heraeus GmbH (Hanau) and by the Rechenzentrum, Universität Freiburg.—Part 3: E. Roland, H. Vahrenkamp, *Organometallics 2* (1983) 183.

Table 1. Distance between heavy atoms in **1** and **2** [a].

| Positions **1** | Distance [pm] | Positions **2** | Distance [pm] |
|---|---|---|---|
| Fe1-Fe2 | 264.2(5) | Ru1-Co1 | 269.0(3) |
| Fe1-Fe3 | 286.4(4) | Ru1-Co2 | 267.5(3) |
| Fe2-Fe3 | 275.0(4) | Ru1-Ru2 | 278.5(2) |
| Fe1-Au1 | 272.2(3) | Co1-Co2 | 249.2(4) |
| Fe2-Au1 | 269.8(4) | Co1-Ru2 | 295.4(3) |
| Fe3-Au1 | 274.6(3) | Co2-Ru2 | 272.3(3) |
| Fe1-Au2 | 267.1(3) | Co1-Au2 | 265.1(3) |
| Fe3-Au2 | 275.0(4) | Co2-Au2 | 286.6(3) |
| Au1-Au2 | 302.0(1) | Ru2-Au2 | 288.7(2) |
| Fe1-S | 221.1(8) | Co1-Au1 | 261.3(3) |
| Fe2-S | 219.4(5) | Ru2-Au1 | 287.2(2) |
| Fe3-S | 219.8(6) | Au2-Au1 | 289.0(1) |
| Au1-P1 | 230.5(6) | Au1-P1 | 229.5(5) |
| Au2-P2 | 230.1(6) | Au2-P2 | 229.9(5) |

[a] Further details on the crystal structure investigation can be obtained from the Fachinformationszentrum Energie Physik Mathematik, D-7514 Eggenstein-Leopoldshafen, by quoting the depository number CSD 50299, the names of the authors and the journal citation.

nondirected way from $[Fe_4(CO)_{13}]^{2-}$, contains the gold atoms in $\mu_4$-positions as components of an octahedral framework. **2** is the first hexanuclear cluster to be constructed stepwise from simple building blocks ($KCo(CO)_4$, $[Ru(Co)_3Cl_2]_2$, $Ph_3PAuCl$), and is hence a unique example for the directed synthesis of clusters.

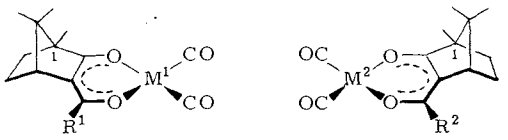
Received: November 18, 1982;
supplemented: December 17, 1982 [Z 203 IE]
German version: *Angew. Chem. 95* (1983) 324
The complete version of this communication appears in:
*Angew. Chem. Suppl. 1983*, 419-426

[1] W. L. Gladfelter, G. L. Geoffroy, *Adv. Organomet. Chem. 18* (1980) 207; M. Tachikawa, E. L. Muetterties, *Prog. Inorg. Chem. 28* (1981) 203.
[2] J. W. Lauher, K. Wald, *J. Am. Chem. Soc. 103* (1981) 7684.
[3] M. Green, K. A. Mead, R. M. Mills, I. D. Salter, F. G. A. Stone, P. Woodward, *J. Chem. Soc. Chem. Commun. 1982*, 51; B. F. G. Johnson, D. A. Kaner, J. Lewis, P. R. Raithby, M. J. Taylor, *ibid. 1982*, 314.
[4] M. J. Mays, P. R. Raithby, P. L. Taylor, K. Henrick, *J. Organomet. Chem. 224* (1982) C45; P. Braunstein, J. Rose, Y. Dusausoy, J. P. Mangeot, *C. R. Acad. Sci. Ser. II 294* (1982) 967.
[11] L. W. Batemann, M. Green, J. A. K. Howard, K. A. Mead, R. M. Mills, I. D. Salter, F. G. A. Stone, P. Woodward, *J. Chem. Soc. Chem. Commun. 1982*, 773; M. I. Bruce, B. K. Nicholson, *ibid. 1982*, 1141.
[12] B. F. G. Johnson, D. A. Kaner, J. Lewis, P. R. Raithby, M. J. Rosales, *J. Organomet. Chem. 231* (1982) C59.

## Construction of an Alternating (Rh, Rh, Ir, Ir)$_\infty$-Columnar Structure *via* a Quasiracemate**

By *Volker Schurig**, *Wolfgang Pille*, and *Werner Winter*

The chiral, square-planar $d^8$ metal chelate dicarbonylrhodium(I) 3-trifluoroacetylcamphorate **1**[1a] has recently been reported as representing an interesting example for the striking influence of the relative chirality of the β-diketonate ligands on cooperative phenomena in the crystalline state[1b]. Thus, whereas the identically configurated molecules in the crystalline *yellow* enantiomers of **1** pack *via* a zig-zag arrangement of the metal atoms, the oppositely configurated molecules in the crystalline *red-green* (dichroic) racemate stack *via* a columnar structure with a one-dimensional metal atom chain.



(1*S*)-**1**: $R^1 = CF_3$, $M^1 = Rh$
(1*R*)-**2**: $R^2 = CH_3$, $M^2 = Rh$
(1*R*)-**3**: $R^2 = CF_3$, $M^2 = Ir$

It has been suggested[1b] that the influence of the heterochiral ligands in the racemate may be exploited to prepare highly ordered solid-state structures with alternating molecular properties by combining *quasienantiomers* of similar structure in a "zipper-like mode" to stable *quasiracemates* ("active racemates"[2]).

Having succeeded in obtaining a red-green (dichroic) quasiracemate from yellow dicarbonylrhodium(I) (1*R*)-3-*acetyl*camphorate (1*R*)-**2** and yellow dicarbonylrhodium(I) (1*S*)-3-*trifluoroacetyl*camphorate (1*S*)-**1**, we attempted to construct a columnar structure with alternately arranged homologous central atoms. When equimolar amounts of the yellow crystalline quasienantiomer dicarbonyl*rhodium*(I) (1*S*)-3-trifluoroacetylcamphorate (1*S*)-**1** and the yellow crystalline quasienantiomer of opposite configuration dicarbonyl*iridium*(I) (1*R*)-3-trifluoroacetylcamphorate (1*R*)-**3** are mixed, a crystalline black-violet (dichroic) quasiracemate forms spontaneously from the solution (*n*-hexane) or by a slow solid-state reaction.

The crystal structure of the quasiracemate (1*S*)-**1**/(1*R*)-**3** (space group C2, $a = 27.808(8)$, $b = 9.384(3)$, $c = 13.486(3)$ Å, $\beta = 117.57(2)°$, $Z = 4$ for the dimeric entity[3a]) is close related to that of the racemate (1*S*)-**1**/(1*R*)-**1** (space group C2/c, $a = 24.726(1)$, $b = 9.365(1)$, $c = 13.447(1)$ Å, $\beta = 91.56(1)°$, $Z = 8$)[3b]: the *b*- and *c*-axes in the quasiracemate and racemate have a similar length, whereas the extended *a*-axis in the quasiracemate corresponds to the [101]-axis in the racemate. In both columnar structures (Fig. 1), *anti*-orientated racemic and quasiracemic pairs of molecules (*R*,*S*), respectively, stack in such a way that an

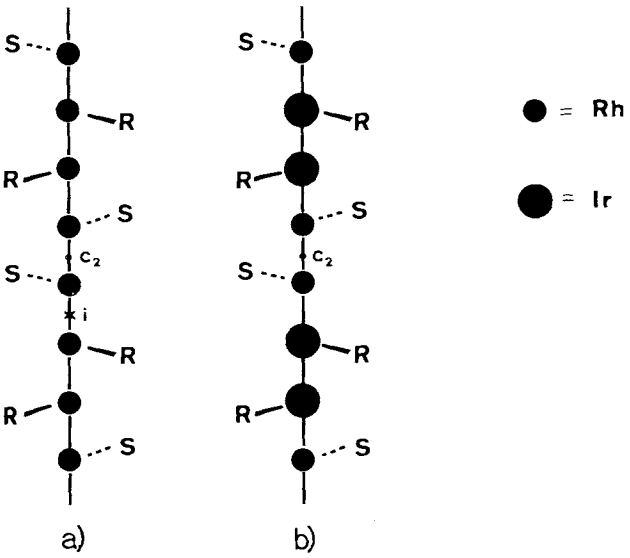



Fig. 1. Construction of an alternating (Rh,Rh,Ir,Ir)$_\infty$ columnar structure (b) *via* control by chiral ligands. Structural comparison between a) racemate [prepared from (1*S*)-**1** and (1*R*)-**1** (1:1)] and b) quasiracemate [prepared from (1*S*)-**1** and (1*R*)-**3** (1:1)].

[*] Prof. Dr. V. Schurig, W. Pille, Prof. Dr. W. Winter [+]
Institut für Organische Chemie der Universität
Auf der Morgenstelle 18, D-7400 Tübingen (Germany)
[+] X-ray structural analysis.
[**] This work was supported by the Fonds der Chemischen Industrie and the Stiftung Volkswagenwerk.

overall alternating arrangement of ligands $(R,R,S,S)_\infty$ along the *c*-crystal axis results[4]. Thus, mixing the pure quasienantiomers (1*S*)-**1** and (1*R*)-**3** produces the quasiracemate as a *highly* ordered columnar structure with a one-dimensional $(Rh,Rh,Ir,Ir)_\infty$ chain of central atoms. The Rh–Rh, Ir–Ir, and Rh–Ir distances are 3.36, 3.36, and 3.43 (±0.02) Å, respectively. In the quasiracemate the metal chain is not strictly linear, since the Rh–Rh and Ir–Ir moieties are slightly displaced in the crystal lattice; the distance between the axes, which contain all Rh and Ir atoms, respectively, is 0.6 Å.

The pair-wise stacking in the crystalline quasiracemate enforced by the chirality of the molecules represents a new type of one-dimensional metal chain[5]. The tailor-made synthesis of quasiracemates appears, therefore, to be a highly promising method for the construction of collective solid-state structures having alternating molecular parameters.

Received: December 1, 1982 [Z 214 IE]
German version: *Angew. Chem. 95* (1983) 327

[1] a) V. Schurig, *Inorg. Chem. 11* (1972) 736; b) *Angew. Chem. 93* (1981) 806; *Angew. Chem. Int. Ed. Engl. 20* (1981) 807.
[2] M. Delepine, *Helv. Chim. Acta 22* (1939) 519.
[3] a) Nonius CAD 4, $Mo_{K\alpha}$ (graphite monochromator), 1697 symmetry-independent reflections with $I \geq 2\sigma(I)$, R = 0.077 (Rh,Ir anisotropic). b) Further details on the crystal structure investigation can be obtained from the Fachinformationszentrum Energie Physik Mathematik, D-7514 Eggenstein-Leopoldshafen, by quoting the depository number CSD 50354, the names of the authors, and journal citation; b) F. Frolow, D. Rabinovich, V. Schurig, unpublished.
[4] A similar arrangement of quasienantiomers in an "active racemate" [2] was detected in the system [(+)-Co(en)$_3$, (−)-Cr(en)$_3$]Cl$_6$·6.1 H$_2$O by X-ray crystallography (P. A. Whuler, C. Brouty, P. Spinat, P. Herpin, *Acta Crystallogr. B 32* (1976) 194.
[5] For other examples of alternating columnar structures cf. J. S. Miller, A. J. Epstein, *Prog. Inorg. Chem. 20* (1976) 1; J. A. Ibers, L. J. Pace, J. Martinson, B. M. Hoffmann, *Struct. Bonding* (Berlin) *50* (1981) 1, and literature cited therein.

## Synthesis of a Tetranuclear Manganese(IV) Cluster with Adamantane Skeleton: $[(C_6H_{15}N_3)_4Mn_4O_6]^{4+}$

By *Karl Wieghardt**, *Ursula Bossek*, and *Walter Gebert*

Stable complexes of manganese(IV) are hardly known in aqueous solution[1]. Some dinuclear μ-oxo-manganese(IV) compounds have been obtained by oxidation of $Mn^{II}$ by $O_2$ in alkaline media[1a]. Oxidation of $H_2O$ to molecular oxygen by tetrameric complexes of $Mn^{IV}$ (4e acceptor) has been discussed in connection with photosynthesis, although until now there were no examples of such compounds[1b].

We have now found that aqueous alkaline solutions of the cyclic amine 1,4,7-triazacyclononane react with manganese dichloride and oxygen to produce black solutions, from which, after addition of NaBr, black crystals of $[(C_6H_{15}N_3)_4Mn_4O_6]Br_{3.5}OH_{0.5}\cdot 6H_2O$, **1**, can be isolated[2]. The X-ray structure analysis of **1** indicates that a tetranuclear, oxo-bridging cation is formed (Fig. 1). The four Mn centers occupy the corners of a tetrahedron, and an O-bridging atom is located above the middle of each of the six edges.

The $Mn_4O_6$ moiety corresponds to an adamantane skeleton, as recently described for $[F_{12}Ta_4O_6]^{4-}$[3]. Each Mn atom is surrounded in a distorted octahedral configuration by three N atoms and three O atoms. The average values of the Mn–N and Mn–O distances are in excellent accord with those in $[(bpy)_2Mn^{IV}O_2Mn^{III}(bpy)_2]^{3+}$[4].

Redox titration of **1** with $[Fe(CN)_6]^{2-}$ at pH 5 indicates consumption of two equivalents per $Mn^{IV}$; this corresponds to the two-electron reduction of $Mn^{II}$. The visible absorption spectrum exhibits two maxima at 552 ($\varepsilon = 2.6\times10^3$ L mol$^{-1}$ cm$^{-1}$ per tetrameric unit) and 336 nm ($1.7\times10^4$). An intense band in the IR spectrum at 730 cm$^{-1}$ is characteristic of vibrations of the $Mn_4O_6$ cluster[5]. The magnetic moment of **1** adheres to the Curie-Weiss law over the range 93–293 K with $\theta = 37$ K and $\mu_{eff} = 3.96(2)\,\mu_B$ per $Mn^{IV}$; this corresponds to the spin-only value for a $d^3$ electron configuration of the $Mn^{IV}$ centers. The cation of **1** is stable in neutral and alkaline solutions.

Received: December 9, 1982 [Z 220 IE]
German version: *Angew. Chem. 95* (1983) 320

[1] a) M. E. Bodini, L. A. Willis, T. L. Reichel, D. T. Sawyer, *Inorg. Chem. 15* (1976) 1538; b) D. T. Sawyer, M. E. Bodini, *J. Am. Chem. Soc. 97* (1975) 6588; c) M. M. Morrison, D. T. Sawyer, *ibid. 99* (1977) 257; L. J. Boucher, C. G. Coe, *Inorg. Chem. 14* (1975) 1289; D. L. Hoof, D. G. Tisley, R. A. Walton, *Inorg. Nucl. Chem. Lett. 9* (1973) 571.

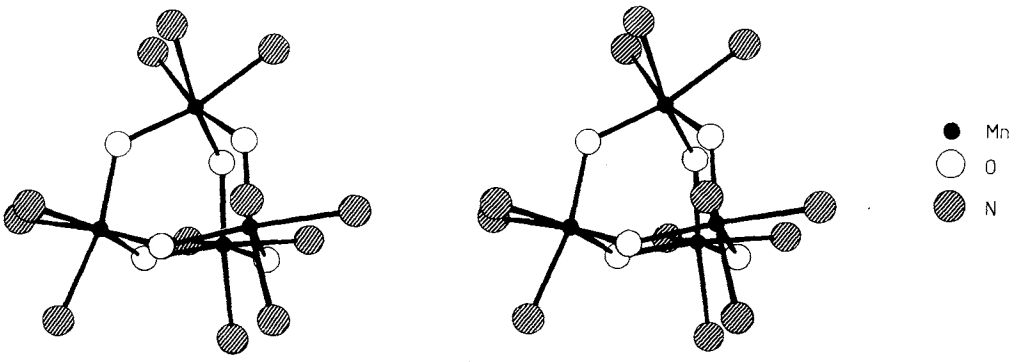



Fig. 1. Structure of $[(C_6H_{15}N_3)_4Mn_4O_6]^{4+}$ in the crystal as a stereoscopic projection (only the framework of N, O, and Mn atoms is shown). Distances and angles (average values): Mn–O 1.79(1), Mn–N 2.08(1), Mn···Mn 3.21(1) Å; MnOMn 128.7(8), NMnN 81(1), OMnO 98(1)°. – Space group $P2_1/n$, $a = 17.52(1)$, $b = 13.05(1)$, $c = 21.58(1)$ Å, $\beta = 105.64(3)°$, $Z = 4$; 6404 independent reflections ($I > 3\sigma(I)$), $R = 0.108$. Further details on the crystal structure investigation can be obtained from the Fachinformationszentrum Energie Physik Mathematik, D-7514 Eggenstein-Leopoldshafen, by quoting the depository number CSD 50374, the name of the authors, and the journal citation.

[*] Prof. Dr. K. Wieghardt, U. Bossek
Lehrstuhl für Anorganische Chemie I der Universität
Postfach 102148, D-4630 Bochum (Germany)
Dr. W. Gebert
Institut für Mineralogie der Universität Bochum (Germany)

[2] Procedure: 1,4,7-Triazacyclononane (0.6 g, 4 mmol) is added to a solution of $MnCl_2\cdot 4H_2O$ (0.8 g, 4 mmol) in 20 mL of $H_2O$, and air is passed into the mixture for 2 h at 20 °C until a clear, black solution forms. After addition of 3 g NaBr and adjustment of the pH value to 8, needle-shaped crystals of **1** (0.6 g, 48%) grow at 0 °C. The sparingly soluble perchlorate

$[(C_6H_{15}N_3)_4Mn_4O_6](ClO_4)\cdot 2H_2O$ can be precipitated from aqueous solutions of **1** by addition of $NaClO_4$.
[3] J. Sala-Pala, J. E. Guerchais, A. J. Edwards, *Angew. Chem. 94* (1982) 876; *Angew. Chem. Int. Ed. Engl. 21* (1982) 870.
[4] P. M. Plaksin, R. C. Stoufer, M. Mathew, G. L. Palenik, *J. Am. Chem. Soc. 94* (1972) 2121.
[5] Interestingly, similar bands were found for the novel clusters $Cp_6Ti_6O_8$, $Cp_5V_5O_6$, $Cp_4Cr_4O_4$ ($Cp^-$ = cyclopentanienide): F. Bottomley, D. E. Paez, P. S. White, *J. Am. Chem. Soc. 104* (1982) 5651. This indicates the structural relationship of these clusters with the cation of **1**.

## $(C_5H_5)_6Ni_2Zn_4$— The First Zinc-Containing Mixed-Metal Cluster**

By *Peter H. M. Budzelaar, Jaap Boersma,* and *Gerrit J. M. van der Kerk**

In previous studies we found that dicyclopentadienylzinc, $Cp_2Zn$, is a useful starting material for the preparation of cyclopentadienylzinc-transition metal compounds[1]. By reaction of $Cp_2Zn$ with $Ni(cod)_2$ (cod = 1,5-cyclooctadiene) we have now been able to prepare $(C_5H_5)_6Ni_2Zn_4$ **1**[2], the first compound with a NiZn bond. This first zinc-containing mixed-metal cluster is extremely sensitive to hydrolysis and oxidation, particularly in solution.

A single-crystal X-ray diffraction study was undertaken in order to unambiguously establish the nature of **1**. It was found that **1** crystallizes in space group $P4_2/mnm$ of the tetragonal system with 2 formula units in a cell of dimensions $a = 9.352(5)$ Å and $c = 16.32(1)$ Å. The molecular framework consists of an octahedral arrangement of 4 equatorial zinc atoms and 2 apical nickel atoms, each having an $\eta^5$-bound cyclopentadienyl group attached to it (Fig. 1a). In accord with this symmetric structure, the $^1H$-NMR spectrum (90 MHz, solvent $C_6D_6$, TMS) shows two singlets ($\delta = 6.23$ and 4.64) in the intensity ratio 2 : 1 due to the cyclopentadienyl groups bound to zinc and nickel, respectively.

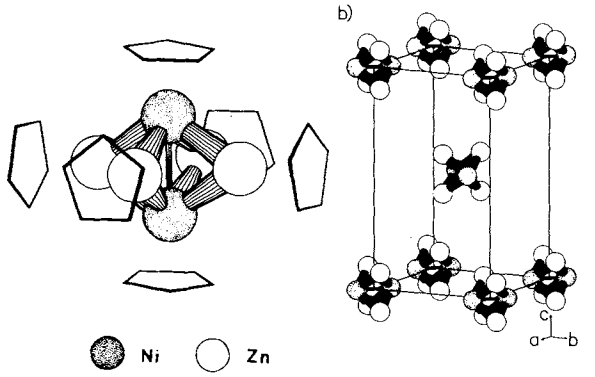



Fig. 1. a) Structure of $Cp_6Ni_2Zn_4$ **1** in the crystal. All cyclopentadienyl groups are disordered; only one orientation of each is shown. b) Packing of the $Ni_2Zn_4$ clusters of **1** in the unit cell [5].

Figure 1b shows the packing of the clusters in the unit cell. The metal octahedron, which has an almost perfect 4/mmm symmetry, is compressed along the NiNi axis; the NiZn distance is 2.40 Å, the NiNi distance 2.56 Å, and the ZnZn distance 2.79 Å. This last distance is very close to the non-bonded ZnZn distance of 2.78 Å found in $(CpZn)_2Co(Cp)PPh_3$[1]. Simple electron-counting, similarly to that used in the case of the iridium-copper cluster $Ir_2Cu_4(PPh_3)_2(C{\equiv}CPh)_8$[3], indicates that the metal framework in **1** is held together by 5 bonds. Since the NiNi distance of 2.56 Å is longer than that found in metallic nickel (2.50 Å) it may be assumed that interaction between the two nickel atoms will not be very strong. This leaves a bond order of between 0.50 and 0.63 for each of the eight NiZn bonds. In view of the close similarity of the covalent radii of nickel and cobalt, the NiZn single bond length should be very similar to the CoZn bond length in $(CpZn)_2Co(Cp)PPh_3$[1] and $Zn[Co(CO)_4]_2$ (2.30 Å)[4]. The significantly larger bond length in **1** is therefore in agreement with the proposed lower bond order.

Received: November 9, 1982 [Z 199 IE]
German version: *Angew. Chem. 95* (1983) 335

[*] Prof. Dr. G. J. M. van der Kerk, Drs. P. H. M. Budzelaar, Dr. J. Boersma
Department of Organic Chemistry, University of Utrecht
Croesestraat 79, NL-3522 AD Utrecht (The Netherlands)

[**] We are grateful to Dr. *A. L. Spek* for collection of the X-ray data and for his aid in solving the structure.

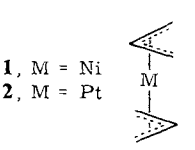
[1] P. H. M. Budzelaar, J. Boersma, G. J. M. van der Kerk, A. L. Spek, A. J. M. Duisenberg, *Inorg. Chem. 21* (1982) 3777.
[2] $Cp_2Zn$ (2.2 g, 11.3 mmol) was added to a solution of $Ni(cod)_2$ (1.0 g, 3.64 mmol) in benzene (30 mL) at room temperature; the mixture was stirred and heated within 1 h to 70 °C. A dark-green solution was formed, from which dark-green crystals separated out on cooling. The supernatant liquor was decanted off and the residue washed with hot cyclohexane to remove excess $Cp_2Zn$. The crude product thus obtained was recrystallized from benzene. Yield: 0.93 g (67%); m.p. > 200 °C.
[3] M. R. Churchill, S. A. Bezman, *Inorg. Chem. 13* (1974) 1418.
[4] B. Lee, J. M. Burlitch, J. L. Hoard, *J. Am. Chem. Soc. 89* (1967) 6362.
[5] Further details of the crystal structure determination can be obtained from the Fachinformationszentrum Energie Physik Mathematik, D-7514 Eggenstein-Leopoldshafen 2 by quoting the number CSD 50328, the name of the author, and the complete citation of the journal.

## Heavy Atom Effect in the Photoelectron Spectra of Transition Metal Complexes**

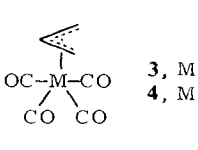
By *Michael C. Böhm* and *Rolf Gleiter**

The bands in photoelectron spectra are frequently assigned exploiting the fact that the intensities of the bands are a sensitive function of the wavelength of the radiation employed [*e.g.* He(I), He(II), Ne(I)] if the ejected electron is prevailingly localized at an element heavier than C (*e.g.* S, Se, Te and Ni, Pd, Pt)[1].

We describe here an alternative approach, namely that of varying the heavier element. This strategy is especially applicable in the case of transition metal compounds (replacement of a 3d atom by an isovalent electronic 4d or 5d atom). To demonstrate the utility of this principle we show in Figure 1 the He(I) PE spectra of the bis($\eta^3$-allyl) com-




**1**, M = Ni
**2**, M = Pt




**3**, M = Mn
**4**, M = Re

[*] Prof. Dr. R. Gleiter, Dr. M. C. Böhm
Organisch-chemisches Institut der Universität
Im Neuenheimer Feld 270, D-6900 Heidelberg 1 (Germany)

[**] Electronic Structure of Organometallic Compounds, Part 24. This work was supported by the Stiftung Volkswagenwerk, the Fonds der Chemischen Industrie, and BASF Aktiengesellschaft Ludwigshafen.—Part 23: M. C. Böhm, R. Gleiter, J. Grobe, D. Le Van, *J. Organomet. Chem.*, in press.

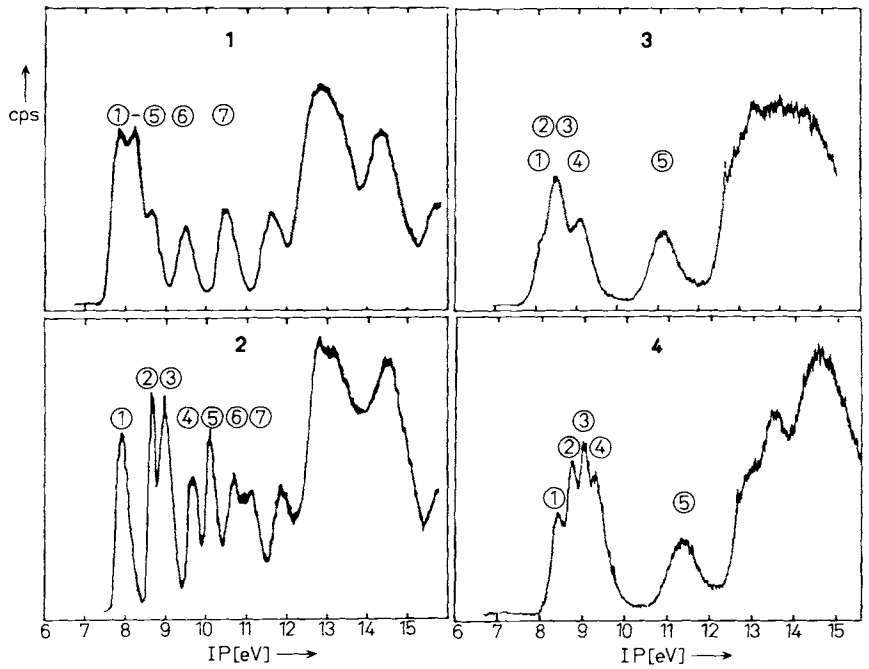



Fig. 1. Comparison of the He(I) PE specra (recorded with a PS18 spectrometer, Perkin Elmer, at room temperature) of the compounds **1** and **2** (left) and **3** and **4** (right).

plexes of Ni and Pt, **1** and **2**[2], as well as those of the $\eta^3$-allyl(tetracarbonyl) complexes of Mn and Re, **3** and **4**, respectively[3]. The ionization energies of these compounds are listed in Table 1. The bands corresponding to ionizations, which are predominantly localized at the metal atom (bands ② to ⑤ in the case of **1** and **2**, and bands ① to ③ in the case of **3** and **4**), split and become sharper when the 3d metal atom is replaced by a 4d or 5d metal atom. The reason for this splitting is the increasing covalent interaction between the nd orbitals (n = 3—5) of the metal atom and the orbitals of the organic ligands, which becomes greater with increasing principal quantum number of the metal atom. Slight differences in the covalent interaction are thereby enhanced. A prerequisite for the use of this heavy atom effect is a low symmetry of the complex, since degenerate levels are additionally propagated as a result of a Jahn-Teller effect and a rigid arrangement of the ligands.

Table 1. Ionization energies (I) of **1** to **4**. In the assignment, only the valence orbitals were considered.

| Compound | Band | $I_{v,j}$ [eV] | Assignment |
|---|---|---|---|
| **1** | | 7.76 | $7a_u$ |
| | | | $13a_g$ |
| | ①—⑤ | 8.19 | $12a_g$ |
| | | | $5b_g$ |
| | | 8.58 | $11a_g$ |
| | ⑥ | 9.40 | $6b_g$ |
| | ⑦ | 10.38 | $11b_u$ |
| **2** | ① | 7.91 | $7a_u$ |
| | ② | 8.64 | $13a_g$ |
| | ③ | 8.95 | $11a_g$ |
| | ④ | 9.65 | $12a_g$ |
| | ⑤ | 10.14 | $5b_g$ |
| | ⑥ | 10.73 | $11b_u$ |
| | ⑦ | 11.15 | $6b_g$ |
| **3** | ① | 8.04 | 19a″ |
| | ② | 8.44 | 20a″ |
| | ③ | | 11a″ |
| | ④ | 9.04 | 12a″ |
| | ⑤ | 11.10 | 18a″ |
| **4** | ① | 8.40 | 19a″ |
| | ② | 8.72 | 20a″ |
| | ③ | 9.00 | 11a″ |
| | ④ | 9.23 | 12a″ |
| | ⑤ | 11.23 | 18a″ |

Received: December 3, 1982;
supplemented: February 7, 1983 [Z 215 IE]
German version: *Angew. Chem. 95* (1983) 334

[1] M. B. Hall, I. H. Hillier, J. A. Connor, M. F. Guest, D. R. Lloyd, *Mol. Phys. 30* (1975) 839; J. A. Connor, M. L. R. Derrick, I. H. Hillier, M. F. Guest, D. R. Lloyd, *ibid. 31* (1976) 23; B. R. Higginson, D. R. Lloyd, S. Evans, A. F. Orchard, *J. Chem. Soc. Faraday Trans. II 71* (1975) 1913; C. Cauletti, J. C. Green, M. R. Kelly, P. Powell, J. van Tilborg, J. Robbins, J. Smart, *J. Electron Spectrosc. Relat. Phenom. 19* (1980) 327.
[2] M. C. Böhm, R. Gleiter, C. D. Batich, *Helv. Chim. Acta 63* (1980) 990.
[3] M. C. Böhm, R. Gleiter, T. A. Albright, V. Sriyunyongwat, *Mol. Phys.*, in press.

## $\mu_2$-($\eta^5$:$\eta^5$-Cyclooctatetraene)-bis($\eta^5$-cyclopentadienylchromium): A "Siamese Twin" of two Half-Open Sandwich Moieties**

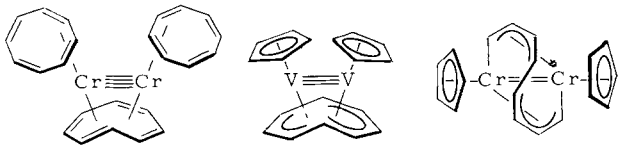
By *Christoph Elschenbroich*, Jürgen Heck, Werner Massa,* and *Roland Schmidt*

Two structure variants for dinuclear complexes of the type $[(C_mH_m)M]_2C_nH_n$, $m \leq n$, can be conceived in which the $(C_mH_m)M$ moieties are either coordinated to opposite sides or to the same side of a bridging $C_nH_n$ ligand. Examples for the first, antifacial variant with $n = 8$ are provided

[*] Prof. Dr. C. Elschenbroich, Dr. W. Massa, R. Schmidt
Fachbereich Chemie der Universität
Hans-Meerwein-Strasse, D-3550 Marburg (Germany)
Dr. J. Heck
Anorganisch-chemisches Institut der Universität
Winterthurer Strasse 190, CH-8057 Zürich (Switzerland)

[**] This work was supported by the Deutsche Forschungsgemeinschaft and the Fonds der Chemischen Industrie.

by the complexes $[(C_8H_8)Ti]_2C_8H_8$ and $[(C_5H_5)Co]_2C_8H_8$, whose bridging $C_8H_8$ rings are, however, nonplanar[1]. The second, synfacial variant is realized in $[(C_8H_8)Cr]_2C_8H_8$ **1**[2a] as well as in the complex $[(C_5H_5)V]_2C_8H_8$ **2**, which we prepared from $VCl_2$, $NaC_5H_5$, and $K_2C_8H_8$[2b]. A compound **3** having the analogous composition to **2**, $[(C_5H_5)Cr]_2C_8H_8$, was previously synthesized using another method $[(C_5H_5)_2Cr + Na_2C_8H_8]$ and characterized by X-ray crystallography[3a]. Surprisingly, in **3** a $C_8$ chain occurs, whose terminal C atoms are σ-bonded to the Cr atoms.




**1** **2** **3**

By allowing $CrCl_2 \cdot THF$ to react with $NaC_5H_5$ and $K_2C_8H_8$[4] we have now obtained compound **4** which, according to its elemental analysis and mass spectrum, also has the composition $C_{18}H_{18}Cr_2$ but which, in contrast to **3**, is characterized by simple NMR spectra [**4** ([D$_8$]toluene, 27 °C); $\delta(^1H) = 4.22$ (s, 10H), 3.89 (s, 8H); $\delta(^{13}C) = 74.53$, 86.55]. The X-ray structure analysis reveals that **4** has an analogous structure to **2**, and is hence an isomer of **3** (Fig. 1)[3b].

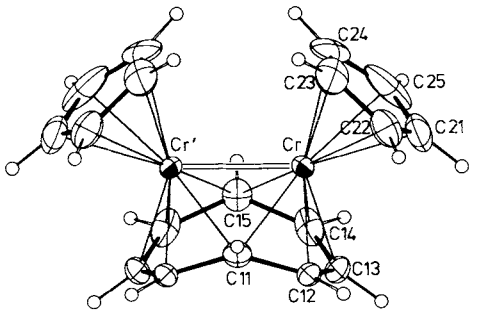
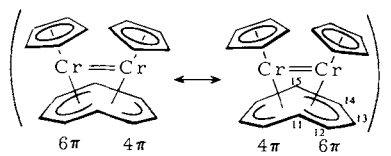
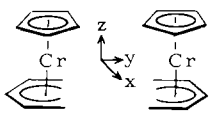



Fig. 1. Structure of **4** in the crystal (ORTEP representation, thermal vibrational ellipsoids with 30% probability). Mirror plane perpendicular to the Cr–Cr axis. Space group Pnma, $a = 1184.9(3)$, $b = 1577.8(3)$, $c = 764.1(2)$ pm, $Z = 4$. $R_w = 0.052$ (weighting $w = 2.6/\sigma^2_{F_o}$) for 693 independent reflections ($I > 2\sigma$; CAD4, Enraf-Nonius, MoK$_\alpha$). Important bond lengths [pm]: Cr–Cr' 239.0(2), Cr–C11 226(1), Cr–C12 207(1), Cr–C13 210(1), Cr–C14 205(1), Cr–C15 225(1), Cr–C21 220(1), Cr–C22 221(1), Cr–C23 219(2), Cr–C24 217(2), Cr–C25 220(2), C11–C12 142(1), C12–C13 141(2), C13–C14 139(2), C14–C15 144(1), C11···C15 310(2). Angles between the "best planes": at C(11)–C(15) axis: 131.4°, between C(11–15) and C(21–25): 16.2°. Distances Cr–C(11–15) 149 pm, Cr–C(21–25) 186 pm. Further details on the crystal structure investigation can be obtained from the Fachinformationszentrum Energie-Physik-Mathematik, D-7514 Eggenstein-Leopoldshafen, by quoting the depository number CSD 50382, the names of the authors and the journal citation.

**4** can be considered as a combination of two "half-open" chromocene molecules[5a], **5**, which share the atoms C11–C15. The dinuclear complex **4**, which as opposed to the paramagnetic monomer chromocene ($S = 1$) is diamagnetic, displays a bond distance $d(Cr{-}Cr) = 239$ pm. Compared to other species with Cr–Cr bonds[5b], this distance suggests a Cr=Cr double bond.




**4**




**5**

A metal-metal bond order of 2 would also result from the interaction of two chromocene moieties of individual electron configuration ... $(e_2; xy, x^2-y^2)^3(a_1; z^2)^1$; the different overlap qualities of the $e_2$ and $a_1$ orbitals in **4** imply an MO sequence which—occupied by $2 \times 4$ electrons—leads to the configuration $(e^2)^4(a_1)^2(a\uparrow)^2$ for **4**. This is corroborated by the finding that the radical cation $\mathbf{4}^{\odot\oplus}$, generated electrochemically from **4**, has an orbitally non-degenerate ground state [$\langle g \rangle$ (dimethoxyethane, 27 °C) = 2.024, $a(^{53}Cr)$ not resolved]. Finally, the formation of **4** as a resonance hybrid secures that in each of the two canonical forms one Cr atom has an 18e shell.

Received: December 13, 1982 [Z 222 IE]
German version: *Angew. Chem. 95* (1983) 319

[1] J. W. Lauher, M. Elian, R. H. Summerville, R. Hoffmann, *J. Am. Chem. Soc. 98* (1976) 3219 and literature cited therein.

[2] a) D. J. Brauer, C. Krüger, *Inorg. Chem. 15* (1976) 2511; b) C. Elschenbroich, J. Heck, W. Massa, E. Nun, R. Schmidt, *J. Am. Chem. Soc.*, in press.

[3] a) W. Geibel, G. Wilke, R. Goddard, C. Krüger, R. Mynott, *J. Organomet. Chem. 160* (1978) 139; b) Thermal rearrangement of **3** also leads to isomer **4** (cf. G. Wilke in M. Tsutsui: *Fundamental Research in Homogeneous Catalysis*, Vol. 3, Plenum, New York 1978, p. 1; R. Goddard, C. Krüger in P. Coppens, G. Hall: *Electron Distributions and the Chemical Bond*, Plenum, New York 1982, p. 297.

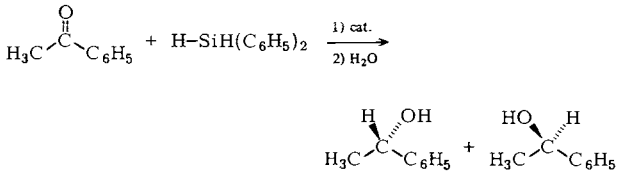
[4] *Procedure:* A solution of $K_2C_8H_8$ (2.0 g, 11 mmol) in 100 mL tetrahydrofuran (THF) is added to a stirred suspension of $CrCl_2 \cdot THF$ (4.39 g, 22.1 mmol) in 120 mL THF at −25 °C, and after 30 min solid $NaC_5H_5$ (1.9 g, 22 mmol) added. After warming to room temperature and 2 h refluxing, the solvent is removed and the residue sublimed at $10^{-4}$ mbar. The first fraction (60 °C) contains a mixture of chromocene and $\eta^5$-cyclopentadienyl-$\eta^6$-cyclooctatetraenechromium (1.92 g). Extraction of the second brown-red fraction (140 °C) with 50 mL petroleum ether 40/60 and crystallization (1 week at 4 °C) leads to the complex **4** as black needles (185 mg (4.9%), decomp. > 180 °C) EI-MS [*m/z* (%): 339 (10.2) $(M+1)^+$, 338 (17.9) $M^+$, 221 (25.8) $(M - C_5H_5Cr)^+$, 195 (12.7) $C_{11}H_{11}Cr^+$, 182 (65.6) $C_{10}H_{10}Cr^+$, 117 (100) $C_5H_5Cr^+$ *etc.*

[5] a) "Open" chromocene: D. R. Wilson, J.-Z. Liu, R. D. Ernst, *J. Am. Chem. Soc. 104* (1982) 1120; U. Giannini, E. Pellino, M. P. Lachi, *J. Organomet. Chem. 12* (1968) 551; b) cf. F. A. Cotton, R. A. Walton: *Multiple Bonds Between Metal Atoms*, Wiley, New York 1982, and literature cited therein.

## Enantioselective Hydrosilylation of Acetophenone with Rhodium/Thiazolidine Catalysts**

By *Henri Brunner*, Georg Riepl,* and *Helgard Weitzer*

We recently reported on the enantioselective hydrosilylation of prochiral ketones with (cod)Rh-pyridine imine catalysts (cod = 1,5-cyclooctadiene)[1]. With the catalyst system $[(cod)RhCl]_2$/**1** (Rh : **1** ≈ 1 : 13) an enantiomeric excess (*ee*) of up to 57.3% was achieved in the reaction acetophenone → 1-phenylethanol (substrate : Rh = 110 : 1)[1].

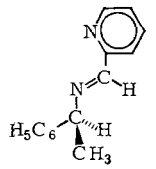



With catalyst systems whose pyridine imine component is obtained from (−)-3-aminomethylpinane and 2-pyridine-

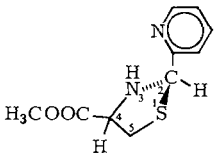
[*] Prof. Dr. H. Brunner, G. Riepl, H. Weitzer
Institut für Anorganische Chemie der Universität
Universitätsstrasse 31, D-8400 Regensburg (Germany)

[**] Asymmetric Catalyses, Part 10. This work was supported by the Deutsche Forschungsgemeinschaft, the Fonds der Chemischen Industrie, and BASF AG.—Part 9: see Ref. [1].

carbaldehyde, the *ee* value can be increased to 78% (substrate : Rh = 100 : 1, Rh : ligand = 1 : 15); L-valine methyl ester and L-alanine methyl ester as amine components in the Schiff base condensation, respectively, yield only slight or no enantiomeric excess. The best catalyst system for the model reaction is obtained from $[(cod)RhCl]_2$ and **2**, the



**1**



**2**

condensation product of L-cysteine methyl ester and 2-pyridinecarbaldehyde. With the Rh/thiazolidine system an enantiomeric excess of up to 86.7% is achievable (Table 1).

Table 1. Enantioselective hydrosilylation of acetophenone with diphenylsilane without solvent. Catalyst system: $[(cod)RhCl]_2$/**2**. The (*R*)-enantiomer is always formed as main product.

| Rh/2 | Rh/ Substrate | $T$ [°C] | $t$ [h] | Yield Chem. [%] | Opt. [% *ee*] |
|---|---|---|---|---|---|
| 1/9 | 1/210 | 0→20 | 38 | 99 | 83.2 |
| 1/5 | 1/210 | 0→20 | 20 | 96 | 80.0 |
| 1/2 | 1/210 | 0→20 | 20 | 96 | 74.7 |
| 1/1.6 | 1/210 | 0→20 | 43 | 95 | 72.3 |
| 1/5 | 1/860 | 0→20 | 65 | 94 | 78.2 |
| 1/5 | 1/1220 | 0→20 | 40 | 93 | 75.0 |
| 1/5 | 1/1710 | 0→20 | 65 | 92 | 78.9 |
| 1/5 | 1/2800 | 0→20 | 40 | 43 | 73.6 |
| 1/5 | 1/210 | −10 | 115 | 79 | 83.6 |
| 1/9 | 1/210 | −15 | 235 | 98 | 86.7 |

The Rh/thiazolidine system is also far superior to the Rh/Schiff base systems with regard to reaction rate and stability. High enantiomeric excesses are possible with the pyridine imine ligands only at substrate-rhodium ratios of up to 200 : 1[1]; in contrast, the Rh/thiazolidine catalyst leads to high conversion *and* high enantiomeric excess under the same conditions at substrate-rhodium ratios of up to 2000 : 1 (Table 1).

In the condensation of 2-pyridinecarbaldehyde with 1-phenylethylamine, 3-aminomethylpinane, alanine methyl ester and valine methyl ester, Schiff bases are formed which show characteristic low chemical shifts of the proton of the CH=N group in the $^1$H-NMR spectrum ($\delta = 8.0-8.7$). The $^1$H-NMR spectrum of the thiazolidine derivative **2** exhibits two doublets for the CHSN protons at $\delta = 5.84$ and 5.66 ($^3J_{HH} = 11.4$ Hz), in the intensity ratio 58 : 42; this finding is attributed to the presence of two diastereomers (the (2*R*,4*S*)-diastereomer is shown in the formula), which differ only in the configuration at C2. The diastereoselectivity in the formation of **2** corresponds to that in the oxazolidine ring closure of aldehydes and ephedrine[2]. It is surprising that an almost stereospecific synthesis of 1-phenylethanol is possible with a 58 : 42 diastereomeric mixture of the thiazolidine **2** and $[(cod)RhCl]_2$.

Received: November 24, 1982 [Z 209 IE]
German version: *Angew. Chem. 95* (1983) 326
The complete version of this communication appears in: *Angew. Chem. Suppl. 1983*, 445–450

[1] H. Brunner, G. Riepl, *Angew. Chem. 94* (1982) 369; *Angew. Chem. Int. Ed. Engl. 21* (1982) 377; *Angew. Chem. Suppl. 1982*, 769.

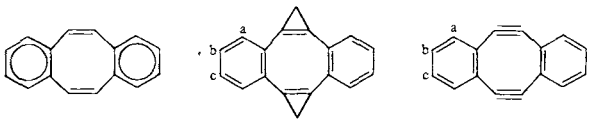
[2] H. Beckett, G. R. Jones, *Tetrahedron 33* (1977) 3313; H. Abdallah, R. Gree, R. Carrie, *Tetrahedron Lett. 23* (1982) 503; P. N. Confalone, G. Pizzolato, E. G. Baggiolini, D. Lollar, M. R. Uskoković, *J. Am. Chem. Soc. 99* (1977) 7020.

## A Novel Planar Antiaromatic Dibenzo[8]annulene**

By *Heinz Dürr**, *Günter Klauck*, *Karl Peters*, and *Hans Georg von Schnering*

*Dedicated to Professor Georg Wittig*

Cyclopropene double bonds are intermediary in character between the normal olefinic CC double bond and the CC triple bond. For this reason dibenzo[*a*,*e*]dicyclopropa[*c*,*g*]cyclooctene **2**, a cyclooctatetraene derivative in which two >C=C< units are each replaced by a cyclo-

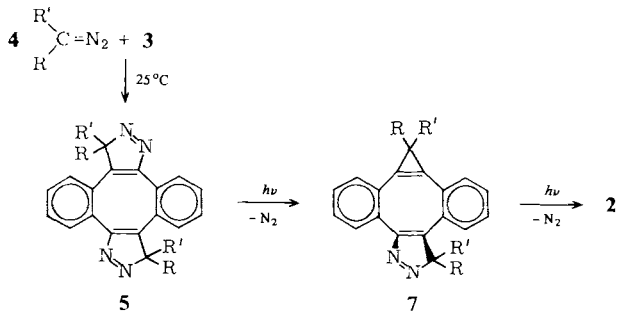


**1** **2** **3**

propene ring, should be ranked between the olefinic dibenzo[*a*,*e*]cyclooctene **1** and the antiaromatic[1] [8]annulene **3**[4]. Compound **3** is planar[5] and relatively stable (transannular interactions see [6]).

We have checked, 1) whether the cyclopropene rings in **2** enforce a planar structure on the framework of **1**; 2) to what extent the planarity in **2** renders an antiaromatic [8]annulene possible.

For the synthesis of **2** the diyne **3** was first allowed to react with the diazo compounds **4a**–**d** to give the bis-3*H*-pyrazoles **5a**, **b** and the bis(spiro-3*H*-pyrazoles) **5c**, **d**.



**5** **7**

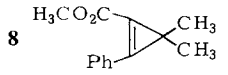
| | R | R′ | 5 Yield [%] | 5 M.p. [°C] | 7 Yield [%] | 7 M.p. [°C] | 2 Yield [%] | 2 M.p. [°C] |
|---|---|---|---|---|---|---|---|---|
| *a* | $CH_3$ | $CH_3$ | 24 | 340 | 8.7 | 153 | 1.8 | 135 |
| *b* | $C_6H_5$ | $C_6H_5$ | 65 | 135 | | | | |
| *c* | —*o*-$C_6H_4$— | —*o*-$C_6H_4$— | 46 | 175 | | | 16 | 230 |
| *d* | —*o*-$C_6H_4$—CO—*o*-$C_6H_4$— | | 64 | 120 | | | 20 | 120 |

[*] Prof. Dr. H. Dürr, G. Klauck
Fachbereich 14, Organische Chemie der Universität
D-6600 Saarbrücken (Germany)
Prof. Dr. G. von Schnering, Dr. K. Peters
Max-Planck-Institut für Festkörperforschung
Heisenbergstr. 1, D-7000 Stuttgart 80 (Germany)

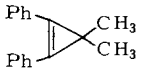
[**] Photochemistry of Small Rings, Part 42. This work was supported by the Deutsche Forschungsgemeinschaft and the Fonds der Chemischen Industrie.—Part 41: E. Lüddeke, H. Rau, H. Dürr, H. Schmitz, *Tetrahedron 33* (1977) 2677.

 © *Verlag Chemie GmbH, 6940 Weinheim, 1983* *0570-0833/83/0404-0332 $ 02.50/0* 

Stepwise photochemical elimination of $N_2$ from **5** ($\lambda > 310$ nm, pyrex filter) then led *via* the cyclopropapyrazoles **7** to the biscyclopropenes **2**. According to an X-ray structure analysis[7] **7a** exists in the boat conformation with the three-membered ring and five-membered ring in *trans* orientation. **7b—d** could not be obtained in analytically pure form.



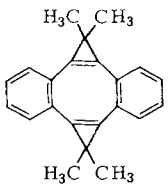
**8**



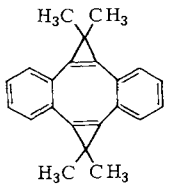
**9**

The $^1$H-NMR signals of the methylcyclopropene protons of **2a** ($\delta = 1.30$) are shifted about $\Delta\delta = 0.18$ upfield compared to those of **8** ($\delta = 1.47$), **9** ($\delta = 1.48$), and **7a** ($\delta = 1.48$). The protons of the benzene rings in **2a** ($\delta = 6.67 - 6.93$) are also shielded compared to those in **7a** ($\delta = 7.04 - 7.80$). This is unequivocally consistent with a paramagnetic ring current in **2a**. Consequently, **2a** appears to exist as a planar, paratropic, antiaromatic dibenzo[8]annulene, for which the resonance structures **2a** and **2a'** apply rather than **2a''**, in the classical sense of the resonance concept.

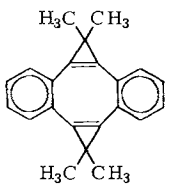
An X-ray structure analysis confirms that **2a** has an almost planar structure[7]. The bond lengths in **2a** and **3** ($C_a-C_b$ and $C_b-C_c$ in **2a**: 139.1 and 137.1 pm, respectively; in **3**: 138.9 and 136.9 pm, respectively) closely resemble each other. Despite structural differences the angular deformations are also essentially similar.



**2a**



**2a'**



**2a''**

Thus, in analogy to **3**, **2a** is to be regarded as a planar antiaromatic [8]annulene. So far, very few planar [8]annulenes have been reported in the literature.

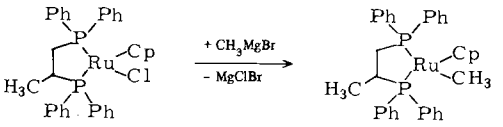
Received: September 21, 1982;
revised: January 21, 1983 [Z 150 IE]
German version: *Angew. Chem. 95* (1983) 321
The complete version of this communication appears in:
*Angew. Chem. Suppl. 1983*, 347—362

[1] H. Günther, M. E. Günther, D. Mondeshka, H. Schmickler, *Liebigs Ann. Chem. 1978*, 165.
[4] F. Sondheimer, H. N. C. Wong, P. J. Garratt, *J. Am. Chem. Soc. 96* (1974) 5604; H. N. C. Wong, F. Sondheimer, *Tetrahedron, R. B. Woodward Memorial Issue 1981*, 99.
[5] R. Destro, T. Pilati, M. Simonetta, *J. Am. Chem. Soc. 97* (1975) 658.
[6] J. Wirtz, *Helv. Chim. Acta 58* (1975) 162; N.-Z. Huang, F. Sondheimer, *Acc. Chem. Res. 15* (1982) 96.
[7] Details of the crystal structure investigation can be obtained on request from the Fachinformationszentrum Energie Physik Mathematik, D-7514 Eggenstein-Leopoldshafen quoting the number CSD 50355, the name of the author, and complete citation of the journal.

## Stereospecific Reactions of Chiral Chlororuthenium(II) Complexes with Grignard Reagents

By *Giambattista Consiglio**, *Franco Morandini*, *Gianfranco Ciani*, and *Angelo Sironi*

Compounds with metal-carbon $\sigma$ bonds are mainly prepared by reaction of halometal complexes with organometallic derivatives of the main group elements. The stereochemical aspects of such "metathesis" reactions are largely unknown. $(-)_{365}$-$[(\eta^5\text{-}C_5H_5)Fe(CO)(PPh_2R^*)I]$ reacts with methyllithium to afford both diastereomeric methyliron complexes in the ratio 68 : 32[1]. On the basis of CD spectra, a reaction path involving retention of the configuration at iron was postulated. Because of the epimerization of the educt during the reaction, it could not be determined whether the reaction proceeds stereoselectively or stereospecifically.




**1**, **2** **3**, **4**

$[(S)_{Ru}, (R)_C]$: **1**, **3**; $[(R)_{Ru}, (R)_C]$: **2**, **4**

We report here that $CH_3MgBr$ reacts stereospecifically and with retention of configuration at Ru with $(S)_{Ru}$, $(R)_C$-[CpRuCl(prophos)] **1** (absolute configuration determined by X-ray structure analysis[2]) or with its diastereomer $(R)_{Ru}$, $(R)_C$-[CpRuCl(prophos)] **2** (prophos = propylenebis(diphenylphosphane)[3], Cp = $\eta^5$-cyclopentadienyl) to give $(S)_{Ru}$, $(R)_C$-[CpRu($CH_3$)(prophos)] **3** or $(R)_{Ru}$, $(R)_C$-[CpRu($CH_3$)(prophos)] **4**. The reaction of **1** [$^{31}$P-NMR (36.43 MHz, [D$_8$]toluene, room temperature): $\delta(P_a) = 86.4$, $\delta(P_b) = 61.3$, $J_{P-P} = 30.2$ Hz[4] with excess (molar ratio $\approx 1:8$) $CH_3MgBr$ ($\approx 2$ M in $Et_2O$) in [D$_8$]toluene under an inert gas atmosphere at room temperature was followed in an NMR tube. **3** [$\delta(P_a) = 100.0$, $\delta(P_b) = 74.1$, $J_{P-P} = 35.2$ Hz[4]; $^1$H-NMR (90 MHz): $\delta(Ru)CH_3 = -0.49$, $J_{P-H} = 5.7$ and 6.5 Hz] is formed quantitatively within 4 h. Complex **4** [$\delta(P_a) = 93.6$, $\delta(P_b) = 85.0$, $J_{P-P} = 32.9$[4]; $\delta(Ru)CH_3 = -0.21$, $J_{P-H} = 4.8$ and 6.4 Hz] is formed analogously from **2** [$\delta(P_a) = 80.9$; $\delta(P_b) = 74.1$, $J_{P-P} = 36.7$ Hz[4]]. Within the limits of detection of the NMR experiment **4** is not formed from **1** nor **3** from **2**.

**1** was also allowed to react with $CH_3MgBr$ on the preparative scale; after removal of the solvent, **3** was dissolved in toluene and crystallized by slow diffusion of *n*-pentane. The crystal structure of **3** (Fig. 1) proves that the configuration of the Ru atom is retained upon alkylation.

As in the case of the $[CpRuCl(PPh_3)_2]$ complex[5], **1** and **2** do not undergo alkylation with *s*-$C_4H_9MgBr$[5]; rather,

[*] Dr. G. Consiglio
Technisch-chemisches Laboratorium der
Eidgenössischen Technischen Hochschule
Universitätstrasse 6, CH-8092 Zürich (Switzerland)
Dr. F. Morandini
CNR, Centro di Studio sulla Stabilità e
Reattività dei Composti di Coordinazione
Istituto di Chimica Analitica
Via Marzolo 1, I-35100 Padova (Italy)
Dr. G. Ciani, Dr. A. Sironi
Centro di Studio per la Sintesi e la Struttura dei
Composti dei Metalli di Transizione nei Bassi Stati di Ossidazione
Via Venezian 21, I-20133 Milano (Italy)

 © *Verlag Chemie GmbH, 6940 Weinheim, 1983* *0570-0833/83/0404-0333 $ 02.50/0* 

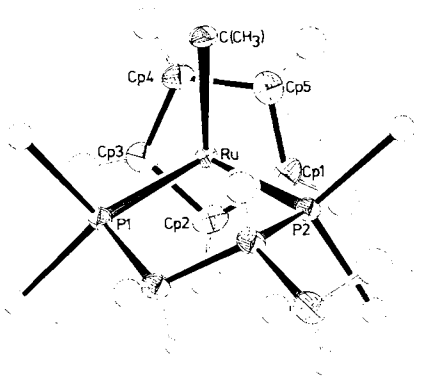



Fig. 1. Structure of complex **3** in the crystal (the phenyl groups are represented by their first C-atoms). Selected bond lengths [Å] and bond angles [°]: RuP1 2.247(2), RuP2 2.229(2), RuC 2.169(6), RuCp (average) 2.246; CRuP1 87.4(2), CRuP2 84.6(2), P1RuP2 84.6(1), P1RuCp* 135.4, P2RuCp* 129.8, CRuCp* 119.0 (Cp* = centroid of the $\eta^5$-$C_5H_5$ ring).

the hydrido complexes [CpRuH(prophos)] **5** [$\delta(P_a)=98.1$, $\delta(P_b)=77.2$, $J_{P-P}=30.0$ Hz[4]; $\delta(Ru)H=-13.22$, $J_{P-H}=29.4$ and 37.5 Hz] and **6** [$\delta(P_a)=104.3$, $\delta(P_b)=85.7$, $J_{P-P}=22.9$ Hz[4]; $\delta(Ru)H=-13.05$, $J_{P-H}=32.0$ Hz], respectively, are formed. These reactions also are stereospecific within the NMR detection limits. The stereochemistry of the β-hydrogen elimination should be clarified by an X-ray structural analysis of **5** or **6**.

Received: November 15, 1982 [Z 202 IE]
German version: *Angew. Chem. 95* (1983) 322

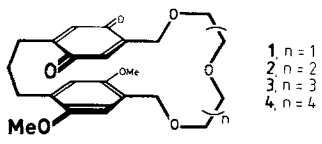
[1] H. Brunner, G. Wallner, *Chem. Ber. 109* (1976) 1053. $PPh_2R^*=(S)$-$Ph_2PN(CH_3)CH(CH_3)Ph$.
[2] G. Consiglio, F. Morandini, G. Ciani, A. Sironi, M. Kretschmer, *J. Am. Chem. Soc.*, in press.
[3] M. D. Fryzuk, B. Bosnich, *J. Am. Chem. Soc. 100* (1978) 5491.
[4] The $^{31}$P-NMR signals were not assigned.
[5] H. Lehmkuhl, J. Grundke, R. Benn, G. Schroth, R. Mynott, *J. Organomet. Chem. 217* (1981) C5.

## Cation-Induced Charge-Transfer Absorption of Intramolecular Quinhydrones with Oligooxaparacyclophane Structure[1]

By *Helmut Bauer, Jan Briaire,* and *Heinz A. Staab**

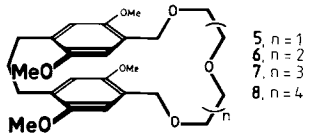
The dependence of the charge-transfer (CT) absorption on distance, orientation, and mutual fixation of donor and acceptor components in quinhydrones of the [n.n]paracyclophanes (n = 2—5) were studied[1,2]. For the intramolecular quinhydrones **1–4**, which are oligooxa derivatives of [3.m]paracyclophanes (m = 9, 12, 15, and 18), it was anticipated that donor and acceptor are not optimally arranged for CT transition due to the width and flexibility of the macrocyclic rings. Because of the crown ether partial structure of these molecules, however, complexation of cations with suitable ionic radius should result in a greater rigidity of the macrocycle and in an approach of donor and acceptor regions; as a consequence, a change in CT-absorption was expected.

The synthesis of **1—4** starts from tetramethoxyoligooxaparacyclophanes **5–8**. **5** (m.p. 85—95 °C, mixture of *pseudoortho* and *pseudogeminal* isomers)[3a] was obtained from 4,4′-trimethylenebis(2,5-dimethoxybenzyl alcohol)[4] and




**1**, n = 1
**2**, n = 2
**3**, n = 3
**4**, n = 4

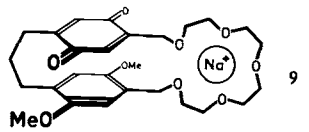
diethylene glycol ditosylate (sodium hydride, tetrahydrofuran, dilution principle; 20% yield). Analogously, reaction of 1,3-bis(4-bromomethyl-2,5-dimethoxyphenyl)propane[4] with tri-, tetra-, and pentaethylene glycol, respectively, led to **6** (m.p. 88—89 °C, 35% yield)[3a], **7** (m.p. 82—85 °C, 21%)[3a], and **8** (m.p. 67—69 °C, 22%)[3a].




**5**, n = 1
**6**, n = 2
**7**, n = 3
**8**, n = 4

Partial oxidative demethylation of **5–8**, respectively, with diammonium hexanitratocerate[5] yielded **1** (42%)[3b], **2** (65%)[3c], **3** (97%)[3d], and **4** (82%)[3e], respectively.

The UV/VIS spectrum of **3** has a CT absorption ($\lambda_{max}=462$ nm, $\varepsilon=324$; in chloroform), which upon complexation with $Na^+$ (NaSCN, chloroform) shows a remarkable increase in intensity ($\varepsilon=874$, Fig. 1), together with a bathochromic shift of 16 nm. This change in the CT absorption, which is also visually easily observable, is reversed by addition of the stronger ligand 4,7,13,16,21-pentaoxa-1,10-diazabicyclo[8.8.5]tricosane (Cryptofix® 221). To explain this complexation effect we assume that the reaction **3** → **9** results in a conformational change which brings the donor and acceptor regions of the molecule closer together. This is supported by the fact that, relative to those of **3**, in **9** the signals of the two benzoquinone protons in the $^1$H-NMR are shifted to highfield by $\Delta\delta=0.10$ and 0.23 ppm (in $CDCl_3$) as a result of a stronger transannular anisotropy effect of the neighboring aromatic ring. Crystals of **9** may be obtained (m.p. 152—153 °C, decomp.) from a solution in chloroform/methanol by precipitation with ether.




**9**

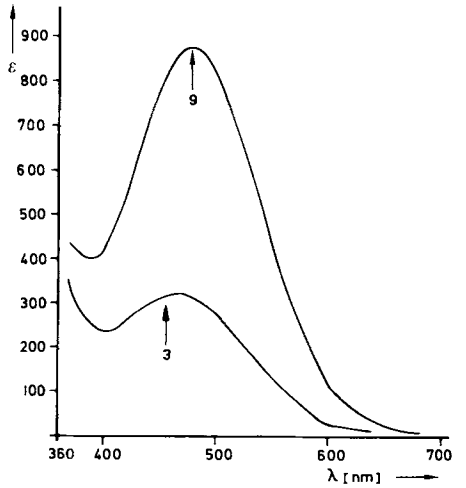



Fig. 1. Absorption spectra of **3** and **9** (conc. $1.72\times10^{-3}$ mol/L in chloroform).

[*] Prof. Dr. H. A. Staab, Prof. Dr. H. Bauer, J. Briaire
Abteilung Organische Chemie
Max-Planck-Institut für medizinische Forschung
Jahnstrasse 29, D-6900 Heidelberg 1 (Germany)

 © Verlag Chemie GmbH, 6940 Weinheim, 1983 0570-0833/83/0404-0334 $ 02.50/0 

With the lower analogues **1** and **2**, $Na^+$ ions do not show any significant effect on the CT absorption; for the higher analogue **4** ($\lambda_{CT}=442$ nm, $\varepsilon=213$) the complexation effect of $Na^+$ with $\Delta\varepsilon=162$ is significantly smaller than for **3**. $K^+$ ions change the CT absorption of **1** and **2** scarcely at all, and that of **3** significantly less than $Na^+$ ions; with **4**, however, they result in an enhancement of the intensity by $\Delta\varepsilon=139$ and in a bathochromic shift of 23 nm. It seems to us that in compounds **1**—**4** a principle of cation-selective ligands with a "built-in CT indicator" is realized which may be of some general interest.

Received: December 8, 1982;
supplemented: February 14, 1983 [Z 219 IE]
German version: *Angew. Chem. 95* (1983) 330

CAS Registry numbers:
**1**, 85083-46-1; **2**, 85083-47-2; **3**, 85083-48-3; **4**, 85083-49-4; **4**·$Na^+$, 85083-44-9; **4**·$K^+$, 85083-45-0; **5**, 85083-50-7; **6**, 85083-51-8; **7**, 85083-52-9; **8**, 85083-53-0; **9**, 85083-54-1.

[1] Electron Donor-Acceptor Compounds, Part 34.—Part 33: H. A. Staab, C. P. Herz, C. Krieger, M. Rentea, *Chem. Ber.*, in press.

[2] H. A. Staab, W. Rebafka, *Chem. Ber. 110* (1977) 3333; H. A. Staab, C. P. Herz, *Angew. Chem. 89* (1977) 839; *Angew. Chem. Int. Ed. Engl. 16* (1977) 799; H. A. Staab, A. Döhling, C. Krieger, *Liebigs Ann. Chem. 1981*, 1052, and references cited therein.

[3] a) Elemental analyses and spectroscopic data correspond to the structure suggested; b) **1**: orange-red crystals, m.p. 120—122 °C (from ethyl acetate/cyclohexane, 2:1); MS: $m/z=416$ (100%, $M^+$); $^1$H-NMR ($CDCl_3$, 80 MHz): $\delta=2.00-3.25$ (m, 6H), 3.62-3.82 (m, 14H), 4.33 (d, $J=2$ Hz, 2H), 4.23, and 4.62 (AB, $J=13$ Hz, 2H), 6.17 (s, 1H), 6.35 (t, $J=2$ Hz, 1H), 6.45 (s, 1H), 6.68 (s, 1H).—c) **2**: orange-red crystals, m.p. 68-70 °C (from ether/*n*-heptane); MS: $m/z=460$ (100%, $M^+$); $^1$H-NMR ($CDCl_3$, 80 MHz): $\delta=2.00-2.80$ (m, 6H), 3.69 (s, 18H), 4.27 (d, $J=2$ Hz, 2H), 4.48 (s, 2H), 6.13 (t, $J=1$ Hz, 1H), 6.41 (t, $J=2$ Hz, 1H), 6.46 (s, 1H), 6.68 (s, 1H).—d) **3**: orange-red prisms, m.p. 71-72 °C (from ether/*n*-heptane); MS: $m/z=504$ (100%, $M^+$); $^1$H-NMR ($CDCl_3$, 80 MHz): $\delta=1.80-2.25$ (m, 2H), 2.25—2.80 (m, 4H), 3.50—3.85 (m, 22H), 4.31 (d, $J=2$ Hz, 2H), 4.52 (s, 2H), 6.31 ('t', $J\approx1$ Hz, 1H), 6.54 (s, 1H), 6.60 (t, $J=2$ Hz, 1H), 6.81 (s, 1H).—e) **4**: orange-yellow crystals, m.p. 88—90 °C (from ethyl acetate/cyclohexane, 3:1); MS: $m/z=548$ (10%, $M^+$), 177 (100%); $^1$H-NMR ($CDCl_3$, 80 MHz): $\delta=1.91$ (quint., $J=7$ Hz, 2H), 2.42 (t, $J=7$ Hz, 2H), 2.86 (t, $J=7$ Hz, 2H), 3.58—3.70 (m, 20H), 3.71 (s, 3H), 3.74 (s, 3H), 4.34 (d, $J=2$ Hz, 2H), 4.52 (s, 2H), 6.42 (t, $J=1$ Hz, 1H), 6.59 (s, 1H), 6.74 (t, $J=2$ Hz, 1H), 6.87 (s, 1H).

[4] Starting from 1,3-bis(2,5-dimethoxyphenyl)propane (R. E. Moser, H. G. Cassidy, *J. Org. Chem. 30* (1965) 2602) chloromethylation and hydrolysis yielded 4,4'-trimethylenebis(2,5-dimethoxybenzyl alcohol) [3a]; bromomethylation yielded 1,3-bis(4-bromomethyl-2,5-dimethoxyphenyl)propane [3a].

[5] General procedure for the synthesis of **1**—**4**: A solution of diammonium hexanitratocerate (0.8 mmol) in 10 mL water was added to a stirred solution of **5**, **6**, **7**, or **8** (0.4 mmol) in 40 mL acetonitrile at room temperature. After 20 min the reaction mixture was extracted with dichloromethane; the extract was dried on magnesium sulfate, evaporated, and the residue chromatographed on silica gel using cyclohexane/ethyl acetate.

# BOOK REVIEWS

**Elektronenstruktur organischer Moleküle. Grundbegriffe quantenchemischer Betrachtungsweisen.** By *Martin Klessinger*. Verlag Chemie, Weinheim 1982. xv, 331 pp., bound, DM 78.—.

This book by *M. Klessinger* is the first volume of a six-part series entitled "Physikalisch Organische Chemie" and treats the current quantum chemical models of theoretical organic chemistry in nine chapters and a detailed appendix. The first chapter deals with the orbital concept in atomic and molecular systems, while the second one introduces the HMO (Hückel molecular orbital) model for simple systems and the third gives a short introduction to the basic principles of group theory and symmetry of fermion systems. The interactions between orbitals in a range of organic molecules are discussed in the fourth chapter and correlated with experimental results (photoelectron spectroscopy). Then the most important aspects of the application of perturbation theory are discussed. The basics of SCF (self-consistent field) models and various types of correlation diagrams (orbital correlation diagrams, configuration and state diagrams) are introduced in the next two chapters. Finally, important MO models of theoretical chemistry are treated together with quantum mechanical aids for the interpretation of such models (population analysis, energy fragmentation, localization procedures *etc.*).

All the chapters are constructed so as to be highly instructive; each time the main points of a theme are presented in a short introduction. The demands on the reader are then increased stepwise, without noticable gaps or jumps in the discussion. The numerous problems at the end of each chapter allow a continuous check on the text that has been worked through. Such an organized layout should make the volume attractive for a potential readership over and above theoretically and physically oriented organic chemists. The subject matter covers, on the one hand, the fundamental principles of quantum mechanics (the variational method, perturbation theory, Hellmann-Feynman relation) and, on the other hand, presents almost all the important models in applied theoretical (organic) chemistry that have been developed in the last 50 years. Many topics are treated at a level of intensity which is not to be found in comparable text books. The explanations of correlation technique (with many up to date references), the treatment of reactions in the ground state and photochemical reactions, the comparison of MO and VB results for reactive systems, together with the discussion of the various types of reaction hypersurfaces are all particularly effective. The layout of the text could perhaps have been made even clearer by combining chapters six and eight.

This textbook can, in any event, be unreservedly recommended to a wide readership. The construction of the book, the diagrams and the layout of the formulas could scarcely be more painstaking. This simplifies, in particular, the working through of the mathematical and quantum mechanical equations. The price of the book is reasonable in view of the amount of information it provides. It is to be hoped that the volumes of "Physikalisch Organische

Chemie" that follow maintain the high instructional quality and, thus, help to fill a considerable informational gap in the chemical literature. A good start has been made with *M. Klessinger*'s book, which deserves to find its way into a large number of textbook collections and private libraries.

*Michael C. Böhm* [NB 583 IE]

**Recent Books**

**The following books have been received by the editor. All the publications listed are available through W & P Buchversand für Wissenschaft und Praxis, Boschstrasse 12, D-6940 Weinheim (Federal Republic of Germany). Tel. (06201) 606-0, Telex 465516 vchwh d, Telefax (06201) 602328.**

**Gmelin. Handbuch der Anorganischen Chemie.** 8th edit. Springer-Verlag, Berlin 1983.
Sn—Organotin Compounds. Part 10: Mono- and Di-organotin-Sulfur Compounds. Organotin-Selenium and Organotin-Tellurium Compounds. xi, 352 pp., bound, DM 993.00.—ISBN 3-540-93468-5
U—Uranium. Supplement Vol. A 6: General Properties, Criticality. xvi, 251 pp., bound, DM 950.00.—ISBN 3-540-93471-5

**Defects in Insulating Crystals.** Edited by *V. M. Tuchkevich* and *K. K. Shvarts*. Springer-Verlag, Berlin 1981. 744 pp., bound, DM 99.00.—ISBN 3-540-10782-7

**Springer Series in Solid-State Sciences: Vol. 28; The Structure and Properties of Matter.** Edited by *T. Matsubara*. Springer-Verlag, Berlin 1982. xi, 446 pp., bound, DM 100.00.—ISBN 3-540-11098-4

**Physikalische Grundlagen der Verfahrenstechnik.** 3rd completely revised edition. By *P. Grassmann*. Otto Salle Verlag/Verlag Sauerländer AG, Frankfurt 1983. 972 pp., bound, DM 280.00.—ISBN 3-7935-5514-3

**Annual Reports in Medicinal Chemistry. Vol. 17.** Edited by *H.-J. Hess*. Academic Press, New York 1982. xiii, 383 pp., bound, $ 32.00.—ISBN 0-12-040517-2

**Proceedings of the First International Symposium on Cyclodextrins.** Edited by *J. Szejtli*. D. Reidel Publishing Company, Dordrecht 1982. xiii, 544 pp., bound, Dfl. 195.00.—ISBN 90-277-1433-9

**Encyclopedia of the Terpenoids.** 2 Volumes: A—H, I—Z. By *J. S. Glasby*. John Wiley, Chichester 1982. 2646 pp. (1—1322, 1323—2646), bound, £ 250.00.—ISBN 0-471-27986-2 (0-471-90031-1 A—H, 0-471-90032-X I—Z)

**Solid Hydrogen. Theory of the Properties of Solid $H_2$, HD, and $D_2$.** By *J. van Kranendonk*. Plenum Press, New York 1983. xv, 306 pp., bound, $ 39.50.—ISBN 0-306-41080-X

**Electron-Atom and Electron-Molecule Collisions.** Edited by *J. Hinze*. Plenum Press, New York 1983. viii, 354 pp., bound, $ 49.50.—ISBN 0-306-41188-1

**Petroanalysis '81. Advances in Analytical Chemistry in the Petroleum Industry.** Edited by *G. B. Crump*. John Wiley, Chichester 1982. xiv, 456 pp., bound, £ 36.00.—ISBN 0-471-26217-X

**Comprehensive Treatise of Electrochemistry. Vol. 6: Electrodics: Transport.** Edited by *E. Yeager, J. O'M. Bockris, B. E. Conway*, and *S. Sarangapani*. Plenum Press, New York 1983. xxiii, 522 pp., bound, $ 67.50.—ISBN 0-306-40942-9

**Umweltforschungskatalog 1981 (UFOKAT '81).** 4th edition. Issued by the Umweltbundesamt. Erich Schmidt Verlag, Bielefeld 1982. xiii, 1724 pp., boards, DM 79.00.—ISBN 3503-02188-4

**Technologie der Reinen Räume.** By *W. Tauscher*. Verlag für Chemische Industrie H. Hiolkowsky KG, Augsburg 1982/83. 441 pp., paperback, DM 48.00.—ISBN 3-87846-106-2

**Nitrat—Nitrit—Nitrosamine in Gewässern.** *Mitteilung III der Kommission für Wasserforschung in Verbindung mit der Kommission zur Prüfung von Lebensmittelzusatz- und Inhaltsstoffen.* A Deutsche Forschungsgemeinschaft publication. acta humaniora der Verlag Chemie GmbH, Weinheim 1982. 240 pp., paperback, DM 70.00.—ISBN 3-527-27305-0

*Registered names, trademarks, etc. used in this journal, even without specific indication thereof, are not to be considered unprotected by law.*

© Verlag Chemie GmbH, D-6940 Weinheim, 1983. - Printed in the Federal Republic of Germany by Zechnersche Buchdruckerei, Speyer/Rhein.

All rights reserved (including those of translation into foreign languages). No part of this issue may be be reproduced in any form - by photoprint, microfilm, or any other means - nor transmitted or translated into a machine language without written permission from the publishers. Only single copies of contributions, or parts thereof, may be reproduced for personal use. Copies reproduced and used other than for private purposes in an industrial or commercial undertaking are subject to copyright and, in such cases, a copyright fee must be paid to the VG WORT, Abteilung Wissenschaft, Goethestr. 49, 8000 München 2, from whom conditions of payment can be obtained on request.

**Valid for users in the USA:** The appearance of the code at the bottom of the first page of an article in this journal (serial) indicates the copyright owner's consent that copies of the article may be made for personal or internal use, or for the personal or internal use of specific clients. This consent is given on the condition, however, that the copier pay the stated per-copy fee through the Copyright Clearance Center, Inc., for copying beyond that permitted by Sections 107 or 108 of the U.S. Copyright Law. This consent does not extend to other kinds of copying, such as copying for general distribution, for advertising or promotional purposes, for creating new collective works, or for resale. For copying from back volumes of this journal see 'Permissions to Photo-Copy: Publisher's Fee List' of the CCC.

**Editorial office:** Pappelallee 3, D-6940 Weinheim, Federal Republic of Germany, Telephone (06201) 602315, Telex 465516 vchwh d, Telefax (06201) 602328.

**Editors:** *P. Gölitz, J. G. Neil, O. Smrekar, A. Stimson.*

**Publishers:** Verlag Chemie GmbH. (Managing Directors: *Prof. Dr. Helmut Grünewald* and *Hans Dirk Köhler*), Pappelallee 3, D-6940 Weinheim, Federal Republic of Germany.
Correspondence concerning advertisements should be addressed to Verlag Chemie GmbH. (Advertising Manager *R. J. Roth*), Pappelallee 3, P.O. Box 1260/1280, D-6940 Weinheim, Federal Republic of Germany, Telephone Weinheim (06201) 602-0, Telex 465516 vchwh d, Telefax (06201) 602328.

ANGEWANDTE CHEMIE
International Edition in English
Volume 22 · Number 5
May 1983
Pages 337–422

# Homolytic Cyclizations of *N*-Chloroalkenylamines

New synthetic methods (38)

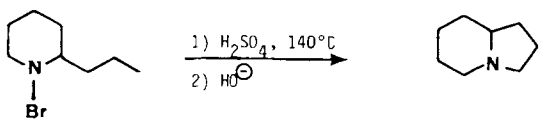
By Lucien Stella*

*Dedicated to Professor Jean-Marie Surzur on the occasion of his 50th birthday*

Many *N*-chloroalkylamines with double bond(s) dissociate homolytically to give chlorine atoms and aminyl radicals which undergo intramolecular cyclization reactions. Here, the nature of the aminyl radicals (neutral, protonated, or complexed to metal salts) appears to be important. The reactivity varies strongly from one species to another, and their selectivities can be different towards addition, substitution, abstraction, or dimerization reactions. A good synthetic tool appears to be the "complexed radical", which is generated under mild conditions. A variety of β-functionalized, substituted, fused, or bridged azaheterocycles with alkaloid part structures thus become easily accessible in high yields, in a regio- and, possibly, stereoselective manner. Many examples are discussed illustrating the synthetic possibilities, limitations, and mechanistic features of this cyclization process.

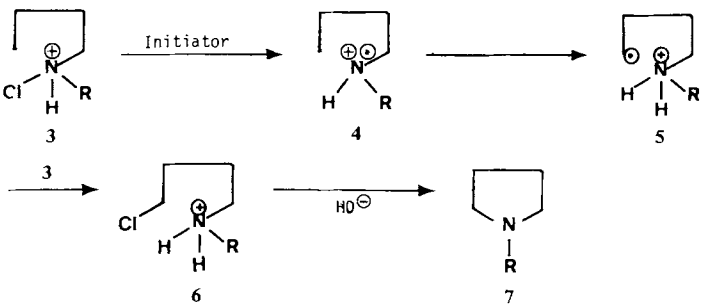
## 1. Introduction

The basis for the use of aminyl free radicals in organic synthesis—although unrecognized as such—was laid almost a hundred years ago. In the period 1881–1885, *Hofmann*[1] made the surprising discovery that the treatment of *N*-bromo-2-propylpiperidine **1**, an *N*-halodialkylamine, with hot sulfuric acid leads to a tertiary amine: this was later shown[2,3] to be octahydroindolizine **2**.




**1** **2**

*Löffler* and *Freytag*[4] extended the Hofmann reaction to simple secondary amines and found it to be a general method for synthesis of pyrrolidines[5]. *Wawzonek* and *Thelen*[6], and later *Corey* and *Hertler*[7] about 70 years after its discovery, established a free radical chain mechanism for this reaction.



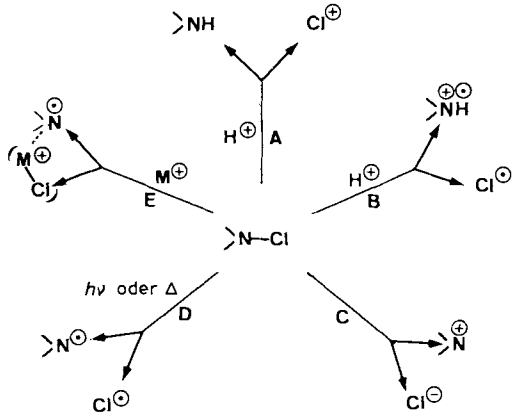

The protonated *N*-chloroamine **3** undergoes homolytic cleavage under the influence of heat, light, or initiators. The protonated aminyl radical **4** obtained intramolecularly abstracts a sterically favorably orientated hydrogen atom to afford, regioselectively, an alkyl radical **5**, which in turn abstracts a chlorine atom to form a chloroalkylammonium ion **6**: this then cyclizes in the presence of base to

[*] Dr. L. Stella
Laboratoire Associé au CNRS n° 109
Université d'Aix-Marseille III
Rue H. Poincaré, F-13397 Marseille Cedex 13 (France)

 © Verlag Chemie GmbH, 6940 Weinheim, 1983 0570-0833/83/0505-0337 $ 02.50/0 

afford the cyclic tertiary amine 7. In 1963 *Wolff*[5] presented a comprehensive survey of this reaction, known today as the Hofmann-Löffler-Freytag reaction.

Besides their selective behavior, which at that time was astonishing, *N*-chloroamines have proved to be useful synthons for ionic or radical aminations and chlorinations. Thus, in protonating media they can lead spontaneously to amine and chlorine(I) ions (Scheme 1, path A) or, in the presence of initiators, to ammoniumyl ions and chlorine atoms (path B). In non-protonating media, solvolysis can produce aminylium and chloride ions by heterolytic dissociation (path C), whereas photolysis or thermolysis afford aminyl radicals and chlorine atoms (path D). Finally, in the presence of reducing metal salts, a redox process generates an aminyl radical complexed to the metal salt, and a chloride ion (path E).




Scheme 1. $>NH^{\oplus\odot}$: Ammoniumyl ion, amine cation or protonated aminyl radical; $>N^{\oplus}$: aminylium ion; $>N^{\odot}$: aminyl radical.

A review article[8] which presented a comprehensive discussion of these various modes of reaction appeared in 1970. More recently, a number of publications[9–13] have stressed the value of the homolytic reactions of *N*-chloroamines in synthetic organic chemistry, especially for the amination of olefinic[9,13] and aromatic[12] compounds, and for the chlorination of saturated aliphatic compounds[12]. As in the Hofmann-Löffler-Freytag reaction, many of these reactions of aminyl radicals do not afford mixtures of products or tars but, in contrast, proceed with very high regioselectivities and good yields. This is, for example, the case when *N*-chloroamines add to alkenes and conjugated dienes[13] under conditions favoring generation of free radicals.

In principle, addition of aminyl radicals to a CC double bond can also occur intramolecularly. The reaction pathways of the alkyl radical thus formed proceed either *via* transfer of a chlorine atom to give β-chloroazaheterocycles, or by addition to strategically located double bonds, or by substitution of aromatic rings to form polycyclization products. These reactions are of interest both for synthesis and for the mechanistic problems they pose. Despite increasing interest in the chemistry of aminyl radicals[16–19], until recently[14,15] the synthetic possibilities presented by their intramolecular addition to CC double bonds remained in the background—in contrast to the well-known corresponding reactions involving carbon-centered radicals[20–23]. The present review points out that, under carefully controlled conditions, homolytic heterocyclizations of *N*-chloroalkenylamines have interesting applications which compete in originality and usefulness with ionic reactions of the same substrates.

This article deals first with the reactions of aminyl radicals as a function of their nature (neutral, protonated, or complexed to a metal salt). The different behavior of monoolefinic *N*-chloroamines under various reaction conditions is then examined, including competition between 1) ionic and radical reactions, 2) between radical abstraction and radical addition reactions, and 3) between radical addition and radical substitution reactions. A number of factors are identified which allow classification of the reactions of aminyl radicals and selection of experimental conditions for organic synthesis: complexed aminyl radicals cyclize to mono- or polycycles. This constitutes a "redox cyclization" of the substrate. Ionic and radical cyclizations of *N*-chloroalkenylamines are compared.

## 2. Characteristic Reactions of Aminyl Radicals

### 2.1. Neutral Aminyl Radicals

Besides thermal or photolytic decomposition of 2-tetrazenes[18,24–27], neutral aminyl radicals can also be generated by photolysis of *N*-chlorodialkylamines in neutral media[28–31]. Generally, neutral dialkylaminyl radicals dimerize to hydrazines and disproportionate to Schiff bases and amines[24–27]. In the presence of olefins they show a strong tendency to abstract hydrogen[25,32,33] in preference to addition reactions. However, they are not useful dehydrogenating agents, since mixture of products are obtained in low yields[26]; intramolecular abstraction of hydrogen (Hofmann-Löffler-Freytag type) is not observed[34]. However, aminyl radicals add to styrene and to α-methylstyrene[35] as well as to arenes[36], but not in the presence of non-aromatically bonded atoms[26,37]. Similarly, addition to ethene (no reactive hydrogen atoms) has been reported[27], but no yields given.

The sluggishness of neutral dialkylaminyl radicals to add to olefins, as well as their strong tendency towards non-selective abstraction of hydrogen seemed to rule out reactions that could be of preparative value.

### 2.2. Protonated Aminyl Radicals

Homolytic decomposition of *N*-chlorodialkylamines in acidic media leads to generation of protonated aminyl radicals[9,10,12], which behave very differently from neutral species. Indeed, the positive charge eliminates the tendency to dimerize or disproportionate. The most important difference is the pronounced tendency of the protonated radicals to add efficiently to many types of unsaturated hydrocarbons[9] and arenes[12,38] in preference to abstracting allylic or benzylic hydrogen atoms. However, protonated aminyl radicals can also abstract hydrogen atoms very selectively in intramolecular[5] (the Hofmann-Löffler-Freytag reaction is faster than intermolecular additions[39]) as well as in intermolecular reactions [$(\omega-1)$ effect[12]]. The homo-

lytic amination of olefins and arenes can be limited or eliminated by the competitive electrophilic chlorination which takes place with electron-rich substrates[9,12].

### 2.3. Aminyl Radicals Complexed to Metal Ions

The decomposition of *N*-chloroamines catalyzed by reducing metal salts in neutral solution generates aminyl radicals complexed to metal ions[13,40]. As in the case of protonation, complexation is presumed to take place *via* the lone pair of electrons of the aminyl radicals. This might increase their electrophilic character and induce a reactivity intermediate between that of neutral and protonated species[41]. Hence, it is not altogether surprising that complexed, like neutral aminyl radicals, do not undergo Hofmann-Löffler-Freytag reactions[34] or selective intermolecular abstractions [$(\omega-1)$ effect is not observed[12]]. Like protonated species, complexed aminyl radicals do not dimerize or disproportionate but add efficiently to dienes, acetylenes, and alkenes[42-45]. Moreover, use of a non-acidic medium in many cases prevents electrophilic chlorination, which is the main limiting reaction of protonated *N*-chloroamines[46,47].

A significant difference in the *cis*- to *trans*-ratios occurs in the adducts of cyclohexene with protonated and complexed aminyl radicals. Thus, addition of *N*-chloropiperidine in acidic media gives a mixture of *cis*- and *trans*-products, whereas in non-acidic solvents mainly the *cis*-isomer is obtained[40]. This stereoselectivity was explained by coordination of the unprotonated radical by the metal salt, which of course is not expected with the protonated species.

Although homolytic substitution of activated aromatic compounds can proceed highly regioselectivity using complexed aminyl radicals[48], strongly acidic media are preferred for highest yields and the low reactivity of the strongly deactivated protonated aromatic amines formed[12].

It is noteworthy that the mild experimental conditions required for generation of complexed aminyl radicals can prevent undesired reactions. This is of particular interest for sensitive systems which could be decomposed by strong acids.

## 3. Synthesis of Monocyclic Compounds

### 3.1. *N*-Chloro-4-alkenylamines

#### 3.1.1. Monosubstituted Double Bonds

*Cyclizations of Neutral Aminyl Radicals:* Unexpectedly, we obtained very strong evidence for intramolecular addition of neutral aminyl radicals[28]. It is clear in this particular case, where the two reacting groups are strategically situated in the same molecule, that very favorable entropy effects come into play. Photolysis of *N*-chloro-*N*-propyl-4-pentenylamine **8a** was studied in various neutral solvents, and the results are shown in Table 1.

In aqueous acetic acid, where *N*-chloroamines exist as free bases[7], photolysis of **8a** gives only 2-chloromethyl-

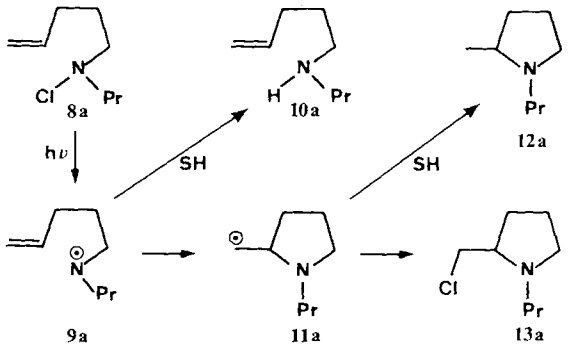
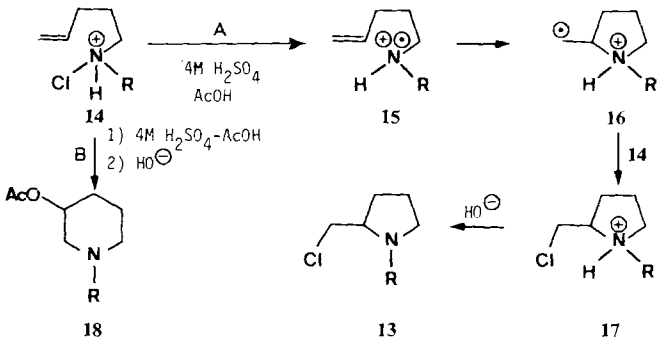



Table 1. Photochemical Cyclization of *N*-chloro-*N*-propyl-4-pentenylamine **8a** in non-protonating solvents (SH), which can function as H donors.

| Solvent | Yield [%] | **10a** : | **12a** : | **13a** |
|---|---|---|---|---|
| AcOH-$H_2O$ (1:1) | 70 | 0 | 0 | 100 |
| MeOH | 72 | 14 | 49 | 37 |
| *i*PrOH | 62 | 29 | 61 | 10 |

pyrrolidine **13** in 70% yield. This appears to be an attractive synthetic method which takes place under quite mild conditions. The relative yields in Table 1 are in good agreement with the participation of the radicals **9a** and **11a**. In particular, 1) formation of **13a** rules out the expected intermolecular reaction of a Cl atom[49], 2) the exclusive formation of the five-membered ring radical **11a** is a characteristic feature of homolytic intramolecular additions of radicals[15], and 3) the reactions of radicals **9a** and **11a** depend only on the ability of the solvent to act as an H donor; the stronger this ability, the higher the amount of **10a** and **12a** produced, and the lower that of **13a**. The hypothesis that the aminyl radical thus generated is not neutral is invalidated by the different behavior of protonated and complexed aminyl radicals (see below), and by the similar behavior of aminyl radicals generated by photolysis of *N*-chloroamines or tetrazenes[18,31].

*Cyclizations of Protonated Aminyl Radicals:* In view of the clear electrophilic character of protonated aminyl radicals, it can be expected that they cyclize more ready than their neutral counterparts. The first systematic investigation of this type of reaction[50] with protonated *N*-chloroamines **14** brings certain characteristic features to light. The main results are collected in Table 2 (see Schemes 2 and 3).

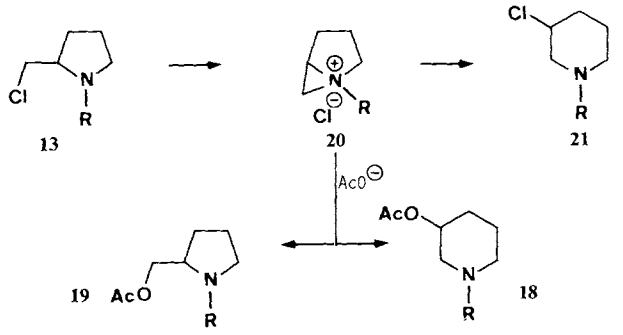



Scheme 2. A: Radical reactions, B: Ionic reactions.

Table 2. Cyclization of alkyl(chloro)-4-pentenylammonium ions **14** in 4 M $H_2SO_4$-AcOH solution.

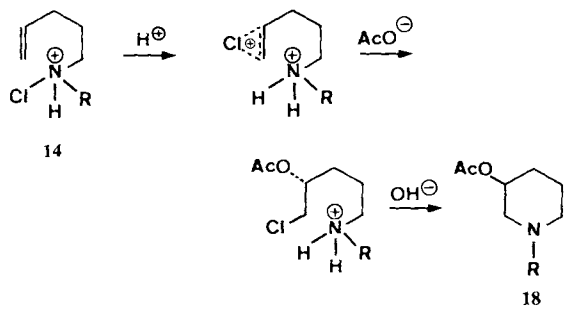
| | R | Conditions | Yield [%] 13 | 18 | 19 |
|---|---|---|---|---|---|
| **14a** | *n*Pr | $FeSO_4/N_2$/25 °C | 66 | 0 | 0 |
| **14a** | *n*Pr | $N_2$/25 °C | 0 | 50 | 0 |
| **14a** | *n*Pr | $N_2$/110 °C | 13 | 33 | 14 |
| **14a** | *n*Pr | *hν*/$N_2$/25 °C | 55 | 0 | 0 |
| **14a** | *n*Pr | $FeSO_4$/air/25 °C | 0 | 50 | 0 |
| **14b** | *n*Bu | $FeSO_4/N_2$/25 °C | 55 | 0 | 0 |
| **14c** | *t*Bu | $FeSO_4/N_2$/25 °C | 57 | 8 | 0 |
| **14c** | *t*Bu | *hν*/$N_2$/25 °C | 60 | 0 | 0 |

Heat, UV light, and metal ions ($Fe^{2+}$) can catalyze the homolytic cyclization; the best yields are obtained with the last two methods mentioned. Intramolecular addition of protonated aminyl radical **15** to **13** is favored by performing the reaction at room temperature in the absence of oxygen and under conditions of relatively high acidity (4 M $H_2SO_4$ in AcOH). As indicated by the inhibitive effect of oxygen and catalytic amounts (1—2%) of metal-ion initiators, the homolysis follows a mechanism with a long reaction-chain propagated by the radical **15**. The exclusive formation of the primary radical **16** resulting from regioselective cyclization to the five-membered ring strongly suggests that the intramolecular addition is kinetically controlled. Initiation of the reaction by heat and/or subsequent work-up at relatively high temperature ($T > 60$ °C) can result in rearrangement of the primary product[51]. Thus, the 2-chloromethylpyrrolidines **13** can undergo the well-known ring expansion[52] to the 3-chloropiperidines **21** *via* the bicyclic aziridinium salt **20**[50], which can also react with nucleophiles other than the chloride ion (acetate ions, for example) leading to a mixture of β-functionalized piperidines **18** and pyrrolidines **19**, whose the ratio is dependent on the nature of the nucleophile (Scheme 3)[53].

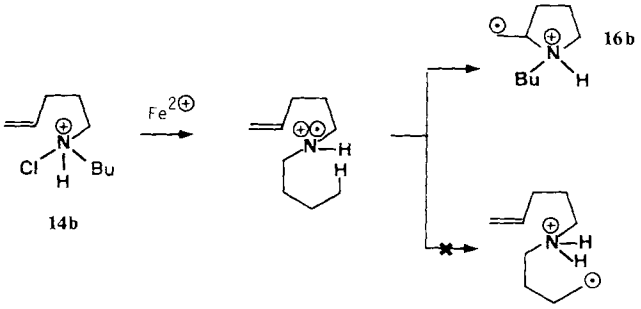


Scheme 3.

In the absence of initiators or in presence of oxygen, **14** reacts exclusively by ionic chlorination leading to **18** (see Scheme 2).



Interestingly, the product resulting from rearrangement of a protonated aminyl radical by a Hofmann-Löffler-Freytag reaction is not formed when intramolecular 1,5-addition to the double bond is possible[54] (Table 2).



Moreover, this is also the case for *N*-chloro-5-alkenylamines when allylic activated δ-hydrogen atoms are present [see **38** → **39** (Section 3.2) and **137** → **138** + **139** (Section 4.5)].

In contrast, *N*-chlorodialkylamines undergo facile Hofmann-Löffler-Freytag rearrangements at the expense of intermolecular free radical addition to simple alkenes[41,55].

*Cyclizations of Aminyl Radicals Complexed to Metal Ions:* When applied to the olefinic *N*-chloroamines **8**, the experimental conditions described by *Minisci et al.* for the intermolecular addition of *N*-chloroamines to olefins in the presence of redox systems[44] gave only very poor yields (less than 20%) of heterocyclic compounds[51]. The search for appropriate conditions for the intramolecular reaction led us to a solvent consisting of 50% aqueous acetic acid[50]. This mixture dissolves the metal salts and the *N*-chloroamines. The best yields of heterocyclization products are obtained using titanium trichloride as reducing agent (Table 3). Due to its high solubility and decoloration when oxidized, this salt allows control of the exact quantities (*ca.* 0.1 equivalents) and time required for complete

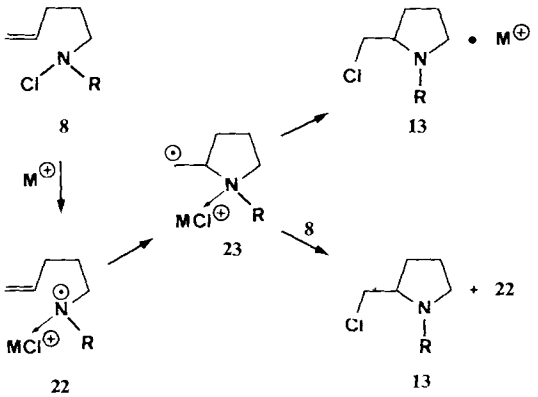


Table 3. Redox cyclizations of *N*-chloro-4-pentenylamines **8** in aqueous acetic acid.

| | R | Metal salt(s) | **13**, Yield [%] |
|---|---|---|---|
| **8a** | *n*Pr | CuCl | 64 [a] |
| **8a** | *n*Pr | CuCl-$CiCl_2$ | 62 |
| **8a** | *n*Pr | $FeSO_4$-$FeCl_3$ | 70 |
| **8a** | *n*Pr | $TiCl_3$ | 81 |
| **8c** | *t*Bu | $TiCl_3$ | 66 |

[a] Together with 9% amine **10a**.

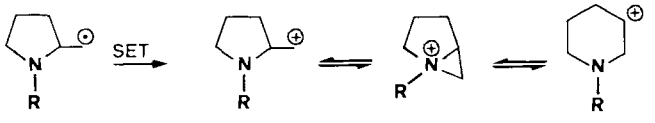
reaction. Although they do not offer the same advantages, copper(I) and iron(II) salts are also suitable reducing agents; however, in order to avoid reducing the aminyl radicals to amines[50] they should be used in the presence of twice as much copper(II) or iron(III) salts. Larger amounts (0.2 to 0.45 equiv.) of metal salts, however, complicate the further work-up.

The mechanism of the reaction depends on the nature of the metal salts: homolytic fission of the N–Cl bond effected by the reducing metal salt produces, in every case, a metal-complexed aminyl radical **22**, which undergoes cyclization by intramolecular addition to the double bond.

Two principal ways for reaction of the resulting carbon-centered radical **23** can be envisaged[13]: 1) reaction with the oxidizing species $(MCl)^+$ in a redox chain process, 2) reaction with the *N*-chloroamine **8** and abstraction of a chlorine atom in a typical radical chain reaction. In both cases catalytic amounts of metal salts are required.

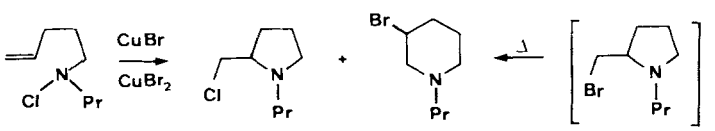
There are two main types of interactions between alkyl radicals and metal salts[56]: the selective transfer of a ligand bonded to the metal ("ligand transfer") and the selective oxidation of the alkyl radical to a carbocation ("electron transfer").

On the basis of extensive investigations by *Kochi*[56], we can expect that, as in intermolecular addition reactions of *N*-chloroamines to alkenes[13], "ligand transfers" are involved when copper(II) and iron(III) chlorides are used. This process is in good agreement with the exclusive formation of the 2-chloromethylpyrrolidine system **13**. "Electron transfer" oxidation of the non-complexed carbon-centered radical **11** should result in a five-membered ring carbocation **24**, which is very prone to rearrange to the piperidine ring species **25** *via* a bicyclic aziridinium ion (cf. **20**)[52] (SET = single electron transfer).




**11** **24** **25**

Furthermore, the use of a stoichiometric amount of copper(II) bromide clearly confirms the "ligand transfer" mechanism. Under these conditions the 3-bromopiperidine **26** resulting from the rearrangement of the initially formed thermally unstable 2-bromomethylpyrrolidine **27** is isolated in 23% yield together with 17% 2-chloromethylpyrrolidine **13a**[34].

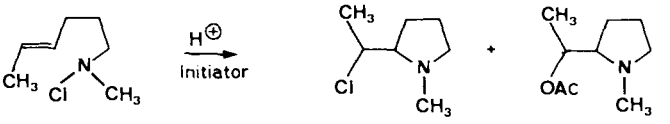



**8a** **13a** **26** **27**

When the reactions are carried out using titanium trichloride, the development of a redox chain mechanism *via* a "ligand transfer" process is unlikely. In this particular case further evidence clearly shows that a typical radical chain reaction takes place (see Section 4.1).

### 3.1.2. *Disubstituted Double Bonds*

In highly acidic media exclusively competitive ionic chlorination becomes important when the double bond of the *N*-chloroalkenylamine is disubstituted by alkyl groups (Table 4).



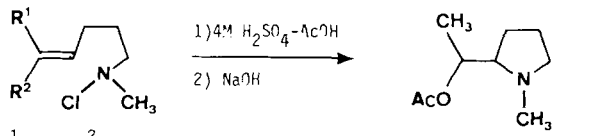

**28** **29** **30**

Table 4. Cyclization of *N*-chloro-*N*-methyl-*trans*-4-hexenylamine **28** in 4 M $H_2SO_4$-AcOH solution.

| Conditions | Yield [%] | |
|---|---|---|
| | **29** | **30** |
| $FeSO_4$, $N_2$, 25 °C | 3 | 47 |
| *hν*, $N_2$, 25 °C | 5 | 50 |
| Δ, $N_2$, 110 °C | 34 | 12 |

With radical initiators the protonated *N*-chloroamine **28** leads to a mixture of *erythro*- and *threo*-2-(1-chloroethyl)-1-methylpyrrolidine **29** and *erythro*-1-(1-methyl-2-pyrrolidinyl)ethyl acetate **30**[57]. It was demonstrated[57,58] that the acetate **30**, which occurs in pure *erythro*-configuration, is not formed from the mixture of chlorides **29** but directly by the ionic pathway (see below)[57,58].

The electrophilic chlorination of *N*-chloroalkenylamines, which competes with the homolytic heterocyclization can also be useful for synthetic purpose because it leads to regio- and stereoselective heterocyclizations[58]. Hence *trans*-*N*-chloro-4-hexenylamine **28** in 4 M $H_2SO_4$–AcOH mixture forms the *erythro*-pyrrolidine **30**[58], whereas under the same conditions the *threo*-pyrrolidine **32** is formed from *cis*-*N*-chloroamine **31**[59].



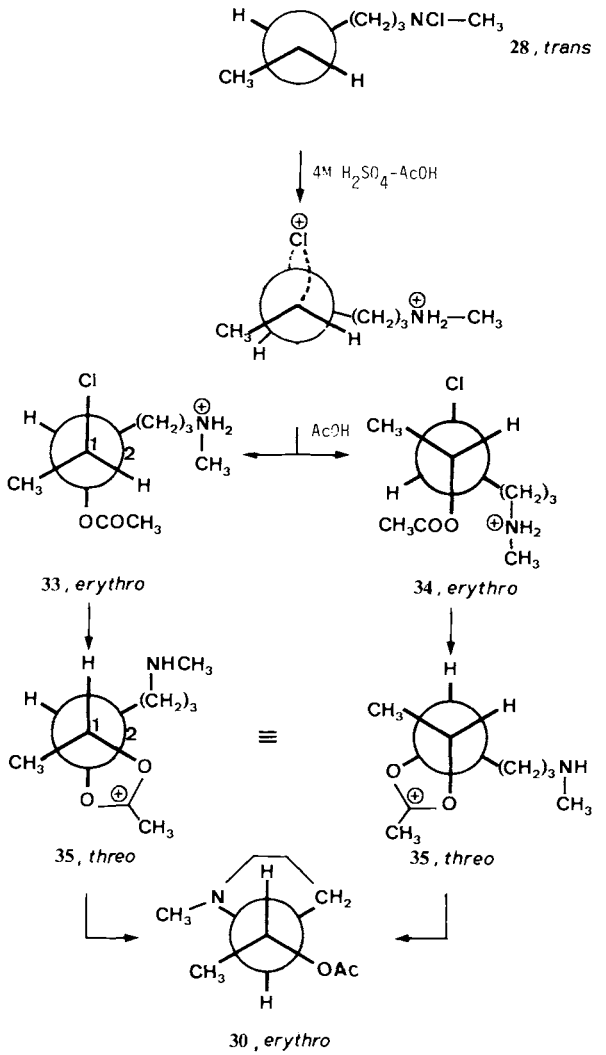

**28**, $R^1$ = H, $R^2$ = $CH_3$
**31**, $R^1$ = $CH_3$, $R^2$ = H

**30**, *erythro*, 42%
**32**, *threo*, 55%

This result can be rationalized as follows[58]. The *trans*-chloroacetylation of the *trans*-double bond of **28** produces two *erythro*-chloroacetates (**33** and **34**). The next two steps consist essentially of two $S_N2$ reactions, which both lead to an inversion, so that the net result is a retention of configuration. For example, starting from the *erythro*-chloroacetate **33**, the *threo*-ion **35** is formed by inversion of the configuration at C-1. The cyclization leading to the *erythro*-aminoacetate **30** then induces inversion of the configuration at C-2.

As for the stereoselectivity, the regioselectivity can be also explained by neighboring group participation with anchimeric assistance; the lowest conformational energy is for the cyclization leading to a five-membered ring[58].

Considering now the redox mechanism of the cyclization of *N*-chloroalkenylamines in non-protonating media, we expect that if the metal in a polydentate complex per-




mitted a relatively rigid transition-state an efficient stereospecific radical reaction should occur. Thus, we employed[60] *trans*- **28** and *cis*-*N*-chloro-*N*-methyl-4-hexenylamine **31** as substrates which react with reducing metal salts to form *erythro*- **29e** and *threo*-2-(1-chloroethyl)-1-methylpyrrolidine **29t** (Table 5).

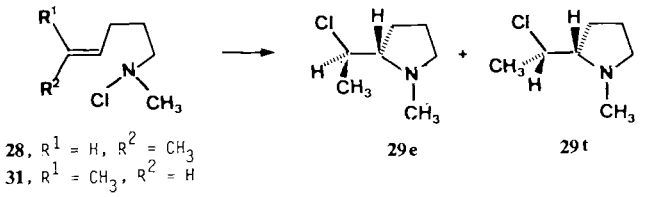
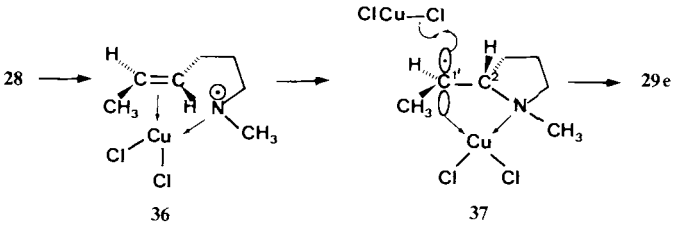



Table 5. Stereoselective cyclization of **28** and **31** with redox systems.

| Substrate | Metal salt(s) | Yield [%] | **29e** | : | **29t** |
|---|---|---|---|---|---|
| **28** | $TiCl_3$ | 74 | 58 | | 42 |
| **28** | $CuCl$-$CuCl_2$ | 81 | 100 | | 0 |
| **28** | $FeCl_2$ | 78 | 100 | | 0 |
| **31** | $TiCl_3$ | 79 | 42 | | 58 |
| **31** | $CuCl$-$CuCl_2$ | 79 | 9 | | 91 |
| **31** | $FeCl_2$ | 76 | 0 | | 100 |

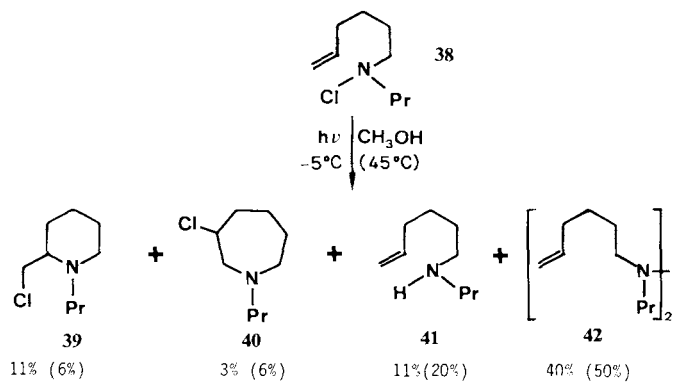
These results are in accord with the following interpretation: the carbon centered radical formed in the cyclization abstracts a Cl atom from the *N*-chloroamine in a typical radical chain reaction, if titanium salts are used, or transfers a Cl atom from copper(II) or iron(III) chloride in a redox chain mechanism. The *cis*-*N*-chloroamine **31** preferentially forms the *threo*-isomer **29t** and the *trans*-*N*-chloroamine **28** the *erythro*-isomer **29e**, *i.e.* the intramolecular addition is *trans (anti)*. This highly stereospecific *trans*-addition strongly suggests hindered rotation about the C2–C1′ bond in the radical **37**, and can be attributed to the coordination of the radical to the metal salt.




The result may also imply that the rate of chlorine transfer, which is higher for redox chain reactions than for typical radical chain reactions[56], controls the extent of stereospecificity. Such stereochemical behavior supports the concept that stereoselective biosyntheses could consist of controlled radical reactions[61].

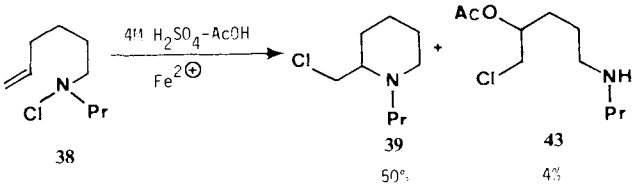
### 3.2. *N*-Chloro-3-alkenyl- and *N*-Chloro-5-alkenylamines

That the absolute rate constants for the cyclization of the neutral *N*-propyl-4-pentenylaminyl radical **9** are not amenable to measurement, indicates clearly that this process is slow ($k_c < 10^3\ s^{-1}$ at 80°)[90]. Nevertheless, on the basis of their main features, the cyclization of neutral alkenylaminyl radicals resembles those of analogous oxygen and non-stabilized carbon-centered radicals[14,15]. Thus, while the photolysis of *N*-chloro-*N*-propyl-3-butenylamine **44** (lower homologue) in methanol leads only to the parent amine[34], the *N*-chloro-*N*-propyl-5-hexenylamine **38** (higher homologue) can cyclize, leading in low yields to a temperature dependent ratio of a mixture of 2-chloromethylpiperidine **39**, 3-chloroazacycloheptane **40**, together with amine **41** and hydrazine **42**[34].




The behavior of *N*-chloro-3-alkenyl- and *N*-chloro-5-alkenylamines was also studied in protonating solvents[57]. With *N*-chloro-3-alkenylamines formation of protonated aminyl radicals does not lead to cyclization but to β-frag-

mentation. With the *N*-chloro-5-alkenyl isomer cyclization, for example, of **38** occurs and gives the 2-chloromethylpiperidine **39** in 50% yield together with a small amount of the β-chloroacetate **43**.

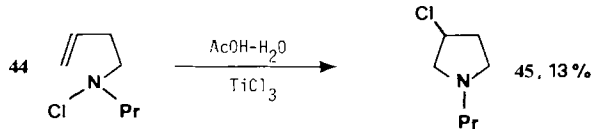



It appears that the intramolecular addition of the protonated aminyl radical is a very efficient process since the Hofmann-Löffler-Freytag reaction, which should be favored in this case by the production of a radical stabilized by allylic conjugation, is not observed[54].

It is noteworthy that the cyclization of protonated *N*-chloro-5-alkenylamine **38** is a little less efficient than that of the 4-alkenyl homologue **14**, but is much more efficient than that of its neutral counterpart.

In a non-protonating medium the clean reaction of **38** with titanium trichloride gives, selectively, the 2-chloromethylpiperidine **39** in 72% yield[34]. Compared with the non-selectivity and low yields obtained by photolysis in neutral solution, this result provides good evidence that aminyl radicals generated in the presence of a redox system are not really free but coordinated to metal salts.

Furthermore, from *N*-chloro-3-butenylamine **44**, which is in general too strained to undergo radical cyclization, the 3-chloropyrrolidine **45** is obtained after complexation, although in lower yield[34].



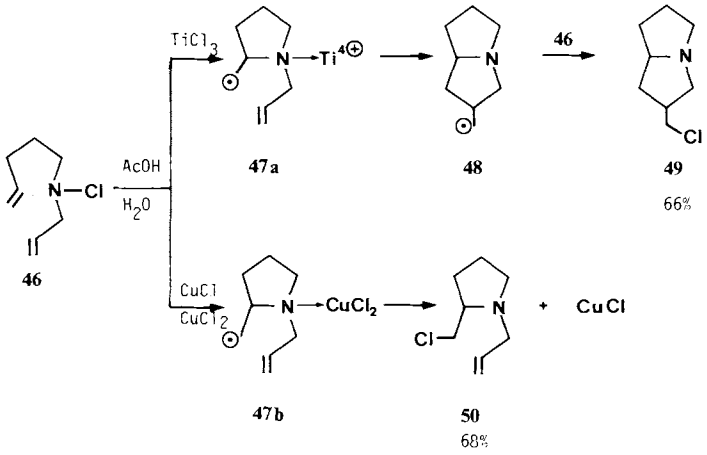

## 4. Synthesis of Polycyclic Compounds

### 4.1. Acyclic *N*-Chloroamines with Two Double Bonds

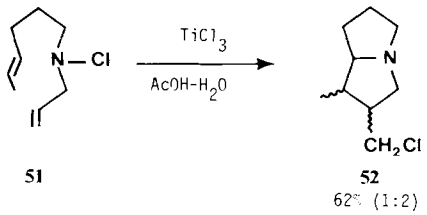
When treated with titanium trichloride in aqueous acetic acid, the readily available *N*-allyl-*N*-chloro-4-pentenylamine **46** leads smoothly to the 2-chloromethylpyrrolizidine **49**[62]. The cyclization of **46** to the five-membered ring leads to the carbon-centered radical **47a**: this undergoes further homolytic cyclization, which appears to be faster than the transfer of chlorine.

This result is a clear indication that the reaction does not proceed *via* a redox chain but rather *via* a typical radical chain mechanism involving transfer of a Cl atom from the *N*-chloroamine **46**. It was indeed well-known that transfer of chlorine from copper(II) chloride, for example, is faster than cyclization of the 5-hexenyl radical[63].

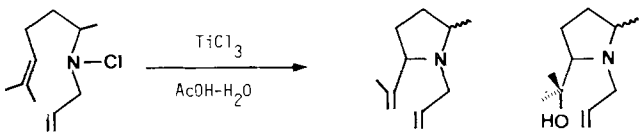
This is also confirmed by **46**[64]: when it is treated in the same solvent with copper(I) chloride in the presence of copper(II) chloride, no bicyclic product **49** can be detected, and *N*-allyl-2-chloromethylpyrrolidine **50** is formed exclusively.



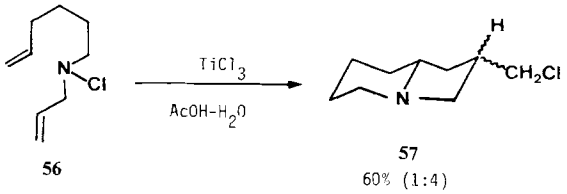

The synthesis of bicyclic products by double intramolecular addition reaps advantage from the radical chain process induced by titanium trichloride. Thus, the *N*-allyl-*N*-chloro-*trans*-4-hexenylamine **51** reacts similarly to **46** with this reducing salt forming a 1:2 mixture of the two diastereoisomeric 2-chloromethyl-1-methylpyrrolizidines **52**[65].




However, the substitution pattern of the double bond of the pentenyl moiety influences the course of the reaction: with the more substituted *N*-allyl-*N*-chloro-1,5-dimethyl-4-hexenylamine **53**, the second radical cyclization does not occur; only monocyclic products **54** and **55** are isolated, resulting, respectively, from dehydrochlorination and hydrolysis of the parent tertiary chloride formed initially[65].



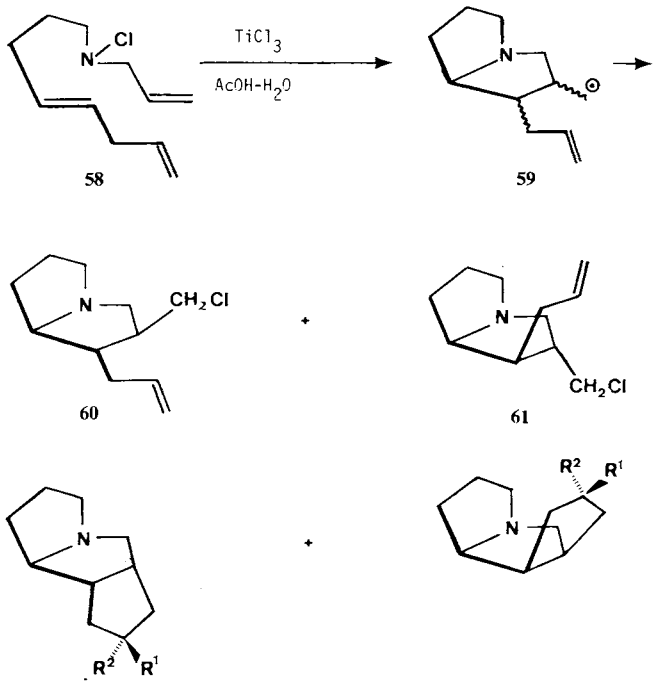

Under the same conditions the higher homologue of **46**, *N*-allyl-*N*-chloro-5-hexenylamine **56**, undergoes an analogous bicyclization to give a 1:4 mixture of the two isolable isomers of 2-chloromethylindolizidine **57**[65].



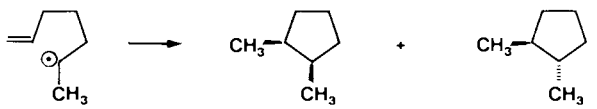

Thus a single synthetic operation, involving two sequential radical cyclizations, provides a direct access to fused azabicyclic systems.

### 4.2. Acyclic *N*-Chloroamines with Three Double Bonds

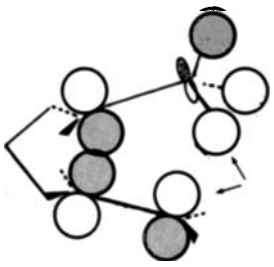
The only known triple homolytic cyclization of a suitable *N*-chloroamine with three double bonds demonstrates the possibility of inducing unexpected stereoselective syntheses with radicals. Excluding the monocyclic product, which has never been obtained using titanium salts, we can expect the two bicycles **60** and **61** and the four tricycles **62**, **63**, **64**, and **65** from the *N*-chloroamine **58**.




In fact we obtained[64], in 75% overall yield, a mixture of six isomeric bicycles and tricycles. Structures have not been assigned to the four minor components (present in 11, 6, 6, and 4% relative yield), but the major components are a tricycle (46%) and a bicycle (27%). It is noteworthy that the tricyclic product represents nearly half of the overall yield. This unexpectedly high amount derives from the favorable stereoselectivity in the second radical cyclization. Thus, for an efficient final cyclization, the intramolecular addition leading to the carbon-centered radical **59** must produce a methylene radical *syn* to the allylic chain. Such stereoselectivity is not altogether surprising in radical cyclizations: for example, in a simpler case, *Beckwith et al.*[66] obtained a mixture of 70% *cis*- **67** and 30% *trans*-dimethylcyclopentane **68**.



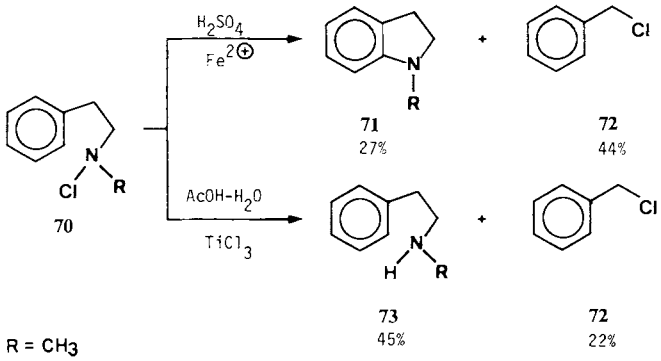

The explanation put forward by *Beckwith et al.*[66] for this surprising *cis*-mode of cyclization also accounts for our results. Orbital symmetry considerations afford a different view to that of simple thermodynamic approaches: hyperconjugative mixing of the half-filled π orbital with the adjacent CH-σ and CH-σ* orbitals produces a modified delocalized orbital which is of similar symmetry to the acceptor π* orbital. Thus, in the transition state **69** leading to the *cis*-disubstituted product, there is a secondary attractive interaction between the alkyl substituent and the olefinic bond which is not available to the transition state for *trans*-cyclization.




In view of the need for stereoselective bond-forming cyclizations, more attention should be given to this polycyclization.

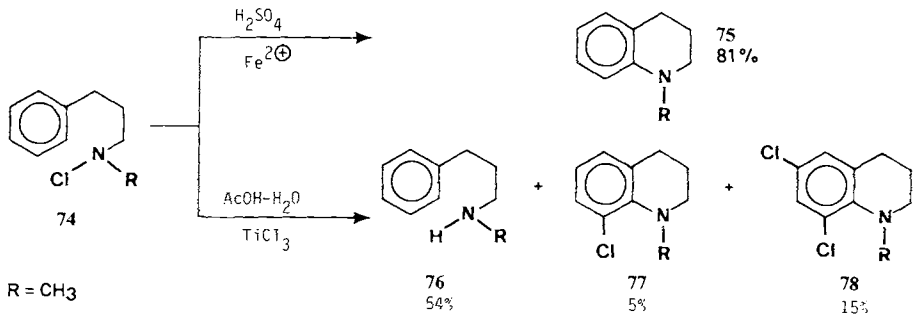
### 4.3. *N*-Chloro(arylalkyl)amines

The cyclizations of *N*-chloroamines are not limited to additions to olefinic bonds: additions to aromatic rings can also occur. Such reactions have been used to synthesize indolines and tetrahydroquinolines. The $Fe^{2+}$ catalyzed decomposition of *N*-chloro-2-phenylethylamine **70** in concentrated sulfuric acid[67] leads to *N*-methyldihydroindole **71** and benzyl chloride **72**, while the mild reaction of titanium trichloride in aqueous acetic acid[34] gives only the amine **73** and benzyl chloride **72**.



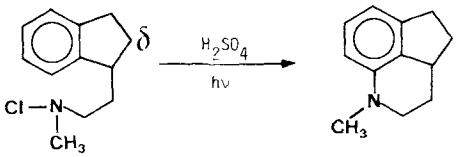

With **70**, which can be compared to *N*-chloro-3-alkenylamines (see Section 3.2), it appears that a protonating is more favorable than a complexing medium. Furthermore, with *N*-chloro-3-phenylpropylamine **74** (similar to *N*-chloro-4-alkenylamines **8** and **14**) no β-scission occurs and the *N*-methyltetrahydroquinoline **75** is formed in 81% yield in concentrated sulfuric acid[67] in presence of $Fe^{2+}$. In contrast, treatment of **74** with titanium trichloride in aqueous acetic acid leads only to low yields of cyclization products **77** and **78**, which result from further electrophilic chlorination of **75**[34].

These results clearly show that when electrophilic chlorination of the substrate does not compete with formation




of protonated aminyl radicals, a strongly acidic medium is more favorable: the radical intermediate cyclizes more efficiently and the protonated aromatic amines formed are deactivated towards further electrophilic reactions.

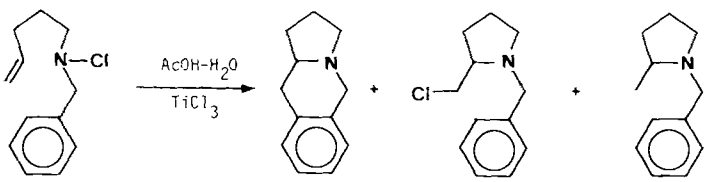
Similarly, photolysis of the *N*-chloroamine **79** in concentrated sulfuric acid gives the *N*-methylhexahydrocyclopentaquinoline **80** in 90% yield[68].



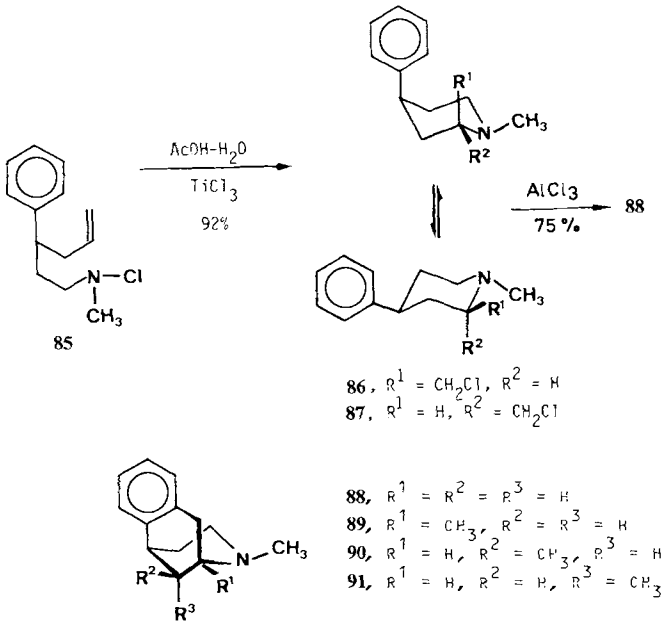

With the *N*-chloroamine **79** δ-hydrogen abstraction by the protonated aminyl radical could have led to a hexahydroindenopyrrole. However, the preference of this intermediate for intramolecular aromatic substitution dominates the reaction, thus leading to **80** as the sole product. This result should be contrasted with the fact that *N*-chlorodialkylamines are known to undergo facile Hofmann-Löffler-Freytag rearrangement at the expense of homolytic intermolecular addition to benzene[12].

### 4.4. *N*-Alkenyl-*N*-chloro(arylalkyl)amines

Two successive radical cyclizations involving an olefinic double bond and an aromatic ring should lead to a new route to benzo-annelated indolizines, such as **82**[62]. In contrast to the reaction **46**→**49**, a mixture of products is obtained in the reaction of *N*-chloro-*N*-benzyl-4-pentenylamine **81** with titanium trichloride. The formation of hexahydropyrrolo[1,2-*b*]isoquinoline **82** involves as a second cyclization step an intramolecular aromatic substitution which is more difficult than intramolecular addition to a double bond. Thus, we also obtained the monocyclization products **83** and **84**, which result from transfer of chlorine and hydrogen.




Using the same strategy a radical approach to *N*-methylbenzomorphan **88**, an analgesic compound related to morphine[69], has been developed. When the *N*-chloroamine **85** is allowed to react with titanium trichloride in aqueous acetic acid, a 4:1 mixture of *cis*- **86** and *trans*-2-chloromethyl-1-methyl-4-phenylpiperidine **87** is obtained in 92% yield[70].



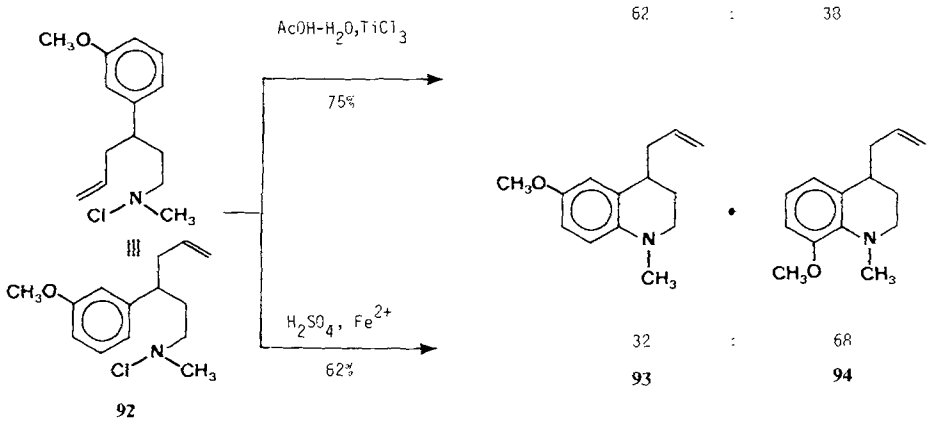

Under these conditions no *N*-benzomorphan **88** can be detected, since the unfavorable diaxial conformation would result in further aromatic substitution of the intermediate carbon centered radical: chlorine atom transfer from **85**, therefore, dominates the reaction.

However, as for *cis*- **86**, which is the major product, inversion of the 2,4-diequatorial to the 2,4-diaxial conformer takes place in boiling cyclohexane and, in the presence of aluminum trichloride the benzomorphan **88** is formed in 75% yield[70].

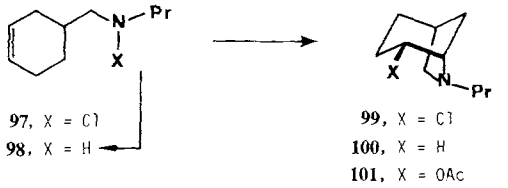
This attractive method, which leads in eight steps from benzaldehyde to benzomorphan, has been used to synthesize 1,2- **89**, 2,9α- **90**, and 2,9β-dimethylbenzomorphan **91**[71].

From these reactions it can be deduced that the complexed aminyl radical exhibits a stronger preference for the double bond than for the benzene ring. But, when the benzene ring is activated by a methoxy group the reverse is observed[71].

The complexed aminyl radical reacts preferentially with the activated aromatic ring and substitution in the *p*-posi-



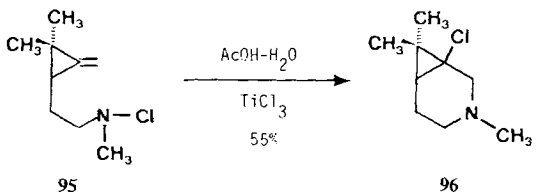

tion is favored. The protonated aminyl radical exhibits the same preference, but the *o/p* regioselectivity is reversed. The same trend is observed in intermolecular aromatic substitutions when instead of complexed[72], protonated aminyl radicals are used[73].




### 4.5. *N*-Chloroamines with Methylcyclopropyl or Cycloalkenyl Groups

Cyclizations of *N*-chloroamines with methylcyclopropyl or cycloalkenyl groups in which the double bond is or not incorporated into a ring can lead to *ortho*-fused and bridged azapolycycles.

Ring-closure of *N*-chloro-*N*-methyl-2-(1,1-dimethyl-2-methylenecyclopropane)ethylamine **95** by titanium trichloride in aqueous acetic acid results in the 3-azabicyclo[4.1.0]heptane derivate **96**[30]. The overall *endo*-regioselectivity observed is in disagreement with Baldwin's rules[74] and with the general behavior of irreversible radical cyclizations[14, 15]. Molecular models clearly show that the five-membered transition state is not favored by the rigid dimethylcyclopropane bridge. However, although steric effects are known to alter regioselectivity[75, 76], such a complete change leading to a six-membered ring was unforeseen.




Depending on the reaction conditions, the *N*-chlorocyclohexenylmethylamine **97** leads to the azabicyclo[3.2.1]octanes **99**, **100**, and/or **101** (Table 6)[29].

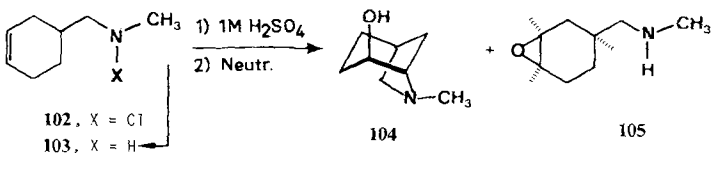
Using titanium trichloride in aqueous acetic acid, the *endo*-chlorinated compound **99** is formed exclusively. Such stereoselectivity is often observed with bridged bicyclic radicals, and is generally interpreted on the basis of steric effects[77]. It appears in this case that the chlorine transfer is easier by *endo*-approach of the *N*-chloroamine to the intermediate bicyclic carbon-centered radical.

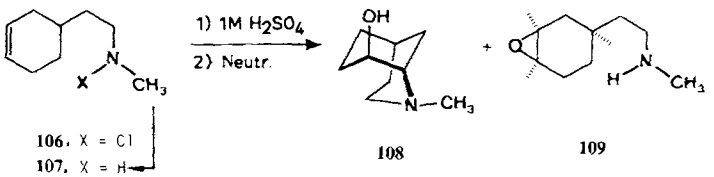
Photolysis in neutral media affords, besides the parent amine **98**, a mixture of compounds **99** and **100** resulting, respectively, from transfer of chlorine and hydrogen.

Table 6. Reactions of *N*-chloro-*N*-propyl-3-cyclohexenylmethylamine **97**.

| Solvent | Conditions | Yield [%] | **98** : | **99** : | **100** : | **101** |
|---|---|---|---|---|---|---|
| AcOH-$H_2O$ | $TiCl_3$ | 77 | 0 | 100 | 0 | 0 |
| MeOH | *hv* | 60 | 23 | 59 | 18 | 0 |
| *i*PrOH | *hv* | 65 | 69 | 5 | 26 | 0 |
| 4M $H_2SO_4$-AcOH | *hv* | 52 | 0 | 23 | 0 | 77 |
| 4M $H_2SO_4$-AcOH | air | 52 | 0 | 17 | 0 | 83 |

In highly acidic media, either with or without photolytic initiation, ionic chlorination of the disubstituted double bond to give acetate **101** is preferred. Similarly, when the *N*-chloroamine **102** is refluxed in 1 M sulfuric acid a mixture of **103**, **104**, and **105** is obtained in the ratio 1 : 13 : 8. Under the same conditions, the *N*-chloroamine **106** leads to a 1 : 4 : 2 mixture of **107**, **108**, and **109**. No yields were given in the last two cases[78].

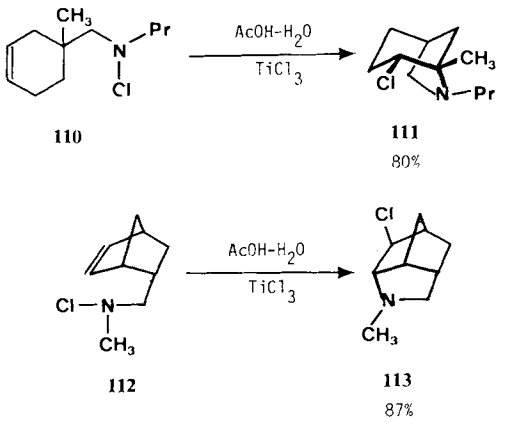


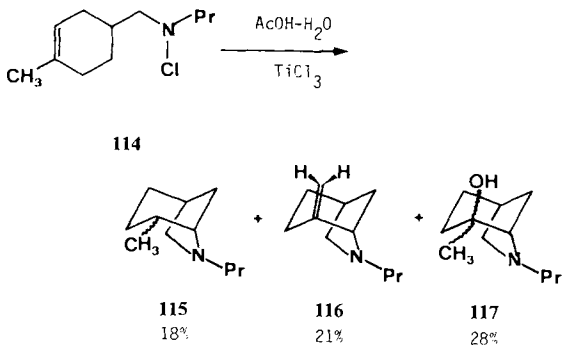

In contrast, electrophilic chlorination of the double bond is never observed in aqueous acetic acid. The following reactions illustrate the scope and limitations of the mild reduction of *N*-chloro-cycloalkenylamines by titanium trichloride.

Starting from **110** the *endo*-chlorinated azabicycle **111** is again obtained[79], while cyclization of **112** results in the

*exo*-chlorinated azatricycle **113**[79]. Mechanistically, this inversion of stereoselectivity can be rationalized on the basis of steric effects.

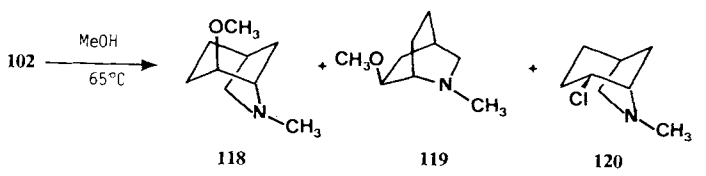



Even when the double bond is trisubstituted, as in **114**, regioselective intramolecular addition of the complexed aminyl radical is observed[79].

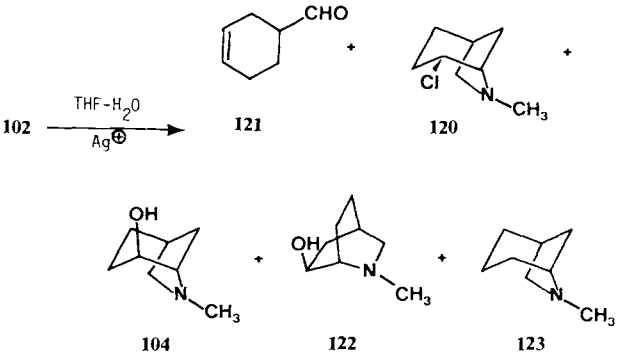



Very probably **115** arises from hydrogen atom transfer, whereas **116** and **117** are formed by dehydrochlorination and solvolysis, respectively, from the parent *endo*-tertiary chloride. Analogously, on photolysis in methanolic solution **114** gives a 45:55 mixture of **115** and **116** in 75% yield[79].

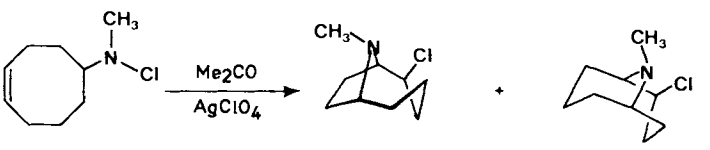
The high regio- and stereoselectivities generally observed when aminyl radicals coordinated to titanium salts are involved contrast with the low yields and complex mixtures of products obtained by thermolysis or ion-catalyzed solvolysis of **102**[80]. Thus, refluxing a methanolic solution of **102** results in the recovery of 40% of the parent amine **103** and formation of three cyclization products **118**, **119**, and **120** in 15, 23, and 13% yields, respectively.

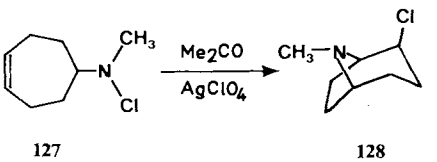



Solvolysis of **102** in aqueous tetrahydrofuran (THF) catalyzed by silver ions gives a more complex mixture of products consisting of **103** (17%), **104** (14%), **120** (12%), **121** (18%), **122** (19%), and **123** (16%).



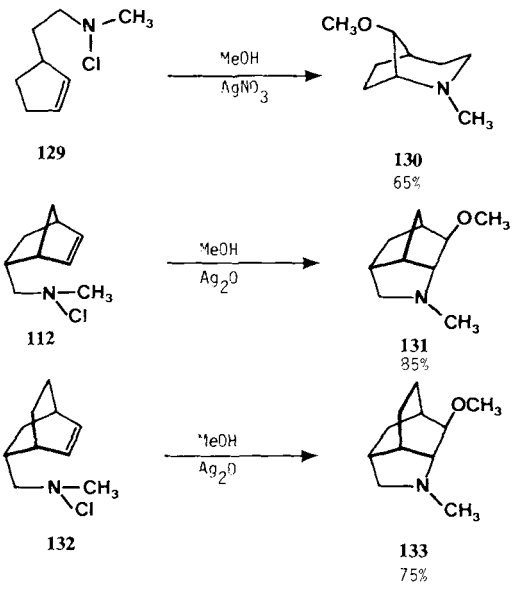

These reactions are unsatisfactory for the synthesis of azabicycles and have been rationalized by *Gassman et al.* as indicating the involvement of triplet and singlet aminylium ions[80,81]. Although it is beyond doubt that both silver ion-promoted and non-catalyzed solvolysis of *N*-chloroamines can proceed *via* aminylium ions[31], it was proposed that under these conditions a homolytic can compete with the heterolytic process to form cyclized products from unsaturated *N*-chloroamines[82]. The following examples were regarded as being consistent with this. Thus[83,84], the reaction of the *N*-chloro-cyclooctenylamine **124** with stoichiometric amounts of silver perchlorate in refluxing acetone yields **125** (25%) and **126** (14%). Under the same conditions, the *N*-chloro-cycloheptenylamine **127** affords a single bicycle **128** in 7.5% yield. To rationalize the stereospecific *cis*-addition of nitrogen and chlorine to the double bond coordination of the catalyst to nitrogen[83] or internal return of chlorine during solvolysis by silver ion[81] have been proposed.




With silver oxide in refluxing chloroform[85], the *N*-chloroamine **112** leads, in 75% yield, to the same *exo*-chlorinated bicycle **113** previously obtained by reaction of **112** with titanium trichloride (see above).

Whatever the importance of the homolytic process may be, the selective transformations **129** → **130**[81,82], **112** → **131**[85], and **132** → **133**[85] illustrate nicely that solvolytic conditions may provide a simple route from *N*-chloro-cycloalkenylamines to bridged azapolycycles containing *trans*-orientated amino and methoxy substituents.

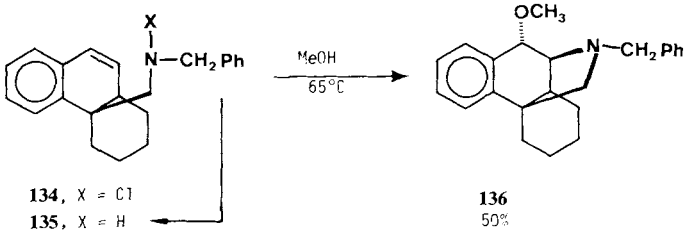



129 → 130 (65%)

112 → 131 (85%)

132 → 133 (75%)

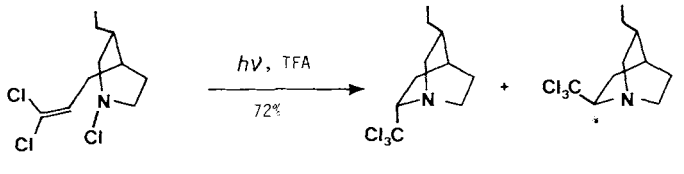
Similarly, refluxing a solution of the *N*-chloroamine **134** in methanol produces 20% amine **135** and 50% *N*-benzyl-10-*trans*-methoxy-D-normorphinan **136**. This compound is the only cyclized product recovered from the reaction[87].




**134**, X = Cl
**135**, X = H

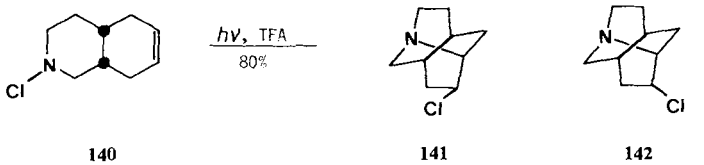
**136**
50%

As in intermolecular reactions of protonated *N*-chloroamines with olefins[41,55], ionic chlorination of the double bond can be eliminated by introducing electron-withdrawing groups. Thus, irradiation of a solution of **137** in trifluoroacetic acid (TFA) affords a 1:1 mixture of trichloromethylquinuclidines **138** and **139**[88]. These substituted quinuclidines were used as intermediates in a total synthesis of *Chinchona* alkaloids.




**137** → **138** + **139**

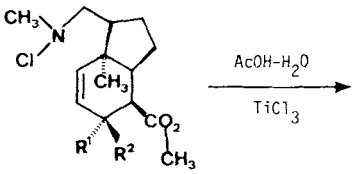
An exception to five-membered ring formation and to the non-ionic pathway in the case of a disubstituted double bond is provided by the homolytic cyclization of *N*-chloro-*cis*-octahydroisoquinoline **140**, leading to a 4:3 mixture of β-chloroazatwistanes **141** and **142**[89].



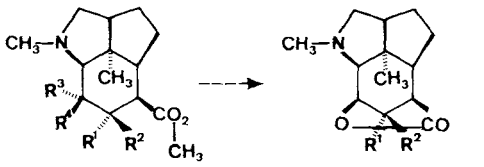

**140** → **141** + **142**

Consideration of models clearly shows that the very propicious closure of the six-membered instead of the five-membered ring is probably due in this particular case to much less important non-bonding interactions in the transition state leading to the staggered azatwistanes **141** and **142** than in that leading to the eclipsed isomer.

In recent attempts to synthesize the natural dendrobine alkaloid **148**, redox cyclization of the *N*-chloroamines **143** and **144** has been examined. In the presence of titanium trichloride the crude chloropyrrolidine derivate **145** was obtained from **143** and allowed to react with lithium iodide in refluxing lutidine to give 8-*epi*-dendrobine **147** (45%)[91]. Under the same conditions **144** reacts in a similar manner leading to **146** (20—30% yield, not optimized).



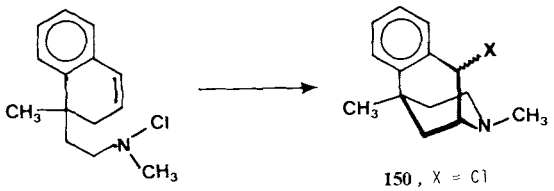

**143**, $R^1$=H, $R^2$=iPr
**144**, $R^1$=iPr, $R^2$=H



**145**, $R^1$=H, $R^2$=iPr, $R^3$,$R^4$=H,Cl
**146**, $R^1$=iPr, $R^2$=H, $R^3$=Cl, $R^4$=H

**147**, $R^1$=H, $R^2$=iPr
**148**, $R^1$=iPr, $R^2$=H

The synthetic approach to benzomorphans discussed in Section 4.4 does not allow further substitution of the benzylic carbon atom by a methyl group[71]. Since this substitution pattern is important for analgesics, we developed another strategy for the synthesis of 2,5-dimethylbenzomorphans. Depending on the reaction conditions (Table 7), *N*-chloroamine **149**, easily obtained in a nine-step sequence from levulinic acid, leads to 2,5-dimethylbenzomorphans **150**, **151** or **152** functionalized in the 8-position[59].



**149**

**150**, X = Cl
**151**, X = OAc
**152**, X = OH

Table 7. Cyclizations of the *N*-chloroamine **149** to benzomorphan derivatives **150–152**.

| Conditions | Product | Yield [%] |
|---|---|---|
| AcOH-$H_2O$, $TiCl_3$ | **150** | 63 |
| 4 M $H_2SO_4$-AcOH | **151** | 82 |
| 4 M $H_2SO_4$-$H_2O$ | **152** | 81 |

The stereochemistry of the C-8 substituents has not yet been assigned, although these reactions probably take place stereoselectively.

## 5. Concluding Remarks

Accumulated evidence points to the synthetic potential of homolytic heterocyclizations of *N*-chloroalkenylamines. From the examples given a set of rules can be derived enabling the behavior of *N*-chloroamines to be classified and predicated in terms of solvent, temperature, catalyst, and the nature of the various functional groups which can react inter- and intramolecularly with aminyl radicals. Particular mention should be made of exclusively *exo*-regioselective cyclizations leading to five- and six-membered ring heterocycles including substituted, fused, and bridged systems (for an exception see the reaction **95** → **96**). In addition to steric, stereoelectronic, and metal salt effects the kinetic control of cyclizations may further influence the outcome, as indicated by many stereoselective syntheses and by one stereospecific synthesis **28** → **29e**; **31** → **29t**). The combination of intramolecular addition of aminyl radicals with other radical cyclizations provides additional possibilities for the synthesis of polycyclic systems.

It therefore appears that aminyl radicals, and especially complexed aminyl radicals, provide the organic chemist with the opportunity of synthesizing complex molecules using mild and simple redox reactions in both a regio- and a stereoselective manner. They are thus good synthetic tools for the synthesis of heterocycles.

*Our own work mentioned in this article was carried out in the laboratory of Professor Jean-Marie Surzur, at the University of Marseille. It is a pleasure to dedicate this review to him in grateful recognition for his inspiration, contribution, and support. I have also great pleasure in expressing thanks to my colleagues who have worked on one or another parts of this program: Drs. Jean-Luc Bougeois, Jean Lacrampe, Robert Nouguier, Bernard Raynier, Jean-Louis Stein, and Prof. Paul Tordo. The financial support of the Centre National de la Recherche Scientifique is gratefully acknowledged.*

Received: April 1, 1982 [A 451 IE]
German version: *Angew. Chem. 95* (1983) 368

[1] A. W. Hofmann, *Ber. Dtsch. Chem. Ges. 14* (1881) 2725; *16* (1883) 558; *18* (1885) 5, 109.
[2] K. Löffler, H. Kaim, *Ber. Dtsch. Chem. Ges. 42* (1909) 94.
[3] E. Lellmann, *Justus Liebigs Ann. Chem. 259* (1880) 193; *Ber. Dtsch. Chem. Ges. 23* (1890) 2141.
[4] K. Löffler, C. Freytag, *Ber. Dtsch. Chem. Ges. 42* (1909) 3427.
[5] M. E. Wolff, *Chem. Rev. 63* (1963) 55.
[6] S. Wawzonek, P. J. Thelen, *J. Am. Chem. Soc. 72* (1950) 2118.
[7] E. J. Corey, W. R. Hertler, *J. Am. Chem. Soc. 82* (1960) 1657.
[8] P. Kovacic, M. K. Lowery, K. W. Field, *Chem. Rev. 70* (1970) 639.
[9] R. S. Neale, *Synthesis 1971*, 1.
[10] C. Deno in E. S. Huyser: *Methods in Free Radical Chemistry*, Marcel Dekker, New York 1972, Vol. *3*, p. 135–154.
[11] G. Sosnovsky, D. I. Rawlinson, *Adv. Free-Radical Chem. 4* (1972) 203.
[12] F. Minisci, *Synthesis 1973*, 1.
[13] F. Minisci, *Acc. Chem. Res. 8* (1975) 165.
[14] A. L. J. Beckwith, K. U. Ingold in P. de Mayo: *Rearrangements in Ground and Excited States*, Academic Press, New York 1980, Vol. *1*, p. 161–310.
[15] J. M. Surzur, *React. Intermed. (Plenum) 2* (1982) 121.
[16] a) J. K. Kochi: *Free Radicals*, Wiley, New York 1973; b) S. F. Nelsen in [16a], Vol. *2*, p. 527–593.
[17] W. C. Danen, F. A. Neugebauer, *Angew. Chem. 87* (1975) 823; *Angew. Chem. Int. Ed. Engl. 14* (1975) 783.
[18] C. Michejda, D. H. Campbell, D. H. Sieh, S. R. Koepke in W. A. Pryor: *Organic Free Radicals*, A. C. S. Symp. Ser. *69*, Am. Chem. Soc., Washington, DC 1978, Vol. *18*, p. 292–308.
[19] Y. L. Chow, *React. Intermed. (Plenum) 1* (1980) 151.
[20] M. Julia, *Pure Appl. Chem. 15* (1967) 167.
[21] A. L. J. Beckwith, *Chem. Soc. Spec. Publ. 24* (1970) 239.
[22] M. Julia, *Acc. Chem. Res. 4* (1971) 386.
[23] J. W. Wilt in [16a], Vol. *1*, p. 333–501.
[24] H. Wieland, H. Fressel, *Justus Liebigs Ann. Chem. 392* (1912) 133.
[25] B. R. Cowley, W. A. Waters, *J. Chem. Soc. 1961*, 1228.
[26] D. Mackay, W. A. Waters, *J. Chem. Soc. C 1966*, 813.
[27] A. Good, J. C. J. Thynne, *J. Chem. Soc. B 1967*, 684.
[28] J. M. Surzur, L. Stella, P. Tordo, *Tetrahedron Lett. 1970*, 3107.
[29] J. M. Surzur, L. Stella, R. Nouguier, *Tetrahedron Lett. 1971*, 903.
[30] J. L. Stein, L. Stella, J. M. Surzur, *Tetrahedron Lett. 21* (1980) 287.
[31] P. G. Gassman, K. Uneyama, J. L. Hahnfeld, *J. Am. Chem. Soc. 99* (1977) 647.
[32] C. H. Bamford, *J. Chem. Soc. 1939*, 17.
[33] G. H. Booth, R. G. W. Norrish, *J. Chem. Soc. 1952*, 188.
[34] L. Stella, *Thesis*, Marseille 1972.
[35] C. J. Michejda, D. H. Campbell, *Tetrahedron Lett. 1977*, 577.
[36] M. Bellas, D. Bryce-Smith, A. Gilbert, *J. Chem. Soc. Chem. Commun. 1967*, 862.
[37] R. E. Jacobson, K. M. Johnston, G. H. Williams, *Chem. Ind. (London) 1967*, 157.
[38] H. Bock, K. L. Kompa, *Angew. Chem. 77* (1965) 807; *Angew. Chem. Int. Ed. Engl. 4* (1965) 783; *Chem. Ber. 99* (1966) 1347, 1357.
[39] R. S. Neale, R. L. Hinman, *J. Am. Chem. Soc. 85* (1963) 2666.
[40] F. Minisci, R. Galli, M. Cecere, *Chim. Ind. (Milano) 48* (1966) 347.
[41] R. S. Neale, N. L. Marcus, *J. Org. Chem. 32* (1967) 3273.
[42] F. Minisci, *Chim. Ind. (Milano) 49* (1967) 705.
[43] F. Minisci, R. Galli, *Tetrahedron Lett. 1964*, 167.
[44] F. Minisci, R. Galli, G. Pollina, *Chim. Ind. (Milano) 47* (1965) 736.
[45] F. Minisci, R. Galli, *Chim. Ind. (Milano) 45* (1963) 1400.
[46] R. S. Neale, *Tetrahedron Lett. 1966*, 483.
[47] F. Minisci, R. Galli, M. Cecere, *Tetrahedron Lett. 1966*, 3163.
[48] F. Minisci, R. Galli, *Tetrahedron Lett. 1965*, 433.
[49] Y. Ogata, Y. Izawa, M. Tomiska, *Tetrahedron 33* (1967) 1509.
[50] J. M. Surzur, L. Stella, P. Tordo, *Bull. Soc. Chim. Fr. 1970*, 115.
[51] J. M. Surzur, P. Tordo, *C. R. Acad. Sci. Ser. C 263* (1966) 446.
[52] R. C. Fuson, C. L. Zirkle, *J. Am. Chem. Soc. 70* (1948) 2760; E. G. Brain, F. P. Doyle, H. D. Mehta, *J. Chem. Soc. 1961*, 663; R. C. Paul, S. Tchelitcheff, *Bull. Soc. Chim. Fr. 1958*, 736; C. F. Hammer, S. R. Heller, *J. Chem. Soc. Chem. Commun. 1966*, 919; C. F. Hammer, S. R. Heller, J. H. Craig, *Tetrahedron 28* (1972) 239.
[53] D. R. Crist, N. J. Leonard, *Angew. Chem. 81* (1969) 953; *Angew. Chem. Int. Ed. Engl. 8* (1969) 962.
[54] J. M. Surzur, L. Stella, P. Tordo, *Bull. Soc. Chim. Fr. 1975*, 1429.
[55] R. S. Neale, *J. Org. Chem. 32* (1967) 3263.
[56] J. K. Kochi in [16a], Vol. *1*, p. 591–683.
[57] J. M. Surzur, L. Stella, P. Tordo, *Bull. Soc. Chim. Fr. 1975*, 1425.
[58] J. M. Surzur, L. Stella, *Bull. Soc. Chim. Fr. 1977*, 255.
[59] J. L. Bourgeois, Thesis, Marseille 1980.
[60] J. L. Bougeois, L. Stella, J. M. Surzur, *Tetrahedron Lett. 22* (1981) 61.
[61] N. A. Porter in W. A. Pryor: *Free Radicals in Biology*, Academic Press, New York 1980, Vol. *4*, p. 261–294.
[62] J. M. Surzur, L. Stella, *Tetrahedron Lett. 1974*, 2191.
[63] C. L. Jenkins, J. K. Kochi, *J. Org. Chem. 36* (1971) 3109.
[64] L. Stella, unpublished results.
[65] J. Lacrampe, Thesis, Marseille 1977.
[66] A. L. J. Beckwith, I. Blair, G. Phillipou, *J. Am. Chem. Soc. 96* (1974) 1613.
[67] F. Minisci, R. Galli, *Tetrahedron Lett. 1966*, 2531.
[68] P. S. Anderson, G. F. Lundell, J. L. Cias, F. M. Robinson, *Tetrahedron Lett. 1971*, 2787.
[69] D. C. Palmer, M. J. Strauss, *Chem. Rev. 77* (1977) 1.
[70] L. Stella, B. Raynier, J. M. Surzur, *Tetrahedron Lett. 1977*, 2721.
[71] L. Stella, B. Raynier, J. M. Surzur, *Tetrahedron 37* (1981) 2843.
[72] F. Minisci, R. Bernardi, L. Grippa, V. Trabucchi, *Chim. Ind. (Milano) 48* (1966) 264.
[73] F. Minisci, R. Galli, M. Cecere, *Tetrahedron Lett. 1965*, 4663.
[74] J. E. Baldwin, *J. Chem. Soc. Chem. Commun. 1976*, 734.
[75] A. L. J. Beckwith, I. Blair, G. Phillipou, *Tetrahedron Lett. 1974*, 2251.
[76] M. Julia, C. Descoins, M. Baillarge, B. Jacquet, D. Uguen, F. A. Groeger, *Tetrahedron 31* (1975) 1737.
[77] P. D. Bartlett, G. N. Kickes, F. C. Haupt, R. Helgeson, *Acc. Chem. Res. 3* (1970) 177.
[78] P. G. Gassman, J. H. Dygos, *Tetrahedron Lett. 1970*, 4749.
[79] R. Nouguier, Thesis, Marseille 1975.

[80] P. G. Gassman, J. H. Dygos, *Tetrahedron Lett. 1970*, 4745.
[81] P. G. Gassman, *Acc. Chem. Res. 3* (1970) 26.
[82] O. E. Edwards, G. Bernath, J. Dixon, J. M. Paton, D. Vocelle, *Can. J. Chem. 52* (1974) 2123.
[83] J. D. Hobson, W. D. Riddell, *J. Chem. Soc. Chem. Commun. 1968*, 1178.
[84] J. W. Bastable, J. D. Hobson, W. D. Riddell, *J. Chem. Soc. Perkin 1 1972*, 2205.
[85] R. Tadayoni, J. Lacrampe, A. Heumann, R. Furstoss, B. Waegell, *Tetrahedron Lett. 1975*, 735; R. Furstoss, R. Tadayoni, B. Waegell, *Nouv. J. Chim. 1* (1977) 167; *J. Org. Chem. 42* (1977) 2844.
[86] P. G. Gassman, F. Hoyda, J. Dygos, *J. Am. Chem. Soc. 90* (1968) 2716.
[87] T. T. Conway, T. W. Doyle, Y. G. Perron, J. Chapuis, B. Belleau, *Can. J. Chem. 53* (1975) 245.
[88] G. Grethe, H. L. Lee, T. Mitt, M. Uskoković, *J. Am. Chem. Soc. 100* (1978) 581.
[89] K. Heusler, *Tetrahedron Lett. 1970*, 97.
[90] Y. Maeda, K. U. Ingold, *J. Am. Chem. Soc. 102* (1980) 328.
[91] R. F. Borch, A. J. Evans, J. J. Wade, *J. Am. Chem. Soc. 97* (1975) 6282; *99* (1977) 1612.
[92] W. R. Roush, *J. Am. Chem. Soc. 102* (1980) 1390.

# Modern Pulse Methods in High-Resolution NMR Spectroscopy

**By Reinhard Benn* and Harald Günther***

The introduction of Fourier transform methods has not only remarkably enhanced the sensitivity of high-resolution NMR spectroscopy, thus allowing measurements to be made on less sensitive nuclei of the Periodic Table, but also has paved the way for the development of a large number of new experimental techniques. On the one hand, procedures already known have been improved and can now be performed more rapidly, and, on the other, completely new experimental approaches have become available. This situation resulted mainly from the introduction of programmable pulse transmitters and the separation of the experiment into preparation, evolution, and detection. In particular, the concept of two-dimensional spectroscopy has opened up new possibilities important for the analysis of complicated spectra and is able to provide information previously not accessible. As elsewhere, optimum application of the techniques and correct interpretation of the results require sound understanding of the underlying physical principles. Since a rigorous mathematical treatment is complicated and does not necessarily improve the comprehensibility, this article attempts to give an illustrative presentation of the new pulse techniques within the framework of the Bloch vector model. After a short introduction covering the basic principles, one-dimensional pulse techniques that can be applied using standard experimental equipment are dealt with. The main areas of application are signal assignment, sensitivity enhancement for measurements on less abundant nuclei, and selective excitation of individual resonances. Subsequently, the various techniques of two-dimensional NMR spectroscopy are treated: these enable shift correlations for different types of nuclei to be made, the presentation of spin multiplets without overlap, and the analysis of geometrical relations as well as of chemical exchange phenomena.

## 1. Introduction

The introduction of pulse Fourier transform methods undoubtedly started a new era of NMR spectroscopy that resulted in an unpredicted and intensive development of new experimental techniques. Whereas at the beginning enhancement of sensitivity was the most important aspect and attention focussed quite naturally on $^{13}C$-NMR spectroscopy, we are now witnessing progress in the NMR spectroscopy of less abundant nuclei[1] and in solid state spectra[2] that nobody would have dreamed of even a few years ago. In addition, NMR spectroscopy of macroscopic systems and NMR imaging techniques have opened completely new applications in physiology and medicine, the potential of which has not yet been fully uncovered[3].

This expansion towards new applications is matched by an equally impressive growth of new experimental techniques which have decisively enlarged the classical repertoire of the NMR spectroscopist and eliminated many of the older CW (continuous wave) techniques. Above all, the more extensive integration of computers into the NMR experiment provided the basis for a large number of investigations that are computer-controlled, since times in the order of ms and μs are involved and the treatment of large quantities of data becomes necessary.

Accordingly, the last few years have seen the development of pulse experiments also in the field of high-resolution NMR spectroscopy, where on the one hand the sensi-

[*] Prof. Dr. H. Günther
FB 8, Organische Chemie II, Universität—Gesamthochschule
Postfach 21 02 09, D-5900 Siegen 21 (Germany)
Dr. R. Benn
Max-Planck-Institut für Kohlenforschung
Kaiser-Wilhelm-Platz 1, D-4330 Mülheim a. d. Ruhr (Germany)

 © Verlag Chemie GmbH, 6940 Weinheim, 1983 0570-0833/83/0505-0350 $ 02.50/0 

tivity problem connected with the NMR measurement of less abundant nuclei was solved and, on the other, spectral information has now become available that was previously difficult to obtain. The potential of these techniques—whose introduction was accompanied by a burgeoning system of shorthand notations not easily deciphered by non-experts—has, however, not yet been fully recognized by the majority of NMR users. The reason for this must be seen both in an insufficient understanding of the physical background and by the fact that these techniques very often have been used for the first time to obtain the NMR spectra of proteins and other macromolecules. While the potential of the new techniques is particularly impressively demonstrated with complicated molecules, the complex structure of these systems and their spectra make the experiments difficult to understand.

In the following progress report an illustrative presentation of the new developments will be given and—using small molecules as examples—we shall try to make the mechanisms of the new pulse techniques and the information they can provide more transparent[4]. In this context the phenomenological presentation of the basic principles within the framework of the Bloch vector model will be emphasized. For obvious reasons a complete literature survey and a comprehensive discussion of the experimental aspects will not be given.

Section 2 deals with *one-dimensional* pulse sequences with different goals (signal assignment, sensitivity enhancement, selective excitation), whereas Section 3 is devoted to *two-dimensional* experiments. Of particular interest here are those techniques that allow correlation of spectral parameters (chemical shifts, spin-spin coupling constants) of different nuclei, for example $^1H$ and $^{13}C$, with the aim of displaying the spectral information without overlap.

### 1.1. The FT-NMR Experiment

Let us first recall the basic principles of the Fourier transform NMR experiment[5]. For the nucleus of interest, the resonance signals of different Larmor frequency present in the spectral window chosen form the so-called *macroscopic magnetization* $\boldsymbol{M}$ of magnitude $M_0$, parallel to the external field $\boldsymbol{B}_0$ (Fig. 1a).

A strong radio frequency field $\boldsymbol{B}_1$, a so-called RF pulse[6], produced by a radio frequency coil on the x-axis, carries $\boldsymbol{M}$ away from the z-axis. The duration and power of the RF pulse determine the direction of $\boldsymbol{M}$ after the pulse. If a so-called $90^\circ_x$ or $\pi/2$ pulse is applied, $\boldsymbol{M}$ points along the positive y-axis (Fig. 1b). The *longitudinal* or *z-magnetization* is thus transformed into a *transverse magnetization*. With the power of the RF sources used in modern spectrometers this process requires 5—20 μs.

The Larmor frequencies of the various nuclear magnetic moments present vary and, as a consequence, the vector $\boldsymbol{M}$ now splits into its components (Fig. 1c). The magnetic vectors rotating in the x,y-plane produce a voltage in the receiver coil that is detected as the NMR signal. If we plot for an individual vector the time dependence of the intensity of its y-component, that is, the voltage, $U$, induced in

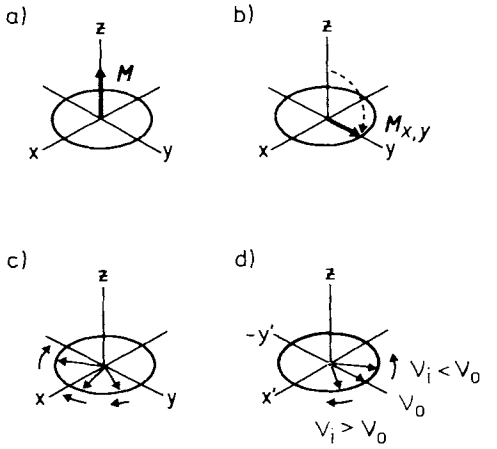



Fig. 1. a) Macroscopic magnetization $\boldsymbol{M}$ in the laboratory frame; b) transverse magnetization $\boldsymbol{M}_{x,y}$ after a $90^\circ_x$ pulse; the effect of pulses is described by the "right-hand rule", where the thumb gives the direction of the pulse and the bent fingers the rotational sense of the magnetization vector; c) Larmor precession of the individual nuclear magnetic moments of different Larmor frequency in the laboratory frame; d) as c), however, in the rotating frame K'(x',y',z) (cf. text).

the receiver coil, and if we take into account transverse relaxation, *i.e.* the loss of transverse magnetization as a consequence of relaxation processes, a damped oscillation of frequency $\nu_i$ results that is known as the *free induction decay* (FID) (Fig. 2).

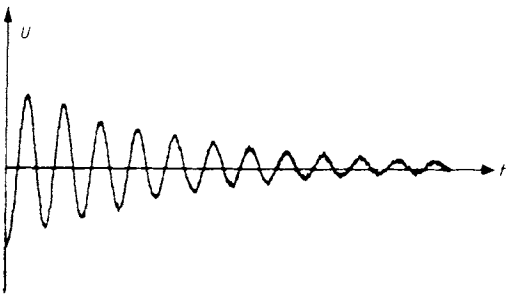



Fig. 2. Free induction decay (FID) or time signal of a NMR line. The damped sine wave is characterized by the time constant $T_2^*$ and the frequency $\nu_i$. $T_2^*$ is the *effective* transverse relaxation time that contains contributions from transverse relaxation and from field inhomogeneity.

Fourier transformation of this time signal yields the well-known NMR signal or spectrum. The frequency measured is the difference between the transmitter or carrier frequency, $\nu_0$, and the Lamor frequency, $\nu_i$, of the particular spin, and is usually in the order of several kHz.

For the description of NMR experiments the concept of the "rotating frame", introduced by *Torrey*[7], is convenient. It uses a coordinate system K' that rotates in the same sense and with the same frequency, $\nu_0$, as the rotating field vector of the RF field. Within the rotating frame vectors that correspond to signals with frequencies $\nu_i > \nu_0$ rotate clockwise, whereas those corresponding to signals with $\nu_i < \nu_0$ rotate anti-clockwise: a signal with $\nu_i = \nu_0$ is static in the rotating frame (Fig. 1d).

Furthermore, it is helpful to remember that each vector is characterized by its Larmor frequency, by its orientation in the rotating frame, and by its lifetime. The Larmor frequency determines the *position of the signal* in the spectrum—that is the chemical shift—whereas the orientation

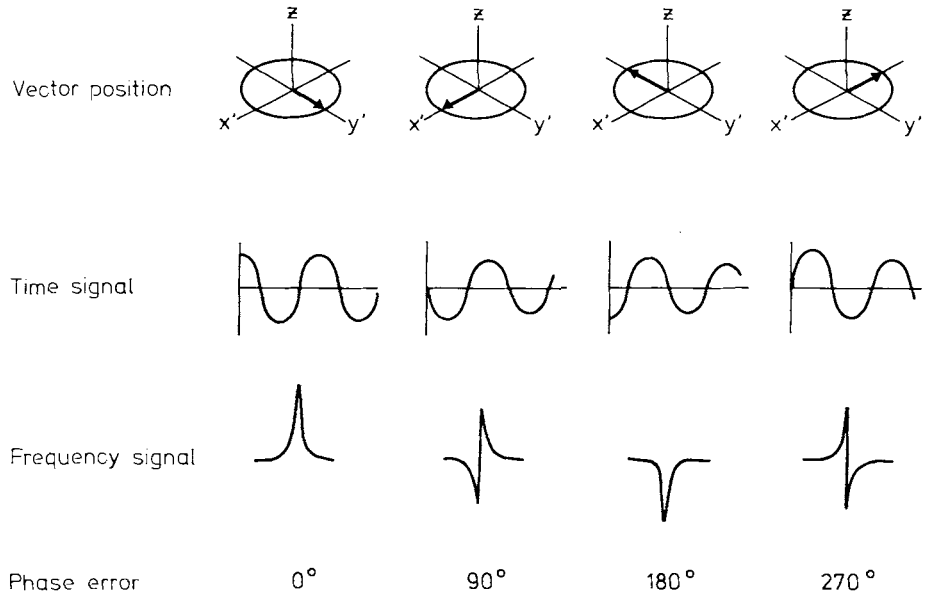



Fig. 3. Precession of transverse magnetization: relation between vector orientation, time signal, frequency signal, and phase error.

at the beginning of data accumulation determines the phase with respect to the rotating frame and, therefore, the *signal phase* (Fig. 3). In this context it is of importance that the detector of the NMR spectrometer is phase-sensitive, since the dispersion signals with phase errors of 90° and 270° can be suppressed. As a consequence, the adjustable detector phase allows the selection of certain components of the transverse magnetization for detection, a vital aspect for many of the pulse experiments to be discussed. Finally, the effective transverse relaxation time $T_2^*$ determines the time dependence of transverse magnetization and, since $\omega_{1/2}=1/\pi T_2^*$, the half-width, $\omega_{1/2}$, of the NMR signal.

### 1.2. The Fate of Transverse Magnetization

In order to understand the principles of the new pulse experiments it is necessary to investigate the time dependence of transverse magnetization more closely. Three effects are important: transverse relaxation, the inhomogeneity of the external magnetic field $\boldsymbol{B}_0$, and spin-spin coupling to neighboring nuclei.

#### *1.2.1. Transverse Relaxation*

Transverse magnetization can be reduced by different relaxation mechanisms. According to $\omega_{1/2}^{(n)}=1/\pi T_2$, the transverse relaxation determines the natural half-width, $\omega_{1/2}^{(n)}$, of the NMR signal. In the following discussion transverse relaxation is always assumed.

#### *1.2.2. Inhomogeneity of the $B_0$ Magnetic Field*

Within the framework of the classical macroscopic description of the NMR experiment, not only is the macroscopic magnetization $\boldsymbol{M}$ a sum of components, but also each individual vector $\boldsymbol{v}_i$ is the vector sum of the various nuclear magnetic moments that have the same chemical environment, and therefore precess with the same Larmor frequency. Since inhomogeneity of the external field $\boldsymbol{B}_0$ cannot be avoided, the ideal situation that all nuclear magnetic moments experience the same field strength $\boldsymbol{B}_0$ does not hold. Rather, the local field varies over the sample volume ($\boldsymbol{B}_{\text{local}}=\boldsymbol{B}_0\pm\Delta\boldsymbol{B}$). After excitation, the individual vectors $\boldsymbol{v}_i$ fan out since, according to the resonance condition $\nu_i=\gamma\boldsymbol{B}_{\text{local}}$, those in areas with $\boldsymbol{B}_{\text{local}}>\boldsymbol{B}_0$ rotate faster and those in areas with $\boldsymbol{B}_{\text{local}}<\boldsymbol{B}_0$ slower than the average. It is easy to appreciate that this process causes transverse magnetization to finally disappear (Fig. 4). The effect of field inhomogeneity is taken into account by introducing an *effective* transverse relaxation time, $T_2^*$, that contains contributions from true relaxation as well as from inhomogeneity. In practice, field inhomogeneity makes by far the most

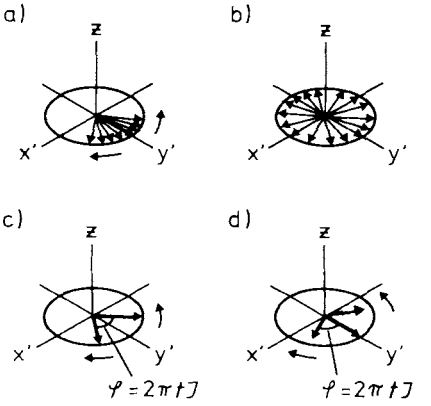



Fig. 4. a) Fanning-out of the transverse magnetization in the rotating frame K' as a consequence of the inhomogeneity of the external field $\boldsymbol{B}_0$; b) after time $T_2^*$ the vector sum in the x,y-plane is zero; c) transverse magnetization of nucleus A under the influence of scalar spin-spin coupling to a neighboring X nucleus (AX system); d) transverse magnetization of nucleus A under the influence of scalar spin-spin coupling to two neighboring $X_2$ nuclei ($AX_2$ system). In the case of c) and d) the frequency of the A nucleus was chosen as the frequency for the rotating frame. The precessional frequencies of the components of the multiplet are, therefore, $\pm\frac{1}{2}J$ and $+J, 0, -J$, respectively; relaxation and inhomogeneity effects are neglected.

important contribution to the disappearance of transverse magnetization and, therefore, to the line-width in high-resolution NMR spectroscopy.

### *1.2.3. Spin-Spin Coupling*

If a nucleus A experiences scalar spin-spin coupling to a neighboring nucleus X[8], the excitation is followed by a separation of its transverse magnetization $M^{A}_{x,y}$ into different vectors corresponding to the various components of the spin multiplet. This situation is depicted in Figures 4c and 4d for a doublet and a triplet, respectively. Spin decoupling causes the vectors of a multiplet to be static within the rotating frame, since their Larmor frequencies become identical if $\nu_A = \nu_0$. The momentary y-magnetization of the vectors is thus "frozen in" by the application of a decoupler field $B_2$, and the magnetization detected at $\nu_A$ is the resultant of the y-components of the individual vectors.

## 1.3. The Spin Echo Experiment

For most of the new pulse methods the spin echo experiment[9] is of central importance. If the fanning-out process of the individual magnetic vectors after the initial 90°$_x$ pulse described above has proceeded for a time $\tau$, the vectors can be inverted by the application of a 180°$_x$ pulse. Since the rotational sense of their motion is unchanged, the vectors refocus along the negative y-axis and a spin echo signal is recorded after time $2\tau$. The amplitude of the signal now differs from the initial value only through true relaxation losses (Fig. 5).

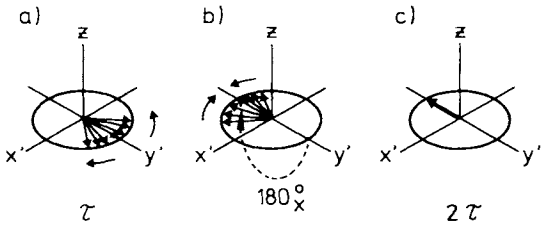



Fig. 5. The spin echo experiment; a) state of the transverse magnetization at time $\tau$ after the 90°$_x$ exitation pulse; b) effect of the 180°$_x$ pulse; c) state of the transverse magnetization after time $2\tau$; since for the pulse width $t_p \ll \tau$ holds (typical values are $t_p = 20$ µs, $\tau = 5$ ms), changes of the spin system during the pulse can be neglected.

It follows that the spin echo experiment causes cancellation of all effects that result from different Larmor frequencies—including those of chemical shifts—and that lead to a fanning-out of the macroscopic transverse magnetization after the exciting pulse. A simple experiment serves to demonstrate this.

For this purpose we use the well-known frequency-dependent phase error that results during the FT experiment if data collection is delayed to a time $t_0$ after the exciting pulse[10]. Due to their divergent Larmor frequencies the precession of the individual magnetic vectors in the rotating frame has progressed by different amounts and the phases of the corresponding NMR signals differ (Figs. 6a and b). If we now apply a 180°$_x$ pulse at $t_0$ and start data collection at $2t_0$, the phase difference is eliminated since the vectors refocus within the second $t_0$ period (Figs. 6c and d).

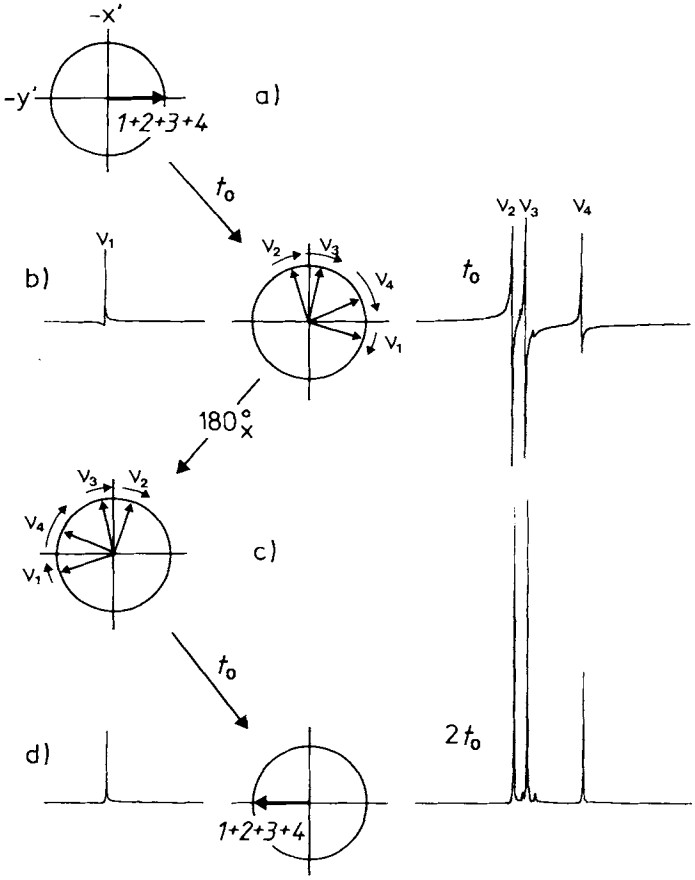



Fig. 6. Phase correction by a spin echo experiment for the aromatic $^{13}C$ resonances of ethylbenzene; a) situation after excitation; b) after a time $t_0$ the precession of the individual components of the macroscopic magnetization around the field axis has progressed by distinct amounts as a consequence of their different Larmor frequencies. Data collection yields a spectrum with frequency-dependent phase errors; c) a 180°$_x$ pulse at $t = t_0$ inverts the vector system and after $t = 2t_0$ again leads to superposition, the spin echo. The phase differences in the experimental spectrum vanish (d). In order to obtain an absorption mode spectrum an additional phase correction of 180° was applied in case d).

A situation distinct from that described above is met if spin-spin coupling to a neighboring nucleus occurs. Since the pulse methods to be discussed almost exclusively rest on the effect of spin-spin coupling, we shall treat this aspect in more detail using the example of a two-spin system. Several situations have to be distinguished.

For a *homonuclear* AX-system the 180°$_x$ pulse is not selective, *i.e.* it is felt by the A as well as by the X nucleus. Within the vector diagram this means that the multiplet vectors are reflected on the x,y-plane: Inversion is accompanied by a change of rotational sense, since the 180°$_x$ pulse also interchanges the spin states of the neighboring nucleus. Refocussing to the spin echo is not observed (Fig. 7a).

In the *heteronuclear* case, *e.g.* with an AX-system consisting of a $^1H$ and a $^{13}C$ nucleus, two variants are possible. If we observe the $^{13}C$ resonance and apply a 180°$_x$ pulse at this frequency, refocussing occurs and—as in the case of the chemical shift—a spin echo is detected after a time $2\tau$

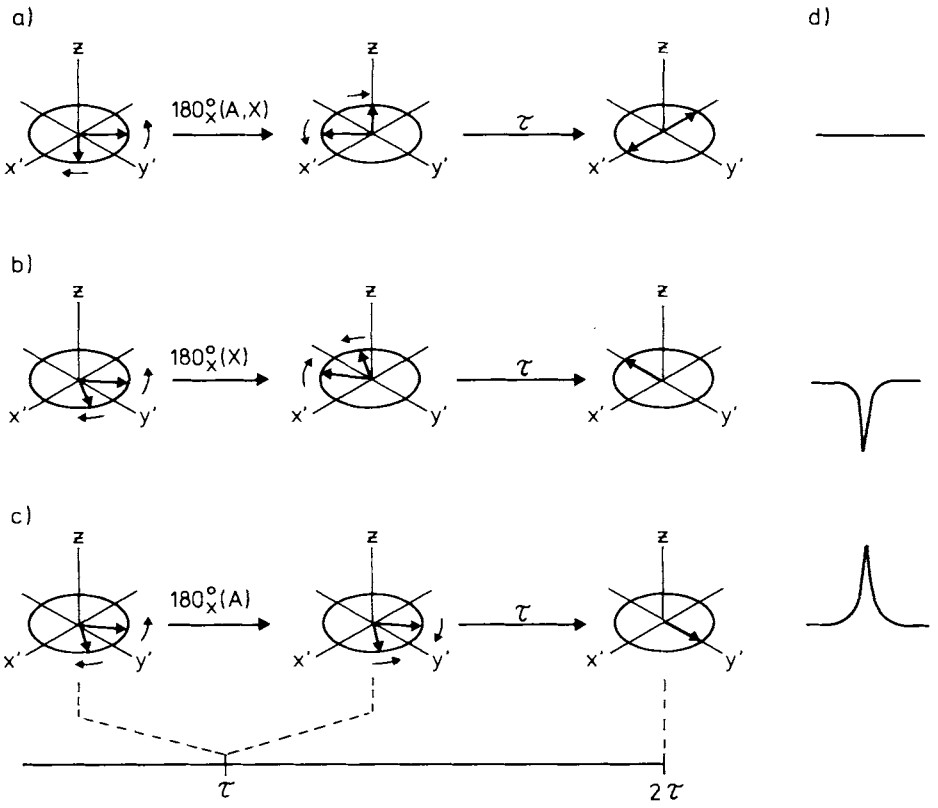



Fig. 7. Spin echo experiment with an AX system; vector diagram for the X nucleus; a) homonuclear case; b) heteronuclear case with $180^\circ_x$ pulse for the X nucleus; c) heteronuclear case with $180^\circ_x$ pulse for the A nucleus; d) X echo at $t=2\tau$ with simultaneous A decoupling.

(Fig. 7b). On the other hand, a $180^\circ_x$ pulse at the frequency of the A nucleus changes the rotational sense of both X vectors and, after a time $2\tau$, also leads to a spin echo signal, whose phase, however, differs by 180° (Fig. 7c). Finally, two $180^\circ_x$ pulses applied simultaneously to the A and X regions lead to a situation that corresponds to that described for the homonuclear case.

These considerations can now be completed by taking into account the effect of inhomogeneity. For each individual X vector in Figure 7 it results in an additional fanning-out process that can, however, be cancelled out by a selective $180^\circ_x$ pulse at the X nucleus. Only the experiments shown in Figures 7a and 7b thus lead to a refocussing of the effects of inhomogeneity and of chemical shifts, which can be treated in the same way as the previously mentioned frequency-dependent phase errors. This is an important practical aspect, since the carrier frequency $\nu_0$ normally is not identical with the Larmor frequency of the X nucleus as has been assumed until now in the simplified treatment presented here.

### 1.4. The Evolution Time

The most important feature of the new pulse experiments is the so-called *evolution time*, $t_1$, during which the spin system—in some cases under the influence of further pulses—evolves. However, the spin system has to be prepared for evolution, and the evolution time is therefore preceded by the *preparation time*. Data collection starts at the end of the evolution period with the *detection time* (Fig. 8)[11].

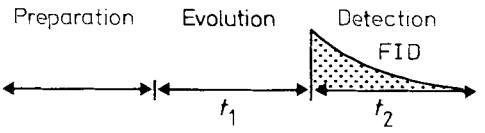



Fig. 8. Time sequence of modern pulse experiments [11].

These time sequences allow the state of the spin system at the start of the detection period to be varied and, therefore, affect the informational content of the whole experiment. For this purpose suitable pulses, whose effects on the magnetization vectors have been discussed earlier, can be used, but, in addition, scalar spin-spin interactions, which can be applied periodically by gating the decoupler channel, are of importance. Alternatively, dipolar couplings or the magnetization transfer between nuclei of different Larmor frequencies arising from dynamic processes can be used. Very often a spin echo sequence is a direct or indirect part of the experiment, which secures that at the end of the evolution period the effects of chemical shifts and of field inhomogeneity are refocussed. In other words, as far as these effects are concerned the spin system is in the same situation when data collection starts as it is in the normal FT experiment directly after the excitation pulse.

## 2. One-Dimensional Pulse Sequences

### 2.1. SEFT[*]: Assignment of $^{13}C$-NMR Signals

The modulation of transverse magnetization through spin-spin coupling[12,13] can be used in a simple manner in $^{13}C$-NMR spectroscopy *via* spin echo experiments with gated $^1H$-decoupling to distinguish between signals of quarternary C atoms, and CH, $CH_2$, and $CH_3$ groups[14–23]. In the case of large molecules this method is superior to the well-known off-resonance $^1H$-decoupling experiment, where strong overlap of partially decoupled multiplets makes the assignment difficult or even impossible. In its simplest form, known as SEFT[14], it yields singlets that differ by 180° in their phase.

The SEFT pulse sequence, which relies on spin echo modulation through $^1J(^{13}C,^1H)$ coupling is shown in Figure 9. The $^1H$-decoupler is active during the first half of

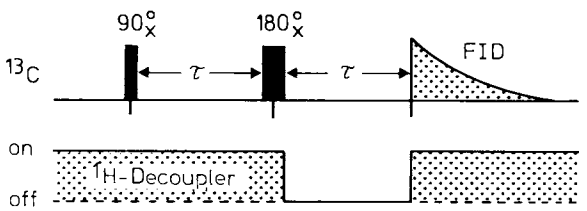



Fig. 9. The SEFT pulse sequence [14].

the spin echo sequence and during data acquisition. In the second $\tau$ period transverse $^{13}C$ magnetization is modulated through spin-spin coupling to the protons. The vector diagrams relevant for the correct choice of time interval $\tau$ are shown in Figure 10. Neglecting relaxation effects, the $\tau$-dependence of the receiver signal, $I$, for CH, $CH_2$, and $CH_3$ groups can be described by a cosine dependence:

$$I(\mathrm{CH}) = I_0 \cos(\pi\tau J)$$
$$I(\mathrm{CH_2}) = \tfrac{1}{2} I_0[1+\cos(2\pi\tau J)]$$
$$I(\mathrm{CH_3}) = \tfrac{1}{4} I_0[3\cos(\pi\tau J)+\cos(3\pi\tau J)]$$

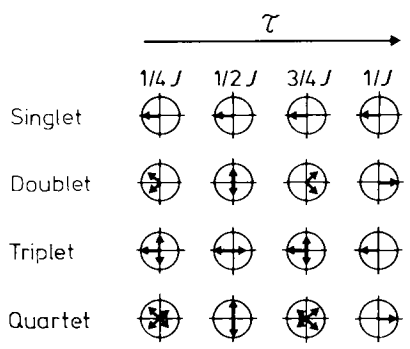



Fig. 10. Vector diagrams for the transverse magnetization of simple first-order spin multiplets for quarternary C atoms, and CH, $CH_2$, and $CH_3$ groups and their dependence on the evolution period $2\tau$. The diagram shows the situation after the 180°x pulse, where the $^1H$-broadband decoupler is switched on again. In the rotating frame the vectors are static and the receiver detects the sum of their y components. For $\tau = 1/J$ the signal phase alternates by 180°, for $\tau = 1/2J$ only the signals of quarternary carbon atoms are detected.

[*] SEFT = *s*pin *e*cho *f*ourier *t*ransform.

The graphical representation (Fig. 11) facilitates the choice of an appropriate $\tau$-value.

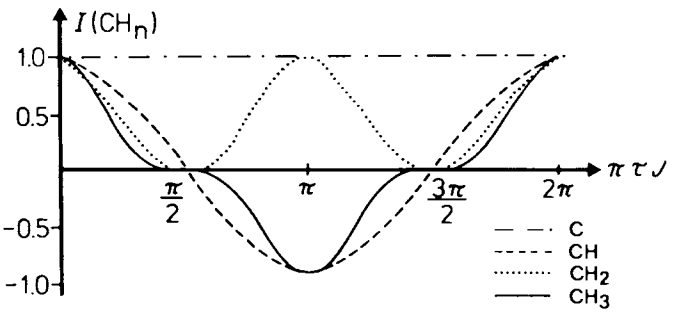



Fig. 11. Time dependence of $^1J(^{13}C,^1H)$-modulated $^{13}C$ magnetization for quarternary C atoms, and CH, $CH_2$, and $CH_3$ groups [21].

As seen from Figure 11, with $\tau = 1/J$ it is possible in only *one* experiment to distinguish between signals of quarternary and methylene C atoms, on the one hand, and those of methine and methyl carbons on the other, since for both groups of resonances a phase difference of 180° exists. The signals of quarternary C atoms and those of $CH_2$ groups have a positive, and those of CH and $CH_3$ groups a negative phase. A further experiment with $\tau = 1/2J$ only yields signals arising from quarternary C atoms. To be able to distinguish CH and $CH_3$ resonances different proposals exist[14–21], none of which, however, is fully satisfactory, since the situation is complicated by changes in the $^1J(^{13}C,^1H)$ values. According to Figure 11, the region $\pi/2 \mp 20\%$ should be appropriate for identifying CH resonances on the basis of their relative intensities and positive or negative phase, respectively (Figure 12).

A practical disadvantage of the SEFT sequence may be seen in the use of 90° pulses, which call for relatively long relaxation delays between individual pulse cycles, and consequently lead to low repetition rates for data accumulation and an increase in the total measurement time. *Patt* and *Shoolery*[22] have eliminated this limitation by the introduction of an additional $\Delta$-180°x-$\Delta$ sequence ($\Delta \approx 1$ ms) which inverts the negative z-magnetization resulting from smaller flip angles.

The application of the SEFT pulse sequence with $^1H$- and $^2H$-decoupling provides an interesting possibility of eliminating the signals from deuterated solvents which often complicate $^{13}C$-NMR spectra. As can be derived from the appropriate vector diagrams for $\tau = 1/3\,^1J(^{13}C,^2H)$ the sum of the y-components of the multiplet lines for CD, $CD_2$, and $CD_3$ groups is zero. Accordingly, the signals of these groups can be eliminated if $^2H$-decoupling is used[24]. An application is given in Figure 13. SEFT pulse sequences that make use of $^2H$- and/or $^1H$-decoupling can also be applied to the analysis of deuterated and partially deuterated compounds, since they allow the $^{13}C$ signals of C, CH, $CH_2$, $CH_3$, CHD, $CHD_2$, $CH_2D$, and $CD_3$ groups to be distinguished[25,26].

Finally, *Bolton*[27] has described a method that can be used to simplify $^1H$ spectra, since only singlets and the central triplet lines are observed. As shown in Figure 10, these lines are independent of the evolution period in a

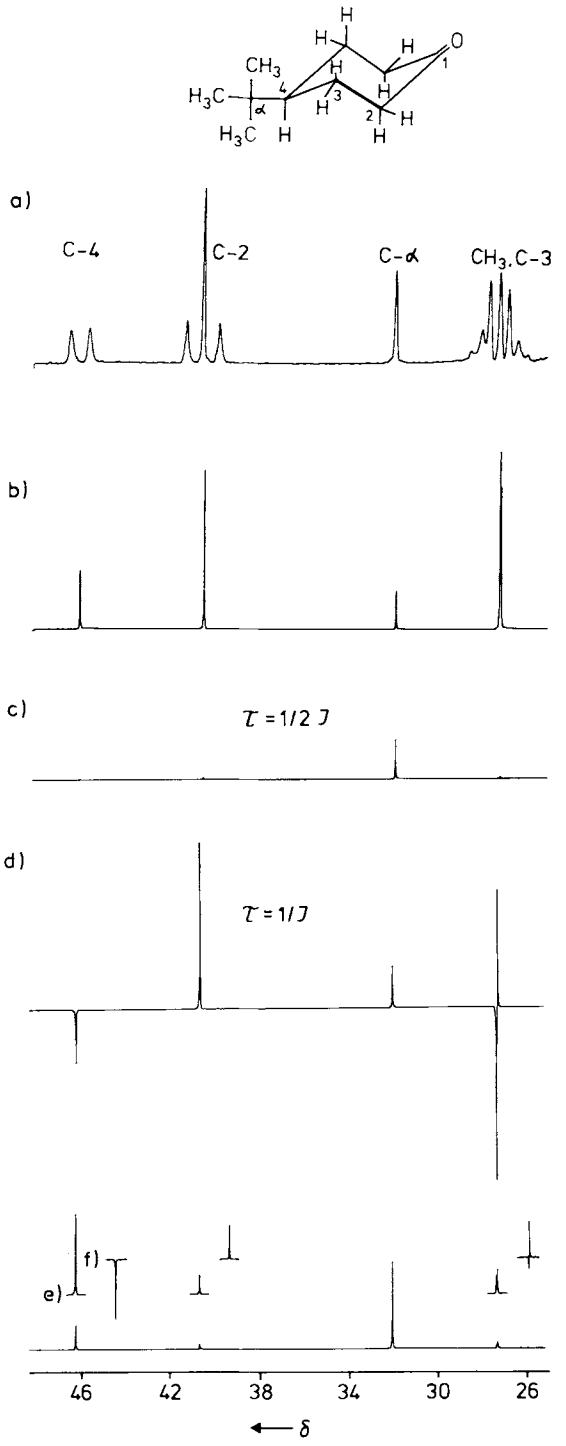



Fig. 12. SEFT experiment on 4-*tert*-butylcyclohexanone; 100.6 MHz $^{13}$C-NMR spectrum, aliphatic region: a) "off-resonance" $^1$H-decoupled; the resonances of C-3 and $CH_3$ are superimposed at $\delta = 27$. b) $^1$H broadband-decoupled. c) SEFT spectrum with $\tau = 1/2J$ ($J = 125$ Hz, $\tau = 4$ ms) for the detection of the resonance of the quarternary carbon $C_\alpha$. d) SEFT spectrum with $\tau = 1/J$ (8 ms); besides the $C_\alpha$ resonance only the signals of $CH_2$ groups show positive phases. The signals superimposed at $\delta = 27$ are now clearly differentiated through phase selection. e) SEFT spectrum for the distinction of CH and $CH_3$ resonances with $\tau = 3.52$ ms. This corresponds to a phase angle of 79° and, according to Figure 11, the signal with the highest relative intensity must be assigned to the methine resonance. An experiment with $\tau = 4.44$ ms ($\theta = 100°$) confirms this (f).

spin echo experiment. By varying $\tau$ in a series of n experiments and summing up the time signals, all absorptions except those mentioned should be averaged out. This has been verified experimentally when n is as low as 4.

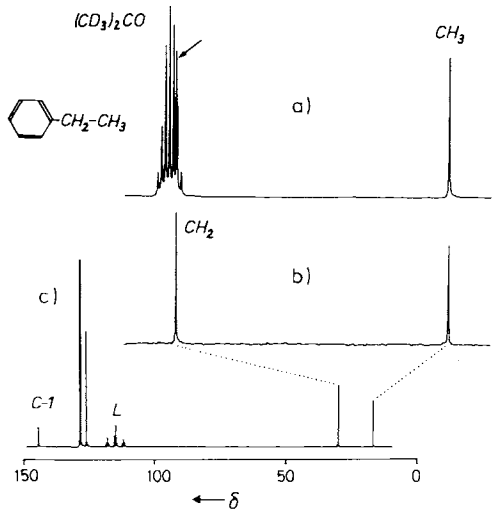



Fig. 13. Elimination of $^{13}$C-NMR signals of [D$_6$]acetone in the spectrum of ethylbenzene; a) superposition of the solvent signal with the signal of the $CH_2$ groups; b) complete elimination of the solvent signal; c) total spectral region; at L, signals of $^{19}$F lock compound 1,2-dibromotetrafluoroethane [24].

## 2.2. Signal Enhancement Through Polarization Transfer

Low sensitivity has always been a shortcoming of NMR spectroscopy. Today, however, the use of high $B_0$ fields and fast data accumulation made possible by the application of the Fourier transform technique have solved this problem for protons and other nuclei with relatively large magnetic moments, such as $^{19}$F, $^{203}$Tl, $^{205}$Tl, and $^{31}$P, in almost 95% of the cases met with in practice. With the exception of $^3$H, however, all other NMR active nuclei are less sensitive than the nuclei mentioned above, and this situation is very often aggregated by low natural abundance and long relaxation times. Methods for enhancing the sensitivity, therefore, continue to be of great importance.

### 2.2.1. *The SPI[*] Experiment*

Let us discuss a two-spin system consisting of a sensitive and an insensitive nucleus, *e.g.* $^1$H,$^{13}$C or $^1$H,$^{15}$N, where the population of the energy levels in equilibrium is given by the Boltzmann law

$$N_q/N_p = \exp(\Delta E/kT) = \exp(-\gamma\hbar B_0/kT) \approx 1 - \frac{\gamma\hbar B_0}{kT}$$

The population difference between two states $E_q$ and $E_p$ is therefore determined by the gyromagnetic ratio $\gamma$ of the nucleus that changes its spin state during the transition $E_p \rightarrow E_q$. For states involving the sensitive nucleus (A, large $\gamma$) a larger population difference results than for those of the less sensitive nucleus (X, small $\gamma$) (Fig. 14).

If through a selective population inversion involving an A transition the respective spin populations are interchanged, the energy level diagram of Figure 14b results, which now shows enhanced absorption and emission for the X transitions. The Boltzmann distribution that deter-

[*] SPI = *s*elective *p*opulation *i*nversion.

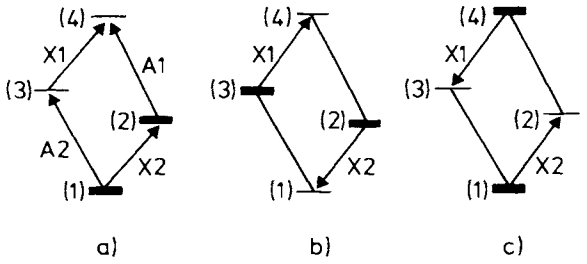



Fig. 14. Population of the energy level diagram of an AX system consisting of a sensitive nucleus (A) and a less sensitive nucleus (X). a) Equilibrium state (the population differences for the X nucleus have been neglected); b) perturbed equilibrium after selective population inversion between the states (1) and (3); for the X lines enhanced absorption (X1) and emission (X2) result; c) as b), however for the states (2) and (4); X1 shows emission and X2 enhanced absorption.

mined the spin populations for the sensitive nucleus now governs those of the less sensitive nucleus. This phenomenon is known as *polarization transfer*.

Experimentally, population inversion can be achieved through a $180^{\circ}_{x}$ pulse applied at the frequency of an A line. Within the framework of Fourier transform methods, however, special techniques are required for selective pulses (see Section 2.4). Yet it proved possible to use the $^1$H-decoupler for this purpose[28].

The method, which became known as the SPI or SPT[*][29] experiment, was first performed with the $^{13}$C,$^1$H spin system of chloroform[28]. It is easily carried out if the $^{13}$C doublet is recorded with the $^1$H-decoupler applied at the frequency of one of the $^{13}$C satellite lines immediately before the $^{13}$C pulse (Fig. 15). The decoupler pulse then leads to a population inversion between those $^1$H levels that are connected by the respective satellite line.

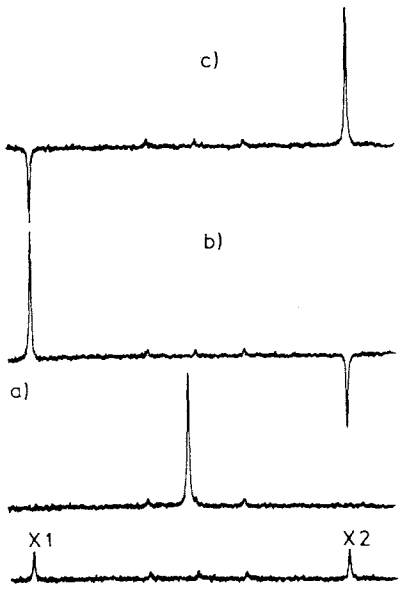



Fig. 15. The SPI experiment with $CHCl_3$ [28]; a) $^1$H-decoupled and $^1$H-coupled $^{13}$C-NMR spectrum; b) and c) with population inversion as Figs. 14b and 14c, respectively.

The SPI experiment is important for signal assignments[30] as well as for measurements of insensitive nuclei[31-34]. In addition, just as the INDOR[**] experiment in CW-NMR spectroscopy, it can be used to determine the relative signs of coupling constants and for spectral analyses[35-40]. Of most general interest is the possibility of sensitivity enhancement of $^1$H-coupled spectra of less abundant nuclei ($^{13}$C[31,33], $^{15}$N[34], $^{29}$Si[32]). The increase in intensity for a first-order $A_nX$-spin system ($A = {}^1H$, $X = {}^{13}C$) is given by comparison with the Pascal triangle, which describes the normal intensity distribution (Fig. 16). An important limitation of the SPI method, however, is to be seen in the fact that only *one* line at a time in the $^1$H spectrum can be perturbed.

| a) | n | b) |
|---|---|---|
| 1 | 0 | 1 |
| 1 1 | 1 | -3 5 |
| 1 2 1 | 2 | -7 2 9 |
| 1 3 3 1 | 3 | -11 -9 15 13 |
| 1 4 6 4 1 | 4 | -15 -28 6 36 17 |
| 1 5 10 10 5 1 | 5 | -19 -55 -30 50 65 21 |
| 1 6 15 20 15 6 1 | 6 | -23 -90 -105 20 135 102 25 |

Fig. 16. Line number and relative intensities for the X multiplet of an $A_nX$ group ($A = {}^1H$) for a Boltzmann distribution (a) and after selective population inversion over one degenerate A line (b) [31].

### 2.2.2. *The INEPT[***] Pulse Sequence*

A crucial step forward was possible after it was recognized that polarization transfer can also be achieved *non-selectively* through a proper pulse sequence[41]. The INEPT method[42] introduced by *Morris* and *Freeman* has this advantage and goes beyond the limits of the SPI experiment.

The basic pulse sequence of the INEPT method is shown in Figure 17 together with the translation into a vector diagram.

The important elements are the modulation of the transverse magnetization of the sensitive nucleus (A) through coupling to the less sensitive nucleus (X) and the simultaneous application of two $180^{\circ}_{x}$ pulses in the A and X frequency regions. The vector arrangement obtained after the evolution period $2\tau$ for the doublet components of the A nucleus can be transformed into the characteristic arrangement of a selectively inverted spin system through application of a $90^{\circ}_{y}$ pulse. Within the energy-level diagram this corresponds to a population inversion of one A line and leads to polarization of the X lines. An example is given in Figure 18 with the $^{15}$N-NMR spectrum of 9-methylpurine. The evolution period of the INEPT pulse sequence is based on one particular AX coupling constant and must be estimated if $J$(A,X) is not known. For $^{15}$N-NMR spectroscopy of unsaturated heterocycles the geminal $^{15}$N,$^1$H coupling constants, which are in the order of 10 Hz ($\tau = 1/40$ s), are suitable for this purpose[43,44]. If NH or $NH_2$ groups are also present, then a second experiment with $\tau = 1/4\,{}^1J({}^{15}N,{}^1H)$ ($\approx 1/250$ s) must be performed.

Typical for INEPT NMR-spectra that display spin-spin coupling is the zero intensity of the central lines of odd

[*] SPT = selective *p*opulation *t*ransfer.

[**] INDOR = *in*ternuclear *do*uble *r*esonance.

[***] INEPT = *i*nsensitive *n*uclei *e*nhanced by *p*olarization *t*ransfer.

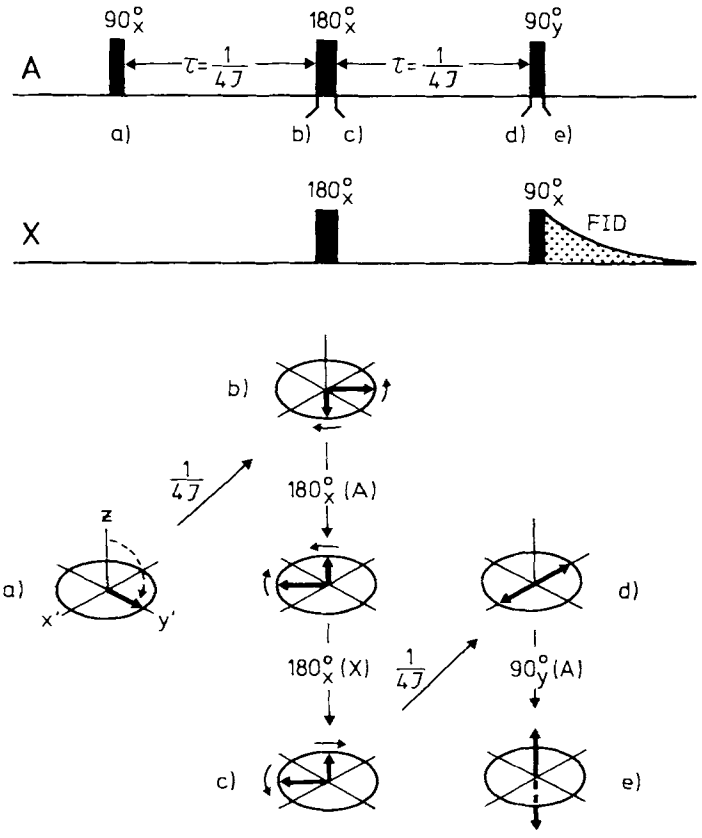



Fig. 17. Pulse sequence of the INEPT method [42] for an AX system (*e.g.* A = $^{1}$H, $^{19}$F, or $^{31}$P; X = $^{13}$C, $^{15}$N, or $^{29}$Si). The vector diagram shows only the A magnetization in the rotating frame ($\nu_0 = \nu_A$). After 90°$_x$ excitation (a) the transverse magnetization of the nucleus A is modulated by spin-spin coupling to the less sensitive nucleus X. After time $\tau = 1/4J$ a phase difference of 90° exists between both doublet vectors (b). A 180°$_x$ pulse in the A as well as in the X frequency region leads to the vector diagram (c) so that after time $2\tau$ state (d) is reached. A 90°$_y$ pulse now inverts the magnetization of one proton line (e). This corresponds to selective population inversion. The polarization of the spin system is detected by a 90°$_x$ pulse in the frequency region of the less sensitive nucleus, whose lines show emission or enhanced absorption. Refocussing is achieved by an additional spin echo sequence, for a doublet 1/4*J*-180°$_x$(A,X)-1/4*J*. The X resonance can then be detected as a positively polarized doublet or—with simultaneous $^{1}$H decoupling during the detection period—as a singlet.

multiplets as well as the inversion of half of the multiplet lines (NH: −1, +1; $NH_2$: −1, 0, +1; $NH_3$: −1, −1, +1, +1). The integrated total intensity of a multiplet in the INEPT spectrum is therefore zero. An additional pulse sequence allows the signals to be refocussed with correct phase so that normal multiplets are observed, or singlets when the protons are decoupled[45,46].

The success of a polarization transfer experiment is determined largely by the relaxation time of the sensitive nucleus: this determines the time necessary for the perturbed spin system to return to the equilibrium state, and must be long enough to prevent reestablishment of the normal Boltzmann distribution during the pulse sequence. Therefore, prolongation of the measurement, as in the refocussing experiment is very often accompanied by sensitivity losses; in the case of macromolecules with short $^{13}$C-$T_2$ and $^{13}$C-$T_1$ values that are shorter than those of the respective protons, the method may even fail[47]. On the other hand, since sensitive nuclei, such as $^{1}$H or $^{19}$F have appreciably shorter relaxation times than *e.g.* $^{13}$C, the repetition rate during data accumulation can be much higher than the less sensitive nucleus would otherwise permit. The total measurement time is therefore reduced; for $^{15}$N measurements, typically by a factor of 2—3.

A further important aspect is that the intensity enhancement in suitable cases can be much larger than that obtained with the well-known nuclear Overhauser effect (NOE). Furthermore, negative $\gamma$ values are not a disadvantage because sensitivity enhancement for NOE experiments is governed by the sum $1+\gamma_A/2\gamma_X$[48], whereas for polarization transfer experiments the ratio $\gamma_A/\gamma_X$ is important[31,33,42]. An additional cumulative effect is observed for degenerate lines.

Interesting INEPT experiments with metal nuclei have been carried out by *Brevard et al.*[49,50]: here protons (for $^{109}$Ag and $^{103}$Rh[49]), but also $^{31}$P nuclei (for $^{57}$Fe, $^{103}$Ru, and $^{183}$W[50]) were used as polarization sources. $^{29}$Si{$^{1}$H} and $^{119}$Sn{$^{1}$H} experiments have been reported by *Doddrell et al.*[51].

Table 1. Maximum signal enhancement factors, $\eta_{NOE}$ and $\eta_{INEPT}$, for nuclear Overhauser and INEPT experiments, respectively, with X{$^{1}$H} spin systems.

| X | $^{11}$B | $^{13}$C | $^{15}$N | $^{29}$Si | $^{57}$Fe | $^{103}$Rh | $^{109}$Ag | $^{119}$Sn | $^{183}$W |
|---|---|---|---|---|---|---|---|---|---|
| $\eta_{NOE}$ | 2.56 | 2.99 | −3.94 | −1.52 | 16.48 | −16.89 | −9.75 | −0.41 | 13.02 |
| $\eta_{INEPT}$ [a] | 3.12 | 3.98 | 9.87 | 5.03 | 30.95 | 31.77 | 21.50 | 2.81 | 24.04 |

[a] For $^{19}$F or $^{31}$P as polarization source (A) these data are reduced by the factor 0.941 ($\gamma_{^{19}F}/\gamma_{^{1}H}$) and 0.407 ($\gamma_{^{31}P}/\gamma_{^{1}H}$), respectively.

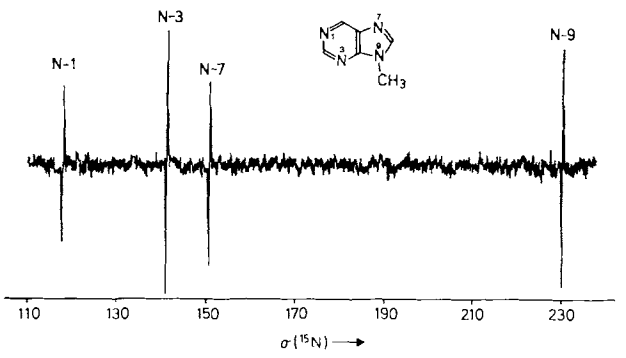



Fig. 18. INEPT-$^{15}$N-NMR spectrum of 9-methylpurine [44]. Frequency 40.53 MHz, 6293 transients, spectral width 6024 Hz, total acquisition time 4.75 h. The $\sigma$-scale refers to external $CD_3{}^{15}NO_3$.

### 2.2.3. *The DEPT[*] Pulse Sequence*

A pulse sequence which is somewhat less critical to the choice of the A,X coupling constant and which yields X multiplets without the artefacts involving relative intensity and line number observed with the INEPT method was recently proposed by *Doddrell et al.*[52]. The method, called DEPT, is characterized in Figure 19: compared to INEPT it differs in the $\tau$-value, which is now $1/2J$, and in the variable length $t_p$ of the last $^{1}$H pulse.

Polarization transfer methods can also be employed for the assignment of resonance signals[53], and the DEPT se-

[*] DEPT = *d*istortionless *e*nhancement by *p*olarization *t*ransfer.

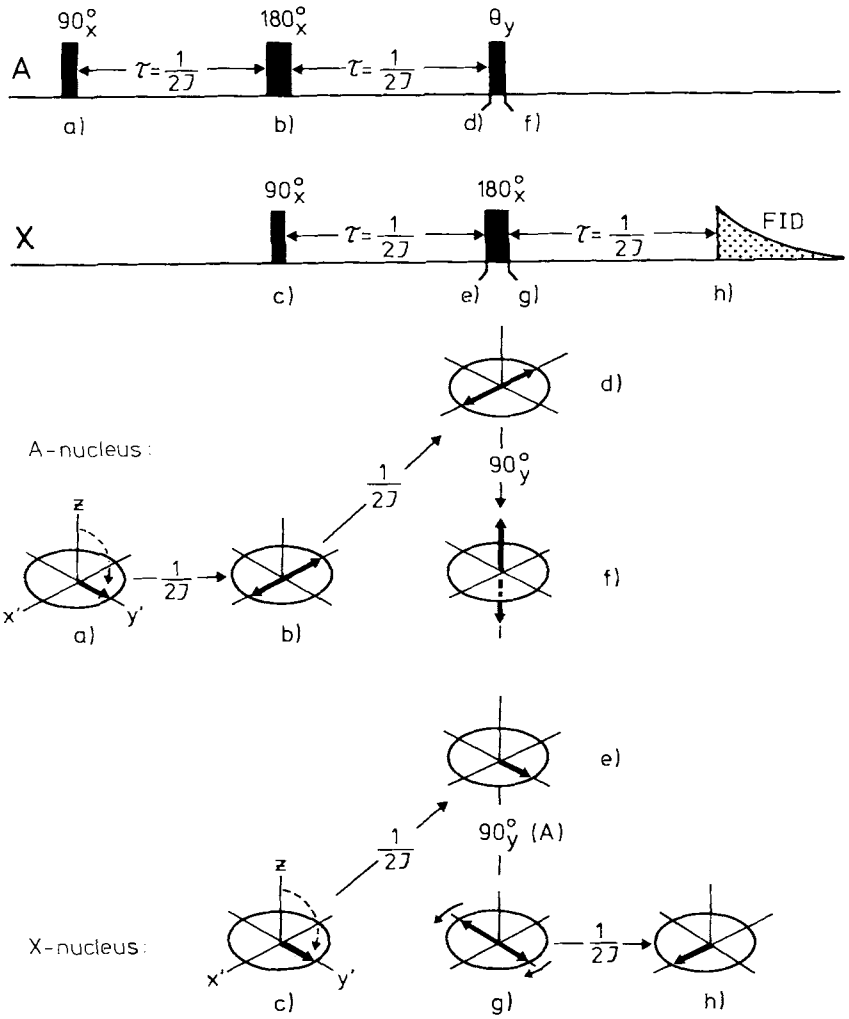



Fig. 19. DEPT pulse sequence [52] and vector diagram for an AX system. After the first 90°$_x$ pulse (a) the transverse A magnetization is modulated through coupling to the X nucleus. After time $\tau = 1/2J$ a phase difference of 180° exists between both doublet vectors (b). A 180°$_x$ pulse in the A region is used for refocussing inhomogeneity contributions. At the same time, a 90°$_x$ pulse in the X region creates transverse $^{13}C$ magnetization (c). Since neither A nor X z-magnetization is present, A and X are practically decoupled. During the next period, $1/2J$, both vectors are static in their rotating frames (d and e, respectively). At $t = 2\tau$ a 90°$_y$ pulse in the A region ($\theta = 90°$) polarizes the A magnetization (f). At the same time this causes polarization of the X magnetization (g). The reestablished z-magnetization in the region of the A nucleus leads *via* spin-spin coupling to refocussing of the X vectors in the last $1/2J$ period (h). X magnetization can now be detected with uniform phase as a doublet or—with simultaneous A decoupling—as a singlet at $t = 3\tau$. If the 90°$_y$ pulse in the A region is neglected, the DEPT pulse sequence consists of two spin echo sequences in the A and X regions, respectively, that are mutually shifted in time. If, on the other hand, the second $\tau$ period and the 180°$_x$ refocussing pulses are eliminated, the INEPT pulse sequence is obtained.

quence seems especially well suited for this purpose[54]. For $^{13}C$-NMR spectra the phase properties of the magnetization of quarternary C atoms and CH, $CH_2$, and $CH_3$ groups were studied and it was shown that pulse angles $\theta$ of $\pi/4$, $\pi/2$, and $3\pi/4$, respectively, for the last $^1H$ pulse enable subspectra to be edited for CH, $CH_2$, and $CH_3$ groups. For the detection of $CH_2$ and $CH_3$ groups, difference spectra must be used. An example is shown in Figure 20.

Other authors have described the selection of $^{13}C$ satellites in $^1H$-NMR spectra[56] and of signals of deuterated carbons in $^{13}C$-NMR spectra[57] using polarization transfer methods. In addition, the INEPT sequence has been used for spin-lattice relaxation time measurements of $^{13}C$[58], $^{29}Si$[59], $^{15}N$[59,60], and was also applied to nuclei with spin quantum numbers $I > 1/2$[61,62]. The advantages and disadvantages of the INEPT and DEPT sequences as well as improvements of these methods for the detection of $^1H$-coupled multiplets in the normal absorption mode have been described recently by *Sørensen* and *Ernst*[63].

### 2.3. INADEQUATE[*]: Determination of $^{13}C,^{13}C$ Spin-Spin Coupling Constants in Molecules with Natural $^{13}C$ Abundance

Spin-spin coupling constants between $^{13}C$ nuclei[64] are of great interest with respect to questions of structure and

[*] INADEQUATE = *i*ncredible *n*atural *a*bundance *d*ouble *qua*ntum *t*ransfer *e*xperiment.

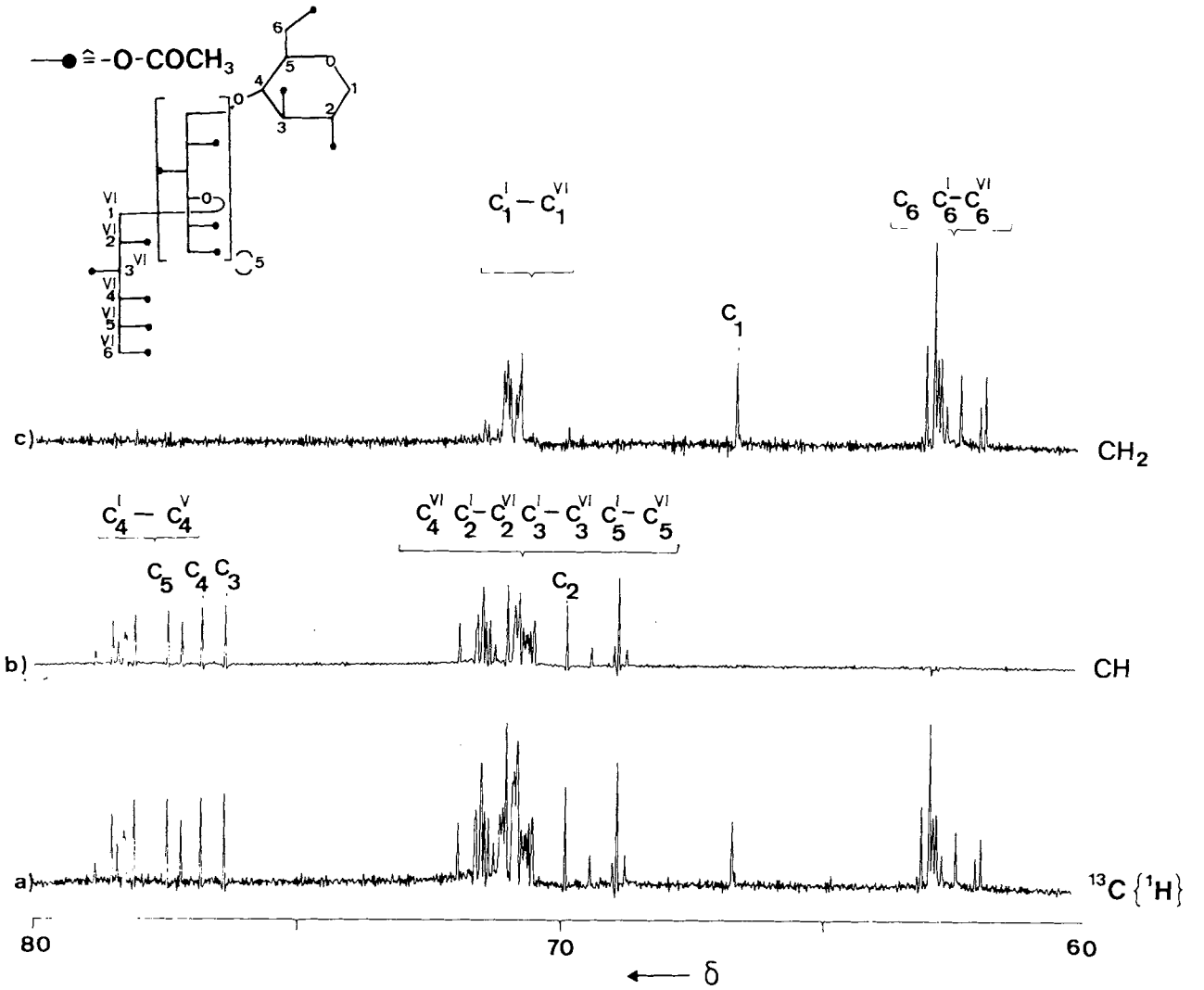



Fig. 20. DEPT $^{13}$C-NMR spectra of a polysaccharide [55]; a) decoupled at 100.6 MHz, $\delta_{TMS}$ scale. For the DEPT sequence the selection of CH and $CH_2$ resonances was achieved with $J = 145$ Hz ($\tau = 3.448$ ms); b) experiment with the phase angle $\theta = 90°$ (see below) for the selective detection of the CH resonances; c) difference spectra of two experiments with phase angles $\theta = 45°$ and 135°, respectively, for the selective detection of $CH_2$ resonances. It would have been difficult to analyze the region around $\delta = 70$ ppm on the basis of a conventional "off-resonance" $^1$H-decoupled spectrum. Signal selection with the DEPT pulse sequence requires measurement of 4 different spectra with pulse angles of $\theta_1 = 45°$, $\theta_2 = 90°$, $\theta_3 = 135°$, and $\theta_4 = 90°$, respectively, for the last $^1$H-pulse using the same number of transients. For the different types of signals the following relations hold[54]: $S(CH)$: $S(\theta_2) + S(\theta_4)$; $S(CH_2)$: $S(\theta_1) - S(\theta_3)$; $S(CH_3)$: $S(\theta_1) + S(\theta_3) + 0.707[S(\theta_2) + S(\theta_4)]$.

bonding in organic chemistry since they yield information directly related to the carbon skeleton of the compound studied. The $^1J(^{13}C,^{13}C)$ data are of particular value because of their dependence on the hybridization of the carbon[64,65] and consequently on the type of CC bond. Furthermore, they can be used to establish connectivities between carbon atoms[66], a central aspect for structure determination which was recognized relatively late, despite successful biochemical studies using $^{13}$C,$^{13}$C double labeling techniques[67]. The reason for this must certainly be seen in the experimental difficulties that prevent routine determination of $^{13}$C,$^{13}$C coupling constants.

The necessary condition for the observation of $^{13}$C,$^{13}$C coupling constants is the presence of two anisochronous $^{13}$C atoms in a molecule. Because of the low natural abundance of $^{13}$C (1.1%) this condition is, however, met only for few molecules in the sample ($\approx 0.011\%$). Line splittings as a result of $^{13}$C,$^{13}$C couplings are present in the $^{13}$C-NMR spectrum only as weak satellites accompanying the intense signals of molecules with one $^{13}$C atom; in particular, small coupling constants are difficult to measure. Since synthetic enrichment is possible only in a few exceptional cases, experimental methods which facilitate the measurement of $J(^{13}C,^{13}C)$ data are of interest.

The pulse sequence INADEQUATE developed by *Freeman et al.*[68] for this purpose is based on the idea that by suitable treatment of the spin system consisting of the AX system of the coupled $^{13}$C nuclei and the intense signal of the parent compound with only one $^{13}$C, the main signal can be suppressed. This is clearly possible if a 90° phase difference exists between the transverse magnetization of the satellites and that of the main signal that allow the selection of the AX magnetization for detection. The pulse sequence shown in Figure 21 achieves this goal. It contains as an important new phenomenon step (d), the so-called *double-quantum coherence*[69].

As shown by *Ernst*, the pulse sequence $90°_x$- $\tau$ -$90°_x$ allows double quantum transitions within the framework of the

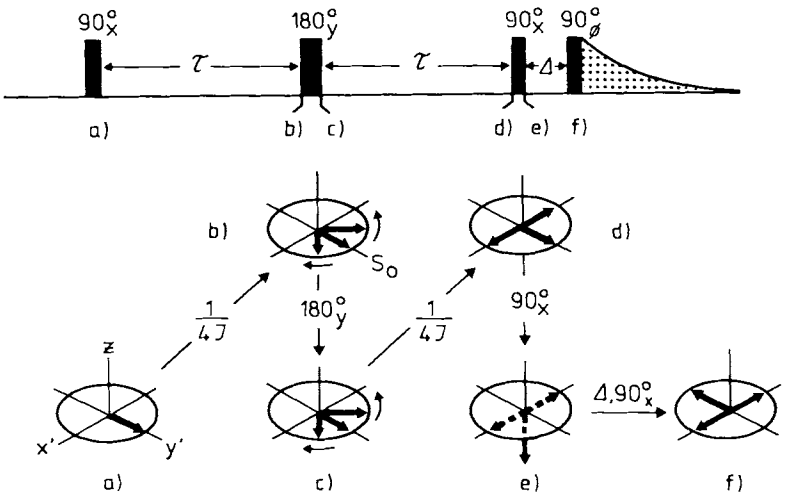



Fig. 21. Pulse sequence of the INADEQUATE experiment[68]. After the initial 90°$_x$ pulse (a) $^{13}C,^{13}C$ coupling leads to a fanning-out of the $^{13}C$ satellites of the A nucleus, which after $\tau = 1/4J$ have a phase difference of 90°, whereas the magnetization $S_0$ of the main signals of molecules with only one $^{13}C$ nucleus is static on the y axis (b). The non-selective 180°$_y$ pulse leaves the rotational sense of the satellites unchanged (c), and after the time $2\tau$, a phase difference of 180° results (d). During this time the main signal retains its direction along the a axis; respective inhomogeneity contributions are refocussed by the 180°$_y$ pulse. The second 90°$_x$ pulse generates double-quantum coherence that cannot be detected directly and directs $S_0$ in the z direction (e). After a short delay $\Delta$ (10 μs), transverse magnetization of the $^{13}C$ satellites is transformed into detectable magnetization by a 90° pulse of variable phase (f) (see Table 2). The doublet components have opposite phase. An additional spin echo sequence $1/4J$- 180°$_x$ - $1/4J$ can be used for refocussing. $^1H$-broadband decoupling is applied during the whole experiment.

Fourier transform method to be excited[70]. This possibility is utilized here, since the 180°$_y$ pulse is only introduced to refocus chemical shift and inhomogeneity contributions. After generation of double quantum coherence, a third 90° pulse of variable phase $\phi$ is applied to prepare the AX magnetization for detection. As shown in Table 2, the detector phase is properly adjusted so that only the AX magnetization can be received.

Table 2. Phase shifts for the selective detection of $^{13}C,^{13}C$-satellites by the INADEQUATE sequence [68] (cf. Fig. 21).

| $\phi$ [a] | $S_0$ [b] | S [c] | $\Psi$ [d] |
|---|---|---|---|
| +x | −y | +x | +x |
| +y | +x | −y | −y |
| −x | +y | −x | −x |
| −y | −x | +y | +y |

[a] Phase of read pulse; [b] Phase of main signal; [c] Phase of satellite magnetization; [d] Detector phase.

The result of an INADEQUATE experiment is shown in Figure 22 for ($\eta^5$-cyclopentadienyl)-$\eta^1,\eta^2$-2,2-dimethyl-3-butenylnickel. Here, an additional $1/4J$-180°$_x$-$1/4J$ sequence[68] was employed to produce absorption signals. The selection of $^{13}C,^{13}C$ coupling constants is achieved by varying the time interval, $\tau$, given by $\tau = 1/4J(^{13}C,^{13}C)$. In the case of unknown compounds $\tau$ must be estimated from the data of similar systems. For the detection of $^{13}C,^{13}C$ coupling constants of different magnitude, a number of experiments with different $\tau$ values are necessary; however, in many cases one $\tau$ value is sufficient to detect two or more coupling constants that differ in magnitude, since the general expression for $\tau$ is given by $(2n+1)/4J(^{13}C,^{13}C)$ $(n = 0, 1, 2)$[71].

If, for an unknown compound the $^1J(^{13}C,^{13}C)$ coupling constants have been determined, the resonances of neighboring C atoms can be assigned through recurrent splittings. The analysis of the spectral data is best carried out using a computer[73]. Since individual C atoms can be recognized with respect to their bonding by the characteristic position of their resonance signals, carbon-carbon connectivity[74] determined by $^1J(^{13}C,^{13}C)$ coupling yields valuable information about chemical structures. The analysis of carbon-carbon linkages is therefore an important area of application for the INADEQUATE pulse sequence, in spite of the fact that a gain in sensitivity is not achieved. In this respect, however, the increasing use of superconducting magnets has a positive effect regarding the amount of compound required, as well as on the total measurement time.

If the delay given in Figure 21 is treated as an additional evolution period, it is possible to detect individual AX systems selectively, since different double quantum frequencies can be used for detection[75]. In this way the assignment of $^{13}C$ resonances and further coupling constants with other nuclei that might be present can be achieved. The selection of AX systems and other signals on the basis of double quantum coherence has also been reported for $^1H$-NMR spectra[76–78].

For non-first order systems (AB) the INADEQUATE sequence is less suitable, and this case has been treated separately[79]. The combination of INADEQUATE with INEPT, which is of interest with regard to sensitivity enhancement, has been described[80] as well as signal selection with the help of $^{13}C,^1H$ coupling constants[81]. Furthermore, the one-dimensional INADEQUATE experiment has been transformed into a two-dimensional experiment by using a variable evolution period (see Section 3.5).

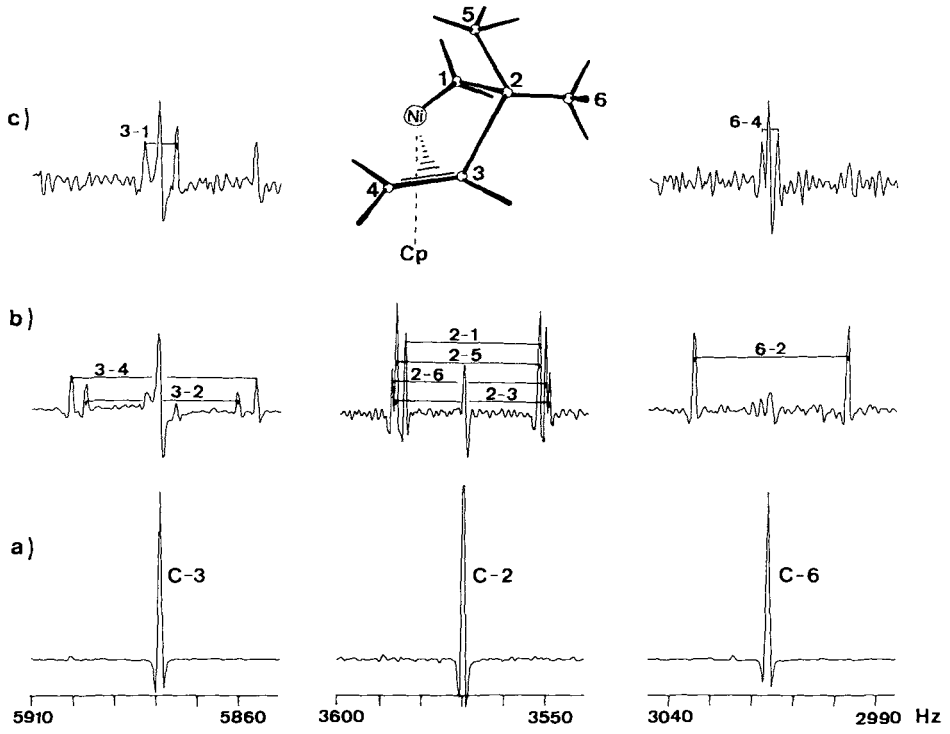



Fig. 22. Use of the INADEQUATE pulse sequence for the determination of $^{13}C,^{13}C$ coupling constants of ($\eta^5$-cyclopentadienyl)-$\eta^1,\eta^2$-2,2-dimethyl-3-butenylnickel [72]; a) signals of C atoms 3, 2, and 6; b) INADEQUATE spectra with $\tau = 6.2$ ms corresponding to $^1J(^{13}C,^{13}C) \approx 40$ Hz; c) as b) with $\tau = 0.08$ s corresponding to geminal and vicinal $J(^{13}C,^{13}C)$ coupling constants; spectral width 5000 Hz, 1600 transients, FID-Gauss multiplication. The result was $^1J(1,2) = 32.1$, $^1J(2,3) = 37.1$, $^1J(2,5) = 34.7$, $^1J(2,6) = 37.1$, $^1J(3,4) = 44.7$, $^2J(1,3) = 8.5$, $^3J(4,6) = 3.2$ Hz.

### 2.4. DANTE[*]: Selective Excitation of $^{13}C$-Resonances

Since pulse excitations are polychromatic, the FT technique has the disadvantage that selective observation of spectral regions is difficult or impossible. Frequency folding leads to problems, and intense solvent lines that may cause data overflow or cover low-intensity signals of interest are not easily eliminated. The possibilities of decreasing the spectral window by suitable frequency filters are limited, and the development of alternative methods for selective excitation was desirable. The techniques proposed[82], known as *tailored excitation*, use excitation functions adapted to the problem under consideration. The necessary software, however, is relatively complicated and practical applications have been rare.

A powerful technique for the selection of individual resonances, which is especially well suited for the analysis of $^1H$-coupled $^{13}C$-NMR spectra where strong overlap of individual multiplets is frequently observed, was introduced by *Freeman et al.*[83]. The idea is that a single $^{13}C$ resonance, whose frequency is determined in the $^1H$-decoupled spectrum, is selectively excited by a special pulse modulation of the RF frequency. $^1H$-coupling is allowed during FID detection, so that the fully coupled multiplet of the $^{13}C$ nucleus in question is recorded without disturbance through overlap with other resonances.

The basis of this method, which is termed DANTE[84], is pulse excitation through a pulse train characterized by small pulse delays $t_r$ and small pulse angles $\alpha$. Such an RF pulse modulation corresponds to a frequency spectrum with sidebands spaced by $1/t_r$, which relative to the pulse frequency $\nu_0$ appear at $\nu_0 \pm 1/t_r$, $\nu_0 \pm 2/t_r$ *etc.*, and which can be regarded as selective pulse transmitters. The correct choice of the transmitter frequency and the repetition rate $t_r$ allow the selective excitation of individual resonances (Fig. 23).

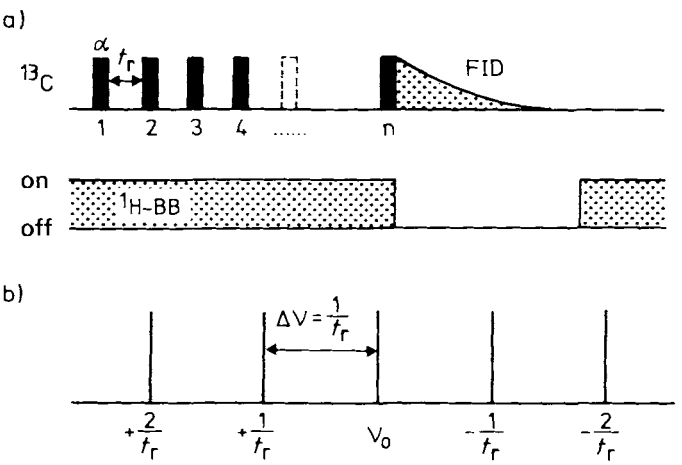



Fig. 23. DANTE pulse sequence for selective excitation of $^{13}C$ resonance [83]. After Fourier transformation small pulse spacings $t_r$ (a) yield the frequency spectrum shown in (b). Using the center band or the first sideband, $^{13}C$-resonances can be selectively excited with simultaneous application of $^1H$ decoupling; $^{13}C,^1H$ coupling is allowed during detection, which results in the measurement of NOE enhanced multiplets. The number of pulses n is chosen in such a way that for the pulse angle, $\alpha = 90°/n$ holds. At the end of the pulse sequence, therefore, a 90° pulse is achieved and the signal intensity at the start of data acquisition is at its maximum. Typical values are $t_r = 2$ µs, $n = 200$, $\alpha = 0.45°$.

[*] DANTE = *d*elays *a*lternating with *n*utation for *t*ailored *e*xcitation.

An application of the DANTE technique is shown in Figure 24 with the $^1$H-coupled $^{13}$C-NMR spectrum of the aromatic carbons of triptycene[85]. At 100.6 MHz the high-field and low-field components of the C-β and C-α multiplets, respectively, are superimposed (Fig. 24a). Selective excitation allows each multiplet to be observed and analyzed separately (Fig. 24b).

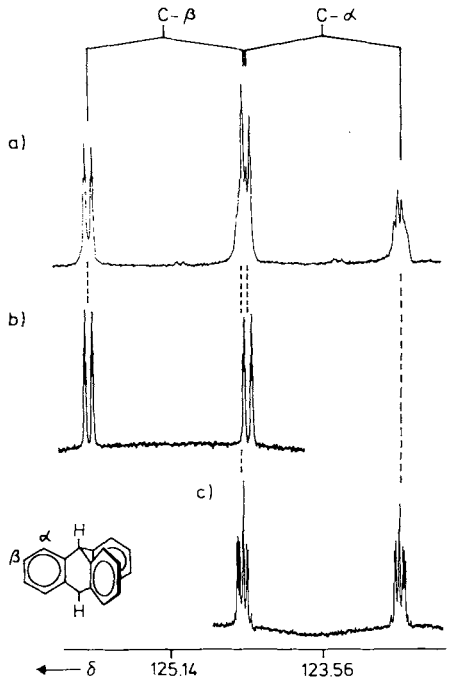



Fig. 24. $^1$H decoupled 100.6 MHz $^{13}$C-NMR spectrum of the aromatic carbon atoms of triptycene [85]; a) conventional spectrum with partial multiplet overlap; b) and c) selective excited C-β and C-α resonances, respectively, with selective decoupling of the benzylic protons. Spectral analysis yields the following $^{13}$C,$^1$H coupling constants: C-α: $^1J = 158.63$, $^2J = 1.54$, $^3J = 8.13$, $^4J = -1.20$ Hz; C-b: $^1J = 159.15$, $^2J_\alpha = 1.13$, $^2J_{\beta'} = 1.32$, $^3J = 7.32$ Hz.

Besides such applications in spectral analysis, the DANTE sequence is a valuable aid for kinetic measurements of reversible first-order reactions on the basis of the saturation transfer method introduced by *Hoffmann* and *Forsén*[86,87]. A detailed discussion of this aspect is given by *Freeman*[83b].

### 2.5. Super Pulse Cycles for Broadband Decoupling

Today, $^1$H-broadband decoupling is a necessary requisite for spectra simplification and intensity enhancement in NMR spectroscopy of heteronuclei. In this respect the increasing use of high-field spectrometers is not without problems, since the enlarged $^1$H-spectral region requires more powerful $^1$H-decouplers. A method recently proposed by *Freeman et al.*[88] is therefore of interest, since it allows the decoupler power to be dissipated over a large frequency range. The basis is again the spin echo experiment (see Fig. 25). As shown in Figure 25a, using a simple diagram for a $^{13}$C, $^1$H pair, detection of $^{13}$C magnetization at intervals $2\tau$, $4\tau$, $6\tau$, *etc.* yields the data of a decoupled multiplet if a 180° ($^1$H) pulse is applied at $\tau$, $3\tau$, $5\tau$, etc. The fact that the doublet components of the X nucleus possess different Larmor frequencies is not "sensed" by the receiver, since magnetization is only sampled when both vectors are superimposed. From Figure 25 it is seen that the receiver detects the spin echo as a non-coupled time signal.

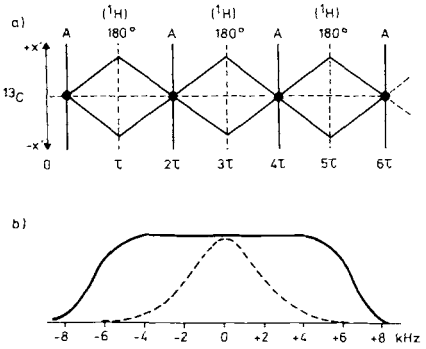



Fig. 25. a) Time dependence of transverse $^{13}$C magnetization of a CH fragment upon application of a sequence of 180° pulses in the $^1$H-spectral region. Data are collected at A and complete $^1$H decoupling is achieved. b) Comparison of the band width of the decoupler field for a conventional modulation technique (curve, ---) and the pulse method described (curve, —). In practice the method described, which is known as MLEV, uses phase cycles for the $^1$H pulses. The choice of the most appropriate phase cycle is presently being investigated [88].

The important practical aspect of this spin-flip method is the fact that, for a given decoupler power, the decoupled spectral region in the $^1$H-NMR spectrum is a factor of 3 larger than that obtained by use of conventional broadband-decoupling modulation techniques (noise modulation, square-wave modulation, *etc.*) (Fig. 25b). This also renders the method interesting for $^{19}$F or $^{31}$P broadband decoupling, since the chemical shift range of these nuclei is much larger than that of protons. Furthermore, maintaining the same frequency region the power of the $B_2$ field can be reduced and the danger of heating the sample is diminished. The nuclear Overhauser effect is established before $^{13}$C excitation. The technique also permits partial decoupling and thus scaling of the respective coupling constants.

## 3. Two-Dimensional (2D-) NMR Spectroscopy

The common feature of the experiments discussed so far was the time sequence *preparation—evolution—detection* shown in Figure 8, where the receiver signal $S(t_2)$ is solely a function of the detection time $t_2$. The same time diagram also forms the basis of two-dimensional NMR spectroscopy[89,90] (2D-NMR); however, with the important difference that the evolution time $t_1$ within a sequence of pulse cycles is now a variable. If over n experiments we increase each evolution period $t_1$ by a constant time increment $\Delta t_1$, the receiver signal will also become dependent on $t_1$. It is thus a function of $t_1$ *and* $t_2$: $S(t_1,t_2)$. Two time-variables imply, however, that the data can be Fourier-transformed twice, *i.e.* with respect to $t_2$ and $t_1$. As a consequence, two frequency variables $F_1$ and $F_2$ are also obtained.

Two-dimensional FT-NMR spectroscopy is always possible if a systematic variation of the evolution period results in a periodic change of a property of the spin system at the end of the evolution time[11]. For example, the origin may be a scalar spin-spin coupling with another nucleus that can be switched on or off by decoupler control during

the evolution period[11,91]. For the signal, which is again decoupled in the detection period, an amplitude- or phase-modulation results. As shown in Figure 26, the first Fourier transformation with respect to $t_2$ yields n conventional spectra, whose data points on the time axis $t_1$ define the modulation frequency, which can be determined by a second Fourier transformation. If, for example, scalar spin-spin coupling during the evolution time results in an amplitude- or phase-modulation through variation of $t_1$, the frequency parameters chemical shift and spin-spin coupling can be separated by a two-dimensional experiment, since the first Fourier transformation with respect to $t_2$ yields the resonance frequency and the second Fourier transformation with respect to $t_1$ the modulation frequency, *i.e.* the coupling constant.

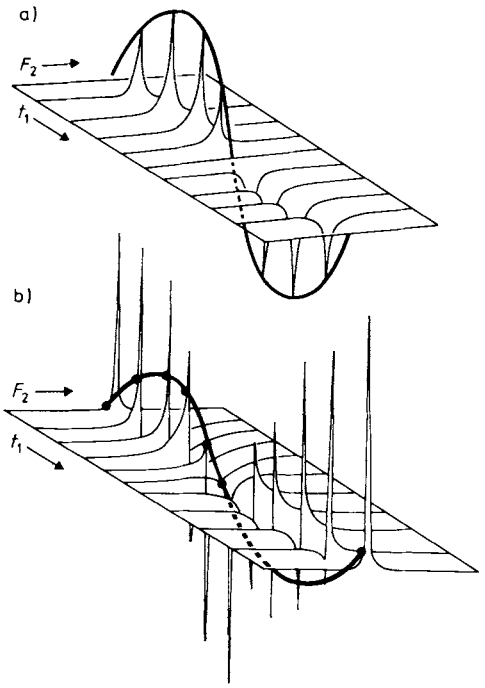



Fig. 26. Two-dimensional NMR spectroscopy through amplitude and phase modulation (a, b, respectively). The figure shows the situation after the first Fourier transformation. The modulation of the signals results from a periodic perturbation of the spin system during the evolution period. Repeated Fourier transformation of the time signal $S(t_1)$ yields the frequency $F_1$.

These relations will be described again for the particular case of a $CH_n$ fragment. We excite the $^{13}C$ resonance with a $90^\circ_x$ pulse and collect the signal information after a variable evolution time $t_1$ with complete proton decoupling[91]. The $t_1$-dependent spin-evolution for a CH and $CH_2$ fragment (doublet and triplet, respectively) is shown in Figure 27. The important point here is that, despite proton decoupling, the coupling information is retained in the detection period, since during the evolution time coupling leads to a periodic change of the amplitude of transverse $^{13}C$ magnetization. The time-domain functions for the doublet and triplet are different, since that of the triplet oscillates at twice the frequency[92] and is positively shifted by a constant amount which results from the central triplet line. Fourier transformation yields in the first case a doublet with lines at $-J/2$, and in the second case a triplet, whose outer lines lie at $\pm J$. This example shows that the $t_1$-dimension contains the scalar coupling constant as an inde-

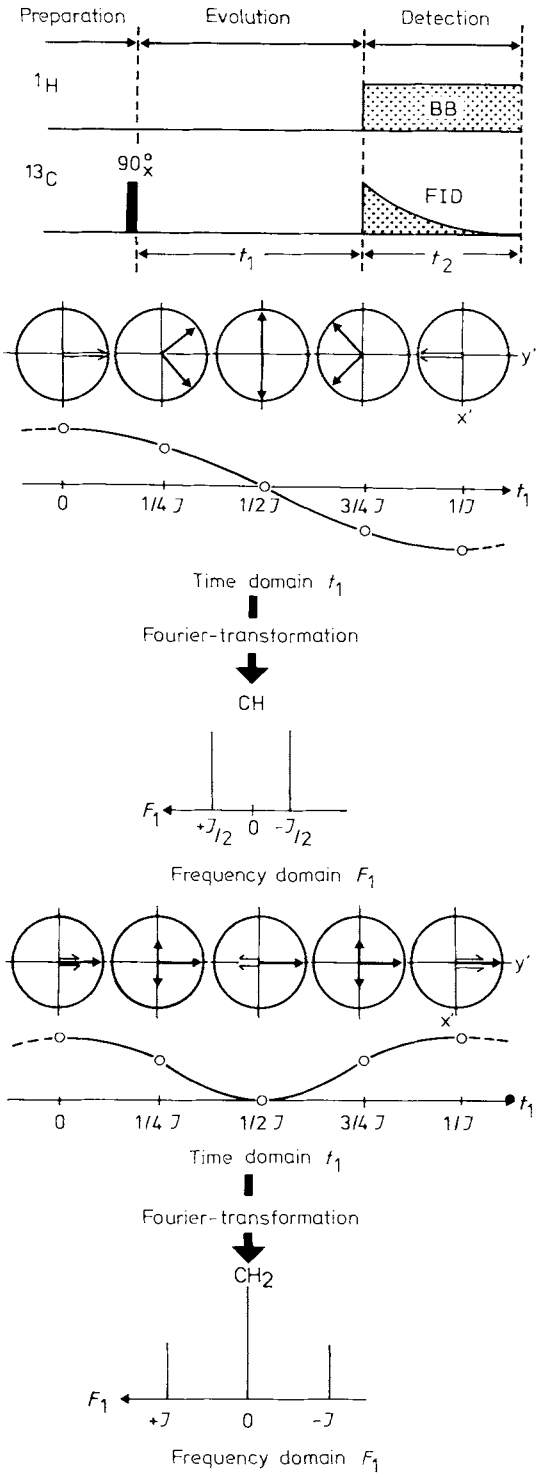



Fig. 27. Simplified time sequence and vector diagram for a *J*-resolved 2D-NMR experiment using the examples of a CH and a $CH_2$ fragment. The vector diagrams in the rotating frame, which has the Larmor frequency of the $^{13}C$ nucleus, show the situation of transverse $^{13}C$ magnetization at the end of the evolution period. $^1H$ decoupling during detection leads to registration of the respective y-components, whose amplitude is modulated as $\cos(\pi J t_1)$ in the case of CH groups, and as $\frac{1}{2}[\cos(2\pi J t_1)+1]$ in the case of $CH_2$ groups. Fourier transformation of the time functions $S(t_1)$ thus defined yields on the $F_1$-axis the frequencies $\pm J/2$ and $+J$, $O$, $-J$, respectively, *i.e.* a doublet and a triplet, since the amplitude-modulated signals can be represented as the sum of two phase-modulated signals of different sign; *e.g.*, for a doublet, $\cos\pi J t_1 = \frac{1}{2}\exp(-i\pi J t_1) + \frac{1}{2}\exp(i\pi J t_1)$ holds. This is equivalent to resolution of the sum $J$ (or $2J$) into its components $\pm\frac{1}{2}J$ (or $\pm J$). The time function $S(t_1)$ of the $CH_2$ fragment is positively shifted by the constant contribution of the center triplet line. Fourier transformation of this constant yields the signal in the center of the $F_1$ axis.

pendent parameter, whereas the chemical shifts are stored in the $t_2$-dimension.

### 3.1. Classification of 2D-Pulse Experiments

In principle, two classes of two-dimensional experiments exist: *J-resolved* and *correlated* 2D spectra. The first type, from which the example discussed above was taken, is characterized by one frequency axis ($F_1$), containing the coupling information, and by another ($F_2$), containing the chemical shifts. In the second type, both frequency axes contain chemical shifts. The connection between the $F_1$ and $F_2$ axes is established through scalar coupling—homonuclear as well as heteronuclear—or through dipolar coupling.

Since two-dimensional NMR spectroscopy is a logical development that starts with the one-dimensional techniques described in the previous section, most 1D experiments can be transformed into 2D experiments by varying the evolution period, and nearly all two-dimensional experiments possess a one-dimensional analog. In Table 3 we have summarized, using a $^{13}C,^1H$ spin system as example, the most important 2D techniques that will be discussed in the following sections, together with the 1D experiments related to them.

corded under the normal conditions for data accumulation. This means that the total acquisition time for the individual $S(t_2)$ signal should not exceed 0.5 h, and for measurements with less sensitive nuclei relatively concentrated samples are necessary[94].

The time-domain signals in the $t_2$ dimension, $S(t_2)$, are transformed by the first Fourier transformation with respect to $t_2$ into the data matrix $S(t_1, F_2)$, where corresponding points on the $F_2$ axis define the time domain function $S(t_1)$. The second Fourier transformation with respect to $t_1$ completes the process $S(t_1,t_2) \rightarrow S(F_1,F_2)$ (Fig. 28). Since even a single Fourier transformation results in a cosine and sine component of the frequency domain signal, phase selection for 2D experiments is relatively complicated.

This problem can be dealt with by using absolute value display, such as is also known for 1D spectra[5]. In this case the signal intensity as a function of the frequency $F_1$ is given by[90]

$$S(F_1) = (u^2 + v^2)^{1/2}$$

where $u$ and $v$ are the cosine and the sine parts, respectively, of the transformed time-domain function. For 2D spectra the following equation holds:

$$S(\pm F_1, F_2) = [(uu \mp vv)^2 + (uv \pm vu)^2]^{1/2}$$

Table 3. Comparison of two-dimensional and one-dimensional pulse sequences and their areas of application in high-resolution NMR spectroscopy (abbreviations, see text).

| 2D-NMR Experiment | Variable $F_1$ | Variable $F_2$ | 1-D-NMR Experiment | Applications, Results |
|---|---|---|---|---|
| homoscalar *J*-resolved | *J*(H,H) | $\delta(^1H)$ | — | |
| heteroscalar *J*-resolved | *J*(X,H) | $\delta$(X) | gated decoupling, selective decoupling, SEFT, INEPT, DEPT | large molecules, isomers, mixtures, X,H spin-spin coupling |
| heteroscalar correlated | $\delta$(X) | $\delta(^1H)$ | selective decoupling, SPI | assignment of $^1H$ and $^{13}C$ resonances |
| homoscalar correlated | | | | |
| COSY | $\delta(^1H)$ | $\delta(^1H)$ | homonuclear decoupling | proton sequences |
| SECSY | $\Delta\delta(^1H)$ | $\delta(^1H)$ | homonuclear decoupling | proton sequences |
| 2D-INADEQUATE | $\nu_{DQ}$ | $\delta(^{13}C)$ | 1D-INADEQUATE | CC connectivity |
| exchange spectra | | | | |
| NOESY | $\delta(^1H)$ | $\delta(^1H)$ | NOE | relation in space |
| chemical exchange | $\delta$(X) | $\delta$(X) | DANTE, DNMR | mechanism and kinetics of reversible reactions |

### 3.2. Data Processing and Graphical Display of 2D-NMR Spectra

A number of important experimental aspects of 2D-NMR spectroscopy will be described in Section 3.7. As a basis for the following discussion only, some remarks concerning data processing and graphical display of 2D-spectra[93] will be made here.

The processing of data obtained from 2D experiments is more demanding for the data system of the spectrometer than is customary with 1D experiments. In order to obtain a satisfactory digital resolution also in the $t_1$ dimension, the number of experiments, which determines the data points in $t_1$, must not be too small. For *J*-resolved spectra 32 time domain signals $S(t_2)$ are often sufficient, which in case of less sensitive nuclei, such as $^{13}C$, have to be recorded under the normal conditions for data accumulation. This means that the total acquisition time for the individual $S(t_2)$ signal should not exceed 0.5 h, and for measurements with less sensitive nuclei relatively concentrated samples are necessary[94].

The time-domain signals in the $t_2$ dimension, $S(t_2)$, are transformed by the first Fourier transformation with respect to $t_2$ into the data matrix $S(t_1, F_2)$, where corresponding points on the $F_2$ axis define the time domain function $S(t_1)$. The second Fourier transformation with respect to $t_1$ completes the process $S(t_1,t_2) \rightarrow S(F_1,F_2)$ (Fig. 28). Since even a single Fourier transformation results in a cosine and sine component of the frequency domain signal, phase selection for 2D experiments is relatively complicated.

This problem can be dealt with by using absolute value display, such as is also known for 1D spectra[5]. In this case the signal intensity as a function of the frequency $F_1$ is given by[90]

$$S(F_1) = (u^2 + v^2)^{1/2}$$

where $u$ and $v$ are the cosine and the sine parts, respectively, of the transformed time-domain function. For 2D spectra the following equation holds:

$$S(\pm F_1, F_2) = [(uu \mp vv)^2 + (uv \pm vu)^2]^{1/2}$$

This strategy has, however, the disadvantage that the signals are broadened at the basis, which complicates spectral analysis if signals of low intensity are close to strong absorption lines. In these cases a line-shape treatment by FID multiplication[95] using an appropriate time function can be helpful.

For the graphical display of 2D-NMR spectra two procedures are currently in use: the *stacked plot* (Fig. 30b)[91,93], which is known from $T_1$ measurements[96], and the *contour plot* (Fig. 30c)[97]. The stacked plot is, in most cases, aesthetically appealing, but often badly arranged and therefore difficult to analyze. In many cases the profile through a cross-section of the 2D diagram[98], however, yields the desired information.

The contour plot is a cross-section through the stacked plot parallel to the x,y-plane at a chosen height. In this

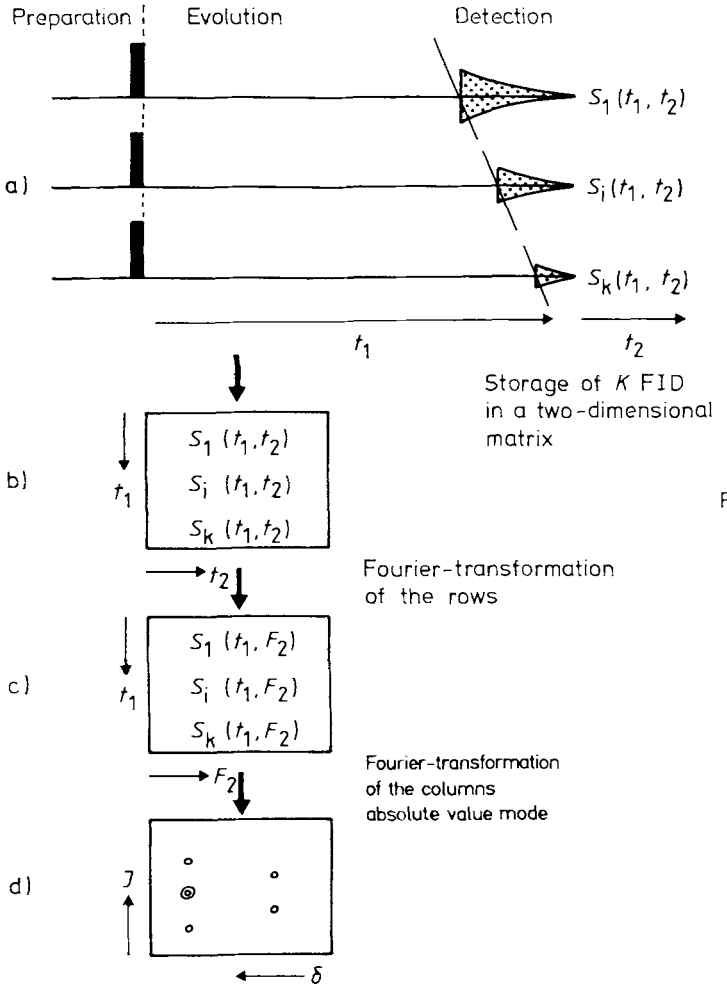



Fig. 28. Data flow in 2D-NMR spectroscopy.

way one obtains a clearly arranged diagram of contour lines that is easy to analyze, in particular for correlated spectra. The use of modern data processing equipment (visual display units, digital plotters) accelerates and facilitates analysis of 2D spectra considerably.

### 3.3. *J*-Resolved 2D-NMR Spectra

As shown in the example mentioned above, a $90°_x$ $^{13}C$ pulse, a variable evolution time, and data acquisition with $^1H$-broadband decoupling are sufficient to perform a heteronuclear 2D *J*-resolved experiment[91]. As already pointed out in the discussion of one-dimensional pulse sequences, additional 180° pulses at the midpoint of the evolution period lead to refocussing of the diverging isochromates. This effect is also used in 2D-NMR spectroscopy. As a consequence of the different effect of a 180° pulse on a hetero- or homonuclear spin system (see Section 1.2.3), the pulse sequences for *J*-resolved $^{13}C$ spectra, where $^{13}C,^1H$ coupling is of interest, are different from those used for $^1H$ spectra, where $^1H,^1H$ coupling is important.

#### *3.3.1. J-Resolved 2D-$^{13}$C-NMR Spectra*

The pulse sequence discussed in Section 3.2 was first used by *Müller, Kumar,* and *Ernst*[91] to separate the parameters $\delta(^{13}C)$ and $J(^{13}C,^1H)$[99]. Of the various versions proposed[93, 100, 101], the *gated decoupler method*[101] is the simplest and that which can be used most generally (Fig. 29). The basis of this pulse sequence is the spin echo experiment as applied to a $^{13}C$,A spin system in the $^{13}C$ region with A decoupling during half of the evolution period. During the preparation period, broadband decoupling can be used on the A channel in order to obtain the necessary NOE enhancement. The pulse sequence is completely identical with that of the SEFT experiment discussed above with the important difference of a variable evolution time $t_1$. In the case of a $^{13}C,^1H$ fragment double Fourier transformation results immediately in a complete separation of the two parameters $\delta(^{13}C)$ and $J(^{13}C,^1H)$.

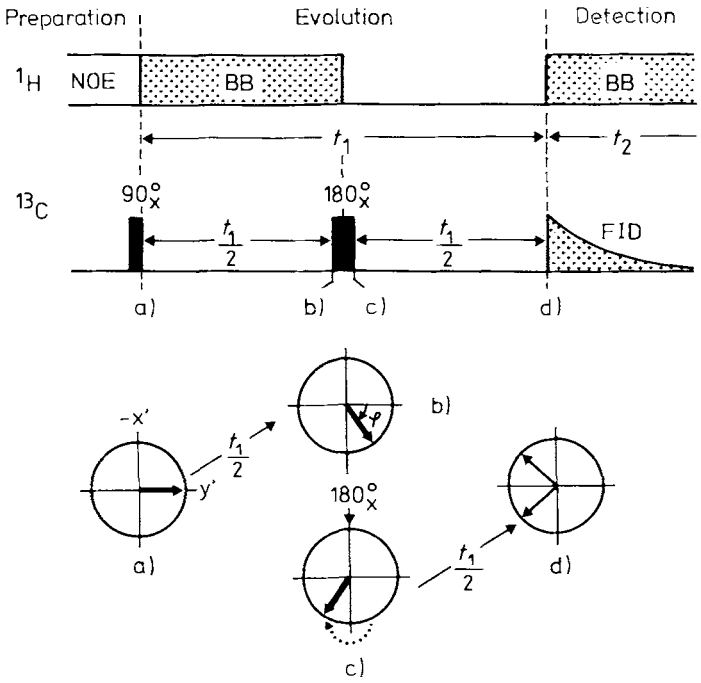



Fig. 29. Pulse sequence and vector representation for *J*-resolved 2D $^{13}C$-NMR spectra using, as example, the gated decoupler method for a CH fragment with $\nu_i > \nu_0$ (see Fig. 1d). At $t_1/2$ the $^{13}C$ magnetization has precessed by the angle $\varphi$ (b). The $180°_x$ pulse shifts the vector into position (c) and allows refocussing of inhomogeneity effects at $t_1$. During the second $t_1/2$ period $^{13}C,^1H$ coupling is allowed. The y-magnetization detected at $t_1$ is $t_1$-dependent (d). $^1H$ decoupling during the preparation period provides nuclear Overhauser enhancement.

For practical applications of this experiment the possibility of disentangling overlapping multiplets is by far the most important aspect. This is convincingly demonstrated using the simple example of a mixture of $\alpha$-deuterated toluenes. As shown in Figure 30, even at 100 MHz the $^1H$-decoupled $^{13}C$ resonances of the $CH_3$, $CH_2D$, $CHD_2$, and $CD_3$ groups are still strongly superimposed. Use of the SEFT sequence with variable $t_1$-time and gated $^2H$-decoupling yields the desired amplitude modulation of the $^{13}C$ signals through $^{13}C,^2H$ spin-spin coupling and, after double Fourier transformation, the $J(^{13}C,^2H)$-resolved 2D $^{13}C$-NMR spectrum, which is shown as a stacked plot in Figure 30b and as contour plot in Figure 30c. It is important to note that the coupling constants on the $F_1$ axis are reduced by half, since the spin multiplets diverge only during half of the evolution period.

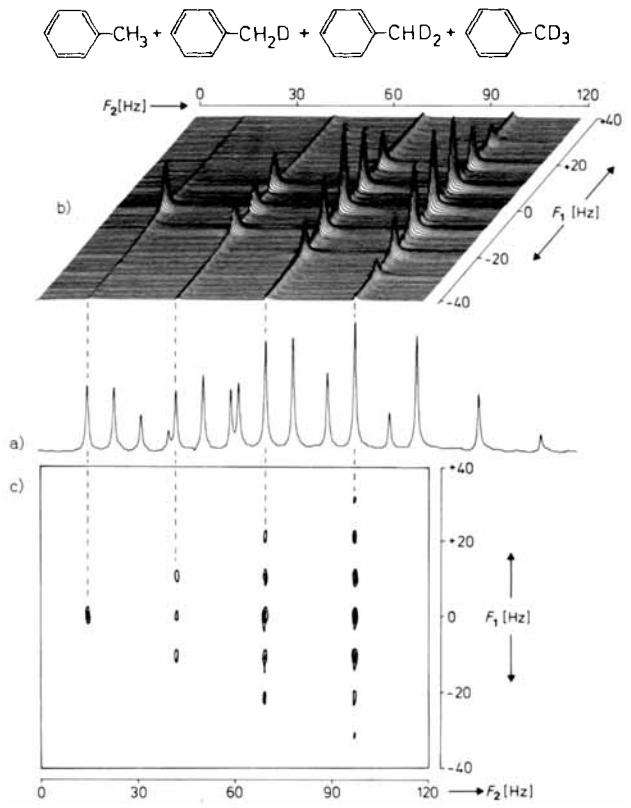



Fig. 30. 100.6 MHz $^{13}$C-NMR spectra of a mixture of toluene, α-[$D_1$]toluene, α-[$D_2$]toluene, and α-[$D_3$]toluene: a) $^1$H-decoupled 1D spectrum; b) stacked plot of the $^1J(^{13}C,^2H)$-resolved 2D spectrum [24] obtained with gated $^2$H-decoupling as stacked plot; c) as b), however as contour diagram.

A straightforward $^{13}$C,$^1$H application from organometallic chemistry is given in Figure 32 (see next page). It deals with the $^{13}$C-NMR spectrum of a mixture of four alkyl-substituted ($\eta^3$-allyl)($\eta^5$-cyclopentadienyl)nickel isomers[102]. The 2D spectra are reproduced as contour diagrams (a) and as stacked plots (b). For comparison, the 1D spectra ($^1$H-decoupled, (c), $^1$H-coupled (d)) are also shown. The desired spectral information can be extracted easily from the contour diagram, where the parameters $\delta(^{13}C)$ and $J(^{13}C,^1H)$ are separated on orthogonal axes. The multiplicities as well as the $^1J(^{13}C,^1H)$ data are obtained by inspection, and differences between $sp^2$- and $sp^3$-hybridized carbon atoms (*e.g.* C-31 and C-34) can immediately be recognized. In striking contrast is the strong overlap of the signals in the conventional $^1$H-coupled spectrum (d). As a further point of importance we note that the result of the experiment does not depend on prior knowledge of the coupling constants, as is the case for applications of one-dimensional pulse sequences, where this information is indispensable for the optimal choice of the evolution period (cf. SEFT, INEPT, and DEPT, Sections 2.1, 2.2.2, and 2.2.3, respectively).

An additional characteristic of this type of 2D spectra is that the multiplets of interest are not superimposed by residual signals of deuterated solvents, since these are treated as singlets with different resonance frequencies. The use of the spin echo technique also has the consequence that the line-width in the $F_2$ dimension is independent of magnetic field inhomogeneity and corresponds to the natural line width of the signals. The resolution of chemical shifts is thus improved relative to one-dimensional experiments. In particular, the gated decoupler method has the advantage that multiplets of strongly coupled spin systems are genuinely reproduced[101b]. This aspect is important, since not only strong coupling[103], but also experimental shortcomings, such as rotational sidebands[104], imprecise pulse-timing, and insufficient pulse power[105] across the spectral window—a difficulty present especially at high fields—lead to artefacts in 2D-NMR spectra.

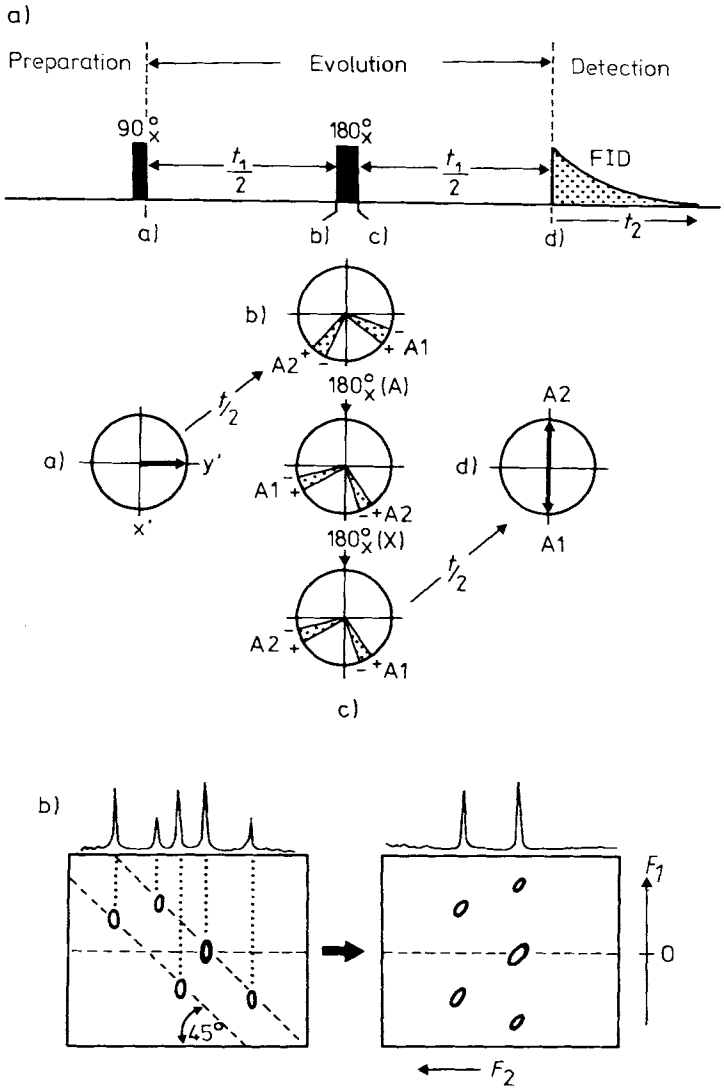



Fig. 32. a) Pulse sequence and vector representation for *J*-resolved 2D $^1$H-NMR spectra using the example of an A nucleus of a homonuclear AX system with $\nu_A > \nu_0$. At a time $t_1/2$ the doublet components A1 and A2 have progressed by different phase angles and at the same time are broadened by field inhomogeneity. The 180°$_x$ pulse inverts A1 and A2 around the x axis, but also changes the spin states of the X nucleus. The Larmor frequencies of the vectors are, therefore, interchanged (see Fig. 7a), and only the inhomogeneity effect refocusses during the second $t_1/2$ period. The y-magnetization detected at $t_1$ is $t_1$-dependent. b) Separation of the parameters $\delta$ and $J$ by tilting the data matrix by 45°.

An interesting variant of the heteroscalar *J*-resolved 2D-NMR experiment is the proton-flip method using a selective 180°$_x$ pulse which inverts only certain $^{13}$C satellites in the $^1$H-NMR spectrum[106]. In this way $^{13}$C,$^1$H long-range couplings can be measured precisely.

### 3.3.2. *J*-Resolved 2D $^1$H-NMR Spectra

For this type of two-dimensional NMR spectra[107] the spin echo experiment is again used, since in the homonuclear case the echo amplitude is a function of the coupling constant $J$(H,H) (cf. Section 1.3). Pulse sequence and vector diagram are given in Figure 31.

Because $^1$H-decoupling is precluded, both spins are also coupled during the detection period. Whereas the $F_1$ dimension contains the coupling information as before, the second frequency variable $F_2$ is now a function of chemical shift *and* spin-spin coupling constant $J$(H,H). An immediate separation of these variables on two frequency axes, therefore, is not possible for *J*-resolved 2D spectra of homonuclear spin systems. As is shown schematically in Figure 31, the individual multiplets lie on a 45° inclined diagonal of the two-dimensional matrix. Rotation of the absolute value spectrum by this angle results, however, in the separation of $\delta$ and $J$, since the projection on the $F_1$ axis now yields the multiplicity and the coupling constants, whereas the projection on the $F_2$-axis gives the chemical shifts[107, 108].

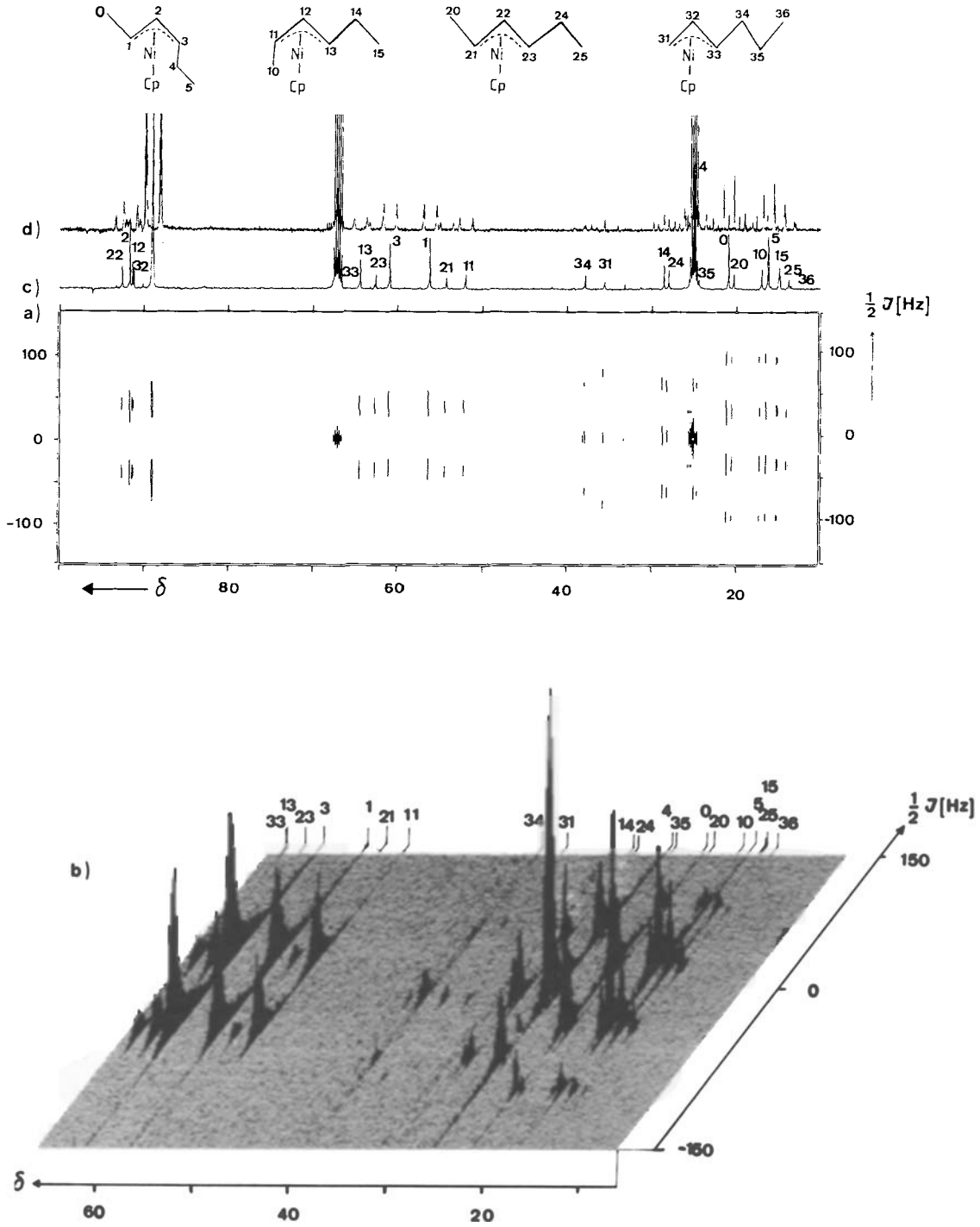



Fig. 31. *J*-resolved 100.6 MHz 2D $^{13}$C-NMR spectrum of a mixture of alkyl-substituted ($\eta^3$-allyl)($\eta^5$-cyclopentadienyl)nickel isomers [102]. a) Contour diagram; b) stacked plot; c) $^1$H-decoupled 1D spectrum; d) $^1$H-coupled 1D spectrum.

An outstanding property of *J*-resolved 2D $^1$H-NMR spectra is the fact that through the projection on the $F_2$-axis a quasi "$^1$H-decoupled $^1$H-NMR spectrum" can be obtained[109]. This type of homonuclear, completely decoupled spectrum is an important aid for spectral analysis, since symmetry arguments on the basis of intensities and line numbers may be used immediately for the interpretation, and the spectra of large molecules can be presented free of overlap. Again, the unravelling of superimposed multiplets is the main application. Here, profiles of suitable cross-sections through the 2D spectrum parallel to the $F_1$-axis allow the representation of individual multiplets to be separated. This is shown in Figure 33 for the mixture of isomeric allylnickel compounds already mentioned above.

In the case of stereoisomers[110], first-order multiplets exist that can also be separated using this technique. Other areas of application are biological macromolecules[111-113], where closely-spaced methyl resonances of amino acids in different positions of the polymer chain can be identified, as well as the relatively complicated $^1$H-NMR spectra of steroids, where the potential of the method has been impressively demonstrated[114]. Finally, the experiment can also be successfully used to separate and assign homonuclear and heteronuclear coupling constants[110, 115, 116]. This rests on the fact that heteronuclear coupling constants are not affected by the pulse sequence and are fully retained in the $F_2$-dimension, as is shown using the example of the $^1$H,$^1$H and $^{31}$P,$^1$H couplings in ($\eta^5$-cyclopentadienyl)(bistriphenylphosphane)vinylruthenium[117] (Fig. 34).

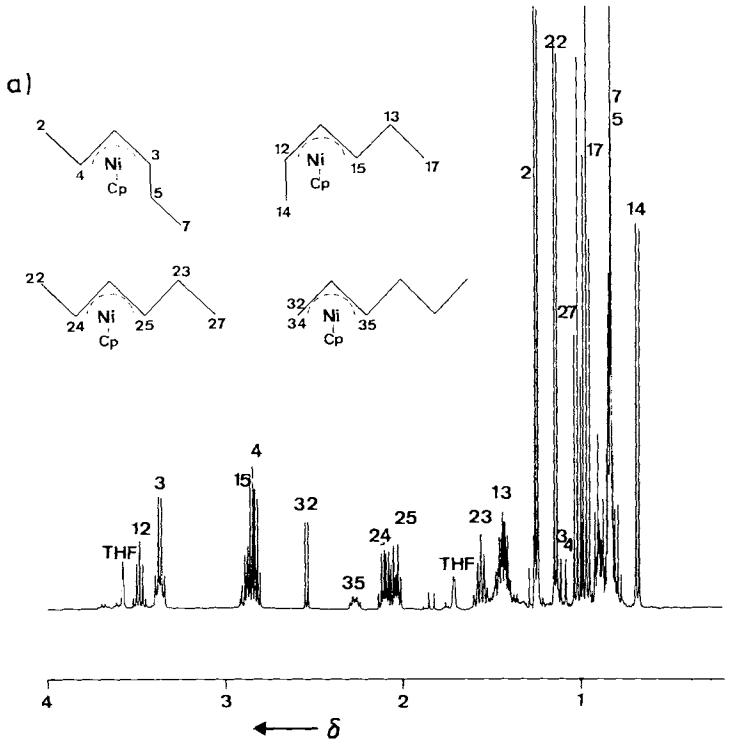



Fig. 33. a) 400 MHz $^1$H-NMR spectrum of alkyl-substituted ($\eta^3$-allyl)($\eta^5$-cyclopentadienyl)nickel isomers; b) selected profiles of cross-sections through the *J*-resolved 2D $^1$H-NMR spectrum that permit representation of individual multiplets free of overlap (cf. *e.g.* the signals of $H^4$ and $H^{15}$, or $H^{24}$ and $H^{25}$).

### 3.4. Correlated 2D-NMR Spectra

So-called correlated 2D-NMR spectra are distinguished from *J*-resolved 2D spectra in that both frequency axes now contain chemical shifts. Experimentally they require an additional time interval, the so-called *mixing time*[98, 118], between evolution and detection period. *Maudsley* and *Ernst*[41] were the first to propose and realize such an experiment. Two types of 2D correlated spectra can be distinguished: both dimensions may be coupled through co-

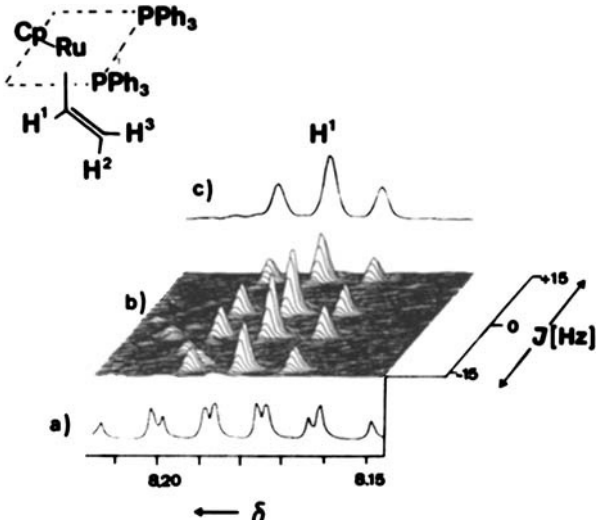



Fig. 34. *J*-resolved 2D $^1$H-NMR spectrum of the vinylic proton H$^1$ of ($\eta^5$-cyclopentadienyl)(bistriphenylphosphane)vinylruthenium [117]. a) Multiplet of the 1D $^1$H-NMR spectrum on the $F_2$-axis yields a triplet due to coupling with two equivalent phosphorus atoms. The doublet of doublets due to H,H coupling with the *cis*- and *trans*-proton is clearly seen on the $F_1$-axis.

herent transfer of transverse magnetization (scalar correlation[89,41]) or through incoherent transfer of magnetization (two-dimensional NOE spectra, two-dimensional chemical exchange spectra[118]).

### *3.4.1. Scalar Correlated 2D-NMR Spectra*

#### *3.4.1.1. Heteroscalar Correlated 2D-NMR Spectra*

If the Larmor frequencies of two different types of nuclei, *e.g.* $^1$H and $^{13}$C, are related through scalar coupling, one refers to heteroscalar correlated 2D-NMR spectra. This method is especially helpful for signal assignments, since it allows one type of nucleus (*e.g.* $^{13}$C) to be assigned from the known assignment of the other type (*e.g.* $^1$H). The pulse sequence generally used to produce heteroscalar correlated spectra contains, as do the INEPT or DEPT methods, a polarization transfer and, therefore, over and above the assignment leads to an enhancement of sensitivity. The fundamental concept is to use the evolution period $t_1$ for the precessional motion of the $^1$H spins, and to

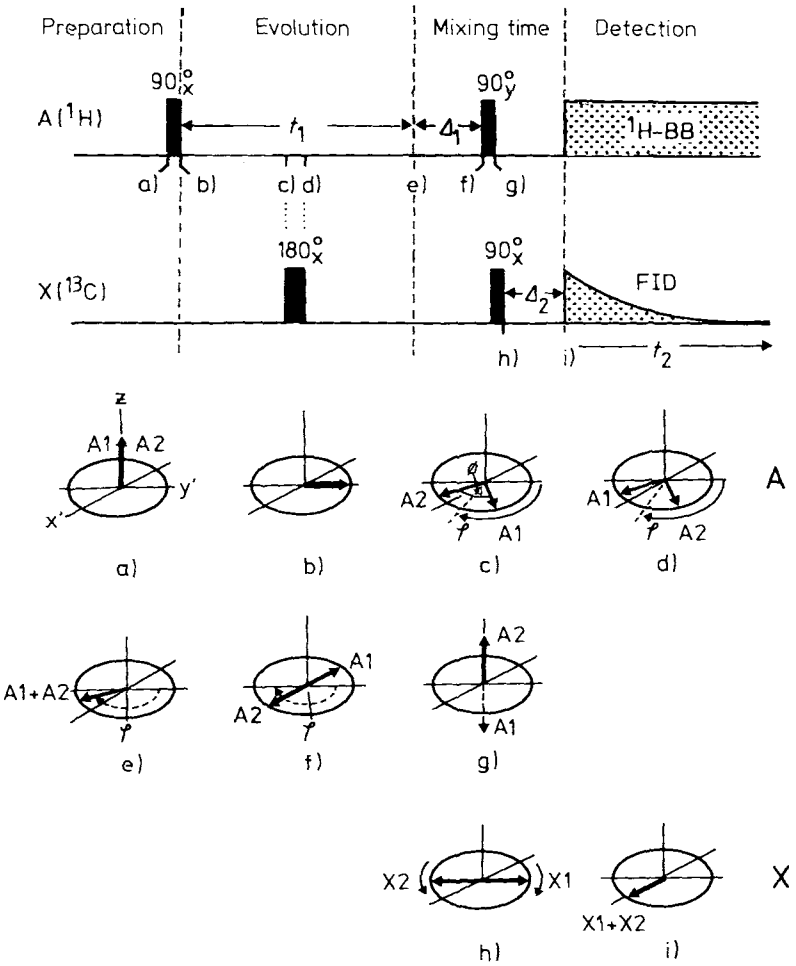



Fig. 35. Pulse sequence and vector representation of a heteroscalar-correlated 2D-NMR experiment using the example of a CH fragment (A = $^1$H, X = $^{13}$C). After a 90°$_x$ $^1$H-pulse both components of the $^1$H doublet rotate in the x,y-plane according to the difference of their frequency to that of the carrier (a–c). A 180°$_x$ $^{13}$C pulse (d) allows for refocussing at (e); $\delta$($^1$H) is retained in form of the angle $\varphi$. This information is transferred to the $^{13}$C nuclei through $^{13}$C,$^1$H spin-spin coupling during the mixing time. Polarization of the $^1$H-magnetization with a 90°$_y$ pulse (g) results in a corresponding polarization of $^{13}$C-magnetization which is transformed into transverse magnetization by the 90°$_x$-$^{13}$C pulse (h). In the remaining mixing time the $^{13}$C vectors precess around their corresponding $^1$H vectors. They are refocussed after $\Delta_2$s and can be detected with simultaneous $^1$H decoupling. The phase modulation obtained depends on the angle $\varphi$.

measure the degree of precession with the $^{13}C$ channel. The transfer of information between protons and carbon-13[119] occurs in the mixing period, which is introduced between the evolution and the detection time. Coupled nuclei yield signals with the coordinates $\delta(A)$, $\delta(X)$.

The pulse sequence for the generation of heteronuclear correlated 2D-NMR spectra is given in Figure 35[119,120]. After the $90^\circ_x$ $^1H$-pulse the components of a CH doublet rotate in the x,y-plane with different Larmor frequencies. The fanning-out angle $\phi$ is determined by the magnitude of the CH coupling, whereas the angle $\varphi$ is determined by the chemical shift of the protons (a—c). The $180^\circ_x$ pulse in the $^{13}C$ channel (d) exchanges the spin states of the protons and, therefore, the relative precessional frequencies of the vectors with the result that they are refocussed at the end of the evolution period $t_1$ (e). Chemical shift information is now contained in the phase angle $\varphi$. After a time $\Delta_1 = 1/2J$ we have $\phi = 180°$. Both vectors are orientated antiparallel and a $90^\circ_y$ pulse transforms them into the $\pm z$-direction, and thus results in a polarization of $^1H$ magnetization. The chemical shift information is now given by the magnitude of the z-components, which depends on the phase angle $\varphi$, since the $90^\circ_y$ pulse only affects the x-components of the vector. For $\varphi = (2N+1)\frac{\pi}{2}$ the longitudinal A magnetization is equal to zero, whereas for $\varphi = 2n\frac{\pi}{2}$ it has its maximum value. As with the SPI experiment, polarization of the protons leads simultaneously to polarization of $^{13}C$ magnetization, which can now be transformed into $\pm y$-magnetization by a $90^\circ_x$ pulse (h). Within the interval $\Delta_2 = 1/2J$, both $^{13}C$ vectors refocus and can be detected as a singlet if $^1H$-decoupling is applied. The polarization achieved, and thus the measured intensity, depends on the phase angle $\varphi$ and is, therefore, a direct function of the Larmor frequency of the protons. In consequence, variation of the evolution period $t_1$ leads to amplitude modulation, which in this case is, however, not a function of the coupling but of the Larmor frequency of the other nucleus. In contrast to the one-dimensional SPI experiment, excitation is non-selective, *i.e.* all resonances of the $^1H$-NMR spectrum are excited at the same time, and polarization transfer is $t_1$-dependent.

The elegance of this type of two-dimensional correlation experiment must be seen in the fact that, using only *one* experiment, connections between two types of nuclei can be established. Previously, this was possible only by means of a series of double-resonance experiments, the results of which are very often difficult to interpret. The correct choice of mixing period allows all the $^{13}C,^1H$ groups of a molecule to be detected. In addition, the problem of line overlap is elegantly eliminated. Especially with large molecules this aspect is of importance[121,122]. As Figure 36 shows, however, also for smaller molecules with less than 20 nonequivalent carbon atoms the assignment of the resonance frequencies becomes unambiguous and is faster than with any other technique.

The correlation character of the method allows an assignment made for one type of nucleus to be transfered immediately to another type. As in all two-dimensional techniques, the elimination of signal overlap is an additional advantage, especially since proton multiplets can now be resolved with the larger dispersion of the $^{13}C$ spectrum. Basically, all nuclei with spin quantum number $I = 1/2$ can be connected in a heteroscalar correlated 2D-NMR experiment. The technique is especially effective in cases where several scalar coupling constants of similar magnitude between protons and less sensitive nuclei exist. Consequently $^{13}C,^1H$[121,122], $^{15}N,^1H$[124], and $^{31}P,^1H$ correlations[125] are of importance in organic chemistry. In organometallic chemistry, phosphorus ligands play an important part, and phosphorus-metal correlations, for instance $^{103}Rh,^{31}P$ or $^{183}W,^{31}P$, will find increasing interest.

### *3.4.1.2. COSY[*] and SECSY[**] Homoscalar-Correlated 2D-NMR Spectra*

Closely related to the SPI and INEPT methods, as well as to heteroscalar correlated NMR spectroscopy discussed in Section 3.4.1.1, are two-dimensional correlations for homonuclear spin systems (for example $A = X = {}^1H$) known as COSY[126] and SECSY[127]. Both frequency axes $F_1$ and $F_2$ now contain the Larmor frequencies of the same nucleus, *e.g.* the $\delta(^1H)$ values.

The basis for COSY spectra is the classical Jeener sequence[11,89] (Fig. 37a), which also results in a magnetization transfer. After the preparation period, a $90^\circ_x$ pulse produces transverse magnetization. The magnetization vectors precess in the x,y-plane according to their Larmor frequency and their spin-spin coupling constants $J$. By analogy to the heteroscalar-correlated 2D experiment the second $90^\circ_x$ $^1H$ pulse can be viewed as the mixing pulse. Since the protons are always coupled, additional mixing times, however, are not necessary.

The second $90^\circ_x$ pulse leads, for a non-coupled A nucleus ($J(A,X) = 0$), to a $t_1$-dependent modulation of the transverse magnetization that depends only on $\nu_A$. The 2D spectrum therefore contains a signal on the diagonal $F_1 = F_2$ (dia peak). For the case $J(A,X) \neq 0$, the A magnetization through the scalar A, X-interaction in the x, y plane also depends on the Larmor frequency $\nu_X$. The 2D spectrum therefore contains the characteristic off-diagonal signals (cross peaks) with coordinates $\delta_A$, $\delta_X$, and $\delta_X$, $\delta_A$, which indicate a scalar spin-spin coupling between A and X. An application of this technique to the field of annulene chemistry is shown in Figure 38 with the correlation diagram for the protons of 9,11-bisdehydrobenzo[18]annulene[128].

Several versions for the Jeener pulse sequence exist. COSY45[126b] uses a $45^\circ_x$ instead of a $90^\circ_x$ mixing pulse and achieves a suppression of signals that are on or near the diagonal. In this method off-diagonal signals are sensitive to the relative signs of the coupling constants. The first to be experimentally verified was the SECSY sequence[127], where the mixing pulse bisects the evolution period (see Fig. 37b). Here, the chemical shifts $\delta_A$ and $\delta_X$ of the normal one-dimensional spectrum appear on the center line of the two-dimensional diagram, and the corresponding cross-peaks have the coordinates $\delta_A$, $(\delta_A - \delta_X)/2$ and $\delta_X$, $(\delta_X - \delta_A)/2$ (Fig. 38b).

[*] COSY = correlated spectroscopy.
[**] SECSY = spin echo correlated spectroscopy.

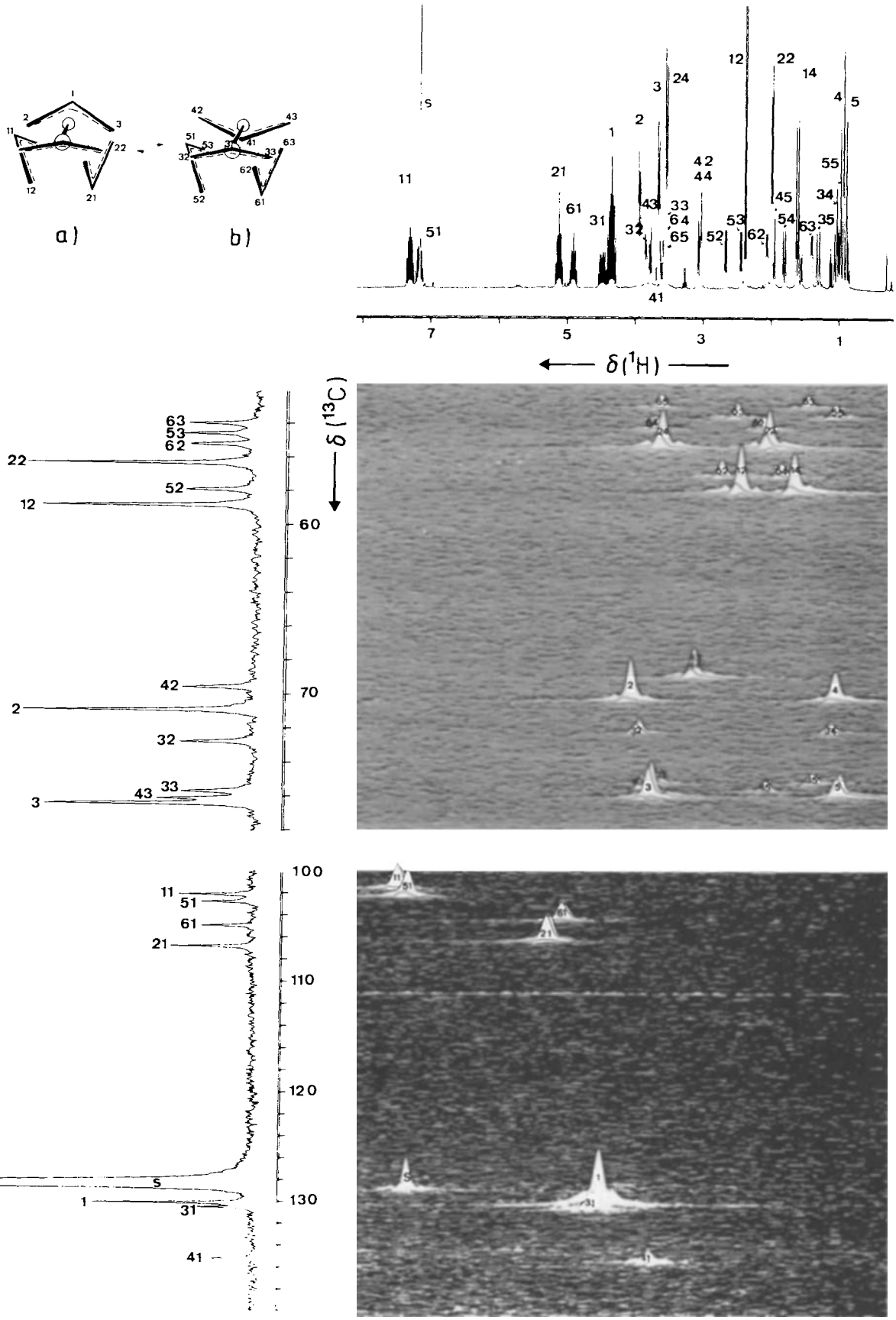



Fig. 36. 2D-$^{13}C,^{1}H$ correlation diagram of *cis*-$(\eta^3$-allyl$)_4Cr_2$ (*a*, signals 1—25) and *trans*-$(\eta^3$-allyl$)_4Cr_2$ (*b*, signals 31—65) in [$D_6$]benzene at 30 °C. The abscissa shows the $\delta(^1H)$- and the ordinate the $\delta(^{13}C)$-values. The 1D-$^1H$ and the $^1H$-decoupled 1D $^{13}C$-NMR spectra are reproduced along the respective frequency axes. The complete assignment of the $^1H$ spectrum has been described[123]. The 2D spectrum confirms this assignment and at the same time allows unambiguous assignment of all $^{13}C$ signals. The digital resolution used for the 2D spectrum led to an extensive loss of the multiplet structure. The signals for the CH fragments 11, 51, 61 and 21 with $\delta(^{13}C) = 100-110$ ppm and $\delta(^1H) = 4.8-7.3$ ppm demonstrate the correlation character of the experiment particularly convincingly ($^{13}C$ measuring frequency 100.6 MHz, acquisition time *ca.* 4 h, dimension of matrix 256 × 4096, dimension of transformation 1024 × 4096.)

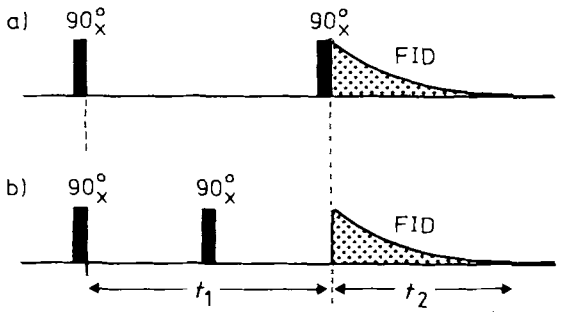



Fig. 37. Pulse sequence for homoscalar correlated 2D-NMR spectroscopy; a) COSY sequence [126]; b) SECSY sequence [127]. With the first 90°x pulse transverse magnetization is generated. The second 90°x pulse has the effect of a mixing pulse and results in an exchange of magnetization between coupled nuclei. The two-dimensional representation of the COSY and SECSY sequences are different (see Fig. 38).

The $F_1$-dimension of the SECSY sequence contains the frequency differences and, therefore, reduces the size of two-dimensional data matrix. The necessary condition is, however, that the Larmor frequencies do not exceed the spectral window, *i.e.* the quantity $\delta_A - \delta_X$ must be smaller than the spectral region for all coupled nuclei.

The advantages of two-dimensional Jeener spectroscopy compared to the classical homonuclear decoupling experiment are that—even in the case of small molecules—less experimental time is required are less, and difficulties arising from small frequency differences between the decoupler field and other resonances in the spectrum are ab-

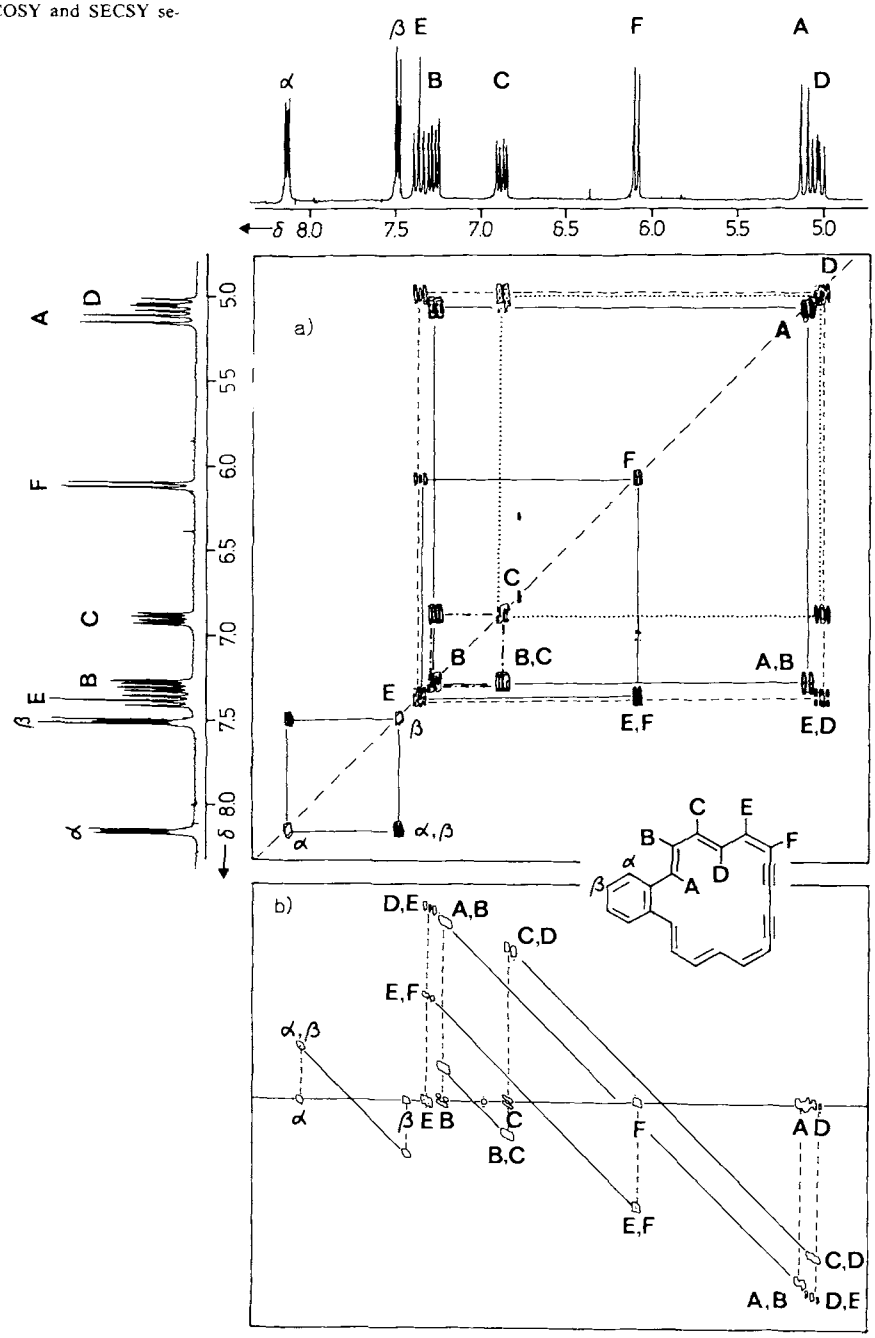



Fig. 38. Homoscalar correlated 2D $^1$H-NMR spectrum of 9,11-bisdehydrobenzo[18]annulene; a) result of a COSY experiment. The cross peaks immediately yield the assignment of the proton sequence in the annulene ring [128]. As an aid in the interpretation, the 1D $^1$H-NMR spectrum is also given (frequency 400 MHz, acquisition time for the 2D experiment *ca.* 4 h, dimension of matrix 256 × 1024, dimension of transformation 256 × 1024). b) Result of a SECSY experiment (acquisition time *ca.* 4 h, dimension of matrix 256 × 1024, dimension of transformation 256 × 1024).

sent. In addition, coupled multiplets are reproduced without overlap (see *e.g.* the contour diagram of Fig. 38). The corresponding one-dimensional experiment—homonuclear decoupling combined with difference spectroscopy—can be complicated by Bloch-Siegert effects[129]. A further advantage is that long-range couplings, which are difficult or even impossible to determine from one-dimensional experiments, can be detected very often easily with the 2D method. By introducing a short constant delay of approximately 0.5 s at the beginning of the evolution period, long-range couplings can be emphasized if the digital resolution is of comparable magnitude to the coupling constants[126b, 130]. A disadvantage of the 2D correlation is that, in many cases, the contour diagrams for large molecules become rather complex. Also, in the COSY45 version many absorptions lie on or near the diagonal, and even at high magnetic field these diagrams are difficult to analyze. This problem can be solved with 2D correlation diagrams based on multiple quantum transitions[11, 71, 131, 132] that allow the suppression or complete elimination of the disturbing diagonal absorptions.

Of special interest is the combination of the Jeener experiment with heteroscalar correlation, since the information obtained from both these experiments yields the carbon skeleton of an organic molecule. Both experiments can be performed either consecutively or within a so-called 2D experiment using correlated coherence (2D-relay-NMR[133]). In the latter case magnetization is first transferred from proton to proton by a Jeener pulse sequence. In the second step this magnetization is transferred to scalar-coupled carbon nuclei. Since the $^{13}$C-NMR spectrum is detected, the larger dispersion of this nucleus is used to check bonding in the molecule through the proton-proton couplings. The problems associated with the accumulation of diagonal signals are thus eliminated.

### 3.5. 2D-INADEQUATE: The Direct Determination of the Carbon Skeleton

As already discussed in Section 2.3, the determination of the $^1J(^{13}C,^{13}C)$ data permits assignment of neighboring carbon atoms for the molecule of interest. This goal is achieved especially elegantly using the two-dimensional version of the INADEQUATE pulse sequence. Here advantage is taken of the fact that the double-quantum frequency $\nu_{DQ}$ of an AX system depends on the transmitter frequency $\nu_0$: $\nu_{DQ} = \nu_A + \nu_X - 2\nu_0$[11, 69]. If we vary the time $t_1$ between the second $90^\circ_x$ pulse, which together with the first produces the double-quantum coherence, and the 90° ($\phi$) read pulse in such a way that $1/t_1$ passes all double-quantum frequencies of the spectrum, the information is obtained as a function of $t_1$ *and* $t_2$ (Fig. 39).

Fourier transformation yields the double-quantum frequencies $\nu_{DQ}$ in the $F_1$-dimension and the normal $^{13}$C chemical shifts in the $F_2$-dimension. Since the $^{13}$C satellite spectrum is detected at the natural abundance level, only 0.01% of the molecules present yield such absorptions, and even if large amounts of compound are available—in the order of several 100 mg—long acquisition times are necessary. It is, therefore, of importance, through the use of quadrature detection, to keep the two-dimensional matrix

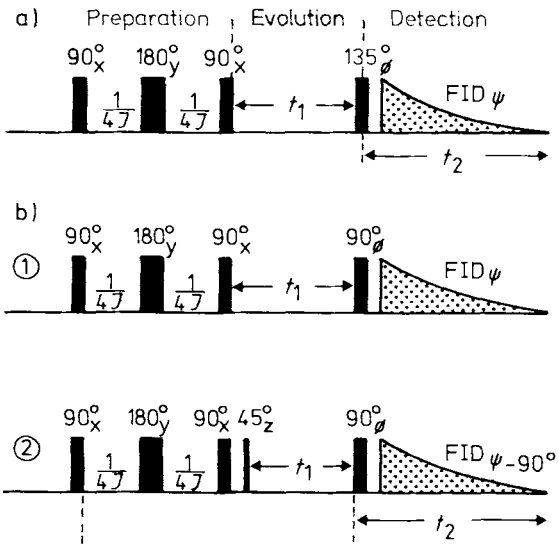



Fig. 39. Pulse sequence for the two-dimensional INADEQUATE experiment with quadrature detection. In case a) positive and negative frequencies are distinguished by a 135° pulse [135]. In case b) the 45° pulse with the sequences ① and ② applied alternately has the same effect [134]; the period $\Delta$ can be neglected if compared to $t_1$.

as small as possible. For this purpose several versions of the INADEQUATE pulse sequence have been proposed[134, 135].

An application of the 2D-INADEQUATE technique is given in Figure 40. In (−)bis[(1*R*,3*R*,4*S*)menthyl]methylphosphane both menthyl groups are diastereotopic and yield ten pairs of $^{13}$C-NMR signals. With the 2D-INADEQUATE experiment it is possible to assign all $^{13}$C resonances of the individual menthyl groups[136]. Subsequently, one can use the $^{31}$P,$^{13}$C couplings to establish the predominant conformation of this molecule at various temperatures; these are of interest in connection with the application of this particular phosphane in the course of catalytic asymmetric syntheses.

The long acquisition time of the 2D experiment compared to the 1D-INADEQUATE experiment is counterbalanced by a number of advantages: strong coupling in the satellite spectra[79] and insufficient suppression of the main signal are less stringent requirements in 2D compared to 1D spectra. In addition—and this is certainly the most important advantage—the analysis of carbon-carbon connectivity can be undertaken without detailed prior information, even if $^1J$(C,C) varies between 30 and 70 Hz, and spectral widths of 20 kHz are necessary[137]. Of course, a prerequisite for such measurements is that solution containing *ca.* 0.5 g of the compound or neat liquids are used.

### 3.6. 2D Exchange Spectroscopy

Two-dimensional exchange spectroscopy[118] is based on transfer of magnetization, such as occurs in the nuclear Overhauser effect (NOE)[48] or in chemical exchange processes[138]. Experiments on the NOE basis are known as NOESY[*].

As with the COSY experiment, the first $90^\circ_x$ pulse produces transverse magnetization that precesses during the

[*] NOESY = *n*uclear *O*verhauser *e*ffect *s*pectroscopy.

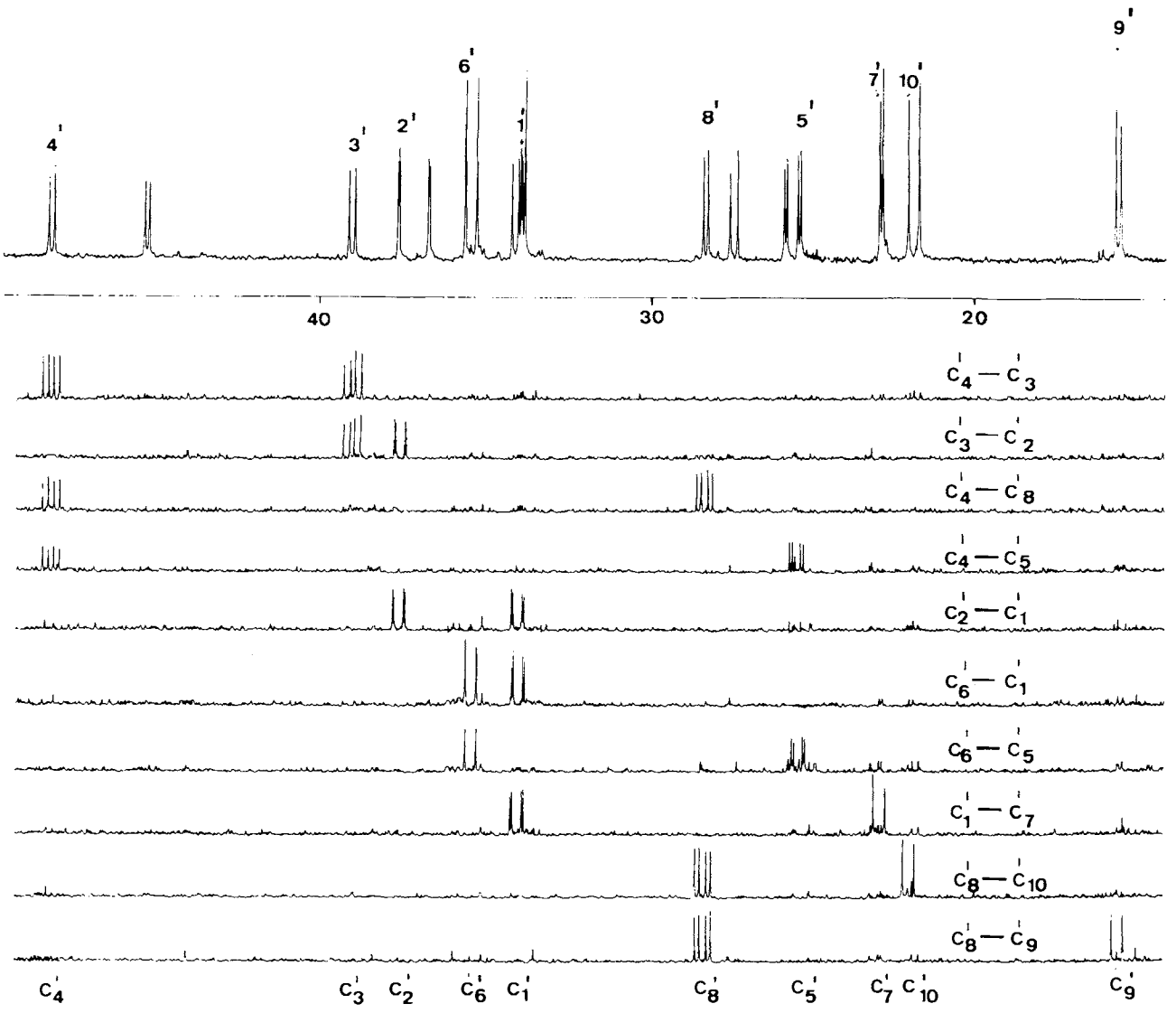
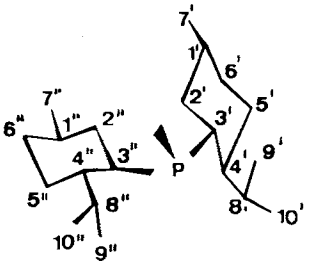



Fig. 40. Two-dimensional INADEQUATE experiment for the $^{13}$C-NMR spectrum of (−)bis[(1*R*,3*R*,4*S*)menthyl]methylphosphane in [$D_6$]benzene at 27 °C [136]. The upper trace shows the $^{13}$C-resonance of 20 different carbon atoms in the $^1$H-decoupled spectrum with the exception of the doublets of the *P*-methyl group. The remaining spectra are $^{13}$C,$^{13}$C satellite spectra of one menthyl group, as obtained from the 2D double quantum diagram. The $^{13}$C main signals for molecules with only one $^{13}$C are completely suppressed. The assignment of all signals to individual menthyl groups is given unambiguously by the double quantum frequency of the individual AX systems and is not based on knowledge of the exact $^1J(^{13}C,^{13}C)$ coupling constants. The $^{13}$C,$^{31}$P coupling constants are retained in the $F_2$-dimension, which also contains the chemical shifts (frequency 100.6 MHz, acquisition time *ca.* 36 h, amount of compound used *ca.* 0.5 g).




evolution period in the x,y-plane. The 90°$_x$ mixing pulse is followed by the mixing time $\Delta$, which is now in the order of the spin-lattice relaxation time $T_1$ or the inverse rate constant of chemical exchange processes. This time is necessary to achieve magnetization transfer arising from dipolar interactions. Scalar interactions, on the other hand, are effective immediately (cf. Section 3.4), and the mixing time varies between 0 (COSY) and $1/J(^{13}C,^1H)$ (heteroscalar correlated). The third 90°$_x$ pulse transforms the resulting z-magnetization into transverse magnetization, which is measured during the detection phase. The 2D data matrix for COSY and NOESY are similar (Fig. 41).

So far, double-resonance methods[5, 139] have been used to investigate geometrical relationships in a molecule with the aid of the nuclear Overhauser effect[48], or to study chemical exchange processes in the region of slow exchange[86]. Both phenomena can be investigated especially effectively and with high sensitivity by difference spectroscopy[123, 140]. Similar advantages hold for two-dimensional exchange spectroscopy, where the total time of measurement can be even shorter.

For medium-sized molecules and at intermediate magnetic field strengths, nuclear Overhauser effects and chemical exchange, respectively, are distinguished in 1D spectra by an increase or decrease in signal intensity. In 2D experiments with nuclei of high isotopic abundance the effect of both phenomena is identical. Where necessary, a differen-

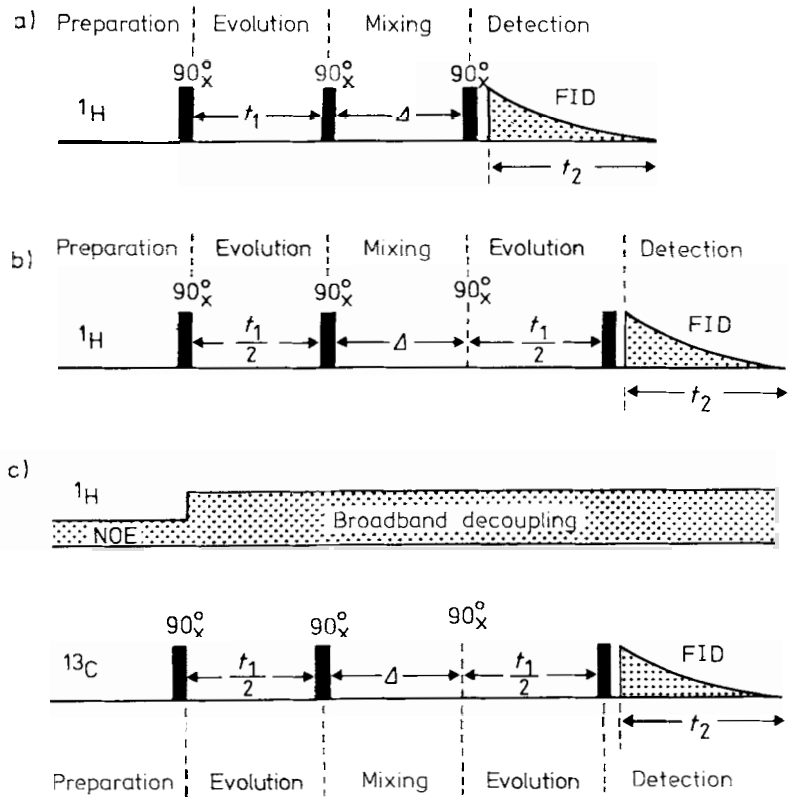



Fig. 41. Pulse sequence for two-dimensional exchange NMR spectroscopy. a) NOESY sequence for 2D $^1$H-NOE spectra with the read pulse at the end of the evolution period (COSY matrix form); b) as a), however with the read pulse at the midpoint of the evolution time (SECSY matrix form); c) shows the pulse sequence for 2D exchange spectra in $^{13}$C-NMR spectroscopy.

tiation can, however, be achieved by variation of the temperature, the mixing time[141], or by phase-sensitive display of 2D spectra. For nuclei with low natural abundance the homonuclear Overhauser effect can be neglected, and the correlation experiment is confined to chemical exchange processes. For protons, 2D-NOE spectroscopy has already been used successfully in a large number of practical applications[142–144].

Turning to chemical exchange, for protons most of the arguments, and for nuclei with $I=1/2$ and relatively low natural abundance, *e.g.* $^{13}$C, nearly all arguments are in favor of the two-dimensional method. In particular, it must be pointed out that the exchange mechanisms very often can be extracted from the 2D matrix by inspection[145,146]. The often lengthy quantitative line-shape calculations that are necessary in 1D-NMR spectroscopy are therefore superfluous with 2D experiments.

As mentioned above, 2D-$^{13}$C exchange spectra lack the possible artefacts arising through nuclear Overhauser effects. The 2D-$^{13}$C exchange spectrum thus appears to be the method of choice for the qualitative investigation of chemical exchange mechanisms, even in the case of small molecules and compounds of moderate solubility. An example of the use of this technique is given in Figure 42.

### 3.7. Experimental Aspects of 2D-NMR Spectroscopy

The absolute value representation of 2D spectra solves the problem of phase correction and at the same time leads to an improvement of the signal-to-noise ratio. It has, however, the disadvantage that the signals are broadened at the basis. This is especially true for *J*-resolved 2D $^1$H-NMR spectra, since because of rotation of the data matrix the absorption and dispersion components overlap. As a consequence, multiplets of components with low concentration are difficult to detect in the presence of intense lines if the absolute value display is used. Apart from certain variations in the experimental **technique**[147], phase programs[148], projection techniques[149], and filter functions[95] play an important role in solving problems of this type in 2D-NMR spectroscopy. Without doubt, the correct choice of preparation time and of suitable filter functions are crucial for the success of a 2D experiment. Filter functions which are symmetric to the midpoint of the time variable $t_2$, so-called pseudoechoes[150], are of special importance in this respect, since they eliminate the symmetrical dispersion components completely and yield centrosymmetric signals. A drawback of such filter functions is the resulting loss of sensitivity; therefore, in many cases phase-shifted sine functions provide a good compromise between sensitivity, resolution, and line shape.

Coupling constants are determined in 2D spectra from profiles of suitable cross-sections. The use of filter functions, absolute-value mode, and spectra of higher order can result in differences between coupling constants derived from 2D spectra and those measured in 1D spectra. In general, however, phase-corrected spectra from phase-sensitive cross-sections lead to complete agreement be-

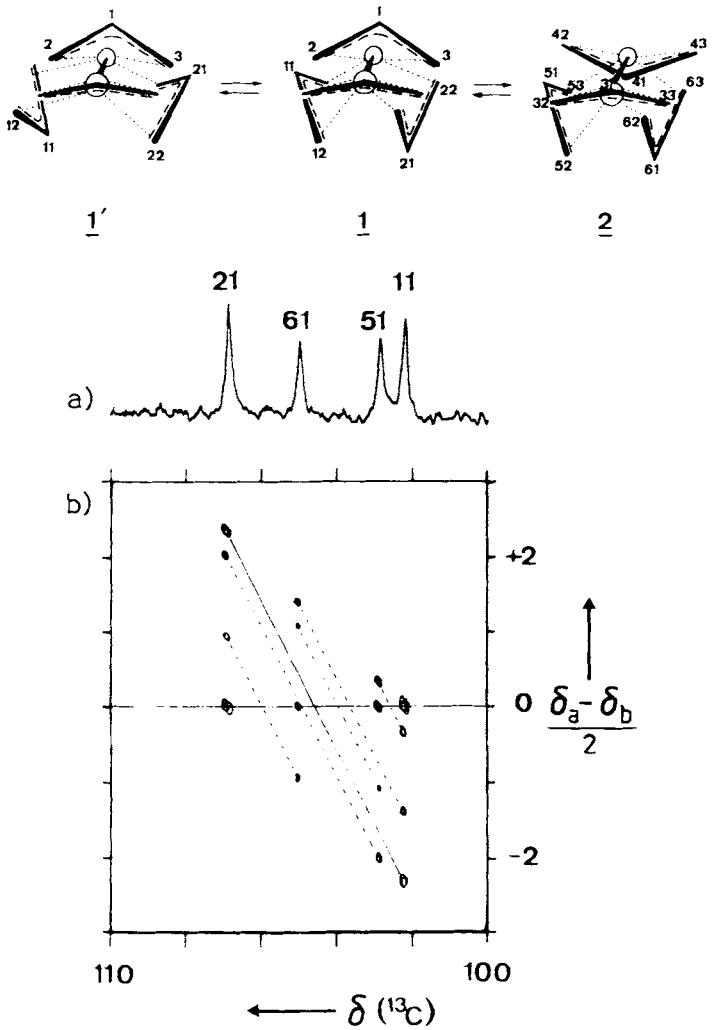



Fig. 42. $^{13}$C-2D exchange NMR spectra for $(\eta^3\text{-allyl})_4Cr_2$ in [D$_6$]benzene [146]. a) 1D-$^{13}$C NMR spectrum at 100.6 MHz; b) correlation diagram obtained with the pulse sequence $90^\circ_x$-$t_1$/2-$90^\circ_y$-$\Delta$-$t_1$/2-$90^\circ_x$-FID; $t_1$ was varied from 0–25.6 ms using 256 increments; the mixing time was 2 s. The horizontal axis ($F_2$-dimension) shows the $^{13}$C-resonances, the vertical axis ($F_1$-dimension) the chemical shift differences. $^{13}$C atoms connected by chemical exchange yield cross signals.

tween the results of both methods[151]. Several procedures for the generation of *J*-resolved 2D absorption spectra are known[149, 152].

Further improvements of the pulse sequence for the detection of *J*-resolved 2D spectra aim at a faster repetition rate[153]. This is especially important for applications involving small molecules and short relaxation times. If fast and sufficiently large data storage is available, the direct acquisition of complete spin echo series can be of advantage[154, 155]. This technique also yields absorption signals relatively easily, requires only short acquisition times, and permits data processing for 2D as well as 1D spectra[155]. The latter aspect is of interest if small molecules are to be detected in the presence of large.

As with conventional 1D spectra, it is of advantage also for 2D heteroscalar correlated spectra to locate both the $^1$H and $^{13}$C pulses in the center of the spectral region. Quadrature detection in the $F_1$- and $F_2$-dimensions requires that negative and positive frequencies be distinguished. The advantage of quadrature detection is the uniform excitation of all signals of one type of nuclei and the reduction of the spectral width. This means that the size of the 2D matrix can be reduced by half, and the signal-to-noise ratio in the $F_1$-dimension is increased by a factor of $\sqrt{2}$, while the acquisition time is decreased by a factor of almost 4. In order to realize this in practice, the phases of both proton pulses and of the receiver are cycled[156]; hence the amplitude modulation produced in the evolution time is transformed into a phase modulation. Generally, heteroscalar correlated 2D experiments use 8 phase cycles[157], which allow quadrature detection in both dimensions and good suppression of erroneous signals, the so-called phantum and ghost peaks.

Similar ideas apply to *J*-resolved[158] and scalar-correlated 2D spectra, such as COSY[126b], SECSY, and NOESY. Here, 16 phase cycles allow quadrature detection and the suppression of ghost peaks[159, 160].

The $^{13}$C-INADEQUATE experiment only detects the satellites; the main signals, which are stronger by a factor of 200, are suppressed. In practice, 32 phase cycles are necessary; however, optimum suppression of the main signals requires 256 phase cycles[80, 130]. A good compromise for 2D-INADEQUATE experiments is 64 phase cycles. In general, phase cycles are of great importance for the elimination of residual magnetization, the suppression of ghost peaks, and faster repetition rate of the experiments.

## 4. Outlook on Practical Applications

As a consequence of the variety of NMR techniques available today, the choice of method best suited to solve the problem at hand is often difficult. In many cases, however, the experimental set-up available enforces restrictions. Therefore, but also for other reasons, 1D techniques will keep their place at the side of 2D methods. 1D spectra normally require shorter acquisition times and can be performed with less sophisticated pulse transmitters. Considering the data systems available today, they also allow better digital resolution. Furthermore the information provided by 1D experiments helps reduce the acquisition time of and the effort required to interpret 2D experiments: 1D information should, therefore, be fully exploited. Practical experience will show quickly where 2D experiments can best be used for particular problems and where they are superior to 1D methods. One should remember that 2D experiments can also be performed using traditional spectrometers at the fields provided by electromagnets, *i.e.* in situations where 1D methods will more often fail than at high fields. Presently, 2D experiments rely less on high field strength than on compounds having good solubility, *i.e.* allowing high sample concentrations to be used.

Polarization transfer, heteronuclear shift correlations, and *J*-resolved 2D-NMR spectra are undoubtedly the most important new techniques that have made considerable contributions to the NMR spectroscopy of less abundant nuclei as well as that of complex natural products. The 2D-$^{13}$C,$^1$H shift correlation is, as far as time requirements are concerned, superior to the 1D technique of selective double resonance. 2D-NOE correlation, on the other hand, improves the methods of detecting neighboring nuclei, not only through the chemical bonds but also through space,

an important step towards complete structure determinations of molecules in solution.

We are certainly not wrong in assuming that the next years will see the development of further experimental techniques—*e.g.* in the field of multiple quantum spectra—and improvements of existing methods with respect to acquisition times and concentration requirements. This development will profit from increasing practical experience gained using the new techniques, which our article may encourage. One thing is already certain: the fascinating physics of spin systems with its numerous practical applications is an important chapter of modern research.

*We are indebted to Dipl.-Chem. P. Schmitt and Dipl.-Chem. J. R. Wesener for performing a number of experiments. Support of our own research by the Deutsche Forschungsgemeinschaft and the Fonds der Chemischen Industrie is gratefully acknowledged. R. B. thanks Prof. Dr. G. Wilke, Mülheim for continuous support. Finally, our thanks are due to Dr. R. Mynott, Mülheim, for improving the English version of this article.*

Received: January 25, 1983 [A 454 IE]
German version: *Angew. Chem. 95* (1983) 381

[1] R. K. Harris, B. E. Mann: *NMR and the Periodic Table,* Academic Press, London 1978; C. Brevard, P. Granger: *Handbook of High-Resolution Multinuclear NMR,* Wiley, New York 1981.
[2] R. E. Wasylishen, C. A. Fyfe, *Annu. Rep. NMR Spectrosc. 12* (1982) 1.
[3] R. E. Gordon, P. E. Hanley, D. Shaw, *Prog. Nucl. Magn. Reson. Spectrosc. 15* (1982) 1; R. A. Iles, A. N. Stevens, J. R. Griffiths, *ibid. 15* (1982) 49; P. Diehl, E. Fluck, R. Kosfeld: *NMR - Basic Principles and Progress,* Bd. *19,* Springer, Berlin 1981; A. M. Gronenborn, K. Roth, *Chem. Unserer Zeit 16* (1982) 1, 35.
[4] Whether we have always succeeded, is at present not clear. Bodenhausen [69] has already characterized the situation for a number of cases with the citation „l'essentiel n'est pas visible" (Saint-Exupéry: *Le Petit Prince*).
[5] a) T. C. Farrar, E. D. Becker: *Pulse and Fourier-Transform NMR,* Academic Press, New York 1971; b) D. Shaw: *Fourier Transform NMR Spectroscopy,* Elsevier, Amsterdam 1976; c) H. Günther: *NMR Spectroscopy,* Wiley, Chichester 1980.
[6] The expression *pulse* implies pulse modulation of the radio frequency field. For the difference between pulse and impulse see [5b].
[7] H. C. Torrey, *Phys. Rev. 76* (1949) 1059.
[8] Here and in the following we always use $\nu_A > \nu_X$; for a heteronuclear spin system it follows that $\gamma_A > \gamma_X$, *i.e.* the A nucleus is the more sensitive.
[9] E. L. Hahn, *Phys. Rev. 80* (1950) 580.
[10] Cf. *e.g.* [5b], p. 139; [5c], p. 321.
[11] W. P. Aue, E. Bartholdi, R. R. Ernst, *J. Chem. Phys. 64* (1976) 2229.
[12] E. L. Hahn, D. E. Maxwell, *Phys. Rev. 88* (1952) 1070.
[13] a) W. Stempfle, E. G. Hoffmann, *Z. Naturforsch 25 A* (1970) 2000; b) I. D. Campbell, C. M. Dobson, R. J. P. Williams, P. F. Wright, *FEBS Lett. 57* (1975) 96.
[14] D. W. Brown, T. T. Nakashima, D. L. Rabenstein, *J. Magn. Reson. 45* (1981) 302; D. L. Rabenstein, T. T. Nakashima, *Anal. Chem. 51* (1979) 1465 A.
[15] M. H. Levitt, R. Freeman, *J. Magn. Reson. 39* (1980) 533.
[16] C. LeCocq, J.-Y. Lallemand, *J. Chem. Soc. Chem. Commun. 1981,* 150.
[17] D. J. Cookson, B. E. Smith, *Org. Magn. Reson. 16* (1981) 111.
[18] M. R. Bendall, D. M. Doddrell, D. T. Pegg, *J. Am. Chem. Soc. 103* (1981) 4603.
[19] J. C. Beloeil, C. LeCocq, J.-Y. Lallemand, *Org. Magn. Reson. 19* (1982) 112.
[20] Pei Feng-hui, R. Freeman, *J. Magn. Reson. 48* (1982) 318.
[21] H. J. Jakobsen, O. W. Sørensen, W. S. Brey, P. Kanyha, *J. Magn. Reson. 48* (1982) 328.
[22] S. L. Patt, J. N. Shoolery, *J. Magn. Reson. 46* (1982) 535.
[23] K.-F. Elgert, R. Kosfeld, *J. Magn. Reson.,* in press.
[24] P. Schmitt, J. R. Wesener, H. Günther, *J. Magn. Reson. 52* (1983) 511.
[25] J. R. Wesener, H. Günther, *Org. Magn. Reson.,* in press.
[26] J. R. Wesener, H. Günther, *J. Am. Chem. Soc.,* submitted for publication.
[27] P. H. Bolton, *J. Magn. Reson. 45* (1981) 418.
[28] K. G. R. Pachler, P. L. Wessels, *J. Magn. Reson. 12* (1973) 337.
[29] S. Sørensen, R. S. Hansen, H. J. Jakobsen, *J. Magn. Reson. 14* (1974) 243.
[30] A. A. Chalmers, K. G. R. Pachler, P. L. Wessels, *Org. Magn. Reson. 6* (1974) 445.
[31] H. J. Jakobsen, S. Aa. Linde, S. Sørensen, *J. Magn. Reson. 15* (1974) 385.
[32] S. Aa. Linde, H. J. Jakobsen, B. J. Kimber, *J. Am. Chem. Soc. 97* (1975) 3219.
[33] K. G. R. Pachler, P. L. Wessels, *Org. Magn. Reson. 9* (1977) 557.
[34] H. J. Jakobsen, W. S. Brey, *J. Am. Chem. Soc. 101* (1979) 774.
[35] A. A. Chalmers, K. G. R. Pachler, P. L. Wessels, *J. Magn. Reson. 15* (1974) 415.
[36] S. Aa. Linde, H. J. Jakobsen, *J. Am. Chem. Soc. 98* (1976) 1041.
[37] K. G. R. Pachler, P. L. Wessels, *Org. Magn. Reson. 13* (1980) 100.
[38] M. L. Martin, M. Trierweiler, V. Galasso, F. Fringuelli, A. Taticchi, *J. Magn. Reson. 42* (1981) 155.
[39] M. Barfield, S. R. Walter, K. A. Clark, G. W. Gribble, K. W. Haden, W. J. Kelly, C. S. Le Houllier, *Org. Magn. Reson. 20* (1982) 92.
[40] For special aspects see H. J. Jakobsen, H. Bildsøe, *J. Magn. Reson. 26* (1977) 183; H. Bildsøe, *ibid. 27* (1977) 393; K. G. R. Pachler, P. L. Wessels, *ibid. 28* (1977) 53; O. W. Sørensen, H. Bildsøe, H. J. Jakobsen, *ibid. 45* (1981) 325; J. Voigt, J. P. Jakobsen, *ibid. 45* (1981) 510.
[41] A. A. Maudsley, R. R. Ernst, *Chem. Phys. Lett. 50* (1977) 368.
[42] G. A. Morris, R. Freeman, *J. Am. Chem. Soc. 101* (1979) 760.
[43] W. Städeli, P. Bigler, W. von Philipsborn, *Org. Magn. Reson. 16* (1981) 170.
[44] M. Schumacher, H. Günther, *Chem. Ber. 116* (1983) 2001.
[45] D. P. Burum, R. R. Ernst, *J. Magn. Reson. 39* (1980) 163.
[46] G. A. Morris, *J. Am. Chem. Soc. 102* (1980) 428.
[47] P. H. Bolton, *J. Magn. Reson. 41* (1980) 287.
[48] J. H. Noggle, R. E. Schirmer: *The Nuclear Overhauser Effect,* Academic Press, New York 1971; cf. also [5c], p. 302.
[49] C. Brevard, G. C. van Stein, G. van Koten, *J. Am. Chem. Soc. 103* (1981) 6746.
[50] C. Brevard, R. Schimpf, *J. Magn. Reson. 47* (1982) 528.
[51] D. M. Doddrell, D. T. Pegg, W. Brooks, M. R. Bendall, *J. Am. Chem. Soc. 103* (1981) 727.
[52] D. M. Doddrell, D. T. Pegg, M. R. Bendall, *J. Magn. Reson. 48* (1982) 323; D. T. Pegg, D. M. Doddrell, M. R. Bendall, *J. Chem. Phys. 77* (1982) 2745.
[53] D. M. Doddrell, D. T. Pegg, *J. Am. Chem. Soc. 102* (1980) 6388.
[54] a) M. R. Bendall, D. T. Pegg, D. M. Doddrell, D. H. Williams, *J. Org. Chem. 47* (1982) 3021; b) M. R. Bendall, D. M. Doddrell, D. T. Pegg, W. E. Hull: *DEPT-Bruker-Information Bulletin,* Bruker Analytische Meßtechnik, Karlsruhe 1982; c) M. R. Bendall, D. T. Pegg, D. M. Doddrell, S. R. Johns, R. I. Willing, *J. C. S. Chem. Comm. 1982,* 1138.
[55] R. Köster, W. Dahlhoff, S. Penades, R. Benn, unpublished results.
[56] R. Freeman, T. H. Mareci, G. A. Morris, *J. Magn. Reson. 42* (1981) 341.
[57] P. L. Rinaldi, N. J. Baldwin, *J. Am. Chem. Soc. 104* (1982) 5791.
[58] G. A. Morris, *J. Magn. Reson. 41* (1980) 185.
[59] J. Kowalewski, G. A. Morris, *J. Magn. Reson. 47* (1982) 331.
[60] D. Marion, C. Garbay-Jauregniberry, B. P. Roques, *J. Am. Chem. Soc. 104* (1982) 5573.
[61] D. M. Doddrell, D. T. Pegg, M. R. Bendall, W. M. Brooks, D. M. Thomas, *J. Magn. Reson. 41* (1980) 492.
[62] D. T. Pegg, D. M. Doddrell, W. M. Brooks, M. R. Bendall, *J. Magn. Reson. 44* (1981) 32.
[63] O. W. Sørensen, R. R. Ernst, *J. Magn. Reson. 51* (1983) 477.
[64] P. E. Hansen, *Annu. Rep. NMR Spectrosc. 11A* (1981) 66; V. Wray, P. E. Hansen, *ibid. 11A* (1981) 99; J. Kowalewski, *Prog. Nucl. Magn. Reson. Spectrosc. 11* (1977) 1.
[65] K. Frei, H. J. Bernstein, *J. Chem. Phys. 38* (1963) 1216; J. M. Schulman, M. D. Newton, *J. Am. Chem. Soc. 96* (1974) 6295; J. Wardeiner, W. Lüttke, R. Bergholz, R. Machinek, *Angew. Chem. 94* (1982) 873; *Angew. Chem. Int. Ed. Engl. 21* (1982) 872.
[66] F. W. Wehrli, T. Wirthlin: *Interpretation of Carbon-13 NMR Spectra,* Heyden, London 1976, S. 121.
[67] H. Seto, T. Sato, H. Yonehara, *J. Am. Chem. Soc. 95* (1973) 8461.
[68] A. Bax, R. Freeman, S. P. Kempsell, *J. Am. Chem. Soc. 102* (1980) 4849.
[69] G. Bodenhausen, *Prog. Nucl. Magn. Reson. Spectrosc. 14* (1980) 113.
[70] A. Wokaun, R. R. Ernst, *Chem. Phys. Lett. 52* (1977) 407.
[71] L. Müller, *J. Am. Chem. Soc. 101* (1979) 4481.
[72] R. Benn, A. Rufinska, *J. Organomet. Chem. 238* (1982) C 27.
[73] R. Richarz, W. Ammann, T. Wirthlin, *J. Magn. Reson. 45* (1981) 270.
[74] R. Richarz, T. Wirthlin: *Varian Information Bulletin Z 13,* Zug 1981.
[75] P. Schmitt, H. Günther, *J. Magn. Reson. 52* (1983) 497.

[76] G. Bodenhausen, C. M. Dobson, *J. Magn. Reson. 44* (1981) 212.
[77] P. J. Hore, E. R. P. Zuiderweg, K. Nicolay, K. Dijkstra, R. Kaptein, *J. Am. Chem. Soc. 104* (1982) 4286.
[78] P. J. Hore, R. M. Scheck, A. Volbeda, R. Kaptein, J. H. van Boom, *J. Magn. Reson. 50* (1982) 328.
[79] A. Bax, R. Freeman, *J. Magn. Reson. 41* (1980) 507.
[80] O. W. Sørensen, R. Freeman, T. Frenkiel, T. H. Mareci, R. Schuck, *J. Magn. Reson. 46* (1982) 180.
[81] R. Benn, *J. Magn. Reson.*, in press.
[82] B. L. Tomlinson, H. D. W. Hill, *J. Chem. Phys. 59* (1973) 1775.
[83] a) G. Bodenhausen, R. Freeman, G. A. Morris, *J. Magn. Reson. 23* (1976) 171; b) G. A. Morros, R. Freeman, *ibid. 29* (1978) 433.
[84] For a literature source cf. [83b].
[85] P. Schmitt, H. Günther, unpublished results.
[86] S. Forsén, R. A. Hoffmann, *J. Chem. Phys. 39* (1963) 2892; R. A. Hoffmann, S. Forsén, *Prog. Nucl. Magn. Reson. Spectrsc. 1* (1966) 15.
[87] E. E. Wille, D. S. Stephenson, P. Capriel, G. Binsch, *J. Am. Chem. Soc. 104* (1982) 405.
[88] R. Freeman, S. P. Kempsell, M. H. Levitt, *J. Magn. Reson. 35* (1979) 447; M. H. Levitt, R. Freeman, *ibid. 43* (1981) 502; M. H. Levitt, R. Freeman, T. Frenkiel, *ibid. 47* (1982) 328; *50* (1982) 157; R. Freeman, T. Frenkiel, M. H. Levitt, *ibid. 50* (1982) 345. - For the theory of broadband decoupling see also J. S. Waugh, *J. Magn. Reson. 49* (1982) 517 and J. W. M. Jacobs, J. W. M. van Os, W. S. Veeman, *ibid. 51* (1983) 56.
[89] The idea of two-dimensional NMR spectroscopy is due to J. Jeener (lecture, Ampère Int. Summer School, Basko Polje, Yugoslavia 1971). R. R. Ernst was the first to recognize its general importance (cf. *Chimia 29* (1975) 179 as well as [11]). An interesting account of the historical development is given in [90a].
[90] Review articles on two-dimensional NMR spectroscopy: a) R. Freeman, G. A. Morris, *Bull. Magn. Reson. 1* (1979) 5; b) G. A. Morris in A. G. Marshall: *Fourier Hadamard and Hilbert Transformations in Chemistry*, Plenum, New York 1982; c) R. Freeman, *Proc. R. Soc. London 373* (1980) 149; d) A. Bax: *Two-Dimensional Nuclear Magnetic Resonance in Liquids*, D. Reidel, Dordrecht 1982.
[91] L. Müller, A. Kumar, R. R. Ernst, *J. Chem. Phys. 63* (1975) 5490.
[92] The splitting relative to the center amounts here to $\pm J$, and for the doublet only to $\pm J/2$.
[93] G. Bodenhausen, R. Freeman, R. Niedermeyer, D. L. Turner, *J. Magn. Reson. 26* (1977) 133.
[94] A comparative discussion of the time requirements for 1D and 2D NMR experiments is given by W. P. Aue, P. Bachmann, A. Wokaun, R. R. Ernst, *J. Magn. Reson. 40* (1980) 175.
[95] J. C. Lindon, A. G. Ferrige, *Prog. Nucl. Magn. Reson. Spectrosc. 14* (1980) 27.
[96] R. R. Ernst, R. Freeman, W. A. Anderson, *J. Chem. Phys. 46* (1967) 1125.
[97] R. K. Hester, J. L. Ackerman, B. L. Neff, J. S. Waugh, *Phys. Rev. Lett. 36* (1967) 1081.
[98] K. Nagayama, P. Bachmann, K. Wüthrich, R. R. Ernst, *J. Magn. Reson. 31* (1978) 133.
[99] The use of $\delta$-values implies the transformation of the frequency parameter $\nu$ [Hz] to the corresponding $\delta$-scale [ppm].
[100] G. Bodenhausen, R. Freeman, R. Niedermeyer, D. L. Turner, *J. Magn. Reson. 24* (1976) 291; L. Müller, A. Kumar, R. R. Ernst, *ibid. 25* (1977) 383.
[101] a) G. Bodenhausen, R. Freeman, D. L. Turner, *J. Chem. Phys. 65* (1976) 839; b) R. Freeman, S. P. Kempsell, M. H. Levitt, *J. Magn. Reson. 34* (1979) 663.
[102] R. Benn, *Z. Naturforsch. B37* (1982) 1054.
[103] R. Freeman, G. Morris, D. L. Turner, *J. Magn. Reson. 26* (1977) 373.
[104] G. Bodenhausen, S. P. Kempsell, R. Freeman, *J. Magn. Reson. 35* (1979) 337.
[105] G. Bodenhausen, D. L. Turner, *J. Magn. Reson. 41* (1981) 200; M. H. Levitt, R. Freeman, *ibid. 43* (1981) 65.
[106] A. Bax, R. Freeman, *J. Am. Chem. Soc. 104* (1982) 1099.
[107] W. P. Aue, J. Karhan, R. R. Ernst, *J. Chem. Phys. 64* (1976) 4226.
[108] A necessary requirement for this and the following discussions are spectra of first-order spin systems. For the influence of strong coupling see [11] or G. Wider, R. Baumann, K. Nagayama, R. R. Ernst, K. Wüthrich, *J. Magn. Reson. 42* (1981) 73.
[109] Analogous information is only obtained from $^1$H-decoupled $^2$H-NMR spectra of molecules with $^2$H natural abundance (0.015%).
[110] R. Benn, W. Riemer, *Z. Naturforsch. B36* (1981) 488.
[111] K. Nagayama, K. Wüthrich, P. Bachmann, R. R. Ernst, *Biochem. Biophys. Res. Commun. 78* (1977) 1.
[112] K. Nagayama, K. Wüthrich, *Eur. J. Biochem. 114* (1981) 365.
[113] K. Nagayama, *Adv. Biophys. 14* (1981) 139.
[114] L. D. Hall, J. K. M. Sanders, *J. Am. Chem. Soc. 102* (1980) 5703; D. Leibfritz, E. Haupt, M. Feigel, W. E. Hull, W.-D. Weber, *Liebigs Ann. Chem. 1982*, 1971.
[115] L. D. Hall, S. Sukumar, *J. Am. Chem. Soc. 101* (1979) 3120.
[116] J. R. Everett, D. W. Hughes, A. D. Bain, R. A. Bell, *J. Am. Chem. Soc. 101* (1979) 6776.
[117] H. Lehmkuhl, J. Grundke, R. Benn, G. Schroth, R. Mynott, *J. Organomet. Chem. 217* (1981) C5.
[118] B. H. Meier, R. R. Ernst, *J. Am. Chem. Soc. 101* (1979) 6441; J. Jeener, B. H. Meier, P. Bachmann, R. R. Ernst, *J. Chem. Phys. 71* (1979) 4546; S. Macura, R. R. Ernst, *Mol. Phys. 41* (1980) 95; A. Kumar, R. R. Ernst, K. Wüthrich, *Biochem. Biophys. Res. Commun. 95* (1980) 1; A. Kumar, G. Wagner, R. R. Ernst, K. Wüthrich, *ibid. 96* (1980) 1156.
[119] A. A. Maudsley, L. Müller, R. R. Ernst, *J. Magn. Reson. 28* (1977) 463; G. Bodenhausen, R. Freeman, *ibid. 28* (1977) 471; *J. Am. Chem. Soc. 100* (1978) 320.
[120] R. Freeman, G. A. Morris, *J. Chem. Soc. Chem. Commun. 1978*, 684.
[121] G. A. Morris, L. D. Hall, *J. Am. Chem. Soc. 103* (1981) 4703.
[122] D. C. Finster, W. C. Hutton, R. N. Grimes, *J. Am. Chem. Soc. 102* (1980) 400.
[123] R. Benn, A. Rufinska, G. Schroth, *J. Organomet. Chem. 217* (1981) 91.
[124] H. Kessler, E. Hehlein, R. Schuck, *J. Am. Chem. Soc. 104* (1982) 4534.
[125] P. H. Bolton, G. Bodenhausen, *J. Am. Chem. Soc. 101* (1979) 1080.
[126] a) A. Bax, R. Freeman, *J. Magn. Reson. 42* (1981) 164; b) *ibid. 44* (1981) 542.
[127] K. Nagayama, A. Kumar, K. Wüthrich, R. R. Ernst, *J. Magn. Reson. 40* (1980) 321.
[128] N. Darby, T. M. Cresp, F. Sondheimer, *J. Org. Chem. 42* (1977) 1960; H. Günther, M.-E. Günther, D. Mondeshka, H. Schmickler, F. Sondheimer, N. Darby, T. M. Cresp, *Chem. Ber. 112* (1979) 71.
[129] J. D. Mersh, J. K. M. Sanders, *J. Magn. Reson. 50* (1982) 289.
[130] W. E. Hull, *Two-Dimensional NMR*, Bruker Analytische Meßtechnik, Karlsruhe, 1982; the brochure contains numerous experimental hints, examples for applications, and a literature survey.
[131] T. H. Mareci, R. Freeman, *J. Magn. Reson. 48* (1982) 158; *Abstr. 6th EENC Super-Nendaz*, Valais 1982, p. 64.
[132] G. Eich, L. Braunschweiler, O. W. Sørensen, G. Bodenhausen, R. R. Ernst, *Abstr. 6th EENC Super-Nendaz*, Valais 1982, p. 14; G. Eich, G. Bodenhausen, R. R. Ernst, unpublished results; U. Piantini, O. W. Sørensen, R. R. Ernst, *J. Am. Chem. Soc. 104* (1982) 6800.
[133] P. H. Bolton, *J. Magn. Reson. 48* (1982) 336; P. H. Bolton, G. Bodenhausen, *Chem. Phys. Lett. 89* (1982) 139.
[134] A. Bax, R. Freeman, T. A. Frenkiel, M. H. Levitt, *J. Magn. Reson. 43* (1981) 478.
[135] T. H. Mareci, R. Freeman, *J. Magn. Reson. 48* (1982) 158.
[136] R. Benn, *Org. Magn. Reson. 21* (1983) 60.
[137] R. Jacquesy, C. Narbonne, W. E. Hull, A. Neszmelyi, G. Lukacs, *J. Chem. Soc. Chem. Commun. 1982*, 409.
[138] G. Binsch, H. Kessler, *Angew. Chem. 92* (1980) 445; *Angew. Chem. Int. Ed. Engl. 19* (1980) 411.
[139] W. von Philipsborn, *Angew. Chem. 83* (1971) 470; *Angew. Chem. Int. Ed. Engl. 10* (1971) 472.
[140] W. E. Hull: *Bruker Report Nr. 1*, Bruker Analytische Meßtechnik, Karlsruhe 1978.
[141] S. Macura, Y. Huang, D. Suter, R. R. Ernst, *J. Magn. Reson. 43* (1981) 259.
[142] C. Bösch, A. Kumar, R. Baumann, R. R. Ernst, K. Wüthrich, *J. Magn. Reson. 42* (1981) 159; G. Wagner, K. Wüthrich, Eur. J. Biochem. 114 (1981) 375; R. Baumann, A. Kumar, R. R. Ernst, K. Wüthrich, *J. Magn. Reson. 44* (1981) 76; S. Macura, K. Wüthrich, R. R. Ernst, *ibid. 46* (1982) 269.
[143] M. S. Broido, D. R. Kearns, *J. Magn. Reson. 41* (1980) 496.
[144] H. Kessler, W. Bermel, A. Friedrich, G. Krack, W. E. Hull, *J. Am. Chem. Soc. 104* (1982) 6297.
[145] Y. Huang, S. Macura, R. R. Ernst, *J. Am. Chem. Soc. 103* (1981) 5327.
[146] R. Benn, *Angew. Chem. 94* (1982) 633; *Angew. Chem. Int. Ed. Engl. 21* (1982) 626.
[147] R. Baumann, W. P. Aue, L. Müller, R. R. Ernst, *J. Magn. Reson. 28* (1977) 29.
[148] M. H. Levitt, R. Freeman, *J. Magn. Reson. 34* (1979) 675.
[149] B. Blümich, D. Ziessow, *J. Magn. Reson. 49* (1982) 151.
[150] A. Bax, R. Freeman, G. A. Morris, *J. Magn. Reson. 43* (1981) 333; A. de Marco, K. Wüthrich, *ibid. 24* (1976) 201.
[151] D. L. Turner, *J. Magn. Reson. 39* (1980) 391.
[152] L. D. Hall, S. Sukumar, *J. Magn. Reson. 38* (1980) 555, 559.
[153] W. Jin-Shan, Z. De. Zheng, J. Tao, H. Xiu-Wen, G. Guo-Bao, *J. Magn. Reson. 48* (1982) 216.
[154] A. Bax, A. F. Mehlkopf, J. Smidt, *J. Magn. Reson. 40* (1980) 213.
[155] L. D. Hall, S. Sukumar, *J. Magn. Reson. 40* (1980) 405.
[156] Modern NMR spectrometers allow the application of independent transmitter and decoupler pulses in 90° steps along the +x, +y, −x, and −y axes, as well as the choice of the detector phase. If the phase program is repeated after n steps, one speaks of a so-called n-step

phase cycle. For multiple quantum investigations smaller phase shifts are of interest, which require, however, further hardware modifications (see *e.g.* M. Hintermann, L. Braunschweiler, G. Bodenhausen, R. R. Ernst, *J. Magn. Reson. 50* (1982) 316).
[157] A. Bax, G. A. Morris, *J. Magn. Reson. 42* (1981) 501.
[158] G. Bodenhausen, R. Freeman, D. L. Turner, *J. Magn. Reson. 27* (1977) 511.
[159] R. Baumann, G. Wider, R. R. Ernst, K. Wüthrich, *J. Magn. Reson. 44* (1981) 76, 402.
[160] J. D. Mersh, J. K. M. Sanders, *J. Magn. Reson. 50* (1982) 171.

# From Environmental Analytical Chemistry to Ecotoxicology—A Plea for More Concepts and Less Monitoring and Testing

**By Werner Stumm, René Schwarzenbach, and Laura Sigg**

The development of cultural and technical civilization has been marked with increasing interference in hydrogeochemical cycles and the production of a growing number of chemicals; this is accompanied by a growing concern on the potential adverse effects of chemicals on biological systems. Assessment of the potential toxicological and ecological effects of pollutants is of central importance. We are of the opinion that this cannot be accomplished by merely evaluating the harmfulness of a substance on the basis of toxicity tests with individual organisms and by monitoring analytically the environment for pollutants. We would like to encourage chemists to participate in the solution of ecotoxicological problems: chemodynamical concepts permit the estimation—on the basis of physical-chemical generalizations and with the help of compound-specific data—of the fate, the distribution, the potential for bioaccumulation in the food chain, and the approximate residence time of pollutants (and thus the attainable residual concentrations) in the environment and therefore to predict the relative risk of different pollutants.

## 1. Introduction

Human society runs on material and energy. In industrialized nations, the anthropogenic energy flow per unit area exceeds biotic energy flux (energy fixed by photosynthesis) by a factor of about ten; organic material produced by industry (*ca.* 150 kg $yr^{-1}$ per inhabitant, or *ca.* 40 g $m^{-2}$ $yr^{-1}$) is within one order of magnitude of that synthesized by nature (net primary production: *ca.* 300 g $m^{-2}$ $yr^{-1}$)[1,2]. The hydrogeochemical cycling of dissolved and suspended materials (*e.g.* phosphorus, heavy metals) is accelerated, and a large number of industrially synthesized chemicals are distributed by various pathways into the environment. Obviously, these anthropogenic activities, considered to be necessary for the maintenance of our civilization and culture, are achieved in many instances not without perturbation of ecosystems and effect on human health. It has been estimated[3] that *ca.* 60000 chemicals are in daily use and that this number increases by 1000 to 1500 substances every year. The evaluation of many of these substances and their impact on nature and human health is among the most important objectives of environmental science.

The *assessment* of this impact of chemical pollution and of the behavior of pollutants in the environment requires qualification and quantification in every respect of the reactions and interactions that occur. In the past, much effort has been directed towards: 1) monitoring the distribution and concentrations of chemical pollutants in the environment; and 2) testing the effects of individual pollutants on individual organisms. However, *monitoring* data can rarely be generalized unless one knows the significant interrelationships and interactions between the parts of an ecological system. Similarly, it is usually very difficult to assess the ecological effects of a given compound from *bioassays* with individual organisms under laboratory conditions.

In view of the great number of existing industrial chemicals, and considering the large amounts of environmental pollutants created every day by human activities, we need to develop and apply general concepts on the behavior and fate of pollutants and to use these concepts as an aid to procuring relevant analytical results. By evaluating the strength of natural and anthropogenic emission sources, and by identifying the relevant pathways, interactions and unit processes that govern the behavior and fate of chemicals in a given natural system, we can improve our ability to understand and predict the future fluxes, distribution,

[*] Prof. Dr. W. Stumm, Dr. R. Schwarzenbach, Dr. L. Sigg
Institut für Gewässerschutz und Wassertechnologie und
Eidgenössische Anstalt für Wasserversorgung, Abwasserreinigung und Gewässerschutz (EAWAG)
Eidgenössische Technische Hochschule Zürich
CH-8600 Dübendorf (Switzerland)

 © Verlag Chemie GmbH, 6940 Weinheim, 1983 0570-0833/83/0505-0380 $ 02.50/0 

and effects of pollutants on ecological systems and on human health. This will be illustrated by some selected examples primarily relevant to the aquatic environment.

Over the years, the gross pollutional load on receiving waters has increased, and its character has changed. Up to a few decades ago, most of our wastes derived predominantly from human and animal excreta and other biogenic components, whereas in recent years they have become increasingly overloaded with the discards of modern industrial society (synthetic chemicals, mining products such as phosphates and metals) and by-products of energy production. This change in waste composition has occurred as a result of industrial activities having grown faster than human populations. Many industrial chemicals reach receiving waters indirectly (*via* households, agricultural drainage, the atmosphere). Some of these substances are refractory (*i.e.* not readily biodegradable) and they progressively accumulate in aquatic ecosystems because self-purification and biological waste treatment are not very effective in eliminating such chemicals. We should remind ourselves that water is the most important linkage in all biogeochemical cycles; it acts as a solvent, catalyst and reagent in most ecosystem reactions and processes. In comparison to terrestrial ecosystems, aquatic systems are particularly sensitive to chemical perturbation[2].

## 2. The Ecotoxicological Task

It is the objective of ecotoxicology to assess the hazards associated with pollutants in the environment. It includes 1) the study of the effects of a given chemical on the environment, especially upon ecology and on human health, and 2) the elucidation of the effect of the environment on the pollutant. As has been pointed out by *Baughman et al.*[4,5] and others[6-11], the second part of this objective, until recently neglected, is of particular importance in any *predictive* environmental assessment.

Figure 1 illustrates synoptically the realms and *perspectives of aquatic ecotoxicology*. We consider first the release of a potential pollutant into the aquatic environment. The transfer of the pollutant into various reservoirs (air, water, soil, biota, *etc.*), its ultimate distribution and residual concentration (activity or fugacity[9]) depend on the physical, chemical and biological *compound-specific properties of the pollutant* (vapor pressure, solubility, functional groups, Henry coefficient, lipophility, adsorbability, chemical and biological degradability) as well as on the *properties of the environment* (flow of water, type of interfaces, transport of particles, photosynthesis and nutrient cycles, redox intensity, presence of other constituents, *etc.*).

### 2.1. From Input to Exposure

Let us follow the various steps from the source to the potential ecological effects of a pollutant released into an aquatic ecosystem. The immission is measured as a flow or load (*capacity* factor; mass per unit time or mass per unit time and volume or area). The resulting concentration is a consequence of dilution, transport, and transformation of this chemical. At any point, the *water condition* is characterized by the entity of interacting physical, chemical, and biological factors which are all *intensity* factors (activity, concentration, redox intensity, velocity gradient, temperature, productivity, *etc.*). These intensive variables, above all

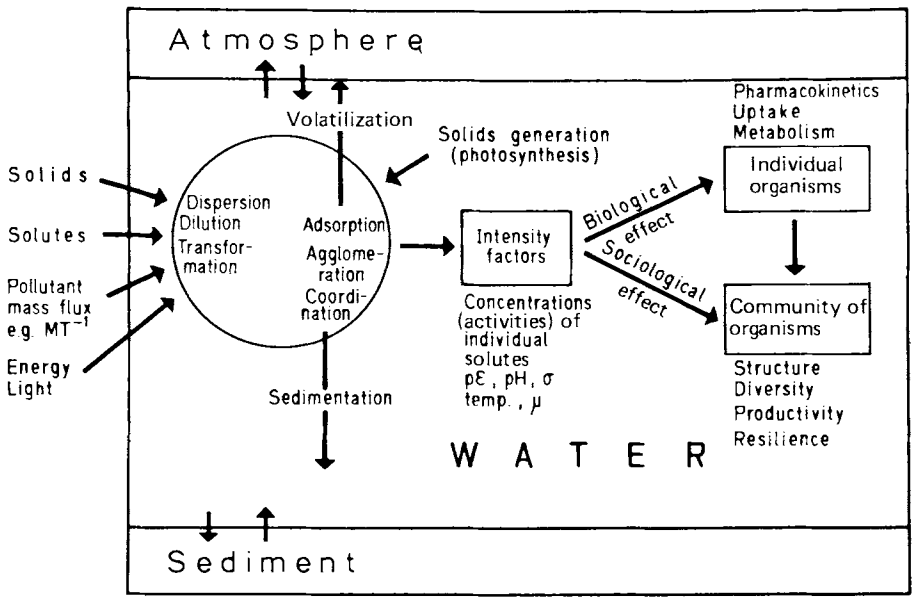



Fig. 1. Aquatic ecosystem transfer and transformation of pollutants by different pathways and various chemical, biological and physical processes. A substance introduced into the system becomes dispersed and diluted: it can become eliminated from the water by adsorption on settling particles or by escape (volatilization) into the atmosphere; it can become transformed chemically or biologically. The residual activities (concentrations) and other intensity factors (pε, velocity gradient, temperature, *etc.*) determine causally physiological, toxicological and sociobiological effects on organisms and their communities.

the concentrations, or, more precisely, the activities of the individual constituents, determine causally the doses (concentration × time) an organism or an ecosystem will receive and thus, in turn, the type of community of organisms present in the ecosystem.

Thus, for an assessment of the exposure and an evaluation of the ecological and hygienic risk, we need to know the residual concentrations of pollutants. An estimate of the ambient concentration of a pollutant based on a prediction of its relevant fate and residence time (considering relevant pathways, exchange processes, biological and chemical conversions) is essential to any hazard assessment. The problem of estimating the dose (activity) is one of the things that distinguishes ecotoxicology from classical toxicology.

The importance of the concentration (activity) of the individual solutes for interpreting the cause/effect relationship depends—in the sense of a simple model—essentially on the thermodynamic statement that, for an equilibrium distribution, the chemical potential (related to the activity) is the same in all phases, *i.e.* in the solution, in the organism, in the sediments, in the gas phase, *etc.*[12]. Under conditions of non-equilibrium, the difference in chemical potential (the activity gradient) is the driving force for the transfer of a substance from one reservoir into another, *e.g.* from water into an organism; but active mechanisms of transport into the inside of a cell are also possible.

### 2.2. The Toxic Effect

The ecological harmfulness of a substance depends on its interaction with organisms or with entire communities of organisms (Fig. 1). The intensity of this interaction depends on the specific structure and on the activity of the substance under consideration; but other factors such as temperature, turbulence, and the presence of other substances are also important. A thorough knowledge of the basic mechanisms by which toxic agents exert their injurious effects (pharmacokinetics, uptake, conversion, degradation and separation, disturbance of regulatory mechanisms in the biological community) is fundamental for an understanding of biological responses. Comparative toxicological research is necessary in order to extrapolate effects observed in laboratory experiments to organisms in nature and from one organism to another or to man.

In evaluating *toxicity,* we need to distinguish between:

1) Substances which have a direct effect on humans, animals and other terrestrial or aquatic organisms (here one often speaks of acute, subacute or chronic toxicity, depending on the time interval within which an effect is observed).
2) Substances which primarily affect the organization and structure of an ecosystem. Here a contaminant may impair the self-regulatory functions of the system or interfere, in a subtle way, with food chains.

*Sociobiological Effects:* While we have some knowledge about the impact of xenobiotic substances on individual organisms, we know less about their impact on ecosystems. In considering biological communities (the biocoenoses) various intra- and inter-species interactions of a sociobiological nature (*e.g.* chemotaxis and chemoreception) have to be taken into account.

The natural distribution of organisms depends primarily on their ability to compete under given conditions and not merely on their ability to survive the physical and chemical environment; a population will be eliminated when its competitive power is reduced to such an extent that it can be replaced by another species[13, 14]. The competitive abilities of an organism are an interplay of its reproductive rates, which are related to food and physiological potential, and the mortality rates from all sources, including predation and imposed toxicity[14]. *Tinbergen*[15] pointed out that there are millions of ways in which an organism can die, but that there is only a very narrow range of ways in which it can survive and leave offspring. Thus, in an ecosystem, a population may be eliminated by the presence of pollutants even at apparently trivial toxicity levels if its competitive ability is marginal, or if it is the most sensitive of the competitors. Often, contaminants at very low concentrations cause changes in the structure of the population by interfering through chemotaxis with interorganismic communication. For example, the survival of a fish population may be rendered impossible by a pollutant (even if it exhibits neither acute nor chronic toxicity to the particular species of fish) if it impairs the food source (zooplankton) or disturbs chemotactical stimuli or mimicks wrong signals (and thus, for example interferes with food finding).

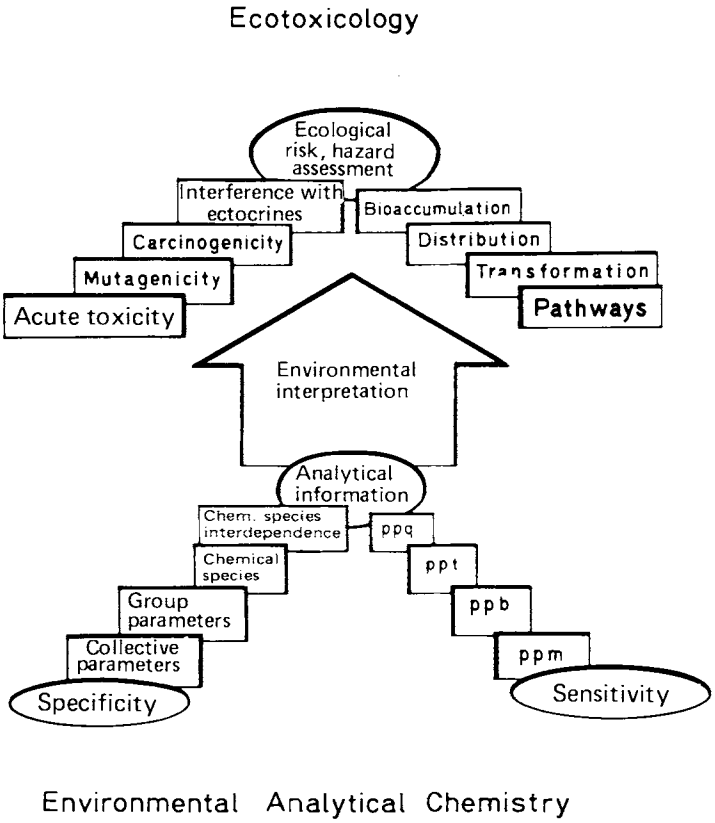



Fig. 2. Interrelationship between environmental analytical chemistry and ecotoxicology; the establishment of cause-effect relationships hinges significantly on the ability to *sensitively* and *selectively* detect individual components in a complex environmental system.

As a consequence of the many microhabitats (niches) that are typically present in a "healthy" water, many species can survive. Because of inter-species competition, most species are present in a low population density. Pollution destroys microhabitats, diminishes the chance of survival for some of the species, and thus in turn reduces the competition; the more tolerant species become more numerous. This shift in the frequency distribution of the species towards a lower diversity of the ecosystem is a general consequence of the chemical impact on waters by substances non-indigeneous to nature[13].

## 3. The Role of Environmental Analytical Chemistry

Figure 2 illustrates the interdependence between environmental analytical chemistry and ecotoxicology, *i.e.* the assessment of the environmental fate and the impact of chemical substances. An understanding of the interaction of chemical compounds in the natural system, that is the mode of their participation in various processes, hinges on the recognition of the compositional complexity of the environment. This requires an adequate analytical methodology, especially the ability to detect individual components (chemical species) *selectively* and to measure them accurately and with the *greatest sensitivity.*

*Specificity:* The environmental behavior and impact of a substance (biological availability, physiological and toxicological effects, adsorbability, chemical, biochemical and geochemical reactivity) are strongly *structure-specific.* Figure 3 illustrates that organic isomers may exhibit remarkable differences in toxicity, chemical reactivity and adsorptivity. The same is true for inorganic constituents. Figure 4 shows the various forms in which metals are thought to occur in natural waters. The different species have different effects. For example $CuCO_3(aq)$ and $Cu(aq)^{2+}$ each affect the growth of algae in quite different ways[16]. Collective

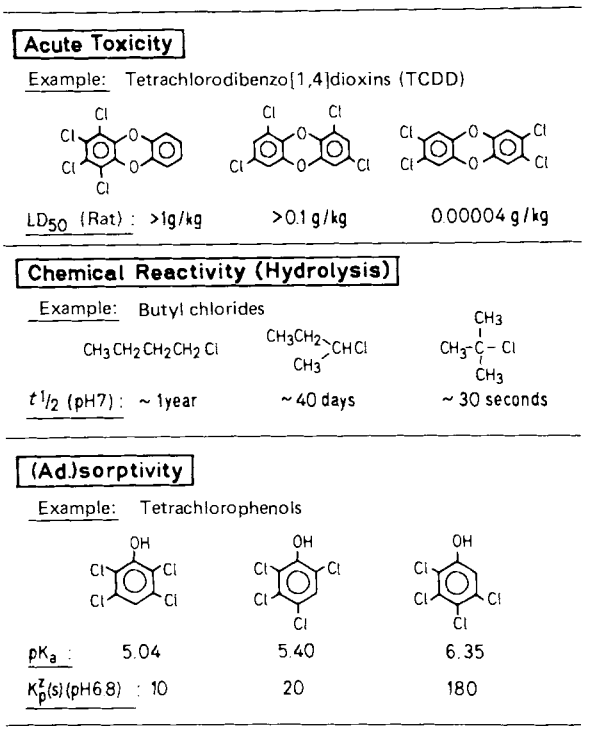



Fig. 3. Chemical and biological reactivity is strongly structure-specific. $LD_{50}$ is the concentration that will produce death in half the population, $t_{1/2}$ is the half-life; $pK_a$ is the neg. log of the acidity constant; $K^z_{p(s)}$ is the distribution coefficient [$m^3\ 10^{-3}\ kg^{-1}$] between a solid (surface) phase (containing 2.9% organic carbon) and the solution.

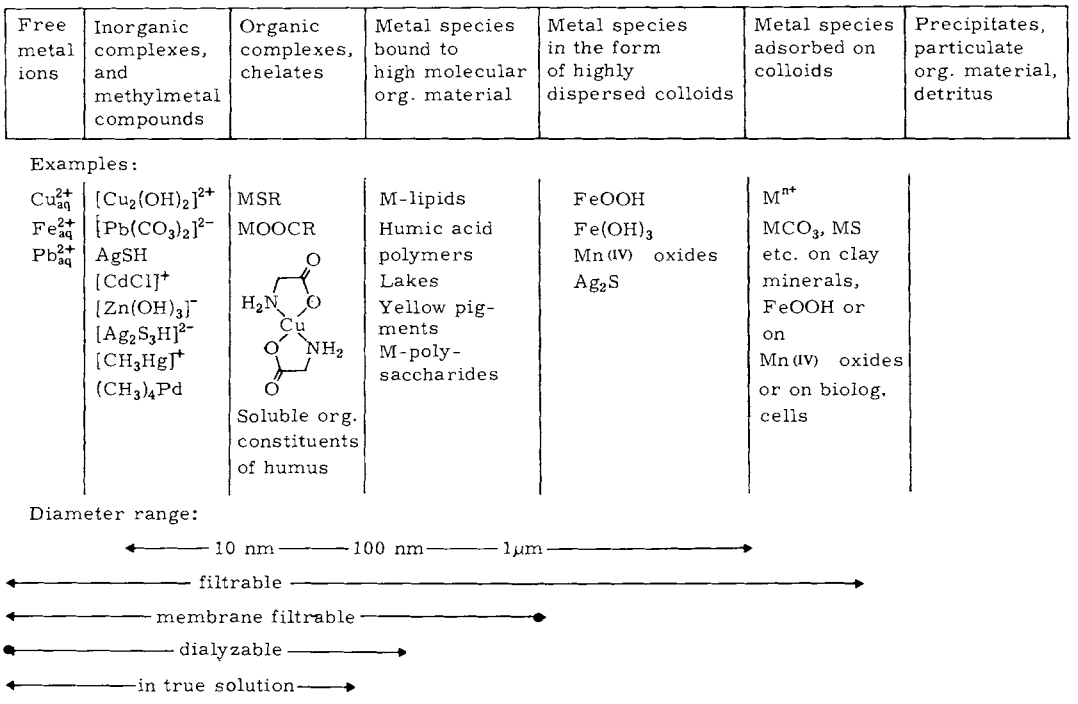



Fig. 4. A knowledge of the forms of occurrence of metals (free metal ion, inorganic or organic complex) is a prerequisite for evaluating biological and chemical effects. It is operationally difficult to distinguish between dissolved and colloidally dispersed substances because membrane filters may not always retain colloids.

parameters such as total organic carbon, copper(II) or total phosphorus, although often useful in establishing total loads, are not suitable for establishing cause-effect relationships between chemistry and biology. For the determination of individual organic chemical species, various methods capable of high selectivity (GC, GC/MS, and HPLC) are available. The specification of metal ions, usually attempted by electrochemical (voltammetric) means is, on the other hand, still a difficult problem.

*Sensitivity:* Analytical chemistry has made remarkable progress in improving the sensitivity of detection down to concentrations of $10^{-11}$ M. This has been a great help for studies on natural water systems, since aquatic ecosystems are more sensitive to chemical perturbation than terrestrial ones. The resorption of a substrate or the uptake of a pollutant by aquatic organisms is controlled by enzymatic processes, and these are affected typically by concentrations lower than $10^{-6}$ M. (The Michaelis constant for enzymatically controlled processes is often between $10^{-5}$ and $10^{-10}$ M.) The growth rate of algae has been shown to be affected by free $Cu^{2+}$ ions at concentrations as low as $10^{-10}$ to $10^{-13}$ M, while concentrations as low as $10^{-8.5}$ M are toxic to daphnia and fish[16] (Fig. 5).

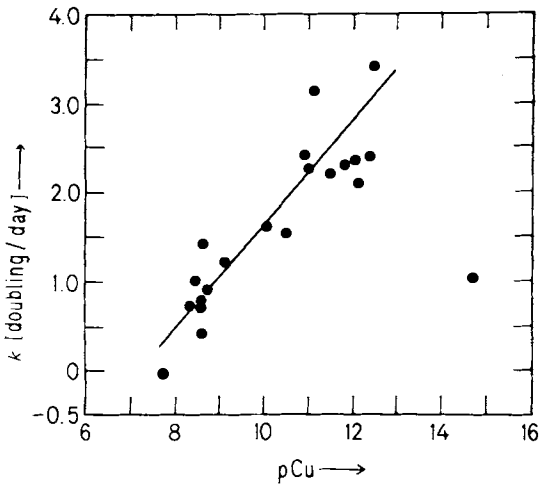



Fig. 5. Effect of "free" $Cu^{2+}_{aq}$ ions on the growth of algae in seawater. pCu was buffered in seawater by $Cu^{II}$ and various complex formers. pCu ($= -\log[Cu^{2+}]$) was calculated from the concentrations of $Cu^{II}$ and complex formers and the pH [16].

*Precision, Accuracy and Sampling:* The decisive prerequisite for any meaningful interpretation is the collection of reliable and accurate data. Because of the extremely low concentrations usually encountered, rather demanding problems have to be met in order to avoid contamination or loss of constituents in all stages, from sampling to sample pretreatment and sample preservation until analytical determination. For example, as shown by *Patterson et al.*[17], most of the results obtained before 1975 for Pb concentrations in seawater were an order of magnitude too high.

## 4. Limitations of Analytical Monitoring and Toxicological Testing

Understandably, the general public requires that the biological effect of pollutants be examined systematically by appropriate toxicity tests and that the environment be surveyed by monitoring programs that search for pollutants and toxicants. Such investigations are important, but we must not overvalue our analytical possibilities and the limited validity of standard toxicity tests.

We are concerned that the present preference and overemphasis of such programs over flexible basic and exploratory research may hinder rather than aid our understanding of nature and of its changing processes[7]. The systematic monitoring of the chemistry of a watershed or of a river or lake is an extremely involved, expensive, and time-consuming enterprise. Because of a lack of understanding of the reciprocal interactions between pollutants and the environment, much of the effort in the past had by necessity to be devoted to measuring, within the momentarily available "analytical window" (for a given methodology), "what is" rather than to projecting "what is likely to be" or "could be made to be". Baseline measurements, as special cases of monitoring, are more promising because they permit recognition of changes in the environment. Unfortunately, baseline records often turn out to be less valuable than one had hoped when the measurements were initiated, because one later realizes that at that time ignorance had prevented both a meaningful definition of the problem and the selection of the best method[17].

Nevertheless, knowledge gained from monitoring data is enhanced significantly if the data can be interpreted in a functional and rational way. To this end, a quantitative knowledge of the hydrological regime (water budget, rainfall, evapo-transpiration, runoff, infiltration) in the area, and information on input and on transformation pathways are required. Field measurements are essential, but they should be supplemented by concurrent laboratory studies on the chemodynamic properties of selected substances of interest in order to establish comparisons between measured field data and concentrations predicted from the "behavior profiles" of chemical species.

*Toxicity tests* are rarely designed to assess chronic toxicity or to evaluate impairment of self-regulatory functions of ecosystems. From an ecological point of view, these latter effects are more important than acute toxicity. Furthermore, one must take into consideration that for each substance (and its degradation intermediates), short and long-term tests with different organisms should be carried out in order to determine whether synergistic and antagonistic effects may occur in presence of other substances or different solution variables. Each negative test result may not mean "zero toxicity".

In addition, the sensitivity of different taxonomic groups to chemicals may vary markedly—even organisms of the same species may respond differently. Thus, results obtained with one kind of organism may not readily be extrapolated to other species. Obviously, new chemicals may be produced and enter the environment faster than they can be tested satisfactorily.

Although we have some knowledge of the effects of xenobiotic substances on individual organisms, our understanding of the impairment of whole aquatic ecosystems is very limited. As we have already seen (Section 2.2), even if no acutely damaging effects on individual organisms are observed, the ecological consequences of such impairment

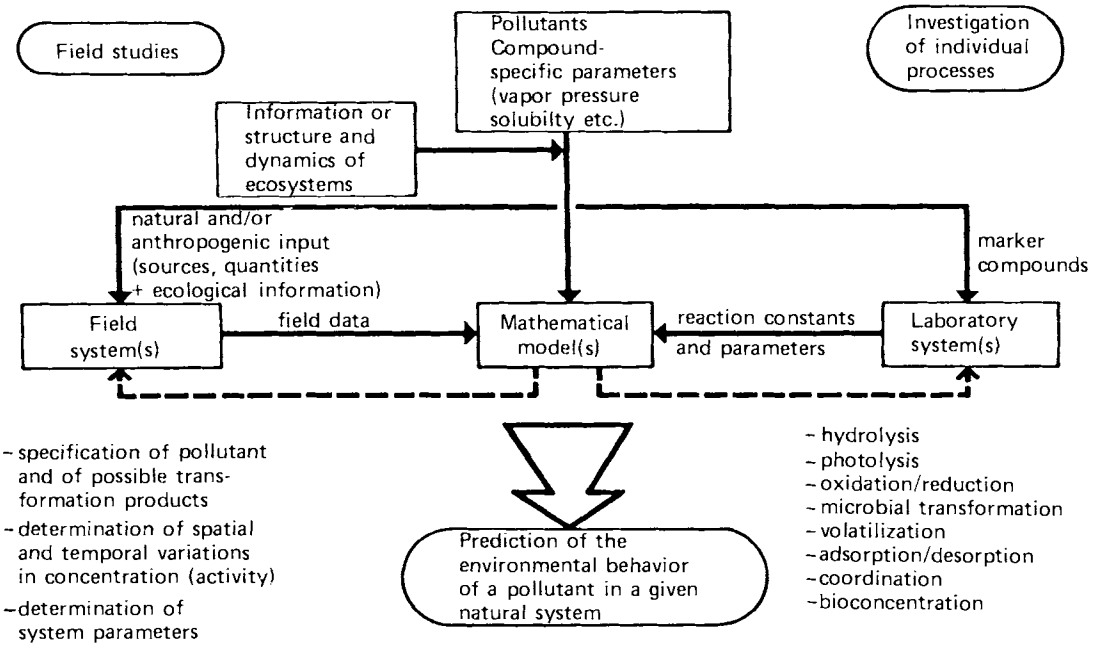



Fig. 6. Development of methods for predicting the environmental behavior of pollutants: General approach. The ecotoxicological and hygienic evaluation of pollutants requires establishing their "behavior profile" in the environment. With the help of simple models, it is in many cases possible to estimate the approximate residual concentrations.

to communities of organisms may often be more detrimental over long time spans than acute toxic effects.

## 5. Concepts for Assessing and Predicting the Environmental Behavior of Pollutants

### 5.1. Development of Predictive Assessment Models

As illustrated in Figure 6, three approaches complement each other in establishing predictive models:

1) A set of data of *compound-specific parameters* (vapor pressure, solubility, lipophility, Henry coefficient, biodegradability, *etc.*) aid in establishing the pollution potential of individual substances and permit one to forecast the manner in which the compounds are distributed in the environment, how fast they may be degraded chemically or biologically, and thus, in turn, to predict their fate and approximate residence time. Thus, a semiquantitative estimate of the ecological impact is obtained. In order to project the distribution of pollutants and how it is influenced by systemic variables, one needs to understand the structure and dynamics of ecosystems and the interactions between the biogeochemical cycles in aquatic ecosystems.

Table 1. Pertinent information to assess fate and residence time of pollutants.

| | *Parameter* | | *Significance* |
|---|---|---|---|
| Transport Paths<br>Mass Flow | production<br>statistics<br>mass balance<br>transport<br>mixing | | immission into environment<br>physical fate |
| Distribution<br>air-water<br>surface-water<br>sediment-water<br>biota-water | (ad)sorption<br>isotherms<br>solubility<br>vapor pressure<br>Henry constant<br>lipophilicity<br>n-octanol-water<br>distribution coeff.<br>mass transfer coefficient | equilibrium | interface transport<br>sedimentation<br>bioconcentration<br>bioaccumulation<br>food chain<br>biolog. retention<br>immission into and from atmosphere<br>dry deposition<br>precipitation scavenging<br>evaporation<br>condensation |
| Molecular<br>Transformation<br>microbial<br>oxidation<br>hydrolysis<br>photolysis | biodegradability<br>equilibrium constants<br>rate constants<br>light absorption | kinetic | residence time<br>half life<br>form of occurrence<br>structure-reactivity<br>correlations<br>photodecomposition |

2) *Laboratory studies* in which individual processes, *e.g.*, with model compounds, can be investigated under conditions where variables are known or kept constant are necessary in order to determine reaction constants and other substance-specific parameters.
3) *Field studies* are necessary in order to determine system parameters and to measure the spatial and temporal distribution of pollutants and to identify the forms of occurrence (species) of these chemicals.

The process of modelling is essential. *Empirical models* require fitting to on-site data and continuous updating with further collection of data. They have low capacity for transferability in time and space and for extrapolation beyond the range of data. *Causal models* based on the principles of physics, chemistry, and biology make possible the explicit incorporation of the effects of changes in land and water environments. In principle, causal models are more readily transferable in space and time. A mixed-model approach will be necessary for predicting the performance of complex systems.

Estimation of the *residence time* of a pollutant in a body of water (or in another reservoir of the environment) with the help of such models is of utmost importance because the residual concentration of the pollutant depends on the residence time. The latter is influenced by hydrological factors (*e.g.*, type of dispersion and loss through the outlet) and by non-hydrological processes (*e.g.* adsorption on settling particles or biomass and chemical and biological transformations).

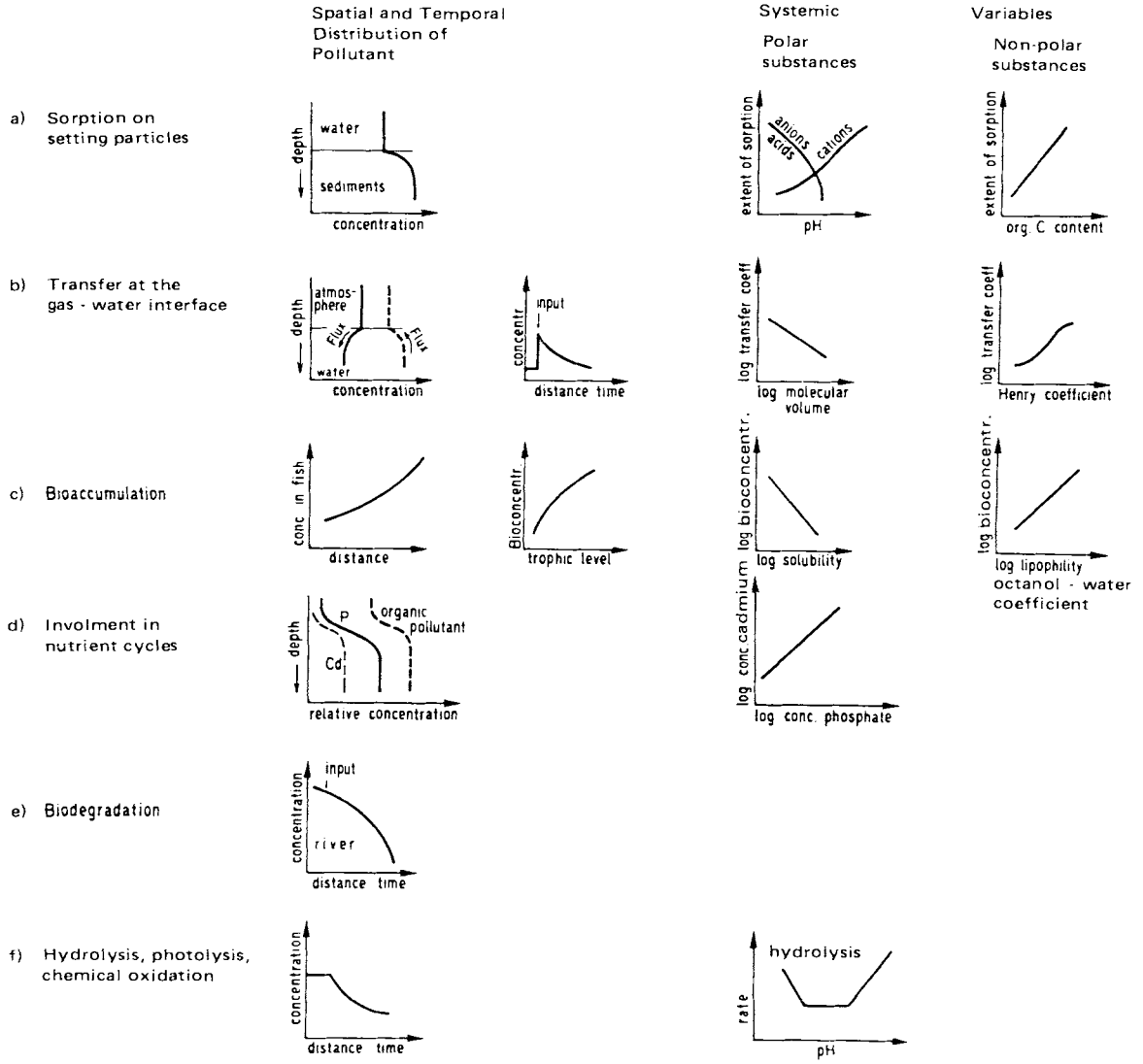



Fig. 7. Illustration of the dependence of spatial and temporal distribution of pollutants on compound-specific and systemic variables: a) The extent of adsorption of polar substances as a function of pH is different for a cationic, anionic or molecular (weak acid) adsorbate; for non-polar lipophilic substances, the extent of adsorption increases with increasing organic C content of the adsorbing particle; b) the concentration gradient at the water/atmosphere interface indicates in which direction the transfer of volatile substances occurs. The specific transfer coefficient is dependent on the Henry coefficient and on the molar volume of the substance as well as on the system-specific parameters such as water turbulence; c) the accumulation of a substance in the food chain is related to its lipophility or to the reciprocal of its solubility; d) nutrients, including certain heavy metals are, for example in oceans, withdrawn from the water during photosynthesis in the top water layers and returned as a consequence of respiration in the same proportions (corresponding to the composition of the biomass) in the deeper water layers; e) biodegradation is autocatalytic and proportional to the microbial biomass available; f) chemical and photochemical transformation processes are influenced by many solution variables, especially pH, light extinction, and concentration of singlet oxygen.

### 5.2. Examples of Relevant Processes

Basic physical, chemical and biological concepts, and unit processes may be modelled in order to predict the behavior of environmental pollutants. Table 1 and Figure 7 identify some of the relevant processes that need to be considered. Some of these processes will be briefly outlined:

*Adsorption:* Particles acting as scrubbing agents by scavenging are important in regulating the concentrations of pollutants. Thus, in water systems, all substances that are strongly adsorbed have small residence times relative to that of $H_2O$. Many xenobiotic substances, hydrophobic substances such as polychlorinated hydrocarbons, as well as polar substances such as lignin sulfonates from the paper industry, or heavy metals, are strongly sorbed to suspended particles. The settling of biogenic particles together with clays is responsible for the dynamic mechanism of elimination of heavy metals in lakes and oceans through transport into the sediments. Surface chemical theory aids in quantifying the extent of the reactions occurring at interfaces[18]. Often, a linear adsorption isotherm

$$[A_{ads}] \approx K_0[A_{aq}]$$

can be used to describe the distribution between solid surface and solution. For polar substances and ions, equilibrium constants have been experimentally determined or approximated from stability constants in electrolyte solutions; the extent of adsorption can thus be predicted as a function of pH and solution variables. The sorption of hydrophobic pollutants on settling particles or sediments and biota can usually be related to the *lipophility* of a substance, *i.e.* the tendency to become soluble in lipids and fats, and the organic carbon content, $f_{oc}$, of the adsorbing particles (Fig. 8). As a measure for lipophility, one usually uses the *n*-octanol/water partition coefficient, $K_{ow}$:

$$K_{ow} = [A_{oct}]/[A_{aq}]$$

As a measure of the distribution coefficient, $K_p$, for many groups of substances, equations of the type

$$K_p = b \cdot f_{oc}(K_{ow})^a$$

may be used[19], where a and b are constants and $K_p$ is expressed in units of volume per mass dry weight and $f_{oc}$ as weight fraction ($f_{oc}$ = organic carbon content of solid material).

*Exchange with the Atmosphere:* Transfer of volatile organic substances from aquatic systems to the atmosphere or *vice versa* can readily be examined in the laboratory. The equilibrium distribution of a compound is given by the Henry coefficient *H:*

$$H = [A_g]/[A_{aq}] = (p_A/RT)/[A_{aq}] = (p_A^0/RT)/[A_{aq}^0]$$

$[A_g]$, $[A_{aq}]$ and $[A_{aq}^0]$ are, respectively, the concentration of A in the gas phase, in aqueous solution and in a saturated solution (=solubility); $p_A$ and $p_A^0$ are, respectively, the partial pressure of A and the vapor pressure of pure A (or the vapor pressure in equilibrium with a solution saturated with A).

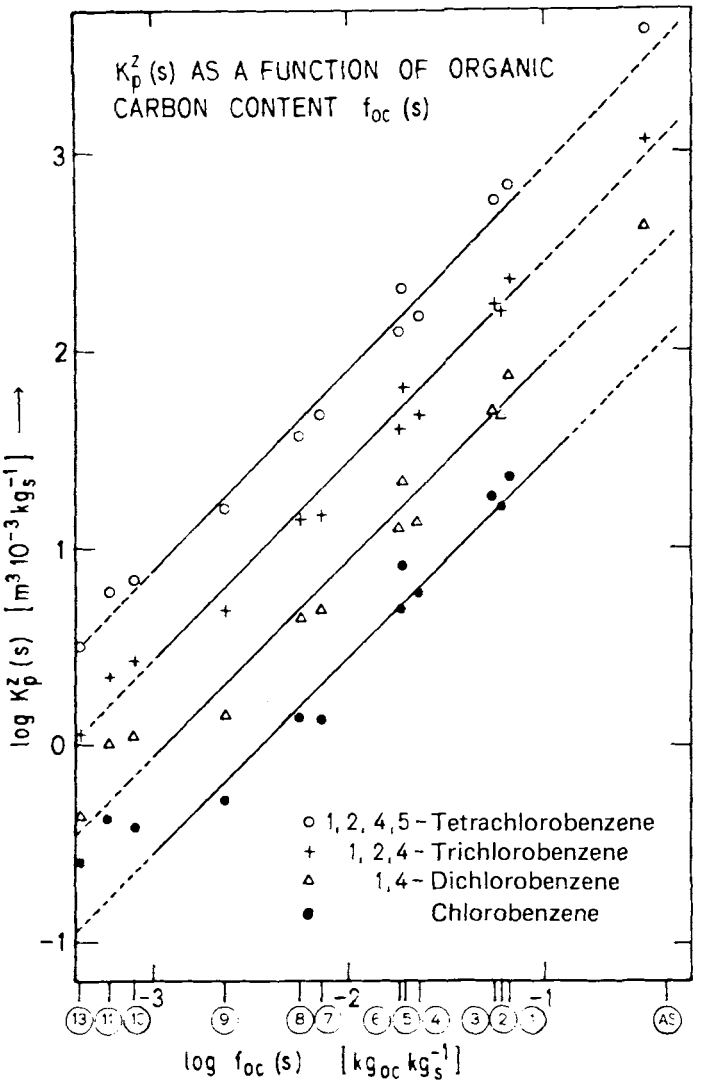



Fig. 8. The distribution of non-polar organic substances between aquatic solids and water (as given by the distribution coefficient $K_p$) is dependent upon the lipophility of the compound and the organic C content of the adsorbing material ($f_{oc}$ = weight fraction). The solid phases considered here are coastal sea and lake sediments (1–5), river sediments (6, 8), solids from aquifers (7, 9–12) and activated sludge (AS). The octanol/water distribution coefficients are, respectively 500, 2400, 11200, and 52000 for chlorobenzene, 1,4-dichlorobenzene, 1,2,4-trichlorobenzene, and 1,2,4,5-tetrachlorobenzene.

The rate of transfer *F* of compound A across the water gas phase boundary can be expressed by

$$F = K_L([A_{aq}] - [A_g]/H)$$

where $K_L$ is the overall gas transfer coefficient ($K_L$ depends on the hydrodynamic conditions; for most volatile substances $K_L$ is of a similar order of magnitude as that of oxygen). Substances having a Henry coefficient larger than *ca.* 0.1 are transferred relatively rapidly from waters of high turbulence to the atmosphere (see example in Fig. 9a). Less volatile compounds (*e.g.* DDT; $H \approx 5 \times 10^{-4}$) have, with regard to gas exchange with the atmosphere, a longer residence time in water; nevertheless, such relatively not very volatile substances "slowly" escape into the atmosphere where they are transported over large distances.

Figure 9b illustrates both; the transfer of a substance from the atmosphere into a lake water, and the "volatilization" of another substance from the lake.

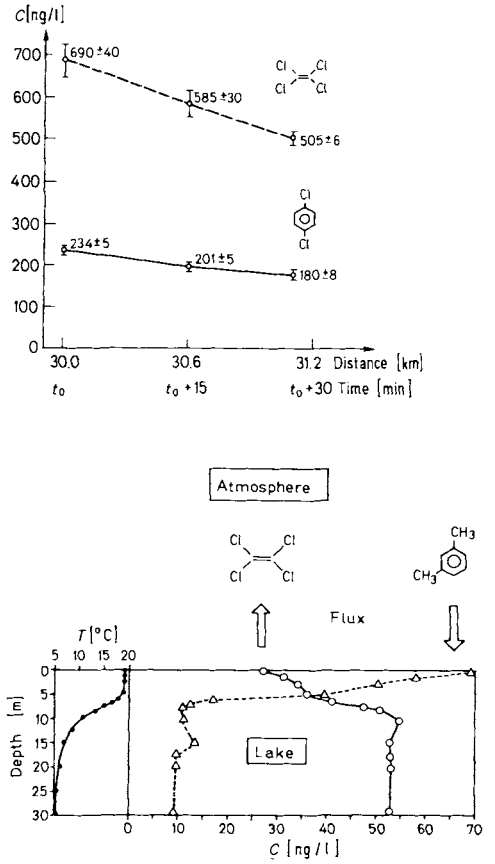



Fig. 9. Gas exchange between surface water and atmosphere is an important process for volatile organic substances. a) Concentration profile of tetrachloroethylene and 1,4-dichlorobenzene along a stretch (1.2 km; average depth 0.42 m) of the River Glatt (Switzerland). Some cascades are responsible for efficient gas exchange. The decrease in concentrations is mainly caused by the escape of these substances into the atmosphere ($t_{1/2}$ (tetrachloroethylene) = 65 min; $t_{1/2}$ (1,4-dichlorobenzene) = 80 min).—b) Exchange of nonpolar organic substances between Lake Zurich and the atmosphere. While 1,3-xylene (a component of gasoline) invades the lake water from the atmosphere, tetrachloroethylene (used in dry cleaning and metal degreasing), a water pollutant, escapes from the water into the atmosphere.

*Microbial Degradation:* Among the molecular transformations, *biodegradability* is one of the most important factors determining the residence time of organic pollutants in the receiving waters. Today, detailed knowledge of the microbiology, the mechanisms and the kinetics of the biotransformation of organic pollutants under natural conditions is still lacking. Many substances are readily altered to the extent that bacteria use their original structural entity, but the metabolites so formed are non- or slowly degradable. For example, as is illustrated in Figure 10, certain nonionic detergents yield ecologically objectionable degradation intermediates that persist in the water much longer than the parent compound[20].

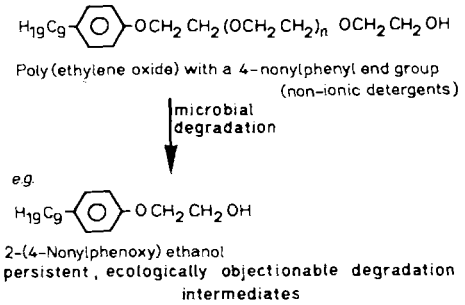



Fig. 10. Example of a group of substances which as a consequence of biological waste treatment is converted into a highly objectionable, relatively refractory degradation intermediate [20].

*Chemical Transformations:* In order to predict the reactivity of organic pollutants, it is often possible to utilize *structure reactivity correlations* because many organic chemicals share common reaction patterns and reactivities among like-structured chemicals; within a class of compounds, the reactivity of a functional group depends on the type and number of substituents. For example, the kinetic hydrolysis constant of organic phosphate esters of the type $(CH_3O)_2P(O)-OR$ can be correlated with the acidity constant of the leaving group ROH[24]. Furthermore, predictions on the dependence of kinetic constants of chemical reactions upon solution variables can often be made (*e.g.*, pH dependence of hydrolysis).

*Bioaccumulation:* Of particular importance in assessing the ecological or toxicological relevance of a pollutant is the question whether the substance is incorporated into the biota. Such incorporation may lead to a retention of the pollutant and its biomagnification in the food chain. Incorporation into biomass is related to the lipophility as measured by the *n*-octanol/water distribution coefficient[21] (Fig. 11). The tendency of certain pollutants to become accumulated in the food chain is much stronger in aquatic ecosystems than in terrestrial ones because the products of photosynthesis are consumed to a much larger extent by herbivores in waters than on land, where the plants are mostly degraded by microorganisms.

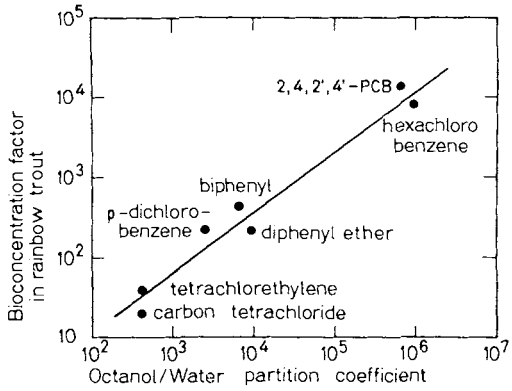



Fig. 11. The lipophility of a substance, as measured by the octanol/water distribution coefficient, is an essential parameter for predicting biomagnification (biostorage and accumulation in the food chain) (calculated from data by *Chiou et al.* [21]). 2,4,2',4'-PCB = 2,4,2',4'-tetrachlorobiphenyl.

## 6. The Consequences

Man's life is accompanied by his concern for safety. The evaluation of ecological and health effects caused by exposure to pollutants is extremely difficult because of our limited knowledge of the impact of chemicals on aquatic ecosystems. As we have tried to show, standard toxicity tests

with single organisms cannot be used to predict the subtle and often chronic impacts of substances on humans and ecology.

As long as our insight into the effect of chemicals on nature is so limited, we must remain very cautious in adopting tolerance levels; in establishing "minimum adverse effect levels", we must demand safety factors that are adequate to protect against the unanticipated effects of yet unsuspected biologically active compounds in the environment. On the other hand, there exists for every substance—even if not accessible experimentally—a certain level of exposure below which damage is highly improbable. The concern for ecosystem protection and safeness cannot exceed a reasonable incremental cost/benefit ratio. The final decision for this balance between ecological and toxicological measures and economics and the public propensity for risk acceptance is after all political; but the environmental scientist should procure better scientific criteria for this decision-making process. Exploratory multidisciplinary research on comparative toxicology, on the cycles of energy and nutrients in ecological communities, and on the impact of chemicals and other stresses upon structure and species distribution frequency can eventually yield criteria that permit the establishment of no adverse effect tolerance levels for substances non-indigeneous to natural systems.

The recommendation made here, *i.e.* to predict, on the basis of substance-specific parameters, the fate, the distribution, the tendency for bioaccumulation and the approximate residence time of potential pollutants, and to estimate their most likely attainable residual concentrations permits a comparison of various substances concerning their relative risks and impairment potential. The confidence in such assessments can be enhanced if field measurements give relative agreement between concentrations predicted and those observed.

Biodegradability and lipophility (lipophilic storage in organisms) are among the most important compound-specific criteria. The best and perhaps most economically feasible way to safeguard aquatic ecosystems and humans against unanticipated effects of organic pollutants is to require: 1) that all substances that are mass-produced and may become dispersed into the environment because they are being used in households, small trades, and agriculture (*e.g.* detergents, cleaning fluids, agrochemicals) have a satisfactory biodegradability; and 2) that in industrial production, the recovery or safe disposal of intermediates and residuals becomes an integral part of the production process.

In establishing priorities on policies in environmental protection, the question arises: What should be of greater concern, human health or "health" of the ecosystem? In answering this question, one needs to consider that the maintenance of resilient ecosystems with a sufficient diversity of organisms, *i.e.* systems that can resist structural and functional displacement, is a prerequisite for the well-being and health of humans.

It is encouraging to find that the ideas and concepts presented here—it may not have been sufficiently evident that much of our ideas have been influenced by the suggestions of *Baughman*[5], *Blumer*[7], *Mackay*[9], *Hapke*[6], *Mill*[10] and *Tinseley*[18]—are, at least partially, gaining some acceptance by the Organization for Economic Cooperation and Development (OECD)[3,22], the American Society for Testing Materials (ASTM)[5], and the US Environmental Protection Agency[23].

The expansion of chemistry will continue to shape our life styles. In the use of chemicals and in further developments, we have to accept the boundary conditions imposed by ecology and human health.

Received: November 12, 1982 [A 453 IE]
German version: *Angew. Chem. 95* (1983) 345

[1] F. Korte: *Ökologische Chemie*, Thieme, Stuttgart 1980.
[2] W. Stumm, J. J. Morgan: *Aquatic Chemistry*, Wiley-Interscience, New York 1981.
[3] OECD Guidelines for Testing of Chemicals, OECD, Paris 1981.
[4] G. L. Baughman, L. A. Burns in O. Hutzinger: *Environmental Chemistry, Vol. 2, Part A*, Springer, Berlin 1980.
[5] G. L. Baughman, R. Lassiter, *Am. Soc. Test. Materials STP 657*, Philadelphia 1978, p. 35.
[6] H. J. Hapke, *Toxicol. Environ. Chem. 3* (1981) 227.
[7] M. Blumer, *Angew. Chem. 87* (1975) 527; *Angew. Chem. Int. Ed. Engl. 14* (1975) 507.
[8] I. J. Tinsley: *Chemical Concepts in Pollutant Behavior*, Wiley-Interscience, New York 1979.
[9] D. Mackay, *Environ. Sci. Technol. 13* (1979) 1218; D. Mackay, S. Paterson, *ibid. 15* (1981) 1006.
[10] T. Mill: *Structure Reactivity Correlations for Environmental Reactions*, U. S. Environ. Protection Agency Reports 560/11-79-012, Washington 1979.
[11] O. Hutzinger, M. Th. M. Tulp, V. Zitko in O. Hutzinger, L. H. van Lelyveld, B. C. J. Zoeterman: *Aquatic Pollutants*, Pergamon, Oxford 1977.
[12] V. A. Filov, A. A. Gobulev, E. I. Liublina, N. A. Tolokontsev: *Quantitative Toxicology*, Wiley-Interscience, New York 1979.
[13] R. M. Patrick, H. Hohn, J. H. Wallace, *Proc. Natl. Acad. Sci. USA 259* (1954) 1.
[14] F. Taub, *Int. J. Environ. Stud. 10* (1976) 23.
[15] N. Tinbergen: *Signals for Survival*, Clarendon Press, Oxford 1970.
[16] G. A. Jackson, J. J. Morgan, *Limnol. Oceanogr. 23* (1978) 268.
[17] M. Burnett, C. C. Patterson in M. Branica, Z. Konrad: *Lead in the Marine Environment*, Pergamon, Oxford 1980.
[18] W. Stumm, R. Kummert, L. Sigg, *Croat. Chim. Acta 53* (1980) 291.
[19] R. P. Schwarzenbach, J. Westall, *Environ. Sci. Technol. 15* (1981) 1360.
[20] E. Stefanou, W. Giger, *Environ. Sci. Technol. 16* (1982) 800.
[21] C. T. Chiou, V. H. Freed, D. W. Schmedding, R. L. Kohnert, *Environ. Sci. Technol. 11* (1977) 475.
[22] F. Schmidt-Bleek, *Toxicol. Environ. Chem. 3* (1981) 265.
[23] J. H. Smith, R. W. Mabey, N. Bohonos, B. R. Holt, S. Lee, T. W. Chow, D. C. Bomberger, T. Mill: *Environmental Pathways of Selected Chemicals in Fresh Water Systems. Part I and II*, U. S. Environ. Protection Agency Reports 600/7-77-113, 600/7-78-074, Washington 1978.
[24] N. L. Wolfe, *Chemosphere 9* (1980) 571.

# Stable Carbodications**

By G. K. Surya Prakash, Tarik N. Rawdah, and George A. Olah*

Methods developed for the generation and study of stable carbomonocations can also be employed for similar investigations on carbodications. Trivalent (classical) as well as hexacoordinate (non-classical) carbodications studied under long-lived ion conditions are reviewed with special emphasis on their structural features, and investigated primarily by $^1$H- and $^{13}$C-NMR spectroscopy.

## 1. Introduction

At the turn of the century, the pioneering work of *Norris, Kehrmann,* and *Baeyer et al.* on triarylcarbenium ions generated wide interest in positively charged carbon compounds[1,2]. However, it was left to later investigators (between 1920—1960) like *Meerwein, Ingold, Hughes, Whitmore, Bartlett,* and *Winstein* to formulate the modern concept of carbocations based primarily on indirect kinetic and stereochemical studies[3]. In the early sixties we found ways to observe carbocations of a wide variety in low nucleophilicity superacidic systems[3]. Presently a remarkable number of carbocations are known and these have not only been detected as transients in chemical reactions, but in most cases have been isolated as long lived species under stable ion low nucleophilicity conditions. The structures of these long lived carbocations have been established by NMR, UV, IR, Raman, and X-ray photoelectron spectroscopy and the subject has been extensively reviewed[3].

Interest in carbocations has largely been confined to monopositive carbon species (carbomonocations). The study of dipositive carbon compounds (carbodications), has only more recently been undertaken, but interest in the area is rapidly growing and a review of this fascinating topic seemed timely. There is still very little information available on carbon multiply positively charged compounds (carbopolycations).

Carbodications have frequently been observed in gas phase mass spectrometric studies (without revealing any structural aspects). The first aryl-stabilized carbodications in solution were independently reported by *Hart et al.*[4] and *Volz et al.*[5] in the early sixties. Alkanediyl dications in which the positive charges are separated by two carbon atoms were first prepared by *Olah et al.*[6] in the mid-sixties. Since then significant experimental and theoretical work has been directed towards investigating carbodications. Although a substantial number of carbodications with widely varied structural features have been studied, their numbers are still relatively small when compared to those of carbomonocations. As in the case of carbomonocations, both classical carbodications (with trivalent carbon) and nonclassical carbodications (with penta and higher coordinated carbon) have been prepared and their structural characteristics have been analyzed primarily by NMR spectroscopy. Aromatic carbodications are known but hitherto no homoaromatic carbodications have been reported.

Our review summarizes the work pertaining to the study of stable carbodications generated under long lived stable ion conditions. We will not discuss either gas phase mass spectrometric observation of carbodications or theoretical quantum mechanical studies relating to dicationic species.

## 2. Generation of Carbodications

The most frequently used route for the generation of carbodications is the ionization of precursor dihalides (fluorides, chlorides) or other suitable precursors in superacids like $HF/SbF_5$, $FSO_3H$, $FSO_3H/SbF_5$ ("magic acid") or $SbF_5$ in low nucleophilicity solvents such as $SO_2ClF$ or $SO_2$. Temperatures in the range 0° to −120 °C are employed. In most cases higher temperatures result in decomposition, polymerization or rearrangement reactions. Ionization of diols in superacids can also lead to carbodications in some specific cases.

A second major route for the production of carbodications involves chemical oxidation of some electron rich compounds. Certain alkenes and arenes undergo two-electron oxidations in $SbF_5$ at low temperatures in solvents like $SO_2$ or $SO_2ClF$. In most cases these reactions occur only if the resulting dipositive species are stabilized by field or resonance effects or if the carbodications formed are Hückel type systems with $(4n+2)$ π electrons.

Electrochemical oxidations in polar aprotic solvents such as nitriles and nitro compounds can also be used for the generation of carbodications. This technique has mainly been employed for the generation of dipositive species from aromatic precursors. In most of these oxidations the cation-radical intermediates can be first detected, so low-temperature voltammetry is especially valuable here since homogeneous chemical reactions of intermediates generated at the electrode are greatly slowed down at low temperatures.

[*] Prof. Dr. G. A. Olah, Dr. G. K. S. Prakash
Hydrocarbon Research Institute and
Department of Chemistry
University of Southern California
University Park, Los Angeles, CA 90089 (USA)
Dr. T. N. Rawdah
Department of Chemistry
University of Petroleum and Minerals
Dharan (Saudi Arabia)

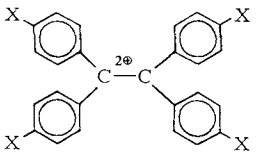
[**] Stable Carbocations, Part 242.—Part 241: G. A. Olah, G. K. S. Prakash, M. Arvanaghi, F. A. L. Anet, *J. Am. Chem. Soc. 104* (1982) 7105.

 © *Verlag Chemie GmbH, 6940 Weinheim, 1983* *0570-0833/83/0505-0390 $ 02.50/0* 

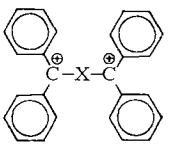
## 3. Classical Carbodications with Trivalent Carbon

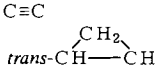
### 3.1. Acyclic Carbodications

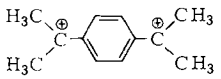
The majority of the acyclic carbodications which are reported in the literature have their positively charged centers stabilized by conjugation with one or more adjacent aromatic rings[4]. Typical representatives[6] of these ions are **1**, **2** and **3**. In all these carbodications the positive charge is substantially delocalized over the aromatic ring(s), as evidenced by the deshielding of the *ortho* and *para* H- and C-atoms and the concomitant downfield shift of the corresponding signals in the $^1$H- and $^{13}$C-NMR spectra.



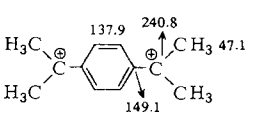
**1a**, X = $OCH_3$
**1b**, X = $N(CH_3)_2$



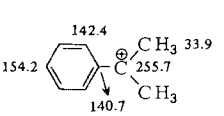
**3a**, X = $CH_2CH_2$
**3b**, X = *trans*-CH=CH
**3c**, X = C≡C
**3d**, X = *trans*- 
**3e**, X = 

**2** 

As an example we will discuss the nature of the dication **2**, in which the positively charged centers are appended to C1 and C4 of a benzene ring. The dication **2** was generated[6] from 2,2′-*p*-phenylenedi-2-propanol in $SbF_5/SO_2ClF$ at −78 °C. The $^1$H-NMR spectrum of the ion consists of only two single peaks at $\delta = 4.46$ and 9.28, while the $^{13}$C-NMR spectrum contains only four peaks at $\delta = 240.8$, 149.1, 137.9, and 42.8 consistent with a symmetrical dicarbenium ion structure **2**. Although the $^{13}$C-NMR chemical shifts of **2** are similar to those of the dimethyl(phenyl)carbenium ion (cumyl cation) **4**[7], charge distribution differences between **2** and **4** are apparent. Most notably, the carbenium carbon in **2** is more shielded than that in **4**, while the reverse is true for the methyl groups. The *ipso* carbon atoms in **2** are also reasonably deshielded. It appears that both positive charges are dispersed to a considerable extent into the neighboring methyl groups through hyperconjugative effects. The charge delocalization into the benzene ring is lowered due to coulombic repulsion. Similar effects are also observed in the case of dications **3b** to **3e**[6].

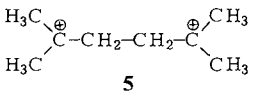



**2**

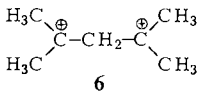



**4**

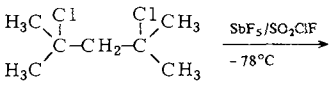
In the absence of aryl stabilization of the positively charged centers, long lived acyclic carbodications can be formed only if the charge bearing carbons are separated by at least two carbon atoms and the carbenium centers are tertiary[6,8]. The 2,2′-ethylenediisopropyl dication **5** prepared by the ionization of 2,5-dichloro-2,5-dimethylhexane in $SbF_5/SO_2ClF$ at −78 °C shows a triplet at $\delta = 4.24$ and a multiplet at $\delta = 5.04$ in the $^1$H-NMR spectrum. The large $J_{HH}$ coupling (3.0 Hz) in **5** between the methyl and methylene protons is characteristic of coupling across a carbenium ion center. The $^{13}$C-NMR spectrum shows three peaks at $\delta = 331.3$, 52.7 and 47.1 consistent with symmetrical carbenium ion structure **5**. The $^{13}$C-NMR shift of the carbenium ion centers in **5** is almost identical to that observed for the ethyldimethylcarbenium ion[9] at $\delta = 333.8$. The additivity of $^{13}$C-NMR chemical shift relationship[11] also shows the regular dicarbenium nature of the species. The total $^{13}$C-NMR chemical shift differences between dications and their parent hydrocarbons are twice as much as those typically observed for classical carbomonocations[11].



**5**

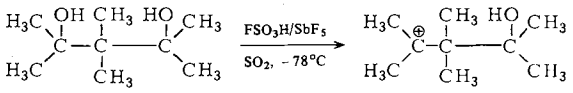


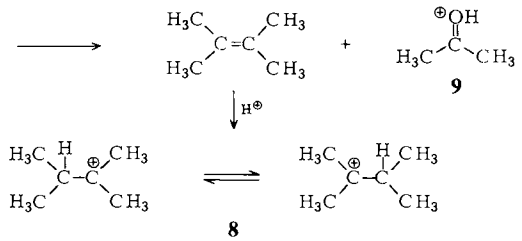
**6**




**7**

Attempts[6] to prepare the 2,2′-methylenediisopropyl dication **6** from 2,4-dichloro-2,4-dimethylpentane led to only the monocation **7**[12]. The potential dicarbenium ion **6** has the two carbenium ion centers separated by only one carbon atom and evidently, if this dication does form, it has only a transient existence, rapidly eliminating a proton to give **7**. Attempted[6] blocking of proton elimination by the ionization of 2,3,3,4-tetramethyl-2,4-pentanediol resulted in quantitative cleavage to the equilibrating isopropyldimethylcarbenium ion **8**[13] and protonated acetone **9**.

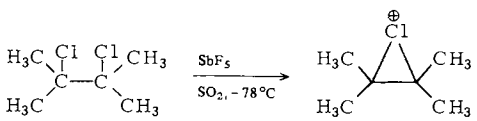


**9**

**8**

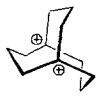
Ionization of 2,3-dichloro-2,3-dimethylbutane, where the two potential carbenium centers are adjacent, gave only the cyclic chloronium ion **10**[14].




**10**

### 3.2. Cyclic and Polycyclic Carbodications

The most interesting examples of bicyclic carbodications are the 1,4-bicyclo[2.2.2]octanediyl[15] and 1,5-bicyclo[3.3.3]undecanediyl[16] dications **11** and **12** respectively, in which the bridgehead C-atoms function as carbenium centers.

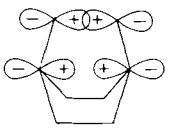
**11**   **12**

The dication **11** is formed from the ionization of 1,4-dichlorobicyclo[2.2.2]octane in $SbF_5/SO_2ClF$ at $-78\,^{\circ}C$. The ion **11** was found to be unstable above $-60\,^{\circ}C$; its dicationic character was established by both $^1H$- and $^{13}C$-NMR spectroscopy. The 60-MHz $^1H$-NMR spectrum of **11** at $-90\,^{\circ}C$ shows a singlet at $\delta = 3.45$. The proton-decoupled $^{13}C$-NMR spectrum shows two absorptions at $\delta = 307$ and 43.5 for the carbenium carbons and the methylene carbons, respectively. The 4-chlorobicyclo[2.2.2]oct-1-yl monocation is formed first, from the dichloride precursor, and the second ionization, which gives a distinctly different spectrum for the dication **11**, depends on the experimental conditions[17a].

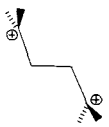
One would expect a strong coulombic repulsion between C1 and C4 carbons, considering the short distance that separates them. Molecular mechanics force-field calculations in which the electrostatic repulsion between the charged centers is included predict the C1–C4 distance in **11** to be 2.34 Å[15, 18]. According to MINDO calculations this distance comes out to be 1.99 Å[15, 19], thus indicating a shortening of the C1–C4 distance by 0.35 Å on going from the hypothetical monocarbenium ion **13** to the dication **11**, and also a shortening of 0.25 Å on going from the uncharged bicyclo[2.2.2]octane **14** to **13**.

**13**   **14**

The shortening of the C1–C4 distance in the dication **11** has been attributed to hyperconjugative transfer of electron density to the cationic centers which then leads to symmetry allowed 1,4 bonding. This can be represented pictorially as in **15**[20]. MINDO/3 calculations show that in

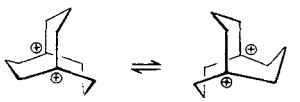
 **15**

 *cis*-**16**

 *trans*-**16**

order to relieve the electrostatic repulsions between the closely located positive charges of **11**, more than half of the total charge is delocalized over the twelve hydrogen atoms; the residual charge is comparable to that in the monocation **13**. The dication **11** can be considered as a doubly charged sphere with the positive charge distributed over its entire surface. Although the 1,4-interaction is favorable in **11**, this does not mean that 1,4-dications prefer a *cis* over a *trans* conformation (see **16**). MINDO/3 calculations indicate that *trans*-**16** is more stable than *cis*-**16** by 11 kcal/mol after corrections are made for ground state energies[15].

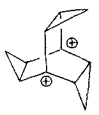
A similar shortening of the C1–C5 distance is predicted in the 1,5-bicyclo[3.3.3]undecanediyl dication **12** (manxanediyl dication) by empirical force field calculations[21]. The bridgehead dication **12** was generated[16] from 1,5-dichloromanxane in $SbF_5/SO_2ClF$ at $-78\,^{\circ}C$. The 60-MHz $^1H$-NMR spectrum of **12** indicates dynamic behavior at $-60\,^{\circ}C$, *i.e.* in this case a rapid bridge-flipping process. This process was frozen out at $-80\,^{\circ}C$ on a 100-MHz instrument indicating an activation energy barrier of about 11 kcal/mol, similar to that observed for the parent hydrocarbon manxane[22]. The $^{13}C$-NMR spectrum shows similar dynamic behavior. At $-85\,^{\circ}C$, there are three carbon resonances at $\delta = 346.2$, 58.7 and 23.5 which are assigned to C1, C2, and C3, respectively.



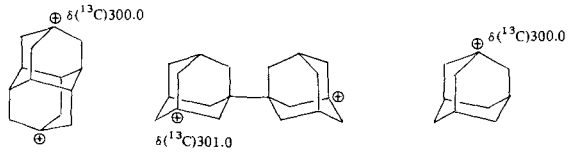
**12** **17**

The manxyl monocation **17** has also been generated[16] for comparison. It shows five $^{13}C$-NMR signals at $\delta = 356.3$, 57.9, 37.0, 32.7 and 35.7, which are assigned to C1, C2, C3, C4 and C5, respectively. It does not show any fluxional behavior in the NMR spectrum between $-30$ to $-135\,^{\circ}C$, indicating either a rapid ring-flipping process with a lower energy barrier than in **12** (faster than can be detected on the NMR time scale) or a very slow inversion of conformation due to the introduction of the $sp^2$ hybridized carbon at C1 only. Contrary to expectations the bridgehead carbons C1 and C5 in **12** are *ca.* $\approx 10$ ppm shielded relative to C1 of the monocation **17**. It appears that the presence of one or two carbocation centers in the manxane system generates subtle conformational variations, as is borne out by the different energy barriers for the bridge-flipping process in the monocation **17** and in the dication **12**. In the case of the monocation **17** the planarization of the bridgehead C1 carbon does not seem to affect the geometry of C5 significantly, as is indicated by its small coupling constant $J_{CH}$ (120 Hz). This implies that the hyperconjugative interaction in the 1,4-bicyclo[2.2.2]octanediyl dication **11**[15], which causes the C1–C4 carbons to move closer together does not seem to be occurring in the case of the manxanediyl dication **12**[11]. Finally, applying the $^{13}C$-NMR additivity relationship to the dipositive ions **11** and **12** in comparison with their hydrocarbon precursors clearly reveals their trivalent dicarbenium ion nature.

The inability to observe the cyclopropane annelated 1,4-bicyclo[2.2.2]octanediyl dication **18**[23] remains unexplained.

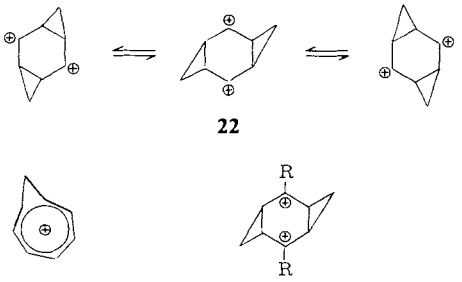
 **18**

Other polycyclic dications such as **19** and **20** have, however, been prepared[17b]. Essentially, they show similar $^{13}$C-NMR spectral characteristics as the monopositive analog, 1-adamantyl cation **21**[17b].




**19** **20** **21**

Attempts to observe circumambulatory rearrangement in the 2,6-*anti*-tricyclo[5.1.0.0$^{3,5}$]octanediyl dication **22** have been unsuccessful[24]. The dication **22** would appear to rearrange instantaneously to the homotropylium ion **23** by proton elimination. However, substituted dications of type **22**, *e.g.* **24**, are quite stable; they are static, and a substantial part of the charge is delocalized into the cyclopropane rings[24].



**22**

**23** **24**, R = $CH_3$, *c*-$C_3H_5$, $C_6H_5$

The effect of introducing two electron deficient centers into the norbornane skeleton has also been explored[25]. These studies are of particular interest in view of the extensive investigations[3b] on the mode of charge delocalization in the parent 2-norbornyl cation. Application of the so-called tool of increasing electron demand[26] (changing the electron demand of the cationic center by gradually changing the charge delocalizing ability of the adjacent aryl ring) to the substituted 2,5-diaryl-2,5-norbornanediyl dications **25** reveals some interesting $^{13}$C-NMR spectral characteristics.

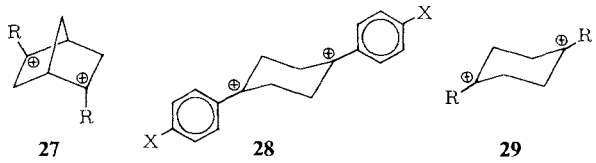


**25** R = $C_6H_5$, 4-$C_6H_4$–$CH_3$, 4-$C_6H_4$–$OCH_3$, 4-$C_6H_4$–$CF_3$, 3,5-$C_6H_3(CF_3)_2$, $C_6F_5$, OH

**26**

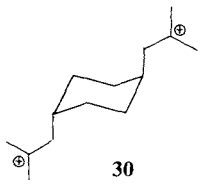
A plot of C1 *vs.* C3 carbon chemical shifts shows an excellent linear fit with a wide variety of substituents, thus indicating **25** as being a normal phenylcarbenium ion. In contrast the monopositive 2-phenyl-2-norbornyl monocations **26** show significant deviations in such a C1 *vs.* C3 plot[27] in the case of electron-withdrawing substituents, due to the onset of nonclassical σ-delocalization. The lack of σ-delocalization in **25** has been rationalized in terms of electronic effects. The coulombic repulsion in **25** is rather significant, and this renders the whole norbornane skeleton electron deficient. However, this effect is partly relieved by the dispersal of charge into the aryl substituents. Charge delocalization into the aryl substituents even in the case of electron withdrawing groups such as 4-$CF_3C_6H_4$, 3,5-$(CF_3)_2C_6H_3$ and $C_6F_5$ is evident from the $^{13}$C-NMR shifts of the *ortho* and *para* C-atoms, which are more strongly deshielded than in the analogous monocations of type **26**[27]. Further evidence for the regular phenylcarbenium ion nature of **25** comes from the observed linear relationship between the chemical shifts of the carbenium centers in **25** and those in 1-aryl-1-cyclopentyl cations[28].

Attempts to generate 2,5-unsubstituted or 2,5-dialkyl-substituted 2,5-norbornanediyl dications **27** have been unsuccessful[25]; on the other hand, it was possible to study the 1,4-diaryl-1,4-cyclohexanediyl dications **28** $^{13}$C-NMR spectroscopically. However, efforts to prepare methyl-substituted and unsubstituted analogs **29** have been futile.



**27** R = $CH_3$, H **28** X = H, $OCH_3$ **29** R = $CH_3$, H

Interestingly, ionization of 1,4-dibutyl-1,4-cyclohexanediol in $SbF_5/SO_2ClF$ at −78 °C resulted only in the rearranged dication **30**, in which the positive charges are separated by six carbon atoms.



**30**

### 3.3. Aromatic Carbodications

#### *3.3.1. Cyclobutadiene Dications*

In contrast to the antiaromatic cyclobutadiene, the cyclobutadiene dication (cyclobutenediyl dication) **31** is predicted by molecular orbital theory and Hückel's rule to have aromatic character and a square planar $D_{4h}$ ground state symmetry **31A**[29]. *Ab initio* molecular orbital calculations[30] suggest that carbodication **31** is not planar but rather prefers a puckered geometry with $D_{2d}$ symmetry **(31B)** instead. This puckering seems to occur despite the loss of resonance energy and the increase in angular strain. The calculated energy difference between the planar and puckered geometries is 2.8 kcal/mol.

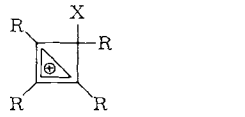


**31A** **31B**

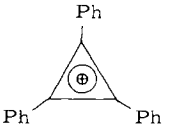
The major reason for the adoption of the puckered geometry **31B** has been attributed to the relief of destabilizing 1,3-interactions which are known to occur in four-membered rings[31]. The *ab initio* calculations indicate that orbital mixing and orbital reorientation which are enhanced through pyramidization also contribute to the stabilization of the puckered form **31B**.

In the gas phase some $C_4H_4^{2+}$ ions have been observed[32,33], and possibly also the unsubstituted carbodication **31**, but their structures could not be determined. As long-lived species in superacid solutions, **31** is still unknown[34]. Attempts to prepare the dication **31** by ionization of 3,4-dichlorocyclobutene in $SbF_5/SO_2ClF$ merely led to the 3-chlorohomocyclopropenyl cation **32** (X = Cl, R = H), which underwent chloride/fluoride exchange at elevated temperatures to give the analogous fluorine derivative.

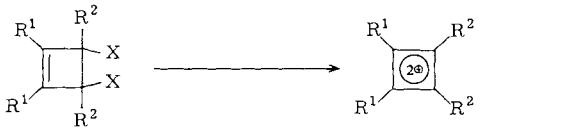
The stability of the cyclobutadiene dication can be greatly enhanced by the introduction of substituents like fluoro, methyl and phenyl groups[30,34]. Earlier attempts to prepare substituted cyclobutadiene dications were either unsuccessful or the postulated dications were later proved to be actually monocation monodonor-acceptor complexes **32**, $X=X\rightarrow MX_n$[35,36]. We later succeeded[34] in generating a variety of cyclobutadiene dications **34** as long-lived species in superacid media.



**32**



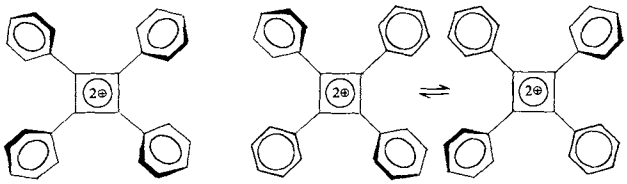
**35**



**33a**, $R^1 = R^2 = Ph$, X = Br
**33b**, $R^1 = R^2 = CH_3$, X = Cl
**33c**, $R^1 = Ph$, $R^2 = H$, X = Br
**33d**, $R^1 = Ph$, $R^2 = X = F$

**34a**, $R^1 = R^2 = Ph$
**34b**, $R^1 = R^2 = CH_3$
**34c**, $R^1 = Ph$, $R^2 = H$
**34d**, $R^1 = Ph$, $R^2 = F$

*Ab initio* calculations on cyclobutadiene dications predict that substituents that are capable of strong π-electron donation render the four-membered ring planar[30]. Thus, the tetrafluorocyclobutadiene dication has been predicted to be planar[30]. The four-membered ring in the tetraphenylcyclobutadiene dication **34a** is most probably planar and, according to the $^1$H- and $^{13}$C-NMR data, *para*-phenyl positions are strongly deshielded, indicating substantial delocalization of the positive charge into the phenyl rings[34]. The dicationic nature of **34a** has been established utilizing the Spiesecke-Schneider relationship (see Section 3.7)[37]. The degree of phenyl conjugation in **34a** proved to be far greater than that in the triphenylcyclopropenylium cation **35**[38]. Due to steric repulsions, the four phenyl rings in **34a** cannot all be coplanar. The existing $^1$H- and $^{13}$C-NMR data can be interpreted in terms of either a static structure **34a**(I) in which all the four phenyl rings are twisted slightly out of the plane of the four-membered ring or alternatively in terms of two dynamically degenerate systems **34a**(II) in which one set of diagonally opposite phenyl substituents are coplanar with the four-membered ring, while the remaining two phenyl rings are rotated out of the plane[34].



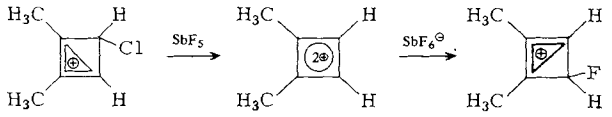
**34a** (I) **34a** (II)

In the 1,2-diphenylcyclobutadiene dications **34c** and **34d** the extent of resonance interaction between the phenyl rings and the double positive charge in the cyclobutadienyl ring[34] is higher than in the tetraphenyl derivative **34a**. Such a strong interaction results in restricted rotation of the phenyl rings in **34c** and **34d** about the *ipso* carbon and four-membered ring carbon bonds. In contrast a free rotation of the phenyl rings is observed in **34a**[34].

The ionization of tetramethyl derivative **33b** in $SbF_5/SO_2ClF$ at −78 °C to the tetramethylcyclobutadiene dication **34b** initially involves the formation of the homocyclopropenylium ion **32** (X = Cl, $R = CH_3$). This intermediate subsequently ionizes to yield the dication **34b**. *Ab initio* quantum mechanical calculations also predict this cation to have puckered geometry with $C_{2v}$ symmetry instead of the $C_{4v}$ planar structure. The energy difference between the two structures is calculated to be 2.3 kcal/mol and is comparable to the 2.8 kcal/mol difference calculated for planar and puckered geometries of the parent dication **31**[30]. Unfortunately, the above two structural possibilities cannot be probed with NMR spectroscopic studies on symmetrical systems. However, with suitably disubstituted cyclobutadiene dications (with substituents such as benzyl or isopropyl), the above possibilities could be proved either by $^1$H- or $^{13}$C-NMR spectroscopy.

In the $^1$H-NMR spectrum, the tetramethylcyclobutadiene dication **34b** shows a sharp singlet at $\delta = 3.68$. In the $^{13}$C-NMR spectrum two signals are observed at $\delta = 209.7$ and 18.8 for the ring C-atoms and methyl C-atoms respectively. Although the methyl substituent effect in **34b** precludes a quantitative interpretation of the π-electron density residing at the cyclobutenediylium carbons from their $^{13}$C-NMR shieldings, comparison of the NMR shieldings ($\delta = 209.7$) with that predicted by the Spiesecke-Schneider relationship[39] for the unsubstituted cyclobutadiene dication **31** ($\delta = 208.8$) certainly support the formulation of **34b** as a dicationic species delocalizing approximately two-π electrons over a four-carbon atom periphery.

Alkyl substituted cyclobutadiene dications seem to be less stable than the aryl analogues. Attempts to generate the 1,2-dimethylcyclobutadiene dication **36** from 3,4-dichloro-1,2-dimethyl-1-cyclobutene result only in the monocation **37**, which at higher temperatures (−20 °C) undergoes halogen exchange reaction with the counter ion; this reaction probably proceeds *via* the dication **36**.

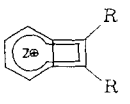


37 36

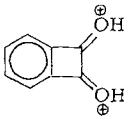
The 1,3-dihydroxy-2,4-diphenylcyclobutadiene dication was first reported by *Farnum* and *Webster* in 1963[40]. There seems to be enough evidence for considering diprotonated cyclobutenediones as 1,2-dihydroxycyclobutadiene dications rather than diprotonated ketones[41].

### 3.3.2. Benzocyclobutadiene Dications

The parent benzocyclobutadiene (cyclobutabenzene) dication **38a** is still unknown despite extensive attempts at its preparation by either two-electron oxidation of the parent benzocyclobutadiene or ionization of some dihalobenzocyclobutenes under long-lived stable ion conditions[42]. However, the 1,2-dimethylbenzocyclobutadiene dication **38b** can be readily generated by the ionization of 1,2-diol precursors in superacid solutions at $-78\,^{\circ}C$[42]. This $6\pi$ aromatic dication shows $^1H$- and $^{13}C$-NMR spectral characteristics comparable to those of the previously described cyclobutadiene dications. The diprotonated benzocyclobutenedione was found to exist predominantly as a dioxonium ion **38c'** rather than as a dihydroxybenzocyclobutadiene dication **38c**[42].

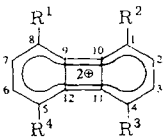


**38a**, R = H
**38b**, R = $CH_3$
**38c**, R = OH



**38c'**

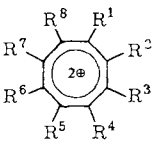
A variety of biphenylene dications **39** have been generated by two-electron oxidations of the corresponding biphenylenes with $SbF_5$ in excess in $SO_2ClF$ solutions at $-10\,^{\circ}C$[42]. The observed $^1H$- and $^{13}C$-NMR deshieldings in these systems confirm the formation of dicationic species. The substantial deshieldings of C2 and C10 and lesser deshielding of C1 indicate that the dications **39a** and **39b** are indeed fully delocalized closed-shell $10\pi$ aromatic biphenylene dications. The unsubstituted dication **39a** has also been observed in some electrochemical studies[43].



**39a**, $R^1 = R^2 = R^3 = R^4 = H$
**39b**, $R^1 = R^2 = R^3 = R^4 = CH_3$
**39c**, $R^1 = R^3 = H$; $R^2 = R^4 = CH_3$
**39d**, $R^1 = R^2 = CH_3$; $R^3 = R^4 = H$

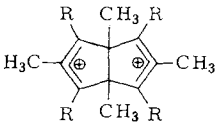
### 3.3.3. Cyclooctatetraene Dications

Several fundamental cationic Hückel-systems have remained elusive of preparation and experimental study. Perhaps the most notable of these is the cyclooctatetraene dication **40a**, which has probably been the subject of more investigations than any other related aromatic dication[44–47]. Basically two synthetic routes have been attempted: one involving two-electron oxidation of the parent cyclooctatetraene by superacids[44,45] or electrochemical methods[46], and the other involving ionization of the well known 8-halohomotropylium ions[44,47].

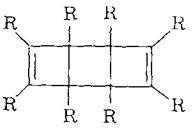


**40a**, $R^1 = R^2 = R^3 = R^4 = R^5 = R^6 = R^7 = R^8 = H$
**40b**, $R^1 = R^4 = CH_3$; $R^2 = R^3 = R^5 = R^6 = R^7 = R^8 = H$
**40c**, $R^1 = R^3 = R^5 = R^7 = CH_3$; $R^2 = R^4 = R^6 = R^8 = H$
**40d**, $R^1 = R^2 = R^3 = R^4 = R^5 = R^6 = R^7 = R^8 = CH_3$
**40e**, $R^1 = R^3 = R^5 = R^7 = Ph$; $R^2 = R^4 = R^6 = R^8 = H$

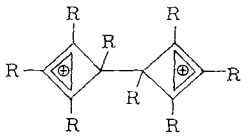
Although the parent cyclooctatetraene dication **40a** itself remains elusive, the methyl (**40b** and **40c**) and phenyl (**40e**) derivatives have successfully been prepared by the two-electron oxidation of the corresponding cyclooctatetraenes in $SbF_5/SO_2ClF$ at $-78\,^{\circ}C$[44]. The $^1H$- and $^{13}C$-NMR data of these dications provide strong evidence that all of these molecules adopt approximately planar geometries[44], despite the excessive strain involved (increased van der Waals repulsion and increase in angular strain[48]). Attempts to generate the octamethyl dication **40d** by two-electron oxidation of the corresponding octamethyl cyclooctatetraene under the experimental conditions which were employed for the preparation of the other cyclooctatetraene dications (**40b**, **40c** and **40e**) resulted in formation of the diallyl dication **41a** instead, and no evidence for **40d** was found. A similar diallyl dication **41b** has been obtained by rearrangement of the dication **40c** above $-20\,^{\circ}C$[44]. Two-electron oxidation of the isomeric *syn*- and *anti*-octamethyltricyclo[4.2.0.0$^{2,5}$]octadiene **42** and octamethylsemibullvalene **43** in $FSO_3H/SbF_5/SO_2$[44] also gives the dication **41a**. Interestingly, two-electron oxidation of **42** in $SbF_5/SO_2ClF$ alone gives the bis(tetramethylhomocyclopropenyl) dication **44**[44b].



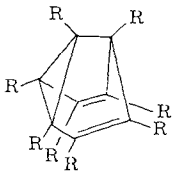
**41a**, R = $CH_3$
**41b**, R = H



**42**, R = $CH_3$

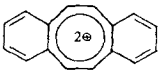


**44**, R = $CH_3$



**43**, R = $CH_3$

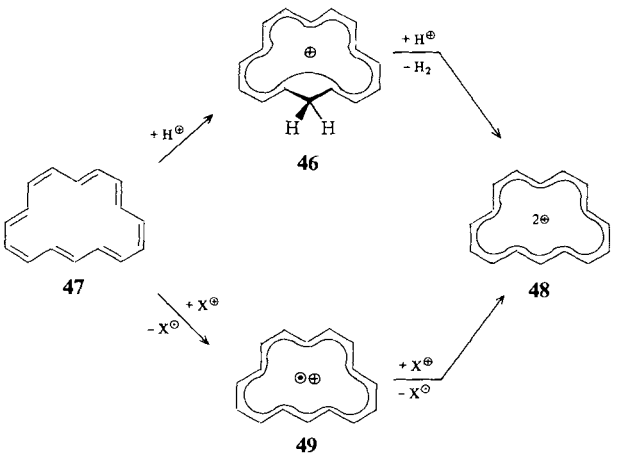
The dibenzo[*a*,*e*]cyclooctene dication **45** has also been prepared by the two-electron oxidation procedure and was found to be relatively stable since it can be heated to at least 0 °C without undergoing any isomerization or thermal decomposition. HMO calculations[49] on **45** indicate that the methine (CH) groups of the central eight-carbon ring are substantially electron deficient relative to the rest of the methine groups. This is also substantiated by the $^1H$-NMR chemical shifts[44a,c].



**45**

### 3.3.4. [16]Annulene Dication

Since the protonation of cyclooctatetraene is known to yield the homotropylium ion, *Schröder et al.* reasoned that the homo[15]annulenyl cation **46** can be formed by protonation of [16]annulene **47**[50]. Instead the [16]annulene dication **48** was obtained along with polymeric products in $FSO_3H/SO_2/CD_2Cl_2$ media at $-80\,^{\circ}C$. The $^1H$- and $^{13}C$-NMR data are consistent with the formation of the dication **48**. Attempts to trap this dication with $NaOAc/CH_3OH$ gave only polymeric products. Two possible mechanisms for the formation of **48** have been considered[50]. The first involves initial protonation to the homo[15]annulenyl cation **46**, which undergoes further protolytic cleavage to the dication **48** (by loss of a molecule of hydrogen). The second route is the stepwise oxidation of **47** by the proton or the conjugate acid of sulfur dioxide ($O{=}S{=}\overset{+}{O}H$), where a radical cation **49** is involved as an intermediate. *Schröder et al.*[50] seem to prefer the second mechanism, since no evolution of hydrogen gas has been observed in the reaction.




## 3.4. Oxidative Generation of Dications from Arenes

The ease of oxidation of polycyclic aromatic hydrocarbons in the gas phase[51] as well as in solution is well documented[52-61]. Monopositive radical ions and/or dipositive ions have been detected in strong acid solutions[60,61]. Similar species have been observed in anodic oxidations of aromatic compounds in non-nucleophilic solvents[52]. Simple Hückel molecular orbital theory predicts that arenes whose highest occupied molecular orbitals (HOMOs) are at higher energy levels should be prone to two-electron oxidation to dipositive ions. On the other hand, the arenes with low lying HOMOs should be more difficult to ionize[60]. Some polycyclic arenes have also been protonated to the corresponding dipositive ions.

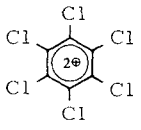
### 3.4.1. Benzene

Benzene itself does not undergo two-electron oxidation upon treatment with $SbF_5/SO_2ClF$, but gives instead the benzenium ion **50**[62] by protonation (due to HF impurity in the system). This behavior is in accordance with the simple Hückel molecular orbital theory, which predicts benzene to be the most difficult member in the arene series to be oxidized[60].

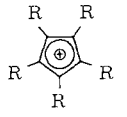
Solid hexachlorobenzene gives a dipositive ion **51** on admixture at room temperature with a viscous solution of $SbF_5$ saturated with $Cl_2$ and subsequent irradiation of the resulting monocation $(C_6Cl_6)^+$ with light of wavelength $\lambda > 3100$ Å at 5 or 77 K[63]. ESR studies on **51** have indicated that this dication is a ground state triplet (or within a few calories/mol of the ground state) as predicted by the simple Hückel method. The two unpaired electrons of **51** occupy degenerate orbitals and the dipositive ion retains the sixfold symmetry of the progenitor hexachlorobenzene itself. The π-electron configuration of **51** is similar to that of the cyclopentadienyl cations **52** which also have triplet ground states[64]. Actually, prolonged irradiation of **51**, particularly with light of wavelength $\lambda > 3100$ Å, yields a species with ESR parameters similar to those of **52b**, and it has been assumed that **51** (or possibly a precursor) under these conditions loses a CCl fragment to produce **52b**[63].




**50**




**51**

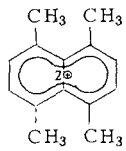


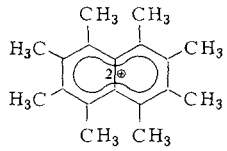

**52a**, R = H
**52b**, R = Cl

### 3.4.2. Naphthalene

Naphthalene gives the corresponding radical monocation upon treatment with $SbF_5/SO_2ClF$ at $-78\,^{\circ}C$; no evidence for further oxidation to the dication has been found[60,61]. However, the presence of methyl substituents on the ring lowers the ionization potential of naphthalene to the point that stable carbodications can be formed. Thus, the tetramethyl- and octamethylnaphthalene dications **53**[61] and **54** have been prepared under superacid conditions from the corresponding arenes.

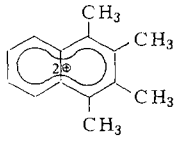
**53**

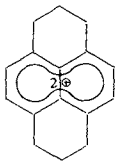



**54**

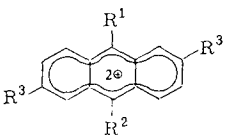
Attempts to prepare the closely related carbodications of 1,2,3,4-tetramethylnaphthalene **55**[61] or hexahydropyrene **56**[61] in superacids led in each case to an equilibrium mixture of the carbodication and the radical monocation. That the dipositive ion **53** is more stable than the isomer **55** has been attributed to the fact that α-methyl substituents stabilize the dipositive charge better than β-methyl substituents. The formation of dication **53** provides relief of *peri*-strain and furnishes an additional driving force for oxidation. Ring closure between the α-carbons in hexahydropyrene apparently prevents complete oxidation to the dication **56**.

55 

 56

### 3.4.3. *Anthracene*

Unlike benzene and naphthalene, anthracene has a relatively low ionization potential and can be converted into the corresponding carbodication **57a** by two-electron oxidation with $SbF_5/SO_2ClF$[60,58,56]. Alternatively, **57a** can be generated by debromination of 9,10-dibromo-9,10-dihydroanthracene in $SbF_5/SO_2ClF$ solution[58]. Stable dipositive ions **57b–f** have also been obtained in superacids from 9-methylanthracene, 9,10-dimethylanthracene, 2,6-dimethylanthracene, 9-bromoanthracene, and 9-chloroanthracene[58].



**57a**, $R^1 = R^2 = R^3 = H$
**57b**, $R^1 = R^3 = H$; $R^2 = CH_3$
**57c**, $R^1 = R^2 = CH_3$; $R^3 = H$
**57d**, $R^1 = R^2 = H$; $R^3 = CH_3$
**57e**, $R^1 = R^3 = H$; $R^2 = Br$
**57f**, $R^1 = R^3 = H$; $R^2 = Cl$

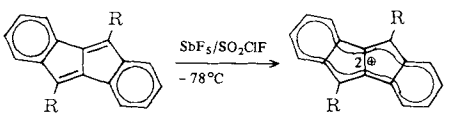
### 3.4.4. *Dibenzopentalene*

Although generation of the 8C-6π aromatic dication **58** of the unknown pentalene **59** has so far proven unsuccessful, *Rabinowitz et al.* have actually been able to prepare the dibenzoannelated derivatives[65].

58 

 59

Upon treatment of dibenzo[*a*,*e*]pentalene (indeno[2,1-*a*]indene) **60** or its 5,10-dimethyl derivative **61** with $SbF_5/SO_2ClF$ at −78 °C, two-electron oxidation furnished the dications **62** and **63**, respectively. The observed $^1H$- and $^{13}C$-NMR spectral deshieldings[65] of **62** and **63** as compared to those of **60** and **61** clearly establishes that **62** and **63** are dications.



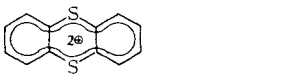

**60**, R = H
**61**, R = $CH_3$

**62**, R = H
**63**, R = $CH_3$

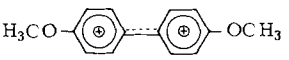
### 3.4.5. *Other Polycyclic Arenes*

Carbodications of higher polycyclic arenes have likewise been generated and studied by $^{13}C$-NMR spectroscopy under superacid conditions[57,58,60,61]. These arenes are listed in Table 1[60]; also listed are systems in which the carbodications are in equilibrium with the radical cations.

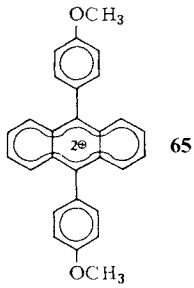
Dipositive ions of arenes have been observed in electrochemical oxidations and have also been assumed to be intermediates in some radical cation reactions[53–55]. *Hammerich* and *Parker*[52] have shown that thianthrene **64**, 9,10-bis(*p*-methoxyphenyl)anthracene **65**, and 4,4′-dimethoxybiphenyl **66** dications can be generated by voltammetric oxidation of the corresponding parent aromatic systems. In solvents such as nitriles, nitro-compounds and dichloromethane, reversible electron transfer behavior for oxidation of these three aromatic compounds to radical cations and dipositive ions was observed[52].



64



66



65

Table 1. Arene species in $SbF_5/SO_2ClF$ solution.

| Arene | $E_{HOMO}$ [β] [a] | Species in $SbF_5/SO_2ClF$ [b] | Color of dication solution |
|---|---|---|---|
| Benzene | 1.0000 | $C_6H_7^+$ | |
| Triphenylene | 0.6840 | (+·) | |
| Naphthalene | 0.6180 | (+·) | |
| Phenanathrene | 0.6052 | (+·) | |
| Coronene | 0.5392 | (+·) | |
| Chrysene | 0.5201 | (+·) | |
| Dibenzo[*g*,*p*]chrysene | 0.5115 | ++ | Blue |
| Picene | 0.5019 | +· ⇌ ++ | Green-black |
| Dibenz[*a*,*c*]anthracene | 0.4991 | +· ⇌ ++ | Blue-black |
| Dibenz[*a*,*h*]anthracene | 0.4735 | ++ | Green |
| Benz[*a*]anthracene | 0.4523 | ++ | Blue-green |
| Pyrene | 0.4450 | ++ | Green-black |
| Benzo[*a*]perylene | 0.4392 | ++ | Purple |
| Anthracene | 0.4142 | ++ | Purple |
| Benzo[*a*]pyrene | 0.3711 | ++ | Blue |
| Perylene | 0.3473 | ++ | Purple |
| Naphthacene | 0.2950 | ++ | Green |
| Pentacene | 0.2197 | ++ [c] | Green |
| Octamethylnaphthalene | | ++ | Red |
| 7,12-Dimethylbenz[*a*]anthracene | | ++ | Blue-green |

[a] Energy of the highest occupied molecular orbital according to the Hückel method. [b] Dication indicated by ++, monocation by +, radical cation by +·. [c] Dication formed in $SbF_5/SO_2$, but not in $SbF_5/SO_2ClF$; $SbF_5/SO_2$ is a weaker oxidizing agent due to complexation of $SbF_5$ with $SO_2$.

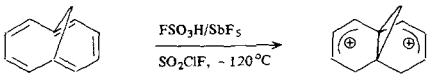
The two consecutive reversible one-electron transfer processes have been reported to occur only if special care is taken to remove residual water from the reaction media. Reaction of the dications **64**, **65**, and **66** with residual water results in irreversibility of the second charge transfer during voltammetry of the corresponding arenes[52].

A wide variety of arene radical cation reactions have been suggested to proceed *via* a mechanism involving reactive dications[53–55]. For example, *Shine* and *Murata*[53] have suggested that the preferable mechanism for the reaction of thianthracene radical cations with water involves a carbodication formed by the disproportionation of the radical cation. A similar mechanism has also been proposed for the anodic reaction between pyridine (Pyr) and anthracene (Ant).

$$\begin{aligned} &\text{Ant} &&\rightleftharpoons \text{Ant}^{\ddagger} + e \\ &2\,\text{Ant}^{\ddagger} &&\rightleftharpoons \text{Ant} + \text{Ant}^{2\oplus} \\ &\text{Ant}^{2\oplus} + \text{Pyr} &&\rightleftharpoons \text{Ant Pyr}^{2\oplus} \\ &\text{Ant Pyr}^{2\oplus} &&\rightleftharpoons \text{Further reactions} \end{aligned}$$

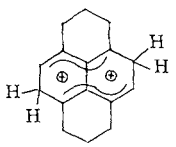
### 3.5. Diprotonation of Arenes

1,6-Methano[10]annulene **67** shows a high reactivity towards sulfonation[66]. This led *Lammertsma* and *Cerfontain*[67] to study protonation of the annulene **67** under superacid conditions. Protonation of the annulene **67** in $FSO_3H/SbF_5/SO_2ClF$ at low temperature gives an interesting cyclopropylenedimethyl dication **68**. It is a diallyl dication in which a substantial portion of the charge is delocalized over the cyclopropane ring.

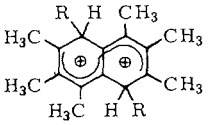



**67** **68**

Recently, *Lammertsma*[68] has also obtained the dication **69** by the protonation of hexahydropyrene with "magic acid" in $SO_2ClF$. The dication **69** is the first example of a β,β′-diprotonated naphthalene derivative. *Koptyug et al.* have studied the α,α′-diprotonated 1,2,3,5,6,7-hexa- and octamethylnaphthalenes **70** and **71** under superacid conditions[69].



**69**



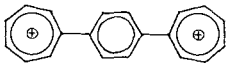
**70**, R = H
**71**, R = $CH_3$

### 3.6. Other Aromatic Dications

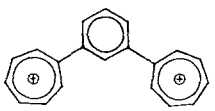
The 6π-aromatic tropylium ion **72** has been well studied by many investigators[70] owing to its unusual stability. *Murray* and *Kaplan*[71] generated the di- and tritropylium ions **73**, **74** and **75** in which the seven-membered rings are separated by a benzene ring. Russian workers[72] have been successful in preparing the dication bitropylium **76** by the direct oxidation of bicycloheptatrienyl in $SbF_5/CCl_4$.



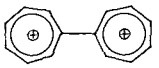
**72**



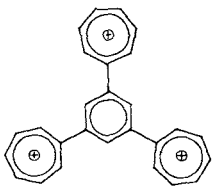
**73**



**74**



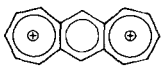
**76**



**75**

The heptalene dication **77**, the benzoditropylium ion **78** and other aromatic dications of this type have been studied theoretically[73], but, despite many attempts, have not been successfully prepared in the laboratory[74].

**77**



**78**

### 3.7. Spiesecke-Schneider Relationship

Although earlier workers[75,76] recognized the possibility of a linear relationship between chemical shift ($\delta$) and charge density ($\rho$), the credit for discovery of a good correlation goes to *Spiesecke* and *Schneider*[37,39]. They correlated the charge densities per methine group of the tropylium ion, benzene and cyclopentadienide ion *vs.* their respective $^1$H- and $^{13}$C-NMR chemical shifts. They observed a linear relationship with slopes of 10 ppm/e (e = electron) and 160 ppm/e for the $^1$H- and $^{13}$C-NMR data respectively.

In the early seventies, *Olah* and *Mateescu*[34c] extended the $^{13}$C-NMR chemical shift correlation to a series of mono- and dipositive ions and again obtained a slope of 160 ppm/e, although many aryl-substituted cationic systems were included in the analysis. *O'Brien et al.*[77] have further extended the correlation to a series of nonconjugated and conjugated anions and cations and have obtained similar slopes (156.3 ppm/e) following the general equation

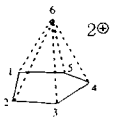
$$\delta_{av} = 289.5 - 156.3\rho_{av}$$

On the other hand, dications by themselves show much larger slopes in such a charge density *vs.* chemical shift plot. In the case of polycyclic arene dications, *Olah* and *Forsyth*[60] obtained a slope of 200 ppm/e. Tetramethylnaphthalene dication **53**[61] shows a deshielding of 192 ppm/e, the octamethylnaphthalene dication **54**[60] an unusual deshielding of 244 ppm/e. This large deshielding has been attributed to steric interactions which might significantly affect chemical shifts in crowded systems. However, monocyclic dications such as tetramethylcyclooctatetraene dication **40c**[44] and [16]annulene dication **48**[50] show much smaller deshieldings of 170 and 153.2 ppm/e, respectively. α,α′-Diprotonated naphthalenes[69] **70** and **71** and the β,β′-diprotonated hexahydropyrene **69** also show deshieldings around 175–180 ppm/e, although they are not Hückel systems with closed shells.

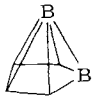
## 4. Hexacoordinate Pyramidal Carbodications

Pioneering investigations to generate carbodications with hexacoordinated carbon atoms have been carried out by *Hogeveen et al.*[78]. The pyramidal dication **79**, which can be considered as structurally related to carborane $C_4B_2C_6$ **80**[79] and ferrocene **81**[80] (following *Williams'* initial suggestion of the pyramidal structure for $C_5H_5^+$ species[79b] based on the $B_5H_{11}$ structure), has resisted attempts at its synthesis, although *ab initio* quantum mechanical

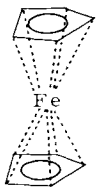
calculations predict this dication to be relatively stable[81]. According to these calculations the most stable structure of **79** is the one in which C6 lies 1.21 Å above the center of the ring[81]. In such a structure the net positive charge on the hydrogen atom of the apical C6 is calculated to be 0.28 units, while 1.71 charge units of the $(CH)_5$ ring is distributed over carbon (0.08 units) and hydrogen (0.28 units).



**79**



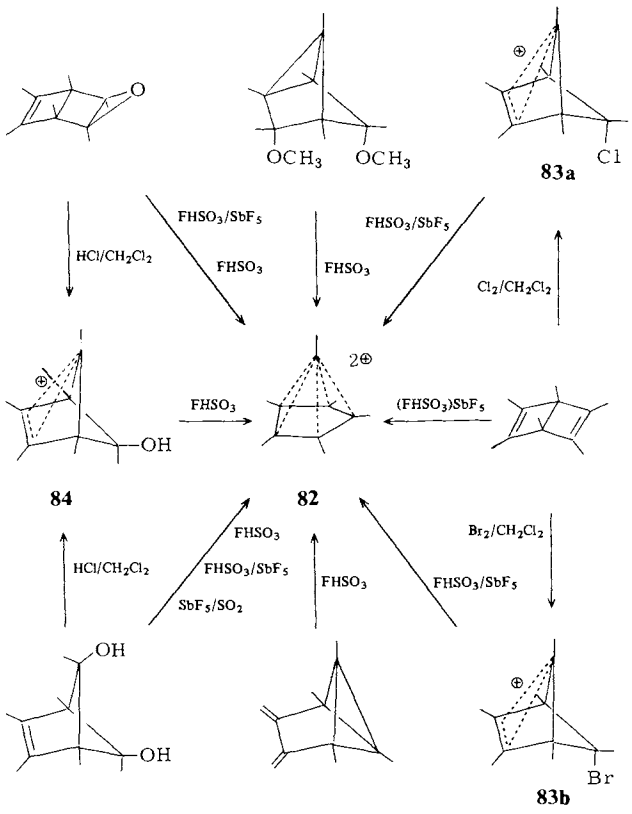
**80**



**81**

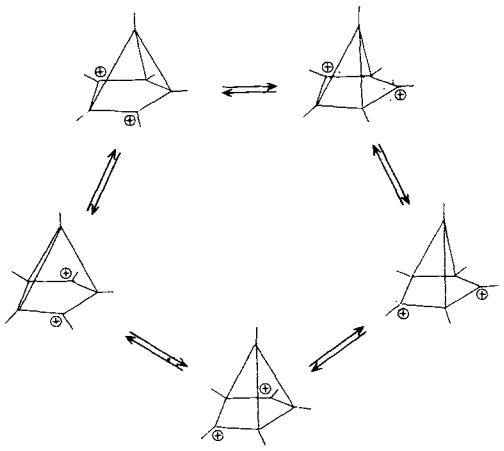
Although the unsubstituted dication **79** is not known, the hexamethyl derivative **82** has been generated at low temperatures from a variety of precursors in superacids[78b].

All synthetic routes have been suggested to involve stepwise ionization *via* the monocations **83** or **84**[78a].




$^1$H- and $^{13}$C-NMR data, the rate of deuterium exchange, the rate of carbonylation and the thermal stability of **82** provide strong evidence for the nonclassical nature of this carbodication[78]. However, the structure can also be considered in terms of the rapidly equilibrating set of structures **85**, which have only one plane of symmetry; during the degenerate process the apical C-atom describes a circle[78].

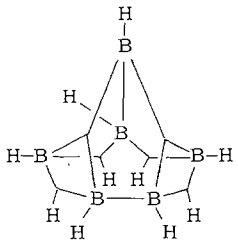
Although the observed $^1$H- and $^{13}$C-NMR data strongly support the bridged nature of the ion **82**, further definite



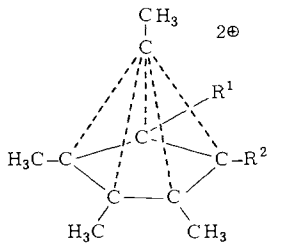
**85**

evidence comes from NMR isotope perturbation studies[82], originally developed by *Saunders et al.*[83] to distinguish classical and nonclassical cations. Very little isotopic perturbation (the degeneracy is not lifted due to $CD_3$ substitution) on the basal carbon signal is observed in the $^{13}$C-NMR spectrum of the dication $[C_6(CH_3)_5CD_3]^{2+}$ indicating that the ion is symmetrically bridged. Other supporting evidence comes from a comparison of the $^{13}$C and $^{11}$B-NMR shifts of the isoelectronic borane $B_6H_{10}$ **86**. *Williams* and *Field*[84] have shown that the $^{13}$C-NMR chemical shifts of a series of nonclassical cations may be compared with the $^{11}$B-NMR chemical shifts of the isoelectronic polyhedral polyboranes.

Recently *Hogeveen et al.*[85] have also prepared the ethyl and isopropyl substituted analogs **87a—d** of the dipositive ion **79**.



**86**



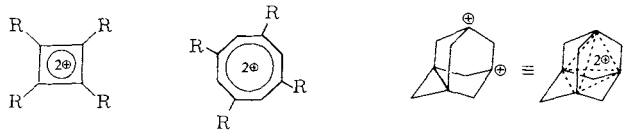
**87a**, $R^1 = CH_3$, $R^2 = C_2H_5$
**87b**, $R^1 = CH_3$, $R^2 = i\text{-}C_3H_7$
**87c**, $R^1 = R^2 = C_2H_5$
**87d**, $R^1 = R^2 = i\text{-}C_3H_7$

## 5. Outlook

In a short span of less than fifteen years the study of carbodications as directly observable, stable intermediates has shown a remarkable development. Many types of dications, including trivalent (classical) as well as hexacoordinate (nonclassical) systems, have been studied, primarily by NMR spectroscopy. This review, as pointed out earlier, is limited to carbodications under long lived conditions. However, it should be emphasized that a powerful technique is being developed for gas phase studies wherein dipositively charged ions can be detected by doubly charged ion mass spectroscopy. This method will clearly lead to generation of many interesting dications; structures will be suggested for these ions on the basis of quantum mechani-

cal calculations[86]. The challenge will be whether these ions can be observed in the condensed state. There are still a number of systems, such as the Hückel dications of cyclobutadiene (**31**) and cyclooctatetraene (**40**), which are inaccessible in solution. One promising route for their generation appears to be the protolytic cleavage of trimethylsilyl groups from the tetrakis(trimethylsilyl) derivatives **88** and **89**.

5,7-Didehydro-1,3-adamantanediyl dication **90** has been predicted by theory to be a possibly stable nonclassical dication. Attempts to prepare it by a variety of methods[87] have, however, been futile so far, but other approaches may succeed.



**88** **89** **90**

R = $Si(CH_3)_3$

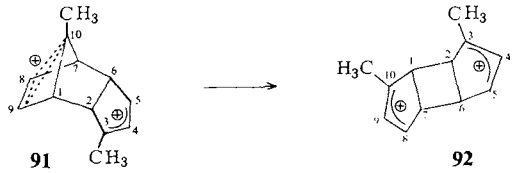
Another powerful technique for elucidating carbodication structures will be by single crystal X-ray structural studies, if single crystals of dication salts can be isolated.

The diversity of dipositive hydrocarbon ions that have been observed and their interesting properties will continue to make this field attractive and the subject of much future research. It also remains to be seen whether dicationic intermediates can be linked to the mechanistic pathway of electrophilic organic transformations and be used as models for specific catalytic reactions.

## 6. Addendum

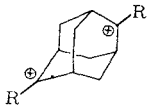
Since this review was written, several interesting dications have been prepared and characterized under long lived conditions, *i.e.* in superacids at low temperatures. Some of those worth mentioning are:

The *endo*-3,10-dimethyltricyclo[5.2.1.$0^{2,6}$]deca-4,8-diene-3,10-diyl dication **91**[88], which has a novel bishomoaromatic/allylic dication structure. At higher temperatures it stereospecifically rearranges to the symmetrical *cis-anti-cis*-3,10-dimethyltricyclo[5.3.0.$0^{2,6}$]deca-4,8-diene-3,10-diyl dication **92**.



**91** **92**

Several 2,6-disubstituted-2,6-adamantanediyl dications **93** have been prepared and characterized[89]. They are stable only when they contain charge delocalizing substituents such as cyclopropyl or phenyl groups.



**93**

*Support of our work on dications was provided by the National Institutes of Health and National Science Foundation. Dr. T. Rawdah thanks the University of Petroleum Minerals, Dhahran, Saudi Arabia for generous financial support.*

Received: November 5, 1981;
revised: January 4, 1983 [A 452 IE]
German version: *Angew. Chem. 95* (1983) 356

[1] J. F. Norris, W. W. Saunders, *J. Am. Chem. Soc. 23* (1901) R85.
[2] a) F. Kehrmann, F. Wentzel, *Ber. Dtsch. Chem. Ges. 34* (1901) 3815; b) M. Gomberg, *ibid. 35* (1902) 1822; c) A. Baeyer, V. Villiger, *ibid. 35* (1902) 1189, 3013.
[3] For detailed reviews see a) G. A. Olah, *Angew. Chem. 85* (1973) 183; *Angew. Chem. Int. Ed. Engl. 12* (1973) 173; b) *Acc. Chem. Res. 9* (1976) 41; c) *Top. Curr. Chem. 80* (1979) 21; d) *Chem. Scr. 18* (1981) 97.
[4] a) H. Hart, T. Sulzberg, R. R. Rafos, *J. Am. Chem. Soc. 85* (1963) 1800; b) H. Hart, T. Sulzberg, R. Schwendeman, R. H. Young, *Tetrahedron Lett. 1967*, 1337; c) H. Hart, C.-Y. Wu, R. H. Schwendeman, R. H. Young, *ibid. 1967*, 1343.
[5] H. Volz, M. J. Volz de Lecea, *Tetrahedron Lett. 1964*, 1871.
[6] G. A. Olah, J. L. Grant, R. J. Spear, J. M. Bollinger, A. Serianz, G. Sipos, *J. Am. Chem. Soc. 98* (1976) 2501.
[7] G. A. Olah, P. W. Westerman, J. Nishimura, *J. Am. Chem. Soc. 96* (1974) 3548.
[8] J. M. Bollinger, C. A. Cupas, K. J. Friday, M. L. Woolfe, G. A. Olah, *J. Am. Chem. Soc. 89* (1967) 156.
[9] G. A. Olah, A. M. White, *J. Am. Chem. Soc. 91* (1969) 5801.
[10] G. A. Olah, C. U. Pittman, Jr., *Adv. Phys. Org. Chem. 1966*, 303.
[11] P. von R. Schleyer, D. Lenoir, P. Mison, G. Liang, G. K. S. Prakash, G. A. Olah, *J. Am. Chem. Soc. 102* (1980) 683.
[12] G. A. Olah, P. R. Clifford, Y. Halpern, R. G. Johanson, *J. Am. Chem. Soc. 93* (1971) 4219 and references cited therein.
[13] G. A. Olah, A. M. White, *J. Am. Chem. Soc. 91* (1969) 5801; G. A. Olah, D. J. Donovan, *ibid. 99* (1977) 5026.
[14] G. A. Olah: *Halonium Ions*, Wiley-Interscience, New York 1975.
[15] G. A. Olah, G. Liang, P. von R. Schleyer, E. M. Engler, M. J. S. Dewar, R. C. Bingham, *J. Am. Chem. Soc. 95* (1973) 6829.
[16] G. A. Olah, G. Liang, P. von R. Schleyer, W. Parker, C. I. F. Watt, *J. Am. Chem. Soc. 99* (1977) 966.
[17] a) G. A. Olah et al., unpublished; b) G. A. Olah, P. von R. Schleyer et al., unpublished.
[18] J. L. Fry, E. M. Engler, P. von R. Schleyer, *J. Am. Chem. Soc. 94* (1972) 4628.
[19] R. C. Bingham, D. H. Lo, M. J. S. Dewar, *J. Am. Chem. Soc. 97* (1975) 1285.
[20] R. Hoffmann, *Acc. Chem. Res. 4* (1971) 1.
[21] a) L. W. K. Chang, Ph. D. Thesis, Princeton University 1977; b) E. M. Engler, J. D. Andose, P. von R. Schleyer, *J. Am. Chem. Soc. 95* (1973) 8005; c) R. C. Bingham, P. von R. Schleyer, *ibid. 93* (1971) 3189.
[22] a) J. C. Coll, D. R. Crist, M. del C. G. Barrio, N. J. Leonard, *J. Am. Chem. Soc. 94* (1972) 7092; b) M. Doyle, W. Parker, P. A. Gunn, J. Martin, D. D. MacNicol, *Tetrahedron Lett. 1970*, 3619.
[23] A. de Meijere, O. Schallner, C. Weitemeyer, W. Spielmann, *Chem. Ber. 112* (1979) 908.
[24] G. A. Olah, G. K. S. Prakash, A. P. Fung, T. N. Rawdah, unpublished.
[25] G. A. Olah, G. K. S. Prakash, T. N. Rawdah, *J. Am. Chem. Soc. 102* (1980) 6127.
[26] G. A. Olah, A. L. Berrier, G. K. S. Prakash, *Proc. Natl. Acad. Sci. USA 78* (1981) 1998 and references cited therein.
[27] G. A. Olah, G. K. S. Prakash, G. Liang, *J. Am. Chem. Soc. 99* (1977) 5683.
[28] D. G. Farnum, R. E. Botto, W. T. Chambers, B. J. Lam, *J. Am. Chem. Soc. 100* (1978) 3847.
[29] a) P. J. Garratt: *Aromaticity*, McGraw-Hill, London 1971; b) C. U. Pittman, Jr., A. Kress, L. D. Kispert, *J. Org. Chem. 39* (1974) 378; c) M. P. Cava, M. J. Mitchell: *Cyclobutadiene and Related Compounds*, Academic Press, New York 1967; d) J. P. Snyder: *Nonbenzenoid Aromatics*, Vol. 2, Academic Press, New York 1971; e) H. Hart, R. W. Fish, *J. Am. Chem. Soc. 82* (1960) 5419; f) G. H. Badger: *Aromatic Character and Aromaticity*, Cambridge University Press, Cambridge 1969.
[30] K. Krogh-Jespersen, P. von R. Schleyer, J. A. Pople, D. Cremer, *J. Am. Chem. Soc. 100* (1978) 4301.
[31] a) J. D. Dunitz, V. Shomaker, *J. Chem. Phys. 20* (1952) 1703; b) J. S. Wright, L. Salem, *J. Am. Chem. Soc. 94* (1972) 322; c) L. Salem, *Chem. Br. 5* (1969) 449; d) J. S. Wright, L. Salem, *Chem. Commun. 1969*, 1370; e) R. Hoffmann, R. B. Davidson, *J. Am. Chem. Soc. 93* (1971) 5699; f) N. L. Bauld, J. Cessac, *ibid. 99* (1977) 942; g) D. Cremer, *ibid. 99* (1977) 1307; h) N. L. Bauld, J. Cessac, R. Holloway, *ibid. 99* (1977) 8140.

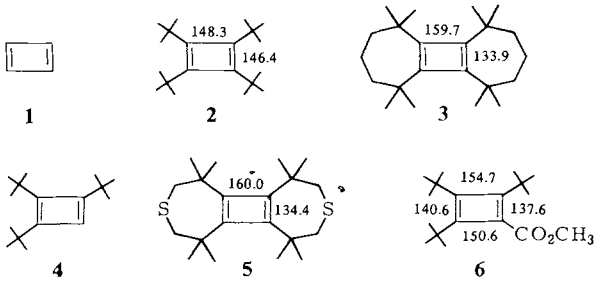
[32] J. H. Beynon, A. Mathias, A. E. Williams, *Org. Mass. Spectrom. 5* (1971) 303.
[33] M. H. Benn, T. S. Sorensen, A. M. Hogg, *Chem. Commun. 1967,* 574.
[34] a) G. A. Olah, J. S. Staral, *J. Am. Chem. Soc. 98* (1976) 6290; b) G. A. Olah, J. M. Bollinger, A. M. White, *ibid. 91* (1969) 3667; c) G. A. Olah, G. D. Mateescu, *ibid. 92* (1970) 1430; d) G. A. Olah, J. S. Staral, R. J. Spear, G. Liang, *ibid. 97* (1975) 5849.
[35] a) H. H. Friedman, A. M. Frantz, Jr., *J. Am. Chem. Soc. 84* (1962) 4165; b) R. F. Bryan, *ibid. 86* (1964) 733.
[36] a) H. H. Friedman, A. E. Young, *J. Am. Chem. Soc. 86* (1964) 734; b) T. J. Katz, J. R. Hall, W. C. Neikam, *ibid. 84* (1962) 3199; c) T. J. Katz, E. G. Gold, *ibid. 86* (1964) 1600.
[37] a) H. Spiesecke, W. G. Schneider, *J. Chem. Phys. 35* (1961) 731; b) *Can. J. Chem. 41* (1963) 966.
[38] G. J. Ray, A. K. Colter, R. J. Kurland, *Chem. Phys. Lett. 2* (1968) 324.
[39] a) H. Spiesecke, W. G. Schneider, *Tetrahedron Lett. 1961,* 468; b) J. B. Stothers: *Carbon-13 NMR Spectroscopy,* Academic Press, New York 1972; c) G. C. Levy, G. L. Nelson: *Carbon-13 Nuclear Magnetic Resonance for Organic Chemists,* Wiley-Interscience, New York 1972.
[40] D. G. Farnum, B. Webster, *J. Am. Chem. Soc. 85* (1963) 3502.
[41] G. A. Olah, J. S. Staral, unpublished results.
[42] G. A. Olah, G. Liang, *J. Am. Chem. Soc. 99* (1977) 6045 and references cited therein.
[43] A. Ronlan, V. D. Parker, *J. Chem. Soc. Chem. Commun. 1974,* 33.
[44] a) G. A. Olah, J. S. Staral, G. Liang, L. A. Paquette, W. P. Melega, M. J. Carmody, *J. Am. Chem. Soc. 99* (1977) 3349; b) G. A. Olah, G. Liang, L. A. Paquette, W. P. Melega, *ibid. 98* (1976) 4327; c) G. A. Olah, J. S. Staral, L. A. Paquette, *ibid. 98* (1976) 1267.
[45] a) D. Bryce-Smith, N. A. Perkins, *J. Chem. Soc. 1962,* 1339; b) M. Finkelstein, R. C. Peterson, S. D. Ross, *Tetrahedron 23* (1967) 3875.
[46] L. E. Berson, K. Nyberg, M. Finkelstein, R. C. Peterson, S. D. Ross, J. J. Uebel, *J. Org. Chem. 32* (1967) 16.
[47] a) G. A. Boche, W. Hecht, H. Huber, R. Huisgen, *J. Am. Chem. Soc. 89* (1967) 3344; b) R. Huisgen, G. A. Boche, H. Huber, *ibid. 89* (1967) 3345; c) R. Huisgen, J. Gasteiger, *Angew. Chem. 84* (1972) 1187; *Angew. Chem. Int. Ed. Engl. 11* (1972) 1104; *Tetrahedron Lett. 1972,* 3361, 3665.
[48] N. L. Allinger, J. T. Strange, C. J. Finder, *Tetrahedron 29* (1973) 2519.
[49] A. Streitwieser, Jr.: *Molecular Orbital Theory for Organic Chemists,* Wiley-Interscience, New York 1961.
[50] J. F. M. Oth, D. M. Smith, U. Prange, G. Schröder, *Angew. Chem. 85* (1973) 352; *Angew. Chem. Int. Ed. Engl. 12* (1973) 327.
[51] F. Borchers, K. Levsen, *Org. Mass Spectrom. 10* (1975) 584 and references cited therein.
[52] O. Hammerich, V. D. Parker, *Electrochim. Acta 18* (1973) 537.
[53] a) H. J. Shine, Y. Murata, *J. Am. Chem. Soc. 91* (1969) 1872; b) Y. Murata, H. J. Shine, *J. Org. Chem. 34* (1969) 3368.
[54] L. S. Marcoux, *J. Am. Chem. Soc. 93* (1971) 537.
[55] I. C. Lewis, L. S. Singer, *J. Chem. Phys. 43* (1965) 2712.
[56] W. I. Aalbersberg, G. J. Hoijtink, E. L. Mackor, W. P. Weijland, *J. Chem. Soc. 1959,* 3055.
[57] W. T. A. M. Vander Lugt, H. M. Buck, L. J. Oosterhoff, *Tetrahedron 24* (1968) 4941.
[58] D. M. Brouwer, J. A. van Doorn, *Recl. Trav. Chim. Pays-Bas 91* (1972) 1110.
[59] a) S. I. Weisman, E. Boer, J. J. Conradi, *J. Chem. Phys. 26* (1957) 963; b) G. J. Hoijtink, W. P. Weijland, *Recl. Trav. Chim. Pays-Bas 76* (1957) 836; c) D. M. Brouwer, *Chem. Ind. (London) 1961,* 177; d) D. M. Brouwer, *J. Catal. 1* (1962) 372; e) J. J. Pooney, R. C. Pink, *Proc. Chem. Soc. 1961,* 70.
[60] G. A. Olah, D. A. Forsyth, *J. Am. Chem. Soc. 98* (1976) 4086.
[61] K. Lammertsma, G. A. Olah, C. M. Berke, A. Streitwieser, *J. Am. Chem. Soc. 101* (1979) 6658.
[62] G. A. Olah, J. S. Staral, G. Asencio, G. Liang, D. A. Forsyth, G. D. Mateescu, *J. Am. Chem. Soc. 100* (1978) 6299.
[63] E. Wasserman, R. S. Hutton, V. J. Kuck, E. A. Chandross, *J. Am. Chem. Soc. 96* (1974) 1965.
[64] a) R. B. Breslow, H. W. Chang, R. Hill, E. Wasserman, *J. Am. Chem. Soc. 89* (1967) 1112; b) M. Saunders, R. Berger, A. Jaffe, J. M. McBride, J. O'Neill, R. Breslow, J. M. Hoffmann, C. Perchonock, E. Wasserman, R. S. Hutton, V. J. Kuck, *ibid. 95* (1973) 3017.
[65] a) I. Willner, M. Rabinovitz, *J. Am. Chem. Soc. 100* (1978) 337; b) I. Willner, J. Y. Becker, M. Rabinovitz, *ibid. 101* (1979) 395.
[66] a) K. Lammertsma, H. Cerfontain, *J. Am. Chem. Soc. 101* (1979) 3618; b) F. Van de Griendt, H. Cerfontain, *Tetrahedron 35* (1979) 2563; c) *ibid. 36* (1980) 317.
[67] a) K. Lammertsma, H. Cerfontain, *J. Am. Chem. Soc. 102* (1980) 3257; b) H. Cerfontain, K. Laali, *J. Org. Chem.*, in press.
[68] K. Lammertsma, *J. Am. Chem. Soc. 103* (1981) 2062.
[69] a) N. V. Bodoev, V. I. Mamatyuk, A. P. Krysin, V. A. Koptyug, *J. Org. Chem. USSR* (Engl. Transl.) **14** (1978) 1789; b) V. I. Mamatyuk, A. P. Krysin, N. V. Bodoev, V. A. Koptyug, *Izv. Akad. Nauk SSSR Ser. Khim. 1974,* 2392; c) N. V. Bodoev, A. P. Krysin, V. I. Mamatyuk, V. A. Koptyug, *ibid. 1976,* 1899.
[70] T. Nozoe in D. Ginsburg: *Non Benzenoid Aromatic Compounds,* Chap. 7, Wiley-Interscience, New York 1959; K. M. Harmon in G. A. Olah, P. von R. Schleyer: *Carbonium Ions,* Vol. *4,* Chap. 29, Wiley-Interscience, New York 1973.
[71] a) R. W. Murray, M. L. Kaplan, *Tetrahedron Lett. 1965,* 2903; b) *ibid. 1967,* 1307.
[72] I. S. Akhrem, E. I. Fedin, B. A. Kvasov, M. E. Volpin, *Tetrahedron Lett. 1967,* 5265.
[73] D. P. Craig, L. Radom, H. F. Scheafer, *Aust. J. Chem. 31* (1978) 261.
[74] a) H. J. Dauben, D. J. Bertelli, *J. Am. Chem. Soc. 83* (1961) 4657, 4659; b) J. Beeby, P. J. Garratt, *J. Org. Chem. 38* (1973) 3051.
[75] G. Fraenkel, R. E. Carter, A. McLachian, J. H. Richards, *J. Am. Chem. Soc. 82* (1960) 5846.
[76] P. C. Lauterbur, *Tetrahedron Lett. 1961,* 274.
[77] D. H. O'Brien, A. J. Hart, C. R. Russel, *J. Am. Chem. Soc. 97* (1975) 4410.
[78] a) H. Hogeveen, P. W. Kwant, *J. Am. Chem. Soc. 96* (1974) 2208 and references cited therein; b) *Acc. Chem. Res. 8* (1975) 413.
[79] a) J. P. Pasinski, R. A. Beaudet, *J. Chem. Soc. Chem. Commun. 1973,* 928; b) R. E. Williams, *Inorg. Chem. 10* (1971) 210; see also H. Schwarz, *Angew. Chem. 93* (1981) 1046; *Angew. Chem. Int. Ed. Engl. 20* (1981) 991.
[80] G. Williamson, M. Rosenblum, M. C. Whiting, R. B. Woodward, *J. Am. Chem. Soc. 74* (1952) 2125.
[81] H. T. Jonkman, W. C. Nieuwport, *Tetrahedron Lett. 1973,* 1671.
[82] H. Hogeveen, E. M. G. A. van Kruchten, *J. Org. Chem. 46* (1981) 1350.
[83] a) M. Saunders, L. Telkowski, M. R. Kates, *J. Am. Chem. Soc. 99* (1977) 8070; b) M. Saunders, M. R. Kates, *ibid. 99* (1977) 8071; c) M. Saunders, M. R. Kates, K. B. Wiberg, W. Pratt, *ibid. 99* (1977) 8072; d) M. Saunders, J. Chandrasekhar, P. von R. Schleyer in P. De Mayo: *Rearrangements in Ground and Excited States,* Vol. *1,* Chap. 1, Academic Press, New York 1980.
[84] R. E. Williams, L. D. Field in R. W. Parry, G. Kodama: *Boron Chemistry,* Pergamon Press, New York 1980.
[85] a) C. Giordano, R. F. Heldeweg, H. Hogeveen, *J. Am. Chem. Soc. 99* (1977) 5181; b) R. F. Heldeweg, Dissertation, Universität Groningen 1977.
[86] P. von R. Schleyer, lecture at the Symposium "Chemistry of Carbocations", Bangor, Wales, September 1981 and references quoted in the lecture.
[87] P. von R. Schleyer, private communication.
[88] G. A. Olah, M. Arvanaghi, G. K. S. Prakash, unpublished results.
[89] G. A. Olah, V. V. Krishnamurthy, M. Arvanaghi, G. K. S. Prakash, unpublished results.

**When submitting manuscripts, authors of articles which are intended for publication as "Communications" are requested to conform to the guidelines reproduced at the beginning of each issue following the list of contents.**

## Three Arguments Supporting a Rectangular Structure for Tetra-*tert*-butylcyclobutadiene**

By *Otto Ermer** and *Edgar Heilbronner*

According to recent theoretical and experimental evidence, cyclobutadiene **1** has a planar rectangular equilibrium structure with $D_{2h}$ symmetry; the optimal square structure ($D_{4h}$) represents a transition state joining two equivalent $D_{2h}$ minima on the potential energy surface[1]. *Irngartinger et al.* interpreted the room temperature X-ray diffraction data of crystalline tetra-*tert*-butylcyclobutadiene **2** in terms of a structure having an almost equilateral four-membered ring[2a]. This led *Borden et al.* to perform quantum mechanical model calculations on **1**, and to conclude that the almost square cyclobutadiene skeleton in the crystal is a plausible equilibrium structure for **2**, since they believed the bulky *tert*-butyl groups to exert a considerable "quadratization effect"[3].




1 2 3 4 5 6

In the formulas, bond lengths determined by X-ray crystallography are given in pm [2].

We give three arguments which, contrary to these conceptions, suggest a rectangular four-membered ring also for **2**:

1. The photoelectron (PE) spectra of **2** to **6**[4] are so closely similar (particularly those of **2** and **3**[4a]) that similar four-membered ring structures may be concluded. Since both the comparison with reliable calculations and the empirical correlation method[4e] lead to an interpretation of the PE spectra of **3** to **6** in terms of the experimentally proven rectangular four-membered ring structures of **3**, **5** and **6**[2], the PE spectrum of **2**[4a] is hardly consistent with a square four-membered ring. In fact, *Schweig* has estimated that a square cyclobutadiene derivative should be approximately 0.7 eV more readily ionizable than a rectangular one. Comparison with other compounds suggests that this estimate is a lower limit.

2. Empirical model calculations based on our force field[5] yield elongations of the double bonds of only 0.6 pm for rectangular **2** and a strain energy reduction of only 1.6 kJ $mol^{-1}$ on going to square **2**. The calculated equidistance of the *tert*-butyl groups also in rectangular **2** is achieved without quadratization essentially by small exocyclic angle deformations at the C atoms of the four-membered ring (C–C=C angles *ca.* 2° larger than C–C–C).

3. The structural model of **2** fitted to the room temperature X-ray intensities is based on *average* atomic positions and has, to a good approximation, $D_{2d}$ symmetry with an almost square four-membered ring[2a]. However, the differences between this $D_{2d}$ structure and the rectangular $D_2$ minimum geometry are so small that the observed structure of higher symmetry may well be a consequence of dynamic or static disorder. In the first case, rectangular $D_2$ minima interconvert in the crystal, *via* the square $D_{2d}$ transition state, to the enantiomeric $D_2$ minima (bond switching), or the disc-shaped molecules execute a (hindered) rotation about the ring axis. In the second case, the crystal contains a statistical distribution of pairs of molecules (with parallel ring planes), in which the partners are mutually rotated by 90° (Fig. 1). The atomic displacements arising from these averaging processes are so small that they are hardly discernible from excessive thermal motion parameters, at least not at room temperature. A rectangular structure for **2** can, therefore, not be ruled out from the available crystallographic results at room temperature. Possibly also low temperature measurements cannot provide a definite answer; such measurements are described by *Irngartinger* and *Nixdorf* in the following communication[2b].

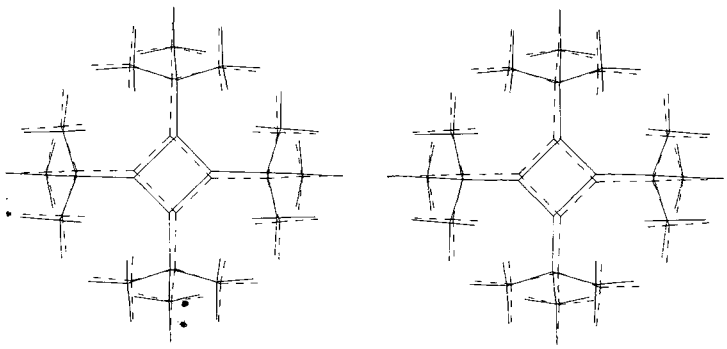


Fig. 1. Proposed disorder model for **2**. The stereoscopic model consists of two calculated rectangular $D_2$ enantiomers mutually rotated by 90° about the ring axis. The averaged structure has $D_{2d}$ symmetry. The distance between the superimposed C atoms of the four-membered rings corresponds to a temperature-factor increase $\Delta U$ of only *ca.* 80 $pm^2$. The remaining atomic positions coincide even more closely.

For the reasons given we conclude that also **2** may have a rectangular four-membered ring structure with dimensions similar to those in **1**, and that the quadratization barriers differ only slightly. The arguments previously put for-

[*] Priv.-Doz. Dr. O. Ermer
Abteilung für Chemie der Universität
Postfach 102148, D-4630 Bochum 1 (Germany)
Prof. Dr. E. Heilbronner
Physikalisch-chemisches Institut der Universität
Klingelbergstrasse 80, CH-4056 Basel (Switzerland)

[**] This work was supported by the Fonds der Chemischen Industrie.

 © Verlag Chemie GmbH, 6940 Weinheim, 1983 0570-0833/83/0505-0402 $ 02.50/0 

ward to support a square structure for **2** are in no way sufficient or convincing.

Received: December 16, 1982;
revised: February 7, 1983 [Z 225 IE]
German version: *Angew. Chem. 95* (1983) 414

CAS Registry number:
**2**, 66809-05-0.

[1] T. Bally, S. Masamune, *Tetrahedron 36* (1980) 343, and literature cited therein.

[2] X-ray structure analysis of a) **2** (room temperature), **3**: H. Irngartinger, N. Riegler, K.-D. Malsch, K.-A. Schneider, G. Maier, *Angew. Chem. 92* (1980) 214; *Angew. Chem. Int. Ed. Engl. 19* (1980) 211; b) **2** (low temperature): H. Irngartinger, M. Nixdorf, *ibid. 95* (1983) 415; *22* (1983) 403; c) **5**: H. Irngartinger, H. Rodewald, *ibid. 86* (1974) 783; **13** (1974) 740; d) **6**: L. T. J. Delbaere, M. N. G. James, N. Nakamura, S. Masamune, *J. Am. Chem. Soc. 97* (1975) 1973.

[3] W. T. Borden, E. R. Davidson, *J. Am. Chem. Soc. 102* (1980) 7958.

[4] PE spectra of a) **2**, **3**: E. Heilbronner, T. B. Jones, A. Krebs, G. Maier, K.-D. Malsch, J. Pocklington, A. Schmelzer, *J. Am. Chem. Soc. 102* (1980) 564; b) **4**: G. Lauer, C. Müller, K.-W. Schulte, A. Schweig, G. Maier, A. Alzérreca, *Angew. Chem. 87* (1975) 194; *Angew. Chem. Int. Ed. Engl. 14* (1975) 172; c) **5**: G. Lauer, C. Müller, K.-W. Schulte, A. Schweig, A. Krebs, *ibid. 86* (1974) 597; *13* (1974) 544; d) **6**: R. S. Brown, S. Masamune, *Can. J. Chem. 53* (1975) 972; e) E. Heilbronner, J. P. Maier in C. R. Brundle, A. D. Baker: *Electron Spectroscopy, Theory, Techniques, and Applications*, Vol. *I*, Academic Press, London 1977.

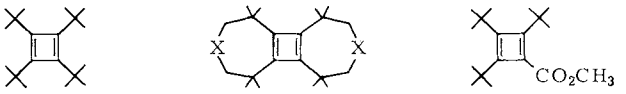
[5] O. Ermer, S. Lifson, *J. Am. Chem. Soc. 95* (1973) 4121.

## Bonding Electron Density Distribution in Tetra-*tert*-butylcyclobutadiene—A Molecule with an Obviously Non-Square Four-Membered ring**

By *Hermann Irngartinger** and *Matthias Nixdorf*

We have found by X-ray structure analysis that the sides of the non-planar four-membered ring in tetra-*tert*-butylcyclobutadiene **1** are almost equal (1.464 and 1.483 Å) at room temperature[1a]. Although the actual differences in length are still significant—being of the order of ten times the standard deviation—markedly greater differences of 0.14–0.26 Å occur in the cyclobutadiene derivatives **2** to **4**[1]. In order to explain this discrepancy, we have carried out low-temperature measurements at −30 and −150 °C on **1** and repeated the room temperature measurement with a second crystal on another diffractometer. The repeat measurement yielded, within the limit of error, the same results as earlier. The values at −30 °C (1.466(2) and 1.491(2), 1.493(2) Å) do not seriously differ from the room temperature data. However, measurements of the bond lengths in the four-membered ring at −150 °C yielded the values 1.441(2) and 1.526(1) and 1.527(2) Å, respectively, with a greater difference of 0.086 Å compared to the room temperature data (Fig. 1). Force field calculations and spectroscopic findings likewise clearly indicate a non-square structure for the four-membered ring[2]. The conformation of **1** in the crystal remains almost unchanged at low temperature; within the error of measurement, the angle at which the four-membered ring is folded remains about the same (169.9°).

On the basis of these results we assume that equilibrating effects are operating in the four-membered ring of **1**



**1** **2**, X = S; **3**, X = $CH_2$ **4**

in the crystal at room temperature, due to static or dynamic disorder. Since the bond lengths in the ring differ significantly at room temperature the molecular arrangement in which the double bond is almost parallel to the twofold rotation axis must be more populated than the arrangement perpendicular to it but with otherwise the same orientation of the molecule. This unequal distribution of the disordered molecules is even more pronounced at −150 °C. Whether a completely ordered structure is achieved, is still unclear.

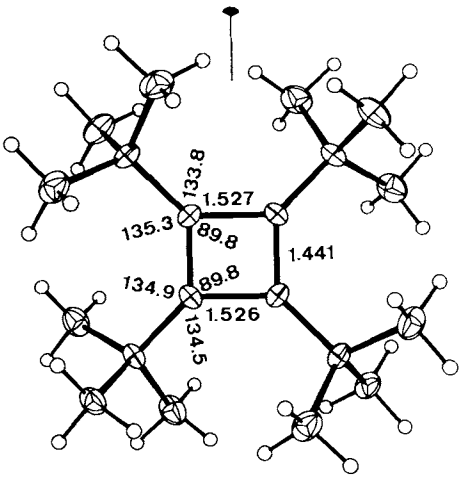



Fig. 1. Bond lengths [Å] and angles [°] of the four-membered ring of **1** at −150 °C; standard deviations 0.002 Å and 0.1° respectively; vibration ellipsoids for 50% probability. Crystallographic data (−150 °C): $a = 17.530(3)$, $b = 9.150(1)$, $c = 11.769(2)$ Å, $\beta = 106.56(2)°$, monoclinic space group C2/c, $Z = 4$. The centric space group derives from statistical tests. Tentative refinement with room temperature data in the space group Cc led to trapezoidal distortion of the four-membered ring. Up to $\sin\theta/\lambda = 1.15$ Å$^{-1}$ ($Mo_{K\alpha}$-radiation) 4813 independent reflections (3184 observed, $I > 3\sigma(I)$); refinement of the C atoms with 953 reflections of higher order ($0.75 < \sin\theta/\lambda < 1.15$ Å$^{-1}$), 11 reflections per variable; $R = 0.048$ [5].

If the low-temperature geometry of the four-membered ring is transferred to the structure at room temperature and an equal population of the two disorder orientations is assumed, then the thermal vibration of 0.0511(5) Å$^2$ vertical to the bisector of the four-membered ring angle and within the ring plane contains a contribution $\Delta U$ of only 0.0009 Å$^2$ (1.8%), thus explaining why no effects of equilibration on the thermal parameters of the four-membered ring atoms were to be observed at room temperature. This value is smaller than that calculated (0.0083 Å$^2$) on the basis of the data for **3**[1a]. The value for **1** has to be set at a higher rate if an incompletely ordered structure is present at low temperatures.

We have experimentally determined the bonding electron density distribution in **1** according to the "X-X" method[3] using the low temperature data (−150 °C) (Fig. 2). The density maxima of the four-membered ring bonds are shifted outwards from the bond axes, so that bent bonds are present, similarly as in the case of **2**[4]. The single bond (with a shift of 0.20 Å) is more strongly bent than the double bond (0.10 Å). Unlike the bond angle of 89.8° (Fig. 1), the angle between the density maxima is 111° (Fig.

[*] Prof. Dr. H. Irngartinger, M. Nixdorf
Organisch-chemisches Institut der Universität
Im Neuenheimer Feld 270, D-6900 Heidelberg 1 (Germany)

[**] This work was supported by the Deutsche Forschungsgemeinschaft and the Fonds der Chemischen Industrie. We thank Prof. G. Maier, Dr. K.-D. Malsch, and Dr. K. A. Schneider (Universität Giessen) for supplying samples.

2). The maxima of electron densities on the single and double bonds have different values (0.37 and 0.57 e/Å$^3$).

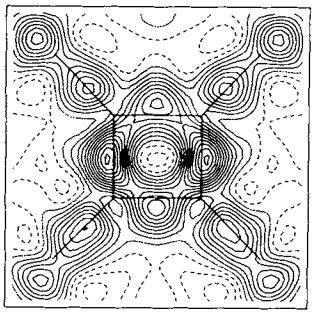


Fig. 2. Deformation densities in the four-membered ring of **1** (2231 $\Delta F$ values from the range $\sin\theta/\lambda < 0.75$ Å$^{-1}$). The contour intervals are 0.05 e/Å$^3$.

Although we cannot rule out equilibration effects also still being effective at low temperatures the differences in the two bond types of the cyclobutadiene system emerge just as clearly in the electron density distribution as in the bond lengths.

Received: December 28, 1982;
revised: February 25, 1983 [Z 233 IE]
German version: *Angew. Chem. 95* (1983) 415

CAS Registry number:
**1**, 66809-05-0.

[1] a) H. Irngartinger, N. Riegler, K.-D. Malsch, K.-A. Schneider, G. Maier, *Angew. Chem. 92* (1980) 214; *Angew. Chem. Int. Ed. Engl. 19* (1980) 211; b) H. Irngartinger, H. Rodewald, *ibid. 86* (1974) 783 and *13* (1974) 740; c) L. T. J. Delbaere, M. N. G. James, N. Nakamura, S. Masamune, *J. Am. Chem. Soc. 97* (1975) 1973; d) Review: T. Bally, S. Masamune, *Tetrahedron 36* (1980) 343.

[2] O. Ermer, E. Heilbronner, *Angew. Chem. 95* (1983) 414; *Angew. Chem. Int. Ed. Engl. 22* (1983) 402.

[3] P. Coppens, *Angew. Chem. 89* (1977) 33; *Angew. Chem. Int. Ed. Engl. 16* (1977) 32.

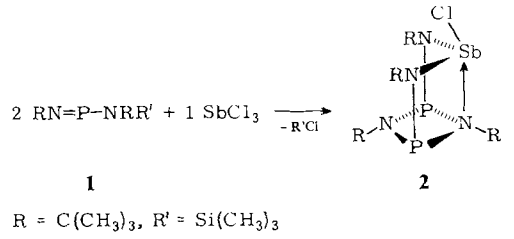
[4] H. Irngartinger, H.-L. Hase, K.-W. Schulte, A. Schweig, *Angew. Chem. 89* (1977) 194; *Angew. Chem. Int. Ed. engl. 16* (1977) 187.

[5] Further details of the crystal structure investigation can be obtained on request from the Fachinformationszentrum Energie Physik Mathematik, D-7514 Eggenstein-Leopoldshafen on quoting the number CSD 50369, the names of the authors, and complete citation of the journal.

## Synthesis and Structure of a Bicyclic SbNP Compound with Intramolecular Donor-Acceptor Bonding**

By *Otto J. Scherer**, *Gotthelf Wolmershäuser*, and *Herbert Conrad*

Amino(imino)phosphanes having at least one $(CH_3)_3Si$ group on the amino nitrogen atom are suitable, among other things, for the preparation of various phosphorus-nitrogen-element heterocycles[1]. Treatment of *tert*-butylimino(*tert*-butyltrimethylsilylamino)phosphane **1** with $SbCl_3$ represents a new variant of this reaction; the four-membered ring compound ClSb(NR)PClNR, which is the product expected by analogy to the reaction with $AsCl_3$[2], is not formed, and the reaction yields the SbNP bicycle **2**[3].




**1**

R = $C(CH_3)_3$, R' = $Si(CH_3)_3$

**2**

**2** forms colorless, air-sensitive crystals [m.p. > 130 °C (decomp.)] which are readily soluble in dichloromethane, benzene, and toluene and moderately soluble in ether and pentane. According to the crystal structure analysis, **2** has a planar $P_2N_2$ four-membered ring, which is bridged by a symmetrical NSbN bridge (Fig. 1). The lone pair of electrons of N3 bond coordinatively to antimony; the considerably larger distances 1.771(4) and 1.772(6) Å for P1–N3 and P2–N3, respectively, can therefore be considered as an ideal model for PN single-bond lengths in molecules with trivalent phosphorus.

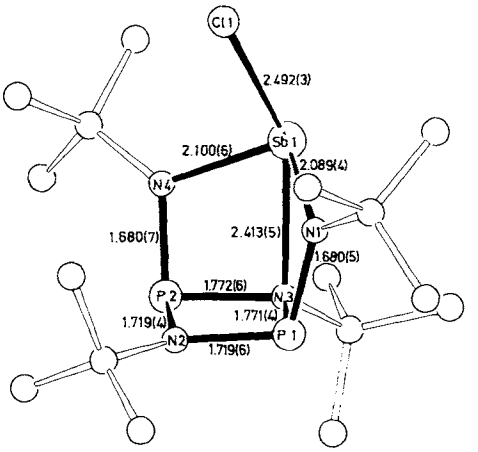


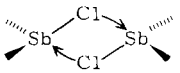

Fig. 1. Molecular structure of **2** (molecule 1) in the crystal. Selected bond angles [°]: Cl1-Sb1-Ne 147.2(1), Cl1-Sb1-N4 95.1(2), Cl1-Sb1-N1 94.5(2), Sb1-N1-P1 107.3(2), Sb1-N4-P2 107.2(2), N1-Sb1-N4 103.5(2), N2-P2-N4 107.3(3), N3-P2-N4 91.8(3), N1-P1-N3 91.6(2), N1-P1-N2 108.0(3), Sb1-N3-P2 92.4(3), Sb1-N3-P1 92.1(2).—Crystal structure data: space group: triclinic $P\bar{1}$: $a = 9.5564(9)$, $b = 9.613(1)$, $c = 31.229(2)$ Å; $\alpha = 79.731(6)$, $\beta = 80.065(6)$, $\gamma = 60.450(8)°$; $V = 2444.0$ Å$^3$, $Z = 4$ (two independent molecules, which do not significantly differ in their individual distances and angles); $\rho_{calc} = 1.369$ g·cm$^{-3}$: 7872 independent reflections, $R = 0.044$, $R_w = 0.050$. Further details of the crystal structure investigation can be obtained from the Fachinformationszentrum Energie, Physik, Mathematik, D-7514 Eggenstein-Leopoldshafen by quoting the depository number CSD 50338, the names of the authors, and the journal citation.

The distorted trigonal-bipyramidal environment at antimony is comparable with that in $Cl_3Sb \cdot H_2NC_6H_5$(A) (A: Sb–$Cl_{(ax)}$ 2.52, Sb–N 2.53 Å, Cl–Sb–N 166.3°[4]). As expected, the greatest difference occurs in the NSbCl axial angle (147.2° in **2**). The $^1$H-NMR spectrum (200 MHz, solvent, $C_7D_8$, TMS int.) exhibits three signal groups at room temperature: $\delta = 1.52$ ("t", $A_9XX'A_9'$ system, 18H (SbN), $|^4J_{PH} + {}^6J_{PH}| = 2.1$ Hz). 1.35 ("t", 9H (PN), $|^4J_{PH} + {}^6J_{PH}| = 1.9$ Hz); 1.25 (s, 9H (PN)). $^{31}$P{$^1$H}-NMR ($C_7D_8$, 85% $H_3PO_4$ ext.): $\delta = 159.8$ (s). Temperature dependent $^1$H-NMR studies of a 30% toluene solution of **2** indicate that the different $(CH_3)_3C$ signals of the $P_2N_2$ four-membered ring coalesce at *ca.* 80 °C, whereas in a 20% solution this occurs at *ca.* 120 °C (extrapolated). This result indicates that the inversion of configuration at anti-

[*] Prof. Dr. O. J. Scherer, Dr. G. Wolmershäuser, H. Conrad
Fachbereich Chemie der Universität
Erwin-Schrödinger-Strasse, D-6750 Kaiserslautern (Germany)

[**] This work was supported by the Fonds der Chemischen Industrie. Prof. Dr. C. Krüger, Max-Planck-Institut für Kohlenforschung, Mülheim, is thanked for the X-ray intensity measurements.

mony does not proceed *via* a classical (intramolecular) mechanism, but *via* intermolecular exchange of halogen[5], which may occur thus:



Received: December 16, 1982 [Z 224 IE]
German version: *Angew. Chem. 95* (1983) 427

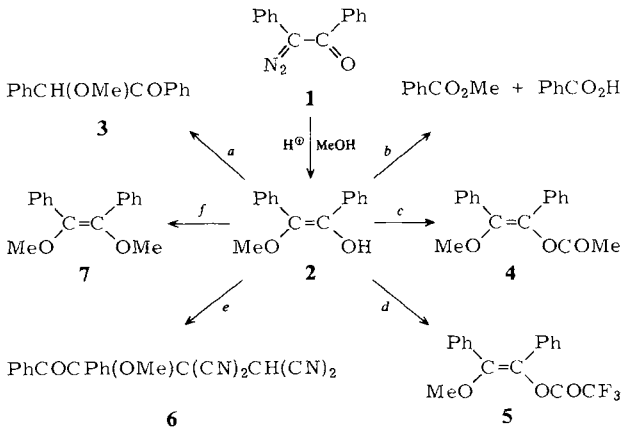
[1] Review: E. Fluck, *Top. Phosphorus Chem. 10* (1980) 194.
[2] O. J. Scherer, G. Schnabl, *Z. Naturforsch. B31* (1976) 142.
[3] *Procedure:* $SbCl_3$ (8.33 g, 36.5 mmol) in 22 mL ether is added dropwise to a solution of **1** (9.0 g, 36.5 mmol) [O. J. Scherer, N. Kuhn, *Angew. Chem. 86* (1974) 899; *Angew. Chem. Int. Ed. Engl. 13* (1974) 811] in 25 mL ether at −35 °C and the sealed apparatus kept for 12–15 d in a refrigerator (6 °C) until **1** had been completely converted (only with a 1:1 stoichiometric mixture; addition of 2 mol **1** shows $^{31}P\{^1H\}$-NMR spectroscopically that *ca.* 1 mol **1** has not reacted). Crystals precipitate out after 1 d at −30 °C and these are dried at −40 °C *in vacuo* (crude yield 4.23 g (46%)). After two recrystallizations (in each case 1 g is dissolved in 20 mL ether at room temperature and the solutions cooled to −30 °C), colorless crystals (2.8 g, 30%) are obtained.
[4] R. Hulme, J. C. Scruton, *J. Chem. Soc. A 1968*, 2448.
[5] Cf. to this problem with phosphorus: B. Fontal, H. Goldwhite, *Tetrahedron 22* (1966) 3275.

## (*Z*)-2-Methoxy-1,2-diphenylvinyl Alcohol, A Remarkably Stable Enol**

By *John F. McGarrity*, Alex Cretton, Alan A. Pinkerton, Dieter Schwarzenbach,* and *Howard D. Flack*

The isolation and structural determination of simple enols has attracted renewed attention recently[1,2]. Until now the only enols isolated have been stabilized by electron-withdrawing or extremely bulky substituents. Less substituted enols such as, *e.g.*, vinyl alcohol[3] have been observed as intermediates in solution, but have not been isolated prior to tautomerization to their more stable keto forms. We now describe the isolation and characterization of (*Z*)-2-methoxy-1,2-diphenylvinyl alcohol **2**, formed stereoselectively under kinetic control.

The acid-catalyzed methanolysis of benzoyl-α-diazotoluene **1** to yield 2-methoxy-1,2-diphenylethanone **3** occurs *via* an intermediate which can be crystallized directly from the reaction mixture. After complete removal of solvent, the intermediate's spectral characteristics [IR: $\nu_{max}$ 3515 $cm^{-1}$ (enol OH); UV: $\lambda_{max}$ 301 nm ($\varepsilon$=4940); $^1$H-NMR (80 MHz, $CDCl_3$, 25 °C, TMS): $\delta$=3.45 (s, 3H), 5.91 (s, 1H), 7.13 (s, 10H)] indicate structure **2**. This assignment was supported by a variety of characteristic reactions (Scheme 1) and by an X-ray structure analysis at −40 °C (Fig. 1).




Scheme 1. Characteristic reactions of **2**. a: $Et_3N$, $10^{-2}$ M in tetrahydrofuran (THF) −30 °C; b: $O_2$, THF; c: $Ac_2O$, $BF_3 \cdot Et_2O$ −50 °C; d: $(CF_3CO)_2O$, $Et_3N$, THF, −30 °C; e: tetracyanoethylene, $CH_2Cl_2$; f: NaH, THF, $(CH_3O)_2SO_2$.

Initial mechanistic studies on the transformation **1**→**2** indicate that protonation on oxygen followed by loss of nitrogen leads to a vinyl cation. The *Z* stereochemistry of the product is a consequence of kinetically controlled attack of

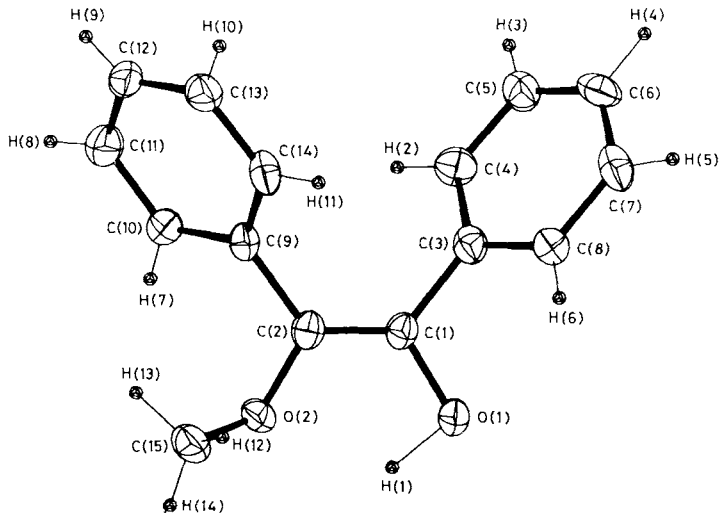



Fig. 2. Crystal structure of **2** · MeOH in the crystal; the solvent atoms are not indicated.

the solvent methanol on the less hindered side of the vinyl cation. Selective attack on this side may also benefit from steering of the incoming nucleophile by hydrogen bonding to the enolic OH group.

Received: November 5, 1982;
revised: March 1, 1983 [Z 196 IE]
German version: *Angew. Chem. 95* (1983) 426
The complete version of this communication appears in:
*Angew. Chem. Suppl. 1983*, 551–563

CAS Registry numbers:
**1**, 3469-17-8; **2**, 85370-23-6; **3**, 3524-62-7; **4**, 85370-24-7; **5**, 85370-25-8; **6**, 85370-26-9; **7**, 34898-74-3; $D_2$, 7782-39-0.

[*] Dr. J. F. McGarrity, Dipl.-Chem. A. Cretton
Institut de chimie organique de l'Université
Rue de la Barre 2, CH-1005 Lausanne (Switzerland)
Dr. A. A. Pinkerton
Institut de chimie minerale et analytique, Université de Lausanne
Prof. Dr. D. Schwarzenbach
Institut de cristallographie, Université de Lausanne
Prof. Dr. H. D. Flack
Laboratoire de cristallographie, Université de Génève

[**] This work was supported by the Swiss National Science Foundation. We wish to thank Prof. H. Dahn for very helpful discussions.

[1] H. Hart, *Chem. Rev. 79* (1979) 515.
[2] Z. Rappoport, S. E. Biali, *Bull. Soc. Chim. Belg. 91* (1982) 388.
[3] B. Capon, D. S. Rycroft, T. W. Watson, C. Zucco, *J. Am. Chem. Soc. 103* (1981) 1761. B. Capon, A. S. Siddhanta, *Tetrahedron Lett. 23* (1982) 3199.

## Synthesis of C-α- and C-β-D-Glucopyranosyl Derivatives from *O*-(α-D-Glucopyranosyl) Trichloroacetimidate**

By *Richard R. Schmidt** and *Michael Hoffmann*

Functionally substituted *C*-glycopyranosides occur as subunits of a variety of natural products. The synthesis of these chiral tetrahydropyran intermediates is therefore of topical preparative importance[1]. Especial interest attaches to the C-α- and C-β-D-glucopyranosyl derivatives, whose synthesis has hitherto presented problems[1,2].

Base-catalyzed reaction of tetra-*O*-benzylglucose **1** with trichloroacetonitrile affords directly and almost quantitatively the *O*-(α-D-glucopyranosyl) trichloroacetimidate **2**, which has proven useful for the synthesis of *O*-glycosides and saccharides[3]. An equally facile and highly stereoselective synthesis of C-α- and C-β-D-glucopyranosyl derivatives has now been achieved with various silylated aliphatic *C*-nucleophiles[4] (see Table 1).

Reaction of **2** with trimethylsilyl cyanide in the presence of boron trifluoride etherate or trimethylsilyl trifluoromethanesulfonate as catalyst affords exclusively the β-D-glucopyranosyl cyanide **3β**. Likewise, with 1,4-bis(ethoxy)-1,4-bis(trimethylsiloxy)-1,3-butadiene predominantly the β-anomer **4β** was obtained. Application of these reaction conditions to enol silyl ethers furnished anomeric mixtures; for example, with the enol silyl ether of acetophenone the anomers **5α**, **β** were formed in the ratio 1 : 1. The tendency for direct formation of the α-anomers to take place with this nucleophile could be exploited for the exclusive formation of **5α** using zinc chloride catalyst. Similarly, with the enol silyl ethers of *tert*-butyl methyl ketone and acetone only the α-anomers **6α** and **7α**, respectively, were obtained. Allyltrimethylsilane as *C*-nucleophile under these reaction conditions led almost exclusively to the important 1-allyl-1-deoxy-α-D-glucopyranose **8α**[1a] (α : β = 10 : 1).

The structure of **8α** was confirmed by comparison[1a]. The structures of **3β**—**5β** and **5α**—**7α** follow from their $^1$H-NMR data, from comparison with each of the other anomers[4,5], and, in the case of **4β**, **5α** and **5β**, also from $^1$H-NMR data of the derivatives obtained by debenzylation and acetylation.

Received: December 21, 1982 [Z 227 IE]
German version: *Angew. Chem. 95* (1983) 417
The complete version of this communication appears in: *Angew. Chem. Suppl. 1983*, 543—550

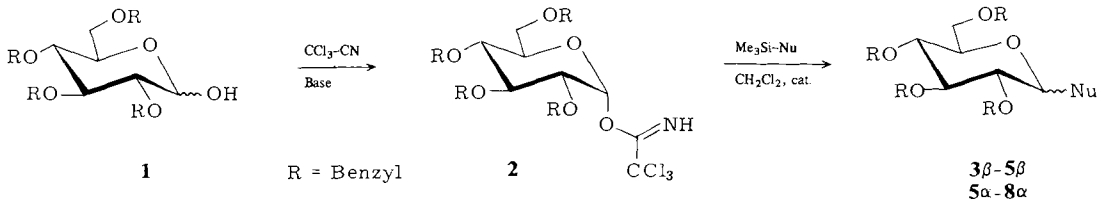
[1] a) M. D. Lewis, J. K. Cha, Y. Kishi, *J. Am. Chem. Soc. 104* (1982) 4976; b) L. A. Reed, III, Y. Ito, S. Masamune, K. B. Sharpless, *ibid. 104* (1982) 6468; c) G. E. Keck, J. B. Yates, *ibid. 104* (1982) 5829, and references cited therein.

[2] For the synthesis of glycosyl cyanides see G. Grynkiewicz, J. N. BeMiller: *XIth Int. Carbohydr. Symp.*, Vancouver 1982; F. G. de las Heras, P. Fernandez-Resa, *J. Chem. Soc. Perkin Trans. 1 1982*, 903; and references cited therein.

[3] R. R. Schmidt, J. Michel, *Angew. Chem. 92* (1980) 763; *Angew. Chem. Int. Ed. Engl. 19* (1980) 731; R. R. Schmidt, M. Stumpp, J. Michel, *Tetrahedron Lett. 23* (1982) 405; and references cited therein.

[4] Phenol ethers have already been successfully converted: R. R. Schmidt, M. Hoffmann, *Tetrahedron Lett. 23* (1982) 409; M. Hoffmann, investigations to be described in a planned dissertation.

[5] P. Boullanger, D. Marmet, G. Descotes, *Tetrahedron 35* (1979) 163.




**1** **2** **3β-5β** **5α-8α**

Table 1. Reaction of **2** with trimethylsilyl nucleophiles under acid-catalysis conditions.

| X—Nu<br>X = $Me_3Si$ | Reaction conditions | Cpd. isolated | Nu | Yield [a] [%] | M.p. [b] [°C] | $[\alpha]_{578}^{22}$ ($CHCl_3$, $c = 1$) |
|---|---|---|---|---|---|---|
| X—CN | [c], 0 °C, 90 min | **3β** [d] | CN | 87 | oil | +33.0 |
| $[XO(EtO)C{=}CH{-}]_2$ | $BF_3 \cdot OEt_2$, 0 °C, 30 min | **4β** [e] | EtOCOCHCH$_2$COOEt | 70 | 69—71 | − 1.0 |
| $CH_2{=}C(Ph)OX$ | $BF_3 \cdot OEt_2$, RT, 5 min | **5α**, **β** [f] | $CH_2COPh$ | 76 | oil | — |
| $CH_2{=}C(Ph)OX$ | $ZnCl_2$, RT, 15 min | **5α** [d] | $CH_2COPh$ | 73 | 72—74 | +48.0 [h] |
| $CH_2{=}C(t\text{Bu})OX$ | $ZnCl_2$, RT, 30 min | **6α** [d] | $CH_2COt\text{Bu}$ | 69 | 89—91 | +49.0 |
| $CH_2{=}C(Me)OX$ | $ZnCl_2$, RT, 15 min | **7α** [d] | $CH_2COMe$ | 68 | 91—94 | +41.0 [h] |
| $CH_2{=}CH{-}CH_2{-}X$ | $ZnCl_2$, RT, 30 min | **8α** [g] | $CH_2CH{=}CH_2$ | 75 | 59—61 | +39.0 |

[a] Analytically pure products. [b] From methanol. [c] $Me_3SiOSO_2CF_3$. [d] In each case the other anomer was not observed thin-layer chromatographically. [e] α : β = 1 : 5. [f] α : β = 1 : 1. [g] α : β = 10 : 1. [h] $c = 0.5$.

[*] Prof. Dr. R. R. Schmidt, M. Hoffmann
Fakultät für Chemie der Universität
Postfach 5560, D-7750 Konstanz (Germany)

[**] Glycosyl Imidates, Part 7.—This work was supported by the Deutsche Forschungsgemeinschaft and the Fonds der Chemischen Industrie.—Part 6: R. R. Schmidt, G. Grundler, *Angew. Chem. 94* (1982) 790; *Angew. Chem. Int. Ed. Engl. 21* (1982) 781; *Angew. Chem. Suppl. 1982*, 1707—1714.

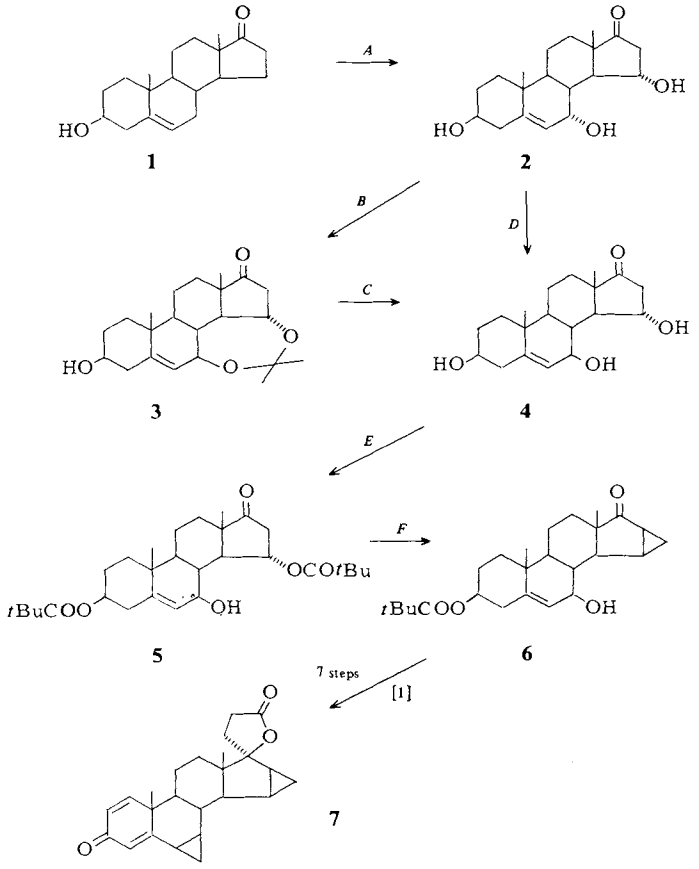
## A Novel Synthetic Route to the Aldosterone-Antagonist Spirorenone

By *Karl Petzoldt**, *Henry Laurent*, and *Rudolf Wiechert*

We recently reported the synthesis of the spirorenone **7**, a novel, highly active aldosterone-antagonist[1]. Starting from 3β-hydroxy-5-androsten-17-one **1**, the title compound **7** was obtained in 1.5% overall yield *via* a 15-step synthesis. We now wish to report an entry to **7** involving unexpected reactions, in which the number of synthetic steps is reduced to 11 and the yield of **7** is increased to 5.6% (Scheme 1).

[*] Dr. K. Petzoldt, Dr. H. Laurent, Prof. Dr. R. Wiechert
Forschungslaboratorien der Schering AG Berlin/Bergkamen
Müllerstrasse 170—178, D-1000 Berlin 65 (Germany)

The first step of the synthesis now consists in a microbiological dihydroxylation using the fungal strain *Colletotrichum lini*, whereby two hydroxy groups are introduced into the 7α- and 15α-position of androstenolone **1** to give **2** in 85% yield. This dihydroxylation has already been performed with microorganism cultures of the species *Gibberella saubinetti*[2] and *Glomerella cingulata*[3].




Scheme 1. *A: Collectotrichum lini*, substrate concentration 1 g/L culture broth, fermentation time 36 h; *B*: $BF_3 \cdot (C_2H_5)_2O$ in acetone, −10 °C, 1 min; *C*: HCl conc. in methanol, 0 °C, 10 min; *D*: 35% $HClO_4$ in methyl isobutyl ketone, RT, 4 h; *E*: $(CH_3)_3CCOCl$, 4-dimethylaminopyridine in pyridine, 50 °C, 4 h; *F*: trimethylsulfoxonium iodide ($(CH_3)_3SO^+I^-$), NaOH in dimethyl sulfoxide, RT, 1 H.—Yields [%], melting points [°C] (Mettler FP11, 2 °C/min) and $[\alpha]_D^{22}$-values ($c = 0.5$ in $CHCl_3$): **2**: 85, 218.2, −45.2; **3**: quant., 168.1, +86; **4**: 95, 189.4, +118.4; **5**: 90, 180.8, +83.4; **6**: 91, 240.3, −48.6.

The isomerization of the allylic 7α-hydroxy function, a further essential step of the synthesis, can be accomplished in two ways: either by preparation and subsequent cleavage of the acetonide **3**, which for steric reasons obviously only exists in the 7β,15α-substituted form, or by direct acid-catalyzed epimerization of **2** in methyl isobutyl ketone, whereupon the equilibrium lies 97% on the side of the 7β-triol **4**.

Surprisingly, **4** can be selectively esterified with pivalic acid chloride in presence of 4-dimethylaminopyridine to give the 3β,15α-dipivalate **5**, which could be directly converted under Corey methylation conditions into the 15β,16β-methylene compound **6**. At this point, the synthesis then follows the previously described preparative route[1] and leads after 7 further synthetic transformations to spirorenone **7**.

Received: December 17, 1982 [Z 226 IE]
German version: *Angew. Chem. 95* (1983) 413

CAS Registry numbers:
**1**, 53-43-0; **2**, 2963-69-1; **3**, 85390-92-7; **4**, 85390-93-8; **5**, 85390-94-9; **6**, 82543-09-7; **7**, 74220-07-8.

[1] D. Bittler, H. Hofmeister, H. Laurent, K. Nickisch, R. Nickolson, K. Petzoldt, R. Wiechert, *Angew. Chem. 94* (1982) 718; *Angew. Chem. Int. Ed. Engl. 21* (1982) 696.
[2] M. Okada, Y. Saito, *Steroids 6* (1965) 651.
[3] K. Kieslich, DOS 2746298 (19. 4. 79), Schering AG; *Chem. Abstr. 91* (1979) 123928v.

## GaGaTe, a Novel Defect Tetrahedral Structure

By *Dieter Fenske* and *Hans Georg von Schnering**

*Dedicated to Professor Harald Schäfer on the occasion of his 70th birthday*

Systematic experiments to prepare ternary quasi (III—V)-phases yield GaGaTe[1], which at the same time was found to be the only stable compound in the ternary system Ga—Ga—Te by *Kra et al.*[2]. GaGeTe crystallizes from a melt of the elements in the form of dull-grey hexagonal crystals, which cleave like graphite parallel to the hexagonal (001) plane (quartz ampoules; melting of the elements at 1150 K; GaGeTe crystallizes peritectically at 1073 K). The compound is stable towards $H_2O$, air and NaOH (25%). In cold hydrochloric acid (10%), colorless crystalline reaction products occur on the cleavage faces after a few days. GaGeTe is a semiconductor with $\Delta E = 1.1$ eV[3]. From the electron balance (VEC = 4.33) and the structural chemistry of the participating elements a defect tetrahedral structure of the type $3_4 4_4 0_1 6_4$[4a] may be expected. This was confirmed by the structure determination[5].

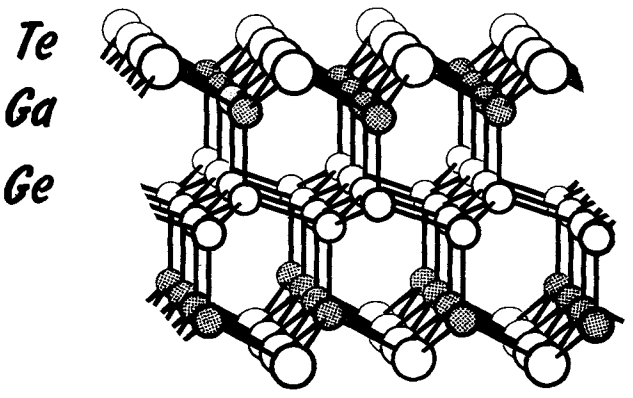



Fig. 1. Two-dimensional structural unit of GaGeTe. Distances [Å]: Ge—Ge = 2.461; Ge—Ga = 2.440; Ga—Te = 2.656; Angles [°]: Ge—Ge—Ge = 110.7, Ge—Ge—Ga = 108.3; Ge—Ga—Te = 118.3; Te—Ga—Te = 99.3; Ga—Te—Ga = 99.3 [5].

GaGeTe presents a novel structure type, characterized by two-dimensional infinite block layers of the type $^2_\infty$[Te—Ga—Ge—Ge—Ga—Te]. The structure (Fig. 1) derives from that of GaSe, $^2_\infty$[Se—Ga—Ga—Se], by insertion of a puckered layer of tetrahedrally bonded Ge-atoms in the form of annelated six-membered rings with chair conformation. The two-dimensional block layers are segments of the diamond structure.

[*] Prof. Dr. H. G. v. Schnering
Max-Planck-Institut für Festkörperforschung
Heisenbergstrasse 1, D-7000 Stuttgart 80 (Germany)
Prof. Dr. D. Fenske
Institut für Anorganische Chemie der Universität
Engesserstrasse Geb. Nr. 3045, D-7500 Karlsruhe (Germany)

Te is bonded to 3 Ga (2.656(3) Å), Ga to 3 Te and 1 Ge (2.440(3) Å) and Ge to 1 Ge and 3 Ge (2.461(3) Å). The intralayer Te–Te distances are 4.048 Å, whereas the interlayer distance is 4.133 Å. The formal description of the compound with $Te^{2-}$, $Ge^{2+}$ and $Ge^0$ takes into account the electronegativities of the elements and shows the relation to the monochalcogenides of gallium. The molecular volume of GaGeTe (49.7 $cm^3\ mol^{-1}$) corresponds exactly to the volume of GaTe and Ge (49.8 $cm^3\ mol^{-1}$), but is noticeably larger than that of the elements (45.8 $cm^3\ mol^{-1}$)[5].

Received: January 13, 1983 [Z 242 IE]
German version: *Angew. Chem. 95* (1983) 420

CAS Registry number:
GaGeTe, 64052-15-9

[1] D. Fenske, unpublished results (1978).
[2] G. Kra, R. Eholie, J. Flahaut, *Ann. Chim. Fr. 1978* (3), 257.
[3] W. Bauhofer, personal communication.
[4] a) E. Parthé: *Cristallochimie des Structures Tétraédriques*, Gordon & Breach, Paris 1972; b) W. Biltz: *Raumchemie der festen Stoffe*, Verlag Leopold Voss, Leipzig 1934.
[5] Crystal structure analysis: R3m (No. 166); hexagonal setting; $a = 4.048(2)$ Å, $c = 34.731(9)$ Å; $Z = 6$; four-circle diffractometer, $Mo_{K\alpha}$ radiation; 151 *hkl* averaged from 586 measured ones; $R(\text{iso}) = 0.081$, $R(\text{aniso}) = 0.071$; atoms at position (00z) with $z(\text{Te}) = 0.11763(6)$, $z(\text{Ga}) = 0.2521(1)$, $z(\text{Ge}) = 0.3224(1)$; $B_i = 0.75(6)$ or 0.72(8) or 0.66(8) $Å^2$ respectively. The deviation from isotropic behavior is negligible. Ga and Ge could definitely be differentiated. Further details of this structural investigation can be obtained on request from the Fachinformationszentrum Energie Physik Mathematik, D-7514 Eggenstein-Leopoldshafen 2 on quoting the number CSD 50363, the name of the author, and complete citation of the journal.

## Are the Previously Described $[ClF_6][CuF_4]$ and $[Cu(H_2O)_4][SiF_6]$ Identical?

By *Hans Georg von Schnering** and *Dong Vu*

*Dedicated to Professor Harald Schäfer on the occasion of his 70th birthday*

In 1980 *Batsanov et al.*[1] published a sensational paper on the occurrence of the compound hexafluorochlorine(VII) tetrafluorocuprate(III) $[ClF_6]^+[CuF_4]^-$. A small portion of crystalline products was obtained, following the shock-wave compression of a mixture of $CuCl_2$ and $CuF_2$. The crystal structure investigation on single crystals revealed square-planar $[CuF_4]$ units and $[ClF_6]$ octahedra. However, the observed paramagnetism and the blue color of the compound significantly contradict the square-planar structure of the $CuF_4$ anions. Instead, diamagnetism and an octahedral $Cu^{II}$-coordination would be expected. Finally, the authors reported, that no chlorine could be detected in the crystalline product on chemical analysis.

Upon discussing these problems[3], aroused by critical comments by *K. O. Christe* at the 10th International Symposium on Fluorine Chemistry in Vancouver (1982), we decided to examine the crystallographic data[1]. First, the determination of the crystal structure seems to be correct ($R = 0.07$). However, we found large discrepancies in the following details: (a) The molar volume was calculated to be 108 $cm^3\ mol^{-1}$, which is unexpectedly large, especially for a high pressure phase (according to *Biltz*[4] it is estimated to be 96 $cm^3\ mol^{-1}$); the experimental density is also 6% smaller than expected. (b) The coefficients of the temperature factors $B$(Cl), $B$(F4) and $B$(F5) are two to three times larger than the values of the corresponding scattering centers of Cu, F1, F2 and F3, respectively; thereby, it is particularly surprising that F4 and F5 form the Cu-coordination.

The following considerations showed that tetraaquacopper(II) hexafluorosilicate $[Cu(H_2O)_4]^{2+}[SiF_6]^{2-}$ would be a perfect candidate to fulfill all of the critia: color, paramagnetism, lack of chlorine, molar volume (an estimated 111 $cm^3\ mol^{-1}$), density, $B_{ij}$ temperature factors, crystal structure and interatomic distances! Since the authors did not report the exact experimental conditions (material of the ampoules, quality of the educt) under which the reaction occurred, we could not reproduce their experiment using a similar apparatus. Therefore, the presence of $H_2O$ and Si is still speculative. We found, that the compound $[Cu(H_2O)_4][SiF_6]$ has been known for a long time and is well characterized[5]. Table 1 shows that lattice constants, space group, and atomic parameters and thus interatomic distances for "$[ClF_6][CuF_4]$"[1] and $[Cu(H_2O)_4][SiF_6]$[5] are identical.

Table 1. Lattice constants and atomic parameters of $[Cu(H_2O)_4][SiF_6]$ **1** and "$[ClF_6][CuF_4]$" **2**. Data of **2** transformed according to *abc*→*cba*.

| **1** | | | **2** | | |
|---|---|---|---|---|---|
| $a$ = 7.22(1) Å | | | $c$ = 7.225(5) Å | | |
| $b$ = 9.64(1) Å | Space group | | $b$ = 9.621(2) Å | Space group | |
| $c$ = 5.36(1) Å | $P2_1/a$ | | $a$ = 5.347(3) Å | $P2_1/a$ | |
| $\beta = 105.2(3)°$ | | | $\beta = 105.2(6)°$ | | |
| Atom | | Positions | Positions | | Atom |
| Cu | *xyz* | 0, 0, 0 | 0, 0, 0 | *zyx* | Cu |
| Si | *xyz* | 1/2, 0, 1/2 | 1/2, 0, 1/2 | *zyx* | Cl |
| F1 | *x* | 0.4565(7) | 0.4542(4) | *z* | F2 |
| | *y* | 0.1047(5) | 0.1056(3) | *y* | |
| | *z* | 0.7303(9) | 0.7346(5) | *x* | |
| F2 | *x* | 0.6122(7) | 0.6125(4) | *z* | F1 |
| | *y* | 0.1328(5) | 0.1348(3) | *y* | |
| | *z* | 0.3907(10) | 0.3933(5) | *x* | |
| F3 | *x* | 0.2917(7) | 0.2906(4) | *z* | F3 |
| | *y* | 0.0484(5) | 0.0503(3) | *y* | |
| | *z* | 0.2967(10) | 0.2969(6) | *x* | |
| O1 | *x* | −0.1224(8) | −0.1205(5) | *z* | F5 |
| | *y* | 0.1596(6) | 0.1586(3) | *y* | |
| | *z* | 0.1252(11) | 0.1228(6) | *x* | |
| O2 | *x* | 0.0815(9) | 0.0800(5) | *z* | F4 |
| | *y* | 0.1248(6) | 0.1258(4) | *y* | |
| | *z* | −0.2402(12) | −0.2412(6) | *x* | |

The fascinating perfluorated cation $[ClF_6]^+$[6] is obviously not obtained in the above mentioned way. For the growth of the crystal $[Cu(H_2O)_4][SiF_6]$ from $CuCl_2$ and $CuF_2$ according to *Batsanov et al.*[1] a small amount of moisture and a quartz-wall are needed.

Received: January 21, 1983 [Z 248 IE]
German version: *Angew. Chem. 95* (1983) 421

CAS Registry numbers:
$[ClF_6][CuF_4]$, 74242-30-1; $[Cu(H_2O)_4][SiF_6]$, 25869-11-8

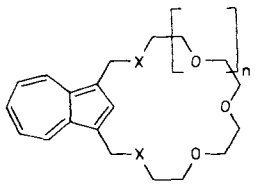
[1] A. S. Batsanov, Yu. T. Struchkov, S. A. Batsanov, *Dokl. Akad. Nauk SSSR Ser. Khim. 251* (1980) 251, 347.
[2] T. Fleischer, R. Hoppe, *Z. Anorg. Allg. Chem. 492* (1982) 76.
[3] 1st Tagung der GDCh-Arbeitsgemeinschaft "Anorganische Chemie", Königstein, October 22–24, 1982.
[4] W. Biltz: *Raumchemie der festen Stoffe*, Verlag Leopold Voss, Leipzig 1934.
[5] M. R. J. Clark, J. E. Fleming, H. Lynton, *Can. J. Chem. 47* (1969) 3859.
[6] I. Q. Roberto, *Inorg. Nucl. Chem. Lett. 8* (1972) 737; K. O. Christie, *ibid. 8* (1972) 741.

[*] Prof. Dr. H. G. von Schnering, Dr. Dong Vu
Max-Planck-Institut für Festkörperforschung
Heisenbergstrasse 1, D-7000 Stuttgart 80 (Germany)

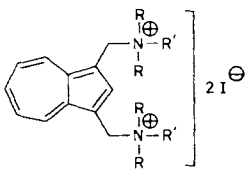
# A Novel Type of Ionic Clathrands for Numerous Inclusion Compounds**

By *Fritz Vögtle**, *Hans-Gerd Löhr*, *Heinrich Puff*, and *Willi Schuh*

For studies of dyestuff ionophores[1] we are interested in crown ethers with azulene building blocks, such as **1**, for whose synthesis[1] *N,N'*-[1,3-azulenylenebis(methylene)]-bis(trimethylammonium) diiodide **2a**[2] has proved valuable.

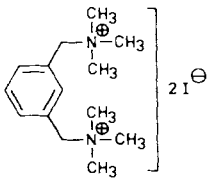


1: X = S,O



2a: R = R' = $CH_3$

2b: R = $CH_3$, R' = $C_2H_5$



3

In the synthesis of **2a** by alkylation of *N,N'*-[1,3-azulenylenebis(methylene)]bis(dimethylamine)[2] with excess iodomethane followed by crystallization from ethanol, varying amounts of iodomethane and ethanol are retained by **2a**. They are not even removed after drying for several days at 25 °C/0.1 torr. Attempts at recrystallization indicate that **2a** incorporates many types of solvent molecules, generally in stoichiometric ratios (cf. Table 1). Because of its ionic structure and colored azulene building block, the diammonium compound **2a** represents a unique example of the still rare clathrate formers (cf.[3]).

Table 1. Clathrates of the novel clathrands **2a** and the comparable host compounds **2b** and **3** (Selection).

| Clathrand | Mol. ratio Host/Guest | Guest molecules |
|---|---|---|
| **2a** | 1:1 | $C_2H_5OH$, 1-$C_3H_7OH$, 2-$C_3H_7OH$, 1-$C_4H_9OH$, 2-$C_4H_9OH$, 1-$C_5H_{11}OH$, 1,2-$C_2H_4(OH)_2$, $C_2H_5SH$, $(CH_3)_2NCHO$, $CHCl_3$, $CCl_4$, $CH_3I$, $C_2H_5I$, $CH_3NO_2$, 2-$C_3H_7NO_2$, *c*-$C_5H_5N$ |
| | 1:2 | $CH_3COOH$ |
| | 1:3 | $BrCCl_3$ |
| | 3:2 | *i*-$C_4H_9OH$, $CH_3CN$, $(CH_3)_2CO$ |
| | nonstoichiom. | $H_2O$, $CH_2Cl_2$ |
| **2b** | ca. 1:2 | $C_2H_5OH$ |
| **3** | 1:1 | $CH_3OH$ |
| | nonstoichiom. | $CH_3CN$, $CH_3COOH$ |

Table 1 shows the violet to red stoichiometric inclusion compounds of the colored [$\lambda_{max}$ = 624 (sh), 567 (sh), 537 nm; in EtOH[2] "clathrands"[4], **2a**, obtained so far. The guest selectivity emerges from the series of homologous alcohols; whereas methanol does not form a stable inclusion compound with **2a**, stoichiometric clathrates are obtained with ethanol to 1-pentanol. Still higher primary *n*-alcohols as well as secondary and branched ones—with the exception of 2-propanol, 2-butanol, and 2-methyl-1-propanol—do not form inclusion compounds. The novel clathrates decompose at temperatures considerably above those of the boiling points of the guest compounds. This, together with the tendency of the clathrates to crystallize well, may result from the ionic lattice of **2a**.

X-ray structure analysis[5] of the iodomethane adduct of **2a** confirms that a lattice inclusion, a clathrate, is encountered. Iodomethane is located in a crystal lattice cavity between two trimethylammonium groups, two iodide ions, and the herring-bone-pattern alternating stacks of layered azulene rings (Fig. 1).

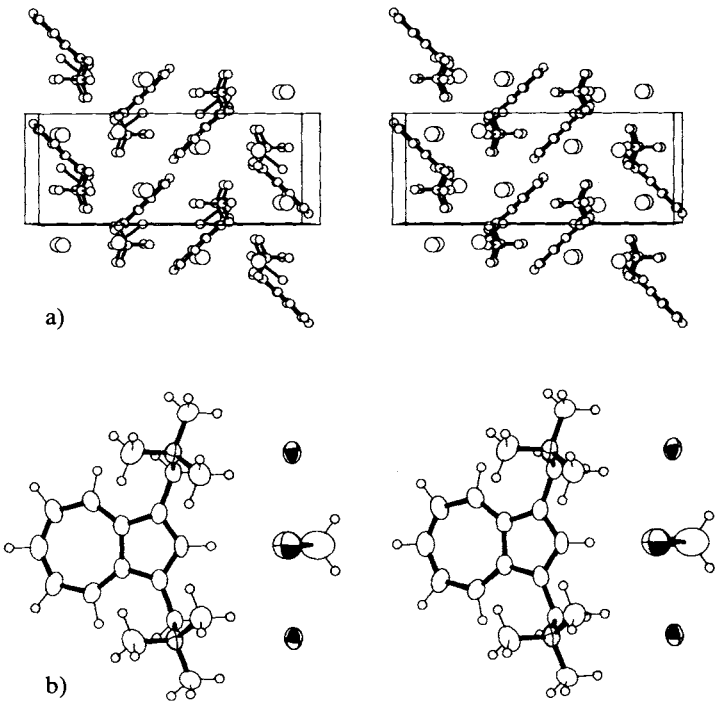


Fig. 1. X-Ray structure of the iodomethane clathrate **2a** · $CH_3I$ (stereoscopic illustrations): a) unit cell, view across the azulene ring planes, b) view perpendicular to the azulene ring plane.

The effect of variations in the host structure of **2a** on its ability to form inclusion compounds was investigated. Under analogous conditions the *m*-phenylenebis(methylene) compound **3**, in fact, yielded inclusion compounds; however with lower stability and with different guest selectivity (Table 1). The bis(ethyldimethylammonium) compound **2b**, prepared by reaction of iodomethane with *N,N'*-[1,3-azulenylenebis(methylene)]bis(dimethylamine) in methanol, crystallizes with difficulty; so far, only with ethanol has an inclusion compound been obtained (Table 1).

[*] Prof. Dr. F. Vögtle, H.-G. Löhr
Institut für Organische Chemie und Biochemie der Universität
Gerhard-Domagk-Strasse 1, D-5300 Bonn 1 (Germany)
Prof. Dr. H. Puff, Dr. W. Schuh
Anorganisch-chemisches Institut der Universität Bonn (Germany)

[**] This work was supported by the Fonds der Chemischen Industrie and by the Deutsche Forschungsgemeinschaft.

Received: January 10, 1983;
revised: March 2, 1983 [Z 232 IE]
German version: *Angew. Chem.* 95 (1983) 425
The complete version of this communication appears in:
*Angew. Chem. Suppl. 1983*, 527-536

CAS Registry numbers:
**2a**, 38303-40-1; **2b**, 85442-75-7; **3**, 85442-76-8; $C_2H_5OH$, 64-17-5; 1-$C_3H_7OH$, 71-23-8; 2-$C_3H_7OH$, 67-63-0; 1-$C_4H_9OH$, 71-36-3; 2-$C_4H_9OH$, 78-

92-2; 1-$C_5H_{11}OH$, 71-41-0; 1,2-$C_2H_4(OH)_2$, 107-21-1; $C_2H_5SH$, 75-08-1; $(CH_3)_2NCHO$, 68-12-2; $CHCl_3$, 67-66-3; $CCl_4$, 56-23-5; $CH_3I$, 74-88-4; $C_2H_5I$, 75-03-6; $CH_3NO_2$, 75-52-5; 2-$C_3H_7NO_2$, 79-46-9; c-$C_5H_5N$, 110-86-1; $CH_3COOH$, 64-19-7; $BrCCl_3$, 75-62-7; i-$C_4H_9OH$, 78-83-1; $CH_3CN$, 75-05-8; $(CH_3)_2CO$, 67-64-1; $H_2O$, 7732-18-5; $CH_2Cl_2$, 75-09-2; $CH_3OH$, 67-56-1; *N,N'*-[1,3-azulenylene-bis(methylene)]bis(dimethylamine), 38300-39-9.


[1] F. Vögtle, G. Hollmann, H.-G. Löhr, 8. Int. Farbensymp., 26.—30. Sept. 1982, Baden-Baden; H.-G. Löhr, Diplomarbeit, Universität Bonn 1982.

[2] M. Mühlstädt, W. Treibs, J. Mohr, *Chem. Ber. 94* (1961) 808; K. Hafner, W. Senf, *Justus Liebigs Ann. Chem. 656* (1962) 34; A. G. Anderson, Jr., R. D. Breazeale, *J. Org. Chem. 34* (1969) 2379.

[3] Review: F. Vögtle, H. Sieger, W. M. Müller, *Top. Curr. Chem. 98* (1981) 109.

[4] E. Weber, H.-P. Josel, *J. Incl. Phenom. 1* (1983), in press.


[5] **2a** · $CH_3I$ crystallizes in violet pyramids with rectangular basal surfaces; unit cell: orthorhombic, $a=1900.7(3)$, $b=1730.5(8)$, $c=755.5(3)$ pm; $Z=4$, Pnma (No. 62); 2098 independent reflections; $R=0.059$ ($R_w=0.070$). Details of the crystal structure investigation can be obtained from the Fachinformationszentrum Energie Physik Mathematik, D-7514 Eggenstein-Leopoldshafen 2 by quoting the depository number CSD 50339, the names of the authors, and the journal citation.

## Twist Conformation of Tetrahydrofuran in the Crystal**


By *Peter Luger** and *Jürgen Buschmann*


The preferred conformation of tetrahydrofuran, a fundamental structural element of carbohydrates and other important biological compounds, is not known. Although theoretical and experimental studies have tackled this question, in the final analysis they do not provide a definitive answer. According to the results of force field[1] and *ab initio* calculations[2], the twist form ($C_2$) should be energetically favored; however, the envelope form ($C_s$ is only slightly less stable (1 kcal/mol). Experimental investigations, such as electron diffraction studies[3,4], suggest almost free pseudorotation in the gas phase, but do not definitely rule out static forms.

We have now determined the conformation at temperatures of $-170\,^{\circ}C$ and $-125\,^{\circ}C$ by single crystal X-ray structure analysis. Tetrahydrofuran (THF) crystallizes in the monoclinic space group C2/c with 4 molecules in the unit cell (lattice constants at $-170\,^{\circ}C$: $a=607.6(9)$, $b=891.4(9)$, $c=774.3(11)$ pm, $\beta=106.11(12)^{\circ}$; at $-125\,^{\circ}C$: $a=618.6(2)$, $b=894.0(2)$, $c=783.5(2)$ pm, $\beta=106.41(2)^{\circ}$). Since a DTA plot between $+20\,^{\circ}C$ and $-140\,^{\circ}C$ contained no further signal below the melting point, and X-ray structure studies down to $-170\,^{\circ}C$ always indicated the same lattice, THF (at least down to $-170\,^{\circ}C$) has no further crystalline phases.

As shown by the structural analysis, the molecule lies on the twofold axis of the space group (Fig. 1). In consequence, the molecule possesses ideal $C_2$ symmetry in the crystal. The puckering parameters after *Cremer* and *Pople*[7] are $q_2=34.8(5)$ ($-170\,^{\circ}C$) and 35.5(4) pm ($-125\,^{\circ}C$), and $\varphi_2=90(-)^{\circ}$. The CO, CC, and CH bond lengths, respectively, (CC and CH determined from two and four independent values, respectively) at $-170\,^{\circ}C$ are 142.9(6), 151.1(7), and 105(5) pm, and at $-125\,^{\circ}C$ 143.5(5), 153.1(10), and 109(5) pm.

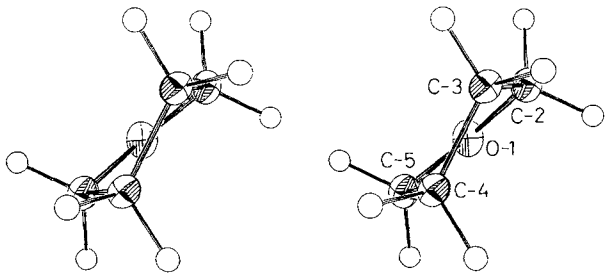



Fig. 1. Molecular model of tetrahydrofuran in the crystal.

Table 2 gives the bond and torsion angles we found; for comparison, the values from electron diffraction studies and from the *ab initio* calculation (4—31G basis set) of *Cremer* and *Pople*[2] are included. The data are in good agreement with each other; only the difference between the COC and the OCC bond angle is not so large in the crystal.

Table 2. Bond angles, torsion angles, and puckering amplitude $q_2$ of tetrahydrofuran determined by X-ray structure analysis (XR), electron diffraction (ED), and *ab initio* calculation (AI).

| | XR (−170 °C) | XR (−125 °C) | ED [3] | ED [4] | AI [2] |
|---|---|---|---|---|---|
| COC [°] | 108.2(4) | 109.8(3) | 110.5 | 111.6 | |
| OCC [°] | 107.4(4) | 106.7(4) | 106.5 | 105.6 | |
| CCC [°] | 102.0(4) | 101.9(3) | 101.8 | 101.9 | |
| C5-O1-C2-C3 [°] | −11.5(4) | −11.7(3) | −11.6 | −11.8 | |
| O1-C2-C3-C4 [°] | 29.7(4) | 29.6(3) | 29.6 | 30.1 | |
| C2-C3-C4-C5 [°] | −34.9(4) | −35.2(4) | −35.0 | −36.0 | |
| $q_2$ [pm] | 34.8(5) | 35.5(4) | 38. | 36.5 | |


Received: December 28, 1982;
revised: February 21, 1983 [Z 235 IE]
German version: *Angew. Chem. 95* (1983) 423
The complete manuscript of this communication appears in: *Angew. Chem. Suppl. 1983*, 537-542

CAS Registry number:
tetrahydrofuran, 109-99-9



[1] H. M. Seip, *Acta Chem. Scand. 23* (1969) 2741.

[2] D. Cremer, J. A. Pople, *J. Am. Chem. Soc. 97* (1975) 1358.

[3] H. J. Geise, W. J. Adams, L. S. Bartell, *Tetrahedron 25* (1969) 3045.

[4] A. Almenningen, H. M. Seip, T. Willadsen, *Acta Chem. Scand. 23* (1969) 2748.

[7] D. Cremer, J. A. Pople, *J. Am. Chem. Soc. 97* (1975) 1354.


## *syn*-Benzene Dioxide/1,4-Dioxocin Systems *via* a Diels-Alder Route


By *Hans-Josef Altenbach, Burkhard Voss,* and *Emanuel Vogel**


In 1968 *Witkop et al.*[1] proved that the arene oxides or arene oxide/oxepin systems[2], which shortly before this had been discovered in the course of experiments directed at verifying the Hückel rule, play a central role in the metabolism of aromatic compounds; as a consequence, the chemistry of these compounds has rapidly become an interdisciplinary area of research. The *syn*-benzene dioxides **1**[3], which were described later and which exist in equilibrium with 1,4-dioxocins, were also recognized to be biochemically relevant[4]; however, they are only accessible


[*] Prof. Dr. P. Luger, Dr. J. Buschmann
Institut für Kristallographie, Fachbereich Chemie,
Freie Universität Berlin
Takustrasse 6, D-1000 Berlin 33 (Germany)

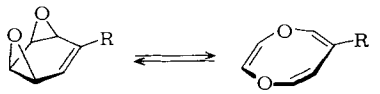


[**] This work was supported by the Deutsche Forschungsgemeinschaft. Dr. W. Dreissig is thanked for assistance in performing the diffraction measurements.



[*] Prof. Dr. E. Vogel, Priv.-Doz. Dr. H.-J. Altenbach, B. Voss
Institut für Organische Chemie der Universität
Greinstrasse 4, D-5000 Köln 41 (Germany)

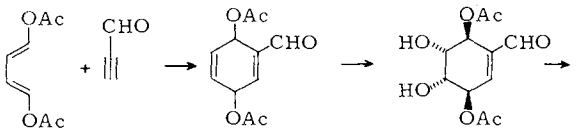
with difficulty. We report here a versatile synthetic pathway leading to *syn*-benzene dioxides and their dioxocin valence tautomers *via* a Diels-Alder route.



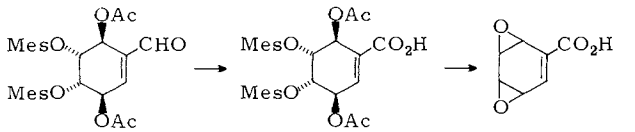
**1** **2**

**a**, R = H [3a]
**b**, R = Br [3b]
**c**, R =  [4]
**d**, R = $CO_2H$
**e**, R = COCl
**f**, R = $CH_2OH$
**g**, R = CHO

*trans,trans*-1,3-Butadienylene diacetate **3**, a valuable diene component for the synthesis of natural products with highly oxygenated cyclohexane-frameworks *via* Diels-Alder routes[5], reacts with excess propiolaldehyde to give the adduct **4** (m.p. = 79—80 °C, 89%). $OsO_4$-catalyzed oxidation of **4** with hydrogen peroxide (cf. Scheme A) leads to *cis*-hydroxylation of the 4,5-double bond to give a diol, to which, based on the assumption that the attack of the oxidant occurs from the sterically more favorable side of the ring, we assign the structure **5** (m.p. = 174—175 °C, 60%). Attempts to convert the bismesylate **6** (decomp. 167 °C, 71%) of the diol **5** with KOH in aqueous methanol into the *syn*-benzene dioxide **1g** afforded aromatic products—presumably as a result of an initial attack of the base at the conjugated double bond in the sense of a Michael reaction. As an alternative, the acid **7**, instead of the aldehyde **6** (Scheme A), or the corresponding alcohol and its isomer **8**, respectively (Scheme B), can be treated with base.



**3** **4** **5**

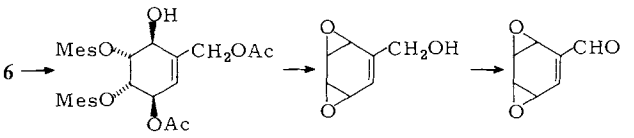


**6** **7** **1d**

Scheme A. **3**→**4**: No solvent, 70 °C, 30 h; **4**→**5**: acetone/$H_2O$, $OsO_4$/30% $H_2O_2$, 0 °C, 72 h; **5**→**6**: $CH_2Cl_2$/$NEt_3$, MesCl, −15 °C/RT, 40 min; **6**→**7**: acetone $CrO_3/H_2SO_4/H_2O$, 0 °C, 30 min; **7**→**1d**: MeOH, $KOH/H_2O$, −10 °C/RT, 30 min.

**6** can best be oxidized to **7** (decomp. 189 °C, 92%) using Jones' reagent. Treatment of **7** with base yields, as uniform product, the *syn*-benzene dioxide carboxylic acid **1d** (m.p. = 145—146 °C, 81%). The dominance of the epoxide ring closure in **7** can be attributed to formation of the carboxylate, which suppresses nucleophilic additions to the double bond. In refluxing tetrachloromethane **1d** isomerizes almost completely within 24 h to 1,4-dioxocin-6-carboxylic acid **2d** (m.p. = 93—94 °C). Heating either **1d** or **2d** in methanol leads to an equilibrium mixture containing the valence tautomers in the ratio 32:68.

Derivatization of the acid **2d** to the methyl ester or amide can advantageously be carried out *via* the acid chloride **2e**, prepared by means of sulfinyl chloride, since this can readily be isolated as a uniform valence tautomer upon recrystallization (m.p. = 32 °C, 90%).



**8** **1f** **1g**

Scheme B. **6**→**8**: $CH_2Cl_2$, $NaBH_4/H_2O$, RT, 3 h; **8**→**1f**: MeOH, $KOH/H_2O$, −10 °C/RT, 30 min; **1f**→**1g**: acetone, $MnO_2$, RT, 45 min.

Contrary to expectations, reduction of the aldehyde **6** with $NaBH_4$ does not afford the corresponding alcohol, but—*via* an acyl migration which does not influence the synthetic concept—the isomeric alcohol **8** (m.p. = 109—110 °C, 75%). This rearrangement apparently proceeds from the alcoholate, which is formed by attack of a hydride ion at the aldehyde function in **6**. As suggested by the behavior of **7**, treatment of **8** with base also leads smoothly to epoxide ring-closure; moreover, the primary OAc group is hydrolyzed, so that **1f** is isolated as the reaction product (m.p. = 93 °C, 60%). **1f** is readily oxidized by $MnO_2$ to **1g** (m.p. = 40 °C, 50%). Finally, heating **1g** in acetone leads quantitatively to the relatively volatile 1,4-dioxin-6-carbaldehyde **2g**, which was proved to be a uniform valence tautomer by NMR spectroscopy (short path distillation, 70 °C bath temp. 0.2 torr, 94%).

**2e** and **2g** are attractive starting materials for the synthesis of the natural product LL-Z1220 **1c**.

Received: December 28, 1982 [Z 236 IE]
German version: *Angew. Chem. 95* (1983) 424
The complete version of this communication appears in:
*Angew. Chem. Suppl. 1983*, 571-582

[1] D. M. Jerina, J. W. Daly, B. Witkop, *J. Am. Chem. Soc. 90* (1968) 6523; D. M. Jerina, J. W. Daly, B. Witkop, P. Zaltzman-Nirenberg, S. Udenfriend, *ibid. 90* (1968) 6525; J. W. Daly, D. M. Jerina, B. Witkop, *Experientia 28* (1972) 1129.

[2] E. Vogel, R. Schubart, W. A. Böll, *Angew. Chem. 76* (1964) 535; *Angew. Chem. Int. Ed. Engl. 3* (1964) 510; E. Vogel, H. Günther, *ibid. 79* (1967) 429; *6* (1967) 385.

[3] a) E. Vogel, H.-J. Altenbach, D. Cremer, *Angew. Chem. 84* (1972) 983; *Angew. Chem. Int. Ed. Engl. 11* (1972) 935; b) H.-J. Altenbach, E. Vogel, *ibid. 84* (1972) 985; *11* (1972) 937.

[4] D. B. Borders, P. Shu, J. E. Lancaster, *J. Am. Chem. Soc. 94* (1972) 2540; D. B. Borders, J. E. Lancaster, *J. Org. Chem. 39* (1974) 435; US-Pat. 3770773 (1973), American Cyanamid Co.

[5] Cf. the syntheses of conduritol-D: R. Criegee, P. Becher, *Chem. Ber. 90* (1957) 2516; shikimic acid: R. McCrindle, K. H. Overton, R. A. Raphael, *J. Chem. Soc. 1960*, 1560; E. E. Smissman, J. T. Suh, M. Oxman, R. Daniels, *J. Am. Chem. Soc. 84* (1962) 1040; pseudo sugars: G. E. McCasland, S. Furuta, L. J. Durham, *J. Org. Chem. 33* (1968) 2835; cf. also the synthesis of *syn*-naphthalene 1,2:3,4-dioxide: R. R. Schmidt, R. Angerbauer, *Angew. Chem. 91* (1979) 325; *Angew. Chem. Int. Ed. Engl. 18* (1979) 304.

## Synthesis and Structure of $(CO)_4W[C(NEt_2)PMePh]$, A Novel Cyclic Carbene Complex[1]

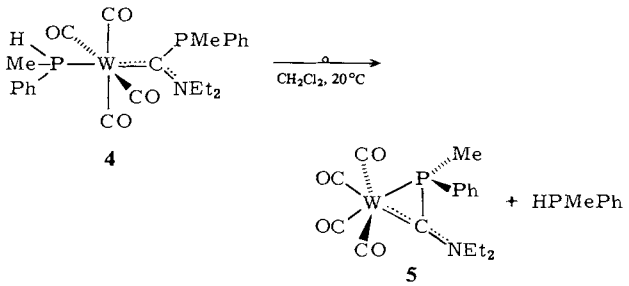
By *Ernst Otto Fischer**, *Rudolf Reitmeier*, and *Klaus Ackermann*

Numerous neutral aminocarbene complexes of the type $[(CO)_5M[C(NEt_2)X]]$, which are usually inaccessible *via*

[*] Prof. Dr. E. O. Fischer, R. Reitmeier, Dr. K. Ackermann
Anorganisch-chemisches Institut der Technischen Universität München
Lichtenbergstr. 4, D-8046 Garching (Germany)

 © *Verlag Chemie GmbH, 6940 Weinheim, 1983* *0570-0833/83/0505-0411 $ 02.50/0* 

conventional direct routes, have been synthesized by addition of anionic nucleophiles $X^-$ to the carbyne carbon atom of the cationic aminocarbyne complex in the compounds $[(CO)_5MCNEt_2]BF_4$ (M = Cr, W)[2,3]. If the same carbyne complexes are allowed to react with strongly reducing nucleophiles such as $R_2E^-$ (R = alkyl, aryl; E = element of the 5th main group) then some completely different types of products can be formed, *e.g.* the μ-bis(aminocarbene) complex $[(CO)_5MCNEt_2]_2$, by reductive $C_\alpha C_\alpha$ coupling of two carbyne fragments[4,5]. With very strongly reducing nucleophiles this reductive dimerization can become the dominating competing reaction over the addition of the nucleophile. Thus, in the reaction of $[(CO)_5WCNEt_2]BF_4$ **1** with potassium methylphenylphosphide the major product is the biscarbene complex $[(CO)_5WCNEt_2]_2$ **2**; as by-products, the mononuclear adduct $[(CO)_5W\{C(NEt_2)PMePh\}]$ **3** and the *trans*-carbene-phosphane complex **4** can also be isolated[5]. On warming in solution, the latter complex exhibits the remarkable property of undergoing dissociation of the phosphane ligand with spontaneous rearrangement to give the novel cyclic carbene complex **5**:




The complex **5**, whose structure has been confirmed spectroscopically as well as X-ray crystallographically, is one of the few compounds in which a carbene ligand is component of a three-membered metallacycle containing a further main group element[9].

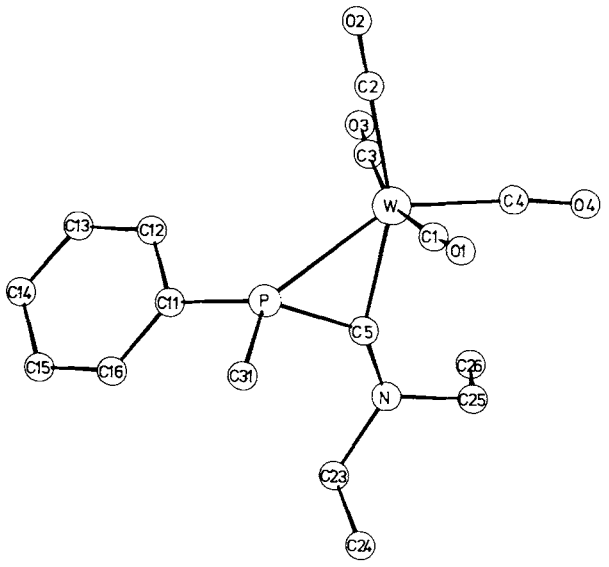



Fig. 1. Molecular structure of tetracarbonyl[$\eta^2$-diethylamino(methylphenylphosphino)carbene]tungsten **5** in the crystal.

Important bond lengths [pm] and angles [°] with standard deviations.

| | | | |
|---|---|---|---|
| W–P | 246.5(3) | W–C5 | 210.8(10) |
| P–C5 | 180.7(10) | N–C5 | 127.7(12) |
| P–W–C5 | 45.7(3) | C5–P–C11 | 114.1(5) |
| W–P–C5 | 56.7(3) | C5–P–C31 | 109.6(5) |
| W–P–C11 | 127.4(3) | W–C5–P | 77.6(4) |
| W–P–C31 | 126.4(4) | N–C5–P | 133.5(8) |
| C11–P–C31 | 105.9(5) | N–C5–W | 148.7(8) |

**5** constitutes the first example of a possible transition state of the carbene-carbyne rearrangement to be characterized by X-ray structure analysis. The PMePh group has not migrated, *i.e.* it is still bound to the carbene carbon atom C5, but its coordination to the metal atom and the elimination of the *trans*-ligand have already taken place. The atomic distances in the three-membered ring are essentially very little different from the corresponding atomic distances in strain-free compounds. Two carbonyl ligands as well as the N, C23, C25 atoms of the amino group lie in the plane of the three-membered ring. Hence, a good overlapping of the orbitals of the metal and nitrogen atoms suitable for π-interactions is guaranteed. The very short C5–N distance makes the amino group seem to be the most important donor in the competition for the vacant orbital of the carbene carbon atom; however, the C5–W bond length is also relatively short in comparison to C–W bond lengths in other tungsten-carbene complexes. Also interesting is the coordination of the phosphorus atom: On the one hand, the tetrahedral angle to C5, C11 and C31 of the starting complex is still recognizable, on the other C31, C11, and W surround the phosphorus atom in an almost trigonal-planar arrangement.

Metallacyclic carbene complexes such as **5** are potential intermediates of the carbene-carbyne rearrangement[3],

$$[(CO)_5M\{C(NR_2)X\}] \longrightarrow trans\text{-}[X(CO)_4MCNR_2]$$

whose mechanism is under investigation.

Received: January 13, 1983 [Z 240 IE]
German version: *Angew. Chem. 95* (1983) 419
The complete version of this communication appears in: *Angew. Chem. Suppl. 1983*, 488–500

CAS Registry numbers:
**4**, 85369-50-2; **5**, 85354-87-6

[1] Transition Metal Carbene Complexes, Part 129.—Part 128: E. O. Fischer, P. Rustemeyer, O. Orama, D. Neugebauer, U. Schubert, *J. Organomet. Chem.*, in press.
[2] E. O. Fischer, D. Wittmann, D. Himmelreich, U. Schubert, K. Ackermann, *Chem. Ber. 115* (1982) 3141, and references cited therein.
[3] H. Fischer, E. O. Fischer, R. Cai, D. Himmelreich, *Chem. Ber.*, in press, and references cited therein.
[4] E. O. Fischer, D. Wittmann, D. Himmelreich, D. Neugebauer, *Angew. Chem. 94* (1982) 451; *Angew. Chem. Int. Ed. Engl. 21* (1982) 444; *Angew. Chem. Suppl. 1982*, 1036–1049.
[5] E. O. Fischer, R. Reitmeier, *Z. Naturforsch. B*, in press.
[9] Cf. F. A. Cotton, L. R. Falvello, R. C. Najjar, *Organometallics 1* (1982) 1640.

## Redox Intercalation Reactions of $VOPO_4 \cdot 2H_2O$

By *Jack W. Johnson** and *Allan J. Jacobson**

The layered, mixed-oxide hydrate $VOPO_4 \cdot 2H_2O$[1] reacts with neutral ligands, such as pyridine, to form intercalation compounds characterized by direct bonding of the ligand to metal atoms of the host layer[2]. However, since $VOPO_4 \cdot 2H_2O$ contains readily reducible $V^{5+}$ ions, it can also undergo redox intercalation reactions analogous to

[*] Dr. J. W. Johnson, Dr. A. J. Jacobson
Corporate Research Science Laboratories,
Exxon Research and Engineering
P.O. Box 45, Linden, NJ 07036 (USA)

those of the reducible binary oxides and the layered dichalcogenides[3].

$VOPO_4 \cdot 2H_2O$ was reduced with a wide variety of mild aqueous reducing agents. In the course of the reduction, cations are incorporated into the interlayer spaces. The basic tetragonal structure of the lattice[1] is maintained; the *a* axis remaining essentially constant at *ca.* 6.2 Å, whereas the *c* axis corresponding to the interlayer spacing is modified.

A convenient reducing agent for intercalation of most monovalent and divalent cations is the aqueous iodide ion [eq. (a)], although other aqueous reducing agents, including $SO_3^{2-}$, $NO_2^-$, $Sn^{2+}$, $Fe^{2+}$, $NH_2OH \cdot HCl$, and $N_2H_4 \cdot 2HCl$, were also effective in forming redox intercalates of $VOPO_4 \cdot 2H_2O$. In Table 1 a series of compounds, $A_xVOPO_4 \cdot yH_2O$, formed by the iodide method are listed. $VOAsO_4 \cdot 2H_2O$ reacts similarly to $VOPO_4 \cdot 2H_2O$[4].

$$VOPO_4 \cdot 2H_2O + \frac{x}{n} M^{n+}I_n + yH_2O \longrightarrow M_{x/n}VOPO_4 \cdot (2+y)H_2O + \frac{x}{2}I \quad (a)$$

Table 1. Intercalation compounds $A_xVOPO_4 \cdot yH_2O$ produced by redox intercalation with iodides in aqueous solution [5].

| A | x | y | c [Å] |
|---|---|---|---|
| Li | 1.0 | 2.1 | 6.41 |
| Na | 0.26 | 2.0 | 6.70 |
| Na | 0.46 | 2.0 | 6.52 |
| Na | 0.68 | 2.0 | 6.53 |
| K | 0.69 | 1.5 | 6.38 |
| Rb | 0.51 | 1.8 | 6.48 |
| Cs | 0.25 | 1.8 | 6.87 |
| Cs | 0.50 | 1.8 | 7.06 |
| Mg | 0.19 | 3.5 | 9.79 |
| Ni | 0.23 | 2.9 | 9.18 (6.61) |
| $NH_4$ | 0.48 | 2.0 | 6.76 |
| $N(CH_3)_4$ | 0.33 | 2.0 | *ca.* 9.2 |

The degree of reduction (x in $A_xVOPO_4 \cdot yH_2O$) depends on the reaction conditions and on the nature of the metal cation. Complete reduction of $V^{5+}$ to $V^{4+}$ is observed for lithium ($x = 1$) but, in general, lower values of x are observed. Both two-phase and single-phase regions are observed as x is varied. For example, intercalation of $Na^+$ ions gives two distinct nonstoichiometric phases with $0.16 \leq x \leq 0.33$ and $0.48 \leq x \leq 0.68$. The layer separations for the sodium phases center on 6.70 and 6.52 Å, respectively. These layer spacings are less than the interlayer separation in $VOPO_4 \cdot 2H_2O$ (7.4 Å) due to the introduction of a strong electrostatic interaction between cations and negatively charged layers upon intercalation. The water contents (y) of the monovalent intercalation compounds at ambient humidity are in the range 1.8 to 2.1 $H_2O/VOPO_4$, the lower values being observed for the larger cations. However, for small divalent cations with charge/radius ratios of greater than 2.59 $Å^{-1}$, two distinct hydrates are formed. For example, $Ni_{0.23}VOPO_4 \cdot yH_2O$ forms hydrates with layer spacings of 6.61 Å and 9.18 Å. Organic and organometallic cations, such as $N(CH_3)_4^+$ and $Co(C_5H_5)_2^+$, also intercalate $VOPO_4 \cdot 2H_2O$ but give products less crystalline than those of the simple cations.

Intercalation of $VOPO_4 \cdot 2H_2O$ and $VOAsO_4 \cdot 2H_2O$ leads to localized $V^{4+}$ sites. The IR spectrum of $VOAsO_4 \cdot 2H_2O$ exhibits a single absorption at 1010 $cm^{-1}$, assigned to the V=O stretching frequency. In $Na_{0.5}VOAsO_4 \cdot 2H_2O$, the vanadyl (V=O) absorption is split into two bands at 1013 and 992 $cm^{-1}$, corresponding to $V^{5+}=O$ and $V^{4+}=O$, respectively. In $VOPO_4 \cdot 2H_2O$ the phosphate bands mask the vanadyl region of the IR spectrum. These are the first intercalation reactions involving transfer of electrons/ions in which the transferred charges are so strongly localized that the process proceeds chemically but not electrochemically.

Received: January 20, 1983 [Z 247 IE]
German version: *Angew. Chem. 95* (1983) 422

CAS Registry numbers:
$VOPO_4$, 12359-27-2; $LiVOPO_4$, 83348-01-0; Na, 7440-23-5; K, 7440-09-7; Rb, 7440-17-7; Cs, 7440-46-2; Mg, 7439-95-4; Ni, 7440-02-0; $NH_4^+$, 14798-03-9; $N(CH_3)_4^+$, 51-92-3; $SO_3^{2-}$, 14265-45-3; $NO_2^-$, 14797-65-0; $Sn^{2+}$, 22541-90-8; $Fe^{2+}$, 15438-31-0; $NH_2OH \cdot HCl$, 5470-11-1; $N_2H_4 \cdot 2HCl$, 5341-61-7; Iodide on, 20461-54-5.

[1] G. Ladwig, *Z. Anorg. Allg. Chem. 338* (1965) 266; H. R. Tietze, *J. Austr. Chem. 34* (1981) 2035; M. Tachez, F. Theobald, J. Bernard, A. W. Hewat, *Rev. Chim. Miner. 19* (1982) 291.

[2] J. W. Johnson, A. J. Jacobson, J. F. Brody, S. M. Rich, *Inorg. Chem. 21* (1982) 3820; J. W. Johnson, A. J. Jacobson, S. M. Rich, J. F. Brody, *Rev. Chim. Miner. 19* (1982) 420.

[3] R. Schöllhorn "Solvated Intercalation Compounds of Layered Chalcogenide and Oxide Bronzes" in M. S. Whittingham, A. J. Jacobson: *Intercalation Chemistry*, Academic Press, New York 1982, pp. 315–360; R. Schöllhorn, *Angew. Chem. 92* (1980) 1015; *Angew. Chem. Int. Ed. Engl. 19* (1980) 983.

[4] The reaction takes place in the course of minutes at room temperature, with the yellow suspension of $VOPO_4 \cdot 2H_2O$ turning green as $V^{4+}$ is produced in the solid phase, whereas the clear supernatant turns red-brown as $I_3^-$ is produced. The amount of solvent ($H_2O$) should be minimized because of the slight solubility of $VOPO_4 \cdot 2H_2O$. The structurally analogous $VOAsO_4 \cdot 2H_2O$ (N. G. Chernorukov, N. P. Egorov, I. A. Korshunov, *Zh. Neorg. Khim. 23* (1978) 2672) reacts similarly to give brown intercalation compounds. Attempts at electrochemical intercalation were unsuccessful due to the low conductivity of both host materials and their intercalation compounds.

[5] The compounds are generally quite crystalline. The layer spacings determined experimentally are equal to the tetragonal *c* axis or *c*/2 when cation order is present. The spacings depend on $H_2O$ activity, those presented in Table 1 being observed under ambient laboratory conditions. The x and n values are determined by microanalysis, redox titrimetry, and thermogravimetric analysis.

## Addition of a Phosphaalkyne to Metal-Metal Multiple Bonds**

By *Gerd Becker, Wolfgang A. Herrmann*, Willibald Kalcher, Gangolf W. Kriechbaum, Claudia Pahl, C. Thomas Wagner,* and *Manfred L. Ziegler*

Following the first demonstration of the existence of phosphorus-carbon multiple bonds (1961) the chemistry of the main group elements took on new dimensions with the synthesis of stable phosphaalkenes **A** and phosphaalkynes **B**[2a,b].

**A** $\ddot{P}=C$ $\quad\quad$ $:P\equiv C-$ **B**

A broad spectrum of complexation chemistry involving these ligands is now also beginning to emerge[4c], thus calling for a more systematic investigation of this class of substances than hithertofore. In this context, and especially with a view to possible metathetic reactions, we have now

[*] Prof. Dr. W. A. Herrmann, W. Kalcher, G. W. Kriechbaum
Institut für Anorganische Chemie der Universität
Niederurseler Hang, D-6000 Frankfurt am Main 50 (Germany)
Prof. Dr. M. L. Ziegler, C. Pahl
Anorganisch-chemisches Institut der Universität Heidelberg (Germany)
Prof. Dr. G. Becker, C. T. Wagner
Institut für Anorganische Chemie der Universität Stuttgart (Germany)

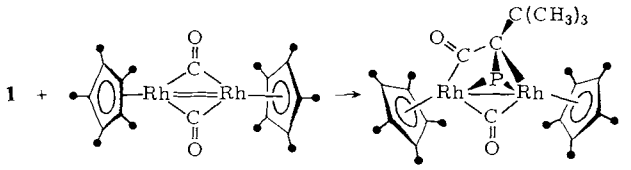
[**] Complex Chemistry of Reactive Organic Compounds, Part 42. This work was supported by the Deutsche Forschungsgemeinschaft and the Fonds der Chemischen Industrie.—Part 41: W. A. Herrmann, M. L. Ziegler, O. Serhadli, *Organometallics*, in press.

examined the conveniently accessible 2,2-dimethylpropylidynephosphane **1**[6] regarding its behavior towards metal-

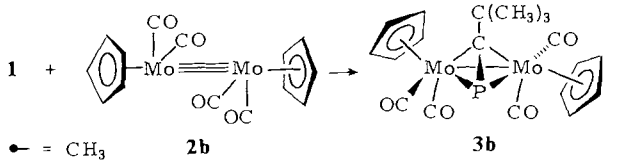
$(CH_3)_3C-C\equiv P$ **1**

metal multiple bonds. The present communication demonstrates for the first time the close analogy between the complex chemistry of phosphaalkynes and that of alkynes.

The phosphaalkyne **1** adds rapidly and quantitatively to the Rh=Rh bond in **2a** and to the Mo≡Mo bond in **2b**, even below −60 °C. The crystalline, air- and moisture-stable products **3a** and **3b** resemble the analogous products



**2a** **3a**



**2b** **3b**

obtained with alkynes regarding their mode of formation and constitution[9].

The addition of **1** to the Rh=Rh bond of **2a** proceeds *via* insertion of the ligand into one of the two Rh–CO bonds, whereby the cyclic structural element of **3a** is formed regiospecifically. Like its phenylacetylene analogue (cf. [9]), **3a** is a rigid molecule ($^{13}C$-NMR data).

The molybdenum complex **3b** (Fig. 1) contains an organometallic tetrahedrane skeleton; the CP moiety added to

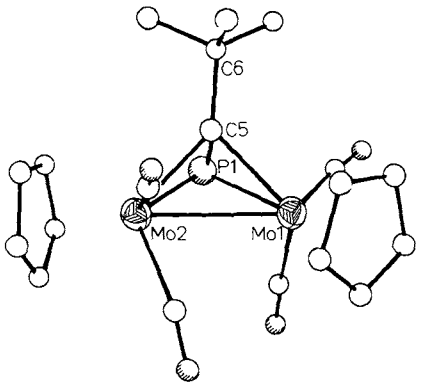



Fig. 1. Structure of the $\mu,\eta^2$-phosphaalkyne complex **3b** in the crystal (H atoms not shown). Monoclinic (from diethyl ether/*n*-hexane 20/80 vol.-%); C2/c, $Z=8$; $a=2702(9)$, $b=882.9(5)$, $c=1695(5)$ pm; $\beta=103.37(2)°$; 3570 independent reflections different from zero ($2° \le 2\theta \le 54°$); $R_{aniso}=0.031$, $R_w=0.027$. Selected bond lengths [pm] and angles [°]: Mo(1)–Mo(2) 301.4(0), Mo(1)–P(1) 249.7(1), Mo(2)–P(1) 244.2(1), Mo(1)–C(5) 222.4(4), Mo(2)–C(5) 222.2(4), P(1)–C(5) 171.9(3), C(5)–C(6) 154.5(6); Mo(1)–P(1)–Mo(2) 75.2(0), Mo(1)–C(5)–Mo(2) 85.3(1), Mo(1)–P(1)–C(5) 60.4(1), Mo(2)–P(1)–C(5) 61.7(1), Mo(1)–C(5)–P(1) 77.4(1), Mo(2)–C(5)–P(1) 75.4(1), Mo(1)–Mo(2)–C(5) 47.4(1), P(1)–C(5)–C(6) 127.9(3).

the Mo≡Mo bond is located vertically above the Mo–Mo bond. The incorporation of **1** into **2b** has the same consequences as the incorporation of alkynes regarding any changes in geometry of the components: The PC bond does not, as formally expected, assume the length of a single bond (182–187 pm), but has the length of a typical double bond (171.9(3) pm). Likewise, only a double bond is formed on addition of C≡C-, M≡C- and As≡As systems to **2b**[21,22].

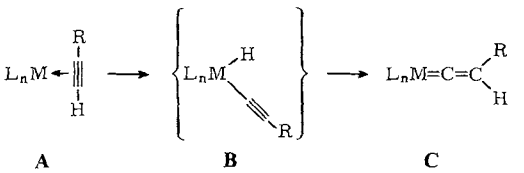
Received: January 25, 1983 [Z 251 IE]
German version: *Angew. Chem. 95* (1983) 417
The complete version of this communication appears in: *Angew. Chem. Suppl. 1983*, 501–526

[2] Summaries: a) R. Appel, F. Knoll, I. Ruppert, *Angew. Chem. 93* (1981) 771; *Angew. Chem. Int. Ed. Engl. 20* (1981) 731; b) G. Becker, W. Becker, O. Mundt, *Phosphorus Sulfur 14* (1983) 267.
[4] c) Recent work: J. C. T. R. Burckett-St. Laurent, P. B. Hitchcock, H. W. Kroto, M. F. Meidine, J. F. Nixon, *J. Organomet. Chem.* **238** (1982) C82; and references cited therein.
[6] G. Becker, G. Gresser, W. Uhl, *Z. Naturforsch. B 36* (1981) 16.
[9] Review: W. A. Herrmann, *J. Organomet. Chem. 250* (1983), in press; and references cited therein.
[21] P. J. Sullivan, A. L. Rheingold, *Organometallics 1* (1982) 1547; and references cited therein.
[22] F. A. Cotton, W. Schwotzer, *Angew. Chem. 94* (1982) 652; *Angew. Chem. Int. Ed. Engl. 21* (1982) 629; and references cited therein.

## Synthesis of $[C_5H_5Rh(PhC\equiv CH)P(iPr)_3]$ and $[C_5H_5Rh(=C=CHPh)P(iPr)_3]$: Mechanism of the Conversion of an Alkyne Ligand into a Vinylidene Ligand

By *Justin Wolf, Helmut Werner*, Ohran Serhadli,* and *Manfred L. Ziegler*

Recently, metal complexes containing the ligands :C=C′RR′ ("vinylidenes"), which are unstable in the free form, have been attracting increasing attention[1]. They are generally prepared by reaction of 1-alkynes with coordinatively unsaturated metal-complex fragments such as $[C_5H_5Mn(CO)_2]$ or $[C_5H_5Fe(CO)_2]^{\oplus}$ generated *in situ*. During these reactions the 1-alkyne is first coordinated to the metal (**A**) and then undergoes transformation in the coordination sphere of the metal, giving the corresponding vinylidene complex (**C**). The question *how* this takes place has hitherto not been answered; in no instance has the postulated intermediate **B** been detected[1c,d].



**A** **B** **C**

In an analogous way to the preparation of the alkyne complexes *trans*-$[RhCl(C_2R_2)(PR'_3)_2]$ (R = Me, Ph; R′ = *i*Pr)[2], we have now synthesized compound **1** (74% yield; yellow, air-sensitive crystals; m.p. 97 °C) by reaction of phenylacetylene with the complex $RhCl[P(iPr)_3]_2$, which is obtained from $[RhCl(C_8H_{14})_2]_2$ and excess $P(iPr)_3$[3]. Due to the position of the $\nu(C\equiv C)$ stretching frequency at 1825 $cm^{-1}$ in the IR spectrum (KBr), we assume **1** to have a

[*] Prof. Dr. H. Werner, J. Wolf
Institut für Anorganische Chemie der Universität
Am Hubland, D-8700 Würzburg (Germany)
Prof. Dr. M. L. Ziegler, O. Serhadli
Anorganisch-chemisches Institut der Universität
Im Neuenheimer Feld 270, D-6900 Heidelberg 1 (Germany)

metallacyclopropene structure (with a 16-electron configuration at the metal). In solution, partial isomerization **1** → **2** takes place, implicating the oxidative addition of the 1-alkyne at the metal. Consequently, in the $^1$H-NMR spectrum (100 MHz, [D$_8$]toluene, 35 °C) one observes two virtual quartets at $\delta = 1.23$ and 1.35 for the phosphane-CH$_3$ protons of **1**/**2**, a doublet at $\delta = 4.07$ ($J$(RhH) = 2.6 Hz) for the PhC$_2$H-proton of **1**, as well as a triplet of doublets at $\delta = -27.70$ ($J$(PH) = 12.7, $J$(RhH) = 42.0 Hz) for the hydrids hydrogen atom of **2**.

Addition of pyridine to an ether solution of **1**/**2** shifts the equilibrium completely, resulting in the formation of the alkynyl(hydrido)-complex **3**[3], for which an octahedral structure is assumed. The colorless crystals are stable under argon, but decompose rather rapidly in solution at room temperature. The $^1$H-NMR spectrum (100 MHz, [D$_8$]toluene, 8 °C) shows two virtual quartets at $\delta = 1.15$ and 1.19 for the diastereotopic PCHC*H*$_3$-protons as well as a pseudo-quartet in the high-field region ($\delta = -17.30$; $J$(PH) = $J$(RhH) = 14.0 Hz) for the hydrido ligand. The appearance of only one signal at $\delta = 36.09$ (d, $J$(RhP) = 96.8 Hz) in the $^{31}$P-NMR spectrum of **3** proves that the two phosphane ligands are in *trans* position.

$$\underset{\mathbf{1}}{RhCl(PhC_2H)(PR'_3)_2} \rightleftharpoons \underset{\mathbf{2}}{RhCl(H)(C_2Ph)(PR'_3)_2} \xrightarrow{py}$$

R' = *i*Pr

$$RhCl(H)(C_2Ph)(PR'_3)_2(py)$$

**3**

Compound **1** reacts with $NaC_5H_5$ in tetrahydrofuran (THF) (*i.e.* under the same conditions as used for the preparation of [$C_5H_5Rh(C_2R_2)P(iPr)_3$] (R = Me, Ph)[2]) to give the alkyne complex **4** (90%; orange colored oil)[3], which is characterized by its *IR* spectrum [$\nu$(C≡C) = 1770 cm$^{-1}$; hexane] and $^1$H-NMR spectrum [100 MHz, $C_6D_6$, 30 °C; $C_5H_5$: $\delta = 5.30$ (d × d, $J$(PH) = 1.4, $J$(RhH) = 0.7 Hz); PhC$_2$*H*: $\delta = 5.58$ (d, $J$(RhH) = 3.2 Hz)] (Scheme 1). If, on the other hand, the pyridine complex **3** is allowed to react with $NaC_5H_5$ in THF, the vinylidene complex **6** (isomeric to **4**) is obtained (65%; orange colored crystals, briefly air-stable; m.p. 95 °C)[3]. The presence of a phenylvinylidene ligand is confirmed by the spectroscopic data [IR (KBr): $\nu$(C=C) = 1615 cm$^{-1}$; $^1$H-NMR (60 MHz, $C_6D_6$, 30 °C): $C_5H_5$: $\delta = 5.23$ (m); C=C*H*Ph: $\delta = 4.42$ (d × d, $J$(PH) = 4.6, $J$(RhH) = 1.6 Hz); $^{13}$C-NMR (90 MHz, $C_6D_6$, 30 °C): *C*=CHPh: $\delta = 316.99$ (d × d, $J$(PC) = 27.7, $J$(RhC) = 67.7 Hz); C=*C*HPh: $\delta = 116.31$ (d × d, $J$(PC) = 4.4, $J$(RhC) = 14.4 Hz)] and the crystal structure analysis[4]. The asymmetric unit contains two independent molecules (Fig. 1), which mainly differ with respect to the RhC and CC bond lengths of the vinylidenerhodium moiety. The RhC bond lengths are significantly shorter than in rhodium-carbene complexes (193.0(11) to 200.6(15) pm)[5], thus indicating, in agreement with the $^{13}$C-NMR data, a high degree of multiple bonding. The RhCC arrangement is almost linear; RhCC angles in the two independent molecules are 173.0(13) and 174.6(14)°.

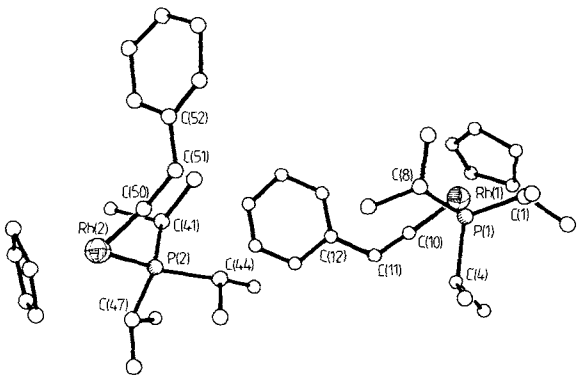
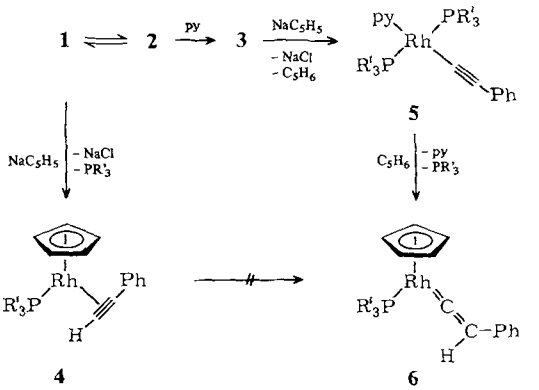



Fig. 1. Structure of **6** in the crystal. The figure shows the two independent molecules in the asymmetric unit. Selected bond lengths [pm]: Rh(1)–P(1) 226.6(6), Rh(1)–C(10) 182.0(16), C(10)–C(11) 129.5(21), Rh(2)–P(2) 227.6(6), Rh(2)–C(50) 175.1(16), C(50)–C(51) 140.6(21).




Scheme 1. R' = *i*Pr.

The mechanism of the reaction of **3** and $NaC_5H_5$ was confirmed by the isolation of the intermediate **5**. According to earlier suggestions[1c,d], we had presumed that replacement of Cl by $C_5H_5$ and elimination of pyridine and P(*i*Pr)$_3$ would lead to intermediary formation of the alkynyl(hydrido)complex [$C_5H_5RhH(C_2Ph)P(iPr)_3$], which, after intramolecular H-shift, would then afford the product **6**. If, however, a solution of **3** in THF is treated rapidly at 0 °C with an equimolar amount of $NaC_5H_5$ and work-up is carried out in the cold, then yellow, air-sensitive crystals of **5** are obtained in 68% yield. The IR spectrum shows, instead of the two bands of **3** at 2180 [$\nu$(RhH)] and 2100 cm$^{-1}$ [$\nu$(C=C)], one frequency at 2055 cm$^{-1}$, which is assigned to the C=C stretching vibration. **5** reacts with $C_5H_6$ at room temperature to give **6** in almost quantitative yield. The rearrangement **4** → **6** is not detectable, either on prolonged standing or on irradiation.

In conclusion, our results show for the first time that a vinylidene ligand is in fact formed from an alkyne ligand *via* an alkynyl(hydrido) intermediate. The mechanism, however, does not involve an intramolecular H shift (from the metal to carbon) but a two-step elimination/addition reaction. The second step involves the protonation of an alkynyl ligand, which has already been used by others for the synthesis of vinylidene complexes[6].

Received: December 21, 1982;
revised: February 21, 1983 [Z 228 IE]
German version: *Angew. Chem.* 95 (1983) 428

[1] a) N. M. Kostic, R. F. Fenske, *Organometallics* **1** (1982) 974; b) B. E. R. Schilling, R. Hoffmann, D. L. Lichtenberger, *J. Am. Chem. Soc. 101* (1979) 585; c) M. I. Bruce, R. C. Wallis, *Aust. J. Chem. 32* (1979) 1471; d) A. B. Antonova, N. E. Kolobova, P. V. Petrovsky, B. V. Lokshin, N. S. Obezyuk, *J. Organomet. Chem. 137* (1977) 55.

[2] H. Werner, J. Wolf, U. Schubert, K. Ackermann, *J. Organomet. Chem. 243* (1983) C63.

[3] Compounds **1** and **3**–**6** gave correct elemental analyses (C, H, N, Rh); **4** and **6** also gave the expected mass spectra [$m/z = 430$ ($M^+$)].

[4] Rhombic (from pentane), space group $Pbc2_1$ ($C_{2v}^5$), $Z=8$; $a=1652.4(4)$, $b=1654.3(3)$, $c=1559.9(5)$ pm; AED; $3° \leq 2\Theta \leq 60°$; 2264 independent reflections with $I > 3.0\sigma(I)$; $R_{iso}=0.045$, $R_{aniso}=0.042$. Further details of the crystal structure investigation can be obtained on request from the Fachinformationszentrum Energie Physik Mathematik, D-7514 Eggenstein-Leopoldshafen by quoting the number CSD 50344, the names of the authors, and full citation of the journal.

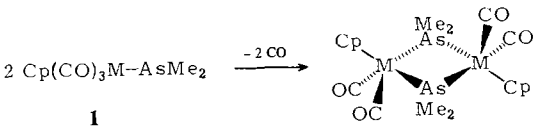
[5] a) K. Itoh, I. Matsuda, F. Ueda, Y. Ishii, J. A. Ibers, *J. Am. Chem. Soc. 99* (1977) 2118; b) M. Cowie, J. A. Ibers, *Inorg. Chem. 15* (1976) 552; c) M. J. Doyle, M. F. Lappert, G. M. McLaughlin, J. McMeeking, *J. Chem. Soc. Dalton Trans. 1974*, 1494, and references cited therein.

[6] a) A. Davison, J. P. Selegue, *J. Am. Chem. Soc. 100* (1978) 7763; b) M. I. Bruce, A. G. Swincer, R. C. Wallis, *J. Organomet. Chem. 171* (1979) C 5; c) H. Berke, *Z. Naturforsch. B35* (1980) 86.

## Dicarbonyl($\eta^5$-cyclopentadienyl)(di-*tert*-butyl-$\lambda^4$-arsanediyl)molybdenum and -tungsten—The First Complexes with a Metal-Arsenic Double Bond**

By *Michael Luksza, Sigrid Himmel,* and *Wolfgang Malisch**

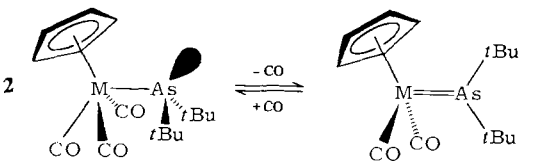
Transition-metal substituted arsanes of type **1**[2a, b] are distinguished from triorganoarsanes by their increased Lewis basicity, which, *e.g.*, is expressed by a marked tendency to coordinate to metallic centers[2b]. A special case of this reaction type is the formation of a four-membered ring with loss of CO, which occurs on heating in toluene or on irradiation[2a] (Cp = $\eta^5$-cyclopentadienyl).




**1**

M = Mo, W

We have now observed that the metalated arsanes **2a, b**[2c], which possess sterically demanding *tert*-butyl ligands at the donor center, lose carbon monoxide already at 60 °C in benzene and that *without* aggregation occurring! The mononuclear complexes **3a, b** are formed in which, for the first time, a metal-arsenic double bond is realized[3].




**a**, M = Mo; **b**, M = W

The blue and deep violet crystals of **3a** and **3b**, respectively, are extremely soluble in benzene and undergo spontaneous addition of carbon monoxide (25 °C, normal pressure, benzene). Their molecular masses have been determined cryoscopically and by mass spectrometry; their constitution follows from the data in Table 1.

The "perpendicular" orientation of the *tert*-butyl groups at the trigonal-planar arsenic atom to the cyclopentadienyl- and $M(CO)_2$ -plane, predicted by *Hoffmann et al.*[4], follows from the anisochronism of the alkyl ligands. This is detectable in the $^1$H-NMR spectrum of **3a/b** below

Table 1. Characteristic data for **3a, b, 7,** and **8**.

**3a**: M.p. = 108–110 °C.—$^1$H-NMR ([D$_8$]toluene, 25/–75 °C): $\delta$ = 5.47/5.55 (s, 5H, $H_5C_5$), 1.60 (s, 18H, $H_3C$)/1.80 (s, 9H, $H_3C$), 1.34 (s, 9H, $H_3C$).—IR (pentane): $\nu CO_s$ = 1947 (vs), $\nu CO_{as}$ = 1873 (s) cm$^{-1}$

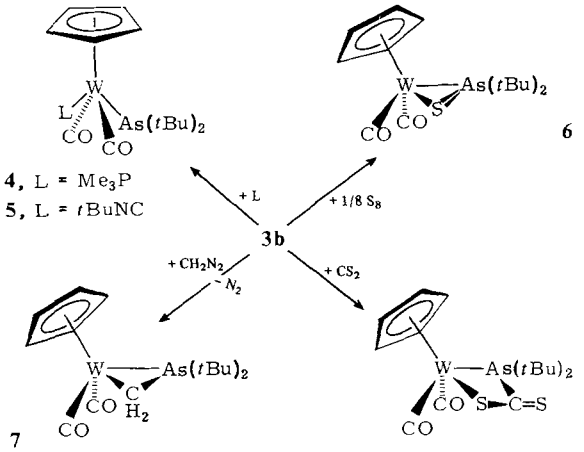
**3b**: M.p. = 125–127 °C.—$^1$H-NMR ([D$_8$]toluene, 25/–60 °C): $\delta$ = 5.13/5.23 (s, 5H, $H_5C_5$), 1.61 (s, 18H, $H_3C$)/1.66 (s, 9H, $H_3C$), 1.24 (s, 9H, $H_3C$).—$^{13}$C-NMR ($^1$H-coupled) ($C_6D_6$): $\delta$ = 231.75 (s, $^1J(^{13}C^{183}W)$ = 180.05 Hz, CO), 90.51 (d, $^1J(HC)$ = 177.64 Hz, $C_5H_5$), 61.42 (s, $CCH_3$), 30.67 (q, $^1J(HC)$ = 123.46 Hz, $CCH_3$).—IR (pentane): $\nu CO_s$ = 1936 (vs), $\nu CO_{as}$ = 1861 (s) cm$^{-1}$

**7**: M.p. = 98 °C (decomp.).—$^1$H-NMR ([D$_8$]toluene, 25/–40 °C): $\delta$ = 5.04/5.08 (s, 5H, $H_5C_5$), 1.15 (s, 18H, $H_3C$)/1.43 (s, 9H, $H_3C$), 1.12 (s, 9H, $H_3C$), 0.64/0.53 (s, 2H, $H_2C$).—IR ($C_6H_6$): $\nu CO_s$ = 1922 (vs), $\nu CO_{as}$ = 1837 (s)

**8**: M.p. = 100–102 °C.—$^1$H-NMR ($C_6H_6$): $\delta$ = 4.90 (s, 5H, $H_5C_5$), 1.49 (s, 9H, $H_3C$), 1.15 (s, 9H, $H_3C$).—$^{13}$C-NMR ($^1$H-coupled) ($C_6D_6$): $\delta$ = 268.24 (s, $CS_2$), 244.38 (s, $^1J(^{13}C^{183}W)$ = 137.33 Hz, CO), 231.25 (s, $^1J(^{13}C^{183}W)$ = 161.75 Hz, CO), 90.64 (d, $^1J(CH)$ = 179.36, $C_5H_5$), 46.59 (s, $CCH_3$), 42.61 (s, $CCH_3$), 29.71 (q, $^1J(CH)$ = 125.91, $CH_3$), 29.41 (q, $^1J(CH)$ = 129.68 Hz, $CH_3$).—IR ($C_6H_6$): $\nu CO_s$ = 1944 (vs), $\nu CO_{as}$ = 1863 (s); $\nu C{=}S$ = 1075 (m) cm$^{-1}$

–48.5/–46 °C, *i.e.* at room temperature rotation relative to the metal-arsenic double bond is rapid: $\Delta G^+$ (224.6/227 K) is 10.9/11.1 kcal/mol. Although **3a, b** prefer this sterically unfavored conformation due to donor-acceptor orbital $\pi$-interaction between the centers of the molecular fragments $Cp(CO)_2M^{\ominus}$ and $(tBu)_2As^{\oplus}$, the reaction **2a, b** → **3a, b** proceeds extremely readily: the *tert*-butyl groups at the sp$^2$ arsenic atom in **3a, b** are considerably less sterically constrained than they would be at the bridging sp$^3$ arsenic atom of the dinuclear compound $[Cp(CO)_2M–As(tBu)_2]_2$.

Participation of the nonbonding lone-pair of electrons on the arsenic of **2a, b** in the MAs double bond of **3a, b** is indicated by the inactivity towards MeI. With HCl in ether, **3b** forms *trans*-$Cp(CO)_2[ClAs(tBu)_2]W–H$[2a]. The nucleophiles $Me_3P$ and *t*BuNC add rapidly and stereospecifically *trans* to the arsenic ligand to form **4** and **5**, respectively[1, 5a]. The "double bond activity" of **3b** is principally expressed by the reaction with sulfur to afford **6**, and with diazomethane to afford **7**, which opens up a completely novel route to three-membered metallacycles[5b].




As shown by [2+2]cycloaddition of $CS_2$ to give **8**, this reaction principle can also be used for the synthesis of larger heterocycles. **6** and **7** are characterized by their dynamic behavior, which has to be attributed to rotation of the $\eta^2$-bonded ligands $(tBu)_2As{=}S$ and $(tBu)_2As–CH_2$, respectively [$\Delta G^+$ (268/248 K) = 15.4/12.4 kcal/mol].

[*] Prof. Dr. W. Malisch, M. Luksza, S. Himmel
Institut für Anorganische Chemie der Universität
Am Hubland, D-8700 Würzburg (Germany)

[**] Transition-Metal Substituted Phosphanes, Arsanes, and Stibanes, Part 35. This work was supported by the Fonds der Chemischen Industrie. Part 34: [1].

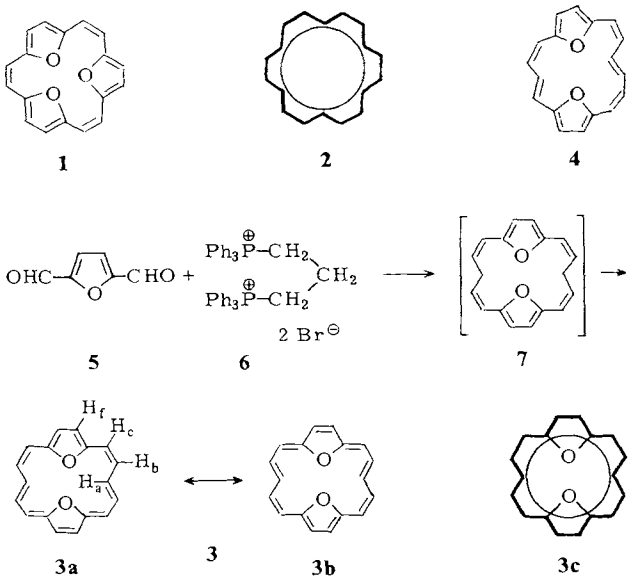
Received: January 25, 1983;
revised: March 1, 1983 [Z 249 IE]
German version: *Angew. Chem. 95* (1983) 418

[1] M. Luksza, K. Fiederling, U. Wanka, W. Malisch, *J. Organomet. Chem. 236* (1982) C1.
[2] a) W. Malisch, M. Kuhn, W. Albert, H. Rößner, *Chem. Ber. 113* (1980) 3318; b) P. Panster, W. Malisch, *ibid. 109* (1976) 3842; c) W. Malisch, M. Luksza, W. S. Sheldrick, *Z. Naturforsch. B36* (1981) 1580.
[3] a) M–As moieties with partial π-bonding character are found in some di- and trinuclear complexes of trigonal planar arsenic, cf. G. Huttner, B. Sigwarth, J. von Seyerl, L. Zsolnai, *Chem. Ber. 115* (1982) 2035; J. von Seyerl, B. Sigwarth, H.-G. Schmid, G. Mohr, A. Frank, M. Marsili, G. Huttner, *ibid. 114* (1981) 1392; b) an M=P double bond was detected in $Cp(CO)_2Mo{=}P\overline{N(Me)CH_2CH_2N(Me)}$: L. D. Hutchins, R. T. Paine, C. F. Campana, *J. Am. Chem. Soc. 102* (1980) 4521.
[4] B. E. R. Schilling, R. Hoffmann, D. L. Lichtenberger, *J. Am. Chem. Soc. 101* (1979) 585; B. E. R. Schilling, R. Hoffmann, J. W. Faller, *ibid. 101* (1979) 592.
[5] a) W. Malisch, H. Rössner, K. Keller, R. Janta, *J. Organomet. Chem. 133* (1977) C21; b) A. Meyer, A. Hartl, W. Malisch, *Chem. Ber. 116* (1983) 348.

## Synthesis of an [18]Annulene Dioxide: An Oxygen-Bridged [18]Annulene Possessing Equivalent Kekulé Structures

By *Haru Ogawa**, *Naomi Sadakari*, *Taiji Imoto*, *Izumi Miyamoto*, *Hidefumi Kato*, and *Yōichi Taniguchi*

The [18]annulene trioxide **1**[1a,b] was characterized, on the basis of the very low field proton resonances and on the remarkably similar electronic spectrum to that of [18]annulene itself, **2**, as a delocalized 18π Hückel arene. We report here on the synthesis and properties of the [18]annulene dioxide **3**, for which two equivalent Kekulé structures (**3a** and **3b**) can be written—as for benzene.




Double Wittig reaction of 2,5-furandialdehyde **5** with trimethylenebis(triphenylphosphonium bromide) **6** (15% excess) in DMF at 85 °C (LiOMe as base) under high-dilution conditions leads, in a "one pot synthesis", to **3** (presumably *via* thermal dehydrogenation of the cycloolefin **7**). **3** was obtained as sole annulene; it could be separated by chromatography on $SiO_2$ (*n*-hexane) as green platelets (m.p. 235 °C, yield 3.0%). The $^{13}$C-NMR spectrum of **3** ($CDCl_3$) exhibited only five resonance lines. The $^1$H-NMR spectrum ($CDCl_3$, 100 MHz) clearly indicates that **3** contains only four types of H-atoms, suggesting the formulation **3c** [$\delta = -5.89$ ($H_a$, 2H, $J_{trans} = 13.5$ Hz), 9.13 ($H_f$, 4H, s), 9.20 ($H_c$, 4H, $J_{cis} = 10.8$ Hz), 10.00 ($H_b$, 4H, q, $J_{cis} = 10.8$ Hz, $J_{trans} = 13.5$ Hz)]. The aromatic character of **3c** was confirmed by the existence of a pronounced diatropic ring current. The observed large chemical shift difference between the inner ($H_a$) and outer ($H_b$) protons is the highest one ever recorded in the [18]-[2], bridged [18]-[3,7], and didehydro[18]annulene series[4]. The electronic spectrum of **3** is remarkably similar to that of [18]annulene **2**.

It may be concluded from these findings that the two oxygen bridges in **3** keep the 18π perimeter in a rigid and planar centrosymmetrical conformation with no bond length alternation. In contrast, another counterpart **4**, consisting of the same building blocks (*i.e.* two furan rings and ten $sp^2$ CH groups) is less planar, and consequently less diatropic[3].

Received: February 11, 1983 [Z 277 IE]
German version: *Angew. Chem. 95* (1983) 412
The complete version of this communication appears in: *Angew. Chem. Suppl. 1983*, 471–479

[1] a) G. M. Badger, J. A. Elix, G. E. Lewis, *Austral. J. Chem. 19* (1966) 1221; b) G. M. Badger: *Aromatic Character and Aromaticity*, Cambridge University Press, Cambridge 1969, p. 103.
[2] J. M. Gilles, J. F. M. Oth, F. Sondheimer, E. P. Woo, *J. Chem. Soc. B 1971*, 2177; $\Delta\delta$ of **2** = 12.13 ppm in the absence of exchange.
[3] H. Ogawa, C. Fukuda, T. Imoto, I. Miyamoto, Y. Taniguchi, T. Koga, Y. Nogami, *Tetrahedron Lett. 24* (1983) 1045.
[4] M. Nakagawa, *Pure and Appl. Chem. 44* (1975) 885; $\Delta\delta$ of tetra-*tert*-butyldidehydro[18]annulene = 14.9 ppm.
[7] W. Wagemann, M. Iyoda, H. M. Deger, J. Sombrock, E. Vogel, *Angew. Chem. 90* (1978) 988; *Angew. Chem. Int. Ed. Engl. 17* (1978) 956.

## Synthesis of Hetero[17]annulene Dioxides and a [16]Annulene Dioxide Using Furan Building Blocks

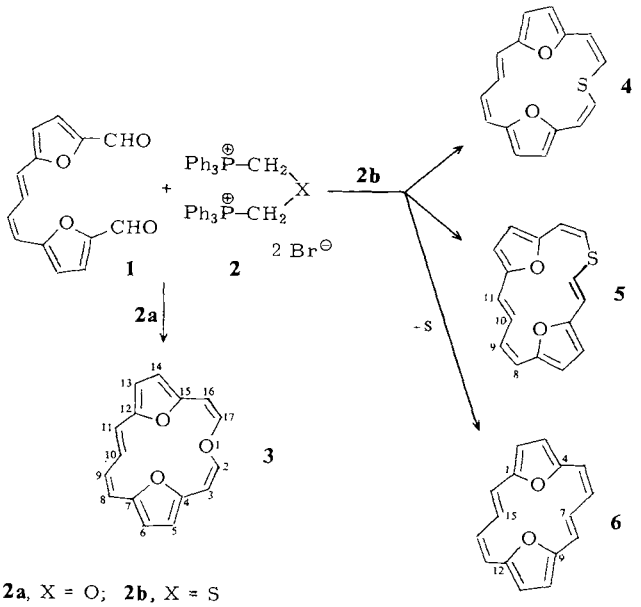
By *Haru Ogawa**, *Chiyuki Fukuda*, *Taiji Imoto*, *Izumi Miyamoto*, *Hidefumi Kato*, and *Yōichi Taniguchi*

Recent investigations of bridged [18]annulenes[1,2] have demonstrated that aromatic π-delocalization is not hampered even by twisting of the perimeter. Results gained from hetero[17]annulenes[3a,4,5] indicated that the diatropicity depends on the structures and that slight structural perturbations may be sufficient to destroy the π-bond delocalization. Therefore, it is of interest to investigate the effect of incorporating furan part structures into hetero[17]annulenes, whose conformations are expected to be considerably twisted. For this purpose we prepared **3**, **4**, and **5** as models.

Double Wittig reaction of the dialdehyde **1**[2] with **2a** gave oxa[17]annulene dioxide **3** as the sole isomer [m.p. 236 °C, yield 8.0%]. In contrast, reaction of **1** with **2b** led to two stereoisomeric thia[17]annulene dioxides **4** (m.p. 227 °C, yield 2.2%) and **5** (m.p. 176 °C, yield 2.0%), together with [16]annulene dioxide **6** (m.p. 182–184 °C, yield 2.0%). The chemical shifts of the H-8, H-9, H-10, and H-11 protons (spin decoupling) showed that **3**, **4** and **5** are 18π-diatropic systems. The signals of the outer protons are

[*] Prof. Dr. H. Ogawa, N. Sadakari, Prof. Dr. T. Imoto
Faculty of Pharmaceutical Sciences, Kyushu University
62, Fukuoka 812 (Japan)
I. Miyamoto, Dr. H. Kato, Prof. Dr. Y. Taniguchi
Department of General Chemistry, National Kurume Technical College
Kurume 830 (Japan)

[*] Prof. Dr. H. Ogawa, C. Fukuda, Prof. Dr. T. Imoto
Faculty of Pharmaceutical Sciences, Kyushu University
62, Fukuoka 812 (Japan)
I. Miyamoto, Dr. H. Kato, Prof. Dr. Y. Taniguchi
Department of General Chemistry, National Kurume Technical College
Komorino Kurume 830 (Japan)



**2a**, X = O; **2b**, X = S

shifted to lower field compared to those of the atropic dihydro[18]annulene dioxide (**4**, $CH_2-CH_2$ instead of S), and those of the inner proton(s) to higher field. The difference in chemical shifts of H-11 and H-10 ($\Delta\delta$) clearly shows that the diamagnetic ring current decreases along the series **5** > **4** > **3** ($\Delta\delta = 4.36$, 3.51, and 1.54 ppm, respectively).

Isomerization **5** → **4** could occur upon heating or simply by acid catalysis ($CF_3COOD$, NMR spectroscopy). Back-isomerization *via* protonated species $\mathbf{4H^+} \rightarrow \mathbf{5H^+}$ was unsuccessful, presumably due to the low $pK_a$ of sulfur. In this respect, the thia[17]annulene system cannot form a "closed" chemical cycle of four sequential steps, as occurs in [15]annulenone dioxide[6] (model of $H^+$-pumping cycle of bacteriorhodopsin).

The structure of **6** was confirmed by $^1H$- and $^{13}C$-NMR spectroscopy. The very low-field resonances of the inner protons (2H, H-7, H-15: $\delta = 17.18$) and the high-field resonances of the outer protons (10H, $\delta = 4.41-4.93$ ppm) observed confirm that **6** is strongly paratropic. The electronic spectrum of **6** is closely similar to that of [16]annulene (broader bands at $\lambda_{max} = 278$ and 530 nm, no vibrational structures), indicating that **6** is a 16π system with alternating bond lengths.

The furan ring, therefore, serves as a useful building block—even more suitable in some cases than acetylenic moieties—for twisted heteroannulenes as well as of [4n+2]- and [4n]annulenes, in which the ring current is to be determined.

Received: June 16, 1981;
revised: February 28, 1983 [Z 418 IE]
German version: *Angew. Chem. 95* (1983) 412
The complete manuscript of this communication appears in:
*Angew. Chem. Suppl. 1983*, 480-487

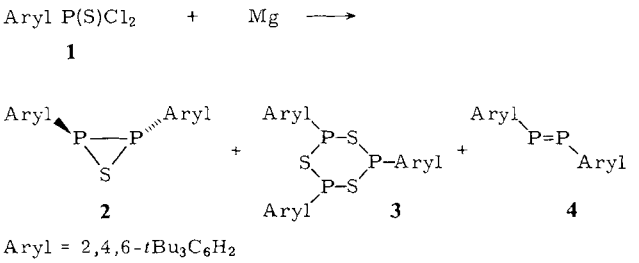
[1] W. Wagemann, M. Iyoda, H. M. Deger, J. Sombroek, E. Vogel, *Angew. Chem. 90* (1978) 988; *Angew. Chem. Int. Ed. Engl. 17* (1978) 956.
[2] H. Ogawa, C. Fukuda, T. Imoto, I. Miyamoto, Y. Taniguchi, T. Koga, Y. Nogami, *Tetrahedron Lett. 24* (1983) 1045.
[3] a) G. Schröder, *Pure Appl. Chem. 44* (1975) 925.
[4] J. M. Brown, F. Sondheimer, *Angew. Chem. 86* (1974) 346; *Angew. Chem. Int. Ed. Engl. 13* (1974) 337.
[5] T. M. Cresp, M. V. Sargent, *J. Chem. Soc. Perkin Trans. I 1973*, 1786.
[6] H. Ogawa, T. Inoue, T. Imoto, I. Miyamoto, H. Kato, Y. Taniguchi, *Angew. Chem. 95* (1983) 244; *Angew. Chem. Int. Ed. Engl. 22* (1983) 253; *Angew. Chem. Suppl. 1983*, 243–253.

## The First X-Ray Structure Analysis of a Thiadiphosphirane**

By *Masaaki Yoshifuji**, *Kaori Ando*, *Katsuhiro Shibayama*, *Naoki Inamoto*, *Ken Hirotsu**, and *Taiichi Higuchi*

Phosphorus-containing small ring systems—particularly three-membered ring compounds—are of topical interest[1a,b]. *Baudler et al.*[1c] have reported the synthesis of 2,3-di-*tert*-butyl-1,2,3-thiadiphosphirane, but so far there have been no reports on the X-ray structure analysis of such compounds.

By using the extremely bulky 2,4,6-tri-*tert*-butylphenyl group to sterically protect a phosphorus-phosphorus double bond we have been able to isolate a true "phosphobenzene", the diphosphene **4**, as a stable compound[2a].



Aryl = 2,4,6-$t$Bu$_3$C$_6$H$_2$

We now wish to report the preparation and characterization of *E*-2,3-bis(2,4,6-tri-*tert*-butylphenyl)-1,2,3-thiadiphosphirane **2** and 2,4,6-tris(2,4,6-tri-*tert*-butylphenyl)-1,3,5-trithia-2,4,6-triphosphorinane **3**[5]. **2** and **3** were obtained by reaction of 2,4,6-tri-*tert*-butylphenylthiophosphonic dichloride **1** with magnesium turnings[2c,3]. **2** is a colorless, odorless, thermally and photolytically insensitive compound, which is quite stable toward atmospheric mois-

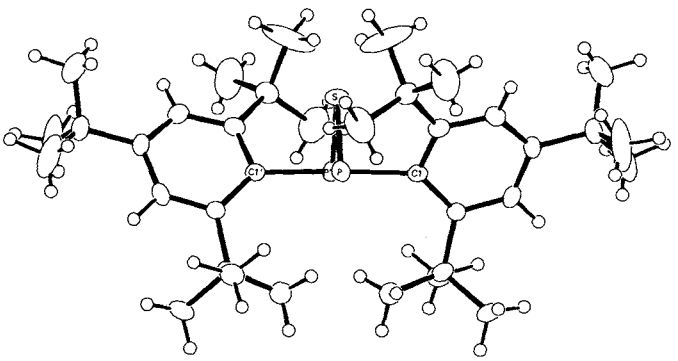


Fig. 1. Structure of **2** in the crystal. Monoclinic, C2/c, $a = 18.529(7)$, $b = 9.506(4)$, $c = 20.760(9)$ Å, $\beta = 100.4(1)°$, $Z = 4$. $Mo_{K\alpha}$-radiation, $\lambda = 0.7107$ Å, $R = 0.059$ for 1107 reflections with $I > 3\sigma(I)$. Important bond lengths and angles: P–P 2.249(3), P–S 2.103(3) Å; ∢ SPP 57.7(1), PSP 64.6(1)°. Further details of the crystal structure investigation can be obtained on request from the Fachinformationszentrum Energie Physik Mathematik, D-7514 Eggenstein-Leopoldshafen by quoting the depository number CSD 50386, the names of the authors, and complete citation of the journal.

[*] Dr. M. Yoshifuji, K. Ando, K. Shibayama, Prof. Dr. N. Inamoto
Department of Chemistry, Faculty of Science,
The University of Tokyo
Hongo, Tokyo 113 (Japan)
Dr. K. Hirotsu, Prof. Dr. T. Higuchi
Department of Chemistry, Faculty of Science, Osaka City University
Sumiyoshi, Osaka 558 (Japan)

[**] This work was supported in part by the Japanese Ministry of Education, Science and Culture (Science Research Grant Nos. 543008 and 57540276).

ture and oxygen over a long period of time[4a]. It was also obtained by reaction of **4** with elemental sulfur (60% yield). Reaction of **2** with chlorine affords 2,4,6-tri-*tert*-butylphenylphosphonic dichloride almost quantitatively after hydrolysis[2a].

The yields of compounds **2**, **3**[4b], and **4** (20—60%, 1—8%, and 1—40%, respectively) depend on the ratio **1** : Mg.

**3** had already been synthesized *via* an alternative route by *Çetinkaya et al.*, who also carried out a crystal structure analysis.

The molecule **2** contains a two-fold crystallographic axis, which bisects the P–S–P angle (Fig. 1). The atoms P, C1, P′, and C1′ form a plane (deviation 0.02 Å); the interplanar angle between a benzene ring and the plane P, C1, P′, C1′ is 59.3°. The benzene rings are distorted to a boat form, in which the largest distortion (14.4°) is a little smaller than in bis(2,4,6-tri-*tert*-butylphenyl)phosphinic chloride (18.5°)[2b].

Received: December 7, 1982 [Z 217 IE]
German version: *Angew. Chem. 95* (1983) 416

[1] a) M. Baudler, *Angew. Chem. 94* (1982) 520; *Angew. Chem. Int. Ed. Engl. 21* (1982) 492; b) H. Quast, *Nachr. Chem. Tech. Lab. 27* (1979) 120; c) M. Baudler, H. Suchomel, G. Fürstenberg, U. Schings, *Angew. Chem. 93* (1981) 1087; *Angew. Chem. Int. Ed. Engl. 20* (1981) 1044.

[2] a) M. Yoshifuji, I. Shima, N. Inamoto, K. Hirotsu, T. Higuchi, *J. Am. Chem. Soc. 103* (1981) 4587; *104* (1982) 6167; b) *Angew. Chem. 92* (1980) 405; *Angew. Chem. Int. Ed. Engl. 19* (1980) 399; M. Yoshifuji, I. Shima, N. Inamoto, T. Aoyama, *Tetrahedron Lett. 22* (1981) 3057; c) M. Yoshifuji, S. Nakayama, R. Okazaki, N. Inamoto, *J. Chem. Soc. Perkin Trans. I 1973*, 2065.

[3] *Procedure:* A solution of **1** (677 mg) in tetrahydrofuran (15 mL) was treated with 44 mg of magnesium turnings, and the mixture heated under reflux for 1 h. After removal of solvent by distillation, chromatographic separation (silica gel, pentane) of the residue furnished 283 mg of **2**, 43 mg of **3**, and 12 mg of **4**.

[4] a) **2**: M.p. 131.5—132 °C; $^{31}$P-NMR ($CDCl_3$): $\delta = -65.1$ (85% $H_3PO_4$ ext.); $^1$H-NMR ($CDCl_3$): $\delta = 7.11$ (s, 4H, arom.), 1.60 (s, 36H, *o*-*t*Bu), 1.25 (s, 18H, *p*-*t*Bu); MS (*m/z*) 584 ($M^+$); $M_r$ ($C_6H_6$): 574.6; UV ($CH_2Cl_2$): $\lambda_{max}$ ($\varepsilon$) = 291 nm (6530); b) **3**: M.p. 170—171 °C; $^{31}$P-NMR ($CDCl_3$): $\delta = 91.0$; $^1$H-NMR ($CDCl_3$): $\delta = 7.35$ (bs, 6H, arom.), 1.63 (s, 54H, *o*-*t*Bu), 1.25 (s, 27H, *p*-*t*Bu); FD-MS (*m/z*) 924 ($M^+$).

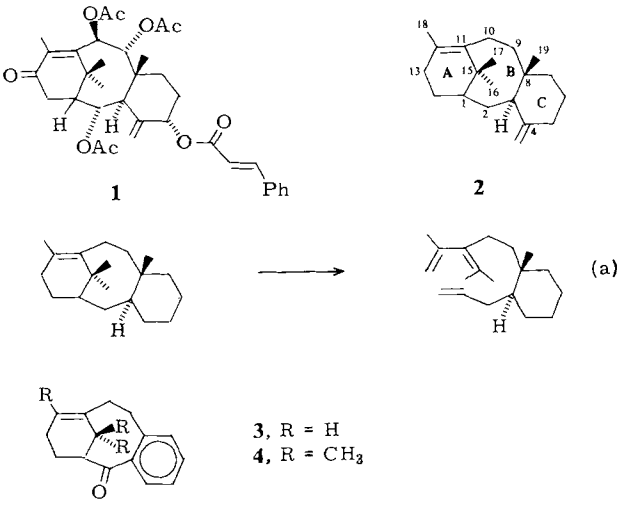
[5] B. Çetinkaya, P. B. Hitchcock, M. F. Lappert, A. J. Thorne, H. Goldwhite, *J. Chem. Soc. Chem. Commun. 1982*, 691.

## The Tricyclo[9.3.1.0$^{3,8}$]pentadecane System—A Short Synthesis of a C-Aromatic Taxane Skeleton

By *Kenneth J. Shea** and *Peter D. Davis*

The taxanes, including taxusin **1**, comprise a group of naturally occurring substances isolated from the European *Taxus baccata*, Japanese *T. cuspidata*, and related species (Taxaceae)[1]. Inspection of the parent taxane ring system **2** reveals a novel fused-bridged tricyclo[9.3.1.0$^{3,8}$]pentadecane ring skeleton that embodies a bridgehead double bond (C11—C12) and a trimethyl-substituted A ring. Neither taxane nor any of the natural derivatives have previously been synthesized[5]. Our approach to the synthesis of the taxane skeleton involves a type II intramolecular Diels-Alder cycloaddition [reaction (a)].

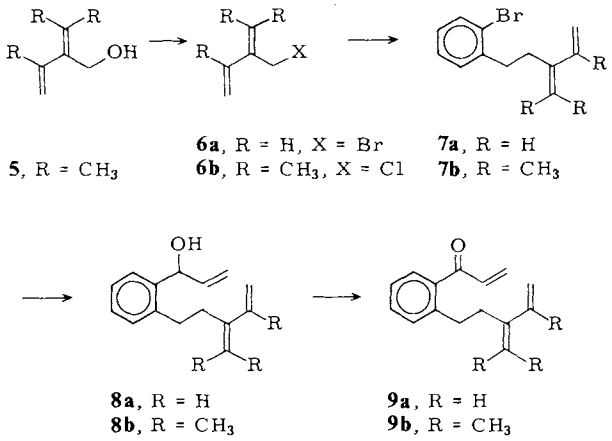
The key intermediates in our synthesis are the trienones **9a** and **9b** (Scheme 1). Their preparation involves reaction of the Grignard reagent **11**, prepared directly from di-




bromide **10**, with the butadiene derivatives **6a** and **6b**, respectively. Thus, when a solution of 2-bromomethyl-1,3-butadiene **6a** in tetrahydrofuran (THF) is treated with a solution of **11** in ether, the bromodiene **7a** is isolated in 54% yield.

To synthesize the taxane derivative **4**, the alcohol **5**[9] was converted quantitatively into the chloride **6b** using Meyers' method. Treatment of **6b** with a two-fold excess of **11** in THF furnished the diene **7b** (43%).

The dienophile moiety of **9** was introduced in two steps from **7**: metalation (*s*BuLi, −78 °C) followed by reaction with acrolein to afford **8**, whose oxidation with pyridinium dichromate in $CH_2Cl_2$ yields the trienones **9a** (50%) and **9b** (63%).



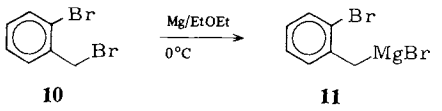

Scheme 1.

When a 1 M solution of the triene **9a** is heated for 1 h in xylene at 185 °C a single cycloadduct is isolated by column chromatography in 70% yield. All spectral data are consistent with structure **3**. **9a** is *ca.* $10^6$ times more reactive than the non-benzannulated derivative **12** [$t_{1/2}$(**9a**) = 1 h (65 °C), $t_{1/2}$(**12**) = 15 h (155 °C)]. The rate increase that results from annulation is probably a general phenomenon of intramolecular Diels-Alder reactions.

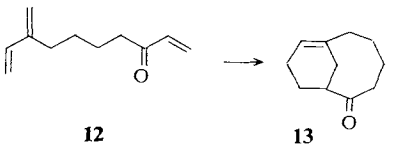
When a 0.1 M solution of **9b** in xylene is heated at 155 °C for 93 h, a single cycloadduct, **4**, is isolated in 70% yield. The vinyl region in the $^1$H-NMR spectrum exhibits three methyl peaks (250 MHz, $CDCl_3$, TMS: $\delta = 1.29$, 1.10, and 0.70). Significantly, the $^{13}$C-NMR spectrum reveals a very low-field doublet (62.89 MHz, $CDCl_3$, TMS: $\delta = 62.9$)

[*] Prof. Dr. K. J. Shea, Dr. P. D. Davis
Department of Chemistry, University of California
Irvine, CA 92717 (USA)

[**] This work was supported by the National Science Foundation and the Petroleum Research Foundation. Prof. P. Lillya, University of Massachusetts, is thanked for a sample of the dienol **5**.




10 11




12 13

attributable to the $sp^3$-bridgehead C atom: the 14.4 ppm shift downfield relative to cycloadduct **3** is consistent with the β-effect produced by *gem*-dimethyl substituents at C-15[14], confirming the regiospecificity of the cycloaddition.

Received: January 12, 1983 [Z 239 IE]
German version: *Angew. Chem. 95* (1983) 422
The complete version of this manuscript appears in: *Angew. Chem. Suppl. 1983*, 564–570

CAS Regsitry numbers:
**3**, 85371-18-2; **4**, 85371-19-3; **5**, 52385-60-1; **6a**, 23691-13-6; **6b**, 85371-20-6; **7a**, 85371-21-7; **7b**, 85371-22-8; **8a**, 85371-23-9; **8b**, 85371-24-0; **9a**, 85371-25-1; **9b**, 85371-26-2; **10**, 3433-80-5; **13**, 85371-27-3; acrolein, 107-02-8.

[1] a) B. Lythgoe in R. H. Manske: *The Alkaloids, Vol. X*, Academic Press, New York 1968, p. 597; b) K. Nakanishi, T. Goto, S. Ito, S. Natori, S. Nozoe: *Natural Products Chemistry, Vol. 1*, Kodansha-Academic Press, Tokyo, Japan 1974, pp. 281–284; c) R. W. Miller, *J. Nat. Prod. 43* (1980) 425.

[5] For recent synthetic efforts related to the taxane problem see: A. S. Kende, M. Benechie, D. P. Curran, P. Fludzinski, *Tetrahedron Lett. 1979*, 4513; B. M. Trost, H. Hiemstra, *J. Am. Chem. Soc. 104* (1982) 886; S. F. Martin, J. B. White, R. Wagner, *J. Org. Chem. 47* (1982) 3192.

[9] a) The alcohol **5** is obtained by reduction of the corresponding diene ester with diisobutylaluminum hydride (I. Alkonyi, D. Szabo, *Chem. Ber. 100* (1967) 2773) (90%) or by ene reaction of tetramethylallene and formaldehyde (R. C. Blume, US-Pat. 3806511 (1974), and 3880669 (1975), Du Pont; *Chem. Abstr. 81* (1975) 3344 and *82* (1975) 172295).

[14] F. W. Wehrli, T. Wirthlin: *Interpretation of Carbon-13 NMR-Spectra*, Heyden, London 1978, p. 22.

# BOOK REVIEWS

**Reactive Intermediates.** Volumes 1 and 2. Edited by *R. A. Abramovitch*. Plenum Press, New York 1980 and 1982. xiii, 522 pp., bound, $ 49.50 and xv, 599 pp., bound, $ 59.50.

It is intended that the series "Reactive Intermediates" shall provide articles concerning relatively new areas of reactive intermediate chemistry, at irregular intervals. In this it complements another series, also entitled "Reactive Intermediates" (edited by *M. Jones Jr.* and *R. A. Moss*, so far two volumes), which reports mainly on advances in well-known intermediates (carbanions, carbonium ions, radicals, carbenes and nitrenes).

The first volume contains contributions on: the preparation and reactions of atomic carbon (*P. B. Shevlin*, 36 pp., the dependence of the products formed on the mode of generation of the atomic carbon is exhaustively discussed); metal atoms as reactive intermediates (*K. J. Klabunde*, 112 pp., deals with experimental techniques, including commercial apparatus, as well as applications in organometallic synthesis and in matrix isolation spectroscopy); aminium radicals (*Y. L. Chow*, 112 pp., surveys chemical, photochemical and electrochemical amine oxidations and the homolysis of *N*-chloramines and *N*-nitrosamines); arylcarbenes in the gas phase (*C. Wentrup*, 56 pp., discusses automerizations and ring contractions that the author has investigated by isotopic labeling); and metal salt-catalyzed carbenoids (*D. S. Wulfman* and *B. Poling*, 191 pp., give a detailed account of the carbenoid concept and the mechanism of methylene transfer together with numerous references to preparative applications of metal salt-catalyzed reactions of diazoalkanes).

Volume 2 contains contributions on: arylnitrenes in solution (*E. F. V. Scriven*, 54 pp., with emphasis on the singlet-triplet problem and the reaction route to azepines); nitrile ylides and nitrenes from 2*H*-azirines (*A. Padwa* and *P. H. J. Carlsen*, 64 pp., *Huisgens'* work on the cycloadditions of nitrile ylides is appraised and photochemical and intramolecular variants are discussed); radical cyclization by intramolecular addition (*J.-M. Surzur*, 174 pp., the influence of substituents, chain length, and heteroatoms on the cyclization of unsaturated radicals is treated in a clearly set-out arrangement of the extensive material. Alongside the kinetic and stereochemical aspects, attention is particularly paid to the synthesis of bicyclic and polycyclic compounds); and the reactions of silicon atoms and silylenes (*Y.-N. Tang*, 70 pp., insertion and addition reactions have analogies with and show differences from carbon atoms and carbenes, *e.g.* the 1,4-addition to conjugated dienes is preferred). There are also contributions on five-membered hetarynes (*M. G. Reinecke*, 160 pp., intermediates with formal triple bonds in furan, pyrrole and thiophene rings are rarer than previously assumed. Many reactions for which such intermediates were postulated take other pathways, which are critically reviewed here; reactions where genuine hetarynes are formed are differentiated) and on the mechanism of the Favorskii rearrangement (*A. Baretta* and *B. Waegell*, 58 pp., where the influence of stereochemistry and of the ring strain of the α-haloketone on the course of the reaction is interpreted by varying participation of cyclopropanone and oxyallyl intermediates).

All the contributions are by experts who have experimental experience in their fields. It is apparent to the reader that the investigation of reactive intermediates is progressing quickly and with high standards, even though the spectacular achievements of the pioneer era are absent. The broad range of topical, thorough and critical reviews makes this work a worthwhile addition to every chemical library. The fact that he must pay the full price, even though only one or two articles may interest him personally, may deter the private purchaser. If he buys inspite of this he will be rewarded by a stimulating view "over the garden fence".

*Wolfgang Kirmse* [NB 581 IE]

**Techniques of Chemistry.** By *A. Weissberger, Vol. 17:* **Applications of Lasers to Chemical Problems.** By *R. Evans.* Wiley-Interscience, Chichester 1982. xii, 291 pp., £ 42.50.

This volume of *"Weissberger"* is a consequence of the fact that, ever since their first technical realization by *Maiman* in 1960, lasers have found their place in analytical chemistry. Considering the continuing active development of laser applications, it is a difficult task to produce a handbook which puts useful information into the hand of the practising chemist.

The first chapter by *J. Wilson,* entitled "Laser Sources", is definitely too short with its 35 pages. The literature is only cited up to 1978. Those intending to use lasers do not find enough helpful information; the reference to the "Laser Focus Buyers Guide" is not sufficient. A reference to the standard volume by *W. Koechner* would have been appropriate in the section on solid state lasers. In the section on dye lasers, the argon-ion laser pumped continuous wave dye laser, which has become a spectroscopist's workhorse, has only been mentioned in passing. There is little about nonlinear optics, and parametric oscillators are only mentioned in connection with a review article from 1969, which is outdated.

The longest chapter with 146 pages, entitled "Applications of Lasers in Analytical Chemistry" by *J. C. Wright,* provides much more information and covers the literature up to 1981 with 394 references. The main attention is focused on spectroscopic methods, particularly on those having extremely high sensitivity: absorption and fluorescence spectroscopy, photoionization and photodissociation methods, coherent Raman spectroscopy and two-photon spectroscopy. A good, comprehensive survey is made of these methods; for example the sensitivities realizable by the various methods are tabulated for 44 elements. In the section on coherent Raman techniques, the numerous possibilities for interactions arising from the nonlinear terms in the expression for the polarizability, are exhaustively discussed. The spectroscopic methods based on these interactions, which may also possess resonant character, *e.g.* CARS (Coherent Anti-Stokes Raman Scattering), are discussed with applications.

The chapter "Ultraviolet and Visible Laser Photochemistry" by *I. R. Evans* complements the contribution to volume 9 of this series by *S. C. Pyke* and *M. W. Windsor* which has the title "Chemical Measurements in the Picosecond and Shorter Time Range". It gives an overview of selected investigations in the nanosecond range. After a rather informative section on experimental techniques, a short section dealing with work on reaction kinetics follows. The rest of the chapter is concerned with multi-photon processes. The choice of examples seems somewhat limited in view of the numerous investigations that have been carried out in this field.

The final chapter by *A. M. Ronn* on "Infrared Laser Photochemistry" may not be very long (46 pages), but it is very readable and offers a clear introduction to the problems of this topic. First the dependence of reaction velocity of bimolecular gas reactions on the selective excitation of molecular vibrational modes by single photons is dealt with. The rest contains a discussion of multi-photon dissociation by infrared photons, giving some typical examples.

Considering the high price of £ 42.50, the book will hardly find its place in a private library, because its contents will be outdated very soon.

*Alexander Müller* [NB 579 IE]

**Industrial Electrochemistry.** By *D. Pletcher.* Chapman & Hall, London 1982. xii, 325 pp., bound, £ 22.50.

Much progress has been made in industrial electrochemistry in the past twenty years. Classical processes such as the electrolysis of water and alkali metal chlorides have been revolutionized by new material technologies. Some entirely new fields have emerged such as fuel cells, the electrochemical synthesis of organic compounds, and the large-scale industrial use of electrodeposition of paint, while other fields, like storage batteries and the electrolytic production of aluminum have remained comparatively little changed. The aim of this book is to depict the present state of industrial electrochemistry, and this aim is well achieved. The author deals with all fields of applied electrochemistry, including some, such as batteries and electrochemical analysis, that would not be expected on the basis of the title. Basically only processes that are actually carried out in industry are discussed, to the exclusion of their historical development and projects now in progress. The literature cited mainly consists of monographs, and key patents are not given as such.

The book is divided into eleven chapters. The electrochemical and chemical process-engineering fundamentals are discussed at the beginning in an elegant and precise manner. The accurate definitions given for the material yield and current efficiency are useful, but the space-time yield is discussed only in general terms, although it is easy to derive a relationship for it.

The next chapters deal with electrolytic processes in inorganic chemistry, including those used for the extraction and purification of metals. In the case of the diaphragm process used in the electrolysis of alkali metal chlorides, the latest electrolyzers are described. It should have been mentioned here that the asbestos suspension is applied to the iron mesh cathodes by a vacuum process. The term "DSA expanded anode" in Table 3.3 does not only mean an expanded-metal structure, but also stretching after fitting to ensure a close contact with the diaphragm.

Organic electrochemical syntheses are still dominated by the Monsanto process. Its new variant, using undivided cells, which was first announced in 1981, is described in detail. In the table summarizing the minor processes, 2,5-dihydrofuran is mistakenly given as the educt in the anodic methoxylation of furan.

The book does justice to the great variety of electrochemical surface treatments practised nowadays, such as electroplating, anodizing, electrodeposition of paint, electroforming and electrochemical machining. Cathodic deposition of paint is now widely used not only in the USA but also in Europe. Equation 7.6 is misleading: according to *Gerischer,* the electrode reaction in cyanide-type silver baths takes place *via* low-coordinated complexes. Further chapters are devoted to anticorrosion measures and to the electrochemical purification of effluents.

This handsome book is richly illustrated, mainly from British sources. It gives a succinct account of the present state of industrial electrochemistry, including its peripheral applications. It is for this reason that it represents a valuable addition to the many existing books in which a more theoretical and fundamental approach has been adopted. A future edition should include production figures and the competing chemical processes. The book describes what there actually is and not what there once was or what might be one day, but then, that was precisely the author's aim.

*Fritz Beck* [NB 576 IE]

## Recent Books

**The following books have been received by the editor. All the publications listed are available through W & P Buchversand für Wissenschaft und Praxis, Boschstrasse 12, D-6940 Weinheim (Federal Republic of Germany). Tel. (06201) 606-0, Telex 465516 vchwh d, Telefax (06201) 602328.**

**Forschung in der Bundesrepublik Deutschland. Beispiele, Kritik, Vorschläge.** A *Deutsche Forschungsgemeinschaft publication.* Verlag Chemie, Weinheim 1983. xvi, 975 pp., bound, DM 92.00.—ISBN 3-527-27001-9

**Clinical Cellular Immunology. Molecular and Therapeutic Reviews.** Edited by *A. A. Luderer* and *H. H. Weetall.* Humana Press, Clifton, NJ 1982. xviii, 391 pp., bound, $ 59.50 (in USA $ 49.50).—ISBN 0-89603-011-3

**Advances in Heterocyclic Chemistry. Vol. 31.** Edited by *A. R. Katritzky.* Academic Press, New York 1982. ix, 350 pp., bound, $ 68.00.—ISBN 0-12-020631-5

**Chemistry and Physics of Carbon. Vol. 18.** Edited by *P. A. Thrower.* Marcel Dekker, Basel 1982. xii, 185 pp., bound, SFr. 135.00.—ISBN 0-8247-1740-6

**Electrical Properties of Polymers.** Edited by *D. A. Seanor.* Academic Press, New York 1982. xii, 379 pp., bound, $ 52.00.—ISBN 0-12-633680-6

**Atomspektrometrische Spurenanalytik. Lectures delivered at the Colloquium "Spurenanalytik mit Atomspektroskopie" in Konstanz (April 1981).** Edited by *B. Welz.* Verlag Chemie, Weinheim 1982. xvi, 564 pp., bound, DM 148.00.—ISBN 3-527-26027-7

**Chemistry and Biology of β-Lactam Antibiotics.** Edited by *R. B. Morin* and *M. Gorman.* Academic Press, New York 1982. Vol. 1: Penicillins and Cephalosporins. xxxix, 553 pp., bound, $ 73.00.—ISBN 0-12-506301-6; Vol. 2: Nontraditional β-Lactam Antibiotics. xiv, 408 pp., bound, $ 64.00.—ISBN 0-12-506302-4

**Chemie der Räucherung.** By *L. Tóth.* A Deutsche Forschungsgemeinschaft publication. Verlag Chemie, Weinheim 1982. xi, 331 pp., bound, DM 68.00.—ISBN 3-527-27501-0

**The Substance Abuse Problems.** By *Sidney Cohen.* The Haworth Press, New York 1981. xiii, 392 pp., Paperback, $ 19.95.—ISBN 0-917724-22-4

**Structure and Activity of Natural Peptides.** Edited by *W. Voelter* and *G. Weitzel.* Walter de Gruyter & Co., Berlin 1981. xii, 634 pp., bound, DM 150.00.—ISBN 3-11-008264-0

**Chemistry of Peptides and Proteins. Vol. 1: Proceedings of the Third USSR-FRG Symposium.** Edited by *W. Voelter, E. Wünsch, Y. Ovchinnikov,* and *V. Ivanov.* Walter de Gruyter & Co., Berlin 1982. xiii, 554 pp., bound, DM 196.00.—ISBN 3-11-008604-2

**Developments in Ionic Polymers—1.** Edited by *A. D. Wilson* and *H. J. Prosser.* Applied Science Publishers, Barking, Essex 1983. ix, 336 pp., bound, £ 34.00.—ISBN 0-85334-159-1

**Biophysics of Water.** Edited by *F. Franks* and *S. Mathias.* John Wiley & Sons, Chichester 1982. xxv, 400 pp., bound, £ 29.95.—ISBN 0-471-10229-6

**Ösophaguschirurgie. Achalasie, Strukturen, Benigne Tumoren, Divertikel, Perforationen.** Edited by *R. Häring.* edition medizin, Weinheim 1982. xxi, 338 pp., stitched, DM 78.00.—ISBN 3-527-15077-3

**Ultraschall-Atlas. Internistische Ultraschalldiagnostik mit schnellen B-Bild-Geräten.** By *H.* und *A. Weiss.* edition medizin, Weinheim 1983. xiv, 423 pp., bound, DM 112.00.—ISBN 3-527-15068-4

**Industrial Crystallization. The State of the Art.** 2nd newly revised edition. By *J. Nývtlt.* Verlag Chemie, Weinheim 1982. vi, 180 pp., bound, DM 62.00.—ISBN 3-527-26065-X

**Advances in Inorganic Chemistry and Radiochemistry. Vol. 25.** Edited by *H. J. Emeléus* and *A. G. Sharpe.* Academic Press, New York 1982. vii, 355 pp., bound, $ 56.00.—ISBN 0-12-023625-7

**Hochdisperse Metalle.** By *W. Romanowski* and *S. Engels.* Verlag Chemie, Weinheim 1982. 171 pp., bound, DM 65.00.—ISBN 3-527-25982-1

**Gaschromatographische Retentionsindices toxikologisch relevanter Verbindungen.** *Mitteilung I der Kommission für klinisch-toxikologische Analytik der Deutschen Forschungsgemeinschaft.* Verlag Chemie, Weinheim 1982. 48 pp., stitched, DM 20.00.—ISBN 3-527-27303-4

*Registered names, trademarks, etc. used in this journal, even without specific indication thereof, are not to be considered unprotected by law.*

© Verlag Chemie GmbH, D-6940 Weinheim, 1983. - Printed in the Federal Republic of Germany by Zechnersche Buchdruckerei, Speyer/Rhein.

All rights reserved (including those of translation into foreign languages). No part of this issue may be be reproduced in any form - by photoprint, microfilm, or any other means - nor transmitted or translated into a machine language without written permission from the publishers. Only single copies of contributions, or parts thereof, may be reproduced for personal use. Copies reproduced and used other than for private purposes in an industrial or commercial undertaking are subject to copyright and, in such cases, a copyright fee must be paid to the VG WORT, Abteilung Wissenschaft, Goethestr. 49, 8000 München 2, from whom conditions of payment can be obtained on request.

**Valid for users in the USA:** The appearance of the code at the bottom of the first page of an article in this journal (serial) indicates the copyright owner's consent that copies of the article may be made for personal or internal use, or for the personal or internal use of specific clients. This consent is given on the condition, however, that the copier pay the stated per-copy fee through the Copyright Clearance Center, Inc., for copying beyond that permitted by Sections 107 or 108 of the U.S. Copyright Law. This consent does not extend to other kinds of copying, such as copying for general distribution, for advertising or promotional purposes, for creating new collective works, or for resale. For copying from back volumes of this journal see 'Permissions to Photo-Copy: Publisher's Fee List' of the CCC.

**Editorial office:** Pappelallee 3, D-6940 Weinheim, Federal Republic of Germany, Telephone (06201) 602315, Telex 465516 vchwh d, Telefax (06201) 602328.

**Editors:** *P. Gölitz, I. G. Neil, O. Smrekar, A. Stimson.*

**Publishers:** Verlag Chemie GmbH. (Managing Directors: *Prof. Dr. Helmut Grünewald* and *Hans Dirk Köhler*), Pappelallee 3, D-6940 Weinheim, Federal Republic of Germany.

Correspondence concerning advertisements should be addressed to Verlag Chemie GmbH. (Advertising Manager *R. J. Roth*), Pappelallee 3. P.O. Box 1260/1280, D-6940 Weinheim, Federal Republic of Germany, Telephone Weinheim (06201) 602-0, Telex 465516 vchwh d, Telefax (06201) 602328.

ANGEWANDTE CHEMIE
International Edition in English
Volume 22 · Number 6
June 1983
Pages 423–506

# Phosphorothioate Analogues of Nucleotides—Tools for the Investigation of Biochemical Processes

By Fritz Eckstein*

Nucleoside phosphorothioates are analogues of nucleotides with a wide range of applications. Thus, on the one hand, in many but not all cases they are more stable against hydrolysis than the unmodified nucleotides—a property which they share with other nucleotide analogues. On the other hand, however, they are good substrates for many, but not all reactions where the nucleotide or the phosphorothioate group is transferred to an acceptor other than $H_2O$. As a consequence, once incorporated into a system such as DNA, phosphorothioates cannot be easily removed.

What makes these compounds unique to a certain extent is the chirality at the phosphorus center if two nonequivalent residues are linked to the phosphorothioate group. This opens the way for the use of these compounds to investigate stereochemical aspects of enzymatic reactions. In addition to these properties, there are those expected from exchange of an oxygen for a sulfur atom in a phosphate group, *e.g.* the increased affinity towards mercury derivatives and the large chemical shift of the $^{31}$P-NMR signals.

If one considers how many biologically interesting compounds contain phosphate groups, the considerable interest in these nucleotide analogues is not surprising.

## 1. Introduction[**]

Nucleoside phosphorothioates are analogues of nucleotides in which a non-bridging oxygen atom of a phosphate group is replaced by sulfur atom. For phosphate groups such as the α- and β-phosphate groups of ATP, which are linked to two non-identical residues, this exchange leads to chirality at phosphorus and thus to the existence of a pair of diastereomers. This property makes the phosphorothioate analogues of nucleotides, in particular those of ATP, interesting compounds for enzymatic phosphoryl and nucleotidyl transfer reactions, since they facilitate the determination of the stereochemical course of the reaction. This development has progressed rapidly in the past five years, as can be seen from the large number of review articles dealing with this subject[1–9]. This use of nucleoside phosphorothioates in bioorganic chemistry has been complemented by those in biochemistry and molecular biology, which are based mainly on the generally higher stability of phosphorothioates towards hydrolytic cleavage relative to the corresponding phosphates. These various developments will be discussed in this progress report.

[*] Prof. Dr. F. Eckstein
Max-Planck-Institut für Experimentelle Medizin, Abteilung Chemie
Hermann-Rein-Strasse 3, D-3400 Göttingen (Germany)

[**] Abbreviations: Ade = adenine; Gua = guanine; Cyt = cytosine; Thy = thymine; Ura = uracil. A = adenosine; G = guanosine; C = cytidine; U = uridine; T = thymidine; N = non-specified nucleoside; NMPS = nucleoside 5′-phosphorothioate; $NDP_\alpha S$ A and B = diastereomers of nucleoside 5′-*O*-(1-thiodiphosphates); $NTP_\alpha S$ A and B = diastereomers of nucleoside 5′-*O*-(1-thiotriphosphates); $NDP_\beta S$ = nucleoside 5′-*O*-(2-thiodiphosphate); $NTP_\gamma S$ = nucleoside 5′-*O*-(3-thiotriphosphate); cNMPS = nucleoside 3′,5′-cyclic phosphorothioate. The prefix d indicates that the corresponding 2′-deoxynucleoside derivative is involved. ATP = adenosine 5′-triphosphate; GTP = guanosine 5′-triphosphate; AMPPNP and GMPPNP = adenylyl and guanylyl imidophosphate; Up(S)A = 5′-*O*-adenosyl 3′-*O*-uridyl phosphorothioate; d[Tp(S)A] = 5′-*O*-(2′-deoxyadenosyl) 3′-*O*-thymidyl phosphorothioate; poly[d(A-T)] = alternating copolymer of dAMP and TMP; poly[d($A_S$T)] = alternating copolymer of dAMP and TMPS; NAD = nicotinamide adenine dinucleotide. The abbreviations apply to dinucleoside phosphorothioates and polymers which consist of other nucleotides. PEP = phosphoenol pyruvate; DEAE = diethylaminoethyl; HPLC = high performance liquid chromatography.

 © *Verlag Chemie GmbH, 6940 Weinheim, 1983* *0570-0833/83/0606-0423 $ 02.50/0* 

## 2. Synthesis and Structure

### 2.1. Nucleoside Di- and Triphosphates

Almost all phosphorothioate analogues of the various ribo- and deoxyribonucleoside 5'-mono-, -di-, and -triphosphates have been synthesized in the meantime (Fig. 1). Their syntheses are straightforward, although the yields

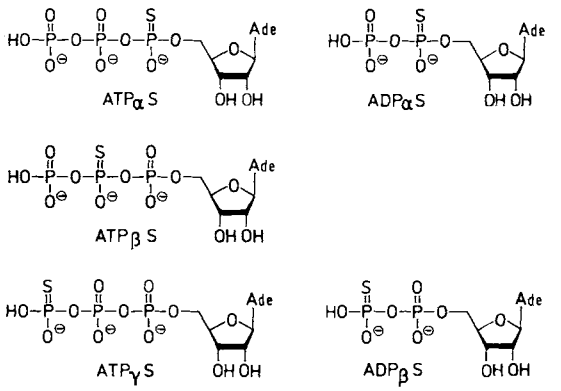



Fig. 1. Structural formulae of the phosphorothioates of ATP and ADP.

are not always satisfactory. For analogues with a terminal phosphorothioate group, such as (d)NTP$_\gamma$S and (d)NDP$_\beta$S, the simplest synthetic route is the activation of *S*-(β-cyanoethyl)phosphorothioate with diphenyl phosphorochloridate and reaction with (d)NDP or (d)NMP, followed by treatment with alkali to cleave the β-cyanoethyl group[10] (Fig. 2). Two routes are available for the synthesis of the

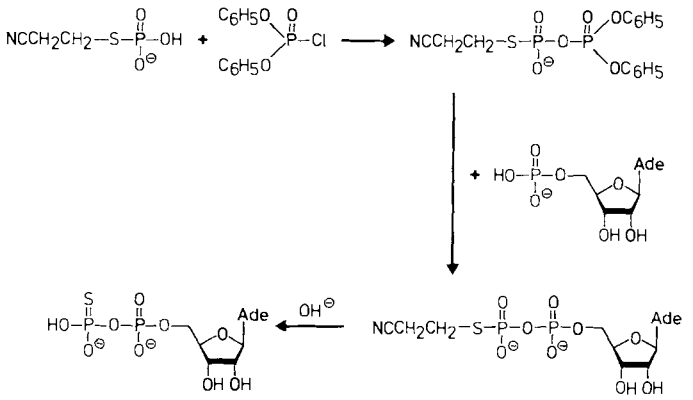



Fig. 2. Synthesis of ADP$_\beta$S. ATP$_\gamma$S is synthesized using ADP instead of AMP.

analogues of (d)NDP or (d)NTP having the phosphorothioate group in the α-position. In both methods the nucleoside is allowed to react with $PSCl_3$ to give (d)NMPS. Subsequent phosphorylation can be accomplished by activation with diphenyl phosphorochloridate and reaction with phosphoric acid or pyrophosphoric acid[11,12], a method which was introduced by *Michelson* for the synthesis of normal nucleoside di- and triphosphates[13] (Fig. 3).

It should be noted that in this reaction the oxygen of the phosphorothioate moiety is more nucleophilic than the sulfur atom. In contrast, on activation with carbonyl diimidazole or dicyclohexylcarbodiimide the sulfur becomes more nucleophilic and complete loss of sulfur is encoun-

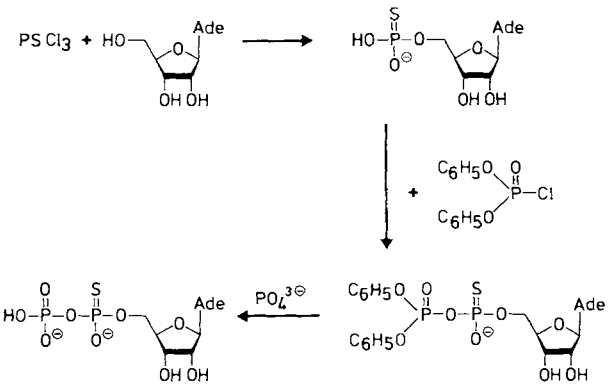



Fig. 3. Synthesis of ADP$_\alpha$S. ATP$_\alpha$S is synthesized using pyrophosphate instead of phosphate.

tered[11]. This synthesis produces both diastereomers of (d)NDP$_\alpha$S or (d)NTP$_\alpha$S in an approximate ratio of 1:1. They can be distinguished by $^{31}$P-NMR spectroscopy[14,15] or separated by HPLC[16,17]. Separation of the mixture of diastereomers can be achieved, at least in some cases, by chromatography on DEAE-Sephadex[16,18]. Where this is not possible, separation can be achieved by selective enzymatic phosphorylation of one of the diastereomers of (d)NDP$_\alpha$S to the corresponding (d)NTP$_\alpha$S by kinases[12,16]. Thus, pyruvate kinase[12], or better phosphoglycerate kinase[19], phosphorylate a diastereomeric mixture of ADP$_\alpha$S selectively to the A-isomer of ATP$_\alpha$S which, if necessary, can be freed of contaminating ATP$_\alpha$S B by reaction with acetyl CoA synthetase[20]. The residual B-isomer of ADP$_\alpha$S can be phosphorylated by creatine kinase to ATP$_\alpha$S B[12], which in turn can be freed of ATP$_\alpha$S A by reaction with hexokinase and glucose[21]. Combinations of enzymatic reactions have also been worked out for the synthesis of the diastereomers of GTP$_\alpha$S[16]. For the preparation of ATP$_\alpha$S A the enzymatic phosphorylation of AMPS with pyruvate kinase and adenylate kinase, which proceeds with very high stereospecificity[14,15], is considerably simpler but, unfortunately, is restricted to the synthesis of this compound (Fig. 4). Despite intensive efforts, no enzyme system has been found so far to synthesize ATP$_\alpha$S B preparatively from AMPS. The diastereomers of (d)NDP$_\alpha$S can be obtained from the diastereomers of (d)NTP$_\alpha$S by hydrolysis with myosin[12].

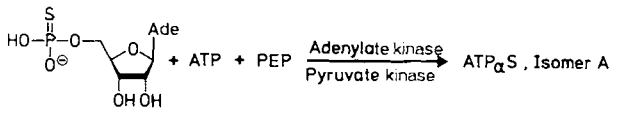



Fig. 4. Enzymatic synthesis of ATP$_\alpha$S A.

An alternative synthesis of dNDP$_\alpha$S, which is particularly attractive for organic chemists, is the condensation of dNMPS after activation with diphenyl phosphorochloridate with AMP protected at the sugar residue, as described for the synthesis of dTTP$_\alpha$S[22] and dCTP$_\alpha$S[23] (Fig. 5). The mixture of isomers resulting from this reaction can readily be separated on DEAE-Sephadex. After removal of the sugar protecting group, the adenosine is removed by oxidation with $NaIO_4$: the separated diastereomers of dNDP$_\alpha$S

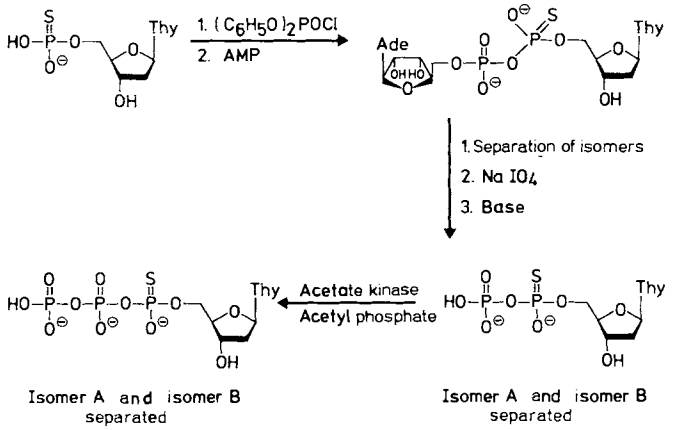



Fig. 5. Synthesis of the diastereomers of dTTP$_\alpha$S. To simplify matters the protecting group on AMP is not shown.

are obtained, which can then easily be phosphorylated enzymatically to the diastereomers of dNTP$_\alpha$S. This method was originally developed for the stereospecific syntheses of [$\alpha$-$^{18}$O]ADP$_\alpha$S, [$\beta$-$^{18}$O]ADP$_\beta$S, and [$\gamma$-$^{18}$O]ATP$_\gamma$S[24,25]. Recently it has also been extended to the preparation of the diastereomers of the phosphorothioate analogue of NAD, in which the phosphorothioate group is localized at the 5'-position of adenosine[26] (Fig. 6).

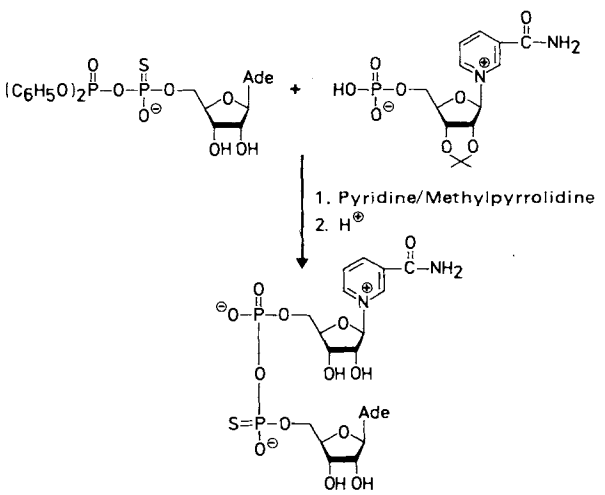



Fig. 6. Synthesis of a phosphorothioate analogue of NAD.

The assignment of the absolute configuration to the A and B diastereomers of ATP$_\alpha$S was accomplished by comparison of their different substrate properties with snake venom phosphodiesterase. Only the B-diastereomer is cleaved by this enzyme[27,28]. Of the isomers of Up(S)A also only one is cleaved, and this forms the *endo*-isomer of uridine 2',3'-cyclophosphorothioate on reaction with RNase A. Since this is the product of transesterification of a substrate with the ($R_p$)-configuration[29,30], the reactive isomer of Up(S)A must also have the ($R_p$)-configuration. It follows that also ATP$_\alpha$S B must have this configuration (Figs. 7, 8). This assignment has been confirmed by a stereospecific synthesis of [$\alpha$-$^{18}$O]ADP$_\alpha$S[31].

The diastereomers of (d)NTP$_\beta$S are prepared by enzymatic phosphorylation of (d)NDP$_\beta$S[12]. On phosphorylating ADP$_\beta$S with pyruvate kinase, the main product is

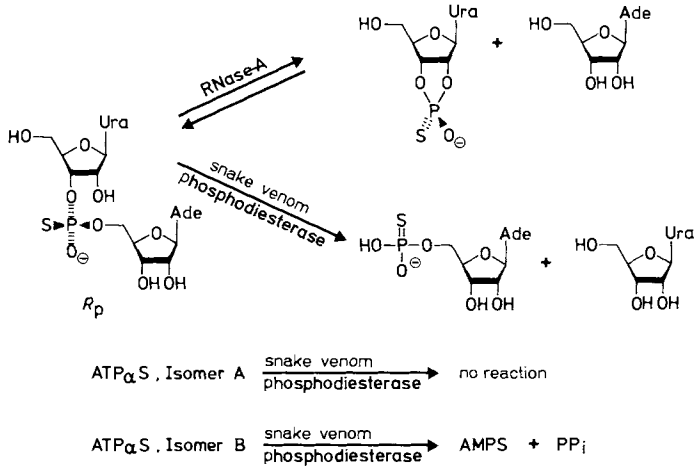



Fig. 7. Enzymatic reactions of Up(S)A and ATP$_\alpha$S for the determination of the absolute configuration of the diastereomers of ATP$_\alpha$S.

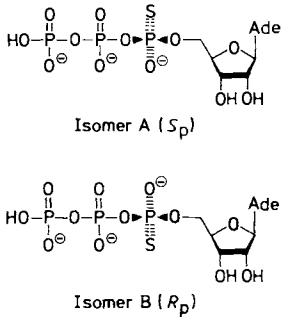



Fig. 8. Absolute configuration of the diastereomers of ATP$_\alpha$S.

ATP$_\beta$S A. The B-isomer can be removed by incubation with hexokinase and glucose[21,32a]. Diastereomerically pure A-isomer can be prepared by phosphorylation with phosphoglycerate kinase[32]. Acetate kinase produces predominantly ATP$_\beta$S B, which can be freed from traces of the A-isomer by reaction with myosin[21] (Fig. 9). The diastereomers can be distinguished by their $^{31}$P-NMR spectra[14,15]. A similar sequence of enzyme reactions has also been worked out for the diastereomers of GTP$_\beta$S[16].

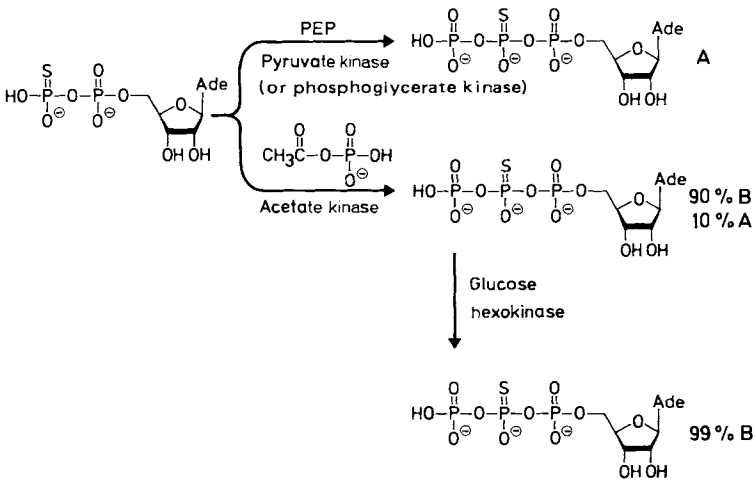



Fig. 9. Enzymatic synthesis of the diastereomers of ATP$_\beta$S.

The configuration of the diastereomers of $ATP_{\beta}S$ is based on comparison of their substrate properties with hexokinase; in the presence of $Mg^{2+}$ only the B-isomer is a substrate[32]. Also, only one of the diastereomers of β,γ-$Co(NH_3)_4ATP$ functions as a substrate[33]. Its configuration was determined as β,γ-Λ by X-ray structural analysis of $Co(NH_3)_4$-triphosphate, which was obtained by removal of the adenosine residue[34]. Since it was assumed that all substrates of a particular enzyme must have the same configuration, $MgATP_{\beta}S$ B also was assigned the Λ-configuration, which corresponds to the ($S_p$)-configuration (Fig. 10). This assignment has been independently confirmed[24].

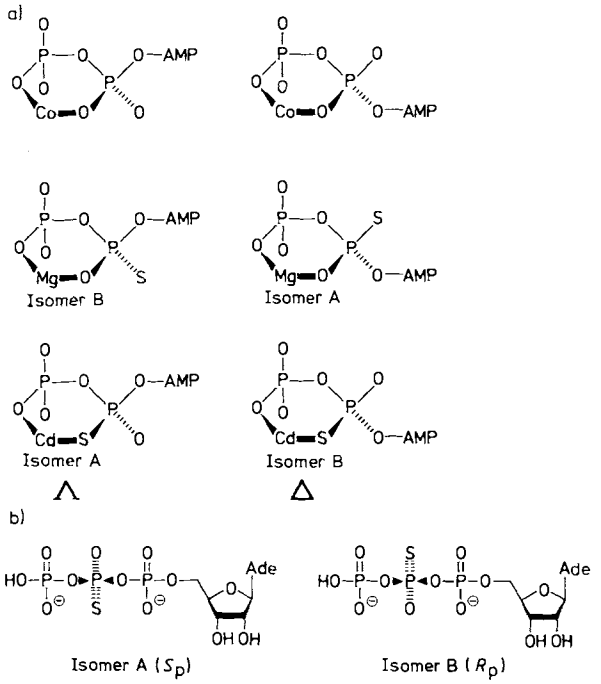



Fig. 10. a) Determination of the absolute configuration of the diastereomers of $ATP_{\beta}S$ by comparison of the substrate properties with those of the diastereomers of $Co(NH_3)_4ATP$ with hexokinase. The isomers in the left half (Λ-configuration) are the substrates. b) Absolute configuration.

## 2.2. Nucleoside 3',5'-Cyclic Phosphorothioates

For enzymatic investigations also the phosphorothioate analogues of nucleoside 3',5'-cyclic phosphates, particularly those of cAMP and cGMP, are of interest. The diastereomers of cAMPS were obtained by conversion of benzoylated cAMP into the anilidate and separation of the diastereomers by preparative thin layer chromatography; reaction with $K/CS_2$ under retention of configuration then leads to the isomers of cAMPS[35]. This has also been extended to the synthesis of the diastereomers of cGMPS[36], cCMPS, and cUMPS[37] (Fig. 11). The configurations were assigned from the $^{31}$P-NMR spectra of the anilidates[35].

A straightforward synthesis of the diastereomers of cAMPS is provided by the cyclization of adenosine 5'-bis(*p*-nitrophenyl)phosphorothioate by potassium *tert*-butoxide[38]. After work-up and chromatographic separation on DEAE-Sephadex, the ($S_p$)-isomer of cAMPS crystallizes out. The assignment of configuration was made using the results of *Stec et al.*[35]. The non-crystalline ($R_p$)-isomer

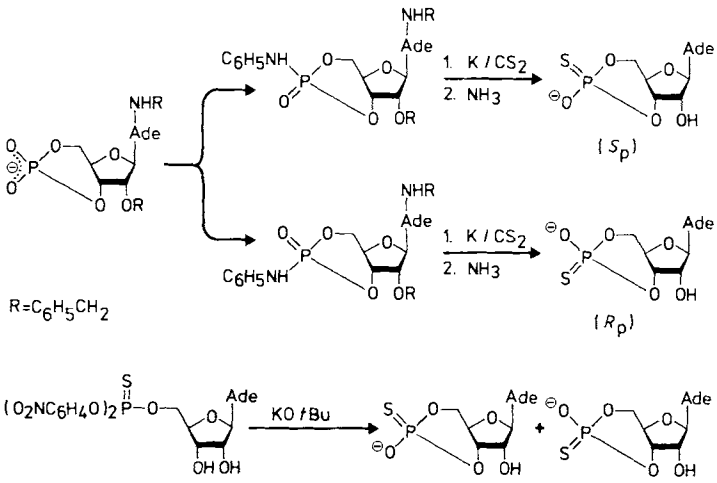



Fig. 11. Synthesis of the diastereomers of cAMPS.

is also obtained but in considerably lower yield. The diastereomers of cUMPS and cCMPS can also be obtained in this way, and the ($S_p$)-isomer of cUMPS is also obtained in crystalline form[23]. cGMPS can be prepared more straightforwardly, albeit in very low yield, by activation of GMPS with diphenyl phosphorochloridate and subsequent cyclization[39].

## 2.3. Dinucleoside Phosphorothioates

The chemical synthesis of the diastereomers of dinucleoside phosphorothioates has, particularly recently, attracted attention for determining the configuration of enzymatically prepared phosphorothioate internucleotidic linkages in polydeoxynucleotides. The first successful separation of such diastereomers was accomplished with a diribonucleoside phosphorothioate, Up(S)A. This was prepared by the triester method using β-cyanoethyl phosphorothioate to thiophosphorylate the 3'-OH group of appropriately protected uridine using triisopropylbenzenesulfonyl chloride as condensing agent in the first step; condensation with the 5'-OH group of appropriately protected adenosine followed in the second step[40]. After removal of the uridine 5'-OH protecting group, the diastereomers could be separated by chromatography on silica gel, and after removal of the β-cyanoethyl group by treatment with triethylamine/$H_2O$ (β-elimination) the diastereomers of Up(S)A were obtained. The configurational assignment was carried out by reaction with RNase A to afford uridine 2',3'-cyclic phosphorothioate (see Section 2.1)[27]. The diastereomers can be distinguished by $^{31}$P-NMR spectroscopy as well as by HPLC. Using this synthetic route *ca.* 20% of the normal dinucleoside phosphate, in this case UpA, is also formed by direct nucleophilic attack at the phosphorus center: this, however, can easily be separated chromatographically. The diastereomers of Tp(S)T[22,41], d[Tp(S)A][42], d[Cp(S)G], and d[Gp(S)C][43] have also been synthesized by this triester method (Fig. 12a), but could only be separated by HPLC after removal of all the protecting groups.

From the experience accumulated so far, it seems that, because of the better yields obtained, the phosphite method is better suited for the synthesis of these compounds. The first synthesis with this method using di-

chloro(phenoxy)phosphane has been described for Up(S)A[44], but the diastereomers could not be separated. Dichloro(methoxy)phosphane has been used successfully for the synthesis of Ap(S)A, and in this case the diastereomers were separated chromatographically[45]. In the meantime, also the diastereomers of Tp(S)T[46], d[Gp(S)A][47], d[Cp(S)T] and d[Gp(S)T][23] have been synthesized by this method using chloro(dimethylamino)methoxyphosphane (Fig. 12b). The configuration was assigned in all cases by hydrolysis with snake venom phosphodiesterase, which only cleaves the ($R_p$)-diastereomer[26], or with nuclease P1, which only cleaves the ($S_p$)-diastereomer[41]. The second method is preferred because the hydrolysis produces considerably cleaner products.

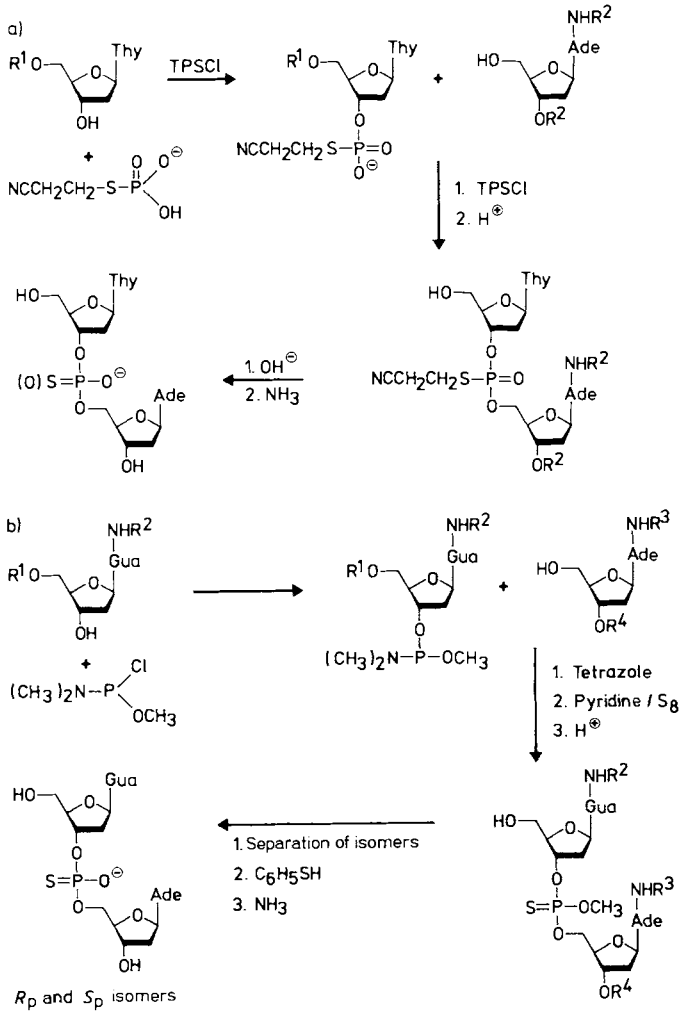



Fig. 12. Synthesis of dinucleoside phosphorothioates examplified by d[Tp(S)A]. a) Triester method. b) Phosphite method.—$R^1$ = dimethoxytrityl; $R^2$ = isobutyryl; $R^3$ = benzoyl; $R^4$ = methoxyacetyl; TPSCl = triisopropylbenzenesulfonyl chloride.

In the meantime sufficient $^{31}$P-NMR and HPLC data are available to postulate that the diastereomer having the larger down-field chemical shift in the $^{31}$P-NMR spectrum and the shorter retention time on reversed phase HPLC columns has the ($R_p$)-configuration.

### 2.4. Exchange of Sulfur by Oxygen Atoms

The diastereomers of the various nucleoside phosphorothioates can be stereospecifically labeled with $^{17}$O or $^{18}$O by reaction with bromocyanogen[48], *N*-bromosuccinimide[49], or bromine[50] in the presence of $H_2{}^{17}O$ or $H_2{}^{18}O$ (Fig. 13). With nucleoside 3′,5′-cyclic phosphorothioates,

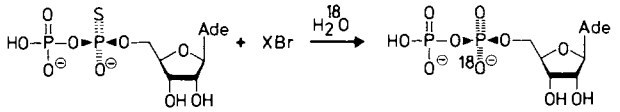



Fig. 13. Exchange of sulfur by oxygen in nucleoside phosphorothioates. X = CN, Br, or succinimide.

such as cAMPS and cTMPS, the two last-mentioned reactions proceed with approximately 80% inversion at phosphorus[49,50,39], but no data are yet available for the reaction of this system with bromocyanogen. When this reaction was performed using *N*-bromosuccinimide and Tp(S)T, the only dinucleoside phosphorothioate with which it has been carried out so far, it proceeded stereospecifically with inversion of configuration at phosphorus[41]. The stereoselectivity of the exchange of sulfur by oxygen in the diastereomers of $ADP_\alpha S$—all three exchange reactions have been performed—cannot easily be determined with sufficient accuracy. It has been determined for the $Co(NH_3)_4$[α-$^{18}$O]ADP complex by $^{31}$P-NMR spectroscopy, where probably up to 10% of the other diastereomer cannot be detected because of poor signal resolution[48,49], or by $^{31}$P-NMR spectroscopy of the diastereomeric methyl esters of [$^{16}$O,$^{17}$O,$^{18}$O]cAMP, obtained by enzymatic hydrolysis of [α-$^{18}$O]ADP in $H_2{}^{17}O$ to give [$^{16}$O,$^{17}$O,$^{18}$O]AMP, followed by cyclization and methylation. Here also the determination of the diastereomeric purity is unsatisfactory[50]. Despite these limitations it was found that all three reactions proceed with inversion of configuration.

A more precise determination, however, has recently become available, and this uses the reaction of $GDP_\alpha S$ A with *N*-bromosuccinimide, since the resulting [α-$^{18}$O]GDP could be used after phosphorylation to [α-$^{18}$O]GTP as substrate for guanylate cyclase. The [$^{18}$O]cGMP obtained in this way consisted of only one isotopomer, as determined with high accuracy by $^{31}$P-NMR spectroscopy of the methyl esters (see Section 3.1, Fig. 18). This result allows it to be concluded that the exchange reaction with $GDP_\alpha S$ as well as the enzymatic cyclization proceed stereospecifically, at least within the limits of detection of this method[39]. This probably also implies that the *N*-bromosuccinimide reaction will proceed similarly with other $NDP_\alpha S$. A more detailed investigation has revealed that the pH value probably plays an important role in all three exchange reactions. Under reaction conditions where the solutions are buffered at pH 7—8, the oxygen is not only introduced at the α-, but also at the β-phosphate group if the β-phosphate group is not protected by a cyanoethyl group. It has been proposed that this "scrambling" involves the formation of intramolecular *cyclo*-diphosphate[51]. When this reaction is performed using $ATP_\alpha S$, oxygen is introduced in all three reactions into the α- as well as the γ-position *via* intermediate formation of a six-membered ring follow-

ing nucleophilic attack of the γ-phosphate on the α-phosphate group[48,49,50]. For this reason in the preparation of [α-$^{18}$O]NTP the corresponding NDP$_\alpha$S is allowed to react with $H_2{}^{18}O$ to afford [α-$^{18}$O]NDP, which is then phosphorylated by a kinase to yield [α-$^{18}$O]NTP.

This method of exchange is also of interest for the stereospecific introduction of $^{17}$O. $^{17}$O-Labeled nucleotides prepared in this way have been used for EPR[52] and $^{17}$O-NMR spectroscopic studies[53,54,55] to determine the structure and configuration of nucleotide metal complexes.

## 3. Application to the Solution of Mechanistic Problems of Enzymatic Reactions

### 3.1. Investigation of the Stereochemical Course of Enzyme Reactions

One of the main applications of nucleoside phosphorothioates is the investigation of the stereochemical course of enzymatic phosphoryl and nucleotidyl transfer reactions[1-9]. Up to now, approximately 40 enzymes have been investigated using the phosphorothioate method (Table 1). The results have been discussed in detail in numerous review articles[5-9], so that only the results of more recent investigations mainly of DNA polymerases will be discussed here. The basic idea of such studies is that information on the stereochemical course of enzymatic transfer reactions should allow distinction to be made between a one-step and a two-step substitution reaction in which a covalent enzyme intermediate occurs. In the first case inversion, and in the second case retention of configuration at the phosphorus atom should be observed.

The stereochemical course of the reactions catalyzed by *E. coli*-DNA-dependent DNA polymerase I (Kornberg enzyme)[55,56,57] as well as by *E. coli*-DNA-dependent RNA polymerase[27] were described relatively early. More recently, other polymerases, such as phage T4 and T7 DNA polymerases[42,58], have been investigated and a rather simple method developed for the determination of the stereochemical course of the reactions catalyzed by these enzymes. Polymerization of TTP and dATP$_\alpha$S, of which so far only the ($S_p$)-isomer has been found to be a substrate on poly[d(A-T)] as template-primer, produces a polymer which contains alternating phosphate and phosphorothioate groups: poly[d(T$_s$A)].

This polymer can be degraded by the 5′→3′ nuclease activity of the Kornberg enzyme, which hydrolyzes only phosphate diesters but not phosphorothioate diesters[55-57] to d[pTp(S)A]. Hydrolysis with alkaline phosphatase produces d[Tp(S)A], whose configuration can be determined by comparison with that of chemically synthesized diastereomers ($^{31}$P-NMR spectroscopy or HPLC) (Fig. 14). Investigations with the enzyme reverse transcriptase have shown that the determination of configuration can also be carried out on the polymers by $^{31}$P-NMR spectroscopy, as long as the chain-lengths are not too long and that they give a sharp signal[22]. All these polymerase-catalyzed reactions proceed by inversion of configuration at phosphorus.

Table 1. Stereochemical course of enzymatic phosphoryl and nucleotidyl transfer reactions.

| Enzyme | Stereochemical Course | Ref. |
|---|---|---|
| A) *Investigations with $^{16}$O-Phosphorothioates* | | |
| Ribonuclease A transesterification step | Inversion | [29, 30] |
| Ribonuclease T$_1$ | Inversion | [180] |
| Ribonuclease T$_2$ | Inversion | [40] |
| *Enterobacter aerogenes* Phosphohydrolase | Inversion | [181] |
| *E.coli* DNA-dependent RNA Polymerase | | |
| Initiation | Inversion | [21] |
| Elongation | Inversion | [27] |
| DNA-dependent DNA Polymerases | | |
| *E. coli* I | Inversion | [56, 57] |
| Phage T4 | Inversion | [42] |
| Phage T7 | Inversion | [58] |
| *M. luteus* | Inversion | [43] |
| Reverse transcriptase | Inversion | [22] |
| Polynucleotide phosphorylase | | |
| Exchange | Retention | [182] |
| Elongation | Inversion | [99] |
| tRNA nucleotidyl transferase | Inversion | [183] |
| RNA ligase, ligation step | Inversion | [184] |
| UDP glucose pyrophosphorylase | Inversion | [185] |
| Galactose-1-phosphate-uridyl transferase | Retention | [185] |
| Adenylate Cyclase | | |
| Bacterial | Inversion | [186] |
| Mammalian | Inversion | [187] |
| B) *Investigations with $^{16}$O,$^{18}$O-Phosphorothioates* | | |
| Ribonuclease A, hydrolytic step | Inversion | [71] |
| Nucleoside diphosphate kinase | Retention | [185] |
| Acetyl CoA synthetase | Inversion | [20, 188] |
| Adenylate kinase | Inversion | [185] |
| Adenosine kinase | Inversion | [189] |
| Nucleoside phosphotransferase | Retention | [190] |
| Nuclease S1 | Inversion | [61] |
| C) *Investigations with $^{16}$O,$^{17}$O,$^{18}$O-Phosphorothioate* | | |
| Myosin ATPase | Inversion | [191] |
| Mitochondrial ATPase | Inversion | [192] |
| ATPase from sarcoplasmatic reticulum | Retention | [193] |
| Elongation factor G GTPase | Inversion | [194] |
| Elongation factor T GTPase | Inversion | [195] |
| Phosphoglycerate kinase | Inversion | [62, 196] |
| Snake venom 5′-nucleotidase | Inversion | [62] |
| Thermophilic bacterium PS3 ATPase | Inversion | [197] |
| D) *Investigations with the phosphorothioate and oxygen isotope method* | | |
| Hexokinase | Inversion | [198, 199, 201] |
| Glycerol kinase | Inversion | [199, 200] |
| Pyruvate kinase | Inversion | [64, 198, 199] |
| Polynucleotide kinase | Inversion | [202, 203] |
| Cyclic phosphodiesterase | Inversion | [204-207] |
| Guanylate cyclase | Inversion | [39] |
| Snake venom phosphodiesterase | Retention | [28, 208-210] |
| Aminoacyl-tRNA synthetases | Inversion | [211, 212] |
| E) *Investigations with the oxygen isotope method* | | |
| Alkaline phosphatase | Retention | [213] |
| Acetate kinase | Inversion | [199] |
| Creatine kinase | Inversion | [214] |
| Staphylococcal nuclease | Inversion | [72] |
| Spleen phosphodiesterase | Retention | [66] |
| Phosphoglycerate mutase | Retention | [215] |
| Nuclease P1 | Inversion | [41] |

The stereochemical course of the reaction catalyzed by a DNA polymerase 3′→5′ exonuclease has also been determined for the phage T4 enzyme by comparison of the configuration of the product [$^{18}$O]dAMPS with that of the substrate [α-$^{18}$O]dATP$_\alpha$S. This was carried out by enzymatic

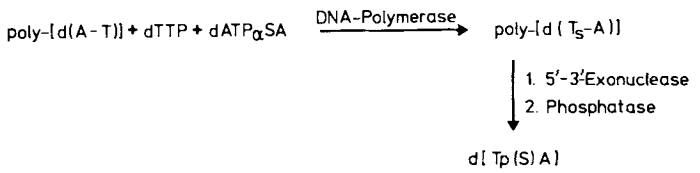



Fig. 14. Determination of the stereochemical course of a reaction catalyzed by a DNA polymerase. The product d[Tp(S)A] is compared by HPLC or NMR spectroscopy with diastereomers synthesized chemically. In all cases the configuration thus determined is $R_p$.

phosphorylation of [$^{18}$O]dAMPS with pyruvate kinase and adenylate kinase to give [α-$^{18}$O]dATP$_\alpha$S having an ($S_p$)-configuration[56]. $^{31}$P-NMR spectroscopy can be used to determine whether the $^{18}$O is localized only at $P_\alpha$ or whether it bridges $P_\alpha$ and $P_\beta$[59,60] (Fig. 15). $^{18}$O was found exclusively at $P_\alpha$ in the product [α-$^{18}$O]dATP$_\alpha$S. This indicates retention of configuration which, since the polymerization reaction proceeds with inversion of configuration, implies inversion of configuration also for the exonuclease reaction[18]. This method of analysis has wide applications and was also used *inter alia* for the determination of the stereochemical course of reactions involving nuclease S1 using the ($S_p$)-isomer of d[Tp(S)A][61].

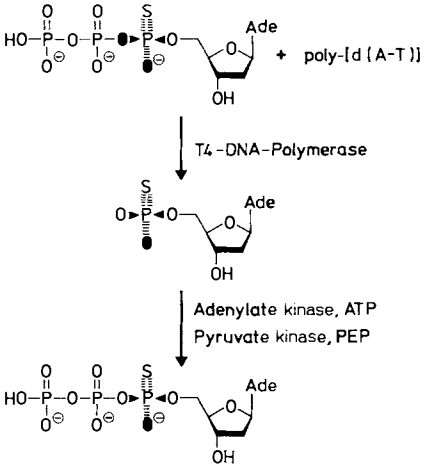



Fig. 15. Determination of the stereochemical course of the reaction catalyzed by the 3'→5' exonuclease of phage T4 DNA polymerase. The configuration of [α-$^{18}$O]dATP$_\alpha$S is analyzed by $^{31}$P-NMR spectroscopy. ● = $^{18}$O.

An elegant application of the phosphorothioates is the investigation of the stereochemical course of ATPase reactions where [γ-$^{18}$O]ATP$_\gamma$S is used in the presence of $H_2{}^{17}O$[9]. The determination of the configuration of the chiral $^{16,17,18}$O-thiophosphate produced in these reactions is carried out by enzymatic incorporation into ATP$_\beta$S, whose configuration can be determined by $^{31}$P-NMR spectroscopy taking advantage of the fact that the quadrupole moment of $^{17}$O broadens the $^{31}$P signals so much that they practically disappear. Thus, the analysis is narrowed down to determining whether $^{18}$O is localized at $P_\beta$ or whether a $P_\gamma$-$^{18}$O-$P_\beta$ bridge is involved[9,62] (Fig. 16). An elegant and impressive analysis!

Of course the question arises with all these stereochemical investigations employing nucleoside phosphorothioates whether the stereochemical course of an enzymatic reaction is different with these analogues than with the normal substrates. This can be clarified by allowing the enzyme to react both with the nucleoside phosphorothioates and with the natural substrate. For investigations involving the natural substrate, the phosphate group to be transferred clearly has to be chiral. This can be achieved by stereospecific incorporation of $^{17}$O and $^{18}$O. *Knowles et al.*[4,63], *Lowe et al.*[64], and *Gerlt et al.*[65] have developed methods for the synthesis of the substrates as well as for the analysis of the products, but this will not be discussed here in detail. One method for the synthesis of such substrates by stereospecific exchange of sulfur by $^{18}$O or $^{17}$O has been discussed in Section 2.4.

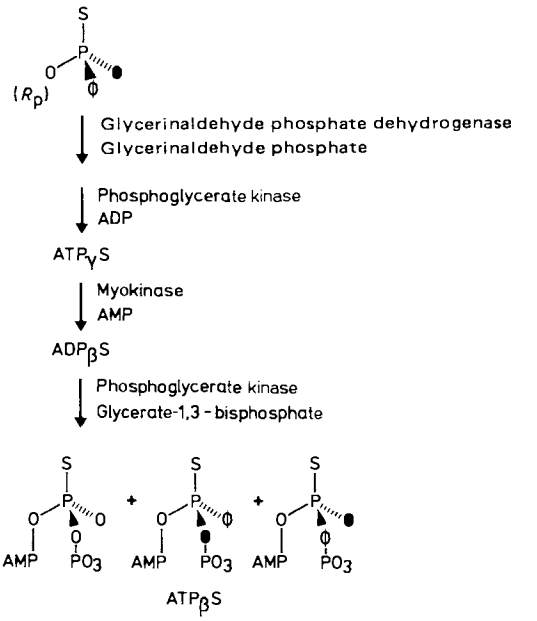



Fig. 16. Determination of the configuration of the ($R_p$)-enantiomer of [$^{16}$O,$^{17}$O,$^{18}$O]thiophosphate. The end product [β-$^{16}$O,$^{17}$O,$^{18}$O]ATP$_\beta$S is analyzed by $^{31}$P-NMR spectroscopy. O = $^{16}$O; Ø = $^{17}$O; ● = $^{18}$O.

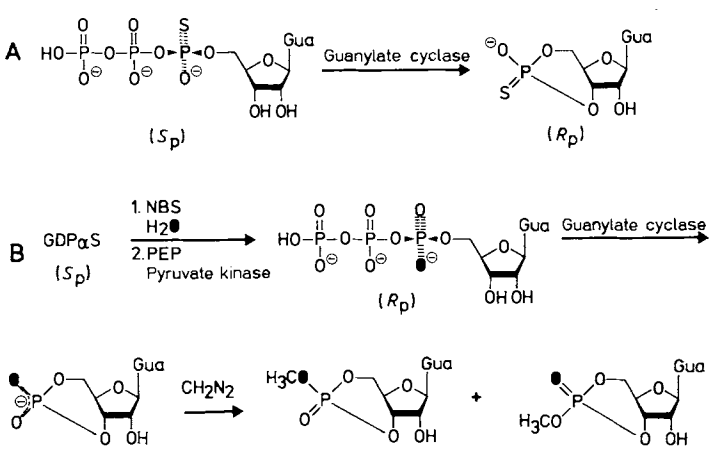



Fig. 17. Determination of the stereochemical course of the reaction catalyzed by guanylate cyclase. ● = $^{18}$O.

For the six enzymes which have been studied by both methods (see also Table 1), and for which guanylate cyclase is described as an example in Figure 17, no difference in the stereochemical course of the reaction could be

detected. This justifies using the results of investigations of the stereochemical course of reactions with phosphorothioates to extrapolate to those of the normal substrates. Phosphorothioates are easier to manipulate than those involving $^{18}O$-compounds because the product analysis is simpler and smaller amounts of material are required. Complications can arise from the slower reaction rates often encountered, particularly when secondary reactions can occur at the substrate or the product, *e.g.* desulfurization has been observed in the reactions with snake venom phosphodiesterase or nuclease S1[27,61]. Up till now there is, however, only one enzyme, spleen phosphodiesterase, where the phosphorothioate method failed; here because of the slow rate of hydrolysis, a transphosphorylation prevails[66].

Of the *ca.* 50 enzymes studied with respect to the stereochemical course of the reactions catalyzed by them, *ca.* 40 show inversion and 10 retention of configuration at the phosphorus atom (Table 1). The simplest interpretation of these results is that 4/5 of the enzyme reactions proceed by a single-step mechanism. This simple interpretation is complicated by the fact that inversion is the result only of substitution reactions at phosphorus in which the incoming nucleophile as well as the leaving group occupy apical positions in the trigonal bipyramidal transition state or intermediate (in-line mechanism). If the incoming group occupies an apical but the leaving group an equatorial position, pseudorotation must occur for the reaction to proceed, and this results in retention of configuration (adjacent mechanism)[67,68] (Fig. 18). Accordingly, retention of configuration does not necessarily have to be the result of two substitution reactions each of which proceeds with inversion. For half of the enzymes which show retention a covalent enzyme intermediate can be detected or is at least plausible, and hence with these enzymes retention of configuration can be interpreted as the result of two subsequent substitution reactions, each proceeding with inversion.

For the other half, a covalent enzyme intermediate has either not yet been found or has not even been sought, so that the possibility still exists that retention is the result of

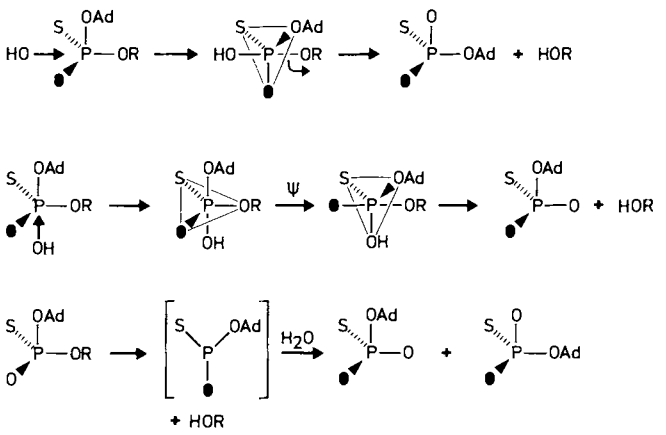


Fig. 18. Stereochemical consequences of substitution reactions at phosphorus in phosphates. Ad = adenosine; ● = $^{18}O$.—Top: in-line mechanism results in inversion of configuration. Middle: adjacent mechanism requires pseudorotation (ψ) and results in retention of configuration. Bottom: elimination-addition mechanism *via* metaphosphate should result in racemization, at least in non-enzymatic reactions.

a single substitution step involving pseudorotation. However, it is considered probable that also for these enzymes the reaction proceeds by a two-step mechanism. Even more complicated interpretations can be considered. Thus, any odd number of substitution reactions of the in-line type leads to inversion, and hence this does not necessarily have to be the result of only one such reaction. In addition, inversion could also be explained by a two-step mechanism the first reaction of which proceeds with inversion but the second with retention, or *vice versa*. However, as long as the simplest interpretations suffice there is no compelling reason to complicate the arguments. For a specific discussion of the importance of the elimination-addition mechanism in enzyme reactions the article by *Knowles*[4] should be consulted.

So far only two X-ray structure analyses of nucleotidyl transfer enzymes, RNase A and staphylococcal nuclease, exist where the structures of the active sites can be described with sufficient precision to enable a mechanism to be delineated[69,70]. The stereochemical analysis of the reactions of both enzymes reveals that inversion of configuration occurs[29,30,71,72], which is in full agreement with the structural analysis (for a detailed discussion of Staphylococcal nuclease see [72]).

### 3.2. Structure of the Mg-ATP Complex in Enzymatic Reactions

Phosphorothioate analogues, particularly those of ATP, have proved to be suitable for the description of the structure of the Mg-ATP complex involved in enzymatic phosphoryl and nucleotidyl transfer reactions[2,3,5,73]. They are therefore useful additions to the exchange-inert $Cr^{III}$- and $Co^{III}$-ATP complexes[74,75]. Phosphorothioate analogues are often considerably better substrates, whereas the $Cr^{III}$ and $Co^{III}$ complexes are more suitable for unambiguous determination of coordination of the metal to the γ-phosphate group.

The use of the phosphorothioate analogues of ATP for studies of this type rests on the observation that in the presence of $Mg^{2+}$ the B-isomer of $ATP_{\beta}S$, and in the presence of $Cd^{2+}$ the A-isomer is the preferred substrate for hexokinase[32]. As already discussed in connection with the configurational assignment of the diastereomers of $ATP_{\beta}S$ (Section 2.1), also only the β,γ-Λ-configuration of the diastereomer of the $Co(NH_3)_4ATP$-complex is a substrate[33]. This result served as the basis for the determination of the configuration of Mg-$ATP_{\beta}S$ B and $CdATP_{\beta}S$ A as β,γ-Λ[32] (Fig. 10a). The different behavior of the diastereomers as substrates in the presence of $Mg^{2+}$ and $Cd^{2+}$ is explained by the preferential coordination of $Mg^{2+}$ to oxygen and of $Cd^{2+}$ to sulfur; this can also be observed by NMR spectroscopy[32]. Other cations such as $Co^{2+}$, $Zn^{2+}$, and $Mn^{2+}$ do not show this preference so strongly; consequently both diastereomers of $ATP_{\beta}S$ are substrates. These results indicate that the cations have to be coordinated to the phosphorothioate group during the enzymatic reaction. If the metal ion were to dissociate and to be replaced, for example, by a positively charged group of the active site of the enzyme, this reversal could not be explained since it is not

Table 2. Structure of the metal-ATP complex at the active site of enzymes as analyzed by the phosphorothioate method.

| Enzyme | $P_\alpha$-Specificity [a] | $P_\beta$-Specificity [a] | Structure of the β,γ-metal-ATP complex [b] | Ref. |
|---|---|---|---|---|
| *E. coli*-DNA polymerase I | $S_p$(Mg–Zn) | $S_p$(Mg)–$R_p$(Zn) | Δ | [56] |
| *E. coli*-DNA-dependent RNA-polymerase | $S_p$(Mg–Cd) | $S_p$(Mg)–$R_p$(Cd) | Δ | [78] |
| Hexokinase, yeast | $S_p$(Mg–Cd) | $R_p$(Mg)–$S_p$(Cd) | Λ | [80] |
| Hexokinase, mammalian | $S_p$(Mg–Cd) | $R_p$(Mg)–$S_p$(Cd) | Λ | [216] |
| Glucokinase | $S_p$(Mg–Cd) | $R_p$(Mg)–$S_p$(Cd) | Λ | [216] |
| Creatine kinase | $R_p$(Mg)–$S_p$(Cd) | $R_p$(Mg)–$S_p$(Cd) | Λ | [76] |
| Arginine kinase | $R_p$(Mg)–$S_p$(Cd) | $R_p$(Mg)–$S_p$(Cd) | Λ | [77] |
| Acetate kinase | $S_p$,$R_p$(Mg,Cd) | $R_p$(Mg)–$S_p$(Cd) | Λ | [217] |
| Adenylate kinase, yeast | $S_p$,$R_p$(Mg,Cd) | $S_p$(Mg)–$R_p$(Cd) | Δ | [82] |
| Myosin | $S_p$,$R_p$(Mg,Cd) | $S_p$(Mg)–$R_p$(Cd) | Δ | [79] |
| Phosphoglycerate kinase | $S_p$(Mg)–$R_p$(Zn) | $S_p$(Mg–Zn) | — | [19] |
| Phe-tRNA synthetase | $S_p$(Mg–Co) | $R_p$(Mg)–$S_p$(Cd) | Λ | [218] |
| Met-tRNA synthetase | $S_p$(Mg) | $S_p$(Mg)–$R_p$(Zn) | Δ | [219] |
| Pyridoxal kinase | $S_p$,$R_p$(Mg,Cd) | $S_p$(Mg)–$R_p$(Cd) | Δ | [129] |
| Protein kinase | — | $S_p$(Mg)–$R_p$(Cd) | Δ | [220] |
| Thermophilic bacterium PS3 ATPase | $S_p$(Mg–Cd) | $S_p$(Mg)–$R_p$(Cd) | Δ | [197] |
| Carbamate kinase | $S_p$,$R_p$(Mg) | $R_p$(Mg,Cd) | — | [221] |
| Glutamine synthetase | $R_p$(Mg)–$S_p$,$R_p$(Co) | $R_p$(Mg)–$S_p$,$R_p$(Co) | Λ | [221] |
| Carbamoylphosphate synthetase | $R_p$(Mg)–$S_p$(Cd) | $S_p$(Mg)–$R_p$(Cd) | — | [221, 222] |
| Phosphoribosylpyrophosphate synthetase | $S_p$(Mg)–$S_p$,$R_p$(Cd) | — | — | [223] |

[a] $S_p$(Mg–Cd) indicates that the enzyme retains the preference for the $S_p$-diastereomer (isomer A) for $ATP_\alpha S$ or $ATP_\beta S$, irrespective of whether $Mg^{2+}$ or $Cd^{2+}$ are used as activating cations; $R_p$(Mg)–$S_p$(Cd) indicates that the enzyme prefers the $R_p$-diastereomer in the presence of $Mg^{2+}$ but the $S_p$-diastereomer in the presence of $Cd^{2+}$ (or $Zn^{2+}$). [b] Δ and Λ indicate the screw sense of the β,γ-metal-ATP complex [33].

clear why this group should in one case bind preferentially to oxygen and in the other to sulfur.

With all the enzyme reactions investigated with the diastereomers of $ATP_\alpha S$ and $ATP_\beta S$ it is always found—with one exception[19]—that reversal of stereoselectivity at the β-phosphate occurs and—with two exceptions[76,77]—that this never occurs at the α-phosphate (Table 2). Therefore, it can be assumed for the β-phosphate that the metal ion is bonded at the β-position, and for the α-phosphate that no coordination of the metal ion to the α-position occurs. This second statement is ambiguous since it is quite conceivable that the geometry of the active site could exert certain constraints on formation of the metal complex, forcing, *e.g.*, an otherwise unfavorable Mg→S coordination upon it. This and similar assumptions must also be made to explain those situations in which the stereoselectivity is very pronounced for one metal ion but not for the other, as, for example, with RNA polymerase[78] where the ratio of activities for $ATP_\beta S$ A/B in the presence of $Mg^{2+}$ is 1.11 and for $Cd^{2+}$ 0.003. A similar situation exists for myosin, where the corresponding values are 3000 and 1.3[79].

A description of the metal-ATP complex on the basis of the results obtained in this way is not entirely straightforward. It can, however, be assumed that the metal ion is bound at some stage of the enzymatic reaction, presumably during the rate determining step, to that phosphorothioate at which reversal of stereoselectivity is observed. Observation of reversal of stereoselectivity only at the β-phosphate usually leads to proposal of a bidentate β,γ-Mg-ATP complex; for thermodynamic reasons a β-monodentate complex is considerably less stable than a six-membered cyclic β,γ-complex. But such a complex cannot be detected with phosphorothioate analogues. This interpretation, however, is consistent with the results obtained from the exchange-inert $Cr^{III}$- and $Co^{III}$-ATP complexes, in as much as comparisons of hexokinase[33,80], creatine kinase[76,81], arginine

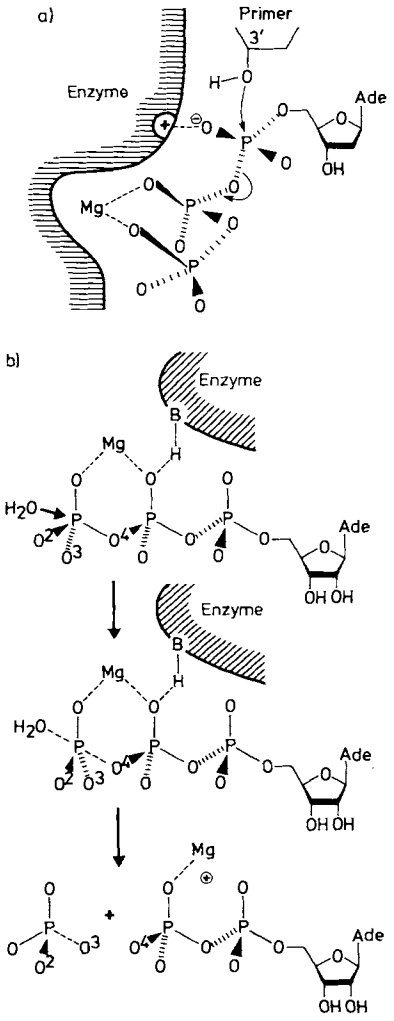



Fig. 19. Structure of the Mg-ATP complex at the active site of a) *E. coli* DNA-dependent DNA polymerase I and b) myosin.—The coordination of the metal to the β-phosphate group of ADP was determined by EPR measurements on [β-$^{17}$O]ADP [84].

kinase[77,81], and adenylate kinase[77,82] are possible. Difficulties arise in the interpretation of the results for creatine and arginine kinase, where reversal is observed at the α- as well as at the β-phosphate of ATP. This could be explained either by the presence of a bidentate α,β- or a β,γ-MgATP complex giving rise to an α,β-ADP complex as product. The solution to the problem seems to be a tridentate α,β,γ-Mg-ATP complex, as deduced from EPR measurements of the [α,β$^{17}$O]ADP-Mn-nitrate-creatine-enzyme complex[52,83]. Such a complex clearly is consistent with a β,γ-ATP structure for the substrate and a α,β-ADP structure for the product. How the results obtained for phosphoglycerate kinase (reversal at α- but not at β-phosphate) can be explained is not yet clear[19].

As seen in Table 2 there is no clear-cut preference for a particular configuration of the metal·ATP complex by these enzymes. It should be mentioned, however, that all DNA and RNA polymerases studied so far accept exclusively the ($S_p$)-isomer as substrate, irrespective of the cation present.

Figure 19 shows the results obtained using the phosphorothioate method to investigate the stereochemical course of the reaction, as well as the structure of the MgATP substrate complex for myosin[79] and DNA polymerase[56]; this shows what a detailed picture of the arrangement of the substrate in the active site can be gained by such studies. Of course, they allow no conclusions to be drawn on the participation and function of functional groups of the protein; this remains the realm of X-ray structure analysis.

## 4. Application to the Solution of Biochemical Problems

### 4.1. Incorporation of Phosphorothioate Groups into DNA

Phosphorothioate groups can easily be incorporated into DNA by enzymatic polymerization of dNTP$_\alpha$S[85]. Of all the DNA polymerases studied so far, *E. coli*-DNA polymerase I[56,57], phage T4 and T7 DNA polymerases[42,58], *M. luteus*-DNA polymerase[43,87], and reverse transcriptase[22] use only the ($S_p$)-isomer of dNTP$_\alpha$S as substrate, and inversion of configuration at phosphorus is always observed. Mammalian DNA polymerase β also polymerizes dNTP$_\alpha$S, although the stereospecificity has not yet been determined[86]. This also applies to *E. coli* cells treated with ether[85]. All systems have in common that the phosphorothioate analogue is incorporated with polymerization rates similar to those of normal triphosphates.

DNA modified by phosphorothioate groups differs in some respects from natural DNA. It was found rather early[85] that double stranded circular ΦX174 or fd DNA in which only the (−)strand had been modified by incorporation of dAMPS instead of dAMP had the same sedimentation coefficient as natural DNA, but that the buoyant density in neutral CsCl was *ca.* 0.4% larger: this might arise from the higher atomic weight of sulfur compared to oxygen. This DNA is infectious and has a $T_m$ value 1-2° below that of unmodified DNA. Lower $T_m$ values have also been observed recently for phosphorothioate analogues of other polymers, such as poly[d(G$_s$C)] ($\Delta T_m$ −2 °C)[43], but also poly[d(A$_s$T)] ($\Delta T_m$ −15 °C) and poly[d(T$_s$A)] ($\Delta T_m$ −5 °C)[87,88]. The reason for this is not clear. The CD spectra, at least of the analogues of poly[d(G-C)], are identical with that of the unmodified polymer[43]. It has not yet been investigated how well DNA modified in this way can serve as a template for DNA-dependent RNA and DNA polymerases. The phosphorothioate groups influence the transition of the polynucleotides from the B to the Z conformation at different rates. Thus, the transition of poly[d(G$_s$C)] is considerably facili-

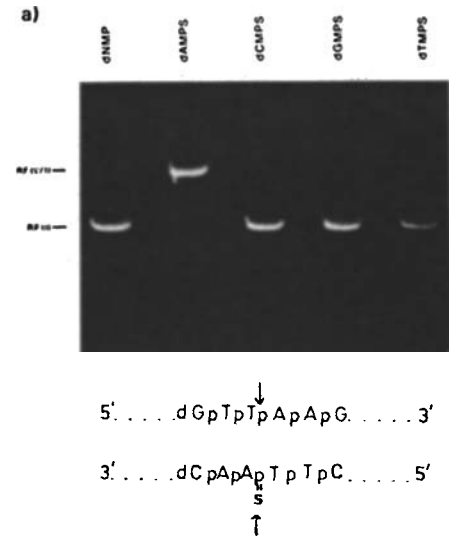



Fig. 20. Inhibition of reactions catalyzed by restriction endonucleases by incorporation of phosphorothioate groups at the site of cleavage. a) Reaction with *Hind*II. b) Reaction with *Hpa*II.—The enzyme *Hind*II cuts fd DNA once to linearize the circular DNA. The enzyme *Hpa*II cuts eight times to yield 8 fragments of different length. The letters A to H describe these fragments. RF IV is circular, covalently closed double-stranded DNA; RF III is double-stranded linear DNA; RF II is circular double-stranded DNA with at least one cut in one of the strands. The fragments were analyzed by gel electrophoresis and stained with ethidium bromide[90].

tated compared to poly[d(G-C)], but practically does not occur with poly[d($C_s$G)].

The transition can be followed by UV, CD, laser-Raman, and $^{31}$P-NMR spectroscopy. Also, poly[d($G_s$C)] is, in contrast to poly[d($C_s$G)], very antigenic and the antibodies produced are specific for Z-DNA. An explanation of this different influence of the phosphorothioate groups is not yet clear[43]. These results indicate a role of the phosphate groups in this conformational change which had previously not been considered, and it is to be hoped that the DNA-analogues will provide deeper insight into the process. The $^{31}$P-NMR spectra of the partially thiophosphorylated polymers poly[d($T_s$A)], poly[d($A_s$T)], poly[d($C_s$G)], and poly[d($G_s$C)] enable assignment of the $^{31}$P-NMR signals in the unmodified polymers to be made, since the signals of the phosphorothioate groups are strongly shifted to lower field[43, 87].

Besides these differences between natural and thiophosphorylated DNA, others are observed in interactions with enzymes. As already mentioned, the phosphorothioate internucleotidic linkage is resistent to the 5′→3′ nuclease of polymerase I (see Section 3.1). This increased stability to nucleases seems to be a rather general phenomenon. Thus, these modified internucleotidic linkages are also not degraded by exonuclease III. This has been used to stabilize 5′-ends of one strand of double-stranded DNA against degradation[89].

Also all restriction enzymes investigated so far hydrolyze phosphorothioate internucleotide linkages more slowly than phosphate linkages. This could be shown for fd DNA molecules where only the (−)strand but not the (+)strand, which had been used as a template for polymerization, was modified[90]. By replacing one deoxynucleoside triphosphate by the corresponding phosphorothioate in the polymerization, four samples were prepared in each of which the 5′-phosphate group of another nucleotide was modified. A comparison of the degradation of these four DNAs by six restriction enzymes shows that, in general, only a modification exactly at the cleavage site, but not in other positions within the recognition sequence, slow down the hydrolysis considerably (Fig. 20). This observation, which has not yet been treated quantitatively, suggests that phosphorothioates might be used to stabilize DNA against degradation by restriction enzymes.

The 3′→5′ nuclease activity of viral and bacterial DNA polymerases is responsible for the excission of non-complementary base pairs during polymerization and is therefore responsible, wholly or partly, for the fidelity of replication in these systems[91] (Fig. 21). If the phosphorothioates were either not or only more slowly degraded by this nuclease, an increase in the error rate in replication would be expected, and an estimation of the contribution of the 3′→5′-nuclease to fidelity should be possible. For the determination of fidelity of replication amber-mutants of circular single-stranded viral DNA which upon incorporation of non-complementary bases during replication, *i.e.* incorrect incorporation, revert to the wild type are particularly well suited (Fig. 22). Even a few revertants can be determined accurately in a large population because each viable virus in a bacterial culture betrays itself by formation of a plaque after being spread on agar film. The number of non-reverted mutants can be estimated in a separate experiment by suppression of the mutation by addition of suppressor tRNA.

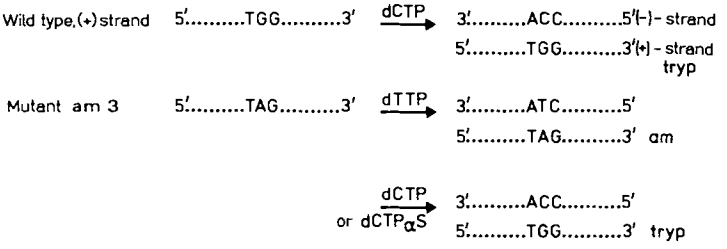



Fig. 22. ΦX174-mutant am3. The positions 586—588 are shown. In the mutant, G is replaced by A. This triplet codes for the amino acid tryptophan (tryp) in the wild-type; in the mutant it is a non-sense codon (cf. also text).

The fidelity of replication of the (+)strand of Φ174 am3 was investigated in such a system in the presence of dCTP$_\alpha$S instead of dCTP[86]. It was found that with *E. coli*-DNA polymerase I the error rate increased by a factor of 20, and with phage T4 DNA polymerase by a factor of 500.

Use of a DNA polymerase which does not possess a 3′→5′ nuclease activity for the polymerization did not influence the error rate. These results show that these nuclease activities play a role in determining the fidelity of replication. They also open the way for target-directed mutagenesis by incorporation of nucleoside phosphorothioates at particular positions, such as at restriction nuclease cleavage sites[92].

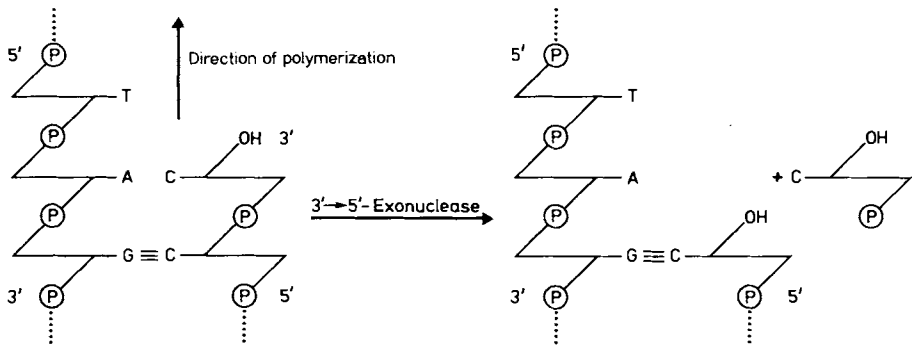



Fig. 21. Schematic representation of the function of the 3′→5′ exonuclease activity of DNA polymerases in preventing incorporation of non-complementary nucleotides.

Because of the impermeability of cell membranes the incorporation of phosphorothioate into the DNA of intact cells *via* deoxynucleoside thiotriphosphates is not possible. However, cells can be made permeable by treatment with ether or toluene[85]. This barrier can also be overcome by the use of thiophosphate. It could be shown with HeLa cells that thiophosphate can be incorporated into nucleotides such as $ATP_\gamma S$ and $GTP_\gamma S$ and subsequently be transferred to other acceptor molecules, *e.g.* histones[93]. In cell cultures of African green monkey cells infected with SV40 it was observed that $ATP_\gamma S$ can also thiophosphorylate thymidine and phosphorothioate, and can thus, after further phosphorylation in the cells to $dTTP_\alpha S$, be incorporated into DNA[94]. Although in these experiments only 3—12 phosphorothioate groups were incorporated into the viral DNA (5226 base pairs), this seemed to have been sufficient to isolate it on Hg-Sepharose!

### 4.2. RNA and DNA Molecules with Terminal Phosphorothioate Groups

Phosphorothioate can also be incorporated into RNA using the corresponding polymerases and $NTP_\alpha S$. So far this seems to have been carried out only for poly-[r(A-U)][78,95,96], the 3′-end of tRNA[97,98], and poly rA[99]. A series of investigations, however, report incorporation of phosphorothioate groups using $ATP_\gamma S$ and $GTP_\gamma S$ into the 5′-end of various RNAs in *Physarum polycephalum* and in isolated nuclei of yeast, mouse myeloma, and *Xenopus'* oocytes, as well as separation of this newly synthesized RNA from endogenous RNA by chromatography on Hg-Sepharose[100-106]. Using various $NTP_\gamma S$ this technique also allows the determination of the nucleotide at the 5′-end of the RNA and makes it possible to determine which promoter starts the RNA synthesis.

Problems can arise from enzymatic transfer of the phosphorothioate group to preexisting RNA molecules, since this gives a wrong picture of the supposedly newly synthesized RNA[107,108]. *Stallcup et al.* had the idea of using

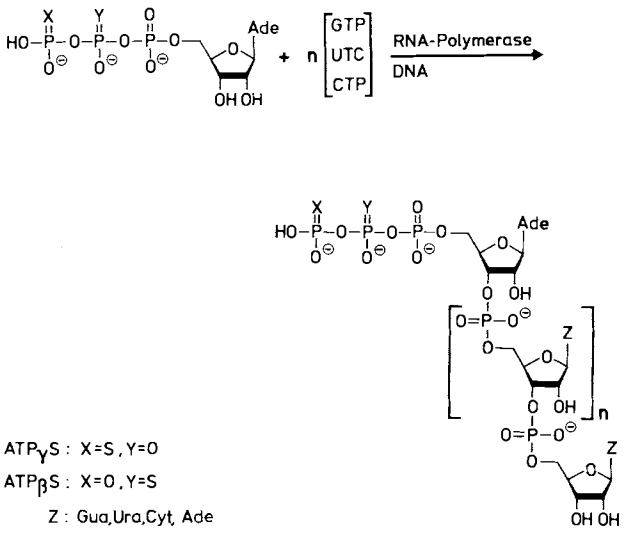



Fig. 23. Incorporation of phosphorothioate groups into the 5′-end of RNA with $ATP_\gamma S$ or $ATP_\beta S$.

$NTP_\beta S$ instead of $NTP_\gamma S$ in the polymerization (Fig. 23) to avoid this transfer[109,110]: these compounds also are good substrates for RNA polymerases[78]. The RNA molecules obtained in this way can also be separated on Hg columns and the transfer of phosphate to other RNA molecules does not interfere, since they are not retained on Hg-Sepharose.

This route is not applicable for the incorporation of terminal phosphorothioate groups into DNA, because DNA polymerases are unable to initiate new chains but can only polymerize onto a 3′-end of an existing polynucleotide. However, the phosphorothioate group of $ATP_\gamma S$ may be transferred to the 5′-end of DNA by polynucleotide kinase[111] (Fig. 24), but this reaction is considerably slower than that with ATP.

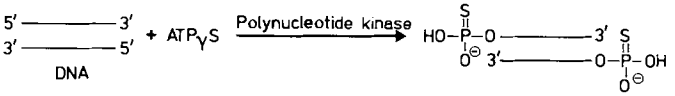



Fig. 24. Incorporation of 5′-phosphorothioate groups into DNA.

### 4.3. Thiophosphorylation of Proteins

Phosphorylation and dephosphorylation of proteins seem to be two of the most frequently used reactions in nature for the regulation of enzyme activity[112,113]. They are catalyzed by protein kinases and phosphatases. Particularly with complex systems it is often difficult to isolate and study proteins in the fully phosphorylated state. Since phosphorothioate esters, such as AMPS, are hydrolyzed extremely slowly by phosphatases it was obvious to examine whether thiophosphorylated proteins are also stable towards phosphatases. This requires that protein kinases accept $ATP_\gamma S$ as a substrate. The first system to be investigated in this connection was glycogen phosphorylase, which is activated by phosphorylation. It turned out that the phosphorothioate residue was transferred by the kinase and that glycogen phosphorylase was activated. The phosphatase could not remove this residue any further so that the phosphorylase was frozen-in in the activated state[114]. This principally demonstrated the applicability of phosphorothioate groups for the study of such problems.

The role played by phosphorylation of the myosin light-chains in smooth muscle for the activation of the enzyme, and thus for the contraction of muscle, was also explained in this way. Muscle contraction is triggered in this system by $Ca^{2+}$ ions, but it was not clear whether this was due to direct interaction between $Ca^{2+}$ and myosin, as in molluscs[115], or whether $Ca^{2+}$ activates a protein kinase, which catalyzes the phosphorylation of the myosin light-chains, and that phosphorylation is the direct trigger of contraction. That the latter is the case could be shown by thiophosphorylation (also on muscle fibers), since the competing dephosphorylation activity which normally complicates such investigations could be suppressed[116-119]. The role of phosphorylation of myosin in skeletal muscle fibers was also investigated in this way[120]. In further studies thiophosphorylation of the myosin light-chains was used for the purification of the phosphatase by affinity

chromatography[121]. Also in cases where phosphorylation of a protein leads to inactivation, such as with pyruvate dehydrogenase, thiophosphorylation can be used for the elucidation of the significance of this step[122]. In addition, for elucidating the significance of the phosphorylation of the receptor and other membrane proteins by the epidermal growth factor thiophosphorylation appears to be interesting because of its increased metabolic stability[123]. Thiophosphorylation may possibly also be of help for studies of phosphorylation of the insulin receptor[124,125] or of the $Ca^{2+}$ transport system in cholinergic synaptic vesicles[126].

Histones are also thiophosphorylated by $ATP_\gamma S$ in the presence of protein kinase. This reaction was not only demonstrated *in vitro*[127], but also (see Section 4.1) *in vivo* with HeLa cells: the $^{35}S$-thiophosphate was first incorporated into $ATP_\gamma S$ and $GTP_\gamma S$ and then transferred to the protein[101]. Thiophosphorylated proteins of this type can be isolated on Hg-Sepharose. This method should be of use for the isolation of other proteins which are normally phosphorylated in the cell. Microtubuli-associated proteins are also thiophosphorylated by $ATP_\gamma S$[128].

Except for the inefficient system of SV40 infected cells there are no known examples for the enzymatic thiophosphorylation of nucleosides and sugars. However, it is reasonably certain that apart from the hitherto described kinases others will also accept $ATP_\gamma S$ as substrate, as the recently published example of pyridoxal kinase demonstrates[129] (Fig. 25).

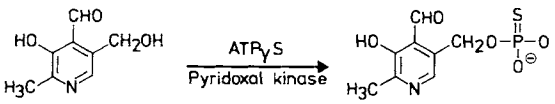



Fig. 25. Enzymatic synthesis of pyridoxal phosphorothioate.

### 4.4. Stabilization of Nucleotide-Protein Complexes with $ATP_\gamma S$ and $GTP_\gamma S$

In coupled reactions in which ATP or GTP are cleaved the question arises how far the reaction would proceed without cleavage of ATP simply by formation of a ATP-enzyme complex, or in other words for which step of the reaction ATP cleavage is necessary. Hydrolytically stable analogues of ATP and GTP should provide the answer to this question. The imido analogues AMPPNP and GMPPNP have been widely used for this purpose[130]. More recently, however, the phosphorothioate analogues $ATP_\gamma S$ and $GTP_\gamma S$ have also been used for studies of such systems.

The first ATPase to be investigated with $ATP_\gamma S$ was myosin[2]. In the kinetic analysis this ATP analogue helped to unambiguously identify the conformational change of the protein on binding of the substrate. This was possible because the actual hydrolysis step for the analogue is considerably slower than that of ATP, so that changes in the fluorescence spectrum of the protein on binding the substrate can be distinguished unambiguously[131,132].

The use of $ATP_\gamma S$ to study reactions catalyzed by recA protein has also turned out to be extremely profitable. This protein is essential for genetic recombination in *E. coli:* in the presence of ATP it catalyzes the *in vitro* hybridization of single-stranded regions with homologous regions in double stranded DNA to form so-called D-loops, which migrate along the DNA until a complete strand exchange takes place (branch migration) (Fig. 26). In addition, in the

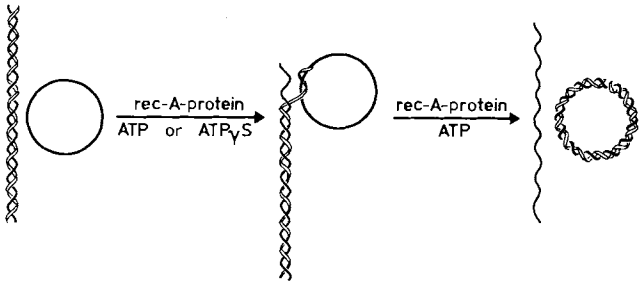



Fig. 26. Function of recA protein as a function of ATP or $ATP_\gamma S$ (cf. also text).

presence of DNA and ATP this protein cleaves various repressors such as λ, lexA, and P22[133,134]. For both reactions it is of interest to know, whether, and if so, for which step ATP hydrolysis is necessary. This question was investigated with $ATP_\gamma S$, since it is resistant to hydrolysis by recA protein. According to these studies the formation of the D-loop does not require ATP hydrolysis but branch migration does[135–138]. The D-loop is so stable in the presence of $ATP_\gamma S$ and recA protein that the complex can be investigated by electron microscopy, which has revealed that in this complex the DNA is unwound, a result[139–141] which had been presumed earlier[142]. The protease activity of recA protein against repressors cannot be observed in the presence of $ATP_\gamma S$, which leads to the conclusion that hydrolysis of ATP is not essential for this activity[143–147].

*E. coli* DNA polymerase III is also not able to cleave $ATP_\gamma S$. With this enzyme cleavage of ATP might be necessary for the formation of a DNA-enzyme complex. In the presence of $ATP_\gamma S$, which cannot be cleaved by this enzyme, the complex dissociates, leading to inhibition of polymerization[148,149]. This suggests that hydrolysis of ATP is necessary for translocation of the enzyme at the replication fork from one primer to the next.

When aminoacylated tRNA binds to the Tu-factor of ribosomes programmed by mRNA another nucleoside triphosphate, in this case GTP, is hydrolyzed. The accuracy of the anticodon-codon recognition determines the accuracy of protein biosynthesis. Comparison of the rate of hydrolysis of GTP with that of $GTP_\gamma S$ indicates that the latter is cleaved *ca.* 2500 times more slowly[150]. A consequence of this is that the complex consisting of $GTP_\gamma S$, Tu-factor, ribosome, and tRNA has a considerably longer lifetime than the corresponding complex with GTP. This leads to a decrease in error rate during translation. Apparently in protein biosynthesis nature puts more emphasis on speed rather than accuracy, at least in this step.

The difference of *ca.* 2500 in the rates of hydrolysis of GTP and $GTP_\gamma S$ in this system is similar to that observed in myosin for ATP and $ATP_\gamma S$ (*ca.* 1000)[131]. Clearly two examples are not sufficient to formulate a rule, but it is interesting to speculate whether this difference might not correspond to the difference in reactivity of γ-phosphate

and γ-phosphorothioate groups towards nucleophilic attack. Detailed fast-kinetic measurements on other ATPases and GTPases are needed to clarify this point. In the non-enzymatic hydrolysis of trialkyl phosphates and trialkyl phosphorothioates a difference of 100 had been found[151].

A GTP binding protein, which consists of two subunits and shows GTPase activity, is also involved in the activation of the hormone-regulated adenylate cyclase[152]. Since GMPPNP and particularly $GTP_\gamma S$ exhibit a practically irreversible and considerably higher activation of the cyclase than GPT this suggests that this effect arises from resistance to the GTPase[153,154]. This idea is inconsistent with a more recent interpretation which suggests that this protein does not show any GTPase activity, and that activation by $GTP_\gamma S$ and GMPPNP is the result of dissociation of the subunits[155]. Since adenylate cyclase is a membrane-bound enzyme, studies of it are often carried out on complex biological systems which are not highly purified. Also, because of their stability, the analogues GMPPNP and $GTP_\gamma S$ are of value here, since there is a possibility that the normal nucleotide GTP is rapidly degraded in this system, and hence its effect cannot be determined accurately. This also applies to GDP, which is assumed not to activate the cyclase but rather to inhibit it by competition with GTP. GDP can readily be degraded to GMP or phosphorylated to GTP so that difficulties arise in unambiguously identifying its effect. A rather stable analogue is $GDP_\beta S$, which is neither degraded by phosphatases nor phosphorylated by kinases. Indeed it could be shown that it inhibits the cyclase[156–160].

The activation of the cyclase by hormone resembles the photo-activation of cyclic phosphodiesterase in the process of vision. In both systems a GTP binding protein transmits the signal from an excited receptor to an enzyme which regulates the cellular concentration of a cyclic nucleotide, cAMP in one and cGMP in the other case. The GTP binding protein involved in the process of vision also shows GTPase activity which puts the enzyme into the non-stimulated stage similar to the protein G/F in the cyclase system. The GTPase activity of both proteins is irreversibly activated by ADP-ribosylation by cholera toxin[161]. Not only GMPPNP but also $GTP_\gamma S$ has been employed in this system as a non-hydrolyzable analogue of GTP, as has $GDP_\beta S$ as an analogue of GDP[161–165]. It is to be expected that these analogues and cGMPS (Section 2.2)[36,39] will be of use for further investigations of this interesting system.

### 4.5. Interaction of cAMPS with Proteins

Also cAMPS differs from cAMP by its greater metabolic stability[38]. Since the last review of the properties of cAMPS[2], the separation of the diastereomers has been achieved (Section 2.2). This made it possible to analyze the products of a previous synthesis of cAMPS[38]. It turns out that the crystalline product obtained in this synthesis is the $(S_p)$-isomer. The $(R_p)$-isomer, which is produced in small amounts, can be separated by chromatography on DEAE-Sephadex. Since all the studies reported in [2] have been carried out with the crystalline isomer, all the results refer to the $(S_p)$-isomer.

Investigations of this type have been extended to other systems and in some cases the different effects of the $(S_p)$- and the $(R_p)$-isomer have been studied, particularly with protein kinases. It was found for protein kinase I that the $(S_p)$-isomer binds better than the $(R_p)$-isomer, but for protein kinase II this trend is reversed[166–168]. The catabolite-activator protein (CAP) also binds the $(S_p)$-isomer[169] and is activated by it, although not as strongly as by cAMP[170]. As described previously[2], cAMPS has been used for studies of chemotaxis in *Dictyostelium discoideum*[171]. Its greater metabolic stability compared to cAMP, its ability to penetrate cells[2,172], and its structural similarity to cAMP should make cAMPS particularly suitable for investigations of the effect of cAMP, and might, under certain circumstances, have advantages over currently used analogues. The availability of the $(S_p)$-isomer commercially will support this development.

### 4.6. Phosphorothioate Analogues of Phospholipids

A new field of application for phosphorothioate analogues is currently being opened up by incorporating phosphorothioate groups into phospholipids. Thus, the two diastereomers of 1,2-dipalmitoyl-*sn*-glycero-3-thiophosphoryl choline (Fig. 27) have been synthesized[173–177]. They can be distinguished by $^{31}P$-NMR; however, their absolute configuration has not yet been determined.

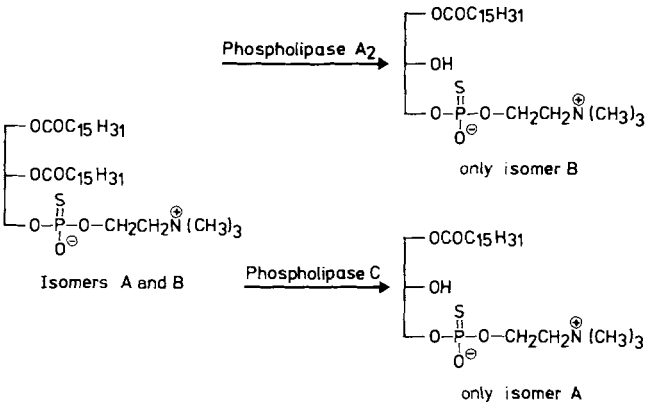



Fig. 27. Separation of diastereomers of 1,2-dipalmitoyl-*sn*-glycero-3-thiophosphoryl choline.

Phospholipase $A_2$ preferentially hydrolyzes that diastereomer whose signal exhibits a shift to low field[175–177]. If this diastereomer is designated B, the product of its hydrolysis is the B-isomer of *lyso*-palmitoyl-thiophosphoryl choline. This can be separated from the A-isomer of the unreacted dipalmitoyl-thiophosphoryl choline by chromatography and then allowed to react with palmitoic acid anhydride to afford the B-isomer of dipalmitoyl-thiophosphoryl choline. This method of separation of the diastereomers using enzymes is reminiscent of the separation of the diastereomers of $ATP_\alpha S$[12] (see Section 2.1). Phospholipase C also shows stereoselectivity, and in this reaction the isomer which is resistant against phospholipase $A_2$ is the preferred substrate[175–177]. These two examples also show that enzymes react stereospecifically or stereoselectively, even if they do not directly attack the chiral phosphorus center.

The phosphorothioate analogues form liposomes, whose transition from gels to the liquid crystalline phase at 44 °C occurs only at slightly higher temperature than that of natural phospholipids (41 °C). $^{31}$P-NMR spectroscopy reveals that aqueous dispersions of phosphorothioate analogues of phospholipids form typical phospholipid bilayers[174]. Since the $^{31}$P-NMR signals of phosphorothioates are shifted strongly to low field relative to those of phosphates, it is expected they can be used to investigate the mobility and structural properties of specific lipids in a mixture. Furthermore, they could be of interest because of their increased metabolic stability in situations where turnover of phospholipids is important for cellular functions. Methods for the incorporation of phosphorothioate analogues into biological membranes are currently being developed. Thus, it was found that *sn*-glycerol-3-phosphorothioate was taken up by the active transport system of *E. coli* strain 8 specifically *via* the active transport system for glycerol phosphate, and incorporated into phospholipids. At higher concentrations this compound is bacteriocidal for strains which have an active transport system for glycerol phosphate[178].

## 5. Conclusion

This progress report indicates that nucleoside phosphorothioates have found wide application in biochemistry. This has arisen because the exchange of oxygen by sulfur in phosphate groups of nucleotides has consequences which are further reaching than initially expected. The existence of diastereomers and the increased affinity of the phosphorothioate groups for $Hg^+$ is not surprising, although the large number of applications of these properties to the solution of biochemical problems is astonishing. What is really remarkable is that the difference between the affinities of nucleotides and nucleoside phosphorothioates towards proteins, if it exists at all, is only very small. This provides further evidence that the active sites of proteins are not rigid but rather, within certain limits, flexible and adaptable structures. At first sight it seems difficult to comprehend that not all enzymatic reactions involving phosphorothioates are slowed down by a similar degree as expected by the lower chemical reactivity of phosphorothioates. Nevertheless, many enzymatic transfer reactions proceed almost as well as the corresponding reactions with the natural substrate (*e.g.* reactions with DNA and RNA polymerases but not with polynucleotide kinase and pyridoxal kinase), but hydrolytic reactions proceed much more slowly (*e.g.* reactions with phosphatases and nucleases). In general it seems that conformational changes in the proteins are rate determining in enzymatic reactions and not in the actual chemical step[179]. Unfortunately, so far only two kinetic studies of enzyme reactions involving nucleoside phosphorothioates have been performed; myosin and Tu-factor[131, 150]. For both of these it has been shown that the chemical step is significantly slower with the analogues, and at least for myosin becomes partially rate determining. Thus, a possible explanation for the similar reaction rates of the enzymes cited above is that the chemical step with the phosphorothioates becomes similar to the normally rate-determining conformational change, so that the steady-state rate is hardly influenced. However, more detailed investigations are clearly required to test this hypothesis.

It is not easy to predict in which direction studies with phosphorothioates will develop. After the investigation of the stereochemical course of approximately 50 enzyme-catalyzed phosphoryl and nucleotidyl transfer reactions this area has lost its novelty appeal. They will probably gain increased significance for investigation of the phosphorylation of proteins, in particular of their regulation. Following current trends, the exploitation of the special properties of phosphorothioate groups in DNA and RNA, particularly their stability against enzymatic degradation, will also probably gain increasing interest. This tendency will certainly be stimulated by the ever increasing number of commercially available nucleoside phosphorothioates, including those with radioactive labels.

What is quite certain is that the development of phosphorothioate analogues of phospholipids is only beginning, and the synthesis of analogues of sugars other than those present in nucleosides has not yet begun.

Nucleoside phosphorothioates seem to be ideally suited for a cooperative effort between chemists, biochemists, biologists, and molecular biologists. On the one hand, through familiarity with these compounds chemists gain access to the biological sciences and, on the other, biological scientists gain insight into problems, whose solution requires structural modifications of the molecules they are interested in. It is to be hoped that nucleoside phosphorothioates will also remain a productive link in the future.

*All the results reported here from my group could only be accomplished through the enthusiastic, stimulating, and critical collaboration of my colleagues Drs. V. W. Armstrong, P. A. Bartlett, P. M. J. Burgers, B. A. Connolly, H. Gindl, R. S. Goody, B. V. L. Potter, P. J. Romaniuk, P. D. Senter, and D. Yee whom I would like to thank for their contributions. These studies were supported, in part, by the Deutsche Forschungsgemeinschaft as well as by the award of fellowships by the Alexander-von-Humboldt Stiftung and the Royal Society. I thank P. Grosse for her patience in typing this manuscript.*

Received: March 9, 1983 [A 457 IE]
German version: *Angew. Chem. 95* (1983) 431

[1] F. Eckstein, *Angew. Chem. 87* (1975) 179; *Angew. Chem. Int. Ed. Engl. 14* (1975) 160.
[2] F. Eckstein, *Acc. Chem. Res. 12* (1979) 204.
[3] F. Eckstein, *Trends Biochem. Sci. 5* (1980) 157.
[4] J. R. Knowles, *Annu. Rev. Biochem. 49* (1980) 877.
[5] P. A. Frey in A. Neuberger, L. L. M. Van Deenen: *New Comprehensive Biochemistry*, Vol. 3, Elsevier Biomedical Press, Amsterdam 1982, p. 201.
[6] P. A. Frey, *Tetrahedron 38* (1982) 1541.
[7] F. Eckstein, P. J. Romaniuk, B. A. Connolly, *Methods Enzymol. 87* (1982) 197.
[8] P. A. Frey, J. P. Richard, H.-T. Ho, R. S. Brody, R. D. Sammons, K.-F. Sheu, *Methods Enzymol. 87* (1982) 213.
[9] M. R. Webb, *Methods Enzymol. 87* (1982) 301.
[10] R. S. Goody, F. Eckstein, *J. Am. Chem. Soc. 93* (1971) 6252.
[11] F. Eckstein, H. Gindl, *Biochim. Biophys. Acta 149* (1967) 35.
[12] F. Eckstein, R. S. Goody, *Biochemistry 15* (1976) 1685.
[13] A. M. Michelson, *Biochim. Biophys. Acta 91* (1964) 1.
[14] K.-F. R. Sheu, P. A. Frey, *J. Biol. Chem. 252* (1977) 4445.

[15] E. K. Jaffe, M. Cohn, *Biochemistry 17* (1978) 652.
[16] B. A. Connolly, P. J. Romanius, F. Eckstein, *Biochemistry 21* (1982) 1983.
[17] F. R. Bryant, S. J. Benkovic, D. Sammons, P. A. Frey, *J. Biol. Chem. 256* (1981) 5965.
[18] A. Guptar, C. De Brosse, S. J. Benkovic, *J. Biol. Chem. 257* (1982) 7689.
[19] E. K. Jaffe, J. Nick, M. Cohn, *J. Biol. Chem. 257* (1982) 7650.
[20] C. F. Midelfort, I. Sarton-Miller, *J. Biol. Chem. 253* (1978) 7127.
[21] D. Yee, V. W. Armstrong, F. Eckstein, *Biochemistry 18* (1979) 4116.
[22] P. A. Bartlett, F. Eckstein, *J. Biol. Chem. 257* (1982) 8879.
[23] F. Eckstein, unpublished results.
[24] J. P. Richard, H.-T. Ho, P. A. Frey, *J. Am. Chem. Soc. 100* (1978) 7756.
[25] J. P. Richard, P. A. Frey, *J. Am. Chem. Soc. 104* (1982) 3476.
[26] Th. Meyer, K. Wilckens, J. Thiem, H. Hilz, unpublished results.
[27] P. M. J. Burgers, F. Eckstein, *Proc. Natl. Acad. Sci. USA 75* (1978) 4798.
[28] F. R. Bryant, S. J. Benkovic, *Biochemistry 18* (1979) 2825.
[29] W. Saenger, D. Suck, F. Eckstein, *Eur. J. Biochem. 46* (1974) 559.
[30] D. A. Usher, E. S. Erenrich, F. Eckstein, *Proc. Natl. Acad. Sci. USA 69* (1972) 115.
[31] R. L. Jarvest, G. Lowe, *J. Chem. Soc. Chem. Commun. 1979,* 364.
[32] a) E. K. Jaffe, M. Cohn, *J. Biol. Chem. 253* (1978) 4823; b) J. Stingelin, D. W. Boyle, E. T. Kaiser, *ibid. 255* (1980) 2022.
[33] R. D. Cornelius, W. W. Cleland, *Biochemistry 17* (1978) 3279.
[34] E. A. Merritt, M. Sundaralingam, R. D. Cornelius, W. W. Cleland, *Biochemistry 17* (1978) 3274.
[35] J. Baraniak, R. W. Kinas, K. Lesiak, W. J. Stec, *J. Chem. Soc. Chem. Commun. 1979,* 940.
[36] J. Baraniak, B. Jastorff, W. J. Stec, personal communication.
[37] J. Baraniak, P. Mejbaum, W. J. Stec, *Pol. J. Chem.*, in press.
[38] F. Eckstein, L. P. Simonson, H. P. Baer, *Biochemistry 13* (1974) 3806.
[39] P. D. Senter, F. Eckstein, A. Mülsch, E. Böhme, *J. Biol. Chem.*, in press.
[40] P. M. J. Burgers, F. Eckstein, *Biochemistry 18* (1978) 592.
[41] B. V. L. Potter, B. A. Connolly, F. Eckstein, *Biochemistry 22* (1983) 1369.
[42] P. J. Romaniuk, F. Eckstein, *J. Biol. Chem. 257* (1982) 7684.
[43] T. Jovin, H. Füldner, F. Eckstein, unpublished results.
[44] P. M. J. Burgers, F. Eckstein, *Tetrahedron Lett. 1978,* 3835.
[45] J. F. Marlier, S. J. Benkovic, *Tetrahedron Lett. 21* (1980) 1121.
[46] B. Uznanski, W. Niewiarowski, W. J. Stec, *Tetrahedron Lett. 23* (1982) 4289.
[47] B. A. Connolly, B. Uznanski, F. Eckstein, unpublished results.
[48] R. D. Sammons, P. A. Frey, *J. Biol. Chem. 257* (1982) 1138.
[49] B. A. Connolly, H. H. Füldner, F. Eckstein, *J. Biol. Chem. 257* (1982) 3382.
[50] G. Lowe, G. Tansley, P. M. Cullis, *J. Chem. Soc. Chem. Commun. 1982,* 595.
[51] R. D. Sammons, H.-T. Ho, P. A. Frey, *J. Am. Chem. Soc. 104* (1982) 5841.
[52] T. S. Leyh, R. D. Sammons, P. A. Frey, G. H. Reed, *J. Biol. Chem. 257* (1982) 15047.
[53] M. D. Tsai, K. Bruzik in L. J. Berliner, J. Reuben: *Biological Magnetic Resonance,* Vol. 5, Plenum, New York 1983.
[54] M. D. Tsai, *Methods Enzymol. 87* (1982) 235.
[55] J. A. Gerlt, P. C. Demon, S. Mehdi, *J. Am. Chem. Soc. 104* (1982) 2848.
[56] P. M. J. Burgers, F. Eckstein, *J. Biol. Chem. 254* (1979) 6889.
[57] R. S. Brody, P. A. Frey, *Biochemistry 20* (1981) 1245.
[58] R. S. Brody, S. Adler, P. Modrich, W. J. Stec, Z. J. Leznikowski, P. A. Frey, *Biochemistry 21* (1982) 2570.
[59] G. Lowe, B. V. L. Potter, B. S. Sproat, W. E. Hull, *J. Chem. Soc. Chem. Commun. 1979,* 733.
[60] M. Cohn, A. Hu, *J. Am. Chem. Soc. 102* (1980) 913.
[61] B. V. L. Potter, P. J. Romaniuk, F. Eckstein, *J. Biol. Chem. 258* (1983) 1758.
[62] M. D. Tsai, T. T. Chang, *J. Am. Chem. Soc. 102* (1980) 5416.
[63] S. L. Buchwald, P. E. Hansen, A. Hassett, J. R. Knowles, *Methods Enzymol. 87* (1982) 279.
[64] G. Lowe, P. M. Cullis, R. L. Jarvest, B. V. L. Potter, B. S. Sproat, *Philos. Trans. R. Soc. London B 293* (1981) 75.
[65] J. A. Gerlt, J. A. Coderre, *J. Am. Chem. Soc. 102* (1980) 4531.
[66] S. Mehdi, J. A. Gerlt, *J. Am. Chem. Soc. 103* (1981) 7018.
[67] F. H. Westheimer, *Acc. Chem. Res. 1* (1968) 70.
[68] F. H. Westheimer in De Mayo: *Rearrangements in Ground and Excited States,* Vol. 2, Academic Press, New York 1980, p. 229.
[69] A. Wlodawer, R. Bott, L. Sjölin, *J. Biol. Chem. 257* (1982) 1325.
[70] F. A. Cotton, E. E. Hazen, M. J. Legg, *Proc. Natl. Acad. Sci. USA 76* (1979) 2551.
[71] D. A. Usher, D. J. Richardson, F. Eckstein, *Nature 228* (1970) 663.
[72] S. Mehdi, J. A. Gerlt, *J. Am. Chem. Soc. 104* (1982) 3223.
[73] M. Cohn, *Acc. Chem. Res. 15* (1982) 326.
[74] W. W. Cleland, *Methods Enzymol. 87* (1982) 159.
[75] J. J. Villafranca, *Methods Enzymol. 87* (1982) 180.
[76] P. M. J. Burgers, F. Eckstein, *J. Biol. Chem. 255* (1980) 8229.
[77] M. Cohn, N. Shih, J. Nick, *J. Biol. Chem. 257* (1982) 7646.
[78] V. W. Armstrong, D. Yee, F. Eckstein, *Biochemistry 18* (1979) 4120.
[79] B. A. Connolly, F. Eckstein, *J. Biol. Chem. 256* (1981) 9450.
[80] E. K. Jaffe, M. Cohn, *J. Biol. Chem. 254* (1979) 10839.
[81] D. Dunaway-Mariano, W. W. Cleland, *Biochemistry 19* (1980) 1506.
[82] A. G. Tomaselli, S. H. Noda, *Fed. Proc. Fed. Am. Soc. Exp. Biol. 40* (1981) 1864.
[83] G. H. Reed, T. S. Leyh, *Biochemistry 19* (1980) 5472.
[84] M. R. Webb, D. E. Ash, T. S. Leyh, D. R. Trentham, G. H. Reed, *J. Biol. Chem. 257* (1982) 3068.
[85] H. P. Vosberg, F. Eckstein, *Biochemistry 16* (1977) 3633.
[86] T. A. Kunkel, F. Eckstein, A. S. Mildvan, R. M. Koplitz, L. Loeb, *Proc. Natl. Acad. Sci. USA 78* (1981) 6734.
[87] F. Eckstein, T. Jovin, *Biochemistry,* in press.
[88] S. Adler, R. S. Brody, P. A. Frey, P. Modrich, unpublished results.
[89] S. Putney, S. Benkovic, P. Schimmel, *Proc. Natl. Acad. Sci. USA 78* (1981) 7350.
[90] H. P. Vosberg, F. Eckstein, *J. Biol. Chem. 257* (1982) 6595.
[91] A. Kornberg: *DNA-Replication,* W. H. Freeman, San Francisco 1980.
[92] D. Shortle, P. Grisafi, S. J. Benkovic, D. Botstein, *Proc. Natl. Acad. Sci. USA 79* (1982) 1588.
[93] I. Y.-C. Sun, V. G. Allfrey, *J. Biol. Chem. 257* (1982) 1347.
[94] I. Y.-C. Sun, V. G. Allfrey, *Proc. Natl. Acad. Sci. USA 79* (1982) 4589.
[95] F. Eckstein, H. Gindl, *Eur. J. Biochem. 13* (1970) 558.
[96] F. Eckstein, K. H. Scheit in G. L. Cantoni, D. R. Davies: *Procedures in Nucleic Acid Research,* Vol. 2, Harper & Row, New York 1971, p. 665.
[97] F. Eckstein, H. Sternbach, F. v. d. Haar, *Biochemistry 16* (1977) 3429.
[98] D. J. Szalda, F. Eckstein, H. Sternbach, S. J. Lippard, *J. Inorg. Biochem. 11* (1979) 279.
[99] P. M. J. Burgers, F. Eckstein, *Biochemistry 18* (1979) 450.
[100] M. M. Smith, A. E. Reeve, R. C. C. Huang, *Cell 15* (1978) 615.
[101] I. Y.-C. Sun, V. G. Allfrey, *J. Biol. Chem. 255* (1980) 742.
[102] R. A. Hipskind, R. H. Reeder, *J. Biol. Chem. 255* (1980) 7896.
[103] G. J. Ide, *Biochemistry 20* (1981) 2633.
[104] E. W. Benz, R. M. Wydro, B. Nadel-Ginard, D. Dina, *Nature 288* (1980) 665.
[105] D. Bunick, R. Weinmann, *Biochim. Biophys. Acta 610* (1980) 331.
[106] S. I. Oskuski, *FEBS Lett. 143* (1982) 119.
[107] M. R. Stallcup, J. C. Ring, D. S. Ucker, K. Yamamoto, *Cold Spring Harbor Conf. Cell Proliferation 7* (1979) 1.
[108] S. Silverman, O. Schmidt, D. Söll, B. Hovemann, *J. Biol. Chem. 254* (1979) 10290.
[109] M. R. Stallcup, L. D. Washington, *J. Biol. Chem. 258* (1983) 2802.
[110] L. D. Washington, M. R. Stallcup, *Nucleic Acids Res. 10* (1982) 8311.
[111] W. R. Beltz, K. J. O'Brien, *Fed. Proc. Fed. Am. Soc. Exp. Biol. 40* (1981) 1849.
[112] P. Greengard, *Science 199* (1978) 146.
[113] P. Cohen, *Nature 296* (1982) 613.
[114] D. Gratecos, E. J. Fischer, *Biochem. Biophys. Res. Commun. 58* (1974) 960.
[115] J. Kendrick-Jones, W. Lehman, A. G. Szent-Györgi, *J. Mol. Biol. 54* (1970) 313.
[116] P. E. Hoar, W. G. L. Kerrick, P. S. Cassidy, *Science 204* (1979) 503.
[117] W. G. L. Kerrick, P. E. Hoar, *Nature 292* (1981) 253.
[118] P. S. Cassidy, P. E. Hoar, W. G. L. Kerrick, *J. Biol. Chem. 254* (1979) 11148.
[119] J. M. F. Sherry, A. Gorecka, M. O. Aksoy, R. Dabrowska, D. J. Hartshorne, *Biochemistry 17* (1978) 4411.
[120] R. Cooke, K. Franks, J. T. Stull, *FEBS Lett. 144* (1982) 33.
[121] M. D. Pato, R. S. Adelstein, *J. Biol. Chem. 255* (1980) 6535.
[122] N. K. Tonks, A. Kearns, P. J. Randle, *Eur. J. Biochem. 122* (1982) 549.
[123] D. Cassel, L. Glaser, *Proc. Natl. Acad. Sci. USA 79* (1982) 2231.
[124] F. Madriaco, T. Urumow, O. H. Wieland, *FEBS Lett. 149* (1982) 96.
[125] J. Avruch, R. A. Nemenoff, P. J. Blackshear, M. W. Pierce, R. Osathanondh, *J. Biol. Chem. 257* (1982) 15162.
[126] A. Rephaeli, S. M. Parsons, *Proc. Natl. Acad. Sci. USA 79* (1982) 5783.
[127] I. Y.-C. Sun, E. M. Johnson, V. G. Allfrey, *J. Biol. Chem. 255* (1980) 742.
[128] D. L. Purich, B. J. Terry, H. D. White, B. A. Coughlin, T. L. Karr, D. Kristofferson, *Cold Spring Harbor Conf. Cell Proliferation 8* (1981) 1143.
[129] J. E. Churdrich, C. Wu, *J. Biol. Chem. 257* (1982) 12136.
[130] R. G. Yount, *Adv. Enzymol. Rel. Areas Mol. Biol. 43* (1975) 1.
[131] C. R. Bagshaw, J. F. Eccleston, D. R. Trentham, D. R. Yates, R. S. Goody, *Cold Spring Harbor Symp. Quant. Biol. 37* (1972) 127.
[132] M. A. Greeves, D. R. Trentham, *Biochemistry 21* (1982) 2782.

[133] C. M. Radding, *Cell 25* (1981) 3.
[134] S. Gottesman, *Cell 23* (1981) 1.
[135] K. McEntee, G. M. Weinstock, I. R. Lehman, *Proc. Natl. Acad. Sci. USA 76* (1979) 2615.
[136] G. M. Weinstock, K. McEntee, I. R. Lehman, *J. Biol. Chem. 256* (1981) 8850.
[137] K. McEntee, G. M. Weinstock, I. R. Lehman, *J. Biol. Chem. 256* (1981) 8835.
[138] M. M. Cox, I. R. Lehman, *Proc. Natl. Acad. Sci. USA 78* (1981) 3433.
[139] A. Stariak, E. Di Capura, *Nature 299* (1982) 185.
[140] K. Dunn, S. Chrysogelos, J. Griffith, *Cell 28* (1982) 757.
[141] J. Flory, C. M. Radding, *Cell 28* (1982) 747.
[142] R. P. Cunningham, T. Shibata, C. DasGupta, C. M. Radding, *Nature 281* (1979) 191.
[143] N. Craig, J. W. Roberts, *J. Biol. Chem. 256* (1981) 8039.
[144] G. M. Weinstock, K. McEntee, *J. Biol. Chem. 256* (1981) 10883.
[145] J. W. Little, D. W. Mount, C. R. Yanish-Pesson, *Proc. Natl. Acad. Sci. USA 78* (1981) 4199.
[146] E. Phizicky, J. W. Roberts, *J. Mol. Biol. 139* (1980) 319.
[147] R. T. Sauer, M. J. Ross, M. Ptashne, *J. Biol. Chem. 257* (1982) 4458.
[148] P. M. J. Burgers, A. Kornberg, *J. Biol. Chem. 257* (1982) 11474.
[149] P. M. J. Burgers, A. Kornberg, *J. Biol. Chem.*, submitted for publication.
[150] R. C. Thompson, A. M. Karim, *Proc. Natl. Acad. Sci. USA 79* (1982) 4922.
[151] J. Ketelaar, H. Gersmann, K. Koopmanns, *Recl. Trav. Chim. Pays-Bas 71* (1952) 1253.
[152] E. M. Ross, A. G. Gilman, *Annu. Rev. Biochem. 49* (1980) 533.
[153] Th. Pfeuffer, E. J. M. Helmreich, *J. Biol. Chem. 250* (1975) 867.
[154] D. Cassel, Z. Selinger, *Biochem. Biophys. Res. Commun. 77* (1977) 868.
[155] J. K. Northrup, M. D. Smigel, A. Gilman, *J. Biol. Chem. 257* (1982) 11416.
[156] F. Eckstein, D. Cassel, H. Lefkowitz, M. Lowe, Z. Selinger, *J. Biol. Chem. 254* (1979) 9829.
[157] D. Cassel, F. Eckstein, M. Lowe, Z. Selinger, *J. Biol. Chem. 254* (1979) 9835.
[158] M. Svoboda, J. Furnelle, F. Eckstein, J. Christophe, *FEBS Lett. 109* (1980) 275.
[159] E. Ezra, Y. Salomon, *J. Biol. Chem. 256* (1981) 5377.
[160] T. H. Hudson, J. F. Roeker, G. L. Johnson, *J. Biol. Chem. 256* (1981) 1459.
[161] M. E. Abood, J. B. Hurley, M.-C. Pappone, H. R. Bourne, L. Stryer, *J. Biol. Chem. 257* (1982) 10450.
[162] A. Fein, D. W. Corson, *Science 212* (1981) 555.
[163] H. Kühn, N. Bennet, M. Michel-Villaz, M. Chabre, *Proc. Natl. Acad. Sci. USA 78* (1981) 6873.
[164] N. Bennet, *Eur. J. Biochem. 123* (1982) 133.
[165] D. Emeis, H. Kühn, J. Reichert, K. P. Hofmann, *FEBS Lett. 143* (1982) 29.
[166] T. S. Yagura, J. P. Miller, *Biochemistry 20* (1981) 879.
[167] C. A. O'Brian, S. O. Roczniak, H. N. Bramson, J. Baraniak, W. J. Stec, E. T. Kaiser, *Biochemistry 21* (1982) 4371.
[168] R. J. W. de Witt, J. Hoppe, W. J. Stec, J. Baraniak, B. Jastorff, *Eur. J. Biochem. 122* (1982) 95.
[169] A. M. Gronenburg, G. M. Clore, *Biochemistry 21* (1982) 4040.
[170] J. Krakow, personal communication.
[171] P. J. M. Van Haastert, B. Jastorff, J. E. Pinas, T. M. Konijin, *J. Bacteriol. 149* (1982) 99.
[172] F. Eckstein, S. Eimerl, M. Schramm, *FEBS Lett. 64* (1976) 92.
[173] E. E. Nifant'ev, D. A. Predvoditelev, H. H. Arlakeon, *Zh. Org. Khim. 14* (1978) 63.
[174] I. Varilenko, B. De Kruijff, A. J. Verkleij, *Biochim. Biophys. Acta 685* (1982) 144.
[175] K. Bruzik, S. M. Gupta, M.-D. Tsai, *J. Am. Chem. Soc. 104* (1982) 4682.
[176] G. A. Orr, C. F. Brewer, G. Heney, *Biochemistry 21* (1982) 3202.
[177] K. Bruzik, R.-T. Jiang, M.-D. Tsai, *Biochemistry*, in press.
[178] G. A. Orr, J. W. Hammelburger, G. Heney, personal communication.
[179] W. W. Cleland, *Acc. Chem. Res. 8* (1975) 145.
[180] F. Eckstein, H. H. Schulz, H. Rüterjans, W. Haar, W. Maurer, *Biochemistry 11* (1972) 3507.
[181] J. A. Gerlt, W. H. Y. Wan, *Biochemistry 18* (1979) 4630.
[182] J. F. Marlier, F. R. Bryant, S. J. Benkovic, *Biochemistry 20* (1981) 2212.
[183] F. Eckstein, H. Sternbach, F. von der Haar, *Biochemistry 16* (1977) 3429.
[184] F. R. Bryant, S. J. Benkovic, *Biochemistry 21* (1982) 5877.
[185] K.-F. R. Sheu, J. P. Richard, P. A. Frey, *Biochemistry 18* (1979) 5548.
[186] J. A. Gerlt, J. A. Coderre, M. S. Wolin, *J. Biol. Chem. 255* (1980) 331.
[187] F. Eckstein, P. J. Romaniuk, W. Heideman, D. R. Storm, *J. Biol. Chem. 256* (1981) 9118.
[188] M.-D. Tsai, *Biochemistry 18* (1979) 1468.
[189] J. P. Richard, M. C. Carr, D. H. Ives, P. A. Frey, *Biochem. Biophys. Res. Commun. 94* (1980) 1052.
[190] J. P. Richard, D. C. Prasher, D. H. Ives, P. A. Frey, *J. Biol. Chem. 254* (1979) 4339.
[191] M. R. Webb, D. R. Trentham, *J. Biol. Chem. 255* (1980) 8629.
[192] M. R. Webb, C. Grubmeyer, H. S. Penefsky, D. R. Trentham, *J. Biol. Chem. 255* (1980) 11637.
[193] M. R. Webb, D. R. Trentham, *J. Biol. Chem. 256* (1981) 4884.
[194] M. R. Webb, J. F. Eccleston, *J. Biol. Chem. 256* (1981) 7734.
[195] J. F. Eccleston, M. R. Webb, *J. Biol. Chem. 257* (1982) 5046.
[196] M. R. Webb, D. R. Trentham, *J. Biol. Chem. 255* (1980) 1775.
[197] P. D. Senter, F. Eckstein, Y. Kagawa, unpublished results.
[198] G. A. Orr, J. Simon, S. R. Jones, G. J. Chin, J. R. Knowles, *Proc. Natl. Acad. Sci. USA 75* (1978) 2230.
[199] W. A. Blättler, J. R. Knowles, *Biochemistry 18* (1979) 3927.
[200] D. H. Pliura, D. Schomburg, J. P. Richard, P. A. Frey, J. R. Knowles, *Biochemistry 19* (1980) 325.
[201] G. Lowe, B. V. L. Potter, *Biochem. J. 199* (1981) 227.
[202] R. L. Jarvest, G. Lowe, *Biochem. J. 199* (1981) 273.
[203] F. R. Bryant, S. J. Benkovic, D. Sammons, P. A. Frey, *J. Biol. Chem. 256* (1981) 5965.
[204] P. M. J. Burgers, F. Eckstein, D. H. Hunneman, J. Baraniak, R. W. Kinas, K. Lesiak, W. J. Stec, *J. Biol. Chem. 254* (1979) 9959.
[205] R. L. Jarvest, G. Lowe, J. Baraniak, W. J. Stec, *Biochem. J. 203* (1982) 461.
[206] P. M. Cullis, R. L. Jarvest, G. Lowe, B. V. L. Potter, *J. Chem. Soc. Chem. Commun. 1981*, 245.
[207] J. A. Coderre, S. Mehdi, J. A. Gerlt, *J. Am. Chem. Soc. 103* (1981) 1872.
[208] P. M. J. Burgers, F. Eckstein, D. H. Huneman, *J. Biol. Chem. 254* (1979) 7476.
[209] R. L. Jarvest, G. Lowe, *Biochem. J. 199* (1981) 447.
[210] S. Mehdi, J. A. Gerlt, *J. Biol. Chem. 256* (1981) 12164.
[211] S. P. Langdon, G. Lowe, *Nature 281* (1979) 320.
[212] G. Lowe, B. S. Sproat, G. Tansley, *Eur. J. Biochem. 130* (1983) 341.
[213] S. J. Jones, L. A. Kindman, J. R. Knowles, *Nature 275* (1978) 564.
[214] D. E. Hansen, J. R. Knowles, *J. Biol. Chem. 256* (1981) 5967.
[215] W. A. Blättler, J. R. Knowles, *Biochemistry 19* (1980) 738.
[216] M. K. Darby, I. P. Trayer, *Eur. J. Biochem. 129* (1982) 555.
[217] P. J. Romaniuk, F. Eckstein, *J. Biol. Chem. 256* (1981) 7322.
[218] B. A. Connolly, F. von der Haar, F. Eckstein, *J. Biol. Chem. 255* (1980) 11301.
[219] L. T. Smith, M. Cohn, *Biochemistry 21* (1982) 1530.
[220] D. W. Bolen, J. Stingelin, H. N. Bramson, E. T. Kaiser, *Biochemistry 19* (1980) 1176.
[221] R. P. Pillai, F. M. Rauschel, J. J. Villafranca, *Arch. Biochem. Biophys. 199* (1980) 7.
[222] F. M. Rauschel, P. M. Anderson, J. J. Villafranca, *J. Biol. Chem. 253* (1978) 6627.
[223] K. J. Gibson, R. L. Switzer, *J. Biol. Chem. 255* (1980) 694.

# Bond-Forming Initiation in Spontaneous Addition and Polymerization Reactions of Alkenes

By H. K. Hall, Jr.*

Spontaneous addition and polymerization reactions of alkenes of different electron-densities result in a wide variety of small organic molecules and high polymers. Tetramethylenes are proposed as key intermediates, *i.e.* resonance hybrids of 1,4-diradical and zwitterionic limiting structures. Their character is determined by the substituents at the terminals: Zwitterionic character is favored by strong donors, such as alkoxy and dialkylamino groups, at the carbenium center and strong acceptors, such as two cyano groups, at the carbanion center; diradical character is favored by acceptor groups, such as diesters and cyano-esters, at the acceptor end, and aryl and vinyl groups as donors. Zwitterionic tetramethylenes initiate ionic homopolymerization, while diradical tetramethylenes initiate alternating copolymerization, thus providing an extremely sensitive technique for the detection and characterization of these intermediates. The effects of the donor and acceptor substituents can be arranged as an "Organic Chemist's Periodic Table", wherein the areas of mechanistic change clearly emerge and which provides predictive capability.—This unifying concept of *bond-forming initiation* is extended to spontaneous addition and polymerization reactions of heteroatom acceptor molecules and 7,7,8,8-tetrasubstituted quinodimethanes and of compounds possessing labile σ-bonds, such as halogens and peroxides. Radical-ion pairs, charge-transfer complexes and adventitious impurities are excluded as significant initiators.

## 1. The Tetramethylene Concept

### 1.1. Introduction

Spontaneous addition and polymerization reactions between alkenes of different electron densities lead to a wide variety of products, including small molecules and polymers. The small molecules include cyclobutanes, 1-butenes, Diels-Alder adducts (from styrenes), ene-reaction products (from alkylethylenes), and pyrans (from unsaturated esters). The modes of formation of the small molecules have been interpreted in terms of 1,4-diradicals, 1,4-zwitterions, and concerted processes. The polymers can be either homopolymers of one or both alkenes, or copolymers. Radical-ion pairs, charge-transfer (CT) complexes, 1,4-diradicals and 1,4-zwitterions have been postulated as intermediates for the polymerizations. Occasionally, CT complexes have been regarded as precursors of free radicals. So far, there has been no concept which could equally interpret both addition as well as polymerization, and enable useful predictions to be made.

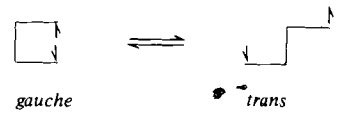
In recent years, tetramethylene intermediates have been extensively studied on a theoretical basis. Tetramethylenes with terminal substituents are currently viewed as resonance hybrids of varying diradical and zwitterionic nature. In this paper we postulate that they frequently function as key intermediates in cycloadditions and polymerizations. This concept can be extended to reactions in which π- and σ-bonds participate.

[*] Prof. H. K. Hall, Jr.
Department of Chemistry, College of Arts and Sciences
The University of Arizona
Tucson, AZ 85721 (USA)

### 1.2. Unsubstituted Tetramethylene

*Hoffmann et al.*[1] first studied theoretically the parent tetramethylene. Later studies showed the existence of two energy minima on the potential energy surface, corresponding to the *gauche* and the *trans* conformers[2].

Different starting compounds furnish tetramethylenes in different conformations; thus, tetramethylenes are formed in the *trans* conformation from two alkenes, but in the *gauche* form on thermolysis of pyridazine[3]. The reactions of the extremely reactive tetramethylenes depend on their origin and conformation[4,5]. Recently, unsubstituted tetramethylene was prepared, and it was confirmed that its subsequent reactions are conformation-dependent[6]. In the case of this species the reactions compete with rotation about the central CC bond.



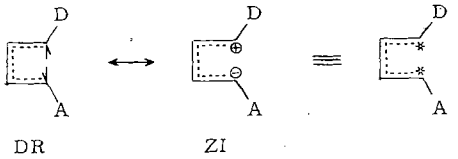

The terminals can interact with each other by "through-bond interaction", analogous to hyperconjugation. "Through-bond coupling makes the terminal centers even in the *trans*-conformation, cognizant of each other"[7]. Even in the extended form, the carbon p-orbitals adopt the 90°-90° conformation to favor maximum through-bond interaction[8]. Recent reviews[9] summarize much of this information.

The identification of tetramethylene intermediates as highly unstable molecules allows us to discuss their chemistry and conformational behavior.

 © Verlag Chemie GmbH, 6940 Weinheim, 1983 0570-0833/83/0606-0440 $ 02.50/0 

### 1.3. Donor-Acceptor-Substituted Tetramethylenes

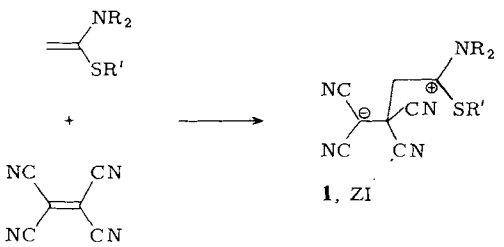
Of great significance is the conclusion drawn by *Salem* and *Rowland*[10], and by *Huisgen*[7] that 1,4-diradical (DR) and 1,4-zwitterionic (ZI) forms of tetramethylene are not different entities, but rather are the extremes of a continuum. The tetramethylene is regarded as a resonance hybrid of the DR- and ZI-forms. An asterisk denotes 0—1 electron or 1—2 electrons. This applies also for the *trans* conformation. The abbreviations A and D mean acceptor and donor substituents, respectively.




The non-commital designation with two asterisks will be used to denote the unused valences of the tetramethylene. Predominant zwitterionic or diradical character will be assigned in each case on the basis of experimental results (see Section 2). The character of the tetramethylene is determined by the nature of the terminal substituents. Although not stated in the literature, it is reasonable to expect that donor and acceptor substituents at the terminals will greatly increase tetramethylene stability by push-pull through-bond interaction.

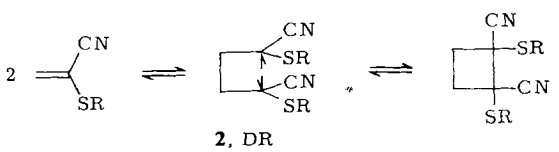
β-Substituents have no influence on the diradical or zwitterionic character of the tetramethylene. However, they play an important role in that they favor the *gauche* conformation of the tetramethylene over the *trans* (extended) form of the parent tetramethylene through the "*gem*-dimethyl" effect. *Gauche* conformations will favor the formation of small molecules because of the proximity of the terminal atoms. Furthermore, steric hindrance by the β-substituents will retard bond formation at that position.

The high reactivity of these tetramethylene intermediates, even in highly stabilized cases, has generally enabled them to escape direct detection or isolation. A stable tetramethylene of type **1** possessing extreme zwitterionic character was prepared by *Gompper et al.*[11] by reaction of ketene *S,N*-acetals with tetracyanoethylene (TCNE); according to *Huisgen* it exists in the *trans*-form[7].




**1**, ZI

Tetramethylenes of type **2** with diradical character are stabilized by captodative substitution[12,13].



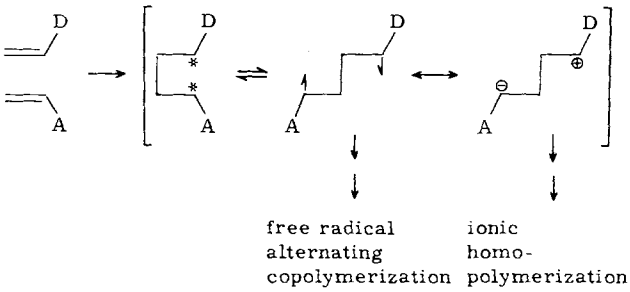

**2**, DR

### 1.4. Indirect Evidence for Tetramethylene Intermediates

Various criteria have been applied to reactions which lead to small molecules. They include detection or trapping of intermediates[7,14-20], stereochemical effects[21], substituent effects and orientation phenomena[21,22], kinetic effects[22-26], effects of solvents[22,27-29] or pressure on the reaction rate[30], and rearrangement of donor substituents[30-34,15,28]. According to *Gompper*[35], detection or trapping is the most decisive evidence for the existence of an intermediate.

### 1.5. Trapping by Initiation of Polymerization

A potentially extremely effective way of trapping an intermediate is by allowing it to initiate polymerization. This technique has great advantages. First: The *amplification*. A small amount of reactive species will lead by chain reaction to an easily detectable yield of polymer. Such a technique should be especially suitable for the detection of very difficultly identifiable intermediates such as tetramethylenes. Second: *The structure of the polymer will diagnose the diradical or zwitterionic nature of the tetramethylene.* Homopolymers of either one or both alkenes indicate the existence of a 1,4-zwitterionic intermediate, while alternating copolymers can only be formed from a diradical intermediate.



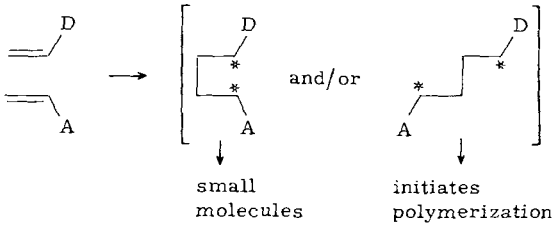

The nature of the polymerization, and of the tetramethylene, can be confirmed by addition of an inhibitor which appropriately suppresses either ionic or radical polymerization. The presence of a third monomer, which can only polymerize *via* a radical mechanism, will support the radical character of the intermediate by formation of terpolymers[36]. Finally, if both small molecules and polymers form competitively from a common intermediate, dilution will favor the former.

## 2. Alkene-Alkene Reactions: Tetramethylenes with All-Carbon Skeleton

The literature was searched for spontaneous addition and polymerization reactions of alkenes with one another. Reactions deliberately initiated by free radical and ionic sources or by irradiation, and many Diels-Alder reactions, were not taken into account. On the other hand, special value was attached to those reactions in which a spontaneously formed polymer is either the sole product or one of the products. This survey is not intended as a complete literature review, but rather as a critical discussion of the

reactions involved. Our goal was to compare the polymerization behavior of various alkene pairs with their behavior in addition reactions, as deduced by the methods of physical organic chemistry.

The alkenes are presented systematically in Table 1, being listed in order of increasing acceptor ability of the acceptor substituents. Within each group, the alkenes are listed in order of increasing electron donor ability of the donor substituents. Table 1 also contains some alkene dimerizations.




*,* denotes +, − and/or ↿, ↾

### 2.1. Dimerizations

Thermal dimerizations have been extensively studied. Ethylene[37] and acrylonitrile[68] cyclodimerize to cyclobutanes, while styrene[38] undergoes [2+2] and [4+2] cycloaddition. Methyl methacrylate and methacrylonitrile[47,48,122] yield mostly unsaturated dimers (ene-reaction) along with cyclobutanes. *Pryor et al.*[19,38] showed that the polymerization kinetics of styrene were bimolecular and postulated the Flory diradical tetramethylene intermediate, which was further supported by other investigators[123]. Kinetic investigations on methyl methacrylate[47,122] and on fluoroalkenes[41] led to the conclusion that diradical tetramethylenes are the intermediates. Since polarity differences play no part in dimerizations, the latter uniformly follow a diradical mechanism.

### 2.2. Cycloadditions and Polymerizations *via* Diradical Tetramethylenes

Spontaneous addition and polymerization reactions between alkenes of different polarity are more rapid than dimerizations. Bimolecular initiation occurs 100 times more rapidly in the cross-initiation between styrene and methyl methacrylate than in the respective homopolymerizations[50]. Bimolecular initiation was also found in the spontaneous polymerization of 1,2-dimethoxyethylene and maleic anhydride[73]. Numerous other examples are given in Table 1.

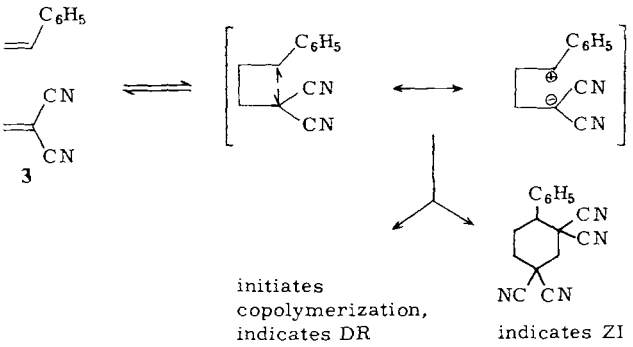
The polar substituents of these diradicals lead to an additional stabilization through the push-pull effect. Polar effects on monoradical behavior are already well known. Even the reaction of dimethyl cyanofumarate and *p*-methoxystyrene still proceeds *via* a diradical mechanism, as witnessed by the formation of copolymer[80].

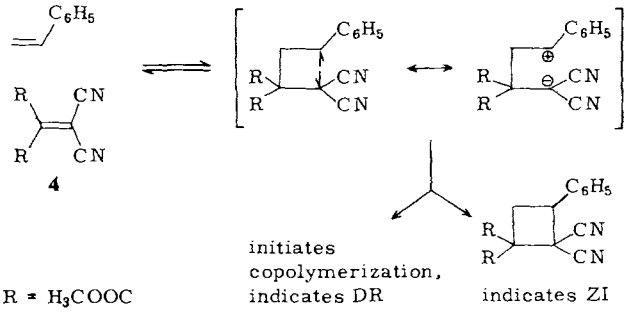
Dilution or addition of solvent causes a shift from copolymer formation to cyclobutane formation in several cases. Typical examples are, *inter alia*, the reactions of dimethyl (dicyanomethylene)malonate with styrene[80], methyl 2,5-dihydro-2,5-dioxo-3-furancarboxylate with styrene[90], and isobutyl vinyl sulfide with trimethyl ethylenetricarboxylate[83]. This is consistent with the intermediacy of a common precursor for the formation of copolymers and small molecules.

A third, non-polar monomer, polymerizable through a free radical mechanism, proves the free radical nature of the copolymer formation by forming terpolymers. Methyl methacrylate as the reaction medium for *p*-methoxystyrene and trisubstituted alkenes possessing cyano and methoxycarbonyl substituents resulted in terpolymers only in those cases in which the tetramethylene had shown diradical character by spontaneous alternating copolymerization[124].

### 2.3. Transition from Diradical to Zwitterionic Behavior

Diradical behavior persists even when the substituents might reasonably have been expected to favor zwitterionic behavior, as in the reaction of dimethyl cyanofumarate or dimethyl dicyanofumarate with *p*-methoxystyrene[98]. Eventual transitional behavior from diradical to zwitterionic is shown by the following alkene pairs: vinylidene cyanide **3** with styrene[103,105] and dimethyl dicyanomethylenemalonate **4** with styrene[80] (for other examples see Table 1).




The orientation of the substituents in these cycloadducts is consistent with zwitterionic behavior of the tetramethylene.

### 2.4. Zwitterionic Tetramethylenes

A very strong donor group at one of the terminal carbons and a very strong acceptor group at the other lead to zwitterionic intermediates. Such donors feature nitrogen substituents, *p*-dimethylaminostyrene, *N*-vinylamines or *N*-

Table 1. Reactions between π-bonds *via* tetramethylenes with all-carbon skeleton. Char.: Predominant character of the tetramethylene. - All substituents on phenyl groups are *para*.

| π-Acceptor | π-Donor | Products: Small Molecules | Products: Polymer | Mechanism | Ref. | Char. |
|---|---|---|---|---|---|---|
|  |  | Cyclobutane | | DR | [37] | ┐, └ |
|  |  | Cyclobutane | | DR | [38] | ┐, └ |
| | | Diels-Alder add. | | Concerted | [38] | |
| | | | Homopol. | Radical from Diels-Alder add. | [38] | [f] |
|  |  | Cyclobutane | Homopol. | DR | [39] | ┐, └ |
| $F_2C{=}CF_2$ | $F_2C{=}CFCl$ | Cyclobutane | | | [40] | ┐, └ |
| |  | Cyclobutane | | DR | [41] | ┐, └ |
| |  | Cyclobutane | | DR | [41] | ┐, └ |
| |  | Cyclobutane | | DR | [41] | ┐, └ |
| $F_2C{=}CFCl$ | $F_2C{=}CFCl$ | Cyclobutane | | DR | [40–43] | ┐, └ |
| $F_2C{=}CCl_2$ | $F_2C{=}CCl_2$ | Cyclobutane | | | [42] | ┐, └ |
| |  | Cyclobutane | | DR | [44, 45] | ┐, └ |
|  |  | Cyclobutane | | ZI | [46] | +, − |
| | | Diels-Alder (C=O) | | ZI | [46] | +, − |

Abbreviations used in Tables 1–4.

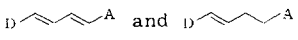
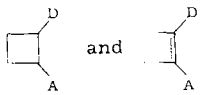
| | |
|---|---|
| Butadiene and 1-Butene |  |
| Concerted | Concerted mechanism |
| Copol. | Copolymer (1:1 alternating) |
| CT | Charge-transfer complex precursor to free radicals |
| Cyclobutane and Cyclobutene |  |
| Cyclohexane | 2:1 Adduct with cyclohexane skeleton |
| Diels-Alder add. | Diels-Alder adduct |
| Diels-Alder (arom.) | Diels-Alder adduct involving the aromatic ring (Wagner-Jauregg adduct) |
| Diels-Alder (C=O) | Diels-Alder adduct involving ester (or ketone) group, hetero Diels-Alder |
| DR | Diradical tetramethylene; *,* denotes ┐, └ |
| ene-reaction | Ene-reaction product |
| Homopol | Homopolymer |
| ion. | Ionic mechanism |
| Metathesis | Metathesis product |
| Poly-combin. | Poly-combination |
| radic. | Radical mechanism |
| Radical from Diels-Alder | Radical formed from Diels-Alder adduct (see Table 4) |
| Radical chain | Radical chain mechanism |
| Random copol. | Random copolymer |
| Rearrang. | Wagner-Meerwein rearranged product |
| Ring opening | Ring-opening polymerization |
| SET | Single electron-transfer |
| ZI | Zwitterionic tetramethylene; *,* denotes +, − |

Table 1 (Continued).

| π-Acceptor | π-Donor | Products: Small Molecules | Products: Polymer | Mechanism | Ref. | Char. |
|---|---|---|---|---|---|---|
|  | $F_2C{=}CF_2$ | Cyclobutane | | DR | [41] | ┐, └ |
|  |  | 1-Butene<br>Cyclobutane | | DR<br>Concerted | [47]<br>[48] | ┐, └ |
| | | | Homopol. | DR | [49] | |
| |  | | Copol. | | [50] | ┐, └ |
| |  | | Copol. | CT | [51] | ┐, └ |
| |  [a] | | Copol. | SET | [52] | ┐, └ |
|  |  | Cyclobutane | Copol. | CT | [53, 54] | ┐, └ |
|  |  | | Copol. | CT | [51] | ┐, └ |
| |  | Cyclobutane | | ZI | [55] | +, − |
| |  | Cyclobutane | | ZI | [56, 57] | +, − |
|  |  | | Copol. | | [58] | ┐, └ |
| |  | | Copol. | CT | [51, 59] | ┐, └ |
| |  | Cyclobutane | | ZI | [55] | +, − |
| |  | Cyclobutane | | ZI | [56, 60] | +, − |
|  |  | | Copol. | SET | [61] | ┐, └ |
| |  | | Copol. | SET | [61] | ┐, └ |
|  |  | 1-Butene | | Concerted | [48] | ┐, └ |
|  |  | Cyclobutane | Copol. | CT | [53, 54] | ┐, └ |
|  | $F_2C{=}CF_2$ | Cyclobutane | | DR | [41, 62] | ┐, └ |
| | $F_2C{=}CFCl$ | Cyclobutane | | DR | [41, 62] | ┐, └ |
| | $F_2C{=}CCl_2$ | Cyclobutane | | DR | [41] | ┐, └ |
| |  | Cyclobutane | | DR | [63] | ┐, └ |
| |  | Cyclobutane | | DR | [64] | ┐, └ |
| |  | Diels-Alder (arom.) | | Concerted | [65] | |
| | | | Copol. | Radical from Diels-Alder add. | [65] | [f] |
| |  | | Copol. | CT | [51] | |
| |  [a] | | Homopol.<br>Copol. | SET | [52, 66] | borderline |
| |  | Cyclobutane | | ZI | [56, 57] | +, − |
| |  | Cyclobutene | | ZI | [11] | +, − |

Table 1 (Continued).

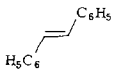
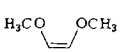
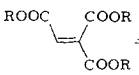
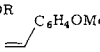
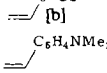
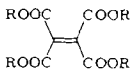
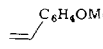
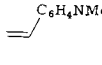
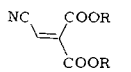
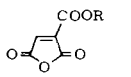
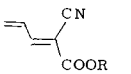
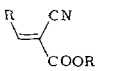
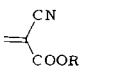
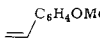
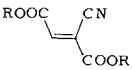
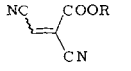
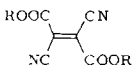
| π-Acceptor | π-Donor | Products: Small Molecules | Products: Polymer | Mechanism | Ref. | Char. |
|---|---|---|---|---|---|---|
|  |  | Cyclobutane | | ZI | [67] | +, − |
| |  [a] | Cyclobutane | Homopol. | ZI | [24] | +, − |
| |  | Cyclobutane | | ZI | [56] | +, − |
|  |  | Diels-Alder (arom.) | | Concerted | [68] | |
| | | | Copol. | CT | [59, 69, 70] | ↿, ↳ |
| | | | | Radical from Diels-Alder add. | [38] | [f] |
| | | | | SET | [71] | |
| |  | | Copol. | | [72] | ↿, ↳ |
| |  | | Copol. | CT | [59, 73, 74] | ↿, ↳ |
| |  | | Copol. | CT | [74, 75] | ↿, ↳ |
| |  | | Copol. | CT | [73] | ↿, ↳ |
| |  | Cyclohexane | | ZI | [76] | +, − |
| |  | | Copol. | CT | [59, 77] | ↿, ↳ |
|  |  | Cyclobutane | Homopol. | ZI | [78] | borderline |
| | | | Copol. | Ring-opening | [78] | |
| |  | Cyclobutane | | ZI | [79] | +, − |
| | | Cyclohexane | | ZI | [79] | |
|  |  | Cyclohexane | | ZI | [56] | +, − |
|  |  | | Copol. | DR | [80] | ↿, ↳ |
| |  | Diels-Alder (C=O) | | Concerted | [81] | |
| | | 1-Butene | Copol. | DR | [81] | ↿, ↳ |
| |  | Diels-Alder (C=O) | | Concerted | [82] | |
| |  | Cyclobutane | | ZI | [83, 84] | ↿, ↳ |
| | | Diels-Alder (C=O) | | Concerted | [84, 85] | |
| | | | Copol. | | [83] | ↿, ↳ |
| |  [b] | Cyclobutane | Homopol. | ZI | [85] | +, − |
| |  | Cyclobutane | | ZI | [86] | +, − |
| |  | Cyclobutane | | ZI | [87] | +, − |
| | | Cyclobutane | | ZI | [87] | +, − |
| | | 1-Butene | | ZI | [87] | +, − |
| |  | Cyclobutane | | | [84] | +, − |
| |  [a] | Cyclobutane 1-Butene | | CT | [88] | +, − |
|  |  | Cyclobutane | | DR | [81] | ↿, ↳ |
| |  | Cyclobutane | | ZI | [89] | +, − |
| |  [b] | Cyclobutane | | ZI | [85] | +, − |
| |  | Cyclobutane | | ZI | [86] | +, − |
| |  | 1-Butene | | ZI | [87] | +, − |
| |  [a] | 1-Butene Cyclobutane | | CT | [88] | +, − |
|  |  | | Copol. | DR | [80] | ↿, ↳ |
| |  | Diels-Alder (arom.) | | Concerted | [90] | |
| | | | Copol. | DR | [90] | ↿, ↳ |
|  |  | Diels-Alder (arom.) | | Concerted | [91] | |
| | | | Copol. | DR | [91] | ↿, ↳ |
| |  | Diels-Alder (C=O) | | Concerted? | [91] | |
| | | | Copol. | DR | [91] | ↿, ↳ |
|  |  | Cyclobutane | | ZI | [92] | +, − |
|  |  | Cyclobutane | | ZI | [93] | +, − |
|  |  | | Copol. | DR | [94–96] | ↿, ↳ |
| |  | Diels-Alder (arom.) | | Concerted | [95] | |
| | | | Copol. | DR | [95] | ↿, ↳ |
| |  | Diels-Alder (C=O) | [c] | Concerted? | [95, 83] | |
| | | | Copol. | | [94] | ↿, ↳ |
|  |  | Diels-Alder (C=O) | | Concerted? | [82] | |
| | | | Copol. | DR | [82, 87] | ↿, ↳ |
| |  | Diels-Alder (C=O) | | Concerted? | [83] | |
| |  [b] | Cyclobutane | Homopol. | ZI | [86] | +, − |
| |  [a] | | Copol. | CT | [97] | ↿, ↳ |
| |  | Cyclobutane | Homopol. | ZI | [85] | +, − |
|  |  | Diels-Alder (C=O) | | Concerted? | [83] | |
| |  | Cyclobutane | | ZI | [85] | +, − |
|  |  | Diels-Alder (C=O) | | Concerted? | [83, 98] | |
| | | | Copol. | DR | [98] | ↿, ↳ |

Table 1 (Continued).

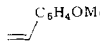
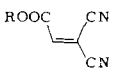
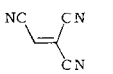
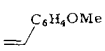
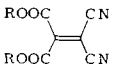
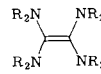
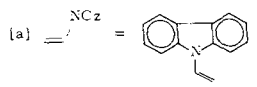
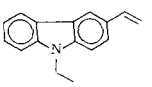
| π-Acceptor | π-Donor | Products: Small Molecules | Products: Polymer | Mechanism | Ref. | Char. |
|---|---|---|---|---|---|---|
| |  | Diels-Alder (C=O) | | Concerted? | [83] | |
|  |  | Cyclobutane | Homopol. | ZI | [99] | +, – |
| |  | Cyclobutane | Homopol. | ZI | [99] | +, – |
| |  | Cyclobutane | Homopol. | ZI | [99] | +, – |
| |  | Cyclobutane | | ZI | [64] | +, – |
|  |  | Cyclobutane | | ZI | [92] | +, – |
|  |  | Cyclobutane | | ZI | [100] | +, – |
| |  | Cyclobutane | | ZI | [101] | +, – |
| |  | Cyclobutane | | ZI | [102] | +, – |
|  |  | Diels-Alder-Add. | | Concerted | [103] | |
| | | | Copol. | | [103] | ↿, ↳ |
| |  | Cyclohexane | Copol. | CT | [103, 104] | borderline |
| |  | Cyclobutane | Homopol. | ZI | [16, 103, 105] | +, – |
| |  | Cyclobutane | Homopol. | ZI | [16, 103] | +, – |
| |  | Cyclohexane | Homopol. | ZI | [16] | +, – |
|  |  | Cyclobutane | Copol. | DR | [81] | ↿, ↳ |
| |  | Cyclobutane | | | [90] | +, – |
|  |  | | Copol. | DR | [81] | ↿, ↳ |
| |  | Cyclobutane | | ZI | [85] | +, – |
| |  | Cyclobutan | | ZI | [85] | +, – |
| |  | Cyclohexane | | ZI | [85] | +, – |
| | | Metathesis | | | [85] | |
| |  [a] | | Homopol. | ZI | [97] | +, – |
|  |  | Butadiene | Homopol. | ZI | [106] | +, – |
| |  | Butadiene | | ZI | [106] | +, – |
|  |  | Cyclobutane | Copol. | borderline | [80] | borderline |
| |  | Cyclobutane | Copol. | borderline | [80] | borderline |

Table 1 (Continued).

| π-Acceptor | π-Donor | Products: Small Molecules | Products: Polymer | Mechanism | Ref. | Char. |
|---|---|---|---|---|---|---|
|  |  | 1-Butene | | ZI | [107] | +, – |
| |  | Cyclobutane | | ZI | [107] | +, – |
| |  | Cyclobutane | | ZI | [107] | +, – |
|  |  | Cyclobutane | | DR | [108] | +, – |
| |  | Cyclobutane | | ZI | [109] | +, – |
| |  | Diels-Alder add. | | Concerted | [109] | |
| |  | Cyclobutane | | ZI | [15] | +, – |
| | | Rearrang. | | ZI | [15] | +, – |
| |  | Cyclobutane | | ZI | [110] | +, – |
| | | Diels-Alder add. | | Concerted | [110, 111] | |
| |  | Cyclobutane | | ZI | [18] | +, – |
| |  | Cyclobutane | | ZI | [112, 28, 34] | +, – |
| |  | Metathesis [d] | | | [29] | |
| | | Diels-Alder add. [e] | | ZI | [113] | |
| |  | Cyclobutane | | ZI | [29, 111] | +, – |
| |  | Cyclobutane | | ZI | [22, 29, 17, 114–116] | +, – |
| |  | 1-Butene | | ZI | [117] | +, – |
| |  | | Homopol. | CT | [118] | +, – |
| |  | Cyclobutane | | ZI | [67] | +, – |
| |  | Cyclobutane | | ZI | [23, 27] | +, – |
| |  | Cyclobutane Butadiene | | ZI | [119] | +, – |
| |  | Butadiene | | ZI | [35] | +, – |
| |  | [g] | | ZI→SET | [120] | +, – |
| |  [a] | Cyclobutane | Homopol. | ZI | [26, 29] | +, – |
| | | | | SET | [25] | |

Table 1 (Continued).

| π-Acceptor | π-Donor | Products: Small Molecules | Products: Polymer | Mechanism | Ref. | Char. |
|---|---|---|---|---|---|---|
| |  | ZI | | ZI | [11] | +, − |
| |  | Ion-Radical-pair | | SET | [121] | |

[a]  [b] 

[c] Inhibited for anionic polymerization. [d] High temperature. [e] High pressure. [f] See Table 4. [g] Heterocycle-formation.

vinylcarbazole. At the acceptor end, two cyano groups favor zwitterionic behavior. Due to Coulombic attraction between the termini, higher yields of small molecules, such as cyclobutanes and 2:1 cyclohexane adducts, are observed in these cases. Homopolymerization is only observed where the propagating ion is highly stabilized. *N*-Vinylcarbazole and vinyl ethers meet this requirement for carbenium ion propagation, nitroethylene and vinylidene cyanide for carbanion propagation.

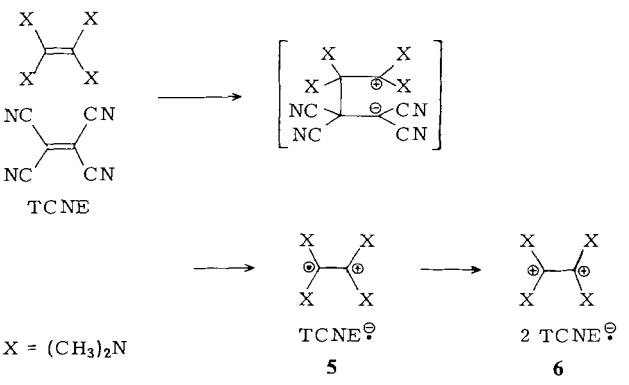
### 2.5. Transition from Zwitterions to Ion-Radical Pairs

When very strong donors and acceptors are present at both termini, single electron transfer takes place. A borderline case is found in the reaction of the enamine of cyclohexanone with tetracyanoethylene[120]. At low temperature, a stable 1,4-zwitterion is formed. At room temperature, electron-transfer gives the radical-ion pair which *via* hydrogen transfer leads to the observed products.

### 2.6. Stable Ion-Radical Pairs

Finally, at the very extremes of donor and acceptor abilities, radical-ion salts are formed, for example **5** and **6**.

The β-substituents hinder bond-formation, and the highly symmetric structures facilitate extensive stabilization of the radical ions[121].




## 3. Reactions of Alkenes with Azo and Carbonyl Compounds

### 3.1. 1,2-Diazatetramethylenes

Our concept of bond-forming initiation can be extended to the reactions of donor molecules with acceptors which contain π-bonded heteroatoms. Extensive studies on the reactions of diethyl azodicarboxylate and 4-phenyl-1,2,4-triazoline-3,5-dione showed that a variety of small molecules and polymers are formed and present a complete analogy to the all-carbon systems (Table 2).

In the reactions of diethyl azodicarboxylate with very electron-rich olefins—*N*-vinylcarbazole and vinyl ethers—zwitterionic intermediates lead to homopolymers or cyclobutanes. With almost all other olefins, hydrogen shift leads to the ene-reaction product. Cyclopentene and cyclohexene are exceptions; here a radical chain reaction is preferred. Bond-forming initiation is *one* possible interpretation for this spontaneous initiation (for other possible interpretations see Section 8.1). Diethyl azodicarboxylate undergoes [4+2] cycloadditions with *cis*-dienes. These various reaction paths correspond completely to those observed in alkene-alkene reactions, namely non-chain small molecule formation, on the one hand, and free radical chain copolymerizations on the other. The $-\overset{*}{N}-COOCH_3$ group is borderline as regards preferred diradical or zwitterionic behavior, comparable to a $-\overset{*}{C}(CN)-COOR$ group in a tetramethylene with carbon skeleton.

4-Phenyl-1,2,4-triazoline-3,5-dione is extremely electrophilic due to its imide structure. Accordingly, it forms a zwitterionic intermediate with most of the alkenes quoted in Table 2. Hydrogen-shift will then lead to the ene-reaction product, or diazacyclobutanes will be formed. With alkenes which contain strong donor groups, the diazacyclobutane formation is reversible. (The copolymers obtained by reaction of triazolinedione with vinyl ethers or *N*-vinylamines are presumably formed by polyrecombination of 1,4-zwitterions, and not *via* a radical mechanism—see Section 8.1.) In several cases, Wagner-Meerwein rearrangements confirm zwitterionic behavior[31,32]. The triazolinedionyl group is similar to two cyano groups at the terminal as regards favoring zwitterionic behavior. With *cis*-dienes, Diels-Alder adducts are formed, although not with 2,5-dimethyl-2,4-hexadiene. Interestingly, an equilibrium between a diradical and zwitterionic diazatetramethylene was postulated; the zwitterion could in fact be trapped with acetic acid[125].

### 3.2. 1-Oxatetramethylenes

The reactions of the very electrophilic hexafluoroacetone with alkenes have been interpreted exclusively in the context of zwitterionic intermediates[126]. The zwitterion could be trapped by inducing cationic polymerization of allyl glycidyl ether. The reactions of bis(trifluoromethyl)ketene with electron-rich alkenes likewise proceed *via* zwitterionic intermediates, as shown by the homopolymerization of the vinyl ether[127]. On the other hand, dimethyl mesoxalate reactions were shown by the deuterium isotope effect to be concerted[128].

Table 2. Reactions between π-bonds *via* heterotetramethylenes. In the case of reactions *via* 1,2-diazatetramethylenes, 1-butene, butadiene, cyclobutane and cyclobutene stand for the corresponding hetero-compounds. – Char.: predominating character of the heterotetramethylene.

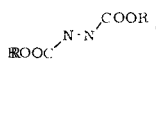
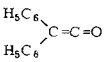
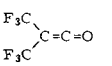
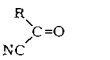
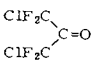
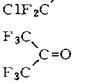
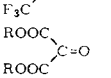
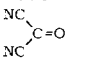
| π-Acceptor | π-Donor | Products: Small Molecules | Products: Polymer | Mechanism | Ref. | Char. |
|---|---|---|---|---|---|---|
|  |  | 1-Butene | | Radical-chain | [129] | ↿, ↳ |
| |  | 1-Butene | | Concerted | [129] | |
| |  | ene reaction | | ZI | [130] | +, – |
| |  | Diels-Alder add. | | Concerted | [130] | |
| |  | 1-Butene | | Concerted | [131] | ↿, ↳ |
| |  | Cyclobutane | | ZI | [132] | +, – |
| |  | Diels-Alder (C=O) | | Concerted | [132] | |
| |  | Diels-Alder (C=O) | | Concerted | [132] | |
| |  | Diels-Alder (C=O) | | Concerted | [133] | |
| |  | 1-Butene | | ZI | [133] | +, – |
| | | Cyclobutane | | ZI | [134] | +, – |
| |  | | Homopol. | CT | [135] | +, – |
|  |  | 1-Butene | | Concerted | [136, 137] | +, – |
| |  | Diels-Alder add. | | Concerted | [125] | |
| |  | [b] | | ZI↔DR | [125] | +, – |
| |  | Cyclobutane | | ZI | [138] | +, – |
| | Indene | Cyclobutane | | ZI | [132] | +, – |
| |  | Diels-Alder (arom.) | | Concerted | [68, 139] | |

Table 2 (Continued).

| π-Acceptor | π-Donor | Products: Small Molecules | Products: Polymer | Mechanism | Ref. | Char. |
|---|---|---|---|---|---|---|
| |  | Rearrang. | | ZI | [140, 141] | +, – |
| | | Cyclobutane | | ZI | [140] | +, – |
| | | | Copol. | Polycombin. | [140] | |
| |  | Cyclobutane | | ZI | [142] | +, – |
| | | | Copol. | Polycombin. | [142] | |
| |  | Cyclobutane | | ZI | [132] | +, – |
| |  | Cyclobutane | | ZI | [143] | +, – |
| | | | Copol. | Polycombin. | [143] | |
| |  | | Copol. | | [144] | ↿, ↳ |
|  |  | Cyclobutane | | ZI | [145, 146] | +, – |
|  |  | Oxetane | | ZI | [127] | +, – |
| | | Cyclobutane | | ZI | [127] | |
| |  | Oxetane | Homopol. | ZI | [127, 147] | +, – |
| $H_2C{=}O$ | β-Pinene | ene reaction | | Concerted | [148] | |
|  |  | Oxetane | | ZI | [149] | +, – |
|  |  | Oxetane | | ZI | [126] | +, – |
|  |  | Oxetane | | ZI | [126] | +, – |
|  |  | ene reaction | | Concerted | [128] | |
|  |  | ene reaction | | ZI | [150] | +, – |
| |  | ene reaction | | ZI | [151] | +, – |
| $ClSO_2N{=}C{=}O$ |  | β-Lactam, ene reaction | | ZI | [152] | +, – |

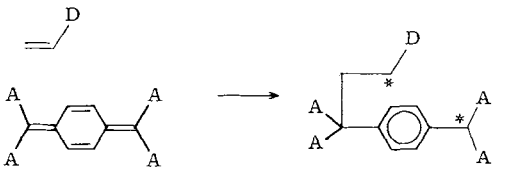
[a] See footnote [a] of Table 1. [b] Acetic acid adduct of tetramethylene

The reactions of donor molecules with acceptor molecules which contain π-bonded heteroatoms follow the same trends as the reactions of the alkenes. Due to the extreme electrophilic character of these nitrogen and oxygen acceptors, the corresponding heterotetramethylenes often have zwitterionic character.

## 4. Reactions of Alkenes with *p*-Quinodimethanes and Quinones

### 4.1. Tetramethylenes Containing *p*-Phenylene Groups

The concept of bond-forming initiation can be further extended to the polymerization reactions of 7,7,8,8-tetra-substituted quinodimethanes (Table 3), which act as acceptors towards some donor alkenes. Here, no small molecules are formed, but the pattern of the observed polymerizations is identical with that observed for acceptor alkenes.

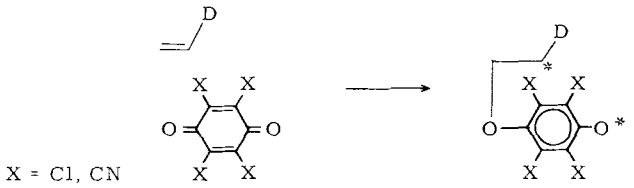


7,7,8,8-Tetrakis(methoxycarbonyl)quinodimethane copolymerizes spontaneously with styrene and other vinyl monomers, suggesting a diradical intermediate. 7,7,8,8-Tetracyanoquinodimethane copolymerizes with styrene. This indicates that a *p*-phenylene-containing tetramethylene has more diradical character than the corresponding alkene-derived tetramethylene, because the former possesses an aryl group at the reactive center. However, 7,7,8,8-tetracyanoquinodimethane induces cationic polymerization of vinyl ethers *via* a zwitterionic intermediate. This intermediate could be trapped with methanol[16, 17]. The more electrophilic 7,7,8,8-tetracyano-2,3,5,6-tetrafluoroquinodimethane can cause the less electron-rich β-chloroethyl vinyl ether to homopolymerize cationically.

With the less electrophilic chloro-substituted quinodimethanes, the copolymers obtained are not alternating, but contain excess quinodimethane. These cases can be considered as borderline between the bond-forming initiation mechanism as proposed here, and the diradical coupling mechanism demonstrated for the parent unsubstituted xylylene[153] (see Section 8.1).

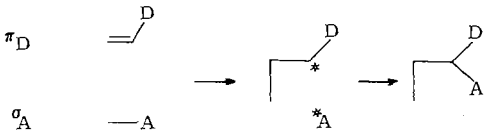
### 4.2. Tetramethylenes Containing *p*-Phenylenedioxy-Groups

The electrophilic quinones, tetrachloro-*p*-benzoquinone (chloranil) and dichlorodicyano-*p*-benzoquinone can copolymerize or induce ionic polymerization of various alkenes. The high electronegativity of the oxygen-substituted *p*-phenylene group favors zwitterion character for the tetramethylene intermediates (Table 3).




## 5. Reactions of Alkenes with Halogens and Peroxides

Some σ-bonds are about as weak as π-bonds. The general picture of bond-forming initiation can be extended to such labile σ-bonds.

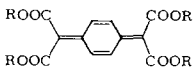



*,* denotes +,− or ↿,↾

Numerous such mechanisms for the reactions of single-bonded molecules with alkenes which spontaneously give rise to free radicals have already been dealt with in reviews by *Pryor*[19] and by *Harmony*[166] under the heading "molecule-assisted homolysis". Molecule-assisted heterolysis is also known, as, *e.g.*, in the reaction of bromine and other reagents with alkenes.

The fragments combine to give small molecules, corresponding to the small molecules in alkene reactions. The character of the *,*-centers must be determined by physical organic methods, *e.g.* by analysis of solvent effects, structural effects, *etc.* However, if the fragments escape the

Table 3. Reactions *via* (hetero)tetramethylenes with *p*-phenylene groups. Char.: Predominating character of the (hetero)tetramethylene.

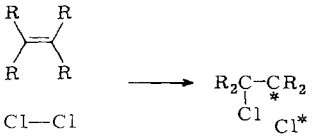
| Acceptor | | Polymers | Mechanism | Ref. | Char. |
|---|---|---|---|---|---|
| *Quinodimethane* | | | | | |
| 7,7,8,8-$Cl_4$ |  | Random copol. | DR Poly combin. | [154] | ↿,↾ |
| 2,5,7,7,8,8-$Cl_6$ |  | Random copol. | DR Poly combin. | [154] | ↿,↾ |
| |  | Random copol. | DR Poly combin. | [154] | ↿,↾ |
| |  | Random copol. | DR Poly combin. | [154] | ↿,↾ |
| 2-CN-7,7,8,8-$Cl_4$ |  | Random copol. | DR Poly combin. | [155] | ↿,↾ |
| 7,7,8,8-$(COOR)_4$ |  | Copol. | CT | [156] | ↿,↾ |
| |  | Copol. | CT | [156] | ↿,↾ |
| |  | Copol. | CT | [156] | ↿,↾ |
| 7,7,8,8-$(CN)_4$ |  | Copol. | CT | [156] | ↿,↾ |
| |  | Copol. | CT | [157] | ↿,↾ |
| |  | Homopol. [b] | CT | [158] | borderline |
| | | Copol. [c] | CT | [158, 159] | |
| |  | Homopol. [d] | SET | [159, 160] | +, − |
| |  | Homopol. | SET | [16, 17] | +, − |
| |  | Homopol. | CT | [161] | +, − |
| |  | Homopol. | CT | [162] | +, − |
| 7,7,8,8-$(CN)_4$, 2,3,5,6-$F_4$ |  | Copol. | CT | [163] | ↿,↾ |
| |  | Copol. | CT | [163] | ↿,↾ |
| |  | Copol. | CT | [163] | ↿,↾ |
| |  | Homopol. | CT | [163] | +, − |
| *Quinone* | | | | | |
| 2,3,5,6-$Cl_4$ |  | Homopol. | ZI | [164] | +, − |
| 2,3-$Cl_2$, 5,6-$(CN)_2$ |  | Copol. | CT | [165] | ↿,↾ |
| |  | Homopol. | SET | [16, 17, 165] | +, − |

[a] See footnote [a] of Table 1. [b] In ethylene carbonate. [c] In acetonitrile. [d] In polar solvent.

solvent cage, they may initiate chain reactions, corresponding to polymerization. *Pryor*[19] and *Harmony*[166] both describe a number of such free radical chain reactions. Just as zwitterion-initiated polymerizations are rarer than diradical ones, we found very few spontaneously initiated ionic chain reactions (see Table 4).

### 5.1. Halogens

*Poutsma*[167] described the spontaneous thermal addition of chlorine to various alkenes. Ionic non-chain addition competes with free radical chain addition. Thus, this is a borderline situation. *Poutsma*'s evidence for the occurrence of these two competing pathways includes: spontaneous reactions even in the dark at −78 °C, no oxygen effect, good structure-property relations, solvent effects, dilution effects, trapping of Cl· by cyclohexane, and the effect of free radical inhibitors.



*,* denotes +,− and/or ↿, ↾

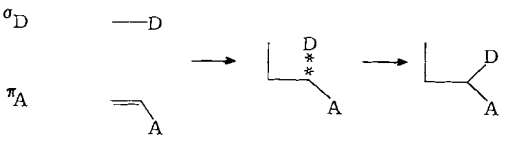
Reactions of bromine with alkenes mostly proceed *via* an ionic pathway[168]. In contrast, iodine reacts with styrene by a radical pathway[169]. Fluorine is so reactive that it could only be studied with tetrachloroethylene, with which it spontaneously forms radicals[170].

### 5.2. Peroxides

Peroxides react spontaneously with alkenes[171]. A "direct reaction", predominantly ionic, is found to compete with a radical chain reaction. Benzoyl peroxide reacts spontaneously with *N*-vinylcarbazole to produce bimodal polymers, one formed ionically and one by a free radical path[172–175]. This may be due to competing ions and radicals from bond-forming initiation. Alternatively in this case, single electron transfer may provide a viable pathway.

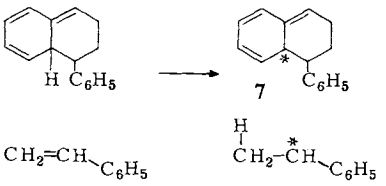
## 6. Reactions of Alkenes with Compounds Containing Aliphatic C–H Bonds

Turning to $\sigma_D+\pi_A$ reactions, a number of cases of hydrogen transfer involve bond-forming initiation. The carbon-hydrogen bond is strong, but its bond energy is regained.

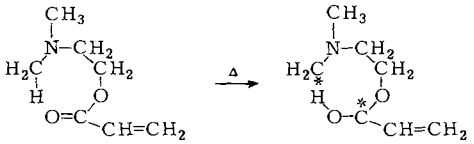


*,* denotes +,− and/or ↿, ↾

The spontaneous polymerization of styrene appears to involve reactions of 1-phenyl-1,2,3,8a-tetrahydronaphthalene (the Diels-Alder adduct of styrene) with other styrene molecules[176–178]. (Only one resonance form of the product **7** is shown.) In this case, the asterisks correspond to radical centers, as shown by the free radical polymerization of styrene.

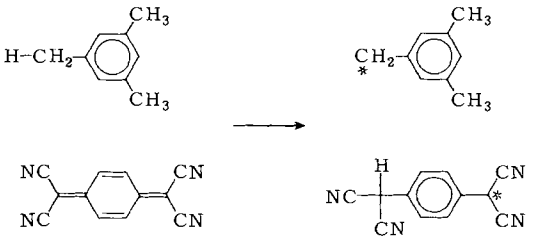


Intramolecular bond-forming initiation occurs in the polymerization of dimethylaminoethyl acrylate[179].

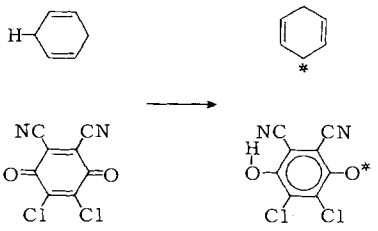


Here the asterisks indicate radicals, as shown by the ready free radical polymerization initiated in this way.

Again, polar character facilitates these reactions. The reaction of tetracyanoquinodimethane with mesitylene[180] or with *p*-methoxytoluene[181] is another case of $\sigma_D+\pi_A$ reaction. Here radical character is displayed, and the reactions proceed readily.



The reaction of dichlorodicyano-*p*-benzoquinone with 1,4-cyclohexadiene[182] can be described in our terms as $\sigma_D+\pi_A$ bond-forming initiation.



Here the asterisks can be identified as +, −, attributable to the electronegativity of oxygen (see Table 4).

Table 4. Reactions involving σ-bonds.

| σ-Acceptor | π-Donor | Mechanism | Ref. |
|---|---|---|---|
| *Halogens* | | | |
| Fluorine | Tetrachloroethylene | radic. | [170] |
| Chlorine | Cyclohexene | radic., ion. | [183, 184] |
| | Butadiene | | |
| | 1-Butene | radic. | [185] |
| | Allyl chloride | | |
| | Styrene | | |
| | Isobutene | ion. | [185] |
| Bromine | Cyclohexene | ion. | [168] |
| Iodine | Styrene | radic. | [169] |
| *t*BuOCl | Styrene | radic. | [186] |
| *Peroxides* | | | |
| Benzoyl peroxide | *N*-Vinylcarbazole | radic., ion. | [172–175] |
| | *N*-Vinylpyrrolidone | radic., ion. | [172] |
| *m*-Bromobenzoyl peroxide | *p,p'*-Dimethoxystilbene | radic., ion. | [171, 187] |
| Phthaloyl peroxide | Stilbene | radic. | [188] |
| Acetyl peroxide | Cyclohexene | radic. | [189] |
| *tert*-Butyl hydroperoxide | Styrene | radic. | [190] |
| Peracids | Alkenes | ion. | [191] |
| σ-Donor | π-Acceptor | | |
| Mesitylene | Tetracyanquinodimethane | radic. | [180] |
| 1,3-Cyclohexadiene | Dichlorodicyano-*p*-benzoquinone | ion. | [182] |
| 1-Phenyl-1,2,3,8a-tetrahydronaphthalene | Styrene | Radical chain | [19] |
| Cyclopentene | Diethyl azodicarboxylate | Radical chain | [192] |
| Dimethylaminoethyl acrylate | | Radical chain | [179] |

## 7. An "Organic Chemist's Periodic Table"

Previous surveys of cycloaddition reactions have not taken into account the results from polymer chemistry. However, the mechanistic information obtained from the polymerization criteria is entirely consistent with the physical organic chemistry data. In particular, *Huisgen*'s expectation[7] that the terminal substituents determine the character of the tetramethylene is abundantly confirmed by our survey. At the donor terminal, phenyl and vinyl groups prefer to stabilize a diradical, while hard donors, such as nitrogen and oxygen, favor a zwitterion. At the acceptor terminal, diester, cyano-ester, anhydride and chlorine favor diradical character, while two cyano-groups favor zwitterionic character.

That the terminal substituents determine tetramethylene character in both organic and polymer reactions, is revealed by systematic presentation in an "Organic Chemist's Periodic Table for Alkenes" (Fig. 1)[84, 193]. In this format, the acceptor alkenes have been listed, as in Table 1, according to increasing acceptor behavior. We found it possible on the basis of general chemical experience to arrange the donor alkenes in such a manner that the Periodic Table shows a region of mechanistic change. In such a presentation covalent bonds would be favored in the center, while ionic bonding would be favored toward the lower and right-hand side. Moreover, increasing reactivity would be expected as one proceeds downwards and to the right.

The Periodic Table also displays monotonically increasing reactivity as we proceed toward more powerful donor and acceptor groups. This is due to the push-pull stabilization of the tetramethylene, whether diradical or zwitterionic. As the reaction partners become respectively more electropositive and electronegative, a transition from covalent to ionic bonding occurs.

This "Periodic Table" enables predictions to be made concerning new reactions. The reactions of azo and carbonyl compounds as well as the other reactions discussed here, can also be included in this "Periodic Table".

## 8. Critique of Method

### 8.1. Remarks on Polymerization

For the polymerization method to be viable, certain criteria must be complied with. The donor and/or acceptor reaction partners must be mono- or 1,1-disubstituted alkenes in order to be homopolymerizable by radical or ionic pathways. Trisubstituted acceptors will copolymerize with monosubstituted donors under free radical conditions, but will not homopolymerize. Tetrasubstituted acceptors copolymerize in only a few cases and do not homopolymerize.

Furthermore, the solvent also must allow polymerization to take place. For free radical polymerizations, most solvents other than those containing halogen- or nitro-groups can be used. For cationic polymerization, dichloromethane, toluene, and benzene are best. Donor solvents must be avoided[194], except for very reactive carbenium ion monomers such as *N*-vinylcarbazole and vinyl ethers, where weak donor solvents such as acetone or acetonitrile can be used. For anionic polymerization tetrahydrofuran, glymes and amide solvents are favored, but protolytic or acceptor solvents cannot be used. For ionic polymerizations, the solvent may affect zwitterion formation and subsequent polymerization differently. A polar non-donor solvent[24, 194] may permit carbenium ion polymerization in cases where a polar donor solvent impedes it. For example, tetracyanoquinodimethane induces cationic polymerization of β-chloroethyl vinyl ether in ethylene carbonate, whereas copolymerization takes place in acetonitrile (see Table 3). Finally, dilution is expected to favor cycloadducts over polymers; this has been found in several cases[90].

For ionic polymerization initiated by a zwitterion, other difficulties arise when we consider the possibility of propagation by carbenium ions in the presence of carbanions or vice versa, or even of simultaneous cationic and anionic polymerization. The latter was observed in the reactions of vinylidene cyanide[16, 103, 105] and of nitroethylene[78]. One of the prerequisites for such a reaction is that the ions are extremely well stabilized by resonance or steric hindrance. Dichlorodicyano-*p*-benzoquinone is able to initiate the cationic polymerization of vinyl ethers, because its anion is highly stabilized[17]. A second contributing factor for simultaneous cationic and anionic polymerizations is phase separation[197] or microphase separation[195, 196], wherein the growing end is preferentially surrounded by like monomer. The third, and probably most important factor, is that the anion can lose an adjacent leaving group, leaving a free carbenium ion to initiate cationic polymerization. Butadienes have been formed in a number of cases where a very stable zwitterion is formed; hydrogen cyanide is elim-

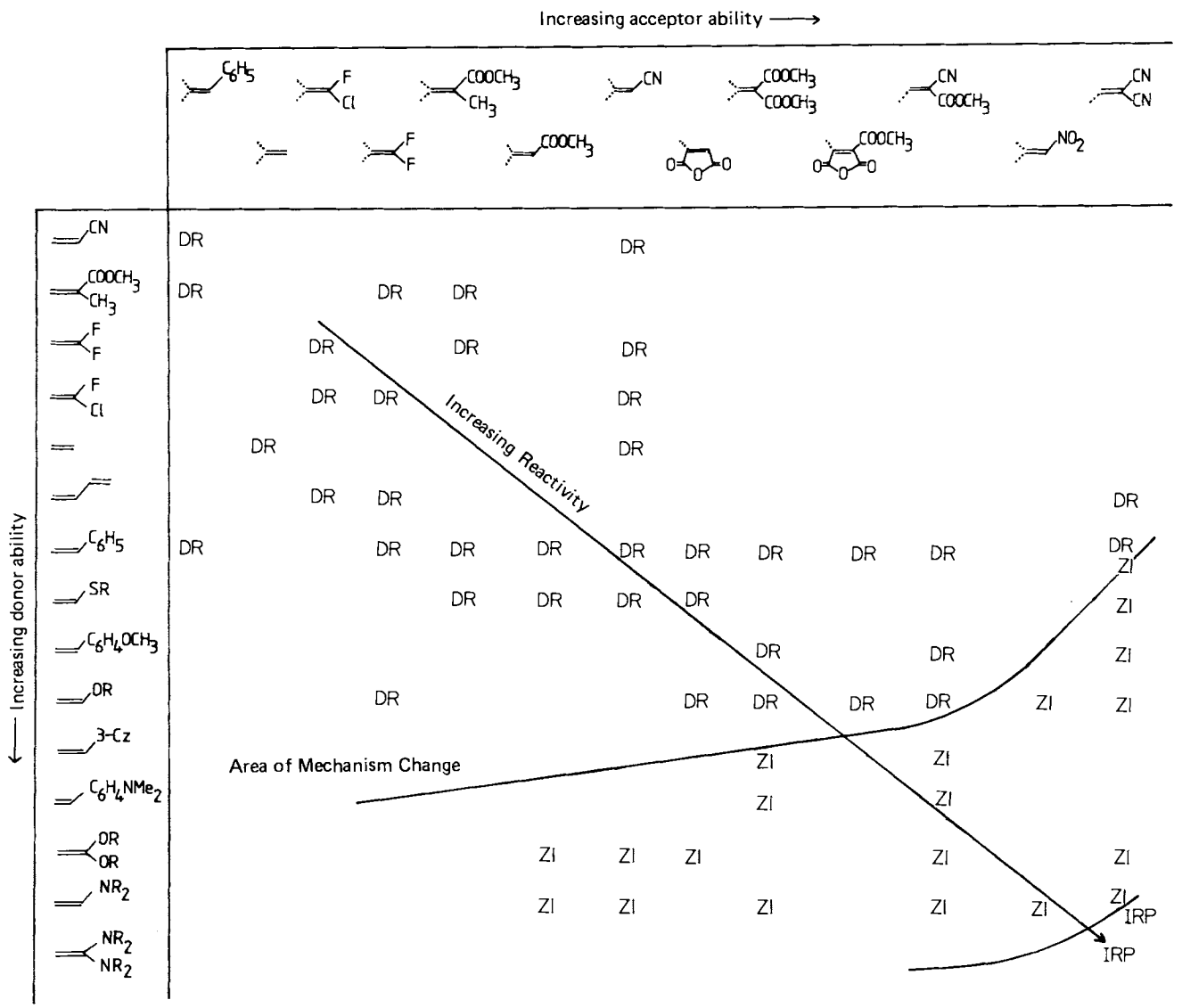
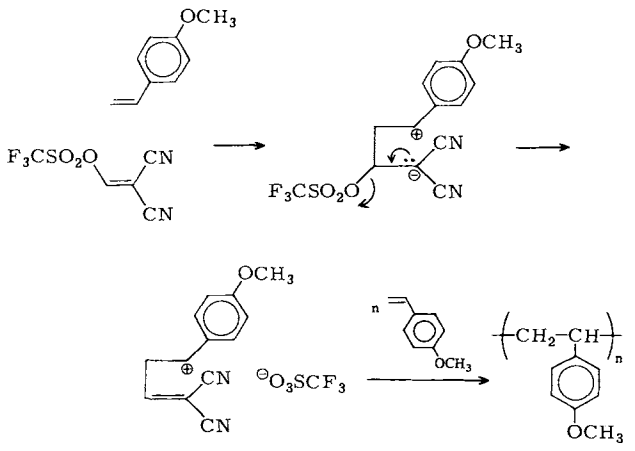



Fig. 1. The Periodic Table of spontaneous reactions of alkenes. DR: diradical mechanism, ZI: zwitterionic mechanism, IRP: mechanism *via* a radical ion pair.

inated in the reaction of *N*-vinylcarbazole and tetracyanoethylene[25], leading to cationic homopolymerization of the former. Cationic polymerizations can be effectively initiated by using di- or tricyanoethylenes containing a β-chloro or β-trifluoromethanesulfonate group as leaving group[198].



Finally, carbenium ions and carbanions can coexist in concentrations suitable to cause polymerization, as seen in radiation polymerizations.

As initiators, diradicals can convert by rotation into the *trans*-conformation, or can be formed in this conformation. Accordingly, they will be more effective initiators than 1,4-zwitterions. In keeping with this idea, far more radical copolymerizations occur in the reactions under discussion than ionic homopolymerizations. As noted by *Huisgen*[7,22], zwitterions are likely to remain in the coiled *gauche*-conformation because of Coulombic attraction. As a result they are likelier to collapse to small molecules, the particular type being determined by the conformation; thus, they may not be very effective initiators for ionic polymerization.

We considered whether coupling of tetramethylenes may contribute to copolymer formation. Polymer formation by coupling of zwitterionic intermediates has been reviewed by *Saegusa*[199]. The very stable zwitterions from 1-phenyl-1,3,4-triazoline-3,5-dione and vinyl ethers were postulated to form copolymers by this route[142]. Coupling

of diradicals contributes to copolymer formation from quinodimethanes. Coupling would be evidenced by head-to-head structures in the former case and by formation of copolymers possessing other than 1 : 1 composition ratios in the latter.

### 8.2. Remarks on the Formation of Small Molecules

The formation of cyclohexenes and ene-reaction products *via* [4+2] and [2+2+2] reactions, respectively, competes with the stepwise [2+2] cycloadditions, which lead to cyclobutanes and 1-butenes. If the donor group is aryl, the Diels-Alder reaction may occur into the ring; in the case of vinyl groups, cyclohexene formation can compete with cyclobutane formation; with alkyl groups, hydrogen shift can lead to ene-reaction products. If the acceptor group is an ester, pyran formation can compete with cyclobutane formation in an inverse electron-demand hetero-Diels-Alder reaction[82].

Current theory postulates a sharp distinction between [2+2] (concerted reaction, disallowed thermally) and [4+2] (concerted reaction, allowed thermally) cycloadditions[200,201]. Nevertheless, other researchers are inclined to consider a range of possibilities, from completely stepwise to completely concerted reactions for the [4+2] cycloadditions. Stepwise hetero[4+2] cycloadditions have been described[46]. For the all-carbon cases, *Gilchrist* and *Storr*[202] describe reactions in which zwitterionic intermediates are so stabilized, that a stepwise [4+2] cycloaddition becomes a viable alternative, and more examples can be found in the literature[18,35,92,203-208]. *Firestone*[209] proposes a spin-paired diradical stepwise mechanism, even for moderately polarized Diels-Alder reactions. Similar considerations apply to ene-reactions[210], which can range from concerted to stepwise in cases where the zwitterion is especially stabilized electronegatively.

It is still not clear for [4+2] reactions where non-concerted reactions end and concerted ones begin[211]. The polymerization criterion may prove useful in further defining the line of demarcation.

### 8.3. Unimportance of Charge-Transfer Complexes and Radical-Ion Pairs in Thermal Initiation

Charge-transfer complexes and radical-ion pairs have been invoked as initiating species (for reviews, see *e.g.* [24,212]). We believe that neither of these contributes significantly, and that the tetramethylenes are the true initiators.

Charge-transfer complexes are certainly formed in many of the reactions we are considering. The same donor-acceptor character facilitating formation of push-pull tetramethylenes also favors formation of charge-transfer complexes. However, such complex formation is only a weak molecular interaction and primarily affects spectral properties rather than reactivity. Nevertheless, charge-transfer complex equilibrium constants between donor and acceptor monomers parallel their increasing reactivity in spontaneous polymerization, as noted by *Iwatsuki* and *Yamashita*[213]. These investigators also noted transitions from copolymerization to ionic polymerizations and then to stable products as the equilibrium constants increased, reminiscent of our "Periodic Table" presentation (above).

With regards to radical-ion pairs as intermediates, *Shirota* and *Mikawa*[24] and *Tazuke* and *Okamura*[66] observe that electron transfer is energetically unfavorable for weak electron-donating and electron-withdrawing monomer pairs.

In the case of alkenes with few substituents, it is very unlikely that a radical-ion pair could be formed without collapsing to a tetramethylene, thereby gaining the whole energy of a chemical bond. If formed, the two should undergo instant radical recombination in the solvent cage, accelerated by Coulombic attraction.

Further evidence against the radical-ion mechanism is offered by the steric effects of the substituents at the β-positions. Trimethyl ethylenetricarboxylate is much more reactive than tetramethyl ethylenetetracarboxylate, even though the latter has a greater electron-affinity as measured by cyclic voltammetry[214]. Similarly, tricyanovinyl trifluoromethanesulfonate is less reactive than 2,2-dicyanovinyl trifluoromethanesulfonate[198].

Even in the case of tetracyanoethylene, which is known to form an extremely stable radical-anion, *Huisgen*[7,22] finds no evidence of single electron transfer in the reaction with vinyl ethers. Still more striking is the formation of a stable zwitterion in the reaction of ketene *S,N*-acetals with tetracyanoethylene with no evidence of single electron transfer[11]. Cycloadditions of vinyl sulfides to tetracyanoethylene proceed through a zwitterionic intermediate, and not through an ion-radical pair[23,27]. Enamines such as dimethylvinylamine add to tetracyanoethylene *via* zwitterionic intermediates[35]. Only in extreme cases, such as the reaction of tetrakis(dimethylamino)ethylene[121,215] or the enamine of cyclohexanone[120] with tetracyanoethylene, does electron transfer occur. Along similar lines, initiation of the reaction of *N*-vinylcarbazole with benzoyl peroxide could involve electron transfer[172]. Such a course is known for the reaction of dimethylaniline with benzoyl peroxide[216].

Finally, evidence against the electron-transfer concept in copolymerization is that when radical cations of a vinyl ether are deliberately synthesized by electrochemical methods, they are known to dimerize[217]. No such products are ever reported in the cycloaddition and polymerization reactions.

On all the above grounds, we can state that single electron transfer will be seen only in the cases where greatly hindered and highly resonance-stabilized radical-ions can be formed.

### 8.4. Impurities, Inhibitors, and Initiators

Trace impurities in a reaction mixture might accelerate the reaction or cause a change of mechanism. Such cases have been encountered on occasion.

Free radical reactions can be accelerated by peroxides, light, or oxygen. For example, the copolymerization of norbornene and sulfur dioxide was formerly believed to proceed *via* coupling of spontaneously formed diradi-

cals[218]. However, this copolymerization was later shown to be initiated by traces of peroxide impurities[219].

With regard to acidic impurities initiating cationic polymerization, *Shirota* and *Mikawa*[24] showed that traces of 2,5,6-trichloro-3-hydroxy-*p*-benzoquinone were the true initiators in the tetrachloro-*p*-benzoquinone-promoted polymerization of *N*-vinylcarbazole. *Stille et al.*[220] described the cationic polymerization of vinyl ether initiated by tricyanoethenol impurity in tetracyanoethylene.

Finally, even diffuse laboratory light induces the radical reactions of nitroso compounds with alkenes[221].

Nevertheless, we exclude impurities or other adventitious effects as responsible for the reactions under discussion. Firstly, impurities are as likely to inhibit as to initiate chain reactions. Secondly, many of the reactions take place rapidly and reproducibly in absence of air or light. Thirdly, the structure-property relation shown in the "Periodic Table" is reassuringly consistent.

Deliberately added inhibitors can, of course, be used to suppress chain reactions in favor of the molecular reactions. Conversely, deliberately added initiators can be used for favoring ionic or radical chain reactions. As noted above, the donor or acceptor character of the solvent can be used to influence ionic polymerizations. In these ways the chemist can control the outcome of the reaction and thus obtain the desired product.

## 9. Outlook

It is well known that reactive particles combine with each other. Thus, free radicals combine or disproportionate at nearly diffusion-controlled rates. Carbenium ions combine very readily with carbanions.

Also well known are reactions in which a reactive particle reacts with a molecule to form a new molecule and a new reactive particle. Such chain reactions are familiar for both free radical and ionic chain carriers.

To round off matters symmetrically, our theory describes reactions of neutral molecules with each other to generate reactive particles. These particles then lead directly to products in non-chain fashion, or can initiate chain reactions, either free radical or ionic. The variety of reactions we have discussed in this article makes it clear that this third process possesses wide generality.

In the future we hope to incorporate all of the cases we have discussed into an extended "Organic Chemist's Periodic Table" for all types of donor and acceptor molecules. Before this can be done much additional experimental information must be obtained.

Other reactions may fall under this scheme, *e.g.* spontaneous reactions of unsaturated molecules such as allenes, alkynes, ketenes, singlet oxygen, sulfur dioxide, and sulfur trioxide. Lewis acids may complex with the acceptor alkene to increase its electrophilicity and shift its position in the "Periodic Table". Oxidation of alkenes and hydrocarbons by electrophiles containing Cr=O and Mn=O bonds may also fit into our scheme.

A quantitative treatment would be highly desirable. As to the reactants, quantitative measures of donor and acceptor ability such as oxidation- and reduction-potentials, nucleophilic- and electrophilic-reactivities, *etc.*, may be considered. Use of Taft constants to correlate reactivities may be useful. As to the tetramethylenes, theoretical studies should be a great help in determining their stabilities and their zwitterionic or diradical nature.

The solvent must also play a crucial role in these reactions, a further facet of this field of chemistry which calls for closer study in the future.

*The author is greatly indebted to his colleagues, Dr. Husam Rasoul, Dr. Mohamet Abdelkader, Dr. Anne Padias, Dr. Pierre Nogues, and Dr. Robert Sentman for their contributions both experimental and interpretative. Generous financial support was provided by the Division of Materials Research of the National Science Foundation, Grant DMR-81-06018.*

*He is also greatly indebted to Professor Hiroshi Sumitomo of Nagoya University and to the "Japan Society for the Promotion of Science" for a Senior Visiting Fellowship, May—July 1981, which provided an opportunity for fruitful discussion with numerous Japanese scientists who have contributed to this field. This work was first presented at the May 1981 Meeting of the Polymer Society of Japan in Kyoto. It was also presented at the Macromolecular Symposium of the International Union of Pure and Applied Chemistry (Amherst, MA, July 1982) and at the Welch Symposium (Houston, TX, November 1982).*

Received: June 9, 1982;
revised: February 1, 1983 [A 456 IE]
German version: *Angew. Chem. 95* (1983) 448

[1] R. Hoffmann, S. Swaminathan, B. G. Odell, R. Gleiter, *J. Am. Chem. Soc. 92* (1970) 7091.
[2] G. A. Segal, *J. Am. Chem. Soc. 96* (1974) 7892.
[3] W. A. Pryor, *Polym. Prepr. Am. Chem. Soc. Div. Polym. Chem. 12* (1971) 49.
[4] L. M. Stephenson, J. I. Brauman, *J. Am. Chem. Soc. 93* (1971) 1988.
[5] P. D. Bartlett, N. A. Porter, *J. Am. Chem. Soc. 90* (1968) 5317.
[6] a) J. S. Chikos, *J. Org. Chem. 44* (1979) 780; b) P. B. Dervan, D. S. Santilli, *J. Am. Chem. Soc. 102* (1980) 3863.
[7] R. Huisgen, *Acc. Chem. Res. 10* (1977) 199.
[8] W. T. Borden, E. R. Davidson, *J. Am. Chem. Soc. 102* (1980) 5409.
[9] a) J. A. Berson in P. de Mayo: *Rearrangements in Ground and Excited States*, Academic Press, New York 1980, p. 311; b) W. T. Borden, *React. Intermed. 2* (1981) 175.
[10] L. Salem, C. Rowland, *Angew. Chem. 84* (1972) 86; *Angew. Chem. Int. Ed. Engl. 11* (1972) 92.
[11] R. Gompper, W. Elser, H. J. Muller, *Angew. Chem. 79* (1967) 473; *Angew. Chem. Int. Ed. Engl. 6* (1967) 453.
[12] H. G. Viehe, R. Merenyi, L. Stella, Z. Janousek, *Angew. Chem. 91* (1979) 982; *Angew. Chem. Int. Ed. Engl. 18* (1979) 917.
[13] K. D. Gundermann, E. Roehrl, *Justus Liebigs Ann. Chem. 1974*, 1661.
[14] R. Huisgen, R. Schug, G. Steiner, *Angew. Chem. 86* (1974) 47; *Angew. Chem. Int. Ed. Engl. 13* (1974) 80.
[15] W. Weber, I. Erden, A. de Meijere, *Angew. Chem. 92* (1980) 387; *Angew. Chem. Int. Ed. Engl. 19* (1980) 387.
[16] J. K. Stille, N. Oguni, D. C. Chung, R. F. Tarvin, S. Aoki, M. Kamachi, *J. Macromol. Sci. Chem. A 9* (1975) 745.
[17] R. F. Tarvin, S. Aoki, J. K. Stille, *Macromolecules 5* (1972) 663.
[18] F. Kataoka, N. Shimizu, S. Nishida, *J. Am. Chem. Soc. 102* (1980) 711.
[19] W. A. Pryor in: W. A. Pryor: *Organic Free Radicals, ACS Symp. Ser. 69* (1978) 33.
[20] A. T. Bottini, L. J. Cabral, V. Dev, *Tetrahedron Lett. 1977*, 615.
[21] P. D. Bartlett, *Q. Rev. Chem. Soc. 24* (1970) 473.
[22] R. Huisgen, *Acc. Chem. Res. 10* (1977) 117.
[23] T. Okuyama, M. Nakada, K. Toyoshima, T. Fueno, *J. Org. Chem. 43* (1978) 4546.
[24] Y. Shirota, H. Mikawa, *J. Macromol. Sci. Rev. Macromol. Chem. C 16* (1977) 129.
[25] C. E. H. Bawn, A. Ledwith, M. Sambhi, *Polymer 12* (1971) 209.

[26] T. Nakamura, M. Soma, T. Onishi, K. Tamaru, *Makromol. Chem. 135* (1970) 241.
[27] H. Graf, R. Huisgen, *J. Org. Chem. 44* (1979) 2594, 2595.
[28] S. Nishida, I. Moritani, T. Teraji, *J. Org. Chem. 38* (1973) 1878.
[29] J. K. Williams, D. W. Wiley, B. C. McKusick, *J. Am. Chem. Soc. 84* (1962) 2210.
[30] F. K. Fleischmann, H. Kelm, *Tetrahedron Lett. 1973,* 3773.
[31] P. J. Wagner, K. C. Liu, Y. Noguchi, *J. Am. Chem. Soc. 103* (1981) 3837.
[32] T. Sasaki, K. Kanematsu, M. Uchide, *Tetrahedron Lett. 1971,* 4855.
[33] W. Adam, O. DeLucchi, D. Scheutzow, *J. Org. Chem. 46* (1981) 4130.
[34] F. Kataoka, S. Nishida, *Chem. Lett. 1980,* 1115.
[35] R. Gompper, *Angew. Chem. 81* (1969) 348; *Angew. Chem. Int. Ed. Engl. 8* (1969) 312.
[36] S. Iwatsuki, Y. Yamashita, *Adv. Polym. Sci. Jpn. 2* (1971) 1.
[37] L. M. Quick, D. A. Knecht, M. H. Back, *Int. J. Chem. Kinet. 4* (1972) 61.
[38] W. A. Pryor, L. D. Laswell, *Adv. Free-Radical Chem. 5* (1975) 27.
[39] W. A. Pryor, M. Iino, G. R. Newkome, *J. Am. Chem. Soc. 99* (1977) 6003.
[40] J. R. Lacher, G. W. Tompkin, J. D. Park, *J. Am. Chem. Soc. 74* (1952) 1693.
[41] W. H. Sharkey, *Fluorine Chem. Rev. 2* (1968) 1.
[42] A. L. Henne, R. P. Ruh, *J. Am. Chem. Soc. 69* (1947) 279.
[43] B. Atkinson, C. Tsiamis, *Int. J. Chem. Kinet. 11* (1979) 585.
[44] P. D. Bartlett, L. K. Montgomery, B. Seidel, *J. Am. Chem. Soc. 86* (1964) 616.
[45] L. K. Montgomery, K. Schueller, P. D. Bartlett, *J. Am. Chem. Soc. 86* (1964) 622.
[46] I. Fleming, M. H. Karger, *J. Chem. Soc. C 1967,* 226.
[47] M. Stickler, G. Meyerhoff, *Polymer 22* (1981) 928.
[48] C. J. Albisetti, D. C. England, M. J. Hogsed, R. M. Joyce, *J. Am. Chem. Soc. 78* (1956) 472.
[49] M. Stickler, G. Meyerhoff, *Makromol. Chem. 181* (1980) 131, 913.
[50] C. Walling, *J. Am. Chem. Soc. 71* (1949) 1930.
[51] H. Inoue, T. Otsu, *Makromol. Chem. 153* (1972) 21.
[52] L. P. Ellinger, *Polymer 5* (1964) 559.
[53] K. Nagai, S. Machida, T. Nonaka, *J. Polym. Sci. Polym. Chem. Ed. 19* (1981) 773.
[54] K. Nagai, S. Machida, *J. Macromol. Sci. Chem. A16* (1981) 965.
[55] K. C. Brannock, R. D. Burpitt, J. G. Thweatt, *J. Org. Chem. 29* (1964) 940.
[56] K. C. Brannock, A. Bell, R. D. Burpitt, C. A. Kelly, *J. Org. Chem. 26* (1961) 625; *29* (1964) 801, 813.
[57] I. Fleming, J. Harley-Mason, *J. Chem. Soc. 1964,* 2165.
[58] C. Walling, E. A. McElhill, *J. Am. Chem. Soc. 73* (1951) 2819.
[59] T. Sato, M. Abe, T. Otsu, *J. Macromol. Sci. Chem. A15* (1981) 367.
[60] F. D. Lewis, T. I. Ho, R. J. De Voe, *J. Org. Chem. 45* (1980) 5283.
[61] H. K. Hall, Jr., Y. Okamoto, A. B. Padias, A. Deutschman, Jr., J. W. Berry, *J. Polym. Sci. Polym. Chem. Ed. 17* (1979) 3889.
[62] A. L. Barney, T. L. Cairns, *J. Am. Chem. Soc. 72* (1950) 3193.
[63] E. C. Coyner, W. S. Hillman, *J. Am. Chem. Soc. 71* (1949) 324.
[64] H. K. Hall, Jr., C. D. Smith, D. E. Plorde, *J. Org. Chem. 38* (1973) 2084.
[65] K. Kirchner, H. Schlapkohl, *Makromol. Chem. 177* (1976) 2031.
[66] S. Tazuke, S. Okamura, *J. Polym. Sci. A-1 6* (1968) 2907.
[67] R. W. Hoffmann, U. Bressel, J. Gehlhaus, H. Häuser, *Chem. Ber. 104* (1971) 873.
[68] Th. Wagner-Jauregg, *Synthesis 1980,* 769.
[69] M. Matsuda, K. Abe, *J. Polym. Sci. A-1 6* (1968) 1441.
[70] T. Sato, M. Abe, T. Otsu, *Makromol. Chem. 178* (1977) 1061.
[71] M. Raetzsch, R. Hoyer, M. Arnold, *Acta Polym. 31* (1980) 572.
[72] Th. Wagner-Jauregg, *Ber. Dtsch. Chem. Ges. 63* (1930) 3213.
[73] T. Kokubo, S. Iwatsuki, Y. Yamashita, *Makromol. Chem. 123* (1969) 256.
[74] T. Kokubo, S. Iwatsuki, Y. Yamashita, *Macromolecules 1* (1968) 482.
[75] S. Iwatsuki, Y. Yamashita, *Makromol. Chem. 89* (1965) 205.
[76] S. M. McElvain, H. Cohen, *J. Am. Chem. Soc. 64* (1942) 260.
[77] T. Otsu, H. Inoue, *Makromol. Chem. 128* (1969) 31.
[78] N. Kushibiki, M. Irie, K. Hayashi, *J. Polym. Sci. Polym. Chem. Ed. 13* (1975) 77.
[79] M. E. Kuehne, L. Foley, *J. Org. Chem. 30* (1965) 4280.
[80] H. K. Hall, Jr., R. C. Sentman, *J. Org. Chem. 47* (1982) 4572.
[81] H. K. Hall, Jr., M. Abdelkader, *J. Org. Chem. 46* (1981) 2948.
[82] H. K. Hall, Jr., H. A. A. Rasoul, M. Gillard, M. Abdelkader, P. Nogues, R. C. Sentman, *Tetrahedron Lett. 23* (1982) 603.
[83] H. K. Hall, Jr., H. Tanaka, unpublished results.
[84] J. K. Hall, Jr., P. Ykman, *J. Am. Chem. Soc. 97* (1975) 800.
[85] M. Abdelkader, H. K. Hall, Jr., *J. Org. Chem. 47* (1982) 292.
[86] H. K. Hall, Jr., L. C. Dunn, A. B. Padias, *J. Org. Chem. 45* (1980) 835.
[87] H. K. Hall, Jr., M. Abdelkader, M. E. Glogowski, *J. Org. Chem. 47* (1982) 3691.
[88] M. E. Glogowski, H. K. Hall, Jr., *J. Macromol. Sci. Chem. A 13* (1979) 369.
[89] R. C. Sentman, Ph. D. Thesis, University of Arizona 1982.
[90] H. K. Hall, Jr., unpublished results.
[91] H. K. Hall, Jr., P. Nogues, J. W. Rhoades, R. C. Sentman, M. Detar, *J. Org. Chem. 47* (1982) 1451.
[92] P. H. J. Ooms, M. A. Bertisen, H. W. Scheeren, R. J. F. Nivard, *J. Chem. Soc. Perkin Trans. 1 1976,* 1538.
[93] P. H. J. Ooms, R. P. Bos, J. W. Scheeren, R. J. F. Nivard, *Recl. J. R. Netherl. Chem. Soc. 96* (1977) 75.
[94] T. Otsu, B. Yamada, S. Kusayama, S. Nagao, *Kobunshi Ronbunshu 36* (1979) 797; *Chem. Abstr. 92* (1979) 94753 x.
[95] H. A. A. Rasoul, H. K. Hall, Jr., *J. Org. Chem. 47* (1982) 2080.
[96] J. B. Kinsinger, J. R. Panchak, R. L. Kelso, J. S. Bartlett, R. K. Graham, *J. Appl. Polym. Sci. 9* (1965) 429.
[97] H. K. Hall, Jr., R. C. Daly, *Macromolecules 8* (1975) 22.
[98] H. K. Hall, Jr., K. Reineke, J. H. Ried, R. C. Sentman, D. Miller, *J. Polym. Sci. Polym. Chem. Ed. 20* (1982) 361.
[99] S. Proskow, H. E. Simmons, T. L. Cairns, *J. Am. Chem. Soc. 88* (1966) 5254.
[100] J. P. Ortega, *Mem. R. Acad. Cienc. Exactas Fis. Nat., Madrid, Ser. Cienc. Fis.-Quim. 9* (1979) 7; *Chem. Abstr. 93* (1980) 45498e.
[101] J. Bitter, J. Leitich, H. Partale, O. E. Polansky, W. Riemer, U. Ritter-Thomas, B. Schlamann, B. Stilkerieg, *Chem. Ber. 113* (1980) 1020.
[102] P. H. J. Ooms, J. W. Scheeren, R. J. F. Nivard, *Synthesis 1975,* 260, 263.
[103] H. Gilbert, F. F. Miller, S. J. Averill, E. J. Carlson, V. L. Folt, H. J. Heller, F. D. Stewart, R. F. Schmidt, H. L. Trumbull, *J. Am. Chem. Soc. 78* (1956) 1669.
[104] J. K. Stille, D. C. Chung, *Macromolecules 8* (1975) 83.
[105] J. K. Stille, D. C. Chung, *Macromolecules 8* (1975) 114.
[106] J. K. Williams, D. W. Wiley, B. C. McKusick, *J. Am. Chem. Soc. 84* (1962) 2216.
[107] W. J. Middleton, *J. Org. Chem. 30* (1965) 1402.
[108] A. T. Blomquist, Y. C. Meinwald, *J. Am. Chem. Soc. 81* (1959) 667.
[109] S. Sarel, A. Felzenstein, J. Yovell, *J. Chem. Soc. Chem. Commun. 1973,* 859.
[110] C. Ruecker, D. Lang, J. Sauer, H. Friege, R. Sustmann, *Chem. Ber. 113* (1980) 1663.
[111] E. Ciganek, W. J. Linn, O. W. Webster in Z. Rappoport: *The Chemistry of the Cyano Group,* Interscience, New York 1970, p. 423.
[112] F. Effenberger, O. Gerlach, *Chem. Ber. 107* (1974) 278.
[113] M. Nakahara, Y. Uosaki, M. Sasaki, J. Osugi, *Rev. Phys. Chem. Jpn. 47* (1977) 119.
[114] M. Sasaki, H. Tsuzuki, J. Osugi, *J. Chem. Soc. Perkin Trans. II 1980,* 1596.
[115] J. von Jouanne, H. Kelm, R. Huisgen, *J. Am. Chem. Soc. 101* (1979) 151.
[116] T. Arimoto, J. Osugi, *Chem. Lett. 1974,* 271.
[117] D. Masilamani, M. E. Reumann, M. M. Rogic, *J. Org. Chem. 45* (1980) 4602.
[118] H. Noguchi, S. Kambara, *J. Polym. Sci. B 3* (1965) 271.
[119] S. Fries, K. Gollnick, *Angew. Chem. 92* (1980) 848; *Angew. Chem. Int. Ed. Engl. 19* (1980) 831.
[120] C. Hubschwerlen, J. P. Fleury, H. Fritz, *Helv. Chim. Acta 60* (1977) 2576.
[121] N. Wiberg, J. W. Buchler, *Chem. Ber. 96* (1963) 3223.
[122] J. Lingnau, M. Stickler, G. Meyerhoff, *Eur. Polym. J. 16* (1980) 785.
[123] N. J. Barr, W. I. Bengough, G. Beveridge, G. B. Park, *Eur. Polym. J. 14* (1978) 245.
[124] H. K. Hall, Jr., H. A. A. Rasoul, M. Gillard, in preparation.
[125] B. T. Gillis, J. D. Hagarty, *J. Org. Chem. 32* (1967) 330.
[126] R. L. Adelman, *J. Org. Chem. 33* (1968) 1400.
[127] D. C. England, C. G. Krespan, *J. Org. Chem. 35* (1970) 3312.
[128] O. Achmatowicz, Jr., J. Szymomiak, *J. Org. Chem. 45* (1980) 4774.
[129] W. A. Thaler, B. Franzus, *J. Org. Chem. 29* (1964) 2226.
[130] B. T. Gillis, P. E. Beck, *J. Org. Chem. 28* (1963) 3177.
[131] R. Huisgen, H. Pohl, *Chem. Ber. 93* (1960) 527.
[132] E. Körner von Gustorf, D. V. White, B. Kim, D. Hess, J. Leitich, *J. Org. Chem. 35* (1970) 1155.
[133] J. H. Hall, M. Wojciechowska, *J. Org. Chem. 43* (1978) 3348.
[134] R. W. Hoffmann, U. Bressel, J. Gehlhaus, H. Hauser, *Chem. Ber. 104* (1971) 873.
[135] S. R. Turner, M. Stolka, *J. Polym. Sci. Polym. Chem. Ed. 16* (1978) 1167.
[136] S. Ohashi, K. Leong, K. Matyjaszewski, G. B. Butler, *J. Org. Chem. 45* (1980) 3467.
[137] S. Ohashi, G. B. Butler, *J. Org. Chem. 45* (1980) 3472.
[138] D. J. Pasto, A. F. T. Chen, *Tetrahedron Lett. 1973,* 713.
[139] K. B. Wagener, S. R. Turner, G. B. Butler, *J. Polym. Sci. Polym. Lett. Ed. 10* (1972) 805.
[140] K. B. Wagener, S. R. Turner, G. B. Butler, *J. Org. Chem. 37* (1972) 1454.

[141] K. B. Wagener, G. B. Butler, *J. Org. Chem. 38* (1973) 3070.
[142] G. B. Butler, L. J. Guilbault, S. R. Turner, *J. Polym. Sci. Polym. Lett. Ed. 9* (1971) 115.
[143] L. J. Guilbault, S. R. Turner, G. B. Butler, *J. Polym. Sci. Polym. Lett. Ed. 10* (1972) 1.
[144] L. J. Guilbault, S. R. Turner, G. B. Butler, *Polym. Prepr., Am. Chem. Soc. Div. Polym. Chem. 13* (1972) 936.
[145] M. E. Kuehne, P. J. Sheeran, *J. Org. Chem. 33* (1968) 4406.
[146] M. Delaunois, L. Ghosez, *Angew. Chem. 81* (1969) 33; *Angew. Chem. Int. Ed. Engl. 8* (1969) 72.
[147] D. C. England, C. G. Krespan, *J. Am. Chem. Soc. 87* (1965) 4019.
[148] R. T. Arnold, P. Veezagu, *J. Am. Chem. Soc. 82* (1960) 5411.
[149] P. H. J. Ooms, H. W. Scheeren, R. J. F. Nivard, *J. Chem. Soc. Perkin Trans. 1 1976*, 1048.
[150] O. Achmatowicz, F. Werner-Zamojska, *Bull. Acad. Pol. Sci. Cl. Troisieme 5* (1957) 923; *Chem. Abstr. 52* (1958) 6333.
[151] O. Achmatowicz, M. Leplawy, A. Zamojski, *Rocz. Chem. 30* (1956) 215; *Chem. Abstr. 51* (1957) 1087.
[152] R. Graf, *Angew. Chem. 80* (1968) 179; *Angew. Chem. Int. Ed. Engl. 7* (1968) 172.
[153] L. A. Errede, M. Szwarc, *Q. Rev. Chem. Soc. 12* (1958) 301.
[154] S. Iwatsuki, H. Kamiya, *Macromolecules 7* (1974) 732.
[155] S. Iwatsuki, K. Inoue, *Macromolecules 10* (1977) 58.
[156] S. Iwatsuki, T. Itoh, *Macromolecules 13* (1980) 983.
[157] S. Iwatsuki, T. Itoh, K. Horiuchi, *Macromolecules 11* (1978) 497.
[158] S. Iwatsuki, T. Itoh, S. Sadaiki, *Macromolecules 14* (1981) 1608.
[159] S. Iwatsuki, T. Itoh, *Macromolecules 12* (1979) 208.
[160] S. Aoki, J. K. Stille, *Macromolecules 3* (1970) 473.
[161] H. Noguchi, S. Kambara, *J. Polym. Sci. B 3* (1965) 271.
[162] H. Scott, G. A. Miller, M. M. Labes, *Tetrahedron Lett. 1963*, 1073.
[163] S. Iwatsuki, T. Itoh, *Macromolecules 15* (1982) 347.
[164] T. Natsuume, M. Nishimura, M. Fujimatsu, M. Shimizu, Y. Shirota, H. Mikawa, *Polym. J. Jpn. 1* (1970) 181.
[165] S. Iwatsuki, T. Itoh, *J. Polym. Sci. Polym. Chem. Ed. 18* (1980) 2971.
[166] J. A. K. Harmony, *Methods Free Radical Chem. 5* (1974) 101.
[167] M. Poutsma, *Science 157* (1967) 997.
[168] G. Belluci, G. Berti, R. Bianchini, G. Ingrosso, R. Ambrosetti, *J. Am. Chem. Soc. 102* (1980) 7480.
[169] G. Fraenkel, P. D. Bartlett, *J. Am. Chem. Soc. 81* (1959) 5582.
[170] W. T. Miller, S. D. Koch, Jr., F. W. McLafferty, *J. Am. Chem. Soc. 78* (1956) 4992.
[171] F. D. Greene, W. W. Rees, *J. Am. Chem. Soc. 80* (1958) 3432.
[172] J. C. Bevington, C. J. Dyball, *Polymer 17* (1976) 742.
[173] J. C. Bevington, C. J. Dyball, *Polymer 16* (1975) 938.
[174] J. C. Bevington, C. J. Dyball, *J. Chem. Soc. Faraday Trans. II, 1975* 2226.
[175] T. Sato, M. Abe, T. Otsu, *Makromol. Chem. 178* (1977) 1259.
[176] F. R. Mayo, *Polym. Prepr. Am. Chem. Soc. Div. Polym. Chem. 2* (1961) 55.
[177] K. Buchholz, K. Kirchner, *Makromol. Chem. 177* (1976) 935.
[178] W. A. Pryor, R. A. Patsiga, *Spectrosc. Lett. 2* (1969) 61, 353.
[179] M. D. Shalati, R. M. Scott, *Macromolecules 8* (1975) 127.
[180] K. Yamasaki, T. Yonezawa, M. Ohashi, *J. Chem. Soc. Perkin Trans. I 1975*, 93.
[181] K. Yamasaki, quoted by S. Inagaki, H. Fujimoto, K. Fukui, *J. Am. Chem. Soc. 97* (1975) 6108.
[182] E. A. Braude, L. M. Jackman, R. P. Linstead, *J. Chem. Soc. 1954*, 3548.
[183] M. L. Poutsma, *J. Am. Chem. Soc. 87* (1965) 2161.
[184] M. L. Poutsma, *J. Org. Chem. 31* (1966) 4167.
[185] J. L. Poutsma, *J. Am. Chem. Soc. 87* (1965) 2172.
[186] C. Walling, L. Heaton, D. D. Tanner, *J. Am. Chem. Soc. 87* (1965) 1715.
[187] F. D. Greene, W. Adam, J. E. Cantrill, *J. Am. Chem. Soc. 83* (1961) 3461.
[188] F. D. Greene, *J. Am. Chem. Soc. 78* (1956) 2250.
[189] J. C. Martin, J. W. Taylor, E. H. Drew, *J. Am. Chem. Soc. 89* (1967) 129.
[190] C. Walling, Y. Chang, *J. Am. Chem. Soc. 76* (1954) 4878.
[191] D. Swern, *J. Am. Chem. Soc. 69* (1947) 1692.
[192] W. A. Thaler, B. Franzus, *J. Org. Chem. 29* (1964) 2226.
[193] H. K. Hall, Jr., *J. Chem. Educ. 57* (1980) 49.
[194] V. Gutmann: *The Donor-Acceptor Approach to Molecular Interactions*, Plenum Press, New York 1978.
[195] N. Oguni, M. Kamachi, J. K. Stille, *Macromolecules 7* (1974) 435.
[196] A. Ledwith, G. Galli, E. Chiellini, R. Solaro, *Polym. Bull. 1* (1979) 491.
[197] G. Burillo, A. Chapiro, Z. Mankowski, *J. Polym. Sci. Polym. Chem. Ed. 18* (1980) 327.
[198] H. A. A. Rasoul, H. K. Hall, Jr.: *Proc. US-Japan Polymer Meetings, Palm Springs 1980*, Marcel Dekker, New York, in press.
[199] T. Saegusa, *Angew. Chem. 89* (1977) 867; *Angew. Chem. Int. Ed. Engl. 16* (1977) 826.
[200] R. B. Woodward, R. Hoffmann: *The Conservation of Orbital Symmetry*, Verlag Chemie, Weinheim 1970; *Angew. Chem. 81* (1969) 797; *Angew. Chem. Int. Ed. Engl. 8* (1969) 781.
[201] K. Fukui in: *Reactivity and Structure Concepts in Organic Chemistry*, Springer, Berlin 1978, Vol. 2.
[202] T. L. Gilchrist, R. C. Storr: *Organic Reactions and Orbital Symmetry*, Cambridge University Press, Cambridge 1979.
[203] J. Sauer, R. Sustmann, *Angew. Chem. 92* (1980) 773; *Angew. Chem. Int. Ed. Engl. 19* (1980) 779.
[204] K. N. Houk in A. P. Marchand, R. E. Lehr: *Pericyclic Reactions*, Academic Press, New York 1977, Vol. 2, p. 181.
[205] C. A. Stewart, *J. Am. Chem. Soc. 84* (1962) 117.
[206] J. C. Little, *J. Am. Chem. Soc. 87* (1965) 4020.
[207] J. J. Eisch, G. R. Husk, *J. Org. Chem. 31* (1966) 589.
[208] W. C. Herndon, J. Feuer, *J. Org. Chem. 33* (1968) 417.
[209] R. A. Firestone, *Tetrahedron 33* (1977) 3009.
[210] W. Oppolzer, V. Snieckus, *Angew. Chem. 90* (1978) 506; *Angew. Chem. Int. Ed. Engl. 17* (1978) 476.
[211] W. A. McEwen, M. A. Hernandez, C. F. Ling, E. Marmugi, R. M. Pradonaggio, C. M. Zepp, III, J. J. Lubinkowski, *J. Org. Chem. 46* (1981) 1656.
[212] J. P. Kennedy, E. Marechal, *J. Polym. Sci. Macromol. Rev. 16* (1981) 123.
[213] S. Iwatsuki, Y. Yamashita, *Prog. Polym. Sci. Jpn. 2*, (1971) 31.
[214] J. E. Mulvaney, R. J. Cramer, H. K. Hall, Jr., *J. Polym. Sci. Polym. Chem. Ed. 21* (1983) 309.
[215] N. Wiberg, *Angew. Chem. 80* (1968) 809; *Angew. Chem. Int. Ed. Engl. 7* (1968) 766.
[216] W. A. Pryor, W. H. Hendrickson, Jr., *J. Am. Chem. Soc. 97* (1975) 1580, 1582.
[217] B. Belleau, Y. K. Au-Young, *Can. J. Chem. 47* (1969) 2117.
[218] N. L. Zutty, C. W. Wilson, G. H. Potter, D. C. Priest, C. J. Whitworth, *J. Polym. Sci. A 3* (1965) 2781.
[219] G. Sartori, R. D. Lundberg, *J. Polym. Sci. Polym. Lett. Ed. 10* (1972) 583.
[220] S. Aoki, R. F. Tarvin, J. K. Stille, *Macromolecules 3* (1970) 472.
[221] C. Chatgilialoglu, K. U. Ingold, *J. Am. Chem. Soc. 103* (1981) 4833.

# Electron Diffraction with the Transmission Electron Microscope as a Phase-Determining Diffractometer— From Spatial Frequency Filtering to the Three-Dimensional Structure Analysis of Ribosomes

By Walter Hoppe*

*Dedicated to Professor Adolf Butenandt on the occasion of his 80th birthday*

Chemists recognize X-ray crystal structure analysis and electron microscopy as powerful methods of analysis. In the last 20 years the basic ideas of X-ray diffraction analysis have been extended to the field of electron microscopy, whereby an image-forming apparatus is converted into an electron diffractometer, and through which an old dream of crystallographers can be realized—the measurement of the phase shift of scattered waves, a prerequisite for the direct calculation of structures. Its most important area of application, like that of the X-ray diffractometer, is in three-dimensional structure analysis—in all fields of science. However, beyond crystallography, aperiodic structures (comparable to crystals with a single unit cell) can also be analyzed three-dimensionally. In this progress report, the development of the first idea (spatial frequency filtering) to the analysis of ribosomal particles is outlined. Attention will be focused primarily on quantitative methods for the measurement of scattered rays, which are also usable beyond the conventional limit of resolution, down to atomic resolution. In the course of this work in 1968, the principle of the three-dimensional analysis of native biological crystal structures using the electron microscope, as worked with today in many laboratories, was developed. In Munich, however, further research focused on the three-dimensional analysis of aperiodic and individual (especially biological) objects. The analysis of 50S-subunits of the procaryotic ribosome of *E. coli* showed surprisingly good reproducibility of the results (although only within the same orientation), allowing the deduction of almost ideal average model structures from a limited number of particles.

## 1. Introduction

It was not easy to find a suitable title for a report on the research work which has been carried out in our laboratory in the field of structural chemistry over the past number of years. "Three-dimensional electron microscopy" soon proved to be too narrow, and missed the important aspect of quantitative analysis, *i.e.*, the measurement of the amplitude and phase of scattered waves, which is important for the determination of the potential distribution (which corresponds to the electron density distribution in X-ray diffraction). If the electron microscope is used as a phase-determining diffractometer, then three-dimensional electron microscopy corresponds in principle to three-dimensional X-ray crystal structure analysis. Different types of diffractometer have been developed using similar basic designs of electron microscope. Aside from the methodological aspects of our work, a selection of the structural findings (especially on ribosomal particles) which are of particular interest to the chemist are outlined, so as to give the reader an idea of the "state of the art" of this technique.

[*] Prof. Dr. W. Hoppe
Max-Planck-Institut für Biochemie, Abteilung Strukturforschung I
Am Klopferspitz, D-8033 Martinsried bei München (Germany)

## 2. The Development of Phase-Determining Diffractometry with the Conventional Transmission Electron Microscope (CTEM)

### 2.1. "Computers" that Work with Light

In the fifties, the light diffractometer was a popular tool of crystallographers. The impetus behind its use stemmed from the "two-wave microscopy" of *Boersch*[1,2], who suggested that masks, fashioned according to the diffraction diagram of a crystal, be brought into the diffraction plane of a microscope working with monochromatic coherent light. Theoretically, an image of the crystal lattice (more exactly, a two dimensional projection of the crystal lattice) should appear in the image plane of the microscope. In two-wave microscopy, the diffraction diagram is created, without using a lens, with the radiation of the first wavelength (X-rays); the function of the lens is reproduced by the radiation of the second wavelength (light). This idea fascinated many people at that time, including *Sir W. L. Bragg*[3].

Two-wavelength microscopy illustrates, in a simple fashion, one of the fundamental features of structural analysis with diffraction methods. The analysis proceeds in two steps. In the first—physically important step—scattered

 © Verlag Chemie GmbH, 6940 Weinheim, 1983 0570-0833/83/0606-0456 $ 02.50/0 

rays are produced which contain the complete information on the structure of the object. In the second step these data are combined, in a way that is equivalent to the mathematical operation of Fourier transformation. The direct result is the structure of the object being investigated. Actually, once the data of the scattered waves have been collected, a physical instrument is no longer needed. The combining of the data can also be done using a suitably programmed computer. Indeed, the coupled light lens has the function of such a computer—the apparatus is therefore commonly referred to as a "light-optical analogue computer".

Although today the much more accurate digital computers (acting as "computer lenses") have taken over this task as well, the light-optical computer has not yet lost its value. It should be remembered that both X-rays and light rays have wave characteristics, and that the wavelength of light is longer than that of X-rays by a factor of about $10^3$. When a light-optical apparatus, corresponding geometrically to an X-ray diffractometer but working with monochromatic light, is built, then in principle the same scattering effects are produced as with X-rays if the objects are enlarged by this factor of about $10^3$. Such an apparatus is called a light diffractometer. The light diffractometer (Fig. 1a) enables rapid checking of structural models. All that is needed is a mask with small holes in the presumed positions of the atoms. Naturally such a check can also be carried out very quickly today with a real computer. Despite this, the light diffractometer has remained useful, especially in electron microscopy (see also Sections 2.5 to 2.7).

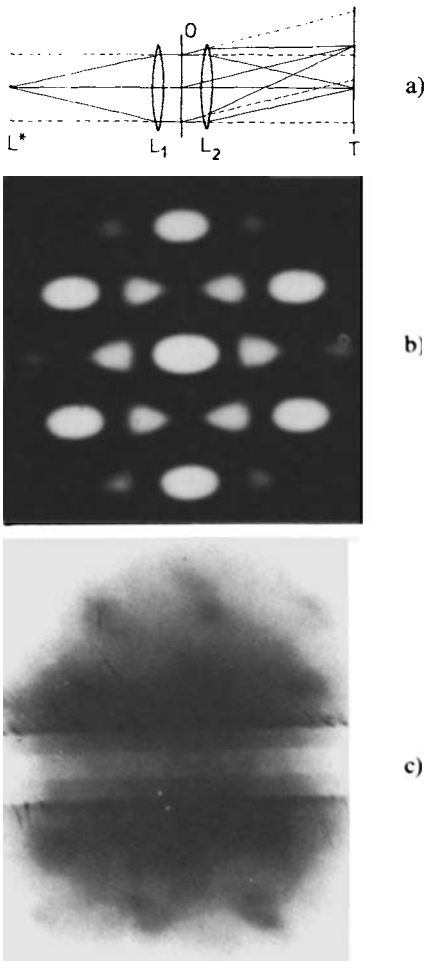



Fig. 1. a) The principle of the light diffractometer. It produces a diffraction image from the object O. The lenses $L_1$ and $L_2$ are unimportant; they should only ensure parallelism of the primary beam and of the scattered rays, despite the relatively short distance to the monochromatic light source L* and the detector (film) T. If they are left out, the distances have to be greatly enlarged. When using X-rays the lenses are left out, but the atomic dimensions of the object are so small that the light source and detector can always be assumed to be infinitely far away. The dashed lines delineate the beam in the absence of the lenses.—b) Light diffractometer diffraction image of a model (mask with holes at the sites of atoms) of naphthalene.—c) Image of the Fourier transform of anthraquinone in the diffuse background scattering of crystals [4]. Because of the geometry of the Weissenberg pictures, the strong "aromatic" maxima lie on lines.

The light diffractometer is especially useful for unravelling the inner symmetries of the object under examination. Thus, for example, owing to the regular hexagonal arrangement of the atoms in arene molecules, characteristic light diffractograms are obtained, typified by the hexagonal positioning of strong scattering maxima (Fig. 1b). However, in the case of a crystal, these molecular scattering diagrams are only seen through the "windows" of the crystal reflections, which makes their investigation difficult. Even as long as thirty years ago, it was shown that they also appear in the continuous scattering background of the X-ray diagrams of single crystals[4]. Figure 1c shows such a molecular scattering diagram in the background of a "Weissenberg" diagram of an anthraquinone crystal. For some time, the study of the diffuse background was relevant to the structural analysis of organic molecules, and was actually used in the constitutional analysis of ecdysone[5]. Since the development of "direct methods", however, the evaluation of additional scattering data (besides the single crystal reflections) is only useful in special cases.

### 2.2. Correction of the Spherical Aberration in the Electron Microscope by Ring Diaphragms

In 1961, a light diffractometer was also to be built in our laboratory for the purpose of studying diffuse X-ray scattering. It was known that one of the main sources of error in the electron microscope is spherical aberration (the refractive power of a magnetic lens increases strongly towards the outer edge, so the outer rays have a shorter focal length than those near to the axis). Therefore, a student named *Menzel* was given the task of testing, through analogous experiments with a home-built light diffractometer, whether the spherical aberration could be eliminated by simply combining a series of exposures which are recorded with ring diaphragms of increasing radius. When this is performed with an electron microscope, the position of the focussing plane would have to be synchronously corrected by changing the objective's current strength. However, we did not attach very great importance to this principle of correcting the spherical aberration. Naturally, the large decrease in the working aperture of the lens is troublesome, since all the scattered rays outside the transmitted rings are lost through shielding. The given task nevertheless fulfilled its purpose, and *Menzel*[6] not only built a good light diffractometer, but also was able to show that sharp image points can indeed be depicted, albeit with additional appearance of a strong background. Strangely enough, the idea of image forming with several ring diaphragms in

electron microscopy has also been discussed in more recent times.

### 2.3. Spatial Frequency Filtering in the Electron Microscope

Although we had never devoted a great deal of effort to this problem, we could not dismiss it: if the temporal sequence of a series of ring diaphragms could be replaced by a spatial sequence of concomitantly operating ring diaphragms, then the intensity of the transmitted light should naturally increase dramatically. At this juncture a little knowledge of wave optics is essential. When a point object—*e.g.* an atom—is irradiated, it acts as the center of a spherical wave. The wavefront is then the surface of a sphere with the point object as its origin. The optical function of a perfect lens is to invert this spherical surface so that a new image-sided spherical wave surface is formed, whose origin is the image-point. The detailed explanation of how the lens does this (in the case of light, by retardation of the waves in the glass) is not necessary for this discussion. The characteristic of an imperfect lens is that it is not able to produce a fully spherical surface. In the extreme case, *i.e.* if no lens is used at all, the wave surface of the object acts at the same time as the wave surface of the image, and this is actually curved in the wrong direction (away from the image point). *Fresnel* had already found that even in this case, an image will be possible if a system of a sequence of ring diaphragms is placed between the object and the image. This Fresnel lens is, of course, of particular interest when working with rays for which there are no lenses, *e.g.* with X-rays. The author had always toyed a little with the idea of building an X-ray microscope with Fresnel lenses, but had soon discovered that the ring distances would have to be of the order of magnitude of atomic distances[*]. On incorporation of a magnetic lens in an electron microscope, the image-sided wave surface is not especially good, but at least it is properly curved. Thus, the idea arose that it should be possible to place a ring plate, working on the principle of the Fresnel lens, between the lens and the image. Owing to the very small discrepancy between real and ideal wave surfaces, in this case, it was to be expected that such a correction plate would show fewer and much wider rings than a real Fresnel lens[7,8]. As shown in Figure 2, this zone correction plate is a "spatial frequency filter".

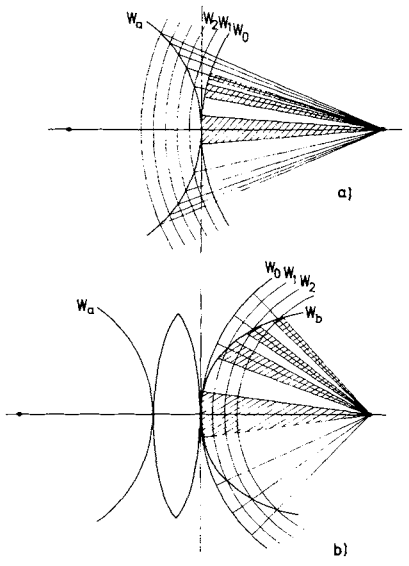



Fig. 2. Principle of the Fresnel lens (a) and of the zone correction plate (b). In (a), the image-side wave surfaces $W_0$, $W_1$, $W_2$ ..., at intervals of $\lambda$ intersect the object-side wave surface $W_a$ at the Fresnel lens and in (b) the defective image-side wave surface $W_b$ at the zone correction plate. In both cases, correct imaging is obtained with a ring-shaped diaphragm system (not shown), which allows passage of in-phase rays (phase shifting $0 \rightarrow \pi$) (shaded), but screens out oppositely phased rays (phase shifting $\pi \rightarrow 2\pi$).

Spatial frequency filtering constitutes one of the most decisive steps which have led to phase-determining diffractometry. In principle, the correction of spherical aberration with the zone correction plate enables improvement of the resolving power of the microscope down to atomic resolution. Right at the outset, plates (with about ten rings) were calculated[7,8], which should allow a resolution of about 0.15 nm (see Section 2.7).

### 2.4. The CTEM—A Diffractometer

A characteristic feature of the conventional transmission electron microscope (CTEM) is that the object is illuminated by a parallel monochromatic primary beam (Fig. 3a). This type of illumination, which would not be feasible with the light microscope because of the appearance of Fresnel fringes (there, a convergent polychromatic light beam is used for illumination), is, in principle, exactly the same as that which the crystallographer uses in his diffractometer. Indeed, if the lower part of Figure 3a, including the lens, is removed, then the scheme is that of a diffractometer: a parallel beam of radiation impinges on an object and sends scattered rays out in all directions. For a complete diffractometer, only one more fitting (a Goniometer) is needed, with which the object can be tilted with respect to the primary ray.

The principal similarity between the construction of an electron microscope and that of an X-ray diffractometer was realized early on by the electron microscopist. If a small crystal is used as the object and the image-forming microscope lenses are omitted, or, put another way, the image of the distribution of the rays is formed on the aperture diaphragm, then instead of photographing the image of the crystal we can photograph its diffraction diagram in the CTEM. The remarkable thing is that the electron microscope—using optical criteria—is actually a poor microscope but an excellent diffractometer. However, as experience in conventional electron microscopy has told us, good microscopy is possible even with this poor microscope if its peculiarities are taken into consideration.

*Boersch* noted in 1947 that atoms can be considered in analogy to phase objects in light optics[9]. Phase objects are structures in which only the refractive index changes but no absorption takes place. They are therefore invisible in the light microscope, but *Zernike* showed that they can be

[*] This idea was later taken up again with respect to an apparatus for far ultraviolet and soft X-rays, after new possibilities for the miniaturization of such a ring diaphragm system became experimentally within reach, at least for wavelengths in the region of 10 nm [G. Schmahl, D. Rudolph, B. Niemann, *Phys. Bl. 38* (1982) 283].

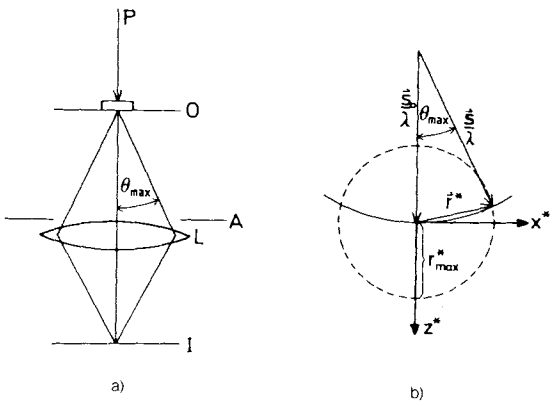



Fig. 3. The "diffractometric" ray path of the conventional transmission electron microscope (CTEM). a) The primary beam P (parallel, monochromatic) penetrates the object O, which scatters rays within a scattering cone with $\theta_{max}$, which are led through the lens L with the aperture A to give the image I. b) Pictorial representation of the scattering in the reciprocal space by Ewald's sphere of propagation: $\vec{s}_0/\lambda$ the vector of the primary wave, $\vec{s}/\lambda$ the vector of the scattered wave, $\vec{r}^*$ the spatial vector in the reciprocal space, $r^*_{max}$ the radius of Ewald's sphere of propagation (dashed), x*, y*, z* the coordinates of the reciprocal space. For very small wavelengths $\lambda$ (for 100 kV electrons, $\lambda$ is only 0.0037 nm!) the scattering angles $\theta$ become very small, and Ewald's sphere can be replaced by its tangential plane. The vectors of the reciprocal space $\vec{r}^*$ then lie in this plane (x*, y* plane). In electron microscopy they are also called spatial frequencies. Each scattered ray therefore corresponds to a reciprocal vector $\vec{r}^*$ (spatial frequency). The amplitude $/F/$ and phase shift $\phi$ of a scattered ray (referred to the primary beam) are designated, in crystal structural analysis (also adopted by us for electron microscopy) as the structural factor $F_{\vec{r}^*} = /F_{\vec{r}^*}/\exp i\phi$. Through the imaging process, $\phi$ becomes $\phi+\gamma$ ($\gamma$ = wave aberration). A "spatial frequency filter" in the ray path of the scattered rays can correct the phase error. The first electron microscopic spatial frequency filter was the zone correction plate. Since phase errors up to the maximum $\pi$ can be allowed in an imaging process, the zone correction plate filters out disturbing spatial frequencies having phase errors between $\pi$ and $2\pi$ (cf. Fig. 2 and Fig. 5). Later, zone correction plates were also developed which corrected the phase error by deceleration of the scattered ray in carbon layers of different thicknesses.

made visible by additionally shifting the mutual phases of irradiating rays and of scattered rays by 90°. This so-called phase contrast method has been an important part of the experimental procedure of light microscopy for decades. It should be mentioned that atoms are also phase objects with respect to X-rays. However, this is of no consequence in crystal structure analysis, because here the primary ray is screened off (*i.e.* one is performing a "dark field operation"). In bright-field electron microscopy with the CTEM one reaches the surprising conclusion, however, that the quest for an ideal lens is actually meaningless: no contrast can be obtained in the imaging of an atomic object. *Zernike*'s trick—of inserting a small plate in the aperture plane of the microscope, and thus enabling modification of the phase between the primary and the scattered rays in the desired way—meets with difficulties in the case of the electron microscope. Surprisingly, however, phase contrast (at least to a certain degree, and certain resolution) can also be produced by replacing the ideal lens by a lens with spherical aberration. This is because the spherical aberration produces an additional phase shift, and one must consider whether this phase shift can be exploited for phase contrast imaging.

With regard to the imaging of atoms, *Scherzer* incorporated into the imaging theory the phase object character of atoms[10]. Since the scattering of electrons is "weak" in the usual voltage range (50–100 kV), the hypothetical atomic images are calculated in a linear approximation[*]. This may seem paradoxical: it is the strong scattering of electrons (orders of magnitude stronger compared to X-rays) which enables the imaging of an object consisting of few atoms. However, the excited scattered rays are still substantially weaker than the exciting primary beam.

The fact that the linear theory suffices for thinner preparations in electron microscopy is of considerable practical importance, similarly as in the X-ray structure analysis of crystals, where the linear theory is known as the kinematic theory. Linear approximations are also used in some—but not all—holographic imaging procedures. One finds for the contrast $g$ in the center of an atomic image,

$$g=(I_0-I)/I_0 \tag{1}$$

the relationships[10]:

$$g=(2\pi e^2/h v_0)\int_0^{\theta_{max}}(Z-f_R)(\sin\gamma)\theta^{-1}\,d\theta \tag{2}$$

$$\gamma=(\pi C_s\theta^4/2\lambda)-(\pi\Delta z\theta^2/\lambda) \tag{3}$$

($I_0$ = bright field intensity, $I$ = intensity in the center of the atom; $e$ = electron charge, $h$ = Planck's constant, $v_0$ = electron velocity; $Z$ = atomic number; $f_R$ = X-ray atomic scattering factor; $\theta$ = scattering angle; $\theta_{max}$ = maximum scattering angle allowed by the lens; $C_s$ = spherical aberration; $\lambda$ = wavelength, $\Delta z$ = defocussing). In optics, $\gamma$ is called the wave aberration (cf. Fig. 3b, see also [7,8]). $\sin\gamma$ is the imaginary part of $\exp i\gamma$; when using amplitude objects, $\sin\gamma$ in (2) has to be replaced by $\cos\gamma$. The function characterizing the spherical aberration, $\exp i\gamma$, corresponds to the pupil function in light optics. Its component describing the imaging properties of weakly scattering objects ($\cos\gamma$ in the case of amplitude objects, $\sin\gamma$ in the case of phase objects) is also called the transfer function. Figure 4 shows $\exp i\gamma$ for a voltage of 100 kV and a rotationally symmetrical magnetic lens with a spherical aberration constant of 1 mm (lenses with spherical aberration constants of this order of magnitude are used in the modern CTEM apparatus), as a function of the scattering angle $\theta$ for different defocussings. Taking case a) first: here the image plane is placed in the focussing plane of the paraxial rays (Gaussian focus). Notice that $\sin\gamma$ is almost zero up to $\theta=5\times10^{-3}$ rad. If an aperture diaphragm were to be placed at this angle, then an atomic object would show no contrast. In this region the lens acts practically as an ideal lens without a *Zernike*'s phase plate, and thus cannot be used for the imaging of phase objects. Only when the scattering angle is larger does $\sin\gamma$ have values larger than zero, so that a contrast is built up in the center of the atom. However, above $\theta\approx9\times10^{-3}$ rad $\sin\gamma$ changes its sign—the integral in (2) becomes smaller with increasing $\theta$. It is therefore advisable to limit the scattering rays building up the image to this angle.

[*] If a large bright-field amplitude $A$ and a small (complex) image amplitude $\rho$ are added, and the intensity is calculated by squaring $((A+\rho)(A+\rho^*)=A^2+A(\rho+\rho^*)+\rho\rho^*)$, then the small term $\rho\rho^*$ can be neglected. The image intensity is proportional to the real part of the amplitude.

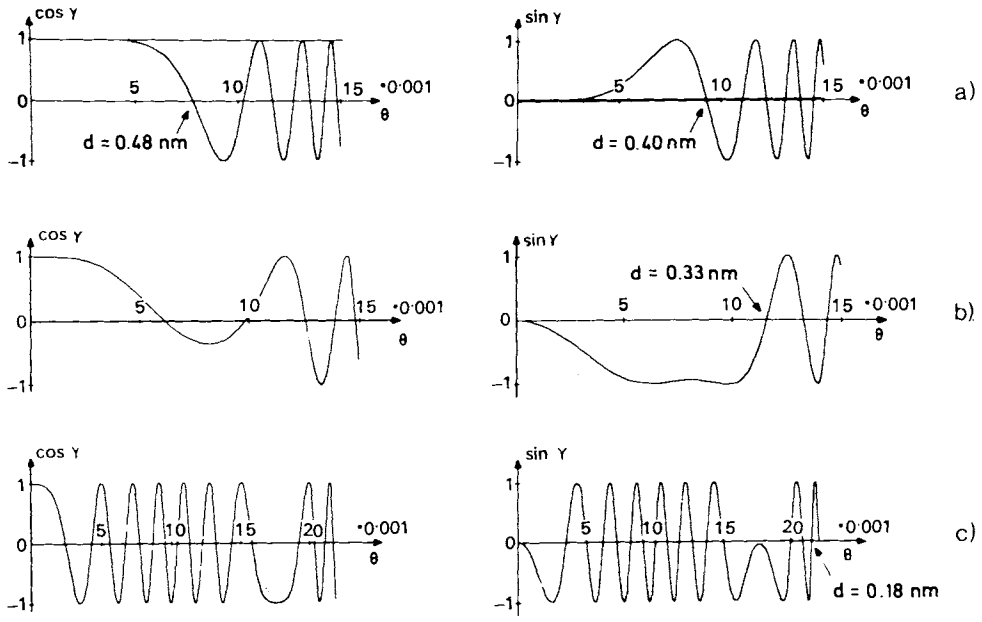



Fig. 4. Pupil functions $\exp i\gamma$ for different defocussings [30]: left, the amplitude component $\cos\gamma$, right, the phase component $\sin\gamma$. Defocussings: a) $\Delta z = 0$ (Gaussian focus), b) $\Delta z = 67{,}5$ nm (Scherzer focus), c) $\Delta z = 310$ nm (zonal correction focus). $U = 100$ kV; $C_s = 1$ mm.

Hence, the phase contrast is indeed produced by the spherical aberration; without the spherical aberration, $\sin\gamma$ would never vary from zero. *Scherzer*[10] tried to improve the contrast by additional defocussing, and succeeded in doing so at a certain value (underfocus) (Fig. 4b): this was found to be 67.5 nm for a spherical aberration of 1 mm; for other spherical aberrations this value changes in accordance with a formula given by *Scherzer*. The range up to the change of sign of $\sin\gamma$ is thereby enlarged, and the scattered rays with low scattering angles can also contribute more to the formation of the image than in the case of the Gaussian focus.

In order to extend the phase contrast principle to our zone correction plate it is necessary to calculate $\sin\gamma$ for even larger defocussings (see image point calculations[11-14]), so that the wave aberration $\gamma$ oscillates strongly (Fig. 4c). If $\sin\gamma$ is now "filtered" through a ring diaphragm system so that the sign is not changed (with gaps in the screened-out places), then in the image point integral (2) all terms of the same sign with increasing $\theta$ are added, and increase both the contrast and the resolution. Figure 5 illustrates how the zone correction plate screens out the unwanted parts of $\sin\gamma$ with opposite sign.

The question then arises of whether the screened-out parts have a disruptive influence on the image. According to image point calculations[11-14], the background variations are somewhat increased, but the form of the image points remains unaffected. Figure 4c shows that with a given defocussing of 310 nm, almost a doubling of the resolution limit compared with Scherzer focus can be reached with 8 oscillations of $\sin\gamma$ (comparable to 8 dark rings). A further increase of resolution, however, soon leads to difficulties, since the number of oscillations increases very rapidly. But, a factor of more than 2 is unnecessary in order to analyze atomic structures. On the other

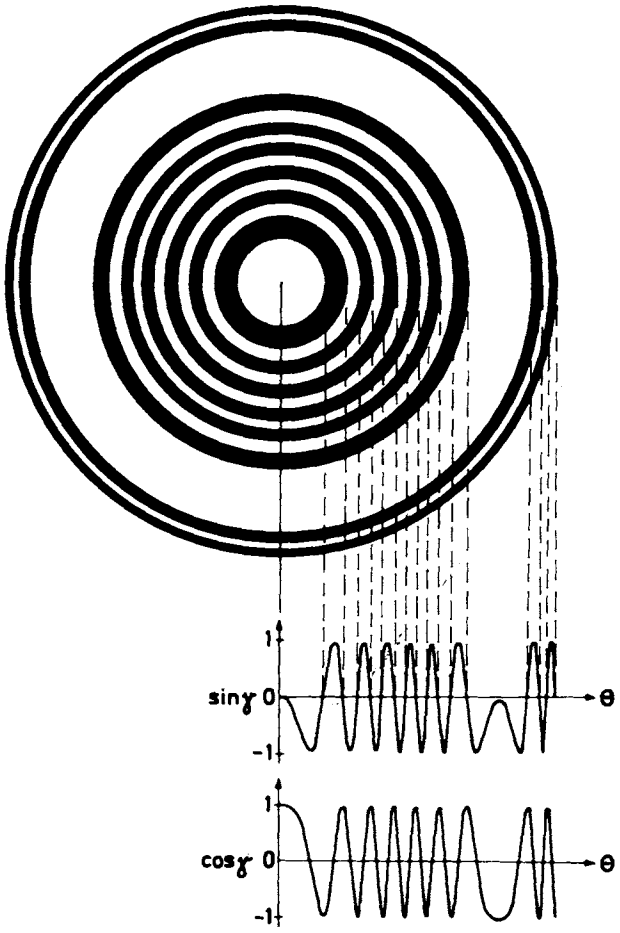



Fig. 5. Phase component of the pupil function (phase contrast transfer function) and design of the zone correction plate. The positive regions of $\sin\gamma$ are screened out. Note that in contrast to the general case (cf. Fig. 2 and Fig. 3), the phase error $\gamma$ (wave aberration) of the transferred structural factors $F_{\vec{r}}$ no longer changes continuously, but jumps from band to band by $\pi$ (three ray interference of the spatial frequency $+\vec{r}^*$, $-\vec{r}^*$, primary ray); the structural factor amplitudes $F_{\vec{r}}$ are therefore weighted by a function $(/\sin\gamma/)$. $U = 100$ kV; $C_s = 1$ mm; $\lambda/\theta_{max} = 0.18$ nm.

hand, the spherical aberration of round magnetic lenses can be pushed only a little under the limit of 1 mm (using 100 kV), (Scherzer's theorem[15]).

### 2.5. The Imaging of the Transfer Function in the Light Diffractogram

As deliberations on the zone correction plate were coming to maturity we still did not possess an electron microscope in our laboratory. On discussing the experimental realization of our ideas, experts told us that secondary errors in electron microscopy (current instability, voltage instability, mechanical drift in the object stage) already made it very difficult to reach double the theoretical minimal image point distance (Scherzer's resolution distance). During a visit to the Siemens' electron microscopy research and development laboratories in Berlin, I was informed about the work of *Thon*, who was studying the dependence of carbon foil granulation on the defocussing of the objective. Electron microscopic investigations on carbon foils had shown that the granular-like image is strongly dependent on the defocussing. *Lenz*[16] had developed a theory explaining the different granulations by changes in the properties of the lens with different defocussing, in which *Thon* incorporated the spherical aberration. To test this theory, the most often occurring distances in many micrographs were measured and their statistical average compared to the theoretical mean[17]. The technical quality of the series of micrographs was excellent. Point distances in the range of Scherzer's resolution distances could be measured. I suggested replacement of the troublesome single measurement of the distances by an investigation of the autocorrelation function (which directly yields a statistic of the distances), or by an investigation of the square of the image Fourier transform (equivalent to the autocorrelation function). This last type of analysis seemed to be especially convenient experimentally. Its execution is simple, if the plate with the electron micrograph is used directly as an object in the light diffractometer. The light diffractometer then directly forms an image of the square of the Fourier transform. *Thon* accepted an invitation to carry out experiments on this in our laboratory. For the experiments, the light diffractometer that *Menzel* had already built was used (see Section 2.2). Even the first pictures showed ring-shaped structures in the light diffractogram. Afterwards *Thon* systematically continued these experiments in Berlin using a light diffractometer with a laser instead of a high-pressure mercury lamp[18]. The light diffractograms showed (as expected from theory) ring-shaped structures modulated by the square of $\sin\gamma$ (see Fig. 6a). These diagrams immediately proved that atoms are phase objects and that the linear theory suffices for the description of the scattering. If the atoms had been amplitude objects (that is, if the electron beam had been absorbed in the atoms), then the light diffractogram would have had to have been modulated by $\cos\gamma$ (cf. left side of Fig. 4). If the linear theory of the phase contrast had not sufficed, then the ring structure would have disappeared.

### 2.6. Spatial Frequency Filtering in the CTEM using the Zone Correction Plate

Some time later, in collaboration with our colleagues in Berlin and Tübingen (we had by then also become involved with experimental electron microscopy), investigations were carried out on filtering by the zone correction plate in the CTEM (see Section 2.3)[19,20]. *Möllenstedt et al.* in Tübingen had developed a special electron-optical technique for etching very fine diaphragm systems[21], which enabled the production of suitable zone correction plates. The direct imaging of $\sin^2\gamma$ in light diffractograms of carbon foils allows adjustment of the filter with control of the proper positioning of the open rings, and rings to be covered up in the light diffractogram. Figure 6 shows the light diffractograms of the same foil before and after the positioning of the zone correction plate; each even-numbered ring zone in Figure 6a is screened off in Figure 6b. Naturally, it is the linear transfer of the real part of the amplitude (see footnote p. 459), after the phase shifting of $\pi/2$ (phase contrast), that enables the direct imaging of the zone correction plate. In Figure 6b, even the clamps on the sides of the rings are pictured.

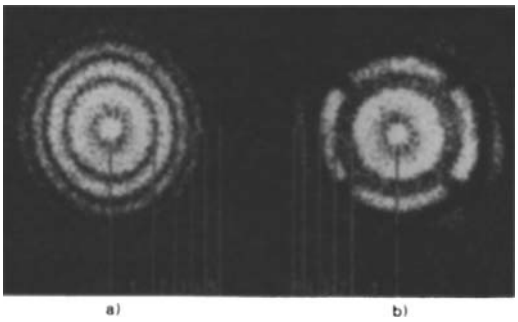



Fig. 6. Light diffractogram of a carbon foil: a) before insertion, b) after insertion of a zone correction plate.

Figure 7 shows one of the first successful spatial frequency filterings in electron microscopy. Here, as in other optics, the resolution is limited by the aperture of the lens, which itself limits the maximum scattering angle $\theta_{max}$. This law has already been used in the discussion of the function $\exp i\gamma$ (pupil function; cf. Fig. 4), where it was shown how the largest usable aperture angle $\theta_{max}$ increases on going from the Gaussian focus to the Scherzer focus, and finally to the spatial frequency filter focus.

The spatial frequency of a scattered ray according to Figure 3, is a two-dimensional vector in the x*,y*-plane. Due to the small scattering angles in electron microscopy, its absolute value corresponds to the scattering angle of the scattered electron beam $\theta$, divided by the wavelength $\lambda$. We always use the reciprocal value of the maximum spatial frequency (the radial limitation in the spatial frequency plane) $\lambda/\theta_{max}$, as the limit of resolution. The resolution defined in this way (dimension length) is also called the crystallographic resolution $d_{cryst}$, since the analogous term is used in crystallography for the definition of resolution (*e.g.* in the crystal structure analysis of proteins). In analogy to light-optical resolution, $d_{cryst}$ corresponds to the smallest distance with which two image points in an image

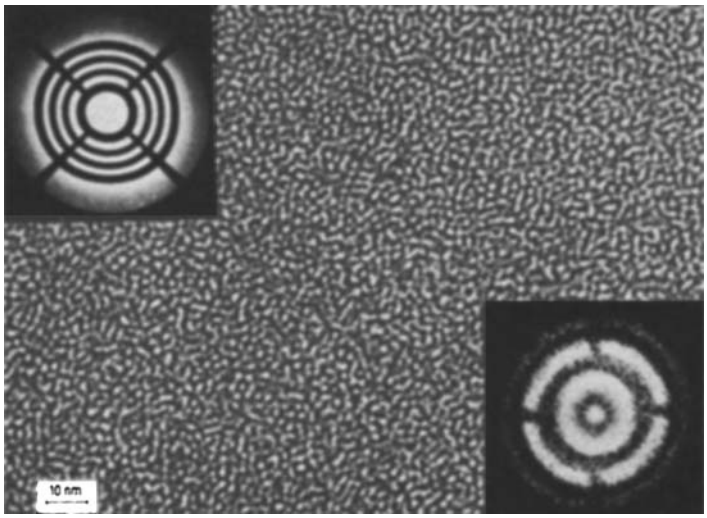



Fig. 7. Spatial frequency filtering in the electron microscope (Elmiscop 101 with a $C_s = 1.35$ mm special objective). Above left: zonal correction plate (after *Möllenstedt et al.*) photographed in the electron diffraction image of the foil; below right: light diffractogram of the foil. The light diffractogram of the foil does *not* encompass the boundaries of the electron diffraction diagram (limited monochromaticity to the thermal cathode).

can be separated. Note, that this definition is somewhat pessimistic, the exact calculation yields an additional factor of 0.85 when using the light-optical definition of resolution for coherent illumination. Sometimes, in electron microscopy publications, even the factor of 0.6 is placed before $\lambda/\theta_{max}$ (called nominal resolution). However, this definition of resolution is somewhat confusing, since this factor corresponds to incoherent illumination, which does not apply in the CTEM. Hence, on studying the literature of electron microscopy, care must be taken that the different definitions of resolution do not lead to false conclusions. The crystallographic resolution has the advantage that it allows the direct comparison between electron microscopy and X-ray crystallography. In the right-hand part of Figure 4 the (crystallographic) limits of resolution under the three different conditions are 0.4, 0.33, and 0.18 nm. When $d_{cryst} = 0.18$ nm, the atomic structure can be excellently interpreted—as protein crystallography has shown—assuming, naturally, that the protein structure has been determined three-dimensionally. Even atomic models down to a resolution of 0.28 nm are routinely constructed; however, the atomic maxima in the electron density synthesis are no longer resolved. Because of the known, and limited, atomic configurations, simple "pattern recognition" models can, however, be established. It follows from this, that with spatial frequency filtering, the barrier to atomic resolution can indeed be broken through.

In Figure 7, however, the light diffractogram (bottom right) of the CTEM-micrographs is only sufficient for a resolution of 0.3 nm (rather than of 0.2 nm). This was disappointing, because we had hoped that contrast would be extended at least to the edge of the strong area of the electron scattering diagram. Since the light diffractogram images the square of the Fourier transform (see Section 2.5), the image will at best give a resolution that corresponds to the reciprocal limit of the light diffractogram. The limit of resolution is not defined by the aperture diaphragm of the objective, but by the expansion of the scattering diagram in the spatial frequency area; beyond this limit, even the best lens cannot improve on the resolution. This effect was investigated in more detail by *Hirt*[22]. The Maxwellian distribution of the electron velocities at the hot cathode prevents the radiation from being totally monochromatic, even with the best possible stabilization. With a larger scattering angle, the scattering intensity will be diminished, and will finally become immeasureably small. By using a cold cathode (field emission gun) the range of speed of the electrons can be narrowed to such an extent that intense scattering appears up to the edges of the zone correction plate. An increase in the accelerating voltage also leads to a better monochromaticity of the radiation; for example, it was possible to demonstrate a crystallographic resolution of 0.18 nm (Scherzer's resolution 0.28 nm) in the light diffractogram using CTEM pictures at 200 kV[23]. For these pictures (Fig. 8) a cryomicroscope was used ($T = 4.2$ K), which offers a further advantage: decreasing of the thermal vibrations of the atoms, and therefore a general increase in the scattering intensities.

### 2.7. Replacement of Light Diffractometry by Computer Calculations

As before, the readily obtainable diffractogram serves as an invaluable aid for the assessment of the quality of an electron micrograph (see Fig. 9).

However, for quantitative analysis, light diffractometry is too imprecise, and has to be replaced by calculations. For this, it is necessary to bring an electron micrograph into a computer retrievable form. The micrograph is therefore scanned, in the course of which the length of the sides of the scanning elements (Pixel) must not surpass half, at most, of the linear resolution. The density of the micrograph in each of these Pixels is determined. Since electron rays, the same as X-rays but in contrast to light rays, increase the density of the photoplate proportionally to the intensity (linear relationship up to a density of $S = 1$), it is possible to determine the intensity profile of the picture with a densitometer. The large amount of data being handled necessitates that the densitometer should scan automatically. Fourier analysis, which can be carried out using a routine program for Fourier transformation, leads to a two-dimensional density diagram that is equivalent to the light diffractogram but which not only produces the square of the Fourier transform, but also the Fourier transform itself (with amplitude and phase).

### 2.8. *A posteriori* Spatial Frequency Filtering Outside the Microscope

Let us look again at Figure 6. As previously explained, in the right-hand part (b), the even numbered (misphased) spatial frequency rings are screened off by the zone correction plate (filtering off), and are therefore missing in the formation of the image. The Fourier transform of a normal bright-field micrograph could also be produced by calculation, and on image formation (by calculation), the mis-

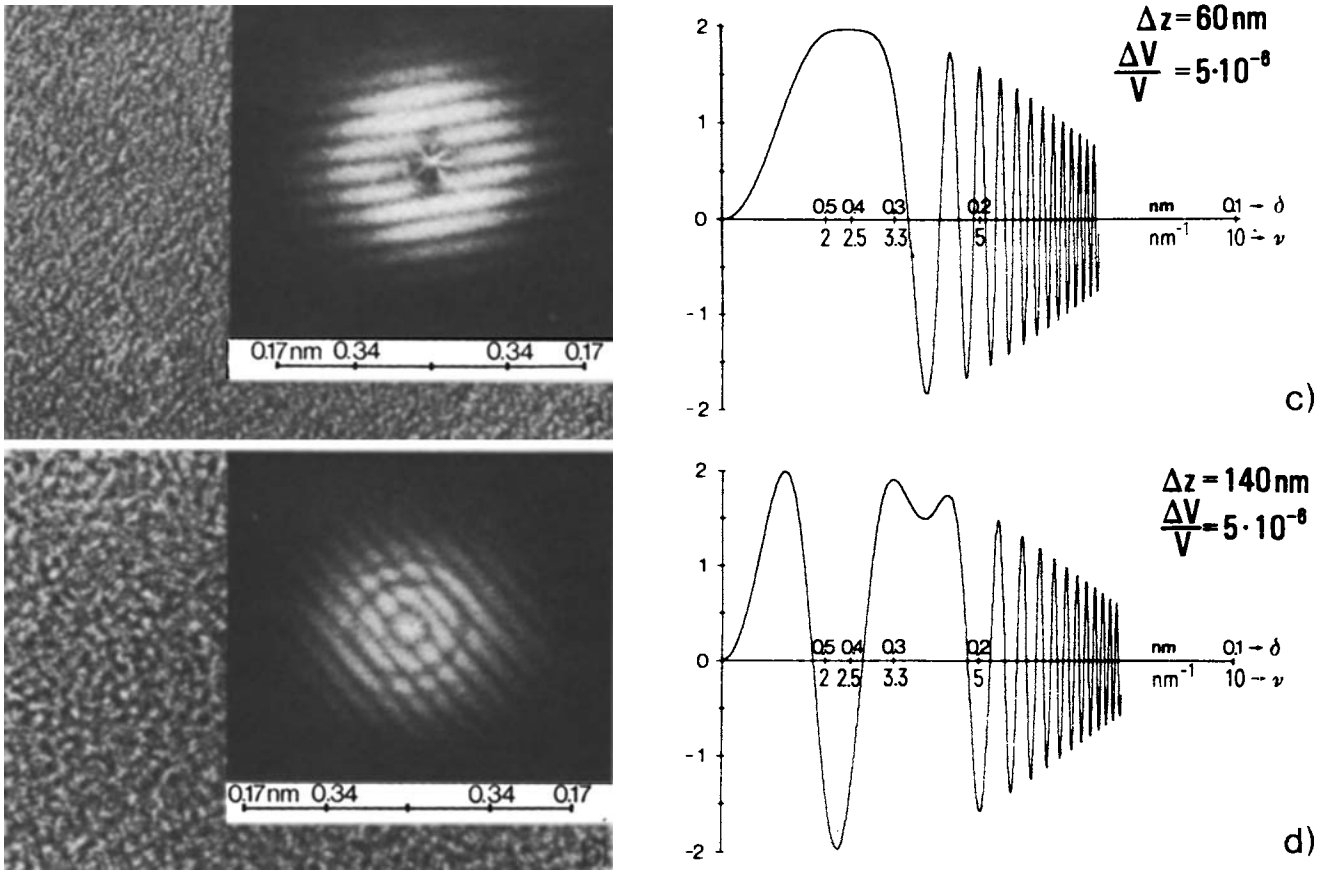



Fig. 8. Exceeding the conventional limit of resolution with central illumination [23] (for inclined illumination, cf. Fig. 11). Photographs taken with the cryomicroscope using an acceleration voltage of 200 kV and $C_s = 1.35$ mm: a) in the proximity of the Scherzer focus ($\Delta z = 40$ nm), b) defocussed for image reconstruction. Note in a) and b) the parallel dark fringes produced by overlaying of two equal, slightly shifted micrographs (resolution test with Young's fringes, see [24b]).—c) and d), phase contrast transfer functions for a) and b). The transfer function c) shows narrow oscillations outside the central region (Scherzer region) that can be scarcely resolved for reconstruction. In contrast to this, the zones in d) are considerably broader (cf. also Fig. 4), which—with regions of sufficient size (see [30])—allows reconstructions. The resolution test with Young's fringes indicates significant regions also in the frequency filtering regions with non-resolvable zones, therefore they are recognizable in a) also outside the strong mid region (Scherzer region). The resolution in the diffractogram (reduction of speckle) can be increased, according to [30], by increasing the illuminated region of the specimen, so that the delineation of the zones (and therefore also the reconstructability) can be improved. An increase in the resolution of the image by reconstruction in case a) should however only be possible to a limited extent, whereas the broad zones in case b) allow reconstruction up to the limit of the Young's fringes (corresponding to 0.18 nm resolution).

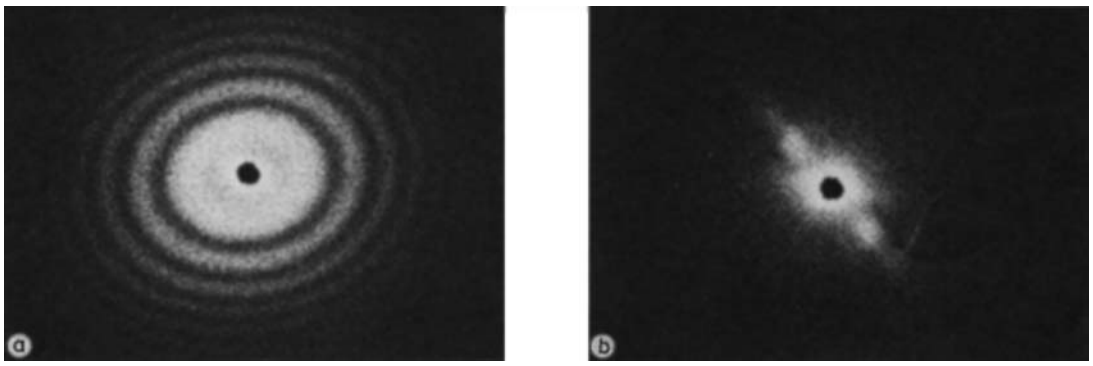


Fig. 9. Light diffractograms for the diagnosis of electron micrographs. a) The light diffractogram has elliptical zones: axial astigmatism (magnetic field non-spherical, adjustment of stigmator inexact); this causes no disturbance with suitable reconstruction. b) Lateral drift of the specimen. Light diffractogram extended in one direction only, micrograph unusable. The reconstructable resolution can be recognized from the extension of the diffractogram. For determination of the absolute limit of significant details (also in non-reconstructable regions), Young's resolution test is necessary (cf. Fig. 8).

phased areas are simply omitted. The picture formed in this way and the image produced by the zonal correction diaphragm should be the same (within the scope of the linear approximation). It is more advantageous to include the misphased scattering areas for the image formation, but then to shift (correct) their phase by the amount $\pi$. In addition, even the weakening of Fourier amplitudes near the zero positions can be compensated for by calculation

(amplitude filtering), but care must be taken, as the noise in these regions is increased at the same time.

Our first calculations of this kind were discussed in 1970 at symposia on new electron microscopic methods in Hirschegg[24] and in London[25]. Soon after the publication of the work on zone correction plates[7,8] *Hanssen et al.*[26] had pointed out that spatial frequency filtering—in the optical instrument and *a posteriori*—had already been developed in light-optics, although for entirely different physical tasks. They applied the light-optical "Linear Transfer Theory" to the situation in the electron miscoscope, whereby essentially the relations inferred by *Scherzer*[10] and ourselves[7,8] had only to be reinterpreted in another way[26]. *Schiske*[27] and *Hanssen*[28] independently proposed transfer of the *a posteriori* filtering from light-optics to electron microscopy. This was realized experimentally in the works previously mentioned[24,25] and in "analogue computations" in a double light diffractometer[29]. A further proposal[27,28] suggested that the corrected image should not be constructed from a single micrograph, but rather from a series of micrographs of the same part of the object taken at a different focus. In this way, the influence of the gaps in the spatial frequency spectrum on the quality of the corrected image should be eliminated (see Section 3.4.2).

## 2.9. A Consistent Theory

Of fundamental significance[30–32] in the use of the electron microscope as a phase-determining diffractometer, is that the microscope is no longer needed to form an image, but is used purely as a measuring instrument for the collection of the characteristic data (structure factors) of the rays scattered by the object under study. As in X-ray structure analysis, these scattering data can be used in various ways.

If it is indeed true that the atoms can be interpreted as pure phase objects, then for electron rays, as with X-rays, Friedel's law applies: the centrosymmetrically related spatial frequencies of a diffractogram show the same intensities, and the corresponding (equally sized) phases have opposite signs. In the case of bright-field image formation, the linear approximation means that, physically, the interferences between the individual scattered rays can be neglected[*]. Therefore, corresponding to the classical definition of the phase in X-ray crystal structure analysis, only the phase difference between the primary and the scattered ray is measured. Luckily, a separate experiment is not necessary for each scattered ray (from the standpoint of the optimal usage of the primary electrons, this would be disastrous); the phases can be determined from the superposition of all the scattered rays with the primary ray by Fourier analysis. However, with a limitation: centrosymmetrically related spatial frequency vectors lead to similar kinds of interference images that coalesce. They can no longer be separated ("three-ray interference"). This can be ignored if Friedel's law is applicable, since the one spatial frequency will be ascribable to the other. The phase-determining diffractometer/electron microscope is therefore basically only suited for scattering diagrams for which Friedel's law applies.

### 2.9.1. *Anomalous Scattering*

It is already known from X-ray crystallography that both sides of the scattering diagrams can show different intensities and phases. This "non-Friedel" case occurs if some of the atoms in the structure scatter anomalously. This concerns heavy atoms which have an absorption edge in the wavelength region of the rays being used. The scattering from these atoms proceeds with a certain (small) phase shift $\eta$ with respect to that of the non-anomalously scattering atoms, and this effect leads to the inequality of both halves of the scattering diagram. Such anomalous scattering also occurs with electron rays, albeit likewise weak, but significantly stronger than with X-rays. In practice, this too is only noticeable with heavy atoms. It was first noticed in the electron diffraction of gases. Similarly as in X-ray diffraction, it can be described by complex atomic scattering factors. However, there is a special case of anomalously scattering atoms in which Friedel's law applies, namely when only one kind of atom is present. The electron microscope is then once again a perfect interferometer which accurately records the diffraction spectrum of the object (naturally, within the limits of the linear approximation). The phase shifting of the anomalous scattering $\eta$ can easily be taken account of if $\gamma$ in equation (3) is replaced by $\gamma-\eta$ (in the special case of a pure amplitude object, with $\eta=\pi/2$)[30].

What do we do when mixed structures, *i.e.* structures with various kinds of atoms are present? This is the case, for example, in the structure analysis of "heavy atom stained" organic compounds. As already mentioned, the centrosymmetrically related spatial frequency vectors of both halves of the diffraction diagram together make a sum whose single components can no longer be discerned. If, however, at least two micrographs with different defocussings are used, then the weighting of the components will be different due to the influence of the transfer function, through which a separation becomes possible[27,30]. This becomes even simpler[31] if only one of the two centrosymmetrically coupled rays is allowed entry to the image plane. If half a plane is covered in the aperture diaphragm, then only half of the diffraction pattern will be recorded, and a second micrograph is necessary for recording the other half, with the complementary half-plane being concealed. Admittedly two micrographs are necessary in order to transfer the complete experimental information, but calculations show that—other than with the central beam bright-field micrograph —no weakening of scattered wave amplitudes takes place. However, all the phases of the Fourier spectrum of the spatial frequencies are now wrong, but by knowing the transfer function, the phase errors can be calculated and corrected. The transfer function can either be determined from a third micrograph (with central beam illumination), or be calculated from both the half-plane micrographs. The latter procedure, however, is only exact in the case of a centrosymmetrical diffraction dia-

[*] They only have to be considered in the case of an approximation to the second order of magnitude.

gram (*e.g.* of a pure phase object), but it should also be possible in other cases, since $\gamma$ is only dependent on a few parameters according to equation (3) (cf. Figures 10 and 11 for procedures with oblique illumination). With the exception of experiments on the discrimination of heavy atoms[36], this possibility has not yet been exhausted in structural analyses, but belongs to the reservoir of methods for the future. Besides determinations of the complex function, the unweighted recording of the amplitude of the scattered rays is of special interest.

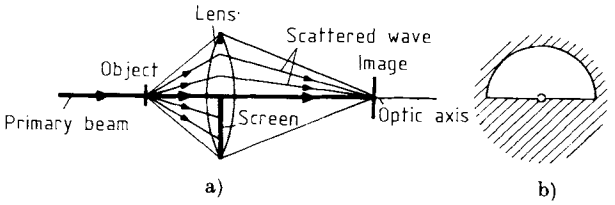



Fig. 10. Complex image reconstruction according to the complementary half-plane procedure [31]. a) Schematic construction of the imaging arrangement.—b) Half-diaphragm (the small ring marks the penetration point of the primary ray). For the second micrograph, the diaphragm must be removed, and a complementary diaphragm inserted.

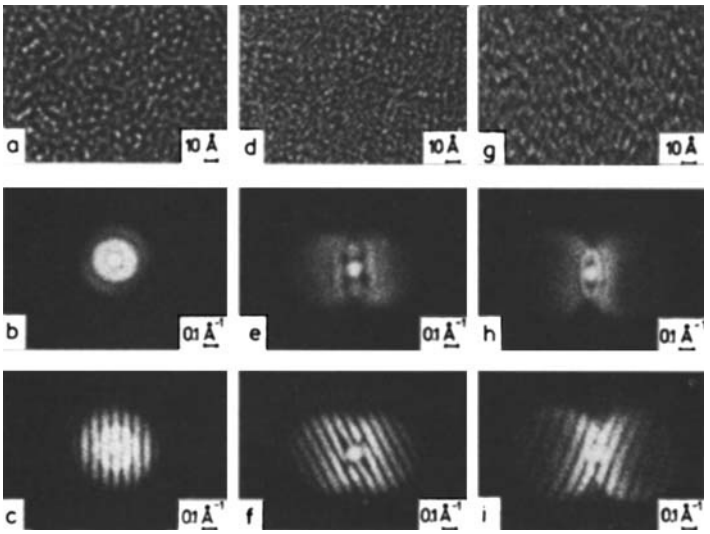



Fig. 11. Complex image reconstruction with inclined illumination [33–35]. Using inclined illumination a resolution down to the atomic limit can be achieved, even with thermic cathodes (with 100 kV). However, the total image must then be compiled from several partial images (synthetic aperture). Light diffractograms reveal the (anisotropic) increase in the transferred spatial frequency area on increasing the angle from 0° (a, b, c) to 0.66° (g, h, i). In the latter case, a limit of resolution of 0.16 nm can be measured. The procedure is complicated and of low intensity, but excellently demonstrates the possibilities that an electron microscope offers on its use as a phase-determining diffractometer.

Another possibility for the analysis of structures with different kinds of atoms is offered by approximation procedures, in which the separation of phase and amplitude parts of the scattering is dispensed with. Such a procedure is usual in X-ray structural analysis, where, however, the influence of anomalous scattering is much smaller. Approximation is also used in our analysis of "heavy atom stained" organic compounds. Here—in contrast to what is usual in light optics—it is important not to discriminate into phase and amplitude objects, but into "differently mixed" objects with the extreme case of the pure phase object (pure amplitude objects do not appear in electron microscopy). In this way, not only is the important link between phase and amplitude parts of anomalously scattering atoms taken into account, but also, the influence on the transfer function can easily be surveyed. Figure 12 shows, for example, the transfer functions at different defocussings for $\eta = 0.25$ (corresponding approximately to platinum according to the table of atomic scattering factors[37]) and for $\eta = 0$ (light atoms). It can be seen that the differences—with the exception of the immediate proximity of the primary ray—are not very great. The experimental zero positions will lie somewhere between the zero transition points of both transfer functions. It can also be seen that the weakening of the amplitudes of the scattered rays near to the zero positions is greatly advantageous here, for the unstable phases, which are anyway in a very narrow range, are associated with a strong weakening of the amplitudes, so that the form of the image is little influenced. Despite renunciation of a complex reconstruction, both heavy atoms as well as light atoms are well reproduced; the errors of this approximation procedure play hardly any role. A short time ago, in our laboratory, *Typke et al.*[38] experimentally determined the magnitude of the anomalous scattering for some heavy atoms (cf. Fig. 13).

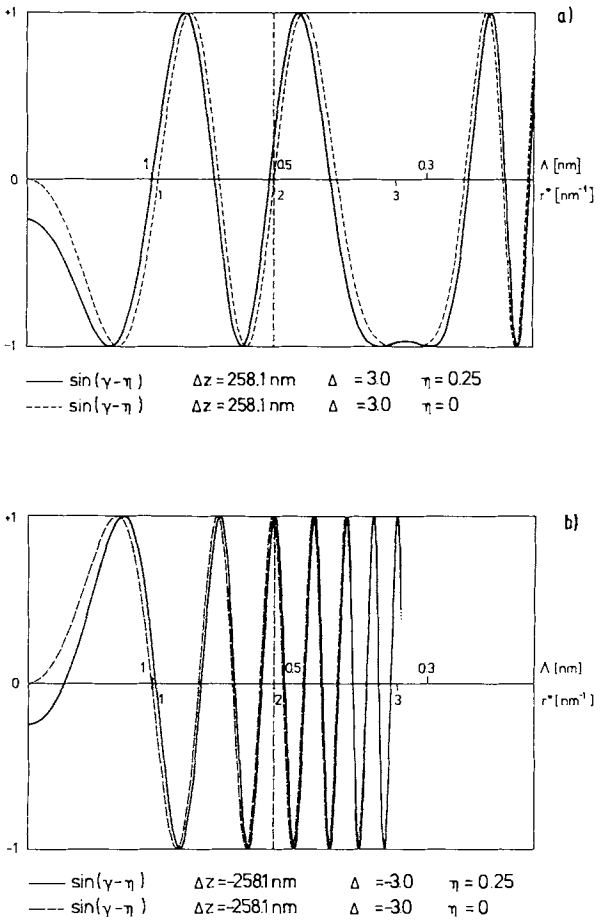



Fig. 12. The function $\sin(\gamma - \eta)$ for $\eta = 0$ and $\eta = 0.25$ (from [36]): a) underfocussed, b) overfocussed.

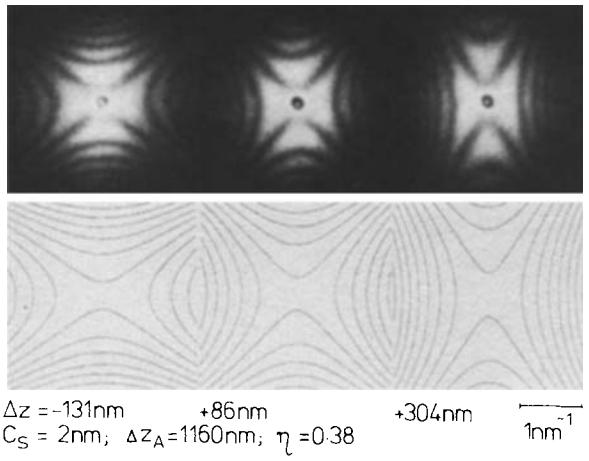



Fig. 13. Light-optical diffractograms of electron micrographs of a carbon foil shadowed with platinum. Due to the relatively large astigmatic difference $\Delta z_A$ (1160 nm), the zero lines in the diffractogram (corresponding to the gaps in the transfer function) are hyperbolic in the inner region (shown for three defocussing values of $\Delta z$ in comparison with the calculated curves). Because of the anomalous scattering of the platinum atoms, this also applies for the innermost zero line, which with a pure weak phase object, would go through the center (cf. [38]). The images show that the electron microscope is also utilizable as a Fourier interferometer for the study of physical parameters (for further refinement of our methods, a more exact knowledge of the anomalous scattering is important).

At the "double symposia" in Hirschegg and in London in 1970, *Erickson* and *Klug* reported on the influence of amplitude filtering on the defocussing-dependency of the reflections of catalase crystals stained with uranyl acetate[39], and thereby experimentally proved[*] the concept which we had formulated the previous year[30-32]. Particularly noteworthy was the finding that the linear theory even remains valid for strongly scattering specimens—we had previously only experimented with light-atom structures.

### 2.9.2. *Consideration of the Curvature of Ewald's Sphere of Propagation*

Discrete formulation with spatial vectors and atomic scattering factors had proven especially useful for the handling of structural analysis problems in X-ray diffraction. Consequently introduced into our work since 1969[30], it led to the separation of "partial amplitude scattering (angle $\eta$)" and "phase scattering"—a separation which would have made little sense in light optics. On extension of the theory of electron diffraction to thick specimens (within the validity of single scattering)[30], the complication arose that the transfer functions of the atoms become dependent on their position along the optical axes of the instrument. This complication could be eliminated by replacement of the two-dimensional spatial frequency area by the three-dimensional reciprocal space (Fourier space)[30]. The Ewald's sphere of propagation (see Fig. 3b) then comes back into play, and thus, electron microscopy becomes now, in every detail, a variant of the diffraction methods in structure research. When dealing with scattering at the surface of the sphere of propagation, complex image reconstruction is unavoidable even with pure phase objects—and one must fall back on the "methods in store" (cf. Figs. 10 and 11). "Phase-determining diffractometry with the electron microscope as a tool" is still a recent method, but the door to three-dimensional analysis down to atomic resolution, in analogy to X-ray structural analysis, is open. This also applies for the aperiodic case; even it can be considered as "crystal structure analysis" in the widest sense, if a small piece of aperiodic material is regarded as a "crystal with one unit cell". The electron microscope thereby loses its property as an image-forming apparatus (however, it can be further used as such for readout and presorting of the submicroscopic entities) and the lens is replaced by the computer for generally three-dimensional images.

### 2.10. Automation of Phase-Determining Diffractometry

The development of the electron microscope into a "robot" is therefore indicated. A robot works not only fast and reliably, but also enables any chemist, biologist, mineralogist *etc.* to carry out complicated physical procedures without any specialist knowledge, using a "black box"[40]. It is remarkable that the prerequisites for the automation of phase-determining diffractometry are even better than in X-ray structure analysis; the phases can be measured directly, whereas in the latter case they have to be determined indirectly. Although the demands on the computer are greater, the incredible advances in computer technology allow for no faint-heartedness even if the conditions of a dedicated computer—now common in X-ray diffraction analysis—are imposed. Of interest is the shift in the problems of development. Whereas formerly, in the case of X-ray structural analysis, the translation of the relatively simple measuring methods into the robot's technology gave difficulties, today these are marginal. On the other hand, articulation of the meticulous adjustment and measuring operations in conformity with robots, which are so difficult in electron microscopy, requires special attention[*].

An electron microscopist of the good old stamp may at first pity the "degradation" of the electron microscope to a measuring instrument. But, is it not true that the computer creates new, incredible, possibilities for the electron microscope? Phase-determining diffractometry is—within the framework of kinematic approximation—just as quantitative a procedure as X-ray crystal structure analysis. Both are based on measurements; it should be noticed that even the density curves of X-rays and electron rays are analogous, and that in both cases quantum-counting direct detectors can also be used[43]. Phase-determining diffractom-

[*] The theoretical basis of this contribution was inaccurate: in the basic equation (5), in which the influence of the light atoms has apparently been neglected, the authors have added the phase part and amplitude part of the heavy atom scattering as if they had been independent of each other, whereby the correct transfer function $\sin(\gamma-\eta)$ is obtained as an approximation. With a small amplitude part, this has scarcely any influence on the numerical results; only when $\eta \approx \pi/4$ (for uranium from about $\theta/\lambda = 7.5\ \mathrm{nm}^{-1}$) do incorrect factors, of the order of magnitude of $\sqrt{2}$, and phase errors, emerge.

[*] It can only be remarked in passing that the on-line diffractometer [41, 42] and the on-line correlation computer [40] are important aids to adjustment.

etry is not limited to periodic structures, and can be used in all areas of chemistry, from inorganic chemistry to biochemistry. It also offers the prospect of atomic analysis—not as a vague presumption, but rather as a precise, theoretically-founded procedure, and one that is, experimentally, already realizable for the most part.

### 2.11. The Scattering Absorption Contrast

Looking back, it seems remarkable that the fundamental relationship between electron microscopy and light-optic phase contrast microscopy was not fully utilized until the sixties, although *Boersch* had already noted in 1947 that atoms scatter and do not absorb[9]. For sure, a reason for this was that, even in the light microscope, the method of phase contrast is not trivial—it is so much easier to view an object as it is (if necessary also after staining). Actually, even thin structures, stained with heavy atoms, show some contrast in the Gaussian focus of the electron microscope at low resolution. Because of the anomalous scattering, heavy atoms are not colorless, but light grey. But strong phase objects (thick objects) can also behave as amplitude objects (non-applicability of the linear approximation, quadratic phase contrast), similarly as to how air bubbles can easily be seen in water when using the light microscope. This becomes more complicated if multiple scattering takes place. In earlier electron microscopy, the source of the contrast was not important, the images being seen "as if" they came from absorbing material. Even today, one must revert to the phenomenological approach if the range of applicability of the linear theory is relinquished; but nowadays, attempts are made when calculating the bright-field intensity, to take the quadratic terms into account.

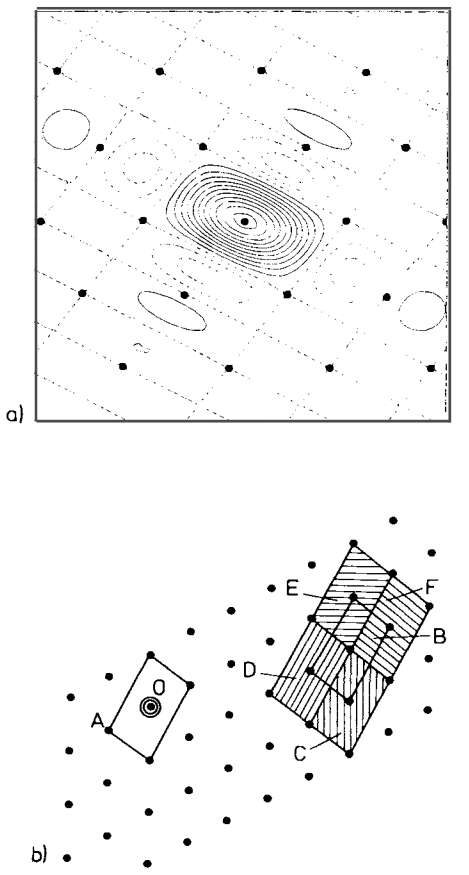



Fig. 14. "Phenomenological" description of a variant of ptychography [46]. In a scanning transmission electron microscope, a structure is impressed, according to a), on the (coherent) scanning probe. The lattice reflections enlarge according to b) to sharply defined spots, which overlap one another (with interference). On scanning, the intensities in the overlapping regions vary in unison with the phase differences of the reflections. For recording the micrographs, the usual one-channel detector has to be replaced by a position-sensitive area detector for electrons (*e.g.* according to [43]).

### 2.12. What is "Ptychography"?

This name describes some (almost forgotten) procedures for determining the amplitudes and phases of scattered electron waves without lenses, which with today's knowledge are especially applicable in the case of crystals[44]. They are based on the mutual interference of scattered rays—in contrast to holography, in which all scattered rays are superimposed with *one* reference wave. A variant of these procedures has recently been realized[45]. Another variant should be relatively easily realizable in the scanning transmission electron microscope, and should enable the evaluation of diffractograms with almost any resolution that is needed (Fig. 14)[46]. In the case of inorganic crystals, and perhaps also in the case of radiation-sensitive organic crystals, these procedures could easily develop into being competitors for the methods described in Sections 2.3—2.10.

### 2.13. Highly Ordered Biological Structures

In crystallography textbooks, the laws of diffraction are usually "amalgamated" with periodicity and symmetry. But, just as the laws of diffraction can be abstracted from periodicity and symmetry[61], using periodic and/or symmetrical patterns, the laws of symmetry can be abstracted from the diffraction theory. X-ray crystallography has led to the study of objects transformed into the reciprocal space (Fourier space). Periodicity and symmetry produce certain Fourier structures in which it does not matter whether the object is an electron density distribution or another—even macroscopic—density distribution. This naturally also applies for micrographs obtained by imaging the respective objects in the electron microscope. Once again, it does not matter whether it is a question of qualitatively correct images, or—as in the extension of the kinematic theory to electron microscopy outlined in this review—of parallel projections of potential distributions.

Qualitative electron microscopical images of contrasted, periodic and symmetrical biostructures have been investigated since the early sixties using Fourier principles, whereby the light diffractometer (see Section 2.1) has served as an especially convenient "calculating machine" for Fourier transformation[47]. By exploiting the Fourier-distribution of the object—known as filtering—certain structural properties are especially accentuated. This filtering, which concerns the object under investigation, has nothing to do with the spatial frequency filtering that we introduced, which concerns the optical properties of the objective. A special kind of "object filtering" is possible in

the case of two-dimensional lattices, whose Fourier transform shows strong, grid-like arranged maxima (corresponding to the periodicity), and a background (arising from individual differences in the unit cell pictures). By filtering out the background, and averaging all the distorted entities by a further Fourier transformation (*e.g.* in a light diffractometer), a strictly periodic structure can be produced. The averaging was first carried out on high-dose micrographs (good electron statistics, but preparation and irradiation artefacts). Electron microscopic work on periodic unstained and native biostructures has been published since 1968 (see Section 3.3).

## 3. Three-Dimensional Analysis

### 3.1. The Problem

Considering the electron microscope and the X-ray diffractometer as analogue instruments already implicates all applications which are possible with a diffractometer. These include, above all, the three-dimensional analysis of the structures under study. In the fifties, X-ray crystal structure analysis of projections (along the edges of the unit cell) was followed by three-dimensional analysis of the electron density in the unit cell, since it was clear that only the true[*] three-dimensional analysis (for which the kinematic theory had afforded the theoretical background) could lead to elucidation of the construction of complicated structures. Fortunately, the tools which were necessary for complex information processing were developed at the same time, namely, automatic measuring machines and electronic calculating machines. In electron microscopy, as in crystal structure analyses, the object specimens are far too thick, relative to the lateral resolution, so that overlapping of the structural details prevents a consequent analysis. Three-dimensional electron microscopy was not simply achieved in an analogous way, but had its origin, in part, in general procedures of image processing[48–50].

This is not surprising, due to the original image-forming character of the electron microscope. The "transfunctionalization" of the bright-field electron microscope into a phase-determining diffractometer for electron diffraction signifies a development away from the admittedly attractive, but only qualitative "peep" microscopy (a term given by *Ernst Ruska*), to quantitative structural research.

### 3.2. Tomographic Procedures

#### *3.2.1. The Polytropic Montage*

In *Hart*'s contribution[49], the term "three-dimensional" does not even appear. He describes his method a "polytropic montage", with which electron micrographs taken at different angles are superimposed on top of one another in such a way that single layers of the specimen are thrown into sharp relief. By changing the overlapping parameters, different layers can be rendered predominant. A similar principle had been referred to much earlier in X-ray diagnostics as "tomography". If X-ray shadow pictures of a body are made at different angles, then they contain projections of all the superimposed layers, which are, however, overlaid using different amounts of shifting. If such pictures are superimposed in such a way that one layer is placed in the same orientation in all the pictures, then this layer will predominate, whilst the other layers are shifted with respect to each other, and, to a certain degree, average themselves out (Fig. 15).

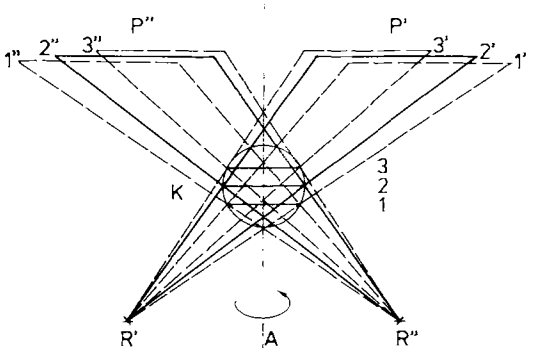



Fig. 15. Principle of circular tomography. The layers of the body K (*e.g.* 1, 2, 3) are imaged with shifts in the X-ray shadow diagram. The shifts depend on the location of the X-ray tube (*e.g.* position R′ or R″). If the pictures P′ and P″ are shifted one over the other in such a way that the layer pictures 2′ and 2″ become congruent, then only 2 is highlighted in the overlapping image. In circular tomography, R rotates about the axis A. In the electron microscope, central projection is replaced by parallel projection (R infinitely far away; imaging of the object at large depth of focus). The change in direction of projection is achieved by tilting of the specimen. The plane of the image (P′, P″) is therefore perpendicular to the direction of the projection. A certain, but easily managable, distortion of the projection images is produced (squares are imaged as rectangles).

#### *3.2.2. Electron Microscopic Computer Tomography*

In the sixties, it was found that disturbances caused by insufficient averaging-out of the unwanted layers in tomography, are largely mathematically correctable, especially when one kept to parallel projections, instead of central projections (which called for new X-ray imaging apparatus). The "reconstruction" of a three-dimensional image of a body becomes especially easy to view if different directions of projection are adjusted by the rotation of the body about one axis; with an asymmetrical body, the axis of choice does not, in principle, matter (computerized tomography, see Figure 16).

This computerized tomography is very well suited for extension to electron microscopy[48]. The parallel projection is guaranteed by image formation with great depth of focus[49], through which superimposed layers of the specimen appear projected over one another in the electron micrograph. Microgoniometers can be used to rotate the specimen (*e.g.* in the way that "tilt cartridges" are used in electron microscopy) and finally, the computerized analysis follows in analogy with calculation methods, if the

[*] This means the substitution of the two-dimensional image function $\rho(x,y)$ (*e.g.* on an electron micrograph) by the three-dimensional image function $\rho(x,y,z)$ (in electron microscopy, z extends along the optical axis). To be distinguished from image stereoscopy, in which a two-dimensional image is replaced by two two-dimensional images slightly tilted towards one another, whose view gives a spatial impression, but does not give the inner construction.

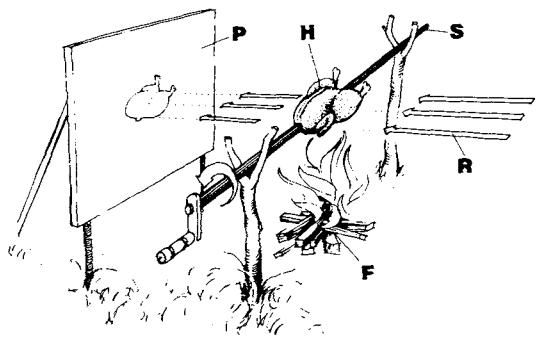



Fig. 16. "Tomographic chicken grill". The chicken H on the skewer S is grilled by the fire F. On turning the skewer, pictures of the chicken at equal angular increments $\Delta\alpha$ are produced on the plates P with parallel X-rays. In electron microscopy, the X-rays are replaced by electron rays; parallel projection is achieved by imaging with great depth of focus. The "grilling" of the "chicken" is (unfortunately) done by the electrons themselves.

image is transformed into a digital field of numbers, *e.g.* by densitometry. The "grilling", which is not normally the case in X-ray tomography, is (unfortunately) brought about by the electron rays themselves: at a dose necessary for image formation, they destroy the organic substance (*e.g.* biological macromolecules), which means that special methods of specimen preparation must be used.

Thus, irradiation-resistant inorganic structures are imprinted on the specimen (positive and negative staining), which allows recognition of the primarily interesting features of the organic structure. They can also be imaged with high irradiation doses, where generally, structural details are only relevant down to the so-called biological resolution ($\geq 1.5$ nm). Care must always be taken, because, even on stabilization of the structure after the very rapid destruction of the organic substance, slow changes cannot be ruled out[51], and the laws of "staining" are in no way trivial—the principle of the filling of gaps with an amorphous heavy-atom glass in negative contrasting is, *e.g.*, certainly only approximate[*].

[*] To define the term "computerized tomography" more precisely (to differentiate it from "diffractometry"): Tomography can be carried out both in real, as well as in reciprocal space, whereby the mathematical procedures of image processing are formally related to the procedures of crystallography. All three-dimensional methods necessitate a set of pictures taken with the illuminating rays in different directions (cf. Fig. 15 and 16 and [50]). There are, however, characteristic differences: (a) Tomography is based on central or parallel projections, (b) in tomography the physics of the imaging process is unimportant.—Tomography can be used in such diverse areas as X-ray diagnostics and radio astronomy (corresponding to (b)). In contrast, in diffractometry the physical imaging process (scattering process) is important; in X-ray diffractometry the requisites of "projections" (see (a), planar sections in the reciprocal space in the case of parallel projections) are only applicable in an approximate way, in special cases (small angle scattering). The reciprocal space is transected by a spherical surface. This also applies in diffractometry using the electron microscope. Of course, it is useful in practice that the spherical surface can be approximated by a plane, owing to the short wavelength of the electrons at a not too high resolution. In a diffractometry theory, there must be a defined correlation between scattering and structure. It can only be applicable to an approximation (neglect of multiple scattering in the kinematic theory, use of linear theory for phase measuring). Using these criteria, the procedure of *DeRosier* and *Klug* [48] is "tomographic", not only because it absolutely necessitates parallel projections, but primarily because here, a phenomenological imaging theory (scattering absorption contrast based on the logarithms of the densities) is used, without taking spherical aberration into account. In our image-point calculations with spatial frequency filtering the kinematic scattering theory and the linear approximation had already been used since 1965 [11—14]. This theory (with spatial frequency filtering), was adopted in Cambridge in 1970 [39]. In electron microscopy, however, consideration of the lens properties is especially important, since different kinds of "images" are obtained using different defocussing. In the Gaussian focus, for example, the linear approximation is not applicable. The first three-dimensional image reconstructions in electron microscopy (fatty acid synthetase [81]) are consistent with diffractometry theory. A phenomenological imaging theory is completely unusable at high resolution (accelerating voltage of the order of magnitude of 100 kV), because, in such a case, the curvature of the sphere of reflection, as well as the change of sign in the spatial frequency spectrum, has to be taken into consideration. However, there are conditions under which work can only be qualitative: thick objects, multiple scattering (see Section 2.11). Qualitative analyses have recently been described [93].

### 3.2.3. *Three-Dimensional Analysis via Symmetry*

The experimental work on three-dimensional electron microscopy by *DeRosier* and *Klug*[48] did not, however, correspond exactly to the model in Figure 16. With respect to the analysis of highly-ordered biological structures (especially helical structures)[48], in the model case the chicken would have to be replaced by a macroscopical helix, *e.g.* a helical spring whose axis is identical to the skewer axis. Simple geometric considerations show that a sinusoidal curve must appear as the image (parallel projection). When the skewer is rotated, the sinusoidal curve retains its shape, but appears to move along the axis, one full turn corresponding to a shift of the sine curve by one period. This means that, in such a case, all tomographic pictures can be derived from a single image, and so, of course, for three-dimensional analysis, one X-ray or electron diffraction picture would suffice. However, if this model is refined to a helix on which identical subunits are threaded like pearls, then identical projections appear merely on rotation through small, discrete angle increments $\Delta\alpha$ (*e.g.* for tobacco mosaic virus $\Delta\alpha = 3.7°$). A discrete set of tomographic pictures is obtained (*e.g.* 49 pictures with tobacco mosaic virus), which, in most cases, suffice for a three-dimensional analysis at biologically-significant resolution. With anglular increments that are too large, intermediate layers can either be taken from images with incidentally different positions of the objects, or the specimen can be tilted inside the region of the anglular increments. The three-dimensional structure of the tail of the T4 phage was determined in this way[48].

The method of producing projections by symmetry relationships (instead of by measuring) can also be used with other highly symmetrical structures (*e.g.* with spherical viruses). The experimental simplicity of the analysis is fascinating, especially in the case of helical structures with small angle increments—no tilting of the specimen is necessary, and the micrographs can be taken with a conventional microscope[52].

This does not yet constitute a three-dimensional analysis in the strictest sense, since the identity of experimentally determined projections and projections deduced *via* symmetry is correct only to a relatively crude approximation. The specimen lies on a foil, and is covered with contrast medium; these components certainly have no helical, nor even cylindrical, structure. The helix in the specimen could also have been squashed; this is not revealed in every case on enlarging the micrograph[*]. Despite these limitations,

these kinds of experiments have yielded a lot of valuable information on the structure and function of macromolecules—*e.g.* on the mechanism of contraction of the phage tails.

Regarding the term "macromolecule", it should be noted that from the standpoint of the content of information (expressed, for example, by the sum of all atomic coordinates), it is of great importance whether a highly symmetrical molecule (*e.g.* tobacco mosaic virus (TMV)), or an unsymmetrical molecule (*e.g.* ribosome), is under study. The content of information in the former case can be lower by orders of magnitude. Often a small subunit (the truly unsymmetrical structure—like the base sequence of the RNA in viruses—is neglected) repeats itself, according to a law of symmetry, which can usually be given with few parameters—in the case of a helix, with its polarity, diameter, pitch, and number of subunits per turn. Their number plays hardly any role compared to the considerably larger numbers of parameters necessary to describe the subunit, so—according to information theory—such a macromolecule can practically be taken as the "subunit molecule". This concept can be extended even further. As already mentioned, a biological helix is a "string of pearls" consisting of "equal" subunits wound in the form of a screw. From the viewpoint of three-dimensional analysis, such a helix can directly be seen as a "tilting device", which brings single subunits into the orientations necessary for structural analysis. This is associated with both an advantage, as well as a disadvantage: on the one hand, many subunits form an image, whereby averaging takes place on artefacts of preparation and irradiation damage (object filtering[47]); on the other hand, this principle apparently functions only for smaller structures—a helix similar to TMV with ribosomes as subunits would be so enormous, that this would go far beyond the applicability of the kinematic theory, because of its thickness. This has the consequence that the proper three-dimensional information—expressed, *e.g.*, as the number of resolution elements N in the "reconstruction volume" of the subunit—is very small (order of magnitude 10) because of the limited biological resolution.

Nevertheless, the aesthetic charm of highly symmetrical helical and spherical ornaments is immense—it is pleasing, in a certain way, that the long-forgotten dreams of *Dorothy Wrinch*, who had postulated extremely symmetrical protein structures in her cyclol theory[53], have come true, at least in this field.

Furthermore, this information-based description of the molecule also applies for the X-ray diffraction experiments of highly symmetrical macromolecules like the TMV protein[54]. However, the high molecular weight complicates the measurement—an immense number of scattering data have to be determined—but the high symmetry facilitates the analysis. On discussing helical structures, the possibility of three-dimensional X-ray analysis of fiber diagrams must be mentioned. It was the precursor of electron microscopic analysis, and could be carried very far, for example, with TMV[55].

[*] Recent investigations on a spherical virus (turnip yellow mosaic virus) seem to confirm these fears.

### 3.3. The Analysis of Native Periodic Structures

The tomographic procedures[48,49] and our contribution[50] to three-dimensional electron microscopy had different origins. Dissatisfaction with the fact that in the case of biological specimens irradiation damage necessitated contrasting tricks, and bad resolution seemed to be inevitable, stimulated a search for ways which could lead, in analogy to X-ray crystallography, to an electron-ray crystallography of native proteins. We immediately directed our attention to the possibility of the diffractometric determination of amplitude and phase of the crystal reflections using electron-microscopic methods, for the methods of spatial frequency filtering, and hence electron-microscopical diffractometry, had been developed in our laboratory.

The first hurdle was specimen preparation. Protein crystals contain about the same amount of solvent as the protein itself. On drying, the crystalline order is almost completely lost. It was therefore necessary to find a vacuum-resistant material that could replace the solvent without disturbing the crystalline order. Of the known embedding materials for electron microscopy, hydrophilic polymers proved to be the most useful. The alternative, that water should be left in the crystal and its evaporation prevented[56] by modified experimental procedures, such as electron microscopy with humid object chambers, or low-temperature microscopy (at $-180\,^{\circ}C$, ice has a vapor pressure of $10^{-20}$ bar), seemed far from promising in the initial stages of research. As test structures, we used crystals of myoglobin and erythrocruorin, and tested the preservation of their structure X-ray crystallographically. For specimen preparation, special procedures were developed (for example, cross-linking of the proteins with glutaraldehyde to render them insoluble).

Figure 17b shows a precession diagram of a myoglobin crystal embedded in Vestopal. Here, it can be seen that the order is much worse than in a water-containing crystal (Fig. 17a). The disturbance of the crystal order takes place only in the last step of the preparation, on transformation of the monomeric embedding material into the polymer; diagrams of the crystal soaked with the monomer show an unchanged order of the protein molecules[57]. It is therefore recommended to lower the vapor pressure by non-covalent forces (lowering of the temperature) instead of by polymerization through covalent cross-linking. The range of materials that can be used as substitutes for water is therefore broader. Of course, water itself—as already mentioned, and as was later proven experimentally[58]—can also be used. Its anomalous behavior on crystallization, however, can only be overcome by certain tricks, for example, by supercooling (shock-like deep-freezing), or by the generation of a non-anomalous ice modification at high pressure[59]. On substitution of the water, new parameters can be varied (vapor pressure curve), and also mixtures (partial distillation) can be tried out. In any case, today there is scarcely any doubt—for ice[58] and organic monomers[57] it has been proven—that a preparation of native structures of biomolecules for high resolution electron microscopy is possible.

As a temporary aim of our work[80], the X-ray crystallographic resolution of 0.8 nm that we reached, was consid-

ered satisfactory (Fig. 17). Electron diffraction on thin layers of crystals prepared without contrasting yielded clear crystal reflections, which on comparison with the X-ray diagrams showed an analogous intensity distribution. These diffraction diagrams using the normal conditions of irradiation in the electron microscope—still without the minimal dose technique introduced by *Williams et al.*[60] (not to be confused with the low dose technique)—were visible for only a few seconds. The poorer resolution in the electron diffraction diagram (1.2 nm instead of 0.8 nm) can perhaps be attributed to radiation damage during the adjustment operation. However, most important was the fact that the possibility of carrying out an electron ray analysis of native proteins (and therefore also that of other biogenic macromolecules) had been demonstrated.

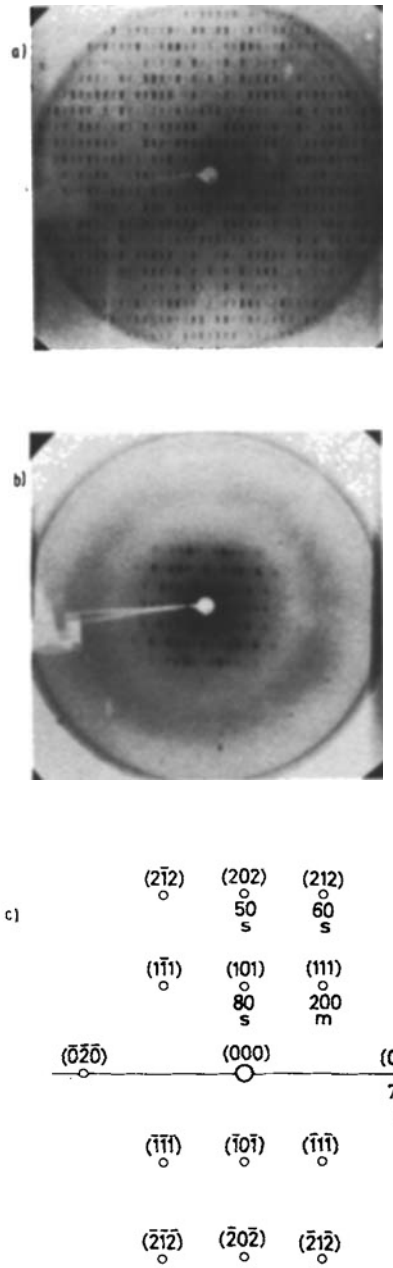



Fig. 17. a) X-ray diffraction diagram (precession diagram) of a sperm whale myoglobin crystal (hk0 projection) in mother liquor. b) Precession diagram after crosslinking of the proteins with glutaraldehyde, and dehydration and embedding in Vestopal (polymerized). c) Electron diffractogram of a thin ultramicrotome section of a crystal embedded in Vestopal (schematic). In addition to the indexing, absolute values of the structural factors measured by X-rays and (beneath) the estimated electron ray intensities (st = strong, m = middle, s = weak) are given (after [50]).—In a "supplement" [57], different embedding materials, primarily water soluble materials, were also tested, and an electron micrograph of an unstained microtome section was shown, which seemed to be unordered ("granulated"), but showed single reflections in the light diffractogram.

A law in structure research, the reciprocity law, states that structural information in one of the two dual spaces—real space and reciprocal space—must always correspond to an analogous information (transformed into the other space). When applied to our problem, it means that the same information on the structure of the crystal must be contained in the image of the native crystal lattice in the electron microscope as in the diffraction diagram. However, it contains information about the phases, which indeed the diffraction diagram also contains, but which is lost on the transformation of the amplitude into intensity (in contrast to the intensity formation in the image plane)[50]. However, the influence of the measuring instrument, the electron microscope (phase object, spherical aberration) must be taken into account (cf. Sections 2.3—2.10). For the changing of direction of the projection (for three-dimensional analysis) differently orientated ultramicrotome sections of the crystal were proposed[50], with which, in electron microscopy also, the whole reciprocal space is accessible. The same goal can be achieved by changing the orientation with the aid of a goniometer ("tilting"), as is otherwise usual in crystallography.

Why a crystal structure analysis of native biogenic macromolecules is possible with the electron microscope is made clear in the following reference[24a]: "Let us first start with a not very encouraging discussion concerning the physical possibility of "molecular microscopy". It is the strong interaction of electrons with atoms which makes it possible to collect in a reasonable time enough scattered electrons for the recognition of single atoms. But there is also the unhappy situation that for light atoms the cross-sections for elastic and inelastic scattering are of the same order of magnitude. That means that the number of elastic and inelastic collisions is approximately the same. In crystal structure analysis there are many equivalent molecules—in a small protein crystal, *e.g.*, $10^{17}$! It is therefore highly improbable that a molecule will be hit more than once by an incident quantum. Therefore the elastically scattered quanta will find untouched molecules and can build up diffraction patterns of the non-distorted molecule". Now, the averaging principle is a fundamental principle of crystallography; it is dealt with in text books[61], is used in the X-ray diffraction analysis of statistical superpositions of molecules with different conformations[62], and is applied to stained electron microscopical molecular pictures, which show differences produced by preparation and radiation damage (high dose pictures)[47,48]. Remarkably, however, it was not until much later that averaging to eliminate irradiation damage was given any attention[50,24a] (work on information theory[63] cited in this context[58] contains no remark on this possibility), perhaps because it only became known later[64] that the ratio of inelastic to elastic collisions with atoms, also in the case of X-rays (substitution of the electrons by X-ray quanta) is very

large. It is actually almost larger by a factor of 10 compared with electron rays, *i.e.* X-rays are very destructive[*].

From 1970 onwards *Glaeser*[58] systematically investigated the radiation damage of organic structures, and demonstrated in computer simulations how the influence of the radiation damage can be reduced by crystallographic averaging. Using these preliminary studies as a basis, *Henderson* and *Unwin* succeeded in performing the diffractometric three-dimensional analysis of a native crystal (purple membrane from *H. halobium*) by the use of spatial frequency filtering (see Sections 2.2—2.10)[**]. Such structural analyses have become very popular in recent years[66]. However, it soon became obvious that preparation of a specimen suitable for high resolution encountered difficulties in the case of very large molecules; even without radiation damage, resolutions of less than or equal to 2 nm are difficult to obtain. Similar difficulties are also encountered in the X-ray crystallography of macromolecular structures. Highly symmetrical organic macromolecules (*e.g.* helical structures) could easily be investigated in their native states using the low-dose technique. Low-dose experiments on stained TMV[67,68] have demonstrated how new details (above all in the nucleic acid sector) become visible on changing to the non-damaged molecule.

### 3.4. Three-Dimensional Electron Microscopy of Individual Structures ("Real" Three-Dimensional Electron Microscopy)

#### *3.4.1. Why "Individual" Structures?*

X-ray crystallography has developed from small beginnings to be one of the most important branches of science. What would our understanding of matter (and therefore, of chemistry) be today if the diffraction method had not given us such a detailed knowledge of the atomic architecture of compounds—up to the proteins? This is true, of course, only for highly ordered, periodic aggregates (like single crystals). However, there also exists the world of individual structures which are not exactly reproducible, but which are of importance not only in biology (although there especially) but also for chemical reactions in the most general sense. How paltry is our knowledge here!

Just think of "platinum black", an inorganic catalyst for reactions of organic molecules, whose particulate form hardly ever repeats itself. Or a biological membrane: its enzyme pattern on the surface leads us to suspect topological interactions, which optimize sequences of enzyme reactions. Enzyme complexes like fatty acid synthetase may be precursors of such "factories". Again, the structure is not repeatable, but its principle of construction is important for biochemistry.

A method which is fundamentally suited to experiments in this problematical sector is to be found in microscopy. For example, cells, which are individually so different, but which also show structural similarities, can be identified under the light microscope. On investigating individual structures by conventional electron microscopy, the molecular, but not of course the atomic region, was approximated. But even this method had in many ways its limitations. One of its most important being the information-destroying restriction to projections of spatial bodies.

Phase-determining diffractometry, with its combination of the principles of structural research and microscopy, promised to provide the most interesting insights into the wide field of aperiodic and individual structures (with possibilities for use in all areas of chemistry).

In Munich, therefore, although X-ray diffraction and neutron diffraction[69]—as well as protein crystal structure analysis in the electron microscope[50]—were not totally ignored, our efforts were concentrated on the further methodological development of electron diffraction for the investigation of individual and aperiodic structures in the electron microscope. Atomic resolution was not attainable using thermal cathodes, or, only incompletely so, (with synthetic aperture techniques[33–35]). The laborious development of better monochromatic field emission guns in our own laboratory would have been unjustified, as such a program of studies was already under way and proving successful elsewhere; today, field emission cathodes are commercially available (although they are costly). Three-dimensional analysis, however, was fascinating at any resolution; it was also to be expected that in lower resolution investigations the general stability problems would be of less trouble. A self-imposed handicap was the concentrating of our efforts on biological structures, for that presented the complex problem of radiation damage. It is not without envy that we look at inorganic electron microscopy, in which, completely conventionally and with incredibly high irradiation doses, imaged crystal projections yield practicable contributions to topological chemical questions[70]. The energy transferred in elastic scattering processes is carried off without damage to the object. But, on the other hand, biochemical and biophysical investigations are especially interesting. Moreover, conventional electron microscopy had already shown what valuable information can be won in spite of radiation damage, if the object is prepared in a suitable way (cf. Fig. 18).

The success of the low-dose analysis of native periodic structures (Section 3.3) has unfortunately misled many into regarding high-dose analysis of contrasted structures as being "retrogressive". However, in the case of individual structures, high-dose analysis must be resorted to. The object to be studied, *e.g.*, a macromolecule, is by no means to be regarded as isolated. In reality, reaction products are observed, from the reactions of the compounds actually of interest with the reagent of preparation, the supporting

[*] A measure of the damage caused by the rays is given by the ratio of inelastic collisions—which are able to but do not have to change a structure—to the elastic collisions. Formerly, the damage caused by the rays was often correlated (also in high-voltage electron microscopy) with the reciprocal scattering cross-section. Naturally, this is meaningless regarding imaging problems, where the number of the scattered quanta (electrons) is important.

[**] Compared to the first experiments on the structure analysis of native crystals[50], it is methodologically noteworthy that the analysis on a two-dimensional crystal (membrane crystal) has been carried out, enabling a link to the methods of analysis for individual structures (cf., *e.g.*, [81]); even the determination of the common origin (after translation into reciprocal space; cf. Section 3.4.2). This holds for three-dimensional crystals (such as in [50]) only with limitations (cf. [77, 96]).

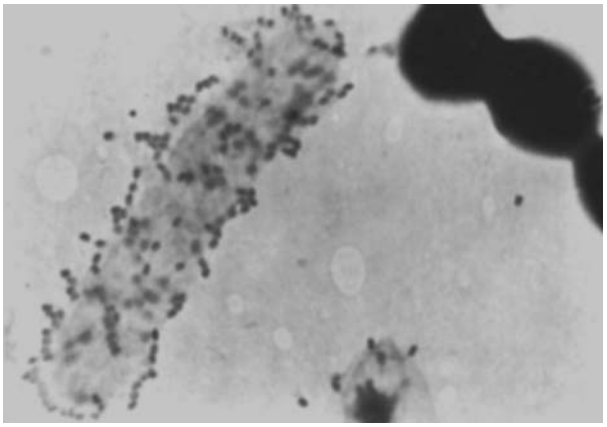


Fig. 18. Discovery of bacteriophages with the electron microscope. As long ago as the 16th December 1939, *H. Ruska* had submitted an article for publication (*Naturwissenschaften 28* (1940) 45) in which it was reported that bacteriophages had been discovered on lysis of *E. coli* cells. The micrograph shown here is reproduced from a later communication (H. Ruska, *Naturwissenschaften 29* (1941) 367) after the phage tails, which were "often pointed into the inside of the bacteria" had been observed for the first time, on the attack of bacteriophages on *Proteus* cells. [I thank *C. Ruska*, Institut für Biophysik der Medizinischen Akademie, Düsseldorf, for permission to reproduce this micrograph.]

foil, and the radiation. "Radiation damage" is also chemistry. Even if the radiation reactions can be eliminated in any way, the preparation reactions are still there. And these can highly influence the structure of the object. Even with identical molecules the reaction product is only reproducible under exactly the same reaction conditions. For comparison: if several people write the letter "a", it can look different in each case, although it is still "a". Here, we are dealing with one of the fundamental problems of computerized character recognition, which in information theory is studied as "pattern recognition". By varying common structural characteristics the concept of the letter "a" is reached. Primitive comparisons and averaging have to be replaced by the ideas of "pattern recognition" in the electron microscopy of individual structures too. As a calculable reaction product, "radiation damage" loses its horror; the electrons are simply a further, although undesired, partner in the reaction. The reaction conditions can be controllably varied, *e.g.* by trapping the emitted electrons with acceptors or by lowering the temperature.

Only three-dimensional investigations lead to inequivocal structural results. For a given projection, as many structures as wanted can be produced by exchanging image elements along the direction of projection. In addition, there are components lying, accidentally, above or beneath this projection (*e.g.* support foil). It is also important that a high enough radiation dose should be used, to ensure significant imaging of the spatial structure. Only then can changes in the structure be assigned to chemical changes, for example, in the distribution of contrasting material. With the necessarily high doses, a slow change of the structure during the exposure (after the rapid destruction of the native structure) cannot be ruled out. The three-dimensional procedure should therefore work in such a way that it yields the average structure (as in conventional microscopy). And finally, the electron microscope itself should be free of errors, otherwise no decision can be made as to whether a structural change is due to the object, or is simulated by the spherical aberration. For this reason, the tomographic procedures are incomplete. Only correct spatial frequency filtering with determination of the structure of the image points, guarantees a sufficiently quantitative procedure.

This is often misunderstood; only recently, it was suggested that individual structures of identical particles should be made more "similar" by reducing the resolution, and thereby reducing the "noise". This is something like proposing to a cell biologist to image his cells less sharply in order to iron out their individual differences (which are designated as "noise"). He can of course do this, and in this way gets a "unit cell" by subsequent superimposition, but all the fine details—*e.g.* in the nucleus—are lost.

The light microscopist, studying his cells individually, can do it better: he does "pattern recognition" intuitively. One only has to bear in mind the really quite crude preparation procedures in order to understand how different "identical" particles can look. However, the rich preparative experience potential collected in conventional electron microscopy, should also not be underestimated. But only by three-dimensional analysis can it be thoroughly explored and made usable. In the future, directed improvements of the preparation methods are therefore to be expected.

Naturally, this should not mean that the averaging of the same kinds of "reaction products" of identical particles is unnecessary. Statistical procedures will always be necessary in order to study the regularities in a population of entities. But the chemistry involved should not be forgotten. From the development of low-dose analysis, it can be seen how errors of judgement in the microscopy of individual structures were made. The individual image consists practically only of real, uninterpretable electron noise. However, for example, the "granulation" so characteristic of each electron micrograph with high resolution (cf. Fig. 23) is not noise, even if the electron microscopist refers to it as "structural noise"[*].

### *3.4.2. Methodological Aspects*

#### *The Necessary Radiation Dose*

On going from two-dimensional diffractometry (fixed direction of the primary ray) to three-dimensional diffractometry, some new questions arise. Thus, it was feared that the large number of pictures on rotating the object (cf. Fig. 16) would result in an extreme radiation load on the speci-

[*] The averaging described concerns particles which were measured to an electron-statistically significant degree. But naturally the integral dose per particle can also be reduced, whereby the single particles show strong electron noise that can only be reduced on averaging. Thereby, the influence of radiation can be studied. In the borderline case of very low radiation doses (analysis of native structures), the projections necessary for the carrying out of the three-dimensional reconstruction can, because of the interchangability of the operations, also be averaged first of all, and afterwards, reconstruction can be made with the averaged projection[94]. This procedure basically corresponds to crystallographic reconstruction (cf. Section 3.3), in which the three-dimensional reconstruction is built up from the averaged (through the crystal) single projections in the same way.

men. We have demonstrated[71] (which was surprising and raised doubts[72]), that for a two-dimensional micrograph (with spatial frequency filtering), about the same amount of electrons are necessary as for a three-dimensional analysis with the same electron-statistical significance. In the first case, the whole dose is applied in the taking of one image, in the second case, it is evenly distributed over the taking of the series of images. "Equally significant" means that in both cases an object detail (*e.g.* a heavy atom group) can be recognized, with the same ratio of signal to noise, whereby in the first case it is assumed that it can be discriminated due to the fanning out in the z-direction (the direction of the optical axis) and also determined in its z-coordinates. In order to understand this[73], think of the object as being divided into a series of thin sections (having the thickness of the z-resolution). A micrograph is made of each section. This is obviously the optimal procedure, because the other sections do not become impaired by the electrons that are necessary for the imaging of one section. Calculation shows that three-dimensional diffractometry works as economically as does two-dimensional analysis (or to be more precise, admittedly, only if the curvature of the sphere of reflection can be neglected). This *Gedanken-experiment*[73] also reveals the source of the misunderstanding[72]. Naturally, the images of the sections are more poorly contrasted than the image of the unsliced thick object. If only the last one is to be seen, then a few electrons suffice. However, then, no details can be seen in the two-dimensional image of the object (electron noise!).

*Determination of the Common Origin*

A second problem concerns the phase correlation of the structural factors of the tilted images. It would not be necessary if—as in tomography—the axis of rotation could be rotated with the exactness of the resolution. This is not possible in electron microscopy—the resolutions lie in the order of magnitude of nanometers, the mechanical precisions in the order of micrometers. We worked out the procedure of cross-correlation of slightly inclined projections for the determination of the common origin of all Fourier sections[74,75], and developed this theory, first of all for the ideal case of point atoms[75] and later for real atoms[76]. Note that it is also used for the analysis of native crystals[65] after translation in the reciprocal space[77].

*Number of Images*

From each picture, the structure factors on a spherical surface in the reciprocal space can be determined (cf. Fig. 3b), which in the case of average resolutions can be approximated by their tangential plane. In three-dimensional analysis, a discrete bundle of such surfaces (cf. Fig. 20) is determined, between which one must interpolate in order to obtain the continuous structural factor distribution in reciprocal space. Use of the Whittaker-Shannon interpolation theorem shows[78] that the minimum number of images is dependent on the resolution and on the size of the object. Our formula for the number of projections[78] was confirmed by *Crowther et al.*[79]. Later, however, this problem proved to be more complicated. These calculations[78] refer to the ideal case of an undisturbed three-dimensional image point that is independent of location. Allowing for the background disturbance increasing a little, or the image points on the edges of the reconstruction area being somewhat more badly resolved than in the middle, the number of projections can be reduced by up to a factor of 2. Thus, in the Cormack procedure known from computerized tomography, which reconstructs a cylindrically shaped body (cylinder axis identical with tilt axis), the region in the proximity of the axis is somewhat more sharply imaged than next to the cylinder surface. We use this procedure—after exact testing of the dependency of the image point on the location—in many of our reconstructions, because the surroundings of the object under study (the reconstruction area is always larger than the particles) are less interesting, and with the present state of the experimental technique, a limitation of the number of images seems to be economically necessary. This is because the whole experiment would be ruined by one, or a few, abortive images of a series (above all in the case of drift, cf. Figure 9b). It can be assumed that with further experimental improvements (above all, by automation), the question of the minimum number of images will be less important.

*Blind Region in Reciprocal Space*

The limitation of the range of rotation in electron microscopy—because it is fundamental—is more crucial. As an illustration, imagine a thin plate (specimen on a support) as the object in the "tomographic grill" (Fig. 16). If this plate stands edgewise, there is no transmission, and, in addition, mountings limit the range of angles. In electron microscopy the preparation can generally be tilted by about $\pm 60°$ away from the horizontal position, *i.e.* the rotation in Figure 16 has to be replaced by a tilting of about $\pm 60°$. This has unfortunate consequences for the image point shape, which in the ideal case should be sphere-like (as in crystallography). From Figure 19 it can be seen that instead of a sphere, an anisotropic pattern is formed, which shows the electron-optical resolution in the direction of the tilting axis ($\Delta y$), perpendicular to this, but determined, not only by the electron-optical resolution, but also by the angle increment $\Delta\alpha$ (in other words, by the number of images). Thereby, the length of the image points in the direction of the optical axis ($\Delta z$) is longer by a factor n than perpendicular to it ($\Delta x$); n depends on the angular range ($n = 1.8$ when $\alpha = \pm 60°$). $\Delta x = \Delta y$ can, of course, always be achieved by reducing $\Delta\alpha$, however, the elongation of $\Delta z$ is always present. Undesirable, are two deep, closely neighboring side minima in the x-direction. Otherwise, however, the background is only slightly disturbed by diffraction ripples. Especially noteworthy is the fact that the weighting of the transfer functions with their zero positions scarcely influences the image point shape and the background noise. After determination of the transfer function for each picture (which can be very different), the real image point of this reconstruction is calculated. Figure 19b shows one result. The cumbersome averaging by a series of focussings[26,27] can therefore be omitted in three-dimensional analysis—the averaging also works with tilted projections.

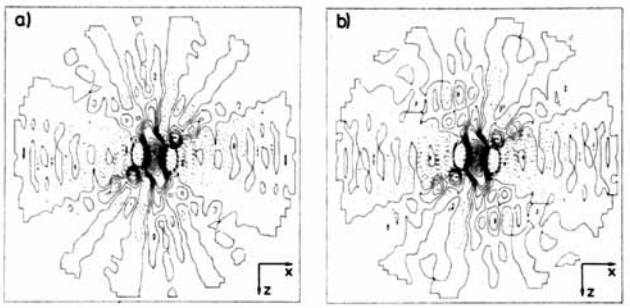



Fig. 19. Image point problems in three-dimensional electron microscopy. Because of finite resolution, an image point is always an extended object, in the ideal case in two dimensions with circular symmetry, in three dimensions (crystallography) with spherical symmetry. The limited range of tilting angle of goniometers is the reason for the asymmetry and the anisotropy. On tilting about an axis, the three-dimensional reconstruction body can be thought of as being divided into a series of layers perpendicular to the tilting axis (y-axis), which are arranged at intervals equal to the y-resolution ($\Delta y$). a) Imaging of the image point in the x,z-plane on tilting between $+60°$ and $-54°$, ideal weight function, contour lines $<0$ dashed, contour line spacing 6% (above the density +30% the contour line spacing increases to 8%). Image point height normalized to 1; background noise well under 10% with the exception of two neighboring side minima. These effect a certain deformation of the reconstructions in the x-direction (cf. test calculations [81c]). Important is that the side minima can only influence the immediate surroundings of the image points, and thus, large falsifications of the total reconstruction are impossible. Naturally, astigmatic distortions have to be taken into consideration when interpreting the analyses. On overlapping of reproducible, equally orientated structures, (with different directions of the tilting axis) the influence of the negative minima largely averages out, whilst the anisotropy along z remains. Unfortunately, an averaging of differently orientated particles (which could produce an almost spherically symmetrical averaged image point) meets with difficulties, owing to orientation effects, at least with current preparation procedures. b) Same image point as in a), but calculated with the aid of experimental transfer functions. Note the surprisingly large similarity to a), which makes the averaging of the influences of spatial frequency gaps according to [26, 27] unnecessary. By weighting the transfer functions, however, the image point height is reduced by about 25% (non-optimal contrast transfer with respect to the hypothetical ideal case (error-free microscope and Zernike plate)).

Does this strongly anisotropic image point suffice? Our situation is similar to that of a person with an astigmatic eye. If the resolution in the direction of the lengthened image point is sufficient, he is able to read; deformations in the other directions are then only slightly disturbing. For application in electron microscopy, this means that $\Delta z$ should be the same size as the required resolution (*i.e.* about 2 nm with stained biological structures). This is not difficult to achieve, since the electron microscopic resolution is always rather high in the case of individual structures. The granulation is always seen, so to speak, in the heavy atom glass, which is not interesting in itself (if its laws are not to be studied), but which helps to reach a sufficient z-resolution. For this reason, we usually work with a $\Delta x$ range of about 1 nm. As test calculations have shown, the negative, closely neighboring minima only disturb the nearest surroundings with very steep edges, (they produce a kind of Fresnel fringe); these fringes, and the randomness of the structure in the directions of sharper reproduction, must be "overlooked". Figure 20 systematically shows the whole reconstruction procedure.

The disturbance by negative minima can be totally eliminated with "conical tilting"[49] using special reconstruction procedures[78b]. Figure 21 shows an image point which is rotationally symmetrical and which already seems to be lengthened by only $n = 1.4$ in the z-direction with 45° tilting. The negative minima have totally disappeared. The image geometry is, however, more complicated than with simple tilting on a single axis (Fig. 19) but should be controllable. Because of this surprisingly convenient form of image point, experiments to replace the flat support foils used in electron microscopy by needles (whiskers)[80], and

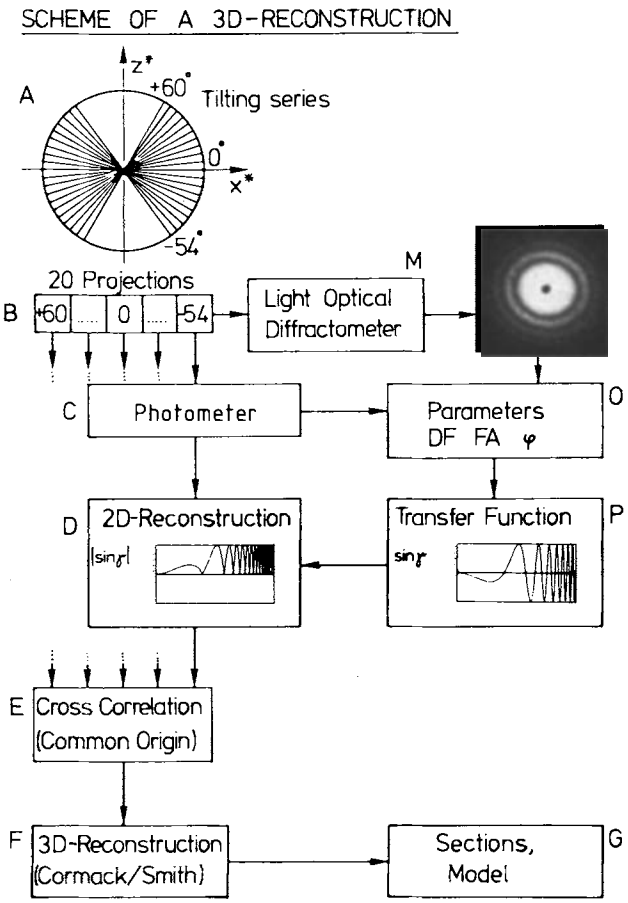



Fig. 20. Flow diagram of a reconstruction on tilting about one axis. A: Occupation of the reciprocal space with Fourier sections; the coordinates x*, y*, z* are parallel to the coordinates x, y, z in the real space, central sections (corresponding to the projections in the real space) are drawn in the tilting angle range of $-54°$ to $+60°$ at angular increments of 6° (projected along y*). Note the "blind" region in the reciprocal space, which is not filled with sections and therefore causes the anisotropies of the image point as discussed in Figure 19. B: Block of micrographs, which are measured in the automatic densitometer C (after testing in the light diffractometer M, which gives the light diffractograms N). From these (semi-quantitative) and from the densitometer data, the parameters O (defocussing, axial astigmatism) are obtained for the correction of the structure factors (transfer functions P). In step D, this correction (two-dimensional image reconstruction, also called image restoration) is made. In the next step, the determination of the common origin of all projections (and hence that of the three-dimensional body) is accomplished. The last step is the actual three-dimensional synthesis (sections G).

thus to reach a kind of "rotating molecule method" with spherical image points, were stopped. In spite of indisputable theoretical advantages, this would have meant a changing of the whole technique of specimen preparation in electron microscopy. Three-dimensional microscopy should, however, be "seamlessly" coupled to conventional microscopy.

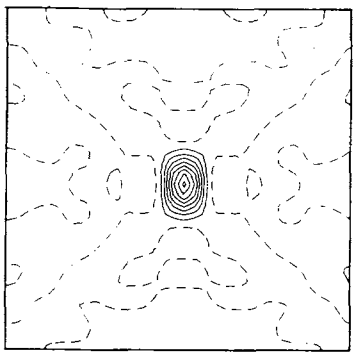


Fig. 21. Image point by conical tilting, If the primary beam is guided onto the surface of a cone, which corresponds to circular tomography in geometry (cf. Fig. 15 and [49]), then, with a modified reconstruction program [78b], an image point can be derived, which is, however, lengthened in the z-direction, but which appears circular in the x,y-plane (think of the figure as being rotated about the z-axis perpendicular to the plane of the paper) and produces no negative minima. If, therefore, the z-resolution $\Delta z$ is properly chosen, then no more problems arise on interpretation than when a spherical image point (diameter $\Delta z$) would be present—the anisotropy actually produces a "reducing" of the image point (in the x,y-direction). Notice, however, that in certain "pathological" occupations of the reciprocal space with structure factors (in which these lie mostly in the non-measured blind region of the reciprocal space), difficulties can arise. With asymmetrical structures, such difficulties are hardly to be expected.

### 3.5. Use of Three-Dimensional Electron Microscopy in the Structural Investigation of Ribosomes

With a resolution of 2 nm, smaller biomolecular particles—for example, the TMV protein, phage proteins, coat proteins of spherical virus molecules, bacteriorhodopsin, *etc.* (molecular weights of the order of 20000)—also show only a few details in three-dimensional analysis (number of image points of the order of 10). The situation is different if (asymmetrical) particles with molecular weights of several millions are being studied—structures are obtained which, even with this low resolution, show the complexity of smaller proteins (resolution 0.2—0.3 nm; more than 1000 image points). Clearly, these are cases in which projections will have to remain uninterpretable.

The first real three-dimensional analysis of an electron-microscopic object was published in 1974[81]. As shown in Section 3.2.3, difficulties might be encountered in investigations with the production of the projections by symmetry operations. The first three-dimensional crystal structure analysis (for which these limitations, with exception of the averaging of similar objects, do not apply) was published in 1975[65]. In collaboration with *Lynen et al.* in Munich, we studied the structure of fatty acid synthetase of yeast ($M_r \approx 2.3 \times 10^6$)[81]. At that time, our experimental technique was not perfected ($\alpha = \pm 45°$, $\Delta\alpha = 10°$), and also the total dose was higher than that required for recording the micrographs (no minimal dose technique). Later, stimulated by work on label triangulation methods (cf. [69]), we turned to the structure analysis of ribosomes (ribosomes of *E. coli*, $M_r \approx 2.7 \times 10^6$). It was no accident that the first investigations in this new field of individual analysis were not carried out on real aperiodic structures[*], but on chemically reproducible, although very large, particles, which could in theory also have been investigated using crystallographic methods. The identical chemical structures enable comparison of the reaction products—dependent on preparation conditions such as orientation towards the support foil, *etc.* Further, in the case of the ribosomes, the strong ionic character of the protein-RNA complex is interesting, which also leads to the assumption of staining of structural details in the inner particle (positive staining). Above all, however, ribosomes are molecular structures which are biologically very important, occur in all forms of life, and through which the synthesis of proteins takes place. They are not only highly differentiated in their (totally asymmetric) structure, but are also highly differentiated in their function. Depending on the cell (prokaryote, eukaryote) and functional assignment (cytoplasm, mitochondria), they can show large differences (*e.g.* in molecular size and form), but—especially as sequence analysis of RNA strands have shown—are closely related to one another. In the last few years ribosomes, especially from *E. coli*, have been intensively investigated chemically; today, for example, practically all the sequences of the approximately 50 (different) ribosomal proteins are known. Characteristic is the capability of the ribosome, after its segregation into the single proteins and nucleic acid strands, to aggregate back into intact and active ribosomes, a capability which is utilized in the label triangulation investigations for the determination of the native protein topology (see [69]). The ribosomes are easily divided into two subunits of different sizes; 30S and 50S subunits[*] for prokaryotes, 40S and 60S subunits for eukaryotes. It is obvious that these subunits should next of all be investigated separately.

#### *3.5.1. Conventional Electron Microscopy of Ribosomes*

Because of the size of the particles, and their relative stability toward preparation procedures with staining, they were investigated electron microscopically fairly early on—actually, they were discovered in this way. But, however, there is hardly any other object with which the limits of conventional electron microscopy are made so drastically clear than with ribosomes—in spite of, or perhaps because of the ingenious experiments to characterize structural details immunologically or with other labels.

It was not only due to their size, but also to the complete lack of symmetry, that—in contrast to the somewhat equally sized spherical viruses (with which the ribosomal particles were first of all compared)—no structural laws could be found, and in the best case, only the outlines of the particles could be recognized. The surroundings and the particles are covered with a general granulation ("structural noise") (cf. Figures 22 and 23). Only a short while ago, (long after the beginning of our analyses) were defined structures inside the particles revealed, by the averaging of micrographs of equally oriented particles[82,83],

[*] Exceptions are investigations on the analysis of the action of complement on vesicles [91], and preliminary high resolution investigations on amorphous carbon [92].

[*] Classification according to the sedimentation constant in the ultracentrifuge.

which, as projections of thick bodies, can tell us little[*]. Even the seemingly simple problem of the determination of the shape found no satisfactory solution. Three-dimensional bodies were tentatively "invented", which—projected in different directions—should explain the different molecular images appearing in the micrographs. In a way, this is a primitive form of the three-dimensional analysis of projections; however the number of projections is extremely low (of the order of 5), and their respective angles are unknown. Furthermore, it is fully unknown, whether structural changes are associated with the different orientations of the specimen. It is understandable that in different laboratories, different models were found.

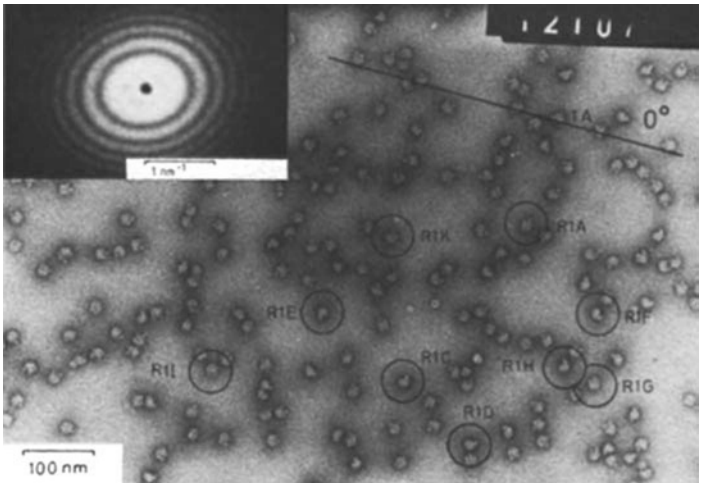



Fig. 22. One of the 21 micrographs (0° tilt) from the +60° to −60° series of micrographs (−60° micrograph discarded due to drift) taken at angular increments of 6°: ribosomal 50S subunits from *E. coli* without L7 and L12 stalks. Enlargement of 79300, mean defocussing $\Delta z = 827$ nm, axial defocussing difference $dz = 386$ nm, dose $\approx 7 \times 10^3$ e/nm$^2$. Reconstructed particles marked, direction of the tilting axis drawn in.

### 3.5.2. *Three-Dimensional Analysis of Stained Ribosomal Particles*

The large experimental expenditure in the case of these specimens[**] makes it necessary to limit the analysis to a few particles. With today's priority of averaging methods in electron microscopy, this would seem to imply a severe limitation, but this is not true. On comparing structures (in the general sense) not only the number of structures, but also the number of structural details are important. A classic example is the "fingerprint" of criminology. Even a comparison of two fingerprints is enough to prove the identity. In the case of the three-dimensional analysis of ribosomes, the number of characteristic details is especially large (corresponding to the volume of the particle), and thus the information content of the analysis is considerable. Of course, it is necessary to choose a high enough radiation dose so that the electron statistical significance suffices for significant recognition of the details. We work with doses of about $1.5 \times 10^5$ e/nm$^2$—this is a factor of about $10^3$ more than in the analysis of native crystals. The results, similarly as in crystallography, can be represented quantitatively in contour maps of the single sections. We chose the contour line distance in such a way that it corresponds to the double or triple amount of the electron statistical standard deviation—differences between reconstructions of different particles are therefore certainly not noise, but are produced chemically (and radiation chemically). To prove that no significant changes occur during a series, we expose a "radiation damage series", under the same conditions but without tilting (at another site on the specimen). The mathematical measure of the similarity of two images is the cross correlation coefficient $C_k$[*]. We test the constancy of the images in the radiation damage series with cross correlation, visual examination, and by calculating the difference. Of course, the organic substance is totally destroyed, even on recording the first micrograph—its skeleton, however, is very stable against further radiation; the reconstruction procedures average out smaller changes (as the theory shows). However, with a dose of about $10^5$ e/nm$^2$, recrystallization of the contrasting material slowly begins[51,84]; therefore, this dose should not be exceeded to any great extent. Since our experiments are done under minimal dose conditions, no further loading occurs through adjustment processes.

Our reconstructions[85] were done on uranyl salt-stained 30S and 50S subunits of *E. coli* in different orientations. 3—5 particles were investigated in each orientation. A simple trick enables us to avoid having to do separate tilting series for each particle. On choosing the proper preparation conditions, relatively many particle projections are imaged (about 500) on a micrograph (magnification about 80000). These micrographs show different "shapes", whose differences are explained by different orientations and by influences of specimen preparation. Often, shapes occur which are especially characteristic and similar in outline, which the electron microscopist—as already mentioned—interprets as different projections of a three-dimensional body. In the literature, they are referred to by different names—*e.g.* asymmetric and symmetric forms with 30S subunits, kidney and crown forms with 50S subunits. In the tilting series, approximately the same number of ribosomes are imaged on each micrograph of the series, so that the three-dimensional preparation under study is actually a population of ribosomes. Subsequently, the single particle pictures to be reconstructed are chosen, and measured in an automatic densitometer. Note the immense information capacity of the photoplate, which will make it difficult to replace it electronically. With the 20 μm scanning raster (diameter of the probe on the specimen 0.25 nm

[*] The experimental averaging in [82] agrees very well with the projection of our 3-D model.

[**] We thank Dr. *M. Stöffler-Meilicke*, Max-Planck-Institut für Molekulare Genetik, Berlin, for the preparation of ribosomal particles and ribosomes from *E. coli*.

[*] $C_k = C_{12}/\sqrt{C_{11}^2 C_{22}^2} \cdot C_{12}$ is the magnitude of the cross-correlation maximum, $C_{11}$ and $C_{22}$ are the magnitudes of the autocorrelation maxima of the structures compared. With the supposition that the cross correlation maximum lies in the zero position (*i.e.* that both images were exactly in line, by correlation), then $C_{12}$ equals the integral over the products of the densities of both images. $C_{11}$ and $C_{22}$ correspond to the integral over the square of the densities of the single images. When both images are the same, $C_k = 1$; with different images $C_k$ decreases. With two random structures, $C_k = 0$.

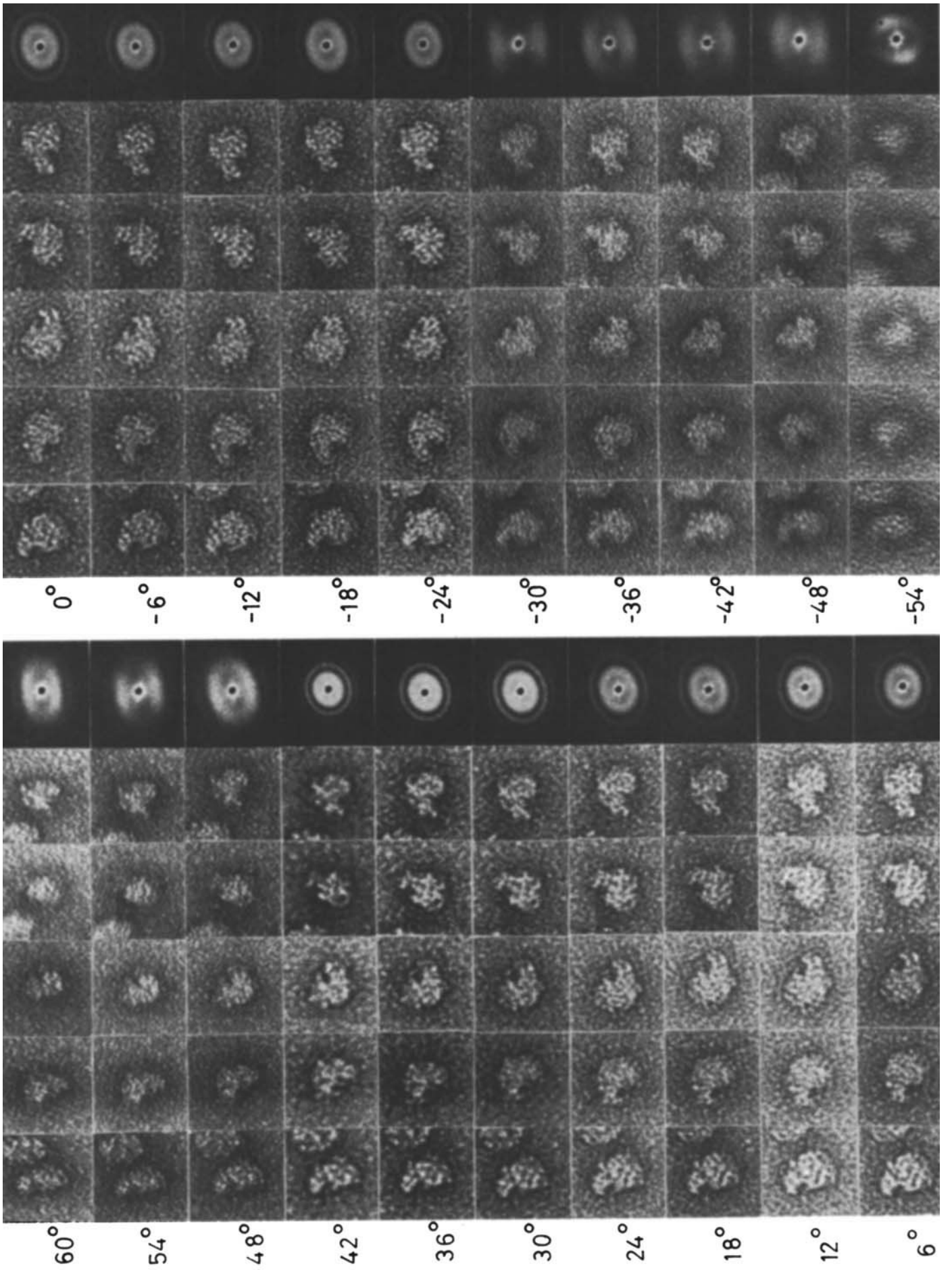



Fig. 23. Gallery of all "kidneys" studied, of the series $\alpha = +60°$ to $-54°$, $\Delta\alpha \approx 6°$, with their respective light diffractograms. Designation, from left to right: R1D, R1C, R1E, R1F, R1H (cf. Fig. 22).

with an enlargement of 80000[*]), which we mostly used, a $6 \times 9$ cm$^2$ photoplate contains $13.5 \times 10^6$ image elements, a series with 20 pictures $2.7 \times 10^8$ image elements! From this information, only a very small fraction is used. With higher tilting angles the defocussing in the preparation changes to a large extent. This does not matter, since it is determined by calculation, and corrected. For the same reason, it is also immaterial whether the focus on the reference position (with which it is adjusted and which is at a distance of several micrometers from the picture position) varies somewhat, due to mechanical inexactness or because of the not completely planar specimen surface.

Figure 22 shows a 0° micrograph taken from a series of 21 micrographs of a population of 50S subunits stained with uranyl formate (z-resolution 2 nm), which were isolated in such a way that two of the 34 proteins of the subunit (L7 and L12) were split off. These proteins—closely related in their chemical structure, and present in up to 4 copies—are located, as comparative conventional analyses had shown, in a lateral rod-shaped protrusion (stalk) of the subunit. We have investigated subunits with and without the stalk, in parallel, since we were interested in how this chemical operation influences the inner structure of the subunit. As already mentioned, artificial and natural modifications of the structure of the ribosomes of different kinds are characteristic of ribosome chemistry—we are dealing here with a simple model case. In the micrograph, the chosen particles of two orientations are marked (kidneys R1C, R1D, R1E, R1F, R1H, crowns R1A, R1G, R1I, R1K). Figure 23 shows a gallery of all micrographs of 5 chosen kidneys, in a tilt series, together with their light diffractograms. The micrographs show such strong, and such random differences, that the experimental evidence could almost be regarded as being obscure. But this is incorrect—on the contrary, it is remarkable how exactly electron optics "draw", if lens aberrations are corrected. The micrograph can perhaps be compared with projections of fruits which are dug up from moist and loamy earth and seem like accidentally formed clumps of earth, but which are highly ordered within.

Generally, it can be said that particles in the same orientation have structures which differ a little in detail (different staining and radiation influences), but which are surprisingly reproducible in their general proportions. They can also be superimposed to give a well resolved average structure, whereby, however, a correlation of the slightly different orientations becomes necessary by laborious three-dimensional correlation procedures. By way of contrast, the structures of differently orientated particles show large differences; the first suspicion, that the particles flatten strongly by surface forces on drying, has fortunately not been confirmed (see also [86]). The staining material forms a ring around the particles (cf., *e.g.*, Fig. 24); with thick specimens, in particular, (*e.g.* oriented in edgewise positions) the staining intensity inside the particle varies

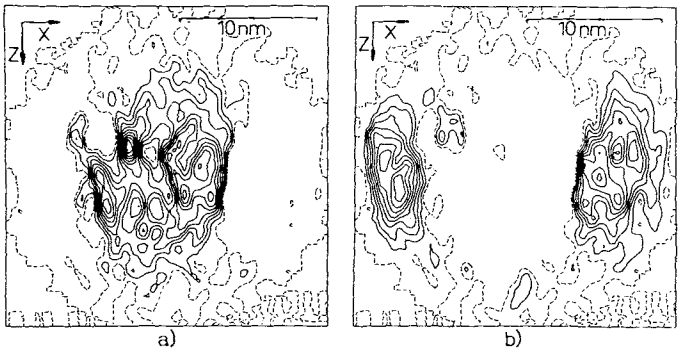



Fig. 24. "Looking around the corner" in three-dimensional electron microscopy. With a three-dimensional body, projections can be calculated in any direction, which can also correspond to micrographs which would not be accessible due to the imaging geometry. A projection of the "kidney" averaged from R1C, R1D, R1E, R1F (cf. Fig. 22) in the direction of the y-axis is shown: a) positive regions, b) negative regions. Note: in a) a general decrease in contrast from the middle plane to above and below, which corresponds to the decrease in contrast in the layers. However, the bordering of the particles above and below can be seen, since the differently structured foils above and below the particles already average themselves out (the projections of the foils appear with lower contrast); in b) primarily the projection of the ring-shaped contrast middle region is conspicuous. The particle area seems "more positive" than the surroundings, due to the normalization, which equates the total integral from the positive densities with the integral of the negative densities.

from above to below. The middle layers are the most strongly stained. All particles show contrasted channel-like regions inside—the assumption arises that, at least for the largest part, positively stained RNA is being dealt with. Note that in the reconstruction the areas of high scattering density are negatively depicted. Because of the normalization (phase contrast!), areas with weak scattering ability seem positive in all reconstructions, whereby positive maxima correspond to areas with especially *low* scattering ability. Up to now we have investigated the 50S subunit more precisely, since with its compactness, drastic changes of form are not likely to appear—in the case of the 30S subunit we see evidence for not inconsiderable orientation-dependent changes of shape.

Naturally, it is not possible to present all the details of these complicated investigations in a progress report. Figure 25 shows a section through 4 contrasted 50S particles in crown form (after correlation of the orientation). For sake of clarity, only the contour lines of the non-contrasted structure are represented—the channel-like contrasted structures therefore appear white. To facilitate the comparison, common negative areas are depicted with "guiding" dots—they are also contained in the mid-structural section AV2. After correlation, the three-dimensional cross-correlation coefficients lie between 0.25 and 0.3. Actually, their values are surprisingly low, considering the really pronounced similarities in Figure 25. The reason for this lies in the great sensitivity of the cross-correlation coefficients towards *all* individual changes. We can try, however, using principles of pattern recognition, to mark out and compare the fundamental structural information—in this case, the special channel-like staining. Here, two steps can be distinguished. In the first step, the same overall structure is demanded (no distortion is allowed); however, the abstraction from details such as, for example, intensity and struc-

[*] From Fourier principles, the scanning elements may maximally have half the diameter of the resolution elements. With the scanning calibration, pictures with a resolution of up to 0.5 nm can therefore be worked with, so that adequate certainty is ensured with the necessary reconstruction resolution of about 1.0 nm (in the x, y plane).

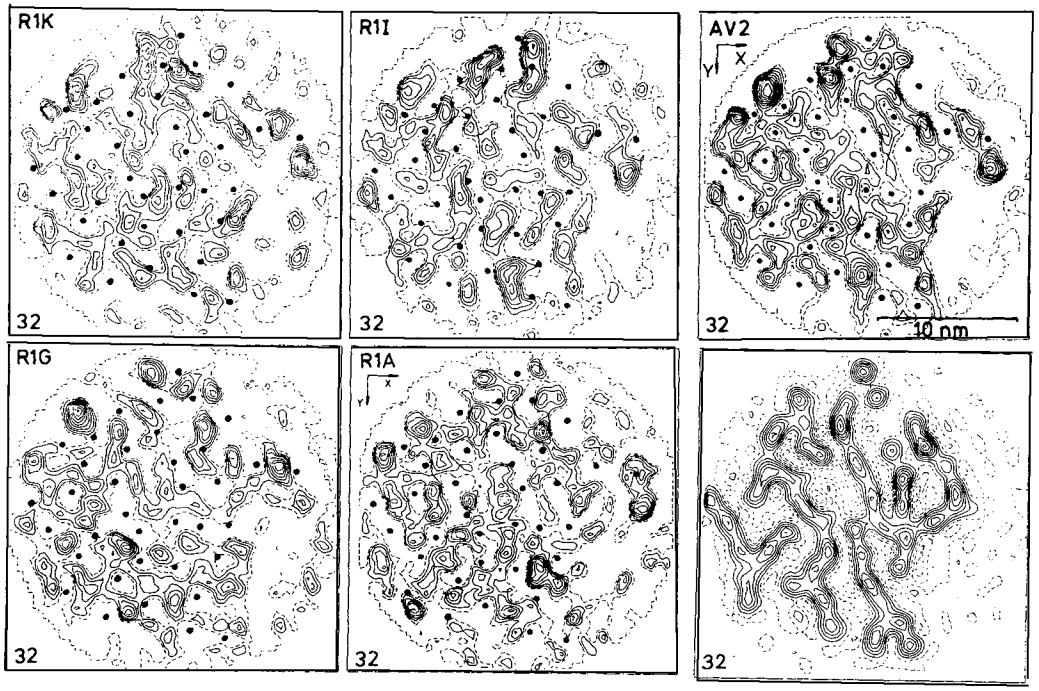



Fig. 25. Analysis of the crown form of ribosomal 50S particles (without stalks). The reconstruction body is a cylinder (extension along the tilting axis (y)) with a diameter of $D = 23.8$ nm and a length of $L = 23.8$ nm. It is divided into cubic scanning elements of edge length $D/64 = 0.37$ nm. The resolution is $\Delta x \approx 1.3$ nm, $\Delta z = 2.0$ nm; $\Delta Y$ equals the mean electron optical resolution, which varies in the micrographs between 0.7 and 1.0 nm (as a standard value we assume that $\Delta y = 1$ nm). The reconstruction body can be cut into layers in any orientation and, for example, 64 x,y-layers are obtained perpendicular to the optical axis (z-axis). For comparison, however, the single particles must be three-dimensionally correlated with one another in respect to location and orientation. In all layers, the comparison shows surprisingly strong similarities. As examples, the most central sections (No. 32) of the "crowns" R1A, R1G, R1I, R1K (cf. Fig. 22) are shown. As already made clear in Figure 24, negative areas correspond to structural elements with high scattering ability, especially with contrasted structures. The use of the zero line for characterization of the separation of weakly contrasted structures (light atomic structures, positive) from strongly contrasted structures (heavy atomic structures) is somewhat arbitrary. For clarity, the contour lines in the negative areas are not shown. To facilitate comparison, the common negative regions of the single particles are marked by guiding dots. The averaged structure AV2 has practically the same resolution (only small distortion of the particles) and now shows even more clearly the channel-like negative regions; in addition, beneath section 32 of AV2, the section 32 of a "model" of the structure of AV2 is shown, which is produced by occupation of the negative regions with points at a distance of 2 nm. If this model is imaged with a resolution of 2 nm, tube-like objects emerge, since neighboring point images blend with each other (see picture). Note that in the model, the contrasted areas are positively marked (not negative as in the contour line charts!). Analogous models of the single particles have cross-correlation coefficients of $\approx 0.7$ with respect to each other (instead of 0.25—0.3).

ture in the stained areas or in the region of the light atom structure is required. The guiding dot concept offers a possibility for this. If guiding dots are arranged at the approximate resolution distance in the negative regions in each single structure, then on Fourier mapping with 1.5 nm resolution (at which the dots become smeared[87]), a tube-like model of the contrasted structure is obtained. Figure 25 (AV2) shows one section. The models obtained from the different structures can be correlated with each other, and a (three-dimensional) correlation coefficient between 0.6 and 0.7 is obtained—a clear indication of how analogous the structures of the single particles really are. However, it should be noted that the simplest method of model building (if no large distortions are present) would actually be an averaging of sufficient single structures—this procedure, however, is very laborious.

Exactly the same analysis was carried out on 50S subunits with the L7, L12 stalk. It can only be referred to as surprising, how exactly the average structure of four subunits with "stalk" AV3 is in agreement with the average structure without "stalk" AV2 (Fig. 26)—the correlation coefficient $C_k$ is about 0.5. As Figure 26 shows, the structure AV4 averaged from AV2 and AV3 (the stalk was cut out by calculation in these comparisons) is now only a little different from AV2 and AV3. The chemical splitting of the stalk therefore does not touch the rest of the structure at all. Incidentally, these two analyses can be interpreted as an excellent consistency test for the method. We are concerned with chemically different, electron microscopically different preparations, and—last but not least—analyses in very different defocussing ranges[*]. During the next analysis steps attempts were made to compare "crowns" and "kidneys" with each other. For the calculations, the tube models were taken because they have a reciprocal space that is filled equally (without blind regions)—an important requirement for a good correlation with large angular differences. The correlation converges very well; however, only a cross-correlation coefficient of $C_k = 0.26$ could be reached, a clear sign of how much the specimen

[*] The second analysis was carried out near to the Scherzer focus. The associated decrease in the lower spatial frequencies led to a lowering of the general contrast of the images.

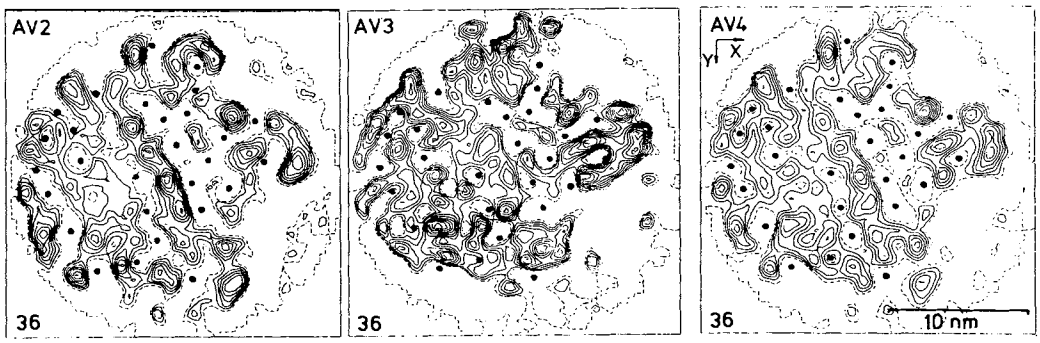



Fig. 26. Comparison of the average structures of each of four 50S subunits "without L7 and L12 stalks" (AV2) and "with L7 and L12 stalks" (AV3) (Sections Nos. 36). In AV3, the stalk is mathematically cut off. The reconstruction body of AV3 was later reduced to the size of the reconstruction body of AV2; the correlation coefficient between AV2 and AV3 is $\approx 0.5$. The structure AV4 averaged from AV2 and AV3 is very similar to AV2 and AV3.

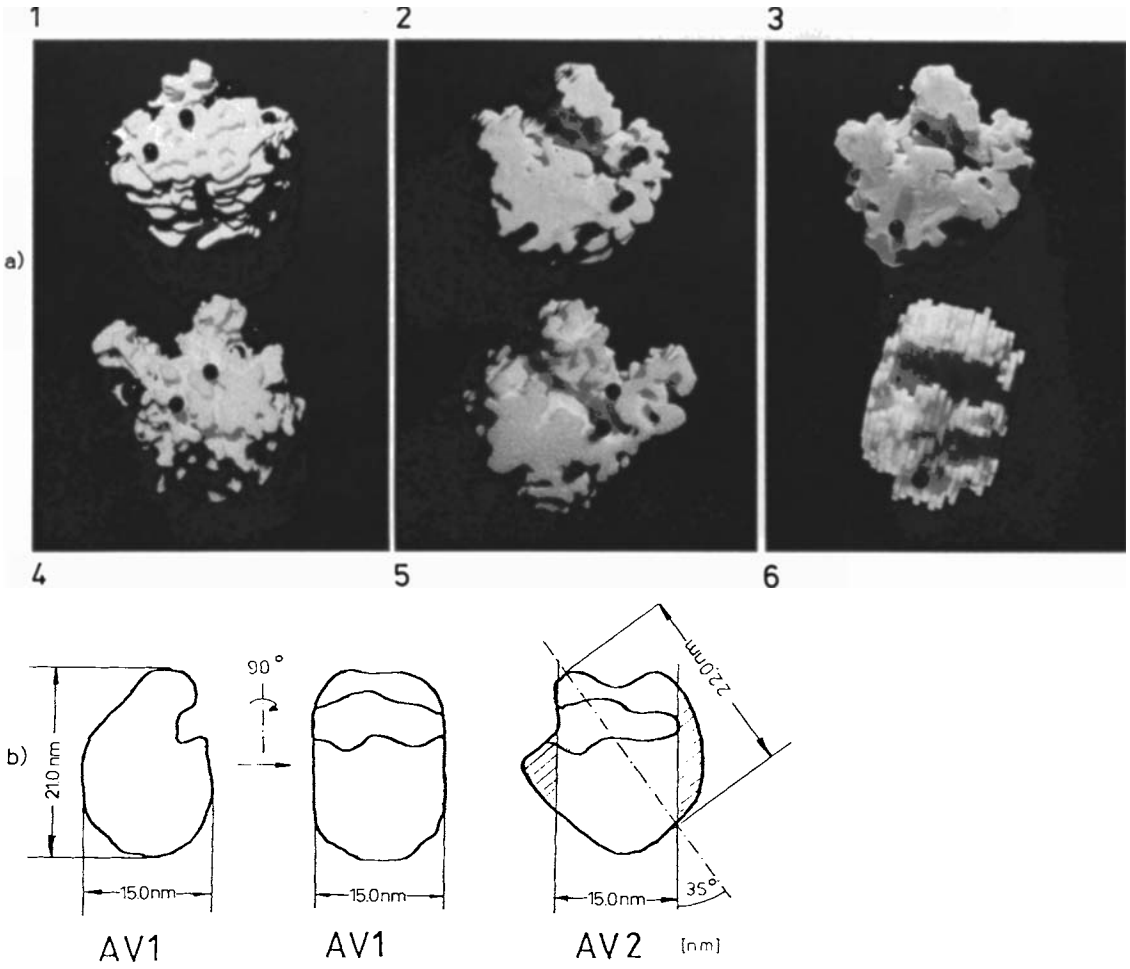



Fig. 27. a) Comparison of the models of the 50S subunit (crown orientation) without stalk [photographed from above (1) and from below (2)] and the 50S subunit (crown orientation) with stalk [photographed from above (4) and from below (5)]; comparison of the model of the "crown" [without stalk (3)] with the "kidney" [without stalk (6)]. Because of the low contrast of the most upper and lower layers, these are not shown in the model of the kidney. The small and large black points indicate areas where channels penetrate the surface. Regions marked by large black points correspond to regions in which the RNA, according to earlier conventional pictures (with marking using respective effectors), comes to the surface. b) Schematic representation of the mutual orientations of "kidney" and "crown" (average structures AV1 and AV2, see Figures 25 and 26). AV1 shows the orientation of the foil; on turning about the longitudinal axis by 90°, AV1′ is obtained. The longitudinal axis of AV1′ is tilted by 35° towards the longitudinal axis of AV2. Areas lying above and below are not easily recognizable in the only weakly contrasted "kidney", and so have not been shown in the model.

preparation conditions influence the structure. As already mentioned, one should not speak of the structure of the ribosomes, but of reaction product structures. However, in spite of this the general deformation is so low that the shape can be derived from the combination of both results. With a reconstruction of crown or kidney alone, the particle borders only partially on the staining material, so that the determination at the bottom (in respect to the support foil) and with sandwich preparations (as in our case) at the top gives difficulties (Fig. 27).

### 3.5.3. *The Structure of the Uranyl-Contrasted 50S Ribosomal Subunit from E. coli in Crown Form*

From our investigations it is clear that the 50S particle is especially well imaged structurally, in its crown form. It lies flat on the base, is well stained, and is easily distinguishable against the staining material. Further, an averaged structure of 8 particles (AV3) is present, and experiments have shown that changes in the inner structure of preparations with and without stalk are negligably small. Since the "accidental" structures of the support foil already averaged out well on the averaging of 8 particles[*], the demarcation "below" and "above" can be well recognized (even though their confirmation by the kidney structure is very valuable). Cross-correlation coefficients can then be calculated in different averaging combinations, which agree well with the statistical expectations. Of particular interest is the cross-correlation coefficient with the (extrapolated) averaging structure from "infinitely" many particles, which is so large with $C_k = 0.8$, that only small differences are to be expected with respect to the structure, determined from an infinite number of particles. This means, however, that practically the same results occur as with a hypothetical "crystal". The tilt of the particles with respect to the z-direction (about 3—4°) is also considered, which cannot be corrected in crystal analysis. Figure 28 shows the complete structure of the averaged particles.

### 3.5.4. *Radiation Damage in Ribosomal Particles*

In a further analysis, we were more closely concerned with the problem of the influence of the radiation[88]. We had produced a tilting series of 30S subunits with a 3° angular increment, which actually consisted of two 6° series tilted against one another by 3°. With this it was possible not only to carry out a reconstruction of larger areas or with higher resolution, but also to compare both 6° series (after correction of the tilting), in order to study the influence of the radiation[**]. However, the radiation load of the second series was much larger than we would normally tolerate. Actually, a comparison shows changes, the cross-correlation coefficient has the order of magnitude $C_k = 0.7$. The reconstructions show, that on comparison of the fine details, care must be taken; migration of heavy atoms occurs on irradiation[*]. It is important (and actually to be expected) that the general proportions do not change—distortions are therefore surely caused largely by the specimen preparation. Note, incidentally, that even with this overloading of radiation the similarity of both structures of the same particle, which have been loaded differently with radiation, is larger than with two different particles of the same orientation.

### 3.5.5. *Pattern Recognition with Consideration of Distortions*

These experiments prove that ribosomal 50S particles in crown form (the same applies for the kidney form) show the general structural relations—otherwise, on averaging, a drastic reduction of the resolution would have to occur. They also explain the jump of the cross-correlation coefficients between single particles, from about 0.25 to about 0.7, if pattern recognition of the first kind (no distortions) is made (cf. Fig. 25). Of particular value are those results for the investigations of aperiodic structures, with which averaging is not possible—it is to be expected that the result can be interpreted in a topologically meaningful way. The analysis of the 30S structure in different orientations should become interesting with such kinds of topologically smoothed models, because the analysis of crowns and kidneys already show clear topological differences. Then, pattern recognition procedures of the second kind have to be worked out, which—somewhat in analogy to the comparison of different types of handwriting—tolerate distortions, too. Then, simple averaging processes do not suffice any longer.

## 4. Outlook

The problems of ribosomal analysis made it especially clear how valuable the further development of the methods are (if possible, with automation). What is really interesting is the function. Structural analyses have no use in themselves but should lead to an understanding of the ribosomal "protein factory". Therefore, we do not believe that a single analysis of a native crystal—as important as it would naturally be—would offer very much for an understanding of ribosomal function. Reactions have to be carried out, and reaction products with small and large partners have to be investigated. Only a born optimist would hope that all the reaction products would be crystallizable. Actually, conventional ribosomal microscopy already shows us the way. The reaction products are studied not only with the preparation reagents, but also with many effectors. The not very helpful two-dimensional methods have only to be replaced by three-dimensional analysis. It is by no means self-evident that the "dirty" ribosomal "dumplings" have shown defined and reproducible structures on the inside in spite of crude preparation and irra-

[*] If the cross-correlation coefficient for two particles equals $C_k$ and the assumption is made that the particles are only disturbed by "white noise" (no changing of the general proportions) then the correlation coefficients can be calculated between the average structure from $n_1$ particles, and the average structure from $n_2$ particles:

$$C_{1,2} = C_k \Big/ \sqrt{\left[C_k + \frac{1}{n_1}(1 - C_k)\right]\left[C_k + \frac{1}{n_2}(1 - C_k)\right]}$$

If $n_2$ equals infinity, then it follows that

$$C_{1,\infty} = \sqrt{C_k / C_k + \frac{1}{n_1}(1 - C_k)}$$

(I thank Dr. *R. Henderson*, Cambridge, for the reference to these statistical relationships). The quasistatistical behavior was tested by calculation of different experimental averagings.

[**] The total dose after the first series was $9.6 \times 10^4$ e/nm$^2$, after the second series $20.1 \times 10^4$ e/nm$^2$. But note that in the first case the effective dose for the imaging is only half as great as the total dose (this applies to all series without preirradiation), since the partial images come from particles irradiated for different times (in the first picture, actually from unirradiated particles) (average load $4.3 \times 10^4$ e/nm$^2$). With the second series this load is about three times as great as in the first series ($14.7 \times 10^4$ e/nm$^2$), because of the pre-irradiation.

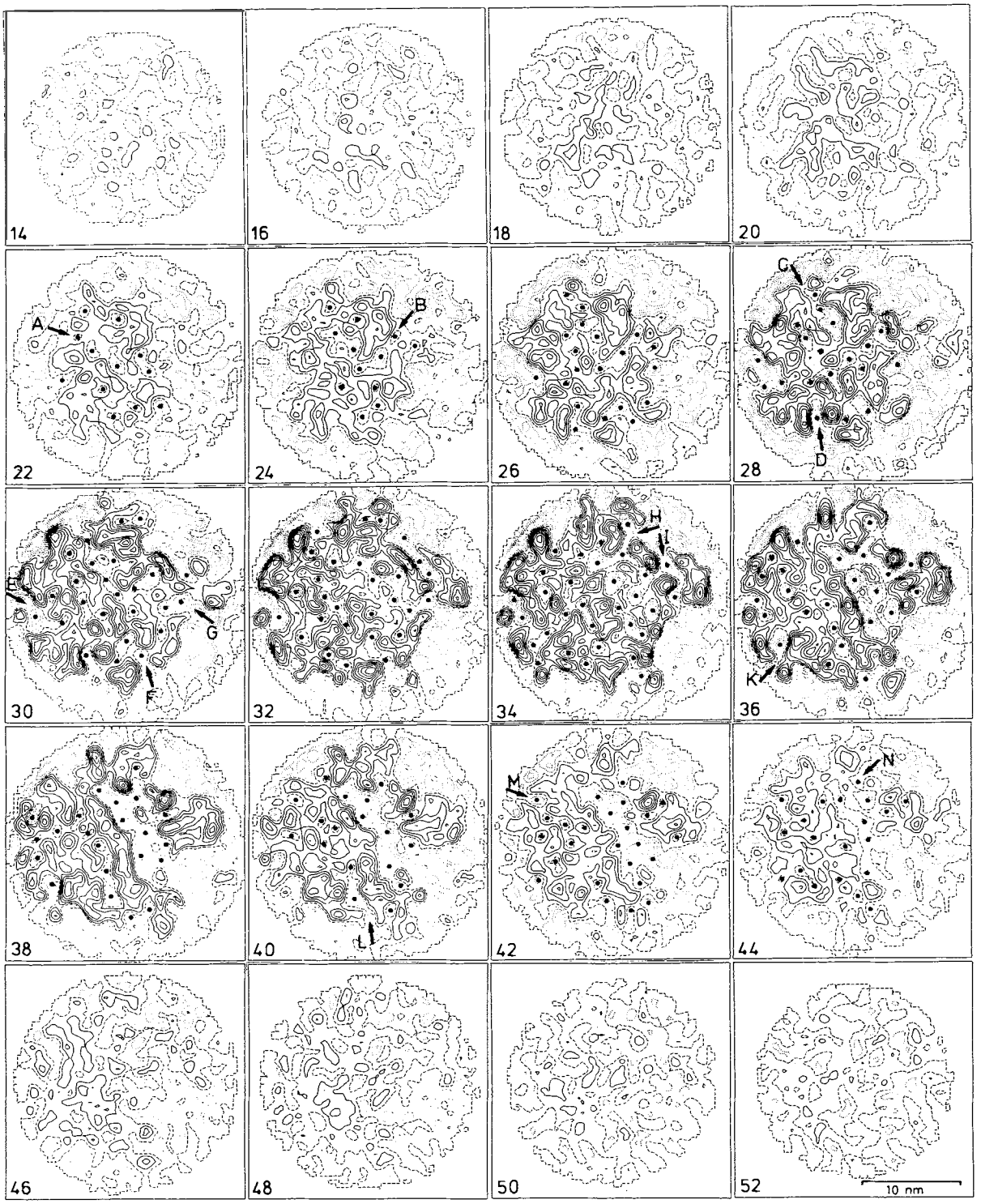



Fig. 28. Almost an "artificial crystal" of the uranyl stained 50S subunit in the crown orientation. The reproducibility of the single particles (dose about $10^5$ e/nm$^2$) is so excellent that even an averaging of 8 particles yields a correlation coefficient for the (hypothetical) "crystal structure" of $C_k = 0.8$. Averaging of a further arbitrary number of particles would not change the model in any major way. Representation of the structure in 64 layers in the distance of 0.4 nm; the even-numbered layers from 14 to 52 are imaged (zero line dashed, positive areas with solid lines, negative areas shown with dots). Positive (negative) contour lines form weak (strong) scattering regions, high positive maxima therefore correspond to especially weakly scattering parts of the structure. The contour line spacing is arbitrary, but the structure corresponds, to a good approximation, to the distribution of potential in the particles distorted by the influence of the image point. Resolution in the z-direction *ca.* 2 nm, in the x,y-plane 1.0 to 1.5 nm. Characteristics: contrasting of different strengths in the single layers, strongest in the middle layers. The particles extend from about layer 20 to layer 46. From layer 22 to layer 44, guiding dots at a spacing of about 2 nm (in the channels) are marked in the negative regions. Their imaging in the 2 nm resolution yields a tube-like model structure (see Fig. 25). The bottom side of the subunit is relatively planar, with a relatively narrow groove, which does not, however, cut through the whole particle. Note the strong contrasting in the groove. The more complicated channel structure on the inside, which should correspond, for the greater part, to the ribosomal RNA, is more weakly contrasted. However, one has to be careful on interpretation, since artefacts of staining can appear (staining variability stronger than radiation-induced variability!). Investigations by other preparative methods are yet to be carried out. The structure shows several penetration points of the stained channels (A to N) to the surface, whereby according to results with conventional labeling microscopy, C should correspond to the 3′ end of the 23S RNA and G to the 3′ end of the 5S RNA. Note, too, the highly differentiated surface, which borders the particles and the negative contrasting material.

diation. They could have been disturbed much more strongly—even then, it would have been a significant result that would have had to be accepted.

But, naturally, it is also desirable to study individual organic structures without the "corset" of heavy atom staining. We believe that in this case, investigations at low temperatures (liquid helium) would help further. At room temperature the real structural catastrophies actually develop secondarily. Bonds become broken, large and small fragments are formed. The small fragments try to break free, and finally, after a mass reduction of about 40%, a skeleton remains, which perhaps (given luck) can still show some relation to the native structure—we do not know.

The experimentally proven advantage of cryomicroscopy is that no mass reduction occurs. We can assume that on the whole, the low molecular fragments keep their place, hence, the spatial architecture should survive. At the moment, there is little sense in speculating on what really happens. Perhaps the idea of trace structure analysis (cf. [46]) can be used, and extrapolated to the native original state. But one can certainly experiment along these lines, since it is now possible to build high-resolution cryomicroscopes (cf. [23]).

A microscope ideal for cryomicroscopy would be one in which the relative change of direction is produced electronically by the tilting of the primary beam (instead of tilting the specimen). In this way, no location errors occur, which necessitate a further determination of the common origin. This is of importance with low radiation doses, with which the present correlation methods may fail. Serious proposals have already been put forward here[89], and attempts have actually been made at their realization[90].

The enhancement of the resolution down to the atomic limit has not yet been mentioned—it goes almost without saying that this will have to be attempted. As this report tries to demonstrate, if the newly-developed field emission guns are used, then experimental methodology is no longer the limiting factor. Admittedly, a great deal of preparative chemistry (not only in the biological field) remains to be learnt. However, atomic resolution must be coupled with three-dimensional analysis. Matter is "porous", only in three dimensions—and only then can one also use structural limitations in the analysis, as we had suggested some time ago[24a]. Cross-checking in the chemical "sense" (bond lengths and angles) will facilitate the analysis.

Finally, a remark for contemplation: It is the strong interaction between atoms and electrons which (in principle) enables the determination of the position of an atom by the scattering of electrons, in an incredibly short time. Centuries of measuring time would be needed to reach the same goal with X-rays. Thus, a great deal of experimental information is obtainable in a very short time—in contrast the volume of experimental data obtainable by using even the most sophisticated X-ray or neutron diffraction analysis is tiny. However, its accomplishment is only possible with very effective computers. Phase-determining electron diffractometry is a real child of our computer age.

*The long period of 20 years, covered in this report, makes it impossible to thank all my co-workers personally. More than 50 diploma and doctoral theses concern our work carried out in the field of electron microscopy—from instrumental techniques to informational theoretical contributions. I therefore ask to be pardoned if I only mention a few collaborators of the last few years: E. Demm, B. Grill, R. Guckenberger, H. Hebert (Guest from the Karolinska Institute, Stockholm), R. Hegerl, U. Jakubowski, V. Knauer, G. Nützel, H. Öttl, H. R. Tietz, D. Typke. With the construction of an He-cryomicroscope, work will be possible in an important part of the subject in our laboratory. I thank Dr. I. Dietrich and her co-workers (Siemens AG, Munich) for their collaboration. I also wish to thank the Deutsche Forschungsgemeinschaft and the Fonds der Chemischen Industrie for financial support.*

Received: January 18, 1983 [A 455 IE]
German version: *Angew. Chem. 95* (1983) 465
Translated by *K. Duffy and Dr. M. Tropschug*, Martinsried (Germany)

[1] H. Boersch, *Z. Tech. Phys. 19* (1938) 337.
[2] H. Boersch, Discussion remarks on a lecture by C. Peters, *Z. Elektrochem. Angew. Phys. Chem. 46* (1940) 449.
[3] W. L. Bragg, *Nature (London) 143* (1939) 678.
[4] W. Hoppe, *Z. Kristallogr. Kristallgeom. Kristallphys. Kristallchem. 107* (1956) 28.
[5] W. Hoppe, R. Huber, *Chem. Ber. 98* (1965) 2353.
[6] M. Menzel, Diplomarbeit, Technische Universität München 1961.
[7] W. Hoppe, *Naturwissenschaften 48* (1961) 736.
[8] W. Hoppe, *Optik (Stuttgart) 20* (1963) 599.
[9] H. Boersch, *Z. Naturforsch. A 2* (1947) 615.
[10] O. Scherzer, *J. Appl. Phys. 20* (1949) 20.
[11] W. Hoppe, R. Langer, Int. Conf. Electron Diffraction and Crystal Defects, Melbourne 1965, *Abstr.* 1 0-5.
[12] R. Langer, W. Hoppe, *Optik (Stuttgart) 24* (1966/1967) 740.
[13] R. Langer, W. Hoppe, *Optik (Stuttgart) 25* (1967) 413.
[14] R. Langer, W. Hoppe, *Optik (Stuttgart) 25* (1967) 507.
[15] O. Scherzer, *Z. Phys. 101* (1936) 593.
[16] F. Lenz, W. Scheffels, *Z. Naturforsch. A 13* (1958) 226.
[17] F. Thon, *Z. Naturforsch. A 20* (1965) 154.
[18] F. Thon, *Z. Naturforsch. A 21* (1966) 476.
[19] G. Möllenstedt, R. Speidel, W. Hoppe, R. Langer, K.-H. Katerbau, F. Thon, *Proc. 4th Eur. Congr. Electron Microsc., Rome 1968*, Vol. *1*, p. 125.
[20] W. Hoppe, K.-H. Katerbau, R. Langer, G. Möllenstedt, R. Speidel, F. Thon, *Siemens Rev. 36* (1969), 3rd Spec. Issue "X-Ray and Electron Microscopy News".
[21] K. H. von Grote, G. Möllenstedt, R. Speidel, *Optik (Stuttgart) 22* (1965) 252.
[22] A. Hirt, R. Langer, W. Hoppe, *Ber. Bunsenges. Phys. Chem. 74* (1970) 1101.
[23] I. Dietrich, F. Fox, E. Knapek, G. Lefranc, K. Nachtrieb, R. Weyl, H. Zerbst, *Ultramicroscopy 2* (1977) 241.
[24] Discussion meeting of the Bunsengesellschaft für Physikalische Chemie, Hirschegg, March 15-18, 1970; cf. also a) W. Hoppe, *Ber. Bunsenges. Phys. Chem. 74* (1970) 1090; b) J. Frank, P. Bussler, R. Langer, W. Hoppe, *ibid. 74* (1970) 1105; c) R. Langer, J. Frank, A. Feltynowski, W. Hoppe, *ibid. 74* (1970) 1120.
[25] Symposium on New Developments in Electron Microscopy, Royal Society, London, March 12, 1970; cf. also W. Hoppe, *Philos. Trans. R. Soc. London B 261* (1971) 71; also in H. E. Huxley, A. Klug: Recent Developments in Electron Microscopy, The Royal Society, London 1971.
[26] K. J. Hanssen, B. Morgenstern, *Z. Angew. Phys. 19* (1965) 215; cf. also (Coherent Light Optics) P. Elias, D. S. Grey, D. Z. Robinson, *J. Opt. Soc. Am. 42* (1952) 127; O. Brynydal, A. Lohmann, *ibid. 58* (1968) 620; A. Maréchal, P. Croce, *C. R. Acad. Sci, 237* (1953) 607.
[27] P. Schiske, *Proc. 4th Eur. Congr. Electron Microsc., Rome 1968, Vol. 1*, p. 145.
[28] K. J. Hanssen, *Proc. 4th Eur. Congr. Electron Microsc., Rome 1968, Vol. 1*, p. 153.
[29] F. Thon, B. M. Siegel, *Ber. Bunsenges. Phys. Chem. 74* (1970) 1116.
[30] W. Hoppe, *Acta Crystallogr. A 26* (1970) 414; cf. also (Anomalous Scattering) L. Reiner, *Z. Naturforsch. A 24* (1969) 377.
[31] W. Hoppe, R. Langer, F. Thon, *Optik (Stuttgart) 30* (1970) 538.
[32] W. Hoppe, R. Langer, F. Thon, Lecture at the joint meeting of the Austrian and German Chemical Societies for Electron Microscopy, Vienna, September 1969.
[33] W. Hoppe, *Z. Naturforsch. A 26* (1971) 1155.

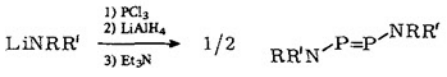
[34] W. Hoppe, D. Köstler, D. Typke, N. Hunsmann, *Optik (Stuttgart) 42* (1975) 43.
[35] a) W. Hoppe, D. Köstler, *Proc. 6th Eur. Congr. Electron Microsc., Jerusalem 1976*, Vol. *1*, p. 99; b) D. Typke, D. Köstler, *Ultramicroscopy 2* (1977) 285.
[36] a) B. Grill, Diplomarbeit, Technische Universität München 1973; b) W. Hoppe, *Naturwissenschaften 61* (1974) 239.
[37] *International Tables for X-Ray Crystallography*, Vol. *4*, p. 176, The Kynoch Press, Birmingham 1974.
[38] D. Typke, M. Radermacher, *Ultramicroscopy 9* (1982) 131.
[39] H. P. Erickson, A. Klug, *Ber. Bunsenges. Phys. Chem. 74* (1970) 1129; *Philos. Trans. R. Soc. London B 261* (1971) 105.
[40] W. Hoppe, *Chem. Scr. 14* (1978/1979) 227; cf. also *Angew. Chem. 77* (1965) 484; *Angew. Chem. Int. Ed. Engl. 4* (1965) 508; *ibid. 78* (1966) 289 and *5* (1966) 267.
[41] V. Witt, H. P. Englmeier, W. Hoppe, *Proc. 5th Eur. Congr. Electron Microsc., Manchester 1972*, Vol. *1*, 632.
[42] F. Thon, DBP 1564658 (1966), Siemens AG.
[43] a) R. Brüders, K. H. Hermann, D. Krahl, H.-P. Rust, *Proc. 6th Eur. Congr. Electron Microsc., Jerusalem 1976*, Vol. *1*, p. 318, 320; b) W. Kerzendorf, Dissertation, Technische Universität München 1979.
[44] W. Hoppe, *Acta Crystallogr. A 25* (1969) 495, 508; W. Hoppe, G. Strube, *ibid. A 25* (1969) 502.
[45] H. Berndt, R. Doll, *Optik (Stuttgart) 51* (1978) 93; *ibid.*, in press.
[46] W. Hoppe, *Ultramicroscopy 10* (1982) 187.
[47] A. Klug, J. E. Berger, *J. Mol. Biol. 10* (1964) 565.
[48] D. J. DeRosier, A. Klug, *Nature (London) 217* (1968) 130.
[49] R. Hart, *Science 159* (1968) 1464.
[50] W. Hoppe, R. Langer, G. Knesch, C. Poppe, *Naturwissenschaften 55* (1968) 333.
[51] P. N. T. Unwin, *Z. Naturforsch. A 29* (1974) 158; *J. Mol. Biol. 87* (1974) 657.
[52] R. A. Crowther, A. Klug, *Annu. Rev. Biochem. 44* (1975) 161.
[53] D. Wrinch, *Nature (London) 157* (1946) 226.
[54] J. N. Champness, A. C. Bloomer, G. Bricogne, P. J. G. Butler, A. Klug, *Nature (London) 259* (1976) 20.
[55] K. C. Holmes, G. J. Stubbs, E. Mandelkow, U. Gallwitz, *Nature (London) 254* (1975) 192.
[56] W. Hoppe, *Naturwissenschaften 55* (1968) 65.
[57] R. Langer, C. Poppe, H. J. Schramm, W. Hoppe, *J. Mol. Biol. 93* (1975) 159.
[58] a) R. M. Glaeser, *J. Ultrastruct. Res. 36* (1971) 466; b) R. M. Glaeser, I. Kuo, T. F. Budinger, *Annu. Proc. Electron Microsc. Soc. Am. 29* (1971) 466; c) R. M. Glaeser in B. Siegel, D. R. Beaman: *Physical Aspects of Electron Microscopy and Microbeam Analysis*, Wiley, New York 1975.
[59] F. Parak, R. L. Mössbauer, W. Hoppe, *Ber. Bunsenges. Phys. Chem. 74* (1970) 1207.
[60] R. C. Williams, H. W. Fisher, *J. Mol. Biol. 52* (1970) 121.
[61] Cf., *e.g.*, W. Hoppe in: *Ullmanns Enzyklopädie der technischen Chemie*, 3rd edit., Vol. *2/1*, Urban und Schwarzenberg, München 1961, p. 529; W. Hoppe in W. Hoppe, W. Lohmann, H. Murkl, H. Ziegler: Biophysik, 2nd Edit., Springer, Berlin 1982, p. 54.
[62] Cf., *e.g.*, A. Gieren, M. Kokkinidis, *Z. Naturforsch. C37* (1982) 977.
[63] J. D. McLachlan, *Proc. Natl. Acad. Sci. USA 44* (1958) 948.
[64] J. R. Breedlove, G. T. Trammel, *Science 170* (1970) 1310.
[65] R. Henderson, P. N. T. Unwin, *Nature (London) 257* (1975) 28.
[66] Cf. also in W. Baumeister, W. Vogell: *Electron Microscopy at Molecular Dimensions*, Springer Verlag, Berlin 1980, p. 353.
[67] W. Hoppe, H. Wenzl, H. J. Schramm, *Proc. 6th Eur. Congr. Electron Microsc., Jerusalem 1976*, Vol. *2*, p. 58.
[68] W. Hoppe, H. Wenzl, H. J. Schramm, *Hoppe-Seyler's Z. Physiol. Chem. 358* (1977) 1069.
[69] W. Hoppe, *Isr. J. Chem. 10* (1972) 321; W. Hoppe, R. May, P. Stöckel, S. Lorenz, V. A. Erdmann, H. G. Wittmann, H. L. Crespi, J. J. Katz, K. Ibel in B. P. Schoenborn: *Neutron Scattering for the Analysis of Biological Structures*, Brookhaven Symposia in Biology No. 27 (1975), p. IV-38.
[70] Cf., *e.g.*, R. Gruehn, W. Mertin, *Angew. Chem. 92* (1980) 531; *Angew. Chem. Int. Ed. Engl. 19* (1980) 505.
[71] R. Hegerl, W. Hoppe, *Z. Naturforsch. A 31* (1976) 1717.
[72] B. E. H. Saxberg, W. O. Saxton, *Ultramicroscopy 6* (1981) 85.
[73] W. Hoppe, R. Hegerl, *Ultramicroscopy 6* (1981) 205.
[74] N. Hunsmann, P. Bussler, W. Hoppe, *Proc. 5th Eur. Congr. Electron Microsc., Manchester 1972*, Vol. *1*, p. 654.
[75] W. Hoppe, *Naturwissenschaften 61* (1974) 534.
[76] R. Guckenberger, *Ultramicroscopy 9* (1982) 167.
[77] Cf. W. Hoppe, *Adv. Struct. Res. Diffr. Methods 7* (1979) 213.
[78] a) W. Hoppe, *Optik (Stuttgart) 29* (1969) 617; b) M. Radermacher, W. Hoppe, *Proc. 9th Int. Congr. Electron Microsc., Toronto 1978*, Vol. *1*, p. 218.
[79] R. A. Crowther, D. J. DeRosier, A. Klug, *Proc. R. Soc. London A 317* (1970) 319.
[80] V. Knauer, Diplomarbeit, Technische Universität München 1975.
[81] W. Hoppe, J. Gassmann, N. Hunsmann, H. J. Schramm, M. Sturm, *Hoppe-Seyler's Z. Physiol. Chem. 355* (1974) 1483; W. Hoppe, H. J. Schramm, M. Sturm, N. Hunsmann, J. Gassmann, *Z. Naturforsch. A 31* (1976) 645, 1370, 1380.
[82] N. A. Kiselev, V. Ya. Stel'mashuk, E. V. Orlowa, V. D. Vasiliev, O. M. Selivanova, *Mol. Biol. Rep. 8* (1982) 191.
[83] J. Frank, A. Verschoor, M. Boublik, J. S. Wall, J. F. Hainfeld, Proc. 10th. Int. Congr. Electron Microsc., Hamburg 1982, Vol. *3*, 97.
[84] W. Kunath, V. Lamvik, *20. Tagung für Elektronenmikroskopie, Innsbruck 1981*, p. 8.
[85] V. Knauer, H. J. Schramm, W. Hoppe, *Proc. 9th Int. Congr. Electron Microsc., Toronto 1978*, Vol. *2*, p. 4; V. Knauer, W. Hoppe, *Proc. 7th Eur. Congr. Electron Microsc., Den Haag 1980*, Vol. *2*, p. 702; W. Hoppe, *Proc. 10th Int. Congr. Electron Microsc., Hamburg 1982*, Vol. *1*, p. 97; V. Knauer, R. Hegerl, W. Hoppe, *J. Mol. Biol. 163* (1983) 409; H. Oettl, R. Hegerl, W. Hoppe, *ibid. 163* (1983) 431.
[86] E. Kellenberger, M. Häner, M. Wurtz, *Ultramicroscopy 9* (1982) 139.
[87] W. Hoppe, H. Oettl, unpublished.
[88] V. Knauer, M. Hintermaier, W. Hoppe, unpublished.
[89] W. Hoppe, *Z. Naturforsch. A 27* (1972) 919; D. Typke, W. Hoppe, *Proc. 5th Eur. Congr. Electron Microsc., Manchester 1972*, Vol. *1*, p. 70; D. Typke, W. Hoppe, W. Sessler, M. Burger, *Proc. 6th Eur. Congr. Electron Microsc., Jerusalem 1976*, Vol. *1*, p. 334; E. Plies, D. Typke, *Z. Naturforsch. A 33* (1978) 1361; E. Plies, *Proc. 9th Int. Congr. Electron Microsc., Toronto 1978*, Vol. *1*, p. 50; D. Typke, *Nucl. Instrum. Methods 187* (1981) 217; E. Plies, *ibid. 187* (1981) 227.
[90] M. Burger, Dissertation, Technische Universität München 1978; D. Typke, M. Burger, N. Lemke, G. Lefranc, *Proc. 7th Eur. Congr. Electron Microsc., Den Haag 1980*, Vol. *1*, p. 82.
[91] E. R. Podack, H. J. Müller-Eberhard, H. Horst, W. Hoppe, *J. Immunol. 128* (1982) 2353.
[92] B. Grill, Dissertation, Technische Universität München 1980.
[93] D. E. Olins, A. L. Olins, H. A. Levy, R. C. Durfee, S. M. Margle, E. P. Tinnel, S. D. Dover, *Science 220* (1983) 498.
[94] J. Frank, W. Goldfarb, D. Eisenberg, T. S. Baker, *Ultramicroscopy 3* (1978) 283.
[95] V. Knauer, unpublished.
[96] W. Hoppe in W. Baumeister, W. Vogell: *Electron Microscopy at Molecular Dimensions*, Springer Verlag, Berlin 1980, p. 278.

**When submitting manuscripts, authors of articles which are intended for publication as "Communications" are requested to conform to the guidelines reproduced at the beginning of each issue following the list of contents.**

## Diaminodiphosphenes—Synthesis, Crystal Structure and Bonding Properties**

By *Edgar Niecke**, *Reinhold Rüger*, *Manfred Lysek*, *Siegfried Pohl*, and *Wolfgang Schoeller*

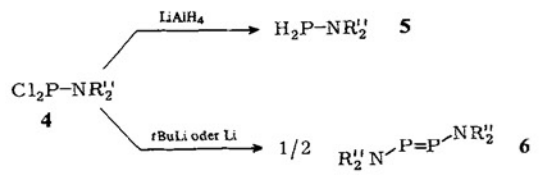
Compounds containing Si=Si and P=P bonds are of current interest[2]. We recently reported on the synthesis of the tetrakis(trimethylsilyl)diaminodiphosphene **1**[2f] by elimination of HCl from 1,2-bis[bis(trimethylsilyl)amino]-1-chlorodiphosphane[3]. We have now found that the diphosphenes **1** and **2** can be obtained directly from the corresponding lithium amides, *i.e.* without previous isolation of the intermediates. Further, it was found that when an equimolar mixture of both lithium amides is present the reaction leads to **3**, the first representative of an unsymmetrically substituted diphosphene, along with **1** and **2** as by-products.




**1**, R = R' = $SiMe_3$
**2**, R = $SiMe_3$, R' = *t*Bu

**3** $(Me_3Si)_2N-P=P-N(tBu)SiMe_3$

Attempts to prepare the diphosphene **6** analogously from the bulky aminodichlorophosphane **4** failed; this reaction afforded only the aminophosphane **5**. However, the tetrakis(*tert*-butyldimethylsilyl)diaminodiphosphene **6** could be obtained by reaction of **4** with lithium or *tert*-butyllithium.




R'' = $tBuMe_2Si$

[*] Prof. Dr. E. Niecke, Dr. R. Rüger, M. Lysek, Priv.-Doz. Dr. S. Pohl, Prof. Dr. W. Schoeller
Fakultät für Chemie der Universität
Postfach 8640, D-4800 Bielefeld 1 (Germany)

[**] This work was supported by the Deutsche Forschungsgemeinschaft and the Fonds der Chemischen Industrie.

The highly pyrophoric diphosphenes **2** and **3** resemble **1** in their reaction behavior—their tendency to undergo dimerization decreases along the series **1** > **3** > **2**. Compound **6**, which is crystalline at room temperature, does not dimerize. A striking feature of all diaminodiphosphenes **1**—**3** and **6** is their thermochemistry, which is characterized by a change in color from intense red (25 °C) to yellow (< −100 °C).

The $^{31}P$-NMR spectra of **2**, **3**, and **6** show the typical strong deshielding of the $^{31}P$ nucleus that is to be expected for this class of compounds (Table 1). The observed upfield shift of the $^{31}P$-NMR signal [$\Delta\delta^{31}P(1,2) = 73$ ppm] on successive replacement of the trimethylsilyl groups by *tert*-butyl groups is possibly due to an increasing population of the coplanar conformation (*vide infra*). This could also explain the temperature-dependence of the $^{31}P$-NMR signal. The PP interaction ($^1J_{PP} = 670$ Hz)—observed for the first time in **3**—reflects an unusual bonding situation for the central PP bond (compared with the values for diphosphanes, especially the value for the *trans*-(*S,R/R,S*)-tetrakis(trimethylsilyl)diaminodiphosphane[3] ($^1J_{PP} = 148$ Hz)).

Table 1. $^{31}P$-NMR data (chemical shifts) of diphosphenes [a].

| Compound | δ value | Ref. |
|---|---|---|
| $[P-C(SiMe_3)_3]_2$ | 599.6 | [2d] |
| | 598.6 | [2e] |
| $[P-N(SiMe_3)_2]_2$ | 572 | [2f] |
| $[P-N(tBuMe_2Si)_2]_2$ **6** | 561 | |
| $P-N(SiMe_3)_2$ | 544 | |
| ‖ **3** | | |
| $P-N(tBu)SiMe_3$ | 507 | |
| $[P-N(tBu)SiMe_3]_2$ **2** | 499 | |
| $[P-C_6H_2-2,4,6-tBu_3]_2$ | 492.4—494 | [2a—d] |
| $[P-C_6H_2-2,4,6-Me_3]_2$ | 492 | [2g] |
| $[P-NC_5H_6-2,2,6,6-Me_4]_2$ | 472 | [2h] |

[a] In solution with $H_3PO_4$ as external standard.

The X-ray structure analysis shows that the PP bond length in **6** is similar to that in the aryl-substituted diphosphene $(2,4,6-tBu_3C_6H_2-P)_2$[2a] (Fig. 1). Unexpected is the almost bisorthogonal conformation in **6** (angle between the normals to the SiNSi and PPN planes: 77.5°). In contrast the isovalent tetrakis(trimethylsilyl)tetrazene[7a] has a coplanar $Si_2N-N=N-NSi_2$ framework[7b]. The associated strongly repulsive interaction between the non-bonding electron pairs on the nitrogen and the phosphorus atoms in **6** is presumably one of the causes for the unusually long PN bond length (176.9 pm).

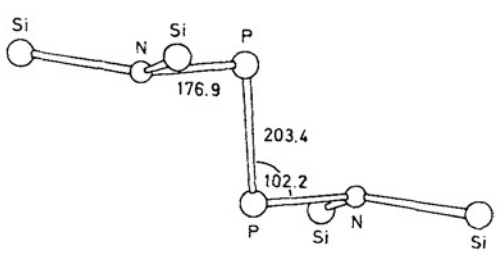



Fig. 1. Central skeleton of tetrakis(*tert*-butyldimethylsilyl)diaminodiphosphene **6** with important bond lengths [pm] and angles [°].

 © Verlag Chemie GmbH, 6940 Weinheim, 1983 0570-0833/83/0606-0486 $ 02.50/0 

According to SCF calculations on the parent compound of the diaminodiphosphene system (Fig. 2) the coplanar conformation (left) is energetically favored compared to the bisorthogonal conformation (right) [STO-3G; $H_2N-P=P-NH_2$: 53 kJ/mol; $H_2N-N=N-NH_2$; 143 kJ/mol]. Both conformations are stabilized on formal re-

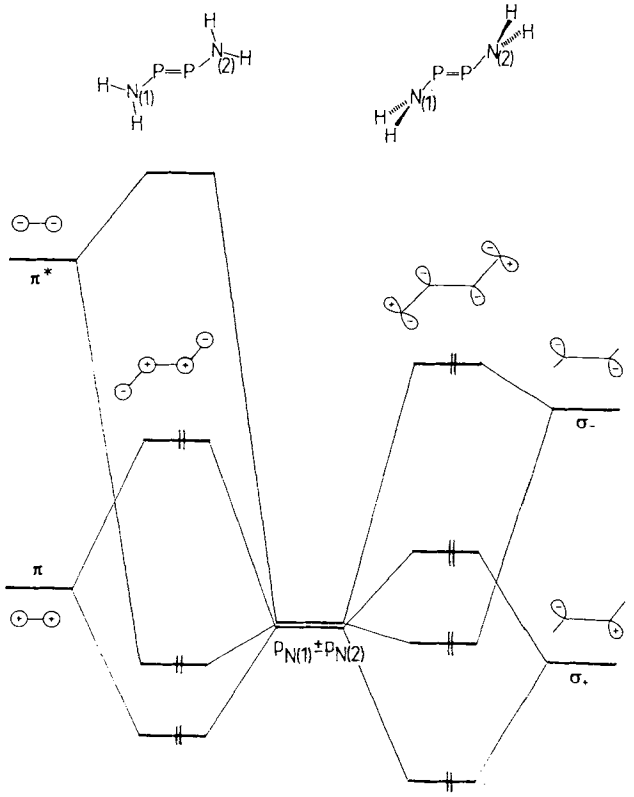



Fig. 2. Interaction diagram of the two non-bonding p-orbitals of the amino groups with the π-orbitals of the PP double bond (left) or the non-bonding electron pairs on the phosphorus atoms (right) forming a coplanar or bisorthogonal diaminodiphosphene.

placement of the hydrogen atoms by silyl groups, owing to the electron-acceptor activity of the latter; however, the bisorthogonal conformation is more highly stabilized, owing to the higher energy of its HOMO. This already leads, in the case of the fully silylated diaminodiphosphene **1**, which has a smaller rotation barrier than the corresponding tetrazene, to preference for the bisorthogonal form in the ground state of the molecule.

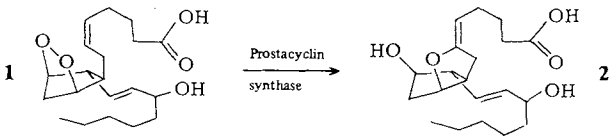
Received: January 14, 1983
revised: March 17, 1983 [Z 243 IE]
German version: *Angew. Chem. 95* (1983) 495
The complete manuscript of this communication appears in: *Angew. Chem. Suppl. 1983*, 639–654

[2] a) M. Yoshifuji, J. Shima, N. Inamoto, *J. Am. Chem. Soc. 103* (1981) 4587; *104* (1982) 6167; b) B. Cetinskaya, P. B. Hitchcock, M. L. Lappert, A. J. Thorne, H. Goldwhite, *J. Chem. Soc. Chem. Commun. 1982*, 691; c) G. Bertrand, C. Couret, J. Escudié, M. Majid, J. P. Majoral, *Tetrahedron Lett. 23* (1982) 3567; d) A. H. Cowley, J. E. Kilduff, T. H. Newman, M. Pakulski, *J. Am. Chem. Soc. 104* (1982) 5820; e) C. Couret, J. Escudié, J. Satgé, *Tetrahedron Lett. 23* (1982) 4941; f) E. Niecke, R. Rüger, *Angew. Chem. 95* (1983) 154; *Angew. Chem. Int. Ed. Engl. 22* (1983) 155; g) H. W. Roesky, private communication; h) M. Lysek, Staatsexamensarbeit, Bielefeld 1983.
[3] E. Niecke, R. Rüger, *Z. Naturforsch. B 37* (1982) 1593.
[7] a) N. Wiberg, *Angew. Chem. 83* (1971) 379; *Angew. Chem. Int. Ed. Engl. 10* (1971) 374; b) M. Veith, *Acta Crystallogr. B 31* (1975) 678.

## Prostacyclin Synthase, a Cytochrome P450 Enzyme

By *Hermann Graf, Hans Heinrich Ruf,* and *Volker Ullrich**

Prostacyclin ($PGI_2$), **2**, is a physiologically highly potent intercellular transmitter substance, which causes relaxation of smooth muscle and platelet aggregation[1]. Its biosynthesis involves an unusual rearrangement of 9,11-epidioxy-15-hydroxy-5,13-eicosadienoic acid ($PGH_2$), **1**.




The mechanism of this enzymatic isomerization is not yet known. Starting out from our work on oxygen activation by cytochrome P450-dependent monooxygenases, we postulated a possible role for a $Fe^{III}$-heme-thiolate center at the catalytic site of $PGI_2$ synthase[2]. Such heme-thiolate containing enzymes are characterized spectroscopically by a typical low-spin EPR signal and by a red-shift of the Soret band of the $Fe^{II}$–CO complex to 450 nm[3]. Since these two spectral properties clearly define a cytochrome P450 enzyme we purified $PGI_2$ synthase in order to test our hypothesis.

$PGI_2$ synthase was obtained in pure form as a homogenous protein of about 49000 d by affinity chromatography of detergent-solubilized pig aorta microsomes. The absorption spectrum of the oxidized enzyme corresponds almost exactly to those of the cytochrome P450 monooxygenases known so far (Fig. 1, A). Reduction of the enzyme by Na-dithionite in the presence of CO shifted the Soret band to 450 nm, although very slowly ($t_{1/2} \approx 5$ min) (Fig. 1, B); complete reduction did not occur. In contrast to microsomal monooxygenase P450 from liver enzymatic reduction by $NADPH_2$ after addition of $NADPH_2$-cytochrome P450 reductase did not occur.

The EPR spectrum of the protein at low temperature is shown in Figure 2, A. For comparison the spectrum of a monooxygenase P450 isolated from liver microsomes is also shown (Fig. 2, B). $PGI_2$ synthase exhibits the typical $g$-values of P450-monooxygenases, although a somewhat larger anisotropy is observed ($g_x = 2.46$; $g_z = 1.90$). Such variations, however, are common with other P450 enzymes[4].

Thus, having established that $PGI_2$ synthase is a cytochrome P450 enzyme, the question of the function of the hemin-thiolate group in the catalysis of the rearrangement arises. In contrast to the P450-monooxygenases this reaction does not require an external source of electrons, and hence the $Fe^{III}$ is not reduced to $Fe^{II}$. This is similar to the non-physiological transfer of an oxygen atom (oxene) from iodosyl benzene[5] or organic peroxides to substrates (RH) of P450 monooxygenases (Scheme 1).

[*] Prof. Dr. V. Ullrich, H. Graf
Fakultät für Biologie der Universität
Postfach 5560, D-7750 Konstanz
H. H. Ruf
Institut für Physiologische Chemie
Universität des Saarlands
D-6650 Homburg-Saar

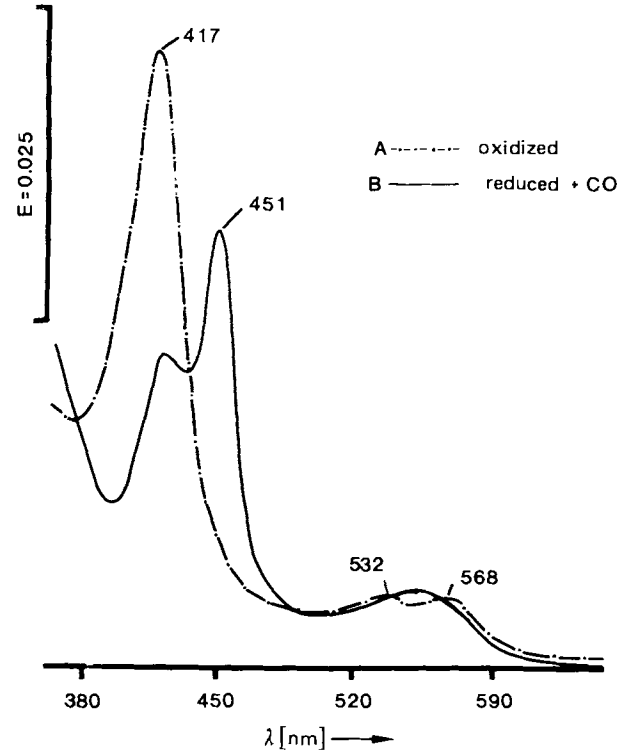



Fig. 1. Absorption spectra of prostacyclin synthase.

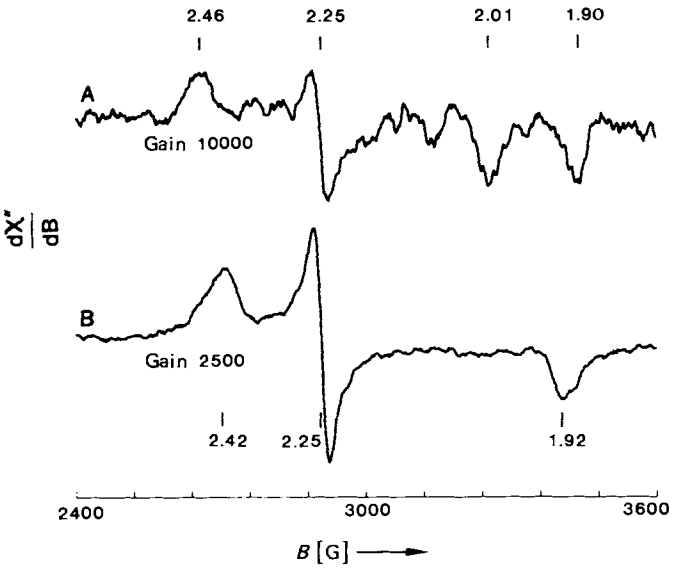
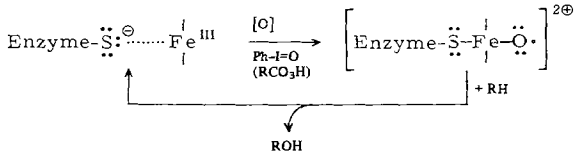
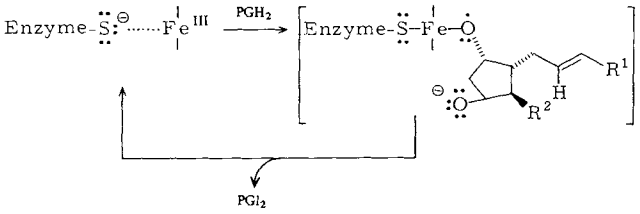



Fig. 2. EPR spectra of prostacyclin synthase (A) and cytochrome P450 of liver microsomes (B).




Scheme 1.

By analogy, the $PGH_2$-isomerization can be formulated as a heterolytic cleavage of the peroxide bond generating an activated 9-O atom (Scheme 2). It appears, therefore, that both cytochrome P450 enzyme systems have in common a mechanism of oxygen activation which apparently relies on the *trans*-thiolate ligand.




Scheme 2.

Received: February 7, 1983 [Z 271 IE]
German version: *Angew. Chem. 95* (1983) 497

[1] S. Moncada, R. Gryglewski, S. Bunting, J. R. Vane, *Nature 263* (1976) 663; W. Bartmann, G. Beck, *Angew. Chem. 94* (1982) 767; *Angew. Chem. Int. Ed. Engl. 21* (1982) 751.
[2] V. Ullrich, L. Castle, P. Weber, *Biochem. Pharmacol. 30* (1981) 2033.
[3] V. Ullrich, *Angew. Chem. 84* (1972) 689; *Angew. Chem. Int. Ed. Engl. 11* (1972) 701.
[4] M. Chevion, J. Peisach, W. E. Blumberg, *J. Biol. Chem. 252* (1977) 3637.
[5] F. Lichtenberger, W. Nastainczyk, V. Ullrich, *Biochem. Biophys. Res. Commun. 70* (1976) 939.

## Through-Bond Interaction *via* Strained σ-Bonds—The Synthesis and PE Spectrum of 1,5-Dimethyltetracyclo[3.3.0.0$^{2,8}$.0$^{4,6}$]octane-3,7-dione**

By *Gerhard Jähne* and *Rolf Gleiter**

The interaction between lone pairs or π-systems *via* the molecular σ-frame depends critically on the relative energies of the corresponding basis orbitals. To increase the σ/n or σ/π interaction highly strained σ-bonds are very effective, as shown by comparison of the PE spectrum of [2.2]paracyclophane with that of [1:2;9:10]bismethano[2.2]paracyclophane[1].

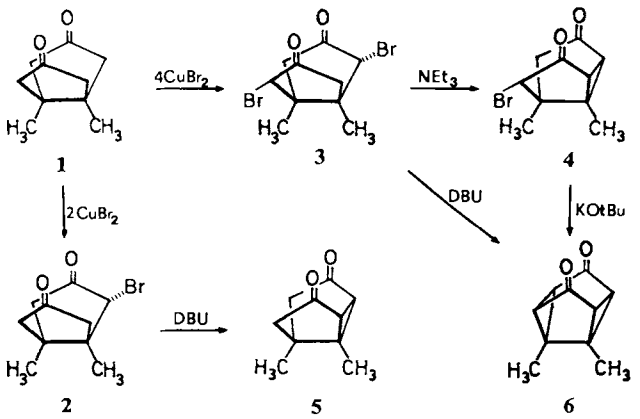
To extend this concept we have synthesized 1,5-dimethyltetracyclo[3.3.0.0$^{2,8}$.0$^{4,6}$]octane-3,7-dione **6** and its tri- and bicyclic precursors **5** and **1**, respectively, as shown in Scheme 1.

The starting point of our synthesis is 1,5-dimethylbicyclo[3.3.0]octane-3,7-dione **1**[2], which when treated with $CuBr_2$ in ethyl acetate/chloroform[3] leads to the *exo*-2-bromo- and the *exo,exo*-2,6-dibromo derivatives **2** and **3** in 60 and 70% yield, respectively. Transannular elimination of HBr can be achieved with 1,5-diazabicyclo[5.4.0]undec-5-ene (DBU) in dry acetonitrile at 50 °C under nitrogen to give **5** (70%, m.p. = 140–142 °C). The conversion of **3** to **6** can be achieved in 80% yield in one step using DBU as base, or in two steps *via* **4**.

In Table 1 we list the ionization energies corresponding to the first two bands of the PE spectra of **1**, **5**, and **6**. For

[*] Prof. Dr. R. Gleiter, G. Jähne
Institut für Organische Chemie der Universität
Im Neuenheimer Feld 270, D-6900 Heidelberg (Germany)

[**] Financial support from the Stiftung Volkswagenwerk and the BASF AG is gratefully acknowledged. We thank Dr. D. Krauss, E. Wallenwein, Dr. P. Kunzelmann, G. Rissmann, G. Schwebel, and W. Haseloff for measurements and discussions concerning the mass- and NMR-spectra.



Scheme 1.

comparison, the splitting ($\Delta n$) between the first two bands in cyclohexane-1,4-dione is 0.1 eV[4], and in bicyclo[3.3.0]octane-3,7-dione 0.33 eV[5].

Table 1. Comparison of the first two measured vertical ionization energies ($I_{v,j}$), the highest occupied MO energies according to MINDO/3 ($\varepsilon_j$), and the energy difference between them ($\Delta n$) for **1**, **5**, and **6**. All values in eV.

| Compound | band | $I_{v,j}$ | $\Delta n$ | Assignment | $\varepsilon_j$ | $\Delta n$ |
|---|---|---|---|---|---|---|
| **1** | ① | 9.31 | 0.27 | 6 $a_2$ ($n_-$) | − 9.62 | 0.29 |
| | ② | 9.58 | | 8 $b_2$ ($n_+$) | − 9.92 | |
| **5** | ① | 9.08 | 0.50 | 13 a″ ($n_-$) | − 9.41 | 0.49 |
| | ② | 9.58 | | 19 a′ ($n_+$) | − 9.90 | |
| **6** | ① | 8.86 | 0.94 | 5 $a_2$ ($n_-$) | − 9.05 | 1.03 |
| | ② | 9.80 | | 8 $b_2$ ($n_+$) | −10.08 | |

We assign the first band to ionization from $n_-$ and the second to ejection of electrons from $n_+$. This assignment is supported by the shape of the bands and by MINDO/3[6] calculations.

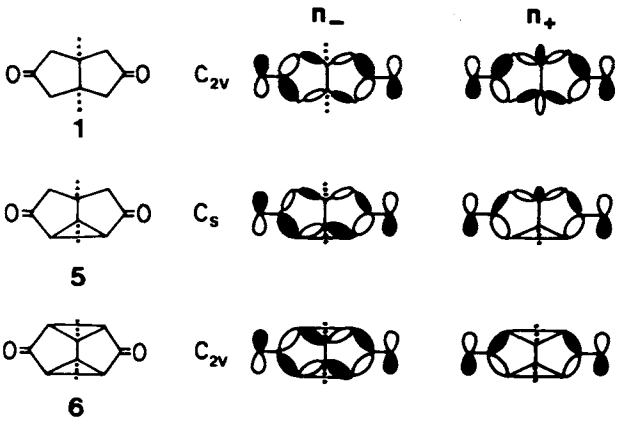


Fig. 2. Schematic representation of the MO's $n_-$ and $n_+$ of **1**, **5**, and **6** according to MINDO/3 calculation.

Figure 2 shows a steady increase (decrease) of the $\sigma/n$ interaction for $n_-$ ($n_+$), and thus explains the increase in the energy difference between the first two bands in the PE spectra of **1**, **5**, and **6**. The calculated distances between the oxygen atoms in **1** (6.2 Å), **5** (5.0 Å), and **6** (4.8 Å) preclude any significant through-space interaction between the 2p lone pairs on oxygen.

Received: February 7, 1983 [Z 273 IE]
German version: *Angew. Chem. 95* (1983) 500
The complete manuscript of this communication appears in:
*Angew. Chem. Suppl. 1983*, 661-667

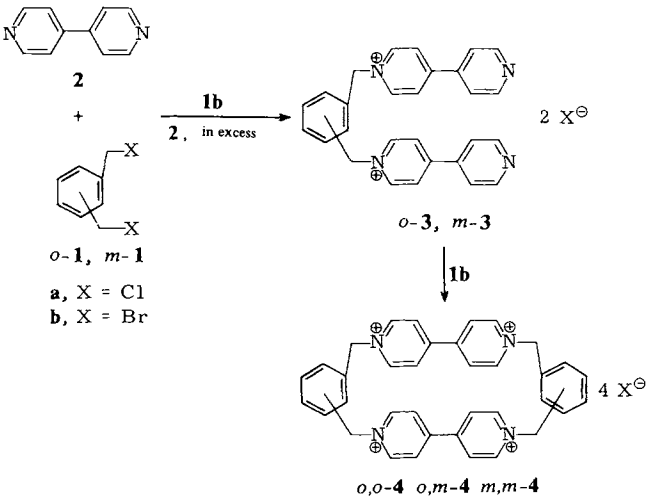
[1] R. Gleiter, M. Eckert-Maksić, W. Schäfer, E. A. Truesdale, *Chem. Ber. 115* (1982) 2009.
[2] U. Weiss, J. M. Edwards, *Tetrahedron Lett. 1968*, 4885.
[4] D. O. Cowan, R. Gleiter, J. A. Hashmall, E. Heilbronner, V. Hornung, *Angew. Chem. 83* (1971) 405; *Angew. Chem. Int. Ed. Engl. 10* (1971) 401.
[5] D. Dougherty, P. Brint, S. P. McGlynn, *J. Am. Chem. Soc. 100* (1978) 5597.
[6] R. Bingham, M. J. S. Dewar, D. H. Lo, *J. Am. Chem. Soc. 97* (1975) 1285; P. Bischof, *ibid. 91* (1969) 5947.

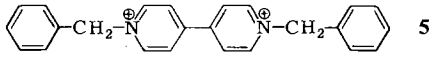
## Phanes with Two 4,4′-Bipyridinium Moieties—A New Class of Compounds**

By *Wolfram Geuder, Siegfried Hünig**, and *Adolf Suchy*

(1,4)Pyridinophanes, *i.e.* phanes in which one of the bridges is bonded to the pyridine nitrogen atom, were, to the best of our knowledge, not previously known. Here, we report for the first time on phanes having two 4,4′-bipyridinium moieties linked *via* two *o*- or two *m*-xylene bridges (*o,o*-**4**; *m,m*-**4**) or *via* one *o*- and one *m*-xylene bridge (*o,m*-**4**).

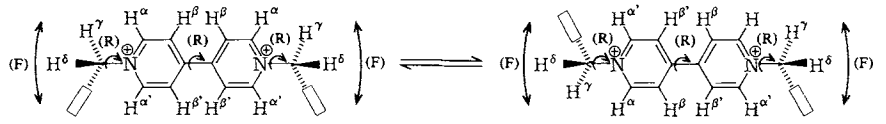
These macrocyclic tetracations could not be synthesized using the usual dilution methods, but could be prepared surprisingly easily by two-phase reaction of aqueous solutions of *o*-**3a** or *m*-**3a** (1 mmol in 10 mL $H_2O$) with 2 mmol of crystalline *o*-**1b** or *m*-**1b** by stirring the suspension at 20 °C. After three weeks *o,o*-**4b** (60%), *o,m*-**4a** (50%) (by reaction of *o*-**1b** with *m*-**3a** or *m*-**1b** with *o*-**3a**), and *m,m*-**4a**





[*] Prof. Dr. S. Hünig, Dr. A. Suchy, W. Geuder
Institut für Organische Chemie der Universität
Am Hubland, D-8700 Würzburg (Germany)

[**] Financial support of the Fonds der Chemischen Industrie and the Stiftung Volkswagenwerk is acknowledged.



*syn*-4 *anti*-4

Table 1. 400 MHz $^1$H-NMR data (δ-values) of **4** and **5** as $PF_6$ salts in [$D_6$] dimethyl sulfoxide at 25 °C. The pyridinium protons appear as doublets ($J$ = 6.5 Hz); geminal coupling of the benzyl protons: $J$ = 15 Hz.

| Compound | $H^\alpha$ | $H^{\alpha'}$ | $H^\beta$ | $H^{\beta'}$ | $H^\gamma$ | $H^\delta$ | Phenylene |
|---|---|---|---|---|---|---|---|
| *syn-o,o*-**4** | 9.43 | 8.27 | 8.52 | 7.97 | 6.49 (d) | 6.09 (d) | 8.07 (mc), 7.91 (mc) |
| *anti-o,o*-**4** | 9.33 | 8.33 | 8.40 | 8.21 | 6.47 (d) | 6.09 (d) | 8.07 (mc), 7.91 (mc) |
| *o,m*-**4** | *o:* 8.90<br>*m:* 9.26 | | *o:* 8.36<br>*m:* 8.57 | | *o:* 6.52 (d; $H^\gamma$), 6.09 (d; $H^\delta$), *m:* 6.06 (s) | | *o:* 8.09 (mc), 7.95 (mc), *m:* 7.71 (mc), 6.26 (s) |
| *m,m*-**4** | 9.37 | | 8.51 | | 6.05 (s) | | 7.86 (d), 7.62 (t), 7.31 (s) (2 : 1 : 1) |
| **5** | 9.50 | | 8.76 | | 6.01 (s) | | 7.62 (s) |

(30%), respectively, were isolated (after precipitation as the $PF_6$ salts and anion-exchange with $Et_4NCl$ in nitromethane)[1]. Using this method *o,o*-**4b** (25%) is formed even from **2** and *o*-**1b**.

The precursors *o*-**3** and *m*-**3**[1], as well as the salt of the ion **5**[1] are readily accessible. The purity of all products was monitored by thin-layer chromatography ($SiO_2$, MeOH/$H_2O$/50% aqueous $EtNH_3Cl$ (6 : 2 : 2). The composition and structure of the three isomers of **4a** were determined by mass spectrometry (FAB-MS[2]: *m/z* 520 (**4**); 555 (**4** + Cl); 590 (**4** + 2Cl) and NMR spectroscopy (also by comparison with the bisbenzylpyridinium ion **5**). In the phanes **4** rotation (R) of the pyridine rings and flipping (F) of the phenyl rings (*syn*- and *anti*-**4**) have to be borne in mind, as indicated by inspection of the upper half of the molecule (Table 1).

$^1$H-NMR spectroscopic studies indeed reveal that the internal mobility of the macrocycles changes dramatically from *o,o*-**4** *via* *o,m*-**4** to *m,m*-**4** with increasing size of the bridges. This is associated with an increase of the separation of the bipyridinium groups from 290 pm *via* 290 pm/510 pm to 510 pm[3].

*o,o*-**4**: Rotation (R) and flipping (F) are frozen-in. The $^1$H-NMR spectrum exhibits two sets of signals for *syn-o,o*-**4** and *anti-o,o*-**4** (2.5 : 1). The assignment reflects the expectation that the para- and diatropic effects of both phenylene bridges increase in *syn*-**4**, but not in *anti*-**4**. Compared to **5** ($H^\alpha$, $\delta$ = 9.50) the large high-field shift of the signal of $H^{\alpha'}$, which lies above the plane of the *o*-phenyl ring, is particularly noticeable [$\delta$ = 8.27 (*syn-o,o*-**4**), 8.33 (*anti-o,o*-**4**)], so that the difference between the chemical shifts of $H^\alpha$ and $H^{\alpha'}$ in *syn-o,o*-**4** increases to 1.16 ppm. In contrast, the ring current of the rotationally hindered pyridinium groups shifts the benzylic $H^\gamma$ signal *ca.* 0.5 ppm to low field relative to that of the model compound **5**, whereas the proton $H^\delta$, which lies over the long axis of the molecule and is orientated outwards, behaves "normally". This assignment is consistent with the fact that in *syn*- and *anti-o,o*-**4** $H^\delta$ has the same chemical shift, whereas the $H^\gamma$-signals differ by approximately 0.02 ppm.

*o,m*-**4**: Even the ring expansion of *ca.* 220 pm on one side is sufficient to reduce the barrier to rotation of all four pyridinium rings. The 2 × 2 doublets ($H^\alpha$, $H^\beta$) arise from the different bridge members. In contrast, the phenylene bridges can only undergo flipping on the *m*-side.

*m,m*-**4**: Introduction of the second *m*-phenylene bridge results in complete (R) and (F) mobility, and hence the signals largely correspond to those of the open-chain model compound. A discrepancy, which confirms the ring structure, arises from the high-field shift of both isolated *m*-phenylene protons: their signal is shifted in *m,m*-**4** to $\delta$ = 7.31 [*m*-**3**: $\delta$ = 7.55]; in the somewhat more narrower *o,m*-**4** the signal of the corresponding proton appears at $\delta$ = 6.26.

*Temperature effects:* In the 90 MHz $^1$H-NMR spectrum the pyridinium signals of *o,o*-**4** coalesce at 50 °C ($CF_3CO_2D$) ($\Delta G^+ \approx 65$ kJ/mol). In *o,m*-**4** rotation of the pyridinium rings adjacent to the *o*-bridge slows down at −40 °C ($CD_3CN$) (broad $H^\alpha$ and $H^\beta$ signals). At +70 °C the rate of flipping of the *o*-bridge increases (very broad $H^\gamma$ and $H^\delta$ signals). Inspection of Stuart-Briegleb and Dreiding molecular models suggests that *o,o*-**4** should have considerably higher barriers to rotation.

Furthermore, the ring systems are interesting as multistep redox systems (possible π-merization of the double radical cations[4]) and as host molecules for inclusion compounds. Using the same synthetic principle the preparation of related phanes having other ring members is being undertaken.

Received: February 21, 1983 [Z 280 IE]
German version: *Angew. Chem.* 95 (1983) 501

[1] All compounds gave correct elemental analyses.

[2] *Fast-Atom-Bombardment-MS*. We wish to thank Finnigan-MAT for performing the measurements.

[3] Distances between the benzylic C atoms, measured on a Dreiding model.

[4] For the term "π-merization" cf. E. M. Kosower in W. A. Pryor: *Free Radicals in Biology*, Vol. II, Academic Press, New York 1976, p. 1.

## 1,2-Benzynes from 6-Halopentafulvenes**

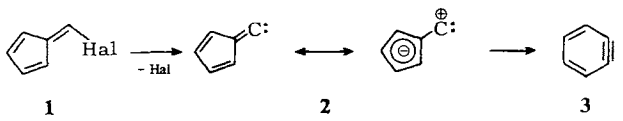
By *Klaus Hafner**, *Hans-Peter Krimmer*, and *Bernd Stowasser*

6-Halopentafulvenes **1** are readily accessible by reaction of acylcyclopentadienes with phosgene or oxalyl halides and have proven very useful as educts for the synthesis of a variety of pentafulvenes functionally substituted at the

[*] Prof. Dr. K. Hafner, H.-P. Krimmer, B. Stowasser
Institut für Organische Chemie der Technischen Hochschule
Petersenstrasse 22, D-6100 Darmstadt (Germany)

[**] This work was supported by the Deutsche Forschungsgemeinschaft and the Fonds der Chemischen Industrie.

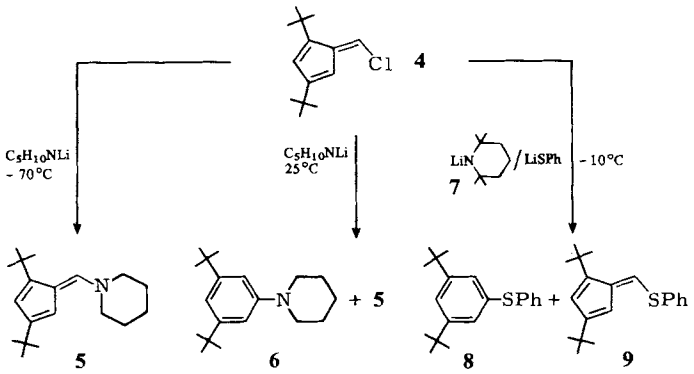
exocyclic C-atom[1]. α-Elimination of hydrogen halide from **1** should furnish the hitherto unknown pentafulvenylidenecarbene **2**.




**1** **2** **3**

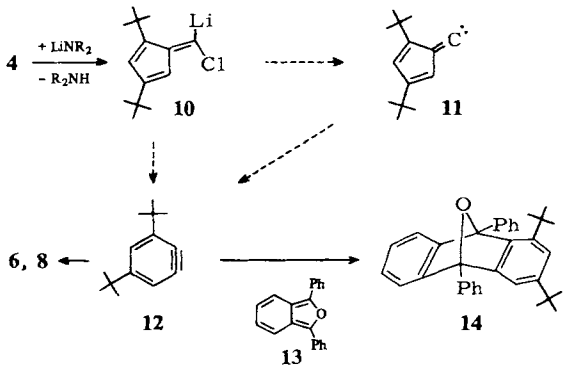
According to quantum chemical calculations by *Apeloig et al.*[2], **2** is expected to be highly electrophilic and undergo rearrangement into the 1,2-benzyne **3**, which should be 14 kcal·mol$^{-1}$ more stable than **2**.

To check this prognosis we have investigated the reaction of the stable 1,3-di-*tert*-butyl-6-chloropentafulvene **4** with bases. Reaction of **4** with lithium piperidide in tetrahydrofuran (THF) at −70 °C affords 1,3-di-*tert*-butyl-6-piperidinopentafulvene **5** in 76% yield[3,4a] with retention of configuration. On the other hand, the same reaction at 25 °C leads to 1,3-di-*tert*-butyl-5-piperidinobenzene **6** in 61% yield[4b] and only 6% of **5**, while reaction with lithium 2,2,6,6-tetramethylpiperidide **7** in presence of an excess of lithium thiophenolate in THF at −10 °C leads to 54% of 3,5-di-*tert*-butyldiphenyl sulfide **8**[4c] and 6% of 1,3-di-*tert*-butyl-6-phenylthiopentafulvene **9**[1].




**5** **6** **8** **9**

These findings confirm the quantum chemical predictions. From **4** the carbenoid **10** can be generated, and from this the carbene **11**, which obviously rapidly rearranges into 3,5-di-*tert*-butyl-1,2-benzyne **12**. This subsequently reacts with nucleophiles[5a], whereupon **6** and **8** are formed regioselectively under the influence of the bulky *tert*-butyl groups. So far, however, it cannot be ruled out that **12** is generated directly from **10** by a rearrangement analogous to the Fritsch-Buttenberg-Wiechell reaction[5b]. Attempts to trap the carbene **11** by [2+1]-cycloaddition have so far remained unsuccessful. On the other hand, by means of 1,3-diphenylisobenzofuran **13** it was possible to trap the 1,2-benzyne **12** formed on reaction of **4** with **7** as the Diels-Alder adduct **14** (50%)[4d].




Received: February 25, 1983 [Z 290 IE]
German version: *Angew. Chem. 95* (1983) 496

[1] K. Hafner, *Pure Appl. Chem. 54* (1982) 939; H.-P. Krimmer, B. Stowasser, K. Hafner, *Tetrahedron Lett. 23* (1982) 5135.
[2] Y. Apeloig, R. Schrieber, P. J. Stang, *Tetrahedron Lett. 21* (1980) 411; P. J. Stang, *Acc. Chem. Res. 15* (1982) 348.
[3] All compounds isolated gave correct elemental analyses.
[4] $^1$H-NMR (in $CDCl_3$); UV (in *n*-hexane). a) **5**: yellow needles, m.p. 110 °C; $^1$H-NMR (300 MHz): $\delta$ = 1.23 (s; 9H, *t*Bu); 1.36 (s; 9H, *t*Bu); 1.70 (m; 6H, $CH_2$–$CH_2$–$CH_2$); 3.56 (m; 4H, $CH_2$–N–$CH_2$); 6.07 (d, $J$ = 2.3 Hz; 1H, H-2); 6.16 (d, $J$ = 2.3 Hz; 1H, H-4); 7.37 (s; 1H, H-6). UV: $\lambda_{max}$(lg$\varepsilon$) = 220 (3.82) sh; 327 (4.47) nm.—b) **6**: colorless platelets m.p. 50 °C; $^1$H-NMR (300 MHz): $\delta$ = 1.31 (s; 18H, *t*Bu); 1.56 (m; 2H, $CH_2$); 1.73 (m; 4H, $CH_2$–$CH_2$–$CH_2$); 3.13 (m; 4H, $CH_2$–N–$CH_2$); 6.83 (d, $J$ = 2 Hz; 2H, H-2, H-6); 6.95 (t, $J$ = 2 Hz; 1H, H-4). UV: $\lambda_{max}$(lg$\varepsilon$) = 217 (4.36); 254 (4.03); 285 (3.20) sh nm.—c) **8**: colorless oil b.p. 85 °C/$10^{-4}$ torr; $^1$H-NMR (60 MHz): $\delta$ = 1.32 (s; 18H, *t*Bu); 7.15–7.45 (m; 8H, arom. H). UV: $\lambda_{max}$(lg$\varepsilon$) = 235 (3.96); 252 (4.08); 276 (3.76) nm.—d) **14**: colorless needles m.p. 245 °C; $^1$H-NMR (300 MHz): $\delta$ = 1.12 (s; 9H, *t*Bu); 1.24 (s; 9H, *t*Bu); 6.98–8.02 (m; 16H, arom. H).
[5] a) R. Huisgen, J. Sauer, *Angew. Chem. 72* (1960) 91; b) G. Köbrich, *Angew. Chem. 79* (1967) 22; *Angew. Chem. Int. Ed. Engl. 6* (1967) 41; *ibid. 84* (1972) 557 and *11* (1972) 473; H. Siegel, *Top. Curr. Chem. 106* (1982) 55.

## The Cation Di-μ-oxo-*trans*-dioxobis[(1,4,7-triazacyclononane)molybdenum(v)](*Mo—Mo*) and its Acid-Catalyzed *cis*-Isomerization**

By *Karl Wieghardt**, *Manfred Hahn*, *Wolfgang Swiridoff*, and *Johannes Weiss*

Dinuclear molybdenum(v) complexes with the central structural element di-μ-oxodioxobis(molybdenum(v)), $Mo_2O_4^{2+}$, are diamagnetic; their short Mo–Mo distance (254–258 pm) is interpreted as originating from a metal-metal single bond[1a–d,f]. The $Mo_2O_2$ four-membered ring is puckered and both terminal oxo groups are always located in a *cis*-arrangement[1a,d,f]. This configuration is apparently the most thermodynamically stable; a structure with *trans*-oxo groups has not previously been reported.

We now report the preparation and structure of the first $Mo_2O_4^{2+}$ complex with *trans*-oxo groups, as well as its irreversible acid-catalyzed conversion into the stable *cis*-form. Hydrolysis of the monomeric, paramagnetic complex **1** in aqueous solution containing $NaHCO_3$ leads to formation of the diamagnetic, green, dinuclear cation **2**. After addition of NaI, the crystalline iodide **2**·2I is obtained. The reaction of aqueous solutions of **2** with dilute perchloric acid under argon affords cherry-red solutions from which red, diamagnetic **3**·2I can be precipitated upon addition of NaI. In solution, **3** undergoes acid-catalyzed reaction to yield **4**, a diamagnetic, yellow, dinuclear μ-oxo complex of molybdenum(v) (for spectroscopic data, see Table 1).

[*] Prof. Dr. K. Wieghardt, M. Hahn
Lehrstuhl Anorganische Chemie I der Universität
Postfach 102148, D-4630 Bochum 1 (Germany)
Prof. Dr. J. Weiss, W. Swiridoff
Anorganisch-chemisches Institut der Universität
Im Neuenheimer Feld 270, D-6900 Heidelberg (Germany)

[**] This work was supported by the Fonds der Chemischen Industrie and by the Deutsche Forschungsgemeinschaft.

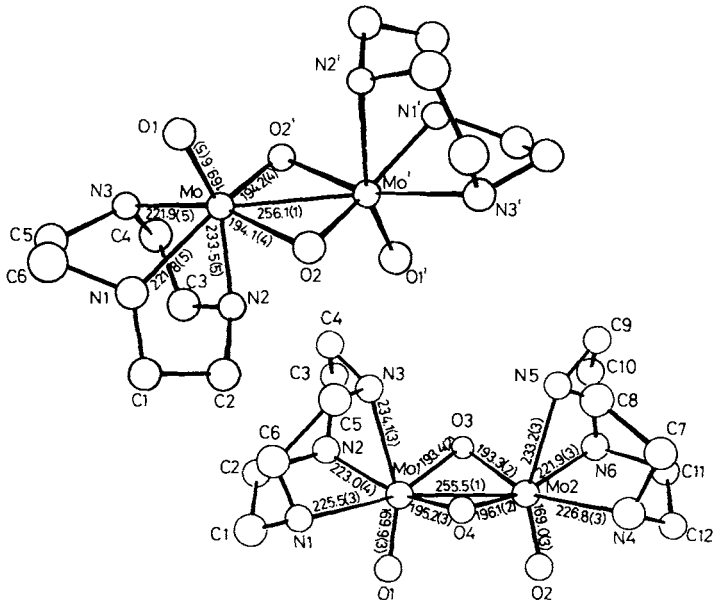



Fig. 1. Top: Structure of the cation in **3**·2I. $P2_1/c$; $a=687.7(3)$, $b=1152.8(4)$, $c=1470.9(7)$ pm, $\beta=90.77(3)°$, $Z=2$, $R=0.06$ (3686 observed reflections). Selected bond angles [°]: Mo–O2–Mo′ 82.6(2), O2–Mo–O2′ 97.5(2), O1–Mo–O2 103.2(2), O1–Mo–O2′ 104.1(2), O1–Mo–N2 163.3(2). Bottom: Structure of the cation in **4**·2SCN·KSCN. $P2_1n$; $a=1045.8(2)$, $b=1220.0(2)$, $c=2077.3(3)$ pm, $\beta=99.52(2)°$, $Z=4$, $R=0.032$ (2614 observed reflections). Selected bond angles [°]: Mo1–O3–Mo2 82.7(1), Mo1–O4–Mo2 81.5(1), O3–Mo1–O4 92.9(1), O3–Mo2–O4 92.6(1), O1–Mo1–O3 108.3(1), O1–Mo1–O4 110.3(1), O2–Mo2–O3 108.9(1), O2–Mo2–O4 108.5(1).

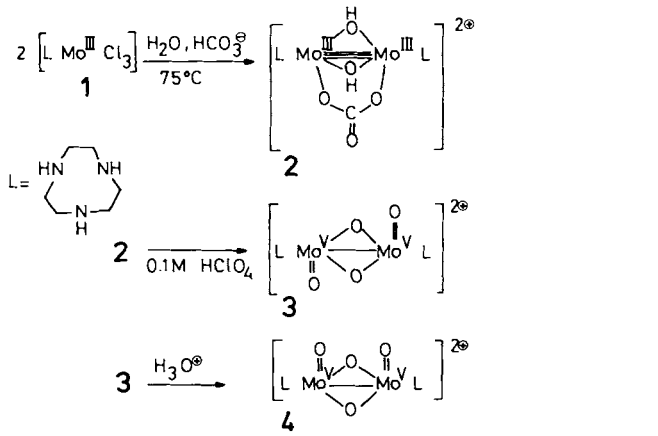



Table 1. UV/VIS ($\lambda_{max}$ [nm]: $\varepsilon$ [$L\,mol^{-1}\,cm^{-1}$]) and selected IR data [$cm^{-1}$] of the complexes **2**–**4** in aqueous solution (pH 7).

| | UV-VIS [a] | IR |
|---|---|---|
| 2 | 735 (sh), 630 (71), 450 (sh), 366 ($1.2\times10^3$) | $\nu$(C=O) 1535, $\nu$(C–O) 1300 |
| 3 | 525 (380), 312 ($3.6\times10^3$) | $\nu$(Mo=O) 909, $\nu_{as}$(Mo–O) 720, $\nu_s$(Mo–O) 410 |
| 4 | 378 (390), 284 ($7.0\times10^3$) | $\nu$(Mo=O) 940, $\nu_{as}$(Mo–O) 735, $\nu_s$(Mo–O) 420 |

[a] The molar absorption coefficients are calculated per dimeric cation (*not* per Mo center).

The crystal structure analysis of **3**·2I proves the existence of a dinuclear molybdenum(v) cation. Each Mo atom has a distorted octahedral environment (two edge-sharing octahedra, Fig. 1a). The terminal oxo ligands occupy *trans*-sites; the $Mo_2O_2$ four-membered ring is planar. In the isomeric **4**·2SCN·KSCN the terminal oxo groups are *cis* and the $Mo_2O_2$-ring is puckered.

The environment of the $Mo^V$ centers in **3** and **4** is almost identical; within the limits of experimental error all the Mo–Mo, Mo–N, Mo–O, and Mo=O bond lengths are the same. Only the O–Mo–O angles in **4** are somewhat larger than those in **3**.

The kinetics of the irreversible *trans-cis*-isomerization indicate that a protonated form of **3** is involved in the rate-determining step. The rate law (30 °C, ionic strength 1.0 mol/L) is

$$\frac{-d[\mathbf{3}]}{dt}=\frac{d[\mathbf{4}]}{dt}=k_{AH}(1+K_{AH}[H^+]^{-1})^{-1}[\mathbf{3}]$$

where $k_{AH}=6.4\times10^{-4}$ L mol$^{-1}$ s$^{-1}$ and $K_{AH}=2.8$ mol L$^{-1}$.

Received: February 21, 1983 [Z 282 IE]
German version: *Angew. Chem. 95* (1983) 499
The complete manuscript of this communication appears in: *Angew. Chem. Suppl. 1983*, 583–598

[1] E. I. Stiefel, *Prog. Inorg. Chem. 22* (1977) 1; b) F. A. Cotton, S. M. Morehouse, *Inorg. Chem. 4* (1965) 1377; c) A. Kojima, S. Ooi, Y. Sasaki, K. Suzuki, K. Saito, H. Kuroya, *Bull. Chem. Soc. Jpn. 54* (1981) 2457; d) F. A. Cotton, W. H. Ilsey, *Inorg. Chim. Acta 59* (1982) 213; f) I. Shibahara, H. Kuroya, K. Matsumoto, S. Ooi, *ibid. 54* (1981) L75.

## Reactions at the Counter Electrode in Electroreductions under Aprotic Conditions in One-Compartment Cells

By *Rainer Engels**, *Cornelis J. Smit*, and *Wim J. M. van Tilborg*

Cathodic syntheses in aprotic media are normally carried out in divided cells so as to avoid reoxidation of the (primary) products at the anode. Such syntheses, however, are usually limited to the laboratory scale owing to the complicated and expensive cell constructions, the high ohmic resistance, and especially the short lifetime of the ion-exchange membrane[1]. We now report on a generally applicable method for solving this problem.

Table 1 (selected data). Reactions at the counter electrode during electroreductions in one-compartment cells.

| No. | Conducting salt/ Substrate | Foot potential [a] [V vs. SCE] | (Primary) Oxidation products |
|---|---|---|---|
| 1 | Bis(tetraethylammonium) oxalate (DTEAOx) [b] | +0.2 | $CO_2$ |
| 5 | Tetraethylammonium formate (TEAForm) [b] | +0.7 | $CO_2+H^+$ |

[a] 0.1 M in acetonitrile, platinum anode. [b] Prepared by neutralization of tetraethylammonium hydroxide with the appropriate acid.

The anodic oxidations of the oxalates[3] and formates listed in Table 1 proceed rapidly at relatively low potentials, independent of the anode material. They are therefore particularly well suited for limiting the counter elec-

[*] Dr. R. Engels[+], Ing. C. J. Smit[+], Dr. W. J. M. van Tilborg[+]
Koninklijke/Shell-Laboratorium
Amsterdam (Shell Research B.V.) (Holland)
[+] New address: Billiton Research B.V.
P.O. Box 38, NL-6800 LH Arnhem (Holland)

Table 2/3 (selected data). Electroreductions in one-component cells [a].

| Starting compound | Products [b] | Current efficiency [%] | | |
|---|---|---|---|---|
| | | DTEAOx Rcn. 1 [c] | TEAForm Rcn. 5 [c] | Divided cell |
| Dimethyl maleate | Trimethyl 1,1,2-ethanetricarboxylate **1** | 5 | 59 | |
| | Tetramethyl 1,1,2,2-ethanetetracarboxylate **2** | 24 | — | |
| | Tetramethyl 1,2,3,4-butanetetracarboxylate **3** | — | 20 | |
| | Pentamethyl 1,1,2,3,4-butanepentacarboxylate **4** | 12 | — | |
| | Hexamethyl 1,1,2,3,4,4-butanehexacarboxylate **5** | 45 | — | 46 [5] |
| 1,3-Butadiene | Methyl 2-butene-1-carboxylate **6** | 48 | 3 [e] | 8 [6] |
| | Dimethyl 2-butene-1,4-dicarboxylate **7** | — | 14 [e] | 18 [6] |
| | Dimethyl 2,6-octadiene-1,8-dicarboxylate **8** | 15 | 56 [e, f] | 5 [6] |
| | Dimethyl 5-vinyl-2-hexene-1,6-dicarboxylate **9** | | | |
| | Dimethyl 2,3-divinylbutane-1,4-dicarboxylate **10** | | | |
| Benzylidene-aniline | (*R,S*)-Methyl α-phenyl-*N*-phenylglycinate **13** | 79 | | 60 [7] |
| Aceto-phenone | Methyl α-phenyllactate **14** | 58 | | |
| | 2,3-Diphenyl-2,3-butanediol **15** | 21 [g] | | |
| 1-Bromo-2-methyl-pentane | Methyl 2-methylpentanecarboxylate **18** | 95 | | |
| 1,10-Ditosyl-1,10-diaza[18]-crown-6 [h, i] | 1,10-Diaza[18]-crown-6 **21** | | 85 [k] | 80 [k] |
| (±)-1,2-Dibromo-1,2-diphenyl-ethane [h] | *cis/trans*-stilbene **22** [i] | 86 | | 85 [10] |

[a] Conditions: glass beaker cell, platinum anode, lead cathode, 0.2—0.4 M starting compound and DTEAOx (0.23 M) or TEAForm (0.46 M) in anhydrous acetonitrile with passage of carbon dioxide, room temperature. [b] Isolated after esterification with methyl iodide [13]. [c] Reaction at the counter electrode, see Table 1. [e] Capillary gap cell, material yield of **6**–**10** based on 1,3-butadiene ≥95%. [f] **8** : **9** : **10** = 7 : 2 : 1. [g] Reduction in methanol at a mercury cathode without additional carbon dioxide furnishes **15** in 61% current yield (94% material yield). [h] Without additional carbon dioxide. [i] In *N,N*-dimethylformamide at a mercury cathode. [k] Material yield, isolated. [l] *cis/trans* = 38/62.

trode potential in reductions. The anodically evolved carbon dioxide can be used in reductive carboxylations, but application of the counter electrode reactions (see Table 2/3) is by no means restricted to carboxylations.

As Table 2/3 shows, the selectivity of the cathodic reaction can strongly depend on the type of counter electrode reaction. Thus, the reductive electrocarboxylation of dimethyl maleate[5] in presence of DTEAOx affords a mixture of the mono- and dicarboxylated monomers (**1**, **2**) and dimers (**4**, **5**), but no hydrodimer **3**. However, the protons formed during the anodic oxidation of TEAForm shift the selectivity of the reaction towards **1** as main product along with **3** as byproduct. A similar change in the selectivity is found in the reductive carboxylation of butadiene[6]. Changing from DTEAOx to TEAForm shifts the selectivity of the reaction in favor of the $C_{10}$-dicarboxylic acids **8**—**10**. In the electrocarboxylation of acetophenone the carboxylated alcohol **14** is formed in moderate amounts along with the pinacol **15**. If, on the other hand, acetophenone is reduced in presence of DTEAOx without additional carbon dioxide under conditions suitable for the pinacolization[11] then only **15** is formed. The cleavage of the tosyl group from 1,10-ditosyl-1,10-diaza[18]crown-6 proceeds in excellent yield, thus providing a simplified route to 1,10-diaza[18]crown-6.

As these examples demonstrate, the oxidations of the oxalates and formates enable a variety of cathodic electrosyntheses to be carried out under anhydrous conditions in one-compartment cells—a prerequisite for scaling-up the reactions to the industrial scale.

Received: May 10, 1982;
revised: April 18, 1983 [Z 37 IE]
German version: *Angew. Chem. 95* (1983) 502
The complete version of this communication appears in:
*Angew. Chem. Suppl. 1983*, 691—702

[1] F. Beck: *Elektroorganische Chemie*, Verlag Chemie, Weinheim 1974, S. 110.
[3] *Savéant et al.* used the oxidation of DTEAOx as the counter-electrode reaction in a divided cell without recognizing the advantages reported here: J. C. Gressin, D. Michelet, L. Nadjo, J. M. Savéant, *Nouv. J. Chim. 3* (1979) 545.
[5] D. A. Tyssee, M. M. Baizer, *J. Org. Chem. 39* (1974) 2819. W. J. M. van Tilborg, C. J. Smit, *Recl. Trav. Chim. Pays-Bas 100* (1981) 437.
[7] N. L. Weinberg, A. K. Hoffmann, T. B. Reddy, *Tetrahedron Lett. 1971*, 2271.
[10] H. Lund, E. Hobolt, *Acta Chem. Scand. B30* (1976) 895.
[11] W. J. M. van Tilborg, C. J. Smit, *Recl. Trav. Chim. Pays-Bas 98* (1979) 532.

## Ketene-Alkyne Conversion using Lewis Acids**

By *Fritz R. Kreissl**, *Werner Sieber*, and *Mathias Wolfgruber*

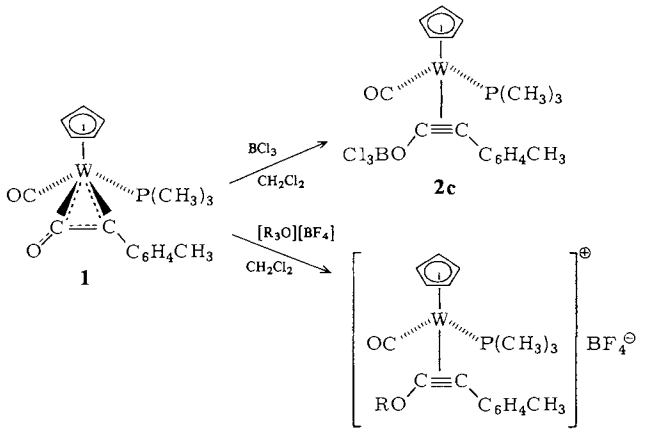
Mild carbonylation of carbyne complexes, *via* CC bond formation, leads to $\eta^1$- and $\eta^2$-ketenyl compounds[2]. These react with Lewis bases, such as phosphanes, carbon monoxide, or isocyanides, to afford $\eta^1$-ketenyl compounds. With halophosphanes and haloarsanes they react to give phosphanyl- and arsanylketene complexes[6], from which an intermediate having a CPW ring system could be isolated. Use of higher pressures of CO leads to deoxygenation of the $\eta^2$-ketenyl *via* the stage of the $\eta^1$-ketenyl compounds to yield σ-bonded alkyne derivatives[8].

In contrast, π-bonded alkyne complexes are formed by reaction of the $\eta^2$-ketenyl compounds with Lewis acids: thus at dry-ice temperature both alkyl cations and boron trichloride add to the ketene oxygen atom of **1** with concomitant conversion of the $\eta^2$-ketenyl into an $\eta^2$-alkynyl ligand. Comparable alkyne complexes have recently been

[*] Priv.-Doz. Dr. F. R. Kreissl, W. Sieber, M. Wolfgruber
Anorganisch-chemisches Institut der Technischen Universität München
Lichtenbergstrasse 4, D-8046 Garching (Germany)

[**] Transition-Metal Ketene Compounds, Part 13. This work was supported by the Deutsche Forschungsgemeinschaft and the Fonds der Chemischen Industrie. Priv.-Doz. Dr. H. G. Alt (Universität Bayreuth) is thanked for the NMR measurements.—Part 12: W. Sieber, M. Wolfgruber, D. Neugebauer, O. Orama, F. R. Kreissl, *Z. Naturforsch. B38* (1983) 67.

obtained in the reaction of $Cl[P(CH_3)_3]_4WCH$ with CO in the presence of aluminum trichloride[9].




The products **2a** and **2b** can be isolated as orange salt-like solids, whereas **2c** is a diamagnetic beige molecular solid; all three compounds are soluble in dichloromethane. The compositions and structures of the products were determined by elemental analysis and by mass-, IR-, and NMR-spectroscopy. In each case the $\nu$CO solution spectrum ($CH_2Cl_2$) exhibits a very intense band at 1975, 1976, and 1970 $cm^{-1}$, respectively. The $^1H$-NMR spectra of the novel acetylene complexes have the expected number of signals in the correct intensity ratios. The $^{13}C\{^1H\}$-NMR spectrum ($CD_2Cl_2$, $\delta$-value rel. $CD_2Cl_2 \triangleq 54.2$ ppm) of **2b** contains 12 signals: W–CO 223.4 [$J$(WC) = 135.0, $J$(PC) = 6.8 Hz]; C≡*C*O 228.8 [$J$(WC) = 66.7, $J$(PC) = 6.0 Hz]; *C*≡CO 193.7 [$J$(WC) = 32.5; $J$(PC) = 6.0 Hz]; $C_6H_4$ 141.6, 133.4, 130.0, 129.4; $C_5H_5$ 93.6; $OCH_2$ 72.3; $P(CH_3)_3$ 21.8 [$J$(PC) = 37.6 Hz]; $CH_3$ 21.5; $CH_2CH_3$ 15.1. The strong deshielding of the alkyne C atoms in **2** suggests a 4π-electron ligand[12], whereas the relatively large WC coupling constants indicate high σ-bond contributions[15] between the central metal atom and the two carbon atoms; a second limiting structure for the description of the complexes, a metallacyclopropene system, therefore, cannot be excluded. In each case the $^{31}P\{^1H\}$-NMR spectra ($CD_2Cl_2$, $\delta$-value rel. ext. $H_3PO_4$) of **2a**–**2c** exhibit a singlet accompanied by tungsten satellites: −17.2 [$J$(WP) = 394.3 Hz], −17.3 [394.3], and −16.0 [399.8], respectively. In the mass spectra (FD) of **2a** and **2b**, the signals of the cations appear at $m/z$ 499 and 513, respectively, in addition to signals at 547 and 561, respectively, whose relative intensities are markedly dependent on the temperature of the emitter; this corresponds to $CO/P(CH_3)_3$ exchange in the cations.

Received: February 17, 1983;
revised: April 11, 1983 [Z 279 IE]
German version: *Angew. Chem. 95* (1983) 503
The complete version of this communication appears in:
*Angew. Chem. Suppl. 1983*, 631–638

CAS Registry numbers:
**1**, 61202-59-3; **2a**, 85748-32-9; **2b**, 85735-54-2; **2c**, 85735-55-3; $[Me_3O][BF_4]$, 420-37-1; $[Et_3O][BF_4]$, 368-39-9.

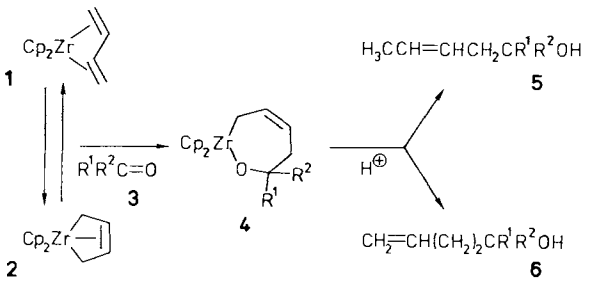
[2] F. R. Kreissl, W. Uedelhoven, K. Eberl, *Angew. Chem. 90* (1978) 908; *Angew. Chem. Int. Ed. Engl. 17* (1978) 859.
[6] F. R. Kreissl, M. Wolfgruber, W. Sieber, H. G. Alt, *Angew. Chem. 95* (1983) 159; *Angew. Chem. Int. Ed. Engl. 22* (1983) 149; *Angew. Chem. Suppl. 1983*, 148.
[8] F. R. Kreissl, K. Eberl, W. Uedelhoven, *Angew. Chem. 90* (1978) 908; *Angew. Chem. Int. Ed. Engl. 17* (1978) 860.
[9] M. R. Churchill, H. J. Wasserman, S. J. Holmes, R. R. Schrock, *Organometallics 1* (1982) 766.
[12] Cf. J. L. Templeton, B. C. Ward, *J. Am. Chem. Soc. 102* (1980) 3288.
[15] Cf. C. G. Kreiter, K. Nist, H. G. Alt, *Chem. Ber. 114* (1981) 1845.

## The Zirconocene-Induced Coupling of Butadiene with Carbonyl Compounds**

By *Gerhard Erker**, *Klaus Engel*, *Jerry L. Atwood*, and *William E. Hunter*

Additions of aldehydes and ketones to alkyltitanium and alkylzirconium compounds are attracting increasing attention as synthetically useful reactions, often with surprisingly high selectivities. Since X-ray structure analyses[2] have shown (*s-cis*-diene)zirconocene complexes exhibit substantial alkylmetal character it was tempting to consider the regioselective coupling of isoprene with aldehydes and ketones at the bis(η-cyclopentadienyl)zirconium unit as being a further example of this reaction type[3].

Reaction of the equilibrium mixture of (*s-trans*- and *s-cis*-$\eta^4$-butadiene)zirconocene **1** ⇌ **2** (25 °C: 45/55) with benzophenone, acetone, cyclododecanone, acetophenone, pinacolone and isobutyraldehyde (**3a**–**f**) leads to the or-




ganometallic products **4a**–**f** having a oxazirconacycloheptene structure; this was confirmed by X-ray structure analysis in the case of **4a** (Fig. 1). Hydrolysis of **4** affords mixtures of the alcohols **5** and **6**.

Addition of **3** to **2** was expected to give directly the seven-membered metallacycles **4** with *cis*-configurated double bond. Surprisingly, however, **4a**–**f** are not formed in this way. In the equilibrium mixture **1** ⇌ **2** the (*s-trans*-$\eta^4$-butadiene)zirconocene **1** reacts more rapidly with **3** than its isomer **2** with **3**, even at room temperature. This becomes impressively confirmed upon reacting the mixture of **1** and **2** (45:55) with benzophenone **3a** at low temperatures. Above −25 °C slow formation [$\tau_{1/2}(-20\,°C) \approx 1$ h] of **4a** is found to take place. The thermally-induced equilibration **1** ⇌ **2** is "frozen in"[2]; reaction of **1** with **3a** is the sole reaction recorded $^1H$-NMR spectroscopically.

[*] Priv.-Doz. Dr. G. Erker, K. Engel
Abteilung für Chemie der Universität
Postfach 102148, D-4630 Bochum 1 (Germany)
Prof. Dr. J. L. Atwood, Dr. W. E. Hunter
Department of Chemistry, University of Alabama
University, Alabama 35486 (USA)

[**] This work was supported by the Minister für Wissenschaft und Forschung des Landes Nordrhein-Westfalen and by the Fonds der Chemischen Industrie.

No thermally-induced reaction is observed at $-50\,^{\circ}C$, even after several hours, whereas **1** reacts photochemically (Philips HPK 125; Pyrex filter) with **3a** within a few minutes. (*s-cis*-Butadiene)zirconocene **2** also proves to be no

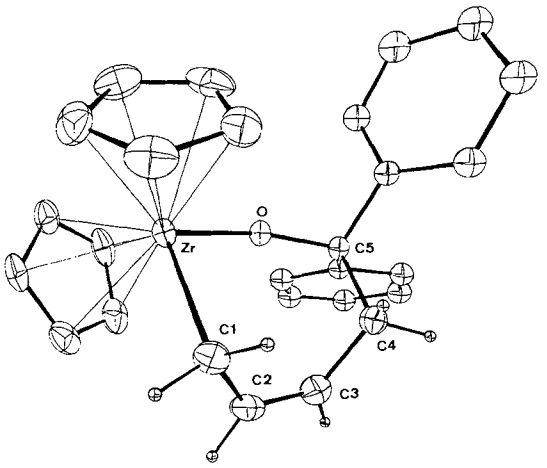
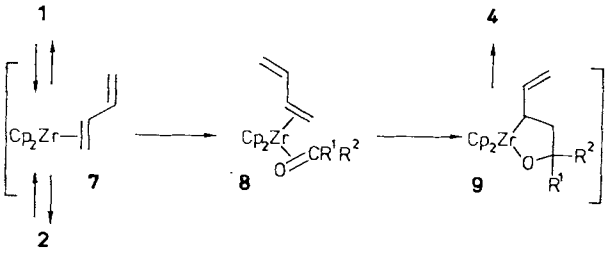



Fig. 1. Structure of **4a** in the crystal. Selected bond lengths [Å]: Zr–O 1.946(4), Zr–Cl 2.311(7), C1–C2 1.468(9), C2–C3 1.351(9), C3–C4 1.498(8); bond angles [°]: Zr–O–C5 150.5(4), O–Zr–Cl 91.9(2).

longer inert towards **3a**: on reaction with the mixture of the isomers **1** and **2**, **2** is consumed at a similar rate as **1**, with formation of **4a**.




These observations suggest that—analogous to the reaction of **1** ⇌ **2** with olefins[4]—**4** is formed from the intermediary product ($\eta^2$-butadiene)zirconocene **7**[9] *via* the intermediates **8** and **9**. Therefore, it appears that the selectivity control of the zirconocene-induced coupling of conjugated dienes with aldehydes and ketones may in some cases depend decisively on the formation and properties of intermediary ($\eta^2$-diene)metallocene complexes[10].


Received: February 2, 1983 [Z 265 IE]
German version: *Angew. Chem. 95* (1983) 506
The complete version of this communication appears in: *Angew. Chem. Suppl. 1983*, 675–690



[2] G. Erker, J. Wicher, K. Engel, F. Rosenfeldt, W. Dietrich, C. Krüger, *J. Am. Chem. Soc. 102* (1980) 6344; G. Erker, J. Wicher, K. Engel, C. Krüger, A.-P. Chiang, *Chem. Ber. 115* (1982) 3300, 3311.

[3] H. Yasuda, Y. Kajihara, K. Mashima, K. Nagasuna, A. Nakamura, *Chem. Lett. 1981*, 671.

[4] G. Erker, K. Engel, U. Dorf, J. L. Atwood, W. E. Hunter, *Angew. Chem. 94* (1982) 915, 916; *Angew. Chem. Int. Ed. Engl. 21* (1982) 913, 913; *Angew. Chem. Suppl. 1982*, 1974, 1984.

[9] U. Dorf, K. Engel, G. Erker, *Organometallics 2* (1983) 462.

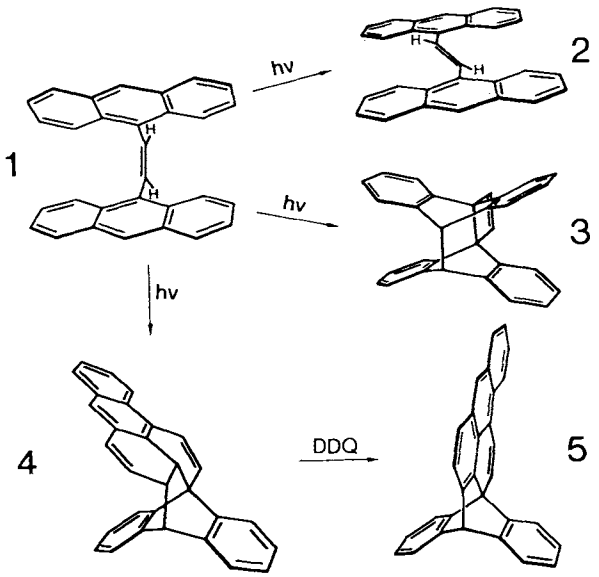
[10] A. Stockis, R. Hoffmann, *J. Am. Chem. Soc. 102* (1980) 2952; V. Skibbe, G. Erker, *J. Organomet. Chem. 241* (1983) 15.


## *cis*-1,2-Di(9-anthryl)ethylene: Photochemical Isomerization by Intramolecular Diels-Alder Reaction


By *Hans-Dieter Becker**, *Kjell Sandros*, and *Kjell Andersson*


*Dedicated to Professor Günther O. Schenck on the occasion of his 70th birthday*

As part of a study of the relationship between molecular geometry and excited state reactivity, we recently prepared *cis*-1,2-di(9-anthryl)ethylene **1** in order to compare its photochemical and photophysical properties with those of its *trans*-isomer **2**[1–3]. Attempts to induce photochemical *trans*→*cis* isomerization were not successful, but irradiation of **1** in cyclohexane ($\lambda > 300$ nm) produced the *trans*-isomer **2** in nearly quantitative yield, together with small amounts of the [4π+4π] cycloaddition product **3**[2]. At low conversion of **1**, however, equal quantum yields (0.0007) were estimated for both the geometrical isomerization to **2** and the cycloaddition to **3**.




We have now investigated the wavelength dependence of the photochemical isomerization of **1** and found a novel intramolecular cycloaddition in which the 1,2-bond of an anthracene π-system participates as a dienophile in a Diels-Alder reaction.

Irradiation of **1** (20 mg) in cyclohexane (900 mL) at 50 °C for 6 h under argon ($\lambda > 392$ nm) results in complete isomerization. After separation of the *trans*-isomer **2** (37% yield) **3** remains and, surprisingly, the novel dissymmetric photo-isomer **4** (50% yield, colorless crystals, m.p. *ca.* 180 °C, decomp.).

The high-resolution mass spectrum, the 270 MHz $^1$H-NMR spectrum, and the electronic absorption spectrum are consistent with the structure **4** (Fig. 3a). Evidence for this structure was also obtained by dehydrogenation with 2,3-dichloro-5,6-dicyanobenzoquinone (DDQ), which afforded the triptycene derivative **5** (yellow crystals, m.p. 293 °C). The structure of **5** is supported by its $^1$H-NMR spectrum and by its electronic absorption spectrum, which


[*] Dr. H.-D. Becker, Dr. K. Sandros, K. Andersson
Departments of Organic and Physical Chemistry
Chalmers University of Technology and University of Gothenburg
S-41296 Gothenburg (Sweden)

is typical of the planar 9-vinylanthracene chromophore [$\lambda_{max}$ ($\varepsilon \times 10^{-3}$): 440 (13), 414 (10.4), 391 (4.9), 371 (1.9), 314 sh (3.2), 271 (66)].

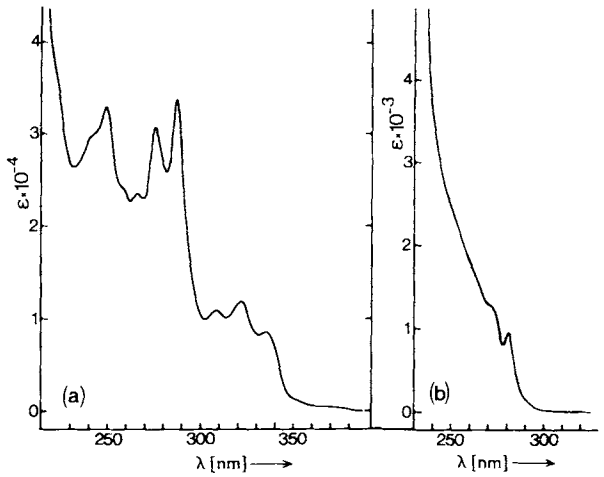



Fig. 3. Electronic absorption spectra of cycloaddition products **4** (a) and **3** (b) in cyclohexane.

Upon photo-excitation ($\lambda < 360$ nm) in cyclohexane, **4** undergoes smooth cycloreversion to give **1**: the quantum yield of this reaction is 0.20, exceeding that of the formation of **4** from **1** by a factor of 300. Hence, **4** can be obtained only when its photo-excitation is prevented by use of appropriate filters. The quantum yield for the photolytic cycloreversion of **3** → **1** is three times as high as that of the reaction **4** → **1**, but its UV spectrum (Fig. 3b) precludes photo-excitation when **1** is irradiated in Pyrex apparatus.

The low concentration of **1** employed in the experiment described above (20 mg in 900 mL cyclohexane) is of critical importance for the photochemical formation of **4**. Numerous attempts to obtain **4** by photochemical isomerization of higher concentrations of **1** in cyclohexane failed since the *trans*-isomer **2**, whose solubility at room temperature is only 2 mg/L, always precipitated soon after commencement of irradiation, and became the major product. Surprisingly, the efficiency of *cis-trans* isomerization surpasses that of the intramolecular cycloaddition **1** → **4** after precipitation of **2** has commenced. Absorption spectroscopy indicates that when most of the incident light is absorbed by crystalline **2** the photochemical formation of **4** from **1** virtually ceases, while the rate of conversion of **1** into **2** is enhanced. The use of other solvents in which **2** is more soluble than in cyclohexane is impaired by the fact that the quantum yield of *cis-trans* isomerization is solvent dependent[2]: specifically in cyclohexane solution can the intramolecular Diels-Alder reaction of **1** to afford **4** compete efficiently with the geometrical isomerization leading to **2**.

Received: February 3, 1983 [Z 266 IE]
German version: *Angew. Chem. 95* (1983) 507
The complete manuscript of this communication appears in:
*Angew. Chem. Suppl. 1983*, 609-619

[1] H.-D. Becker, *Pure Appl. Chem. 54* (1982) 1589.
[2] H.-D. Becker, L. Hansen, K. Andersson, *J. Org. Chem. 46* (1981) 5419.
[3] H.-D. Becker, K. Sandros, L. Hansen, *J. Org. Chem. 46* (1981) 821.

## $(PhC{\equiv}CLi)_4(tmhda)_2$, A Polymeric Organolithium Compound with Cubic $Li_4C_4$ Structural Units**

By *Bernd Schubert* and *Erwin Weiss**

For systematic investigations on the structure of organolithium compounds we prepared some phenylethynyllithium compounds containing additional diamine ligands: [(PhC≡CL)$_2$tmeda], [(PhC≡Li)tmpda]$_2$ **1** and [(PhC≡CLi)$_4$(tmhda)$_2$] **2** (tmeda = *N,N,N',N'*-tetramethylethylenediamine, $Me_2N(CH_2)_2NMe_2$; tmpda = *N,N,N',N'*-tetramethylpropanediamine, $Me_2N(CH_2)_3NMe_2$; tmhda = *N,N,N',N'*-tetramethylhexanediamine, $Me_2N(CH_2)_6NMe_2$).

The length of the diamine ligand obviously has a large influence on the composition and structure of these compounds. Thus, **1** is a dimer with two phenylethynyl bridges[1], isostructural to the phenyl compound (PhLi·tmeda)$_2$[2].

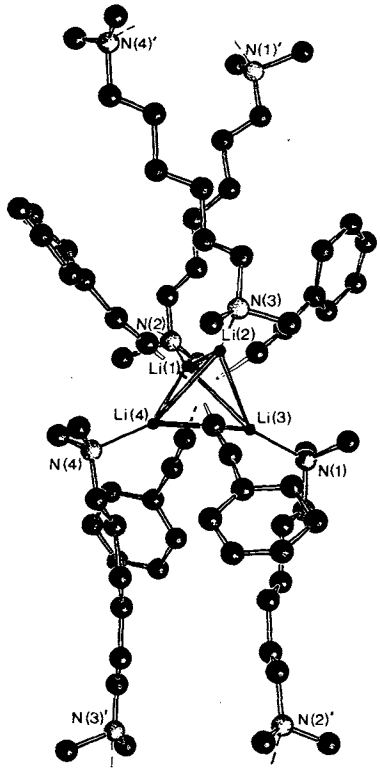



Fig. 1. SCHAKAL diagram of the structure of **2** in the crystal. Monoclinic, $P2_1/n$, $a = 1574.7(9)$, $b = 1563.9(9)$, $c = 2140.3(8)$ pm, $\beta = 102.87(4)°$, $\rho_r = 1.003$ g cm$^{-3}$, $Z = 4$; $Mo_{K\alpha}$-radiation, solution by direct methods (MULTAN 78), refinement (SHEL X) to $R = 0.092$ with 1515 reflections (anisotropic temperature factors, H not determined). Most important distances (pm, average values): Li–Li 272(2), Li–C 220(1), Li–N 211(2), C≡C 124(2) pm [6].

The longer chain diamine tmhda adds to PhC≡CLi with formation of the 1:2 compound **2**. Surprisingly, the X-ray structure analysis (Fig. 1) revealed that **2** contains a distorted cubic $Li_4C_4$-unit similarly as in $(CH_3Li)_4$ and $(CH_3Li)_4(tmeda)_2$ **3**[4]. Structurally analogous are the

[*] Prof. Dr. E. Weiss, Dr. B. Schubert
Institut für Anorganische und Angewandte Chemie
der Universität
Martin-Luther-King-Platz 6, D-2000 Hamburg 13 (Germany)

[**] Metal-Alkyl and -Aryl Compounds, Part 31. This work was supported by the Deutsche Forschungsgemeinschaft.—Part 30: [1].

$Li_4O_4$-units in Li-enolates[5]. Adjacent $(PhC{\equiv}CLi)_4$-units in **2** are each bound by pairs of tmhda ligands, giving rise to high polymer strands with helix-like structure. In **3**, tmeda links the $(CH_3Li)_4$-unit in a different way, with formation of a three-dimensional network structure.

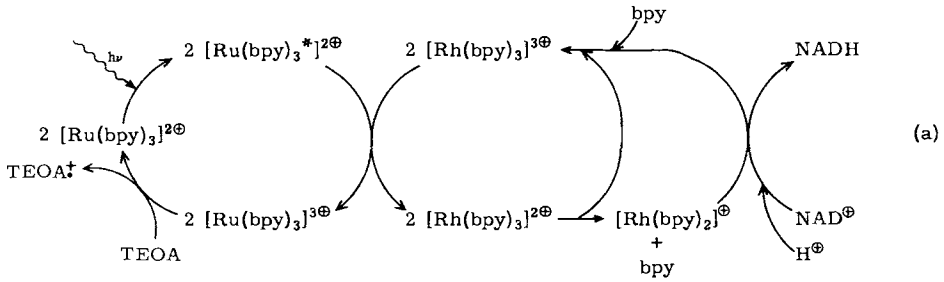
Received: February 1, 1983
revised: March 24, 1983 [Z 262 IE]
German version: *Angew. Chem. 95* (1983) 499
The complete manuscript of this communication appears in: *Angew. Chem. Suppl. 1983,* 703–709

[1] B. Schubert, E. Weiss, *Chem. Ber.*, in press.
[2] D. Thönnes, E. Weiss, *Chem. Ber. 111* (1978) 3157.
[4] H. Köster, D. Thönnes, E. Weiss, *J. Organomet. Chem. 160* (1978) 1.
[5] R. Amstutz, W. B. Schweizer, D. Seebach, J. W. Dunitz, *Helv. Chim. Acta 64* (1981) 2617.
[6] Further details of the crystal structure investigation can be obtained on request from the Fachinformationszentrum Energie Physik Mathematik, D-7514 Eggenstein-Leopoldshafen by quoting the number CSD 50359, the names of the authors, and complete citation of the journal.

## Selective Generation of NADH by Visible Light**

By *Rainer Wienkamp* and *Eberhard Steckhan**

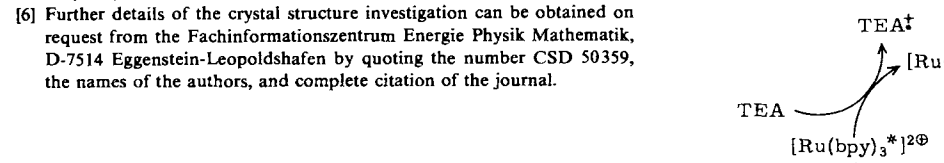
We recently reported on the reduction of $NAD^{\oplus}$ to NADH by the electrochemically generated two-electron transfer agent $[Rh(bpy)_2]^{\oplus}$[1]. In this way, the rhodium complex suppresses formation of enzyme-inactive dimers, which normally are formed in direct electrochemical reductions. We have now succeeded in preparing enzyme-active NADH from $NAD^{\oplus}$ using visible light in the presence of the photochemically generated bipyridinerhodium(I) complex. In this reaction tris(2,2′-bipyridine)ruthenium(II) functions as the sensitizer and 2,2′,2″-nitrilotriethanol (triethanolamine, TEOA) as an electron donor in the usual way[2] [eq. (a)]. The quantum yield for the photoproduct $[Rh(bpy)_2]^{\oplus}$ is 0.13[2b].




(a)

A 0.42 M aqueous solution of TEOA (80 mL) containing 200 μmol $[Rh(bpy)_3]_2(SO_4)_3$, 100 μmol $[Ru(bpy)_3]SO_4$, and 300 μmol $NAD^{\oplus}$ was adjusted to pH 9.7 with concentrated $H_2SO_4$; this mixture was then irradiated with a slide projector (300 W halogen lamp) and a circular 25 W fluorescent lamp without a lense system to focus the beam and in the absence of a filter. After 4 h 60 μmol, after 6.75 h 90 μmol, and after 24 h 230 μmol NADH formed (established after filtration over Dowex 50 WX4 by enzymatic reduction of cyclohexanone with horse liver alcohol dehydrogenase). At a detection limit of *ca.* 0.5 μmol NAD dimers could not be observed. In the absence of the relay compound $[Rh(bpy)_3]^{3\oplus}$ photoreduction of $NAD^{\oplus}$ to NADH did not occur. Aliphatic ketones were neither reduced by $[Ru(bpy)_3^*]^{2\oplus}$ nor by $[Rh(bpy)_2]^{\oplus}$. At higher concentrations of $NAD^{\oplus}$ conversion rates of 10 to 15 μmol/h were maintained, however, because of its photosensitivity NADH formation is reduced at irradiation times of longer than 24 h. In future experiments the UV irradiation ($\lambda < 400$ nm) must, therefore, be filtered out.

The recent proposal by *Kiwi*[3] to store solar energy by reducing $NAD^{\oplus}$ using the strong reducing agent $[Ru(bpy)_3]^{\oplus}$, formed from photochemically excited $[Ru(bpy)_3^*]^{2\oplus}$ and triethylamine (TEA) in $CH_3CN/H_2O$ (7 : 3) as electron donor leads, in contrast to the statements of the author, not to enzyme-active NADH but to NAD dimers [eq. (b)]. The alleged formation of NADH was studied exclusively by absorption spectroscopy at 340 nm ($\varepsilon_{NADH} = 6220\ M^{-1}\ cm^{-1}$). We have established that the NAD radicals, generated by one-electron reduction, react as described in the literature [4] practically exclusively to afford enzyme-inactive NAD dimers, which can be detected by thin-layer chromatography. No enzyme activity was observed in the presence of horse liver alcohol dehydrogenase with cyclohexanone as substrate. Since both NADH and the NAD dimer absorb at 340 nm ($\varepsilon_{NAD_2} = 6650\ M^{-1}\ cm^{-1}$), this method of detecting NADH is unsuitable. Because of the instability of the photoproduct $[Ru(bpy)_3]^{\oplus}$ under the reaction conditions, the bipyridineruthenium(II) complex used by *Kiwi* has only a moderate lifetime.




(b)

Since oxidation of TEOA leads to formation of aldehydes, our system is not yet suitable for the continuous internal regeneration of NADH in the presence of an alcohol dehydrogenase with a carbonyl compound as substrate. Use of other donors and the possibilities of electrochemical regeneration of the $Ru^{II}$ complex from the $Ru^{III}$ compound could improve the system.

Received: January 31, 1983 [Z 258 IE]
German version: *Angew. Chem. 95* (1982) 508

[*] Prof. Dr. E. Steckhan, R. Wienkamp
Institut für Organische Chemie und Biochemie der Universität
Gerhard-Domagk-Strasse 1, D-5300 Bonn 1 (Germany)

[**] This work was supported by the Deutsche Forschungsgemeinschaft, the Fonds der Chemischen Industrie, and BASF AG.

[1] R. Wienkamp, E. Steckhan, *Angew. Chem. 94* (1982) 786; *Angew. Chem. Int. Ed. Engl. 21* (1982) 782; *Angew. Chem. Suppl. 1982,* 1739.
[2] a) M. Kirch, J.-M. Lehn, J.-P. Sauvage, *Helv. Chim. Acta 62* (1979) 1345; b) S. F. Chan, M. Chou, C. Creutz, T. Matsubara, N. Sutin, *J. Am. Chem. Soc. 103* (1981) 369.
[3] J. Kiwi, *J. Photochem. 16* (1981) 193.
[4] C. O. Schmakel, K. S. V. Santhanam, P. J. Elving, *J. Am. Chem. Soc. 97* (1975) 5083; H. Jaegfeldt, *Bioelectrochem. Bioenerg. 8* (1981) 355.

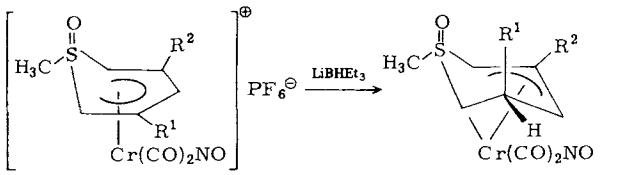
 © *Verlag Chemie GmbH, 6940 Weinheim, 1983* *0570-0833/83/0606-0497 $ 02.50/0* 

## Novel $\eta^3,\sigma$-Sulfur Double-Ylide Chromium Complexes by *endo*-Hydride Addition to Cationic ($\lambda^6$-Thiabenzene 1-Oxide)chromium Complexes**

By *Lothar Weber** and *Roland Boese*

The unsaturated hydrocarbon ligands of cationic transition-metal complexes have electrophilic character and add nucleophiles *via* kinetically controlled *exo*-addition[1].

In the reaction of the cations **1a—d** with $LiBHEt_3$ we observed the rare case of *endo*-addition of hydride to a $\pi$-bonded organic ligand[3]. As a result compounds **2**, having a novel double-ylidic ligand, are formed from the cationic ($\lambda^6$-thiabenzene 1-oxide)chromium complexes [(1-oxo-$\lambda^6$-thiin)chromium) complexes] **1**[7].




**1a-d** **2a-d**

| 1, 2 | a | b | c | d |
|---|---|---|---|---|
| $R^1$ | Ph | Me | Me | *t*Bu |
| $R^2$ | Ph | Ph | Me | Ph |

The *exo*-position of the 3-*tert*-butyl group in **2d**, determined by X-ray structure analysis (Fig. 1), establishes *endo*-addition of the hydride. In addition, the double-ylidic heterocycle is coordinated as a 4—6$\eta$,2$\sigma$ ligand to the $Cr(CO)_2(NO)$ fragment.

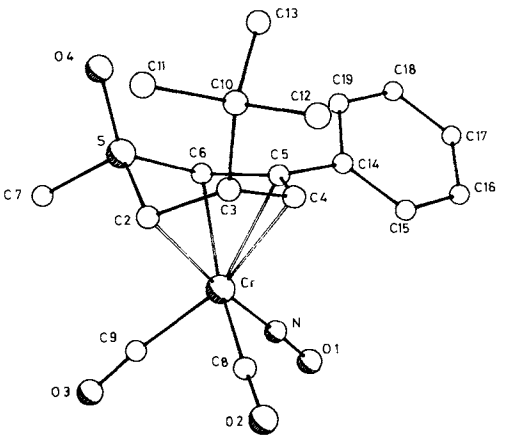
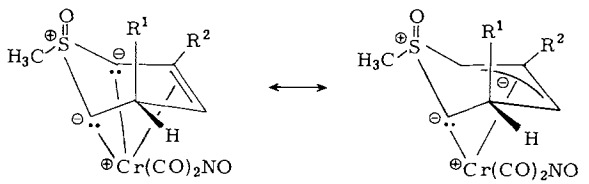



Fig. 1. Structure of the complex **2d** in the crystal [4]. Selected distances [pm] and angles [°]: Cr-S 283.9(1), Cr-C2 221.9(4), Cr-C4 224.7(4), Cr-C5 219.3(4), Cr-C6 217.1(4), S-O4 145.6(3), S-C2 171.0(4), S-C6 169.8(4), S-C7 177.9(4), C2-C3 152.2(5), C3-C4 150.3(5), C4-C5 138.2(5), C5-C6 145.6(5); C2-S-C6 95.0(2), S-C2-C3 114.9(3), C2-C3-C4 103.2(3), C3-C4-C5 123.8(3), C4-C5-C6 121.8(3), C5-C6-S 117.8(3).

The $\eta^3$-allyl moiety is considerably distorted, and hence the bond relationships can be reproduced best by the resonance structures **A** and **B**.




In contrast to phosphorus ylides, double-ylide ligands with sulfonium centers are rare. Compound **2d** is the first complex having such a ligand which has been characterized by X-ray structure analysis[9].

Received: February 7, 1983;
revised: March 28, 1983 [Z 270 IE]
German version: *Angew. Chem. 95* (1983) 510
The complete manuscript of this communication appears in: *Angew. Chem. Suppl. 1983*, 620–630

CAS Registry numbers:
**1a**, 76831-13-5, **1b**, 85762-74-9, **1c**, 85762-76-1, **1d**, 85762-78-3, **2a**, 85762-79-4, **2b**, 85762-80-7, **2c**, 85762-81-8, **2d**, 85781-10-8, *syn*-tricarbonyl(1,3-dimethyl-5-phenyl-$\lambda^6$-thiabenzene 1-oxide)chromium(0), 85762-82-9, *syn*-tricarbonyl(1,3,5-trimethyl-$\lambda^6$-thiabenzene 1-oxide)chromium(0), 85762-83-0, *syn*-(3-*tert*-butyl-1-methyl-5-phenyl-$\lambda^6$-thiabenzene 1-oxide)tricarbonylchromium(0), 85762-84-1.

[*] Priv.-Doz. Dr. L. Weber, Dr. R. Boese
Institut für Anorganische Chemie der Universität
Universitätsstrasse 5—7, D-4300 Essen 1 (Germany)

[**] Transition-Metal Sulfur Ylide Complexes, Part 19. This work was supported by the Deutsche Forschungsgemeinschaft and the Fonds der Chemischen Industrie.—Part 18: L. Weber, *Chem. Ber. 116* (1983) 2022.

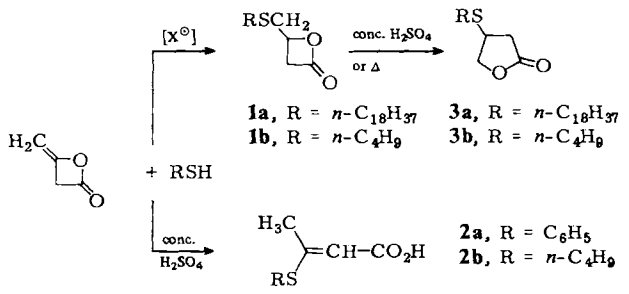
[1] S. G. Davies, M. L. H. Green, D. M. P. Mingos, *Tetrahedron 34* (1978) 3047; P. L. Pauson, *J. Organomet. Chem. 200* (1980) 207.
[3] *endo*-Addition of hydride has been reported in only one other case: A. J. Birch, I. D. Jenkins in H. Alper: *Transition Metal Organometallics in Organic Synthesis. Vol. 1*, p. 69, Academic Press, New York 1976.
[4] **2d**: Space group Pbcn; $a=903.0(1)$, $b=1763.3(2)$, $c=2406.6(4)$ pm, $V=3.832(1)\times10^9$ pm$^3$; $Z=8$, $R=0.048$. Further details can be obtained from the Fachinformationszentrum Energie Physik Mathematik, D-7514 Eggenstein-Leopoldshafen 2, by quoting the depository number CSD 50427, the names of the authors, and the journal citation.
[7] The term double-ylides signifies not only species which contain two carbanion functions on one onium center ($\bar{C}-\dot{E}-\bar{C}$), but also those having the combination of two onium carbanion moieties ($\bar{C}-\dot{E}\frown\bar{C}-\dot{E}$). This applies, by analogy, also for triple-ylides.
[9] The sulfur double-ylide ligands $[(CH_2)_2S(O)CH_3]^-$ and $[(CH_2)_2SCH_3]^-$ have been described: O. I. Kolodyazhnyi, *Zh. Obshch. Khim. 45* (1973) 704; H. Schmidbaur, W. Richter, *Z. Anorg. Allg. Chem. 429* (1977) 222; H. Schmidbaur, W. Kapp, *Chem. Ber. 105* (1972) 1203; P. Bravo, G. Fronza, G. Ticozzi, *J. Organomet. Chem. 118* (1976) C78; F. B. McCormick, J. A. Gladysz, *ibid. 218* (1981) C57.

## Addition of Alkanethiols to Diketene—a Correction

By *John G. Dingwall** and *Brian Tuck*

*Hertenstein*[1] has recently reported that the acid catalyzed addition of alkanethiols to diketene gives $\beta$-lactones **1**, in contrast to the previously reported formation of the crotonic acid derivative **2a** from the acid catalyzed addition of thiophenol to diketene[2]. The thermal stability and spectral data reported by *Hertenstein* are inconsistent with the literature values[3,4] for 4-(alkylthiomethyl)oxetan-2-ones **1** and with our own observations. The IR and the NMR data (Table 1) led us to believe that the products isolated were the thermally stable isomeric $\gamma$-lactones **3**, one of which, **3a**, was previously observed[3] as a product of the thermal decomposition of $\beta$-lactone **1a**.

[*] Dr. J. G. Dingwall, Dr. B. Tuck
Central Research Laboratories Ciba-Geigy (UK) Limited,
Tenax Road, Trafford Park, Manchester M17 1WT (England)



**1a**, R = *n*-$C_{18}H_{37}$ **3a**, R = *n*-$C_{18}H_{37}$
**1b**, R = *n*-$C_4H_9$ **3b**, R = *n*-$C_4H_9$

**2a**, R = $C_6H_5$
**2b**, R = *n*-$C_4H_9$

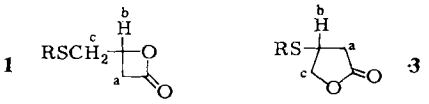
Table 1. Selected data for the β- and γ-lactones **1** and **3**, respectively.

| Comp. | B.p. [°C/torr] | IR [$cm^{-1}$] $\nu$(C=O) | $^1$H-NMR ($\delta$-values, $J$ [Hz]) a | b | c |
|---|---|---|---|---|---|
| **1a** [3] | dec. | 1820 | 3.24, 3.56 (AB, 2d of d, $J_{AB}=16.25$, $J_{AX}=5.5$, $J_{BX}=4.5$ Hz) | 4.64 m, X of ABXCD | 2.80, 3.00 (CD, 2d of d, $J_{CD}=14.0$, $J_{CX}=6.75$, $J_{DX}=5.5$ Hz) |
| **1b** | dec. | 1820 | 3.11, 3.45 (AB, 2d of d, $J_{AB}=16$, $J_{AX}=6$, $J_{BX}=5$ Hz) | 4.49 m, X of ABXCD | 2.64, 2.79 (CD, 2d of d, $J_{CD}=16.0$, $J_{CX}=6.0$, $J_{DX}=7.5$ Hz) |
| **3a** [3] | — | 1785 | 2.42, 2.87 (AB, 2d of d, $J_{AB}=18.5$, $J_{AX}=8.0$, $J_{BX}=7.5$ Hz) | 3.59 m, X of ABXCD | 4.10, 4.54 (CD, 2d of d, $J_{CD}=10.0$, $J_{CX}=7.0$, $J_{DX}=6.5$ Hz) |
| **3b** | 98–102°/0.01 | 1780 | 2.38, 2.92 (AB, 2d of d, $J_{A,B}=17.5$, $J_{AX}=7.5$, $J_{BX}=6.5$ Hz) | 3.70 m, X of ABXCD | 4.17, 4.57 (CD, 2d of d, $J_{CD}=9.0$, $J_{CX}=7.0$, $J_{DX}=5.5$ Hz) |
| [a] | 111–115°/0.06 | 1780 | 2.25–3.00 m (4H) | 3.55 m | 4.25, 4.26 ($J_{AB}=12.3$ Hz) |

[a] Compound **3a** from [1], considered there to be a β-lactone (≡ **1b**). According to the data presented here, however, it is identical to the γ-lactone **3b**.

We have reinvestigated the reaction of butanethiol with diketene under the conditions outlined by *Hertenstein*[1], and have found that the product can be either γ-lactone **3b** or the crotonic acid derivative **2b**.

Addition of butanethiol to a solution of diketene in ether at 0–5 °C generally resulted in a spontaneous, mildly exothermic radical reaction giving β-lactone **1b** in high yield. The structure of the β-lactone was confirmed by its IR and NMR (Table 1) spectra. Attempted distillation of **1b** resulted in its rapid decomposition at 80–90 °C to give a mixture containing γ-lactone **3b** (12% isolated yield). Similarly, treatment of a solution of **1b** in ether with concentrated sulphuric acid at 0–5 °C gave a mixture from which the γ-lactone **3b** was obtained in 19% yield.



The spectral data in Table 1 for **1** and **3** exhibit features characteristic of β-lactones [$\nu$(C=O), 1820 $cm^{-1}$, $\delta(H_b)$ *ca.* 4.5] and of γ-lactones [$\nu$(C=O), 1780 $cm^{-1}$, $\delta(H_b)$ *ca.* 3.6], respectively. The thermal stability and spectral data of *Hertenstein*'s lactones are clearly more consistent with the γ-lactone structure, suggesting that he isolated further reaction products of initially formed β-lactones (radical products).

When the radical reaction was suppressed by an inhibitor (*tert*-butylcatechol), addition of concentrated sulphuric acid to a mixture of butanethiol and diketone gave the crotonic acid derivative **2b**[5], analogous to the product **2a** obtained from thiophenol and diketene. The IR spectrum of the crude reaction mixture revealed that neither β- nor γ-lactones were formed.

Received: August 11, 1980 [Z 419 IE]
German version: *Angew. Chem. 95* (1983) 504

[1] U. Hertenstein, *Angew. Chem. 92* (1980) 123; *Angew. Chem. Int. Ed. Engl. 19* (1980) 127.
[2] N. F. Yaggi, K. T. Douglas, *J. Chem. Soc. Chem. Commun. 1977*, 609.
[3] G. A. Hull, F. A. Daniher, T. F. Conway, *J. Org. Chem. 37* (1972) 1837.
[4] C. W. Theobald, US-Pat. 2675392 (1954), Du Pont.
[5] Diketene (21.0 g, 0.25 mol) is added to a cooled (0–5 °C) solution of butanethiol (22.5 g, 0.25 mol) and *tert*-butylcatechol (0.25 g) in ether (100 mL). Concentrated $H_2SO_4$ (25.0 g) is then added dropwise with stirring. On warming to room temperature, an exothermic reaction occurs and the mixture is left for a further 2 h at room temperature. The ether solution is washed with water, dried ($MgSO_4$), and the product distilled or crystallized from petroleum ether to give 3-butylthiocrotonic acid **2b** (30%), m.p. 78–80 °C; IR (Nujol): $\nu$(C=O) = 1645 $cm^{-1}$, $\nu$(C=C) = 1565 $cm^{-1}$; $^1$H-NMR ($CDCl_3$): $\delta$ = 0.95 (m, 3H), 1.56 (m, 4H), 2.82 (m, 2H), 2.41 (d, $J$ = 1 Hz, 3H, $CH_3-C=$), 5.52 (d, $J$ = 1 Hz, 1H, $-CH=$), 12.25 (s, 1H, $CO_2H$).

## 2D-NMR Spectroscopy in Annulene Chemistry: Complete Assignment of the $^{13}$C-NMR Spectrum of 9,11-Bisdehydrobenzo[18]annulene by $^1$H,$^{13}$C Shift Correlation

By *Peter Schmitt* and *Harald Günther**

*In memoriam Franz Sondheimer*

The unambiguous assignment of $^{13}$C resonances in the $^{13}$C-NMR spectra of annulenes and their ions is of vital importance for the study of bonding and charge density. However, most of the traditional assignment techniques[1] fail, since the various methine fragments have insufficiently different spin-spin coupling constants and relaxation times. Selective $^1$H-decoupling is time consuming and, in view of the signal overlap that usually exists, of limited value, especially at lower magnetic field strengths.

Here it is shown that two-dimensional (2D)-$^1$H,$^{13}$C shift correlation[2] is the method of choice to solve this problem, since the $^1$H assignment, which can be derived very often in a straightforward manner from ring current effects and $^1$H,$^1$H coupling constants, may be transferred in only one experiment to the $^{13}$C-NMR spectrum, thus identifying each $^1$H,$^{13}$C pair. The basis of this method is magnetization transfer due to heteroscalar $^{13}$C,$^1$H spin-spin coupling through one bond.

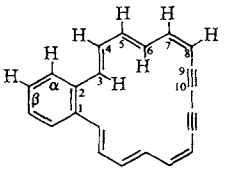


Figure 1a shows the 1D-$^{13}$C-NMR spectrum of 9,11-bisdehydrobenzo[18]annulene **1**[3] with the chemical shift as-

[*] Prof. Dr. H. Günther, P. Schmitt
FB 8, Organische Chemie II, Universität–Gesamthochschule
Postfach 210209, D-5900 Siegen 21 (Germany)

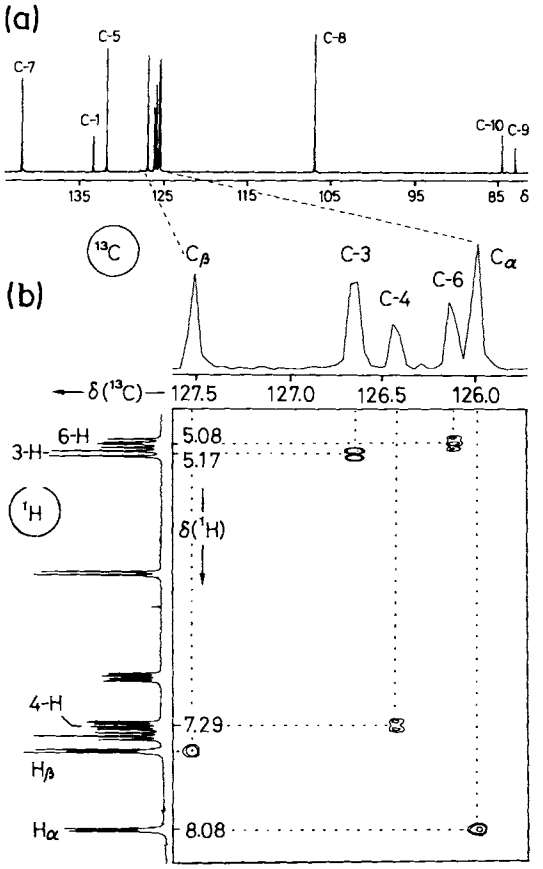



Fig. 1. a) 100.6 MHz $^{13}$C-NMR spectrum of 9,11-bisdehydrobenzo[18]annulene (0.1 M in $CDCl_3$) at 40 °C with $^{1}$H broadband decoupling (sweep width 16 kHz, 64 K data points, acquisition time 2 s, relaxation delay 4 s, 8504 transients, total acquisition time 14 h); b) section of the heteroscalar $^{1}$H,$^{13}$C correlated 2D spectrum (contour diagram) with the 400 MHz $^{1}$H-NMR 1D spectrum [3b] as ordinate and the projection of the 2D-$^{13}$C-NMR spectrum onto the abscissa; pulse sequence after [2] with $^{1}$H phase cycles [4] and a mixing time of 3 ms ($\approx 1/2\,{}^{1}J(^{13}C,^{1}H)$); data matrix format 128 × 2048, 128 accumulations, acquisition time 0.26 s, relaxation delay 3.6 s, sweep widths 4 kHz ($^{13}$C) and 1400 Hz ($^{1}$H), total time of measurement 17.8 h.

signment derived from the 2D correlation experiment. The power of the 2D technique is convincingly demonstrated by considering a section of the $\delta(^{1}H)/\delta(^{13}C)$ correlation diagram covering the $^{13}$C resonances between 126 and 128 ppm that amply illustrates the direct $^{1}$H,$^{13}$C assignment transfer. The assignment of the quarternary carbons C-1, C-9, and C-10 was made from the conventional $^{1}$H-coupled spectrum, which yields a singlet for C-1 and, due to geminal and vicinal $^{13}$C,$^{1}$H coupling, a doublet of doublets for C-9 (X part of an ABX system), together with a doublet ($^{3}J = 14.4$ Hz) for C-10. This spectrum also provided all the $^{1}J(^{13}C,^{1}H)$ data. The results are collected in Table 1.

Table 1. $^{13}$C resonances ($\delta_{TMS}$ values) and $^{1}J(^{13}C,^{1}H)$ coupling constants [Hz] for **1**.

| | $C_\alpha$ | $C_\beta$ | C-1 | C-3 | C-4 | C-5 |
|---|---|---|---|---|---|---|
| $\delta(^{13}C)$ | 125.98 | 127.52 | 134.20 | 126.71 | 126.46 | 132.56 |
| $^{1}J(^{13}C,^{1}H)$ | 151 | 160.5 | — | 149.9 | 152.6 | 153.8 |
| | C-6 | C-7 | C-8 | C-9 | C-10 | |
| $\delta(^{13}C)$ | 126.13 | 142.97 | 107.12 | 82.56 | 84.16 | |
| $^{1}J(^{13}C,^{1}H)$ | 151.6 | 158.3 | 169.0 | — | — | |

Received: February 7, 1983 [Z 269 IE]
German version: *Angew. Chem. 95* (1983) 509

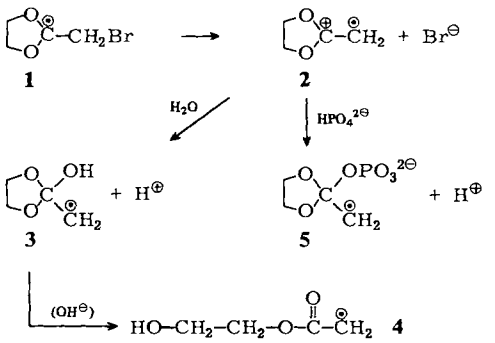
[1] F. W. Wehrli, T. Wirthlin: *Interpretation of Carbon-13 NMR Spectra*, Heyden, London 1976.
[2] a) A. A. Maudsley, L. Müller, R. R. Ernst, *J. Magn. Reson. 28* (1977) 463; b) G. Bodenhausen, R. Freeman, *ibid. 28* (1977) 471; c) G. Bodenhausen, R. Freeman, *J. Am. Chem. Soc. 100* (1978) 320; d) for a review see R. Benn, H. Günther, *Angew. Chem. 95* (1983) 381; *Angew. Chem. Int. Ed. Engl. 22* (1983) 350.
[3] a) N. Darby, T. N. Cresp, F. Sondheimer, *J. Org. Chem. 42* (1977) 1960; b) H. Günther, M.-E. Günther, D. Mondeshka, H. Schmickler, F. Sondheimer, N. Darby, T. M. Cresp, *Chem. Ber. 112* (1979) 71.
[4] A. Bax, G. A. Morris, *J. Magn. Reson. 42* (1981) 501.

## 1,1-Dialkoxytrimethylene Radical Cations

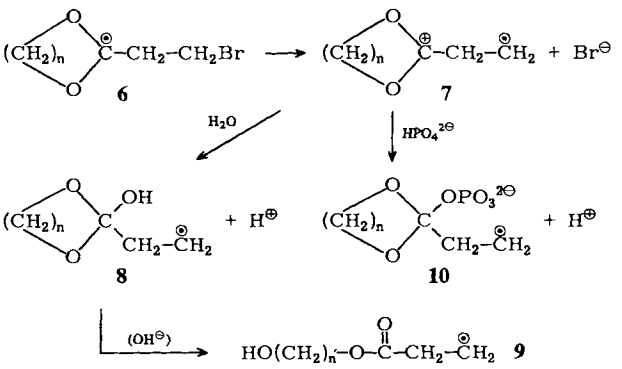
By *Günther Koltzenburg, Günther Behrens,* and *Dietrich Schulte-Frohlinde**

*Dedicated to Professor Günther O. Schenck on the occasion of his 70th birthday*

In aqueous solution the radical **1** dissociates very rapidly into $Br^{\ominus}$ and the 1,1-dialkoxyethylene radical cation **2**, which can be detected by ESR spectroscopy and which reacts with $H_2O$, $OH^{\ominus}$, and $HPO_4^{2\ominus}$ to afford the radicals **3**, **4**, and **5**, respectively[1].




We have now found that radical **6a**, which is homologous to **1**, surprisingly decomposes under similar conditions to give the radicals **8a–10a** (Table 1), which are homologues of **3–5**. The 1,1-dialkoxytrimethylene radical cation **7a** is assumed to be an intermediate. The ring-homologous radical **6b** behaves analogously.




**6a–10a**, n = 2; **6b–10b**, n = 3

[*] Prof. Dr. D. Schulte-Frohlinde, Dr. G. K. Koltzenburg, Dr. G. Behrens
Max-Planck-Institut für Strahlenchemie
Stiftstrasse 34–36, D-4330 Mülheim a. d. Ruhr 1 (Germany)

 © Verlag Chemie GmbH, 6940 Weinheim, 1983 0570-0833/83/0606-0500 $ 02.50/0 

Table 1. ESR spectroscopic results on aqueous solutions of 2-(2-bromoethyl)-1,3-dioxolane and -1,3-dioxane, $10^{-2}$ M, 3 °C, H-abstraction by $SO_4^{\ominus}$ radical anions (generated from $S_2O_8^{2-}$ in a photolytic flow system [1]). Borate ($10^{-2}$ M) was used as a buffer at pH 9 and 10.

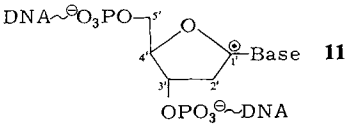
| Additional Conditions | Precursor Radicals | Observed Radicals [a] | Hyperfine Splittings [mT] 2H(α) | 2H(β) |
|---|---|---|---|---|
| pH 4.5 | **6a** | **8a** [b] | 2.23 | 2.58 |
| | **6b** | **8b** | 2.23 | 2.59 |
| pH 10 | **6a** | **9a** | 2.23 | 2.72 |
| | **6b** | **9b** | 2.23 | 2.73 |
| pH 9 | **6** | [9] > [8] [c] | | |
| pH 10 and $10^{-2}$ M $HPO_4^{2-}$ | **6a** | [10] ≈ [9] [c] | 2.22 | 2.64 (**10a**) |
| | **6b** | | 2.22 | 2.63 (**10b**) |
| pH 10 and $10^{-1}$ M $HPO_4^{2-}$ | **6** | [10] ≫ [9] [c] | | |

[a] Additionally, small signals were observed from radicals formed by H abstraction from ring positions. [b] $g = 2.0026$. [c] **8**, **9**, and **10**: steady-state concentrations of the species **8a**, **b**, **9a**, **b**, and **10a**, **b**, respectively.

$H^{\oplus}$ and $Br^{\ominus}$ were determined acidimetrically and argentometrically, respectively. For both radicals **6a** and **6b**, generated by pulse radiolysis, a half-life of $(6 \pm 1) \times 10^{-6}$ s at 20 °C was determined by measurement of the conductivity changes (for method see [1]). This half-life is assigned to the formation of **7** from **6**, which is followed by a more rapid reaction with water to yield **8** and $H^{\oplus}$. In alkaline solution a ring opening reaction (**8** → **9** ensues (Table 1).

In the presence of phosphate a competing reaction (**7** → **10**) occurs; at pH 10 and $10^{-2}M$ phosphate both the radicals **9** and **10** are formed in equal concentration (Table 1); hence, the reactions (**7** → **8**) and (**7** → **10**) have approximately the same rate. Thus, $k(HPO_4^{2\ominus}) \cdot [HPO_4^{2\ominus}] = k(H_2O)$. Assuming that the reaction with phosphate is diffusion controlled [$k(HPO_4^{2\ominus}) \approx 5 \times 10^9\ M^{-1}\ s^{-1}$] a half-life of the order of $10^{-8}$ s is obtained, which we assign to the lifetime of the trimethylene radical cations **7** in water. Cations of the type $ArylC^{\oplus}(CH_3)OCH_3$ have lifetimes of this order of magnitude in water[2]; the cations $(CH_3O)_3C^{\oplus}$ and $ArylC^{\oplus}(OCH_2)_2$ are longer lived[3].

Loss of a halogen anion at C-3 of an alkyl radical with the unpaired electron at C-1 has not been described previously. It remains an open question whether the loss of $Br^{\ominus}$ is preceded by a 3,1-migration[4] of bromine. Formation of the ions $Br^{\ominus}$ and **7** in water is made possible by solvation. Deprotonation of the radical cations to form alkyl radicals was not observed.




**11**

The loss of $Br^{\ominus}$ from **6** is considered to be a further model reaction for radical-induced strand breaks of DNA in water[5]; thus, possibly also DNA-1'-radicals **11** might undergo strand breaks by the loss of a phosphate group from the 3'-position (or in further analogy from the 5'-position).

Received: Februar 22, 1983;
revised: April 15, 1983 [Z 281 IE]
German version: *Angew. Chem. 95* (1983) 511

[1] $\tau_{1/2}(\mathbf{1}) \leq 4 \times 10^{-8}$ s, since **1** is not trapped by $O_2$; $\tau_{1/2}(\mathbf{2}) = 10^{-4}$ s in $H_2O$: G. Behrens, E. Bothe, G. Koltzenburg, D. Schulte-Frohlinde, *J. Chem. Soc. Perkin Trans. II 1980*, 883; *ibid. 1981*, 143. In this study only the dissociation of the radicals with $Cl^{\ominus}$ as leaving group was performed; radicals with $Br^{\ominus}$ (**1**) or $F^{\ominus}$ as leaving group also behave in this way.

[2] P. R. Young, W. P. Jencks, *J. Am. Chem. Soc. 99* (1977) 8238; lifetimes determined by scavenging reactions.

[3] R. A. McClelland, M. Ahmad, *J. Am. Chem. Soc. 100* (1978) 7031; extrapolated lifetimes from stopped-flow experiments in strongly acidic solutions.

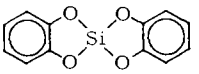
[4] The 1,3-migration of a CN group in a radical has recently been described: A. Bury, P. Bougeard, S. J. Corker, M. D. Johnson, M. Perlmann, *J. Chem. Soc. Perkin Trans. II 1982*, 1367.

[5] Model reactions for strand breaks of DNA-4'-radicals: G. Behrens, G. Koltzenburg, D. Schulte-Frohlinde, *Z. Naturforsch. C37* (1982) 1205.

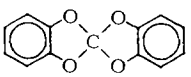
## The Crystal and Molecular Structure of Bis(1,8-naphthalenedioxy)silane—A Contribution to the Controversy over Planar, Four-Coordinated Silicon in Orthosilicic Acid Esters**

By *W. Bibber, C. L. Barnes, D. van der Helm,* and *Jerold J. Zuckerman**

A controversy has developed in this journal concerning the structure of bis(*o*-phenylenedioxy)silane **1**, which was synthesized directly from elemental silicon by one of us twenty years ago[1].




**1**




**2**

The glassy, probably polymeric product has recently been crystallized with difficulty and shown to have a space group ($P2_1/c$), which is different from that of its orthocarbonic acid ester analogue **2** (Pccn). The latter contains the expected tetrahedral *spiro*-C atom (∢O-C-O 108.3—111.7°), but the structure of **1** could not be determined because the crystals were not stable enough. However, it was claimed that the two Si atoms in the unit cell (assuming the space group assignment is correct) must sit on centers of symmetry requiring that the $SiO_4$ system be planar[2]. This conclusion is supported by theoretical arguments which predict only a small energy difference between tetrahedral and planar silicon[2,3]. It has been claimed that the π-system of pyrocatechol should facilitate the planarization[2].

These claims have been challenged on the basis that if **1** were to have a P2/c space group, this would not require planar silicon; that possible disorder in the crystal would preclude assignment of molecular symmetry from the space group; and that it was the hydrolysis product, pyrocatechol, which has similar unit cell dimensions, that was actually examined[4]. Counter-arguments are also available[5].

We report here the structure of bis(1,8-naphthalenedioxy)silane **3** (Fig. 1).

The angles at the spiro-Si atom of **3** are tetrahedral [mean ∢O-Si-O 109.48(6)°; range 106.90(6)—111.61(6)°]. There are no short intermolecular contacts to suggest

[*] Prof. J. J. Zuckerman, Dr. J. W. Bibber, Dr. C. L. Barnes, Prof. D. van der Helm
Department of Chemistry, University of Oklahoma
Norman, OK 73019 (USA)

[**] Our work was supported by the U. S. Office of Naval Research, by the U. S. National Science Foundation (Grant CHE-78-26548, J. J. Z.), and by the U. S. National Cancer Institute (Grant CA-17562, D. v. d. H.). We thank the University of Oklahoma for providing computer time.

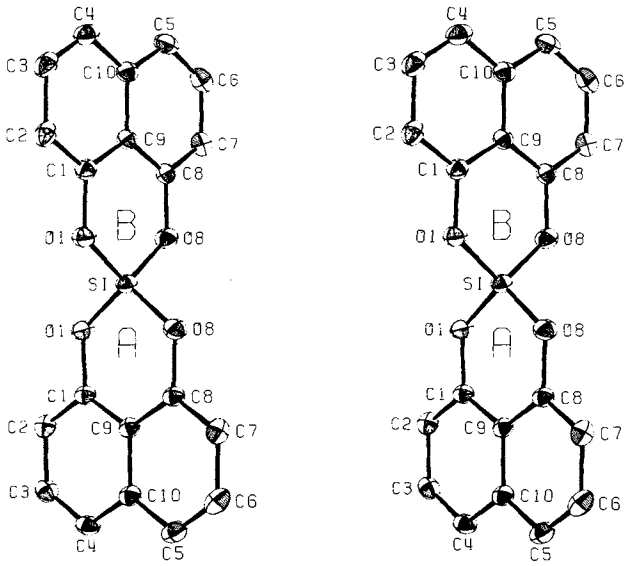



Fig. 1. Stereoview of the structure of the orthosilicic acid ester **3** in the crystal.

transformation to an octahedral geometry at silicon by interaction with donor orbitals of the oxygen atoms of neighboring molecules. The 1,8-dioxy system is held planar by the naphthalene group to give the six-membered ring homologue of **1**. The intramolecular distances in **3** are O1–O8 2.601(2) Å (mean) [2.250 Å in **2**[2]], O(1A)–O(1B) 2.676(2) Å, and O(8A)–O(8B) 2.646(2) Å [in **2**: 2.285 Å[2]], O(1A)–O(8B) and O(1B)–O(8A) 2.655(2) and 2.668(2) Å, respectively.

Thus definitive evidence for a planar, four-coordinated silicon atom remains elusive[8].

Received: November 5, 1982 [Z 195 IE]
German version: *Angew. Chem. 95* (1983) 498
The complete version of this communication appears in:
*Angew. Chem. Suppl. 1983*, 668–674

[1] J. J. Zuckerman, *J. Chem. Soc. 1962*, 837.
[2] H. Meyer, G. Nagorsen, *Angew. Chem. 91* (1979) 587; *Angew. Chem. Int. Ed. Engl. 18* (1979) 551.
[3] E. U. Würthwein, P. V. R. Schleyer, *Angew. Chem. 91* (1979) 588; *Angew. Chem. Int. Ed. Engl. 18* (1979) 553.
[4] J. D. Dunitz, *Angew. Chem. 92* (1980) 1070; *Angew. Chem. Int. Ed. Engl. 19* (1980) 1034.
[5] G. Nagorsen, H. Meyer, *Angew. Chem. 92* (1980) 1970; *Angew. Chem. Int. Ed. Engl. 19* (1980) 1034.
[8] The recently reported crystal structure of bis(tetramethylethylenedioxy)silane is similarly disappointing (mean ∢O-Si-O 106.9°; range 98.3–116.3°) [9].
[9] D. Schomberg, *Angew. Chem. 95* (1983) 52; *Angew. Chem. Int. Ed. Engl. 22* (1983) 65.

## Aerial Oxidation of Benzene in the Presence of Electrochemically Generated $Cu^+$ Ions

By *Tatsuyuki Kinoshita, Junji Harada, Sotaro Ito,* and *Kazuo Sasaki**

Recently, the oxidation of aromatic compounds using Fenton's reagent has attracted growing interest[1,2,4–6]. *Walling et al.*[2] and *Steckhan et al.*[3] reported that phenol can be produced continuously by means of electrolytic regeneration of $Fe^{2+}$ ions. In these studies is was noted that the presence of $Cu^{2+}$ ions improves the efficiency of Fenton's reagent. Recently, we showed[8] that in the presence of $Cu^+$ ions $O_2$ oxidizes benzene very efficiently; the presence of $H_2O_2$ is not necessary. Here we wish to report that the reaction can be operated continuously when the active species, $Cu^+$ ions, are regenerated electrochemically.

A small H-shaped glass cell having a sintered glass separator was used as the reaction vessel. The cathode (working electrode) material was a graphite rod (surface area 9.3 $cm^2$). The cathode potential was adjusted with a potentiostat to 0.1 V (*vs.* SCE). At this potential, $Cu^{2+}$ ions are selectively reduced to $Cu^+$: in order to stabilize the $Cu^+$ ions, a solvent consisting of 0.1 N $H_2SO_4$ and acetonitrile (9 : 1 (v/v)) was used. Benzene (1 mL) was added to the catholyte (16 mL) and air was bubbled in at controlled rates. The average current varied from 30–100 mA, depending on the $CuSO_4$ concentration. The reaction products were analyzed by HPLC.

The major product was phenol; hydroquinone and catechol were also formed together with a few unidentified compounds; biphenyl could not be detected. The ratio phenol : hydroquinone varied depending on the concentration of $CuSO_4$ (Table 1). The coulombic efficiency (mol product per *F*) is *ca.* 10% at 10 mmol/L $CuSO_4$ and 6 – 7% at 100 mmol/L $CuSO_4$.

Table 1. Yield of phenol and hydroquinone (HQ) together with coulombic efficiency (in parenthesis) as a function of the $Cu^{2+}$ concentration and air flow rate.

| $Cu^{2+}$ [mmol/L] | Air [mL/min] | Phenol [mmol/L] | HQ [mmol/L] |
|---|---|---|---|
| 10 | 7 | 5.13 (9.9) | 2.05 (4.0) |
| 20 | 7 | 5.07 (9.8) | 2.11 (4.1) |
| 50 | 7 | 4.82 (9.3) | 1.03 (2.0) |
| 50 | 21 | 4.52 (8.7) | 1.36 (2.6) |
| 100 | 7 | 4.57 (8.8) | 0.66 (1.3) |
| 100 | 21 | 2.34 (4.5) | 0.38 (0.7) |
| 200 | 7 | 3.19 (6.1) | 0.21 (0.4) |
| 500 | 7 | 0.68 (1.3) | 0 |
| 500 | 21 | 0.90 (1.7) | 0 |

The reaction is highly pH-dependent, and pH control during the electrolysis is necessary. When the glass frit separator was replaced by a cation exchange membrane and a hydrogen electrode employed as counter electrode, the operational characteristics were much improved. Under these conditions, the coulombic efficiency remained constant at 8% throughout the entire electrolysis, in the course of which 500 mAh was passed.

Received: December 30, 1982;
revised: April 5, 1983 [Z 237 IE]
German version: *Angew. Chem. 95* (1983) 504
The complete version of this communication appears in:
*Angew. Chem. Suppl. 1983*, 599–608

[*] Prof. Dr. K. Sasaki, T. Kinoshita, J. Harada, Assoc. Prof. Dr. S. Ito
Department of Applied Chemistry, Faculty of Engineering
Hiroshima University
Higashi-Hiroshima-shi 724 (Japan)

[1] C. Walling, *Acc. Chem. Res. 8* (1975) 125.
[2] C. Walling, R. A. Johnson, *J. Am. Chem. Soc. 97* (1975) 363.
[4] J. Wellmann, E. Steckhan, *Chem. Ber. 110* (1977) 3561.
[5] T. Matsue, M. Fujihira, T. Osa, *J. Electrochem. Soc. 128* (1981) 2565.
[6] M. Fujihira, Y. Sato, T. Osa, *Bull. Chem. Soc. Jpn. 55* (1982) 665.
[8] K. Sasaki, S. Ito, Y. Saheki, T. Kinoshita, T. Yamasaki, J. Harada, *Chem. Lett. 1983*, 37.

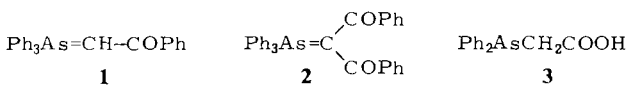
## Novel Nickel-Oligomerization Catalysts with Arsenic-Oxygen Chelate Ligands**

By *Wilhelm Keim**, *Arno Behr*, *Brigitte Limbäcker*, and *Carl Krüger*

Chelate ligands have an unusual controlling effect on nickel catalyzed oligomerization and polymerization of ethylene[1,2]. In this communication arsenic-containing chelate ligands are presented for the first time as oligomerization-catalysts.

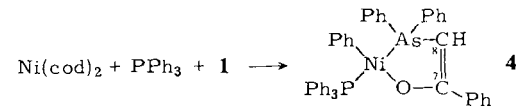
Reaction of benzoylmethylenetriphenyl-$\lambda^5$-arsane **1** with bis(1,5-cyclooctadiene)nickel [Ni(cod)$_2$] in toluene yields an in-situ catalyst which oligomerizes ethylene under mild conditions ($T$=40 °C, $p$=15 bar). Almost exclusively linear olefins (>95%) are formed at conversions of up to 70%; the proportion of α-products exceeds 70%. Activities of 1600 mol ethylene per mol nickel and per hour are achieved.

If the methine proton in **1** is replaced by a further electrophilic benzoyl group one obtains dibenzoylmethylenetriphenyl-$\lambda^5$-arsane **2**. Reaction of Ni(cod)$_2$, **2** and triphenylarsane in the molar ratio 1 : 1 : 1 yields a catalyst system which oligomerizes ethylene with conversions of up to 99.9%. This increase in conversion is due to the strong resonance stabilization in the ylide **2** compared to in **1**. However, the linearty of the products obtained with **2** is only 60 to 80%. The arsenic-containing chelate ligands **1** and **2** show a higher ionic interaction between ligand and central atom than the analogous phosphorus compounds. This difference, however, is counter-balanced by an increased π-portion in the chelate ligand, *e.g.* by incorporation of a further benzoyl group (**2**).




Unusual is the behavior of the chelate ligand diphenylarsinoacetic acid **3**. Diphenylphosphinoacetic acid leads to good ethylene conversions and almost 100% linearity and 99% α-fraction[3], whereas with **3** only butenes and hexenes are obtained with a conversion below 1%. This difference can be explained in terms of the size of the chelate ring. Diphenylphosphinoacetic acid reacts with nickel to give a five-membered ring chelate[3]; diphenylphosphinopropionic acid (with an additional $CH_2$-group) can form only a six-membered ring chelate. Surprisingly, this complex is completely inactive. In the ligand **3** the arsenic atom, which is larger than the phosphorus atom, can now likewise lead to an expansion of the five-membered ring and thus to lower catalyst activity.

The isolation of a catalytically active complex was possible in the case of the ligand **1**. In the stoichiometric reaction of Ni(cod)$_2$, **1** and triphenylphosphane in toluene at room temperature (12 h), the complex **4** could be isolated (yellow-brown crystals, m.p. 165 °C, yield 52%). The spectroscopic data and crystal structure analysis[4,5] show that the arsenic ylide complex **4** is constructed analogously to the phosphorus ylide complex[1]. The ylide ligand in **4** is also planar (C7: −0.017 Å, C8: 0.015 Å). Other than in the case of the phosphorus ylide complex[1], however, the nickel atom tends to deviate from planarity in the direction towards tetrahedral coordination. Furthermore, a marked shortening of the Ni–P distance *trans* to the arsenic (2.208(1) Å) compared to 2.230 in the phosphorus ylide complex is observable[5].




Received: January 26, 1983;
revised: March 24, 1983 [Z 252 IE]
German version: *Angew. Chem. 95* (1983) 505
The complete version of this communication appears in:
*Angew. Chem. Suppl. 1983*, 655–660

CAS Registry numbers:
**1**, 20691-73-0; **2**, 85735-23-5; **3**, 41006-47-7; **4**, 85735-24-6; Ni(cod)$_2$, 57776-90-6; $PPh_3$, 603-35-0; $AsPh_3$, 603-32-7; ethylene, 74-85-1.

[1] W. Keim, F. H. Kowaldt, R. Goddard, C. Krüger, *Angew. Chem. 90* (1978) 493; *Angew. Chem. Int. Ed. Engl. 17* (1978) 466.
[2] W. Keim, R. Appel, A. Storeck, C. Krüger, R. Goddard, *Angew. Chem. 93* (1981) 91; *Angew. Chem. Int. Ed. Engl. 20* (1981) 116.
[3] W. Keim, M. Peuckert, *Organometallics*, in press.
[4] $a$=9.6262(6), $b$=35.065(1), $c$=11.0344(3) Å, $\beta$=98.6673(3)°, $V$=3682.03 Å$^3$, $d_c$=1.344 g cm$^{-3}$, $\mu$=24.077, $Z$=4; space group $P2_1/a$; total number of reflections: 7530, observed reflections: 5855, refined parameters: 433, $R$=0.0384, $R_w$=0.0502.
[5] Further details of the crystal structure investigation can be obtained on request from the Fachinformationszentrum Energie Physik Mathematik by quoting the depository number CSD 50345, the authors names, and complete citation of the journal.

[*] Prof. Dr. W. Keim, Dr. A. Behr, Dr. B. Limbäcker
Institut für Technische Chemie und Petrolchemie der Technischen Hochschule
Worringer Weg 1, D-5100 Aachen (Germany)
Prof. Dr. C. Krüger
Max-Planck-Institut für Kohlenforschung
Lembkestrasse 5, D-4330 Mülheim a. d. Ruhr 1 (Germany)

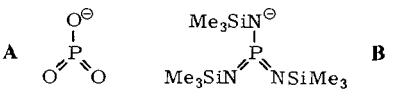
[**] This work was partly supported by the Deutsche Forschungsgemeinschaft and by the Ministerium für Wissenschaft und Forschung des Landes Nordrhein-Westfalen.

## $P(NSiMe_3)_3^{\ominus}$ — A Derivative of the Monomeric Metaphosphate Ion as Building Block for a Tricyclic Rhenium Complex**

By *Otto J. Scherer**, *Jürgen Kerth*, and *Manfred L. Ziegler*

*Dedicated to Professor Ulrich Wannagat on the occasion of his 60th birthday*

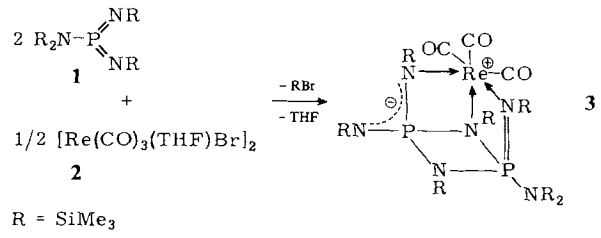
The synthesis of $R_2N-P(=NR)_2$, R = $SiMe_3$ **1**[1], the first derivative of the monomeric metaphosphoric acid $HOPO_2$ stable at room temperature[2], immediately raised the question whether the derivative **B**, formally corresponding to the monomeric metaphosphate ion **A**, could also be prepared.




Starting from $[Re(CO)_3(THF)Br]_2$ **2** and **1** we obtained the tricyclic rhenium complex **3**[4], which could be for-

[*] Prof. Dr. O. J. Scherer, J. Kerth
Fachbereich Chemie der Universität
Erwin-Schrödinger-Strasse, D-6750 Kaiserslautern (Germany)
Prof. Dr. M. L. Ziegler
Anorganisch-chemisches Institut der Universität
Im Neuenheimer Feld 270, D-6900 Heidelberg 1 (Germany)

[**] This work was supported by the Fonds der Chemischen Industrie through a grant to J. K.




mally derived from the monomeric $Re(CO)_3(THF)Br$ by replacing $Br^-$ by ligand **B** and the tetrahydrofuran (THF) by the double ylide **1** as 4-electron donor, and coupling the two ylide units together. Attempts to prepare **3** under the same conditions from **2** and the dimer of **1**[3a] met without success.

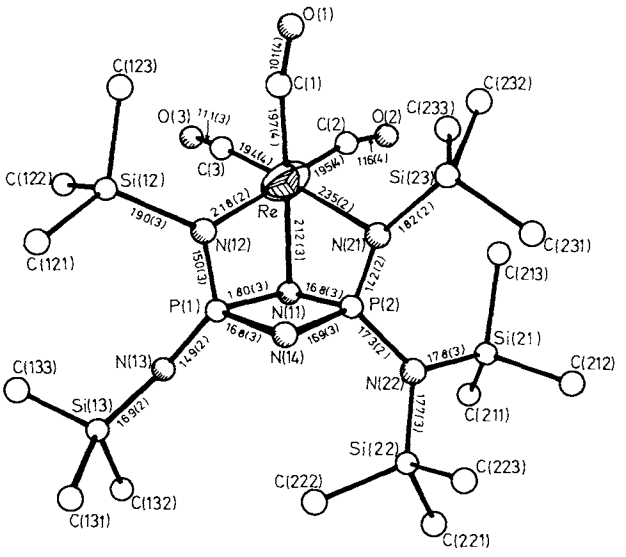



Fig. 1. Structure of 3 in the crystal (the $Me_3Si$ groups at N11 and N14 have been omitted for clarity). Bond lengths in pm. Selected bond angles [°]: N11-Re-N12 65.8(9), N11-Re-N21 64.1(9), N12-Re-N21 89.6(9), P1-N12-Re 106.1(13), P1-N11-Re 98.0(12), N11-P1-N12 89.8(13), P2-N21-Re 96.6(11), P2-N11-Re 97.7(11), N11-P2-N21 100.3(14), N11-P1-N14 85.0(13), N11-P2-N14 88.8(13), P1-N11-P2 90.8(14), P1-N14-P2 94.7(15).

**3** forms bright yellow crystals which are sensitive to hydrolysis and are readily soluble in pentane, benzene, and $CH_2Cl_2$. The $^1$H-NMR spectrum[4b] contains signals for protons of seven different $(CH_3)_3Si$ groups; this is consistent with an additional hindrance to rotation about the $R_2N-P$ bond.

The crystal structure analysis[5] confirms that **3** forms a distorted cube with a missing corner (Fig. 1). The P2–N21 bond length of 142(2) pm is unusually short; it comes within $3\sigma$ of the lowest limiting value of the shortest P=N bond length of 150.5(4) found so far[3b] in monophosphazenes. Due to the poor quality and high sensitivity of the crystals, the structure determination is relatively inaccurate. This short P=N bond length ($U$ value of P2 ($U_{eq}$) and N21: 0.042(4) and 0.042(7) Å$^2$, respectively) should therefore not be overvalued. Worth mentioning is the almost linear arrangement of the exocyclic $Me_3Si-N=P$-moiety (Si13–N13–P1 173.9(19)°).

Received: February 7, 1983 [Z 272 IE]
German version: *Angew. Chem.* 95 (1983) 510

[1] a) E. Niecke, W. Flick, *Angew. Chem. 86* (1974) 128; *Angew. Chem. Int. Ed. Engl. 13* (1974) 134; b) O. J. Scherer, N. Kuhn, *Chem. Ber. 107* (1974) 2123.

[2] Review: F. H. Westheimer, *Chem. Rev. 81* (1981) 313.

[3] a) R. Appel, M. Halstenberg, *J. Organomet. Chem. 121* (1976) C47; b) S. Pohl, *ibid. 142* (1977) 195.

[4] a) **3**: A solution of **2** (635 mg, 0.75 mmol) in $CH_2Cl_2$ (10 mL) is added dropwise at room temperature to a solution of freshly distilled **1** [1b] (1100 mg, 3 mmol) in anhydrous $CH_2Cl_2$ (5 mL) and the mixture stirred for 15 min. After removal of solvent the yellow oily residue is washed with 8 mL pentane (*ca.* 10 min, with gentle heating and stirring), filtered over filter flocs and cooled for 1 d at −30 °C and 1 d at −90 °C. After separation, the bright yellow crystals are washed with 1 mL cold pentane and dried for 1 h at 0.01 torr; yield 490 mg (35%).—b) $^1$H-NMR (200 MHz, $C_6D_6$, TMS int.): $\delta = 0.648$ (s), 0.540 (s), 0.482 (s), 0.36 (d, $^4J_{PH} = 0.75$ Hz), 0.355 (s), 0.347 (s), 0.329 (s); $^{13}$C{$^1$H}-NMR ([$D_8$]toluene, TMS int., 183 K): $\delta = 199.3$ (s), 195.8 (s), 195.6 (s) (3 CO); $^{31}$P{$^1$H}-NMR ($C_6D_6$, $H_3PO_4$ ext.): $\delta = 10.3$ (d), −18.6 (d, $^2J_{PP} = 16.9$ Hz); IR (pentane): $\nu$(CO) = 2018, 1915, 1895 cm$^{-1}$.

[5] Monoclinic, space group $C_2^2$-$P2_1$, $Z = 2$; $a = 1105.5(5)$, $b = 1763.2(7)$, $c = 1171.5(5)$ pm, $\beta = 103.98(8)°$; 2151 independent reflections with $I > 2.5\sigma(I)$; $R_w = 0.079$. Further details of the crystal structure investigation can be obtained on request from the Fachinformationszentrum Energie Physik Mathematik by quoting the number CSD 50385, the names of the authors, and complete citation of the journal.

# BOOK REVIEWS

**Chemical and Enzymatic Synthesis of Gene Fragments. A Laboratory Manual.** Edited by *H. G. Gassen* and *A. Lang*. Verlag Chemie, Weinheim 1982. x, 250 pp., bound, DM 78.00.

This book, which consists essentially of the edited protocols of an EMBO course, describes the current situation in the chemical and enzymatic synthesis of DNA. The book fills a gap by particularly emphasizing the methodological and experimental aspects and therefore is a valuable collection of methods for the synthesis, purification and analysis of DNA and RNA fragments. The chemical section surveys the synthesis of protected 2′-deoxyribonucleosides, the synthesis of DNA dimers and the synthesis of oligodeoxynucleotides on polymer carriers, according to the phosphate triester and phosphite triester methods. The biochemical section describes, *inter alia*, the ligation of DNA fragments, the construction of recombinant plasmids and the use of RNA-ligase for the synthesis of oligonucleotides. Finally, there is a chapter on the purification and analysis of DNA and RNA fragments by chromatography and sequencing techniques.

Because of the nature of the subject the choice of themes in this volume lacks uniformity. In spite of this it contains a great deal of valuable information, so that it constitutes a veritable handbook for those who wish to take up DNA synthesis.

The editors mention in the foreword that the methods have now become so simple that they can be employed by

non-chemists. The reviewer believes this statement to be overoptimistic. Even chemists, who are not themselves experienced in nucleotide chemistry, will not directly be able to synthesize, purify, analyze and enzymically ligate defined, oligonucleotide chains solely by having this excellent collection of experimental data at hand. However, anyone who wishes to initiate work on the synthesis of DNA is recommended to study this book.

*Hubert Köster* [NB 588 IE]

**Carbocationic Polymerization.** By *J. P. Kennedy* and *E. Maréchal*. John Wiley and Sons, Chichester 1982. xx, 510 pp., bound, £ 55.50.

On the one hand, the technical preparation of polymers by cationic polymerization is limited to a few monomers *e.g.* isobutylene, vinyl ether and trioxane. On the other hand, about 5—7% of all scientific publications on polymers are concerned with the mechanism, kinetics or thermodynamics of cationic homo- and copolymerization, with monomer or oligomer synthesis.

It is, therefore, to be welcomed, that two competent authors, with many years of experience in the field, have now produced a broad-based review of this constantly developing area.

The two introductory chapters pay special attention to the individualities of cationic polymerization, as well as explaining some general concepts and the nomenclature. Compounds are defined as "cationic monomers" that are "cationizable" and able to cationize other molecules of the same compound, independent of whether a high molecular weight polymer is formed thereby. About 200 compounds (with few exceptions, unsaturated hydrocarbons), which conform to this definition, are assembled in a table. Most of them, however, only form oligomers. Unfortunately, literature references are not included in the table; the reader is referred to an earlier book by *J. P. Kennedy* (Cationic Polymerization of Olefins: A Critical Inventory; Wiley, Chichester 1975). Further tables list commonly used initiators, of the Brønstedt acid, carbocation salt and Friedel-Craft compound types. The chemistry of carbocationic polymerization is dealt with very thoroughly in Chapter 4. For the most thoroughly investigated monomers such as styrene, isobutylene, vinyl ether and some of the longer chain α-olefins, the initiation reactions (including photo- and electroinitiation), the propagation, termination and transfer reactions and the "inifer method" developed by *Kennedy* are described. The emphasis in all this is on the chemical aspects. A relatively short chapter on kinetics follows.

Chapters 6 and 8 on the formation of copolymers are worth particular mention. After a critical discussion of the methods of parameter determination follows a table encompassing 643 polymerization systems (oxacycles are excluded) with $r_1$ and $r_2$ values taken from the literature and after recalculation according to the Kelen-Tüdös method. Then follows a discussion of theoretical considerations for the calculation of the reactivity together with the effect of experimental conditions as well as of steric and electronic factors. The chapter on block and graft copolymers prepared by carbocationic reactions is very stimulating. The chapter on "macromolecular engineering" conveys the impression that this field is in a state of flux and that all the possibilities have not yet been exploited. The last chapter gives a short outline of the industrial application and technical aspects with emphasis on polyisobutylene and polyvinyl ether. A short section by *R. W. Lenz* and *J. E. Chandler* describes step-growth polymerizations proceeding *via* a Friedel-Craft alkylation mechanism, by reference to a few examples.

Each chapter is accompanied by a comprehensive list of references, arranged according to the authors (numbered references would have been much more appropriate here). The subject index is adequately comprehensive and very helpful. The printing and formulae are good and free from all but minor errors. The formulae on page 437 do not correspond to the text; isobutylene and PiB have to be substituted for styrene and PSt. The discussion of vinylamine on page 33 is superfluous, since this monomer does not exist.

This book can be heartily recommended to all who are active in polymer chemistry or who would like to achieve a quick, comprehensive survey. It is to be desired that advanced students have access to it in their departmental libraries and are, thus, stimulated to study it.

*Rolf C. Schulz* [NB 590 IE]

**Topics in Current Chemistry 103: Preparative Organic Photochemistry.** By *P. Margaretha*. Springer Verlag, Berlin 1982. x, 89 pp., bound, DM 48.00.

The lively development of organic photochemistry and its successful application in the synthesis of natural products makes a topical review of synthetically attractive phototransformations desirable. *Margaretha* attempts to supplement the book of the same title by *A. Schönberg* published in 1968. However, as the author states in the introduction, it would be a difficult task to present the current state of organic photochemistry, which has, in the meantime, acquired an interdisciplinary character, according to this example. A subjective selection has been made of the plethora of examples of application and an attempt has been made to fill in gaps in the literature. This has been partially successful. This little book commands the attention of the practising chemist with a sceptical attitude to photochemistry and, furthermore, it offers the beginner an easy entry to the field.

After a general introduction to photochemistry follow chapters on cleavage, addition and substitution reactions. Next the multitude of rearrangements are treated as are reactions with singlet oxygen. The book terminates with references to experimental technique. The shortest possible, theoretical treatment of photochemistry in the introduction conveys some of the fascination of the mechanistic aspects. The subjective choice of the examples has led to some of the chapters being too short, so there are limits to their representative nature. For example the subsection on nitrogen extrusion, alongside the transformations treated there are also important applications in the field of natural product synthesis. It is also noticeable that the work of important groups, such as that of *G. Berson*, is not represented. A final criticism is concerned with the guidelines contained in the addendum which summarize the experimental techniques. Because of their brevity they do not contain very much information and do not refer to indispensable reference works like that of *Calvert* and *Pitts*.

In spite of the faults mentioned the book fulfils the desired aim. Its strength lies in the clear presentation which quickly brings the reader into contact with the important

aspects of the subject. It indicates very well, how the wealth of mechanistic knowledge enables photochemical reactions to be incorporated into directed, synthetic sequences. It will not only interest students but also help the practising chemist to break new ground.

*Martin Demuth* [NB 584 IE]

**Recent Books**

The following books have been received by the editor. All the publications listed are available through W & P Buchversand für Wissenschaft und Praxis, Boschstrasse 12, D-6940 Weinheim (Federal Republic of Germany). Tel. (06201) 606-0, Telex 465516 vchwh d, Telefax (06201) 602328.

**Catalysis. Science and Technology. Vol. 3.** Edited by *J. R. Anderson* and *M. Boudart*. Springer-Verlag, Berlin 1982. x, 289 pp., bound, DM 128.00.—ISBN 3-540-11534-6

**Crystals. Growth, Properties and Applications. Vol. 8: Silicon Chemical Etching.** Springer-Verlag, Berlin 1982. vii, 226 pp., bound, DM 144.00.—ISBN 3-540-11862-4

**Reactivity and Structure. Concepts in Organic Chemistry 14: Silicon Reagents for Organic Synthesis.** By *W. P. Weber*. Springer-Verlag, Berlin 1983. xviii, 430 pp., bound, DM 224.00.—ISBN 3-540-11675-3

**Reactivity and Structure. Concepts in Organic Chemistry 15: The Anomeric Effect and Related Stereoelectronic Effects at Oxygen.** By *A. J. Kirby*. Springer-Verlag, Berlin 1983. viii, 149 pp., bound, DM 114.00.—ISBN 3-540-11684-2

**Biochemie. Einführung in die Chemie des Stoffwechsels.** By *H.-J. Flechtner (dec.)*. 3rd edition. Newly revised by *S. Flemming*. S. Hirzel Verlag, Stuttgart 1982. 367 pp., Paperback, DM 48.00. — ISBN 3-7776-0376-7

**Chemistry Made Easy. Parts 1 and 2.** By *J. A. Nentwig, M. Kreuder,* and *K. Morgenstern*. Verlag Chemie, Weinheim 1983. xviii, 652 pp./xiv, 674 pp., Paperback, DM 38.00/45.00.—ISBN 3-527-25931-7/3-527-25932-5

**ICC Studies, Vol. 6: German Industrial Property, Copyright and Antitrust Laws.** Edited by *F.-K. Beier, G. Schricker,* and *W. Fikentscher*. Verlag Chemie, Weinheim 1982. ix, 222 pp., paperback, DM 76.00. — ISBN 3-537-26000-5

**Phase Transfer Catalysis.** Edited by *E. Dehmlow* and *S. Dehmlow*. Verlag Chemie, Weinheim 1983. 2nd imp. edit. xiv, 386 pp., bound, DM 138.00. — ISBN 3-537-25897-3

**Nuclear Fuel Cycle. Vol. 2.** Edited by *F. Baumgärtner, K. Ebert, E. Gelfort,* and *K. H. Lieser*. Verlag Chemie, Weinheim 1983. xiv, 352 pp., paperback, DM 130.00. — ISBN 3-527-25947-3

**Maximum Concentrations at the Workplace and Biological Tolerance Values for Working Materials 1982.** Issued by the Deutsche Forschungsgemeinschaft. Verlag Chemie, Weinheim 1982. 90 pp., paperback, DM 12.50. — ISBN 3-527-27302-6

**Principles of the Theory of Lattice Dynamics.** By *H. Böttger*. Physik Verlag, Weinheim 1983. 332 pp., bound, DM 96.00. — ISBN 3-87664-064-4

**Methods of Enzymatic Analysis. Vol. 1: Fundamentals.** Edited by *H. U. Bergmeyer*. Verlag Chemie, Weinheim 1983. xxii, 580 pp., bound, subscription price until 31. 12. 1983 DM 170.00 (later DM 198.00), as individual volume DM 230.00. — ISBN 3-527-26041-2

**Industrial Crystallization. The State of the Art.** By *J. Nývlt*. Verlag Chemie, Weinheim 1982. vi, 180 pp., paperback, DM 62.00. — ISBN 3-527-26065-X

**Liebigs Experimentalvorlesung. Vorlesungsbuch und Kekulés Mitschrift.** Edited and commented on by *P. Krätz* and *C. Priesner*. Verlag Chemie, Weinheim 1983. xii, 498 pp., bound, DM 160.00. — ISBN 3-527-25885-X

**Der Brief im Zeitalter der Renaissance.** Edited by *F. J. Worstbrock*. A publication of the Deutsche Forschungsgemeinschaft. Acta humaniora im Verlag Chemie, Weinheim 1983. 225 pp., sewed, DM 62.00. — ISBN 3-527-17002-2

*Registered names, trademarks, etc. used in this journal, even without specific indication thereof, are not to be considered unprotected by law.*

© Verlag Chemie GmbH, D-6940 Weinheim, 1983. - Printed in the Federal Republic of Germany by Zechnersche Buchdruckerei, Speyer/Rhein.

All rights reserved (including those of translation into foreign languages). No part of this issue may be be reproduced in any form - by photoprint, microfilm, or any other means - nor transmitted or translated into a machine language without written permission from the publishers. Only single copies of contributions, or parts thereof, may be reproduced for personal use. Copies reproduced and used other than for private purposes in an industrial or commercial undertaking are subject to copyright and, in such cases, a copyright fee must be paid to the VG WORT, Abteilung Wissenschaft, Goethestr. 49, 8000 München 2, from whom conditions of payment can be obtained on request.

**Valid for users in the USA:** The appearance of the code at the bottom of the first page of an article in this journal (serial) indicates the copyright owner's consent that copies of the article may be made for personal or internal use, or for the personal or internal use of specific clients. This consent is given on the condition, however, that the copier pay the stated per-copy fee through the Copyright Clearance Center, Inc., for copying beyond that permitted by Sections 107 or 108 of the U.S. Copyright Law. This consent does not extend to other kinds of copying, such as copying for general distribution, for advertising or promotional purposes, for creating new collective works, or for resale. For copying from back volumes of this journal see 'Permissions to Photo-Copy: Publisher's Fee List' of the CCC.

**Editorial office:** Pappelallee 3, D-6940 Weinheim, Federal Republic of Germany, Telephone (06201) 60 23 15, Telex 465516 vchwh d, Telefax (06201) 602328.

**Editors:** *P. Gölitz, I. G. Neil, O. Smrekar, A. Stimson.*

**Publishers:** Verlag Chemie GmbH. (Managing Directors: *Prof. Dr. Helmut Grünewald* and *Hans Dirk Köhler*), Pappelallee 3, D-6940 Weinheim, Federal Republic of Germany.
Correspondence concerning advertisements should be addressed to Verlag Chemie GmbH. (Advertising Manager *R. J. Roth*), Pappelallee 3, P.O. Box 1260/1280, D-6940 Weinheim, Federal Republic of Germany, Telephone Weinheim (06201) 602-0, Telex 465516 vchwh d, Telefax (06201) 602328.

ANGEWANDTE CHEMIE
International Edition in English
Volume 22 · Number 7
July 1983
Pages 507–564

# A Quarter Century of Thin-Layer Chromatography—An Interim Report

By Egon Stahl*

*Dedicated to Professor Wilhelm Fresenius on the occasion of his 70th birthday*

Thin-layer chromatography (TLC) has been in general use since 1958. The prerequisites were the use of very small particle size material in the layers and the demonstration that not only lipophilic mixtures but also mixtures of cardiac glycosides, alkaloids, sugars, and amino acids could be separated quickly and simply on silica gel layers. The impressive separations obtained using the method later encouraged attempts to use adsorbants having such, narrow-range small particles in column chromatography. In order to achieve sufficient flow rates the use of high pressures was necessary. Thus, high pressure or high performance liquid chromatography (HPLC) was born, whose godfather, as far as instrumental development is concerned, was gas chromatography (GC). Today, chromatography is classified according to the nature of the transport phase: liquid, gas, or "electro" chromatography. Sample preparation often requires more time than the actual separation. Rapid thermal separation and application techniques (TAS, TFG) have brought advantages to TLC. As before, the art of chromatography consists in choosing the appropriate mobile phase, stationary phase, and separation technique. Gradient TLC offers new possibilities; for example, gradient layers make it possible to obtain selective information on the individual components of a mixture and also allow significant focussing effects to be achieved. Sequential and centrifugal TLC have paved the way for further advances. The questions arise whether the standard conditions, formulated 25 years ago, are still applicable and how the variations which have been introduced should be judged. Group- and substance-specific methods of detection are discussed in addition to universal methods. Quantitation is critically discussed and it is concluded that HPLC has the better chance in the future. Combination and coupling techniques ease the positive identification of individual substances. Finally, it is discussed why TLC is the simplest, most versatile, most cost effective, and most widely used chromatographic method and reasons are proposed as to why it will remain so for the foreseeable future.

## 1. Historical Introduction

The principle of thin-layer chromatography, that is a thin, separating layer on a glass plate, has been known for almost 100 years (cf. Table 1). The question arises as to why neither the pioneering research of *Beyerinck*[1] nor subsequent contributions led to the general adoption of the method. My first contribution to this physico-chemical separation technique, with the publication in 1956 of an article[6] entitled "Dünnschicht-Chromatographie" (thin-layer chromatography), a term which was new at the time,

[*] Prof. Dr. E. Stahl
Pharmakognosie und Analytische Phytochemie der Universität
D-6600 Saarbrücken (Germany)

 © Verlag Chemie GmbH, 6940 Weinheim, 1983 0570-0833/83/0707-0507 $ 2.50/0 

was ignored just as much as its predecessors. The breakthrough only occurred when Merck was persuaded to produce a special grade of silica gel for thin-layer chromatography (TLC) and Desaga to manufacture the basic equipment and accessories. These were both first presented in 1958 at the International Chemistry Exhibition (ACHEMA) in Frankfurt am Main, and aroused great interest.

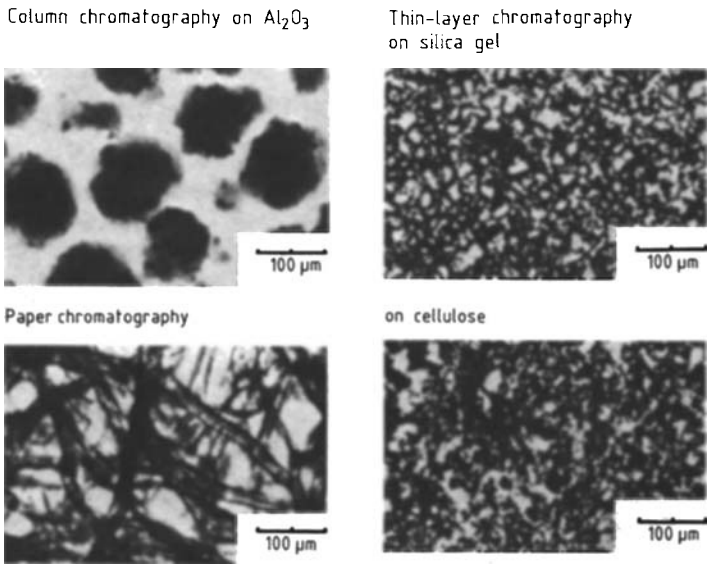



Fig. 1. Comparison of particle sizes of adsorbents for classical column chromatography, paper chromatography, and thin-layer chromatography.

Thin-layer chromatography was soon in general use under the recommended standard conditions[7]. The real scientific advance, however, was not the possibility of manufacturing thin layers, but the use, based on our years of investigation, of a much finer particle-sized material than previously had been used as a stationary phase in chromatography (cf. Fig. 1). The first commercial adsorbents for TLC, however, left something to be desired; the problem was the difficult manufacturing technique required to produce fine particle sizes and narrow fractions.

The fact that TLC was not limited to the separation of terpenes[4], but that a form of partition chromatography of *e.g.* cardiac glycosides, saponins, alkaloids, amino acids, and sugars is also possible on thin silica layers, was also a further advance. The range of applications could, therefore, be extended to numerous separation problems in chemistry, biology, and medicine. The first laboratory handbook on thin-layer chromatography appeared in 1962, under the combined authorship of a group of specialists, and led to a further dissemination of the method[8].

Table 1. Development of thin- layer chromatography.

| Year | Authors | Method designation | Ref. |
|---|---|---|---|
| 1889 | Beyerinck | Simple diffusion experiment | [1] |
| 1938 | Izmailov, Schraiber | Drop-chromatography | [2] |
| 1949 | Meinhard, Hall | Surface chromatography | [3] |
| 1951 | Kirchner, Miller, Keller | Chromatostrip technique | [4] |
| 1954 | Reitsema | Chromatoplate technique | [5] |
| 1956 | Stahl | Thin-layer chromatography | [6] |
| 1958 | Stahl | TLC standardization, basic equipment, Kieselgel G Merck | [7] |
| 1962 | Stahl (Edit.), Bolliger, Brenner, Gänshirt, Mangold, Seiler, Waldi | TLC Laboratory Handbook | [8] |

The instrumental development of gas chromatography (GC) occurred almost in parallel with the further development of thin-layer chromatography, but it was some time before it was realized that GC is not a universal separation method and that the classical Tswett column chromatography also exists. The separating capacity of fine particle size layers used in thin-layer chromatography stimulated attempts to pack columns with these materials. Since almost nothing would pass through such closely packed columns it was necessary to force the solvent through by the application of pressure. Thus, high pressure liquid chromatography was a necessary consequence of the fine particle size of the packing. Thin-layer chromatography has, in this manner, undoubtedly decisively influenced the further development of chromatographic techniques. A caricaturist might see the development as shown in Figure 2.

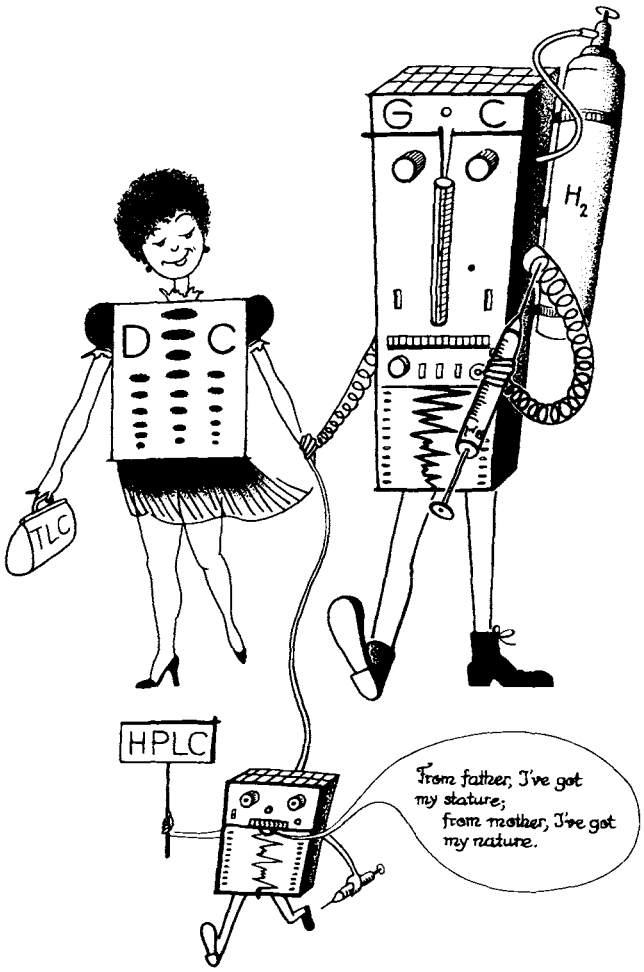



Fig. 2. A happy family.

## 2. Chromatographic Techniques Today

To obtain a topical view of chromatographic processes it is appropriate to classify them into three large groups according to the "transport phase"; that is into liquid, gas

and electro chromatography (Fig. 3). Liquid chromatography includes classical column chromatography, paper chromatography, thin-layer chromatography, and high pressure liquid chromatography, as well as exclusion chromatography.

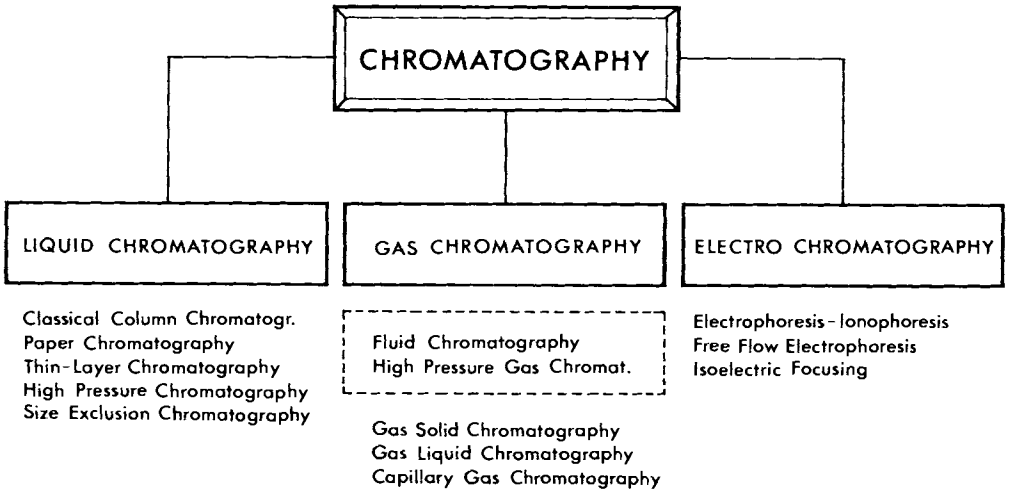



Fig. 3. Classification of chromatographic methods according to the mobile phase.

If one wishes to compare the advances made in chromatography it is first necessary to divide these methods, which are intrinsically complex, into their three components and to analyze each of these individually. The scheme shown in Figure 4 indicates the three main components of each chromatographic method together with the preceding and following steps. Advances of varying degrees have been made in all five chromatographic steps in the last few years.

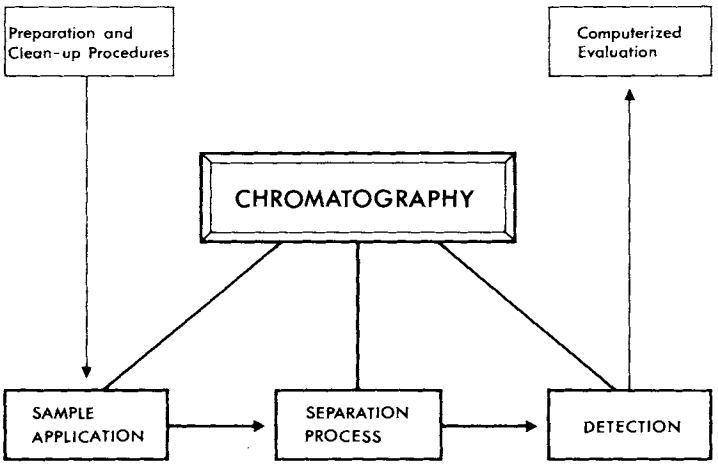



Fig. 4. Chromatography is a three-stage process; sample preparation and quantitative evaluation are also involved.

Experience has shown that sample preparation, clean-up, and preparation of the application- or injection-solution are often more time consuming than the actual chromatography. Since 1968, we have, therefore, developed methods for transporting the substances from the sample directly "on line" onto the thin layer without the use of solvents. Suitable for this purpose are, *inter alia*, thermal techniques and microextraction with supercritical gases. The thermo-micro application of substances (TAS) technique can be used to transport essential oils from drugs and many other substances directly, within 1 or 2 minutes, onto the thin layer[9, 10]. Further development led to thermofractography[11], a technique that has seen relatively little application until now.

## 3. Chromatographic Parameters

The first step, *sample application* (cf. Fig. 4), is important for the success of chromatography. It must be adapted to the particular problem and to the sensitivity of detection. The amount of sample may be more and more reduced, but it must be remembered, that trace components will then, in most cases, be undetectable, because the sensitivity of detection is inadequate. As a rule of thumb, when the purity of a substance is to be checked a relatively large sample should be used in order to detect trace components; if, however, a mixture of substances is to be investigated the amount applied should be reduced in order to provide a better overview. The sample applicator should be as cheap as possible conformable with the desired success. It is remarkable that manual application in a streak, as recommended in most cases by the European Pharmacopeia, leads to improved chromatograms and allows clear, qualitative evaluation.

The actual heart of the chromatographic process is the *separation* itself (Fig. 4). Figure 5 presents schematically the range of variables available in thin-layer chromatography. It rests on the skill of the user to adjust and compensate the manifold possibilities in order to achieve an optimal separation.

The scheme indicates that three main parameters must be considered; the choice of the *stationary* and the *mobile phases* and of the most suitable *separation technique*. The particular advantage of thin-layer chromatography is that it is simple to adjust these parameters with respect to each other and to check the success of the separation. The introduction of pre-manufactured separation layers at the be-

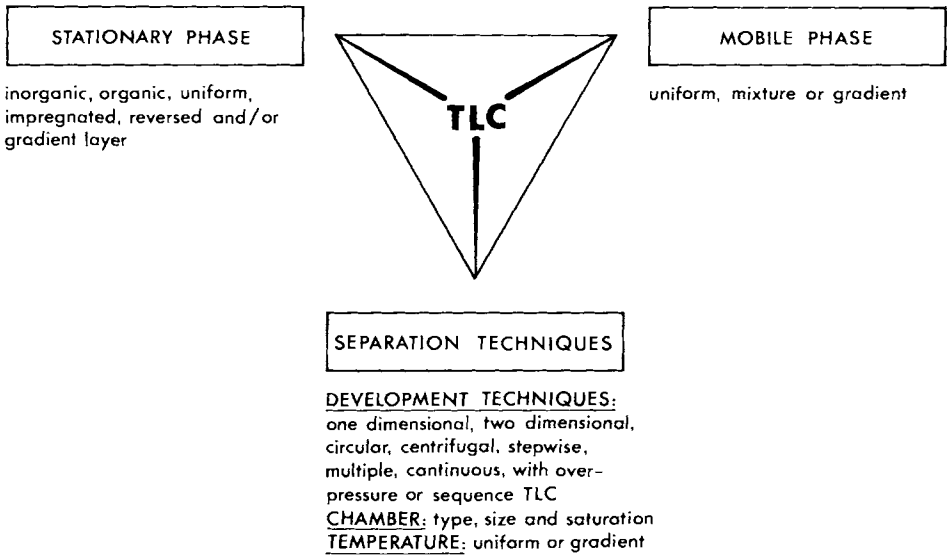



Fig. 5. The multitude of variable parameters in thin layer chromatography which must be mutually adjusted to achieve optimal conditions.

ginning of the 1960s was certainly a success as far as further dissemination of the method was concerned. It is to be hoped that even more and diverse layers with different separating properties will come onto the market. The industrial manufacture of derivatized silicas (RP phases) that allow reversed phase chromatography without impregnating the layer is a step in the right direction. A successful future can be predicted for such adsorbents and ready-prepared layers. Industrially manufactured gradient layers would be desirable: layers with so-called concentration zones are a step in this direction. The introduction of gradient layers was a milestone in the further evolution of thin-layer chromatography[12-14]. The new possibilities it opened up will be demonstrated with the aid of the following examples.

As is well-known, a gradient layer can be developed in three directions: the chromatogram can be developed across the gradient or in two directions along it. The pH

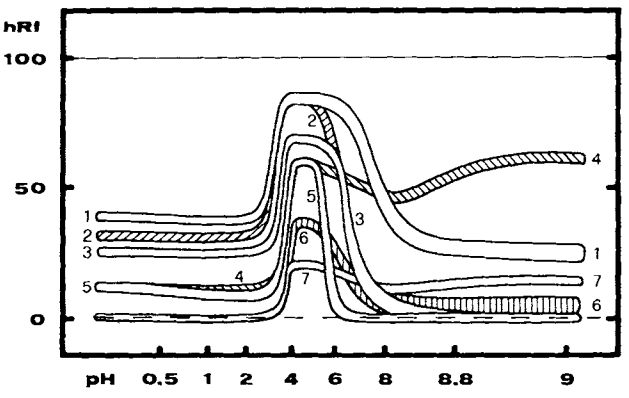



Fig. 6. pH-*T*-gradient TLC of seven sulphonamides: 1 sulfaphenazole, 2 sulfisoxazole, 3 sulfacetamide, 4 sulfanilamide, 5 sulfathiazole, 6 sulfisomidine, 7 sulfaguanidine. Mobile phase: benzene-2-propanol (80+20), 2×12 cm, chamber saturation. Detection: fluorescamine, $UV_{365}$.

gradient layers are particularly interesting. If, for example, a mixture of seven sulfonamides is chromatographed, it can be seen from the shape of the curves that, apart from sulfanilamide and sulfaguanidine, they are amphoteric substances. The pH-*T*-chromatogram (Fig. 6) shows, furthermore, that no pH region exists where all seven substances can be separated from each other.

The separation of the seven most common benzodiazepines on a pH-*T*-gradient layer is also interesting[15]. In the developed chromatogram (Fig. 7) the basic character of the substances is evident; the separation takes place in the sequence of the $pK_a$ values.

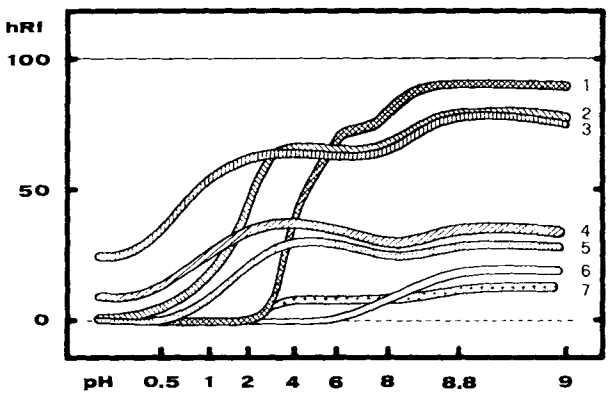



Fig. 7. pH-*T*-gradient TLC of seven benzodiazepines viewed under long wavelength UV light after being sprayed with sulfuric acid: 1 medazepam, 2 diazepam, 3 flunitrazepam, 4 clonazepam, 5 nitazepam, 6 flurazepam, 7 chlordiazepoxide. Mobile phase chloroform-acetone (90+10), 2×10 cm, chamber saturation. Detection: 8 N sulfuric acid, $UV_{365}$.

Such pH-*T*-gradients are very well suited to the study of decomposition phenomena, for metabolic studies, and for the detection of impurities in syntheses. No other technique enables such subtle differences to be detected. A fur-

ther possibility is to develop the plate along the gradient. We have discovered a focussing effect in this mode[14, 16]. Whereas with increasing developing distances the zones normally become broader, in TLC-focussing, by analogy to the phenomenon of isoelectric focussing, narrowing, on occasions pronounced, of the bands occurs. As shown in Figure 8, more than 20 components can be detected in a mixture (developed in the acidic to basic direction) on a gradient, whereas only 9 components are resolved in conventional chromatography on a uniform layer. The problems associated with manufacturing gradient plates can surely be overcome.

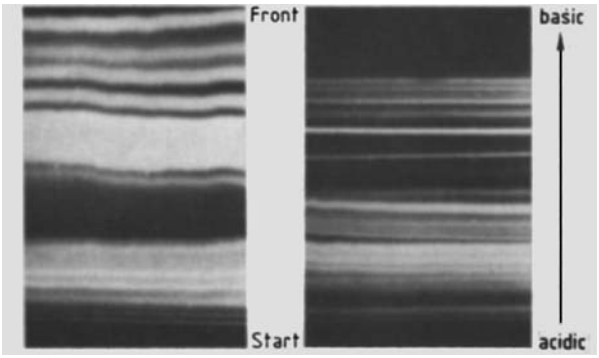



Fig. 8. Focussing of a mixture of fluorescent dyestuffs by thin-layer chromatography on a gradient from "acidic" to "basic" (on the right); for purposes of comparison, a standard, uniform silica gel layer is shown on the left.

Adhesive stability and abrasion resistance are important for both gradient and normal, monotonic layers. These parameters must be neither too high nor too low. A special apparatus for measuring the abrasion resistance of layers has proved of value in testing binders[17]. An "abrasive weight" of 200 g seems optimal. As before, suitable organic plastic binders are, unfortunately, not available commercially for those who wish to manufacture their own TLC layers.

There have not been any spectacular developments in *mobile phases*. The eluotropic series has proven itself in adsorption TLC and the classification of solvents according to polarity and approximately according to dielectric constant can be advantageous. Benzene should not be used as a solvent on account of its established toxicity; toluene or the somewhat more polar dichloromethane should be employed instead. An attempt to market solvent mixtures with increasing dielectric constants did not meet with success. The old proven technique of gradient elution has also failed to establish itself in thin-layer chromatography.

The largest number of degrees of freedom in thin-layer chromatography are available in choosing the *separation technique*. Alongside the possibilities of ascending development and descending development there is also the possibility of horizontal development in special chambers. Further variations are two-dimensional, centrifugal and radial development. Stepwise development has also proven very useful, as has multiple development. Recently, horizontal development in so-called mini-chambers, which enable economies to be made on solvents, has aroused renewed interest. A pressurized TLC chamber (Chrompres 10)[18] and the ingenious "sequence TLC"[19] are new. All these techniques offer particular advantages, and it is necessary to understand them properly in order to utilize them to advantage.

The classical TLC development troughs have seen little change. Very small chambers have come into use and are used as dipping chambers[20]. As well as the established low temperature TLC[21], use of a temperature gradient during development[22] has been investigated. The temperature gradient causes increasing evaporation of solvent and, hence, focussing of the zones[23, 24]. In order to separate substances that are almost insoluble at room temperature, as for example many organic dyes and pigments, TLC at 150 °C on silica gel using suitable solvents that can be classified according to their elution effect can be recommended[25]. Centrifugal TLC has attracted great interest in the last few years and has led to the development of the "Chromatotron" in the United States. In this device the mixture is separated on a spinning disc (Ø 24 cm), which carries a thin separating layer of 1 to 4 mm thickness. The advantage of centrifugal TLC lies in its ability to rapidly separate preparative quantities of from 0.1 to 1 g (Fig. 9). We also have investigated this method[26] in order to establish its advantages and disadvantages.

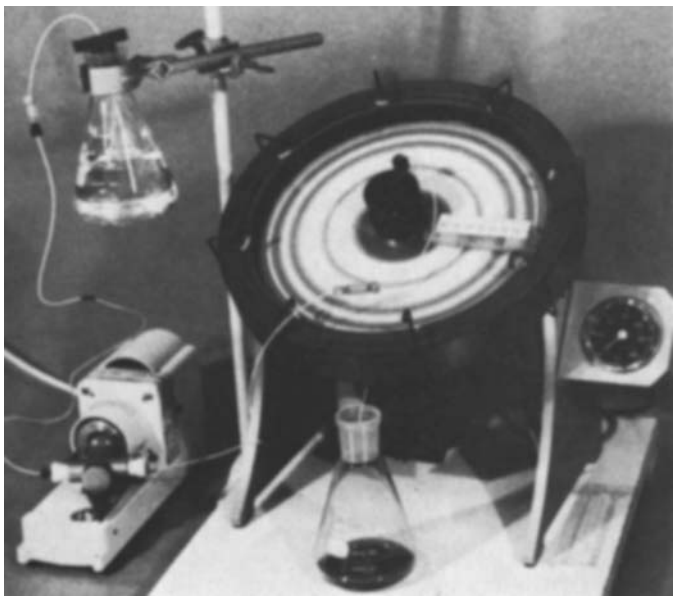


Fig. 9. Centrifugal TLC with the Chromatotron for preparative separation of a mixture of substances.

## 4. Standard Conditions and Variations

Our discussion of the three parameters of thin-layer chromatography raises the question of whether the standard conditions formulated 25 years ago are still valid today. The scheme laid out in Figure 10 shows the variations put forward up till now. In choosing the standard conditions we were striving for a handy, square plate which was versatile enough to accommodate all possibilities. We suggested 20 × 20 cm for its size, a layer thickness of 0.25 mm, and a 10 cm long separation zone. The early introduction of these standard conditions for TLC has simplified the

task of all manufacturers producing accessories, up to and including expensive scanners.

The standard conditions have been modified in five ways (cf. Fig. 10). For example, for preparative purposes the plates have been increased to a width of 100 cm and the layer thickness to 1–2 mm; this technique was christened "preparative TLC" or "layer chromatography"[27]. Nowadays, however, the tendency is more and more to use standard 20 × 20 cm plates for preparative work[28].

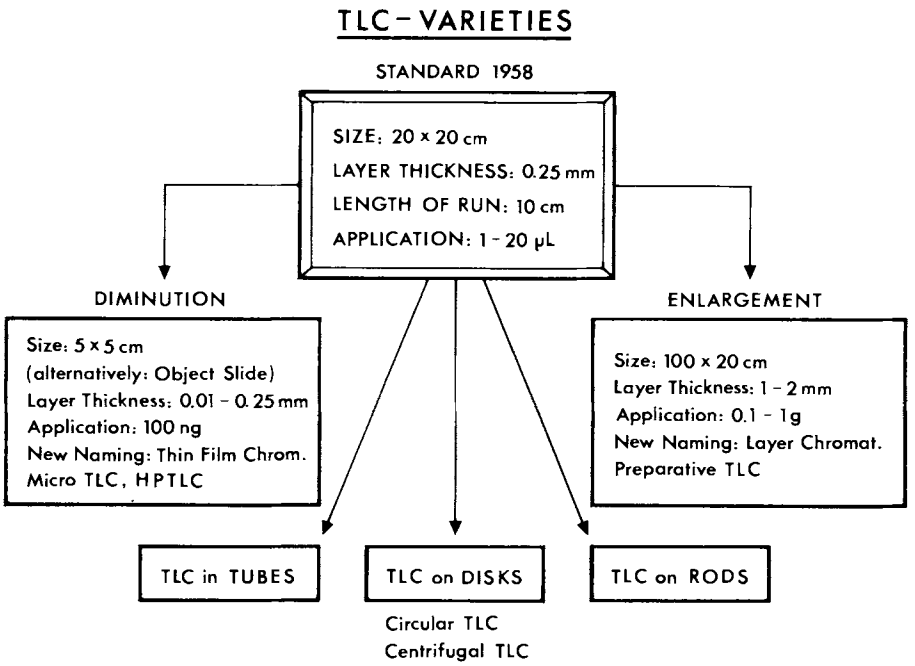



Fig. 10. Variations to the standard conditions for TLC formulated in 1958.

Another development has been to reduce the format to that of a microscope slide or a projection slide (5 × 5 mm). This raises the question of whether the separation zone is long enough. The advantages and disadvantages of this micro TLC or thin-film chromatography[29], which recently has come to include HPTLC or nano-TLC[30], must also be considered from the point of view of costs. Sometimes it is forgotten that subsequent coupling processes often require µg amounts of substance, which cannot be provided by a nano-TLC method. The future will decide whether the time is yet ripe for a smaller format. If it is, then the work of *Szekely*[31], who indicated that this can be done economically by dividing normal commercial 20 × 20 cm plates into four handy 10 × 10 cm plates, should be remembered. Suitable solvent-saving developing troughs are commercially available.

TLC in *tubes* was also advocated at one time; this variant, however, is now almost forgotten. TLC on glass *rods* is also scarcely utilized. For the historical record, I would like to interpolate that 33 years ago I performed chromatography on magnesia rods and grooves, and it was this that ultimately led me to TLC. TLC on plates also includes the circular TLC proposed by *Ismailov* and *Schraiber*[2], which preceded "circular filter paper chromatography". The attempts of many authors—ourselves included—have, as yet, failed to achieve the breakthrough for this method.

## 5. Detection in Thin-Layer Chromatography

Detection of the separated substances is essential in every chromatographic method. It is possible today to separate chromatographically molecule A from molecule B or molecule C; it is, however, not always possible to demonstrate such a separation because the detectors are too insensitive.

The detection problems are very different in the various chromatographic methods. In gas chromatography and high pressure liquid chromatography the separated substances are detected at some expense in a flowing system. This requires flow-through detectors and potentiometric recorders. The number of possible methods in these techniques is, therefore, strictly limited. The situation for TLC is quite different. Here, detection is performed after all the components have been separated, *i.e.* under stationary conditions. The possibilities here are enormous and this is an extraordinary advantage of the method.

As well as destructive methods using aggressive reagents, many non-destructive detection methods are available in TLC. As a rule, it has been found advantageous to initially use one or more non-destructive detection methods, *e.g.* examination of the chromatogram with several wavelengths of UV light—possibly using a fluorescent layer—and only then to resort to one or more destructive reactions that cause, for example, coloration.

For objective evaluation, the numerous detection reactions can be divided into three large groups (Fig. 11). Depending on the problem, either one or other of them will be preferred or they will be used consecutively. For mixtures of unknown composition, techniques capable of detecting as many of the components as possible are required; a universal detector is needed. This aim is only partially realizable with TLC, *e.g.* by UV absorption on

fluorescent layers or by oxidation reactions that produce coloration and ultimately carbonize all organic materials.

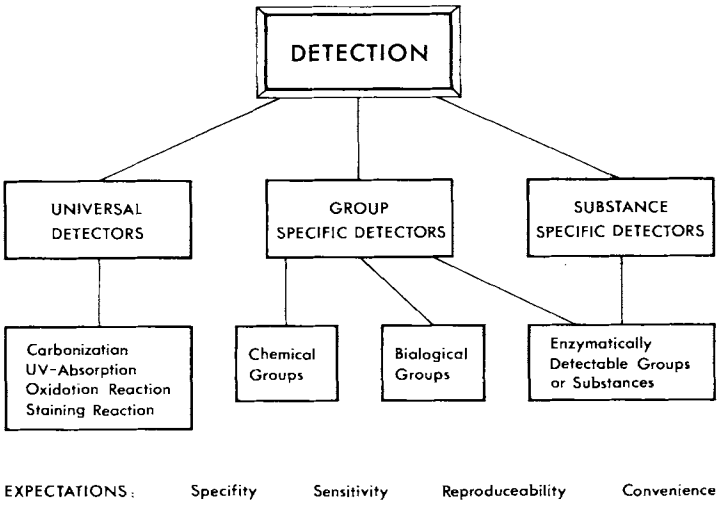



Fig. 11. Arrangement and classification of the numerous possibilities for visualization (detectors!) in TLC.

Currently, sulfuric acid-aldehyde reagents are most frequently used for detecting the separation of mixtures of natural products. It has recently been shown that the reaction takes place stepwise, and that anisaldehyde is the most suitable of the many aldehydes investigated[32]. The application of the ANSA reagent (8-anilino-1-naphthalenesulfonic acid) represented a great step forward in the detection of unreactive lipids, hydrocarbons, fats, and plasticizers[33]. Only at the end of last year an improvement on this, in itself a sensitive reagent, was suggested; the TNS reagent[34] (6-*p*-toluidino-2-naphthalenesulfonic acid). The INPTC reagent, a tetrazolium chloride derivative which reacts with plasticizers, long-chain fatty acids, higher aliphatic aldehydes, and other substances to produce different colors[35], is also worth mentioning here.

After the "universal" reagents the group-specific detection methods claim attention. One class reacts specifically with particular functional groups, for example with phenolic, alcoholic or carbonyl groups; the other class can be designated as "biological detectors".

Of all the reagents that react with chemical groups fluorescamine (Fluram Roche) has undoubtedly excited the greatest interest in the last decade. It was described by *Weigele et al.* for the detection of primary amino groups, and partially displaced the classical ninhydrin reaction. The possibilities for its application (*e.g.* [37–40]) have in no way been exhausted, as may be demonstrated by the following example. In the last few years, in Spain 300 people have died and more than ten thousand have become ill as a result of consuming cooking oil contaminated with aniline (2 ppm) and with anilides (up to 2000 ppm). Aniline and, in particular, the anilides could only be detected with difficulty. On the one hand, complicated sample preparation was followed by analysis and detection by GC-MS, and, on the other, non-specific TLC detection was used, *e.g.* using potassium permanganate. Only later was it shown, using only a 10 μL sample, that the anilides can be thermally cleaved in 90 sec with soda lime (TAS method) and that the aniline formed can be reliably detected at concentrations down to 1 ppm using the fluorescamine reagent[41]. The fluorescence reaction of aniline with *o*-phthalaldehyde is slightly less sensitive. If this method had been available at the beginning of the catastrophy then it would have been possible to analyze hundreds of samples per day and to quickly confiscate large amounts of the oil.

A further group-specific reagent, the long-established 4-nitrobenzylpyridine (NBP), is very interesting in this context; using it, it is possible to detect alkylating agents on the chromatogram[42–45]. It is widely known that alkylating agents, such as epichlorohydrin, are strongly carcinogenic; recently, *Braun et al.* have demonstrated the alkylating activity of valepotriates in valerian species[46] using this simple method.

Further advances in the field of TLC detectors can be made by systematically developing reagents that react with functional groups to form colored or fluorescent products.

The application of so-called biological detectors is very useful in certain problems, since certain biological activities can be established on the microgram scale using certain techniques. For example, using TLC it can be established what substances in a microbiological culture have antibiotic activity and against which microorganisms they are active. Parallel investigations can establish which of the substances on the chromatogram are hemolytic (cf. [47]).

The field of application of such biological detectors is a very broad one. The use of small organisms such as aedes larvae as "guinea pigs" to detect the insecticidal activity of synthetically modified pyrethrum compounds by TLC (TRT method)[48] is only one example.

The advantages of substance-specific detection in TLC have been largely neglected. The solution of some problems is facilitated when it is possible to detect one substance in a mixture, specifically, for example glucose in a mixture of sugars. This can be realized using a fermentation reaction catalyzed by glucose oxidase. The possibility of detecting specific substances in this manner will probably be restricted to enzymatic detection systems even in the future.

*Geike*[49,50], in particular, has made considerable advances in detecting plant protection agents with enzymic detectors. He was able, for example, to detect insecticidal carbamates enzymatically, recognize phosphatase inhibitors, and discover trace metals by this method. The area has been reviewed up to 1974 by *Mendoza*[51].

In this connection, a new investigation of a sensitive, enzyme-catalyzed color reaction for the detection of hydrogen peroxide and other peroxides on TLC plates ought to be mentioned[52]. The technique of allowing substrates to react with enzymes at the point of application, followed by TLC separation, is also of interest. TLC plates with concentration zones have been used successfully in this context. A contribution towards elucidating the structures of high molecular weight glycosphingolipids has been made on TLC layers using this method[53].

Finally, it is appropriate to make some observations on the sensitivity of detection in TLC. In spite of the relatively simple facts the situation is often unclear. The sensitivity

of the detection system used for a substance can vary by as much as a factor of 100 or even 1000. A simple diagram illustrates this (Fig. 12). A mixture of the four substances A,

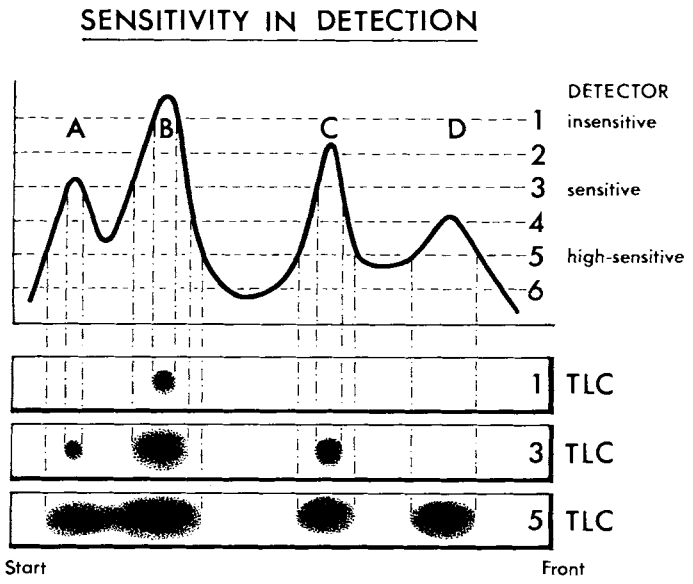



Fig. 12. Schematic representation of the sensitivity of detection using the example of a mixture of four substances and visualizing reactions of varying sensitivities.

B, C, and D at different concentrations is separated and the substances visualized using three reagents of varying sensitivity (1, 3, and 5). With sensitive reagent No. 3, three zones can be made out, as shown in the scheme; however, with the less sensitive reagent No. 1, only one is detected. The very sensitive reagent No. 5 indicates that substances A and B overlap, and that next to C there is a small amount of highly diluted substance D. Depending on the problem posed one can choose what one wants to see.

## 6. Quantitative Evaluation of TLC

In addition to simply scraping off the separated zone and eluting the substance, which is subsequently determined quantitatively, photometers were used right from the beginning of thin-layer chromatography, just as they were for the evaluation of paper chromatograms and electrophoresis strips. In the 1960s, special photometers were manufactured for TLC and were further developed in the 1970s. A top-quality instrument in this field was the computer-controlled TLC spectrophotometer from Zeiss. The high cost of such sophisticated machines and the development of HPLC raise the question as to which method is preferable for routine purposes. Without doubt, the evaluation by TLC has the advantage that many samples can be run on a chromatogram alongside each other, whereas HPLC can only cope with one sample at a time. However, sample removal and quantitative evaluation are an integral part of the instrument in HPLC and it is not necessary to set up an expensive measuring station. In my opinion, the argument lies in favor of HPLC. It is strengthened by the possibility of round-the-clock, automatic sample injection.

Consideration of all the facts leads to the conclusion that complicated, computer-controlled instrumentation does not represent a realistic, long-term solution for TLC. It is my belief that the simple, cheap, visual comparison of zone sizes is more suitable than an expensive instrument. Some specialists who possess such an instrument and the manufacturers will criticize this opinion, but not the majority of scientists who utilize chromatographic methods and are not tied to one particular technique. In my opinion, the various chromatographic techniques are complementary in the hands of a competent analyst, who is able to use them as a conductor uses his orchestra.

## 7. Combination and Coupling Techniques

The $R_f$ values in TLC are coefficients, but not physicochemical constants. Thus, they are only of limited value for identification purposes. For this reason, the combination or coupling of TLC with other more conclusive methods is of particular importance. In the simplest case, it can be seen that performing and observing one or more color reactions, which are often used for detection, already constitutes another criterion for identification. This is, however, insufficient for identification purposes. In addition, TLC can be combined with other chromatographic techniques. These should be chosen so that the separation takes place according to different principles; *e.g.* after adsorption TLC, partition TLC or reversed-phase TLC should be used, or occassionally also TLC on a layer impregnated with silver nitrate. Depending on the problem at hand, TLC and GC can, of course, also be coupled.

Coupling with spectroscopic techniques is particularly desirable. The simplest case is coupling with UV-VIS spectroscopy, which enables the spectrum of the zone in question to be recorded. Coupling with IR spectroscopy after microtransfer of the particular zone is, however, much more informative. The easiest method of performing the transfer from the layer is to use the commercially available, compressed, potassium bromide pyramids ("Wick Stick", "Spectro-Tip").

Coupling with mass spectrometry is particularly powerful in terms of positive identification; however, manual transfer is essential. The amount of material available per TLC zone is important in all these methods. All the combination and coupling techniques mentioned can be realized using standard TLC methods and loadings in the µg range.

The importance and esteem in which a method is held can be estimated both by the number of publications and the number of books which have appeared on it. In the 1960s, it was more or less possible to keep abreast of the exponentially increasing numbers of publications in which TLC was used. The method then became a general-purpose tool, which was perhaps mentioned in the experimental section of a publication. The situation with books is different[8, 29, 30, 54–85]. I deliberately subtitled the first book on TLC ("Dünnschicht-Chromatographie") a "Laboratory Handbook". Written together with six colleagues, who contributed their individual experience, it became a best seller and was translated into several languages. When the

developments mentioned above necessitated a second edition it required 24 co-authors, who presented a summary and critique of the greatly increased body of information in the various fields.

In the meantime, special literature compilations and annual special issues devoted to the method are published in leading journals or appear separately. After the appearance of the 2nd edition, which encompassed 1000 pages, it did not appear necessary to produce a 3rd edition of the Laboratory Handbook. My co-workers and I have devoted almost a decade to the development of microthermal techniques that can be coupled with TLC. Additionally, I have investigated the extraction of natural products with supercritical gases; here, too, the initial work was a combination of the technique with thin-layer chromatography.

## 8. Retrospect and Outlook

It may sound presumptuous, but TLC has enriched science and medicine enormously. Chemical reactions, increases in concentration, and isolations can be followed visually. Pharmacognosists do not have to limit themselves to the microscopic analysis of the "packaging material", but can quickly separate and visualize the active components of the drugs.

Finally, it remains to discuss the future of TLC. TLC is the most employed separation technique for the following reasons:

1. It offers the greatest freedom in the easy choice of stationary and mobile phases.
2. It offers a large number of different development techniques.
3. It offers the largest number of methods of detection.
4. It is possible to separate and visualize many samples and reference mixtures simultaneously.
5. Simple methods are available for combining and coupling with microextraction and identification techniques.
6. Thin-layer chromatography is the simplest and most economical chromatographic technique for fast separation and visual evaluation.

These and other advantages justify the prediction that TLC will retain its place in the world's laboratories and increase in importance. It is not a very spectacular technique, but it is extraordinarily useful. It only remains to say that the hectic development of chromatography and spectroscopy in the last 25 years has placed tools in our hands, which until now could only be used to a small extent because of the multiplicity of unsolved problems. A large chasm has opened between the arsenal of modern, available techniques and the results that have been gained using them. If we seize our chances, success will not evade us!

Received: March 31, 1983 [A 458 IE]
German version: *Angew. Chem. 95* (1983) 515

[1] M. W. Beyerinck, *Z. Phys. Chem. 3* (1889) 110.
[2] N. A. Izmailov, M. S. Schraiber, *Farmatsiya 3 (Moscow)* (1938) 1.
[3] I. E. Meinhard, N. F. Hall, *Anal. Chem. 21* (1949) 185.
[4] I. G. Kirchner, I. M. Miller, G. I. Keller, *Anal. Chem. 23* (1951) 420.
[5] R. H. Reitsema, *Anal. Chem. 26* (1954) 960.
[6] E. Stahl, *Pharmazie 11* (1956) 633.
[7] E. Stahl, *Chem.-Ztg. 82* (1958) 323.
[8] E. Stahl: *Dünnschicht-Chromatographie, ein Laboratoriumshandbuch*, Springer-Verlag, Berlin 1962 (2nd edit. 1967).
[9] E. Stahl, *J. Chromatogr. 37* (1968) 99.
[10] E. Stahl, *Analyst (London) 94* (1969) 723.
[11] E. Stahl, *Acc. Chem. Res. 9* (1976) 75.
[12] E. Stahl, *Chem. Ing. Tech. 36* (1964) 941.
[13] E. Stahl, J. Müller, *J. Chromatogr. 189* (1980) 293.
[14] E. Stahl, J. Müller, *GIT Fachz. Lab. 24* (1980) 649.
[15] E. Stahl, J. Müller, *J. Chromatogr. 209* (1981) 484.
[16] E. Stahl, J. Müller, *J. Liq. Chromatogr. 3 (6)* (1980) 775.
[17] E. Stahl, *Chromatographia 14* (1981) 673.
[18] Bender & Hobein GmbH, Lindwurmstrasse 71, D-8000 München.
[19] P. Buncak, *GIT Fachz. Lab., Chromatogr. Suppl. July 1982*, 3.
[20] Desaga GmbH, *GIT Fachz. Lab., Chromatogr. Suppl. July 1982*, 49.
[21] E. Stahl, *Angew. Chem. Int. Ed. Engl. 3* (1964) 784.
[22] S. Turina, Z. Soljic, V. Marjanovic, *J. Chromatogr. 39* (1969) 81.
[23] S. Turina, V. Jamnicki, *Anal. Chem. 44* (1972) 1892.
[24] I. Kupęc, S. Turina, *Chromatographia 10* (1977) 157.
[25] G. Szekely, P. Baumgartner, *J. Chromatogr. 186* (1979) 575.
[26] E. Stahl, J. Müller, *Chromatographia 15* (1982) 493.
[27] H. Halpapp, *Chem. Ztg. Chem. Appar. 89* (1965) 835.
[28] E. Stahl, *Z. Anal. Chem. 236* (1968) 294.
[29] E. V. Truter: *Thin Film Chromatography*, Cleaver-Hume Press, London 1963.
[30] A. Zlatkis, R. E. Kaiser: *High Performance Thin-Layer Chromatography*, Elsevier, Amsterdam 1977.
[31] R. Delley, G. Szekely, *Chimia 32* (1978) 261.
[32] E. Stahl, A. Glatz, *J. Chromatogr. 240* (1982) 518; *243* (1982) 139.
[33] J. A. Vinson, J. E. Hooyman, *J. Chromatogr. 135* (1977) 226.
[34] M. Jones, R. W. Keenan, P. Horowitz, *J. Chromatogr. 237* (1982) 522.
[35] N. M. Rascher, J. H. Onley, *J. Chromatogr. 140* (1977) 109.
[36] M. Weigele, S. L. DeBernardo, J. P. Teng, *J. Am. Chem. Soc. 94* (1972) 5927.
[37] S. Udenfriend, S. Stein, P. Böhlen, W. Leimgruber, W. Weigele, *Science 178* (1972) 871.
[38] K. Imai, P. Böhlen, S. Stein, S. Udenfriend, *Arch. Biochem. Biophys. 161* (1974) 161.
[39] A. M. Felix, M. H. Jimenez, *J. Chromatogr. 89* (1974) 361.
[40] H. Nakamura, *J. Chromatogr. 121* (1976) 33, 79; *131* (1977) 215; *152* (1978) 153; *154* (1978) 51; *175* (1979) 153; *200* (1980) 324.
[41] E. Stahl, C. Zimmer, S. Juell, *Z. Lebensm. Unters. Forsch. 175* (1982) 88.
[42] I. Epstein, R. W. Rosenthal, R. I. Ess, *Anal. Chem. 27* (1955) 1435.
[43] I. A. Guth, L. P. Manner, *J. Chromatogr. 30* (1967) 514.
[44] K. Norpoth, H. Schriewer, H. M. Rauen, *Arzneim. Forsch. 21* (1971) 1718.
[45] R. Braun, W. Dittmar, M. Machut, S. Weickmann, *Dtsch. Apoth. Ztg. 122* (1982) 1109.
[46] R. Braun, personal communication.
[47] E. Stahl, P. J. Schorn in [8], p. 401.
[48] E. Stahl, *Arch. Pharm. (Weinheim, Ger.) 293* (1960) 531.
[49] F. Geike, *J. Chromatogr. 44* (1969) 95; *52* (1970) 447; *53* (1970) 269; *58* (1971) 257; *61* (1971) 279; *63* (1971) 343; *64* (1972) 383; *67* (1972) 343; *72* (1972) 153, 333; *87* (1973) 199.
[50] F. Geike, *Z. Anal. Chem. 255* (1971) 134; *256* (1971) 203; *258* (1972) 284; *261* (1972) 397; *266* (1973) 286; *270* (1974) 366, 367; *276* (1975) 77.
[51] C. E. Mendoza, *Res. Rev. 43* (1972) 105; *50* (1974) 43.
[52] W. M. Draper, D. G. Crosby, *J. Chromatogr. 216* (1981) 413.
[53] M. Doerr, Dissertation, Universität Saarbrücken 1983.
[54] K. Randerath: *Dünnschicht-Chromatographie*, Verlag Chemie, Weinheim 1963.
[55] J. M. Bobbitt: *Thin-Layer Chromatography*, Reinhold, New York 1963.
[56] G. B. Marini-Bettolo: *Thin-Layer Chromatography*, Elsevier, Amsterdam 1964.
[57] K. Macek, I. M. Hais: *Stationary Phase in Paper and Thin-Layer Chromatography*, Publ. House Czech. Acad. Sci., Prag 1965.
[58] L. Labler, V. Schwarz: *Chromatografie na Tenke Vrstve*, Czech. Acad. Sci., Prague 1965.
[59] G. Pataki: *Dünnschichtchromatographie in der Aminosäure- und Peptid-Chemie*, de Gruyter, Berlin 1966.
[60] J. Kirchner: *Thin-Layer Chromatography*, Wiley-Interscience, New York 1967.
[61] M. Šaršunova, V. Schwarz, C, Michalec: *Chromatografie na Tenkych Vrstvach vo Farmacii a v Klinickej Biochemii*, Obzor 1968.
[62] J. Opienska-Blauth, H. Kraczkowski, H. Brzuskiewicz: *Zarys Chromatografii Cienkowarstwowej*, Panstwowetto Wyd. Rolnicze, Warsaw 1967.
[63] M. Ishikawa, S. Hara, T. Furuya, Y. Nakazawa: *Thin-Layer Chromatography. Theory and Practice* (Japanese), Nanzando, Tokyo 1968.

[64] E. J. Shellard: *Quantitative Paper and Thin-Layer Chromatography*, Academic Press, New York 1968.
[65] G. Vernin: *La Chromatographie en Couche Mince*, Dunod, Paris 1970.
[66] A. Niederwieser, G. Pataki, *Prog. Thin-Layer Chromatogr. Relat. Methods 1* (1970); *2* (1972), Ann Arbor-Humphrey Science Publ.
[67] E. Stahl: *Chromatographische und mikroskopische Analyse von Drogen*, Gustav Fischer Verlag, Stuttgart 1970 (suppl. reprint 1978).
[68] F. Geiss: *Die Parameter der Dünnschicht-Chromatographie*, Vieweg, Braunschweig 1972.
[69] K. Macek: *Pharmaceutical Applications of Thin-Layer and Paper Chromatography*, Elsevier, Amsterdam 1972.
[70] R. M. Scott: *Thin-Layer Chromatography Abstracts 1968-1971*, Ann Arbor Science Publ. 1972.
[71] W. Christen: *Dünnschicht-Chromatographie*, GIT, Darmstadt 1975.
[72] H. Auterhoff, K. A. Kovar: *Identifizierung von Arzneistoffen*, Wissenschaftliche Verlagsgesellschaft, Stuttgart 1971.
[73] S. Dominguez: *Cromatografia en Papel y en Capa Delgada*, Selbstverlag, Monterrey 1978.
[74] J. Gasparic, J. Churacek: *Laboratory Handbook of Paper and Thin-Layer Chromatography*, Wiley, New York 1978.
[75] W. Götz, A. Sachs, H. Wimmer: *Dünnschicht-Chromatographie*, Gustav Fischer Verlag, Stuttgart 1978.
[76] J. Touchstone, M. Dobbins: *Practice of Thin-Layer Chromatography*, Wiley, New York 1978.
[77] E. Stahl, W. Schild: *Pharmazeutische Biologie*, Bd. *4*, Gustav Fischer Verlag, Stuttgart 1981.
[78] H. Jork, H. Wimmer: *Quantitative Auswertung von Dünnschicht-Chromatogrammen* (Literatursammlung), GIT, Darmstadt 1982.
[79] P. Pachaly: *Dünnschichtchromatographie in der Apotheke*, Wissenschaftliche Verlagsgesellschaft, Stuttgart 1982.
[80] J. Touchstone: *Advances in Thin-Layer Chromatography*, Wiley, New York 1982.
[81] H. Wagner, S. Bladt, E. M. Zgainski: *Drogenanalyse, Dünnschicht-chromatographische Analyse von Arzneidrogen*, Springer-Verlag, Berlin 1983.
[82] A. Baerheim Svendsen, R. Verpoorte: *Chromatography of Alkaloids, Part A: Thin Layer Chromatography*, Elsevier, Amsterdam 1983.
[83] D. Jänchen: *TLC-Abstracts 1965-1977*, Selbstverlag Camag, Muttenz 1977.
[84] O. H. Masek, M. J. Saxby: *TLC-Abstracts 1971-1979*, PRM Science and Technology, London 1979.
[85] M. Lederer: Abstracts in *J. Chromatogr.*, since 1964.

# Metal Complexes of Sulfur Ylides: Coordination Chemistry, Preparative Organic Chemistry, and Biochemistry

**By Lothar Weber***

In recent years both acyclic and cyclic sulfur ylides have proved to be interesting and versatile ligands in preparative organometallic chemistry. In addition to paralleling the coordination chemistry of their phosphorus analogues, sulfur ylide complexes show specific structural and chemical features; they are becoming more important in preparative inorganic and organic chemistry, and may also be biochemically relevant as methylene transfer agents. Recent studies of the complexes of the ylidic $\lambda^4$-thiabenzenes and $\lambda^6$-thiabenzene 1-oxides have frequently demonstrated unexpected and novel reactions, and thereby enriched the chemistry both of ylides and of carbonylmetals.

## 1. Introduction

Phosphorus ylides[1] belonged to the synthetic armoury of organic chemists for 20 years before inorganic chemists began to take an increased interest in them. As powerful electron donors, these exceptionally versatile ligands form with almost all metals a wide range of complexes having surprisingly stable metal-carbon bonds. Ylide complexes enrich our knowledge of structural chemistry; in addition, several exhibit exceptional catalytic activity or are of pharmacological importance. The coordination chemistry of phosphorus ylides has been reviewed by *Schmidbaur*[2], *Weber*[3], and *Kaska*[4].

A similar fate awaited sulfur ylides. Some fifteen years after their introduction as synthetic reagents in organic chemistry, *Trost* described them in a monograph as "emerging synthetic intermediates"[5]. Only then did some research groups begin to study the ligand properties of these fascinating compounds, which had long since become indispensable reagents to the organic chemist[6].

This article reports on the synthesis, structure, and chemical properties of sulfur ylide complexes, underlines their relevance in preparative organic and organometallic chemistry, and presents comparisons to, and contrasts with, the chemistry of phosphorus ylides.

## 2. Sulfur Ylides as σ-Ligands

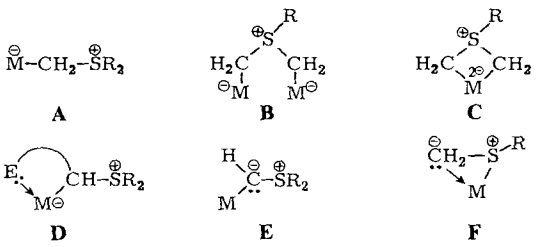
### 2.1. Metal Complexes of Acyclic Sulfur Ylides

Sulfur ylides are zwitterions in which a carbanion center is stabilized by a directly neighboring sulfonium center. Open-chain sulfur ylides can be coordinated as terminal ligands to a metal center (**A**), in the same way as phosphorus ylides. Their monoanions can coordinate as bridging double ylides (**B**) or as chelating ligands (**C**). Chelate com-

[*] Priv.-Doz. Dr. L. Weber
Institut für Anorganische Chemie der Universität—Gesamthochschule
Postfach 10 37 64, D-4300 Essen 1 (Germany)

 © Verlag Chemie GmbH, 6940 Weinheim, 1983 0570-0833/83/0707-0516 $ 02.50/0 

plexes are also formed if, in addition to the ylide function, a further donor atom is present in the molecule (**D**). The ylide function itself may be substituted with metal atoms at the carbanion center (**E**), or a complexed metal may additionally act as substituent at the sulfonium center (**F**), whereby in the last-mentioned case this substituent can also function as an intramolecular coordination center.

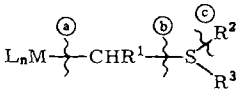


**A** **B** **C**

**D** **E** **F**

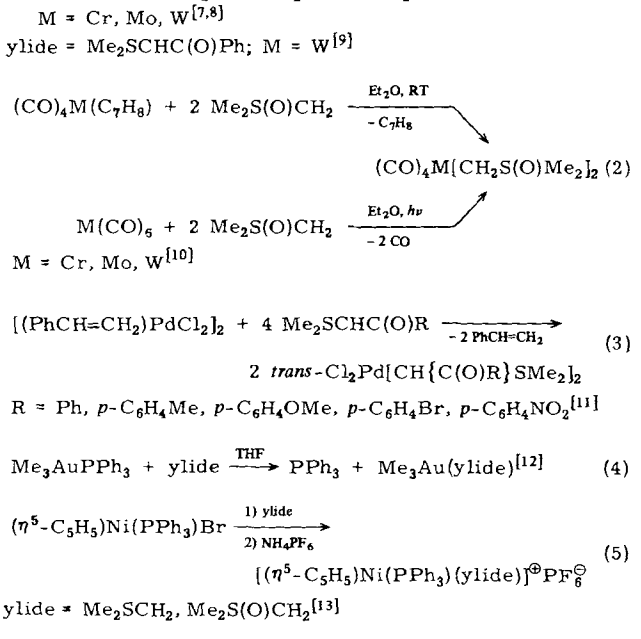
### 2.1.1. Terminal Ligands

Complexes of type (**A**) are generally synthesized by forming the bonds ⓐ, ⓑ, or ⓒ (cf. Scheme 1); the indirect routes *via* ⓑ and ⓒ are not dependent on the ability of the free ylide to exist separately. This enables unstable ylides to be synthesized at a protecting metal center.



Scheme 1. Routes to ylide complexes of type **A**.

*Bond Formation* ⓐ: Most complexes of the type discussed here are prepared by ligand exchange reactions, normally of labile ligands such as ethers, alkenes, nitriles, halides, or even tertiary phosphanes. Exchange of CO is usually achieved photochemically.



THF = tetrahydrofuran
ylide = $Me_2S(O)CH_2$, $Me(Me_2N)S(O)CH_2$;
M = Cr, Mo, W[7,8]
ylide = $Me_2SCHC(O)Ph$; M = W[9]



M = Cr, Mo, W[10]



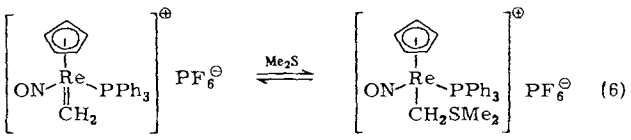
R = Ph, *p*-$C_6H_4Me$, *p*-$C_6H_4OMe$, *p*-$C_6H_4Br$, *p*-$C_6H_4NO_2$[11]





ylide = $Me_2SCH_2$, $Me_2S(O)CH_2$[13]

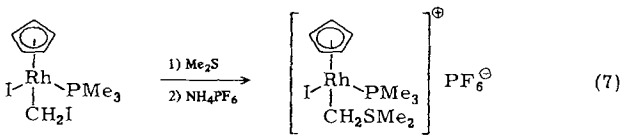
*Bond Formation* ⓑ: In the protecting coordination spheres of transition metals, the synthesis and stabilization of thermolabile $Me_2SCH_2$ is achieved by sulfane addition to carbene complexes[22a].



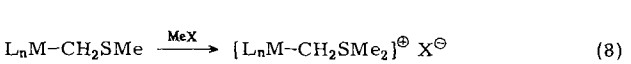
**1**

Here, the ylide complex **1** is in equilibrium with the starting materials. The formation of complexes of this type is determined, in general, by the size and basicity of the sulfane and by the size and electrophilicity of the alkylidene ligand[22a]. In contrast, only very electron-rich phosphorus ylide complexes tend to decompose to phosphane and alkylidene complexes[22b-e] (for the reversible reaction of Fischer carbene-metal complexes with phosphanes cf. [3,39f]).

The rhodium-$CH_2SMe_2$ unit can be synthesized by substitution of the corresponding iodomethyl complex[23].



*Bond Formation* ⓒ: The alkylation of alkylthiomethyl complexes leads in many cases to complexes of sulfur ylides.



| $L_nM$ | $Cp(CO)_2Fe$[24] | $Cl(Ph_3P)_2(CO)_2Os$[25] |
|---|---|---|
| MeX | $(Me_3O)BF_4$, $MeSO_3F$ | $MeSO_3CF_3$ |

| $L_nM$ | $ClL_2Pt$ (L = $PPh_3$, $PPh_2Me$)[26] |
|---|---|
| MeX | $MeSO_3F$ |

*Bonding and Molecular structure:* In the compounds discussed in this section, the ylide ligand is always linked to the metal atom by a σ-bond. As in the analogous complexes of phosphorus ylides, the metal-carbon σ-bond is remarkably stable, both chemically and thermally. In general, phosphorus ylides are stronger donor ligands than the corresponding sulfur ylides, as revealed by a comparison of IR data for $(CO)_5Cr$(ylide) [ylide = $Ph_3PCH_2$, $Ph_2MePCH_2$, $PhMe_2PCH_2$, $(MeO)_3PCH_2$, $Me_2S(O)CH_2$,

$Me(Me_2N)S(O)CH_2$[27]] and by ESCA measurements on $Me_3Au(ylide)$ [ylide = $Me_3PCH_2$, $Ph_3PCH_2$, $Me_2SCH_2$, $Me_2S(O)CH_2$[12b]].

X-Ray structure analysis of $Me_3Au[CH_2S(O)Me_2]$[12b], as well as of $[(tBuCH_2)_2SMe]^{\oplus}[(tBuCH_2)_2SCH_2ZnI_3]^{\ominus}$[28], $[(\eta^5\text{-}C_5H_5)(CO)_2FeCH_2SMe_2]^{\oplus}[SO_3F]^{\ominus}$[24b], and (±)-*trans*-$Cl_2Pd[CH\{C(O)Ph\}SMe_2]_2$[11] demonstrates the existence of metal-carbon single bonds.

### 2.1.2. Bridging and Chelating Ligands

In contrast to the analogous phosphorus ylide compounds, coordination compounds of sulfonium double-ylide

$$[(PhCH{=}CH_2)PdCl_2]_2 \xrightarrow[\text{DMSO}]{4\ Me_2S(O)CH_2/2\ NaI} \text{(Me, CH}_2\text{, I, Pd, Pd, I, CH}_2\text{, O, S, CH}_2\text{, CH}_2\text{, S, Me)} + 2\ NaCl + 2\ (Me_3SO)Cl + 2\ PhCH{=}CH_2 \quad (9)$$

DMSO = dimethylsulfoxide

derivatives (type **B** or **C**) are rare. The anions $[(CH_2)_2S(O)Me]^{\ominus}$ and $[(CH_2)_2SMe_2]^{\ominus}$ can act as bridging or chelating ligands. The deprotonation of the ylide occurs by transylidation[11].

Metalalkyl compounds contain strongly basic ligands, which can deprotonate coordinated $Me_2S(O)CH_2$. However, the products are usually coordination polymers, whose structures could not be determined[14,29].

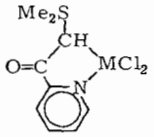
$$nR_2M + 2\,n\ Me_2S(O)CH_2 \longrightarrow \left[\text{(O, Me, S, CH}_2\text{, CH}_2\text{, M, M, CH}_2\text{, CH}_2\text{, S, Me, O)}\right]_n + 2n\ RH \quad (10)$$

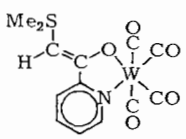
| M | Zn | Cd |
|---|---|---|
| R | Et | Me, $Me_3SiCH_2$ |

A dinuclear rhenium complex with a bridging sulfur double ylide can be synthesized indirectly by twofold addition of a methylene complex to a methanethiolate ion[22a].

$$2\left[\text{(ON, Re, PPh}_3\text{, CH}_2\text{)}\right]^{\oplus} \xrightarrow{\ominus SCH_3} \left[\text{(ON, Re, PPh}_3\text{, ON, Re, PPh}_3\text{, CH}_2\text{, S, CH}_2\text{, CH}_3\text{)}\right]^{\oplus} \quad (11)$$

Chelate complexes of type **D** can also be formed if the sulfur ylide carries a further donor atom. Dimethylsulfonio-2-picolinoylmethanide forms palladium and platinum




M = Pd, Pt

complexes in which it is bonded to the metal *via* the ylide group and the pyridine N atom; in a tungsten complex, however, the donor atoms are pyridine N and "carbonyl" oxygen[9,30,31].

### 2.1.3. Metal-Substituted Ylides

Whereas numerous phosphorus ylides have a metal substituent at the carbanion center[3], few metal-substituted sulfur ylides (type **E**), such as **2a**–**2c**, have been reported[32,33].

$$Me_2S(O)CH_2 \xrightarrow[-\ nBuH]{+\ nBuLi} \text{(Me, CH}_2\text{, S, O, CH}_2\text{, Li}^{\oplus}\text{)} \xrightarrow[-\ LiCl]{+\ Me_3GeCl} \text{(Me, CHGeMe}_3\text{, S, O, CH}_3\text{)} \quad \textbf{2a} \quad (12)$$

$$3\ Me(Me_2N)S(O)CH_2 + 2\ Me_3MCl \longrightarrow 2\ [Me_2(Me_2N)S(O)]Cl + \text{(Me}_2\text{N, C(MMe}_3\text{)}_2\text{, S, O, CH}_3\text{)} \quad \begin{matrix}\textbf{2b},\ M = Ge\\ \textbf{2c},\ M = Sn\end{matrix} \quad (13)$$

Transition-metal-substituted sulfur ylide complexes of the form **2d** are unknown. They might be regarded as carbyne complexes stabilized by a sulfane and would be of interest synthetically as methylidyne transfer agents. This would be analogous to alkylidene transfer by sulfur ylide complexes (see Section 2.3).

$$L_nM\text{–}C(R^1){=}SR_2^2 \xrightarrow[-\ R_2^2S]{} [L_nM{\equiv}CR^1]$$

**2d**

### 2.1.4. $\eta^2$-Methylthiomethyl Complexes

Compounds containing the structural group **F** can be formally regarded as ylide complexes. A carbanion center occupies the α-position to a sulfonium center, at which the metal atom acts as a substituent (and as acceptor). Such compounds are accessible by intramolecular ligand exchange from $\eta^1$-methylthiomethyl complexes.

$$L'L_nM\text{–}CH_2SMe \xrightarrow[-\ L']{\Delta\ \text{or}\ h\nu} \text{(L}_n\text{M, CH}_2\text{, S, Me)} \quad (14)$$

| $L_nM$ | $(PPh_3)_2Pd$[34] | $(CO)_4Mn$[35] | $Cp(CO)_2M$ (M = Mo, W)[35] |
|---|---|---|---|
| L' | Cl | CO | CO |

*S*-Methylation of $\eta^2$-thioformaldehyde ligands also leads to cationic complexes of type **F**[25].

$$(\eta^2\text{-}CH_2S)Os(CO)_2(PPh_3)_2 \xrightarrow{CF_3SO_3Me} \left[\text{(O, PPh}_3\text{, C, S–CH}_3\text{, Os, O, C, CH}_2\text{, PPh}_3\text{)}\right] CF_3SO_3^{\ominus} \quad (15)$$

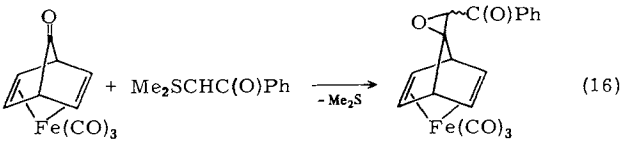
The existence of three-membered metallacycles with CS single bonds has been confirmed by X-ray crystallographic analysis[36,37].

## 2.2. Reactions of Coordinated Ligands with Acyclic Sulfur Ylides

Transition-metal centers have an appreciable and varied influence on organic molecules: they can behave as protecting groups by coordinating to polyfunctional species, thus allowing selective reactions[38]; thermolabile moieties can be stabilized by complex formation, and hence made available for directed reactions[39]. Metal atoms can also often activate ligands and catalyze many processes[40]. The reactions described in this section involve nucleophilic attack of sulfur ylides on the Lewis acid centers of a number of molecules in the coordination sphere of metal complexes.

### 2.2.1. *Aldehydic and Ketonic Carbonyl Groups*

Norbornadien-7-one is stabilized by the $Fe(CO)_3$ fragment; the chemistry of its CO group can thus be studied[41].




(16)

Reactions of this type involving sulfur ylides have been little studied, but seem very promising. It might be possible, for instance, to allow the 2,4-cyclohexadienone ligand (isomeric with phenol) of tricarbonyl(cyclohexadienone)iron[42a-c] to react with ylides, a reaction impossible with free phenol[42d]. α,β-Unsaturated carbonyl compounds usually form cyclopropanes on reaction with sulfur ylides; this reaction would be blocked by coordination at a metal center, possibly opening the way for the alternative epoxidation. Acylferrocenes can be converted in good yield into other derivatives using $Me_2SCH_2$[43].

$$Fc\text{–}C(O)R \xrightarrow[DMSO/THF]{Me_2SCH_2} Fc\text{–}CHR\text{–}CHO \qquad (17)$$

Fc = $(\eta^5\text{-}C_5H_5)Fe(\eta^5\text{-}C_5H_4)$; R = H, Me, Ph

### 2.2.2. *Carbonyl Ligands*

In contrast to the more strongly nucleophilic phosphorus ylides, such as $Ph_3PCH_2$ or $Me_3PCH_2$[44], sulfur ylides do not add to the CO ligands of $M(CO)_6$ (M = Cr, Mo, W). The force constants of the CO stretching vibrations provide a measure of the electrophilicity of coordinated carbon monoxide ($k$ = 16.49, 16.42, 16.41 mdyn/Å for $[M(CO)_6]$, M = Cr, Mo, W, respectively[45]). The higher electrophilicity of the CO ligands in $Fe(CO)_5$ ($k_{ax}$ = 17.0, $k_{eq}$ = 16.4 mdyn/Å) and $[(\eta^5\text{-}C_5H_5)Fe(CO)_3]^{\oplus}$ ($k$ = 17.6 mdyn/Å[46]), allows $Me_2S(O)CH_2$ to add to the carbonyl group, followed by its rapid transylidation[27,47].

$$Fe(CO)_5 + 2\ Me_2S(O)CH_2 \longrightarrow (Me_3SO)^{\oplus}[(CO)_4Fe{=}C(O)CHS(O)Me_2]^{\ominus} \qquad (18)$$

$$[(\eta^5\text{-}C_5H_5)Fe(CO)_3]^{\oplus}PF_6^{\ominus} + 2\ Me_2S(O)CH_2 \longrightarrow (Me_3SO)PF_6 + (\eta^5\text{-}C_5H_5)(CO)_2Fe[C(O)CHS(O)Me_2] \qquad (19)$$

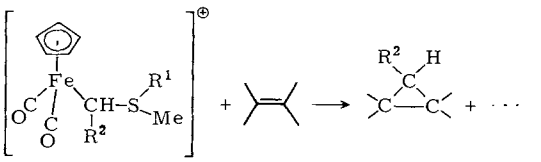
The products can be regarded as sulfonioacyl-metal complexes or as sulfur ylides substituted by ferriocarbonyl moieties.

Apart from the reaction of $Me_2S(O)CH_2$ with the SiCl function of chlorosilyliron complexes[48], periphery reactions of sulfur ylides with small ligands remain largely uninvestigated. The results of reactions of carbene, carbyne, olefin, and isocyanide complexes with phosphorus ylides[49] may serve as guidelines for the corresponding reactions of sulfur ylides.

## 2.3. Sulfur Ylide Complexes as Synthetic Building Blocks

### 2.3.1. *Cyclopropanation*

Sulfur ylides normally form cyclopropane derivatives only with activated alkenes; however, stereospecific alkylidene-transfer to electron-rich olefins is possible using complexed ylides[24,50].



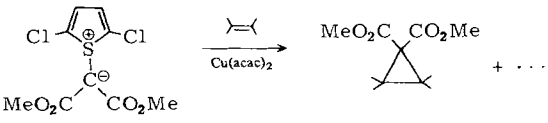

(20)

$R^1$ = Me, Ph; $R^2$ = H, Me

Unlike other reagents for cyclopropanation, ylide-iron complexes are readily accessible and easy to handle. The reaction conditions are largely determined by the leaving group properties of the sulfane.

*McCormick* and *Gladysz*[22a] have shown that sulfur ylide complexes are in equilibrium with the free sulfanes and reactive alkylidene complexes. It is, therefore, reasonable to assume that the reactive species in cyclopropanation is a carbene complex: cyclopropanations using carbene complexes have been described frequently in the literature[51].

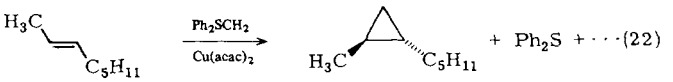
In this context, analogies between sulfur ylide complexes and diazoalkanes are apparent[52]. *Salomon* and *Kochi*[52a] use a sulfur ylide complex as a model for cyclopropanation reactions[52a]. *Tamblyn et al.*[53] demonstrated a relationship between formation of sulfur ylides and catalytic cyclopropanation with ethyl diazoacetate, both of which occur *via* carbenemetal complexes[53]. *Porter et al.*[54] reported that the metal-catalyzed (Cu, Rh) cyclopropanation of olefins with a sulfur ylide is appreciably more efficient than with the corresponding dimethyl diazomalonate.

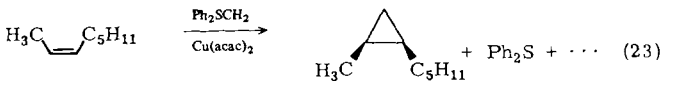



(21)

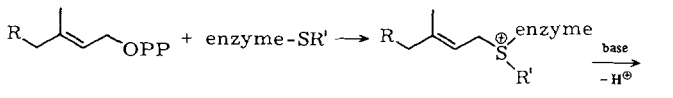
The ease and safety in preparing and handling sulfur ylides make them, in combination with copper salts, attrac-

tive cyclopropanation reagents. Furthermore, unlike $N_2$, the sulfane leaving group can be modified to control the reactivity of the ylide-copper complex. There is evidence that sulfonium salts and sulfur ylides are important in the biosynthesis of cyclopropanes[55-57]. *Cohen et al.* discovered that (diphenylsulfonio)methanide, which is inert to olefins such as *cis*- and *trans*-2-octene, forms the corresponding cyclopropanes stereospecifically in the presence of copper salts[58].

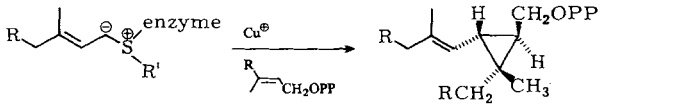



Since ylide formation is possible even under physiological conditions, a metabolic pathway involving sulfur ylide complexes of copper has been proposed for the biosynthesis of presqualene pyrophosphate[58].



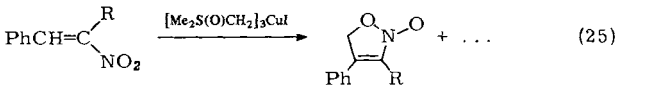

(24)




R = geranyl; PPO = pyrophosphate

### 2.3.2. Synthesis of Heterocycles

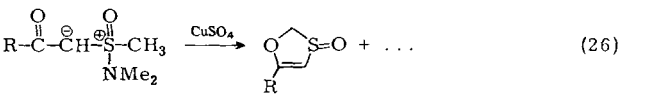
Although β-nitrostyrenes are converted into resins by free $Me_2S(O)CH_2$, they react with a copper complex of the ylide to give good yields of 2-isoxazoline *N*-oxides[59a].




(25)

R = H, Me

*Johnson et al.* have reported the conversion of carbonyl-stabilized [(dialkylamino)methyl(oxo)sulphonio]methanides into 1,3-oxathiol *S*-oxides, catalyzed by $CuSO_4$. Here, again, an ylide complex is postulated as reactive intermediate[59b].

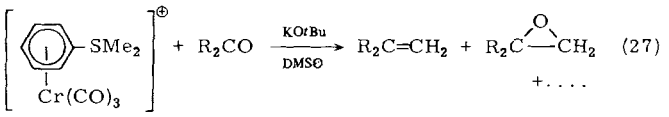



(26)

R = Me, Ph, *p*-$C_6H_4Cl$, *p*-$C_6H_4NO_2$, $PhCH_2$

### 2.3.3. Wittig Reactions

Unlike phosphorus ylides, which react with carbonyl groups to afford olefins, sulfur ylides react with aldehydes and ketones to give oxiranes. The coordination of the arene moiety of $Ph(Me)SCH_2$ to the $Cr(CO)_3$ group drastically alters this behavior of the ylide: with diaryl ketones the main products are alkenes[60].



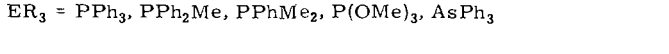

(27)

R = Ph, *p*-$C_6H_4NMe_2$

Electron withdrawal by the $Cr(CO)_3$ group increases the electrophilicity of the sulfonium center and allows deoxygenation of the primary adduct. This synthetic method is, however, confined to benzophenone derivatives, because of the reduced carbanion activity in the ylide complex. In addition, it is believed that the transition state leading to olefin formation is considerably stabilized by two aryl substituents.

### 2.3.4. Coordination Compounds of Unstable Ylides

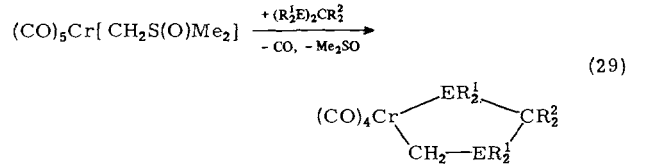
Alkylidenemetal fragments can be transferred from sulfur ylide complexes to phosphanes and arsanes[61].




(28)

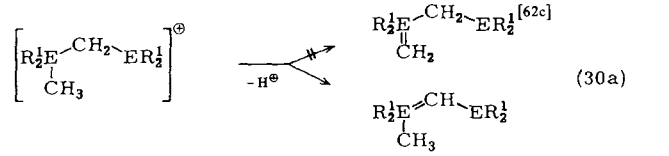
$ER_3$ = $PPh_3$, $PPh_2Me$, $PPhMe_2$, $P(OMe)_3$, $AsPh_3$

This process is relevant to the synthesis of complexes of unstable ylides, such as $(MeO)_3PCH_2$. Compounds of the form $(R^1_2E)_2CR^2_2$ give chelate complexes of ylide ligands that are unstable in the free state and subject to rearrangements[62a,b].

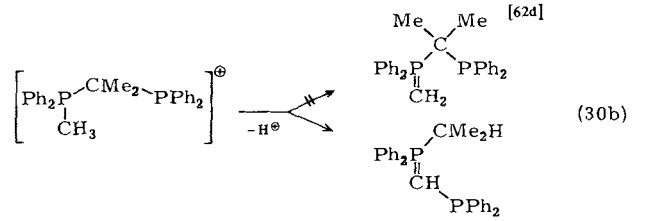



(29)

| $ER^1_2$ | $PPh_2$ | $PMe_2$ | $P(NMe_2)_2$ | $AsPh_2$ | $PPh_2$ |
|---|---|---|---|---|---|
| $R^2$ | H | H | H | H | $CH_3$ |

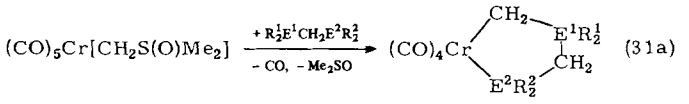



[62c] (30a)

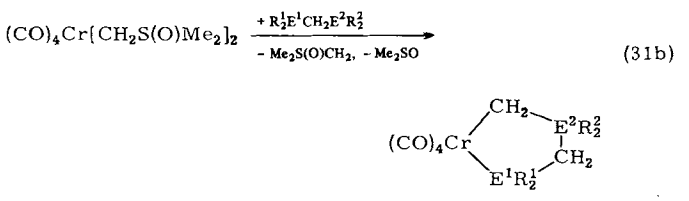



[62d] (30b)

The use of non-symmetrically substituted reagents allows regioselectivity of chelate synthesis by suitable choice of the sulfur ylide complex.



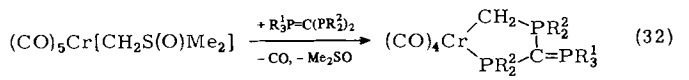
(31a)



(31b)

The first step in reaction (31a) is the displacement of $Me_2SO$ by $E^1R_2^1$, the more nucleophilic end group of $R_2^1E^1CH_2E^2R_2^2$; formation of product in reaction (31b) consists of attack of $E^1R_2^1$ on the chromium atom of the coordinatively unsaturated species $\{(CO)_4Cr[CH_2S(O)Me_2]\}$[62b].

The use of diphosphino-substituted ylides[62f,g] facilitates the synthesis of novel polyfunctional ylide ligands (reaction (32))[62e].

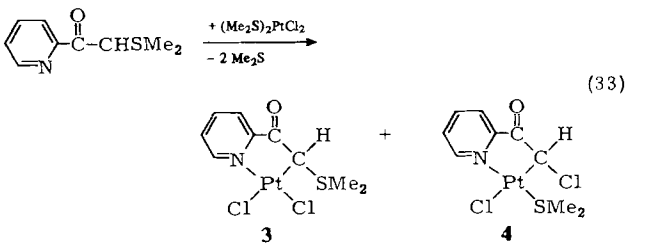


(32)

| $R^1$ | Me | Ph | Ph |
|---|---|---|---|
| $R^2$ | Me | Ph | Me |

### 2.3.5. α-Haloalkyl Complexes

Both the ylide complex **3** and the isomeric chelate complex **4**, with the (2-picolinoyl)chloromethyl ligand, can be isolated from the reaction of $PtCl_2(SMe_2)_2$ with $Me_2SCHC(O)-C_5H_4N$. Compound **4** is formed from **3** by removal and complexation of $Me_2S$, and 1,2-migration of a chloride ion from the metal to the neighboring carbon atom.



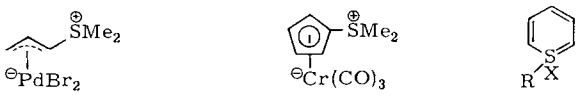
(33)

**3** **4**

This corresponds to the retrosynthesis of sulfur ylide complexes from halomethyl complexes and sulfanes (cf. reaction (7)).

## 3. Sulfur Ylides as π-Ligands

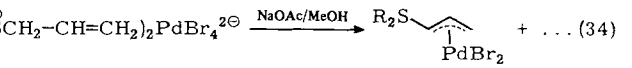
If the carbanion function is stabilized by mesomerism with vinyl substituents or by incorporation into a cyclic diene system, the resulting sulfur ylide can behave as an $\eta^3$- or $\eta^5$-ligand in π-interactions with metal centers.



The $\lambda^4$-thiabenzenes[64] (X = lone pair) and their oxides (X = O) differ from the sulfoniocyclopentadienides[63] in that the onium center is a ring member. The nature of $\lambda^4$-thiabenzenes was formerly disputed. *Price et al.* considered $\lambda^4$-thiabenzenes[66a,c,e], $\lambda^4$-thianaphthalenes[66b,d], and $\lambda^4$-thiaanthracenes[66b] to be novel aromatic species, but *Hortmann et al.*[64a] and *Mislow et al.*[64b,c] showed that at least some of *Price*'s compounds were polymers, and that aryl-substituted $\lambda^4$-thiabenzenes are extremely thermolabile species with ylidic character. MO calculations on the parent compound[67], and NMR[64b,c,68] and X-ray crystallographic data[69] on substituted thianaphthalenes confirm the ylidic nature of these non-planar heterocycles.

### 3.1. $\eta^3$-Sulfoniopropenide Ligands

(Dialkylsulfonio)-2-propenides (-"allylides") are unstable and undergo [2,3]sigmatropic rearrangements with allylic inversion[5]. *Nishiyama* managed to fix and stabilize species of this type at a palladium template[70].



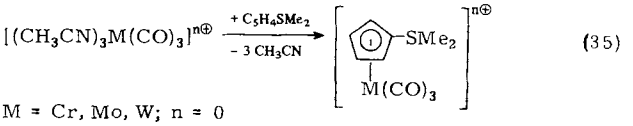
(34)

R = Me
$R_2$ = $(CH_2)_4$

These complexes decompose at 70 °C in $[D_6]$-$Me_2SO$ to afford 1,3,5-hexatriene.

### 3.2. $\eta^5$-Sulfoniocyclopentadienide Ligands

The different electronic shielding of the ring protons in $C_5H_4SMe_2$ are balanced out by complexation to $M(CO)_3$ (M = Cr, Mo, W, $Mn^+$, $Re^+$). The synthesis of the complexes proceeds by exchange of labile acetonitrile ligands in the corresponding starting materials.



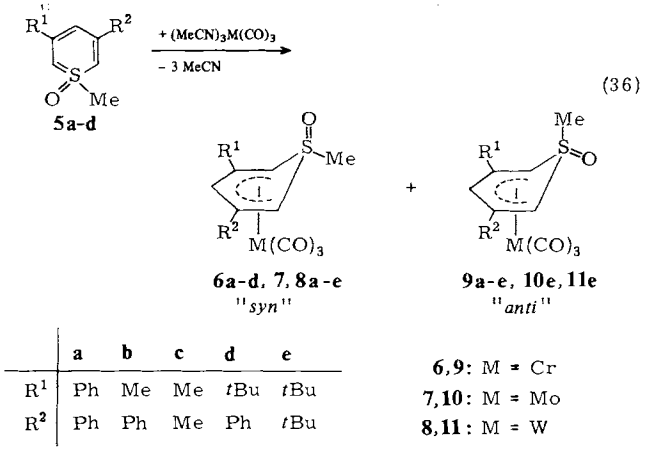
(35)

M = Cr, Mo, W; n = 0
M = Mn, Re; n = 1

The crystal structure of the chromium complex shows that there are no bonding interactions between the metal and the sulfonium center[71].

### 3.3. Preparation and Structure of λ⁶-Thiabenzene 1-Oxide Complexes

The $\lambda^6$-thiabenzene 1-oxides **5a—5d** act as $\eta^5$-6π-ligands towards $M(CO)_3$ fragments (M = Cr, Mo, W). The formation of two isomers, differing in the relative orientation of metal and oxosulfonium center, is observed only for chromium[72,73].

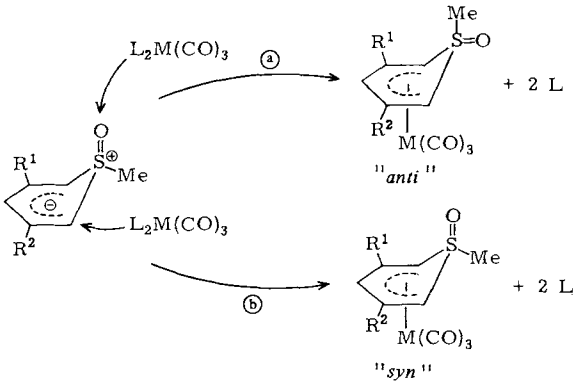



(36)

| | a | b | c | d | e |
|---|---|---|---|---|---|
| $R^1$ | Ph | Me | Me | *t*Bu | *t*Bu |
| $R^2$ | Ph | Ph | Me | Ph | *t*Bu |

In contrast, the di-*tert*-butyl derivative **5e** affords only the *anti*-isomer **9e**[*] with $Cr(CO)_3$, but both *syn*- and *anti*-isomers **7e**, **8e**, **10e**, and **11e** with $Mo(CO)_3$ and $W(CO)_3$[73].

The formation of the *anti*-complexes probably starts with attack of coordinatively unsaturated species, such as $(MeCN)_2M(CO)_3$, on the "hard" oxygen of the oxosulfonium center (Scheme 2, pathway ⓐ), whereas attack on the "soft" π-system leads to the *syn*-configurated compound (pathway ⓑ).




Scheme 2. Reaction pathways leading to *syn*- and *anti*-isomers of $\lambda^6$-thiabenzene 1-oxide complexes.

This would also explain why chromium, as the hardest metal, also forms *anti*-complexes. In **5e** the small chromium atom of $[(MeCN)_2Cr(CO)_3]$ is sterically blocked from the π-system, and thus only the *anti*-compound **9e** is formed. The spatial demands of the bulky *tert*-butyl groups in **5e** force the larger and "softer" molybdenum and tungsten also to proceed by the otherwise unfavorable reaction pathway ⓐ, again leading to *anti*-isomers.

The crystal structures of the free ylide **5a**[74] and the isomeric chromium complexes **6a** and **9a**[72] confirm the $\eta^5$-coordination of all five coplanar carbon atoms of the non-planar heterocycle at the metal center. **5a** adopts the *"syn"*-configuration in the crystal, the sulfur atom laying 39.5 pm above the plane of the carbon atoms[75]. In the two $Cr(CO)_3$ complexes the sulfur atoms move a further 36 and 23 pm, respectively, away from this plane.

[*] Complexes with the *syn*-configuration have the 1-alkyl group and the metal atom on the same side of the ring; in the *anti*-configuration, they are on opposite sides.

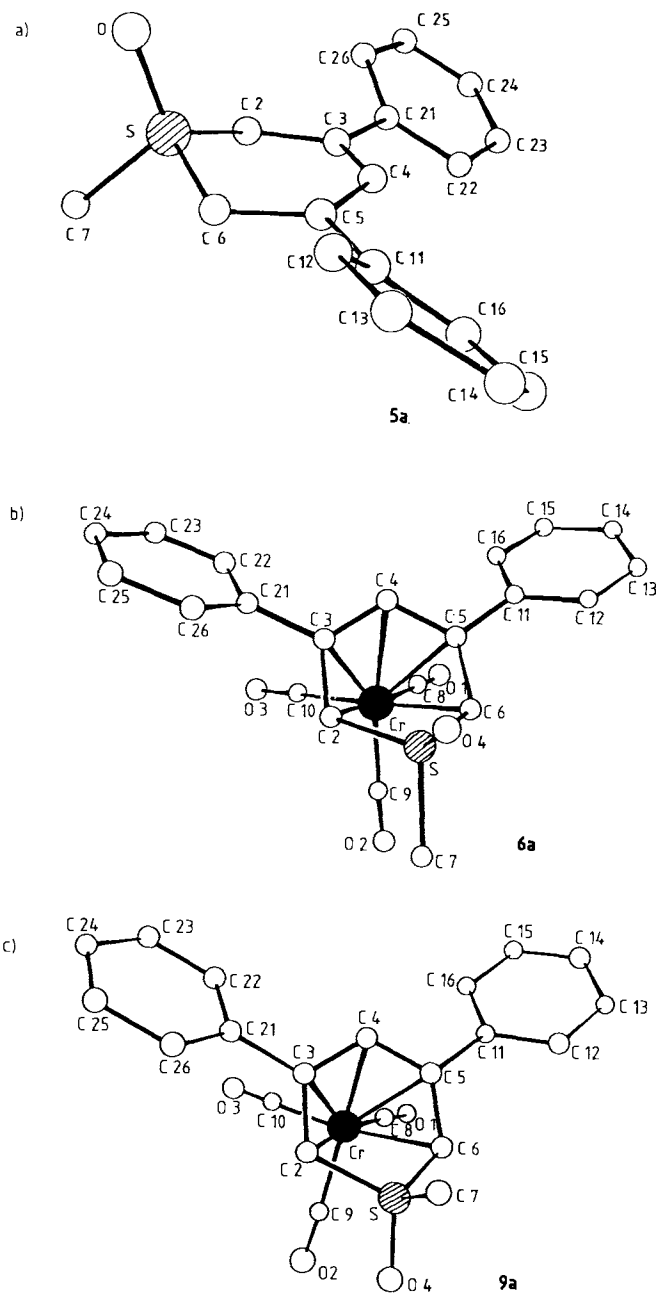



Fig. 1. Structures of molecules **5a**, **6a** and **9a** in the crystal. Selected bond parameters (distances [pm], angles [°]):

| | **5a** | **6a** | **9a** |
|---|---|---|---|
| Cr...S | — | 289.8(2) | 280.7(1) |
| S–O4 | 147.6(5) | 144.6(7) | 144.9(1) |
| S–C2 | 166.2(6) | 171.1(8) | 172.0(2) |
| S–C6 | 169.3(6) | 169.5(8) | 170.6(2) |
| S–C7 | 182.1(7) | 181.1(9) | 177.1(2) |
| C2–C3 | 142.9(8) | 142.2(10) | 142.5(3) |
| C3–C4 | 136.6(9) | 141.1(9) | 141.2(3) |
| C4–C5 | 139.8(9) | 140.7(10) | 140.8(3) |
| C5–C6 | 141.0(9) | 143.2(10) | 142.8(3) |
| planar ($C_2-C_6$) | 39.5 | 76 | 63 |
| Interplanar angle | 157.8° | 146° | 137° |

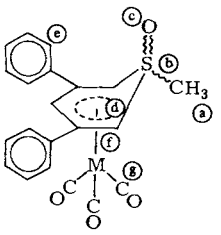
These structures are noteworthy in view of the coordination behavior of $\lambda^5$-phosphabenzenes[76]. The loss of planarity of the free heterocycles on complexing to $Cr(CO)_3$[76f] shows that in their complex chemistry $\lambda^5$-phosphabenzenes, like $\lambda^6$-thiabenzene 1-oxides, behave as

ylidic ligands, whose onium centers are not involved in bonding with the metal atom[77].

### 3.4 Chemical Properties of λ⁶-Thiabenzene 1-Oxide Complexes

Reports on λ⁶-thiabenzene 1-oxides have mostly been restricted to the preparation of the rings, but their chemistry has not been intensively investigated: reports have included their reduction[64a–c,65i], H/D exchange[65b,h–k], bromination and nitration[65h,i], and reactions at substituents[65b,k].

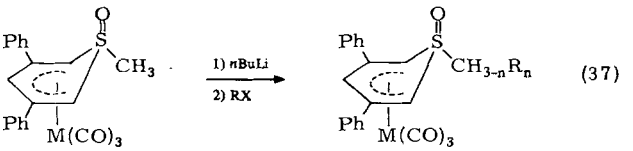
The electron density of the ring is appreciably reduced by coordination to the $M(CO)_3$ group and transferred to the metal. This electronic modification of both structural elements of the complexes makes possible a series of reactions that cannot be carried out with the free ligand or with the $M(CO)_3$ group in other chemical environments. The chemical properties of polyfunctional λ⁶-thiabenzene 1-oxide complexes are usually investigated with the 3,5-diphenyl derivatives; here reactions at positions ⓐ–ⓖ are possible (Scheme 3).



Scheme 3. Reactive centers of λ⁶-thiabenzene 1-oxide complexes.

#### 3.4.1. Alkylation of the $SCH_3$ Group

The influence of the electron-withdrawing $M(CO)_3$ unit markedly increases the acidity of the hydrogen atoms of the $SCH_3$ group (Scheme 3: ⓐ), facilitating alkylations in the two-phase system aqueous $NaOH/CH_2Cl_2$[78]. The $SCH_3$ group can also be lithiated with $n$-$C_4H_9Li$, and the resulting organolithium compound treated with a variety of electrophiles RX[78].



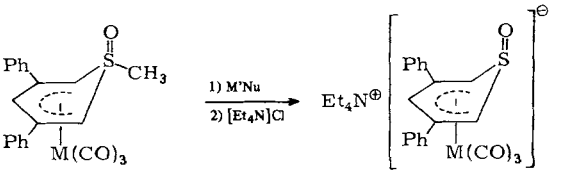
RX = MeI, $C_3H_5Br$, $PhCH_2Br$, $Me_3SiCl$, $Me_3GeCl$, $Me_3SnCl$, MeHgCl

n = 1,2

Chlorination of the *S*-alkyl group can be achieved by reaction of the lithium derivatives with $Cl_3CCN$[78].

#### 3.4.2. Demethylation to η⁵-Thiacyclohexadienyl 1-Oxide Complexes

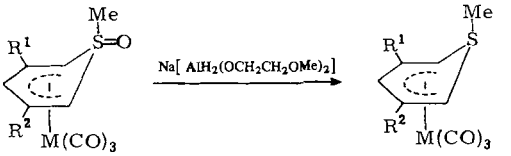
λ⁶-Thiabenzene 1-oxide complexes having the *syn*-configuration are demethylated by "soft" nucleophiles such as $Na_2[Fe(CO)_4]$, $LiPPh_2$, $Li[BHEt_3]$; the products can be converted into stable tetraethylammonium salts by metathesis with $[Et_4N]Cl$. The anions contain the novel thiacyclohexadienyl 1-oxide ligand[79,80], which is a weaker donor than the familiar η⁵-cyclopentadienyl ligand.



M'Nu = $Na_2[Fe(CO)_4]$, $LiPPh_2$, $Li[BHEt_3]$

#### 3.4.3. Deoxygenation to λ⁴-Thiabenzene Complexes

The complex hydride $Na[AlH_2(OCH_2CH_2OMe)_2]$ reacts differently than $Li[BHEt_3]$ with λ⁶-thiabenzene 1-oxide complexes: whereas the *syn*-complexes, in an uncharacteristic way, decompose, the *anti* complexes are reduced to λ⁴-thiabenzene complexes **12**[81].

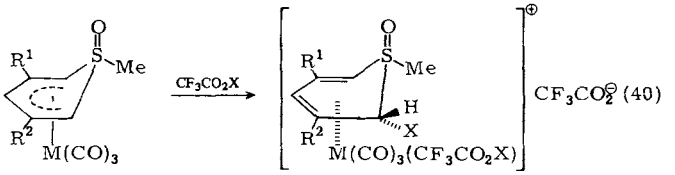


**9–11** **12**

The reduction of **5a** with $Cl_3SiH$ or $LiAlH_4$, however, gives thiopyrans and not the unstable λ⁴-thiabenzenes[64a]. The presence of the $M(CO)_3$ protecting group is necessary to stabilize the cyclic ylide.

#### 3.4.4. Protonation

The relatively long wavelength ν(CO) absorption bands indicate appreciable accumulation of electron density at the metal carbonyl groups in λ⁶-thiabenzene 1-oxide complexes **6**–**8**[72]. In order to investigate the basicity of the metal atoms, the complexes were dissolved in $CF_3CO_2H$; the molybdenum and tungsten derivatives were protonated at the α-position of the ring (relative to the oxosulfonium center)[82]. Deuteration experiments indicate *endo*-addition to the ring, presumably *via* prior protonation of the metal. In the tricarbonyl(cyclopentadienylide) complexes, on the other hand, the metal-hydrogen bond remains stable[83].

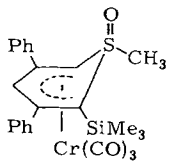


X = H, D

*Silylation of the Ring*

The reaction of **6a** with excess $n$-$C_4H_9Li$, followed by reaction with $Me_3SiCl$ and chromatographic separation on

$SiO_2$, leads, in a manner analogous to reaction (37), to complex **13**, with the silyl group in the α-position of the ring.



**13**

*endo-Hydride Addition*

The coordination of the $\lambda^6$-thiabenzene 1-oxide to the $(CO)_2Cr(NO)$ cation (see Scheme 3: ⑧) brings about a marked decrease in electron density at the 3- and 5-positions of the ring; these thus acquire electrophilic characteristics. Complexes of novel double ylide sulfonium compounds[85] can then be formed by *endo*-hydride addition reactions of unusual reaction type[84]. Figure 2 shows the molecular structure of **14d**.

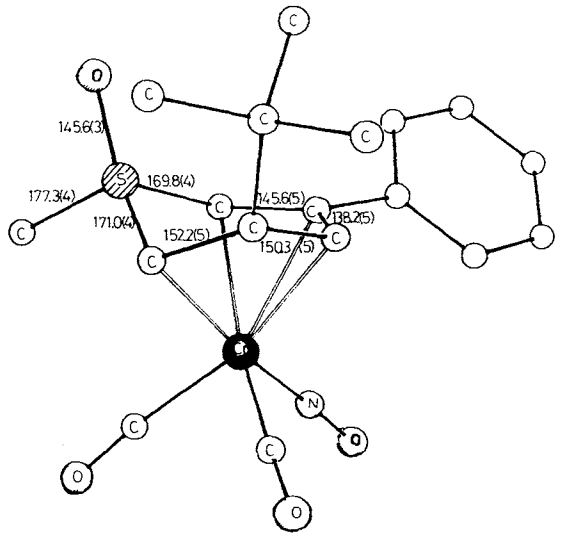
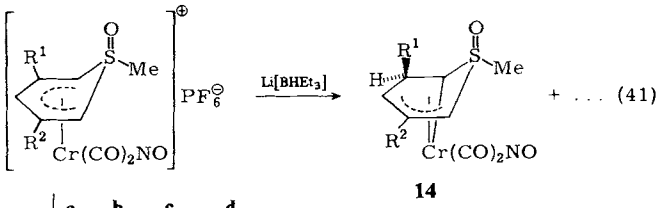


Fig. 2. Molecular structure of **14d** with selected bond lengths.

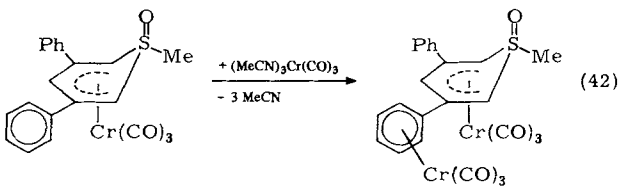


| | a | b | c | d |
|---|---|---|---|---|
| $R^1$ | Ph | Me | Me | *t*Bu |
| $R^2$ | Ph | Ph | Me | Ph |

**14**

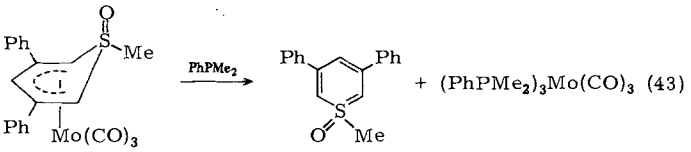
*3.4.5. Complex Formation at Phenyl Substituents*

The phenyl substituents of $\lambda^6$-thiabenzene 1-oxide ligands also exhibit donor properties, although coordination of the phenyl group (Scheme 3: ⑥) prior to that of the central heterocycle is never observed[27].



*3.4.6. Rupture of the Metal-Ring Bond*

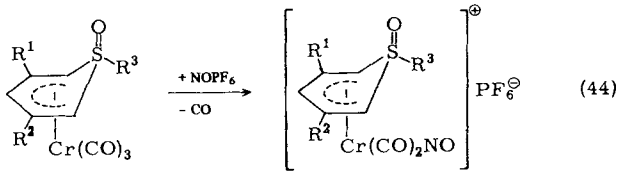
If the electron density of the $\lambda^6$-thiabenzene 1-oxide has been modified by coordination to a metal, and the activated species subsequently allowed to react further, the last step in the cycle is often the removal of the chemically altered ligand. **5a** is quantitatively displaced from complexes by excess $PhPMe_2$ in boiling THF[27].



**5a**

*3.4.7. Displacement of CO*

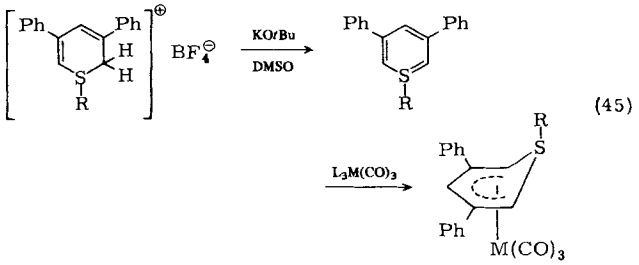
In the *syn*-configurated ($\lambda^6$-thiabenzene 1-oxide)chromium complexes **6**, a CO ligand can easily be replaced by the isoelectronic $NO^+$ ion, without breaking the metal-ring bonds[86].



Cationic arene(dicarbonyl)nitrosyl complexes of molybdenum and tungsten are, as yet, unknown; all attempts to prepare them have led to loss of the arene ligand[87]. Use of electron-donating or bulky groups ($R^1=R^2=Ph$; $R^3=CH(SiMe_3)_2$, $CH(CH_2Ph)_2$; $R^1=R^2=t$Bu, $R^3=Me$) on the $\lambda^6$-thiabenzene 1-oxide ligand stabilizes the metal-ring bond to such an extent that cationic dicarbonyl(nitrosyl)molybdenum and -tungsten complexes with organic 6π-ligands become accessible[86].

### 3.5. Preparation and Structure of $\lambda^4$-Thiabenzene Complexes

$\lambda^4$-Thiabenzene complexes of type **12** are accessible by deoxygenation of $\lambda^6$-thiabenzene 1-oxide complexes (cf. Section 3.4.3). This process is, however, dependent on the existence of complexes, such as **9**—**11**, having the *anti*-



R = Me, Et; M = Cr, L = MeCN; M = Mo, W, $L_3 = C_7H_8$

configuration. In some cases the synthesis can be achieved by trapping $\lambda^4$-thiabenzenes generated *in situ*[88].

Structural changes associated with the coordination of the $\lambda^6$-thiabenzene 1-oxide **5a** to the $Cr(CO)_3$ group are known. Information on the structure of the thermolabile $\lambda^4$-thiabenzene derivative analogous to **5a** can be obtained from the X-ray structure analysis of its $Cr(CO)_3$ complex **12a** and by comparison with data for **5a**, **6a**, and **9a**. In the stable, crystalline **12a** (Fig. 3) the heterocycle is bonded to the chromium atom through the five coplanar carbon atoms (as in the *anti*-complex **9a**). The sulfur atom lies 75 pm above this plane and is directed away from the chromium ($d$(Cr–S) = 288 pm). The methyl group occupies the axial *"anti"*-position at the pyramidal sulfur: *syn/anti* isomerism has not been detected. The ylidic nature of these heterocycles is thus established by means of their coordination chemistry. It is possible that the free ligand has a similar configuration.

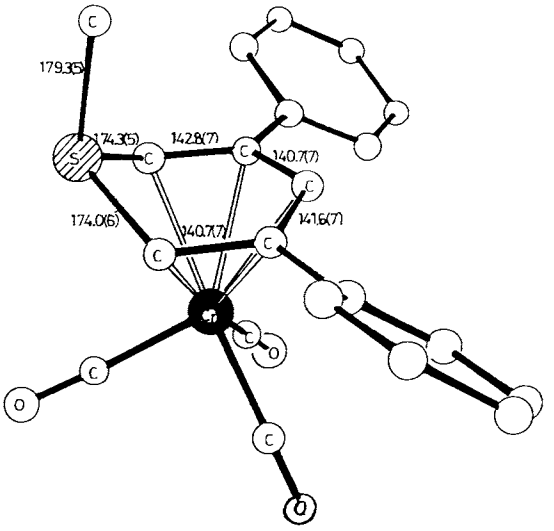


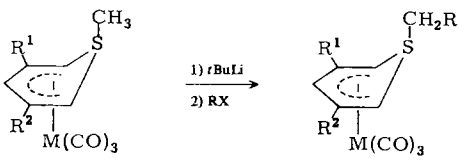

Fig. 3. Molecular structure of **12a** with selected bond lengths.

### 3.6. Chemical Properties of $\lambda^4$-Thiabenzene Complexes

Because of their thermolability, the chemistry of $\lambda^4$-thiabenzene complexes has been little investigated[64a,89–91]. The stabilizing influence of the $M(CO)_3$ template should, as with $\lambda^6$-thiabenzene 1-oxide complexes, allow a wide variety of reactions of $\lambda^4$-thiabenzenes to be investigated; some preliminary results have been obtained.

#### *3.6.1. Metalation and Alkylation of the $SCH_3$ Group*

The hydrogen atoms of the $SCH_3$ group are sufficiently acidic to allow lithiation and subsequent reaction with electrophiles. The $\lambda^4$-thiabenzene ligands thus formed have not yet been obtained by other methods[88b].

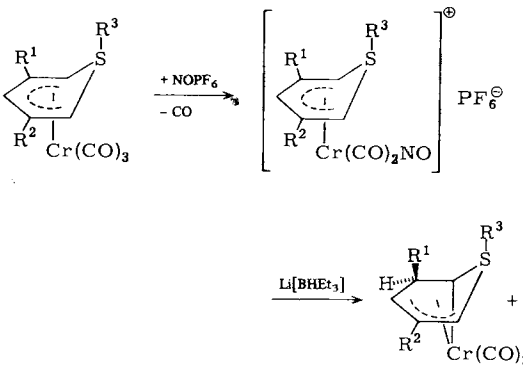



(46)

RX = MeI, $C_3H_5Br$, $PhCH_2Br$, $Me_3SiCl$, $Me_3GeCl$

#### *3.6.2. Nitrosylation*

Cationic $\lambda^4$-thiabenzene complexes are obtained by substitution of CO by $NO^+$; the ring ligand exhibits electrophilic properties and, in preliminary studies, has been shown to add hydride ion (cf. reaction (41))[92].



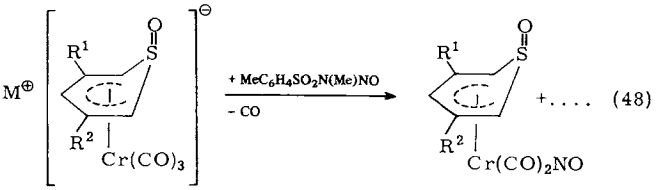

(47)

### 3.7. Chemical Properties of $\eta^5$-Thiacyclohexadienyl 1-Oxide Complexes

The $\eta^5$-thiacyclohexadienyl 1-oxide complexes synthesized as described in Section 3.4.2 possess structures similar to those of the corresponding *syn*-$\lambda^6$-thiabenzene 1-oxide complexes **6**—**8**. Demethylation appreciably increases the nucleophilicity of the complexes. Like other complex anions, they are valuable synthetic building blocks in organometallic chemistry.

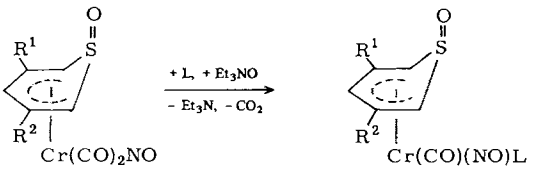
#### *3.7.1. Ligand Displacement*

The chromium complexes are easily nitrosylated to give neutral complexes[93].




(48)

A further ligand L can be introduced by the amine oxide method to give chiral complexes[93].

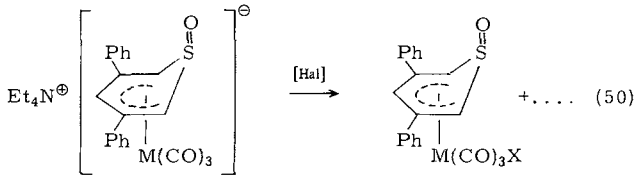



(49)

L = $PPh_3$, $PPh_2Me$, $PPhMe_2$, $C_5H_5N$

#### *3.7.2. Halogenation*

The molybdenum and tungsten complexes are halogenated by $PhICl_2$, $C_5H_5N \cdot Br_2$, or $I_2$[80].

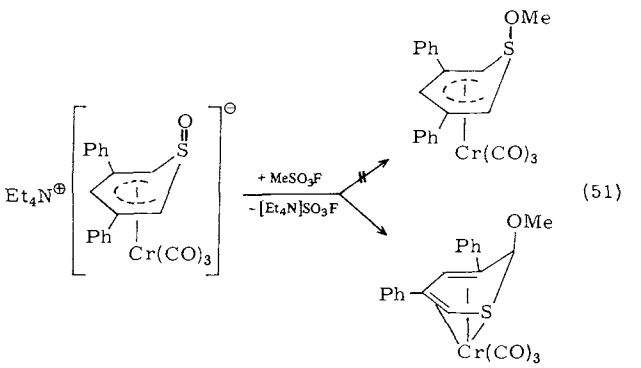


M = Mo, W
[Hal] = $PhICl_2$, $C_5H_5N{\cdot}Br_2$, $I_2$; X = Cl, Br, I

(50)

### 3.7.3. Alkylation

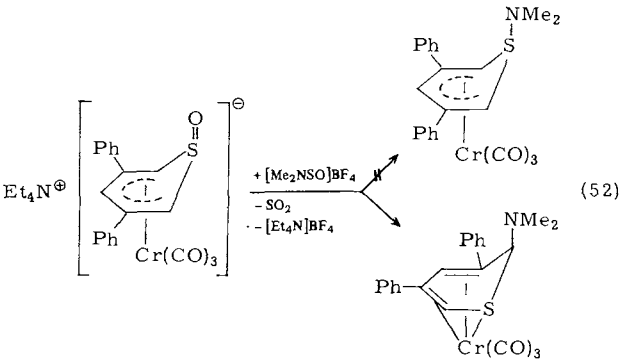
"Hard" alkylating agents attack the oxosulfonium center. A 2*H*-thiopyran complex is isolated, rather than the expected isomeric *S*-methoxylated $\lambda^4$-thiabenzene complex[94].



(51)

### 3.7.4. Amination

By analogy to the work of *Kresze et al.*[95], it should be possible to synthesize 1-amino-$\lambda^4$-thiabenzene complexes by reaction with $[Me_2NSO]^+BF_4^-$. Here also, however, only the isomeric 2*H*-thiopyran complex can be isolated, whose structure is confirmed by X-ray crystallography[94].



(52)

The rearrangements described in reactions (51) and (52) are novel in organometallic chemistry and may perhaps best be compared with the Pummerer rearrangement. The chirality of the complexes obtained from reactions (48), (49), (51), and (52) raises the question of whether asymmetric syntheses are possible.

## 4. Summary and Prospects

The coordination chemistry of open-chain sulfur ylides show similarities to, but also clear differences from, the chemistry of phosphorus ylides. The differences arise, as in the organic chemistry of these compounds, from the greater leaving-group tendency of diorganosulfanes or sulfoxides. Thus, some sulfur ylide complexes function as metal-alkylidene transfer reagents. Whereas free sulfur ylides can cyclopropanate only activated olefinic double bonds, they undergo an umpolung upon complexing to metals; in so doing they acquire electrophilic properties, and are then able to cyclopropanate electron-rich olefins. This reaction type is also feasible *in vivo* and may be of biochemical relevance. The tendency of sulfoxides to act as good leaving groups enables (formally) the $[(CO)_4Cr{=}CH_2]$ fragment to be transferred from the ylide complexes $(CO)_4Cr[CH_2S(O)Me]_2$ and $(CO)_5Cr[CH_2S(O)Me_2]$ to methylenebisphosphanes and -arsanes, thus forming coordination compounds of unstable phosphorus ylides. The regiospecificity of this reaction is clearly determined by the nature of the organometallic complex. The thermolabile $\lambda^4$-thiabenzenes can act as ylidic $\eta^5$-ligands at suitable metal centers, and can thus be stabilized. This is achieved by trapping the free rings *in situ* or by reduction of *anti*-$\lambda^6$-thiabenzene 1-oxide complexes. The crystal structure of the $Cr(CO)_3$ complex rules out any heteroaromaticity of the ligand ring and suggests a structure similar to that of the corresponding oxide for the free ylide ligand.

$\lambda^6$-Thiabenzene 1-oxides form a series of structurally fascinating complexes with $M(CO)_3$ (M = Cr, Mo, W); these undergo a variety of interesting reactions, which enrich our knowledge of organometallic chemistry. $\eta^5$-Thiacyclohexadienyl 1-oxide complexes display an interesting rearrangement of the coordinated ligand, comparable to the Pummerer rearrangement, on reaction with "hard" electrophiles.

The chemistry of organometallic complexes and sulfur ylides as reaction partners is, hence, far from exhausted; indeed, the reactions with coordinated ligands have been scarcely investigated. It should also be noted that, despite the wide range of known sulfur ylides, only a few have been studied as ligands. This is clearly due, at least in part, to their high reactivity; but this also suggests the possibility of generating reactive metal ylide complexes and thus extending the synthetic tools of the preparative chemist.

*I should like to thank Prof. Dr. Günter Schmid for generous support of our work. Frau D. Vehreschild-Yzermann, Frl. M. Stoffel, Frl. M. Utzat, Herr D. Wewers, and Herr U. Meyer are thanked for committed and conscientious collaboration; Dr. R. Boese and Prof. Dr. C. Krüger (Mülheim a. d. Ruhr) and their co-workers for X-ray analyses; and Prof. Dr. B. M. Trost for hospitality during my stay at the University of Wisconsin, Madison. The Deutsche Forschungsgemeinschaft, the Fonds der Chemischen Industrie, and Degussa (Hanau) and Hoechst AG (Werk Knapsack) provided financial support.*

Received: April 25, 1983 [A 460 IE]
German version: *Angew. Chem. 95* (1983) 539

[1] A. W. Johnson: *Ylid Chemistry*, Academic Press, New York 1966, and references cited therein.
[2] H. Schmidbaur, *Acc. Chem. Res. 8* (1975) 62; *Pure Appl. Chem. 50* (1978) 19.

[3] L. Weber "Synthesis of Ylide Complexes" in F. R. Hartley, S. Patai: *The Chemistry of the Metal-Carbon Bond,* Wiley, Chichester 1982, p. 91.
[4] W. C. Kaska, *Coord. Chem. Rev. 48* (1983) 1.
[5] B. M. Trost, L. M. Melvin Jr.: *Sulfur Ylides, Emerging Synthetic Intermediates,* Academic Press, New York 1975.
[6] a) A. W. Johnson in D. H. Reid: *Organic Compounds of Sulphur, Selenium, and Tellurium* (Specialist Periodical Reports, Vol. 3), The Chemical Society, London 1975, p. 322; b) E. Block, M. Haake in D. R. Hogg: *Organic Compounds of Sulphur, Selenium, and Tellurium* (Specialist Periodical Reports, Vol. 4 und 5), The Chemical Society, London 1977 and 1979, p. 78, p. 70, respectively; c) E. Block, D. L. J. Clive, N. Furukawa, S. Oae in D. R. Hogg: *Organic Compounds of Sulphur, Selenium, and Tellurium* (Specialist Periodical Reports, Vol. 6), The Royal Society of Chemistry, London 1981, p. 79; d) E. Block: *Reactions of Organosulfur Compounds,* Academic Press, New York 1978, p. 91; e) A. C. Knipe "Reactivity of Sulphonium Salts" in C. J. M. Stirling, S. Patai: *The Chemistry of the Sulphonium Group,* Vol. *1,* Wiley, Chichester 1981, p. 313; f) E. Block "Synthetic Applications of Sulphonium Salts and Sulphonium Ylides" in C. J. M. Stirling, S. Patai: *The Chemistry of the Sulphonium Group,* Vol. *2,* Wiley, Chichester 1981, p. 673.
[7] L. Weber, *J. Organomet. Chem. 105* (1976) C9.
[8] L. Weber, *J. Organomet. Chem. 142* (1977) 309.
[9] I. Kawafune, G. Matsubayashi, *Inorg. Chim. Acta 70* (1983) 1.
[10] L. Weber, *Z. Naturforsch. B 31* (1976) 780.
[11] P. Bravo, G. Fronza, C. Ticozzi, G. Gaudiano, *J. Organomet. Chem. 74* (1974) 143.
[12] a) J. P. Fackler, C. Paparizos, *J. Am. Chem. Soc. 99* (1977) 2363; b) J. Stein, J. P. Fackler, C. Paparizos, H. W. Chen, *ibid. 103* (1981) 2192.
[13] B. L. Booth, K. G. Smith, *J. Organomet. Chem. 220* (1981) 219.
[14] H. Schmidbaur, W. Richter, *Z. Anorg. Allg. Chem. 429* (1977) 222.
[15] L. Weber, unpublished results.
[16] H. Koezuka, G. Matsubayashi, T. Tanaka, *Inorg. Chem. 13* (1974) 443.
[17] H. Koezuka, G. Matsubayashi, T. Tanaka, *Inorg. Chem. 15* (1976) 417.
[18] M. Okunaka, G. Matsubayashi, T. Tanaka, *Inorg. Nucl. Chem. Lett. 12* (1976) 813.
[19] M. Seno, S. Tsuchiya, *J. Chem. Soc. Dalton Trans. 1977,* 751.
[20] M. Onishi, Y. Ohama, K. Hiraki, H. Shintani, *Polyhedron 1* (1982) 539.
[21] E. T. Weleski Jr., J. L. Silver, M. D. Janson, J. L. Burmeister, *J. Organomet. Chem. 102* (1975) 365.
[22] a) F. B. McCormick, J. A. Gladysz, *J. Organomet. Chem. 218* (1981) C57; b) N. J. Copper, M. L. H. Green, *J. Chem. Soc. Chem. Commun. 1974,* 208, 761; *J. Chem. Soc. Dalton Trans. 1979,* 1121; c) M. Canestrari, M. L. H. Green, *J. Chem. Soc. Chem. Commun. 1979,* 913; d) P. R. Sharp, R. R. Schrock, *J. Organomet. Chem. 171* (1979) 43; e) J. Schwartz, K. I. Gell, *ibid. 184* (1980) C1.
[23] H. Werner, R. Feser, W. Paul, L. Hofmann, *J. Organomet. Chem. 219* (1981) C29.
[24] a) S. Brandt, P. Helquist, *J. Am. Chem. Soc. 101* (1979) 6473; b) E. J. O'Connor, P. Helquist, *ibid. 104* (1982) 1869.
[25] a) T. J. Collins, W. R. Roper, *J. Chem. Soc. Chem. Commun. 1977,* 901; *J. Organomet. Chem. 159* (1978) 73; b) W. Paul, H. Werner, *Angew. Chem. 95* (1983) 333; *Angew. Chem. Int. Ed. Engl. 22* (1983) 316.
[26] G. Yoshida, H. Kurosawa, R. Okawara, *J. Organomet. Chem. 131* (1977) 309.
[27] L. Weber, Habilitationsschrift, Universität Essen 1982.
[28] B. T. Kilbourn, D. Felix, *J. Chem. Soc. A 1969,* 163.
[29] O. I. Kolodyazhnyi, *Zh. Obshch. Khim. 45* (1975) 704.
[30] G. Matsubayashi, Y. Kondo, T. Tanaka, S. Nishigaki, K. Nakatsu, *Chem. Lett. 1979,* 375.
[31] G. Matsubayashi, I. Kawafune, T. Tanaka, S. Nishigaki, K. Nakatsu, *J. Organomet. Chem. 187* (1980) 113.
[32] H. Schmidbaur, W. Kapp, *Chem. Ber. 105* (1972) 1203.
[33] H. Schmidbaur, G. Kammel, *Chem. Ber. 104* (1971) 3252.
[34] G. Yoshida, H. Kurosawa, R. Okawara, *J. Organomet. Chem. 113* (1976) 85.
[35] R. B. King, M. B. Bisnette, *J. Am. Chem. Soc. 86* (1964) 1267; *Inorg. Chem. 4* (1965) 486.
[36] E. R. de Gil, L. F. Dahl, *J. Am. Chem. Soc. 91* (1969) 3751.
[37] K. Miki, Y. Kai, N. Yasuoka, N. Kasai, *J. Organomet. Chem. 135* (1977) 53.
[38] H. W. Whitlock Jr., C. Reich, W. D. Woessner, *J. Am. Chem. Soc. 93* (1971) 2483.
[39] a) E. R. Biehl, P. C. Reeves, *Synthesis 1974,* 883; b) G. Berens, F. Kaplan, R. Rimerman, B. W. Roberts, A. Wissner, *J. Am. Chem. Soc. 97* (1975) 7076; c) E. E. Nunn, *Aust. J. Chem. 29* (1976) 2549; d) M. B. Stringer, D. Wege, *Tetrahedron Lett. 1977,* 65; e) F. A. Kaplan, B. W. Bryan, *J. Am. Chem. Soc. 99* (1977) 513; f) H. Fischer "Synthesis of Transition Metal-Carbene Complexes" in F. R. Hartley, S. Patai: *The Chemistry of the Metal-Carbon Bond,* Wiley, Chichester 1982, S. 181.
[40] See e.g. G. Jaouen "Arene Complexes in Organic Synthesis" in H. Alper: *Transition Metal Organometallics in Organic Synthesis,* Vol. *2,* Academic Press, New York 1978, p. 65.
[41] J. M. Landesberg, J. Sieczkowski, *J. Am. Chem. Soc. 93* (1971) 972.
[42] a) A. J. Birch, P. E. Cross, J. Lewis, D. A. White, S. B. Wild, *J. Chem. Soc. A 1968,* 332; b) A. J. Birch, K. B. Chamberlain, M. A. Haas, D. J. Thompson, *J. Chem. Soc. Perkin Trans. I 1973,* 1882; c) A. J. Birch, K. B. Chamberlain, D. J. Thompson, *ibid. I 1973,* 1900; d) Phenols are *O*-methylated by $Me_2S(O)CH_2$: H. König, H. Metzger, K. Seelert, *Chem. Ber. 98* (1965) 3724; *ibid., Tetrahedron Lett. 1964,* 867.
[43] J. P. Sevenair, D. H. Lewis, B. W. Ponder, *J. Org. Chem. 37* (1972) 4061.
[44] W. C. Kaska, D. K. Mitchell, R. F. Reichelderfer, W. D. Korte, *J. Am. Chem. Soc. 96* (1974) 2847.
[45] D. J. Darensbourg, M. Y. Darensbourg, *Inorg. Chem. 9* (1970) 1691.
[46] R. J. Angelici, L. J. Blacik, *Inorg. Chem. 11* (1972) 1754.
[47] L. Weber, *J. Organomet. Chem. 122* (1976) 69.
[48] W. Malisch, *J. Organomet. Chem. 61* (1973) C15; *82* (1974) 185.
[49] a) C. P. Casey, T. J. Burkhardt, *J. Am. Chem. Soc. 94* (1972) 6543; b) C. W. Rees, E. v. Angerer, *J. Chem. Soc. Chem. Commun. 1972,* 420; c) T. L. Gilchrist, R. Livingston, C. W. Rees, E. v. Angerer, *J. Chem. Soc. Perkin Trans. I 1973,* 2535; d) P. Lennon, A. M. Rosan, M. Rosenblum, *J. Am. Chem. Soc. 99* (1977) 8426; e) D. L. Reger, E. G. Culbertson, *J. Organomet. Chem. 131* (1977) 297.
[50] K. A. M. Kremer, P. Helquist, R. C. Kerber, *J. Am. Chem. Soc. 103* (1981) 1862.
[51] a) M. Brookhart, M. B. Humphrey, H. J. Kratzer, G. O. Nelson, *J. Am. Chem. Soc. 102* (1980) 7802; b) C. P. Casey, S. W. Polichnowski, *ibid. 99* (1977) 6097; c) F. N. Tebbe, G. W. Parshall, G. S. Reddy, *ibid. 100* (1978) 3611; d) K. H. Dötz, *Naturwissenschaften 62* (1975) 365; e) C. P. Casey, W. W. Miles, H. Tukada, J. M. O'Connor, *J. Am. Chem. Soc. 104* (1982) 3761.
[52] a) R. G. Salomon, J. K. Kochi, *J. Am. Chem. Soc. 95* (1973) 3300; b) B. M. Trost, *ibid. 89* (1967) 138.
[53] W. H. Tamblyn, S. R. Hoffmann, M. P. Doyle, *J. Organomet. Chem. 216* (1981) C64.
[54] J. Cuffe, R. J. Gillespie, A. E. A. Porter, *J. Chem. Soc. Chem. Commun. 1978,* 641.
[55] J. H. Law, *Acc. Chem. Res. 4* (1971) 199.
[56] G. A. Maw "The Biochemistry of Sulphonium Salts" in C. J. M. Stirling, S. Patai: *The Chemistry of the Sulphonium Group,* Vol. *2,* Wiley, Chichester 1981, p. 703.
[57] G. Pattenden, R. Storer, *Tetrahedron Lett. 1973,* 3473.
[58] T. Cohen, G. Herman, T. M. Chapman, D. Kuhn, *J. Am. Chem. Soc. 96* (1974) 5627.
[59] a) M. Clagett, A. Gooch, P. Graham, N. Holy, B. Mains, J. Strunk, *J. Org. Chem. 41* (1976) 4033; b) C. R. Johnson, P. E. Rogers, *J. Org. Chem. 38* (1973) 1978.
[60] A. Ceccon, F. Miconi, A. Venzo, *J. Organomet. Chem. 181* (1979) C4.
[61] L. Weber, *J. Organomet. Chem. 131* (1977) 49.
[62] a) L. Weber, R. Boese, W. Meyer, *Angew. Chem. 94* (1982) 938; *Angew. Chem. Int. Ed. Engl. 21* (1982) 926; b) L. Weber, R. Boese, D. Wewers, W. Meyer, *Chemiedozententagung Dortmund 1983, Abstr. B 36,* p. 103; c) M. S. Hussain, H. Schmidbaur, *Z. Naturforsch. B 31* (1976) 721; d) H. Schmidbaur, A. Wohlleben-Hammer, *Chem. Ber. 112* (1979) 510; e) L. Weber, D. Wewers, unpublished; f) K. Issleib, R. Lindner, *Liebigs Ann. Chem. 699* (1966) 40; g) H. H. Karsch, *Chem. Ber. 115* (1982) 1956.
[63] Z. Yoshida, S. Yoneda, M. Hazama, *J. Org. Chem. 37* (1972) 1364.
[64] a) A. G. Hortmann, R. L. Harris, J. A. Miles, *J. Am. Chem. Soc. 96* (1974) 6119; b) B. E. Maryanoff, J. Stackhouse, G. H. Senkler Jr., K. Mislow, *ibid. 97* (1975) 2718; c) G. H. Senkler Jr., B. E. Maryanoff, J. Stackhouse, J. D. Andose, K. Mislow, in C. J. M. Stirling: *Organic Sulphur Chemistry,* Butterworths, London 1975, p. 157; d) M. Hori, H. Shimizu, *Farumashia 12* (1976) 468; *Chem. Abstr. 85* (1976) 122731q; e) D. C. Dittmer, B. H. Patwardhan "Cyclic Sulphonium Salts" in C. J. M. Stirling, S. Patai: *The Chemistry of Sulphonium Group,* Vol. 2, Wiley, Chichester 1981, p. 477.
[65] a) A. G. Hortmann, *J. Am. Chem. Soc. 87* (1965) 4972; b) A. G. Hortmann, R. L. Harris, *ibid. 93* (1971) 2471; c) Y. Kishida, J. Ide, *Chem. Pharm. Bull. (Tokyo) 15* (1967) 360; d) C. Tamira, S. Sato, Y. Kishida, *Tetrahedron Lett. 1968,* 2379; e) T. M. Harris, C. M. Harris, J. C. Cleary, *ibid. 1968,* 1427; *J. Org. Chem. 39* (1974) 72; f) B. Holt, J. Howard, P. A. Lowe, *Tetrahedron Lett. 1969,* 4937; g) Y. Tamura, T. Miyamoto, H. Taniguchi, K. Sumoto, M. Ikeda, *ibid. 1973,* 1729; h) Y. Tamura, H. Taniguchi, T. Miyamoto, M. Tsunekawa, M. Ikeda, *J. Org. Chem. 39* (1974) 3519; i) Y. Tamura, M. Tsunekawa, H. Taniguchi, T. Miyamoto, M. Ikeda, T. Fujiwara, T. Hombo, K. Tomita, *Heterocycles 9* (1978) 131; k) M. Watanabe, T. Kinoshita, S. Furukawa, *Chem. Pharm. Bull. (Tokyo) 23* (1975) 258.
[66] a) G. Suld, C. C. Price, *J. Am. Chem. Soc. 83* (1961) 1770; *84* (1962) 2090, 2094; b) C. C. Price, M. Hori, T. Parasaran, M. Polk, *ibid. 85* (1963) 2278; c) M. Polk, M. Siskin, C. C. Price, *ibid. 91* (1969) 1206; d) C. C. Price, D. H. Follweiler, *J. Org. Chem. 34* (1969) 3202; e) C. C. Price, H. Pirelahi, *ibid. 37* (1972) 1718.
[67] F. Bernardi, N. D. Epiotis, S. S. Shaik, K. Mislow, *Tetrahedron 33* (1977) 3061.

[68] M. Hori, T. Kataoka, H. Shimizu, K. Narita, S. Ohno, H. Aoki, *Chem. Lett. 1974,* 1101.
[69] M. Hori, T. Kataoka, H. Shimizu, S. Ohno, K. Narita, H. Takayanagi, G. Ogura, Y. Iitaka, *Tetrahedron Lett. 1979,* 1603.
[70] H. Nishiyama, *J. Organomet. Chem. 165* (1979) 407.
[71] a) V. I. Zdanovitch, A. Zh. Zhakaeva, V. N. Setkina, D. N. Kursanov, *J. Organomet. Chem. 64* (1974) C25; b) V. N. Setkina, V. I. Zdanovitch, A. Zh. Zhakaeva, Yu. S. Nekrasov, N. I. Vasynkova, D. N. Kursanov, *Dokl. Akad. Nauk SSSR Ser. Khim. 219* (1974) 1137; c) A. N. Nesmeyanov, N. L. Kolobova, V. I. Zdanovitch, A. Zh. Zhakaeva, *J. Organomet. Chem. 107* (1976) 319; d) V. N. Setkina, A. Zh. Zhakaeva, G. A. Panosyan, V. I. Zdanovitch, P. V. Petrovskii, D. N. Kursanov, *ibid. 129* (1977) 361; e) V. G. Andrianov, Yu. T. Struchkov, V. N. Setkina, A. Zh. Zhakaeva, V. I. Zdanovitch, *ibid. 140* (1977) 169; f) V. I. Zdanovitch, N. E. Kolobova, N. I. Vasynkova, Yu. S. Nekrasov, G. A. Panosyan, P. V. Petrovskii, A. Zh. Zhakaeva, *ibid. 148* (1978) 63.
[72] L. Weber, C. Krüger, Y.-H. Tsay, *Chem. Ber. 111* (1978) 1709.
[73] L. Weber, D. Wewers, *Chem. Ber. 116* (1983) 1327.
[74] R. Boese, L. Weber, unpublished.
[75] For crystal structure analyses of other $\lambda^6$-Thiabenzene 1-oxides cf. [65d] and T. Fujiwara, T. Hombo, K. Tomita, Y. Tamura, M. Ikeda, *J. Chem. Soc. Chem. Commun. 1978,* 197.
[76] a) K. Dimroth, *Fortschr. Chem. Forsch. 38* (1973) 1; *Acc. Chem. Res. 15* (1982) 58; b) M. Lückoff, K. Dimroth, *Angew. Chem. 88* (1976) 543; *Angew. Chem. Int. Ed. Engl. 15* (1976) 503; c) K. Dimroth, H. Kaletsch, *ibid. 93* (1981) 898 and *20* (1981) 871; d) K. Dimroth, S. Berger, H. Kaletsch, *Phosphorus Sulfur 10* (1981) 295, 305; e) K. Dimroth, M. Lückoff, H. Kaletsch, *ibid. 10* (1981) 285; f) T. Debaerdemaeker, *Acta Crystallogr. B35* (1979) 1686.
[77] For metal complexes of sulfonium ions cf. a) R. D. Adams, D. F. Chodosh, *J. Am. Chem. Soc. 100* (1978) 812; b) C. A. Stein, H. Taube, *ibid. 100* (1978) 336; c) in $[Me_2SC(CN)_2]_2PdCl_2$ Pd-S coordination has been suggested: H. Koezuka, G. Matsubayashi, T. Tanaka, *Inorg. Chem. 14* (1975) 253.
[78] L. Weber, *Chem. Ber. 112* (1979) 3828.
[79] L. Weber, *Chem. Ber. 112* (1979) 99.
[80] L. Weber, D. Wewers, *Z. Naturforsch. B 37* (1982) 68.
[81] L. Weber, *Chem. Ber. 116* (1983) 2022.
[82] L. Weber, unpublished results.
[83] J. C. Kotz, D. G. Pedrotty, *J. Organomet. Chem. 22* (1970) 425.
[84] The addition of nucleophiles to arene ligands in cationic 18e transition-metal complexes usually occurs from the *exo*-position. a) S. G. Davies, M. L. H. Green, D. M. P. Mingos, *Tetrahedron 34* (1978) 3047; b) P. L. Pauson, *J. Organomet. Chem. 200* (1980) 207; c) N. G. Connelly, R. L. Kelly, *J. Chem. Soc. Dalton Trans. 1974,* 2334. Only two other cases of *endo*-hydride addition have been observed: d) A. J. Birch, I. D. Jenkins "Transition Metal Complexes of Olefinic Compounds" in H. Alper: *Transition Metal Organometallics* in *Organic Synthesis,* Vol. *1,* Academic Press, New York 1976, p. 69.
[84a] Y. K. Chung, H. S. Choe, D. A. Sweigrt, N. G. Connelly, *J. Am. Soc. 104* (1982) 4245.
[85] L. Weber, R. Boese, *Angew. Chem. 95* (1983) 510; *Angew. Chem. Int. Ed. Engl. 22* (1983) 498; *Angew. Chem. Suppl. 1983,* 620.
[86] L. Weber, *Chem. Ber. 114* (1981) 1.
[87] a) N. G. Connelly, personal communication; b) B. W. S. Kolthammer, P. Legzdins, T. J. Malito, *Inorg. Chem. 16* (1977) 3173; c) A. M. Bond, R. Colton, J. J. Jackowski, *ibid. 18* (1979) 1977.
[88] a) L. Weber, *Angew. Chem. 93* (1981) 304; *Angew. Chem. Int. Ed. Engl. 20* (1981) 297; b) L. Weber, R. Boese, *Chem. Ber. 115* (1982) 1775.
[89] Under mild conditions thiabenzenes, -naphthalenes, and anthracenes undergo the Stevens rearrangement: cf. [64b, c, e, 66a, e, 68].
[90] Thianaphthalenes and -anthracenes react as dipoles with acetylenedicarboxylic acid dimethyl ester, diphenylcyclopropenone, diphenylcyclopropenethione, and tetracyanoethylene: see [68] and a) M. Hori, T. Kataoka, H. Shimizu, H. Aoki, *Heterocycles 6* (1976) 413; b) M. Hori, T. Kataoka, H. Shimizu, S. Ohno, *ibid. 7* (1977) 863.
[91] For the decomposition of thiabenzene derivatives with oxygen cf. [66a, e] and M. Hori, H. Kataoka, H. Shimizu, S. Ohno, K. Narita, *Tetrahedron Lett. 1978,* 251.
[92] L. Weber, R. Boese, *Chem. Ber. 116* (1983) 197.
[93] L. Weber, D. Vehreschild-Yzermann, C. Krüger, G. Wolmershäuser, *Z. Naturforsch. B36* (1981) 198.
[94] L. Weber, R. Boese, *Chem. Ber. 116* (1983) 514.
[95] a) G. Kresze, M. Rössert, *Angew. Chem. 90* (1978) 61; *Angew. Chem. Int. Ed. Engl. 17* (1978) 64; b) A. Schwöbel, M. A. Pérez, M. Rössert, G. Kresze, *Liebigs Ann. Chem. 1982,* 723.

# Four-Membered Ring Peroxides as Excited State Equivalents: A New Dimension in Bioorganic Chemistry

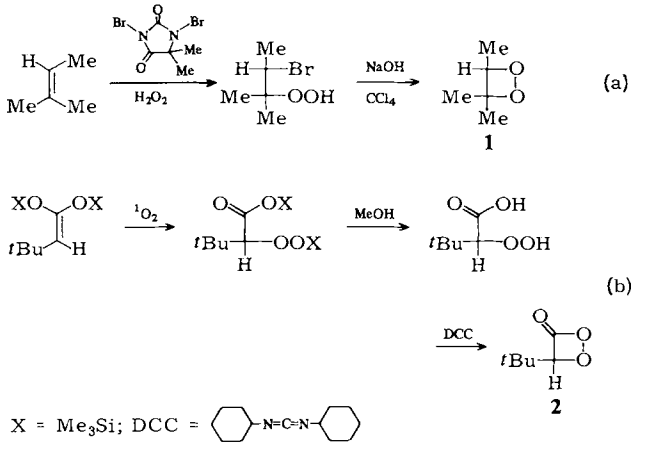
**By Waldemar Adam* and Giuseppe Cilento**

*Dedicated to Professor Günther O. Schenck on the occasion of his 70th birthday*

Consideration of chemiluminescent and bioluminescent processes invariably brings to mind the four-membered ring peroxides, 1,2-dioxetanes and α-peroxylactones. Nevertheless, while chemiluminescence and bioluminescence are well established fields of scientific study, isolable and characterized "high-energy" molecules such as the 1,2-dioxetanes and α-peroxylactones are of relatively recent vintage, about a decade. These intriguing compounds produce electronically excited products which manifest themselves by light emission during their thermal decay; more importantly, these transformations are involved in luminescent as well as dark enzymatic processes. It is not our intention to present a comprehensive overview in this progress report, but rather to focus on those aspects which require further study.

## 1. Synthesis

The isolation of the first stable 1,2-dioxetane, the trimethyl derivative **3**, prepared by the Kopecky sequence [reaction (a)], was reported in 1969[3], while the first α-peroxylactone (1,2-dioxetanone), the *tert*-butyl derivative **2**, was obtained in 1972 [reaction (b)][2]. Since then, well over a hundred dioxetanes **3** and about a dozen α-peroxylactones **4** have been isolated and characterized.




Besides reactions (a) and (b), which have become established classical routes, photooxygenation has proved to be a method of quite general synthetic utility. Provided ene-reactions and Diels-Alder additions do not figure as menacing side reactions, photosensitized singlet oxygenation of olefins and ketenes [reaction (c)] constitutes a convenient and facile approach to the four-membered cyclic peroxides **3** and **4**[3]. Substituents used include alkyl, aryl, alkoxy, aryloxy, dialkylamino, and recently even thioalkyl[4,5] and thioaryl groups[4], leading to the first sulfur-substituted 1,2-dioxetanes **5** and **6**, respectively. In **5** and **6** the spiroadamantane substitution stabilizes the dioxetane ring sufficiently to allow spectroscopic characterization of these labile species.



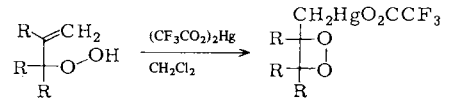
**5** **6**

The advantages of the singlet oxygenation method [reaction (c)] over the classical Kopecky route [reaction (a)] are the usually higher yields, mild conditions, and low temperatures. Most importantly, by using an appropriate sensitizer (tetraphenylporphine, polymer-bound rose bengal, *etc.*) and deuterated solvents (chloroform, dichloromethane, acetone, *etc.*) very labile dioxetanes and α-peroxylactones can be detected by $^1$H- or $^{13}$C-NMR spectroscopy without requiring isolation.

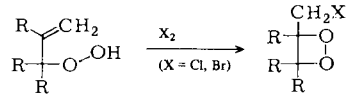
Methods of more limited scope include peroxymercuration[6], peroxyhalogenation[7], silica gel-catalyzed rearrangement of *endo*-peroxides[8], electrochemical oxygenations[9], and ozonation of vinylsilanes[10]. A method of promising synthetic potential entails base-catalyzed ring-opening of epoxides[11], leading to hydroxy-substituted dioxetanes **12**. The functionalized dioxetanes **7**, **8**, **11**, and **12** should provide opportunities of preparing derivatives bound to biomolecules such as sugars, steroids, fatty acids, proteins, pyrimidines, purines, *etc.*, which should be interesting substrates for biological testing.

This summarizes the repertoire of synthetic methods for 1,2-dioxetanes and α-peroxylactones. As is typical for the preparation of four-membered rings, the yields are low

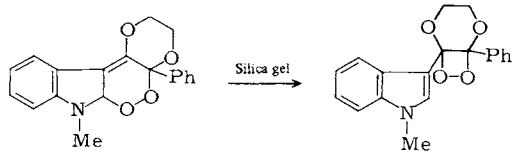
[*] Prof. Dr. W. Adam
Institut für Organische Chemie der Universität
Am Hubland, D-8700 Würzburg (Germany)
and Departamento de Quimica, Universidad de Puerto Rico
Rio Piedras, PR 00931 (USA)
Prof. Dr. G. Cilento
Departamento de Bioquimica, Instituto de Quimica
Universidade de São Paulo, C.P. 20.780, São Paulo (Brazil)



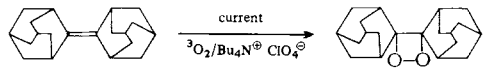

7



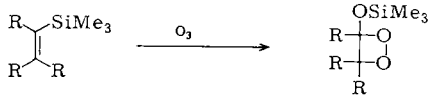

8



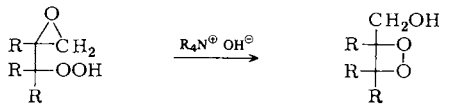

9




10

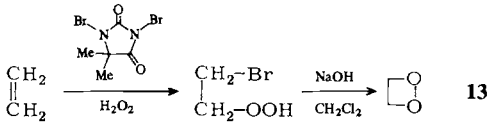



11




12

and the methods limited. In addition, these "high-energy" compounds are thermally and photolytically labile and undergo acid- and base-catalyzed decomposition, nucleophilic and electrophilic attack, and worst of all, dissociation by traces of transition-metal ions.

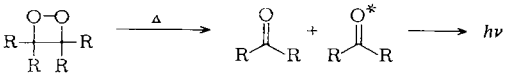



13

Consequently, much pioneering and challenging work awaits synthetic chemists to improve this unfavorable situation, especially if biologically relevant four-membered ring peroxides are to be prepared. But even simple species for mechanistic scrutiny, for example the parent dioxetane **13**, present a formidable synthetic challenge. Its transitory existence is claimed on the basis of the observed formaldehyde chemiluminescence in the gas phase singlet oxygenation of ethylene[12]. Attempts to prepare isolable quantities by low-temperature photosensitized singlet oxygenation of a solution of ethylene in $CFCl_3$ failed. Not even traces of peroxidic material was detected. However, after persistent efforts, *ca.* 10 mg of the parent 1,2-dioxetane **13** was recently isolated *via* the classical Kopecky route. The observed chemiluminescence on thermal decomposition and the characteristic NMR spectra support this success[13].

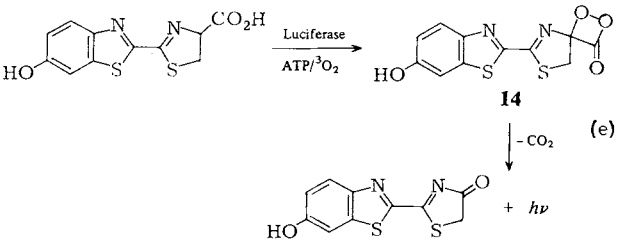
## 2. Characterization

The most characteristic property of four-membered ring peroxides is their ability to emit light upon decomposition [reaction (d)]. In chemistry this is referred to as chemiluminescence and in biology as bioluminescence. One of the best studied and mechanistically most understood bioluminescent reactions is firefly bioluminescence [reaction (e)],




(d)

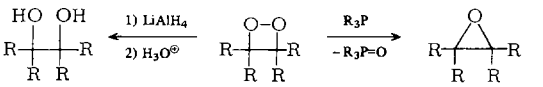
in which luciferin is converted enzymatically by luciferase and ATP into the corresponding carbonyl product (oxyluciferin), $CO_2$, and light *via* the intermediary α-peroxylactone **14**[14]. However, although all dioxetanes and α-peroxylactones emit light, even if often only rather feebly, the corollary is far from true that all luminescent chemical or biological autoxidations involve four-membered ring peroxides. While in chemistry it is, at least in principle, possible to isolate the suspected dioxetane and α-peroxylactone, or synthesize them independently, in biology the evidence is indirect and circumstantial. To the best of our knowledge no genuine biologically derived dioxetane or α-peroxylactone has yet been isolated or independently synthesized. Unquestionably, demanding but potentially rewarding work lies ahead on this score.




(e)

Even if the four-membered ring peroxides in question can be prepared and isolated, what criteria other than light emission [reaction (d)] can be employed for their definitive characterization? In view of the large volume of accumulated data[15], spectroscopic identification is convenient and reliable. The carbonyl frequency at *ca.* 1870 $cm^{-1}$ is particularly characteristic of α-peroxylactones, whereas for dioxetanes NMR spectroscopy is usually helpful. Dioxetanyl protons usually lie in the chemical shift range $\delta = 4.5$–5.5 and the ring carbon atoms between $\delta = 80$ and 110.

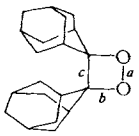
For their chemical identification several criteria can be useful. Of course, besides light emission on thermolysis, the products are usually the expected carbonyl fragments. Reduction of dioxetanes by $LiAlH_4$ to the respective 1,2-diols and deoxygenation to the corresponding epoxides by phosphanes are helpful procedures [reaction (f)], but other reliable and general chemical transformations need to be developed.



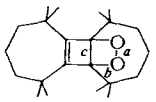

(f)

By far the most rigorous method, providing important structural parameters such as bond lengths and bond angles, is X-ray structure analysis. However, its general use is limited. On the one hand, the dioxetane must be crystalline and have good reflecting properties; on the other, since dioxetanes are radiation sensitive, the crystals must survive X-ray exposure. Despite these limitations, considerable progress has been made along these lines. The first X-ray structures reported concern the "superstable" dioxetanes

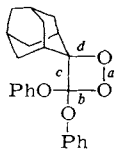
**10**[16] and **15**[17], derived from 2,2-biadamantylidene and the sterically hindered cyclobutadiene, respectively. More recently we have added the dioxetanes **16**—**21** and even the bisdioxetane **22** to the list[18]. The latter compound is interesting in that the two dioxetane rings are arranged *anti* to another and are considerably puckered, but the dioxane ring is planar. This is particularly surprising in view of the dioxetanes **17**—**19**, in which the reverse applies. Thus,



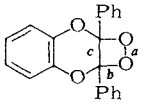
**10**



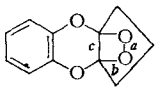
**15**



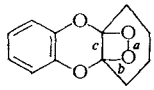
**16**



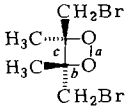
**17**



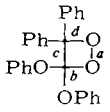
**18**



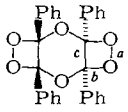
**19**



**20**



**21**



**22**

Table 1. Bond lengths [pm] and twist angles [°] in dioxetane rings, and rate constants for decomposition [$s^{-1}$] of the annelated dioxetanes **17**–**19** [a].

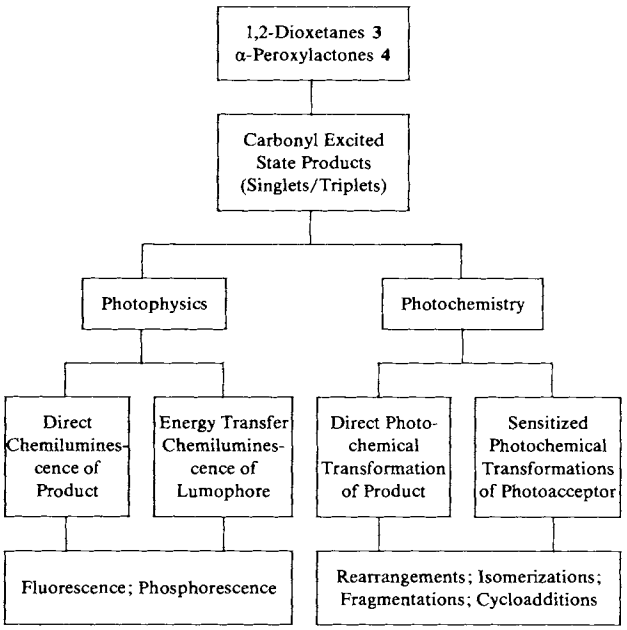
| Dioxetane | Bonds a | b | c | d | Angle | $10^3\,k$ |
|---|---|---|---|---|---|---|
| **10** | 148 | 147.5 | 155 | | 21.3 | |
| **15** | 149 | 149 | 155 | | 0 | |
| **16** | 147 | 148 | 148 | 151 | 11.7 | |
| **17** | 155 | 144 | 161 | | 0.8 | 1.00±0.5 |
| **18** | 158 | 144 | 158 | | 0 | 8.30±0.5 |
| **19** | 149 | 149 | 150.5 | | 0 | 6.00±2.0 |
| **20** | 144 | 148 | 151 | | 15.3 | |
| **21** | 150.5 | 148 | 155 | 143 | 9.6 | |
| **22** | 150 | 144 | 155.5 | | 16.3 | |

[a] $10^3\,k$ (370.2 K), determined by chemiluminescence measurements under isothermal conditions [18b].

here the dioxetane ring is essentially planar, but the dihydrodioxin ring boat-like. The greatest degree of puckering is observed in **10**; this arises to a large extent from steric interactions of the adamantyl groups (see Section 4). Of course, **15** is necessarily planar in view of the fused cyclobutene ring. In the future one can expect to see intensified activity in acquiring structural data of this type, particularly since the few examples discussed here do not allow *a priori* predictions to be made concerning the degree of dioxetane ring puckering. It must be stressed at this point that no X-ray structure analyses of α-peroxylactones have been reported so far since stable α-peroxylactones of good crystalline quality have not yet been isolated.

## 3. Excitation Yields

We have seen that a characteristic feature of four-membered ring peroxides is their ability to generate electronically excited carbonyl products, *e.g.* aldehydes, ketones, esters, carboxylic acids, and anhydrides. In this sense we consider these "high-energy" molecules as *excited state equivalents*, since they serve as chemical or even biological precursors to excited states. Such chemienergized excited states derived from four-membered ring peroxides behave identically to their photoenergized equivalents in their photophysical and photochemical properties. Thus, among the known photophysical phenomena, excited states of this type display direct chemiluminescence (DC) in the form of fluorescence (singlet states) and phosphorescence (triplet states), or undergo energy transfer chemiluminescence (ETC) with an appropriate luminescing photoacceptor (lumophore), which subsequently either fluoresces or phosphoresces (Scheme 1). In this respect it is completely immaterial whether the four-membered ring peroxide is of chemical or biological origin, except that in the latter cases such emissions are termed bioluminescence. The chemienergized carbonyl product can undergo direct photochemical transformations such as rearrangements, isomerizations, fragmentations, or cycloadditions, but can also sensitize such photochemical transformations *via* energy transfer to an appropriate photoactive acceptor (Scheme 1).




Scheme 1.

One of the central analytical problems concerns the determination of the excitation parameters, *i.e.* the efficiency of singlet ($\phi^S$) and triplet ($\phi^T$) excited state generation during decomposition of 1,2-dioxetanes or α-peroxylactones. Specifically, for mechanistic reasons it is desirable to know the total chemiexcitation efficiency ($\phi^T+\phi^S$) and the efficiency of spin state selection ($\phi^T/\phi^S$). Of course, for this purpose either the quantum yield of the photophysical processes can be measured or the chemical yield of the photochemical reactions determined (Scheme 1). These methods have been described in detail[19], and only the salient features and problems, especially with enzymatically generated excited states, will be considered here.

### 3.1. Luminescence Probes

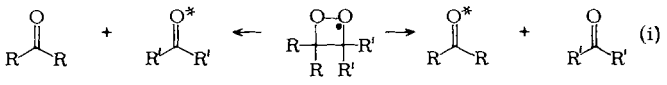
For luminescence techniques, by means of which the quantum yield is experimentally established, the key mathematical relationships for direct (DC) and energy transfer (ETC) chemiluminescence are given in equations (g) and (h), respectively. In the case of DC, the chief prerequisite is that the identity of the excited carbonyl product is

$$\phi_{DC} = \phi_{exc} \cdot \phi_{lum} \quad (g)$$

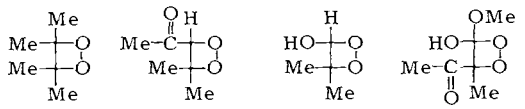
$$\phi_{ETC} = \phi_{exc} \cdot \phi_{ET} \cdot \phi_{lum} \quad (h)$$

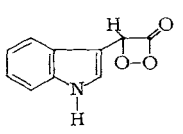
$\phi_{DC}$ = direct chemiluminescence yield; $\phi_{ETC}$ = energy transfer chemiluminescence yield; $\phi_{exc}$ = chemiexcitation yield ($\phi^S$ for singlets and $\phi^T$ for triplets); $\phi_{lum}$ = luminescence yield of excited carbonyl product or lumophore; fluorescence yield ($\phi_{fl}$) for singlets and phosphorescence yield ($\phi_{ph}$) for triplets; $\phi_{ET}$ = energy transfer efficiency of excited carbonyl product to the lumophore

known. This is not a trivial matter, especially for unsymmetrically substituted dioxetanes, which can chemienergize either or both of the possible carbonyl fragments [reaction (i)], particularly in biological molecules in which


(i)

the dioxetane has been postulated as a transient intermediate. If, however, the chemiexcited carbonyl excited state is known with certainty and its luminescence efficiency available or determinable, then to determine the desired $\phi_{exc}$ it is only necessary to measure $\phi_{DC}$ by the usual photometric methods[19]. Since under normal conditions the observed emission is usually fluorescence, this provides direct access to singlet quantum yields ($\phi^S$). Only under special circumstances can triplet excitation yields ($\phi^T$) be measured by direct phosphorescence. For example, under degassed conditions the triplet yield of acetone from tetramethyl-1,2-dioxetane **23** has been reported[20], and the triplet yield of methylglyoxal from dioxetane **24**[21] could be determined directly, since such α-dicarbonyl excited states undergo direct phosphorescence. Significantly, the direct emission observed in the enzymatic autoxidation of isobutyraldehyde by horseradish peroxidase (HRP) in the presence of a chelating ligand (EDTA, pyrophosphate) has been identified as derived from triplet acetone produced from the hypothetical intermediary dioxetane **25**[22]. However, when the HRP enzyme is replaced by hemin, autoxidation of isobutyraldehyde to triplet excited acetone still occurs, except that its phosphorescence can no longer be observed directly[23]. Consequently, it was postulated that in the HRP-catalyzed autoxidation the triplet acetone was screened by the enzyme against quenching by oxygen, but in the hemin-catalyzed autoxidation of isobutyraldehyde it was not. An intermediate case is the HRP-catalyzed autoxidation of methyl 2-methylacetoacetate, which affords triplet biacetyl, presumably *via* the dioxetane **26**, as indicated by its directly observable phosphorescence[24]. Here, the triplet biacetyl is also not screened by the enzyme against quenching by oxygen; but since, compared to triplet acetone, triplet biacetyl phosphoresces quite efficiently, its phosphorescence can be observed directly near oxygen completion. These unusual results are of considerable biological significance.

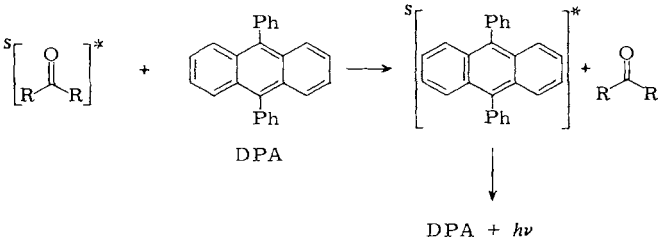

**23** **24** **25** **26**


**27**

In general, it can be said that DC is a convenient method, but has limited scope. The most serious disadvantages are that triplet yields can seldom be determined, the excited-state product must be known, and the fluorescence and phosphorescence yields must be sufficiently large to enable quantitative determination[19].

Energy transfer chemiluminescence (ETC) has by now established itself as the most popular technique for the determination of excitation yields. It was pioneered by the Russian school[25] for monitoring the excited carbonyl products responsible in the chemiluminescence accompanying hydrocarbon autoxidation. With the proper choice of lumophore to which the excitation energy of the chemienergized carbonyl excited state is transferred, singlet ($\phi^S$) and triplet ($\phi^T$) yields can be obtained photometrically[26].

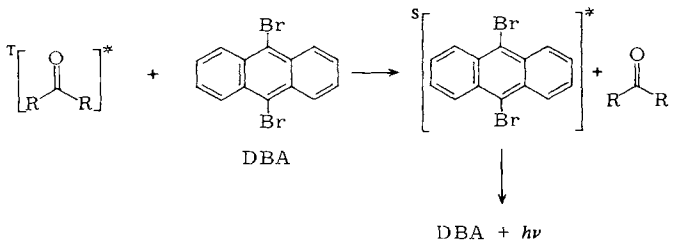
For studying singlet excited states 9,10-diphenylanthracene (DPA) is frequently used as a lumophore; its fluorescence is sensitized *via* singlet-singlet energy transfer by the chemienergized carbonyl product. In practice the DPA quantum yield ($\phi_{ETC}^{DPA}$) is measured at infinite DPA concentrations under conditions where Stern-Volmer kinetics apply ($\phi_{ET}^{DPA} = 1.00$), and since the fluorescence yield of DPA is known, the singlet quantum yield ($\phi^S$) can be calculated from eq. (h)[19].



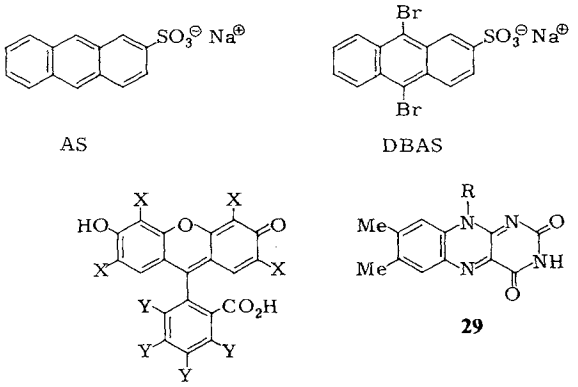

9,10-Dibromoanthracene (DBA) has been widely used to study triplet excited states. Through spin-orbital coupling the bromine atoms catalyze the spin-forbidden triplet-singlet energy transfer from the chemienergized triplet carbonyl product to DBA, thereby sensitizing its fluorescence. Here the DBA quantum yield ($\phi_{ETC}^{DBA}$) is determined at infinite DBA concentration using Stern-Volmer kinetics ($\phi_{ET}^{DBA} = 0.25$), and since the fluorescence yield of DBA is known, the triplet yield ($\phi^T$) can be obtained from eq. (h)[19].

The convenience of these luminescent techniques cannot be overemphasized. They are simple to carry out, sensitiv-

ity is merely limited by the quality of the photometric equipment on hand, and most importantly the exact nature of the chemienergized excited states involved in the energy transfer need not to be known. It should, therefore, not be surprising that such methods are extensively used in assessing excitation yields, particularly in biological systems[27].

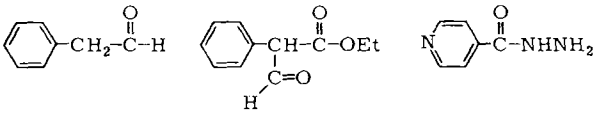



For this purpose water-soluble lumophores have been developed, such as sodium 2-anthracenesulfonate (AS) and sodium 9,10-dibromo-2-anthracenesulfonate (DBAS). Thus, in the HRP-catalyzed autoxidation of isobutyraldehyde, generation of triplet acetone was confirmed by showing that fluorescence of DBAS, but not of AS, could be sensitized[22]. In addition, fluorescence of **28a—c**[28] and flavins **29**[29] could be stimulated effectively by triplet acetone generated from HRP-catalyzed autoxidation of isobutyraldehyde (**28a**: fluorescein; **28b**: eosin; **28c**: rose bengal).



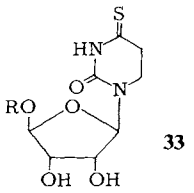

Similarly, the lumophores **28** and **29** could be sensitized by HRP-catalyzed autoxidation of straight-chain aldehydes, which presumably occurs *via* triplet aldehydes derived from intermediary dioxetanols such as **25**[30]. However, triplet excited 3-indolecarbaldehyde, produced in the HRP-catalyzed autoxidation of 3-indolacetic acid *via* the postulated α-peroxylactone **27**[31], could not be detected with flavins. When this enzymatic autoxidation was carried out in the presence of micelle-solubilized chlorophylls, these lumophores fluoresced strongly, thus indicating that electronically excited 3-indolecarboxaldehyde occurs as an intermediate[32]. Cationic (CTAB), anionic (SDS), and neutral (Brij-35 and Triton X-100) micellar solutions of chlorophylls all gave excellent results.

Thus, this novel detection system holds great promise for the search of enzymatically generated triplet carbonyl products *via* peroxidase-catalyzed autoxidation of appropriate substrates, provided a chemically induced electron exchange luminescence (CIEEL) process can be excluded. For example, using micellar solutions of chlorophylls it was possible to detect triplet carbonyl products in the HRP-catalyzed autoxidation of phenylacetaldehyde **30**[33], ethyl 2-formyl-2-phenylethylacetate **31**[34], and isonicotinic acid hydrazide **32**[35].



**30** **31** **32**

Even complex biomolecules can serve as lumophores to monitor enzyme-generated triplet excited carbonyl products. Thus, in the HRP-catalyzed autoxidation of 3-indoleacetic acid in the presence of $tRNA^{Phe}$, emission from the 4-thiouridine moiety **33** could be sensitized[36]. In a control



**33**

experiment it was shown that photoenergized 3-indolecarboxaldehyde sensitized the same emission. When $tRNA^{Phe}$ is replaced by yeast tRNA, which lacks the thiouridine group, no sensitization is observed. More recently it has been found that triplet acetone, triplet straight-chain carbaldehydes, and triplet 3-indolecarbaldehyde, all generated from the appropriate substrate *via* HRP-catalyzed autoxidation, elicit red emission from intact chloroplasts[37]. Processes other than energy transfer could be excluded.

After having presented the advantages of energy-transfer chemiluminescence (ETC) to detect and quantitate chemically and/or biologically generated excited states, its limitations should now also be pointed out. Clearly, in order to be efficient, the excitation energy of the lumophore must be low enough to cause exothermic energy transfer. For simple carbonyl excited states, such as acetone, benzaldehyde, methyl benzoate, *etc.*, the choice of an appropriate lumophore is not difficult, because all of these species have relatively high excitation energies. Even DPA and DBA or AS and DBAS suffice, although their singlet excitation energies are as high as *ca.* 70 kcal/mol. However, for extensively conjugated carbonyl excited states whose singlet excitation energies lie below 50 kcal/mol and triplet excitation energies below 30 kcal/mol, the choice of appropriate lumophore is problematic. If lumophores with sufficiently low excitation energies are used, *e.g.* porphines or rubrene, an electron exchange luminescence (CIEEL) mechanism may be promoted[38]. Satisfactory solutions to these analytical problems have not yet been provided.

### 3.2. Chemical Titrations

As outlined in Scheme 1, in this type of detection system the chemienergized excited state undergoes a known photochemical transformation either directly or *via* energy transfer. The mathematical relationships for the determination of the excited state yields are given by eqs. (j) and (k). In practice the chemical yield ($\phi_{chem}$) of photoproduct

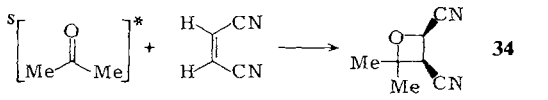
$$\phi_{chem} = \phi_{exc} \cdot \phi_{photo} \quad (j)$$

$$\phi_{chem} = \phi_{exc} \cdot \phi_{ET} \cdot \phi_{photo} \quad (k)$$

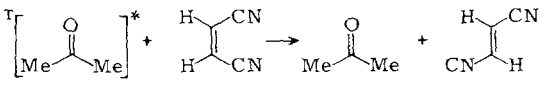
$\phi_{chem}$ = direct or sensitized yield of chemienergized photoproduct; $\phi_{exc}$ = chemiexcitation yield ($\phi^S$ for singlets and $\phi^T$ for triplets); $\phi_{photo}$ = yield of photoenergized photoproduct; $\phi_{ET}$ = energy transfer efficiency

must be determined either spectroscopically or chromatographically; the photochemical yield ($\phi_{photo}$) is usually known or can be determined readily by the usual photomechanistic techniques for photochemical reactions. For sensitized photochemical reactions, the energy transfer efficiency is determined at infinite concentration of photoacceptor under Stern-Volmer kinetics ($\phi_{ET} = 1.0$). All the necessary experimental data is, therefore, available to calculate $\phi_{exc}$ either from eq. (j) or (k). If the direct or sensitized photochemical transformation is singlet-state specific, singlet yields ($\phi^S$) are obtained, but if it is triplet-state specific, then triplet yields ($\phi^T$) are obtained. Such photochemical determination of excitation yields is commonly referred to as "chemical titration" of chemienergized excited states.

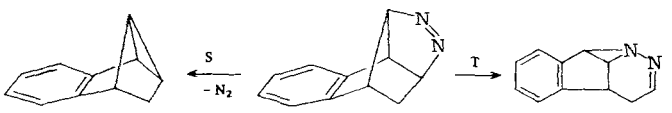
The now classical example of sensitized chemical titration by energy transfer is shown in reaction (l). Thus, singlet and triplet excited acetone react with maleonitrile to give the oxetane **34** and fumaronitrile[39]. Hence, $\phi^S$ and $\phi^T$ can be determined in one experiment from eq. (k) by quantifying the chemical yield of the photoproducts.




(l)



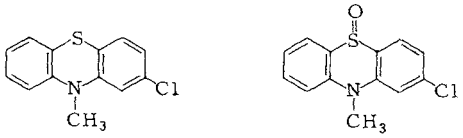

A more recent spin state-specific chemical titrant of chemienergized singlet and triplet excited carbonyl products is the azo compound **35**, which on singlet sensitization gives the tetracyclic hydrocarbon **36**, and on triplet sensitization the aziridine **37**[40]. Numerous other examples of such sensitized and direct chemical titrations of chemienergized carbonyl excited states have been compiled[19].




**36** **35** **37**

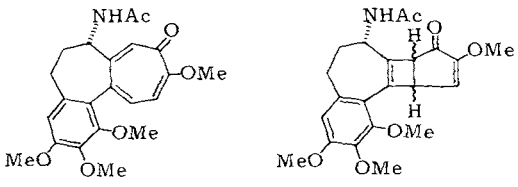
The major advantage of these chemical titrations is that no special photometric equipment is necessary to measure quantum yields. Instead, the chemical yield of photoproduct is determined by standard spectroscopic and chromatographic techniques. Furthermore, one has at one's disposal a wide range of photochemical transformations. Again, sensitized chemical titrations are more convenient than the direct, since in the former the exact nature of the chemienergized excited state need not to be known. Moreover, in direct chemical titrations for each specific case a specific dioxetane or α-peroxylactone needs to be synthesized as an excited state equivalent. In sensitized chemical titrations, however, only a suitable photoacceptor needs to be sought, whose excitation energy, of course, must lie below that of the chemienergized excited state so that energy transfer is efficient. It is not surprising, therefore, that sensitized chemical titrations of this type have been used to monitor enzymatically generated excited states. For example, the 7% yield of isopropyl alcohol found when the HRP-catalyzed autoxidation of isobutyraldehyde is carried out in ethanol has been attributed to reduction of the intermediary triplet acetone by ethanol[22d].

In the meantime a number of such dark photobiological transformations have been reported[27]. For example, HRP-catalyzed autoxidation of isobutyraldehyde in the presence of chloropromazine **38** affords the sulfoxide **39** and the radical cation of **38**[41]. It is known that chloropromazine is

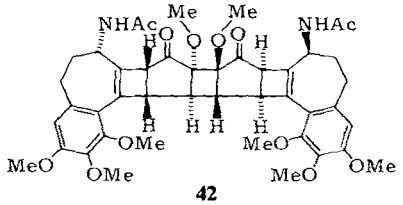



**38** **39**

photooxidized *via* triplet sensitization[42], implicating triplet-triplet energy transfer from enzymatically produced triplet acetone. In this respect DBAS serves as inhibitor, presumably by quenching triplet acetone. Quantitative estimates indicate that the yield of triplet acetone in this peroxidase-catalyzed autoxidation is almost 100%. Similarly, the interconversion of the phytochromes $P_R$ and $P_F$ is sensitized by enzymatically generated triplet acetone derived from HRP-catalyzed autoxidation of isobutyraldehyde[43].



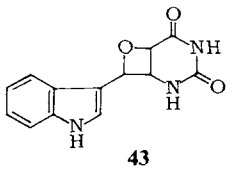

**40** **41**




**42**

One of the most intriguing and significant studies along these lines entails sensitized conversion of colchicine **40**

into β- and γ- **41** and α-lumicolchicine **42** by triplet acetone generated in the HRP-catalyzed autoxidation of isobutyraldehyde[44]. The chemical yield ($\phi_{chem}$) is approximately 7%. What is especially significant is that this photochemical transformation takes place in *Colchicum autumnale L.*, even in parts not exposed to light[45]. It is, therefore, conceivable that in the living organism triplet excited states are produced endogenously, which sensitize the colchicine-lumicolchicine conversion by energy transfer. The fact that α-lumicolchicine **42**, a photodimer of β-lumicolchicine **41**, is produced under biological conditions in the dark has important implications for dimerization of thymine mediated by endogenously generated excited states. In this connection a photoadduct between lysozyme and riboflavin has recently been isolated from the HRP-catalyzed autoxidation of isobutyraldehyde[46]; formation of the Paterno-Büchi adduct **43** between enzymatically generated triplet 3-indolecarbaldehyde and the uridine group of tRNA has been demonstrated[36b]. From this chemical titration it was estimated that the triplet excitation yield ($\phi^T$) of 3-indolecarbaldehyde in the HRP-catalyzed autoxidation of 3-indoleacetic acid approaches *ca.* 20%.



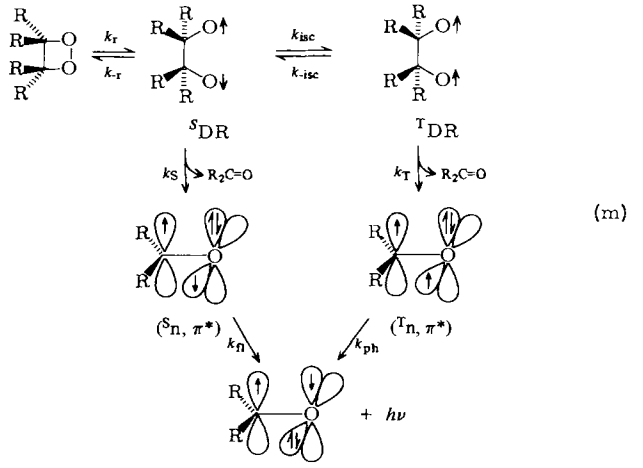
**43**

Clearly, chemical titration techniques provide a powerful and convenient tool for the detection and quantitation of enzymatically generated excited states allegedly derived from intermediary 1,2-dioxetanes and α-peroxylactones. Together with the luminescent probes, they provide a wide spectrum of generally applicable analytical methods. The future should witness further intensified activity in this still virgin territory of bioorganic chemistry.

## 4. Mechanistic Incognita

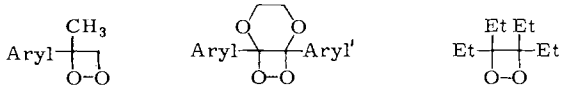
To account for the thermal stability of dioxetanes and α-peroxylactones, and to explain their ability to generate electronically excited states, a thorough understanding of the mechanism of their thermal decomposition is essential. It is, therefore, hardly surprising that since the discovery of dioxetanes intensive efforts have been expended on this perplexing mechanistic problem[15]. Two extreme mechanistic views have persisted over the last decade, each backed up by convincing experimental data. Based on thermokinetic calculations[47], the diradical mechanism (m) was proposed as the best explanation of the thermal stability of dioxetanes (eq.m). Furthermore, the high propensity of triplet state generation, *i.e.* the ($^T$n,π*) state of the carbonyl product, can be accounted for by imposing the kinetic conditions $k_{isc} > k_S$ and $k_T > k_{-isc}$.

Recently, evidence to support the diradical mechanism has been presented which uses Hammett correlations of substituent effects on the decomposition rates of 3-aryl-3-methyl-1,2-dioxetanes **44**[48] and 2a,6a-diarylperhydro[1,2]dioxeto[3,4-*b*][1,4]dioxins **45**[49], and the influence



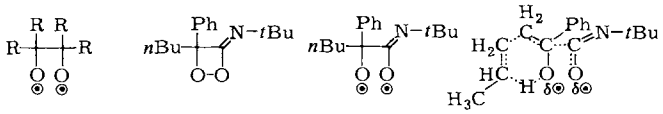
(m)

of steric effects on the rates of thermolysis of 3,3-dialkyl- and trialkyl-1,2-dioxetanes[50]. However, one of the biggest drawbacks of the diradical mechanism is its failure to account for the unusual stability of the tetraethyl-1,2-dioxetane **46**[51].



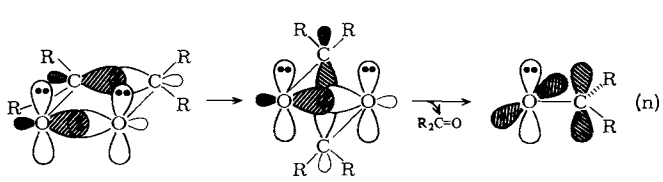
**44** **45** **46**

Trapping experiments would constitute the most unequivocal proof for the involvement of diradical intermediates such as **47** in the thermolysis of 1,2-dioxetanes. However, although no positive results have been reported yet, an interesting observation concerns the formation of acetophenone and propene in the thermolysis of the dioxetane derivative **48**. The diradical **49**, which fragments *via* the transition state **49**$^{\ddagger}$, was proposed as precursor of the observed product[52].



**47** **48** **49** **49**$^{\ddagger}$

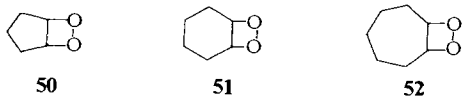
Neither has it been possible so far to detect dioxetane diradicals spectroscopically. For example, multiphoton infrared excitation of tetramethyl-1,2-dioxetane in the gas phase did not result in detection of diradical intermediates, thus limiting their lifetimes to less than 5 ns[53]. Still more convincing evidence that such diradicals, if indeed formed, must be extremely short-lived (less than 10 ps) is provided by the fact that they were not even detected by picosecond spectroscopy in the 264 nm pulsed photolysis of tetramethyldioxetane in acetonitrile using a mode-locked neodymium phosphate laser[54].



(n)

In the alternative mechanism (n), which involves simultaneous oxygen-oxygen and carbon-carbon bond scission, dioxetane decomposition occurs concertedly[55] (eq. n). Puckering of the four-membered ring allows optimal alignment of the hatched orbitals shown in the formulae to form an n,π* excited state of the carbonyl product. To explain the high yield of triplet excited product it has been proposed that enhanced spin-orbital coupling occurs during puckering[56].

Recent evidence in favor of this decomposition mode is provided by the series of dioxetanes **50**—**52**[57]: the activation parameters (Table 2) clearly show that the fused six-membered ring dioxetane **51** is considerably more thermally unstable than the homologues **50** and **52**[58]. This dependence of the thermal stability on ring size can hardly be explained in terms of the diradical mechanism (m). It was argued[57] that in dioxetane **51** the four-membered ring is puckered and thus already partway along the decomposition coordinate of the concerted mechanism (n), whereas in dioxetanes **50** and **52** the four-membered rings can be planar, and thus require greater thermal activation to acquire the twisted transition state. Examination of Dreiding models corroborates this proposal.



**50** **51** **52**

Table 2. Activation parameters of the bicyclic 1,2-dioxetanes **50**–**52** [a].

| Dioxetane | $\Delta H^{+}$ [kcal/mol] | $\Delta S^{+}$ [cal/mol/K] | $\Delta G^{+}$ (333.2 K) [kcal/mol] | $10^4\,k$ (333.2 K) [$s^{-1}$] |
|---|---|---|---|---|
| **50** | 25.3±0.3 | +1.6 | 24.8 | 3.8 |
| **51** | 21.9±0.3 | −2.1 | 22.5 | 110 |
| **52** | 25.4±0.3 | +1.9 | 24.8 | 4.0 |

[a] Determined by chemiluminescence measurements under isothermal conditions [58].

To test this hypothesis, the set of crystalline dioxetanes **17**—**19** were prepared and their activation parameters and crystal structures determined[18b]. As the structural data show (Table 1), the dihydrobenzodioxin annelation unfortunately necessitates essentially planar four-membered rings in all three dioxetanes. It is, therefore, not surprising that the rate constants for their decomposition are almost the same (Table 1). Challenging work lies ahead to synthesize a set of crystalline dioxetanes with fixed puckered or planar geometries, *e.g.* of type **53** and **54**. It is known that **53** is considerably more thermally labile than **54**[59]. Crystal structure analysis might provide an answer to this interesting mechanistic problem.

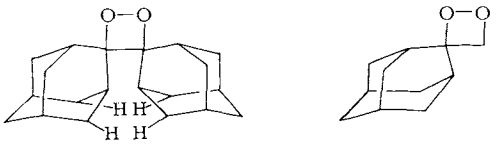


**53** **54**

Clearly, experimental evidence has been amassed both for and against the diradical and concerted mechanisms[15]. To resolve this dichotomy, a number of studies on the thermal stability and excitation parameters have recently been performed. For example, the complete set of methylated 1,2-dioxetanes **1**, **13**, **23**, and **55**—**57** have been prepared and their activation parameters determined (Table 3)[13]. The principal intention here was to test the substituent effect of one particular alkyl group, in this case methyl, by measuring the activation parameters under identical conditions in the same laboratory, and thus avoid the great divergence in results of this type as indicated by a recent compilation[60]. The rate constants in Table 3 display a pronounced substituent effect, *e.g.* the parent 1,2-dioxetane **13** decomposes about 75 times faster than the tetramethyl-1,2-dioxetane **23** at 343.2 °K, and the change in activation enthalpy ($\Delta H^{+}$) per methyl substituent is *ca.* 1 kcal/mol. While this significant substituent effect provides evidence in favor of the concerted mechanism, thermokinetic calculations[47] assuming a diradical decomposition pathway also predict a monotonic increase in the thermal stability of 1,2-dioxetanes on increasing methylation.

It is also interesting to mention that the efficiency of chemienergization increases with increasing methylation, the increase being mainly in the triplet yield. This is consistent with the empirical trend that the triplet yield ($\phi^{T}$) increases with the activation energy[61].

A persisting problem is to provide an explanation for the unusual thermal stability of the 1,2-dioxetane **10** with two spiroadamantane moieties. Even a single spiroadamantane moiety significantly stabilizes such dioxetanes against thermolysis[4,62]. Because of the rigid geometry of



**10** **58**

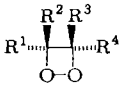


Table 3. Activation parameters of the methyl-substituted 1,2-dioxetanes [a].

| Dioxetane | $R^1$ | $R^2$ | $R^3$ | $R^4$ | $\Delta H^{+}$ [cal/mol$^{-1}$ K$^{-1}$] | $\Delta S^{+}$ [cal mol/K] | $\Delta G^{+}$ (343.2 K) [kcal/mol] | $10^4\,k$ (343.2 K) [$s^{-1}$] |
|---|---|---|---|---|---|---|---|---|
| **13** | H | H | H | H | 19.1±1.7 | −3.0±1.0 | 19.9±1.9 | 150±10 |
| **55** | Me | H | H | H | 21.5±0.6 | −1.4±0.5 | 21.9±0.7 | 85±5 |
| **56** | Me | Me | H | H | 22.5±0.2 | −1.3±0.2 | 22.9±0.3 | 26±3 |
| **57a** | Me | H | Me | H | 21.6±0.6 | −1.8±0.8 | 22.1±0.7 | 35±3 |
| **57b** | Me | H | H | Me | 22.1±1.0 | −1.6±0.8 | 22.6±1.2 | 27±3 |
| **1** | Me | Me | Me | H | 24.5±1.5 | −1.0±0.5 | 24.8±1.5 | 8.6±0.5 |
| **23** | Me | Me | Me | Me | 24.9±0.6 | −0.8±0.4 | 25.1±0.6 | 2.0±0.2 |

[a] Determined by chemiluminescence measurements under isothermal conditions [13].

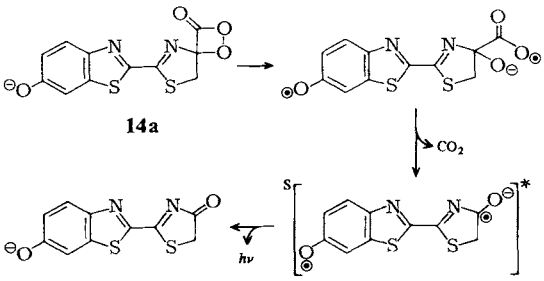
the adamantyl group, the four equatorial methylene H atoms in **10** are interlocked[16].

One consequence of this is that **10** has one of the most puckered dioxetane rings (torsional angle *ca.* 21.3°). The interlocking of these H atoms prevents further twisting of the four-membered ring, and the diradical mechanism, therefore, seems to be the more plausible. In this context it would be important to investigate the, as yet unknown, spiro[adamantanedioxetane] **58**, since in this molecule such stabilization arising from interlocking of H atoms is not possible.

It should be evident that a mechanistic explanation for even such a straightforward molecular property as the thermal stability of these intriguing dioxetanes has not been satisfactorily solved experimentally. The dichotomy of diradical and concerted pathways persists! Considerable mechanistic work is essential to resolve these problems. Theoretical studies have provided some progress. The most recent and sophisticated calculations[63] suggest the diradical mechanism; however, irrespective of their sophistication, all quantum-mechanical methods used predict a puckered transition state, both for the concerted as well as for diradical decomposition[60]. Consequently, theoreticans also have plenty of food for thought. Apart from accounting for the thermal stability of these "high-energy" compounds, a still more significant problem is to provide an explanation for the efficiency of generation of excited states in terms of their structures. A novel and provocative hypothesis is that an exciplex between the two carbonyl fragments is formed as the initial excited-state species in the decomposition of 1,2-dioxetanes[48]. In fact, exciplex emission has been observed for indole-substituted dioxetanes[64]. Such effects might also account for a number of poorly understood empirical trends in the excitation parameters[19]. Clearly, molecular spectroscopists should also get involved here.

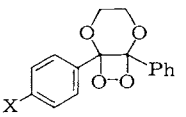
Still more perplexing is the unusual ability of dioxetanes to chemienergize preferentially triplet excited carbonyl products. Of significance and importance in this context is the still poorly understood phenomenon of energy-surface crossings. A qualitative treatment[65] emphasizes the potential of such a view, and more intensive action along these lines appears mandatory.

Mechanistic work on the decomposition of four-membered ring peroxides of biological importance is even more difficult because compounds of this type are too labile to be isolated. Nevertheless, significant progress has been made in understanding the mechanism of luciferin bioluminescence[14], especially that of the firefly [reaction (e)]. With the recognition of the phenomenon of chemically induced electron exchange chemiluminescence (CIEEL) between peroxides and easily oxidized fluorescers[38], model studies confirmed that the catalyzed luminescent decomposition of α-peroxylactones belonged to this novel category of chemiluminescence reactions [reaction (o)][66]. This then enabled the high quantum yield (*ca.* 90%) of singlet excited states observed in luciferin bioluminescence to be rationalized. Thus, reaction (p) represents an intramolecular version of the model process (o)[67]. Significant in this context is the long-known fact[68] that efficient production of singlet excited states requires the phenolate form **14a** of the α-peroxylactone **14**. In **14a** the benzenethiazole group




(p)

behaves as the electron donor and the α-peroxylactone moiety as the electron acceptor; however, since this takes place intramolecularly, electronically excited oxyluciferin is produced efficiently after decarboxylation. In fact, a recent model study[69] of the dioxetane **59** provides convincing evidence for this hypothesis. Thus, while the unsubstituted dioxetane **59** (X = H) gave a large triplet yield of excited product, the phenolate derivate **59** ($X = O^{\ominus}$) gave predominantly a singlet excited product. Clearly, intramolecular CIEEL must also operate here analogously to the α-peroxylactone **14** of firefly luciferin. In the future other examples of such intramolecular electron exchange chemiluminescence will surely be discovered.



**59**, X = H, OH, OMe, $O^{\ominus}$

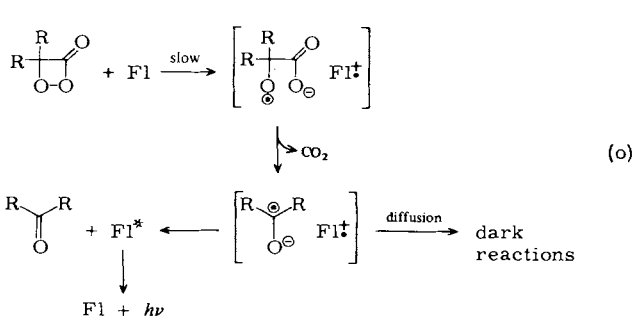
Another area of biological investigation in which important progress has been made are energy-transfer phenomena involving enzymatically generated excited states[27]. Only some of the recent highlights will be presented here. For example, in normal triplet-singlet energy transfer involving free collisions [eq. (q)], the Stern-Volmer constant [eq. (r)] for triplet acetone quenching should not exceed that ob-

$$^{T}D^{*} + A_0 \longrightarrow D_0 + {}^{S}A^{*} \qquad (q)$$

$$K_{SV} = k_{ET} \cdot \tau_0 \qquad (r)$$

D = Donor; A = acceptor; $k_{ET}$ = effective rate constant of energy transfer; $\tau_0$ = unquenched donor lifetime

served for molecular oxygen, *i.e.* $K_{SV}$ is *ca.* $2 \times 10^{-3}$ to $5 \times 10^{3}$ L mol$^{-1}$. Frequently, however, $K_{SV} \geqq 10^{4}$ L mol$^{-1}$. Since the Förster criteria[70] for long-range triplet-singlet energy transfer are not met in all cases, one may infer from these high $K_{SV}$ values that the acceptor is very near the ac-




(o)

tive site prior to excitation by the donor. This proximity, therefore, facilitates triplet-triplet energy transfer [eq. (s)]. This mechanism may even apply when the Förster overlap

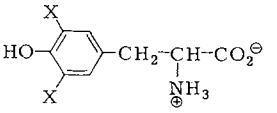
$$^{T}D^{*} + A_0 \longrightarrow D_0 + {}^{T}A^{*} \qquad (s)$$

criterion is met. Such a case appears to be the quenching of enzymatically generated acetone phosphorescence by the xanthene dyes **28**[28]. When the integrated sensitized dye emissions and the fluorescence yields are taken into account, the relative efficiencies of populating the singlet excited state of the dye are found to be 1 : 15 : 100, respectively, for fluorescein, eosin, and rose bengal. The significantly greater $S_1$ yield with rose bengal most probably arises because the triplet energy of the acetone donor is first transferred to an upper triplet state of the dye acceptor: the iodine atoms (heavy atom effect) in the rose bengal favor formation of its singlet excited state *via* enhanced intersystem-crossing [eq. (t)]. If only the traditional Förster mechanism [eq. (q)] were to operate, fluorescein would have had the highest relative efficiency.

$$\begin{aligned} {}^{T}D^{*} + A_0 &\longrightarrow D_0 + {}^{T_2}A^{*} \\ {}^{T_2}A^{*} &\longrightarrow {}^{S}A^{*} \\ {}^{S}A^{*} &\longrightarrow A_0 + h\nu \end{aligned} \qquad (t)$$

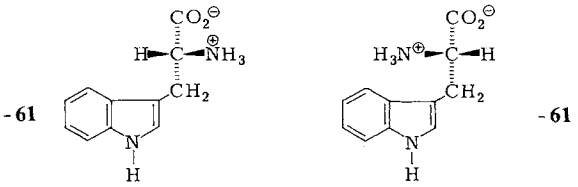
Evidence in support of this hypothesis is provided by the chemienergized fluorescence of DBA by triplet acetone generated thermally from tetramethyldioxetane. By analogy to eq. (t), an upper triplet state ($T_2$) of DBA is first produced *via* allowed triplet-triplet energy transfer; subsequently, the intramolecular heavy atom effect enhances intersystem-crossing from the $T_2$ to the $S_1$ state[71]. This mechanism appears also to apply to the energy transfer from enzymatically generated triplet acetone to DBAS as acceptor. In this context it is of interest to mention that energy transfer to AS occurs as efficiently as to DBAS; however, no fluorescence is observed with AS since it lacks the bromine atoms of DBAS to promote intersystem-crossing of the $T_2$ to the $S_1$ state. Instead, internal conversion of the $T_2$ to the $T_1$ state of AS is favored; the $T_1$ state, however, does not emit.

A further interesting case of energy transfer concerns the tyrosine derivatives **60**. Thus, when triplet acetone is chemienergized by thermolysis of tetramethyldioxetane in the presence of these tyrosines, the Stern-Volmer quenching plots (monitored by DBAS) are linear[72]. Except for the parent tyrosine, **60a**, the quenching rate constants approach those operating under diffusion control conditions. Presumably the energies of the $T_2$ states are too high, so that the $T_1$ states of the tyrosines **60b—d** are energized directly. The intramolecular heavy atom effect cannot, therefore, be observed experimentally for these quenchers, since the energy transfer process of eq. (t) is not accessible energetically. However, if triplet acetone is generated enzymatically *via* HRP-catalyzed autoxidation of isobutyraldehyde, the Stern-Volmer quenching plots for the parent tyrosine **60a** and its dichloro derivative **60b** are almost linear, whereas for the dibromo **60c** and especially for the diiodo **60d** derivatives, the corresponding plots have a marked upward curvature. A heavy atom effect is also discernible with **60c** and **60d**. A static contribution to quenching in the presence of the enzyme involving enzyme-protected triplet acetone seems to operate.



**60a**, X = H
**60b**, X = Cl
**60c**, X = Br
**60d**, X = I

The protective role of the enzyme is most convincingly demonstrated in the quenching of enzymatically generated acetone phosphorescence by D- and L-tryptophan **61**[73]. Thus, when D-tryptophan is present, competitive quenching by L-tryptophan is very inefficient; however, when the converse applies, quenching by D-tryptophan is still observed. This chiral discrimination precludes the possibility that triplet acetone and the quencher exist freely in solution under these conditions, since triplet acetone generated by thermolysis of tetramethyldioxetane is quenched equally efficiently by D- and by L-tryptophan. The chiral discrimination by the enzymatically generated triplet acetone probably involves a collisional complex of the quencher and the active site of the enzyme prior to energy transfer.



-61 -61

*D*-61 *L*-61

Several features about these unusual results with enzymatically generated triplet acetone still remain unsolved. For example, complete quenching by quinones can be observed even at concentrations much lower than that of the enzyme[74]. Under these conditions the quencher can encounter at most one acetone triplet during the lifetime of the latter (*ca.* $10^{-5}$ s). Quenching by long range energy transfer must, therefore, operate. In this respect the Förster overlap criterium is fulfilled for some, but not all quinones. Quenching by electron transfer or charge transfer interaction is unlikely because both triplet acetone and quinones are electron acceptors.

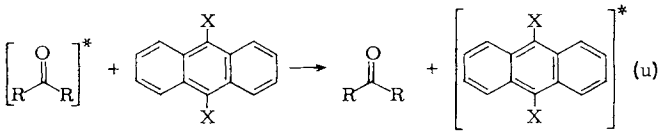
A further important unresolved question concerns how the excited species transfers energy to organelles such as chloroplasts and to acceptors in micelles. When the triplet energy donor is shielded by the protecting enzyme, energy transfer may require the intermediacy of exposed groups of the macromolecule or of the organelle. For micelles the acceptor presumably resides at or near the micellar surface. No doubt, interesting results should be forthcoming in this fascinating bioorganic discipline.

## 5. Photological Divertissement

The fact that 1,2-dioxetanes and α-peroxylactones are masked electronically excited states, defined here as "excited state equivalents", clearly has important consequences in the elucidation of photophysical, photochemi-

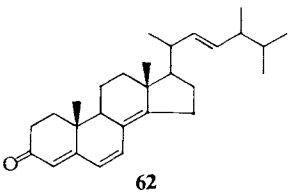
cal, and photobiological phenomena[*]. As implied in Scheme 1, chemically and biologically photoenergized excited states behave in the same way as excited states generated by the action of light. Clearly, chemi- and bioenergization provide fascinating opportunities to study photological problems in an unconventional manner, also referred to as photochemistry[75] and photobiology[76] in the dark. The fundamental difference, however, in these two approaches is that photoenergized generation of excited states competes with photoabsorption by the substrate, whereas chemi- and bioenergization entail straightforward conventional techniques, with the proviso, however, that the four-membered ring peroxides must first be synthesized. This is frequently not a trivial task and presumably has restricted more frequent use of these "high-energy" molecules. Nevertheless, the preparation of the stable dioxetane **10** is an undergraduate laboratory experiment[77], and the synthesis of the more labile tetramethyldioxetane **23** can be mastered by a proficient laboratory technician in a few days. Consequently, there are no excuses for not employing these interesting molecules.

As a divertissement, a number of photophysical, photochemical, and photobiological problems will be presented in which 1,2-dioxetanes and α-peroxylactones have been employed as "excited state equivalents". This selection should serve to encourage more intensive activity in this promising area. In this context a number of problems will be outlined that could possibly be tackled with the aid of four-membered ring peroxides.

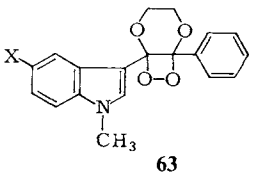



In photophysics, dioxetanes lend themselves particularly well to energy transfer studies. By means of photoenergization it would be difficult to transfer excitation energy from a weakly absorbing donor to a strongly absorbing acceptor, especially if the absorption bands extensively overlap. A specific example is given in eq. (u), in which an excited carbonyl compound (weakly absorbing donor) transfers its excitation energy to the 9,10-disubstituted anthracene (strongly absorbing acceptor) (X = Ph: DPA; X = Br: DBA). Clearly, with conventional photoenergization all the light is preferentially absorbed by anthracene. However, by heating the appropriate dioxetane in the presence of the anthracene acceptor the desired excited carbonyl product is generated *via* chemienergization, and competitive photoabsorption problems are, therefore, circumvented. Hence, important photophysical data, which were previously difficult to obtain, can be acquired for the triplet-singlet energy transfer of chemienergized acetone to 9,10-dibromoanthracene (DBA) in solution and in polymer matrices[71,78]. The singlet-singlet energy transfer of chemienergized acetone to ergostatetraenone **62** could also be studied in an analogous way[78g].

[*] No collective term exists in the dictionary for photobiology, photochemistry, and photophysics, so that we shall define the term photology, as the *science* (logia) of *light* (phos).



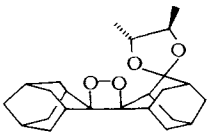
**62**



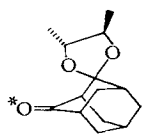

**63**

Unconventional energy transfer studies of this type hold great promise for biologically important acceptors. Even macromolecules and organelles (chloroplasts) can be selectively energized by four-membered ring peroxides. The feasibility of such studies has already been demonstrated with enzymatically generated excited states[37], but authentic dioxetanes should prove more convenient.

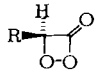
With the observation of exciplex emission[64] in the direct chemiluminescence of the indolyldioxetanes **63** and the suggestion that exciplex formation might be quite general in dioxetane decomposition[48], a number of stimulating problems present themselves. For example, the optically active dioxetane **64** causes circularly polarized fluorescence of the chiral adamantanone **65**[79]. In fact, circularly polarized bioluminescence has been observed for the firefly[80] arising from the achiral oxyluciferin [reactions (e) and (p)], while the adamantanone **65** possesses a permanent chiral center. A chiral excited state of the oxyluciferin arising from exciplex formation might possibly be the cause of circularly polarized bioluminescence in the firefly. Consequently, it would be of interest to synthesize an optically active α-peroxylactone **66**, or for that matter a 1,2-dioxetane, which subsequently leads to an achiral product, but whose intervening chiral excited state (presumably an exciplex) might emit polarized chemiluminescence. An interesting luminescent probe for elucidating excited state geometries thus presents itself.




**64**



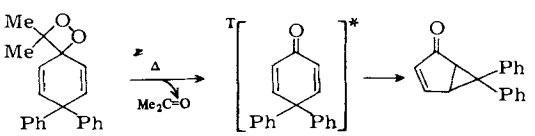

**65**




**66**

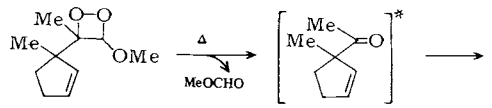
Bisdioxetanes, for example the benzoic acid anhydride dimer **22**[81], should be excellent precursors for the thermal generation of upper excited states, since each dioxetane ring represents the equivalent of a trapped photon. Possibly "biphotonic" processes might be included in such unconventional studies.

In photochemistry, use of chemienergization to tackle mechanistic problems has been surprisingly rare. The value of dioxetanes is clearly evident in the decomposition of **67**, where they chemienergize the formation of enone **69** *via* the $^3n,\pi^*$ excited state of dienone **68**[82]. In this manner a long standing photomechanistic problem of whether $n,\pi^*$ or $\pi,\pi^*$ triplet states are involved in dienone rearrangement could be resolved.

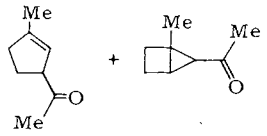



**67** **68** **69**

By analogy, the dioxetane **70** proved useful in elucidating the photomechanistic details of the rearrangement of the excited enone **71** to **72** and **73**[83]. Comparison of the yields of the 1,3-acyl shift product **72** with those of the oxa-di-π-methane (ODPM) product **73** of the chemi- and photoenergized enone **71** leads to the conclusion that a n,π* triplet is the principal precursor for the 1,3-acyl shift and a π,π* triplet for the ODPM process.

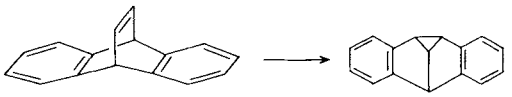



**70** **71**




**72** **73**

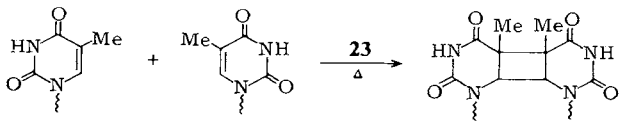
In this exploitation of chemienergization the specific excited-state equivalents, dioxetanes **67** and **70**, had to be synthesized. Of course, this is not always a simple task as already mentioned in Section 1. It is considerably more convenient to sensitize a particular photochemical reaction by energy transfer *via* a chemienergized carbonyl excited state as donor. For example, using tetramethyl-1,2-dioxetane **23**, a clean source of triplet acetone, it could be confirmed that the rearrangement of azoalkane **35** to aziridene **37** is a spin-specific triplet reaction[40]. Similarly, using chemienergized triplet acetone the di-π-methane rearrangement of dibenzobarrelene **74** to afford semibullvalene **75** was also shown to be a spin-specific triplet process[84]. In the future such photochemical applications of dioxetanes should certainly become more frequent.



**74** **75**

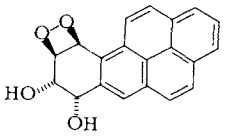
For the application of four-membered ring peroxides to photobiological problems a rather extensive compilation of the possibilities was made right at the beginning of this field[75,85]. Significant progress was achieved once enzymatic generation of electronically excited triplet states was established[27]. A number of problems have been solved, but many still remain.

Thus, considerable attention has been devoted to photodamage of DNA by thymine dimerization in view of its connection with carcinogenesis[86]. A key experiment[87] was the demonstration that chemienergized triplet acetone, generated from the tetramethyl-1,2-dioxetane **23**, caused formation of thymine dimers **76** in DNA. Subsequently, it




**76**

was shown that bioenergized triplet acetone, generated by HRP-catalyzed autoxidation of isobutyraldehyde, promoted single strand breaks[88] and altered the circular dichroism[89] in DNA. As supporting evidence that enzymatically produced triplet acetone was the damaging species, is the fact that such damage can, in part, be inhibited by DBAS. That a metabolic system can generate excited states *in situ* from intermediary dioxetanes has recently been demonstrated in the degradation of benzo[a]pyrene by liver microsomes. The accompanying weak chemiluminescence was attributed to the intervening dioxetane **77**[90].




**77**

If chemi- and bioenergized triplet excited states can lead, *via* energy transfer, to thymine dimerization in DNA, the photochemical reversion of such damage should, in principle, also be reasible in this manner. Indeed, model studies reveal that photoenergized excited indoles[91] and quinones[92], species that can be generated enzymatically in the dark, induce splitting of thymine dimers **76**.

Another area of great challenge and potential is photoaffinity labeling[94]. For example, the carbonyl functions of hormonal ligands, *e.g.* steroidal ketones, could be masked in the form of dioxetanes or α-peroxylactones. After complexation with the receptor, decomposition of the dioxetane would release the electronically excited ligand, which would become permanently bound to the receptor, thereby revealing the specific binding site. The advantage of such "photoaffinity labeling in the dark" is that it could be performed *in vivo* in aqueous systems.

Stimulating problems of bioorganic significance in which "excited state equivalents" should prove of interest concern photoregulation mediated by phytochromes[95], plant growth hormones involving 3-indoleacetic acid[96], the conversion of ergosterol into vitamin D[97,98], and the isomerization of retinal[99], *etc.* In addition, the opportunity of creating a radically new line of chemotherapeutic agents presents itself.

We shall close with the following citation[100], which best describes our contention that the fun has just begun: "Already today preparative photochemistry plays its own role within the methods of chemistry in view of the special possibilities it offers. However, its real importance arises from the abundant interdisciplinary connections, through which chemical problems caused by biological radiation become especially typical".

*The authors wish to express their deep gratitude to Professor Frank H. Quina (Universidáde de São Paulo) for his unfailing and unselfish assistance. Appreciation is extended to former and present students for their dedicated, diligent, and stimulating collaboration. Generous financial support by the Financiadora de Estudios e Projetos (Rio de Janeiro), the Conselho Nacional de Desenvolvimento Científico e Tecnologico (Brasilia), Fundacáo de Ampazo á Pesquisa do Estado de São Paulo (São Paulo), the Deutsche Forschungsge-*

*meinschaft, the Fonds der Chemischen Industrie, the Fritz Thyssen Stiftung, the Alexander von Humboldt Stiftung, and the Volkswagenwerk Stiftung is acknowledged. The latter deserves special emphasis since it presently sponsors the collaborative efforts of the Brazilian and German groups.*

Received: March 25, 1983 [A 459 IE]
German version: *Angew. Chem. 95* (1983) 525

[1] K. R. Kopecky, C. Mumford, *Can. J. Chem. 47* (1969) 709.
[2] W. Adam, J.-C. Liu, *J. Am. Chem. Soc. 94* (1972) 2894.
[3] W. Adam, G. Cilento: *Chemical and Biological Generation of Electronically Excited States*, Academic Press, New York 1982.
[4] W. Adam, L. A. Arias, *Chem. Ber. 115* (1982) 2592.
[5] G. G. Geller, C. S. Foote, D. B. Pechman, *Tetrahedron Lett. 24* (1983) 673.
[6] W. Adam, K. Sakanishi, *J. Am. Chem. Soc. 100* (1978) 3965.
[7] A. Zahn, Diplomarbeit, Universität Würzburg, September 1981.
[8] H. Nakamura, T. Goto, *Heterocycles 15* (1981) 1119.
[9] a) S. F. Nelsen, R. Akaba, *J. Am. Chem. Soc. 103* (1981) 2096; b) E. L. Clennan, W. Simmons, C. W. Almgreen, *ibid. 103* (1981) 2098.
[10] G. Büchi, W. Wüest, *J. Am. Chem. Soc. 100* (1978) 294.
[11] D. Leclercq, J.-P. Bats, P. Picard, J. Moulines, *Synthesis 1982*, 778.
[12] D. Bogan in [3], Chap. 1.
[13] W. Baader, Dissertation, Universität Würzburg, July 1983.
[14] O. Shimomura in [3], Chap. 8.
[15] W. Adam in S. Patai: *The Chemistry of the Peroxide Bond*, Wiley, New York 1983.
[16] H. Numan, J. H. Wieringa, H. Wynberg, J. Hess, A. Vos, *J. Chem. Soc. Chem. Commun. 1977*, 591.
[17] A. Krebs, H. Schmalstieg, O. Jarchow, K.-H. Klaska, *Tetrahedron Lett. 21* (1980) 3171.
[18] a) W. Adam, L. A. Arias, A. Zahn, K. Zinner, E.-M. Peters, K. Peters, H. G. von Schnering, *Tetrahedron Lett. 23* (1982) 3251; b) W. Adam, E. Schmidt, E.-M. Peters, K. Peters, H. G. von Schnering, unpublished results.
[19] W. Adam in [3], Chap. 4.
[20] N. J. Turro, P. Lechtken, N. E. Schore, G. Schuster, H.-C. Steinmetzer, A. Yekta, *Acc. Chem. Res. 7* (1974) 97.
[21] K. A. Horn, G. B. Schuster, *J. Am. Chem. Soc. 100* (1978) 6649.
[22] a) N. Durán, O. M. M. Faria Oliveira, M. Haun, G. Cilento, *J. Chem. Soc. Chem. Commun. 1977*, 442; b) O. M. M. Faria Oliveira, M. Haun, N. Durán, P. J. O'Brien, E. J. H. Bechara, G. Cilento, *J. Biol. Chem. 253* (1978) 4707; c) G. Cilento, N. Durán, K. Zinner, C. C. C. Vidigal, O. M. M. Faria Oliveira, M. Haun, A. Faljoni, O. Augusto, R. Casadei de Baptista, E. J. H. Bechara, *Photochem. Photobiol. 28* (1978) 445; d) E. J. H. Bechara, O. M. M. Faria Oliveira, N. Durán, R. Casadei de Baptista, G. Cilento, *ibid. 30* (1979) 101.
[23] O. Augusto, E. J. H. Bechara, *Biochem. Biophys. Res. Commun. 631* (1980) 203.
[24] C. H. L. Soares, E. J. H. Bechara, *Photochem. Photobiol. 36* (1982) 117.
[25] V. A. Belyakov, R. F. Vasil'ev, *Photochem. Photobiol. 11* (1970) 179.
[26] N. J. Turro, P. Lechtken, G. Orell, H.-C. Steinmetzer, W. Adam, *J. Am. Chem. Soc. 96* (1974) 1627.
[27] G. Cilento in [3], Chap. 9.
[28] N. Durán, G. Cilento, *Photochem. Photobiol. 32* (1980) 113.
[29] M. Haun, N. Durán, G. Cilento, *Biochem. Biophys. Res. Commun. 81* (1978) 779.
[30] M. Haun, N. Durán, O. Augusto, G. Cilento, *Arch. Biochem. Biophys. 200* (1980) 245.
[31] a) C. C. C. Vidigal, K. Zinner, N. Durán, E. J. H. Bechara, G. Cilento, *Biochem. Biophys. Res. Commun. 65* (1975) 138; b) N. Durán, K. Zinner, R. Casadei de Baptista, C. C. C. Vidigal, G. Cilento, *Photochem. Photobiol. 24* (1976) 383; c) C. C. C. Vidigal, A. Faljoni-Alário, N. Durán, K. Zinner, Y. Shimizu, G. Cilento, *ibid. 30* (1979) 195.
[32] I. L. Brunetti, G. Cilenti, L. Nassi, Photochem. Photobiol., in press.
[33] N. Durán, K. Zinner, C. C. C. Vidigal, G. Cilento, *Biochem. Biophys. Res. Commun. 74* (1977) 1146.
[34] V. S. Kalyanaraman, S. Mahdevan, S. A. Kumar, *Biochem. J. 149* (1975) 565.
[35] K. Zinner, C. C. C. Vidigal, N. Durán, G. Cilento, *Arch. Biochem. Biophys. 180* (1977) 452.
[36] a) M. P. De Mello, S. M. De Toledo, M. Haun, G. Cilento, N. Durán, *Biochemistry 19* (1980) 5270; b) M. P. De Mello, S. M. De Toledo, H. Aoyama, H. K. Sarkar, G. Cilento, N. Durán, *Photochem. Photobiol. 36* (1982) 21.
[37] L. Nassi, G. Cilento, *Photochem. Photobiol. 37* (1983) 233.
[38] G. B. Schuster in [3], Chap. 6.
[39] N. J. Turro, P. Lechtken, *J. Am. Chem. Soc. 94* (1972) 2886.
[40] W. Adam, K. Hannemann, *J. Am. Chem. Soc. 105* (1983) 714.
[41] N. Durán, M. Haun, A. Faljoni, G. Cilento, *Biochem. Biophys. Res. Commun. 81* (1978) 785.
[42] S. Ates, G. Somer, *J. Chem. Soc. Faraday Trans. 1 77* (1981) 859.
[43] O. Augusto, G. Cilento, J. Jung, P.-S. Song, *Biochem. Biophys. Res. Commun. 83* (1978) 963.
[44] I. L. Brunetti, E. J. H. Bechara, G. Cilento, E. H. White, *Photochem. Photobiol. 36* (1982) 245.
[45] H. Poteschlová, J. Hrbek, Jr., F. Santavý, *Collect. Czech. Chem. Commun. 32* (1967) 141.
[46] N. Durán, M. Haun, S. M. De Toledo, G. Cilento, E. Silva, *Photochem. Photobiol. 37* (1983) 247.
[47] a) H. E. O'Neal, W. H. Richardson, *J. Am. Chem. Soc. 92* (1970) 6553; *93* (1971) 1828; b) W. H. Richardson, H. E. O'Neal, *ibid. 94* (1972) 8665.
[48] W. H. Richardson, D. L. Stiggall-Estberg, *J. Am. Chem. Soc. 104* (1982) 4173.
[49] A. P. Schaap, S. D. Gagnon, K. A. Zaklika, *Tetrahedron Lett. 23* (1982) 2943.
[50] A. L. Baumstark, T. Dumas, *J. Org. Chem. 47* (1982) 3754.
[51] E. J. H. Bechara, T. Wilson, *J. Org. Chem. 45* (1980) 5261.
[52] Y. Ito, H. Yokoya, K. Kyono, S. Yamamura, Y. Yamada, T. Matsuura, *J. Chem. Soc. Chem. Commun. 1980*, 898.
[53] a) Y. Haas, G. Lahav, *J. Am. Chem. Soc. 100* (1978) 4885; b) *Chem. Phys. Lett. 48* (1977) 63; c) W. E. Farnetz, G. Flynn, R. Slater, N. J. Turro, *J. Am. Chem. Soc. 98* (1976) 7877; d) B. D. Cannon, F. F. Crim, *ibid. 103* (1981) 6722.
[54] a) K. K. Smith, J.-Y. Koo, G. B. Schuster, K. J. Kaufmann, *J. Phys. Chem. 82* (1978) 2291; b) D. C. Doetschman, J. L. Fish, P. Lechtken, D. Negus, *Chem. Phys. 51* (1980) 89.
[55] N.-J. Turro, P. Lechtken, *Pure Appl. Chem. 33* (1973) 363.
[56] a) A.-C. Steinmetzer, P. Lechtken, N. J. Turro, *Justus Liebigs Ann. Chem. 1973*, 1984; b) H.-C. Steinmetzer, A. Yekta, N. J. Turro, *J. Am. Chem. Soc. 96* (1974) 282.
[57] A. L. Baumstark, C. E. Wilson, *Tetrahedron Lett. 22* (1981) 4363.
[58] C. Babatsikos, Diplomarbeit, Universität Würzburg, September 1981.
[59] K. R. Kopecky, P. A. Lockwood, R. R. Gomez, J.-Y. Ding, *Can. J. Chem. 59* (1981) 851.
[60] W. Adam, K. Zinner in [3], Chap. 5.
[61] W. H. Richardson, J. H. Burns, M. E. Price, R. Crawford, M. Forster, P. Slusser, J. H. Anderegg, *J. Am. Chem. Soc. 100* (1978) 7596.
[62] W. Adam, L. A. Arias Encarnación, K. Zinner, *Chem. Ber. 116* (1983) 839.
[63] a) L. B. Harding, W. A. Goddard, III, *J. Am. Chem. Soc. 99* (1977) 4520; b) S. P. Schmidt, M. A. Vincent, C. E. Dykstra, G. B. Schuster, *ibid. 103* (1981) 1292.
[64] H. Nakamura, T. Goto, *Photochem. Photobiol. 30* (1979) 27.
[65] N. J. Turro, A. Devaquet, *J. Am. Chem. Soc. 97* (1975) 3859.
[66] a) S. P. Schmidt, G. B. Schuster, *J. Am. Chem. Soc. 102* (1980) 306, 7100; b) W. Adam, O. Cueto, *ibid. 101* (1979) 6511.
[67] a) J.-Y. Koo, S. P. Schmidt, G. B. Schuster, *Proc. Natl. Acad. Sci. USA 75* (1978) 30; b) F. McCapra, *J. Chem. Soc. Chem. Commun. 1977*, 946.
[68] a) E. H. White, E. Rapaport, H. H. Seliger, T. A. Hopkins, *Bioorg. Chem. 1* (1971) 92; b) E. H. White, H. Wörther, H. H. Seliger, W. D. McElroy, *J. Am. Chem. Soc. 88* (1966) 2015.
[69] A. P. Schaap, S. D. Gagnon, *J. Am. Chem. Soc. 104* (1982) 3504.
[70] T. Förster, *Comp. Biochem. Physiol. 22* (1967) 61.
[71] a) T. Wilson, A. M. Halpern, J. Am. Chem. Soc. 102 (1980) 7272; b) R. Schmidt, H. Kelm, H.-D. Brauer, *Ber. Bunsenges. Phys. Chem. 81* (1977) 402.
[72] E. Rivas-Suárez, L. H. Catalani, E. J. H. Bechara, G. Cilento, *Photochem. Photobiol. 37* (1983) 93.
[73] E. Rivas-Suárez, G. Cilento, *Biochemistry 20* (1981) 7329.
[74] E. Rivas-Suárez, O. Augusto, G. Cilento, *Photochem. Photobiol. 33* (1981) 279.
[75] E. H. White, J. D. Miano, C. J. Watkins, E. J. Breaux, *Angew. Chem. 86* (1974) 292; *Angew. Chem. Int. Ed. Engl. 13* (1974) 229.
[76] G. Cilento, *Photochem. Photobiol. Rev. 5* (1980) 199.
[77] E. W. Meijere, W. Wynberg, *J. Chem. Educ. 59* (1982) 1071.
[78] a) R. Schmidt, H.-D. Brauer, W. Adam, K. Zinner, *Z. Phys. Chem. (Frankfurt am Main) 131* (1982) 129; b) W. Adam, G. Cilento, K. Zinner, *Photochem. Photobiol. 32* (1980) 87; c) W. Adam, O. Rodriguez, K. Zinner, *J. Org. Chem. 43* (1978) 4495.; d) W. Adam, E. M. Cancio, O. Rodriguez, *Photochem. Photobiol. 27* (1978) 617; e) N. J. Turro, I. E. Kochevar, Y. Noguchi, M.-F. Chow, *J. Am. Chem. Soc. 100* (1978) 3170; f) N. J. Turro, *Pure Appl. Chem. 49* (1977) 405; g) W. Adam, G. Cilento, L. O. Rodriguez, O. Rodriguez, A. S. Sarma, K. Zinner, *Photochem. Photobiol. 26* (1977) 299.
[79] W. Wynberg, H. Numan, H. P. J. M. Dekkers, *J. Am. Chem. Soc. 99* (1977) 3870.
[80] H. Wynberg, E. W. Meijere, J. C. Hummelen, *Nature (London) 265* (1980) 641.

[81] W. Adam, C.-C. Cheng, O. Cueto, I. Erden, K. Zinner, *J. Am. Chem. Soc. 101* (1979) 4735.
[82] H. E. Zimmerman, G. E. Keck, J. L. Pflederer, *J. Am. Chem. Soc. 98* (1976) 5574.
[83] M. J. Mirbach, A. Henne, K. Schaffner, *J. Am. Chem. Soc. 100* (1978) 7127.
[84] W. Adam, O. De Lucchi, K. Peters, E.-M. Peters, H. G. von Schnering, *J. Am. Chem. Soc. 104* (1982) 5747.
[85] a) G. Cilento, *Q. Rev. Biophys. 6* (1973) 485; b) *J. Theor. Biol. 55* (1975) 471.
[86] W. Wisseroth, *Chem.-Ztg. 107* (1983) 1.
[87] A. Lamola, *Biochem. Biophys. Res. Commun. 43* (1971) 893.
[88] R. Meneghini, M. E. Hoffmann, N. Durán, A. Faljoni, G. Cilento, *Biochim. Biophys. Acta 518* (1978) 177.
[89] A. Faljoni, M. Haun, M. E. Hoffmann, R. Meneghini, N. Durán, C. Cilento, *Biochem. Biophys. Res. Commun. 80* (1978) 490.
[90] H. H. Seliger, A. Thompson, J. P. Hammann, G. H. Posner, *Photochem. Photobiol. 36* (1982) 359.
[91] C. Hélène, M. Charlier, *Photochem. Photobiol. 25* (1977) 429.
[92] a) S. Sasson, D. Elad, *J. Org. Chem. 37* (1977) 3164; b) H. D. Roth, H. H. Lamola, *J. Am. Chem. Soc. 94* (1972) 1013.
[93] J. A. Montgomery, *J. Med. Chem. 23* (1980) 1063.
[94] a) W. Chowdhry, F. H. Westheimer, *Annu. Rev. Biochem. 48* (1979) 293; b) J. R. Knowles, *Acc. Chem. Res. 5* (1972) 155.
[95] W. Shropshire in K. C. Smith: *The Science of Photobiology*, Plenum Press, New York 1977, p. 281–312.
[96] P. J. Davies, A. W. Galston, *Plant Physiol. 47* (1971) 435.
[97] E. F. Ullman, US-Pat. 3689391; *Chem. Abstr. 78* (1972) 3585r.
[98] G. A. Blondin, B. D. Kulkarni, W. R. Nes, *Comp. Biochem. Physiol. 20* (1967) 379.
[99] W. H. Waddell, R. Crouch, K. Nakanishi, N. J. Turro, *J. Am. Chem. Soc. 98* (1976) 4189.
[100] G. O. Schenck, *Angew. Chem. 69* (1957) 579.

# COMMUNICATIONS

**When submitting manuscripts, authors of articles which are intended for publication as "Communications" are requested to conform to the guidelines reproduced at the beginning of each issue following the list of contents.**

## 1,2-Cyclohexadiene**

By *Curt Wentrup**, *Gerhard Gross*, *André Maquestiau*, and *Robert Flammang*

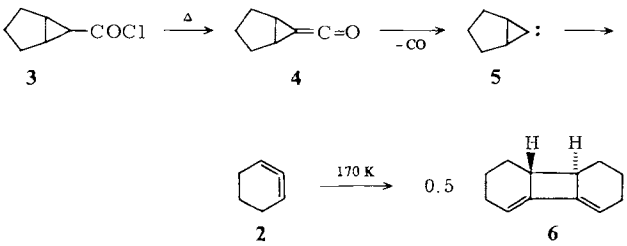
The structure of 1,2-cyclohexadiene has been a matter of controversy. Calculations and experiments have suggested a planar zwitterionic or diradicaloid ground state **1**[1]. However, it was recently shown in elegant trapping experiments that the species is chiral in solution at room temperature, but that optical activity is lost at 80 °C[2]. This indicates that the trapped species is the nonplanar allene **2** and that at 80 °C it either interconverts with the planar structure **1** or racemizes *via* a planar transition state.



1 2

* signifies ⊕/⊖ or ⊙

We now wish to report the direct spectroscopic observation of **2**, which conclusively proves that the ground state of 1,2-cyclohexadiene is an allene. **2** was generated by vacuum pyrolysis of bicyclo[3.1.0]hexane-6-carbonyl chloride **3** at 800 °C/$10^{-4}$ torr. This leads initially to the ketene **4** ($\nu = 2126\ cm^{-1}$), which under the reaction conditions rapidly loses CO, presumably to give the carbene **5**. The latter undergoes ring opening to the allene **2**, which was collected on a KBr window and characterized by a sharp and strong infrared absorption at 1886 $cm^{-1}$, persisting at temperatures between 11 K (Ar matrix) and 170 K (neat substance). The absorption disappeared at the latter temperature with concomitant formation of the dimer **6**, which has previously been isolated during a preparation of **5** in solution by an alternative route[3]. **6** was isolated by preparative gas chromatography and identified by direct comparison with an authentic sample.




3 4 5

2 6

The identity of **2** was also ascertained by pyrolyzing **3** in a reactor placed immediately before the ion source of a Varian MAT 311A mass spectrometer. The CID-MIKE mass spectrum demonstrated the formation of an ion ($m/z = 80$) whose intensity increased with increasing temperature. At the same time, the intensities of peaks due to the starting material **3** diminished.

Confirmation of the reaction pathway **3** → **2** may also be obtained from the analogous formation of allene by pyrolysis of cyclopropanecarbonyl chloride, as observed by IR and mass spectrometry in the present study and previously by photoelectron spectroscopy[4].

The observation of an allenic absorption for **2** at 1886 $cm^{-1}$ clearly identifies this molecule as a ground state allene. Ring strain and an obvious deviation from linearity causes a shift by approximately 70 $cm^{-1}$ from the normal position of the C=C stretching vibration in allenes. This conclusion is also supported by very recent *ab initio* calculations[5].

Received: February 22, 1983 [Z 283 IE]
German version: *Angew. Chem. 95* (1983) 551

CAS Registry numbers:
**2**, 14847-23-5; **3**, 85763-23-1; **4**, 85763-24-2; **6**, 28229-15-4.

[*] Prof. Dr. C. Wentrup, G. Gross
Fachbereich Chemie der Universität
Lahnberge, D-3550 Marburg (Germany)
Prof. Dr. A. Maquestiau, Dr. R. Flammang
Laboratoire de Chimie Organique, Université d'Etat
B-7000 Mons (Belgium)

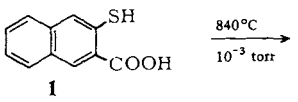
[**] Presented, in part, at the Chemiedozententagung in Kaiserslautern (Germany), March 22—26, 1982. This work was supported by the Deutsche Forschungsgemeinschaft and the Fonds der Chemischen Industrie.

[1] P. W. Dillon, G. R. Underwood, *J. Am. Chem. Soc. 96* (1974) 779. For early experimental work, see G. Wittig, P. Fritze, *Justus Liebigs Ann. Chem. 711* (1968) 82.
[2] M. Balci, W. M. Jones, *J. Am. Chem. Soc. 102* (1980) 7607.
[3] W. R. Moore, W. R. Moser, *J. Am. Chem. Soc. 92* (1970) 5469.
[4] H. Bock, T. Hirabayashi, S. Mohmand, *Chem. Ber. 114* (1981) 2595.
[5] M. W. Schmidt, R. O. Angus, Jr., R. P. Johnson, *J. Am. Chem. Soc. 104* (1982) 6838.

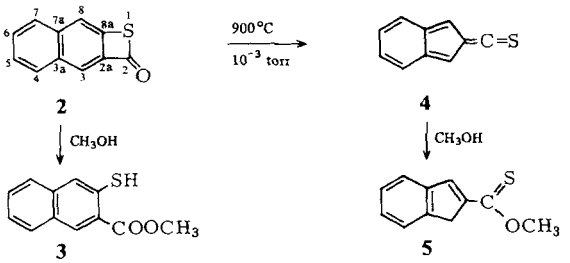
## Thietones, Oxetones, and Azetones**

By *Curt Wentrup** and *Gerhard Gross*

Unsaturated four-membered heterocycles are rare, and no substantiated preparations of stable thietones, oxetones, or azetones have been described. We now wish to report the first isolation of a stable thietone, namely naphtho[2,3-*b*]thiet-2-one **2**, obtained in 25% yield as yellow crystals, m.p. 85 °C, by flash vacuum pyrolysis of 3-mercapto-2-naphthoic acid **1** at 840 °C/$10^{-3}$ torr. The structure of **2** is established by elemental analysis and spectroscopic properties[1]. **2** is indefinitely stable in the crystalline state, but a mixture of dimers and trimers slowly precipitates from solutions at room temperature. Reaction with methanol gives the methyl ester **3** in quantitative yield, and pyrolysis at 900 °C/$10^{-3}$ torr leads to elimination of CO and formation of 2-thiocarbonyl-2*H*-indene **4**, isolated on a KBr window at −196 °C. Compound **4** absorbs in the IR at 1742 $cm^{-1}$, disappears above −100 °C, and reacts with methanol at −120 °C to give the methyl ester **5**.

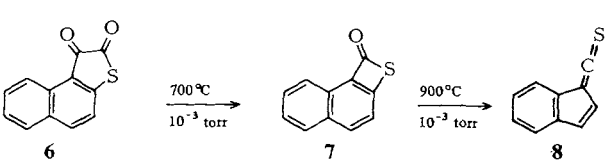



1




2 4 3 5

The corresponding naphtho[2,1-*b*]thiet-2-one **7** was obtained in quantitative yield by pyrolysis of the dione **6**[2]. **7** is less stable than **2**, dimerizing within 30 min at room temperature. A solution of **7** in $CH_2Cl_2$ reacts with methanol at −40 °C to give the methyl ester of 2-mercapto-1-naphthoic acid in quantitative yield. Pyrolysis of **6** at 900 °C/$10^{-3}$ torr gives the thioketene **8** (IR: 1739 $cm^{-1}$), which is stable below −40 °C and reacts with methanol to furnish *O*-methyl 3-indenethiocarboxylate.

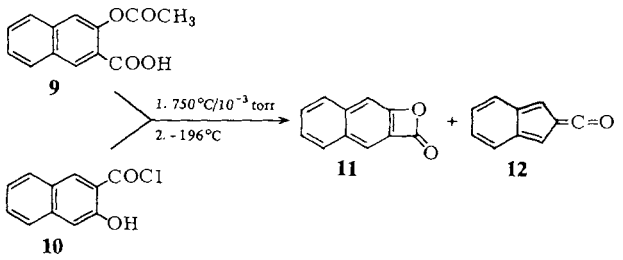



6 7 8

[*] Prof. Dr. C. Wentrup, G. Gross
Fachbereich Chemie der Universität
Lahnberge, D-3550 Marburg (Germany)

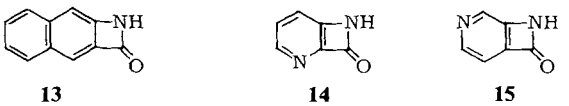
[**] This work was supported by the Deutsche Forschungsgemeinschaft and the Fonds der Chemischen Industrie.

The naphthothietones are considerably more stable than benzothietone, the latter having been observed only in a low-temperature matrix[3a] and in the gas-phase using photoelectron spectroscopy[3b]. Also benzoxetone is reported to be unstable[4], but naphtho[2,3-*b*]oxetone has been described as a stable crystalline compound[5]. The compound described is certainly not monomeric. The real naphtho[2,3-*b*]oxetone, the monomer **11**, is obtained by pyrolysis of either **9** or **10** at 750 °C/$10^{-3}$ torr, absorbs in the IR at 1893 and 1874 $cm^{-1}$, is stable till −40 °C, and reacts at this temperature with methanol to give methyl 3-hydroxy-2-naphthoate in 20% isolated yield. In the pyrolyses of **9** and **10** a further, weak IR absorption due to the ketene **12** is observed at 2127 $cm^{-1}$, increasing in intensity with increasing temperature, and also obtained by pyrolysis of methyl 2-indenecarboxylate to which it reverts below −100 °C in the presence of methanol.




9 11 12 10

Naphtho[2,3-*b*]azet-2(1*H*)-one **13** (1778 $cm^{-1}$; stable till 0 °C), azeto[3,2-*b*]pyridin-2(1*H*)-one **14** (1807 $cm^{-1}$; stable till −40 °C), and azeto[2,3-*c*]pyridine-2(1*H*)-one **15** (1809 $cm^{-1}$; stable till 0 °C) were generated by analogous pyrolyses (750 °C/$10^{-3}$ torr) of the corresponding aminocarboxylic acids or esters thereof.



13 14 15

Received: February 25, 1983 [Z 287 IE]
German version: *Angew. Chem. 95* (1983) 552

[1] **2**: IR: 1800 $cm^{-1}$; MS: *m/z* 186 ($M^+$); $^1$H-NMR ($CDCl_3$, 400 MHz): $\delta = 7.40$ (t, $J = 8$ Hz), 7.43 (s), 7.46 (s), 7.55 (t, $J = 8$ Hz), 7.67 (d, $J = 8$ Hz), 7.78 (d, $J = 8$ Hz); $^{13}$C-NMR ($CDCl_3$, 100.6 MHz) (multiplicity, incl. long range couplings): $\delta = 177.7$ (s; C-2), 146.1 (s; C-2a), 138.3 (s; C-7a), 135.7 (s; C-3a), 131.4 (s; C-8a), 130.8 (dt), 129.6 (dd), 127.1 (dt), 125.9 (dd), 120.8 (dd), 118.9 (dd).
[2] **7**: IR: 1793 $cm^{-1}$; MS: *m/z* 186 ($M^+$); $^1$H-NMR ($CDCl_3$, 400 MHz, −40 °C): $\delta = 7.38$ (t, $J = 8$ Hz), 7.42 (d, $J = 8$ Hz), 7.56 (t, $J = 8$ Hz), 7.76 (d, $J = 8$ Hz), 7.80 (d, $J = 8$ Hz), 7.90 (d, $J = 8$ Hz).
[3] a) O. L. Chapman, C. L. McIntosh, *J. Am. Chem. Soc. 92* (1970) 7001; b) R. Schulz, A. Schweig, *Tetrahedron Lett. 1979*, 59.
[4] O. L. Chapman, C. L. McIntosh, J. Pacansky, G. V. Calder, G. Orr, *J. Am. Chem. Soc. 95* (1973) 4061.
[5] J. W. Airan, S. V. Shah, *J. Indian Chem. Soc. 19* (1942) 333.

## 1,3,5,7-Tetrazocines**

By *Rudolf Gompper** and *Marie-Luise Schwarzensteiner*

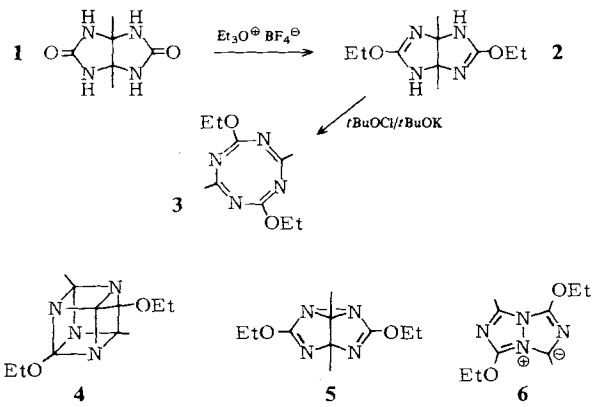
The prognosis that donor-substituted semibullvalenes have a bishomoaromatic ground state is corroborated

[*] Prof. Dr. R. Gompper, M.-L. Schwarzensteiner
Institut für Organische Chemie der Universität
Karlstrasse 23, D-8000 München 2 (Germany)

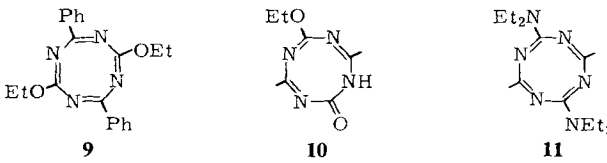
[**] This work was supported by the Deutsche Forschungsgemeinschaft and the Fonds der Chemischen Industrie.

neither by tetramethyl 3,7-diacetoxy-1,5-dimethyltricyclo[3.3.0.0$^{2,8}$]octa-3,6-diene-2,4,6,8-tetracarboxylate[2] nor by similar compounds[3]. Even with a 2,6-diazasemibullvalene[4] only a rapid Cope rearrangement was observed. However, because of the relatively weak NN bond, 1,5-dialkyl-2,4,6,8-tetraazasemibullvalenes should represent the best models for bishomoaromatic semibullvalenes. We report here on attempts to synthesize systems of this type.

Based on our experience gained in synthesizing the above-mentioned semibullvalenetetracarboxylic acid esters, 1,5-dimethylglycoluril should be an appropriate educt[2]. 3,7-Diethoxy-1,5-dimethyl-2,4,6,8-tetraazabicyclo[3.3.0]octa-3,7-diene, **2**, is obtained upon heating **1** and triethyloxonium tetrafluoroborate to 90–100 °C (yield 20–25%; m.p. = 248 °C). **2** reacts with *tert*-butyl hypochlorite and potassium *tert*-butoxide to afford a compound (yield 50%; colorless crystals, m.p. = 26 °C) having the empirical formula $C_{10}H_{16}N_4O_2$. From the spectroscopic data [$^1$H-NMR: solvent $CDCl_3$, room temperature, 60 MHz): $\delta = 1.32$ (t, $J = 6$ Hz; 6H, $OCH_2CH_3$), 2.11 (s; 6H, $CH_3$), 4.20 (q, $J = 6$ Hz; 4H, $OCH_2CH_3$); $^{13}$C-NMR ($CDCl_3$, 80 MHz): $\delta = 14.02$ ($CH_3$), 23.99 ($OCH_2CH_3$), 64.33 ($OCH_2CH_3$), 160.29 (=C–$CH_3$), 173.40 (=C–OEt); $^{15}$N-NMR ($CDCl_3$, 200 MHz): $\delta = 206$], which indicate the presence of only sp$^2$-hybridized framework C atoms, only one type of vinyl $CH_3$-group, and N atoms, neither the tetraazasemibullvalene **5**, the structures **4** and **6**, nor bicyclooctatriene derivatives are involved. Consequently, the compound must be 2,6-diethoxy-4,8-dimethyl-1,3,5,7-tetrazocine **3**.




2,6-Diethoxy-4,8-diphenyl-1,3,5,7-tetrazocine, **9**, can be prepared using the same method (yield 65%; m.p. = 151 °C). According to an X-ray structure analysis[8], **9** has the boat conformation. Compounds **3** and **9** represent the first tetraazacyclooctatetraenes. Previous attempts to prepare these types of compounds have always led to isolation of tetraazapentalenes[9].




When a solution of **3** in ether is stirred for a few days in the presence of silica gel 6-ethoxy-4,8-dimethyl-1,3,5,7-tetrazocin-2(1*H*)-one **10** (m.p. = 86 °C) results. Heating **3** and diethylamine gives the tetrazocine **11** (yield 81%; b.p. = 130 °C/0.01 mbar).


Received: February 28, 1983 [Z 295 IE]
German version: *Angew. Chem. 95* (1983) 553
The complete version of this manuscript appears in:
*Angew. Chem. Suppl. 1983*, 812–817

CAS Registry numbers:
**1**, 28115-25-5; **2**, 86162-03-0; **3**, 86146-62-5; **7**, 5157-15-3; **8**, 86146-63-6; **9**, 86146-64-7; **10**, 86146-65-8; **11**, 86146-66-9.



[2] R. Gompper, M.-L. Schwarzensteiner, *Angew. Chem. 94* (1982) 447; *Angew. Chem. Int. Ed. Engl. 21* (1982) 438; *Angew. Chem. Suppl. 1982*, 1028.

[3] a) D. Paske, R. Ringshandl, I. Sellner, H. Sichert, J. Sauer, *Angew. Chem. 92* (1980) 464; *Angew. Chem. Int. Ed. Engl. 19* (1980) 456; b) L. S. Miller, K. Grohmann, J. J. Dannenberg, L. Todaro, *J. Am. Chem. Soc. 103* (1981) 6249; c) R. Askani, M. Littmann, *Tetrahedron Lett. 23* (1982) 3651; d) H. Quast, J. Christ, Y. Görlach, W. von der Saal, *ibid. 23* (1982) 3653.

[4] C. Schnieders, H.-J. Altenbach, K. Müllen, *Angew. Chem. 94* (1982) 638; *Angew. Chem. Int. Ed. Engl. 21* (1982) 637; *Angew. Chem. Suppl. 1982*, 1353.

[8] H. Nöth, H.-U. Wagner, unpublished results.

[9] C. A. Ramsden, *Tetrahedron 33* (1977) 3203.


## Photolysis of the Cyclopentadienyl(hydrido) Complexes $C_5H_5M(CO)_3H$ (M = Cr, Mo, W) in Matrices and in Solution: Characterization of $[C_5H_5W(CO)_2H]_2$ and $[C_5Me_5W(CO)_2H]_2$**


By *Helmut G. Alt**, *Khalil A. Mahmoud*, and *Antony J. Rest*


The dissociation energy of transition metal-hydrogen bonds is considerably higher than that of the corresponding transition metal-carbon single-bonds[1]. In the photolysis of carbonylhydrido complexes it is, therefore, to be expected that the initial step should involve removal of the carbonyl ligands and formation of highly reactive hydrido complex fragments. We have irradiated ($\lambda > 300$ nm) the compounds $C_5H_5M(CO)_3H$ (M = Cr, Mo, W) in solution and isolated the subsequent reaction products. To account for the primary step, the photolysis was also performed in gas matrices (Ar, $CH_4$, $N_2$, CO) at 12 K; the photolysis products were characterized by IR spectroscopy. In all cases, with the exception of the CO matrix, the initial step of the photoreaction, the removal of a CO ligand and the formation of the 16e-fragment $C_5H_5M(CO)_2H$, could be detected.

$$C_5H_5M(CO)_3H \underset{\lambda > 370\ nm}{\overset{290 < \lambda < 370\ nm}{\rightleftharpoons}} C_5H_5M(CO)_2H + CO$$

[*e.g.* $C_5H_5W(CO)_3H$: $\nu(CO) = 2025.5$, 1939.5, 1935.1 cm$^{-1}$, $\lambda_{max} = 305$ nm; $C_5H_5W(CO)_2H$: $\nu(CO) = 1956.4$, 1872.0 cm$^{-1}$; free CO: $\nu(CO) = 2138.0$ cm$^{-1}$; in argon matrix at 12 K]. The reaction can be reversed if the products of the initial step are irradiated with visible light ($\lambda > 370$ nm). The fragments $C_5H_5M(CO)_2H$ can be stabilized in the matrix by ligands L (L = $N_2$, $C_2H_4$, $^{13}$CO) or in solution (L = $C_2H_4$, THF, $PMe_3$), leading to formation of *cis/trans*-


[*] Priv.-Doz. Dr. H. G. Alt
Laboratorium für Anorganische Chemie der Universität
Universitätsstrasse 30, D-8580 Bayreuth (Germany)

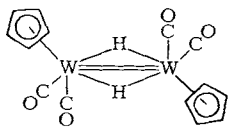
Dr. A. J. Rest, K. A. Mahmoud
Department of Chemistry, The University,
Southampton, SO9 5NH (England)



[**] This work was supported by the Deutsche Forschungsgemeinschaft and the Fonds der Chemischen Industrie.

isomers of $C_5H_5M(CO)_2(L)H$[3]. In the CO matrix at 12 K we observed, furthermore, the formation of the radicals $C_5H_5M(CO)_3$ and CHO[4], which indicate the photoinduced removal of the metal-hydrogen bond.

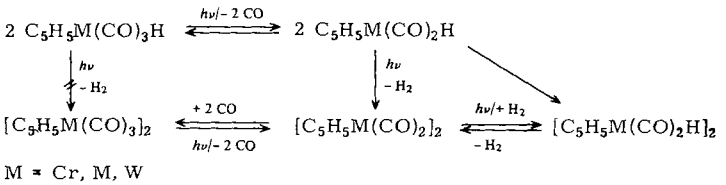
Photolysis of the three carbonylhydrido complexes $C_5H_5M(CO)_3H$ (M = Cr, Mo, W; *ca.* 2 mmol in 300 mL pentane) at 15 °C leads to various products. The yellow, highly air-sensitive $C_5H_5Cr(CO)_3H$ is completely converted within 20 min into $[C_5H_5Cr(CO)_2]_2$, and CO and $H_2$ are evolved. No intermediates were detected upon investigation of the reaction by $^1$H-NMR spectroscopy in [$D_8$]-toluene at −40 °C. $C_5H_5Mo(CO)_3H$ is considerably more photostable than the Cr derivative, and complete photoinduced dehydrogenation requires *ca.* 3 h. The major product $[C_5H_5Mo(CO)_3]_2$ and a minor product $[C_5H_5Mo(CO)_2]_2$ could be isolated. Upon UV irradiation for 5 h the extent of reaction of the colorless $C_5H_5W(CO)_3H$ is only *ca.* 80%. Predominantly $[C_5H_5W(CO)_2]_2$ is found in the reaction solution in addition to small amounts of $[C_5H_5W(CO)_3]_2$, although the major product is a dark brown precipitate [decomp. 115 °C (under $N_2$); yield *ca.* 55%], whose IR, NMR, and mass spectrum indicate a dinuclear complex $[C_5H_5W(CO)_2H]_2$ [MS: *m/z* 612 ($M^+$) relative to $^{184}$W]. We propose the following structure for the complex which dissociates in solution.



The nature of the two bridging hydrido ligands can be clearly determined from the $^1$H-NMR spectrum [$\delta$(WHW) = −13.24, [$D_6$]acetone, −30 °C] due to the intensity of the tungsten satellites [$J$(W,H) = 83.1 Hz; 24% of the signal intensity]. The two $C_5H_5$ ligands exhibit only one singlet ($\delta$ = 6.14). Only two CO-bands occur in the IR spectrum (1930 and 1860 cm$^{-1}$, in toluene), thus confirming the symmetric structure of the dinuclear complex. Comparable data are known for the osmium complex $[C_5Me_5Os(CO)H]_2$[7].

The photolysis of a solution of the pentamethylcyclopentadienyl derivative $C_5Me_5W(CO)_3H$ in pentane proceeds analogously: the major product, the red-brown complex $[C_5Me_5W(CO)_2H]_2$ is eluted from the chromatographic column by toluene [m.p. > 300 °C; yield 65%. IR (pentane): $\nu$(CO) = 1920, 1848 cm$^{-1}$; $^1$H-NMR ([$D_6$]-acetone): $\delta$ = 1.85 (s, 15), −9.30 (s, 1), $J$(W,H) = 82.8 Hz; $^{13}$C-NMR ([$D_6$]-acetone: $\delta$ = 102.3 ($C_5$), 9.9 ($Me_5$), 225.1 (CO); MS: *m/z* 752 ($M^+$) relative to $^{184}$W].

The diamagnetic compounds $[C_5H_5W(CO)_2H]_2$ and $[C_5Me_5W(CO)_2H]_2$ are the first examples of doubly hydrido-bridged neutral complexes which formally possess a W=W bond. We presume that photolysis of the educt $C_5H_5M(CO)_3H$ in solution proceeds according to:




The fragment $C_5H_5M(CO)_2H$, which is generated initially, predominantly undergoes photoinduced dehydrogenation; the radicals thus formed may dimerize to give $[C_5H_5M(CO)_2]_2$, which in turn adds hydrogen photochemically. This assumption is corroborated experimentally: $[C_5Me_5Mo(CO)_2]_2$ rapidly takes up hydrogen upon being UV irradiated to form the 1 : 1 adduct $[C_5Me_5Mo(CO)_2H]_2$ [IR (pentane): $\nu$(CO) = 1929, 1858 cm$^{-1}$; $^1$H-NMR ([$D_6$]acetone): $\delta$ = 1.90 (Me), −10.01 (MoHMo)], which could not be detected in the photolysis of $C_5Me_5Mo(CO)_3H$. Since photolysis of $C_5H_5Cr(CO)_3H$ and $C_5Me_5Cr(CO)_3H$, respectively, in solution leads only to observation of $[C_5H_5Cr(CO)_2]_2$ and $[C_5Me_5Cr(CO)_2]_2$, direct photoinduced dehydrogenation of the parent complexes is precluded. In contrast to the Mo and W derivatives, $[C_5H_5Cr(CO)_2]_2$ and $[C_5Me_5Cr(CO)_2]_2$ are not able to add CO at standard pressure[10].

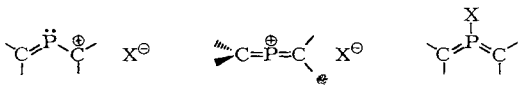
Received: February 25, 1983;
revised: April 8, 1983 [Z 289 IE]
German version: *Angew. Chem. 95* (1983) 569
The complete version of this communication appears in:
*Angew. Chem. Suppl. 1983*, 803–811

[1] J. A. Connor, M. T. Zafarani-Moattar, J. Bickerton, N. I. El Saied, S. Suradi, R. Carson, G. Al Takhin, H. A. Skinner, *Organometallics 1* (1982) 1166; J. Halpern, *Acc. Chem. Res. 15* (1982) 238.
[3] K. A. Mahmoud, A. J. Rest, H. G. Alt, *J. Chem. Soc. Dalton Trans.*, in press.
[4] K. A. Mahmoud, A. J. Rest, H. G. Alt, *J. Organomet. Chem. 246* (1983) C37.
[7] J. K. Hoyano, W. A. G. Graham, *J. Am. Chem. Soc. 104* (1982) 3722.
[10] D. S. Ginley, C. R. Bock, M. S. Wrighton, *Inorg. Chim. Acta 23* (1977) 85.

## 2-Phosphaallyl Cations by Formal Insertion of P$^\oplus$ into the C=C Double Bond**

By *Alfred Schmidpeter**, *Siegfried Lochschmidt*, and *Angela Willhalm*

Isoelectronic substitution of the central carbon atom of (linear) allenes by N$^\oplus$ leads to 2-azaallyl cations, whose structures, depending on the nature of the substituents, are either bent or linear. In addition to these alternatives **A** and **B**, a covalent form **C** is also feasible for the corresponding 2-phosphaallyl halides.



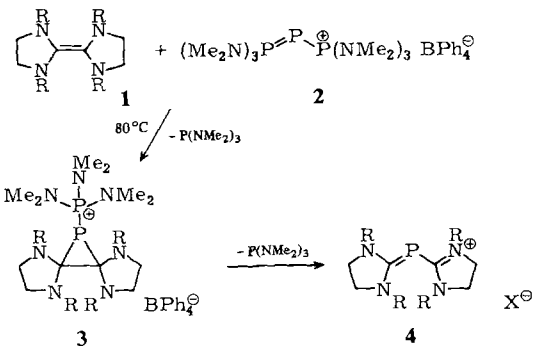
**A** **B** **C**

Electron-donating substituents should favor form **A**, whereas electron-attracting substituents should favor form **C**. Examples of **A** are the classical phosphamethine cyanines, in which the carbon atoms are members of heterocycles. One example for **C**, (X = Cl), having $Me_3Si$-substituted carbon atoms is also known.

Particularly form **B** makes one think that phosphaallyl cations could formally be accessible by insertion of P$^\oplus$ into an olefin. A comparable insertion of the C atom isoelectronic to P$^\oplus$ occurs in the conversion of an olefin into an allene[7]. By analogy, the conversion of an olefin into a phosphaallyl cation could commence from $PCl_3$, which in the course of the reaction would have to be reduced to P$^\oplus$. As we have previously reported, this reduction can be per-

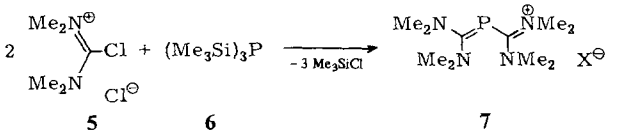
[*] Prof. Dr. A. Schmidpeter, S. Lochschmidt, A. Willhalm
Institut für Anorganische Chemie der Universität
Meiserstrasse 1, D-8000 München 2 (Germany)
[**] This work was supported by the Deutsche Forschungsgemeinschaft and the Fonds der Chemischen Industrie.

formed separately and the $P^{\oplus}$ stabilized as a bisphosphane complex[10]. The complex with tris(dimethylamino)phosphane, the 1,1,1,3,3,3-hexakis(dimethylamino)-1$\lambda^5$,3$\lambda^5$-triphospha-2-enium tetraphenylborate **2**, is particularly easy to handle[11]. In order to accept $P^{\oplus}$ from **2**, however, the olefin must be particularly electron-rich. Thus, the biimidazolidinylidene **1** reacts with **2** in the way suggested to afford the phosphaallyl tetraphenylborates **4** (X = $BPh_4$; R = Me, Et), displacing two equivalents of tris(dimethylamino)phosphane.



The reaction could commence by electrophilic attack of **2** and proceed *via* a phosphiranylphosphonium intermediate, which, however, has not yet been detected.

There is a second, more general and more effective route to amino-substituted 2-phosphaallyl cations[14]: for example, tetramethylchloroformamidinium chloride, **5**, reacts with tris(trimethylsilyl)phosphane, **6**, to form tetrakis(dimethylamino)phosphaallyl chloride, **7**, X = Cl[15].



In the same way the phosphaallyl chloride, **4**, (X = Cl, R = Me) is formed from 2-chloro-1,3-dimethylimidazolidinium chloride.

All of the products **4** and **7** are remarkably insensitive towards oxidation and hydrolysis. In compounds with X = Cl the chloride can be exchanged by other anions without significant alteration of the chemical shifts in the resulting NMR spectra. This result confirms their ionic character. In **4**, $\delta(^{31}P)$ is −93, but in **7**, in contrast, −20, which indicates that in the second case the positive charge is less strongly transferred to the nitrogens. Irrespective of the differences in degree, however, both cases should be of the structural alternative **A**.

Received: February 28, 1983;
revised: March 28, 1983 [Z 294 IE]
German version: *Angew. Chem. 95* (1983) 561
The complete version of this manuscript appears in:
*Angew. Chem. Suppl. 1983*, 710–717

[7] Cf. W. Kirmse: *Carbene, Carbenoide und Carbenanaloge*, Verlag Chemie, Weinheim 1969.

[10] A. Schmidpeter, S. Lochschmidt, W. S. Sheldrick, *Angew. Chem. 94* (1982) 72; *Angew. Chem. Int. Ed. Engl. 21* (1982) 63.

[11] A. Schmidpeter, S. Lochschmidt, unpublished results.

[14] A third route to 2-phosphaallyl cations could be opened by alkylating the tris(trimethylsilyl)phosphane carbodiimide adducts (cf. K. Issleib, H. Schmidt, C. Wirkner, *Synth. React. Inorg. Met.-Org. Chem. 11* (1981) 279) in as far as this occurs at the nitrogen and not (as would be expected) at the phosphorus atom.

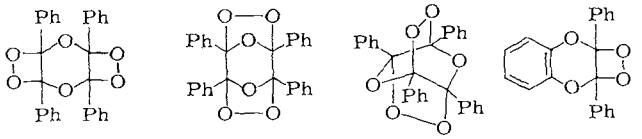
[15] The reaction of the fluorine compound corresponding to **5**, *i.e.* of bis(dimethylamino)difluoromethane, with **6** was recently described by other workers. This leads to the 1 : 1 product, $(Me_2N)_2C{=}P{-}SiMe_3$, not observed by us in the reaction of **5** with **6**: L. N. Markovskii, K. D. Romanenko, T. I. Pidvarko, *Zh. Obshch. Khim. 52* (1982) 1925.

## Crystal Structure of 2,4,5,7,9,10-Hexaoxa-1,3,6,8-tetraphenyltricyclo[6.2.0.0$^{3,6}$]decane: An Authentic Bisdioxetane**

By *Waldemar Adam**, *Ernst Schmidt*, *Eva-Maria Peters*, *Karl Peters*, and *Hans Georg von Schnering*

*Dedicated to Professor Giuseppe Cilento on the occasion of his 60th birthday*

The stable product of the photooxygenation of tetraphenyl-1,4-dioxin was assigned the bisdioxetane structure **1**[1], since it thermally decomposed with formation of benzoic anhydride and emission of light. Elemental analysis and



iodometric peroxide titration were consistent with the empirical formula $C_{28}H_{20}O_6$. While chemiluminescence is indicative but not necessarily definitive for 1,2-dioxetanes[2], the cited evidence is in principle also consistent with the alternative structures **2** and **3** for this unusual "benzoic anhydride dimer"[3]. $^1$H-NMR is uninformative in this structural problem and $^{13}$C-NMR ($\delta$ = 107.80 ppm for the dioxetane carbon) cannot differentiate between the possible alternatives. Since **1** is the first bisdioxetane[4] to be reported, it was essential that an X-ray structure analysis be carried out. Aside from confirming the bisdioxetane structure **1**, we expected information about the stereochemical arrangement of the two dioxetane rings, *i.e.* whether they are oriented *syn* or *anti* with respect to each other.

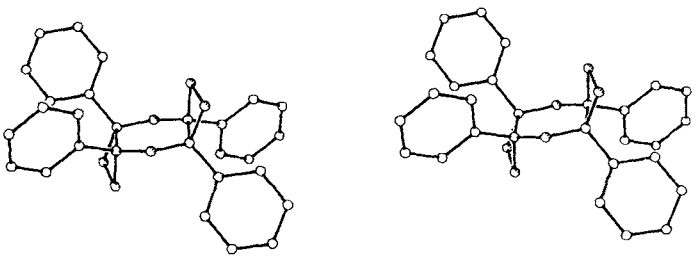


Fig. 1. Stereodiagram of the structure of **1**. Space group $P2_1/n$; $a$ = 1417.3, $b$ = 766.6, $c$ = 1036.7 pm, $\beta$ = 90.00°, $Z$ = 2, $\rho_{calc.}$ = 1.304 g·cm$^{-3}$, 1653 $F > 3\sigma(F)$, R = 0.062.

The $C_{28}H_{20}O_6$ product was prepared as described[1], and well defined crystals were grown by low-temperature re-

[*] Prof. Dr. W. Adam, E. Schmidt
Institut für Organische Chemie der Universität
Am Hubland, D-8700 Würzburg (Germany)
Dr. E.-M. Peters, Dr. K. Peters, Prof. Dr. H. G. von Schnering
Max-Planck-Institut für Festkörperforschung
Heisenbergstrasse 1, D-7000 Stuttgart 80 (Germany)

[**] Generous financial support from the Deutsche Forschungsgesellschaft, the Fonds der Chemischen Industrie, and Volkswagenstiftung is gratefully acknowledged.

crystallization from petroleum ether/dichloromethane (m.p. 111 °C, pale yellow prisms). X-ray structure analysis[5] confirmed beyond any doubt (Fig. 1) that this product is the "benzoic anhydride dimer" **1**, the first authentic bis-dioxetane. As expected, the dioxetane rings are arranged *anti* to each other. Surprisingly, however, they are appreciably puckered (dihedral angle *ca.* 16.3°). The dioxane ring is almost planar; it has a markedly flattened chair conformation (all atoms deviate about 8 pm from the equalizing plane). Presumably, in an almost planar dioxane ring the non-bonding repulsive forces between the dioxetane oxygen atoms and the *syn*-oriented phenyl groups are minimal (inspection of Dreiding models indeed suggest this to be the case).

On the other hand, the related dioxetane **4** (m.p. 113–116 °C, pale yellow prisms from *n*-pentane), prepared by singlet oxygenation of diphenylbenzodioxin[6] (Fig. 2) has

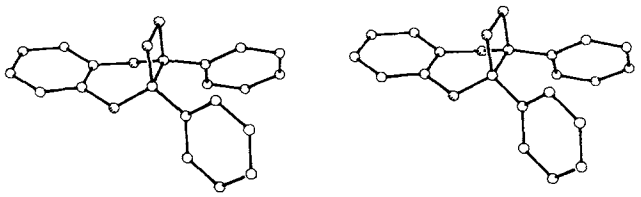


Fig. 2. Stereodiagram of the structure of **4**. Space group $P2_1/a$; $a = 1923.2$, $b = 1239.3$, $c = 1320.6$ pm, $\beta = 93.44°$, $Z = 8$, $\rho_{calc} = 1.346$ g·cm$^{-3}$, 2332 $F > 3\sigma(F)$, $R = 0.084$.

an almost planar dioxetane ring (dihedral angle *ca.* 0.8°) and a puckered dihydro-1,4-dioxin ring. In **1** and **4** the oxygen-oxygen bond lengths are 150.0 and 155 pm, respectively, the dioxetane carbon-carbon bond lengths 155.5 and 161 pm, respectively.

Received: March 21, 1983 [Z 317 IE]
German version: *Angew. Chem. 95* (1983) 566

[1] W. Adam, C.-C. Cheng, O. Cueto, I. Erden, K. Zinner, *J. Am. Chem. Soc. 101* (1979) 4735.
[2] W. Adam, G. Cilento: *Chemical and Biological Generation of Electronically Excited States*, Academic Press, New York 1982.
[3] The compound is not polymeric, since it is crystalline and has a well defined melting point.
[4] Since this type of "high energy" molecule contains two dioxetane rings, *higher* excited states could be formed on thermal decomposition.
[5] Details of the crystal structure investigation can be obtained on request from the Fachinformationszentrum Energie Physik Mathematik, D-7514 Eggenstein-Leopoldshafen, by quoting the depository number CSD 50458, the names of the authors, and full citation of the journal.
[6] W. Adam, O. Cueto, E. Schmidt, K. Takayama, *Angew. Chem. 93* (1981) 1100; *Angew. Chem. Int. Ed. Engl. 20* (1981) 1031.

## Lithiumcarbamoyl-bis(ethene)nickel(0)

By *Klaus Pörschke**, *Günther Wilke*, and *Carl Krüger*

Reaction of (cdt)NiCO **1**[1] with organolithium compounds or lithium amides in ether/pmdta as solvent leads to formation of the thermolabile lithiumacyl- or lithiumcarbamoyl-nickel(0) complexes {(pmdta)LiO(R)C}Ni(cdt) (R = $CH_3$ (**2**), $C_6H_5$ (**3**), $NMe_2$ (**4**))[2], which may be regarded as precursors of *carbonyl-free* and *olefin-containing* carbene complexes. We have now been able to replace the triene ligand cdt in **4** by ethene and to isolate the 16e-complex **5** in crystalline form.

$$\underset{\mathbf{1}}{(cdt)NiCO} + (pmdta)LiNMe_2 \xrightarrow[-40°C]{Ether} (pmdta)LiOC(NMe_2)Ni(cdt)\ \mathbf{4}$$

$$\mathbf{4} + 2\ C_2H_4 \xrightarrow[-10°C]{Ether} (pmdta)LiOC(NMe_2)Ni(C_2H_4)_2 + cdt\ \ \mathbf{5}$$

cdt = *trans,trans,trans*-1,5,9-cyclododecatriene
cod = 1,5-cyclooctadiene
cot = cyclooctatetraene
pmdta = pentamethyldiethylenetriamine
tmeda = tetramethylethylenediamine

The yellow-brown crystals of the pmdta-stabilized lithiumcarbamoyl-bis(ethene)nickel(0) **5**, which are stable at room temperature, are readily soluble in polar organic solvents such as ether, tetrahydrofuran (THF) and acetonitrile, moderately soluble in toluene, and only sparingly soluble in pentane. As shown by the NMR spectra, the pmdta ligand is released on dissolution of **5** in THF; the slight electrical conductivity of such a solution ($\Lambda = 0.014$ cm$^{-2}/\Omega$M; 0.1 M, 0 °C) infers a very weak dissociation into ions.

Methanolysis of **5** in presence of cod yields dimethylamine, which was detected gas-chromatographically, and the expected amounts of ethene, as well as CO, $Ni(CO)_4$ and $Ni(cod)_2$. Apparently, the nitrogen atom in **5** is protonated by weak acids, with dissociation of the carbamoyl group. The bonded ethene in **5** is quantitatively liberated by cot. An exchange between bonded and excess ethene cannot be detected by NMR spectroscopy at room temperature. **5** reacts with CO at −78 °C, the CO replacing the ethene to give the 18e-complex **6**, which can also be prepared from $Ni(CO)_4$ or **4**[2].

$$\mathbf{5} + 3\ CO \xrightarrow[-78°C \rightarrow 0°C]{Ether} (pmdta)LiOC(NMe_2)Ni(CO)_3 + 2\ C_2H_4\ \ \mathbf{6}$$

The 400-MHz $^1$H- and 75.5-MHz $^{13}$C-NMR spectra of a solution of **5** in [$D_8$]-THF are temperature-dependent between +20 °C and −80 °C, and show a remarkable complexity at −80 °C. At 20 °C they are consistent with a trigonal-planar coordination of the nickel atom by the two ethene ligands and the carbamoyl ligand, whereby—referred to the NMR time scale—all ligands freely rotate about the axis of coordination, while rotation of the $NMe_2$ group about the bond to the carbamoyl C-atom is appreciably restricted. The strong shielding of the ethene C-atoms and H-atoms in **5**, which compares with that in {(pmdta)$LiCH_3$}Ni($C_2H_4$)$_2$ **7**[3] in [$D_8$]-THF, points to a high negative charge on the bis(ethene)nickel moiety of the complex through the lithiumcarbamoyl ligand. Lowering of the temperature leads to freezing-in of the ethene rotation (< −20 °C) and to the appearance at −80 °C of two detectable isomers, A and B (*ca.* 1 : 1.5), which presumably differ in the bonding of the lithium atom to the carbamoyl ligand (Li–O- and Li–N contacts).

**5** is present in only one form in the crystalline state. As shown by X-ray structure analysis (Fig. 1), the planar bis(ethene)nickel moiety, whose structural data are already known[3,4], is linked to the likewise planar carbamoyl moiety *via* a short Ni–C bond. The plane of the carbamoyl system is nearly perpendicular (84°) to the trigonal coordination plane of the transition metal. The geometry of the carbamoyl ligand deviates only slightly from that of formamide and its complexed derivatives. The lithium atom, which is surrounded by a highly distorted tetrahedral array

[*] Dr. K. Pörschke, Prof. Dr. G. Wilke, Prof. Dr. C. Krüger [**]
Max-Planck-Institut für Kohlenforschung
Kaiser-Wilhelm-Platz 1, D-4330 Mülheim a. d. Ruhr 1 (Germany)
[**] X-ray structure analysis.

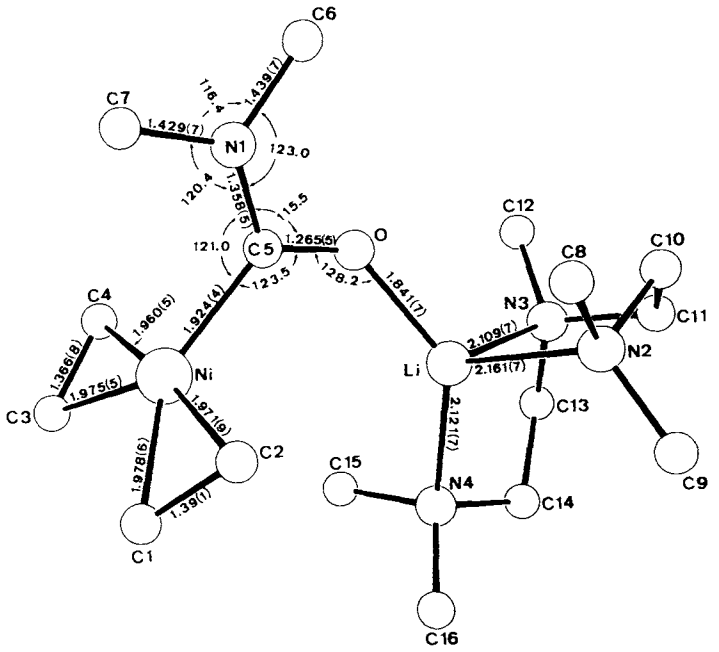



Fig. 1. Molecular structure of the complex **5** in the crystal. Further details of the crystal structure investigation can be obtained on request from the Fachinformationszentrum Energie Physik Mathematik, D-7514 Eggenstein-Leopoldshafen, by quoting the depository number CSD 50337, the names of the authors, and full citation of the journal.

of nitrogen atoms, is bonded to the carbonyl group *via* a free electron pair (C5–O–Li: 128.2°). All intramolecular distances appear inconsistent with **5** being formulated as a carbene complex.

Received: March 14, 1983 [Z 312 IE]
German version: *Angew. Chem. 95* (1983) 564
The complete version of this manuscript appears in:
*Angew. Chem. Suppl. 1983*, 786–793

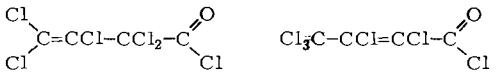
[1] B. Bogdanović, M. Kröner, G. Wilke, *Liebigs Ann. Chem. 699* (1966) 1.
[2] K. Pörschke, G. Wilke, *Chem. Ber.*, in press.
[3] K. Pörschke, K. Jonas, G. Wilke, R. Benn, R. Mynott, R. Goddard, C. Krüger, *Chem. Ber.*, in press.
[4] K. Jonas, K. Pörschke, C. Krüger, Y.-H. Tsay, *Angew. Chem. 88* (1976) 682; *Angew. Chem. Int. Ed. Engl. 15* (1976) 621; K. Jonas, C. Krüger, *ibid. 92* (1980) 513 and *19* (1980) 520.

## Structure Determination by $^{13}$C-NMR Spectroscopy Using an INADEQUATE Pulse Sequence: Differentiation of Heteroatom-Substituted Organic Constitutional Isomers by means of $^{13}$C-$^{13}$C Coupling Constants**

By *Joachim Buddrus**, *Hans Bauer*, *Hans Gotthardt*, and *Rüdiger Jung*

The differentiation of constitutional isomers of organic compounds whose hydrogen atoms are largely or completely substituted by heteroatoms often presents difficulties. Conventional $^{13}$C-NMR spectroscopy certainly provides signals; however, in many cases these cannot be interpreted unambiguously. Here we show that by analyzing the $^{13}$C-$^{13}$C satellites of a $^{13}$C-NMR spectrum the bonding pattern of C atoms can be obtained, thus enabling the different constitutions of such compounds to be distinguished. To measure the satellites the main $^{13}$C-NMR signals were reduced in intensity using the double quantum coherence technique (INADEQUATE pulse sequence[1]); this method was introduced by *Freeman et al.*[2], but previously has been rarely used[3] to solve constitutional problems.

Chlorination of 1-ethoxypentachlorobutadiene leads to formation of pentachloro-3-butenoyl chloride, **1**, or pentachloro-2-butenoyl chloride **2**[4].




**1** **2**

The $^{13}$C-NMR signal of the aliphatic C atom at $\delta = 86.8$ is shown in Figure 1; it consists of two pairs of satellites with coupling constants of 67.3 and 62.6 Hz, which also are observed on the signal of the carbonyl C atom and on that of an olefinic C atom, respectively. This result is consistent only with structure **1**, which is also consonant with the results of IR and UV studies[5].

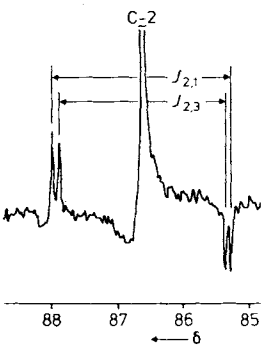
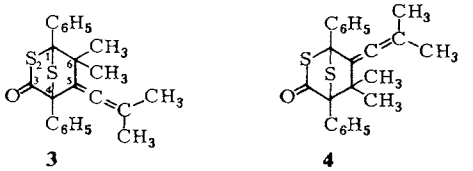



Fig. 1. Part of the one-dimensional $^{13}$C-INADEQUATE-NMR spectrum of **1** at 25 MHz (JEOL FX-100). Sample solution: 2.5 mL **1**, 0.3 mL $CDCl_3$, and *ca.* 10 mg $Cr(acac)_3$ (as relaxation reagent). Pulse sequence: 90°(x)-$\tau$-180°(±y)-$\tau$-90°(x)-$\Delta$-90°($\phi$)—accumulation of data; $\tau$ adjusted for $J_{CC} = 65$ Hz. 12704 sweeps, repetition time 5 s (total measurement time 16 h).

The 1,3-dipolar cycloaddition of 2,5-dimethyl-2,3,4-hexatriene to 2,5-diphenyl-1,3-dithiolylium-4-olate affords the heterobicyclic constitutional isomers **3** and **4**, which can be separated, but not differentiated by conventional spectroscopic methods.




**3** **4**

The $^{13}$C-NMR signals of the two bridgehead C atoms of the major isomer are shown in Figure 2. The signal at $\delta = 79.6$ exhibits two pairs of satellites with coupling constants 31.9 and 49.7 Hz, which also occur on the signal of the aliphatic quaternary C atom and on that of an aromatic C atom, respectively. The signal at $\delta = 75.6$ exhibits three

[*] Priv.-Doz. Dr. J. Buddrus, Dr. H. Bauer
Institut für Spektrochemie und angewandte Spektroskopie
Bunsen-Kirchhoff-Strasse 11, D-4600 Dortmund 1 (Germany)
Prof. Dr. H. Gotthardt, R. Jung
Lehrstuhl für Organische Chemie der Universität-Gesamthochschule
Gaussstrasse 20, D-5600 Wuppertal 1 (Germany)

[**] This work was supported by the Minister für Wissenschaft und Forschung des Landes Nordrhein-Westfalen and by the Minister für Forschung und Technologie der Bundesrepublik Deutschland (J. B., H. B.), as well as by the Fonds der Chemischen Industrie (H. G.). J. B. and H. B. thank Dr. W. Auf der Heyde and Dr. W. Kimpenhaus, Chemische Werke Marl-Hüls for supplying a sample of pentachloro-3-butenoyl chloride.

pairs of satellites (in part, overlaid) with coupling constants 41.8, 42.6, and 52.3 Hz: the first coupling constant is also observed on the signal of the carbonyl C atom, the second on that of an allenic C atom, and the third on that of an aromatic C atom. These results are consistent only with structure **3**.

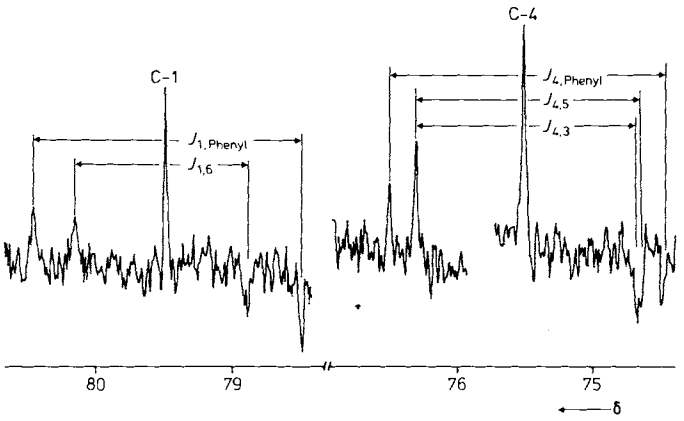



Fig. 2. Part of the one-dimensional $^{13}$C-INADEQUATE-NMR spectrum of **3** at 25 MHz. Sample solution: 1 g **3** and *ca.* 10 mg Cr(acac)$_3$ in 1.5 mL $CDCl_3$. Pulse sequence as in Fig. 1; $\tau$ adjusted for $J_{CC}=45$ Hz. 33 400 sweeps, repetition time 6.1 s (total measurement time 57 h). The residual signals of the solvent were not recorded.

The advantage of the INADEQUATE pulse sequence is that it enables structures such as **1** and **2**, or **3** and **4** to be differentiated unequivocally, without having to draw upon reference compounds.

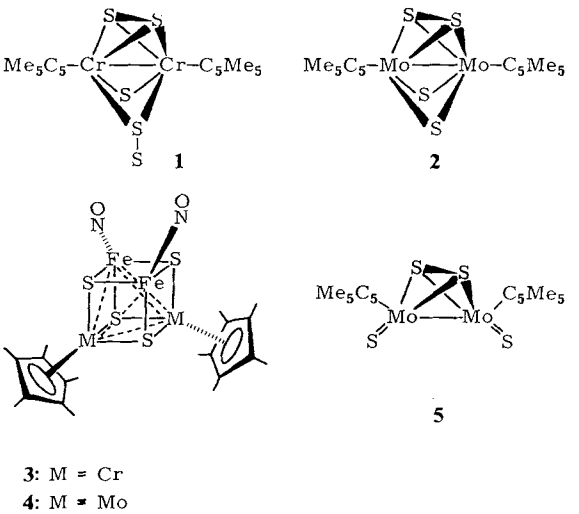
Received: March 9, 1983 [Z 308 IE]
German version: *Angew. Chem. 95* (1983) 565

[1] R. Benn, H. Günther, *Angew. Chem. 95* (1983) 381; *Angew. Chem. Int. Ed. Engl. 22* (1983) 350.
[2] A. Bax, R. Freeman, S. P. Kempsell, *J. Am. Chem. Soc. 102* (1980) 4849.
[3] R. Freeman, T. Frenkiel, M. B. Rubin, *J. Am. Chem. Soc. 104* (1982) 5545; A. C. Pinto, S. K. Do Prado, R. B. Filho, W. E. Hull, A. Neszmelyi, G. Lukacs, *Tetrahedron Lett. 23* (1982) 5267.
[4] A. Roedig, P. Bernemann, *Justus Liebigs Ann. Chem. 600* (1956) 1; G. Maahs, *Angew. Chem. 75* (1963) 451; *Angew. Chem. Int. Ed. Engl. 2* (1963) 394; *ibid. 77* (1965) 811; *4* (1965) 787.
[5] A. Roedig, W. Wenzel, *Justus Liebigs Ann. Chem. 728* (1969) 1.

## A General Method for the Synthesis of Heterometal Clusters of the $M_2Fe_2S_4$-Cubane Type (M = Cr, Mo)

By *Henri Brunner, Heike Kauermann,* and *Joachim Wachter**

Interest in the cubane-like molecules $Cp_4M_4S_4$ (Cp = $\eta^5$-$C_5H_5$; M = Cr, Mo, Fe, Co) has so far been directed at the problem of the metal-metal bond[1] rather than at expanding the system with new ligand-metal combinations. The multifarious properties of cubane-like $Fe_3MoS_4$ clusters[2] stimulated a search for generally applicable methods for the synthesis of such heterometal clusters. Expansion of a precursor containing four sulfur atoms and two cyclopentadienyl-6A metal groups by two each of the isoelectronic groups MCp (M = Cr, Mo), $Mn(CO)_2$, Fe(NO) or Co(CO) offers a facile entry to the $M_4S_4$ skeletal framework. This concept was successfully tested by reaction of the sulfur-rich pentamethylcyclopentadienyl complexes $Cp'_2Cr_2S_5$ **1** and $Cp'_2Mo_2S_4$ **2** with $Co_2(CO)_8$ to give $Cp'_2M_2Co_2S_4(CO)_2$ ($Cp' = \eta^5$-$C_5Me_5$; M = Cr, Mo)[3].




**3**: M = Cr
**4**: M = Mo

We have now been able to confirm the general validity of the concept: Irradiation of the green and blue solutions, respectively, of **1** and **2** in tetrahydrofuran in the presence of two equivalents of $[Fe(CO)_3NO][Ph_3PNPPh_3]$ affords the red-brown diamagnetic complexes **3** and **4**, respectively, in 40–50% yield[4a]. The isomer of **2** containing terminal sulfur ligands, complex **5**, also reacts analogously. The composition of the products $Cp'_2M_2Fe_2S_4(NO)_2$ is confirmed by elemental analysis and mass spectra. Since we have so far been unable to grow single crystals of the products, the confirmation of the structure rests primarily on spectroscopic data. The 70 eV mass spectrum of **4** shows the molecular ion and the successive cleavage of all ligands from the $Mo_2Fe_2S_4$ skeleton, with appearance also of the doubly positively charged ion for each fragment, whereas the molecular ion **3** can be observed only in the field-desorption mass spectrum (from toluene solution). A single sharp methyl signal appears in each of the $^1$H-NMR spectra, at $\delta = 1.90$ in the case of **3** and at 1.96 in the case of **4** ($CDCl_3$ solution). The IR spectra[4b] contain absorption bands for the NO- and the $C_5Me_5$-groups, but no further metal-ligand vibration bands. The disappearance of the strong $\nu$(Mo=S) bands of **5** (485 cm$^{-1}$) and of the absorptions of the $\mu_2,\eta^2$-$S_2$- and $\mu_2,\eta^1$-$S_2$-ligands in **1** (599, 495, 445 cm$^{-1}$) in favor of a weak absorption at 386 cm$^{-1}$ can best be interpreted in terms of an equal distribution of four S-atoms over all metal centers in the form of $\mu_3$-ligands.

The novel heterometal clusters **3** and **4** represent a link between the $Cp_4Mo_4S_4$ cluster, for which MO considerations point to metal-metal interactions[5a], and the isoelectronic $(NO)_4Fe_4S_4$ complex, for which X-ray structure investigations have confirmed a distorted cubane-structure with four Fe–Fe bonds[5b].

Received: February 23, 1983 [Z 288 IE]
German version: *Angew. Chem. 95* (1983) 567

[*] Dr. J. Wachter, Prof. Dr. H. Brunner, H. Kauermann
Institut für Anorganische Chemie der Universität
Universitätsstr. 31, D-8400 Regensburg (Germany)

[1] H. Vahrenkamp, *Angew. Chem. 87* (1975) 363; *Angew. Chem. Int. Ed. Engl. 14* (1975) 332.
[2] R. H. Holm, *Chem. Soc. Rev. 10* (1981) 455 and references cited therein; W. H. Armstrong, P. K. Mascharak, R. H. Holm, *Inorg. Chem. 21* (1982) 1699.
[3] H. Brunner, J. Wachter, *J. Organomet. Chem. 240* (1982) C41.
[4] a) General procedure: A solution of 0.5 mmol of **1** or **2**, respectively, and 708 mg (1.0 mmol) of $[Fe(CO)_3NO][Ph_3PNPPh_3]$ in 230 mL of THF is ir-

radiated for 20 h in an immersion lamp apparatus (125 W Hg-lamp). The reaction mixture is concentrated and chromatographed on $SiO_2$ (40 × 3.5 cm column), the complexes **3** and **4**, respectively, being eluted as red-brown zones with toluene. Recrystallization from toluene/pentane (6 : 1) furnishes analytically pure amorphous crystals.—b) IR (KBr, $cm^{-1}$): **3**: $\nu_{NO}$ = 1738, 1712 vs (toluene 1725), $\nu_{Cr-NO}$ = 592 w, $\nu_{CH}$ = 1373, 1017 s; **4**: $\nu_{NO}$ = 1734, 1708 vs (toluene 1720), $\nu_{Mo-NO}$ = 595 w, $\nu_{CH}$ = 1374, 1022 s.

[5] a) T. Toan, R. Broach, L. F. Dahl, Abstr. 6th ICOMC, Amherst 1973; W. Danzer, Dissertation, Universität München 1976. Reaction of **1** or **2** with $[CpM(CO)_2]_2$ (M = Cr, Mo) under analogous conditions offers a convenient entry to this class of compounds.—b) C. T.-W. Chu, F. Y.-K. Lo, L. F. Dahl, *J. Am. Chem. Soc. 104* (1982) 3409.

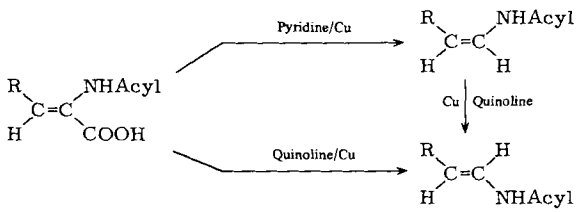
## Biomimetic Synthesis of Primary Enamides by Decarboxylation of α,β-Dehydroamino Acids**

By *Ulrich Schmidt** and *Albrecht Lieberknecht*

*Dedicated to Professor Adolf Steinhofer on the occasion of his 75th birthday*

Primary enamides[1] are produced by lower organisms from amino acids, probably by decarboxylation of α,β-dehydroamino acids. We have also succeeded in performing this reaction *in vitro*. Decarboxylation of aliphatic and aromatic *N*-acyldehydroamino acids[2] offers the simplest route to primary enamides; it is superior to previously described methods[3] and, in addition, opens the possibility of synthesizing (*E*)- and (*Z*)-enamides stereoselectively.

Aromatic and aliphatic *N*-acyldehydroamino acids[4] decarboxylate within an hour at 145 °C in the presence of bases and copper powder to afford enamides in 50—75% yield. On the whole, the reaction can be stereoselectively controlled (exceptions: examples 5 and 10 in Table 1): solutions of aromatic (*Z*)-*N*-acyldehydroamino acids in diglyme react with copper powder and pyridine to give predominantly (*Z*)-enamides ($Z : E \approx 80 : 20$); in contrast, with quinoline and copper powder predominantly (*E*)-enamides are obtained ($Z : E \approx 10 : 90$). Under these conditions (*Z*)-enamides rearrange to (*E*)-enamides. The decarboxylation can also be performed on dehydropeptides (examples 7 and 8).




### *Procedure*

A solution of α-(*N*-acetylamino)cinnamic acid (205 mg), copper powder (200 mg), and quinoline (166 mg) in 5 mL diglyme under nitrogen is heated to 145 °C in an oil bath. The volatile components are subsequently removed *in vacuo*: the residue is taken up in chloroform, filtered, and extracted with $KHSO_4$ solution. After medium pressure chromatography on silica gel Lichroprep Si60 (15—25 μ) using ethyl acetate/petroleum ether 19 mg *cis*- and 102 mg *trans*-β-acetylaminostyrene were isolated.

Table 1. Decarboxylation of *N*-acyldehydroamino acids to afford enamides [a].

| No. | R | Acyl | Catalyst | Yield [%] | *Z* : *E* |
|---|---|---|---|---|---|
| 1 | $C_6H_5$ | $CH_3CO$ | Py/Cu | 67 | 84 : 16 |
| 2 | $C_6H_5$ | $CH_3CO$ | Quin/Cu | 75 | 16 : 84 |
| 3 | 4-$CH_3O$-$C_6H_4$ | $CH_3CO$ | Py/Cu | 50 | 71 : 29 |
| 4 | 4-$CH_3O$-$C_6H_4$ | $CH_3CO$ | Quin/Cu | 77 | 20 : 80 |
| 5 | 3,4-$(CH_3O)_2C_6H_3$ | $CH_3CO$ | Py/Cu | 60 | 0 : 100 |
| 6 | 3,4-$(CH_3O)_2C_6H_3$ | $CH_3CO$ | Quin/Cu | 60 | 0 : 100 |
| 7 | $C_6H_5$ | Boc-Ile | Quin/Cu | 68 | 14 : 86 |
| 8 | 3,4,5-$(CH_3O)_3C_6H_2$ | Boc-Trp | Quin/Cu | 63 | 22 : 78 |
| 9 | $iC_5H_{11}$ | $C_6H_5CO$ | Quin/Cu | 45 | 0 : 100 |
| 10 | $nC_5H_{11}$ [b] | $CH_3CO$ | Quin/Cu | 51 | 73 : 27 |

[a] 1 mmol dehydroamino acid, 200 mg copper powder, 1.2 mmol pyridine (Py) or quinoline (Quin), 5 mL diglyme, autoclave with glass insert, 60 min, 145 °C. [b] 1 mmol dehydroamino acid, 200 mg copper powder, 1.2 mmol quinoline, 5 mL dioxane, autoclave with glass insert, 60 min, 145 °C.

Received: August 24, 1982;
revised: January 20, 1983 [Z 139 IE]
publication delayed at authors' request
German version: *Angew. Chem. 95* (1983) 575

[1] Occurrence of primary enamides: (a) in rhamnaceae and stericuliacae: review: R. Tschesche, E. V. Kaussmann in R. H. F. Manske: *The Alkaloids, Vol. XV*, Academic Press, New York 1975, p. 165; (b) in sponges: R. J. Stonard, R. J. Andersen, *J. Org. Chem. 45* (1980) 3687 and literature cited therein; (c) in *Peripterygia marginata*: R. Hocquemiller, A. Cavé, H. P. Husson, *Tetrahedron 33* (1977) 645.

[2] U. Schmidt, A. Lieberknecht, U. Schanbacher, Th. Beuttler, J. Wild, *Angew. Chem. 94* (1982) 797; *Angew. Chem. Int. Ed. Engl. 21* (1982) 776; *Angew. Chem. Suppl. 1982*, 1682.

[3] Synthesis of primary enamides: Review: G. R. Lenz, *Synthesis 1978*, 489; J. K. Stille, Y. Becker, *J. Org. Chem. 45* (1980) 2139; St. Jendrzejewski, W. Steglich, *Chem. Ber. 114* (1981) 1337; U. Redeker, N. Engel, W. Steglich, *Tetrahedron Lett. 22* (1981) 4263; total synthesis of Clionamide: U. Schmidt, A. Lieberknecht, H. Griesser, H. Bökens, *ibid. 23* (1982) 4911.

[4] Review on dehydroamino acids: U. Schmidt, E. Öhler, J. Häusler, H. Poisel, *Fortschr. Chem. Org. Naturst. 37* (1979) 251.

## Asymmetry of Emission Quenching and Product Formation in an Asymmetrically Sensitized Photoreaction**

By *Hermann Rau** and *Richard Ratz*

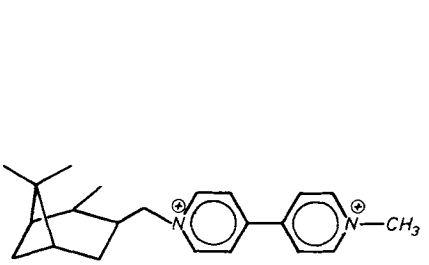
Asymmetry in photoreactions of chiral molecules sensitized by one enantiomer of a chiral donor may be monitored by determining the asymmetry of emission quenching and the optical induction found in the remaining educt and/or in the photoproduct[1]. *Irie et al.*[2] have observed asymmetries ($\kappa = k_q(S-R)/k_q(R-R)$) in electron-transfer emission quenching of (−)-(*R*)-1,1′-binaphthyl by enantiomeric pairs of optically active amines to the extent of up to $\kappa = 7.9$ at −10 °C. The highest asymmetry observed at room temperature ($\kappa = 4.0$), if maintained in an overall photochemical decomposition reaction, would lead to an enantiomeric purity of the educt $P_{en} = (c_R - c_S)/(c_R + c_S)$ of more than 60% at 63% extent of reaction. If this could be realized, then asymmetric photochemistry would become a viable preparative method.

[*] Prof. Dr. U. Schmidt, Dr. A. Lieberknecht
Institut für Organische Chemie, Biochemie und Isotopenforschung der Universität
Pfaffenwaldring 55, D-7000 Stuttgart 80 (Germany)

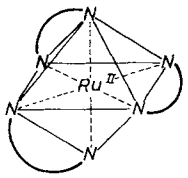
[**] Dehydroamino Acids, Part 17. Amino Acids and Peptides, Part 39. This work was supported by BASF AG, the Fonds der Chemischen Industrie, and the Deutsche Forschungsgemeinschaft.—Part 16: [2]; Part 38: U. Schmidt, H. Bökens, A. Lieberknecht, H. Griesser, *Liebigs Ann. Chem.*, in press.

[*] Prof. Dr. H. Rau, R. Ratz
FG Physikalische Chemie, Institut für Chemie, Universität Hohenheim
Garbenstrasse 30, D-7000 Stuttgart 70 (Germany)

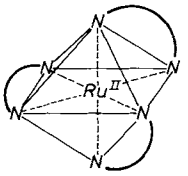
[**] This work was supported by the Deutsche Forschungsgemeinschaft and the Fonds der Chemischen Industrie. We thank Dr. W. Himmele (BASF) for providing (3*S*/3*R*)-formylpinane.



(3S)-(-)



Λ

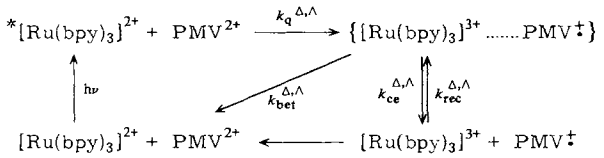


Δ

N ⌒ N = 2,2'-bpy

In order to compare the degree of asymmetry of the quenching reaction and the photoreaction we selected a well-known photoredox system[3], tris(bipyridyl)ruthenium(II)/viologen. Δ-(−)-$[Ru(bpy)_3]Cl_2$ and Λ-(+)-$[Ru(bpy)_3]Cl_2$ were used as donors and 1-methyl-1'-[(3*S*)-(−)-3-pinanylmethyl]-4,4',bipyridinium dichloride ($PMV\text{-}Cl_2$) as an acceptor.

According to *Kalyanasundaram* and *Neumann-Spallart*[4] the reaction proceeds as shown in Scheme 1. These authors found that the yield of dissociated radicals $\phi_{redox} = k_{ce}/(k_{ce}+k_{ret}) = 0.25$.



Scheme 1.

We have determined the asymmetry of the emission quenching using both steady state and dynamic emission quenching techniques[5] and Stern-Volmer evaluation: $k_q(\Delta\text{-}[Ru(bpy)_3]^{2+}/S\text{-}PMV^{2+}) = 2.02\times10^8$ dm$^3$ mol$^{-1}$ s$^{-1}$ and $k_q(\Lambda\text{-}[Ru(bpy)_3]^{2+}/S\text{-}PMV^{2+}) = 3.34\times10^8$ dm$^3$ mol$^{-1}$ s$^{-1}$ were found. From this $\kappa = k_q^{\Lambda}/k_q^{\Delta} = 1.66$. Since the enantiomeric purity of the donors was 92% (Δ) and 54% (Λ), respectively, the calculated value of $\kappa$ for pure enantiomers is 1.95.

The asymmetry of the product formation can be determined from the different ellipticities of $PMV^{+\cdot}$ in the reactions of the two diastereomeric combinations. Electron transfer leading to re-formation of the educts ($k_{bet}$) can be prevented partially and concomitantly the formation of the product $PMV^{+\cdot}$ can be favored if a large amount of ethylenediaminetetraacetic acid as the Na salt is added. Under the chosen conditions, the latter is irreversibly reduced more rapidly than $PMV^{+\cdot}$ by $[Ru(bpy)_3]^{3+}$ generated in the photoreaction. Unfortunately, the molar ellipticity of the $PMV^{+\cdot}$ radical ion (which may be generated by reduction with Zn in high concentration) is so small that there is no possibility of determining the ellipticity of $PMV^{+\cdot}$ in experiments starting from racemic $PMV^{2+}$[1]. Hence, we used the transient absorption[5] of $PMV^{+\cdot}$ immediately after the laser flash to determine the asymmetry of the photoreaction. We obtained $\kappa = (k_q^{\Lambda}/k_q^{\Delta})(\phi_{redox}^{\Lambda}/\phi_{redox}^{\Delta}) = 1.12\pm0.05$ for both the combinations Δ-$[Ru(bpy)_3]^{2+}/S\text{-}PMV^{2+}$ and Λ-$[Ru(bpy)_3]^{2+}/S\text{-}PMV^{2+}$. Extrapolation to the pure enantiomers gives $\kappa = 1.32$ ($\kappa - 1$: ±40%).

The results indicate that a considerable amount of the asymmetry found in the quenching step is lost in the competing back electron transfer ($k_{bet}$) and ion pair dissociation ($k_{ce}$) steps. The diastereomeric ion pair formed preferentially ($k_q^{\Lambda} \approx 2k_q^{\Delta}$), has a 1.5 times higher rate of electron back transfer, too. Currently we are investigating other systems to determine whether the phenomenon described here is more general.

Received: January 31, 1983 [Z 259 IE]
German version: *Angew. Chem. 95* (1983) 552

CAS Registry numbers:
Δ-(−)-$[Ru(bpy)_3]Cl_2$: 85908-80-1; Λ-(+)-$[Ru(bpy)_3]Cl_2$: 85893-99-8; $PMV\text{-}Cl_2$: 85893-98-7

[1] H. Rau, *Chem. Rev.*, in press.
[2] M. Irie, T. Yorozu, K. Hayashi, *J. Am. Chem. Soc. 100* (1978) 2236; T. Yorozu, K. Hayashi, M. Irie, *ibid. 103* (1981) 5480.
[3] C. R. Bock, T. J. Meyer, D. G. Whitten, *J. Am. Chem. Soc. 96* (1974) 4710.
[4] K. Kalyanasundaram, M. Neumann-Spallart, *Chem. Phys. Lett. 88* (1982) 7.
[5] Instrumentation: a) emission quenching: (steady state) Farrand MK 1 spectrofluorimeter and (dynamic) excimer laser EMG 500 (Lambda Physik) irradiation 337 nm, Tektronix storage oscilloscope No. 7834. b) Transient absorption: excimer laser, irradiation 337 nm, monitored for laser intensity, xenon flash probe 395 nm, storage oscilloscope. All samples degassed by Ar flushing.

## Deuteroporphyrin-IX Dimethyl Ester: Assignment of the $^1$H-NMR Spectrum by NOE Measurements in Presence of a Diamagnetic Shift Reagent

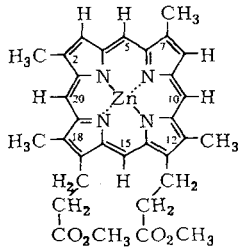
By *Klaus Witthohn* and *Hans Brockmann Jr.**

Repeated attempts have been made to assign the $^1$H-NMR signals of natural porphyrins[1,2]. The use of intramolecular Nuclear Overhauser Effects for this purpose has only seldom met with success[3,4], since overlapping in the region of the methyl- and bridge-methine protons frequently preclude selective irradiation experiments.

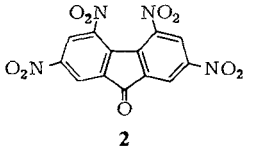
In the presence of electron-acceptors such as tetranitrofluorenone **2**, zinc deuteroporphyrin-IX dimethyl ester **1a**

[*] Prof. Dr. H. Brockmann Jr., Dr. K. Witthohn
Fakultät für Chemie der Universität
Universitätsstrasse, D-4800 Bielefeld 1 (Germany)

 © *Verlag Chemie GmbH, 6940 Weinheim, 1983* *0570-0833/83/0707-0551 $ 02.50/0* 



**1a**
**1b**, 2 H instead of Zn



**2**

as well as the zinc-free porphyrin **1b** form donor-acceptor complexes with greatly altered $^1$H-NMR spectra[9]. Owing to the rapid establishment of equilibrium between complex and free donor and acceptor, **2** can be used as NMR shift reagent for porphyrins which removes signal overlapping at suitable concentrations and enables NOE studies to be carried out (Fig. 2).

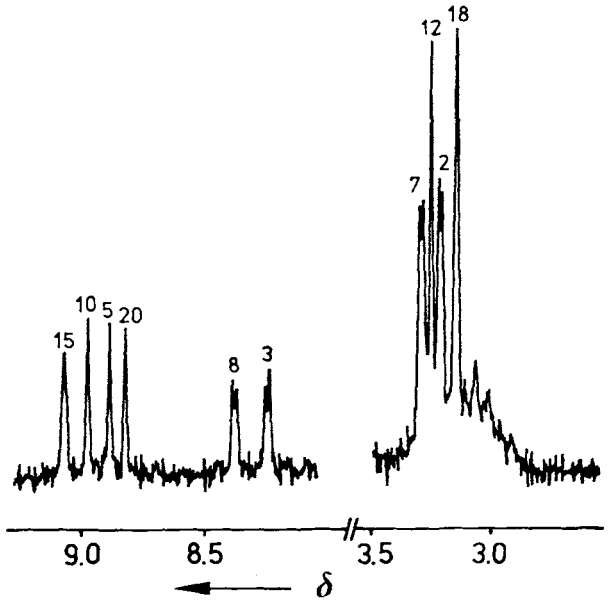



Fig. 2. 80-MHz $^1$H-NMR part spectrum of **1a** in presence of **2**; $CDCl_3$, TMS int. standard, 309 K.

We have performed NOE experiments on an equimolar solution of **1a** and **2** in $CDCl_3$. Irradiation at the resonances of the methyl- as well as the α-located methylene protons of **1a** causes integral increases of individual bridge-methine proton signals of between 15 and 25 percent (Table 1).

In addition, in the normal homonuclear decoupling experiment the allyl coupling ($J = 1.5$ Hz) between the methyl protons and 3-H and 8-H is removed.

Table 1 (selected data). $^1$H-NMR NOE double resonance experiments (80 MHz), $CDCl_3$, δ-values, 309 K.

| | Irradiation | Integral increase |
|---|---|---|
| | 4.00 | 9.07 (16%) |
| | 3.36 | 8.85 (15%) |
| **1a** + **2** | 3.28 | 8.95 (25%) |
| | 3.20 | 8.78 (25%) |
| | 3.14 | 8.78 (16%) |

These results, and those of the investigations on **1b** and **2**, unequivocally lead to the signal assignments listed in Table 2. Moreover, they can be extended to the interpretation of the $^1$H-NMR spectra of pure **1a** and **1b** if the alteration of the individual signals with concentration of shift reagent is taken into account (Table 2). These assignments

Table 2. Assignment of the $^1$H-NMR spectra (80 MHz) of the porphyrins **1a** and **1b**, δ-values referred to TMS, 309 K [a].

| H-Position | **1a** + **2** | **1b** + **2** | **1a** | **1b** |
|---|---|---|---|---|
| 5 | 8.85 | 9.71 | 9.27 | 10.05 |
| 10 | 8.95 | 9.62 | 9.32 | 10.01 |
| 15 | 9.07 | 9.94 | 9.10 | 10.09 |
| 20 | 8.78 | 9.74 | 9.10 | 10.11 |
| 3 | 8.23 | 8.82 | 8.50 | 9.09 |
| 8 | 8.37 | 8.86 | 8.66 | 9.09 |
| $13^1$ | 4.00 | 4.37 | 4.13 | 4.44 |
| $17^1$ | 4.00 | 4.37 | 4.05 | 4.44 |
| $13^3$-$OCH_3$ | 3.79 | 3.80 | 3.67 | 3.67 |
| $17^3$-$OCH_3$ | 3.77 | 3.80 | 3.65 | 3.67 |
| 2 | 3.20 | 3.60 | 3.40 | 3.73 |
| 7 | 3.36 | 3.60 | 3.51 | 3.73 |
| 12 | 3.28 | 3.52 | 3.40 | 3.62 |
| 18 | 3.14 | 3.55 | 3.25 | 3.64 |
| $13^2$ | 3.08 | 3.37 | 3.09 | 3.30 |
| $17^2$ | 3.08 | 3.37 | 3.09 | 3.30 |

[a] Measurements with WP80 (Bruker) multinuclear spectrometer; all solutions were degassed and purged with nitrogen; concentration in each case: $2 \times 10^{-2}$ mol/L of porphyrin and shift reagent.

can also be checked, at least in part, by NOE measurements on solutions of pure **1a** and **1b**. Further investigations have shown that the method used here can also be extended to other tetrapyrrole pigments.

Received: March 4, 1983;
revised: May 19, 1983 [Z 303 IE]
German version: *Angew. Chem. 95* (1983) 563
The complete version of this communication appears in:
*Angew. Chem. Suppl. 1983*, 778-785

[1] T. R. Janson, J. J. Katz, *J. Magn. Reson. 6* (1972) 209.
[2] R. J. Abraham, F. Eivazi, R. Nagyir-Mazhir, H. Pearson, K. M. Smith, *Org. Magn. Reson. 11* (1978) 52.
[3] J. K. M. Sanders, J. C. Waterton, I. S. Denniss, *J. Chem. Soc. Perkin Trans. 1 1978*, 1150.
[4] A. Pfaltz, B. Jaun, A. Fässler, A. Eschenmoser, R. Jaenchen, H. H. Gilles, G. Diekert, R. K. Thauer, *Helv. Chim. Acta 65* (1982) 828.
[9] K. Witthohn, Dissertation, Universität Bielefeld 1982.

## Azatriphosphetidines as Cyclotrimers of an Iminophosphane—Synthesis and Crystal Structure**

By *Edgar Niecke**, *Reinhold Rüger*, *Bernt Krebs*, and *Mechthild Dartmann*

*Dedicated to Professor Ulrich Wannagat on the occasion of his 60th birthday*

Frontier orbital theory predicts that on passing from methylenephosphane **A** to iminophosphane **B** an orbital crossing [**A**: HOMO = $\pi_{(P=C)}$/LUMO = $\pi^*_{(P=C)}$, **B**:

[*] Prof. Dr. E. Niecke, Dr. R. Rüger
Fakultät für Chemie der Universität
Postfach 8640, D-4800 Bielefeld 1 (Germany)
Prof. Dr. B. Krebs, M. Dartmann
Anorganisch-chemisches Institut der Universität
Corrensstrasse 36, D-4400 Münster (Germany)

[**] Phosphazenes of Coordination Number 2 and 3, Part 24. This work was supported by the Deutsche Forschungsgemeinschaft and the Fonds der Chemischen Industrie.—Part 23: [1b].

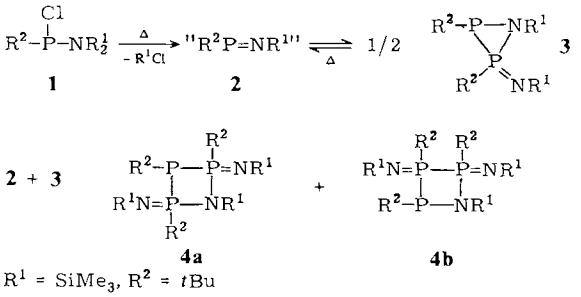
HOMO = $\sigma_{(P)}$/LUMO = $\pi^*_{(P=N)}$] occurs[1a]. We recently found experimental evidence for this prediction; reversible formation of an iminophosphane from its dimer, formed by [2 + 1] cycloaddition[1b].



A B

By means of insertion reactions the "carbene-like"[2] iminophosphanes should act as synthetic building blocks for phosphorus heterocycles.

We have now found that the azadiphosphirane **3**[3a], which is readily accessible from **1** by elimination of chloro(trimethyl)silane, undergoes an insertion reaction at 140 °C with the intermediate *tert*-butyl(trimethylsilylimino)phosphane **2** to afford the two isomers **4a** and **4b**, which possess the previously unknown azatriphosphetidine framework.



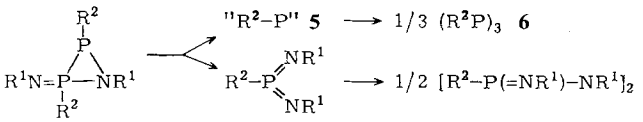
**1** **2** **3**

**2 + 3** **4a** + **4b**

$R^1$ = $SiMe_3$, $R^2$ = *t*Bu

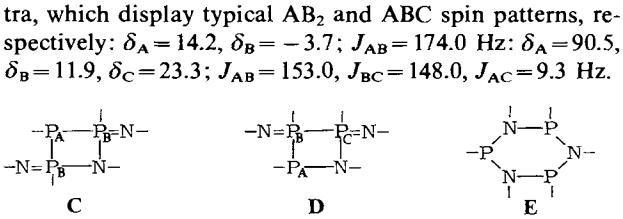
The preferred formation of **4a** (**4a** : **4b** = 6 : 1) and, hence, the insertion of **2** into the $\lambda^3$–PN bond of **3** suggests that the "carbene analogues", **2**, have electrophilic character, as predicted by theoretical studies[3b].

Side products of the reaction (< 25%), arising by fragmentation of **3**, are the cyclotriphosphane **6**[3c], as well as *cis*- and *trans*-diazadiphosphetidine **8**[3d], which are, respectively, stable oligomers of *tert*-butylphosphanediyl, **5**, and *tert*-butylbis(trimethylsilylimino)phosphorane **7**[3d].



**3** **7** **8**

Pure **4a**, which can be isolated from the reaction mixture, is a crystalline, readily oxidizable solid; its composition has been determined by elemental analysis and molecular weight determination[4]. Its constitution and that of **4b** as 1,2$\lambda^5$,3,4$\lambda^5$-azatriphosphetidine (**C**) and 1,2$\lambda^5$,3$\lambda^5$,4-azatriphosphetidine (**D**)—isomers of the cyclo-$\lambda^3$-triphosphazane system (**E**)—are derived from the $^{31}P\{^1H\}$-NMR spectra, which display typical $AB_2$ and ABC spin patterns, respectively: $\delta_A = 14.2$, $\delta_B = -3.7$; $J_{AB} = 174.0$ Hz: $\delta_A = 90.5$, $\delta_B = 11.9$, $\delta_C = 23.3$; $J_{AB} = 153.0$, $J_{BC} = 148.0$, $J_{AC} = 9.3$ Hz.



**C** **D** **E**

The configuration of **4a**, with *trans*/*trans*-arrangement of the *tert*-butyl groups at the $\lambda^5$-phosphorus atom relative to the substituents at the $\lambda^3$-phosphorus atom in an almost planar four-membered ring, was proved by X-ray structure analysis (Fig. 1).

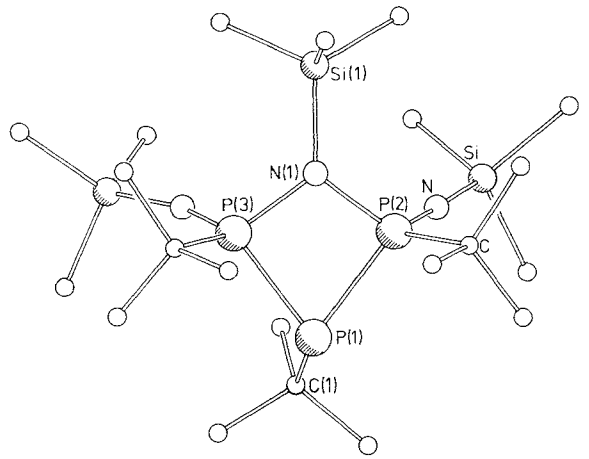



Fig. 1. Molecular structure of **4a** (without H atoms) in the crystal [monoclinic, $P2_1/m$, $a = 969.7(2)$, $b = 1922.9(4)$, $c = 901.9(2)$ pm, $\beta = 106.0(2)°$, $V = 1616.4 \times 10^6$ pm$^3$, $\rho_{calc.} = 1.08$ g/cm$^3$, $Z = 2$ measured at −130 °C]. The structure was determined by direct methods (MULTAN) from 2716 single-crystal diffractometer data and refined to $R = 0.067$ [3a]. Most important bond lengths [pm] and angles [°]: P(1)–P(2) 223.2(4), P(1)–P(3) 219.5(4), N(1)–P(2) 172.7(9), N(1)–P(3) 170.9(9), P(1)–C(1) 186.8(8), N(1)–Si(1) 179.5(6); P(2)–P(1)–P(3) 74.8(2), P(2)–N(1)–P(3) 103.0(4), P(1)–P(2)–N(1) 87.7(3), P(1)–P(3)–N(1) 89.4(3), P(2)–N(1)–Si(1) 126.5(5), P(3)–N(1)–Si(1) 126.0(5).

Received: March 3, 1983 [Z 299 IE]
German version: *Angew. Chem. 95* (1983) 570

CAS Registry numbers:
**3**, 86239-08-9; **4a**, 86259-40-7; **4b**, 86239-05-6; **5**, 86239-06-7; *cis*-**8**, 86239-07-8; *trans*-**8**, 86239-09-0

[1] a) W. W. Schoeller, E. Niecke, *J. Chem. Soc. Chem. Commun. 1982*, 569; see also: G. Trinquier, *J. Am. Chem. Soc. 104* (1982) 6969; b) E. Niecke, R. Rüger, W. W. Schoeller, *Angew. Chem. 93* (1981) 1110; *Angew. Chem. Int. Ed. Engl. 20* (1981) 1034.

[2] In their frontier orbital properties such iminophosphanes are isolobal with singlet carbenes: cf. R. Hoffmann, *Angew. Chem. 94* (1982) 725; *Angew. Chem. Int. Ed. Engl. 21* (1982) 711.

[3] a) E. Niecke, R. Rüger, B. Winckler, B. Krebs, unpublished results; b) T. Dabisch, Diplomarbeit, Universität Bielefeld 1983; c) M. Baudler, C. Gruner, *Z. Naturforsch. B31* (1976) 1305; d) H. G. Schäfer, Dissertation, Universität Bielefeld 1981.

[4] Procedure: **3** (21 g, 60 mmol) is heated to 140 °C in a glass bomb tube for 1 h. The cooled reaction mixture is dissolved in 5 mL pentane and stored at −30 °C until crystallization has occurred (4–5 d). After decanting the mother liquor and one recrystallization from a small amount of pentane, pure **4a** is obtained (7.5 g, 35%); decomp. 250–255 °C. Based on $^{31}P$-NMR findings, the mother liquor still contains **4b** (20%), **5** (15%), and *cis*/*trans*-**8** (20%). Data for **4a**: $M_+$ (cryoscopic in $C_6H_{12}$): 516, 520 (calc. 525); $^1H$-NMR (30% in $CDCl_3$, TMS int.): $\delta = 0.05$ (P=NSiMe$_3$); 1.19 (*t*BuP=N), $^3J_{HP} = 18.5$, $^4J_{HP} = 1.0$ Hz, 1.43 (*t*BuP), $^3J_{HP} = 15.0$, $^4J_{HP} = 3.2$ Hz.

## 1-(1,3-Butadienyl)triazoles from 1-Vinyltriazoles and Electron-Rich Alkynes—Cleavage to "Push-Pull" 1,3-Butadienes**

By *Hans Schubert* and *Manfred Regitz**

1-Vinyl-1,2,3-triazoles exhibit typical azolide reactivity and, as mild vinylating reagents, *e.g.* of methylenephosphoranes, have found valuable use in synthetic chemistry[3]. Their synthetic potential can be considerably increased by insertion of electron-rich alkynes, either between the nucleus and the side-chain or in the side-chain itself.

[*] Prof. Dr. M. Regitz, Dr. H. Schubert
Fachbereich Chemie der Universität
Erwin-Schrödinger-Strasse, D-6750 Kaiserslautern (Germany)

[**] This work was supported by the Deutsche Forschungsgemeinschaft and the Fonds der Chemischen Industrie.

Reaction of the triazole **1a** with the alkynylamine **3a** or alkynyl ether **3b** in chloroform leads to formation of the title compounds **6a** and **7a** or **6b**, respectively. The α-diazoimidate **2b** (which must be in equilibrium with small amounts of **1b**[4]) reacts with **3a** to give **6c** and **7c**. **6a/7a** and **6c/7c** can be separated by column chromatography and identified by mass spectrometry and $^1$H-NMR spectroscopy (for typical data of **6a** and **7a** see Table 1).

We assume that branching in the reaction starts from the charge stabilized dipole **4**; it either rearranges to **6** (main reaction, route B)[5] or undergoes ring-close to give **5**, followed by electrocyclic ring-opening to give **7** (side-reaction, route A).

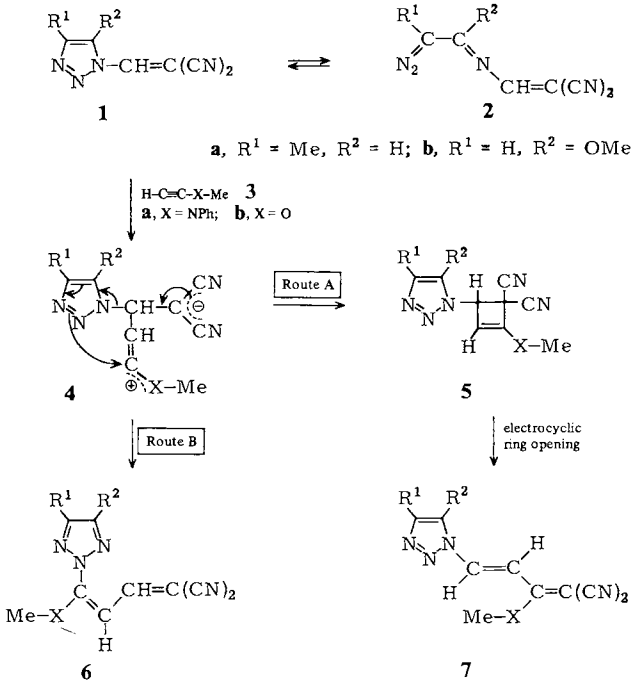



Table 1 (selected data). 1-(1,3-Butadienyl)triazoles **6** and **7** that have been synthesized.

| Triazole | $R^1$ | $R^2$ | X | Yield [%] | M.p. [°C] |
|---|---|---|---|---|---|
| **6a** [a, b] | Me | H | NPh | 45 | 137 |
| **7a** [a, b] | Me | H | NPh | 21 | 184 (dec.) |
| **6b** | Me | H | O | 50 | 122 |
| **6c** | H | OMe | NPh | 31 | 114 |
| **7c** | H | OMe | NPh | 20 | 161 (dec.) |

[a] MS (70 eV): **6**: $m/z$ 290 (62%, $M^+$), as expected no peak for $M^+ - N_2$; **7a**: $m/z$ 262 (41%, $M^+ - N_2$) but only weak molecular peak (5%). [b] $^1$H-NMR ($CDCl_3$, 200 MHz): **6a**: $\delta = 5.85$ (d, 1H, $^3J_{H,H} = 12.3$ Hz, H-2); **7a**: $\delta = 6.47$ (d, 1H, $^3J_{H,H} = 14.4$ Hz, H-2).

The insertion reaction **1** → **6** can be used for the preparation of "push-pull" 1,3-butadienes[6]: cleavage of **6b** with sodium methoxide affords **8a**; reaction with sodium methoxide and sodium isopropoxide in ethanol and isopropanol, respectively, with additional displacement of the $OCH_3$ group, leads to formation of the butadienes **8b** and **8c**, respectively. Cleavage with sodium salts of *N*-methylaniline and diethylamine provides access to the mixed-substituted 1,3-butadienes **8d** and **8e** (Table 2).

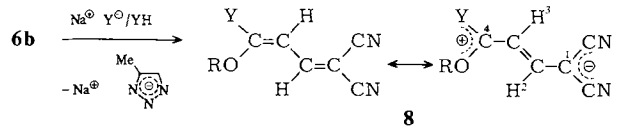



Table 2 (selected data). "Push-Pull" 1,3-butadienes that have been synthesized.

| Butadiene | R | Y | Yield [%] | M.p. [°C] |
|---|---|---|---|---|
| **8a** | Me | OMe | 58 | 102–102 |
| **8b** [a] | Et | OEt | 68 | 108 |
| **8c** | *i*Pr | O*i*Pr | 52 | 57–58 |
| **8d** | Me | N(Me)(Ph) | 61 | 109–110 |
| **8e** | Me | $NEt_2$ | 39 | 33–34 |

[a] $\mu = 9.2 \pm 0.3$ D (dioxane); $^1$H-NMR ($CDCl_3$, 200 MHz): $\delta = 5.08$ (d, 1H, $^3J_{H,H} = 12.3$ Hz, $H^3$); 7.85 (d, 1H, $^3J_{H,H} = 12.3$ Hz, $H^2$). $^{13}$C-NMR ($CDCl_3$, 200 MHz): $\delta = 66.34$ ($C^1$); 169.38 ($C^4$).

Some of the data affording proof of the constitution of the yellow **8b** are given in Table 2. Particular attention is drawn to the high dipole moment, as well as the upfield and downfield positions, respectively, of $C^1$ and $C^4$.


Received: March 4, 1983 [Z 304 IE]
German version: *Angew. Chem. 95* (1983) 564
The complete version of this communication appears in: *Angew. Chem. Suppl. 1983*, 726–733



[3] H. Schubert, M. Regitz, *Synthesis 1982*, 149. The triazole **6** described in this article is the 4-methyl isomer **1a**, which is irrelevant regarding vinylation.

[4] For the α-diazoimine/1,2,3-triazole equilibrium see M. Regitz, *Diazoalkanes*, Thieme, Stuttgart 1977, p. 216ff.

[5] The only other reaction comparable to this is that of 1,5-dibenzoyl-4-diethylamino-3-methylpyrazole with 1-diethylaminopropyne: R. Huisgen, M. P. B. Verderol, A. Gieren, V. Lamm, *Angew. Chem. 93* (1981) 710; *Angew. Chem. Int. Ed. Engl. 20* (1981) 694.

[6] Other syntheses preferably afford 2,3-disubstituted or 2- and 3-monosubstituted compounds of this type: R. Gompper, W. Elser, *Justus Liebigs Ann. Chem. 725* (1969) 73; K. Peseke, *Z. Chem. 17* (1977) 288; W. Kantlehner, J. C. Ivanov, W. W. Mergen, H. Bredereck, *Liebigs Ann. Chem. 1980*, 372.


## Synthesis and Structure of $[\{[CH_3C(CH_2PPh_2)_3]IrP_3\}_3Cu_5Br_4]CuBr_2$—A 21 Atom Ir/Cu/P/Br Cluster


By *Franco Cecconi, Carlo A. Ghilardi*, Stefano Midollini,* and *Annabella Orlandini*


We recently reported that the reaction between (triphos)$CoP_3$[3] (triphos = $CH_3C(CH_2PPh_2)_3$) and copper(I) bromide (molar ratio 1:3) yields the adduct $[\{(triphos)CoP_3\}_2(CuBr)_6]$[5], which contains an unprecedented hexagonal $Cu_6$-unit held together by two (triphos)$CoP_3$-fragments[5]. We now report that when (triphos)$IrP_3$[6] is allowed to react with CuBr in the molar ratio 1:2, a novel ionic compound, $[\{(triphos)IrP_3\}_3Cu_5Br_4]CuBr_2$, is obtained.

The title compound was prepared by allowing a suspension of CuBr (1 mmol) in $CH_2Cl_2$ (10 mL) to react with a continuously stirred solution of (triphos)$IrP_3$ (0.5 mmol) in the same solvent (30 mL) for *ca.* 30 min at room temperature. Evaporation of the solvent gave orange crystals, which were recrystallized from nitroethane/*n*-butanol. The


[*] Dr. C. A. Ghilardi, F. Cecconi, Dr. S. Midollini, Dr. A. Orlandini
Istituto per lo Studio della Stereochimica ed Energetica dei Composti di Coordinazione del CNR
27 Via F. D. Guerrazzi, I-50132 Firenze (Italy)

compound, which is air-stable, behaves as a 1 : 1 electrolyte in nitroethane.

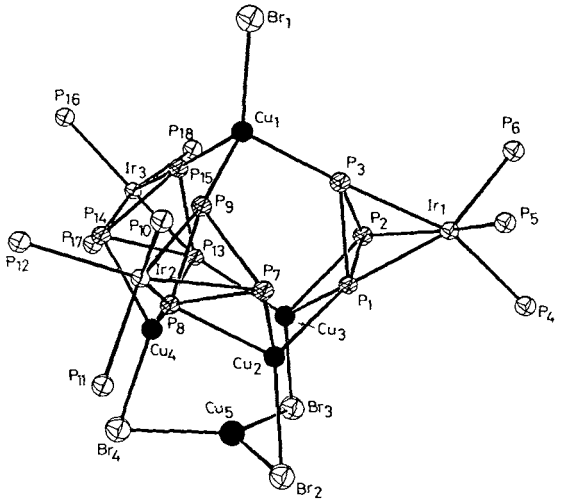



Fig. 1. Framework of the cluster cation $[\{(triphos)IrP_3\}_3Cu_5Br_4]^+$ in the crystal. Monoclinic, space group $P2_1/a$; $a = 44.558(22)$, $b = 18.869(9)$, $c = 17.361(8)$ Å, $\beta = 93.80(4)$, $\rho_{calc.} = 1.637$ g cm$^{-3}$ for $Z = 4$. The structure was solved by the heavy-atom method and refined to $R = 0.067$ and $R_w = 0.072$ for 10065 reflections with $I \geq 3\sigma(I)$ ($2\theta \leq 100°$); $Cu_{K\alpha}$ irradiation. Further details on the crystal structure investigation can be obtained from the Fachinformationszentrum Energie Physik Mathematik, D-7514 Eggenstein-Leopoldshafen 2, by quoting the depository number CSD 50434, the names of the authors, and the journal citation.

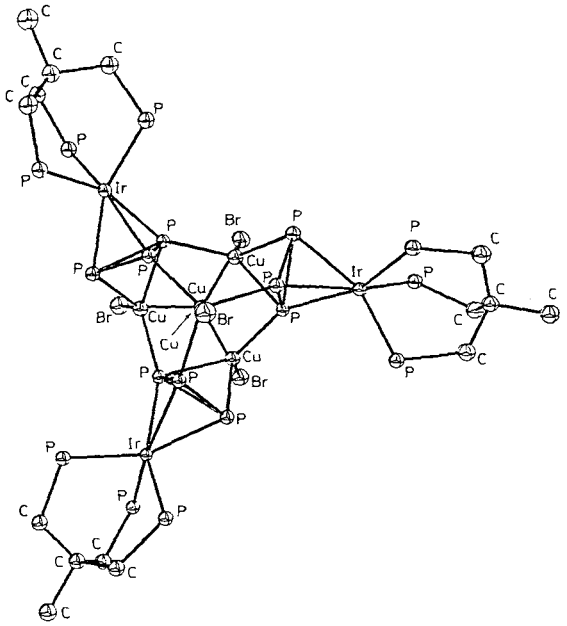



Fig. 2. Perspective view of the $[\{(triphos)IrP_3\}_3Cu_5Br_4]^+$ cation along the pseudo threefold axis passing through Br1, Cu1, and Cu5. For the sake of clarity the phenyl rings have been omitted. Selected distances (average values): CuCu (upper edge) 4.637(2), CuCu (lower edge) 2.795(13), CuCu (equatorial edge) 3.017(28), CuBr (tetrahedral) 2.360(3), CuBr (trigonal) 2.396(10), CuBr (digonal) 2.221(10), IrP(triphos) 2.292(3), IrP($P_3$) 2.427(10), CuP 2.308(6)–2.422(6) Å.

In the cluster cation, whose inner core possesses a pseudo threefold axis of symmetry (Figs. 1, 2), three molecules of (triphos)$IrP_3$ are held together *via* the $P_3$-groups by the central $Cu_5Br_4$-framework. The five Cu atoms are at the vertices of a distorted trigonal bipyramid, whose upper edge (4.637(2) Å (av)) is much longer than both the lower and the equatorial edges, (average lengths: 2.795(13) Å and 3.017(28) Å, respectively). The overall inner core geometry may be described in terms of a $Cu_5$-trigonal bipyramid, whose lower edges are bridged by Br atoms, while each upper triangular face is unsymmetrically capped by the $P_3$-group of one (triphos)$IrP_3$ fragment.

The Cu atoms display three different coordination geometries with four different geometric environments; the Cu atom at the lower vertex bridges three Br atoms trigonally, its displacement from the $Br_3$-plane being 0.08 Å. Each equatorial Cu atom is tetrahedrally coordinated by one bridging Br atom and by three P atoms of two different $P_3$-groups. The fifth Cu atom, which lies at the apex of the elongated pyramid, is tetrahedrally coordinated by one terminal Br atom and by three P atoms of three $P_3$-groups. Finally, the $CuBr_2^-$ anion is almost linear (Br–Cu–Br = 178.4(3)°).


Received: March 7, 1983;
revised: April 11, 1983 [Z 305 IE]
German version: *Angew. Chem. 95* (1983) 554
The complete version of this communication appears in: *Angew. Chem. Suppl. 1983*, 718–725

CAS Registry numbers:
$[\{(triphos)IrP_3\}_3Cu_5Br_4]CuBr_2$, 86238-21-3; (triphos)$IrP_3$, 73663-54-4; $CuBr_2$, 7787-70-4



[3] M. Di Vaira, C. A. Ghilardi, S. Midollini, L. Sacconi, *J. Am. Chem. Soc. 100* (1978) 2550; review: M. Di Vaira, L. Sacconi, *Angew. Chem. 94* (1982) 338; *Angew. Chem. Int. Ed. Engl. 21* (1982) 330.

[5] F. Cecconi, C. A. Ghilardi, S. Midollini, A. Orlandini, *J. Chem. Soc. Chem. Commun. 1982*, 229.

[6] C. Bianchini, C. Mealli, A. Meli, L. Sacconi, *Inorg. Chim. Acta 37* (1979) L543.


## Topotactic Redox and Exchange Reactions of Ruthenium(III) Halides


By *Robert Schöllhorn**, *Robert Steffen*, and *Klaus Wagner*


A large variety of transition metal chalcogenides and oxides with low dimensional structures are known to represent suitable host lattices for reversible intercalation reactions *via* topotactic electron/ion transfer[1,2]. We report here on intercalation reactions of α-$RuCl_3$ (layered structure) and $RuBr_3$ (chain structure) which demonstrate that binary metal halides with appropriate structure and electronic properties are principally able to undergo reactions similar to those of the host lattice types mentioned above.

α-$RuCl_3$ is an anisotropic semiconductor with a layered structure of the $AlCl_3$-type[3] in which intercalation of solvated and unsolvated guest ions can be accomplished either by electrochemical or chemical techniques. Cathodic reduction of α-$RuCl_3$ in aqueous electrolytes containing alkali, alkaline earth or transition metal ions leads to the uptake of solvated guest ions into the van der Waals gap between the $(RuCl_3)_\infty$ units with a corresponding increase in the interlayer spacing $d$ (Table 1).

$$RuCl_3 + \frac{x}{n}A^{n+} + x\,e^- + y\,H_2O \rightleftharpoons A^{n+}_{x/n}(H_2O)_y[RuCl_3]^{x-} \quad (1)$$


[*] Prof. Dr. R. Schöllhorn, R. Steffen, K. Wagner
Anorganisch-chemisches Institut der Universität
Corrensstrasse 36, D-4400 Münster (Germany)

Table 1. Intercalation compounds of α-$RuCl_3$: Dependence of interlayer spacing $d$ upon guest species [atomic ions hydrated, or solvated with dimethyl sulfoxide (DMSO) or formamide (FA); molecular guest ions unsolvated; Cp = cyclopentadienyl ligand]; interlayer spacing in empty host lattice $d = 573$ pm.

| Guest species | $d$ [pm] | Guest species | $d$ [pm] | Guest species | $d$ [pm] |
|---|---|---|---|---|---|
| $Li^+$ | 1103 | $Mg^{2+}$ | 1118 | $Zn^{2+}$ | 1078 |
| $Na^+$ | 1115 | $Ca^{2+}$ | 1125 | $Cd^{2+}$ | 1132 |
| $K^+$ | 826 | $Sr^{2+}$ | 1136 | $Na^+$/DMSO | 1598 |
| $Rb^+$ | 828 | $Mn^{2+}$ | 1096 | $Na^+$/FA | 1592 |
| $Cs^+$ | 870 | $Co^{2+}$ | 1075 | $Cp_2Co^+$ | 1085 |
| $NH_4^+$ | 828 | $Ni^{2+}$ | 1082 | $CH_3NH_3^+$ | 827 |

The hexagonal lattice parameters of the black $K^+$- and $Na^+$-compounds are $a = 610$, $c = 2478$, $d = c/3 = 826$ pm and $a = 605$, $c = 3345$, $d = c/3 = 1115$ pm, respectively. The maximum charge transfer to the $RuCl_3$ layers corresponds to $x = 0.5$ (*e.g.* $K_{0.5}^+(H_2O)_y[RuCl_3]^{0.5-}$); the reaction proceeds *via* a two-phase and a one-phase region (occurrence of nonstoichiometric compounds with $1/3 \leq x \leq 1/2$). As observed in the case of the hydrated chalcogenides[1,4], cations with a charge/radius ratio of $z/r > 100$ pm$^{-1}$ form bilayer hydrates ($d \approx 1100$ pm), while for cations with $z/r < 100$ pm$^{-1}$ only monolayer hydrates are stable ($d \approx 800$ pm). The hydrated phases are able to undergo rapid ion-exchange with atomic and molecular ions, which offers an alternative route for the preparation of a large number of new compounds. Similarly, solvate exchange reactions with neutral polar molecules is possible. The products of cathodic reduction in aqueous acids depend strongly upon the acid concentration. Hydrogen bronzes $H_xRuCl_3$ are obtained from $H_2SO_4$ solutions (*ca.* 70 wt-%); with decreasing acid concentration a series of hydrated hydronium phases $(H_3O)_x^+(H_2O)_y[RuCl_3]^{x-}$ with $x_{max} = 0.5$ can be isolated: monolayer hydrate ($d = 874$ pm), double layer hydrate ($d = 1126$ pm), triple layer hydrate ($d = 1538$ pm).

Unsolvated cations such as $Na^+$, $Cu^+$, $Ag^+$ can be intercalated by cathodic reduction of α-$RuCl_3$ in organic aprotic electrolytes (propylene carbonate, acetonitrile *etc.*), leading to formation of ternary phases [eq. (1) for $y = 0$]. Intercalation of $Ag^+$ leads to $Ag_{0.4}^+[RuCl_3]^{0.4-}$, while two phases $Cu_{0.5}^+[RuCl_3]^{0.5-}$ and $Cu_1^+[RuCl_3]^{1-}$ are found on intercalation of $Cu^+$. $CuRuCl_3$ shows a slight contraction of the $c$-axis as compared to the host lattice; hexagonal lattice parameters are $a = 609$, $c = 1678$, $d = c/3 = 559$ pm. α-$RuCl_3$ can be considered as a variant of the $CdI_2$-type structure $\square_{1/3}Ru_{2/3}Cl_2$ with regular defects (□) on octahedral sites within the layers. We assume, therefore, that small or "soft" ions such as $H^+$, $Li^+$, $Cu^+$ may occupy lattice sites (octahedral or tetrahedral, respectively) *within* the layers[5].

The reactions discussed above are reversible; on anodic oxidation the "empty" host lattice α-$RuCl_3$ is regenerated. Chemical intercalation is possible with reducing agents as the electron donors, *e.g.* dithionite or hydrazine. The reaction of α-$RuCl_3$ with aqueous solutions of $Na_2S_2O_4$ results in the formation of a black phase identical with that described for cathodic reduction in aqueous $Na^+/H_2O$. It is interesting to note that on prolonged exposure of the host lattice to $Na_2S_2O_4$ solution a drastic reversible color change is observed to a yellow transparent phase ($x \approx 1$) which cannot be obtained by the electrochemical technique, obviously because of an electronic transition. The fact that $Na_2S_2O_4$ may enforce a higher reduction stage is attributed to the Donnan equilibrium. A small but finite concentration of reducing anions is present inside the interlayer space, so that electron transfer from the outer surface to the bulk of the solid is not limited under these conditions by the electronic transport properties of the host matrix units.

An interesting point is that α-$RuCl_3$ is able to react with neutral Lewis bases (*e.g.* $NH_3$, pyridine, alkylamines) at room temperature to form intercalation compounds, *e.g.* $(NH_3)_xRuCl_3$ ($d = 850$ pm, $x_{max} = 1.5$), $(C_5H_5N)_xRuCl_3$ ($d = 1147$ pm, $x_{max} = 0.7$). Similar reactions of chalcogenide host lattices were shown earlier to be correlated with partial redox disproportionation of the guest species and formation of ionic species[1,4].

$RuBr_3$ has an orthorhombic structure of the $TiI_3$ type and can be described as consisting of $(RuBr_3)_\infty$ chains of face-sharing $RuBr_6$ octahedra with rather short metal/metal distances[3]. Electrochemical or chemical reduction in electrolytes containing atomic or molecular cations leads to reversible intercalation of solvated or unsolvated guest species, depending upon the polarity of the solvent, with a corresponding increase in the interchain distances. The maximum charge transfer for $Cu^+$ and $Ag^+$ intercalation (aprotic electrolyte) corresponds to $[RuBr_3]^{0.5-}$. Orthorhombic lattice parameters of $Ag_{0.5}RuBr_3$ are $a = 687$, $b = 1171$, $c = 584$ pm. The interchain distance of the hydrated black-violet products is dependent upon the ambient water vapor pressure. The hydronium phase shows strong two-dimensional lattice disorder and yields colloid solutions upon the influence of shear forces. Pronounced line broadening is observed on reoxidation of the intercalated products to $RuBr_3$.

The reactions discussed above provide access to an interesting and promising new field in the chemistry of intercalation compounds, since many transition metal halides exhibit structures and electronic properties related to those of the ruthenium compounds.

Received: March 7, 1983;
revised: May 24, 1983 [Z 306 IE]
German version: *Angew. Chem. 95* (1983) 559

[1] R. Schöllhorn, *Angew. Chem. 92* (1980) 1015; *Angew. Chem. Int. Ed. Engl. 19* (1980) 983; R. Schöllhorn in J. L. Atwood, J. E. D. Davies, D. D. MacNicol: *Inclusion Compounds*, Academic Press, New York, in press.
[2] a) M. S. Whittingham, A. J. Jacobson: *Intercalation Chemistry*, Academic Press, New York 1982; b) M. S. Whittingham, *Prog. Solid State Chem. 12* (1978) 41; J. Rouxel, *Rev. Inorg. Chem. 1* (1979) 245.
[3] G. Thiele, K. Brodersen, *Fortschr. Chem. Forsch. 10* (1968) 631; L. Binotto, J. Pollini, G. Spinolo, *Phys. Status Solidi B 44* (1971) 245.
[4] A. Lerf, R. Schöllhorn, *Inorg. Chem. 16* (1977) 2950; R. Schöllhorn in [2a], p. 315.
[5] For an example of hydrogen in chalcogenide layers cf.: C. Riekel, H. G. Reznik, R. Schöllhorn, C. J. Wright, *J. Chem. Phys. 70* (1979) 5203.

## Efficient Method for Generation of Radical Anions from Benzene Derivatives of Low Electron Affinity**

By *Fabian Gerson** and *René Heckendorn*

In the past two decades, the radical anions of numerous benzene derivatives in solution have been characterized by ESR spectroscopy[1]. Nevertheless, hyperfine data are still

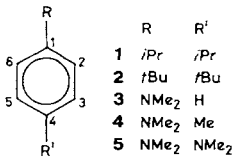
[*] Prof. Dr. F. Gerson, R. Heckendorn
Physikalisch-chemisches Institut der Universität
Klingelbergstrasse 80, CH-4056 Basel (Switzerland)
[**] This work was supported by the Swiss National Science Foundation.

missing for the radical anions of several simple mono- and *p*-disubstituted benzenes of low electron affinity. The equilibrium of the reaction of such a derivative **X** with solvated electrons

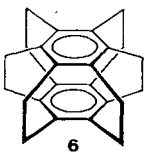
$$\mathbf{X} + e_{solv.} \rightleftharpoons \mathbf{X}^{\ominus}$$

lies largely to the left, so that the concentration of the radical anion is too low for spectroscopic studies. A shift of the equilibrium to the right can be achieved by lowering the temperature[2a]; however, this procedure is limited by the freezing point of the solution. More effectively, $[\mathbf{X}^{\ominus}]$ is increased by raising the concentrations of **X** and $e_{solv.}$. While **[X]** is readily increased by starting with a larger amount of **X**, a ten- to hundredfold increase in $[e_{solv.}]$ can be accomplished by irradiating the deep-blue solution of potassium in 1,2-dimethoxyethane at low temperatures[2b]. It is known[2b,c] that the blue color arises from a diamagnetic species, in which an electron pair is attached to the cation $K^{\oplus}$, and which is usually referred to as the anion $K^{\ominus}$. In contrast to $[K^{\ominus}]$, $[e_{solv.}]$ is rather small, as indicated by the low intensity of the pertinent ESR signal ($g = 2.0021 \pm 0.0001$). Irradiation of the solution by visible light leads to the fading of the blue color and to an increase in $[e_{solv.}]$, manifested by a strikingly large enhancement of the ESR signal[2b]. When a compound **X** is present in the solution, this signal of $e_{solv.}$ is partly or completely replaced by the ESR spectrum of $\mathbf{X}^{\ominus}$, due to the reaction of **X** with $e_{solv.}$.

To begin with, this method was tested on mesitylene, which, hitherto, could be converted into its radical anion only under special conditions[3]. The coupling constants of the ring and methyl protons (0.282 and 0.493 mT, respectively) measured by us agree with those reported previously[3]. Subsequently, the radical anions of *p*-diisopropylbenzene **1**, *p*-di-*tert*-butylbenzene **2**, *N,N*-dimethylaniline **3**, *N,N*-dimethyl-*p*-toluidine **4**, and *N,N,N',N'*-tetramethyl-*p*-phenylendiamine **5** were generated for the first time[4].

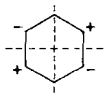



| | R | R' |
|---|---|---|
| **1** | *i*Pr | *i*Pr |
| **2** | *t*Bu | *t*Bu |
| **3** | $NMe_2$ | H |
| **4** | $NMe_2$ | Me |
| **5** | $NMe_2$ | $NMe_2$ |



**6**

The data provided by the ESR spectra of these radical anions are given in Table 1. They point to a single occupancy of an orbital which correlates with the "antisymmetric" benzene-LUMO, as is expected in view of the substituent effects.




The method can also be applied to other compounds of low electron affinity—for example, "superphane" **6** which is not reduced by standard procedures[5]. A coupling constant of $0.185 \pm 0.005$ mT for 12 equivalent protons was derived from the ESR spectrum of the radical anion of **6** ($g = 2.0030 \pm 0.0002$); this result means that, on the hyperfine time-scale, the unpaired electron is localized in one benzene ring.

Table 1. $^1$H- and $^{14}$N-coupling constants (mT) and *g* values for the radical anions of **1**–**5**.

| Cpd. | H(2,6) [a] | H(3,5) [a] | H(4) [b] | Substituent [b] | *g* [c] |
|---|---|---|---|---|---|
| **1** | 0.525 | 0.525 | — | [d] | 2.0028 |
| **2** | 0.480 | 0.480 | — | 0.014 (18 H) [e] | 2.0028 |
| **3** | 0.515 | 0.585 [f] | 0.032 | 0.019 (1 N) [g] | 2.0029 |
| **4** | 0.530 | 0.575 | — | 0.019 (1 N) [g]<br>0.054 (3 H) | 2.0029 |
| **5** | 0.540 | 0.540 | — | [d] | 2.0029 |

[a] Experimental error ±0.005 mT. [b] Experimental error ±0.002 mT. [c] Experimental error ±0.0001. [d] Unresolved. [e] Additional coupling of $0.014 \pm 0.002$ mT with the $^{39}$K nucleus of the counterion. [f] Assignment by deuteration. [g] Coupling to the *N*-methyl protons unresolved.

Received: March 11, 1983;
revised: April 11, 1983 [Z 310 IE]
German version: *Angew. Chem. 95* (1983) 571

[1] See, *e.g.*, Landolt-Börnstein: *Magnetic Properties of Free Radicals*, Volumes 1 and 9 (part d1), Springer, Heidelberg, 1965 and 1980.

[2] a) F. Gerson, E. Heilbronner, J. Heinzer, *Tetrahedron Lett. 1966*, 2095. b) S. H. Glarum, J. H. Marshall, *J. Chem. Phys. 52* (1970) 5555. c) I. Hurley, T. R. Tuttle, Jr., S. Golden, *Pure Appl. Chem. 26* (1969) 449. J. L. Dye, C. W. Andrews, S. E. Mathews, *J. Phys. Chem. 79* (1975) 3065, and further references therein.

[3] G. V. Nelson and A. von Zelewsky, *J. Am. Chem. Soc. 97* (1975) 6279. These authors reduced neat mesitylene with potassium in the presence of [18]crown-6. They found an additional coupling (0.018 mT) to 6 protons of the ether. Instead of this, we observed a hyperfine splitting ($0.024 \pm 0.002$ mT) from the $^{39}$K nucleus of the counterion ($g = 2.0029 \pm 0.0001$).

[4] The photolytic apparatus followed the description by H. Paul, H. Fischer, *Helv. Chim. Acta 56* (1973) 1575. The solutions were irradiated in Pyrex cells, which are transparent for $\lambda > 330$ nm, with a high-pressure Hg-lamp (Philips-1000W). Since the compounds do not absorb above 330 nm, it is improbable that their electronic affinity is enhanced by excitation.

[5] F. Gerson, J. Lopez, V. Boekelheide, H. Hopf, *Helv. Chim. Acta 65* (1982) 1391.

## Tetrakis(trimethylsilyl)plumbane, The First Organosilicon-Lead Compound**

By *Lutz Rösch** and *Uwe Starke*

Molecules with Si–Pb bonding were hitherto unknown. This is surprising since organometallic compounds of both lead[1] as well as of silicon[2] with bonding to all other elements of the 4th main group are well known. We have now been able to obtain the first organosilylplumbane by reaction of $PbCl_2$ with $Mg(SiMe_3)_2 \cdot DME$ (DME = 1,2-dimethoxyethane)[3].

$$2\,PbCl_2 + 2\,Mg(SiMe_3)_2 \xrightarrow{Et_2O,\ -78\,^{\circ}C} Pb(SiMe_3)_4 + Pb + 2\,MgCl_2$$

$Pb(SiMe_3)_4$ can be isolated as pale yellow, moderately light-sensitive crystals, which are soluble in hydrocarbons and in ethers. The solutions are stable for several hours at room temperature. On heating, the crystals start to decompose at 80 °C. The composition of the new compound was confirmed by elemental analysis and by its IR, Raman, $^1$H-NMR, and mass spectra. The mass spectrum contains the ion with calculated isotopic pattern and the expected frag-

[*] Priv.-Doz. Dr. L. Rösch, U. Starke
Institut für Anorganische und Analytische Chemie
der Technischen Universität
Strasse des 17. Juni 135, D-1000 Berlin 12 (Germany)

[**] This work was supported by the Deutsche Forschungsgemeinschaft and the Fonds der Chemischen Industrie. We thank Prof. J. Müller for recording the mass spectra.

ment ions. The $^1$H-NMR spectrum (benzene solution) shows a singlet in the neighborhood of the TMS standard, flanked by Si- and Pb-satellites.

The IR and Raman spectra are consistent with the spectra of the homologous compounds $E(SiMe_3)_4$ (with E = C, Si, Ge, Sn) investigated by *Bürger et al.*[2]. As expected, the lead compound has the two lowest $ESi_4$ valence vibrations (305, 302 $cm^{-1}$) of this series; however, the shift is small compared to the corresponding bands of $Sn(SiMe_3)_4$ (325, 311 $cm^{-1}$)[2] and gives no indication of a particular weakening of the Pb–Si bond.

Our synthesis of $Pb(SiMe_3)_4$ started from a $Pb^{II}$ compound. In analogy to the synthesis of tetraorganolead compounds it may be assumed that $Pb(SiMe_3)_2$ and $Pb_2(SiMe_3)_6$ occur as intermediates.

$$PbCl_2 + Mg(SiMe_3)_2 \longrightarrow Pb(SiMe_3)_2 + MgCl_2$$
$$3\,Pb(SiMe_3)_2 \longrightarrow (Me_3Si)_3Pb{-}Pb(SiMe_3)_3 + Pb$$
$$2\,Pb_2(SiMe_3)_6 \longrightarrow 3\,Pb(SiMe_3)_4 + Pb$$
$$\text{or: } Pb_2(SiMe_3)_6 \longrightarrow Pb(SiMe_3)_4 + Pb(SiMe_3)_2$$

$Pb(SiMe_3)_2$ has so far never been detected, whereas the occurrence of $Pb_2(SiMe_3)_6$ could be confirmed mass spectroscopically[4].

Received: March 14, 1983 [Z 311 IE]
German version: *Angew. Chem. 95* (1983) 572

CAS Registry numbers:
$Pb(SiMe_3)_4$, 86196-55-6; $Mg(SiMe_3)_2$, 61218-55-1; $PbCl_2$, 7758-95-4

[1] Cf. *e.g.* L. C. Willemsens, G. J. M. van der Kerk, *J. Organomet. Chem. 2* (1964) 260.

[2] Cf. *e.g.* H. Bürger, U. Götze, W. Sawodny, *Spectrochim. Acta A 26* (1970) 685.

[3] Procedure [all operations carried out under repurified argon as inert gas in complete absence of air and moisture (BASF catalyst, $P_4O_{10}$)]: 5.2 g (20 mmol) of $Mg(SiMe_3)_2 \cdot DME$ [5] was dissolved in 100 mL of anhydrous ether and the solution cooled to −78 °C. On portionwise addition of 5.34 g (20 mmol) of $PbCl_2$ the solution immediately turned gray, and then, after 15 min, deep black. After 8 hours' stirring at −78 °C the mixture was allowed to slowly warm to room temperature, and stirring was continued for a further 5 h. After settling, the solution was first removed by decantation, and then the readily volatile components by suction at the oil-pump. Subsequent extraction of the residue with pentane followed by evaporation and cooling afforded $Pb(SiMe_3)_4$ as pale yellow crystals, yield 8.4 g (84%), dec. 80 °C.

[4] MS: *m/z* 854, $Pb_2(SiMe_3)_6^+$; 781, $Pb_2(SiMe_3)_5^+$; 708, $Pb_2(SiMe_3)_4^+$; 635, $Pb_2(SiMe_3)_3^+$; 562, $Pb_2(SiMe_3)_2$.

[5] L. Rösch, *Angew. Chem. 89* (1977) 497; *Angew. Chem. Int. Ed. Engl. 16* (1977) 247.

## Novel Surface-Modified Solids by Topochemical Oxidation of Zintl Anions**

By *Robert C. Haushalter**

Although Zintl phases[1] and Zintl anions[2,10,11] have been known for many years, their chemical reactivity has rarely been investigated[10]. We have found that many Zintl anions can be topochemically oxidized by reducible solids to give a large class of new surface-modified materials. Thus, *e.g.*, it was possible to metallize certain organic polymers (polyimide, polyacetylene) non-electrochemically *via* a novel reduction-intercalation-deposition scheme[3] (cf. Fig. 1: steps ⓐ and ⓑ). We now report that many anisotropic inorganic solids, and even certain metals, can be surface-metallized with Zintl anions by a similar mechanism. Furthermore, unique bimetallic surfaces can be prepared by utilizing the reducing power of the solids obtained from the reduction-intercalation-deposition reaction to reduce metal cations from solution (Fig. 1: step ⓒ).

When single crystals of graphite are treated with ethylenediamine (en) solutions of $K_4Sn_9$[10] (36 h, 25 °C), elemental analysis of the product shows an Sn/K ratio ≈ 2; scanning electron microscopy (SEM), electron microprobe/energy dispersive X-ray analysis (EM/EDX) and powder X-ray diffraction (XRD) show that crystalline tin is deposited only on the edges of the graphite layers. This anisotropic metallization is presumably due to the much greater rates of diffusion of $K^+$ between the graphite layers in the crystals compared to diffusion rates perpendicular to the layers. Thus, the Sn crystals are deposited on the surface where the Zintl anion ($Sn_9^{4-}$) is oxidized and the cations ($K^+$) are intercalated in the graphite lattice. The electrons and $K^+$ can be removed from the graphite lattice by treatment with oxidants (*e.g.* treatment with benzophenone generates the $K^+$ salt of the blue benzophenone radical anion; see Fig. 1: step ⓓ).

Likewise, golden metallic $HfTe_2$ crystals rapidly turn silver-gray when treated with $K_4Sn_9$ in en-solution, and SEM and EM/EDX again show tin deposited primarily on edges of the flat crystals.

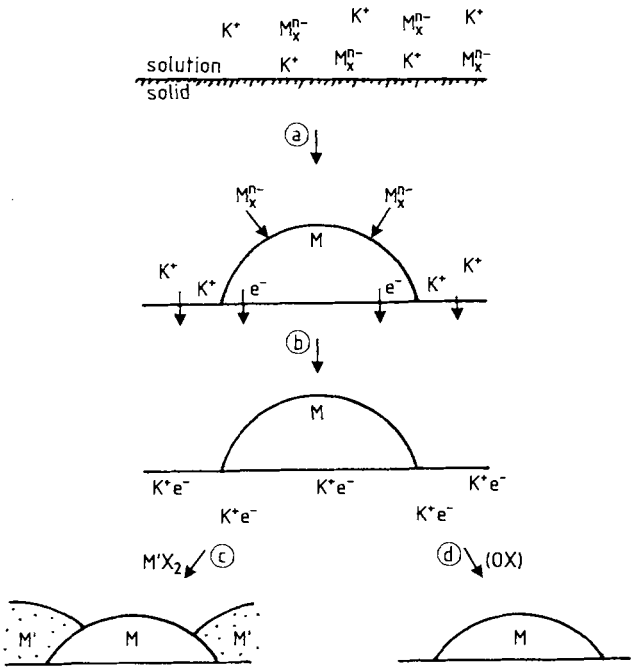



Fig. 1. Schematic illustration of the surface modification of solids by the oxidation of Zintl anions (for example $K_4M_9$): ⓐ Treatment of a solid surface with a Zintl anion in a solution of the polyanion. ⓑ Once a nucleation site forms, a metal crystal grows on the surface of the solid by the decomposition of the Zintl $M_x^{n-}$. The Zintl anion's electrons are transferred through the growing metal crystal to reduce the solid while the Zintl anion's counterions combine with the substrate to balance the charge from the reduction. ⓒ The now oxidizable potassium-containing solid enables reduction of a metal salt ($M'X_2$) with formation of a bimetallic surface. ⓓ A "pure" surface metal crystal obtained by action of an electron acceptor in connection with ⓑ.

[*] Dr. R. C. Haushalter
Materials Science and Technology Division
Argonne National Laboratory
9700 South Cass Avenue, Argonne, IL 60439 (USA)

[**] This work was supported by the U. S. Department of Energy (Contract No. W-31-109-Eng-38). I thank B. Tani for assistance with the SEM analysis.

Some of the more electronegative transition metals can also be surface metallized by Zintl anions *via* a similar mechanism. Treatment of Pt foil with $K_4Pb_9$ in en (24—48 h, 25 °C) gives lead crystals surrounded by a potassium-rich phase (XRD, SEM, EM/EDX). The potassium-rich phase is not present as $K^+$ as it retains considerable reducing power. Reaction of this K/Pb surface with reducible metal cations, like $Pd^{2+}$, leads to deposition of the metal onto the surface to give a bimetallic surface, and $K^+$ goes into solution (Fig. 1: ⓒ). Other transition metal substrates (*e.g.* Au), and other Zintl anions and reducible metal cations can be used similarly to form many bimetallic surfaces. The second stage of the formation of these bimetallic surfaces, *i.e.* reduction of the cation $M^{n+}$ (cf. Fig. 2b) can be viewed conceptually as the reverse of the oxidation of the Zintl anion $M_x^{n-}$ at a solid surface (Fig. 2a).

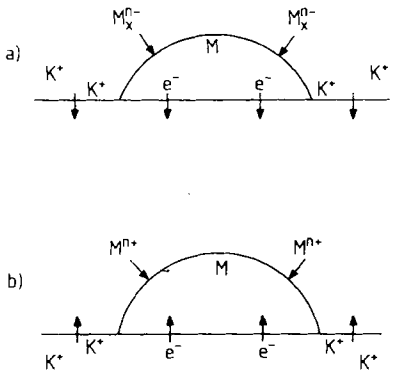



Fig. 2. Contrast of the surface oxidation of Zintl anions with the reduction of metal cations by reduced, intercalated solid. a) The oxidation of Zintl anions to the metal with simultaneous reduction, intercalation of the solid, b) reduction of metal cations accompanied by oxidation, deintercalation of the solid.

The common feature of these reactions is the deposition of metal crystals on the surface of a solid by oxidation of Zintl anions on the surface of the growing metal crystal, transfer of the electrons through the metal crystal to the substrate, which is then intercalcated by cations to balance the charge. The reaction type is general and has allowed the preparation of many surface-modified materials not accessible by other preparative techniques.

Received: January 28, 1983;
revised: May 19, 1983 [Z 257 IE]
German version: *Angew. Chem. 95* (1983) 560
The complete version of this communication appears in:
*Angew. Chem. Suppl. 1983*, 766-777

[1] H. Schäfer, B. Eisenmann, W. Müller, *Angew. Chem. 85* (1973) 742; *Angew. Chem. Int. Ed. Engl. 12* (1973) 694; G. Cordier, H. Schäfer, *ibid. 93* (1981) 474 and *20* (1981) 466.

[2] J. Corbett, S. Critchlow, R. Burns, "Polyatomic Zintl Anions Stabilized Through Crypt Complexation of the Cations" in A. Cowley: Proc. Ralph Rudolph Memorial Symp. Main Group Clusters, *ACS Symp. Ser.*, in press.

[3] L. Krause, R. Haushalter, *Thin Solid Films 102* (1983) 161.

[10] D. Kummer, L. Diehl, *Angew. Chem. 82* (1970) 881; *Angew. Chem. Int. Ed. Engl. 9* (1970) 895; cf. also L. Diehl, K. Khodadadeh, D. Kummer, J. Strähle, *Z. Naturforsch. B 31* (1976) 522; *Chem. Ber. 109* (1976) 3404.

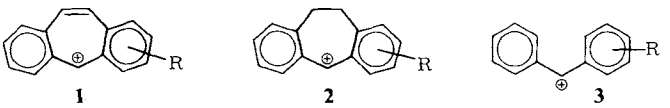
[11] H. G. von Schnering "Catenation of Phosphorus Atoms" in A. L. Rheingold: *Homoatomic Rings, Chains and Macromolecules of Main Group Elements*, Elsevier, Amsterdam 1977, p. 317.

## Quenching of the Aromaticity of the 5-Dibenzo[*a,d*]cycloheptenylium Ion by Complexing with $(CO)_3Cr$

By *Alberto Ceccon, Alessandro Gambaro, Annamaria Romanin,* and *Alfonso Venzo**

Thermodynamic and kinetic data[1] show that the π-coordination of an aryl ring by a tricarbonylchromium group anchimerically stabilizes benzylic carbenium ions; this has been demonstrated, primarily, by NMR spectroscopic data[2]. Tropylium ions are, as suggested by the $pK_{R^+}$ values, likewise stabilized by $(CO)_3Cr$ groups—albeit by a different mechanism[1c]. We report here on the $pK_{R^+}$ values and $^1$H-NMR spectra of the free and of the $(CO)_3Cr$-complexed 5-dibenzo[*a,d*]cycloheptenylium ions **1** and the 10,11-dihydro analog **2**.

We compare UV data and $pK_{R^+}$ values for the free and complexed ions, obtained by ionization of the corresponding alcohols in trifluoracetic acid/$H_2O$, with the data for the diphenylcarbenium ion **3**. The coordination with the $(CO)_3Cr$-residue stabilizes the cation **2a** ($\Delta pK_{R^+} = +3.5$) almost as equally as well as **3a** ($\Delta pK_{R^+} = +3.3$). A quite different behavior is observed, however, in the case of **1a**;




**1** **2** **3**

**a**, R = H; **b**, R = $(CO)_3Cr$

here the thermodynamic stability is strongly reduced on complexation with $(CO)_3Cr$ ($\Delta pK_{R^+} = -2.4$). Since the free ion **1a** is about 5 $pK_{R^+}$ units more stable than the dehydro analog **2a**, the complexed ions **1b** and **2b** show a comparable stability. These findings, which are not consistent with the effects usually induced by the $(CO)_3Cr$ group, can be explained on the basis of $^1$H-NMR data.

For the $^1$H-NMR investigations, solutions of the carbenium ions were obtained by protonation of the corresponding alcohols in $CD_2Cl_2$ at 200 K with $HSO_3F$. The 5-H singlets were assigned by comparison with the $^1$H-NMR spectra of 5-deuterio derivatives. In the case of the uncomplexed ions it is found that in **2a** the positive charge is delocalized over the aryl rings, whereas in **1a** it is not. In **1a** the 5-H signal is shifted further downfield than in **2a** (Table 2); this is attributed to a strong diatropic ring current in the central ring of **1a**[7]. This is also responsible for the large downfield shift of the signals of the olefinic protons; with $\delta = 9.18$ these signals lie in the same region as the signal of tropylium tetrafluoroborate ($\delta = 9.30$).

The coordination with $(CO)_3Cr$ causes an upfield shift of all signals in both carbenium ions (see Δ-values in Table 2). For **2b** the complexation effects closely resemble those found for the $(CO)_3Cr$-complex of the di(*p*-tolyl)carbenium ion[2a]: The signals of the complexed aryl ring and the 5-H signal are shifted further upfield than the signals of the $CH_2$ groups and the uncomplexed aryl ring. The

[*] Prof. Dr. A. Ceccon, Prof. Dr. A. Gambaro, Dr. A. Romanin, Dr. A. Venzo
Istituto di Chimica Fisica, Università di Padova
I-35100 Padova (Italy)

Table 2 (selected data). $^1$H-NMR chemical shifts [a] of **1a**, **b** and **2a**, **b** [b, c].

| | 1-H | 2-H | 3-H | 4-H | 5-H | 6-H | 7-H | 8-H | 9-H | 10-H | 11-H |
|---|---|---|---|---|---|---|---|---|---|---|---|
| **1a** | 8.81 | 8.79 | 8.56 | 9.03 | 10.45 | 9.03 | 8.56 | 8.79 | 8.81 | 9.18 | 9.18 |
| **1b** | 6.02 | 5.77 | 6.83 | 6.10 | 8.12 | 8.19 | 7.94 | 8.15 | 7.90 | 7.57 | 7.20 |
| $\Delta_{1b-1a}$ [d] | −2.79 | −3.02 | −1.73 | −2.93 | −2.33 | −0.84 | −0.62 | −0.64 | −0.91 | −1.61 | −1.98 |
| **2a** | 7.72 | 8.27 | 7.83 | 8.30 | 9.39 | 8.30 | 7.83 | 8.27 | 7.72 | 3.44 | 3.44 |
| **2b** | 5.95 | 6.65 | 5.99 | 6.19 | 7.42 | 7.79 | 7.57 | 7.72 | 7.45 | 2.7÷3.7 [e] | |
| $\Delta_{2b-2a}$ | −1.77 | −1.62 | −1.84 | −2.11 | −1.97 | −0.51 | −0.26 | −0.55 | −0.27 | −0.24 [f] | |

[a] $\delta$-values referred to TMS; 90 MHz. [b] In $CD_2Cl_2$ saturated with $HSO_3F$; $T = 243$ K. [c] The $(CO)_3Cr$ is bonded to the ring bearing the 1-H—4-H atoms. [d] $\Delta_{1b-1a} = \delta_{1b} - \delta_{1a}$. [e] Complicated multiplet. [f] Mean difference.

smaller charge delocalization into the uncomplexed ring is also revealed in the alternating Δ-values ($\Delta^9_{2b-2a} \approx \Delta^7_{2b-2a} < \Delta^8_{2b-2a} \approx \Delta^6_{2b-2a}$; $\Delta^1_{2b-2a} = \delta^1_{2b} - \delta^1_{2a}$). The most striking effect caused by introduction of the $(CO)_3Cr$ group is the large upfield shift of the "side chain" protons 10, 11-H (of the same order of magnitude as in the case of the 1-H—5-H signals). Moreover, all $\Delta_{1b-1a}$ values are greater than the corresponding $\Delta_{2a-2b}$ values. The $\Delta_{1b-1a}$ values of the protons of the uncomplexed aryl ring are not alternating ($\Delta^6_{1b-1a} \approx \Delta^9_{1b-1a} < \Delta^7_{1b-1a} \approx \Delta^8_{1b-1a}$).

We assume that the diatropic character of the central ring in **1a** is substantially reduced on complexation with $(CO)_3Cr$; this explains the decrease in thermodynamic stability in the transition **1a** → **1b**.

Comparison of the results obtained on the aromatic 5-dibenzo[*a*,*d*]cycloheptenylium ion **1a** with those of the antiaromatic anion 5-dibenzo[*a*,*d*]cycloheptenide[10] reveals that complexation of an aryl ring with $(CO)_3Cr$ causes a dramatic decrease in the extended diatropic or paratropic ring current; the aromatic species is destabilized, the antiaromatic is stabilized.

Received: March 4, 1983;
revised: May 18, 1983 [Z 301 IE]
German version: *Angew. Chem. 95* (1983) 572
The complete version of this communication appears in:
*Angew. Chem. Suppl. 1983*, 734–746

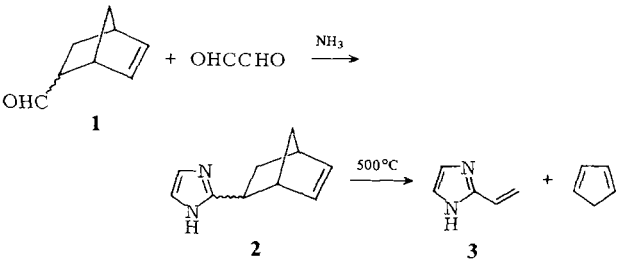
[1] a) A. Ceccon, A. Gobbo, A. Venzo, *J. Organomet. Chem. 162* (1978) 311, and references cited therein; b) P. C. Reeves, *ibid. 215* (1981) 215; c) J. C. Holmes, D. A. K. Jones, R. Pettit, *ibid. 4* (1965) 324; d) A. Ceccon, *ibid. 29* (1971) C 19.
[2] a) M. Acampora, A. Ceccon, M. Dal Farra, G. Giacometti, *J. Chem. Soc. Chem. Commun. 1975*, 871; b) M. Acampora, A. Ceccon, M. Dal Farra, G. Giacometti, G. Rigatti, *J. Chem. Soc. Perkin Trans. II 1977*, 483; c) G. A. Olah, S. H. Yu, *J. Org. Chem. 41* (1976) 1694; d) D. Seyferth, J. S. Merola, C. Scott Eschbach, *J. Am. Chem. Soc. 100* (1978) 4124.
[7] G. A. Olah, G. Liang, *J. Org. Chem. 40* (1975) 2108.
[10] a) A. Ceccon, A. Gambaro, L. Pizzato, A. M. Romanin, A. Venzo, *J. Chem. Soc. Chem. Commun. 1982*, 907.

## A Simple Route to 2-Vinylimidazoles

By *Alan S. Rothenberg**, *David L. Dauplaise*, and *Hans P. Panzer*

2-Vinylimidazoles are an interesting class of compounds because of their unique polymerization characteristics, which set them apart from the more familiar 1-vinylimidazoles[1]. They have previously been available only by a lengthy and tedious sequence involving condensation of β-hydroxypropionimidate with an aminoacetaldehyde dimethyl acetal, followed by dehydration of the resulting 2-(β-hydroxyethyl)imidazole[2]. Alternatively, the hydroxyethylimidazole could be converted into the corresponding β-bromide and dehydrobrominated to 2-vinylimidazole[3]. Since low yields of 2-vinylimidazoles result from either of these routes, only limited quantities of 2-vinylimidazoles have previously been available, and little is known about their polymerization behavior.

We now wish to report the first practical laboratory method for the preparation of significant quantities of 2-vinylimidazoles. This route uses the classical condensation of an aldehyde and an α-dicarbonyl compound with ammonia to provide the imidazole ring system[4, 5]. However, by using 5-norbornene-2-carbaldehyde **1**, the Diels-Alder adduct of acrolein and cyclopentadiene, as the aldehyde component, a 2-(5-norbornen-2-yl)imidazole **2** is obtained which is readily convertible into the 2-vinylimidazole **3** and cyclopentadiene by a retro-Diels-Alder reaction. Various α-dicarbonyl compounds can be used to prepare differently substituted 2-vinylimidazoles; however, best results are obtained in reactions using glyoxal. In this case, yields of about 90% are achieved in each of the two steps.




*Procedure*

**2**: Anhydrous ammonia (25.5 g, 1.5 mol) is added dropwise to a vigorously stirred mixture of **1** (61 g, 0.5 mol; *endo*/*exo* = 80/20) and 80% glyoxal powder (36.25 g, 0.5 mol) in methanol (150 mL) at −10 °C. The temperature is maintained at −10 °C, stirring is continued for four hours, and the reaction temperature is then allowed to rise to ambient temperature. The product is poured into water (2 L) and the precipitated solid collected on a filter, washed with water and vacuum dried to provide 74 g (90%) of **2** as a white solid, m.p. 209–210 °C.

**3**: A 20% solution of **2** in methanol is continuously fed at a rate of up to 3 mL/min to the top of a 60 cm long vertically mounted pyrolysis tube, 30 cm of which is packed with ceramic beads. The tube is heated to 500 °C and the vapors are swept through the apparatus by a flow of $N_2$ (200 mL/min) from top to bottom, with the methanolic

[*] Dr. A. S. Rothenberg, Dr. D. L. Dauplaise, Dr. H. P. Panzer
American Cyanamid Company, Chemical Research Division
1937 West Main St., P.O. Box 60, Stamford, CT 06904-0060 (USA)

 © Verlag Chemie GmbH, 6940 Weinheim, 1983 0570-0833/83/0707-0560 $ 02.50/0 

product being condensed and collected in an ice-cooled receiver. The product is inhibited with *p*-methoxyphenol (500 ppm) and stripped of methanol and cyclopentadiene on a rotary evaporator keeping the temperature below 40 °C. Crystallization of the crude product from toluene/hexane with carbon decolorization provides **3**, m.p. 130–131 °C in 85–90% yield; $^1$H-NMR ($CDCl_3$, 60 MHz): $\delta = 5.36$ (ABq, $J_{AB} = 1.4$ Hz, $J_{BC} = 11$ Hz, 1H), 5.96 (ABq, $J_{AB} = 1.4$, $J_{BC} = 18$ Hz, 1H), 6.75 (ABq, $J_{AC} = 11$, $J_{BC} = 18$ Hz, 1H), 7.13 (s, 2H); $^{13}$C-NMR ($CDCl_3$, 100 MHz): $\delta = 116.46$ ($CH{=}\mathit{C}H_2$), 122.62 (C-4,5), 125.83 ($\mathit{C}H{=}CH_2$), 146.51 (C-2).

Received: March 23, 1983 [Z 319 IE]
German version: *Angew. Chem. 95* (1983) 573

[1] a) H. P. Panzer, A. S. Rothenberg, D. L. Dauplaise, *Abstr. Fourteenth Akron Polym. Conf. on Hydrophilic Polymers: Synth., Characterization, Appl.*, May 19, 20, 1983; b) C. H. Bamford, E. Schofield, *Polymer 22* (1981) 1227.
[2] J. K. Lawson, *J. Am. Chem. Soc. 75* (1953) 3398.
[3] C. G. Overberger, K. Gerberding, *J. Polym. Sci. Polym. Lett. Ed. 11* (1973) 465.
[4] B. Radziszewski, *Ber. Dtsch. Chem. Ges. 15* (1882) 1493.
[5] M. Akiyama, Y. Hara, M. Tanabe, *J. Chem. Soc. Perkin Trans. II 1978*, 288.

## $[Cl_2FeS_2MoO(S_2)]^{2-}$, a Novel Bimetallic Complex with Unusual Electronic Structure and a Substituted Tetrachalcogenometalate as "Ligand"

By *Achim Müller*, Sabyasachi Sarkar, Hartmut Bögge, Rainer Jostes, Alfred Trautwein,* and *Uschi Lauer*

Heterometal complexes and clusters which can be of biochemical importance (*e.g.* in connection with the elucidation of the structure of the FeMoS cluster of nitrogenase[1,2]), are, *in general,* rarely accessible *via* conventional preparative routes. In special cases $d^0$-thiometalates of the type $MO_{4-n}S_n^{2-}$ (M = Mo, W; n = 2, 3, 4), which have unique ligand properties, have proven to be ideal synthetic reagents[2]. We have now been able to synthesize a heterometal complex which *formally* contains a substituted thiometalate, the chelate ligand $[S_2MoO(S_2)]^{2-}$, **1**. Substituted thiomolybdates have so far never been isolated.

Reaction of $MoOS_3^{2-}$ with $FeCl_2$ and sulfur ($S_8$) in dimethylformamide (DMF) leads to formation of black-green $(PPh_4)_2[Cl_2FeS_2MoO(S_2)]\cdot DMF$, which we characterized by elemental analysis, magnetic measurements, $^{57}$Fe-Mössbauer, IR, and UV/VIS spectra, MO calculations, and a complete crystal structure analysis. The complex anion $[Cl_2FeS_2MoO(S_2)]^{2-}$, **2** (Fig. 1), contains a distorted tetrahedrally coordinated Fe central atom with two chloro ligands and the novel bidentate "perthiomolybdato" ligand, **2**, derived from the "tetrahedrally shaped" $MoOS_3^{2-}$ by $S^{2-} \rightarrow S_2^{2-}$ substitution. The FeCl distances almost correspond to those observed in $[Cl_2Fe(MoS_4)]^{2-}$ and $[Cl_2Fe(MoS_4)FeCl_2]^{2-}$. The $FeS_2MoO(S_2)$ group in **2** is similar in structure to the $MoS_2MoO(S_2)$ moiety in $[(S_2)OMo^VS_2Mo^VO(S_2)]^{2-}$, **3** (dihedral angles $FeS_2Mo$ 158.5° and $MoS_2Mo$ 148.8°). The FeMo distance is 275.2(2) pm.

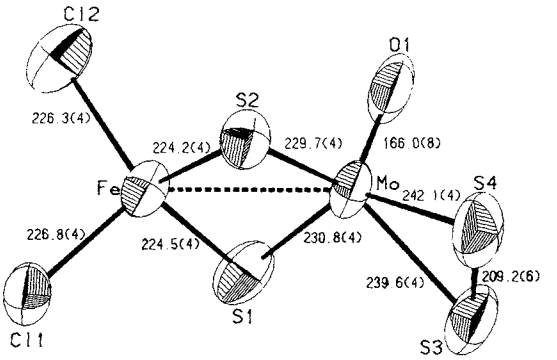
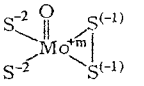



Fig. 1. Structure of the anionic complex **2** in crystals of $(PPh_4)_2[Cl_2FeS_2MoO(S_2)]\cdot DMF$. Atomic distances in pm.

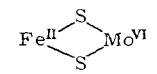
Substitutions of thiomolybdates(VI) have so far proved impossible, because reactions with both nucleophiles (*e.g.* $CN^-$) as well as with electrophiles (*e.g.* sulfur or $H^+$) lead to reduction of the $Mo^{VI}$[2], yielding predominantly multinuclear Mo compounds.

The $^{57}$Fe-Mössbauer spectrum ($IS = 0.40 \pm 0.01$, $QS = 1.75 \pm 0.01$ mm/s at room temperature rel. to α-Fe), which is characteristic for $Fe^{II}$-"high-spin" complexes with tetrahedral coordination and *extraordinarily strong acceptor ligands,* reveals interesting electronic properties of **2**. A comparison of the isomeric shift with that of $[Cl_2Fe(MoS_4)]^{2-}$ ($IS = 0.48$, $QS = 2.10$ mm/s) shows that the ligand **1** effects a more pronounced Fe→L electron delocalization than $MoS_4^{2-}$[2]. In **1** the (unoccupied) MOs with Mo-4d character lie, in part, energetically much lower relative to the non-bonding S-3p level than they do in $MoS_4^{2-}$. Whereas the $M'(S_{br})_2M$ moieties in known thiometalato complexes are almost planar[2], in **2** an FeMo distance typical for $Fe(S_{br})_2Mo$ systems is realized (despite the longer $MoS_{br}$ bonds) by bending of the $FeS_2$- and $S_2Mo$-planes, owing to relatively strong Fe-Mo interaction.

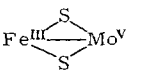
It seems important in the bio-inorganic chemistry of molybdenum that the "fragment" **1**




(with m = 5 in the case of **3**, and between 5 and 6 in the case of **2**) can manifestly exist with different electron populations. In the case of **2** the electronic structure can best be described in terms of the "valence structures" (therefore the designation "ligand" for **1** can be considered only in a formal sense). This would indicate that a re-




and




[*] Prof. Dr. A. Müller, Dr. S. Sarkar, Dr. H. Bögge, R. Jostes
Fakultät für Chemie der Universität
Postfach 8640, D-4800 Bielefeld 1 (Germany)
Prof. Dr. A. Trautwein, U. Lauer
Fachbereich für Angewandte Physik der Universität
D-6600 Saarbrücken (Germany)

 © *Verlag Chemie GmbH, 6940 Weinheim, 1983* *0570-0833/83/0707-0561 $ 02.50/0* 

markable type of bonding ensues in the bimetallic complex **2**. Metal-metal interactions as observed in **2** are of general interest in connection with the electronic structure of heterometal clusters in proteins.

Received: December 28, 1981;
revised: May 18, 1983 [Z 420 IE]
German version: *Angew. Chem. 95* (1983) 574
Publication delayed at authors' request
The complete version of this communication appears in:
*Angew. Chem. Suppl. 1983*, 747-765

CAS Registry numbers:
$(PPh_4)_2[Cl_2FeS_2MoO(S_2)]\cdot DMF$, 86238-48-4

[1] A. Müller, W. E. Newton: *Nitrogen Fixation: The Chemical-Biochemical-Genetic Interface*, Plenum Press, New York 1983.
[2] A. Müller, E. Diemann, R. Jostes, H. Bögge, *Angew. Chem. 93* (1981) 957; *Angew. Chem. Int. Ed. Engl. 20* (1981) 934.

## Selective Reductive Dehalogenation of Tertiary and Benzylic Halides with $Zn(BH_4)_2$ in Diethyl Ether**

By *Sunggak Kim**, *Chang Yong Hong*, and *Sungbong Yang*

The reductive dehalogenation of organic halides is an important reaction which is frequently used in organic synthesis, and considerable progress has been made in the development of various synthetic methods for such conversion[1]. $Zn(BH_4)_2$ is a well-known useful reagent for the reduction of alkali-sensitive compounds[2a], the selective 1,2-reduction of enones[2b], and the stereoselective reduction of β-keto esters[2c]. However, no successful report has appeared about the application of $Zn(BH_4)_2$ for the reduction of organic halides[3]. Here, we describe an efficient method for the selective reduction of tertiary and benzylic halides to afford the corresponding hydrocarbons using zinc borohydride; hereby, primary and secondary alkyl halides, and aryl halides are not attacked[4].

Addition of $Zn(BH_4)_2$ in dimethoxyethane to tertiary alkyl halides such as **1** gives only *ca.* 5% of the alkane in 24 h at room temperature; however, the reaction proceeds smoothly when diethyl ether is used as solvent.

$$RX + Zn(BH_4)_2 \xrightarrow{Et_2O} RH$$

R = tertiary or benzylic alkyl moiety; X = Cl, Br

The tertiary halides **1**, **2**, **4**, and **5** are rapidly reduced in excellent yields. Of special synthetic significance is that no eliminations occur, in contrast to what is often encountered in $S_N1$ reactions. Surprisingly, the tertiary trifluoroacetate **3** is recovered unchanged after 1 h reaction. Secondary benzyl halides such as **6** and **7** are reduced to the corresponding hydrocarbons within 1 h, whereas primary benzyl halides such as **8** and **9** are reduced rather slowly. Allyl and vinyl halides such as **10** and **11** are not reduced to the corresponding alkenes, but polymerize almost instantly[5]. $Zn(BH_4)_2$ in diethyl ether is inert towards primary and secondary alkyl halides such as **12** and **13**, and aryl halides such as **9**. 1,2-Dibromo-1-phenylethane is exclusively reduced to 1-bromo-2-phenylethane; this opens up a general route to β-arylethyl halides.

Table 1. Reduction of organic halides by $Zn(BH_4)_2$ in diethyl ether at room temperature.

| Educt | *t* [h] | Product | Yield [%] [a] |
|---|---|---|---|
| $n$-$C_4H_9CBr(C_2H_5)_2$ **1** | 0.2 | $n$-$C_4H_9CH(C_2H_5)_2$ | 90 (98) |
| $n$-$C_4H_9CCl(C_2H_5)_2$ **2** | 0.2 | $n$-$C_4H_9CH(C_2H_5)_2$ | 89 (97) |
| $n$-$C_4H_9C(OCOCF_3)(C_2H_5)_2$ **3** | 1 | $n$-$C_4H_9CH(C_2H_5)_2$ | 0 [b] |
| 1-Bromoadamantane **4** | 4 | Adamantane | 94 |
| $(C_6H_5)_3CBr$ **5** | 0.2 | $(C_6H_5)_3CH$ | 94 |
| $(C_6H_5)_2CHBr$ **6** | 0.2 | $(C_6H_5)_2CH_2$ | 99 |
| $C_6H_5CHBrCH_3$ **7** | 1 | $C_6H_5CH_2CH_3$ | 91 |
| $C_6H_5CH_2Br$ **8** | 36 | $C_6H_5CH_3$ | (93) |
| $p$-$BrC_6H_4CH_2Br$ **9** | 48 | $p$-$BrC_6H_4CH_3$ | 90 |
| $C_6H_5CH{=}CHCH_2Br$ **10** | 0.2 | $C_6H_5CH{=}CH{-}CH_3$ | 0 [c] |
| $C_6H_5CH{=}CHBr$ **11** | 0.2 | $C_6H_5CH{=}CH_2$ | 0 [c] |
| $CH_3(CH_2)_7CH_2Br$ **12** | 24 | $CH_3(CH_2)_7CH_3$ | 0 [b] |
| $CH_3(CH_2)_8CHBrCH_3$ **13** | 24 | $CH_3(CH_2)_9CH_3$ | 0 [b] |
| $C_6H_5CHBrCH_2Br$ **14** | 24 | $C_6H_5CH_2CH_2Br$ | 81 |

[a] The yields refer to isolated products. The numbers in parentheses indicate the GLC yields. [b] The educts are recovered in essentially quantitative yields. [c] The halides are completely converted into polymeric products.

### *Experimental*

Reduction of 1-bromoadamantane **4**: To a stirred solution of 1-bromoadamantane (430 mg, 2 mmol) in anhydrous $Et_2O$ (6 mL) is added a 0.5 M solution of $Zn(BH_4)_2$ (4 mL) in ether at room temperature. The reaction mixture is stirred at room temperature under a nitrogen atmosphere for 4 h and then hydrolyzed with a saturated aqueous $NH_4Cl$ solution (1 mL). After addition of $Et_2O$ (20 mL) the mixture is washed with $H_2O$ (10 mL) and saturated NaCl solution (20 mL), and dried over $MgSO_4$. Adamantane (255 mg, 94%) is obtained as the only product after removal of solvent.

Received: February 28, 1983 [Z 291 IE]
German version: *Angew. Chem. 95* (1983) 568

[*] Prof. Dr. S. Kim, C. Y. Hong, S. Yang
Department of Chemistry,
Korea Advanced Institute of Science and Technology
Seoul 131 (Korea)
[**] This work was supported by the Korea Science and Engineering Foundation.

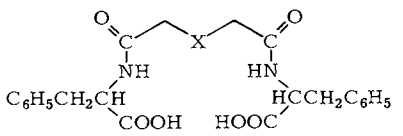
[1] Recent review: A. R. Pinder, *Synthesis 1980*, 425.
[2] a) W. J. Gensler, F. Johnson, A. D. B. Sloan, *J. Am. Chem. Soc. 82* (1960) 6074; b) E. J. Corey, N. H. Anderson, R. M. Carlson, J. Paust, E. Vedejs, I. Vlattas, R. E. K. Winter, *J. Am. Chem. Soc. 90* (1968) 3245; c) J. Canceill, J.-J. Basselier, J. Jocques, *Bull. Soc. Chim. Fr. 1967*, 1024; J. Canceill, J. Jacque, *ibid. 1970*, 2180; T. Nakata, T. Tanaka, T. Oichi, *Tetrahedron Lett. 22* (1981) 4723; T. Nakata, T. Oishi, *ibid. 21* (1980) 1641.
[3] For the solvolysis of tertiary alkyl halides with zinc salts, see: a) S. Anandaraman, K. N. Gurudutt, C. P. Natarajan, B. Ravindranath, *Tetrahedron Lett. 21* (1980) 2189; b) K. N. Gurudutt, B. Rabindranath, S. Srinivas, *Tetrahedron 38* (1982) 1843.
[4] For the selective reduction of tertiary, benzylic, and allylic halides, see: H. Toi, Y. Yamamoto, A. Sonoda, S.-I. Murahashi, *Tetrahedron 37* (1981) 2261, and references cited therein.
[5] Allyl bromide **10** is reduced by $Zn(BH_4)_2$ in dimethoxyethane at a reasonable rate (approximately 60% conversion in 24 h) without polymerizing.

 © *Verlag Chemie GmbH, 6940 Weinheim, 1983* *0570-0833/83/0707-0562 $ 02.50/0* 

## Highly Selective Extraction of Uranyl Ions by Acyclic Ligands Containing L-Phenylalanine Moieties**

By *Maurizio Delcanale, Rosangela Marchelli*, Alessandro Mangia, Arnaldo Dossena,* and *Giuseppe Casnati*

Selective extraction of uranyl ions from aqueous solutions containing other ionic species is an interesting subject theoretically and has great practical significance[1]. We recently reported the synthesis[4] and complexing properties[5] of the ligands **1–4**, in which two L-phenylalanine moieties are linked by oligoethylene oxide bridges. Here we report that these ligands are particularly effective and selective in extracting uranyl ions from aqueous solutions into an organic phase (dichloromethane).



**1**, X = O
**2**, X = O O
**3**, X = O O O
**4**, X = O O O O

The extraction was performed by stirring a solution of ligands **2—4** in $CH_2Cl_2$ ($10^{-2}$—$10^{-3}$ M) for 2 h with an aqueous solution of $UO_2(NO_3)_2$ or $UO_2(OAc)_2$ over a wide concentration range ($10^{-2}$—$10^{-5}$ M) at various pH values and different $L/UO_2^{2+}$ ratios. The degree of extraction is influenced by the concentration of the ligand and increases with the ligand/$UO_2^{2+}$ molar ratio to give complete extraction (98%) with a 70-fold excess of ligand. The anion has little effect on the extraction. Extraction efficiency reaches a maximum when the pH of the aqueous phase is *ca.* 4.

The high selectivity of the ligands **2—4** for $UO_2^{2+}$ was ascertained by competition experiments with other cations. Of all metals present, either in the same concentration ($Cu^{2+}$, $Ni^{2+}$) or in large excess (1000 ppm : 1 ppm; $Na^+$, $K^+$, $Mg^{2+}$, $Ca^{2+}$), only $Cu^{2+}$ was extracted in traces (2.7%); the total percentage of $UO_2^{2+}$ extracted remained unchanged. The complexed $UO_2^{2+}$ ions can be totally liberated from the organic phase by treatment with 0.1 M HCl for a few minutes. The recovery of the ligand is very satisfactory, *ca.* 90% remaining practically unaltered in the organic phase.

$UO_2^{2+}$ forms at least two types of complexes with the ligands **1—4**, whereby the ligands occur as dianion: 1:1 complexes (greatest amount at pH ≈ 3.5) and 2:1 complexes (greatest amount at pH 4.5). The former complexes are more stable than the latter by 2—3 $\log K$ units: $\log K_1$ 5.44 (**1**), 6.10 (**2**), 5.28 (**3**), 5.43 (**4**).

The $^{13}C$-NMR spectra of the free ligands and of the complexes in methanol show that the amide- and carboxy-CO groups are involved in complexation to $UO_2^{2+}$; in the presence of $UO_2^{2+}$ ions the corresponding signals undergo significant downfield shifts (*ca.* 1 ppm), whereas the signals of the C atoms adjacent to the ether O atoms show no or very small changes in shift (*ca.* 0.2 ppm). This, therefore, indicates that the $UO_2^{2+}$ ion is complexed preferentially by compounds having carboxylate groups than by those with crown ether moieties[9].

In conclusion, compounds **1—4** are effective and selective ligands for the extraction of $UO_2^{2+}$; since they also readily release the $UO_2^{2+}$ ions again they could be used, *e.g.,* in the field of decontamination.

Received: March 1, 1983;
revised: April 19, 1983 [Z 298 IE]
German version: *Angew. Chem. 95* (1983) 562
The complete version of this communication appears in:
*Angew. Chem. Suppl. 1983,* 794–802

[*] Prof. Dr. R. Marchelli, Dr. M. Delcanale, Dr. A. Dossena, Prof. Dr. G. Casnati
Istituto di Chimica Organica dell'Università
Via M. D'Azeglio 85, I-43 100 Parma (Italy)
Prof. Dr. A. Mangia
Istituto di Chimica Generale dell'Università
Via M. D'Azeglio 85, I-43 100 Parma (Italy)

[**] This work was supported by the Ministero Pubblica Instruzione (Italy).

[1] I. Tabushi, Y. Kobuke, T. Nishiya, *Nature (London) 280* (1979) 665.
[4] T. Lodi, R. Marchelli, A. Dossena, E. Dradi, G. Casnati, *Tetrahedron 38* (1982) 2055.
[5] R. Marchelli, E. Dradi, A. Dossena, G. Casnati, *Tetrahedron 38* (1982) 2061.
[9] P. G. Eller, R. A. Penneman, *Inorg. Chem. 15* (1976) 2439.

# BOOK REVIEWS

**Multiple Bonds between Metal Atoms.** By *F. A. Cotton* and *F. R. Walton.* John Wiley and Sons Ltd., Chichester 1982, xiv, 466 pp., bound, £ 35.00.

The authors report on a new area of chemistry, in whose opening up and development they were decisively involved, on multiple bonds between transition metal atoms. Cotton explained the very short ReRe distance in the $Rh_2Cl_8^{2-}$ ion in 1964 by assuming a quadruple bond between the metal atoms. This was later confirmed and the idea was extended to dinuclear complexes of other metals; fifteen years later the trickle has become a flood, with almost a 100 publications a year from many research groups. For this reason the time was ripe for assembling the multitude of individual reports, which are now too unwieldy to cover completely, into a monograph.

The first section is devoted to a historical synopsis (and to the clarification of priority). The treatment of individual systems is undertaken in six sections occupying a total of 300 pages: quadruple bonds between Re and Tc atoms, between Mo and W atoms as well as between Cr atoms; triple bonds, double bonds and finally single bonds in dirhodium complexes and complexes isoelectronic with them. A final section, entitled "Physical, spectroscopic and theoretical results", summarizes the present, quantitative picture concerning the stability, the structure and the chemical bonding of this type of MM bonded dinuclear

complexes. The monograph presents a comprehensive survey of the preparation and structural characterization, and the chemical reactions and catalytic activity of a fascinating class of substances, in the light of modern understanding of chemical bonding. In the process, what is already understood is treated and that which is, until now, unclarified is adequately mentioned. Thus, the MM bond does not exhibit a simple correlation between bond order and length, like that familiar to every chemist for the main group elements.

It is usual to outline the possible *readership*. The theme and presentation make this book of interest to every chemist, whether he is only taking a general interest in what is possible over and above the CC triple bond or if he is seeking details of a new class of compound. The reviewer sees a limitation of the possible *purchasers* of the book only in its price, which is high; but that applies, nowadays, to every specialist book.

It is also usual to offer criticism in a review. In this instance little is required; at most the fact that the discussion of supershort CrCr bonds (*ca.* 185 pm) is carried out in several sections of the book and that a chapter is devoted to chromium without even mentioning the short bond in $Cr_2$ of 168 pm, which is interpreted as a six-fold linkage (*J. Phys. Chem. 86* (1982) 3914).

*Arndt Simon* [NB 586 IE]

**Ullmanns Encyklopädie der technischen Chemie.** Edited by *E. Bartholomé, E. Biekert, H. Hellmann, H. Ley* (deceased), *W. M. Weigert* (deceased), and *E. Weise*. Verlag Chemie, Weinheim 1982. 4th edit., vol. 21: Schwefel bis Sprengstoffe [Sulfur to Explosives]. xiv, 697 pp., bound, DM 525.00.

With entries on sulfur, silicon, and their compounds this volume of the 4th edition of Ullmann[*] covers important areas of industrial inorganic chemistry, although these entries also extend into organic chemistry, as in the case of silicones and sulfur dyes. Other inorganic subjects are discussed in the entries on selenium and its compounds (8 pages), rare earths (37 pages), silver and its compounds and alloys (54 pages), and sintered iron and steel (29 pages). The book also offers entries on silk (7 pages), soap (18 pages), sorbic acid (5 pages), sera and vaccines (38 pages), and spasmolytics (13 pages). Four entries from the field of applications deal with cutting and welding (22 pages), solar technology (37 pages), mirrors (4 pages), and explosives (61 pages). This last list illustrates the large and diverse field in which chemistry has found applications. Although each application also contains elements of several other branches of science, it is interesting to see how much chemistry is needed in various fields, whether classical, such as the production of mirrors, or topical, such as solar technology.

As for the production and presentation, this volume too has the well-known Ullmann quality, which has by now become a byword.

*Ulfert Onken* [NB 574 IE]

[*] Cf. *Angew. Chem. 94* (1982) 563; *Angew. Chem. Int. Ed. Engl. 21* (1982) 553.

**Recent Books**

**The following books have been received by the editor. All the publications listed are available through W & P Buchversand für Wissenschaft und Praxis, Boschstrasse 12, D-6940 Weinheim (Federal Republic of Germany). Tel. (06201) 606-0, Telex 465516 vchwh d, Telefax (06201) 602328.**

**Protein Folding.** By *C. Ghélis* and *J. Yon*. Academic Press, New York 1982. xiii, 562 pp., bound, $ 74.50.—ISBN 0-12-281520-3

**Advances in Quantum Chemistry.** Edited by *P.-O. Löwdin*. Academic Press, New York 1982. **Vol. 15:** x, 277 pp., bound, $ 54.00.—ISBN 0-12-034815-2. **Vol. 16:** x, 285 pp., bound, $ 56.00.—ISBN 0-12-034816-0

**Enrichment Techniques for Inorganic Trace Analysis. Chemical Laboratory Practice.** By *A. Mizuike*. Springer-Verlag, Berlin 1983. viii, 144 pp., bound, DM 72.00.—ISBN 3-540-12051-3

**Advances in Polymer Science.** Edited by *H.-J. Cantow, G. Dall'Asta, K. Dušek, J. D. Ferry, H. Fujita, M. Gordon, J. P. Kennedy, W. Kern, S. Okamura, C. G. Overberger, T. Saegusa, G. V. Schulz, W. P. Slichter,* and *J. K. Stille*. Springer-Verlag, Berlin 1983. **Vol. 48: Light Scattering from Polymers.** v, 167 pp., bound, DM 98.00.—ISBN 3-540-12030-0; **Vol. 49: Living Polymers and Mechanisms of Anionic Polymerization.** v, 187 pp., bound, DM 112.00.—ISBN 3-540-12047-5; **Vol. 50: Unusual Properties of New Polymers.** v, 149 pp., bound, DM 92.00.—ISBN 3-540-12048-3

*Registered names, trademarks, etc. used in this journal, even without specific indication thereof, are not to be considered unprotected by law.*

© Verlag Chemie GmbH, D-6940 Weinheim, 1983. - Printed in the Federal Republic of Germany by Zechnersche Buchdruckerei, Speyer/Rhein.

All rights reserved (including those of translation into foreign languages). No part of this issue may be be reproduced in any form - by photoprint, microfilm, or any other means - nor transmitted or translated into a machine language without written permission from the publishers. Only single copies of contributions, or parts thereof, may be reproduced for personal use. Copies reproduced and used other than for private purposes in an industrial or commercial undertaking are subject to copyright and, in such cases, a copyright fee must be paid to the VG WORT, Abteilung Wissenschaft, Goethestr. 49, 8000 München 2, from whom conditions of payment can be obtained on request.

**Valid for users in the USA:** The appearance of the code at the bottom of the first page of an article in this journal (serial) indicates the copyright owner's consent that copies of the article may be made for personal or internal use, or for the personal or internal use of specific clients. This consent is given on the condition, however, that the copier pay the stated per-copy fee through the Copyright Clearance Center, Inc., for copying beyond that permitted by Sections 107 or 108 of the U.S. Copyright Law. This consent does not extend to other kinds of copying, such as copying for general distribution, for advertising or promotional purposes, for creating new collective works, or for resale. For copying from back volumes of this journal see 'Permissions to Photo-Copy: Publisher's Fee List' of the CCC.

**Editorial office:** Pappelallee 3, D-6940 Weinheim, Federal Republic of Germany, Telephone (06201) 602315, Telex 465516 vchwh d, Telefax (06201) 602328.

**Editors:** *P. Gölitz, I. G. Neil, O. Smrekar, A. Stimson.*

**Publishers:** Verlag Chemie GmbH. (Managing Directors: *Prof. Dr. Helmut Grünewald* and *Hans Dirk Köhler*), Pappelallee 3, D-6940 Weinheim, Federal Republic of Germany.

Correspondence concerning advertisements should be addressed to Verlag Chemie GmbH. (Advertising Manager *R. J. Roth*), Boschstr. 12. P.O. Box 1260/1280, D-6940 Weinheim, Federal Republic of Germany. Telephone Weinheim (06201) 602-0, Telex 465516 vchwh d, Telefax (06201) 602328.

ANGEWANDTE CHEMIE
International Edition in English
Volume 22 · Number 8
August 1983
Pages 565–636

# From Macromolecules to Biological Assemblies (Nobel Lecture)**

By Aaron Klug

## 1. Introduction

Within a living cell there take place a large number and variety of biochemical processes, almost all of which involve, or are controlled by, large molecules, the main examples of which are proteins and nucleic acids. These macromolecules do not of course function in isolation but often interact to form ordered aggregates or macromolecular complexes, sometimes so distinctive in form and function as to deserve the name of organelles. The properties of the individual macromolecules in a cell are often expressed in such biological assemblies. It is on some of these assemblies on which I have worked for over 25 years and which now form the subject of this lecture.

The aim of our field of structural molecular biology is to describe the biological machinery, in molecular, *i.e.* chemical, detail. The beginnings of this field were marked just over 20 years ago in 1962 when *Max Perutz* and *John Kendrew* received the Nobel prize for Chemistry for the first solution of the structure of proteins. In the same year *Francis Crick, James Watson,* and *Maurice Wilkins* were likewise honoured, having received the Nobel prize for Medicine for elucidating the structure of the double helix of DNA. In his Nobel lecture *Perutz* recalled how 40 years earlier, in 1922, *Sir Lawrence Bragg,* whose pupil he had been, came here to thank the Academy for the Nobel prize awarded to himself and his father, *Sir William Bragg,* for having founded the new science of X-ray crystallography, by which the atomic structure of simple compounds and small molecules could be unravelled. These men have not only been my predecessors, but some of them have been something like scientific elder brothers to me, and I feel very proud that it should now be my turn to have this supreme honour bestowed upon me. For the main subjects of my work have been both nucleic acids and proteins, the interactions between them, and the development of methods necessary to study the large macromolecular complexes arising from these interactions.

In seeking to understand how proteins and nucleic acids interact, one has to begin with a particular problem, and I can claim no credit for the choice of my first subject, tobacco mosaic virus. It was the late *Rosalind Franklin* who introduced me to the study of viruses and whom I was lucky to meet when I joined *J. D. Bernal*'s department in London in 1954. She had just switched from studying DNA to tobacco mosaic virus (TMV), X-ray studies of which had been begun by *Bernal* in 1936. It was *Rosalind Franklin* who set me the example of tackling large and difficult problems. Had her life not been cut tragically short, she might well have stood in this place on an earlier occasion.

## 2. Tobacco Mosaic Virus

Tobacco mosaic virus (TMV) is a simple virus consisting only of a single type of protein molecule and of RNA, the carrier of the genetic information. Its simple rod shape results from its design, namely a regular helical array of these protein molecules, or subunits, in which is embedded a single molecule of RNA. This general picture (Fig. 1) was already complete by 1958 when *Rosalind Franklin* died. It is clear that the protein ultimately determines the architecture of the virus, an arrangement of $16\frac{1}{3}$ subunits per turn

[*] Prof. Dr. A. Klug
Laboratory of Molecular Biology, Medical Research Council Centre
University Medical School
Hills Road, Cambridge CB2 2QH (England)

[**] Copyright © The Nobel Foundation 1983.—We thank the Nobel-Foundation, Stockholm, for permission to publish this lecture.

of a rather flat helix with adjacent turns in contact. The RNA is intercalated between these turns with three nucleotide residues per protein subunit and is situated at a radial distance of 40 Å from the central axis and is therefore isolated from the outside world by the coat protein. The geometry of the protein arrangement forces the RNA backbone into a moderately extended single-strand configuration. Running up the central axis of the virus particle is a cylindrical hole of diameter 40 Å, which we then thought to be a trivial consequence of the protein packing, but which later turned out to figure prominently in the story of the assembly.

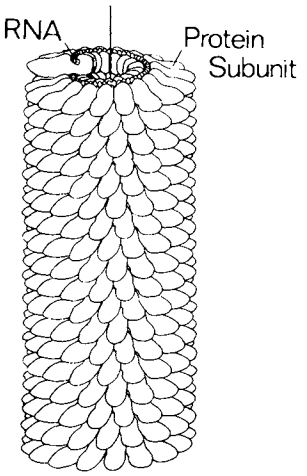



Fig. 1. Diagram summarizing the results of the first stage of the structure analysis of tobacco mosaic virus [71]. There are three nucleotides per protein subunit and 16⅓ subunits per turn of the helix. Only about one-sixth of the length of a complete particle is shown.

At first sight, the growth of a helical structure like that of TMV presents no problem of comprehension. Each protein subunit makes identical contacts with its neighbours so that the bonding between them repeats over and over again. Subunits can have a precise built in geometry so that they can assemble themselves like steps in a spiral staircase in a unique way. Subunits would simply add one or a few at a time onto the step at the end of a growing helix, entrapping the RNA that would protrude there and generating a new step, and so on. It was in retrospect thus not too surprising when the classic experiments of *Fraenkel-Conrat* and *Williams* in 1955[6] demonstrated that TMV could be reassembled from its isolated protein and nucleic acid components. They showed that, upon simple remixing, infectious virus particles were formed that were structurally indistinguishable from the original virus. Thus, all the information necessary to assemble the particle must be contained in its components, that is, the virus "self assembles". Later experiments[7] showed that the reassembly was fairly specific for the viral RNA, occurring most readily with the RNA homologous to the coat protein.

All this was very satisfactory but there were yet some features which gave cause for doubt. First, other experiments[8] showed that foreign RNAs could be incorporated into virus-like rods and these cast doubt on the belief that specificity *in vivo* was actually achieved during the assembly itself. Another feature about the reassembly that suggested that there were still missing elements in the story was its slow rate. Times of 8 to 24 hours were required to give maximum yields of assembled particles. This seemed to us rather slow for the assembly of a virus *in vivo*, since the nucleic acid is fully protected only on completion. These doubts, however, lay in the future and before we come to their resolution, I return to the structural analysis of the virus and the virus protein.

### 2.1. X-Ray Analysis of TMV: The Protein Disk

After *Franklin*'s death, *Holmes* and I continued the X-ray analysis of the virus. Specimens for X-ray work can be prepared in the form of gels in which the particles are oriented parallel to each other, but randomly rotated about their own axes. These gels give good X-ray diffraction patterns but because of their nature the three-dimensional X-ray information is scrambled into two dimensions. Unscrambling these data to reconstruct the three-dimensional structure has proved to be a major undertaking, and it was only in 1965 that *Holmes* and I obtained the first three-dimensional Fourier maps to a resolution of about 12 Å. In fact, only recently has the analysis by *Holmes* and his colleagues in Heidelberg (where he moved in 1968) reached a resolution approaching 4 Å in the best regions of the electron density map, but falling off significantly in other parts[9]. At this resolution it is not possible to identify individual amino-acid residues with any certainty and ambiguities are too great to build unique atomic models. However, the map, taken together with the detailed map of the subunit we obtained in Cambridge (see below) yields a considerable amount of information about the nature of the contacts with RNA[10].

These difficulties in the X-ray analysis of the virus were foreseen, and by the early 1960's I came to realise that the way around this difficulty was to try to crystallize the isolated protein subunit of the virus, solve its structure by X-ray diffraction and then try to relate this to the virus structure solved to low resolution. We therefore began to try to crystallize the protein monomer. In order to frustrate the natural tendency of the protein to aggregate into a helix, *Leberman* introduced various chemical modifications in the hope of blocking the normal contact sites, but none of these modified proteins crystallized. The second approach was to try to crystallize small aggregates of the unmodified protein subunits. It had been known for some time, particularly from the work of *Schramm* and *Zillig*[11], that the protein on its own, free of RNA, can aggregate into a number of distinct forms, besides that of the helix. I chose conditions under which the protein appeared to be mainly aggregated in a form with a sedimentation constant of about 4S, identified by *Caspar* as a trimer[12]. We obtained crystals almost immediately but we found[13] them to contain not the small aggregate hoped for, but a large one, corresponding to an aggregate with a sedimentation constant of 20S. The X-ray analysis showed that this was built from two juxtaposed layers, or rings, of 17 subunits each and we named this form the two-layer disk (Figs. 2 and 4). Our initial dismay in being faced with such a large structure, of molecular weight 600000, was tempered by the fact that

the geometry of the disk was clearly related to that of the virus particle. The cylindrical rings contained 17 subunits each compared with $16\frac{1}{3}$ units per turn of the virus helix, so that the lateral bonding within the disks was therefore likely to be closely related to that in the virus. We also showed, by analysing electron micrographs, that the disk was polar, *i. e.* that its two rings faced in the same direction as do successive turns of the virus helix.

### 2.2. Protein Polymorphism

These results on the structure of the disk which showed that it was fairly closely related to the virus helix made me wonder whether the disk aggregate might not be fulfilling some vital biological role. It had been easy to dismiss it as perhaps an adventitious aggregate of a sticky protein or a storage form. The polymorphism of TMV protein was first

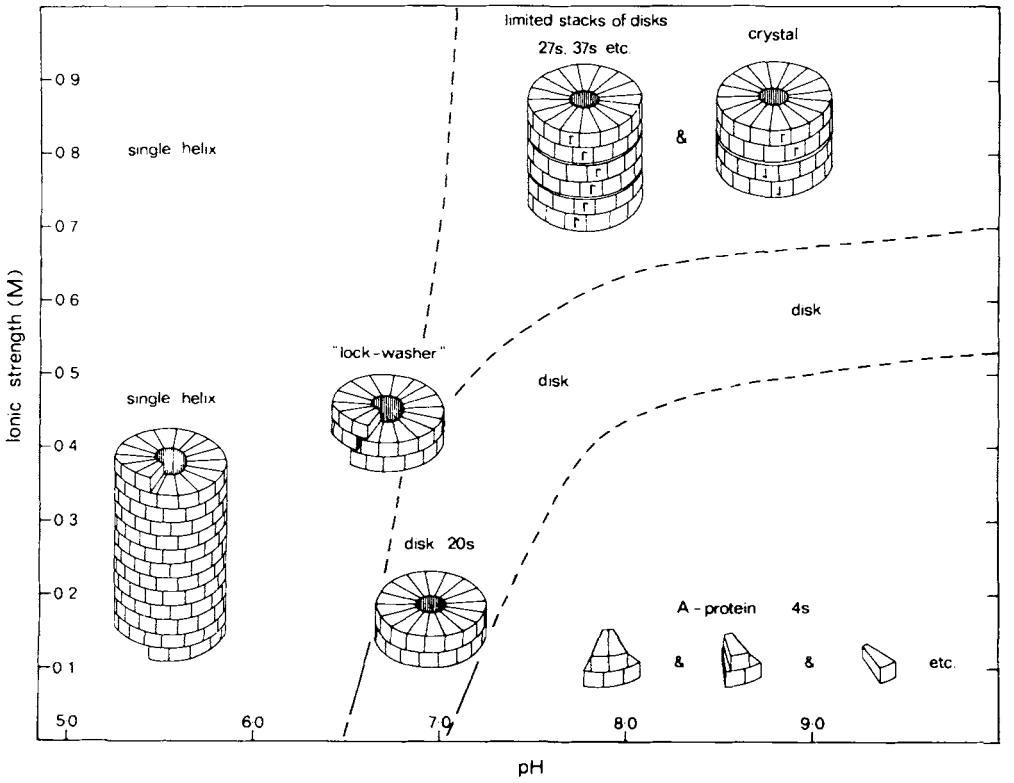



Fig. 2. Diagram showing the ranges over which particular forms of TMV protein participate significantly in the equilibrium in dependence of pH and ionic strength [17]. This is not a conventional phase diagram: a boundary is drawn where a larger species becomes detectable and does not imply that the smaller species disappears sharply. The "lock-washer" indicated on the boundary between the 20S disk and the helix is not well defined and represents a metastable transitory state observed when disks are converted into helices by abrupt lowering of the pH.

This was the first very large structure ever to be tackled in detail by X-ray analysis and it took about a dozen years to carry through the analysis to high resolution. The formidable technical problems were overcome only after the development in our laboratory of more powerful X-ray tubes and of special apparatus (cameras, computer-linked densitometers) for data collection from a structure of this magnitude. (In fact we had begun building better X-ray tubes in London to use on weakly diffracting objects like viruses.) The 17-fold rotational symmetry of the disk also gives rise to redundant information in the X-ray data, which was exploited in the final analysis[14], to improve and extend the resolution of a map based originally on only one heavy atom derivative. The map at 2.8 Å resolution[15] has been interpreted in terms of a detailed atomic model for the protein (Figs. 3 and 4), although the individual interactions upon RNA binding have yet to be deduced.

considered in some detail by *Caspar* in 1963[12] who foresaw that some of the aggregation states might give insight into the way the protein functions. Quantitative studies of aggregation started by *Lauffer* in the 1950's[16] concentrated upon a rather narrow range of conditions, the main interest being in understanding the forces driving the aggregation (these are largely entropic). Because of the scattered nature of the earlier observations, *Durham, Finch* and I began a systematic survey of the aggregation states as a result of which the broad outline became clear[17,18]. The results can be summarised as a phase diagram (Fig. 2).

At low or acid pH, the protein alone will form helices of indefinite lengths that are structurally very similar to the virus except for the lack of the RNA. Above neutrality the protein tends to exist as a mixture of smaller aggregates from about trimer upwards, in rapid equilibrium with each other, commonly referred to as A-protein. Near pH 7 and at about room temperature the dominant form present is

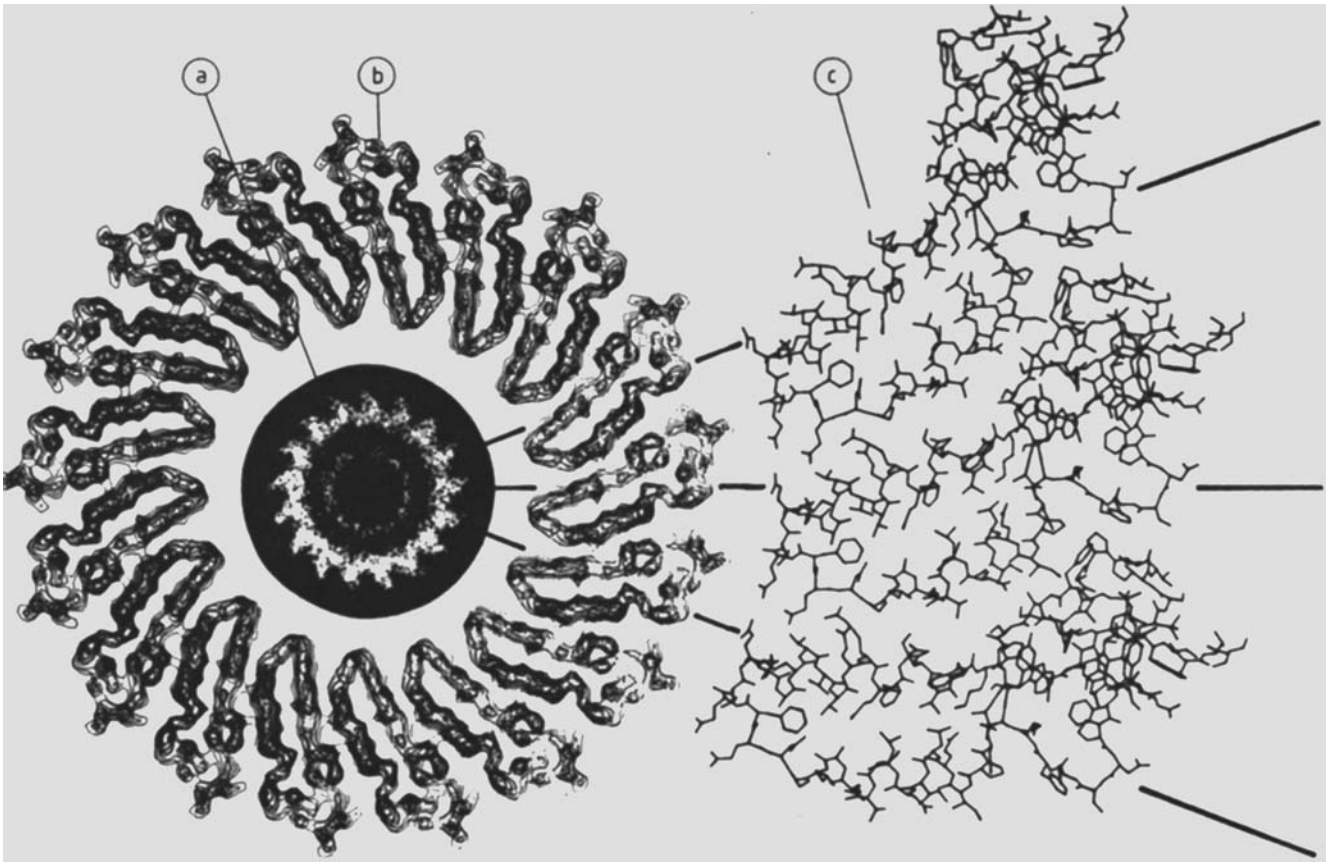



Fig. 3. The disk viewed from above at successive stages of resolution. From the centre outward there follow: ⓐ a rotationally filtered electron microscope image at about 25 Å resolution [72]; ⓑ a slice through the 5 Å electron density map of the disk obtained by X-ray analysis, showing rod-like α-helices [26]; ⓒ part of the atomic model built from the 2.8 Å map [15].

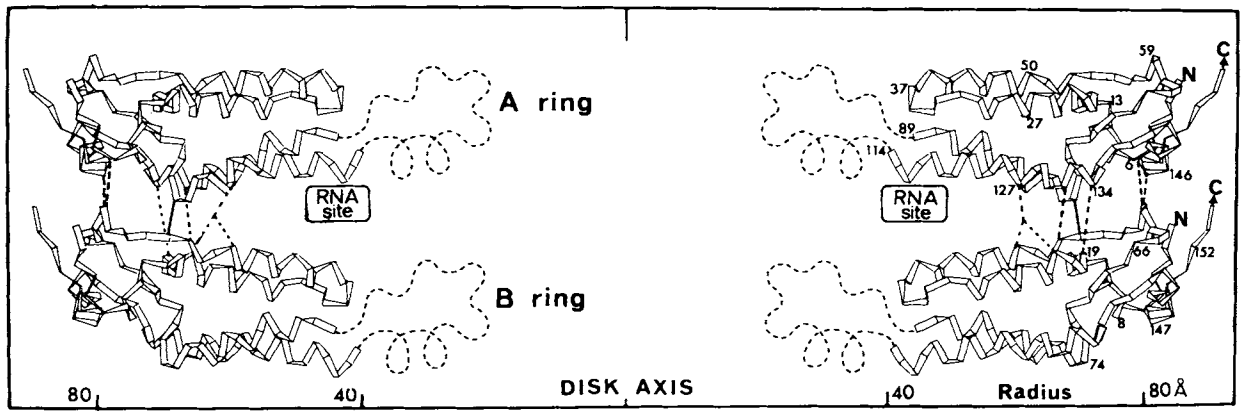



Fig. 4. Section through a disk along its axis reconstructed from the results of X-ray analysis to a resolution of 2.8 Å [15]. The ribbons show the path of the polypeptide chain of the protein subunits. Subunits of the two rings can be seen touching over a small area toward the outside of the disk but opening up into the "jaws" toward the centre. The dashed lines at low radius indicate schematically the mobile portion of the protein in the disk, extending in from near the RNA binding site to the edge of the central hole.

the disk which is in a relatively slow equilibrium with the A-form in the ratio of about 4 : 1. The dominant factor controlling the state of aggregation of the coat protein is thus the pH. The control is mediated through groups, probably carboxylic acid residues, as identified by *Caspar*[12], that bind protons abnormally in the helical state, but not in the A-form. Thus, the helical structure can be stabilised either in the virus by the interaction of the RNA with the protein, or, in the case of the free protein, by protonating the acid groups. These groups thus act as a "negative switch", ensuring that under physiological conditions the helix is not formed, and thus that enough protein in the form of disks or A-protein is available to interact with the RNA during virus assembly.

### 2.3. A Role for the Disk

The disk aggregate of the protein therefore has a number of significant properties. It is not only closely related to the virus helix, but also is the dominant form of the protein under "physiological" conditions; moreover, disk forms had also been observed for other helical viruses. These strengthened my conviction that the disk form was not adventitious but might play a significant role in the assembly of the virus. What could this role be?

Assembly of any large aggregate of identical units such as a crystal can be considered from the physical point of view in two stages: first nucleation and then the subsequent growth, or, in more biochemical language, as initiation and subsequent elongation. The process of nucleation—or, crudely, getting started—is frequently more difficult than the growth. Thus, a simple mode of initiation in which the free RNA interacts with individual protein subunits does pose problems in getting started. At least 17 separate subunits would have to bind to the flexible RNA molecule before the assembling linear structure could close round on itself to form the first turn of the virus helix. This difficulty could be avoided if a preformed disk were to serve as a jig upon which the first few turns of the viral helix could assemble to reach sufficient size to be stable. This mode of nucleation of helix assembly could also furnish a mechanism for the recognition by the protein of its homologous RNA. The surface of the disk presents a set of 51 ($=17\times3$) nucleotide binding sites which could interact with a special long run of bases, resulting in an amplified discrimination that might not be possible with a few nucleotides. It thus seemed that the disk could solve both the physical and biological requirements for initiating virus growth and conferring specificity on the interaction. This hypothesis is illustrated in Figure 5. It turned out that all the details in this diagram are wrong, but yet the spirit is correct. As *A. N. Whitehead* once observed, it is more important that an idea should be fruitful than it should be true.

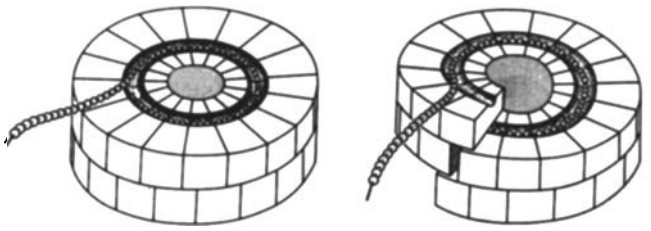


Fig. 5. The role of the disk as originally conceived: the specific recognition of a special (terminal) sequence of TMV-RNA initiates conversion of the disk form of the protein (left) into two turns of a helix (right). (See Fig. 7, for the mechanism finally established.)

This proposed mechanism of nucleation required that the disk be able to dislocate into a two-turn helix to form the beginning of the growing nucleoprotein rod. To test this, we carried out a very simple experiment, the pH drop experiment[19]. This showed that an abrupt lowering of the pH would convert disks directly, within seconds, into short helices—or lock-washers (Fig. 2), which stack on each other to give longer nicked helices, which in due course anneal to give more perfect helices. This conversion is an *in situ* one, not requiring dissociation and then reassociation into a different form. The success of this experiment encouraged us to proceed to experiments with RNA itself, the natural "substrate" of the virus protein.

The first reconstitution experiments carried out by *Butler* and myself proved to be dramatic[20]. When a mixture was made at pH 7 of the viral RNA and a disk preparation, complete virus particles were formed within 10 to 15 minutes, rather than over a period of hours, as was the case in the early reassembly experiments in which protein had been used in the disaggregated form[6].

The notion that disks are involved in the natural biological process of initiation was strengthened by companion experiments[20] in which assembly was carried out with RNAs from different sources. These showed a preference, by several orders of magnitude, of disks for the viral RNA over foreign RNAs or synthetic polynucleotides of simple sequence. It is thus the disk state of the protein that is needed to achieve specificity in the interaction with the RNA. In the experiments cited earlier, in which virus-like rods were made containing TMV A-protein and foreign RNA[8], reactions were carried out at an acid pH, and under these artificial conditions the protein alone would tend to form helical rods and so could entrap any RNA present.

Besides this effect of disks on the rate of initiation, which had been predicted, we also found to our surprise that the disks appeared to enhance the rate of elongation, and we concluded that they must be therefore actively involved in growth. This result has been questioned by some other workers in the field and is still the subject of argument[21,22], but recent discoveries on the configuration of RNA during incorporation into a growing particle (see Section 2.5) have made the involvement of disks in the elongation, as well as in nucleation, much more intelligible.

The disk form of the protein therefore provided the elements which were missing from the simple reconstitution experiments using disaggregated protein, namely speed and specificity. We now knew what the disk did, the next question was how did it do it?

### 2.4. The Interaction of the Protein Disk with the Initiation Sequence on the RNA

Specificity in initiation ensures that only the viral RNA is picked out for coating by the viral protein. This must be brought about by the presence of a unique sequence on the viral RNA for interaction with the protein disk. *Zimmern* and *Butler* isolated the nucleation region containing this site by supplying limited quantities of disk protein, sufficient to allow nucleation to proceed, but not subsequent growth, then digesting away the uncoated RNA with nuclease[23,24]. With the varying protein : RNA ratios and different digestion conditions, they found they could isolate a series of RNA fragments, all of which contained a unique common core sequence with variable extents of elongation at either end. These fragments could be rebound to the coat protein when it was in the form of disks. Among this population of fragments was a fragment only about 60 nucleotides long—just over the length necessary to bind

round a single disk—and it appeared to represent the minimum protected core. Because of the strong rebinding of this fragment back to the disk, it seemed likely that it constituted the "origin of assembly", where the normal nucleation reaction began.

However, the work on the RNA produced, in turn, another puzzle: the obvious expectation that the nucleation region would be near one end of the RNA turned out to be wrong. The nucleation occurs about one sixth of the way along the RNA from the 3′ end[25], so that over 5000 nucleotides have to be coated in the major direction of elongation (3′—5′) and 1000 have to be coated in the opposite direction. Yet growing nucleoprotein rods observed in the electron microscope[20] were always found to have all the uncoated RNA only at one end: why were rods never seen with a tail at each end? The resolution of this conundrum came from considering the structure of the protein disk, to which I now turn.

Although the structure of the disk was solved in detail only in 1977, an earlier stage in the X-ray analysis gave the clue as to how it might interact with the RNA. At 5 Å resolution[26] the course of the polypeptide chain could be traced and the basic design of the disk established (cf. Fig. 4). The subunits of the upper ring of the disk lie in a plane perpendicular to the disk axis while those of the lower ring are tilted downward towards the centre, so that the two rings touch only towards the outside of the disk. In the neighbourhood of the central hole they are thus far apart, like an open pair of jaws which could, as it were, "bite" a stretch of RNA entering through the central hole. Moreover, entry through the centre would be facilitated because the inner region of the protein, from around the RNA binding site inward, was found to be disordered and not packed into a regular structure.

It therefore looked very much as though the disk was designed to permit the RNA to enter through the central hole, effectively enlarged by the flexibility of the inner loop of protein, and intercalate between its two layers. The RNA which would enter thus would of course be the nucleation sequence which lies rather far from an end of the RNA molecule. This could, however, be achieved if the RNA doubled back on itself at a point near the origin of assembly and so entered as a hairpin loop. Indeed, the smallest RNA fragment that is protected during nucleation has a base sequence which can fold into a weakly paired double-helical stem with a loop at the top, that is a hairpin (Fig. 6). This was proposed by *Zimmern*[24]. The loop and top of the stem have an unusual sequence, containing a repeating motif of three nucleotides, with guanine (G) in one specific position, and usually adenine (A) or sometimes uracil (U) in the other two. Since there are three nucleotide binding sites per protein subunit, such a triplet repeat pattern will place a specific base in a particular site on the protein molecule and could well lead to the recognition of the exposed RNA loop by the disk during the nucleation process.

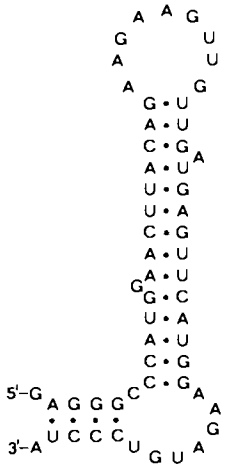


Fig. 6. Postulated secondary structure of the RNA in the nucleation region [24]. This gives a weakly bonded double-helical stem and a loop at the top which is probably the actual origin of assembly. The sequence at and near the top contains a repeating motif of three bases having G in the middle position and A, or U in the outer positions.

### 2.5. Nucleation and Growth

The hypothesis for nucleation[27] is then that the special RNA hairpin would insert through the central hole of the disk into the jaws formed by the two layers of protein subunits (Fig. 7). The dimensions are quite suitable for this to occur and the open loop could then bind to the RNA binding sites on the protein. More of the rather unstable double helical stem would melt out and be opened as more of the RNA was bound within the jaws of the nucleating disk. Some, as yet unknown, feature of this interaction would cause the disk to dislocate into a short helical segment, entrapping the RNA and, after the rapid addition of a few more disks[23], would provide the first stable nucleoprotein particle.

The subsequent events after nucleation can be called growth and as stated above there is a controversy about the particular way in which this proceeds. Our view is that elongation in the major direction of growth very likely takes place through the addition of further disks, as indeed our first reconstitution experiments drove us to conclude. The special configuration generated during the insertion of the loop into the middle of the disk must be perpetuated as the rod grows, by pulling further RNA up through the central hole. Thus, elongation could occur by a substantially similar mechanism to nucleation, only now, rather than requiring the specific nucleation loop of the RNA, it occurs by means of a "travelling loop" which can be inserted into the centre of the next incoming disk. This mechanism therefore overcomes the main difficulty in envisaging how a whole disk of protein subunits could interact with the RNA in the growing helix. There is now more evidence for growth by incorporation of blocks of subunits of roughly disk size[22], but the subject is still controversial and I will therefore not proceed further with it.

On the other hand, there is now clear experimental confirmation of our hypothesis for the mechanism of nucleation. This predicts (i) that two tails of the RNA will be left at one end of the growing nucleoprotein rod formed, and (ii) that one of these tails would project directly from one end but the other would be doubled back all the way from the active growing point at the far end of the rod down the central hole of the growing rod. Both of these predictions

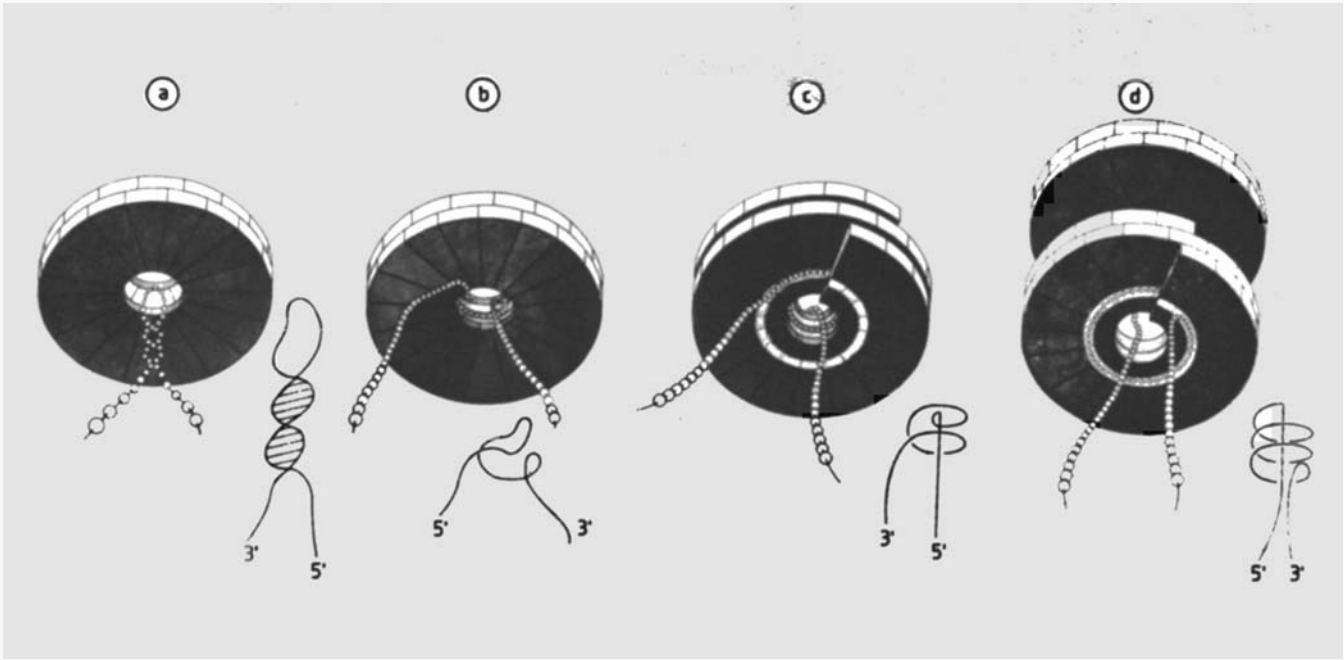



Fig. 7. Nucleation of virus assembly occurs by the insertion of a hairpin of RNA (see Fig. 6) into the central hole of the protein disk and between the two layers of subunits ⓐ. The loop at the top of the hairpin binds to form part of the first turn, opening up the base-paired stem as it does so ⓑ, and causes the disk to dislocate into a short helix ⓒ. This presumably "closes the jaws", entraining the RNA between the turns of protein subunits, and gives a start to the nucleoprotein helix (which can then elongate rapidly to some minimum stable size) ⓓ.

have now been confirmed. *Hirth*'s group in Strasbourg has obtained electron micrographs of growing rods in which the RNA is spread by partial denaturation, and many particles show two tails protruding from the same end[28]. In Cambridge my colleagues have used high resolution electron microscopy, in which the two ends of the rods can be identified by their shapes to show that it is indeed the longer tail that is doubled back through the growing rod[29]. Other experiments show that the RNA configuration has a substantial effect on the rate of assembly[29].

### 2.6. Design and Construction: Physical and Biological Requirements

We have seen that the protein disk is the key to the mechanism of the assembly of TMV. The protein subunit is designed not to form an endless helix, but a closed two-layer variant of it, the disk, which is stable and which can be readily converted into the lock-washer or helix-going form. The disk therefore represents an intermediate sub-assembly by means of which the entropically difficult problem of nucleating helical growth is overcome. At the same time the nucleation by the disk sub-assembly furnishes a mechanism for recognition of the homologous viral RNA (and rejection of foreign RNAs) by providing a long stretch of nucleotide binding sites for interaction with the special sequence of bases on the RNA. The disk is thus an obligatory intermediate in the assembly of the virus, which simultaneously fulfills the physical requirement for nucleating the growth of the helical particle and the biological requirement for specific recognition of the viral RNA. TMV is self-assembling, self-nucleating and self-checking.

There are a number of morals to be derived from the story of TMV assembly[1]. The first is that one must distinguish between the design of a structure and the construction process used to achieve it. That is, while TMV looks like a helical crystal and its design lends itself to a process of simple addition of subunits, its construction actually follows a more complex path that is highly controlled. It illustrates the point that function is inextricably linked with structure and how much can be done by one single protein. A most intricate structural mechanism has been evolved to give the assembly an efficiency and purposefulness whose basis we now understand. The general moral of all this is that not merely does nature once again confound our obvious preconceptions, but it has left enough clues for us to be able to puzzle out finally what is happening. As *Einstein* once put it, "Raffiniert ist der Herrgott, aber bösartig ist er nicht: The Lord is subtle, but he is not malicious".

## 3. Crystallographic or Fourier Electron Microscopy

In 1955, *Finch* and I in London, and *Caspar*, then in Cambridge, took up the X-ray analysis of crystals of spherical viruses. These had first been investigated by *Bernal* and his colleagues just before and after the war, using "powder" and "still" photography. *Finch* and I worked on Turnip Yellow Mosaic Virus (TYMV) and its associated empty shell, and *Caspar* on Tomato Bushy Stunt virus (TBSV). *Crick* and *Watson* had predicted that spherical viruses ought to have one of the forms of cubic symmetry, and we showed that both viruses had icosahedral symmetry. Later, when *Finch* and I showed that polio virus also had the same symmetry, we realised that there was some

underlying principle at work, and this eventually led *Caspar* and I to formulate our theory of virus shell structure[30].

When my research group moved to Cambridge in 1962, we turned to electron microscopy for the speed with which it enables one to tackle new subjects, and also because it produces a direct image, or so we thought. Armed with a theory of virus design and some X-ray data, we had some notion of how spherical shells of viruses might be constructed and thought we would be able to see the fine detail in electron micrographs. Thus, we knew what we were looking *for*, but we soon found that we did not understand what we were looking *at*: the micrographs did not present simple direct images of the specimens. We soon discovered the limitations of electron microscopy. First, there were preparation artefacts and also radiation damage during observation. Secondly, artificial means of contrast enhancement had to be used as the majority of atoms in biological specimens have an atomic number too low to give sufficient contrast on their own. Thirdly, the image formed depends on the operating conditions of the microscope and on the focussing conditions and aberrations present. Above all, because of the large depth of focus of the conventional microscope, all features along the direction of view are superimposed in the image. Finally, in the case of strongly scattering or thick specimens, there is multiple scattering within the specimen, which can destroy even this relation between object and image.

For these reasons, the detail one sees in a raw image is often unreliable and not easily interpretable without methods which correct for the operating conditions of the microscope and which can separate contributions to the image from different levels of the specimen. It is also important to be able to assess the degree of specimen preservation in each particular case. These procedures for image processing of electron micrographs were developed by myself and my colleagues over a period of about 10 years. Their aim is to extract from the information recorded in electron micrographs the maximum amount of reliable information about the two- or three-dimensional structures which are being examined. Some applications of these methods to various problems studied in the Medical Research Council Laboratory, Cambridge, over the first 15 years are given in Table 1. Electron microscopy combined with image reconstruction, supplemented wherever possible by X-ray studies on wet, intact material, has provided what are now generally accepted models of the structural organisation of a large number of biological systems such as those listed in Table 1. Here, I will describe only a limited number of examples which serve to demonstrate the power of various techniques and the nature of the results they can give. Fuller accounts of the methods and the theory are given elsewhere[2,3], but I would like to emphasize that these methods arose out of practical concerns and grew in the course of tackling concrete problems; nevertheless they have proved to be of wide application.

Table 1. Some applications of electron microscope image reconstruction in the MRC Laboratory of Molecular Biology, Cambridge, 1964–1979.

| Viruses | Organelles | Enzymes |
|---|---|---|
| Helical<br>TMV, TMV protein disk, Paramyxoviruses | Microtubules from flagellar doublets and brain; tubulin sheets | Haemocyanin<br>Glutamic dehydrogenase |
| Icosahedral<br>Polyoma, wart, TBSV, TYMV, R17, Nudaurelia, CPMV | Muscle filaments: actin; actin + tropomyosin; actin + myosin + tropomyosin (inhibited and relaxed) | Catalase; crystals and tubes<br>Sickle cell haemoglobin fibres |
| Adenovirus hexon<br>Aberrant hexagonal and pentagonal tubes of polyoma | Bacterial flagella;<br>Bacterial cell walls | Purple membrane (Bacteriorhodopsin) |
| Phage T2 and T4<br>Head and its tubular variants (polyheads)<br>Tail: sheath + core<br>Baseplate | Ribosome crystals<br>Chromatin: crystals of nucleosome cores; tubes of histone octamers<br>Gap junctions | Cytochrome oxidase |

### 3.1. Two-Dimensional Reconstruction: Digital Computer Image Processing

We began our studies on viruses, both spherical and helical, using the method of negative staining which had recently been introduced by *Huxley*, and by *Brenner* and *Horne*[31]. In this method the specimen is embedded in a thin amorphous layer of a heavy metal salt which simultaneously preserves and maps out the shape of the regions from which it is excluded. Much fine detail was to be seen, but one could not easily make sense of it in most cases. People simply thought that the specimens were being disordered, because it was assumed that the negative stain gave, as it were, a footprint of the particle. We gradually came to realise that the confusion arose, not so much because of the disorder that the stain produced, but because there was a superposition of detail from the front and back of the particle; *i.e.*, the stain was enveloping the whole particle, so forming a cast rather than a footprint. This interpretation was proved in two different ways which proceeded in parallel. First, in the case of the spherical viruses, one could build a model and compute or otherwise display it in projection and we found that this could account for many if not all of the previous uninterpretable images[32]. The uniqueness of the model could be proved by tilting experiments in which the specimens on the grid and the model were tilted in the same manner through large angles (cf. Fig. 10 and ref. [73]). The second approach was applied to helical structures, which are translationally periodic and therefore lend themselves to a direct image analysis, which I shall now illustrate.

Figure 8a shows an electron micrograph of a negatively stained specimen of a "polyhead", which is a variant of the head of T4 bacteriophage, consisting mainly of the major head protein. The particle has been flattened and so its original tubular form lost. The image clearly shows some structural periodicities, but these are difficult to discern and such interpretations used to be left to subjective judgement. I realised that the optical (Fraunhofer) diffraction pattern produced from such an image would allow an objective analysis of all the periodicities present to be made[33]. This is shown in Figure 8b. Here clear diffraction maxima can be seen: these fall into two sets which can be accounted for as arising respectively from the near and far

sides of the specimen. In this way it was established that the negative stain was producing a complete cast of the particle rather than a one-sided footprint of it[33]. Since this is a helically periodic structure, the diffraction maxima tend to lie on a lattice and so they pick out genuine repeating features within the structure. In this case the regular diffraction maxima extended to a spacing of about 20 Å which demonstrated that the long range order in the specimen was preserved to this resolution, which is indeed sufficient to resolve individual protein molecules.

The essence of image processing of this type is that it is a two-step procedure after the first image has been obtained. First the Fourier transform of the raw image is produced. Fourier coefficients are then manipulated or otherwise corrected and then transformed back again to reproduce the reconstructed image. These operations can be carried out most easily on a digital computer, and digital image-processing as first introduced by *DeRosier* and myself[36] allows a much greater flexibility than our original optical method and makes three-dimensional procedures possible.

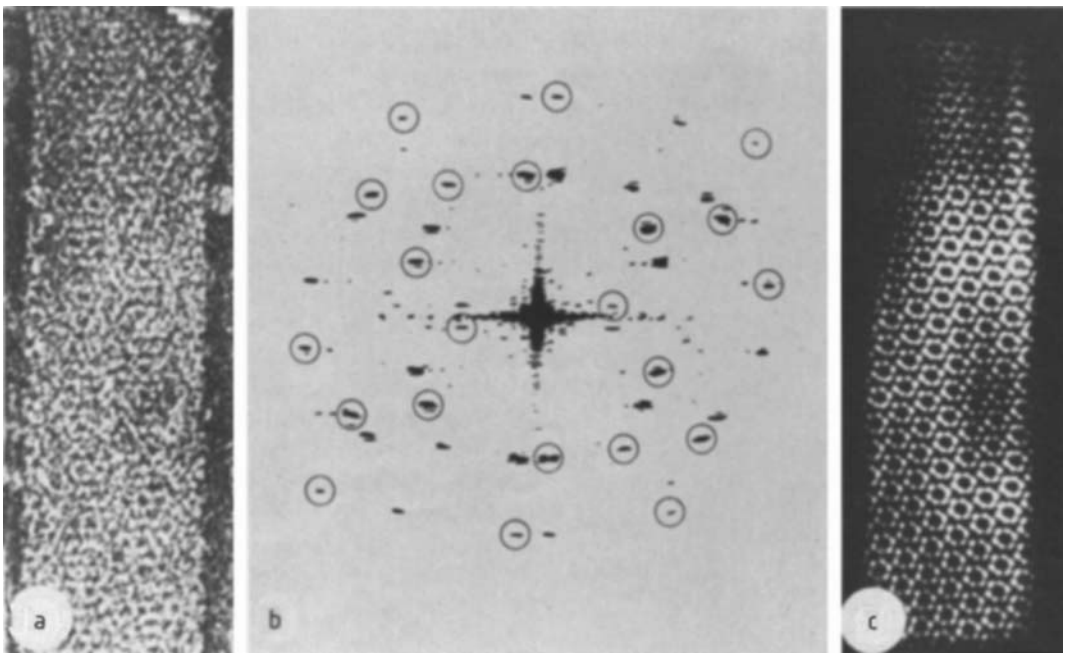



Fig. 8. Optical diffraction and image filtering of the tubular structures known as "polyheads", consisting of the major head protein of T4 bacteriophage [35]. ⓐ Electron micrograph of negatively stained flattened particle; magnification × 200000. ⓑ Optical diffraction pattern of ⓐ, with circles drawn around one set of diffraction peaks corresponding to one layer of the structure. ⓒ Filtered image of one layer in ⓐ using the diffraction mask shown in ⓑ. The apertures in the mask are chosen so that the averaging here extends locally only over a few unit cells. Individual molecules arranged in hexamers can be seen.

The confusion in the image is largely due to the superposition of the near and far sides of the particle, and any one such side can be filtered out in an optical system by a suitably positioned mask which transmits only the desired diffracted rays[34]. The filtered image, Figure 8c, is immediately interpretable in terms of a particular arrangement of protein molecules[35].

The clarity of the processed image derives also from the fact that the background noise in the diffraction pattern has been filtered out. This noise arises because of the individual variations between molecules in the specimen, *i.e.* the disorder, and these contribute randomly in all parts of the diffraction pattern. Indeed, what has been done is that the signal-to-noise ratio in the image has been enhanced by averaging over the copies of the molecules present in the arrangement. This idea of averaging over many copies of a repeated motif is central to the most powerful techniques developed so far for producing reliable images of biological specimens, and the three-dimensional procedures which I will describe later can also use this technique.

### 3.2. Three-Dimensional Image Reconstruction

The first example I have given (Fig. 8) is of a relatively simple case where the problem is essentially that of separating contributions from two overlapping crystalline layers and we have seen how the method of Fourier analysis resolves the superposition in real space into separated sets of contributions in Fourier space. It was, however, already clear from the simple analysis of spherical viruses that in order to get a unique or reliable picture of a three-dimensional structure one must be able to view the specimen from very many different directions[32]. These different views were often provided by specimens lying in different orientations but they can also be realised by tilting the specimen in the electron microscope (see Section 3.1). Originally, as described, the different views were interpreted by the building of models, but eventually I saw that a set of transmission images taken in different views could be combined objectively to give a reconstruction of a three-dimensional object.

This happened when *DeRosier* and I were studying the

tail of bacteriophage T4 and our analysis showed that there were contributions to the image from the internal structure as well as from the front and back surfaces[36]. To work in three dimensions a generalised form of the two-dimensional filtering process had to be found, and—by making a connection with X-ray analysis—I realised that what was required was a three-dimensional Fourier synthesis. In the analysis of the X-ray diffraction patterns of TMV, I had used the idea that a helical structure could be built up mathematically out of a set of cylindrical harmonic functions; there is a relation between the number of functions that could be obtained and the number of different views available. Each new view would give additional harmonics of higher spatial frequency, and so, if one had enough views, one could build up the complete structure. Later, we recognized[36] that this synthesis was only a special case of a general theorem known to crystallographers as the projection theorem.

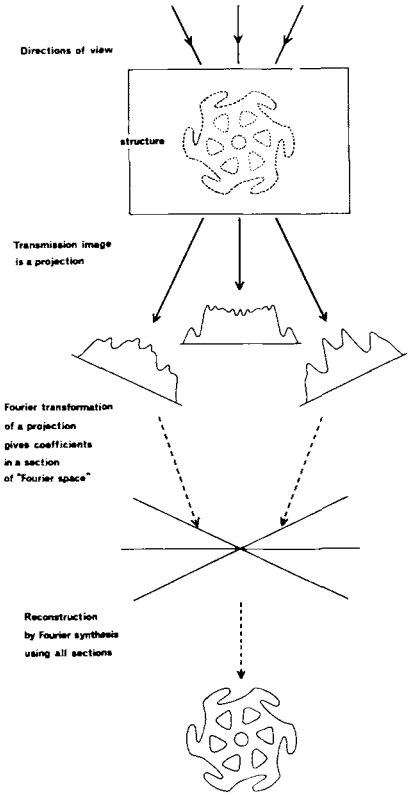



Fig. 9. General scheme for the process of 3-D reconstruction of an object from a set of 2-D projections [36].

The general method of reconstruction which we developed (Fig. 9) is based on the projection theorem, which states that the two-dimensional Fourier transform of a plane projection of a three-dimensional density distribution is identical to the corresponding central section of the three-dimensional transform normal to the direction of view. The three-dimensional transform can therefore be built up section by section using transforms of different views of the object, and the three-dimensional reconstruction then produced by Fourier inverstion. The important feature of the method is that it tells one how many different views are needed for a required resolution and how these are to be recombined into a three-dimensional map of the object[36,37]. The process is both quantitative and free from arbitrary assumptions. The approach is similar to conventional X-ray crystallography, except that the phases of the X-ray diffraction pattern cannot be measured directly, whereas here they can be computed from a digitised image. Were it not for radiation damage, the different views could be collected from a single particle by using a tilting stage in the microscope, but more realistically one must use several particles in different but identifiable orientations. In general, it is desirable to combine data from different particles so that imperfections can be averaged out.

The Fourier method is only one of several ways for solving the sets of mathematical equations which relate the unknown three-dimensional density distribution with known projections in different directions[37], but in fact no other reliable method has been shown to be superior and it is used in computer tomography. Moreover, the Fourier method has the advantage that because it is carried out in steps, *i.e.* formation of the two-dimensional transforms, and then recombination in three dimensions, it is possible as described above, to assess, select, and correct the data going into the final reconstruction.

Many applications have been made. The first application was in fact to the phage tail of T4, the problem in which it had arisen. Particles with helical symmetry are the most straightforward to reconstruct, because a reconstruction can be made from a single view of the whole particle, to a limited resolution, set by the helix symmetry. In physical terms, this is because a single image of a helical particle presents many different views of the repeating subunit, and it was this simplification that led us to use the phage tail as a first specimen for 3-D image reconsruction. Generally, more than one view is necessary, but any symmetry present will reduce the number required. Typically, for small icosahedral viruses, three or four views are sufficient, but many more specimens must be investigated before the appropriate number can be found and averaging carried out[38]. Figure 10 shows two electron micrographs and the three-dimensional reconstruction of human wart virus (HWV), which was investigated by *Crowther* and *Amos*[39].

### 3.3. Phase Contrast Microscopy

Electron microscopy, combined with some method of image analysis, when applied to negatively stained specimens, has proved ideal for determining the arrangement and shape of small protein subunits within natural or artificial arrays, including two-dimensional crystals and macromolecular assemblies such as viruses and microtubules[2]. The structural information obtainable has proved to be highly reliable with respect to detail down to about the 20 Å or 15 Å level. It became clear, however, that the degree of detail revealed was limited by the granularity of the negative stain and the fidelity with which it follows the surface of the specimen[40]. To obtain much higher resolution information, better than about 10 Å, one should dispense with the stain and view the protein itself. At high resolution, there is a second problem: irradiation damage. This

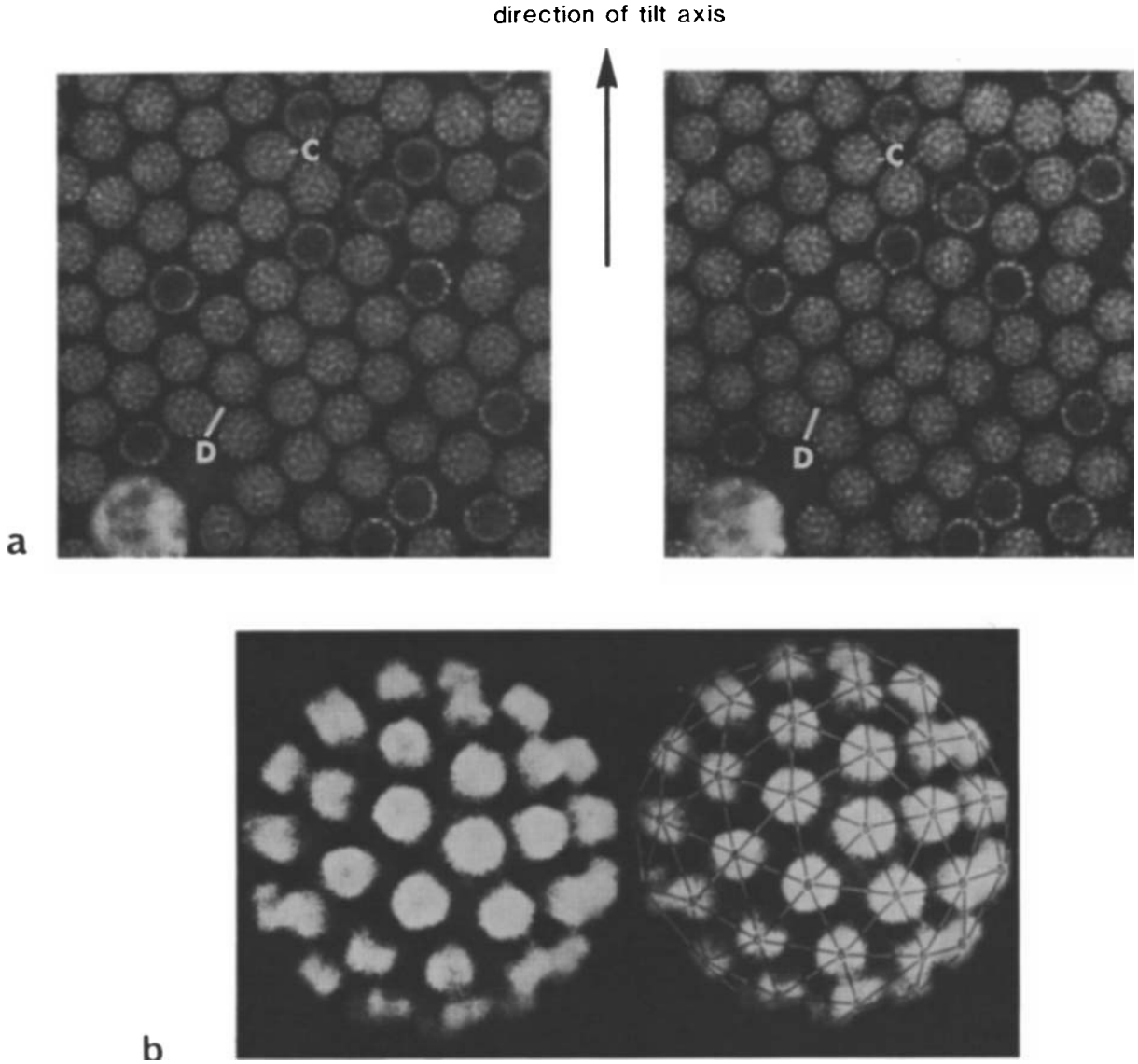



Fig. 10. ⓐ Electron micrographs of the same field of negatively-stained close-packed particles of human wart virus (HWV), (left) before, and (right) after tilting the specimen grid through an angle close to 18° [73]. × 140000. ⓑ A three-dimensional reconstructed image of human wart virus [39]. Alongside is shown the underlying icosahedral surface lattice [30] with the fivefold and sixfold symmetry axes marked.

can be reduced by cutting down the illuminating beam, but the statistical noise is then increased, and the raw image becomes less and less reliable. However, this difficulty can be overcome satisfactorily by imaging ordered arrays of molecules, so that the information from the different molecules can be averaged, as described above, to give a statistically significant picture. The first problem of replacing the negative stain, yet avoiding dehydration, can be solved in two ways. One, now being intensively studied, is to use frozen hydrated specimens[41]. The second, tried method is that of *Unwin* and *Henderson*, who, in their radical approach to determining the structure of unstained biological specimens by electron microscopy[42,43], used a dried-down solution of glucose to preserve the material.

The question then arose as to how this unstained specimen, effectively transparent to electrons, is to be visualised. In the light microscopy of transparent specimens the well-known Zernike phase contrast method is used. Here the phases of the scattered beams relative to the unscattered beam are shifted by means of a phase plate and then the scattered and unscattered beams are allowed to interfere in the image plane to produce an image. A successful electrostatic phase contrast device for electron microscopy, quite analogous to the phase plate used in light microscopy, was constructed by *Unwin*[44], but it is not easy to make or use. A practical way of producing phase contrast in the electron microscope is simply to record the image, with the objective lens underfocussed, and this was the method used by *Unwin* and *Henderson*.

The defocussing phase contrast method arose out of an academic study by *Erickson* and myself of image formation in the electron microscope[45]. This was undertaken because of a controversy that had developed concerning the nature of the raw image itself. When three-dimensional image reconstruction was introduced and applied to biological particles embedded in negative stain, objections were raised by various workers in the field of materials science, accustomed to dynamical effects in strongly scat-

tering materials, to the premise that the image essentially represented the simple projection of the distribution of stain. It was asked whether multiple or dynamical scattering might not vitiate this assumption. To investigate this question, *Erickson* and I undertook an experimental study of negatively stained thin crystals of catalase as a function of the depth of focussing[45]. We found that a linear or first order theory of image formation would explain almost entirely the changes in the Fourier transform of the image. We concluded that the direct image, using a suitable value of underfocus dependent on the frequency range of interest, is a valid picture of the projection of the object density. When greater values of underfocus were used to enhance the contrast, the image could be corrected to give a valid picture.

This study, although confined to the medium resolution range, included a practical demonstration that *a-posteriori* digital image processing could be used to measure and compensate for the effects of defocussing, and we suggested that this approach could be directly extended to high resolution to compensate for the effects of spherical aberration as well as defocussing. It also provided a convenient way of producing phase contrast in the electron microscope in the case of unstained specimens. The image is recorded with the objective lens underfocussed, so changing the phases of the scattered beams relative to the unscattered (or zero order) beam. Defocussing does not however act as a perfect phase plate analogous to that of *Zernike,* since the phases are not all changed by the same amount, and successive bands of spatial frequencies contribute to the image with alternately positive and negative contrast. In order to produce a "true" image, the electron image must be processed to correct for the phase contrast transfer of the microscope so that all spatial frequencies contribute with the same sign of contrast.

To produce their spectacular three-dimensional reconstructed image of the purple membrane of *Halobacterium* to a resolution of about 7 Å[44], *Henderson* and *Unwin* took a series of very low-dose images of different pieces of membrane tilted at different angles. The final map represented an average over some 100000 molecules. The small amount of contrast present in the individual micrographs was produced by underfocussing which was then compensated for in the computer reconstruction by the method described above. For the first time the internal structure of a protein molecule was "seen" by electron microscopy.

## 4. The Structure of Chromatin

The work on viruses has given results not only of intrinsic interest, but as indicated above, the difficulties in tackling large molecular aggregates led to the development of methods and techniques which could be applied to other systems. A recent example of this approach, and one which I think would not have gone so fast without our earlier experience, is that of the investigation of chromatin. Chromatin is the name given to the chromosomal material when extracted. It consists mainly of DNA, tightly associated with an equal weight of a small set of rather basic proteins called histones. We took up the study of chromatin in Cambridge about ten years ago when the protein chemists had shown that there were only five main types of histones, the apparent proliferation of species being due to post-synthetic modifications, so that the structural problem appeared tractable.

The DNA of the eukaryotic chromosome is probably a single molecule, amounting to several centimeters in length if laid out straight, and it must be highly folded to make the compact structure one can see in a chromosome. At the same time it is organised into separate genetic or functional units, and the manner in which this folding is achieved, genes organised and their expression controlled, is the subject of intense study throughout the world. The aim of our research group has been to try to understand the structural organisation of chromatin at various levels and to see what connections could be made with functional controls.

The high concentrations in which histones occur in the cell nucleus suggested that their role was structural, and it was shown over the years 1972—1975 that the four histones H2A, H2B, H3 and H4 are responsible for the first level of structural organisation in chromatin. They fold successive segments of the DNA about 200 base pairs long into compact bodies of about 100 Å in diameter, called nucleosomes. A string of nucleosomes or repeating units is thus created and when these are closely packed they form a filament about 100 Å in diameter. The role of the fifth histone H1 was at first not clear. It is much more variable in sequence than the other four, being species and tissue specific. In the years 1975—1976 we showed that H1 is concerned with the folding of the nucleosome filament into the next higher level of organisation, and later how it performed this role.

This is not the place to relate in detail how this picture of the basic organisation of chromatin emerged[4], but the idea of a nucleosome arose from the convergence of several different lines of work. The first indications for a regular structure came from X-ray diffraction studies on chromatin which showed that there must be some sort of repeating unit, albeit not well ordered, on the scale of about 100 Å[46,47]. The first biochemical evidence for regularity came from the work of *Hewish* and *Burgoyne*[48], who showed that an endogenous nuclease in rat liver could cut the DNA into multiples of a unit size, which was later shown by *Noll,* using a different enzyme, *Micrococcus* nuclease, to be about 200 base pairs[49]. The fact that the nuclease cuts the DNA of chromatin at regularly spaced sites, quite unlike its action on free DNA, is attributed to the fact that the DNA is folded in such a way as to make only short stretches of free DNA between these folded units available to the enzyme. The third piece of evidence which led to the idea of a nucleosome was the observation by *Kornberg* and *Thomas*[50] that the two highly conserved histones, H3 and H4, existed in solution as a specific oligomer, the tetramer $(H3)_2(H4)_2$, which behaved rather like an ordinary multi-subunit globular protein. On the basis of these different lines of evidence, *Kornberg* in 1974[51] proposed a definite model for the basic unit of chromatin as a bead of about 100 Å diameter, containing a stretch of DNA 200 base pairs long condensed around the protein core made out of eight histone molecules, namely the

$(H3)_2(H4)_2$ tetramer and two each of H2A and H2B. The fifth histone, H1, was somehow associated with the outside of each nucleosome. A quite unexpected feature of the model was that it was the DNA which "coated" the histones rather than the reverse.

However, in 1972, when *Kornberg* came to Cambridge, all this lay in the future. We began using X-ray diffraction to follow the reconstitution of histones and DNA, because the X-ray pattern given by nuclei, or by chromatin isolated from them, limited as it was, was the only assay then available to follow the ordered packaging of the DNA. These X-ray studies showed that almost 90% reconstitution could be achieved when the DNA was simply mixed with an unfractionated total histone preparation, but all attempts to reconstitute chromatin by mixing DNA with a set of all four purified single species of histone failed, as if the process whereby the histones were being separated were denaturing them. We therefore looked for milder methods of histone extraction and found that the native structure could be reformed readily if the four histones were kept together in two pairs, H3 and H4 together, and H2A and H2B together, but not once they had been taken apart. It was this work which led *Kornberg* to investigate further the physicochemical properties of the histones and to the discovery[50] of the histone tetramer $(H3)_2(H4)_2$, which in turn led him to the model of the nucleosome described above.

### 4.1. The Structure of the Nucleosome

Approaches such as nuclease digestion and X-ray scattering on unoriented specimens of chromatin or nucleosomes in solution could reveal certain features of the nucleosome, but a full description of the structure can only come from crystallographic analysis, which gives complete three-dimensional structural information. In the summer of 1975 my colleagues and I therefore set about trying to prepare nucleosomes in forms suitable for crystallization. Nucleosomes purified from the products of *Micrococcus* nuclease digestion contain an average of about 200 nucleotide pairs of DNA, but there is a rather wide distribution about the average, and such preparations are not homogeneous enough to crystallize. However, this variability in size can be eliminated by further digestion with *Micrococcus* nuclease. While the action of *Micrococcus* nuclease on chromatin is first to cleave between nucleosomes, it subsequently acts as an exonuclease on the excised nucleosome, shortening the DNA first to about 166 base pairs, where there is a brief pause in the digestion[52], and then to about 146 base pairs, where there is a clear plateau in the course of digestion, before more degradation occurs. During this last stage the histone H1 is released[52], leaving as a major metastable intermediate a particle containing 146 base pairs of DNA complexed with a set of eight histone molecules. This enzymatically reduced form of the nucleosome is called the core particle and its DNA content was found to be constant over many different species. The DNA removed by the prolonged digestion, which had previously joined one nucleosome to the next, is called the linker DNA.

A core particle therefore contains a well-defined length of DNA and is homogeneous in its protein composition. We naturally tried to crystallize preparations of core particles, but we were not at first successful, probably because of small traces of the fifth histone H1. Eventually my colleague *Leonard Lutter* found a way to produce exceptionally homogeneous preparations of nucleosome core particles, and these formed good single crystals[53]. The conditions for growing the crystals were based on our previous experience in crystallizing transfer-RNA, because we reasoned that a good part of the nucleosome core surface would consist of DNA. These experiments perhaps surprised biologists in showing dramatically that almost all the DNA in the nucleus is organised in a highly regular manner.

The derivation of a three-dimensional structure from a crystal of a large molecular complex is, as for the TMV disk, a process that can take many years. We have therefore concentrated on obtaining a picture of the nucleosome core particle at low resolution by a combination of X-ray diffraction and electron microscopy, supplemented where possible by biochemical and physicochemical studies. We first solved the packing in the crystals by analysing electron micrographs of thin crystals and then obtained projections of the electron density along the three principal axes of the crystals, using X-ray diffraction amplitudes and electron microscope phases[53, 54]. The nucleosome core particle turned out to be a flat disk-shaped object, about 110 Å by 110 Å by 57 Å, somewhat wedge-shaped, and strongly divided into two layers. We proposed a model in which the DNA was wound into about $1\frac{3}{4}$ turns of a shallow superhelix of pitch about 27 Å around the histone octamer. There are thus about 80 nucleotides in each turn of the superhelix. This model for the organisation of DNA in a nucleosome core also provided an explanation for the results of certain enzyme digestion studies on chromatin[53, 55], thus showing that what we had crystallized was essentially the native structure.

The first crystals we obtained were found to have the histone proteins within them partly proteolysed, but their physicochemical properties remained very similar to those of the intact particle. We have since grown crystals from intact nucleosome cores which diffract to a resolution of about 5 Å and a detailed analysis is in progress[56]. Over the years *Daniela Rhodes, Ray Brown,* and *Barbara Rushton* have grown crystals of core particles prepared from seven different organisms: all give essentially identical X-ray patterns testifying to the universality of nucleosomes. There is a dyad axis of symmetry within the particle, which is not surprising since the eight histones occur in pairs and DNA is studded with local dyad axes. High angle diffuse X-ray scattering from the crystals shows that the DNA of the core particle is in the B-form.

An electron density map of one of the principal projections of the crystal is shown in Figure 11a. This map gives the total density in the nucleosome, the density of the DNA not being distinguished from that of the protein. The contributions of protein and DNA can be distinguished by using neutron scattering combined with the method of contrast variation and such a study was therefore begun by *John Finch* and a group at the Laue-Langevin Institute, Grenoble, when sufficiently large crystals were available[57]. The obtained maps of the DNA and protein along

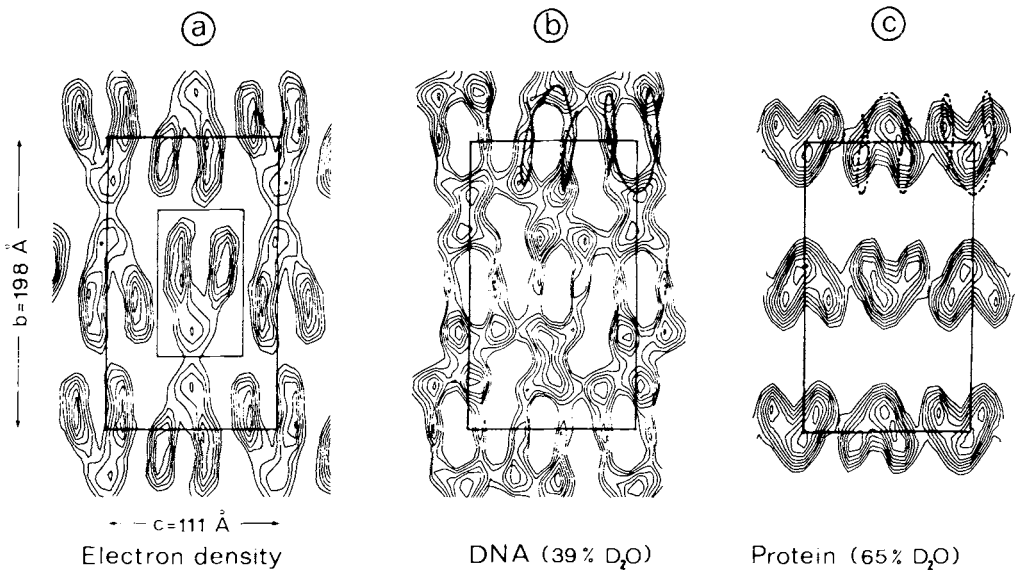



Fig. 11. Fourier projection maps of the nucleosome core particle. ⓐ Map calculated from X-ray data [56]; ⓑ and ⓒ calculated from neutron scattering data using contrast variation [57]. ⓑ The DNA component with the path of the superhelix drawn superimposed on the density. ⓒ The protein core component.

the three principal axes (see Figs. 11b and 11c). The map of the DNA is consistent with the projection of about $1\frac{3}{4}$ superhelical turns as proposed earlier, and the map of the protein shows that the histone octamer itself has a wedge shape.

### 4.2. Three-Dimensional Image Reconstruction of the Histone Octamer and the Spatial Arrangement of the Inner Histones

An alternative to separating the contributions of the DNA and the protein by neutron diffraction is to study the histone octamer directly. The histone octamer which forms the protein core of the nucleosome can exist in that form free in solution at high salt concentration, which displaces the DNA[58]. In the course of attempts to crystallize it, we obtained ordered aggregates—hollow tubular structures—which were investigated by electron microscopy[59]. The image reconstruction method described in Section 3.2 was used to produce a low resolution three-dimensional map and model of the octamer (Fig. 12a). As a check that the removal of DNA had not led to a change in the structure of the histone octamer, projections of this model were calculated and compared with the projections of the protein core of the nucleosome obtained from the neutron scattering study mentioned above. There was a good agreement between the three maps showing that the gross structure was not altered.

At the resolution of the analysis (20 Å) it was shown that the histone octamer possesses a two-fold axis of symmetry, just as the nucleosome core particle itself. Like the nucleosome core, the histone octamer is a wedge-shaped particle of bipartite character. Its periphery shows a system of ridges which form a more or less continuous helical ramp of external diameter 70 Å and pitch about 27 Å, exactly suitable for it to act as a spool on which could be wound about $1\frac{3}{4}$ turns of superhelix of DNA in the appropriate dimensions (Fig. 12b).

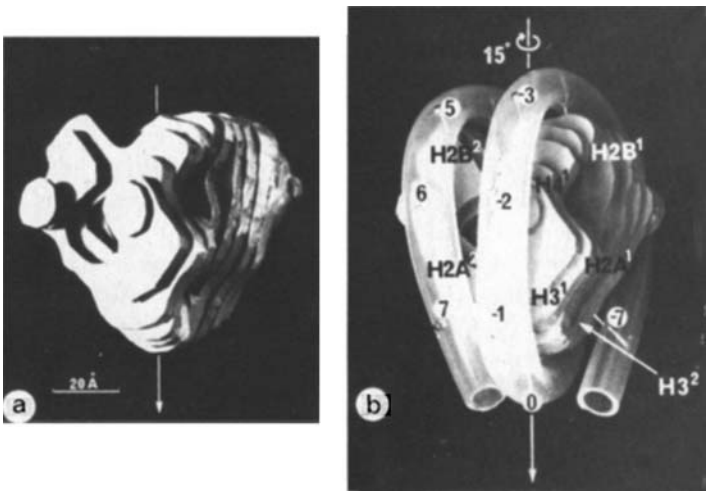



Fig. 12. ⓐ Model of the histone octamer obtained by three-dimensional image reconstruction from electron micrographs [59]. The dyad axis is marked. The ridges on the periphery of the model form a left-handed helical ramp on which $1\frac{3}{4}$ to 2 turns of a superhelix of DNA could be wound. ⓑ The histone octamer structure ⓐ with two turns of a DNA superhelix wound around it. (Note that for clarity, the diameter of the plastic tube has been chosen smaller than the true scale for DNA.) Distances along the DNA are indicated by the numbers $-7$ to $+7$, taking the dyad axis as origin, to mark the 14 repeats of the double helix contained in the 146 base pairs of the nucleosome core. The assignment of the individual histones to various locations on the model is described in the text.

The resolution of the octamer map is too low to define individual histone molecules, but we have exploited the relation of the octamer to the superhelix of DNA to interpret them in terms of individual histones[59]. This interpretation uses the results of *Mirzabekov* and his colleagues[60] on the chemical cross-linking of histones to nucleosomal DNA, and also information on histone/histone proximities given by protein cross-linking. This data cannot be interpreted

reliably without a three-dimensional model because a knowledge of the points of contact of histones along a strand of the DNA is not sufficient to fix a spatial arrangement of the histones in the nucleosome core. Furthermore, because the two superhelical turns of DNA are close together the pattern of histone/DNA cross-links need not directly reflect the linear order of histones along the DNA. The three-dimensional density map restricts the number of possibilities and enables choices to be made.

In the spatial arrangement proposed, the helical ramp of density in the octamer map is composed of a particular sequence of the eight histones, in the order H2A-H2B-H4-H3-H3-H4-H2B-H2A, with a dyad in the middle. The $(H3)_2(H4)_2$ tetramer has the shape of a dislocated disk or single turn of a helicoid, which defines the central turn of a DNA superhelix. The structure of the histone tetramer explains the findings of many workers, expanding on the original observations of *Felsenfeld*[61], that H3 and H4 alone, in the absence of H2A and H2B, can confer nucleosome-like properties on DNA, in particular supercoiling and resistance to *Micrococcus* nuclease digestion, whereas H2A and H2B alone cannot. It also explains the asymmetric dissociation of the histone octamer when the salt concentration is lowered: the octamer dissociates, through a hexameric intermediate, into a $(H3)_2(H4)_2$ tetramer and two H2A·H2B dimers[58,62].

### 4.3. The Role of Histone H1 and Higher Order Structures

These studies have given a fairly detailed picture of the internal structure of the nucleosome, but until 1975 there was still no clear idea of the relation of one nucleosome to another along the nucleosome chain or basic chromatin filament, nor of the next higher level of organisation. It had been known for some time that the thickness of fibres observed in electron microscopical studies of whole-mount chromosome specimens varied from about 100 to 250 Å in diameter, depending on whether chelating agents had been used or not in the preparation. Taking this as a clue, *Finch* and I carried out some experiments *in vitro* on short lengths of chromatin prepared by brief micrococcal digestion of nuclei[63]. In the presence of chelating agents this native chromatin appeared as fairly uniform filaments of 100 Å diameter. When $Mg^{2+}$ ions were added, these coiled up into thicker, knobbly fibres about 250–300 Å in diameter, which are transversely striated at intervals of about 120–150 Å, corresponding apparently to the turns of an ordered, but not perfectly regular helix or supercoil. Since the term "supercoil" had already been used in a different context, we called it a solenoid, because the turns were spaced close together. On the basis of these micrographs and companion X-ray studies[64], we suggested that the second level of folding of chromatin was achieved by the winding of the nucleosome filament into a helical fibre with about six nucleosomes per turn. Moreover, we found that when the same experiments were carried out on H1-depleted chromatin, only irregular clumps were formed, showing that the fifth histone H1 is needed for the formation or stabilisation of the ordered fibre structure.

These experiments told us the level at which H1 performs its function of condensing chromatin, but the way in which the H1 molecule mediates the coiling of the 100 Å filament into the 300 Å fibre only became clear later by putting together evidence from the biochemistry, from the crystallographic analysis, and from more refined electron microscopic observations.

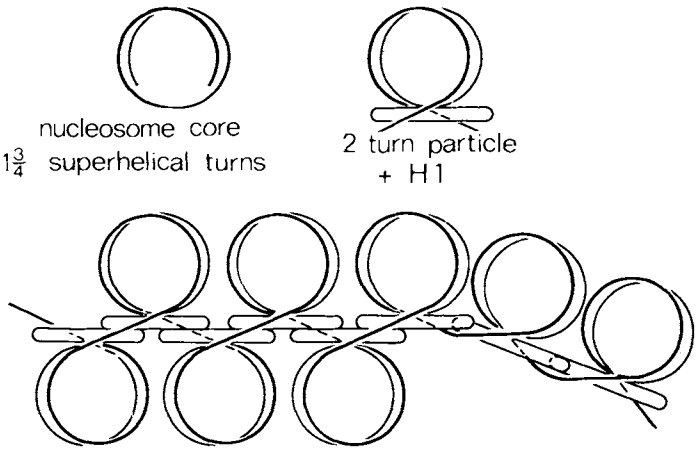



Fig. 13. (Top) If the 146 base pairs of DNA in the nucleosome core correspond to $1\frac{3}{4}$ superhelical turns, then the 166 base particle corresponds to about 2 full superhelical turns. Since the 166 base pair particle is the limit point for the retention of H1 [52], it must be located as shown. (Bottom) Schematic diagram of the nucleosome filament at low ionic strength, showing origin of the zigzag structure (cf. Fig. 14). At the right of the drawing is shown a variant of the zigzag structure which is often observed: this is formed by flipping a nucleosome by 180° about the filament axis.

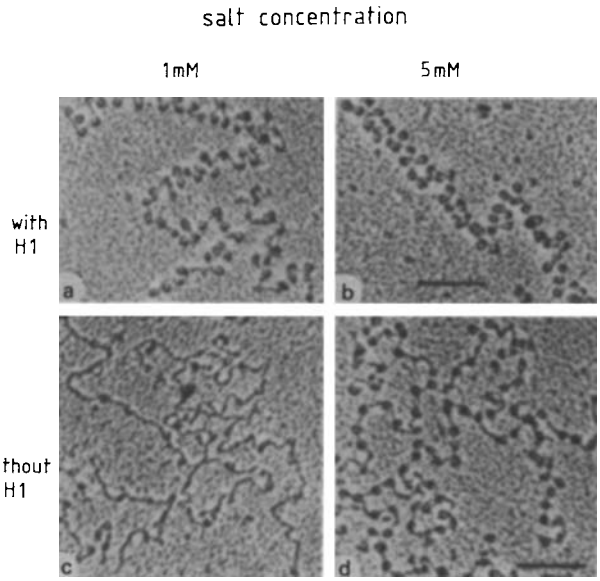



Fig. 14. The appearance of chromatin with and without H1 at low ionic strength [66]. When H1 is present the first recognizable ordered structure is ⓐ a loose zigzag in which the DNA enters and leaves the nucleosome at sites close together; at a somewhat higher salt concentration ⓑ the zigzag is tighter. In the absence of H1, there is no order in the sense of a defined filament direction. At the lower salt concentration ⓒ, nucleosome beads are no longer visible, the structure having opened to produce a fibre of DNA coated with histones. At somewhat higher salt concentration ⓓ, beads are again visible but the DNA enters and leaves the nucleosome more or less at random. The bar represents 100 nm.

From observations on the course of nuclease digestion, taken in conjunction with the known X-ray structure of the

nucleosome core, one can deduce where the H1 might be on the complete nucleosome. I have already mentioned in Section 4.1 that there is an intermediate in the digestion of chromatin by *Micrococcus* nuclease at about 166 base pairs of DNA and it is during this step from 166 to 146 base pairs that H1 is released[52]. Since the 146 base pairs of the particle correspond to $1\frac{3}{4}$ superhelical turns, we therefore suggested that the 166 base pair particle contains two full turns of DNA[53]. This brings the two ends of the DNA on the nucleosome close together so that both can be associated with the same single molecule of H1 (Fig. 13). A particle consisting of the histone octamer and 166 base pairs has been called the chromatosome[65] and has been suggested by us and others to constitute the basic structural element of chromatin. In this particle, the H1 would therefore be on the side of the nucleosome in the region of the entry and exit of the DNA superhelix.

This location follows in logic: but was histone H1 really there? Although H1 is too small a molecule to be seen directly by electron microscopy, its position in the nucleosome can be inferred from its effect on the appearance of chromatin, in the intermediate range of folding between the 100 Å nucleosome filament and the 300 Å solenoidal fibre. These intermediate stages were exposed in the course of a systematic study by *Thoma* and *Koller*[66], of the folding of chromatin with increasing ionic strength. By employing monovalent salts rather than divalent ones, they exposed a range of structures showing increasing degrees of compaction as the ionic strength was raised. Thus, from the filament of nucleosomes around 1 mM, the extent of structure increased through a family of intermediate helical structures until, by 60 mM, the compact 300 Å fibre structure was formed, in all respects identical to that originally observed by *Finch* and myself.

The location of H1 can be deduced by considering the difference between the structures observed in the range of ionic strength 1—5 mM in the presence or absence of H1 (Fig. 14). In chromatin containing H1, an ordered structure is seen in which the nucleosomes are arranged in a regular zigzag with their flat faces down on the supporting grid. The zigzag form arises because the DNA enters and leaves the nucleosome at sites close together, as one would expect from the combination of X-ray and biochemical evidence (Fig. 13). In chromatin depleted of H1, entrance and exit points are more or less on opposite sides and in any case randomly located. Indeed, at very low ionic strength, the nucleosomal structure unravels into a linearised form in which individual beads are no longer seen. When H1 is present this is prevented from happening. We therefore concluded that H1, or strictly part of it, must be located at, and stabilises, the region where DNA enters and leaves the nucleosome, as was predicted.

In the zigzag intermediates the H1 regions on adjacent nucleosomes appear to be close together or touching. We therefore suggested that, with increasing ionic strength, more of the H1 regions interact with one another, eventually aggregating into a helical polymer along the centre of the solenoid and thus accounting for its geometrical form. Polymers of H1 have indeed been shown to exist by chemical cross-linking experiments at both low and high ionic strength[61], but it remains to be shown that they are located in the centre of the fibre. The important point, however, is that it appears to be the aggregation of H1 which accompanies, and indeed may control, the formation of the 300 Å fibre.

### 4.4. The Roles of the Histones

From the spatial arrangements of molecules proposed for the histone octamer and from the location deduced for histone H1, one can see [59] the roles of the individual histones in folding the DNA on the nucleosome (Fig. 15). The $(H3)_2(H4)_2$ tetramer has the shape of roughly a single turn of a helicoid and this defines the central turn of the DNA superhelix. H2A and H2B add as two heterodimers,

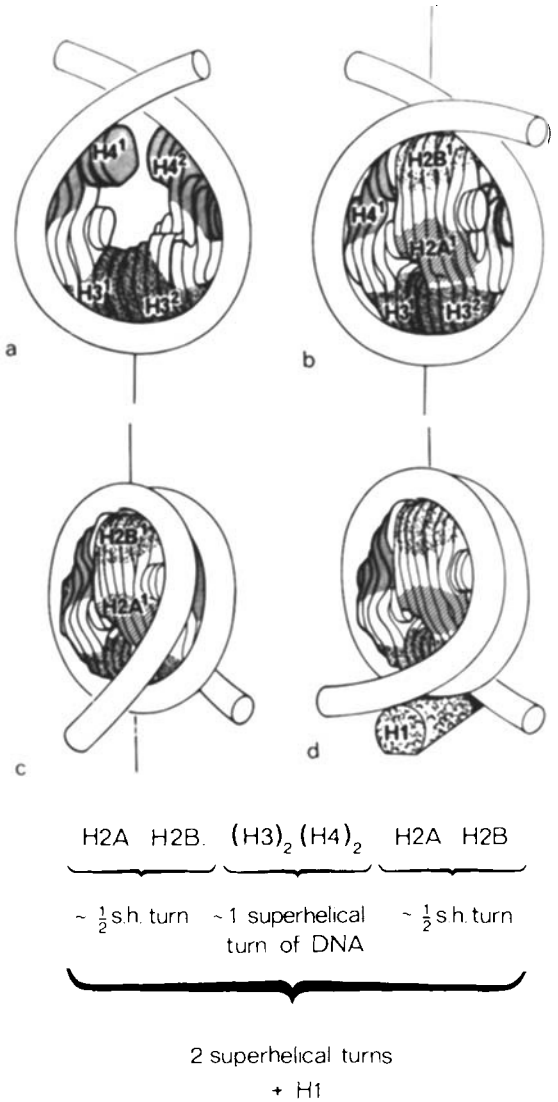



Fig. 15. "Exploded" views of the nucleosome, showing the roles of the constituent histones. The patches on the histone core indicate locations of individual histone molecules, but the boundaries between them are not known and are thus left unmarked. ⓐ the $(H3)_2(H4)_2$ tetramer has the shape of a lock-washer and can act as a spool for 70–80 base pairs of DNA, forming about one superhelical turn. ⓑ An H2A·H2B dimer associates with one face of the tetramer. ⓒ H2A·H2B dimers on opposite faces each bind 30—40 base pairs of DNA, or one-half a superhelical turn, to give a complete 2-turn particle. ⓓ The histone H1 interacts with the unique configuration of DNA at the entry and exit points to seal off the nucleosome.

H2A/H2B, one on each face of the H3-H4 tetramer, each binding one extra half-turn of the DNA, thereby completing the two-turn superhelix. Finally, H1 then binds to the unique region at the side of the two-turn particle where three segments of DNA come together, stabilising and "sealing off" the nucleosome, and also mediating the folding to the next level of organisation. Such a sequence of events in time would provide a structural rationale for the temporal order of assembly of histones onto newly replicated DNA[68-70].

We now have arrived at a moderately detailed model of the nucleosome and a description for the next higher level of folding. There is thus a firm structural and chemical framework in which to consider the dynamic processes which take place in chromatin in the cell, that is, transcription, replication and mitosis.

## 5. Concluding Remarks

I particularly wanted to outline the chromatin work because it may serve as a contemporary paradigm for structural studies which try to connect the cellular and the molecular. One studies a complex system by dissecting it out physically, chemically, or in this case enzymatically, and then tries to obtain a detailed picture of its parts by X-ray analysis and chemical studies, and an overall picture of the intact assembly by electron microscopy. There is, however, a sense in which viruses and chromatin, which I have described here, are still relatively simple systems. Much more complex systems, ribosomes, the mitotic apparatus, lie before us and future generations will recognise that their study is a formidable task, in some respects only just begun. I am glad to have had a hand in the beginnings of the foundation of structural molecular biology.

*It will be obvious that I could not have accomplished all that has been summarized here without the help of many highly able and valued colleagues and collaborators. After Rosalind Franklin's death, I was able to continue and extend the virus work with John Finch and Kenneth Holmes, who were then students, and who became colleagues. Over the years I have had a transatlantic association with Donald Caspar and have benefitted from his advice, criticism and insights. I can mention here only some of the names of my other collaborators in the several branches in which I have been involved: in the study of virus chemistry and assembly, Reuben Leberman, Tony Durham, Jo Butler and David Zimmern; in virus crystallography, William Longley, Peter Gilbert, John Champness, Gerard Bricogne and Anne Bloomer; in electron microscopy and image reconstruction, David DeRosier, Harold Erickson, Tony Crowther, Linda Amos, Jan Mellema, Nigel Unwin and, throughout, John Finch; in the structural studies on transfer RNA, Brian Clark, who provided the biochemical background without which the work could not have begun, Jon Robertus, Jane Ladner and Tony Jack; in chromatin, Roger Kornberg, whose skill and insight transformed a "messy" project into a clear problem, Markus Noll, Len Lutter, and also Daniela Rhodes and Ray Brown, who fruitfully transferred their experience from tRNA to nucleosomes, and finally Tim Richmond and John Finch who are engaged in the higher resolution X-ray studies now in progress.*

Received: April 25, 1983 [A 463 IE]
German version: *Angew. Chem. 95* (1983) 579

Reviews:

[1] A. Klug: "The Assembly of Tobacco Mosaic Virus: Structure and Specificity". *Harvey Lect. 74* (1979) 141-162.
[2] R. A. Crowther, A. Klug: "Structural Analysis of Macromolecular Assemblies by Image Reconstruction from Electron Micrographs". *Annu. Rev. Biochem. 44* (1975) 161-182.
[3] A. Klug: "Image Analysis and Reconstruction in the Electron Microscopy of Biological Macromolecules". *Chem. Scr. 14* (1979) 245-256.
[4] a) R. D. Kornberg: "Structure of Chromatin". *Annu. Rev. Biochem. 46* (1977) 931-954; b) R. D. Kornberg, A. Klug: "The Nucleosome". *Sci. Am. 244* (1981) 52-64.
[5] P. J. G. Butler, A. Klug: "The Structure of Nucleosomes and Chromatin" in F. Palmieri: *Horizons in Biochemistry and Biophysics*. Wiley, Chichester 1983, in press.

Original publications:

[6] H. Fraenkel-Conrat, R. C. Williams, *Proc. Natl. Acad. Sci. USA 41* (1955) 690-698.
[7] H. Fraenkel-Conrat, B. Singer, *Biochim. Biophys. Acta 33* (1959) 359-370.
[8] R. E. F. Matthews, *Virology 30* (1966) 82-96.
[9] G. Stubbs, S. Warren, K. Holmes, *Nature London 267* (1977) 216-221.
[10] K. C. Holmes, *J. Supramol. Struct. 12* (1979) 305-320.
[11] G. Schramm, W. Zillig, *Z. Naturforsch. B 10* (1955) 493-498.
[12] D. L. D. Caspar, *Adv. Protein Chem. 18* (1963) 37-121.
[13] J. T. Finch, R. Leberman, Y.-S. Chang, A. Klug, *Nature London 212* (1966) 349-350.
[14] G. Bricogne, *Acta Crystallogr. Sect. A 32* (1976) 832-847.
[15] A. C. Bloomer, J. N. Champness, G. Bricogne, R. Staden, A. Klug, *Nature London 276* (1978) 362-368.
[16] M. A. Lauffer, C. L. Stevens, *Adv. Virus Res. 13* (1968) 1-63.
[17] A. C. H. Durham, J. T. Finch, A. Klug, *Nature London, New Biol. 229* (1971) 37-42.
[18] A. C. H. Durham, A. Klug, *Nature London, New Biol. 229* (1971) 42-46.
[19] A. Klug, A. C. H. Durham, *Cold Spring Harbor Symp. Quant. Biol. 36* (1971) 449-460.
[20] P. J. G. Butler, A. Klug, *Nature London, New Biol. 229* (1971) 47-50.
[21] M. Fukuda, T. Ohno, Y. Okada, Y. Otsuki, I. Takebe, Proc. Natl. Acad. Sci. USA 75 (1978) 1727-1730.
[22] P. J. G. Butler, G. P. Lomonossoff, *Biophys. J. 32* (1980) 295-312.
[23] D. Zimmern, P. J. G. Butler, *Cell 11* (1977) 455-462.
[24] D. Zimmern, *Cell 11* (1977) 463-482.
[25] D. Zimmern, T. M. A. Wilson, *FEBS Lett. 71* (1976) 294-298.
[26] J. N. Champness, A. C. Bloomer, G. Bricogne, P. J. G. Butler, A. Klug, *Nature London 259* (1976) 20-24.
[27] P. J. G. Butler, A. C. Bloomer, G. Bricogne, J. N. Champness, J. Graham, H. Guilley, A. Klug, D. Zimmern in R. Markham, R. W. Horne: *Structure-Function Relationships of Proteins*, Elsevier, Amsterdam 1976, p. 101-110.
[28] G. Lebeurier, A. Nicolaieff, K. E. Richards, *Proc. Natl. Acad. Sci. USA 74* (1977) 149-153.
[29] P. J. G. Butler, J. T. Finch, D. Zimmern, *Nature London 265* (1977) 217-219.
[30] D. L. D. Caspar, A. Klug, *Cold Spring Harbor Symp. Quant. Biol. 27* (1962) 1-24.
[31] S. Brenner, R. W. Horne, *Biochim. Biophys. Acta 34* (1959) 103-110.
[32] A. Klug, J. T. Finch, *J. Mol. Biol. 11* (1965) 403-423.
[33] A. Klug, J. E. Berger, *J. Mol. Biol. 10* (1964) 565-569.
[34] A. Klug, D. J. DeRosier, *Nature London 212* (1966) 29-32.
[35] D. J. DeRosier, A. Klug, *J. Mol. Biol. 65* (1972) 469-488.
[36] D. J. DeRosier, A. Klug, *Nature London 217* (1968) 130-134.
[37] R. A. Crowther, D. J. DeRosier, A. Klug, *Proc. R. Soc. London Ser. A 317* (1970) 319-340.
[38] R. A. Crowther, L. A. Amos, J. T. Finch, D. J. DeRosier, A. Klug, *Nature London 226* (1970) 421-425.
[39] R. A. Crowther, L. A. Amos, *Cold Spring Harbor Symp. Quant. Biol. 36* (1971) 489-494.
[40] P. N. T. Unwin, *J. Mol. Biol. 87* (1974) 657-670.
[41] K. A. Taylor, R. M. Glaeser, *J. Ultrastruct. Res. 55* (1976) 448-456.
[42] P. N. T. Unwin, R. Henderson, *J. Mol. Biol. 94* (1975) 425-440.
[43] R. Henderson, P. N. T. Unwin, *Nature 257* (1975) 28-32.
[44] P. N. T. Unwin, *Proc. R. Soc. London Ser. A 329* (1972) 327-359.
[45] H. P. Ericksòn, A. Klug, *Ber. Bunsenges. Phys. Chem. 74* (1970) 1129-1137; *Philos. Trans. R. Soc. London Ser. B 261* (1971) 105-118.

[46] M. H. F. Wilkins, G. Zubay, H. R. Wilson, *J. Mol. Biol. 1* (1959) 179–185.
[47] V. Luzzati, A. Nicolaieff, *J. Mol. Biol. 1* (1959) 127–133.
[48] D. R. Hewish, L. A. Burgoyne, *Biochem. Biophys. Res. Commun. 52* (1973) 504–510.
[49] M. Noll, *Nature London 251* (1974) 249–251.
[50] R. D. Kornberg, J. O. Thomas, *Science 184* (1974) 865–868.
[51] R. D. Kornberg, *Science 184* (1974) 868–871.
[52] M. Noll, R. D. Kornberg, *J. Mol. Biol. 109* (1977) 393–404.
[53] J. T. Finch, L. C. Lutter, D. Rhodes, R. S. Brown, B. Rushton, M. Levitt, A. Klug, *Nature London 269* (1977) 29–36.
[54] J. T. Finch, A. Klug, *Cold Spring Harbor Symp. Quant. Biol. 42* (1978) 1–15.
[55] L. C. Lutter, *J. Mol. Biol. 124* (1978) 391–420.
[56] J. T. Finch, R. S. Brown, D. Rhodes, T. Richmond, B. Rushton, L. C. Lutter, A. Klug, *J. Mol. Biol. 145* (1981) 757–769.
[57] J. T. Finch, A. Lewit-Bentley, G. A. Bentley, M. Roth, P. A. Timmins, *Philos. Trans. R. Soc. London Ser. B 290* (1980) 635–638.
[58] J. O. Thomas, R. D. Kornberg, *Proc. Natl. Acad. Sci. USA 72* (1975) 2626–2630.
[59] A. Klug, D. Rhodes, J. Smith, J. T. Finch, J. O. Thomas, *Nature London 287* (1980) 509–516.
[60] A. D. Mirzabekov, V. V. Shick, A. V. Belyavsky, S. G. Bavykin, *Proc. Natl. Acad. Sci. USA 75* (1978) 4184–4188.
[61] R. D. Camerini-Otero, G. Felsenfeld, *Nucleic Acids Res. 4* (1977) 1159–1181.
[62] J. O. Thomas, R. D. Kornberg, *FEBS Lett. 58* (1975) 353–358.
[63] J. T. Finch, A. Klug, *Proc. Natl. Acad. Sci. USA 73* (1976) 1897–1901.
[64] L. Sperling, A. Klug, *J. Mol. Biol. 112* (1977) 253–263.
[65] R. T. Simpson, *Biochemistry 17* (1978) 5524–5531.
[66] F. Thoma, Th. Koller, A. Klug, *J. Cell Biol. 83* (1979) 403–427.
[67] J. O. Thomas, A. J. A. Khabaza, *Eur. J. Biochem. 112* (1980) 501–511.
[68] A. Worcel, S. Han, M. L. Wong, *Cell 15* (1978) 969–977.
[69] T. Senshu, M. Fukuda, M. Ohashi, *J. Biochem. Tokyo 84* (1978) 985–988.
[70] C. Cremisi, M. Yaniv, *Biochem. Biophys. Res. Commun. 92* (1980) 1117–1123.
[71] A. Klug, D. L. D. Caspar, *Adv. Virus Res. 7* (1960) 225–325.
[72] R. C. Crowther, L. A. Amos, *J. Mol. Biol. 60* (1971) 123–130.
[73] A. Klug, J. T. Finch, *J. Mol. Biol. 31* (1968) 1–12.

# Holographic Methods for the Investigation of Photochemical and Photophysical Properties of Molecules

**New analytical methods (23)**

**By Christoph Bräuchle* and Donald M. Burland***

Holography is most frequently thought of as a method of photography that results in three-dimensional images of the object being photographed. It is certainly true that this is the most visually spectacular aspect. But holography can also be used as a powerful tool for the investigation of a variety of photochemical and photophysical processes. These experimental techniques rely on the fact that small spatial modulations of a material's optical properties (index of refraction and absorption coefficient) can deflect an incident light beam into another direction. By following the growth or decay in intensity of this deflected beam, one can follow the underlying photochemical and photophysical processes producing the changes in optical properties. If a CW laser is used to produce the hologram one can use the technique to investigate solid state photochemistry. If a pulsed laser is used one can investigate a broad range of time dependent processes; energy transfer, diffusion, rotational relaxation, charge transport *etc.* Compared to conventional spectroscopic techniques the holographic method shows various advantages. So for example it is a highly sensitive zero-background technique and permits free choice of detection wavelength and detection beam intensity.

As a result of information obtained using the holographic technique as a scientific tool, one can also find new classes of materials for the recording of holograms. This is the way in which two-photon four-level systems for hologram recording in the infrared were discovered. Materials of this type are self-developing, can have the recording process gated on and off with an auxiliary source, and can be read with the infrared recording laser with no erasing of the hologram.

## 1. Introduction

Holography is most widely known as a technique for producing a three-dimensional picture. According to *Gabor*'s original idea[1], for which he received the Nobel prize in 1971, a picture or more generally information can be stored as an interference pattern generated from an object and reference wave. Although the production of a three-dimensional picture[2] was one of the most impressive initial results of holography[3–5], applications of the technique have since spread over a variety of different areas. For example, holographic interferometry[6,7] can be used to measure very small deformations of an object which is put under mechanical stress. In this way holography represents an important advance in nondestructive material testing. Medical and biomedical applications[8] are a growing field for holographic methods. A great amount of effort has also gone into the assessment of the potential usefulness of holograms in optical memories[9,10]. In this application holograms containing binary information are produced in a two- or three-dimensional array. Holograms can play an important role in coherent optical data processing[11,12].

[*] Dr. habil. C. Bräuchle
Institut für Physikalische Chemie der Universität
Sophienstr. 11, D-8000 München 2 (Germany)
Dr. D. M. Burland
IBM Research Laboratory
5600 Cottle Road, San José, CA 95193 (USA)

 © Verlag Chemie GmbH, 6940 Weinheim, 1983 0570-0833/83/0808-0582 $ 02.50/0 

Perhaps in the future holograms will be most widely used for the production of a variety of kinds of optical elements for focusing and deflecting light[13, 14]. Holographic optical elements are currently being considered for applications as passive devices in the fast growing area of integrated optics[15] and optical communication technologies[16].

In all of these cases the basic principle[3-5] is the same: An object wave which carries complete information about the object in the modulation of its intensity and phase is overlapped with a reference wave (see Fig. 1a) which is frequently a plane wave. If both waves are mutually *coherent* in space and time, *i.e.*, if there are fixed phase relationships between both waves during the recording period, a stationary interference pattern is produced. This pattern can be impressed photochemically into a photosensitive recording medium. The photochemically stored interference pattern is called the hologram. It consists of a complex pattern of irregularly arranged bright and dark regions of microscopic dimensions representing the interference fringes. Because of this irregularity such a hologram at first sight seems to contain no information at all. However, if it is illuminated with the reference wave only (see Fig. 1b), the recorded interference fringes diffract part of the reference wave in such a way that an image wave is reconstructed as an exact replica of the original object wave. Since not only the intensity (as in photography) but also the absolute value of the phase of the object wave is reconstructed correctly, the technique is called holography, originating from the Greek word "ὅλος" meaning "the whole". In a sense the whole pictorial information is stored in a hologram, permitting one to reconstruct a complete three-dimensional image of the original object.

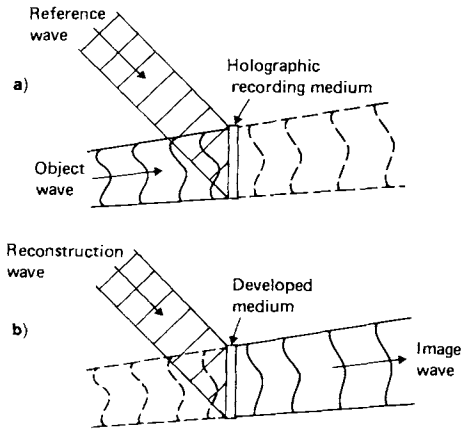



Fig. 1. Schematic representation (a) of the holographic recording and (b) reconstruction procedures.

From this brief description of holography it is obvious that *coherence* of the object and reference wave is a prerequisite. Therefore after the invention of holography[1] in 1948 its rapid development had to await the development of the laser[17] as a source of coherent light. The close relationship between laser technology and holographic development holds to the present day. So, for example, new lasers such as the semiconductor lasers[18] have stimulated a search for new holographic recording materials in the infrared.

In this review we will concentrate on two aspects of holography. First we want to discuss the application of holography as a powerful scientific tool for the investigation of photochemical and photophysical processes. Because the hologram recording process involves photochemical and photophysical changes of the photosensitive molecules in the recording medium, it is possible to use holography in order to follow these processes. In this way, holography can serve as an extremely sensitive tool for fundamental photochemical and photophysical investigations. The second aspect of holography that we wish to discuss is the search for new holographic recording materials. We will show how fundamental investigations using holographic photochemistry can yield new kinds of holographic recording materials. These new materials rely on a two-photon four-level (2P4L) photochemical reaction scheme and a comparison with conventional one-photon two-level (1P2L) photochemical recording systems will demonstrate that the 2P4L systems have many significant advantages. The use of these new materials in a range of holographic applications will be discussed.

## 2. The Use of Holography to Investigate Photochemical and Photophysical Processes

### 2.1. The Principle

In order to investigate photochemical and photophysical processes by holography it is reasonable to use the simplest of holograms, *i.e.*, a plane wave hologram[3-5]. This will avoid unnecessary complications. The production of such a plane wave hologram is shown in Figure 2. Two coherent waves (reference and object wave) with the intensities $I_R$ and $I_O$ and the same wavelength overlap at the holographic sample. Since both waves are plane waves the interference pattern is a simple cosine modulation of intensity $I(x)$ in the $x$-direction across the sample,

$$I(x)=(I_R+I_O)\left[1+V\cos\left(\frac{2\pi x}{\Lambda}\right)\right] \quad (1)$$

where $V=2\sqrt{I_R I_O}/(I_R+I_O)$ accounts for the contrast or fringe visibility and $\Lambda=\lambda/(2\sin\theta)$ gives the fringe spacing which is dependent on the wavelength $\lambda$ and the angle of incidence $\theta$. With both beams having the same intensity ($I_R=I_O$), $V$ equals unity and totally dark and maximally bright stripes occur in the interference pattern (cf. Fig. 2).

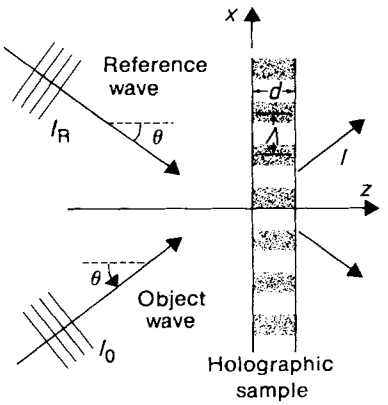



Fig. 2. The production of a plane wave hologram. For meanings of symbols see text.

If the holographic sample contains molecules that are photochemically or photophysically sensitive to the incident light they will change their chemical or physical properties. This change will be strongest in the brightest regions of the interference pattern and absent in the dark regions. In cases where these photochemical or photophysical changes are related to corresponding changes of the index of refraction $n$ or the absorption coefficient $a$ of the molecules, a spatial modulation of the index of refraction

$$n(x)=n_0+n_1\cos\left(\frac{2\pi x}{\Lambda}\right) \tag{2a}$$

and the absorption coefficient

$$a(x)=a_0+a_1\cos\left(\frac{2\pi x}{\Lambda}\right) \tag{2b}$$

will be produced by the interfering light beams. This modulation has the same periodic behavior as the intensity pattern $I(x)$ in Eq. (1). $n_0$ and $a_0$ in Eqs. (2) are the average values of the index of refraction and the absorption coefficient whereas $n_1$ and $a_1$ are the corresponding amplitudes of modulation. This photochemically or photophysically impressed variation of the index of refraction or the absorption coefficient of the holographic sample represents the process of plane wave hologram formation. Because of its regular spatial variation and its analogies to optical gratings it has also been called a holographic grating. When a reading beam strikes such a plane wave hologram along the direction of the reference wave, some of the light from this beam will be diffracted by the holographic grating and the absent object wave will be reconstructed.

A hologram can be characterized by its diffraction efficiency[3] which is defined as the intensity $I$ of the diffracted beam divided by the intensity $I_R$ of the reading beam. *Kogelnik*[19] has obtained an important expression for the diffraction efficiency $\eta$ of a plane wave hologram of thickness $d$:

$$\eta=\frac{I}{I_R}=\left[\sin^2\left(\frac{\pi n_1 d}{\lambda\cos\theta}\right)+\sinh^2\left(\frac{a_1 d}{2\cos\theta}\right)\right]\exp\left(-\frac{2a_0 d}{\cos\theta}\right) \tag{3a}$$

This expression was derived for thick or volume plane wave holograms for which the relation $d\gg\Lambda$ holds. Generally, in all cases treated in this review, thick holograms are obtained.

In order to give an interpretation of Eq. (3a) it is important to emphasize that the two terms inside the square bracket of Eq. (3a) represent two different mechanisms of hologram formation. The first term describes hologram formation as a result of changes in the index of refraction and connects the diffraction efficiency with the amplitude $n_1$ in Eq. (2a). Holograms of this type are called *phase holograms*[3] because the diffraction is caused by phase changes of the reading beam due to the modulation of the optical path lengths by $n(x)$. The second term describes holograms resulting from changes in the absorption according to Eq. (2b). These holograms are called *amplitude holograms*[3]. For these holograms the diffraction occurs because the reading beam sees a quasi-multislit grating produced by $a(x)$. The exponential factor in Eq. (3a) accounts for the absorption of the reconstruction wave as it passes through the sample. This factor is responsible for the low maximum theoretical diffraction efficiency[3] of 3.7% for a pure amplitude hologram. On the other hand, for pure phase holograms the efficiency may theoretically approach 100% if the reading wavelength $\lambda'$ is not absorbed ($a_0=0$, $a_1=0$). For photochemical reactions it can be shown[20] that even in cases where some absorption is present the effect of the phase hologram generally exceeds that of the amplitude hologram. For these cases, in a first approximation it is often possible to consider the phase holograms only.

Equation (3a) is the central formula for the holography described in this review. It is obvious from this equation that changes in the photochemical or photophysical properties of molecules in the holographic sample can cause changes in the diffraction efficiency $\eta$ if these properties are related to corresponding changes in the index of refraction or absorbance. In Sections 2.2–2.3 a new holographic method is described which measures the change of molecular parameters by following the change of the diffraction efficiency. Since, in most applications of this holographic technique, the total diffraction efficiency is small ($\eta\leq 0.01$) Eq. (3a) can be accurately approximated by Eq. (3b):

$$\eta=\left[\left(\frac{\pi n_1 d}{\lambda\cos\theta}\right)^2+\left(\frac{a_1 d}{2\cos\theta}\right)^2\right]\exp\left(-\frac{2a_0 d}{\cos\theta}\right) \tag{3b}$$

In these cases, $\eta$ is directly proportional to the *square* of the amplitudes $n_1$ and $a_1$.

## 2.2. The Holographic Method with Continuous Wave (CW) Lasers

### 2.2.1. Determination of Photochemical Rate Constants

If the holographic sample (Fig. 2) consists of photochemically active molecules dispersed in a polymer film or any other glassy or crystalline matrix these molecules will react in the brightly illuminated regions of the sample but not in the dark regions. As a result, a spatial variation of the photochemical product formation occurs which changes the index of refraction and the absorption coefficient of the sample. The change in the index of refraction can be obtained from the photochemical changes by using the Lorentz-Lorenz relation[21], which gives for the amplitude $n_1$ after some manipulations[20]:

$$n_1=\frac{(n_0^2+2)^2}{6000 n_0}\sum_i R_i\Delta C_i(t) \tag{4a}$$

where $R_i$ is the molar refraction and $\Delta C_i(t)$ gives the time dependent changes of the concentration at the maxima of the interference pattern. The subscript i runs over all components of the reaction. A similar formula can be obtained for the changes in the absorption coefficient caused by a photochemical reaction

$$a_1(\lambda)=2.30\sum_i \varepsilon_i(\lambda)\Delta C_i(t) \tag{4b}$$

where $\varepsilon_i(\lambda)$ is the molar extinction coefficient of the *i*th component of the reaction.

For a simple one-step reaction

$$A_1 \xrightarrow{k} A_2 \tag{5}$$

with the overall reaction rate $k$ the changes of the concentrations of $A_1$ and $A_2$ with time are well known from the kinetic rate equations[22]

$$C_1(t) = C_1(0)\,e^{-kt} \tag{6a}$$
$$C_2(t) = C_1(0) - C_1(0)\,e^{-kt} \tag{6b}$$

where $t$ equals time and $C_1(0)$ is the initial concentration of $A_1$. Considering a pure phase hologram and putting Eqs. (6) in (4a) and (4a) in (3) gives a relationship for the efficiency as a function of time[20,23–26]. For the early stages of the hologram formation, where $\eta$ is very low, Eq. (3b) can be used instead of Eq. (3a) giving the simple result[25]:

$$\eta = (F \cdot C \cdot k)^2 t^2. \tag{7}$$

In Eq. (7)

$$F = \frac{\pi d}{\lambda' \cos\theta} \quad \text{and} \quad C = \frac{(n_0^2+2)^2}{6000 n_0}(R_2 - R_1)C_1(0)$$

are constants representing geometrical and material specific parameters. From an experimental observation of $\eta$ as a function of time it can thus be seen that one can obtain the overall rate constant $k$. Curves showing $\eta$ as a function of time are called hologram growth curves. The remainder of this section will indicate how one can obtain important information about photochemical and photophysical processes from such curves.

### 2.2.2. Experimental Observation of Hologram Growth Curves

Experimentally, hologram growth curves are obtained with an apparatus[20,23–27] similar to the one shown in Figure 3. The light from a laser is split into reference and object waves which produce the interference pattern at the sample. The formation of the hologram can be observed in two ways. First the light from a second laser (most conveniently a HeNe laser) can be used to read the hologram. If the light of this second laser strikes the sample with the intensity $I_R$ it will be diffracted by the hologram. The intensity $I$ of the diffracted beam can be modulated, measured with a photodiode and recorded with a lock-in amplifier. It is directly proportional to the diffraction efficiency $\eta = I/I_R$ and provides a record of the hologram growth as a function of time. If one chooses the wavelength of this second laser so that it is not absorbed by the sample a pure phase hologram is observed. It has to be mentioned, however, that in cases where the reading wavelength $\lambda'$ differs from the writing wavelength $\lambda$ a different angle of incidence $\theta'$ for the reading beam must be used for the maximum intensity $I$. This angle should satisfy the Bragg relation[3]:

$$2\Lambda \sin\theta' = \lambda' \tag{8}$$

In Eq. (8) $\Lambda$ is fixed once the hologram is impressed.

A second method of detection is to use the light of the argon laser itself. In this case a chopper is used in the object beam. When the chopper blocks the object beam, only the reference wave strikes the sample. Then light of this wavelength is deflected into the direction of the object wave as the hologram grows and can be detected with a photodiode which is connected to a boxcar integrator. The reference of the chopper opens the gate of the signal input of the boxcar integrator only during the periods when the object beam is blocked so that hologram growth (open period of the chopper) and hologram detection (closed period) follow each other at the frequency of the chopper. In this way the Bragg relation is automatically satisfied.

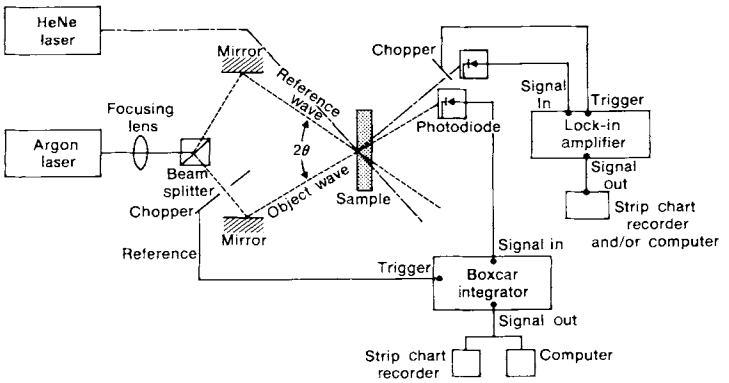



Fig. 3. A schematic representation of the apparatus for the recording of holographic growth curves. The detection method using a third HeNe laser is indicated by the dash-dotted line. The method using a chopper in the object beam is shown by the dashed line.

The setup in Figure 3 illustrates several advantages of the holographic technique. It is truly a zero-background technique. Until the hologram begins to form no light is received at the photodiode. If one uses a HeNe laser for detecting the hologram, scattered light from the writing laser can be reduced by placing a narrow band pass filter before the photodiode allowing only 632.8 nm light to reach the detection. The HeNe laser beam has very little divergence so that one can further eliminate interference from scattered light simply by moving the detector well away from the sample. With such an experimental arrangement hologram efficiencies of less than $10^{-9}$ can be detected.

### 2.2.3. Analysis of Hologram Growth Curves to Obtain Quantum Yields and the Number of Mechanistically Necessary Photons

With the experimental setup described above hologram growth curves[23–27] as shown in Figure 4 can be obtained. All curves show a quadratic time dependence in good agreement with Eq. (7). For each curve in the figure, *i.e.*, for each intensity of the hologram producing beams, an overall rate constant $k$ can be obtained according to Eq. (7).

The dependence of the overall rate constant $k$ on the intensity can be explained by referring to the energy level

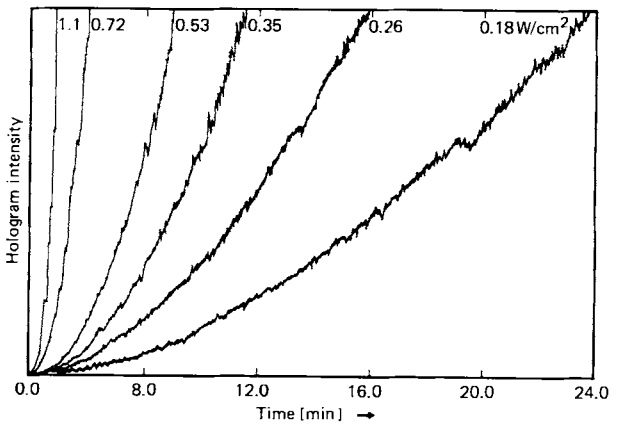



Fig. 4. Hologram growth curves for different intensities of the hologram forming beams. Only the early stages of the hologram growth are shown. These results were obtained with a sample of dimethyl-*s*-tetrazine in polyvinylcarbazole using the 514.5 nm line from an argon ion laser.

schemes in Figure 5. On the left side of Figure 5 a one-photon two-level (1P2L) process is shown. Here the absorption of one photon excites the molecule into the reactive state $A_1^*$. The right side of Figure 5 illustrates a two-photon four-level (2P4L) scheme indicating that two photons are necessary to reach the reactive state $A_2^*$. Since the rate constant $k$ obtained above describes only the overall reaction process ($A_1 \rightarrow A_2$ for the left side or $A_1 \rightarrow A_3$ for the right side of Fig. 5), it involves the intensity-dependent "absorption rates" $I_a$. In the steady state approximation it can be easily shown that $k$ is related to the intensity $I$ according to

$$k = \xi I^r \tag{9}$$

where $r$ gives the number of mechanistically necessary photons and $\xi$ contains all other photochemical and photophysical constants. For the one-photon process ($r = 1$) in Figure 5 one gets[23]

$$\xi = 2303 \cdot \varepsilon_1 \phi_p \tag{10a}$$

with $\varepsilon_1$ the molar extinction coefficient and $\phi_p$ the photochemical quantum yield, whereas for the two-photon process ($r = 2$)

$$\xi = (2303)^2 \cdot \varepsilon_1 \varepsilon_2 \tau_2 \phi_2 \phi_p \tag{10b}$$

with $\varepsilon_1$, $\varepsilon_2$ the molar extinction coefficients of the two absorption steps, $\tau_2$ the lifetime and $\phi_2$ the quantum yield for

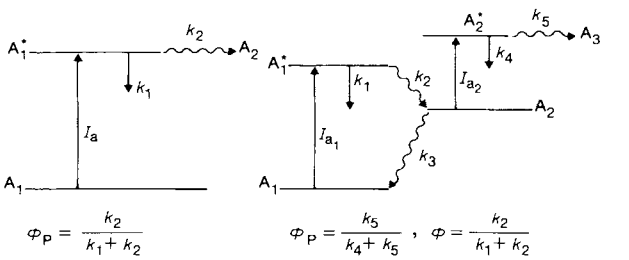



Fig. 5. Energy level diagrams for a one-photon two-level (left side) and a two-photon four-level (right side) photoreaction. The rate constants and the quantum yields for the kinetic processes are indicated as are expressions for the quantum yields.

population of state $A_2$. $\phi_p$ is the photochemical quantum yield.

A plot of $\log k$ as a function of $\log I$ gives $r$ as the slope and $\log \xi$ as the intercept according to Eq. (9). Such a plot is shown in Figure 6 for the holographically observed photoreaction of *o*-nitrobenzaldehyde (ONB)[25,28] dissolved in a polymethylmethacrylate (PMMA) film. Since $r = 1.04$ the use of Eq. (10a) with the easily obtained value of $\varepsilon_1$ gives the photochemical quantum yield $\phi_p = 0.17 \pm 0.05$ for this reaction in very good agreement with the value determined by optical absorption spectroscopy. Thus, the holographic method provides information about the overall photochemical reaction scheme (see Fig. 5) through the value of $r$, and provides information about the ratio between the rates of excited state photochemistry and photophysical relaxation processes through $\phi_p$. In Section 2.2.6 the advantages of the holographic technique are discussed in more detail; however, it is already obvious from this example that important parameters such as $r$ and $\phi_p$ can be obtained quite easily by this technique.

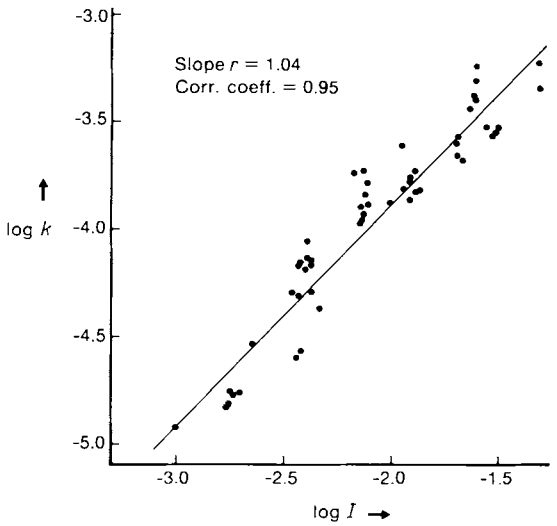



Fig. 6. A double logarithmic plot of the overall rate constant $k$ as a function of intensity $I$ for the holographically observed photoreaction of *o*-nitrobenzaldehyde.

Several other reactions have been investigated using the holographic technique sketched above. In the field of ketone photochemistry, hydrogen abstraction by benzophenone in a PMMA matrix has been studied[29]. It has been shown that a two-photon consecutive reaction is the major pathway in the solid (see also Section 2.2.4) in contrast to solution where this pathway is a minor one[30–32]. The reaction steps involve two photons probably because of a cage effect in the solid matrix[29,33]. Another example is the holographic investigation of dimethyl-*s*-tetrazine[23,24,34] which dissociates in a two-photon reaction[35,36]. A so far unidentified intermediate plays an important part in this reaction. There have been several attempts to characterize this intermediate[37–39]. The holographic method has shown[34] that the intermediate which is responsible for the two-photon nature of the reaction has an absorption in the same range as dimethyl-*s*-tetrazine itself (see also Section 2.2.5).

### 2.2.4. *Computer Modelling of Hologram Growth Curves*

Hologram growth curves can have different shapes[20,29] according to the reaction mechanism underlying the production of the hologram. It is instructive to compare calculated hologram growth curves with experimentally obtained ones, for one can obtain valuable information about reaction mechanisms in this way. The bases for such a calculation are Eqs. (3) and (4). Since these equations connect the time dependent change of the concentrations $\Delta C_i(t)$ of each component of the reaction with the hologram efficiency $\eta$ the hologram growth curves can be calculated for all types of kinetic rate equations. Therefore, having an expression for the kinetic rate equations of a particular reaction scheme, the appropriate growth curve can, in principle, be simulated.

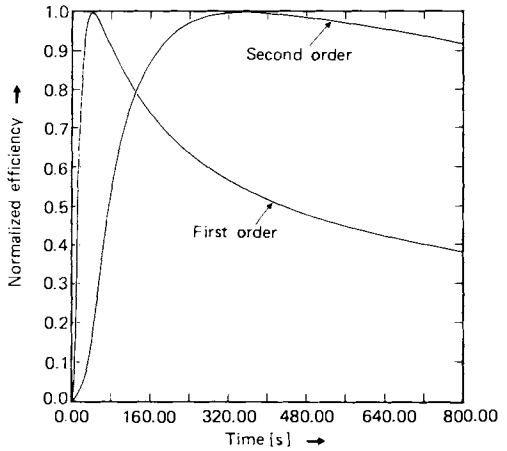



Fig. 7. Calculated hologram growth curves for first and second order holograms. Both curves have been normalized to maximum efficiencies of unity.

Figure 7 shows such calculated hologram growth curves for first and second order holograms of a simple one-step reaction $A_1 \rightarrow A_2$ as in Eq. (5)[20]. The second order hologram can be observed at an angle $2\theta$. It is weaker than the first order hologram and results primarily from the fact that after prolonged irradiation times the change of the index of refraction reaches saturation due to bleaching of the photoactive material in the bright parts of the interference pattern. This can be seen in Figure 8 where the change of the index of refraction is calculated for increasing reaction times. As a result of the bleaching process, $n(x)$ must be described by a Fourier expansion for longer reaction times instead of the simple two term expression in Eq. (2). Higher order holograms are then due to higher order coefficients of $n(x)$ in the Fourier expansion.

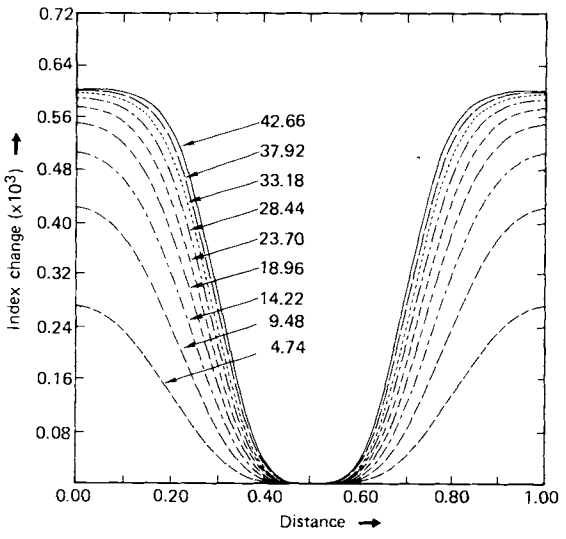



Fig. 8. The change in index of refraction across one period $\Lambda$ of the holographic grating for a one-step photoreaction for various illuminations times. (The distance is in units of $\Lambda$.)

The experimentally observed curves in Figure 4 for a one-step reaction are obtained only for the very first part of hologram growth well before saturation begins. If one expands the timescale in Figure 7, a clear quadratic time dependence is found for the early stages of hologram growth as observed experimentally and described by Eq. (7).

Hologram growth curves can be calculated for more complex kinetic schemes. For example, a consecutive reaction

$$A_1 \xrightarrow{k_1} A_2 \xrightarrow{k_2} A_3 \tag{11}$$

has been treated[20]. Results for such a calculation are shown in Figure 9. For the reaction scheme outlined in Eq. (11), one can, according to Eq. (4a), write

$$n_1 \sim \Delta C_2 R_2 + \Delta C_3 R_3 - (\Delta C_2 + \Delta C_3) R_1 . \tag{12}$$

For the case shown in Figure 9b, $R_1 > R_2 > R_3$; thus, $n_1$ is negative throughout the reaction. In this case we expect the hologram to grow initially at a rate characteristic of the $A_1 \rightarrow A_2$ reaction but eventually to grow with the $A_2 \rightarrow A_3$ rate. This is exactly what occurs, as shown in Figure 9b.

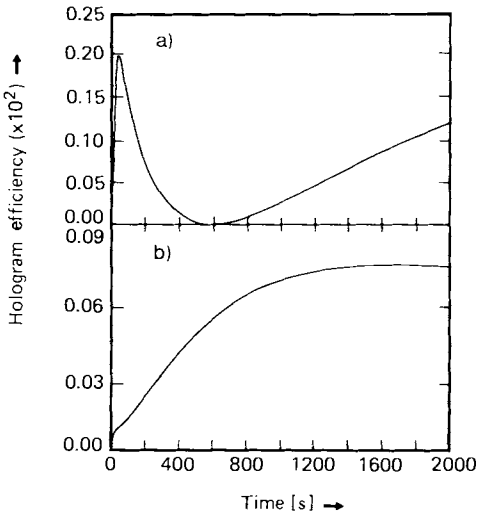



Fig. 9. Calculated hologram efficiency *versus* time for a consecutive reaction scheme $A_1 \rightarrow A_2 \rightarrow A_3$: (a) Subtractive and (b) additive behavior of the change in the index of refraction in the two reaction steps.

If, perhaps in another wavelength region, $R_2 > R_1 > R_3$ the result in Figure 9a is obtained. During the initial stage of the reaction while $A_1$ is being converted into $A_2$, the hologram grows at a rate characteristic of this reaction. But

as the reaction proceeds further $A_2$ is replaced by $A_3$ and since $R_3 < R_1$ this means that $n_1$ must eventually become negative. Following $n_1$ as a function of time, we find that $n_1$ begins to decrease during the second phase of the photochemistry, passing through zero and eventually becoming negative. Since the hologram efficiency depends only on the square of the quantity $n_1$, the expected hologram growth pattern is as shown in Figure 9a.

Such hologram growth curves have been observed for the consecutive photoreaction scheme of benzophenone in PMMA[20,29]. Results at two different wavelengths corresponding to the two cases discussed above (cf. Fig. 9) are shown in Figure 10.

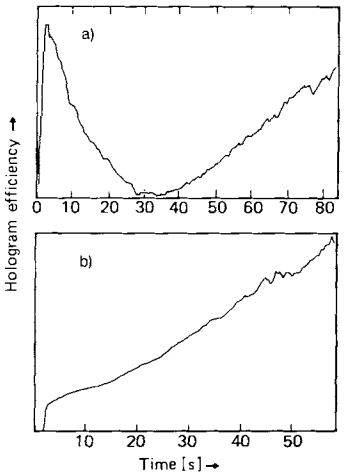



Fig. 10. Experimental hologram efficiency *versus* time for a 250-μm thick sample of 5% by weight benzophenone in PMMA. The hologram was produced using the UV-lines of an $Ar^+$ laser and read with (a) the UV lines and (b) the 514 nm line.

These examples show that characteristic shapes of hologram growth curves occur for different types of reactions. As long as expressions for the kinetic rate equations are available these shapes can be calculated and compared to the experimentally observed features. In this way they can help to prove the underlying reaction mechanism, and, in principle, a fit can give the kinetic parameters.

### 2.2.5. *Observation of a Photochemical Action Spectrum Using Holography*

As a final example of the use of the CW holographic technique in photochemical investigations the observation of a photochemical action spectrum will be discussed[29,34,40]. Many examples exist of photochemistry that occurs when a molecule in its lowest metastable triplet state is excited to a higher triplet state[41]. The holographic technique is particularly useful for studying such processes because it can be used even in cases where interfering reactions occur from the lowest triplet state.

To illustrate the use of holography in this context, we consider the first step in the benzophenone hydrogen abstraction process[29]. As discussed in Section 2.2.3, this process involves the consecutive absorption of two photons. The first photon at a frequency $\omega_1$ excites the $S_0 \rightarrow S_1$ absorption as shown in Figure 11. After intersystem crossing, the lowest triplet state $T_1$ is produced. Absorption of a second photon at $\omega_1$ produces $T_3$. As a result of photochemistry undergone by $T_3$, a product known as the light absorbing transient (LAT)[30-32] is produced.

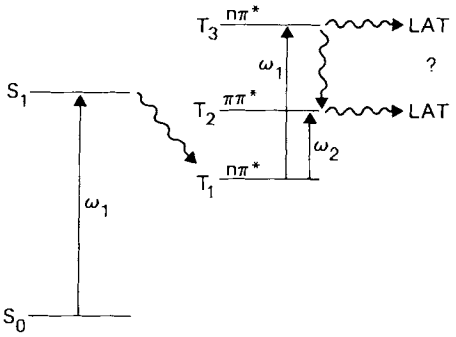



Fig. 11. The energy level diagram for the first step of the photoreaction of benzophenone to the light absorbing transient (LAT) involving the absorption of two photons. Two possible pathways to the LAT are suggested.

The question arises as to which excited states are responsible for the photochemical reaction, $T_3$ itself or an intermediate triplet state $T_2$ that is reached by radiationless relaxation from $T_3$. The holographic technique is ideally suited to answer questions like this. Figure 12 indicates how this might be done. A UV source that need not be coherent excites the benzophenone molecules at $\omega_1$ ultimately producing molecules in the $T_1$ state. Note that even if this irradiation results in photochemistry no hologram is produced since there is no interference pattern.

If two interfering beams at a frequency $\omega_2$ now strike the sample, they can excite the benzophenone molecules to a higher triplet state. If photochemistry occurs from this higher state, then a hologram will be formed. By varying the frequency $\omega_2$ and following the hologram growth rate, a photochemical action spectrum may be obtained. For benzophenone these results indicate that, referring to Figure 11, the nπ* state $T_3$ is reactive, but the ππ* $T_2$ is not.

Investigations using this technique have also been performed for the N–H bond cleavage reaction of carbazole[40] and the previously discussed photodissociation of dimethyl-*s*-tetrazine[34].

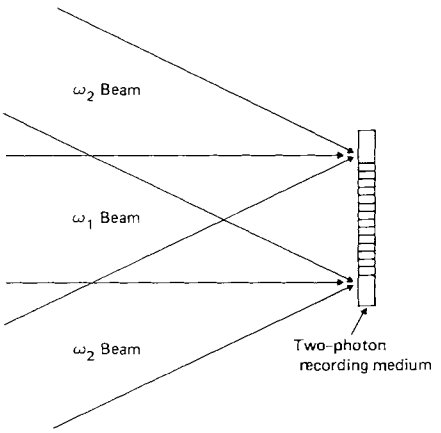



Fig. 12. A three-beam experiment using two different light sources. Only the beams at $\omega_2$ need to be coherent, and only these beams can produce a hologram.

### 2.2.6. *Comparison of the Holographic Method with Conventional Absorption Spectroscopy*

It is perhaps useful at this point to compare the holographic method with other spectroscopic methods, such as conventional optical absorption spectroscopy.

One advantage of the holographic technique is that only small sample areas are needed. Since the fringe spacing of the interference pattern are in the range of a few microns a sample area with a diameter of less than 100 μm contains more than enough fringes to give a well-defined diffraction pattern. Due to the low divergence of laser beams it is easy to focus the light onto such small sample areas. Thus, for materials which are available in small quantities or difficult to align on large surfaces (biological samples, crystals *etc.*) the holographic technique is very suitable.

Further, the holographic technique is sensitive to changes in *both* the index of refraction and absorption. Thus, this technique encompasses both *dispersion* and *absorption* spectroscopy. To illustrate this important point, Figure 13 shows the absorption curve $a(\omega)$ and the related dispersion curve $n(\omega)$ for an optical transition with a maximum at the frequency $\omega_0$[42]. It is obvious from Figure 13 that in the holographic technique the wavelength for the observation of a photochemical reaction is not restricted to the range of absorption but can, in principle, be chosen anywhere in the optical region. This free choice of the detection wavelength has the advantage that overlapping absorption bands do not prevent the investigation of the kinetics of a reaction. Complicated reaction schemes (*e.g.* $A \rightarrow B \rightarrow C \cdots$) can be observed at a *single* wavelength and *without* interruption even when the reaction components have totally different regions of absorption. Further, the detection wavelength can be chosen in a spectral range where the detection system has high sensitivity or where convenient laser sources are available.

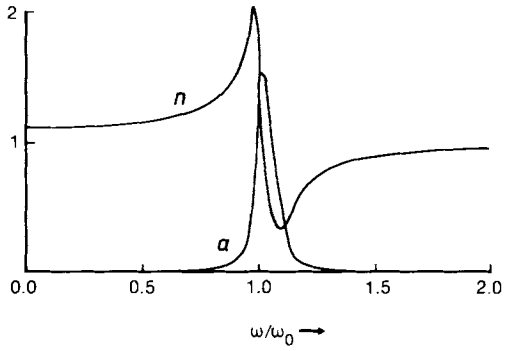



Fig. 13. The dispersion curve *n versus* $\omega$ and the absorption curve *a versus* $\omega$ for an optical transition at frequency $\omega_0$. The abscissa is in units of $\omega/\omega_0$.

If one considers a pure phase hologram the detection beam is *not* absorbed and one has the additional advantage of being able to choose the intensity of the detection beam. Using high power in this beam does not destroy the sample but can give highly improved sensitivity. It should be emphasized that the use of the phase hologram in the holographic technique adds a powerful dispersion method to the spectroscopic tools in the optical region. With the exception of optical rotatory dispersion spectroscopy[43] for optically active materials there exists no other useful dispersion technique.

As mentioned previously (cf. Section 2.2.2) the holographic technique is a zero-background technique, *i.e.* the hologram grows out of the dark. This is in contrast to conventional optical absorption spectroscopy where attenuations, *i.e.* differences in light intensities have to be measured. Since a weak attenuation of a light beam is always much more difficult to measure than the small absolute light intensity of a deflected beam itself the holographic technique is more sensitive than conventional absorption spectroscopy[44-47]. Index changes of $10^{-7}$ or optical absorption changes of $10^{-5}$ are sufficient to cause an easily detected diffracted beam[47].

In the examples of the holographic technique shown so far, the characteristics of the spatial orientation of the fringe pattern relative to a distinct spatial axis of the sample have not been used. However, it is easy to imagine that for anisotropic processes like lattice controlled photoreactions or diffusion processes the orientation of the fringe pattern can reveal the corresponding tensor components quite easily. In Section 2.3 some examples will be discussed. In conventional optical absorption spectroscopy such experiments are impossible.

The advantages discussed above for holography with continuous wave lasers can also be attributed to the pulsed holographic technique described in the following sections. However the limitations of the technique have to be mentioned too. Thus, for example, the observation of photochemical reactions using continuous wave irradiation is confined to reactions in the solid state and an identification of the photoproducts is not possible. Conventional absorption spectroscopy can, however, help to identify photoproducts if the products show characteristic absorption bands.

## 2.3. The Holographic Method with Pulsed Lasers – Transient Gratings

### 2.3.1. *Creation and Detection of Transient Gratings*

Lasers can be run not only in the continuous wave (CW) mode, but can also be used as pulsed light sources giving very short light pulses with a pulse width ranging from about a picosecond up to several nanoseconds[48]. These pulses can be selected as single pulses out of a pulse train or can be obtained at a high repetition rate. If such a laser pulse is split by a beam splitter, as indicated in Figure 3, then, provided the path lengths are equal, two laser pulses arrive at the sample simultaneously but from different directions. Because both pulses originate from the same laser and are thus coherent, an interference pattern is created at the sample which exists for a duration approximately equal to the pulse width. Due to photochemical or photophysical processes involving the molecules in the sample, a holographic grating is induced quasi-instantaneously. After the pulses have left the sample, this grating may decay because of relaxation processes in the sample.

This decay can easily be observed by using a probe pulse with variable time delay. The probe pulse will be diffracted by the grating and its diffracted intensity as a function of

delay time will give the time dependent decay of the grating. An experimental setup[45,49–52] with pulsed lasers can be run at a high repetition rate (*e.g.* 500 Hz) measuring the diffracted probe pulse intensity averaged over many pulses, while slowly varying the time delay between excitation and probe pulses. The time resolution of such an apparatus is given approximately by the pulse width of the laser pulses. The decay of such a grating can, of course, also be observed by a diffracted CW-detection beam whose time dependent intensity shows the decay of the grating. Since the above described holographic grating exists only for a short period of time the holographic method using pulsed lasers is often called the transient grating technique[45,49–51]. (The expression "Forced Rayleigh Scattering" is also used for this technique[52].)

Unlike the CW-holographic method, the transient grating technique is not restricted to investigations of molecules in the solid state but can also be used for molecules in the liquid phase. A wide variety of time dependent phenomena can be observed by this technique. Examples include processes like the relaxation of excited states[44,53,54], photoreactions from excited states, energy transfer across the fringe pattern[56], energy trapping[46], diffusion processes of molecules[44,47,54,57–59], carrier transport in semiconductors[50,60], optical generation and detection of ultrasonic waves[45], and thermal diffusion[44,51]. In the following sections, we will concentrate on a few examples of the technique.

### 2.3.2. *Excited State Dynamics: Lifetimes, Photoreactions and Energy Transfer*

In this section, we want to concentrate on transient gratings produced by time dependent phenomena involving excited states of molecules excluding any effect which may result from the diffusion of the molecules themselves. Thus, we are first restricting our discussion to transient grating effects involving molecules in the solid state or where the relaxation times of interest are much shorter than any observable molecular diffusion process. We will discuss three cases dealing with lifetimes of excited states, photoreactions and energy transfer.

If molecules in the holographic sample are excited by two interfering laser pulses to higher electronic or vibrational states, the index of refraction and the absorbance of the sample will change. The index changes are due to rearrangements in the electronic structure of the molecules[61] whereas the change in the absorption results from a partial depopulation of the ground state. Thus, a holographic grating will be produced in the same general manner as discussed in Section 2.1. Since the change in the index of refraction and absorption coefficient is proportional to the number of molecules excited, the diffraction efficiency $\eta$ depends on $(N_1)^2$, *i.e.*, the square of the number of the excited states at the grating peaks. Here, the simple Eq. (3b) has been used because of the low hologram efficiency produced by the excited states. In the absence of any other processes besides the relaxation of the excited states to the ground state, the time dependence of the intensity $I(t)$ of a diffracted probe beam will be determined by the excited state lifetime $\tau$:

$$I(t)=A\exp\left(-\frac{2}{\tau}t\right). \tag{13}$$

In Eq. (13), $A$ is a constant gathering together all time independent holographic parameters. A plot of $\log I(t)$ against time $t$ will give the decay rate $k=2/\tau$ as the slope and $A$ as the intercept. Thus, lifetimes of excited states can be obtained easily with the transient grating technique[45,50,53]. This can be important for states that decay without the emission of radiation and which cannot thus be investigated by optical emission techniques. Further, from the value of $A$ in Eq. (13), the differences of the molar refractions of the ground and excited states can be elucidated. This gives, in principle, the possibility of determining polarizabilities of excited molecules[62].

Besides the radiationless or radiative relaxation of excited states, a photoreaction can also occur from these transient states as discussed in Section 2.2. It is of interest to see if any complementary information can be obtained by the transient grating technique that cannot be obtained by the CW-holographic method. Without going into details and restricting ourselves to the simple case of a one-photon two-level reaction scheme (see Fig. 5), it can be shown that the time dependence of the diffraction efficiency should be given by [55]

$$\eta(t)=(K_1+K_2\exp[-(k_1+k_2)t])^2 \tag{14}$$

In this equation, $K_1$ and $K_2$ are time independent constants whereas $k_1$ and $k_2$ are rate constants for the decay of the excited state and the photochemical step respectively as indicated in Figure 5. Assuming that the population in the excited state is established instantaneously by the two interfering laser pulses, $k_1$ describes the decay of the transient grating while $k_2$ characterizes the time dependent increase of the modulation depth of the grating due to the creation of photochemical products. Thus, in this case, a photophysical hologram decays and a photochemical hologram grows. The sum of the rate constants for both processes $(k_1+k_2)$ can be obtained from the experimental measurements. The seperate rate constants $k_1$ and $k_2$ cannot be obtained from the pulsed holographic measurements alone. However, if this result is *combined* with the photochemical quantum yield $\phi_p=k_2/(k_1+k_2)$ obtained from the CW-holographic experiment the lifetime of the excited state $\tau=1/k_1$ and the rate constant $k_2$ of the photochemical step can be determined. Thus, a combination of both CW and pulsed holographic methods can provide a detailed picture of the photochemical reaction. It is also possible to obtain $k_1$ and $k_2$ from the application of one of the holographic methods and a spectroscopic lifetime measurement.

Starting again from the modulated pattern of excited states created by two interfering laser pulses, as a third example, one can describe the subsequent dynamics of an excited state not only by radiative and radiationless relaxation to the ground state but also by energy transfer[63,64] to neighboring molecules. For these processes, molecular crystals[65] provide an important example. Their energy transfer has been studied at least in part as a model for energy transfer in biological systems[66,67]. In molecular crys-

tals, energy transfer results from intermolecular interactions and can be thought of as a migration of an excited state by hopping from molecule to molecule in the time before relaxation to the ground state. Because intermolecular interactions are anisotropic, the transfer of energy is very often easier along some crystallographic directions than others. If a transient grating is created in such a crystal, its decay will thus depend on two processes: First the excited state lifetime $\tau$ will reduce the amplitude of the fringe pattern as discussed above and second, the migration of the excited states perpendicular to the fringes will wash out the modulation pattern. Assuming that the energy transport can be described as a diffusion process with a diffusion constant $D$, the observed signal intensity $I(t)$ of the diffracted probe beam should show an exponential decay as in Eq. (13); however, the decay rate $k$ must be modified by a second term describing the diffusion process[56]:

$$k = 2/\tau + (16\pi^2 D/\lambda^2)\theta^2. \qquad (15)$$

Since the effect of the diffusion process on the overall decay depends on $D$ and in addition on the fringe spacing $\Lambda$ (see Eq. (1)), the second term in Eq. (15) depends on $\lambda$ and $\theta$. Performing transient grating experiments with different fringe spacings, *i.e.*, by varying $\theta$, a set of decay constants $k$ can be measured. From the slope of a plot of $k$ as a function of $\theta^2$, the diffusion constant $D$ can be calculated, whereas the intercept of the plot yields the lifetime $\tau$. Thus, transient grating experiments with variable fringe distances are capable of *separating* lifetime and diffusion effects quite easily.

Such measurements have been done by several workers[50,56,68]. In Figure 14, the results of *Siegman et al.*[56] are shown. They investigated a single crystal of *p*-terphenyl doped with $10^{-3}$ mol/mol of pentacene. Obtaining $k$ from decay curves as in Figure 14a and plotting $k$ as a function of $\theta^2$ (see Fig. 14b), they obtained a diffusion constant $D = 2 \pm 0.1$ cm$^2$ s$^{-1}$ for the energy transfer along the crystallographic $b$ axis. The intercept $2/\tau$ was in good agreement with the independently measured lifetime of $\tau = 9.5 \pm 0.3$ nsec. Since such measurements can be done along different crystallographic directions by simply rotating the holographic sample the anisotropy of energy transfer and thus of intermolecular interactions can be studied in a very direct manner.

It should be emphasized that the transient grating technique with variable fringe distances is not just restricted to diffusion by energy transfer. In principle, any diffusive process that reduces the peaks and fills the nulls of the modulation pattern can be investigated. Thus, for example, transient gratings have been produced in *semiconductors*[50,60,69]. In these materials, the gratings are due to the formation of free carriers and the decay of the grating gives the characteristic diffusion constant for the movement of the free carriers. Other systems in which light induced charge transport is of great importance include *electro-optic crystals* such as $LiNbO_3$ and $LiTaO_3$ doped with transition metals. These materials have been considered as potential candidates for holographic information storage[10] and have a variety of other applications in modern optics. The photoinduced electron and hole transport in

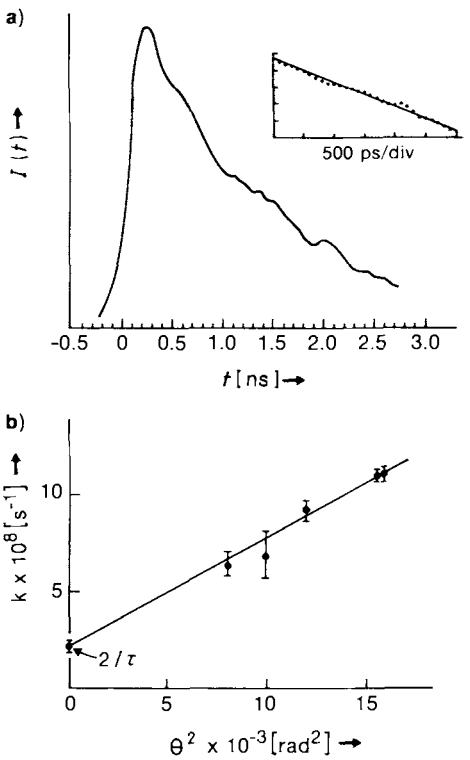



Fig. 14. (a) The decay of the diffracted probe pulse intensity *versus* probe pulse delay time. The inlay shows the logarithmic plot giving the decay rate $k$ as the slope. (b) The transient grating decay rate $k$ *versus* the square of the angle of incidence $\theta^2$ giving the diffusion constant $D$ as the slope and $2/\tau$ as the intercept. After [56].

these materials has been investigated by holographic methods[70]. So far, mainly CW-holographic methods have been used[71]; however, for systems with shorter decay times the transient grating method is suitable as well.

### 2.3.3. *Rotational and Translational Diffusion Processes in Liquid Solutions*

In the sections above, it was assumed that the molecules under investigation had fixed positions relative to the polarization of the exciting as well as the detecting light pulses because they were incorporated in an ordered or unordered way in a crystalline or glassy matrix. However, if the experiments are performed in liquid solution, the molecules can diffuse within the sample showing rotational as well as translational diffusion. Since laser light is linearly polarized, the two interfering light pulses will preferentially excite molecules with a transition moment parallel to the electric vector of the light waves. So not only a spatial modulation pattern of excited states is created by the interference of the two light pulses but also a photoselection of preferentially oriented molecules. For these molecules in a liquid solution, it is possible to follow rotational diffusion if the polarization of the delayed probe pulses relative to the exciting laser pulses is taken into account[44,54]. Since rotation of molecules in solution will occur much faster than noticeable diffusion of excited molecules from the peaks into the nulls of the grating, it is the rotational and not the translational diffusion which is observed first using linearly polarized laser light as a probe beam. As in time resolved fluorescence depolarization ex-

periments[72, 73] the decay of the transient grating is measured with two time dependent signals[54] $I_{\parallel}(t)$ and $I_{\perp}(t)$ which are obtained for parallel or perpendicular orientation of the polarization of the probe pulse relative to that of the excitation pulses. A detailed analysis[44, 54] of the time dependence of the signals $I_{\parallel}(t)$ and $I_{\perp}(t)$ shows that the sum $S(t)$ of both signals gives an exponential decay with a decay constant $k = 1/\tau$ where $\tau$ is the lifetime of the excited state. Computing the difference $D(t)$ of both signals $I_{\parallel}(t)$ and $I_{\perp}(t)$ and taking the ratio $R(t) = D(t)/S(t)$ it can be shown that $R(t)$ gives an exponential decay too; however, the decay constant $k_R = 1/\tau_R$ yields the rotational reorientation time $\tau_R$. So, by performing two time dependent measurements, $I_{\parallel}(t)$ and $I_{\perp}(t)$, it is possible to *separate* the lifetime effect from the reorientation of the molecules. In Figure 15a, the two time dependent signals $I_{\parallel}(t)$ and $I_{\perp}(t)$ are shown for a sample of Rhodamine B in *n*-propanol as obtained by *Fayer et al.*[54]. Figure 15b shows the corresponding logarithmic plot of $S(t)$ and $R(t)$ giving the excited state lifetime $\tau$ and the rotational reorientation time $\tau_R$, respectively.

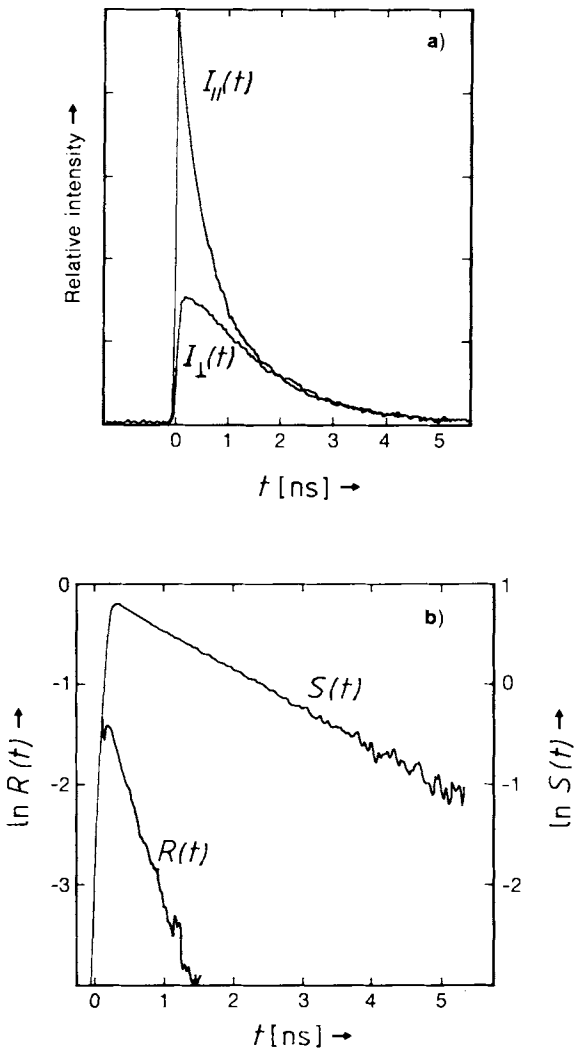



Fig. 15. (a) The decay of the transient grating signal with probe pulse polarization parallel to ($I_{\parallel}(t)$) and perpendicular to ($I_{\perp}(t)$) the excitation polarization for a sample of rhodamine B in *n*-propanol. (b) $S(t)$ and $R(t)$ curves calculated from the data presented in (a). The straight line fits yield values of the excited state lifetime $\tau$ and the orientational reorientation time $\tau_R$. After [54].

It is interesting to note that the above obtained excited state lifetime can be checked in a third experiment. Setting the polarization of the probe beam at 54.7° (the "magic angle") relative to the excitation polarization, it can be shown that the observed decay is independent of rotational dynamics. In this case, the exponential decay of the signal $I_M(t)$ gives directly the excited state lifetime $\tau$. So both independently obtained values for $\tau$ can be compared[44, 54].

In principle, diffusion of molecules perpendicular to the grating can also be observed in liquids. However, for this translational diffusion process the lifetime of the excited states of the molecules must be in the range of the diffusion time necessary to give noticeable equilibration between the peaks and the nulls of the grating. This limitation can be circumvented if the molecules are labeled by forming photoproducts[47, 74]. For the observation of very slow diffusion processes, as discussed in Section 2.3.4, this is of great importance.

The investigation of rotational reorientation and translational diffusion of molecules in liquid solvents is helpful in discussing solute conformations, solvent-solute interactions and local solvent structure[72–77]. In particular, the predictions of the Debye-Stokes-Einstein hydrodynamic theory[78] can be examined yielding the effective volume of the rotating molecule as a characteristic parameter. So far, such investigations have been done by applying time resolved absorption[79] or fluorescence depolarization spectroscopy[72, 73] in the picosecond time regime. With the transient grating technique, an additional, very accurate technique is available. If this technique is combined with fluorescence depolarization measurements differences in the excited state and ground state rotation times $\tau_R$ can be obtained. Values of up to 30% are estimated for these differences.

### 2.3.4. *Holographic Investigations of Polymers*

A recently very active field of research is the study of chain dynamics in polymer solutions or in pure polymers. It was pointed out that one has to distinguish carefully between individual and collective chain motions, *i.e.*, monomer motions respectively with or without relative displacement of the center of mass of the chains[80]. Whereas the collective motions can be observed quite well with, *e.g.* dynamic light scattering[81], for the individual chain motion described by a self-diffusion process no suitable technique has been available until recently. The reason was the very slow diffusion process with diffusion constants $D$ in the range of $10^{-7}$ to $10^{-11}$ cm$^2$ s$^{-1}$. Since the duration of the experiment is proportional to the square of the diffusion length, classical tracer techniques[82] using macroscopic diffusion distances (0.1–1 cm) imply extremely long detection times of the orders of several days or weeks. However, if the diffusion length is diminished to the microscopic fringe distances of an interference pattern (1–10 μm) the observation time will be reduced by up to 8 orders of magnitude. *Léger* and *Rondelez et al.*[47, 57, 58] have investigated successfully the self-diffusion of polystyrene chains in benzene with the holographic technique using a photochromic label on the polymer chains. After the holographic excitation pulses, the labels indicate the peaks and the nulls of the grating

which are then equilibrated by diffusion. Thus, *very slow* diffusion processes can be observed efficiently by the holographic technique. This is not only of interest for polymers in solution but also for, *e.g.*, diffusion of polymer chains—especially of low molecular weight additives like plasticizers—in a pure polymer network[59], or for biological processes such as protein diffusion on cell surfaces[83].

Another application of the holographic technique is the determination of the chain length of polymers. For example, the polymerization of butadiene single crystals has recently been observed with a holographic setup[84]. The disappearance of the hologram due to the growth of polymeric chains across the fringe pattern was investigated. So far, the chain length did not exceed the spatial resolution of the holographic grating so that only an upper limit on chain length could be determined. These investigations have been done using a CW holographic technique but could also have been done with the transient grating technique[62].

### 2.3.5. *Optical Generation of Ultrasonic Waves by Transient Gratings*

So far, local heating by the *absorption* of the two interfering light pulses has not been taken into account. With low laser power, this effect is negligible[44]. However, if high laser power is concentrated in short laser pulses considerable heating can occur in the sample[44,45,50,51,85–87]. Since this heating is due to radiationless relaxation processes of the excited molecules, it is concentrated at the local maxima of the transient interference pattern and causes a thermal expansion in this region of the sample. Thus, the density in the peaks of the grating is reduced whereas the density in the nulls is increased. As a result, a counterpropagating density wave (a standing density wave) is created, which is present even after the two exciting pulses have left the sample. In this way, an ultrasonic wave can be generated optically in the medium. It is obvious that the wavelength of this wave is determined by the fringe distance $\Lambda$. Since $\Lambda$ can be varied easily, in a broad range from about 1 mm to 0.1 μm (cf. Eq. (1)) tunable acoustic frequencies from about 3 MHz to 3 GHz can be generated by simply changing the angle of incidence $\theta$ [45]. Since the oscillating density changes of the ultrasonic wave cause oscillations of the amplitude $n_1$ of the index of refraction, the ultrasonic wave can be detected with diffracted time delayed probe pulses in the ordinary manner. Results are shown in Figure 16c for a $5 \times 10^{-5}$ M solution of malachite green in ethanol[45], where the excitation wavelength was chosen in the absorption region of malachite green.

Another mechanism for generating ultrasonic waves by transient gratings uses stimulated Brillouin scattering instead of absorption[88,89]. This mechanism is similar to stimulated Raman scattering. A higher frequency photon in one of the two interfering beams is cancelled and a lower frequency photon in the other beam is created. The result is an acoustic phonon with a frequency equal to the difference of the frequencies of the two photons. In addition to the conservation of energy, the conservation of momentum has to be satisfied. The spread in frequency in the two interfering pulses is always broad enough to allow efficient phonon generation at any angle of intersection of the two interfering beams. It has to be emphasized that in this mechanism, *no absorption* and therefore no heating occurs. There is a direct coupling of the optical electromagnetic field to the material acoustic field. Thus, this effect can be observed without absorption of the interfering beams as shown in Figure 16a for a solution of pure ethanol[45]. A more detailed description[45,88,89] of the heating effect and the stimulated Brillouin scattering shows that different time dependences of the diffracted signal arise which allow a separation of the two mechanisms. In Figure 16b, an intermediate case is shown where both mechanisms are visible because of the very low concentration of malachite green[45]. Both of the above mentioned mechanisms have to be taken into account when decaying signals of transient gratings as described in the foregoing sections show an oscillating behavior[56,85,87,89].

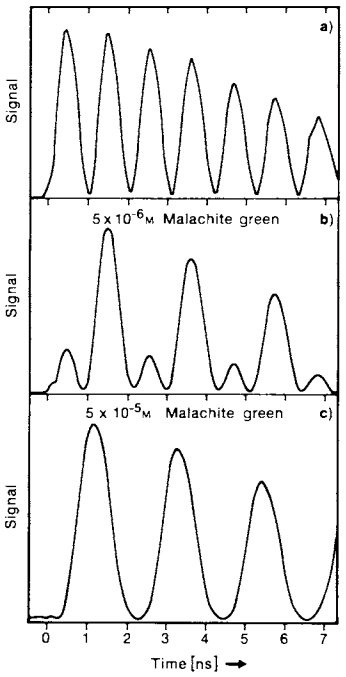



Fig. 16. Optically generated ultrasonic waves detected in (a) pure ethanol, (b) and (c) malachite green in ethanol (increasing concentrations). In pure ethanol the Brillouin scattering is responsible, whereas in concentrated solutions of malachite green, the heating effect due to absorption accounts for the generation of ultrasonic waves; (b) represents an intermediate case. After [45].

Since the ultrasonic waves can be optically generated in liquids and in solids, there are a wide variety of applications[45,50]. The technique can be used for nondestructive acoustic testing of materials, for measuring anisotropic elastic constants, acoustic attenuation, isotropic and anisotropic thermal diffusion, photoelastic constants, and a variety of other interesting material parameters.

## 3. New Materials for Holography

### 3.1. Conventional Holographic Materials

In the preceding discussion we have shown how the development and decay of a hologram can be used to obtain

information on a variety of chemical and physical processes. We will now turn this approach around and show how these studies of solid state chemistry can result in the development of new classes of holographic recording materials.

A variety of materials have been considered for holographic recording. Table 1 lists a few of these materials and the subject has been treated in a number of reviews[90,91]. One can list several desirable criteria for holographic materials. A reasonably high efficiency is desirable, but efficiencies approaching 100% are not necessary. The photosensitivity should be high, *i.e.*, the time required to reach maximum efficiency should be as short as possible. The recording material should be sensitive in wavelength regions accessible to commercially available lasers. The hologram must not be erased during reading, so some method of fixing the recorded interference pattern is necessary.

Table 1 illustrates the point that no material satisfies all of these requirements. On the other hand, a material like dichromated gelatin is perfectly adequate for many applications and has proven quite useful[92].

Table 1. Properties of some holographic recording materials.

| Material | Advantage | Disadvantage |
|---|---|---|
| dichromated gelatin | large $n_1$<br>high hologram efficiency<br>thin coatings | spectral sensitivity<br>recording speed<br>passivation<br>shelf life |
| photopolymer | light induced developing<br>no shrinkage<br>inert<br>coating ease | small $n_1$<br>thick coatings<br>spectral sensitivity<br>low hologram efficiency |
| photographic film | spectral sensitivity<br>chemical amplification<br>reproducibility | medium efficiency<br>substrate choices<br>resolution |
| photoresist | high hologram efficiency<br>coating ease<br>stability | spectral sensitivity<br>recording speed<br>linearity |
| thermoplastic | "self-developing"<br>high sensitivity<br>erasibility | spectral sensitivity<br>low hologram efficiency<br>resolution |

One severe limitation in all of the currently available materials is their spectral sensitivity. This sharply limits the number of possible laser sources that can be used directly. Dichromated gelatin, for example, cannot be used at wavelengths longer than 500 nm[92]. Responses to wavelengths as long as 748 nm have been obtained using photographic film such as Kodak 649F or 120-01[93]. Attempts to spectrally sensitize dichromated gelatin or holographic quality photographic film to longer wavelengths have so far produced unsatisfactory results. At present no single-photon volume holographic recording material with response at wavelengths longer than 750 nm exists. This is unfortunate because it means that there are no holographic materials compatible with the convenient and inexpensive injection diode lasers such as GaAlAs (800—900 nm) or GaInAsP (1.2—1.6 μm).

As a result of some of the photochemical investigations described in the first part of this paper, a new technique has been developed involving *two-photon four-level photochemistry* for the production of holograms in the red and infrared[94,95]. In addition to their spectral sensitivity, these materials have the advantage that they are self-developing and require no fixing step. Furthermore, the hologram can be gated off and on by utilizing an auxiliary light source.

### 3.2. Two-Photon Four-Level (2P4L) Photochemistry for Holographic Recording

Most holographic recording materials utilize photochemical reactions in which the rate of product formation depends linearly on laser light intensity. The corresponding 1P2L scheme has already been shown in Figure 5. Only two levels of the molecule $A_1$ are involved in the photochemistry. It can be shown[23] that the overall rate constant $k$ for product formation is proportional to the molar extinction coefficient $\varepsilon$ and is linear in laser intensity $I$ as previously indicated:

$$k \sim \varepsilon I. \tag{16}$$

Now consider using such a two-level medium for holographic recording. Such an experiment is shown schematically in Figures 1 and 5. Normally the reconstruction wave will be at the same wavelength as the object and reference waves. This means that the reconstruction wave itself can also produce photochemistry. This photochemistry will result in gradual erasure of the hologram. There are two ways of eliminating or minimizing the effect of erasure during reading for 1P2L materials. The first, and less satisfactory method, is simply to reduce the reading light intensity so that the photochemistry that occurs during reading is reduced to an acceptable level. This is, of course, impractical when the hologram is meant to be semi-permanent. The most commonly used method of eliminating erasure is to fix the holographic image permanently. This is done in dichromated gelatin and silver halide films by wet chemical processes.

Another disadvantage of 1P2L materials arises when one considers extending their sensitivity into the red and infrared regions. All of the energy used to produce photochemistry must come from *one* absorbed photon (cf. Fig. 5). Very few systems undergo efficient photochemistry in the red or infrared, and those few systems that do also tend to be thermally unstable. This point is illustrated in Table 2, where laser wavelengths and bond energies are compared. Both AIBN and hexaphenylethane shown in the table are thermally unstable.

It has been recognized by previous workers that many of the problems with the one-photon systems are either not present or are significantly reduced in importance when the hologram forming photochemical process involves the absorption of two or more photons[96,97]. These investigators employed a two-photon three-level (2P3L) system. The energy level diagram for such a system is similar to the four level scheme shown in Figure 5 with the difference that $A_1^*$ and $A_2$ have now been combined into a single level. In a three-level system, the recording medium is simul-

Table 2. Bond energy and related wavelengths of various lasers.

| Bond | Bond-Energy [a] [kJ/mol] | Wavelength [nm] | Laser | Wavelength range [nm] |
|---|---|---|---|---|
| C–H | 410 | 291.7 | | |
| C–C | 347.3 | 344.5 | $Ar^+$ (UV) | 334-364 |
| Cl–Cl | 239.3 | 499.9 | $Ar^+$ (VIS) | 458-529 |
| Br–Br | 189.1 | 632.8 | HeNe | 632.8 |
| | 140.6 | 850 | GaAlAs | 800-900 |
| AIBN | 129.7 | 992 | | |
| | 112.6 | 1064 | Nd-YAG<br>Nd-Glass | 1064 |
| $(C_6H_5)_3C-C(C_6H_5)_3$ | 50.2 | 1906 | | |

[a] Value for azobisisobutyronitrile (AIBN) from F. M. Lewis, M. S. Matheson, *J. Am. Chem. Soc. 71* (1949) 747. All other values from S. W. Benson, *J. Chem. Educ. 42* (1965) 503.

taneously exposed to radiation at two different optical frequencies $\omega_1$ and $\omega_2$ with intensities $I_1$ and $I_2$. The rate constant $k$ for product formation is now given by

$$k \propto \varepsilon_1 I_1 \varepsilon_2 I_2 \tau \tag{17}$$

where $\varepsilon_1$ and $\varepsilon_2$ are the respective molar extinction coefficients at the two frequencies $\omega_1$ and $\omega_2$. $\tau$ is the lifetime of the intermediate state.

Consider the simple case where $\omega_1 = \omega_2$. The photochemistry is then proportional to $I_1^2$. Any reduction in the laser intensity during reading would have its effect on hologram erasure reduced by the square of this factor. In addition, the energy to produce photochemistry is now supplied by two laser photons and it should not be difficult to find thermally stable two-photon systems that could be used with red or infrared radiation.

Perhaps a more interesting case is when $\omega_1 > \omega_2$, *i.e.* when the energy from the ground level to the intermediate level is greater than from the intermediate level to the final level. The medium is illuminated by reference and object beams at a frequency $\omega_2$, as well as by an additional uniform and not necessarily coherent beam at $\omega_1$. Note that we have treated this case in another context in the discussion associated with Figure 12. Holograms formed using this approach have several advantageous properties. As for the case where $\omega_1 = \omega_2$, these materials can be written with red or infrared lasers. Most of the energy needed to produce photochemistry is supplied by the $\omega_1$ photon which can be in the ultraviolet. Another important advantage is that the recording medium is sensitive to the $\omega_2$ radiation only when $\omega_1$ radiation is present. Thus, during the reconstruction of the image for readout no additional deleterious exposure of the recording medium takes place. Also, temporal or spatial gating of the recording can be achieved by masking or modulating the $\omega_1$ beam.

The first demonstrations of two-photon holographic recording were in $LiNbO_3$ and KTN ($KTa_xNb_{1-x}O_3$), where the recording process was the multi-photon photorefractive effect[96,97]. This effect involves the excitation of carriers within the crystal lattice to produce a macroscopic polarization change that induces a modulation of the index of refraction *via* the electro-optic effect. The major disadvantage of these materials is the lack of real intermediate energy levels between the ground and final states. Since a resonant enhancement from these intermediate levels is not present, the two-photon absorption processes are extremely weak and peak exposure intensities greater than 5 $MW/cm^2$ are necessary. A factor of 100 improvement in sensitivity was demonstrated by doping the $LiNbO_3$ crystal with $Cr^{3+}$, thereby converting the intermediate level from a virtual to a real level with a 500 ns lifetime[98]. The resulting sensitivity, however, was still several orders of magnitude too low for CW two-photon holography.

It can be shown[95] that *no* 2P3L system can be sensitive enough to be used for holographic recording with CW lasers. This can be seen qualitatively by considering the role played by the intermediate state. For optimum production of photochemical products one wants the population in this state to be as large as possible. This means that the extinction coefficient $\varepsilon_1$ should be large and the lifetime $\tau$ of this state should be long. However, these two quantities are not independent since lifetime and absorption strength are inversely proportional to each other. There is thus an upper limit to the rate $k$ that one can obtain for a 2P3L system.

To produce two-photon holographic systems that can be used with CW laser sources, one must circumvent these constraints. One way of doing this is to use the two-photon four-level system (Fig. 5). There are now two intermediate levels $A_1^*$ and $A_2$. Level $A_1^*$ may have a large oscillator strength with respect to transitions from the ground state, while level $A_2$ may have a long lifetime. It thus should be possible to find a two-photon four-level system with which one can produce holograms using only a few milliwatts of CW laser power.

A variety of organic materials have energy level systems arranged as shown in Figure 5. States $A_1$ and $A_1^*$ are the lowest ground state and an excited singlet state of the molecule, respectively. $A_2$ and $A_2^*$ may be ground and excited states of an isomeric form of the molecule or they can be excited triplet states. In fact, such systems are described in Section 2.2.5. In that earlier discussion we were interested in using holography to investigate excited state photochemistry. Here we note that benzophenone[29] and carbazole[94] can be used in two-photon four-level holographic recording materials.

The holographic system that has been most thoroughly investigated in this context is biacetyl dissolved in a polymer host matrix[95]. The relevant absorption spectra of biacetyl are shown in Figure 17. The initial photon excites the

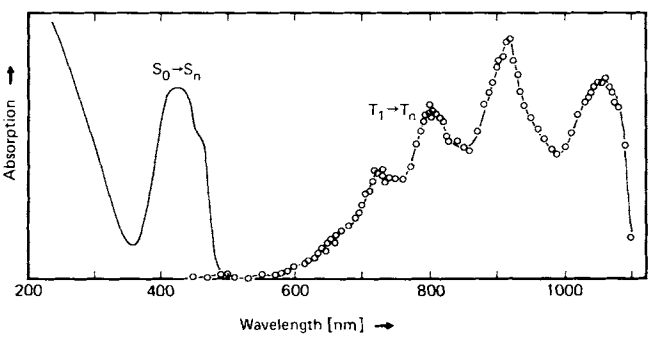



Fig. 17. The $S_0 \rightarrow S_n$ and $T_1 \rightarrow T_n$ absorption spectra for biacetyl. The $S_0 \rightarrow S_n$ absorption is for a 15% concentration of biacetyl in a 300-μm thick sample of polycyanoacrylate and the $T_1 \rightarrow T_n$ absorption is for a $3.9 \times 10^{-2}$ M solution of biacetyl in carbon tetrachloride.

biacetyl molecule from its ground state to an excited singlet state $S_n$. This can be done according to the figure, provided the exciting wavelength is shorter than 500 nm. The second photon produces the hologram by exciting the biacetyl from $T_1 \rightarrow T_n$. This occurs if the second wavelength is between 600 and 1100 nm. The hologram is produced as a result of a photochemical reaction that occurs from $T_n$. Hologram formation in biacetyl[95] is illustrated in Figure 18. The experimental arrangement was similar to the one

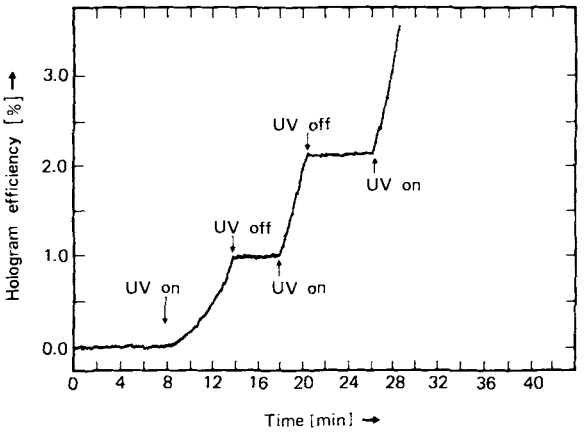



Fig. 18. Gating of a hologram in a 15% biacetyl in polycyanoacrylate sample.

sketched in Figure 12. The matrix in which the biacetyl was dissolved for these experiments was a polycyanoacrylate polymer. Irradiation at $\omega_1$ was provided in the UV by a medium pressure Hg-lamp. The infrared source at $\omega_2$ was a krypton laser operating at 752.5 nm. At time $t=0$ only the IR source illuminates the sample. Since this light is not absorbed by a ground state biacetyl molecule, no hologram is produced. When the UV source is turned on hologram formation begins. When it is turned off the hologram growth is gated off. Holograms formed in this way require no chemical development step. They are "developed" simply by turning off the UV source.

### 3.3. Applications of 2P4L Materials

In this section we will illustrate several applications of two-photon four-level infrared holographic materials. The most familiar application for materials of this type is in the production of three-dimensional images. The recording of an extended image using the biacetyl/polycyanoacrylate system is shown in Figure 19[99]. The hologram was produced and reconstructed at 752.5 nm. The advantage of recording extended holographic images in this way lies in the possibility of spatially or temporally gating the process. By spatially gating hologram formation one can imagine the production of holographic movies with frame to frame exposures gated on and off with the UV source. Temporal gating, of course, provides the potential for recording holograms at precisely well-defined instants in time.

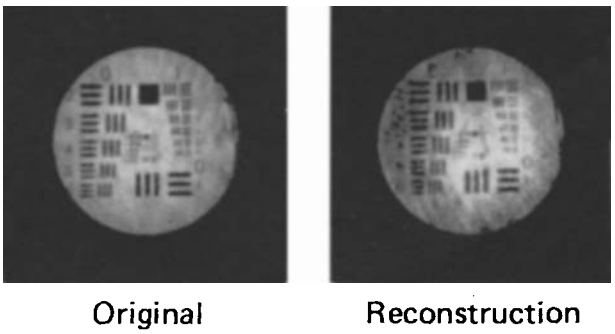



Fig. 19. Two-photon hologram of a resolution chart.

In the future holograms will probably be most widely used for the production of a variety of kinds of optical elements for the deflection and focusing of light. Holographic optical elements (HOEs) utilize the fact that a hologram is capable of transforming a family of incident waves. The simplest example of a HOE is the holographic grating formed by the interference of plane object and reference waves. This type of HOE was described in Section 2.1, and later its use for monitoring photochemistry was treated. Another example is the holographic lens that is formed by the interference of a spherical object wave with a spherical or plane reference wave. Figure 20 shows the recording geometry for the production of an off-axis holographic lens. A hologram is produced from the "real" glass lens. If this hologram is illuminated it will work like a lens; thus a copy of the lens is obtained. The properties and applications of HOEs have been the subject of several recent reviews[100].

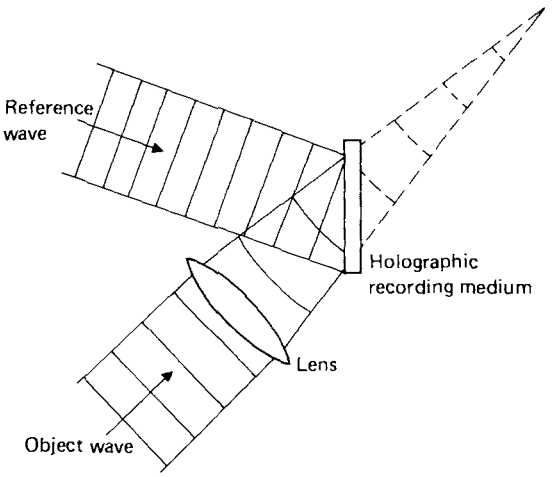



Fig. 20. The arrangement of the coherent light waves necessary to record the holographic image of a lens.

The fundamental advantage of HOEs is that a complex and expensive optical system can be replaced by a cheap and simply fabricated piece of plastic. This is a particularly important consideration when one wishes to use the HOE with an inexpensive injection diode laser.

As a final example of the use of the infrared hologram recording technique described above, we consider the fabrication of integrated optical devices[101]. The general principal of these devices is illustrated in Figure 21. The two interfering infrared beams intersect inside a narrow dielectric waveguide formed from a thin biacetyl/polycyanoacrylate layer between glass plates. Since the infrared beams are confined within a several micron thick dielectric layer, power densities can be quite high. Input powers of a few milliwatts can result in waveguide power densities of a few

kilowatts/cm$^2$. This is particularly important for the two-photon four-level materials that tend to have low recording sensitivities. Optical waveguide directional couplers have been produced in this way[102].

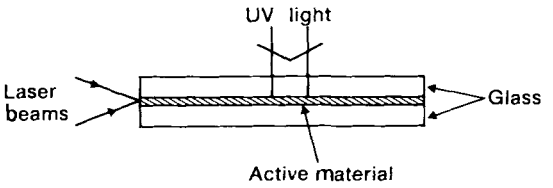



Fig. 21. Formation of a thin-film waveguide directional coupler, whose active material is suitable for two-photon four-level photochemistry.

## 4. Conclusion and Outlook

In this review we have discussed a variety of material parameters that can be studied using holographic grating techniques. Excited state photochemistry, energy transfer, rotational relaxation, charge transport and polymerization can all be conveniently studied by holography. One can use CW or pulsed versions of the technique.

The holographic technique has several distinct advantages over conventional spectroscopic methods. The CW technique is ideally suited for investigating solid state photochemical reactions such as photopolymerization, and photodegradation. Pulsed holography can be used to follow dynamic processes such as diffusion. Because extremely small sample areas are used for these measurements, the method can for example be used to follow energy transfer or diffusion in biological systems.

The holographic technique measures diffusion or energy transport in directions perpendicular to the fringe planes. Because this direction can be varied by varying the incident plane formed by the interfering beams, holography can be used in a variety of applications where diffusion or energy transport is anisotropic. The use of pulsed holography to produce ultrasonic waves permits one to obtain values for the elastic constants and acoustic attenuation. In this way holography can be used as a non-destructive testing method.

In addition to the above uses of holography for physical measurements, we have shown in this paper, how the fundamental holographic technique can be used to suggest new classes of holographic recording materials. This point has been illustrated by a discussion of infrared sensitive two-photon four-level holographic recording materials. Because the recording process in these materials can be gated on or off, they offer new possibilities for holographic information recording. In addition they are sensitive in the wavelength regime of the widely used semiconductor lasers. These new holographic materials can be used as passive elements in integrated optics and optical communication. Current two-photon four-level photochemical recording materials are not yet sensitive enough to be widely practical. Much work needs to be done to understand this two-photon recording process and to identify more sensitive materials.

*The authors would like to acknowledge fruitful collaboration with a number of co-workers whose names appear in the references. C. B. thanks the VW-Stiftung and the Fonds der Chemischen Industrie for financial support. DMB is grateful to the Office of Naval Research and the U. S. Army Research Office for partial financial support.*

Received: May 10, 1983 [A 464 IE]
German version: *Angew. Chem. 95* (1983) 612

[1] D. Gabor, *Nature (London) 151* (1948) 777; *Proc. R. Soc. London A 197* (1949) 454; *Proc. Phys. Soc. London B64* (1951) 449.
[2] E. N. Leith, J. Upatnieks, *J. Opt. Soc. Am. 52* (1962) 1123; *54* (1964) 1295.
[3] R. J. Collier, C. B. Burckhardt, L. H. Lin: *Optical Holography*, Academic Press, New York 1971.
[4] H. M. Smith: *Principles of Holography*, Wiley-Interscience, New York 1969.
[5] H. Kiemle, D. Röss: *Einführung in die Technik der Holographie*, Akademische Verlagsgesellschaft, Frankfurt am Main 1969.
[6] Y. I. Ostrovsky, M. M. Butusov, G. V. Ostrovskaya: *Interferometry by Holography*, Springer Series in Optical Sciences, Vol. 20, Springer, Berlin 1980.
[7] W. Schuman, M. Dubas: *Holographic Interferometry*, Springer Series in Optical Sciences, Vol. 16, Springer, Berlin 1979.
[8] G. von Bally: *Holography in Medicine and Biology*, Springer Series in Optical Sciences, Vol. 18, Springer, Berlin 1979.
[9] B. Hill in N. H. Farhat: *Advances in Holography*, Vol. 3, Marcel Dekker, New York 1977.
[10] D. L. Staebler, in H. M. Smith: *Holographic Recording Materials*, Top. Appl. Phys., Vol. 20, Springer, Berlin 1977.
[11] D. Casasent: *Optical Data Processing*, Top. Appl. Phys., Vol. 23, Springer, Berlin 1978.
[12] S. H. Lee: *Optical Information Processing*, Top. Appl. Phys., Vol. 48, Springer, Berlin 1981.
[13] B. J. Chang, C. D. Leonard, *Appl. Opt. 18* (1979) 2407.
[14] D. H. Close, *Opt. Eng. 14* (1975) 408.
[15] V. E. Wood, N. F. Hartman, C. M. Verber, R. P. Kenan, *J. Appl. Phys. 46* (1975) 1214; W. J. Tomlinson, H. P. Webber, C. A. Pryde, E. A. Chandross, *Appl. Phys. Lett. 26* (1975) 303; T. Tamir: *Integrated Optics*, Top. Appl. Phys. Vol. 7, Springer, Berlin 1979; A. Wuthrich, W. Lukosz, *Appl. Phys. 21* (1980) 55.
[16] W. S. Boyle, *Sci. Am. 237* (1977) No. 2, 40.
[17] A. L. Schawlow, C. H. Townes, *Phys. Rev. 112* (1958) 1940.
[18] E. Garmire in T. Tamir: *Integrated Optics*, Top. Appl. Phys. Vol. 7, Springer, Berlin 1979.
[19] H. Kogelnik, *Bell Syst. Tech. J. 48* (1969) 2909.
[20] D. M. Burland, C. Bräuchle, *J. Chem. Phys. 76* (1982) 4502.
[21] J. D. Jackson: *Classical Electrodynamics*, Wiley, New York 1962, p. 155.
[22] Z. G. Szabo in C. H. Bamford, C. F. H. Tipper: *Theory of Kinetics*, Elsevier, Amsterdam 1969.
[23] G. C. Bjorklund, D. M. Burland, D. C. Alvarez, *J. Chem. Phys. 73* (1980) 4321.
[24] D. M. Burland, G. C. Bjorklund, D. C. Alvarez, *J. Am. Chem. Soc. 102* (1980) 7117.
[25] F. W. Deeg, J. Pinsl, C. Bräuchle, J. Voitländer, *J. Chem. Phys. 79* (1983), No. 2, in press.
[26] C. Bräuchle, *Mol. Cryst. Liq. Cryst.*, in press.
[27] C. Bräuchle, *Nachr. Chem. Tech. Lab. 29* (1981) 603.
[28] M. V. George, J. C. Scaiano, *J. Phys. Chem. 84* (1980) 492; J. N. Pitts Jr., J. K. S. Wan, E. A. Schuck, *J. Am. Chem. Soc. 86* (1964) 3006.
[29] C. Bräuchle, D. M. Burland, G. C. Bjorklund, *J. Phys. Chem. 85* (1981) 123, 618.
[30] G. O. Schenk, M. Cziesla, K. Eppinger, G. Matthias, M. Pape, *Tetrahedron Lett. 1967*, 193; G. O. Schenk, G. Matthias, *ibid. 1967*, 699.
[31] N. Filipescu, F. L. Minn, *J. Am. Chem. Soc. 90* (1968) 1544.
[32] J. Chilton, L. Giering, C. Steel, *J. Am. Chem. Soc. 98* (1976) 1865.
[33] H. Murai, K. Obi, *J. Phys. Chem. 79* (1975) 2446; H. Murai, M. Jinguji, K. Obi, *ibid. 82* (1978) 38.
[34] C. Bräuchle, D. M. Burland, G. C. Bjorklund, *J. Am. Chem. Soc. 103* (1981) 2515.
[35] D. M. Burland, *Proc. Soc. Photo-Opt. Instrum. Eng. 113* (1977) 151; D. M. Burland, F. Carmona, J. Pacansky, *Chem. Phys. Lett. 56* (1978) 221.
[36] B. Dellinger, M. A. Paczkowski, R. M. Hochstrasser, A. B. Smith III, *J. Am. Chem. Soc. 100* (1978) 3242.
[37] D. M. Burland, F. Carmona, *Mol. Cryst. Liq. Cryst. 50* (1979) 279.
[38] H. de Vries, D. A. Wiersma, *J. Chem. Phys. 72* (1980) 1851.
[39] M. A. Paczkowski, R. Pierce, A. B. Smith III, R. M. Hochstrasser, *Chem. Phys. Lett. 72* (1980) 5.
[40] U. Schmitt, D. M. Burland, *J. Phys. Chem. 87* (1983) 720.

[41] N. J. Turro, V. Ramamurthy, W. Cherry, W. Farneth, *Chem. Rev. 78* (1978) 125.
[42] R. Loudon: *The Quantum Theory of Light*, Clarendon Press, Oxford 1973, p. 56ff.
[43] P. Crabbé: *ORD and CD in Chemistry and Biochemistry*, Academic Press, New York 1972; K. B. Kagan: *Stereochemistry*, Vol. 2, Thieme, Stuttgart 1977.
[44] A. von Jena, H. E. Lessing, *Opt. Quant. Elect. 11* (1979) 419 and references cited therein.
[45] M. D. Fayer, *Annu. Rev. Phys. Chem. 33* (1982) 63 and references cited therein.
[46] D. R. Lutz, K. A. Nelson, C. R. Gochanour, M. D. Fayer, *Chem. Phys. 58* (1981) 325.
[47] H. Hervet, W. Urbach, F. Rondelez, *J. Chem. Phys. 68* (1978) 2725.
[48] S. L. Shapiro: *Ultrashort Light Pulses*, Top. Appl. Phys., Vol. 18, Springer, Berlin 1977.
[49] D. W. Phillion, D. J. Kuizenga, E. A. Siegman, *Appl. Phys. Lett. 27* (1975) 85 and references cited therein.
[50] H. J. Eichler, *Opt. Acta 24* (1977) 631 and references cited therein.
[51] H. J. Eichler, G. Salje, H. Stahl, *J. Appl. Phys. 44* (1973) 5383.
[52] D. W. Pohl, S. E. Schwarz, V. Irniger, *Phys. Rev. Lett. 31* (1973) 32.
[53] H. J. Eichler, P. Glotzbach, B. Kluzowski, *Z. Angew. Phys. 28* (1970) 303.
[54] R. S. Moog, M. D. Ediger, S. G. Boxer, M. D. Fayer, *J. Phys. Chem. 86* (1982) 4694.
[55] F. W. Deeg, J. Pinsl, C. Bräuchle, unpublished results.
[56] J. R. Salcedo, A. E. Siegmann, D. D. Dlott, M. D. Fayer, *Phys. Rev. Lett. 41* (1978) 131.
[57] H. Hervet, L. Léger, F. Rondelez, *Phys. Rev. Lett. 42* (1979) 1681.
[58] L. Léger, H. Hervet, F. Rondelez, *Macromolecules 14* (1981) 1732.
[59] J. Constandin, H. Sillescu, R. Voelkel, *Macromol. Chem. Rapid Commun. 3* (1982) 649.
[60] R. Baltramiejunas, K. Jarasinomas, J. Vaitkus, D. Veleckas, *Opt. Commun. 18* (1976) 47.
[61] D. M. Friedrich, S. A. Klem, *Chem. Phys. 41* (1979) 153.
[62] C. Bräuchle, Habilitationsschrift, Universität München 1982.
[63] A. S. Davydov: *Theory of Molecular Excitons*, Plenum Press, New York 1971.
[64] I. Berlman: *Energy Transport Properties of Aromatic Compounds*, Academic Press, New York 1973.
[65] D. M. Burland, A. H. Zewail, *Adv. Chem. Phys. 40* (1979) 369.
[66] T. Markvart, *J. Theor. Biol. 72* (1978) 91.
[67] J. R. Norris, M. E. Druyan, J. J. Katz, *J. Am. Chem. Soc. 95* (1973) 1680; F. K. Fong, *Appl. Phys. 6* (1975) 151; M. C. Thurnaver, J. J. Katz, J. R. Norris, *Proc. Natl. Acad. Sci. USA 72* (1975) 3270.
[68] H. G. Danielmeyer, *J. Appl. Phys. 42* (1971) 3125.
[69] D. R. Dean, J. R. Collins, *J. Appl. Phys. 44* (1973) 5455.
[70] R. Orlowski, E. Krätzig, *Solid State Commun. 27* (1978) 1351; *Ferroelectrics 26* (1980) 831; *27* (1980) 241.
[71] R. Orlowski, *Phys. Bl. 37* (1981) 365.
[72] G. R. Fleming, J. M. Morris, G. W. Robinson, *Chem. Phys. 17* (1976) 91.
[73] S. A. Rice, G. A. Kenney-Wallace, *Chem. Phys. 47* (1980) 161.
[74] C. Bräuchle, unpublished results.
[75] G. R. Fleming, A. E. Knight, J. M. Morris, R. J. Robbins, G. W. Robinson, *Chem. Phys. Lett. 49* (1977) 1.
[76] A. von Jena, H. E. Lessing, *Chem. Phys. 40* (1979) 245; *Chem. Phys. Lett. 78* (1981) 187.
[77] G. S. Beddard, T. Doust, J. Hudales, *Nature (London) 294* (1981) 145.
[78] A. Einstein, *Ann. Phys. 19* (1906) 371.
[79] K. B. Eisenthal, K. H. Drexhage, *J. Chem. Phys. 51* (1969) 5720.
[80] P. G. de Gennes: *Scaling Concepts in Polymer Physics*, Cornell University Press, Ithaca, NY 1979, Chap. III.
[81] W. Burchard, *Adv. Polym. Sci. 48* (1983) 1.
[82] J. Klein, B. J. Briscoe, *Polymer 17* (1976) 481; F. Rondelez, *Solid State Commun. 14* (1974) 815.
[83] M. Edidin, *Annu. Rev. Biophys. Bioeng. 3* (1974) 179.
[84] K. H. Richter, W. Güttler, M. Schwoerer, *Chem. Phys. Lett. 92* (1982) 4.
[85] K. A. Nelson, M. D. Fayer, *J. Chem. Phys. 72* (1980) 5202.
[86] J. R. Andrews, R. M. Hochstrasser, *Chem. Phys. Lett. 76* (1980) 213.
[87] K. A. Nelson, R. Casalegno, R. J. D. Miller, M. D. Fayer, *J. Chem. Phys. 77* (1982) 1144.
[88] D. Pohl, M. Maier, W. Kaiser, *Phys. Rev. Lett. 20* (1968) 366.
[89] K. A. Nelson, D. R. Lutz, M. D. Fayer, *Phys. Rev. B 24* (1981) 3261.
[90] M. R. B. Forshaw, *Opt. Laser Technol. 1974*, No. 2, p. 28; R. L. Kurtz, R. B. Owen, *Opt. Eng. 14* (1974) 393; P. Hariharan, *ibid. 19* (1980) 636.
[91] W. J. Tomlinson, E. A. Chandross, *Adv. Photochem. 12* (1980) 201.
[92] B. J. Chang, *Opt. Eng. 19* (1980) 642.
[93] K. Tatsuno, A. Arimoto, *Appl. Opt. 19* (1980) 2096.
[94] G. C. Bjorklund, C. Bräuchle, D. M. Burland, D. C. Alvarez, *Opt. Lett. 6* (1981) 159.
[95] C. Bräuchle, U. P. Wild, D. M. Burland, G. C. Bjorklund, D. C. Alvarez, *Opt. Lett. 7* (1982) 177; *IBM J. Res. Dev. 26* (1982) 217.
[96] D. von der Linde, A. M. Glass, K. F. Rodgers, *Appl. Phys. Lett. 25* (1974) 155.
[97] D. von der Linde, A. M. Glass, K. F. Rodgers, *Appl. Phys. Lett. 26* (1974) 22.
[98] D. von der Linde, A. M. Glass, K. F. Rodgers, *J. Appl. Phys. 47* (1976) 217.
[99] V. Gerbig, R. K. Grygier, D. M. Burland, G. Sincerbox, *Opt. L. 8* (1983) 404.
[100] D. H. Close, *Opt. Eng. 14* (1975) 408; B. J. Chang, C. D. Leonard, *Appl. Opt. 18* (1979) 2407; Yu. S. Mosyakin, G. V. Skrotski, *Sov. J. Quantum Electron 2* (1972) 199; C. S. Ih, *Appl. Opt. 17* (1978) 748; R. V. Pole, H. W. Werlich, R. J. Krusche, *ibid. 17* (1978) 3249; S. K. Case, V. Gerbig, *Opt. Eng. 19* (1980) 711.
[101] P. K. Tien, *Appl. Opt. 10* (1971) 2395; W. S. C. Chang, *IEEE Trans. Microwave Theory Tech. MTT21* (1973) 755.
[102] V. Gerbig, R. K. Grygier, D. M. Burland, G. Sincerbox, unpublished results.

# Complex Reducing Agents (CRA's)— Versatile, Novel Ways of Using Sodium Hydride in Organic Synthesis

**New synthetic methods (39)**

By Paul Caubère*

Why do we hardly use the simplest and, at the same time, inexpensive reducing agent sodium hydride in organic chemistry? To this question the answer is invariably: "It is too basic". In this progress report we describe work we have performed aimed at controlling the basicity of NaH using sodium alcoholates and metal salts. The *c*omplex *r*educing *a*gents (CRA's) developed (symbolized NaH-RONa-$MX_n$) allow organic halides, alkenes, alkynes and ketones to be reduced selectively. Highly regioselective 1,4- and 1,2-reductions of α,β-unsaturated ketones are easily performed using appropriate metal salts. Modified CRA's have proved to be excellent hydrosilylating reagents for carbonyl groups, non-pyrophoric heterogeneous hydrogenation catalysts, coupling reagents for aryl and vinyl halides, and reagents for the carbonylation of organic halides under very mild conditions. The study of these reactions opened up the field to phase-transfer-catalyzed photostimulated carbonylations as well as to $S_{RN}1$ reactions of metalates.—Thus, starting from the simple sodium hydride a large number of useful reagents have become accessible.

## 1. Introduction

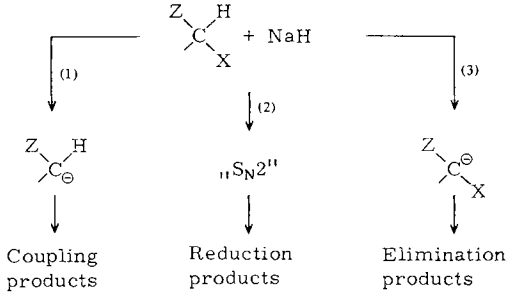
### 1.1. General Considerations

Sodium hydride is a long-known, inexpensive reagent easily prepared on a large scale from sodium and hydrogen. It is generally used in organic chemistry only as a base for proton abstraction[1]. Although a few substrates may be reduced by NaH, the reactions are often slow and the yields far from excellent[1,2]; nevertheless, these reductions indicate the potential reducing properties of NaH which, unfortunately, are masked by the basic ones.

Thus to be able to use this reagent for reductions the following have to be achieved: 1) its ability to undergo one-electron transfer must be increased and 2) its basic properties must be masked. In the present review we shall describe how these problems could be solved using a combination of observations, experiments, and intuition.

### 1.2. Reducing Properties of Sodium Hydride in Aprotic Solvents

During investigations on base-promoted eliminations in hexamethylphosphoric triamide (HMPA)[3] (Warning: suspected carcinogen[4]) it was observed that NaH reacted with benzyl bromide to give bibenzyl and a small amount of toluene (reduction product), instead of the expected *trans*-stilbene (elimination product). This unexpected reaction was thoroughly studied using substrates possessing, simultaneously, a reactive halogen and hydrogens of varying acidity. With less acidic hydrogens the soft base[5] $H^{\ominus}$ attacks the halogen atom (soft acid) and the halogen-substituted carbon atom, leading to couplings (reaction (1)) and reductions (reaction (2)), respectively. On the other hand, if sufficiently acidic hydrogens are present normal acid-base reactions occur (reaction (3))[6,7]. Mechanistic studies[6] led us to propose an ionic mechanism (Scheme 1).

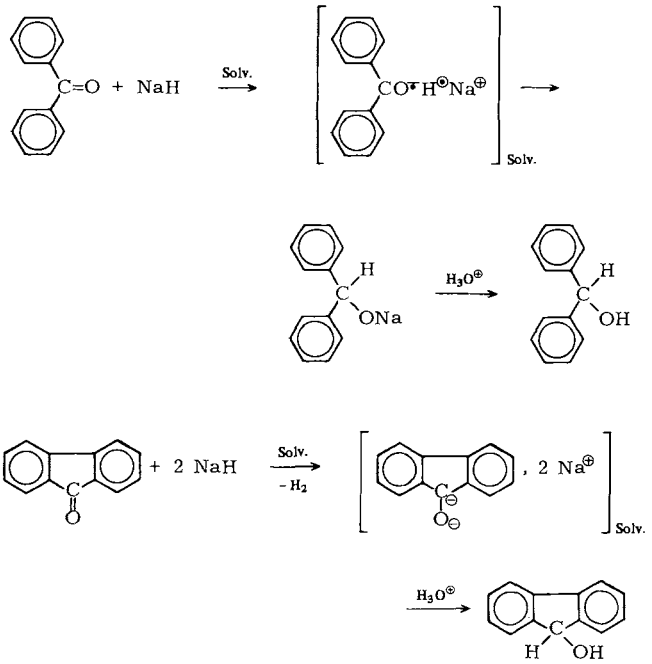



Scheme 1. X = halogen.

One-electron transfer from $H^{\ominus}$ to the substrate is presumably the preliminary step to halide loss. To confirm this hypothesis we studied the reaction of NaH with *gem*-dihalocyclopropanes in HMPA: a reaction which has been well explored in connection with radical and "ionic" reductions[8]. We found[6,9] that dibromides could be reduced to monobromides and that the reductions could take place by way of radicals trapped in solvent cages. Support for one-electron transfer from $H^{\ominus}$ was provided by the reduction of carbonyl derivatives in aprotic solvents[10]. Indeed, ketyl radicals were detected by ESR spectroscopy in the reduction of benzophenone and fluorenone. Moreover, benzophenone incorporated an electron and a hydrogen atom from NaH, but fluorenone accepted two electrons to form a dianion. These experiments are concordant with the mechanism depicted in Scheme 2.

An extremely unusual observation convinced us of the propensity of NaH to undergo one-electron transfer reactions: careful addition of aqueous HMPA to a suspension of NaH (free from Na) in HMPA led to blue solutions of solvated electrons[6]. This indicates that in the presence of water solvated by HMPA hydride ions could lose electrons, which in turn are solvated by HMPA (for interpretation of this reaction, see Section 2.10).

[*] Prof. Dr. P. Caubère
Laboratoire de Chimie Organique I, ERA CNRS n° 476,
Université de Nancy I,
B.P. 239, 54506 Vandœuvre-les-Nancy Cédex (France)

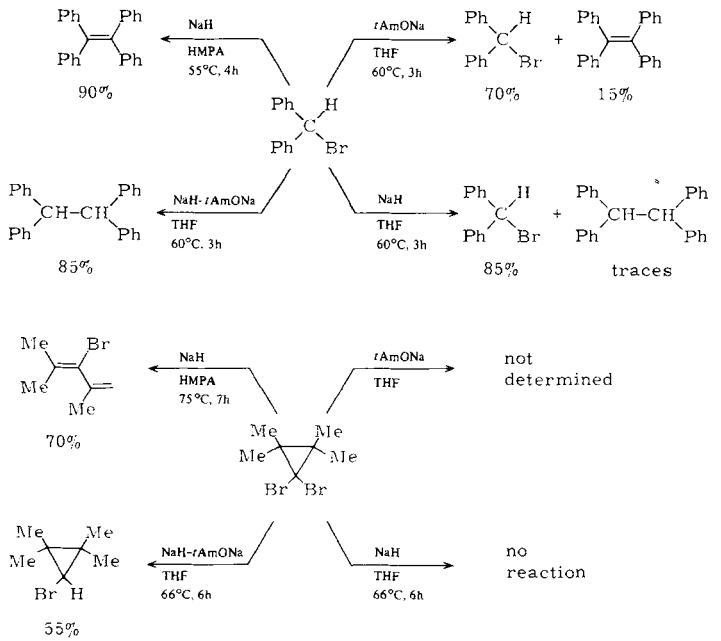


Scheme 2. Solv. = solvent = HMPA.

### 1.3. Activated Sodium Hydride "NaH-RONa"

In addition to investigating the reducing properties of NaH, we studied the system NaH-RONa (we term the alcoholate RONa an activating agent). Indeed, at that time we had already established the concept of the synergism of bases and had shown that $NaNH_2$-RONa ("complex bases"[11]) had properties remarkably different from those of the individual components. If such a synergism were to occur between NaH and RONa, a parallel increase of the basic or reducing properties would result.

Major differences appeared between the properties of activated NaH (NaH-RONa (2:1)), which is as readily prepared as complex bases[11], and those of NaH and



Scheme 3.

RONa. The following features emerged[7,9,10,12]: 1) sodium *tert*-amylalcoholate (*t*AmONa) was found to be an excellent activating agent; 2) in HMPA, NaH-*t*AmONa was a stronger base than either NaH or *t*AmONa; 3) although NaH was very weakly reactive in tetrahydrofuran (THF), NaH-*t*AmONa showed marked reducing properties (Scheme 3); 4) other things being equal, NaH-*t*AmONa in THF had comparable or even better reducing properties than NaH in HMPA (Scheme 3). Finally, since ketyl radicals were observed during the reduction of aromatic ketones by NaH-*t*AmONa in THF[10] we concluded that in THF one-electron transfer from NaH could be amplified by sodium alcoholates.

Unfortunately, all the results obtained up to this point, interesting though they were, did not give us any hope of finding general synthetic applications for the reagent; indeed, even in THF, NaH-RONa was still too basic. Fortunately, as we shall see later, a solution was found to this problem in the course of investigations directed towards a somewhat different target.

## 2. Complex Reducing Agents (CRA's) "NaH-RONa-$MX_n$" and Related Reagents

### 2.1. Introductory Remarks

In the hope of preparing transition-metal hydride derivatives, we studied the reactivity of NaH with Cu salts. The results were disappointing and difficult to reproduce. We therefore tested whether NaH-*t*AmONa could be used in place of NaH. Moreover, it was felt that the presence of alcoholates in the reagent might enhance its reducing properties.

This time we were not disappointed. First experiments[13] showed that addition of copper salts to NaH-*t*AmONa at 50–60 °C in THF reproducibly led to formation of brown-black reagents which slowly reduced aromatic halides. Since these first results the number of reagents and applications have grown considerably.

Nomenclature: *c*omplex *r*educing *a*gents will be abbreviated as CRA's or MCRA's (metal atom specified) or as RONa·MCRA's (alcoholate and metal atom specified); if necessary, we symbolize RONa·MCRA as NaH-RONa-$MX_n$, although, of course, $MX_n$ is not present as such in the reagent. The abbreviation RONa·MCRA(x/y/z) indicates that NaH/RONa/$MX_n$ (in that order) is equal to the molar ratio x/y/z. This ratio refers to the ratios of the starting reagents and has nothing to do with the actual constitution of the CRA (see Section 2.10).

### 2.2. Main Characteristics of CRA's

CRA's are readily prepared from commercial reagents. Thus, it is sufficient to add, in the chosen solvent, anhydrous $MX_n$ to NaH-RONa, or to add the alcohol to the suspension obtained by mixing NaH and $MX_n$. After warming, the reagents are ready for use[14]. CRA's are heterogeneous reagents, whose reactive moiety seems, generally, to be located in the solid fraction. Their reactivity is a function of the solvent; the ratio of the reagents; the na-

ture of the alcoholate; and, above all, the nature of the metal salt. Advantage may be reaped from this: a palette of reducing agents with graduated properties can be obtained. Considering the large number of metal salts which led to CRA's and their various areas of application, we are presently far from having exhausted all the possibilities. The properties of CRA's[14-17] are briefly summarized below.

CRA's can be prepared starting from the halides or acetates of Ti, V, Cr, Mn, Fe, Co, Ni, Cu, Zn, Cd, Zr, Mo, Pd, and W. Using the chosen test reaction, the reduction of 1-bromonaphthalene, we observed that, besides naphthalene, noticeable amounts of 1,1'-binaphtyl were formed with Fe-, Cu-, Cd-, and ZnCRA's.

The influence of the solvent is not easy to predict; however it may be stated that dimethoxyethane (DME) usually leads to more reactive CRA's than THF. In general, it appears that the reducing properties decrease with the polarity of the solvent (from DME, THF to benzene and cyclohexane).

When metal complexes are used as starting materials instead of salts, the ligands seem to have a strong influence on the properties of CRA's. For example, the CRA prepared from NaH, *t*AmONa, and $NiCl_2$ reacted poorly with 1-bromonaphthalene, whereas the reagent obtained from $(Ph_3P)_2NiCl_2$ led to very good yields of naphthalene and binaphtyl. The formation of large amounts of binaphtyl was surprising, since all other reagents prepared from Ni salts, such as $Ni(OAc)_2$, only afforded naphthalene. The following interpretation is proposed: during preparation of CRA from Ni salts, low oxidation-state Ni species are formed which occur as reducing species later in the reaction. On the other hand, in the presence of $Ph_3P$ [from $(Ph_3P)_2NiCl_2$] a fraction of the low oxidation-state metal species must be trapped as complexes capable of coupling with organic halides. Thus, in the presence of sufficient amounts of appropriate ligands formation of CRA's could lead to formation of new reagents possessing properties other than reducing. This hypothesis has been verified experimentally (see Sections 2.4 and 2.9).

We must now underline a very important point concerning the complexes thus obtained. Even if they are well-known complexes it must be borne in mind that they are generated in a somewhat unusual environment! Thus, completely unexpected properties may occur. For an example see Section 2.9.

For CRA's themselves, the influence of reactant ratios has been determined experimentally for each type of reaction. Presently we are only at the initial stages of their interpretation (Section 2.10).

For alcoholates a short study showed that the variation of activating properties follows a trend which resembles that found for complex bases[11]. Thus *t*AmONa, *t*BuONa, *i*PrONa, and $Et(OCH_2CH_2)_2ONa$ exhibit excellent activating properties. Most of the reactions studied were performed using tertiary alcoholates to avoid possible redox side reactions.

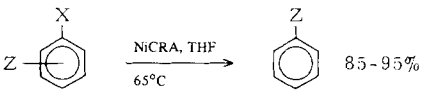
Interestingly, a number of CRA's reactions may be performed catalytically or semi-catalytically.

Finally, it should be noted that the basicity of CRA's appears to be weakened—a very important point for synthetic uses.

### 2.3. Reduction of Organic Halides by CRA's

All reagents used in this section were prepared from *t*AmONa.

NiCRA(4/2/1) (NaH, *t*AmONa, and $Ni(OAc)_2$ in molar ratio 4:2:1) reduced aromatic iodides, bromides, chlorides, and even fluorides under mild conditions and in good yields (Scheme 4)[15]. CoCRA (4/2/1) did not reduce fluorides and reduced chlorides slowly, although in good yields.



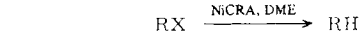

| X | Z | *t* [h] | X | Z | *t* [h] |
|---|---|---|---|---|---|
| F | H | 6 | Br | 4-Me | 1 |
| F | 4-MeO | 12 | Br | 2-MeO | 1 |
| Cl | 2-Me | 1 | Br | 4-MeO | 1 |
| Cl | 3-Me | 1 | Br | 2-COOH | 1-2 |
| Cl | 4-Me | 1.5 | Br | 3-COOH | 1-2 |
| | | | Br | 4-COOH | 12-18 |

Scheme 4. Reaction times *t* are for comparable amounts of substrate.

*gem*-Dibromocyclopropanes were easily reduced to the corresponding monobromo derivatives by NiCRA and CoCRA. Even the reduction of 7,7-dichloronorcarane took place under mild conditions with NiCRA (4/2/1)[16]. The values of the *cis/trans*-ratios of 7-bromonorcaranes obtained from 7,7-dibromonorcarane varied between 2.3 and 3, indicating the intervention of free radicals[8] in the reductions. It was also shown that these reductions could be performed with catalytic amounts of metal salts (yields were *ca.* 400% with Co and *ca.* 500% with Ni).

Finally, the reduction and selective reduction of alkyl, vinyl, benzyl, and allyl halides[17,18] were examined in more detail. The following salient features emerged:

Of the CRA's capable of reducing alkyl halides under mild conditions (particularly CRA's containing V, Fe, Co, Ni, Zn, and Cd), NiCRA(4/2/1) and ZnCRA(4/2/1) were selected: the reactions were performed in THF or DME.




| R | X | *T* [°C] | *t* [h] | Yield [%] |
|---|---|---|---|---|
| 1-Octyl | Br | 20 | 0.5 | 90-95 |
| 1-Octyl | Cl | 65 | 0.5 | 100 |
| 2-Octyl | Br | 20 | 0.33 | 90-100 |
| Cyclopentyl | Cl | 20 | 1.5 | 90 |
| Cyclopentyl | Cl | 65 | 0.25 | 91 |
| Cyclohexyl | Br | 20 | 0.5 | 95 |
| 1-Adamantyl | Br | 20 | 1 | 95 |
| 1-Adamantyl | Br | 65 | 0.25 | 95 |
| 1-Adamantyl | Cl | 20 | 4 | 95 |
| 1-Adamantyl | Cl | 65 | 0.75 | 92 |
| 1,1-Dimethylundecyl | Cl | 65 | 48 | 90 |
| 1-Methylcyclohexyl | Br | 65 | 0.05 | 66 [a] |
| 1-Methylcyclohexyl | Cl | 20 | 2 | 60 [a] |
| Benzyl [b] | Br | 20 | 0.5 | 85-100 |
| Benzyl [b] | Cl | 65 | 3 | 85-100 |
| 2-Cyclohexenyl | Br | −40 | 0.08 | 90 |

[a] In addition, 30-40% 1-methylcyclohexene is formed. [b] Reduction with ZnCRA in THF.

Scheme 5. Reaction times *t* are for comparable amounts of substrate.

With NiCRA, the general reactivity followed the trends RI > RBr > RCl and primary, secondary > tertiary. It is noteworthy that even tertiary halides were reduced under rather mild conditions. ZnCRA reduced only primary halides, following the trend RI > RBr ≫ RCl.

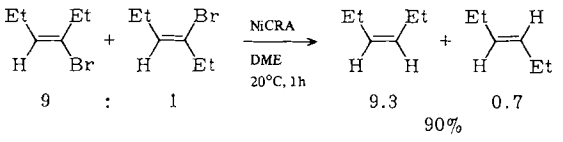
Benzyl and allyl halides were reduced by NiCRA and ZnCRA. In Scheme 5 some significant examples are given.

Vinyl chlorides and bromides were reduced highly stereoselectively under extremely mild conditions in excellent yields by NiCRA (Scheme 6).

Reductions could be performed with NiCRA but not with ZnCRA in the presence of catalytic amounts of metal salts.

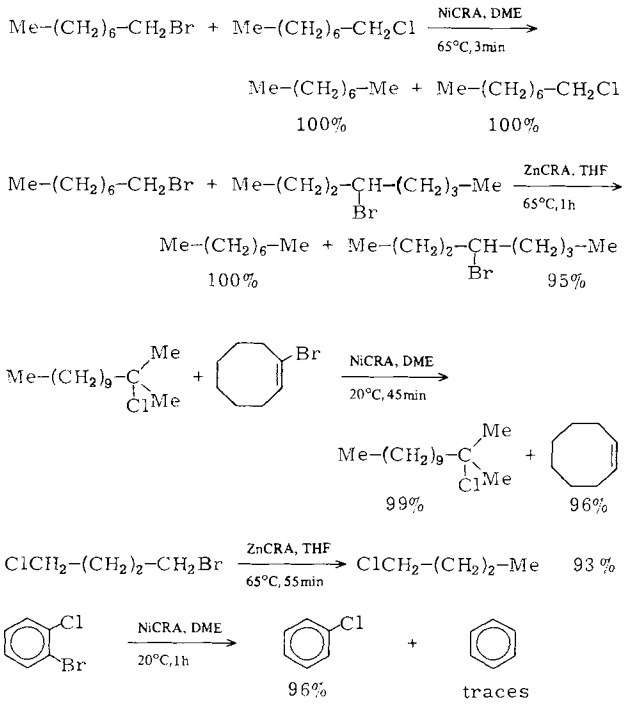



| R | X | n | $T$ [°C] | $t$ [min] |
|---|---|---|---|---|
| H | Br | 2 | 20 | 30 |
| H | Br | 3 | 20 | 60 |
| H | Cl | 2 | 45 | 25 |
| 4-Me | Cl | 2 | 45 | 10 |



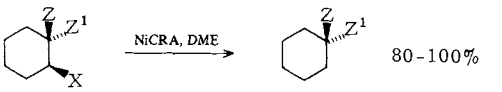

Scheme 6.

The differences in reactivity between the various halides were sufficient to permit selective reductions (Scheme 7). Particularly striking was the reduction of *o*-bromochlorobenzene to chlorobenzene, which took place readily without formation of benzyne.

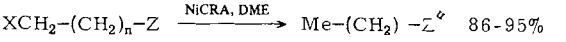



Scheme 7.

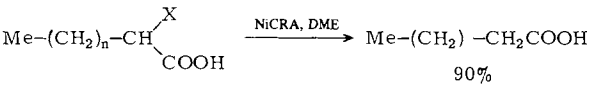
Finally, the unique reactivity of NiCRA and ZnCRA with organic halides is such that carbon-halogen bonds can be selectively reduced in the presence of numerous functional groups (Scheme 8).



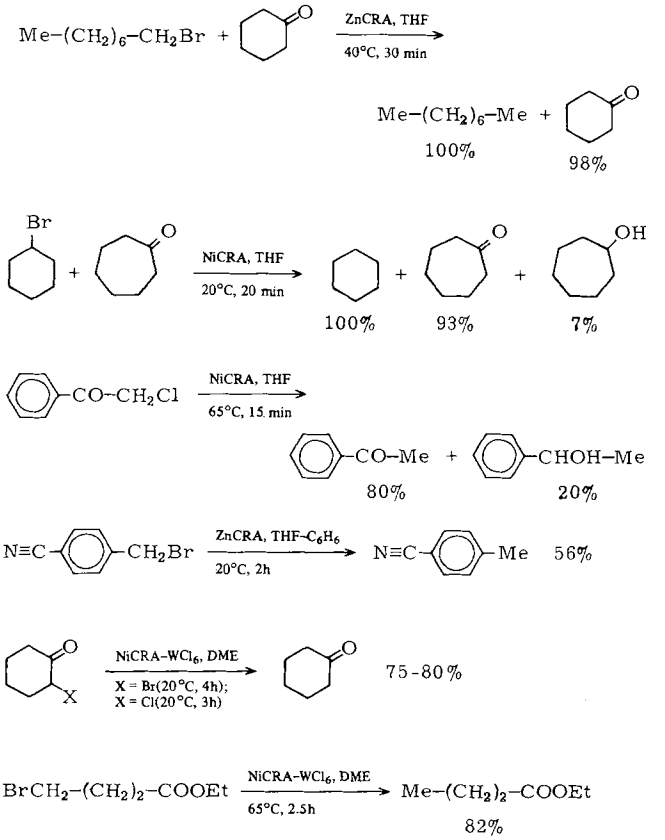

| X | Z | Z¹ | $T$ [°C] | $t$ [min] |
|---|---|---|---|---|
| Br | H | OTetrahydropyranyl | 65 | 5 |
| Br | H | OMe | 65 | 5 |
| Br | | -O-(CH2)2-O- | 65 | 5 |
| Cl | | -O-(CH2)2-O- | 65 | 20 |




| X | Z | n | $T$ [°C] | $t$ [min] |
|---|---|---|---|---|
| Br | OH | 10 | 65 | 5 |
| Br | COOH | 9 | 20 | 2 |
| Cl | COOH | 3 | 20 | 20 |




| X | n | $T$ [°C] | $t$ [min] |
|---|---|---|---|
| Br | 8 | 20 | 2 |
| Cl | 1 | 20 | 30 |




Scheme 8. Reaction times $t$ are for comparable amounts of substrate.

It is notable that no eliminations were observed in the reduction of β-haloethers and α-haloketals. A number of α-haloketones and γ-haloesters were too sensitive to be reduced by the usual CRA's; addition of $WCl_6$ to NiCRA enabled "normal" reductions to be performed (cf. the last two equations of Scheme 8), but the role played by $WCl_6$ remains obscure.

How should CRA's be classified among other known reducing agents?

Considerable effort has been devoted to the use of metal hydrides as reducing agents for organic halides[19a]; alkali metal aluminum hydrides have been extensively studied[19]. $LiAlH_4$ itself readily reduces reactive halides and, less readily, secondary bromides, *e.g.* bromocyclohexane is particularly resistant to reduction. Tertiary, aromatic, and alkenyl halides are reduced with difficulty, unless they are iodides. More efficient are a number of alkoxyaluminum hydrides[19a, i, n], but these are of limited value for the reduction of tertiary, vinyl, and aromatic halides.

Finally, the ability of aluminum hydrides to reduce numerous functional groups limits their use for the selective removal of halogen atoms.

The less reactive borohydrides $LiBH_4$ and $NaBH_4$[19a, b, g-i] are more selective, but more drastic conditions are often necessary[19a, h, 20a-c]. Note that with these reagents "indirect reduction" (dehydrohalogenation-hydroboration) may be observed[19a, h]; these hydrides lead to low yields of reduction products with a number of bromides, chlorides and, above all, with aromatic and alkenyl halides.

Modification of simple borohydrides leads to more efficient reducing agents such as $M[BH_3CN]$ (M = Na, K, $Bu_4N$), 9-BBNCN (9-cyano-9-hydrido-9-borabicyclo[3.3.1]nonane), or $Li[BHEt_3]$ (superhydride).

In HMPA[4] benzyl, allyl, as well as primary and secondary halides are reduced by an excess of cyanoborohydrides[20e] (treatment for 24 h at 70–100 °C is necessary with the less reactive halides). These hydrides are much less successful in reducing alkenyl, aromatic, and a number of tertiary halides. On the other hand, they are selective, since most other functional groups do not react under the conditions used.

Note that reducing agents such as the ate-complex prepared from 9-borabicyclo[3.3.1]nonane selectively reduce benzyl, allyl, and tertiary halides. There is evidence to suggest formation of a carbocation intermediate[20f]. $Li[BHEt_3]$[19a, g-i] is a convenient reagent for the reduction of reactive halides. Tertiary halides are reduced slowly, since elimination can be a competing reaction and vinyl or aryl halides are inert.

$Cr^{II}$ salts[19a, 21] and organotin hydrides[19a, 22] are valuable reagents for the selective reduction of aliphatic and reactive halides, but are much less reactive with alkenyl and aromatic halides. Moreover, a number of $Cr^{II}$ salts are unstable and use of tin hydrides often necessitates high reduction temperatures. Also, some problems can arise in disposing of the tin residues (see the comments given in [19f]).

The results given in Schemes 4–8 show that CRA's compare favorably with the above reducing agents. Generally, our reagents are more efficient with less reactive halides; in their selectivity they appear, with a few exceptions, to be as selective as other reducing agents.

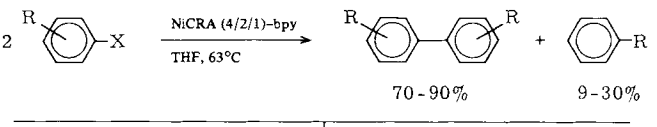
A large number of transition-metal species have also been reported to reduce organic halides[19a, 23]; among these the reagents obtained by addition of metal salts to aluminum hydrides or borohydrides are directly comparable to CRA's.

Lithium copper hydrides $Li_nCuH_{n+1}$ (from MeLi, CuI, and $LiAlH_4$)[24a] exhibit different reactivities. $Li_4CuH_5$ (the most reactive) reduces cyclohexyl, vinyl, and aryl chlorides poorly at room temperature, even after 24 h. The reagents obtained by addition of a series of transition-metal salts to $LiAlH_4$[24b, c] reduce aliphatic as well as aromatic halides, including chlorides; however, unreactive halides necessitate long reaction times, and no selective reductions have been studied. The reagent prepared from $Li[AlH(OMe)_3]$ and CuI[24d] essentially reduces organic bromides. Parallel experiments have been performed with $NaBH_4$[19a, 25]. The most reactive reagents were obtained with $Ni^0$[25b] and, above all, Pd derivatives[25a]; however, weakly reactive halides, such as arenes, require a very large excess of $NaBH_4$ and reaction conditions conducive to the decomposition of the borohydride[25a]. More reactive is the reagent obtained from $K[BHsBu_3]$ and CuI[25e]; however, it must be used in large excess with aromatic chlorides and also reduces keto and ester groups.

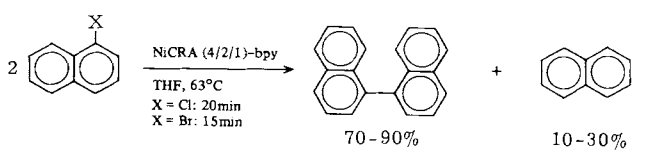
Here too, it seems that CRA's compare favorably with the last mentioned reagents. As a general comment it must be underlined that CRA's can be prepared readily from commercial starting materials and are, on the whole, less expensive than most other reducing agents.

### 2.4. Use of Ligand-Modified MCRA's (MCRAL's) to Couple Organic Halides

Stimulated by the reactions observed with $(Ph_3P)_2NiCl_2$ (Section 2.2), we first prepared *t*AmONa · NiCRA(4/2/1) in the presence of $Ph_3P$. The addition of 1-bromonaphthalene to the reagent thus obtained led to 70% of 1,1'-binaphthyl and to only 25% of naphthalene[17]. In order to avoid side reactions, such as transfer of phenyl from $Ph_3P$, the latter was replaced by 2,2'-bipyridine, leading to satisfying results (Scheme 9)[17, 26].



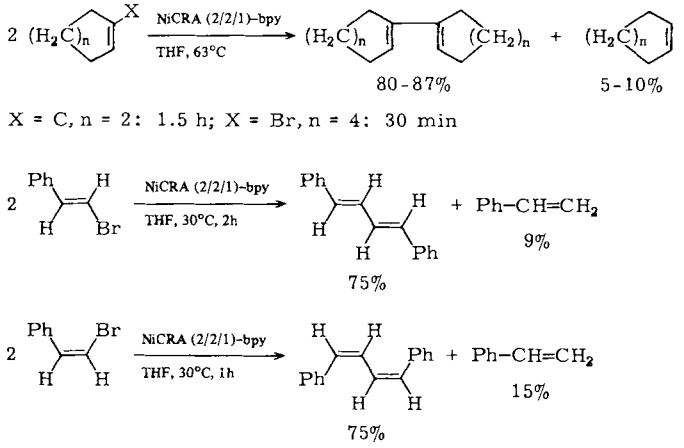

| X | R | *t* [h] | X | R | *t* [h] |
|---|---|---|---|---|---|
| Br | H | 0.5 | Cl | H | 2.5 |
| Br | 2-MeO | 0.5 | Cl | 2-Me | 8 |
| Br | 3-MeO | 0.5 | Cl | 3-Me | 8 |
| Br | 4-MeO | 0.5 | Cl | 4-Me | 8 |




Scheme 9. Reaction times *t* are for comparable amounts of substrate.

A comparison of Schemes 4 and 9 underlines the substantial difference between CRA's and the new reagents, which we term MCRAL (L = ligand).

Some problems arose with NiCRAL and their reactions with vinyl halides: NiCRA is too powerful a reducing agent. Since NiCRA (4/2/1) contains NaH (see Section 2.10) but NiCRA (2/2/1) does not, we used the latter reagent and succeeded in performing coupling reactions (Scheme 10)[26b].




Scheme 10.

It is noteworthy that the reactions took place without isomerization.

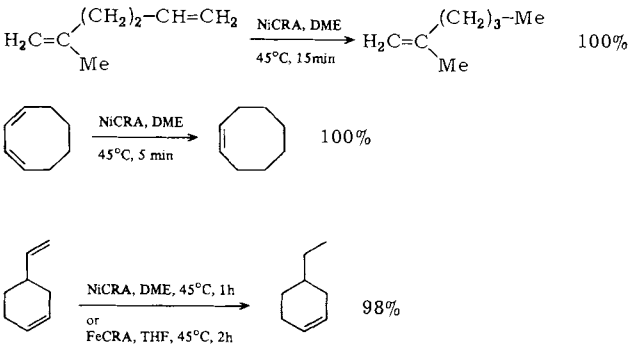
Although our studies of coupling reactions are only just beginning, comparison with the literature is very encouraging. Coupling of aryl or vinyl halides by $Ni^0$ complexes or $Ni^0$ species generated *in situ* has been described (see *e.g.* [27]). Not only are NiCRAL's much more thermally stable and less air-sensitive than conventional $Ni^0$ complexes, but they are also more efficient in coupling bromides and, above all, chlorides. Moreover, the coupling of simple alkenyl bromides appears to be stereospecific with NiCRAL but not with $Ni^0$ complexes[27d].

### 2.5. Reduction of Alkynes and Alkenes by CRA's

Here we shall elaborate only upon those results which throw light on the nature of CRA's. Mono- and disubstituted alkynes are smoothly reduced to the corresponding alkanes by *t*AmONa·NiCRA (4/2/1) and *t*BuONa·FeCRA (4/2/1) (from $FeCl_3$) in THF or anisole[28]. Moreover, the use of FeCRA avoids the inconvenience presented by NaH-$FeCl_3$, which necessitates a large excess of NaH and of $FeCl_3$ and causes oligomerization of monosubstituted alkynes[29a]. This result emphasizes the improvement wrought by addition of alcoholates.

Interestingly, using appropriate conditions NiCRA allows the reduction of alkynes to alkenes. The alkenes obtained from disubstituted alkynes were predominantly *cis*, corresponding to a *syn*-addition of the reagent. With monosubstituted alkynes small amounts of 2-alkenes arising from isomerization of 1-alkenes were detected. These observations strongly suggest the presence of nickel hydride species[30].

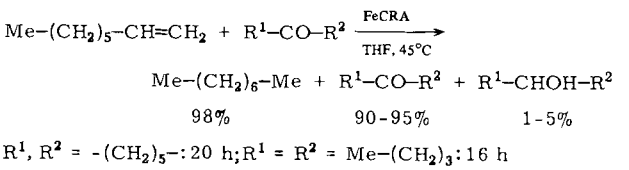
NiCRA and FeCRA also reduce alkenes[28]. Depending on the environment of the double bond they behave differently, thus permitting selective reductions (Scheme 11)[28b,31a].




Scheme 11.

Careful study of the reaction with NiCRA led to an intriguing observation: reductions of alkenes are catalytic with respect to Ni only if stoichiometric amounts of the alcoholate and alkene are used; they are catalytic with respect to alcoholate only if stoichiometric amounts of Ni and alkene are used[31b].

Finally, even though NaH-$FeCl_3$ reduces ketones[29b], FeCRA does not: this permits selective reductions (Scheme 12)[28b].




Scheme 12.

CRA's are as efficient as reagents containing $LiAlH_4$ or $NaBH_4$ and a metal salt [216, 32]. Their selectivity in competitive reduction of alkenes is also comparable. On the other hand, CRA's as well as $LiAlH_4$-containing systems[32a] are more selective than $NaBH_4$-containing reagents[32b] in the reduction of alkynes to alkenes. Finally CRA's are much more efficient than LiH-metal salt systems in which the very reactive and pyrophoric LiH is prepared from *t*BuLi and hydrogen[2e].

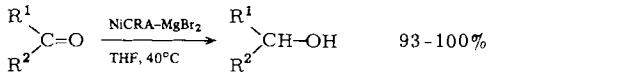
### 2.6. Reduction of Ketones and Aldehydes and Regioselective Reduction of α,β-Unsaturated Ketones by CRA's

Ketones and aldehydes, whose reductions are of synthetic interest, constitute ideal substrates to ascertain whether the basic properties of CRA's really have been controlled.

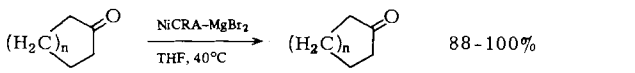
Exploratory experiments performed with *t*AmONa·NiCRA (4/1/1)[28a] showed that enolizable ketones might be reduced; however, these reductions suffer from long reaction times, only moderate yields with some substrates, and retro-reactions of varying rate (reoxidation of the alcoholate produced). We were able to show[33] that reoxidation was due to decomposition of transition-metal alcoholates[23,34] (formed in addition to sodium alcoholate), leading to ketones and metal hydrides. These results suggested that the addition of alkali metal or alkaline earth cations could increase the reduction rates by electrophilic assist-

ance; moreover, these cations might efficiently compete with $Ni^{II}$ for complexation at the oxygen atom, hence, helping to limit reoxidation. Among others, Li and Mg halides were found to be particularly suited for this purpose. They allowed fast NiCRA reduction of ketones in excellent yields, and dramatically retarded the reoxidation process (Scheme 13). Among other CRA's examined under the same conditions, *t*AmONa·CdCRA (4/1/1) and, particularly, *t*AmONa·ZnCRA (4/1/1), were found to be very efficient reducing agents for ketones.

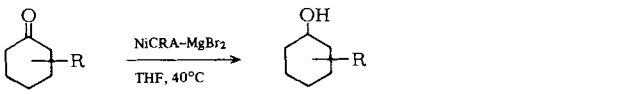
Reduction of aromatic or α-alkylated aliphatic aldehydes by NiCRA (with Li or Mg salts) presented no difficulties, but low yields of reduction products were obtained with primary aliphatic aldehydes. In these cases, satisfying results were obtained using ZnCRA in the absence of added salts (Scheme 13)[33].



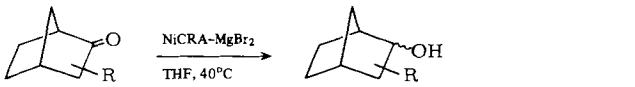

| $R^1$ | $R^2$ | *t* [h] | $R^1$ | $R^2$ | *t* [h] |
|---|---|---|---|---|---|
| *n*Bu | *n*Bu | 0.75 | *t*Bu | *t*Bu | 6.5 |
| *i*Pr | *i*Pr | 2.5 | Me | Ph | 0.5 |



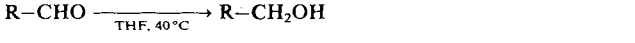

| n | *t* [h] | n | *t* [h] |
|---|---|---|---|
| 2 | 0.5 | 4 | 1 |
| 3 | 0.25 | 8 | 0.5 |




| R | *t* [h] | Yield [%] | Isomer ratio |
|---|---|---|---|
| 2-Me | 1 | 98 | 25*c* : 75*t* |
| 4-*t*Bu | 1 | 95 | 25*c* : 75*t* |
| 3,3,5-$Me_3$ | 23 | 83 | 60*ax* : 40*eq* |
| 3,3,5,5-$Me_4$ | 3 | 85 | |




| R | *t* [h] | Yield [%] | *exo* : *endo* |
|---|---|---|---|
| H | 0.5 | 100 | 32 : 68 |
| 1,7,7-$Me_3$ | 5 | 98 | 50 : 50 |



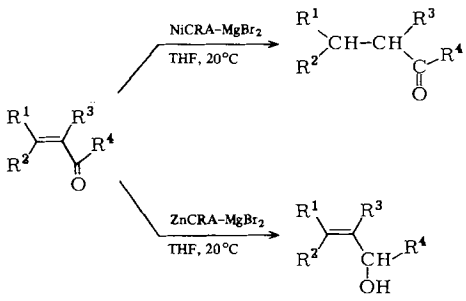

| R | Reagent | *t* [h] | Yield [%] |
|---|---|---|---|
| Ph | NiCRA–LiCl | 1 | 98 |
| 1-Methylbutyl | NiCRA–$MgBr_2$ | 2.5 | 98 |
| Cyclohexyl | NiCRA–$MgBr_2$ | 1 | 98 |
| Hexyl | ZnCRA | 3 | 60 |

Scheme 13. Reaction times *t* are for comparable amounts of substrate.

It was also shown that reductions performed with NiCRA could be catalytic with respect to Ni, *t*AmONa, and $MgBr_2$[33]. On the other hand, with ZnCRA yields were never higher than 180% relative to Zn[31b].

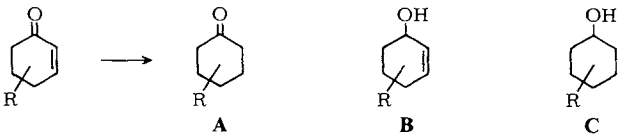
Among the myriad of reagents able to reduce ketones and aldehydes [see *e.g.* [19b, h, n, 20d, 21b]] CRA's occupy a consolidated position among those species capable of operating at not too low a temperature. However, their stereoselectivity has to be improved. We already know that it is possible to modify the stereochemistry of the reduction by varying the nature of the alcoholate, and this, therefore, constitutes one of the ways we have at our disposal to improve the performance of these reagents.

It should be noted that CRA's are much more efficient than NaH-$FeCl_2$, NaH-$FeCl_3$[29b], or LiH-transition-metal salt systems[2e]; moreover, commercial NaH is much less

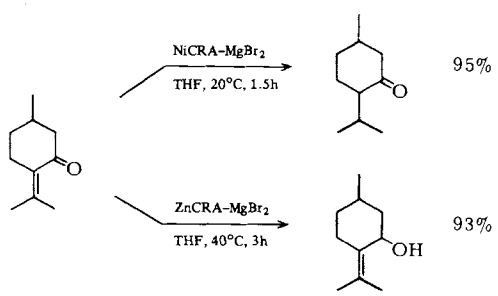



| $R^1$ | $R^2$ | $R^3$ | $R^4$ | M = Ni | | M = Zn | |
|---|---|---|---|---|---|---|---|
| | | | | *t* [h] | Yield [%] | *t* [h] | Yield [%] |
| Me | H | H | Me | 0.5 | 30 | 0.5 | 55-60[a] |
| *t*Bu | H | H | *t*Bu | 2.5 | 93 | 3 | 93 |
| Me | Me | H | Me | 0.25 | 98 | 2 | 98[a] |
| Ph | H | H | Me | 0.25 | 85 | 20 [a] | 45-50[a] |
| Me | Me | Me | Me | 0.75 | 99 | 2 | 93 [b] |
| Ph | H | H | Ph | 3.5 | 50 | 4 | 98 [a] |

[a] 20 °C. [b] 40 °C




| R | Reagent | *T* [°C] | *t* [h] | Yield [%] A | B | C |
|---|---|---|---|---|---|---|
| H | NiCRA–$MgBr_2$ | 20 | 0.5 | 98 | — | — |
| H | ZnCRA–$MgBr_2$ | 20 | 6 | — | 50 | 25 |
| 3,5,5-$Me_3$ | NiCRA–$MgBr_2$, THF | 40 | 0.5 | 93 | — | 5 |
| 3,5,5-$Me_3$ | ZnCRA–$MgBr_2$, THF | 40 | 3.5 | — | 90 | — |




Scheme 14. Reaction times *t* are for comparable amounts of substrate.

expensive and easier to handle than the very reactive, highly pyrophoric LiH used by *Ashby et al.*

The results obtained in reducing alkenes and saturated ketones encouraged us to attempt the regioselective reduction of α,β-unsaturated ketones. Under the conditions found to be satisfactory for saturated ketones it was discovered that highly regioselective reductions could be performed using NiCRA, leading to saturated ketones, and with ZnCRA leading to allylic alcohols (Scheme 14)[35].

It is noteworthy that, with two exceptions, saturated alcohols are formed, if at all, only in trace amounts.

Broadly speaking, reagents which reduce α,β-unsaturated carbonyl compounds may be divided into three groups:

The first contains reducing agents which mainly or exclusively lead to saturated carbonyl compounds in moderate to excellent yields: among them are $M^{\oplus}[HFe(CO)_4]^{\ominus}$ or $M^{\oplus}[HFe_2(CO)_8]^{\ominus}$ (see *e.g.* literature cited in [19b] and [23]), $R_3SiH$-$F_3CCOOH$[36], $NaBH_4$-pyridine[37], NaHTe (from tellurium powder and $NaBH_4$)[38], $LiBHEt_3$[19h], RCuHLi[39], or $LiAlH_4$-CuI[40].

The second group contains reagents which give excellent yields of allyl alcohols. Here are found reagents such as 9-BBN[41] or $NaBH_4$-lanthanoid chlorides[42].

The third group comprises reagents which regioselectively reduce α,β-unsaturated carbonyl derivatives to varying extents and/or whose regioselectivity depends on the structure of the carbonyl compound, on the experimental conditions, or on the nature of the reagent. In this group are a number of aluminum hydrides and borohydrides, either with or without transition-metal salts[19b,n,23,41,43–46], as well as alkylaluminums[47], $Li_nCuH_{n+1}$[24a], NaH-$Fe^{II}$ or NaH-$Fe^{II}$[29a].

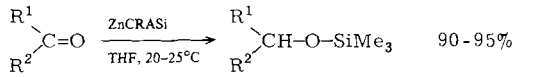
Comparison of the results shown in Scheme 14 with the data given in the above cited literature references indicates that 1) the regioselectivity of the inexpensive NiCRA and ZnCRA reagents is such that they may be classified among the best reducing agents of the first and the second groups, respectively, and 2) that, on average, the overall yields with CRA's must be considered as very good.

### 2.7. Hydrosilylation of Carbonyl Groups in Saturated and α,β-Unsaturated Ketones and Aldehydes by $Me_3SiCl$-Modified MCRA's (MCRASi's)

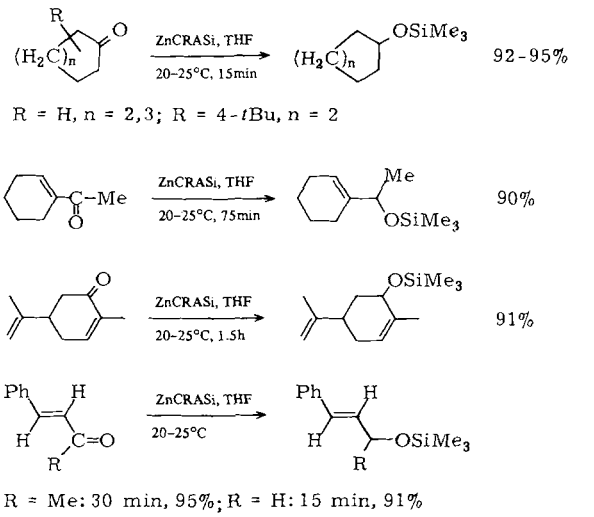
Condensation of three equivalents of $Me_3SiCl$ with *t*AmONa·ZnCRA (4/1/1) led to a new reagent (ZnCRASi) which hydrosilylated carbonyl groups[48]. The active silicon component appears to be bound to the reactive aggregates. ZnCRASi, an inexpensive reagent, rapidly reduces ketones and aldehydes to give excellent yields of trimethylsilyl ethers. This reagent specifically reduces carbonyl groups and does not reduce or isomerize CC double bonds (Scheme 15).

These results indicate that ZnCRASi is one of the best reducing reagent for the selective reduction of the carbonyl group of α,β-unsaturated carbonyl derivatives.

The most general method of hydrosilylating carbonyl groups is the reaction of alkyl, aryl or alkoxysilanes[49] catalyzed by group VIII metal derivatives. The common drawbacks of these reactions lie in the use of generally ex-




| $R^1$ | $R^2$ | *t* [min] |
|---|---|---|
| Me | $Me-(CH_2)_7$ | 20 |
| Me | $Me_2C=CH-(CH_2)_2$ | 15 |
| Me | Ph | 45 |
| H | $Me-(CH_2)_5$ | 15 |
| H | Ph | 15 |
| H | *p*-$ClC_6H_4$ | 15 |




Scheme 15. Reaction times *t* refer to comparable amounts of substrate.

pensive reagents, of frequently high reaction temperatures, and the lack of selectivity towards CC double bonds in unsaturated carbonyl derivatives. Recently[49b] an interesting highly regioselective hydrosilylation of α,β-unsaturated carbonyl compounds has been described: with $R_3SiH$–$(Ph_3P)_3RhCl$ 1,4-addition products are formed and with $R_2SiH_2$–$(Ph_3P)_3RhCl$ 1,2-addition products. ZnCRASi compares favorably with the second system and is much less expensive.

### 2.8. Use of MCRA's in the Preparation of Selective Catalysts (Mc's) for Heterogeneous Hydrogenation

Our results suggest that CRA's could behave like metal hydride species (see Section 2.5). Considering that M–H bond formation is one of the postulated key steps in numerous catalytic hydrogenations[34b], it might be anticipated that CRA's could be sources of new hydrogenation catalysts: exploratory experiments[50] performed with *t*AmONa·NiCRA (4/2/1) were successful. Catalysts obtained from CRA's are abbreviated "Mc's" (M = metal).

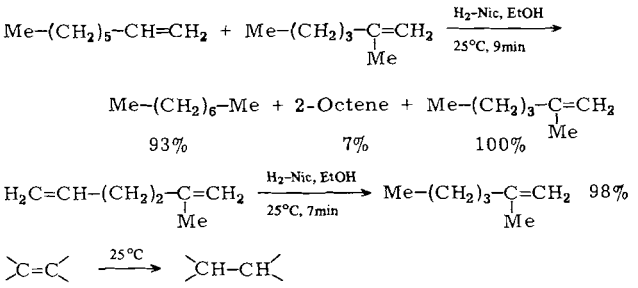
Nic's are NiCRA's (4/2/1) prepared at temperatures lower than usual, in which residual NaH has been neutralized[51]. In special cases, soluble alcoholates may be removed easily by washing ($Nic_w$).

Even when dry, Nic's are not pyrophoric. Nickel constitutes 60 to 70% (by weight) of the ethanol-washed catalyst. Thus alcoholates, on which the efficiency of Nic's depends, could be included as part of the catalyst framework. Nic's may be used in protic (MeOH, EtOH, *etc.*) or aprotic

(AcOEt, THF, toluene, *etc.*) solvents. Interestingly, they are only very slightly sensitive to catalyst poisoning and lead to good results with Ni/substrate ratios varying from 1:20 to 1:200. Finally, in the presence of NaH and under an inert atmosphere they are stable for long periods.

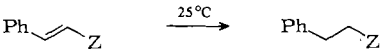
### 2.8.1. Hydrogenation of CC Double Bonds by tAmONa Containing Nic at Standard Pressure[51,52]

Nic is very sensitive to the environment of the alkene double bond, and selective hydrogenations are easily performed. Moreover, hydrogenation of CC double bonds can be performed without difficulty in the presence of various functional groups (Scheme 16). It is noteworthy that although carbonyl groups may be reduced by Nic (see Section 2.8.3), its affinity for the CC double bond is strong enough to allow selective hydrogenation of α,β-unsaturated ketones.

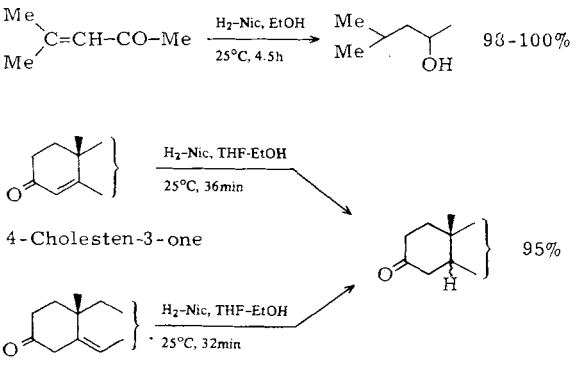



| Educt | Reagent | *t* [min] | Product | Yiled [%] |
|---|---|---|---|---|
| 4-Vinylcyclohexene | [a] | 7.5 | 4-Ethylcyclohexene | 98 |
| 1,3-Cyclohexadiene | [a] | 12 | Cyclohexene | 98 |
| 1,5-Cyclooctadiene | [a] | 14 | Cyclooctene | 93 |
| 1,3-Cyclooctadiene | [a] | 10.5 | Cyclooctene | 98 |
| Allylamine | [b] | 22 | Propylamine | 95 |
| Ethyl crotonate | [b] | 21 | Ethyl butyrate | 100 |

[a] $H_2$–Nic, EtOH. [b] $H_2$–$Nic_w$, MeOH.



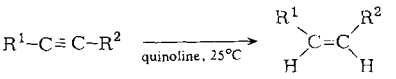

| Z | Reagent | *t* [min] | Yield [%] |
|---|---|---|---|
| $CH_2OH$ | $H_2$–$Nic_w$, EtOH | 25 | 92 |
| CHO | $H_2$–$Nic_w$ or Nic, EtOH | 95 | 83 |
| COMe | $H_2$–$Nic_w$ or Nic, EtOH | 12 | 94 |
| COOH | $H_2$–$Nic_w$ or Nic, EtOH | 58 | 97 |




Scheme 16. Reaction times *t* refer to comparable amounts of substrate.

### 2.8.2. Partial Hydrogenation of CC Triple Bonds by tAmONa Containing Nic at Standard Pressure[51,52]

Complete hydrogenation of mono- and disubstituted alkynes is readily performed using Nic. The reaction proceeds in two steps; the catalyst preferentially complexes the alkyne[53]. Taking advantage of this, partial hydrogenations of alkyne derivatives can be performed in excellent yields in the presence of quinoline (Scheme 17).




| $R^1$ | $R^2$ | Reagent | Yield [%] | Purity [%] |
|---|---|---|---|---|
| Pr | Me | $H_2$–$Nic_w$, MeOH | 82 | 96 |
| Et | Et | $H_2$–$Nic_w$, MeOH | 80 | 97 |
| Ph | Me | $H_2$–$Nic_w$, EtOH | 80 | 90 |
| $Et_2NCH_2$ | Et | $H_2$–$Nic_w$, MeOH | 93 | 97 |
| $HOCH_2$ | $CH_2OH$ | $H_2$–$Nic_w$, EtOH | 80 | 95 |
| Ph | H | $H_2$–$Nic_w$, EtOH | 86 | 91 |
| $Et_2NCH_2$ | H | $H_2$–$Nic_w$, MeOH | 90 | 90 |
| Et–C(OH)(Me) | H | $H_2$–Nic, EtOH | 90 | 81 |
| 1-cyclohexenyl | H | $H_2$–Nic, EtOH | 84 | 80 |

Scheme 17. In most cases the impurity was the saturated product.

Taking into account that the yields in Scheme 17 refer to isolated products, it should be noted that a number of results obtained with Nic (particularly with 1,4-butynediol[54] and 1-ethynylcyclohexene[55]) compare favorably with those obtained with Lindlar palladium. Nic is superior to Raney nickel[55b].

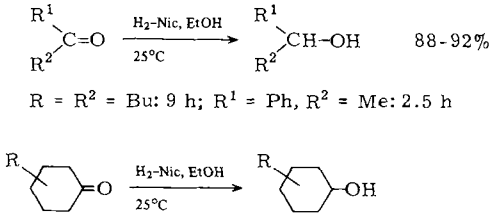
### 2.8.3. Hydrogenation of CO Double Bonds by tAmONa Containing Nic at Standard Pressure[51,52]

It is well known that only a few nickel catalysts allow the reduction of carbonyl compounds under mild conditions[56]. Among the more efficient are $W_7$-, $W_6$- and modified $W_4$-Raney nickels; however, $W_7$- and $W_6$-Raney nickels have very poor storage stability, $W_6$-Raney nickel appears to be hazardous[56], and the modifications of $W_4$-Raney nickel needed for hydrogenations of carbonyl groups are not simple to prepare[57].

Nic does not suffer from these drawbacks and is able to reduce carbonyl groups under mild conditions, frequently regioselectively (Scheme 18).

### 2.8.4. Comparison of Mc's with other Hydrogenation Catalysts

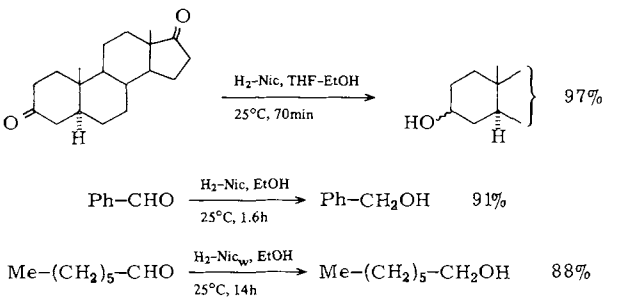
Nic's are easily and reproducibly prepared, are non-pyrophoric, can be stored, and are nonhazardous; they allow selective reduction of double bonds, partial hydrogenation of triple bonds and hydrogenation of carbonyl groups under ambient conditions. The affinity of Nic's for CC double bonds and carbonyl groups is sufficiently different, on







| R | t [h] | Yield [%] |
|---|---|---|
| 2-Me | 4.5 | 83 |
| 3-Me | 4.2 | 82 |
| 4-Me | 3.8 | 82 |
| 4-*t*Bu | 4 | 92 |
| 2-cyclohexyl | 20 | 94 |
| 2,6-$Me_2$ | 16 | 85 |
| 3,3,5-$Me_3$ | 6 | 88 |
| 3,3,5,5-$Me_4$ | 16 | 90 |




Scheme 18. Reaction times *t* refer to comparable amounts of substrate.

the whole, to allow selective hydrogenation of the CC double bonds of unsaturated ketones or aldehydes.

As far as efficiency, selectivity and handling are concerned, Nic's are more interesting than Raney nickels. The properties of Nic's are more directly comparable with those of *Brown*'s $P_1$- and $P_2$-nickel[56c,58], although their compositions are completely different (P-nickels contain large amounts of nickel boride[59]). In fact, to a certain degree, they are complementary; P-nickels and Nic's are very sensitive to the environment of the double bond, show rather low propensity toward isomerization or hydrogenolysis, and are not subject to poisoning by amines[59,60]. Use of $P_2$-nickel, however, allows hydrogenation of unsaturated nitriles to saturated ones[60], whereas use of Nic's does not[61]. In contrast, carboxyl groups (as sodium salts) do not prevent hydrogenations by Nic's, whereas cinnamic acid cannot be reduced using $P_2$-nickel[62].

P-nickels[56c,58,59,63] and Nic's permit selective hydrogenation of alkenes, but their respective selectivity toward cycloalkenes is different. On the other hand, unlike $P_2$-nickel[56c], Nic's do not have a propensity to disproportionate.

Partial hydrogenation of acetylenes can be performed highly selectively. However, in the presence of ethylenediamine $P_2$-nickel[64] could be slightly better for hydrogenating disubstituted alkynes, whereas Nic's could be slightly better with 1-alkynes.

P-nickels promote hydrogenation of carbonyl groups only very slowly[59,65], whereas Nic's do so fairly rapidly, thereby allowing carbonyl hydrogenations to be performed under mild conditions. Nic's promote, even in difficult cases, selective hydrogenation of the CC double bond of unsaturated ketones; however, perhaps $P_2$-nickel is more selective in special cases.

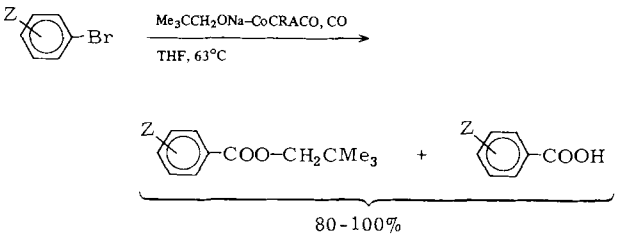
Since Nic's are prepared from NaH-RONa, their properties can be varied simply by changing the activating alcoholates. Moreover, many other catalysts may be prepared in a similar manner to Nic, and some of them (Coc, Pdc[52]) appear to be very promising for selective hydrogenations.

## 2.9. Carbonylation of Halogen Derivatives with CO-Modified MCRA's (MCRACO's) at Standard Pressure

### *2.9.1. Carbonylation of Aryl Halides with CoCRACO — Consequences for Phase Transfer Catalyzed Carbonylations*

Starting from the same ideas as in Section 2.4, we examined the preparation of CRA's using CO at atmospheric pressure. For the following reasons we chose to study the possible preparation of carbonylcobalt compounds and their ability to carbonylate aromatic halides: 1) the preparation of carbonylcobalt compounds from Co salts in aprotic media under mild conditions was rare in the literature[66a]; 2) contrary to an erroneous statement[66b], extreme reaction conditions are required for carbonylation of aryl halides in the presence of Co species[66c].

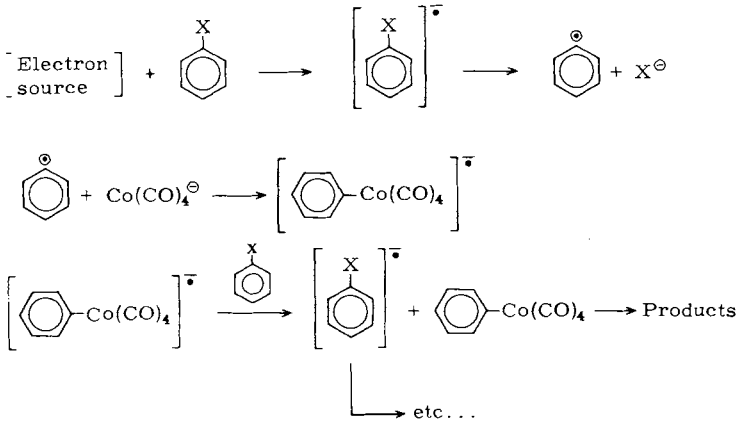
After careful systematic study[67] we succeeded in preparing a series of reagents (termed CoCRACO's) from CoCRA's (4/2/1), which reproducibly carbonylated aryl halides at atmospheric pressure of CO (Scheme 19). In the presence of amines, amides were obtained in moderate to good yields, and the carbonylations were found to be catalytic with respect to Co.




Z = H: 10 h; 2-Me: 25 h; 3-Me: 20 h; 4-Me: 20 h; 2-MeO: 15 h; 3-MeO: 15 h; 4-MeO: 15 h; 4-F: 20 h; 4-MeCO: 25 h

Scheme 19. Reaction times *t* refer to comparable amounts of substrates.

Investigations of the constitution of CoCRACO's led to the following conclusions: 1) *ca.* 90% of the cobalt was in solution; 2) only a fraction (*ca.* 13%) of the soluble cobalt was present as a carbonyl species; 3) the only carbonylcobalt species present was $NaCo(CO)_4$[68]. However, this anion alone does not carbonylate aryl halides under mild conditions[69]. We showed that this apparent contradiction was due to an $S_{RN}1$[70]-initiated process (one-electron transfer from $H^{\ominus}$). This result was confirmed when we were able to photostimulate the carbonylation of aryl halides in the presence of $NaCo(CO)_4$-*t*AmONa[68]. From these results, reactions involving CoCRACO's should proceed as depicted in Scheme 20.




Scheme 20.

The ability of $Co(CO)_4^{\ominus}$ to react *via* an $S_{RN}1$ process has an interesting consequence. It is known that $Co(CO)_4^{\ominus}$ might be generated from $Co_2(CO)_8$ in a PTC process[71]; however, under these conditions only organic halides which are particularly reactive in $S_N2$ processes can be carbonylated. These results led us to think that simple irradiation of such systems might allow the carbonylation of aryl and vinyl halides. This was in fact the case, and we can now perform numerous reactions of this type (Scheme 21) by irradiating a PTC system in a pyrex reaction flask with a simple commercial "sun lamp"[72]!

RX ⟶ RCOOH

| R | X | Reagent and conditions | $t$ [h] | Yield [%] |
|---|---|---|---|---|
| $C_6H_5$ | Br | [a] | 1–2 | 95–96 |
| 2-$MeC_6H_4$ | Br | [a] | 1–2 | 96 |
| 4-$MeC_6H_4$ | Br | [a] | 1 | 97 |
| 4-$MeOC_6H_4$ | Br | [a] | 2 | 98 |
| 4-$FC_6H_4$ | Br | [a] | 2 | 97 |
| 4-$ClC_6H_4$ | Br | [a] | 1 | 98 |
| 1-cyclohexenyl | Cl | [b] | 2.5 | 98 |
| 1-cyclohexenyl | Br | [b] | 2.5 | 98 |
| 1-cyclooctenyl | Br | [b] | 4.5 | 97 |
| $Me_3C-C(=CH_2)$ | Cl | [b] | 2 | 95 |

[a] 1. $Co_2(CO)_8$ (catalyst), CO, benzene/NaOH (aq) or NaOH (aq), $Bu_4NBr$, *hν* (sun lamp), 63 °C; 2. $H_3O^{\oplus}$. [b] 1. $Co_2(CO)_8$ (catalyst), CO; benzene/NaOH (aq), $Bu_4NBr$, *hν* (sun lamp), 65 °C; 2. $H_3O^{\oplus}$.

Scheme 21.

### 2.9.2. *Carbonylation of Organic Halides with FeCRACO*

FeCRACO is prepared from *t*AmONa·FeCRA (4/2/1) using CO at 1 bar pressure. The soluble fraction contains mainly $Na_2Fe(CO)_4$ and some $Na_2Fe_2(CO)_8$[73]. Interestingly, this $Na_2Fe(CO)_4$ behaves very differently to pure $Na_2Fe(CO)_4$, which has been thoroughly studied by *Collman et al.*[23,74]. Thus, using FeCRACO primary, secondary, and even tertiary bromides and chlorides can be carbonylated, whereas under normal conditions $Na_2Fe(CO)_4$ is moderately reactive with secondary halides; however, no reaction is observed with 1-bromoadamantane after 9 days. Although these carbonylations have to be improved, some excellent results have already been obtained (Scheme 22)[73]. It should be noted that the carbonylations of primary and secondary halides are catalytic with respect to the metal[73].

$$RX \xrightarrow[DME,\ then\ H_3O^{\oplus}]{FeCRACO,\ CO} \underset{\mathbf{A}}{RCOOH} + \underset{\mathbf{B}}{RCOOtAm} + \underset{\mathbf{C}}{RCHO}$$

| R | X | $T$ [°C] | $t$ [h] | Yield [%] |
|---|---|---|---|---|
| $Me-(CH_2)_7$ | Br | 20 | 20 | 75 [a] |
| $Me-CH(-(CH_2)_5-Me)$ | Br | 20 | 53 | 68 [a] |
| $Me-CH(-(CH_2)_5-Me)$ | Cl | 65–70 | 13 | 60 [a] |
| Cyclohexyl | Br | 30 | 40 | 70 [b] |
| Cyclohexyl | Cl | 65–70 | 36 | 75 [b] |
| 1-Adamantyl | Br | 40 | 84 | 88 [b] |
| 1-Adamantyl | Cl | 65–70 | 80 | 80 [b] |

[a] Relative yields **A** + **B** 58–90%, **C** 38–10%. [b] Only **A** + **B** are formed.

Scheme 22. Reaction times $t$ refer to comparable amounts of substrate.

Of course, a radical mechanism must be suspected for most of these carbonylations. This is supported by the carbonylation of $C_6H_5Br$ by FeCRACO under CO (40% yield), the first example of carbonylation of bromobenzene by $Na_2Fe(CO)_4$.

### 2.10. Structure and Mode of Action of CRA's

The determination of the constitution of CRA's is a very difficult task. However, interesting data have been obtained for *t*BuONa·NiCRA (4/2/1) and *t*AmONa·ZnCRA (4/1/1)[75].

An analysis of the gas evolved during preparation of CRA's and their hydrolyses, and of the phase distribution of their main constituents yielded important information, which is briefly summarized in Scheme 23; the notation defined in Section 2.1 is used. In both cases, the amount of hydrogen evolved during the preparation was 10 mmol in excess of that expected for the reaction of NaH and ROH.

For NiCRA the excess of $H_2$ arises from the reaction

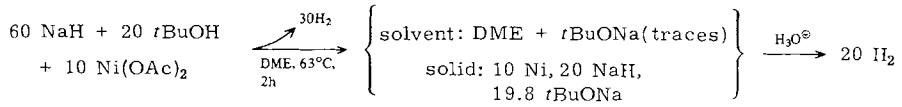
$$2H^{\ominus} + Ni^{II} \longrightarrow Ni^0 + H_2$$

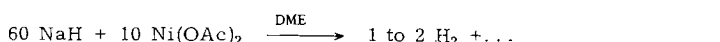
No reduction took place without alcoholate. The crucial part played by the alcoholate may have two explanations: 1) activation of NaH (Section 1.3), and/or 2) formation of nickel alcoholates with concomitant favorable shift of the $Ni^{II}$ reduction potential[76], or electron relay between $H^{\ominus}$ and $M^{n\oplus}$. Both phenomena probably occur. Indeed, the addition of NaH to $RONa-Ni(OAc)_2$ in THF or DME leads to a reagent similar to NiCRA, but the rate of formation is lower[31b]. Likewise, *t*AmONa–$Co(OAc)_2$ reacts with NaH and CO to give $NaCo(CO)_4$; in contrast, $Co(OAc)_2$ does not[68].

The amount of hydrogen evolved in the hydrolysis of NiCRA is consistent with that expected from the "free" hydride. It is, further, noteworthy that *t*BuONa was found only in the solid fraction despite its high solubility in DME.

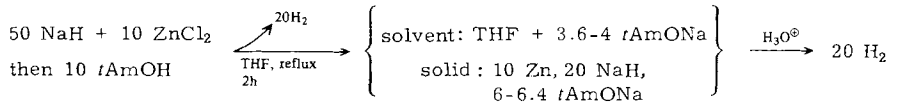
Comparison of X-ray powder patterns of the solid fractions with those of the possible constituents or precursors leads to the following conclusions[75]: 1) at least some NiCRA (if not all) is crystalline; 2) NiCRA consists of new

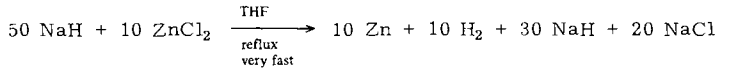
NiCRA (4/2/1)



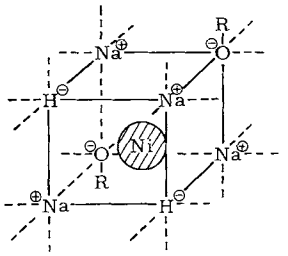

ZnCRA (4/1/1)




Scheme 23. Above: the NiCRA (4/2/1) shown here consists of NaH, *t*BuONa, and $Ni(OAc)_2$ in the molar ratio 4:2:1.—Below: the ZnCRA (4/1/1) shown here consists of NaH, *t*AmONa, and $ZnCl_2$ in the molar ratio 4:1:1 (numerical values in scheme: mmol).

species in which each constituent (or precursor) has lost its own characteristics and participates in the formation of new structures. From the data, NiCRA appears to be constituted of aggregates formed by association of matrices (see Scheme 24) consisting of Ni atoms surrounded by $Na^{\oplus}$, $H^{\ominus}$, $tBuO^{\ominus}$, and perhaps $AcO^{\ominus}$.




Scheme 24.

The results for ZnCRA[75] are interesting. The excess of $H_2$ observed in the preparation (Scheme 23) arises from the reaction:

$$2H^{\ominus} + Zn^{II} \longrightarrow Zn^{0} + H_2$$

consistent with the results of *Ashby et al.*[77]. Since ZnCRA may be obtained by addition of *t*AmOH to the suspension obtained after $ZnCl_2$ has been allowed to react with excess of NaH, this suggests that ZnCRA is formed by the reaction of *t*AmOH with Zn–NaH! Moreover, *t*AmOH does not react with Zn (prepared from NaH and $ZnCl_2$), and the metal was found in the solid fraction. In contrast to *t*BuONa with NiCRA about one third of *t*AmONa remained in solution with ZnCRA.

Analysis of the X-ray powder patterns study led to the following conclusions: 1) most of the NaH and about 30% of Zn are present as such; 2) the remaining Zn and *t*AmONa form new species. In other words, ZnCRA has to be considered as an association of Zn metal, NaH, and species tentatively formulated as $[(tAmO)_xZnNa_x]_n$. Why should this mixture be so efficient in reducing substrates such as carbonyl compounds? In trying to answer this question we noted the following observations[75]: 1) "$[(tAmO)_xZnNa_x]_n$" obtained from NaH-*t*AmONa-$ZnCl_2$ (3/1/1) does not reduce ketones; 2) Zn prepared from $ZnCl_2$–NaH (1/2) does not reduce ketones either; 3) curiously, Zn–NaH obtained from $ZnCl_2$–NaH (1/5) slowly reduces ketones such as cyclohexanone, but is much less efficient than ZnCRA.

From these observations it appears that ZnCRA could be tentatively considered as a mixture of NaH, $[(tAmO)_xZn(Na)_x]_n$, a small amount of $[(tAmO)_y(H)_zZn(Na)_{y+z}]_n$ (the active part), and some Zn metal. Reductions would take place at the active part, which could be regenerated from NaH and $[(tAmO)_xZnNa_x]_n$.

For chemists not intimately concerned with it, the work described in this review may appear to be more akin to alchemy than chemistry. This is not completely true. In fact, a unifying principle has directed the greater part of the research on complex bases and on CRA's, and I shall attempt to rationalize this beginning with complex bases.

The activation of ionic bases or nucleophiles by alcoholates must arise from formation of aggregates of the type $(-M^{\oplus}-Nu^{\ominus}-M^{\oplus}-\overset{\ominus}{O}R-)_n$. Of course, $Nu^{\ominus}M^{\oplus}$ also activates $RO^{\ominus}M^{\oplus}$, and once the aggregates are formed they must be viewed as a single entity. I postulate that these "supermolecules" presumably possess structures with marked electron delocalization and strong one-electron transfer tendencies. More generally, if $Nu^{\ominus}M^{\oplus}$ is a potential one-electron transfer reagent, an aggregation with appropriate ion pairs (or with itself) would lead to new species with much higher one-electron transfer abilities. It should be noted that one-electron transfer from $NaNH_2$–*t*BuONa has been recently demonstrated[78].

The active part of CRA's must also be viewed as consisting of NaH-RONa supermolecules, whose framework contains low oxidation-state metal cores. The metal species must be stabilized by the surrounding ionic framework and amplify the one-electron transfer ability of the whole.

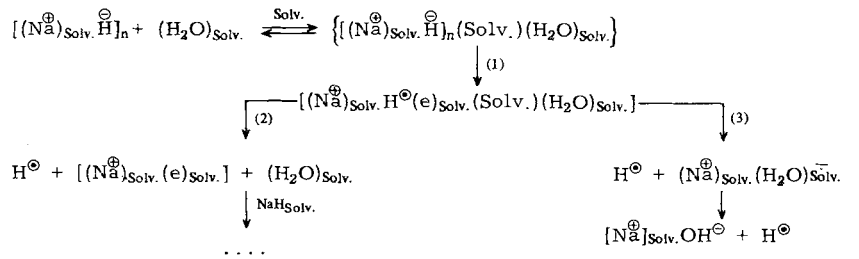
Moreover, they must also participate in anchoring the substrates during the electron transfer process.

If this description is accepted, CRA's appear to be complex polymeric hydrides with strong one-electron transfer abilities. The reduction steps could then be: 1) fixation to the "polymer"; 2) one-electron transfer; 3) hydrogen abstraction. The hydrogen source for the last step is of particular interest. The low yields of coupled products in the reductions support the conclusion that free radicals are not very abundant. However, some current experiments show that some of the hydrogen fixed on the reduced substrates must be supplied by the solvent. The absence of coupling could indicate that the radicals formed on the aggregates are still strongly bound to the reagent until the hydrogen abstraction step.

Thus, it appears plausible that in the reduction of substrates by CRA's radical species are formed on the polymer. A small fraction of these radicals may be liberated, resulting in coupling reactions and abstraction of hydrogen from the solvent. Other radicals strongly bound to the reagent abstract hydrogen from the polymeric hydride. The remaining fraction, consisting of more loosely bound radicals, abstracts hydrogen from the solvent. Presumably the lower the amount of free NaH, the greater the degree of solvent participation.

In view of what is known about reactions between organic substrates and low oxidation-state metal species[79], together with the recent results obtained by *Ashby et al.* on electron transfer from hydrides (and other reagents)[19l, 80], the view of CRA's presented above appears to be a good rationale.

Finally, in Section 1.2 we mentioned the generation of solvated electrons in HMPA in the reaction between NaH and water (or alcohols). This reaction, in my opinion, may be related to the activation hypothesis. Indeed, in HMPA the active part of NaH must take the form $(H^{\ominus}\text{--}Na^{\oplus}\text{--}\overset{\ominus}{O}\text{--}\overset{\oplus}{P}\!\!<)_n$ (which resembles the aggregates in complex bases or activated NaH), whose one-electron transfer ability is increased. Electron transfer through HMPA from active NaH towards a protic substrate (bound to HMPA) must be the first step of the reaction (step 1, Scheme 25). HMPA, a good electron stabilizing solvent[81], may trap some of the electrons (step (2)), while the others follow the normal pathway (step (3)).




Scheme 25. Solv. = solvent = HMPA.

To generalize this view, it is proposed that in an appropriate medium radical formation as well as numerous "ionic reactions" could be initiated by an electron transfer through electron-transmitting, separated nucleophile-electrophile ion pairs.

## 3. Conclusions

Before examining possible future developments of CRA's, some remarks must be made.

After we had published our first results on CRA's[15], some work appeared describing reducing agents involving NaH-metal salt systems. Thus, *Fujisawa et al.*[29] showed that NaH–$FeCl_2$ and NaH–$FeCl_3$ were able to reduce CC double bonds and carboxy groups. However, long reaction times and a considerable excess of reagents had to be used. On the other hand, *Ashby et al.*[2e], who attempted to reduce 1-octene with NaH in the presence of a series of metal salts, concluded their work with the following sentence: "It was somewhat disappointing that NaH did not produce yields of octane larger than 5%, since NaH is much less expensive than LiH and is easier to handle". It must be noted that even the highly reactive LiH did not lead to very efficient reducing agents.

In fact, in the course of the hundred or so control experiments we performed with the NaH-metal salts systems we also observed unsatisfactory reactivity in most cases; however, with some substrates high yields of reduction products were obtained. Nevertheless, the reactions were not very reproducible, and above all, substitution of the substrate by a similar one led to very low, or to no, yields of reduction product.

It, therefore, appears that NaH alone can donate its electrons, but its proton affinity impedes it with a few exceptions; activated by alcoholates or some metal salts its tendency to electron transfer becomes better but erratic. Moreover, the basicity of NaH-RONa still constitutes a formidable drawback.

In CRA's NaH, RONa and metal species occur together, and a synergism between the constituents seems to arise which concentrates their efforts toward a goal: to donate electrons to organic substrates.

In the future some work which should be performed is dictated by these observations. I am convinced that the study of physical properties of solid CRA's, such as conductivity and magnetic behavior, should lead to important information and perhaps show that they constitute a new class of electronic materials. Moreover, it is not unreasonable to assume that CRA's could be the first members of a new generation of electron or hydrogen reservoirs.

Of course, the initial studies on the constitution of CRA's, which we have performed on NiCRA and ZnCRA, must be extended.

The role played by the activating agents is so important that it appears of paramount importance to continue the

study of the influence of alcoholates on the properties of CRA's. Above all, activating agents with heteroatoms other than oxygen should be studied. Presumably elements such as sulfur, for example, should be excellent electron regulators. The use of "chelating" and polymeric activating agents would also lead to new CRA's.

A further point must be raised. We showed in Section 2.6 that CRA's containing two different metals have interesting properties. It is clear that the association of two (or more?) complementary metals should open new possibilities for application of CRA's. Use of these multimetal-containing CRA's to obtain new catalysts should also be investigated.

For elucidating the mechanism of reduction by CRA's, reactions with NaD should be very informative. Currently, the greatest problem is to find pure NaD. Sodium deuteride is very expensive since it has few uses. If deuteration were possible with CRA's, NaD would become less expensive than other deuterides. It should also be noted that NaH, which is relatively cheap, would become still less expensive if proper packaging were available to facilitate its use in industry, and extend its use as a reducing agent.

Among the problems which must still be considered is the investigation of the possibilities offered by CRA's to oligomerize or polymerize vinyl or dienyl monomers[17]. The use of asymmetric activating agents would also be of interest to induce asymmetric reductions as well as asymmetric coupling reactions or carbonylations.

Carbonylations must also be developed further in aprotic media and under phase transfer catalysis conditions. Specifically the concept of $S_{RN}1$-condensation of metalates should be extended.

To conclude it can said that the study of CRA's and related reagents is far from completion. If all the working hypotheses expressed in the work covered in this review are correct, then we have achieved the expected results in a designed way. If, on the contrary they are wrong, then we have been very lucky!

*I express my sincere appreciation to my coworkers who are individually identified in the references, particularly to J. J. Brunet. I am indebted to them for their experimental as well as intellectual contributions. Our work has been financially aided by the Centre National de la Recherche Scientifique, as E.R.A., DGRST (Proscom), Hoechst France, and Société Nationale Elf Aquitaine (Production). I am very grateful to Professor K. G. Taylor, visiting Professor in Nancy University, for helpful discussions.*

Received: February 18, 1983 [A 461 IE]
German version: *Angew. Chem. 95* (1983) 597

[1] J. Plesek, S. Hermanek: *Sodium Hydride,* Iliffe, London 1968.
[2] See *e.g.* a) . M. Z. Gladych, R. Hornby, *Chem. Ind. (London) 1970,* 652; b) M. Natsume, S. Kumadaki, Y. Kanda, K. Kiuchi, *Tetrahedron Lett. 1973,* 2335; c) Y. J. Lee, W. D. Closson, *ibid. 1974,* 381; d) R. B. Nelson, G. W. Gribble, *J. Org. Chem. 39* (1974) 1425; e) E. C. Ashby, S. A. Noding, *ibid. 45* (1980) 1041.
[3] P. Caubère, *Bull. Soc. Chim. Fr. 1966,* 1293.
[4] HMPA is now thought to be a potent chemical carcinogen and should be handled with extreme care; H. Spencer, *Chem. Ind. (London) 1979,* 728; On toxicity see also R. Kimbrough, T. B. Gaines, *Nature (London) 211* (1966) 146.
[5] R. G. Pearson, J. Songstad, *J. Am. Chem. Soc. 89* (1967) 1827.
[6] P. Caubère, J. Moreau, *Tetrahedron 25* (1969) 2469.
[7] P. Caubère, J. Moreau, *Bull. Soc. Chim. Fr. 1970,* 1986.
[8] H. G. Kuivila, O. F. Beumel, *J. Am. Chem. Soc. 80* (1958) 3798; H. G. Kuivila, *ibid. 84* (1962) 3584; R. Barlet, Y. Vo Quang, *Bull. Soc. Chim. Fr. 1969,* 3729 Review; C. L. Osborn, T. C. Shields, B. A. Shoulders, C. G. Gardenas, P. D. Gardner, *Chem. Ind. (London) 1965,* 766.
[9] J. Moreau, P. Caubère, *Tetrahedron 27* (1971) 5741.
[10] P. Caubère, J. Moreau, *Bull. Soc. Chim. Fr. 1971,* 3270; *1971,* 3276.
[11] P. Caubère, *Acc. Chem. Res. 7* (1974) 301; *Top. Curr. Chem. 73* (1978) 50; For recent applications 1) Generation of carbanions: G. Ndebeka, Thèse d'Etat, Nancy (France) (1979) (registered at CDST Centre National de la Recherche Scientifique) 2) Anionic polymerizations: S. Raynal, S. Lecolier, G. Ndebeka, P. Caubère, *Polymer 23* (1982) 283, and references cited therein.
[12] P. Caubère, J. Moreau, *Tetrahedron 26* (1970) 2637.
[13] P. Caubère, unpublished results.
[14] J. J. Brunet, R. Vanderesse, P. Caubère, *J. Organomet. Chem. 157* (1978) 125.
[15] G. Guillaumet, L. Mordenti, P. Caubère, *J. Organomet. Chem. 92* (1975) 43.
[16] G. Guillaumet, L. Mordenti, P. Caubère, *J. Organomet. Chem. 102* (1975) 353.
[17] B. Loubinoux, R. Vanderesse, P. Caubère, *Tetrahedron Lett. 1977,* 3951.
[18] R. Vanderesse, J. J. Brunet, P. Caubère, *J. Org. Chem. 46* (1981) 1270.
[19] a) A. R. Pinder, *Synthesis 1980,* 425; b) A. Hajos: *Complex Hydrides and Related Reducing Agents in Organic Synthesis,* Elsevier, Amsterdam 1979; c) J. E. Johnson, R. H. Blizzard, H. W. Carhart, *J. Am. Chem. Soc. 70* (1948) 3664; d) L. W. Trevoy, W. G. Brown, *ibid. 71* (1949) 1675; e) H. C. Brown, S. Krishnamurthy, *J. Org. Chem. 34* (1969) 3918; f) C. W. Jefford, D. Kirkpatrick, F. Delay, *J. Am. Chem. Soc. 94* (1972) 8905; g) H. C. Brown, S. Krishnamurthy, *ibid. 95* (1973) 1669; h) *Tetrahedron 35* (1979) 567; i) S. Krishnamurthy, H. C. Brown, *J. Org. Chem. 45* (1980) 849; j) S. K. Chung, *ibid. 45* (1980) 3513; k) P. R. Singh, A. Nigam, J. M. Khurana, *Tetrahedron Lett. 21* (1980) 4753; l) E. C. Ashby, R. N. de Priest, A. B. Goel, *ibid. 22* (1981) 1763; m) S. Krishnamurthy, H. C. Brown, *J. Org. Chem. 47* (1982) 276; n) J. Malek, M. Cerny, *Synthesis 1972,* 217.
[20] a) H. M. Bell, C. W. Vanduslice, A. Spechar, *J. Org. Chem. 34* (1969) 3923; b) R. O. Hutchins, D. Hoke, J. Keogh, D. Koharski, *Tetrahedron Lett. 1969,* 3495; c) R. O. Hutchins, R. J. Bertsch, D. Hoke, *J. Org. Chem. 36* (1971) 1568; d) C. F. Lane, *Synthesis 1975,* 135; e) R. O. Hutchins, D. Kandasamy, C. A. Maryanoff, D. Masilamani, B. E. Maryanoff, *J. Org. Chem. 42* (1977) 82; f) H. Toi, Y. Yamamoto, A. Sonoda, S. I. Murahashi, *Tetrahedron 37* (1981) 2261.
[21] a) J. R. Hanson, *Synthesis 1974,* 1; b) Tse-Lok Ho, *ibid. 1979,* 1.
[22] H. G. Kuivila, L. W. Menapace, *J. Org. Chem. 28* (1963) 2161; H. G. Kuivila, *Acc. Chem. Res. 1* (1968) 299.
[23] J. P. Collman, L. S. Hegedus: *Principles and Applications of Organo-Transition Metal Chemistry,* University Science Books, Mill Valley, CA 1980.
[24] a) E. C. Ashby, J. J. Lin, A. B. Goel, *J. Org. Chem. 43* (1978) 183; b) E. C. Ashby, J. J. Lin, *Tetrahedron Lett. 1977,* 4481; c) *J. Org. Chem. 43* (1978) 1263; d) S. Masamune, P. A. Rossy, G. S. Bates, *J. Am. Chem. Soc. 95* (1973) 6452.
[25] a) R. A. Egli, *Helv. Chim. Acta 51* (1968) 2090; b) S. T. Lin, J. A. Roth, *J. Org. Chem. 44* (1979) 309; c) I. D. Entwistle, P. Bochm, R. A. W. Johnstone, R. P. Telford, *J. Chem. Soc. Perkin Trans. 1 1980,* 27; d) B. Meunier, *J. Organomet. Chem. 204* (1981) 345; e) T. Yoshida, E. I. Negishi, *J. Chem. Soc. Chem. Commun. 1974,* 762.
[26] a) R. Vanderesse, Thèse d'Etat, Université de Nancy 1981 (CDST Centre National de la Recherche Scientifique); b) R. Vanderesse, J. J. Brunet, P. Caubère, to be published.
[27] a) A. S. Kende, L. S. Liebeskind, D. M. Braitsch, *Tetrahedron Lett. 1975,* 3375; b) M. Zembayashi, K. Tamao, J. Yoshida, M. Kumada, *ibid. 1977,* 4089; c) T. T. Tsou, J. K. Kochi, *J. Am. Chem. Soc. 101* (1979) 7547, and references cited therein. d) M. F. Semmelhack, P. Helquist, L. D. Jones, L. Keller, L. Mendelson, L. Speltz Ryono, J. Gorzynski Smith, R. D. Stauffer, *ibid. 103* (1981) 6460, and references cited therein.
[28] a) J. J. Brunet, L. Mordenti, B. Loubinoux, P. Caubère, *Tetrahedron Lett. 1977,* 1069; b) J. J. Brunet, P. Caubère, *ibid. 1977,* 3947.
[29] a) T. Fujisawa, K. Sugimoto, H. Ohta, *Chem. Lett. 1976,* 581; b) *J. Org. Chem. 41* (1976) 1667; T. Fujisawa, K. Sugimoto, H. Ota, *Japan Kokai* 7691, 202, *Chem. Abstr. 85* (1976) 142299w.
[30] P. W. Jolly, G. Wilke: *The Organic Chemistry of Nickel,* Vol. 2, Academic Press, London 1975.
[31] a) P. Jacob, DEA, Université de Nancy 1979; b) D. Besozzi, Thèse 3e cycle, Université de Nancy 1982 (CDST Centre National de la Recherche Scientifique).
[32] a) E. C. Ashby, J. J. Lin, *J. Org. Chem. 43* (1978) 2567; b) S. K. Chung, *ibid. 44* (1979) 1014.
[33] J. J. Brunet, L. Mordenti, P. Caubère, *J. Org. Chem. 43* (1978) 4804.

[34] a) H. D. Kaesz, R. B. Saillant, *Chem. Rev. 72* (1972) 231; b) P. W/ Jolly, G. Wilke: *The Organic Chemistry of Nickel*, Vol. *1*, Academic Press, New York 1974.
[35] L. Mordenti, J. J. Brunet, P. Caubère, *J. Org. Chem. 44* (1979) 2203.
[36] D. N. Kursanov, Z. N. Parnes, N. M. Loim, *Synthesis 1974*, 633.
[37] W. R. Jackson, A. Zuraiyah, *J. Chem. Soc. 1965*, 5280.
[38] M. Yamashita, Y. Kato, R. Suemitsu, *Chem. Lett. 1980*, 847.
[39] S. Masamune, G. S. Bates, P. E. Georghiou, *J. Am. Chem. Soc. 96* (1974) 3686.
[40] E. C. Ashby, J. J. Lin, R. Kovar, *J. Org. Chem. 41* (1976) 1939.
[41] S. Krisnamurthy, H. C. Brown, *J. Org. Chem. 40* (1975) 1864, and references cited therein.
[42] J. L. Luche, L. Rodriguez-Hahn, P. Crabbe, *J. Chem. Soc. Chem. Commun. 1978*, 601; J. L. Luche, *J. Am. Chem. Soc. 100* (1978) 2226; A. L. Gemal, J. L. Luche, *ibid. 103* (1981) 5454.
[43] M. R. Johnson, B. Rickborn, *J. Org. Chem. 35* (1970) 1041.
[44] M. F. Semmelhack, R. D. Stauffer, A. Yamashita, *J. Org. Chem. 42* (1977) 3180.
[45] R. O. Hutchins, D. Kandasamy, *J. Org. Chem. 40* (1975) 2530.
[46] J. M. Fortunato, B. Ganen, *J. Org. Chem. 41* (1976) 2194.
[47] A. M. Caporusso, G. Giaconelli, L. Lardicci, *J. Org. Chem. 47* (1982) 4640.
[48] J. J. Brunet, D. Besozzi, P. Caubère, *Synthesis 1982*, 721.
[49] See *e.g.* a) H. Matsumoto, Y. Hoshino, Y. Nagai, *Bull. Chem. Soc. Jpn. 54* (1981) 1279, and references cited therein; b) I. Ojima, T. Kogue, *Organometallics 1* (1982) 1390, and references cited therein; c) C. Chuit, R. J. P. Corriu, R. Perz, C. Reye, *Synthesis 1982*, 981, and references cited therein.
[50] J. J. Brunet, P. Gallois, P. Caubère, *Tetrahedron Lett. 1977*, 3955.
[51] J. J. Brunet, P. Gallois, P. Caubère, *J. Org. Chem. 45* (1980) 1937.
[52] P. Gallois, J. J. Brunet, P. Caubère, *J. Org. Chem. 45* (1980) 1946.
[53] R. J. Card, C. E. Liesner, D. C. Neckers, *J. Org. Chem. 44* (1979) 1095, and references cited therein.
[54] See *e.g.* R. Romanet, *C. R. Acad. Sci. 236* (1953) 1044, and references cited therein; R. J. Tedeschi, G. Clark, *J. Org. Chem. 27* (1962) 4323.
[55] a) E. N. Marvell, J. Tashiro, *J. Org. Chem. 30* (1965) 3991; b) E. N. Marvell, T. Li, *Synthesis 1973*, 457.
[56] a) R. L. Augustine: *Catalytic Hydrogenations*, Marcel Dekker, New York 1965; b) M. Friefelder: *Practical Catalytic Hydrogenation*, Wiley-Interscience, New York 1971; c) C. A. Brown, V. K. Ahuja, *J. Org. Chem. 38* (1973) 2226.
[57] A. A. Pavlic, H. Adkins, *J. Am. Chem. Soc. 68* (1946) 1471, and references cited therein
[58] H. C. Brown, C. A. Brown, *J. Am. Chem. Soc. 85* (1963) 1003; C. A. Brown, *J. Org. Chem. 35* (1970) 1900.
[59] For an excellent review on $NaBH_4$-reduced Co and Ni systems see R. C. Wade, D. G. Olah, A. N. Hughes, B. C. Hui, *Catal. Rev.-Sci. Eng. 14* (2) (1976) 211.
[60] T. W. Russell, R. C. Hoy, J. E. Cornelius, *J. Org. Chem. 37* (1972) 3552.
[61] P. Gallois, Thèse Dr. Ing., Université de Nancy 1979 (CDST Centre National de la Recherche Scientifique).
[62] T. W. Russell, R. C. Hoy, *J. Org. Chem. 36* (1971) 2018.
[63] W. Strohmeier, H. Steigerwald, *Z. Naturforsch. B 30* (1975) 816.
[64] C. A. Brown, V. K. Ahuja, *J. Chem. Soc. Chem. Commun. 1973*, 553.
[65] T. W. Russell, D. M. Duncan, S. C. Hansen, *J. Org. Chem. 42* (1977) 551.
[66] a) F. Calderazzo, R. Ercoli, G. Natta in I. Wender, P. Pino: *Organic Syntheses via Metal Carbonyls*, Vol. *1*, Interscience, New York 1968, p. 1; L. Cassar, G. P. Chiusoli, Ital. Pat. 868994 (1969); *Chem. Abstr. 78* (1973) 147583; b) A. Mullen in J. Falbe: *New Syntheses with Carbon Monoxide*, Springer, Berlin 1980, p. 295; references given deal with benzyl halids *Chem. Abstr. 85* (1976) 32638k; c) see [67] and references cited therein.
[67] J. J. Brunet, C. Sidot, B. Loubinoux, P. Caubère, *J. Org. Chem. 44* (1979) 2199.
[68] J. J. Brunet, C. Sidot, P. Caubère, *J. Organomet. Chem. 204* (1980) 229.
[69] I. Wender, P. Pino: *Organic Syntheses via Metal Carbonyls*, Vol. *1* and *2*, Wiley-Interscience, New York 1968 and 1977; R. B. King, *Acc. Chem. Res. 3* (1970) 417, and references cited therein (we verified this lack of reactivity).
[70] For review on $S_{RN}1$ reactions, see J. F. Bunnett, *Acc. Chem. Res. 11* (1978) 413; R. A. Rossi, *ibid. 15* (1982) 164.
[71] Review: H. Alper, *Adv. Organomet. Chem. 19* (1981) 183.
[72] J. J. Brunet, C. Sidot, P. Caubère, *Tetrahedron Lett. 22* (1981) 1013; C. Sidot, Thèse d'Etat, Université de Nancy 1982 (CDST Centre National de la Recherche Scientifique); J. J. Brunet, C. Sidot, P. Caubère, *J. Org. Chem. 48* (1983) 1166; *ibid. 48* (1983) 1919.
[73] J. J. Brunet, C. Sidot, P. Caubère, *J. Org. Chem. 46* (1981) 3147.
[74] See *e.g.* J. P. Collman, *Acc. Chem. Res. 8* (1965) 342; J. P. Collman, R. G. Finke, J. N. Cawse, J. I. Brauman, *J. Am. Chem. Soc. 99* (1977) 2515, and references cited therein.
[75] J. J. Brunet, D. Besozzi, A. Courtois, P. Caubère, *J. Am. Chem. Soc. 104* (1982) 7130.
[76] For such ligands effects, see *e.g.* M. Mikuiya, M. Nakamura, H. Okawa, S. Kida, *Chem. Lett. 1982*, 839, and references cited therein
[77] J. J. Watkins, E. C. Ashby, *Inorg. Chem. 13* (1974) 2350, and references cited therein.
[78] M. Perdicakis, J. Bessiere, *C. R. Acad. Sci. 295*, II (1982) 879.
[79] See *e.g.* J. K. Kochi: *Organometallic Mechanisms and Catalysis*, Academic Press, New York 1978.
[80] See *e.g.* E. C. Ashby, A. B. Goel, R. N. de Priest, *J. Am. Chem. Soc. 102* (1980) 7779; *Tetrahedron Lett. 22* (1981) 3729; E. C. Ashby, A. B. Goel, *ibid. 22* (1981) 1879, 4783; E. C. Ashby, A. G. Goel, R. N. de Priest, H. S. Prasad, *J. Am. Chem. Soc. 103* (1981) 973, and references cited therein.
[81] H. Normant, *Bull. Soc. Chim. Fr. 1968*, 791; J. K. Kochi: *Free Radicals*, Wiley-Interscience, New York 1973.

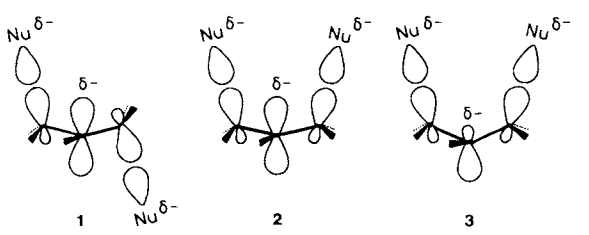
# COMMUNICATIONS

**When submitting manuscripts, authors of articles which are intended for publication as "Communications" are requested to conform to the guidelines reproduced at the beginning of each issue following the list of contents.**

## On the Stereochemistry of the $S_N2'$ Reaction

By *Wolf-Dieter Stohrer**

In bimolecular nucleophilic substitution with allyl rearrangement ($S_N2'$ reaction) the entering and the leaving nucleophile (Nu) can be oriented antiplanar (*anti*-reaction *via* the transition state **1**) or synplanar (*syn*-reaction *via* the transition state **2**). Of the $S_N2'$ reactions so far investigated stereochemically the overwhelming majority proceeded with high *syn*-preference[1].



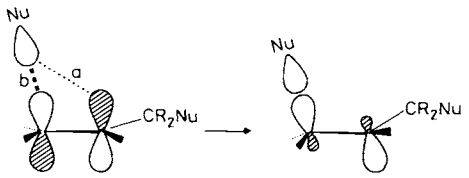

In most of the theoretical investigations[2] on the stereochemistry of the $S_N2'$ reaction this *syn*-preference is rationalized, in that the quasi-cyclic transition state **2** (as a Hückel arene) is sufficiently favored stereoelectronically compared to the non-cyclic transition state **1**, although

[*] Prof. Dr. W.-D. Stohrer
Fachbereich 2, Studiengang Chemie der Universität
Postfach, D-2800 Bremen 33 (Germany)

MO calculations[3] strengthen the obvious suspicion that the greater steric—and in the case of (negatively) charged transition states also electrostatic—repulsion between the two nucleophiles in **2** compared to in **1** compensates the stereoelectronic stabilization.

In this communication attention is drawn to a further stereoelectronic factor favoring the *syn*-reaction which has hitherto never been taken into consideration[4]. The central C atom, which does not directly participate in the reaction, and which in the transition state—regardless if charged or not—accumulates *more or less negative charge*, is planar in the *anti*-transition state **1** (as shown), *i.e.* $sp^2$-hybridized, but (other than previously assumed and other than shown in **2**) non-planar in the *syn*-transition state, and—because of the *partial negative charge on this C atom energetically more favorably*—$sp^n$ hybridized ($2<n<3$). The bigger of the two orbital lobes lies (as shown in **3**) on the side opposite to that of the two nucleophiles.

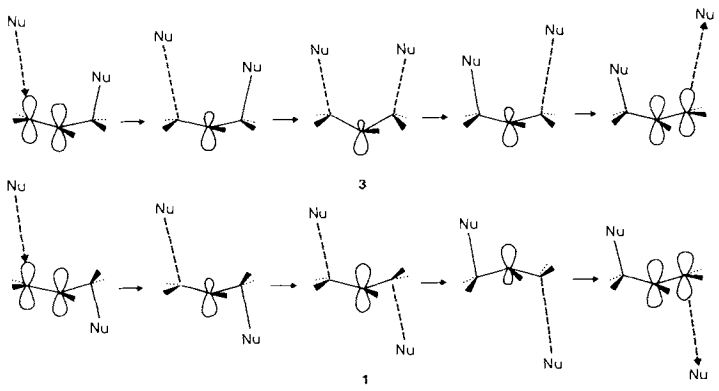
These different hybridizations at the central C atom (C-2) of the two transition states can be readily explained in terms of the frontier orbital model: the entering nucleophile interacts with maximal stabilization with the LUMO of the double bond, *i.e.* for optimization of the direct bonding interaction b and for minimization of the antibonding interaction a the nuclear framework distorts itself such that the bigger orbital lobe of the $sp^n$-hybridized central C atom develops on the side opposite to that of the entering nucleophile.




Based on the principle of microscopic reversibility, this correspondingly also applies to the leaving nucleophile, *i.e.*:

—in the *syn*-reaction (*via* **3**) the bigger orbital lobe on C-2 remains on the same side of the molecule along the whole reaction coordinate;

—in the *anti*-reaction (*via* **1**) the bigger orbital lobe on C-2 must change "sides" during the reaction, *i.e.* an energetically more or less unfavorable inversion must take place at the central atom, which is partially negatively charged during the reaction.




This inversion barrier reduces *a priori* the chance of the *anti*-reaction all the more with increasing accumulation of negative charge at C-2 in the transition state, *i.e.* the longer the 'bond breaking' of the leaving nucleophile lags behind the 'bond forming' of the entering nucleophile; and *vice versa!* Thus, other things being equal, a difficultly cleavable nucleophile should favor the *syn*-reaction, an easily cleavable nucleophile the *anti*-reaction. The height of this barrier, which depends on the nature of the nucleophiles, can still be increased (in favor of the *syn*-reaction) or lowered (in favor of the *anti*-reaction) by commonly known steric and/or electronic factors.

Received: April 12, 1983 [Z 344 IE]
German version: *Angew. Chem. 95* (1983) 642

[1] R. M. Magid, *Tetrahedron 36* (1980) 1901.

[2] N. Cheng, B. Zhon, *Fenzi Kexue Xuebao 1982*, 119; *Chem. Abstr. 97* (1982) 197541j; W. S. Murphy, B. O'Mahony, *Tetrahedron Lett. 22* (1981) 585, and references cited therein.

[3] a) R. L. Yates, N. D. Epiotis, F. Bernardi, *J. Am. Chem. Soc. 97* (1975) 6615; b) W.-D. Stohrer, unpublished results of a series of different semiempirical calculations and *ab-initio* calculations (with various basis sets) for the transition states **1** and **2**.

[4] The model presented here differs fundamentally from the, at first glance, apparently similar "Orbital Distortion Model" of C. L. Liotta, *Tetrahedron Lett. 1975*, 523. Liotta uses the statistical distortion of the LUMO to predict the preferred nucleophilic attack; in the model presented here the dynamic distortion of the nuclear framework along the reaction coordinate is investigated.

## Probing the Environment of Al Atoms in Noncrystalline Solids: $Al_2O_3$–$SiO_2$ Gels, Soda Glass, and Mullite Precursors**

By *John M. Thomas**, *Jacek Klinowski*, *Paul A. Wright*, and *Rustum Roy*

Very few techniques are available for ascertaining the coordination of atoms within amorphous or quasi-crystalline solids. One recently developed approach is based on magic-angle spinning NMR (MAS-NMR) which, especially in crystalline specimens[1], can readily identify the immediate environment of atoms. Tetra- and hexacoordinated Al and Si are directly distinguishable in various minerals and their synthetic analogues using $^{27}Al$ and $^{29}Si$ MAS-NMR spectroscopy. Moreover, tri- and tetracoordinated B in borosilicate glasses[2a]; different kinds of tetracoordinated Si in silica gels[2b] and cements[2c] have been characterized.

A disadvantage of $^{29}Si$ MAS-NMR for nuclei having spin 1/2 in amorphous solids are long spin-lattice relaxation times, which we have found to be of the order of several hours in some high-purity glasses[3]. Relaxation of quadrupolar nuclei, such as $^{27}Al$ with spin 5/2, proceeds by a different mechanism from those with spin 1/2 and is generally very fast. Recycle times of 0.1 sec give quantitatively reliable spectra; another important advantage of $^{27}Al$ is its 100% isotopic abundance, which makes $^{27}Al$-NMR a very sensitive probe. Al atoms can, for example, be

[*] Prof. J. M. Thomas, Dr. J. Klinowski, P. A. Wright
Department of Physical Chemistry, University of Cambridge
Lensfield Road, Cambridge, CB2 1EP (UK)
Prof. R. Roy
Materials Research Laboratory, The Pennsylvania State University
University Park, PA 16802 (USA)

[**] We wish to thank the University of Cambridge for support and experimental assistance, Prof. C. A. Fyfe (Ontario) for recording the $^{27}Al$-MAS-NMR spectra, Dr. S. R. Elliott for preparing the soda glass, and Dr. W. E. Hull and Dr. D. Müller for their experimental help. We are grateful for the support of the Science and Engineering Research Council and B.P. Co. Ltd. The Sol-gel research of Rustum Roy is supported by NSF Grant No. DMR-8110476.

quantitatively detected[4] even in materials with Si/Al ratios as large as 10000. $^{27}$Al-MAS-NMR can be used to distinguish four- and six-coordinated Al, the former resonating at $\delta \approx 50$—90 ppm, and the latter at 0—20 ppm (relative to $Al(H_2O)_6^{3+}$). It is advantageous to employ high magnetic field strengths, since the second-order quadrupolar interaction is inversely proportional to the field strength. $^{27}$Al-MAS-NMR spectra were recorded at 104.22 MHz and 130.32 MHz using Bruker WH-400 and AM-500 spectrometers; the latter instrument uses the highest currently available persistent magnetic field. Delrin rotors were spun at rates up to 4 kHz.

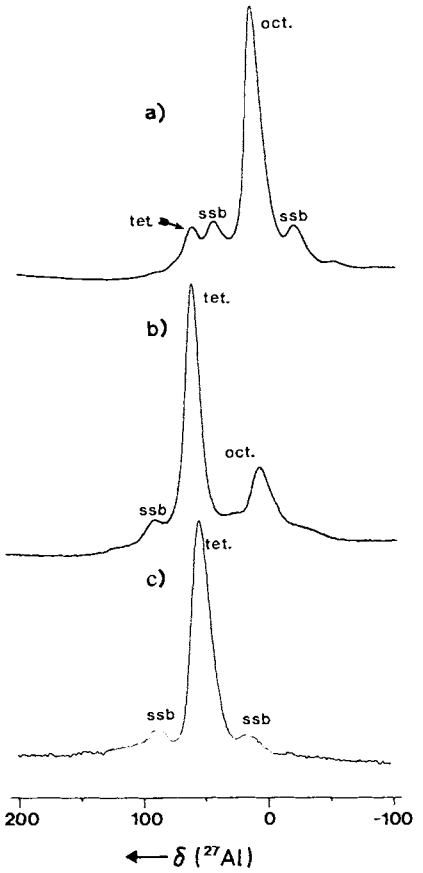



Fig. 1. $^{27}$Al-MAS-NMR spectra at 104.22 MHz: a) $Al_2O_3$—$SiO_2$ gel with 75% $Al_2O_3$; b) $Al_2O_3$—$SiO_2$ gel with 28% $Al_2O_3$; c) Soda glass (15% $Na_2O$ + 85% $SiO_2$) containing only traces of $Al_2O_3$: ssb = spinning of sidebands, oct. = octahedral, tet. = tetrahedral.

In the gel containing *ca.* 28% $Al_2O_3$ most Al atoms are tetracoordinated, while in the gel with *ca.* 75% $Al_2O_3$ most Al is hexacoordinated (octahedral); indeed, the spectrum of this gel is almost indistinguishable from that of commercial $Al_2O_3$. Figure 1(c) shows the spectrum of soda glass containing 15% $Na_2O$, 85% $SiO_2$ and only traces of Al: all the Al atoms in soda glass are tetrahedrally bound. This is also the case in borosilicate glass containing traces of $Al_2O_3$. In all cases the NMR signals are relatively broad, indicating that Al is present in a variety of environments, *i.e.* is disordered. It appears that Al functions as an "environmental probe", in that it adopts the preferred coordination of the dominant component of the gel.

We have used $^{27}$Al-MAS-NMR to study the crystallization of mullite from a $SiO_2$—$Al_2O_3$ xerogel precursor. Mullite (nominally $3Al_2O_3 \cdot 2SiO_2$, with a variable composition close to Al : Si = 3 : 1) is a very stable phase, whose structure has not yet been unambiguously established, but is loosely based on the ordered sillimanite structure involving chains of Al octahedra parallel to the z-axis, cross-linked by tetrahedra containing both Si and Al[5]. By analogy with Al-substituted sillimanite we would expect that two unit cells of mullite contain twelve sites, four of which are octahedral and eight tetrahedral. Since in mullite Si is tetracoordinated it follows that two unit cells of mullite (with the ideal composition) contain four octahedral and five tetrahedral Al atoms, and three tetrahedral Si atoms. Mullite xerogel precursor was prepared by mixing 15 g of $Al(NO_3)_3 \cdot 9H_2O$, 10 mL of ethanol, 5 mL of water, and 2.2 mL of $Si(OC_2H_5)_4$. The gel (amorphous to X-rays) was warmed in a water bath (4 h, 75 °C), subsequently air dried for 15 d, and finally heated to 450 °C. Crystallization of mullite was monitored by heating the gel to various temperatures in the range 1000 to 1400 °C and recording X-ray diffractograms and $^{27}$Al-MAS-NMR spectra (Fig. 2) of the products.

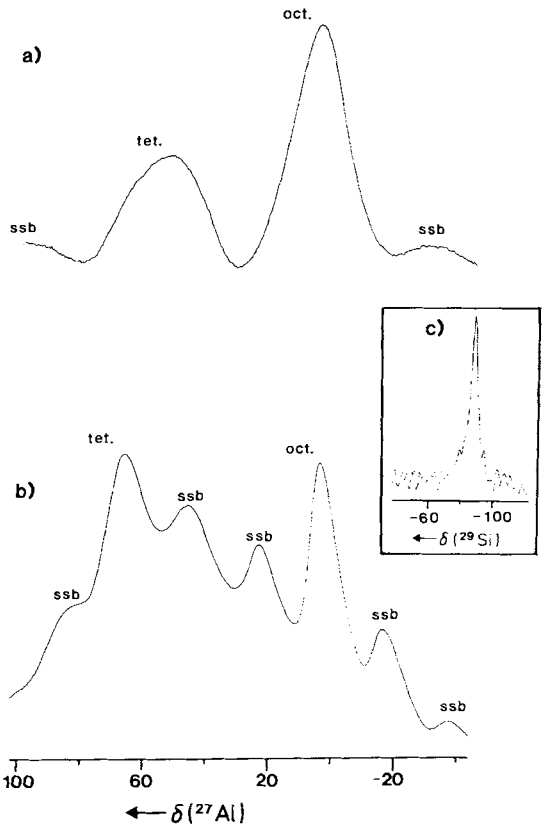



Fig. 2. $^{27}$Al-MAS-NMR spectra at 130.32 MHz; a) mullite xerogel; b) crystalline mullite; c) $^{29}$Si-MAS-NMR spectrum of crystalline mullite at 59.60 MHz.

The $^{27}$Al spectrum of the parent xerogel (Fig. 2a) is well resolved and yields a ratio of tetrahedral to octahedral Al of 0.63, in good agreement with the spectra in Figures 1a and 1b. Since the corresponding ratio in mullite is 1.25 (see above) its crystallization from the gel must involve extensive conversion of hexacoordinated to tetracoordinated Al. This was indeed observed by $^{27}$Al-MAS-NMR. X-ray diffraction studies identify $\gamma$-$Al_2O_3$ as an intermediate product in samples heated to lower than 1400 °C. The $^{29}$Si-MAS-NMR spectrum of crystalline mullite (Fig. 2a; $T_1$ in the order of several seconds) features a *single* signal at $\delta = -86.0 \pm 1$ (rel. to TMS), indicating that all Si atoms are in an identical intracrystalline environment. The assign-

ment of the resonance to Si(4Al) is consistent with the structural model described above.

Received: February 28, 1983 [Z 293 IE]
German version: *Angew. Chem. 95* (1983) 643

CAS Registry Numbers:
Al: 7429-90-5; mullite: 1302-93-8.

[1] a) E. R. Andrew, *Intl. Rev. Phys. Chem. 1* (1981) 195; b) C. A. Fyfe, J. M. Thomas, J. Klinowski, G. C. Gobbi, *Angew. Chem. 95* (1983) 257; *Angew. Chem. Int. Ed. Engl. 22* (1983) 259 and literature cited therein.

[2] a) C. A. Fyfe, G. C. Gobbi, unpublished results; S. Schramm, E. Oldfield, *J. Chem. Soc. Chem. Commun. 1982*, 980; b) D. W. Sindorf, G. E. Maciel, *J. Am. Chem. Soc. 102* (1980) 7606; *ibid. 103* (1981) 4263; *J. Phys. Chem. 86* (1982) 5218; G. E. Maciel, D. W. Sindorf, V. J. Bartuska, *J. Chromatogr. 205* (1981) 438; C. A. Fyfe, G. C. Gobbi, G. J. Kennedy, unpublished results; c) E. Lippmaa, M. Mägi, M. Tarmak, W. Wieker, A.-R. Grimmer, *Cement Concrete Res. 12* (1982) 597.

[3] J. Klinowski, J. M. Thomas, C. A. Fyfe, G. C. Gobbi, unpublished results.

[4] C. A. Fyfe, G. C. Gobbi, J. Klinowski, J. M. Thomas, S. Ramdas, *Nature (London) 296* (1982) 530.

[5] W. A. Deer, R. A. Howie, J. Zussman: *An Introduction to the Rock-Forming Minerals*, Longman, London (1966).

## Surfactants with Novel Structural Characteristics**

By *Edwin Weber**

A typical surfactant molecule consists of a lipophilic and hydrophilic part[1]. Here we report on surfactants having a novel construction principle which at the same time exhibits the characteristics of neutral ligands[2]. The oligotopic crown ethers **1**—**11** attracted our attention because of their remarkable solubility behavior. Unexpectedly, the six-armed (**1**, **2**) and some trisubstituted species (**5**, **8**, **9**) (cf. Table 1) are highly soluble in water and other polar solvents (methanol, ethanol, dimethylformamide, dimethyl sulfoxide), but as a rule only possess limited solubility in less polar solvents (including chloroform). Aqueous solutions of these compounds readily wet a contiguous glass wall (*e.g.* $\gamma = 47$ mN/m for **1**, 42 for **8**, each in $5 \times 10^{-4}$ M solution, $T = 23$ °C). Upon concentrating the solutions the viscosity and the foaming ability increase markedly until a reversible opaque and almost immobile gel results. The surfactant character is illustrated even more clearly by the occurrence of cloud points in water[1,3] (Table 1), which are directly related to the molecular structure: the cloud point decreases with increasing conformational flexibility of the molecular framework and *vice versa* (cf. **1** with **2**, **8** with **9**, **9** with **11**). A typical characteristic of these compounds is that upon evenly warming samples of these compounds in glass vessels the clouding always starts at the glass/water/air interface.

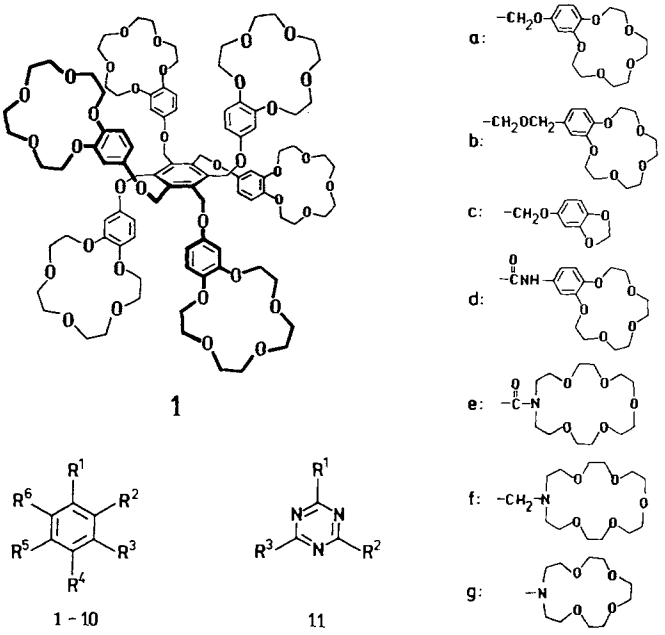



Table 1. Selected data for the synthesized compounds [a].

| No. | $R^1$—$R^6$ | M.p. [°C] | CP [°C] [b] |
|---|---|---|---|
| 1 | $R^1$—$R^6$ = **a** | 195—198 | 52—54 |
| 2 | $R^1$—$R^6$ = **b** | 85 (decomp.) | 36—38 |
| 3 | $R^1$—$R^6$ = **c** | 214—216 | [c] |
| 4 | $R^1$, $R^2$, $R^4$, $R^5$ = **a**; $R^3$, $R^6$ = H | 183—185 | [c] |
| 5 | $R^1$, $R^3$, $R^5$ = **a**; $R^2$, $R^4$, $R^6$ = H | (glassy) | 27—29 |
| 6 | $R^1$, $R^3$, $R^5$ = **a**; $R^2$, $R^4$, $R^6$ = $CH_3$ | 192—195 | [c] |
| 7 | $R^1$, $R^3$, $R^5$ = **d**; $R^2$, $R^4$, $R^6$ = H | 117—120 (decomp.) | [c] |
| 8 | $R^1$, $R^3$, $R^5$ = **e**; $R^2$, $R^4$, $R^6$ = H | oil | [d] |
| 9 | $R^1$, $R^3$, $R^5$ = **f**; $R^2$, $R^4$, $R^6$ = H | oil | 24—26 |
| 10 | $R^1$, $R^3$ = **a**; $R^2$, $R^4$, $R^5$, $R^6$ = H | (glassy) | [c] |
| 11 | $R^1$—$R^3$ = **g** | 107—108 | 83—85 |

[a] Elemental analyses and spectroscopic data are consistent with the given structures; melting points are not corrected. [b] Cloud point in water, $10^{-3}$ M solution. [c] Low soluble in water. [d] No clouding up to 100 °C.

The clouding phenomenon described above indicates that in the chosen concentration range micellar solutions are present[3]. Using light scattering methods, critical concentrations for micelle formation of $1.3 \times 10^{4}$ and $5.4 \times 10^{-4}$ mol/L were determined for **1** and **9**, respectively ($T = 23$ °C)—values which are typical for non-ionic surfactants[3]. The aggregation number of the micelles of **8** at $c = 5 \times 10^{-4}$ mol/L is 76; for **1** the value is 50, which seems to correspond to the increased number of ligand arms.

Solvent- and temperature-specific short-range order data of the dissolved surfactants can also be gathered from the $^1$H-NMR spectra[4].

Since numerous biological reactions proceed and/or are catalyzed in aqueous (lyotropic) systems, and because of the enzyme model character of crown ethers[5], the novel surfactant structures should provide highly promising starting points for biomimetic catalysis. The interactions of complexing agents with surfactants are also decisive in the washing process[1b].

Received: December 20, 1979;
revised: June 13, 1983 [Z 900 IE]
German version: *Angew. Chem. 95* (1983) 632
The complete manuscript of this communication appears in: *Angew. Chem. Suppl. 1983*, 840-850

CAS Registry Numbers:
**1**, 86422-12-0; **2**, 86422-13-1; **3**, 86422-14-2; **4**, 86436-09-1; **5**, 86436-10-4; **6**, 86422-15-3; **7**, 86422-16-4; **8**, 86422-11-5; **9**, 86422-18-6; **10**, 86436-11-5; **11**, 86422-19-7; **12**, 3095-73-6; **13**, 15442-91-8; **14**, 18226-42-1; **15**, 3849-01-2; **16**, 626-15-3; **17**, 4422-95-1; **18**, 86422-20-0; **19**, 46421-67-3; **20**, 65558-67-0; **21**, 60835-71-4; **22**, 66943-05-3; **23**, 33941-15-0.

[*] Dr. E. Weber
Institut für Organische Chemie und Biochemie der Universität
Gerhard-Domagk-Str. 1, D-5300 Bonn 1 (Germany)

[**] The author thanks E. Kloppe and W. M. Müller for their experimental help, and Henkel KGaG, Düsseldorf-Holthausen for carrying out the physical measurements.

[1] a) H. Bueren, H. Grossmann: *Grenzflächenaktive Substanzen*, Verlag Chemie, Weinheim 1971; b) Henkel & Cie GmbH, Düsseldorf: *Waschmittelchemie*, Hüthig, Heidelberg 1976.

[2] E. Weber, F. Vögtle, *Top. Curr. Chem. 98* (1981) 1.
[3] N. Schönfeldt: *Grenzflächenaktive Äthylenoxid-Addukte*, Wissenschaftliche Verlagsgesellschaft, Stuttgart 1976.
[4] B. Lindman, H. Wennerström, *Top. Curr. Chem. 87* (1980) 1; C. L. Khetraphal, A. C. Kunwar, A. S. Tracey, P. Diehl, *NMR 9* (1975).
[5] J. H. Fendler, E. J. Fendler: *Catalysis in Micellar and Macromolecular Systems*, Academic Press, New York 1975.

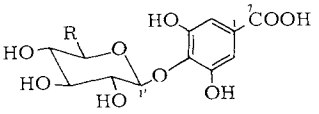
## A New Phytohormone from *Mimosa pudica L.***

By *Hermann Schildknecht** and *Wolfgang Bender*

The extract of *M. pudica L.* contains, aside from 4-*O*-(6-*O*-sulfo-β-D-glucopyranosyl)gallic acid **1** (M-LMF4)[1], a further leaf movement factor called M-LMF5. Preliminary UV and $^1$H-NMR spectroscopic investigations on small amounts of sample immediately showed a high degree of similarity in the arene- and sugar-moieties of the two mimosa hormones. However, subsequent comparative TLC and HPLC studies revealed distinct differences in the polarity and chemical behavior of the two compounds. It followed from these investigations that the sugar moiety of M-LMF5 must contain an acid group whose p$K_a$ value compares with that of acetic acid. An improvement in the previously used separation technique enabled isolation of sufficient amounts of the compound for elucidation of the structure.

The IR spectrum of M-LMF5 (KBr microdisk) shows a pronounced band between 1660 and 1730 cm$^{-1}$, which is caused by superposition of two carbonyl absorptions: that of the gallic acid CO group and that of an aliphatic CO group. The $^{13}$C-resonances at $\delta = -175.7$ (C-6′) and $-172.3$ (C-7) confirm the presence of the acid groups in the molecule. Both groups must be free since large downfield shifts occurred in the dipotassium salt. The signals observed between $\delta = -110$ and $-160$ could be assigned to the ring atoms of gallic acid (3,4,5-trihydroxybenzoic acid). The singlet of H-2,6 at $\delta = 7.07$ in the $^1$H-NMR spectrum points to symmetrical substitution of the aglycone moiety. The $^{13}$C-NMR signal at $\delta = -106.8$ is characteristic for C-1′ of a β-D-*O*-glucosidically linked pyranose. The large coupling constant of $J_{1,2} = 7.5$ Hz observed for the anomeric doublet in the $^1$H-NMR spectrum confirms the β-pyranose configuration, the chemical shift of H-1′ ($\delta = 5.08$) the 1′-*O*-glycosidic linkage. Separated from the multiplet of three protons ($\delta = 3.69$), there appears a doublet from H-5′ at $\delta = 3.97$ ($J_{4,5} = 8.5$ Hz), typical for hexauronic acids. Since also this signal is split by diaxial coupling, the β-D-glucopyranosiduronic acid in M-LMF5 must be 1′-*O*-glucosidically linked with the 4-OH group of the gallic acid.

The structures of the sugar and aglycone of the phytohormone could be confirmed by GC and GC/MS analysis after acid hydrolysis and silylation. All the mass spectra (EI and CI) were identical with those of the authentic reference substances trimethylsilyl 3,4,5-tris(trimethylsiloxy)benzoate and tris(trimethylsilyl)-α,β-glucurono-3,6-lactone. The data obtained on mass spectrometric investigation of the unhydrolyzed molecule were also consistent with the proposed structure. The low-resolution FAB (fast atom bombardment) measurement shows *m/z* 345 for $M-1$ in the spectrum of the negative ions. In the high-resolution MS of persilylated M-LMF 5 we have obtained $M-CH_3$ as highest mass (*m/z* 835.3065, $C_{33}H_{67}O_{11}Si_7$, error 0.3 mmu). The 4-*O*-(β-D-glucopyranosiduronyl)gallic acid **2** synthesized by us in a modified Koenigs-Knorr reaction was identical with natural M-LMF5 in all chromatographic and spectroscopic properties. The compound, which occurs only in hormonal amounts in the mimosa, still triggers the specific stimulation reaction at a concentration of $3 \times 10^{-6}$ mol/L, and is a further low-molecular phytohormone.




**1**, R = $CH_2OSO_3H$ (M-LMF 4)
**2**, R = COOH (M-LMF 5)

This new leaf movement factor of the mimosa (M-LMF5, **2**) is only apparently similar to the already known factors such as **1**[1, 13], since its chemical and biological behavior are largely determined by the carboxy group in the sugar moiety, which is much less weakly acidic than the sulfuric acid ester group. It would be interesting to know whether this second natural structural variation of the leaf movement substances also occurs in other plants or is only to be found in *M. pudica L.*

Received: March 23, 1983 [Z 318 IE]
German version: *Angew. Chem. 95* (1983) 634
The complete version of this manuscript appears in: *Angew. Chem. Suppl. 1983*, 818–834

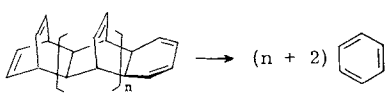
CAS Registry numbers:
**2**, 86568-69-6; **3**, 21085-72-3; **4**, 83553-80-4; **5**, 86563-26-0.

[1] H. Schildknecht, W. Bender, *Chem.-Ztg. 107* (1983) 111.
[13] H. Schildknecht, K. Schumacher, *Pure Appl. Chem. 54* (1982) 2501.

## *p*-(*o*,*p*)-*o*-Tribenzene and *p*-(*o*,*p*)-(*o*,*o*)-*p*-Tetrabenzene, Diels-Alder Oligomers of Benzene

By *Wolfram Grimme** and *Gerd Reinhardt*

Benzene comprises both functionalities necessary for a Diels-Alder reaction—a diene and an ene—and, like other difunctional compounds, should, therefore, be capable of forming oligomeric and polymeric structures. The direct cycloaddition of benzene is precluded by its high resonance energy, which on the other hand causes the ready decomposition of adducts obtained *via* indirect pathways. Hence, *p*-*o*-dibenzene, **1a**, is only known as a ligand in a tricarbonyliron complex[1], which decomposes at $-20$ °C upon removal of the iron. This readiness to undergo retrocleavage reactions should not be so pronounced in the higher homologues of the series **1**, since now only one of the cleavage products exhibits aromatic resonance. We now report on *p*-(*o*,*p*)-*o*-tribenzene, **1b**, which is stable at room temperature and is suitable for the addition of further benzene moieties.




**1a**, n = 0; **1b**, n = 1

[*] Prof. Dr. H. Schildknecht, W. Bender
Organisch-chemisches Institut der Universität
Im Neuenheimer Feld 270, D-6900 Heidelberg I (Germany)

[**] Plant Defense Substances, Part 19; Part 18: [1]. On the Biological Chemistry of the Mimosaceae, Part 10. Part 9: [1].

[*] Prof. Dr. W. Grimme, Dr. G. Reinhardt
Institut für Organische Chemie der Universität
Greinstrasse 4, D-5000 Köln 41 (Germany)

The cycloadduct **2**[2] of *p*-benzoquinone and cyclooctatetraene can be transformed by standard methods (reduction of the carbonyl-flanked double bond with zinc in acetic acid, and deoxygenation *via* the bistosylhydrazone[3]) into the benzene adduct **3** of cyclooctatetraene. Compound **3** decomposes at 132 °C into its components and cannot, therefore, be transformed by a thermal Diels-Alder reaction into its dimer **4**. In contrast, in the presence of 12 mol% tris(*p*-bromophenyl)ammoniumyl hexachloroantimonate as catalyst the reaction proceeds in $CHCl_3$ at room temperature within 20 min[4]. In **4** both cyclobutene rings can be simultaneously removed by double cycloaddition of *o*-chloranil and subsequent photolysis to afford **5**, CO, and tetrachlorobenzene[5]. The heptacycle **5** is a tetrabenzene $(CH)_{24}$ in which, in contrast to the principle of construction of the series **1**, the cyclohexadiene ring of the part structure **1b** functions as a dienophile towards benzene. On heating the *p*-(*o*,*p*)-(*o*,*o*)-*p*-tetrabenzene **5** for 12 h at 50 °C, the "wrongly" associated benzene ring is selectively cleaved off, leading to the *p*-(*o*,*p*)-*o*-tribenzene, **1b**. The assignment of the *endo*-configuration to both rings annelated to the central bicyclooctene moiety is based on the chemical shifts of the protons at the ring junctions in **1b** and in the model compounds **7** and **8** (Table 1).

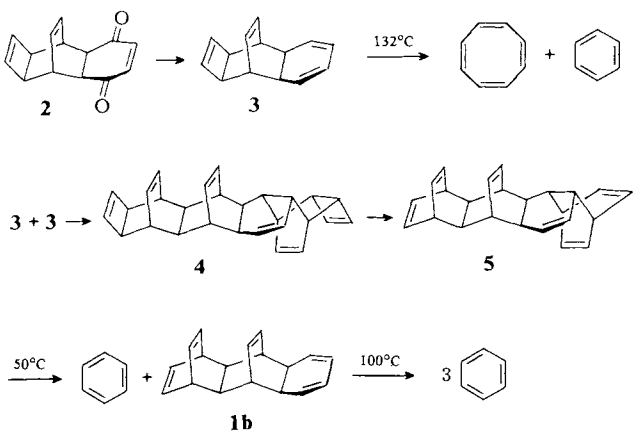



Table 1. Physical data for compounds **1b** and **3**—**8**. $^1$H-NMR spectra ($\delta$-values) were recorded at 90 MHz in $CCl_4$.

**1b**, m.p. = 95 °C; $^1$H-NMR: 6.62 (m, 2H), 5.77 (m, 4H), 5.27 (AA'BB', 4H), 3.25 (m, 2H), 2.73 (s, 2H), 2.33 (m, 2H), 1.98 (s, 2H)

**3**, m.p. = 77 °C; $^1$H-NMR: 5.93 (m, 2H), 5.79 (s, 2H), 5.38 (AA'BB', 4H), 2.67 (m, 2H), 2.63 (s, 2H), 2.52 (m, 2H)

**4**, m.p. = 180 °C; $^1$H-NMR: 6.1—5.4 (12H), 2.8—1.4 (16H); MS: *m/z* 364 ($M^+$), 260 ($M^+ - C_8H_8$), 104 ($C_8H_8^+$, 100%), 78 ($C_6H_6^+$, 25)

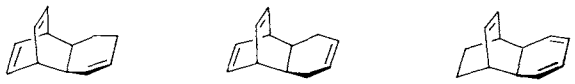
**5**, m.p. = 96 °C (decomp.); $^1$H-NMR: 6.3—6.0 (m, 6H), 5.8—5.2 (m, 6H), 3.35 (m, 4H), 2.8—1.2 (m, 8H)

**6**, $^1$H-NMR: 6.30 (t, 2H), 6.20 (t, 2H), 5.67 (AB, $J$ = 9.5 Hz, 2H), 3.45 (m, 2H), 1.85 (m, 5H), 1.12 (m, 1H)

**7**, $^1$H-NMR: $\delta$ = 6.36 (m, 4H), 5.73 (m, 2H), 3.28 (quint, 2H), 1.93 (m, 6H)

**8**, m.p. = 58 °C; $^1$H-NMR: 6.28 (m, 2H), 5.28 (AA'BB', 4H), 2.82 (s, 2H), 2.42 (m, 2H), 1.40 (AA'BB', 4H)

The tribenzene, **1b**, decomposes at 100 °C into its components; the obligatory dibenzene intermediate, **1a**, cannot be detected. The question at which end of the cyclooligomeric benzenes of type **1** the retro-cleavage occurs can be answered by means of the model adducts **6** to **8**: **6** and **7**, in which benzene is the diene-component, decompose more rapidly than **8**, in which benzene is the ene-component. Furthermore, as comparison of **6** and **7** indicates, the conjugated ene-component 1,3-cyclohexadiene is more readily removed from the cycloadducts with *p*-bonded benzene than its 1,4-isomer (Table 2). On the one hand this leads to an explanation of the selective cleavage of the "wrongly" attached benzene ring of the tetrabenzene **5**, since in this case a conjugated diene is cleaved from a *p*-bonded benzene. On the other hand it is clear that in the decomposition of **1b** the *p*-bonded benzene is removed first.



6 7 8

Table 2. Free energies of activation for the thermal cycloreversion.

| | | *p*-bonded benzene | | | *o*-bonded benzene | |
|---|---|---|---|---|---|---|
| Cpd. | **1b** | **5** | **6** | **7** | **3** | **8** |
| $\Delta G^+$ [kcal/mol] [a] | 29.3 [b] | 25.1 [c] | 26.9 [c] | 28.5 [b] | 31.8 [b] | 35.8 [d] |

[a] At 110.8 °C; error limit ≤ 1.0 kcal/mol. [b] In $CCl_4$. [c] In *n*-dodecane. [d] In $C_2D_2Cl_4$.

For the higher members of the series **1**, it is expected that the *p*-bonded benzene units are cleaved off stepwise with equal activation energies and that the heat of reaction of *ca.* 6 kcal/mol for each benzene extrusion might raise the reaction rate to the explosion limit.

Received: March 20, 1983 [Z 324 IE]
German version: *Angew. Chem. 95* (1983) 636

CAS Registry numbers:
**1b**, 86471-42-3; **2**, 86471-43-4; **3**, 86471-44-5; **4**, 86471-45-6; **5**, 86471-46-7; **6**, 86471-47-8; **7**, 86471-48-9; **8**, 86471-49-0;

[1] W. Grimme, E. Schneider, *Angew. Chem. 89* (1977) 754; *Angew. Chem. Int. Ed. Engl. 16* (1977) 717.
[2] W. Reppe, O. Schlichting, K. Klager, T. Toepel, *Justus Liebigs Ann. Chem. 560* (1948) 1.
[3] R. H. Shapiro, M. J. Heath, *J. Am. Chem. Soc. 89* (1967) 5734.
[4] D. J. Bellville, N. L. Bauld, *J. Am. Chem. Soc. 103* (1981) 718; *104* (1982) 2665.
[5] E. E. Nunn, W. S. Wilson, R. N. Warrener, *Tetrahedron Lett. 1972*, 175.

## Synthesis of Acylpolyamines: Acetylspermidines and $C_{12:0}$-Acarnidine**

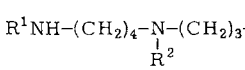
By *John Boukouvalas, Bernard T. Golding*, Richard W. McCabe,* and *Pritpal K. Slaich*

Naturally occurring acylpolyamines [*e.g.* the $N^8$- and $N^1$-acetylspermidines **1a** and **1b**[1], the alkaloid maytenine, **1c**, the siderophore parabactin **1d**, and the acarnidines, **2a**—**2c**, from the sponge *Acarnus erithacus*[4]] have potential clinical applications. Efficient synthetic routes to these compounds and their analogues are, therefore, required[5]. We describe a general, convergent route to acylpolyamines, which is illustrated by the syntheses of **1a** and **1b** and of the $C_{12:0}$-acarnidine **2a**. In the synthesis of **2a** the value

[*] Dr. B. T. Golding, Dr. J. Boukouvalas, Dr. R. W. McCabe, P. K. Slaich
Department of Chemistry and Molecular Sciences,
University of Warwick, Coventry CV4 7AL (England)

[**] This work was supported by the SERC and Ciba-Geigy. B. T. G. thanks Prof. R. Keese and Prof. R. Scheffold, Bern, for laboratory facilities, where the electrochemistry described was carried out. We thank Prof. K. L. Rinehart, Illinois, and Dr. M. H. G. Munro, Christchurch, for unpublished information about acarnidines.

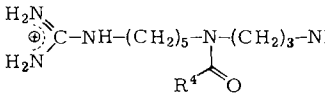
of reductive, electrolytic de-protection of a nitroguanidine is demonstrated.



$R^1NH-(CH_2)_4-N(R^2)-(CH_2)_3-NHR^3$ **1**

**1a**, $R^1$ = MeCO, $R^2$ = $R^3$ = H; **1b**, $R^1$ = $R^2$ = H, $R^3$ = MeCO

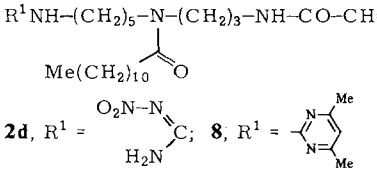
**1c**, $R^1$ = $R^3$ = PhCH=$^{E}$=CHCO, $R^2$ = H



**2a–c**

**2a**, $R^4$ = $Me(CH_2)_{10}$; **2b**, $R^4$ = $Me(CH_2)_5CH=^{Z}=CH(CH_2)_3$

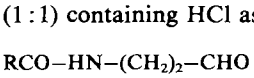
**2c**, $R^4$ = $EtCH=^{Z}=CHCH_2CH=^{Z}=CH(CH_2)_2CH=^{Z}=CH(CH_2)_2$



$R^1NH-(CH_2)_5-N(Me(CH_2)_{10}CO)-(CH_2)_3-NH-CO-CH=CMe_2$ **2d**, **8**

**2d**, $R^1$ = $O_2N-N=C(NH_2)-$; **8**, $R^1$ = 1,4,6-trimethylpyrimidin-2-yl

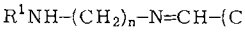
The propanals **3a—3c** were prepared [yields: *e.g.* 77% for **3b**] by acylating 3,3-diethoxypropylamine and hydrolyzing the resulting acylamidoacetal with aqueous dioxane (1 : 1) containing HCl as catalyst.



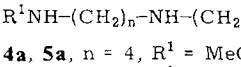
$RCO-HN-(CH_2)_2-CHO$ **3**

**3a**, R = $PhCH_2O$; **3b**, R = Me; **3c**, R = $Me_2C=CH$

*Synthesis of 1a and 1b:* Condensation of **3a** with *N*-(4-aminobutyl)acetamide (molar ratio 1 : 1) in $CH_2Cl_2$ gave the Schiff base **4a**, which was immediately reduced with $NaBH_4$ to afford amine **5a** [47% relative to **3a**]. Hydrogenolysis of **5a** gave **1a** (70%), which was isolated as its dihydrochloride. A similar strategy was used to prepare the dihydrochloride of **1b** [41% relative to **3b**].



$R^1NH-(CH_2)_n-N=CH-(CH_2)_2-NHR^3$ **4**



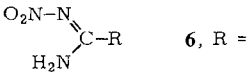
$R^1NH-(CH_2)_n-NH-(CH_2)_3-NHR^3$ **5**

**4a**, **5a**, n = 4, $R^1$ = MeCO, $R^3$ = $PhCH_2OCO$

**4b**, **5b**, n = 4, $R^1$ = $PhCH_2OCO$, $R^3$ = MeCO

**4c**, **5c**, n = 5, $R^1$ = $O_2N-N=C(NH_2)-$, $R^3$ = $Me_2C=CHCO$

*$C_{12:0}$-Acarnidine, 2a: Blunt et al.*[13] have recently described a synthesis of acarnidine **2a** and analogous structures. In our approach to acarnidine **2a** we protected the guanidino function by an *N*-nitro group. This strategy removes the troublesome basicity of the guanidino group, and has also been used to protect arginine residues in peptides[14]. Furthermore, the de-protection, for which many methods employing either reducing agents or acidic reagents have been described, is conveniently the last step of the synthesis.



$O_2N-N=C(NH_2)-R$ **6**, R = 1,4,6-trimethylpyrimidin-2-yl; **7**, R = $NH-(CH_2)_5-NH_2$

We found that dropwise addition of a solution of amine **6** in dioxane (molar ratio 1 : 1) to 1,5-diaminopentane in dioxane gave *N*-(5-aminopentyl)-*N'*-nitroguanidine **7**, which precipitated directly from the reaction mixture (5.5 h, 20 °C) in 64% yield. Condensation of **7** with aldehyde **3c** (molar ratio 1 : 1) in $CH_2Cl_2$ gave, after 1.5 h at 20 °C, the imine **4c**. This was immediately reduced (excess $NaBH_4$ in MeOH) to amine **5c** (50% relative to **3c**), which was acylated with *p*-nitrophenyl laurate and 1-hydroxybenzotriazole (molar ratio 1 : 1 : 2) in dimethylformamide to give nitro-substituted $C_{12:0}$-acarnidine **2d** [80%]. Attempts to remove the nitro group from **2d** using either $SnCl_2$ or $TiCl_3$ failed. We avoided strong acidic reagents (*e.g.* HF) or catalytic hydrogenation for this de-protection, since these reactions would probably affect the dimethylacryloyl residue of acarnidines and/or the unsaturated fatty acyl groups of acarnidines **2b** and **2c**. In a model experiment we determined that *N*-benzyl-*N'*-nitroguanidine was cleanly converted into *N*-benzylguanidine (isolated as its hydrogen carbonate in 52% yield) when reduced at a mercury cathode (−0.9 V *vs.* SCE) in tetrahydrofuran/0.5 M aq. $H_2SO_4$ (1 : 1).

Application of this method to nitro compound **2d** gave $C_{12:0}$-acarnidine, **2a**, which was isolated as its sulphate by removing THF from the electrolyzed solution. The product contained an impurity (*ca.* 20%), which was removed by preparative layer chromatography.

Reaction of $C_{12:0}$-acarnidine, **2a**, with acetylacetone gave pyrimidine, **8**, isolated as a colorless oil in 55% yield. Its $^1$H-NMR spectrum is consistent with the assigned structure, and its EI mass spectrum exhibits all the structurally significant peaks reported in [4].

Warming solutions of **2d** and **2a** from 294 to 333 K results in the collapse of several of the $^1$H-NMR resonances. We ascribe this behavior to the existence of rotamers about the tertiary *N*-lauroyl bond for compounds **2a** and **2d**.

Received: February 2, 1983;
revised: June 3, 1983 [Z 263 IE]
German version: *Angew. Chem. 93* (1983) 646
The complete manuscript of this communication appears in: *Angew. Chem. Suppl. 1983*, 860–873

CAS Registry numbers:
**1a**, 13431-24-8; **1a**·2HCl, 34450-15-2; **1b**·2HCl, 34450-16-3; **2a**, 67534-25-2; **2a**·sulfate, 86550-20-1; **2a**·HCl, 86550-21-2; **2d**, 86550-22-3; **3a**, 65564-05-8; **3b**, 73323-68-9; **3c**, 83686-11-7; **3c** DNP, 86550-30-3; **4a**, 86550-23-4; **4b**, 86550-24-5; **4c**, 86550-25-6; **5a**, 86563-01-1; **5b**, 86550-26-7; **5c**, 86550-27-8; **6**, 2946-89-6; **7**, 86550-28-9; **8**, 67534-28-5; 3,3-diethoxypropylamine, 41365-75-7; *N*-(4-aminobutyl)acetamide, 5699-41-2; *N*-(4-aminobutyl)benzyl carbamate, 86550-29-0; 1,5-diaminopentane, 462-94-2; *p*-nitrophenyl laurate, 1956-11-2; *N*-benzyl-*N'*-nitroguanidine, 5415-72-5; 3-chloro-1,1-diethoxypropane, 35573-93-4; acetylacetone, 123-54-6; *N,N'*tetramethylene bis(benzyl carbamate), 18807-69-7; benzylguanidinium hydrogen carbonate, 86550-31-4.

[1] H. Tabor, C. W. Tabor, *Methods Enzymol. 17 B* (1971) 829.
[4] G. T. Carter, K. L. Rinehart, *J. Am. Chem. Soc. 100* (1978) 4302.
[5] Review: B. Ganem, *Acc. Chem. Res. 15* (1982) 290.
[13] J. W. Blunt, M. H. G. Munro, S. C. Yorke, *Tetrahedron Lett. 23* (1982) 2793.
[14] P. M. Scopes, K. Walshaw, M. Welford, G. T. Young, *J. Chem. Soc. 1965*, 782.

## Dephosphorylating "Ylide Diketone"-Rearrangement of the Arylcarbonyloxyalkylidenephosphoranes**

By *Ernst Anders** and *Thomas Gassner*

As recently reported[1], reaction of the arenecarboxylic acid chlorides **1**, aldehydes **2** and triphenylphosphane **4**

[*] Priv.-Doz. Dr. E. Anders, T. Gassner
Institut für Organische Chemie der Universität Erlangen-Nürnberg
Henkestrasse 42, D-8520 Erlangen (Germany)

[**] This work was supported by the Deutsche Forschungsgemeinschaft and the Fonds der Chemischen Industrie.

leads to formation of the 1-(arylcarbonyloxy)alkyltriphenylphosphonium salts **5**[2], which can be converted by reaction with strong bases [sodium bis(trimethylsilyl)amide **6a**[3a], lithium diisopropylamide **6b**[3b]] into the corresponding 1-(arylcarbonyloxy)alkylidenetriphenylphosphoranes **7**. The highly reactive ylides **7** (they undergo Wittig reactions even at $-50\,^{\circ}C$) have surprising properties: when their solutions are heated from $-60\,^{\circ}C$ to room temperature, the unsymmetrically substituted 1,2-diketones **9** and triphenylphosphane **4** are obtained.

We presume that the carbanionic center initially reacts with the acyl moiety in **7** with formation of the zwitterions **8**, which split off **4** to give the diketones **9** (ylide diketone rearrangement). The results of a crossover experiment are consistent with the formation of **8** and, thus, with an *intra*molecular reaction: an equimolar mixture of the salts **5a** and **5b** (Table 1) leads, according to the general procedure for **9**[4] to formation of the diketones **9a** and **9b**. The amount of crossover product **9c** expected from conceivable intermolecular reaction mechanisms is at most 1%[5]. Since the salts **5** are obtainable in good yields for a wide variety of the aromatic moieties $R^1$ and $R^2$[1], the synthetic route presented here constitutes a novel method for the preparation of unsymmetrically substituted 1,2-diketones.

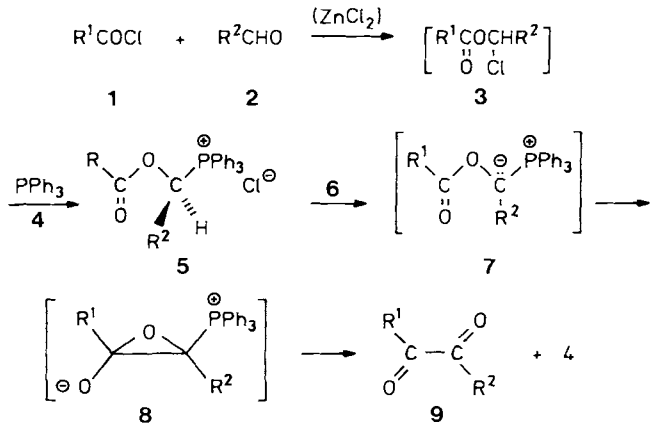


Table 1. 1,2-Diketones **9** from **5**.

| 9 | $R^1$ | $R^2$ | Yield [%] [a] | M.p. [°C] | |
|---|---|---|---|---|---|
| **a** | $C_6H_5$ | $C_6H_5$ | 51, 50 [b] | 92 | (92–96 [6a]) |
| **b** | $p$-$CH_3C_6H_4$ | $p$-$CH_3C_6H_4$ | 35 | 99–100 | (102 [6a]) |
| **c** | $C_6H_5$ | $p$-$CH_3C_6H_4$ | 39, 53 [c] | 31–32 | (31 [6b]) |
| **d** | $p$-$CH_3C_6H_4$ | $p$-$ClC_6H_4$ | 34 | 116–117 | — |
| **e** | $C_6H_5$ | 1-Naphthyl | 31, 51 [c] | 97–98 | (102.5–103 [6c]) |
| **f** | $C_6H_5$ | 1-Thienyl | 34 | 57–58 | (59–60 [6d]) |

[a] The yields have not been optimized; all compounds gave correct elemental analyses. [b] Reaction with **6b**. [c] Results when working at greater dilution (here: 500 mL THF/13.5 mmol **5** [4], otherwise: 200 mL THF/40 mmol **5**, cf. [1]) after 6 h at $-30\,^{\circ}C$.

Received: April 5, 1983;
revised: May 16, 1983 [Z 332 IE]
German version: *Angew. Chem. 95* (1983) 635

[1] E. Anders, T. Gassner, *Angew. Chem. 94* (1982) 292; *Angew. Chem. Int. Ed. Engl. 21* (1982) 289; *Angew. Chem. Suppl. 1982*, 675.

[2] Isolation of the intermediate **3** (cf. P. Bigler, M. Neuenschwander, *Helv. Chim. Acta 61* (1978) 2381) is unnecessary.

[3] a) H.-J. Bestmann, W. Stransky, O. Vostrowsky, *Chem. Ber. 109* (1976) 1694; b) K. Deuchert, U. Hertenstein, S. Hünig, G. Wehner, *ibid. 112* (1979) 2045.

[4] The salt **5** (13.5 mmol) is added to a solution of **6a** (2.76 g, 15 mmol) in tetrahydrofuran (THF) (500 mL) under nitrogen. The mixture is dispersed for 15–30 min (20000 r.p.m., cf. [1]) and subsequently stirred for 6 h at $-30\,^{\circ}C$ (5000 r.p.m.). The solvent is removed *in vacuo* and the residue taken up in a mixture of ether (200 mL) and hydrochloric acid (60 mL). After separation of the aqueous phase, the ethereal phase is successively washed with 1N hydrochloric acid (60 mL), water (100 mL), and saturated $NaHCO_3$ solution (100 mL), and then dried over $MgSO_4$. The ether is removed *in vacuo* and the residue purified by column chromatography (20 cm × 1.8 cm, silica gel 60 (Merck) 70–230 mesh; benzene/cyclohexane 1:1). After separation of the front (**4**), **9c** and **9e** are eluted in analytically pure form; **9a**, **9b** and **9d** are recrystallized from ethanol, **9f** from petroleum ether.

[5] Result of the gas-chromatographic analysis of the crude product after separation of **4** (Packard 472, separation column: 1.8 m × 3 mm, Diatoport s; 4% OV 17%, 175 °C, 0.9 kp/cm² $N_2$). The components were identified on the basis of the retention times of authentic material. Included are **9a** ($t_R$ = 25 min) and **9b** ($t_R$ = 73 min); the amount of **9c** ($t_R$ = 43 min) is < 1% (referred to **9a** plus **9b**).

[6] a) B. Klein, *J. Am. Chem. Soc.* **63** (1941) 1474; b) H. H. Hatt, A. Pilgrim, W. J. Hurran, *J. Chem. Soc. 1936*, 93; c) A. McKenzie, A. Kellman, *J. Chem. Soc. 1934*, 412; d) J. H. Biel, E. P. Sprengeler, H. A. Leiser, J. Horner, A. Drukker, H. L. Friedman, *J. Am. Chem. Soc. 77* (1955) 2250.

## $\eta^6$-Bonded Alkylbenzenes as Novel Bridging Ligands in Dinuclear Complexes of Iron and Cobalt

By *Klaus Jonas**, *Gerd Koepe*, *Ludwig Schieferstein*, *Richard Mynott*, *Carl Krüger*, and *Yi-Hung Tsay*

We have recently prepared $(CpVH)_2C_6H_6$ as well as $(CpV)_2C_6H_6$, $(CpV)_2C_6H_5CH_3$, $(CpV)_2C_6H_5C_3H_7$, and $(CpV)_2C_6H_3(CH_3)_3$ ($Cp = \eta^5$-$C_5H_5$), a series of novel dinuclear complexes that are the first reported examples in which $\eta^6$-arene ligands are bonded to two metal centers[1]. While the two vanadium atoms in the hydrido vanadium compound $(CpVH)_2C_6H_6$ are located on the same side of a non-planar $C_6H_6$ ring (Fig. 1a), in the other four complexes the six-membered rings are planar with the metal atoms on opposite sides (Fig. 1b).

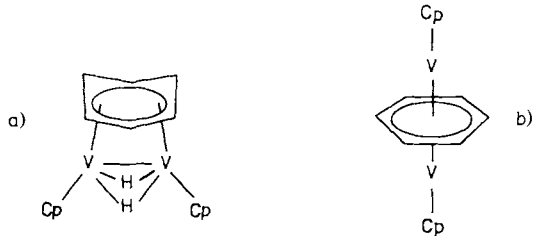


Fig. 1. The compounds (a) $(CpVH)_2C_6H_6$ and (b) $(CpV)_2C_6H_6$ (and analogous alkylbenzene complexes).

A common feature of these vanadium complexes is that their six-membered ring bridging ligands contain six equal or approximately equal CC bond lengths. We now report the iron complexes **2a**, **2b**, and the cobalt complex **4**, all of which contain six-membered ring ligands with unequal CC bond lengths. These bridging ligands are non-planar, as found in $(CpVH)_2C_6H_6$.

Starting material for the synthesis of the iron complexes **2** is CpFe(cod) **1** (cod = 1,5-cyclooctadiene), a monomeric 17-electron metal complex with an unpaired electron, which was prepared from Li[CpFe(cod)] and trityl chlo-

[*] Priv.-Doz. Dr. K. Jonas, G. Koepe, Dr. L. Schieferstein, Dr. R. Mynott
Dr. R. Mynott [+], Prof. Dr. C. Krüger [++], Dr. Y.-H. Tsay [++]
Max-Planck-Institut für Kohlenforschung
Kaiser-Wilhelm-Platz 1, D-4330 Mülheim a. d. Ruhr 1 (Germany)

[+] NMR spectroscopy.

[++] X-ray structure analysis.

 © Verlag Chemie GmbH, 6940 Weinheim, 1983 0570-0833/83/0808-0620 $ 02.50/0 

ride[2]. **1** reacts with 2-butyne or 3-hexyne in the molar ratio 2:3 in ether or pentane at 0 °C to give **2a** (Fig. 2) or **2b**,

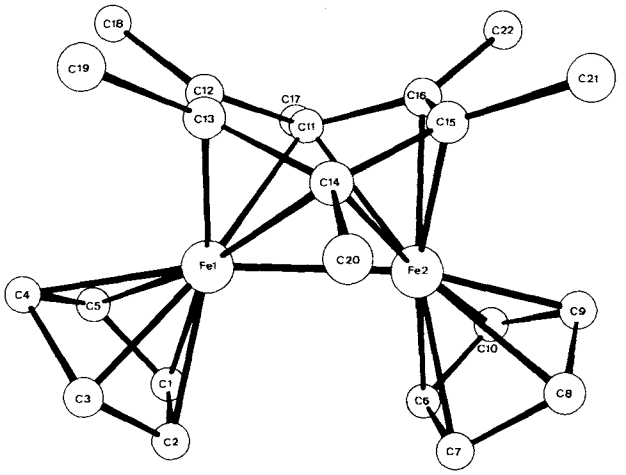



Fig. 2. Molecular structure of **2a** in the crystal [5, 10].

respectively. **2a** and **2b** are fluxional and display antiferromagnetic behavior.

$$2\,\mathrm{CpFe(cod)} + 3\,C_2R_2 \longrightarrow (\mathrm{CpFe})_2C_6R_6 + 2\,\mathrm{cod}$$

**1** — **2a**: R = $CH_3$; **2b**: R = $C_2H_5$

The mononuclear cobalt complex **3**, prepared by hydrocobaltation of *p*-xylene[8], was used as starting material for the synthesis of the dinuclear cobalt complex **4** (Fig. 4).

$$2\,(Cy_2PC_2H_4PCy_2)Co[\eta^5\text{-}C_6H_5(CH_3)_2] \xrightarrow[20\,^\circ C]{-\,C_6H_4(CH_3)_2,\ -\,2\,H^\oplus} [(Cy_2PC_2H_4PCy_2)Co]_2[C_6H_4(CH_3)_2]$$

**3** — **4**

Cy = Cyclohexyl; $[\eta^5\text{-}C_6H_5(CH_3)_2]$ = Dimethylcyclohexadienyl

When a solution of **3** in *p*-xylene is diluted with *n*-hexane and then allowed to stand at room temperature, **4** precipitates as dark red crystals.

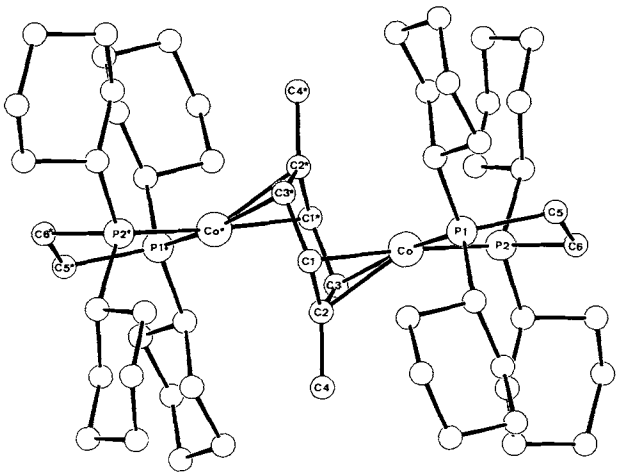



Fig. 4. Molecular structure of **4** in the crystal [9, 10].

The synthesis and structures of these new dinuclear complexes of vanadium, iron, and cobalt, demonstrate that $\eta^6$-arene bridging ligands are capable of bonding two metal centers in at least four different ways.


Received: March 24, 1983 [Z 321 IE]
German version: *Angew. Chem. 95* (1983) 637
The complete version of this communication appears in: *Angew. Chem. Suppl. 1983*, 920–928

CAS Registry numbers:
**1**, 70713-60-9; **2a**, 86497-09-6; **2b**, 86497-08-7; **3**, 86481-03-0; 4, 86481-04-1; $(Cy_2PC_2H_4PCy_2)Co(\eta^3\text{-}C_3H_5)$, 86481-05-2; $C_2(CH_3)_2$, 503-17-3; $C_2(C_2H_5)_2$, 928-49-4; $C_6H_4(CH_3)_2$, 106-42-3.



[1] a) K. Jonas, V. Wiskamp, C. Krüger, Y.-H. Tsay, *J. Am. Chem. Soc.*, in press; b) A. W. Duff, K. Jonas, R. Goddard, H.-J. Kraus, C. Krüger, *J. Am. Chem. Soc.*, in press.

[2] K. Jonas, L. Schieferstein, *Angew. Chem. 91* (1979) 590; *Angew. Chem. Int. Ed. Engl. 18* (1979) 549.

[5] Crystallographic data: $a = 8.059(1)$, $b = 8.059(1)$, $c = 25.187(3)$ Å, $\alpha = 90.0$, $\beta = 90.0$, $\gamma = 120.0°$, $Z = 3$, $V = 1416.69$ Å$^3$, $\rho_{calc} = 1.421$ g cm$^{-3}$, $\mu = 15.36$ cm$^{-1}$, $\lambda = 0.71069$ Å, space group: $P3_1$ (No. 144), $R = 0.0635$, $R_w = 0.0629$, for 3570 observed reflections ($2\sigma$, measured: 7387 reflections) and 273 parameters.

[8] K. Jonas, G. Koepe, unpublished results.

[9] Crystallographic data: $a = 10.764(1)$, $b = 11.546(1)$, $c = 13.233(1)$ Å, $\alpha = 74.682(5)$, $\beta = 72.630(6)$, $\gamma = 84.017(8)°$, $V = 1513.28$ Å$^3$, $\rho_{calc} = 1.173$ g cm$^{-3}$, $\mu = 6.841$ cm$^{-1}$, $Z = 1$, space group: $P\bar{1}$, 6825 reflections, 5167 of which observed ($2\sigma$), 298 refined parameters (without H atoms), $R = 0.039$, $R_w = 0.048$.

[10] Further details of the crystal structure determination are available on request from the Fachinformationszentrum Energie Physik Mathematik, D-7514 Eggenstein-Leopoldshafen, by quoting the depository number CSD 50407, the names of the authors, and full citation of the journal.

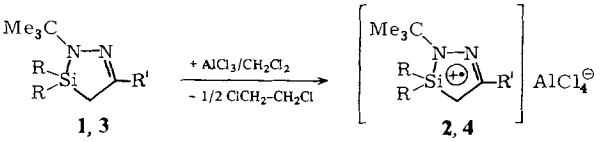

## The One-Electron Oxidation of Diazasilacyclopentenes**


By *Onno Graalmann, Michael Hesse, Uwe Klingebiel*, William Clegg, Martin Haase,* and *George M. Sheldrick**


*Dedicated to Professor Ulrich Wannagat on the occasion of his 60th birthday*

Following our reports on substitution and elimination reactions at the reactive centers of diazasilacyclopentenes[1,6]—the silyl and the methylene groups—we now turn to the one-electron oxidation of the ring system[7]. As oxidizing agent we chose $AlCl_3/CH_2Cl_2$, which oxidizes compounds with vertical first oxidation potentials of < 8 eV in solution to radical cations[7].

2-*tert*-Butyl-3,3,5-trimethyl-1,2-diaza-3-sila-5-cyclopentene **1** reacts with $AlCl_3/CH_2Cl_2$ with cleavage of 1,2-dichloroethane to give a colorless solid **2**; no ESR signal was found for **2**. The cryoscopic determination of the molar mass of **2** indicated dimerization of an initially formed radical cation. Since a radical cation with bulky substituents should not dimerize so readily we synthesized **3** and oxidized it analogously.




**1, 3** — **2, 4**

**1, 2**, R = R' = Me, **3, 4**, R = $CHMe_2$, R' = $CMe_3$

Colorless crystals of **4** were isolated. Its constitution as a salt of a radical cation was established, *inter alia*, by sig-


[*] Prof. Dr. U. Klingebiel, O. Graalmann, M. Hesse
Prof. G. M. Sheldrick, Dr. W. Clegg, M. Haase
Institut für Anorganische Chemie der Universität
Tammannstrasse 4, D-3400 Göttingen (Germany)



[**] This work was supported by the Deutsche Forschungsgemeinschaft and the Fonds der Chemischen Industrie.

nals in a complicated ESR spectrum and by a crystal structure analysis (Fig. 1).

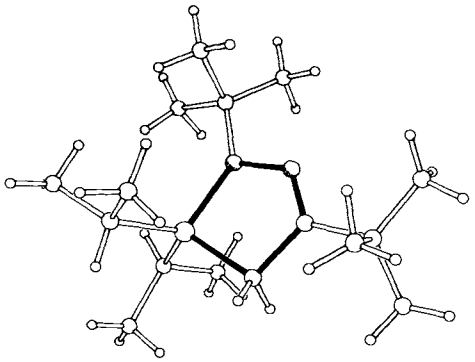


Fig. 1. Structure of the cation of **4** in the crystal. Bond lengths [pm] and bond angles [°] in the inner ring: NN 142.4(12), NSi 178.1(9), SiC 188.6(12), CC 152.3(15), CN 124.5(14); NNSi 108.1(6), NSiC 91.4(5), SiCC 102.7(7), CCN 116.3(9); CNN 119.6(9).

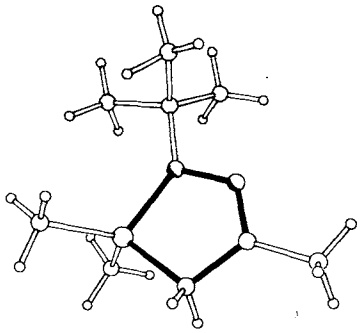
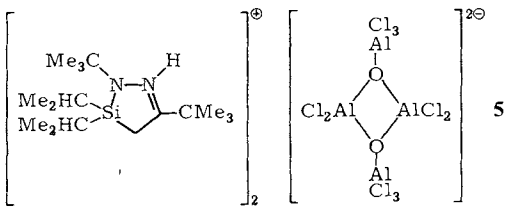


Fig. 2. Structure of the cation of **2** in the crystal.

A change in conformation during the transition from neutral compounds to radical cation was not observed. According to a subsequent X-ray structure analysis, **2** also contains a monomeric cation in the crystal (Fig. 2). **2** and **4** are very sensitive to hydrolysis. During repeated recrystallization of **4**, the formation of a partially hydrolyzed product **5** could not be avoided. X-ray structure analysis shows




that **5** is a protonated diazasilylcyclopentene with a recently described chlorooxoaluminate as counterion[9].

Received: April 11, 1983;
revised: June 15, 1983 [Z 336 IE]
German version: *Angew. Chem. 95* (1983) 630
The complete version of this manuscript appears in:
*Angew. Chem. Suppl. 1983*, 874–886

CAS Registry numbers:
**1**, 76616-34-7; **2**, 86508-14-7; **3**, 86508-18-1; **4**, 86508-16-9; **5**, 86508-17-0.

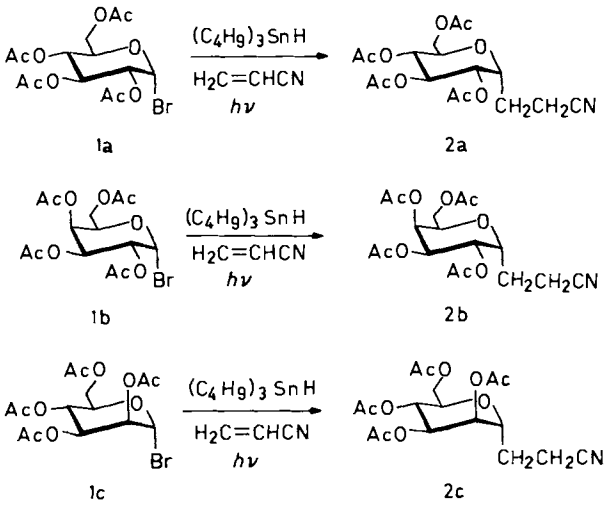
[1] U. Klingebiel, S. Pohlmann, P. Werner, *Z. Anorg. Allg. Chem. 482* (1981) 65.
[6] W. Clegg, M. Haase, M. Hesse, U. Klingebiel, G. M. Sheldrick, *Angew. Chem. 94* (1982) 461; *Angew. Chem. Int. Ed. Engl. 21* (1982) 445; *Angew. Chem. Suppl. 1982*, 1009.
[7] H. Bock, G. Brähler, G. Fritz, E. Matern, *Angew. Chem. 88* (1976) 765; *Angew. Chem. Int. Ed. Engl. 15* (1976) 669.
[9] U. Thewalt, F. Stollmaier, *Angew. Chem. 94* (1982) 137; *Angew. Chem. Int. Ed. Engl. 21* (1982) 133; *Angew. Chem. Suppl. 1982*, 209.

## Diastereoselective Syntheses of *C*-Glycopyranosides**

By *Bernd Giese** and *Jacques Dupuis*

*Dedicated to Professor Sir Derek Barton on the occasion of his 65th birthday*

*C*-Glycosides occur as subunits of natural products[1a] and as enzyme inhibitors[1b], and are of great preparative interest as potential, chiral synthetic building blocks[2a]. The linking of the axial CC bond in the formation of *C*-glycopyranosides such as, *e.g.*, in palytoxin is of special interest[2b]. We have now elaborated a diastereoselective one-pot synthesis of the axial *C*-glycopyranosides **2a–c**, starting from α-D-glycopyranosyl bromides **1a–c**.




10% solutions of **1a–c** with tributyltin hydride (molar ratio 1.0 : 1.0–1.5) and acrylonitrile (10- to 20-fold excess) in boiling ether were photolyzed for 6–12 h. The *C*-glycopyranoside **2a** crystallized out directly in 72% yield (m.p. 120–121 °C). For isolation of the *C*-galactopyranoside **2b** (yield 70%; m.p. 79–80 °C) and of the *C*-mannopyranoside **2c** (yield 65%; oil) the tin salts were precipitated with potassium fluoride and the oily residues chromatographed. The structure assignment can be unequivocally resolved from the $^1$H-NMR spectra[3]. The coupling constants decrease from 6.8–8.5 Hz for diaxial, through 3.1–5.2 Hz for axial/equatorial, to 1.7 Hz for diequatorial arrangements of the vicinal H-atoms on the tetrahydropyran ring.

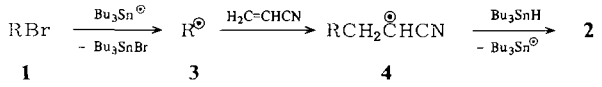
The NMR spectra contain no indication of the occurrence of equatorial *C*-glycopyranosides; consequently these CC-coupling reactions must proceed very selectively.

As in the reduction of halides with tributyltin hydride[4a], alkyl radicals **3** should also be formed on reaction of gly-

[*] Prof. Dr. B. Giese, J. Dupuis
Institut für Organische Chemie und Biochemie
der Technischen Hochschule
Petersenstrasse 22, D-6100 Darmstadt (Germany)

[**] This work was supported by the Fonds der Chemischen Industrie.

cosyl bromides **1**. These radicals react with acrylonitrile[4c] in competition with H-trapping[4b] to give the adduct radicals **4**. H-Transfer yields the *C*-glycosides **2** and the chain-carrying trialkylstannyl radical.



**1** **3** **4**

The formation of the sterically unfavored α-anomers **2** indicates that either an anomeric effect is effective in the radical CC-bond formation or that σ-radicals are formed which are trapped before their inversion by acrylonitrile. Because of the large variety of possible CC-bond formations *via* radical additions to alkenes[5], this diastereoselective synthesis opens up a wide entry to variously substituted *C*-glycosides with axial alkyl groups on C-1.

Received: March 31, 1983 [Z 331 IE]
German version: *Angew. Chem. 95* (1983) 633

CAS Registry numbers:
**1a**, 572-09-8; **1b**, 3068-32-4; **1c**, 13242-50-3; **2a**, 86563-27-1; **2b**, 86563-28-2; **2c**, 86563-29-3; $H_2C$=CH-CN, 107-131.

[1] a) D. T. Connor, R. C. Greenough, M. J. von Strandtmann, *J. Org. Chem. 42* (1977) 3664; R. E. Moore, G. J. Bartoline, *J. Am. Chem. Soc. 103* (1981) 2491; b) M. L. Shulmann, S. D. Shilyan, A. Y. Khorlin, *Carbohydr. Res.* **33** (1974) 229; M. Chmielewski, J. N. BeMiller, D. P. Cerretti, *ibid. 97* (1981) C1.

[2] a) S. Hanessian, H. C. Pernet, *Adv. Carbohydr. Chem. Biochem. 33* (1976) 111; b) A. P. Kozikowski, K. L. Sorgi, *Tetrahedron Lett. 23* (1982) 2281; M. D. Lewis, J. K. Cha, Y. Kishi, *J. Am. Chem. Soc. 104* (1982) 4976; L. A. Reed, Y. Ito, S. Masamune, K. B. Sharpless, *ibid. 104* (1982) 6468; R. R. Schmidt, M. Hoffmann, *Angew. Chem. 95* (1983) 417; *Angew. Chem. Int. Ed. Engl. 22* (1983) 406.

[3] The coupling constants of the ring protons were taken from partly decoupled $^1$H-NMR spectra (300 MHz). The C-atoms have been numbered as in the case of the glycosyl bromides. **2a**: $J_{1,2}=5.2$; $J_{2,3}=J_{3,4}=J_{4,5}=8.5$ Hz. **2b**: $J_{1,2}=4.2$; $J_{2,3}=8.1$; $J_{3,4}=J_{4,5}=3.1$ Hz. **2c**: $J_{1,2}=1.7$; $J_{2,3}=3.2$; $J_{3,4}=6.8$; $J_{4,5}=8.4$ Hz.

[4] a) H. G. Kuivila, *Synthesis 1970*, 499; b) P. Kocienski, C. Pant, *Carbohydr. Res. 110* (1982) 330; c) G. Stork, N. H. Baine, *J. Am. Chem. Soc. 104* (1982) 2321; S. D. Burke, W. B. Fobare, D. M. Armistead, *J. Org. Chem. 47* (1982) 3348.

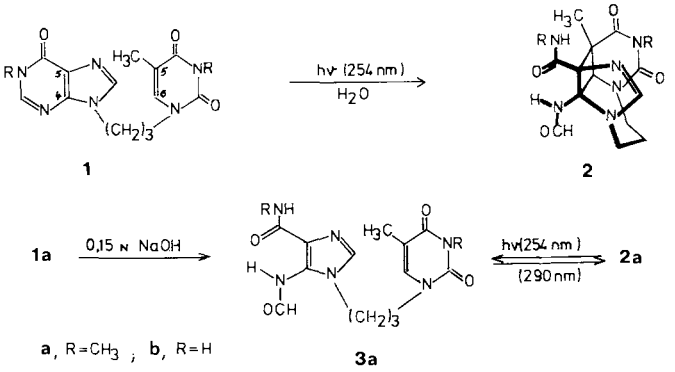
[5] B. Giese, J. Meister, *Chem. Ber. 110* (1977) 2588; B. Giese, J. Meixner, *ibid. 114* (1981) 2138.

## Photocycloaddition of 6-Oxopurines and Thymine to Products with Cyclobutane Part Structures

By *Grażyna Wenska, Stefan Paszyc**, and *Bohdan Skalski*

Previously, it has generally been accepted that among purine and pyrimidine constituents of nucleic acids only the latter can undergo photochemical cycloaddition reactions[1a]. Using dinucleotide analogues in which various purines are linked to pyrimidine by a trimethylene chain, we have observed novel photocycloadducts in which the purine residue is covalently bonded to pyrimidine[1b]. We wish to report here the hitherto unknown, thermally stable cyclobutane photoproducts isolated from low-pressure mercury lamp irradiation of aqueous solutions of **1a** and **1b** ($10^{-3}$ M, ca. 30% conversion of starting materials, 10 min)[2]. Photoproducts **2a** and **2b**[3] were isolated in 80–90% yields (based on amount of **1a** and **1b** consumed).

The absence of CC double bonds in **2a** and **2b** is indicated by their UV and 90 MHz $^1$H-NMR spectra. As expected, only two signals, arising, respectively, from one H, are observed in the low-field region after treating the samples with $D_2O$. The opening of the pyrimidine ring in the purine moiety is also clearly indicated by $^1$H-NMR spectroscopy. Thus, as demanded by the structure of **2a**, one of the N–$CH_3$ resonances appears as a doublet due to coupling with an additional proton at nitrogen.



**1** **2**

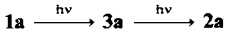
**1a** **3a** **2a**

**a**, R=$CH_3$ ; **b**, R=H

Photoproducts **2a** and **2b** undergo a reversible photochemical reaction. Irradiation with light of wavelength $\lambda=254$ nm cleaves a cyclobutane ring. The identity of the resulting product, **3a**, is based on its spectral properties[3] and is further confirmed by comparison with a sample synthesized independently from **1a** by mild alkaline hydrolysis. Irradiation of **3a** with light of wavelength $\lambda>290$ nm gives **2a** as the sole product.

Careful inspection of Dreiding models suggests *cis-syn* geometry for **2a** and **2b** due to the shortness of the trimethylene chain[4].

The formation of **2** could be accounted for by initial photocycloaddition of the CC double bonds $C^5=C^6$ of the thymine and $C^4=C^5$ of the hypoxanthine moiety. In a subsequent dark reaction a water molecule adds to the C=N bond of the 4,5-dihydropyrimidine moiety of hypoxanthine, followed by a ring opening reaction[5]. The reverse sequence



does not occur here since no reaction has been observed upon irradiation of aqueous solutions of 9-propylhypoxanthine with light of wavelength $\lambda=254$ nm.

Received: March 28, 1983;
revised: June 21, 1983 [Z 323 IE]
German version: *Angew. Chem. 95* (1983) 642

CAS Registry numbers:
**1a**, 86543-43-3; **1b**, 80655-37-4; **2a**, 86543-44-4; **2b**, 86543-45-5; **3a**, 86543-46-6.

[1] a) S. Y. Wang: *Photochemistry and Photobiology of Nucleic Acids, Vol. 1*, Academic Press, New York 1976; b) S. Paszyc, B. Skalski, G. Wenska, *Tetrahedron Lett. 1976*, 449.

[2] No reaction is observed upon irradiation through pyrex glass (150 W high-pressure mercury lamp, 4 h). ε (300 nm) ≈ 250 for **1a** and **1b**.

[3] All new compounds (**1a**, **1b**, **2a**, **2b**, and **3a**) exhibit consistent spectra ($^1$H-NMR, UV, IR, MS) and elemental analyses; **2a**: UV ($H_2O$): $\lambda=222$ nm ($\varepsilon=7400$); $^1$H-NMR ($CDCl_3$): $\delta=9.68$ (s, 1H, NH), 8.34 (d, $J=1.5$ Hz, 1H, CHO), 7.02 (s, 1H, HC=N), 6.65 (br. s, 1H, $CH_3NH$), 3.20 (s, 3H, $NCH_3$), 2.83 (d, $J=5$ Hz, 3H, $HNCH_3$); MS: $M^+$ calc. 348.1546, found 348.1545; **3a**: UV ($H_2O$): $\lambda=250$ nm ($\varepsilon=11800$), 267 nm (sh 10300); $^1$H-NMR ([$D_6$]-DMSO): $\delta=10.00$ and 9.70 (br. s, total 1H, NH), 8.26 and 8.16 (2d, $J=1.2$ Hz and 12 Hz, total 1H, CHO), 7.85 (br. s, 1H, $CH_3NH$), 7.75 (s, 1H, N=CH), 7.56 (s, 1H, C=CH), 3.18 (s, 3H, $NCH_3$), 2.68 (d, $J=5$ Hz, 3H, $HNCH_3$).

[*] Prof. Dr. S. Paszyc, Dr. G. Wenska, Dr. B. Skalski
Department of Chemistry, A. Mickiewicz University
Grunwaldzka 6, PL-60-780 Poznań (Poland)

[4] The nomenclature used here is that generally used for pyrimidine dimers; see [1a], p. 227.

[5] Nucleophilic addition of a water molecule to the C=N bond and ring opening are well-established reactions for 5,6-dihydro-4-oxopyrimidines: V. Skaric, B. Gaspert, *Croat. Chem. Acta 39* (1967) 65.

## Solution-Phase Metal Atom Preparation of Catalytically Active Zeolite-Encapsulated Metal Clusters; Characterization and Application to the Selective Reduction of CO to Butene**

By *Linda F. Nazar, Geoffrey A. Ozin*, François Hugues, John Godber,* and *Denis Rancourt*

Here, we wish to report a new, versatile technique for the preparation of zeolite-encapsulated, zerovalent metal clusters under extremely mild conditions: the method relies on the *in situ* formation of a highly labile organometallic in solution (solvated metal-atom reagents) using rotary metal-vapor, solution-phase synthetic techniques, and is applicable to a wide variety of metals. The choice of the organometallic species that acts as the metal atom carrier is governed by the dimensions and stability of the molecule, which must be sufficiently small to permit access to the α-cage of the zeolite through the outer window (this "opening" is 7.4 Å in diameter for NaY), and must also be sufficiently labile to allow facile dissociation of the organic ligand at or below room temperature. These requirements are fulfilled by the bis(toluene)metal(0) complexes of iron and cobalt, whose dimensions are approximately 7 Å along the longest axis, and which decompose at *ca.* −30 and −50 °C, respectively[1].

The Mössbauer spectra of a representative freshly prepared sample of $Fe_n^0$/NaY with $^{57}Fe$ enrichment, and of a deliberately oxidized sample show that Fe is no longer present as bis(toluene)iron(0)[2], that no oxidation has occurred during the preparation of the sample, that the average size of the $Fe_n^0$ particles is quite small, and that they are superparamagnetic. The Mössbauer doublets for $Fe_n^0$/NaY show different line intensities and line widths, and can adequately be fitted assuming only a distribution of isomer shifts and quadrupole splittings, although relaxation and Gol'Danskii-Karyagin effects cannot be discounted as contributing towards the observed line asymmetry.

The diameters of the iron clusters were calculated from the magnetization curves of the various $Fe_n^0$/NaY samples, using the low field ($d_{LF}$) and high field ($d_{HF}$) approximations of the Langevin function for superparamagnetic particles. The $\bar{d}_{LF}$ and $\bar{d}_{HF}$ diameters of the superparamagnetic $Fe_n^0$ clusters lie between 4 and 11 Å, with an average value of $\bar{d} \approx 6-7$ Å. Furthermore, from the Mössbauer spectra it can be estimated that *ca.* 80–90% of the iron is present in the form of these very small iron clusters. It is also interesting that most of the $Fe_n^0$ clusters formed by the bis(toluene)iron(0) method have diameters less than 12 Å, the diameter of the supercage of zeolite Y. Although this cannot be taken as proof that the iron clusters lie within the zeolite α-cages, the very large quadrupole splittings observed in the Mössbauer spectra strongly suggest that this is indeed the case.

Metal analysis of $Fe_n^0$/NaY and $Co_n^0$/NaY samples showed that there is a decided preference by a factor of about 5 for adsorption of the organometallic in the α-cage over that of the toluene; we presume that this originates from the greater interaction between the $Na^+$ cations of the zeolite and complexed toluene rings rather than with free toluene[12].

Preliminary results on samples of $Fe_n^0$/NaY and $Co_n^0$/NaY containing *ca.* 0.5% Fe and 2.4% Co by weight, respectively, indicated they were catalytically active for the Fischer-Tropsch synthesis (above 230 °C, 1 atm pressure, flow microreactor/on-line gas chromatograph system).

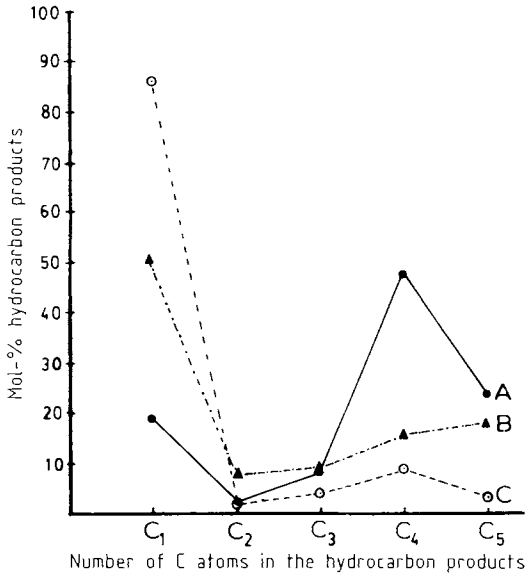



Fig. 4 I. Distribution of products in the Fischer-Tropsch synthesis with $Fe_n^0$/NaY catalysts. A) Normal sample (see Supplement), 250 °C, $CO/H_2 = 1:2$, 0.15% conversion; 1-butene: 10.4 mol-%, isobutene: 5.0%, *trans*-2-butene: 16.2%, *cis*-2-butene: 15.4%. B) Normal sample, 300 °C, $CO/H_2 = 1:2$, 0.10% conversion. C) Sample P, 250 °C, $CO/H_2 = 1:2$, 0.02% conversion.

The resultant hydrocarbon distribution with $Fe_n^0$/NaY and $Co_n^0$/NaY samples at *ca.* 250 °C do not follow Schulz-Flory (SF) behavior[13]. A high selectivity for $C_4$ hydrocarbons is evident, corresponding to *ca.* 50 and 70 mol% of the total hydrocarbons for the iron and cobalt catalysts, respectively, with little $CH_4$ being formed (Fig. 4 I A and 4 II A). When the reaction was carried out at *ca.* 290–300 °C, however, the fraction of $CH_4$ increased, less $C_4$ hydrocarbon was formed, and selectivity decreased (Fig. 4 I B and Fig. 4 II B). Furthermore, a zeolite sample which had been specifically prepared to contain large clusters of iron on the external zeolite surface, by allowing the bis(toluene)iron(0)/zeolite slurry to warm to RT during filtration (sample P), showed very high levels of $CH_4$ at 250 °C and a small amount of $C_4$ hydrocarbon (Fig. 4 I C). The data at *ca.* 250 °C are consistent with the presence of very small $Fe_n^0$ and $Co_n^0$ clusters in the zeolite super-cages, giving rise to the observed product selectivity. As the temperature is raised, migration and sintering of metal clusters occurs, resulting in larger clusters, probably on the zeolite external surface and, hence, in higher levels of $CH_4$.

[*] Prof. G. A. Ozin, Dr. F. Hugues, J. Godber, L. F. Nazar
Lash Miller Chemistry Department, University of Toronto
80 St. George Street, Toronto, Ontario M5S 1A1 (Canada)
D. Rancourt
Physics Department, University of Toronto
Ontario M5S 1A1 (Canada)

[**] This work was supported by the National Sciences and Engineering Research Council of Canada's Strategic Energy Grants Programme. *F. H.* acknowledges the French-Canadian Cultural Exchange Programme for assistance with his research leave at the University of Toronto. L. F. N. thanks NSERC for a graduate fellowship during her research work. We especially wish to thank Dr. *W. Pearce* and Dr. *J. Daniels*, Toronto, for the use of their magnetic and Mössbauer equipment and for their invaluable advice.

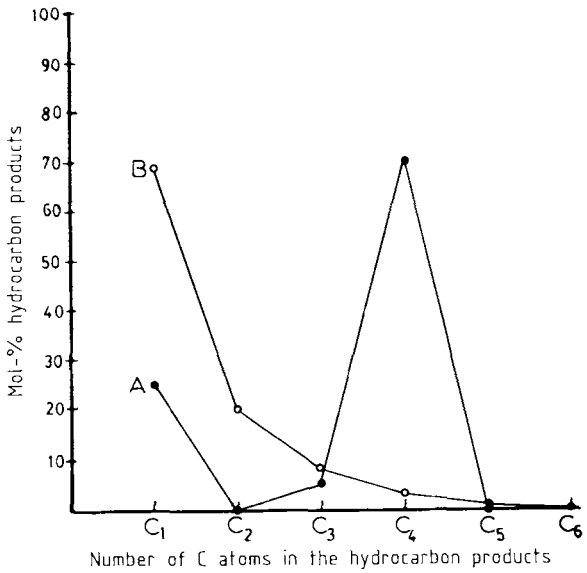



Fig. 4 II. Distribution of products in the Fischer-Tropsch synthesis with $Co_n^0/NaY$ catalysts. A) Normal sample, 247 °C, $CO/H_2 = 1:2$, 0.02% conversion, 1-butene: 33 mol-%, isobutene: 3%, *trans*-2-butene: 18.5%, *cis*-2-butene: 15.5%. B) Normal sample, 290 °C, $CO/H_2 = 1:2$, 0.04% conversion.

In summary, $Fe_n^0/NaY$ and $Co_n^0/NaY$ clusters encapsulated in zeolites have proven to be interesting catalysts for the conversion of $CO/H_2$ mixtures into low carbon number olefins with a propensity towards $C_4$ products. The results reinforce the hypothesis of *Jacob et al.*[15] that Fischer-Tropsch product distributions are directly dependent on metal particle size.

Received: March 1, 1983 [Z 297 IE]
German version: *Angew. Chem. 95* (1983) 645
The complete manuscript of this communication appears in: *Angew. Chem. Suppl. 1983*, 898-919

CAS Registry numbers:
Fe, 7439-89-6; Co, 7440-48-4; CO, 630-08-0; butene, 25167-67-3.

[1] L. F. Nazar, G. A. Ozin, C. G. Francis, M. P. Andrews, H. X. Huber, *J. Am. Chem. Soc. 103* (1981) 2453; L. F. Nazar, G. A. Ozin, P. A. Montano, unpublished results; J. Godber, G. A. Ozin, unpublished results; A. L. Shobert, *Diss. Abstr. 1982*, 367.

[2] P. Michaud, J. P. Mariot, F. Varret, D. Astruc, *J. Chem. Soc. Chem. Comm. 1982*, 1383.

[12] H. Lechert, K. P. Wittern, *Ber. Bunsenges. Phys. Chem. 82* (1978) 1054; H. Lechert, K. P. Wittern, W. Schweitzer, *Acta Phys. Chem. 24* (1978) 201.

[13] P. Biloen, W. M. H. Sachtler, *Adv. Catalysis 30* (1981) 165, and references cited therein.

[15] P. A. Jacobs, H. H. Nijs, *J. Catal. 65* (1980) 328.

## Detonation of Benzyl(triethyl)ammonium Permanganate

By *Jürgen Graefe* and *Roland Rienäcker**

Although several groups have already reported on the danger of benzyl(triethyl)ammonium permanganate[1-3], a recent incident in our laboratory gives cause for a renewed warning that utmost care must be taken when handling this compound.

[*] Dr. R. Rienäcker, Dr. J. Graefe
Max-Planck-Institut für Kohlenforschung
Kaiser-Wilhelm-Platz 1, D-4330 Mülheim a. d. Ruhr (Germany)

Crystalline benzyl(triethyl)ammonium permanganate (*ca.* 50 g) was prepared from benzyl(triethyl)ammonium chloride and potassium permanganate according to the method described by *Schäfer et al.*[4], but instead of drying the crystals as prescribed, *i.e.* at 40 °C in a vacuum drier[5], they were dried in a high vacuum at 20 °C over 36 h. On pouring these dried crystals from a wide-necked Erlenmeyer flask into another vessel, they ignited explosively with formation of a flame about 1 m in length.

Thus, contrary to previous reports, benzyl(triethyl)ammonium permanganate can decompose explosively even at room temperature, so very strict safety measures should be taken when using this oxidizing agent in the dry state.

Received: June 13, 1983 [Z 421 IE]
German version: *Angew. Chem. 95* (1983) 634

CAS Registry number:
Benzyl(triethyl)ammonium permanganate, 68844-25-7.

[1] H. H. Jäger, J. Lütolf, M. W. Meyer, *Angew. Chem. 91* (1979) 852; *Angew. Chem. Int. Ed. Engl. 18* (1979) 786.

[2] H.-J. Schmidt, H. J. Schäfer, *Angew. Chem. 91* (1979) 852; *Angew. Chem. Int. Ed. Engl. 18* (1979) 787.

[3] B. P. Leddy, M. A. McKervey, P. McSweeney, *Tetrahedron Lett. 21* (1980) 2261.

[4] H.-J. Schmidt, H. J. Schäfer, *Angew. Chem. 91* (1979) 77; *Angew. Chem. Int. Ed. Engl. 18* (1979) 68; H.-J. Schmidt, Dissertation, Universität Münster 1980.

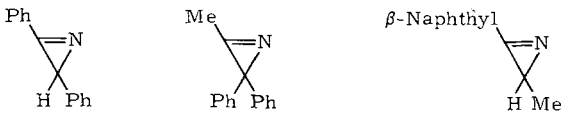
[5] H. J. Schäfer *et al.* have been using this compound, even in large amounts (200 g), in their work over the past 6 years and have never observed a detonation when drying the reagent in a vacuum drier (max. 40 °C, *ca.* 20 torr) or a dessicator (RT, 15 torr, Sicapent) (private communication).

## Kinetics of the Reaction of Electron Deficient Olefins with Nitrile Ylides Generated by Laser Flash Photolysis of Substituted Azirines**

By *Nicholas J. Turro**, *David A. Hrovat*, *Ian R. Gould*, *Albert Padwa*, *William Dent*, and *Robert J. Rosenthal*

*Dedicated to Professor G. O. Schenck on the occasion of his 70th birthday*

In view of the traditional importance of nitrile ylides as intermediates in azirine photochemistry[1] and the new attention that these species have acquired as possible intermediates in carbene chemistry[2], we have initiated a pulsed laser transient absorption study of a series of azirines **1**—**3**. The nitrile ylides derived from these azirines have been characterized both in terms of their optical absorption spectra and absolute rates of reactivity, and as possible intermediates in carbene chemistry.




**1** **2** **3**

[*] Prof. Dr. N. J. Turro, D. A. Hrovat, I. R. Gould
Department of Chemistry, Columbia University
New York, NY 10027 (USA)
Prof. Dr. A. Padwa, W. Dent, R. J. Rosenthal
Department of Chemistry, Emory University
Atlanta, GA 30322 (USA)

[**] The authors at Columbia thank the Air Force Office of Scientific Research and the National Science Foundation for their generous support of this research. The authors at Emory acknowledge the support of the National Science Foundation.

Pulsed laser photolysis of Ar-purged isooctane solutions of **1**—**3** at 25 °C resulted in the production of intense, long-lived ($\tau > 100$ μs) absorptions over the range 250—400 nm. Absorption spectra taken *ca.* 5 μs after the laser pulse are in excellent agreement with those obtained at 77 K (Table 1). While laser photolysis of azirines **1** and **3** gave rise to absorptions attributable to nitrile ylides only, azirine **2** yielded a signal of an additional short-lived intermediate in the range 300—320 nm. This species, unlike the ylides, was quenched by $O_2$ ($k_q = 2 \times 10^9$ M$^{-1}$ s$^{-1}$), thus allowing us to obtain the spectrum of the ylide alone. Subtraction of the $O_2$-purged spectrum from the Ar-purged spectrum (after normalization at 370 nm) resulted in a spectrum of the short-lived intermediate with $\lambda_{max} = ca.$ 305 nm; this corresponds well with that of diphenyl carbene produced by other routes[3]. It is important that the ylide absorption obtained from azirine **2** is not observed upon pulsed laser photolysis of diphenyl carbene precursors in acetonitrile solvent. This is in contrast to the observation of an ylide, formed by addition of the free carbene to the nitrile solvent, upon laser flash photolysis of 9-diazofluorene in acetonitrile[2]. Evidently, the rate constant for reaction of acetonitrile with diphenyl carbene is significantly smaller than that of acetonitrile with fluorenylidene.

Table 1. Absorption maxima and rate constants of the subsequent reactions of the primary photolysis products of azirines **1**—**3**.

| Azirine | $\lambda_{max}$ (77 K) [nm] [a] | $\lambda_{max}$ (298 K) [nm] [b] | $k_q$ [d] (acrylonitrile) [M$^{-1}$ s$^{-1}$] | $k_q$ [d] (fumaronitrile) [M$^{-1}$ s$^{-1}$] | $k_{rel}$ (acrylonitrile, fumaronitrile) |
|---|---|---|---|---|---|
| **1** | 346 | 345 | $(1.22 \pm 0.03) \times 10^6$ | $(1.09 \pm 0.07) \times 10^9$ | $890 \pm 100$ |
| **2** | 368 | 305 [c], 360 | $(1.0 \pm 0.3) \times 10^6$ | $(5.4 \pm 0.3) \times 10^8$ | $540 \pm 200$ |
| **3** | 277 | 280 | $(5.4 \pm 0.3) \times 10^6$ | $(7.4 \pm 0.8) \times 10^9$ | $1370 \pm 200$ |

[a] Steady-state photolysis (1000 W Xe/Hg arc lamp equipped with a high intensity monochromator; $\lambda_{ex} = 248 \pm 10$ nm) of *ca.* $10^{-5}$ M azirine in Ar-purged 3-methylpentane. [b] Laser flash photolysis (Lambda Physik EMG 101 Excimer Laser, 248 nm, 15 ns pulse width) of *ca.* $10^{-5}$ M azirine in Ar-purged isooctane. [c] This absorption is quenched by $O_2$ (see text). [d] Conditions are the same as in [b], except that azirine, **1**, was excited at 308 nm (20 ns pulse width).

In the absence of quenchers the observed transient decays for each ylide exhibit both first and second order components; however, pulsed laser photolysis of azirines **1**—**3** in the presence of electron deficient olefins in $O_2$-saturated isooctane solution resulted in quenching of the transient absorption. At sufficiently high olefin concentrations, the decay of the transient obeyed clean first-order kinetics. Under these experimental conditions, plots of the observed first-order rate for ylide decay as a function of olefin concentration were linear, and their slopes gave the bimolecular quenching rate constant, $k_q$. The rate constants for quenching by acrylonitrile and fumaronitrile are listed in Table 1. For azirine **1** the relative quenching rates of fumaronitrile and acrylonitrile have been reported in the literature from steady-state trapping experiments[4]. This value ($1070 \pm 100$) is the same, within experimental error, as that obtained from our absolute rate constants ($890 \pm 100$).

The rate constants $k_q$ for the reaction of the nitrile ylide derived from **1** with methyl acrylate and diethyl fumarate were studied as a function of temperature. The resulting Arrhenius plots after correction for solvent contraction indicate that $k_q$ for methyl acrylate is essentially insensitive to temperature ($E_a \approx 0$ kcal/mol), while the quenching rate constant for diethyl fumarate initially increases with decreasing temperature ($E_a \approx -1.5$ kcal/mol) and begins to decrease at temperatures below *ca.* −65 °C. This type of Arrhenius behavior has been observed previously for the quenching of phosphorescence from ketones, carbenes, and singlet oxygen[5]. A kinetic scheme which fits this behavior is given in eq. (a), where NY is the nitrile ylide and NY/olefin is a nitrile ylide/olefin complex:

$$\text{NY} + \text{olefin} \underset{k_{-1}}{\overset{k_1}{\rightleftharpoons}} \text{NY/olefin} \xrightarrow{k_2} \text{product} \qquad \text{(a)}$$

Assuming steady-state kinetic behavior for the complex, the observed first-order quenching rate constant, $k_q$, can be expressed in terms of the above rate constants to give eq. (b):

$$k_q = \frac{k_1 k_2}{k_{-1} + k_2} \qquad \text{(b)}$$

Rearrangement of this equation gives the ratio of the rates for dissociation and collapse to product for the ylide/olefin complex [eq. (c)]. Assuming that complex formation is diffusion controlled (*i.e.*, $k_1 = k_{diff}$), calculation of the diffusion rate constant at the temperatures at which $k_q$ was obtained yields values for the ratio $k_{-1}/k_2$ from eq. (c):

$$k_{-1}/k_2 = \frac{k_1 - k_q}{k_q} \qquad \text{(c)}$$

A plot of $\lg k_{-1}/k_2$ *versus* 1/T was found to yield a straight line (Fig. 1), whose slope yields the difference in the activation parameters for product formation and dissociation of the complex (*i.e.*, $\Delta\Delta G^{\neq} = \Delta G^{\neq}_{prod} - \Delta G^{\neq}_{diss}$). As expected, the free energy requirement for reaction *versus* dissociation is greater for the slower quencher methyl acrylate

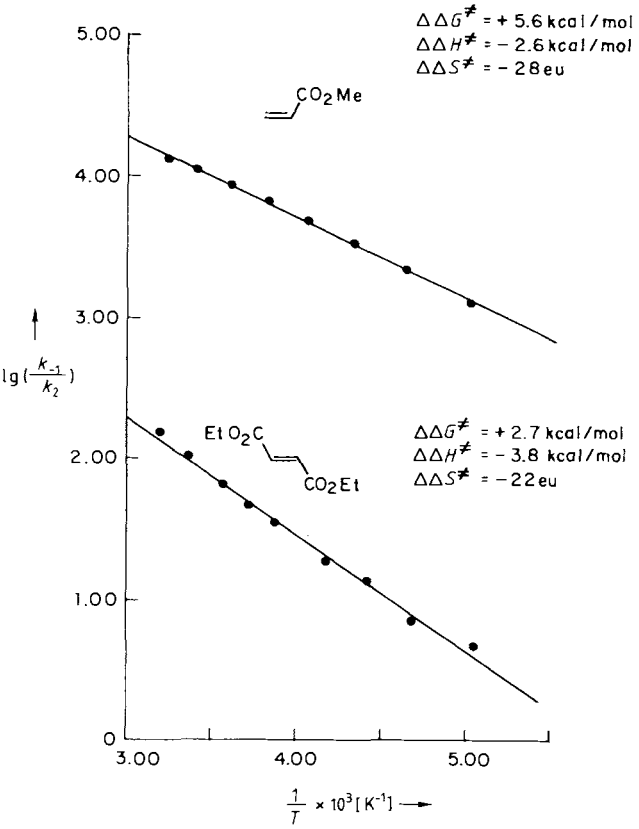



Fig. 1. Plot of $\lg(k_{-1}/k_2)$ against $1/T$ ($\Delta\Delta G^{\neq}$ calculated at $T = 298$ K).

 © Verlag Chemie GmbH, 6940 Weinheim, 1983 0570-0833/83/0808-0626 $ 02.50/0 

than for the faster quencher, diethyl fumarate; however, it is noteworthy that the bulk of this free energy difference, $\Delta\Delta G^{+}$, results from differences in the activation entropy rather than enthalpy.

Received: April 12, 1983 [Z 345 IE]
German version: *Angew. Chem. 95* (1983) 647

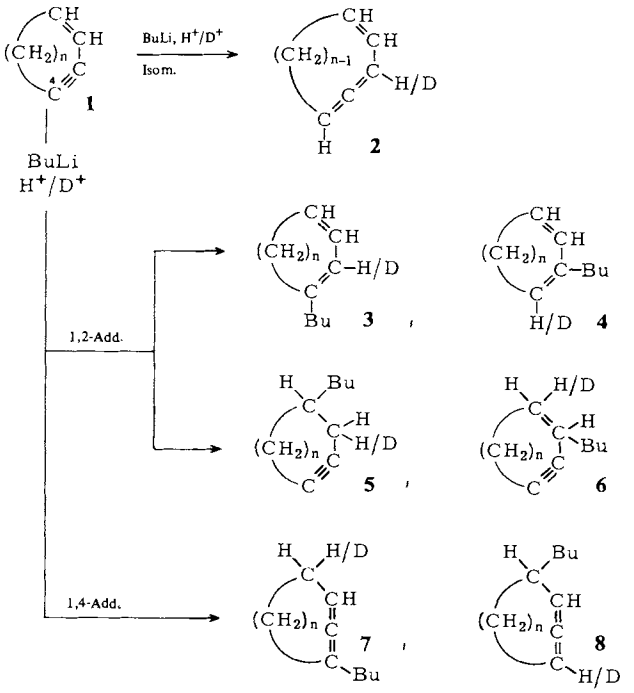
CAS Registry numbers:
**1**, 16483-98-0; **2**, 65817-54-1; **3**, 51051-84-4; acrylonitrile, 107-13-1; fumaronitrile, 764-42-1; methyl acrylate, 96-33-3; diethyl fumarate, 623-91-6.

[1] a) A. Padwa, *Acc. Chem. Res. 9* (1976) 371; b) A. Orahovats, H. Heimgartner, H. Schmid, W. Heinzelmann, *Helv. Chim. Acta 58* (1975) 2662.
[2] D. Griller, C. R. Montgomery, J. C. Scaiano, M. S. Platz, L. Hadel, *J. Am. Chem. Soc. 104* (1982) 6813.
[3] A. M. Trozzolo, W. A. Gibbons, *J. Am. Chem. Soc. 89* (1967) 239.
[4] A. Padwa, M. Dharan, J. Smolanoff, S. I. Wetmore, Jr., *Pure Appl. Chem. 33* (1973) 269.
[5] a) U. Maharaj, M. A. Winnik, *J. Am. Chem. Soc. 103* (1981) 2328; b) N. J. Turro, G. F. Lehr, J. A. Butcher, R. A. Moss, W. Guo, *ibid. 104* (1982) 1754; c) A. A. Gorman, I. R. Gould, I. Hamblett, *ibid. 104* (1982) 7098.

## Base-Induced Isomerization of Cycloalkenynes in Competition with Addition Reactions**

By *Johannes Zountsas, Matthias Kreuzer,* and *Herbert Meier**

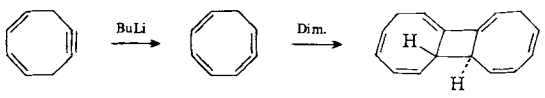
The recently discovered group of substances the cycloalkenynes, such as **1**[3,4], offer interesting possibilities for reaction with bases. Besides isomerization to cyclic allenes **2**, with bases—such as alkyllithium compounds—addition reactions must also be considered; here, the regioselectivity is decisive for preparative applications. Isotopic labeling with deuterium has proved of value in elucidating the course of the reaction.




Bu = *n*-$C_4H_9$, *t*-$C_4H_9$
**1a**, **3a**, **4a**: n = 4
**1c**,**c'**, **2c**, *trans*-**3c**, **8c**: n = 8

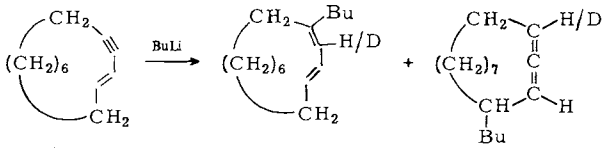
All variants of the eight-membered ring system **1** lower the geometrical ring-strain energy $E_g$. 1,2-Addition to the triple bond is thermodynamically most favorable, since only in **3** and **4** is $E_g = 0$. 1-Cycloocten-3-yne, **1a**, adds to butyllithium, used in *ca.* threefold excess, to afford exclusively **3a** and **4a**. Here, in contrast to *cycloadditions* of **1a**, a regioselectivity in favor of **3a** is observed (*n*BuLi, **3a** + **4a** = 80%, **3a** : **4a** = 80 : 20, *t*BuLi, **3a** + **4a** = 80%, **3a** : **4a** = 76 : 24). This orientation corresponds to the distribution of charge estimated from the $^{13}$C-NMR signals. Thus, in **1a** the electron density at C-4 is smaller than at C-3; the $C_4H_9^{\ominus}$ ion therefore favors addition at C-4.

1,3-Cyclooctadien-6-yne, **1b**, behaves differently. Base-catalyzed isomerization results first in 1,2,4,6-cyclooctatetraene, **2b**, which dimerizes regio- and stereospecifically to afford **9** (yield with *n*BuLi and *t*BuLi, 72%)[6]. The stereochemistry of the addition was determined from the 4-phenyl-1,2,4-triazolin-3,5-dione adducts.




**1b** **2b** **9**

The two highly strained eight-membered ring alkynes **1a** and **1b**, therefore, behave quite differently with butyllithium. For comparison we examined the strained twelve-membered ring *trans*-enyne, **1c**, and its *cis*-isomer, **1c'**, with $E_g = 0$[4]. Although in analogy to **1a**, **1c** forms the 1,2-adduct **3c** (30%), the main reaction is, nevertheless, a regiospecific 1,4-addition to give **8c** (57%).




**1c** **3c** **8c**

In contrast, only 13% **8c** is formed from **1c'**; isomerization to **2c** (54%) is preferred. At room temperature, **2c** rearranges by suprafacial [1,5-H]-shift to afford the (*E,Z,E*)-1,3,5-cyclododecatriene, **13**, which undergoes thermally allowed, disrotatory ring closure to yield the bicycle **14**. The isomerization **2c** → **13** → **14** proceeds quantitatively; at room temperature which of the three products is isolated depends only on the reaction time. Heating **14** for several hours lead to its dehydrogenation and to formation of **15** (60%).

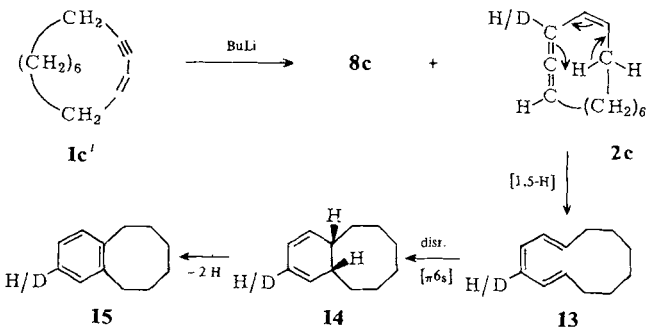
The four modes of reaction of the cycloalkenynes (**1a**, **b**, **c**, **c'**) with butyllithium should serve to indicate the synthetic potential of the reactions.—Open-chain enynes are less reactive[10].

High-field measurements and double resonance experiments permit the products described here to be characterized from their $^1$H- and $^{13}$C-NMR data.

[*] Prof. Dr. H. Meier[+], M. Kreuzer, J. Zountsas
Institut für Organische Chemie der Universität
Auf der Morgenstelle 18, D-7400 Tübingen (Germany)

[**] This work was supported by the Deutsche Forschungsgemeinschaft and the Fonds der Chemischen Industrie.

[+] New Address: Institut für Organische Chemie der Universität, J.-J.-Becher-Weg 18—22, D-6500 Mainz (Germany)



Received: March 30, 1983 [Z 328 IE]
German version: *Angew. Chem. 95* (1983) 638
The complete version of this communication appears in: *Angew. Chem. Suppl. 1983*, 851–859

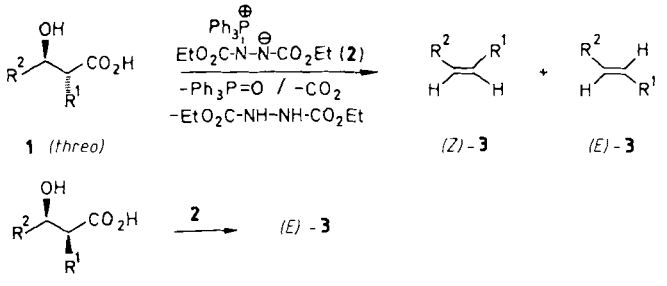
CAS Registry numbers:
**1a**, 75029-45-7; **1b**, 80339-91-9; **1c**, 92969-50-4; **1c'**, 66633-30-5; **2b**, 86471-50-3; **2c**-H, 86471-51-4; **2c**-D, 86471-52-5; *n*-Bu-**3a**-H, 66633-29-2; *t*-Bu-**3a**-H, 86471-53-6; *n*-Bu-**3a**-D, 75349-86-9; *t*-Bu-**3a**-D, 86471-54-7; **3c**-H, 86471-55-8; *n*-Bu-**4a**-H, 86471-56-9; *t*-Bu-**4a**-H, 16240-44-1; *n*-Bu-**4a**-D, 86471-57-0; *t*-Bu-**4a**-D, 86471-58-1; **8c**-H, 86471-59-2; **9**, 86471-60-5; **12**, 86471-61-6; **13**-H, 86471-62-7; **13**-D, 86471-63-8; **14**-H, 86471-64-9; **14**-D, 86471-65-0; **15**-H, 1076-69-3; **15**-D, 86471-66-1; *n*-BuLi, 109-72-8; *t*-BuLi, 594-19-4; PTD, 4233-33-4.

[3] H. Meier, T. Echter, *Angew. Chem. 94* (1982) 68; *Angew. Chem. Int. Ed. Engl. 21* (1982) 67; *Angew. Chem. Suppl. 1982*, 91.
[4] J. Zountsas, H. Meier, *Liebigs Ann. Chem. 1982*, 1366.
[6] Presumably **9** is identical to the compound $C_{16}H_{16}$ obtained in the Bamford-Stevens reaction of the sodium salt of 2,3-homotropontosylhydrazone[7], although the spectroscopic data only conform to a moderate extent.
[7] M. Oda, Y. Ito, Y. Kitahara, *Tetrahedron Lett. 1975*, 2587.
[10] B. Mauzé, *J. Organomet. Chem. 131* (1977) 321, and references cited therein.

## Olefins from β-Hydroxycarboxylic Acids—Synthesis of Isomerically Pure α- and β-Asarone**

By *Johann Mulzer** and *Ortrud Lammer*

The dehydrative decarboxylation of β-hydroxycarboxylic acids (**1**, **4**) with the adduct **2** has proven useful for the synthesis of olefins[7b]. We report here on the steric course of the reaction, and, as an application, we describe the synthesis of isomerically pure α- and β-asarone (**11** and **13**, respectively).



**1** *(threo)* *(Z)*-**3** *(E)*-**3**



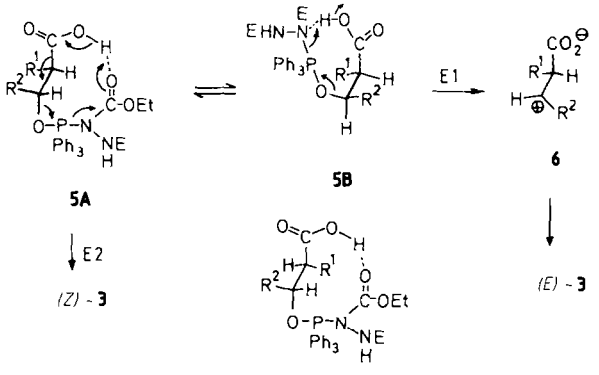
**4** *(erythro)*

In the *threo* series[8] (Table 1) the isomeric distribution shifts with increasing +M effect of $R^2$ from pure (*Z*)-**3** to pure (*E*)-**3**. The residue $R^2$ can be catagorized into three groups. I: $R^2$ with small +M effect. In these cases pure (>98%) (*Z*)-**3** is formed. II: $R^2$ with medium +M effect. (*Z*)- and (*E*)-**3** are both formed in varying amounts. III: $R^2$ with large +M effect. Up to >98% (*E*) is obtained. Compared to $R^2$, $R^1$ is of minor significance and merely shows an influence on the acids in group II. The *erythro* acids **4a—c**, **h—m** (notation analogous to **1**, see Table 1) always afford >98% (*E*)-**3** in yields of 80—95%, independent of the nature of $R^1$ and $R^2$.

Table 1. Steric course of the reaction of **1** with **2** (tetrahydrofuran, 22°C, 5 min). Presumed mechanism: group I: E2; group II: E2 and E1; group III: E1.

| **1** | $R^1$ | $R^2$ | **3** *Z* : *E* [a] | Yield [b] | Group |
|---|---|---|---|---|---|
| **a** | Ph | Me | >98 : 2 | 73 | |
| **b** | Ph | Et | >98 : 2 | 82 | |
| **c** | Ph | *i*Pr | >98 : 2 | 92 | I |
| **d** | *t*Bu | Et | >98 : 2 | 60 | |
| **e** | OPh | Et | >98 : 2 | 85 | |
| **f** | OPh | *n*Pr | >98 : 2 | 84 | |
| **g** | Ph | Vinyl | 94 : 6 | 91 | |
| **h** | Me | Ph | 85 : 15 | 82 | |
| **i** | Et | Ph | 73 : 27 | 87 | |
| **j** | Ph | Ph | 55 : 45 | 82 | II |
| **k** | *i*Pr | Ph | 24 : 76 | 81 | |
| **l** | *t*Bu | Ph | < 2 : 98 | 82 | |
| **m** | | | | | |
| **n** | Ph | 2-Furyl | < 2 : 98 | 96 | |
| **o** | Ph | 4-$MeOC_6H_4$ | < 2 : 98 | 87 | III |
| **p** | Ph | 4-$Me_2NC_6H_4$ | < 2 : 98 | 92 | |

[a] **a—m**: Determined by GC; **n—p**: determined by $^1$H-NMR (60 MHz, $CDCl_3$). [b] Aside from **3**, *ca.* 10% β-lactone is also formed from **1a—d**, **h—m**.



**5A** **5B** **6** **7**

Scheme 1. E = $CO_2Et$.

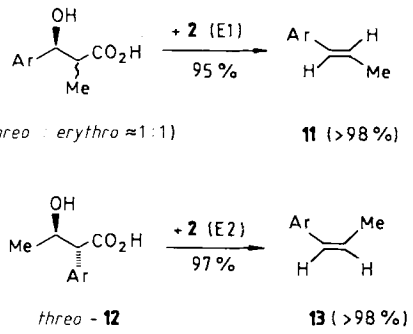
These results find a mechanistic rationalization in the hydroxy-activated intermediates **5** (from **1**) and **7** (from **4**), which decompose *via* E2- or E1-fragmentation, depending on the electron supply from $R^2$ (Scheme 1). In the *threo* series these two mechanisms lead to sterically different products. The E2-reaction is coupled with the *anti*-conformation **5A** and furnishes (*Z*)-**3**. The E1-route, on the other hand, proceeds *via* the conformer **5B**, sterically favored by the larger $R^1$—$R^2$ distance, and **6** to (*E*)-**3**. Thus, the data in Table 1 can be interpreted to the effect that group I is operated by the E2-mechanism and group III by the E1-mechanism. In group II, on the other hand, both mechanisms depend on the position of equilibrium **5A** ⇌ **5B**; the E1-decomposition being favored more and more with increasing bulkiness of $R^1$ (**h—m**). In the *erythro* series the all-*anti* arrangement **7** is the optimal intermediate for both mechanism; hence, (*E*)-**3** becomes the sole possible isomer.

*Synthesis of α- and β-asarone 11 and 13*, respectively: Asarone **13**, a constituent of calamus oil, was first recognized in 1977 as a novel chemosterilizing insecticide[11]. The activity

[*] Prof. Dr. J. Mulzer, O. Lammer
Institut für Organische Chemie der Universität
Universitätsstrasse 1, D-4000 Düsseldorf 1 (Germany)

[**] This work was supported by the Deutsche Forschungsgemeinschaft and the Fonds der Chemischen Industrie.

is connected with the (*Z*)-geometry[11]. **11** and **13** cannot be prepared in isomerically pure form by Wittig reaction[12], and they are almost unseparable even by TLC.




Scheme 2. Ar = 2,4,5-trimethylphenyl.

As an easy access to **11** and **13** we chose the reaction of **10** and **12** with **2** (Scheme 2). The electron-rich aryl group ($R^2$) in **10** enforces the E1 elimination and, quite consistently, **11** is formed from **10** in >98% yield. In the case of **12**, on the other hand, the methyl group induces an E2-mechanism; up to >98% of **13** is isolated. The transition from **10** to **12** corresponds to an interchange of substituents $R^1$ and $R^2$ with largely differing +M effects. The character of elimination is—in complete agreement with our interpretation—thereby completely shifted from E1 to E2.

Received: 18, 1983 [Z 350 IE]
German version: *Angew. Chem. 95* (1983) 629
The complete version of this communication appears in:
*Angew. Chem. Suppl. 1983*, 887-897

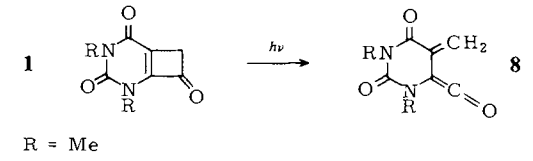
[7b] J. Mulzer, A. Pointner, A. Chucholowski, G. Brüntrup, *J. Chem. Soc. Chem. Commun. 1979*, 52.
[8] (Abstract) The use of *threo-erythro* descriptors for β-hydroxycarbonyl compounds is contradictory to the original convention derived from threose and erythrose. However, since more recent alternative descriptors do likewise not offer an ideal solution to the problem we stay by *threo-erythro* and—despite all reservations—define these configurations according to C. H. Heathcock, C. T. White, J. J. Mirrison, D. VanDerveer, *J. Org. Chem. 46* (1981) 1296.
[11] B. P. Saxena, O. Koul, K. Tikku, C. K. Atal, *Nature 270* (1977) 512.
[12] *Chem. Eng. News 1979*, April 16, p. 24.

## Photocycloaddition of 6-Cyanouracil to Ketene Diethyl Acetal: Synthesis of a Uracil Derivative Possessing a Cyclobutenone Framework

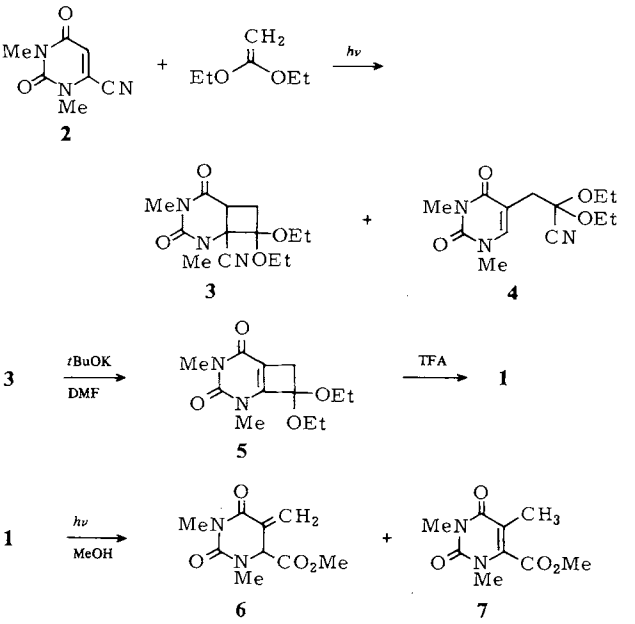
By *Isao Saito*, Fuyuhiko Kubota, Koji Shimozono,* and *Teruo Matsuura**

*Dedicated to Professor G. O. Schenck on the occasion of his 70th birthday*

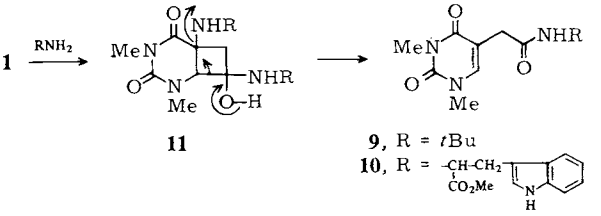
The synthesis of highly photochemically reactive pyrimidine bases is of special importance for photochemical modification of nucleic acids[1]. Upon irradiation, pyrimidine bases possessing cyclobutenone frameworks are expected to exhibit high reactivity toward nucleophiles, since photochemical ring-opening of cyclobutenone may produce highly reactive vinylketene derivatives[2]. We describe here the synthesis of 2,4-diazabicyclo[4.2.0]oct-1(6)-en-3,5,8-trione **1**, the first uracil derivative possessing a cyclobutenone framework, utilizing photocycloaddition as a key step.




Irradiation of 6-cyano-1,3-dimethyluracil, **2**, and excess ketene diethyl acetal in acetonitrile at −25 °C using a high-pressure mercury lamp (Pyrex filter) gave cycloadduct **3** (40%) and rearranged product **4** (23%). The formation of rearranged adducts such as **4** has previously been shown to occur in the photoaddition of **2** to other olefins[4]. Conversion of **3** into **5** (80%) was readily accomplished by reaction with potassium *t*-butoxide in dimethylformamide. Treatment of acetal **5** with 90% trifluoroacetic acid (TFA) gave cyclobutenone **1** (77%) [m.p. = 108—110 °C; $^1$H-NMR ($CDCl_3$): $\delta$ = 3.38 (s, 3H), 3.40 (s, 3H), 3.67 (s, 2H)].




Cyclobutenone **1** is stable at ambient temperature in the usual organic solvents, including alcohols; however, irradiation of methanolic solutions of **1** resulted in rapid formation of **6** (55%) and **7** (21%). **7** also formed by prolonged irradiation of **6**, whereas the latter probably originates from the trapping of vinylketene **8** by methanol.




Unexpectedly, cyclobutenone **1** reacts smoothly with primary amines without irradiation at ambient temperature to give 5-substituted uracil derivatives in high yields. For example, treatment of **1** with *t*-butylamine gave **9** quantitatively. When a solution of **1** and tryptophan methyl ester

[*] Prof. Dr. I. Saito, F. Kubota, K. Shimozono, Prof. Dr. T. Matsuura
Department of Synthetic Chemistry, Faculty of Engineering
Kyoto University, Kyoto 606 (Japan)

in acetonitrile was stirred at room temperature, the adduct **10** precipitated (76%). Thus the cyclobutenone **1** can be used as a synthon for the preparation of 5-substituted uracil derivatives under neutral conditions. In view of the high reactivity of the CC double bond of cyclobutenones toward nucleophiles[2], **9** is assumed to arise from ring-opening of the amine adduct **11**[5].

Received: April 26, 1983 [Z 356 IE]
German version: *Angew. Chem. 95* (1983) 639
The complete manuscript of this communication appears in: *Angew. Chem. Suppl. 1983*, 835-839

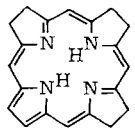
CAS Registry numbers:
**1**, 86436-22-8; **2**, 49846-86-8; **3**, 86436-23-9; **4**, 86436-24-0; **5**, 86436-25-1; **6**, 85436-26-2; **7**, 83174-95-2; **9**, 86436-27-3; **10**, 86436-28-4; ketene diethyl acetal, 2678-54-8; tryptophan methyl ester, 4299-70-1.

[1] I. Saito, H. Sugiyama, T. Matsuura, *J. Am. Chem. Soc. 105* (1983) 956, and references cited therein.
[2] R. Huisgen, H. Mayr, *J. Chem. Soc. Chem. Commun. 1976*, 55.
[4] I. Saito, K. Shimozono, T. Matsuura, *J. Am. Chem. Soc. 102* (1980) 3948; *ibid. 105* (1983) 936.
[5] For an analogous reaction, see A. Wexler, R. J. Balchunis, J. S. Swenton, *J. Chem. Soc. Chem. Commun. 1975*, 601.

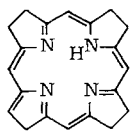
## The Chemistry of Pyrrocorphins: Stereoselectivity in the Porphyrinogen→Pyrrocorphin Tautomerization**

By *Rudolf Waditschatka* and *Albert Eschenmoser**

As originally surmised[1], and recently demonstrated[2], the corphinoids play a central role in the biosynthesis of vitamin $B_{12}$. We report here new findings on the chemistry of the pyrrocorphins[3].



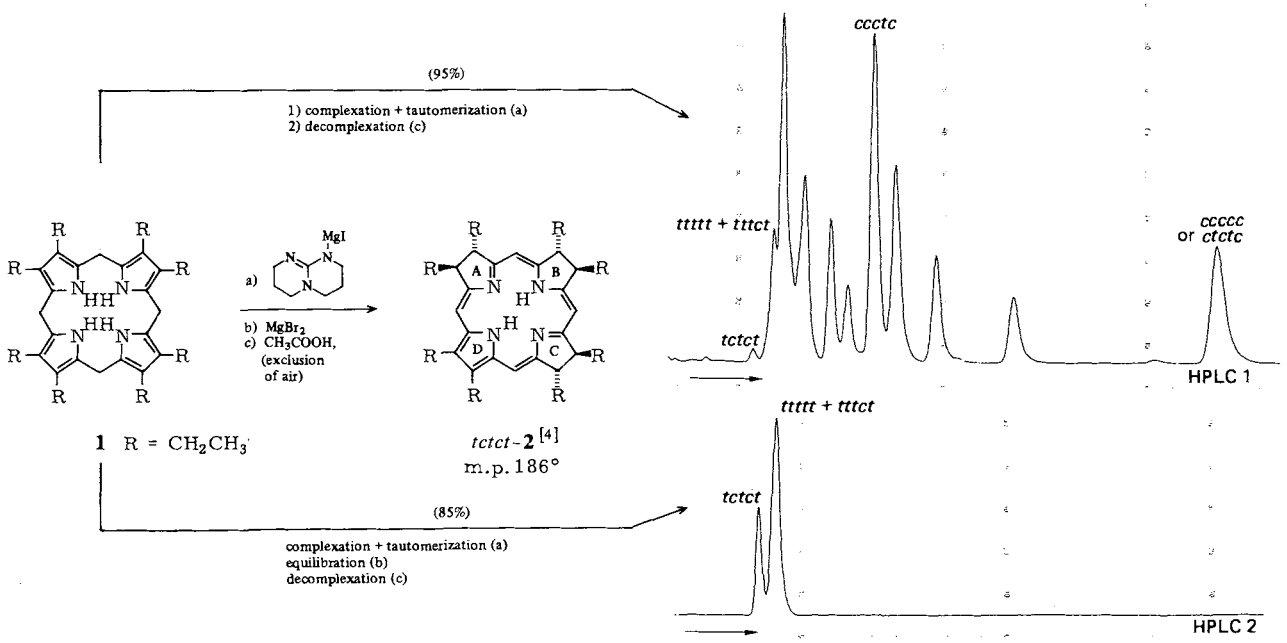
Pyrrocorphin[3]



Corphin[1]

Optimized reaction conditions have now been found for the previously reported[3a] porphyrinogen→pyrrocorphin tautomerization. Thus, treatment of octaethylporphyrinogen **1** with the MgI salt of 1,5,7-triazabicyclo[4.4.0]-dec-5-ene (TBD) directly followed by decomplexation with acetic acid (see legend to Scheme 1), provided a mixture of diastereomers of the octaethylpyrrocorphins **2** in practically quantitative yield. This endergonic isomerization proceeds *via* the non-isolated mixture of diastereomeric Mg pyrrocorphinate complexes (assumed to be decomplexed under conditions of kinetic control)[3a]. HPLC of the non-equilibrated mixture of pyrrocorphins resulted in detection of at least 12 of the 20 possible diastereomers (UV/VIS, HPLC 1), the configurations of three of which have been assigned. Normally, the *cctc* isomer[3a,4] makes up the main part (15–20%) of such mixtures.

If the mixture is allowed to equilibrate between the tautomerization and the decomplexation steps, or the 12-component mixture is subjected to such conditions, a mixture of diastereomers is obtained in 85% yield, HPLC of which now shows only two fractions (HPLC 2). The first fraction (*ca.* 30% of the total mixture) is the readily crystallized




Scheme 1. R = Et. a) $8 \times 10^{-3}$ M **1** in xylene, 15 equiv. TBD, 5 equiv. EtMgI, 16 h, 85°, under $N_2$. Work-up with saturated NaCl/$H_2O$ (or c directly). b) $2 \times 10^{-3}$ M Mg-complex of **2** in wet benzene, 12 equiv. $MgBr_2$, RT, 15 min. c) 10% $CH_3COOH$ in saturated NaCl/$H_2O$, 1 min, *ca.* 20°C. All operations conducted in glove box (< 5 ppm $O_2$). HPLC Partisil 5; pentane + 1.5 vol.-% $Et_3N$, detection 340 nm. For experimental details see *R. Waditschatka*, Dissertation ETH Zürich (in preparation), and [5c].

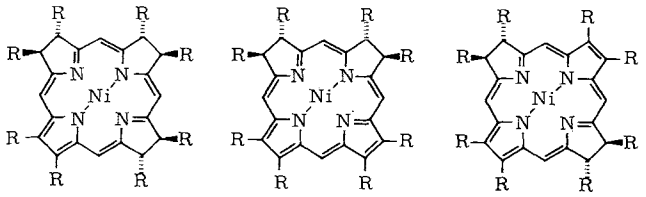
isomer *tctct*-**2** (m.p. = 186°C). The second fraction is a binary (not crystallized) mixture of isomers *ttttt*-**2** (*ca.* 25%) and *tttct*-**2** (*ca.* 45%). Thus, *tctct*-**2**, a crystalline representative having the pyrrocorphin structure, can be prepared in 20–25% yield directly from octaethylporphyrinogen.

The configurational assignment of *tctct*-**2** rests on the complexation with nickel(II) acetate (acetic acid, 110°C, 5

[*] Prof. Dr. A. Eschenmoser, R. Waditschatka
Laboratorium für Organische Chemie der
Eidgenössischen Technischen Hochschule, ETH-Zentrum
Universitätstrasse 16, CH-8092 Zürich (Switzerland)

[**] This work was supported by the Schweizerische Nationalfonds zur Förderung der wissenschaftlichen Forschung. We thank Dr. *D. Livingston* for translating the German manuscript and Dr. *E. Zass* for his assistance in the preparation of the final version.

min), which gives the known[3a] nickel(II) pyrrocorphinate *tctct*-**3** as the sole product (HPLC, $^1$H-NMR, UV/VIS). Incorporation of nickel into the second fraction of HPLC 2 gives, in contrast, two nickel pyrrocorphinates, easily separable by HPLC. Dehydrogenation in air (4 d, RT, hexane) transforms one of these into a binary mixture (1 : 2.5), composed of the known[5] nickel(II) isobacteriochlorinate, *ttt*-**4**, and the known[5c] nickel(II) bacteriochlorinate, *ttt*-**5**, (UV/VIS, HPLC). Analogous dehydrogenation of the other nickel pyrrocorphinate provides a mixture of the known isobacteriochlorinates *tct*-**4**[5] and *ttt*-**4**[5] (3.5 : 1), together with small amounts of a nickel bacteriochlorinate. The second pyrrocorphin fraction from HPLC 2 is, therefore, composed of the diastereomers *ttttt*-**2** and *tttct*-**2**.



*tctct*-**3** *tct*-**4** *ttt*-**5**

The three diastereomers present in the equilibrated mixture of pyrrocorphins **2** have a trans arrangement for each of the vicinal sets of ethyl groups. The equilibration occurs at the stage of the magnesium complexes, which are assumed to be mutually interconverted by protonation and deprotonation of the corresponding magnesium corphinates[3c].

Received: April 11, 1983 [Z 340 IE]
German version: *Angew. Chem. 95* (1983) 639

CAS Registry numbers:
**1**, 24477-51-8; *tttct*-**2**, 86594-50-5; *tctct*-**2**, 86594-51-6; *ttttt*-**2**, 86594-52-7.

[1] A. P. Johnson, P. Wehrli, D. Fletcher, A. Eschenmoser, *Angew. Chem. 80* (1968) 622; *Angew. Chem. Int. Ed. Engl. 7* (1968) 623.

[2] H. C. Uzar, A. R. Battersby, *J. Chem. Soc. Chem. Commun. 1982*, 1204.

[3] a) J. E. Johansen, V. Piermattie, C. Angst, E. Diener, C. Kratky, A. Eschenmoser, *Angew. Chem. 93* (1981) 273; *Angew. Chem. Int. Ed. Engl. 20* (1981) 261; b) R. Schwesinger, R. Waditschatka, J. Rigby, R. Nordmann, W. B. Schweizer, E. Zass, A. Eschenmoser, *Helv. Chim. Acta 65* (1982) 600; c) see also R. Waditschatka, E. Diener, A. Eschenmoser, *Angew. Chem. 95* (1983) 641; *Angew. Chem. Int. Ed. Engl. 22* (1983) 631.

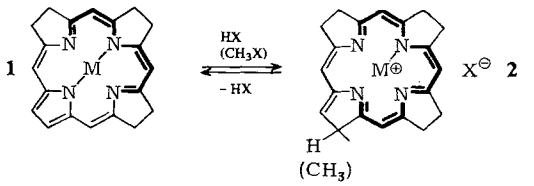
[4] Designation of configuration (*c* = *cis*, *t* = *trans*) beginning with ring A and proceeding clockwise.

[5] a) J. E. Johansen, C. Angst, C. Kratky, A. Eschenmoser, *Angew. Chem. 92* (1980) 141; *Angew. Chem. Int. Ed. Engl. 19* (1980) 141; b) C. Kratky, C. Angst, J. E. Johansen, *ibid. 93* (1981) 204; *20* (1981) 211; c) C. Angst, Dissertation, ETH Zürich No. 6783 (1981), pp. 45 and 145.

## The Chemistry of Pyrrocorphins: *C*-Methylation of Pyrrocorphinates at the Ligand Periphery**

By *Rudolf Waditschatka, Eva Diener,* and *Albert Eschenmoser**

The pyrrocorphin **1** and corphin **2** chromophores can be interconverted by protonation and deprotonation, respectively[1]. We report here that *the magnesium and zinc pyrrocorphin complexes are C-methylated selectively at the ligand periphery with methyl iodide to give the corphin complexes.* Thus, the pyrrocorphin ligand system promises to provide an entry to the (long sought[2]) biomimetic introduction of methyl groups into the construction of peripherically methylated porphinoids and corrinoids.

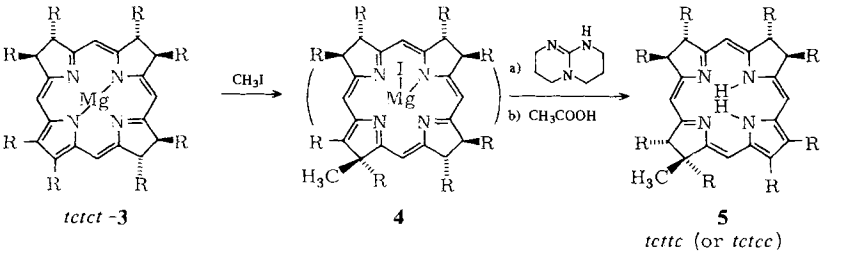



Upon treatment with excess EtMgI in tetrahydrofuran (THF) (70 °C, 10 min), *tctct*-octaethylpyrrocorphin[1a] is transformed into the (extremely oxygen-sensitive) magnesium complex **3** (Scheme 1; $\lambda_{max}$ = 354 (rel. int. = 1.00), 392 (0.66), 408 (0.84), 533 (0.10), 593 (0.18), 646 nm (0.66) in hexane). Brief heating of rigorously dried **3** in benzene/$CH_3I$ (2 : 1), followed by work-up with $H_2O$/NaCl gives the magnesium corphinates **4** (mixture of diastereomers, $\lambda_{max}$ = 308 (0.78), 363 (1.00), 540 (0.20), 566 (0.20) in hexane). Deprotonation with 1,5,7-triazabicyclo[4.4.0]dec-5-ene[1c] in benzene (5 min, RT), followed immediately by decomplexation (dilute acetic acid, a few min at RT) provides a mixture of monomethylated pyrrocorphins of constitution **5**, **6**, and **7** (combined yield *ca.* 90%)[3]. Of the three main fractions detected by HPLC, one could be isolated and characterized as isomer **5** (*tcttc* or *tctcc*)[4]. Its structural assignment, **5**, stems from its characteristic pyrrocorphinoid UV/VIS spectrum (cf. [1]), its $^1$H-NMR spectrum (4 vinyl proton signals at $\delta$ = 6.06, 6.12, 6.61, 6.73, 300 MHz, $CS_2/C_6D_6$ 9 : 1), and its mass spectrum ($m/z$ = 554 (100%, $M^+$); its nuclear Overhauser effect (NOE) $^1$H-NMR difference spectrum shows a strong NOE from the singlet of the angular methyl group ($\delta$ = 1.48) to the vinyl proton singlet at $\delta$ = 6.61, which fixes the position of the pyrrole ring relative to the methyl group. The *cis*-configuration of the ethyl groups on the methylated ring[4] is apparent from a strong NOE between the methyl singlet and a methine multiplet centered around $\delta$ = 3.0, and is confirmed by conversion of **5** into the nickel(II) *cis*-chlorinate **8b**. The remaining two HPLC main fractions (spectra recorded as a mixture; $M^+$, $m/z$ = 554 (100%); UV/VIS as **5**) contain three pyrrocorphins of constitution **6** and **7**[4]. The $^1$H-NMR spectrum shows three methyl singlets ($\delta$ = 1.149, 1.154, 1.271, *ca.* 3 : 1 : 4, 300 MHz in $C_6D_6$) and three groups of four (partially overlapping) vinyl proton signals. The possibility that these pyrrocorphins are diastereomers of **5** is precluded by NOE's observed from the methyl signals to three upfield vinyl proton signals.

Direct complexation of the crude methylation mixture from **3** with nickel acetate ($CH_3COOH$, 105 °C, 5 min) gives four main fractions readily separated by HPLC: a (38%), b (23%), c (15%), and d (19%). Fractions b, c, and d are UV/VIS and $^1$H-NMR spectroscopically uniform nickel(II) pyrrocorphinates of constitution **7**, **5**, and **6** (c identical with the Ni complex from pure **5**); fraction a contains two components (2.5 : 1), the main component being a *cis*-isomer of **7**[4]. Upon autoxidation in air, c and d produce the UV/VIS spectrum of a nickel(II) bacteriochlorinate/isobacteriochlorinate mixture; in contrast, a and b produce

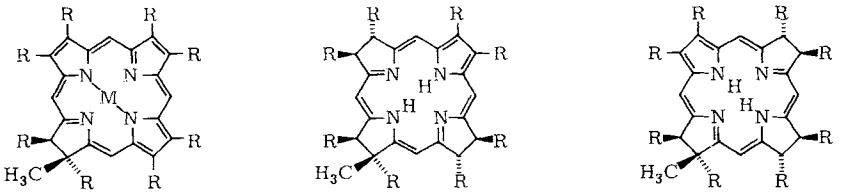
[*] Prof. Dr. A. Eschenmoser, R. Waditschatka, E. Diener
Laboratorium für Organische Chemie der
Eidgenössischen Technischen Hochschule, ETH-Zentrum
Universitätstrasse 16, CH-8092 Zürich (Switzerland)

[**] This work was supported by the Schweizerische Nationalfonds zur Förderung der wissenschaftlichen Forschung. We thank Dr. *D. Livingston* for translating the German manuscript and Dr. *E. Zass* for his assistance in preparing the final version.




*tctct*-3 4 5 *tcttc* (or *tctcc*)

**8a**, M = Ni, *trans* (R,R)
**8b**, M = Ni, *cis* (R,R)
**9a**, M = H/H, *trans* (R,R)
**9b**, M = H/H, *cis* (R,R)



7 6

Scheme 1. R = Et. For experimental details, see *R. Waditschatka*, Disserta tion, ETH Zürich (in preparation).

a clean isobacteriochlorinate spectrum. Upon dehydrogenation (*o*-chloranil, hexane-ether, RT), b and d give the *trans*-chlorinate **8a**, and a and c the *cis*-chlorinate **8b** (UV/VIS, HPLC).

In exploratory investigations with the total mixture of diastereomers **3**, described in [1c], we observed that zinc pyrrocorphinates react analogously with methyl iodide (THF, 80°C, $ZnI_2$). Here, the methylation products were identified by deprotonation, decomplexation ($CF_3COOH$, $CH_3CN$, RT), dehydrogenation (*o*-chloranil, benzene, RT), and chromatography to give the monomethylated chlorins **9a** (m.p. = 193°) and **9b** (m.p. = 203°)[5].

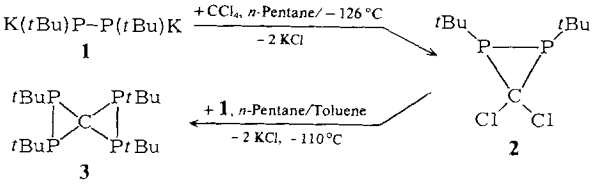
The peripheral *C*-methylation of pyrrocorphins extends the conjugation of the *bis*-vinamidine system of the starting chromophore (cf. **1**) to a corrinoid *tris*-vinamidine system (cf. **2**). We presume that this is the reason for the occurrence of peripheral *C*-methylation. The methylation step and the pyrrocorphinate-regenerating deprotonation step (**3**→**4**→**5**) are separable. This should stimulate attempts to perform sequential methylations of pyrrocorphins starting from porphyrinogens, as well as to explore the regio- and stereoselectivity problems thereby presented.

Received: April 11, 1983 [Z 341 IE]
German version: *Angew. Chem. 95* (1983) 641

## $(tBuP)_2C(tBuP)_2$— The First Tetraphosphaspiro[2.2]pentane**

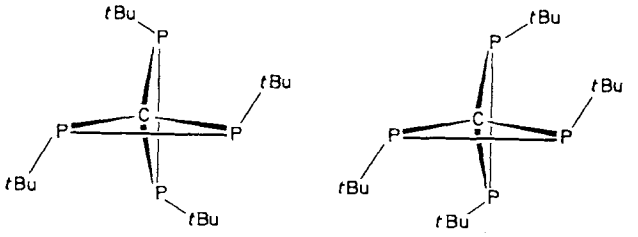
By *Marianne Baudler** and *Wolfgang Leonhardt*

[2+1]-Cyclocondensation of 1,2-dipotassium 1,2-di-*tert*-butyldiphosphide **1** with geminal dihaloalkanes leads to formation of diphosphiranes $(tBuP)_2CR_2$[1]. Reaction of the phosphide with silicon tetrachloride (2:0.9) furnishes the tetraphosphasilaspiro[2.2]pentane $(tBuP)_2Si(tBuP)_2$[2]. We report here on the reaction of **1** with tetrachloromethane, in which, aside from polymeric solids and *tert*-butylcyclophosphanes $(tBuP)_n$ (n = 4, 3), the novel phosphorus three-membered ring compounds 1,2-di-*tert*-butyl-3,3-dichlorodiphosphirane **2** and tetra-*tert*-butyltetraphosphaspiro[2.2]pentane **3** are formed.




**1** **2** **3**

The spirocycle **3**, the proportion of which in the soluble products amounts to *ca.* 5 mol-%[3], is formed as a mixture of the isomers **3a** and **3b** (85:15), which differ from each



**3a** **3b**

[*] Prof. Dr. M. Baudler, W. Leonhardt
Institut für Anorganische Chemie der Universität
Greinstrasse 6, D-5000 Köln 41 (Germany)

[**] Contributions to the Chemistry of Phosphorus, Part 130. This work was supported by the Deutsche Forschungsgemeinschaft and the Fonds der Chemischen Industrie.—Part 129: M. Baudler, H. Suchomel, *Z. Anorg. Allg. Chem.*, in press.

[1] a) R. Waditschatka, A. Eschenmoser, *Angew. Chem. 95* (1983) 639; *Angew. Chem. Int. Ed. Engl. 22* (1983) 630; b) R. Schwesinger, R. Waditschatka, J. Rigby, R. Nordmann, W. B. Schweizer, E. Zass, A. Eschenmoser, *Helv. Chim. Acta 65* (1982) 600; c) J. E. Johansen, V. Piermattie, C. Angst, E. Diener, C. Kratky, A. Eschenmoser, *Angew. Chem. 93* (1981) 273; *Angew. Chem. Int. Ed. Engl. 20* (1981) 261.

[2] a) Cf. A. W. Johnson in H. C. Heinrich: *Vitamin $B_{12}$ and Intrinsic Factor*, Enke, Stuttgart 1962, p. 1; b) D. P. Arnold, A. W. Johnson, *J. Chem. Soc. Chem. Commun. 1977*, 787; c) K. Hosaka, A. P. Johnson, A. W. Johnson, *Tetrahedron Lett. 1978*, 2959.

[3] All reactions and work-ups were carried out in a glove box under nitrogen (< 5 ppm $O_2$).

[4] The configuration of the angular methyl group relative to the ethyl groups on the unmethylated rings has not been established.

[5] $^1$H-NMR (300 MHz, $C_6D_6$): *s*, the $CH_3$ from **9a**: $\delta = 2.03$, from **9b**: $\delta = 1.96$. $^{13}$C-NMR (75 MHz, $C_6D_6$); *q* the angular $CH_3$ group of **9a**: $\delta = 22.21$, from **9b**: $\delta = 28.11$.

other in the relative arrangement of the *trans*-oriented *tert*-butyl groups at the two three-membered rings. Whereas **3a** could be isolated as colorless stable crystals (m.p. 141–143 °C, reversible)[5], **3b** slowly rearranges at room temperature to **3a**. Owing to its thermal decomposability, the diphosphirane **2** could be enriched to only 80 mol-%.

**3a,b** and **2** were identified by their molecular masses (MS: **3a,b**: *m/z* 364; **2**: *m/z* 258) and nuclear magnetic resonance spectra[4], and, in the case of **3a**, also by elemental analysis. Proof of the structure of **3a,b** and **2** is provided by the $^{31}$P-NMR signals observed in the high-field region characteristic for phosphorus three-membered ring compounds[2b]. The spirocyclic molecular framework of **3** follows from the $^{13}C\{^1H\}$-NMR spectrum of **3a**, which, as a result of C,P-coupling, shows two triplets of triplets for the *tert*-butyl groups and a quintet with $^1J(CP) = 80.6$ Hz for the spiro carbon atom. Of the two singlets in the $^{31}P\{^1H\}$-NMR spectrum of **3**, the downfield signal of lower intensity is ascribable to the isomer **3b**, since here the transannular steric interaction of the *tert*-butyl substituents leads to a downfield shift as a result of widening of the exocyclic C–P–C bond angles.

Remarkable in the case of **3a** is its low sensitivity towards air and moisture, and the finding that the $P_4C$ ring skeleton does not fragment during the mass spectrometric investigation, even at 70 eV.

Received: April 14, 1983 [Z 346 IE]
German version: *Angew. Chem. 95* (1983) 633

CAS Registry numbers:
**1**, 66874-44-0; **2**, 86508-26-1; **3a**, 86508-27-2; **3b**, 86560-61-4; $CCl_4$, 56-23-5.

[1] M. Baudler, F. Saykowski, *Z. Naturforsch. B 33* (1978) 1208; *Z. Anorg. Allg. Chem. 486* (1982) 39.

[2] a) M. Baudler, T. Pontzen, *Z. Anorg. Allg. Chem. 491* (1982) 27; b) M. Baudler, *Angew. Chem. 94* (1982) 520; *Angew. Chem. Int. Ed. Engl. 21* (1982) 492.

[3] Optimized by means of $^{31}$P-NMR spectroscopic monitoring.

[4] $^{31}P\{^1H\}$-NMR: **2** (purity 80%, *n*-pentane): $\delta = -76.1$ (s, 2P); **3a** (*n*-hexane): $\delta = -132.0$ (s, 4P); **3b** (mixture with **3a** and $(t\text{BuP})_n$, *n*-hexane): $\delta = -109.7$ (s, 4P).—$^{13}C\{^1H,^{31}P\}$-NMR: **3a** (benzene/[D$_6$]-benzene): $\delta = 30.42$ (s, 4C, PC), 29.89 (s, 12C, PCC), 24.46 (s, 1C, $P_4C$).—$^1H\{^{31}P\}$-NMR: **3a** (benzene/[D$_6$]-benzene): $\delta = 1.25$ (s, 36H).

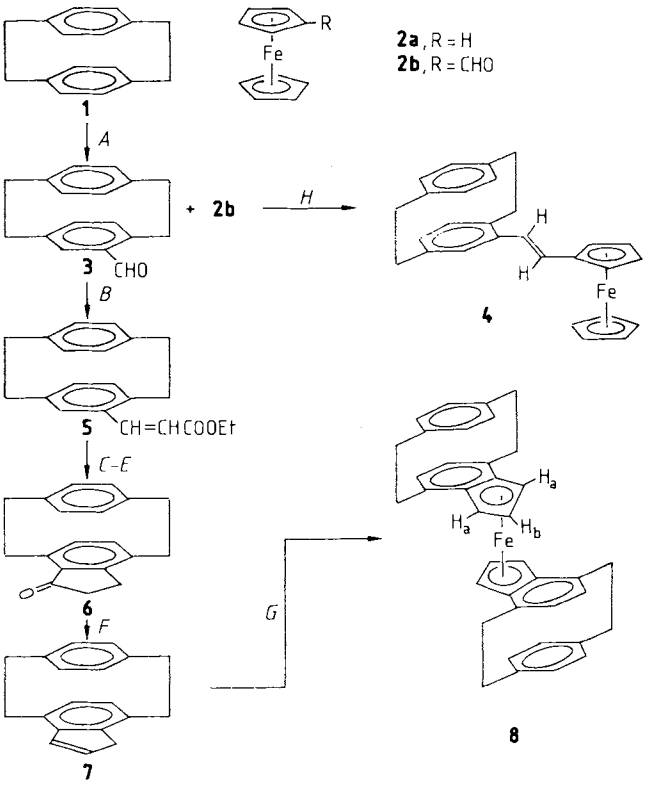
[5] *One-pot reaction for* **3a**: A solution of tetrachloromethane (10.3 g, 67 mmol) in toluene (60 mL) is cooled to −78 °C and added dropwise (2–4 drops/s) to a stirred suspension of **1** (17.6 g, 60 mmol) in 150 mL of *n*-pentane/toluene (1 : 1) at −110 °C. The mixture is stirred for a further 5 h at −78 °C, after which time the precipitate is filtered off under suction in the cold and then washed three times each with 20 mL toluene. The combined filtrates are evaporated down at room temperature and the black-brown viscous residue is chromatographed on $Al_2O_3$ (heated *in vacuo*) with *n*-hexane. The fractions with the highest content of **3** are combined, the solvent is removed by evaporation, and the residue successively recrystallized from *n*-hexane (*ca.* 9 times), dioxane (*ca.* 3 times), and methanol (*ca.* 2 times) with concomitant $^{31}$P-NMR spectroscopic monitoring; yield 0.19 g (2%) **3a**, purity >99% (trace of $(t\text{BuP})_4$, $^{31}$P-NMR).

## New Link between Cyclophane and Ferrocene Chemistry**

By *Sayed El-Tamany, Friedrich-Wilhelm Raulfs,* and *Henning Hopf**

[2.2]Paracyclophane **1** and ferrocene **2a** are prototypes of multilayered organic and organometallic molecules, respectively. We were interested in whether multilayer systems consisting of alternating organic and organometallic components can be synthesized from these two sandwich compounds. In order to achieve the greatest electronic interaction between "layers" it is recommendable to link **1** and **2** either by unsaturated structural units or by direct annelation[1].

A coupling of the first type may be achieved by reacting the commercially available product **2b** with the aldehyde **3**, which is readily obtainable from **1** by Rieche formylation[2], using the coupling method described by *McMurry* (Lenoir variant)[3]. Besides the main product **4** (33%, brown-red needles from ethanol/chloroform, m.p. 175–177 °C), dimers of **3** (7%) and **2b** (24%) are also formed, which, however, can be easily separated from **4** by chromatography. The $^1$H-coupling constant between the two olefinic protons ($\delta = 6.77$ and 6.56) of 16.0 Hz is consistent with the *E*-configuration[4].




*A:* $Cl_2CHOCH_3/TiCl_4$, $CH_2Cl_2$ (92%); *B:* $(EtO)_2P(O)CH_2CO_2Et$/NaH, tetrahydrofuran (THF) (85%); *C:* 1. NaOH, 2. HCl (91%); *D:* Pd/C, $H_2$, ethyl acetate (91%); *E:* polyphosphoric acid, 120 °C (79%); *F:* 1. $H_2NNHTs$, $H^+$, EtOH (86%), 2. Na, $HOCH_2CH_2OH$, reflux (79%); *G:* 1. Na (suspension), THF, 2. $FeCl_2$, THF (14%); *H:* $TiCl_4$/Zn, pyridine/THF (33%).

**3** can also be used as starting material for the second type of coupling: The aldehyde is converted by Wittig-Horner reaction into the unsaturated ester **5**, which can be cyclized by conventional methods to the five-membered ring ketone **6**. Bamford-Stevens elimination affords the olefin **7**, which is subsequently allowed to react in analogy to a synthesis of bisindenyliron to give **8**[5]. Proof of the structure of this four-layered molecule, which on sublimation (200–220 °C/$10^{-3}$ torr) yields dark-violet crystals, is based on spectroscopic data[4]. Noteworthy is the chemical shift of the five-membered ring protons $H_b$ and $H_a$ in **8** compared to that observed in the model substance bisindenyliron[5]: Whereas $H_b$ in both ferrocene derivatives ab-

[*] Prof. Dr. H. Hopf, S. El-Tamany, F.-W. Raulfs
Institut für Organische Chemie der Technischen Universität
Schleinitzstrasse, D-3300 Braunschweig (Germany)

[**] Cyclophanes, Part 20. This work was supported by the Fonds der Chemischen Industrie and the Stiftung Volkswagenwerk (Project "Chemie und Physik unkonventioneller Materialien").—Part 19: S. El-Tamany, H. Hopf, *Chem. Ber. 116* (1983) 1682.

sorbs at almost the same position ($\Delta\delta = 0.11$) the protons $H_a$ in **8** are so strongly shifted upfield through the magnetic anisotropy of the bridging benzene ring that the order of the signals is reversed ($\Delta\delta = 0.79$).

Received: April 18, 1983 [Z 349 IE]
German version: *Angew. Chem. 95* (1983) 631

CAS Registry numbers:
**1**, 1633-22-3; **2b**, 12093-10-6; **3**, 729-30-6; **4**, 86421-38-7; **5**, 86409-80-5; **6**, 86409-81-6; **7**, 86409-82-7; **8**, 86409-83-8.

[1] The complexation of cyclophanes with the ($\eta^5$-cyclopentadienyl)iron unit is well-known: A. R. Koray, *J. Organomet. Chem. 232* (1982) 345, and references cited therein, particularly E. D. Laganis, R. G. Finke, V. Boekelheide, *Proc. Natl. Acad. Sci. USA 78* (1981) 2657. The 1:1 and 1:2 adducts that are formed, however, no longer contain intact ferrocene units. Moreover, in the 2:1 products the surfaces of the cyclophanes capable of complexation are complexed, so that there is no direct possibility for the construction of oligomeric structures. This limitation does not exist in the case of the coupling possibilities presented here; the requisite dialdehydes of **1** and [2.2]indenophane have already been prepared (S. Ehrhardt, F.-W. Raulfs, H. Hopf, unpublished results).

[2] A. Rieche, H. Gross, E. Höft, *Chem. Ber. 93* (1960) 88.

[3] D. Lenoir, *Synthesis 1977*, 553.

[4] **4**: UV (acetonitrile): $\lambda_{max} = 456$ ($\varepsilon = 1200$), 319 (16400), 236 (sh, 17300), 207 nm (34700); **8**: $^1$H-NMR ($CDCl_3$, int. TMS): $\delta = 6.32$ (s, 4H), 6.12 (s, 4H), 5.63 (s, 4H), 3.75 (t, $J = 2.3$ Hz, 2H, $H_b$), 3.67 (d, $J = 2.3$ Hz, 4H, $H_a$), 2.85 (ps-t, 4H), 2.72–2.52 (m, 12H, bridge-$CH_2$); IR (KBr): 3005 w, 2940 w, 2920 m, 2850 m, 1498 m, 1435 m, 1100 w, 853 m, 800 m, 792 cm$^{-1}$; UV (cyclohexane): $\lambda_{max} = 530$ ($\varepsilon = 500$), 418 (1100), 300 (16000), 216 nm (37000). – The spectroscopic and analytical data of all the new substances prepared here are consistent with the given structures.

[5] a) I. J. Eisch, R. B. King: *Organometallic Synthesis*, Vol. *1*, Academic Press, New York 1965, p. 73ff.; b) G. Wilkinson, *Org. Synth. 36* (1956) 31.

# BOOK REVIEWS

**World Energy Supply: Resources, Technologies, Perspectives.** By *Manfred Grathwohl*. Walter de Gruyter & Co., Berlin 1982. 450 pp., bound, DM 120.00.

This book needs to be read selectively. Portions of it are well thought out and convey useful information in a useful way. Other portions are close to unreadable; they consist of an accumulation of information from dozens of sources, frequently selected and reproduced with little discrimination, and presented to the reader with scarcely more input by the author than goes into compiling a telephone directory. This is a pity, for the book bears all the evidence of very hard work over a prolonged period.

The task is, of course, enormous. It calls for an ability to deal intelligently with the major aspects of fossil energy, nuclear, solar and everything in between. It would be a big job for a committee. It is apt to overwhelm a single author, and I am afraid in this instance it has almost done that. Over and over the author is reduced to merely citing the literature. I have not made a count, but the number of sentences that begin with "According to ..." is large. What emerges is a hybrid between a reproduction of statistics and diagrams, a physics textbook, a geography textbook, and an occasional policy recommendation that expresses more the author's own philosophy or moral suasion than a conclusion from the data presented.

The book is meticulously organized along logical lines. It proceeds from a brief, largely introductory chapter, entitled "Primary sources and world economics" to a discussion of the world's energy potential (which contains segments on each of the primary sources) to a very extensive chapter on energy supply systems, by which are meant basically the non-primary sources—nuclear, solar, electricity, synthetic fuels, etc. It next deals with question of the environment and with safety and closes with a brief chapter in which conclusions are drawn.

Of these chapters, by far the best are those dealing with energy supply systems, or what I would call "secondary sources". Here one has the feeling that the author is at home, comfortable with the subject matter and far less inclined to lean, often uncritically, on the literature as his main support. Within this area, nuclear matters are especially well discussed, and so is solar energy.

Had the author been less ambitious and just published the second half of the book, he would merit high marks. Unfortunately, the first half in no way measures up to the second. Some of the reasons are inherent in his self-imposed limitation to supply. They are inherent in that it is very hard, if not unproductive, to deal merely with the supply side. Indeed, one senses that the authors feels the same way, for he finds himself compelled to bring in demand if only for the purpose of assessing adequacy of resources. But, of course, he cannot usefully do that without discussing price. Adequacy or inadequacy exists only at a stipulated price. Without it there cannot be too much or too little. Yet, demand and price are treated, if at all, in a highly incidental fashion. This removes much of the discussion from reality. If I may mention the four most discussed energy books that were published in the United States in 1979 and 1980: *Energy in America's Future, Energy Future, Energy: The Next Twenty Years,* and *Energy in Transition* (only one of which, incidentally, is mentioned in the author's references, as best I can tell), they dealt, without exception, equally with supply and demand and with price as the link.

Still, as I have said, demand sneaks in. So do discussions of population growth, income differences among countries, famine, and the like – none of these themes being developed and discussed with the authority that stems from knowledge. They are obviously subjects that fascinate him, but self-discipline should have kept him from (as an old editor-friend of mine used to say) chasing too many rabbits at the same time. Too many *obiter dicta*.

Concept and structure of the book apart, much of the first half or so of the book (chapters 2 and 3) is, moreover, quite unsatisfactory on its own merit. Two points stick out. First, there is the author's above-mentioned indiscriminate use of sources, a practice that proves only that he had access to a wide range of books and articles. What is missing is evaluation. They are presented as, or turned into, tables and graphs, regardless of the time the data were first published, or without revealing to the reader the background of the data, so that he has to take them on faith, and second-hand at that. This is particularly distressing when most of these data are not hard facts but estimates, so that

the assumptions behind them are at least as interesting and certainly as important to understanding as the data themselves. Here the author simply lets the reader down. If I want to read a new book on energy, I am interested in what the author makes of this vast arsenal of numbers. Otherwise I go to the original source.

What adds to the discomfort is that much of the material is badly, at times fatally, out of date. To be sure, there are reasons: the time it takes to translate such a long, complex volume, the speed with which the energy scene is changing, the slowness with which some of the data become available. But it goes beyond that. For example, most of the production and consumption data on the United States—the area I am most familiar with—are drawn from publications that are four and five years old. One of these is, for example, a 1977 report by the Congressional Research Service, a compilation of separate articles by some twenty authors. How far out of date it is, can be seen when we look at the U. S. energy consumption and oil import projections for 1985—then seven years in the future—and compare them with the 1982 reality. Consumption, then conjectured to rise from 74 quads in 1976 to 95 quads in 1985 had instead dropped to 71 quads in 1982! No reason to believe it will reach even 80 by 1985. Oil imports then projected to rise from 8.1 million barrels per day in 1976 to 11.8 million berrels per day in 1985 have instead declined to 5 million barrels per day in 1982. These are hardly small differences, nor is this an atypical example. Nuclear energy projections, for instance, and with them uranium requirements, are taken from sources prior to the beginning of the big slide in plans and construction of new plants.

In the face of an abundance of timely data from governmental, industrial and academic sources this is not excusable. As a result, recent trends and projections are for the most part not just useless but misleading. Though less so, obsolescence also penetrates the technology portion. To cite an especially glaring example, the author reports plans for a U. S. scheme to produce shale oil through the explosion of nuclear devices. Puzzled what he had in mind I consulted the source reference at the back of the book: an article in a German journal written in 1965! Surely, it would not have been difficult to track the relevance of that statement and above all not to present it as though this was a contemporary plan. Again, this is not an isolated instance. The Energy Research and Development Administration (ERDA) which was dissolved in 1978, figures as a live agency. Its estimates, now several years old, are presented as valid now. This is especially disturbing when a projection of solar energy reaching 25 percent of total U. S. energy in 2000 is ascribed to that organization (this was a one-time "goal" put forward by President Carter in early 1977), followed by the observation that "recent projections are even higher". Recent, when? The oil price did not quadruple in two years after 1973, but in one year (p. 59). Coal slurry pipelines are not in the "research and pilot" stage in the U. S. (p. 90). One, carrying coal from Arizona to California, has been operating for several years, and an earlier one, in Ohio, carried coal for some 160 km for many years, before it succumbed to competition from the railroad. A 1400 mile line will begin to be built in 1984 and is expected to go into operation in 1986. Expectations for steady increases in enhanced oil recovery have been steadily declining and reliance on non-conventional sources of natural gas has been relegated to a more distant horizon.

Various experts' or organizations' cost estimates for new sources or processes are based on costs and prices long exceeded, and much of the time it is not clear whether we are dealing in current or constant monetary units. The word "presently" used frequently remains generally undefined.

Some peculiarities may be due to language difficulties. For example, anthracite is a small portion of U. S. coal, yet it is repeatedly used to characterize all U. S. coal. Indeed, for some reason anthracite and bituminous coal are at times treated as synonymous. That there are "vast" coal fields available for strip-mining in the Middle West is equally confusing. They are in the *West*, not the *Middle* West, nor is there any anthracite in Kentucky (p. 54). The *imbalance* between production and consumption is persistently referred to as *discrepancy*, a term that threw me off until I sensed the error.

Given the enormous effort that must have gone into writing this book, the care with which the glossary, the index and the referencing has been done, it is indeed a pity that the outcome is not more useful. It would be my advice to take with a large pinch of salt the offerings in chapter 2 and 3 and concentrate on the balance of the book, even though here too, caution is advised.

*Hans H. Landsberg* [NB 593 IE]

**Electrons in Chemical Reactions; First Principles.** By *L. Salem*. Wiley-Interscience, Chichester 1982. xii, 260 pp., bound, £ 27.25.

Anyone who has read and followed *Lionel Salem's* numerous, original and pioneering publications will note with disbelief and regret that he has turned his back on chemistry, in order to devote himself in future to banking. The present volume is thus—if another U turn does not follow—something of a going-away present to his colleages and a summary of current thinking concerning the electronic theory of chemical reactions as seen by a scientist, who has made fruitful contributions to the field.

The text is written from a lofty standpoint and assumes a solid background in theoretical chemistry on the part of the reader, at least enough that he can recognize the importance of and complete the numerous, almost impressionistically sketched definitions. This is in no way the introduction at an elementary level that the subtitle "First Principles" seems to suggest.

The choice and treatment of the individual themes (energy hypersurfaces; the electronic structure of excited molecules and intermediates; orbital and state symmetries; reaction paths; the role of electron spin; solvent effects) distinctly bear the stamp of the predilections and style of an author who likes to work out the solution of a problem using a theoretical-chemical "catch as catch can" technique, which extends from the use of naive, resonance considerations to the use of quantum-chemical methods of considerable sophistication. The result is a sometimes uneven but demanding text, that is always stimulating and readable but which challenges contradiction on occasions. Furthermore, since the text leans on the interests and work of the author, there are necessarily gaps which some readers will deplore. The few trivial errors, such as the wrong quadricyclane or benzvalene formulas on p. 113 and 122 will scarcely cause misunderstanding.

Taken as a whole this book constitutes an exceedingly stimulating piece of work that is suited as a "mise au point" as well as a basis and source of information for postgraduate seminars and discussions at a higher level. From the latter point of view its rather personal approach is an added attraction.

*Edgar Heilbronner* [NB 589 IE]

## Recent Books

The following books have been received by the editor. All the publications listed are available through W & P Buchversand für Wissenschaft und Praxis, Boschstrasse 12, D-6940 Weinheim (Federal Republic of Germany). Tel. (06201) 606-0, Telex 465516 vchwh d, Telefax (06201) 602328.

**Peptides. Syntheses. Physical Data.** By *W. Voelter*. Thieme, Stuttgart 1983. **Vol. 1: Amino Acids.** *Ca.* 320 pp., bound, *ca.* DM 98.00.—ISBN 3-13-639201-9; **Vol. 6: Subject Index.** *Ca.* 155 pp., bound, *ca.* DM 48.00.—ISBN 3-13-639701-0

**Moderne photographische Systeme. Wirkprinzipien, Prozesse, Materialien.** By *H. Böttcher* and *J. Epperlein*. VEB Deutscher Verlag für Grundstoffindustrie, Leipzig 1983. 360 pp., bound, *ca.* DM 65.00.—Bestell-Nr. 541698 2

**Chemikaliengesetz. 3. Ergänzungslieferung.** By *M. Nöthlichs* and *R. Anzinger*. Erich Schmidt Verlag, Bielefeld 1983. Pages 3002–3431, loose-leaf edition. Basic text including 3rd supplementary installment, 828 pp., DM 86.00

**Vom Atom zum Makromolekül. Organische Chemie—Biochemie—Technische Anwendungen.** By *H. Kiechle* and *H. R. Christen*. Verlag Diesterweg/Salle-Sauerländer, Frankfurt am Main 1982. vii, 424 pp., sewed, DM 58.00.—ISBN 3-425-05403-1

**Computeranwendungen in der Chemie. Eine Einführung in das Arbeiten mit Kleinrechnern.** By *K. Ebert* and *H. Ederer*. Verlag Chemie, Weinheim 1983. ix, 359 pp., bound, DM 63.00.—ISBN 3-527-26021-8

**Mobility and Recognition in Cell Biology.** Edited by *H. Sund* and *C. Veeger*. de Gruyter, Berlin 1983. xix, 586 pp., bound, DM 190.00.—ISBN 3-11-009536-X

**Stereospecific Polymerization of Isoprene.** By *E. Ceausescu*. Pergamon Press, Oxford 1983. x, 280 pp., bound, $ 60.00.—ISBN 0-08-029987-3

**Studienführer Chemie.** Published by the Gesellschaft Deutscher Chemiker. Verlag Chemie, Weinheim 1983. xx, 456 pp., brochure, DM 25.00.—ISBN 3-527-26036-6

**Moleküle und Molekülanhäufungen. Eine Einführung in die physikalische Chemie.** By *H.-D. Försterling* and *H. Kuhn*. Springer-Verlag, Berlin 1983. xvi, 369 pp., bound, DM 49.00.—ISBN 3-540-11541-2

**Advances in Heterocyclic Chemistry. Vol. 32.** Edited by *A. R. Katritzky*. Academic Press, New York 1982. ix, 404 pp., bound, $ 74.50.—ISBN 0-12-020632-3

**Advances in Magnetic Resonance. Vol. 10.** Edited by *J. S. Waugh*. Academic Press, New York 1983. xi, 223 pp., bound, $ 35.00.—ISBN 0-12-025510-3

**Adhäsion. Theoretische und experimentelle Grundlagen.** By *C. Bischoff* and *W. Possart*. Akademie-Verlag, Berlin 1983. 272 pp., brochure, *ca.* DM 68.00.—Bestell-Nr. 763056-0 (66676)

**Pergamon Series in Analytical Chemistry. Vol. 6: Computers in Analytical Chemistry.** By *P. Barker*. Pergamon Press, Oxford 1983. xvi, 472 pp., bound, £ 37.50.—ISBN 0-08-024008-9

**Fortschrittsberichte aus Naturwissenschaft und Medizin.** Edited by *H. A. Staab, W. Gerok, H. Markl, W. Martienssen,* and *H. Gibian*. Wissenschaftliche Verlagsgesellschaft mbH, Stuttgart 1983. 352 pp., paperback, DM 32.00.—ISSN 0172-0651

**Springer Advanced Texts in Chemistry. Protein Purification. Principles and Practice.** By *R. K. Scopes*. Springer-Verlag, Berlin 1982. xiii, 282 pp., bound, DM 79.00.—ISBN 3-540-90726-2

**Ellis Horwood Series in Physical Chemistry. Adsorption.** By *J. Ościk*. Ellis Horwood Ltd., Chichester 1983. xv, 206 pp., bound, £ 22.50.—ISBN 0-85312-166-4

**Conformation in Biology.** Edited by *R. Srinivasan* and *R. H. Sarma*. Adenine Press, Guilderland NY 1983. xvii, 483 pp., bound, $ 89.00.—ISBN 0-940030-05-5

**Molecular Theory of Evolution. Outline of a Physico-Chemical Theory of the Origin of Life.** By *B.-O. Küppers*. Springer-Verlag, Berlin 1983. ix, 321 pp., bound, DM 79.00.—ISBN 3-540-12080-7

**Structure and Bonding. Vol. 53: Copper, Molybdenum, and Vanadium in Biological Systems.** Edited by *M. J. Clarke, J. B. Goodenough, P. Hemmerich, J. A. Ibers, C. K. Jørgensen, J. B. Neilands, D. Reinen, R. Weiss,* and *R. J. P. Williams*. Springer-Verlag, Berlin 1983. v, 166 pp., bound, DM 88.00.—ISBN 3-540-12042-4

*Registered names, trademarks, etc. used in this journal, even without specific indication thereof, are not to be considered unprotected by law.*

© Verlag Chemie GmbH, D-6940 Weinheim, 1983. - Printed in the Federal Republic of Germany by Zechnersche Buchdruckerei, Speyer/Rhein.

All rights reserved (including those of translation into foreign languages). No part of this issue may be be reproduced in any form – by photoprint, microfilm, or any other means – nor transmitted or translated into a machine language without written permission from the publishers. Only single copies of contributions, or parts thereof, may be reproduced for personal use. Copies reproduced and used other than for private purposes in an industrial or commercial undertaking are subject to copyright and, in such cases, a copyright fee must be paid to the VG WORT, Abteilung Wissenschaft, Goethestr. 49, 8000 München 2, from whom conditions of payment can be obtained on request.

**Valid for users in the USA:** The appearance of the code at the bottom of the first page of an article in this journal (serial) indicates the copyright owner's consent that copies of the article may be made for personal or internal use, or for the personal or internal use of specific clients. This consent is given on the condition, however, that the copier pay the stated per-copy fee through the Copyright Clearance Center, Inc., for copying beyond that permitted by Sections 107 or 108 of the U.S. Copyright Law. This consent does not extend to other kinds of copying, such as copying for general distribution, for advertising or promotional purposes, for creating new collective works, or for resale. For copying from back volumes of this journal see 'Permissions to Photo-Copy: Publisher's Fee List' of the CCC.

**Editorial office:** Pappelallee 3, D-6940 Weinheim, Federal Republic of Germany, Telephone (06201) 602315, Telex 465516 vchwh d, Telefax (06201) 602328.

**Editors:** *P. Gölitz, I. G. Neil, O. Smrekar, A. Stimson.*

**Publishers:** Verlag Chemie GmbH. (Managing Directors: *Prof. Dr. Helmut Grünewald* and *Hans Dirk Köhler*), Pappelallee 3, D-6940 Weinheim, Federal Republic of Germany.

Correspondence concerning advertisements should be addressed to Verlag Chemie GmbH. (Advertising Manager *R. J. Roth*), Boschstr. 12, P.O. Box 1260/1280, D-6940 Weinheim, Federal Republic of Germany. Telephone Weinheim (06201) 602-0, Telex 465516 vchwh d, Telefax (06201) 602328.

ANGEWANDTE CHEMIE
International Edition in English
Volume 22 · Number 9
September 1983
Pages 637–740

# Stereoselective Synthesis of Enantiomerically Pure Natural Products—Estrone as Example**

By Gerhard Quinkert* and Herbert Stark

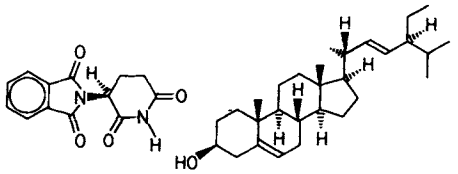
*Dedicated to Sir Derek Barton on the occasion of his 65th birthday*

Natural products have been synthesized for billions of years in animals, plants, and microorganisms. As a rule they occur enantiomerically pure. Their chiral character corroborates their use in metabolism or as biologically active agents. Natural products may be insufficient in quality or quantity. They have recently begun to become accessible, either unchanged or modified, by biological synthesis; here, too, they are obtained enantiomerically pure. In the last twenty years chemical synthesis has become a major concern of organic chemists. Their target compounds are primarily enantiomerically pure natural products or biologically active variants thereof.

## 1. Current Problems in the Chemical Synthesis of Natural Products

### 1.1. The Fundamentally Different Routes to Enantiomerically Pure Target Compounds

At the threshold of synthetic biology[3] one of the main challenges of synthetic chemistry is to find routes which satisfy the demands of industrial applicability to enantiomerically pure compounds with biologically important properties. As the "thalidomide case"[5] shows, the application of enantiomerically pure active agents is no matter for esoteric players of the "glass-bead game"[***]. According to recent investigations, only (*S*)-(−)-thalidomide **1** behaves teratogenically when administered intraperitoneally to mice and rats; it is claimed that (*R*)-(+)-thalidomide (*ent*-**1**), even at the highest doses, causes no deformity in animals used in the experiments[6].



**1** **2**

Scheme 1. (*S*)-(−)-thalidomide **1** and stigmasterol, (3β,22*E*)-5,22-stigmastadien-3-ol **2**.

Enantiomerically pure target compounds are now accessible by three routes *via* chemical synthesis. Whenever possible, the synthetic chemist resorts to optically active natural products as starting materials[7]. By conducting a synthesis intelligently, use can be made of the evolutionary preference for one enantiomer in the selection operations yet to be performed, so that on introduction of further centers of chirality a choice between two diastereomers, and never one between two enantiomers is involved.

It is left very much to the imagination of the synthetic chemist to decide what natural products are suitable starting materials in a particular instance. Previously, in natural product synthesis it was generally attempted to select both starting material and target molecule from the same class of compounds. Thus, for example, the Mexican barbas-

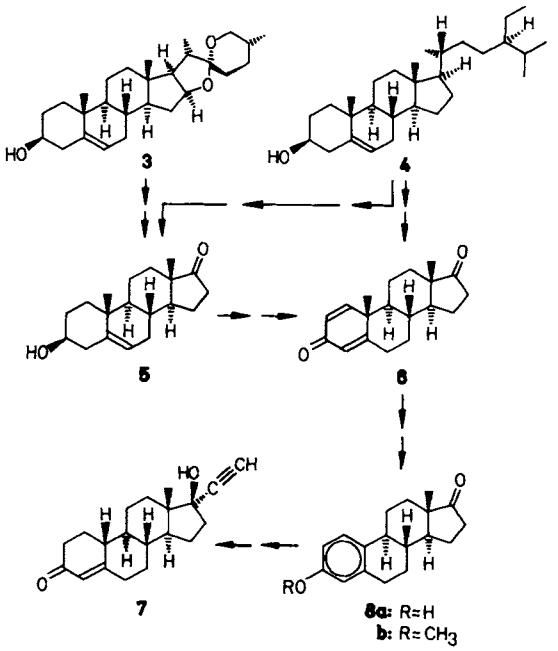
[*] Prof. Dr. G. Quinkert, Dr. H. Stark [+]
Institut für Organische Chemie der Universität
Niederurseler Hang, D-6000 Frankfurt am Main 50 (Germany)
[+] Current address: Pflanzenschutz, Hoechst AG, D-6230 Frankfurt am Main 80 (Germany)

[**] 11th Essay on Light Induced Reactions and 4th Essay on Chemical Synthesis. – 10th Essay: [1]; 3rd Essay: [2].

[***] Cf. *The Glass.Bead Game*, H. Hesse.

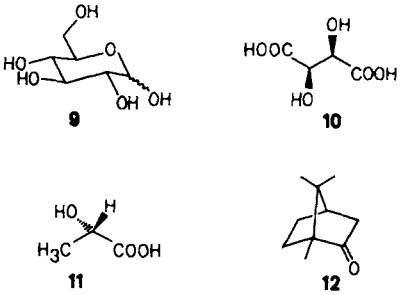
 © *Verlag Chemie GmbH, 6940 Weinheim, 1983* *0570-0833/83/0909-0637 $ 02.50/0* 

co[9], which contains diosgenin **3**, was used for some time as the raw material for the partial synthesis of steroids with the C-17 side chain shortened or even absent, as in the naturally occurring hormone estrone **8a** or the synthetically produced progestin fraction of the oral contraceptive norethindrone **7**. In the meantime, sitosterol **4** or stigmasterol **2** have supplanted **3**. This substitution was provoked by politico-economic circumstances[11] and made possible by recent technological progress[12].



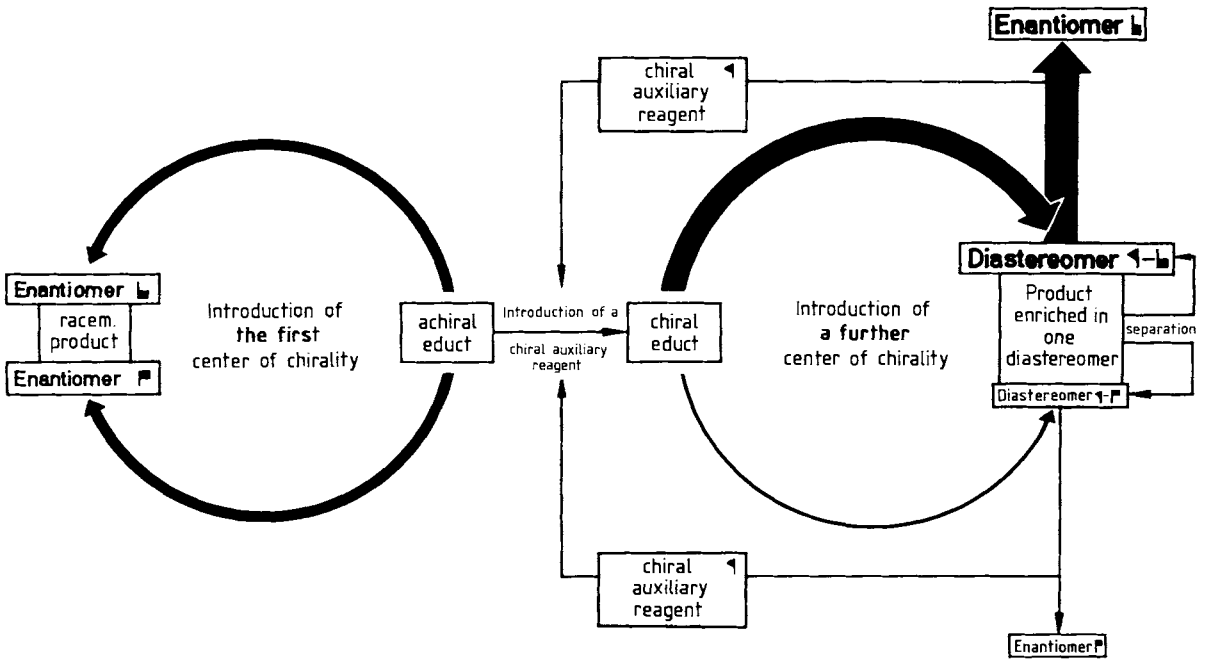

Scheme 2. Partial synthesis of pharmacologically interesting 19-norsteroids such as norethindrone **7** or estrone **8a** from diosgenin **3** or sitosterinol = (3β)-5-stigmasten-3-ol **4**.

The trend is moving towards the use as starting materials of those natural products that, as far as possible, are available from cultivated plants or microorganisms; examples are (+)-glucose **9**[14], (+)-tartaric acid **10**[16], (+)-lactic acid **11**[18], and (+)-camphor **12**[20]. Their structural relationship with the target compounds is generally obvious only at a second glance. It is not enough that they are available cheaply; in addition they must fit into a synthetic scheme which preserves the introduced optical activity and guarantees the desired sense of chirality. Yet only rarely do natural products directly correspond to the starting materials. Generally, structural modifications are necessary; here the result of stereoselection, which occurred in the course of biosynthesis without the chemist's cooperation and culminated in the actual absolute configuration produced, must not be spoiled.




Scheme 3. (+)-Glucose **9**, (2*R*,3*R*)-(+)-tartaric acid **10**, (*S*)-(+)-lactic acid **11**, or (1*R*)-(+)-camphor **12**; important optically active natural products that are possible chiral starting materials, either directly or after structural modification.

From the early days, the conventional method for chemists to obtain enantiomerically pure target compounds has been the resolution of racemates[22]. To separate enantiomers at the end of a multistep synthesis is almost fatal; indeed more than 50% of a laboriously constructed synthetic product is thus lost. Resolution of a racemate at the start of a synthesis is much more acceptable, certainly in those cases when the other enantiomer can either be used in the




Scheme 4. Mode of action of a chiral auxiliary reagent, which converts an achiral into a chiral educt; instead of a racemic product, a diastereomerically enriched product is obtained. This can be converted into pure enantiomers by separation of the diastereomers and recovery of the chiral auxiliary reagent. The flag symbols (see [17]) are two-dimensionally chiral figures.

synthesis or converted into the synthetically useful isomer[26]. In the past, many chemists have regarded their synthesis as accomplished when a racemic mixture was obtained, only half of which consists of the target compound. This may well have contributed to the fact that it has too often been ignored that the enantiomers of active agents can differ in their biological activity.

The forward-looking approach to enantiomerically pure compounds makes use of kinetic stereoselection and includes a so-called asymmetric step in the synthesis. Such a plan is based on the insight that each reaction step in which a center of chirality is formed produces two stereoisomers (Scheme 4). On introduction of the first center of chirality two reaction paths having the same width lead from the achiral educt to two enantiomeric product components, whereas on introduction of every further center of chirality two reaction paths having different widths connect the now chiral educt to two diastereomeric product components. Therefore, formation of the first center of chirality must be avoided under all circumstances. The *imperative of asymmetric synthesis* expresses this requirement in its classical form (see Scheme 5).

Imperative of asymmetric synthesis

Whenever stereo-isomers arise, avoid enantiomers!

Scheme 5. "Imperative of asymmetric synthesis" which, in its classical form, goes back to *Emil Fischer* [27].

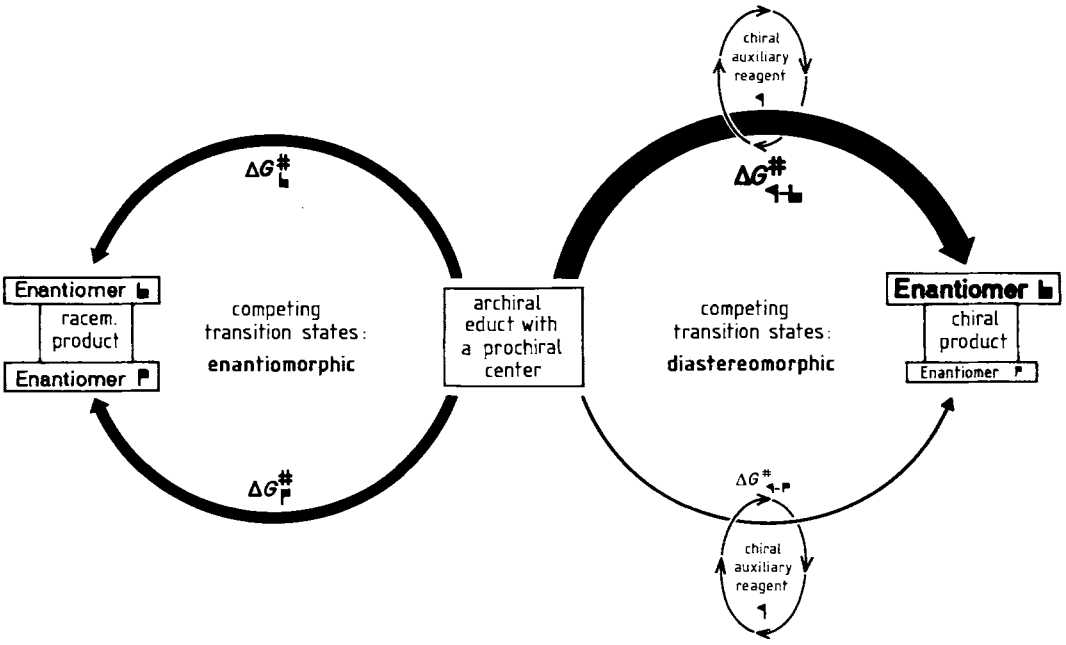
The problem thus imposed is, therefore, to ensure that a chiral auxiliary reagent is incorporated into the achiral educt (see Scheme 4). Any center of chirality formed in a subsequent reaction cannot be the first one, of course, and the resulting two diastereomers, which usually are produced in different amounts, can generally readily be separated. After recovery of the chiral auxiliary reagent (which can be used again for stereoselection), the product enantiomers are available in a pure state. "In this way optical activity is propagated from molecule to molecule as life is passed on from cell to cell". In 1894, Emil Fischer used these words[27] to comment on the principle of asymmetric synthesis which he had formulated. Since then our understanding of the course of chemical reactions has grown, and stereoselection is understood as the preference for one of two transition states which compete with one another. In its updated version the *imperative of asymmetric synthesis* (see Scheme 6) demands:

Imperative of asymmetric synthesis

Select enantiomers via diastereomorphic transition states!

Scheme 6. "Imperative of asymmetric synthesis" in its updated form.

If the chiral auxiliary reagent is only transiently incorporated into the competing transition states and, furthermore, is perhaps only needed in catalytic quantities, then the ideal version of asymmetric synthesis has been achieved:




Scheme 7. Possible mode of action of a chiral auxiliary reagent (if catalytically effective) which transforms competing enantiomorphic into diastereomorphic transition states. Instead of a racemic product, an enantiomer-enriched product results. The flag symbols (see [17]) are two-dimensionally chiral figures.

An achiral educt with a prochiral center gives rise, *via* two competing diastereomorphic transition states, to a chiral product in which one of the two enantiomers predominates. The degree of selectivity is determined by the difference in the free energies of activation $\Delta G^{\ddagger}_{\blacksquare} - \Delta G^{\ddagger}_{\blacksquare}$ (see Scheme 7). To achieve, for example, an enantiomeric excess of 92% (*i.e.* a ratio of ■ to ■ of 96 : 4) this difference need only to amount to 1.5 kcal/mol.

### 1.2. The Classification of Natural Product Total Syntheses

Today, selectivity is the watchword of the synthetic chemist. Indeed the progress of synthetic chemistry can be judged by the precision with which a single, quite definite, chemical species can be synthesized among the many possible isomers, in particular the many possible stereoisomers. If the accumulated fund of natural product total syntheses of the last 50 years is considered, it follows that the criterion of *stereoselection* enables a sensible classification of natural product synthesis.

*Category I*

Little or no stereoselectivity on the introduction of centers of chirality

Time-consuming separations, including racemate resolution

Scheme 8. Typical pre-1950 natural product syntheses: low selectivity of the absolute configuration of the target compound.

To *Category I* (Scheme 8) belong those syntheses which are characterized by little or no stereoselectivity in the introduction of the required centers of chirality. They are associated with time-consuming separations, including racemate resolution, and on this account are of little practical use. The natural product syntheses known in the first half of this century are practically without exception to be included in this category.

*Category II*

High stereoselectivity on introduction of every center of chirality, except the first

Racemate resolution at any rate

Scheme 9. Natural product total syntheses in the third quarter of this century: high selectivity for the relative configuration of the synthetic target compound.

Then syntheses appeared on the scene which were distinguished by high stereoselectivity on introduction of each center of chirality, with the exception of the first one. In many cases the cost of separation could be so far reduced that practical application began to be considered. The representatives of *Category II* (see Scheme 9) are handicapped by the fact that the envisaged target compounds can only be obtained with the correct relative configuration and, hence, an enantiomer separation still has to conclude the synthesis.

*Category III*

High stereoselectivity on introduction of center of chirality, including the first

Limited effort on separation-no racemate resolution

Scheme 10. Natural product total syntheses as they ought to be today with high selectivity for the absolute configuration of the synthetic target compound.

*Category III* (Scheme 10) comprises total syntheses that before 1970 at best existed only on paper: syntheses of enantiomerically pure target compounds without a subsequent racemate resolution. To this class belong all total syntheses that begin with an optically active starting material or in which an optically active intermediate occurs as early as possible in the synthesis. Those syntheses in which the chiral building blocks arise from asymmetry inducing reactions are worthy of special note.

### 1.3. The Unambiguous Use of Configurational Formulas in Characterizing Enantiomers and Enantiomeric Mixtures

Reaction steps in which asymmetry is introduced lead either directly (see Scheme 7) or, *via* initially resulting diastereomers (Scheme 4), to mixtures in which two enantiomers can appear in any arbitrary ratio. In order to work out the factors of stereoselection in different cases, a simple and unambiguous notation is needed. The indiscriminate use of one and the same configurational formula for different configurational problems makes it more difficult for chemists to understand one another and turns out to be a considerable barrier in discussing stereochemical problems with non-chemists. Thus accounts of syntheses can be found in which a particular configurational formula not only characterizes the absolute configuration depicted by the formula, but also that of its enantiomer and/or mixtures of both enantiomers. Therefore in the following we shall take the literal meaning of a configurational formula,

even with respect to the absolute configuration, and use the Arabic numeral representing the chemical formula in the text only for that enantiomer expressed by the configurational formula.



**12** **13**

**13** ≡ *ent*-**12**

**12**/*ent*-**12** = 1:1 ≡ *rac*-**12**

Scheme 11. Systematic use of configurational formulas. **12** describes only the dextrorotatory enantiomer of camphor. If the other camphor enantiomer is being dealt with, the mirror image formula **13** is not shown and *ent*-**12** is written instead of **13**. Mixtures of both enantiomers are easily and unambiguously described. In the case of the racemate, the expression *rac*-**12** is used.

If instead of a chiral compound, whose configurational formula has been depicted, its enantiomer is being discussed, we shall omit the formula of the latter (see Scheme 11). To indicate that enantiomer, the Arabic numeral, a synonym of the depicted configurational formula, is prefixed by *ent*. Mixtures in which one enantiomer prevails are specified by the unprefixed Arabic numeral and by the same numeral prefixed by *ent*. Thus it is easy to distinguish those cases in which the ratio of the enantiomers is not known (but $\neq 1$), those for which it is simply known what enantiomer predominates ($>1$ or $<1$), and those in which the numerical ratio could be determined precisely [(100 − n) : n]. For the frequently encountered special case in which the enantiomers are present in exactly the same proportion, the prefix *rac* is placed before the Arabic numeral synonymous with the configurational formula that represents one of the enantiomers. This emphasizes the special position that racemic mixtures occupy among mixtures of enantiomers.

If in a flow chart describing a natural product synthesis, not only the enantiomer whose absolute configuration is correctly depicted appears but also the corresponding racemic mixture, the latter is not characterized by a chemical formula. Instead, an Arabic number prefixed by *rac* is used which has previously been assigned to a chemical formula outside the flow chart (see, *e.g.*, Scheme 28). Before the foregoing proposal for notation is dismissed by the perplexed reader, it should be recalled that less than 25 years ago *Fieser*[28], in publications in *J. Am. Chem. Soc.*, suggested the use of boldface Arabic, in place of the previously usual Roman numerals as convenient "representatives" of chemical compounds. What far-sighted editors allowed experimentally in those days could not be dispensed with today by authors and readers of chemical publications.

From the development of stereochemical nomenclature it can be clearly seen how chemists have delved ever deeper into more and more complex stereochemical problems. At the beginning of organic chemistry it was *steric factors* that determined the ground state. Then followed a phase in which *stereoelectronic factors* that influenced transition states were postulated. Today *factors of stereoselection*, either of steric, electronic, or stereoelectronic origin, loom large in considerations of chemical synthesis of natural products.

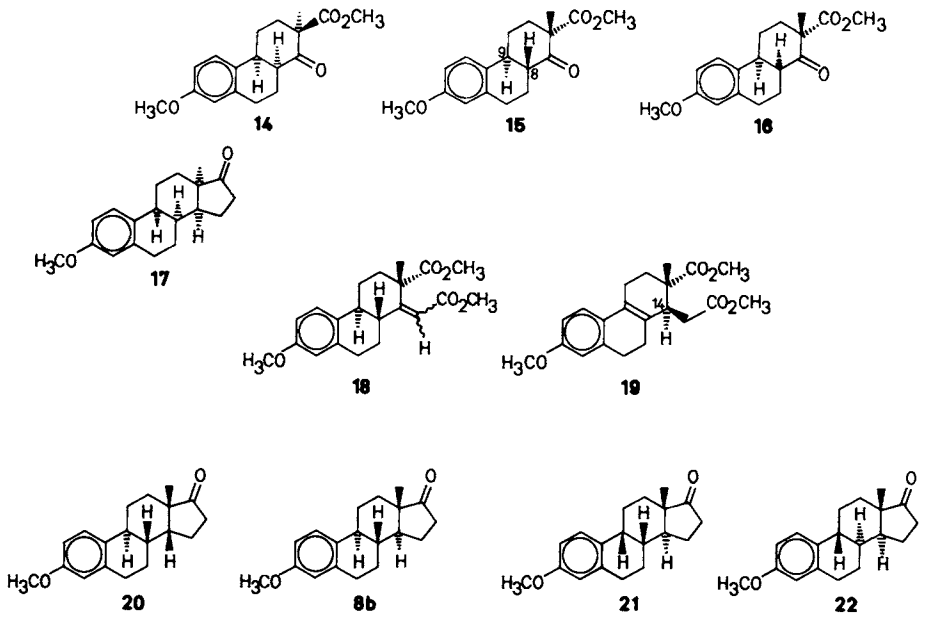
## 2. The Development of Natural Product Synthesis Exemplified by Estrone

The development of chemical syntheses of natural products is best clarified using selected target compounds. Here we shall avail ourselves of the synthesis of estrone as example: the synthesis of estrone, in general, and the *photochemical* synthesis of estrone (see Section 3), in particular. Numerous variations on the theme of "estrone synthesis" have been devised and realized in university and industrial laboratories over the last forty years. A systematic grouping of such syntheses does not correspond to the historical development. Much more useful is the classification of natural product total syntheses in terms of the *criterion of stereoselection* referred to in Section 1.2.

### 2.1. Category I Estrone Syntheses

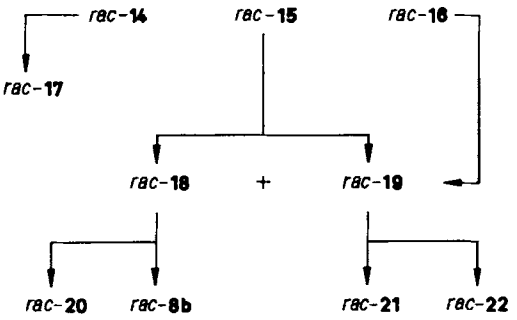
The first total synthesis of estrone was published in 1948 by *Anner* and *Miescher*[30]. It follows the A→AB→ABC →ABCD construction principle. Here, *rac*-**15** (see Scheme 12) plays a key role. This racemate is one of four possible racemates, three of which were in fact isolated (*rac*-**14**, *rac*-**15**, and *rac*-**16**). It was obtained through a series of reactions based on preliminary work by *Robinson et al.*[31] and *Bachmann et al.*[32]. In the mixture of stereoisomeric racemates *rac*-**15** is the main component and is easily separated from the others by fractional crystallization. The subsequent route to estrone makes quite clear the problems of selection that appear in category I syntheses. As if it were not enough that the selectivity upon introduction of the fourth asymmetric center was very low, even the stereochemical information already present was partly lost under the reaction conditions used.

From the outset, the configuration at C-8, labile under basic conditions, cannot be maintained. After Reformatzky reaction and subsequent elimination of water, a mixture of both unsaturated esters *rac*-**18** and *rac*-**19** was isolated. The formation of *rac*-**19** indicates a complex reaction path involving epimerization of C-8 and also places the stereostructural information at C-9 in question. Thus a large part of the selection achieved in *rac*-**15** is destroyed. The primary elimination product with an endocyclic double bond is isomerized to the thermodynamically more stable styrene derivative *rac*-**19**. Hydrogenation of *rac*-**18** leads, as expected, to two esters, epimeric at C-14, which could be separated by fractional crystallization. Under the same conditions *rac*-**19** also affords two saturated esters, the formation of only one of which can be explained by a further double bond shift. The relative configuration was finally established by hydrogenation of the unsaturated esters *rac*-**18** and *rac*-**19**. Arndt-Eistert homologation of the acetic acid side chains of the four products of hydrogenation, followed by cyclization of the resultant dicarboxylic acids in the presence of $Pb(CO_3)_2$, and subsequent decarboxylation of the cyclization product finally gave four racemates having the constitution of the methyl ether of estrone: *rac*-**8b**,



Scheme 12. Total synthesis of estrone after *Anner* and *Miescher* [30] (see Scheme 13).

*rac*-**20**, *rac*-**21**, and *rac*-**22**. Resolution of the corresponding menthyloxyacetates of *rac*-**8b** gave a pure enantiomer, whose melting point and optical rotation were identical to those of natural **8a**. The absolute configuration of the synthetic product was, thus, substantiated. The relative configurations of the three remaining racemates having the estrone constitution were not definitely determined until 1958 by *Johnson* et al.[33], after all eight possible racemates had been synthesized.

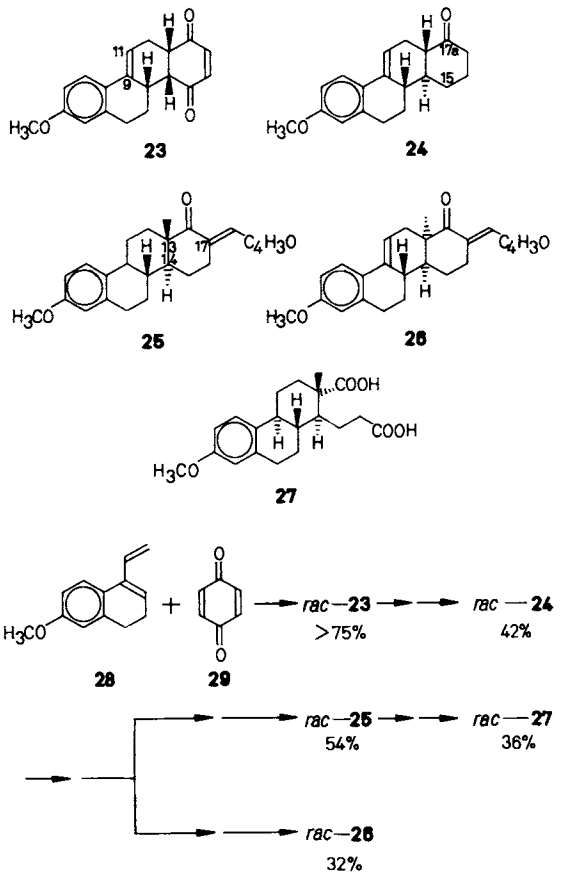



Scheme 13. Flow chart for the total synthesis of estrone after *Anner* and *Miescher* [30] (see Scheme 12).

## 2.2. Category II Estrone Syntheses

The estrone synthesis of *Johnson et al.*[34] belongs to category II (see Scheme 9). It follows the AB + D → ABCD construction principle and in order to achieve the necessary *trans*-fusion of the rings C and D leads first to a D-homoestrone derivative. An intermolecular Diels-Alder reaction serves as the key step (see Scheme 14).

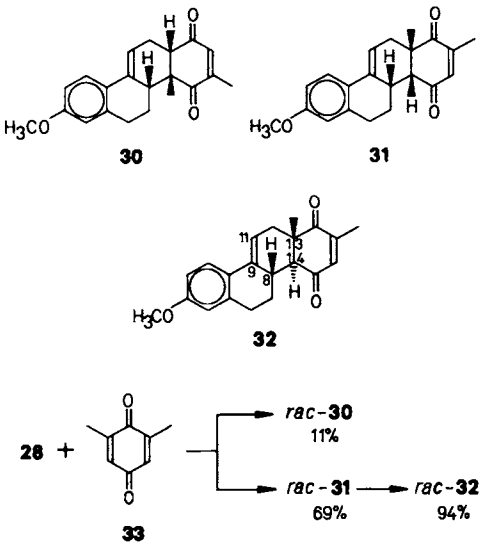
The achiral AB unit **28** reacts with *p*-benzoquinone **29** to give the tetracyclic adduct *rac*-**23**. Of the three possible racemates only the one with the relative *syn*/*cis* configuration was formed. Since **29** was chosen as a constitutionally symmetric dienophile, no regioisomers occurred. After hydrogenation of the ring D double bond of *rac*-**23** and selective reduction of the 17a-keto group to the alcohol, the desired *anti* arrangement of the hydrogen atoms on C-8 and C-14 occurs under the basic reaction conditions necessary for deoxygenation of the 15-keto group, and *rac*-**24** was obtained by subsequent oxidation of the 17a-OH group.




Scheme 14. Synthesis of *rac*-estrone, *rac*-**8a** after *Johnson*, *Walker* et al. [34].

The selective introduction of the angular methyl group at C-13 proved somewhat puzzling; studies by *Johnson* and *Allen* on model compounds[35] had shown that if a C-9,C-11 double bond is present, predominantly *trans* alkylation is to be expected. To avoid formation of regioisomeric methyl ketones, the 17-position in ring D of *rac*-**24** was blocked by condensation with furfural. In fact, on methylation of the resulting furfurylidene ketone with potassium *tert*-butoxide/methyl iodide the 13β-methyl compound was predominantly obtained. However, the β/α selectivity of 3 : 2 is still relatively small. Reduction of the 9,11-double bond of *rac*-**26** with sodium in liquid ammonia led in high stereoselectivity to the thermodynamically more stable *trans* arrangement of rings B and C. The usual reaction sequence to contract ring D completed the synthesis of *rac*-**8a**.

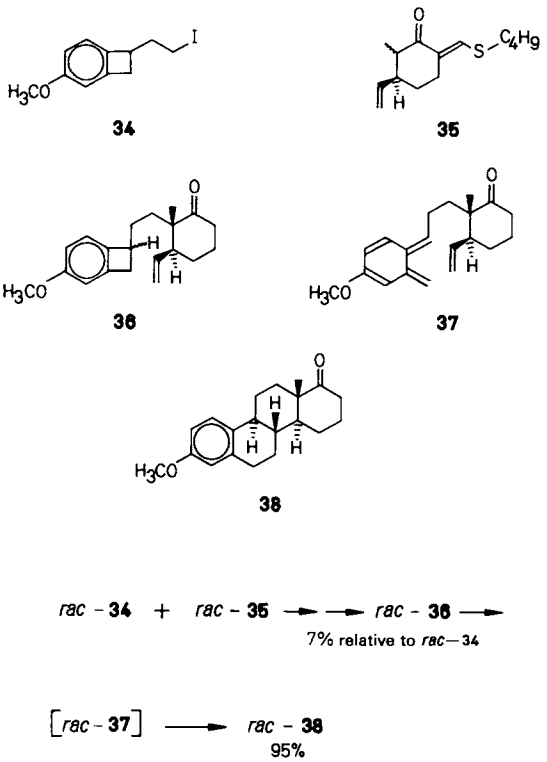
The improvement in the selective construction of the C-8, C-9, and C-14 centers of chirality is striking compared to category I syntheses. The introduction of the angular methyl group still leaves something to be desired. This shortcoming has been remedied in a variant by *Valenta et al.*[36] (see Scheme 15): they managed to exploit the synthetic potential of the Diels-Alder reaction even better than *Johnson et al.* As dienophile they used **33**, which already bears the methyl group later to be incorporated at C-13. On the assumption that the cycloaddition follows the *endo*-rule, the relative *syn/cis* configuration would arise at the future C-8, C-14, and C-13 centers but would later be modified to the relative *anti/trans* configuration. In the past, the realization of such a plan had failed: the Diels-Alder reaction of **28** with **33** had indeed led to the "wrong" constitutional isomer, *rac*-**30**. *Valenta et al.*[36] were now able to show that this cycloaddition proceeds regioselectively in the presence of Lewis acids. With 1.3 equivalents of $BF_3$-ether at −15 °C, the desired regioisomer predominates (*rac*-**31** : *rac*-**30** = 6 : 1). Base-catalyzed epimerization at C-14 and catalytic hydrogenation of the 9(11)-double bond of *rac*-**32** (palladium/calcium carbonate) established the relative configuration of the remaining asymmetric centers in the desired sense. A new procedure for ring contraction led finally to *rac*-**8a**. This total synthesis satisfies to a large measure the demands for selection of category II. It is unsatisfactory only in that to establish the *trans*-fusion of rings C and D the multistep detour via the D-homosteroid skeleton has to be undertaken.




Scheme 15. Synthesis of *rac*-estrone (*rac*-**8a**) after *Valenta et al.* [36].

Yet the synthetic potential of the Diels-Alder reaction is still not exhausted; the intramolecular variant allows the construction of the carbon skeleton in a straightforward manner with optimal control of the stereochemistry. Constitutional isomers do not occur on completion of the steroid skeleton because the short linkage between diene and dienophile moieties precludes incorrect orientations, only formally possible.

Since then, numerous syntheses of 19-norsteroids have been published which follow the particularly clear-cut A + D → AD → ABCD construction principle using kinetically unstable *o*-quinodimethanes[37]. They are impressive, above all, for the ease with which the relative *trans/anti/trans*-configuration at the C-9, C-8, C-14, and C-13 centers can be achieved.

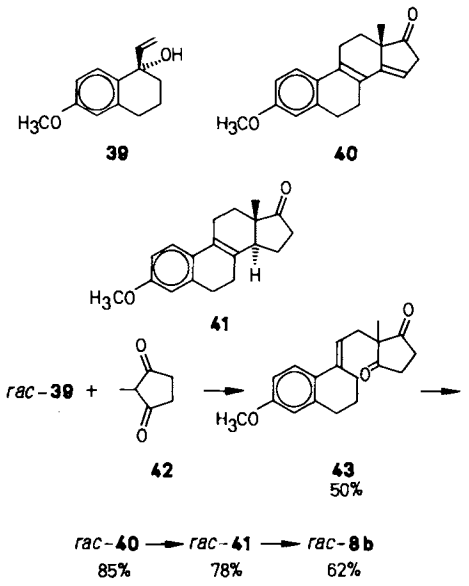



Scheme 16. Synthesis of *rac*-D-homoestrone methyl ether (*rac*-**38**) after *Kametani et al.* [38].

For *Kametani et al.*[38], *rac*-**36** functioned as a latent *o*-quinodimethanoid derivative. It was accessible by alkylating the enolate of *rac*-**35** with *rac*-**34**. To achieve the regioselective coupling of the ring A and ring D units, a protecting group was temporarily introduced, which otherwise has no further function. One must commiserate with the Japanese authors that they did not succeed in the corresponding conversion with the five-membered homologue of *rac*-**35** (later a ring A unit was alkylated, as an achiral α-nitrile anion, with a five-membered, chiral ring D unit (see Section 2.3)). The heat-induced isomerization of *rac*-**36** *via* *rac*-**37** to *rac*-**38** occurred in high chemical yield. Since *rac*-**38** had already been converted into *rac*-**8a**, the sequence of

reactions sketched out in Scheme 16 constitutes a formal total synthesis of *rac*-**8a**.

The total syntheses developed in the laboratories of *Johnson, Valenta,* and *Kametani* have enormous didactic value. They teach that it pays to develop systematically the key reaction of a synthetic scheme—here the Diels-Alder reaction. *Kametani*'s synthesis, moreover, illustrates an all too common case: the efficiency of the key reaction is impressively demonstrated, yet the other conversions are not optimized with the same care. A total synthesis that in terms of composition and execution can serve as a model must satisfy the requirement that it be fully developed.



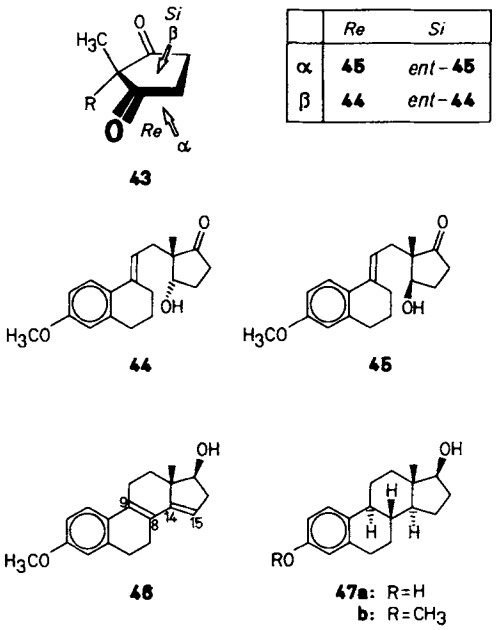

Scheme 17. Synthesis of *rac*-estrone (*rac*-**8a**) after *Torgov, Ananchenko et al.* [39].

The synthetic target compound can be attained without detours using the concept outlined by *Torgov et al.*[39] in 1963. This follows the AB+D→ABD→ABCD construction pattern (see Scheme 17); the AB unit, *rac*-**39**, obtained by treating 6-methoxytetralone with vinylmagnesium halide, reacts under acid catalysis with 2-methyl-1,3-cyclopentanedione **42** to give the achiral diketone **43**. *Kuo, Taub,* and *Wendler*[40] found that the acidity of **42** alone is sufficient to bring about the condensation. **43** cyclizes in the presence of *p*-toluenesulfonic acid to give *rac*-**40**. The tetracyclic reaction product already contains the complete steroid skeleton but only one of the necessary asymmetric C atoms. The three remaining centers of asymmetry are easily introduced along with the *trans*-fusion of rings C and D (*rac*-**41**) or the *trans/anti/trans* configuration of the BCD ring system (*rac*-**8b**) by catalytic hydrogenation of *rac*-**40** from the less hindered side using palladium/calcium carbonate, or by reducing *rac*-**41** with potassium and aniline in liquid ammonia *via* the thermodynamically more stable radical anion transients.

The synthetic concept proposed by *Torgov et al.* has, even today, lost none of its startling simplicity. It would play a significant role among the estrone syntheses of category III if **40** instead of *rac*-**40** were produced.

### 2.3. Category III Estrone Syntheses

The first total synthesis of enantiomerically pure estrone without racemate resolution draws, as expected, on *Torgov*'s concept (see Scheme 17). It sets out from the diketone **43**, achiral but equipped with a prochiral center, which is the source compound for the four stereoisomeric hydroxyketones **44**, *ent*-**44**, **45**, and *ent*-**45** (see Scheme 18). If an achiral hydrogenating agent attacks one of the two enantiotopic carbonyl groups from both diastereotopic sides of the molecule [see **43**], then, albeit with different probabilities of formation, *rac*-**44** and *rac*-**45** will result simultaneously. In fact, the bulky lithium *tert*-butoxyaluminum hydride attacked selectively from the less hindered β-side, on which the methyl group lies, to afford the partially hydrogenated product *rac*-**44** in 85–90% yield[40].

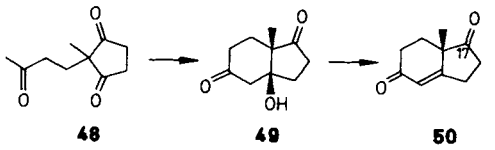



Scheme 18. Microbiological reduction of the diketone **43** (R=2-(6-methoxy-1,2,3,4-tetrahydronaphthylidene)ethyl]) and the conversion into (+)-17β-estradiol **47a** [41].

To avoid a racemate, a chiral hydrogenating agent had to be employed which, furthermore, selectively reacted with only one of the two carbonyl groups. Hydrogenating enzymes or microorganisms that contain such reductases were considered. Since the conformation of the enzyme-bound substrate not only can differ from case to case, but, moreover, is known in no single example, model studies were required. It turned out that of 160 microorganisms—bacteria, yeasts or fungi—that were tested in preliminary investigations[41], most were capable of partially hydrogenating **43**, and 37 of these came in for closer consideration; one group produced principally **44**, another group afforded mainly *ent*-**45**, and, finally, a third group resulted in a mixture of both diastereomers. With *Saccharomyces uvarum (CBS 1508) ent*-**45** could be obtained on a technical scale in 74% yield[41]; its subsequent cyclization (with HCl in methanol) led to **46** (see Scheme 18). Catalytic hydrogenation ($Pd/CaCO_3$) of the C-14,C-15 double bond of the resulting cyclisation product, followed by chemical reduc-

tion (K and aniline in liquid $NH_3$) of the generated dihydro product afforded 3-methoxy-1,3,5(10)-estratrien-17-ol **47b** in 37% overall yield (based on *ent*-**45**)[42,43].

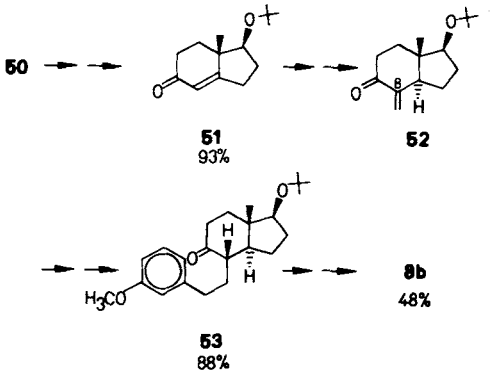
The remarkable total synthesis of 19-norsteroids with a microbiological key step was to be outdone shortly after its realization through the exclusive application of cheaper reagents of known structure. Two industrial laboratories that had mounted a joint research program independently discovered a simple route to the optically active synthetic building block **50** (see Scheme 19)[44]: they observed that the triketone **48**, achiral but fitted out with a prochiral center, cyclized to the aldol in the presence of (*S*)-(−)-proline (3 mol%) with a high preference for **49** over *ent*-**49**. On subsequent dehydration **50** was obtained in over 90% chemical and optical yields.




Scheme 19. Preparation of the optically active CD building block **50** by asymmetric cyclization of the triketone **49**, catalyzed by (−)-(*S*)-proline [44].

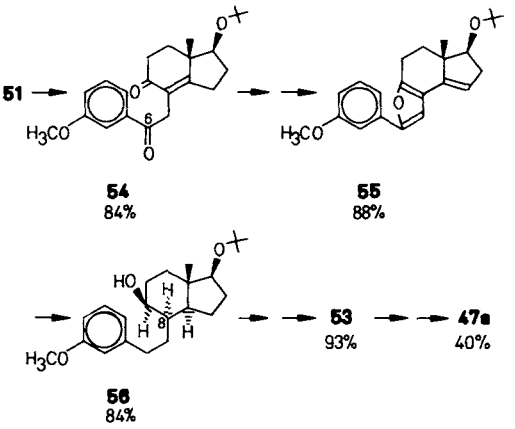
In spite of profound mechanistic considerations and adroit manipulation of the experimental parameters the parties involved[44–46] have not yet succeeded in deciphering the structure of the competing diastereomorphic transition states (cf. Scheme 7). The remarkable finding[45] that in the presence of (*S*)-(−)-proline **48** cyclizes preferentially to **49**, whereas in the presence of (*S*)-(+)-homoproline (side-chain lengthened by one $CH_2$ group) it cyclizes preferentially to *ent*-**49**, has since become the touchstone for every attempt to interpret the asymmetry-inducing aldol addition.

The total syntheses of 19-norsteroids starting from **50** follow the A+CD→ACD→ABCD construction pattern. The estrone synthesis developed by Hoffmann-La Roche (Basel and Nutley, NJ, USA)[47] (see Scheme 20) proceeds *via* the α-methylene ketone **52**. First the 17-keto group of **50** was reduced and the resultant alcohol converted into the *tert*-butyl ether. Methylmagnesium carbonate was used




Scheme 20. Synthesis of (+)-estrone methyl ether **8b** developed by chemists from Hoffmann-La Roche [47]. No yields were given for the conversion **51**→**52**.

to introduce a carboxyl group at C-8. On hydrogenation of the β-keto acid, which has been opened out by hydrogen bonding, stereoselective attack of the catalyst from the sterically less hindered α-side is observed; at any rate, in the dihydro product the rings are fused *trans* to one another. **52** was finally reached by a decarboxylating Mannich condensation. From here, **53** is obtained by 1,4-addition of *m*-methoxybenzylmagnesium chloride and stereochemical correction of the primary reaction product. Ring B was closed by cyclodehydration. The resultant mixture of olefins contains as its main component the 9,11-unsaturated steroid. The latter can be catalytically hydrogenated with the customary high stereoselectivity. Cleavage of the *tert*-butyl ether and oxidation of the now unprotected hydroxy group finally afforded **8b**.

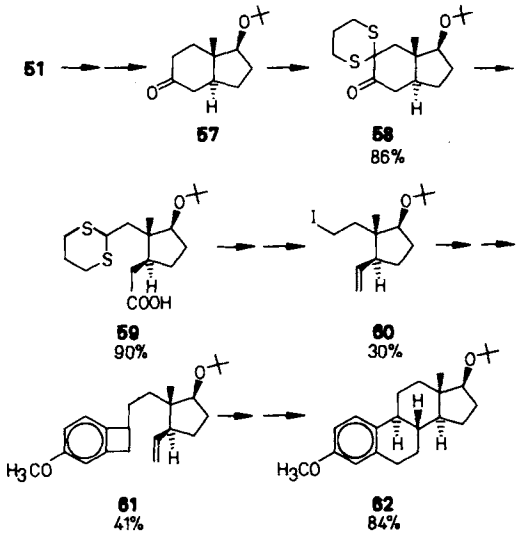



Scheme 21. Synthesis of (+)-17β-estradiol **47a** by chemists from Schering AG [48].

The route worked out by *Wiechert et al.* (Schering AG Berlin)[48] to 17β-estradiol **47a** (see Scheme 21) avoids the detour from **51** to **52**. Instead **51** was directly alkylated to **54** with *m*-methoxyphenacyl bromide. Treatment of the dimethyl ketal obtained by selective conversion of the C-6 keto group with *p*-toluenesulfonic acid furnished the furan derivative **55**. Catalytic hydrogenation of **55** generated **56** with *trans*-fused rings C and D; Jones oxidation and subsequent correction of configuration at C-8 led to the previously known compound **53** (see Scheme 20) and thus to **47a** or, if desired, to **8a**.

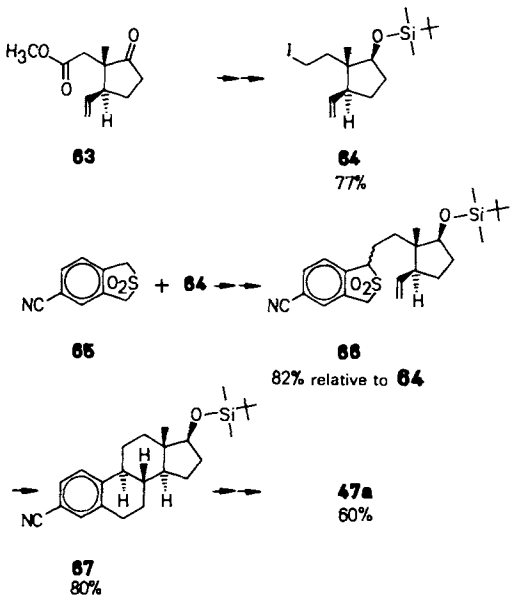
With the syntheses of enantiomerically pure 19-norsteroids (see Schemes 20 and 21) the chemists of the Roche and Schering groups changed the synthetic panorama in more than one respect: they overcame a psychological barrier that, more or less consciously, had stood in the way of the cultivation of asymmetric synthesis. With **50** they, moreover, enriched the pool of versatile chiral synthetic building blocks[49].

As shown in Scheme 22, *Kametani et al.*[51] have applied the synthetic unit **51**, easily generated from **50**, to the construction of **61**. The benzocyclobutene derivative **61** is better suited than *rac*-**36** (see Scheme 16) to function as a latent *o*-quinodimethane derivative: firstly because it occurs as the enantiomer with the necessary absolute configuration and secondly because it already contains the five-membered ring D.



Scheme 22. The synthesis of (+)-17β-estradiol **47a** from the optically active CD building block **51** (see Scheme 20) after *Kametani et al.* [51]. No yields were given for the conversion **51**→**57**.

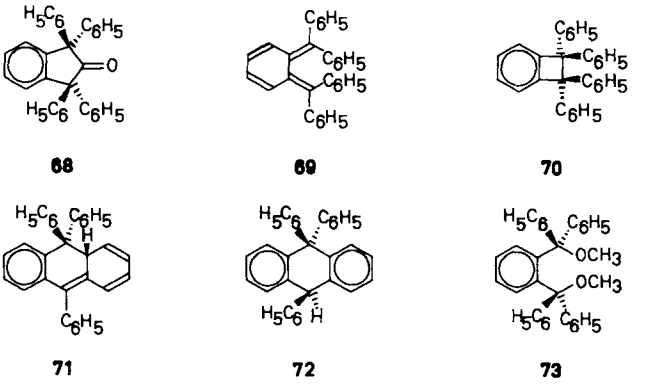
Of course, the route from **51** to **60** is much too long for practical purposes. It is somewhat better to rely on the route (see Scheme 23) developed by *Oppolzer et al.*[52], even though a racemate resolution must be accomplished, fortunately quite early in the synthesis.

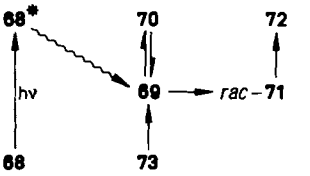


Scheme 23. Synthesis of (+)-17β-estradiol **47a** after *Oppolzer et al.* [52].

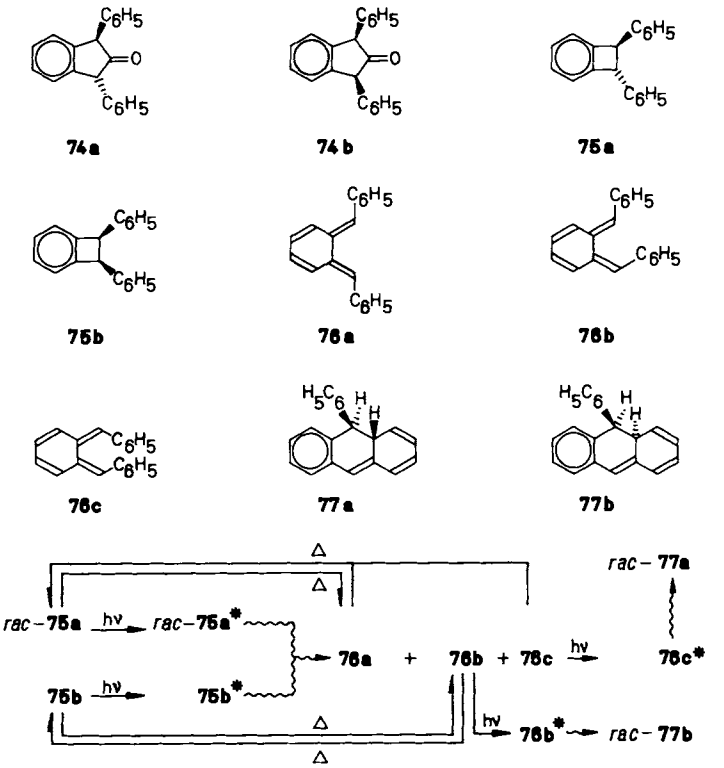
## 3. The Photochemical Synthesis of Estrone

Work in our laboratory has the aim of developing photochemical reactions to the point where they can be considered as key reactions in natural product total syntheses. Precisely why photochemical conversions should interest us is quickly explained: light is a clean "reagent", whose intensity and energy content can be finely controlled and which makes kinetically unstable transients with great synthetic potential from many conveniently accessible key compounds.





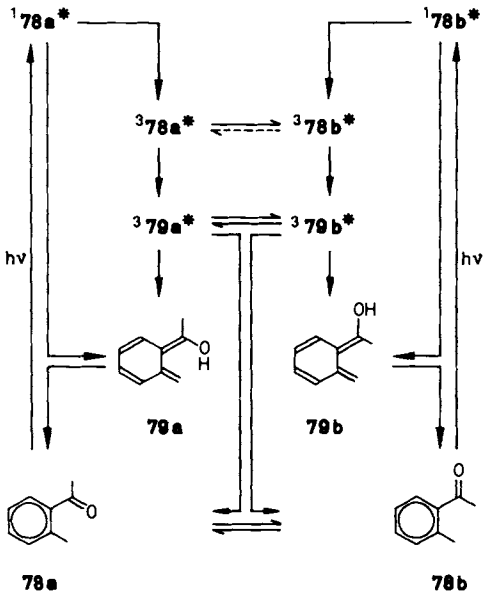
Scheme 24. Preparation of tetraphenyl-*o*-quinodimethane **69** by photodecarbonylation [53a] of **68** [53b]: characterized by electron absorption spectroscopy at low temperature [53c, d] or by kinetic spectrophotometry [53e] at room temperature. **69** cyclizes to the kinetically favored benzocyclobutene derivative **70** or to the thermodynamically favored isodihydroanthracene derivative *rac*-**71** [53d, e, 54].



Scheme 25. Preparation of **76a** and **76c** by photodecarbonylation [53a] of *rac*-**74a** or **74b** [56a—d]: characterized by electron absorption spectroscopy at low temperature [56e] or by kinetic spectrophotometry at room temperature [53e]. Intermolecular Diels-Alder reaction [56b] and cyclization of **76a** or **76c** or **76b** to give *rac*-**75a** or **75b** [56b, e], and of **76b** or **76c** to afford *rac*-**77b** or *rac*-**77a** [56e].

The decision to construct the carbon skeleton of 19-norsteroids by intramolecular Diels-Alder reaction of a suitably substituted vinyl group with a photochemically generated *o*-quinodimethane derivative *(vide infra)* was preceded by years of study of *o*-quinodimethane derivatives. Schemes 24 and 25 summarize the experience gained.

*o*-Quinodimethanes with a hydroxyl group in the chromophore system, often also described indiscriminately as photoenols, are accessible from *o*-alkyl substituted acetophenone derivatives by light induced isomerism. Scheme 26 shows the complex relationships that exist between the




Scheme 26. Thermally reversible [59] adiabatic photoenolization [57] of *o*-methyl-substituted acetophenone derivatives **78a** ⇌ **78b** after *Haag, Wirz,* and *Wagner* [60].

educt conformers **78a** or **78b** and the transient configurations **79a** or **79b**.

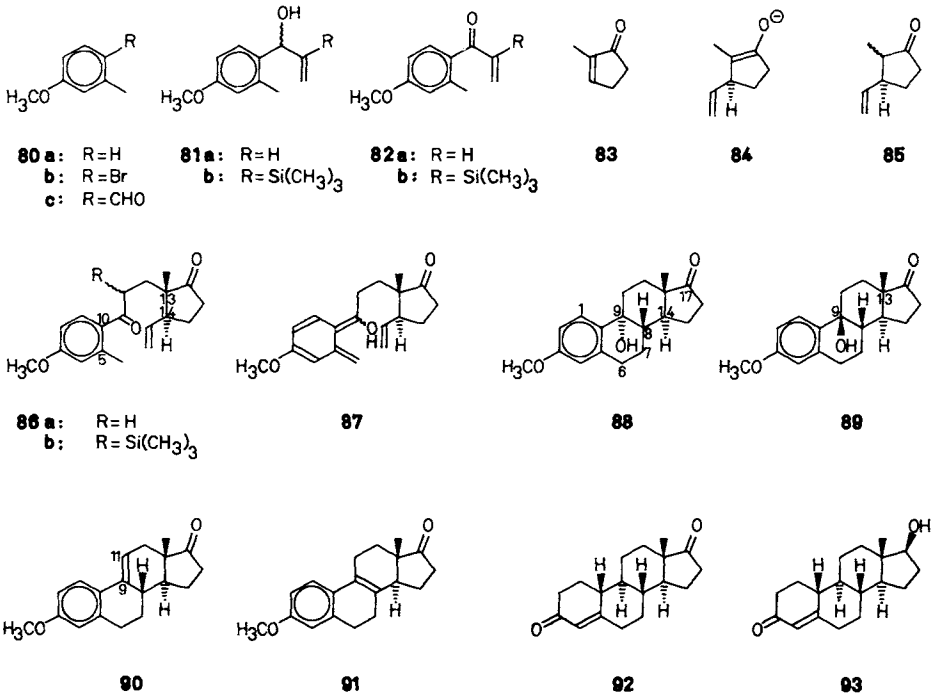
Since *o*-quinodimethanoid phototransients appear in both cases as mixtures of stereoisomers, pragmatic reasons selected photoenolization of **86a** (see Scheme 27) and not the light-induced ring opening *e.g.* of **61** (see Scheme 22): the acetophenone derivative is more readily accessible and, because of its absorption at longer wavelength, more conveniently photoactivated than the benzocyclobutene derivative.

### 3.1. Racemic Target Compounds[58]

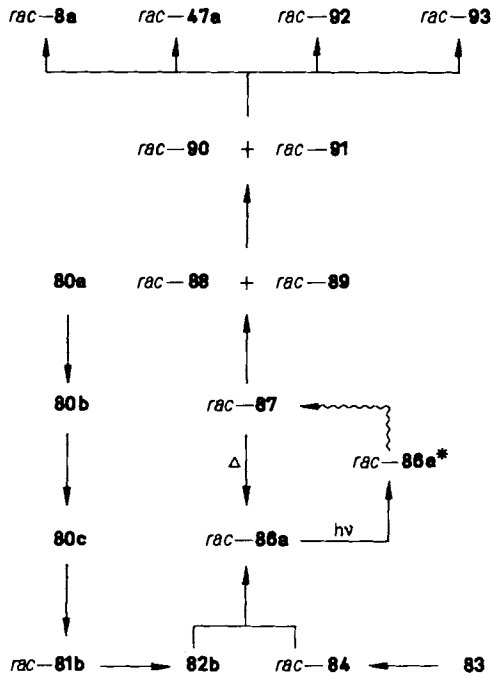
The synthesis of 19-norsteroids proceeding *via* an *o*-quinodimethanoid phototransient and which follows the A + D → AD → ABCD construction pattern (see Section 2.2) is convergent in its initial phase and typified by the separate production of both ring A and ring D units.

The ring A unit **82b** is formed in an overall 56% yield by a conventional reaction sequence which begins with *m*-cresol methyl ether **80a** (see Scheme 28); **80a** can be converted into **80b** with bromine in carbon tetrachloride below 0°C in the presence of iron filings. The Grignard reagent formed from **80b** affords the aldehyde **80c** on reaction with *N,N*-dimethylformamide in tetrahydrofuran at temperatures below −20°C. Reaction of the Grignard reagent from (1-bromovinyl)trimethylsilane with **80c** in tetrahydrofuran below room temperature gives *rac*-**81b**, which on subsequent chromic acid oxidation in the water/ether two phase system affords the achiral Michael acceptor **82b**.

The corresponding Michael donor, *rac*-**84**, which plays the part of the ring D unit, is formed directly by $Cu^{III}$-catalyzed, 1,4-addition of vinyllithium to **83**[63] and reacts *in situ* with **82b**. In the racemic series a problem of stereosel-




Scheme 27. Total synthesis of 19-norsteroids using a photochemical key reaction [50, 58].




Scheme 28. The total synthesis of racemic 19-norsteroids (cf. Scheme 27; a thermally reversible photoisomerization system [61] plays a key role [58].

ection is encountered for the first time with the Michael addition: the newly formed C-12,C-13 bond lies either on the same or on the opposite side of the vinyl group at C-14. The AD adduct *rac*-**86a**, of course, is the desired one, for which not only the indicated constitution but also the specified relative configuration are correct. This racemate would already contain a five-membered ring D and would have the methyl group at C-13 oriented *trans*, once and for all, to the H atom at C-14.

In fact, *rac*-**86a** was successfully isolated, free of isomers, in 70% yield[65]. The trimethylsilyl group, which is removed from the primary Michael adduct *rac*-**86b** on acid work-up, amplifies the effect of selection which occurs in any case. **82b** approaches **84** from the less hindered side to an even greater extent than **82a**, and possibly the Michael addition, reversible when **82a** is used, becomes irreversible if **82b** is the starting material (see Section 2 of [50]). The relative configuration of *rac*-**86a** was determined by NMR spectroscopy by comparison of the chemical shifts either of the protons of the angular methyl group or of C-13 and C-14 with the corresponding data for suitable reference compounds[66].

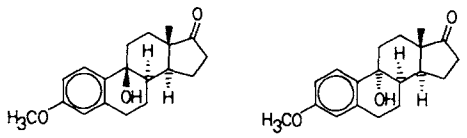
The disecosteroidal Michael adduct *rac*-**86a** already possesses all the carbon atoms of the future 19-norsteroids; as yet the bonds between C-6 and C-7 and between C-8 and C-9 are absent. To complete the carbon skeleton of the target compound, the AD adduct *rac*-**86a** was isomerized to an *o*-quinodimethanoid photo-transient, *rac*-**87**, and the latter to an ABCD cycloadduct. In our steroid synthesis (see Scheme 28) a key role is played by a thermally reversible photoisomerization system with a trappable intermediate[61] (here by intramolecular Diels-Alder reaction). The reketonization of the photoenol *rac*-**87** seems at first sight rather undesirable since it reduces the quantum yield of the photochemically initiated overall reaction. However, on optimization of the reaction conditions, which at the end sounded rather alchemical, it turned out to be very useful precisely for the case when the generated phototransient cannot be trapped by intramolecular Diels-Alder reaction, and the desired cycloadduct cannot, therefore, be isolated. When on UV irradiation of *rac*-**86a** in a mixture of $C_6D_6$ and $CD_3OD$ the $CH_3$-group at C-5 was converted to a $CD_3$ group, it was concluded that the acidic photoenol definitely must have been present as an intermediate.

In the elaborated version of the synthesis, the Michael adduct *rac*-**86a** is converted into a mixture of constitutionally isomeric styrene derivatives, *rac*-**90**/*rac*-**91**, in 65% overall yield. It turned out to be expedient not to isolate the kinetically unstable components of the ABCD cycloadduct with the constitution 9-hydroxy-3-methoxy-1,3,5(10)-estratrien-17-one, but rather to dehydrate it using oxalic acid in dry benzene.

The irradiation was eventually carried out

- in methylcyclohexane (optically transparent with boiling point 100.9 °C) at 95 °C
- with light of wavelength >340 nm (to avoid absorption by the nonconjugated keto group and resultant loss of stereochemical integrity at C-13)
- in the presence of 2,6-di- or 2,4,6-trimethylphenol (to protect the initially formed ABCD cycloadduct from light-induced decomposition) as well as
- in the presence of pyridine (which raises the barrier to reketonization and, hence, the lifetime of the (*Z*)-photoenol)

Photoenolization of the AD adduct was followed by thermal cyclization of the resulting phototransient of an ABCD cycloadduct. The latter was converted without purification into a mixture of 95% *rac*-**90** and 5% *rac*-**91**[69].

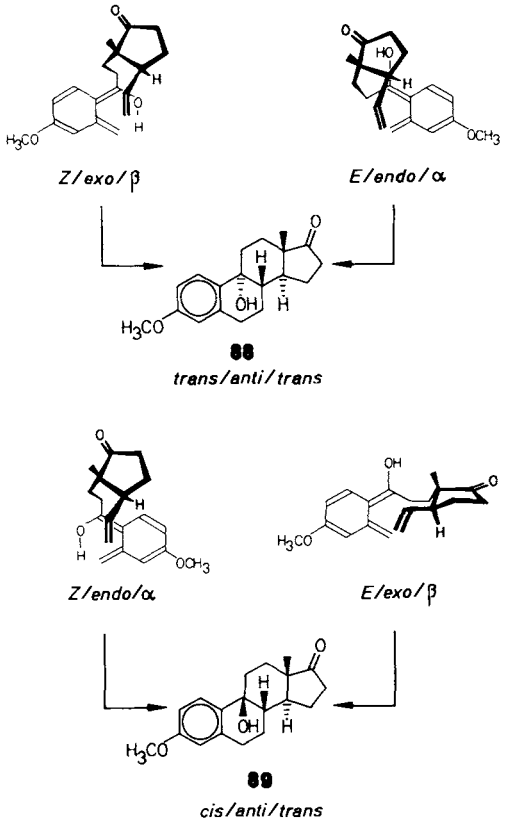



**94** **95**

Scheme 29. **94** and **95**, the other members, beside **88** and **89** (see Scheme 27), of the group of 9-hydroxy-3-methoxy-1,3,5(10)-estratrien-17-ones stereoisomeric at C-8 and C-9.

In the racemic series of compounds the conversion of the AD adduct into the ABCD cycloadduct poses, for the second time, a problem of stereoselection: since the *trans* fusion of the rings C and D is present already in *rac*-**86a**, altogether four relative configurations are feasible: *trans/anti/trans rac*-**88**, *cis/anti/trans rac*-**89**, *trans/syn/trans rac*-**94**, or *cis/syn/trans rac*-**95** (see Scheme 29). To establish their structures both cycloadduct components were isolated, albeit in low yield. All the chemical shifts and coupling constants were determined by two-dimensional FT-NMR analysis for the major isomer[70]. In the latter the *trans* diaxial coupling between H-14α and H-8β (11.5 Hz) and between H-7α and H-8β (12.6 Hz) indicates the desired *trans/anti/trans*-configuration, *rac*-**88**. This relative confi-

guration can only have resulted from the least strained of all possible transition states: the vinyl group approaches the diene, whose enolic double bond has the *Z*-configuration, from the β-side and with an *exo*-orientation (see Scheme 30). The alternative approach of the vinyl group from the α-side but *endo*-orientated to the diene with the enolic double bond in the *E*-configuration is much too strained to be considered seriously.




Scheme 30. How *rac*-**87** reacts to give the ABCD cycloadducts *rac*-**88** and *rac*-**89**; *rac*-**88** indeed arises from the least strained of all possible transition structures with the enolic CC double bond *Z*-orientated and *exo* approach of the dienophile region to the diene moiety from the α-side. Whether *rac*-**89** arises from the transition state in which the enolic CC double bond is *Z*-orientated and the dienophile region *endo*-approaches the diene moiety from the α-side or from the transition state with *E*-orientation of the enolic CC double bond and *exo*-approach of the dienophilic region to the diene moiety from the β-side cannot be decided from mere inspection of molecular models [58].

The minor isomer has the relative configuration *cis/anti/trans* of *rac*-**89**. Under conditions that admittedly lead to a mixture of *rac*-**90** and *rac*-**91**, but not to an equilibrium mixture[69], *rac*-**89**, and for that matter *rac*-**88** also, dehydrates to the styrene derivative *rac*-**90**. *rac*-**90** contains a double bond between C-9 and C-11 and the original *anti/trans*-configuration is still intact.

For *rac*-**89** it is not so easy to imagine the structure of the appropriate transition state. Certainly, regioselectivity favoring the constitution of the steroid skeleton is exceedingly high: in the conversion of the AD adduct into the ABCD cycloadduct the short bridge between C-9 and C-13 allows CC bond formation only between C-9 and C-8 and between C-6 and C-7. Whether the vinyl group, a poor nucleophile, approaches the *Z*-configurated *o*-quinodimethane from the α-side in an *endo*-orientation and/or the *E*-configurated *o*-quinodimethane from the β-side in an *exo*-orientation cannot be reliably estimated merely by inspection of molecular models. It should be recalled that in the synthetic routine the AD adduct *rac*-**86a** is converted in remarkable overall yield into a mixture of the styrene derivatives *rac*-**90**/*rac*-**91**. Intermediates need not be isolated and the resulting olefinic mixture need not be separated. Due to the pioneering investigations of *H. Smith et al.*[71], those reduction conditions which lead from a mixture of *rac*-**90**/*rac*-**91** optionally to *rac*-**8a**, *rac*-**47a**, *rac*-**92** or *rac*-**93** are precisely known[72].

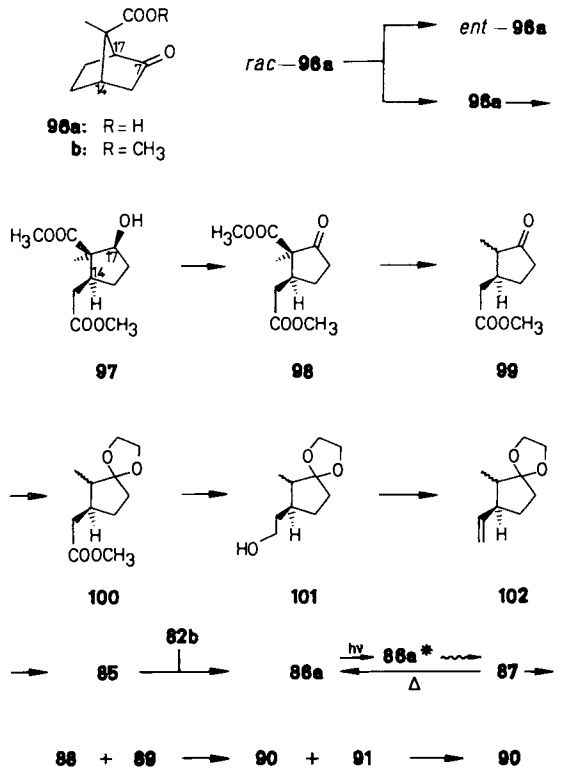
Since efficient syntheses to give access to enantiomerically pure compounds with biologically important properties have been demanded *(vide supra)*, the photochemical synthesis of estrone must not stop with racemic products. Further development has to commence at that point in the course of the synthesis where a racemic synthetic building block is introduced for the first time (see Scheme 28): in our case with the ring D unit. Enantiomerically pure 19-norsteroids would be accessible if, instead of *rac*-**84**, the enantiometer **84** were available.

### 3.2. Enantiomerically Pure Target Compounds

#### *3.2.1. The Chiral Ring D Building Block by Racemate Resolution of a Synthetic Precursor*[73]

A possible route to the enantiomerically pure ring D component **85** and thence to the enantiomerically pure steroid **90** (see Scheme 31) starts with the readily available[74] keto carboxylic acid *rac*-**96a**, the resolution of whose racemate has been thoroughly studied[75].

Which of the two separated enantiomers must be represented by **96a**, and which by *ent*-**96a** has been determined by trial and error[77]. The constitutional relationship between **96a** and **85** becomes obvious as soon as the C-17,C-7 bond is opened (numbering of the C atoms in **96a**, **b** reflects their position in the steroid eventually formed) by Baeyer-Villiger oxidation and hydrolysis of the initially formed lactone. The hydroxyl group at C-17 thus produced may be oxidized to a keto group. The desired vinyl group is obtained from the acetic acid side chain at C-14 by a standard procedure[78] without damaging the stereostructural integrity of the chiral center at C-14 (see Scheme 31). **85** represents a mixture of diastereomers; this was converted into the enolate **84**, as in the racemic series, and then into a mixture of the styrene derivatives **90** and **91**. The main components of **85**, which has the methyl group at C-13 *trans*-orientated to the H atom of C-14, and of **90**/**91**, which has the double bond between C-9 and C-11, were purified by chromatography and characterized by their chiroptical data. Since **90** is accessible from natural (+)-estrone by etherification and dehydration[79], natural and synthetic samples could be compared; the values of the optical rotations and the CD spectra leave no doubt that the samples are identical, and thus that C-14 of **96a** has (*S*)-chirality. It was precisely this last point that had prompted the synthesis of 3-methoxy-1,3,5(10),9(11)-estratetraen-17-one **90** shown in Scheme 31: authentic samples of **85**, **86a**, and **90**[73] would then be available to stereostructurally control the total synthesis of enantiomerically pure 19-norsteroids which uses a chiral ring D building



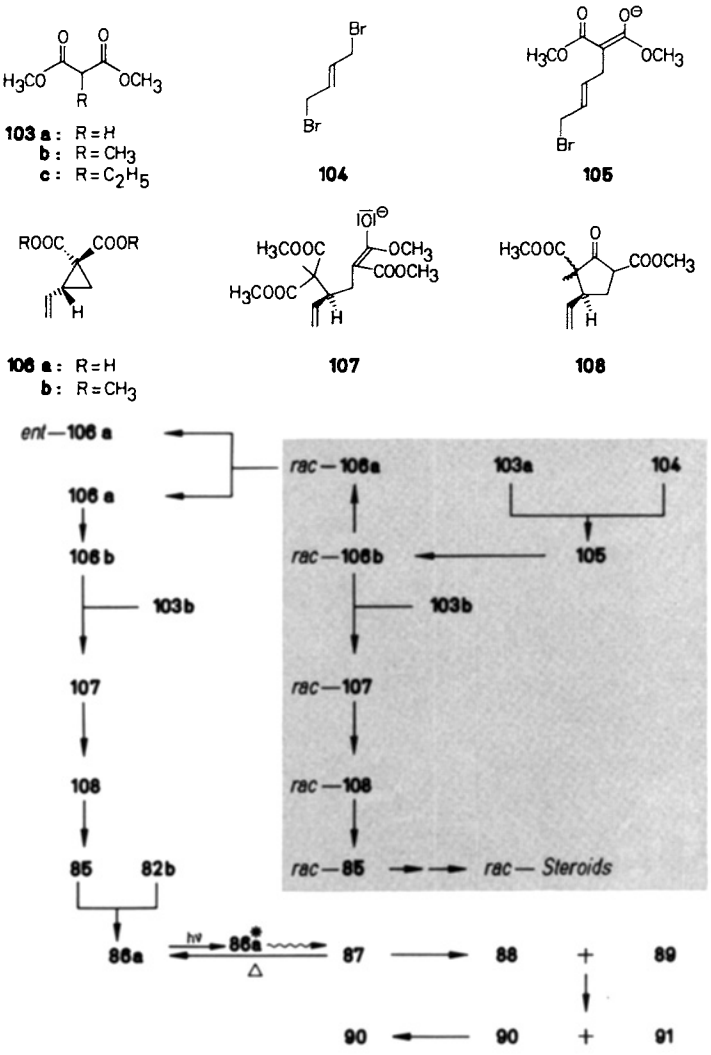
Scheme 31. Synthesis of the enantiomerically pure estrone derivative **90**; after racemate resolution of *rac*-**96a**, **96b** is converted into the mixture of enantiomerically pure diastereomers of type **85** [75]; **90** is obtained from **85** [76].

block obtained by asymmetric induction (see Section 3.2.2). Before this total synthesis, which dispenses with resolution of racemates, is more closely examined, the ring D unit should be logistically safeguarded.

*Perkin*[81], *Linstead*[82], and *Danishefsky*[83] and their respective co-workers have established the conditions whereby dimethyl *rac*-2-vinylcyclopropane-1,1-dicarboxylate *rac*-**106b** is

- conveniently accessible by intermolecular alkylation of the enolate of **103a** with (*E*)-1,4-dibromo-2-butene **104** and subsequent $S_{eN'}$ reaction (cyclization by vinylogous nucleophilic substitution)[84] of the intermediate enolate **105** (see Scheme 32),
- ring opened on nucleophilic substitution of the vinyl-substituted C atom by the enolate anion of dimethyl methylmalonate **103b**, whereupon the resultant enolate *rac*-**107** cyclizes in a Dieckmann condensation, and the β keto diester *rac*-**108** arising from alkoxide-initiated elimination of dimethyl carbonate gives *rac*-**85** after hydrolysis and decarboxylation (see Scheme 32).

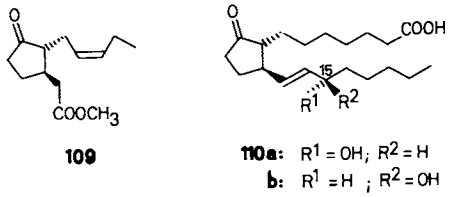
If the dextrorotatory enantiomer **106b** is substituted for *rac*-**106b** in the synthetic sequence, the enantiomerically pure steroid **90** can be obtained *via* the chiral ring D unit **85** and the optically active AD adduct **86a**. It will be remembered that the compounds specified, in as far as they contain a five-membered ring, have already been prepared as reference compounds; there are, thus, three test points in the synthesis at which the enantiomeric purity of intermediates can be checked. The result[80] is convincing; no-



Scheme 32. Synthesis of *rac*-**8a**, *rac*-**47a**, *rac*-**92**, or *rac*-**93** from **103a**, **104** and **103b** via *rac*-**85**; area in grey [85]; synthesis of **90** via **85** from **106a**, after the resolution of *rac*-**106a** with (−)-brucine [66b, 86]: area not in grey; see [87].

where—including the conversion of **106b** to **85**—is stereostructural information lost: *ent*-**106b**[88] is transformed into enantiomerically pure methyl jasmonate **109**[90,91] or (−)-11-deoxyprostaglandin $E_1$ **110a**, or (−)-15-*epi*-11-deoxyprostaglandin $E_1$ **110b**[89]. In all these cases (see Scheme 33) it is assumed that inversion[92] of configuration at the center of substitution occurs simultaneously with opening of the cyclopropane ring.

With the four chiral reference compounds **106**, **85**, **86a**, and **90** in hand, the preparations for a total synthesis of



Scheme 33. Enantiomerically pure target compounds whose synthesis began with *ent*-**106b** [88] as chiral starting material; for **109** see [90] and for **110a** and **110b** see [89].

19-norsteroids were complete. What was still missing was the preparation of the enantiomerically pure synthetic building block **106b** by an asymmetry-inducing step.

### *3.2.2. The Chiral Ring D Unit by Application of an Asymmetry-Inducing Step*

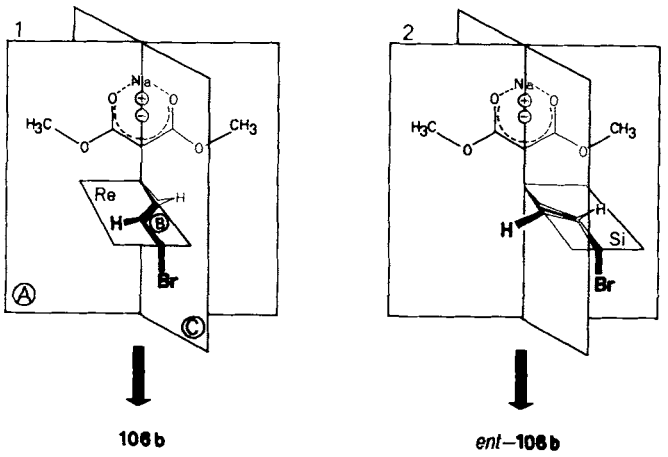
The enolate of the monosubstituted dimethyl malonate **105** (see Scheme 32) reacts *via* an $S_{cN'}$ reaction[84] to give *rac*-**106b**. The formation of a cyclopropane ring can also be rationalized as an intramolecular addition of a nucleophile to an electrophile, arising from elimination and concomitant allylic rearrangement. The central C atom of **105** functions here as a nucleophilic center; the halogen-distant C atom with coordination number 3 from the haloallyl group as an electrophilic center. At **105** the reaction path branches and separate routes lead to the two enantiomers **106b** and *ent*-**106b**. The corresponding transition states are at least enantiomorphic. Yet what detailed structure lies behind them? An analysis of the course of the reaction requires that conformational flexibility of **105** be limited. Scheme 34 sketches the reacting compound and lays stress equally on the malonate moiety, on the region of the halogen-containing substituent, and on their mutual orientation.

As a bidentate ligand, the enolate of a malonate diester is able to chelate a suitable cation[93]. By this means this structural element, which is otherwise "floppy", is tightly locked in a U-shaped conformation: the chelate ring and both methoxy groups lie more or less in a single plane (plane Ⓐ in Scheme 34)[94].

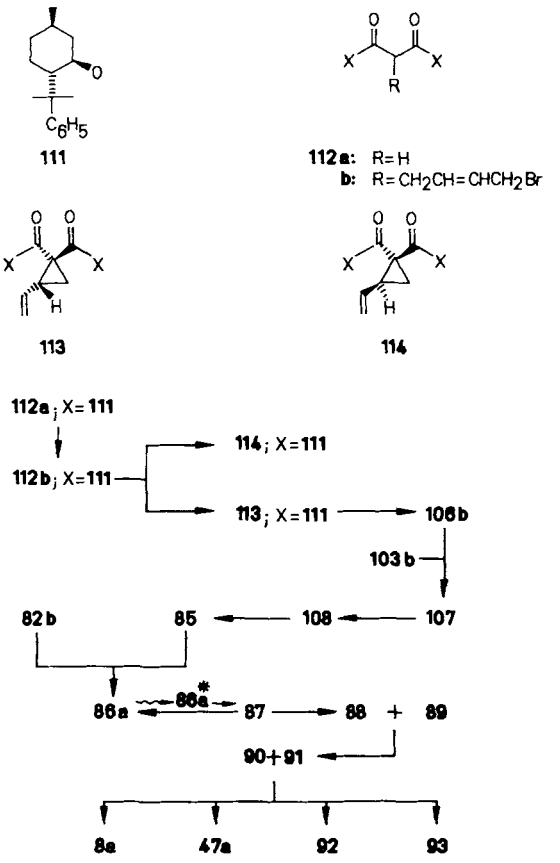
In the halogen-containing substituent the carbon atoms of the CC double bond and the central atoms of their ligands are likewise oriented in a plane (plane Ⓑ). In the transition state of the $S_{cN'}$ reaction, the two parts of the molecule are so mutually oriented that optimal overlap of the orbitals is achieved. This is the case when the axes of the anionic donor orbital and the olefinic acceptor orbital lie in the plane (plane Ⓒ) which also contains the centers of the future three-membered ring. In short: the conformations depicted in Schemes 34.1 and 34.2 satisfy the stereoelectronic requirements of the $S_{cN'}$ reaction.

The formation of the cyclopropane ring occurs in one of the two half-spaces into which plane B has divided three-dimensional space (see Scheme 34). If it occurs in the *Re* half-space[96] the (*R*)-enantiomer **106b** results, and if in the *Si* half-space the (*S*)-enantiomer *ent*-**106b** is obtained. Since the conformations of the competing transition states are enantiomorphic and, hence, have the same potential energy, the racemate *rac*-**106b** is formed. In order to obtain three-membered ring diastereomers, which are easier to separate than the three-membered ring enantiomers (see Scheme 4), the *imperative of asymmetric synthesis* may be invoked (see Scheme 5) and a chiral auxiliary reagent introduced into the hitherto achiral educt **105**, *e.g.* by using the alkoxide residue of a chiral alcohol instead of the methoxide residue. In the following discussion (−)-8-phenylmenthol (hydride of **111**) plays the role of the optically active auxiliary reagent. This alcohol is accessible from (+)-pulegone[97], can be esterified with malonic acid, and can be recovered from the corresponding ester of **106a**[50]. It is, as will be shown, superbly suited to assist in the generation of enantiomerically pure dimethyl 2-vinylcyclopropane-1,1-dicarboxylate **106b** (see Scheme 35).

Scheme 36 shows at a glance that the representations 36.1 and 36.2 are diastereomorphic[96]. The reaction paths that branch from **112a** (X = **111**; see Schemes 4 and 7) dif-

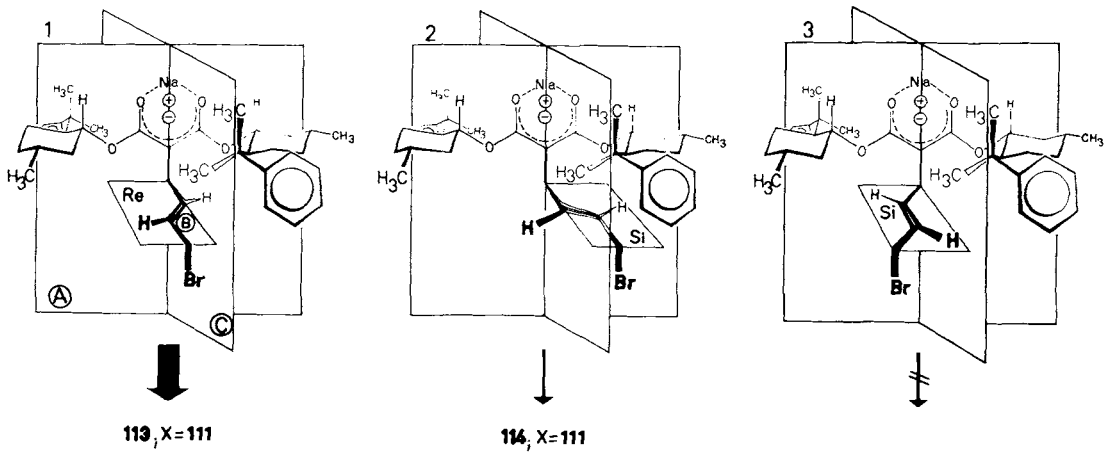



Scheme 34. $S_{cN'}$ reaction via enantiomorphic transition states of the same potential energy gives *rac*-**106b** (see Scheme 32). Cyclopropyl ring formation in the *Re* half-space (Scheme 34.1) gives **106b**, whereas cyclization in the *Si* half-space (Scheme 34.2) gives *ent*-**106b**.




Scheme 35. Asymmetric synthesis of **8a**, **47a**, **92** or **93** from **104** (see Scheme 32) or the corresponding dichloro compound and **112a** (X = **111**). After optimization [98] enantiomerically pure **113** (X = **111**) was obtained in 67% yield and thence—with recovery of the chiral alcohol (the hydride of **111**)—**106b** was isolated in 65% yield [99].

fer in width and provide unequal amounts of **113** (X = **111**) or **114** (X = 111). The chemical yield of **113** (X = **111**) should be higher than that of its epimer **114** (X = **111**), thanks to the steric hindrance between the dimethylbenzyl group of the chiral alcohol moiety and the $C_4H_6Br$ ligand. This interaction exists practically only in the transition state between **112b** (X = **111**) and **114** (X = **111**) (see Scheme 36.2), not, however, in the transition state between **112b** (X = **111**) and **113** (X = **111**) (see Scheme 36.1).




Scheme 36. $S_{cN'}$ reaction via diastereomorphic transition states of unequal potential energy gives predominantly **113** (X = **111**) and only a very limited amount of **114** (X = **111**) (see Scheme 35). **113** arises from cyclopropane ring formation in the *Re* half-space (Scheme 36.1), whereas **114** (X = **111**) arises from cyclization in the *Si* half-space (Scheme 36.2 but not 36.3).

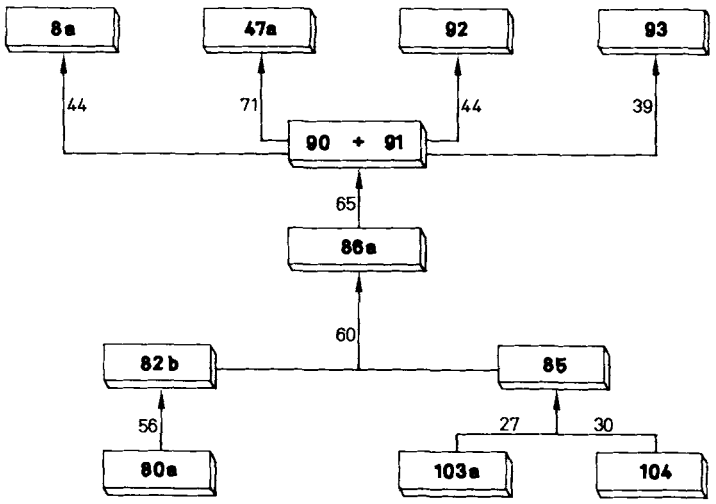
If the representations 36.2 and 36.3 are compared, it is immediately seen that the bromine-containing ligand can very easily flip over from the congested (see Scheme 36.2) to the empty quadrant (see Scheme 36.3) by rotation of both parts of the **112b** molecule around the central CC single bond. Thus it might be expected that the three-membered ring closure would also be possible in the *Si* half-space without significant steric hindrance, and in consequence, that substantial molecular selection would be questionable. Such a conclusion, however, disregards the stereoelectronic requirements of the $S_{cN'}$ reaction. Ultimately, cyclization in the *Si* half-space to afford diastereomer **114** (X = **111**) with a newly created center of (*S*)-chirality is handicapped compared to cyclopropanation in the *Re* half-space. Before the experimental results are reported, a word about a hitherto neglected detail of the $S_{cN'}$ reaction mechanism is in order: Opinions still differ[100] as to whether the nucleophilic center and the leaving group in the transition-state structure of an $S_{cN'}$ reaction are orientated *syn* or *anti* to one another. The antiplanar conformation is shown in Schemes 34 and 36 simply for the sake of convenience of representation. It is to be expected, however, that the synperiplanar orientation dominates[101]. The arguments developed above in favor of **113** (X = **111**) and against **114** (X = **111**) (Scheme 36) would then carry even more weight.

If **112a** (X = **111**) (see Scheme 35) is treated with (*E*)-1,4-dihalobutene in the presence of tricaprylammonium chloride in the *n*-hexane/50% aqueous sodium hydroxide two phase system at room temperature, enantiomerically pure **113** (X = **111**) is obtained in 67% yield after HPLC purification. Vigorous hydrolysis (KOH/MeOH/$H_2O$) and treatment of the resultant crude acid with excess $CH_2N_2$ gave **106b** (see Scheme 35) in 65% yield.

This is an example in which stereoselection has been successfully directed during introduction of the first center of chirality. In order to draw the correct conclusions for analogous cases in the future, the essential points of this stereoselection should be summarized: For a compound to fulfill the task of selection, it must, within a definite type of conformation, adopt one of two competing diastereomorphic conformations. The type of conformation is determined in each case by stereoelectronic factors which are specific for the reaction in question. In the present case the chelate effect exerts an additional influence. Selection in favor of one of two competing diastereomorphic transition states arises from involvement of a chiral auxiliary reagent. Which enantiomer of the latter should be used, follows from a comparative conformational analysis in which the least possible steric hindrance between different parts of the molecule is decisive.

To proceed beyond a mere formal synthesis, the three-membered ring compound **106b**, obtained by an asymmetry-inducing step, was converted by ring expansion into the ring D building block **85** (see Scheme 35), which was then transformed *via* Michael adduct **86a** and a mixture of constitutionally isomeric steroids **90** and **91** into the various target compounds **8a**, **47a**, **92**, or **93** (see Scheme 35)[50]. Scheme 37 presents an overview and details the chemical yields of the individual sections of the synthesis.

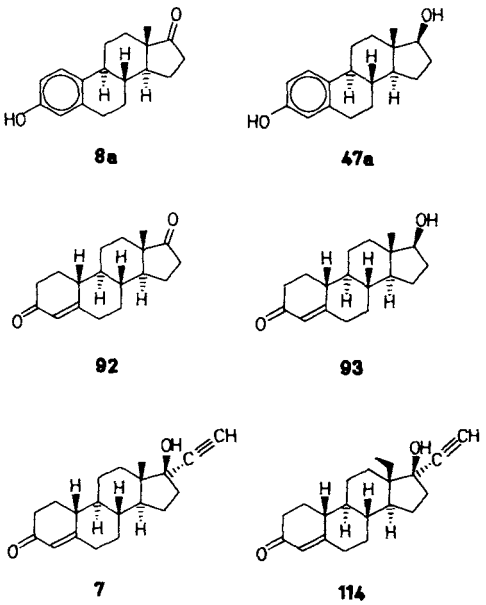
Thus, the aim of preparing enantiomerically pure 19-norsteroids stereoselectively has been achieved by a total synthesis that uses a photochemical key reaction and cheap industrial chemicals, dispenses with racemate resolution, and does not depend on the tedious use of protective groups.




Scheme 37. At a glance: the chemical yields for the individual sections of the asymmetric total synthesis of diverse enantiomerically pure 19-norsteroids from *m*-cresol methyl ether **80a** (see Fig. 27), dimethyl malonate **103a** and (*E*)-1,4-dibromo-2-butene **104** (see Scheme 32) via a photochemical key reaction.

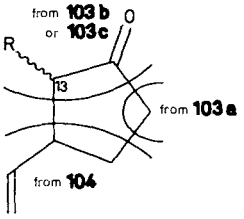
Depending on preference, the photochemical synthesis of estrone leads

- to 19-norsteroidal natural products which contain a benzenoid ring A (**8a**, **47a**; see Fig. 38) and exhibit estrogenic activity;
- to 19-norsteroidal gestagens having no benzenoid ring A (**92**, **93**, **7**; see Scheme 38) which, while themselves not natural products, can easily be prepared from them;
- to 19-norsteroidal gestagens which are methylated at C-18 (norgestrol **115**; see Scheme 38) and are more readily obtained by total synthesis from cheap industrial chemicals than by partial synthesis from available natural products.




Scheme 38. Biologically active 19-norsteroids which are accessible via the photochemical synthesis of estrone. While for **7**, **8a**, **47a**, **92** or **93** partial and total syntheses compete, for **115** total synthesis is clearly favored.

The last-cited case reveals the flexibility of the photochemical synthesis of estrone. If the synthesis of the ring D building block **85** from three components is recalled (see Scheme 39), the structural scope for target compounds of topical interest becomes clear; if instead of **103b** the homologous compound **103c** is used along with **103a** and **104**, steroidal derivatives with an ethyl, rather than a methyl, group at C-13 are obtained[102].




Scheme 39. The ring D building block with $R=CH_3$ or with $R=C_2H_5$ arises from the components **103a**, **104** and either **103b** or **103c**.

The chiral ring D building block **85** could also be used for total syntheses that follow the A+D→AD→ABCD construction principle and include thermally induced *o*-quinodimethanes. These syntheses, developed in other laboratories, have, hitherto, led only to racemic 19-norsteroids[103].

Natural products are one of the few *de novo* sources of drug discovery and the target compounds of chemical synthesis. In an area where research is carried out to cultivate synthetic methodology and to study structure-activity relationship, industrial chemists on the whole are more interested in new products, whereas chemists in the academic world for the most part are more interested in new synthetic methods. The development of the total synthesis of 19-norsteroids illustrates what a "concerted effort" can achive for the stereoselective synthesis of enantiomerically pure natural products.

These days, the art of synthesis is linked to a productive technology of synthesizing. One after another, synthetic methods are refined until they correspond to *Emil Fischer's* concept of asymmetric synthesis. In view of the results expected from biological synthesis, the conspicuous growth in potential of chemical synthesis has occurred just in time. Chemical synthesis will certainly profit from competition with developing recombinant DNA technology.

*Wolf-Dietrich Weber, Ulrich Schwartz, Herbert Stark, Friedhelm Adam, Helmut Baier, Stefan Gross, and Gudrun Frank were involved as undergraduates, postgraduates, or postdoctorals in the synthetic work in our laboratory mentioned here. Gerd Dürner has many years experience of analytical and preparative HPLC. His cooperation, supported by Marlies Dürr and Gabriele Stracke, has lent our statements the degree of security they enjoy. Prof. D. Rehm and Priv.-Doz. Dr. F. P. Montforts performed online-dialog computer search in data banks. As always, Helga Zimmermann took care of the illustrations, and Anneliese Dlabal was responsible for the many versions up to the final manuscript. Our work has been generously supported by the Deutsche Forschungsgemeinschaft and the Fonds der Chemischen Industrie, and promoted by donations of valuable samples, numer-*

*ous chemicals and considerable quantities of solvents from the chemical industry in this country. The above-mentioned ladies and gentlemen and the institutions referred to all deserve our sincere gratitude.*

Received: April 20, 1983 [A 466 IE]
German version: *Angew. Chem.* 651
Translated by Dr. C. Probert, Berlin

[1] G. Quinkert in W. Bartmann, E. Winterfeldt: *Stereoselective Synthesis of Natural Products, Workshop Conferences Hoechst, Vol. 7*; Excerpta Medica, Amsterdam 1979.

[2] G. Quinkert in "Lectures on the occasion of the 60th birthday of Prof. Dr. Klaus Weissermel", Hoechst AG Frankfurt am Main 1982

[3] "Synthetic biology" is used here as an extension of "synthetic chemistry", synonymous with "natural product synthesis by gene technology". For the synthesis of chemical compounds by in vitro recombination and in vivo transformation see [4].

[4] a) Recombinant DNA, *Science 209* (1980) Nr. 4463; b) J. D. Watson, J. Tooze: *The DNA Story*. Freeman, San Francisco 1981; c) H. G. Gassen, A. Lang: *Chemical and Enzymatic Synthesis of Gene Fragments*, Verlag Chemie, Weinheim 1982; d) S. A. Narang, *Tetrahedron 39* (1983) 3; e) J. E. Davies, H. G. Gassen, *Angew. Chem. 95* (1983) 26; *Angew. Chem. Int. Ed. Engl. 22* (1983) 13; f) Biotechnology, *Science 219* (1983) No. 4585.

[5] a) W. Lenz, *Ann. N. Y. Acad. Sci. 123* (1965) 228; b) G. Schreiber, *Dtsch. Apoth.-Ztg. 108* (1968) 675.

[6] G. Blaschke, *Angew. Chem. 92* (1980) 14; *Angew. Chem. Int. Ed. Engl. 19* (1980) 13.

[7] a) See p. 579 in [8]; b) D. Seebach, H.-O. Kalinowski, *Nachr. Chem. Techn. Lab. 24* (1976) 415.

[8] F. Ebel in K. Freudenberg: *Stereochemie*. Franz Deuticke, Leipzig 1933, p. 579.

[9] For an astonishing account of someone who set out into the interior of Mexico to find steroids with degradable side chains and was successful, see [10].

[10] R. Witzemann: *Schlüssel des Lebens - Die Steuerung biologischer Vorgänge durch Steroide*. Molden, Wien 1977, p. 202ff.

[11] W. Müller-Haeseler, *Frankfurter Allgemeine Zeitung 36* (1976) No. 62 (13th March, 1976), p. 15.

[12] For the adaptation of the partial synthesis of contraceptive 19-norsteroids to the respective economically attractive raw material sources see [13].

[13] a) R. Wiechert, *Angew. Chem. 92* (1970) 331; *Angew. Chem. Int. Ed. Engl. 9* (1970) 321; b) *ibid. 89* (1977) 513; and **16** (1977) 506.

[14] D-(+)-glucose **9**, free or bound, is the most abundant of all organic compounds on our planet. This sugar is readily accessible and is a renewable resource. Thanks to its accumulation of functional groups and chiral centers it is a convenient starting material for the synthesis of many enantiomerically pure target compounds; [15] is a leading reference.

[15] A. Vasella in R. Scheffold: *Modern Synthetic Methods. Vol. 2*, Salle+Sauerländer, Frankfurt am Main 1980, p. 173.

[16] Of the two commercially available enantiomers of tartaric acid, (*R,R*)-(+)-tartaric acid **10** is the cheaper, but (*S,S*)-(−)-tartaric acid (*ent*-**10**) can certainly be used for laboratory scale syntheses; see [17].

[17] D. Seebach, E. Hungerbühler in R. Scheffold: *Modern Synthetic Methods. Vol. 2*, Salle+Sauerländer, Frankfurt am Main 1980, p. 91.

[18] (*R*)-2-hydroxypropanoic acid (D-lactic acid) **11**, (*S*)-2-hydroxypropanoic acid (L-lactic acid) *ent*-**11**, and (±)-2-hydrocypropanoic acid (DL-lactic acid) *rac*-**11** all occur naturally. A computer search in the SDC Chemical Abstracts data bank for the period 1967–1982 (*Chem. Abstr.* (1982) No. 97, issue 20) in the file segment ORGCHEM with the search word "SYNTHE#S/TI" produced 26 publications in which either **11** (10326-41-7/RN) and/or *ent*-**11** (Registry No. 79-33-4) or their methyl esters, respectively (17392-83-5; 27871-49-4), or ethyl esters, respectively (7699-00-5; 687-47-8), were used. In [19a–f] one of these chiral compounds was used directly as a synthetic building block. The conversion into other chiral synthetic units is described in [19g–i].

[19] a) M. Imfeld, M. Suchy, P. Vogt, T. Kukac, M. Schlageter, E. Widmer, *Helv. Chim. Acta 65* (1982) 1233; b) S. W. Baldwin, M. T. Crimmins, *J. Am. Chem. Soc. 104* (1982) 1132; c) H. R. Pfaendler, *Spec. Publ. R. Soc. Chem. 38 (Recent Adv. Chem. β-Lactam Antibiot.)* (1980) 368; d) K. Hintzer, R. Weber, V. Schurig, *Tetrahedron Lett. 22* (1981) 55; e) H. J. Nestler, H. Bieringer, *Z. Naturforsch. B35* (1980) 366; f) B. D. Johnston, K. N. Slessor, *Can. J. Chem. 57* (1979) 233; g) B. Seuring, D. Seebach, *Helv. Chim. Acta 60 (1977) 1175*; h) V. Schurig, B. Koppenhöfer, W. Bürkle, *Angew. Chem. 90* (1978) 993; *Angew. Chem. Int. Ed. Engl. 17* (1978) 937; i) B. T. Golding, D. R. Hall, S. Sakrikar, *J. Chem. Soc. Perkin Trans. I 1973*, 1214.

[20] (1*R*)-(+)-Camphor **12**, (1*S*)-(−)-camphor *ent*-**12**, and (±)-camphor *rac*-**12** all occur naturally. A computer search in the SDC Chemical Abstracts data bank for the period 1967–1982 (*Chem. Abstr. 97* (1982) No. 18) with the registry numbers of **12** (464-49-3) and/or *ent*-**12** (464-48-2) using the search word "SYNTHES#S/TI" in the file segment ORGCHEM produced 32 publications; of these, those given under [21a–g] were concerned with natural product synthesis starting from optically active camphor. The publications given under [21h–l] also belong to this category: we, but not the computer remembered them.

[21] a) H. Shibuya, K. Hiromichi, A. Kajiware, Y. Yamamoto, I. Kitagawa, *Chem. Pharm. Bull. 30* (1982) 1271; b) I. Kitagawa, H. Shibuya, H. Fujioka, A. Kajiwara, Y. Yamamoto, S. Tsujii, A. Takagi, M. Hori, *ibid. 29* (1981) 2540; c) I. Kitagawa, H. Shibuya, H. Fujioka, A. Kajiwara, S. Tsujii, Y. Yamamoto, A. Takagi, *Chem. Lett. 1980*, 1001; d) N. Ching-Yu Lame, thesis, University of British Columbia, Vancouver 1979 (*Diss. Abstr. Int. B 1980*, 40 (11) 5275); e) M. S. Allen, N. Lamb, T. Money, P. Salisbury, *J. Chem. Soc. Chem. Commun. 1979*, 112; f) N. Darby, N. Lamb, T. Money, *Can. J. Chem. 57* (1979) 742; g) R. V. Stevens, F. C. A. Gaeta, *J. Am. Chem. Soc. 99* (1977) 6105; h) J. W. Cornforth in J. W. ApSimon: *The Total Synthesis of Natural Products. Vol. 1*, Wiley-Interscience, New York 1973, p. 266; i) R. B. Woodward, *Pure Appl. Chem. 17* (1968) 519; j) A. K. Chopra, G. P. Moss, B. C. L. Weedon, *J. Chem. Soc. Chem. Comm. 1977*, 467; k) R. V. Stevens in B. Zagalak, W. Friedrich: *Vitamin B-12*, de Gruyter, Berlin 1979, S. 119–135; l) W. A. Szabo, H. T. Lee, *Aldrichimica Acta 13* (1980) 13.

[22] See [8], p. 564.

[23] Eschenmoser's synthesis of cobyric acid is also a teaching model in this respect; it comprises 37 steps [24]; a racemic Diels/Alder adduct is obtained at the second step and the two isomers separated using (+)- or (−)-phenylethylamine. While the dextrorotatory isomer was developed into suitable A, B or C ring units, the chiral ring D unit arose from the levorotatory enantiomer [25].

[24] A. Eschenmoser, *Nova Acta Leopold. Neue Folge 55* (1982) 5.

[25] A. Eschenmoser, 23. Int. Congr. Boston, *Suppl. Pure Appl. Chem. 2* (1971) 69.

[26] a) M. Gerecke, J.-P. Zimmermann, W. Aschwanden, *Helv. Chim. Acta 53* (1970) 991; b) A. Fischli, M. Klaus, H. Mayr, P. Schönholzer, R. Rüegg, *ibid. 58* (1975) 564; c) B. M. Trost, J. M. Timko, J. L. Stanton, *J. Chem. Soc. Chem. Commun. 1978*, 436; d) N. Cohen, R. J. Lopresti, C. Neukom, *J. Org. Chem. 46* (1981) 2445.

[27] E. Fischer, *Ber. Dtsch. Chem. Ges. 27* (1894) 3189.

[28] See footnote 1 in [29].

[29] L. F. Fieser, W.-Y. Huang, T. Goto, *J. Am. Chem. Soc. 82* (1960) 1688.

[30] a) G. Anner, K. Miescher, *Helv. Chim. Acta 31* (1948) 2173; b) *ibid. 32* (1949) 1957; c) *ibid. 33* (1950) 1379.

[31] F. Litvan, R. Robinson, *J. Chem. Soc. 1938*, 1997.

[32] a) W. E. Bachmann, W. Cole, A. L. Wilds, *J. Am. Chem. Soc. 62* (1940) 824; b) W. E. Bachmann, S. Kushner, A. C. Stevenson, *ibid. 64* (1942) 974.

[33] a) W. S. Johnson, R. G. Christiansen, R. E. Ireland, *J. Am. Chem. Soc. 79* (1957) 1995; b) W. S. Johnson, I. A. David, H. C. Dehm, R. J. Highet, E. W. Warnhoff, W. D. Wood, E. T. Jones, *ibid. 80* (1958) 661.

[34] J. E. Cole, W. S. Johnson, P. A. Robin, J. Walker, *J. Chem. Soc. 1962*, 244.

[35] W. S. Johnson, D. S. Allen, Jr., *J. Am. Chem. Soc. 79* (1957) 1261.

[36] a) R. A. Dickinson, R. Kubela, G. A. MacAlpine, Z. Stojanac, Z. Valenta, *Can. J. Chem. 50* (1972) 2378; b) J. Das, R. Kubela, G. A. MacAlpine, Z. Stojanac, Z. Valenta, *ibid. 57* (1979) 3308.

[37] For the total synthesis of 19-norsteroids via *o*-quinodimethane transients see SYNFORM No. 3 (1983).

[38] a) T. Kametani, H. Nemoto, H. Fukumoto, J. Ishikawa, K. Shiroyama, K. Fukumoto, *J. Am. Chem. Soc. 98* (1976) 3378; b) T. Kametani, H. Nemoto, H. Ishikawa, K. Shiroyama, H. Matsumoto, K. Fukumoto, *ibid. 99* (1977) 3461.

[39] a) S. N. Ananchenko, I. V. Torgov, *Tetrahedron Lett. 1963*, 1553; b) A. V. Zakharichev, S. N. Ananchenko, I. V. Torgov, *ibid. 1964*, 171; c) A. V. Zakharychev, I. Hora, S. N. Ananchenko, I. V. Torgov, *ibid. 1966*, 3585.

[40] C. H. Kuo, D. Taub, N. L. Wendler, *J. Org. Chem. 33* (1968) 3126.

[41] a) H. Gibian, K. Kieslich, H.-J. Koch, H. Kosmol, C. Rufer, E. Schröder, R. Vössing, *Tetrahedron Lett. 1966*, 2321; b) H. Kosmol, K. Kieslich, R. Vössing, H.-J. Koch, K. Petzoldt, H. Gibian, *Justus Liebigs Ann. Chem. 701* (1967) 199.

[42] C. Rufer, E. Schröder, H. Gibian, *Justus Liebigs Ann. Chem. 701* (1967) 206.

[43] If **46** was acylated before catalytic hydrogenation and the dihydro product subsequently hydrolyzed, the overall yield for the conversion of *ent*-**45** to **47b** rose to more than 50%; see [42].

[44] a) U. Eder, G. Sauer, R. Wiechert, *Angew. Chem. 83* (1971) 492; *Angew. Chem. Int. Ed. Engl. 10* (1971) 496; b) Z. G. Hajos, D. R. Parrish, *J. Org. Chem. 39* (1974) 1615.

[45] a) P. Buchschacher, J.-M. Casal, A. Fürst, W. Meier, *Helv. Chim. Acta 60* (1977) 2747; b) T. Wakabayashi, K. Watanabe, J. Kato, *Synth. Commun. 7* (1977) 239; c) S. Danishefsky, P. Cain, *J. Am. Chem. Soc. 98* (1976) 4975; d) Review: N. Cohen, *Acc. Chem. Res. 9* (1976) 412.
[46] K. L. Brown, L. Damm, J. D. Dunitz, A. Eschenmoser, R. Hobi, C. Kratky, *Helv. Chim. Acta 61* (1978) 3108.
[47] a) R. A. Micheli, Z. G. Hajos, N. Cohen, D. R. Parrish, L. A. Portland, W. Sciamanna, M. A. Scott, P. A. Wehrli, *J. Org. Chem. 40* (1975) 675; b) N. Cohen, B. L. Banner, W. F. Eichel, D. R. Parrish, G. Saucy, *ibid. 40* (1975) 681.
[48] U. Eder, H. Gibian, G. Haffer, G. Neef, G. Sauer, R. Wiechert, *Chem. Ber. 109* (1976) 2948.
[49] See footnote 35 in [50].
[50] G. Quinkert, U. Schwartz, H. Stark, W.-D. Weber, F. Adam, H. Baier, G. Frank, G. Dürner, *Liebigs Ann. Chem. 1982,* 1999.
[51] a) T. Kametani, H. Matsumoto, H. Nemoto, K. Fukumoto, *Tetrahedron Lett. 1978,* 2425; b) *J. Am. Chem. Soc. 100* (1978) 6218.
[52] a) W. Oppolzer, D. A. Roberts, *Helv. Chim. Acta 63* (1980) 1703; b) W. Oppolzer, K. Bättig, M. Petrzilka, *ibid. 61* (1978) 1945.
[53] a) G. Quinkert, K. Opitz, W.-W. Wiersdorff, J. Weinlich, *Tetrahedron Lett. 1963,* 1863; b) G. Quinkert, W.-W. Wiersdorff, M. Finke, K. Opitz, *ibid. 1966,* 2193; c) G. Quinkert, *Photochem. Photobiol. 7* (1968) 783; d) G. Quinkert, W.-W. Wiersdorff, M. Finke, K. Opitz, F.-G. von der Haar, *Chem. Ber. 101* (1968) 2302; e) K. H. Grellmann, J. Palmowski, G. Quinkert, *Angew. Chem. 83* (1971) 209; *Angew. Chem. Int. Ed. Engl. 10* (1971) 196.
[54] *G. Wittig* and *M. Leo* [55a] reported the intensive efforts expended to convert **73** into **69** or into **70** by reductive ether cleavage; they isolated **72** and originally inferred that **69** was involved as an intermediate. Later in [55b] it was assumed that **70** had occurred as a transient and isomerized to **72**, it was taken for granted that the reader is familiar with the *seco/cyclo*-isomerization of **70** and *rac*-**71** to **69**, and with the irreversible isomerization of *rac*-**71** to **72** [53d].
[55] a) G. Wittig, M. Leo, *Ber. Dtsch. Chem. Ges. 64* (1931) 2395; b) G. Wittig, *Angew. Chem. 92* (1980) 671; *Science 210* (1980) 600.
[56] a) G. Quinkert, H.-P. Lorenz, W.-W. Wiersdorff, *Chem. Ber. 102* (1969) 1597; b) G. Quinkert, K. Opitz, W.-W. Wiersdorff, M. Finke, *Justus Liebigs Ann. Chem. 693* (1966) 44; c) G. Quinkert, J. Palmowski, H.-P. Lorenz, W.-W. Wiersdorff, M. Finke, *Angew. Chem. 83* (1971) 210; *Angew. Chem. Int. Ed. Engl. 10* (1971) 198; d) G. Quinkert, T. Tabata, E. A. J. Hickmann, W. Dobrat, *ibid. 83* (1971) 212; *10* (1971) 199; e) G. Quinkert, M. Finke, J. Palmowski, W.-M. Wiersdorff, *Mol. Photochem. 1* (1969) 433.
[57] See footnote 33 in [58].
[58] G. Quinkert, W.-D. Weber, U. Schwartz, H. Stark, H. Baier, G. Dürner, *Liebigs Ann. Chem. 1981,* 2335.
[59] K.-H. Grellmann, H. Weller, E. Tauber, *Chem. Phys. Lett. 95* (1983) 195.
[60] R. Haag, J. Wirz, P. J.Wagner, *Helv. Chim. Acta 60* (1977) 2595.
[61] G. Quinkert, *Angew. Chem. 84* (1972) 1157; *Angew. Chem. Int. Ed. Engl. 11* (1972) 1072.
[62] G. H. Posner: *An Introduction to Synthesis Using Organocopper Reagents.* Wiley, New York 1980.
[63] For the preparation of **83** see [64a]; we [64b] followed [64c].
[64] a) R. L. Funk, *Synthesis* **1980,** 118; b) H.-G. Schmalz, Diplomarbeit 1983, Universität Frankfurt am Main; c) A. Fischli, M. Klaus, H. Mayer, P. Schönholzer, R. Rüegg, *Helv. Chim. Acta 58* (1975) 564.
[65] See Section 5.3.3 in [58].
[66] a) See Table 2 in [58]; b) F. Adam, Dissertation, Universität Frankfurt am Main 1982.
[67] See Section 2 in [61].
[68] See Section 3.4 in [58].
[69] The equilibrium mixture contains 65% *rac*-**90** and 35% *rac*-**91**.
[70] D. Leibfritz, E. Haupt, M. Feigel, W. E. Hull, W.-D. Weber, *Liebigs Ann. Chem. 1982,* 1971.
[71] G. H. Douglas, J. M. H. Graves, D. Hartley, G. A. Hughes, B. J. McLoughlin, J. Siddall, H. Smith, *J. Chem. Soc. 1963,* 5072.
[72] See Section 5.6 in [58].
[73] See Section 3 in [50].
[74] H. Stark, Dissertation, Universität Frankfurt am Main 1981.
[75] See Section 3.3 in [50].
[76] See Sections 6.2.1.2 and 6.3.1.3 in [50].
[77] See footnote [29] in [50].
[78] See footnote [57] in [58].
[79] See Section 5.8.1 in [58].
[80] See Table 1 and Figure 4C in [50].
[81] W. A. Bone, W. H. Perkin, *J. Chem. Soc. 67* (1895) 108.
[82] R. W. Kwierstead, R. P. Linstead, B. C. L. Weedon, *J. Chem. Soc. 1952,* 3610, 3616.
[83] S. Danishefsky, *Acc. Chem. Res. 12* (1979) 66, and references cited therein.
[84] G. Stork, A. R. Schoofs, *J. Am. Chem. Soc. 101* (1979) 5081.
[85] See Sections 5.2.1, 5.3.1, 5.5 and 5.6 in [58].
[86] G. C. Rovnyak, Ph. D. Thesis, University of Pittsburgh 1970.
[87] See Sections 6.1.2, 6.2.1.2, and 6.3.1.2 in [50].
[88] *ent*-**106b** was obtained from *rac*-**106b** as described [89] and according to [90] from (*S*)-2-vinylcyclopropane-1,1-dicarboxylic acid-bis [(1*R*,2*S*,5*R*)-2-(1-methyl-)phenylethyl)-5-methylcyclohexyl ester] by hydrolysis and treatment of the ensuing dicarboxylic acid with diazomethane.
[89] N. A. Abraham *Tetrahedron Lett. 1974,* 1393; although work up was as in [86], *ent*-**106b** was obtained instead of **106b**.
[90] G. Quinkert, F. Adam, G. Dürner, *Angew. Chem. 92* (1982) 866; *Angew. Chem. Int. Ed. Engl. 21* (1982) 856; *Angew. Chem. Suppl. 1982,* 1777.
[91] Natural methyl jasmonate consists of 90% **109** and of 10% methyl [(*Z*, 1*R*, 2*S*)-3-oxo-2-(2-pentenyl)cyclopentyl]acetate; see [90].
[92] S. Danishefsky, G. Rovnyak, *J. Chem. Soc. Chem. Commun. 1972,* 821.
[93] L. M. Jackman, B. C. Lange, *Tetrahedron 33* (1977) 2737.
[94] For the conformations of esters see [95].
[95] a) A. McL. Mathieson, *Tetrahedron Lett. 1965,* 4137; b) R. Schmierer, Dissertation, Universität Stuttgart 1980; c) W. B. Schweizer, J. D. Dunitz, *Helv. Chim. Acta 65* (1982) 1547.
[96] V. Prelog, G. Helmchen, *Helv. Chim. Acta 55* (1972) 2581.
[97] a) E. J. Corey, H. E. Ensley, *J. Am. Chem. Soc. 97* (1975) 6908; b) H. E. Ensley, C. A. Parnell, E. J. Corey, *J. Org. Chem. 43* (1978) 1610.
[98] See Sections 2 and 6.1.1.1.1 in [50].
[99] Careful analysis revealed that **113** (X = **111**) and **114** (X = **111**) occur in a ratio of 98:2 on cyclopropanation (see Figure 3 in [50]). The diastereomer formed in smaller amounts was completely removed during purification of the crude cyclization product under the optimized conditions of the synthesis.
[100] K. H. Overton, Chem. Soc. Rev. 8 (1979) 447 and references cited both there and in [84].
[101] W. D. Stohrer, *Angew. Chem. 95* (1983) 647; *Angew. Chem. Int. Ed. Engl. 22* (1983) 613.
[102] The asymmetric total synthesis of enantiomerically pure norgestrol **115** using a photochemical key reaction is in progress in our laboratory. H. Baier, G. Quinkert, unpublished results.
[103] The enolate *rac*-**84** plays a role in: a) R. L. Funk, K. P. C. Vollhardt, *J. Am. Chem. Soc. 102* (1980) 5253; b) Y. Ito, M. Kakatsuka, T. Saegusa, *ibid. 103* (1981) 476; c) W. Oppolzer, M. Petrzilka, K. Bättig, *Helv. Chim. Acta 60* (1977) 2694; d) S. Sjuric, T. Sarkar, P. Magnus, *J. Am. Chem. Soc. 102* (1980) 6885; e) T. Kametani, H. Nemeto, *Tetrahedron Lett. 1979,* 27; f) K. C. Nicolaou, W. E. Barnette, P. Ma, *J. Org. Chem. 45* (1980) 1463.
[104] G. Quinkert, *Angew. Chem. 90* (1978) 503; *Angew. Chem. Int. Ed. Engl. 17* (1978) 473.

# Solution Conformations, Photophysics, and Photochemistry of Bile Pigments; Bilirubin and Biliverdin Dimethyl Esters and Related Linear Tetrapyrroles

**By Silvia E. Braslavsky, Alfred R. Holzwarth, and Kurt Schaffner***

*Dedicated to Professor Günther O. Schenck on the occasion of his 70th birthday*

Bilirubin and biliverdin dimethyl esters (BRE and BVE, respectively) and related linear tetrapyrroles have been studied using a combination of photochemical and spectroscopic techniques, the latter including absorption, fluorescence, fluorescence excitation, medium-induced circular dichroism, and proton magnetic resonance. Both types of tetrapyrroles form mixtures of different topological isomers in very dilute solutions. In the case of the bilirubins the heterogeneity of the solutions is caused by two coexisting conformers with different orientations of the A/B and C/D pyrromethenone moieties with respect to each other. The spectral properties of one conformer resemble the isolated parent pyrromethenone, whereas those of the other result from electronic coupling of the two subchromophores presumably held in a "ridge tile"-like orientation. C–C rotations at the C-5 and C-15 bridges substantially compete in both components with the photochemical channels ($E \rightarrow Z$ isomerization and lumirubin formation) for the radiationless deactivation of the excited singlet state. The more rigid "ridge tile" component additionally undergoes hydrogen bond-mediated deactivation, and it photoisomerizes more efficiently. The situation is markedly more complex with the biliverdins. In order to obtain a more detailed insight into the mechanisms of the radiationless excited-state processes, time-resolved optoacoustic spectroscopy and ultrafast absorption (pump-probe) and fluorescence detection (single-photon-timing) techniques were used to supplement the stationary methods. The solution mixtures are composed of a (family of) helically coiled all-*Z*,all-*syn* species, and of species differing from the former by stretched arrangements of the rings B and C around the central C-10 bridge (*E-anti, E-syn,* and *Z-anti*). Two excited singlet states with picosecond lifetimes are attributed to either one or two coiled ground-state forms, and two remarkably long-lived nanosecond excited states arise each from a stretched ground state. The radiationless deactivation of the shorter-lived of the picosecond states is brought about by ultrafast intramolecular proton transfer between the B/C nitrogen atoms, in addition to the C–C rotational modes operative in both. $Z \rightarrow E$ photoisomerization is also an appreciable deactivation channel of excited biliverdin dimethyl ester. It is confined to the central C-10 double bond and selectively affords a stretched isomer (10*E-anti*), which thermally reforms the coiled starting material at room temperature *via* a sequence of tautomerization and C–C rotation. Heating or ultrasonic treatment can reverse this sequence and drive it farther to populate another stretched isomer (10*E-syn*) which is thermally stable at room temperature. This stretched form aggregates (presumably to dimers) already at concentrations at which the coiled species still appears to be fully monomeric.

## 1. Introduction[**]

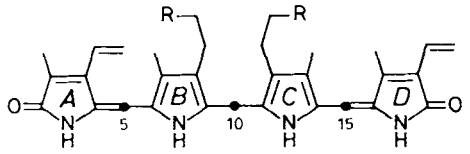
Linear, open-chain tetrapyrroles (cf. Scheme 1) are synthesized in nature from δ-aminolevulinic acid *via* the porphyrins which are oxidatively cleaved at either of two (α and γ) of the four methine linkages[1]. While in higher organisms iron has to be removed prior to the cleavage, the porphyrins of plants and lower algae are cleaved directly. Linear tetrapyrroles are found in nature as catabolic products (*e.g.*, the neurotoxic bilirubin in the bile fluid), as the chromophores of biliproteins performing important photobiological functions, and as pigments in lepidopters (*e.g.*, biliverdin IXγ = pterobilin).

The linear tetrapyrroles also attract attention for several other reasons. They are chromophores of remarkably high flexibility, and they may potentially adopt a large number of configurational, conformational, and tautomeric forms. Some interconversions of such forms can be expected to occur exclusively in the photoexcited state, in particular

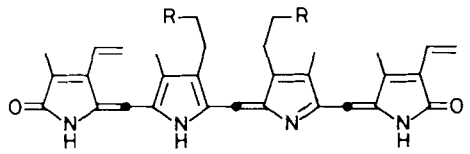
[*] Prof. Dr. K. Schaffner, Prof. Dr. S. E. Braslavsky, Dr. A. R. Holzwarth
Max-Planck-Institut für Strahlenchemie
Stiftstrasse 34–36, D-4330 Mülheim a. d. Ruhr (Germany)

[**] Abbreviations: BVE-H$^+$, monoprotonated biliverdin dimethyl ester; $D_{UV}/D_{Vis}$, ratio of the dipole strengths of the UV and Vis absorption and fluorescence excitation bands; DPL, dipalmitoyl lecithin; EYL, egg yolk lecithin; LIOAS, laser-induced optoacoustic spectroscopy; NBVE-IXδ, neobiliverdin IXδ dimethyl ester; SICD, medium(solvent, membrane)-induced circular dichroism; PP, picosecond pump-probe; SA, serum albumin; SPT, single-photon timing; ZnBVE, Zn complex of biliverdin dimethyl ester; see also Schemes 1, 2, 4, 6, and 8.

 © Verlag Chemie GmbH, 6940 Weinheim, 1983 0570-0833/83/0909-0656 $ 02.50/0 



**BR** (R = $CO_2H$) Bilirubin (IXα)
**BRE** (R = $CO_2CH_3$) Bilirubin dimethyl ester (IXα)



**BVE** (R = $CO_2CH_3$) Biliverdin dimethyl ester (IXα)

Scheme 1. Constitution of BR, BRE, and BVE [*].

the $E \rightleftharpoons Z$ isomerizations of the exocyclic double bonds. Others such as rotations around C–C single bonds are characteristic ground-state processes, and still others such as intramolecular transfers of protons or hydrogens are *a priori* possible in either state. In the fully conjugated BVE, furthermore, proton transfers between the two central rings B and C would merely lead to a temporary shift of the ground-state equilibrium between two very similar tautomers—a change in population of only two in a mixture of possibly several more components which would be very difficult to directly differentiate spectroscopically. Rather, demonstration of such a proton transfer possibly would remain restricted to experimental detection as a non-radiative deactivation channel.

In view of the structural features, which are of quite general interest, and the biological relevance of the linear tetrapyrroles, their photophysics and photochemistry have been widely studied in recent years[2]. For example, the $Z \rightarrow E$ photoisomerization of BR has been found to be the crucial step in the phototherapy used routinely in hospitals for treating the jaundice of the newly-born (neonatal hyperbilirubinemia)[3], and BVE has roused interest as a model chromophore for the photochromic plant chromoprotein phytochrome and for the light-harvesting (antennae) pigments of cyanobacteria, red algae, and cryptophyceae.

This article will focus on our investigations of recent years into the solution conformation, the photophysics and photochemistry of BRE, BVE and related compounds. At room temperature in liquid solution, fully conjugated linear tetrapyrroles such as BVE appear to be photochemically unreactive at first sight, and the luminescence[4–6] and intersystem crossing[5,7,8] quantum yields are very small. Radiationless deactivation processes ("energy wasting") must therefore be of particular importance in this type of molecules. It is appropriate at this juncture to recall that radiationless deactivation of an electronically excited molecule can occur by intersystem crossing, which is a transition between states of different spin multiplicities (*e.g.*, triplet excited to ground state), by internal conversion, which is a transition between states of the same spin multiplicity (*e.g.*, excited singlet to ground state), and/or by photochemical reaction. "Energy wasting" channels are pathways by which ground-state starting compounds are regenerated after photoexcitation. Photochemical reactions meet with this requirement only when the photoproduct is thermally labile and returns to the starting material. The problems posed in the investigation of such processes together with the finding that the linear compounds in solution quite generally exist as mixtures of several forms with different photophysical and photochemical properties, rendered the studies particularly challenging and exciting. The final goal of this investigation is the understanding of the factors controlling specific relaxation processes, *i.e.*, the routing of the excitation energy into radiative, radiationless, and photochemical channels.

## 2. The Rubins

### 2.1. Spectroscopy of Bilirubin Dimethyl Ester in Solution. Coexistence of Different Forms

A combination of absorption, luminescence, SICD and $^1$H-NMR studies has established that BRE can adopt various forms of aggregation and of monomeric species such as conformers and/or tautomers depending on concentration, solvent and temperature[9]. BR and its dianion appear to behave qualitatively in a similar way, as judged from their solvatochromic and thermochromic properties in absorption and fluorescence[9–12]. For dilute solutions of BRE (*ca.* $10^{-5}$ M) the situation is exemplified in Figures 1–3 which clearly indicate the presence of at least two species[9]. Either or both of these species may in fact represent groups, each of which is composed of several components similar in spectral and conformational respects. For the sake of simplicity we shall continue here, nevertheless, to use the expressions "two species" or "two forms".

The absorption bands of BRE in different solvents at room temperature exhibit quite different intensity ratios. For example, in ethanol there is a maximum at 448 nm with a shoulder at 408 nm, and in 2-methyltetrahydrofuran a maximum at 397 nm with a shoulder at 445 nm (Fig. 1B). However, the fluorescence spectra in these solvents at the same temperature are still very similar (Figs. 1A and 1B). The emission of one species—with $\lambda_{max}^{exc} = 450$ nm at room temperature and 481 nm at 77 K—strongly predominates in ethanol over the entire temperature range. While the other species—with $\lambda_{max}^{exc} = 395$ and 420 nm, respectively—is detected in ethanol only at 77 K as a very small fraction (Fig. 2), appreciable contributions of both species to the fluorescence are observed in ethyl lactate at room temperature (Fig. 1C and 1C′) and in 2-methyltetrahydrofuran at 77 K (Fig. 2)[9].

When evaluating the quantitative aspects of fluorescence, it is important to recall that *the ground-state fraction*

[*] Trivial names are used throughout this article. In accordance with the IUPAC nomenclature suggested for the bile pigments [*Pure Appl. Chem. 51* (1979) 2251] the Fischer IXα notation for the carbon skeletons of BR, BRE and BVE is omitted while the full Fischer nomenclature is retained for the constitutional isomers. Furthermore, all-*Z*,all-*syn* conformations are not specified. Only diastereoisomers with at least one *E* double bond and/or *anti* arrangement of the nitrogen atoms are designated as such.

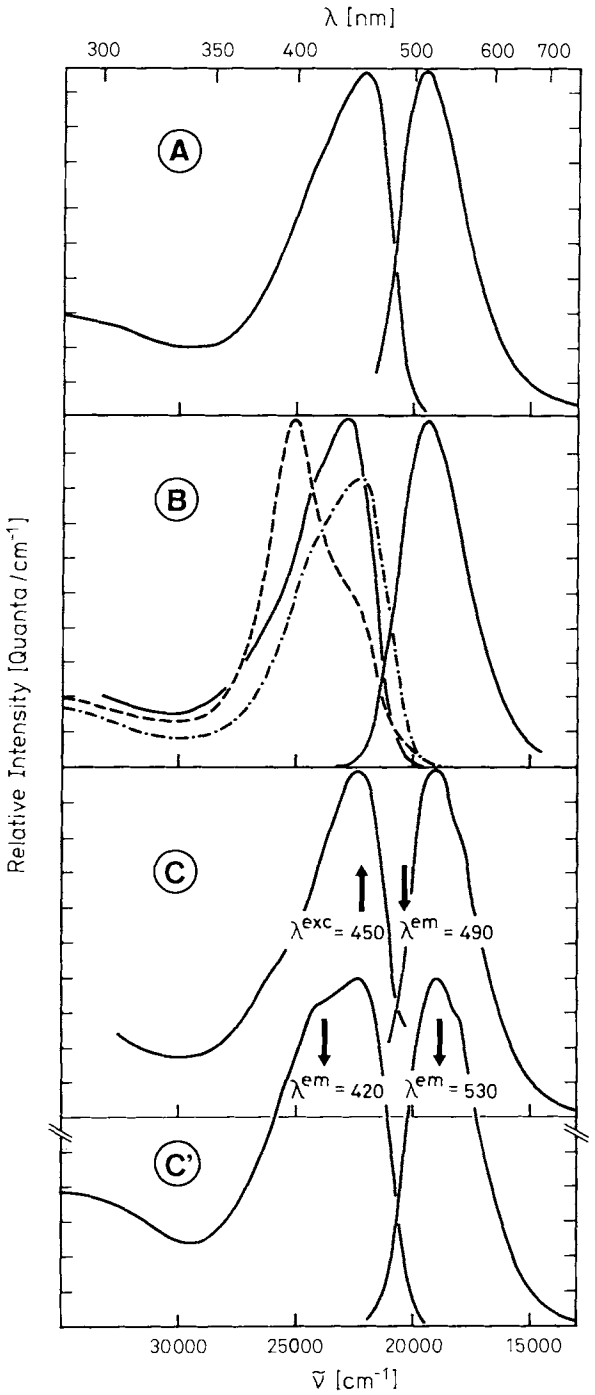



Fig. 1. Corrected room temperature fluorescence and fluorescence excitation spectra of BRE in ethanol (A), 2-methyltetrahydrofuran (B), and ethyl lactate (C and C). While in A and B the spectra are essentially independent of $\lambda^{exc}$ and $\lambda^{em}$, they clearly arise from different components of a mixture in C and C where $\lambda^{exc}$ and $\lambda^{em}$ were varied. The room temperature absorption spectra in ethanol (---) and in 2-methyltetrahydrofuran (----) are also given in B for comparison [9].

*of a fluorescing component in a mixture, i. e., the molar fraction $X_i$, is often difficult to determine.* Since the relative fluorescence intensity is proportional to the product of $X_i$ times individual fluorescence quantum yield, $\Phi_{f(i)}$, the comparison of the fluorescence bands therefore does not give a direct measure of $X_i$ unless $\Phi_{f(i)}$ is known as well. In investigations such as discussed here, however, the measurement of $\Phi_{f(i)}$ values is normally difficult if at all possible.

Fluorescence lifetime and SICD measurements in optically active solvents confirm the presence of two BRE species[9]. For example, in ethanol at 77 K fluorescence lifetimes of 1.9 ns for the predominant "450 nm" and 11.9 ns

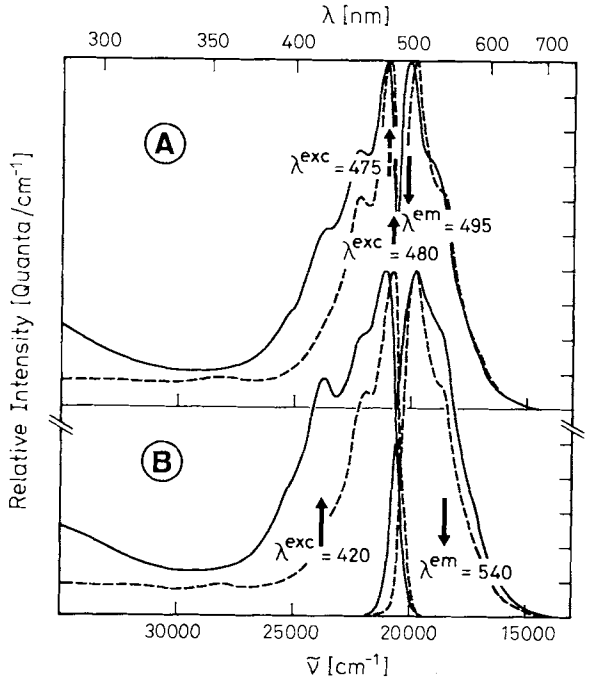



Fig. 2. Corrected 77 K fluorescence and fluorescence excitation spectra of BRE in ethanol (---) and in 2-methyltetrahydrofuran (—). A: $\lambda^{exc}$ = 475 (ethanol) and 480 nm (2-methyltetrahydrofuran), $\lambda^{em}$ = 495 nm (both solvents); B: $\lambda^{exc}$ = 420 nm, $\lambda^{em}$ = 540 nm (both solvents) [9].

for the minor "395 nm" component of the dual emission were obtained. The relative lifetimes are reversed at room temperature. Thus, from the room temperature data (Table 1) a *circa* tenfold lower fluorescence quantum yield, and hence a correspondingly shorter lifetime has been estimated for the minor species than was measured for the major component. The BR form which spectrally corresponds to the "450 nm" BRE species, was found to have a lifetime of about 20 ps in organic solvents at room temperature[13, 14]. Lifetimes in the nanosecond range, found for BR in various media and initially attributed to the *E,Z* photoisomers[15], now appear more likely to belong to secondary photoproducts such as lumirubin and isolumirubin (see Section 2.3 and Schemes 3 and 4). The *E,Z* isomers have much lower fluorescence quantum yields[14] and hence should possess correspondingly shorter lifetimes than BR.

In ethyl (*S*)-(−)-lactate and (*R,R*)-(−)-2,3-butanediol at room temperature, where the absorptions of BRE lie between the two extremes shown in Figure 1B, the SICD spectrum exhibits two bands of opposite signs in the Vis region (Figs. 3A and 3B). While the wavelength positions of the SICD maxima are almost independent of the solvent, their relative intensities and signs respond to solvent changes. The most simple explanation for this behavior is to attribute the two bands to different species. However, one cannot rule out the alternative that one of the BRE

Table 1. Fluorescence quantum yields of some rubins, verdins, and model chromophores in solution [a].

| Cpd. | see Scheme | Concentration [$10^5$ mol $L^{-1}$] | $\lambda^{exc}$ [nm] | Temp. [K] | $\Phi_f$ | Ref. |
|---|---|---|---|---|---|---|
| IPRE | 2 | 10 | 410 | 298 | 0.04 | [18] |
| IPRE | 2 | 10 | 410 | 77 | 0.81 | [18] |
| PRE | 2 | 10 | 410 | 298 | 0.0015 | [18] |
| PRE | 2 | 10 | 410 | 77 | 0.37 | [18] |
| BR | 1 | 50 | 430 | 293 | 0.0005 [b] | [20] |
| BR | 1 | 50 | 430 | 293 | 0.33 [c] | [20] |
| BRE | 1 | 0.2 | 390 | 298 | 0.0076 | [4] |
| BRE | 1 | 0.4 | 390 | 77 | 0.31 | [4] |
| 1 | 2 | 0.8 | 390 | 298 | 0.00096 | [4] |
| 1 | 2 | 0.16 | 390 | 77 | 0.44 | [4] |
| BVE | 1 | 3 | 390 | 298 | 0.00011 [d] | [4] |
| BVE | 1 | 3 | 390 | 77 | 0.00050 [d] | [4] |
| BVE | 1 | 3 | 593 | 298 | 0.00057 [e] | [67b] |
| BVE | 1 | [f] | 593 | 298 | 0.004 [d] | [67b] |
| BVE | 1 | [g] | 593 | 298 | 0.0023 [d] | [67b] |
| BVE-$H^+$ | | 3 [h] | 390 | 298 | 0.00027 | [4] |
| BVE-$H^+$ | | 3 [h] | 390 | 77 | 0.026 | [4] |
| ZnBVE | | 3.3 | 593 | 298 | 0.036 | [67b] |
| 4 | 7 | 1.2 | 430 | 298 | 0.00026 | [4] |
| 4 | 7 | 1.2 | 430 | 77 | 0.0051 | [4] |
| 5 | 7 | 0.14 | 371 | 298 | 0.00043 | [4] |
| 5 | 7 | 0.028 | 371 | 77 | 0.088 | [4] |
| 6 [i] | 7 | 0.29 | 390 | 298 | 0.31 | [4] |
| 6 [i] | 7 | 0.29 | 390 | 77 | 0.37 | [4] |

[a] All measurements in ethanol unless otherwise specified. [b] In ethyl acetate. 1: Neoxanthobilirubinic acid methyl ester; 4: 4,4'-diethyl-3,3',5,5'-tetramethyl-4-pyrromethene. [c] In poly(methylmethacrylate). [d] $\Phi_f$ Value close to that of the helically coiled form. [e] $\Phi_f$ Value from excitation of more stretched components than in [d]. [f] In EYL liposomes immediately after incubation. [g] In DPL liposomes after incubation with BVE. [h] [HCl] *ca.* $10^{-3}$ M. [i] See [21] for similar data of additional difluoroborylpyrromethene complexes.

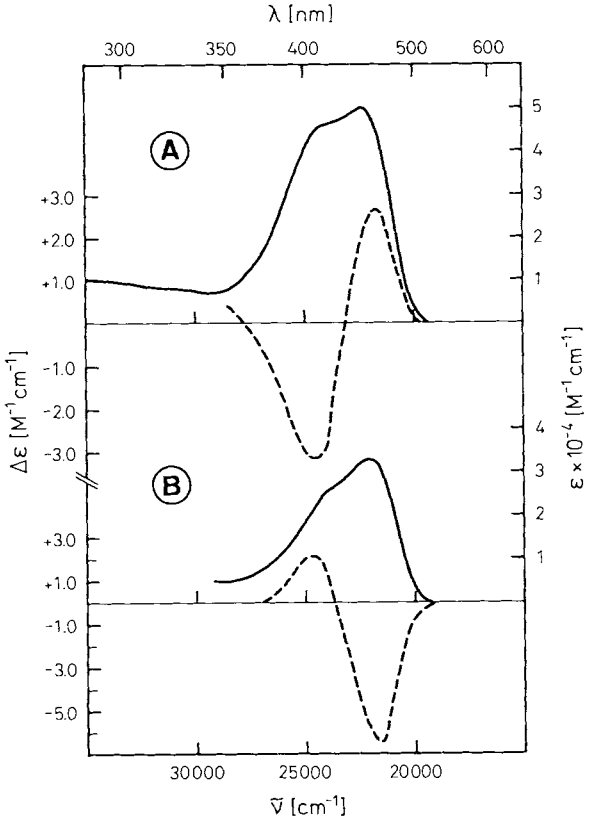



Fig. 3. Room temperature absorption (—) and SICD (---) spectra of BRE in ethyl (*S*)-(−)-lactate Ⓐ and (*R,R*)-(−)-2,3-butanediol Ⓑ [9].

forms has an intrinsic bisignate Cotton effect[*] owing to exciton coupling, and that this spectrum is superimposed by an additional single CD band belonging to the second BRE form. The two Cotton effects of SA-bound BR, again of opposite signs, can be ascribed either to a bisignate effect due to exciton coupling as proposed previously[16], or to a conformational inhomogeneity of BR. The latter perhaps is complexed only with one half of the molecule so that much of it might still be able to adopt different conformations[11]. This last point, however, is still under debate[17]. The former alternative finds some support in the fact that the BR populations in solution and when bound to SA, as judged from the absorption spectra, appear to be more homogeneous than are those of BRE in various solvents[9].

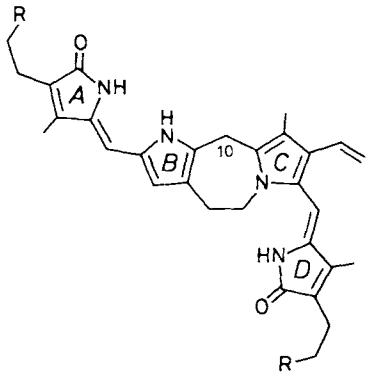
### 2.2. The Nature of the Coexisting Ground-State Forms. Phorcarubin and Isophorcarubin Dimethyl Esters

For an evaluation of the nature of the two prevailing forms of BRE in dilute solutions it is best to first consider analogous results obtained for PRE and IPRE (Scheme 2)[18]. Both isomers possess more rigid tetrapyrrole backbones than does the parent BRE. The fusion of the central rings B and C forces the two pyrromethenone partial structures into a stretched (though not necessarily planar) alignment with the nitrogens in an *anti* arrangement. While in PRE the pyrromethenones are still conformationally and configurationally flexible around the C-5–C-6 and C-14–C-15 bonds, the constraints are greater in IPRE, with one of the pyrromethenones (rings C/D) fixed by intramolecular cyclization in the *Z-anti* form. Coalescence of the C-10 methylene proton signals in the NMR spectra of PRE and IPRE at room temperature shows that the central seven-membered ring has retained some degree of conformational mobility in both compounds. In contrast, the fused tricyclic C/D chromophore of IPRE must be more rigid, and only the A/B part is as flexible as in BRE and the parent pyrromethenone 1.

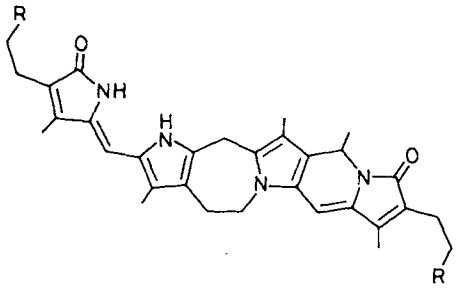
This rigidity is reflected for IPRE, on the one hand, in some structure of the UV absorption even at ambient temperature, whereas the coexistence of several conformers of the more flexible bilirubins gives rise to broad and unstructured bands. On the other hand, it is even more clearly reflected in the fluorescence quantum yields of the rubins and of 1 in fluid solution (Table 1). IPRE exhibits by far the highest fluorescence efficiency of all. This can be attributed to the C/D chromophore and its lack of conformational mobility. Such mobility is known to provide an efficient mode for radiationless deactivation in other chromophoric systems[19] (see also the verdins, Section 3[4]).

The absorption, fluorescence and fluorescence excitation properties of both PRE and IPRE qualitatively resemble those of BRE. In each case, they again clearly arise

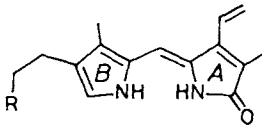
[*] An intrinsic bisignate Cotton effect is a couplet, *i.e.*, two close-lying Cotton effects with opposite signs. Such couplets are observed in the CD of coupled oscillators with sufficiently large electrical transition moments; cf. [82].



**PRE** Phorcarubin dimethyl ester



**IPRE** Isophorcarubin dimethyl ester



**1**

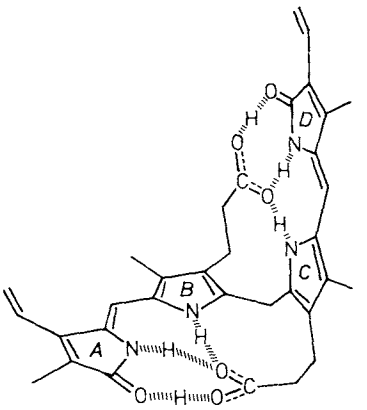
$R = CO_2CH_3$

Scheme 2. The constitution of PRE and IPRE possessing constrained conformational mobilities, and the parent ring A/B model chromophore (**1**) of BRE.

from at least two species, and the composition again strongly depends on concentration, solvent and temperature[9, 18]. The nature of the two forms prevailing at low concentrations has not yet been rigorously elucidated, but a conformational isomerism is the most likely. A lactam-lactim tautomerism, which has been ruled out for BRE[22, 23], seems less probable, and aggregation, preferred in apolar solvents at sufficiently high concentrations[23], had been excluded for the low-concentration experiments with BRE, PRE, and IPRE[9, 18]. In view of the similarity in fluorescence and fluorescence excitation it was suggested[18] that the origin of the spectral heterogeneity is also common to all three compounds. It is attributed to different relative orientations of the A/B and C/D subchromophores around the central C-10 methylene carbon which in PRE and IPRE is contained in the still flexible seven-membered ring (see above). The alternative would be that the different forms arise from different orientations of the individual rings with respect to each other, *i.e.*, within the A/B and C/D pyrromethenone moieties. This possibility is ruled out by the negligible contribution at room temperature of the non-cyclized pyrromethenone moiety to the total emission of IPRE. An important general conclusion then is that *the major contribution to the heterogeneity in fluorescence comes from the different orientations of the A/B and C/D pyrromethenone moieties with respect to each other.*

It is in accord with this conclusion that the spectral properties of the "395 nm" species of BRE, on the one hand, resemble those of the isolated parent chromophore **1**[24, 25]. A geometry with minimum electronic interaction between the two halves of the BRE molecule was consequently assigned to this species[25]. On the other hand, the spectrum of the "450 nm" form cannot be extrapolated straightforwardly from the spectra of the separate partial chromophores. Rather, it must arise from an electronic coupling of the two subchromophoric moieties of BRE, presumably owing to a particular geometric orientation. Analogous assignments can also be made for the two forms of BR.

Calculations on the BR-SA complex[16] using CD and the absorption data which essentially correspond to those of the "450 nm" species predicted a conformation similar to the "ridge tile" arrangement (Scheme 3) found subsequently for the BR crystal structure[26]. We shall see in Section 2.4 that this is also the most likely arrangement for the electronically coupled "450 nm" forms of BR and BRE in organic solvents.



Scheme 3. Intramolecularly hydrogen-bonded "ridge tile" conformation of BR in the crystal structure [26]. The "450 nm" forms of BR and BRE in organic solvents presumably possess a similar conformation.

### 2.3. The Photochemistry of Bilirubin and Bilirubin Dimethyl Ester

Under anaerobic conditions, two types of photoisomerizations have been encountered[20, 27-33]: A rapid configurational $Z \rightarrow E$ isomerization of either of the exocyclic C=C double bonds has been found with BR and BRE, as well as with similar tetrapyrroles and model compounds[34], and BR has also been shown to undergo a less efficient cyclization to form lumiproducts. Other photoreactions such as addition reactions, formation of positional isomers, and oxidative degradation of BR do not noticeably interfere with $Z \rightarrow E$ isomerization and lumiproduct formation, since

they proceed with quantum yields that are at most a tenth of that of the predominant isomerization near room temperature. The oxidation reactions, moreover, require aerated solutions[35].

Several studies show that the $Z \rightarrow E$ double bond photoisomerization occurs in the lowest excited singlet state of BR. The evidence can be summarized as follows:

1) The quantum yields of fluorescence and $Z \rightarrow E$ isomerization of SA-bound BR exhibit a reciprocal relation as the temperature is varied. The fluorescence yield increases from about 0.0002 at room temperature to 0.44 at 77 K, while the isomerization yield drops from 0.20 to $\leq 0.01$[14].

2) The yield of triplet state BR near room temperature strongly varies with the nature of the solvent, but it consistently is lower than the isomerization yield[5,7,8]. The fluorescence yields under the same conditions are about ten times lower[5,14], indicating that electronic relaxation of excited singlet BR at this temperature proceeds predominantly *via* radiationless pathways other than intersystem crossing to the triplet state.

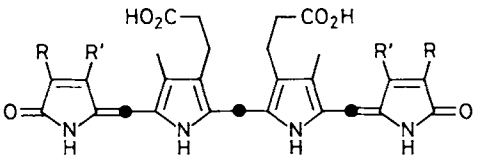
3) In organic and aqueous solvents, in vesicles and when bound to SA the $S_1$ state of BR with a lifetime in the range of 12—70 ps was observed at 295 K by fluorescence ($\lambda^{em} = 525$ nm)[13] and absorption detection[14]. Similar lifetimes were also obtained for BR-IIIα and the pyrromethenone **2** (Scheme 4)[13]. The assignment of the absorption decay to the $S_1$ state is confirmed for BR-SA by the parallel temperature dependence of this decay and of the fluorescence quantum yield[14].

The three configurational photoisomers of BR[31,32] and BRE[28,29,36] are unstable and revert to the (4*Z*,15*Z*)-isomer, both photochemically and thermally. Equation (a) summarizes these interconversions[31]:

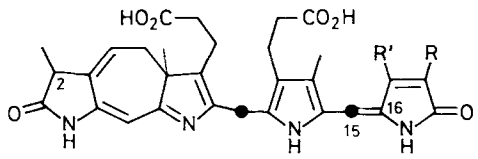
$$4Z,15Z \rightleftharpoons (4E,15Z + 4Z,15E) \rightleftharpoons 4E,15E \qquad \text{(a)}$$

The anaerobic photochemical transformations of BR, both in solution and bound to human and rat SA, have been studied in some detail. The results did not differ qualitatively. While the symmetrical BR-IIIα rapidly reaches a photostationary equilibrium with its (*E*,*Z*) and (*E*,*E*) isomers[31], the $Z \rightarrow E$ isomerization of BR and BR-XIIIα is accompanied in each case by the slower photocyclization to the C(-2)-epimeric lumirubins LR and ILR[33] (Scheme 4). On further irradiation of the lumirubins an $E \rightleftharpoons Z$ equilibrium at the C-15=C-16 double bond is established without detectable reversion to the parent bilirubins. Since the lumirubin formation is not inhibited by molecular oxygen, it was suggested that the reaction occurs also from the excited singlet state. It appears, furthermore, that the cyclization is a single-photon process *not* requiring the (*E*,*Z*)-bilirubins as intermediates[33].

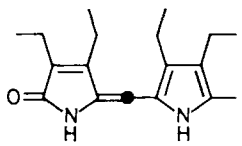
It is not surprising in the light of the heterogeneous composition of BRE solutions (Sections 2.1 and 2.2) that the anaerobic photochemistry proved dependent on the excitation wavelength[36]. The "395 nm" species has a lower quantum yield of photoisomerization than the "450 nm" conformer. Moreover, the distributions of the products formed, at very low conversions, from the two components and their reactivities in the secondary phototransformations are different. The results can be summarized by extending the reaction scheme (a) to (b) which represents a *minimum* scheme for the $E \rightleftharpoons Z$ isomerizations of the "395 nm" and "450 nm" solution forms of BRE. Additional transformations not included in this scheme (*e.g.*, conversions diagonally across the scheme (b) such as *Z,Z*-BRE′ $\rightleftharpoons$ *Z,E*-BRE″ *etc.*) are also conceivable provided that the preferences for the reaction pathways are maintained.



**BR-IIIα** (R = CH=CH$_2$, R′ = CH$_3$) Bilirubin IIIα
**BR-XIIIα** (R = CH$_3$, R′ = CH=CH$_2$) Bilirubin XIIIα

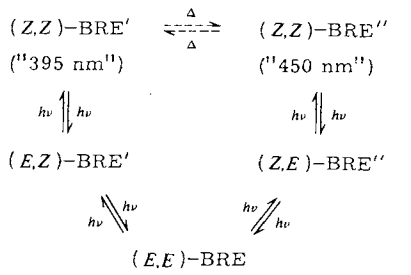


*(E)*- and *(Z)*-**LR** Lumirubins
*(E)*- and *(Z)*-**ILR** Isolumirubins (C2 epimers)



**2**

Scheme 4. Constitution of BR-IIIα, BR-XIIIα, the lumiproducts, LR and ILR, formed photochemically from BR and BR-XIIIα, respectively, and the pyrromethenone **2**.




(b)

### 2.4. Radiationless Deactivation (Internal Conversion)

Rotation modes around the C—C and C=C bonds at C-5 and C-15 play a substantial role in the direct deactivation of the first singlet excited state of BR and BRE at room temperature. This conclusion is based on the overall quantum efficiency associated with the $Z \rightarrow E$ photoisomerization (*i.e.*, with the relaxation by $k_1$ and $k_2$ of the twisted excited singlet state, $^1S_1$, to both the *Z,Z* and *E,Z* isomers;

see Fig. 4), which is probably not much greater than 0.4 in solution (see below)[27,37,38], and the fact that an important part of the wasting channels for the remainder (almost 0.6, with emission being negligible) is turned into fluorescence upon lowering the temperature or upon embedding the molecule in a solid matrix at room temperature (Table 1). This points to substantial energy dissipation in fluid media at room temperature by rotations around C–C single bonds, which are strongly inhibited in solid matrices. The rotations are restricted to the C-5 and C-15 bridges, *i.e.*, to within the pyrromethenone subchromophores. The evidence has already been partially given in Sections 2.1 and 2.2. It comprises the behavior of the emission with temperature or viscosity, the comparison with PRE and IPRE, and the increase of fluorescence[39], singlet lifetime, and singlet yield[15] upon disruption of the intramolecular hydrogen bonds. Such bonds, between the carbomethoxy carbonyls and the pyrrole nitrogens similar to those found in the crystal structure of BR[26] (Scheme 3), are presumably attained also in organic solvents[12,40–42]. Results with SA-bound BR confirm this assignment. At room temperature, the fluorescence yield increases upon binding by a factor of about 25 over that in chloroform solution, while the photoisomerization remains essentially unaffected[14,28]. Although the fluorescence yield of the BR-SA system at room temperature reaches only about a fifth of the yield at 77 K in ethanol, the trends followed upon binding to SA and upon cooling are parallel. Moreover, the photoisomerization is obviously not subject to the same environmental control. An analogous situation is also indicated for the pyrromethenone **1**, the fluorescence of which increases by a similar margin upon binding to SA[17].

These considerations refer particularly to the electronically coupled "450 nm" species since it is the predominant form of BR and BRE under the conditions studied. The relative fluorescence quantum yields of the two BRE species (low for the "395 nm" and high for the "450 nm" form at room temperature) and their opposite trends with the lowering of temperature indicate that the latter is the more rigid one. The greater rigidity may derive, in BR, from a conformational fixation through intramolecular hydrogen bonds, *i.e.*, the "450 nm" form of BR may correspond to an arrangement as shown in Scheme 4. According to NMR measurements, the activation barrier associated with the unzipping of the six hydrogen bonds of BR is *ca.* 75 kJ/mol in chloroform[42]. The internal bonding restricts the rotational freedom of the molecule, and it slows down the excited-state twisting towards the $Z \rightarrow E$ photoisomerization[20,28], with a barrier of *ca.* 30 kJ/mol[43]. In SA-bound BR which lacks the hydrogen bridging between the two halves of the pigment, the barrier is lowered to 23 kJ/mol[20].

The "450 nm" species of BRE may well be subject to similar constraints, albeit less important since there are fewer hydrogen bonds involved in the diester. Thus, the overall rate of isomerization of BRE is faster than that of BR in the same solvent[28]. Reversible intramolecular proton transfer processes remain available for alternative channels of energy wasting. This deactivation mode should be less affected thermally and by viscosity than that induced by the C–C rotation modes, and it should thus assume a more important role at low temperature. The more flexible "395 nm" species presumably lacks similar intramolecular hydrogen bridges, and it consequently is more readily subjected to deactivation induced by rotations around C–C bonds and less so to hydrogen bond-mediated deactivation.

In conclusion we may extend somewhat the kinetic scheme of an earlier[14] diagram of the potential energy levels and deactivation routes of BR and BRE (Fig. 4). The sums of rotational and hydrogen bridge-mediated deactivation rate constants, $k_{d(1)}$ and $k_{d(2)}$, of the $S_1$ states of BR, BRE and the *E,Z* photoisomers are included as an important competition to fluorescence. In the BR-SA system the $Z \rightarrow E$ isomerization quantum yield and the proportion of the *E,Z* isomer in the photoequilibrium at room temperature are about equal (*ca.* 0.2) when excited at the isosbestic point of 465 nm[14,30]. In terms of the rate constants $k_{d(1,2)}$, $k_{I,II}$ and $k_{1,2}$ two limiting situations can be envisaged. On the one hand, it has been suggested[20] that the twisted singlet state, $^tS_1$, is formed with nearly total efficiency from both the *E,Z* and *Z,Z* $S_1$ states ($k_I/k_{II}$ at $\lambda^{irr} = 465$ nm). This assumption would result in a $k_1/k_2$ ratio of *ca.* 4 and would leave no room for direct radiationless deactivation to the ground state. It should be pointed out that the rate constants of all C–C and C=C rotational modes, $k_I$, $k_{II}$, $k_{d(1)}$, and $k_{d(2)}$ can be expected to be strongly viscosity and/or temperature dependent, for they involve large-amplitude intramolecular motions (cf. also Section 3). The *a priori* assumption in [20] that $k_d$ is *independent* of temperature and/or viscosity is lacking experimental verification. The reciprocal relation between the yields of fluorescence and photoisomerization are insufficient evidence for establishing constancy of $k_d$. Our arguments are further supported by the finding that in frozen matrix $Z \rightarrow E$ photoi-

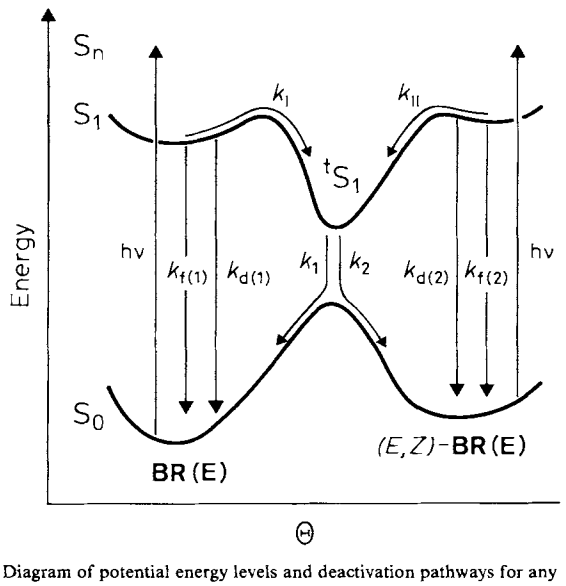



Fig. 4. Diagram of potential energy levels and deactivation pathways for any given conformer of BR and BRE and their *E,Z* photoisomers. $\Theta$ designates the twist angle about one of the exocyclic double bonds, $k_{d(1)}$ and $k_{d(2)}$ are the sums of the rate constants for deactivation by C–C rotation and hydrogen bridge-mediated processes, $k_{f(1)}$ and $k_{f(2)}$ are the rate constants for fluorescence, $k_I$ and $k_{II}$ for twisting around a double bond, and $k_1$ and $k_2$ for relaxation of the twisted excited state, $^tS_1$, to starting material and photoproduct, respectively. The activation energies required for $k_{d(1)}$ and $k_{d(2)}$ and the reaction paths for the cyclization to the LR's and ILR's, the mechanism of which is still under debate, are not depicted (cf. [14]).

somerization is negligible and yet the fluorescence quantum yield does not reach unity. We therefore prefer an alternative situation approaching the other extreme in which the ratio $k_I/k_2$ is close to 1. This implies that the efficiency of $^1S_1$ formation is considerably less than unity and different for the two $S_1$ states (*i.e.*, $k_I/k_{II}$ *ca.* 4:1 at $\lambda^{irr}=465$ nm). The remainder would thus be available for direct deactivation of the $S_1$ states *via* $k_{d(1)}$ and $k_{d(2)}$, respectively, as discussed above. The second model also fully accommodates the above-mentioned different responses of fluorescence and photoisomerization of BR upon complexation with SA.

## 3. The Verdins

### 3.1. Spectroscopy of Biliverdin Dimethyl Ester in Solution. Coexistence of Helically Coiled and Stretched C-10 Isomers

A combination of stationary spectroscopic techniques similar to that used for BRE served also for the initial investigation of BVE. It was subsequently supplemented by time-resolved methods (LIOAS, PP, SPT) which afford a better insight into the relationship between structure and radiationless processes of individual species.

The solution spectra of BVE, at low concentrations, also exhibit distinct thermochromic and solvatochromic properties which again have been interpreted in terms of predominantly two forms coexisting in solution (as an illustration see Fig. 5)[4,44,45]. Aggregation at low concentrations (*e.g.*, $\leq 10^{-5}$ M in ethanol; for a discussion of aggregation see Section 3.5) and lactam-lactim tautomerism can be discarded[46]. The intensity ratio of the two first emission bands varies quite appreciably in the various solvents. In methanol and ethyl lactate the absolute maximum is at *ca.* 660 nm, and in ethanol, chloroform and 2-methyltetrahydrofuran at around 710 nm.

The "660 nm" form, with its relatively small values for the SICD Cotton effect, the Stokes shift and the $D_{UV}/D_{Vis}$ ratio in the fluorescence excitation spectrum has been assigned a stretched form[4,44,47]. Furthermore, the stretched partial structure can be localized around the C-10 bridge (Scheme 5)[47,48] (see Section 3.4 for the evidence). Although our term "form" may, as for the rubins, just as well cover members of families of closely related spatial arrangements rather than individual forms, the vibrationally

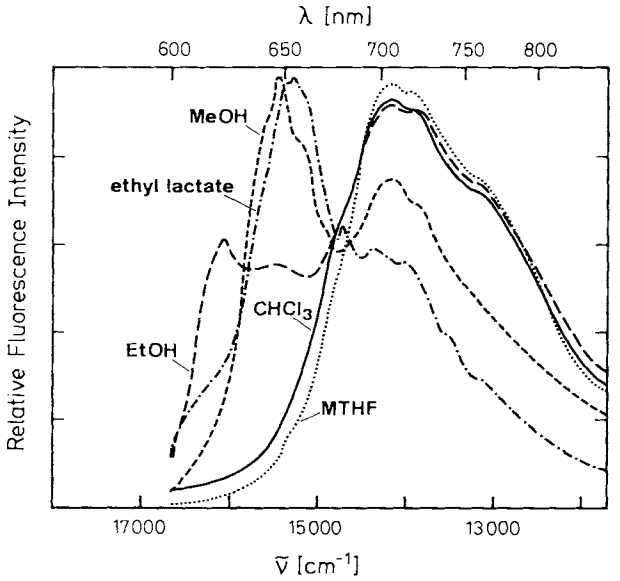
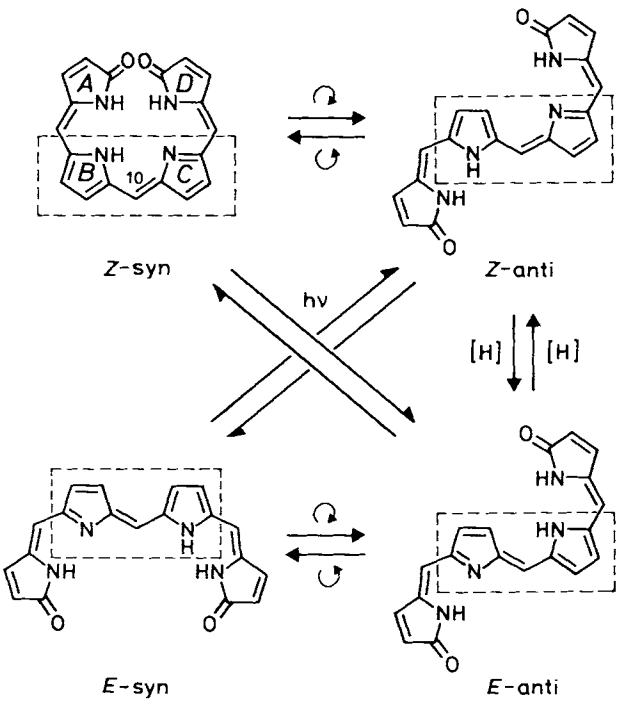



Fig. 5. Corrected fluorescence spectra of BVE in different solvents at room temperature; $\lambda^{exc}=580$ nm; concentration $1\times10^{-5}$ M [47]. MTHF = 2-methyltetrahydrofuran. Prior to the measurement, the solutions were subjected to a *short* ultrasonic treatment in order to ensure better reproducibility. There are slight quantitative differences in composition between the sonicated and the corresponding non-sonicated solutions (cf. Section 3.3).




Scheme 5. The helically coiled all-*Z*,all-*syn* and the three stretched *E-anti*, *E-syn* and *Z-anti* forms of bilatriene with interconversion paths involving proton transfer processes (tautomerizations) between the B/C nitrogens ([H]) and rotation around the C-9–C-10 single bond (⌒) in the electronic ground state, and $E \rightleftharpoons Z$ isomerization of the C-10=C-11 double bond in the excited state (*hν*). Given the unsymmetric IXα substitution pattern of BVE, the overall number of these forms doubles to eight [*] (cf. Scheme 9).

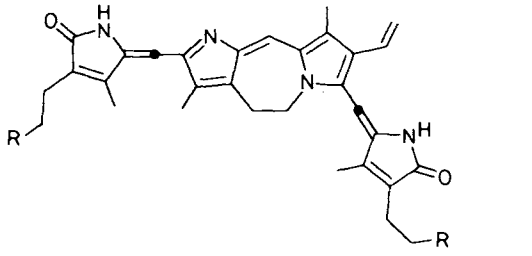
[*] In order to simplify the nomenclature in this article, we shall use generally applicable terms such as "form" and "species" in the discussion of the possible spatial arrangements of BVE, in lieu of "conformation" as a general topological definition or "conformation" and "configuration" as energetically distinguished terms for rotational isomerism. Scheme 5 lists the forms of the constitutionally symmetrical bilatriene, which are still possible after motions within the A/B and C/D halves of the molecule have been excluded. A justification of this restriction in the context of this article is given in Section 3.4. The diverse forms, which equilibrate only slowly at room temperature, can be divided into two categories: the *Z-syn* form on the one hand, and the three stretched forms *E-anti*, *E-syn* and *Z-anti* on the other hand. These species form two pairs of configurational isomers (*E-anti*/*Z-syn* and *E-syn*/*Z-anti*), the components of which are formally interconvertible. Such interconversions can be effected in both a one-step $E\rightarrow Z$ isomerization of the C-10=C-11 double bond and in two steps comprising a rotation around the C-9–C-10 single bond and a proton transfer between the B and C nitrogen atoms. The two-step transformation proceeds, in each case, *via* the *anti* component of the alternate pair (cf. Scheme 5). When the unsymmetrical IXα substitution of rings A and D is introduced, each of the forms of Scheme 5 is supplemented by a further constitutional isomer (tautomer) as shown in Scheme 9.

structured narrow bands of the "660 nm" species (cf. Figs. 5 and 10C) point to a well defined unique species.

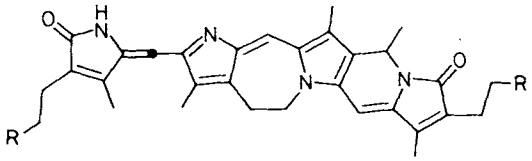
The "710 nm" form, with a longer-wavelength emission, a broader first excitation band, and larger values for rotational strength, Stokes shift and $D_{UV}/D_{Vis}$ ratio, was identified as a helically coiled all-*syn*-type orientation similar to the conformation found in the crystal lattice[49]. This form is quite generally the more abundant in organic solvents[44,45,50]. A thermal barrier of 42 kJ/mol was measured, in a $^1$H-NMR kinetic study of the centrochiral methanol adduct **3** (Scheme 6)[51], for the interconversion of the two diastereoisomeric bilatriene all-*syn* helices.

The conformational assignment is based on a detailed $^1$H-NMR study of the all-*syn* form in chloroform solution[45], and it is in accord with the prediction of semiempirical calculations that the ratio $D_{UV}/D_{Vis}$ of the two main absorption bands of the verdins is a function of molecular extension. A decrease of this ratio indicates a change from a helically coiled to a more stretched form[16,52-57]. This trend analysis is supported by the fact that the conformationally rigid stretched verdins BVE-IXδ (Scheme 8), PBE and IPBE (Scheme 6)[58-60] have a very much smaller UV absorption band than BVE.

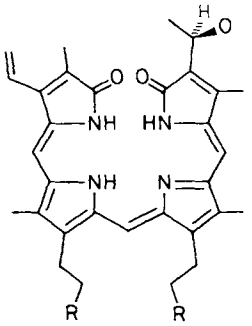
SICD measurements in optically active solvents corroborate the conclusions drawn from the emission results. Structurally related compounds such as tetraphenylporphyrin, protoporphyrin, and dipyrromethenes do not exhibit any such SICD. The observed effects therefore reflect mainly an inherent chiral property of BVE. At room temperature, the positions of the two main absorption bands, and particularly the position of the Vis maximum, are solvent-dependent, whereas the SICD bands invariably appear at the same wavelength. They either coincide with the absorption, which is an envelope of the individual absorptions of the various forms, or they are red-shifted (Fig. 6A). Such red shifts are due to the fact that the most abundant species in most solvents is the coiled form which absorbs at the longer wavelengths. These findings confirm the



**PBE** Phorcabilin dimethyl ester



**IPBE** Isophorcabilin dimethyl ester



**3**

$R = CO_2CH_3$

Scheme 6. Constitutional formulas of PBE and IPBE possessing constrained conformational mobilities, and of the methanol adduct **3**, for which the interconversion barrier of the bilatriene helix was determined.

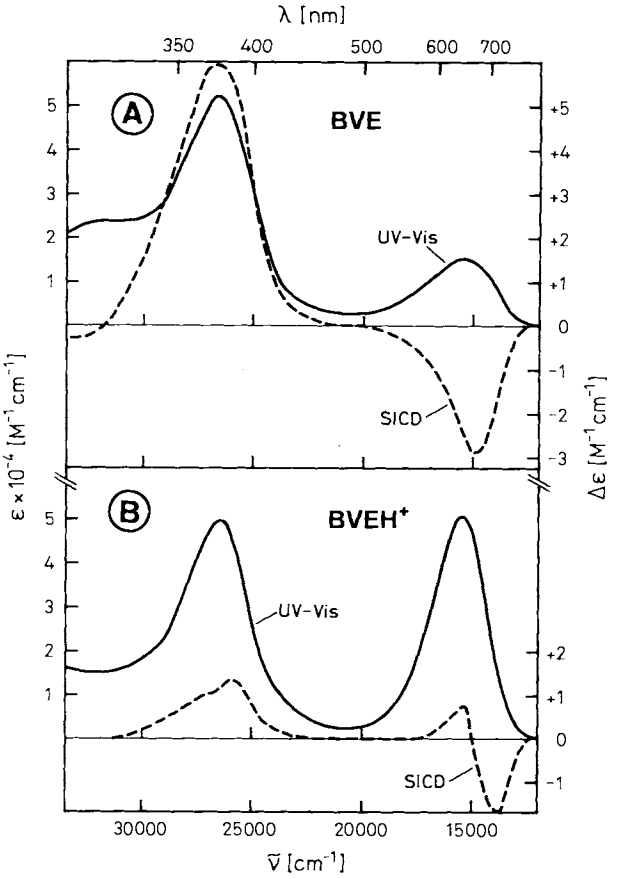



Fig. 6. UV/Vis absorption and SICD spectra at 298 K Ⓐ of BVE and Ⓑ of BVE-H$^+$ in ethyl (*S*)-(−)-lactate; concentration $3.3 \times 10^{-5}$ M [44].

coexistence of at least two forms. Their relative populations vary with the nature of the solvent, and they differ in their contributions to rotational strength, absorption, and fluorescence. The SICD spectrum of BVE-H$^+$, which exhibits the same general spectroscopic characteristics as BVE (Table 1), reveals even more clearly the composite nature of the solution. Only one component of BVE-H$^+$ similar to the "660 nm" species of BVE is seen by fluorescence at

room temperature in ethyl lactate. Nevertheless, the visible SICD is shifted to longer wavelengths relative to the corresponding absorption (Fig. 6B), and the rotational strengths of both bands are markedly lower than those of BVE. Furthermore, the visible SICD shows two Cotton effects of opposite signs. The interpretation necessarily is as ambiguous as it is in the case of BR (Section 2.1). Rather than attributing the phenomenon to exciton splitting alone, we prefer again to attribute it to a composed SICD split either into two single-band components of opposite signs or into one single-band component superimposed onto another one which is bisignate. The shorter-wavelength component is assigned to the predominant stretched species possessing an intrinsically small rotational strength. The red-shifted SICD component then is of the coiled form with an intrinsically larger rotational strength which is present in too small an amount for absorption and fluorescence detection.

### 3.2. Picosecond Kinetics of Excited State Relaxation in Biliverdin Dimethyl Ester

The study of detailed aspects of the radiationless relaxation processes by fluorescence quantum yield determinations and LIOAS (see below) has been particularly impaired by the considerable overlap of the absorption and fluorescence spectra of the individual BVE forms. These difficulties have recently been overcome by an investigation[47] which combined picosecond absorption and fluorescence detection using the PP and SPT techniques, respectively, and a synchronously pumped mode-locked dye laser system[61]. It proved much superior to previous single-shot picosecond measurements of etiobiliverdin with transient absorption and fluorescence detection[62]. The results obtained are supplementary to the data obtained by the stationary (absorption, fluorescence, SICD) and limited-time resolution methods (LIOAS) which have previously led to the postulate of the coexistence of two (families of) BVE ground-state forms in solution.

In general, a greater number of decay components could be found by the SPT technique (Table 2, Fig. 7 and Fig. 8) than by transient absorption spectroscopy (PP, Table 3). This is due to the considerably larger dynamic range covered by the former (>3 orders of magnitude) than by the latter (*ca.* 1—2 orders of magnitudes). Apart from this, the results obtained by the two techniques are in excellent agreement. They show that, in fact, the situation is even more complex for dissolved BVE than previously recognized. *Up to four fluorescing species, two short-lived (picosecond range) and two long-lived ones (nanosecond range), are detected (Tables 2 and 3). These four excited states can be attributed to either three or four ground-state species.*

The nanosecond decay components $\tau_3$ and $\tau_4$ originate from the stretched "660 nm" form(s). Lifetimes in the nanosecond range are remarkably long for BVE in liquid solution. In accordance with the narrow fluorescence and excitation bands, their partially resolved vibrational structure, and the small Stokes shift these long lifetimes indicate that the species should possess a relatively rigid and uniform conformation and a high fluorescence quantum

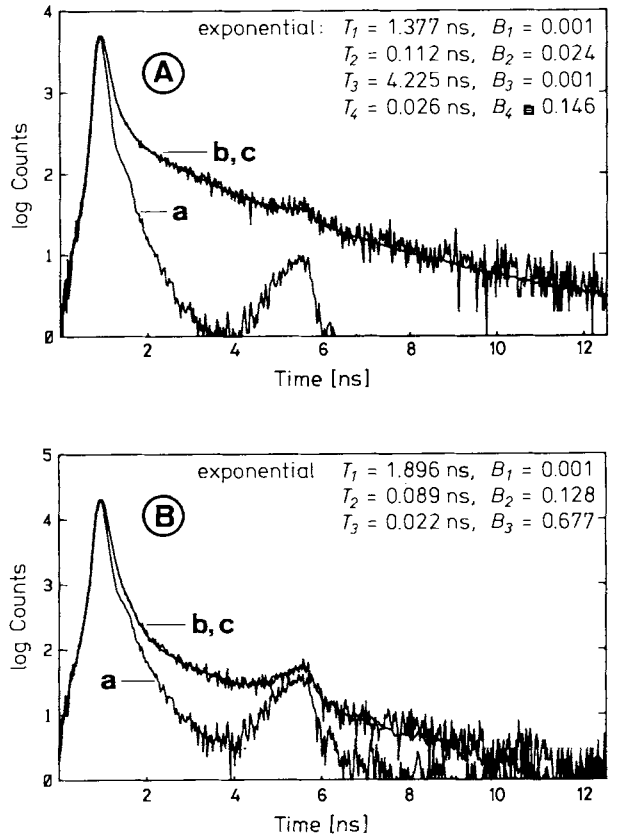



Fig. 7. Semilogarithmic plots of fluorescence decay of BVE in 2-methyltetrahydrofuran at room temperature, as determined by the SPT technique; (A): $\lambda^{exc}$ = 580 nm, $\lambda^{em}$ = 650 nm; (B): $\lambda^{exc}$ = 580 nm, $\lambda^{em}$ = 710 nm (cf. Table 2) [47]. *Note:* The semilogarithmic plots of the exciting pulse (a), the measured decay (b), and the decay function calculated from the best-fit kinetic parameters (c) are shown. In the inset the calculated lifetimes $T_1 \ldots T_n$ and amplitudes $B_1 \ldots B_n$ of the decay components are given.

Table 2. Lifetimes and relative yields of the fluorescence decay components of BVE measured at 298 K by the single-photon timing technique [47].

| Solvent [a] | $\lambda^{exc}$ [nm] | $\lambda^{em}$ [nm] | Lifetimes [ps] [b] | | | | Normalized rel. yields [%] | | | |
|---|---|---|---|---|---|---|---|---|---|---|
| | | | $\tau_1$ | $\tau_2$ | $\tau_3$ | $\tau_4$ | $\varphi_1$ | $\varphi_2$ | $\varphi_3$ | $\varphi_4$ |
| MTHF [c] | 580 | 650 | 26 | 112 | 1377 | 4225 | 34 | 23 | 11 | 32 |
| MTHF [d] | 580 | 710 | 22 | 89 | 1896 | — | 54 | 42 | 4 | — |
| MTHF | 640 | 660 | — | 94 | 1685 | 4545 | — | 12 | 9 | 79 |
| MTHF | 640 | 710 | — | 78 | 968 | 4183 | — | 62 | 10 | 28 |
| $CHCl_3$ | 580 | 650 | 21 | 183 | 1151 | — | 69 | 18 | 13 | — |
| $CHCl_3$ | 580 | 710 | 12 | 71 | 1406 | — | 66 | 31 | 3 | — |
| $CHCl_3$ | 640 | 660 | — | 69 | 940 | 3883 | — | 25 | 10 | 65 |
| $CHCl_3$ | 640 | 710 | — | 62 | 1009 | 3365 | — | 73 | 7 | 20 |
| MeOH | 580 | 650 | — | 140 | — | 4678 | — | 2 | — | 98 |
| MeOH | 580 | 710 | — | 52 | — | 4589 | — | 6 | — | 94 |
| MeOH [e] | 640 | 660 | — | — | — | 4612 | — | — | — | 100 |
| MeOH [f] | 640 | 710 | 38 | — | 630 | 4592 | 8 | — | 3 | 89 |
| EtOH | 580 | 650 | 19 | 249 | 1639 | 4601 | 15 | 11 | 16 | 58 |
| EtOH | 580 | 710 | 10 | 112 | 910 | 3997 | 57 | 9 | 8 | 26 |
| EtOH | 640 | 660 | — | 97 | 879 | 4610 | — | 4 | 27 | 69 |
| EtOH | 640 | 710 | — | 56 | 710 | 4043 | — | 40 | 25 | 35 |
| Ethyl lactate | 580 | 650 | 39 | 239 | 894 | 4150 | 8 | 16 | 12 | 64 |
| | 580 | 710 | 20 | 124 | 659 | 3902 | 29 | 22 | 13 | 37 |
| Ethyl lactate | 640 | 660 | — | 126 | 2140 | 4470 | — | 4 | 21 | 75 |
| | 640 | 710 | — | 108 | 681 | 4250 | — | 5 | 13 | 82 |

[a] Concentration $1 \times 10^{-5}$ M in all measurements; MTHF, 2-methyltetrahydrofuran. [b] The $\tau$ values correspond to the $T$ values given in the insets of Figs. 7 and 8. The ordering $\tau_1 \ldots \tau_n$ (increasing lifetimes) does not correspond to the ordering $T_1 \ldots T_n$. Errors in lifetimes are ±10% or ±5 ps, whichever is larger, except for the single-exponential analysis in which the error is ±1%. For components with a relative yield of less than 5% the errors in lifetime may be up to ±20%. [c] See Fig. 7A. [d] See Fig. 7B. [e] See Fig. 8A. [f] See Fig. 8B.

yield. The long lifetime and the high fluorescence yield are best compatible with an arrangement of rings B and C which prevents rapid deactivation by intramolecular proton transfer between the central nitrogen atoms. While any other than the *Z-syn* form would satisfy this condition alone (cf. Scheme 5), the rigidity appears feasible only by intramolecular hydrogen bonding in a fashion similar to the "ridge tile"-type stabilization (Scheme 3) of BRE, which requires an *anti* arrangement of the B/C nitrogen atoms. As will be shown in Section 3.4, this conclusion is strongly and independently supported by the photochemical results with BVE-IXγ and -IXδ[48].

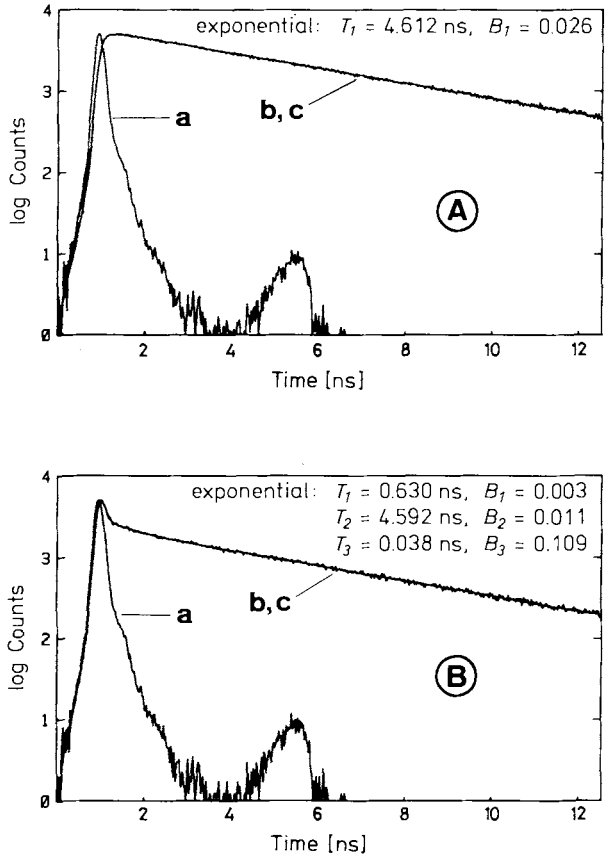



Fig. 8. Semilogarithmic plots of fluorescence decay of BVE in methanol at room temperature, as determined by the SPT technique; Ⓐ: $\lambda^{exc}$ = 640 nm, $\lambda^{em}$ = 660 nm; Ⓑ: $\lambda^{exc}$ = 640 nm, $\lambda^{em}$ = 710 nm (cf. Table 2) [47]. See also the Note of Figure 7.

Table 3. Lifetimes of excited-state BVE measured at 298 K by the PP technique [47].

| Solvent [a] | Excitation-detection wavelength $\lambda^d$ [nm] | Lifetimes [ps] [b] $\tau_1$ | $\tau_2$ | $\tau_3$ | Rel. amplitudes $\tau_1/\tau_2$ |
|---|---|---|---|---|---|
| EtOH | 605 | 19 | 73 | — | 1.7 |
| $EtO^2H$ | 605 | 17 | 57 | — | 1.5 |
| EtOH [c] | 643 | 12 | 68 | — | 3 |
| $EtO^2H$ | 643 | 15 | 55 | — | 5 |
| MeOH | 640 | — | 51 [d] | 1200 [e] | 1.3 [f] |
| MTHF | 640 | 20 | 64 | — | 0.5 |

[a] Concentration $3\text{-}7 \times 10^{-4}$ M in all measurements; MTHF, 2-methyltetrahydrofuran. [b] Maximum errors ± 10%. [c] Cf. data point x in Fig. 9. [d] This lifetime possibly represents an average value of two components. [e] Lower limit to the actual lifetime of a nanosecond component. [f] $\tau_2/\tau_3$.

The spectral properties of stretched BVE are quite reminiscent of those of native phytochrome and phycobiliproteins, especially the phycocyanines. The chromophores of these proteins have also been assigned stretched conformations[2a] in analogy to previous conclusions about BVE[44] and to the absorptions of PBE and IPBE[63]. Inasmuch as analogies between the biliprotein chromophores and BVE are valid, it is of a general photobiological interest to note that BVE can adopt an *inherently rigid* stretched conformation even at room temperature in solution. Intramolecular stabilizing forces evidently suffice. Stabilizing interaction with the protein is, therefore, not necessarily an *a priori* condition for the conformational rigidity of BVE-like tetrapyrroles in biliproteins, in contrast to the generally accepted previous view.

The picosecond decay components are related to the coiled "710 nm" species. The different responses of their decay rates to temperature (Fig. 9) indicates that two mechanisms are responsible for the ultrarapid radiationless deactivation. Relaxation induced by rotation around the single bonds of the methine bridges is presumed to be common to both components. Intramolecular proton transfer, most probably between the central B and C nitrogen atoms as predicted also for *Z-syn*-dipyrroles[64], contributes additionally to the deactivation of the faster ($\tau_1$) of the two decay components. Thus, the relaxation data of the shorter-lived picosecond species are independent of temperature below *ca.* 260 K in $EtO^2H$. The $\log k_1$ *vs.* $1/T$ function consequently is a sum of temperature-dependent and -independent processes, *i.e.*, rotations around C–C bonds and proton transfer, respectively. The latter (long dashes in Fig. 9) brings about radiationless deactivation at a rate of $3.5 \times 10^{10}\ s^{-1}$, and it parallels the temperature-(or rather, viscosity-)dependent relaxation induced by C–C rotations (short dashes). The activation energy for the rotations is in the range of the solvent viscosity activation energy, with an estimated lower limit of *ca.* 12 kJ/mol.

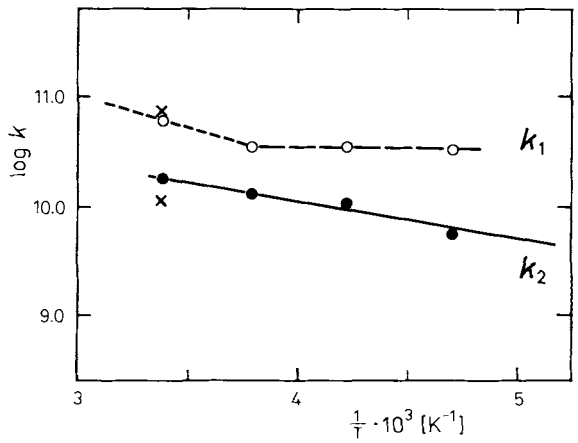
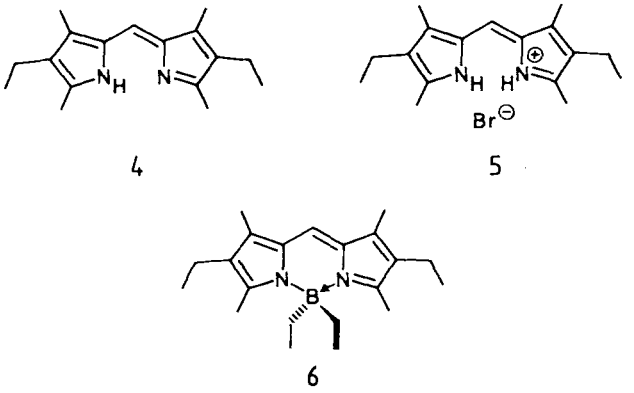



Fig. 9. Temperature dependence of the picosecond decay rate constants $k_1$ and $k_2$ of the BVE transients $\tau_1$ and $\tau_2$, respectively, in $EtO^2H$, determined by the PP technique; $\lambda^d$ = 643 nm. ○: short-lived component $\tau_1$; ●: long-lived component $\tau_2$; ×: room temperature data in EtOH (see Table 3). The short dashes denominate the temperature-(viscosity-)dependent part of the decay of $\tau_1$, and the longer dashes denominate the temperature-independent proton transfer in the $\tau_1$ component [47].

The temperature dependence of the longer-lived component, $\tau_2$, can be smoothly fitted to a straight line (cf. $k_2$ in Fig. 9). Ultrafast intramolecular proton transfer plays no role in the relaxation of this state, and the small activation energy of about 6 kJ/mol must solely be due to intramolecular barriers to other relaxation modes through, *e.g.*, C–C rotation.



Scheme 7. Models used as reference compounds in the evaluation of the deactivation modes induced by C–C rotations and intramolecular proton transfer.

The comparison of the fluorescence quantum yields of BVE at 77 K and room temperature with those of ZnBVE, BVE-$H^+$ and compounds **4**–**6** (Scheme 7 and Table 1) suggests that intramolecular proton transfer between the nitrogens (of rings B and C in the verdins) and C–C rotations are important in inducing the radiationless deactivation of BVE. An appreciable N–H/$^2$H isotope effect on the fluorescence yield was therefore expected. However, no such effect, even at 77 K[4], could be observed in EtOH/EtO$^2$H. The model of picosecond relaxation mechanisms now also offers a rationale for the failure of these attempts. At room temperature the radiationless decay rate of the $\tau_1$ component, and thus also its fluorescence yield, is still largely determined by the conformational relaxation rather than by the proton transfer. At very low temperatures the increase in the overall fluorescence yield may be mostly due to an increase in fluorescence yield of the longer-lived components ($\tau_2 - \tau_4$) which are not affected by the proton transfer. This argument presumes that the unproportionally large increase in fluorescence yield overrides the partial loss of stretched species incurring upon cooling. Therefore, the contribution of the proton transfer to the fluorescence yield is relatively small at the two temperature extremes, evidently ranging within the experimental error of the continuous excitation method.

Our results clearly show that in solution, depending on the conditions, at least three species of BVE can occur in the electronic ground state. They include two stretched forms with long-lived $S_1$ states ($\tau_3$, $\tau_4$). The results give no straightforward indication, however, as to whether the two picosecond decays ($\tau_1$, $\tau_2$) are related to only one or to several ground state species. From a conformational viewpoint the first possibility appears more plausible. However, one may expect anyway, in accordance with Ramachandran[56,65], force field[66] and MO calculations[53,55-57], the potential energy minima to be quite flat and the separating activation barriers small in comparison with the thermal energy.

The fluorescence lifetimes now provide also a rough estimate of the relative fluorescence quantum yields of coiled and stretched BVE in solution. The absorption coefficient of the long-wavelength band, which was excited in the lifetime determinations, is only about four times larger for the stretched than for the coiled form. The fluorescence yield is consequently about two orders of magnitude larger for the former.

### 3.3. The Thermal Interconversion of the Helically Coiled and Stretched Forms of Biliverdin Dimethyl Ester. Influence of the Medium

The differences between the static spectra of the two forms of BVE are best illustrated by the observations—using fluorescence, fluorescence excitation, and SICD in optically active membranes—upon the incorporation of BVE into the lipophilic part of the bilayer of liposome membranes[67].

When the incubation of intact liposomes with BVE is carried out at room temperature without ultrasonic or thermal perturbation, the fluorescence of the helically coiled form initially predominates in all cases. It persists in the gel-type liposomes, *e.g.*, in DPL membranes, the phase transition of which is above room temperature (315 K; Fig. 10A). It changes, however, to the emission of the stretched species on standing when incorporated in more fluid liquid-crystalline liposomes (*e.g.*, in EYL which has a phase transition temperature of 268 K). The same irreversible change can also be effected by heating the BVE-DPL liposomes to a temperature above the phase transition, and by sonication of the BVE-containing liposomes (Fig. 10B). Stretched species consequently are the only form(s) demonstrable by fluorescence in liposomes which have been prepared by cosonication of BVE and lipid (Fig. 10C). These findings show that the population of stretched species of BVE is favored in the membranes and that, however, a minimum fluidity of the local environment is prerequisite for spontaneous stretching in the membranes.

Again, SICD measurements—in the optically active EYL membrane—confirm the emission-based conclusions about the BVE forms in liposomes. The development of the CD band at 650 nm with time—its increase in intensity during the first phase after incubation, followed by gradual disappearance—and its dependence on the method of incorporation parallel those of the emission.

The stretching of coiled BVE in the liquid-crystalline membranes is facilitated by the ordered medium as long as it is not too rigid. A similar *stretching in solution at room temperature occurs only very slowly*[48,68]. Dimethyl sulfoxide, even in catalytic amounts, provides for the lowest activation energy observed so far. In other solvents stretching requires activation energies in the order of about 20 kJ/mol, which is in the range of solvent viscosity activation. It can only be effected upon sonication or heating of such solutions, up to a limit which is determined by the

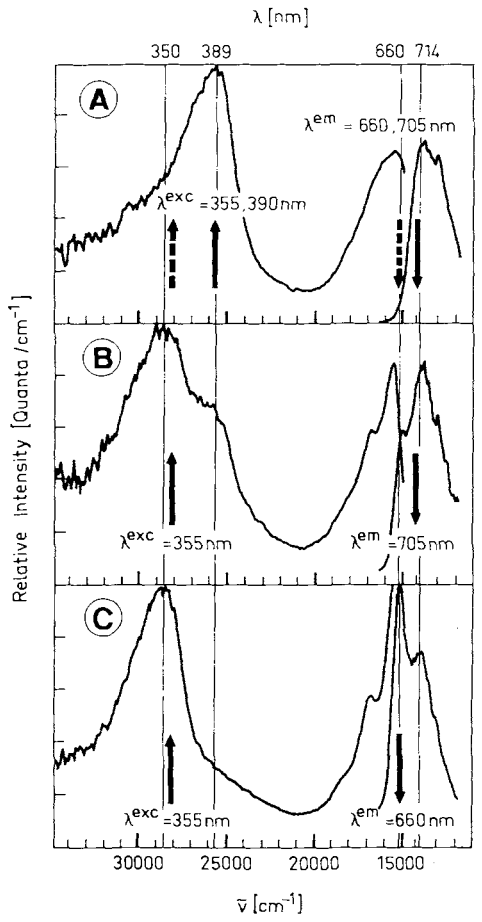



Fig. 10. Corrected fluorescence and fluorescence excitation spectra of BVE-DPL liposomes at 298 K, Ⓐ from a sample prepared by incubation of preformed DPL liposomes with BVE, Ⓑ after subsequent *short* sonication, and Ⓒ from liposomes prepared by cosonication of BVE and DPL. The spectra Ⓐ, which were wavelength independent in emission and excitation, are those of the coiled "710 nm" species, Ⓑ shows the grow-in of the stretched "660 nm" form on ultrasonic perturbation, and Ⓒ exhibits the "660 nm" spectra essentially uncontaminated with the "710 nm" species. Note that $\lambda^{em}$ of the "710 nm" species is shifted in DPL to *ca.* 730 nm [67].

maximum temperature reached, the rate of cooling, and the solvent nature. The largest populations of the stretched form have been obtained so far in dimethyl sulfoxide, somewhat smaller ones in protic solvents (alcohols), and the smallest in aromatic hydrocarbons[68]. It is interesting to note that, by comparison, the barrier between the two conformers of BRE (the "395 nm" and "450 nm" forms; Section 2) must be substantially lower.

The results of fluorescence and LIOAS during the first hours after incubation of the liposomes with BVE afford some insight into the process of incorporation into the membranes and the nonradiative energy dissipation of BVE in these media[67]. The fluorescence quantum yields of coiled and stretched BVE in the EYL and DPL liposomes are all similar and about 5—8 times higher than $\Phi_f$ of stretched BVE in ethanol at room temperature (Table 1). This increase evidently reflects the greater constraints exerted by the more rigid membranes on the vibrational and rotational degrees of freedom, *i.e.*, the overall rate of radiationless relaxation processes of incorporated BVE is reduced. One may therefore expect a concomitant decrease of the LIOAS signal which is a measure of all nonradiative nonphotochemical decay modes[69]. In the case of BVE-DPL such a decrease is indeed observed. It is 2/3 or less of the minimum "prompt" heat dissipation yield $\alpha$ (which is defined as the fraction of absorbed energy converted into the acoustic wave)[70, 71] measured for BVE in ethanol (Fig. 13)[67, 71].

The LIOAS study of the incorporation of BVE into liposome membranes revealed also a facet of a more direct photochemical interest[67]. In the case of DPL the LIOAS intensity decreased during the first 20 hours after incubation (Fig. 11B), finally reaching *ca.* 30% of the initial value. One should have anticipated, *a priori*, a correspondingly large increase in fluorescence yield. However, a mere 5—20% increase is observed (Fig. 11A). Moreover, the time scales of the two observations are different, with only two hours to reach a constant $\Phi_f$ value. The portion of decrease in LIOAS, which correlates with the increase in $\Phi_f$, is obviously overridden by a similar but much larger effect. The origin for this large LIOAS deficit is likely to be photochemistry. Since no permanent photochemical change is observed in BVE-DPL, such a photoreaction of BVE must

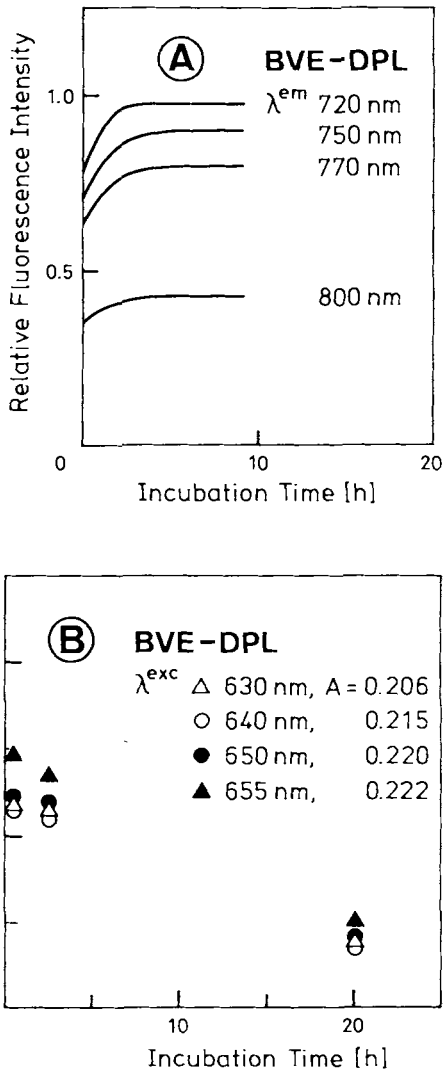



Fig. 11. Incubation of preformed DPL liposomes with BVE: Ⓐ Increase of fluorescence intensity at several emission wavelengths, and Ⓑ decrease of the LIOAS signal intensity (measured 9 μs after the laser pulse) at several excitation wavelengths, both as a function of the time elapsed after incubation [67b].

revert thermally on a time scale too long ($>1$ μs) to be registered by LIOAS. The lower limit for the lifetime of the photoproduct is given by the time required for generating the acoustic wave.

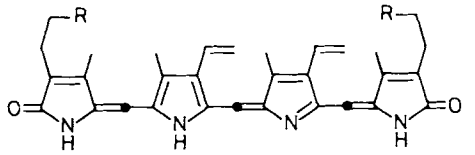
The fluorescence increase after the incubation of the EYL liposomes with BVE is of similar magnitude as that observed for DPL (Table 1), but the LIOAS intensity does not change significantly in this instance. A photochemical $Z \rightarrow E$ isomerization and thermal reversion—although not directly in evidence—is again consistent with these observations. They would require that in the "soft" EYL membranes the thermal reversion of the photoproduct is faster ($<1$ μs) than in the more rigid DPL liposomes, which is plausible.

One of the possible ways to visualize the events upon the incubation of liposomes with BVE is now as follows. When added in a concentrated tetrahydrofuran solution to the aqueous liposome dispersion, the BVE is deposited on the membrane surface in an aggregated form (cf. Section 3.5). In the process of intrusion into the membrane the aggregates will split into the monomers, which then are finally found as the preferentially coiled or stretched species depending on the lipid viscosity. The concomitant increase in fluorescence intensity possibly reflects a somewhat less efficient radiationless deactivation of the monomers, unless it is not simply a concentration effect caused by the deposition of aggregates on the membrane surface. In any event, the monomers undergo the—thermally reversible—photoisomerization significantly more efficiently as indicated by the increase in LIOAS deficit.

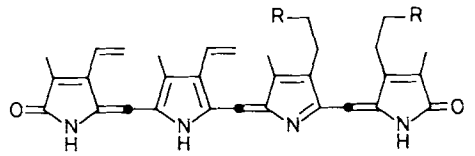
### 3.4. The Photochemistry of Biliverdin Dimethyl Ester. The Conformation-Selective Photocyclization of the Biliverdin IXγ and IXδ Dimethyl Esters

Inspection of molecular models suggests that the coiled all-*Z*,all-*syn* BVE molecule can be transformed into many different stretched forms by rotations around any of the C-5, C-10 and/or C-15 single and double bonds. No specific differentiation in regard of this multiple choice of stretched forms has yet been made in the preceding Sections, except for Scheme 5 and the footnote on p. 663 where it was assumed that the difference between the coiled and stretched forms is exclusively localized within the ring B/C partial structure, *i.e.*, that rotations are limited to the bonds of the central bridge C-10. In the following, arguments supporting this assignment shall be derived from the photochemical results obtained with BVE and its XIIIα, IXγ, and IXδ isomers (Scheme 8).

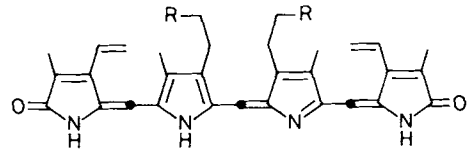
Since the constitutional isomers BVE, BVE-IXγ, BVE-IXδ and BVE-XIIIα exhibit generally similar spectral properties, it is reasonable to assume that their electronic ground and excited states are also similar rather than being drastically affected by the different substitution patterns. Furthermore, the individual sets of dual fluorescence and fluorescence excitation spectra indicate that the solutions of all these biliverdins are heterogeneous and have similar compositions, with the coiled all-*Z*,all-*syn* forms emitting at the longer wavelengths and the stretched forms emitting at the shorter wavelengths. The spectral similarity suggests,



**BVE-IXγ** Biliverdin IXγ dimethyl ester



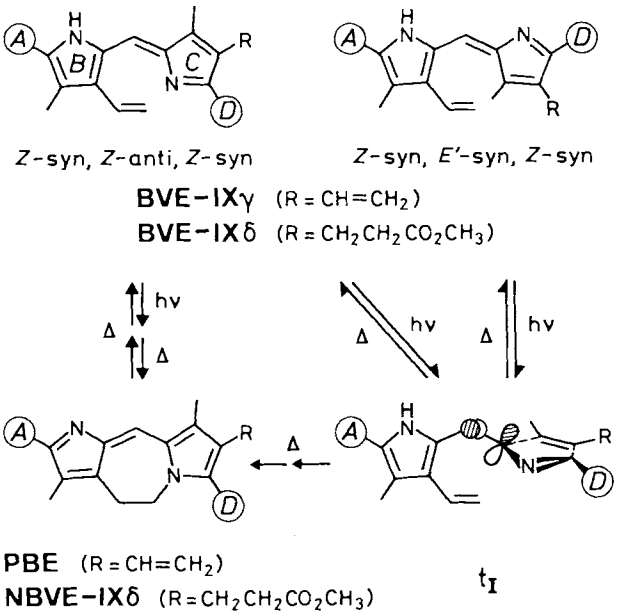
**BVE-IXδ** Biliverdin IXδ dimethyl ester



**BVE-XIIIα** Biliverdin XIIIα dimethyl ester

$R = CO_2CH_3$

Scheme 8. Constitutional formulas of BVE-IXγ, BVE-IXδ, and BVE-XIIIα.




Scheme 9. Possible primary steps of the photocyclization of stretched forms of BVE-IXγ and BVE-IXδ to PBE and NBVE-IXδ, respectively. Ⓐ and Ⓓ stand for the correspondingly IXγ- and IXδ-substituted partial structures. For the *E'-syn* notation cf. Scheme 10.

moreover, that the stretched forms have similar arrangements around all three methine bridges.

BVE-IXγ and BVE-IXδ cyclize thermally and photochemically to PBE and NBVE-IXδ, respectively (Scheme 9)[58,60]. An analogous ring closure across one of the lateral

bridges (C-5 and C-15) is not observed, neither in BVE-IXγ and BVE-IXδ as an alternative to the closure in the central part, nor in BVE and BVE-XIIIα which have one and two vinyl groups, respectively, exclusively adjacent to lateral bridges. One may expect on the basis of structural and mechanistic considerations that the cyclization can occur in several possible ways, which all should exhibit a distinct selectivity for the stretched conformation of the starting material. For example, the ring closure may be effected directly from the twisted excited state intermediate, $^t$I, of the photochemical interconversion of the *E'-syn* and *Z-anti* isomers (cf. Scheme 10), in competition to relaxation to either (Scheme 9). Excited state processes other than twisting, *e.g.*, a direct electrocyclic ring closure, may also be visualized as responsible for the primary photochemical step. In either case the formation of the final product will require some sort of a hydrogen relocation subsequent to the cyclization. A stretched conformation is prerequisite for any of these or alternative primary reactions to occur in BVE-IXγ and BVE-IXδ. And indeed, a marked dependence of the quantum yields of the photoreaction on the irradiation wavelength strongly suggests a distinct selectivity favoring reaction in one particular conformation[48]. Thus, the highest quantum yields are achieved with irradiation wavelengths in the region of 575–600 nm where absorption by the stretched forms is relatively important. Above this range, where the relative importance of the absorption by the coiled form increases, the reaction efficiency declines sharply (Fig. 12).

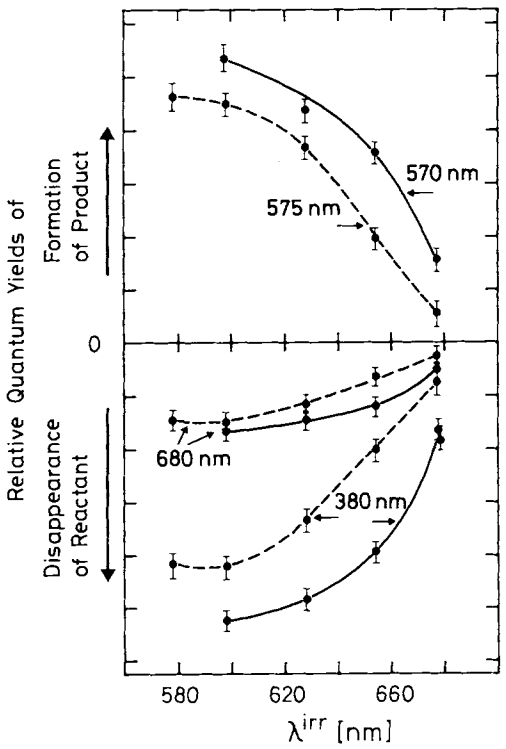


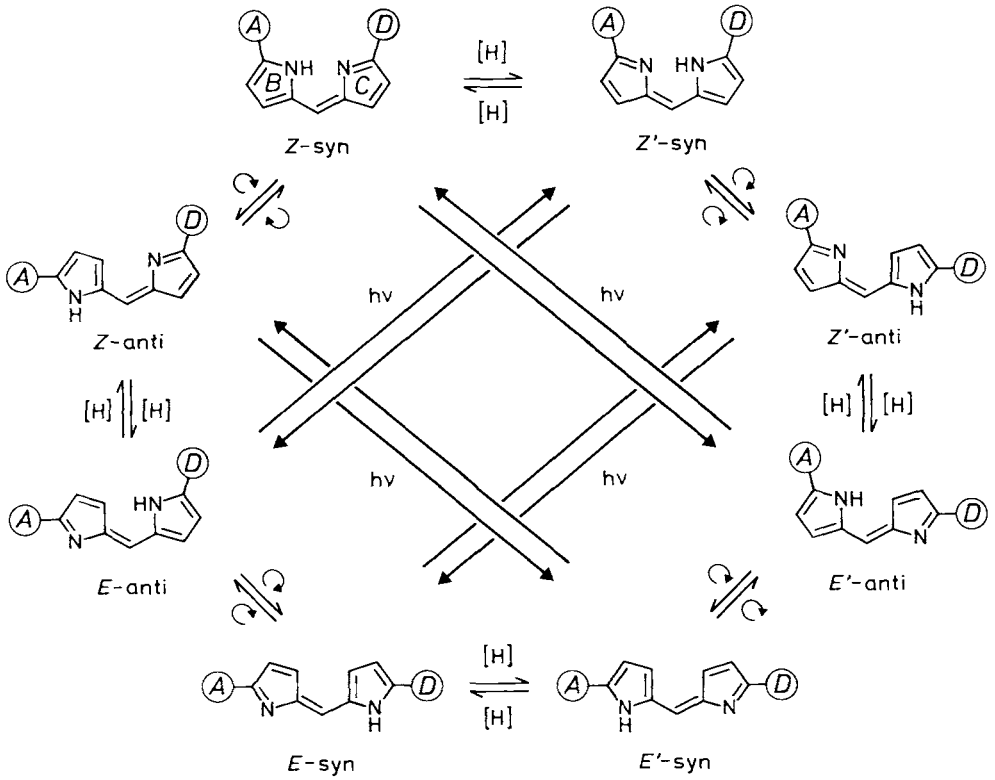

Fig. 12. Relative quantum yields, plotted as a function of irradiation wavelength, of the disappearance of BVE-IXγ (—) and BVE-IXδ (---) (bottom), and of the cyclization to PBE (—) and NBVE-IXδ (---) (top), respectively. For each transformation, the measurements were carried out at the wavelengths of the three extrema in the difference spectrum obtained upon irradiation in dimethyl sulfoxide. The initial concentrations of BVE-IXγ and BVE-IXδ were in the order of $10^{-5}$ M [48].

For a better understanding of the above arguments based on the absorption properties of the diverse species, we should reiterate that the Stokes shifts are large for the coiled and small for the stretched forms. This means that the absorption of the stretched form is relatively narrow (560–660 nm in ethanol) and superimposed onto the short-wavelength flank of the much broader absorption band of the coiled species. In fact, the absorption of the coiled species is adequately represented by the normal absorption spectrum, since this species is the more abundant in most solvents, apparently independent of concentration (see Section 3.5). The absorption of the stretched species is only accessible in the excitation spectrum of the short-wavelength fluorescence.

The photochemical results obtained with the four isomers can be rationalized comprehensively when it is assumed that in each case *the stretching of the coiled form is confined to thermal and photochemical transformations within the B/C moiety, while the Z-syn geometry of the A/B and C/D partial structures is retained as shown in Scheme 5.* An inspection of the eight possible C(10)-isomeric forms of an unsymmetrically substituted biliverdin reveals that one can discern three topologically different groups, comprising: 1) two coiled $Z^{(\prime)}$-*syn* forms, 2) two stretched $E^{(\prime)}$-*syn* forms, and 3) four stretched *anti* forms (Scheme 10). The coiled ($Z^{(\prime)}$-*syn*) and the stretched $E^{(\prime)}$-*anti* forms selectively interconvert by direct $E \rightleftharpoons Z$ photoisomerization, whereas the four other stretched isomers cannot directly photoisomerize to the coiled forms, and vice versa.

Irradiation of BVE in ethanol at 173 K ($\lambda^{irr} = 560$ and 700 nm) affords a photostationary equilibrium in which the composition is shifted towards a larger population of stretched forms[44]. The initial ground state-controlled composition is reestablished when the irradiated solution is warmed up to room temperature, where neither a similarly lasting photochemical change[44,60,71] nor any transient absorptions in the microsecond range[7,72] can be detected. However, a LIOAS study[71] has revealed that BVE does in fact undergo photoisomerization also under these conditions. Considerable losses of "prompt" heat dissipation, $\alpha$, are registered upon irradiation of low BVE concentrations ($10^{-6}$ M; see Fig. 13), which give a measure of the formation of a photoproduct reverting back to BVE on the microsecond time scale. Analogous findings have already been described for BVE incorporated in the liposomes (Section 3.3). It is also interesting to note that the *E,Z,Z* and *Z,Z,E* isomers[46] give $\alpha$ values larger than 1 (*e.g.*, $\alpha = 1.3$ at $\lambda^{irr}$ 640 nm)[71] indicating an immediate heat release upon photoisomerization to the all-*Z* BVE. The net energy release of this overall exothermic process is thus *ca.* 40 kJ/mol.

The thermal stabilities of stretched BVE formed from the coiled form upon heating or ultrasonic perturbation (Section 3.3) and of that formed photochemically are evidently different. The interconversion paths shown in Scheme 10 suggest an explanation of this apparent discrepancy. The photochemical stretching of the coiled BVE affords directly the $E^{(\prime)}$-*anti* forms, whereas the thermal treatments of the coiled species may drive the transformations farther and populate also the stretched $E^{(\prime)}$-*syn* conformations. The implication then is that C–C rotation in




Scheme 10. Interconversions which link the eight possible C-10 isomers of BVE, involving proton transfer processes ([H]), rotation around the C-9–C-10 single bond (↷), and $E \rightleftarrows Z$ isomerization of the C-10=C-11 double bond ($h\nu$). This Scheme derives from Scheme 5 upon the introduction of the asymmetrical IXα substitution pattern of rings A and D, again not allowing for a change in geometry within the A/B and C/D partial structures.

the latter is the rate determining step for the reformation of coiled BVE. We should note in this context that it cannot yet be predicted which of the two C–C rotations involved will be the rate determining activation barrier in the reverse direction, *i.e.* the thermal stretching of coiled BVE to the $E^{(\prime)}$-*syn* form.

In view of the photochemical behavior of BVE and its IXγ and IXδ isomers it appears plausible to expect that *10E→10Z photoisomerization may play an appreciable role as a deactivation channel of excited BVE.* It is important in this connection to recall two collateral aspects of bilatriene photochemistry. One concerns the remarkable change in the photochemical behavior of BVE either when adsorbed on alumina[46,73] or in solution in the presence of strong electron donors[74]. Under these conditions 'bilirubin-type" processes are in fact observed. Reaction now occurs selectively at C-4 and C-15, and the *E,Z,Z* and *Z,Z,E* isomers are formed. These isomers are more stable thermally than the *Z,E,Z* isomers and, if formed, they would not have escaped detection after the irradiations in inert solvents. The striking difference in the photochemistry has been ascribed to strong interaction by a donor with C-10 or even to the intervening addition of a nucleophile to this position. It is brought about by the extensive delocalization through the symmetrical hydrogen bridge between the nitrogens in rings B and C[76], which renders C-10 the lowest-electron density carbon in the biliverdins and susceptible to such nucleophilic attacks[4,75]. The resulting bilirubin-type intermediates are capable of undergoing the observed photoreactions at C-5 and C-15 and, being much more efficient emitters than the verdins at low temperatures (cf. Table 1), they have also been recognized[4] as the trace sources of the so-called "blue" or "anomalous" fluorescence of BVE[4,77] and of phytochrome[25]. The step sequence has been confirmed for the parent 2,3-dihydrobilatriene model chromophore of phytochrome. After the deliberate addition of 2-mercaptoethanol to C-10 the dipyrromethenone partial structure could be selectively $Z \rightarrow E$ photoisomerized[46], whereas the irradiation of the intact 2,3-dihydrobilatriene in the presence of iodine (as an oxidant) and pyridine effects addition of the latter to C-5[78].

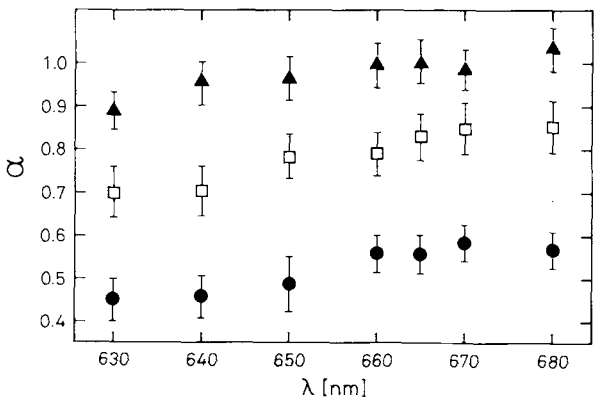



Fig. 13. LIOAS of BVE in ethanol: "prompt" heat dissipation fractions $\alpha$; ● = $1.0 \times 10^{-6}$ M, □ = $2.0 \times 10^{-6}$ M, ▲ = $1.3 \times 10^{-5}$ M [71].

The second aspect concerns the question why in the absence of medium-induced processes the *E-Z* photoisomerization of BVE is confined to C-10. On the basis of calculations and studies of appropriate model compounds[79] it

has been concluded that the excited-state twisting preferentially involves the double bond with the greatest out-of-plane distortion in the ground state. This is demonstrated, *e.g.*, by results with etiobiliverdins which are *N*-methylated in rings A and/or D. Steric crowding by the methyl substituents forces the rings out of the dipyrromethenone plane and destabilizes the subchromophores. As a consequence, $Z \rightarrow E$ photoisomerization occurs, already in inert solvents, selectively about the double bond adjacent to the substituted ring in the monomethylated, and about either of the two double bonds in the dimethylated derivative[79].

### 3.5. The Formation of Aggregates

The tendency of BVE to aggregate, already referred to in Section 3.1, can manifest itself in various ways. One is to form strong adducts of varying stoichiometry with solvents such as tetrahydrofuran, acetonitrile, and ethyl lactate[80]. Another one is shown by the LIOAS results in Figure 13. Static inhibition of the formation of the *Z,E,Z* photoisomers through some sort of association of an unidentified quencher with ground-state BVE was proposed[71] to cause the concentration dependence of $\alpha$, without noticeably effecting a deviation from the Lambert-Beer law in the long-wavelength absorption. It could only recently be demonstrated that the association in fact involves like BVE molecules[68]. As seen in Figure 14, the emission maximum at $10^{-4}$ M in methanol is around 735 nm. On dilution its intensity drops, and there is a shift towards shorter wavelengths, accompanied by the growing-in of a band at around 650 nm. At concentrations of $10^{-6}$ M the long-wavelength emission has disappeared, while bands around 650 and 700 nm are persisting. The quantitative evaluation of the three emission bands was associated with large errors since the measurements were approaching the limits of instrumental sensitivity. Nevertheless, the fluorescence band at *ca.* 700 nm, which is that of the coiled monomer, proved largely independent of concentration. On the other hand, the emission intensities of the stretched form at 650 nm and of the 735 nm band followed opposite trends

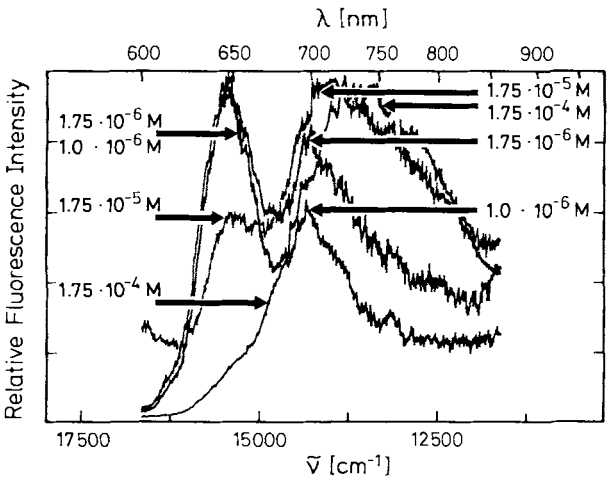



Fig. 14. Concentration dependence of the fluorescence of BVE in methanol at room temperature; $\lambda^{irr} = 580$ nm. The stock solution ($1.75 \times 10^{-4}$ M) had been prepared without warming or sonication. The maximum of each spectrum is normalized [68].

with the changing of concentration. In other words, the association selectively involves the dimerization of the stretched *Z-syn,E(ʹ)-anti,Z-syn* forms. In accord with this conclusion, the excitation spectra of the emissions of Figure 14 exhibit with increasing concentration a distinct broadening of both bands, together with a hypsochromic shift of the Vis maximum from 635 nm to about 600 nm, and a bathochromic shift of the UV maximum from 345 nm to about 380 nm.

## 4. Conclusions and Outlook

The present knowledge of the rather complex picture of the ground- and excited-state behavior of BRE and BVE is based on a large array of diverse experimental and theoretical studies, all of which could not adequately be incorporated into this article[81]. The variety of coexisting forms in organic solvents as well as the variable responses of the individual components—in their electronic ground and first excited singlet states—to medium, temperature and concentration are, generally speaking, common to BRE and BVE, even though important differences may be found with regard to certain aspects. It should also be reiterated in this connection that not all details are yet fully understood. The hitherto most elaborate investigation has been carried out with BVE, owing to the supplementing of the static spectroscopic methods with methods of limited (LIOAS) and highest possible time resolution (PP, SPT). It has afforded a far-reaching insight into the structural and dynamic properties of the diverse components, their selective interconversions upon photochemical and thermal excitation, and the deactivation channels of the individual singlet excited states.

It has already been pointed out in Section 1 that the *in vitro* physical and (photo)chemical properties of the linear tetrapyrroles alone would justify the relatively expensive spectroscopic study of these compounds and the concurrent instrumental and methodological developments (see, *e.g.*,[61,71]). Beyond this, however, the expectation has been amply confirmed that the resulting knowledge constitutes an essential contribution to the studies of the molecular foundations of biological systems containing such pigments. The elucidation of the anaerobic photochemistry of BR in connection with neonatal jaundice, and the further development of the phototherapy was of great importance. The significance, for the biliproteins, of the conclusions drawn from the picosecond kinetics and photochemical studies of BVE has already been alluded to in Sections 3.2 and 3.4. Undoubtedly, other such results will still be forthcoming[81] and lend further support in the even more exacting investigations of the processes in biological systems. This is to be expected in particular from studies with linear tetrapyrroles of the dihydrobilindione type, which are even more closely related in structure to the biliproteinic chromophores, and with the native chromophores linked to oligopeptidic residues as accessible from partial degradation of the proteins. A further approach towards *in vivo* conditions is seen in experiments modelled after the experiences with BVE in solution but carried out in combination with biologically more relevant media (*e.g.*, membranes). In ad-

dition, decisive advances in the *in vivo* studies appear feasible with the application of spectroscopic methods which have been developed, *inter alia*, in connection with studies of the tetrapyrrole models (*e.g.*, laser-induced optoacoustic spectroscopy and single-photon-timing with multi-component resolution capacity in a dynamic range over >3 orders of magnitude).

*Our work described here greatly profited from collaboration with friends and colleagues of other laboratories, notably with Dr. W. Kufer and Professor H. Scheer of the Universität München, Dr. A. A. Lamola of Bell Laboratories, Murray Hill, Professor D. A. Lightner of the University of Nevada, Reno, and Dr. V. Sundström, Mr. Å. Sandström, and Dr. T. Gillbro of the University of Umeå. It would not have been possible at all, however, without the efforts of the team at the Mülheim institute, the first director of which this article is dedicated to. The team includes, among others, the scientists Dr. H. Al-Ekabi, Dr. S. Culshaw, Dr. R. M. Ellul, Dr. H. Lehner, Dr. J. I. Matthews, Professor C. Nicolau, Dr. C. Pétrier, Dr. I.-M. Tegmo-Larsson, Professor R. G. Weiss (while on leave from Georgetown University), and Mr. J. Wendler, the technical staff members Mr. H.-J. Herbert, Miss A. Keil, Miss G. Koc, Miss D. Kreft, Mr. W. Riemer, Mr. W. Schuster, Mr. V. Seeling, and Mrs. G. Wojciechowski, the staff of the computer center, and that of the electronic and mechanical workshops.*

Received: May 13, 1983 [A 467 IE]
German version: *Angew. Chem. 95* (1983) 670

[1] R. F. Troxler, A. Brown, *Biochim. Biophys. Acta 215* (1970) 503; R. F. Troxler, J. M. Dokos, *Plant Physiol. 51* (1973) 72.
[2] For recent reviews see a) H. Scheer, *Angew. Chem. 93* (1981) 230; *Angew. Chem. Int. Ed. Engl. 20* (1981) 241; b) H. Scheer in F. K. Fong: *Molecular Biology, Biochemistry and Biophysics, Vol. 35*, Springer, Berlin 1982, p. 7.
[3] A. F. McDonagh, L. A. Palma, D. A. Lightner, *Science 208* (1980) 145; S. Onishi, K. Isobe, S. Itoh, N. Kawade, S. Sugiyama, *Biochem. J. 190* (1980) 533; A. A. Lamola, W. E. Blumberg, R. McClead, A. Fanaroff, *Proc. Natl. Acad. Sci. USA 78* (1981) 1882.
[4] A. R. Holzwarth, H. Lehner, S. E. Braslavsky, K. Schaffner, *Liebigs Ann. Chem. 1978*, 2002; S. E. Braslavsky, A. R. Holzwarth, H. Lehner, K. Schaffner, *Helv. Chim. Acta 61* (1978) 2219.
[5] R. W. Sloper, T. G. Truscott, *Photochem. Photobiol. 31* (1980) 445.
[6] R. F. Chen in A. A. Thaer, M. Sernetz: *Fluorescence Techniques in Cell Biology*, Springer, New York 1973, p. 273; A. A. Lamola, J. Eisinger, W. E. Blumberg, S. C. Patel, J. Flores, *Anal. Biochem. 100* (1979) 25.
[7] E. J. Land, *Photochem. Photobiol. 24* (1976) 475; *29* (1979) 483.
[8] I. B. C. Matheson, N. U. Curry, J. Lee, *Photochem. Photobiol. 31* (1980) 115.
[9] A. R. Holzwarth, E. Langer, H. Lehner, K. Schaffner, *J. Mol. Struct. 60* (1980) 367; *Photochem. Photobiol. 32* (1980) 17.
[10] M. Jirsa, J. P. Dickinson, G. H. Lathe, *Nature 22* (1968) 1322; C. C. Kuenzle, *Biochem. J. 119* (1970) 395; A. Cu, G. Bellah, D. A. Lightner, *J. Am. Chem. Soc. 97* (1975) 2579; M. Carey, A. P. Koretzky, *Biochem. J. 179* (1979) 675; J. Dalton, L. R. Milgrom, R. Bonnett, *Chem. Phys. Lett. 61* (1979) 242.
[11] R. Brødersen, *J. Biol. Chem. 254* (1979) 2364.
[12] C. C. Kuenzle, M. H. Weibel, R. R. Pelloni, P. Hemmerich, *Biochem. J. 133* (1973) 364.
[13] C. D. Tran, G. S. Beddard, *Biochim. Biophys. Acta 678* (1981) 497.
[14] B. I. Greene, A. A. Lamola, C. V. Shank, *Proc. Natl. Acad. Sci. USA 78* (1981) 2008.
[15] C. D. Tran, G. S. Beddard, *J. Am. Chem. Soc. 104* (1982) 6741.
[16] G. Blauer, D. Harmatz, A. Naparstek, *FEBS Lett. 9* (1970) 53; G. Blauer, D. Harmatz, J. Snir, *Biochim. Biophys. Acta 278* (1972) 68; G. Blauer, D. Harmatz, *ibid. 278* (1972) 89; G. H. Beaven, A. d'Albis, W. B. Gratzer, *Eur. J. Biochem. 33* (1973) 500; G. Blauer, G. Wagnière, *J. Am. Chem. Soc. 97* (1975) 1949.
[17] A. A. Lamola, S. E. Braslavsky, K. Schaffner, D. A. Lightner, *Photochem. Photobiol. 37* (1983) 263.
[18] W. Kufer, H. Scheer, A. R. Holzwarth, *Isr. J. Chem. 23* (1983), in press.
[19] W. West, B. H. Carroll in C. E. K. Mees, T. H. James: *Theory of the Photographic Process*, Macmillan, New York 1966, 3rd edit., p. 243; G. Calzaferri, H. Gugger, S. Leutwyler, *Helv. Chim. Acta 59* (1976) 1969; W. Windhager, S. Schneider, F. Dörr, *Z. Naturforsch. A 32* (1977) 876; G. Beddard, T. Doust, M. Windsor in R. M. Hochstrasser, W. Kaiser, C. V. Shank: *Picosecond Phenomena*, Springer, Berlin 1980, Vol. *II*, p. 166; V. Sundström, T. Gillbro, *Chem. Phys. 61* (1981) 257; A. D. Osborne, *J. Chem. Soc. Faraday Trans. II 76* (1980) 1638.
[20] A. A. Lamola, J. Flores, *J. Am. Chem. Soc. 104* (1982) 2530.
[21] E. Vos de Wael, J. A. Pardoen, J. A. van Koeveringe, J. Lugtenburg, *Recl. Trav. Chim. Pays-Bas 96* (1977) 306.
[22] H. Falk, S. Gergely, K. Grubmayr, *Monatsh. Chem. 107* (1976) 987.
[23] H. Falk, N. Müller, *Monatsh. Chem. 113* (1982) 111.
[24] H. Falk, F. Neufingerl, *Monatsh. Chem. 110* (1979) 987.
[25] A. R. Holzwarth, S. E. Braslavsky, S. Culshaw, K. Schaffner, *Photochem. Photobiol. 36* (1982) 581.
[26] R. Bonnett, J. E. Davies, M. B. Hursthouse, G. M. Sheldrick, *Proc. R. Soc. London B 202* (1978) 249.
[27] D. A. Lightner, T. A. Wooldridge, A. F. McDonagh, *Proc. Natl. Acad. Sci. USA 76* (1979) 29.
[28] A. F. McDonagh, D. A. Lightner, T. A. Wooldridge, *J. Chem. Soc. Chem. Commun. 1979*, 110.
[29] D. A. Lightner, T. A. Wooldridge, A. F. McDonagh, *Biochem. Biophys. Res. Commun. 86* (1979) 235.
[30] A. A. Lamola, J. Flores, F. H. Doleiden, *Photochem. Photobiol. 35* (1982) 649.
[31] A. F. McDonagh, L. A. Palma, F. R. Trull, D. A. Lightner, *J. Am. Chem. Soc. 104* (1982) 6865.
[32] H. Falk, N. Müller, M. Ratzenhofer, K. Winsauer, *Monatsh. Chem. 113* (1982) 1421.
[33] A. F. McDonagh, L. A. Palma, D. A. Lightner, *J. Am. Chem. Soc. 104* (1982) 6867.
[34] G. L. Landen, Y.-T. Park, D. A. Lightner, *Tetrahedron 33* (1983), in press; J. A. de Groot, R. van der Steen, R. Fokkens, J. Lugtenburg, *Recl. Trav. Chim. Pays-Bas 101* (1982) 35, 219; A. Hori, S. Mangani, G. Pèpe, E. F. Meyer, Jr., D. L. Cullen, H. Falk, K. Grubmayr, *J. Chem. Soc. Perkin Trans. II 1981*, 1525; H. Falk, K. Grubmayr, G. Höllbacher, O. Hofer, A. Leodolter, F. Neufingerl, J. M. Ribo, *Monatsh. Chem. 108* (1977) 1113; W. S. Sheldrick, A. Borkenstein, M. Blacha-Puller, A. Gossauer, *Acta Crystallogr. 33* (1977) 3625; D. A. Lightner, Y.-T. Park, *J. Heterocycl. Chem. 14* (1977) 415; H. Falk, K. Grubmayr, V. Herzig, O. Hofer, *Tetrahedron Lett. 1975*, 559.
[35] D. A. Lightner, *Photochem. Photobiol. 26* (1977) 427.
[36] A. R. Holzwarth, K. Schaffner, *Photochem. Photobiol. 33* (1981) 635.
[37] R. E. Davies, S. J. Keohane, *Photochem. Photobiol. 17* (1973) 303.
[38] R. W. Sloper, T. G. Truscott, *Photochem. Photobiol. 35* (1982) 743.
[39] J. J. Lee, G. D. Gillispie, *Photochem. Photobiol. 33* (1981) 757.
[40] A. J. Knell, F. Hancock, D. W. Hutchinson in A. F. Bakken, J. Fog: *Metabolism and Chemistry of Bilirubin and Related Tetrapyrroles*, Pediat. Res. Inst., Rikshospitalet, Oslo 1 1975, p. 234.
[41] D. Kaplan, G. Navon, *Biochem. J. 201* (1981) 605; *J. Chem. Soc. Perkin Trans. II 1981*, 1374.
[42] P. Manitto, D. Monti, *J. Chem. Soc. Chem. Commun. 1976*, 122.
[43] G. Favini, D. Pitea, P. Manitto, *Nouv. J. Chim. 3* (1979) 299.
[44] S. E. Braslavsky, A. R. Holzwarth, E. Langer, H. Lehner, J. I. Matthews, K. Schaffner, *Isr. J. Chem. 20* (1980) 196; see also *idem*, in J. De Greef: *Photoreceptors and Plant Development, Proc. Ann. Eur. Symp. Plant Photomorphogenesis*, Antwerpen University Press 1980, p. 89.
[45] H. Lehner, S. E. Braslavsky, K. Schaffner, *Liebigs Ann. Chem. 1978*, 1990.
[46] H. Falk, K. Grubmayr, E. Haslinger, T. Schlederer, K. Thirring, *Monatsh. Chem. 109* (1978) 1451.
[47] A. R. Holzwarth, J. Wendler, K. Schaffner, V. Sundström, Å. Sandström, T. Gillbro in T. Doust, M. A. West: *Picosecond Chemistry and Biology*, Science Reviews, Northwood 1983, in press; *Isr. J. Chem.* (1983), in press.
[48] S. E. Braslavsky, H. Al-Ekabi, C. Pétrier, K. Schaffner, unpublished results.
[49] W. S. Sheldrick, *J. Chem. Soc. Perkin Trans. II 1976*, 1457; H. Lehner, S. E. Braslavsky, K. Schaffner, *Angew. Chem. 90* (1978) 1012; *Angew. Chem. Int. Ed. Engl. 17* (1978) 948.
[50] H. Falk, G. Höllbacher, *Monatsh. Chem. 109* (1978) 1429.
[51] H. Lehner, W. Riemer, K. Schaffner, *Liebigs Ann. Chem. 1979*, 1798.
[52] G. Wagnière, G. Blauer, *J. Am. Chem. Soc. 98* (1976) 7806.
[53] M. J. Burke, D. C. Pratt, A. Moscowitz, *Biochemistry 11* (1972) 4052.
[54] Q. Chae, P.-S. Song, *J. Am. Chem. Soc. 97* (1975) 4176; T. Sugimoto, K. Ishikawa, H. Suzuki, *J. Phys. Soc. Jpn. 40* (1976) 258.
[55] R. Pasternak, G. Wagnière, *J. Am. Chem. Soc. 101* (1979) 1662.
[56] H. Scheer, H. Formanek, S. Schneider, *Photochem. Photobiol. 36* (1982) 259.
[57] H. Falk, N. Müller, *Monatsh. Chem. 112* (1981) 791.

[58] M. Choussy, M. Barbier, *Helv. Chim. Acta 58* (1975) 2651.
[59] M. Bois-Choussy, M. Barbier, *Heterocycles 9* (1978) 677.
[60] M. Choussy, M. Barbier, *C. R. Acad. Sci. Paris C 282* (1976) 619.
[61] J. Wendler, A. R. Holzwarth, unpublished results; cf. A. R. Holzwarth, J. Wendler, W. Wehrmeyer, *Photochem. Photobiol. 36* (1982) 479.
[62] M. E. Lippitsch, A. Leitner, M. Riegler, F. R. Aussenegg, *Springer's Series in Chemical Physics 14* (1980) 327; *23* (1982) 323; *7th Vavilov Conference on Nonlinear Optics*, Akademgorodok/Novosibirsk 1981.
[63] C. Pétrier, P. Jardon, C. Dupuy, R. Gautron, *J. Chim. Phys. 78* (1981) 519.
[64] H. Falk, K. Grubmayr, F. Neufingerl, *Monatsh. Chem. 110* (1979) 1127.
[65] H. Scheer, H. Formanek, W. Rüdiger, *Z. Naturforsch. C34* (1979) 1085.
[66] H. Falk, G. Höllbacher, O. Hofer, N. Müller, *Monatsh. Chem. 112* (1981) 391.
[67] a) I.-M. Tegmo-Larsson, S. E. Braslavsky, C. Nicolau, K. Schaffner, *Biophys. Struct. Mechn., Suppl. to Vol. 6* (1980) 112; b) I.-M. Tegmo-Larsson, S. E. Braslavsky, S. Culshaw, R. M. Ellul, C. Nicolau, K. Schaffner, *J. Am. Chem. Soc. 103* (1981) 7152.
[68] S. E. Braslavsky, I.-M. Tegmo-Larsson, H. Al-Ekabi, K. Schaffner, unpublished results.
[69] Photoacoustic spectroscopy has only begun to attract the attention of modern spectroscopists, instrumental analysts and photochemists about 100 years after the effect was first described by A. G. Bell [*Phil. Mag. 11* (1881) 510]. It is appropriate here to recall that in this century one of the very early photoacoustic investigations was conducted in Professor Schenck's institute and reported in 1967 by E. Hey and K. Gollnick before the International Conference on Photochemistry in Munich [abstracted in: *Ber. Bunsenges. 72* (1968) 263; cf. also *J. Photoacoustics 1* (1982) 1]. - Note that we follow common practice referring to *opto*acoustic spectroscopy when laser excitation is employed.
[70] A. M. Bonch-Bruevich, T. K. Razumova, I. O. Starobogatov, *Opt. Spectrosc. (USSR) 42* (1977) 45, and references cited therein.
[71] S. E. Braslavsky, R. M. Ellul, R. G. Weiss, H. Al-Ekabi, K. Schaffner, *Tetrahedron 39* (1983) 1909.
[72] C. K. N. Patel, A. C. Tam, *Rev. Mod. Phys. 53* (1981) 517.
[73] H. Falk, K. Grubmayr, *Angew. Chem. 89* (1977) 487; *Angew. Chem. Int. Ed. Engl. 16* (1977) 470.
[74] W. Kufer, E. Cmiel, F. Thümmler, W. Rüdiger, S. Schneider, H. Scheer, *Photochem. Photobiol. 36* (1982) 603.
[75] H. Falk, T. Schlederer, *Monatsh. Chem. 109* (1978) 1013; H. Falk, N. Müller, T. Schlederer, *ibid. 111* (1980) 159; T. Manitto, D. Monti, *Experientia 35* (1979) 1418; W. Kufer, H. Scheer, *Hoppe-Seyler's Z. Physiol. Chem. 360* (1979) 935; *Z. Naturforsch. C37* (1982) 179.
[76] B. Pullman, A.-M. Pérault, *Proc. Natl. Acad. Sci. USA 45* (1959) 1476; J.-H. Fuhrhop, J. Subramian, *Philos. Trans. R. Soc. London B273* (1976) 335; V. Wray, A. Gossauer, B. Grüning, G. Reifenstahl, H. Zilch, *J. Chem. Soc., Perkin Trans. II* (1979), 1558.
[77] P.-S. Song, Q. Chae, D. A. Lightner, W. R. Briggs, D. Hopkins, *J. Am. Chem. Soc. 95* (1973) 7892.
[78] C. Krauss, C. Bubenzer, H. Scheer, *Photochem. Photobiol. 30* (1979) 473.
[79] H. Falk, K. Thirring, *Z. Naturforsch. B34* (1979) 1448, 1600; *B35* (1980) 376.
[80] S. E. Braslavsky, H.-J. Herbert, A. R. Holzwarth, K. Schaffner, *J. Chromatogr. 205* (1981) 85.
[81] In this context, see also a most recently published series of papers in *Tetrahedron;* cf. in particular H. Falk, N. Müller, *Tetrahedron 39* (1983) 1875; A. Gossauer, *ibid. 39* (1983) 1933; F. Thümmler, W. Rüdiger, *ibid. 39* (1983) 1943. See furthermore: H. Falk, W. Grubmayr, G. Kapl, N. Müller, U. Zrunek, *Monatsh. Chem. 114* (1983) 753; H. Falk, G. Kapl, N. Müller, *ibid. 114* (1983) 773.
[82] J. A. Schellman, *Acc. Chem. Res. 1* (1968) 144; G. Haas, P. B. Hulbert; W. Klyne, V. Prelog, G. Snatzke, *Helv. Chim. Acta* 54 (1971) 491.

# Ligand-Free Metal Clusters

**By Geoffrey A. Ozin* and Steven A. Mitchell**

Recent advances in the synthesis and spectroscopic characterization of ligand-free metal clusters immobilized in cryogenic rare gas matrices have contributed greatly to the understanding of electronic, geometric, dynamic, and chemical bonding properties of a wide range of uni- and bimetallic clusters as a function of nuclearity and metal type. The knowledge accumulated on molecular metal aggregates devoid of ligands and isolated on various supports will form an important data base for gauging the reliability of quantum chemical calculations on metal clusters, as well as for comprehending certain aspects of chemisorption on, and catalysis by, supported metal clusters. It can be envisaged that information on ligand-free metal clusters entrapped in a wide range of matrix environments in conjunction with the data for these same metal clusters in the gas phase and in molecular beams will probably contribute towards understanding metal-support interactions and to the designed synthesis of a new breed of high-technology heterogeneous catalysts in the not too distant future.

## 1. Introduction to Zerovalent "Naked" Metal Clusters

In a recent review of the structure and diversity of metal clusters[1], the smallest group by far consisted of neutral metal clusters devoid of ligands. On the other hand, the theory of cluster models is usually applied to just such kinds of "ligand-free" metal aggregates, because they are thought to represent the most chemically and physically realistic bridge between isolated metal atoms and the extended arrays of metal atoms found in bulk metals[2]. Not surprisingly, therefore, theoretical studies of the size dependence of electronic, magnetic, structural, bonding, and reactivity properties of ligand-free metal clusters currently far outnumber experimental work, mainly because of the considerable technical difficulties in preparing sufficient quantities of representative metal clusters. However, this situation is changing rapidly, and the main purpose of this

[*] Prof. G. A. Ozin,
Lash Miller Chemical Laboratories, University of Toronto
80 St. George Street, Toronto, Ontario M5S 1A1 (Canada)
Dr. S. A. Mitchell
Chemistry Division, National Research Council
Sussex Drive, Ottawa, Ontario K1A 0R6 (Canada)

 © Verlag Chemie GmbH, 6940 Weinheim, 1983 0570-0833/83/0909-0674 $ 02.50/0 

review article is to examine the current status of experimental work on naked metal clusters. Attention will be directed mainly towards the technique of matrix isolation, with only a cursory glance at the corresponding gas phase data and at the theory of cluster models. Because of the burgeoning activity in the area over the past five years, an exhaustive coverage of naked metal cluster research is beyond the scope of this article, and only key experiments and underlying principles will be illustrated.

Over the past decade, experimental techniques for preparing and spectroscopically probing specific naked metal clusters of nuclearities spanning the range from atom to the bulk solid have increasingly attracted the attentions of a multidisciplinary group of scientists. Molecular beam and matrix isolation methods have emerged as the methods of choice to study ligand-free metal clusters in the gas and condensed phases, respectivity[3]. In the ideal, collision-free environment of a molecular beam, the metal cluster can be considered to be truly isolated from cluster-substrate interactions. Therefore, it can be argued that spectroscopic methods capable of selectively extracting information from molecular beams of metal clusters hold great promise for studying diverse size-dependent properties of aggregates of metal atoms in their equilibrium configurations. Co-condensation of metal atoms and/or metal clusters and rare gases from either jets or beams at cryogenic temperatures represents the other main approach for observing nucleation phenomena from isolated metal atoms to bulk metal agglomerates in a weakly interacting solid support. In this way, the metal dispersion as well as the thermal and photolytic behavior of particular metal atomic and cluster species can be evaluated spectroscopically. The spectra obtained reflect not only the properties of the cluster "guests" but also their interaction with the host[10]. Because the size requirement of up to *ca.* ten metal atoms is of great practical significance to the spectroscopic, chemical and catalytic properties of supported metal clusters in both weakly and strongly interacting environments[4], it is important to study very small metal clusters both in various types of substrates and in the gas phase. In this way, it is hoped to be able to develop a scale of metal-support effects (guest-host interactions) and to evaluate the role that they play in diverse phenomena[5].

In this overview, we shall concentrate on some of the more recent experimental advances in the field of naked metal clusters immobilized in rare gas solid supports. Although such experiments are certainly of a fairly recent vintage, they can be considered to have evolved as a natural extension of the original matrix isolation method. A brief introduction to matrix isolation will, therefore, be discussed in the following section.

## 2. The Cryogenic Matrix Trapping Experiment

Matrix isolation is a technique whereby solids formed at low-temperature are used as media for stabilizing reactive chemical species for the purpose of spectroscopic study. The modern practice of matrix isolation, involving the use of monatomic rare gases as matrix materials in the temperature range 4–20 K, was pioneered by *Pimentel et al.*[6] in the early 1950's. The experimental technique typically involves condensation of gaseous atomic or molecular species together with a large excess of an inert gas matrix on a suitable substrate at cryogenic temperatures. A very attractive feature of this method is that normally unstable or highly reactive species may be isolated for long periods of time, allowing relatively leisurely spectroscopic investigation. It is often the case that the interaction between the guest species and the host matrix is sufficiently weak that electronic, vibrational, and ESR spectra differ only slightly from those expected from a simple model of a nonrotating, but otherwise unperturbed, gaseous species having internal degrees of freedom (apart from rotation) in equilibrium at the temperature of the matrix. Thus the low temperature of the solid matrix serves not only to stabilize the species of interest but also to simplify its spectra. The number of species which can be studied spectroscopically by matrix isolation techniques is very large, being limited only by the requirement that the species itself or a suitable photolytic precursor can be produced initially in the gaseous state. Fruitful areas of application include free radicals, molecular ions, and high-temperature species found in the vapor above refractory materials such as metal oxides, carbides, nitrides, halides, and the metals themselves. The most commonly used probes are IR, Raman, UV/VIS, laser-induced fluorescence, and ESR spectroscopy[7–11].

Chemical applications of matrix isolation began to be investigated following their early development by *Skell et al.*[12] and *Timms*[13]. An early example of an application of low-temperature condensation of high-temperature species as a synthetic technique is the work of *Skell* and *Wescott*[12] on reactions of carbon species with organic compounds on a surface cooled with liquid nitrogen. The first example of the use of matrix isolation for *in situ* spectroscopic characterization of reaction products formed by co-condensation of gaseous reactants and a rare gas diluent at a temperature below 77 K is a study by *Andrews* and *Pimentel*[14] of the reaction of Li atoms and NO to form LiON in an argon matrix. Matrix cryochemistry has since undergone extensive development, with applications in inorganic, organometallic, and organic chemistry[15–18]. An especially fruitful area has been the chemistry of elemental vapors, in particular of metal vapors[15–17]. The reaction of main group and transition-metal atoms with small inorganic and organic molecules in inert gas matrices have been extensively investigated, and in many cases detailed vibrational and electronic spectroscopic studies of the products carried out. In addition to providing information on the reactivity and general chemical properties of metal vapors, and on the structures and electronic properties of many new and interesting metal-containing molecular species, these studies are often relevant to problems in chemical synthesis and homogeneous and heterogeneous catalysis[15, 19].

An important consideration in certain matrix isolation experiments is to what extent the gaseous species of interest becomes isolated and free from interactions with other guest molecules in the host matrix. In many applications it is desirable to minimize guest-guest interactions, but, since the species of interest are often thermodynamically unstable with respect to dimerization or polymerization, significant quantities of polymers are also often isolated in the

matrix along with the monomer. Measures which may be taken to minimize this effect include the use of very low temperatures and very high dilution with inert gas. Whereas the formation of aggregates is frequently an undesirable side effect, the resultant species are often interesting in their own right; it then becomes of interest to take steps to control the aggregation process and, hence, produce specific cluster species for spectroscopic characterization. This technique of "designed relaxation" of matrix isolation conditions has been used to obtain vibrational spectra of clusters such as $(H_2O)_n$ $(n=1-4)$[20]; $(SiO)_n$ $(n=1-3)$[21]; and $(MX)_n$ (M = Cu or Ag; X = Cl or Br; $n=1-8$)[22]. In addition, there are many examples of matrix isolation spectroscopic studies of metal cluster species: a selection of these forms the subject of this progress report.

## 3. Metal Atom Clusters

A remarkable feature of the structure of metals is the role played by the extended crystal lattice in determining the overall electronic properties and stability of the bulk phase. The question of how the physical and chemical properties of metals change in the limit of very small particle sizes has recently become the focus of increasing investigation[3,4,23,24]. This interdisciplinary area of research is motivated by both fundamental and applied interests. Very small metal particles are employed as catalysts in a broad range of industrially and commercially important chemical processes[25]. The nature of the catalysts used in these systems is often only poorly understood, and it is hoped that experimental and theoretical studies directed at elucidating the general properties of highly dispersed metals will provide a basis for the more rational selection and testing of catalysts. Metal clusters containing only a few metal atoms are particularly interesting from a fundamental viewpoint, since at this level one may expect the most marked deviations from the properties of the bulk phase. A striking experimental demonstration of this is the study by *Montano* and *Dyson*[124] of the evolution of iron clusters from atom to bulk metal using Mössbauer matrix spectroscopy. The dependence of the isomer shift on cluster size for $Fe_n$ $(n=1$ to 8) is shown in Figure 1. Here, it is seen that the isomer shift undergoes a large change on proceeding from a single iron atom to the dimer; the maximum value of the isomer shift occurs at the dimer and trimer level, and then gradually diminishes to the value of α-iron for a cluster of eight iron atoms. Concomitant reductions in the magnitude of the quadrupole splitting with cluster size are also observed (see Section 8.7).

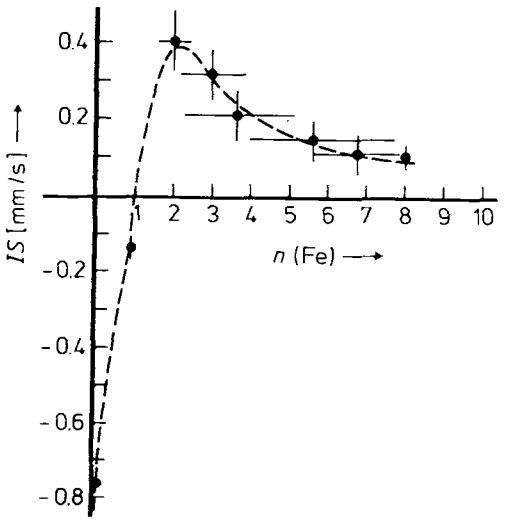



Fig. 1. Variation of isomer shift in the Mössbauer spectra of $Fe_n$ clusters in solid Ar at 4.2 K with the number of nearest-neighbor Fe atoms [124].

A large number of reports dealing with theoretical studies of the evolution of the electronic structure of uni- and bimetallic metal clusters to that of the bulk metal have also appeared[2,3,23,24]. Studies of this type should aid in understanding the structure and properties of metals and alloys and in elucidating the electronic properties of highly dispersed metallic clusters.

## 4. Metal Clusters in the Gas Phase

Experimental investigations of metal clusters with low numbers of atoms have been actively pursued along a number of different directions. The equilibrium vapors above heated metals are in most cases predominantly atomic, as, for example, metals of the first transition series; mass spectrometric studies have shown that their vapors consist of more than 99% atoms[26]. Detection of the diatomic molecules of these metals under equilibrium conditions has, nevertheless, permitted measurements of the diatomic bond dissociation energies[26]: this technique has been extended to include measurements of the atomization energies of certain metal cluster species[3], including $Cu_3$ and $Ag_3$[27]. Recently, a number of methods have been used to produce metal vapors which contain higher proportions of clusters than occur in the pure equilibrium vapors: these include; 1) bombardment of solid metals with energetic rare gas ions (sputtering techniques)[29,29]; 2) vapor phase nucleation of the metal in the presence of a relatively high pressure of inert gas at low temperature (gas evaporation methods)[30,31]; 3) supersonic expansion of either the pure metal vapor[32–35] or of an inert gas to which a small amount of the metal vapor has been added[36]; 4) pulsed laser vaporization of metals[37]; and 5) laser-induced decomposition of organometallic complexes of metal clusters[38,39]. The role of the low-temperature inert gas in the above techniques is to cool the metal vapor and, hence, to produce a condition of supersaturation, thus promoting formation of clusters. For the methods involving supersonic expansion, the cooling is achieved by adiabatic expansion of the vapor from a high pressure region through a small orifice into a vacuum. Although the usefulness of these methods for producing metal clusters has been demonstrated by means of mass spectrometric measurements, to date, only very few spectroscopic studies of metal clusters in the gas phase have been performed. *Sontag* and *Weber*[132a] have studied $Sb_2$ isotopomers by laser-induced fluorescence and determined the spectroscopic constants in various molecular states. *Schumacher et al.*[34] have reported the formation of pure and mixed alkali metal clusters of the type $Na_n$ $(n \leq 16)$, $K_n$ $(n \leq 12)$, and

$K_nNa_m$ ($n+m \leqq 6$) in experiments involving supersonic expansion of the metal vapors. These workers used a single photon photoionization technique in conjunction with mass spectrometric detection to measure ionization potentials of the clusters, and reported data for each of the individual members of the series $Na_n$ ($n \leqq 14$) and $K_n$ ($n \leqq 8$): at the time, these data represented the longest continuous series of any cluster property yet known. These studies have more recently been extended to include seeded beam expansions of high-temperature sodium vapor in He, Ne, Ar, Kr, and $N_2$ carrier gases[36]. In contrast to conventional supersonic expansions, which display an exponential decrease of the abundance of clusters with nuclearity up to $Na_{16}$, the seeded sodium beams produce much larger clusters; at least up to $Na_{65}$ (the upper detection limit of the mass spectrometer) with unprecedented mass abundancies at $Na_8$, $Na_{19}$, $Na_{38}$: these possibly correspond to particularly stable sodium clusters or to an artifact of the cluster growth process. Using a technique involving two-color laser photoionization of sodium clusters in a supersonic sodium beam[*] and mass-selective detection of $Na_3^+$, *Schumacher et al.*[40] were able to generate a spectrum which is in certain respects equivalent to an electronic absorption spectrum of $Na_3$.

A most significant series of experiments has recently been reported for transition-metal molecular beams by *Smalley et al.*[36a,68c]. Here, transition-metals were vaporized with a pulsed laser (Q-switched Nd: YAG second harmonic, 532 nm) and combined with a pulsed supersonic helium expansion. In this way (pulsed supersonic nozzle), large concentrations of ultracold clusters were produced (cf. Fig. 2), including even those of the most refractory metals such as molybdenum and tungsten containing up to 25 atoms[68c]. Very recently *Kaldor et al.*[38] have generated beams of $Fe_n$($n=2$–$23$) and $Ni_n$, ($n=2$–$25$) clusters in a similar manner. From the dependence of the ionizing laser intensity of the time-of-flight mass spectrometric signals, it was found that the cluster ionization potentials exhibited oscillations as a function of cluster size, rather than a monotonic decrease towards the bulk metal work function. Moreover, even for clusters as large as $Fe_{23}$ and $Ni_{25}$ the values had not converged to the work function of the bulk metal. Oscillatory structures of this type had previously been observed in the mass spectra of alkali and group Ib metal clusters and were attributed to the paired/unpaired nature of the S-band. Such a simple explanation cannot, however, be invoked to rationalize the situation for the more complex Fe($3d^64s^2$) and Ni($3d^84s^2$) metals. Thus, the structure has been construed as evidence for unique geometrical and/or electronic porperties for $Fe_n$ and $Ni_n$ clusters and suggests chemical properties which may differ vastly from those of the bulk metal. These results indicate a promising future for the application of supersonic beam and laser spectroscopic techniques to gas-phase metal cluster studies. However, it must be recognized that the requirement for rather complicated experimental techniques is a significant factor which may well retard the expected progress.

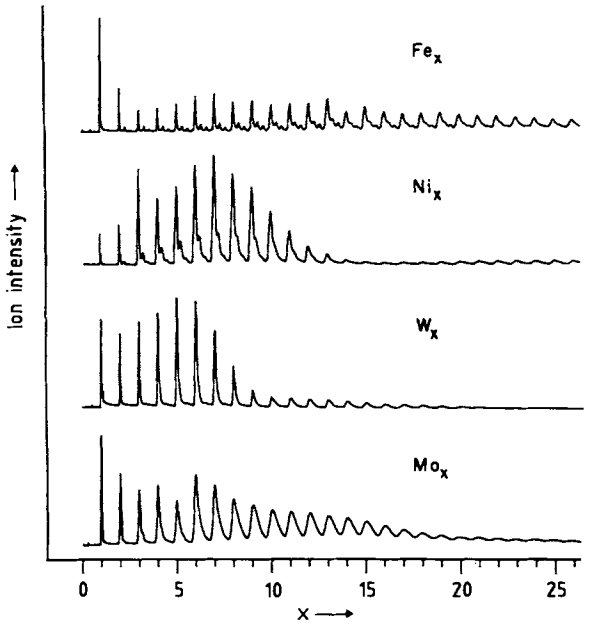



Fig. 2. Time-of-flight mass spectra illustrating cluster size distributions obtained for beams of iron, nickel, tungsten, and molybdenum. Ions were produced by photoionization using an ArF (193 nm) excimer laser with a brightness of *ca.* 1 mJ/cm$^2$. The nozzle backing pressure was 8 bar He, which expanded through a 1 mm orifice. The mass spectra of $Fe_x$ and $Ni_x$ contain additional features due to metal oxides $M_xO_y$. The features in the $Mo_x$ mass spectrum are broadened by the various isotopomers arising from the seven naturally occurring molybdenum isotopes [68c].

## 5. Supported Metal Clusters

The use of refractory solids, such as alumina or silica, or porous materials, such as zeolites, to stabilize metal clusters and small metal particles is widespread and forms the basis of much of the current practice in heterogeneous catalysis by metals[25]. Physical methods of analysis such as X-ray scattering, electron microscopy, magnetization measurements, Mössbauer, photoelectron, ESR and more recently solid-state metal NMR spectroscopy have been used extensively in conjunction with chemisorption studies to characterize supported metal particle arrays. Many examples of such studies may be found in the proceedings of several recent international conferences on the growth and properties of metal clusters[3,4,23,24]. A recent development in this rapidly growing area is the introduction of a new technique which is useful for examining the structures of supported metal particles: this involves analysis of the fine structure extending beyond an X-ray absorption edge, EXAFS (extended X-ray absorption fine structure)[*]. As discussed by *Teo*[41], the fine structure is sensitive to the immediate environment of the atom absorbing the X-ray irradiation, and yields information on the number, type, and distances of the atoms in the first few coordination spheres of the absorber. An example of an interesting application of this method is the comparison of the interatomic distances in bulk platinum metal and zeolite-entrapped pla-

[*] The term "supersonic molecular beam" gives no information about the velocities involved. Under certain conditions (pressure differences of approximately 10 torr, geometry of the jet) phenomena can occur in gas expansion experiments of this type which can formally be accounted by those of ultrasound.

[*] 50 years ago it was observed that the fine structure of an absorption edge extended over a region *ca.* 1000 eV beyond that of an edge.

tinum particles of about 10 Å diameter (corresponding to less than 100 metal atoms per particle) by *Moraweck et al.*[42]. The characteristic interatomic distance for the platinum particles was found to be *ca.* 4% less than the corresponding distance in the bulk metal. The combination of EXAFS and high-resolution electron microscopy (with a resolution of better than 2.5 Å)[43] should enable the size distribution and morphology of supported metal particles to be characterized in considerable detail. Considering that certain features of electronic structure are amenable to study by photoelectron, Mössbauer, and fluorescence spectroscopy, and that chemical properties may be probed by chemisorption and catalytic studies, it is apparent that considerable potential exists for examining trends in cluster properties as a function of particle size, shape, and the nature of the support. The metal clusters which are accessible by preparative methods using solid supports at room temperature typically contain more than one hundred metal atoms, and these systems are most often studied using the above techniques. As discussed below, matrix isolation is a widely applicable method for stabilizing clusters of fewer than ten metal atoms in a form suitable for investigation by a variety of spectroscopic methods.

## 6. Metal Clusters in Rare Gas Matrices—How It All Began

From early studies of the electronic absorption spectra of metal atoms such as Hg, Cd, Mg, and Na isolated in rare gas matrices, it was recognized that under certain conditions significant quantities of homonuclear diatomic metal molecules were co-isolated in the solid matrix with the metal atoms and exhibited distinct UV/VIS bands[44]. Subsequent investigations showed that the extent to which diatomic metal molecules were formed depended in a very sensitive way on the dilution ratio of the metal atom/rare gas atom; the choice of rare gas; and the temperature of the cold substrate during the deposition process[45–48]. It was suggested that the formation of metal dimers and polymers occurred because the metal atoms are highly mobile before they dissipate their kinetic energy in the newly condensing surface layers of the matrix; thereby, aggregation processes can occur for a brief period before solidification of the new layers and immobilization of the metal atoms. This idea has recently been put into the form of a simple kinetic model for the metal atom aggregation processes[49–51]. The model predicts that for a constant inert gas deposition rate the ratio of the absorbance of a metal molecule with n atoms to that of the metal atom should be proportional to the $(n-1)$th power of the metal deposition rate. By means of a quartz crystal microbalance to accurately monitor metal deposition rates, experimental data were obtained which were in accord with this prediction[51,52]. This development contributed to a growing interest in the cryochemical synthesis of diatomic and polyatomic metal molecules: matrix-absorption spectra have been reported for a variety of homo- and heteronuclear diatomic transition-metal molecules, including several whose corresponding gas phase spectra are not available[51–54]. Matrix-isolated metal cluster species whose UV/VIS absorption spectra have been reported include $Na_{3,4}$[55,56], $Mg_{3,4}$[57], $Co_3$[58], $Ni_3$[59], $Cu_{3,4}$[60], $Cr_3$, $Mo_3$, $Cr_nMo_{3-n}$[61a], $Ag_{3-6}$[62,63], and $Cr_nAg_m$[61b].

## 7. Bridging the Gap between Naked Metal Clusters in the Gas Phase and in Matrices

The generation of a distribution of metal clusters in a molecular beam, followed by selective separation of a cluster of specific nuclearity and its subsequent trapping in a rare gas matrix for spectroscopic observation have recently been realized in an elegant experiment by *Schumacher et al.*[127]. In essence, this was achieved by incorporating a Stern-Gerlach magnet into an experimental set-up designed to immobilize pre-formed, spectrally and mass spectrometrically analyzed cluster beams in an inert gas matrix at 4 K. For $Na_x$ ($x = 1, 2, 3$) beams, it was possible to separate paramagnetic $Na_1$ and $Na_3$ magnetically from diamagnetic $Na_2$ and, hence, obtain the UV/VIS spectrum of high purity $Na_2$ dimers in a krypton matrix. Furthermore, by cocondensing the separated partial beam through a mask with Kr onto a cooled sapphire target, it was also possible to obtain the optical spectrum of low density $Na_3$ in solid krypton.

It has recently been demonstrated by *Scoles et al.*[139] that rare-gas cluster hosts containing a single guest molecule can be produced using free-jet expansions and molecular beam techniques. For example, Ar clusters containing a single $SF_6$ or $CH_3F$ molecule have been generated using nozzles with very small orifices and high-dilution mixtures of gases. Using this method it has proved possible to spectroscopically study the seeded molecule as a function of cluster size and temperature. In the limit of large cluster size, this form of spectroscopy in the gas phase would become equivalent to normal matrix spectroscopy. In this way, *Scoles et al.*[139] succeeded in proving that the IR spectra obtained in the limit of large clusters for $(Ar)_nSF_6$ and $(Ar)_nCH_3F$ were remarkably similar to the infrared spectra of the same molecules deposited in an Ar matrix. Clearly the extension of this technique to $(Ar)_nM_x$ as a function of n and x would be a rather elegant way of determining line-shifts and -shapes, and, hence, would be a new method of probing metal-support interactions (cf. Sections 9, 12, and 13).

It seems clear from these pioneering experiments that the combination of size-specific absorption spectroscopy in metal cluster beams with mass-selective separation and techniques of collecting rare-gas solids offers exciting possibilities for in-depth study of the properties of individual particles in mixtures of metal clusters using both gas and matrix phase spectroscopy: the method, thus, offers a new way of studying the perturbation of metal cluster properties by a host support.

## 8. Spectroscopic Methods of Studying Naked Metal Clusters in Solids at Low Temperatures

A variety of spectroscopic methods have been employed to study metal clusters in rare gas matrices. A brief survey of the most important results is presented in the following sections.

### 8.1. Laser-Induced Fluorescence, Raman, and Resonance Raman Spectroscopy

Characteristically, in the electronic absorption spectra of many matrix-isolated metal atomic species the absorption bands are quite broad, with half-widths in the range 100—500 $cm^{-1}$[64]. The UV/VIS absorption bands observed for matrix-isolated diatomic metal molecules are often similarly broad, and in many cases the vibrational structure of the electronic absorption bands is either poorly resolved or not detected[45,48,51,54]. The technique of laser-induced fluorescence (LIF) offers some important advantages in studying the electronic spectra of these systems. The narrow band width and high intensity of the stimulating radiation enable high-resolution spectra to be recorded. In those cases where absorption bands are inhomogeneously broadened due to the occurrence of a multiplicity of slightly different matrix trapping sites, laser excitation may selectively pick out one or a narrow distribution of trapping sites, and thereby produce fluorescence spectra with greatly diminished line-broadening. Laser-induced fluorescence techniques have recently been used to measure the ground-state vibrational frequencies and first anharmonicity constants of molecules such as $Ti_2$, $V_2$[65], $Ni_2$[66], $Fe_2$[67], and $Mo_2$[68] isolated in rare gas matrices. Studies of the electronic absorption spectra of these systems have provided information on certain excited-state vibrational frequencies and on the electronic energy levels[52–54]. Experimental measurements of vibrational frequencies and electronic transition energies are valuable for comparisons with theoretical predictions, and useful insights into the nature of the chemical bonding may be gained by examining trends in these data, especially in conjunction with related data such as bond dissociation energies[65].

With the new LIF data for $Mo_2$[68a] and $Cr_2$[68b] in cryoscopic matrices, and a recent report of resonant two-photon ionization spectra for these same species in a rotationally cold supersonic beam of metal clusters[68c], the topical issue of metal-metal multiple bonding[68d] in these dimers has taken on a new perspective. This began in 1974 with the report by *Efremov et al.*[68e] of a rotationally resolved transient absorption around 460 nm produced by flash photolysis of gaseous $Cr(CO)_6$, and assigned to $Cr_2$ with an "amazingly" short bond length of 1.68 Å in the electronic ground state ($v=0$). Support for this assignment came first in 1975 from the work of *Ozin et al.*[68f], who used quantitative concentration studies of Cr atoms in an argon matrix to identify $Cr_2$ absorptions at 455 and 260 nm. This report was followed in 1977 by the first definitive characterization of UV/VIS transitions of $Mo_2$ and CrMo in rare gas matrices[68g]. At this time *Ozin et al.*[68h] and *Gray et al.*[68i], on the basis of semiempirical MO calculations, independently proposed that the high spin $3d^54s^1$ and $4d^55s^1(^7S)$ ground states of Cr and Mo atoms, respectively, could be considered to be bonded through two single 4sσ and 3dσ bonds, and two 3dπ and two 3dσ bonds, yielding tightly bound, closed shell $^1\Sigma_g^+$ electronic ground states for both $Cr_2$ and $Mo_2$. The proposal of a sextuple metal-metal bond in the $Cr_2$ and $Mo_2$ dimers stimulated a number of *ab initio* calculations[68j] which produced effective bond orders ranging from 0 to >4. Hence, it was highly significant that the LIF matrix studies of *Gruen et al.*[68a] on $Mo_2$, and *Moskovits et al.*[68b] on $Cr_2$ yielded very high vibrational frequencies (475.7 $cm^{-1}$ and 427.5 $cm^{-1}$, respectively) with exceedingly short empirically estimated bond lengths (1.9 Å and 1.7 Å, respectively). For $Mo_2$, *Gruen et al.*[68a] observed time-resolved LIF spectra for this species isolated in argon and krypton matrices (Fig. 3). Here, two separate vibrational progressions were observed, each having long (m sec) but distinct lifetimes (exponential and biexponential, respectively), with spacings $\omega_e = 475.7 \pm 4.5$ $cm^{-1}$; these originate from $Mo_2$ in two slightly different matrix sites. Minimal perturbation of the vibrational states of $Mo_2$ by the surrounding rare gas atoms was indicated by the invariance of $\omega_e$ in Ar and Kr.

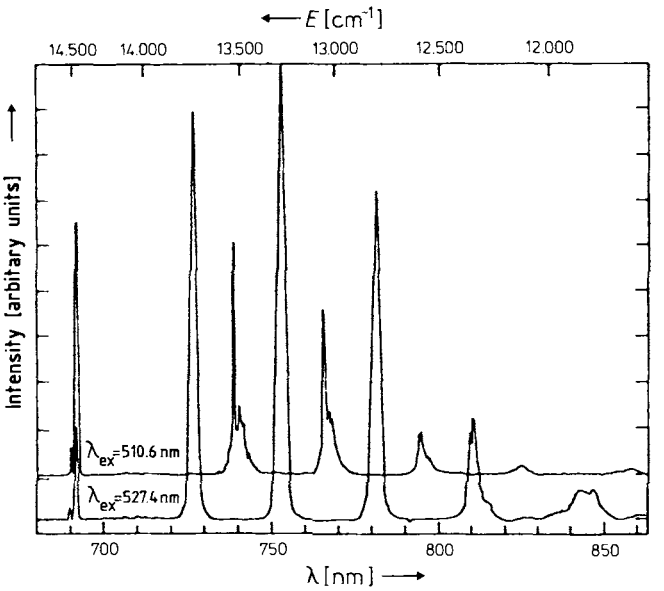



Fig. 3. Emission spectrum of $Mo_2$ in solid krypton. The upper curve is observed for 510.6 nm excitation and the lower for 527.1 nm excitation [68a].

A pivotal experiment, which provided a direct determination of the metal-metal bond length and electronic ground state in $Cr_2$ and $Mo_2$, has recently been reported by *Smalley et al.*[68a]. They used a pulsed-laser metal vaporization source to produce supersonic beams of chromium and molybdenum clusters. With resonant two-photon ionization, mass-selective detection techniques, rotationally resolved absorptions at *ca.* 460 nm and 530 nm were observed for $Cr_2$ and $Mo_2$ isotopomers, respectively. The rotational structure found for each species was that expected for a $^1\Sigma_u^+ \leftarrow {}^1\Sigma_g^+$ transition. Rotational constants yielded bond lengths of 1.68 Å and 1.94 Å for $Cr_2$ and $Mo_2$, respectively, in the v = 0 level of the $^1\Sigma_g^+$ state[68]. Moreover, the vibronic analysis indicates that $Cr_2$ and $Mo_2$ have the same electronic structure. The available experimental data can, therefore, be considered to vindicate the original proposal by *Efremov et al.*[68e] of a short bond for gas phase $Cr_2$, as well as the conclusion by *Ozin et al.* of similar electronic and bonding properties for $Cr_2$, CrMo, and $Mo_2$ isolated in rare gas matrices[68g,h]. Since naked $Cr_2$, with its internuclear separation of 1.68 Å, now boasts the shortest homonuclear bond of any element (Cr bulk, 2.5 Å, $Cr_2^{4+}$ complexes, 1.83 Å[68k]), the controversial issue of the existence

of effective metal-metal bond orders of $>4$ can be considered to have received new fuel.

*Miller* and *Andrews* have made extensive studies of the electronic absorption and LIF spectra of homonuclear and heteronuclear group IIa and IIb diatomic metal molecules isolated in rare gas matrices[69]. The advantages of combining matrix and gas phase studies of the electronic spectra of molecules such as $Pb_2$, $Cu_2$ and $Bi_2$ has been demonstrated by *Bondybey et al.*[70a], *Gole et al.*[70b], and *Nixon et al.*[71].

Recently, Raman and resonance Raman data have been published on tri- and multi-atomic metal clusters, exemplified by $Cr_3$, $Ni_3$, $Cu_3$, $Ag_3$, $Pb_3$, $Sb_3$, $Sb_4$, and $Pb_4$ in rare gas matrices[72,74,133,134]. On the basis of analysis of the isotopic fine structure of laser-excited emissions of $Ni_3$ molecules isolated in an argon matrix (Fig. 4), *Moskovits* and *DiLella*[72] proposed that this species has a bent structure with an apex angle of between 90° and 100°. The frequency of the symmetric stretching vibration of $Ni_3$ was reported to be 232 $cm^{-1}$; the comparable value for $Ni_2$ is 381 $cm^{-1}$[66].

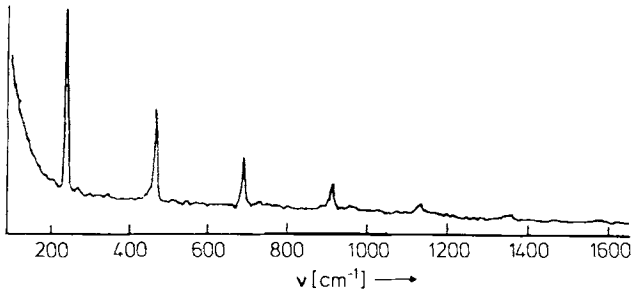



Fig. 4. Resonance Raman spectrum of a solid argon matrix containing nickel excited with 488 nm $Ar^+$ laser radiation, and assigned to $Ni_3$ [72].

Raman and resonance Raman spectra have recently been obtained for $Cr_3$ in argon matrices, and a bent structure with an estimated apex angle of *ca.* 60° was proposed[72]. The resonance Raman spectrum of $Cu_3$ in solid Ar (excitation center *ca.* 16810 $cm^{-1}$) has been found to display an irregularly spaced progression of lines (major series 355, 710, 1063, 1430 $cm^{-1}$; minor series 404, 760, 1115 $cm^{-1}$) with vibrational components possessing an unexpected form of isotopic structure thought to be diagnostic of a pseudorotating $Cu_3$ molecule[133] (see calculations on $Li_3$[88] and ESR data[129]). Briefly, the assignment of fluxionality to $Cu_3$ was based, in part, on the observation of vibrational features arising only from $^{63}Cu_3$ and $^{65}Cu_3$, but not from $^{63}Cu_2{}^{65}Cu$ and $^{63}Cu^{65}Cu_2$ isotopomers. This was explained by proposing that the degenerate vibrational ground (and possibly excited) state of $D_{3h}$ ($^2E'$) of $^{63}Cu_3$ is removed in $C_{2v}$ ($^2B_2 + {}^2A_1$), $^{63}Cu_2{}^{65}Cu$. Such splittings could possibly put the $^{63}Cu_2{}^{65}Cu$ isotopomer out of resonance with the exciting laser frequency. Also, changes in selection rules could make the dipole-allowed electronic excitation in $^{63}Cu_3$ forbidden in $^{63}Cu_2{}^{65}Cu$. Either or both of these effects could lead to the absence of $^{63}Cu_2{}^{65}Cu/{}^{63}Cu^{65}Cu_2$ vibronic components in the resonance Raman spectrum of the $Cu_3$ molecule undergoing dynamic Jahn-Teller distorsions[133].

For the first time, a complete vibrational spectrum of $Sb_4$ has been observed in rare gas matrices by non-resonant Raman scattering[132b]. Samples were prepared by quenching antimony vapor (deposited under Langmuir evaporation conditions, which favor $Sb_4$ as the major component) with, for example, Ar at *ca.* 13 K. The Raman spectra shown in Figure 5 were obtained using visible laser

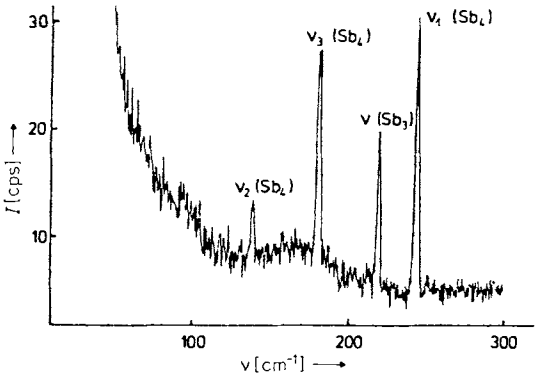



Fig. 5. Raman spectrum of $Sb_4$ in argon at 13 K. A resonance Raman line assigned to $Sb_3$ is also present in this sample, as well as a broad background around 160 $cm^{-1}$ assigned to larger $Sb_n$ clusters [132].

excitation. The observation of three vibrational modes at 241.5, 178.5 and 137.1 $cm^{-1}$, the first being strongly polarized, the second and third being completely depolarized (all lines displaying only $\omega^4$ intensity variation without enhancement), is consistent with the symmetry assignment $\nu_1(A_1)$, $\nu_3(T_2)$, and $\nu_2(E)$, respectively, for an $Sb_4$ molecule with $T_d$ symmetry; none of the modes is subject to resonance enhancement. A resonance Raman spectrum of an antimony cluster ascribed to $Sb_3$ was also observed in this study; however, no structural conclusions could be drawn.

Laser-excited emissions attributable to tetrahedral $Bi_4$ in a neon matrix have been observed by *Bondybey* and *English*[73], who were able to extract all three fundamental vibrational frequencies of this molecule from their data. *Stranz* and *Khanna*[74] reported vibrational frequencies from emission spectra which they tentatively assigned to a trigonal ($D_{3h}$) $Pb_3$ molecule isolated in a xenon matrix.

## 8.2. Fourier Transform Far-Infrared (FT-FarIR) Spectroscopy

Whereas Raman and resonance Raman methods alone may establish cluster geometry, ambiguities can arise from scattering or resonance enhancement by only specific isotopomers and/or structural isomers, as well as non-observation of inactive or weakly active Raman or resonance Raman bands. Uncertainties of this type can, in principle, be clarified by complementary low frequency IR spectroscopic data. Very recently, we devised an experiment in which metal clusters isolated in a rare gas were generated directly inside a far-FIR vacuum interferometer[75]. In this way, the first IR spectroscopic data for ligand-free metal triatomics were obtained. The results for $Cr_3$ immobilized in argon and xenon matrices have revealed that, depending on the metal concentration and thermal treatment condi-

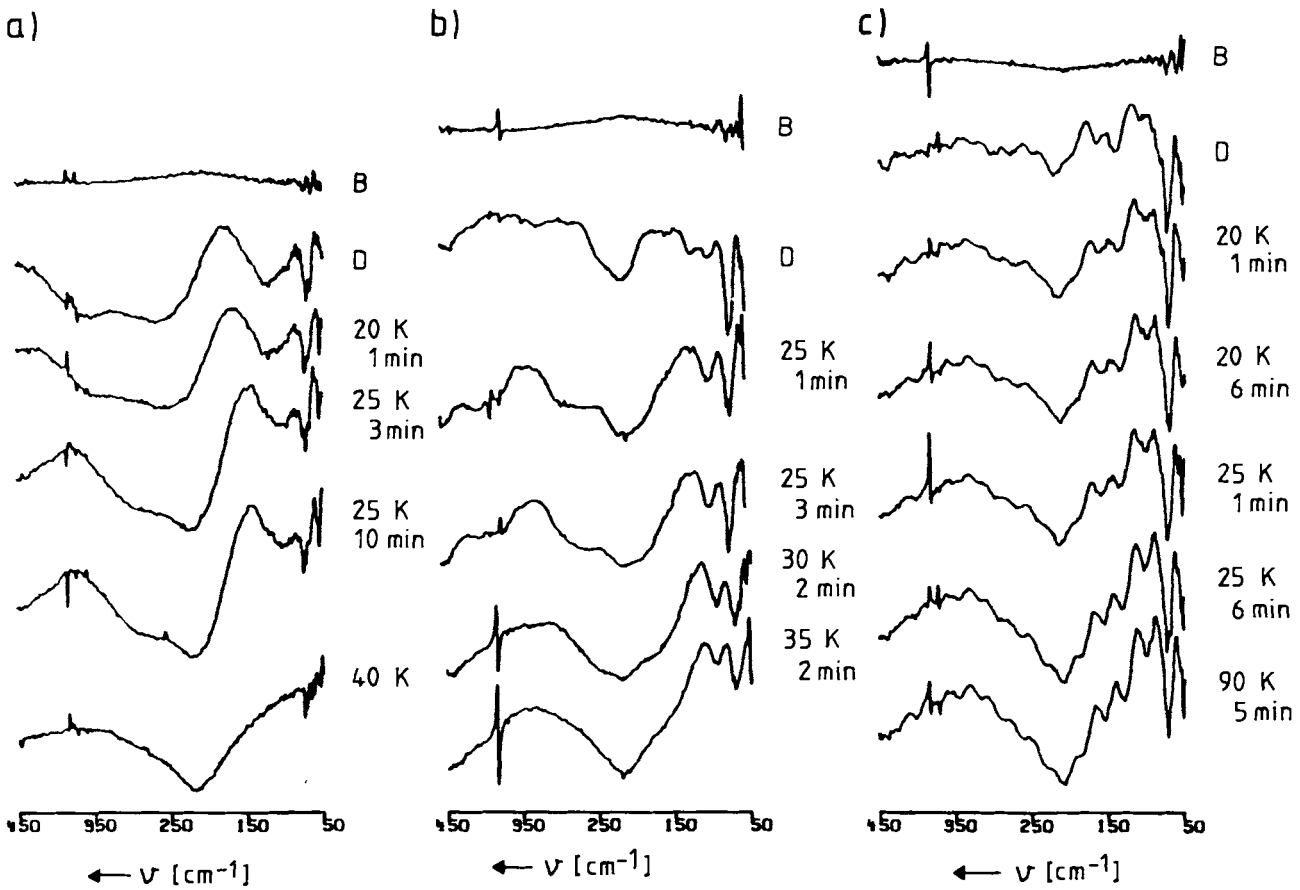
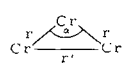



Fig. 6. FT far-IR spectra for Cr/Ar ratios of a) $\approx 1/10^3$, b) $\approx 2.5/10^4$, c) $\approx 1/10^4$ deposited at 12 K and annealed at the temperatures indicated. Peak to peak noise at 200 $cm^{-1}$ *ca.* 0.5% [75].

Table 1. Observed and calculated far-IR active vibrational modes of $Cr_3$ [a, b].

| Calculated [c, d] | | | | | | | | | | | Observed [e] | Assignment [f] |
|---|---|---|---|---|---|---|---|---|---|---|---|---|
| 60° | 70° | 80° | 90° | 100° | 110° | 120° | 130° | 140° | 150° | 160° | | |
| (335) | | | | | | | | | | | 340–360 | $Cr_3$ (60) (≥ 140) |
| | 329 | | | | | | | | | | 325 | $Cr_3$ (70–80) |
| | | 322 | 313 | | | | | | | 308 | 315 | $Cr_3$ (90) |
| | | | | 304 | | | | 299 | 304 | | 295 | $Cr_3$ (100) (110) (130) |
| | | | | | | | 292 | | | | | |
| | | | | | 293 | 284 | | | | | 285 | $Cr_3$ (100) (120) |
| | | | | | 275 | 281 | | | | | | |
| | | | | 265 | | | 268 | | | | 270 | $Cr_3$ (100) |
| | | | 254 | | | | | 253 | | | 260 | $Cr_3$ (90) |
| | | 243 | | | | | | | 239 | | | |
| | 231 | | | | | | | | | | 232 | $Cr_3$ (70–80) |
| 220 | | | | | | | | | | 223 | 215 | $Cr_3$ (60) |
| | 203 | | | | | | | | | | 187 | $Cr_3$ (70–80) |
| | | 185 | | | | | | | | | | |
| | | | 166 | | | | | | | | 155 | $Cr_3$ (90) |
| | | | | 147 | | | | | | | 135 | $Cr_3$ (100) |
| | | | | | 127 | | | | | | 130 | $Cr_3$ (110) |
| | | | | | | 107 | | | | | 105 | $Cr_3$ (120) |
| | | | | | | | 87 | | | | 95 | $Cr_3$ (130) |
| | | | | | | | | 66 | | | | |
| | | | | | | | | | 46 | | | |
| | | | | | | | | | | 27 | | |




[a] All frequency units in $cm^{-1}$. [b] Frequencies refer to argon matrices. [c] Stretching force constants and interaction constants in mdyn $Å^{-1}$, where $f_r = 1.00, f_{rr} = 0.05$, $f_r = 1.00\gamma, f_{rr} = 0.05\gamma$; $\gamma = (180 - \alpha)/120$. [d] Frequencies in parenthesis denote Raman-only active modes. [e] Summary of data from a collection of concentration and annealing experiments (Cr/Ar $\approx 1/10^4$ to $1/10^3$ and 12–40 K, respectively), which are conducive to the formation of $Cr_3$. A sharp absorption observed around 75 $cm^{-1}$ for Cr/Ar and 60 $cm^{-1}$ for Cr/Xe matrices is thought to originate from a localized Cr atom-rare gas cage vibration, rather than a chromium cluster vibration. [f] Numbers in parenthesis refer to the bond angle $\alpha$.

tions, molecular geometries ranging from that of an equilateral triangle to that of an almost linear triatomic molecule can be trapped and identified (cf. Fig. 6 and Table 1).

It is evident from these data that the $Cr_3$ cluster must have a rather shallow potential energy surface for the framework deformation and that, for a particular selection

of experimental conditions, extremely subtle perturbations can profoundly influence cluster geometry. These results are significant because they underscore that even a "weak" metal-support interaction can markedly influence the electronic, vibrational, and geometrical properties of a supported metal cluster. It is clear from these results that FT far-IR spectroscopic data will form a valuable adjunct to the complementary information emerging from laser Raman, resonance Raman, and resonance fluorescence spectroscopy.

### 8.3. Magnetic Circular Dichroism (MCD) Spectroscopy

Magnetic circular dichroism (MCD) spectroscopy has recently been applied to study the electronic absorption spectra of $Cu_{2,3}$, $Ag_{2,3}$, $Mg_{2,3,4}$, $Ca_2$, $Sr_2$, $Mn_2$, and $Ni_n$ isolated in rare gas matrices[57,76,117,118]. This technique involves measurement of the differential absorption of left and right circularly polarized light propagating along the direction of an externally applied magnetic field, and yields information on the degeneracy of the electronic states involved in optical transitions. The MCD spectra of certain paramagnetic molecules exhibit a characteristic temperature dependence which is diagnostic of the presence of unpaired electron spins. *Grinter et al.*[76] reported temperature-dependent MCD spectra for an absorption band at 246 nm (cf. Fig. 7) which had previously been assigned to paramagnetic $Ag_3$ in an argon matrix, thus supporting the previous assignment[109]. Their results were also suggestive of orbital degeneracy in the excited electronic state, consistent with a $^2\Pi \leftarrow ^2\Sigma$ assignment for the electronic transition and, therefore, indicating a linear $Ag_3$ molecule: this is also consistent with the results of a recent Raman spectroscopic study of $Ag_3$ molecules isolated in a krypton matrix[77]. *Miller et al.*[57] have reported the MCD spectra of $Mg_3$ and $Mg_4$ clusters isolated in argon matrices: a detailed analysis of these spectra provided evidence for a triangular ($D_{3h}$) structure for $Mg_3$ and a tetrahedral structure for $Mg_4$.

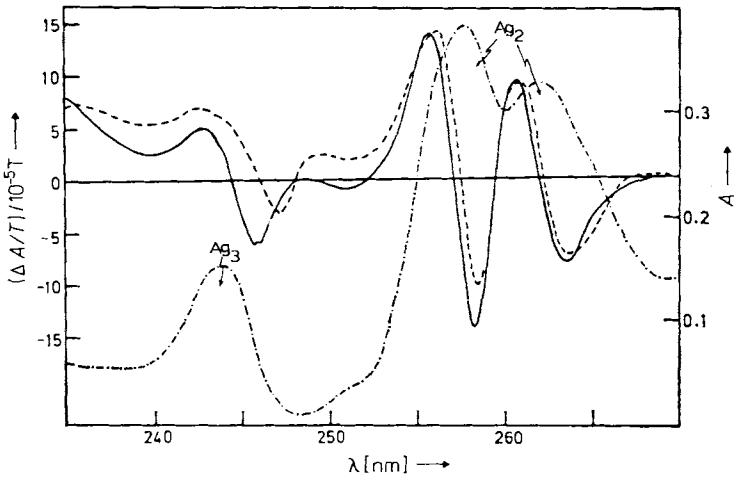



Fig. 7. Absorption and MCD spectra of silver in an argon matrix. Features in the region of 246 nm and 254–270 nm are assigned to $Ag_3$ and $Ag_2$ molecules, respectively. The MCD spectra were measured at a field of 6 T. Absorption spectrum at 10 K (-·-·-·); MCD spectrum at 10 K (——) and 20 K (– – –) [76].

In an early study of Ni atoms in an argon matrix[119], it was reported that 325 nm excitation of one of the $3d^84s^2 \rightarrow 3d^84s^14p^1$ Ni atomic resonance absorptions causes aggregation to $Ni_2$ and $Ni_3$ clusters, which absorb in the range 350–530 nm[119]. Prolonged photolysis caused these bands to disappear and be replaced by new absorptions at *ca.* 240 nm, which were ascribed to $Ni_n$ clusters ($n>3$). In a recent MCD study of Ni/Kr matrices subjected to prolonged atomic photolysis, absorption by a $Ni_n$ cluster was observed at *ca.* 235 nm[118]. This probably corresponds to the same $Ni_n$ cluster observed in an argon matrix at *ca.* 240 nm. Further work will be required to establish the value of n. In this context, it should be noted that recent matrix vacuum-UV/VIS studies of Ni atoms in rare gas solids have shown that the electronic ground-state configuration of the isolated Ni atom can be changed by the matrix; for example it is $3d^84s^2$ in Ne and in the gas phase, but $3d^94s^1$ in Ar, Kr, and Xe. The important point is that repulsive matrix-dopant interactions in Ar, Kr, and Xe are sufficiently lowered in the $3d^94s^1$ configuration of Ni to overcompensate for the 205 $cm^{-1}$ energy difference by which the $3d^94s^1$ level lies above the $3d^84s^2$ level in Ne an in the free atom[136].

Temperature-dependent transitions (347 and 331 nm) in the optical absorption and MCD spectra of Mn atoms in argon matrices over the range 13–27 K have been assigned recently to the $Mn_2$ molecule[117]. The data confirm the earlier theoretical proposal by *Nesbet*[89] that $Mn_2$ should be a weakly bound, antiferromagnetic molecule with a $^1\Sigma_g^+$ ground state. The exchange energy for ground state $Mn_2$ was determined to be $-10.3 \pm 0.6$ $cm^{-1}$, which is identical to the value[86] obtained by *Weltner et al.* from ESR measurements (cf. Section 8.5), and is consistent with the calculated value of $-4$ $cm^{-1}$[89].

### 8.4. UV-Photoelectron Spectroscopy (UPS)

*Jacobi et al.* have recently shown that UV-photoelectron spectroscopy is a highly useful technique for the study of matrix isolated species[78], such as atoms and clusters of Ni and Cu. Rare gas matrices of 50 Å thickness were deposited onto a thin film of Ga on a flat copper block as cryosurface, taking advantage of the featureless UPS of gallium in the energy range of interest. At binding energies below 8 eV, He($II_\beta$) excitation of Cu/Kr $\approx 1/10^3$ produced a new peak at 5.1 eV, which is not observed in a pure krypton matrix (Fig. 8a), and which is ascribed to atomic Cu (Fig. 8b): all bond energies are relative to the Fermi level of the gallium substrate. For Cu/Kr $\approx 1/10^2$, a broad emission at *ca.* 4 eV is assigned to matrix entrapped $Cu_n$ clusters (Fig. 8c). These data are quite distinct from those of bulk Cu (Fig. 8d). Both the invariant Cu atom emission at *ca.* 5.1 eV in various matrices (Ar, Kr, and Xe), assigned to a $3d^94s^1$ final state, and the corresponding gas to matrix relaxation shifts of 1.3 eV confirm that the ground state of Cu atoms in the matrix is the same as in the gas phase, namely $4d^{10}4s^1$; furthermore, the mechanism of relaxation in the matrix is solely intra-atomic, being determined by the Cu 4s electron. The discrepancy between the emissions of small $Cu_n$ clusters at *ca.* 4 eV and that of bulk Cu at *ca.* 2.5 eV is at variance with some electronic structure calcula-

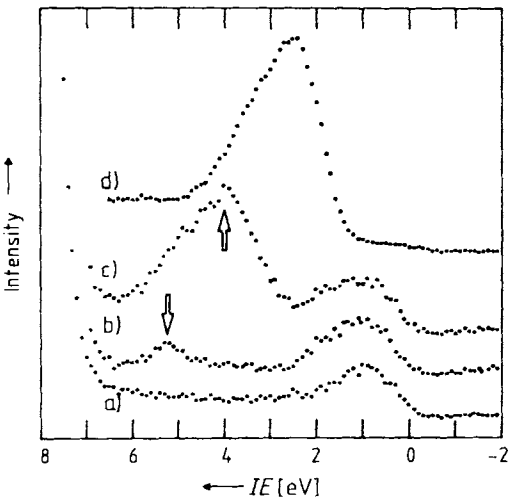



Fig. 8. UPS of a) a pure krypton matrix, b) Cu atoms isolated in krypton and c) Cu clusters isolated in krypton. For comparison the spectrum of bulk Cu is also shown in d). Excitation: $He(II_\beta)$; $T = 7$ K [78].

tions[79] which indicate that copper clusters with as few as 6 to 13 atoms display d-band energies similar to those of bulk Cu. The UPS data imply that to achieve acceptable convergence of metal cluster electronic properties and those of the bulk metal, nuclearities higher than those previously treated by theory will probably have to be considered. It is interesting to note that although the emission spectra of Cu and $Cu_n$ are independent of the matrix gas, emission from the np orbitals of the rare gas host atoms was markedly modified by the copper guests; for example, two kinds of Xe $5p_{1/2,3/2}$ emissions are observed in $Cu_n$/Xe matrices, one of which is identical with that of pure Xe and the other, whose intensity is dependent on the concentration of Cu, is red-shifted by 0.8 eV. The data imply that the atomic relaxation process for an Xe atom in the proximity of a Cu or $Cu_n$ guest is dominated by relaxation effects in the metal rather than in the surrounding Xe atoms. In this sense the UPS data of Cu-doped rare gas solids are similar to those observed for physisorbed rare gases[80].

More recently, *Jacobi et al.* have extended their UPS studies of $Cu_n$ and $Ni_n$ clusters isolated in rare gas matrices to include reactive matrices such as CO and $O_2$[120]. In these experiments they compared the adsorption of CO and $O_2$ on Cu and Ni films with that on small $Cu_n$ and $Ni_n$ clusters and, hence, introduced a novel method of studying chemisorption and catalysis by small metal particles. For $Cu_n$ in CO, for example, a new emission was observed at 1.5 eV, which was not present in the UPS of $Cu_n$ isolated in rare gas matrices. This new signal was assigned to a photoemission from the $2\pi^*$ orbital of CO, which is unoccupied in the free molecule, but partly occupied by charge transfer from $Cu_n$. A similar peak is observed for CO adsorbed on Cu films and surfaces, and has been taken to be diagnostic of $Cu \rightarrow CO(2\pi^*)$ charge transfer; an interaction which plays a central role in Cu–CO bond formation.

### 8.5. Electron Spin Resonance (ESR) Spectroscopy

Matrix-isolated diatomic metal molecules such as $Mn_2$, $Sc_2$, CrCu, and clusters such as $Li_3$, $Na_3$, $K_3$, $Ag_3$, $Cu_3$, CuAgCu, $Cu_5$, $Mn_5$, $Ag_5$, $Na_7$, and $K_7$ have been studied by electron spin resonance (ESR) spectroscopy[81–87, 121, 129, 130, 140].

The ESR spectra reported by *Lindsay et al.*[81–83] for $Na_3$ and $K_3$ isolated in argon matrices indicated linear or slightly bent structures for these systems, and provided direct evidence for covalent rather than ionic or van der Waals' bonding in $M_3$ molecules. In addition, evidence was found for a second form of $K_3$ exhibiting a dynamic structure which fluctuates between three equivalent bent forms of the molecule; the three potassium atoms alternatively occupying the apical position. Fluxionality of this type has been predicted theoretically for the $Li_3$ molecule by *Gerber* and *Schumacher*[88].

Subsequently, ESR spectra assigned to pseudorotating $^6Li_3$ and $^7Li_3$ molecules were observed[129] following photoaggregation at 30 K of $^6Li$ and $^7Li$ atoms, respectively, which were isolated initially in argon matrices at 4.2 K. A typical spectrum for $^6Li_3$ in solid argon is shown in Figure 9. Unlike matrix-isolated $Na_3$ and $K_3$[81–83], the ESR spectra of $Li_3$ showed no alternating line-width behavior in the range 30–40 K, and no stationary $Li_3$ spectra were found between 4.2–40 K. Instead, the observation of seven equally spaced hyperfine transitions with measured intensities close to 1:3:6:7:6:3:1 is consistent with the coupling of the unpaired electron with three equivalent $I = 1$ nuclei and, hence, with assignment to pseudorotating $^6Li_3$ (Fig. 9). The observation of a ten line ESR spectrum (with two components obscured) in the analogous $^7Li$/Ar photoaggregation experiment is in accord with that expected for three equivalent $I = 3/2$ nuclei in a pseudorotating $^7Li_3$ molecule[129]. The absence of a stationary ESR spectrum of the trimer was taken as evidence that $Li_3$ has a relatively "non-localized" ground vibronic state. An average isotropic spin population in $Li_3$ of $\bar{\rho} = 0.225$ was obtained from the ESR data: this value is in excellent accord with *ab initio* calculations for $Li_3$[131]. Moreover, the total isotropic spin population of $3\bar{\rho} \approx 0.68$ indicates approximately 30% p-character in the unpaired electron wavefunction and, hence, significant sp hybridization in the $Li_3$ molecule. In general, the ESR spectra of $Li_3$ are consistent with a $(E' \times e')$ vibronic ground state having $^2E'$ symmetry. On the ESR time scale, the trimer appears to pseudorotate, for example, by tunneling between three equivalent electronic potential energy wells of $^2B_2$ symmetry which are insufficiently deep to support a vibrational level; that is, a completely fluxional $Li_3$ molecule as originally predicted theoretically by *Gerber et al.*[88].

In this same vein, *Lindsay et al.* have recently reported ESR spectra for $Na_7$ and $K_7$ septemers. These spectra display large isotropic hyperfine splittings from two equivalent alkali nuclei plus a much smaller splitting from at least five additional equivalent nuclei. The most likely structure for these $M_7$ clusters appears to be a pentagonal bipyramid; the most compact geometry for seven interacting spheres.

A recent report by *Howard et al.* described the ESR spectrum of $Ag_3$ molecules isolated in solid benzene[84]. The spectrum was interpreted as indicating a slightly bent structure for $Ag_3$. These same authors have recently obtained ESR spectra for $Cu_3$, CuAgCu, and $Cu_5$ trapped in various organic matrices[121]; for example, $^{63}Cu_3$ was trap-

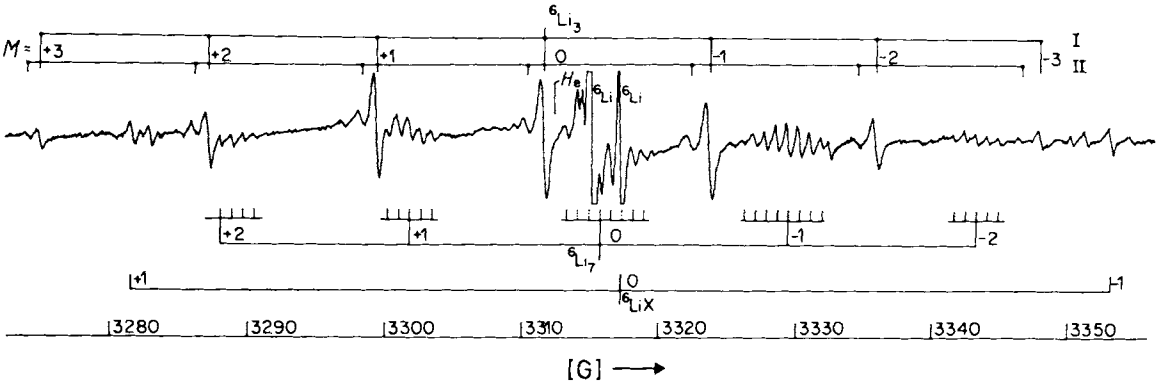



Fig. 9. ESR spectrum of pseudorotating $^6Li_3$ in an argon matrix at 28.5 K. Roman numerals designate matrix sites. Also shown are atomic lithium, $^6Li_7$, and a radical, designated $^6LiX$ [129].

ped in an adamantane matrix at 77 K. Its ESR spectrum displayed 16 sets of quartets with $a_2 = 625.5$, $a_1 = 55.6$ G and $\langle g \rangle = 1.9925$ (obtained from an exact solution of the isotropic spin Hamiltonian using the Breit-Rabi equation). The spectrum was ascribed to a single unpaired electron having equal and large isotropic hyperfine interactions with two equivalent $^{63}Cu$ atoms and a further small interaction with a third $^{63}Cu$ atom. By analogy to that of $Ag_3$ in solid benzene[84], it was suggested that the structure of $Cu_3$ was slightly bent with a $^2B_2$ electronic ground state. Using $^{63}Cu/^{107}Ag/C_6D_6$ codepositions at 77 K, *Howard et al.* observed an ESR spectrum consisting of sixteen doublets with a large hyperfine splitting from two equivalent $^{63}Cu$ nuclei ($I = 3/2$, $a_2 = 880.5$ G) and a smaller hyperfine splitting from one $^{107}Ag$ nucleus ($I = 1/2$, $a_1 = 35.5$ G), with $\langle g \rangle = 1.962$. Analysis of the data led to assignment to the mixed triatomic cluster $^{63}Cu^{107}Ag^{63}Cu$, which probably has an obtuse triangular structure with a $^2B_2$ electronic ground state. In a related study, *Howard et al.*[121] co-condensed $^{63}Cu$ and $C_6D_{12}$ with simultaneous *in situ* photochemical excitation at $\lambda > 320$ nm. The ESR spectrum of the sample at 77 K was highly impressive, displaying a 16 line pattern, each component of which was subsplit into a 13 line multiplet. The unequally spaced 16 lines were assigned to a large hyperfine splitting from two equivalent $^{63}Cu$ atoms and were fitted with the Breit-Rabi equation. This yielded an $a_2$ value of 608 G and a $\langle g \rangle$ value of 2.055. Each of the large lines was further split into 13 lines with an intensity distribution close to that expected for two equivalent Cu atoms with a hyperfine interaction of 15 G and a third Cu atom having twice this interaction. An assignment to $Cu_5$ was clearly indicated. Of the five structures considered by *Howard*[121] for $Cu_5$: linear $D_{\infty h}$; trigonal bipyramidal $D_{3h}$; square pyramidal $C_{4v}$; body centered square $D_{4h}$; and pentagonal $D_{5h}$ the final three species are immediately precluded since they do not contain three distinct types of Cu atom as required by the ESR data. The linear structure is predicted to have the highest spin density on the central Cu atom followed closely by that on the two terminal Cu atoms, with the two intermediate Cu atoms having much smaller values. Since the ESR spectra of $Cu_5$ showed two equivalent Cu atoms with large hyperfine splittings and three with small, the $D_{3h}$ trigonal bipyramidal structure was favored[121]. Molecular orbital calculations on $Cu_5$ suggest that the unpaired electron occupies an e′ orbital formed by a linear combination of equatorial Cu orbitals[97,98]. The $^2E'$ electronic ground state of $Cu_5$ is, therefore, degenerate; however, Jahn-Teller distortion is expected to remove this degeneracy and, thereby, lower the total energy. The distorted $Cu_5$ structures that result are described as $C_{2v}$ "compressed" and $C_{2v}$ "opened". Quite different electron spin distributions are expected for the relevant $a_1$ and $b_2$ HOMO's of the respective $Cu_5$ ($C_{2v}$) clusters which correlate with the degenerate e′ HOMO of the $Cu_5$ ($D_{3h}$) cluster. Proceeding in this way the ESR spectra of $Cu_5$ were interpreted in terms of a trigonal bipyramidal skeleton with a Jahn-Teller distortion towards the $C_{2v}$ "open" arrangement of five copper atoms.

Similar results have also recently been obtained by *Howard et al.*[121] for the neutral cluster $^{107}Ag_5$, generated at 77 K from $^{107}Ag$ by photolysis during deposition in $C_6D_{12}$, followed by careful annealing to remove the transitions belonging to $^{107}Ag$ and $^{107}Ag_3$ from the overall spectrum; what remains is a reasonably clean ESR spectrum which is assigned to $^{107}Ag_5$ (Fig. 10). The signal intensity shows reversible temperature dependence, suggesting either dynamic behavior or a matrix orientation effect. The spectrum consists principally of a triplet of multiplets, indicating two equivalent $^{107}Ag$ nuclei ($I = 1/2$) with $a_2 = 204.6$ G and $\langle g \rangle = 2.081$. The sub-splittings associated with each line of the triplet were best fitted by proposing coupling to three additional $^{107}Ag$ atoms, two being equivalent with $a_2 = 5.5$ G, and the third having $a_1 = 11$ G. In this way the ESR spectrum shown in Figure 10 was assigned. By analogy to the reasoning described previously for $Cu_5$, the

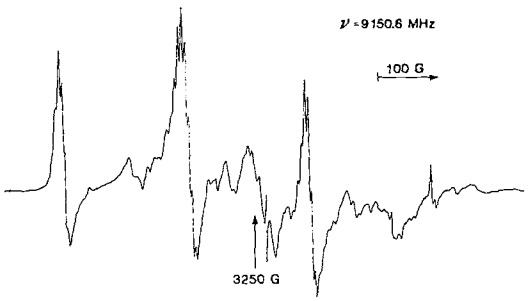



Fig. 10. ESR spectrum of $^{107}Ag_5$ in $C_6D_{12}$ at 77 K following careful annealing to remove most of the $^{107}Ag$ and $^{107}Ag_3$ [121].

trigonal bipyramidal structure with Jahn-Teller distortion was assigned to $^{107}Ag_5$. Using $^{107}Ag$ one-electron parameters, the isotropic hyperfine interactions in $^{107}Ag_5$ yielded the following unpaired spin populations: 62% for two equatorial $^{107}Ag$ nuclei; 1.7% for the unique equatorial $^{107}Ag$; and 0.8% for the remaining two axial $^{107}Ag$ nuclei. These are similar in magnitude to the spin-populations on the copper nuclei of $Cu_5$. The data imply that in $^{107}Ag_5$ *ca.* 60% of the unpaired spin-population resides in 5s orbitals, with as much as 40% spin density in p and/or d orbitals.

The interesting diatomic molecules CrCu[85], $Sc_2$[140], and $Mn_2$[86] have been prepared in rare gas matrices and studied by ESR spectroscopy by *Weltner et al.*: for $Sc_2$ and CrCu high spin $^5\Sigma$ and $^6\Sigma$ ground states, respectively, were suggested. Although a diamagnetic ground state was indicated for $Mn_2$, in agreement with an earlier theoretical prediction[89], evidence was found for a series of regularly spaced higher spin states, some of which were found to be thermally accessible for $Mn_2$ in a krypton matrix at 50 K (Fig. 11). For example, in krypton at 4.2 K only Mn atom signals were observed, displaying six lines of equal intensity centered at *ca.* 3350 G of hyperfine splitting *ca.* 28 G. At 10 K an 11 line pattern of intensity ratio 1:2:3:4:5:6:5:4:3:2:1 and hyperfine splitting 15 G begins to emerge at 2511 G (Fig. 11). The observed ESR

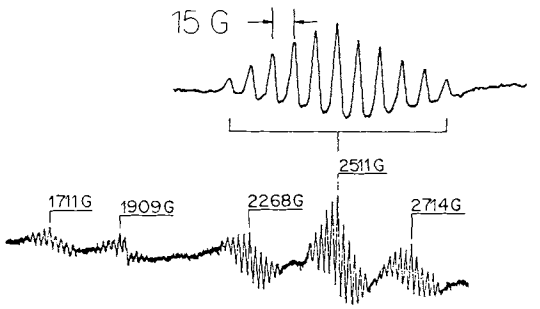



Fig. 11. ESR spectrum of the $Mn_2$ antiferromagnetically exchange-coupled dimer isolated in a Kr matrix at a temperature of *ca.* 50 K, $\nu = 9.3840$ GHz [86].

spectra and their temperature dependence identified lines at 1711, 2511, 4305 G with $S = 2$ and 1909, 2268, 2714, 4050 G with $S = 3$ total spin states; these were analyzed assuming a spin Hamiltonian of the form

$$\mathscr{H} = \beta H \cdot g \cdot S - (J/2)[S(S+1) - S_i(S_i+1) - S_j(S_j+1)] + D_z[S_z^2 - 1/3\,S(S+1)] + (A/2)S \cdot (I_i + I_j)$$

where $J$ is the isotropic exchange energy; $S = S_i + S_j$ is the total spin with values $S_i + S_j$, $S_i + S_j - 1, \ldots 0$; $A$ is the hyperfine interaction constant for the isolated atom; and $D_z$ is an effective zero-field splitting parameter expected to be dependent on the $S$ value. The ESR spectra of $Mn_2$ are thus analyzed in terms of an antiferromagnetically exchange-coupled dimer which takes on thermally accessible and increasing values of $S$ as the temperature increases from 4.2 to 50 K. Support for this fascinating proposal would stem from the observation of the $S = 4$ signals, which are expected to evolve at *ca.* 65 K, a temperature which was unfortunately inaccessible in *Weltner*'s study[86]. The temperature variation of the absorption and MCD

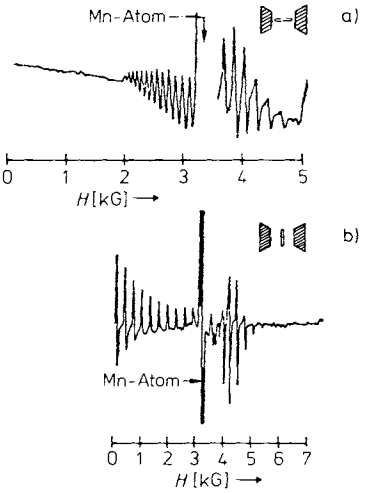



Fig. 12. ESR spectrum of the $Mn_5$ molecule in solid krypton at 4 K ($\nu = 9.378$ GHz). Strong preferential orientation of the $Mn_5$ molecules is indicated by the different spectra observed when the flat face of the sapphire rod is parallel (top spectrum) and perpendicular (bottom spectrum) to the magnetic field direction [87].

spectra of $Mn_2$ in solid argon described in earlier work[117] are consistent with the conclusions drawn from the ESR study of $Mn_2$ in solid krypton[86].

Finally, an interesting example of a metal cluster in a high spin state is $Mn_5$, for which a recent matrix-isolation ESR study[87] suggested a total electronic spin $S = 25/2$ (corresponding to five unpaired spins on each Mn atom) and a pentagonal planar geometry (Fig. 12).

### 8.6. X-Ray (EXAFS) Spectroscopy

The presence of incompletely filled atomic d orbitals in transition metals gives rise to a rather dense manifold of low-lying electronic states for diatomic metal molecules. The relative stabilities of these low-lying electronic states are a matter of considerable interest to problems involving the electronic structures of metals and the electronic configurations and bonding capabilities of the diatomic metal subunits of binuclear metal complexes with neutral or ionic ligands. The chemistry and catalytic activity of many of these binuclear metal complexes are currently being actively investigated[90]. Several recent theoretical studies of diatomic transition-metal molecules point out the difficulties associated with treating electron correlation and exchange effects adequately[91–99]. It is clear that experimental results on these systems are crucial for the development of reliable theoretical treatments. Of particular importance are the properties of the ground electronic state, including, in addition to the vibrational frequency and dissociation energy, the internuclear distance, spin multiplicity, and orbital state symmetry. The recent EXAFS[100] and Mössbauer spectroscopic studies[101] of $Fe_2$ in argon matrices by *Montano et al.* may be noted in this connection. From the EXAFS data a bond distance of 1.87 Å was deduced for $Fe_2$ in argon, and the Mössbauer results were indicative of a $^7\Sigma$ electronic ground state. Similar Mössbauer studies have been reported for the heteronuclear diatomics FeNi, FeMn, FeCu, and FeCo[101]. Currently available experi-

mental and theoretical results suggest stable states of high spin multiplicity for diatomic transition-metal molecules.

In a recent study, *Montano et al.* obtained EXAFS and XANES (X-ray absorption near edge structure) data for small $Fe_n$ molecules in neon matrices (Fig. 13) over a wide range of Fe concentrations[102]. By averaging the Fe–Fe distances over a narrow range of $Fe_n$ multimers, a significant contraction of the Fe–Fe distance was observed: 2.48 Å for α-Fe; 2.30 Å for $Fe_n(n>5)$; 2.05 Å for $Fe_2$, $Fe_3$, and $Fe_4$; and 2.02 Å at extreme dilutions, for mainly $Fe_2$. It is fascinating to note that similar nuclearity-dependent metal-metal interatomic distances are beginning to emerge from related studies of metal clusters on more strongly interacting supports, such as those reported by *Moraweck et al.*[42] ($Pt_n$/zeolites) and *Apai et al.*[103] ($Cu_n$ and $Ni_n$ on carbon and oxides, respectively). The XANES spectra of $Fe_n$/Ne solids also show considerable metal concentration dependence near edge structures (Fig. 13b). A K-edge shift of $3\pm1$ eV for Fe atoms compared to that of bulk Fe is consistent with the expected higher binding energies for $3d^64s^2$ Fe monomers compared to the $3d^74s$ configuration of the bulk metal[102]. The near edge absorptions observed for $Fe_n$ multimers were tentatively assigned to

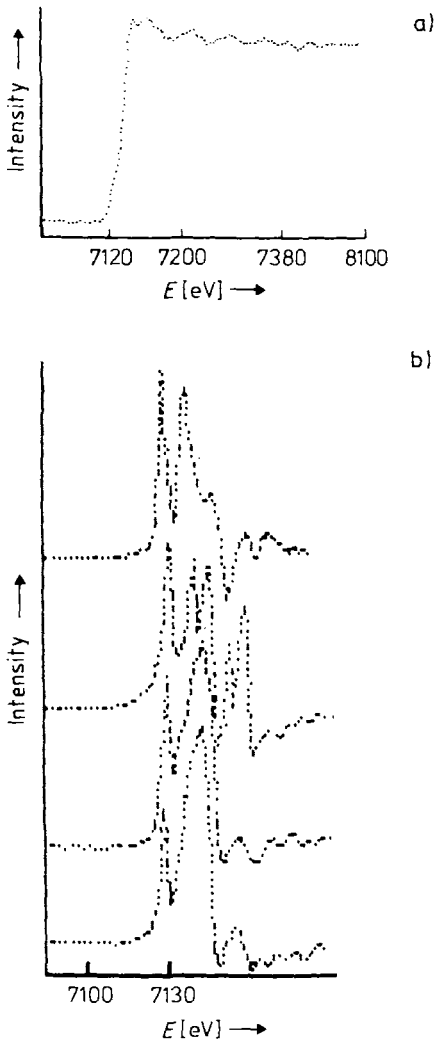



Fig. 13. a) X-ray absorption spectrum (EXAFS) of a sample containing 0.4 at-% Fe in Ne at 4.2 K. b) Derivative of the XANES spectra of (a) Fe foil; (b) 1.5 at% Fe in Ne; (c) 0.5 at% Fe in Ne; and (d) 0.4 at% Fe in Ne at 4.2 K [102].

1s→3d,4s,4p,np transitions. However, a firmer theoretical understanding of XANES will be necessary to quantify metal cluster data of the above type.

### 8.7. Mössbauer Spectroscopy

Mössbauer spectra of matrix-isolated $Fe_xCo_y$ molecules have recently been obtained[122]. A number of samples were investigated with metal concentrations varying from 0.1 to 25 at-%. From symmetry considerations and the magnitude of the electric field gradient, the electronic ground state of the FeCo molecule was found to be $^6\Sigma$. In addition to FeCo, the trimeric clusters $Fe_2Co$ and $FeCo_2$ were identified and their Mössbauer parameters determined[122]. Definitive conclusions on the structure of these triatomic, bimetallic clusters were not made in this study; however, using higher metal concentrations and Monte Carlo methods to estimate the cluster size and composition, the variation of the isomer shift of Fe with the number of cobalt nearest neighors in $Fe_xCo_y$ clusters could be established[122]. Similar kinds of experiments have been performed for $Fe_n$[124]. It was found that the isomer shift approached the value obtained for iron in a cobalt matrix for about twelve Co nearest neighbors. For one Co nearest neighbor a maximum in the isomer shift of Fe was observed, indicating a change in the configuration of the iron atom with a subsequent decrease of the s electron density at the $^{57}$Fe nucleus. As the number of surrounding Co atoms increased, the isomer shift was observed to decrease from this maximum value, suggesting an increase in the s electron density at the nucleus arising from 3d electron delocalization effects. It is interesting that the Mössbauer spectra obtained for a metal concentration of 5 at-% with Fe : Co = 1 : 3 already showed the six lines characteristic of magnetic hyperfine splitting[122]. Monte Carlo analysis of these samples predicts the formation of clusters containing only four to five metal atoms: $Fe_2Co_2$, $FeCo_3$, $FeCo_4$, $Fe_3Co_2$, and $Fe_2Co_3$. At 25 at-% the observed magnetic hyperfine field was the same as that observed for disordered iron-cobalt alloys of the same composition.

From this brief look at the Mössbauer spectroscopic investigation of the Fe/Co matrix (as well as the $Fe_n$ study described previously, cf. Fig. 1) it can be deduced that such studies have great potential for probing subtle electronic and bonding interactions between metal atoms, and provide a means of following the evolution of bulk metallic properties from those of the metal atom to those of the small metal cluster.

Very recently, $^{119}$Sn and $^{57}$Fe Mössbauer spectra (Fig. 14) have been employed to study small bimetallic clusters of $Fe_xSn_y$ in solid argon[104, 123]. The use of two γ-resonance probes in a single sample of clusters, and self-consistent assignment of isomer shifts, quadrupole splittings, line widths, and relative intensities of the $^{119}$Sn and $^{57}$Fe lines led to identification of FeSn, $Fe_2Sn$, $Fe_2Sn_2$, $FeSn_3$, $Fe_2Sn_3$ and $FeSn_4$ molecules; provided geometrical clues concerning the mixed trimers; gave relative reactivity information for Fe and Sn atoms and dimers in nucleation processes occurring during matrix condensation; and enabled some conclusions to be drawn about the Fe–Sn bond in ligand-free $Fe_xSn_y$ clusters.

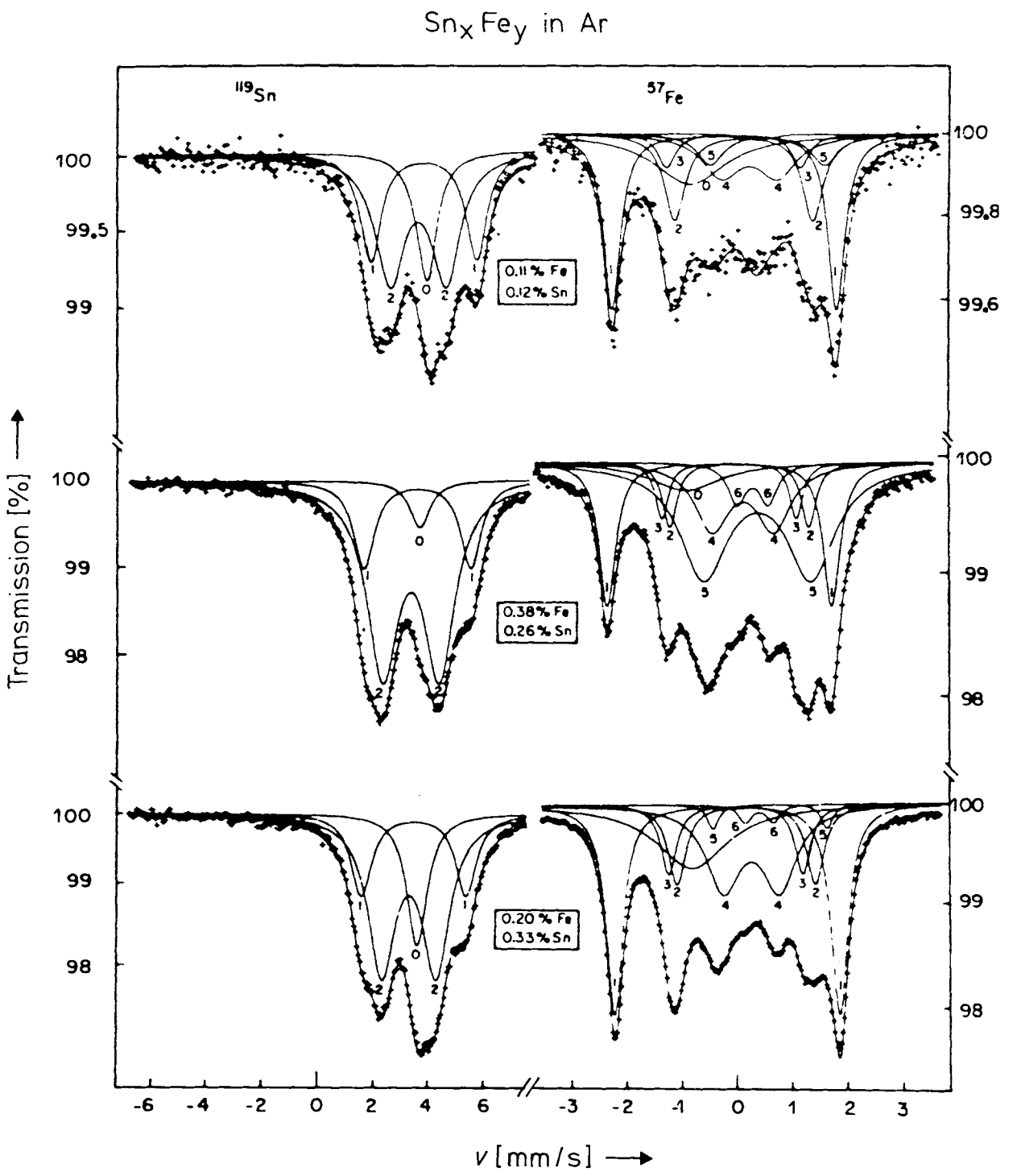


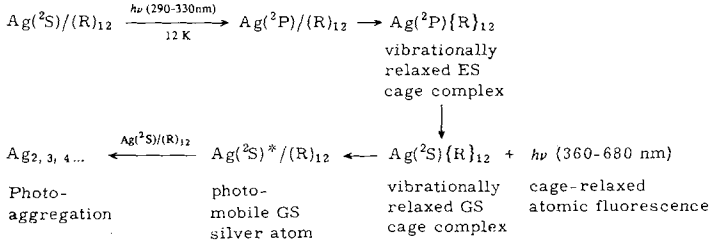

Fig. 14. Two γ-resonance $^{57}$Fe and $^{119}$Sn Mössbauer absorption spectra for various metal to argon ratios at 4.5 K. The solid lines are a least squares fit of the experimental spectra. Six and three components were characterized for $^{57}$Fe and $^{119}$Sn, respectively. Notation: 0 = $Fe^0$, 1 = $Fe_2$, 2 = FeSn, 3 = $FeSn_2$, 4 = SnFeSn, 5 = $Fe_2Sn$, 6 = $Fe_3$ and 0 = $Sn^0$, 1 = $Sn_2$, 3 = $Sn_xFe_y$ [104].

### 8.8. UV/VIS Absorption and Emission Spectroscopy

Experimental studies of metal clusters are subject to an inherent difficulty, since it is generally not feasible to selectively produce specific cluster species. Conditions leading to formation of significant quantities of any given cluster may, in general, be expected to lead also to formation of comparable quantities of both larger and smaller clusters. In the absence of methods to selectively excite or detect one cluster, therefore, it is generally necessary to deconvolute spectroscopic data into contributions from several clusters. It is, thus, highly desirable to work with well characterized cluster distributions, and to be able to easily change the cluster distribution in a designed way. As noted earlier, the general mechanism of metal cluster formation in cryoscopic matrices is aggregation of the metal atoms in the mobile surface layers of the matrix during the deposition process. The degree of aggregation is controlled by

factors such as the metal atom/rare gas atom dilution ratio, the temperature of the cold substrate, and the atomic weight of the matrix gas; all of which may be varied to optimize the cluster distribution. Further agglomeration of the metal species in the deposited matrix may, in certain cases, be induced by thermal annealing[63]. UV/VIS absorption measurements provide a convenient and fairly sensitive means of detecting entrapped metal clusters. Matrix-isolated metal atoms typically exhibit very intense UV/VIS absorption bands; hence, it is not unexpected that diatomic metal molecules and small clusters also show absorptions in this region. Under conditions of carefully controlled metal atom aggregation, quantitative metal deposition techniques may be used in conjunction with optical absorption measurements to estimate relative extinction coefficients of isolated atoms and of diatomic and triatomic metal molecules[49]. Measurements of this type are very useful, since they serve to define the experimental conditions under which at least partly understood metal cluster distributions may be produced.

A new method for producing silver clusters in rare gas matrices has recently been reported by *Ozin* and *Huber*[63]. This involves photoinduced diffusion and aggregation of entrapped silver atoms promoted by narrow-band illumination of the matrix at a wavelength corresponding to the strong resonance absorption band of the silver atoms. Similar metal atom photoaggregation effects have been observed for matrix-isolated sodium, nickel, copper, chromium, molybdenum, and rhodium atoms[19, 58, 61, 105, 118, 125]. In this context, the fluorescence emission and excitation spectra of metal atoms and small clusters immobilized in cryogenic matrices exhibit a specificity which, for sometime, has been recognized as a sensitive probe of the microscopic environment of the entrapped guest signalling subtle changes in its surroundings as well as specific guest-host interactions in its ground and excited states[105–108, 128]. Here, a striking resemblence between the optical spectra of silver atoms isolated in rare gases and faujasite zeolites, and those of small clusters of silver atoms has been noted and interpreted in terms of a weak metal-support interaction for the silver guests in the zeolitic host[5].

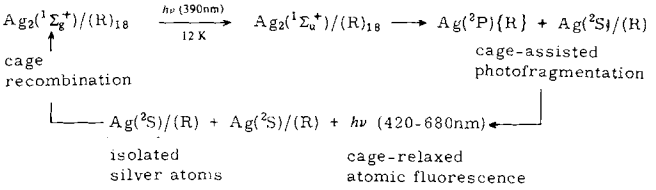



Scheme 1. Photoprocesses of silver atoms isolated in rare gas matrices. $(R)_{12}$ represents the twelve nearest-neighbor rare gas atoms (R = Ar, Kr, Xe) around a cubooctahedral, substitutional Ag atom trapping site.

Studies of the energetics and dynamics of Ag, $Ag_2$, $Ag_3$, Cu, and $Cu_2$ in rare gas solids have been undertaken[63, 105–111]. The absorption and fluorescence spectra are indicative of strong guest-host interactions in the low lying excited states of these species. A summary of the observed radiative and non-radiative relaxation processes of VIS- and UV-photoexcited Ag, $Ag_2$ and $Ag_3$ in rare gas solids is shown in Schemes 1–3.

The most pertinent feature of the spectroscopy and photoprocesses of Ag atoms isolated in rare gas matrices are the strong guest-host interactions in the optically excited, vibronically active $^2P$ state of Ag, which results in fast vibrational relaxation of the rare gas cage atoms surrounding the Ag($^2$P) atom followed by cage-relaxed (strongly red-shifted) atomic fluorescence. It is thought that the destabilization caused by formation of a Ag($^2$S) ground state in the vibrationally relaxed excited state cage-configuration provides the driving force for photoinduced diffusion of the Ag atom leading to photoaggregation[63, 107].

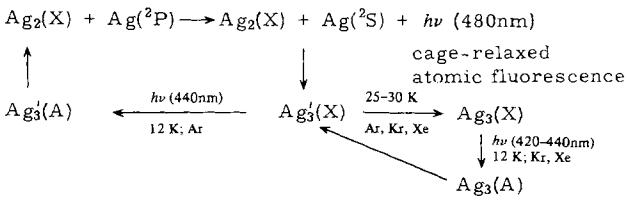
The optical absorption and fluorescence spectra of $Ag_2$ in rare gas solids[108] are also clearly indicative of strong guest-host interactions involving the A ($^1\Sigma_u^+$) and C ($^1\Pi_u$) states of $Ag_2$ (cf. Scheme 2).




Scheme 2. Photoprocesses of silver dimers isolated in rare gas matrices. $(R)_{18}$ represents the eighteeen nearest-neighbor rare gas atoms (R = Ar, Kr, Xe) around a $D_{2h}$ disubstitutional $Ag_2$ trapping site.

The atomic emission spectrum produced by A←X excitation of $Ag_2$ at 390 nm in argon, krypton, and xenon matrices is interpreted in terms of dissociation of an excited state of $Ag_2$. This involves strong destabilization of the A state of $Ag_2$ (bound in the gas phase) and strong stabilization of the Ag($^2$P) + Ag($^2$S) fragments by matrix-cage relaxation effects (cf. Scheme 2). The net "cage-assisted" photofragmentation yield is only *ca.* 10%[110] due to the short-range repulsive constraints of the matrix cage, which result in efficient recombination of the ground state Ag fragments (Scheme 1).

The optical absorption and fluorescence spectra and photochemical properties of $Ag_3$ provide clear evidence for the occurrence of two distinct forms of $Ag_3$ in each of the three rare gas matrices[5, 106, 109, 111]. These observations show that the matrix environment stabilizes distinct isomeric forms of this species. It appears that the normal form of $Ag_3$ is produced in argon, krypton and xenon matrices, and a structurally distinct yet normal form, denoted $Ag_3'$, by photoinduced aggregation of Ag in argon matrices and by 420–440 nm photoisomerization of $Ag_3$ in krypton and xenon matrices[111]. The results available for $Ag_3$ and $Ag_3'$ in rare gas solids are summarized in Scheme 3.




Scheme 3. Photoprocesses of silver trimers isolated in rare gas matrices.

For the $Ag_3'$ isomer in solid argon, the spectroscopic and photochemical results indicate that an efficient photodissociative-recombination process $Ag_3 \rightleftharpoons Ag_2 + Ag$ occurs in the matrix cage. However, for the $Ag_3$ isomer in solid krypton and xenon, the available data lean heavily in favor of a photoisomerization to the $Ag_3'$ structural form within a deformable matrix cage, rather than a photodissociation or photoionization process.

## 9. Matrix Effects on the Spectroscopic Properties and Structure of Naked Metal Clusters

As described previously, isomeric forms have been proposed for $Ni_3$[72], $Cr_3$[75], and $FeSn_2$[104] in rare gas solids. Recently, three forms of $Cu_3$ have been identified in solid xenon[60b]. These are significant discoveries because they represent direct experimental evidence that the environment in a rare gas solid can exert a decisive influence on the energetic, dynamic, and structural properties of entrapped molecular metal clusters. Thus, in certain cases it may not be appropriate to directly compare the results of spectroscopic and structural studies of immobilized metal clusters with predictions based on calculations on the corresponding clusters in the gas phase. Of course, a great deal of very useful and interesting information can be obtained from such spectroscopic studies, even if the clusters are significantly perturbed by the matrix support, because such interactions are expected to be of importance in most experiments involving metal clusters, especially those involving chemical or catalytic processes. It is perhaps not surprising that such matrix interactions are important for $Ag_3$ because, on the basis of accurate SCF-CI-MO calculations on the $Ag_3$ molecule, *Basch*[112] has concluded that the energy difference between a linear and strongly bent form of $Ag_3$ is only 0.14 eV (3.2 kcal·mol$^{-1}$). This energy difference is of the same order of magnitude as the spectral shift of the $Ag_3$ absorption bands on changing from argon to xenon matrices, and can be taken as a rough measure of the magnitude of the $Ag_3$-rare gas interaction energy. Similar MO calculations have shown an energy difference of only 0.04 eV between the linear, obtuse, and acute forms of $Cu_3$[137]. Thus, even a weak metal-support effect can exert a significant influence on the energetic, structural, and dynamic properties of entrapped cluster guests. It is thus of paramount importance to evaluate the metal-support interactions for a range of metal clusters in a wide variety of supports.

## 10. Loosely Coupled Groups of Metal Atoms and Clusters

The UV/VIS absorption, fluorescence emission, and excitation spectra of Cu atoms in xenon matrices[115] have recently revealed the existence of a weakly coupled copper dimer ($Cu_2''$) which co-exists with the "normal" diatomic copper molecule ($Cu_2'$) (Fig. 15a). Kinetic and spectroscopic studies (Fig. 15b) have shown that photoexcitation of $Cu_2''$ with visible light induces an irreversible first-order transformation to form the normal dicopper molecule,

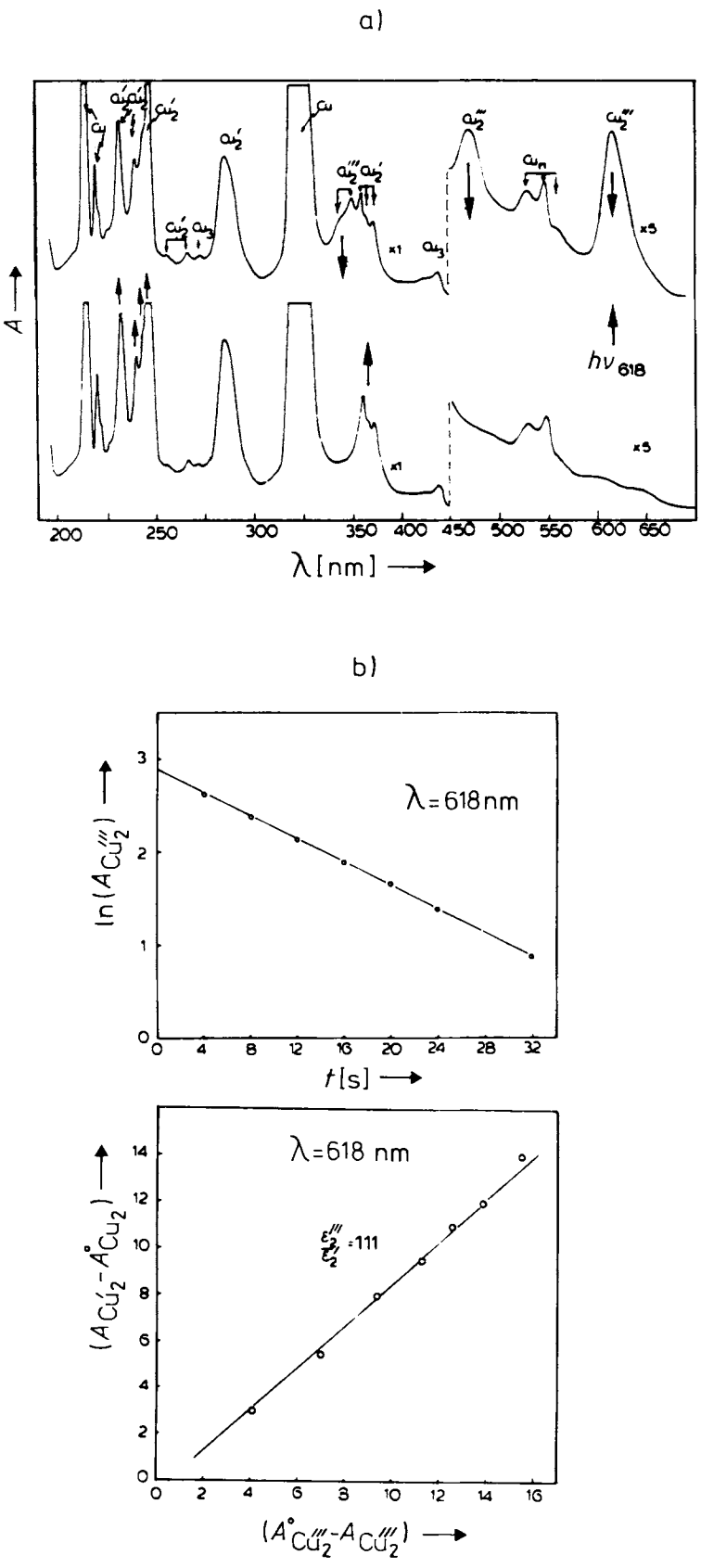



Fig. 15. a) Top: UV/VIS absorption spectrum of Cu/Xe ≈ 1/10$^3$ at 10–12 K; Bottom: Following photoexcitation at 618 nm for 5 min showing photoconversion of the weakly coupled $Cu_2''$ molecule to the normal $Cu_2'$ molecule. Similar effects are observed for the 474 nm absorption of $Cu_2''$.

b) Photoconversion $Cu_2'' \xrightarrow{h\nu(618\,nm)} Cu_2'$ showing well behaved first-order kinetics (top) and direct proportionality to the growth of $Cu_2'$ (bottom). The latter yields a value of the extinction coefficient ratio $\varepsilon_2''/\varepsilon_2'$ of *ca.* 1 [115].

$Cu_2'$. SCF-Xα-SW-MO calculations of the spectroscopic properties of copper dimers, modelled to fit the nearest-neighbor and next nearest-neighbor disubstitutional vacancy sites of solid xenon, were compared with the experimental observations[115]. These calculations suggest that the weakly coupled copper dimer can be considered to have arisen from the trapping and stabilization of copper atoms in next nearest-neighbor disubstitutional vacancy sites as the $D_{4h}$, $Cu_2''''\{Xe\}_{20}$ "cage-complex" (Fig. 16a), which is unique to the xenon lattice and has no detectable counterparts in solid argon or krypton[105]. Photochemical or thermal excitation of $Cu_2''''\{Xe\}_{20}$ binuclear species produces the normal $D_{2h}$, $Cu_2'\{Xe\}_{18}$ dimer (Fig. 16b), containing copper atoms trapped in nearest-neighbor disubstitutional vacancy sites, separated by the gas-phase $Cu_2$ internuclear distance.

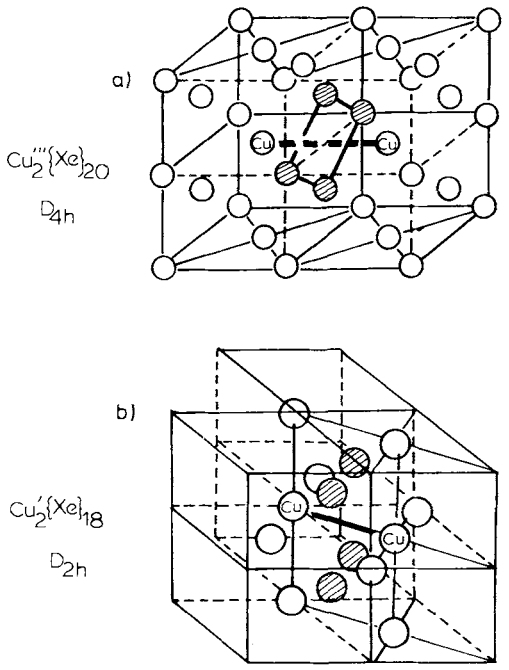



Fig. 16. Illustration of a) the weakly-coupled $D_{4h}$, $Cu_2''''\{Xe\}_{20}$ copper dimer cage-complex and b) the normal $D_{2h}$, $Cu_2'\{Xe\}_{18}$ copper dimer cage-complex, isolated in the fcc lattice of xenon at 12 K [115].

In view of the discovery of weakly coupled copper atom pairs in solid xenon, it is now clear that extreme care must be exercised in analyzing spectroscopic, photochemical and kinetic studies of metal clusters immobilized in weakly and strongly interacting supports. It seems highly likely that unexplained lines and effects observed in the spectra and reactions of entrapped metal clusters, which might have been presumed to originate from metal aggregates bound in a "normal" covalent fashion, may instead arise from loosely coupled groups of metal atoms (and clusters). These concepts should be kept firmly in mind in future work on metal clusters. It is believed that the loosely coupled "cage-complex", $Cu_2''''\{Xe\}_{20}$, may be analogous to the $F_2$ color-center in alkali halides, which comprises two neighboring anionic vacancies, each containing a single trapped electron. The alkali halide $F_2$ color center is well-known and is of considerable interest for broadly tunable, optically pumped, "dye-like", continuous wave, solid-state lasers[116]. Immobilized metal atoms and clusters may, therefore, find an application in lasers in the near future.

## 11. Surface Effects in Raman Spectroscopy (SERS)

Finally, the highly popular but not yet fully understood technique of surface enhanced Raman spectroscopy (SERS) will be briefly examined from the point of view of matrix-isolation metal cluster spectroscopy. Since the first observation of highly intense Raman emissions from adsorbents on rough silver surfaces[113a], many experiments and much theoretical work have been directed towards exploring the origin of the effect. Three recent reviews have been written on the subject[113b]. Two theoretical models appear to have attracted most attention: One involves coupling with surface plasmons, the other considers coupling to localized electronic states induced by chemisorption. Both consider the role played by the size and shape of the adsorbate on the Raman enhancement. Experiments using well-defined single crystal grating surfaces, colloidal metal particles, and molecular metal clusters as model substrates have been designed to evaluate these effects[113b]. Matrix isolation methods are, therefore, useful in evaluating SERS, since the technique of matrix trapping is useful for generating and stabilizing size- and shape-controlled metal agglomerates with dimensions varying from atomic, to molecular, to colloidal, to that of the bulk microcrystal.

Most of the Raman studies of molecules on or near colloidal metal surfaces have involved CO, pyridine, $C_2H_2$, or $C_2H_4$ and silver. These experiments have demonstrated that SERS depends on the excitation of surface plasmons involving only the first layer of adsorbed molecules chemically bonded to the surface. In essence, the excitation profile of the enhancement appears, in a general, to follow the spectral behavior of the surface plasmon. This has been interpreted in terms of a model in which the adsorbent vibrations couple with the conduction-electron surface plasmon mode by charge-transfer between the adsorbent and the metal, synchronous with the vibration[113b].

Recently, Raman enhancement studies due to chemical effects alone have been studied on the silver clusters $Ag_2$ and $Ag_3$ entrapped in rare gas solid films in the presence and absence of pyridine[114a]. Complementary IR studies have also subsequently appeared[114b]. Interestingly, both the ligand and $\nu$(Ag–N) stretching regions were found to be quite similar to those of pyridine chemisorbed on silver electrodes. Although the luminescence of naked silver clusters[106–108, 128] was found to be markedly perturbed by the presence of pyridine, neither the vibration frequencies of the pyridine ring nor those of the $\nu$(Ag–Ag) stretching modes of $Ag_2$ or $Ag_3$[77] were significantly shifted. It would appear, therefore, that the last word has not yet been spoken on the major effects contributing to the surface enhancement mechanism. Nevertheless, matrix isolation of metal cluster and colloidal metal particles, either with or without a reactive ligand, is important for the study of SERS as well as other spectroscopic and chemical phenomena which depend on the nuclearity of the metal[106].

## 12. Limitations and Strengths of the Matrix Isolation Technique

When assessing the spectroscopic data for naked metal clusters embedded in low temperature matrix supports, it is advisable to bear in mind the difficulties involved in generating well defined cluster distributions as well as those characteristics arising from the solid state, both of which can influence, complicate, and confuse spectroscopic analyses.

On the positive side, the matrix isolation method enables high concentrations of metal clusters, even those of refractory metals, to be stabilized in a low temperature environment for leisurely spectroscopic study. As described previously in this article, the technique has been extensively used to investigate a wide range of transition-metal dimers as well as higher uni- and bimetallic clusters. Thermal excitation of low-lying excited electronic states is usually quenched at cryogenic temperatures, thereby simplifying the absorption spectra of metal dimers and clusters compared those expected at the temperatures needed to vaporize the metals. These low temperatures are conducive to detailed rotational analysis of metal clusters in, for example, the collision-free environment of a supersonic molecular beam. However, isolation of the clusters in a solid support generally results in loss of rotational structure, thereby imposing certain limits on the spectroscopic determination of, for example, electronic symmetry species and bond lengths and geometries. On the other hand, these "frozen gas" cluster samples can display pronounced band sharpening, enhancement of vibrational structure and metal isotope bands, as well as a rich hyperfine structure. From this information, the guest can be identified, permitting evaluation of vibrational frequencies; first anharmonicity constants; estimates of bond dissociation energies; and even structural determination of the metal cluster carrier. Furthermore, in an isotropic frozen solid the randomly oriented, rigidly held cluster also permits fruitful exploitation of photoselection techniques and polarization spectroscopy, which have great value for cluster identification and in the assignment of electronic and vibrational symmetry species.

The advantages offered by the "frozen gas" are somewhat offset by loss of some of the finer details of spectroscopic structure due to inhomogeneous broadening and perturbations induced by the matrix host. The latter effects may be manifest as gas to matrix spectral shifts (as much as 1000 $cm^{-1}$, depending on the spectroscopic technique), and as band shape and intensity changes; they generally depend on the host matrix. Effects of this type do, however, carry useful information on guest-host interaction potentials in the ground and excited states of entrapped clusters, which are of increasing interest for studies of metal-support effects important in catalysis.

Splittings of spectral lines can arise from a myriad of solid state and electronic effects; the most commonly encountered being multiple trapping sites, low site symmetries, metal isotopes in natural abundance, crystal field perturbations, phonon, spin-orbit and vibronic coupling, as well as extraneous impurity centers. In many instances, multiple trapping site effects may either arise from different host cage geometries or guest structures or a combination thereof.

A thorough spectroscopic analysis of an immobilized naked metal cluster, therefore, requires a judicious choice of control experiments to assess the importance of matrix perturbations and effects mentioned above. These commonly involve variations of the host substrate, its temperature and of the metal concentration in combination with metal isotope enrichment studies, impurity doping experiments (usually atmospheric and typical high temperature metal source contaminants such as $O_2$, $N_2$, CO, $CO_2$, $CH_4$, and $H_2O$) and possibly photochemical treatment. In this way, authentic band splittings can be distinguished from extraneous matrix effects, thereby greatly enhancing the value of matrix isolation data for the characterization of ligand-free metal clusters.

In the matrix isolation experiment it is important to bear in mind that the identification of metal clusters of specific nuclearity, produced either by co-condensing metal atoms and matrix gases, or by photoaggregating metal atoms in solid matrices, relies heavily on the use of approximate statistical models and nucleation kinetic techniques designed to describe the metal cluster growth processes and resulting metal cluster distributions for a particular set of experimental conditions. (Cluster distributions can be subsequently manipulated by thermal annealing and photochemical methods, and certainly aid in identifying species and in spectral interpretation.) These "indirect" methods for defining metal cluster nuclearity and cluster concentrations are limited to about 1–5 at-% of metal, which is equivalent to a cluster of about six metal atoms. This approach is clearly less straightforward than "direct" mass spectrometric observation of a cluster distribution, as is commonly used in the characterization of gas phase cluster samples. It is worth noting that cryogenic secondary-ion mass spectroscopy (SIMS), recently pioneered by *Michl et al.*, is likely to help in alleviating this particular weakness of the matrix isolation experiment[126]. Clearly, the entrappment of metal clusters in solid supports is not a panacea for the characterization of arrays of metal atoms. Matrix isolation studies have their place together with gas phase molecular beam studies. Useful information can be gleaned from each method, and both are interesting in their own right.

For the matrix trapping experiment one can conclude by saying that when metal and matrix gas depositions are precisely controlled using *in situ* mass monitors, mass flow meters and/or laser interference film thickness devices, a quantitative metal concentration and/or photoaggregation experiment can be used in conjunction with statistical and kinetic cluster growth models to pinpoint, with a fair degree of certainty, the identity and concentration of the metal cluster species present. The increasing number of cryogenic matrix studies of naked metal clusters using different spectroscopic probes, the results of which support each other, attests to the reliability and value of the method and establishes a permanent place and ongoing role for matrix isolation spectroscopy as one of the two methods of choice for understanding the physicochemical properties of ligand-free metal clusters.

## 13. Future Prospects

Over the last few years an impressive array of new synthetic techniques and powerful spectroscopic probes have been applied to the study of ligand-free metal clusters in rare gas matrices. The spectroscopic methods used in these investigations now include ESR, MCD, UPS, EXAFS, XANES, Mössbauer, FT far-IR, Raman, resonance Raman and LIF spectroscopy: A list of acronyms almost as impressive as those found in surface science! These studies are yielding a wealth of new electronic, vibrational, structural and bonding information for what can be regarded as the simplest, yet theoretically most challenging form of metal aggregate. With these kinds of data, the characterization of certain physical and chemical properties of a wide range of metal clusters in different solid supports is now a realistic goal. In conjunction with emerging gas phase data for ligand-free metal clusters, a unique opportunity now exists for assessing the strength of metal-support interactions and for monitoring subtle alterations in electronic charge density and structure at the anchoring site of a supported metal cluster.

Experimental and theoretical breakthroughs that are much needed in the field of ligand-free metal clusters and which one can look forward to in the near future include:

a) The development of new techniques and improvement of existing methods for the size-selective generation of $M_n$ molecules in the gas phase and in the matrix, as well as in solid inorganic and organic supports of relevance to heterogeneous catalysis.
b) The perfection of sources and separation devices for generating well defined, high nuclearity metal clusters ($6 \leqq n \leqq 500$) for elucidating the effect of cluster size on physical properties on proceeding from molecular metal clusters to bulk metals, and to study size effects in small metal clusters.
c) The development of higher sensitivity and better resolved spectroscopic probes for elucidating molecular electronic, geometrical, and bonding details of naked metal clusters in both the gas phase and solid supports; these methods could permit an evaluation of metal-support interactions of great importance in chemisorption and catalytic phenomena.
d) Continuing improvement of molecular electronic structure calculations including configuration, interaction, and relativistic effects of small $M_n$ clusters of the 1st to 3rd transition series. This would develop an interplay with available experimental data, enabling extensions to larger $M_n$ clusters. Calculations of this type are of great interest because they provide ideal test cases of metal-metal bonding free from the complexities introduced by metal-ligand and intraligand bonding.
e) The application of increasingly sophisticated experimental and theoretical methods to the study of precisely defined $M_n$ clusters interacting with ligands of interest in surface chemistry. In this way, the interface between "supercoordinately" unsaturated $M_nL$ complexes and L chemisorbed on the bulk metal can be explored, thereby enhancing our understanding of chemisorption phenomena and, possibly, of surface catalytic processes.
f) More detailed studies of heteronuclear metal aggregates as a function of size and composition. These studies are relevant to bimetallic cluster catalysis, to examinations of the evolution of the chemical and physical properties of bulk alloys from those of molecular "alloy" clusters, and for the study of metal atom components classified in the bulk phase diagram as miscible or immiscible.
g) Further investigations of static and dynamic Jahn-Teller effects of the type observed for $Li_3$, $Na_3$, $K_3$, and $Cu_3$, and predicted theoretically for $Li_3$. Studies of this type are valuable because they contribute to our understanding of potential energy surfaces and the symmetry of the distortions of non-rigid naked metal clusters. They should also serve as a stringent testing ground for relaxation theories of fluxional metal clusters in disparate time scales, and should enable differentiation of localized vibronic ground states with quantum mechanical tunneling from completely fluxional schemes. The concepts derived from studies of fluxional, ligand-free metal clusters of low nuclearity will aid our comprehension of larger non-rigid metal clusters. This in turn is relevant to dynamic effects of metal surfaces, as well as to non-rigidity in other classes of metal clusters containing ligands; for example, carbonylmetal clusters, organometallic complexes containing multiple metal-metal bonds, and compounds containing metal-metal bonds involving metals in high oxidation states.

*Financial assistance from the Natural Sciences and Engineering Research Council of Canada's Strategic Energy Programme, and a Special Research Grant from the Connaught Foundation of the University of Toronto are both greatly appreciated. S. A. M. acknowledges NSERC and Noranda for graduate scholarships at various times during his research at the University of Toronto. We should like to express our gratitude to V. E. Bondybey, P. A. Montano, R. Grinter, J. A. Howard, D. M. Lindsay, A. Kaldor, and R. E. Smalley for helpful comments on this manuscript and for preprints of their recent research in this field.*

Received: November 26, 1982;
revised: March 7, 1983 [A 462 IE]
German version: *Angew. Chem. 95* (1983) 706

[1] E. L. Muetterties, *Chem. Eng. News 60* (1982) Nr. 35, p. 28; cf. also E. L. Muetterties, M. J. Krause, *Angew. Chem. 95* (1983) 135; *Angew. Chem. Int. Ed. Engl. 22* (1983) 135.
[2] R. P. Messmer „Cluster Model Theory" in T. N. Rhodin, G. Ertl: *The Nature of the Surface Chemical Bond*, North Holland, Amsterdam 1979, p. 51.
[3] „Proc. 2nd Int. Meet. Small Particles and Inorganic Clusters", *Surf. Sci. 106* (1981).
[4] J. Bourdon: *Growth and Properties of Metal Clusters*, Elsevier, Amsterdam 1980.
[5] G. A. Ozin, F. Hugues, D. F. McIntosh, S. Mattar „Intrazeolitic and Rare Gas Isolated Silver Atom and Silver Cluster Spectroscopy, Photoprocesses and Support Interactions" in G. Stucky: *Intrazeolitic Chemistry*, ACS Spec. Symp. Ser., 218 Washington 1983, p. 409.
[6] E. Whittle, D. A. Dows, G. C. Pimentel, *J. Chem. Phys. 22* (1954) 1943; cf. G. C. Pimentel, *Angew. Chem. 87* (1975) 220; *Angew. Chem. Int. Ed. Engl. 14* (1975) 199.
[7] B. Meyer: *Low Temperature Spectroscopy*, Elsevier, New York 1971.

[8] H. E. Hallam: *Vibrational Spectra of Trapped Species*, Wiley, New York 1973.
[9] S. Craddock, A. J. Hinchcliffe: *Matrix Isolation*, Cambridge University Press, Cambridge 1975.
[10] V. E. Bondybey, L. E. Brus, *Adv. Chem. Phys. 41* (1980) 269.
[11] A. J. Barnes, W. J. Orville-Thomas, A. Müller, R. Gaufrès: *Matrix Isolation Spectroscopy*, D. Reidel, Dordrecht 1981.
[12] P. S. Skell, L. D. Wescott Jr., *J. Am. Chem. Soc. 85* (1963) 1023; cf. also P. S. Skell, M. J. McGlinchey, *Angew. Chem. 87* (1975) 215; *Angew. Chem. Int. Ed. Engl. 14* (1975) 195.
[13] P. L. Timms, *J. Am. Chem. Soc. 89* (1967) 1629; cf. also *Angew. Chem. 87* (1975) 295; *Angew. Chem. Int. Ed. Engl. 14* (1975) 273.
[14] W. L. S. Andrews, G. C. Pimentel, *J. Chem. Phys. 44* (1966) 2361.
[15] M. Moskovits, G. A. Ozin: *Cryochemistry*, Wiley, New York 1976.
[16] G. A. Ozin, A. Vander Voet, *Prog. Inorg. Chem. 19* (1975) 105; E. P. Kündig, M. Moskovits, G. A. Ozin, *Angew. Chem. 87* (1975) 314; *Angew. Chem. Int. Ed. Engl. 14* (1975) 292.
[17] W. J. Power, G. A. Ozin, *Adv. Inorg. Chem. Radiochem. 23* (1980) 79.
[18] I. R. Dunkin, *Chem. Soc. Rev. 9* (1980) 1.
[19] G. A. Ozin, *Acc. Chem. Res. 10* (1977) 21; *Cat. Rev. Sci. Eng. 16* (1977) 191; *Coord. Chem. Rev. 28* (1979) 117; *48* (1983) 203; *J. Macromol. Sci. A 16* (1981) 167; and literature cited therein.
[20] R. M. Bentwood, A. J. Barnes, W. J. Orville-Thomas, *J. Mol. Spectrosc. 84* (1980) 391.
[21] R. K. Khanna, D. D. Stranz, B. Donn, *J. Chem. Phys. 74* (1981) 2108.
[22] T. P. Martin, H. Schaber, *J. Chem. Phys. 73* (1980) 3541.
[23] „Diatomic Metals and Metallic Clusters", *Faraday Symp. Chem. Soc. 14* (1980).
[24] „Int. Meet. Small Particles and Inorganic Clusters", *J. Phys. (Paris) 38* (1977) C-2.
[25] J. R. Anderson: *Structure of Metallic Catalysts*, Academic Press, New York 1975.
[26] K. A. Gingerich, *Faraday Symp. Chem. Soc. 14* (1980) 109; and literature cited therein.
[27] K. Hilpert, K. A. Gingerich, *Ber. Bunsenges. Phys. Chem. 84* (1980) 739.
[28] G. Hortig, M. Müller, *Z. Phys. 221* (1969) 119.
[29] N. Winograd, D. E. Harrison Jr., B. J. Garrison, *Surf. Sci. 78* (1978) 467.
[30] K. Sattler, J. Muhlbach, E. Recknagel, *Phys. Rev. Lett. 45* (1980) 821.
[31] H. Abe, W. Schulze, B. Tesche, *Chem. Phys. 47* (1980) 95.
[32] P. J. Foster, R. E. Leckenby, E. J. Robbins, *J. Phys. B 2* (1969) 478; S. J. Riley, E. K. Parks, C. R. Mao, L. G. Popp, S. Wexler, *J. Phys. Chem. 86* (1982) 3911.
[33] A. Herrmann, S. Leutwyler, E. Schumacher, L. Wöste, *Helv. Chim. Acta 61* (1978) 453.
[34] A. Herrmann, E. Schumacher, L. Wöste, *J. Chem. Phys. 68* (1978) 2327.
[35] D. R. Preuss, S. A. Pace, J. L. Gole, *J. Chem. Phys. 71* (1979) 3553; J. L. Gole, G. J. Green, S. A. Pace, D. R. Preuss, *ibid. 76* (1982) 2247.
[36] a) T. G. Dietz, M. A. Duncan, D. E. Powers, R. E. Smalley, *J. Chem. Phys. 74* (1981) 6511; b) M. M. Kappes, R. W. Kunz, E. Schumacher, *Chem. Phys. Lett. 91* (1982) 413.
[37] V. E. Bondybey, J. H. English, *J. Chem. Phys. 74* (1981) 6978; D. E. Powers, S. G. Hansen, M. E. Geusic, A. C. Pulu, J. B. Hopkins, T. G. Dietz, M. A. Duncan, P. R. R. Langridge-Smith, R. E. Smalley, *J. Phys. Chem. 86* (1982) 2556.
[38] S. Leutwyler, U. Even, *Chem. Phys. Lett. 84* (1981) 188.
[39] V. Vaida, N. J. Cooper, R. J. Hemley, D. G. Leopold, *J. Am. Chem. Soc. 103* (1981) 7022.
[40] A. Herrmann, M. Hofmann, S. Leutwyler, E. Schumacher, L. Wöste, *Chem. Phys. Lett. 62* (1979) 216.
[41] B.-K. Teo, *Acc. Chem. Res. 13* (1980) 412.
[42] B. Moraweck, G. Clugnet, A. J. Renouprez, *Surf. Sci. 81* (1979) L631.
[43] E. B. Prestridge, G. H. Via, J. H. Sinfelt, *J. Catal. 50* (1977) 115.
[44] L. Brewer, B. Meyer, G. D. Brabson, *J. Chem. Phys. 43* (1965) 3973.
[45] L. Andrews, G. C. Pimentel, *J. Chem. Phys. 47* (1967) 2905.
[46] L. Brewer, J. L. F. Wang, *J. Mol. Spectrosc. 40* (1971) 95.
[47] L. Brewer, C. Chang, *J. Chem. Phys. 56* (1972) 1728.
[48] J. E. Francis Jr., S. E. Webber, *J. Chem. Phys. 56* (1972) 5879.
[49] M. Moskovits, G. A. Ozin, in [15], chpt. 9.
[50] M. Moskovits, J. E. Hulse, *J. Chem. Soc. Faraday Trans. 2 73* (1977) 471.
[51] E. P. Kündig, M. Moskovits, G. A. Ozin, *Nature (London) 254* (1975) 503.
[52] T. A. Ford, H. Huber, W. Klotzbücher, E. P. Kündig, M. Moskovits, G. A. Ozin, *J. Chem. Phys. 66* (1977) 524.
[53] R. Busby, W. Klotzbücher, G. A. Ozin, *J. Am. Chem. Soc. 98* (1976) 4013.
[54] T. C. De Vore, A. Ewing, H. F. Franzen, V. Calder, *Chem. Phys. Lett. 35* (1975) 78.
[55] M. Hofmann, S. Leutwyler, W. Schulze, *Chem. Phys. 40* (1979) 145.
[56] G. A. Ozin, H. Huber, *Inorg. Chem. 18* (1979) 1402.
[57] J. C. Miller, R. L. Mowery, E. R. Krausz, S. M. Jacobs, H. W. Kim, P. N. Schatz, L. Andrews, *J. Chem. Phys. 74* (1981) 6349.
[58] G. A. Ozin, A. J. L. Hanlan, *Inorg. Chem. 18* (1979) 1781.
[59] M. Moskovits, J. E. Hulse, *J. Chem. Phys. 66* (1977) 3988.
[60] a) M. Moskovits, J. E. Hulse, *J. Chem. Phys. 67* (1977) 4271; G. A. Ozin, S. A. Mitchell, J. Carcia-Prieto, *J. Phys. Chem.*, in press.
[61] a) W. E. Klotzbücher, G. A. Ozin, *J. Am. Chem. Soc. 100* (1978) 2262; b) *Inorg. Chem. 18* (1979) 2101.
[62] W. Schulze, H. U. Becker, H. Abe, *Chem. Phys. 35* (1978) 177.
[63] G. A. Ozin, H. Huber, *Inorg. Chem. 17* (1978) 155.
[64] D. M. Gruen in [15], chpt. 10.
[65] C. Cosse, M. Fouassier, T. Mejean, M. Tranquille, D. P. DiLella, M. Moskovits, *J. Chem. Phys. 73* (1980) 6076.
[66] F. Ahmed, E. R. Nixon, *J. Chem. Phys. 71* (1979) 3547.
[67] M. Moskovits, D. P. DiLella, *J. Chem. Phys. 73* (1980) 4917.
[68] a) M. J. Pellin, T. Foosnoes, D. M. Gruen, *J. Chem. Phys. 74* (1981) 5547; b) D. P. DiLella, R. H. Lipson, M. Moskovits, K. Taylor „Resonance Raman Studies of Metal Dimers and Metal Clusters", *Proc. 8th Raman Conf. Bordeaux 1982*; c) D. L. Michalopoulos, M. E. Geusic, S. G. Hansen, D. E. Powers, R. E. Smalley, *J. Phys. Chem. 86* (1982) 3915; J. B. Hopkins, P. R. R. Langridge-Smith, M. D. Morse, R. E. Smalley, *J. Chem. Phys. 78* (1983) 1627; d) F. A. Cotton, *Acc. Chem. Res. 6* (1973) 368; *11* (1978) 225; F. A. Cotton, M. H. Chisholm, *Chem. Eng. News 60* (1982) No. 26, p. 40; W. C. Trogler, H. B. Gray, *Acc. Chem. Res. 11* (1978) 233; e) Yu. Efremov, A. N. Samoilova, L. Gurrich, *Opt. Spectrosc. 36* (1974) 381; f) cf. [51]; g) G. A. Ozin, W. Klotzbücher, J. G. Norman Jr., H. J. Kolari, *Inorg. Chem. 16* (1977) 2871; h) G. A. Ozin, W. Klotzbücher, *ibid. 16* (1977) 984; i) J. G. Norman Jr., H. J. Kolari, H. B. Gray, W. C. Trogler, *ibid. 16* (1977) 987; j) J. Harris, R. O. Jones, *J. Chem. Phys. 70* (1979) 830; M. M. Goodgame, W. A. Goddard, *J. Phys. Chem. 85* (1981) 215; *Phys. Rev. Lett. 48* (1982) 135; C. Wood, M. Doran, I. H. Hillier, M. F. Guest, *Faraday Symp. Chem. Soc. 14* (1980) 159; C. de Mello, W. D. Edwards, M. C. Zerner, *J. Am. Chem. Soc. 104* (1982) 1440; k) A. W. Hull, *Phys. Rev. 14* (1919) 540; A. Bino, F. A. Cotton, W. Kaim, *J. Am. Chem. Soc. 101* (1979) 2506.
[69] J. C. Miller, L. Andrews, *Appl. Spectrosc. Rev. 16* (1980) 1.
[70] a) V. E. Bondybey, J. H. English, *J. Chem. Phys. 67* (1977) 3405; b) J. L. Gole, J. H. English, V. E. Bondybey, *J. Phys. Chem. 86* (1982) 2560.
[71] F. Ahmed, E. R. Nixon, *J. Chem. Phys. 74* (1981) 2156.
[72] M. Moskovits, D. P. DiLella, *J. Chem. Phys. 72* (1980) 2267; *77* (1982) 5263.
[73] V. E. Bondybey, J. H. English, *J. Chem. Phys. 73* (1980) 42.
[74] D. D. Stranz, R. K. Khanna, *J. Chem. Phys. 74* (1981) 2116.
[75] G. A. Ozin, M. D. Baker, S. A. Mitchell, D. F. McIntosh, *Angew. Chem. 95* (1983) 157; *Angew. Chem. Int. Ed. Engl. 22* (1983) 166.
[76] R. Grinter, S. Armstrong, U. A. Jayasooriya, J. McCombie, D. Norris, J. P. Springall, *Faraday Symp. Chem. Soc. 14* (1980) 94.
[77] W. Schulze, H. U. Becker, R. Minkwitz, K. Manzel, *Chem. Phys. Lett. 55* (1978) 59.
[78] K. Jacobi, D. Schmeisser, D. M. Kolb, *Chem. Phys. Lett. 69* (1980) 113; *J. Chem. Phys. 75* (1981) 5300.
[79] N. Rösch, D. Menzel, *Chem. Phys. 13* (1976) 243; R. P. Messmer, S. K. Knudsen, K. H. Johnson, J. B. Diamond, C. Y. Yang, *Phys. Rev. 1313* (1976) 1396.
[80] G. Kaindl, T. C. Chaing, D. E. Eastman, F. J. Himpsel, *Phys. Rev. Lett. 45* (1980) 1808.
[81] D. M. Lindsay, D. R. Herschbach, A. L. Kwiram, *Mol. Phys. 32* (1976) 1199.
[82] G. A. Thompson, D. M. Lindsay, *J. Chem. Phys. 74* (1981) 959.
[83] G. A. Thompson, F. Tischler, D. Garland, D. M. Lindsay, *Surf. Sci. 106* (1981) 408.
[84] J. A. Howard, K. F. Preston, B. Mile, *J. Am. Chem. Soc. 103* (1981) 6226.
[85] R. J. Van Zee, W. Weltner Jr., *J. Chem. Phys. 74* (1981) 4330.
[86] R. J. Van Zee, C. A. Baumann, W. Weltner Jr., *J. Chem. Phys. 74* (1981) 6977.
[87] R. J. Van Zee, C. A. Baumann, S. V. Bhat, W. Weltner Jr., *J. Chem. Phys. 76* (1982) 5636.
[88] W. H. Gerber, E. Schumacher, *J. Chem. Phys. 69* (1978) 1692.
[89] R. K. Nesbet, *Phys. Rev. A 135* (1964) 460.
[90] M. H. Chisholm: *Reactivity of Metal-Metal Bonds*, ACS Symp. Ser. No. 155 (1981).
[91] I. Shim, K. A. Gingerich, *J. Chem. Phys. 77* (1982) 2490.
[92] P. M. Atha, I. H. Hillier, *Mol. Phys. 45* (1982) 285.
[93] M. M. Goodgame, W. A. Goddard III, *J. Phys. Chem. 85* (1981) 215.
[94] L. Noodleman, *J. Chem. Phys. 74* (1981) 5737.
[95] A. Wolf, H. H. Schmidtke, *Int. J. Quantum Chem. 18* (1980) 1187.
[96] J. Harris, R. O. Jones, *J. Chem. Phys. 70* (1979) 830.
[97] J. Demuynek, M. M. Rohmer, A. Strich, A. Veillard, *J. Chem. Phys. 75* (1981) 3443.
[98] H. Tatewaki, E. Miyoshi, T. Nakamura, *J. Chem. Phys. 76* (1982) 5073.

[99] C. W. Bauschlicher Jr., S. P. Walch, P. E. M. Siegbahn, *J. Chem. Phys. 76* (1982) 6015.
[100] P. A. Montano, G. K. Shenoy, *Solid State Commun. 35* (1980) 53.
[101] P. A. Montano, *Faraday Symp. Chem. Soc. 14* (1980) 79.
[102] H. Purdum, P. A. Montano, G. K. Shenoy, T. Morrison, *Phys. Rev. B 25* (1982) 4412.
[103] G. Apai, J. F. Hamilton, J. Stöhr, A. Thompson, *Phys. Rev. Lett. 43* (1979) 165.
[104] S. Shamai, M. Pasternak, H. Micklitz, *Phys. Rev. B 26* (1982) 3031.
[105] G. A. Ozin, S. A. Mitchell, J. Garcia-Prieto, *J. Phys. Chem. 86* (1982) 473.
[106] G. A. Ozin, *Faraday Symp. Chem. Soc. 14* (1980) 7.
[107] G. A. Ozin, S. A. Mitchell, J. Farrell, G. Kenney-Wallace, *J. Am. Chem. Soc. 102* (1980) 7702.
[108] G. A. Ozin, S. A. Mitchell, J. Farrell, G. Kenney-Wallace, *J. Am. Chem. Soc. 103* (1981) 6030.
[109] G. A. Ozin, H. Huber, S. A. Mitchell, *Inorg. Chem. 18* (1979) 2932.
[110] G. A. Ozin, H. Huber, D. F. McIntosh, S. A. Mitchell, J. G. Norman Jr., L. Noodleman, *J. Am. Chem. Soc. 101* (1979) 3504.
[111] S. A. Mitchell, *Ph. D. Thesis*, University of Toronto 1982.
[112] H. Basch, *J. Am. Chem. Soc. 103* (1981) 4657.
[113] a) M. Fleishmann, P. J. Hendra, A. J. McQuillan, *Chem. Phys. Lett. 26* (1974) 163; b) J. E. Furtak, J. Reyes, *Surf. Sci. 93* (1980) 351; A. Otto, *Appl. Surf. Sci. 6* (1980) 309; M. Moskovits in J. E. Furtak, R. Chang: *Surface Enhanced Raman Scattering*, Plenum, New York 1981; and literature cited therein.
[114] a) W. Krasser, U. Kettler, P. S. Bechthold, *Chem. Phys. Lett. 86* (1982) 223; b) D. E. Trevault, R. R. Smardzewski, *J. Chem. Phys. 77* (1982) 2221.
[115] G. A. Ozin, S. A. Mitchell, D. F. McIntosh, S. Mattar, J. Garcia-Prieto, *Int. Conf. Organomet. Chem. Toronto 1981*, Pap. 2E20; *J. Phys. Chem.*, in press.
[116] L. F. Mollenauer, *Opt. Lett. 1* (1977) 164; *J. Appl. Phys.*, in press.
[117] J. C. Rivoal, J. S. Emampour, K. J. Zeringne, M. Vala, *Chem. Phys. Lett. 92* (1982) 313.
[118] R. Grinter, personal communication.
[119] M. Moskovits, J. E. Hulse, *J. Chem. Phys. 66* (1977) 3988.
[120] D. Schmeisser, K. Jacobi, D. M. Kolb, *J. Vac. Sci. Technol. 20* (3) (1982) 647.
[121] J. A. Howard, K. F. Preston, R. Sutcliffe, B. Mile, J. S. Tse, *Chem. Phys. Lett. 94* (1983) 561; *J. Phys. Chem. 87* (1983) 2268; and personal communication.
[122] W. Dyson, P. A. Montano, *Phys. Rev. B 20* (1979) 3619.
[123] H. M. Nagarathna, P. A. Montano, *J. Chem. Soc. Faraday Trans. 2 78* (1982) 923.
[124] W. Dyson, P. A. Montano, *Solid State Commun. 33* (1980) 191.
[125] G. A. Ozin, H. Huber, *Inorg. Chem. 18* (1979) 1402.
[126] H. T. Jonkman, J. Michl, *J. Chem. Soc. Chem. Commun. 1978*, 751.
[127] E. Schumacher, W. H. Gerber, H. P. Härri, M. Hofmann, E. Scholl in J. L. Gole, W. C. Stwalley: *Metal Bonding and Interactions in High Temperature Systems*, ACS Symp. Ser. No. 179 (1982), p. 83.
[128] D. Leutloff, D. M. Kolb, *Ber. Bunsenges. Phys. Chem. 83* (1979) 666.
[129] D. A. Garland, D. M. Lindsay, *J. Chem. Phys. 78* (1983) 2813.
[130] G. A. Thompson, F. Tischler, D. M. Lindsay, *J. Chem. Phys.*, in press.
[131] D. M. Lindsay, D. R. Herschbach, A. L. Kwiram, *Mol. Phys. 39* (1980) 529; J. Kendrick, *ibid. 35* (1978) 593.
[132] a) H. Sontag, R. Weber, *J. Mol. Spectrosc. 91* (1982) 72; b) *Chem. Phys. 70* (1982) 23.
[133] D. P. DiLella, K. V. Taylor, M. Moskovits, *J. Phys. Chem. 87* (1983) 524.
[134] W. Schulze, H. U. Becker, *Chem. Phys. Lett. 35* (1978) 177.
[135] H. Sontag, B. Eberle, R. Weber, *J. Chem. Phys.*, in press.
[136] B. Breithaupt, J. E. Hulse, D. M. Kolbe, H. H. Rotermund, W. Schroeder, W. Schrittenlacher, *Chem. Phys. Lett. 95* (1983) 1483.
[137] G. H. Jeung, M. Pelissier, J. C. Bonthelat, *Chem. Phys. Lett. 97* (1983) 369.
[138] E. A. Rohlfing, D. M. Cox, A. Kaldor, *J. Phys. Chem.* (in press) and *Chem. Phys. Lett.* (in press).
[139] T.-E. Gough, D. G. Knight, G. Scoles, *Chem. Phys. Lett. 97* (1983) 155.
[140] L. B. Knight, Jr., R. J. Van Zee, W. Weltner, Jr., *Chem. Phys. Lett. 94* (1983) 296.

# Turgorins, Hormones of the Endogeneous Daily Rhythms of Higher Organized Plants— Detection, Isolation, Structure, Synthesis, and Activity**

By Hermann Schildknecht*

*Dedicated to Professor Adolf Butenandt on the occasion of his 80th birthday*

Probably the most fascinating biological phenomenon is the movement which is so impressively observed in higher organized plants when, *e.g.*, in a sort of "quick retreat", the sensitive plant apparently vanishes on touching, or when all the pinnules of an acacia fold together pairwise at dusk, as though the whole tree were going to "sleep". Such plants and trees do not possess muscles for the movement of their organs; instead of the contraction of a "still primitive" actomyosin system, in this movement the hydrostatic internal pressure of the vacuoles—the turgor—in the parenchymal cells of the motile organs is often drastically and unilaterally reduced. After preception of an external stimulus there follows a gradual or sudden change in the semipermeability of the boundary plasma layers, and, mediated by a stimulus conduction, also of all the symplasts of a multicellular plant organism. The phytohormones which form the molecular basis of the physiology of movement discussed here have now been isolated and structurally elucidated. The chemical agonists of phytodynamics, referred to as turgorins, elicit leaf movement; moreover, they very probably also regulate—perhaps together with other phytohormones—the mechanism of change of aperture in stomatal transpiration. Hence, the turgorins facilitate not only a regulation of temperature, but even their own transport in the sap of the whole plant body.

## 1. Introduction

*Alexander the Great,* amidst all military enterprises, paid great regard to the spread of civilization by the furtherance of literary and scientific research. During his campaigns to subjugate the Persian empire—a task left to him by his father, *Philip of Macedon*—he ordered his generals on their respective expeditions to carefully record the local "histories", *i.e.* to write accounts of the flora and fauna *etc.* at the places they visited—or the "ιστορίαι" as they were called by the Ionians some centuries previously. Afterwards, all these records were collected in the imperial archive at Babylon, intended by Alexander to be the principal city on the founding of the new empire. It was here also that compedia important for the learned world were prepared which later stimulated *Theophrastus* to write his excellent "Plant Geography"[2], in which he comprehensively and expertly compiled the botanical accounts of Alexander the Great's expeditions, and outlined for the first time the "physiognomy" and "behavior" of all the flora of the orient. *Theophrastus* paid particular attention to the trees bearing pinnate leaves—with their scanty shade—and described these with the word τό πτερυγῶδες[3].

*Mimosa asperata L.*, the sensitive plant of the Ancients, has leaves of the same shape—even twofold, *i.e.* bipinnate leaves. As *Theophrastus* aptly said, "...and it is thus possible for the wonderful Mimosa of Memphis to collapse on being touched—it wilts! But after a while it recovers in all its grandeur"[4].

Thus, *Theophrastus* had for the very first time described plant mimicry, further examples of which have since been found in the orchids and the insect attracting plants[5].

That even the ancient Greeks, who are known to have been excellent observers, associated the closing and opening of leaves with the relaxation of cell pressure—of the turgor—and renewed tension of the cell sap is borne out by the expression "ἀφαυαινόμενα" (dying or parched with thirst)[4].

From this pre-Christian era to the present the sensitive plant has been the object of investigation and experiment for generations of naturalists of the western world, who have hoped to throw light on the phenomenon of the turgor movement of fixed plants.

## 2. Ecological Plant Physiology

The objective of this relatively young scientific discipline[6] is to explain the existence of a plant and its adaptation to the environment in physiological and biological terms in such a way that all aspects, even at the molecular level, are taken into account, and thus, in particular, that the *active principles* of "chemical plant ecology" are taken into consideration.

It is now known that the growth and development processes of higher plants are influenced by photohormones[7]. Like the hormones in human and animal organisms they can be formed in certain tissues and then translocated to the active centers, *i.e.* to the target organs. But this is not always so. There are several examples where the so-called

[*] Prof. Dr. H. Schildknecht
Organisch-chemisches Institut der Universität
Im Neuenheimer Feld 270, D-6900 Heidelberg (Germany)

[**] Plant Defense Substances, Part 21.—Part 20: [56].

 © *Verlag Chemie GmbH, 6940 Weinheim, 1983* *0570-0833/83/0909-0695 $ 02.50/0* 

hormones are also active "on the spot", *i.e.* where they are released. One could compare such "tissue hormones" with the prostaglandins of the animal organism. However, because of the ambiguity of the term hormone, it would be incorrect to designate these phytohormones as effectors, since this would include herbicides, which can also react hormonally but do not occur in nature, as *e.g.* the synthetic growth regulator 2,4-dichlorophenoxyacetic acid.

### 2.1. Phytohormones

Unlike the animal hormones, plant hormones are less specific, and many physiological processes are influenced at one and the same time by several hormones. For an overview of the complex hormonal system of higher plants one distinguishes four important classes of hormones on the basis of their structure and activity, namely the auxins, gibberellins, cytokinins, and abscisins (cf. Table 5). Aside from these, however, the chemically most simple growth factor, ethylene, must also be mentioned. Ethylene occupies a special position insofar as it not only influences growth processes but also the germination of seeds, the formation of buds, flowers, and roots, and the ripening of fruit—in intimate interaction with the aforementioned hormones.

All phytohormones have a common physiological property: they act on and *via* plasma membranes. This holds true in particular for the hormones responsible for the rapid movement of fixed plants; the chemical structure of these hormones was, however, unknown until just a few years ago. This is virtually unbelievable when one considers that their activity has been known for centuries.

### 2.2. Phytodynamics

According to the historian *Julius Sachs*[8], the climax in the development of phytodynamics was reached with "A treatise by Ernst Wilhelm Brücke on the movement of mimosa leaves (1848), which has become an accepted model for all further investigations in this field". Methodologically important for an explanation of the phytodynamics involved in plant movement was a clear interpretation of the potential set up between the vascular bundle and the turgescent parenchymal sheath, and ascription of the periodically stimulated movements to movement of water in the parenchyma.

The movements observed in fixed higher plants can only arise by movement of water and the accompanying changes in pressure in the motile organs, since the muscular system typically found in animals is missing.

Actually, contractile proteins have been isolated from motile organs[9], but these do not exhibit the same biochemical properties as the proteins isolated from muscles. Also our attempts[10] to detect cytochemically contractile elements with fluorescein-stained phalloidin and cytochalasin B using the method of *Th. Wieland et al.*[11] gave inconclusive results, probably because the reagents are unable to penetrate into the plant cells.

There are thus osmotic forces which lead to the plant turgor- or variation-movements through changes in cell turgidity.

#### 2.2.1. *Turgor Movements*

An increase or decrease of the turgor alone leads to shortening or lengthening of the cells, *i.e.* to cell movement. In fact, the turgor merely needs to change on one side of an organ to bring about movement. In stomatal movement, which is vital for plant life, an increase of turgor leads to flexion, a decrease of turgor to stretching of the guard cells.

Visible leaf movements have been and still are of special importance for studies on the physiology of plant movements. Such movements are made possible through pulvini or leaf joints (hinge effect), whose anatomical structure determines the pattern of movement—independently of the stimulus direction. In this case one speaks of a nastic movement, which is variously designated depending upon the type of stimulus triggering the movement: seismonastic (shaking), thigmonastic (touching), traumatonastic (wounding), photonastic (light), and thermonastic (heat).

#### 2.2.2. *The Pulvinus—The Motor Organ of Leaf Movements*

After *Brücke* had recognized[12] that the movement of the leaf's joints—the pulvini (cf. Figs. 3 and 4)—was caused by a change of turgor, the observed relaxation of the highly turgescent abaxial and adaxial motile tissue by exudation of cell fluid into the intercellular space prior to the movement was explained[13]. The sudden loss of turgor in all excitable cells of the pulvinus causes a measurable shortening of the thin-walled abaxial motor tissue. The essentially thicker adaxial tissue, on the other hand, hardly experiences any change in length and functions as a sort of hinge joint[14] (cf. Fig. 4).

On the *Physiology of the Motile Cells in the Pulvini:* The motile cells contain a tannin vacuole and a central vacuole[15]. During movement, *i.e.* change of shape of the two vacuoles, a migration of $Ca^{2+}$ takes place[16]. At the same time large amounts of $K^+$ and $Cl^-$ ions are released into the intercellular space and give rise to an action potential[17]. In the following reconstitution phase the tannin vacuole assumes its original spherical shape. The refractory period for the rest potential lies between 2 and 3 minutes[14], while up to 20 minutes can elapse before the pulvini have regained their normal daily position.

As long ago as 1912, *Pfeffer* proposed that rapid loss of turgor is caused by an active contraction of the protoplasts, coupled with a simultaneous increase in membrane permeability. Several authors have therefore tried to demonstrate a participation of the ATP-ATPase system in leaf movement after the fashion of muscle contraction in animals[19]. *Driessche*[20] observed a closing of the pinnules on application of mersalyl, an ATPase blocking agent, to opened primary leaves. This rather indicates, however, an energy-consuming system, which is necessary for the maintenance of the turgor and, thus, of the opened daily position.

#### 2.2.3. *Stimulus Conduction in* Mimosa pudica L.

The mechanism of rapid stimulus conduction is still a controversial topic in Mimosa research.

As already pointed out, differences in the turgor between guard cells and their companion cells determine the degree of opening or the aperture of the stomata. One may assume that turgor differences propagate in vast dimensions. Thus, even before the turn of the century it was assumed by various authors[21] that the stimulus, in the form of a change of pressure in a network of "tube cells"[22] traversing the phloem[*], is transmitted throughout the whole plant body. However, this theory became untenable following the experiment carried out by *Macdougal*[42], who connected the basal ends of cut shoots to a pressure pump and observed no reaction at all on suddenly changing the pressure.

As the electrophysiologist *Bose*[23] of Calcutta showed—when experimenting with *M. pudica L.* and other sensitive and non-sensitive plants—the propagation of differences in electric potential is a further possibility for communication between cells or organs. *Bose* found that the irritation is accompanied by an action potential, which is rapidly transmitted through stem and leaf stalk. He thus came to the conclusion that the stimulus is transmitted through plants in the same way as it is in the animal nervous system.

*Ricca*'s stimulus conduction theory for the transport of a "wound hormone" in the transpirational stream came under violent attack. *Herbert*[24] observed stimulus conduction in a primary leaf stalk, even though he had severed the xylem[*]; hence, the stimulus must have passed through the still intact phloem.

Even as early as 1908 *Linsbauer*[25] had been able to measure various rates of conduction on changing the intensity and type of stimulus; some rates even reached an order of magnitude of 10—40 cm/s. These values were later confirmed in further electrophysiological investigations carried out by *Bose*[23,26] and *Umrath*[27]. *Snow*[28,29], who determined the rates of chemonastic stimulus conduction with stained mimosa extracts, quoted highest values of 8 to 20 cm/min.

*Houwink* was undoubtedly the first to attempt to combine the chemical and electrical conduction of stimuli (chemo-electric sensory transduction)[30]. He found two sorts of stimulus conduction: a very rapid single action flow, which cannot continue in dead parts of tissue, and a stimulus flow, with a much slower rate, which even traverses dead zones of tissue. He called the latter "variation".

*Sibaoka*[31] confirmed the different rates of stimulus conduction and designated them the s-wave (slow wave, a few mm/s), the m-wave (middle wave, 5—40 mm/s), and the r-wave, already recognized by *Houwink* (r = rapid, 60 mm/s). It was also *Houwink* who described stimulus conduction in the following way: The stimulant transported in the xylem sap stream elicits a response in the neighboring tissue in the form of a variation potential (s-wave). Either the signal substance itself or the variation potential generated by it triggers a rapid action potential (m- or r-wave), which can travel ahead of the slower variation potential.

[*] The phloem is the sieve part, the xylem the woody part of the vascular bundle.

## 3. The Sleep Movements of Plants

Perhaps the most wondrous observation ever made in plant physiology was that by Alexander the Great's admiral, *Androsthenes* of Thasos, on the Bahrein island Tylos in 325 BC: He noticed the nyctitropic movements of the pinnules of *Tamarindus indica L.* (Fig. 1)[32]. *Androsthenes* was deeply impressed by the fact that even plants can move, and, even more so, by the observation that the pinnate leaves of a large tree, directed by some still unknown inner life, can gently fold together from dusk until dawn, such that one can say that the tree sleeps: καθεύδει.



Fig. 1. *Tamarindus indica L.* during the day (left) and at night (right).

When *Androsthenes,* like his predecessor *Archias of Pella,* decided not to attempt circumnavigation of the treacherous, surf buffeted Cape Musandam and nearby dangerous rocky islands in the Persian Gulf with a thirty-oar galley, he instead examined, with outstanding scientific interest, the flora of an until then unknown coast in the wonderland of Arabia. For two thousand years, his report remained the sole scientific record of the flora of this paradisaic group of islands. Unfortunately, the original report was lost at a very early date, but we find an excellent transcript of it in *Theophrastus'* Plant Geography[4].

*Androsthenes* outlined the daily periodic movement of the pinnate leaves of the tamarind in their four stages so masterfully that his description of this plant movement phenomenon has never been surpassed. It is the first documentary record of plant sleep, which only some two thousand years later was to become generally known through the behavior of *M. pudica L.,* when, fittingly enough, the astronomer *de Mairan* in 1729 observed that the daily periodic movements of leaves do not implicitly comply with changes in daylight.

### 3.1. The Physiological Clock

As *de Mairan* found out by experiment, the sensitive plant *M. pudica L.* closes and opens its pinnules at the usual time, even in continuous darkness. According to a communique by *du Fay*[33] in the Histoire de L'Academie Royal des Sciences Paris, "The sensitive feel the sun even without seeing it". And thus, the "inner clock" of the plant

kingdom was "brought to light"; the regular rotation of our planet in the course of evolution has so impressed itself upon plants that its day-night rhythm, now inherited by them, is autonomously simulated.

30 years later, in 1759, *Zinn*[34], with his experiments on the bean, and then, in 1832, *de Condolle*[35] with his experiments on *Mimosa, Oxalis,* and *Phaseolus,* confirmed that periodic leaf movements can also take place in continous daylight. The interest of almost all eminent plant physiologists of the second half of the nineteenth century—*Darwin, Dutrochet, Hofmeister, Sachs,* and *Pfeffer*[8]—was now aroused in the patterns of motion of pinnate leaves. These scientists were concerned with how movements were executed, but also with why they existed and what caused their periodicity.

It was to be expected that this basic research work would also lead to discoveries of fundamental importance. Thus, in his experiments on the sensitivity of mimosa leaves, *Pfeffer* discovered that a "remarkably high hydrostatic pressure was involved", and this prompted him to explore the physical causes of such a phenomenon, which he outlined in his famous "Osmotic Studies" in 1877. Even the very first of *Pfeffer*'s models of the cell, never missing in elementary scientific lectures, subsequently formed the basis of *van't Hoffs* theory of solutions.

#### *3.1.1. Circadian Rhythms*

"Circadian rhythms" was the expression suggested by *Halberg*[36] to define the endogenous or autonomous daily rhythms of plants, for these rhythms are observed to continue under constant conditions, especially constant temperature, in continuous light or continuous darkness, but with a periodicity of only approximately 24 hours (*circa* = approximately, *diem* = day; hence circadian).

Interest in these rhythms has increased tremendously in the last few years, since it was recognized that the phenomena are of importance not only in biology. Numerous biological observations of such rhythms have been made, as can be gathered from the book "Die physiologische Uhr" by *Bünning,* one of the pioneers in this field[37]. However, the final active principle of endogenous rhythms remains, as before, unknown.

### 3.2. Endogenous Chemonasty

When *Linné* in 1755 was studying the periodic movement of leaves it sufficed him when describing this phenomenon, which he observed in numerous types of plants, to call it simply "plant sleep". *Pfeffer* in 1875 summed up the same phenomena under the heading "nyctinasty" and suggested that "even chemical stimuli play a prominent role in the autoregulatory control of internal sensory transmission and, thus, also of autonomous (endogenous) movement". His tutor, *Sachs,* had already surmised the participation of "internal factors" in visible plant rhythms as early as 1863. We may therefore speak of an "endogenous chemonasty" when a movement, uninfluenced in its direction, is induced by active principles that are generated in the plant itself.

This gave us very good reason some 30 years ago to search for the presumed endogenous active principle—later designated as the "Leaf Movement Factor" (LMF)—or perhaps even a new phytohormone. Such active principles could possibly be the chemical initiators of many plant movements.

#### *3.2.1. Bioassay of the Active Principles of Seismonasty and Nyctinasty*

It was *Ricca*[38], who in 1916 first attempted to detect stimulants in *Mimosa pudica L.* in his well-known glass tube experiments. He connected the two parts of a cut shoot of mimosa *via* a small glass tube filled with a salt solution or water. According to *Ricca* a stimulation of one part of the shoot is transduced and conducted as stimulant through the solution and into the other part of the shoot, where it triggers the well-known movement reaction of the pinnules.

We have repeatedly tried over the past ten years to reproduce *Ricca*'s pioneering experiment, but have never met with success. However, the glass tube experiment at least served as a model for a bioassay of turgor active movement factors which is still in use today. From the point of view of a natural products chemist it cannot be overemphasized that the demonstration of an active principle is characteristically influenced by the choice of bioassay. Nature is being interrogated—sometimes in a biased way—and the sort of answer we get is already asserted by the disposition of a given object in the test. Moreover, as quoted by *Dörfflings*[7], "hormones are chemical signals to which the living system responds in various ways depending on the disposition of the system or depending on how strong the signal is or from which direction it comes". We believe that the bioassay chosen by us, *i.e.* the bioassay of a single leaf, enables one to detect the sought after phytohormones with regards to function just as well if not better than with a whole plant. Two criteria important for the hormone activity are combined—transport to the target organ and visible triggering of the physiological effect at the target organ.

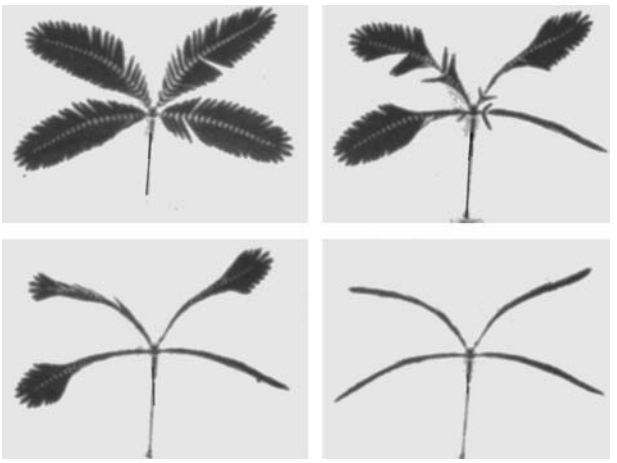


Fig. 2. Bioassay for the detection of turgor active phytohormones. The supposed active principle is placed in a small glass vase and is drawn up by the rachis of the *M. pudica L.* leaf. After a short time the pinnules fold together.

When a leaf is separated from the mimosa plant, and, after restoration, is placed in a solution of the supposed active principle (Fig. 2), the sap stream, influenced to some extent by the external temperature and pressure, transports the phytohormone to the active site, *i.e.* to the pulvini, where (Fig. 3) the biomembranes respond so strongly that each pair of pinnules rapidly fold up through visible turgor changes until the whole leaf has assumed the typical irritated posture.

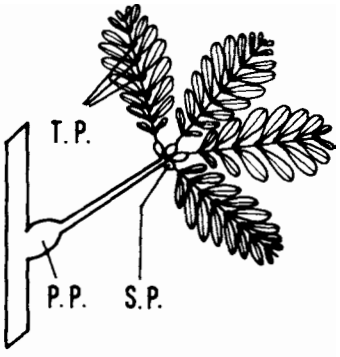



Fig. 3. Schematic drawing of a mimosa leaf showing the primary (P.P.), secondary (S.P.) and tertiary pulvini (T.P.).

The primary as well as the tertiary pulvini are irritated by these substances. The response of the primary pulvinus is manifested by a drooping of the whole leaf stalk (Fig. 4). We have also observed that the pulvini usually react one after the other corresponding to their position and the acropetal progress of the chemonastic stimulus (cf. Fig. 5 and 6). The dilution at which the stimulatory action is still evident may be regarded as a further criterium for the hormonal character of the irritant. As long ago as 1936 *Fitting* reported[39] that an extract of 1 g fresh mimosa leaves, dissolved in 500 g, or even in 5000 g of water under optimal conditions, triggers the specific mimosa reaction in the leaf-test. Accordingly, the movements recognizable in the test are by no means the result of an all-or-nothing reaction; *Fitting* actually reported a usable relationship between strength of stimulus and response. In the movement reactions observed by us we have even demonstrated a quantitative relationship between degree of stimulation and response. On recording a dose-response curve (Fig. 7)

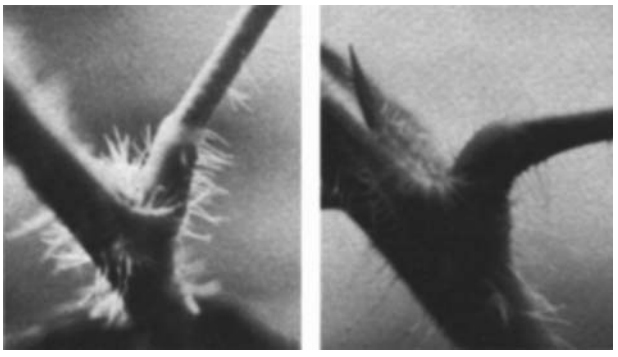


Fig. 4. Primary pulvinus on a mimosa shoot, before (left) and after (right) irritation.



Fig. 5. Test situation with a mimosa shoot

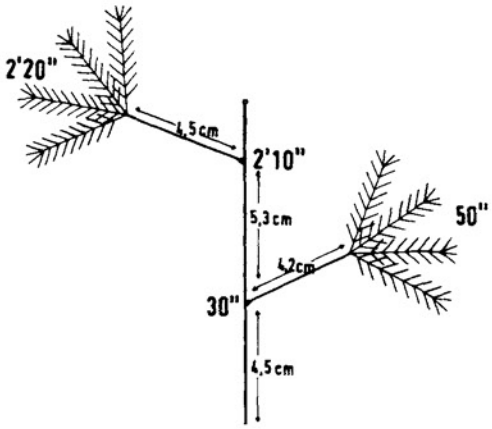



Fig. 6. Rate of stimulus conduction in a leafed shoot of *M. pudica L.* after a chemonastic irritation.

we were able to confirm the hyperbolic dependence of the response time on the concentration of mimosa extract reported by *Sibaoka*[40], and have successfully applied it to the control of fractionation and enrichment in the isolation of the natural product. The exposure time of the pinnate

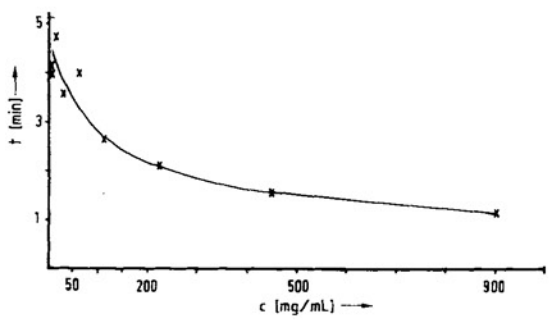



Fig. 7. Dose-response curve of a crude extract of *M. pudica L*

leaves is often several minutes, so that the recorded curve not only reflects the intensity of the stimulation but also the duration of activity (amount of stimulation = intensity × time)[41].

### 3.2.2. *The First Irritants from M. pudica L.*

*Umrath*[27] was the first to point out that the same class of chemical compounds occur in several types of mimosaceae active principles. *Fitting*[43] tested more than 1000 substances regarding their chemonastic activity in the sensitive plant. His most important finding was that some amino acids and anthraquinone derivatives are stimulative down to a concentration of $10^{-3}$ to $10^{-4}$ mol/L, while a mimosa extract is still active at a dilution of 1:5000.

Despite extensive attempts at purification, the results of *Fitting*[39] as well as those of *Soltys* and *Umrath et al.*[44] were only modestly informative: the supposed active principle had to be a "perhaps nitrogen-containing, and probably monobasic oxyacid with a molecular weight of between 300 and 500". Resigned, *Fitting* remarked, "further efforts to isolate the mimosa hormone in pure form must, in my opinion, be carried out by chemists, for they alone have the appropriate aids at their command and can master the modern methods of separation that are obviously required"[39].

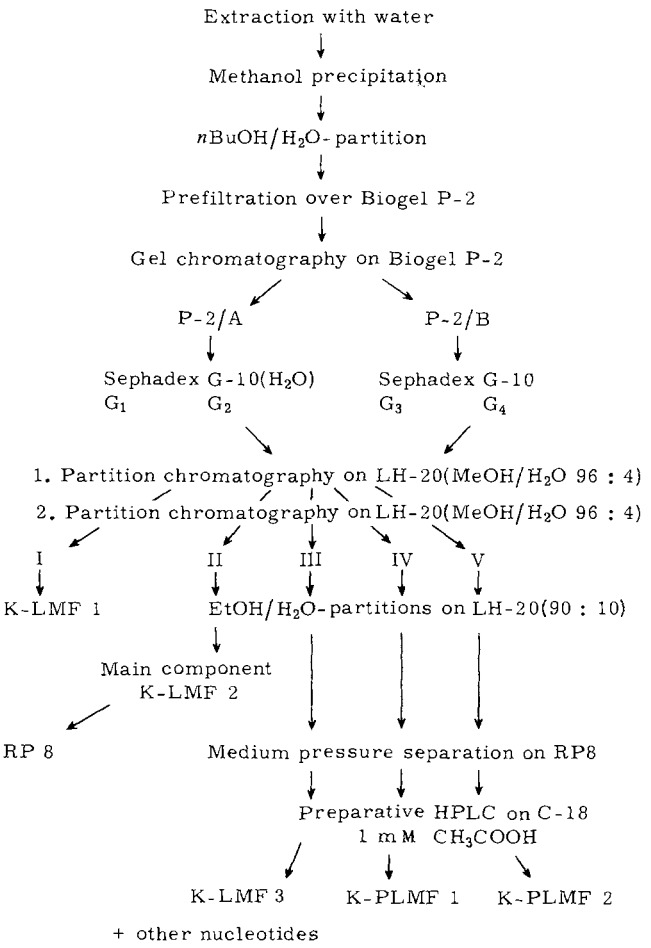
The challenge was accepted. But progress was slow, and it was not until 1980 that the supposed phytohormones could be isolated in pure form by highly developed Tswett column chromatography and their structures elucidated by modern instrumental techniques of analysis.

## 4. Leaf Movement Factors (LMFs)

When a plant with pinnate leaves exhibits the abovementioned "sleep movement", and its pinnules are joined to the stalk by pulvini, the leaf extract will most certainly react chemonastically in the aforementioned bioassay. This holds true especially in the case of acacia plants, even though they may only react nyctinastically and not seismonastically.

The South African plant *Acacia karroo* is not "sensitive", but even it folds its leaves together pairwise when it reacts nyctinastically, or even only thermonastically; and it then looks just like a "sleeping" mimosa plant (Fig. 8).

After having collected convincing evidence that the hormones found in the mimosa plant also occur in the extract from *A. karroo*[45,46]—and probably in substantially higher concentration than in the mimosa—we concentrated our efforts on developing a method of separation which would ensure isolation of the active substances in pure form (cf. Scheme 1)[46].



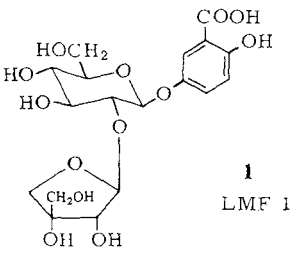

Scheme 1. Separation process for isolation of the chemonastically active hormones from *Acacia karroo* (cf. Figs. 9 and 10). Separation by medium pressure reverse phase chromatography.



Fig. 8. *A. karroo*; the pinnate leaves of one branch are partly irritated thermonastically (Stellenbosch, South Africa).

The results obtained on using this multistep and painstaking method of separation confirm that the complex phenomenon of movement in plants involves a chain of stimuli with participation of various active substances. On working up the crude extract from *A. karroo* we obtained five, almost pure, active fractions (I to V). However, despite the high degree of purity, on further chromatographic separation only substances of limited activity could be isolated, apart from the much more highly active factors K-PLMF 1 and 2.

We should only mention here the Leaf Movement Factor isolated from *M. pudica L.* (M-LMF 1) **1** and its synthesis[47,48], for we are still unable to state its position in a chain of stimuli, even though we have isolated it again as K-LMF1 from *A. karroo*.

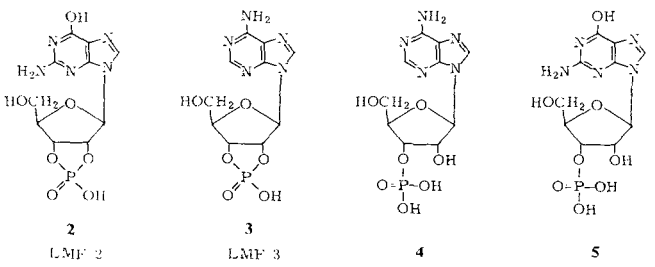


1
LMF 1

### 4.1. Nucleotides as Leaf Movement Cofactors

On purifying a dry crude extract from 4.5 kg of *M. pudica L.* by dissolution/precipitation with methanol, ion-exchange chromatography and filtration over polyacrylamide we obtained a solution of active substances free of amino acids, from which, after further purification by chromatography on Sephadex LH 20, we were able to isolate crystalline M-LMF 2 and 3[49]. Preliminary analysis of these active substances pointed to cyclic nucleotides, which were first detected in plant tissue only a few years ago. This finding called for an intensive spectroscopic analysis of the substances. The absorption maxima at 254 and 275 nm and the positive Cotton effect already showed M-LMF 2 to be a guanosine derivative, which was identified by a detailed IR investigation and PFT-$^1$H-NMR spectroscopy as 2',3'-guanosine cyclomonophosphate **2**. M-LMF 3 correspondingly proved to be 2',3'-adenosine cyclomonophosphate **3**. From a highly active fraction obtained on separation of the *A. karroo* extract (cf. Scheme 1) we isolated the pure substances K-LMF 2 and 3. On the basis of their $^1$H-NMR spectra alone it was evident that these were the same cyclic nucleotides found in *M. pudica L.*

An extended and thorough analysis of all movement factors, *i.e.* also of cofactors, revealed two further nucleotides in the region typical for the above nucleotides (HPLC), which according to the UV, IR, and $^1$H-NMR spectra could only be 3'-adenosine monophosphate **4** and 3'-guanosine monophosphate **5** (cf. Table 1).



2 LMF 2 | 3 LMF 3 | 4 | 5

Table 1. Comparison of the retention times (HPLC) of the nucleotides from *M. pudica L.* and *A. karroo*. Column: 25 × 0.8 cm, Nucleosil C-18, 5 μm, 1 mM $CH_3COOH$, 165 bar, 5 mL/min. UV: $\lambda = 254$ nm.

| | Nucleotides | Authentic substances $t_r$ [min] | *M. pudica* | *A. karroo* |
|---|---|---|---|---|
| 3 | 2',3'-cAMP | 10.3 | 10.4 | 10.3 |
| 4 | 3'-AMP | 8.6 | 8.7 | 8.7 |
| 2 | 2',3'-cGMP | 4.25 | 4.3 | 4.3 |
| 5 | 3'-GMP | 3.6 | 3.65 | 3.6 |

### 4.2. Periodic Leaf Movement Factors (PLMFs) from *A. karroo* (K-PLMF)

The latter-mentioned components found in a mixture of active principles of the nyctinastically reacting African plant *A. karroo* flank factors which in purest form are also chemonastically active. We have designated them as Periodic Leaf Movement Factors (PLMF), so as to point out, using the same nomenclature, that they are the endogenous factors of the daily periodic leaf movements—of a plant not irritable by touching or shaking.

As shown in Scheme 1, the fractions I to V obtained by partition chromatography led, on further separation by medium pressure reverse phase chromatography, to the factors K-PLMF 1 and 2 in almost pure form. However, without any impurities K-PLMF 1, *e.g.*, can only be isolated by HPLC on C-18-alkylated silica gel (cf. Fig. 9).

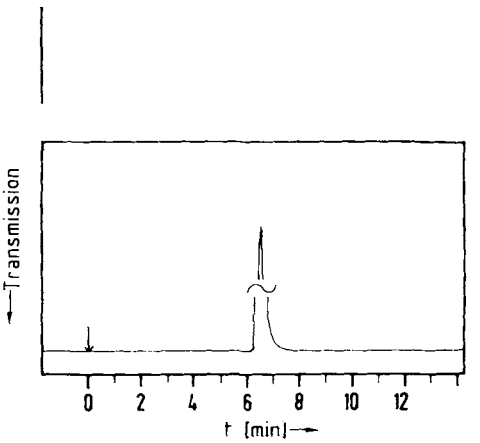



Fig. 9. HPLC diagram of K-PLMF 1 on Nucleosil C-18, 5 μm; column 25 × 0.8 cm, 1 mM $CH_3COOH$, 165 bar, 5 mL/min. Ordinate: transmission at $\lambda = 210$ nm.

#### *4.2.1. Structure Analysis of K-PLMF 1 and 2*

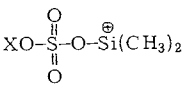
The first relevant information on the structure of these factors was provided by the UV absorption spectrum, which indicated the presence of a gallic acid derivative. The analysis of barely visible amounts of the active principle with a high resolution mass spectrometer confirmed the presence of gallic acid by virtue of the recorded $m/z$ values 79, 107, 125, 126, 153, and 170. Of special significance, however, was the fragment $m/z = 63.9609$—which corresponds to the $SO_2^+$ ion—since this is the first time that an $SO_2$-group has been detected in a molecule of active principle, alongside glucose and the aforementioned aglycone (cf. Table 2).

An extensive mass spectrometric analysis of the trimethylsilyl derivative of K-PLMF 1 provided a clear insight into its structure (cf. Fig. 10). The replacement of the organic sulfate by the derivatizing agent was especially informative.

The fragment with $m/z = 227.0229$ (standard deviation 0.8 mmu) contains a complete sulfate group. In this connection the fragment with $m/z = 573.2371$ ($C_{24}H_{45}O_7Si_4$) is of special interest, since it indicates presence of a free carboxy group in the molecule.

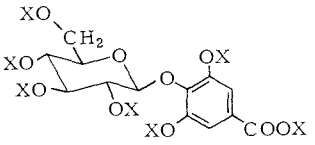
Table 2. Mass spectrometry of K-PLMF 1. Direct inlet, sample temperature 300 °C, ZAB 2F high resolution mass spectrometer.

| *m/z* | Exact mass | Elemental composition | Standard deviation (mmu) |
|---|---|---|---|
| 64 | 63.9609 | $SO_2$ | +1.0 |
| 79 | 79.0178 | $C_5H_3O$ | +0.6 |
| 80 | 80.0266 | $C_5H_4O$ | −0.4 |
| 95 | 95.0105 | $C_5H_3O_2$ | +2.8 |
| 97 | 97.0276 | $C_5H_5O_2$ | +1.3 |
| 107 | 107.0131 | $C_6H_3O_2$ | +0.2 |
| 108 | 108.0219 | $C_6H_4O_2$ | −0.8 |
| 110 | 110.0371 | $C_6H_6O_2$ | −0.3 |
| 125 | 125.0242 | $C_6H_5O_3$ | −0.3 |
| 126 | 126.0337 | $C_6H_6O_3$ | −2.0 |
| 153 | 153.0199 | $C_7H_5O_4$ | −1.1 |
| 170 | 170.0197 | $C_7H_6O_5$ | +1.8 |



*m/z* 227

X = $Si(CH_3)_3$



*M* 836

alcohols. We thus had indication of a sugar sulfate, which, however, was first detected by FAB (fast atomic bombardment) mass spectrometry with negative ions[50]. The key fragment $m/z = 411$ (Fig. 11) points to the presumed sulfate of a gallic acid glucoside, the fragment $m/z = 241$ to the glucose sulfate moiety, and the fragment $m/z = 169$ to gallic acid. Such fragments are not found in an FAB spectrum of a mixture of glucose and potassium hydrogen sulfate.

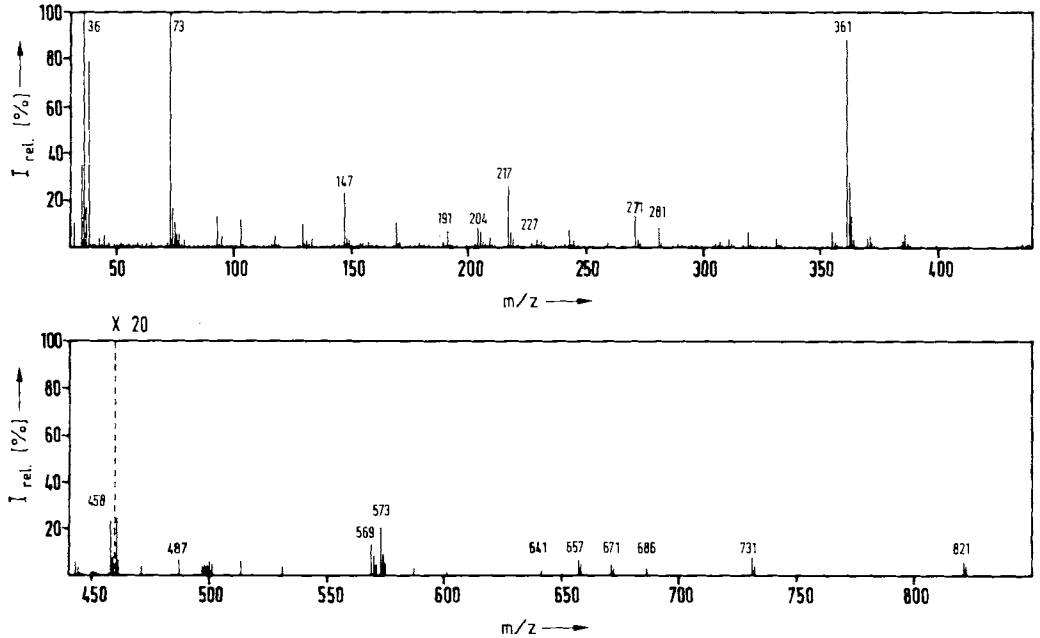



Fig. 10. EI mass spectrum of persilylated K-PLMF 1; direct inlet.

Consistent with the mass spectrometric finding, the IR absorption spectrum of K-PLMF 1 shows a band at 1284 $cm^{-1}$ for an S=O stretching vibration and one at 818 $cm^{-1}$ (γC–O–S), which is characteristic for sulfates of primary

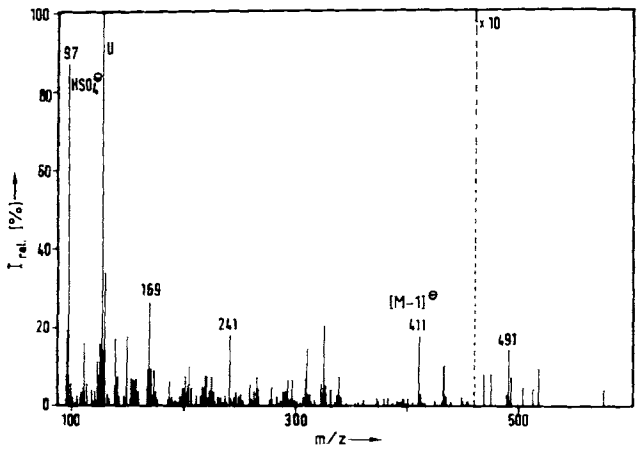
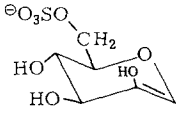
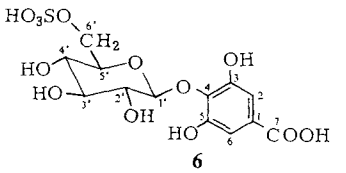



Fig. 11. FAB mass spectrum of K-PLMF 1, obtained with negative ions.

The structure of a 4-*O*-(6-*O*-sulfo-β-D-glucopyranosyl)gallic acid **6** for K-PLMF 1 could be unequivocally confirmed by $^{13}$C-NMR spectroscopy (Fig. 12). It is well-known that the downfield shift of the $^{13}$C-NMR signal of



*m/z* 241

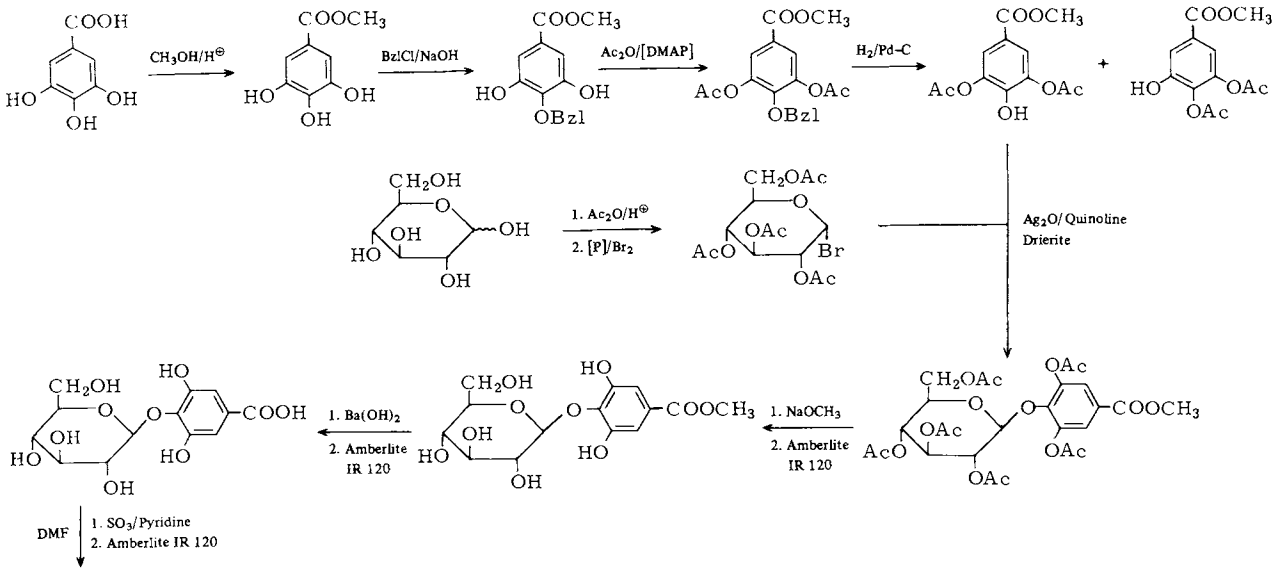


**6**

K-PLMF 1

C-6′ by about $\Delta\delta = 6$ clearly points to esterification of the primary alcoholic group of the glucose. We therefore expected the corresponding signal of K-PLMF 1 between $\delta = 68$ and 70. Consistent with this we found a triplet at $\delta = 69.4$ in the off-resonance spectrum.

Elucidation of the structure of K-PLMF 2 was aided by this finding[51]. Even its IR absorption spectrum was quite




similar to that of K-PLMF 1. Gallic acid and glucose could also be detected gas-chromatographically in the hydrolyzates of both movement factors. As in the case of K-PLMF 1 it was possible, after hydrolysis of K-PLMF 2 with 2 N hydrochloric acid, to collect the sulfate as barium sulfate in substance and to identify it by the Debye-Scherrer diagram.

The first indication that K-PLMF 2 could contain two sulfate groups was revealed by high-pressure liquid chromatography, according to which K-PLMF 2 appears to be

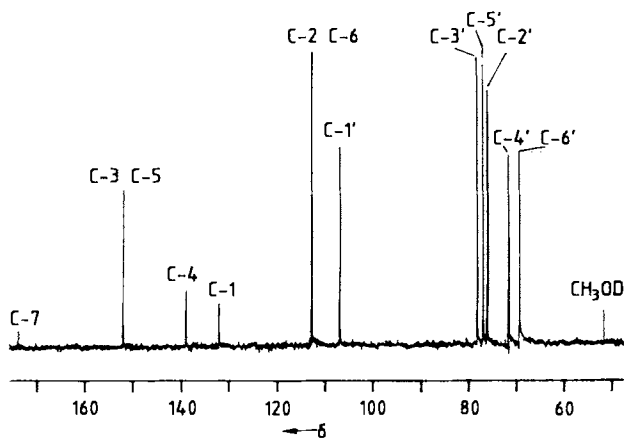
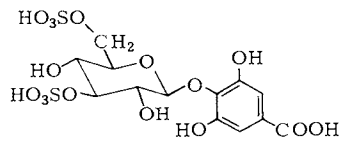



Fig. 12. 75.46-MHz $^{13}$C-NMR spectrum of K-PLMF 1 in $D_2O$ (480000 scans); techique: broad band coupling; reference signal: $CH_3OD$.

much more polar than K-PLMF 1. The highly resolved spectrum of silylated K-PLMF 2 shows all ions corresponding to those of silylated 4-*O*-glucosylgallic acid. But only the $^{13}$C-NMR spectrum confirmed that the hydroxy groups on C-6′ and C-3′ are each esterified by a sulfate group, thus giving K-PLMF 2 the structure **7**.



7
K-PLMF 2

### 4.2.2. *Synthesis and Biological Activity of K-PLMF 1*

The synthesis of K-PLMF 1 was not only important as a final proof of structure; we also wanted to check the biological activity of the synthetic active substance. At the same time, however, the synthetic route should serve as a model example for the preparation of other similar compounds, in order to investigate structure-activity relationships.

We have glucosidized gallic acid as methyl 3,5-di-*O*-acetylgallate, which had been prepared in a four-step reaction sequence. The protected aglycone was reacted with 2,3,4,6-tetra-*O*-acetyl-α-D-glucopyranosyl bromide, silver oxide and quinoline in a "classical" Koenigs-Knorr reaction to give the peracetylated methyl glucosylgallate. Cleavage of the acetyl groups and hydrolysis of the ester group affords free 4-*O*-(β-D-glucopyranosyl)gallic acid, which is reacted with $SO_3$/pyridine complex to give the sulfate. Sulfation at the unprotected glucoside to give the 6′-sulfate is facilitated by the increased reactivity of the primary 6′-OH group compared to the remaining secondary OH-groups.

In this way, a natural leaf movement factor has been prepared by *Milde* for the first time in a laboratory[52]. Not

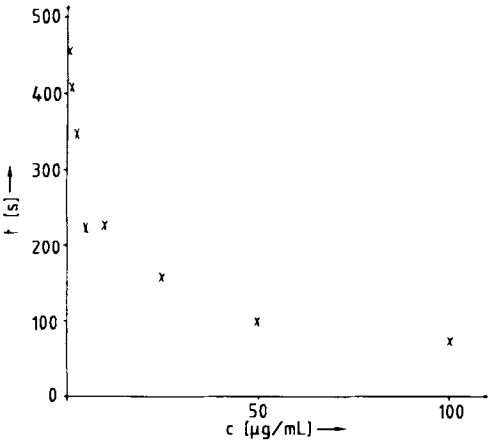



Fig. 13. Dose-response curve of synthetic K-PLMF 1 (**6**); cf. Fig. 7.

only all the spectroscopic properties, but also the biological properties of the synthetic product are in excellent agreement with those of the natural substance. Thus, in the bioassay (cf. Fig. 2) we obtained the same dose-response curves (cf. Fig. 7) as we had determined for the acid extract of the sensitive plant. The 6′-sulfate **6** which was synthesized also elicited the previously described leaf movement response, even at a concentration of $2 \times 10^{-7}$ mol/L.

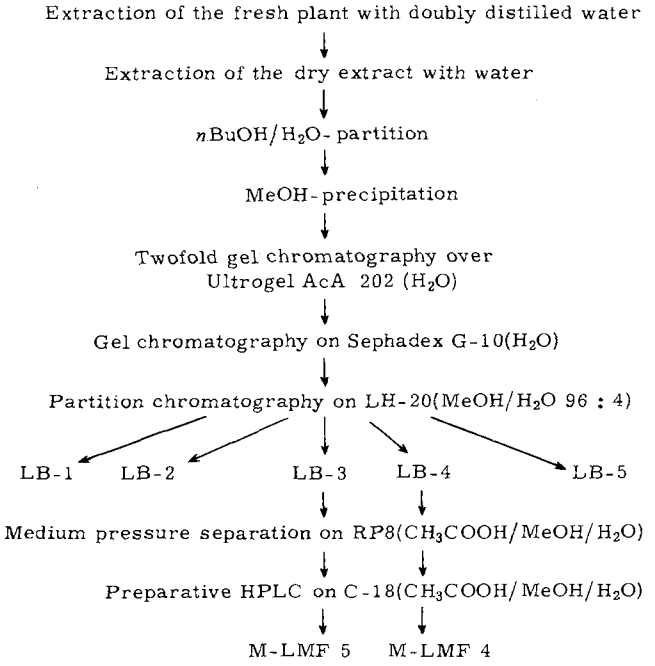
### 4.3. Detection of LMFs in Several Families of Plants

Despite all the intensive work on the non-sensitive *A. karroo*, the sensitive plant *M. pudica L.* still remains an important object for our research work on the movement phenomena of plants.

#### *4.3.1. LMFs from* M. pudica L.

By an unavoidably lengthy, yet rational separation process (Scheme 2), we were able to isolate from 23 kg of fresh mimosa from our plantation at Hainsbachweg in Heidelberg 0.8 mg of a compound which, in its pure state, also exhibited a considerable nastic activity[53]. Preliminary chromatographic and spectroscopic studies indicated that the active substance of mimosa was very probably identical with **6**, the K-PLMF 1 isolated from *Acacia karroo*. The structure was finally proven by an NMR spectroscopic analysis.

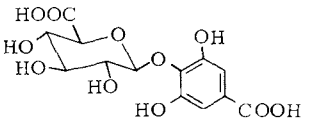
The extract of *M. pudica L.* contains, aside from 4-*O*-(6-*O*-sulfo-β-D-glucopyranosyl)gallic acid **6** (M-LMF 4), a further movement factor called M-LMF 5[1,54]. UV and $^1$H-NMR spectroscopic investigations on small amounts of the new compound already showed a high degree of similarity in the arene and sugar moieties of the two mimosa




Scheme 2. Isolation of the LMF from *M. pudica L.* Separation by medium pressure reverse phase chromatography on Merck Lithoprep RP8, HPLC separation on Polygosil C-18.5 μm.

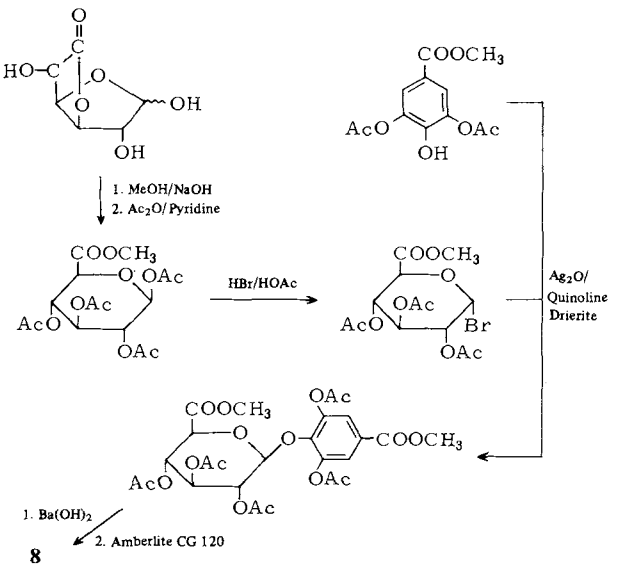
hormones. Subsequent comparative TLC and HPLC studies, however, revealed marked differences in the polarity and chemical properties of the two compounds. All the data indicated that M-LMF 5 must contain an acid group in the sugar moiety of its molecule whose $pK_s$ value is comparable to that of acetic acid.

Decisive for the proposed structure of the new leaf movement factor from the sensitive plant were the NMR spectroscopic data. The acid groups of the molecule are confirmed by the $^{13}$C-resonances at $\delta = 175.7$ (C-6′) and 172.3 (C-7). Both groups must be free, since marked downfield shifts occur in the dipotassium salt. The signals between $\delta = 110$ and 160 could be assigned to the ring atoms of the gallic acid. The signal at $\delta = 106.8$ is characteristic for C-1′ of a β-D-glucosidically linked pyranose. In the $^1$H-NMR spectrum, the singlet of the two protons H-2,6 at $\delta = 7.07$ suggests symmetric substitution of the aglycone. The large coupling constant of $J_{1,2} = 7.5$ Hz in the anomeric doublet confirms the β-pyranose configuration, the chemical shift of H-1′ ($\delta = 5.08$) the 1′-glucosidic linkage. Separated from the multiplet of three protons ($\delta = 3.69$) there appears at $\delta = 3.97$ the doublet of H-5′ ($J_{4,5} = 8.5$ Hz) typical for hexuronic acids. Since this signal is also split by diaxial coupling, the β-D-glucopyranosideuronic acid in M-LMF 5 must be 1′-glucosidically linked with the 4-OH group of the gallic acid.




**8**
M-LMF 5

All the chromatographic and spectroscopic data of the 4-*O*-(β-D-glucopyranosideuronyl)gallic acid **8** synthesized by us by a modified Koenigs-Knorr reaction[1] were identical with those of natural M-LMF 5. The compound, which occurs only in hormonal amounts in mimosa, still triggers the specific stimulation reaction at a concentration of $3 \times 10^{-6}$ mol/L and is thus a further, low-molecular leaf movement factor.




**8**
M-LMF 5

M-LMF 5 **8** is only apparently similar to the leaf movement factors K-PLMF 1 and 2 (**6** and **7**, respectively); the chemical and biological behavior of the active substance **8** are determined by the carboxy function in the C-6′ position, which is much less acidic than the sulfuric acid ester function. It would be interesting to know whether this second variation of the structure of natural leaf movement substances also occurs in other plants or is only to be found in *M. pudica L.*

### 4.3.2. *A Leaf Movement Factor from a Malvaceae*

Not only after we had isolated, structurally identified, and synthesized the first biologically very active leaf movement factor from *A. karroo* did we ask ourselves whether or not there were other fixed, higher organized plants which react nyctinastically, using the same or a chemically similar active principle. Thus, we had already also observed the movements of *Abutilon grandiflorum*, whose leaves were found to fold together and its leaf stalks droop downwards, even at midday (Fig. 14).



Fig. 14. *Abutilon grandiflorum* in the midday heat at Hainsbachweg in Heidelberg.

Table 3. Occurrence of K-PLMF 1 in *Fabaceae, Oxalidaceae,* and *Malvaceae; t* = reaction time of on extract. K-PLMF 1 **6** is identical with M-LMF 4 and with S-PLMF 1 (see Section 4.3.3).

| Plant | *t* [s] | K-PLMF 1 | Ref. |
|---|---|---|---|
| *Mimosa pudica L.* | 25 | + | [54] |
| *Acacia karroo* | 30 | + | [51] |
| *Acacia dealbata* | 40 | + | [68] |
| *Albizia julibrissin* | 50 | + | [58] |
| *Gleditsia triacanthos* | 60 | + | [69] |
| *Robinia pseudacacia* | 60 | + | [70] |
| *Oxalis acetosella* | 50 | ? | [67] |
| *Oxalis stricta* | 40 | + | [56] |
| *Oxalis deppei* | 40 | + | [67] |
| *Abutilon grandiflorum* | 25 | + | [55] |

We were, however, astounded at also being able to isolate K-PLMF 1 from this flowering plant of the family *Malvaceae*[55], but not surprised to find it also in plants of the family *Fabaceae* (Table 3).

### 4.3.3. *LMFs of the Oxalidaceae*

It has been known since *Pliny the elder*'s time that oxalis-type plants also behave nyctinastically, and under certain circumstances even react thigmonastically or seismonastically. This is observed particularly nicely in the case of *Oxalis deppei,* the four-leaf clover, which folds its four leaves together like an umbrella, not only at night but also in full sunshine (Fig. 15).

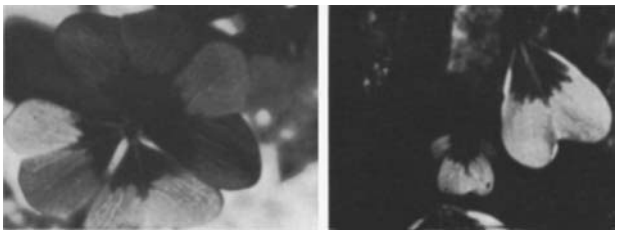


Fig. 15. *Oxalis deppei* at 16.07 (left) and at 21.14 hours (right) on July 11, 1982.

The first attempts made in the search for LMF in this family of plants, which are quite different from the *Fabaceae,* have revealed that here also the chemical principles underlying nyctinastic movement are compounds at least related to the already known factors.

Thus, it is not surprising that we have isolated a leaf movement factor S-PLMF 1 from *Oxalis stricta,* the sorrel, which is identical with K-PLMF 1[56]. A second factor S-PLMF 2, which could be isolated by the usual methods of enrichment, exhibited in a bioassay the well-known leaf movement reaction, and, following preliminary spectroscopic studies, it could be concluded that it was likewise chemically related to the previously described LMFs (cf. also Table 4).

Table 4. Comparison of the retention times (HPLC) of diverse PLMFs. Column: 25 × 0.8 cm Nucleosil C-18, 5 μm; detection: $\lambda = 210$ nm; System I: 20% $CH_3OH$/0.05% $CH_3COOH$; 3 mL/min; System II: 1 mM $CH_3COOH$; 5 mL/min.

| | | $t_r$ [min] System I | $t_r$ [min] System II |
|---|---|---|---|
| **6** | S-PLMF 1 | 15.1 | 5.8 |
| **6** | K-PLMF 1 | 15.3 | 5.9 |
| **9** | S-PLMF 2 | 11.9 | 4.3 |
| **7** | K-PLMF 2 | 42.2 | 3.1 |

By means of GC-MS investigations on the silylated hydrolyzate we found that the aglycone of S-PLMF 2 was not gallic acid but protocatechuic acid, with one less hydroxy group. Glucose was also found to be a structural unit of S-PLMF 2. As in the case of the other LMFs, the total structure of S-PLMF 2 has been determined NMR spectroscopically (cf. Fig. 16). Typical coupling patterns of a 1,3,4-substituted arene are recognizable in the downfield region of the spectrum: two doublets and the doublet of doublets.

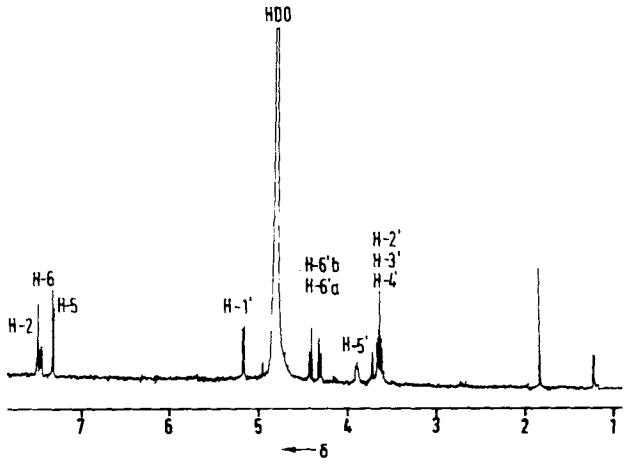
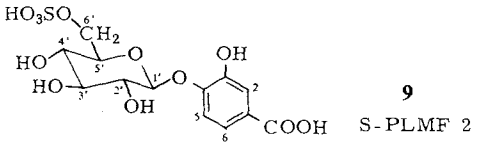



Fig. 16. 500-MHz $^1$H-NMR spectrum of S-PLMF 2 in $D_2O$ (500 scans), calibration: HDO = 4.77 ppm.

The splitting of the H-5 signal at $\delta = 7.2$ ($J = 8.1$ Hz) is brought about by the *ortho*-coupling with H-6. This in turn additionally couples with the *meta* H-2 ($J = 2.0$ Hz). Since the methyl protons of the glucopyranoside have experienced a significant downfield shift of about $\Delta\delta = 0.5$ compared to unsubstituted glucosides it must be concluded that an electron-attracting substituent is located on C-6'. According to data in the literature, and our proton resonance spectroscopic findings on LMFs that have already been identified, especially K-PLMF 1, the polar group could be a sulfate ester. Unequivocal proof of this was not possible, even from the $^{13}$C-NMR spectrum, since a total of not more than 0.8 mg of the active substance was available for all the analytical and spectroscopic investigations. Hence, here once again the synthesis served as a means for proof of the structure; the end product, 4-*O*-(6-*O*-sulfo-β-D-glucopyranosyl)protocatechuic acid **9**, proved to be identical with the natural substance, both spectroscopically and in the bioassay[56].




**9** S-PLMF 2

This structural variant of K-PLMF 1 exhibited specific activity at a concentration of 0.001 to 0.005 mg/L in the biological test system (Fig. 2); the absence of an hydroxy group in the aglycone obviously leads to a reduction of the activity by a factor of more than 10.

### 4.4. Phenomena-Oriented Consideration of the LMFs

Studies on the day-night periodicity of leaf movements led to the discovery of the circadian rhythms of plants[57]. The movements are caused by a change in the turgescent tension in the tissues of the motile organs made up of parenchymic cells. We may assume that the change of turgor is the consequence of changes in the water permeability of boundary plasma layers, caused by turgor active endogenous factors, the leaf movement factors.

#### *4.4.1. PLMFs as Final Active Principles of the "Circadian Rhythms" of* Albizia lophanta

*Hein*[58] was able to demonstrate on the pinnate leaves of *A. lophanta*, whose daily periodic movements are illustrated quite vividly in Figure 17, that leaves placed in an aqueous solution of K-PLMF 1 **6** (0.05 mM) "sleep" earlier than the control plants.

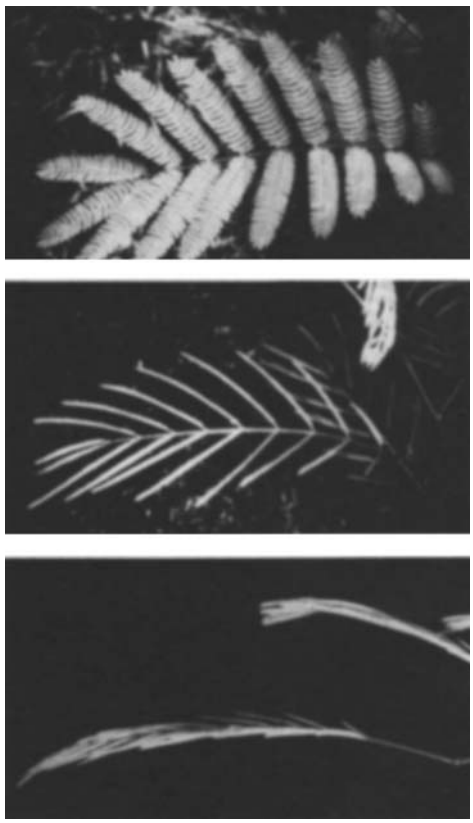
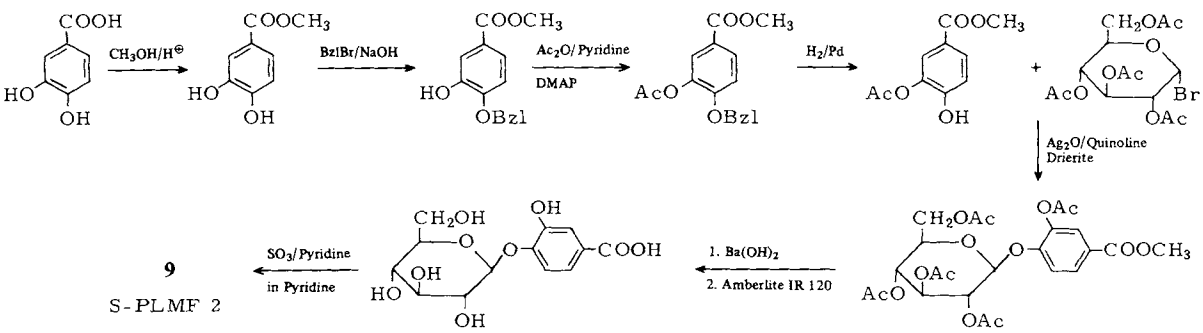


Fig. 17. Pinnate leaf of *A. lophanta*, photographed at 19.23 (top), 21.53 (center), and about 22.22 hours CET (bottom) on July 15, 1981.



An unexpected finding was that the pinnules close together later under the influence of 2′,3′-*c*AMP **3** and 2′,3′-*c*GMP **2** (3 mM). Furthermore, the cyclic nucleotides remarkably influence the time of opening of the pinnules after four hours' action in the morning. The activity of all three factors also depends on the time of the day. Thus, earlier as well as later "sleeping" of the test leaves can be initiated by combination of the PLMF with the cyclic nucleotides.

#### *4.4.2. PLMFs as Final Active Principles of the Nastic Movements of Stomatal Opening*

Stomatal opening on the underside of the leaves of higher organized plants regulates transpiration and gas exchange as a result of the turgor movement of their guard cells. Stomatal opening (Fig. 18) provides communication

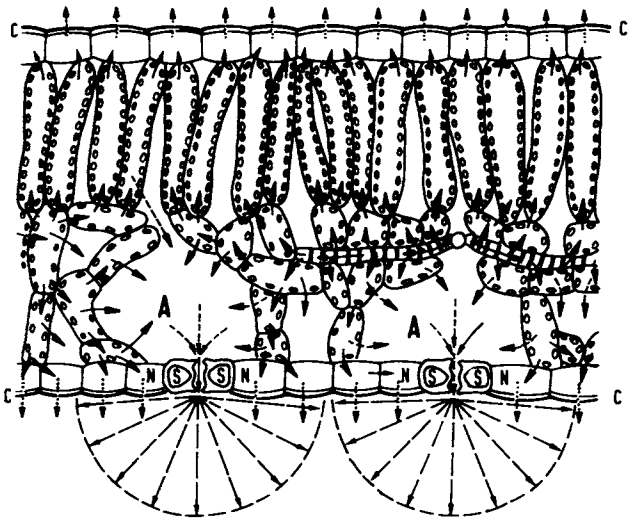
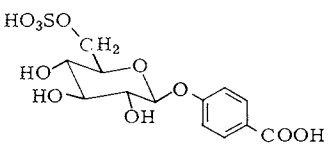



Fig. 18. Stomatal and cuticular transpiration of a leaf, altered after *Nultsch* [41]; S = guard cells, N = companion cells, A = breathing holes (stomatal openings), C = cuticula; arrows indicate the direction of flow of water.

between the external air and the intercellular system of the subepidermal tissue. It has long been known that each increase in the turgor of the guard cells relative to the companion cells leads to opening of the stomatal slit, each decrease in turgor to closing of the stomatal slit[59]. Although turgor changes can come about in various ways, we may, following our experiences with LMFs, assume that here also PLMF 1 **6** is the final active principle.

In fact it has emerged from experiments carried out by *H. Ziegler et al.*[60] that M-LMF 5 **8**, synthetic 4-*O*-(6-*O*-sulfo-β-D-glucopyranosyl-*p*-hydroxybenzoic acid **10**[61], and, above all, K-PLMF 1 and 2 (**6** and **7**, respectively) can make guard cell protoplasts of broad beans *(Vicia faba)* rapidly shrink after previously being brought to




**10**

swelling with $K^+$ ions. This means that the sulfate-containing turgorins, in particular, rapidly increase the permeability of the plasma membrane. As a rule, they have a closing effect on the guard cells in isolated but intact Vicia leaf epiderma. This observation by *Ziegler* and *Schnabl* is in agreement with the experimental results obtained by *Jung*[62]: in a barley leaf segment bioassay on the influence of leaf ageing and stomatal movement, K-LMF 1 promotes leaf senescence and stomatal closure.

## 5. Turgorins—A New Class of Phytohormones

It was already pointed out in Section 2 that the first four classes of phytohormones listed in Table 5, like the superhormone ethylene, are important agonists in ecological plant physiology. Following the identification of K-LMF 1—exactly 50 years after the discovery of the first phytohormone by *Kögl* in 1931[7]—we must extend the list.

Like all phytohormones, the trugorins are transported from the place where they are formed through the sap stream to the target organ, where they depolarize a biomembrane and so alter its permeability that the turgor diminishes. The pinnate leaves close and open and the whole mimosa tree goes to "sleep" and "wakes up" again—together with a likewise hormone-regulated "Venus pudica", who, in an allegoric portrayal by an unknown artist, takes a look at a new day (Fig. 19).

Her beauty is due in part to a phenol, which of course K-PLMF 1 also is. But, more by good luck than good management the artist has cunningly represented the mutuality of hormone-regulated life forms—a human person and a

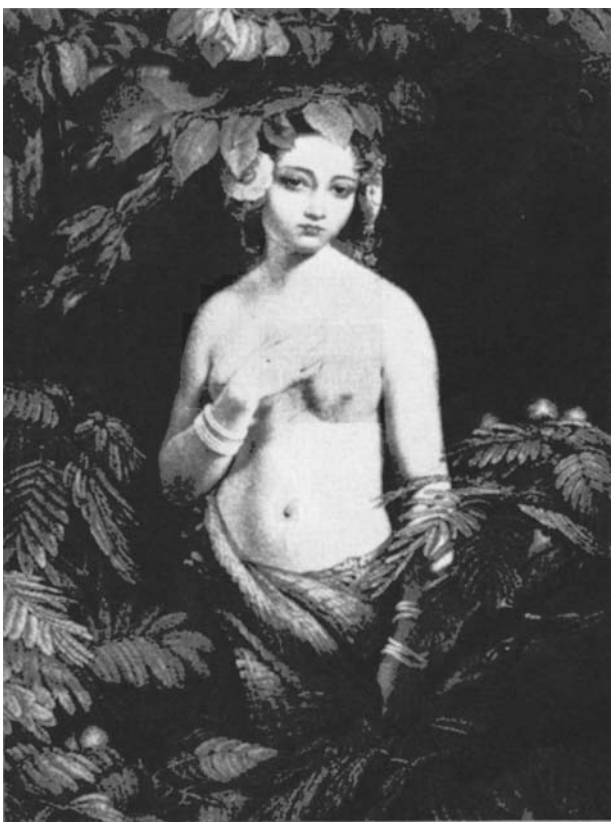
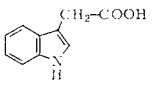
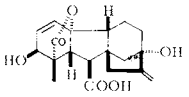
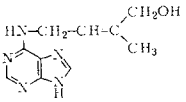
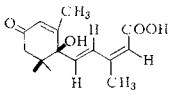
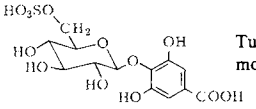


Fig. 19. "Venus pudica" in the mimosa jungle—xylograph of a picture of the late, romantic cum classic period [63].

Table 5. The most important classes of hormones in higher organized plants.

| Hormone Class | Structure | Activity | Discovery |
|---|---|---|---|
| Auxins<br>Example:<br>3-Indolyl-acetic acid |  | Longitudinal growth | 1931 |
| Gibberellins<br>Example:<br>Gibberellin-acid $GA_3$ |  | Longitudinal growth | 1935 |
| Cytokinins<br>Example:<br>Zeatin |  | Cell division - Cytokinesis | 1955 |
| Abscisins<br>Example:<br>(+)-Abscinic acid |  | Abscission - Stomatal opening movement | 1970 |
| Turgorins<br>Example:<br>K-PLMF 1 **6** |  | Turgor movement | 1981 |

plant. The female sexual hormone estradiol promotes *inter alia,* a growth movement of the breast glands, the turgorin K-PLMF 1 promotes the sleep movement of a mimosa.

## 6. Discussion and Outlook

In his "Plant Geography"—a work such as has never been surpassed in antiquity—the Greek philosopher *Theophrastus* already compared the phenomenon of "plant sleep" with the phenomenon of movement of the sensitive plant, and thus, unknowingly presented mimosa as the index plant for all later research work (Fig. 20) on the power of movement in plants (after *Darwin*[64]). Thus, one can understand that *Pfeffer*'s warning remained for a long time unheeded. In § 3 of the "Nature of Stimulation Processes" in his Pflanzenphysiologie[65] he says: "Accordingly, even in special cases, *e.g.* sudden stimulation reactions (such as the folding together of the leaves of the sensitive plant), are of little general significance compared to the army of slow and continually effective reactions and regulations".

This claim was—so far as the stimuli of sleep movements are concerned—first given justice in 1981, when we isolated and elucidated the structure of the first turgorin from *Acacia karroo,* a non-sensitive plant[51].

### 6.1. Dissemination of the Turgorins

The relatively wide dissemination of the turgorins is now recognized (cf. Table 3). But we are still tormented by the question of whether all nyctinastically responsive plants have essentially only K-PLMF 1 **6** at their disposal, or whether or not compounds other than turgorins can be effective.

We must first wait for the analytical results obtained on the rain tree (*Pithecolobium saman,* Fabaceae), the flame tree (*Delonix regia,* Ceasalpinaceae), the calliandra (*C. fulgens* and *C. Haematocephala,* Mimosaceae), and the bauhinia (*Bauhinia* spec., Caesalpinaceae). *Hein*[58] has, already found that K-PLMF 1 does in fact occur in *Albizia julibrissin* (cf. Table 3), but not in a near relative, *Albizia lophanta*. From *A. julibrissin* we isolated a complex mixture of over 20 saponins, which were obtained in pure form by HPLC. These saponins consist of a pentacyclic triterpenic acid, linked to two sugar chains containing up to seven monosaccharide units. Almost all of these saponins are also coupled in an ester-like fashion with two α,β-unsaturated monoterpenic acids. Small variations in the triterpene, sugar, or monosaccharide moieties of the molecules give rise to numerous possible structures. Although, in principle, they are very similar in structure it was surprising that only two of the individual components proved to be highly active in the bioassay. In the most favorable case 3 mg/L sufficed, at a molecular weight of *ca.* 2000, to stimulate a leaf movement. By a detailed NMR spectroscopic analysis of the individual components, in which 2D-techniques have proven especially valuable, it has been shown



Fig. 20. *M. pudica L.*, photographed in the mimosa plantation, Heidelberg-Hainsbachweg, during the day (left), at night (center), and after touching (right).

that even a small change in one of the monoterpenes can lead to a drop in the activity by a factor of about 1000. Thus, the activity is in no way a general property of the saponin; rather, it is coupled with definite structural requirements in which the monoterpenes play an important role.

Also surprising are the results which *Koch*[66] obtained with the leaves of *Glycine max.*, the soya bean: derivatives of *p*-hydroxycinnamic acid occur, which appear to be esterified with a sugar acid.

Of importance for an overview of the new class of hormones are also the investigations with oxalidaceae, not only because they represent other families than the Fabaceae, but also because an extract from the bulb of the four-leaf clover *(Oxalis deppei)*—which in all probability contains K-PLMF 1—stimulates the leaves of some plants to "sleep". *Backfisch*[67] found a new chemonastically active factor in the South African plants *Oxalis compressa* and *O. obtusa*, which according to their chromatographic behavior must be substantially more polar then K-PLMF 1. Because of the inducible variation in potential in the vine, *Vitus gongylodes*, *Houwink*[30] assumed that a stimulating substance was also effective here, as in the mimosa. Whether in this case the turgorins described by us are involved will be clarified by a bioassay.

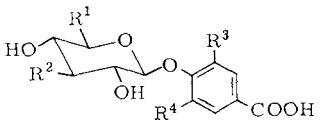
### 6.2. Mechanism of Stimulus Perception and Its Inductive Character

At the slightest touch, the sensitive hairs on the pulvini of *M. pudica L.* stimulate movement of the hinge cells in the leaf joints. We may assume that the first step of the physiological process is the—perhaps enzymatic—activation of the turgorins.

#### *6.2.1. Stimulation Reactions at the Biomembrane*

As agonists of turgor bending and thus of the associated changes in permeability of the biomembranes, the turgorins provide the causal connection between irritation and movement. As in the case of acetylcholine, the neurotransmitter in animal synapses, a receptor also participates in plant stimulation phenomena; this was previously recognized by us by the fact that the turgorins exhibit a distinct structure-activity relationship (cf. Table 6). The activity decreases when the free phenolic OH-groups are absent.

Table 6. Structure-activity relationship of the turgorins.




| | Turgorin | Structure $R^1$ | $R^2$ | $R^3$ | $R^4$ | Activity min. Conc. [g/L] |
|---|---|---|---|---|---|---|
| **6** | K-PLMF 1 [a] | $CH_2OSO_3H$ | OH | OH | OH | $10^{-4}$ |
| **7** | K-PLMF 2 | $CH_2OSO_3H$ | $OSO_3H$ | OH | OH | $10^{-4}$ |
| **9** | S-PLMF 2 | $CH_2OSO_3H$ | OH | OH | H | $10^{-3}$ |
| **8** | M-LMF 5 | COOH | OH | OH | OH | $10^{-3}$ |
| | PLMF-synth. | $CH_2OSO_3H$ | OH | H | H | $10^{-2}$ |
| | LMF-synth. | COOH | OH | H | H | $5 \times 10^{-1}$ |

[a] Identical with M-LMF 4 and S-PLMF 1.

However, alone on the basis of investigations on the role of 3′,5′-*c*AMP in plant "sleep"[71], the PLMFs must still be discussed together with the aforementioned cyclic nucleotides as additional members of a stimulation chain.

Perhaps, with the endogenous cofactors 2′,3′-*c*AMP and 2′,3′-*c*GMP (**3** and **2**, respectively, Table 1), we have further "second messengers" of the higher plants.

#### *6.2.2. Stimulation Conduction*

The above-mentioned, easily controlled turgorin syntheses will enable us to study both the receptor as well as stimulus conduction with the aid of $^{13}C$-labeled active substances.

The inductive effect of a stimulus on movement is nowhere more conspicuous than in hormone-carrying stimulus conduction. Provisionally, we can only corroborate *Houwink*'s hypothesis[30], according to which a specific irritant—in our way of thinking a turgorin—is transported in the channels from the induced vacuole to the typically structured target organ. In this process a variation potential (10 cm/min) occurs. In principle, we make no distinction between the endogenous movements controlled by external stimulation and those controlled by an internal mechanism, *e.g.* the sleep movements, which obey a physiological clock.

## 7. Epilogue

> *Das logische Wissen kann wahr nur sein, wenn es allumfassend ist.*
>
> *K. Jaspers, Von der Wahrheit*[73]

Although trees, for the very sake of their unsurpassable size have remained fixed, they are not on this count wholly immovable; just like the plants with regard to their external appearance and the mechanics of their movements they demonstrate incomparably greater diversity than animals—despite the absence of a developed musculator.

But how can a fixed plant manage its highly systemized organic structure, or even alone its circulation, without muscles and thus without a heart? Actually, only by a subtle control of the turgor in the motor and guard cells (cf. also Figs. 18 and 21). In end effect, it is thus the "water balance" of the whole plant organism which controls, *via* biomembranes and thus by turgorins, the temperature regulation in the plant body and makes its firmness possible.

If one was previously of the opinion that cuticular exchange (Fig. 18) is not regulatable[41], then one should again reflect on turgor-controlled movement, at least of the papilionaceous plants with their daily periodic leaf movements.

Alone the idea of a common chemical basis for all turgor-controlled movements suggests that cuticular as well as stomatal transpiration is influenced by the sleep movements of the leaves, *i.e.* likewise hormonally controlled.

In the comparison just drawn between plants and animals we presume a similar, even though primitive actomyosin system in the ancient forms of both types of life, from

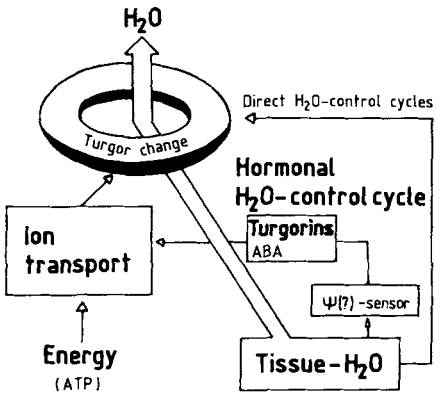



Fig. 21. Regulatory mechanism of the water balance of higher terrestial plants; simplified according to *Haupt* [72]. The guard cells are depicted schematically above. ABA signifies abscissinic acid; ψ-sensor signifies sensor for the water potential (ψ) in a tissue.

which the animal muscles could have developed. But we are still lacking the appropriate analogue to the animal nervous system in the plants, in which *e.g.* one even misses the synapses. The neutrotransmitter, however, should now be compared with the turgorins, or perhaps also with new phytohormones not yet chemically identified beyond doubt.

*When, as is the case here, the author has been granted the privilege, after thirty years of research, to present a comprehensive account of such a fascinating area of phytochemistry – framed by historical, artistic and philosophical considerations – then he owes his gratitude to an unusually large number of highly able and valued colleagues and collaborators, both technical and scientific. They have shown a high degree of skill and expertise at manipulating barely visible amounts of natural products in the quest to interpret a natural phenomenon on a sound chemical basis. This has naturally entailed a resort to modern and sophisticated instrumental analysis, the apparatus for which, like many other things, could not have been acquired or realized without appreciative and generous financial support from the Deutsche Forschungsgemeinschaft and the Fonds der Chemischen Industrie. I am deeply indebted to Brigitte Schmich for the layout of the diagrams and to Patricia Bock, my secretary, for her remarkable engagement in the preparation of the manuscript. And last but not least I also wish to thank Dr. Karl Friedrich (Brazil) and Prof. U. Burger (South Africa) for their continued help in placing tropical plants at my disposal.*

Received: June 6, 1983 [A 465 IE]
German version: *Angew. Chem. 95* (1983) 689

[1] H. Schildknecht, W. Bender, *Angew. Chem. 95* (1983) 634; *Angew. Chem. Int. Ed. Engl. 22* (1983) 617; *Angew. Chem. Suppl. 1983*, 818.
[2] O. Kirchner "Die botanischen Schriften des Theophrast von Eresos", *Jahrb. für class. Philologie, 7. Suppl.-Bd. 1874*, 449–539.
[3] Theophrast hist. pl. IV 7,8.
[4] Theophrast hist. pl. IV 2,11.
[5] W. Wickler: *Mimikry, Nachahmung und Täuschung in der Natur*, Kindlers Universitäts-Bibliothek, Munich 1968.
[6] O. L. Lange, P. S. Nobel, C. B. Osmond, H. Ziegler: *Encyclopedia of Plant Physiology, New Series, Vol. 12A*, Springer, Berlin 1981, p. 1.
[7] K. Dörffling: *Das Hormonsystem der Pflanzen*, Thieme, Stuttgart 1981.
[8] J. Sachs: *Geschichte der Botanik vom 16. Jahrhundert bis 1860*, Georg Olms Verlagsbuchhandlung, Hildesheim 1966.
[9] G. Roblin, *Biol. Rev. Cambridge Philos. Soc. 54* (1979) 135.
[10] W. Bender, Diplomarbeit, Universität Heidelberg 1981.
[11] E. Wulf, A. Deboben, F. A. Bautz, H. Faulstich, Th. Wieland, *Proc. Natl. Acad. Sci. USA 76* (1979) 4498.
[12] E. Brücke, *Arch. Anat. Physiol. Wiss. Med. 1848*, 434–455.
[13] V. H. Blackman, S. G. Paine, *Ann. Bot. (London) 32* (1918) 69.
[14] T. Abe, *Shokubutsugaku Zasshi (Bot. Mag.) Tokyo 93* (1980) 247.
[15] H. Toriyama, *Cytologia 36* (1971) 359.
[16] H. Toriyama, M. J. Jaffe, *Plant Physiol. 49* (1972) 72.
[17] M. Samejima, T. Sibaoka, *Plant Cell Physiol. 21* (1980) 467.
[18] W. Pfeffer: *Physiologie végétale*, Steinheil, Paris 1912, p. 900ff.
[19] T. Vandem Driessche, *Arch. Biol. 89* (1978) 435.
[20] T. Vandem Driessche, *Ann. Physiol. Vég. Univ. Bruxelles 8* (1963) 101.
[21] J. Sachs: *Handbuch der Experimental-Physiologie*, Leipzig 1865, p. 479.
[22] G. Haberland: *Das Reizleitende Gewebesystem der Sinnpflanze*, Leipzig 1865.
[23] J. C. Bose: *The Nervous Mechanism in Plants*, Longmans, Green & Co., London 1926.
[24] D. A. Herbert, *Proc. R. Soc. Queensl. 36* (1925) 121.
[25] K. Linsbauer: *Über Reizleitungsgeschwindigkeit und Latenzzeit bei Mimosa pudica*, Wiesner-Festschrift 1908, p. 396.
[26] J. C. Bose: *The Motor Mechanism of Plants*, Longmans, Green & Co., London 1928.
[27] K. Umrath, *Biol. Gen. 1* (1925) 396.
[28] R. Snow, *Proc. R. Soc. London 96* (1924) 349.
[29] R. Snow, *Proc. R. Soc. London 98* (1926) 188.
[30] A. L. Houwink, *Recl. Trav. Bot. Neerl. 32* (1945) 51.
[31] T. Sibaoka, *Annu. Rev. Plant Physiol. 20* (1969) 165.
[32] H. Bretzl: *Botanische Forschungen des Alexanderzuges*, Verlag B. G. Teubner, Leipzig 1903.
[33] Observation bonatique. Histoire de L'Academie Royale des Sciences Paris 1729, p. 35.
[34] J. G. Zinn, *Hamburger Magazin 22* (1759) 40–50.
[35] A. P. de Candolle: *Physiologie végétale*, Paris 1832.
[36] F. Halberg, A. Reinberg: *Rythmes circadians et rythmes de bas fréquences en physiologie humaine*, Masson, Paris 1968.
[37] E. Bünning: *Die physiologische Uhr*, 3rd edit., Springer, Berlin 1977.
[38] U. Ricca, *Nuovo G. Bot. Ital. (Nuova Seria) 23* (1916) 51.
[39] H. Fitting, *Jahrb. Wiss. Bot. 83* (1936) 270.
[40] T. Sibaoka, *Sci. Rep. Tohoku Univ. Ser. 4 (Biol.) 20* (1953) 72.
[41] W. Nultsch: *Allgemeine Botanik*, 7th edit. Thieme, Stuttgart 1982, p. 443.
[42] D. T. Macdougal, Bot. gaz. *22* (1976) 293.
[43] H. Fitting, *Jahrb. Wiss. Bot. 72* (1930) 701.
[44] A. Soltys, K. Umrath, C. Umrath, *Protoplasma 31* (1938) 454.
[45] H. Schildknecht, K. Schumacher, *Chem.-Ztg. 106* (1981) 287.
[46] H. Schildknecht, K. Schumacher, *Chem.-Ztg. 106* (1982) 421.
[47] P. Hettinger, Dissertation, Universität Heidelberg 1982.
[48] H. Schildknecht, K. Schumacher, *Pure Appl. Chem. 54* (1982) 2501.
[49] G. Esswein, Dissertation, Universität Heidelberg 1981.
[50] H. Schildknecht, P. Hettinger, D. Krauss, F. Mayer, R. Söllner, K. Schumacher, P. Farrow, 15th Meeting of the Working Group for Mass Spectrometry, Bielefeld, June 2–4, 1982, Lecture by D. Krauss.
[51] K. Schumacher, Dissertation, Universität Heidelberg 1982.
[52] R. Milde, Diplomarbeit, Universität Heidelberg 1982.
[53] H. Schildknecht, W. Bender, *Chem.-Ztg. 107* (1983) 111.
[54] W. Bender, Dissertation, Universität Heidelberg 1983.
[55] T. Kramer, Diplomarbeit, Universität Heidelberg 1983.
[56] H. Schildknecht, K. Schumacher, R. Söllner, *Chem.-Ztg. 107* (1983) 233.
[57] J. Aschoff: *Circadian Clocks*, North Holland, Amsterdam 1965.
[58] M. Hein, Dissertation, Universität Heidelberg 1983.
[59] J. F. Gmelin: *Allgemeine Geschichte der Pflanzengifte*. 2nd edit., in the Raspeschen Buchhandlung, Nürnberg 1803.
[60] H. Ziegler, H. Schnabl, private communication 1983.
[61] R. Muley, Diplomarbeit, Universität Heidelberg 1982.
[62] J. Jung, BASF, private communication 1983.
[63] P. A. Riedel, Heidelberg, private communication 1983.
[64] Ch. Darwin: *The Power of Movement in Plants*, John Murray, London 1880.
[65] W. Pfeffer: *Pflanzenphysiologie*, 2nd edit., *vol. 1*, Wilhelm Engelmann, Leipzig 1897, p. 19.
[66] G. Koch, Dissertation, Universität Heidelberg 1983.
[67] G. Backfisch, Diplomarbeit, Universität Heidelberg 1982.
[68] T. Markert, Diplomarbeit, Universität Heidelberg 1981.
[69] G. Kresbach, Diplomarbeit, Universität Heidelberg 1981.
[70] F. Mayer, Dissertation, Universität Heidelberg 1983.
[71] I. Bollig, K. Mayer, W.-E. Mayer, W. Engelmann, *Planta 141* (1978) 225.
[72] W. Haupt: *Bewegungsphysiologie der Pflanzen*, Thieme, Stuttgart 1977.
[73] K. Jaspers: *Von der Wahrheit*, Piper, München 1968, p. 3.

**When submitting manuscripts, authors of articles which are intended for publication as "Communications" are requested to conform to the guidelines reproduced at the beginning of each issue following the list of contents.**

## Synthesis of the Chiral Synthetic Building Block (1*R*,5*S*)-3-Phenyl-4-oxa-2,6-diazabicyclo[3.2.0]hept-2-en-7-one from 6-Aminopenicillanic Acid

By *Dieter Häbich**

The isolation and determination of the structure of thienamycin together with the discovery of the monobactam antibiotics gave renewed impetus to the synthesis of β-lactams.

The previously unknown oxazolines **1**, which have no substituents at N-6, should be particularly useful building blocks for syntheses of this type and be accessible by analogy to the corresponding thiazolines[5]. The synthetic potential of compounds **1** has already been recognized. For example, *Stoodley* reported the unsuccessful attempt to isolate the enantiomer of **1b** using another route[7].

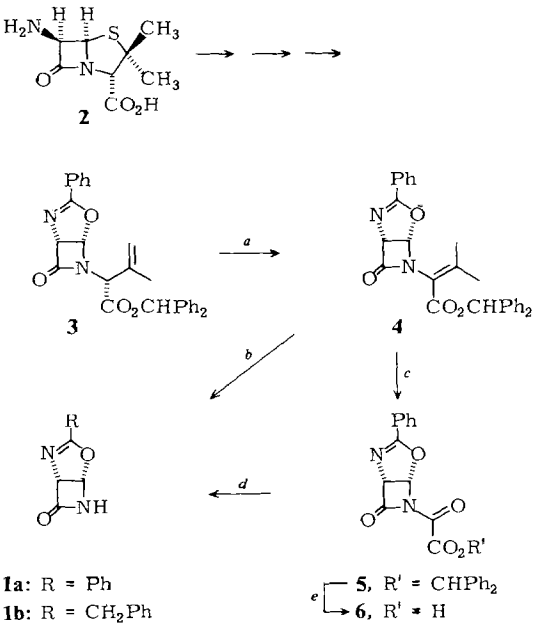
*Aoki et al.* used the stereoselective intramolecular ring-opening of *N*-substituted annelated oxazolines to synthesize oxacephems[8]. *Woodward et al.* employed the reaction of free azetidinones with electrophiles in the total synthesis of cephalosporin C[9]. Oxazolines **1** should permit reactions of both types.

We have now synthesized (1*R*,5*S*)-3-phenyl-4-oxa-2,6-diazabicyclo[3.2.0]hept-2-en-7-one **1a** (alternatively: 2-phenyl-3a,5a-dihydroazet[3,2-*d*]oxazol-5-one) as well as some of its *N*-substituted derivatives (Scheme 1).

The *epi*-secopenicillin **3**, accessible in four steps from 6-aminopenicillanic acid **2**, can be isomerized to **4** using the base-catalyzed method described by *Maki et al.*[11]. Oxidative cleavage of the side chain to afford **1a** proceeds directly with potassium permanganate[5]. Higher yields can be obtained using the route *via* **5**, obtained by ozonolysis of **4**. Methanolysis of **5** in the presence of silica gel or sodium methoxide as catalyst yields the crystalline oxazoline **1a**, $[\alpha]_D^{20} = -114.8$ (0.836% in acetone).

Surprisingly, acid **6** can be formed from ester **5**, although its IR band at 1832 $cm^{-1}$ suggests a highly reactive β-lactam ring.

Crystalline **6** is stable [m.p. = 148–150 °C (decomp.)]; however, in solution (DMSO-$D_2O$-$NaHCO_3$) it rapidly decomposes at 37 °C. Neither **6** nor **1a** exhibit antibiotic activity or inhibit β-lactamases.




Scheme 1. *a:* cat. $NEt_3$, $CH_2Cl_2$, 6 h RT (84%). *b:* $KMnO_4$-acetone-water, pH 7 (19%). *c:* $O_3$, $CH_2Cl_2$ −70 °C; $Me_2S$ (70%). *d:* $SiO_2$, $CH_3HO$, 8 min RT (62%) *or* cat. $NaOCH_3$, $HOCH_3$, 15 min RT (46%). *e:* $CF_3COOH$, anisole, $CH_2Cl_2$, 20 min 0 °C (68%).

Received: September 28, 1982;
revised: November 8, 1982;
withheld from publication at the author's request [Z 160 IE]
German version: *Angew. Chem. 95* (1983) 755
The complete version of this communication appears in:
*Angew. Chem. Suppl. 1983*, 1035–1044

[5] E. G. Brain, A. Eglington, J. H. C. Nayler, M. J. Pearson, R. Southgate, *J. Chem. Soc. Chem. Commun. 1972*, 229.
[7] R. J. Stoodley, *Proc. Seventh Workshop Conf. Hoechst, Schloss Reisenburg* 1978, p. 193; R. J. Stoodley in J. Elks: *Recent Advances in the Chemistry of β-Lactam Antibiotics*, Chem. Soc. Spec. Publ. No. 28 (1977) p. 189.
[8] T. Aoki, M. Yoshioka, S. Kamata, T. Konoike, N. Haga, W. Nagata, *Heterocycles 15* (1981) 409.
[9] R. B. Woodward, K. Heusler, J. Gostelli, P. Naegeli, W. Oppolzer, R. Ramage, S. Ranganathan, H. Vorbrüggen, *J. Am. Chem. Soc.* **88** (1966) 852.
[10] Y. Hamashima, S. Yamamoto, S. Uyeo, M. Yoshioka, M. Murakami, H. Ona, Y. Nishitani, W. Nagata, *Tetrahedron Lett. 1979*, 2595.
[11] Y. Maki, N. Mitsumori, M. Sako, M. Suzuki, *J. Chem. Soc. Perkin Trans. 1* (1981) 2087.

## The Photooxygenation of Estrogens: a New Synthesis of 19-Norsteroids

By *Pilar Lupón, José Gómez,* and *Juan-Julio Bonet**

*Dedicated to Professor Günther O. Schenck on the occasion of his 70th birthday*

Since the pioneering work of *G. O. Schenck*, photooxygenation has been widely used as the key step of many organic syntheses[3], some of which have been conducted

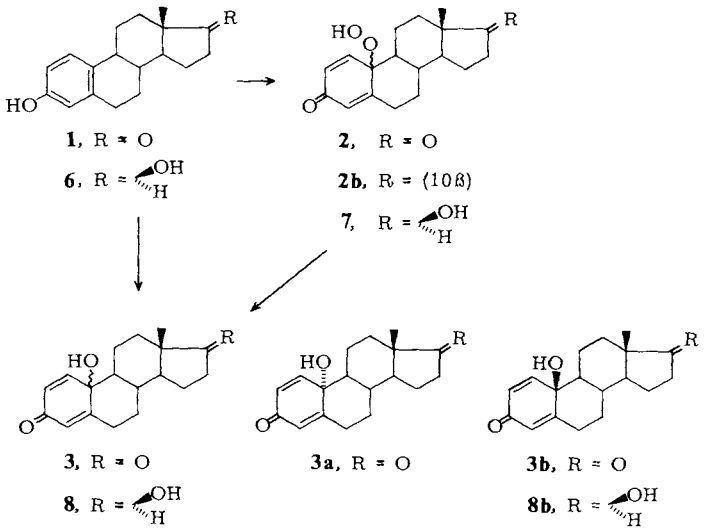
[*] Dr. D. Häbich
Chemisch-wissenschaftliches Labor Pharma der Bayer AG
Postfach 101709, D-5600 Wuppertal 1 (Germany)

[*] Prof. Dr. J.-J. Bonet, Dr. J. Gómez, P. Lupón
Department of Organic Chemistry
Instituto Químico de Sarriá
Barcelona-17 (Spain)

even on a technical scale. Classical examples are the synthesis of the anthelmintic ascaridole by 1,4-cycloaddition of singlet oxygen to α-terpinene[5], and the ene-reaction between citronellol and singlet oxygen to form rose oxide[6].

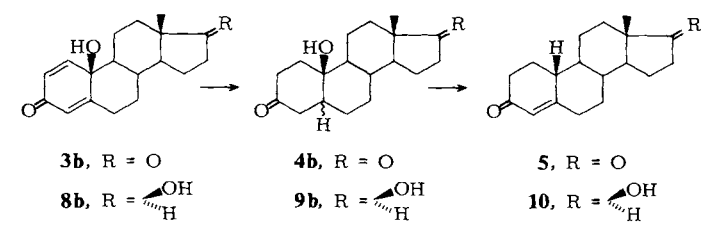
We now report a new application of photooxygenation to the synthesis of 19-norsteroids. These compounds, of considerable importance due to their biological activity, have been traditionally prepared by Birch reduction of estradiol derivatives[8]—a very remarkable procedure that, nevertheless, has some limitations[8].

Our procedure is based on the known photooxygenation of *p*-substituted phenols to the corresponding 4-hydroperoxy-2,5-cyclohexadienones[12], which we have applied to the synthesis of estrogens. The main advantages of this reaction are that it can be carried out directly with the free phenols; that no solubility problems arise; that keto groups remain unchanged; and that the operation is simple, affording the required products in good yield.




Scheme 1.

The photosensitized oxygenation of estrone **1** in methanol using rose bengal as sensitizer led to a mixture of hydroperoxide **2** and alcohol **3** (Scheme 1), which was separated by silica gel chromatography: estradiol **6** was photooxygenated under the same conditions to give **7** and **8**. The isolated hydroperoxides **2** and **7** are white crystalline solids which decompose slowly at room temperature; the alcohols **3** and **8** are stable white crystalline solids. Reduction of the crude mixtures of the photooxygenation of **1** and **6** with iodine in methanol yielded, preferentially, the alcohols **3b** (76%) and **8b** (78%), respectively; with **1** the less stable 10α-isomer **3a** (2.5%) was also isolated as a minor component. Yields are not optimized.




Scheme 2.

Transformation of the unsaturated alcohols into 19-norsteroids was carried out in two steps (Scheme 2). Catalytic hydrogenation ($PtO_2$) of **3b** and **8b** afforded in practically quantitative yield the saturated alcohols **4b** and **9b**, respectively. Dehydration of solutions of **4b** and **9b** in methanol was carried out in the presence of perchloric acid (70%) as catalyst on silica gel at 90°C. In this way, 19-nor-4-androstene-3,17-dione **5** and 19-nortestosterone **10** were obtained in 51% and 60% yield, respectively (not optimized).


Received: April 27, 1983;
revised: July 4, 1983 [Z 362 IE]
German version: *Angew. Chem. 95* (1983) 757
The complete manuscript of this communication appears in:
*Angew. Chem. Suppl. 1983*, 1025–1034



[3] A. Schönberg, G. O. Schenck, O.-A. Neumüller, *Preparative Organic Photochemistry*, Springer, Berlin 1968.
[5] G. O. Schenck, K. Ziegler, *Naturwissenschaften 32* (1944) 157.
[6] F. Ohloff, E. Klein, G. O. Schenck, *Angew. Chem. 73* (1961) 578.
[8] H. L. Dryden, Jr., "Reductions of Steroids by Metal-Ammonia Solutions", in J. Fried, J. A. Edwards: *Organic Reactions in Steroid Chemistry*, Vol. 1, Van Nostrand Reinhold, New York 1972; F. J. Kakis, "The Birch Reduction and the Partial Synthesis of 19-Norsteroids", in C. Djerassi: *Steroid Reactions*, Holden-Day, San Francisco 1963.
[12] I. Saito, T. Matsuura, "The Oxidations of Electron-Rich Aromatic Compounds", in H. H. Wasserman, R. W. Murray: *Singlet Oxygen*, Academic Press, New York 1979.

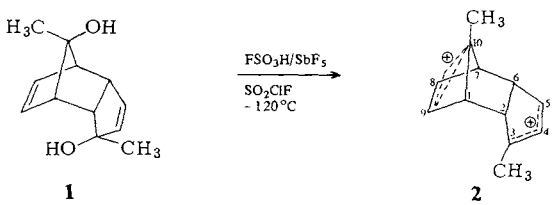

## The *endo*-3,10-Dimethyltricyclo[5.2.1.$0^{2,6}$]deca-4,8-dien-3,10-diyl Dication, A Novel Bishomoaromatic/Allylic Dication and its Rearrangement to the Symmetrical *cis-anti-cis*-3,10-Dimethyltricyclo[5.3.0.$0^{2,6}$]deca-4,8-dien-3,10-diyl Dication**


By *George A. Olah**, *Massoud Arvanaghi*, and *G. K. Surya Prakash*


Although the chemistry of carbocations has largely been confined to the study of carbomonocations, interest in carbodications is growing rapidly. Several intriguing experimental and theoretical studies have been undertaken on carbodications, including classical carbodications with three-coordinate C atoms and non-classical carbodications with hexacoordinate C atoms[1].

In our continued interest in carbodications, we now report the generation and NMR spectroscopic study of *endo*-3,10-dimethyltricyclo[5.2.1.$0^{2,6}$]deca-4,8-dien-3,10-diyl dication **2**, a novel bishomoaromatic, allylic dication.

Dissolution of a slurry of 3-*exo*-10-*syn*-dimethyltricyclo[5.2.1.$0^{2,6}$]deca-4,8-diene-3,10-diol **1**[2] in $SO_2ClF$ in $FSO_3H:SbF_5/SO_2ClF$ at −120°C (liquid nitrogen/ethanol slush bath) resulted in a dark orange solution.



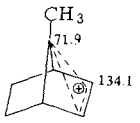


[*] Prof. Dr. G. A. Olah, Dr. M. Arvanaghi, Dr. G. K. S. Prakash
Hydrocarbon Research Institute and Department of Chemistry
University of Southern California, Los Angeles, CA 90089 (USA)

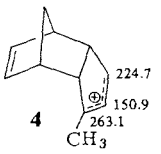


[**] Stable Carbocations. Part 248. Support of our work by the National Science Foundation and the National Institutes of Health is gratefully acknowledged. Presented at the 185th National Meeting of American Chemical Society, Organic Division, Seattle, WA, March 1983.

The $^{13}$C-NMR spectrum of the resulting solution exhibited twelve major absorptions (Table 1). Based on the chemical shifts and multiplicities the ion is unequivocally assigned the dicationic structure **2**. The dication has a bishomoaromatic/allylic dication framework, and the observed chemical shifts correspond closely to those of the monocations **3**[3a] and **4**[3b]; however, the bishomoaromatic moiety in **2** is unsymmetrical. The observed $^1$H-NMR spectrum is also compatible with structure **2** (Table 1). **2** is stable only below $-100\,^\circ$C; at higher temperatures it slowly rearranges irreversibly to a new species.




**3**




**4**

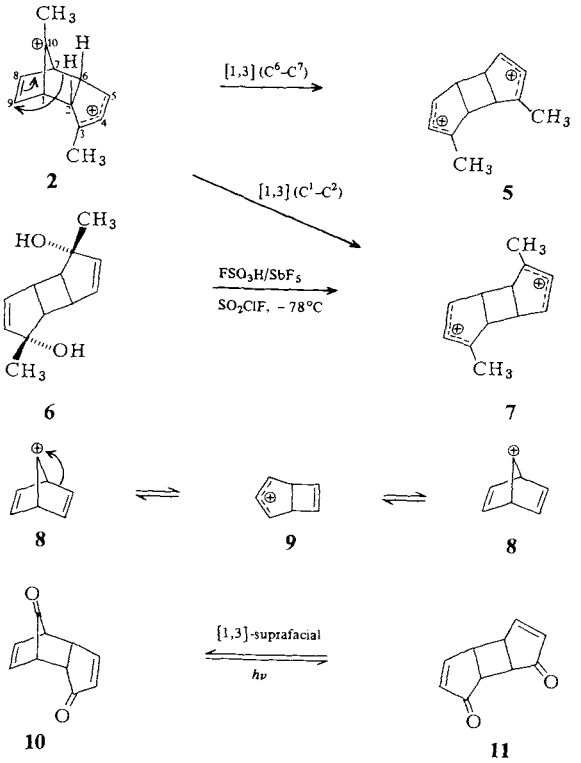
Warming a solution of **2** to $-40\,^\circ$C results in formation of a species with only six absorptions in the $^{13}$C-NMR spectrum, indicating the formation of a very symmetrical dicationic system. The observed chemical shifts and multiplicities suggest formation of a tertiary bisallylic dication. The $^1$H-NMR chemical shifts in the allylic region at $\delta = 9.25$ and 8.12 also corroborate this structure. The rearrangement of the unsymmetrical dication **2** to a symmetrical new dicationic system can occur *via* a 1,3-sigmatropic shift. In fact, a 1,3-shift of either the $C^6$–$C^7$ bond or the $C^1$–$C^2$ bond results in two symmetrical bisallylic tertiary dicationic systems **5** or **7**. The structure of the rearranged species is unequivocally assigned to the *cis-anti-cis*-3,10-dimethyltricyclo[5.3.0.0$^{2,6}$]deca-4,8-dien-3,10-diyl dication **5**: formation of *cis-anti-anti*-dication **7** was excluded by its independent synthesis involving ionization of the 3,8-diol **6**[4] in $FSO_3H/SO_2ClF$ at $-78\,^\circ$C. It appears that the $C^6$–$C^7$ bond migrates preferentially since it is farther from the tertiary allylic cationic center than the $C^1$–$C^2$ bond. There is precedence for similar rearrangements in the literature: the 7-norbornadienyl cation **8** undergoes rapid 1,2-sigmatropic shift (through the intermediacy of bicyclo[3.2.0]heptadienyl cation **9**), resulting in scrambling of carbon and hydrogen atoms[5a]. The photochemical conversion of tricyclic diendione **10** into *cis-anti-cis*-tricyclic dienedione **11** has also been reported[5b], although we were unable to reproduce this result satisfactorily.

Dications **5** and **7** show similar $^{13}$C-NMR chemical shifts, although there are some apparent differences in the chemical shifts of the allylic carbon atoms. This is as a consequence of the separation of the tertiary cationic centers by only two C atoms in **5**, compared to three C atoms in **7**.

Table 1. $^{13}$C- and $^1$H-NMR spectroscopic data of the tricyclic carbodications **2**, **5**, and **7** [a].

| Dication | $\delta(^{13}C)$ | $\delta(^1H)$ |
|---|---|---|
| **2** | 263.6 (C-3), 220.5 (C-5), 152.1 (C-4), 132.9 (C-9), 131.5 (C-8), 89.4 (C-10), 63.2 (C-2), 60.5 (C-6), 58.6 (C-1), 52.3 (C-7), 30.5 (3-$CH_3$), 13.2 (10-$CH_3$) | 9.8 (d, $J$=5.0 Hz, H-5), 7.82 (d, $J$=5.0 Hz, H-4), 7.16 (br., H-8,9), 5.02 (br., H-2,6), 4.58 (m, br., H-1,7), 3.37 (s, 3-$CH_3$), 2.13 (s, 10-$CH_3$) |
| **5** | 256.4 (C-3,10), 207.2 (C-5,8), 156.8 (C-4,9), 58.6 (C-1,2), 55.6 (C-6,7), 28.7 ($CH_3$) | 9.25 (d, $J$=4.7 Hz, H-5,8), 8.12 (m, br., H-4,9), 5.46 (m, H-1,2,6,7), 3.35 (s, $CH_3$) |
| **7** | 261.00 (C-3,8), 217.1 (C-5,10), 151.7 (C-4,9), 57.3 (C-2,7), 54.4 (C-1,6), 28.4 ($CH_3$) | |

[a] Chemical shifts relative to ext. tetramethylsilane.




Received: April 6, 1983 [Z 333 IE]
German version: *Angew. Chem. 95* (1983) 726

[1] Review: G. K. S. Prakash, T. N. Rawdah, G. A. Olah, *Angew. Chem. 95* (1983) 356; *Angew. Chem. Int. Ed. Engl. 22* (1983) 390.
[2] The diol was prepared by the addition of methyllithium to the *endo*-tricyclo[5.2.1.0$^{2,6}$]deca-4,8-diene-3,10-dione in diethyl ether.
[3] a) G. A. Olah, G. Liang, *J. Am. Chem. Soc. 97* (1975) 6803; b) G. A. Olah, G. K. S. Prakash, G. Liang, *J. Org. Chem. 41* (1976) 2820.
[4] The diol was prepared by the addition of methyllithium to *cis-anti-anti*-tricyclo[5.3.0.0$^{2,6}$]deca-4,9-diene-3,8-dione. The dienedione was prepared from cyclopentenone in five steps following the procedure of P. E. Eaton (*J. Am. Chem. Soc. 84* (1962) 2344). Attempts to prepare the *cis-anti-cis*-diendione **11** by a similar procedure were, however, unsuccessful.
[5] a) R. K. Lustgarten, M. Brookhart, S. Winstein, *J. Am. Chem. Soc. 89* (1967) 6350; b) U. Klinsmann, J. Gauthier, K. Schaffner, M. Pasternak, B. Fuchs, *Helv. Chim. Acta 55* (1972) 2643.

## Organometallic Variants of the Wittig Reaction: Synthesis and Structure of *trans*-μ-(2-5; 8-11-η-Dodecapentaene)bis(tricarbonyliron)**

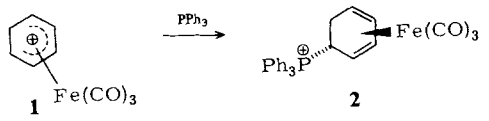
By *Andreas Hafner, Jost H. Bieri, Roland Prewo, Wolfgang von Philipsborn,* and *Albrecht Salzer**

Cationic metal complexes of type **1** react readily with nucleophiles, which generally attack the dienyl system at the terminal carbon atom and approach from the *anti*-side. The synthetic potential of this reaction has been exploited[1]. Using tertiary phosphanes, metal-coordinated

[*] Priv.-Doz. Dr. A. Salzer
Anorganisch-chemisches Institut der Universität
Winterthurerstrasse 190, CH-8057 Zürich (Switzerland)
Prof. Dr. W. von Philipsborn, A. Hafner, Dr. J. H. Bieri, R. Prewo
Organisch-chemisches Institut der Universität Zürich

[**] Reactions with Metal-Coordinated Olefins, Part 2.—Part 1: [2b].

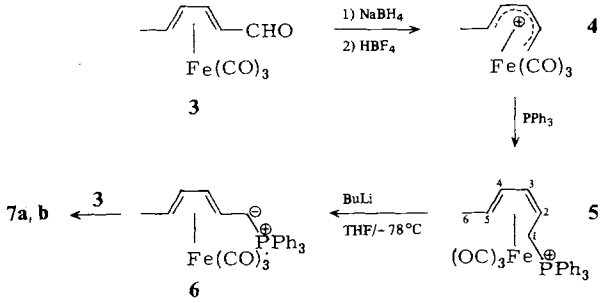
phosphonium derivatives of type **2**[2a], which are hardly accessible by other routes, are formed quantitatively.




**1** **2**

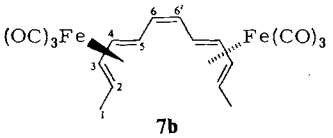
They can be oxidatively decomplexed[2b]; **2** itself cannot be converted into a stable ylide[2a]. This occurs only when dimethyl(phenyl)phosphane is used[2c].

Our investigations now indicate that reaction of acyclic dienyl systems such as **4**[1] with triphenylphosphane and subsequent deprotonation with n-butyllithium lead to formation of stable deep-red solutions of ylide complex **6**, which smoothly undergo a Wittig reaction with **3**[3] to form the two isomeric polyene complexes **7a** and **7b** in the ratio 1:3[4].




**3** **6**

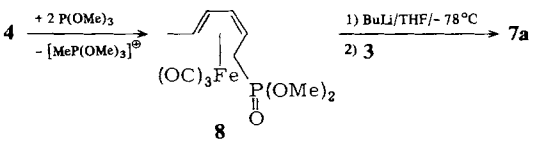
The products **7a** and **7b** have the empirical formula $C_{12}H_{16}Fe_2(CO)_6$; their $^{13}$C-NMR spectra are consistent with symmetrical structures with four coordinated and one non-coordinated double bond[4]. Because of the symmetry and the fixed (*E,E*)-configuration of **3**, they can, therefore, only differ in configuration at C-6, C-6′. On the basis of the coupling $^3J$(*C*-5, *H*C-6′), obtained from selectively {$^1$H}-decoupled $^{13}$C-INEPT spectra, we assign an (*E*)-configuration to **7a** and, in contrast, a (*Z*)-configuration to **7b** for the middle double bond.




**7b**

Both molecules have two (degenerate) chiral moieties; they therefore occur as an enantiomeric pair or as a *meso*-form. No stereochemical assignment can be made from the spectroscopic data of **7a** and **7b**; however, it appears that both molecules most probably have a *transoid* arrangement of the two $Fe(CO)_3$ groups. This is confirmed for **7a** by X-ray structure analysis (Fig. 1). The polyene chain is almost planar, but exhibits the usual slight distorsion of the terminal CC bonds of complexed *s-cis*-dienes.

Compounds **7a** and **7b** are, on the whole, air-stable and even at higher temperatures are configurationally stable.




**8**

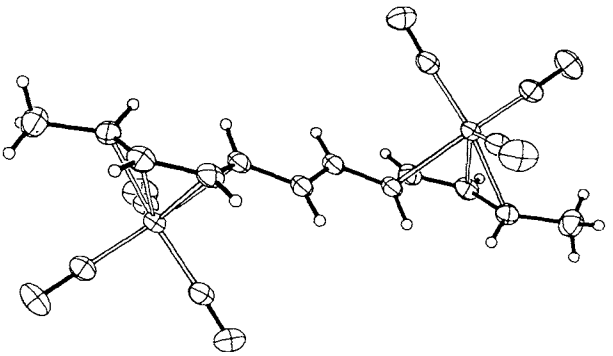


Fig. 1. Molecular structure of complex **7a** in the crystal. Structural data (at ca. −140 °C): $P2_1/c$; $a = 7.389(1)$, $b = 12.230(1)$, $c = 11.923(1)$ Å, $\beta = 117.83(1)°$, $Z = 2$; 3448 symmetry-independent reflections; $(\sin\theta)/\lambda \leq 0.76$ Å$^{-1}$; $R = 0.036$, no absorption correction. Further details on the crystal structure investigation can be obtained from the Fachinformationszentrum Energie Physik Mathematik, D-7514 Eggenstein-Leopoldshafen by quoting the depository number CSD 50485, the names of the authors, and the journal citation.

They are moderately soluble in aliphatic solvents, but readily soluble in toluene or $CHCl_3$. Deprotonation of **5** with potassium *tert*-butoxide affords **7a**, exclusively, just as in the Wittig-Horner variant, which upon reaction of **4** with trimethyl phosphite and subsequent spontaneous Michaelis-Arbuzov reaction of the primary adduct leads to **8**.

The Wittig carbonyl olefination is a key reaction in preparative organic polyene chemistry[5a,b], but is also occasionally used to extend the chain length of diene-$Fe(CO)_3$ complexes[5c]. The reactions described here differ from conventional methods in three ways:

1. The reaction of cationic dienyl-$Fe(CO)_3$ complexes with triphenylphosphane or trimethylphosphite affords in regeiospecific addition otherwise only difficultly accessible dienylphosphonium salts or dienylphosphonates.
2. The *cisoid*-ylides formed initially upon deprotonation of **5** or **8** are apparently unstable; they isomerize completely at C-2. In fact, **5** rearranges to the isomeric (*E,E*)-phosphonium complex with deuteration at C-1 in the presence of catalytic amounts of $CD_3ONa$ in $CD_3OD$[2b]. Cyclic systems such as **2** do not have this stabilization possibility and cannot, therefore, be converted into stable ylides at the complex.
3. Formation of the ylide from **5** using *n*BuLi and subsequent reaction with **3** do not lead to the high (*E*)-selectivity normally observed, but to the preferred formation of the (*Z*)-isomer. Use of *t*BuOK as described by *Schlosser*[5d], in turn unexpectedly affords exclusively the (*E*)-isomer **7a**. In contrast, the Wittig-Horner reaction displays the normal (*E*)-selectivity[5b].

Received: April 28, 1983 [Z 364 IE]
German version: *Angew. Chem. 95* (1983) 736

[1] Cf. *Nachr. Chem. Tech. Lab. 30* (1982) 706; A. J. Birch, I. D. Jenkins in H. Alper: *Transition Metal Organometallics in Organic Synthesis*, Vol. *1*, Academic Press, New York 1976.

[2] a) J. Evans, D. V. Howe, B. F. G. Johnson, J. Lewis, *J. Organomet. Chem. 61* (1973) C48; b) A. Hafner, A. Salzer, *Helv. Chim. Acta*, in press; c) G. Jaouen, B. F. G. Johnson, J. Lewis, *J. Organomet. Chem. 231* (1982) C21.

[3] *Gmelin Handbook of Inorganic Chemistry*, Organoiron Compounds, Part *B 6*, Springer, Berlin 1981.

[4] **7a** and **7b** separated using Lobar chromatography: LiChroprep Si 60 (15–25 μm), heptane. $^{13}$C-NMR (25.2 MHz, 25 °C, $CDCl_3$, int. TMS,

proton noise decoupled): **7a**: $\delta(CH_3)=19.2$, $\delta$(C-2)=57.0, $\delta$(C-3,4)=80.8, 85.0, $\delta$(C-5)=62.1, $\delta$(C-6)=132.4; **7b**: $\delta(CH_3)=19.3$, $\delta$(C-2,5)=56.2, 57.5, $\delta$(C-3,4)=82.4, 85.9, $\delta$(C-6)=131.7.

[5] a) H. Pommer, *Angew. Chem. 89* (1977) 437; *Angew. Chem. Int. Ed. Engl. 16* (1977) 423; b) H. J. Bestmann, *Pure Appl. Chem. 51* (1979) 515; c) R. C. Kerber in E. A. Koerner von Gustorf, F. W. Grevels, I. Fischler: *The Organic Chemistry of Iron*, Vol. 2, Academic Press, New York 1981; d) M. Schlosser, K. F. Christmann, *Liebigs Ann. Chem. 708* (1967) 1.

## Inclusion Complexes between a Macrocyclic Host Molecule and Aromatic Hydrocarbons in Aqueous Solution

By *François Diederich** and *Klaus Dick*

We are interested in cyclophane-like macrocycles which possess a hydrophobic cavity of definite size and which permit the formation of stoichiometric inclusion complexes with apolar substrates in aqueous solution at room temperature at pH ≈ 7[2]. The key reaction in the synthesis of the novel host molecule **1** is the cyclization of two equivalents each of **7** and **8** to the macrocycle **9**, which proceeds in 18% yield; **1** is obtained in good yield after four subsequent steps[3]. Over the range $2\times10^{-4}$—$7\times10^{-3}$ M, the $^1$H-NMR signals of **1** in $D_2O$ (303 K, see Table 1) are independent of concentration and are highly resolved. The critical micellar concentration (CMC) of **1** in water was found to be $7.5\times10^{-3}$ M by $^1$H-NMR spectroscopy.

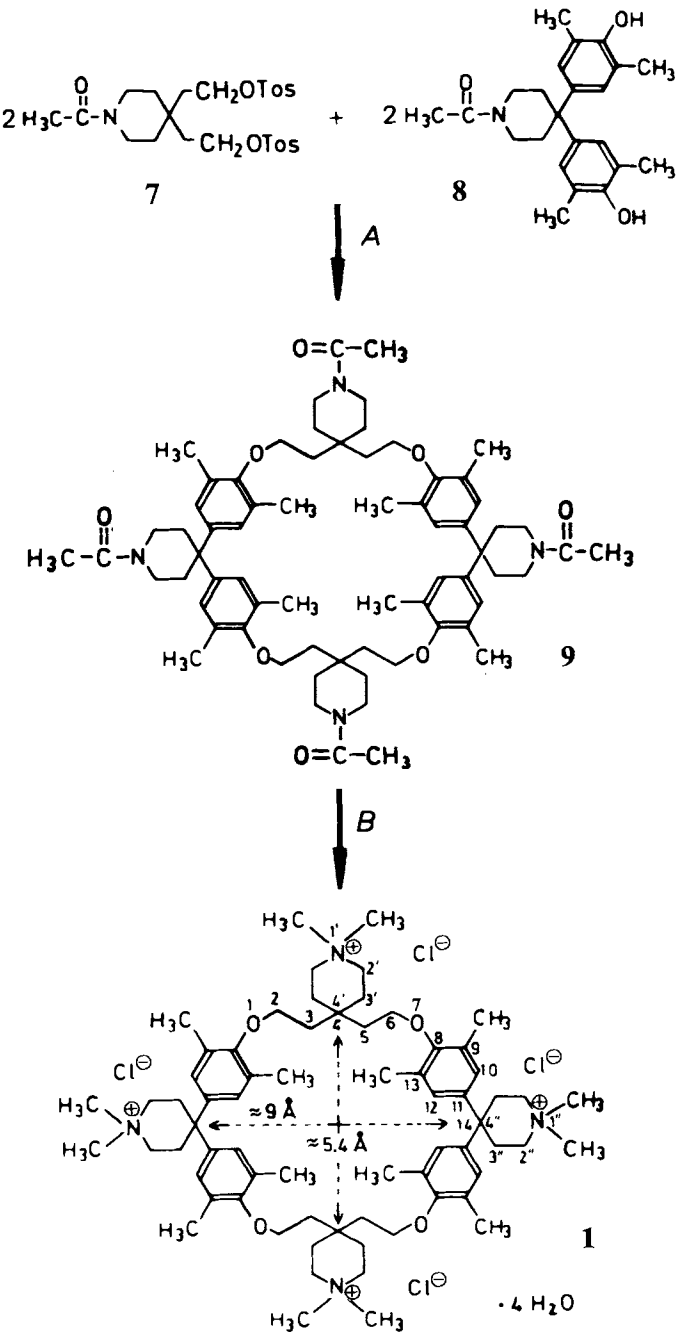
If a suspension of solid pyrene prepared by ultrasonification is stirred or shaken with a $2\times10^{-5}$ M aqueous solution of **1** and then centrifuged and filtered, the solution exhibits the intense fluorescence of monomeric pyrene.

In this solid-liquid extraction an inclusion complex between pyrene and **1**, which possesses a hydrophobic cavity of complementary size, is formed. A solution of **13** (with smaller cavity) is considerably less effective. A $2\times10^{-5}$ M solution of γ-cyclodextrin has an even weaker effect, and a $2\times10^{-4}$ M solution of **12** produces no increase in fluorescence intensity compared to the extraction with water.

Aqueous solutions of the complex of **1**-pyrene can also be prepared by liquid-liquid extraction: *e.g.* a $10^{-2}$ M solution of pyrene in *n*-heptane is shaken with a $2\times10^{-5}$ M aqueous solution of **1**.

Multiple extraction of an aqueous solution of the **1**-pyrene complex with *n*-hexane results in quantitative transfer of pyrene into the organic phase; the concentration of **1** before complex formation can be determined from the absorption spectrum of the aqueous phase. The concentration of the complex is obtained from the concentration of pyrene in the organic phase on consideration of the solubility of pyrene in water[10]. Using a $5.5\times10^{-3}$ M solution of **1**, a concentration of complex of $2.9\times10^{-3}$ M was achieved.

Evidence for the 1:1-stoichiometry and information about the geometry of the **1**-pyrene complex in aqueous solution were obtained by $^1$H-NMR spectroscopy (Table 1). The large difference in chemical shift between the solution of the complex and the solutions of the components can best be explained by the following favored geometry of the complex: the long pyrene $C_2$-axis through C(2) and C(7) lies along the direction of the $C_2$-axis passing through the cavity of **1** perpendicular to the mean molecular plane.




*A:* KOH, [18]crown-6, tetrahydrofuran, 48 h, 65°C, 18%; *B:* 1) NaOH, $CH_3OCH_2CH_2OH$, 124°C, 85%; 2) HCHO, HCOOH, 100°C, 91%; 3) $FSO_3CH_3$, $CHCl_3$, 25°C, 82%; 4) Dowex 1×8 $Cl^\ominus$, 79%.

Pyrene only then fits completely into the cavity if its short $C_2$-axis, which intersects the C(4)—C(5) and C(9)—C(10) bonds, runs in the direction of the $C_2$-axis of **1** through the spiro carbon atoms of the two diphenylmethane moieties. In this way, H-2,7 of pyrene project out of the cavity and are shifted to the smallest extent; in contrast, H-1,3,6,8 and H-4,5,9,10 are directed towards the diphenylmethane moieties and are shifted markedly to high field.

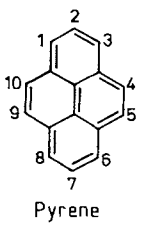
The proposed geometry for the complex is corroborated by the low-field shift of the protons of **1** in the pyrene molecular plane and by the high-field shift of the protons perpendicular to this plane. The unexpected high-field shift of H-2′ and N(1′)—$CH_3$ can be explained by the conformational mobility of the $C_5$ bridges bearing the piperidinium

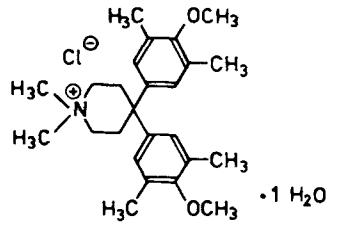
[*] Dr. F. Diederich, K. Dick
Abteilung Organische Chemie
Max-Planck-Institut für Medizinische Forschung
Jahnstrasse 29, D-6900 Heidelberg 1 (Germany)

Table 1. $^1$H-NMR spectra (360 MHz) of the complex **1**-pyrene in $D_2O$ ([**1**] = $5.5 \times 10^{-3}$ M, [**1**-pyrene] = $2.9 \times 10^{-3}$ M; $\delta$ relative to sodium 2,2,3,3-tetradeuterio-3-(trimethylsilyl)propionate (TSP) in $D_2O$ as ext. standard) and, for comparison, of pyrene ($\delta$ relative to $TSP_{ext.}$ in [$D_4$]methanol) and **1** ([**1**] = $2 \times 10^{-4}$—$7 \times 10^{-3}$ M, $\delta$ relative to $TSP_{ext.}$ in $D_2O$]). $J$ in Hz.

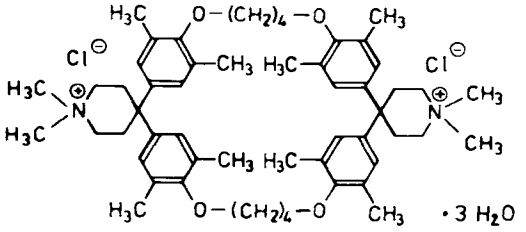
| | Pyrene in [$D_4$]Methanol | | Complex **1**-Pyrene in $D_2O$ | |
|---|---|---|---|---|
| | *303 K* | | *303 K* | *353 K* |
| H-1 | 8.21 (d, $J$=7.6, 4H) | | 7.19 (d, $J$=7.5, 4H) | 7.19 |
| H-2 | 8.02 (t, $J$=7.6, 2H) | | 7.58 (t, $J$=7.5, 2H) | 7.54 |
| H-4 | 8.10 (s, 4H) | | 6.95 (s, 4H) | 6.95 |
| | **1** in $D_2O$ | | | |
| | *303 K* | *353 K* | | |
| H-3′ | 1.87 (m, 8H) | 1.87 | 1.13 (m, br, 8H) | 1.17 (m, 8H) |
| H-3 | 1.96 ("t", $J$=7, 8H) | 1.96 | 1.47 (m, br, 8H) | 1.45 ("t", $J$=7.5, 8H) |
| Aryl-$CH_3$ | 2.08 (s, 24H) | 2.08 | 2.10 (s, 24H) | 2.09 (s, 24H) |
| H-3″ | 2.73 (m, 8H) | 2.68 | [a] | 2.86 (m, 8H) |
| N(1′)-$CH_3$ | 3.16 (s, 24H) | 3.15 | 2.96 (s, 12H) | 2.96 (s, 12H) |
| N(1″)-$CH_3$ | | | 3.18 (s, 12H) | 3.17 (s, 12H) |
| H-2′ | 3.43 (m, 16H) | 3.41 | [a] | 2.94 (m, 8H) |
| H-2″ | | | 3.50 (m, 8H) | 3.48 ("t", $J$=5.2, 8H) |
| H-2 | 3.88 ("t", $J$=7, 8H) | 3.88 | [a] | 3.10 ("t", $J$=7.5, 8H) |
| H-10 | 7.01 (s, 8H) | 6.95 | 7.30 (s, br, 8H) | 7.23 (s, 8H) |

[a] These signals are very broad and collapse at $\delta$ = 2.6—3.1.




**12**




**13**

rings which, favored by additional hydrophobic interactions, can approach the pyrene. In contrast to the highly resolved pyrene signals between 273 and 353 K, the signals of **1** in the complex are very broad below 333 K. This probably arises from the exchange of pyrene on the $^1$H-NMR time scale with the host molecules present in excess[16].

By analogy, inclusion complexes were prepared from **1** and water-insoluble aromatic hydrocarbons such as perylene, fluoranthene, naphthalene, and durene. $^1$H-NMR and optical spectra confirm the results obtained from the complexation of pyrene.

Received: April 28, 1983 [Z 363 IE]
German version: *Angew. Chem. 95* (1983) 730
The complete manuscript of this communication appears in: *Angew. Chem. Suppl. 1983*, 730

CAS Registry numbers:
**1**, 86765-98-2; **2**, 32161-06-1; **3**, 86748-13-2; **4**, 86748-15-4; **5**, 86748-16-5; **6**, 86748-17-6; **7**, 86748-18-7; **8**, 86748-12-1; **9**, 86748-19-8; **10**, 86748-20-1; **11**, 86748-21-2; **11** · $4FSO_3CH_3$, 86765-97-1; **12**, 86748-22-3; **13**, 86748-23-4; 2,6-dimethylphenol, 576-26-1; ethyl cyanoacetate, 105-56-6; piperidine-4,4-diacetic acid, 86748-14-3; pyrene, 129-00-0; γ-cyclodextrin, 17465-86-0.

[2] F. Diederich, K. Dick, *Tetrahedron Lett. 23* (1982) 3167.
[3] Correct analytical results and appropriate spectra were obtained for these compounds.
[10] A $8 \times 10^{-7}$ M (0.162 mg/L) aqueous solution of pyrene can be prepared at room temperature using the method described; this value, obtained photometrically, is completely consistent with the literature data: H. B. Klevens, *J. Phys. Chem. 54* (1950) 283; W. W. Davis, M. E. Krahl, G. H. A. Clowes, *J. Am. Chem. Soc. 64* (1942) 108.
[16] The $^1$H-NMR experiment was performed using a similar concentration ratio [**1**]:[pyrene] and a concentration of complex of $5.5 \times 10^{-5}$ M (303 K); here, almost identical chemical shifts (e.g. of the pyrene protons at $\delta$ = 7.57, 7.19, and 6.95) and similar line widths for the signals of **1** are obtained—an important piece of evidence for the same complex form at concentrations below the CMC of **1**.

## Synthesis and Reactions of $\eta^5$-Cyclopentadienylbis(ethene)cobalt

By *Klaus Jonas**, *Etienne Deffense*, and *Dietrich Habermann*

Metallocenes react with alkali metals and olefins, with elimination of alkali-metal cyclopentadienides, to give transition metal-olefin or alkali metal-transition metal-olefin complexes[3]. Thus, reaction of cobaltocene ($Cp_2Co$) with potassium and ethene in diethyl ether leads to formation of the bis(ethene) complex **1**.

$$Cp_2Co + K + 2C_2H_4 \xrightarrow[-20 \text{ to } 0\,^\circ C]{Et_2O} \underset{\mathbf{1}}{CpCo(C_2H_4)_2} + KCp$$

This unusually facile entry to **1** (one-step synthesis, yield 85%), whose ethene ligands are readily replaceable, makes **1** a very useful starting material in organometallic chemistry (*cf.* Supplement). Of particular interest are the reactions of **1** with alkynes or nitriles since, with $CpCo(CO)_2$ or $CpCo(C_8H_{12})$ at temperatures $>100\,^\circ C$, cobalt-catalyzed alkyne cyclotrimerization[25] or cocyclization of alkynes and nitriles to afford pyridine derivatives occurs[26].

At $-10\,^\circ C$, **1** reacts with 2-butyne in *n*-hexane to afford a new deep-red complex, which can be recrystallized from boiling *n*-hexane, and which, according to the elemental analysis and mass spectrum, has the composition **9**.

$$\underset{\mathbf{1}}{CpCo(C_2H_4)_2} + 3\,C_2(CH_3)_2 \xrightarrow[-10\,^\circ C]{n\text{-}C_6H_{14}} \underset{\mathbf{9}}{CpCo\{C_6(CH_3)_6\}} + 2C_2H_4$$

The product **9** (yield 46%) was investigated crystallographically but, because of disorder in the crystal lattice, an accurate description of the molecular geometry could not be obtained. However, these results indicate that the cobalt atom in **9** is sandwiched between a cyclopentadienyl ring and a hexamethylbenzene ring[18]. The magnetic moment, $\mu_{eff} = 2.85\,\mu_B$, of solid **9** is almost exactly that expected for two unpaired electrons according to the spin-only formula. We assume, therefore, that **9** exists as $\eta^5$-$C_5H_5Co$-$\eta^6$-$C_6(CH_3)_6$, which is isoelectronic with the cation of $[\{C_6(CH_3)_6\}_2Co]PF_6$[27], and in which the krypton electronic configuration is exceeded by two electrons. This probably accounts for the ease of displacement of the hexamethylbenzene ligand, *e.g.*, with CO, and why **9** is the first reported $(C_5H_5)Co$-compound that can catalyze the cyclotrimerization of alkynes and cocyclization of alkynes and nitriles at *room temperature*.

[*] Priv.-Doz. K. Jonas, Dr. E. Deffense, Dr. D. Habermann
Max-Planck-Institut für Kohlenforschung
Postfach 01 13 25, D-4330 Mülheim an der Ruhr 1 (Germany)

$$CpCo\{C_6(CH_3)_6\} \xrightarrow[20\,^\circ C]{CO\ (1\ atm.)} CpCo(CO)_2 + C_6(CH_3)_6$$

**9**

$$3\,C_2H_2 \xrightarrow[20\text{–}40\,^\circ C]{9} C_6H_6$$

$$3\,C_2(CH_3)_2 \xrightarrow[20\,^\circ C]{9} C_6(CH_3)_6$$

$$2\,C_2H_2 + C_2H_5CN \xrightarrow[20\text{–}40\,^\circ C]{9} C_5H_4NC_2H_5$$

Received: April 25, 1983 [Z 353 IE]
German version: *Angew. Chem. 95* (1983) 729
The complete version of this communication appears in:
*Angew. Chem. Suppl. 1983, 1005–1016*

[3] K. Jonas, C. Krüger, *Angew. Chem. 92* (1980) 513; *Angew. Chem. Int. Ed. Engl. 19* (1980) 520.
[18] C. Krüger *et al.*, unpublished results.
[25] K. P. C. Vollhardt, *Acc. Chem. Res. 10* (1977) 1.
[26] H. Bönnemann, *Angew. Chem. 90* (1978) 517; *Angew. Chem. Int. Ed. Engl. 17* (1978) 505.
[27] E. O. Fischer, H. H. Lindner, *J. Organomet. Chem. 1* (1964) 307; M. R. Thompson, C. S. Day, V. W. Day, R. I. Mink, E. L. Muetterties, *J. Am. Chem. Soc. 102* (1980) 2979.

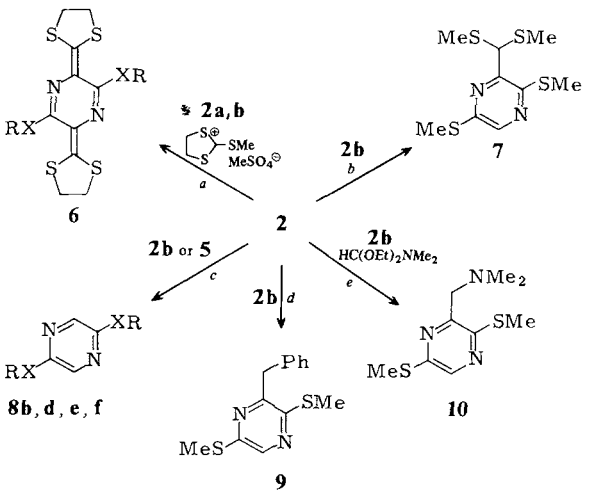
## Diazaquinodimethanes, Donor-Substituted Pyrazines, and Dihydropyrazines**

By *Rudolf Gompper** and *Walter Breitschaft*

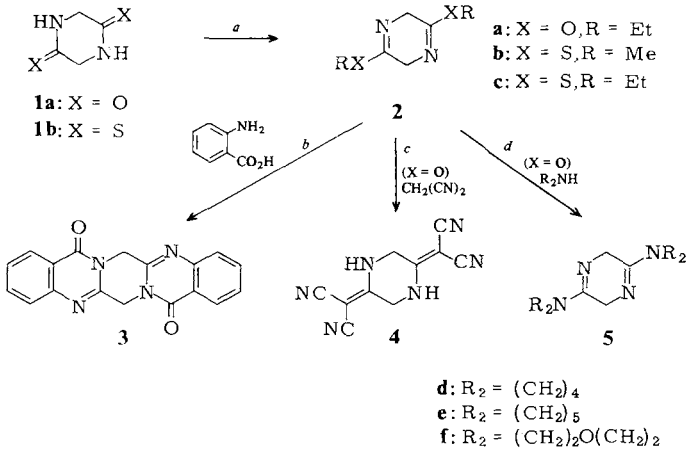
*Dedicated to Professor Harald Jensen on the occasion of his 60th birthday*

Previously, the influence of ring N-atoms on the properties of quinodimethanes has only been studied with azaquinodimethanes[1a]. With one exception[2a], diazaquinodimethanes have not yet been described. Since diethoxydihydropyrazines can be converted into carbanions[2b], it might be expected that compounds of this type and aryl- and pyridylmalononitriles[1] would react with cyclic carbenium salts to afford diazoquinodimethanes.

The syntheses start from the dihydropyrazines **2** [by analogy to the formation of **2a** from **1a**[3], **2b,c** can be prepared from **1b**; **2b**: yield 77%, m.p. = 103–104 °C; **2c**: 63%, b.p. = 150 °C/0.01 torr, m.p. = 30–32 °C]. The diaminodihydropyrazines **5** are formed from **2a** on reaction with secondary amines [**5d**: 78%, m.p. = 143–144 °C (decomp.); **5e**: 52%, decomp. above 126 °C; **5f**: 48%, m.p. = 165.5 °C (decomp.)]. In the presence of anthranilic acid as the amine component the sparingly soluble 7,15-dihydropyrazino[2,1-*b*:5,4-*b'*]-diquinazoline-5,13-dione **3** [54%, ocher-colored platelets, m.p. = 298 °C] is obtained from **2a,b**. The structure type **3** also occurs in the piperazine derivative **4** (m.p. > 300 °C), which forms almost quantitatively from **2a** and malononitrile. The desired diazaquinodimethanes **6**, which correspond to the bis(ethylenedithio)-*p*-quinodimethanes[4], are formed by reaction of **2** with 2-methylthio-1,3-dithiolanylium methyl sulfate [**6a**: 43%, yellow needles, m.p. = 218–219 °C; **6b**: 21%, orange needles, m.p. = 285 °C (decomp.)]. — Addition of tetrafluoroboric acid-ether to **6a** yields the bis(tetrafluoroborate) of **6a** as a brick-red powder.




*a*: AcOH-pyridine, Δ, 30 min; *b*: 1) 2*n*BuLi, THF, −78 °C, 2) $CS_2$, 3) MeI, −78→25 °C; *c*: chloranil, toluene, Δ, 3 h; *d*: 1) *n*BuLi, THF, −78 °C, 2) PhCHO, 3) AcOH, −78→25 °C, 4) 150 °C/0.01 bar or benzene, TosOH, Δ; *e*: 130 °C, 1 h.




*a*: 1) $R_3O^{\oplus}BF_4^{\ominus}$, $CH_2Cl_2$, Δ, 3 d, 2) $Na_2HPO_4/NaH_2PO_4$, $H_2O$; *b*: 150–200 °C, 1 h; *c*: 120 °C, 1 h; *d*: $CHCl_3$, toluene or xylene, Δ, 15–60 h.

3-Dimethylaminomethyl-2,5-bis(methylthio)pyrazine **10** [42%, yellow oil, b.p. = 170/0.01 torr] is formed upon heating **2b** with *N,N*-dimethylformamide diethyl acetal in dimethylformamide. Apparently, the CH-acidity of **10** is insufficient to cause further reaction to a quinodimethane such as **6**. Also the action of carbon disulfide on the Li salt of **2b** results only in formation of a monoadduct. Methylation of the latter affords 3-[bis(methylthio)methyl]-2,5-bis(methylthio)pyrazine **7** [39%, m.p. = 77–78 °C]. Reaction of the Li salt of **2b** with benzaldehyde proceeds similarly. The 1:1-adduct (not isolated, cf.[3]) formed after hydrolysis can be converted into 3-benzyl-2,5-bis(methylthio)pyrazine **9** (44%, m.p. = 56.5–58.5 °C).

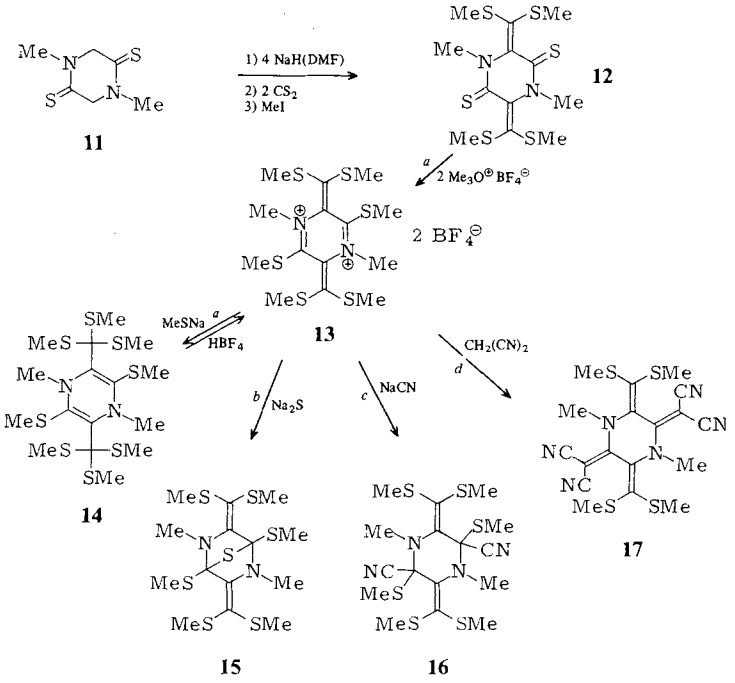
The new compounds **7**, **9**, and **10** are to be considered as electron-rich pyrazines. Further compounds of the general type **8** can be prepared, by analogy to the oxidation of **2a**[3], by heating **2b** and **5d–f** with chloranil in toluene [**8b**: 42%, pale yellow needles, m.p. = 105–107 °C; **8d**: 52%, m.p. = 172.5–173 °C; **8e**: 16%, m.p. = 123–123.5 °C; **8f**: 70%, m.p. = 182–182.5 °C].

The electron acceptor properties of **6** should be increased by twofold quaternization. **6**, however, does not react with alkylating agents. We, therefore, prepared the ketene thioacetal **12** [59%, orange rhomohedra,

[*] Prof. Dr. R. Gompper, W. Breitschaft,
Institut für Organische Chemie der Universität
Karlstrasse 23, D-8000 München 2 (Germany)

[**] This work was supported by the Deutsche Forschungsgemeinschaft and the Fonds der Chemische Industrie.

m.p. = 123—125 °C] from **11**. **12** reacts with trimethyloxonium tetrafluoroborate to yield 3,6-bis[bis(methylthio)methylene]-1,4-dimethyl-2,5-bis(methylthio)3,6-dihydropyrazindium bis(tetrafluoroborate) **13** [83%, orange needles, blackens above 225 °C; UV/VIS ($CH_3CN$): $\lambda_{max}$ (lg $\varepsilon$) = 205 (4.15), 300 (sh, 4.09), 447 nm (4.21)].



*a*: $CH_2Cl_2$, 25 °C, 15 h; *b*: $CH_2Cl_2/H_2O$, 25 °C, 2 h; *c*: $CH_3CN$, 25 °C, 15 h; *d*: pyridine, Δ, 1 h.

**13** contains two ambifunctional azaallyl cation moieties. Heating with malononitrile in pyridine gives the tetrakis(methylene)piperazine derivative **17** [80%, yellow needles, m.p. = 189.5—191 °C; UV/VIS ($CH_3CN$): $\lambda_{max}$ (lg $\varepsilon$) = 225 (4.10), 274 (4.30), 360 nm (4.40)], and this is the product expected from the charge distribution in **13**. The site at which malononitrile attacks the C atom of the C=N bonds is confirmed by the fact that the salt obtained from **12** and triethyloxonium fluoroborate also reacts with malononitrile to afford **17**. In the same way, **13** reacts with sodium cyanide and sodium sulfide to yield **16** [29%, m.p. = 162.5—163 °C] and the episulfide **15** [57%, m.p. = 170.5—171 °C (decomp.)], respectively, which is interesting *inter alia* because of its structural relationship with the 3,6-epithio-2,5-piperazinediones (cf.[5]).

Remarkably, sodium methanethiolate reacts with **13** to give the dihydropyrazine **14** [66%, pale yellow parallelepipeds (from hexane), m.p. = 136—137.5 °C]. In view of the formal antiaromaticity of **14** (cf.[6]), which represents a novel type of stable dihydropyrazines, its great tendency to form is striking. Addition of tetrafluoroboric acid-ether to a solution of **14** in dichloromethane leads to re-formation of **13**.

Received: April 11, 1983 [Z 342/343 IE]
revised: June 6, 1983
German version: *Angew. Chem. 95* (1983) 727

[1] H.-U. Wagner, R. Gompper, *Angew. Chem. 81* (1969) 1004; *Angew. Chem. Int. Ed. Engl. 8* (1969) 986; b) R. Gompper, E. Kutter, H.-U. Wagner, *ibid. 78* (1966) 545; *ibid. 5* (1966) 517; R. Gompper, E. Kutter, H. Kast, *ibid. 79* (1967) 147; *6* (1967) 171.

[2] a) R. E. Bowman, R. J. Islip, J. M. Lockhart, K. E. Richards, M. Wright, *J. Chem. Soc. 1965*, 1080; b) U. Schöllkopf, W. Hartwig, U. Groth, *Angew. Chem. 91* (1979) 922; *Angew. Chem. Int. Ed. Engl. 18* (1979) 863; cfl. also D. Hoppe, *Nachr. Chem. Tech. Lab. 30* (1982) 852.

[3] K. W. Blake, A. E. A. Porter, P. G. Sames, *J. Chem. Soc. Perkin Trans. 1, 1972*, 2494; J. L. Markham, P. G. Sammes, *ibid. 1, 1979*, 1889.

[4] H. Bock, G. Brähler, U. Henkel, R. Schlecker, D. Seebach, *Chem. Ber. 113* (1980) 289.

[5] A. Srinivasan, A. J. Kolar, R. K. Olsen, *H. Heterocycl. Chem. 18* (1981) 1545.

[6] W. Kaim, *Angew. Chem. 95* (1983) 201; *Angew. Chem. Int. Ed. Engl. 22* (1983) 171.

## Photochemistry of Previtamin $D_3$ at 92 K: Formation of an Unstable Tachysterol$_3$ Rotamer**

By *Paul A. Maessen, Harry J. C. Jacobs*, Jan Cornelisse,* and *Egbert Havinga*

*Dedicated to Professor G. O. Schenck on the occasion of his 70th birthday*

The principle of non-equilibration of excited rotamers (NEER)[2] predicts that on irradiation of previtamin $D_3$(P) (at least) two species are generated, *tZc*-P* and *cZc*-P*, each of which yields its specific assortment of photoproducts. As products of *cis/trans*-isomerization, one expects the formation of the *tEc* and *cEc* rotamers of tachysterol$_3$ (T) from *tZc*-P* and *cZc*-P*, respectively (Fig. 1+2).

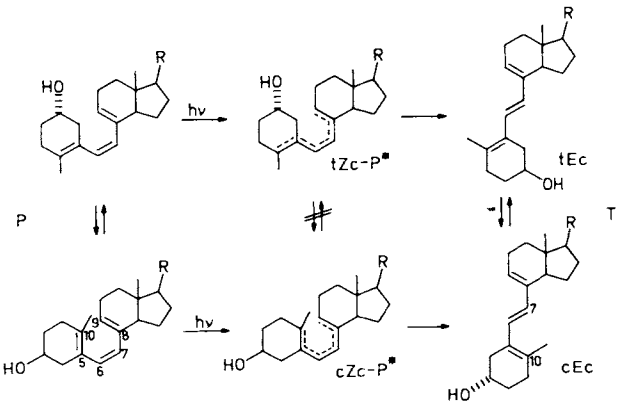


Fig. 1+2 (extract). Non-equilibration of excited rotamers (P*) and photochemical *cis/trans* isomerization of previtamin $D_3$(P) and tachysterol$_3$ (T). R = $CH(CH_3)(CH_2)_3CH(CH_3)_2$.

The *cEc* rotamer, which is destabilized by steric interaction between 10-$CH_3$ and 7-H, can be observed only when the conversion into the more stable *tEc* and *tEt* rotamers is impeded. We, therefore, turned our attention to low-temperature irradiation, and monitored the reaction by UV and CD spectroscopy.

At temperatures down to 125 K the irradiation of previtamin $D_3$ appears to proceed essentially as observed at room temperature, the rapid formation of tachysterol$_3$ being indicated by the characteristic UV[5] and CD absorption spectra. A different behavior is manifest when the ir-

[*] Dr. H. J. C. Jacobs, Dr. P. A. Maessen, Prof. Dr. J. Cornelisse, Prof. Dr. E. Havinga
State University at Leiden, Department of Chemistry
Gorlaeus Laboratories
P. O. Box 9502, NL-2300 RA Leiden (Netherlands)

[**] Studies of Vitamin D and Related Compounds, Part 30.—Part 29: [1].

radiation is conducted at 92 K. Irradiation in ether/isopentane/alcohol 5:5:1 (EPA) solution (Fig. 4) produces a species exhibiting a broad, almost structureless absorption band that is red-shifted relative to the absorption of previtamin $D_3$ and tachysterol$_3$. The Cotton effect is large and negative.

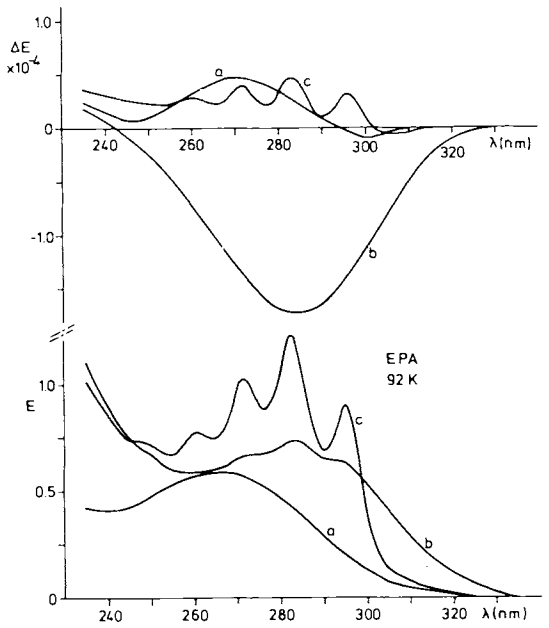



Fig. 4. UV and CD spectra of previtamin $D_3$ (EPA, 92 K). a) Before irradiation; b) after irradiation for 1 to 3 min; c) after irradiation for 1 to 3 min the mixture is warmed to 105 K and then cooled to 92 K.

The spectra remain the same as long as the solution is kept at 92 K in the dark; however, on warming the sample to 100—105 K in the dark, the spectra slowly change and take on the appearance of those of tachysterol$_3$ obtained by irradiation at 125 K. Irradiation at 92 K in the less viscous methylcyclohexane/isopentane 1:5 (MIP) solution proceeds similarly, but the intermediate is less stable and is gradually converted into tachysterol$_3$ upon standing in the dark at 92 K. From the rate of disappearance a free energy of activation of 27 kJ mol$^{-1}$ (6.5 kcal mol$^{-1}$) ± 10% is calculated for the decay process.

The intensity and $\lambda_{max}$ of the UV and CD spectra suggest a conjugated triene; the configuration of the central double bond must be *trans*, since only a low energy barrier separates the intermediate from the *E*-triene tachysterol$_3$. We therefore identify the transient species with the higher-energy *cEc* rotamer of tachysterol$_3$. The activation energy includes a viscosity-dependent contribution, whose value is an upper limit for the intrinsic barrier to twisting about the single bond. It compares favorably with the energy barrier separating s-*cis*- from s-*trans*-butadiene (3.9 kcal mol$^{-1}$)[9]. Similarly, the difference in the UV absorption curves b and c (Fig. 4) corresponds to the change observed upon conversion of s-*cis*- to s-*trans*-butadiene[9].

We note that apart from cyclization *cis/trans* isomerization apparently is an important pathway of relaxation for an excited *cZc* triene. Furthermore, the formation of the *cEc* rotamer as a primary photoproduct in the *cis/trans* isomerization nicely illustrates the operation of the NEER principle in the photochemistry of conjugated polyenes.

Received: May 2, 1983;
revised: August 1, 1983 [Z 371 IE]
German version: *Angew. Chem. 95* (1983) 752
The complete version of this communication appears in:
*Angew. Chem. Suppl. 1983*, 994-1004

[1] H. J. C. Jacobs, J. W. J. Gielen, E. Havinga, *Tetrahedron Lett. 22* (1981) 4013.
[2] E. Havinga, J. L. M. A. Schlatmann, *Tetrahedron 16* (1961) 146; H. J. C. Jacobs, E. Havinga, *Adv. Photochem. 11* (1979) 305.
[5] R. J. de Kock, G. van der Kuip, A. Verloop, E. Havinga, *Recl. Trav. Chim. Pays-Bas 80* (1961) 20; E. Havinga, R. J. de Kock, M. P. Rappoldt, *Tetrahedron 11* (1960) 276.
[9] M. E. Squillacote, R. S. Sheridan, O. L. Chapman, F. A. L. Anet, *J. Am. Chem. Soc. 101* (1979) 3657.

## Regiocontrolled Prenylations and Alkylations of Furans: Preparation of Rosefuran and Novel Analogues**

By *Zeinhom M. Ismail* and *H. M. R. Hoffmann**

Friedel-Crafts alkylation is one of the most important reactions undergone by aromatic rings. In contrast, heteroaromatic systems have been studied less. We have previously obtained a variety of 2-allylfurans by silver-ion promoted heterolysis of allylic iodides in the presence of furans[2], and related work has been reported by other groups[3]. Using improved methodology for generating electrophilic carbon intermediates[4], we now describe novel alkylations of furans **1a**, **b**. It turns out that prenylation[5] of 3-methylfuran **1a** is feasible in one step without polymerization to give rosefuran **3** and the previously unknown isomer **4** (Table 1).

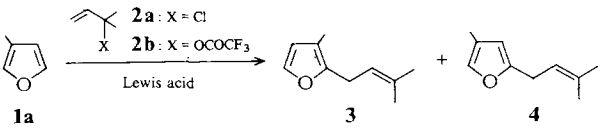



Table 1. Preparation of rosefuran **3** and its isomer (**4**) *via* prenylation of 3-methylfuran **1a**.

| No. | Experimental Conditions | Ratio 3 : 4 | Yield [%] 3 + 4 |
|---|---|---|---|
| 1 | **2a** [a], $AgOCOCF_3$, pentane, RT, 17 h | 80 : 20 | 5 [b] |
| 2 | **2a**, $ZnCl_2 \cdot Et_2O$ [c], $CH_2Cl_2$, −40 °C, 1 h | 80 : 20 | 30 [d] |
| 3 | **2b**, $ZnI_2$, $CH_2Cl_2$, reflux, 2 h | 74 : 26 [e] | 73 |
| 4 | **2b**, $ZnI_2$, $CH_2Cl_2$, RT, 18 h | 89 : 11 [e] | 73 |

[a] A. J. Ultée, *J. Chem. Soc. 1948*, 530. [b] Conversion of 3-methylfuran **1a** was very low, and most of **1a** was recovered. Polymerization of products was not observed. [c] See [5a]. [d] Unidentified products with longer GC retention time were formed also. When the reaction was carried out at room temperature for 10 min, the conversion (**3** + **4**) was 17% (GC). Longer reaction times gave tarry material. [e] Product ratios determined by GC and, independently, by $^1$H-NMR.

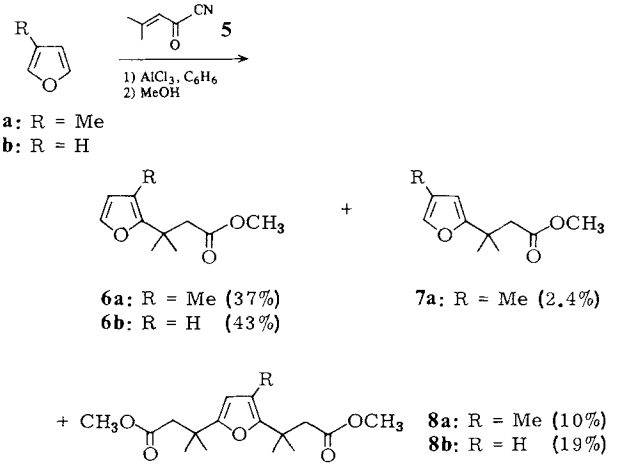
Initial experiments with **2a** and silver trifluoroacetate led to **3** and **4** in low yields (5% after 17 h; cf. Table 1, No.

[*] Prof. H. M. R. Hoffmann, Dr. Z. M. Ismail
Institut für Organische Chemie, Universität Hannover
Schneiderberg 1 B, D-3000 Hannover 1 (Germany)

[**] This work was supported by the Niedersächsische Minister für Wissenschaft und Kunst, the Deutsche Forschungsgemeinschaft, and the Fonds der Chemischen Industrie. We thank Dr. F. J. Hammerschmidt of Dragoco for GC-MS measurements and Dr. E. J. Brunke for the sensory evaluations. Note added in proof (Aug. 12, 1983): After submission of our manuscript, G. A. Kraus and P. Gottshalk (*Tetrahedron Lett. 24* (1983) 2727) reported vinylogous additions of furans to enones mediated by iodotrimethylsilane.

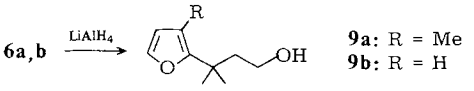
1): apparently, **2a** is not reactive enough. Formation of the desired isomer **3** dominated over that of **4** by the ratio 4:1. The same ratio of isomers was obtained with zinc chloride-ether[5a] (No. 2); although this reaction was carried out at −40°C, some of the product decomposed at longer reaction times. We therefore activated the allylic alcohol by trifluoroacetylation to afford **2b** and found that prenylation was feasible in refluxing dichloromethane (No. 3). Interestingly, on lowering the temperature to 25°C prenylation was more regioselective; formation of **3** was preferred still more (**3**:**4** = 89:11; No. 4). The total isolated yield of **3** + **4** was 73%. Products arising from attack of the tertiary allylic terminus on **1a** were not detected.

We found, however, that tertiary alkyl groups can be introduced into furans by a different method, *i. e.* by reaction with 4-methyl-2-oxo-3-pentenenitrile **5**[7] in the presence of aluminum chloride in benzene (Scheme 1). This reagent is




Scheme 1. Tertiary alkylation of **1a, b** with 4-methyl-2-oxo-3-pentenenitrile 5 in the presence of $AlCl_3$.

more regioselective than the prenylation reagent; the ratio **6a**:**7a** was 94:6. Compound **6a**, which is of the *cis*-jasmone type, has an interesting herbal, sweet, floral odor. **6a** and **6b** have also been reduced to the corresponding alcohols **9a** and **9b**.




The introduction of *functionalized* tertiary alkyl groups into furans by our second procedure goes beyond the recently described introduction of the simple *t*-butyl group[8]. Clearly, decomposition and polymerization need no longer be the necessary result of electrophilic alkylations of furans such as **1a**, **b**. Finally, regioselective control has been achieved both with respect to the site of attack in furan and also with respect to the ambident electrophile.

Received: April 29, 1983 [Z 370 IE]
German version: *Angew. Chem. 95* (1983) 737
The complete manuscript of this communication appears in:
*Angew. Chem. Suppl. 1983*, 985–993

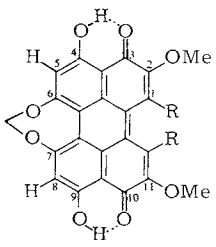
[2] H. M. R. Hoffmann, N. F. Janes, *J. Chem. Soc. C 1969*, 1456.
[3] a) P. H. Boyle, J. H. Coy, H. N. Dobbs, *J. Chem. Soc. Perkin Trans. I 1972*, 1617; b) M. Elliott, N. F. Janes, B. C. Pearson, *J. Chem. Soc. C 1971*, 2251; c) P. G. Wiering, H. Steinberg, Th. J. de Boer, *Rec. Trav. Chim. Pays Bas 96* (1977) 119.
[4] a) H. M. R. Hoffmann, J. Matthei, *Chem. Ber. 113* (1980) 3837; b) R. Henning, H. M. R. Hoffmann, *Tetrahedron Lett. 23* (1982) 2305; c) H. M. R. Hoffmann, R. Henning, *Helv. Chim. Acta. 66* (1983) 828.
[5] a) Cf. also H. Klein, A. Erbe, H. Mayr, *Angew. Chem. 94* (1982) 63; *Angew. Chem. Int. Ed. Engl. 21* (1982) 82; *Angew. Chem. Suppl. 1982*, 105; b) M. T. Reetz, *ibid. 94* (1982) 97; *21* (1982) 96 and references cited therein.
[7] a) Cf. H. M. R. Hoffmann, K. Haase, Z. M. Ismail, S. Preftitsi, A. Weber, *Chem. Ber. 115* (1982) 3880; b) Z. M. Ismail, H. M. R. Hoffmann, *Angew. Chem. 94* (1982) 862; *Angew. Chem. Int. Ed. Engl. 21* (1982) 859; *Angew. Chem. Suppl. 1982*, 1819; c) A. Jellal, M. Santelli, *Tetrahedron Lett. 21* (1980) 4487.
[8] J. E. Fitzpatrick, D. J. Milner, P. White, *Synth. Commun. 12* (1982) 489; D. N. Munro, D. J. Milner, *Chem. Ind. (London) 1982*, 603.

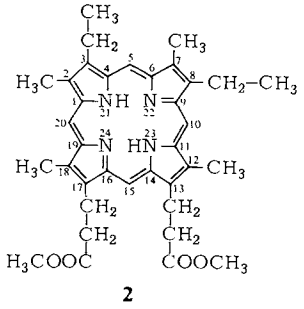
## Cercosporin, a Singlet Oxygen Generator**

By *Diane C. Dobrowolski* and *Christopher S. Foote**

*Dedicated to Prof. Günther O. Schenck on the occasion of his 70th birthday*

The photodynamic fungal pigment cercosporin **1**[1] is a nonspecific toxin which kills plant cells *in vitro* in the presence of light by lipid peroxidation[2, 3a]. The requirement for light, the cercosporin-sensitized formation of the characteristic $^1O_2$ oxidation product of cholesterol (the 5α-hydroperoxide), and the inhibition of the effects of cercosporin by β-carotene and other $^1O_2$ quenchers suggest that the mechanism of action involves production of $^1O_2$ sensitized by **1**[3]. We now report direct evidence for $^1O_2$ formation by observation of the characteristic $^1O_2$-luminescence at 1270 nm sensitized by cercosporin. This is the first time that a plant photodynamic sensitizer has been shown unequivocally to produce singlet oxygen. The quantum yield of $^1O_2$ formation is large: 0.81 ± 0.07 (95% confidence level).




R = $CH_2CHOHCH_3$

Samples of **1** ($1.0 \times 10^{-4}$ M, $A_{532} = 1.25$) or meso-porphyrin IX dimethyl ester **2** ($3.0 \times 10^{-4}$ M, $A_{532} = 1.15$) in $C_6D_6$ were irradiated with a Nd:YAG laser ($\lambda = 532$ nm)[6]. Luminescence was detected with a germanium photodiode[4]. The luminescence intensity at 1270 nm was the same in air or oxygen for both sensitizers, indicating that triplet states alone are involved in $^1O_2$ formation. The lifetime of the luminescence at 1270 nm (617 μs) and its quenching on addi-

[*] Prof. C. S. Foote, Ms. D. C. Dobrowolski
Department of Chemistry and Biochemistry
University of California
Los Angeles, CA 90024 (USA)

[**] Chemistry of Singlet Oxygen, Part 46. This work was supported by NSF grant CHE 80-20140. We thank Dr. *M. E. Daub* for helpful discussions and a sample of cercosporin.—Part 45: J.-J. Liang, C.-L. Gu, M. L. Kacher, C. S. Foote, *J. Am. Chem. Soc. 105* (1983) 4717.

tion of 2,3-dimethyl-2-butene further confirmed its identity as $^1O_2$.

After correction for differing sensitizer optical densities, the maximum intensities of **1**- and **2**-sensitized $^1O_2$ luminescence were compared. Since the quantum yield of triplet formation from **2** is 0.81[5], and this state is efficiently quenched by oxygen to form $^1O_2$[5], the absolute quantum yield of cercosporin-sensitized formation of $^1O_2$ could be determined. Based on four independent determinations, the relative ratio of luminescence produced from **2** to that produced from **1** was found to be $1.01 \pm 0.04$. Two separate determinations of the relative rates of photooxygenation of 2-methyl-2-pentene in benzene sensitized by **2** and **1** gave the ratio $1.00 \pm 0.12$. Both ratios indicate that the quantum yield of formation of $^1O_2$ sensitized by **1** is $0.81 \pm 0.07$.

This large quantum yield strongly supports the suggestion that singlet oxygen is the toxic agent in host plants. This is a striking example of the use of a chemical mechanism by a parasite to gain an "environmental advantage".

Received: April 26, 1983;
revised: July 12, 1983 [Z 358 IE]
German version: *Angew. Chem. 95* (1983) 729

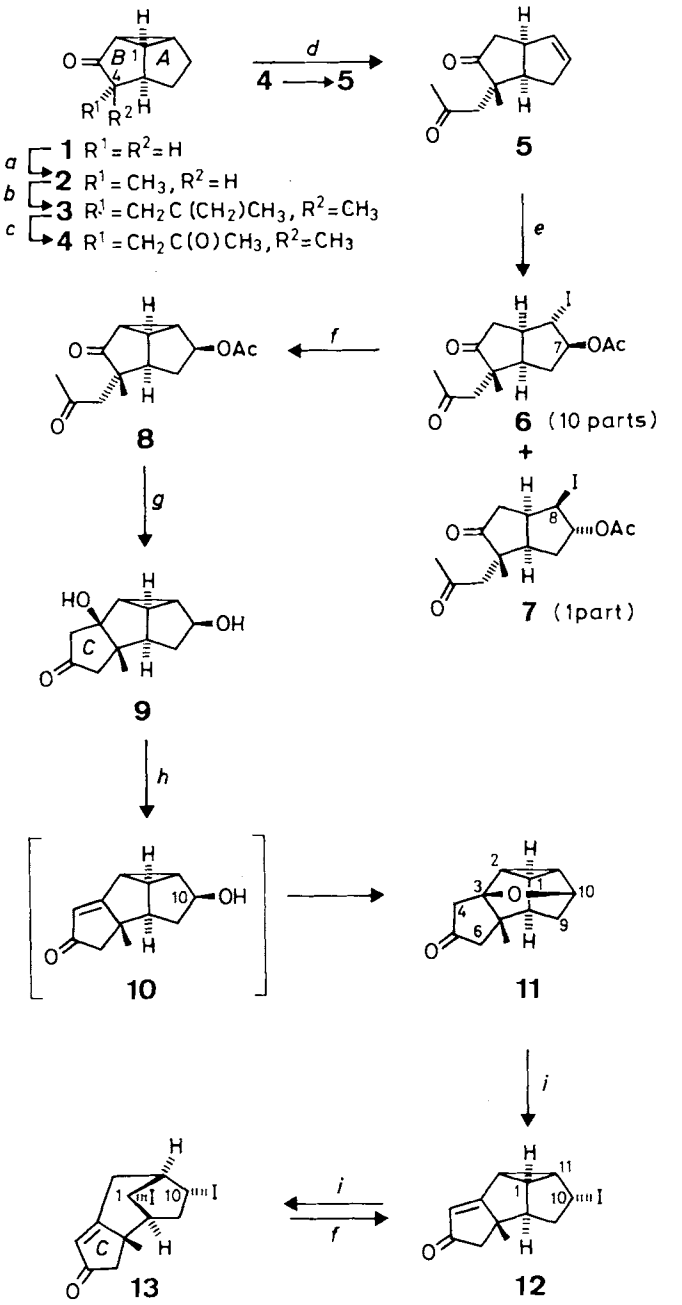
[1] S. Yamazaki, T. Ogawa, *Agr. Biol. Chem. 36* (1972) 1707; R. J. J. C. Lonsberg, U. Weiss, C. A. Salemink, A. Arnone, L. Merlini, G. Nasini, *Chem. Commun. 1971*, 1463.
[2] M. E. Daub, *Plant Physiol. 69* (1982) 1361.
[3] a) M. E. Daub, *Phytopathology 72* (1982) 370; b) M. E. Daub, personal communication.
[4] a) P. R. Ogilby, C. S. Foote, *J. Am. Chem. Soc. 104* (1982) 2069; b) *ibid. 105* (1983) 3423.
[5] R. Bonnett, A. A. Charalambides, E. J. Land, R. S. Sinclair, D. Tait, T. G. Truscott, *J. Chem. Soc. Farad. Trans. I 76* (1980) 852.
[6] Cercosporin was provided by Dr. *M. E. Daub*, Michigan State University. Its structure and purity were confirmed by comparison of the absorption and NMR spectra with published data[1]. 2-Methyl-2-pentene (Aldrich) was purified by column chromatography on basic $Al_2O_3$. $C_6H_6$ (Mallinckrodt) was distilled from $P_2O_5$ immediately before use. **2** (Sigma) and $C_6H_6$ (Cambridge Isotope Laboratories) were used as received.—The apparatus used to observe $^1O_2$ luminescence has been described previously [4].

## Synthesis and Structure of a Linearly *anti*-Annelated Tetracycloundecane. A Potential Precursor for a Coriolin Synthesis

By *Martin Demuth**, *Antonio Cánovas*, *Eva Weigt*, *Carl Krüger*, and *Yi-Hung Tsay*

*Dedicated to Professor Günther O. Schenck on the occasion of his 70th birthday*

We recently presented a widely applicable concept for the synthesis of cyclopentanoid natural products based on the utilization of tricyclo[3.3.0.0$^{2,8}$]octan-3-one **1** as central optically active building block[1,2]. Scheme 1 outlines the strategy (AB+C principle) now chosen by us for the preparation of the tetracycloundecanes **9** and **12**, which are potential precursors for the synthesis of coriolins[1]. The most important step in the sequence involves the previously only indirectly demonstrated[3] *anti*-annelation of a third five-membered ring to **1**. The desired *anti*-configuration of the rings A and C in **13** could be confirmed by an X-ray structure analysis.




Scheme 1. a: NaH, MeI, tetrahydrofuran, 50 °C. b: 3-chloro-2-methylpropene, KBr, tBuOK, tBuOH, toluene, 80°C. c: $OsO_4$, $NaIO_4$, dioxane, $H_2O$, room temperature. d: Nafion-TMS (perfluorinated trimethylsilyl sulfonate resin), toluene, 80°C. e: AcOAg, $I_2$, toluene, room temperature. f: 1,5-diazabicyclo[4.3.0]non-5-ene, toluene, room temperature. g: tBuOK, tBuOH, toluene, 80°C, 5 min. h: as g but 12 h or TosOH cat., $CH_3OH$, room temperature. i: iodotrimethylsilane, $CH_2Cl_2$, room temperature. The numbering in **10**—**13** is that generally employed in coriolin chemistry.

The alkylation **2**→**3** proceeds in 86% yield and just as selectively as the preceding methylation **1**→**2**[2,3]. Oxidative degradation (**3**→**4**; 82%) and subsequent isomerization **4**→**5** (60%)[4] afforded a suitable starting material for further functionalization of ring A. The Prévost addition of acetyl hypoiodate to the double bond of **5** yields **6** and **7** with equally high selectivity (10 : 1) as has already been observed in an analogous case[1,3]. After re-formation of the three-membered ring (**6**→**8**; 77%, annelation of the ring C

[*] Dr. M. Demuth, Dr. A. Cánovas, E. Weigt
Max-Planck-Institut für Strahlenchemie
Stiftstrasse 34—36, D-4330 Mülheim a. d. Ruhr (Germany)
Prof. Dr. C. Krüger, Dr. Y.-H. Tsay (X-ray structure analysis)
Max-Planck-Institut für Kohlenforschung
Kaiser-Wilhelm-Platz 1, D-4330 Mülheim a. d. Ruhr (Germany)

(**8**→**9**, **11**) was achieved with potassium *tert*-butoxide in *tert*-butyl alcohol and toluene at 80°C. Interruption of this reaction after 5 min permitted isolation of the primary aldol product **9**; the end product after 12 h was the pentacyclic ether **11** (93%). The labile primary product **9** readily cyclizes to **11** in the presence of traces of bases or acids, the presumed intermediary enone **10** not being detectable (for model considerations cf. [1]). Since **9** and **10** proved to be of no synthetic value we searched for a stable derivative having basically similar features and which is readily accessible from **11**. To avoid the undesired internal ether formation, it seemed desirable that C10 be either *exo*-substituted with oxygen or bear a readily modifiable group not containing oxygen. The latter variant could be achieved by treatment of **11** with iodotrimethylsilane (TMSI)[5]; this afforded the crystalline diiodo compound **13** as major product (64%) (Fig. 1). Re-formation of the three-membered

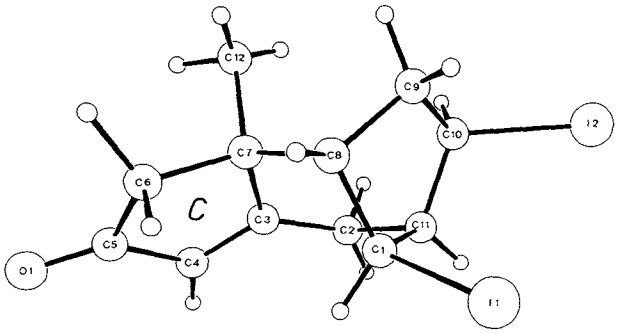



Fig. 1. Structure of the diiodo compound **13** in the crystal. $a=7.789(1)$, $b=13.772(3)$, $c=14.293(1)$ Å, $\alpha=64.51(1)$, $\beta=89.353(7)$, $\gamma=73.98(1)°$, $V=1319.90$ Å, $\rho_{calc}=2.154$ g cm$^{-3}$, $Mo_{K\alpha}$, $\mu=46.9$ cm$^{-1}$, $Z=4$, space group $P\bar{1}$, 5960 reflections, 5010 observed (2σ), 271 refined parameters, $R=0.0565$, $R_w=0.696$. Further details of the crystal structure investigation are obtainable on request from the Fachinformationszentrum Energie Physik Mathematik, D-7154 Eggenstein-Leopoldshafen by quoting the depository number CSD 50466, the names of the authors, and full citation of the journal.

ring (→ **12**; 72%) was accomplished by reaction of **13** with diazabicyclo[4.3.0]non-5-ene; thus a stable *anti*-annelated tetracycloundecane with appropriate ring A substitution was prepared for the first time. As initial step of the ring-opening **11**→**13** we postulate cleavage of the ether by $S_N2$ substitution with iodide at C10 and concomitant formation of the enone (→ **12**). The opening of the cyclopropane ring of **12** taking place in the second step does not occur at C11, but, because of steric interaction with the 10-*exo* iodide, selectively at C1. As has also been found in other examples, the iodide addition at C1 occurs with inversion[4].

Received: May 25, 1983 [Z 395 IE]
German version: *Angew. Chem. 95* (1983) 747
The complete manuscript of this communication appears in: *Angew. Chem. Suppl. 1983*, 1053-1065

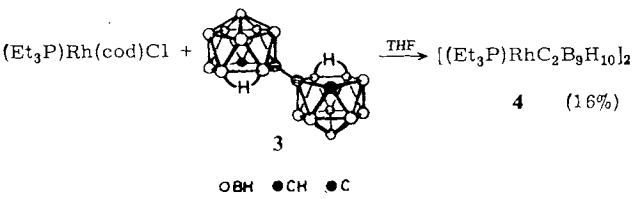
[1] M. Demuth, K. Schaffner, *Angew. Chem. 94* (1982) 809; *Angew. Chem. Int. Ed. Engl. 21* (1982) 820.
[2] M. Demuth, S. Chandrasekhar, K. Schaffner, *J. Am. Chem. Soc.*, in press.
[3] M. Demuth, S. Chandrasekhar, K. Nakano, P. R. Raghavan, K. Schaffner, *Helv. Chim. Acta 63* (1980) 2440.
[4] M. Demuth, G. Mikhail, *Tetrahedron 39* (1983) 991.
[5] Review: G. A. Olah, S. C. Narang, *Tetrahedron 38* (1982) 2225.

## Synthesis and Structure Determination of $[(PEt_3)RhC_2B_9H_{10}]_2$— A Binuclear Rhodacarborane Containing Four Bonds Between Two Icosahedra**

By *Paul E. Behnken, Carolyn B. Knobler,* and *M. Frederick Hawthorne**

In the course of our studies of the homogeneous catalysis of olefin hydrogenation by *closo*-3,3-$(PPh_3)_2$-3-(H)-3,1,2-$RhC_2B_9H_{11}$ **1**[1], we characterized and reported the molecular structure of $[(PPh_3)RhC_2B_9H_{11}]_2$ **2**[2], a binuclear (phosphane)rhodacarborane complex formed by formal loss of $H_2$ and two phosphane ligands from two molecules of **1**. Of interest were the Rh—H—B interactions supporting the Rh—Rh bond and the stereospecificity of their formation. The two terminal B—H bonds involved in the Rh—H—B interactions determine a specific stereoisomer: of the six possibilities only **2** is observed with both enantiomers present in the unit cell.

In an attempt to further probe the nature of these interactions, cyclooctadiene(triethylphosphane)rhodium(I) chloride was allowed to react with $Cs_2[7\text{-}(7'\text{-}7',8'\text{-}C_2B_9H_{11})\text{-}7,8\text{-}C_2B_9H_{11}]$ **3**[3] (15 h reflux) to produce a dark blue compound **4** in 16% yield.




Crystals of **4** (Fig. 1) contain two icosahedral rhodacarborane fragments joined symmetrically at three vertices. Carbon atoms C1 and C1′ are covalently bonded as in the

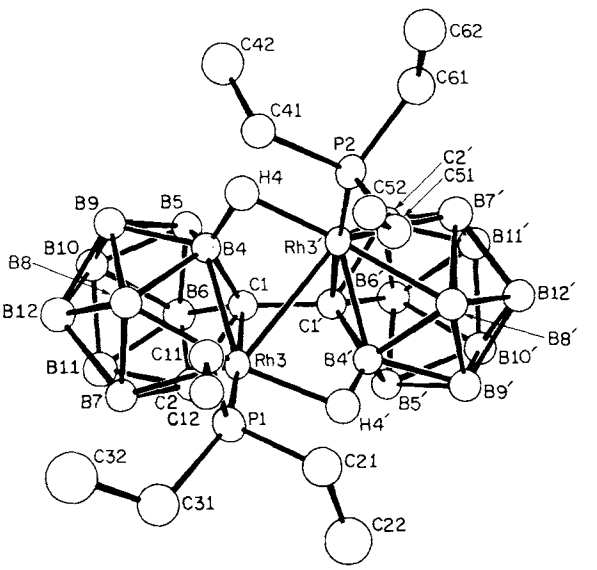



Fig. 1. ORTEP projection of the binuclear rhodium complex $[(Et_3P)RhC_2B_9H_{10}]_2$ **4**. H atoms other than those involved in bridging are omitted for clarity. For details of the crystal structure analysis ($R_w=0.036$), see Supplement.

[*] Prof. M. F. Hawthorne, P. E. Behnken, Dr. C. B. Knobler
Department of Chemistry and Biochemistry,
University of California
Los Angeles, CA 90024 (USA)

[**] This work was supported by the U. S. National Science Foundation.

carborane precursor. Each $C_2B_9$ fragment sequesters a rhodium vertex, (Rh3 and Rh3′) with a Rh–Rh distance of 2.725(1) Å, in the range of a Rh–Rh single bond[4] and comparable to that of 2.763(1) Å in **2**.

The Rh–Rh bond is further supported by two Rh–H–B three-center interactions between Rh3, H4′, B4′ and Rh3′, H4, B4 with Rh–B distances of 2.306(7) and 2.323(7) Å, respectively. The Rh–H distances are 1.92(7) Å for Rh3–H4′ and 1.85(7) Å for Rh3′–H4. These distances are comparable to those observed in **2**.

The molecule **4** has $C_2$ symmetry with the axis of rotation bisecting the Rh3–Rh3′ and C1–C1′ bonds. Unlike the asymmetric structure of **2**, the symmetry in **4** is attributed to the C1–C1′ bond which limits the Rh–H–B interactions to the B4 and B4′ vertices adjacent to C1 and C1′, respectively.

Interestingly, the carborane ligand **3** is diastereomeric by virtue of the asymmetry of the $C_2B_9H_{11}$ fragment. The mirror-plane symmetry of each carborane fragment is destroyed by substitution at one of the carbon vertices, and the carborane precursor **3** contains two chemically distinct isomers, detectable by $^{11}$B-NMR spectroscopy, which differ in the configuration of one $C_2B_9H_{11}$ moiety. The $^{31}$P-NMR spectrum of chromatographed **4** contains resonances attributable to **4** ($\delta = 34.4$, $J_{P-Rh} = 173$ Hz) as well as those of an unsymmetrical compound ($\delta = 32.3$, $J_{P-Rh} = 177$ Hz; $\delta = 29.2$, $J_{P-Rh} = 149$, $^3J_{P-P} = 6.6$ Hz) derived from the diastereomeric carborane ligand containing icosahedral fragments of opposite configuration. A hypothetical structure of the unsymmetric isomer structurally analogous to **4** would contain a Rh–H–C as well as a Rh–H–B interaction. Inversion of one $C_2B_9H_{11}$ fragment maintaining the C1–C1′ and Rh3–Rh3′ bonds would result in an interaction between C2 and Rh3′. Interactions of this type have been characterized structurally[5].

Received: April 26, 1983 [Z 355 IE]
German version: *Angew. Chem.* *95* (1983) 738
The complete manuscript of this communication appears in: *Angew. Chem. Suppl. 1983*, 929-944

[1] T. E. Paxson, M. F. Hawthorne, *J. Am. Chem. Soc.* *96* (1974) 4674.
[2] R. T. Baker, R. E. King III, C. B. Knobler, C. A. O'Con, M. F. Hawthorne, *J. Am. Chem. Soc.* *100* (1978) 8266.
[3] M. F. Hawthorne, D. A. Owen, J. W. Wiggins, *Inorg. Chem.* *10* (1971) 1304.
[4] F. A. Cotton, T. R. Felthouse, *Inorg. Chem.* *20* (1981) 584.
[5] Y. W. Yared, S. L. Miles, R. Bau, C. A. Reed, *J. Am. Chem. Soc.* *99* (1977) 7076.

## Pentacarbonylrhenium Complexes with Thiazylamide Ligands**

By *Gabriele Hartmann, Rüdiger Mews**, and *George M. Sheldrick*

Whereas *N,N′*-dialkylsulfurdiimides R–NSN–R′ **1** and *N,N*-dialkyl(thionitroso)amines RR′N–NS **2** have been known for some time, *N,N*-dialkyl(thiazyl)amides NS–NRR′ **3**, which are isomeric to both classes of compounds, could not previously be detected. **1**[5] and **2**[6] can be incorporated into transition-metal complexes by ligand exchange. Complexes having thiazylamides as ligands are accessible by substitution of fluorine in thiazylfluoride coordinated to a transition metal. The cation $[Re(CO)_5(NSF)]^+$, which is also highly stable in solution, has proved to be particularly suitable for reactions of this type[9]:

$$\underset{\mathbf{4}}{[(OC)_5Re(NSF)]^+}\ AsF_6^- + \underset{\mathbf{5}}{Me_3SiNMe_2} \xrightarrow[SO_2]{-30\,^\circ C} \underset{\mathbf{6}}{[(OC)_5Re(NSNMe_2)]^+}AsF_6^- + Me_3SiF \qquad (1)$$

$$\mathbf{4} + \underset{\mathbf{7}}{(Me_3Si)_2NMe} \xrightarrow[SO_2]{-30\,^\circ C} \left\{\left[(OC)_5Re\left(NSN\begin{matrix}Me\\SiMe_3\end{matrix}\right)\right]^+ AsF_6^-\right\}_{\mathbf{8}} + Me_3SiF$$

$$\mathbf{8} + \mathbf{4} \longrightarrow \left[(OC)_5Re\left(NS\text{–}\underset{Me}{N}\text{–}SN\right)Re(CO)_5\right]^{2+}_{\mathbf{9}}(AsF_6^-)_2 + Me_3SiF \qquad (2)$$

At −30 °C in liquid $SO_2$, reaction (1) leads quantitatively to **6**, in which the structure of the starting complex **4** is retained. Side reactions occur at higher temperatures. In reaction (2) **4** reacts analogously with the bisilylated amine **7** at −30 °C. The product **8**, which cannot be isolated pure, reacts with excess **4** to afford a dinuclear complex **9**, which contains the methylbis(thiazyl)amide as bridging ligand. If **4** and **7** are only present in the molar ratio 1 : 1, the $AsF_6^-$ anion attacks the cation in **8** (above −15 °C) to form products that have not yet been unequivocally identified.

The X-ray crystal structure of the complex cation in **6** (Fig. 1) was determined on single crystals obtained from acetone/*n*-pentane.

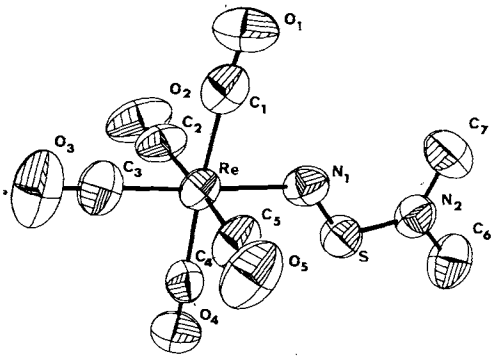


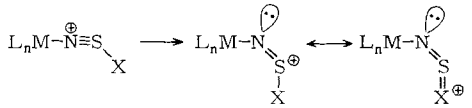

Fig. 1. Crystal structure of the mononuclear cation $[Re(CO)_5(NSNMe_2)]^+$ in **6**. All atoms (apart from H) are represented by 50% probability vibrational ellipsoids (50% location probability). **6** crystallizes in the orthorhombic system, Pbca, $a = 1136.8(4)$, $b = 2497.6(6)$, $c = 1139.8(4)$ pm, $Z = 8$, $\mu = 9.84$ mm$^{-1}$ ($Mo_{K\alpha}$). Structure determination from diffractometer data using the Patterson method. Refinement using absorption- and extinction-corrected structure factors from 2173 reflections [$F > 4\sigma(F)$] to $R = 0.044$.

The bond lengths N1–S (144.7 pm) and S–N2 (158.1 pm) characterize the novel ligands as thiazylamide, and the Re–N1 distance (216.1 pm) corresponds to that of a single bond. The M–N–S angle of 130° in **6** is considerably smaller than that in complexes of other thiazyl derivatives ($[M(NSF)_6]^{2+}$: M = Co[8a] 170.5°, M = Ni[8b] 168.6°; $[Ni\{N\text{-}SON(CF_3)_2\}_6]^{2+}$[10] 161.7°); the N1–S distances in these other complexes are somewhat shorter (140–144 pm). The

[*] Prof. Dr. R. Mews, G. Hartmann, Prof. G. M. Sheldrick
Institut für Anorganische Chemie der Universität
Tammannstrasse 4, D-3400 Göttingen (Germany)

[**] This work was supported by the Deutsche Forschungsgemeinschaft and the Fonds der Chemischen Industrie.

contraction of the angle and the increase in the N1–S distance can be accounted for by an increase in $sp^2$ character of the coordinating nitrogen atom:



Received: November 29, 1982;
revised: April 5, 1983 [Z 212]
German version: *Angew. Chem. 95* (1983) 753
The complete manuscript of this communication appears in:
*Angew. Chem. Suppl. 1983*, 945–956

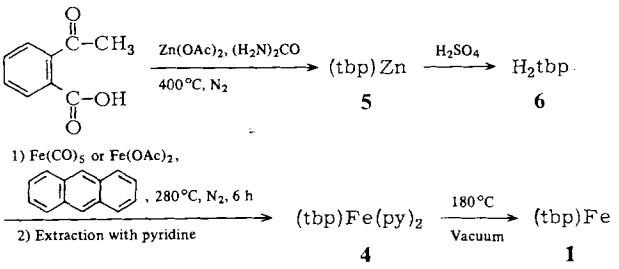
[5] Review: K. Vrieze, G. van Koten, *Recl. Trav. Chim. Pays-Bas 99* (1980) 145.
[6] H. W. Roesky, R. Emmert, W. Clegg, W. Isenberg, G. M. Sheldrick, *Angew. Chem. 93* (1981) 623; *Angew. Chem. Int. Ed. Engl. 20* (1981) 591.
[8] a) B. Buss, P. G. Jones, R. Mews, M. Noltemeyer, G. M. Sheldrick, *Angew. Chem. 91* (1979) 253; *Angew. Chem. Int. Ed. Engl. 18* (1979) 231; *Acty Crystallogr. B 36* (1980) 141; b) G. Hartmann, P. G. Jones, R. Mews, G. M. Sheldrick, *Z. Naturforsch. B 35* (1980) 1191.
[9] R. Mews, C. S. Liu, *Angew. Chem. 95* (1983) 156; *Angew. Chem. Int. Ed. Engl. 22* (1983) 158.
[10] G. Hartmann, R. Mews, G. M. Sheldrick, *J. Organomet. Chem.*, in press.

## Preparation and Properties of Tetrabenzoporphyrinatoiron(II) and Its Isocyanide Complexes

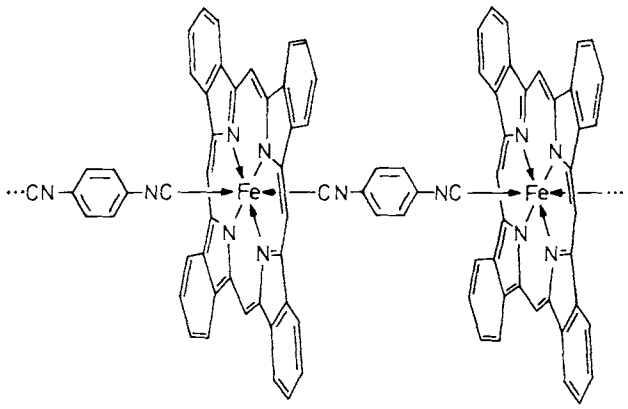
By *Konrad Fischer* and *Michael Hanack**

In contrast to hexacoordinated bisaxially bridged phthalocyaninato-transition metal compounds[1], the corresponding tetrabenzoporphyrinato (tbp) complexes have so far been the subject of very few investigations. Bisaxially bridged (tbp)M compounds should exhibit interesting properties—*e.g.* high electrical conductivity.

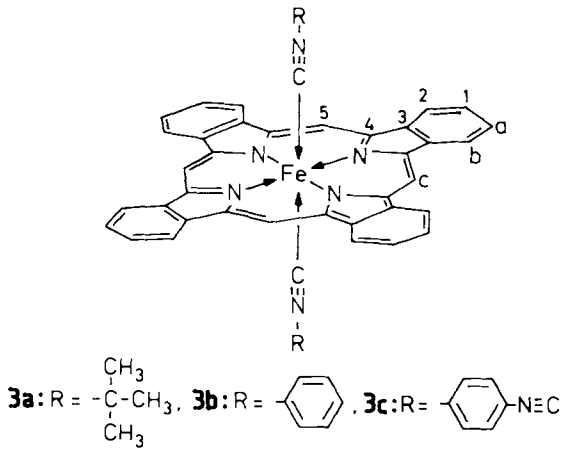
We were able to prepare tetrabenzoporphyrinatoiron(II) **1**, for the first time, by thermal cleavage of the axial pyridine ligand (180 °C, vacuum) from the known[8] bis(pyridine)tetrabenzoporphyrinatoiron(II) **4**, which, however, was




obtained *via* a new route. $H_2$tbp reacts with pentacarbonyliron or iron(II) acetate in an anthracene melt to give almost quantitative yields of **1**, which was isolated as (tbp)Fe(py)$_2$ from the crude product by Soxhlet extraction with pyridine. **1** can be converted by reaction with isocyanides into the monomeric derivatives (tbp)Fe(CNR)$_2$ **3** and by reaction with 1,4-diisocyanobenzene (dib) into the polymeric derivative [(tbp)Fe(dib)]$_n$ **2**. For the reaction leading to the monomeric isocyanide complexes **3a** and **3b**, merely excess ligand suffices as solvent, whereas for the reaction furnishing **3c** and its polymer **2**, anhydrous chloroform was found to be the best solvent. The complexes **1**, **2** and **3** were characterized by elemental, differential thermal, and thermogravimetric analysis, as well as by UV/VIS, IR, and $^1$H-NMR spectroscopy.




**2**




The bands occurring at 690, 718, 1190, 1212, 1440 and 1480 cm$^{-1}$ in the IR spectrum of **4** are no longer observable in the spectrum of **1**, while the rest of the absorptions remain unchanged. Owing to the solubility of **1** in pyridine leading to formation of **4**, both the $^1$H-NMR as well as $^{13}$C-NMR spectra could be measured in [$D_5$]-pyridine. The $^{13}$C-NMR data ($C^1$: $\delta = 127.2$, $C^2$: 121.8, $C^3$: 139.6, $C^4$: 144.7, $C^5$: 95.0) are in agreement with the values found for **5**[3c].

The complex **3a** obtained from **1** and *tert*-butyl isocyanide is not stable in solution but partially dissociates into its components; after addition of excess isocyanide, the $^1$H-NMR signal of the *tert*-butyl group of the coordinated ligand can also be observed: owing to the diamagnetic ring current of the macrocycle it is shifted upfield by about $\Delta\delta = 2.25$ compared to the signal of the free ligand. The spectrum of pure monomeric **3c** can likewise only be measured in presence of excess ligand, since, otherwise, partial double cleavage leads to formation of the dimer and oligomers, which are also soluble in $CDCl_3$; the signal of the α-proton of the bridge ligand is shifted about $\Delta\delta = 2.57$, that of the β-proton about $\Delta\delta = 1.11$ upfield. Unlike **3a** and **3c**, **3b** can be investigated $^1$H-NMR spectroscopically

[*] Prof. Dr. M. Hanack, K. Fischer
Institut für Organische Chemie (Lehrstuhl II) der Universität
Auf der Morgenstelle 18, D-7400 Tübingen 1 (Germany)

 © Verlag Chemie GmbH, 6940 Weinheim, 1983 0570-0833/83/0909-0724 $ 02.50/0 

without addition of free phenyl isocyanide; the same upfield shift is found for the α- and β-protons as in **3c**.

A characteristic feature of each of the IR spectra of the isocyanide complexes is the very intense $\nu$(CN) band. In the case of **3a** it appears in the same region as for the free ligand; *i.e.* π-bonding becomes increasingly more significant over pure σ-bonding in these complexes compared to the analogous phthalocyaninatoiron(II) compounds. As expected, the mesomeric ligands dib and CNPh exhibit even stronger π-acceptor behavior, as evidenced by the shift of the CN stretching vibration frequency by, respectively, 20 and 30 $cm^{-1}$ to lower energy. On proceeding from the monomer **3c** to the polymer **2**, $\nu$(CN) shifts a further 10 $cm^{-1}$ to lower energy, and the bands at 700, 1190 and 1595 $cm^{-1}$ are absent; otherwise only a few intensities change.

The pyridine complex **4** has an electrical conductivity of $\sigma_{RT} = 2 \times 10^{-9}$ S·cm$^{-1}$ (powder pellet, 1 kbar). In the case of "ligand-free" **1** it increases similarly as in the case of **2**, which is polymerized by dib bridges, *i.e.* it increases by three orders of magnitude to $2 \times 10^{-6}$ S·cm$^{-1}$. **1** and **2** can be oxidatively doped with two equivalents of iodine in benzene suspension. The compounds (tbp)Fe$I_{1.5}$ and $[(tbp)Fe(dib)I_{1.7}]_n$ are formed which have electrical conductivities of $\sigma_{RT} = 2 \times 10^{-2}$ and $9 \times 10^{-3}$ S·cm$^{-1}$, respectively, and are stable up to 120 °C. Thus, the electrical conductivity of (tbp)Fe$I_{1.5}$ is an order of magnitude higher than that of the corresponding phthalocyaninato-Fe$^{II}$ compound[11].

Received: May 25, 1983 [Z 396 IE]
German version: *Angew. Chem. 95* (1983) 741
The complete version of this communication appears in: *Angew. Chem. Suppl. 1983*, 1017–1024

[1] M. Hanack, *Chimia 37* (1983) 238; M. Hanack, G. Pawlowski, *Naturwissenschaften 69* (1982) 266.
[3] c) D. E. Remy, *Tetrahedron Lett. 24* (1983) 1451.
[8] A. Vogler, H. Kunkely, B. Rethwisch, *Inorg. Chim. Acta 46* (1980) 101.
[11] J. L. Petersen, C. S. Schramm, D. R. Stojakovic, B. M. Hoffman, T. J. Marks, *J. Am. Chem. Soc. 99* (1977) 286.

## $[Me_3Si(py)]^{\oplus}X^{\ominus}$ (X = Br, I): X-Ray Structural Analysis of the 1:1-Adducts of Bromo- or Iodotrimethylsilane and Pyridine

By *Karl Hensen**, *Thomas Zengerly*, *Peter Pickel*, and *Gerhard Klebe*

*Dedicated to Professor Ulrich Wannagat on the occasion of his 60th birthday*

As Lewis acids, silicon halides and their alkyl derivatives react with tertiary organic nitrogen bases such as pyridine, bipyridine, or trialkylamines in nonpolar solvents to afford, in general, sparingly soluble addition compounds[1]. In contrast to the numerous 1:2-adducts, $Me_2SiBr_2$, $Me_3SiBr$[2a], $Me_2SiI_2$, and $Me_3SiI$[2b] give only 1:1-adducts with pyridine. All of the compounds are readily hydrolyzable. Previously, only $SiF_4 \cdot 2$py has been studied by X-ray crystallography[3a]. In this compound the silicon atom has a slightly distorted octahedral coordination and the pyridine rings are *trans*-orientated.

[*] Prof. Dr. K. Henson, T. Zengerly, Dr. P. Pickel
Institut für Physikalische und Theoretische Chemie der Universität
Niederurseler Hang
D-6000 Frankfurt am Main 50 (Germany)
Dr. G. Klebe
Institut für Kristallographie
der Universität Frankfurt am Main

In the 1:1-adduct of germanium tetrachloride and trimethylamine the amine ligand occupies an axial position in the trigonal-bipyramidal complex[3d].

We have now succeeded in growing suitable crystals of the 1:1-pyridine adducts of $Me_3SiBr$ (m.p. ≈ 27 °C) and $Me_3SiI$ (m.p. > 100 °C) by sublimation in glass capillaries, and have investigated the structures in the solid state.

These compounds do not occur as increased coordination complexes, rather the Lewis base displaces a halide ion from the first coordination sphere of the silicon atom, and ionic structures $[Me_3Si(py)]^{\oplus}X^{\ominus}$ occur in the solid state (cf. Fig. 1). The Si–Br and Si–I distances of 4.359 and 4.559 Å, respectively, are *ca.* 0.5 Å longer than the sum of the van der Waals' radii of the atoms concerned[4] and more *ca.* 2 Å longer than the sum of the covalent radii[4a].

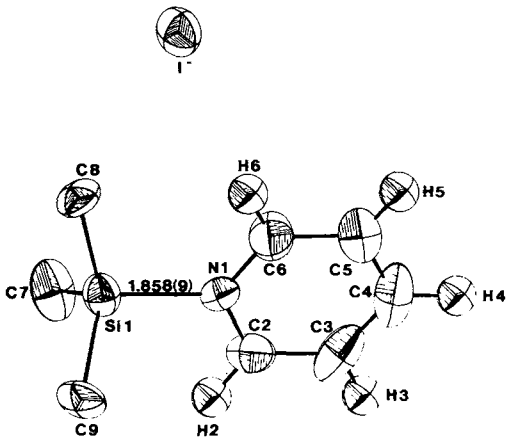



Fig. 1. ORTEP representation of the asymmetric moiety $[(CH_3)_3Si(py)]^{\oplus}I^{\ominus}$: $P2_1/c$, $a = 8.288(2)$, $b = 10.997(2)$, $c = 13.538(4)$ Å, $\beta = 110.80(2)°$, $Z = 4$; 2020 reflections, $R_w = 0.040$; Si–N 1.858(9) Å.—$[(CH_3)_3Si(py)]^{\oplus}Br^{\ominus}$: $P2_1/c$, $a = 12.008(4)$, $b = 7.206(2)$, $c = 13.518(4)$ Å, $\beta = 111.47(3)°$, $Z = 4$; 1630 reflections, $R_w = 0.076$; Si–N 1.856(7) Å.—Further details on the crystal structure investigations can be obtained from the Fachinformationszentrum Energie Physik Mathematik, D-7514 Eggenstein-Leopoldshafen, by quoting the depository number CSD 50506, the names of the authors, and the journal citation.

The CSiC angles are up to ca. 6° greater, and the CSiN angles ca. 6° smaller, than the ideal tetrahedral angle, *i.e.* considerable distorsion to trigonal pyramidal structures occurs. Within the standard deviation, the pyridine ring is planar.

Notable is the Si–N distance of 1.86(1) Å. All the previously studied compounds with tetracoordinated silicon exhibit shorter Si–N distances (mainly *ca.* 1.75 Å)[5a,b]. Comparison with corresponding cations is not possible since the structures discussed here represent the first examples of this type. *Sheldrick et al.* found a similar Si–N distance of 1.857(4) Å in a pentacoordinated silicon compound[5b]; all other increased coordination silicon compounds have values longer than 1.91 Å[3,5c,d]. The Si–C distances correspond to normal single bond values.

The formation of ionic structures apparently favors 1:1-compounds of halosilanes and pyridine in the solid state. Hence, the melting-point diagram of the system $Me_3SiCl$-pyridine[2a] gives no information about formation of an adduct. Presumably ionic structures also occur in the adducts of bromo- or iodotrimethylsilane and hexamethylphosphoric triamide (HMPT) investigated by *Chojnowski et al.*[5f]; in contrast, even with HMPT, which is a stronger Lewis base than pyridine[5g], chlorotrimethylsilane does not form a solid adduct at room temperature.

Received: May 6, 1983 [Z 379 IE]
German version: *Angew. Chem. 95* (1983) 739
The complete manuscript of this communication appears in:
*Angew. Chem. Suppl. 1983*, 973-984

[1] Cf. the reports by *U. Wannagat et al.* „Über Verbindungen von Nichtmetallhalogeniden mit Pyridin und seinen Homologen" (1954–1969), Part 10: *Monatsh. Chem. 100* (1969) 1127.
[2] a) K. Hensen, R. Busch, *Z. Naturforsch. B 37* (1982) 1174; b) H. J. Campbell-Ferguson, E. A. V. Ebsworth, *J. Chem. Soc. A 1966*, 1508; *1967*, 705.
[3] a) V. A. Bain, R. C. G. Killean, M. Webster, *Acta Crystallogr. B 25* (1969) 156; –d) M. S. Bilton, M. Webster, *J. Chem. Soc. Dalton Trans. 1972*, 722.
[4] a) L. Pauling: The Nature of the Chemical Bond, 3rd ed., Cornell University Press, Ithaca, NY 1960; b) A. Bondi, *J. Phys. Chem. 68* (1964) 441.
[5] a) G. Klebe, K. Hensen, H. Fuess, *Chem. Ber.*, in press; b) W. S. Sheldrick, W. Wolfsberger, *Z. Naturforsch. B 32* (1977) 22; c) G. Sawitzki, H. G. von Schnering, D. Kummer, T. Seshadri, *Chem. Ber. 111* (1978) 3705; d) G. Klebe, J. W. Bats, K. Hensen, *Z. Naturforsch. B 38* (1983), in press. – f) J. Chojnowski, M. Cypryk, J. Michałski, *J. Organomet. Chem. 161* (1978) C31; g) W. B. Jensen, *Chem. Rev. 78* (1978) 1.

## [4+2]-Cycloaddition of Singlet Oxygen to 2,5-Dimethylfuran: Isolation and Reactions of the Monomeric and Dimeric Endoperoxides**

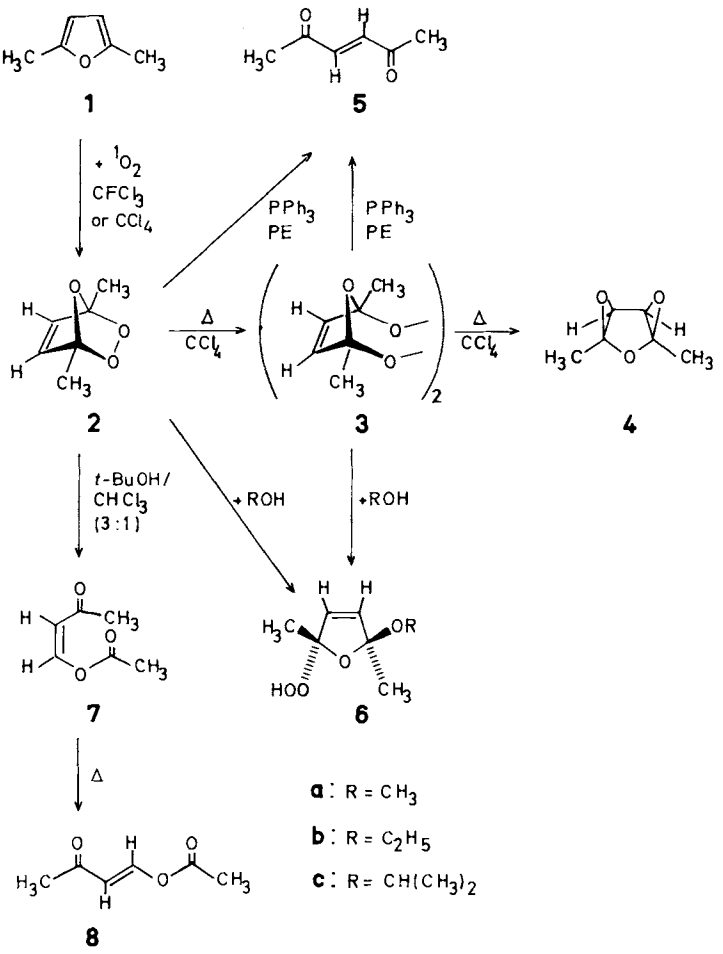
By *Klaus Gollnick** and *Axel Griesbeck*

*Dedicated to Professor Günther O. Schenck on the occasion of his 70th birthday*

The endoperoxide **2**, postulated by *G. O. Schenck et al.*[1] to be the primary product of the photosensitized oxygenation of 2,5-dimethylfuran **1**, has not yet been isolated. Here, we report the first isolation of monomeric **2**. **2** was obtained by tetraphenylporphin-photosensitized oxygenation (singlet oxygen reaction) of **1** in Freon 11 ($CFCl_3$) at room temperature, followed by removal of the solvent *in vacuo* and distillation of the residue at 5 °C/$10^{-3}$ torr into a cold trap at −78 °C[2a,b]. Solvent-free **2** always gives rise to explosions if handled in amounts greater than *ca.* 100 mg; however, in inert solvents like benzene or $CCl_4$ at room temperature it slowly *dimerizes* to the previously observed[1] **3**[2c], but at 55–60 °C the reaction is fast and quantitative[3]. If the temperature is raised further, the *cis*-bisepoxide **4**[2d], so far observed only in solution[4b], is obtained together with polymeric material (*ca.* 4:1).

Solutions of the *monomeric* endoperoxide **2** and the *dimeric* endoperoxide **3** in benzene or $CCl_4$ are reduced by triphenylphosphane in petroleum ether (PE) to give diketone **5**[2e] and triphenylphosphane oxide. Only one of the two possible *cis-trans* isomeric alkoxy hydroperoxides (presumably the *trans* isomer) **6a–c**[2f] is formed if **2** is dissolved in methanol, ethanol, or isopropanol, respectively, as indicated by the proton-decoupled $^{13}C$-NMR spectra of **6a** and **6b**. Alkoxy hydroperoxides **6a–c** may be prepared directly by reaction of $^1O_2$ with **1** in the corresponding alcohol, as has been known for some time for **6a**[1]. Interestingly, the same alkoxy hydroperoxides are obtained if the *dimeric* endoperoxide **3** is dissolved in these alcohols, probably *via* trapping of the *monomeric* endoperoxide **2** that may be in equilibrium with **3**.

*tert*-Butyl alcohol does not add to endoperoxide **2**; instead, **2** rearranges to the previously unknown *cis*-3-oxo-1-butenyl acetate **7**[2g] in *t*BuOH/$CHCl_3$ (3:1). **7**, which rearranges to the *trans* isomer **8**[2h,5] on heating, is also synthesized directly *via* reaction of $^1O_2$ with **1** in *t*-BuOH/$CHCl_3$ (3:1). Addition of *t*-butyl alcohol to **2** is sterically hindered and replaced here by a Baeyer-Villiger-type reaction in which vinyl group migration is preferred over methyl group migration[6].




Received: May 2, 1983;
revised: June 10, 1983 [Z 374 IE]
German version: *Angew. Chem. 95* (1983) 751

[1] C. S. Foote, M. T. Wuesthoff, S. Wexler, I. G. Burstain, R. Denny, G. O. Schenck, K. H. Schulte-Elte, *Tetrahedron 23* (1967) 2583.
[2] a) Elemental analyses and spectroscopic data are in accord with the given structures. – b) **2**: yellowish oil; MW: 128.1 (calc.), 144 (osmometric in benzene); $^1H$-NMR ($CCl_4$, 80 MHz): $\delta$ = 1.70 (s, 2 $CH_3$), 6.25 (s, 2 olef. H); $^{13}C$-NMR ($CDCl_3$, 80 MHz): $\delta$ = 13.48 (q, 2 $CH_3$), 112.34 (s, 2 $C_2CO_2$), 124.12 (d, −CH=). – c) **3**: yellowish solid; m.p. = 143 °C (decomp.) (from ether/petroleum ether, 1:1); MW: 256.2 (calc.), 254 (osmometric in acetone); $^1H$-NMR: $\delta$ = 1.81 (s, 4 $CH_3$), 6.31 (s, 4 olef. H). – d) **4**: colorless liquid; $^1H$-NMR: $\delta$ = 1.58 (s, 2 $CH_3$), 3.42 (s, 2 tert. H). – e) **5**: colorless needles (subl.); m.p. = 83 °C (78 °C [1]); $^1H$-NMR: $\delta$ = 2.28 (s, 2 $CH_3$), 6.67 (s, 2 olef. H). – f) **6a**: colorless crystals; m.p. = 81 °C (76 °C [1]); $^1H$-NMR: $\delta$ = 1.47 (s, $CH_3$), 1.53 (s, $CH_3$), 3.33 (s, $OCH_3$), 5.99 (AB system, 2 olef. H), 8.63 (s, OOH); $^{13}C$-NMR: $\delta$ = 22.26 (q, $CH_3$), 25.11 (q, $CH_3$), 51.01 (q, $OCH_3$), 131.64 (d, −CH=), 134.63 (d, −CH=), 111.55 (s, $C_2CO_2$), 114.16 (s, $C_2CO_2$). The proton-decoupled spectrum showed only one set of $^{13}C$ signals. – **6b**: colorless oil; $^1H$-NMR: $\delta$ = 1.17 (t, $OCH_2CH_3$, $J$ = 7 Hz), 1.49 (s, $CH_3$), 1.55 (s, $CH_3$), 3.63 (m, $OCH_2CH_3$), 5.95 (AB system, 2 olef. H); $^{13}C$-NMR: $\delta$ = 15.51 (q, $OCH_2CH_3$), 22.35 (q, $CH_3$), 25.59 (q, $CH_3$), 58.85 (t, $OCH_2CH_3$), 131.33 (d, −CH=), 135.09 (d, −CH=), 111.22 (s, $C_2CO_2$), 114.07 (s, $C_2CO_2$). The proton-decoupled

[*] Prof. Dr. K. Gollnick, A. Griesbeck
Institut für Organische Chemie der Universität
Karlstrasse 23, D-8000 München 2 (Germany)

[**] This work was supported by the Fonds der Chemischen Industrie.

spectrum showed only one set of $^{13}C$ signals.—**6c**: colorless oil; $^1H$-NMR: $\delta = 1.18$ (d, $OCH(CH_3)_2$), 1.54 (broad s, 2 $CH_3$), 4.00 (sept., $OCH(CH_3)_2$, $J = 6$ Hz), 5.93 (AB system, 2 olef. H).—g) **7**: yellowish liquid; b.p. = 67—70°C/10 torr; $^1H$-NMR: $\delta = 2.29$ (s, $CH_3$), 2.41 (s, $CH_3$), 5.45 (d, olef. H, $J = 7$ Hz), 7.60 (d, olef. H, $J = 7$ Hz).—h) **8**: yellowish liquid; b.p. ≈ 74—76°C/10 torr (71—72°C/10 torr [5]), $^1H$-NMR: $\delta = 2.25$ (s, $CH_3$), 3.31 (s, $CH_3$), 5.86 (d, olef. H, $J = 13$ Hz), 8.10 (d, olef. H, $J = 13$ Hz).


[3] Recently, two different $^1H$-NMR spectra of **2** in $CCl_4$ were reported [4a, b]. According to our results, the compound observed by *Adam et al.* [4a] is indeed the *monomeric* **2**, whereas it appears more likely that *Graziano et al.* [4b] observed the *dimeric* **3**.

[4] a) W. Adam, K. Takayama, *J. Org. Chem.* **44** (1979) 1727; b) M. L. Graziano, M. R. Iesce, R. Scarpati, *J. Chem. Soc. Perkin I 1982*, 2007.

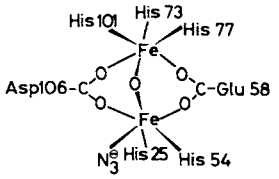
[5] L. R. Fedor, N. C. De, S. K. Gurwara, *J. Am. Chem. Soc. 95* (1973) 2906.

[6] I. Saito, A. Nakata, T. Matsuura, *Tetrahedron Lett. 22* (1981) 1697 found that the endoperoxide of 1,3-di-*tert*-butylisobenzofuran underwent an analogous rearrangement of the Baeyer-Villiger type.


## $[\{(C_6H_{15}N_3)Fe\}_2(\mu\text{-}O)(\mu\text{-}CH_3CO_2)_2]^{2+}$, a Dinuclear Iron(III) Complex with a Metazidohemerythrin-Type Structure**


By *Karl Wieghardt*, Klaus Pohl,* and *Walter Gebert*


Hemerythrins are iron-containing, $O_2$-transporting proteins; the methemerythrins are formed by redox reaction $2Fe^{II}/O_2 \rightarrow 2Fe^{III}/O_2^{2-}$ and replacement of the coordinated peroxide by other ligands ($N_3^-$, $OH^-$, $H_2O$)[1a]. The coordination geometry of the four dinuclear $Fe^{III}$ structural units was determined by magnetic[1b] and UV spectroscopic[1c] measurements, by EXAFS investigations[1d], and by X-ray structure analyses of metaquo-[2a] and metazidohemerythrin[2b] (cf. **1**). Dinuclear $Fe^{III}$-complexes with this type of structure (an angular oxo-bridge and two carboxylato-bridges) have so far never been reported in the literature[2b].




**1**

Hydrolysis of the monomeric neutral complex (tacn)$FeCl_3$ (tacn = 1,4,7-triazacyclononane) in aqueous ammonium acetate solution and addition of NaI leads to precipitation of orange-brown crystals of the composition

$[(C_6H_{15}N_3)_2Fe_2O(CH_3CO_2)_2]I_2 \cdot 0.5\,NaI \cdot 3\,H_2O$ **2**[3].

The X-ray structure analysis of **2** shows that a dinuclear complex is formed (Fig. 1). The two $Fe^{III}$ centers are each surrounded by a distorted octahedral array of one *fac*-coordinated triamine, one μ-oxo ligand and two almost symmetrical μ-acetato ligands. This corresponds to the structure type **1** of the protein metazidohemerythrin[2b]. The Fe—O distances of the oxo-bridge (178(1) pm) are shorter than those of the acetato-bridges (203(2) pm); they indicate considerable π-bonding[4]. The Fe—N bonds *trans* to the O-atom of the oxo-bridge are somewhat longer (221(2) pm) than those *trans* to the O-atoms of the acetato-bridges (216(1) pm). This suggests a *trans*-effect of the oxo-bridge. The Fe...Fe distance (306.4(5) pm) is markedly shorter than has been found in all previous structural investigations on methemerythrin[1,2]; interpretation of the EXAFS measurements[1d] gives an Fe...Fe distance of 349(8) pm, whereas the Fe—O distance thus determined for the oxo-bridge (180 pm) is in very good agreement with our data.

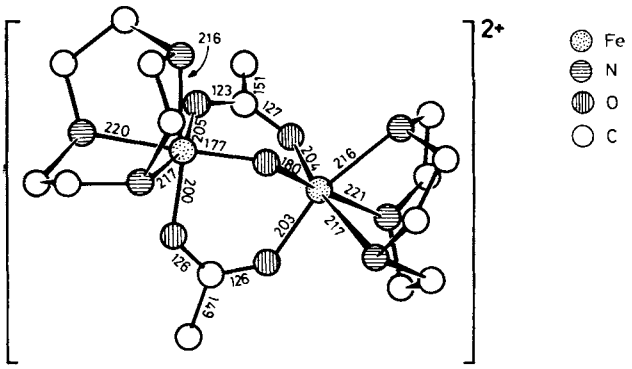



Fig. 1. Structure of the complex cation in the salt **2** (distances in pm with average standard deviation of 2 pm). Fe...Fe distance 306.4(5) pm; FeOFe angle 118.3(5)°. Space group $P2_1/c$, $a = 1323.4(7)$, $b = 1754.5(6)$, $c = 1525.0(4)$ pm, $\beta = 114.23(3)°$, $Z = 4$; 6050 independent reflections ($I > 3\sigma(I)$), $R = 0.062$. Further details of the crystal structure investigation are available on request from the Fachinformation Energie Physik Mathematik, D-7514 Eggenstein-Leopoldshafen on quoting the depository number CSD 50477, the names of the authors, and full citation of the journal.

The $Fe^{III}$ centers in **2** are coupled antiferromagnetically (temperature-dependent effective magnetic moment of 0.89 $\mu_B$ at 100 K and 1.84 $\mu_B$ at 283 K per $Fe^{III}$ center). This is in good agreement with the magnetic behavior of metaquohemerythrin[1b], for which antiferromagnetic coupling of two high-spin $Fe^{III}$ centers is assumed. The UV/VIS spectrum of **2** [286 nm ($\varepsilon = 2.5 \times 10^3$ L mol$^{-1}$ cm$^{-1}$ per Fe-atom) 412 (sh), 450 (350), 484 (sh), 711 (19)] is similar to that of metazidohemerythrin. An FeOFe-vibration is observed at 730 cm$^{-1}$ in **2**.


Received: May 16, 1983 [Z 386 IE]
German version: *Angew. Chem. 95* (1983) 739

CAS Registry numbers:
**2**, 86823-89-4; (tacn)$FeCl_3$, 86823-88-3.



[*] Prof. Dr. K. Wieghardt, K. Pohl
Lehrstuhl für Anorganische Chemie I der Universität
Postfach 102148, D-4630 Bochum (Germany)
Dr. W. Gebert
Institut für Mineralogie der Universität Bochum (Germany)



[**] This work was supported by the Deutsche Forschungsgemeinschaft and the Fonds der Chemischen Industrie.



[1] a) R. G. Wilkins, P. C. Harrington, *Adv. Inorg. Biochem.*, in press; b) J. W. Dawson, H. B. Gray, H. E. Hoenig, G. R. Rossman, J. M. Schredder, R.-H. Wang, *Biochemistry 11* (1972) 461; c) J. Sanders-Loehr, T. M. Loehr, A. G. Mauk, H. B. Gray, *J. Am. Chem. Soc. 102* (1980) 6992; d) W. T. Elam, E. A. Stern, J. D. McCallum, J. Sanders-Loehr, *ibid. 104* (1982) 6369.

[2] a) R. E. Stenkamp, L. C. Sieker, L. H. Jensen, J. Sanders-Loehr, *Nature (London) 291* (1981) 263; b) R. E. Stenkamp, L. C. Sieker, L. H. Jensen, *J. Inorg. Biochem.*, in press.

[3] *Procedure:* 12 mL of an ethanolic 1 M solution of 1,4,7-triazacyclononane (tacn) is added to a solution of $FeCl_3 \cdot 6\,H_2O$ (3.5 g) in ethanol (100 mL). The resulting bright yellow precipitate of (tacn)$FeCl_3$ is filtered off, washed with ethanol, and air-dried (3 g). 0.5 g of (tacn)$FeCl_3$ is dissolved with gentle warming in a saturated aqueous $NH_4OAc$ solution (20 mL). NaI (5 g) is added to the clear brown solution. After 12 h at 0°C the brown, crystalline precipitate of **2** is filtered off and air-dried (0.4 g). $ClO_4^-$ and $PF_6^-$ salts with the cation of **2** can also be obtained.

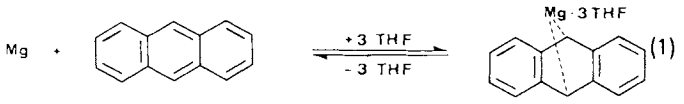
[4] K. S. Murray, *Coord. Chem. Rev. 12* (1974) 1.

# "Organically Solvated" Magnesium for the Synthesis of Transition-Metal Complexes and Catalysts

By *Helmut Bönnemann*, Borislav Bogdanović*, Rainer Brinkmann, Da-Wei He,* and *Bernd Spliethoff*

The method that has proved most useful for the synthesis of the species in the title is the reaction of transition-metal salts with reducing agents in the presence of suitable ligands[1]. The most suitable reducing agent is magnesium metal[2a], whose reactivity strongly depends on the size and purity of its active surface[2b]. Although numerous attempts have been made to improve the activity of elemental magnesium by additives[2c], no generally applicable method for the preparation of transition-metal complexes using magnesium as reducing agent has so far been reported in the literature.

Starting from the observation[3] that addition of a catalytic amount of anthracene to magnesium powder in tetrahydrofuran (THF) produces a highly reactive organically solvated magnesium (equilibrium (1)), we have worked out a simple preparative route to transition-metal complexes which for the first time allows magnesium powder to be used for the reductive synthesis of all preparatively important compounds of this type[4].



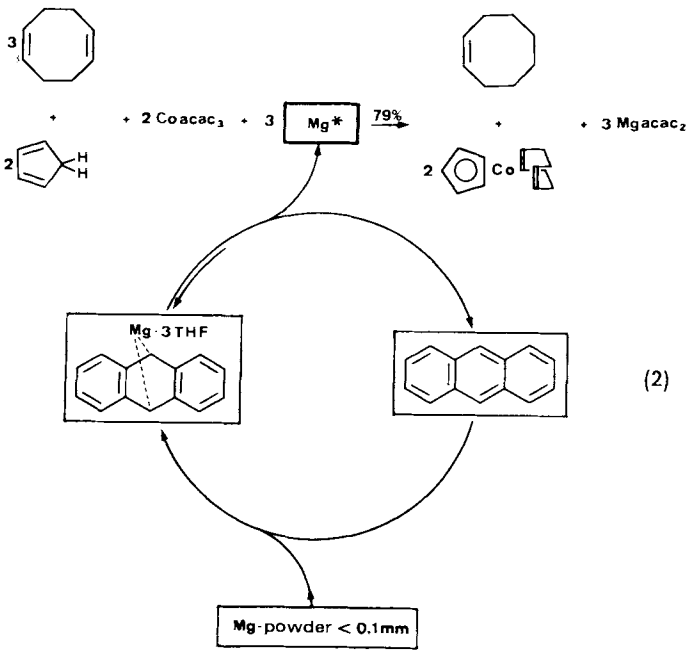
(1)

The reaction cycle depicted in (2) illustrates the catalytic function of the anthracene in the activation of magnesium powder: the hydrocarbon first reacts with the alkaline earth metal in THF to give a sparingly soluble adduct (for the structure cf. [3c]). The adduct formation is reversible[3b], *i.e.* in the equilibrium quasi-atomic magnesium is continually produced in solution. This means that the anthracene is acting as a phase-transfer catalyst[5]. The highly active magnesium so formed reacts exothermally with the transition-metal salt, which in the presence of electron donors is converted into the corresponding complex.

Cobalt salts, 1,5-cyclooctadiene (COD) and cyclopentadiene derivatives react smoothly to give, in one step, $\eta^5$-cyclopentadienylcobalt half-sandwich complexes which are of importance as catalysts for the synthesis of pyridines from alkynes and nitriles[6]. An excess of COD takes up the active hydrogen from the cyclopentadiene to give cyclooctene.

Decisive for the success of the synthesis is that the catalyst continually supplies highly reactive magnesium. One of the main advantages of this direct synthesis of transition-metal complexes using anthracene-activated magnesium is its extraordinary variability. Thus, we have so far also been able to prepare metallocenes ($Cp_2V$, $Cp_2Fe$, $Cp_2Co$), $\eta^3$-allyl complexes of Co and Ni, olefinmetal(0) compounds ($Ni(COD)_2$, $Pt(COD)_2$, $Mo(butadiene)_3$), as well as phosphane complexes ($Pd(PPh_3)_4$, $Ni(C_2H_4)[P(OC_6H_4Me)_3]_2$). All these species are active catalysts for organic reactions.

*Typical Procedure:* Magnesium powder (7.2 g, 300 mmol; particle size $<0.1$ mm) is treated in an inert atmosphere (argon) with 1.1 g (6.2 mmol) anthracene, 300 mL THF (purified over $NaAlEt_4/LiAlH_4$) and 0.1 mL methyl iodide. On stirring at 23 °C a yellow-green solution is formed, from which orange colored anthracenemagnesium separates in *ca.* 1—2 h. The mixture is subjected to an ultrasonic bath treatment for 3 h and heated with stirring to 65 °C. After addition of 27.0 g (250 mmol) COD and 7.3 g (111 mmol) monomeric cyclopentadiene, the source of heat is removed and solid cobalt(III) acetylacetonate (35.6 g, 100 mmol) is added portionwise to the continually stirred solution over 15 min, whereby the solution vigorously boils. After cooling to 20 °C and filtration through a G3 glass frit, the clear filtrate is evaporated to dryness in a high vacuum. The residue is taken up in 500 mL pentane and the solution filtered once again through a G3 glass frit. The complex (COD)CoCp crystallizes from the clear solution at $-80$ °C. The orange-brown crystals are washed with cold pentane and dried *in vacuo*; yield 18.4 g (79.1%).



(2)

Received: May 19, 1983 [Z 391]
German version: *Angew. Chem. 95* (1983) 749

[*] Prof. Dr. H. Bönnemann, Prof. Dr. B. Bogdanović, R. Brinkmann, D.-W. He, B. Spliethoff
Max-Planck-Institut für Kohlenforschung
Postfach 011325, D-4330 Mülheim a. d. Ruhr 1 (Germany)

[1] G. Wilke et al., DBP 1 191 375 (20. 04. 60/16. 12. 65), Studiengesellschaft Kohle m.b.H.; *Chem. Abstr. 63* (1965) 7045; P. W. Jolly in *Ullmanns Encyklopädie der technischen Chemie*, 4th Edit., Vol. *16*, p. 587, Verlag Chemie, Weinheim 1978.

[2] a) H.-F. Klein, H. H. Karsch, *Chem. Ber. 108* (1975) 944; W. Gausing, G. Wilke, *Angew. Chem. 93* (1981) 201; *Angew. Chem. Int. Ed. Engl. 20* (1981) 186; b) J. R. Blackborow, D. Young: *Metal Vapour Synthesis in Organometallic Chemistry*, p. 179, Springer, Berlin 1979; c) Y.-H. Lai, *Synthesis 1981*, 585.

[3] a) B. Bogdanović, S.-T. Liao, M. Schwickardi, P. Sikorsky, B. Spliethoff, *Angew. Chem. 92* (1980) 845; *Angew. Chem. Int. Ed. Engl. 19* (1980) 818; b) B. Bogdanović, S.-T. Liao, K. Schlichte, *3rd Int. Symp. Homogeneous Catalysis, Abstr. C 32* (1982) 104; c) B. Bogdanović, S.-T. Liao, R. Mynott, K. Schlichte, U. Westeppe, *Chem. Ber.*, in press.

[4] H. Bönnemann, B. Bogdanović, DBP 3 205 550.1 (Prior. 17. 02. 82); Eur. Pat. 83 101 246.3 (10. 02. 83), Studiengesellschaft Kohle m.b.H.

[5] According to V. Dehmlow in a discussion at the Chemiedozententagung 1983 in Dortmund, this is an example of a zero-valent transferred metal.

[6] H. Bönnemann, *Angew. Chem. 90* (1978) 517; *Angew. Chem. Int. Ed. Engl. 17* (1978) 505; H. Bönnemann, M. Samson, DBP 2 840 460 (16. 09. 78), Studiengesellschaft Kohle m.b.H.; H. Bönnemann, B. Bogdanović, W. Brijoux, R. Mynott: *Catalysis in Organic Chemistry*, Marcel Dekker, New York 1983; H. Bönnemann, W. Brijoux "The Cobalt-catalyzed Synthesis of Pyridine and its Derivatives" in R. Ugo: *Aspects of Homogeneous Catalysis*, Vol. *5*, D. Reidel, Dordrecht, in press.

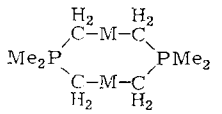
 © *Verlag Chemie GmbH, 6940 Weinheim, 1983* *0570-0833/83/0909-0728 $ 02.50/0* 

# Coinage Metal Complexes of Hexaphenylcarbodiphosphorane—Organometallic Compounds with Coordination Number 2

By *Hubert Schmidbaur**, *Christian E. Zybill*, *Gerhard Müller*, and *Carl Krüger*

*Dedicated to Professor Ulrich Wannagat on the occasion of his 60th birthday*

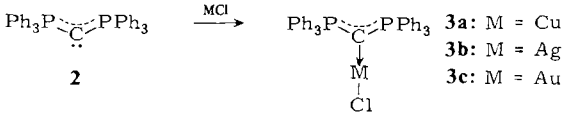
In organometallic compounds with gold in the oxidation state +1 the coordination number never as a rule exceeds 2, whereas with the lighter "coinage metals" this lower coordination number is exceptionally rare[1]. Among the few structurally characterized copper compounds with simple aliphatic ligands we find, besides the (trimethylsilylmethyl)copper(I) tetramer[2], also the dinuclear ylide complex **1a**[3a], in which two linear $CH_2CuCH_2$ groups are arranged parallel to each other. The corresponding silver and gold compounds **1b** and **1c**, respectively, have an analogous structure[3b].



**1a**: M = Cu
**1b**: M = Ag
**1c**: M = Au

We now report on the synthesis of coinage metal complexes of the double ylide[4] hexaphenylcarbodiphosphorane **2**, in which the strictly linear twofold coordination is ensured in all cases by the specific (especially steric) effect of the new ligand, even although the second ligand is a halide capable of functioning as a donor.

Suspensions of anhydrous CuCl or AgCl in tetrahydrofuran rapidly clarify on addition of a solution of **2** in the same solvent, and the reaction products **3a** and **3b**, respectively, crystallize from the mixtures on cooling. For the preparation of **3c** it is more advantageous to use (CO)AuCl as starting material, with removal of CO.



**2**

**3a**: M = Cu
**3b**: M = Ag
**3c**: M = Au

None of the three products[5a] is sensitive to air, and all are thermally stable up to *ca.* 200°C. Solutions of **3a**, **3b** and **3c** in $CD_2Cl_2$ show $^{31}P\{^1H\}$-NMR singlet signals at $\delta = 16.5$, 16.5, and 13.7, respectively. In the $^{13}C$-NMR spectra the signal of the ylidic C-atom is not observable; the phenyl signals conform to expectation [*e.g.* **3b**: $\delta = 132.6$, AA'X, $N = 95.7$ Hz, C-1; 127.9(4.9), C-2; 132.3, br, C-3; 130.8(4.9), C-4].

The X-ray structure analysis of **3a** shows[5b] that discrete molecules are present in the crystal, between which there are no unusually short contacts (Fig. 1). The ligand arrangement at the copper atom is practically linear with Cl–Cu–C1 = 178.2(1)°, while that at the ylidic carbon atom (C1) is trigonal planar. C1 is only 0.056 Å outside of the CuP1P2 plane, whereas the chlorine atom lies, within the standard deviation, in the plane (Fig. 2). The angles P1–C1–Cu and P2–C1–Cu, however, are very different

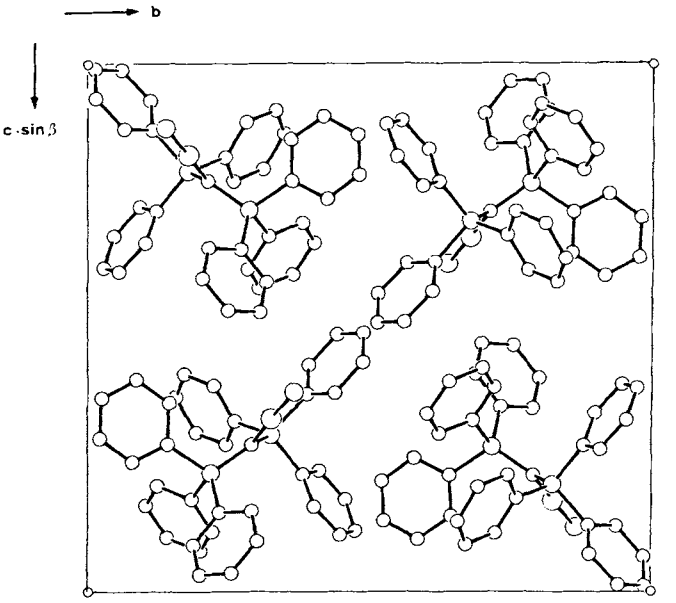



Fig. 1. Projection of a section from the crystal lattice of the copper complex **3a**.

(122.1(1) and 113.7(1)°, respectively); P1–C1–P2 is 123.8(1)° and is thus smaller than the corresponding angle in **2**. The especially interesting C1–Cu distance of 1.906(2) Å corresponds to a Cu–C($sp^2$) bond, as also exists, for example, in the bis(mesityl)copper(1–) ion (1.915(9) Å[6a]).

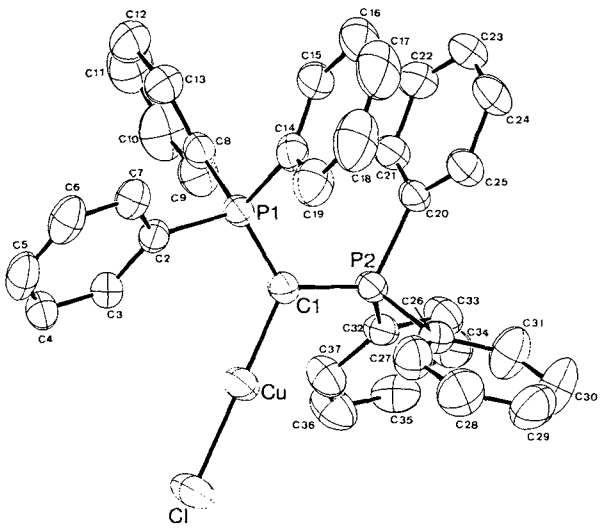
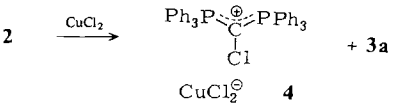



Fig. 2. Molecular structure of **3a** in the crystal [5b]. Some bond distances and angles are given in the text.

The compounds **3** are especially suitable for the synthesis of further lower coordinated organometallic derivatives.

Reaction of anhydrous $CuCl_2$ with **2** does not lead to $Cu^{II}$ coordination compounds but to reduction of the copper and oxidative halogenation of the carbodiphosphorane to give the salt **4**[5a] [$\delta(P) = 26.8$, s; $\delta(PCP) = 192$, t, $^2J(^{13}P^{13}C) = 113.3$ Hz[6b]; $\nu(CuCl_2) = 385$ cm$^{-1}$].



**4**

[*] Prof. Dr. H. Schmidbaur, Dr. C. E. Zybill
Anorganisch-chemisches Institut der Technischen Universität München
Lichtenbergstr. 4, D-8046 Garching (Germany)
Prof. Dr. C. Krüger, Dr. G. Müller
Max-Planck-Institut für Kohlenforschung
Kaiser-Wilhelm-Platz 1, D-4330 Mülheim a. d. Ruhr (Germany)

This behavior of **2** is in complete contrast to that of the simple ylides, which under comparable conditions undergo oxidative coupling to give bisphosphonium salts[6c].

Received: May 2, 1983 [Z 372 IE]
German version: *Angew. Chem. 95* (1983) 753

[1] Gold, silver: *Gmelin Handbuch der Anorganischen Chemie*, 8th Edit., Springer, Berlin 1975 and 1980; Copper: A. E. Jukes, *Adv. Organomet. Chem. 12* (1974) 215; F. H. Jardine, *Adv. Inorg. Chem. Radiochem. 17* (1975) 116.

[2] M. F. Lappert, R. Pearce, *J. Chem. Soc. Chem. Commun. 1973*, 24; J. A. J. Jarvis, B. T. Kilbourn, R. Pearce, M. F. Lappert, *ibid. 1973*, 475.

[3] a) H. Schmidbaur, J. Adlkofer, M. Heimann, *Chem. Ber. 107* (1974) 3697; H. Schmidbaur, J. Adlkofer, W. Buchner, *Angew. Chem. 85* (1973) 448; *Angew. Chem. Int. Ed. Engl. 12* (1973) 415; P. K. Mehrotra, R. Hoffmann, *Inorg. Chem. 17* (1978) 2187; G. Nardin, L. Randaccio, E. Zangrando, *J. Organomet. Chem. 74* (1974) C 23; - b) H. Schmidbaur, W. Richter, *Chem. Ber. 108* (1975) 2656; Y. Yamamoto, H. Schmidbaur, *J. Organomet. Chem. 96* (1975) 133; *97* (1975) 479; H. Schmidbaur, J. R. Mandl, W. Richter, V. Bejenke, A. Frank, G. Huttner, *Chem. Ber. 110* (1977) 2236; J. Stein, J. P. Fackler, C. Paparizos, H. W. Chen, *J. Am. Chem. Soc. 103* (1981) 2192.

[4] H. Schmidbaur, *Nachr. Chem. Tech. Lab. 27* (1979) 620.

[5] a) Procedure: A solution of **2** (444 mg, 0.83 mmol) in tetrahydrofuran (THF) (30 mL) is added dropwise to a suspension of anhydrous CuCl (82 mg, 0.83 mmol) in THF (10 mL), whereupon the CuCl almost completely dissolves. After filtration and cooling to 0°C, **3a** crystallizes as yellow cubes, m.p. 241°C (decomp.), yield 486 mg (92%).—**3b** is obtained in an analogous way, but as the THF-monoadduct, m.p. 234°C, yield 90%.—Colorless crystals of the THF-monoadduct of **3c** (decomp. 250°C, yield 87%) are likewise formed on reaction of (CO)AuCl and **2** in THF.—The preparation of **4** is analogous to that of **3a**. The product is very sparingly soluble in THF and is recrystallized from dichloromethane. Colorless cubic crystals ($CH_2Cl_2$-monoadduct), m.p. 210—212 (decomp.), yield 63%. b) Crystallographic data: $C_{37}H_{30}ClCuP_2$ (635.5983); P2$_1$/c, $Z=4$; $a=9.540(2)$, $b=18.741(3)$, $c=17.935(1)$ Å, $\beta=100.663(7)°$, $V=3151.35$ Å$^3$, $\rho_{calc.}=1.3396$ g cm$^{-3}$; $Mo_{K\alpha}$, $\lambda=0.71069$ Å, $T=21°C$, scan $\omega-2\vartheta$, $1.0<\vartheta<28.9°$, 8289 independent reflections, 2895 unobserved ($I<2\sigma(I)$), heavy atom method (SHELX-76), H atoms observed at $R=0.059$; from 490 refined parameters $R=0.0395$, $R_w=0.0464$. Further details of the crystal structure investigation are obtainable on request from the Fachinformationszentrum Energie Physik Mathematik, D-7514 Eggenstein-Leopoldshafen, on quoting the depository number CSD 50442, the names of the authors, and full citation of the journal.

[6] a) P. Leoni, M. Pasquali, C. A. Ghilardi, *J. Chem. Soc. Chem. Commun. 1983*, 240; b) R. Appel, F. Knoll, W. Michel, W. Morbach, H. D. Wihler, H. Veltmann, *Chem. Ber. 109* (1976) 58; c) G. A. Bowmaker, C. Dörzbach, H. Schmidbaur, unpublished.

## $(FMe_2Si)_2CF_2$: Synthesis and Reactions**

By *Gerhard Fritz** and *Heinz Bauer*

*Dedicated to Professor Ulrich Wannagat on the occasion of his 60th birthday*

The synthesis and reactive behavior of organosilicon compounds containing $CF_2$ groups have to our knowledge never been described in the literature. Reports have appeared, however, on NMR investigations of perfluoroalkylsilanes[1a] obtained by reaction of $CF_3I$ with $SiF_2$[1b].

*C*-Fluorinated carbasilanes are of interest in view of the known reactions of *C*-chlorinated compounds such as $(Cl_3Si)_2CCl_2$[2a] or $(Cl_2Si-CCl_2)_3$[2b]; *e.g.*, lithiation of the $CCl_2$ group in $(Cl_2Si-CCl_2)_3$ leads to ring contraction and ring opening[2b], and in the case of $ClMe_2Si(Me_3Si)CCl_2$ to ring closure with formation of a 2,4-disilabicyclo[1.1.0]butane[2c].

[*] Prof. Dr. G. Fritz, H. Bauer
Institut für Anorganische Chemie der Universität
Postfach 6380, D-7500 Karlsruhe 1 (Germany)

[**] This work was supported by the Deutsche Forschungsgemeinschaft.

Insertion of the carbene $CF_2$, generated by thermolysis of $Me_3SnCF_3$[3a], into the SiSi bond of $(FMe_2Si)_2$[3b] leads according to

$$FMe_2Si-SiMe_2F + :CF_2 \longrightarrow \underset{\mathbf{1}}{FMe_2Si-CF_2-SiMe_2F}$$

to formation of the new compound **1**, which we were able to isolate from the reaction mixture by gas chromatography[4]. At room temperature, and in the absence of air and moisture, **1** is a stable, colorless liquid, b.p. 161.6°C (extrapolated from the vapor pressure curve).

Unlike the corresponding *C*-chlorinated carbasilanes, **1** reacts with MeMgCl or MeLi, even at low temperatures, not with *C*-metalation but with *Si*-alkylation to give the products **2** and **3**[4]. Reaction of **1** with PhMgBr or PhLi analogously yields the phenyl derivatives **4** and **5**. That is, neither a CF- nor a CSi-cleavage takes place. Reaction of **1** with $LiAlH_4$ leads, depending upon the molar ratio, to **6** and **7**[4]. In all cases the $CF_2$ group remains inert.

| $RMe_2Si-CF_2-SiMe_2F$ | $RMe_2Si-CF_2-SiMe_2R$ |
|---|---|
| **2**: R = Me | **3**: R = Me |
| **4**: R = Ph | **5**: R = Ph |
| **6**: R = H | **7**: R = H |

Table 1. Spectroscopic data of the compounds **1**–**8**.

**1**: MS (EI): $m/z$ $Si_2C_5H_{12}F_4$ 204.04 deviation—1.1; $^1$H-NMR: $\delta=0.32$ (m), higher order; $^{13}C\{^1H\}$-NMR: $\delta=103.0$ (t) $CH_3$, −24.0 (d) $CF_2$, $^1J_{CF}=260$, $^2J_{CF}=25.9$ Hz; $^{19}$F-NMR: $\delta=144.7$ (m) FC, 166.0 (m) FSi, spin system $XA_6Y_2X'A'_6$; $^{29}Si\{^1H\}$-NMR: $\delta=20.35$ (m), $^1J_{SiF}=290.4$, $^2J_{SiF}=36.0$ Hz

**2**: $m/z$ 200.07, deviation 2.0; $\delta(^1H)=0.18$ (m) $Me_3Si$, 0.28 (dt) $Me_2Si$, $^3J_{HF}=8.2$, $^4J_{HF}=0.8$ Hz; $\delta(^{13}C\{^1H\})=97.2$ (dt) $CF_2$, −25.0 (dt) $Me_3Si$, −25.4 (dt) $Me_2Si$, $^1J_{CF}=255$, $^2J_{CF}=26$, $^2J_{MeF}=13$ Hz; $\delta(^{19}F)=141$ (d) FC, 165 (sept) FSi, $^3J_{FH}=8.2$, $^4J_{FH}=0.8$, $^3J_{FF}=6.8$ Hz; $\delta(^{29}Si\{^1H\})=1.43$ (t) $SiMe_3$, 20.43 (dt) $SiMe_2$, $^1J_{SiF}=285$, $^2J_{SiF}=37.5$ and 27.8 Hz

**3**: $m/z$ 196.02, deviation −1.0; $\delta(^1H)=0.10$ (t), $^4J_{HF}=0.7$ Hz; $\delta(^{19}F)=136.4$ (m)

**4**: $\delta(^1H)=0.43$ (dm) $Me_2SiF$, 0.15 (m) $Me_2SiPh$, 7.49 (m) Ph, $^3J_{HF}=7.2$ Hz; $\delta(^{19}F)=143.1$ (d) FC, 159.0 (3 × 7) FSi, $^3J_{FH}=7.2$, $^3J_{FF}=6.4$ Hz

**5**: $\delta(^1H)=0.18$ (t) Me, 7.32 (m) Ph, $^4J_{HF}=0.6$ Hz; $\delta(^{19}F)=133.5$ (m)

**6**: $\delta(^1H)=0.4$ (d) $Me_2SiF$, 0.12 (d) $Me_2SiH$, 4.08 (3 × 7) HSi, $^3J_{HF}=4.6$, $^3J_{HH}=3.7$, $^3J_{HF}=7.6$ Hz; $\delta(^{19}F)=137.3$ (dd) FC, 156.0 (sept) FSi, $^3J_{FF}=6.8$ Hz

**7**: $\delta(^1H)=0.2$ (d) $Me_2Si$, 4.03 (m) HSi, $^3J_{HH}=3.8$, $^3J_{HF}=11$ Hz; $\delta(^{19}F)=135.7$ (t)

**8**: $\delta(^1H)=0.41$ (d) $Me_2Si$, 1.28 (ddt) $Me_2PC$, 0.92 (ddt) $Me_2PP$, $^3J_{HF}=7.2$, $^2J_{HP}=11.6$ and 5.1, $^3J_{HP}=16.1$ and 3.9 Hz; $\delta(^{31}P\{^1H\})=9.1$ (dt) P=C, −59.5 (dm) PP, $^1J_{PP}=212.8$, $^3J_{PF}=2.6$ Hz

NMR data measured on **1** and **2** in $C_6D_6/CCl_4/C_6F_6$, on **3** to **7** in $Et_2O/C_6D_6/C_6F_6$, on **8** in $C_6H_6/C_6D_6$ [$^1$H (80 and 300 MHz); $^{13}$C (75.46 MHz), $^{29}$Si (59.26 MHz), $^{31}$P (121.49 MHz); $^{19}$F (84.6 MHz)]

It is well known that *C*-chlorinated carbasilanes cleave the SiP bond in silylphosphanes with formation of the ylide[5a]. Thus, $(Cl_3Si)_2CCl_2$ reacts with $Me_3Si-PMe_2$ to give $(Cl_3Si)_2C=PMe_2Cl$. The $CF_2$ group in **1** is also capable of undergoing this reaction, as is shown by the formation of the ylide **8**.

$$\underset{\mathbf{1}}{(FMe_2Si)_2CF_2} \xrightarrow[-\,Me_3SiF]{+\,Me_3SiPMe_2} \underset{\mathbf{9}}{\{(FMe_2Si)_2CF-PMe_2\}}$$

$$\underset{\mathbf{8}}{(FMe_2Si)_2C=PMe_2-PMe_2} \xleftarrow[-\,Me_3SiF]{+\,Me_3SiPMe_2} \underset{\mathbf{10}}{\{(FMe_2Si)_2C=PMe_2F\}}$$

 © Verlag Chemie GmbH, 6940 Weinheim, 1983 0570-0833/83/0909-0730 $ 02.50/0 

The intermediate **9** immediately rearranges to **10**. The reactions of **1** and **10** correspond to those of the analogous chloro compounds[5b], but take place only at elevated temperatures[4]. The reactivity of the $CF_2$ group can be attributed to the formation of the energetically favorable SiF bond.

Received: May 9, 1983 [Z 381 IE]
German version: *Angew. Chem. 95* (1983) 740

[1] a) K. G. Sharp, S. Li, R. B. Johannsen, *Inorg. Chem. 15* (1976) 2295; b) J. L. Margrave, K. G. Sharp, P. W. Wilson, *J. Inorg. Nucl. Chem. 32* (1970) 1817; K. G. Sharp, T. D. Coyle, *J. Fluorine Chem. 1* (1971) 249; *Inorg. Chem. 11* (1972) 1259.

[2] a) G. Fritz, W. Himmel, *Z. Anorg. Allg. Chem. 448* (1979) 40, 55; G. Fritz, S. Wartanessian, *J. Organomet. Chem. 178* (1979) 11; b) G. Fritz, N. Braunagel, *Z. Anorg. Allg. Chem. 399* (1973) 280; c) G. Fritz, S. Wartanessian, E. Matern, *ibid. 475* (1981) 87.

[3] a) E. Hengge, S. Waldhör, *Monatsh. Chem. 105* (1974) 671; K. G. Sharp, P. A. Sutor, *J. Am. Chem. Soc. 99* (1977) 8046; b) H. C. Clark, C. J. Willis, *ibid. 82* (1960) 1888; H. D. Kaesz, J. R. Philipps, F. G. A. Stone, *ibid. 82* (1960) 6229.

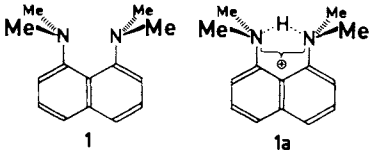
[4] Experimental: For the synthesis of **1**, a mixture of 6.1 g (26 mmol) of $Me_3SnCF_3$ and 4.0 g (26 mmol) of $(FMe_2Si)_2$ was heated in a sealed glass ampule (100 mL) at 160 °C for 3 d. After opening the ampule, the volatile reaction products were condensed in a cold trap (−196 °C). In addition to components that are gaseous at room temperature ($CHF_3$, $F_2C{=}CF_2$, $Me_2SiF_2$, $Me_3SiF$; total 0.06 g), liquid (**1**, $Me_4Si_2F_2$, $SnMe_4$, $Me_3SiF$; total 5.31 g) and solid ($Me_3SnF$; 4.7 g) components are also obtained. The liquid components can be separated gas chromatographically (column packing: silica gel with 5% SE 52, 120 °C, 0.4—0.6 bar, He), the yield of **1** being *ca.* 76%.—For the reaction of **1** (500 mg) in tetrahydrofuran with MeLi (1—2 M solution), the mixture prepared at −50 °C is warmed slowly to 20 °C; after separation of LiF there remain NMR spectroscopically pure Si-methylation products. The reactions with MeMgCl, PhMgBr, PhLi, and $LiAlH_4$ (in $Et_2O$) are carried out analogously; however, in the case of the phenyl compounds the temperature must be raised to 50 °C. For the reaction of **1** with $Me_3SiPMe_2$ the mixture must be heated in benzene for at least 6 h at 75 °C to initiate the reaction; consequently, compounds other than **8** are formed, especially $P_2Me_4$. The corresponding reaction of $(ClMe_2Si)_2CCl_2$ already takes place at 25 °C.

[5] a) G. Fritz, U. Braun, W. Schick, W. Hönle, H. G. von Schnering, *Z. Anorg. Allg. Chem. 472* (1981) 45; b) G. Fritz, W. Schick, unpublished results.

## 4,5-Bis(dimethylamino)fluorene, a New "Proton Sponge"

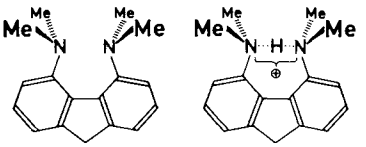
By *Heinz A. Staab**, *Thomas Saupe*, and *Claus Krieger*

According to *Alder et al.*[1], 1,8-bis(dimethylamino)naphthalene **1** ("proton sponge"[2]) is several orders of magnitude more basic than normal aromatic amines (**1**: $pK_a = 12.34$; *N,N*-dimethylaniline: $pK_a = 5.1$). This unusual basicity of **1** has been ascribed to the steric interaction of the two *peri*-dimethylamino groups and to the formation of a very strong N···H···N hydrogen bond in monoprotonated **1a**[1,3]. The search for similar "proton sponges" has previously been confined primarily to a variation of the 1,8-diaminonaphthalene system of **1** by substitution[4].



**1** **1a**

A model estimation shows, however, that the steric factors to which the specific basicity of **1** was attributed should be even more pronounced in 4,5-bis(dimethylamino)fluorene **2**: Based on the structures of naphthalene and fluorene, and assuming planarity for **1** and **2** with $C_{Aryl}-N$ bond lengths of 140 pm[3c], a significantly shorter N···N distance (231 pm) is derived for **2** than for **1** (245 pm). Corresponding steric interactions between the $Me_2N$ groups should likewise be preserved if the N···N distance in **2** is increased by deviations of the $C_{Aryl}-N$ bonds to opposite sides of the aromatic plane, as shown for **1** by X-ray structure analysis[3c]. A further difference between **1** and **2** should exist insofar as in the latter the lone pairs of electrons of the two nitrogen atoms, more so than in **1**, should be directed towards each other along the N···N connecting line. Therefore, in contrast to **1a** (N···H···N angle: *ca.* 140°)[3a], an approximately linear hydrogen bond was expected for monoprotonated **2a**.



**2** **2a**

4,5-Diaminofluorene[5a], by analogy to a procedure described for the synthesis of **1**[5b], was methylated with dimethyl sulfate (sodium hydride, tetrahydrofuran, 6 h reflux) to afford **2**[6] (m.p. = 69—69.5 °C) which, despite considerable steric hindrance, was obtained in 80% yield.

With perchloric acid, **2** forms **2a** · perchlorate[6] (m.p. = 295—296 °C, dec.); with excess perchloric acid double protonation of **2** was not observed. In the $^1$H-NMR spectrum of **2a** · perchlorate (360 MHz, [$D_6$]dimethyl sulfoxide) the four methyl groups of **2a** give rise to a singlet at $\delta = 3.19$, which through coupling to the proton of the hydrogen bond is split into a doublet with $J = 2.03$ Hz; a significantly higher coupling constant than is observed for **1a** · perchlorate[6] ($J = 1.92$ Hz). Compared to **2**, all fluorene protons of **2a** are shifted to higher $\delta$-values due to the positive charge on the nitrogen atoms. The proton of the hydrogen bond gives a strongly down-field shifted, broad singlet at $\delta = 18.25$.

The stronger basicity of **2** in comparison to **1** was shown by simple deprotonation experiments: Addition of **1a** · perchlorate to a solution containing an equimolar amount of **2** in [$D_6$]dimethyl sulfoxide gave rise to $^1$H-NMR signals of **1**, and those of **2** became correspondingly weaker. Integration of the signals of the $Me_2N$-protons (**1**: $\delta = 2.73$; **2**: $\delta = 2.62$; **1a**: $\delta = 3.11$; **2a**: $\delta = 3.19$; 360 MHz) in the equilibrium mixture indicates a **1**/**2**-ratio of *ca.* 4:1 (at 33 °C). Thus, **2** is able to deprotonate **1a**. On the basis of the $pK_a$ value of **1**, a $pK_a$ of *ca.* 13.5 is estimated for **2**.

An X-ray structure analysis of **2a** · perchlorate indicated that **2a** has $C_2$ symmetry and that the $C_2$ axis (in the direction of the crystallographic *b* axis) passes through C(9) and the midpoint of C(4A)–C(4A′) in the fluorene plane. **2a** and the perchlorate anions are stacked alternatingly along *b*. The atoms C(4) and C(4′) deviate by 10 pm from the mean plane of the remaining carbon atoms of the fluorene framework; the nitrogen atoms lie on opposite sides of this plane and deviate from it by 23 pm. The bond angles at nitrogen indicate that with inclusion of the hydrogen bond the bonds at the two nitrogens are arranged tetrahedrally. As expected, the N···N distance of 262.6(2) pm is very

[*] Prof. Dr. H. A. Staab, T. Saupe, C. Krieger
Abteilung Organische Chemie
Max-Planck-Institut für medizinische Forschung
Jahnstrasse 29, D-6900 Heidelberg 1 (Germany)

 © *Verlag Chemie GmbH, 6940 Weinheim, 1983* *0570-0833/83/0909-0731 $ 02.50/0* 

short; in contrast to **1a**, the N···H···N hydrogen bond is almost linear (178°).

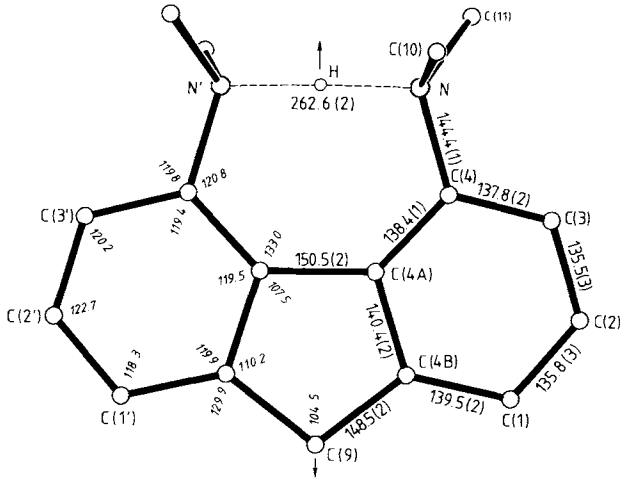



Fig. 1. Crystal structure of the **2a**-moiety of **2a**-perchlorate; view onto the fluorene plane: $a=843.7(1)$, $b=2554.5(2)$, $c=829.2(1)$ pm, $\beta=102.12(2)°$; space group C2/c, $Z=4$; 2206 measured, 1212 observed reflections; $R=0.061$. C(4)–N–C(10): 110.9; C(4)–N–C(11): 114.4; C(10)–N–C(11): 109.4; C(4)–N···N 105.0; C(10)–N···N: 107.0; C(11)–N···N: 109.8°. Further details of the crystal structure investigation can be obtained from the Fachinformationszentrum Energie Physik Mathematik, D-7514 Eggenstein-Leopoldshafen, by quoting the depository number CSD 50498, the names of the authors, and the journal citation.

Comparison of **1a** and **2a** clearly demonstrates the influence of steric factors on the N···H···N hydrogen bond. From the dependence found here for the 4,5-bis(dimethylamino) derivatives of 9,10-dihydrophenanthrene and—if accessible—of phenanthrene, interesting "proton sponge" properties may be expected.

Received: May 24, 1983 [Z 393 IE]
German version: *Angew. Chem. 95* (1983) 748

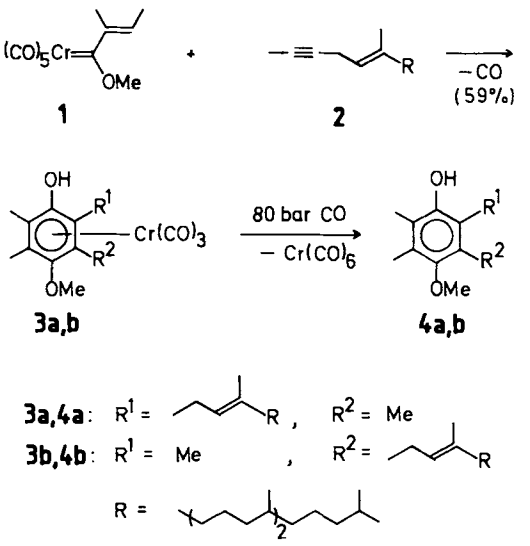
[1] R. W. Alder, P. S. Bowman, W. R. S. Steele, D. R. Winterman, *J. Chem. Soc. Chem. Commun. 1968*, 723.
[2] Trade name, *Aldrich Chemicals Co.*, Milwaukee, WI.
[3] a) M. R. Truter, B. L. Vickery, *J. Chem. Soc. Dalton Trans. 1972*, 395;—b) E. Haselbach, A. Henriksson, F. Jachimowicz, J. Wirz, *Helv. Chim. Acta 55* (1972) 1757;—c) H. Einspahr, J.-B. Robert, R. E. Marsh, J. D. Roberts, *Acta Crystallogr. B 29* (1973) 1611.
[4] Cf. R. W. Alder, M. R. Bryce, N. C. Goode, N. Miller, J. Owen, *J. Chem. Soc. Perkin Trans. 1 1981*, 2840 and references cited therein.
[5] a) Prepared by partial modification of the synthesis described by E. K. Weisburger, J. H. Weisburger, *J. Org. Chem. 20* (1955) 1396; E. K. Weisburger, *ibid. 21* (1956) 698; b) H. Quast, W. Risler, G. Döllscher, *Synthesis 1972*, 558.
[7] For these compounds correct elemental analyses were obtained. **2**: $^1$H-NMR (360 MHz, $CDCl_3$): $\delta=2.69$ (s, 12H), 3.90 (s, 2H), 6.96 (d, $J\approx7.8$ Hz, 2H), 7.08 (dd, $J\approx7.3$ and 0.7 Hz, 2H), 7.21 (dd, $J\approx7.3$ and 7.8 Hz, 2H); MS: $m/z=252$ (100%, $M^+$), 237 (50), 222 (36), 221 (78), 208 (30), 206 (58)]. **2a**·perchlorate: $^1$H-NMR (360 MHz, [D$_6$]dimethyl sulfoxide): $\delta=3.19$ (d, $J=2.03$ Hz, 12H), 4.10 (s, 2H), 7.61 (dd, $J=8.0$ and 7.4 Hz, 2H), 7.71 (d, $J=7.4$ Hz, 2H), 7.83 (d, $J=8.0$ Hz, 2H), 18.25 (br. s, 1H).

## A Carbene-Complex Route to Vitamin E**

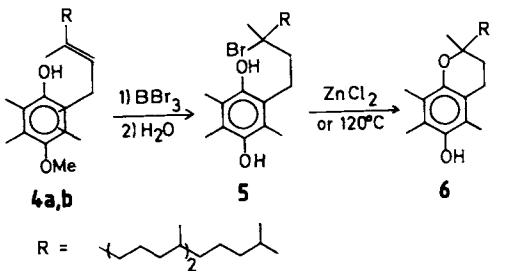
By *Karl Heinz Dötz** and *Werner Kuhn*

Alkyne, carbonyl, and unsaturated carbene ligands can cyclize in the coordination sphere of chromium(0) to afford metal-coordinated arenes[1,3]. Following the use of this type of reaction for the synthesis of compounds in the vitamin K series[5], we have turned our attention to vitamin E.

The carbene complex pentacarbonyl[(*E*)-1-methoxy-2-methyl-2-butenylidene]chromium **1** reacts with (*E*)-6,10,14,18-tetramethyl-5-nonadecen-2-yne (methylphytylacetylene) **2** to yield the metal-coordinated hydroquinone derivative **3** as the isomeric mixture **a** : **b** = 70 : 30, which can be separated by column chromatography on silica gel. The tricarbonylchromium residue can be cleaved at room temperature using CO under pressure: in this way the hexacarbonylchromium required for preparation of the carbene complex **1** is re-formed.




In order to be able to use both hydroquinone isomers (**4a** and **4b**) for the cyclization to the chroman framework, the 4-position is demethylated using boron tribromide[10]; hydrobromination of the allyl function to afford **5** occurs




simultaneously. The subsequent condensation step occurs, as is well-known, with Lewis acids such as anhydrous zinc chloride[11]. More advantageous, however, proved to be the thermally induced ring closure which leads practically quantitatively to α-tocopherol (vitamin E) **6**.

Received: April 5, 1983;
revised: July 4, 1983 [Z 384 IE]
German version: *Angew. Chem. 95* (1983) 750
The complete manuscript of this communication appears in: *Angew. Chem. Suppl. 1983*, 1045–1052

[*] Priv.-Doz. Dr. K. H. Dötz, W. Kuhn
Anorganisch-chemisches Institut der Technischen Universität München
Lichtenbergstrasse 4, D-8046 Garching (Germany)

[**] Vitamin Syntheses *via* Carbene Complexes, Part 5.—Part 4: [1].

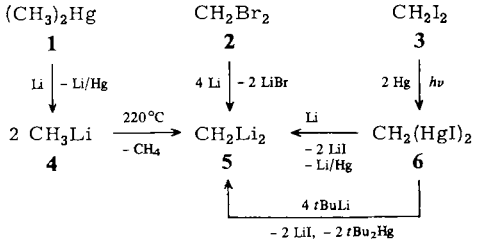
[1] K. H. Dötz, W. Kuhn, *J. Organomet. Chem.*, in press.
[3] K. H. Dötz, R. Dietz, *Chem. Ber. 111* (1978) 2517.
[5] K. H. Dötz, I. Pruskil, J. Mühlemeier, *Chem. Ber. 115* (1982) 1278.
[10] J. F. W. McOmie, D. E. West, *Org. Synth. Coll. Vol. V 1973*, 412.
[11] P. Karrer, H. Fritzsche, B. H. Ringier, H. Salomon, *Helv. Chim. Acta 21* (1938) 520.

 © *Verlag Chemie GmbH, 6940 Weinheim, 1983* *0570-0833/83/0909-0732 $ 02.50/0* 

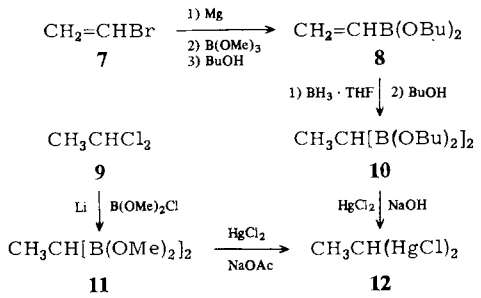
## 1,1-Dilithioethane**

By *Adalbert Maercker**, *Manfred Theis*, *Alexander J. Kos*, and *Paul von Ragué Schleyer*

Until now, dilithiomethane **5** was the only known geminal dilithioalkane. It was first obtained by *West* and *Rochow*[1a] from dibromomethane **2** and lithium in 6% yield. The yield was improved by *Lagow et al.*[1b] using a specially devised apparatus; however, mixtures of polylithio compounds were always formed that could not be separated. The best synthesis of **5** is the pyrolysis of salt-free methyllithium **4** described by *Ziegler et al.*[1c], but, unfortunately, this method does not lend itself to the preparation of higher dilithioalkanes.

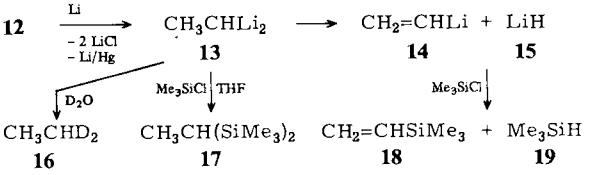



We have now found that the reaction of bis(iodomercurio)methane **6**[2] with lithium powder gives access to **5**; the method also permits the synthesis of higher 1,1-dilithioalkanes for the first time. 1,1-Bis(chloromercurio)ethane **12**, which is accessible by two routes, serves as starting material for the preparation of 1,1-dilithioethane **13**. Rather than starting from vinyl bromide **7**[3a], **12** can be obtained more straightforwardly from 1,1-dichloroethane **9**. This synthesis was elaborated from a known method[3b].




**12** reacts in diethyl ether at room temperature with lithium powder (2 h, molar ratio ≈ 1:20) to afford a black suspension. Immediate addition of this suspension, which consists of 1,1-dilithioethane **13**, lithium chloride, and lithium amalgam, to $D_2O$ gives pure 1,1-dideuterioethane **16**, in almost quantitative yield, and mercury[4].

The starting material **12** or possible intermediates, such as ethylmercury chloride or diethylmercury, do not react with lithium under these conditions of hydrolysis. Treatment of **13** directly after its preparation with chlorotrimethylsilane/tetrahydrofuran (*ca.* 1:1) (reaction time 24 h at room temperature) gives 1,1-bis(trimethylsilyl)ethane **17** (30%) in addition to trimethylsilane **19** (15%) and reduction products of trimethylvinylsilane **18**. This suggests partial decomposition of **13** into vinyllithium **14** and lithium hydride **15**.




If the reaction product from **12** and lithium is first filtered off and refluxed with chlorotrimethylsilane in the absence of solvent, exclusively **18** and **19** are formed. Under these conditions **18** is not reduced, although lithium was present in considerable excess. As no organolithium compounds were detectable in the filtrate, **13** must have decomposed by loss of lithium hydride only after filtration since, as is well-known, vinyllithium is soluble in diethyl ether. In contrast to 1,1-dilithioethane **13**, dilithiomethane **5** decomposes slowly into lithium hydride **15** and lithium acetylide[1c], since a 1,2-elimination of lithium hydride is not possible.

The dilithio compound **5** can be obtained free of lithium amalgam if **6** is allowed to react with excess *tert*-butyllithium in hexane instead of with lithium powder. In contrast, 1,1-dilithioethane **13** is not accessible by this route: vinyllithium **14** immediately forms.

The thermodynamic stability and structure of **13** can be discussed by considering hypothetical gas phase monomers, which can be satisfactorily described by *ab initio* calculations at the 3—21 G basis set level[5].

**13** is destabilized relative to ethyllithium **20** due to the presence of the second lithium atom, as revealed by the following formal disproportionation:

$$\underset{\mathbf{20}}{2CH_3CH_2Li} \longrightarrow \underset{\mathbf{13}}{CH_3CHLi_2} + C_2H_6 \qquad 6.1\ \text{kcal/mol}$$

The methyl group, which destabilizes ethyl- relative to methyllithium, also has an unfavorable effect in **13**[6a]:

$$\underset{\mathbf{5}}{CH_2Li_2} + C_2H_6 \longrightarrow \underset{\mathbf{13}}{CH_3CHLi_2} + CH_4 \qquad 12.4\ \text{kcal/mol}$$

The difficulties experienced in the preparation of **13** can, in part, be attributed to this destabilizing effect. Because of lithium-hydrogen interactions, which lead to a partially double-bridged structure, the isomeric 1,2-dilithioethane **21** is much lower in energy[6b]:

$$\underset{\mathbf{13}}{CH_3CHLi_2} \longrightarrow \underset{\mathbf{21}}{LiCH_2CH_2Li} \qquad -17.6\ \text{kcal/mol}$$

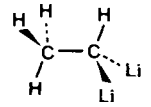
At room temperature **13** decomposes quantitatively within 8 h to afford lithium hydride and vinyllithium. It has been suggested that this reaction proceeds *via* a vinyllithium-lithium hydride complex **22**, which is more stable than the monomers **14** and **15**[6c]:

$$\underset{\mathbf{14}}{CH_2{=}CHLi} + \underset{\mathbf{15}}{LiH} \longrightarrow \underset{\mathbf{22}}{CH_2{=}CHLi_2H} \qquad -51.0\ \text{kcal/mol}$$

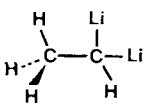
**13** and **21** are less stable than **22** by 47.5 and 29.8 kcal/mol, respectively.

[*] Prof. Dr. A. Maercker, M. Theis
Institut für Organische Chemie der Universität
Adolf-Reichwein-Strasse, D-5900 Siegen 21 (Germany)
Prof. Dr. P. von R. Schleyer, Dr. A. J. Kos
Institut für Organische Chemie der Universität Erlangen-Nürnberg
Henkestrasse 42, D-8520 Erlangen (Germany)

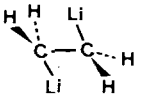
[**] This work was supported by the Fonds der Chemischen Industrie. Professor Dr. D. Seebach, Zürich, is thanked for helpful discussions.



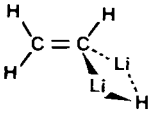
13a



13b



21



22

The structure of **13** optimized using the 3–21 G basis set is "classical" and exhibits no special Li···H or Li··Li interactions. The C–Li bond in **13a** (2.007 Å) is calculated to be only slightly shorter than that in ethyllithium **20** (2.017 Å), the length of the C–C bond is 1.581 and 1.563 Å, respectively. In addition, the energy difference between the staggered and eclipsed conformations of **13** also suggests no special Li···H interaction.

The 1,1-dilithioethane conformer **13b** is only 1.1 kcal/mol less stable than **13a** and displays a strong Li···H interaction. **13b** could, therefore, be an intermediate arising from elimination of LiH.

Received: March 1, 1983;
revised: July 13, 1983 [Z 296/315 IE]
German version: *Angew. Chem. 95* (1983) 755

[1] a) R. West, E. G. Rochow, *J. Org. Chem. 18* (1953) 1739; b) J. A. Gurak, J. W. Chinn, Jr., R. J. Lagow, *J. Am. Chem. Soc. 104* (1982) 2637; c) K. Ziegler, K. Nagel, M. Patheiger, *Z. Anorg. Allg. Chem. 282* (1955) 345.

[2] J. Sakurai, *J. Chem. Soc. 39* (1881) 485.

[3] a) D. S. Matteson, J. G. Shdo, *J. Org. Chem. 29* (1964) 2742; b) R. B. Castle, D. S. Matteson, *J. Organomet. Chem. 20* (1969) 19; A. Mendoza, D. S. Matteson, *ibid. 152* (1978) 1.

[4] Procedure: **12** (1.0 g, 2 mmol) is added to a suspension of lithium powder (0.6 g, 80 mmol, 2% sodium) in anhydrous diethyl ether (20 mL) under argon, and the mixture stirred for 2 h at room temperature; during this time the initial grey color becomes black. For the derivatization the mixture is immediately added to 20 mL $D_2O$ at 0°C and stirred vigorously: the 1,1-dideuterioethane **16** formed is trapped at −196°C. Gas analysis was carried out using a GC/MS coupling (glass column, Porapak Q 100/120 mesh, Ø 5 mm, length 70 cm). The precipitated mercury (0.7 g, 88%) was determined gravimetrically.

[5] J. S. Binkley, J. A. Pople, W. J. Hehre, *J. Am. Chem. Soc. 102* (1980) 939; J. S. Binkley, R. Whiteside, R. Krishnan, R. Seeger, H. B. Schlegel, D. J. DeFrees, J. A. Pople, *QCPE 11* (1981) 406.

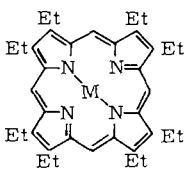
[6] a) P. von R. Schleyer, J. Chandrasekhar, A. J. Kos, T. Clark, G. W. Spitznagel, *J. Chem. Soc. Chem. Commun. 1981*, 882; b) A. J. Kos, E. D. Jemmis, P. von R. Schleyer, R. Gleiter, U. Fischbach, J. A. Pople, *J. Am. Chem. Soc. 103* (1981) 4996; c) P. von R. Schleyer, A. J. Kos, E. Kaufmann, *ibid.*, in press.

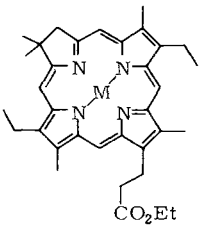
## Novel Methods for Demetalating Tetrapyrrolic Metallo-Macrocycles**

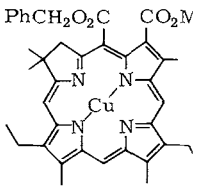
By *Alan R. Battersby*, Keith Jones,* and *Roger J. Snow*

Many natural tetrapyrrolic pigments occur as complexes with metal ions; this applies to most porphyrins, chlorins, bacteriochlorins, and corrins[1,2]. In addition, several synthetic routes to such macrocyclic systems generate metallo-complexes, *e.g.*, the $Cu^{II}$-promoted cyclization of dimethyl-*a,c*-biladienes, which is very effective for the synthesis of $Cu^{II}$-porphyrins[3]. Often it is desirable to eliminate the metal ion from the metallo-complexes in order to release the sequestering organic macrocycle in its free form: this is normally achieved by treating the metallo-complex with protic acids[4]. Removal of the metal ion in this way from the porphyrin complexes may be facile as, for example, with $Zn^{II}$ and $Mg^{II}$; however, in other cases demetalation may be difficult, and examples are common where either repetitive treatment with strong acids or forcing conditions such as dissolution in 100% sulfuric acid are necessary[4]. Clearly, these methods would cause difficulties if the macrocycle carries sensitive groups. Accordingly, we sought methods which might achieve rapid, relatively mild demetalation.

We reasoned that a promising approach would be to combine a protic acid with a reagent expected to precipitate or complex the liberated metal ion. This led to trifluoroacetic acid (TFA) with either 1,2-ethanedithiol or 1,3-propanedithiol as the preferred reagents; a solution of $H_2S$ in TFA is also effective but, in the cases studied so far, reacts more slowly.







6

**1**, M = $Cu^{II}$
**2**, M = H, H
**3**, M = $Ni^{II}$
**4**, M = $Cu^{II}$
**5**, M = H, H

Typical conditions for demetalation are as follows: The $Cu^{II}$-complex **1** (25 mg) of octaethylporphyrin (OEP) was treated at *ca.* 20°C in TFA (5 mL) with 1,2-ethanedithiol (40 µL); demetalation was complete in < 10 min as shown by UV/VIS spectroscopy; the reaction mixture was diluted with chloroform, shaken with 1 M sodium hydroxide, and the product from the chloroform layer was chromatographed to give pure OEP **2** in 97% yield. Increasing the quantity of thiol accelerated still further the demetalation. Use of 1,3-propanedithiol (10 µL for 1 mL TFA) also led to essentially quantitative removal of copper, in 25 min. The alternative method involved suspending $Cu^{II}$-OEP **1** (5 mg) in TFA (2 mL) through which $H_2S$ was bubbled for 2 min and then sealing the flask. Demetalation was complete in 1.5 h.

The nickel porphyrin **3** was also successfully demetalated, the only difference being the slightly slower rate of reaction with the thiols; the times for completion under the same conditions as used above were 20 min (1,2-ethanedithiol), 35 min (1,3-propanedithiol), and 1 h ($H_2S$). The complete removal of $Ni^{II}$ using these methods contrasts with the results using protic acids. Treatment of $Ni^{II}$-OEP **3** (1 mg) with neat TFA (1 mL) gave 50% demetalation after 15 min and 70% after 1 h, this being unchanged after 6 h. Similarly, TFA-$H_2SO_4$ gave 70% demetalation after 10 min and the same value after 1 h. Clearly an equilibrium is reached which is displaced by the thiols or $H_2S$[5].

Finally, the $Cu^{II}$-chlorins[6] **4** and **6** were demetalated essentially quantitatively using TFA-$H_2S$. For example, **4** (5 mg) in TFA (6 mL) was saturated with $H_2S$ and the mixture kept at *ca.* 20°C for 18 h; work-up and chromatography gave the metal-free chlorin **5** in 71% isolated yield.

[*] Prof. Dr. A. R. Battersby, Dr. K. Jones, Dr. R. J. Snow
University Chemical Laboratory
Lensfield Road, Cambridge, CB2 1EW (England)

[**] This work was supported by the Science and Engineering Research Council.

We believe these reagents, especially those based on dithiols, have considerable potential and warrant wider exploration.

Received: April 29, 1983 [Z 365 IE]
German version: *Angew. Chem. 95* (1983) 742

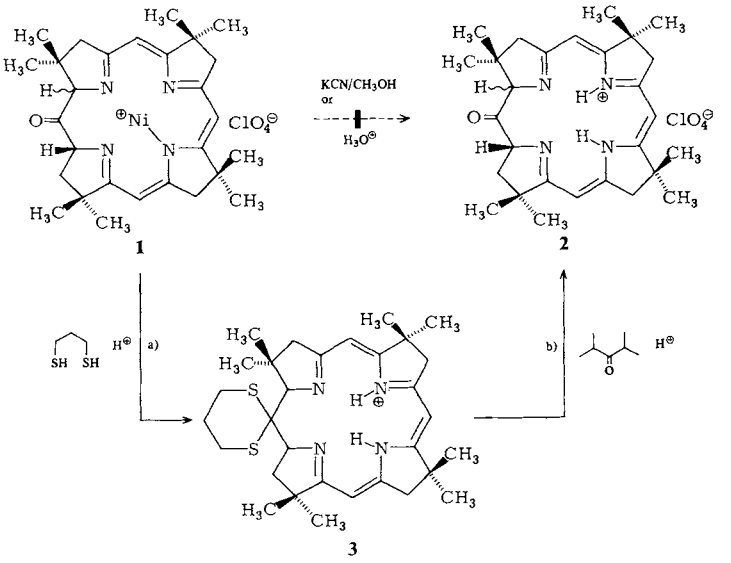
[1] K. M. Smith: *Porphyrins and Metalloporphyrins*, Elsevier, Amsterdam 1975.
[2] D. Dolphin: *The Porphyrins*. Vols. I and II, Academic Press, New York 1978.
[3] A. W. Johnson, I. T. Kay, *J. Chem. Soc. 1961*, 2418; I. D. Dicker, R. Grigg, A. W. Johnson, I. T. Kay, *J. Chem. Soc. C 1971*, 536.
[4] J. W. Buchler in [1], p. 157 and in [2], *Vol. I*, p. 390.
[5] After developing these reagents, we learned that 1,2-ethanedithiol had been tried independently for $Cu^{II}$-demetalation (P. S. Clezy, A. J. Liepa, N. W. Webb, *Aust. J. Chem. 25* (1972) 1991), but for the compound of interest to the authors offered no advantage over the $H_2SO_4$ method [4].
[6] R. J. Snow, C. J. R. Fookes, A. R. Battersby, *J. Chem. Soc. Chem. Commun. 1981*, 524.

## Acid-Catalyzed Demetalation of Nickel-Hydrocorphin and Cobalt-Corrin Complexes with 1,3-Propanedithiol**

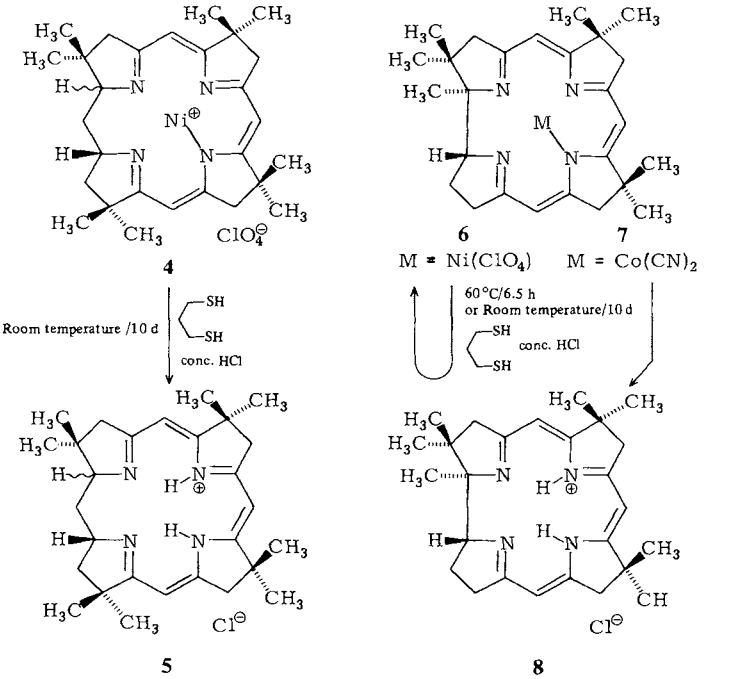
By *Norman J. Lewis, Andreas Pfaltz,* and *Albert Eschenmoser**

In investigating the chemistry of the hydrocorphinol→corrin rearrangement, we attempted to obtain the metal-free ligand system of the 20-keto-tetrahydrocorphin **2** by demetalation of the nickel(II) hydrocorphinate **1**[1] (see Scheme 1) in order to examine the possibility of A/D ring contraction. Both acids and cyanide ion were unsuccessful in effecting such a decomplexation, *e.g.*, treatment of **1** with KCN in degassed methanol at 100°C left the nickel complex essentially unchanged even after several hours[2]. Attempts at decomplexation with strong acids gave either starting material or complex mixtures of products. In striking contrast was the result obtained with 1,3-propanedithiol, which *Battersby et al.*[3] had used to decomplex a nickel-isobacteriochlorinate: By allowing **1** to stand for several days in (degassed) concentrated hydrochloric acid in the presence of excess 1,3-propanedithiol, we obtained the metal-free (crystalline) dithioketal **3** in 60% yield. The target compound **2** was then produced by acid-catalyzed transacetalization.

Subsequently, we carried out decomplexation experiments with 1,3-propanedithiol in the corrin series, where demetalation of nickel and cobalt complexes had not been achieved without destruction of the ligand system (cf. lit. in [3] and Scheme 2). Conditions which decomplexed the nickel(II)*tetrahydrocorphinate* **4**[4] cleanly to the free ligand **5** (UV/VIS) left the nickel(II) *corrinate* **6**[4] unchanged, even at 60°C. *In contrast, the cobalt(III) corrin complex* **7**[4] *was smoothly decomplexed with 1,3-propanedithiol.* The metal-free corrin, isolated in 83% yield as the crystalline hydrochloride **8**, was characterized by UV/VIS (Fig. 1), fluorescence, $^1$H-NMR, and mass spectroscopy. Among the reaction conditions that effected smooth demetalation of **7** (but not of **6**), were the following: 1,2-ethanedithiol instead of 1,3-propanedithiol or (!) 1-propanethiol in degassed $CHCl_3$ (but not $CH_3OH$) containing HCl (g), at room temperature for 5 days. This is remarkable in view of the vigorous conditions used to prepare the cobalt complex **7** from its 15-cyano derivative in over 85% yield[4] (40 h, 230°C, degassed 0.1 N hydrochloric acid).




Scheme 1. a) **1** (20 mg) in 10 mL conc. HCl + 0.1 mL 1,3-propanedithiol degassed in sealed tube, RT, 11 d in the dark; worked-up with 0.1 N $HClO_4$, short-column chromatography on silica gel (1% $NaClO_4$), $CH_2Cl_2$/ether (10:1); **3**: red crystals from $CH_2Cl_2/CH_3COOCH_3$, m.p. = 283°C, yield 60%.—b) **3** (10 mg) in 5 mL diisopropyl ketone/conc. HCl (1:1) degassed in sealed tube, RT, 2 d in the dark; worked-up with 0.1 N $HClO_4$, short-column chromatography on silica gel (1% $NaClO_4$), $CH_2Cl_2$/ether (10:1); **2**: red crystals from $CH_2Cl_2/CH_3COOCH_3$/hexane, m.p. = 174°C, yield *ca.* 30% (not optimized).




Scheme 2. a) **7** (25 mg) in 12 mL conc. HCl + 0.1 mL (≈*ca.* 20 molar equiv.) 1,3-propanedithiol degassed in sealed tube, heated 6.5 h, 60°C. **8**: dark orange crystals from $CH_2Cl_2/CH_3COOC_2H_5$ under argon, m.p. > 165°C (decomp.), yield 83%.

[*] Prof. Dr. A. Eschenmoser, Dr. N. J. Lewis [+], Dr. A. Pfaltz
Laboratorium für Organische Chemie
der Eidgenössischen Technischen Hochschule
ETH-Zentrum, Universitätstrasse 16, CH-8092 Zürich (Switzerland)
[+] Current address: Smith Kline & French
Old Powder Mill, Near Leigh, Tonbridge, Kent (England)

[**] This work was supported by the Schweizerischer Nationalfonds zur Förderung der wissenschaftlichen Forschung. *N. J. L.* thanks the Royal Society, London, for a postdoctoral fellowship under the European Science Exchange Program. We thank Dr. *D. A. Livingston* for translating the German manuscript and Prof. *Battersby* for a personal communication (cf. [3]).

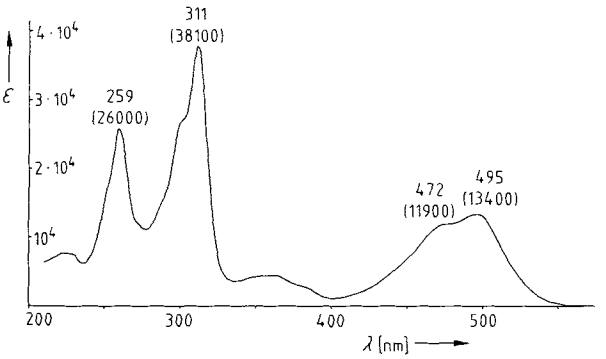



Fig. 1. UV/VIS spectrum of **8** in $CH_3OH$. $c = 4.55 \times 10^{-5}$ M. $\lambda_{max} = 259$ ($\varepsilon = 26000$), 286 (sh, 14000), 300 (sh, 27000), 311 (38100), 346 (sh, 4200), 360 (4400), 384 (2600), 472 (sh, 11900), 495 (13400) nm.

The differing behavior of the nickel(II) complexes **4** and **6**, whose ligand systems have similar chromophores but dissimilar carbon-nitrogen skeletons, presents further evidence that the corrin system is sterically a better ligand for $Ni^{2+}$ than hydroporphinoid systems[5]. The difference in the behavior of the nickel and cobalt corrin complexes corresponds to a known trend in the chemistry of the two transition metal ions (Co(III) is likely to be reduced to Co(II) before decomplexation). Moreover, the decomplexation of a cobalt corrin complex is a *novum*, which promotes the original synthesis of corrin complexes *via* A/B ring closure[4c] to a synthesis of metal-free corrins (see, however, [6]).

Received: April 29, 1983 [Z 366 IE]
German version: *Angew. Chem. 95* (1983) 743

[1] a) A. Fässler, A. Pfaltz, P. M. Müller, S. Farooq, C. Kratky, B. Kräutler, A. Eschenmoser, *Helv. Chim. Acta 65* (1982) 812; b) P. M. Müller, S. Farooq, B. Hardegger, W. S. Salmond, A. Eschenmoser, *Angew. Chem. 85* (1973) 954; *Angew. Chem. Int. Ed. Engl. 12* (1973) 914; c) P. M. Müller, Dissertation, ETH Nr. 5135, Juris Druck + Verlag, Zürich 1973; d) V. Rasetti, K. Hilpert, A. Fässler, A. Pfaltz, A. Eschenmoser, *Angew. Chem. 93* (1981) 1108; *Angew. Chem. Int. Ed. Engl. 20* (1981) 1058.

[2] Cf. the decomplexation of the corresponding nickel(II) A/D-secocorrinate by cyanide at room temperature within minutes; A. Eschenmoser, *Pure Appl. Chem. 20* (1969) 1, 11. See also J. W. Buchler in K. M. Smith: *Porphyrins and Metalloporphyrins*, Elsevier, Amsterdam 1975, pp. 157–231.

[3] Prof. Battersby, personal communication 1980; cf. A. R. Battersby, K. Jones, R. J. Snow, *Angew. Chem. 95* (1983) 742; *Angew. Chem. Int. Ed. Engl. 22* (1983) 734.

[4] Origin of the complexes **4**, **6**, and **7**: a) **4**: Sample from P. M. Müller [1c] (pp. 43 and 140–144), see also footnote 8 in [1a]; b) **6**: produced by complexation of **8** with 6 molar equiv. $NiCl_2 \cdot 6H_2O$ and excess NaCl in $CH_3CN$ at 65 °C for 5 h; m.p. = 172 °C, yield 56%; see also [2a], where the UV/VIS spectrum of **6** is reproduced; c) **7**: I. Felner, A. Fischli, A. Wick, M. Pesaro, D. Bormann, E. L. Winnacker, A. Eschenmoser, *Angew. Chem. 79* (1967) 863; *Angew. Chem. Int. Ed. Engl. 6* (1967) 864; experimental details in E. L. Winnacker, Dissertation ETH Nr. 4177, Juris Druck + Verlag, Zürich 1968 (p. 70); A. Eschenmoser, *Q. Rev. Chem. Soc. 24* (1970) 366.

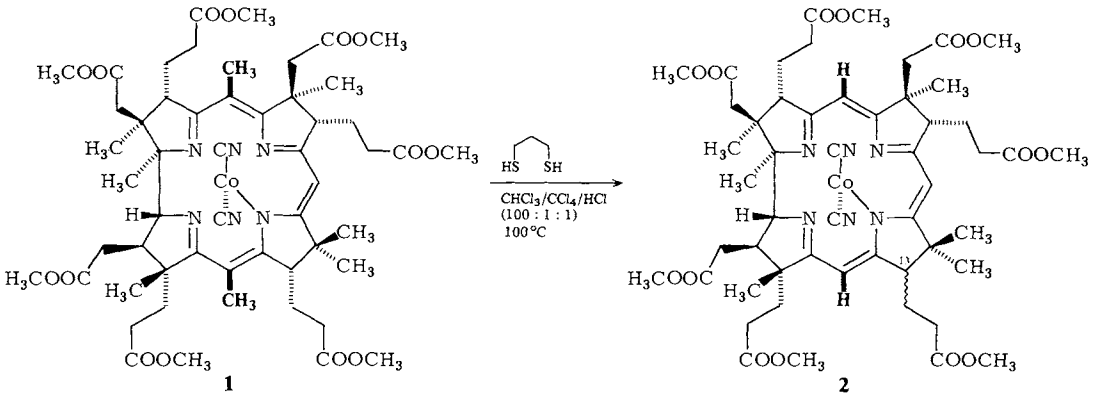
[5] J. E. Johansen, V. Piermattie, Ch. Angst, E. Diener, Ch. Kratky, A. Eschenmoser, *Angew. Chem. 93* (1981) 273; *Angew. Chem. Int. Ed. Engl. 20* (1981) 261; C. Angst, C. Kratky, A. Eschenmoser, *ibid. 93* (1981) 275; *20* (1981) 263: see also J. W. Buchler in D. Dolphin: *The Porphyrins, Vol. IA*, Academic Press, New York 1978, p. 389, particularly p. 472.

[6] N. J. Lewis, R. Nussberger, B. Kräutler, A. Eschenmoser, *Angew. Chem. 95* (1983) 744; *Angew. Chem. Int. Ed. Engl. 22* (1983) 736.

## 5,15-Bisnorcobester: an Unexpected Mode of Formation**

By *Norman J. Lewis, Rolf Nussberger, Bernhard Kräutler,* and *Albert Eschenmoser**

The decomplexation of a cobalt(III) corrin complex[1], led us to also attempt a demetalation in the vitamin $B_{12}$ series. This was not successful, but in the course of our attempts we discovered a remarkable reaction of the cobester (heptamethylcobyrinate) **1**[2].




Scheme 1. a) **1** (20.00 mg) in 20 mL $CHCl_3$, satd. at 0 °C with HCl(g) (ca. 1 wt-%) + 0.2 mL $CCl_4$ + 0.1 mL 1,3-propanedithiol, degassed (−190 °C, 2×) and sealed in an ampule (0.5 torr), heated for 4.5 d at 100 °C. Crude product methanolyzed at 65 °C in 30 mL $CH_3OH$/7 vol-% $H_2SO_4$, under argon, 2 d (reconstitution of the methoxycarbonyl groups). Chromatography on silica gel and (3×) crystallization ($CH_3CO_2CH_3$/hexane), m.p. = 114 °C, yield 56% (experimental details in R. Nussberger, Disseration ETH Zürich, in preparation).

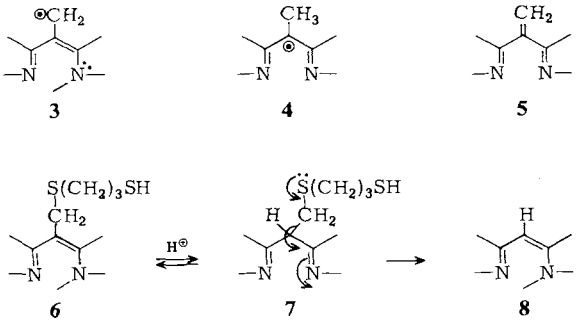
Reaction of 1,3-propanedithiol in concentrated hydrochloric acid with cobester resulted in complex (water soluble) product mixtures with considerable loss of chromophore, but without any indication of demetalation. *Anhydrous* reaction conditions (1,3-propanedithiol + HCl(g) in $CHCl_3$, exlusion of air) led to cobalt(II)-corrinoids. Use of drastic reaction conditions (100 °C, 4 d) led to a particularly interesting result: after reoxidation of the reaction mixture with KCN/air ($Co^{II} \rightarrow Co^{III}$) and chromatographic purification of the products, a fraction with the hypsochromically

[*] Prof. Dr. A. Eschenmoser, Dr. N. J. Lewis [+], Dr. B. Kräutler, R. Nussberger
Laborarotium für Organische Chemie
der Eidgenössischen Technischen Hochschule
ETH-Zentrum, Universitätstrasse 16, CH-8092 Zürich (Switzerland)

[+] Present address: Smith Kline & French
Old Powder Mill, Near Leigh, Tonbridge, Kent (England)

[**] This work was supported by the Schweizerischer Nationalfonds zur Förderung der wissenschaftlichen Forschung. *N. J. L.* thanks the Royal Society, London for a postdoctoral fellowship as part of the European Science Exchange Programme.

shifted UV/VIS spectrum of the chromophore of 5,15-bisnorcobester **2**[3] was observed. The reaction is only reproducible in the presence of small amounts of $CCl_4$. Under optimized conditions (Scheme 1) the didemethylation proceeds almost quantitatively (UV/VIS spectroscopy). The crystalline product (56%) had identical UV/VIS, CD, IR, $^1H$- and $^{13}C$-NMR, as well as mass spectra (fast-atom bombardement technique) as a sample of a (1:1) crystallizate of 13α- and 13β-5,15-bisnorcobester **2** (spectra shown in[3]) obtained earlier in this laboratory by total synthesis[3a,b].

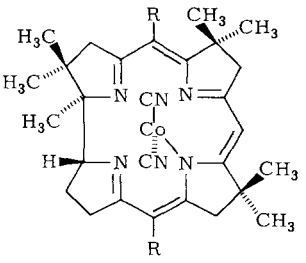


**3** **4** **5**

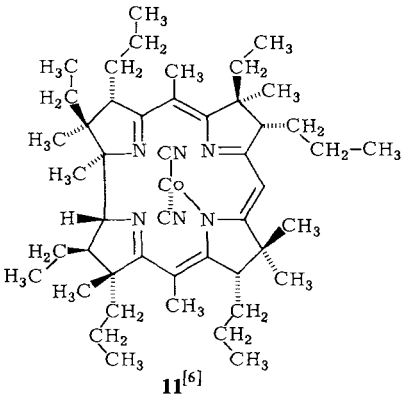


**6** **7** **8**

The demethylation of cobester has precedence in the $KMnO_4$ oxidation of the *meso*-methyl groups of $B_{12}$ derivatives to carboxyl functions, observed by *Rapp et al.*[3d]. Diastereomerically pure 5,15-bisnorcobester[3a,b], obtained (in 4% overall yield) from this source upon decarboxylation and methanolysis, served as a reference compound in the vitamin $B_{12}$ synthesis[3b,c]. The demethylation **1**→**2** is also likely to proceed by oxidative attack on the *meso*-methyl groups and may lead *via* (stabilized) radicals of type **3** and/or **4** to a dehydrocorrinoid intermediate of type **5**, electrophilic at the *exo*-methylidene carbon. Addition of $CCl_4$ to the reaction mixture seems to ensure the formation of the necessary oxidizing agent. The hypothetical dealkylation scheme **6**→**7**→**8** corresponds to a reversal of the thiomethylation which served to introduce the *meso*-methyl groups in the cobyric acid synthesis[3b,c,4]. An alternative, stepwise procedure for the demethylation of cobester to 5,15-bisnorcobester is described by *Nussbaumer* and *Arigoni*[5].



**9**, R = H[1]
**10**, R = $CH_3$[4]



**11**[6]

When cobester was subjected to the reaction conditions shown in Scheme 1 *but without addition of $CCl_4$*, neither demethylation nor demetalation occured. After methanolysis and chromatography, cobester was recovered in 70% yield as a crystalline 13α,β-mixture. The discrepancy between cobester and the heptamethylcorrin **9**[1] in their decomplexation behavior is not caused by the two *meso*-methyl groups: the nonamethylcorrin complex **10**[4] is demetalated as easily as **9** by 1,3-propanedithiol (conc. HCl, 60 °C, 7 h or $CHCl_3$/HCl, 20 °C, 3 d). Neither is the discrepancy a consequence of the methoxycarbonyl groups of cobester, since we found that *Gossauer*'s corrin complex **11**[6] also resisted demetalation (1,3-propanedithiol in $CHCl_3$, *without $CCl_4$*, HCl, 70 °C, 1 month). These findings support the view that the additional substituents of the natural corrinoids compared to **9** or **10** hamper the transient protrusion of the nitrogen atoms from the coordination plane during decomplexation. The challenge to find a preparative route for demetalation of vitamin $B_{12}$ and its derivatives still remains.

Received: April 29, 1983 [Z 367 IE]
German version: *Angew. Chem. 95* (1983) 744

[1] N. J. Lewis, A. Pfaltz, A. Eschenmoser, *Angew. Chem. 95* (1983) 743; *Angew. Chem. Int. Ed. Engl. 22* (1983) 735.
[2] L. Werthemann, Dissertation ETH Nr. 4097, Juris Druck + Verlag, Zürich 1968, p. 67.
[3] a) P. Schneider, Disseration ETH Nr. 4819, Juris Druck + Verlag, Zürich 1972, p. 135–141; b) H. Maag, Disseration ETH Nr. 5173, Juris Druck + Verlag, Zürich 1973, p. 64–90; A. Eschenmoser, *Pure Appl. Chem. Suppl.* IUPAC Congress, Boston, *1971*, 69; c) R. B. Woodward, *Pure Appl. Chem. 25*, 283 (1971), *ibid.* 33 (1973) 145; d) D. Jauernig, P. Rapp, G. Ruoff, *Hoppe-Seylers Z. Physiol. Chem. 354* (1973) 957.
[4] E. L. Winnacker, Disseration ETH Nr. 4177, Juris Druck + Verlag, Zürich 1968; A. Eschenmoser, *Quart. Revs. Chem. Soc. 24* (1970) 366.
[5] C. Nussbaumer, D. Arigoni, *Angew. Chem. 95* (1983) 746; *Angew. Chem. Int. Ed. Engl. 22* (1983) 737.
[6] B. Grüning, A. Gossauer, *Tetrahedron Letters 1979*, 3497.

## A Simple Route to 5-Nor, 15-Nor-, and 5,15-Bisnorcobesters**

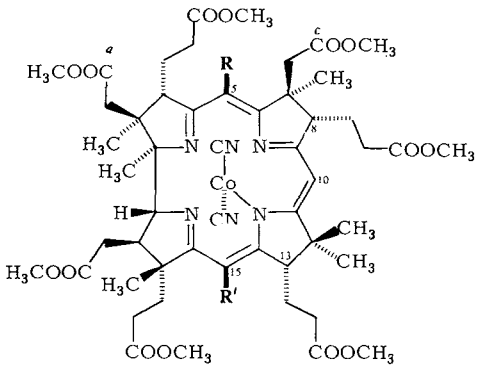
By *Cornelius Nussbaumer* and *Duilio Arigoni**

Derivatives of vitamin $B_{12}$ lacking methyl groups at positions 5 and 15 have played an important role in the total synthesis of the vitamin[1]; they are or interest in connection with current investigations on the biosynthesis of naturally occurring corrins and studies on the mode of action of the $B_{12}$-coenzyme. Diasteromerically pure 5,15-bisnorcobester **2** has been prepared previously from the 5,15-diacids, which are formed in low yield on oxidation of $B_{12}$-derivatives with $KMnO_4$[1c,d]; an unexpected mode of formation of **2** in a (1:1)-mixture with its 13β-epimer is re-

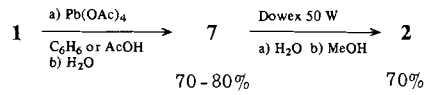
[*] Prof. Dr. D. Arigoni, C. Nussbaumer
Laboratorium für Organische Chemie
der Eidgenössischen Technischen Hochschule
ETH-Zentrum, Universitätstrasse 16, CH-8092 Zürich (Switzerland)

[**] We are grateful to Sandoz AG, Basel, for financial support and to Prof. *H. H. Inhoffen* for a generous gift of cobester.

ported by *Lewis et al.*[2]. Here we describe a stepwise efficient new procedure for converting **1** into **2**, which, in addition, is also a route to the two mononor-derivatives **3** and **4**.

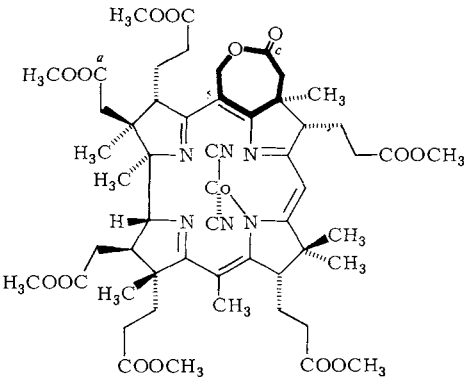


| | R | R' | UV/VIS λ[nm] (α-band, MeOH) |
|---|---|---|---|
| **1** | $CH_3$ | $CH_3$ | 582 |
| **2** | H | H | 561 |
| **3** | H | $CH_3$ | 572 |
| **4** | $CH_3$ | H | 569 |
| **5** | $CH_2OH$ | $CH_3$ | 576 |
| **6** | $CH_3$ | $CH_2OH$ | 575 |
| **7** | $CH_2OH$ | $CH_2OH$ | 571 |
| **8** | $CH_2OCH_3$ | $CH_2OCH_3$ | 570 |




Treatment of cobester **1** with $Pb(OAc)_4$ (3 eq. of a $2.4 \times 10^{-2}$ M solution in benzene, 24 h, RT) generated a mixture of labile acetoxymethyl compounds, mild hydrolysis of which (acetone/$H_2O$ 1:10, trace $CH_3COOH$, 4 h, RT), followed by purification, gave the two monohydroxylated derivatives **5** (11%) and **6** (31%) as well as the 5,15-bishydroxymethyl compound **7** (46%), all in crystalline form. Reaction of **1** with 5 equivalents of the reagent (40 h, RT) and subsequent methanolysis (2 h reflux) of the crude product afforded the crystalline 5,15-bismethoxymethyl compound **8** in 75% yield after chromatographic purification. Use of excess $Pb(OAc)_4$ in boiling benzene caused additional oxidation at C-8 and gave a mixture from which on methanolysis variable amounts of **8** and of the corresponding *c*,8-lactone could be isolated. In contrast to a previous report[3], no products arising from electrophilic attack of the reagent at C-10 of the substrate could be detected.

On treatment with zinc in acetic acid at room temperature each of the three hydroxylated compounds **5**—**7** was reduced cleanly to the starting material **1**. An initial assignment of the structures of the two isomeric compounds **5** and **6** was made by carrying out the reduction in $CH_3COOD$ and comparing the $^1H$- and $^{13}C$-NMR spectra of the resulting regiospecifically monodeuterated cobester samples with the spectra of the unlabeled material, which have been analyzed in detail[4a, b]. Conclusive evidence corroborating these assignments was provided by the facile transformation (acetone/0.1 M phosphate buffer 1:10, pH 8, 4 h, RT) of **6** into the seven-membered lactone **9**, which could be reduced with Zn in acetic acid to the known cobester-*c*-acid. A similar tendency towards lactone formation was also observed for **7**, whereas the 15-hydroxymethyl derivative **6** was unaffected under the same reaction conditions.



**9**

Smooth elimination of the two hydroxymethyl groups of **7** was achieved by using Dowex® 50 W as catalyst[5]. After chromatographic separation, the desired product **2** was isolated in crystalline form (70%); according to the $^1H$- and $^{13}C$-NMR analyses, contamination by the 13β-epimer did not exceed 10%. Extension of the same procedure to the monohydroxylated compounds **5** and **6** afforded in good yields the 5-norcobester **3** and the 15-norcobester **4**, respectively, both crystalline and free from diastereomeric impurities. Similar 5-nor- and 15-nor-compounds had been prepared previously by more involved and less efficient routes[1c, d], and their structures assigned tentatively from spectroscopic data. The established structures of **3** and **4** now provide a basis for unambiguous correlations.

Received: April 29, 1983 [Z 368 1E]
German version: *Angew. Chem. 95* (1983) 746

CAS Registry numbers:
**1**, 86834-33-5; **2**, 86834-34-6; **3**, 86834-35-7; **4**, 86834-36-8; **5**, 86834-37-9; **6**, 86834-38-0; **7**, 86834-39-1; **8**, 86834-40-4.

[1] a) A. Eschenmoser, *Pure Appl. Chem. Suppl.*, IUPAC Congress Boston *1971*, 69; b) R. B. Woodward, *Pure Appl. Chem. 25* (1971) 283, *ibid. 33* (1973) 145; c) D. Jauernig, P. Rapp, G. Ruoff, *Hoppe-Seylers Z. Physiol. Chem. 354* (1973) 957; d) H. Maag, Disseration ETH Nr. 5173, Juris Druck + Verlag, Zürich 1973.

[2] N. J. Lewis, R. Nussberger, B. Kräutler, A. Eschenmoser, *Angew. Chem. 25* (1983) 744; *Angew. Chem. Int. Ed. Engl. 22* (1983) 736.

[3] H. H. Inhoffen, A. Gossauer, K. P. Heise, H. Laas, *Phil. Trans. R. Soc. Lond. B 273* (1976) 327.

[4] a) L. Ernst, *Liebigs Ann. Chem. 1981*, 376; b) A. R. Battersby, C. Edington, C. J. R. Fookes, J. M. Hook, *J. Chem. Soc. Perkin Trans. I 1982*, 2265.

[5] Procedure **2**: **7** (40 mg) in 1 mL AcOH/2 mL $H_2O$ is heated for 30 min at 50 °C, adsorbed on 4 g Dowex® 50 W, and then heated for 22 h at 75 °C in 20 mL degassed $H_2O$; the $H_2O$ is displaced with 20 mL MeOH and the solution kept under argon for 24 h at RT. After neutralization (4 mL 5% $NH_3$ in MeOH), elution with aqueous KCN and MeOH, extraction with $CCl_4$, chromatography (silica gel, hexane/isopropanol/MeOH 5:2:1 + 0.02% HCN), and crystallization from methyl acetate/hexane the product (26 mg, 69%) is obtained (for additional details and data cf. C. Nussbaumer, Disseration, in preparation).

 © Verlag Chemie GmbH, 6940 Weinheim, 1983 0570-0833/83/0909-0738 $ 02.50/0 

**Contemporary Heterocyclic Chemistry: Syntheses, Reactions and Applications.** By *G. R. Newkome* and *W. W. Paudler*. John Wiley – Sons, Chichester 1982. x, 422 pp., bound, £ 30.80.

To present such a complex subject as heterocyclic chemistry in a 422 page monograph is not the simplest of tasks. The authors' aim is to cover heterocyclic chemistry with particular emphasis on heteroarene chemistry.

The subject is divided into π-excessive and π-deficient heteroarenes, according to the classical concept of *Adrien Albert*, in order to allow its presentation as an entity. After a (too brief) introduction to the nomenclature, a subject which requires particular care because of the "arbitrary growth" in several areas, the basic concept of this volume is presented including MO calculations, dipole moment and NMR studies (some tables showing electronic densities, dipole moments, $^{1}$H-, $^{13}$C-, and $^{15}$N-NMR data, p$K_a$ values, UV data, bond lengths and MS fragmentation schemes of customary heterocycles are collected at the end of the volume). The main part of the book consists of a discussion of the five-membered π-excessive and the six-membered π-deficient heteroarenes, together with their benzo-annelated analogues and derivatives, to which ten and nine chapters, respectively, are devoted. Successful classical methods and modern developments are always dealt with side by side. A great deal of space is devoted to the [2+1]- and the [4+2]-cycloadditions and to the additions of singlet oxygen to five-membered heteroarenes and the subsequent reactions. Alongside pyridine, the six-membered heterocycles treated are the pyridazines, pyrimidines (significantly under-represented in comparison to their importance), pyrazines, triazines, tetrazines and their benzo derivatives.

Further chapters deal with $S_N$ and $S_E$ reactions as well as radical reactions and photochemical transformations. Among the nucleophilic reactions described in detail are the $E_A$ (heteroaryne) and the ANRORC mechanisms. They are followed by photoinduced valence isomerizations, "ring scrambling" and [4+4]-dimerizations of pyridines, pyrazines and pyrimidines. Each class of compound has a chapter on natural products and (a few) pharmaceutically important compounds, devoted to it.

Heterocondensed heteroarenes are treated in a chapter of their own. There then follows a comprehensive treatment of mesoionic heterocycles (sydnones, munchnones, 1,3-oxazolium-5-olates, 1,3-oxathioliumolates, 1,3-diazoliumolates and amides, 1,2,3,4-tetrazolium-5-thiolates) and their manifold, synthetic potential. Particular attention is paid to the three- and four-membered heterocycles; it is noticeable that the photochemical C–C cleavage of epoxides to carbonyl ylides is not mentioned. Finally, two chapters are concerned with some classical azepine, (benzo)diazepine and thiepin syntheses, together with methods of producing some azocines and diheterocines; however, the recently successful cycloaddition-ring enlargement reactions are practically ignored.

References up to 1980 are included; the principal sources quoted are monographs and review articles. Half of the citations come from the last two decades. In spite of this, one searches in vain for notions such as intramolecular cycloadditions, frontier orbitals, or regio- and enantioselectivity. The literature citations are listed at the end of each chapter which is irksome during intensive study. The formulas often look awkward because of the greatly varying bond lengths sometimes used. Better quality is to be expected in a monograph of this price class.

Altogether this lucidly constructed monograph takes its place between a text book and a progress report and guarantees, in an exemplary fashion, the chemistry student, the chemist in research and in industry, as well as the scientist of neighboring disciplines, an excellent and speedy introduction to current chapters of modern heterocyclic chemistry by means of a clear conception and ample literature citation. This book can be warmly recommended to all in industry or university who are concerned with the chemistry of heteroarenes.

*Heinrich Wamhoff* [NB 580 IE]
Institut für Organische Chemie
und Biochemie der Universität Bonn

**Non-formal Kinetics.** By *R. Schmid* and *V. N. Sapunov*. Verlag Chemie, Weinheim 1982. xi, 199 pp., bound, DM 98.00.

The authors first introduce the reaction kinetic method with the aid of simple examples. Elementary quantities, such as the reaction rate constant or the half-life, are described in terms of the concentration-time curve, invariances I and II are also defined with the aid of linear transformations. Starting from these simplest cases and *via* parallel and series reactions, ever more complex, kinetic systems are treated. The kinetics of simple, catalyzed reactions are the starting point for the analysis of complicated, catalyzed reaction paths, particularly with reference to biochemical applications.

In the second part of the book the authors introduce a method of analysis of complex kinetics on the basis of the kinetic techniques described, which proceeds largely without assumptions. Invariances I and II, described at the beginning of the book, afford an opportunity to obtain preliminary information. The differentiated form of the rate-time curve plays a central role in the further analysis. A procedure is described that allows a numerical expression for the kinetic equations to be formulated by repeated correction of the rate-time diagram, even in the case of fractional orders of reaction and for catalyzed reactions. The development of reaction mechanisms from the equations so discribed is discussed.

Following the actual, kinetic analysis there is a chapter concerning the influence of temperature on the rate constant. The Arrhenius equation and the Eyring equation are compared and discussed in terms of the transition state theory. Further chapters treat the influence of pressure, of the solvent (with emphasis on empirical scales of polarity) and of substituents. The appendix is concerned with free enthalpy relationships and with the Exner analysis for the determination of isokinetic relationships.

The book is useful both to the advanced student and to the experienced practitioner, since it offers the one a summary of kinetic methods and the other a wealth of useful details, which is systematized. The mathematical relationships in kinetic statements are clearly and distinctly formulated. The derivation of the Bodenstein principle might be mentioned as an example. The effect of errors in measurement on the results of kinetic measurements is perhaps treated too briefly; but it may be that this lies outside the

scope of the book. Even in the future, intuition will have to play its part in the elucidation of complex reactions. However, the authors have succeeded in systematizing, for practical application, the available, kinetic methods. This book will enrich anyone who is concerned with reaction mechanisms.

*Heinz Langhals* [NB 585 IE]
Chemisches Laboratorium der Universität Freiburg

**Recent Books**

**The following books have been received by the editor. All the publications listed are available through W & P Buchversand für Wissenschaft und Praxis, Boschstrasse 12, D-6940 Weinheim (Federal Republic of Germany). Tel. (06201) 606-0, Telex 465516 vchwh d, Telefax (06201) 602328.**

**The Fischer Indole Synthesis.** By *B. Robinson.* John Wiley, Chichester 1982. xiii, 923 pp., bound, £ 95.00.—ISBN 0-471-10009-0

**Chronopharmakologie. Tagesrhythmen und Arzneimittelwirkung.** By *B. Lemmer.* Wissenschaftliche Verlagsgesellschaft mbH, Stuttgart 1983. 100 pp., paperback, DM 29.00.—ISBN 3-8047-0725-4

**Chemical Engineering. Vol. 6. An Introduction to Chemical Engineering Design.** By *J. M. Coulson, J. F. Richardson,* and *R. K. Sinnott.* Pergamon Press, Oxford 1983. xvi, 838 pp., paperback, £ 13.50, bound, £ 37.50.—ISBN 0-08-022970-0/0-08-022969-7

**User Guide on Process Integration for the Efficient Use of Energy.** Published by the Institution of Chemical Engineers. By *B. Linnhoff, D. W. Townsend, D. Boland, G. F. Hewitt, B. E. A. Thomas, A. R. Guy,* and *R. H. Marsland.* Pergamon Press, Oxford 1982. v, 247 pp., paperback, £ 12.50.—ISBN 0-08-030245-9

**Einführung in die praktische Biochemie.** 3rd., completely new and revised edition. By *H. Aebi, U. Brodbeck, H. Kohler, K. Lauber, G. Pfleiderer, J. P. von Wartburg,* and *S. Wyss.* Karger, Basel 1982. xii, 462 pp., paperback, SFr. 75.00.—ISBN 3-8055-3448-5

**Grundlagen der technischen Anorganischen Chemie.** By *H.-H. Emons, G. Bräutigam, P. Hellmold, H. Holldorf, R. Kümmel,* and *H. Martens.* Salle+Sauerländer, Frankfurt am Main 1983. 444 pp., bound, DM 58.00.—ISBN 3-7935-5484-8

**Encyclopedia of the Alkaloids. Vol. 4.** By *J. S. Glasby.* Plenum Press, New York 1983. 391 pp., bound, $ 65.00.—ISBN 0-306-41217-9

**Advances in Organometallic Chemistry. Vol. 21.** Edited by *F. G. A. Stone* and *R. West.* Academic Press, New York 1982. vii, 304 pp., bound, $ 52.00.—ISBN 0-12-031121-6

**Advances in Chemical Physics. Vol. 52.** Edited by *I. Prigogine* and *S. A. Rice.* John Wiley, Chichester 1983. ix, 528 pp., bound, £ 62.00.—ISBN 0-471-86845-0

**Current Trends in Organic Synthesis. Proceedings of the Fourth International Conference on Organic Synthesis. Tokyo, Japan, August 22—27, 1982.** A IUPAC Title. Edited by *H. Nozaki.* Pergamon Press, Oxford 1983. xii, 429 pp., bound, £ 45.00.—ISBN 0-08-029217-8

**Books on Soils and the Environment: Soil. Analysis, Instrumental Techniques and Related Procedures.** Edited by *K. A. Smith. Marcel Dekker, Basel 1983. 576 pp., bound, SFr. 198.00.—ISBN 0-8247-1844-5*

**Topics in Current Chemistry.** Edited by *F. L. Boschke.* Springer-Verlag, Berlin 1983. **Vol. 100: Radicals in Biochemistry.** vii, 140 pp., bound, DM 68.00.—ISBN 3-540-11846-2. **Vol. 107: Plasma Chemistry IV.** viii, 186 pp., bound, DM 76.00.—ISBN 3-540-11828-4

**Adsorption from Solution.** Edited by *R. H. Ottewill, C. H. Rochester,* and *A. L. Smith.* Academic Press, London 1983. xiii, 315 pp., bound, £ 18.00.—ISBN 0-12-530980-5

**Ion-Selective Electrode Reviews. Vol. 4.** Edited by *J. D. R. Thomas.* Pergamon Press, Oxford 1982. v, 286 pp., bound, £ 46.50.—ISBN 0-08-030414-1

*Registered names, trademarks, etc. used in this journal, even without specific indication thereof, are not to be considered unprotected by law.*

© Verlag Chemie GmbH, D-6940 Weinheim, 1983. - Printed in the Federal Republic of Germany by Zechnersche Buchdruckerei, Speyer/Rhein.

All rights reserved (including those of translation into foreign languages). No part of this issue may be be reproduced in any form - by photoprint, microfilm, or any other means - nor transmitted or translated into a machine language without written permission from the publishers. Only single copies of contributions, or parts thereof, may be reproduced for personal use. Copies reproduced and used other than for private purposes in an industrial or commercial undertaking are subject to copyright and, in such cases, a copyright fee must be paid to the VG WORT, Abteilung Wissenschaft, Goethestr. 49, 8000 München 2, from whom conditions of payment can be obtained on request.

**Valid for users in the USA:** The appearance of the code at the bottom of the first page of an article in this journal (serial) indicates the copyright owner's consent that copies of the article may be made for personal or internal use, or for the personal or internal use of specific clients. This consent is given on the condition, however, that the copier pay the stated per-copy fee through the Copyright Clearance Center, Inc., for copying beyond that permitted by Sections 107 or 108 of the U.S. Copyright Law. This consent does not extend to other kinds of copying, such as copying for general distribution, for advertising or promotional purposes, for creating new collective works, or for resale. For copying from back volumes of this journal see 'Permissions to Photo-Copy: Publisher's Fee List' of the CCC.

**Editorial office:** Pappelallee 3, D-6940 Weinheim, Federal Republic of Germany, Telephone (06201) 602315, Telex 465516 vchwh d, Telefax (06201) 602328.

**Editors:** *P. Gölitz, I. G. Neil, O. Smrekar, A. Stimson.*

**Publishers:** Verlag Chemie GmbH. (Managing Directors: *Prof. Dr. Helmut Grünewald* and *Hans Dirk Köhler*), Pappelallee 3, D-6940 Weinheim, Federal Republic of Germany.

Correspondence concerning advertisements should be addressed to Verlag Chemie GmbH. (Advertising Manager *R. J. Roth*), Boschstr. 12. P.O. Box 1260/1280, D-6940 Weinheim, Federal Republic of Germany, Telephone Weinheim (06201) 602-0, Telex 465516 vchwh d, Telefax (06201) 602328.

ANGEWANDTE CHEMIE
International Edition in English
Volume 22 · Number 10
October 1983
Pages 741–804

# Adventures and Excursions in Bioassay: The Stepping Stones to Prostacyclin (Nobel Lecture)**

By John R. Vane*

Physiology has spawned many biological sciences, amongst them my own field of pharmacology. No man has made a more important contribution to the fields of physiology and pharmacology than *Sir Henry Dale* (1875–1968, Nobel Laureate in Physiology or Medicine in 1936). *Dale* had a great influence not only on British pharmacology in general but also on my own scientific endeavours. Indeed, I can put forward a strong case for considering myself as one of *Dale*'s scientific grandchildren. My early days as a pharmacologist were influenced not only by *Dale* himself but also by his own school of colleagues, including *Burn*, *Gaddum* and *von Euler*. It was *Burn* who taught me the principles and practice of bioassay. Some of *Gaddum*'s first publications were on the development of specific and sensitive methods for biological assay, and he maintained a deep interest in this subject for the rest of his life[1]. In 1964 he said "the pharmacologist has been a 'jack of all trades' borrowing from physiology, biochemistry, pathology, microbiology and statistics—but he has developed one technique of his own, and that is the technique of bioassay"[2].

Expensive, powerful and sophisticated chemical methods, such as gas chromatography and mass spectrometry, have been developed and perfected for detection and quantification of prostaglandins (PGs) and related substances. One should not forget, however, that starting with the discovery and isolation of prostaglandins by *von Euler*[3a]; see also text of the Nobel lecture by *Bergström*[3b]), biological techniques and bioassay have contributed very substantially to the development of the field. Bioassay has provided crucial information on the role of the lungs in the removal of circulating prostaglandins[4], the participation of prostaglandins in inflammatory reactions[5,6], the contribution of prostaglandins to the autoregulation and maintenance of blood flow to the kidney[7–9], the inhibitory effect of aspirin-like drugs on the biosynthesis of prostaglandins[10–12], the mediation of pyrogen fever by prostaglandins[13], and the release of rabbit aorta-contracting substance (RCS; now identified as thromboxane $A_2$, $TXA_2$) from lungs during anaphylaxis[14,15]. Moreover, in 1976 bioassay made possible the discovery of PGX, now renamed prostacyclin ($PGI_2$), the latest member of the prostaglandin family[16–19]. Indeed, it is doubtful whether the biological significance of any of the unstable products of arachidonic acid metabolism would have been recognised without bioassay techniques. With extraordinary simplicity and convenience, by its very nature, bioassay distinguishes between the important biologically active compounds and their closely related but biologically unimportant metabolites.

In this review I shall discuss the development of the cascade superfusion bioassay technique and some of the discoveries and concepts which arose from its application, leading up to the discovery and development of prostacyclin. The effects of prostacyclin in man and its clinical assessment (another application of bioassay) will also be discussed.

[*] Dr. J. R. Vane
Wellcome Research Laboratories
Langley Court, Beckenham, Kent (England)

[**] Copyright © The Nobel Foundation 1983.—We thank the author and the Nobel Foundation, Stockholm, for permission to publish this lecture.

## 1. Cascade Superfusion Bioassay

### 1.1. Development

Most uses of bioassay involving smooth muscle demand high sensitivity and specificity. These aspects have been achieved first, by limiting the volume of fluid bathing the isolated tissue and second, by using an assay organ sensitive to, and relatively specific for, the test substances under study. Further specificity can be achieved by using a combination of several tissues which present a characteristic pattern of response to the test substance or substances. This takes advantage of the principle of parallel pharmacological assay, regarded by *Gaddum*[20] as strong evidence for the identity of a compound.

*Magnus*[21] introduced the idea of suspending an isolated portion of smooth muscle in a chamber containing a nutrient fluid and measuring changes in tissue tone. The organ baths used today are modified versions of that used by *Dale*[22]. *Gaddum*[23] applied the experimental design developed by *Finkleman*[24] to the assay of minute amounts of biologically active substances. He called his technique "superfusion" in contrast to perfusion. This consisted of bathing an assay tissue with a stream of fluid which was momentarily stopped at the moment of addition of the test substance. *Vane*[25] introduced the idea of superfusing several tissues in cascade (generally up to six, arranged in two banks; Fig. 1). Besides being useful for the parallel assay of individually injected samples, this arrangement also allows parallel analysis of the active components present in a fluid stream (most commonly Krebs' solution) taken from the outflow of a perfused organ.

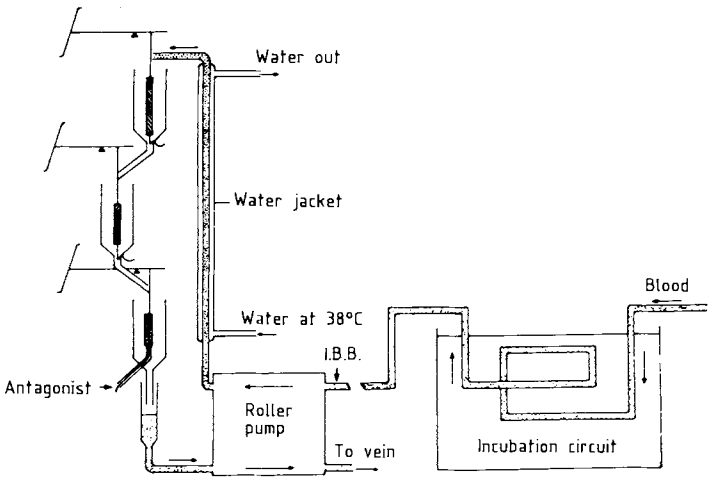



Fig. 1. Diagram of the blood-bathed organ technique. Blood is continuously withdrawn from a convenient blood vessel by a roller pump, kept at 37°C by a water jacket and then allowed to superfuse a series of isolated organs, the longitudinal movements of which are recorded. The blood is then collected in a reservoir and returned to the animal. In some experiments the blood flows through a length of silicone tubing in a water bath (incubating circuit) before superfusing the isolated tissues. Drugs can be applied directly to the isolated tissues by infusions or injections into the bathing blood (I.B.B.) or with a time delay into the incubating circuit (from *Vane* [33], by permission of the *Br. J. Pharmacol.*).

Another innovation introduced by *Vane*[25] was to use blood as the superfusion medium (the blood-bathed organ technique). The anaesthetised animal is heparinised and blood is continuously removed at a constant rate of 10—15 mL/min (dogs, cats and rabbits). Lower rates can be used from guinea pigs[26]. The blood (either from a vein or from an artery) superfuses the assay tissues and is then returned by gravity to a large vein.

Plainly, when perfusate from an organ or blood from an animal is used for superfusion, substances can reach the assay tissues within a few seconds of generation or release. This element of "instantaneity" is an important aspect of cascade superfusion bioassay in that it detects the biological activity of chemically unstable compounds whose activity would otherwise be lost in an extraction process. Another important feature of the method is that it gives the maximum opportunity for serendipity. The dynamic nature of the assay also allows the measurement of inactivation of an infused substance across a particular vascular bed. Further modifications of the bioassay technique have been developed by *Collier*[27], *Ferreira* and *Souza Costa*[28] and *Gryglewski et al.*[29].

### 1.2. Choice of Bioassay Tissues

It is usually possible to find a piece of smooth muscle which is particularly sensitive to the hormone under investigation and relatively insensitive to other substances. Indeed, think of any part of the body and you can be sure that the pharmacologist has cut it out, put it into an isolated organ bath, or perfused its vessels in order to study the effects of drugs. For bioassay, segments of the gastrointestinal tract or spirally cut strips of vascular tissue have mainly been used. Such procedures are the backbone not only of bioassay but also of classical pharmacology.

Figure 2 depicts the reactions of some superfused isolated tissues to various endogenous substances in concentrations likely to be found in circulating blood. It should be remembered that when blood is used as the superfusing medium, some smooth muscle preparations (but not others) exhibit an increased resting tone often lasting for the

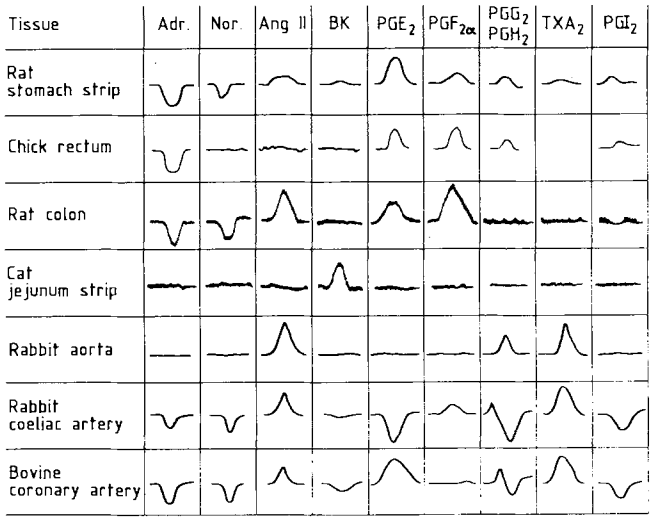



Fig. 2. Diagram showing the reactions of some blood-bathed organs to various endogenous substances in concentrations of 0.1—5.0 ng/mL. The actions of the catecholamines, 5-hydroxytryptamine and histamine can be abolished by treatment with suitable blocking agents (Adr = adrenaline, Nor = noradrenaline, Ang = angiotensin, BK = bradykinin).

duration of the experiment. Such increased tone reduces sensitivity to substances which cause contraction but increases sensitivity to those which induce relaxation.

For detection of the classical prostaglandins, the most useful combination of assay tissues is the rat stomach strip, rat colon, and chick rectum. For PG endoperoxides and later for prostacyclin, vascular tissues were added such as strips of coeliac or mesenteric artery[30]. Strips of bovine coronary artery[31] were especially useful for they contracted to $PGE_2$ but relaxed to prostacyclin (Fig. 2).

The specificity of a bioassay can be increased still further by the use of antagonists. For instance, contractions of the rat stomach strip induced by 5-hydroxytryptamine can be abolished by a specific antagonist such as methysergide, thereby leaving the preparation more specifically sensitive to the prostaglandins. The rat colon is relaxed by catecholamines but contracted by angiotensin II; when both are present in the superfusion fluid, the catecholamines reduce the contraction produced by angiotensin. This unwanted interference is prevented by blocking the actions of catecholamines with a β-receptor antagonist. When blood is used as the superfusion fluid, the antagonist can be perfused through the closed lumen (Fig. 1) of, say, the rat colon[32] thus localising the blocking agent to the assay tissue and minimising its effects on the whole animal. For a detailed discussion of the limitations of the cascade superfusion bioassay technique, the reader is referred to *Vane*[33] and to *Moncada, Ferreira* and *Vane*[34].

### 1.3. Measurement of Substances by Cascade Superfusion Bioassay

The technique is well suited for measuring substances released into the circulation, such as catecholamines or angiotensin II, and also for determining the fate of substances released or infused into different parts of the circulation.

#### *1.3.1. Release of Substances in Response to Stimuli*

Release of catecholamines from the adrenal medulla can be detected and quantitated by use of a rat stomach strip and chick rectum. This technique was used to demonstrate that circulating catecholamines appeared to play little or no part in arterial baroreceptor reflexes[25] and also that catecholamines are released into the circulation during anaphylaxis[35]. Of the substances released during the anaphylactic reaction, histamine, bradykinin and slow reacting substance in anaphylaxis (SRS-A) will all in turn release adrenaline when injected intravenously, although there may be species differences in the mechanisms of action and in the sensitivity of the adrenal medulla[36–38].

An early use of the blood-bathed organ technique was to show the sequential release of angiotensin II and catecholamines during haemorrhage[39]. Release of bradykinin into the blood stream by the intravenous injection of kallikrein or by contact of the blood with glass was easily demonstrated[40] but we consistently failed to demonstrate with this technique the endogenous release of bradykinin by physiological manipulation. However, circulating kinins were demonstrated during hypotension due to haemorrhage in the dog and the concentrations detected in the bloodstream were sufficient to lower a normal blood pressure[41].

#### *1.3.2. Inactivation of Circulating Vasoactive Substances*

By comparing the effects on the blood-bathed assay organs of infusions of a substance over several minutes into a particular vascular bed with the effects of similar infusions given into the effluent of the vascular bed, it is possible to assay the percentage of the substance disappearing in one circulation through that vascular bed (Fig. 3). This technique allowed the demonstration of the inactivation of several vasoactive substances as they passed through vascular beds such as the hind legs, the liver and the lungs.

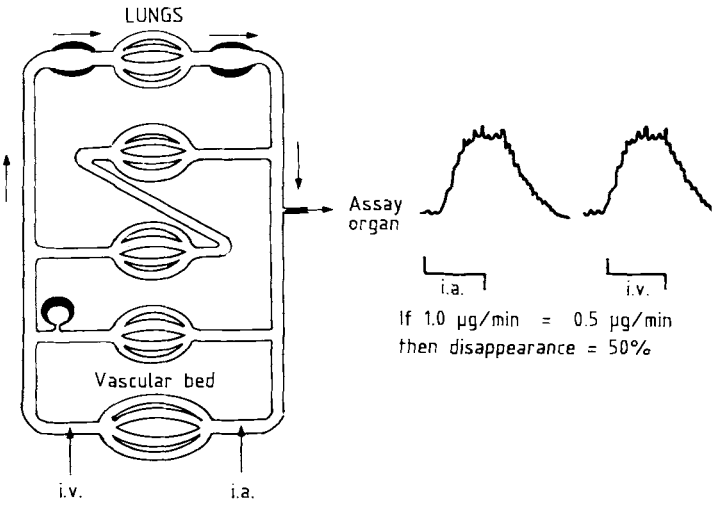



Fig. 3. Diagram showing principle of bioassay of the degree of disappearance across a vascular bed. The differences in responses of the blood-bathed organs to infusions made intraarterially (i.a.) or intravenously (i.v.) represent the degree of removal of the substance in one passage through the vascular bed.

Angiotensin II, for example, is unaffected by passage through the pulmonary circulation, either *in vivo* or in isolated lungs of all species studied, including rats, dogs, guinea pigs, cats and man (for review see *Bakhle* and *Vane*[42]). However, the same substance is substantially inactivated (50—70%) in one passage through peripheral vascular beds such as the liver, the kidneys and the hind legs[43].

We also studied the fate of adrenaline and noradrenaline and found in both cats and dogs that 70—95% of an intraarterial infusion of adrenaline or noradrenaline disappeared in one passage through the hindquarters. The lungs, however, inactivated up to 30% of an infusion of noradrenaline without interfering with the passage of adrenaline[44,45].

Bradykinin is fairly rapidly destroyed in blood and has a half-life in the blood stream of cat or dog of about 17 seconds. *Ferreira* and *Vane*[46] showed that, whereas the liver inactivated about 50%, the lungs inactivated about 80% of the bradykinin infusion.

It was observations such as these that drew our attention to the metabolic and pharmacokinetic function of the pul-

monary circulation. The selectivity of the pulmonary inactivation mechanism is strikingly demonstrated by the way in which the lungs inactivate bradykinin, but allow other peptides such as eledoisin, substance P, physalaemin, vasopressin and oxytocin to pass through without change[42].

The metabolism of prostaglandins in the pulmonary circulation *in vivo* was first studied by *Vane et al.*[4,47] who showed that almost all of an infusion of $PGE_1$, $PGE_2$ or $PGF_{2\alpha}$ was inactivated in one passage through the lungs. *McGiff et al.*[48] confirmed that $PGE_1$ and $PGE_2$ were avidly removed by dog lung *in vivo* but further showed that $PGA_1$ and $PGA_2$ survived the passage through the lungs without change. Thus, within this very closely related group of substances, the inactivation process can distinguish between the individual members. Interestingly, after the discovery of prostacyclin, we also found[49] that prostacyclin (unlike $PGE_2$, see Fig. 4) survived passage through

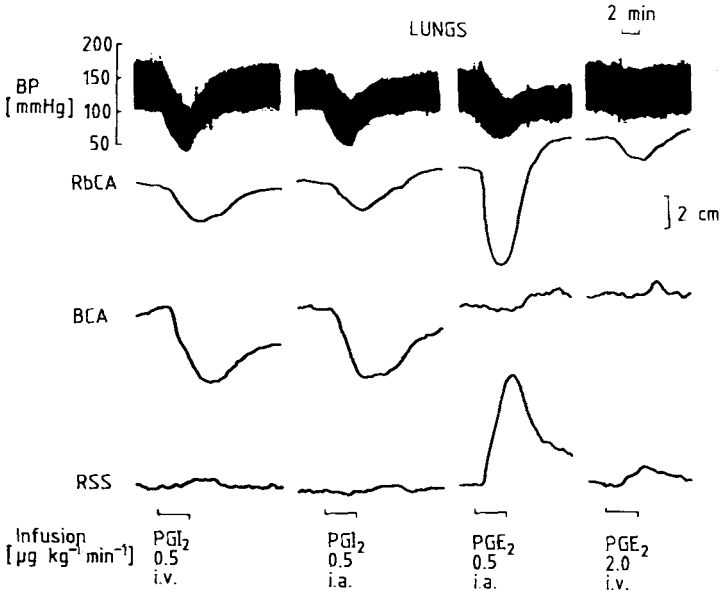



Fig. 4. Passage of prostacyclin ($PGI_2$) and prostaglandin $E_2$ ($PGE_2$) across the lungs. Spiral strips of rabbit coeliac artery (RbCA), bovine coronary artery (BCA) and rat stomach strip (RSS) were bathed in arterial blood from a dog. $PGI_2$ infused intravenously (i.v.) caused similar effects on the bioassay tissues and blood pressure (BP) as infusion into the root of the aorta (i.a.), indicating that $PGI_2$ did not disappear across the lungs. In contrast, much more than 75% of $PGE_2$ was inactivated in passage through the pulmonary circulation (see *Dusting, Moncada* and *Vane*, 1978 [49], by permission of the *Br. J. Pharmacol.*).

the pulmonary circulation without change. In other vascular beds, the inactivation of prostacyclin in a single passage (50—70%) was comparable to that of $PGE_2$. Thus, the hindquarters, and particularly the liver, removed some of the prostacyclin which reaches those beds.

Overall, the inactivation of prostacyclin in one circulation was about 50%, giving a metabolic half-life of one circulation time (30s) as compared with the chemical half-life of 2—3 min. The inactivation mechanisms for $PGE_2$ and prostacyclin[50] are similarly dependent on prostaglandin 15-hydroxydehydrogenase (PGDH). However, the disappearance of prostaglandins in the pulmonary circulation depends on two mechanisms, namely uptake and attack by the enzyme PGDH, so our results suggested that prostacyclin is not a substrate for the PG uptake mechanism.

From the differential removal of vasoactive hormones by the pulmonary circulation we proposed that they could be divided into at least two types—"local" and "circulating" hormones. The local hormones are those which are largely removed by the lungs and if they have a physiological function, it is probably localised at or near to the site of release. It is intriguing to think that venous blood may be full of potent, as yet unidentified, chemicals released by peripheral vascular beds but removed by the lungs before they can cause effects in the arterial circulation. Interestingly, in 1970, *Gryglewski* and *Vane* described the release of an unidentified substance into the venous blood after infusion of isoprenaline into the hind legs of dogs[51]. The pattern of activity of this substance on the blood-bathed assay tissues was unlike that of any prostaglandin known at that time, but it can now be clearly identified as prostacyclin.

Circulating hormones are those which pass through the lungs, either unchanged (adrenaline, histamine, vasopressin, prostacyclin) or with an actual increase in activity. One such demonstration of an increase in activity on passage through the pulmonary circulation was associated with the renin-angiotensin system. We showed[52] that, contrary to popular belief, conversion of angiotensin I into angiotensin II did not take place in the bloodstream, but was largely accomplished in the pulmonary circulation. This was demonstrated both *in vivo*[52–54] and *in vitro* (Fig. 5).

### 1.3.3. *Our Studies of Substances Released during Anaphylaxis*

*Piper* and *Vane*[14,55,56] investigated the release of mediators from perfused lungs isolated from sensitised guinea pigs. We found, as expected, that there was a large release of histamine when the lungs were challenged with antigen.

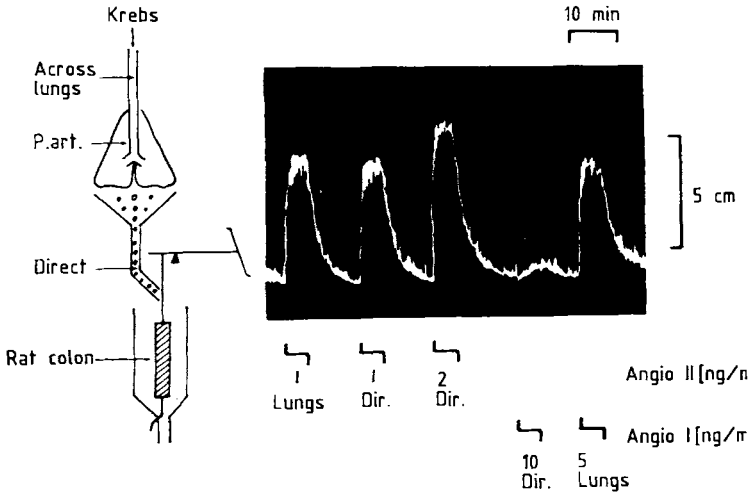



Fig. 5. Increased activity of angiotensin I when passed through guinea pig isolated lungs. The diagram on the left shows the experimental procedure (Krebs = Krebs solution, P. art. = pulmonary artery). Infusions of angiotensin II (Angio II) through the lungs or direct to the rat colon (Dir.) gave the same response of the rat colon, showing that there was no destruction in the lungs. An infusion of angiotensin I (Angio I) at 10 ng/mL direct to the rat colon gave a minimal response, but when half this concentration (5 ng/mL) was infused through the lungs there was a much greater contraction of the rat colon (after *Vane* [33], by permission of the *Br. J. Pharmacol.*).

As also expected, we found a release of SRS-A. However, we were excited at that time to find the release of three other substances which had not previously been associated with anaphylaxis (Fig. 6). We detected the release of prostaglandin-like substances with our bioassay systems and were later able to show by thin layer chromatography that prostaglandins $E_2$ and $F_{2\alpha}$ were present in the effluent. Even more exciting was the detection of the release of a previously undescribed substance which caused a strong contraction of strips of rabbit aorta and which we called, because of this effect "rabbit aorta contracting substance" or RCS. Two properties of RCS intrigued us. First, it was chemically unstable and if we introduced a delay coil of a few minutes before the lung effluent reached the assay tissues the activity had disappeared, although that of histamine, $PGE_2$, $PGF_{2\alpha}$ and SRS-A was still present. Second, we found that the release of RCS during anaphylaxis was selectively prevented by aspirin and other similar compounds. *Piper* and *Vane*[14] postulated that RCS may be involved in causing those symptoms which aspirin relieves. Isolated lungs also released prostaglandins into the perfusate when particles ($\leq 120\ \mu m$) were infused into the pulmonary artery[57].

At this time we were also becoming interested in prostaglandin release from other tissues. Mammalian cells of all types disgorge prostaglandins at the slightest provocation, but the tissue content of prostaglandins is very low compared with the release. This is well illustrated in the dog spleen, from which less than 1 μg (or 7 ng per g wet weight) can be extracted; however, the spleen can release up to 10 μg of prostaglandin (assayed as $PGE_2$) per minute when it is stimulated. *Horton et al.*[58] were the first to demonstrate that $PGE_2$ was released into splenic venous blood following splenic nerve stimulation in the dog. We became interested in the characteristics of this release and further showed that the output ($PGE_2$ and $PGF_{2\alpha}$) was associated with contraction of the spleen, for it could be induced by adrenaline and prevented by α-adrenoreceptor antagonists. Interestingly, as in the lungs, we found that prostaglandins were released by the spleen in response to infusions of particles[59].

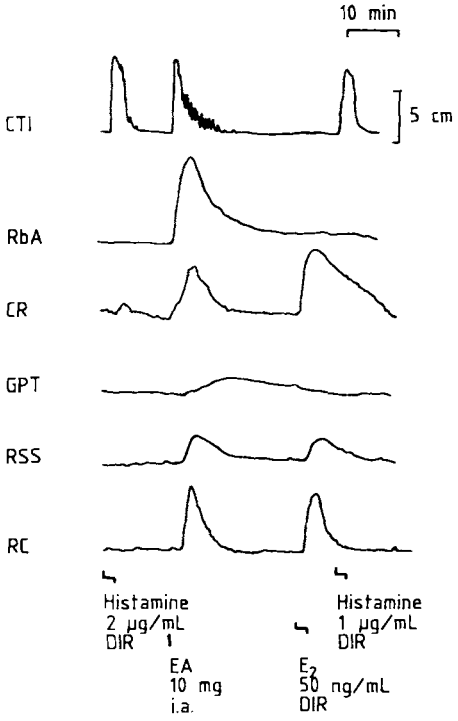



Fig. 6. Release of mediators from isolated lungs of sensitized guinea pigs. The lungs were perfused through the pulmonary artery with Krebs' solution and the effluent superfused a cat terminal ileum (CTI), rabbit aorta spiral strip (RbA), chick rectum (CR), guinea pig trachea (GPT), rat stomach strip (RSS) and rat colon (RC). All tissues except CTI were blocked with antagonists to 5HT, catecholamines and histamine. Infusions of histamine (2 μg and 1 μg/mL) DIR) and of prostaglandin $E_2$ ($E_2$, 50 ng/mL DIR) directly to the assay tissues demonstrated the selective sensitivity of the assay system. Anaphylaxis was induced in the lungs by injecting ovalbumen intraarterially (EA 10 mg I.A.). Contractions of CTI demonstrated release of histamine, RbA release of RCS, GPT release of SRS-A and CR, RSS and RC release of prostaglandins (*Piper* and *Vane* in [163], by permission of Churchill Livingstone).

## 2. Aspirin and Prostaglandin Biosynthesis

In research there is always a "climate" of experience which acts as a background to important discoveries. I have tried to indicate the "climate" in our laboratory at The Royal College of Surgeons of England around the year 1970. We had a major interest in the release and fate of vasoactive hormones and were pursuing this with especial reference to the lungs. We had discovered RCS as an unstable substance released from lungs during anaphylaxis and we knew that its release was inhibited by aspirin and other aspirin-like drugs. We had become interested in the prostaglandins and had come to the idea that any tissue which was distorted or disturbed or traumatised would release prostaglandins. In this context, it seemed to me that each distention of the lungs might cause a prostaglandin release which could help to adjust the regional pulmonary blood flow. Indeed, the idea that a prostaglandin release might be important in controlling regional blood flow in the lungs had also been suggested by *Liljestrand*[60]. With over-distention, any prostaglandins released might be detected in the arterial blood stream. I started a series of experiments using the blood-bathed organ technique to test this hypothesis. In anaesthetised dogs it was easy to show that when they were hyperventilated, there was an output into the arterial blood from the pulmonary circulation of an RCS-like substance and of $PGE_2$ and $PGF_{2\alpha}$ (*Vane*, unpublished). It was at this time that I was impressed by the effects of an infusion of aspirin into the hyperventilated dog, for not only was the associated hypotension reduced, but there was also a strong inhibition of the prostaglandin release. It was this experiment that led me to the idea (over a weekend) that aspirin might be interfering with prostaglandin biosynthesis. On the Monday morning I said to *Sergio Ferreira* and *Priscilla Piper* "I think I know how aspirin works" and set about doing an experiment. *Anggard* and *Samuelsson*[61] had described a preparation of guinea pig lungs in which a crude cell-free homogenate was used to convert arachidonic acid into $PGE_2$ and $PGF_{2\alpha}$. Although I was inexperienced in working with biochemical techniques, for I have always believed in using whole animals or organs whenever possible, I homogenised some guinea pig lungs, spun off the cell debris, divided the su-

pernatant into test-tubes, added arachidonic acid and measured by bioassay the amounts of $PGE_2$ and $PGF_{2\alpha}$ formed. To some of the tubes was added aspirin, indomethacin or morphine. By the end of that day I was convinced that aspirin and indomethacin (but not morphine) strongly inhibited the formation of prostaglandins from arachidonic acid (see Fig. 7).

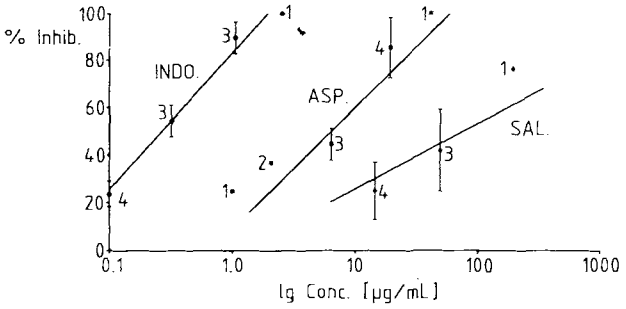



Fig. 7. Concentration (µg/mL) of indomethacin (INDO.), aspirin (ASP.) and salicylate (SAL.) plotted on a log scale against the percentage inhibition of prostaglandin synthesis (assayed as $PGF_{2\alpha}$ on rat colons). The lines are those calculated for best fit. Numbers by the points indicate number of experiments. When three or more estimates were averaged, the standard error of the mean is shown (from *Vane* [10], by permission of *Nature*).

During the time that I was confirming and extending this first experiment, *Ferreira* and *Moncada*[12] began to study the effects of aspirin and indomethacin on prostaglandin release from the spleen (Fig. 8). Independently of

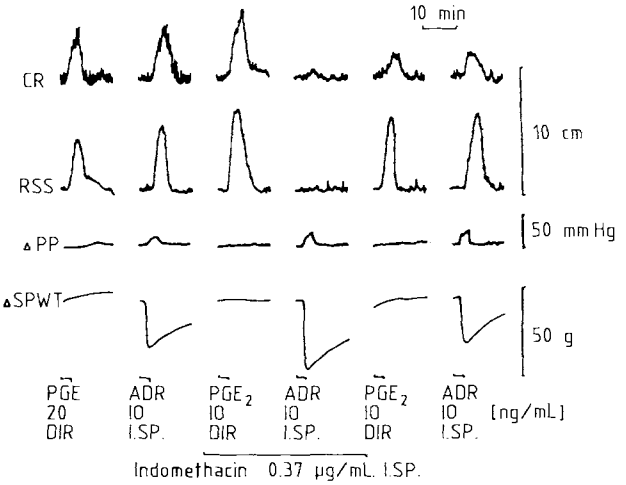



Fig. 8. A spleen from a dog was perfused with Krebs'-dextran solution at a rate of 20 mL/min. A continuous sample (10 mL/min) of the splenic outflow, with antagonists to histamine, 5HT and catecholamines added, was used to superfuse the assay tissues. The figure shows the effects of prostaglandins on a chick rectum (CR; top) and a rat stomach strip (RSS). The next two tracings (bottom) show changes in perfusion pressure (ΔPP) and spleen weight (ΔSP, WT). Except when infused into the spleen indomethacin was added to the splenic outflow to give a concentration of 0.37 µg/mL. The first panel shows contractions of CR and RSS induced by prostaglandin $E_2$ (20 ng/mL DIR). Next an adrenaline infusion into the spleen (ADR 10 ng/mL I. SP) induced a rise in perfusion pressure, a fall in spleen weight and an output of prostaglandins equivalent to $PGE_2$ at about 20 ng/mL. Indomethacin (0.37 µg/mL) was then infused into the spleen. During the next 25 min the assay tissues relaxed (not shown) and were then more sensitive to $PGE_2$ (10 ng/mL DIR). Adrenaline (40 min after start of indomethacin) now caused a greater increase in perfusion pressure, a greater decrease in spleen weight, but no output of prostaglandin. After stopping the indomethacin infusion into the spleen, the reactivity of the assay tissues gradually decreased and the output of prostaglandin induced by adrenaline infusion into the spleen gradually returned. The adrenaline stimulation shown was made 70 min after stopping the indomethacin (from *Ferreira, Moncada* and *Vane* [12], by permission of *Nature*).

these observations, *Smith* and *Willis* were using platelets to measure the effects of aspirin on prostaglandin formation. The results of these three studies were published simultaneously in 1971[10–12]. *Vane*[10] developed the hypothesis that this biochemical intervention in prostaglandin formation by the aspirin-like drugs is the basis of their therapeutic action.

An explanation of the therapeutic action of aspirin and its congeners had long been sought in terms of inhibition of a specific enzyme or biological function. Although these drugs inhibited a wide variety of enzymic reactions *in vitro*, no convincing relationship could be established between such inhibition and their known anti-inflammatory, antipyretic and analgesic actions. This was largely because of the high concentrations needed for enzyme inhibition. At the time we discovered that aspirin-like drugs inhibited the biosynthesis of prostaglandins in low concentrations, there was some evidence that the prostaglandins participated in the pathogenesis of inflammation and fever, and this reinforced the suggestion that inhibition of prostaglandin biosynthesis could explain the clinical action of these drugs. In the years which have elapsed since the original observations, a considerable body of evidence has accumulated which supports this hypothesis. Our knowledge about the inflammatory process has also increased, and the way in which prostaglandins participate in this process has been considerably clarified.

Inhibition of prostaglandin biosynthesis is a property peculiar to the aspirin-like drugs, since many otherwise pharmacologically active agents are inactive against this enzyme system, including the opiates, antihistamines, α- and β-adrenoreceptor blocking agents and antagonists of acetylcholine and 5HT. The anti-inflammatory steroids are also inactive against this enzyme although they can reduce prostaglandin production by inhibition of phospholipase $A_2$ (for review see *Flower, Blackwell, DiRosa* and *Parente*[62]).

Any hypothesis which purports to explain the action of a drug in terms of an anti-enzyme action must satisfy at least two basic criteria. First, the free concentrations achieved in plasma during therapy must be sufficient to inhibit the enzyme in question. Second, there must be a reasonable correlation between the level of anti-enzyme activity and the therapeutic potency. Clearly, there is abundant evidence to show that both these criteria are satisfied and there is also good evidence that therapeutic dosage reduces prostaglandin biosynthesis in man (for review, see *Vane, Flower* and *Salmon*[63]).

## 3. Prostacyclin

### 3.1. The Advent of the Prostaglandin Endoperoxides and the Discovery of Prostacyclin

The isolation of the prostaglandin endoperoxides by *Samuelsson et al.* in the early 1970's was a major step forward in prostaglandin research (see text of the Nobel lecture by *Samuelsson*[64]). The demonstration that the endoperoxides caused platelet aggregation and that they were transformed in platelets to $TXA_2$ led us and others to the con-

clusion that most of the activity associated with RCS was due to $TXA_2$[65a,b] (Fig. 9).

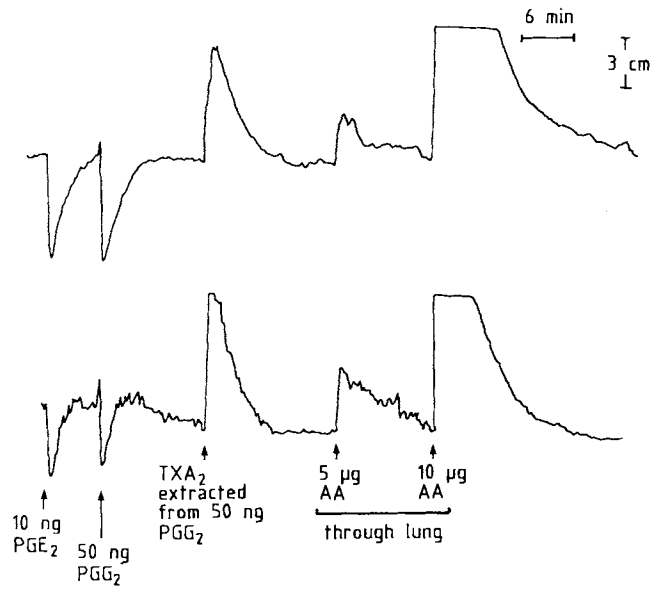



Fig. 9. Rabbit coeliac (above) and mesenteric (below) artery strips were superfused with the outflow of a pair of guinea pig lungs perfused with Krebs' solution at 10 mL/min. Prostaglandin $E_2$ (10 ng) relaxes the two tissues as does $PGG_2$. Thromboxane $A_2$ generated from 50 ng $PGG_2$ produced a contraction. Challenge of the lungs with arachidonic acid (AA 5 and 10 µg) produces a dose-dependent release of $TXA_2$-like material (from *Moncada* and *Vane* [65b], by permission of Academic Press).

From *Samuelsson*'s work we knew that $TXA_2$ could be released by platelets. We isolated the enzyme from the "microsomal" fraction of platelets and showed by our bioassay techniques that endoperoxides, when incubated with this fraction (even at 0°C), were rapidly transformed into $TXA_2$ which potently contracted rabbit aorta and induced platelet aggregation. This enzyme, which we called "thromboxane synthetase"[66,67] is now an important therapeutic target for the development of compounds with antithrombotic potential.

*Moncada, Gryglewski* and *Bunting* then began to look at other tissues to determine whether they also could generate $TXA_2$. To do this, they took microsomal fractions of several different tissues and measured, again with the superfusion cascade bioassay, formation of either the classical stable prostaglandins $E_2$ and $F_{2\alpha}$, or of $TXA_2$. It was *Moncada*'s suggestion that we should look into the biosynthetic system of vascular tissue, since vascular endothelium and platelets might share some structural features. Indeed, after several weeks of work we found that microsomal fractions of pig aorta incubated with the endoperoxide did not generate classical prostaglandins even though the endoperoxide activity (measured as RCS) disappeared. We eventually came to the conclusion that the endoperoxide was being transformed into an unknown prostaglandin and began to refer to this substance as PGX. By using recently-developed bioassay tissues such as the rabbit coeliac and mesenteric arteries[30] we were able to distinguish between the endoperoxides (which have a biphasic effect) and PGX (which has a relaxing effect). Importantly, PGX, in contrast to $TXA_2$, inhibited the clumping of platelets. Like $TXA_2$, it was also unstable, with a half-life of two minutes at 37°C. Boiling the solution for 15 seconds destroyed all measured activity.

The first paper on PGX was published by *Moncada, Gryglewski, Bunting* and *Vane* in *Nature* in October 1976[16]. Although the structure was then unknown, many of the characteristics of PGX were described, together with some important concepts. PGX was different from the other products of PG endoperoxides, and its biological activity on isolated tissues, its instability and its potent anti-aggregatory activity distinguished it from $PGD_2$, $PGE_2$, $PGF_{2\alpha}$, $TXA_2$ and $TXB_2$. PGX relaxed strips of rabbit mesenteric and coeliac arteries, but contracted rat stomach strip, chick rectum, guinea pig tracheal chain and guinea pig ileum, although its contractile potency on these tissues was less than that of the classical prostaglandins. The rat colon was not contracted by PGX: indeed, spontaneous movement was decreased.

In this first paper, the transformation of the PG endoperoxides by platelets to $TXA_2$, which caused platelet aggregation and vascular contraction, was contrasted with their transformation by blood vessel microsomes to PGX, which had potent anti-aggregatory properties and relaxed vascular strips. Thus, the concept was suggested that a balance between the amounts of $TXA_2$ formed by platelets and PGX formed by blood vessel walls might be critical for thrombus formation. Indeed, in the light of the discovery of this anti-thrombotic property associated with arterial walls, we recalled the pre-*Lister* vitalistic view that in some way the arteries kept the blood fluid.

We also developed the concept that platelets attempting to stick to vessels may release endoperoxides which are then used by the blood vessel wall to generate PGX, thus limiting or preventing further platelet clumping. We also suggested that plaque formation on the arterial wall could hinder access of platelet endoperoxides to the PGX generating system. These important properties and concepts are now well established and developed (for review, see *Moncada* and *Vane*[68]).

The structure of PGX was established through a collaborative research programme between scientists at the Upjohn Company in Kalamazoo and The Wellcome Foundation Ltd. in Beckenham[19]. This also led to the first chemical syntheses of the substance which was renamed prostacyclin ($PGI_2$)[19,69].

There is now a plethora of names for prostacyclin. The IUPAC name is 5-[(1*S*,3*Z*,5*R*,6*R*,7*R*)-7-hydroxy-6-[(1*E*,3*S*)-3-hydroxy-1-octenyl]-2-oxabicyclo[3.3.0]oct-3-ylidene]pentanoic acid. As a freeze-dried pharmaceutical preparation, the approved name is Epoprostenol, and the trade names are Flolan (Wellcome) and Cyclo-prostin (Upjohn). To maintain consistency in the scientific literature, the trivial name, prostacyclin, should be used whenever possible.

### 3.2. The Formation and Properties of Prostacyclin

Prostacyclin is the main product of arachidonic acid in all vascular tissues so far tested, including those of man (Fig. 10). The ability of the large vessel wall to synthesise prostacyclin is greatest at the intimal surface and progressively decreases toward the adventitia[70]. Culture of cells

from vessel walls also shows that endothelial cells are the most active producers of prostacyclin[71,72].

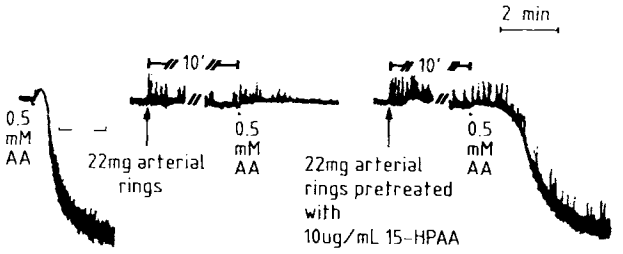



Fig. 10. Inhibition of platelet aggregation by rings of human vascular tissue. Cut rings (15–30 mg), when incubated at 37°C in human platelet rich plasma (P.R.P.) for 10 min, inhibited the aggregation produced by 0.5 mmol arachidonic acid (AA). When the rings were pretreated by incubation with 15 hydroperoxyarachidonic acid (15-HPAA) (10 μg/mL) for 5 min at 22°C, and then added to the P.R.P., aggregation was once more observed after addition of 0.5 mmol AA (from *Moncada, Higgs* and *Vane* [164], by permission of *The Lancet*).

Prostacyclin relaxes isolated vascular strips and is a strong hypotensive agent through vasodilation of all vascular beds studied, including the pulmonary and cerebral circulations (for review, see *Moncada* and *Vane*[73]). Several authors have suggested that prostacyclin generation participates in or accounts for functional hyperaemia[74,75].

Prostacyclin is the most potent endogenous inhibitor of platelet aggregation yet discovered. This effect is short-lasting *in vivo*, disappearing within 30 minutes of cessation of intravenous administration. Prostacyclin disperses platelet aggregates *in vitro*[16,76] and in the circulation of man[77]. Moreover, it inhibits thrombus formation in models using the carotid artery of the rabbit[76] and the coronary artery of the dog[78], protects against sudden death (thought to be due to platelet clumping) induced by intravenous arachidonic acid in rabbits[79], and inhibits platelet aggregation in pial venules of the mouse when applied locally[80].

Prostacyclin inhibits platelet aggregation by stimulating adenylate cyclase, leading to an increase in cAMP levels in the platelets[81,82]. In this respect prostacyclin is much more potent than either $PGE_1$ or $PGD_2$ and its effect is longer-lasting. In contrast to $TXA_2$, prostacyclin enhances $Ca^{2+}$ sequestration in platelet membranes[83]. Moreover, inhibitory effects on platelet phospholipase[84,85] and platelet cyclo-oxygenase[86] have been described. All these effects are related to its ability to increase cAMP in platelets. Prostacyclin, by inhibiting several steps in the activation of the arachidonic acid metabolic cascade, exerts an overall control of platelet aggregability.

Prostacyclin increases cAMP levels in cells other than platelets (for review, see *Moncada*[87]), raising the possibility that in these cells a balance with the thromboxane system exerts a homeostatic control of cell behaviour similar to that observed in platelets. Thus, the prostacyclin/$TXA_2$ system may have wider biological significance in cell regulation. An example is that prostacyclin inhibits white cell adherence to the vessel wall[88,89], to nylon fibres, and to endothelial monolayers *in vitro*[90]. Prostacyclin increases cAMP in the endothelial cell itself, suggesting a negative feedback control for prostacyclin production by the endothelium[91–93].

One of the functional characteristics of the intact vascular endothelium is its non-reactivity to platelets; clearly, prostacyclin generation could contribute to this thromboresistance. Moreover, prostacyclin inhibits platelet aggregation (platelet-platelet interaction) at much lower concentrations than those needed to inhibit adhesion (platelet-collagen interaction)[94]. Thus, prostacyclin may permit platelets to stick to vascular tissue and to interact with it, so allowing platelets to participate in the repair of a damaged vessel wall while at the same time preventing or limiting thrombus formation.

### 3.3. Prostacyclin and Cytoprotection

In addition to its well-known vasodilating and anti-aggregating actions, prostacyclin shares with other prostaglandins a "cytoprotective activity", as yet not clearly defined. This activity has usually been studied on gastric ulcers[95]. We have suggested[68,96] that this third property may be important in explaining certain therapeutic effects of prostacyclin. For instance, in models of myocardial infarction, prostacyclin reduces infarct size[97–99], arrhythmias[100], oxygen demand[99], and enzyme release from infarcted areas[101]. In sheep, prostacyclin protected the lungs against injury induced by endotoxin[102]. There was also a beneficial effect in endotoxin shock in the dog[103] and cat[104], where prostacyclin improves splanchnic blood flow and reduces the formation and release of lysosomal hydrolases. The effects of hypoxic damage in the isolated perfused liver of the cat are also substantially reduced by prostacyclin[105]. Canine livers can be preserved *ex vivo* for up to 48 hours and then successfully transplanted using a combination of refrigeration, Sacks' solution and prostacyclin[106].

All these effects could be related to a result obtained recently by *Moncada et al.*[107]. The addition of prostacyclin to platelets during their separation from blood and subsequent washing substantially improves their immediate functionality *in vitro*. In addition, whereas platelets normally are functional for about 6 h, when prepared with the addition of prostacyclin they remain functional for more than 72 h[107]. This extended viability of platelets *in vitro* is not accompanied by a prolonged increase in levels of cAMP, thus separating the effect from the classical anti-aggregating activity[108]. Interestingly, there has been a study demonstrating a dissociation between anti-aggregating and cytoprotective effects of a prostacyclin analogue in a model of acute myocardial ischaemia[109].

All these results suggest that some of the therapeutic effects of prostacyclin might be related to this cytoprotective effect and point to even wider indications for prostacyclin in cell or tissue preservation *in vivo* and *in vitro*.

### 3.4. Prostacyclin and Atherosclerosis

Lipid peroxides, such as 15-hydroperoxy arachidonic acid (15-HPAA), are potent and selective inhibitors of

prostacyclin generation by vessel wall microsomes or by fresh vascular tissue (see Fig. 10)[17, 18, 110, 111]. There are high concentrations of lipid peroxides in advanced atherosclerotic lesions[112]. Lipid peroxidation induced by free radical formation occurs in vitamin E deficiency, the ageing process, and perhaps also in hyperlipidaemia accompanying atherosclerosis[113]. Accumulation of lipid peroxides in atheromatous plaques could predispose to thrombus formation by inhibiting generation of prostacyclin by the vessel wall without reducing $TXA_2$ production by platelets. Moreover, platelet aggregation is induced by 15-HPAA and this aggregation is not inhibited by adenosine or $PGE_1$[114]. Human atheromatous plaques do not produce prostacyclin[115, 116]. In normal rabbits the production of prostacyclin by the luminal surface of the aorta is abolished by de-endothelialisation and slowly recovers with re-endothelialisation over a period of about 70 days. However, the recovery of prostacyclin formation did not occur in rabbits made moderately hypercholesterolaemic by diet[117]. These results suggest that it would be worth exploring whether attempts to reduce lipid peroxide formation by inhibiting peroxidation influence the development of atherosclerosis and arterial thrombosis. Vitamin E acts as an antioxidant and perhaps its empirical use in arterial disease in the past[118–120] had, in fact, a biochemical rationale. For discussion of the implication of prostacyclin and $TXA_2$ in diseases other than atherosclerosis see *Moncada* and *Vane*[68].

### 3.5. Clinical Applications of Prostacyclin

Prostacyclin is available as a stable freeze-dried preparation (Epoprostenol) for administration to man. Intravenous infusion of prostacyclin in healthy volunteers leads to a dose-related inhibition of platelet aggregation, dispersal of circulating platelet aggregates, arteriolar vasodilatation, increases in skin temperature, facial flushing and sometimes headache[87, 121]. Infusion of prostacyclin into patients susceptible to migraine or cluster headache induces, in most cases, a headache different from those usually experienced[122].

Extracorporeal circulation of blood brings it into contact with artificial surfaces which cannot generate prostacyclin. In the course of such procedures thrombocytopaenia and loss of platelet haemostatic function occur and make an important contribution to the bleeding problems following charcoal haemoperfusion and prolonged cardiopulmonary bypass in man. Formation of microemboli during cardiopulmonary bypass may also contribute to the cerebral complications which sometimes follow this procedure. Platelet damage and thrombocytopaenia were prevented by prostacyclin both in animal models of extracorporeal circulation[87, 121] and in man.

In patients with fulminant hepatic failure undergoing charcoal haemoperfusion[123], prostacyclin infusion prevented the fall in platelet count and elevation of β-thromboglobulin seen in the control patients. *Gimson et al.*[124] have made almost 200 charcoal haemoperfusions on a daily basis using prostacyclin for platelet protection in the treatment of 76 patients with fulminant hepatic failure. Remarkable survival rates (65%) were obtained in the 31 patients who had been referred early and in whom the serial haemoperfusions were started whilst the signs of grade III encephalopathy were still apparent (not rousable but may or may not respond to painful stimuli). The authors thought that this was probably the major factor in the improved survival rate, a reflection of the better biocompatibility of the system because prostacyclin was used, allowing the patients to be treated at an earlier stage. In the group treated later, with Grade IV encephalopathy already present, 20% survived, so that the overall survival rate from the 76 patients was 38%. These results (especially those treated early) compare favourably with a survival rate of 15% in patients under standard intensive care measures.

Several double-blind clinical trials of prostacyclin in cardiopulmonary bypass have been published[125–131]. The treatment groups showed a preservation of platelet number and function, with a reduction in the blood loss in the first 18 hours after operation. In the trial by *Longmore et al.*[130] the blood loss was halved. In that by *Walker et al.*[129], filters were used and the formation of platelet aggregates on the filters from the placebo group contrasted strikingly with the lack of platelet adhesion to those from patients treated with prostacyclin (Fig. 11). The heparin-sparing effect of prostacyclin was confirmed and the vasodilator effects were not troublesome; indeed, *Noback et al.*[131] suggest that these effects may be utilised in controlling intra-bypass hypertension. Clearly, the use of prostacyclin or an analogue should allow improvements in the methodology of extracorporeal circulations.

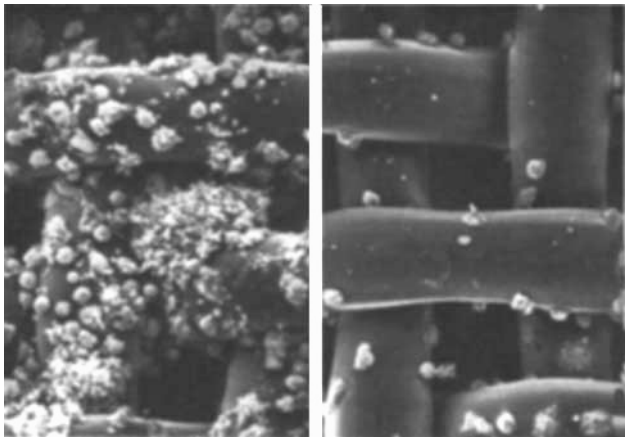


Fig. 11. Electron micrographs of the downstream face of filters taken from the arterial lines of cardio-pulmonary bypass operations in man. The left-hand picture (patient receiving placebo) shows formation of platelet aggregates, some clogging the pores ($40 \pm 5$ μ) of the filter. The right-hand picture (patient receiving prostacyclin) shows lack of platelet adhesion. The few cells sticking to the filter are leucocytes (Electron micrographs kindly provided by Dr. *N. Read* and Mr. *P. J. Astbury*, Wellcome Research Laboratories).

Therapeutic assessment of prostacyclin is still in its infancy with many trials in progress. The results are, therefore, still preliminary, but nevertheless they point the way to conditions in which prostacyclin therapy may be useful. In open trials, prostacyclin was of benefit to patients with peripheral vascular disease both through relief of ischaemic pain and improved ulcer healing[132–137]. Placebo controlled blind trials are now in progress and the results of the first to be analysed[138] are encouraging. In the 13

patients infused intravenously for 4 days with placebo, 3 showed reduction in rest pain at 5 days, 2 at 1 month and 1 at 6 months. After 6 months, 3 had died and 5 others had received surgical intervention. Of those 15 patients who were infused with prostacyclin for 4 days (average 7 ng/kg/min intravenously), at 5 days, all had reduction in rest pain. At 1 month, 9 still showed a substantial improvement, which was also evident in 7 patients at 6 months. By this time, two other patients in the group had received surgical intervention and one had died. *Zygulska-Mach et al.*[139] infused prostacyclin into 3 patients with sudden blockage of central retinal veins. Improvement was observed in those two patients who were treated within the first 48 hours.

Prostacyclin also induces long-lasting improvements in Raynaud's phenomenon. Intravenous infusion of the drug for 72 hours produced striking reductions in the frequency, duration and severity of the disease in 21 of 24 patients. The improvement lasted for a mean of 9–10 weeks, and in 3 patients subjective improvement was still reported 6 months after the infusion. Pain relief was a striking feature, presumably associated with the increased blood flow as indicated by increased temperature of the hands and fingers[140]. *Belch et al.*[141] have also reported successful treatment in 4 out of 5 patients, and a double-blind clinical trial[142] has now confirmed these results in Raynaud's phenomenon. There was an overall improvement still present at 6 weeks in 6 of 7 patients receiving prostacyclin, but only in 1 of 7 receiving placebo. The prostacyclin patients had a significant fall in the number and duration of attacks over the 6 weeks period post infusion, whereas there was no change in the placebo group.

*Gryglewski et al.* in Cracow, who first demonstrated the beneficial effects of infusion of prostacyclin in ischaemic disease of the legs, have now obtained dramatic improvements following prostacyclin infusion in 10 patients with ischaemic stroke[143]. Patients with transient ischaemic attacks and haemorrhagic stroke were excluded. With prostacyclin treatment there was a reversal of symptoms strikingly sooner in all 10 patients than could have been expected and in 6 patients during the first 6 hour infusion. One patient died 2 weeks later of a second stroke, but the other 9 have maintained return of function for (so far) up to 6 months.

Prostacyclin has been successfully used in a few cases of pulmonary hypertension and is more effective than $PGE_1$[144–146]. Single case studies have suggested that prostacyclin may be useful in the treatment of patent ductus arteriosus[147] and pre-eclamptic toxaemia[148].

Beneficial effects of intravenous infusion of prostacyclin were obtained in 9 patients with severe congestive heart failure refractory to digitalis and diuretics[149]. Mean pulmonary and systemic pressures and vascular resistances were reduced, and heart rate, cardiac index and stroke index were all increased during the infusion, with facial flushing as the only side effect.

*Bergman et al.*[150] gave an intravenous infusion of prostacyclin to patients with coronary artery disease with no deleterious effects. Heart rate and cardiac index were increased, and mean blood pressure, as well as systemic and pulmonary resistance all fell. Mean atrial pacing time to angina rose from 142 to 241 seconds. The authors concluded that acute administration of prostacyclin was beneficial in angina pectoris, having effects similar to those of the short-acting nitrates. In 5 patients with coronary artery disease, prostacyclin was safely infused directly into diseased coronary arteries[151] and there was a beneficial effect of intravenous prostacyclin infusions in patients with unstable angina[137]. However, prostacyclin had no effect on the number, severity and duration of ischaemic episodes in 8 of 9 patients with variant angina, although consistent relief was seen in the ninth patient[152].

A prostacyclin deficiency has been reported in thrombotic thrombocytopaenic purpura (TTP)[153]. Infusion of prostacyclin into two patients with TTP did not produce an increase in circulating platelet count[153, 154]. However, *FitzGerald et al.*[155] have reported an increase in platelet count and an improvement in the neurological status of one such patient during 18 days of prostacyclin infusion. They were sufficiently encouraged to conclude that the controlled evaluation of prostacyclin in TTP was warranted.

Infusion of prostacyclin protects transplanted kidneys from hyperimmune rejection in dogs[156] and is also protective in patients with chronic renal transplant rejection[157].

Clearly, there are many clinical conditions which may respond to prostacyclin treatment and its place (or that of chemically stable analogues) in therapeutics will be defined in the next few years. Some of these conditions are pre-eclamptic toxaemia[158], haemolytic uraemic syndrome[159], peptic ulceration[160], the thrombotic complications associated with transplant rejection[156], the prevention of tumour metastasis[161] and the treatment of pulmonary embolism[162].

*Over the years I have had a remarkably talented and productive group of colleagues. They have come from many parts of the world, including Australia (Greg Dusting, Bob Hodge), Belgium (Arnold Herman), Brazil (Sergio Ferreira), Great Britain (Mick Bakhle, Rod Flower, Gerry and Annie Higgs, John Hughes, Robert Lowe, Priscilla Piper, John Salmon, Ivor Williams), Holland (Franz Nijkamp), Honduras (Salvador Moncada), Italy (Domenico Regoli), Poland (Krystyna Herbaczynska-Cedro, Richard Gryglewski, Janina Staszewska-Barczak), Singapore (Kevin Ng), and the United States (Jim Aiken, Alan Block, Nobby Gilmore, Jack McGiff, Phil Needleman). Some of these have returned to my laboratory several times. Others have started as technicians and are still with me as Ph.D.'s. All (and many others) have contributed to the work which I have described. In particular, the discovery of prostacyclin was made in the Prostaglandin Research Department of the Wellcome Research Laboratories under the direction of Dr. Salvador Moncada and with the co-operation of Richard Gryglewski and Stuart Bunting. The further pre-clinical development of prostacyclin in our laboratories was also largely directed by Dr. Salvador Moncada. I would like to thank all of these friends and colleagues for their help and collaboration over the years. Their participation in the work described in this article is gratefully acknowledged.*

*I would also like to thank Mrs. A. Higgs and Mrs. A. Skinner for their help in the preparation of this manuscript.*

Received: May 31, 1983 [A 469 IE]
German version: *Angew. Chem. 95* (1983) 782

[1] W. Feldberg: *John Henry Gaddum, Biogr. Mem. Fellows R. Soc. 13* (1967) 57.
[2] J. H. Gaddum in P. Talalay: *Drugs in our Society*, The John Hopkins Press, Baltimore, MD, USA 1964, pp. 17–26.
[3] a) U. S. von Euler, *Biochim. Biophys. Acta 499* (1936) 48; b) S. Bergström, *Angew. Chem. 95* (1983), in press; *Angew. Chem. Int. Ed. Engl. 22* (1983), in press.
[4] S. H. Ferreira, J. R. Vane, *Nature London 216* (1967) 868.
[5] A. L. Willis, *J. Pharm. Pharmacol. 21* (1969) 126.
[6] A. L. Willis in P. Mantegazza, E. W. Horton: *Prostaglandins, Peptides and Amines*, Academic Press, New York 1969, pp. 31–38.
[7] K. Herbaczynska-Cedro, J. R. Vane, *Circ. Res. 33* (1973) 428.
[8] A. J. Lonigro, H. D. Itskovitz, K. Crowshaw, J. C. McGiff, *Circ. Res. 32* (1973) 712.
[9] A. J. Lonigro, N. A. Terragno, K. U. Malik, J. C. McGiff, *Prostaglandins 3* (1973) 595.
[10] J. R. Vane, *Nature New Biol. 231* (1971) 232.
[11] J. B. Smith, A. L. Willis, *Nature New Biol. 231* (1971) 235.
[12] S. H. Ferreira, S. Moncada, J. R. Vane, *Nature New Biol. 231* (1971) 237.
[13] W. Feldberg, K. P. Gupta, A. S. Milton, S. Wendlandt, *J. Physiol. London 234* (1973) 279.
[14] P. J. Piper, J. R. Vane, *Nature London 223* (1969) 29.
[15] M. Hamberg, J. Svensson, B. Samuelsson, *Proc. Natl. Acad. Sci. USA 72* (1975) 2994.
[16] S. Moncada, R. J. Gryglewski, S. Bunting, J. R. Vane, *Nature London 263* (1976) 663.
[17] R. J. Gryglewski, S. Bunting, S. Moncada, R. J. Flower, J. R. Vane, *Prostaglandins 12* (1976) 685.
[18] S. Moncada, R. J. Gryglewski, S. Bunting, J. R. Vane, *Prostaglandins 12* (1976) 715.
[19] R. A. Johnson, D. R. Morton, J. H. Kinner, R. R. Gorman, J. R. McGuire, F. F. Sun, N. Whittaker, S. Bunting, J. Salmon, S. Moncada, J. R. Vane, *Prostaglandins 12* (1976) 915.
[20] J. H. Gaddum, *Pharmacol. Rev. 11* (1959) 241.
[21] R. Magnus, *Ergeb. Physiol. Biol. Chem. Exp. Pharmakol. 2* (1903) 637.
[22] H. H. Dale, *J. Pharmacol. Exp. Ther. 4* (1912) 167.
[23] J. H. Gaddum, *Br. J. Pharmacol. Chemother. 8* (1953) 321.
[24] B. Finkleman, *J. Physiol. London 70* (1930) 145.
[25] J. R. Vane, *Br. J. Pharmacol. 23* (1964) 360.
[26] M. A. Palmer, P. J. Piper, J. R. Vane, *Br. J. Pharmacol. 49* (1973) 226.
[27] J. G. Collier, *Br. J. Pharmacol. 44* (1972) 383.
[28] S. H. Ferreira, F. S. Souza Costa, *Eur. J. Pharmacol. 39* (1976) 379.
[29] R. J. Gryglewski, R. Korbut, A. C. Ocetkiewicz, *Nature London 273* (1968) 765.
[30] S. Bunting, S. Moncada, J. R. Vane, *Br. J. Pharmacol. 57* (1976) 462P.
[31] P. Needleman, S. D. Bronson, A. Wyche, M. Sivakoff, K. C. Nicolaou, *J. Clin. Invest. 61* (1978) 839.
[32] R. L. Hodge, R. D. Lowe, J. R. Vane, *J. Physiol. London 185* (1966) 613.
[33] J. R. Vane, *Br. J. Pharmacol. 35* (1969) 209.
[34] S. Moncada, S. H. Ferreira, J. R. Vane, *Adv. Prostaglandin Thromboxane Res. 5* (1978) 211.
[35] P. J. Piper, H. O. Collier, J. R. Vane, *Nature London 213* (1967) 838.
[36] J. Staszewska-Barczak, J. R. Vane, *J. Physiol. London 177* (1965) 57P.
[37] J. Staszewska-Barczak, J. R. Vane, *Br. J. Pharmacol. Chemother. 25* (1965) 728.
[38] J. Staszewska-Barczak, J. R. Vane, *Br. J. Pharmacol. Chemother. 30* (1967) 655.
[39] D. Regoli, J. R. Vane, *J. Physiol. London 183* (1966) 513.
[40] S. H. Ferreira, J. R. Vane, *Br. J. Pharmacol. Chemother. 29* (1967) 367.
[41] H. E. Berry, J. G. Collier, J. R. Vane, *Clin. Sci. 39* (1970) 349.
[42] Y. S. Bakhle, J. R. Vane, *Physiol. Rev. 54* (1974) 1007.
[43] R. L. Hodge, K. K. F. Ng, J. R. Vane, *Nature London 215* (1967) 138.
[44] J. R. Vane, *Pharmacol. Rev. 18* (1966) 317.
[45] R. W. Ginn, J. R. Vane, *Nature London 219* (1968) 740.
[46] S. H. Ferreira, J. R. Vane, *Br. J. Pharmacol. Chemother. 30* (1967) 417.
[47] P. J. Piper, J. R. Vane, J. H. Wyllie, *Nature London 225* (1970) 600.
[48] J. C. McGiff, N. A. Terragno, J. C. Strand, J. B. Lee, A. J. Lonigro, K. K. F. Ng, *Nature London 223* (1969) 742.
[49] G. J. Dusting, S. Moncada, J. R. Vane, *Br. J. Pharmacol. 64* (1978) 315.
[50] J. C. McGuire, F. F. Sun, *Arch. Biochem. Biophys. 189* (1978) 92.
[51] R. Gryglewski, J. R. Vane, *Br. J. Pharmacol. 39* (1970) 573.
[52] K. K. F. Ng, J. R. Vane, *Nature London 216* (1967) 762.
[53] K. K. F. Ng, J. R. Vane, *Naunyn-Schmiedeberg's Arch. Pharmakol. Exp. Pathol. 259* (1968) 2.
[54] K. K. F. Ng, J. R. Vane, *Nature London 218* (1968) 144.
[55] P. J. Piper, J. R. Vane in P. Mantegazza, E. W. Horton: *Prostaglandins, Peptides and Amines*, Academic Press, New York 1969, pp. 15–19.
[56] P. Piper, J. R. Vane, *Ann. N. Y. Acad. Sci. 180* (1971) 363.
[57] H. E. Lindsey, J. H. Wyllie, *Br. J. Surg. 57* (1970) 738.
[58] B. N. Davis, E. W. Horton, P. G. Withrington, *Br. J. Pharmacol. 32* (1968) 127.
[59] N. Gilmore, J. R. Vane, J. H. Wyllie in P. Mantegazza, E. W. Horton: *Prostaglandins, Peptides and Amines*, Academic Press, New York 1969, pp. 21–29.
[60] G. Liljestrand in S. Bergström, B. Samuelsson: *Nobel Symposium 2, Prostaglandins*, Almqvist and Wiksell Stockholm 1967, pp. 107–108.
[61] E. Anggard, B. Samuelsson, *J. Biol. Chem. 239* (1964) 4097.
[62] R. J. Flower, G. Blackwell, M. DiRosa, L. Parente, in G. P. Lewis, M. Ginsburg: *Mechanisms of Steroid Action*. Macmillan Press Ltd., London 1981, pp. 97–114.
[63] J. R. Vane, R. J. Flower, J. A. Salmon, *Prostaglandins Rel. Lipids 2* (1982) 21.
[64] B. Samuelsson, *Angew. Chem. 95* (1983) No. 11; *Angew. Chem. Int. Ed. Engl. 22* (1983) No. 11.
[65] a) J. Svensson, M. Hamberg, B. Samuelsson, *Acta Physiol. Scand. 94* (1975) 222; b) S. Moncada, J. R. Vane in N. Karasch, J. Fried: *Biochemical Aspects of Prostaglandins and Thromboxanes*, Academic Press, New York 1977, pp. 155–177.
[66] P. Needleman, S. Moncada, S. Bunting, J. R. Vane, M. Hamberg, B. Samuelsson, *Nature London 261* (1976) 558.
[67] S. Moncada, P. Needleman, S. Bunting, J. R. Vane, *Prostaglandins 12* (1976) 323.
[68] S. Moncada, J. R. Vane in *Harvard Medical School Bicentennial Celebration Proceedings*, Wiley, Chichester 1983, in press.
[69] N. Whittaker, *Tetrahedron Lett. 1977*, 2805.
[70] S. Moncada, A. G. Herman, E. A. Higgs, J. R. Vane, *Thromb. Res. 11* (1977) 323.
[71] B. B. Weksler, A. J. Marcus, E. A. Jaffe, *Proc. Natl. Acad. Sci. USA 74* (1977) 3922.
[72] D. E. MacIntyre, J. D. Pearson, J. L. Gordon, *Nature London 271* (1978) 549.
[73] S. Moncada, J. R. Vane, *Pharmacol. Rev. 30* (1979) 293.
[74] B. J. R. Whittle in L. P. Fielding: *Gastro-intestinal Mucosal Blood Flow*, Churchill Livingstone, London 1980, pp. 180–191.
[75] L. Axelrod, L. Levine, *Diabetes 30* (1981) 163.
[76] F. B. Ubatuba, S. Moncada, J. R. Vane, *Thromb. Diath. Haemorrh. 41* (1979) 425.
[77] A. Szczeklik, R. J. Gryglewski, R. Nizankowski, J. Musial, R. Pieton, J. Mruk, *Pharmacol. Res. Commun. 10* (1978) 545.
[78] J. W. Aiken, R. R. Gorman, R. J. Shebuski, *Prostaglandins 17* (1979) 483.
[79] B.-L. Bayer, K. E. Blass, W. Forster, *Br. J. Pharmacol. 66* (1979) 10.
[80] W. I. Rosenblum, F. El Sabban, *Stroke 10* (1979) 399.
[81] R. R. Gorman, S. Bunting, O. V. Miller, *Prostaglandins 13* (1977) 377.
[82] J. E. Tateson, S. Moncada, J. R. Vane, *Prostaglandins 13* (1977) 389.
[83] R. Kaser-Glanzmann, M. Jakabova, J. George, E. Luscher, *Biochim. Biophys. Acta 466* (1977) 429.
[84] E. G. Lapetina, C. J. Schmitges, K. Chandrabose, P. Cuatrecasas, *Biochem. Biophys. Res. Commun. 76* (1977) 828.
[85] M. Minkes, M. Standford, M. Chi, G. Roth, A. Raz, P. Needleman, P. Majerus, *J. Clin. Invest. 59* (1977) 449.
[86] C. Malmsten, E. Granström, B. Samuelsson, *Biochem. Biophys. Res. Commun. 68* (1976) 569.
[87] S. Moncada, *Br. J. Pharmacol. 76* (1982) 3.
[88] G. A. Higgs, S. Moncada, J. R. Vane, *J. Physiol. London 280* (1978) 55P.
[89] G. A. Higgs in A. G. Herman, P. M. Vanhoutte, H. Demolin, A. Goossens: *Cardiovascular Pharmacology of the Prostaglandins*, Raven Press, New York 1982, pp. 315–325.
[90] L. A. Boxer, J. M. Allen, M. Schmidt, M. Yoder, R. L. Baehner, *J. Lab. Clin. Med. 95* (1980) 672.
[91] N. K. Hopkins, R. R. Gorman, *J. Clin. Invest. 67* (1981) 540.
[92] A. I. Schafer, M. A. Gimbrone Jr., R. I. Handin, *Biochem. Biophys. Res. Commun. 96* (1980) 1640.
[93] A. A. F. Brotherton, J. C. Hoak, *Proc. Natl. Acad. Sci. USA 79* (1982) 495.
[94] E. A. Higgs, S. Moncada, J. R. Vane, J. P. Caen, H. Michel, G. Tobelem, *Prostaglandins 16* (1978) 17.
[95] B. J. R. Whittle, *Brain Res. Bull. 5, Suppl. 1* (1980) 7.
[96] J. R. Vane, *Adv. Prostaglandin, Thromboxane Leukotriene Res. 11* (1983) 449.

[97] B. F. Jugdutt, G. M. Hutchins, B. H. Bulkley, L. C. Becker, *Clin. Res. 27* (1979) 177A.
[98] M. L. Ogletree, A. M. Lefer, J. B. Smith, K. C. Nicolaou, *Eur. J. Pharmacol. 56* (1979) 95.
[99] L. G. T. Ribeiro, T. A. Brandon, D. G. Hopkins, L. A. Reduto, A. A. Taylor, R. R. Miller, *Am. J. Cardiol. 47* (1981) 835.
[100] V. A. Starnes, R. K. Primm, R. L. Woolsey, J. A. Oates, J. W. Hammon, *J. Cardiovasc. Pharmacol. 4* (1982) 765.
[101] R. Ohlendorf, E. Perzborn, K. Schrör, *Thromb. Res. 19* (1980) 447.
[102] R. H. Demling, M. Smith, R. Gunther, M. Gee, J. Flynn, *Surgery 89* (1981) 257.
[103] J. R. Fletcher, P. W. Ramwell, *Circ. Shock 7* (1980) 299.
[104] A. M. Lefer, J. Tabas, E. F. Smith III, *Pharmacology 21* (1980) 206.
[105] H. Araki, A. M. Lefer, *Am. J. Physiol. 238* (1980) H176.
[106] M. Monden, J. G. Fortner, *Ann. Surg. 196* (1982) 38.
[107] S. Moncada, M. Radomski, J. R. Vargas, *Br. J. Pharmacol. 75* (1982) 165P.
[108] G. J. Blackwell, M. Radomski, J. R. Vargas, S. Moncada, *Biochim. Biophys. Acta 718* (1982) 60.
[109] K. Schrör, R. Ohlendorf, H. Darius, *J. Pharmacol. Exp. Ther. 219* (1981) 243.
[110] S. Bunting, R. Gryglewski, S. Moncada, J. R. Vane, *Prostaglandins 12* (1976) 897.
[111] J. A. Salmon, D. R. Smith, R. J. Flower, S. Moncada, J. R. Vane, *Biochim. Biophys. Acta 523* (1978) 250.
[112] J. Glavind, S. Hartmann, J. Clemmesen, K. E. Jessen, H. Dam, *Acta Pathol. Microbiol. Scand. 30* (1952) 1.
[113] T. F. Slater: *Free Radical Mechanisms in Tissue Injury*, Pion, London 1972.
[114] H. S. Mickel, J. Horbar, *Lipids 9* (1974) 68.
[115] V. D'Angelo, S. Villa, M. Mysliwiec, M. B. Donati, G. De Gaetano, *Thromb. Diath. Haemorrh. 39* (1978) 535.
[116] H. Sinzinger, W. Feigl, K. Silberbauer, *Lancet II* (1979) 469.
[117] A. Eldor, D. J. Falcone, D. P. Hajjar, C. R. Minick, B. B. Weksler, *Am. J. Pathol. 107* (1982) 186.
[118] A. M. Boyd, J. Marks, *Angiology 14* (1963) 198.
[119] K. Haeger, *Vasc. Dis. 5* (1968) 199.
[120] J. Marks, *Vitam. Horm. 20* (1962) 573.
[121] J. R. Vane, *J. Endocrinol. 95* (1982) 3P.
[122] R. C. Peatfield, M. J. Gawel, F. Clifford Rose, *Headache 21* (1981) 190.
[123] A. E. S. Gimson, R. D. Hughes, P. J. Mellon, H. F. Woods, P. G. Langley, J. Canalese, R. Williams, M. J. Weston, *Lancet I* (1980) 173.
[124] A. E. S. Gimson, S. Braude, P. J. Mellon, J. Canalese, R. Williams, *Lancet II* (1982) 681.
[125] J. G. Bennett, D. B. Longmore, J. O'Grady in P. J. Lewis, J. O'Grady: *Clinical Pharmacology of Prostacyclin*, Raven Press, New York 1981, pp. 201–208.
[126] S. Bunting, J. O'Grady, J.-N. Fabiani, E. Terrier, S. Moncada, J. R. Vane in P. J. Lewis, J. O'Grady: *Clinical Pharmacology of Prostacyclin*. Raven Press, New York 1981, pp. 181–193.
[127] J. Chelly, A. Tricot, A. Garcia, J.-C. Boucherie, J.-N. Fabiani, J. Passelecq, Ch. Dubost in P. J. Lewis, J. O'Grady: *Clinical Pharmacology of Prostacyclin*, Raven Press, New York 1981, pp. 209.
[128] K. Radegran, N. Egberg, C. Papaconstantinou, *Scand. J. Thoracic Cardiovasc. Surg. 15* (1981) 263.
[129] I. D. Walker, J. F. Davidson, A. Faichney, D. Wheatley, K. Davidson in P. J. Lewis, J. O'Grady: *Clinical Pharmacology of Prostacyclin*, Raven Press, New York 1981, pp. 195–199.
[130] D. B. Longmore, J. G. Bennett, P. M. Hoyle, M. A. Smith, A. Gregory, T. Osivand, W. A. Jones, *Lancet I* (1981) 800.
[131] C. R. Noback, J. H. Tinker, M. P. Kaye, G. R. Holcomb, J. R. Pluth, *Circulation 62, Suppl. 3* (1980) 1242.
[132] D. Negus in R. M. Greenhaugh: *Hormones and Vascular Disease*, Pitman Medical, London 1981, p. 181.
[133] A. G. Olsson, *Lancet II* (1980) 1076.
[134] B. J. H. Pardy, J. D. Lewis, H. H. G. Eastcott, *Surgery 88* (1980) 826.
[135] O. Soreide, L. Segadahl, A. Trippestad, H. Engedal, *Scand. J. Thoracic Cardiovasc. Surg. 16* (1982) 71.
[136] A. Szczeklik, R. Nizankowski, S. Skawinski, J. Szczeklik, P. Gluszko, R. J. Gryglewski, *Lancet I* (1979) 1111.
[137] A. Szczeklik, R. Gryglewski in P. J. Lewis, J. O'Grady: *Clinical Pharmacology of Prostacyclin*, Raven Press, New York 1981, p. 159–167.
[138] J. J. F. Belch, A. McKay, B. McArdle, P. Lieberman, J. G. Pollock, G. D. O. Lowe, C. D. Forbes, C. R. M. Prentice, *Lancet I* (1983) 315.
[139] H. Zygulska-Mach, E. Kostka-Trabka, A. Niton, R. J. Gryglewski, *Lancet II* (1980) 1075.
[140] P. M. Dowd, M. F. R. Martin, E. D. Cooke, S. A. Bowcock, R. Jones, P. A. Dieppe, J. D. T. Kirby, *Br. J. Dermatol. 106* (1982) 81.
[141] J. J. F. Belch, P. Newman, J. K. Drury, H. Capell, P. Leiberman, W. B. James, C. D. Forbes, C. R. M. Prentice, *Thromb. Haemostasis 45* (1981) 255.
[142] J. J. F. Belch, P. Newman, J. K. Drury, F. McKenzie, H. Capell, P. Leiberman, C. D. Forbes, C. R. M. Prentice, *Lancet I* (1983) 313.
[143] R. J. Gryglewski, S. Nowak, E. Kostka-Trabka, K. Bieron, A. Dembinska-Kiec, B. Blaszczyk, J. Kusmiderski, E. Markowska, S. Szmatola, *Pharmacol. Res. Common. 14* (1982) 879.
[144] W. D. Watkins, M. B. Peterson, R. K. Crone, D. C. Shannon, L. Levine, *Lancet I* (1980) 1083.
[145] L. J. Rubin, B. M. Groves, J. T. Reeves, M. Frosolono, F. Handel, A. E. Cato, *Circulation 66* (1982) 334.
[146] J. Szczeklik, A. Szczeklik, R. Nizankowski, *Lancet II* (1980) 1076.
[147] J. E. Lock, P. M. Olley, F. Coceani, P. R. Swyer, R. D. Rowe, *Lancet I* (1979) 1343.
[148] J. Fidler, M. J. Bennett, M. de Swiet, C. Ellis, P. J. Lewis, *Lancet II* (1980) 31.
[149] Y. Yui, H. Nakajima, C. Kawai, T. Murakami, *Am. J. Cardiol. 50* (1982) 320.
[150] G. Bergman, R. Daly, L. Atkinson, M. Rothman, P. J. Richardson, G. Jackson, D. E. Jewitt, *Lancet I* (1981) 569.
[151] R. J. C. Hall, H. A. Dewar, *Lancet I* (1981) 949.
[152] S. Chierchia, C. Patrono, F. Crea, G. Ciabattoni, R. de Caterina, G. A. Cinotti, A. Distante, A. Maseri, *Circulation 65* (1982) 470.
[153] C. N. Hensby, P. J. Lewis, P. Hilgard, G. J. Mufti, J. Hows, J. Webster, *Lancet II* (1979) 748.
[154] G. T. Budd, R. M. Bukowski, F. V. Lucas, A. E. Cato, D. M. Cocchetto, *Lancet II* (1980) 915.
[155] G. A. FitzGerald, L. J. Roberts II, D. Maas, A. R. Brash, J. A. Oates in P. J. Lewis, J. O'Grady: *Clinical Pharmacology of Prostacyclin*, Raven Press, New York 1981, p. 81.
[156] A. R. Mundy, M. Bewick, S. Moncada, J. R. Vane, *Prostaglandins 19* (1980) 595.
[157] C. Leithner, H. Sinzinger, M. Schwarz, *Prostaglandins 22* (1981) 783.
[158] J. Fidler, C. Ellis, M. J. Bennett, M. de Swiet, P. J. Lewis in P. J. Lewis, J. O'Grady: *Clinical Pharmacology of Prostacyclin*, Raven Press, New York 1981, pp. 141–143.
[159] J. Webster, L. K. Borysiewicz, A. J. Rees, P. J. Lewis in P. J. Lewis, J. O'Grady: *Clinical Pharmacology of Prostacyclin*, Raven Press, New York 1981, pp. 77–80.
[160] B. J. R. Whittle, G. L. Kauffman, S. Moncada, *Nature London 292* (1981) 472.
[161] K. V. Honn, B. Cicone, A. Skoff, *Science 212* (1981) 1270.
[162] T. Utsunomiya, M. M. Krausz, C. R. Valeri, D. Shepro, and H. B. Hechtman, *Surgery 88* (1980) 25.
[163] J. R. Vane in R. Porter, J. Birch: *Identification of Asthma*, Churchill Livingstone, Edinburgh 1971, pp. 121–131.
[164] S. Moncada, E. A. Higgs, J. R. Vane, *Lancet I* (1977) 18.

# Formation of CC Bonds by Addition of Free Radicals to Alkenes

**By Bernd Giese***

*Dedicated to Professor Karl Winnacker on the occasion of his 80th birthday*

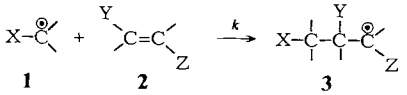
There are many reactions in which CC bonds are formed by addition of free radicals to alkenes. Information about the mechanism is important for the synthesis of specific target molecules. The rate of addition of alkyl radicals to alkenes is controlled by steric and polar effects. The stabilities of the educts and products are of only limited importance, since the transition states for these exothermic reactions occur very early on the reaction coordinate. Variations in reactivity and selectivity can be described using frontier orbital theory: for nucleophilic radicals the dominant interactions are those between SOMO's and LUMO's, and for electrophilic radicals those between SOMO's and HOMO's. The large differences in the steric effects of α- and β-substituents of alkenes can be explained by postulating an unsymmetrical transition state—the radical approaches one of the C atoms preferentially. Regio- and stereoselectivities can be predicted and are determined, in general, by steric effects.

## 1. Introduction

In recent years increasing use has been made of free radical reactions in the synthesis of organic compounds[1]. This development was made possible by mechanistic studies in which the influence of substituents on the reactivity and selectivity of free radicals was established. The most important industrial application of free radical chemistry in organic synthesis is radical-induced polymerization. This reaction involves the synthesis of a carbon skeleton by addition of alkyl radicals to alkenes. The synthesis of tailor-made polymers requires that their mechanism of formation be known: studies of the influence of substituents on the addition of alkyl radicals to alkenes were, therefore, carried out very early[2]. The development of new methods of measurement and theories has led to such advances in this area that the influence of substituents at the alkene and at the radical center on reactivity, regioselectivity, and stereoselectivity is to a large extent understood.

## 2. Influence of Substituents on the Rate of Addition of Free Radicals to Alkenes

The rates of addition of free radicals to alkenes are determined, on the one hand, by the substituents X at the radical **1** and, on the other, by the substituents Y and Z at the alkene **2**.

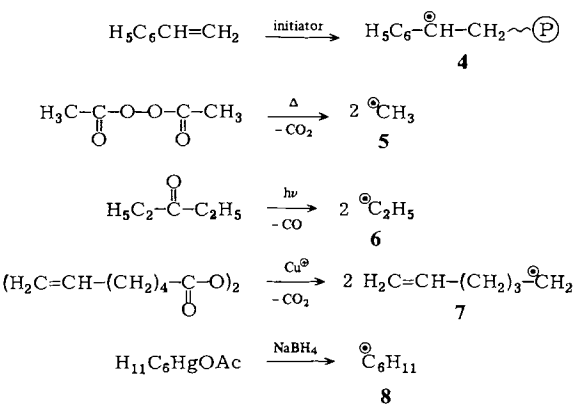


**1** **2** **3**

The alkene substituents Y and Z affect the rate of formation of the radical adduct **3** in very different ways. In order to distinguish between these substituents the group Y, which is bound to the carbon atom of the alkene **2** that is attacked by the radical, is denoted as the α-substituent and the neighboring group Z as the β-substituent. These substituents then exert α- and β-effects, respectively.

### 2.1. The β-Effect of Alkene Substituents

Almost forty years ago *Mayo, Lewis,* and *Walling et al.*[2,3] concluded from an analysis of free radical copolymerizations that the rate of addition of polymeric benzyl radicals **4** to monomers increases when the alkenes bear electron-withdrawing substituents. *Szwarc et al.*[4] came to the same conclusion in studies of competition kinetics using methyl radicals **5** generated from diacetyl peroxide. *James et al.*[5] determined the relative reactivities of ethyl radicals **6**, formed on photolysis of diethyl ketone. *Minisci et al.*[6] used metal salts to liberate the primary radical **7** from, for example, diacyl peroxides and to measure its relative and absolute reactivities towards alkenes. *Giese*[7] used cyclohexyl radicals **8**, formed by reaction of alkylmercury salts and $NaBH_4$, to determine the influence of substituents on the rate of addition.



**4** **5** **6** **7** **8**

The relative rates of addition of the alkyl radicals **4**—**8** to monosubstituted alkenes **9**, which are attacked to more than 98% at the terminal group, are summarized in Table 1[2-8].

Table 1 shows that the rate of addition of radicals **4**—**8** increases with the electron-withdrawing ability of the sub-

[*] Prof. Dr. B. Giese
Institut für Organische Chemie und Biochemie
der Technischen Hochschule
Petersenstrasse 22, D-6100 Darmstadt (Germany)

 © *Verlag Chemie GmbH, 6940 Weinheim, 1983* *0570-0833/83/1010-0753 $ 02.50/0* 

$$R^{\odot} + H_2C{=}CHZ \xrightarrow{k_{rel}} RCH_2{-}\overset{\odot}{C}HZ$$

**4–8** **9** **10**

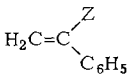
Table 1. Influence of the substituents Z on the rate of addition of radicals **4–8** to monsubstituted alkenes **9**.

| Alkene **9** Z | $k_{rel}$ for addition of the radicals **4** (60°C) | **5** (65°C) | **6** (100°C) | **7** (69°C) | **8** (20°C) |
|---|---|---|---|---|---|
| CHO | | | | | 34 |
| CN | 2.5 | 2.2 | 5.1 | 7.5 | 24 |
| $COCH_3$ | 3.5 | 2.3 | | 5.8 | 13 |
| $CO_2H$ | | | | 4.7 | |
| $CO_2CH_3$ | | 1.3 | 1.9 | 3.5 | 6.7 |
| $CONH_2$ | | | | | 1.1 |
| $C_6H_5$ | ≡1.0 | ≡1.0 | ≡1.0 | ≡1.0 | ≡1.0 |
| Cl | 0.06 | | | | 0.12 |
| $OCOCH_3$ | 0.02 | | 0.05 | | 0.016 |
| H | | | | | (0.015) [a] |
| $n$-$C_4H_9$ | | | | | 0.004 |
| $OC_2H_5$ | 0.01 | | | | |

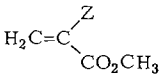
[a] Extrapolated from the Hammett relationship.

stituent Z at the alkene **9**. Thus, the rate of addition of the cyclohexyl radical **8** at 20°C increases by almost four orders of magnitude when the reaction is carried out using acrolein instead of 1-hexene. This substituent effect decreases at higher temperatures or if primary radicals (*e.g.* **5**—**7**) are used.

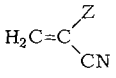
A similar increase in the rate of addition is caused by the presence of electron-withdrawing substituents Z in the substituted styrenes **11**, methyl acrylates **12**, and acrylonitriles **13** (Table 2)[7].



**11**



**12**



**13**

Table 2. Influence of the substituents **Z** on the rate of addition of cyclohexyl radicals **8** to styrenes **11**, methyl acrylates **12** and acrylonitriles **13** at 20°C.

| Alkenes **11–13** Z | $k_{rel}$ for the addition to alkenes **11** | **12** | **13** |
|---|---|---|---|
| CN | 66 | 310 | |
| $CO_2CH_3$ | 6.4 | 150 | 310 |
| $CF_3$ | | 40 | |
| Cl | | 12 | 31 |
| $SeC_6H_5$ | | 9.9 | |
| $CH_2Cl$ | | 7.7 | |
| $C_6H_5$ | 0.51 | 6.4 | 66 |
| $SC(CH_3)_3$ | | 5.6 | |
| $CH_2CO_2C_2H_5$ | | 1.4 | |
| H | 0.15 | ≡1.0 | 3.6 |
| $CH_3$ | 0.14 | 0.75 | 2.0 |
| $C(CH_3)_3$ | | 0.26 | 0.9 |
| $OC_2H_5$ | | | 0.5 |
| $OCH_3$ | | 0.16 | |
| Morpholino | | | 2.5 |

Plots of the relative reactivities of the cyclohexyl radical **8** from Tables 1 and 2 against $\sigma^-$ and $\sigma$-values[10], respectively, give straight lines with correlation coefficients of 0.91—0.99. The $\rho$-values calculated from the gradients lie between 3.1 and 3.8 at 20°C[8,9].

The positive sign of these $\rho$-values indicates that alkyl radicals are nucleophilic. This is remarkable since the attacking radical **1** has an electron septet which forms an octet upon generation of the adduct radical **3**. This apparent contradiction is resolved by frontier orbital theory (see Section 3).

The widest substituent variation was carried out with the methyl acrylates **12**. Figure 1 shows that there is a good correlation between the relative reactivities of **12** and the Hammett $\sigma$-values for Z. Neither radical-stabilizing substituents such as the phenyl group or a combination of captodative substituents[11] (*e.g.* $OCH_3$ and $CO_2CH_3$) nor the bulky $C(CH_3)_3$ group lead to an appreciable deviation from the straight line.

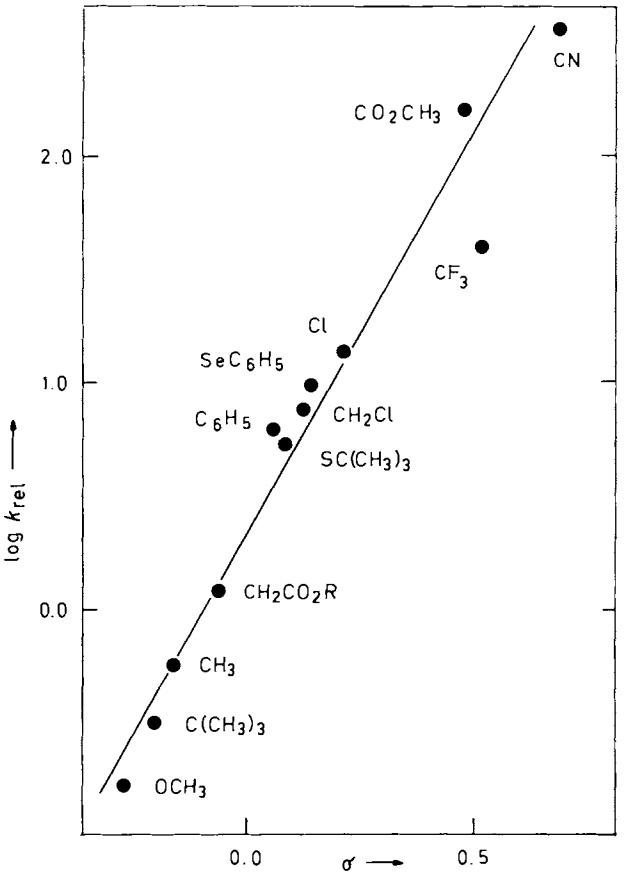



Fig. 1. Correlation of the relative reactivities of the cyclohexyl radical **8** with Hammett $\sigma$-parameters for substituents Z in methyl acrylates **12**. R = $C_2H_5$.

However, an increasing influence of the radical-stabilizing phenyl effect is observed on proceeding from the styrenes **11** ($k_{C_6H_5}/k_H = 3.4$) *via* the methyl acrylates **12** ($k_{C_6H_5}/k_H = 6.4$) and acrylonitriles **13** ($k_{C_6H_5}/k_H = 18$) to the monosubstituted alkenes **9** ($k_{C_6H_5}/k_H = 67$). This cannot be due solely to the differences in the $\rho$-values. The increasing influence of the phenyl group is probably partly due to an increase in the planarity of the $\pi$-system when the size of the geminal substituents decreases. This interpretation is supported by the fact that *trans*-substituted alkenes react faster with cyclohexyl radicals than do *cis*-substituted alkenes, and that this effect increases with increasing repulsive interaction between the vicinal substituents (Table 3)[12].

The methyl radical **5** showed a similar rate variation[13]. The unusually high reactivity of maleic anhydride is also certainly mainly due to the planarity of this *cis*-alkene[14].

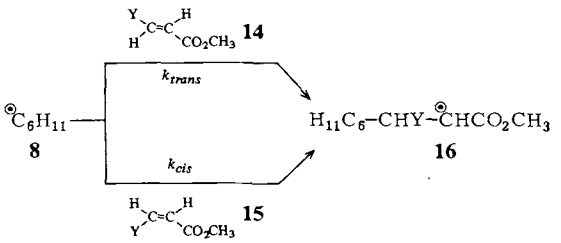


Table 3. Influence of the substituents Y on the rate ratio ($k_{trans}/k_{cis}$) for addition of cyclohexyl radicals **8** to *trans*- and *cis*-acrylic esters **14** and **15** at 20°C.

| Alkenes **14** and **15** Y | $k_{trans}/k_{cis}$ |
|---|---|
| H | 1.0 |
| CN | 1.4 |
| $CH_3$ | 1.4 |
| Cl | 1.6 |
| $C_6H_5$ | 5.0 |
| $CO_2CH_3$ | 10 |

The phenyl effect reaches its largest value ($k_{C_6H_5}/k_H = 67$) in monosubstituted alkenes **9**[8]. However, cyclohexyl radicals react 34 times faster with acrolein than with styrene at 20°C (Table 1), although free radicals are less stabilized by carbonyl groups than by phenyl substituents[15]. Thus, radical-stabilizing effects are much less important than polar effects.

The slight rate-reducing effect of bulky β-substituents is also very surprising. Thus, at 20°C the rate of addition of cyclohexyl radicals **8** decreases only by a factor of 2.2 and 2.9, respectively, when the substituent $Z = CH_3$ in acrylonitriles **13** or methylacrylates **12** is replaced by $Z = C(CH_3)_3$ (Table 2)[8, 16]. The shielding of the alkenes **12** and **13** in reactions with the cyclohexyl radical is even smaller than these values suggest, since the diminution in rate is partly caused by the electron-releasing effect and partly by the twisting of the π-system due to the repulsive interaction of the geminal substituents.

To sum up: *Substituents at the carbon atom of the alkene that is not attacked (β-substituents) exert, on the whole, only polar effects on the rate of addition of free radicals.* Radical-stabilizing and space-filling β-substituents influence the rate of addition only slightly.

### 2.2. The α-Effect of Alkene Substituents

That substituents at the vinylic carbon atom undergoing attack (α-substituents) and at the neighboring carbon atom (β-substituents) of the alkene have markedly different effects is shown by comparison of the rates of addition of cyclohexyl radicals **8** to acrylic esters **12** and **14**. Whereas 2-substituted acrylic esters **12** are attacked solely at the methylene group, addition occurs at both vinylic carbon atoms of the esters **14**. Analysis of the product mixtures allows the determination of the $k_\alpha$ value, which is statistically corrected[*] for $Y = CO_2CH_3$[9, 12] (cf. also Table 11).

[*] Since the fumaric ester has two equivalent olefinic C atoms, the rate constants are divided by 2.

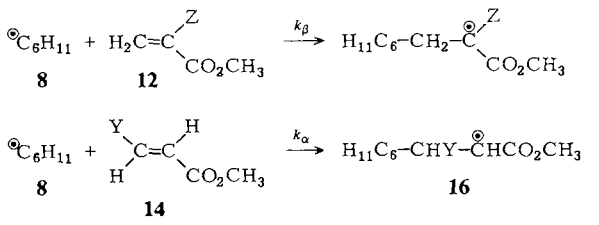


Table 4. Comparison of the relative rates $k_\beta$ and $k_\alpha$ for the addition of cyclohexyl radicals **8** to acrylic esters **12** and **14** at 20°C.

| Alkenes **12** and **14** Z or Y | $k_\beta$ | $k_\alpha$ | $k_\beta/k_\alpha$ |
|---|---|---|---|
| CN | 310 | 6.0 | 51 |
| $CO_2CH_3$ | 150 | 5.0 | 30 |
| Cl | 10 | 0.067 | 149 |
| $C_6H_5$ | 6.4 | 0.009 | 710 |
| H | ≡1.0 | ≡1.0 | 1.0 |
| $CH_3$ | 0.7 | 0.011 | 64 |

Table 4 shows that for a given substituent $k_\alpha$ is always smaller than $k_\beta$. The order of the α-effect is also completely different from that of the β-effect, so that no correlation can be made between $\log k_\alpha$ and $\sigma^-$ or σ-values. This is because substituents Y at the vinylic carbon atom of **14** undergoing attack sterically hinder the approach of free radicals. To quantify this steric effect, alkyl groups of differing steric demands were introduced into the acrylic esters **12** and **14**[12, 16]. A *tert*-butyl substituent at the vinylic carbon of alkene **12** that is not attacked (β-substituent,

Table 5. Influence of alkyl substituents Z or Y on the relative rates $k_\beta$ and $k_\alpha$ for the addition of cyclohexyl radicals **8** to acrylic esters **12** and. **14** at 20°C.

| Alkenes **12** and **14** Z or Y | $10^3\ k_\beta$ | $10^3\ k_\alpha$ | $k_\beta/k_\alpha$ |
|---|---|---|---|
| H | ≡1000 | ≡1000 | 1.0 |
| $CH_3$ | 710 | 11 | 65 |
| $C_2H_5$ | 550 | 6.6 | 83 |
| $i$-$C_3H_7$ | 430 | 1.5 | 290 |
| $t$-$C_4H_9$ | 240 | 0.05 | 4800 |

$Z = t\text{-}C_4H_9$) decreases the reaction rate of cyclohexyl radicals only by a factor of 4.2; however, the same substituent variation at the vinylic carbon atom of **14** that is attacked (α-substituent, $Y = t\text{-}C_4H_9$) decreases the rate by a factor of 20000 (Table 5). In contrast to the small steric β-effects, the steric α-effects are thus very large. This is also shown by the different slopes ($\delta = 0.28$ and 1.4, respectively) of the correlation lines in Figure 2, in which the relative reactivities are plotted against the Taft steric parameters $E_S$[10] for the substituents Z and Y.

If the alkyl groups are replaced by substituents which exhibit completely different polar effects, the polar α-effects can be determined from the deviations from the steric correlation. The $E_S$ values for Y = Cl and CN are known. After correction for the steric interactions, polar α-effects of 4.3 for Cl and 92 for CN are obtained from the rate constants. A comparison with the influence of β-substituents shows that the polar α-effects are somewhat smaller than the polar β-effects (Table 6).

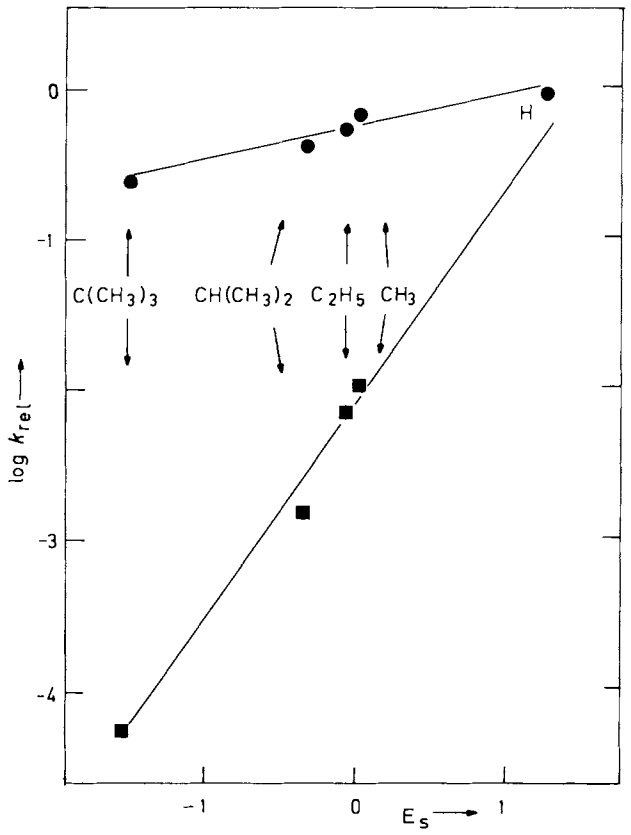



Fig. 2. Correlation between the relative reactivities of the cyclohexyl radical **8** at 20°C and the Taft $E_S$ parameters for substituents Z (●) and Y (■) in alkenes **12** and **14**.

The α-substituents Y are bonded to carbon atoms which change their hybridization from $sp^2$ to $sp^3$ during the reaction. Thus, the influence of Y on the stability of the alkenes[17] is removed during formation of the CC bond. If this hybridization change makes itself felt in the transition state for the free radical addition reaction, an α-phenyl substituent should exert a further rate-reducing effect in addition to the steric one. The phenyl group of the cinnamic ester **14** ($Y=C_6H_5$) retards the rate of addition of cyclohexyl radicals **8** to the α-carbon atom by a factor of 110[18]. Thus, the addition occurs 1.4 and 6.7 times faster than at the α-carbon atom of the ethyl- and isopropyl-substituted acrylic esters **14**, respectively ($Y=C_2H_5$ and *i*-$C_3H_7$, respectively). Since the steric effect of the phenyl group lies between that of the ethyl and isopropyl groups, and the rate-increasing polar β-effect of the phenyl group in the acrylic esters **12** is 6.4, it follows that the alkene-stabilizing effect of a phenyl group has almost no influence on the rate of addition.

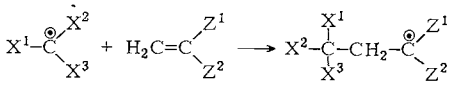
Table 6. Comparison of the polar β- and α-effects for addition of cyclohexyl radicals **8** to acrylic esters **12** and **14** at 20°C.

| Alkenes **12** and **14** Z or Y | Polar contribution to the rate of addition $k_\beta$ | $k_\alpha$ | $k_\beta/k_\alpha$ |
|---|---|---|---|
| H | ≡1.0 | ≡1.0 | 1.0 |
| Cl | 12 | 4.3 | 2.8 |
| CN | 310 | 92 | 3.4 |

To sum up: *Substituents at that carbon atom of the alkene which is attacked (α-substituents) exert both polar and steric effects on the rate of addition of free radicals.* The polar α-effect is somewhat smaller than the polar β-effect. Alkene-stabilizing substituents exert no additional effect on the rate of addition.

### 2.3. The Effect of Radical Substituents

Radical substituents also influence the rate of addition in a characteristic manner. Thus, *Minisci et al.*[19] and *Roberts et al.*[20] observed that alkyl groups X increase the reactivity of radicals **17** in addition reactions with the electron-deficient alkenes **9** and **18** (Table 7).



**17** **18**

Table 7. Influence of the substituents X on the rate of addition of radical **17** to alkenes $H_2C=CHZ$ **9**.

| Radicals **17** $X^1$ | $X^2$ | $X^3$ | Alkenes **9** Z | $k$ [L·mol$^{-1}$·s$^{-1}$] | $T$ [°C] |
|---|---|---|---|---|---|
| H | H | H | $PO(OEt)_2$ | $2.5\cdot10^3$ | −40 |
| $CH_3$ | H | H | $PO(OEt)_2$ | $2.6\cdot10^3$ | −40 |
| *n*-$C_3H_7$ | H | H | $PO(OEt)_2$ | $5.0\cdot10^3$ | −40 |
| $CH_3O$ | H | H | $PO(OEt)_2$ | $6.8\cdot10^3$ | −40 |
| $CH_3$ | $CH_3$ | H | $PO(OEt)_2$ | $1.2\cdot10^4$ | −40 |
| $CH_3$ | $CH_3$ | $CH_3$ | $PO(OEt)_2$ | $5.9\cdot10^4$ | −40 |
| *n*-$C_6H_{13}$ | H | H | CN | $5.9\cdot10^5$ | 0 |
| $CH_3$ | $CH_3$ | H | CN | $4.3\cdot10^6$ | 0 |
| OAc | $CH_3$ | H | CN | $1.1\cdot10^5$ | 25 |
| CN | alkyl | H | CN | $10^2$–$10^3$ | 25 |

The diethyl vinylphosphonate **9** ($Z=PO(OEt)_2$) reacts 24 times faster with *tert*-butyl than with methyl radicals, and acrylonitrile **9** (Z=CN) 7.5 times faster with isopropyl than with 1-heptyl radicals (Table 7). This increase in the reactivity of the radicals with the number of alkyl substituents X is remarkable since, at the same time, the stability of the reacting radicals **17** increases and that of the newly formed σ-bond decreases[15]. Thus, for these relatively small alkyl substituents the polar effects, which increase the nucleophilicity of the radical with increasing number of alkyl groups at the radical center, are apparently more important than the substituent effects on the stability of the radicals. Alkoxy substituents, which are more strongly electron-releasing than alkyl groups, further increase the reactivity of the radicals in addition reactions with electron-deficient alkenes (Table 7)[20]. In contrast, electron-attracting substituents such as X=OAc[21] or X=CN[22] decrease the rate of addition of free radicals **17** to acrylonitriles (Table 7). It is interesting to note that the reactivity and selectivity of the radicals **17** change in the same sense[23]. On proceeding from the primary 1-hexyl *via* the secondary cyclohexyl to the *tert*-butyl radical, the ρ-value for addition to acrylic esters **12** increases from 2.4 to 3.1 to 4.1[9,24], and in the fumaric esters series from 2.2 to 2.5 to 2.9[25]. A primary, alkoxy-substituted radical is just as selective as the *tert*-butyl radical[25], and a tertiary, acyl-

oxy-substituted radical just as selective as the primary 1-hexyl radical[24].

The nucleophilic reactivity and the nucleophilic selectivity of radicals **17** are thus influenced in the same sense by substituents. An explanation for this proportionality between reactivity and selectivity, which contradicts the classical reactivity-selectivity principle[26], is provided by frontier orbital theory (Section 3).

Strongly electron-withdrawing substituents can even reverse the polarity of the radicals. Thus, *Boldt et al.*[27] have shown that the reactivity of the dicyanomethyl radical increases when electron-releasing alkyl groups are introduced into alkenes. *Tedder*[28] demonstrated in very detailed studies the electrophilic properties of perfluoroalkyl and trichloromethyl radicals. For these species the rate of addition is increased by an electron-releasing methyl group and decreased by an electron-withdrawing trifluoromethyl substituent at the alkene (Table 8)[30]. This influence of substituents on the polarity of the radicals, which can lead to a change from nucleophilic to electrophilic behavior, is of paramount importance for copolymerization[31].

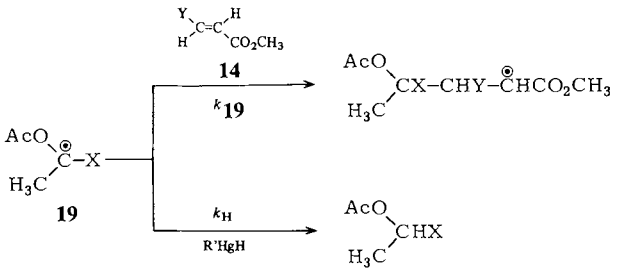
Table 8. Influence of β-substituents Z on the relative rates of addition of electrophilic radicals to alkenes **18**.

| Alkenes **18** | | $k_{rel}$ for addition of the radicals | | |
|---|---|---|---|---|
| $Z^1$ | $Z^2$ | $\overset{\oplus}{C}F_3$ (164 °C) | $\overset{\oplus}{C}F(CF_3)_2$ (164 °C) | $\overset{\oplus}{C}H(CN)_2$ (28 °C) |
| $CF_3$ | H | 0.4 | 0.13 | |
| H | H | ≡1.0 | ≡1.0 | |
| $CH_3$ | H | 2.3 | 5.6 | ≡1.0 |
| $CH_3$ | $n$-$C_3H_7$ | | | 16 |

Substituents X exert not only polar but also steric effects on the reactivity and selectivity of the radicals. The influence of the size of the group X can be studied in radicals of type **19**, which in competition with addition to the alkene **14** react with the alkylmercury hydride formed as intermediate[32]. Since hydrogen abstraction is much less dependent on the size of the substituents X than the addition to alkenes[32,33], the selectivity data in Table 9 reflect the influence of the steric variations on the reactivity of the radicals **19** in additions.

However, the influence of X on the H-abstraction cannot be completely neglected, so that the steric effect on the rate variation is even larger than that on the selectivity variation (Table 9). Substitution of a $CH_3$ by a $C(CH_3)_3$ group in the radical **19** thus decreases the rate of addition to fumaric ester by a factor of *at least* 260. As is to be expected, the steric effect is larger for reactions of fumaric esters than for those of acrylic esters, since the latter are attacked at the less shielded, unsubstituted methylene group.

Just as for the α- and β-alkene substituents Y and Z, respectively, the stabilizing influence of a radical substituent X has but little effect on the rate of addition. Thus alkyl and alkoxy substituents increase the reactivity of the radicals (Table 7), although they also stabilize them to a small extent[15]. A phenyl substituent, however, decreases the rate of addition. It can be shown from polymerization experiments, for example, that benzyl radicals react almost as slowly with acrylonitrile as do electrophilic, nitrile-substituted radicals[31]. The mesomeric stabilizing effect of a phenyl group thus retards the rate of addition of radicals to acrylonitrile just as strongly as the polar effect of a nitrile substituent.




**a**: X = $CH_3$; **b**: X = $i$-$C_3H_7$; **c**: X = $t$-$C_4H_9$

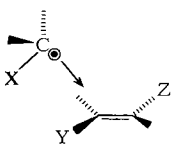
Table 9. Steric effects of alkyl groups on the selectivity ($k_{19}/k_H$) of radicals **19** at 20°C.

| Radicals **19** X | Alkenes **14** Y | Selectivity $10^3 \cdot k_{19}/k_H$ |
|---|---|---|
| $CH_3$ | H | ≡1000 |
| $i$-$C_3H_7$ | H | 250 |
| $t$-$C_4H_9$ | H | 50 |
| $CH_3$ | $CO_2CH_3$ | ≡1000 |
| $i$-$C_3H_7$ | $CO_2CH_3$ | 110 |
| $t$-$C_4H_9$ | $CO_2CH_3$ | 3.8 |

To sum up: *Substituents at the radical center exert polar and steric effects on the rate of addition to alkenes.* Radical-stabilizing substituents have comparatively little influence: only substituents which exert a strong stabilizing effect, such as X = $C_6H_5$, reduce the rate of addition.

## 3. The Reaction Mechanism

Additions of alkyl radicals to alkenes are strongly exothermic, since a σ-bond is formed and a π-bond is broken[34]. According to the Hammond postulate[35], the transition states should lie very early on the reaction coordinate, so that bond making and breaking are not far advanced. This is supported by the measured enthalpies of activation, which lie generally between 3 and 8 kcal/mol[36], and by theoretical calculations, according to which the distance between the methyl radical and ethylene in the transition state is *ca.* 230 pm[37]. All calculations favor an unsymmetrical transition state **20** in which the distances between the attacking radical and the two vinylic carbon atoms of the alkene are unequal[37,38]. There is no evidence that bridged radicals ("non-classical radicals"), whose existence has been discussed for addition reactions involving hetero radicals[39], are formed. An unsymmetrical transition state **20** readily explains the difference in the steric α- and β-effects summarized in Table 5. The distance between the β-alkene substituent Z and the radical is so large in the transition state that steric effects cannot become effective. The α-substituent Y is, however, oriented towards the attacking radical and thus exerts repulsive forces. The steric effects of the α-




**20**

alkene substituent Y and the radical substituent X are of similar magnitude (see Tables 5 and 9). This unsymmetrical transition state is also the reason for the favored formation of five-membered rings in intramolecular free radical additions[40].

The existence of early transition states and the absence of steric β-effects led us to expect that the polar effects in free radical additions can be described in terms of frontier orbital theory. To a first approximation, this theory states that the energy differences between the highest occupied molecular orbitals (HOMO's) and the lowest unoccupied molecular orbitals (LUMO's) of the reacting species are decisive in determining rate variations[41]. The smaller the energy difference between these frontier orbitals, the larger is the stabilizing effect when the reactants approach one another. The frontier orbital of a free radical is the SOMO (singly occupied molecular orbital). Thus, the interaction between the SOMO of the free radical and the LUMO and HOMO of the alkene should play a decisive role in the interpretation and prediction of polar effects[41] (Fig. 3).

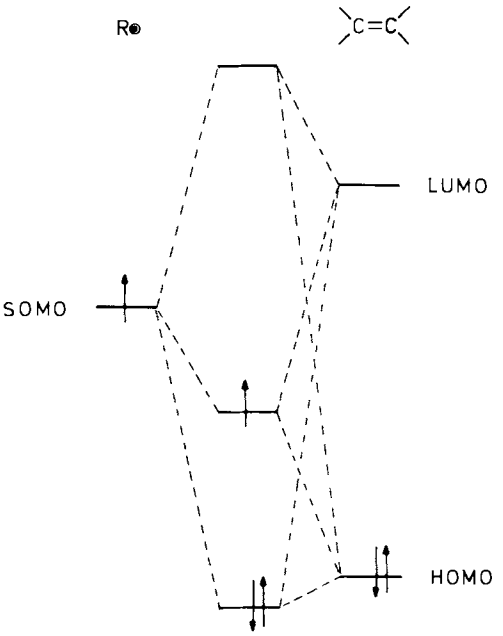



Fig. 3. Interaction between the SOMO of a free radical and the HOMO and LUMO of an alkene.

The SOMO-LUMO interaction is decisive in reactions of alkyl radicals containing electron-donating groups, which increase the energy of the SOMO[42]. The incorporation of electron-withdrawing substituents into the alkene decreases the SOMO-LUMO energy difference, and thus increases the rate of addition of the free radicals. This explains the nucleophilicity of alkyl radicals: their nucleophilic reactivity increases when electron-donating substituents are incorporated into the radical, since these decrease the SOMO-LUMO energy difference. Thus, the *tert*-butyl radical reacts more rapidly with electron-deficient alkenes than does a secondary or a primary radical (Table 7).

The variation of reactivity and selectivity in the same sense can also be understood on the basis of frontier orbital theory. The SOMO-LUMO energy difference is small for a *tert*-butyl radical, so that variation of the substituents at the alkene exerts a large effect. In comparison, the SOMO-LUMO energy difference is larger for the primary 1-hexyl radical, and, hence, the same variation of substituents at the alkene has less influence on the rate of addition. The *tert*-butyl radical is, thus, not only more reactive, but also more selective than the primary hexyl radical.

Strongly electron-withdrawing substituents decrease the SOMO energy of the radical to such an extent that the SOMO-HOMO interaction becomes dominant[43]. The radicals then lose their nucleophilic properties and become electrophilic. This change is expressed below the isokinetic temperature[44] in the form of negative ρ-values, which are typical of nitrogen-, oxygen-, and sulfur-centered radicals[45]. Just as in the carbene series[46], free radicals also exhibit nucleophilic and electrophilic behavior. Which property dominates is determined by the SOMO-HOMO and SOMO-LUMO energy differences and, thus, by the substituents at the radical center and at the alkene.

This interpretation of the polar effects is valid not only for β-substituents but also, when the steric interactions are taken into account, for α-substituents. Both electron-withdrawing α- and β-substituents lower the LUMO energies of alkenes; however, electron-withdrawing α-substituents appear to exert somewhat smaller effects than β-substituents (see Table 6). This is because not only the energies of the frontier orbitals but also the coefficients of the corresponding atomic orbitals are of importance in the interaction[41]. The rate of a reaction involving bond formation between two atoms increases with the orbital coefficients of these atoms. For the LUMOs of alkenes electron-withdrawing substituents decrease the orbital coefficients at a substituted α-carbon atom and increase those at an unsubstituted β-carbon atom[41]. Thus, the polar α-effect of electron-withdrawing groups is smaller than their β-effect (Table 6).

The LUMO of alkynes lies higher, and the HOMO lower, than in alkenes[47]. The interaction between the SOMO of the free radical and the frontier orbitals of the π-system is smaller for alkynes than for alkenes. Hence, both nucleophilic[48] and electrophilic[49] radicals react faster with alkenes **2** than with alkynes **21** (Table 10).

In contrast to free radicals, nucleophiles with non-bonding electron pairs attack triple bonds faster than double

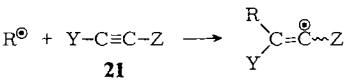



Table 10. Ratio of reactivities of alkenes **2** and alkynes **21** ($k_{alkene}/k_{alkyne}$) for additions involving nucleophilic and electrophilic radicals.

| Alkenes **2** | Alkynes **21** | $k_{Alkene}/k_{alkyne}$ for the radicals | | | |
|---|---|---|---|---|---|
| Y | Z | $\overset{\odot}{C}(CH_3)_3$ (20°C) | $\overset{\odot}{C}_6H_{11}$ (20°C) | $\overset{\odot}{C}F_3$ (164°C) | $\overset{\odot}{C}F_3$ (65°C) |
| H | H | | | 2.4 | 12 |
| H | $CH_3$ | | | | 24 |
| H | $CO_2CH_3$ | | 3.0 | | |
| H | $CF_3$ | | | 2.0 | |
| H | $C_6H_5$ | | 3.5 | | 36 |
| $CH_3$ | $CH_3$ | | | | 94 |
| $CO_2CH_3$ | $CO_2CH_3$ | 2.5 | | | |

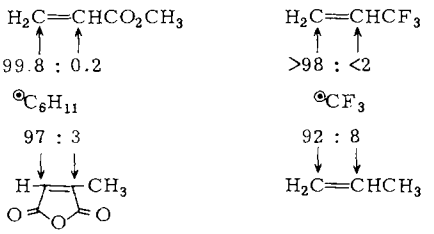
bonds. The transition states of these reactions lie so late on the reaction coordinate that the rate of addition is determined by the rehybridization of the resulting carbanion rather than by the interactions of the frontier orbitals[50]. Competition experiments using the alkyne/alkene system can, thus, be used to distinguish between free radical and ionic nucleophilicity[48,50].

To sum up: *The transition states for addition of alkyl radicals to alkenes lie so early on the reaction coordinate that the polar substituent effects can be described in terms of frontier orbital theory. The unsymmetric transition state explains the absence of steric β-effects.*

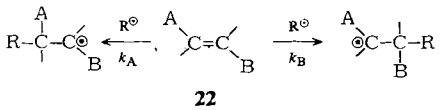
## 4. Selectivity Effects

### 4.1. Regioselectivity

Free radicals preferentially attack the less-substituted carbon atoms of alkenes. Thus, the electron-donating methyl group in methylmaleic anhydride directs attack by cyclohexyl radicals **8** to the non-methylated vinylic carbon atom[51]. The electron-withdrawing ester group in methyl acrylate has a similar influence on the regioselectivity[16]. The same substituent influence is also observed for attack by electrophilic radicals, as shown by *Haszeldine et al.*[52] and *Tedder et al.*[28,53] in detailed studies involving fluorine-containing free radicals.




*Walling*[54], *Rüchardt*[55] and *Tedder et al.*[28,29,53] pointed out the dominant influence of steric parameters on the regioselectivity of free radical addition[56]. However, many textbooks explain the favored addition at the less-substituted vinylic carbon atom in terms of the differences in stabilities of the newly formed radical centers. This argument is not convincing, since when the alkene substituents are varied the stabilities of the radicals formed play only a minor role in determining the rate of free radical addition to alkenes (Section 2).




**22**

The regioselectivity for attack by radicals $R^{\odot}$ at alkene **22** is equal to $k_A:k_B$. The rate constants $k_A$ and $k_B$ are determined by the α-effect of the substituent A plus the β-effect of the substituent B and by the β-effect of A plus the α-effect of B, respectively. Since α- and β-substituents exert polar effects of similar magnitude, $k_A:k_B$ reflects to a first approximation only the differences in the steric effects of the substituents A and B. The regioselectivity of the addition of cyclohexyl radicals **8** to the acrylic esters **14** makes this clear (Table 11)[16].

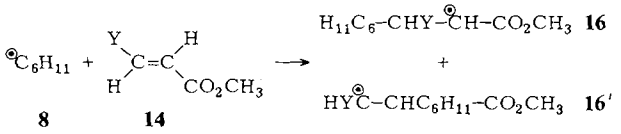
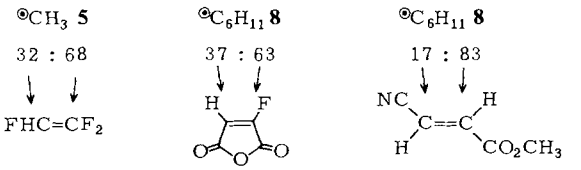



Table 11. Influence of the substituents Y on the regioselectivity of addition of cyclohexyl radicals **8** to acrylic esters **14**.

| Alkenes **14** Y | Regioselectivity **16** : **16'** | **16/16'** |
|---|---|---|
| H | 99.8 : 0.2 | 499 |
| $CH_3$ | 92 : 8 | 11.5 |
| $C_2H_5$ | 88 : 12 | 7.3 |
| $i$-$C_3H_7$ | 75 : 25 | 3 |
| $t$-$C_4H_9$ | 20 : 80 | 0.25 |

The tendency of free radicals to attack the ester-substituted vinylic carbon atom of **14** increases with the bulkiness of Y, leading to formation of **16'** Whereas the unsubstituted acrylic ester (Y = H) reacts almost solely at the methylene group to afford **16**, the *tert*-butyl-substituted acrylic ester (Y = $t$-$C_4H_9$) is attacked predominantly at the ester-substituted vinylic carbon atom. The variation in regioselectivity from 499 to 0.25 compares well with the variation of the rate ratio $k_\beta:k_\alpha$ (Table 5). Thus, the regioselectivity changes on proceeding from Y = H *via* $CH_3$, $C_2H_5$, and $i$-$C_3H_7$ to $t$-$C_4H_9$ in the acrylic esters **14** (Table 11) by factors of 43, 68, 166, and 2000, respectively. The ratios of the steric β- and α-effects ($k_\beta/k_\alpha$, see Table 5) increase in a similar manner by factors of 65, 83, 290, and 4800. As expected, the regioselectivity decreases somewhat with increasing temperature[57] and on changing to the more reactive phenyl radical[58].

The addition of free radicals to alkenes proceeds highly regioselectively when the difference in the steric bulk of the groups at the vinylic carbon atoms is large. Since all substituents are larger than hydrogen, free radicals preferentially attack the less-substituted carbon atom of alkenes. Fluorine is almost the same size as hydrogen[10], and the regioselectivity for free radical addition to fluorine-substituted alkenes is in fact often small. Trifluoroethylene[28] and fluoromaleic anhydride[59] are even preferentially attacked at the more highly substituted vinylic carbon atom.



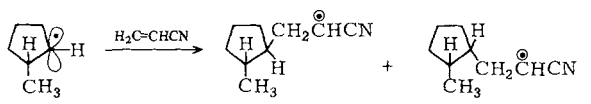

This reversal of the regioselectivity is probably due to an increase of the LUMO coefficient at the α-carbon caused by the mesomerically electron-donating[60] fluorine atom[61]. Electron-withdrawing substituents, however, increase the LUMO coefficients at the β-carbon atom. This

explains the preferential attack of the cyclohexyl radical **8** at the ester-substituted carbon atom of methyl-3-nitriloacrylate[12]. Sterically, an ester group hinders α-attack of the free radical somewhat more than a nitrile substituent; however, this is more than compensated for by the increase of the β-coefficient caused by the cyano group, which is a more effective electron acceptor than the ester substituent.

To sum up: *The regioselectivity is mainly determined by steric effects.* An exact prediction of the regioselectivity requires that the difference between the polar α- and β-effects be taken into account.

### 4.2. Stereoselectivity

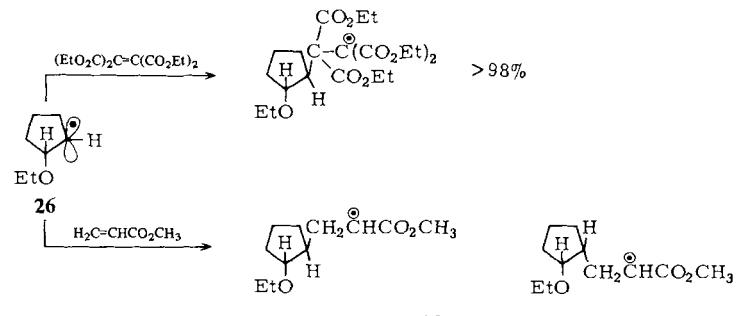
The rate of addition of free radicals to alkenes depends on the steric effects of the substituents at the radical center and at the alkene (Section 2). When the two lobes of the orbitals containing the p-electrons in radicals or alkenes are shielded to a different extent, free radical addition occurs with a stereoselectivity corresponding to the difference in the steric substituent effects. Thus, the radical **23** reacts with acrylonitrile to give a 92:8 mixture of the adduct radicals **24** and **25**[62].



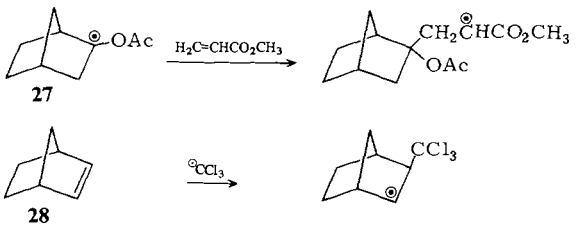

**23** **24** 92 : 8 **25**

One side of the singly occupied p-orbital of **23** is shielded by a neighboring methyl group and a hydrogen atom, and the other side only by two hydrogen atoms. This difference should correspond approximately to the steric substituent effect on the rate of addition which occurs on proceeding from the methyl-substituted radical **19a** to the isopropyl- or *tert*-butyl-substituted radicals **19b** and **19c**, respectively. The 12:1 stereoselectivity of radical **23** does, in fact, lie between the rate effects for the addition of the radicals **19a—c** to acrylic esters (Table 9); $k_{19a}:k_{19b}$ is 4:1 and $k_{19a}:k_{19c}$ 20:1.

Table 9 shows that the steric substituent effects of the radicals are amplified when the alkene is substituted at the carbon atom which is attacked. Thus, the observations that the radical **26** is attacked by the tetrasubstituted alkene exclusively *trans* to the ethoxy group[62], whereas methyl acrylate reacts with noticeably lower selectivity[63], correspond to the expected behavior.




The reactions of the norbornyl radical **27**[33] and of norbornene **28**[64] show that bulky substituents at free radical centers and at alkenes exert similar effects. In both cases, *exo*-addition occurs to more than 98%, although in **27** the p-electron of the free radical and in **28** the π-electrons of the alkene are shielded to different extents.

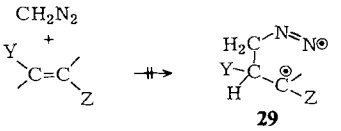



## 5. Applications

### 5.1. Studies of Reaction Mechanisms

In studies of reaction mechanisms, the questions as to whether an intermediate is involved and, if so, whether it is a free radical must often be resolved. Here, information regarding the substituent effects on the rate and selectivity of the addition of free radicals to alkenes can be useful.

Thus, comparison of the rates of additions of the cyclohexyl radical **8** and of cycloadditions of diazomethane[65] shows that the reactivity and regioselectivity of these reactions are influenced in a completely different way by alkene substituents: this suggests that the diradical **29** is not involved in the cycloaddition.




The difference between the "one-bond reactivity" of free radical additions and the "two-bond reactivity" of one-step cycloadditions makes itself felt in a highly characteristic way when substituents are introduced successively into alkenes (Table 12).

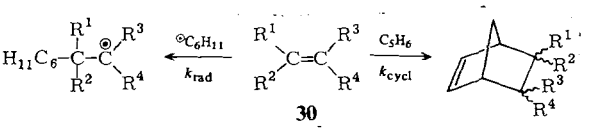


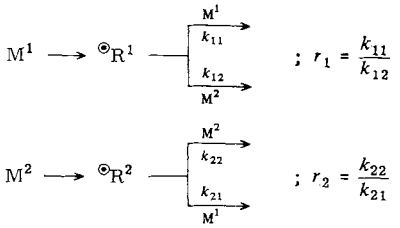

Table 12. Influence of the substituents $R^1$–$R^4$ on the rates of addition of cyclohexyl radicals **8** ($k_{rad}$) and of cycloaddition of cyclopentadiene ($k_{cycl}$) to alkenes **30** at 20°C.

| Alkenes **30** | | | | $k_{rad}$ | $k_{cycl}$ |
|---|---|---|---|---|---|
| $R^1$ | $R^2$ | $R^3$ | $R^4$ | | |
| H | H | H | $CO_2CH_3$ | ≡1.0 | |
| $CO_2CH_3$ | H | H | $CO_2CH_3$ | 6.2 | |
| H | H | $CO_2CH_3$ | $CO_2CH_3$ | 150 | |
| H | $CO_2C_2H_5$ | $CO_2C_2H_5$ | $CO_2C_2H_5$ | 25 | |
| $CO_2C_2H_5$ | $CO_2C_2H_5$ | $CO_2C_2H_5$ | $CO_2C_2H_5$ | 1.1 | |
| H | H | H | CN | | ≡1.0 |
| CN | H | H | CN | | 78 |
| H | H | CN | CN | | 43500 |
| H | CN | CN | CN | | 460000 |
| CN | CN | CN | CN | | 4150000 |

Whereas the rate of cycloaddition of cyclopentadiene increases with the number of electron-withdrawing substituents at the alkene[67], the rate of addition of the cyclohexyl radical passes through a maximum[18]; the 1,1-disubstituted alkene reacts fastest with cyclohexyl radicals **8**. Due to steric α-effects, substituents at the vinylic carbon atom which is attacked influence the rate of free radical addition to such an extent that the alkene **30**, with four ester groups, does not react faster than the monosubstituted acrylic ester[18]. In contrast, the rate of one-step cycloaddition[68] with cyclopentadiene is markedly increased by introduction of electron-withdrawing substituents at both vinylic carbon atoms. However, the validity of this comparison is diminished by the fact that ester groups exert larger vicinal, and also geminal, effects than do nitrile groups.

### 5.2. Free Radical Polymerization

In free radical polymerizations, carbon chains are formed by addition of alkyl radicals to alkenes. Thus, substituent effects which direct radical additions are of prime importance for free radical polymerization. If two monomers $M^1$ and $M^2$ which give rise to the polymer radicals $^{\odot}R^1$ and $^{\odot}R^2$ are copolymerized, the copolymerization parameters $r_1$ and $r_2$ and the $Q_j$ and $e_j$ values in the Alfrey-Price relationship (a)[69] can be correlated with the rates of addition of cyclohexyl radicals to alkenes[70].

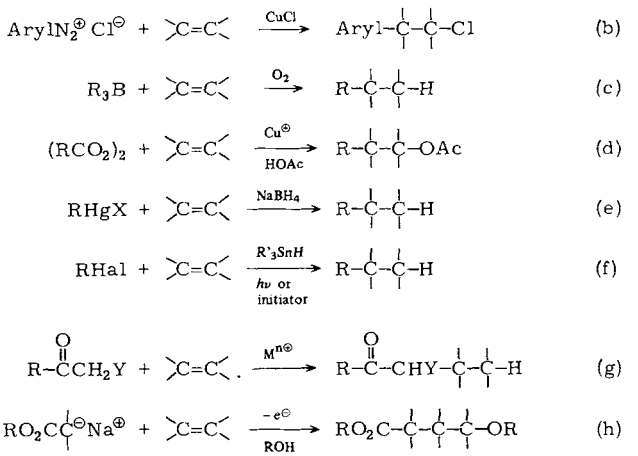


$$k_{ij} = P_i \cdot Q_j \cdot e^{-e_i \cdot e_j} \qquad \text{(a)}$$

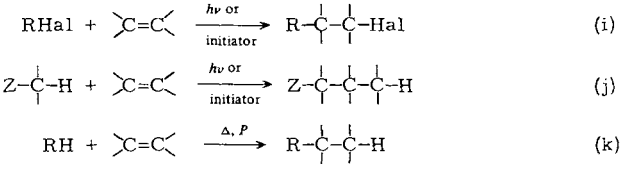
In this way, the polymerization parameters $r$ can be determined without carrying out polymerization experiments. It is also possible to measure $Q_j$ and $e_j$ values for alkenes when one of the $r$ values tends to zero. Thus, the $Q_j$ and $e_j$ values of methyl α-trifluoromethylacrylate **12** ($Z=CF_3$), which is of interest as a photoresist, cannot be measured in free radical copolymerization experiments with methyl methacrylate **12** ($Z=CH_3$) since $r_1=0$[71]. However, the $Q_j$ and $e_j$ values for **12** ($Z=CF_3$) can be calculated from the correlation between the reactivities of cyclohexyl radicals (Table 2) and the polymerization parameters of alkenes as given by equation (a)[70] using the known value of $r_2$ of 2.36: the values thus obtained are 0.74 and 2.50, respectively[72].

### 5.3. Syntheses involving CC Bond Formation

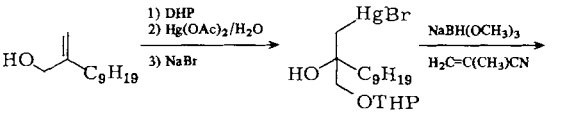
Information about the effects of substituents on the reactivity and selectivity of free radical additions can be used to predict yields and product ratios in syntheses involving the formation of CC bonds by addition of free radicals to alkenes. Examples of such syntheses are the Meerwein reaction[73] of diazonium salts (b); the Brown reaction[74] involving trialkylboranes (c); the copper-catalyzed Minisci reaction (d)[6,75]; reductive alkylation involving alkylmercury salts (e)[7,33,76] or alkyl halides (f)[77,78]; the metal salt-catalyzed reactions of carbonyl-, nitrile- or alkoxycarbonyl-substituted alkanes (g)[79]; and, to a lesser extent, the electrochemical reaction (h) involving carbanions[80].



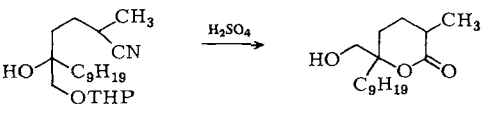
A number of halogenated hydrocarbons (i)[81] or compounds with weak CH bonds (j)[82] can add thermally or photochemically to alkenes; these reactions involve free radicals. As a final example, even the addition of unactivated hydrocarbons to alkenes (k) at high temperatures and pressures can proceed *via* free radicals[57,83].



A few examples will demonstrate the wide range of possibilities offered by these methods. *Kozikowski et al.*[84] prepared the antibiotic malyngolide **32** in only a few steps from the allylic alcohol **31**: solvomercuration, reductive addition to methacrylonitrile, and, finally, solvolysis. The 1:1 mixture of diastereomers obtained could be separated by chromatography (DHP: dihydropyran, THP: tetrahydropyranyl).

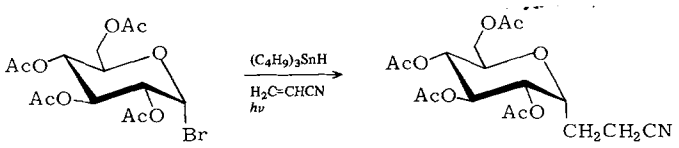


**31** 45%



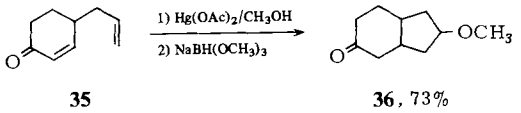
49% **32**

The exclusive formation of the 3-(α-*C*-glucopyranosyl)propionitrile **34** in the reaction of the glucosyl bromide **33** with acrylonitrile and tributyltin hydride[78] indicates that CC bond formation involving free radicals can proceed with a high degree of stereoselectivity.



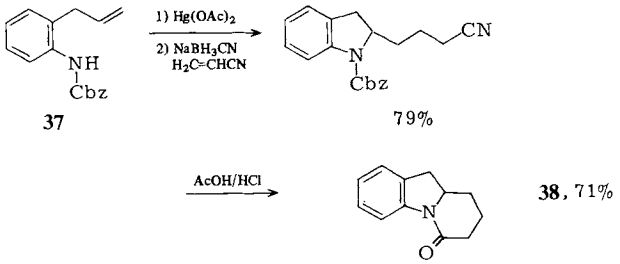

**33** **34**, 72%

*Danishefsky et al.*[85] used an intramolecular addition to carry out CC bond formation in the synthesis of the bicyclic ketone **36** from diene **35**.



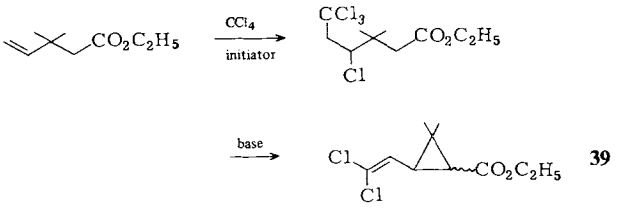

**35** **36**, 73%

However, the two cyclization steps to benzo[*b*]indolizidinone **38** precede or follow the radical reaction[86] (Cbz = benzyloxycarbonyl).




**37** 79% **38**, 71%

Electrophilic radicals have also been used in the synthesis of target molecules, as is demonstrated by several syntheses of ethyl permethrinate **39**[87].




**39**

## 6. Perspectives

The effects of substituents at the radical and at the alkene on the reactivity and selectivity of addition of free radicals to alkenes are, in general, known and predictable. Their description in terms of frontier orbital theory (Section 3) suggests that there should exist not only nucleophilic and electrophilic but also ambiphilic radicals[88], for which there will be no linear correlation between the σ-parameters of the substituents at the alkene and the free radical reactivity. Instead, the equally important interactions between the free radical SOMO and the LUMO and HOMO of the alkene will lead to a parabolic curve when free radical reactivity is plotted against the substituent parameters, just as has been described for cycloadditions[68,69]. Studies of the homolytic arylation of arenes[90] have provided evidence that free radical reactivity is increased both by electron-withdrawing and by electron-donating substituents at the π-system. However, the transition states in these reactions are so late that the stability of the product radicals is also of importance. In contrast, free radical addition to alkenes, a reaction involving early transition states, should be suitable for demonstrating the existence of ambiphilic radicals.

Recently, metal-catalyzed reactions of alkyl halides and alkenes have opened up new possibilities for the formation of CC bonds[91]. It is still unclear whether these syntheses involve free radicals. Comparison of the reactivity and selectivity with the data in Tables 1–11 could provide an answer to this question.

The correlation between free radical reactivities and copolymerization parameters (Section 5.2) indicates that *r*-, *Q*- and *e*-values will in the future be carried out to an increasing extent *via* direct measurement of the rates of addition of free radicals to alkenes. Studies of the "penultimate unit" effect[92] (*i.e.* the influence of substituents which are not attached to the radical center) are particularly interesting in this connection.

Finally, use of free radical chemistry for the synthesis of carbon skeletons (Section 5.3) enriches the potential of preparative organic chemistry. Specific syntheses involving free radicals require detailed knowledge of the reaction mechanism. In addition, the radicals should react *via* a chain mechanism, and, hence, be continually trapped and regenerated. Both these preconditions are fulfilled in the addition of free radicals to alkenes. Because of the high chemoselectivity of alkyl radicals (with which carbonyl, hydroxy, and halogen substituents do not interfere), free radical reactions could be particularly suitable for the synthesis of polyfunctional molecules such as carbohydrates[78,93].

*Our own work in this area was made possible by the generous support of the Deutsche Forschungsgemeinschaft and the Fonds der Chemischen Industrie and by the dedicated efforts of my co-workers, whose names are to be found in the literature references. I wish, in addition, to express my grateful thanks to the Karl Winnacker Foundation.*

Received: April 5, 1983 [A 468 IE]
German version: *Angew. Chem. 95* (1983) 771
Translated by *T. N. Mitchell*, Dortmund

[1] F. Minisci, A. Citterio, *Adv. Free Radical Chem. 6* (1980) 65; P. Brun, B. Waegell, *React. Intermediates 3* (1983) 367.
[2] F. R. Mayo, F. M. Lewis, *J. Am. Chem. Soc. 66* (1944) 1594; F. M. Lewis, F. R. Mayo, W. F. Hulse, *ibid. 67* (1945) 1701; F. R. Mayo, F. M. Lewis, C. Walling, *ibid. 70* (1948) 1529.
[3] F. R. Mayo, F. M. Lewis, C. Walling, *Discuss. Faraday Soc. 2 1947*, 285.
[4] M. Szwarc, *J. Polymer Sci. 16* (1955) 367; F. Leavitt, M. Levy, M. Szwarc, V. Stannett, *J. Am. Chem. Soc. 77* (1955) 5493.
[5] D. G. L. James, T. Ogawa, *Can. J. Chem. 43* (1965) 640.
[6] F. Minisci, P. Zammori, R. Bernadi, M. Cecere, R. Galli, *Tetrahedron 26* (1970) 4153; A. Citterio, F. Minisci, A. Arnoldi, R. Pagano, A. Parravicini, O. Porta, *J. Chem. Soc. Perkin Trans. 2 1978*, 519; A. Citterio, A. Arnoldi, F. Minisci, *J. Org. Chem. 44* (1979) 2674.
[7] B. Giese, J. Meister, *Chem. Ber. 110* (1977) 2558; *Angew. Chem. 89* (1977) 178; *Angew. Chem. Int. Ed. Engl. 10* (1977) 178.

[8] B. Giese, G. Kretzschmar, *Chem. Ber. 116* (1983) 3267.
[9] B. Giese, J. Meixner, *Chem. Ber. 114* (1981) 2138.
[10] Substituent constants were taken from C. Hansch, A. J. Leo: *Substituent Constants for Correlation Analysis in Chemistry and Biology*, Wiley, New York 1979.
[11] H. G. Viehe, R. Merenyi, L. Stella, Z. Janousek, *Angew. Chem. 91* (1979) 982; *Angew. Chem. Int. Ed. Engl. 18* (1979) 917.
[12] S. Lachhein, Dissertation, Technische Hochschule Darmstadt 1982.
[13] A. R. Bader, R. P. Buckley, F. Leavitt, M. Szwarc, *J. Am. Chem. Soc. 79* (1957) 5621.
[14] B. Giese, G. Kretzschmar, *Chem. Ber. 115* (1982) 2012.
[15] K. W. Egger, A. T. Cocks, *Helv. Chim. Acta 56* (1973) 1537; F. Zabel, S. W. Benson, D. M. Golden, *Int. J. Chem. Kinet. 10* (1978) 295; C. Rüchardt, H. D. Beckhaus, *Angew. Chem. 92* (1980) 417; *Angew. Chem. Int. Ed. Engl. 19* (1980) 429.
[16] B. Giese, S. Lachhein, *Angew. Chem. 93* (1981) 1016; *Angew. Chem. Int. Ed. Engl. 20* (1981) 967.
[17] J. Hine: *Structural Effects on Equilibria in Organic Chemistry*, Wiley, New York 1975.
[18] J. Meixner, Dissertation, Technische Hochschule Darmstadt 1980.
[19] T. Caronna, A. Citterio, M. Ghirardini, F. Minisci, *Tetrahedron 33* (1977) 793.
[20] J. A. Baban, B. P. Roberts, *J. Chem. Soc. Perkin Trans. 2 1981*, 161.
[21] H. Shiraishi, B. Ranby, *Chem. Sci. 12* (1977) 118.
[22] R. Korus, K. F. O'Driscoll in J. Brandrup, E. H. Immergut: *Polymer Handbook*, Wiley, New York 1975, p. II-45.
[23] B. Giese, G. Kretzschmar, J. Meixner, *Chem. Ber. 113* (1980) 2787.
[24] R. Fischkal, Diplomarbeit, Technische Hochschule Darmstadt 1981.
[25] B. Giese, J. Dupuis, T. Haßkerl, J. Meixner, *Tetrahedron Lett. 24* (1983) 703.
[26] B. Giese, *Angew. Chem. 89* (1977) 162; *Angew. Chem. Int. Ed. Engl. 16* (1977) 125; A. Pross, *Adv. Phys. Org. Chem. 14* (1977) 69.
[27] R. Riemschneider, E. Drechsel-Grau, P. Boldt, *Tetrahedron Lett. 1979*, 185.
[28] J. M. Tedder, J. C. Walton, *Tetrahedron 36* (1980) 701.
[29] See also: M. M. Martin, G. J. Gleicher, *J. Am. Chem. Soc. 86* (1964) 233.
[30] L. L. T. Vertommen, J. M. Tedder, J. C. Walton, *J. Chem. Res. (S) 1977*, 18.
[31] A. D. Jenkins in A. D. Jenkins, A. Ledwith: *Reactivity, Mechanism and Structure in Polymer Chemistry*, Wiley, London 1974, p. 117.
[32] H. Harnisch, planned Dissertation, Technische Hochschule Darmstadt 1983.
[33] B. Giese, U. Erfort, *Chem. Ber. 116* (1983) 1240.
[34] R. M. Marshall, N. D. Page, *Int. J. Chem. Kinet. 11* (1979) 199; H. E. O'Neal, S. W. Benson in J. K. Kochi: *Free Radicals, Vol. 2*, Wiley, New York 1973, p. 275.
[35] G. S. Hammond, *J. Am. Chem. Soc. 77* (1955) 334.
[36] P. I. Abell in C. H. Bamford, C. F. H. Tipper: *Comprehensive Chemical Kinetics, Vol. 18*, Elsevier, Amsterdam 1976, p. 111.
[37] M. V. Basilevsky, I. E. Chlenov, *Theor. Chim. Acta 15* (1969) 174; J. R. Hoyland, *ibid. 22* (1971) 229; D. T. Clark, I. E. Scalan, J. C. Walton, *Chem. Phys. Lett. 55* (1978) 102; M. J. S. Dewar, S. Olivella, *J. Am. Chem. Soc. 100* (1978) 5290; E. Gey, W. Kühnel, *Collect. Czech. Chem. Commun. 44* (1979) 3649; M. N. Paddon-Row, N. G. Rondan, K. N. Houk, *J. Am. Chem. Soc. 104* (1982) 7162.
[38] S. Nagase, K. Takatsuka, T. Fueno, *J. Am. Chem. Soc. 98* (1976) 3838; V. Bonačić-Koutecký, J. Koutecký, L. Salem, *ibid. 99* (1977) 842.
[39] P. S. Skell, K. J. Shea in J. K. Kochi: *Free Radicals, Vol. 2*, Wiley, New York 1973, p. 809.
[40] A. L. J. Beckwith, K. U. Ingold in P. de Mayo: *Rearrangements in Ground and Excited States, Vol. 1*, Academic Press, New York 1980, p. 161.
[41] K. Fukui, *Fortschr. Chem. Forsch. 15* (1970) 1; H. Fujimoto, S. Yamabe, T. Minato, K. Fukui, *J. Am. Chem. Soc. 94* (1972) 9205; I. Fleming: *Frontier Orbitals and Organic Chemical Reactions*, Wiley, London 1976.
[42] A. Citterio, F. Minisci, O. Porta, G. Sesana, *J. Am. Chem. Soc. 99* (1977) 7960; B. Giese, J. Meixner, *Angew. Chem. 91* (1979) 167; *Angew. Chem. Int. Ed. Engl. 17* (1979) 154.
[43] J. Sorba, J. Fossey, D. Lefort, *Bull. Soc. Chim. Fr. 1977*, 967; K. Riemschneider, H. Bartels, W. Eichel, P. Boldt, *Tetrahedron Lett. 1979*, 189; S. V. Volvik, G. G. Dyadyusha, V. I. Staninets, *Theor. Exp. Chem. USSR 16* (1980) 107; *Chem. Abstr. 93* (1980) 70512.
[44] J. E. Leffler, E. Grunwald: *Rates and Equilibria of Organic Reactions*, Wiley, New York 1963; A. G. Shostenko, V. E. Myshkin, N. P. Tarasova, V. Kim, *Org. React. USSR 15* (1978) 308; *Chem. Abstr. 91* (1978) 19444.
[45] T. Mojelsky, Y. L. Chow, *J. Am. Chem. Soc. 96* (1974) 4549, and literature cited therein.
[46] R. A. Moss, *Acc. Chem. Res. 13* (1980) 58.
[47] K. D. Jordan, P. D. Burrow, *Acc. Chem. Res. 11* (1978) 341.
[48] B. Giese, S. Lachhein, *Angew. Chem. 94* (1982) 780; *Angew. Chem. Int. Ed. Engl. 21* (1982) 768.
[49] G. E. Owen, J. M. Pearson, M. Szwarc, *J. Chem. Soc. Trans. Faraday Soc. 61* (1965) 1722; A. ElSoueni, J. M. Tedder, J. C. Walton, *J. Chem. Soc. Faraday Trans. 1 1981*, 89.
[50] K. N. Houk in W. A. Pryor: *Frontiers of Free Radical Chemistry*, Academic Press, New York 1980, p. 43; K. N. Houk, R. W. Strozier, M. D. Rozeboom, S. Nagase, *J. Am. Chem. Soc. 104* (1982) 323; see also S. Nagase, C. W. Kern, *ibid. 102* (1980) 4513.
[51] B. Giese, J. Meixner, *Tetrahedron Lett. 1977*, 2779.
[52] R. N. Haszeldine, *J. Chem. Soc. 1952*, 2504; R. N. Haszeldine, B. R. Steele, *ibid. 1953*, 1199; R. N. Haszeldine, *ibid. 1953*, 3559, 3565; R. N. Haszeldine, B. R. Steele, *ibid. 1954*, 923; *1957*, 2193, 2800.
[53] J. M. Tedder, J. C. Walton, *Acc. Chem. Res. 9* (1976) 183.
[54] C. Walling: *Free Radicals in Solution*, Wiley, New York 1957.
[55] C. Rüchardt, *Angew. Chem. 82* (1970) 845; *Angew. Chem. Int. Ed. Engl. 9* (1970) 830.
[56] See also: M. H. Treder, H. Kratzin, H. Lübbecke, C. Y. Yang, P. Boldt, *J. Chem. Res. (S) 1977*, 165.
[57] J. O. Metzger, Habilitationsarbeit, Universität Oldenburg 1982.
[58] A. Citterio, F. Minisci, E. Vismara, *J. Org. Chem. 47* (1982) 81.
[59] G. Kretzschmar, Dissertation, Technische Hochschule Darmstadt 1983.
[60] F. Bernardi, A. Mangini, N. D. Epiotis, J. R. Larson, S. Shaik, *J. Am. Chem. Soc. 99* (1977) 7465; E. R. Vorpagel, J. Streitwieser, Jr., S. D. Alexandros, *ibid. 103* (1981) 3777.
[61] An interpretation where steric effects play a more important role is given by J. M. Tedder, *Angew. Chem. 94* (1982) 433; *Angew. Chem. Int. Ed. Engl. 21* (1982) 401.
[62] U. Lüning, planned Dissertation, Technische Hochschule Darmstadt 1983.
[63] B. Giese, H. Lenhardt, U. Lüning, *Chem. Ber.*, in press.
[64] D. I. Davies in: *Essays on Free-Radical Chemistry*. Special Publication No. 24 of the Chemical Society, London 1970, p. 201.
[65] J. Geittner, R. Huisgen, R. Sustmann, *Tetrahedron Lett. 1977*, 881.
[66] B. Giese, S. Lachhein, J. Meixner, *Tetrahedron Lett. 21* (1980) 2505.
[67] J. Sauer, *Angew. Chem. 79* (1967) 16; *Angew. Chem. Int. Ed. Engl. 6* (1967) 76.
[68] J. Sauer, R. Sustmann, *Angew. Chem. 92* (1980) 773; *Angew. Chem. Int. Ed. Engl. 19* (1980) 779.
[69] T. Alfrey, C. C. Price, *J. Polym. Sci. 2* (1947) 101.
[70] B. Giese, J. Meixner, *Angew. Chem. 92* (1980) 215; *Angew. Chem. Int. Ed. Engl. 19* (1980) 207; *Polymer Bull. 2* (1980) 805.
[71] H. Ito, D. C. Miller, C. G. Willson, *Macromolecules 15* (1982) 915.
[72] H. Ito, R. Engelbrecht, B. Giese, *Macromolecules*, in press.
[73] C. S. Rondestvedt, *Org. React. 24* (1976) 225.
[74] H. C. Brown, M. M. Midland, *Angew. Chem. 84* (1972) 702; *Angew. Chem. Int. Ed. Engl. 11* (1972) 692.
[75] F. Minisci, *Acc. Chem. Res. 8* (1975) 165.
[76] B. Giese, K. Heuck, *Chem. Ber. 112* (1979) 3759; B. Giese, W. Zwick, *ibid. 112* (1979) 3766; B. Giese, G. Kretzschmar, *Angew. Chem. 93* (1981) 1015; *Angew. Chem. Int. Ed. Engl. 20* (1981) 965; B. Giese, H. Horler, W. Zwick, *Tetrahedron Lett. 23* (1982) 931; B. Giese, J. A. González Gómez, *ibid. 23* (1982) 2765.
[77] G. Stork, N. H. Baine, *J. Am. Chem. Soc. 104* (1982) 2321; S. D. Burke, W. B. Fobare, D. M. Armistaed, *J. Org. Chem. 47* (1982) 3348.
[78] B. Giese, J. Dupuis, *Angew. Chem. 95* (1983) 633; *Angew. Chem. Int. Ed. Engl. 22* (1983) 622.
[79] J. B. Bush, N. Fingbeiner, *J. Am. Chem. Soc. 90* (1969) 5903; H. H. Vogel, *Synthesis 1970*, 99; E. I. Heiba, R. M. Dessau, *J. Am. Chem. Soc. 93* (1971) 995; M. Okano, *Chem. Lett. 1973*, 165; G. I. Nikishin, M. G. Vinogradov, T. M. Fedorova, *J. Chem. Soc. Chem. Commun. 1973*, 693; W. J. de Klein, *Recl. Trav. Chim. Pays-Bas 94* (1975) 48; R. B. Mane, G. S. K. Rao, *J. Chem. Soc. Perkin Trans. 1 1975*, 1235; F. J. McQuillin, M. Wood, *ibid. 1976*, 1762; J. Y. Lallemand, *Tetrahedron Lett. 1975*, 1217; M. Hajek, J. Malek, *Collect. Czech. Chem. Commun. 42* (1977) 2388.
[80] H. Schäfer, A. Alazrak, *Angew. Chem. 80* (1968) 485; *Angew. Chem. Int. Ed. Engl. 7* (1968) 474.
[81] C. Walling, E. S. Huyser, *Org. React. 13* (1963) 91.
[82] D. Elad in O. L. Chapmann: *Organic Photochemistry, Vol. 2*, Marcel Dekker, New York 1969, p. 168.
[83] F. E. Frey, H. J. Hepp, *Ind. Eng. Chem. 28* (1936) 1139; K. Alder, O. Wolff, *Justus Liebigs Ann. Chem. 576* (1952) 182; L. K. Freidlin, N. M. Nazarova, D. L. Badalova, *Neftekhimiya 4* (1964) 839; translation: *Pet. Chem. USSR 1964*, 317; H. Pines, J. T. Arrigo, *J. Am. Chem. Soc. 79* (1957) 4958; J. O. Metzger, J. Hartmanns, P. Köll, *Tetrahedron Lett. 22* (1981) 1891.
[84] A. P. Kozikowski, T. R. Nieduzak, J. Scripko, *Organometallics 1* (1982) 675.
[85] S. Danishefsky, S. Chackalamannil, B. J. Uang, *J. Org. Chem. 47* (1982) 2231.
[86] S. Danishefsky, E. Taniyama, R. R. Webb, *Tetrahedron Lett. 24* (1983) 11.

[87] D. Arlt, M. Jautelat, R. Lantzsch, *Angew. Chem. 93* (1981) 719; *Angew. Chem. Int. Ed. Engl. 20* (1981) 703.
[88] This term, suggested by *Moss* [46] for carbenes, should also be applicable to free radicals.
[89] R. Sustmann, *Tetrahedron Lett. 1971*, 2717; *Pure Appl. Chem. 40* (1974) 569; W. C. Herndon, *Chem. Rev. 72* (1972) 152; R. Huisgen, *J. Org. Chem. 41* (1976) 403.
[90] M. J. Perkins in J. K. Kochi: *Free Radicals, Vol. 2*, Wiley, New York 1973, p. 231.
[91] P. Martin, E. Steiner, D. Bellus, *Helv. Chim. Acta 63* (1980) 1937; R. Scheffold, M. Dike, S. Dike, T. Herold, L. Walder, *J. Am. Chem. Soc. 102* (1980) 3642.
[92] H. G. Elias: *Makromoleküle*, Hüthig and Wepf, Basel 1975.
[93] The reduction of alcohols using the method developed by *Barton* demonstrates how free radicals can be effectively used in carbohydrate chemistry: D. H. R. Barton, W. Hartwig, W. B. Motherwell, *J. Chem. Soc. Chem. Commun. 1982*, 447.

# Raw Materials and Energy: A Challenge for Polymer Research**

**By Klaus Weissermel* and Harald Cherdron***

*Dedicated to Professor Karl Winnacker on the occasion of his 80th birthday*

The substantial rapid growth of synthetic polymers—plastics, man-made fibers, films, rubbers, and coatings—which continued unabated over many years, suffered a severe setback for the first time in 1973–1974 followed by another in 1980. A major cause of these reverses was the changed situation with respect to raw materials and energy. For industrial polymer research, in particular, this presents a fresh challenge with considerably changed priorities. The individual ways of meeting this challenge are highlighted and illustrated by examples: the search for alternative raw material sources for monomers; the development of economic methods for the production and processing of polymers; the recycling of polymers; and finally the development of new raw material-saving and energy-saving technologies based on the use of polymers. In the future, the applications of polymers to new technologies such as communication- and information-systems or biotechnology will join the traditional uses. But the efforts required in research and development to achieve this demand wide-ranging interdisciplinary cooperation on an even greater scale than hitherto.

## 1. The Current Situation Regarding Raw Materials and Energy

With some 85% of all primary chemicals currently used for the manufacture of polymers whose organic constituents are almost completely based on petroleum and/or natural gas, it is understandable that all the problems of availability and pricing are felt especially keenly in the polymer production sector. Thus, the two oil crises were reflected not only in the reduced demand for the primary chemicals ethylene, propene, and BTX aromatics, but, parallel to this, also in the world consumption of synthetic organic polymers in the years following 1973 and 1979 (Fig. 1).

After rapid growth, annual consumption of polymers reached 50 million t by 1974, and then, after the decline in 1975, climbed to the highest level so far of 66 million t in 1979; only to fall back sharply again in 1981.

There can be little doubt that the squandering of petroleum and natural gas for energy generation ought to be reduced[1] in favor of upgrading them into higher grade

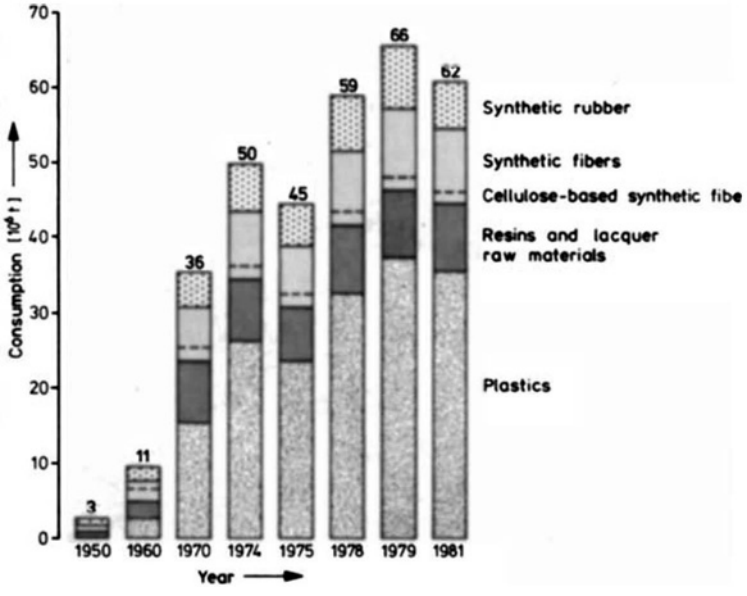



Fig. 1. World consumption of synthetic polymers in million t from 1950—1981 (excluding East block countries and China).

[*] Prof. K. Weissermel, Prof. H. Cherdron
Hoechst Aktiengesellschaft
Postfach 80 03 20, D-6230 Frankfurt am Main (Germany)

[**] Based on a plenary lecture delivered at the 25th anniversary celebrations of the Society of Polymer Science, Japan, Tokyo, 29th May, 1982.

 © Verlag Chemie GmbH, 6940 Weinheim, 1983 0570-0833/83/1010-0764 $ 02.50/0 

products, especially for use in the polymer sector. This poses three questions for polymer research and development and also sets new tasks:

- In the foreseeable future is there a possibility of finding sources of raw materials other than petroleum to ensure that the demand for monomers is met?
- In what way can polymer production and processing participate in saving raw materials and energy?
- Can the development of special polymers make a contribution to technologies that economize on raw materials and energy?

These three questions will be discussed in the following sections of this article.

## 2. Alternative Sources of Raw Materials for Monomers

The limited availability and continuing high price of petroleum raises the question as to whether it will continue to occupy the leading role as a highly important basis for chemical products. The answer to this should be given in the first place by the energy producers, as the major users of petroleum: the requirements in the transport, industrial, electricity generation, and domestic sectors currently account for approximately 89–94% of total petroleum consumption. The only alternative source of energy at present is nuclear energy, which is technically fully developed. The substitution potential of a nuclear reactor the size of the Biblis reactor is shown in Figure 2.

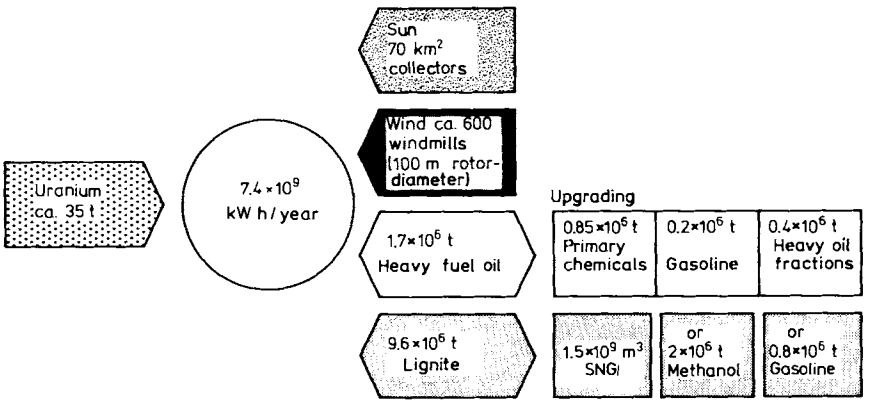



Fig. 2. Substitution potential of a 1200 megawatt nuclear power station [1a]. SNG = synthesis gas.

For electricity generation, such a nuclear power station is equivalent to an oil-fired power station with an annual consumption of 1.7 million t of fuel oil or a coal-fired power station with an annual consumption of 9.6 million t of lignite. This comparison shows how nuclear energy can be a direct or indirect replacement for oil, gas, or coal in the energy sector.

Furthermore, a nuclear power station has an effective output equivalent to 70 $km^2$ of solar collectors or 600 windmills with rotor diameters of 100 meters.

Nuclear energy could, therefore, provide an appreciable relief for the supply of energy and thus help to decelerate the wasteful exploitation of fossil fuels. These would thus become available for the more useful task of manufacturing high-grade products.

Coal and biomass as possible alternative raw materials for chemical upgrading pose fresh problems compared to petroleum as far as production of specific monomers is concerned.

### 2.1. Coal as a Source of Raw Materials

On the long term, coal and, especially, lignite will gain in importance for the chemical industry.

Compared with the outlay involved in the processing of petroleum and natural gas, all coal upgrading processes are many times more complicated and, thus, many times more expensive. For technological, economic, and ecological reasons, entry into the field of coal upgrading will very probably be gained *via* coal gasification. Lignite is the easiest to gasify and is the least expensive type of coal. Hence, synthesis gas ($CO+H_2$) produced from lignite has the greatest likelihood of becoming an economic reality in the foreseeable future.

In this context, the processing sequence "coal—synthesis gas—methanol—acetic acid—derived products" is the most tried and tested and the easiest to justify economically. In the medium term, this coal basis might also increase in significance for formaldehyde, *e.g.* for the manufacture of polyacetals and thermosets. On the other hand, the much studied catalytic conversion of ethanol into ethylene is far from being economically viable, as also is the step for the conversion of synthesis gas into polyethylene (Fig. 3).

The capital expenditure and gross requirement on raw materials for the production of 1 million t of ethylene increase steadily from ethane through naphtha to heavy fuel oil. However, the cost of raw materials and increase in capital expenditure first begin to escalate when the switch is made to coal. The reason for this is that petroleum and natural gas have a far more favorable (*i.e.* higher) hydrogen : carbon ratio than coal. Although this ratio is not of vital importance for the generation of thermal energy, process heat, or electricity, it is essential in upgrading to primary chemicals and gasoline. Only by the use of substantial quantities of energy by further consumption of lignite

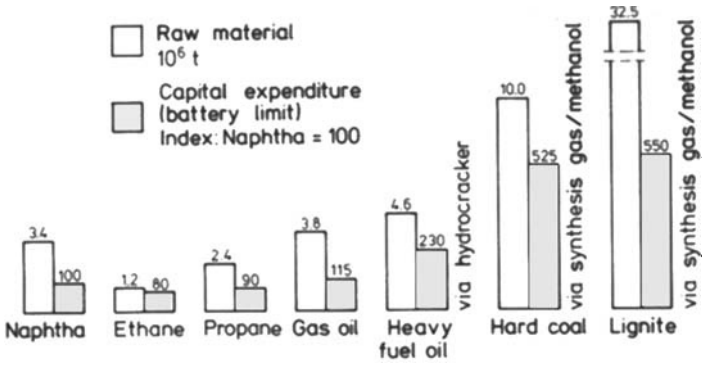



Fig. 3. Capital expenditure and gross requirement on raw materials for production of 1 million t of ethylene per annum from various starting material [1a].

is it possible to produce the hydrogen required for ethylene production (*e.g.* on the basis of lignite). This shows clearly that the slogan "Get away from oil" is inappropriate, at least for this form of upgrading. Gigantic misinvestments would result if we were to ignore suitability for upgrading in our deliberations over the future.

### 2.2. Biomass as a Source of Raw Materials

Among other possibilities, biomass could be used as an alternative source of raw materials. But in industrialized countries, in particular, even this regenerative source is subject to severe limitations. In tropical regions with large arable areas and rapid regeneration of the raw materials, bioalcohol based on carbohydrates is growing increasingly in importance as a source of energy and as a raw material for syntheses. One example of this is provided by Brazil. Yet even there an area the size of Belgium is required for sugarcane planting to replace only 20% of the gasoline requirement.

In heavily populated industrialized countries the use of valuable agricultural land to plant sugar beet would be totally uneconomic. Even to replace a mere 4.5% of the current gasoline demand (equivalent to 1 million t *per annum* in the Federal Republic of Germany), 4000 $km^2$ of land would have to be planted to yield the bioalcohol equivalent.

Furthermore, if nearly 40 mass-% were lost, for example, in dehydration to obtain ethylene from bioalcohol, it is clear that even regenerative biomass can hardly be a substitute for petroleum and can, therefore, provide no argument for continuing to use petroleum in a carefree manner in the major consumer sectors.

## 3. More Economic Methods for the Manufacture and Processing of Polymers

In the preceding section the problems associated with an economic breakthrough in alternative sources of monomers in the foreseeable future were highlighted. We now want to investigate the contributions being made by polymer research and development towards solving these problems by making economies in raw materials and energy.

### 3.1. New or Improved Polymerization Methods

The deteriorating situation with respect to raw materials and energy has undoubtedly done much to accelerate the development of improved or of new manufacturing methods. Mention should first be made of the so-called mass process, *i.e.* processes carried out without solvents or diluents. To the extent that the basic chemical and technological conditions exist, and the desired product properties are attainable, in many instances they afford advantages over the solution or dispersion processes.

As representative of these efforts, a number of examples dealing with olefin polymerization with Ziegler catalysts will be mentioned.

Polymerizations initiated by organometallic substances represent a classic example illustrating that progress in process technology is impossible without progress being made in the catalysts.

#### *3.1.1. Progress in the Development of Ziegler Catalysts*

The original Ziegler catalysts[2] consist of organometallic complexes produced by reaction of a transition-metal compound with an alkylaluminum compound. Their activity, *i.e.* the amount of polymer formed per gram of catalyst, is relatively low. Consequently, the crude polymers formed in such processes contain high amounts of residual catalyst which impairs the properties of the polymer; the crude polymer subsequently has to be upgraded using a process which is very expensive in terms of energy. Moreover, in the polymerization of propene an extraction stage is needed to remove atactic polypropylene formed because of the insufficient stereoselectivity of the catalyst. The last few years have witnessed the development of a new generation of Ziegler catalysts[3] which are notable for the following features:

- High activity ($\geq$ 1000 kg/g catalyst), which obviates the need for removal of residual catalyst from the polymer.
- High stereoselectivity ($\geq$95%), which obviates removal of atactic polypropylene.
- High selectivity with respect to the relative molecular weights of the product, *i.e.*, the molecular weight distribution can be varied within wide limits only by chemically modifing the catalyst.

Catalysts for the polymerization of ethylene[4] which meet these requirements are the so-called supported catalysts, obtained, for example, by reaction of titanium tetrachloride with a suitable solid (support) and subsequent activation with an alkylaluminum compound. These supported catalysts can be broadly divided into two groups: In the first group, the structure of the support is (largely) retained in the reaction with $TiCl_4$ (*e.g.* magnesium hydroxide supported catalysts), whereas in the second, the crystal lattice and, hence, the morphology are altered (*e.g.* magnesium alcoholate-supported catalysts).

The new supported catalysts differ from the original Ziegler catalysts in having, *inter alia*, a large specific surface area of *ca.* 60 $m^2/g$ and a very large pore volume

which does not change markedly during the polymerization process. Monomer is thus readily accessible to the polymerization-active centers over an extended period of time and, therefore, gives rise to a high conversion (Fig. 4). Associated with this is the high level of exploitation of titanium: 60 to 80% of the bound titanium is polymerization active (compared with *ca.* 10% in the classical Ziegler catalysts).

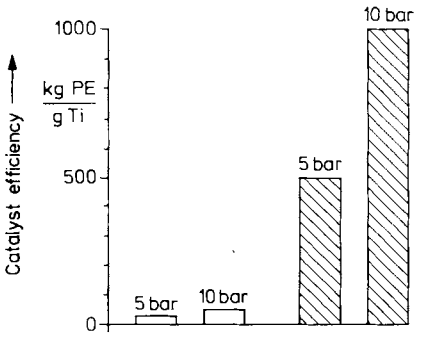



Fig. 4. Efficiency of Ziegler catalyst in the suspension polymerization of ethylene (PE = polyethylene): □ conventional catalysts, ▨ second generation catalysts.

Although long considered improbable, catalysts that possess both high activity and high stereoselectivity have also recently been discovered for the polymerization of propylene[5]. These are obtained by allowing, for example, titanium tetrachloride to react with specially pretreated magnesium chloride followed by activation with trialkylaluminum in the presence of so-called stereoregulators.

These new catalysts have not only made it possible to improve the existing dissolution or suspension processes but have also been the key to the development of totally new olefin polymerization processes[6], such as the liquid phase process for polypropylene and the gas phase process for polyethylene and polypropylene.

### *3.1.2. Progress in the Development of Processes for Polymerization with Ziegler Catalysts*

Progress in the production of polyolefins using a combination of new catalysts with new technologies is exemplified by polypropylene. Nowadays, polypropylene is produced industrially by three main methods (Fig. 5):

- Suspension process (in aliphatic hydrocarbons)
- Liquid-phase process (suspension process in liquid monomers)
- Gas-phase process

From the flow chart in Figure 5 it is clear that the use of new catalysts also enables the suspension process to be simplified because the catalyst no longer has to be removed. The mass polymerization processes (liquid-phase process and gas-phase process) have even fewer processing stages because the removal and return of the suspension agent are eliminated. Of course, these simplifications in processing contribute substantially to reducing energy consumption, although this is reflected only to a small extent in production costs, since 70% of the latter are now accounted for by the cost of the raw materials.

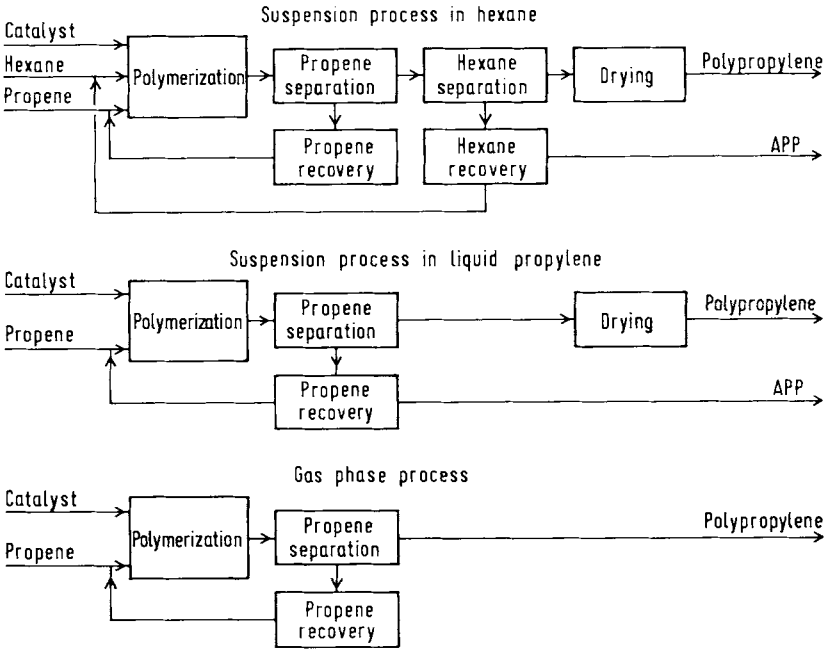



Fig. 5. Flow chart showing the various processes for production of polypropylene with Ziegler catalysts. APP = amorphous polypropylene.

## 3.2. New or Improved Processing Methods

In the sequence monomer-polymer-finished article, the processing methods, *i.e.* the conversion of the polymer powder or granules into a functional end product, are very important from the point of view of energy consumption. Thus, all processes that exploit the thermoplasticity of polymers require substantial amounts of energy, both to melt the polymer and to extrude the high-viscosity melts through nozzles or to shape them in molds. However, processing methods involving use of solutions also con-

sume large amounts of energy at the dissolution and solvent recovery stages.

As a result, considerable efforts have been, and continue to be, made to optimize existing processing methods or to develop completely new ones[7]. Examples of this include:

- Direct spinning processes for fibers,
- Improved or new nonwoven processes,
- Co-extrusion of films,
- Transfer molding processes for expanded polystyrene,
- SMC (sheet molding compounding) method for fiber-reinforced, unsaturated polyesters,
- RIM (reaction injection molding) and RRIM (reinforced reaction injection molding), *e.g.* for polyurethanes,
- New coating methods.

A number of new coating methods will be described to typify these developments.

The most important and universally applicable industrial coating methods involve use of solutions or of dispersions of a polymer. From the point of view of energy, evaporation and recovery of the organic solvent are important factors in the process. Consequently, major efforts have been made to develop alternative coating methods[8,9].

One group of methods operates without solvents (*e.g.* coating with polymer powders or radiation curing of liquid monomers), whereas the second group uses water as solvent or dispersing liquid. This includes the electrophoretic coating methods.

Today, electrophoretic coating (also known as electrodeposition coating) is used, for example, on a large scale for priming vehicle bodywork. For this purpose the coating resin, present in aqueous solution as a polyelectrolyte, is deposited on an immersed metal part by applying a direct current (anaphoretic or cataphoretic coating).

### 3.2.1. *Anaphoretic Coating*

For the coating resin, anodic deposition requires a water-soluble polyanion which can be coagulated by protons on the workpiece connected as the anode in the circuit (Fig. 6). The protons are formed by electrolysis of the water.

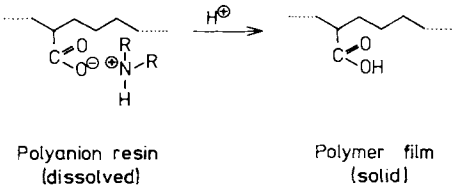



Fig. 6. Film formation in anaphoretic coating (schematic).

Suitable polyanions include, for example, low-molecular weight resins with carboxyl groups rendered water-soluble by neutralization with bases. After deposition on the workpiece, the solid film (thickness $\leq 20\ \mu m$) is crosslinked at elevated temperature in the presence of reactive compounds.

### 3.2.2. *Cataphoretic Coating*

Cathodic deposition requires a water-soluble polycation which can be coagulated by hydroxyl ions on the workpiece connected as the cathode in the circuit. The hydroxyl ions are formed by electrolysis of the water (Fig. 7).

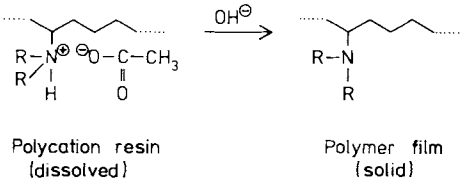



Fig. 7. Film formation in cataphoretic coating (schematic).

The solid film deposited on the workpiece (thickness $\leq 20\ \mu m$) is crosslinked by heating to 180—190 °C in the presence of catalysts.

The main advantages of the electrophoretic coating methods are the following:

- Only very small quantities of organic solvents are required;
- Optimum utilization of the polyelectrolytes in the coating baths;
- Possibility of automating the entire coating process;
- Uniform coating, even of complicated workpieces and cavities;
- Greatly improved protection against corrosion.

In addition to anaphoresis and cataphoresis, two other aqueous coating processes are being developed; namely, autophoresis and electrolytic powder coating, in which water also functions as solvent or dispersing liquid.

## 4. Recycling of Polymers

The main problems in devising a method for recycling plastics, films, fibers, and elastomers, and which is suitable for both industrial waste and communal refuse, lie in the collection and separation of the various polymers. It is thus understandable that the polymer-processing industry was the first to concern itself with re-utilization, since collection and classification within the industry can be organized relatively simply. For example, for many years in the processing of thermoplastics the scrap produced from the trimming of edges in film production or from sprue in injection molding has been ground and returned to the processing operation. Recently, as a result of the changed situation with respect to raw materials, increased attention has also been given to the recycling of polymers from communal refuse. In the Federal Republic of Germany this highly complex subject was studied under the auspices of the Association of the Plastics Manufacturing Industry (VKE) and with support of the Federal Ministry for Research and Technology (BMFT), and involved cooperation between various groups in universities and from industry. The results of this project, which covered not only the separation of polymers from other forms of refuse and their classification, but also re-utilization, have been published[10]. The following processes appear to be suitable for

the recycling of polymers—after their separation and classification:

- Direct re-utilization of polymers,
- Hydrolysis,
- Pyrolysis.

### 4.1. Direct Re-Utilization of Polymers

The direct re-utilization of polymers is dependent to a large extent on how completely it is possible to separate polymers from other materials and classify them according to type. This is particularly true if it is intended to manufacture further high-grade articles from polymer scrap by thermoplastic processing. This requirement becomes comprehensible if it is borne in mind that the great majority of polymers are not miscible, with the result that, for example, small amounts of polystyrene in polyethylene markedly affect the latter's solid-state properties[*].

An interesting example in which technical solutions have been found for the re-use of a polymer from communal refuse is provided by the recycling of polyethylene-terephthalate (PET) bottles. The process comprises the following steps[11]: The collected bottles are ground and then subjected to a number of separating processes in which paper (from the labels), aluminum (from the screw caps), and polyethylene (from the bottle bases) are removed. The PET granules after being segregated in this way are then dried carefully and can subsequently be processed to medium-quality fibers by melt-spinning, provided the polymer melt is cleaned by filtration.

To produce high-grade fibers or films, the PET granules are subjected to partial glycolysis to give low viscosity PET, which is simpler to purify; the molecular weight can subsequently be adjusted to the desired value by polycondensation. Finally, there is the third possibility: The total methanolysis or total hydrolysis of the PET to give ethylene glycol and either dimethyl terephthalate or terephthalic acid, which can be purified and polycondensed by the usual methods.

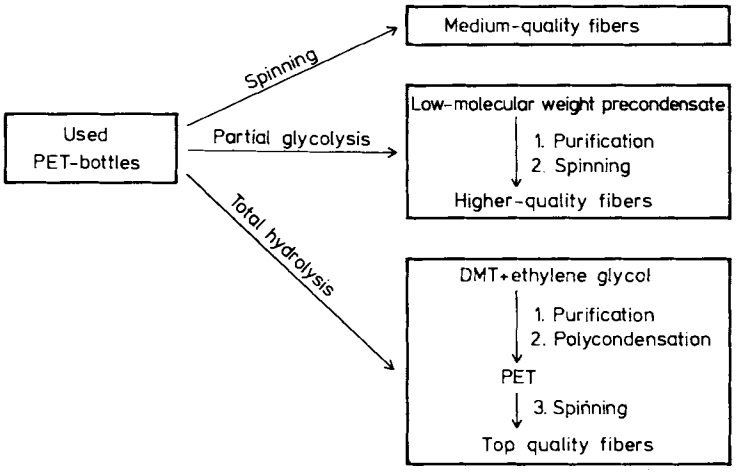



Fig. 8. Schematic representation of the possibilities for recycling polyethylene terephthalate (PET). DMT = dimethyl terephthalate.

[*] The materials known as polymer blends or polymer alloys are certainly multi-phase systems, but their favorable properties are achieved only by a defined phase morphology which requires special measures to be taken in the production of both the individual components and of the corresponding polymer blends.

### 4.2. Hydrolysis of Polymers

The re-isolation of the starting monomers by hydrolysis is possible, in principle, with many classes of polymers, *e.g.*, polyesters, polyamides, polycarbonates, and polyurethanes. For polyurethane foams[10,12], a method has been developed on a pilot plant scale in which foam-plastic scrap is hydrolyzed to polyethers and diamines in a twin-screw extruder. The reaction proceeds at 200—300 °C and 15—30 bar in the presence of water in 10 to 20 min in 90% yield. The only by-product formed is carbon dioxide. The diamine can be converted by reaction with phosgene into the corresponding diisocyanate, which then reacts with the polyether to yield a polyurethane foam.

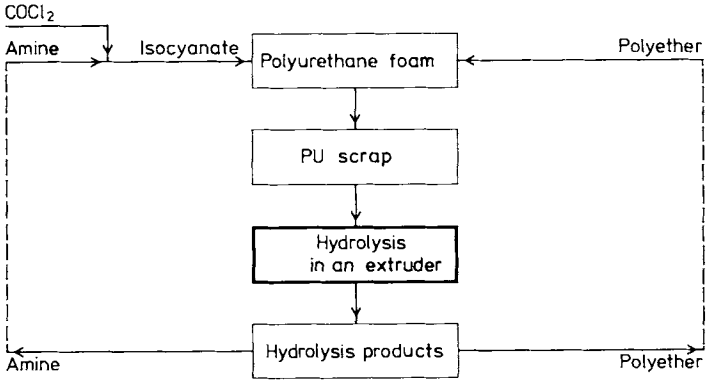



Fig. 9. Schematic representation of the recycling of scrap polyurethane foam by hydrolysis.

### 4.3. Pyrolysis of Polymers

Because it is not limited to particular structures, pyrolysis is a very widespread method of recycling polymer scrap in the form of pyrolysis products. Pyrolysis in a fluidized bed layer has proved to be a particularly elegant and versatile method[13,14].

The centerpiece of this method is a fluidized bed reactor which uses quartz sand as the fluidized medium. Fluidization is achieved by blowing in hot pyrolysis gases at 400 °C. The pyrolysis temperature of 600—900 °C is attained by means of heating coils which project into the fluidized bed and are also heated by pyrolysis gas. The polymers to be pyrolyzed are introduced into the fluidized bed in pulverized form[*]. The hot pyrolysis gases are freed from dust and soot in a cyclone, and after cooling to 30—50 °C are passed through an oil washer in which the liquid components separate out.

The composition of the pyrolysis products can be controlled by the choice of well-defined decomposition conditions (temperature, particle size, residence time, throughput rate). Examples of the material balance are shown in Table 1.

[*] Experiments with non-pulverized vehicle tires were also successful.

Table 1. Composition of the pyrolysis product of polyethylene (PE), polypropylene (PP), and a mixture (3:1:1) of PE, PP and polystyrene (PS) from a fluidized bed reactor; pyrolysis temperature: 740 °C.

| Pyrolysis products [% by weight] | Starting product PE | PP | PE/PP/PS |
|---|---|---|---|
| Hydrogen | 0.75 | 0.63 | 0.62 |
| Aliphatics | 59.52 | 52.04 | 52.01 |
| comprising methane | 23.58 | 20.60 | 20.46 |
| ethylene | 19.84 | 13.32 | 17.49 |
| propylene | 5.52 | 7.09 | 4.57 |
| Aromatics | 35.35 | 44.60 | 47.43 |
| comprising benzene | 19.07 | 18.12 | 14.80 |
| toluene | 3.86 | 6.67 | 6.41 |
| Tar | 2.76 | 5.87 | 5.91 |
| Total gases ($H_2$, $C_1$–$C_4$) | 58.56 | 49.62 | 50.69 |
| Total oils ($>C_4$) | 38.88 | 46.94 | 46.59 |
| Soot | 1.75 | 1.61 | 1.40 |

Up to 50% of the pyrolysis products are liquid and correspond to a mixture of light gasoline and tar, with a very high proportion of aromatics. The gaseous products (50–60%) are chiefly methane, ethane, ethene, and propene, and have a calorific value of $50 \times 10^6$ J/Nm$^3$. Less than half of this gaseous mixture is sufficient to heat the plant. The pilot plant experiments at the University of Hamburg are proving to be highly successful. Consequently, at the present time a plant capable of pyrolyzing 8000 t of old vehicle tires per annum is being constructed. This, too, is self-sufficient with respect to energy, *i.e.* the pyrolysis gases formed suffice to heat the reactor.

## 5. Raw Material- and Energy-Saving Technologies Using Polymers

The enormous growth in synthetic polymers in the last thirty years can be attributed to the following reasons:

- Synthetic polymers frequently have properties or combinations of properties that are attainable with known natural polymers only with difficulty, if at all;
- The properties of synthetic polymers can be "tailored" by specific measures during synthesis;
- Many of the synthetic polymers are thermoplastic and consequently can be processed considerably more easily with lower energy input.

As a result, synthetic polymers are a welcome addition to natural polymers and expand substantially the range of organic materials.

Undoubtedly, synthetic polymers are likely to make major contributions to inovations, especially the newer materials: highly heat-resistant polymers[15], high-modulus/high-tenacity polymers[15], high-grade polymer alloys[16], and polymer composites[16]. These allow, for example, lightweight construction in motor vehicles and aircraft[17], thereby contributing much to reduction of fuel consumption.

Besides "traditional" applications, such as in automobile and equipment construction and in the building, packaging and clothing industries, in the future polymers will find increasing applications in new technologies aimed at conserving raw materials and energy. Among these are:

- Tertiary recovery of petroleum
- Information and communication systems
- Biotechnology.

Although the amount of polymers used as a constituent in these applications is relatively small, it nevertheless represents an essential component of such systems, which would not function without them.

### 5.1. Polymers for the Tertiary Recovery of Petroleum

Synthetic polymers have long been used in petroleum recovery as drilling auxiliaries and as thickeners in so-called primary and secondary recovery. Despite all the improvements made in these two recovery techniques, *ca.* 70% of the petroleum still remains in the bore hole. As a result, considerable efforts have been made to reduce the quantity of oil retained in the rock capillaries (an improvement of a mere 1% in oil extraction at the present rate of world production would be equivalent to *ca.* 3 billion t of additional oil!). Among the various techniques grouped under the generic term tertiary recovery, surfactant- and polymer-flooding[18] have excellent potential. These processes require water-soluble polymers with extremely high molecular weight (several $10^6$ g/mol) which, nevertheless, are not decomposed by shearing or hydrolysis even at high temperatures, and whose solution viscosities are only slightly dependent on the salt content and p*H* value.

### 5.2. Polymers for Communication and Information Systems

The vital contributions made by photoreactive polymers to the development of new printing and copying processes are well known[19]. Furthermore, the surge in the development of electronics and microelectronics would have been impossible without the indispensable contribution made by polymers[20]. Here the trend towards increasingly short switching times ($<0.05$ µs) and increasingly high storage densities presents a new challenge to photolithography, and thus also to polymer chemistry.

The application potential of liquid crystalline polymers is difficult to estimate[21,22]. For low-molecular liquid crystals this extends from familiar uses (*e.g.* displays) to information storage.

Also at the initial stages of their development are polymers with special optical or electronic properties[23], whose potential applications include those as light conductors, electric conductors, or as building blocks for novel storage media.

### 5.3. Polymers for Biotechnical Applications

The wide-ranging field of biotechnology is also increasingly drawing upon the methods of polymer chemistry to optimize biocatalysts. In particular, mention should be

made here of the immobilization[24,25] of enzymes, of cofactors, and of entire cells. Two techniques of immobilization are used at present:

- The adsorptive or covalent bonding of enzymes to the surface of polymeric carriers;
- The inclusion of enzymes, cells or microorganisms into polymer networks or microcapsules.

The most important advantages of the immobilized biocatalysts are the following:

- Ease of separation of the solid catalyst from the liquid reaction medium;
- Multiple reuse;
- No contamination of the reaction products with the biocatalyst;
- Possibility of tailoring the polymer carrier/biocatalyst system and thus for methodical optimization of the entire process.

Immobilized biocatalysts have already been put to numerous uses in industrial processes. These include, for example, the isomerization of glucose to fructose, the production of L-amino acids by the selective cleavage of *N*-acyl-DL-amino acids with immobilized L-aminoacylase, or the production of 6-aminopenicillanic acid from penicillin G using immobilized penicillin amidase.

As knowledge concerning the highly complex requirements imposed on immobilized biocatalysts and the chemical reactions they initiate increases, this field will undoubtedly receive considerable additional stimuli.

## 3. Prospects

The innovative power of polymer research *on its own* is certainly not sufficient to change the present unsatisfactory economic situation in the polymer industry, but it is a crucial requirement in this respect.

Industrial polymer research, however—as can be understood against this economic background—is presently concentrating on solving short-term and medium-term problems such as optimization of production processes and processing methods, as well as modification of known polymers. This means that research into totally new fields, which requires substantial investment of time and money and is associated with a high degree of risk, is of necessity being forced into the background. To recreate the necessary leeway to reverse this trend, joint efforts from various quarters are essential: besides the reorientation of industrial research and development which is already taking place, the basic polymer research being conducted at the universities must be promoted and intensified in specific areas. In addition, an even closer symbiosis between basic university research and applied research in industrial laboratories should be strived for.

By harnessing all available resources in pure and applied research in a spirit of interdisciplinary cooperation, it ought to be possible to meet the new challenge presented to polymer research successfully, even on the long term.

Received: April 13, 1983 [A 470 IE]
German version: *Angew. Chem. 95* (1983) 763

[1] a) K. Weissermel, W. H. Müller, *Chem. Ind. (Düsseldorf) 33* (1981) 773-778; b) cf. also K. Weissermel, *Angew. Chem. 92* (1980) 75; *Angew. Chem. Int. Ed. Engl. 19* (1980) 79.
[2] K. Ziegler, E. Holzkamp, H. Breil, H. Martin, *Angew. Chem. 67* (1955) 426, 541.
[3] Cf. papers from the GDCh-Fachgruppe Makromolekulare Chemie in *Angew. Makromol. Chem. 94* (1981) 1-213.
[4] L. L. Böhm, *Angew. Makromol. Chem. 89* (1980) 1.
[5] P. Galli, L. Luciani, G. Cecchin, *Angew. Makromol. Chem. 94* (1981) 63.
[6] B. Diedrich in K. Winnacker, L. Küchler: *Chemische Technologie*, 4th edit., Hanser, München 1982, Vol. 6, p. 353.
[7] H. Beuschel in K. Winnacker, L. Küchler: *Chemische Technologie*, 4th edit., Hanser, München 1982, Vol. 6, p. 455.
[8] R. Zimmermann, *FATIPEC-Handb. 2* (1982) 43.
[9] H. J. König in K. Winnacker, L. Küchler: *Chemische Technologie*, 4th edit., Hanser, München 1982, Vol. 6, p. 792.
[10] *Ergebnisberichte VKE-Forschungsprogramm "Wiederverwertung von Kunststoffabfällen"*, Verband Kunststofferzeugende Industrie, Frankfurt am Main 1981.
[11] P. Klein, *Reprints 2nd Int. Seminar "PET-Bottles"*, Society of Plastics Engineers, Antwerpen 1981.
[12] E. Grigat, *Kunststoffe 68* (1978) 5.
[13] H. Sinn, W. Kaminsky, J. Janning, *Angew. Chem. 88* (1976) 737; *Angew. Chem. Int. Ed. Engl. 15* (1976) 660.
[14] W. Kaminsky, H. Sinn, *DECHEMA-Monogr. 86* (1980) 181.
[15] Cf. papers presented at the seminar organized by the GDCh-Fachgruppe Makromolekulare Chemie in *Angew. Makromol. Chem. 109/110* (1982) 1-295.
[16] Cf. review articles in *Kunststoffe 73* (1983), in press.
[17] See review in *Kunststoffe 72* (1982) 7.
[18] V. Martin, J. Klein, *Erdoel Erdgas Z. 95* (1979) 164.
[19] H. W. Vollmann, *Angew. Chem. 92* (1980) 95; *Angew. Chem. Int. Ed. Engl. 19* (1980) 99.
[20] H. Steppan, G. Buhr, H. W. Vollmann, *Angew. Chem. 94* (1982) 471; *Angew. Chem. Int. Ed. Engl. 21* (1982) 455.
[21] H. Ringsdorf, H. Schneller, *Br. Polym. J. 13* (1981) 43.
[22] H. Finkelmann, G. Rehage, *Makromol. Chem. Rapid Commun. 1* (1980) 31.
[23] G. Wegner, *Angew. Chem. 93* (1981) 352; *Angew. Chem. Int. Ed. Engl. 20* (1981) 361.
[24] G. Manecke, W. Storck, *Angew. Chem. 90* (1978) 691; *Angew. Chem. Int. Ed. Engl. 17* (1978) 657.
[25] B. P. Sharma, L. F. Bailey, R. A. Messing, *Angew. Chem. 94* (1982) 836; *Angew. Chem. Int. Ed. Engl. 21* (1982) 837.

**When submitting manuscripts, authors of articles which are intended for publication as "Communications" are requested to conform to the guidelines reproduced at the beginning of each issue following the list of contents.**

## Derivatization-Free Enantiomer Resolution of Chiral Alcohols and Ketones by High-Resolution Complexation Gas Chromatography**

By *Volker Schurig** and *Roland Weber*

Complexation gas chromatography offers a method of precisely determining the enantiomeric purity of volatile chiral natural products as well as of products of enantioselective reactions *without derivatization*[1g].

Previously used separation systems for underivatized alcohols and ketones[1g] have the disadvantage of extremely long retention times (several hours) and markedly asymmetric peaks arising either from insufficient pretreatment of the capillary inner wall (coating efficiency $<20\%$, high surface activity) and/or from unfavorable properties of the stationary phase (poor chiral recognition, insufficient temperature stability).

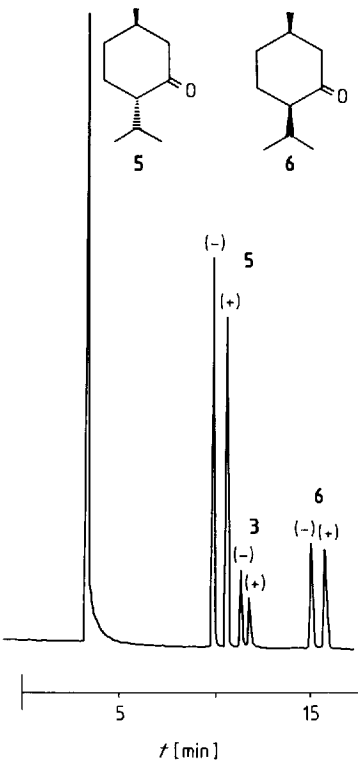



Fig. 2. Enantiomer resolution of menthone **5**, menthol **3**, and isomenthone **6** on nickel(II) bis[3-heptafluorobutyryl-(1*R*)-camphorate] (0.08 M in the methyl silicone fluid OV 101) at 133 °C; carrier gas: 1.0 bar $N_2$; Duran glass capillary (37 m × 0.75 mm).

[*] Prof. Dr. V. Schurig, Dr. R. Weber
Institut für Organische Chemie der Universität
Auf der Morgenstelle 18, D-7400 Tübingen 1 (Germany)

[**] This work was supported by the Deutsche Forschungsgemeinschaft and by the Fonds der Chemischen Industrie. Haarmann & Reimer and Dragoco, Holzminden, are thanked for samples of terpenes.

Here, we report a highly promising further development of complexation gas chromatography using high resolution glass and quartz capillary techniques. By deactivating the glass or quartz surface (thermal cross-linking of Carbowax 20 M[3a] or OV 101[3b]) and using methylsilicone OV 101 as solvent for the optically active metal chelates, it has proved possible to make capillary columns having a coating efficiency of $>80\%$. Using these columns, we were able to resolve quantitatively alcohols and ketones such as *e.g.*, menthol, menthone, and isomethane into their enantiomers without derivatization within 20 minutes (Fig. 2).

In this way, particularly using the combination complexation gas chromatography/"selected-ion" mass spectrometry[4], the rapid, straightforward, and precise determination of the enantiomeric composition of natural products from complex mixtures can be performed directly[4]. The enantiomer resolution of volatile chiral alcohols and ketones by complexation gas chromatography is superior to the recently described resolution as urethane-, acyl-, or oxime-derivatives[5], since the disadvantages of derivatization (sample preparation, incomplete reaction, occurrence of by-products, and products of isomerization and racemization) can be avoided.

Received: May 18, 1983 [Z 388 IE]
German version: *Angew. Chem. 95* (1983) 797
The complete manuscript of this communication appears in: *Angew. Chem. Suppl. 1983*, 1130–1137

[1] g) Cf. also V. Schurig, W. Bürkle, *J. Am. Chem. Soc. 104* (1982) 7573, and literature cited therein.
[3] a) D. A. Cronin, *J. Chromatogr. 97* (1974) 263; b) G. Schomburg, J. Husmann, F. Weeke, *Chromatographia 10* (1977) 580.
[4] V. Schurig, R. Weber, D. Klimetzek, U. Kohnle, K. Mori, *Naturwissenschaften 69* (1982) 602; V. Schurig, R. Weber, G. J. Nicholson, A. C. Oehlschlager, H. Pierce Jr., A. M. Pierce, J. H. Borden, L. C. Ryker, *ibid. 70* (1983) 92; R. Weber, V. Schurig, F. Jüttner, unpublished results.
[5] W. A. König, W. Francke, I. Benecke, *J. Chromatogr. 239* (1982) 227; W. A. König, I. Benecke, K. Ernst, *ibid. 253* (1982) 267.

## Quantitative Separation of Deuterated Tetrahydrofurans $C_4H_{4(\beta)}H_{4-n(\alpha)}D_{n(\alpha)}O$ by Complexation Gas Chromatography on a Cobalt(II) Complex**

By *Volker Schurig** and *Dorothee Wistuba*

Complexation gas chromatography[1] uses the rapid and reversible coordinative interaction between a mobile substrate and a stationary metal complex to solve particularly difficult analytical separation problems. Whereas, previously, the enantiomer resolution of chiral donor molecules with heteroatoms having donor capabilities (O,S,N) was of prime interest[1b], we are now investigating the efficiency of the method for the quantitative separation of protio/deuterio isomers of Lewis bases with mass difference 1.

[*] Prof. Dr. V. Schurig, D. Wistuba
Institut für Organische Chemie der Universität
Auf der Morgenstelle 18, D-7400 Tübingen 1 (Germany)

[**] This work was supported by the Deutsche Forschungsgemeinschaft and the Fonds der Chemischen Industrie.

 © Verlag Chemie GmbH, 6940 Weinheim, 1983 0570-0833/83/1010-0772 $ 02.50/0 

Selective separations of isotopomers by complexation gas chromatography were previously only known for deuterated alkenes (*e.g.* $C_2H_{4-n}D_n$) on $AgNO_3$/ethylene glycol[2a] and on $(CO)_2Rh$(3-trifluoroacetylcamphorate)/squalane[2b]. In addition, a slight difference in the retention times of 2-butanol and (2-D)-2-butanol was reported for gas chromatography on $Eu(fod)_3$/squalane[2c]. A decisive prerequisite for the *complete* and *rapid* separation of isotopomers which only differ by one mass unit is the further development of complexation gas chromatography using high resolution glass or quartz capillary techniques with a coating efficiency of *ca.* 95%[3].

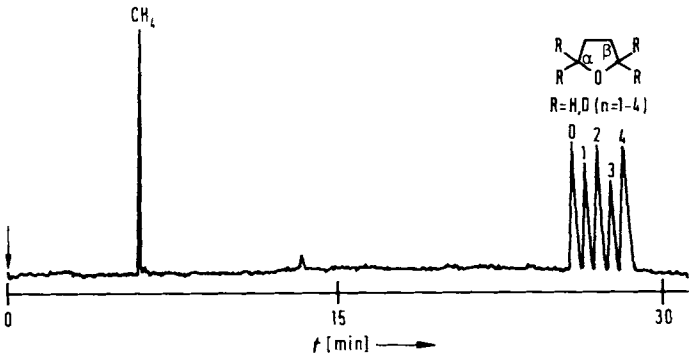
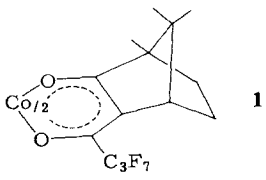



Fig. 1. Complexation gas chromatogram of α-deuterated tetrahydrofurans (0.1 M **1** in methylsilicone OV 101, deactivated [3] glass capillary (60 m × 0.25 mm), 70 °C, carrier gas: 1.9 bar $N_2$; split 1:50). Order of elution; $(D_0)$-THF, $(\alpha\text{-}D_1)$-THF, $(D_2)$-THF (all isomers), $(\alpha,\alpha,\alpha'\text{-}D_3)$-THF, $(\alpha,\alpha,\alpha',\alpha'\text{-}D_4)$-THF (peak classification corresponds to the number of deuterium atoms at the α-position). Peak assignment by GC-MS (Varian MAT 112S).

As shown in Figure 1, we succeeded for the first time in separating the isotopomers of deuterated cyclic ethers with full base line separation for all five isomers of tetrahydrofuran (THF) $C_4H_{4(\beta)}H_{4-n(\alpha)}D_{n(\alpha)}O$[4] using complexation glass capillary chromatography on cobalt(II) bis(3-heptafluorobutyrylcamphorate) **1** in less than 30 min at 70 °C. The separation factors $\alpha$ are logarithmically additive [$\alpha(70\,°C) = (1.03)^n$, n = number of deuterium atoms, $\alpha = t'_D/t'_H$, $t'$ = net retention time]. The separation depends on a marked "inverse" ($K_D > K_H$) secondary isotope effect, whose thermodynamic parameters for $(D_0)$-THF and $(\alpha,\alpha,\alpha',\alpha'\text{-}D_4)$-THF on **1** (0.1 M in squalane) were determined to be $\Delta_{D,H}\Delta H^0 = -0.2$ kcal mol$^{-1}$ and $\Delta_{D,H}\Delta S^0 = -0.4$ cal K$^{-1}$ mol$^{-1}$ between 50 and 80 °C[1a], and which rapidly decreases with the distance to the coordinating oxygen atom (no separation of $(D_8)$-THF and $(\alpha,\alpha,\alpha',\alpha'\text{-}D_4)$-THF).




**1**

The choice of cobalt as the central atom in **1** proved to be optimal, since with the corresponding nickel complex the coordinative interaction $K$ with cyclic ethers is too strong and with the manganese complex, too weak[5]. There are three configuration isomers of $(2,5\text{-}D_2)$-THF. Neither separation of the *meso/rac*-diastereomeric pair nor enantiomeric resolution of the *rac*-form on the enantiomerically pure cobalt complex (1*R*)-**1** was observed (cf. Fig. 1, peak 2).

We have also found similar "inverse" secondary isotope effects in the complexation of α-deuterated tetrahydropyrans and deuterated dioxanes on **1**. The separation factors are expected to double for the tritiated substrates. From the present findings it can be concluded that the introduction of chemical selectivity into the chromatographic separation process is a useful parameter for achieving higher separation efficiencies.


Received: March 4, 1983 [Z 302 IE]
publication delayed at authors' request
German version: *Angew. Chem. 95* (1983) 798


CAS Registry numbers:
**1**, 83664-34-0; $(\alpha\text{-}D_1)$-THF, 87174-62-7; $(D_2)$-THF, 87174-64-9; $(\alpha,\alpha,\alpha'\text{-}D_3)$-THF, 87174-63-8; $(\alpha,\alpha,\alpha',\alpha'\text{-}D_4)$-THF, 20665-63-8; $(D_0)$-THF, 109-99-9


[1] a) V. Schurig, *Chromatographia 13* (1980) 263, and literature cited therein; b) V. Schurig, W. Bürkle, *J. Am. Chem. Soc. 104* (1982) 7573.

[2] a) J. G. Atkinson, A. A. Russell, R. S. Stuart, *Can. J. Chem. 45* (1967) 1963, and literature cited therein; b) V. Schurig, *Angew. Chem. 88* (1976) 336; *Angew. Chem. Int. Ed. Engl. 15* (1976) 304; c) J. J. Books, R. E. Sievers, *J. Chromatogr. Sci. 11* (1973) 303.

[3] V. Schurig, R. Weber, *Angew. Chem. 95* (1983) 797; *Angew. Chem. Int. Ed. Engl. 22* (1983) 772.

[4] The isotopically labeled tetrahydrofurans were synthesized by acid-catalyzed ring closure of deuterated 1,4-butanediols obtained by reduction of the corresponding carbonyl compound with $LiAlD_4$ or a $LiAlD_4/LiAlH_4$ mixture (E. R. Bissell, M. Finger, *J. Org. Chem. 24* (1959) 1259). Characterization of the compounds was performed by mass spectrometry.

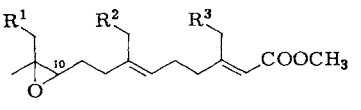
[5] V. Schurig, R. C. Chang, A. Zlatkis, B. Feibush, *J. Chromatogr. 99* (1974) 147.


## Reversal of the Enantioselectivity in the Enzymatic Hydrolysis of Juvenile Hormone as a Consequence of a Protein Fractionation**

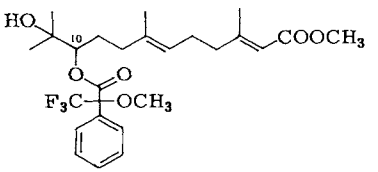

By *Martin G. Peter**, *Hans-Peter Stupp*, and *Klaus-Ulrich Lentes*


*Dedicated to Professor Peter Karlson on the occasion of his 65th birthday*

The juvenile hormones **1a**—**c** are hydrolyzed enzymatically in the blood of insects to afford biologically inactive acids. A conversion of 40—60% is observed after the hydrolysis of racemic **1c** in the blood of *Locusta migratoria*[1]. The unconverted educt contains an excess of naturally configurated (10*R*)-**1c** (*e.e.* 47.2%). We have shown previously that the hormone-binding protein present in the




**1a**: $R^1 = R^2 = CH_3$; $R^3 = H$
**1b**: $R^1 = CH_3$; $R^2 = R^3 = H$
**1c**: $R^1 = R^2 = R^3 = H$




**2a**: C-10 : *R*
**2b**: C-10 : *S*


[*] Priv.-Doz. Dr. M. G. Peter, H.-P. Stupp, K.-U. Lentes
Institut für Organische Chemie und Biochemie der Universität
Gerhard-Domagk-Strasse 1, D-5300 Bonn 1 (Germany)



[**] This work was supported by the Deutsche Forschungsgemeinschaft.

hemolymph preferentially associates with (10*R*)-**1c**. The configuration was determined with established methods[2] using racemic [10-$^3$H] **1c** and involving the diastereomeric derivatives **2**, which can be separated by HPLC on a silica gel column.

After incubation of the hemolymph of *Locusta migratoria* with 2-mercaptoethanol we have now separated an esterase from the hormone-binding protein (HPLC, 0.7 × 60 cm, TSK-G-3000-SW gel permeation column, elution with 0.1 M potassium phosphate buffer pH 6.8; 0.2 mL/min); this esterase catalyzes the hydrolysis of **1c**. Surprisingly, the purified esterase reacts preferentially with (10*R*)-**1c**: the hormone recovered after partial hydrolysis of racemic **1c** contains an excess of (10*S*)-**1c** (*e.e.* 34.4%). Accordingly, the esterase has a chiral binding site which recognizes the configuration of the oxirane quite remote from the active site. The preferential degradation of the natural enantiomer, therefore, arises from the higher affinity of the enzyme for this molecular species. In the presence of the hormone-binding protein, which is also enantioselective, the rate of hydrolysis of the natural enantiomer is markedly reduced, and the enzyme preferentially hydrolyzes the unbound hormone containing an excess of (10*S*)-**1c**. With racemic **1c** the sense of chirality (*R* or *S*) of the enzymatic reaction is, therefore, reversed in the presence of the hormone-binding protein. The result indicates that the enantioselectivity observed with a purified enzyme does not necessarily have to be identical with that of the reaction *in vivo*.

The higher homologue (10*R*,11*S*)-**1a** has not yet been detected in *Locusta migratoria*. The hormone-binding protein does not discriminate between the enantiomers of **1a**[1]. In the enzymatic partial hydrolysis of racemic **1a** either in the presence of the hormone-binding protein or with the purified esterase, (10*S*,11*R*)-**1a** predominates in the recovered educt (*e.e.* ≤ 70%). Hence, the hormone-binding protein does not change the sense of chirality in the enantioselective enzymatic hydrolysis of racemic **1a**.

The esterase found in the blood of *Locusta migratoria* is the first example of an enantioselective enzyme involved in the deactivation of juvenile hormone. Previously, in the Colorado potato beetle, *Leptinotarsa decemlineata*[2b], and in the tobacco horn worm, *Manduca sexta*[3], we found only non-enantioselective esterases. All previously studied insect species have enantioselective hormone-binding proteins whose substrate specificity correlates with the naturally occurring homologues[1,2b,3,4]. Studies of the substrate specificity of esterases and hormone-binding proteins may possibly assist in understanding the considerable species-specificity observed in testing analogues of juvenile hormones as potential insecticides[5].

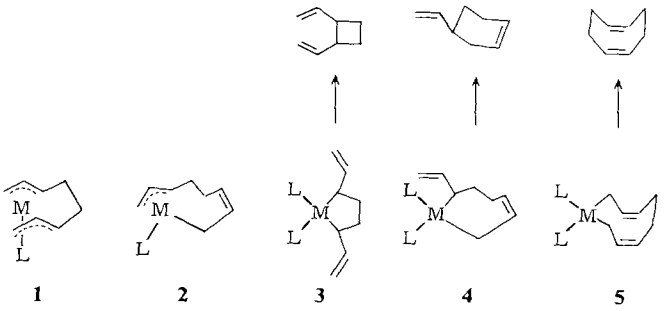
Received: May 10, 1983;
revised: July 22, 1983 [Z 385 IE]
German version: *Angew. Chem. 95* (1983) 794

[1] M. G. Peter, S. Gunawan, G. Gellissen, H. Emmerich, *Z. Naturforsch. C34* (1979) 588.
[2] a) M. G. Peter, P. D. Shirk, K. H. Dahm, H. Röller, *Z. Naturforsch. C36* (1981) 579; b) C. A. D. de Kort, M. G. Peter, A. B. Koopmanschap, *Insect. Biochem. 13* (1983), in press.
[3] M. G. Peter in F. Sehnal, A. Zabza, J. J. Menn, B. Cymborowski: *Regulation of Insect Development and Behaviour*, Politechnika Wrocławska Poland, Wrocław 1981, p. 237.
[4] D. A. Schooley, B. J. Bergot, W. Goodman, L. I. Gilbert, *Biochem. Biophys. Res. Commun. 81* (1978) 743.
[5] J. J. Menn, M. Beroza: *Insect Juvenile Hormones*, Academic Press, New York 1972.

## Phosphane-Induced, Stepwise Rearrangement of an Octadienediyl Palladium Complex to Seven- and Nine-Membered Metallacycles**

By *Holger Michael Büch, Paul Binger*, Reinhard Benn, Carl Krüger,* and *Anna Rufińska*

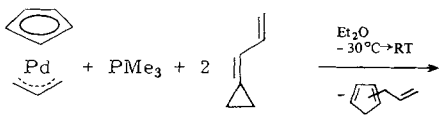
The octadienediyl metal complexes (**1**, **2**) of nickel and palladium[1], obtained by stoichiometric reactions with 1,3-dienes, are of importance in understanding the catalytic dimerization of these dienes. The bis-σ-allyl complexes **3**–**5** could be the last stages before the respective reductive eliminations to the various cyclodimers. Previously, only one platinacyclopentane derivative, analogous to **3**, having *trans*-arrangement of the vinyl groups has been isolated and characterized[2].



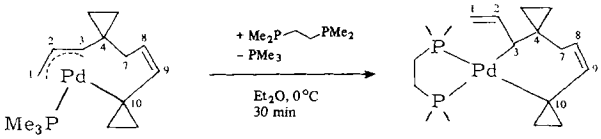
**1** **2** **3** **4** **5**

In the course of studies[3] of catalytic and stoichiometric reactions of the allylidenecyclopropane **6**, we have, for the first time, isolated metallacycles of type **4** and **5**; we have also been able to show that the *cis,cis*-metallacyclononadiene **5** can be formed *via* the α-vinyl metallacycloheptene **4** by interaction of a further ligand with the *syn*-π-allyl-σ-allyl form **2**.

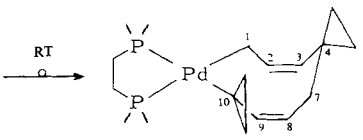
Reaction of dark-red ($\eta^3$-allyl)($\eta^5$-cyclopentadienyl)palladium with trimethylphosphane and allylidenecyclopropane at −30 °C to room temperature leads, upon cleavage of allylcyclopentadiene[4], to the octadienediyl complex **7** (yellow crystals, m.p. = 94.5 °C) in 81% yield.



**6**



**7** **8**



**9**

[*] Priv.-Doz. Dr. P. Binger, Dr. H. M. Büch, Dr. R. Benn, Prof. Dr. C. Krüger, Dr. A. Rufińska
Max-Planck-Institut für Kohlenforschung
Postfach 01 13 25, D-4330 Mülheim a. d. Ruhr 1 (Germany)

[**] Metallacycloalkanes, Part 7.—Part 6: P. Binger, M. J. Doyle, R. Benn, *Chem. Ber. 116* (1983) 1.

 © *Verlag Chemie GmbH, 6940 Weinheim, 1983* *0570-0833/83/1010-0774 $ 02.50/0* 

7 was identified from its spectroscopic data[5]. In particular, the typical shifts and splitting pattern of a *syn*-substituted $\pi$-allyl ligand and a *cis*-double bond can be detected in the $^1$H-NMR spectrum (400 MHz); the exact conformation of the $C_8$-chain was determined by X-ray structure analysis (Fig. 1). It should be noted that the double bond lies out of the Pd-coordination plane relative to the *syn*-position of the allyl group.

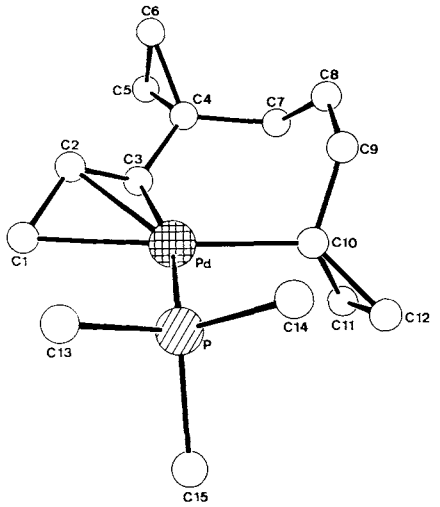



Fig. 1. Crystal structure of 7. Monoclinic, $P2_1/n$, $a = 8.7279(7)$, $b = 17.236(2)$, $c = 11.3139(6)$ Å, $\beta = 110.409(6)°$, $\rho_{calc} = 1.425$ g/cm$^{-3}$, $Z = 4$, $Mo_{K\alpha}$ radiation, $R = 0.034$ (3977 observed reflections, 154 refined parameters). Selected distances [Å] and angles [°]: Pd–P 2.265(1), Pd–C1 2.215(4), Pd–C2 2.179(3), Pd–C3 2.250(3), Pd–C10 2.094(3), C1–C2 1.414(5), C2–C3 1.399(4), C3–C4 1.488(4), C4–C7 1.539(5), C7–C8 1.491(5), C8–C9 1.333(5), C9–C10 1.470(4), P–Pd–C1 101.1(1), P–Pd–C10 96.7(1), C1–Pd–C3 66.9(1), C3–Pd–C10 95.1(1). Further details of the crystal structure investigations can be obtained from the Fachinformationszentrum Energie Physik Mathematik, D-7514 Eggenstein-Leopoldshafen 2, by quoting the depository number CSD 50538, the names of the authors, and the journal citation.

Reaction of a solution of 7 in diethyl ether with one equivalent of ethylenebis(dimethylphosphane) at 0°C leads to quantitative precipitation of almost colorless microcrystals of **8**, which can be isolated by filtration. Within a few hours at room temperature, **8** rearranges quantitatively and irreversibly to afford **9** (pale yellow needles, m.p. = 128°C).

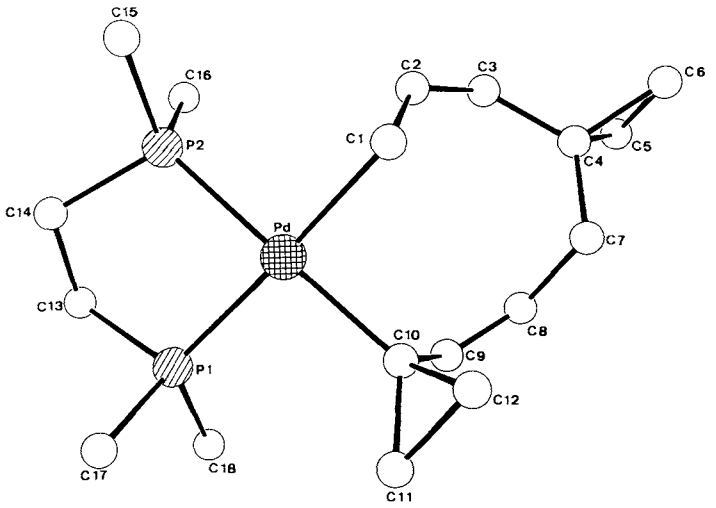



Fig. 2. Crystal structure of **9**. Monoclinic, $P2_1/c$, $a = 9.162(2)$, $b = 20.452(5)$, $c = 11.511(1)$ Å, $\beta = 111.65(1)°$, $\rho_{calc} = 1.379$ g cm$^{-3}$, $Z = 4$, $Mo_{K\alpha}$ radiation, $R = 0.028$ (3734 observed reflections, 190 refined parameters). Selected distances [Å] and angles [°]: Pd–P1 2.305(1), Pd–P2 2.303(1), P1–Pd–P2 84.6(1), Pd–C1 2.130(3), Pd–C10 2.101(3), C1–Pd–C10 87.3(1), C1–C2 1.477(4), C2–C3 1.335(5), C3–C4 1.491(5), C4–C7 1.518(5), C7–C8 1.506(5), C8–C9 1.335(5), C9–C10 1.486(4).

**8** and **9** were characterized from their $^1$H- and $^{13}$C-NMR spectra[5]. Based on the magnitude of the coupling constants $^2J(PC_\alpha)$, the Pd atom in both complexes has an almost square-planar environment. In **8** an uncomplexed vinyl group and a *cis*-double bond can be detected. The structure of the nine-membered ring in **9** can be deduced from the low temperature NMR spectra and was confirmed by X-ray crystallography (Fig. 2). Conformational changes occur at higher temperatures: the protons at $C_1$ and $C_7$ become equivalent as a consequence of inversion of the nine-membered metallacycle; simultaneously, exchange of each of the two geminal $CH_3$ groups as well as of the $CH_2$ groups of the two three-membered rings occur, whereas the C atoms of the chelate bridge remain inequivalent ($C_1$ and $C_{10}$ retain their P couplings).


Received: June 8, 1983;
revised: July 27, 1983 [Z 416 IE]
German version: *Angew. Chem. 95* (1983) 814

CAS Registry numbers:
**6**, 80119-20-6; **7**, 87174-44-5; **8**, 87174-45-6; **9**, 87174-46-7; ($\eta^5$-2,4-cyclopentadien-1-yl)($\eta^3$-2-propenyl)palladium, 1271-03-0



[1] R. Benn, B. Büssemeier, S. Holle, P. W. Jolly, R. Mynott, I. Tkatschenko, G. Wilke, *Z. Naturforsch. B*, in press; A. Döhring, P. W. Jolly, R. Mynott, K.-P. Schick, G. Wilke, *ibid. 36* (1981) 1198.

[2] G. K. Barker, M. Green, J. A. K. Howard, J. L. Spencer, F. G. A. Stone, *J. Chem. Soc. Dalton Trans. 1978*, 1839.

[3] P. Binger, A. Germer, *Chem. Ber. 114* (1981) 3325; H. M. Büch, Dissertation, Universität Kaiserslautern 1982.

[4] H. Werner, *Adv. Organomet. Chem. 19* (1981) 155 and literature cited therein.

[5] **7**: $^{31}$P-NMR (32 MHz, [D$_8$]toluene, $T = 193$ K): $\delta = -15.1$; $^{13}$C-NMR (75 MHz, [D$_8$]toluene, $T = 300$ K, selection): $\delta$(C1) = 56.20 ($J_P = 1.0$), $\delta$(C2) = 115.86 ($J_P = 3.1$), $\delta$(C3) = 80.09 ($J_P = 31.5$), $\delta$(C4) = 17.92, $\delta$(C7) = 31.54, $\delta$(C8) = 114.61, $\delta$(C9) = 140.32, $\delta$(C10) = 13.72 ($J_P = 15.8$ Hz); $^1$H-NMR (400 MHz, [D$_8$]toluene, $T = 300$ K, selection): $\delta$(H1a) = 3.06, $\delta$(H1b) = 2.30, $\delta$(H2) = 4.48 ($^3J_{1b,2} = 13.1$), $\delta$(H3) = 3.09 ($^3J_{2,3} = 12.3$), $\delta$(H8) = 4.87, $\delta$(H9) = 6.08 ($^3J_{8,9} = 9{,}8$ Hz). – **8**: $^{31}$P-NMR (32 MHz, [D$_8$]toluene, $T = 193$ K): $\delta = 20.6$ and 17.7 ($J_{PP} = 13.1$ Hz); $^{13}$C-NMR (100 MHz, [D$_8$]THF, $T = 193$ K, selection): $\delta$(C1) = 99.46 ($J_P = 8.0$), $\delta$(C2) = 148.08 ($J_P = 7.2$), $\delta$(C3) = 38.66 ($J_P = 98.6$ and 6.0), $\delta$(C10) = 14.75 ($J_P = 127.1$ and 11.2 Hz); $^1$H-NMR (400 MHz, [D$_8$]THF, $T = 193$ K, selection): $^3J_{1,2} = 10.1$ *(cis)* and 16.8 *(trans)*, $^3J_{8,9} = 9.5$ Hz *(cis)*. – **9**: $^{31}$P-NMR (32 MHz, [D$_8$]toluene, $T = 300$ K): $\delta = 14.2$ and 12.1 ($J_{PP} = 11.6$ Hz); $^{13}$C-NMR (100 MHz, [D$_8$]THF, $T = 193$ K, selection): $\delta$(C1) = 25.70 ($J_P = 90.5$ and 6.9), $\delta$(C10) = 19.10 ($J_P = 126.0$ and 10.8 Hz); $^1$H-NMR (400 MHz, [D$_8$]THF, $T = 193$ K, selection): $\delta$(H2) = 5.44, $\delta$(H3) = 4.05 ($^3J_{2,3} = 11.8$ *(cis)*), $\delta$(H8) = 5.04, $\delta$(H9) = 5.64 ($^3J_{8,9} = 10.4$ Hz *(cis)*).


## ($t$BuP)$_8$Si$_2$— A Novel Dispirocyclic Silaphosphane**

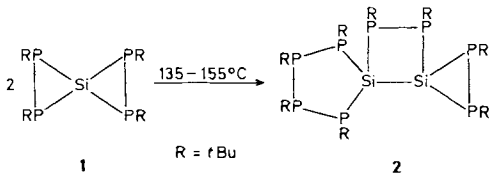

By *Marianne Baudler**, *Thomas Pontzen*, *Ulrike Schings*, *Karl-Friedrich Tebbe*, and *Magda Fehér*


Cyclocondensation of 1,2-dipotassium 1,2-di-*tert*-butyldiphosphide with silicon tetrachloride leads to formation of the tetraphosphasilaspiro[2.2]pentane **1** as a mixture of

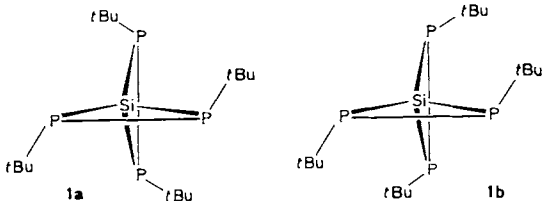

[*] Prof. Dr. M. Baudler, Dr. T. Pontzen, U. Schings, Prof. Dr. K.-F. Tebbe, Dr. M. Fehér
Institut für Anorganische Chemie der Universität
Greinstrasse 6, D-5000 Köln 41 (Germany)



[**] Contributions to the Chemistry of Phosphorus, Part 133. This work was supported by the Deutsche Forschungsgemeinschaft and the Fonds der Chemischen Industrie.—Part 132: M. Baudler, T. Pontzen, *Z. Naturforsch. B*, in press.




**1a** and **1b**, which can be isolated separately[1]. At room temperature **1b** slowly rearranges into the sterically more favorable isomer **1a**.




We have now found that in the melt **1a** or also **1a**, **b** dimerizes almost quantitatively to afford the novel silaphosphane **2**; in the mixture, the rearrangement **1b** → **1a** occurs initially. As by-products tetra-*tert*-butylcyclotetraphosphane[2a], 1,2-di-*tert*-butyldiphosphane[2b], and other nonidentified compounds are formed. Instead of the expected dispiro compound consisting of a three-, six-, and three-membered ring, 1,2,5,6,7,8,9,10-octa-*tert*-butyl-1,2,5,6,7,8,9,10-octaphospha-3,4-disiladispiro[2.0.4.2]decane **2** immediately forms. The carbocyclic analogue is not yet known.

The lemon yellow, prismatic crystals of **2**[3] (decomposition at 265 °C with concomitant red-brown coloration and agglomeration) are only slightly air- and moisture-sensitive, but in solution (toluene, tetrahydrofuran) are rapidly hydrolyzed. Their composition is established from the correct elemental analysis and mass spectrum (field ionization, 200 °C) in which only $M^+$ ($m/z$ 760–762) occurs. The constitution is based on the NMR data, principally, the $^{31}$P-NMR parameters[4]. From these, the molecule has $C_1$ symmetry, and the phosphorus atoms form two two-membered bridges and a four-membered bridge, which are parts of three-, four-, and five-membered structural elements. The high-field position of the $^{29}$Si-NMR signal of the silicon atom of the three-membered ring is comparable with that in **1**[1a].

The X-ray structure analysis[5] confirms the constitution of **2** with the configuration shown in Figure 1. The strongly distorted four-membered ring is, as expected, folded ($|\bar{\tau}| = 13.1°$); the five-membered ring has flat twisted envelope conformation (sequence of the torsion angles from Si: 4.6, −13.9, 18.4, −14.8, 6.2°). Remarkable are the unequal Si–P bond lengths in the four-membered ring, which may principally be attributable to the different size of the substituents at the two silicon atoms.

Received: June 13, 1983 [Z 419 IE]
German version: *Angew. Chem. 95* (1983) 803

CAS Registry numbers:
**1**, 87205-48-9; **2**, 97156-18-1

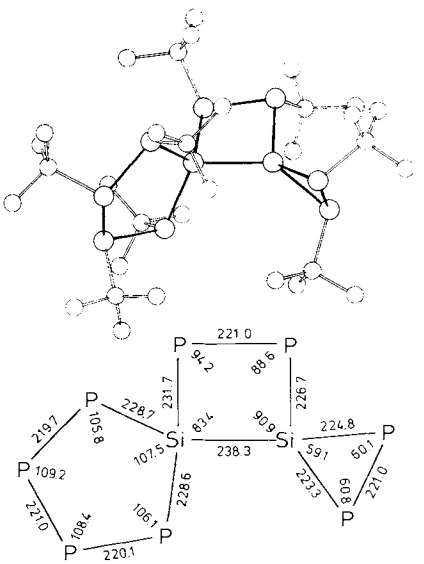



Fig. 1. Molecular structure of **2** in the crystal [5]; top: ORTEP representation; bottom: $P_8Si_2$ framework with bond lengths in pm ($\sigma \leq 0.2$ pm) and endocyclic bond angles in degrees ($\sigma \leq 0.1°$).

[1] a) M. Baudler, T. Pontzen, *Z. Anorg. Allg. Chem. 491* (1982) 27; b) M. Baudler, *Angew. Chem. 94* (1982) 520; *Angew. Chem. Int. Ed. Engl. 21* (1982) 492.

[2] a) K. Issleib, M. Hoffmann, *Chem. Ber. 99* (1966) 1320; b) M. Baudler, C. Gruner, H. Tschäbunin, J. Hahn, *Chem. Ber. 115* (1982) 1739.

[3] *Procedure:* **1a**, **b** (2.74 g, 7.2 mmol) is heated for 1 h at 135–140 °C and then for 20 min at 155 °C. After cooling, the bright orange solid is taken up in 10 mL of *n*-pentane; **2** either forms as a lemon yellow, crystalline powder or precipitates after concentration of the supersaturated solution to 5 mL. The crude product is filtered off, washed with pentane (4 × 2 mL), and recrystallized three times from toluene (the last fraction is washed in a little pentane at −78 °C); yield 143 mg (5%) **2**, purity > 99.9% ($^{31}$P-, $^1$H-NMR).

[4] $^{31}$P{$^1$H}-NMR ([D$_8$]toluene, saturated, 24 °C, parameters estimated from 121.497 MHz spectrum using 1st order rules): $\delta = 52.1$ (t, $^1J = -306$, −311 Hz), 37.9 (t, $^1J = -306$, −317 Hz), 15.9 (d, $^1J = -317$ Hz), 12.6 (d, $^1J = -311$ Hz) (five-membered ring), −11.7 (d, $^1J = -206$ Hz), −30.7 (d, $^1J = -206$ Hz) (four-membered ring), −72.0 (d, $^1J = -146$ Hz), −102.9 (d, $^1J = -146$ Hz) (three-membered ring).—$^{29}$Si{$^1$H}-NMR ([D$_8$]toluene, saturated. 0.1 M Cr(acac)$_3$, 24 °C): $\delta = 43.0$ (m, four-membered/five-membered rings), −62.4 (m, three-membered/four-membered rings).—$^{13}$C{$^1$H,$^{31}$P}-NMR ([D$_8$]toluene, saturated, 24 °C): $\delta = 36.52$, 36.41, 36.27, 34.22, 32.92, 32.52, 32.30, 31.94 (in each case s, 1C, PC), 34.94, 33.57, 32.97, 32.90, 32.01, 31.68 (in each case s, 3C, PCC), 31.35 (s, 6C, PCC).—$^1$H{$^{31}$P}-NMR ([D$_6$]benzene, 50%, 24 °C): $\delta = 1.75$, 1.74, 1.64, 1.56, 1.50, 1.45, 1.38, 1.33 (in each case s, 9H, *t*Bu).

[5] Monoclinic, C2/c, $a = 3529.6(10)$, $b = 1444.2(3)$, $c = 1850.1(6)$ pm, $\beta = 105.37(2)°$, $Z = 8$, 6716 reflections, 3863 of which with $I \geq 1.96\sigma(I)$, $R = 0.047$, $R_w = 0.044$ (anisotropically, geometrically fixed H positions). For further details on the crystal structure investigation, see: M. Fehér, K.-F. Tebbe, *Acta Crystallogr. C*, in press.

## Synthesis of a Tetrasaccharide of the Core Region of *O*-Glycoproteins**

By *Richard R. Schmidt** and *Gerhard Grundler*

*Dedicated to Professor Karl Winnacker on the occasion of his 80th birthday*

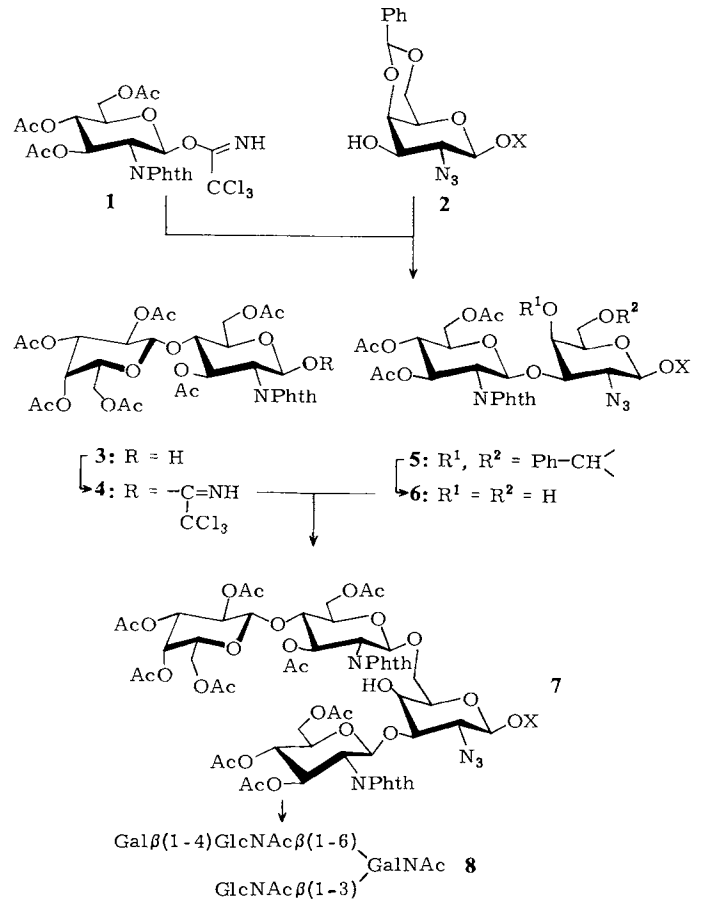
Oligosaccharides which are *O*-glycosidically linked to the serine- or threonine-side chains of proteins *via* *N*-acetylgalactosamine occur, *e.g.*, in the glycoproteins from epithelial mucous secretions, but also in classic blood-group substances[1]. These glycoproteins are designated mucine-type; here the tetrasaccharide **8** functions, *inter alia*, as the core region; α-glycosidically bound to serine, it is a component of the glycoproteins of the bronchial mucous of pa-

[*] Prof. Dr. R. R. Schmidt, G. Grundler
Fakultät Chemie der Universität
Postfach 5560, D-7750 Konstanz (Germany)

[**] Glycosyl Imidates, Part 9. This work was supported by the Deutsche Forschungsgemeinschaft and by the Fonds der Chemischen Industrie. *G. G.* is grateful for the award of a Chemiefonds-Stipendium.—Part 8: R. R. Schmidt, M. Stumpp, *Liebigs Ann. Chem. 1983*, 1249.

tients suffering from cystic fibrosis[1]. Using the trichloroacetimidate method developed previously by us[2], we have now synthesized **8** from the disaccharide building blocks **4** and **6** using a method which dispenses with halogenoses and heavy metal salts[3].

Upon treatment with trichloroacetonitrile and sodium hydride, *N*-phthaloyl-3,4,6-tri-*O*-acetylglucosamine[4] afforded the *O*-(β-glycosyl) trichloroacetimidate **1** (76%, m.p. = 146 °C); the galactose derivative **2** with unprotected 3-OH group ($[\alpha]_{578}^{25}$ −10, $c$ = 1.0 in $CHCl_3$) was obtained by azidonitration of 3,4,6-tri-*O*-acetylgalactal and silylation of the free (anomeric) 1-OH group with *tert*-butyldimethylsilyl chloride (X—Cl)/imidazole (69%), deacetylation with sodium methoxide (88%), and benzylidenation with benzaldehyde dimethyl acetal/*p*-toluenesulfonic acid (78%). Under boron trifluoride-ether catalysis **1** and **2** react in dichloromethane at −20 °C to afford the β(1—3)-linked disaccharide **5**[5] (69%, m.p. = 238 °C (decomp.), $[\alpha]_{578}^{25}$ −22, $c$ = 1.0 in $CHCl_3$), which upon treatment with trifluoroacetic acid can be converted into the 4,6-unprotected disaccharide **6** (88%, m.p. = 203 °).




X = $(CH_3)_2SiC(CH_3)_3$

The lactosamine building block **3** was obtained from the peracetylated lactal by azidonitration, silylation of the anomeric 1-OH group with X—Cl/imidazole (63%), hydrogenation of the azido group with hydrogen, phthaloylation of the amino group with phthalic anhydride, treatment of the resultant compound with acetic anhydride/pyridine (73%), and cleavage of the silyl group with tetrabutylammonium fluoride (88%, $[\alpha]_{578}^{25}$ +39, $c$ = 1.0 in $CHCl_3$ after 2 h). **3** reacts with trichloroacetonitrile and sodium hydride to give the *O*-(2-amino-2-deoxylactosyl) trichloroacetimidate **4** (72%, $[\alpha]_{578}^{25}$ +43, $c$ = 0.5 in $CHCl_3$).

Under boron trifluoride-ether catalysis in dichloromethane at −20 °C the disaccharides **4** and **6** led exclusively to β(1—6)-coupling[5] and, hence, to the tetrasaccharide **7** (71%, m.p. = 168—170 °C, $[\alpha]_{578}^{25}$ +10, $c$ = 0.5 in $CHCl_3$). The phthaloyl group was removed first from **7** with hydrazine. Acetylation using acetic anhydride/pyridine (64%) and desilylation with tetrabutylammonium fluoride (74%) yielded an intermediate which could be used to glycosylate serine and threonine. 1-*O*-Acetylation with acetic anhydride/pyridine, reduction of the azido group with $NiCl_2/NaBH_4$, and *N*-acetylation with acetic anhydride afforded the completely acetylated tetrasaccharide as a 1:1 anomeric mixture [33%; $^1$H-NMR (250 MHz, $CDCl_3$, TMS): $\delta$ = 6.14 (d, α-1-H, $J_{1,2}$ = 3.7 Hz); 5.69 (d, β-1-H, $J_{1,2}$ = 8.9 Hz)]. The unprotected tetrasaccharide **8** ($[\alpha]_{578}^{25}$ = −5, $c$ = 0.2 in $H_2O$ after 2 h) was obtained by cleaving the *O*-acetyl groups with potassium carbonate in methanol (70%).

Received: June 20, 1983 [Z 425 IE]
German version: *Angew. Chem. 95* (1983) 805

CAS Registry numbers:
**1**, 87190-67-8; **2**, 87190-68-9; **3**, 81243-76-7; **4**, 87190-71-4; **5**, 87190-69-0; **6**, 87190-70-3; **7**, 87206-73-3; **8**, 87190-73-6; β-**8** peracetate, 87248-21-3; α-**8** peracetate, 87190-72-5; *N*-phthaloyl-3,4,6-tri-*o*-acetylglucosamine, 87190-66-7; trichloracetonitrile, 545-06-2

[1] H. van Halbeek, L. Dorland, J. F. G. Vliegenhart, W. E. Hull, G. Lamblin, M. Lhermitte, A. Boersma, P. Roussel, *Eur. J. Biochem. 127* (1982) 7, and literature cited therein.

[2] R. R. Schmidt, J. Michel, *Angew. Chem. 92* (1980) 763; *94* (1982) 77; *Angew. Chem. Int. Ed. Engl. 19* (1980) 731; *Angew. Chem. Int. Ed. Engl. 21* (1982) 77; G. Grundler, planned dissertation, Universität Konstanz.—All compounds were characterized by IR, $^1$H-NMR (250 MHz) and $^{13}$C-NMR (62.97 MHz) spectroscopy, and by elemental analysis.

[3] Synthesis of the partially protected trisaccharide moiety

GlcNAcβ(1—6)
GlcNAcβ(1—3) > GalNAcα(1-*O*-Bzl)

using the Koenigs-Knorr method: S. A. Abbas, J. J. Barlow, K. L. Matta, *Carbohydr. Res. 113* (1983) 63.

[4] Synthesis after S. Akiya, T. Osawa, *Chem. Pharm. Bull. 8* (1960) 583.

[5] The β-selectivity is attributable to the neighboring group activity of the *N*-phthaloyl group: H. Paulsen, *Angew. Chem. 94* (1982) 184; *Angew. Chem. Int. Ed. Engl. 21* (1982) 155, and literature cited therein.

## Reversal of the Regioselectivity in the Zirconocene-Induced Coupling of a Ketone with Isoprene**

By *Gerhard Erker** and *Ulrich Dorf*

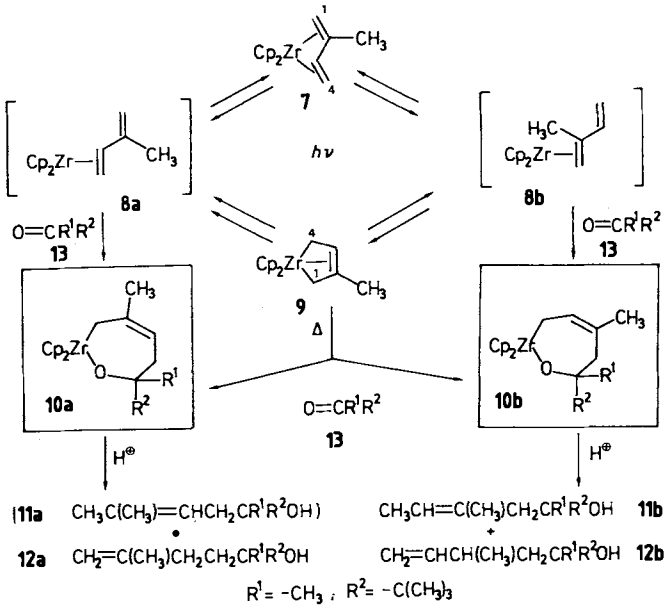
The reaction of (*s-cis*-isoprene)zirconocene **9** with organic carbonyl compounds often leads to regioselective CC coupling at the diene terminus C1 adjacent to the methyl group[3]. Recently, we showed that (*s-trans*-η$^4$-butadiene)zirconocene reacts much faster with aldehydes and ketones than the *s-cis*-isomer, with which it exists in equilibrium[6]. It was, therefore, expected that starting from (isoprene)zirconocene the course of the reaction and, hence, the regioselectivity of the CC coupling would also

[*] Priv.-Doz. Dr. G. Erker, U. Dorf
Abteilung für Chemie der Universität
Postfach 102148, D-4630 Bochum 1 (Germany)

[**] This work was supported by the Minister für Wissenschaft und Forschung des Landes Nordrhein-Westfalen and by the Fonds der Chemischen Industrie.

change if it were allowed to react with ketones under conditions allowing participation of the *s-trans*-isomer[5].

We have now treated (isoprene)zirconocene **9** with 3,3-dimethyl-2-butanone **13**. The major product (≈80%) of the thermally induced reaction (benzene, 60°C, 2 h) is the oxazirconacycloheptene **10b**, which can be hydrolyzed to give alcohols **11b** and **12b**. Photolysis of **9** and **13** in toluene solution leads to competitive formation of both **10b** and its isomer **10a**. The amount of **10a** increases as the temperature of the photolysis is lowered (Table 1). **10a** is also formed as the major product (≈75%) in the thermally induced reaction of (*s-trans*-η⁴-isoprene)zirconocene **7** and **13** at −70°C. Upon hydrolysis, only **12a** is obtained. (See Scheme II.)




Scheme II

Table 1. Reaction of (isoprene)zirconocene **9** with the ketone **13**: product ratio **10b**/**10a** as a function of the reaction conditions.

| | Δ | | | *hν* | |
|---|---|---|---|---|---|
| | +60°C | +37°C | 0°C | −40°C | −78°C |
| **10b** | 86 | 81 | 56 | 37 | 22 |
| **10a** | 14 | 19 | 44 | 63 | 78 |

The regioselectivity achieved [product ratio (**11b** + **12b**)/**12a**] was determined by gas chromatography (Table 1). In the thermally induced reaction of **9** and **13**, CC coupling at C1 of the diene is favored by >80/<20 relative to coupling at C4. When the irradiation is carried out at lower temperatures, the pathway *via* the very reactive intermediate (η²-isoprene)zirconocene complexes **8** becomes increasingly important[2b,6,7]. Here, the ketone couples preferentially with the less substituted olefin moiety. Irradiation of the reaction mixture at sufficiently low temperatures or reaction of the pure (*s-trans*-η⁴-isoprene)zirconocene isomer **7** eventually results in reversal of the observed regioselectivity: with 22/78 the product **10a** arising from coupling at C4 of the isoprene unit, *i.e.* away from the methyl group, is formed predominantly.

Received: June 1, 1983 [Z 406 IE]
German version: *Angew. Chem. 95* (1983) 800
The complete manuscript of this communication appears in: *Angew. Chem. Suppl. 1983*, 1120–1129

CAS Registry numbers:
**7**, 75361-73-8; **9**, 87185-18-0; **10a**, 87185-19-1; **10b**, 87185-20-4; **11b**, 87185-22-6; **12a**, 87185-21-5; **12b**, 87185-23-7; **13**, 75-97-8; isoprene, 78-79-5; zirconocene, 12116-83-5

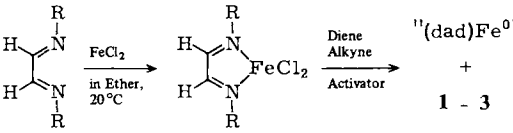
[2] b) U. Dorf, K. Engel, G. Erker, *Organometallics 2* (1983) 462.
[3] H. Yasuda, Y. Kajihara, K. Mashima, K. Nagasuna, A. Nakamura, *Chem. Lett. 1981*, 671; M. Akita, H. Yasuda, A. Nakamura, *ibid. 1983*, 217.
[5] G. Erker, J. Wicher, K. Engel, C. Krüger, *Chem. Ber. 115* (1982) 3300.
[6] G. Erker, K. Engel, J. L. Atwood, W. E. Hunter, *Angew. Chem. 95* (1983) 506; *Angew. Chem. Int. Ed. Engl. 22* (1983) 494; *Angew. Chem. Suppl. 1983*, 675.
[7] G. Erker, K. Engel, U. Dorf, J. L. Atwood, W. E. Hunter, *Angew. Chem. 94* (1982) 915; *Angew. Chem. Int. Ed. Engl. 21* (1982) 913; *Angew. Chem. Suppl. 1982*, 1974.

## Diels-Alder Reactions of Dienes with Alkynes Catalyzed by Diazadieneiron

By *Heindirk tom Dieck** and *Reiner Diercks*

*Dedicated to Professor Karl Winnacker on the occasion of his 80th birthday*

Diels-Alder reactions between simple dienes and alkynes proceed thermally only under somewhat drastic conditions. We have now found that iron compounds modified by 1,4-diaza-1,3-dienes (dad) **4** as directive ligands catalyze the [4+2]cycloaddition of simple dienes with nonterminal alkynes at room temperature (R in dad, see Table 1). The same substrates yield 2:1 adducts or 2:2- and 1:2-cooligomers with ligand-nickel catalysts[3]. With bis(cyclooctatetraene)iron as catalyst, 1:1-adducts have been described[4].

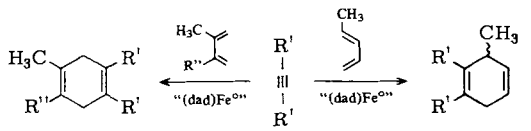



The readily accessible complexes (dad)$FeCl_2$ **5** are activated in the presence of diene and alkyne using reducing agents such as triethylaluminum, alkylmagnesium halides, or magnesium-isoprene·2THF. Bis(diazadiene)iron, $(dad)_2Fe$ **6c**, also gives rise to an active catalyst with $AlEt_3$ at 90°C, just as do the multicomponent systems $Fe(acac)_3$/2dad/4$AlEt_3$ **7a** or $Fe(acac)_3$/2dad/6EtMgBr **8a**.

Table 1 indicates that the results depend on the substituents R on the ligand **4**. Under the conditions investigated to date, only *N,N'*-dialkyldiazadienes are active; in contrast, *N,N'*-diaryldiazadienes, which are highly active in diene cyclodimerizations, are not[1]. Since in the reaction of *trans*-1,3-pentadiene with 3-hexyne to afford **2** a center of chirality is formed, complexes with chiral dad (**4g**—**i**) were also used. Although **2** is also formed in good yield with **5g**—**i**, optical induction—in contrast to diene cyclodimerization using the same precatalyst[1]—could not be detected.

[*] Prof. Dr. H. tom Dieck, R. Diercks
Institut für Anorganische und Angewandte Chemie der Universität
Martin-Luther-King-Platz 6, D-2000 Hamburg 13 (Germany)

[**] This work was supported by the Deutsche Forschungsgemeinschaft. *R. D.* thanks the Fonds der Chemischen Industrie for a grant. Prof. *A. Krebs* and Hoechst AG are thanked for samples of cyclooctyne and *trans*-1,3-pentadiene, respectively.




**1**, $R'' = H$
**3**, $R'' = CH_3$

**2**

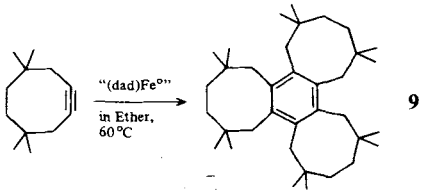
Table 1. Cycloaddition of dienes and alkynes R'C≡CR' in ether or tetrahydrofuran. Ratio of iron catalyst: diene : alkyne = 1 : 100 : 100.

| R' | R in dad | Catalyst components | t [h] | T [°C] | Product | Select./ yields [%] [a] |
|---|---|---|---|---|---|---|
| *Reaction with isoprene:* | | | | | | |
| Et | $CH(iPr)_2$ | **5a**, 4 $AlEt_3$ | 96 | 90 | **1b** | 82/16 |
| Me | $CH(iPr)_2$ | **5a**, 4 EtMgBr | 20 | 20 | **1a** | 97/13 |
| Et | *t*Bu | **5b**, 4 EtMgBr | 24 | 20 | **1b** | 96/[b] |
| Et | $CH(iPr)_2$ | **5a**, 4 EtMgBr | 96 | 20 | **1b** | 95/33 |
| Et | *c*-$C_6H_{11}$ | **5c**, 4 EtMgBr | 24 | 20 | **1b** | 87/[b] |
| Et | 4-$MeOC_6H_4$ | **5d**, 4 EtMgBr | 24 | 20 | — | —/— |
| Et | 2,6-$Me_2C_6H_3$ | **5e**, 4 EtMgBr | 24 | 20 | — | —/— |
| Et | 2,6-$(iPr)_2C_6H_3$ | **5f**, 4 EtMgBr | 24 | 20 | — | —/— |
| $SiMe_3$ | $CH(iPr)_2$ | **5a**, 4 EtMgBr | 48 | 60 | **1c** | [b]/14 |
| Et | $CH(iPr)_2$ | **5a**, Mg·$C_5H_8$ | 72 | 60 | **1b** | 95/50 |
| Et | *c*-$C_6H_{11}$ | **6c**, 4 $AlEt_3$ | 48 | 90 | **1b** | 96/72 |
| Et | $CH(iPr)_2$ | **7a** | 72 | 90 | **1b** | 91/20 |
| Et | $CH(iPr)_2$ | **8a** | 96 | 20 | **1b** | 97/19 |
| *Reaction with trans-1,3-pentadiene:* | | | | | | |
| Et | [c] | **5g**, 4 EtMgBr | 24 | 20 | **2** | 87/[b] |
| Et | [d] | **5h**, 4 EtMgBr | 48 | 20 | **2** | 84/49 |
| Et | [e] | **5i**, 4 EtMgBr | 72 | 20 | **2** | 95/64 |
| *Reaction with 2,3-dimethylbutadiene:* | | | | | | |
| Et | *c*-$C_6H_{11}$ | **6c**, 4 $AlEt_3$ | 48 | 90 | **3** | 93/80 |

[a] Selectivity: mol-% **1**, **2** or **3** relative to volatile products; yield relative to diene, not optimized. [b] Not determined. [c] R in dad is (*R*)-$CH(CH_3)C_6H_5$. [d] R in dad is (1*S*, 2*S*, 3*S*, 5*R*)-3-pinanylmethyl. [e] R in dad is (1*R*, 3*R*, 4*S*)-3-menthyl.

In the presence of the catalyst, non-terminal unstrained alkynes do not react at room temperature. Diene dimers, which in the absence of alkynes are rapidly formed by the catalyst, also do not arise[1]; the only by-products found were alkyne trimers in low yields and, presumably as a secondary product of the work-up, the aromatic oxidation products of cyclohexadienes.

With the non-optimized reaction conditions given in Table 1, the conversion is 13—80%; however, in most cases the selectivity of formation of cyclohexadiene exceeds 90%. Up to 90 °C, neither cyclic dienes such as 1,3-cyclohexadiene or 1,3-cyclooctadiene nor the sterically demanding 2,5-dimethyl-2,4-hexadiene react with 3-hexyne. Experiments directed at the cycloaddition of isoprene to the strained 4,4,7,7-tetramethylcyclooctyne led only to isolation of good yields of the benzene derivative **9** as sole product[9].




**9**

Whereas with phosphanenickel catalysts the alkyne cooligomerization substrate of the diene is incorporated into the product after formation of the $C_8$ chain[3], with the (dad)iron system a normal, *i.e.*, unstrained, alkyne apparently prevents attack by a second diene molecule. In the absence of the alkyne, the dimerization of the diene is usually faster than the [4+2]cycloaddition investigated here. A (dad)iron($\eta^4$-diene)($\eta^2$-alkyne) could be a relatively stable intermediate, whose secondary reaction to afford the cyclohexadiene complex would be the rate determining step in the catalytic reaction.


Received: June 6, 1983 [Z 407 IE]
German version: *Angew. Chem. 95* (1983) 801
The complete manuscript of this communication appears in: *Angew. Chem. Suppl. 1983*, 1138–1146


CAS Registry numbers:
**1a**, 72985-36-5; **1b**, 87226-79-7; **1c**, 87226-80-0; **2**, 87226-81-1; **3**, 87226-82-2; **5a**, 87226-73-1; **5b**, 87226-74-2; **5c**, 87226-75-3; **5g**, 87226-77-5; **5h**, 87249-26-1; **5i**, 87226-78-6; **6c**, 87226-76-4; **9**, 87249-27-2; isoprene, 78-79-5; *trans*-1,3-pentadiene, 2004-70-8; 2,3-dimethyl-1,3-butadiene, 513-81-5; dimethylacetylene, 503-17-3; diethylacetylene, 928-49-4; 4,4,7,7-tetramethylcyclooctyne, 20965-37-1; iron(II) chloride, 7758-94-3


[1] Diazadienes as Directive Ligands in Homogeneous Catalysis, Part 6.— Part 5: H. tom Dieck, J. Dietrich, *Chem. Ber.*, in press.
[3] P. W. Jolly, G. Wilke: *The Organic Chemistry of Nickel*, Academic Press, New York 1975, Vol. 2, p. 167; W. Keim, A. Behr, M. Röper in G. Wilkinson, F. G. A. Stone, E. W. Abel: *Comprehensive Organometallic Chemistry*, Pergamon Press, London 1982, Vol. 8, p. 371; P. W. Jolly, *ibid.* p. 649.
[4] A. Carbonaro, A. Greco, G. Dall'Asta, *J. Org. Chem. 33* (1968) 3948; *J. Organomet. Chem. 20* (1969) 117.
[9] The trimerization on $Pd^{II}$ has also been described by *A. Krebs* and *K.-D. Seidel*; A. Krebs, personal communication.


## $^{27}$Al-NMR Spectroscopy: A Probe for Three-, Four-, Five-, and Sixfold Coordinated Al Atoms in Organoaluminum Compounds


By *Reinhard Benn**, *Anna Rufińska*, *Herbert Lehmkuhl*, *Edo Janssen*, and *Carl Krüger*


$^{27}$Al, like $^{10}$B and $^{11}$B, is suitable for NMR investigations of organometallic compounds of the 3rd main group elements because of its sensitivity and relatively favorable ratio of line width to spectral range. On the basis of the different chemical shifts $\delta(^{27}Al)$ of octahedrally and tetrahedrally coordinated aluminum salts, it has been assumed[1] that a connection exists between $\delta(^{27}Al)$ and the ligand symmetry at the metal. We show here that, in general, a simple correlation exists between coordination number and $\delta(^{27}Al)$ in organoaluminum compounds and that this can be used as an analytical aid to detect tri- and the much discussed pentacoordination[2] of Al atoms.

The NMR parameters of typical compounds together with their respective coordination number (C. N.) are given in Table 1. In contrast to earlier postulates[1], the high $\delta$-values of compounds **1**—**3** can be attributed to the tricoordination of the Al atom and not to substituent effects. In the dimeric compounds **4**—**6** the chemical shifts of the tetrahedrally coordinated Al atoms are found at approximately 153 ppm. With larger alkyl ligands (**6**) or higher degrees of association (**7**, **10a**), the linewidth increases markedly. Replacement of the terminal alkyl ligands by groups having α-heteroatoms can substantially alter $\delta(^{27}Al)$, *e.g.*, 140 for $(EtAlCl_2)_2$ and 95 for $(Cl_3Al)_2$. In contrast, $\delta(^{27}Al)$ for compounds (**4**—**11**) with tetracoordination is apparently insensitive to the type of ligand involved in the multicentered bonding. Ligands which have two do-


[*] Dr. R. Benn, Dr. A. Rufińska, Prof. Dr. H. Lehmkuhl, E. Janssen, Prof. Dr. C. Krüger
Max-Planck-Institut für Kohlenforschung
Postfach 011325, D-4330 Mülheim a. d. Ruhr 1 (Germany)

Table 1. $^{27}$Al-NMR parameters of organoaluminum compounds. Frequency 104.2 MHz, external standard sat. sol. $(acac)_3Al$ in [D$_6$]benzene, $T = 300$ K, 20–50% solutions in [D$_8$]toluene, degree of association $\alpha$ (cf. [3, 4]).

| | Compound [3] | $\alpha$ | $\delta(^{27}Al)$ | $\omega_{1/2}$ [Hz] | C. N. |
|---|---|---|---|---|---|
| **1** | $iPr_3Al$ | 1 | 256 | 5900 | 3 |
| **2** | $iBu_3Al$ | 1 | 276 | 6300 | 3 |
| **3** | $tBu_3Al$ | 1 | 255 | 6100 | 3 |
| **4** | $Me_3Al$ | 2 | 153 | 850 | 4 |
| **5** | $Et_3Al$ | 2 | 154 | 2550 | 4 |
| **6** | $nBu_3Al$ | 2 | 152 | 7800 | 4 |
| **7** | $Et_2AlH$ | 3 | 157 | 4500 | 4 |
| **8** | $Et_2AlCl$ | 2 | 167 | 3300 | 4 |
| **9** | $Et_2AlNEt_2$ | 2 | 160 | 1220 | 4 |
| **10a** | $Et_2AlOMe$ | 3 | 146 | 3400 | 4 |
| **10b** | $Et_2AlOEt$ | 2 | 151 | 2450 | 4 |
| **11** | $Et_2AlO(CH_2)_3OEt$ | 2 | 150 | 7200 | 4 |
| **12** | $Me_2AlO(CH_2)_2OMe$ | 2 | 121 | 1830 | 5 |
| **13** | $Et_2AlO(CH_2)_2OMe$ | 2 | 121 | 5600 | 5 |
| **14** | $Et_2AlO(CH_2)_2OEt$ | 2 | 126 | 6000 | 5 |
| **15** | $Et_2AlO(CH_2)_2NEt_2$ | 2 | 112 | 7200 | 5 |
| **16** | $(acac)_3Al$ | | 0 | 100 | 6 |

nor atoms (*e.g.* acetylacetonate or molecules containing $O(CH_2)_2XR_n$ groups (X = O, N)) can occupy an additional coordination site at the Al atom. In the dimeric, associated complexes **12**–**15**[4] $\delta(^{27}Al)$ lies at around 120 and we attribute this as arising from pentacoordination. In **12**, $\delta(^{27}Al)$ does not change up to 100 °C, and, hence, marked dissociation to tetracoordinated species[5] is precluded. Pentacoordination of the Al atoms has been confirmed by X-ray structural analysis of **12** (Fig. 1). The coordination geometry in **12** can be described as a distorted trigonal bipyramid in which two methyl groups and an oxygen atom (O1) are located in the equatorial plane. O1 is sited over a center of inversion and occupies an apical site of the second Al* atom with a longer Al*–O1 distance (+0.065 Å). Since the bond distance Al–O2 is 0.442 Å longer than the Al–O1 distance, O2 is apparently even more weakly bonded to aluminum.

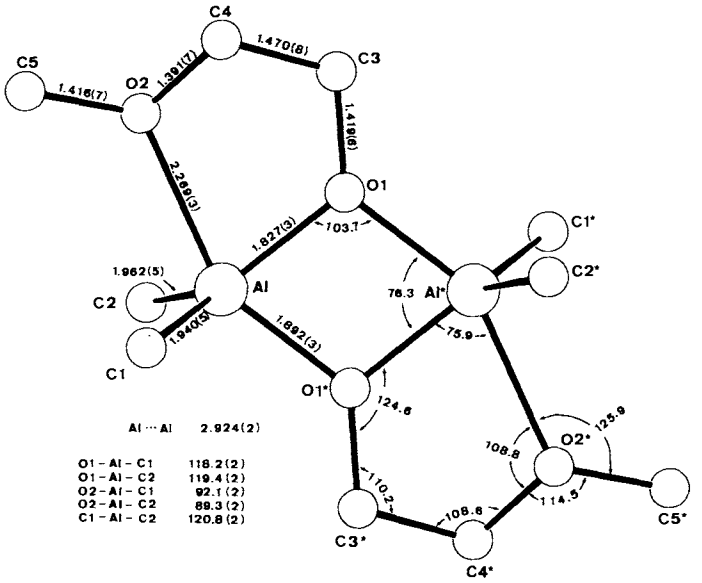



Fig. 1. Crystal structure of **12** with selected distances [Å] and angles [°]. Crystal data: Space group $P2_1/n$ (No. 14) $a = 7.4857(6)$, $b = 14.318(1)$, $c = 7.8940(4)$ Å, $\beta = 102.223(5)°$, $\rho_{calc} = 1.061$ g cm$^{-3}$, $Z = 2$, $\mu = 15.795$ ($Cu_{K\alpha}$), $\lambda = 1.5418$ Å, $R = 0.0614$, $R_w = 0.0776$ (998 observed reflections $I > 2\sigma(I)$, 1396 measured reflections, 73 refined parameters). Further details on the crystal structure determination can be obtained from the Fachinformationszentrum Energie Physik Mathematik, D-7514 Eggenstein-Leopoldshafen 2, by quoting the depository number CSD 50545, the names of the authors, and the journal citation.

Moieties containing three or more $CH_2$-units between the two O atoms function as monodentate ligands and lead to tetracoordinated Al atoms, as in **11** ($\delta(^{27}Al) = 150$).

Aluminum tris(acetylacetonate) **16** has an octahedral structure. In accord with the hexacoordination, $\delta(^{27}Al)$ is located at lower frequency and has a relatively small width at half-height ($\omega_{1/2}$). Accociates which formally correspond to the dialkoxy(alkyl)aluminum compounds $(R(RO)_2Al)_n$, and which until now have not been studied in detail, exhibit signals in the region of tetra- and hexacoordinated Al atoms. We therefore characterize these compounds as mixtures of the tetramers $R_nAl_4(OR)_{12-n}$ (R = Et, n = 1,...6), each of which has a central, hexacoordinated Al atom; this is also consistent with the results of mass spectroscopic studies.

Depending on the coordination number (3, 4, 5, or 6), organoaluminum compounds having similar terminal ligands thus exhibit characteristic chemical shifts, $\delta(^{27}Al)$. This property should be of importance for solving structural and analytical problems and together with the linewidths provide information upon degrees of association and equilibria.

Received: June 23, 1983;
revised: August 8, 1983 [Z 426 IE]
German version: *Angew. Chem.* 95 (1983) 808

CAS Registry number:
Al, 7429-90-5

[1] J. W. Akitt, *Annu. Rep. NMR Spectrosc. VA* (1972) 465; R. K. Harris, B. E. Mann: *NMR and the Periodic Table*, Academic Press, New York 1978, p. 279 ff.; H. Nöth, R. Rurländer, P. Wolfgardt, *Z. Naturforsch. B 37* (1982) 29; M. Dalibart, J. Derouault, P. Granger, *Inorg. Chem. 21* (1982) 2241.

[2] For examples of organoaluminum complexes in which the central atom is pentacoordinated see: S. J. Rettig, A. Storr, B. S. Thomas, J. Trotter, *Acta Crystallogr. B30* (1974) 666; R. A. Forder, K. Prout, *ibid. B30* (1974) 2312; Y. Kai, N. Yasoka, N. Kasei, M. Kakudo, *Bull. Chem. Soc. Jpn. 45* (1972) 3397.

[3] For preparation of the compounds see K. Ziegler, H. Lehmkuhl in: *Houben-Weyl-Müller: Methoden der Organischen Chemie*, Bd. *XIII/4*. Thieme, Stuttgart 1970, pp. 23–53 (for **1**–**7**), pp. 59–66 (for **8**), p. 92 (for **9**), pp. 78–80 (for **10**); for **12**: H. Lehmkuhl, R. Schäfer, *Liebigs Ann. Chem. 705* (1967) 23. Compounds **11**, **13**–**15** were prepared by reaction of trialkylaluminum with the corresponding alkoxy- or dialkylamino-alcohols in the molar ratio 1:1.

[4] E. G. Hoffmann, *Liebigs Ann. Chem. 629* (1960) 104; H. Lehmkuhl, E. Janssen, unpublished results.

[5] O. T. Brachley, K. C. Racette, *Inorg. Chem. 15* (1976) 2110.

## A Novel Synthesis of Macrocyclic Lactones

By *Hans Jürgen Bestmann** and *Rainer Schobert*

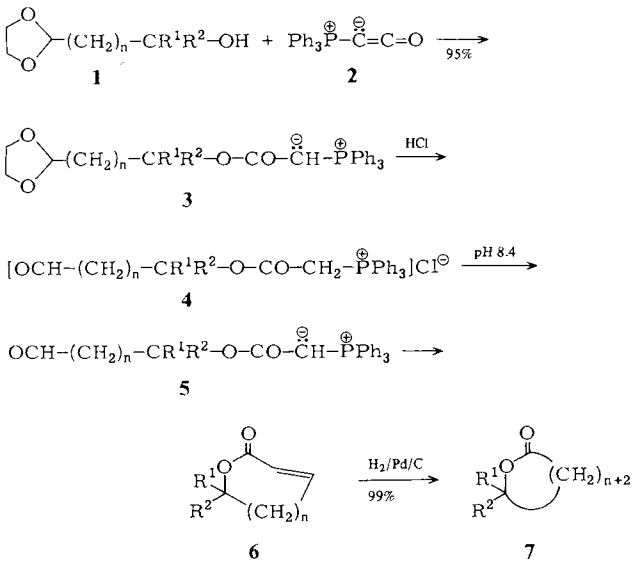
*Dedicated to Professor Karl Winnacker on the occasion of his 80th birthday*

The readily accessible ketenylidenetriphenylphosphorane **2**[1] reacts with acetals of long-chain hydroxyaldehydes **1** to give ylides **3**. Dissolution of these in an equivalent amount of 0.1 N aqueous HCl leads to cleavage of the acetal moieties and formation of the phosphonium salts **4**. Slow dropwise addition of a solution of **4** into a buffer (pH 8.4) affords the ylides **5**, which are converted by intramolecular Wittig reaction[2] into α,β-unsaturated macrocyclic lactones **6** (Table 1). Consistent with our concepts of the mechanism of the Wittig reaction, the cycliza-

[*] Prof. Dr. H. J. Bestmann, R. Schobert
Institut für Organische Chemie der Universität Erlangen-Nürnberg
Henkestr. 42, D-8520 Erlangen (Germany)

tion proceeds *E*-selectively[3] (gas chromatographically determined amount of *Z*-isomer 5–8%).

Compounds **6** are reduced to the saturated lactones **7**; **7f** is the well-known exaltolide, **7g** a further natural product obtainable from galbanum oil (Scheme 1).



Scheme 1.

Table 1. Macrocyclic lactones **6** [a].

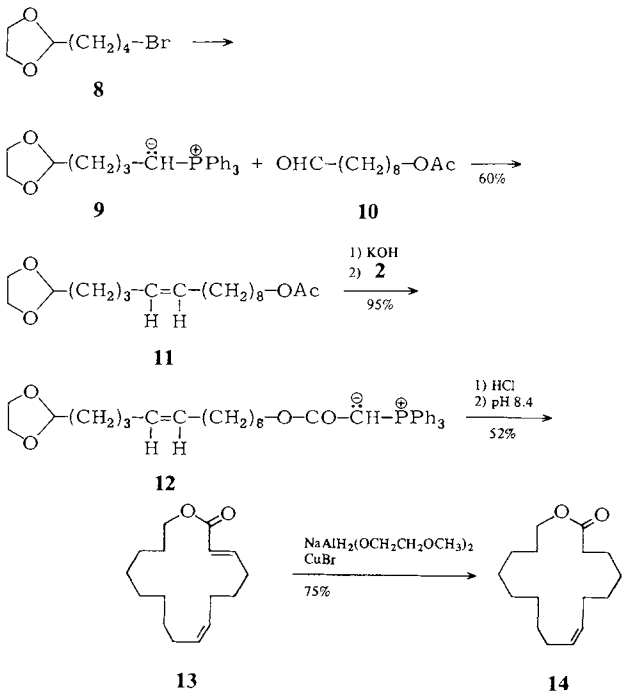
| 6 | n | $R^1$ | $R^2$ | Yield [%] [b] | B.p. [°C/torr] [c] |
|---|---|---|---|---|---|
| **a** | 7 | H | H | 65 | 58/0.01 |
| **b** | 7 | H | $CH_3$ | 60 | 50/0.05 (K) |
| **c** | 7 | H | *n*-$C_3H_7$ | 60 | 81/0.01 |
| **d** | 7 | $CH_3$ | $C_2H_5$ | 55 | 74–76/0.01 (K) |
| **e** | 9 | H | H | 65 | 78.5/0.02 |
| **f** | 11 | H | H | 60 | 76–78/0.05 (K) |
| **g** | 11 | H | $CH_3$ | 60 | 100/0.05 |

[a] A solution of **2** (3.02 g, 10 mmol) and **1** (10 mmol) in anhydrous toluene (100 mL) is heated under reflux (prim., sec. or tert. alcohol 2, 3 or 10d, respectively). After removal of solvent by evaporation, the oily residue (**3**) is dissolved in 101 mL 0.1 N aqueous HCl saturated with nitrogen (in the case of longer chains with 5% tetrahydrofuran), the solution allowed to stand for 1 h at RT, and then added dropwise (20 mL per h) to a well stirred two-phase mixture of 2 L aqueous buffer (3.68 g LiOH, 5.68 g 85% $H_3PO_4$, 2.96 g glacial acetic acid, 3.04 g $B(OH)_3$) and 1 L toluene. The phases are then separated; the aqueous phase is washed with toluene and the organic phase is dried over $Na_2SO_4$. After removal of the solvent by distillation, the residue is chromatographed on 20 g silica gel 60 with 200 mL hexane/ether (1:1); the eluate is evaporated down and distilled *in vacuo*. [b] Yield referred to **3**. [c] (K) signifies purification by Kugelrohr distillation; the temperature of the air-bath is quoted.

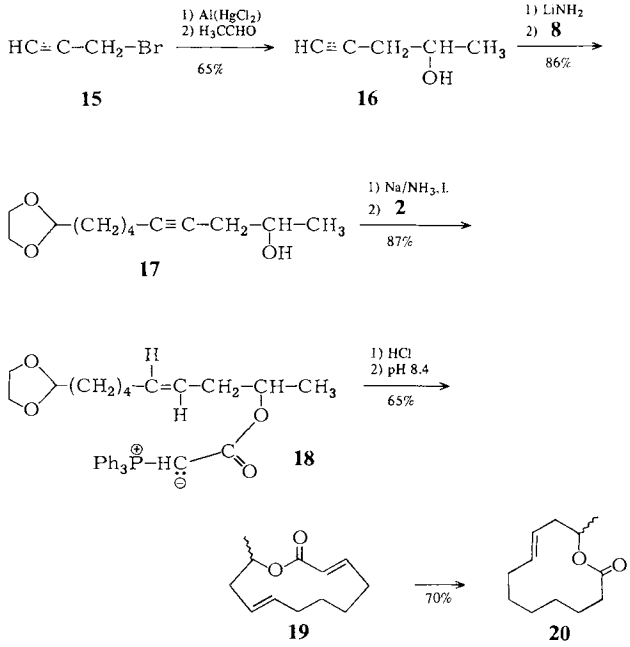
The 'musk ambrette' ambrettolide **14** was obtained as shown in Scheme 2.

5-Bromo-1-pentanol was oxidized to the aldehyde; reaction of its acetal **8** with triphenylphosphane furnishes the phosphonium salt. The corresponding ylide **9** reacts *Z*-selectively with 8-formyloctyl acetate **10** (readily accessible by ozone cleavage from oleyl acetate)[3] to give **11**; subsequent hydrolysis and reaction with **2** affords **12**, which is cyclized analogously to **3**→**6**. The resulting doubly unsaturated lactone **13** can be reduced selectively with Red-Al/CuBr[4] to **14**.

Recifeiolide **20**[5], which has been isolated from cultures of *Cephalosporium recifei*, could be synthesized in the *RS*-form *via* the route shown in Scheme 3.



Scheme 2. **11**, b.p. 104°C/0.03 torr; **13**, b.p. 99°C/0.02 torr; **14**, b.p. 154°C/1 torr.



Scheme 3. **16**, b.p. 127.3°C; **17**, b.p. 115°C/0.3 torr; **19**, b.p. 84°C/0.2 torr; **20**, b.p. 52.5°C/0.02 torr. Yield of **19** based on **17**.

The product formed from propargyl bromide **15** and aluminum in the presence of $HgCl_2$ reacts with acetaldehyde to give the yne-ol **16**, whose Li-salt can be converted with **8** into **17**. *E*-Specific reduction with sodium in liquid ammonia and subsequent reaction with **2** affords the ylide **18**, which is cyclized analogously to **3**→**6**. The macrocyclic *E,E*-diene **19** is isolated and selectively reduced analogously to **13**→**14** to give (*RS*)-**20**.

Received: March 31, 1983 [Z 330 IE]
German version: *Angew. Chem. 95* (1983) 810

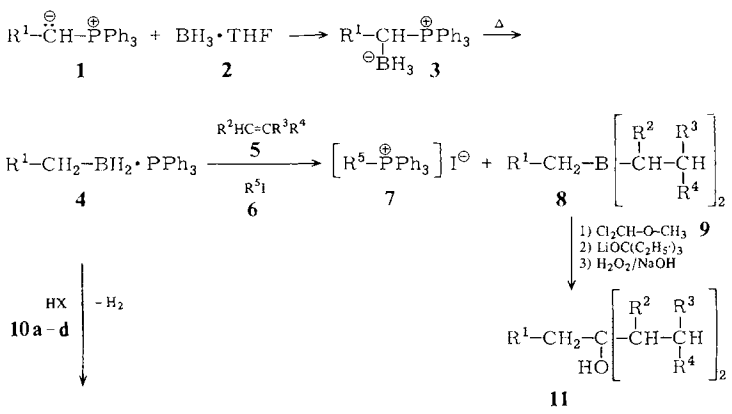
[1] H. J. Bestmann, D. Sandmeier, *Chem. Ber. 113* (1980) 274; review: H. J. Bestmann, *Angew. Chem. 89* (1977) 361; *Angew. Chem. Int. Ed. Engl. 16* (1977) 349.
[2] For cyclizations according to the phosphonate method cf. G. Stork, E. Nakamura, *J. Org. Chem. 44* (1979) 4010.
[3] H. J. Bestmann, *Pure Appl. Chem. 52* (1980) 771.
[4] M. F. Semmelhack, R. D. Stauffer, A. Yamashita, *J. Org. Chem. 42* (1977) 3180.
[5] R. F. Vesonder, F. H. Stodola, L. J. Wickerham, J. J. Ellis, W. K. Rohwedder, *Can. J. Chem. 49* (1971) 2029.

## A Method for the Synthesis of Ketones from Phosphorus Ylides and Olefins *via* "Mixed" Diorganoborinates

By *Hans Jürgen Bestmann** and *Thomas Röder*

*Dedicated to Professor Karl Winnacker on the occasion of his 80th birthday*

We recently reported that the phosphonioborates **3** obtainable from phosphorus ylides **1** and the borane-tetrahydrofuran adduct **2** rearrange on heating to give the monoalkylborane-triphenylphosphane adducts **4**[1]. Reaction of **4** with olefins **5** in the presence of methyl or benzyl iodide **6** affords, aside from the phosphonium salts **7**, "mixed" trialkylboranes **8**, which can be converted by the DCME (dichloromethyl methyl ether) method[2] into the tertiary alcohols **11**.



**6**: $R^5$ = $CH_3$, $C_6H_5$–$CH_2$

**10, 12, 13**: **a**, X = Cl; **b**, X = $OCH_3$, **c**, X = $OC_6H_5$, **d**, X = o-

We have now carried out the reaction of **4** with X–H acidic compounds **10a—d**; even on prolonged reaction, only one mol of $H_2$ is evolved per mol of **4**. The monoalkylborinate-triphenylphosphane adducts thus formed were expected to react with **5** and **6** to give the salts **7** and the dialkylborinates **14** and be finally converted by the DCME method into the unsymmetrical ketones **15**[2,3].

[*] Prof. Dr. H. J. Bestmann, Th. Röder
Institut für Organische Chemie der Universität Erlangen-Nürnberg
Henkestr. 42, D-8520 Erlangen (Germany)

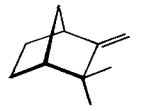
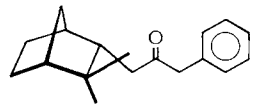
Table 1. Ketones **15** prepared from **3** by thermal rearrangement and successive reactions with **10d**, **6**, and **5** to **14** and subsequent reaction with DCME [2].

| 15 | $R^1$ | $R^2$ | $R^3$ | $R^4$ | B.p. [°C/torr] [a] | Yield [%] [b] |
|---|---|---|---|---|---|---|
| **a** | $n$-$C_5H_{11}$ | H | H | $n$-$C_5H_{11}$ | 90/0.4 | 41 |
| **b** | $n$-$C_5H_{11}$ | H | $CH_3$ | $n$-$C_4H_9$ | 85/0.4 | 43 |
| **c** | $C_6H_5$ | –$(CH_2)_4$– | | H | 85/0.1 | 40 |
| **d** | $CH_3$ | H | H | $HC(CH_3)$–$C_2H_5$ | 84/35 | 36 [c] |
| **e** | $CH_3$ | H | H | $n$-$C_5H_{11}$ | 83/17 | 40 [d] |
| **f** [e] | $CH_3$ | H | H | $n$-$C_9H_{19}$ | 102/0.6 | 45 |

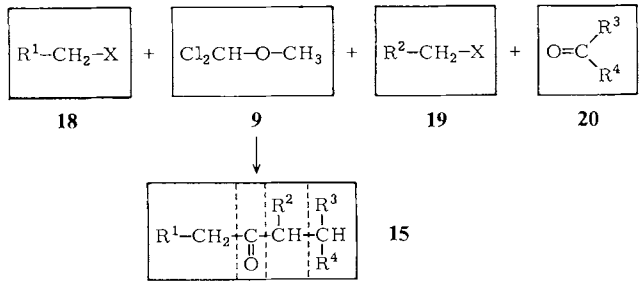
[a] Bath temperature during Kugelrohr distillation. [b] Yields referred to **3**, not optimized. [c] Purification by preparative medium pressure liquid chromatography (MPLC) on a silica gel column (Merck, Lobar size B), elution with $n$-hexane/acetone 6:1. [d] As for [c] but elution with $n$-hexane/ethyl acetate 88:12. [e] Procedure for 3-tetradecanone **15f**: A solution of **3** (20 mmol), $R^1$=$CH_3$, in chlorobenzene (50 mL) is heated for 30 min at 131°C. The solvent is removed *in vacuo* and replaced by 50 mL of THF. A solution of **10d** (22 mmol), 1-undecene (20 mmol) and methyl iodide (20 mmol) in THF (10 mL) is then rapidly added dropwise at room temperature. After 48 hours' stirring at RT, the mixture is filtered to remove salt **7**; the filtrate is allowed to react with DCME and then oxidized [2]. The organic phase is freed of solvent, taken up in a little pentane, and extracted several times with 3 N NaOH to remove **10d**. After drying and removal of solvent, the residue is distilled in a Kugelrohr (analogously as in the case of **15a—c**, **17**). In the case of the lower boiling ketones **15d** and **15e** the residue is worked-up by preparative MPLC and Kugelrohr distillation.

We found that **12a—c** undergo considerable disproportionation to **13a—c** and **4**, especially on prolonged heating[4]. Reaction with **5** and **6** and subsequent DCME reaction led to a mixture of ketone **15** and tertiary alcohol **11**. If, however, the adduct **4** is treated in tetrahydrofuran with a solution of the bulky 2,4,6-trimethylphenol **10d**, an olefin **5** and methyl or benzyl iodide **6**, the disproportionation of **12** is completely suppressed. The borinate **12d** reacts immediately with **5** and **6** to give **14**. When $R^2$ = H, this hydroboration proceeds regioselectively at the terminal position. The conversion of **14** into the ketones **15** by reaction with **9** proceeds without difficulties (Table 1)[5].

Starting from benzylidenetriphenylphosphane **1** ($R^1$ = $C_6H_5$) we obtained from camphene **16**, *via* the intermediates **3** to **14**, the ketone **17**, which according to the $^1$H- and $^{13}$C-NMR data consists of 80% of the *endo* and 20% of the *exo* form, *i.e.* the hydroboration proceeds largely stereoselectively (yield 44%, b.p. 105°C/0.05 torr).

16   17

Since ylides are prepared from alkyl halides (or tosylates) and the olefins are accessible by Wittig reaction from carbonyl compounds, this method of synthesis for ketones can be regarded as based on two alkyl halides **18** and **19**, a carbonyl compound **20** and DCME **9** as fundamental building blocks.



The method which is also suitable for monoalkylboranes not accessible by hydroboration (*e. g.* $CH_3BH_2$, $C_6H_5CH_2BH_2$)[1], can also be regarded as a "reductive acylation" of olefins.

Received: May 24, 1983
revised: July 28, 1983 [Z 394 IE]
German version: *Angew. Chem. 95* (1983) 812

CAS Registry numbers:
**1** ($R'=C_6H_5$), 16721-45-2; **4** ($R'=n$-$C_5H_{11}$), 87115-42-2; **4** ($R'=C_6H_5$), 87115-44-4; **4** ($R'=CH_3$), 87115-45-5; **5** ($R^2=R^3=H$; $R^4=n$-$C_5H_{11}$), 592-76-7; **5** ($R^2=H$; $R^3=CH_3$; $R^4=n$-$C_4H_9$), 6094-02-6; **5** ($R^2R^3=-(CH_2)_4-$; $R^4=H$), 110-83-8; **5** ($R^2=R^3=H$; $R^4=HC(CH_3)C_2H_5$), 760-20-3; **5** ($R^2=R^3=H$; $R^4=n$-$C_9H_{19}$), 821-95-4; **9**, 4885-02-3; **10a**, 7647-01-0; **10b**, 67-56-1; **10c**, 108-95-2; **10d**, 527-60-6; **12a** ($R'=n$-$C_5H_{11}$), 87115-46-6; **12a** ($R'=C_6H_5$), 87115-48-8; **12a** ($R'=CH_3$), 87115-50-2; **12b** ($R'=n$-$C_5H_{11}$), 87115-52-4; **12b** ($R'=C_6H_5$), 87115-87-5; **12b** ($R'=CH_3$), 87115-65-9; **12c** ($R'=n$-$C_5H_{11}$), 87115-67-1; **12c** ($R'=C_6H_5$), 87115-69-3; **12c** ($R'=CH_3$), 87115-71-7; **12d** ($R'=n$-$C_5H_{11}$), 87115-73-9; **12d** ($R'=C_6H_5$), 87115-75-1; **12d** ($R'=CH_3$), 87115-77-3; **13a** ($R'=n$-$C_5H_{11}$), 87115-53-5; **13a** ($R'=C_6H_5$), 87115-54-6; **13a** ($R'=CH_3$), 87115-55-7; **13b** ($R'=n$-$C_5H_{11}$), 87115-78-4; **13b** ($R'=C_6H_5$), 87115-79-5; **13b** ($R'=CH_3$), 87115-80-8; **13c** ($R'=n$-$C_5H_{11}$), 87115-82-0; **13c** ($R'=C_6H_5$), 87115-84-2; **13c** ($R'=CH_3$), 87115-85-3; **14a**, 87115-56-8; **14b**, 87115-57-9; **14c**, 87115-58-0; **14d**, 87115-59-1; **14e**, 87115-60-4; **14f**, 87115-61-5; **15a**, 6137-34-4; **15b**, 87115-62-6; **15c**, 61259-29-8; **15d**, 36808-98-7; **15e**, 928-80-3; **15f**, 629-23-2; **16**, 79-92-5; *endo*-**17**, 87115-63-7; *exo*-**17**, 87115-88-6; $CH_3I$, 74-88-4; $PhCH_2I$, 620-05-3.

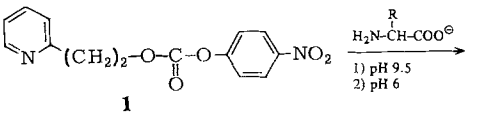
[1] H. J. Bestmann, K. Süss, Th. Röder, *Angew. Chem. 93* (1981) 1098; *Angew. Chem. Int. Ed. Engl. 20* (1981) 1038.
[2] B. A. Carlson, H. C. Brown, *J. Am. Chem. Soc. 95* (1973) 6876; H. C. Brown, B. A. Carlson, *J. Org. Chem. 38* (1973) 2422.
[3] Cf. also S. U. Kulkarni, H. D. Lee, H. C. Brown, *J. Org. Chem. 45* (1980) 4542; G. Zweifel, N. R. Pearson, *J. Am. Chem. Soc. 102* (1980) 5919.
[4] An analogous disproportionation has been described for chloro(thexyl)borane: H. C. Brown, J. A. Sikorski, S. U. Kulkarni, H. D. Lee, *J. Org. Chem. 45* (1980) 4540.
[5] **15d** (6-methyl-3-octanone), **15e** (3-decanone) and **15f** (3-tetradecanone) belong to the alarm pheromones which are exuded by ants on disturbance in the neighborhood of the nest. Thus, **15d** has been detected in seven of ten species of *Myrmica* investigated, **15e** in their subspecies *Mamica*, and **15f** in a lasius species, as components in the alarm pheromone complex: E. Priesner, *Fortschr. Zool. 22* (1973) 49.

## The 2-(2-Pyridyl)ethoxycarbonyl-(Pyoc) Residue—An Acid- and Base-Stable, Hydrophilic Protecting Group for the Amino Function in Peptide Synthesis**

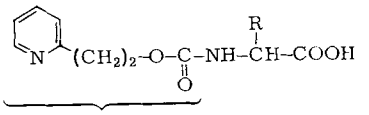
By *Horst Kunz** and *Regina Barthels*

*Dedicated to Professor Theodor Wieland on the occasion of his 70th birthday*

In the search for polarophilic, safe-to-handle, but nevertheless, readily removable amino protecting groups for the synthesis of peptides and glycopeptides[1], we developed the 2-(2-pyridyl)ethoxycarbonyl(Pyoc) group. It can be introduced most favorably by allowing the hydrochloride of the 2-(2-pyridyl)ethyl-*p*-nitrophenyl carbonate **1**, obtained straightforwardly from 2-(2-pyridyl)ethanol and *p*-nitrophenyl chloroformate, to react with amino acids in acetonitrile/water (1 : 1) at pH 9.5. The Pyoc-amino acids **2**[2] are isolated in good yields; the nitrophenol is extracted into ether at pH 6, and the aqueous solutions are concentrated. The more hydrophobic compounds Pyoc-leucine, Pyoc-phenylalanine, and even Pyoc-alanine are separated from sodium chloride by recrystallization from acetone, and the more hydrophilic compounds such as Pyoc-serine by recrystallization of the hydrochloride from isopropyl alcohol.




**1**



Pyoc

**2**, 85-100%

Peptide syntheses are performed with Pyoc-amino acids **2** using the mixed anhydride method[3] in dichloromethane. Thus, *e.g.*, **2a** and triethylamine are treated at −15 °C with an equivalent amount of ethyl chloroformate, and after 2 h at 0 °C the mixture is cooled to −15 °C and the amino acid-*tert*-butyl ester added dropwise. The Pyoc-dipeptide esters such as **3a** are purified by chromatography on silica gel (chloroform/methanol 12 : 1).

Pyoc-Phe-OH + H-Leu-O*t*Bu $\xrightarrow[NEt_3/CH_2Cl_2]{Cl-CO-OEt}$ Pyoc-Phe-Leu-O*t*Bu

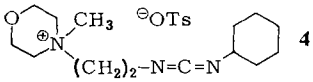
**2a** **3a**, 76%

Also suitable for the preparation of the Pyoc-dipeptide ester **3** is the modified carbodiimide method[4] using *N*-hydroxysuccinimide (HO–SU). After removal of most of the dicyclohexylurea by filtration, any residues of this together with unreacted amino acid esters are separated chromatographically on silica gel.

Pyoc-Ser-OH + H-Ile-O*t*Bu $\xrightarrow[CH_2Cl_2/0°C]{DCC/HO-SU}$ Pyoc-Ser-Ile-O*t*Bu

**2b** **3b**, 83%

Pyoc-amino acids **2**, which are highly soluble in water, enable an effective peptide synthesis to be performed in water; the soluble carbodiimide **4** in the presence of 1-hydroxybenzotriazole (HOBT)[5] serves as the reagent[5].



**4**

Chromatography on silica gel affords the dipeptide esters **3** in good yield.

Pyoc-Ile-OH + H-PHe-O*t*Bu $\xrightarrow[HOBT/H_2O]{4}$ Pyoc-Ile-Phe-O*t*Bu

**2c** **3c**, 82%

The Pyoc group combines the advantages of solubility in water with those of stability to acids and bases. Cleave of the *tert*-butyl ester, *e.g.* from **3a**, with excess trifluoroacetic acid in dichloromethane leads (after neutralization) smoothly to zwitterionic Pyoc-dipeptides such as **5**. With an additional amino acid-*tert*-butyl ester, compounds of this type can be transformed (*e.g.* according to [4]) into tripeptides such as **6**.

**3a** $\xrightarrow[CH_2Cl_2/0°C]{CF_3COOH}$ Pyoc-Phe-Leu-OH

**5**, 88%

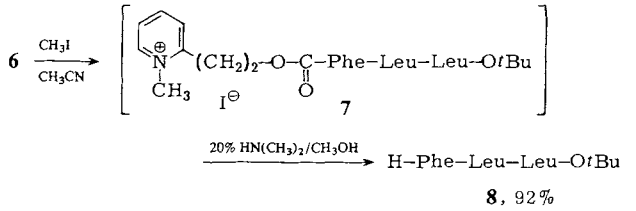
$\xrightarrow[DCC/CH_2Cl_2/HO-SU]{H\text{-}Leu\text{-}O\textit{t}Bu}$ Pyoc-Phe-Leu-Leu-O*t*Bu

**6**, 95%

For removal, the "safety form" of the protecting group is converted at room temperature with methyl iodide in acetonitrile into the pyridinium form **7**, which can be decomposed *via* an E1cB reaction in the presence of mild base to release the protected amino function (example: **6** → **7** → **8**).

[*] Prof. Dr. H. Kunz, Dr. R. Barthels
Institut für Organische Chemie der Universität
Postfach 3980, D-6500 Mainz (Germany)

[**] This work was supported by the Deutsche Forschungsgemeinschaft and by the Fonds der Chemischen Industrie.



Using this modification the initially insensitive, readily manipulable, polarophilic protecting group can, therefore, be removed from the blocked peptide using mild conditions.—The method is not suitable for amino acids such as cysteine or methionine which are readily attacked by methyl iodide.

Received: May 30, 1983; revised: August 10, 1983 [Z 399 IE]
German version: *Angew. Chem. 95* (1983) 799

CAS Registry numbers:
1·HCl, 77637-87-7; **2a**, 87136-59-2; **2b**, 87136-60-5; **2c**, 87136-61-6; **3a**, 87136-62-7; **3b**, 87136-63-8; **3c**, 87136-64-9; **4**, 2491-17-0; **5**, 87136-65-0; **6**, 87136-66-1; **8**, 87136-67-2; H-Leu-O*t*Bu, 21691-53-2; H-Ile-O*t*Bu, 16874-08-1; H-Phe-O*t*Bu, 16874-17-2; L-phenylalanine, 63-91-2; L-serine, 56-45-1; L-isoleucine, 73-32-5; 2-(2-pyridyl)ethanol, 103-74-2; *p*-nitrophenyl chloroformate, 7693-46-1

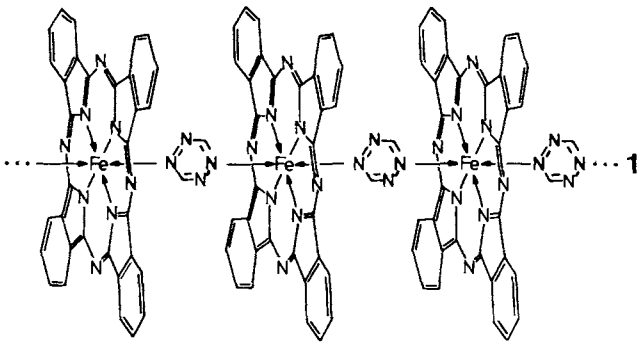
[1] H. Kunz, H. Kauth, *Liebigs Ann. Chem. 1983*, 337, 360.
[2] $^1$H-NMR: $\delta \approx 8.4$ (d, H-6, $J \approx 4$ Hz); $\approx 7.6$ (m, H-4), $\approx 7.1$ (m, H-3,5), $\approx 4.3$ (t, 2 ethylene-H, $J \approx 6$ Hz), $\approx 3.2$ (t, 2 ethylene-H, $J \approx 6$ Hz).
[3] Th. Wieland, J. Fasel, H. Faulstich, *Liebigs Ann. Chem. 713* (1968) 201.
[4] F. Weygand, D. Hoffmann, E. Wünsch, *Z. Naturforsch. B 21* (1966) 426.
[5] W. König, R. Geiger, *Chem. Ber. 103* (1970) 788.

## Polymeric Electrically Conductive Phthalocyaninato(μ-s-tetrazine)iron**

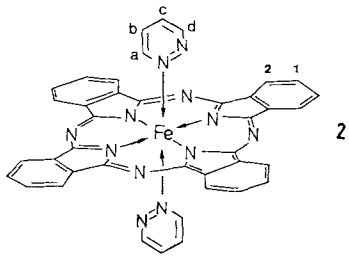
By *Otto Schneider** and *Michael Hanack*

We have already reported on several occasions about the synthesis and properties of phthalocyaninato(Pc)-metal compounds $[PcML]_n$ which are one-dimensionally polymerized *via* bridging ligands L containing π-electrons[1]. In some cases the polymers $[PcML]_n$ exhibit a much higher electrical conductivity than the corresponding monomers PcML or $PcML_2$. Attempts have been made by a process of systematic variation to determine the influences of the three components of the polymer (macrocycle, central metal atom, bridging ligand) on its specific electrical conductivity σ.

Reaction analogously to the synthesis of the pyrazine(pyz) polymer $[PcFe(pyz)]_n$[1a,b], but with 1,2,4,5-tetrazine (tz)[2] as bridging ligand, affords the polymer $[PcFe(tz)]_n$ **1** as a blue, insoluble powder. The product **1** was characterized by elemental analysis, as well as simultaneous TG/DTA and IR measurements[3].



In contrast, with pyridazine (pdz) as ligand, formation of a polymer is not possible for steric reasons. The monomeric complex $PcFe(pdz)_2$ **2** is so soluble in $CDCl_3$ that its structure can be determined $^1$H-NMR spectroscopically. Due to the ring current of the aromatic Pc macrocycle, the signals of the pdz protons of **2** are shifted markedly upfield compared to those of the free ligand (cf. [1b]); a concomitant coordination of both nitrogen atoms of the ligand to the iron atom in PcFe can, on the basis of the NMR data[3], be ruled out. Our proposed structure for **1** is supported by this finding.



The electrical conductivity was measured on pressed-powder tablets (13 mm diameter, *ca.* 1 mm thick) by the 4-point technique at a pressure of $1 \times 10^8$ Pa (1 kbar). The tetrazine derivative **1** (without additional doping) has an electrical conductivity of $\sigma_{RT} = 1 \times 10^{-1}$ S/cm, the highest value so far recorded (cf. [1]) for a coordination polymer; activation energies $E_a$ of 95 meV (in the range 155—330 K) and 120 meV (in the range 80—155 K) are calculated from its temperature dependence using the expression $\sigma_T = \sigma_0(\exp -E_a/kT)$. Compound **1** thus exhibits semiconductor behavior.

We have also found high conductivities in undoped coordination polymers with cyanide as bridging ligand, for example in $[HPcFe(CN)]_n$ or $[PcFe(CN)]_n$ and $[PcCo(CN)]_n$[1c,d], whereas in a number of other one-dimensionally polymerized phthalocyaninatometal systems conductivities of $\sigma_{RT} > 10^{-3}$ S/cm are only achieved after doping (*e.g.* with iodine)[4].

Both **1** as well as the above mentioned cyanide derivatives are stable towards air and moisture and are thermally more stable than the iodine-doped polymers $[(PcMO)I_y]_n$ (M = Si, Ge) and $[(PcMF)I_y]_n$ (M = Al, Ga, Cr)[5a]. An accidental doping of **1** with oxygen cannot, of course, be ruled out; however, it is known that "doping" of PcFe with $O_2$ leads to a reduction in conductivity[5b].

Received: June 20, 1983 [Z 424 IE]
German version: *Angew. Chem. 95* (1983) 804

CAS Registry numbers:
**1**, 87156-20-5; **2**, 87174-18-3

[*] Prof. Dr. M. Hanack, Dr. O. Schneider
Institut für Organische Chemie (Lehrstuhl II) der Universität
Auf der Morgenstelle 18, D-7400 Tübingen 1 (Germany)

[**] This work was supported by the Bundesministerium für Forschung und Technologie (BMFT).

[1] a) O. Schneider, M. Hanack, *Angew. Chem. 94* (1982) 68; *Angew. Chem. Int. Ed. Engl. 21* (1982) 79; *Angew. Chem. Suppl. 1982*, 41; b) *Chem. Ber. 116* (1983) 2088 and references cited therein; c) cf. J. Metz, M. Hanack, *J. Am. Chem. Soc. 105* (1983) 828; d) O. Schneider, M. Hanack, *Z. Naturforsch.*, in press.
[2] G. H. Spencer, P. C. Cross, K. B. Wiberg, *J. Chem. Phys. 35* (1961) 1939.
[3] Thermoanalytically determined cleavage of the ligands. Rate of heating 2 K/min: **1**: TG 220—310°C, reduction in mass 13.0% (calc. 12.6%); DTA exotherm. **2**: TG 205—285°C, reduction in mass 23.1% (calc. 22.0%); DTA endotherm.—$^1$H-NMR data of **2** (in $CDCl_3$): $\delta = 7.93$ (H-1, m, 8H), 9.31 (H-2, m, 8H), 2.80 ($H^a$, m, 2H), 5.5, 6.35, 6.68 ($H^b$, $H^c$, $H^d$, m, each 2H).
[4] T. J. Marks, D. W. Kalina in B. Miller: *Extended Linear Chain Compounds*, Vol. 1, Plenum Press, New York 1982, p. 197.

[5] a) C. W. Dirk, T. Inabe, K. F. Schoch Jr., T. J. Marks, *J. Am. Chem. Soc. 105* (1983) 1539; K. J. Wynne, R. S. Nohr, *Mol. Cryst. Liq. Cryst. 81* (1982) 243; b) K. J. Beales, D. D. Eley, D. J. Hazeldine, T. F. Palmer in H. Kropf, F. Steinbach: *Katalyse an Phthalocyaninen*, Thieme, Stuttgart 1973, p. 1.

## Cyanoformyl Chloride

By *Rolf Appel** and *Mustafa Siray*

The carbonyl cyanide $CO(CN)_2$[1] and the mixed fluoride cyanide CO(CN)F **8**[2] are the only cyano-substituted carboxylic acids to have been previously reported in the literature. Herein we report the chloride cyanide (cyanoformyl chloride) CO(CN)Cl **2**. It is formed in high yield together with sulfur dichloride on heating 2-chloro-2-(chlorothioimino)acetyl chloride **1**[3] in vacuo (Hg diffusion pump) at 800 °C. The pyrolyzate is collected in a cold trap; sulfur dichloride is converted with ethylene into bis(2-chloroethyl) sulfide and separated from **2** by recondensation[4].

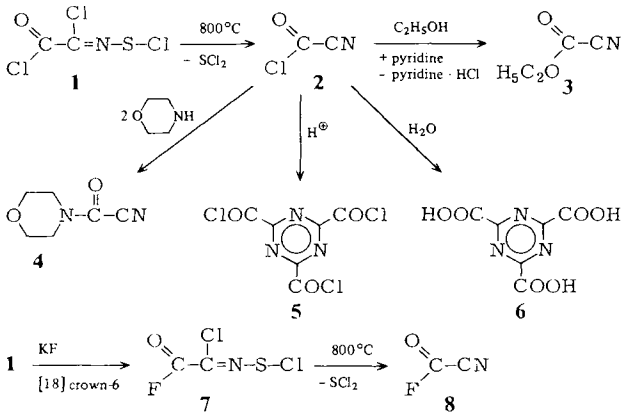



Table 1. Characteristic data of **2** and **8**.

**2**: Yield 3.6 g (88%); b.p. 20.3 °C; m.p. −89 °C; $^{13}C\{^1H\}$-NMR ([D$_8$]toluene, −20 °C): $\delta = 142.7$ (CO), 109.4 (CN); MS (20 eV): $m/z = 89$ (3%, $M^+$), 63 (54%, $M^+ - CN$), 61 (100%, ClCN), 54 (67%, $M^+ - Cl$); molecular weight: 82 (Victor Meyer)

**8**: Yield 2.7 g (74%); b.p. −49 °C; $^{19}F$-NMR (toluene/$CFCl_3$): $\delta = 23.0$; MS (70 eV): $m/z = 73$ (100%, $M^+$), 54 (34%, $M^+ - F$), 47 (59%, $M^+ - CN$), 45 (24%, FCN)

The structure of **2** is confirmed by correct elemental analysis, molecular weight determinations, by characteristic $^{13}C$-NMR and MS data (see also Table 1), and by its reaction with ethanol/pyridine and morpholine—in which the cyanoformyl derivatives **3** and **4**[5a] are formed. **2** can be stored without decomposition at −78 °C; at room temperature, however, slow and irreversible disproportion to the symmetric products phosgene and carbonyl cyanide takes place. In presence of acids, **2** is irreversibly converted within four days into the triazinetricarboxylic acid chloride **5**, while its violent reaction with $H_2O$ leads to the triazinetricarboxylic acid **6**[5b].

Cyanoformyl fluoride **8** could likewise be prepared from **1** by halogen exchange at the chlorocarbonyl function with KF/[18]crown-6[3] to give **7**, followed by pyrolysis. In contrast to **2**, **8** remains monomeric and shows no tendency to "symmetrize" into $COF_2$ and $CO(CN)_2$[4].

Received: June 16, 1983 [Z 423 IE]
German version: *Angew. Chem. 95* (1983) 807

[*] Prof. Dr. R. Appel, M. Siray
Anorganisch-chemisches Institut der Universität
Gerhard-Domagk-Str. 1, D-5300 Bonn 1 (Germany)

CAS Registry numbers:
**1**, 87145-63-9; **2**, 4474-17-3; **3**, 623-49-4; **4**, 87145-64-0; **5**, 87145-65-1; **6**, 87145-66-2; **7**, 87145-67-3; **8**, 683-55-6

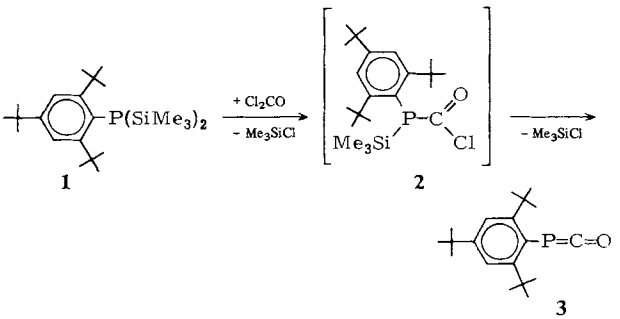
[1] R. Malachowski, L. Jurkiewicz, J. Wojtowicz, *Ber. Dtsch. Chem. Ges. 70* (1937) 1012.
[2] C. W. Tollock, D. D. Caffman, *J. Org. Chem. 25* (1960) 2016.
[3] R. Appel, M. Siray, unpublished results.
[4] *Procedure:* A quartz tube (25 mm diameter), packed in the hot zone with quartz wool, is preheated in a controllable, 10 cm-long ring oven to 800 °C. From a condenser cooled to 10 °C (**2**) or to −30 °C (**8**), 10 g of **1** or **7**, respectively, is passed within 15h under vacuum (Hg diffusion pump) through the ring oven; the pyrolyzates are collected in a cold trap at −196 °C. The conversion is 90%. Ethylene is fed into the condensate, whereupon the color of the solution changes from red to bright yellow. **2** and **8** are finally recondensed from the receiver.
[5] a) M. E. Childs, W. P. Weber, *J. Org. Chem. 41* (1976) 3486; b) C. Grundmann, E. Kober, *ibid. 21* (1956) 1392.

## The First Stable Phosphaketene**

By *Rolf Appel** and *Wilfried Paulen*

pπ–pπ-Multiple bonds between elements of the first and second short periods are a central theme in current main group chemistry. Iminophosphanes, phosphaalkenes, phosphaalkynes, even compounds with Si=Si and P=P double bonds are stable and have been prepared in large numbers during recent years[1]. The classical double bond rule could thus be abolished. On the other hand, only a few systems with cumulative double bonds and containing P=C sequences are known; these compounds, moreover, have a tendency to undergo self-addition. Thus, *tert*-butylphosphaketene, the first phosphaketene to be unequivocally detected, is stable as monomer only below −60 °C[2]. At higher temperatures it dimerizes to the diphosphetanedione.

We have now found that the first phosphaketene stable at room temperature, namely **3**, can be prepared by introduction of the unusually bulky tri-*tert*-butylphenyl moiety. It is formed on reaction of the disilylated phosphane **1** with phosgene, and can be isolated from the solution as orange crystals.




According to NMR investigations[3], molecular weight determination, elemental analysis, and IR and mass spectra, **3** clearly exists in monomeric form. Characteristic is the $^{31}P$-NMR signal, which, as in the case of *t*BuPCO[2] and *t*BuP=C=N*t*Bu[4], appears in the high field region at $\delta = -207.4$. Likewise, the IR band for the unsymmetric stretching vibration of the PCO group at 1953 $cm^{-1}$ is comparable with that of other cumulative double bond systems.

[*] Prof. Dr. R. Appel, W. Paulen
Anorganisch-chemisches Institut der Universität
Gerhard-Domagk-Str. 1, D-5300 Bonn 1 (Germany)

[**] Part 23 of Lower Coordinated Phosphorus Compounds.—Part 22: R. Appel, R. Zimmermann, *Tetrahedron Lett.*, in press.

The monocondensation product **2**, which, in the case of the *tert*-butyl derivative could be detected $^{31}$P-NMR-spectroscopically in the reaction solution at $-90\,^{\circ}C$[2], cannot be observed during the synthesis of **3**, apparently because of the drastic reaction conditions[5].

Received: June 29, 1983 [Z 434 IE]
German version: *Angew. Chem. 95* (1983) 807

CAS Registry numbers:
**1**, 87174-74-1; **3**, 87174-75-2

[1] R. Appel, F. Knoll, I. Ruppert, *Angew. Chem. 93* (1981) 771; *Angew. Chem. Int. Ed. Engl. 20* (1981) 731; P. Jutzi, *Chem. Unserer Zeit 15* (1981) 149.

[2] R. Appel, W. Paulen, *Tetrahedron Lett. 24* (1983) 2639.

[3] $^1$H-NMR ($C_6D_6$, 60 MHz, TMS int.): $\delta = 1.23$ (s, 9H, *t*Bu), 1.66 (s, 18H, *t*Bu), 7.67 (d, $^4J(PH) = 2.6$ Hz, 2 arom. H); $^{31}$P{$^1$H}-NMR ($C_6D_6$, 32.2 MHz, $H_3PO_4$ ext.): $\delta = -207.4$ (s).

[4] O. J. Kolodiazhnyi, *Tetrahedron Lett. 23* (1982) 4933.

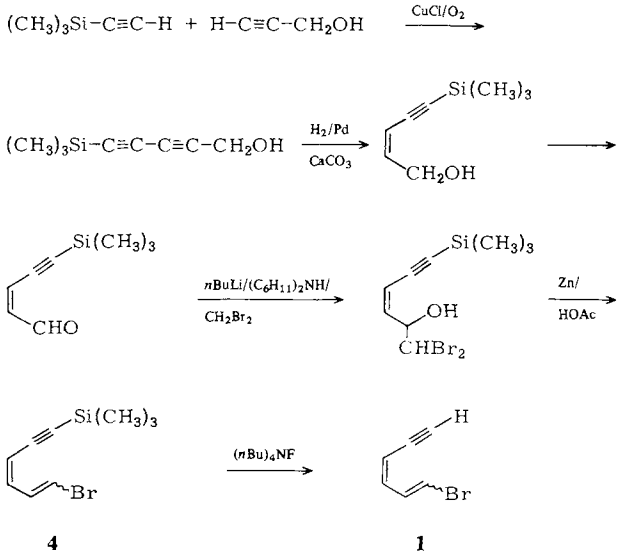
[5] *Procedure:* All operations were carried out under inert gas and with rigorous exclusion of light. A solution of **1** (3.2 g, 7.5 mmol) in toluene (8 mL) at 15 °C (water cooling) is treated dropwise, but relatively rapidly, with an 18% solution of phosgene (3% excess) in toluene. The cooling bath is then removed. After 5 minutes' heating to 40–45 °C, the reaction solution is immediately concentrated under vacuum (oil pump) and the residue quickly recrystallized from toluene at about 60 °C. Complete crystallization is achieved in the refrigerator (−2 °C). The orange crystals are filtered off, washed with a little *n*-pentane and dried in a vacuum (oil pump). Yield 0.8 g (35%), m.p. 115–117 °C.

## Generation of the Phenyl Cation by Dissociative Ionization of a Dienynyl Bromide in the Gas Phase**

By *Gisbert Depke, Michael Hanack, Wolfgang Hümmer,* and *Helmut Schwarz**

*Dedicated to Professor Fred W. McLafferty on the occasion of his 60th birthday*

We recently reported[1] a novel route for the generation of substituted phenyl cations by anchimeric participation of a triple bond in the solvolysis of acyclic dienynyl trifluoromethanesulfonates. We now describe an experiment in which for the first time unsubstituted phenyl cation **3** has also been generated from a dienynyl derivative by dissociative ionization in the gas phase with participation of a triple bond[2]. The dienynyl bromides **1** and **4** employed in this experiment were prepared *via* the route given in Scheme 1.




Scheme 1.

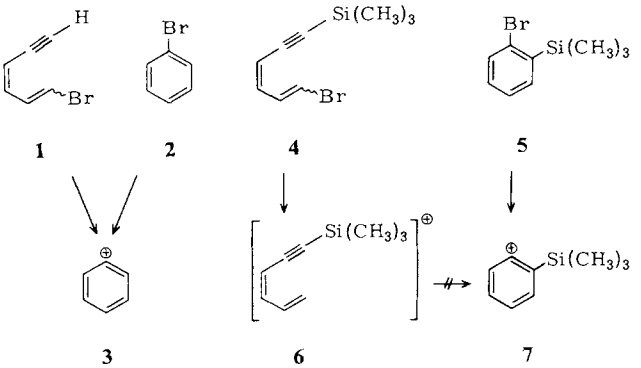
Electron impact ionization (70 eV) of **1** with loss of $Br^{\odot}$ furnished a $C_6H_5^{\oplus}$ ion whose collisional activation mass spectrum (CAMS)[3] is identical in all respects with the CA mass spectrum of a $C_6H_5^{\oplus}$ ion which is accessible either by loss of $Br^{\odot}$ from the molecular ion of **2** or by elimination of HBr from protonated **2**. Since dehalogenation of **2** under the conditions of chemical ionization (CI)[4] leads directly to the phenyl cation **3**[5], it must be concluded from the identity of the CA mass spectra that **1** likewise yields **3** during the cleavage of $Br^{\odot}$—in a previously unobserved reaction. That **1** does not cyclize concomitantly with the formation of the molecular ions, but only after rupture of the C–Br bond, is evidenced by the following findings:

1) The CA mass spectra of the molecular ions of **1** and **2** are different[6];
2) The kinetic energy, $T_k$, released on decomposition of $\mathbf{1}^{\oplus\odot}$ and $\mathbf{2}^{\oplus\odot}$ to $C_6H_5^{\oplus}$ is different in each case.

The $T_k$ values for **1** and **2** are 0.37 kcal/mol and 0.55 kcal/mol, respectively, and were determined from the half-widths of the transient signals for

$$\underset{\mathbf{2}^{\oplus\odot}}{C_6H_5Br^{\oplus\odot}} \longrightarrow \underset{\mathbf{3}}{C_6H_5^{\oplus}} + Br^{\odot}$$

Furthermore, **1** gives a signal that no Gauss function satifies, whereas the signal for **2** corresponds to a Gauss function with $n = 1.8$.




The silylated compounds **4** and **5** likewise decompose under EI and CI conditions with rupture of the C–Br bond; however, the respective ions **6** and **7** thus formed furnish CA mass spectra which are so different that ionization to a common structure, *e.g.* **7**, can be completely ruled out.

Received: June 27, 1983 [Z 430 IE]
German version: *Angew. Chem. 95* (1983) 806

[*] Prof. Dr. H. Schwarz, G. Depke
Institut für Organische Chemie der Technischen Universität Berlin
Strasse des 17. Juni 135, D-1000 Berlin 12 (Germany)
Prof. Dr. M. Hanack, W. Hümmer
Institut für Organische Chemie (Lehrstuhl II) der Universität
Auf der Morgenstelle 18, D-7400 Tübingen (Germany)

[**] Vinyl Cations, Part 41; Mass Spectrometric Investigations of Acetylene Compounds, Part 28. This work was supported by the Deutsche Forschungsgemeinschaft and the Fonds der Chemischen Industrie.—Part 40: M. Hanack, K.-A. Fuchs, C. J. Collins, *J. Am. Chem. Soc. 105* (1983) 4008; Part 27: K. Eckart, H. Schwarz, S. Kobayashi, H. Taniguchi, *Org. Mass Spectr. 17* (1982) 458.

CAS Registry numbers:
**1**, 87184-12-1; **2**, 108-86-1; **3**, 17333-73-2; **4**, 87184-13-2; **5**, 17878-37-4; **6**, 87184-14-3; 7, 87184-15-4


[1] M. Hanack, U. Michel, *Angew. Chem. 91* (1979) 928; *Angew. Chem. Int. Ed. Engl. 18* (1979) 870; M. Hanack, W. Holweger, *J. Chem. Soc. Chem. Commun. 1981*, 713; W. Holweger, M. Hanack, *Chem. Ber.*, in press.

[2] For the gas-phase chemistry and characterization of **3** by several methods see: a) R. G. Cooks, J. H. Beynon, J. F. Litton, *Org. Mass Spectrom. 10* (1975) 503; b) F. Borchers, K. Levsen, *ibid. 10* (1975) 584; c) K. Levsen, E. Hilt, *Liebigs Ann. Chem. 1976*, 257; d) C. Lifshitz, D. Gibson, K. Levsen, *Int. J. Mass Spectrom. Ion Phys. 35* (1980) 365; e) G. Angelini, S. Fornarini, M. Speranza, *J. Am. Chem. Soc. 104* (1982) 4773.

[3] Most recent review in: K. Levsen, H. Schwarz, *Q. Rev. Mass Spectrom. 1983*, 77.

[4] W. J. Richter, H. Schwarz, *Angew. Chem. 90* (1978) 449; *Angew. Chem. Int. Ed. Engl. 17* (1978) 424.

[5] a) M. Speranza, M. D. Sefcik, J. M. S. Henis, P. P. Gaspar, *J. Am. Chem. Soc. 99* (1977) 5583; b) H.-W. Lung, H. Ichikawa, A. G. Harrison, *ibid. 100* (1978) 2479; c) F. W. McLafferty, F. M. Bockhoff, *Org. Mass Spectrom. 14* (1979) 181.

[6] For those interested, the complete spectral data recorded are available from the authors on request.

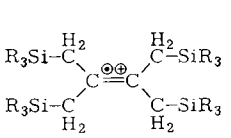

# $^{29}$Si-E(lectron)N(uclear)DO(uble)R(esonance)**

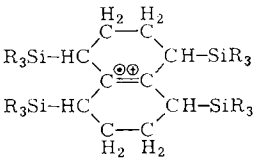

By *Hans Bock**, *Bernhard Hierholzer*, *Harry Kurreck**, and *Wolfgang Lubitz*

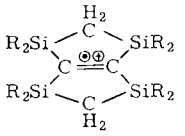

*Dedicated to Professor Ulrich Wannagat on the occasion of his 60th birthday*

NMR double resonance methods have revealed—in the truest sense of the word—a multidimensional range of valuable information about diamagnetic molecules[2]. ESR spectroscopy, an established technique for the investigation of paramagnetic molecules $M^{\odot\oplus}$, $M^{\odot}$, and $M^{\odot\ominus}$ can likewise be extended to multiple resonance methods if the electron-nucleus hyperfine interaction is probed at the individual nuclei and not at the "unpaired" electron: The NMR transitions are measured *via* changes in absorption of a concomitantly irradiated radical specific ESR transition[3]. In further analogy to NMR spectroscopy numerous nuclei with nuclear spins $I \neq 0$ are suitable for ENDOR and TRIPLE resonance measurements; the influence of the nuclear properties on the ENDOR effect is predictable[4]. However, as a result of "critical" temperature- and solvent-dependence there is often only a "narrow window" open for observation of the frequently short-lived molecular radicals.

Herein we report on the first $^{29}$Si-ENDOR and TRIPLE resonance measurements on alkylsilyl-substituted radical ions[5] with natural isotopic abundance (4.70% $^{29}$Si) and, at the same time, demonstrate that the selective, oxygen-free oxidation system $AlCl_3/H_2CCl_2$[5] has the added advantage of being "ENDOR capable". Of the radical cations and radical anions investigated[5] (cf. Supplement, R = $CH_3$), the







example selected here is the radical cation of 1,4,5,8-tetrakis(trimethylsilyl)-1,2,3,4,5,6,7,8-octahydronaphthalene, whose ESR spectrum contains for $^1$H and $^{29}$Si nuclei a total of $5\times5\times5\times37+2(5\times5\times5\times5\times37)=13875$ (!) signals. The sterically shielded radical cation is persistent even at room temperature, and exhibits a dynamic behavior caused by $(-H_2C-CH_2-)$-wagging vibrations[6]. The ESR spectrum (Fig. 1: A) is dominated by the quintet signal of the four H($CSiR_3$)-protons; the satellites flanking both sides of this quintet arise from the corresponding quintet of a radical with a single $^{29}$Si nucleus present in $4.70\times4=18.8\%$ natural abundance. On irradiation into the $^1$H main signal, the $^1$H-ENDOR spectrum results (Fig. 1: B), on saturation of the satellite signal the $^{29}$Si($+^1$H)-ENDOR spectrum (Fig. 1: C).

A comparison of the spectra (Fig. 1) immediately reveals the advantages of $^1$H and $^{29}$Si ENDOR experiments over conventional ESR measurements:

1) In the ENDOR experiment each set of equivalent nuclei furnish only one signal pair: the "37 tet" becomes one pair of lines and the total of 13875 ESR signals of the $C_{22}H_{48}Si_4$ radical cation are reduced to 5 ENDOR line pairs (Fig. 1: Ⓑ and Ⓒ), corresponding to the four different protons and $^{29}$Si. The gain in resolution ESR⇒ENDOR amounts to several orders of magnitude.

2) The ENDOR technique enables the hyperfine coupling constants to be determined even when the ESR spectrum is either only incompletely resolved (Fig. 1: Ⓐ) or unresolved. Even the spin distribution for large organosilicon radicals of lower symmetry can be derived from the "hyperfine information"—including that from $^{29}$Si-ENDOR measurements (Fig. 1: Ⓒ).

3) In the case of small $^{29}$Si couplings or poorly resolved ESR satellite spectra, these should be detectable in the ENDOR experiment by systematic changes in position of the external magnetic field in the ESR spectrum (Fig. 1: Ⓐ and Ⓒ). As important additional information the relative signs of the $^1$H and $^{29}$Si couplings can be determined by TRIPLE resonance measurements (see caption of Fig. 1 and Supplement). Since the $^{29}$Si nucleus has a negative magnetic moment, the positive s-spin density at the Si center demonstrated here corresponds to a negative $^{29}$Si coupling.

4) The hyperfine couplings, which are easily and unambiguously measurable by means of the ENDOR technique, can be monitored as a function of experimental parameters such as solvent or temperature: thus, in the tetrakis(trimethylsilyl)octahydronaphthalene radical cation $a_{^{29}Si}$ decreases and $a_H^{CH}$ increases with increasing temperature, from which it follows for the molecular dynamics that, on the ENDOR time scale and contrary to steric demands, the H($CSiR_3$) protons have a higher probability of being located in the axial position favoring hyperconjugation.


[*] Prof. Dr. H. Bock, B. Hierholzer
Institut für Anorganische Chemie der Universität
Niederurseler Hang, D-6000 Frankfurt am Main 50 (Germany)
Prof. Dr. H. Kurreck, Dr. W. Lubitz
Institut für Organische Chemie der Freien Universität
Takustr. 2, D-1000 Berlin 33 (Germany)


[**] Radical Ions, Part 58.—Part 57: W. Kaim, U. Lechner-Knoblauch, P. Hänel, H. Bock, *J. Org. Chem.*, in press; cf. also W. Lubitz, W. Brosser, B. Kirste, H. Kurreck, K. Schubert, *Z. Naturforsch. A 33* (1978) 1072.

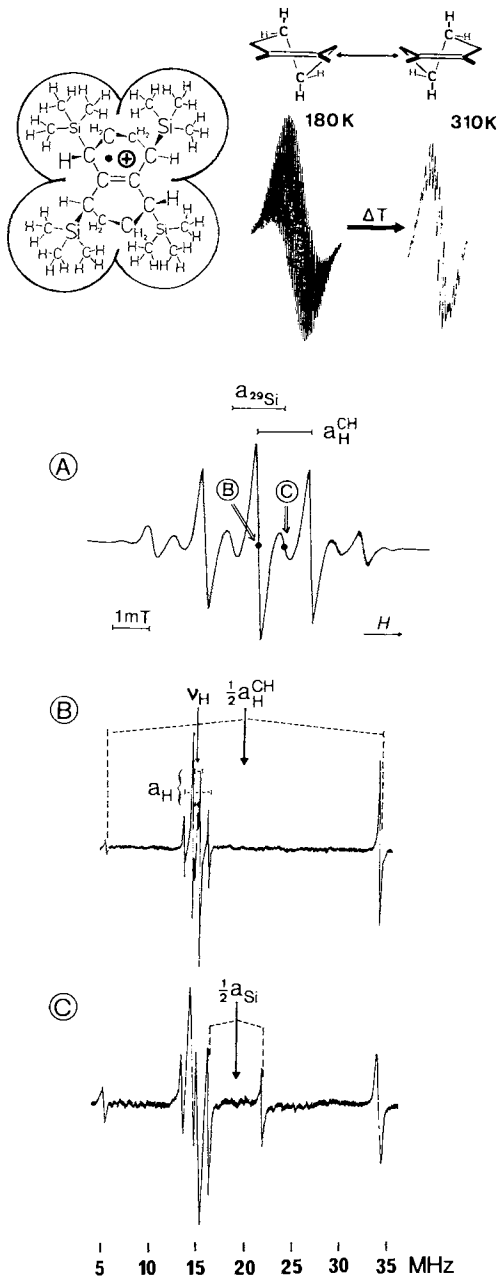



Fig. 1. ESR and ENDOR spectra of the radical cation of 1,4,5,8-tetrakis(trimethylsilyl)-1,2,3,4,5,6,7,8-octahydronaphthalene generated with $AlCl_3/H_2CCl_2$ (for details of the recording conditions cf. Supplement). Ⓐ ESR spectra at 200 K together with a section showing the *T*-dependence at 180 K (vibration frozen-in) and 310 K (vibration activated). Ⓑ $^1$H-ENDOR spectrum at 235 K: All couplings are resolved (signs from TRIPLE resonance measurements: $a_H^{CH} = +39$ MHz≙1.35 mT (!), $a_H^{NH} = +0.094$, $a_H^{SiR_3} = +0.026$, $a_H^{CH_3} - 0.011$ mT). Ⓒ $^{29}$Si-ENDOR spectrum ($a_{^{29}Si} = -37.8$ MHz≙1.33 mT).

5) ENDOR line amplitudes and widths and their dependence on experimental parameters provide additional information on the structure and molecular dynamics of the radicals investigated in solution (cf. Supplement): Thus, for an optimum $^{29}$Si-ENDOR effect the rotation correlation time is $\tau_R = 0.3$ ns at a hyperfine anisotropy of $TrA_{Si}^2 = 3$ MHz$^2$.

Summarizing, the ENDOR effect of the $^{29}$Si nuclei in the radical cation studied here is comparable with that of the protons. Measurement problems could be encountered if the radical contains only one Si nucleus, or if the π spin density at the Si center is rather large. In other cases ENDOR and TRIPLE resonance experiments on $^{29}$Si nuclei in natural abundance should decisively extend the measuring technique and generally contribute to a better understanding of the structure and dynamics of radical cations which are especially accessible in large numbers from π systems containing $R_3SiCH_2$ donor substituents[5].

Received: June 29, 1983 [Z 435 IE]
German version: *Angew. Chem. 95* (1983) 817
The complete version of this communication appears in:
*Angew. Chem. Suppl. 1983*, 1088–1105

[2] Cf. *e.g.* H. Kessler, D. Ziessow, *Nachr. Chem. Tech. Lab. 30* (1982) 488, and references cited therein; K. Roth, R. Richarz, *ibid. 30* (1982) 1014.
[3] K. Möbius, M. Plato, W. Lubitz, *Phys. Rep. 87* (1982) 171; H. Kurreck, B. Kirste, W. Lubitz, *Angew. Chem.* and *Angew. Chem. Int. Ed. Engl.*, in press.
[4] M. Plato, W. Lubitz, K. Möbius, *J. Phys. Chem. 85* (1981) 1202.
[5] H. Bock, W. Kaim, *Acc. Chem. Res. 15* (1982) 9.
[6] H. Bock, W. Kaim, *J. Am. Chem. Soc. 102* (1980) 4429.

## Stereoselective Aldol Reaction with (*R*)-*N*-Acetyl-α-phenylglycinol**

By *Manfred Braun** and *Ralf Devant*

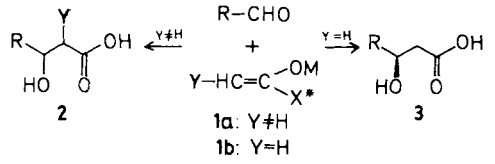
Chiral enolates **1a** facilitate aldol reactions with very high selectivity with formation of almost diastereomerically and enantiomerically pure products **2**. The prerequisite for such reactions, apart from an effective chiral auxiliary group X* and a suitable metal M, is a substituent Y in the α-position of **1a**[1]. The problem of stereoselective addition of an (α-unsubstituted) acetate enolate **1b** to prochiral carbonyl compounds to give enantiomerically pure β-hydroxycarboxylic acids **3** cannot be satisfactorily resolved with the chiral auxiliary groups X* previously employed in **1b**[2].

We have now investigated whether (*R*)-*N*-acetyl-α-phenylglycinol **4a** offers a solution to the problem. The trilithium compound **5**, obtainable from **4a** by threefold deprotonation with *n*-butyllithium, reacts with aldehydes RCHO at −70 °C to give mixed adducts **6**/**7**, the composition of which, however, cannot be determined by $^1$H-NMR spectroscopy. To determine the diastereoselectivity in the addition step we cleaved the crude adducts **6**/**7** into the β-hydroxycarboxylic acids **3a**–**d** and (*R*)-α-phenylglycinol by heating with methanolic potassium hydroxide[3]. The enantiomeric excess (*e.e.*) of the acids **3** has been determined by a comparison of the specific rotations and by $^1$H-NMR spectroscopic investigations of the methyl esters obtained with diazomethane in the presence of chiral shift reagents. From the results can be deduced the diastereomeric ratio **6**:**7** in the addition of **5** (Table 1).

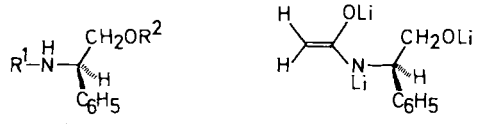
It emerges that **5** shows a distinctly higher diastereoselectivity in the reaction with prochiral carbonyl compounds[4] than the previously investigated acetate enolates **1b**[1]. Moreover, this method enables the isolation of enantiomerically pure β-hydroxy carboxylic acids **3a**–**d**: In each case the diastereomer in excess can be obtained in isomerically pure form from the spontaneously crystalliz-

[*] Priv.-Doz. Dr. M. Braun, R. Devant
Institut für Organische Chemie der Universität
Richard-Willstätter-Allee 2, D-7500 Karlsruhe (Germany)

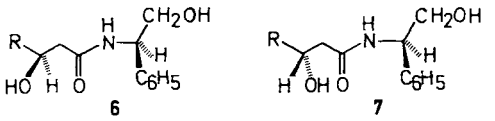
[**] This work was supported by the Fonds der Chemischen Industrie and the Deutsche Forschungsgemeinschaft (Br 604/5-1). *M. B.* thanks the DFG for a Heisenberg fellowship.



2 1a: Y≠H 1b: Y=H 3



4a: $R^1$=$COCH_3$, $R^2$=H
4b: $R^1$=$R^2$=H
4c: $R^1$=$R^2$=$COCH_3$ 5



6 7

3, 6, 7: a: R = $C_6H_5$, b: R = $C(CH_3)_3$, c: R = $CH(CH_3)_2$, d: R = $(CH_2)_2CH_3$

Table 1. Adducts **6/7** and carboxylic acid **3**.

| | 6 : 7 | 6 + 7 [a] Yield [%] | Yield [%] | 6 [b] M.p. [°C] | $[\alpha]_D^{25}$ (c, $CH_3OH$) | 3 Yield [%] | Conf. |
|---|---|---|---|---|---|---|---|
| a | 80 : 20 | 96 | 43 | 136–137 | −21.35 (1.11) | 84 | *R* [c] |
| b | 85 : 15 | 98 | 35 | 118–119 | −44.47 (0.98) | 85 | *R* |
| c | 77 : 23 | 82 | 24 | 117–118 | −51.03 (0.97) | 88 | *R* |
| d | 78 : 22 | 93 | 25 | 86–88 | −65.13 (2.49) | 86 | *S* [d] |

[a] Mixture of crude adducts. [b] Yield after recrystallization, referred to **4a**, not optimized. [c] Procedure for (*R*)-**3a**: A stirred solution of **4a** (1.8 g, 10.0 mmol) in 1,2-dimethoxyethane is treated under $N_2$ at 0°C with 30 mL of a 1.6 M solution of *n*-butyllithium in *n*-hexane and stirred for 15 h at 0°C. After cooling to −78°C and addition of 1.0 mL (10.0 mmol) benzaldehyde, the reaction mixture is stirred for a further 30 min at −78°C and poured into a saturated $NH_4Cl$ solution. Several extractions with $CHCl_3$, drying over $Na_2SO_4$ and removal of the solvent affords 2.74 g of a colorless crude mixture of **6a/7a**, which on recrystallization from $CH_2Cl_2$ yields 1.22 g of **6a**.—A mixture of **6a** (1.22 g, 4.30 mmol), methanol (60 mL), water (30 mL) and KOH (2.4 g, 43 mmol) is heated under reflux for 15 h. The methanol is distilled off, the residue washed with $CHCl_3$, rendered acid (pH 2) with dilute hydrochloric acid, and extracted with ether. After removal of the solvent there remains 0.60 g of **3a**, colorless crystals, m.p. 116–118°C, $[\alpha]_D^{25}$ = +17.9 (*c* = 2.33, ethanol) (116–118°C and +18.2°, resp. (*c* = 4.95, ethanol) after D. S. Noyce, C. A. Lane, *J. Am. Chem. Soc. 84* (1962) 1635). The enantiomeric purity of the methyl ester of **3a** (obtained with diazomethane) is greater than 97% ($^1$H-NMR in presence of Eu(tfc)$_3$). [d] Change of sign of configuration, since *n*-propyl—other than the groups R in **3a–c**—has a lower order than $CH_2COOH$.

ing crude adducts **6/7** by a single recrystallization; alkaline hydrolysis leads to the carboxylic acid **3** with optical purities of more than 97%. Concomitantly, the chiral auxiliary agent **4b** is liberated, from which **4a** can be regenerated by conversion of **4b** into the diacetyl compound **4c** and subsequent ester hydrolysis[5]. As a rule, **4b** is readily accessible by reduction of α-phenylglycine. Since both optical antipodes of this amino acid are commercially available, enantiomerically pure β-hydroxy carboxylic acids can be synthesized in any desired configuration. We have proven the absolute configuration of **3b** by conversion into (*R*)-2,2-dimethyl-3-hydroxypentane.

Received: June 7, 1983 [Z 412 IE]
German version: *Angew. Chem. 95* (1983) 802

[1] D. A. Evans, J. V. Nelson, T. R. Taber, *Top. Stereochem. 13* (1982) 1, and references cited therein.
[2] See [1], especially p. 95f.—With enolates of α-sulfinyl esters (chiral substituent Y) the products **3** can be obtained in high enantiomeric excesses—albeit with loss of the chiral auxiliary agent: C. Mioskowski, G. Solladié, *Tetrahedron 36* (1980) 227.
[3] The acid hydrolysis of amides of *N*-phenylglycinol described by *Helmchen et al.* is not suitable, since **3** racemizes in acid media: G. Helmchen, G. Nill, D. Flockerzi, M. S. K. Youssef, *Angew. Chem. 91* (1979) 65; *Angew. Chem. Int. Ed. Engl. 18* (1979) 63.
[4] In the reaction of **5** with acetophenone a diastereomeric ratio of 81 : 19 is achieved.
[5] M. Kuna, G. Ovakimian, P. A. Levene, *J. Biol. Chem. 137* (1941) 337.

## A New Route to Tellurium-Nitrogen Compounds**

By *Joseph S. Thrasher* and *Konrad Seppelt**

Whereas there is a vast chemistry of sulfur-nitrogen compounds, very little is known about the corresponding tellurium-nitrogen systems. A few Te–N compounds have been prepared by replacement of an F atom in $TeF_6$ by nitrogen-containing groups, resulting, *e.g.*, in $H_2N-TeF_5$[1]. However, the possibilities offered by this method seem to have been exhausted.

We have now found that $TeF_5-Cl$ can add photolytically to nitriles with retention of the $TeF_5$ group.

$$TeF_5Cl + RC{\equiv}N \xrightarrow{h\nu;\ 20°C} F_5Te-N{=}CRCl + ClRC{=}N-N{=}CRCl + \cdots$$

R = Cl, $CF_3$

$F_5Te-N{=}CCl_2$, pentafluorotellurium isocyanidedichloride is obtained as a colorless liquid in 32% yield; $Cl_2C{=}N-N{=}CCl_2$[2] is formed as a by-product (9%), probably as a result of the decomposition of $F_5Te-N{=}CCl_2$. No evidence could be found for the formation of the unknown $Te_2F_{10}$, although $S_2F_{10}$ is observed in the reaction of $SF_5Cl$ with nitriles[3]; instead, both $TeF_4$ and $TeF_6$ are formed.

The reaction of $F_5Te-N{=}CCl_2$ with excess HF gives the amine $F_5Te-NH-CF_3$ as a clear liquid in 90% yield. The anion $[F_5Te-N-CF_3]^-$ can be generated directly from $F_5Te-N{=}CCl_2$ by reaction with caesium fluoride. The caesium salt is a crystalline solid which is readily soluble in acetonitrile.

$$F_5Te-N{=}CCl_2 \xrightarrow[-HCl]{HF;\ 40–50°C} F_5Te-NH-CF_3$$

$$F_5Te-N{=}CCl_2 \xrightarrow{CsF;\ 70°C} Cs^+[F_5Te-N-CF_3]^-$$

$F_5Te-N{=}CF_2$ is produced by pyrolysis of the salt formed between $F_5Te-NH-CF_3$ and KF in 35% yield. Unlike the corresponding sulfur compound, it does not isomerize to $F_4Te{=}N-CF_3$[3]. This is explained by the inability of tellurium(VI) to form five-coordinated species[4].

A mercury derivative, $Hg[N(CF_3)TeF_5]_2$, has also been obtained by reaction of $HgF_2$ with $F_5Te-NH-CF_3$. This

[*] Prof. Dr. K. Seppelt, Dr. J. Thrasher
Institut für Anorganische und Analytische Chemie
Freie Universität Berlin
Fabeckstrasse 34–36, D-1000 Berlin 33 (Germany)

[**] This work was supported by the Deutsche Forschungsgemeinschaft and the Fonds der Chemischen Industrie.

colorless, crystalline, sublimable mercury derivative serves for the preparation of other Te–N compounds:

$$F_5Te-NH-CF_3 \xrightarrow{HgF_2,\ 70-80\,^\circ C} Hg[N(CF_3)TeF_5]_2$$

$$Hg[N(CF_3)TeF_5]_2 \xrightarrow{2XF} HgF_2 + 2X-N(CF_3)TeF_5$$

$X = Cl, Br$

Both chlor- and bromamine compounds are surprisingly stable; however, they decompose under UV-irradiation to yield the first compound with two tellurium atoms bonded to the same nitrogen atom.

$$2Cl-N(CF_3)TeF_5 \xrightarrow{hv;\ 20\,^\circ C} Cl_2 + CF_3N(TeF_5)_2 + \cdots$$

All new compounds have been identified by spectroscopic methods and by elemental analysis where possible. In all cases the $^{19}F$-NMR spectra exhibit an $AB_4$ pattern with $^{125}Te$ satellites, which is characteristic of $TeF_5$ groups.

The analogous reactions with $SeF_5Cl$ gave no evidence for formation of $F_5Se-N$ compounds and, hence, once again no light is thrown on selenium-nitrogen chemistry of this type.

Received: May 31, 1983 [Z 404 IE]
German version: *Angew. Chem. 95* (1983) 813
The complete manuscript of this communication appears in: *Angew. Chem. Suppl. 1983*, 1106–1119

CAS Registry numbers:
$TeF_5Cl$, 21975-44-0; $TeF_5N{=}CCl_2$, 87191-36-4; $TeF_5-N{=}CCl-CF_3$, 87191-37-5; $TeF_5-NH-CF_3$, 87206-80-2; $Cs^+[TeF_5-N-CF_3]^-$, 87191-38-6; $Hg[N(CF_3)TeF_5]_2$, 87191-39-7; $Cl-N(CF_3)TeF_5$, 87191-40-0; $Br-N(CF_3)TeF_5$, 87191-41-1; $CF_3N(TeF_5)_2$, 87191-42-2; $Cl-C{\equiv}N$, 506-77-4; $CF_3-C{\equiv}N$, 353-85-5.

[1] K. Seppelt, *Inorg. Chem. 12* (1973) 2837; H. Hartl, P. Huppmann, D. Lentz, K. Seppelt, *ibid. 22* (1983) 2183.
[2] J. T. Hackmann, W. P. Tromper, DOS 2037612 (1972).
[3] C. W. Tullock, D. D. Coffman, E. L. Muetterties, *J. Am. Chem. Soc. 86* (1964) 357.
[4] K. Seppelt, *Angew. Chem. 91* (1979) 199; *Angew. Chem. Int. Ed. Engl. 18* (1979) 186.

## Unprecedented Oxidative Addition of the $P_4S_3$ Cage Molecule with Phosphorus-Phosphorus Bond Cleavage; Synthesis and Molecular Structure of $[Ir(\mu\text{-}P_4S_3)(PPh_3)Cl(CO)]_2$

By *Carlo A. Ghilardi, Stefano Midollini,* and *Annabella Orlandini**

As part of a study[1] on the synthesis and characterization of transition-metal complexes containing the $P_4$ molecule or its derivatives as ligands, we studied the reaction of the $P_4S_3$ cage molecule with the $d^8$-square planar $IrCl(CO)(PPh_3)_2$ (*Vaska*'s complex), whose ability to undergo oxidative additions with a variety of molecules is well-known. In $Mo(CO)_5P_4S_3$ the $P_4S_3$ cage was found to coordinate the metal *via* the apical P atom[2]. A metal-promoted fragmentation of this cage has been reported recently, leading to the triangular $P_2S$ unit[3].

When a solution of $P_4S_3$ in benzene is allowed to react with an equimolar solution of $IrCl(CO)(PPh_3)_2$ in the same solvent at *ca.* 60 °C, the solution rapidly turns red-brown and green crystals slowly precipitate. The complex formed, $\{Ir(P_4S_3)(PPh_3)Cl(CO)\}$, is air stable and practically insoluble in common organic solvents; its IR spectrum (Nujol) exhibits $\nu$(CO) at 2055 $cm^{-1}$. The increase of the $\nu$(CO) relative to *Vaska*'s complex (1965 $cm^{-1}$) is consistent with oxidation of the metal on adduct formation.

As indicated by the X-ray structure analysis (Fig. 1), the title compound is a dimeric iridium(III) derivative, the $P_3$ ring of the $P_4S_3$ molecule has opened, and one $PPh_3$ group *per* metal center has been displaced. To our knowledge no oxidative addition involving the rupture of a PP bond has previously been reported.

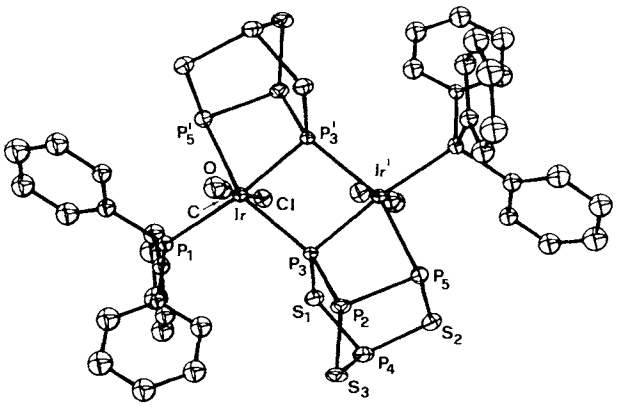



Fig. 1. Crystal structure of $[Ir(\mu\text{-}P_4S_3)(PPh_3)Cl(CO)]_2$. ORTEP representation with 30% probability ellipsoids. Monoclinic, space group $P2_1/n$, $a = 16.252(8)$, $b = 11.421(5)$, $c = 14.443(7)$ Å, $\beta = 97.53(4)°$, $Z = 2$. The structure was solved by the heavy atom method and refined to $R = 0.048$ and $R_w = 0.046$ for 2933 reflections having $I \geq 3\sigma(I)$. Selected bond distances: Ir–Cl 2.396(4), Ir–P1 2.421(4), Ir–P3 2.433(4), Ir–P3′ 2.356(4), Ir–P5′ 2.422(4), Ir–C 1.88(2), C–O 1.11(2), Ir...Ir 3.691(1) Å.

In the centrosymmetric, dimeric complex the two Ir atoms are held together by two $P_4S_3$ groups; each $P_4S_3$ cage functions as a bidentate ligand and bridges the two Ir atoms through one P atom, while another P atom is linked to only one Ir atom. The distorted octahedral geometry of each Ir atom is completed by a $PPh_3$ ligand, a Cl atom, and a CO group; Cl and CO are *trans* to each other (Cl–Ir–CO 177.1(6)°). The distortions from the idealized octahedral geometry are mainly due to the steric requirements of the $P_4S_3$ group, which although strongly distorted upon coordination, nevertheless, retains its rigidity. Due to the presence of the inversion center between the two Ir atoms, the $Ir_2P_2$ unit is strictly planar with an Ir...Ir separation of 3.691(1) Å and an Ir–P3–Ir′ angle of 100.8(1)°.

The $P_4S_3$ group, in contrast to compounds in which it behaves as a monodentate ligand, is significantly distorted compared to the uncoordinated molecule[5]. In fact, due to the bidentate coordination the $P_4S_3$ unit no longer has $C_{3v}$ symmetry: the P5–P2–P3 angle opens from 60.0° to 84.8(2)° and the P5–P3 bond is cleaved. It follows that the P3···P5 separation is 3.055(5) Å, whereas the P2–P3 and P2–P5 distances (2.249(5) and 2.281(6) Å, respectively) are only a little longer than the average value of 2.235 Å reported for the free ligand.—It is noteworthy that a

[*] Dr. A. Orlandini, Dr. C. A. Ghilardi, Dr. S. Midollini
Istituto per lo Studio della Stereochimica ed Energetica
dei Composti di Coordinazione del CNR
Via F. D. Guerrazzi 27, I-50132 Firenze (Italy)

 © Verlag Chemie GmbH, 6940 Weinheim, 1983 0570-0833/83/1010-0790 $ 02.50/0 

four-membered metallocycle was obtained by oxidative addition of the triphenylcyclopropenium cation to $IrCl(CO)(PMe_3)$ with CC bond cleavage[7].

Received: June 6, 1983 [Z 409 IE]
German version: *Angew. Chem. 95* (1983) 801
The complete manuscript of this communication appears in: *Angew. Chem. Suppl. 1983*, 1066–1074

[1] M. Di Vaira, C. A. Ghilardi, S. Midollini, L. Sacconi, *J. Am. Chem. Soc. 100* (1978) 2550; P. Dapporto, S. Midollini, L. Sacconi, *Angew. Chem. 91* (1979) 510; *Angew. Chem. Int. Ed. Engl. 18* (1979) 469; F. Cecconi, C. A. Ghilardi, S. Midollini, A. Orlandini, *J. Chem. Soc. Chem. Commun. 1982*, 229; F. Cecconi, C. A. Ghilardi, S. Midollini, A. Orlandini, *Angew. Chem. 95* (1983) 554; *Angew. Chem. Int. Ed. Engl. 22* (1983) 554; *Angew. Chem. Suppl. 1983*, 718.
[2] A. W. Cordes, R. D. Joyner, R. D. Shores, E. D. Dill, *Inorg. Chem. 13* (1974) 132.
[3] M. Di Vaira, M. Peruzzini, P. Stoppioni, *J. Chem. Soc. Chem. Commun. 1982*, 894.
[5] Y. C. Leung, J. Waser, S. Van Houten, A. Vos, G. A. Wiegers, E. H. Wiebenga, *Acta Crystallogr. 10* (1957) 574.
[7] R. M. Tuggle, D. L. Weaver, *Inorg. Chem. 11* (1972) 2237.

## Fourier Transform Far-Infrared (FT-Far-IR) Spectroscopy of Silver Atoms and Silver Clusters Entrapped in Zeolite NaY**

By *Geoffrey A. Ozin**, *Mark D. Baker*, and *J. Mark Parnis*

Metal clusters entrapped within zeolite cages are of catalytic importance[7]. Crystallographic data on silver atoms and silver clusters in zeolites have made them an attractive system for detailed spectroscopic study, since they are in a well defined setting as found for metal clusters entrapped in rare gas matrices[18–20].

Here, we wish to report the FT-far-IR spectra (400 to 30 $cm^{-1}$) of Ag atoms and clusters entrapped within the cages of zeolite NaY (Fig. 2). The spectrum of the zeolite recorded before cation exchange but after dehydration at 600°C is very similar to that reported by *Peuker et al.*[19]. All the bands below 200 $cm^{-1}$ are assigned to vibrations of sodium ions at different sites in the zeolite lattice. The strong doublet at 190 and 150 $cm^{-1}$ has been assigned to cationic occupancy of site II and site I, respectively, and the band at 100 $cm^{-1}$ to a site I′ sodium ion.

As shown in Figure 2 new features appear below 170 $cm^{-1}$ for the ion-exchanged zeolites; this is striking, and we can immediately assign these to vibrational modes involving silver species. Investigations by *Brodskii et al.*[18] of zeolites exchanged with Na, K, Rb, and Cs have shown that the vibrational frequencies of cationic modes (at the same sites) are proportional to $m^{-1/2}R^{-3/2}$, where $m$ = cation mass and $R$ = cationic radius. Application of this empirical formula to $Ag^+$ located at sites I and II indicates that $Na^+/Ag^+$ exchange should give rise to bands shifted by *ca.* 120 $cm^{-1}$ to lower frequency. We therefore tentatively assign the bands at 60 and 30 $cm^{-1}$ in the $Ag_{55}Y$ spectrum (Fig. 2c) to vibrational modes of $Ag^+$ in sites I and II, respectively. This then allows us to assign the bands above 60 $cm^{-1}$ to either Ag atom vibrations or to $Ag_n$ cluster modes.

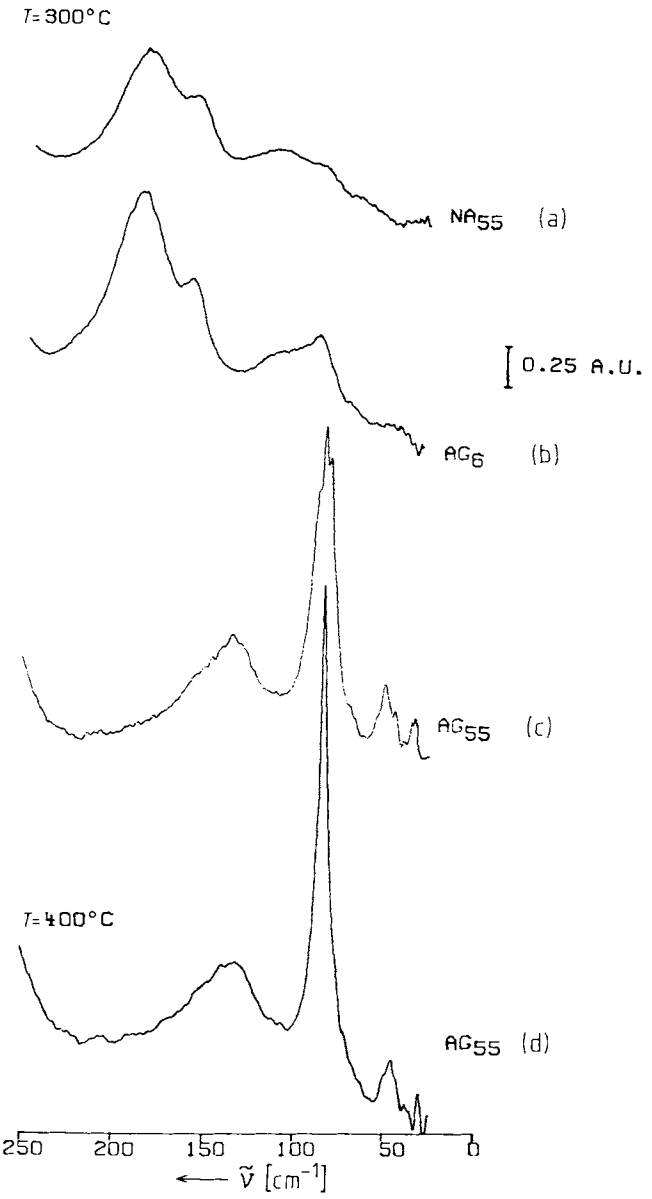



Fig. 2. FT-far-IR spectra of the zeolites $Na_{55}Y$ (a), $Ag_6Na_{49}Y$ (b), and $Ag_{55}Y$ (c: at 300°C, d: at 400°C).

It has been conclusively shown[23] that the thermal treatment of $Na^+/Ag^+$ exchanged Y zeolites *in vacuo* induces autoreduction and clustering processes which give rise to the charged silver clusters $Ag_2^+$ (sites I and I′) and $Ag_n^{q+}$ (n = 5–13; α-cage), as well as $Ag^0$ (site I). For $Ag_6Na_{49}Y$, the majority of species are $Ag^0$ and $Ag_n^{q+}$, whereas with the fully exchanged $Ag_{55}Y$, $Ag_2^+$ is also present. For $Ag_2^+$ the vibrational spectrum of the parent $Ag^0$ at site I will be perturbed by the approach of a $Ag^+$ at site I′. We assign the sharp multicomponent band at 80 $cm^{-1}$ to $Ag^0$ and $Ag_2^+$, and the band at 130 $cm^{-1}$ to the larger cluster in the α-cage. Annealing the $Ag_{55}Y$ (300→400°C) has the effect of removing the splitting of the 80 $cm^{-1}$ band and of sharpening this peak. This result indicates that the band splittings are probably not due to site effects associated with the Si/Al distribution around sites I and I′, and do not arise

[*] Prof. G. A. Ozin, Dr. M. D. Baker, J. M. Parnis
Lash Miller Chemistry Department, University of Toronto
80 St. George Street, Toronto, Ontario M5S 1A1 (Canada)

[**] The generous financial assistance of the Natural Sciences and Engineering Research Council of Canada's Operating, Major Equipment and Strategic Energy Programmes, and the Connaught Fund of the University of Toronto is gratefully acknowledged. *J. M. P.* expresses his gratitude for an NSERC graduate scholarship. The assistance of *K. Molnar* and *T. Higson* in designing the *in situ* FT-far-IR zeolite cell was invaluable.

from $^{107}Ag/^{109}Ag$ isotopes. A more plausible explanation is to ascribe the multiplet structure to a perturbation of the $Ag^0$ or $Ag_2^+$ cage vibration modes by residual intrazeolitic $H_2O$ in the α- or β-cage ($H_2O$ is present at 300°C but absent at 400°C).

This study demonstrates that it is viable to investigate the infrared vibrational spectra of metal atoms and clusters immobilized in zeolite supports. This will provide new insights into the nature of their interaction with the surroundings (metal-support effects). An extension of this study in combination with other spectroscopic studies should certainly increase the amount of information.

Received: June, 1983; revised: August 9, 1983 [Z 408 IE]
German version: *Angew. Chem. 95* (1983) 813
The complete manuscript of this communication appears in: *Angew. Chem. Suppl. 1983*, 1075–1087

CAS Registry number:
1, 7440-22-4

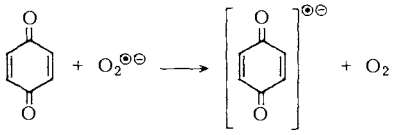
[7] R. A. Schoonheydt, L. J. Vandamme, P. A. Jacobs, J. B. Uytterhoeven, *J. Catal. 43* (1976) 292.
[18] I. A. Brodskii, S. P. Zhdanor, A. E. Stanevich, *Sov. Phys. Solid State 15* (1974) 1771.
[19] C. Peuker, D. Kunath, *J. Chem. Soc. Faraday Trans. I 77* (1981) 2079.
[20] W. M. Butler, C. L. Angell, W. McAllister, W. M. Risen, *J. Phys. Chem. 81* (1977) 2061.
[23] P. A. Jacobs, J. B. Uytterhoeven, H. K. Beyer, *J. Chem. Soc. Faraday Trans. I 75* (1979) 56.

## Efficiency of the Physical Quenching of Singlet Oxygen with Benzoquinone Derivatives**

By *Ernst Gassmann, Titus A. Jenny,* and *André M. Braun** 

*Dedicated to Professor Günther O. Schenk on the occasion of his 70th birthday*

*p*-Benzoquinone and some of its derivatives are readily reduced by hyperoxide (superoxide) to the corresponding semiquinone radical anions (a). Since the product of reduction absorbs in the visible spectral region this reaction provides a very suitable means of analyzing the hyperoxide[1].

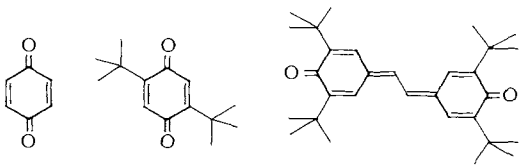


(a)

We have also used this reaction as a basis for working out an analytical method for the differentiation and parallel determination of singlet oxygen and hyperoxide[1]. It can be shown by hydrophobization of the benzoquinone to be reduced that solvated electrons can only penetrate the hydrophilic/hydrophobic interface of microemulsions formed with ionic surfactants under certain experimental conditions. An analogous transfer reaction of $O_2^{\odot\ominus}$ can be practically ruled out[1].

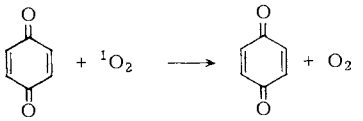
[*] Priv.-Doz. Dr. A. M. Braun, E. Gassmann
Institut de Chimie Physique,
Ecole Polytechnique Fédérale de Lausanne
Ecublens, CH-1015 Lausanne (Switzerland)
Dr. T. A. Jenny
Institut de Chimie Organique, Université de Lausanne

[**] This work was supported by the Schweizerische Nationalfonds zur Förderung der wissenschaftlichen Forschung (Project 2.027-0.81).



1 2 3

The parallel analysis of singlet oxygen and hyperoxide requires that the reagents to be used are physically and chemically specific. This means for the benzoquinones **1** and **2** that their chemical reactivity and their efficiency as physical quenchers can be neglected as far as singlet oxygen is concerned. We have already described the experimental conditions under which the former mentioned requirement is fulfilled[1]; we now report on the efficiency of the physical quenching of singlet oxygen caused by *p*-benzoquinone **1** or 2,5-di-*tert*-butyl-*p*-benzoquinone **2** (b).



(b)

When an aerobic solution of tetraphenylporphyrin ($5 \times 10^{-5}$ M) in tetrachloromethane is excited with monochromatic light of wavelength $\lambda = 546$ nm (HgXe 1000 W, monochromator), the phosphorescence of the $^1\Delta_g$-$O_2$ at 1270 nm can be measured[2a]. Measurements of signal intensity as a function of the concentration of a given quencher enable the product of the constants $k_q\tau$ to be calculated according to the Stern-Volmer equation (c).

$$I_0/I = 1 + k_q\tau[Q] \qquad (c)$$

$I_0$ is the signal intensity of solutions in the absence of quencher, $I$ that of solutions in the presence of quencher, $k_q$ is the rate constant of the physical quenching (b), and $\tau$ is the lifetime of the singlet oxygen in $CCl_4$ ($3 \times 10^{-2}$ s[2b]). For relatively large quencher concentrations [Q], deviations from the linearity required by equation (c) are observed (Fig. 1). Assuming that a steady state quenching must also be taken into consideration at these concentrations, equation (d) holds for $I_0/I = f([Q])$[3], in which we interpret $V$ as the equilibrium constant for complexation of oxygen and quencher.

$$(I_0/I)e^{-V[Q]} = 1 + k_q\tau[Q] \qquad (d)$$

This constant is so chosen that (d) yields a linear function in the range of [Q] ($V = 2\,M^{-1}$; Fig. 1). The constant $k_q = 2900\ M^{-1}\ s^{-1}$ for **1** calculated from $k_q\tau$ is about a factor of $10^4$ smaller than the value ($3.4 \times 10^7\ M^{-1}\ s^{-1}$) published by *Koka* and *Song*[4a].

To check our method of measurement we have determined the constant $k_q$ of a physical quencher of analogous chemical constitution whose value lies in the range $10^7$–$10^8\ M^{-1}\ s^{-1}$. *Taimr* and *Prospisil* found an almost diffusion-controlled quenching for the bisquinomethane **3** in dichloromethane[4b]; according to our measurements the rate constant for $^1O_2$-quenching in $CCl_4$ is $2 \times 10^8\ M^{-1}\ s^{-1}$ (cf. Fig. 2). The $k_q$ of $400\ M^{-1}\ s^{-1}$ found for the hydrophobicized benzoquinone **2** used by us as specific reagent for hyperoxide in the oil phase is, once again, to be classed in the range of very small quenching constants (Fig. 1)[1].

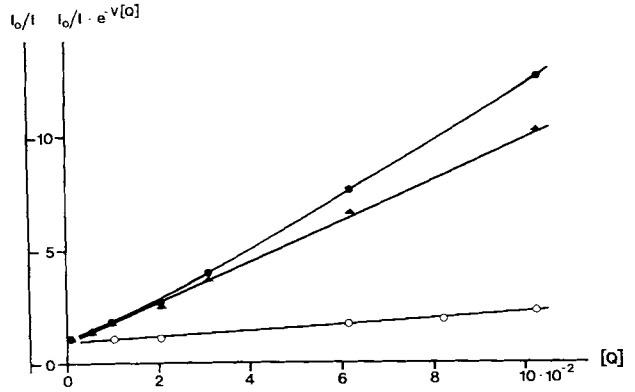



Fig. 1. Stern-Volmer function for the physical quenching of singlet oxygen with **1** (● (c), ▲ (d): $k_q\tau = 87\ M^{-1}$) and with **2** (○ (c): $k_q\tau = 12\ M^{-1}$).

The quenching constant quoted by *Koka* and *Song* has already been interpreted in the appendix to the publication[4a] as a rate constant of an electron transfer reaction *(C. S. Foote, I. Kraljic)*. With a value of $3.4 \times 10^7\ M^{-1}\ s^{-1}$ it lies in the range of the rate constants found by us for the electron transfer (a) from $O_2^{\odot\ominus}$ to **1**[1]. Since the generation of hyperoxide as main reaction during a sensitization with

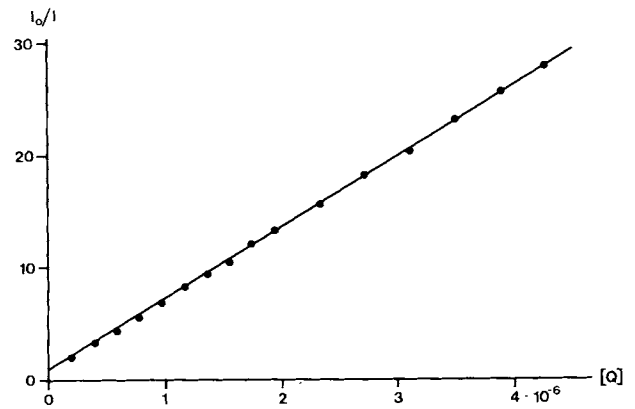



Fig. 2. Stern-Volmer function for the physical quenching of singlet oxygen with **3** ((c): $k_q\tau = 6.0 \times 10^6\ M^{-1}$).

rose bengal (RB) can be ruled out[5], an electron transfer from sensitizer to **1** is likely. This reaction (e) would, as observed by *Koka* and *Song*, compete with the generation of singlet oxygen and, thus, also with the photooxidation of chlorophyll a. A direct triplet quenching (f) can, on the other hand, be ruled out on grounds of the triplet energy of **1** ($E = 50$ kcal/mol).

$$\mathbf{1} + {}^3RB \longrightarrow \mathbf{1}^{\odot\ominus} + RB^{\odot\oplus} \quad (e)$$

$$\mathbf{1} + {}^3RB \longrightarrow {}^3\mathbf{1} + RB \quad (f)$$

Our data confirm the tentative suggestion made by *Foote* (cf. [4a]) that *p*-benzoquinone **1** is a very inefficient physical quencher for singlet oxygen; the quenching constant has the same order of magnitude as that of the commonly used solvent. The same holds for the hydrophobicized derivative **2**. Thus, the specificity of these reagents for hyperoxide[1] has been confirmed experimentally.

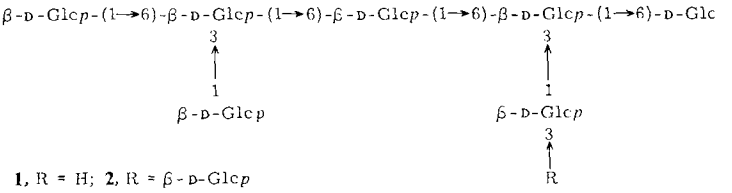
Received: June 24, 1983; revised: August 17, 1983 [Z 428 IE]
German version: *Angew. Chem. 95* (1983) 816

[1] M.-T. Maurette, E. Oliveros, P. P. Infelta, K. Ramsteiner, A. M. Braun, *Helv. Chim. Acta 66* (1983) 722, and references cited therein.
[2] a) J. R. Hurst, J. D. McDonald, G. B. Schuster, *J. Am. Chem. Soc. 104* (1982) 2065; M. A. J. Rodgers, *Photochem. Photobiol. 37* (1983) 99; b) T. A. Jenny, N. J. Turro, *Tetrahedron Lett. 23* (1982) 2923.
[3] M. R. Eftink, C. A. Ghiron, *J. Phys. Chem. 80* (1976) 486.
[4] a) P. Koka, P.-S. Song, *Photochem. Photobiol. 28* (1978) 509; b) L. Taimr, J. Prospisil, *Angew. Makromol. Chem. 52* (1976) 31.
[5] V. S. Srinivasan, D. Podolski, N. J. Westrick, D. C. Neckers, *J. Am. Chem. Soc. 100* (1978) 6513.

## Syntheses of a Branched Hepta- and an Octasaccharide with Phytoalexin-Elicitor Activity

By *Petra Ossowski, Åke Pilotti, Per J. Garegg*, and Bengt Lindberg*

When soybean tissue is infected with certain fungi, *e.g. Phytophthora megasperma* var. *sojae*, the formation of phytoalexins, *e.g.* glyceollin, is initiated by the action of an elicitor, a fungal glucan present in the mycelium[1]. *Albersheim et al.*[1,2] have isolated elicitor-active oligosaccharides by degradation of this glucan by consecutive enzymic and acidic hydrolysis, followed by extensive fractionation. The smallest of these oligosaccharides are a heptasaccharide and an octasaccharide for which the structures **1** and **2**, respectively, have been suggested. Due to difficulties in obtaining pure oligosaccharides in sufficient quantities, these structures were regarded as tentative only.

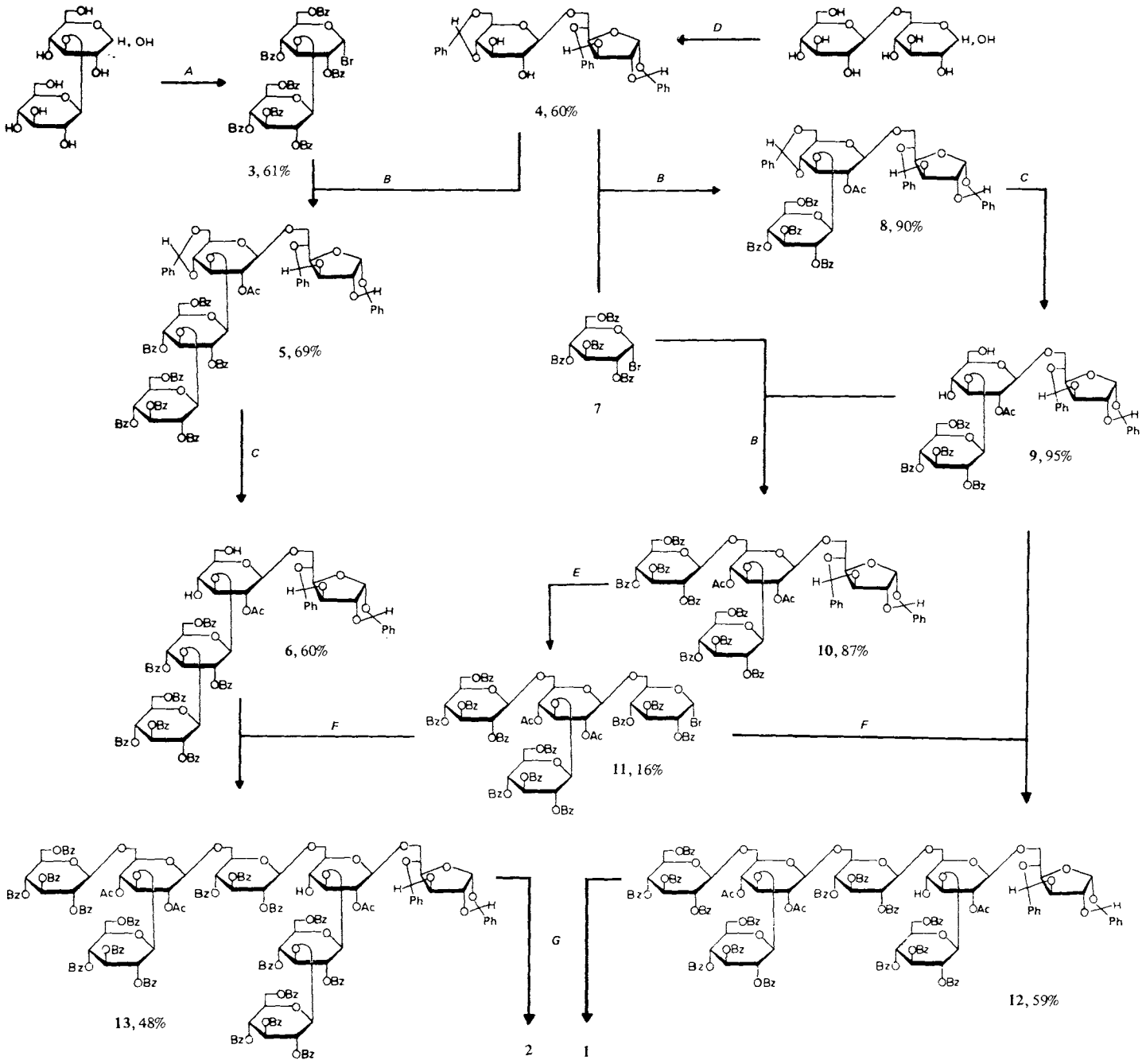



**1**, R = H; **2**, R = β-D-Glcp

We now report the syntheses of **1** and **2** by unambiguous methods. Silver triflate promoted condensations of benzoylated glycosyl bromides[3] with the appropriate hydroxy compounds were used throughout. Regioselective glycosidation of dihydroxy compounds ("open" syntheses) were used to obtain efficient routes. Good yields were obtained in all steps, except for that of the preparation of the tetrasaccharide bromide **11**, which due to degradation during the treatment of its precursor **10** with hydrogen bromide in acetic acid had to be purified by chromatography. The structures of the various intermediates and the final products were confirmed by appropriate analyses and by 400 MHz $^1$H-NMR spectroscopy. The final products **1** and **2** gave the expected results on methylation analysis of the sodium borohydride-reduced products[4].

As shown in Scheme 1 the benzoylated laminaribiosyl bromide **3** was condensed with the gentiobiose derivative **4**; the product was acetylated to give **5**, which was regio-

[*] Prof. Dr. P. J. Garegg, Dr. P. Ossowski, Dr. Å. Pilotti, Prof. Dr. B. Lindberg
Department of Organic Chemistry, Arrhenius Laboratory
University of Stockholm, S-10691 Stockholm (Sweden)




Scheme 1. Bz = benzoyl. *A*) 1. BzCl/pyridine, 2. HBr/HOAc; *B*) 1. Ag-triflate, 2. $Ac_2O$/pyridine; *C*) 80% $CHCl_2COOH$/HOAc; *D*) PhCHO/$ZnCl_2$; *E*) 1. $CF_3COOH$, 2. BzCl/pyridine, 3. HBr/HOAc/$CH_2Cl_2$; *F*) Ag-triflate; *G*) 1. $CF_3COOH$, 2. NaOMe/MeOH. All benzylidene compounds are *exo-endo* isomeric mixtures differing in configuration at the acetal carbon atom of the dioxolane ring.

selectively deblocked at C-4′ and C-6′ to give the intermediate **6**. Similarly, condensation of **7** with **4** and acetylation to **8** was followed by deblocking at C-4′ and C-6′ to give the intermediate **9**. Condensation of part of **9** with **7** afforded the tetrasaccharide **10**, which was converted into the tetrasaccharide bromide **11**. Condensations of this bromide with the hydroxy compounds **9** and **6** afforded the protected heptasaccharide **12** and the octasaccharide **13**, respectively. These were deblocked to give the heptasaccharide **1** and the octasaccharide **2**, respectively.

*Sharp* and *Albersheim*[5] have shown that the synthetic heptasaccharide **1** has elicitor activity equivalent to that of the natural product, whereas **2** is less active.

Received: May 31, 1983 [Z 403 IE]
German version: *Angew. Chem. 95* (1983) 809

CAS Registry numbers:
**1**, 87102-55-4; **2**, 87102-56-5; **3**, 87102-57-6; **4**, 87102-58-7; **5**, 87114-34-9; **6**, 87102-59-8; **7**, 14213-11-2; **8**, 87102-60-1; **9**, 87102-61-2; **10**, 87102-62-3; **11**, 87102-63-4; **12**, 87114-35-0; **13**, 87226-17-3; D-glucose-3-*o*-β-D-glucopyranosyl, 34980-39-7; D-glucose-6-*o*-β-D-glucopyranosyl, 554-91-6;

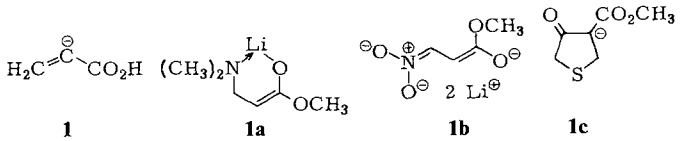
[1] P. Albersheim, B. S. Valent, *Cell Biol. 78* (1978) 627.
[2] P. Albersheim, personal communication.
[3] P. J. Garegg, T. Norberg, *Acta Chem. Scand. B33* (1979) 116; P. J. Garegg, B. Lindberg, T. Norberg, *ibid. B33* (1979) 449.
[4] P.-E. Jansson, L. Kenne, H. Liedgren, B. Lindberg, J. Lönngren, *Chem. Commun. Univ. Stockholm 1976*, No. 8.
[5] J. K. Sharp, P. Albersheim, personal communication.

 © Verlag Chemie GmbH, 6940 Weinheim, 1983 0570-0833/83/1010-0794 $ 02.50/0 

# Preparation of 2-(1-Hydroxyalkyl)acrylic Esters; Simple Three-Step Synthesis of Mikanecic Acid**

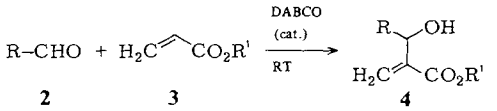
By *H. M. R. Hoffmann** and *Jürgen Rabe*

In recent years a variety of reagents and methods have been developed for generating α-acrylate synthons **1**. Reagents published during the last two years include the lithium salts **1a**[1a] and **1b**[1b] and the heterocyclic anion **1c**[1c]. Numerous older synthons have been listed by *Helquist et al.*[1a]. Many of these, however, proved to be unsatisfactory for the synthesis of specially functionalized



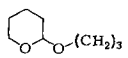
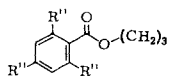
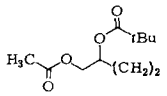
**1** **1a** **1b** **1c**

acrylic esters. We now report that acrylate esters **3** can be coupled readily at the α-position with a wide variety of aldehydes, also sensitive and functionalized representatives, in the presence of catalytic amounts of DABCO (1,4-diazabicyclo[2.2.2]octane)[2] at room temperature[3] (Table 1).



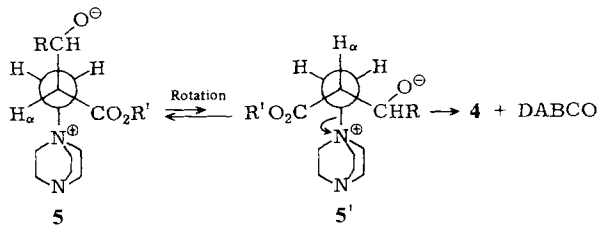
**2** **3** **4**

Table 1. DABCO-catalyzed coupling of functionalized aldehydes **2a**—**k** and acrylic esters **3** to form 2-(1-hydroxyalkyl)acrylic esters **4a**—**k** [a].

| | R | R' | *t* [b] | Yield [%] |
|---|---|---|---|---|
| **a** | $CH_3$ | *t*Bu | 7 d | 89 |
| **b** |  | Me | 7 d | 87 |
| **c** |  R''=H | Me | 7 d | 95 |
| **d** | R''=$CH_3$ | Me | 7 d | 87 |
| **e** |  | Me | 7 d | 89 |
| **f** | $Cl(CH_2)_3$ | Me | 7 d | ≈60 [c] |
| **g** | $CCl_3$ | Me | 20 h | >55 |
| **h** | $C_6H_5$ | Me | 6 d | 39 |
| **i** | 2-Furyl | Me | 18 h | 63 |
| **j** | 3-Pyridyl | Me | 4 h | >82 |
| **k** | $H_2C=C(CH_3)$ | Me | 20 d | 33 |

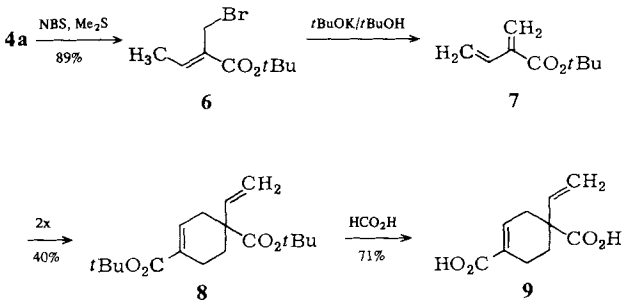
[a] All products were identified spectroscopically. Characteristically, in the $^1$H-NMR spectrum of **4** the two olefinic protons appear between $\delta=5.8$ and 6.2 as approximately two singlets which are well separated (the olefinic protons of the parent acrylic ester appear as a complex ABX system); see also ref. [5]. Yields are not optimized except for adduct **4c**; **4g**, **h**, **j**, **k** were purified by evaporating the remaining starting materials together with the solvent (oil pump) (**4h**, **j** are crystalline); **4i** was purified by chromatography. [b] Reaction mixture allowed to stand at room temperature until the aldehyde had disappeared. [c] Yield reduced by partial quaternization of DABCO.

Less reactive aldehydes such as benzaldehyde **2h** and methacrolein **2k** can also be coupled with acrylic ester. Remarkably, furfural **2i** and especially nicotinaldehyde (**2j**) react much more rapidly than the other aldehydes. We assume that reaction of **2** and **3** initially leads to formation of the intermediate zwitterion **5**, which is in equilibrium with the less favorable conformer **5'** (two gauche interactions). Only conformation **5'** allows an antiperiplanar departure of the crucial $H_\alpha$ proton and DABCO. The various proton migrations that are necessary to complete coupling, are aided by basic heteroatoms on the aldehyde as in **2j** and, less so, **2i**.



**5** **5'**

The new adducts **4** are highly versatile intermediates in organic synthesis and may be used, *inter alia*, for preparing 2-methylene-3-butenoic esters such as **7**[4]. Thus, a short and efficient route to mikanecic acid **9**[5] starts from acetaldehyde **2a** and *tert*-butyl acrylate **3**, R'=*t*Bu. The resulting ester **4a** undergoes allylic rearrangement on reaction with *N*-bromosuccinimide(NBS)/dimethyl sulfide to cleanly give the *Z*-isomer **6**. Following the lead given by *Dreiding et al.*[5] HBr was eliminated to generate *tert*-butyl 2-methylene-3-butenoate **7**, which dimerized *in situ* to the di-*tert*-butyl ester **8** of mikanecic acid. Previously, the diethyl ester of mikanecic has been saponified with base, giving mikanecic acid accompanied by monoester and diester,



**6** **7** **8** **9**

which cannot easily be separated[5a]. Thanks to the possibility of introducing two *tert*-butyl ester groups by our procedure, acid catalyzed ester cleavage in **8** is facile and clean, giving *free* mikanecic acid **9**, which is readily isolated.

Received: June 7, 1983; revised: July 18, 1983 [Z 413 IE]
German version: *Angew. Chem.* 95 (1983) 795

[*] Prof. H. M. R. Hoffmann, Dr. J. Rabe
Institut für Organische Chemie der Universität
Schneiderberg 1B, D-3000 Hannover 1 (Germany)

[**] DABCO-Catalyzed Coupling of Aldehydes with Activated Double Bonds, Part 1. This work was supported by the Fonds der Chemischen Industrie and by BASF AG, Ludwigshafen. We thank *W. Hasel* and *W. Poly* for experimental contributions.

CAS Registry numbers:
**2a**, 75-07-0; **2b**, 54911-85-2; **2c**, 22927-31-7; **2d**, 87102-03-2; **2e**, 87114-19-0; **2f**, 6139-84-0; **2g**, 75-87-6; **2h**, 100-52-7; **2i**, 98-01-1; **2j**, 500-22-1; **2k**, 78-85-3; **3** (R'=*t*-Bu), 1663-39-4; **3** (R'=Me), 96-33-3; **4a**, 87102-04-3; **4b**, 87102-05-4; **4c**, 87050-30-4; **4d**, 87102-06-5; **4e**, 87102-07-6; **4f**, 87102-08-7; **4g**, 87102-09-8; **4h**, 18020-59-2; **4i**, 87102-10-1; **4j**, 87102-11-2; **4k**, 87102-12-3; (*Z*)-**6**, 87102-13-4; **7**, 44985-61-7; **8**, 87102-14-5; **9**, 512-74-3;

 © *Verlag Chemie GmbH, 6940 Weinheim, 1983* *0570-0833/83/1010-0795 $ 02.50/0* 

[1] a) L. C. Yu, P. Helquist, *J. Org. Chem. 41* (1981) 4536; b) D. Seebach, R. Henning, T. Mukhopadhyay, *Chem. Ber. 115* (1982) 1705; c) P. G. Baraldi, A. Barco, S. Benetti, F. Moroder, G. P. Pollini, D. Simoni, V. Zanirato, *J. Chem. Soc. Chem. Commun. 1982*, 1265.

[2] Cf. A. B. Baylis, M. E. D. Hillman, *German Patent* 2155113 (1972); see *Chem. Abstr. 77* (1972) 34174q; see also K. Morita, Z. Suzuki, H. Hirose, *Bull. Chem. Soc. Jpn. 41* (1968) 2815.

[3] Typical example: (3-Formylpropyl)benzoate **2c** (19.2 g, 0.1 mol) was mixed with methyl acrylate **3** (13 g; 14 mL; 0.15 mol). After addition of DABCO (1.6 g, 0.015 mol) the resulting homogeneous mixture was allowed to stand at room temperature until **2c** was no longer detectable (*ca.* 7 days). The remaining methyl acrylate was removed on a rotary evaporator, the residue taken up in ether (100 mL) and washed with 10% aqueous hydrochloric acid (50 mL), and the ether phase washed with water and dried over $MgSO_4$. After removal of the solvent spectroscopically pure product **4c** (26.4 g, 95%) remained.—90 MHz $^1$H-NMR ($CDCl_3$, TMS): $\delta = 1.68-2.02$ (m, 4H, $CH_2CH_2$), 2.90 (bs, 1H, OH), 3.76 (s, 3H, $CH_3O$), 4.25–4.55 (m, 3H, OC*H* and $OCH_2$), 5.84 (t, $J = 1$ Hz, 1H, *H*C=C), 6.24 (s, 1H, *H*C=C), 7.32–7.60 (m, 3H, aromatic H), 7.98–8.12 (dd, $J = 7$ Hz, $J = 1.5$ Hz, 2H, aromatic H); $^{13}$C-NMR ($CDCl_3$): $\delta = 166.35$ (s, COOMe), 142.61 (s, *C*=$CH_2$), 69.70 (d, *C*HOH), 32.32 (t, CHOH–*C*$H_2$), 24.62 (t, $CH_2CH_2CH_2$), 64.40 (t, *C*$H_2$O), 124.37 (t, C=*C*$H_2$), 51.28 (q, $OCH_3$), 166.17 (s, C(O)Ph), 129.91 (s), 127.88 (d), 129.07 (d), 132.43 (d) (aromatic C).

[4] Cf. H. Düttmann, P. Weyerstahl, *Chem. Ber. 112* (1979) 3480.

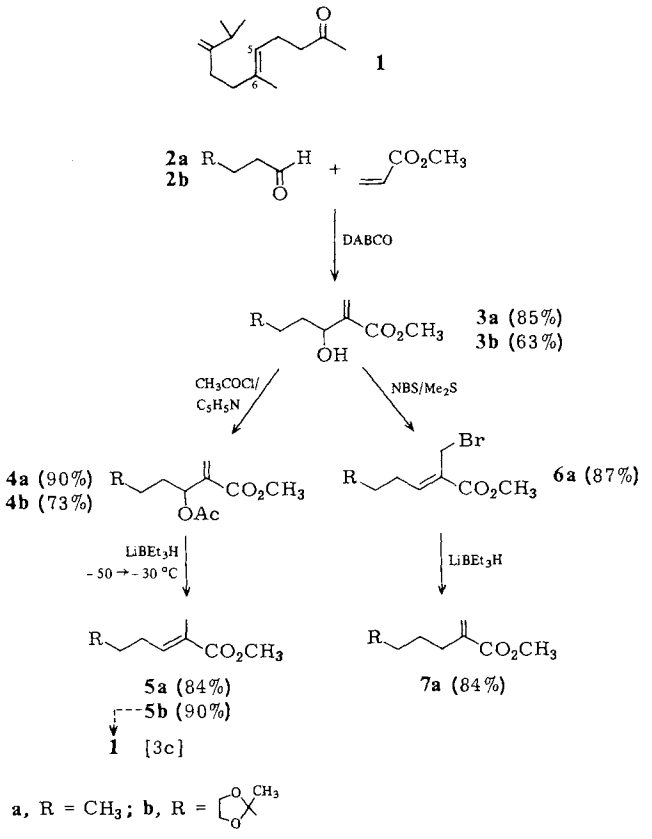
[5] a) O. Goldberg, A. S. Dreiding, *Helv. Chim. Acta 59* (1976) 1904; b) L. K. Sydnes, L. Skattebøl, C. B. Chapleo, D. G. Leppard, K. L. Svanholt, A. S. Dreiding, *ibid. 58* (1975) 2061.

## A New, Efficient and Stereocontrolled Synthesis of Trisubstituted Alkenes *via* Functionalized Acrylic Esters**

By *Jürgen Rabe* and *H. M. R. Hoffmann**

The acrylic acid moiety is an integral feature of a large number of natural products, some of which—like the sesquiterpenoid α-methylene-γ-butyrolactones and related compounds—possess useful biological activity[2]. In reduced form, acrylates are equally important and occur as allylic alcohols and related isoprene units. Described herein is a reaction sequence which starts from inexpensive aldehydes and acrylic ester, and stereoselectively affords trisubstituted olefins.

As the first of several synthetic targets for our procedure we chose novel terpenoid $C_{14}$ ketone **1**, a constituent of costus root oil and presumably a metabolite of the irones, olfactory components of the violet[3a]. A general difficulty in the synthesis of **1** and related terpenes is the stereoselective construction of the central *E*-configurated C(5)–C(6) double bond. In previous preparations of **1** this critical step proceeded with an $E:Z$ ratio of $2:1$[3a], $1.5:1$[3b] and $1.7:1$[3c]. DABCO(1,4-diazabicyclo[2.2.2]octane)-catalyzed coupling of butyraldehyde **2a** or the protected levulinic aldehyde **2b** with methyl acrylate gave adducts **3a** and **3b**, respectively, in good to excellent yield. Interestingly, the sensitive aldehyde **2b** does not—as *e.g.* in chlorinated solvents—rearrange to the isomeric acetal-ketone[4a] under these conditions. After a standard acetylation of **3a**, **b** the resulting acetates **4a**, **b** were reduced with lithium triethylhydridoborate ("Super Hydride")[4b], resulting in clean allylic transposition to give **5a**, **b**. The methoxycarbonyl group of **4a**, **b** was not attacked. Thus, this reduction is not only chemoselective, but also regio- and *trans*-selective, no *Z*-isomer being discernible by $^1$H-NMR. Sterically hindered leaving groups, such as pivaloate[4c,d] and bulky benzoates, which have been used frequently in the past to induce $S_N2'$ displacements on allylic substrates[4d], were not necessary in our case. Note also that the reaction proceeds at −50 °C, although acetate is a comparatively poor leaving group in nucleophilic substitutions. In view of the conversion of **5b** into **1** by *Morizur* and *Tortajada*[3c] the preparation of ketal-acrylic ester **5b** completes a simple *trans*-selective synthesis of **1**[5a].




In a second reaction sequence **3a** was transformed cleanly into **6a**, another useful building block which here was reduced with $LiBEt_3H$ to give **7a**. Such α-alkylacrylic esters cannot be obtained directly from acrylic esters and alkyl halides in the presence of DABCO, because the catalyst is inactivated by quaternization.

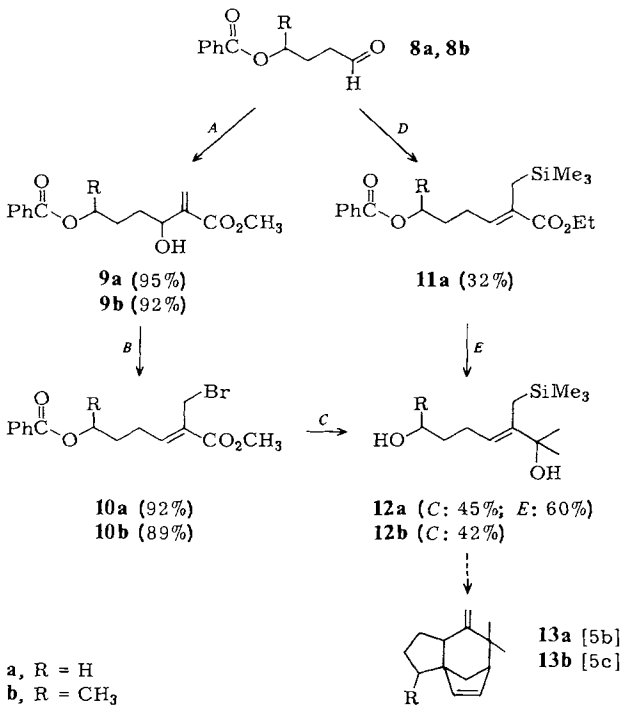
As further examples we prepared the crystalline $C_9$- and $C_{10}$-diols **12a** and **12b**, respectively; they are key precursors in the synthesis of the strained tricyclic dehydronorzizaene **13a**[5b] and dehydrozizaene **13b**[5c], respectively. In our reaction sequence **8**→**9**→**10**→**12** the allylic OH group of **9a**, **b** ist not "wasted", as in the above examples, by simple replacement with hydride ion. Step *B* proceeds *trans*-stereoselectively and in high yield; Step *C* consists in the $S_N2$-like introduction of the $Cl_3Si$ anion[5d] followed by quenching with methyllithium.

Hitherto, functionalized α,β-unsaturated acrylic esters such as **11a** have been prepared mainly by the Horner-Wittig reaction (cf. Step *D*[5b]). Starting from **8a** the Horner-Wittig route furnishes **12a** in 19% yield, a figure which could not be improved upon despite many experiments, also with other aldehydes[5b,c]. Typically, the $Z:E$ selectivity is *ca.* 4:1, and the undesired *E*-isomer, with the ester group *cis* to the alkyl chain, must be separated by column

[*] Prof. H. M. R. Hoffmann, Dr. J. Rabe
Institut für Organische Chemie der Universität
Schneiderberg 1B, D-3000 Hannover 1 (Germany)

[**] DABCO-Catalyzed Coupling of Aldehydes with Activated Double Bonds, Part 2. This work was supported by the Fonds der Chemischen Industrie.—Part 1: see [1].

 © Verlag Chemie GmbH, 6940 Weinheim, 1983 0570-0833/83/1010-0796 $ 02.50/0 




Scheme 1. *A*) acrylic ester, DABCO (cat.). RT; *B*) NBS (*N*-bromosuccinimide), $Me_2S$; *C*) 1. $HSiCl_3$, $NEt_3$, CuI, 0°C→RT [5d]; 2. 8 Equiv. MeLi, −60→0°C; *D*) **8a** was added to the Horner reagent prepared as follows: 1. $(EtO)_2P(O)CH_2CO_2Et$ + NaH in 1,2-dimethoxyethane; 2. $Me_3SiCH_2I$, 70°C, 4 h; 3. NaH, 0°C→RT, thereafter 0°C (and addition of **8a**, 0°C→RT, 16 h); *E*) 5 MeLi, −60→0°C.

chromatography. In contrast the new route is not only *trans*-selective, but uses simpler starting materials, proceeds under milder conditions, and allows a doubling of the overall yield (*ca.* 37% for the steps **8**→**9**→**10**→**12**).

Received: June 7, 1983; revised: July 18, 1983 [Z 414 IE]
German version: *Angew. Chem. 95* (1983) 796

CAS Registry numbers:
**1**, 64854-44-0; **2a**, 123-72-8; **2b**, 24108-29-0; **3a**, 18020-64-9; **3b**, 87050-26-8; **4a**, 87050-27-9; **4b**, 87050-28-0; **5a**, 16493-96-2; **5b**, 34312-78-2; **6a**, 87050-38-2; **7a**, 3070-68-6; **8a**, 22927-31-7; **8b**, 87050-29-1; **9a**, 87050-30-4; **9b**, 87050-31-5; **10a**, 87050-32-6; **10b**, 87050-33-7; **11a**, 87050-34-8; **12a**, 87050-35-9; **12b**, 87050-36-0; **13a**, 87098-85-9; **13b**, 87050-37-1; DABCO, 280-57-9; methyl acrylate, 96-33-3

[1] H. M. R. Hoffmann, J. Rabe, *Angew. Chem. 95* (1983) 795; *Angew. Chem. Int. Ed. Engl. 22* (1983) 795.
[2] See *e.g.* E. Rodriguez, G. H. N. Towers, J. C. Mitchell, *Phytochemistry 15* (1976) 1573.
[3] a) B. Maurer, G. Ohloff, *J. Chem. Soc. Chem. Commun. 1977*, 353; b) P. Dubs, H. P. Schenk, *Helv. Chim. Acta 61* (1978) 984; c) J. P. Morizur, J. Tortajada, *Tetrahedron Lett. 23* (1982) 5275; d) see also L. C. Rohela, R. C. Anand, *Indian J. Chem. 16B* (1978) 1121.
[4] a) Cf. J. A. Bulat, H. J. Liu, *Can. J. Chem. 54* (1976) 3869. Oxidation of the alcohol to the aldehyde was simplified by using buffered pyridinium chlorochromate; b) S. Krishnamurty, H. C. Brown, *J. Org. Chem. 45* (1980) 849; see also S. Krishnamurty, *Aldrichim. Acta 7* (1974) 55; c) H. J. Liu, L. K. Ho, *Can. J. Chem. 61* (1983) 632; d) review: R. M. Magid, *Tetrahedron 36* (1980) 1901.
[5] a) Newer methods for the synthesis of trisubstituted double bonds: A. Marfat, P. R. McGuirk, P. Helquist, *J. Org. Chem. 44* (1979) 3888 and references therein; J. F. Normant, A. Alexakis, *Synthesis 1981*, 841; J. E. McMurry, J. R. Matz, *Tetrahedron Lett. 23* (1982) 2723; b) H. M. R. Hoffmann, R. Henning, *Helv. Chim. Acta 66* (1983) 828; c) J. Rabe, Dissertation, Universität Hannover 1983; d) H. Nishiyama, H. Yokoyama, S. Narimatsu, K. Itoh, *Tetrahedron Lett. 23* (1982) 1267.

# BOOK REVIEWS

**Comprehensive Organometallic Chemistry.** *The Synthesis, Reactions and Structures of Organometallic Compounds.* Nine Volumes. Editors *G. Wilkinson, F. G. A. Stone, E. W. Abel,* Pergamon Press, Oxford 1982. Total *ca.* 8500 pp., bound, £ 1075.00.

*Volume 1*

The first volume (754 pp) of this exceptional work deals with the organoelement compounds of the 1st to the 3rd main groups of the periodic table. Even though the most spectacular developments since 1950 have been more in the area of the transition metals, the chemistry of the main group elements has also developed very rapidly and has stood in need of an adequate modern treatment for some time. Although the aim of the authors to provide a comprehensive coverage of a given field is of its nature unattainable, they have, nevertheless, performed an excellent service within the framework of this series.

Fourteen authors have contributed to this first volume, most of whom are especially active workers in their respective fields. Astonishingly the result is a work with a rather homogeneous style, evidently attributable to the editors. The volume begins with an informative chapter by *M. E. O'Neill* and *K. Wade* (University of Durham): Structural and Bonding Relationships among Main Group Organometallic Compounds (42 pages, 207 references). The most important structural and bonding types for organometallic compounds of the main group elements are presented using examples. Emphasis is placed on the bridge structures of the oligomeric organolithium and organoaluminum compounds, and on the polyhedral structures characteristic of the carbaboranes and metallacarbaboranes. The subsequent chapters deal with the chemistry of the individual elements: *J. L. Wardell* (University of Aberdeen): Alkali Metals (78 pages, 321 references); *N. A. Bell* (Sheffield City Polytechnic): Beryllium (34 pages, 260 references); *W. E. Lindsell* (Heriot-Watt University): Magnesium, Calcium, Strontium and Barium (98 pages, 635 references); *J. D. Odom* (University of South Carolina): Non-cyclic Three and Four Coordinated Boron Compounds (58 pages, 591 references); *J. H. Morris* (University of Strathclyde): Boron in Ring Systems (70 pages, 484 references); *G. E. Herberich* (Technische Hochschule Aachen): Boron Ring Systems as Ligands to Metals (30 pages, 90 refer-

ences); *T. Onak* (California State University): Polyhedral Organoboranes (48 pages, 247 references); *R. N. Grimes* (University of Virginia): Metallacarboranes and Metallaboranes (84 pages, 260 references); *L. J. Todd* (Indiana University): Heterocarboranes (12 pages, 71 references); *J. J. Eisch* (State University of New York): Aluminum (128 pages, 742 references); *D. G. Tuck* (University of Windsor): Gallium and Indium (52 pages, 282 references); *H. Kurosawa* (Osaka University): Thallium (29 pages, 143 references). Each chapter ends with a reference list covering the literature up to about 1980. The whole is a somewhat capricious, but nevertheless very useful compilation of very variable profundity. The compounds of Li, Mg, B, and Al are emphasized as becomes their importance. It should also be taken into account that their application in organic synthesis is the subject of most of Volume 7.

The contributions do not follow any regular pattern, but, nonetheless, regularly contain sections on the formation, structure and reactions of the compounds concerned. More detailed information concerning synthesis is still to be found in the relevant volume of "Houben-Weyl"; here, as also with "Gmelin", there is a not yet complete but updated new edition covering organoboron chemistry. A particularly valuable feature of Volume 1 of "Comprehensive Organometallic Chemistry"—and this applies to the other volumes too—is the information concerning questions of structure and bonding. Taken with the extraordinarily useful index volume the book is a regular treasure-trove and stimulates to repeated delving and reading. The stated intention of the editors to initiate new ideas and further discoveries is likely to meet with real success. The whole work is aimed at the worker engaged in basic research. Over and above this it will be a first-class source of information for all chemists and that for a long time to come. The desirable dissemination of the work is, however, impossible at a total price of more than DM 5000.—. The opportunity to buy individual volumes is, therefore, urgently necessary.

*Erwin Weiss*
Institut für Anorganische und Angewandte Chemie
der Universität Hamburg

*Volume 2*

The second volume of this nine-volume work comprises thirteen chapters dealing with very different areas of organoelement chemistry, so that the volume seems, at first sight, to be very heterogeneous. This is because of its character as a reference work which does not offer a systematic treatment of the material. However, this first impression is soon forgotten as a consequence of the quality and the independence of the individual sections.

The first four chapters are devoted to organosilicon chemistry: *D. A. Armitage* (University of London): Organosilanes (203 pages, 752 references); *T. J. Barton* (Iowa State University): Carbacyclic Silanes (99 pages, 415 references) *R. West* (University of Wisconsin): Organopolysilanes (33 pages, 136 references); *F. O. Stark et al.* (Dow Corning Corporation): Silicones (59 pages, 193 references). This arrangement seems somewhat arbitrary and naturally leads to overlapping. However, since almost every author has been successfully active in his respective field, the contributions are so stamped with a genuine understanding that their study is, nevertheless, of great value in each case. This is also particularly true for the article on the present state of silicone chemistry in industry, which emphasizes the practical importance of organosilicon compounds and summarizes the newest technical developments, briefly but informatively.

The chapters on the organometallic compounds of germanium (120 pages, 716 references) by *J. Satgé et al.* (Université Paul Sabatier, Toulouse), tin (109 pages, 722 references) by *A. G. Davies* and *P. J. Smith* (University College, London, and ITRI, Greenford) and lead (52 pages, 419 references) by *P. G. Harrison* (University of Nottingham) come likewise from laboratories which have made significant contributions to the developments discussed. Naturally only the highlights of the literature could be included: After all organotin chemistry now fills fifteen volumes of Gmelin!

The organoelement compounds of arsenic, antimony and bismuth are described (by *J. L. Wardell,* University of Aberdeen) on only 27 pages (179 references), which necessarily leads to a loss of quality. The expectations of the reader are greatly disappointed in this section; the relative importance of this area is not properly represented, a fact which affects the value of the whole work. Perhaps arsenic (and antimony) should rather have been omitted altogether.

The coinage metals copper, silver and gold are treated in a manner which takes account of the rapidly increasing importance of these elements; the first two by *J. G. Noltes* and *G. van Koten* (TNO Utrecht and University of Amsterdam and the third by *R. J. Puddephatt* (University of Western Ontario), in 55 pages (187 references) and 57 pages (227 references) respectively; here again the competence of the authors is happily apparent. The workers mentioned had already produced the previous leading monographs on the same topics. Finally, there are chapters on the organometallic compounds of zinc and cadmium (*J. Boersma,* Universität Utrecht; 40 pages, 163 references) and mercury (*J. L. Wardell,* University of Aberdeen; 116 pages, 545 references) which are certainly correctly placed alongside the coinage metals.

A concluding contribution from *P. J. Craig* (Leicester Polytechnic): Environmental Aspects of Oranometallic Chemistry (42 pages, 319 references) attempts to set out the more important aspects of the occurrence and effects of toxic (natural and anthropogenic) organometallic derivatives in the environment. Unfortunately the well-known "black sheep", mercury, lead, tin and arsenic, steal so much of the limelight that the desire for information concerning the environmental problems caused by the other elements is scarcely considered. Nevertheless, this chapter is worthy of note and is quite useful as a basis for teaching courses.

The external appearance of the volume, together with the quality of the print, are impeccable, and study is simplified by the attractive distribution of text, formulas, figures and tables. The literature is cited up to the most recent times in most of the contributions, so that this collected work will retain its topicality for some years. The inevitable transcription and typesetting errors (*e.g.* wrongly spelled names in the author index) have been kept to a minimum. Even the surname of the reviewer, which is particularly at risk, was rarely incorrectly spelled.

*Hubert Schmidbaur*
Anorganisch-chemisches Institut der
Technischen Universität München

*Volume 3*

The third volume (1384 pages) comprises ten chapters, of which the first two are devoted to general problems and the others to the organometallic compounds of the elements of the 3rd to 6th subgroups of the periodic table as well as of the lanthanoids and actinoids. This mass of ma-

terial is successfully crammed in, thanks largely to the expertise of most of the authors.

Volume 3 begins with a contribution from *D. M. P. Mingos* (Oxford University): Bonding of Unsaturated Organic Molecules to Transition Metals (88 pages, 551 references), which is mainly classified according to the type of ligands. Metal carbonyls, sandwich compounds, olefin- and alkyne-complexes, alkyl-, carbene- and carbyne-metal compounds are dealt with in separate sections. In addition, important types of reaction such as oxidative addition and reductive elimination, CO and alkene insertion, Ziegler-Natta polymerization and olefin metathesis are discussed. The author presents modern concepts in an instructive manner starting from simple bonding concepts (*e.g.* those of Dewar, Chatt and Duncanson for metal-olefin complexes) and compares the results of calculations (both ab initio and semi-empirical) with experimental data, from UPS measurements for example. Correlations, like those which emerge through the isolobal principle, are also mentioned.

*B. E. Mann* (University of Sheffield): Non-rigidity in Organometallic Compounds (83 pages, 185 references) in the second chapter deals first of all with the methods of studying fluxional structures. The extensive information that follows concerning the results obtained up to now (mostly in tabulated form) covers not only the rotation of $C_1$ (alkyl, carbene) but also of $C_n$ ligands (alkene, alkyne, di- and triene, allyl, cyclopentadienyl, arene) about the axis of the metal-ligand bond, together with intramolecular ligand exchange, the dynamics of σ-allyl and σ-cyclopentadienyl compounds, the rearrangement of $\eta^2$- to $\eta^6$-cyclic ligands (*e.g.* $C_7H_7$, $C_8H_8$, $C_8H_{10}$) at metals and, above all, the fluxional behavior of organic groups on metal clusters. Mechanistic considerations are mentioned, but their understanding requires a careful study of the cited literature.

The other eight "systematic" chapters are arranged according to the placing of the metal in the periodic table. It is pleasant to see that the elements scandium, yttrium, lanthanum as well as the lanthanoids and actinoids are not treated as exotica and pushed into a corner, but that they are given the place they now deserve. The organometallic compounds of the 4f and 5f elements have come into the sphere of general interest more than almost any other area in the last decade, and that largely because of the work of one of the authors, *T. J. Marks*. Of the remaining *ca.* 1100 pages about 280 are devoted to titanium and about 600 pages to the elements of the 6th subgroup (Cr, Mo, W); thus, the extent of this presentation alone reflects the technological importance of the organometallic compounds concerned. The flood of information (*e.g.* just on compounds derived from $(C_5H_5)_2TiCl_2$ or $Cr(CO)_6$) is also presented in part in tabular form, thus facilitating a general overview. The section on "Ziegler-Natta Catalysis" is particularly worthy of mention (pp. 475—547) and deals not only with industrially important aspects but also with the results of model studies and mechanistic considerations. It is also pleasing that even the, as yet, not so well developed fields, such as the compounds of zirconium, hafnium or of niobium and tantalum, have attracted prominent authors (such as *M. F. Lappert* and *J. A. Labinger*) who have played a leading part in the development.

The general impression given by this herculean publication: First-rate! Competent, comprehensive, well-illustrated (with, however, some superfluous ORTEP diagrams) with few printing errors (mainly in the literature references). It is to be hoped by all those who are interested—in industry and in university—that, in spite of the present miserable financial climate, this work will soon be available in all libraries.

*Helmut Werner*
Institut für Anorganische Chemie
der Universität Würzburg

*Volume 4*

The fourth volume fits perfectly into this monumental work and comprises seventeen chapters (1064 pages). *P. M. Treichel* (University of Wisconsin-Madison) describes the organometallic chemistry of manganese in a well laid out manner and with a sure nose for quality and balance (147 pages, 649 references). The treatment of the homologous elements technetium and rhenium (80 pages, 532 references) by *N. M. Boag* and *H. D. Kaesz* (University of California at Los Angeles) is of its very nature more modest but, nevertheless, competent and informative. Apart from the little studied technetium, there are numerous excellent examples of the vast differences in chemical behavior between the corresponding manganese and rhenium compounds. In view of the tidal wave of data which has poured out concerning iron since the renaissance in organometallic chemistry, the editors were well advised in their decision to divide it into five chapters. *D. F. Shriver* (Northwestern University, Evanston), *K. H. Whitmire, A. D. Johnson* (University College London), *A. J. Deeming* (University College London), *W. P. Fehlhammer, H. Stolzenberg* (University of Erlangen-Nürnberg) and *J. L. Davidson* (Heriot-Watt-University) put across the substantial essence over 400 pages (1477 references), whereby the individual treatments of iron complexes with various hydrocarbon ligands complement each other well and seldom overlap unnecessarily. The chemistry of organoruthenium compounds is divided between *M. I. Bruce* (University of Adelaide) and *M. A. Bennett* (Australian National University), who present their chosen classes of compound with experienced pens. Each of these nine contributions (Chap. 32.1—32.9) is rich in content but, thanks to the strict classification, easy to read. The chapter dealing with the chemistry of dodecacarbonyltriruthenium could be taken as a model for disciplined selection of material. The contribution by *M. A. Bennett* and *T. W. Matheson* (Chap. 32.9) gives an almost textbook review of the manifold, catalytic aspects of organometallic ruthenium complexes. Volume 4 finishes with the element osmium: *R. D. Adams* (Yale University) and *J. E. Selegue* (University of Kentucky) expertly describe, in particular, the modern aspects of this chemistry, using the same sensible classification system (carbonyl complexes, mononuclear complexes, cluster complexes) used in the previous chapters as a framework, whereby the treatment of trinuclear carbonyl derivatives is worth particular attention and is a regular treasure-trove of current results. The description of the fascinating osmium clusters of higher nuclearity (Section 33.3.6) could have been more detailed.

Not only the good scientific quality of this volume is impressive but also its presentation, with the exception of the occasional overlarge formulas (*e.g.* pp. 644, 647). The multinuclear complexes with complicated ligands, in particular, should have been drawn in perspective, which would often make understanding easier for the reader (*e.g.* pp. 899, 901, 905). The preparatively oriented chemist will sometimes miss an explicit recommendation of the best synthetic route; in this connection the key compound $(\eta^5\text{-}C_5H_5)Mn(CO)_3$ is incorrectly reported (p. 124; cf. G.

Bauer: *Handbuch der Präparativen Anorganischen Chemie*, 3rd edition, Vol. 3, p. 1866ff, Enke, Stuttgart 1982). In general, however, the fourth volume lives up to the proud record of this modern encyclopedia—indispensable for the specialist, helpful to those in related fields, a masterpiece!

*Wolfgang A. Herrmann*
Institut für Anorganische Chemie
der Universität Frankfurt am Main

*Volume 5*

The fifth volume (628 pages) of the series reviews the organometallic chemistry of cobalt (276 pages, 809 references), rhodium (264 pages, 1311 references) and iridium (88 pages, 512 references); the authors are *R. D. W. Kemmitt* and *D. R. Russel* (University of Leicester), *R. P. Hughes* (Dartmouth College) and *G. J. Leigh* and *R. L. Richards* (University of Sussex) respectively.

The chapters dealing with cobalt and rhodium compounds begin with a suitable historical retrospect. All three chapters are essentially based on the following scheme: carbonyl, carbonyl hydride, thiocarbonyl, carbon disulfide, isocyanide, nitrosyl complexes, divided each time into mono- and multi-nuclear compounds, then follow the complexes with σ-bonded hydrocarbons (alkyl and aryl compounds), carbene, alkylidene as well as carbyne and alkylidyne complexes and then, finally, the compounds with π-bonded hydrocarbons, classified according to the number of carbon atoms which are bonded to the metal (alkene, alkyne, allyl, diene and cyclobutadiene, cyclopentadienyl, arene ligands). The individual sections are, in the main, subdivided according to preparation, structure, properties and the reactivities of the compounds. The literature is covered for the 25 years up to the end of 1979 together with some references from 1980. Organocobalt(III) systems (cobaloximes) are discussed in detail as models for vitamin $B_{12}$. The many tables (more than 100) in which analogous compounds are summarized together with their methods of preparation, spectroscopic data (IR, NMR) are particularly valuable, as are the large numbers (1816) of clear illustrations of formulas and schemes concerning the structure, synthesis and reactivities of the compounds. Catalytic aspects are treated only briefly; these are dealt with in Volume 8.

This series illustrates once more the stormy development of organometallic chemistry since the discovery of ferrocene. The authors and editors have performed excellent work in their critical sifting of the immense body of results, it could scarcely have been done better. Volume 5 is at the moment probably the best source of information in its field for both newcomer and initiate. A treasure-trove of stimulation and, without question, a standard work for every library.

*Wolfgang Beck*
Institut für Anorganische Chemie
der Universität München

*Volume 6*

Two thirds of the sixth volume (1114 pages) are filled with complexes of the Ni, Pd, Pt triad. The rest is devoted to compounds containing heteronuclear bonds between different metals.

All three chapters concerning the organometallic chemistry of nickel, palladium and platinum are written by well-known authors, who had already made names for themselves in the early seventies with monographs devoted to their favorite metal. This explains, on the one hand, the retention with only slight modifications of the well-established classification of the material and, on the other hand, the concentration on the latest results and tendencies. Thus in the first chapter (231 pages, 50 tables), *P. W. Jolly* (Max-Planck-Institut für Kohlenforschung, Mülheim a. d. Ruhr) has deliberately built upon the foundations of Volume 1 of *"The Organic Chemistry of Nickel"* (*P. W. Jolly* and *G. Wilke*, Academic Press, New York 1974); in many of the tables it is noted that earlier work is reviewed in this book. Also the second chapter (237 pages, 13 tables) written by *P. M. Maitlis*, (University of Sheffield), *P. Espinet* (University of Saragossa) and *M. J. H. Russell* (Johnson Matthey Research Centre) is obviously built on the foundations of Volume One of *"The Organic Chemistry of Palladium"* (*P. M. Maitlis*, Academic Press, New York 1971). Similarly in the third chapter (289 pages, 47 tables) *F. R. Hartley* (Royal Military College of Science, Shrivenham) can refer to his monograph *"The Chemistry of Platinum and Palladium"* (Applied Science, London 1973). These contributions are excellently written and well illustrated by formulas; the density of information is very high. Although members of a large team the authors have been able to retain their own personal styles and their individual methods of presentation. Thus, the fifty tables of the first chapter give a quick picture of the known organonickel complexes (with appropriate references). In contrast the tables in both the following contributions serve more to present spectroscopic and other data pertaining to selected palladium and platinum complexes. The chapters on nickel and palladium offer the literature references portionwise at the end of each of the nine sections, while for the chapter on platinum they are collected together into one comprehensive list (1702 references). The fact that the editors did obviously not try to exert a levelling influence on their authors makes a favorable impression; the three individual chapters can certainly be considered as small, independent monographs. (Incidentally the use of nickel and palladium in organic synthesis is described separately in Chapter 8.)

In the last part of Volume 6 the dilemma becomes evident which is necessarily faced on considering the systematics of complexes with two or more different metals, as long as the chemistry of organometallic compounds is classified according to the metal. The problem of heteronuclear compounds has, however, been elegantly solved—without arbitrary definitions of priority. Compounds with heteronuclear bonds between transition metals are dealt with in a detailed chapter (115 pages, 13 tables) by *D. A. Roberts* and *G. L. Geoffroy* (Pennsylvania State University); the emphasis is not on individual complexes but on general synthetic procedures, spectroscopic methods and the (at the moment rather sparse) investigations of reactivity. The main body of information is collected in three long tables at the end of the chapter, which—divided into binuclear complexes, oligomeric compounds and clusters—contain data on all heteronuclear complexes with at least one bond between two different transition metals known before August 1980. These tables and the pertinent references take up 49 pages (42% of the total chapter); they seem likely to become a much cited literature source, since heterometal complexes are of topical importance as potential catalysts. However, it is by no means easy to confirm unequivocally the presence of a metal-metal bond in all cases. The last three chapters offer reviews, taking up 235 pages, of multinuclear complexes, where the bonding of a transition metal occurs to a representative element, such as boron (*K. B. Gilbert, S. K. Boocock*, and *S. G. Shore*, Ohio

State University), aluminum, gallium, indium, and thallium (*S. K. Boocock* and *S. G. Shore*), mercury, cadmium, zinc and magnesium (*J. M. Burlitch*, Cornell University) or silicon, germanium, tin and lead (*K. M. Mackay* and *B. K. Nicholson*, University of Waikato). The order of the sections is not particularly evident. The separation of boron (Chap. 41.1; 67 pages, 22 tables, 289 references) is justified by the structural variety of the boron-containing ligands; structures with up to 18 boron atoms are described. In comparison with boron the organometallic chemistry of its heavier homologues is significantly restricted, although many interesting bond types occur.

*Max Herberhold*
Laboratorium für Anorganische Chemie
der Universität Bayreuth

*Volume 7*

Volume 7 (729 pages) of the series is devoted to the use of organometallic reagents in organic synthesis. Lithium-, alkali- and alkaline earth-containing reagents are dealt with by *B. J. Wakefield* (University of Salford), and the application of organoboron compounds by authors from *H. C. Brown*'s school, namely *E. I. Negishi* (Purdue University) and *M. Zaidlewicz* (N. Copernicus University, Thorn). Organoaluminum compounds are reviewed by *J. R. Zietz, G. C. Robinson* and *K. L. Lindsay* (Ethyl Corporation), while the use of thallium compounds is dealt with by the protagonists of the field, *R. McKillop* (University of East Anglia) and *E. C. Taylor* (Princeton University). A further chapter is devoted to a comprehensive treatment of organosilicon compounds by *P. D. Magnus, T. Sarkar* and *S. Djuric* (Ohio State University). The work concludes with an overview of the applications of zinc, cadmium, mercury, copper, silver and gold compounds in organic synthesis by *W. Carruthers* (University of Exeter). Of the monohapto organometallic derivatives which have acquired wider preparative importance, those of tin and titanium are notably absent.

The volume is divided according to the key metals and to the reagents derived from them. This classification principle assumes that the reader already has a basic knowledge of the typical reactivities of these reagents. For, if he does not know, *e.g.*, that alkyl cuprates add particularly well to alkynes, when searching for such a reaction he is unlikely to stumble across it in Chapter 49, whether he uses the index or not. On the hand, if already armed with this knowledge before consulting the present volume, he will find a concise and precise exposition of the possibilities and limits for the use of the well-known homo- and hetero-cuprates and analogous copper(I) derivatives, which is precisely the information that is of help to him as a potential user. Such assistance is necessary in view of the enormous progress made in the last 25 years with organometallic reagents in organic synthesis: A look at the detailed documentation of "Houben-Weyl" or "Gmelin" in the case of organoboron chemistry illustrates how extensive the results already are. This is just where the utility of the present volume becomes apparent; it enables one to quickly familiarize oneself with the areas it deals with. Commendable are the chapters on organolithium, organoboron and organosilicon compounds; despite the flood of original publications cited they are still comprehensible and readable. Individually the text and the formulas make up a well balanced whole, and the numbers of mistakes in the formulas are minimal. Most of the chapters are written in such a manner as to stimulate voluntary reading which is rewarded with information and ideas that had previously been overlooked. The editors have, therefore, fulfilled their intention of creating a compendium which is very stimulating to study. Since this volume provides an ideal method of quick orientation in the application of organometallic reagents to organic synthesis, most organic chemists would be pleased to have at hand, if not the whole series, at least Volumes 7 and 8. However, only a few of them are likely to have a patron in the background and so most of them will have to use the well-thumbed library copy.

*Reinhard W. Hoffmann*
Fachbereich Chemie der Universität Marburg

*Volume 8*

The eighth volume (1106 pages) contains the following contributions: *R. P. A. Sneeden* (C.N.R.S., Villeurbanne): Preparation and Purification of Carbon Dioxide and Carbon Monoxide (17 pages, 44 references); *R. P. A. Sneeden:* Organic Syntheses where Carbon Monoxide is the Unique Source of Carbon (82 pages, 343 references); *I. Tkatchenko* (C.N.R.S., Villeurbanne): Synthesis with Carbon Monoxide and a Petroleum Product (123 pages, 185 references); *R. P. A. Sneeden:* Reactions of Carbon Dioxide (58 pages, 202 references); *B. R. James* (University of British Columbia): Addition of Hydrogen and Hydrogen Cyanide to Carbon-Carbon Double and Triple Bonds (85 pages, 525 references); *W. Keim, A. Behr, M. Roeper* (Technische Hochschule Aachen): Alkene and Alkyne Oligomerization Cooligomerization and Telomerization Reactions (91 pages, 491 references); *H. B. Kagan* (Université Paris-Sud): Asymmetric Synthesis using Organometallic Catalysts (36 pages, 125 references); *R. H. Grubbs* (California Institute of Technology): Alkene and Alkyne Metathesis Reactions (53 pages, 146 references); *C. U. Pittman Jr.* (University of Alabama): Polymer Supported Catalysts (58 pages, 346 references); *P. W. Jolly* (Max-Planck-Institut für Kohlenforschung, Mülheim a. d. Ruhr): Organonickel Compounds in Organic Synthesis (182 pages, 1210 references); *B. M. Trost, T. R. Verhoeven* (University of Wisconsin and Merck, Sharp and Dohme Research Laboratories, Rahway): Organopalladium Compounds in Organic Synthesis and in Catalysis (140 pages, 805 references); *A. J. Pearson* (University of Cambridge): Organoiron Compounds in Stoichiometric Organic Synthesis (73 pages, 231 references); *W. E. Watts* (New University of Ulster): The Organic Chemistry of Metal-coordinated Cyclopentadienyl and Arene Ligands (59 pages, 355 references); *J. R. Dilworth, R. L. Richards* (A.R.C. Unit of Nitrogen Fixation, University of Sussex): Reactions of Dinitrogen Promoted by Transition Metal Compounds (34 pages, 119 references).

As can be seen from the list of contents, Volume 8 is mainly concerned with very topical applications of transition metal compounds, both as stoichiometric reagents and as catalysts in organic synthesis. In spite of the size of the volume and the fact that two related chapters (Ziegler-Natta catalysis and the catalytic applications of ruthenium complexes) are dealt with in other volumes (3 and 4) of the work the perspective is incomplete. Some topics, *e.g.* oxidation, isomerization, rearrangement reactions and other synthetic steps with organometallic compounds of the first row transition metals, are only dealt with (if at all) in a cursory manner. The division of the contents into chapters that describe either reaction types or the use of particular metals results in some repetition and overlapping; this,

however, is not serious. The individual contributions are from competent authors. The already enormous numbers of references at the ends of the chapters are further augmented by references in the many tables. The patent literature is also included.

The three most important aspects of the product-orientated application of transition metal compounds are expounded upon: catalytic reactions, the modes of action of metal catalysts and reactions at coordinated organic (and inorganic) ligands; stereochemical aspects are discussed.

It is not possible to say that this volume is indispensable, because there are many excellent monographs which cover some of the topics discussed. However, because of the choice of the contributions, their quality, and the growing interdisciplinary importance of the material, this work will be an enrichment for every chemical library and an invaluable aid for many chemists.

*Giambattista Consiglio*
Technisch-chemisches Laboratorium der ETH Zürich

*Volume 9*

The ninth, last and thickest volume (1570 pages) of the series is intended to make the information in the other eight volumes easily available on the basis of several search criteria. The user has the choice of five indexes for this purpose: Subject Index (440 pages), Formula Index (382 pages), Author Index (386 pages), Index of Structures Determined by Diffraction Methods (312 pages), Index of Review Articles and Specialist Texts on Organometallic Chemistry (50 pages).

The Subject Index encompasses 30000 key-words, the Formula Index more than 32000 typical compounds with at least one metal-carbon bond ($\sigma$ or $\pi$; classified according to a modified Hill system). The Author Index contains more than 30000 names from about 40000 literature references. The two following indexes can be used independently of the main work and constitute a useful addition. Thus, the Structure Index compiled by *M. I. Bruce* (University of Adelaide) is a guide to thousands of organometallic structures elucidated during the period from 1927 to 1981 by X-ray, neutron or electron diffraction. Finally, interdisciplinary interest is excited by the presentation of a multifaceted collection of secondary and tertiary literature (*G. B. Young,* Imperial College of Science and Technology, University of London) covering all aspects of the chemistry of organometallic compounds.

All in all the chemist who works in university or in industry, or who sits at an editor's desk has had placed in his hands an extremely useful (yet very expensive and "unelectronic") tool.

*Otto Smrekar*
Angewandte Chemie, Weinheim

**Experimental Methods in Photochemistry and Photophysics.** By *J. F. Rabek.* John Wiley, Chichester 1982, 2 Volumes together 1098 pp., bound, £ 89.95

This book made a good impression on me at first glance. The many illustrations awoke the expectation that here a really versatile and experienced experimentalist had written something useful for experimental work in photochemistry and photophysics. Closer inspection quickly revealed, however, that the author is by no means an experienced experimentalist, but that, following a doubtful plan, he has made a book out of a heterogeneous literature collection.

The aims of this book and the way in which it has been made are set out by the author in the preface: "...This book is an up-to-date survey of the majority of available methods and commercially available equipment applied in the study of photochemical and photophysical reactions. Each major topic is introduced separately and is self-contained.... The material collected in this book has been prepared from hundreds of books, papers, catalogues and private information from laboratories round the world and from my own twenty years experience in experimental work in the photochemistry of polymers. My task was limited to the selection and arrangement of respective information to assist scientists, people from industry and students working in the field of experimental photochemistry and photophysics ...".

The sources of the material in the book can actually be identified as (1) catalogues, (2) books and (3) journals, because the source of each figure or table is usually (but not always) cited. The book also contains material that (4) cannot be traced to a single source or (5) does not refer to experimental methods.

(1) *Catalogs:* Here the author is, de facto, advertising for particular manufacturers. He does not shrink from using their texts as well as their illustrations and tables. Examples: Chapter 4, "Optical Systems", is largely identical with the catalog "Optics Guide" issued by the Melles Griot company, and Chapter 12.2.2, "Photomultiplier Tubes", is, to a large extent, identical with the catalog of the same name issued by the Hamamatsu company. The fact that there are also competing companies, here, for instance, Oriel, RCA and EMI, goes unmentioned.

(2) *Books:* Here the author seems to have inhibitions about reproducing texts without alterations. If he has nothing to add himself then he alters about every other sentence slightly, whereby the text is sometimes weakened or even falsified. Example: Chapter 27.2.2.1, "Potassium Ferrioxalate Actinometer", is, essentially, identical with chapter 7-4B-2 of the book "Photochemistry" by *Calvert* and *Pitts.* The names *Parker* and *Hatchard* are not mentioned in this book (names are not mentioned in the text, on principle) and of the two investigations cited in the original, the author cites only the first. The original sentence "The solid can be stored in the dark for long periods of time without change" has been altered in "the reagent can be stored in a dark bottle for long periods of time." The original sentence "Parker and Hatchard recommended that ... a standard calibration graph ... be prepared" has been altered in "for the preparation of a calibration graph ... it is necessary to prepare a standard calibration graph".

(3) *Journals:* Here the author usually limits himself to reproducing figures and tables with a few lines of text as commentary. Example: Chapter 19.3.3, "Frequency Mixing Technique (Part II)", reports on two publications, [1] "Generation of Vacuum Ultraviolet Radiation in Phase-Matched Cd Vapor", A. H. Kung et al., *Phys. Rev. Lett. 29* (1972) 985, and [2] "Tunable Coherent Vacuum-Ultraviolet Generation in Atomic Vapors", R. T. Hodgson et al., ibid. *32* (1973) 343. What has *Rabek* made out of these publications? The commentary is only 12 lines long. The physical basis of the method is not explained. Fig. 1 is taken from both [1] and [2] and *altered* without specific mention. The reader is left to assume that these are the original figures. The alteration in Fig. 1 of [1] has resulted in the loss of the important words "heat pipe oven" and the vacuum UV detection part. In Fig. 1 from [2] part of the block diagram of

the experiment has been altered and thereby made unintelligible; further, a "Glan Prism" has been turned into a "Glen Thompson Prism" (does *Rabek* think that *Thompson*'s christian name was Glen?), "Sr Oven" has become "heat pipe oven", and the nitrogen laser wavelength, the mention of the opposite circular polarizations of the dye laser beams and the detection part have been lost. Apart from this the mutilated figures take up more than twice as much space in the book as the original figures. *Rabek* took Table 1 out of [2], but left out a line, thus making the following line of the table unintelligible.—For comparison it should be mentioned that a competent author like *Demtröder* describes the same two publications also on two pages, but in such a manner that the reader receives a reasonable idea of the principle and the realization of the method (W. Demtröder: Laser Spectroscopy—Basic Concepts and Instrumentation, Springer 1981, pp. 366 and 367).

(4) *Multiple Sources:* Chapter 10.1 "Spectrometers" and Chapter 10.2 "Monochromators" may be taken as examples. *Rabek* has used the catalog "Das PI-Optische System" issued by Physik Instrumente GmbH to illustrate the construction of various types of spectrometers. On p. 193 of this catalog there are diagrams of five spectrometers. For three of them photographs show how they can be realized by using PI components. For typographical reasons the diagrams and the photographs are not printed side by side. *Rabek* did not notice this and proceeded to make two mistakes: Fig. 10.8 shows the catalog figure E instead of G, and Fig. 10.12 shows G; the photograph that ought to be shown in Fig. 10.12, does not at all exist in the catalog. The section 10.1.5, "Diffraction Gratings" is scanty. It is not even properly explained what is meant by the blaze angle of a diffraction grating. The probably most important manufacturer of optical diffraction gratings, the Jobin Yvon company, is not even mentioned and naturally neither is the instructive handbook on ruled and holographic diffraction gratings, published by this company. *Rabek*'s incompetence reveals itself in Chapter 10.2 "Monochromators". In Fig. 10.16 two setups are shown that are purported to illustrate a prism and a grating monochromator. What one sees, however, is something that looks like a prism spectrograph, and a transmission grating set up, with just the zeroth order going through the exit slit (both setups with lens optics). Nothing is said about the two normal types of grating drive (sine drive for linear wavelength change and cosecant drive for linear wavenumber change), nothing about problems with stray light, multiple diffraction, higher order diffraction, *etc.* Ten monochromator types are listed, four of them with incorrect spelling. This enumeration is useless anyway because nothing is said about the peculiarities of each monochromator type. The twelve literature references are, for the most part, useless: eight refer to special constructions for the vacuum ultra-violet and for space applications; the remaining four refer to an application of the smallest Jobin Yvon concave-grating double-monochromator, a publication from 1965 and two commercial leaflets. The Jobin Yvon company is not even mentioned here, although it produces the largest range of grating monochromators, and although its "high luminosity" concave grating monochromator should be suitable for many photochemical investigations.

(5) Even the two nonexperimental chapters 1 and 20 contain errors and many inaccuracies. In 1 "Nature and Properties of Light", the wave number $\bar{\nu}$ is defined as $(\text{wavelength})^{-1}$ instead of $(\text{wavelength in vacuo})^{-1}$. In Chapter 20, "Electronically Excited States" p. 732, final paragraph, it says: "In an isolated molecule in a very dilute *solution* ($\sim 10^{-6}$ M) or in low-pressure vapor, the fluorescence occurs from the vibronic state ($S_1^\dagger$) initially excited or ..." Thus the exact opposite of *Kasha's rule* is maintained.

An annotated list of all the mistakes and deficiencies would add another volume to the two that have been published. The author has failed to achieve a single one of his aims. Because of the arbitrary choice of manufacturers and the uncritical representation, the book offers no assistance in the purchase of a piece of equipment. It is not up-to-date, because often the very limited capability of a particular commercial instrument is identified with the state of the art. It is useless as a laboratory handbook, because one must be always prepared for a distorting account of the original literature. The book is only of limited use as a collection of literature references, as was illustrated by the example in (4). In conclusion my advice is not to buy this book, not to read it and not to quote it (always read and quote the original publications) and to warn students explicitly about it.

*Bernhard Nickel* [NB 596 IE]
Max-Planck-Institut für
Biophysikalische Chemie, Göttingen

**Advanced Sugar Chemistry. Principles of Sugar Stereochemistry.** By *R. S. Shallenberger.* Ellis Horwood Ltd., Chichester 1982. xx, 323 pp., bound, £ 31.50

The title of this book is somewhat misleading because it suggests to the reader a general treatment of advanced sugar chemistry; the subtitle "Principles of Sugar Stereochemistry" describes the book's content much better. It does not constitute a rival to the well-established textbooks; *Shallenberger* describes rather more the structure of carbohydrates, steric questions and connections such as conformational relationships. With the exception of the phenomenon of mutarotation none of the reactions of saccharides are mentioned, so that the book is in competition with the well-known work "Stereochemistry of Carbohydrates" by *Stoddart* that appeared in 1971 and, at the time, filled an important gap. If the books are compared with each other then that by Stoddart is seen to have the greater depth in places. *Shallenberger*'s book is, in that the material has gelled in the last ten years, better constructed didactically. It is easier to read and patiently introduces the beginner to the complicated stereochemical questions of carbohydrate chemistry.

Chapters 1 to 3 deal with nomenclature, structure and development of the monosaccharides, with stereochemical questions particularly the question of chirality well to the fore. Acyclic systems and their properties are discussed in Chapter 4. Chapters 5 and 6 explain the semiacetal construction of sugars and describe the attendant conformational complications in detail. The optical activity and structure of sugars are brought together in an excellent and detailed manner in Chapter 7. Chapter 8 deals extensively with mutarotation and anhydride formation. Chapter 9 contains many oligosaccharide formulas. It is a fault, however, that there is no discussion of oligosaccharide conformations, a topic which has particularly developed in the last few years. It is debatable whether Chapter 10 on the sweetness of sugars is necessary, since this topic is very speculative at the moment.

All in all the book is very suitable for chemists who are not directly involved with carbohydrate chemistry or for

biochemists and biologists who want an introduction to stereochemistry and the effects it causes. The often difficult or obscure relationships and connections are set down with almost moving patience, which greatly eases the process of understanding them.

*Hans Paulsen* [NB 598 IE]
Institute für Organische Chemie
und Biochemie der Universität Hamburg

**Recent Books**

**The following books have been received by the editor. All the publications listed are available through W & P Buchversand für Wissenschaft und Praxis, Boschstrasse 12, D-6940 Weinheim (Federal Republic of Germany). Tel. (06201) 606-0, Telex 465516 vchwh d, Telefax (06201) 602328.**

**Structure and Dynamics: Nucleic Acids & Proteins.** Edited by *E. Clementi* and *R. H. Sarma*. Adenine Press, Guilderland 1983. xi, 487 pp., bound, $ 49.00.—ISBN 0-940030-04-7

**Advances in Infrared and Raman Spectroscopy. Vol. 10.** Edited by *R. J. H. Clark* and *R. E. Hester*. John Wiley, Chichester 1983. xv, 454 pp., bound, $ 99.00.—ISBN 0-471-26216-1

**NMR and Chemistry. An Introduction to the Fourier Transform-Multinuclear Era.** 2nd Edition. By *J. W. Akitt*. Chapman & Hall, Ltd., London 1983. xiii, 263 pp., paperback, £ 7.95 (bound, £ 17.50).—ISBN 0-412-24020-3 (0-412-24010-6)

**Controlled Release Delivery Systems.** Edited by *T. J. Roseman* and *S. Z. Mansdorf*. Marcel Dekker, Basel 1983. xv, 402 pp., bound, SFr 153.00.—ISBN 0-8247-1728-7

**Pesticide Chemistry. Human Welfare and the Environment.** In four volumes. Edited by *J. Miyamoto* and *P. C. Kearney*. Pergamon Press, Oxford 1983.—**Vol. 1: Synthesis and Structure-Activity Relationships.** ix, 383 pp., bound.—**Vol. 2: Natural Products.** ix, 372 pp., bound.—**Vol. 3: Mode of Action, Metabolism and Toxicology.** xi, 569 pp., bound.—**Vol. 4: Pesticide Residues and Formulation Chemistry.** xi, 429 pp., bound.—£ 195.00 (complete 4 volumes).—ISBN 0-08-029219-4 (Vol. 1: 0-08-029222-4, Vol. 2: 0-08-029223-2, Vol. 3: 0-08-029224-0, Vol. 4: 0-08-029225-9)

**Chemistry and Technology of Water-Soluble Polymers.** Edited by *C. A. Finch*. Plenum Press, New York 1983. xvi, 358 pp., bound, $ 55.00.—ISBN 0-306-41251-9

**Advances in Chromatography. Vol. 21.** Edited by *J. Calvin Giddings, E. Grushka, J. Cazes,* and *P. R. Brown*. Marcel Dekker, Basel 1983. xvi, 341 pp., bound, SFr 148.00.—ISBN 0-8247-1679-5

**Metal Ions in Biological Systems. Vol. 15: Zinc and its Role in Biology and Nutrition.** Edited by *H. Sigel*. Marcel Dekker, Basel 1983. xxii, 493 pp., bound, SFr. 198.00.—ISBN 0-8247-1750-3

**Information Theoretic Indices for Characterization of Chemical Structures.** By *D. Bonchev*. Research Studies Press, Chichester 1983. xiv, 249 pp., bound, £ 29.40.—ISBN 0-471-90087-7

**Progress in Analytical Atomic Spectroscopy. Vol. 5.** Edited by *C. L. Chakrabarti* and *R. E. Sturgeon*. Pergamon Press, Oxford 1983. v, 478 pp., bound, £ 63.00.—ISBN 0-08-030418-4

**The Chemistry of Functional Groups. Supplement C: The chemistry of triple-bonded functional groups. Part 1 and 2.** Edited by *S. Patai* and *Z. Rappoport*. Wiley Interscience, Chichester 1983. Part 1: xiv, pp. 1—736/Part 2: xiv, pp. 737–1522, bound. complete £ 199.00.—ISBN Part 1: 0-471-28030-5, Part 2: 0-471-28031-3, complete 0-471-28032-1

**Organic Synthesis. Concepts, Methods, Starting Materials.** By *J. Fuhrhop* and *G. Penzlin*. Verlag Chemie, Weinheim 1983. xi, 355 pp., bound, DM 78.00.—ISBN 3-527-25879-5

*Registered names, trademarks, etc. used in this journal, even without specific indication thereof, are not to be considered unprotected by law.*

© Verlag Chemie GmbH. D-6940 Weinheim, 1983. - Printed in the Federal Republic of Germany by Zechnersche Buchdruckerei, Speyer/Rhein.

All rights reserved (including those of translation into foreign languages). No part of this issue may be be reproduced in any form - by photoprint, microfilm, or any other means - nor transmitted or translated into a machine language without written permission from the publishers. Only single copies of contributions, or parts thereof, may be reproduced for personal use. Copies reproduced and used other than for private purposes in an industrial or commercial undertaking are subject to copyright and, in such cases, a copyright fee must be paid to the VG WORT, Abteilung Wissenschaft, Goethestr. 49, 8000 München 2, from whom conditions of payment can be obtained on request.

**Valid for users in the USA:** The appearance of the code at the bottom of the first page of an article in this journal (serial) indicates the copyright owner's consent that copies of the article may be made for personal or internal use, or for the personal or internal use of specific clients. This consent is given on the condition, however, that the copier pay the stated per-copy fee through the Copyright Clearance Center, Inc., for copying beyond that permitted by Sections 107 or 108 of the U.S. Copyright Law. This consent does not extend to other kinds of copying, such as copying for general distribution, for advertising or promotional purposes, for creating new collective works, or for resale. For copying from back volumes of this journal see 'Permissions to Photo-Copy: Publisher's Fee List' of the CCC.

**Editorial office:** Pappelallee 3, D-6940 Weinheim, Federal Republic of Germany, Telephone (06201) 602315, Telex 465516 vchwh d, Telefax (06201) 602328.

**Editors:** *P. Gölitz, I. G. Neil, O. Smrekar, A. Stimson.*

**Publishers:** Verlag Chemie GmbH. (Managing Directors: *Prof. Dr. Helmut Grünewald* and *Hans Dirk Köhler*), Pappelallee 3, D-6940 Weinheim, Federal Republic of Germany.

Correspondence concerning advertisements should be addressed to Verlag Chemie GmbH. (Advertising Manager *R. J. Roth*), Boschstr. 12, P.O. Box 1260/1280, D-6940 Weinheim, Federal Republic of Germany, Telephone Weinheim (06201) 602-0, Telex 465516 vchwh d, Telefax (06201) 602328.

ANGEWANDTE CHEMIE
International Edition in English
Volume 22 · Number 11
November 1983
Pages 805–896

# From Studies of Biochemical Mechanism to Novel Biological Mediators: Prostaglandin Endoperoxides, Thromboxanes, and Leukotrienes (Nobel Lecture)**

By Bengt Samuelsson*

## 1. Introduction

Following the completion of the structural work on the prostaglandins with *Sune Bergström et al.* (for review articles see [1–3]), I was very fortunate to be able to spend a year in the Chemistry Department at Harvard University, Cambridge, MA. During this stay I had the opportunity of studying both theoretical and synthetic organic chemistry. The year in Cambridge had a profound effect on my future research. At this time *Konrad Bloch, E. J. Corey, Frank Westheimer, Robert B. Woodward,* and several other prominent scientists were among the faculty members of the department, and it was indeed a stimulating place for a young doctor of medicine interested in chemistry. I worked in *E. J. Corey*'s laboratory, and we have continued to collaborate in several areas ever since.

In 1964 it was established that there was a biogenetic relationship between polyunsaturated fatty acids and prostaglandins[4,5]. This finding was of considerable biological interest, and, since the mechanisms of the reactions involved were unknown, I decided to study this problem in my newly established laboratory.

## 2. Mechanism of Biosynthesis of Prostaglandins

The conversion of 8,11,14-eicosatrienoic acid into prostaglandin $E_1$ ($PGE_1$) involves introduction of two hydroxyl groups and one keto group. Incubation of 8,11,14-eicosatrienoic acid in an atmosphere of $^{18}O_2$ showed that the oxygen atoms of the hydroxyl groups were derived from oxygen gas, whereas the keto oxygen did not contain any $^{18}O$[6,7]. That this was due to oxygen exchange between the keto group and water was shown later[8]. In these studies the keto group was reduced immediately with $BH_4^-$, and the resulting trihydroxy acid derivative was shown to contain three $^{18}O$ atoms. These experiments were extended by carrying out the reaction in a $^{18}O_2/^{16}O_2$ mixture[8]. The reduced product was converted into the trimethoxy derivative, and the side chain carrying a hydroxyl group was cleaved off by oxidation with permanganate/periodate. The resulting dicarboxylic acid ester contained the two oxygen atoms that were introduced into the five-membered ring during the biosynthesis. Analysis of this molecule by mass spectrometry showed that the ring contained either two atoms of $^{18}O$ or two atoms of $^{16}O$, and that molecules with one atom of $^{18}O$ and one atom of $^{16}O$ in the ring were virtually absent. The experiment demonstrated that the oxygen atom of the C-11 hydroxyl group and of the C-9 keto group originated from the same molecule of oxygen (Fig. 1).

It was also shown that the hydrogen atoms at C-8, C-11, and C-12 remain fixed during the conversion of 8,11,14-eicosatrienoic acid into $PGE_1$, which is in agreement with the proposed mechanism. Experiments with the hypothetical intermediates, 15-hydroperoxy-8,11,13-eicosatrienoic acid and 15-hydroxy-8,11,13-eicosatrienoic acid, indicated that the initial reaction consisted of the introduction of the oxygen atoms into the ring[9,10]. However, two mechanisms seemed possible[9–11]: either the oxygen is added across C-9 and C-11 with concomitant formation of the new carbon-carbon bond between C-8 and C-12, or a lipoxygenase-like reaction is involved with formation of 11-hydroperoxy-8,12,14-eicosatrienoic acid in the initial step. In both pathways leading to the cyclic intermediate one hydrogen atom at C-13 is removed. In the second pathway the initial step

[*] Prof. Dr. B. Samuelsson
Department of Physiological Chemistry
Karolinska Institutet, S-10405 Stockholm (Sweden)

[**] Copyright © The Nobel Foundation 1983. – The Nobel Foundation is thanked for permission to print this article.

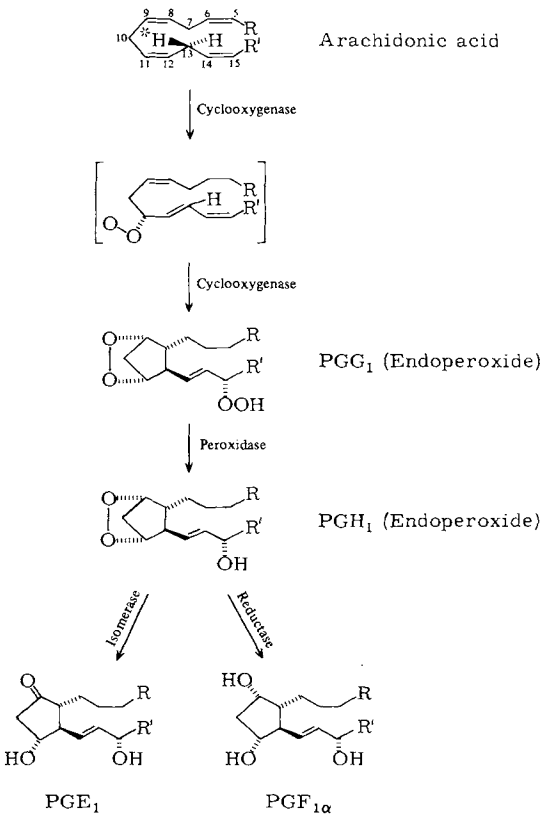



Fig. 1. Mechanism of prostaglandin biosynthesis based on the conversion of 8,11,14-eicosatrienoic acid. R = $(CH_2)_3COOH$, R' = $(CH_2)_4CH_3$.

probably involves removal of the hydrogen atom at C-13, whereas removal of this hydrogen atom occurs later in the first pathway. It was thus conceivable that removal of the hydrogen was the rate-determining step, and that substitution of tritium for hydrogen in the precursor should produce a kinetic isotope effect. In the second pathway the resulting enrichment should occur in the precursor acid, whereas in the first pathway the tritium enrichment should occur in an oxygenated intermediate. Precursor acids stereospecifically labeled with tritium at C-13 and labeled with $^{14}C$ at C-3 were therefore synthesized[10].

The conversion of the doubly labeled acids into $PGE_1$ was catalyzed by a vesicular gland preparation, and the $^3H/^{14}C$ ratio determined in the precursor, product, and in the precursor re-isolated after the reaction. It was found that 13 D-13-$^3$H-3-$^{14}$C-8,11,14-eicosatrienoic acid retained the tritium label throughout the conversion into $PGE_1$. The 13 L-13-$^3$H-3-$^{14}$C-8,11,14-eicosatrienoic acid, however, was transformed into $PGE_1$ with essentially complete loss of tritium. The precursor isolated after 75% conversion was significantly enriched (284% retention) with respect to tritium. Thus, the initial step in the transformation of 8,11,14-eicosatrienoic acid into prostaglandin is the stereospecific elimination of the 13 L-hydrogen atom. This is followed by introduction of oxygen at C-11 *via* a lipoxygenase-like reaction to give 11-hydroperoxy-8,12,13-eicosatrienoic acid[10,12]. It is of interest in this context that soybean lipoxygenase removes the same hydrogen both regio- and stereospecifically[9]. However, the plant lipoxygenase introduces the oxygen molecule at the ω6 position, whereas the lipoxygenase, which is a component of the prostaglandin synthetase, introduces the oxygen at the ω10 position[9]. The 11-peroxy-8,12,13-eicosatrienoic acid, conceived to be formed in the initial oxygenation, is subsequently transformed into an endoperoxide[8] by a concerted reaction involving addition of oxygen at C-15, isomerization of the $\Delta^{13}$-double bond, formation of the new CC bond between C-8 and C-12, and attack of the oxygen radical at C-9. Indirect evidence indicates a free radical mechanism[13,14]. The endoperoxide is transformed into $PGE_1$ by removal of a hydrogen atom at C-9 or into $PGF_{1\alpha}$ by reductive cleavage.

When washed microsomes are used as the enzyme source, eicosatrienoic acid gives rise to other products[15-17]. These cannot act as precursors in the biosynthesis of prostaglandins; however, their structures and the fate of $^3H$ in labeled precursors provided additional evidence for the proposed reaction mechanism. The monohydroxy acid fraction obtained from an incubation with eicosatrienoic acid was shown to consist of 11-hydroxy-8,12,14-eicosatrienoic acid, 15-hydroxy-8,11,13-eicosatrienoic acid, and (8*E*,10*E*)-12-hydroxy-8,10-heptadecadienoic acid. The mechanism of formation of the $C_{17}$ acid was studied using 3-$^{14}$C-eicosatrienoic acid which also contained a tritium label at C-9, C-10, or C-11[16]. These experiments showed that the conversion resulted in loss of the tritium labels in these three positions. Furthermore, malonaldehyde could be identified by condensation with L-arginine to give δ-N-2-(pyrimidinyl)-L-ornithine or with urea to give 2-hydroxypyrimidine. The derivatives of malonaldehyde contained the $^3H$ label from the 9-$^3$H and 11-$^3$H labeled precursors, whereas $^3H$ originally in position C-10 was lost by enolization of the malonaldehyde.

Additionally, it was found that a compound having chromatographic properties similar to those of $PGE_1$ and which was transformed into $PGF_{1\alpha}$ by $BH_4^-$ reduction was formed from eicosatrienoic acid[17]. The structure of the new product was found to be 9α,15-dihydroxy-11-keto-prosta-13-enoic acid (11-dehydro-$PGF_{1\alpha}$)[18]. In the conversion of 9-$^3$H,3-$^{14}$C- and 11-$^3$H,2-$^{14}$C-8,11,14-eicosatrienoic acids into 11-dehydro-$PGF_{1\alpha}$, only the second precursor lost the $^3H$ label. These experiments on the structures of the various products from eicosatrienoic acid and the fate of the $^3H$ labels in their formation provided strong evidence for the existence of the endoperoxide intermediate.

## 3. Isolation and Characterization of Prostaglandin Endoperoxides

Subsequently, it was possible to detect and isolate an endoperoxide obtained from rapid incubation of arachidonic acid with the microsomal fraction of homogenates of sheep vesicular glands[19]. The incubation mixtures were treated with $Sn^{II}Cl_2$ in ethanol to reduce endoperoxide to $PGF_{2\alpha}$. This was followed by $BD_4^-$ reduction and determination of the resulting $PGF_2$ species by mass spectroscopic analysis. Using this method it was possible to assay $PGE_2$ as well as 11-dehydro-$PGF_{2\alpha}$ and $PGF_{2\alpha}$. It was of particular interest that $PGF_{2\alpha}$ appeared in the initial stages of the incubation period. No metabolic transformation of

PGF compounds in preparations of sheep vesicular gland had previously been observed, and it was thus unlikely that $PGF_{2\alpha}$ could be formed enzymatically, followed by rapid metabolic degradation. Furthermore, when the $Sn^{II}Cl_2$ and $BD\bar{4}$ reduction was omitted no $PGF_{2\alpha}$ was detected, indicating that this species was formed by chemical reduction of an oxygenated derivative present in the initial phase of incubation. That an oxygenated intermediate was formed and temporarily accumulated was also suggested by the finding that the rate of $PGE_2$ formation was slower than the rate of oxygenation of the precursor acid.

Additional support for the existence of an oxygenated intermediate that was convertible into $PGF_{2\alpha}$ by $Sn^{II}Cl_2$ reduction came from experiments in which reduced glutathione or *p*-mercuribenzoate was added to the microsomal suspension: reduced glutathione increased the rate of formation of $PGE_2$ and suppressed formation of $PGF_{2\alpha}$, whereas reduced *p*-mercuribenzoate decreased the rate of formation of $PGE_2$ and resulted in a simultaneous increase in the amount of $PGF_{2\alpha}$. The oxygenated intermediate detected in these experiments was also isolated. On thin-layer radiochromatographic analysis of the product (methyl esters) isolated after short incubation (30 sec) of labeled arachidonic acid with microsomes in the presence of *p*-mercuribenzoate, a new radioactive derivative appeared. This was identified as the methyl ester of the previously postulated endoperoxide. In an extension of these studies the endoperoxide was obtained as the free acid; in addition, an endoperoxide with a hydroperoxy group at C-15 was isolated[20,21]. We suggested the trivial names $PGG_2$ for the less polar endoperoxide (15-hydroperoxy-9α,11α-epidioxyprosta-5,13-dienoic acid) and $PGH_2$ for the more polar endoperoxide (15-hydroxy-9α,11α-epidioxyprosta-5,13-dienoic acid). The structure of $PGG_2$ was established in three separate ways. Treatment of $PGG_2$ with mild reducing agents, such as $SnCl_2$ and triphenylphosphane, gave $PGF_{2\alpha}$ as the major product. This showed the presence of the epidioxy bridge between C-9 and C-11, but did not discriminate between a hydroxy and a hydroperoxy group at C-15 since the reagents used reduce the latter group into the former. In a second experiment, $PGG_2$ was treated with lead tetraacetate in benzene and subsequently with triphenylphosphane: in this case, 15-keto-$PGF_{2\alpha}$ was the major product. Lead tetraacetate dehydrates hydroperoxides to ketones and, hence, formation of a 15-ketoprostaglandin from $PGG_2$ in this way strongly indicates the presence of a hydroperoxy group at C-15; isomerization of $PGG_2$ to 15-hydroperoxy-$PGE_2$ in aqueous media provided independent evidence.

Two reactions are involved in the conversion of $PGG_2$ into $PGE_2$ (see also Fig. 1): reduction of the hydroperoxy group at C-15 to a hydroxy group (peroxidase) and isomerization of the endoperoxide structure to a β-hydroxyketone (endoperoxide isomerase). The endoperoxide isomerase was found to be almost entirely associated with the microsomal fraction. The enzymic activity was stimulated by reduced glutathione.

The endoperoxides were quite unstable ($t_{1/2} = 5$ min); however, when stored under anhydrous conditions in acetone they could be kept for several weeks. When their biological activity was tested on *in vitro* preparations it was found that the effects of the endoperoxides on gastrointestinal smooth muscle were comparable to those of $PGE_2$ and $PGF_{2\alpha}$. On the other hand, the effects on vascular (rabbit aorta) and airway (guinea pig trachea) smooth muscle were considerably greater than those of $PGE_2$ and $PGF_{2\alpha}$, respectively[22]. Both endoperoxides were potent contractors of the isolated human umbilical artery[23]. Administration of $PGG_2$ and $PGH_2$ intravenously to guinea pigs[22] produced an increase in insufflation pressure, which was more marked than that caused by comparable doses of $PGF_{2\alpha}$. The cardiovascular effects of the endoperoxides showed a complex pattern. The blood pressure response was triphasic, *i.e.*, a transient fall, consistently followed by a short-term rise, and then by a sustained reduction. These studies on vascular and airway smooth muscle demonstrated that the endoperoxides produced effects that could not be attributed to conversion into the stable prostaglandins.

Additional studies in our laboratory showed that both endoperoxides, $PGG_2$ and $PGH_2$, induced rapid and irreversible aggregation of human blood platelets[19,20,24].

## 4. Discovery of the Unstable Aggregating Factor and Thromboxanes

The biological effects of the pure endoperoxides were of particular interest in relation to other studies which demonstrated that arachidonic acid caused aggregation when added to human platelets[25,26], and that labile aggregating material (LASS) was formed from this acid when it was incubated with preparations of sheep vesicular glands[27-29]. Furthermore, the potency of the endoperoxides in causing contractions of the isolated rabbit aorta was of particular interest in relation to the so-called rabbit-aorta contracting substance (RCS)[30]. RCS was reported to be formed in guinea-pig lung during anaphylaxis and was later suggested to be due to the endoperoxide intermediate in prostaglandin biosynthesis[31]. We found that material with similar biological properties was formed after addition of arachidonic acid to human platelets. However, the rabbit-aorta contracting substance isolated from guinea-pig lung and platelets was found to consist of one major component with a $t_{1/2}$ of *ca.* 30 secs and a minor component ($PGG_2$ and/or $PGF_2$) with a $t_{1/2}$ of 4—5 min[32]. The short-lived major component of RCS could be generated by addition of arachidonic acid to platelets.

To obtain structural information about RCS we, therefore, incubated 1-$^{14}$C-arachidonic acid with suspensions of washed human platelets. Three major metabolites were isolated[33]: one of them was found to be (12*S*)-12-hydroxy-5,8,10,14-eicosatetraenoic acid (12-HETE) (Fig. 2). The corresponding hydroperoxide (HPETE) could be isolated after incubation of arachidonic acid with sonicated plates. Formation of 12-HETE from arachidonic acid was also reported to occur in bovine platelets[34]. A more polar metabolite was identified as (12*S*)-12-hydroxy-5,8,10-heptadecatrienoic acid (HHT), whereas a third component was found to be the hemiacetal derivative of (12*S*)-8-(1-hydroxy-3-oxopropyl)-9-12-dihydroxy-5,10-heptadecadienoic acid (thromboxane $B_2$, PHD). 1-$^{14}$C-$PGG_2$ added to sus-

pensions of human platelets was rapidly converted into HHT and thromboxane $B_2$.

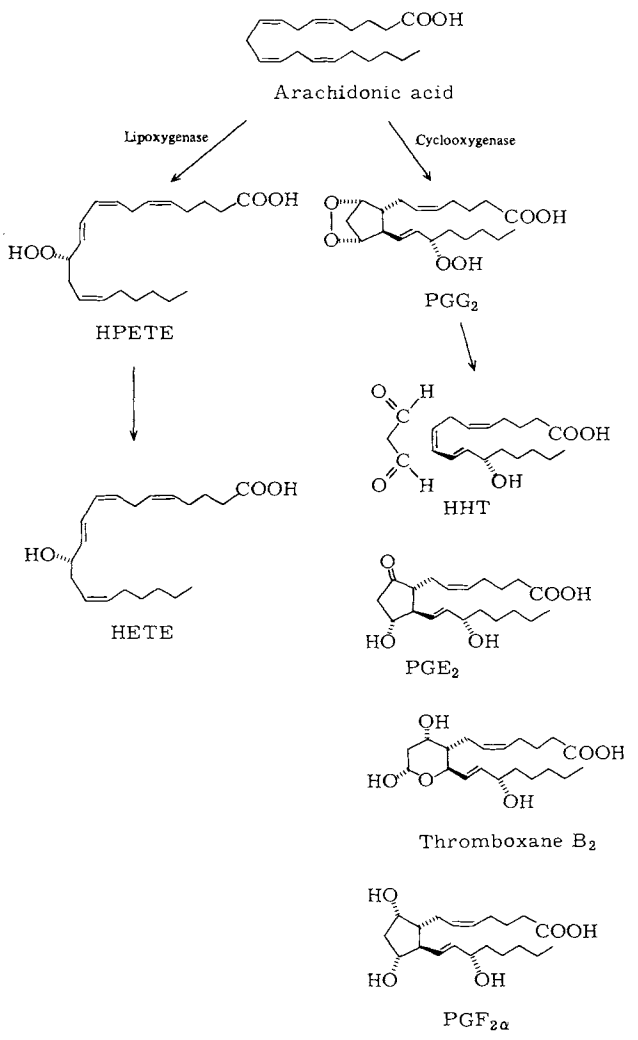



Fig. 2. Transformation of arachidonic acid in human platelets.

All the identified metabolites of arachidonic acid were stable compounds and could therefore not be identical to the very unstable RCS ($t_{1/2}=30$ sec). Additional biological work with the platelets involving characterization of the material formed from arachidonic acid was therefore carried out. When arachidonic acid was incubated with washed platelets and an aliquot of the incubate transferred to a suspension of platelets preincubated with indomethacin, aggregation took place. This was not due to $PGG_2$ or $PGH_2$, since the amounts found were only *ca.* 1% of those required to account for the response. A more detailed analysis of the appearance of the aggregating factor and the endoperoxides showed that the amount of endoperoxides was highest during the very early phase of the incubation period, whereas the aggregating factor reached a maximum later[35] (Fig. 3). Experiments using filtrates of incubates showed that the aggregating factor was very unstable. When the logarithm of the dose (arbitrary units) was plotted against the incubation time at 37 °C, a linear relationship was obtained. The half-life of the aggregating factor was 33–46 seconds. A factor with similar properties was also generated from the endoperoxide $PGG_2$. In addition to inducing irreversible aggregation, the unstable factor also caused release of serotonin from platelets.

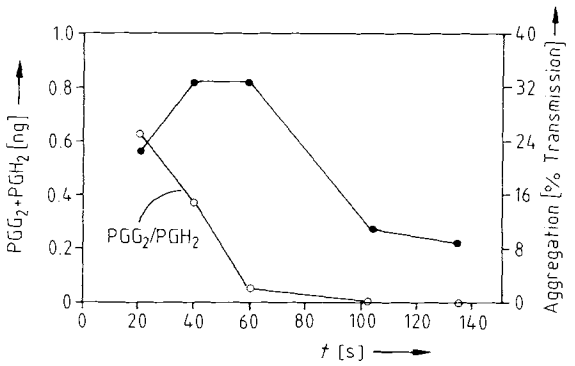



Fig. 3. Maximum aggregation induced by 0.1 mL of suspensions of washed platelets incubated for different times with 120 ng of arachidonic acid (●—●). The content of $PGG_2+PGH_2$ in these samples is also given (○—○). The platelet suspension in the aggregometer tube was preincubated for 2 min with $1.4\times10^{5}$ M indomethacin.

Further work involving experiments with $^{18}O_2$ suggested that thromboxane $B_2$ was formed from $PGG_2$ by rearrangement and subsequent incorporation of one molecule of $H_2O$[33]. It was, therefore, conceivable that if the rearranged intermediate had an appreciable lifetime it should be trapped by nucleophiles[36]: this was found to be the case. Addition of 25 volumes of methanol to washed platelets incubated with arachidonic acid for 20 seconds gave two derivatives that were less polar than thromboxane $B_2$. The mass spectral data indicated that these two compounds were epimers of thromboxane $B_2$ methylated at the hemiacetal hydroxyl group (Fig. 4). The two epimers were also formed when methanol was added to platelets incubated with $PGG_2$ for 30 seconds. Addition of ethanol to platelets incubated with arachidonic acid for 30 seconds analogously gave rise to epimers of thromboxane $B_2$ ethylated at the hemiacetal hydroxyl group. Finally, addition of 5 volumes of 5 M sodium azide to platelets incubated with arachidonic acid gave the corresponding azide (Fig.

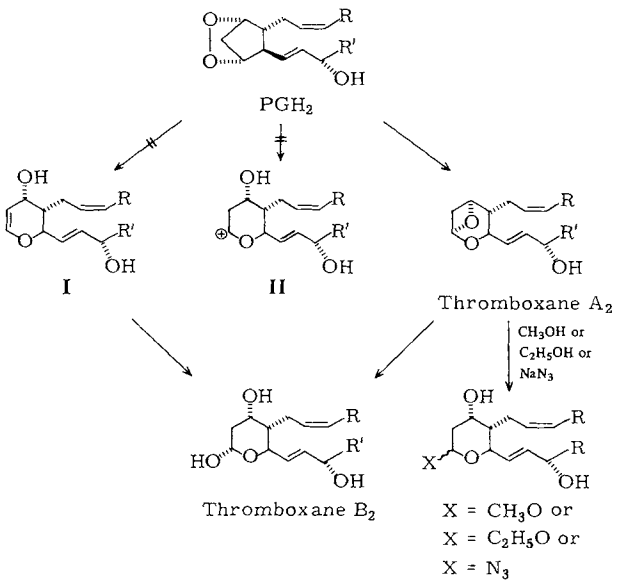



Fig. 4. Transformation of $PGH_2$ into thromboxane derivatives. $R=(CH_2)_3COOH$, $R'=(CH_2)_4CH_3$.

4). The trapping experiments showed the existence of a very unstable intermediate in the conversion of $PGG_2$ into thromboxane $B_2$.

In order to determine the half-life of the intermediate, the platelet suspension was incubated with 1-$^{14}$C-arachidonic acid for 45 seconds and the reaction was stopped by filtration. The clear, essentially platelet-free filtrate was kept at 37 °C, and aliquots were removed after different times and immediately added to 25 mL of methanol containing tritium-labeled monomethylthromboxane $B_2$. A straight line relationship between the logarithms of the $^{14}C/^{3}H$ ratios of the purified methyl ester of monomethylthromboxane $B_2$ and the incubation times was found; the half-life thus obtained was $32 \pm 2$ seconds.

Figure 4 shows the structure proposed for the unstable intermediate (thromboxane $A_2$). The acetal carbon atom should be susceptible to nucleophilic attack, *e.g.*, by $H_2O$ (giving thromboxane $B_2$) as well as by $CH_3OH$, $C_2H_5OH$, and $N_3^-$ (giving the derivatives of thromboxane $B_2$ described above). Addition of $CH_3O^2H$ to platelets incubated with arachidonic acid led to formation of monomethylated thromboxane $B_2$ with no carbon-bound $^2H$. This finding precluded an alternative structure for the unstable intermediate, *i.e.*, a 3,4-dihydro-2*H*-pyran derivative (**I** in Fig. 4). Furthermore, the $t_{1/2}$ of thromboxane $A_2$ seemed to preclude involvement of a carbonium ion structure (**II** in Fig. 4), which in aqueous media should be considerably less stable.

The available evidence indicated that the aggregating factor and RCS were one and the same compound. Thus, they were both derived from arachidonic acid or $PGG_2$, their formation from arachidonic acid was blocked by indomethacin, and their half-lives were similar. It was proposed that this material is identical to the unstable intermediate detected chemically in platelets (Fig. 4).

Because of their structure and origin, the new "oxane" derivatives were named thromboxanes. Thromboxane $A_2$ is a highly unstable bicyclic compound, and thromboxane $B_2$ is a stable derivative, provisionally named PHD. The subscript indicates the number of double bonds, as in the prostaglandin nomenclature. The structure of thromboxane $B_2$ has been confirmed by synthesis[37-40].

Thromboxane $A_2$ has been shown to be highly biologically active: Some of the better known of these effects are induction of platelet aggregation and the release reaction[36,40], as well as the strong constricting effects on vascular smooth muscle. The first blood vessel to be studied in this respect was the rabbit aorta[30,32]; later, similar contractile responses were observed in other blood vessels, such as coronary arteries[42-46], the mesenteric and celiac arteries[47,48], and the umbilical artery[23], *etc.*

These dual effects of $TXA_2$, induction of vasoconstriction and platelet aggregation, both come into operation after a blood vessel has been injured. They indicate that $TXA_2$ probably plays a role in normal hemostasis *in vivo* as well as in pathological conditions with an increased tendency to vasospasm and/or thrombosis. Several reviews have appeared on the biological effects and possible roles of thromboxanes *in vivo*[41,50]. Thromboxane $A_2$ also has potent contractile effects on airways, demonstrable both *in vitro* and *in vivo*[51].

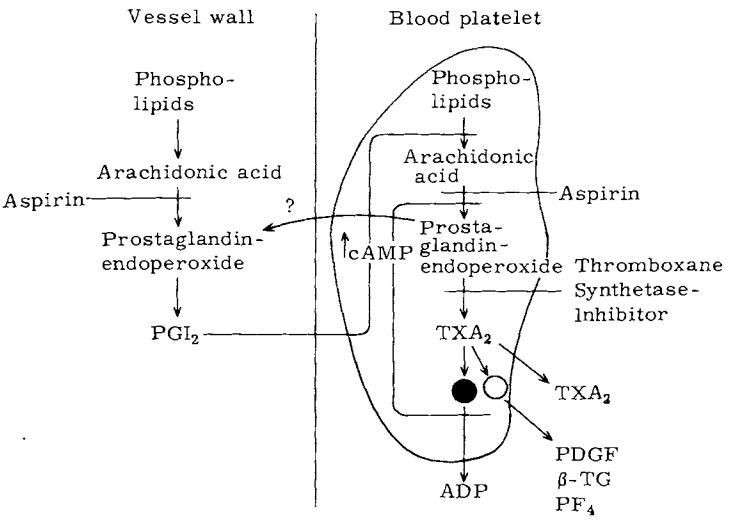



Fig. 5. Interaction between platelets and the blood vessel wall. PDGF = Platelet Derived Growth Factor; β-TG = β-Thromboglobin; $PF_4$ = Platelet Factor 4.

Following the isolation of the endoperoxides and the discovery of thromboxane $A_2$ it was found that arterial tissue converts the endoperoxide into a product with the opposite effects[52]. Structural work demonstrated that it was an enol ether derivative[53]. This vasodilator and antiaggregating compound was named $PGI_2$, or prostacyclin. Thromboxane $A_2$ and prostacyclin together probably form a hemostatic mechanism for controlling the tonus of blood vessels and the aggregation of platelets *in vivo*. These platelet and vessel wall reactions, which are of considerable interest in antithrombotic therapy, are summarized in Figure 5. The main focus is now on the development of specific thromboxane synthetase inhibitors. For a recent review see[54].

## 5. Discovery of the Leukotrienes

The role played by prostaglandins in inflammation was brought into focus by the discovery by *Vane et al.* that nonsteroidal anti-inflammatory drugs such as aspirin inhibit the enzyme (cyclooxygenase) responsible for conversion of arachidonic acid into prostaglandins and thromboxanes[55]. Anti-inflammatory steroids also inhibit the formation of prostaglandins; however, the mechanism of action is different. The steroids inhibit the formation of prostaglandins by blocking the release of arachidonic acid from the phospholipids. Since aspirin-like drugs and steroids have different anti-inflammatory effects it seemed conceivable to us that some of these differences might be due to formation of additional pro-inflammatory derivatives of arachidonic acid. Studies of the transformation of arachidonic acid in leukocytes which were carried out to test this hypothesis have recently resulted in the recognition of a novel group of compounds: the leukotrienes. These compounds seem to be of importance in both immediate hypersensitivity reactions and in inflammation.

When arachidonic acid was incubated with polymorphonuclear leukocytes it was found that the major meta-

bolite was a new lipoxygenase, (5*S*)-5-hydroxy-6,8,11,14-eicosatetraenoic acid (5-HETE)[56]. Additional studies also demonstrated the formation of (5*S*,12*R*)-5,12-dihydroxy-6,8,10,14-eicosatetraenoic acid (major product) (leukotriene $B_4$, see below), two additional (5*S*)-5,12-dihydroxy-6,8,10,14-eicosatetraenoic acids [(*E*,*E*,*E*,*Z*)-C-12 epimeric] and two isomeric 5,6-dihydroxy-7,9,11,14-eicosatetraenoic acids (Fig. 6)[57,58].

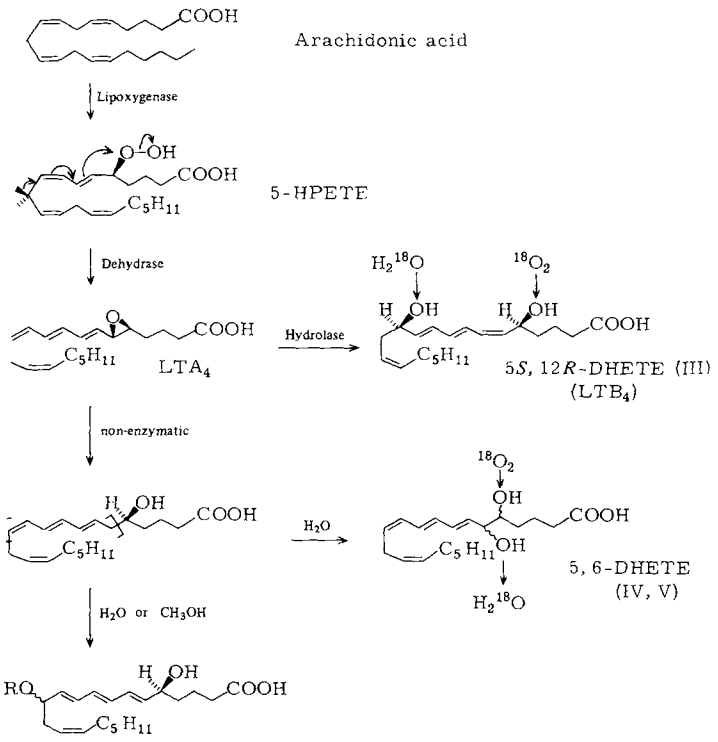



Fig. 6. Formation of dihydroxy derivatives *via* unstable intermediates. Origin of oxygen and trapping experiments.

Stereochemical studies, demonstrating formation of two acids with all-*trans* conjugated trienes which are epimeric at C-12 and of one major isomer (12*R*) with a different configuration of the triene, raised the question of the mechanism of formation[58]. Using $^{18}O_2$ and $H_2{}^{18}O$, it was demonstrated that the oxygen of the hydroxy group at C-5 originated from molecular oxygen, whereas the oxygen of the hydroxy group at C-12 was derived from water (Fig. 6)[59]. These observations led us to propose that leukocytes generated an unstable intermediate which could undergo attack by nucleophiles such as water, alcohols, *etc.* Leukocytes were therefore incubated for 30 seconds with arachidonic acid followed by addition of 10 volumes of methanol, 10 volumes of ethanol, or 0.2 volumes of N hydrochloric acid. Trapping with methanol (or ethanol) yielded two new less polar compounds, present in equal amounts and having ultraviolet spectra identical to those of compounds I and II (Fig. 6). IR spectroscopy indicated that the conjugated trienes had the all-*trans* geometry. Mass spectrometric analyses of the two compounds showed that they were isomeric and had hydroxy groups at C-5 and methoxy groups at C-12. Since C-5 in both cases had the (*S*)-configuration, it was clear that the compounds were the C-12 epimers of (5*S*)-5-hydroxy-12-methoxy-(6*E*,8*E*,10*E*,14*Z*)-eicosatetraenoic acid (Fig. 6).

These experiments demonstrated that leukocytes generate a metabolite of arachidonic acid which can undergo a facile nucleophilic reaction with alcohols. Analysis of samples obtained from trapping experiments performed under different conditions always showed inverse relationships between the amount of compounds I and II and their 12-*O*-alkyl derivatives. This result suggested that compounds I and II and the 12-*O*-alkyl derivatives were formed nonenzymatically from the same intermediate.

The stability of the intermediate was determined by incubating leukocytes with arachidonic acid for 45 seconds; the enzyme was then inactivated by addition of 1 volume of acetone. After different time intervals aliquots of the mixture were transferred to flasks containing 15 volumes of methanol. Chromatographic analysis showed that the $t_{1/2}$ of the intermediate, determined as the 12-*O*-methyl derivative, was 3–4 min. Concomitant with the decrease in the concentration of the intermediate, the concentrations of compounds I, II, IV, and V increased; in contrast, the concentrations of compound III and of 5-hydroxy-6,8,11,14-eicosatetraenoic acid remained constant. These data suggested that the epimeric 5,12- and 5,6-dihydroxy acids (compounds I, II, and IV, and V) are formed by nonenzymatic hydrolysis of a common unstable intermediate, whereas compound III is generated by enzymatic hydrolysis of the same intermediate (Fig. 6). Similar experiments performed at acidic and alkaline pH showed that the intermediate was acid labile, but considerably more stable under alkaline conditions. It was also found that the two 5,6-dihydroxy derivatives (IV and V) were formed nonenzymatically from the same intermediate as the enzymatic product, (5*S*,12*R*)-5,12-dihydroxyeicosatetraenoic acid, and that $^{18}O$ from molecular oxygen was exclusively retained at C-5 of these derivatives; in contrast, $^{18}O$ from water was introduced at C-6 or C-12. On the basis of these experimental data, the structure (5*S*)-5,6-epoxy-7,9,11,14-eicosatetraenoic acid (leukotriene $A_4$, $LTA_4$) (Fig. 6) was proposed for the intermediate[59].

The formation of compounds I–V from the epoxide intermediate is shown in Figure 6. With the exception of compound III, these are formed by chemical hydrolysis of the epoxide *via* a mechanism involving a carbonium ion intermediate, which adds hydroxyl anion preferentially at C-6 and C-12 to yield four isomeric products containing the stable conjugated triene structural moiety. The formation of compound III is enzymatic since it is not racemic at C-12 and is only formed by nondenatured cell preparations.

The structure proposed for leukotriene $A_4$[59] has subsequently been confirmed by chemical synthesis[60]. The (5*S*, 12*R*)-5,12-dihydroxy acid formed enzymatically was earlier shown to contain one *cis* and two *trans* double bonds in the conjugated triene. The location of the *cis*-double bond ($\Delta^6$-position) was recently established by synthesis[61]. The intermediate allylic epoxide $LTA_4$ can exist in free form, since it has been isolated from human polymorphonuclear leukocytes[62]. The suggested mechanism for the biosynthesis of the epoxide from arachidonic acid (Fig. 6) involves initial formation of 5-hydroperoxy-6,8,11,14-ei-

cosatetraenoic acid (5-HPETE); epoxide formation follows by subsequent abstraction of the pro-*R* hydrogen atom at C-10 and elimination of hydroxide ion from the hydroperoxy group[63]. The dehydration reaction is catalyzed by a soluble enzyme, which was recently isolated from leukocytes[64].

## 6. Slow Reacting Substance of Anaphylaxis (SRS-A)

The occurrence of a smooth muscle stimulating factor (SRS) in the perfusate of guinea pig lung treated with cobra venom was described in 1938[65]. The factor was also shown to be released by immunological challenge[66]. Biological studies of SRS suggested that it might be an important mediator of anaphylactic and other immediate hypersensitivity reactions[67,68]. Characterization of SRS indicated that it was a polar lipid which absorbed in the UV and that it might contain sulfur[69–71]. Studies with labeled arachidonic acid suggested that this acid might be incorporated into SRS[72,73].

Studies in our laboratory showed that treatment of human neutrophils with the ionophore A23 187 resulted in stimulation of the synthesis of the 5,12-dihydroxy acid ($LTB_4$) described in the previous section[58]. On the basis of the stimulatory effect of the ionophore on both SRS production[74] and $LTB_4$ formation, the UV absorbance data, and other considerations we developed the hypothesis that there was a biogenetic relationship between the unstable allylic epoxide intermediate in neutrophils and SRS generated in a variety of systems.

For formation of relatively large amounts of SRS we found that murine mastocytoma cells (CXBGABMCT-1) stimulated with the calcium ionophore A23 187 were more suitable than previously described systems[75]. The SRS was purified by high performance liquid chromatography. The purified material showed an absorbance maximum at 280 nm and gave a typical contraction of guinea pig ileum which was reversed by FPL-55712[75]. The UV characteristics resembled those of the dihydroxy acids; however, the maximum was shifted 10 nm to higher wavelength. This was in accord with the presence of a sulfur substituent in the α-position to a conjugated triene. Labeled arachidonic acid and cysteine were incorporated into the product.

Degradation of SRS by Raney nickel desulfurization gave 5-hydroxyeicosanoic acid, indicating that the arachidonic acid derivative and cysteine were linked by a thioether bond (Fig. 7). This finding also supported the hypothesis that there was a biogenetic relationship between the 5-lipoxygenase pathway in leukocytes and SRS. The positions of the double bonds in SRS were determined by reductive ozonolysis. Isolation of 1-hexanol among the products indicated that the $\Delta^{14}$-double bond of arachidonic acid had been retained. The approach used for locating the conjugated triene was based on previous studies in our laboratory which had shown that arachidonic acid and related fatty acids containing two *cis* double bonds at the ω6 and ω9 positions separated by a methylene group are oxygenated to give derivatives in which the ω6 double bond has isomerized to ω7. Incubation of the isolated SRS with lipoxygenase resulted in isomerization of the $\Delta^{14}$-double bond to form a conjugated tetraene, since a bathochromic shift of 30 nm was observed. This finding indicated that SRS contained a $\Delta^{11}$-*cis* double bond and additional double bonds at Δ7 and Δ9. The structural work at this stage showed that SRS was a derivative of 5-hydroxy-7,9,11,14-eicosatetraenoic acid with a cysteine-containing substituent thioether-linked at C-6. That the cysteine is derivatized was suggested by the failure to isolate alanine after desulfurization. The cysteine-containing substituent was, therefore, referred to as RSH[75–77]. Further studies involving amino acid analyses of acid hydrolyzed SRS demonstrated that, in addition to cysteine, one mol of glycine and one mol of glutamic acid were present per mol of SRS. End group (dansyl method and hydrazinolysis) and sequence analyses (dansyl-Edman procedure) of the peptide showed that it was γ-glutamylcysteinylglycine (glutathione). The structure of the SRS from murine mastocytoma cells was therefore 6-*S*-glutathionyl-5-hydroxy-7,9,11,14-eicosatetraenoic acid, leukotriene $C_4$ ($LTC_4$) (Fig. 7)[78]. The structure was confirmed by comparison with synthetic material. This represented the first structure de-

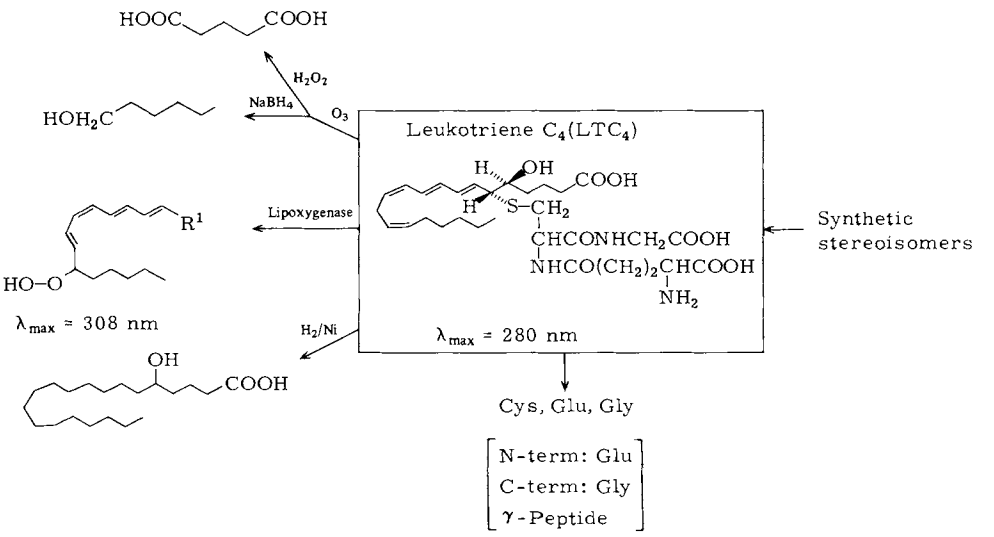



Fig. 7. Some transformations in structural studies on SRS.

termination of an SRS-A[78]. The preparation and some properties of the cysteinylglycine ($LTD_4$) and cysteinyl derivatives ($LTE_4$) were also reported at the same time[78]. These compounds were later isolated from natural sources (see below). The stereochemistry proposed for $LTC_4$ was confirmed and unambiguously assigned by total synthesis, including preparation of stereoisomers of $LTC_4$[79], by *E. J. Corey et al.*: $LTC_4$ is thus (5*S*,6*R*)-6-*S*-glutathionyl-5-hydroxy-(7*E*,9*E*,11*E*,14*Z*)-eicosatetraenoic acid.

Later studies using a different cell type, RBL-1 cells, showed that the major slow reacting substance was $LTD_4$ [(5*S*,6*R*)-6*S*-cysteinylglycine-5-hydroxy-(7*E*,9*E*,11*Z*,14*Z*)-eicosatetraenoic acid][80].

Following the structure determination of SRS from mastocytoma cells[75,78] and the synthesis of $LTC_4$, $LTD_4$, and $LTE_4$[78], all of these cysteine-containing leukotrienes (Fig. 8) were identified in a variety of biological systems using comparison with synthetic material or partial characterization by chemical or physical methods (Table 1). SRS-A is thus a mixture of leukotrienes containing cysteine, *e.g.*, the parent compound $LTC_4$ and the metabolites $LTD_4$ and $LTE_4$.

Transformation of $LTA_4$ into $LTC_4$ by enzymatic addition of glutathione has been demonstrated in both mastocytoma cells and human leukocytes pretreated with the inhibitor of arachidonic acid metabolism, BW755[81]. These studies confirm the originally proposed biosynthetic pathway for SRS, *i.e.*, formation of $LTA_4$ from arachidonic acid *via* 5-HPETE, followed by addition of glutathione to $LTA_4$ and cleavage of the epoxide ring at the allylic position C-6 to give $LTC_4$[75].

The biological significance of the biosynthetic pathways described and the cumbersome systematic names of the compounds involved suggested the introduction of a trivial name for these entities[76]. The term "leukotriene" was chosen because the compounds were discovered in leukocytes and the common structural feature is a conjugated triene. Various members of the group have been designated alphabetically: leukotriene A is a 5,6-epoxy-(7*E*,9*E*,11*Z*)-, leukotriene B a (5*S*,12*R*)-5,12-dihydroxy-(6*Z*,8*E*,10*E*)-, leukotriene C, a (5*S*,6*R*)-5-*S*-glutathionyl-5-hydroxy-(7*E*,9*E*,11*Z*)-, and leukotriene E a (5*S*,6*R*)-6-*S*-cysteinyl-5-hydroxy-(7*E*,9*E*,11*Z*)-eicosapolyenoic acid. Since precursor acids containing the $\Delta^5$-double bond system (*e.g.* 5,8,11-eicosatrienoic acid, arachidonic acid, and 5,8,11,14,17-eicosapentaenoic acid) can be converted into leukotrienes containing 3—5 double bonds, a subscript denoting this number is used[82]. Leukotriene $A_4$ is thus the epoxy derivative of arachidonic acid and can be further transformed into leukotrienes $LTB_4$, $LTC_4$, and $LTE_4$.

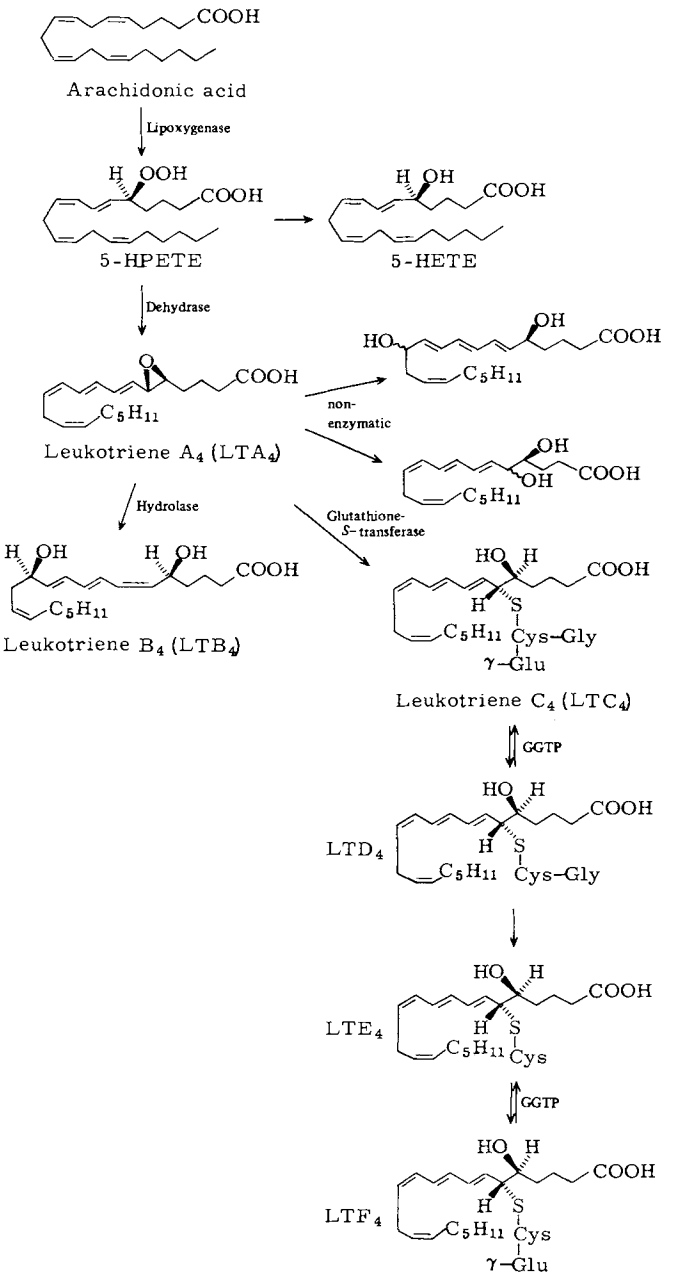



Fig. 8. Formation of leukotrienes from arachidonic acid *via* the 5-lipoxygenase pathway.

Table 1. Identification of leukotrienes (LT) from different sources.

| Source | $LTA_4$ | $LTB_4$ | $LTC_4$ | $LTD_4$ | $LTE_4$ | Ref. |
|---|---|---|---|---|---|---|
| Rabbit peritoneal leukocytes | + | + | | | | [57, 59] |
| Human peripheral leukocytes | + | + | + | | | [86, 119, 120] |
| Mouse mastocytoma cells | + | | + | | | [75, 77, 121] |
| Rat basophilic leukemia cells | | | | + | + | [80, 122, 123] |
| Rat peritoneal cells | | | + | + | + | [124, 126] |
| Rat leukocytes | | + | | | | [127, 128] |
| Rat macrophages | | + | | | | [129] |
| Mouse macrophages | | | + | | | [130] |
| Human lung | | | + | + | | [131] |
| Guinea pig lung | | | | + | | [132] |
| Cat paws | | | | + | + | [133] |

Leukotriene $C_4$ is metabolized to leukotriene $D_4$ by enzymatic elimination of glutamic acid by γ-glutamyl transpeptidase (GGTP)[80]. The remaining peptide bond in leukotriene $D_4$ is hydrolyzed by a renal dipeptidase to give leukotriene $E_4$[83]. It has recently been found that $LTE_4$ can also function as an acceptor for γ-glutamic acid, forming a γ-glutamylcysteinyl derivative, $LTF_4$[84,85] (Fig. 8).

In addition to the 5-lipoxygenase, leukocyte preparations contain enzymes catalyzing introduction of oxygen at C-12 and C-15[86]. Recently, evidence has been obtained for leukotriene formation after initial oxygenation at either of these positions[87–91].

## 7. Biological Effects of the Leukotrienes

Studies with pure leukotrienes have provided detailed information about the effects of this group of compounds in different biological systems. The leukotrienes containing cystein ($LTC_4$, $LTD_4$, and $LTE_4$) are potent bronchoconstrictors in several species, including humans, and seem to have specific effects on the peripheral airways[92–99]. They also show potent vasoconstrictor activity and have negative ionotropic effects on cardiac contractions[100].

In recent studies using bronchi from atopic patients sensitive to birch pollen[101], the relative importance of the leukotrienes as mediators of anaphylaxis has been demonstrated. Treatment of the preparation with a histamine antagonist (mepyramine) and a cyclooxygenase inhibitor (indomethacin) did not reduce the response to the specific allergen; however, benoxaprofen and a prostacyclin derivative (U-60257), both of which block leukotriene formation[102,103], inhibited the anaphylactic contraction in bronchi from asthmatics induced by birch pollen. Incubation of the atopic lung tissue with antigen resulted in release of $LTC_4$, $LTD_4$, and $LTE_4$, which could be inhibited by the prostacyclin derivative U-60257[101]. These studies indicate that the leukotrienes containing cysteine ($LTC_4$, $LTD_4$, and $LTE_4$) are major mediators of airway anaphylaxis; the finding that inhibition of leukotriene formation blocks ascaris-induced asthma in monkeys also indicates that leukotriene antagonists or inhibitors of their formation could be of therapeutic value in the treatment of bronchial asthma[102].

When injected intradermally into guinea pigs, $LTC_4$ and $LTD_4$ cause extravasation of Evan's blue[92,96,98]. More recent studies involving intravital microscopy of the cheek pouch of the hamster *(Mesocricetus sauratus)* have demonstrated that these leukotrienes have specific effects on the permeability of the post-capillary venules[104]. According to dose-response curves, $LTC_4$ and $LTD_4$ both induce a significant increase of vascular permeability at much lower concentrations than histamine. Leukotriene $C_4$ is approximately 5000 times more potent than histamine in this respect. The cysteinyl-containing leukotrienes seem to increase the vascular permeability by direct action on the blood vessel wall, since it occurs rapidly and does not require release of histamine or prostaglandins or the participation of polymorphonuclear leukocytes. Leukotriene $B_4$ also causes extravasation of plasma, although at higher concentrations. The reaction occurs with some latency and requires adhering leukocytes. Administration of a vasodilator together with leukotrienes potentiates the increase in plasma leakage caused by a submaximal dose of leukotrienes, as has been reported for $PGE_2$ and $LTD_4$ in guinea pigs[105] and for $PGE_2$ and $LTB_4$ in guinea pigs, rabbits, and rats[106,107].

When $LTB_4$ was administered to the hamster cheek pouch in the same dose-range as $LTC_4$ it caused a dramatic increase in the adhesion of leukocytes to the endothelium in small venules[104]. Increased adherence of human leukocytes caused by $LTB_4$ has also been demonstrated *in vitro* using a column of nylon fibers[108].

During superfusion with $LTB_4$ (6—10 min) the number of interstitial white cells increased. This finding is consistent with the chemotactic stimulant property of $LTB_4$, and has been shown *in vitro* using either the Boyden chamber technique or migration under agarose[109–112]. *In vivo* this effect has been monitored by determining white cell accumulation in the peritoneal cavity of guinea pigs following intraperitoneal injection of $LTB_4$[113]. The studies described above indicate that $LTB_4$ might be a mediator in the migration of leukocytes from the blood to areas of inflammation. Recent work has also demonstrated that $LTB_4$ activates neutrophils. Addition of nanomolar concentrations of $LTB_4$ to the cells results in rapid aggregation, degranulation, superoxide generation, and mobilization of membrane-associated calcium[114–116].

Studies of the mechanism of action of anti-inflammatory steroids indicate that they inhibit the release of the precursor, arachidonic acid, whereas cyclooxygenase inhibitors, such as aspirin, block the transformation of this acid into prostaglandins and thromboxanes (Fig. 9). The steroid induced inhibition of arachidonic acid release, proposed to be due to formation of peptide inhibitors of phospholipase $A_2$, prevent formation not only of prostaglandins and thromboxanes but also of leukotrienes and other oxygenated derivatives[117,118]. Some of the therapeutic effects of steroids which are not shared by aspirin-type drugs might, therefore, be due to inhibition of leukotriene formation.

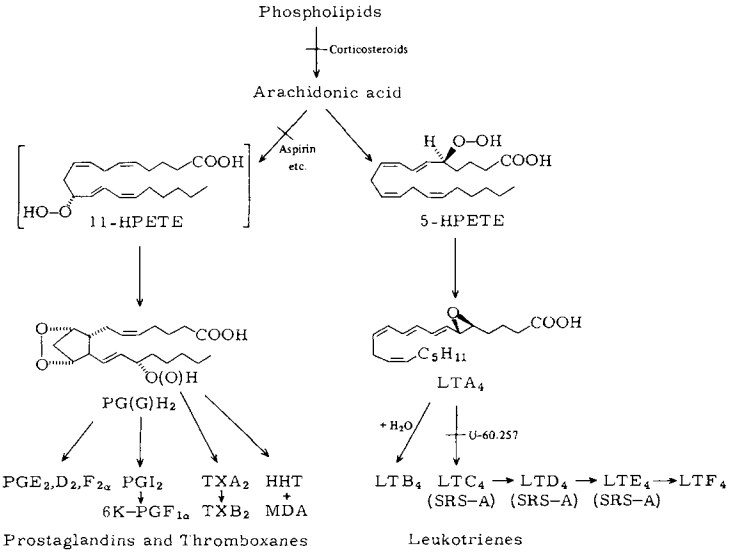



Fig. 9. Formation of prostaglandins, thromboxanes and leukotrienes from phospholipids.

The recent increase in knowledge about the transformation of arachidonic acid and the biological effects of the metabolites appear to provide new possibilities of developing novel and more specific therapeutic agents.

*It is a pleasure to acknowledge the important contributions of my associates who participated in the research described in this article. The work from the author's laboratory was supported by the Swedish Medical Research Council (project 03X-217) and the Knut and Alice Wallenberg Foundation.*

Received: May 31, 1983 [A 471 IE]
German version: *Angew. Chem. 95* (1983) 854

[1] S. Bergström, B. Samuelsson, *Annu. Rev. Biochem. 34* (1965) 101.
[2] B. Samuelsson, *Angew. Chem. 77* (1965) 445; *Angew. Chem. Int. Ed. Engl. 4* (1965) 410.
[3] S. Bergström, *Angew. Chem. 95* (1983) 865 11, Angew. Chem. Int. Ed. Engl. 22 (1983) No. 11.
[4] S. Bergström, H. Danielsson, B. Samuelsson, *Biochim. Biophys. Acta 90* (1964) 207.
[5] D. A. Van Dorp, R. K. Beerthuis, D. H. Nugteren, H. Vonkeman, *Biochim. Biophys. Acta 90* (1964) 104.
[6] D. H. Nugteren, D. A. Van Dorp, *Biochim. Biophys. Acta 98* (1965) 645.
[7] R. Ryhage, B. Samuelsson, *Biochem. Biophys. Res. Commun. 19* (1965) 279.
[8] B. Samuelsson, *J. Am. Chem. Soc. 87* (1965) 3011.
[9] M. Hamberg, B. Samuelsson, *J. Biol. Chem. 242* (1967) 5329.
[10] M. Hamberg, B. Samuelsson, *J. Biol. Chem. 242* (1967) 5344.
[11] B. Samuelsson, *Progr. Biochem. Pharmacol.* 1967.
[12] M. Hamberg, *Eur. J. Biochem. 6* (1958) 135.
[13] D. H. Nugteren, R. K. Beerthuis, D. A. van Dorp in S. Bergström, B. Samuelsson: *Nobel Symposium, 2. Prostaglandins,* Almqvist & Wiksell, Stockholm 1967, p. 45-50.
[14] B. Samuelsson, E. Granström, M. Hamberg in S. Bergström, B. Samuelsson: *Nobel Symposium 2. Prostaglandins,* Almqvist & Wiksell, Stockholm 1967, p. 45-50.
[15] M. Hamberg, B. Samuelsson, *J. Am. Chem. Soc. 88* (1966) 2349.
[16] M. Hamberg, B. Samuelsson, *J. Biol. Chem. 24* (1967) 5344.
[17] D. H. Nugteren, R. K. Beerthuis, D. A. van Dorp, *Recl. Trav. Chim. Pays-Bas 85* (1966) 405.
[18] E. Granström, W. E. M. Lands, B. Samuelsson, *J. Biol. Chem. 243* (1968) 4104.
[19] M. Hamberg, B. Samuelsson, *Proc. Natl. Acad. Sci. USA 70* (1973) 899.
[20] M. Hamberg, J. Svensson, T. Wakabayashi, B. Samuelsson, *Proc. Natl. Acad. Sci. USA 71* (1974) 345.
[21] D. H. Nugteren, E. Hazelhof, *Biochim. Biophys. Acta 326* (1973) 448.
[22] M. Hamberg, P. Hedqvist, K. Strandberg, J. Svensson, B. Samuelsson, *Life Sci. 16* (1975) 451.
[23] T. Tuvemo, K. Strandberg, M. Hamberg, B. Samuelsson, *Acta Physiol. Scand. 96* (1976) 145.
[24] B. Samuelsson, M. Hamberg in H. J. Robinson, J. R. Vane: *Prostaglandin Synthetase Inhibitors,* Raven Press, New York 1974, p. 107.
[25] B. B. Vargaftig, P. Zirinis, *Nature London New Biol. 244* (1973) 114.
[26] M. J. Silver, J. B. Smith, C. Ingerman, J. J. Kocsis, *Prostaglandins 4* (1973) 863.
[27] A. L. Willis, *Science 183* (1974) 325.
[28] A. L. Willis, *Prostaglandins 5* (1974) 1.
[29] A. L. Willis, F. M. Vane, D. C. Kuhn, C. G. Scott, M. Petrin, *Prostaglandins 8* (1974) 453.
[30] P. J. Piper, J. R. Vane, *Nature London 223* (1969) 29.
[31] R. J. Gryglewski, J. R. Vane, *Br. J. Pharmacol. 45* (1972) 37.
[32] J. Svensson, M. Hamberg, B. Samuelsson, *Acta Physiol. Scand. 94* (1975) 222.
[33] M. Hamberg, B. Samuelsson, *Proc. Natl. Acad. Sci. USA 71* (1974) 3400.
[34] D. H. Nugteren, *Biochim. Biophys. Acta 380* (1975) 299.
[35] B. Samuelsson in B. Samuelsson, R. Paoletti: *Advances in Prostaglandin and Thromboxane Research,* Vol. 1, Raven Press, New York 1976, p. 1.
[36] M. Hamberg, J. Svensson, B. Samuelsson, *Proc. Natl. Acad. Sci. USA 72* (1975) 2994.
[37] N. A. Nelson, R. W. Jackson, *Tetrahedron Lett. 1976,* 3275.
[38] R. C. Kelly, I. Schettler, S. J. Stein, *Tetrahedron Lett. 1976,* 3279.
[39] W. P. Schneider, R. A. Morge, *Tetrahedron Lett. 1976,* 3283.
[40] E. J. Corey, M. Schibasaki, J. Knolle, *Tetrahedron Lett. 1977,* 1625.
[41] S. Moncada, J. R. Vane, *Pharmacol. Rev. 30* (1979) 293.
[42] E. F. Ellis, O. Oelz, L. J. Roberts II, N. A. Payne, B. J. Sweetman, A. S. Nies, J. A. Oates, *Science 193* (1976) 1135.
[43] P. Needleman, O. S. Kulkarni, A. Raz, *Science 195* (1977) 4090.
[44] J. Svensson, M. Hamberg, *Prostaglandins 12* (1976) 943.
[45] Z. Terashita, H. Fukkui, K. Nishikawa, M. Hirat, S. Kikuchi, *Eur. J. Pharmacol. 53* (1978) 49.
[46] H. H. Wang, P. S. Kulkarni, K. E. Eakins, *Eur. J. Pharmacol. 66* (1980) 31.
[47] S. Bunting, S. Moncada, J. R. Vane, *Br. J. Pharmacol. 57* (1976) 462.
[48] S. Moncada, S. H. Ferreira, J. R. Vane in J. C. Frölich: *Advances in Prostaglandin and Thromboxane Research,* Vol. 5, Raven Press, New York 1978, p. 211.
[49] T. Tuvemo, K. Strandberg, H. Hamberg, B. Samuelsson in B. Samuelsson, R. Paoletti: *Advances in Prostaglandin and Thromboxane Research,* Vol. 1, Raven Press, New York 1976, p. 425.
[50] R. J. Gryglewski, A. Dembinska-Kiec, R. Korbut, *Acta Biol. Med. Ger. 37* (1978) 715.
[51] J. Svensson, K. Strandberg, T. Tuvemoto, M. Hamberg, *Prostaglandins 14* (1977) 425.
[52] S. Moncada, R. J. Gryglewski, S. Bunting, J. R. Vane, *Nature London 263* (1976) 663.
[53] R. A. Johnson, D. R. Morton, J. H. Kinner, R. R. Gorman, J. C. McGuire, F. F. Sun, N. Whittaker, S. Bunting, J. Salmon, S. Moncada, J. R. Vane, *Prostaglandins 12* (1976) 915.
[54] E. Granström, U. Diczfalusy, M. Hamberg, G. Hansson, C. Malmsten, B. Samuelsson in J. A. Oates: *Advances in Prostaglandin. Thromboxane and Leukotriene Research,* Vol. 10, Raven Press, New York 1982, p. 15.
[55] J. R. Vane in B. Samuelsson, R. Paoletti: *Advances in Prostaglandins and Thromboxane Research,* Vol. 2, Raven Press, New York 1976, p. 791.
[56] P. Borgeat, M. Hamberg, B. Samuelsson, *J. Biol. Chem. 251* (1976) 7816.
[57] P. Borgeat, B. Samuelsson, *J. Biol. Chem. 254* (1979) 2643.
[58] P. Borgeat, B. Samuelsson, *J. Biol. Chem. 254* (1979) 7865.
[59] P. Borgeat, B. Samuelsson, *Proc. Natl. Acad. Sci. USA 76* (1979) 3213.
[60] O. Rådmark, C. Malmsten, B. Samuelsson, D. A. Clark, G. Giichi, A. Marfat, E. J. Corey, *Biochem. Biophys. Res. Commun. 9* (1980) 954.
[61] E. J. Corey, A. Marfat, G. Goto, F. Brion, *J. Am. Chem. Soc. 102* (1981) 7984.
[62] O. Rådmark, C. Malmsten, B. Samuelsson, G. Goto, A. Marfat, E. J. Corey, *J. Biol. Chem. 255* (1980) 11828.
[63] A. Panossian, M. Hamberg, B. Samuelsson, *FEBS Lett. 150* (1982) 511.
[64] O. Rådmark, T. Shimizu, unpublished.
[65] W. Feldberg, C. H. Kellaway, *J. Physiol. London 94* (1938) 187.
[66] C. H. Kellaway, E. R. Trethewie, *Q. J. Exp. Physiol. 30* (1940) 121.
[67] K. F. Austen, *J. Immunol. 121* (1978) 793.
[68] W. E. Brocklehurst, *J. Physiol. London 120* (1953) 16P.
[69] H. R. Morris, G. W. Taylor, P. J. Piper, O. Sirois, J. R. Tippins, *FEBS Lett. 87* (1978) 203.
[70] R. P. Orange, R. C. Murphy, M. L. Karnovsky, K. F. Austen, *J. Immunol. 110* (1973) 760.
[71] K. Strandberg, B. Uvnäs, *Acta Physiol. Scand. 82* (1971) 359.
[72] M. K. Bach, J. R. Brashler, R. R. Gorman, *Prostaglandins 14* (1977) 21.
[73] B. A. Jakschik, S. Falkenhein, C. W. Parker, *Proc. Natl. Acad. Sci. USA 74* (1977) 4577.
[74] M. C. Conroy, R. P. Orange, L. M. Lichtenstein, *J. Immunol. 116* (1976) 1677.
[75] R. C. Murphy, S. Hammarström, B. Samuelsson, *Proc. Natl. Acad. Sci. USA 76* (1979) 4275.
[76] B. Samuelsson, P. Borgeat, S. Hammarström, R. C. Murphy, *Prostaglandins 17* (1979) 785.
[77] B. Samuelsson, P. Borgeat, S. Hammarström, R. C. Murphy in B. Samuelsson, P. Ramwell, R. Paoletti: *Advances in Prostaglandin and Thromboxane Research,* Vol. 6, Raven Press, New York 1980, p. 1.
[78] S. Hammarström, R. C. Murphy, B. Samuelsson, D. A. Clark, C. Mioskowski, E. J. Corey, *Biochem. Biophys. Res. Commun. 91* (1980) 1266.
[79] S. Hammarström, B. Samuelsson, D. A. Clark, G. Goto, A. Marfat, C. Mioskowski, E. J. Corey, *Biochem. Biophys. Res. Commun. 92* (1980) 946.
[80] L. Örning, S. Hammarström, B. Samuelsson, *Proc. Natl. Acad. Sci. USA 77* (1980) 2014.
[81] O. Rådmark, C. Malmsten, B. Samuelsson, *FEBS Lett. 110* (1981) 213.
[82] B. Samuelsson, S. Hammarström, *Prostaglandins 19* (1980) 645.
[83] K. Bernström, S. Hammarström, *J. Biol. Chem. 256* (1981) 9579.
[84] M. E. Anderson, R. D. Allison, A. Meister, *Proc. Natl. Acad. Sci. USA 79* (1982) 1088.
[85] N. Uehara, K. Ormstad, S. Orrenois, L. Örning, S. Hammarström in B. Samuelsson, P. Ramwell, R. Paoletti: *Advances in Prostaglandin,*

*Thromboxane and Leukotriene Research*, Vol. 11, Raven Press, New York 1983, in press.
[86] P. Borgeat, B. Samuelsson, *Proc. Natl. Acad. Sci. USA 76* (1979) 2148.
[87] W. Jubiz, O. Rådmark, J. Å. Lindgren, C. Malmsten, B. Samuelsson, *Biochem. Biophys. Res. Commun. 99* (1981) 976.
[88] J. Å. Lindgren, B. Samuelsson, unpublished.
[89] U. Lundberg, O. Rådmark, C. Malmsten, B. Samuelsson, *FEBS Lett. 126* (1981) 127.
[90] O. Rådmark, U. Lundberg, W. Jubiz, C. Malmsten, B. Samuelsson in B. Samuelsson, R. Paoletti: *Advances in Prostaglandin, Thromboxane and Leukotriene Research*, Vol. 9, Raven Press, New York 1982, p. 61.
[91] R. L. Haas, A. R. Brash, J. A. Oates in B. Samuelsson, R. Paoletti: *Advances in Prostaglandin, Thromboxane and Leukotriene Research*, Vol. 9, Raven Press, New York 1983, p. 29.
[92] S.-E. Dahlén, P. Hedqvist, S. Hammarström, B. Samuelsson, *Nature London 288* (1980) 484.
[93] P. Hedqvist, S.-E. Dahlén, L. Gustafsson, S. Hammarström, B. Samuelsson, *Acta Physiol. Scand. 110* (1980) 331.
[94] R. A. Lewis, F. K. Austen, J. M. Drazen, M. A. Soter, J. C. Figueiredo, E. J. Corey in B. Samuelsson, R. Paoletti: *Advances in Prostaglandin. Thromboxane and Leukotriene Research*, Vol. 9, Raven Press, New York 1982, p. 137.
[95] R. A. Lewis, C. W. Lee, L. Levine, R. A. Morgan, J. W. Weiss, J. M. Drazen, H. Oh, D. Hoover, E. J. Corey, K. F. Austen in B. Samuelsson, P. Ramwell, R. Paoletti: *Advances in Prostaglandin, Thromboxane and Leukotriene Research*, Vol. 11, Raven Press, New York 1983, in press.
[96] P. J. Piper, J. R. Tippins in B. Samuelsson, P. Ramwell, R. Paoletti: *Advances in Prostaglandin, Thromboxane and Leukotriene Research*, Vol. 9, Raven Press, New York 1982, p. 183.
[97] G. Smedegård, P. Hedqvist, S.-E. Dahlén, B. Revenas, S. Hammarström, B. Samuelsson, *Nature London 295* (1982) 327.
[98] J. M. Drazen, F. K. Austen, R. A. Lewis, D. A. Clark, G. Goto, A. Marfat, E. J. Corey, *Proc. Natl. Acad. Sci USA 77* (1980) 4345.
[99] J. W. Weiss, J. M. Drazen, N. Coles, E. R. McFadden, P. W. Weller, E. J. Corey, R. A. Lewis, K. F. Austen, *Science 216* (1982) 196.
[100] R. Levi, J. A. Burke, E. J. Corey in B. Samuelsson, R. Paoletti: *Advances in Prostaglandin, Thromboxane and Leukotriene Research*, Vol. 9, Raven Press, New York 1982, p. 215.
[101] G. Hansson, T. Björck, S.-E. Dahlén, P. Hedqvist, E. Granström, B. Dahlén in B. Samuelsson, P. Ramwell, R. Paoletti: *Advances in Prostaglandin, Thromboxane and Leukotriene Research*, Vol. 11, Raven Press, New York 1983, in press.
[102] M. K. Bach, J. R. Brashler, F. A. Fitzpatrick, R. L. Griffin, S. S. Iden, H. G. Johnson, M. L. McNee, J. C. McGuire, H. W. Smith, R. J. Smith, F. F. Sun, M. A. Wasserman in B. Samuelsson, P. Ramwell, R. Paoletti: *Advances in Prostaglandin, Thromboxane and Leukotriene Research*, Vol. 11, Raven Press, New York 1983, in press.
[103] W. Dawson, J. R. Boot, J. Harvey, J. R. Walker, *Eur. J. Chem. Rheumatol. Inflammation 5* (1982) 61.
[104] S.-E. Dahlén, P. Hedqvist, S. Hammarström, B. Samuelsson, *Nature London 288* (1980) 484.
[105] M. J. Peck, P. J. Piper, T. J. Williams, *Prostaglandins 20* (1980) 863.
[106] M. A. Bray, F. M. Cunningham, A. W. Ford-Hutchinson, M. J. H. Smith, *Br. J. Pharmacol. 72* (1981) 483.
[107] C. V. Wedmore, T. J. Williams, *Nature London 289* (1981) 658.
[108] J. Palmblad, C. L. Malmsten, A.-M. Udén, O. Rådmark, L. Engstedt, B. Samuelsson, *Blood 58* (1981) 658.
[109] A. W. Ford-Hutchinson, M. A. Bray, M. V. Doig, M. E. Shipley, M. J. H. Smith, *Nature London 286* (1980) 264.
[110] C. L. Malmsten, J. Palmblad, A.-M. Udén, O. Rådmark, L. Engstedt, B. Samuelsson, *Acta Physiol. Scand. 110* (1980) 449.
[111] R. M. J. Palmer, R. J. Stephney, G. A. Higgs, K. E. Eakins, *Prostaglandins 20* (1980) 411.
[112] E. J. Goetzl, W. C. Pickett, *J. Immunol. 125* (1980) 1789.
[113] M. J. H. Smith, A. W. Ford-Hutchinson, M. A. Bray, *J. Pharm. Pharmacol. 32* (1980) 517.
[114] C. N. Serhan, J. Fridovich, E. J. Goetzl, P. B. Dunham, G. Weissmann, *J. Biol. Chem. 257* (1982) 4746.
[115] S. J. Feinmark, J. Å. Lindgren, H.-E. Claesson, C. Malmsten, B. Samuelsson, *FEBS Lett. 136* (1981) 141.
6116] C. N. Serhan, A. Radin, J. E. Smolen, H. Korchak, D. Samuelsson, G. Weissmann, *Biochem. Biophys. Res. Commun. 107* (1982) 1006.
[117] G. J. Blackwell, R. Carnuccion, M. Di Rosa, R. J. Flower, L. Parente, P. Persico, *Nature London 287* (1980) 147.
[118] F. Hirata, E. Shiffmann, K. Venkatasubramanian, D. Salomon, J. Axelrod, *Proc. Natl. Acad. Sci. USA 77* (1980) 2533.
[119] O. Rådmark, C. L. Malmsten, B. Samuelsson, G. Goto, A. Marfat, E. J. Corey, *J. Biol. Chem. 255* (1980) 11828.
[120] G. Hansson, O. Rådmark, *FEBS Lett. 122* (1980) 87.
[121] S. Hammarström, B. Samuelsson, *FEBS Lett. 122* (1980) 83.
[122] H. R. Morris, G. W. Taylor, P. J. Piper, M. N. Samhoun, J. R. Tippins, *Prostaglandins 19* (1980) 185.
[123] C. W. Parker, S. F. Falkenhein, M. M. Huber, *Prostaglandins 20* (1980) 863.
[124] M. K. Bach, J. R. Brashler, S. Hammarström, B. Samuelsson, *J. Immunol. 125* (1980) 115.
[125] M. K. Bach, J. R. Brashler, S. Hammarström, B. Samuelsson, *Biochem. Biophys. Res. Commun. 93* (1980) 1121.
[126] R. A. Lewis, J. M. Drazen, K. F. Austen, D. A. Clark, E. J. Corey, *Biochem. Biophys. Res. Commun. 96* (1980) 271.
[127] A. W. Ford-Hutchinson, M. A. Bray, F. M. Cunningham, E. M. Davidson, M. J. H. Smith, *Prostaglandins 21* (1981) 143.
[128] M. I. Siegel, R. T. McConnell, R. W. Bonser, P. Cautrecasas, *Prostaglandins 21* (1981) 123.
[129] M. V. Doig, A. W. Ford-Hutchinson, *Prostaglandins 20* (1980) 1007.
[130] C. A. Rouzer, W. H. Scott, Z. A. Cohn, P. Blackburn, J. M. Manning, *Proc. Natl. Acad. Sci. USA 77* (1980) 4928.
[131] R. A. Lewis, K. F. Austen, J. M. Drazen, D. A. Clark, A. Marfat, E. J. Corey, *Proc. Natl. Acad. Sci. USA 77* (1980) 3710.
[132] H. R. Morris, G. W. Taylor, P. J. Piper, J. R. Tippins, *Nature London 285* (1980) 104.
[133] J. Hoglum, J.-K. Pai, V. Atrache, K.-E. Sok, C. J. Sih, *Proc. Natl. Acad. Sci. USA 77* (1980) 5688.

# New Naturally Occurring Amino Acids**

**By Ingrid Wagner and Hans Musso***

*Dedicated to Professor Hans Brockman on the occasion of his 80th birthday*

The majority of the 500 or so naturally occurring amino acids known today were discovered during the last 30 years, for example during the search for new antibiotics in the culture media of microorganisms, or as components of the antibiotics in fungi, seeds, in numerous plants and fruits, and in the body fluids of animals. Some 240 of these amino acids occur free in nature, some only as intermediates in metabolism. This article provides an overview of the developments that have taken place in this area since 1956 when the last review appeared. Summary accounts are presented, dealing with new unsaturated amino acids, cyclopropane- and cyclobutane-amino acids, heterocyclic amino acids, halogen-containing amino acids, sulfur-, selenium- and phosphorus-containing amino acids as well as aliphatic amino acids. In a few cases, *e.g.* betalamic acid and muscaflavin, the biosynthesis is described in detail.

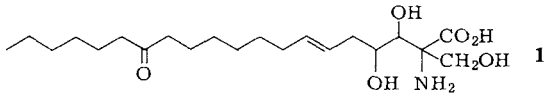
## 1. Historical Introduction

In 1820 glycine was isolated from gelatin hydrolyzates. In the following 100 years the remaining twenty amino acids, which are normally found in proteins, were identified. Only four more were found between 1920 and 1940. With the development of chromatographic methods the number of known naturally occurring amino acids increased rapidly. In 1956 alone over 60 new ones were reported[1]. At the moment 500 are known, of which *ca.* 240 occur free in nature. Still further naturally occurring amino acids are being found each year[2,3].

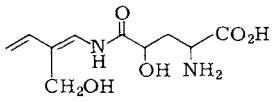
The methods of detection and determination of structure have improved so much in recent years that traces of a new fluorescent spot can be discerned in the two dimensional chromatogram of the dansyl derivatives (dansyl = 5-dimethylamino-1-naphthylsulfonyl)[4–6]. Combined GC-MS of the *N*-trifluoroacetyl-methyl ester derivatives[7] confirms that the sample is homogeneous and provides an empirical formula and often a hint as to the structure, which can be corroborated by $^1$H- and $^{13}$C-NMR on a few mg of the amino acid. In particularly difficult cases, such as for example streptolidin[8a], an X-ray structure analysis is also necessary[8b]. Nowadays one can determine the enantiomeric purity, usually to better than 0.1%, by gas chromatography of volatile amino acid derivatives on a peptide-ester stationary phase. Equally good results are obtained by chromatography of the free amino acids as diastereoisomeric copper complexes with L-proline on octadecylated silica-gel with aqueous eluents[9]. The absolute configuration can be easily determined from CD spectra if a characteristic longwave transition can be produced by making a complex[10a] or a dinitrophenyl derivative[10b]. If there are a number of chiral centers the unambiguous assignment of all the isomers is possible through stereospecific synthesis, as for example in the case of 3-hydroxyprolines[11] (cf. **39** in Section 4.1) or (−)-*S*-(2-carboxypropyl)-L-cysteine[12] (cf. **151** in Section 6).

## 2. Unsaturated Amino Acids

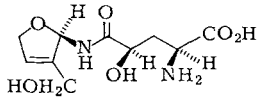
Thermocymocidin **1** from a thermophilic Eumyces species[2b,3l,13] and myriocin from the thermophilic fungus *Myriococcum albomyces*[14] are identical, both in their constitution, with a *trans* double-bond, and in their activity towards molds.




**1**




**2**




**3**

From the seeds of the bush *Staphylea pinnata* are obtained pinnatanine **2** and oxypinnatanine **3**; the absolute configuration of the dihydrofuran moiety of the latter has been established by X-ray analysis[3i].

α-Methylene-β-alanine is toxic and is found as its *N*-acetyl derivative in Hawaian sponges[15]; β-methylene-L-norvaline is found in the fungus *Lactarius helvus*[3b], β-methylene-L-norleucine in *Amanita vaginata*[2a] and (2*S*,3*S*)-3-hydroxy-4-methyleneglutamic acid in *Gleditsia caspica*[3g]. γ-Propylidene-L-glutamic acid was isolated from *Mycena pura* together with γ-methylene- and γ-ethylideneglutamic acid[3i]. Amino acids with methylenecyclopropyl units like **13–15** will be mentioned in Section 3. Further unsaturated naturally occurring amino acids, mostly not bound to proteins, are presented in Table 1.

Together with the amino acids containing one or more double bonds there are also some with triple bonds. The

[*] Prof. Dr. H. Musso, I. Wagner
Institut für Organische Chemie der Universität
Richard-Willstätter-Allee 2, D-7500 Karlsruhe (Germany)

[**] For many of the new amino acids a collective reference, or one to the most recent synthetic work, is given when possible.

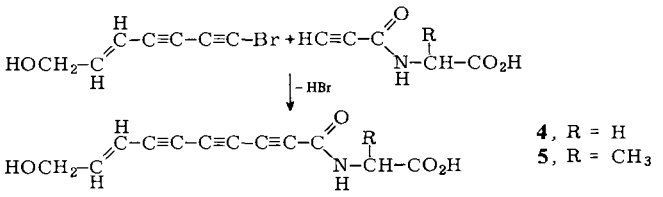
 © Verlag Chemie GmbH, 6940 Weinheim, 1983 0570-0833/83/1111-0816 $ 02.50/0 

Table 1. New unsaturated amino acids.

| Unsaturated Amino Acid | Isolated from | Ref. |
|---|---|---|
| L-2-Amino-4-(2-aminoethoxy)-*trans*-3-butenoic acid | Unidentified streptomyces | [3g] |
| 2-Amino-4-(2-amino-3-hydroxypropoxy)-*trans*-3-butenoic acid | *Rhizobium japonicum* | [3e] |
| 4-Acetamido-2-butenoic acid | *Fusarium graminearum* | [3j] |
| L-2-Amino-3-formyl-3-pentenoic acid | *Bankera fulgineoalba* | [3a] |
| L-2-Amino-3-hydroxymethyl-3-pentenoic acid | *Bankera fulgineoalba* | [3a] |
| L-2-Amino-4-chlor-4-pentenoic acid | *Amanita pseudoporphyria* | [3g] |
| *trans*-2-Amino-5-chlor-4-hexenoic acid | *Amanita solitaria* | [3e] |
| 2-Amino-4-methyl-5-hexenoic acid | *Tricholomopsis rutilans* | [16] |
| 2-Amino-5-methyl-4-hexenoic acid | *Leucocortinarius bulbiger* | [3a] |
| 2-Amino-4-methyl-4-hexenoic acid | *Aesculus californicus* | |
| 2-Amino-6-hydroxy-4-methyl-4-hexenoic acid | *Aesculus californicus* | [3a] |
| L-2-Amino-6-hydroxy-5-methyl-4-hexenoic acid | *Blighia unijugata* | [2b] |
| 2-Amino-4,5-hexadienoic acid [a] | *Amanita solitaria* | [3e] |
| 2-Amino-4-methyl-5-hexynoic acid | | [3b] |
| 2-Amino-4-hydroxy-6-heptynoic acid | *Euphoria longan* | [3b] |
| 2-Amino-4-hydroxymethyl-5-hexynoic acid | | [3b] |
| 2-Amino-3-hydroxy-4-hexynoic acid | *Tricholomopsis rutilans* | [3f,g] |
| 2-Amino-4-hexynoic acid | a New-Guinea fungus | [3e] |

[a] This hexadienoic acid can be regarded as a precursor in the biosynthesis of hypoglycine A **14**.

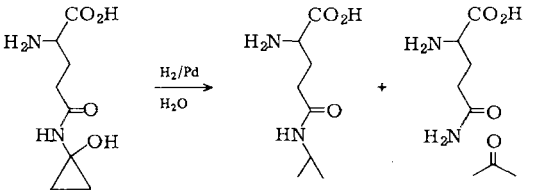
poly-yne amino acids **4** and **5**, which are produced by the fungus *Fayodia bisphaerigera* in its advanced stage of growth[17], and which are isolated as the methyl esters, are rather special. It is assumed that they are formed in nature by acylation of the amino acids with the hydroxyenetriynoic acid since this acid is found together with **4** and **5** in the same fungi. The synthesis was accomplished by coupling of the propiolylated amino acid with the hydroxyenediyne bromide.




**4**, R = H
**5**, R = $CH_3$

## 3. Cyclopropane and Cyclobutane Derivatives

1-Aminocyclopropanecarboxylic acid **7** was first discovered in the late 1950s, bound to cranberry protein, and later in apples and pears[18]. This amino acid is an intermediate in the biosynthesis of ethylene[19,20], which acts as a plant growth regulator. In this process methionine is converted enzymatically *via* an adenosine complex **6** into **7** and methylthioadenosine; **7** is not, however, released but is immediately split into ethylene and glycine—most probably while complexed with an enzyme. In addition, **7** serves as sole source of nitrogen for the bacterium *Pseudomonas sp. ACP* and for the yeast *Hansenula saturnus*, which deaminate it enzymatically to α-oxobutyric acid **8**[20]. On hydrogenation with Pt in glacial acetic acid, α-aminoisobutyric acid **9** is formed predominantly owing to the substituent effect[21], whereas in alcoholic ammonia, α-aminobutyric acid **10** is the main product[22]. Similarly, in the hydrogenation of coprin **11** the $CH_2$–$CH_2$ bond in the cyclopropane is opened to give **12**. This amino acid was isolated from *Coprinus atramentarius*[23] and is responsible for the antabuse effect of this fungus[*].

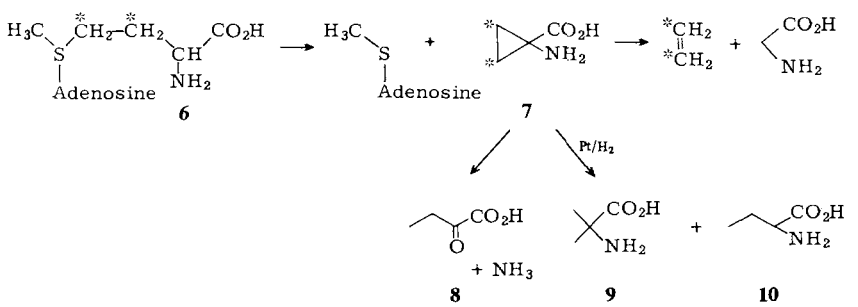



**11** **12**

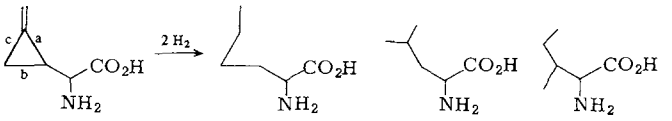
1-Amino-2-ethyl-1-cyclopropanecarboxylic acid, also known as coronamic acid, is a component of the toxin coronatin found in *Pseudomonas coronafacience var. atropurpurea*[24].

α-(Methylenecyclopropyl)glycine **13**, the corresponding alanine derivative hypoglycine A **14**, and hypoglycine B

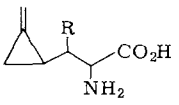
[*] The antabuse effect is the sensitization and intolerance of an organism towards alcohol caused by a drug.



(the dipeptide from **14** and Glu[25]) have been isolated from the unripe fruit of *Blighia sapida* and from litchi seeds[2b]. Compounds **13** and **14** reduce the blood-sugar concentration so drastically that eating the unripe fruit can lead to lethal hypoglycemia. Catalytic hydrogenation of **13** gave norleucine, leucine, and isoleucine (a, b, and c).

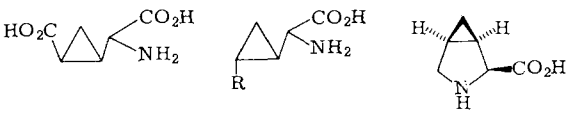


**13** a b c

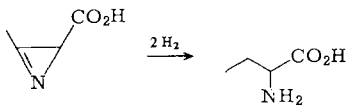


**14**, R = H
**15**, R = $CH_3$

β-(Methylenecyclopropyl)-β-methylalanine **15** has been found in the seeds of *Aesculus californica*[3a], while *cis*- and *trans*-α-(carboxycyclopropyl)glycine, **16** and **17**, can be isolated from the seeds of *Aesculus parviflora* and *Blighia sapida* respectively[3a]. *Blighia unijugata* contains the homologous carboxymethyl derivative **18** as well as L-*exo(cis)*-3,4-methanoproline **19**. The broad-spectrum antibiotic azirinomycin **20**[3d] from *Streptomyces aureus* is, as expected, unstable in concentrated solutions; catalytic hydrogenation of **20** gives L-α-aminobutyric acid.

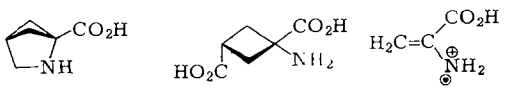


**16** **17**, R = $CO_2H$ **19**
**18**, R = $CH_2$–$CO_2H$

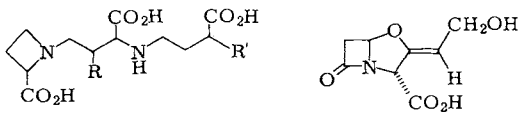


**20**

2,4-Methanoproline **21** and 2,4-methanoglutamic acid **22** from the seeds of the legume *Ateleia Herbert Smithii*[26,27] both have the base peak corresponding to **23** together with other common fragment peaks in their mass spectra.



**21** **22** **23**



**24**, R = H, R' = $NH_2$
**25**, R = R' = OH

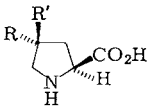
**26**

Other new azetidine derivatives have been reported such as nicotianamine **24** from the leaves of *Nicotiana tabacum*, mugineic acid **25** from oat roots[29], and clavulanic acid **26** from *Streptomyces clavuligerus*[30]. Nicotianamine has also been shown to be the normalization-factor in tomato mutants[28], while **26** acts as a β-lactamase inhibitor[30].

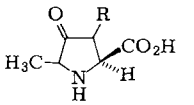
## 4. Heterocyclic Amino Acids

### 4.1. Proline Derivatives

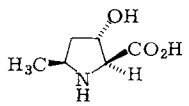
Besides 4-hydroxy-L-proline **27** and the 4-allohydroxy-L-proline **28** with *cis*-L-configuration, already discovered by *H. Wieland* and *B. Witkop* in 1940[31], the D-form *ent*-**28** has also been noted as a structural unit in the antibiotic etamycin[32]. 4-Hydroxymethylproline **29** has been isolated



| | R | R' |
|---|---|---|
| **27** | OH | H |
| **28** | H | OH |
| **29** | H | $CH_2OH$ |
| **30** | = $CH_2$ | |



**31**, R = H
**32**, R = OH



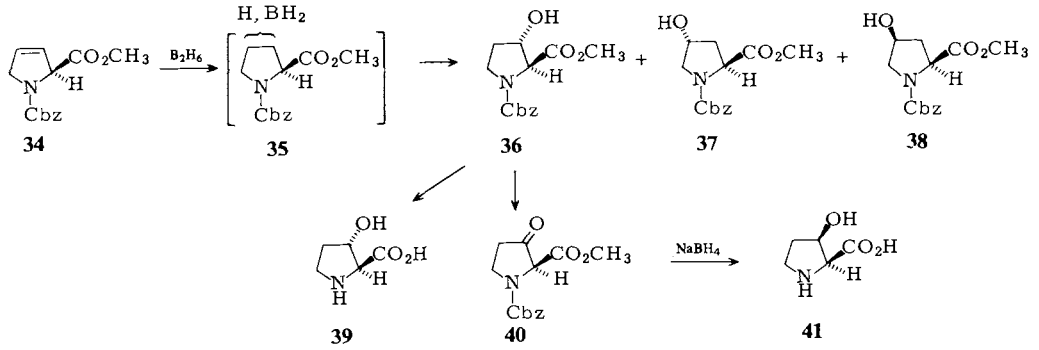
**33**

from apples[33] and from *Eriobotrya japonica*[2b], as has also 4-methylene-D,L-proline **30**/*ent*-**30**. Both 5-methyl-4-oxoprolines **31** and **32** and 3-hydroxy-5-methylproline **33** were found in the peptide lactone ring of the antibiotic actinomycin $Z_1$[11,2f], while 5-methylproline has been found in actinomycin $Z_5$[3f]. *N*-Methyl-4-hydroxyproline **27**, with $NCH_3$ replacing NH and also known as betonicin, occurs in many plants, one of which is yarrow[34,35].

To illustrate how configuration can be established by stereoselective synthesis we shall outline the case of *trans*-3-hydroxyproline **39**, isolated by ion-exchange chromatography from collagen hydrolyzate. **39** was later also found in Mediterranean sponges as well as in the antibiotic telomycin; the *cis*-isomer **41** is found only in the antibiotic[36,37].

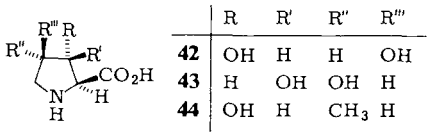
In the hydroboration of *N*-benzoyloxycarbonyl-3,4-dehydro-D,L-proline methyl ester **34**/*ent*-**34** the molecule is attacked preferentially from the back side; oxidation with alkaline hydrogen peroxide gives a mixture of 68% *trans*-3-hydroxyproline **36**/*ent*-**36**, 10% *trans*-4-hydroxyproline **37**/*ent*-**37** and a trace of *cis*-4-hydroxyproline **38**/*ent*-**38**, in each case as the *N*-protected derivative. Oxidation of **36** with chromic acid gives the keto ester **40** which is also attacked from the rear by $NaBH_4$. Alkaline ester hydrolysis and catalytic hydrogenolysis of the protecting group on the nitrogen gives the pure amino acids **39** and **41** (from **36** and **40** respectively).

The *N*-methyl derivatives of *trans*- and *cis*-3-hydroxyprolines **39** and **41**, with $NCH_3$ replacing NH, have been isolated from the ripe fruits of *Courbonia virgata*[38]; the *trans-trans*-3,4-dihydroxyproline **42** is one of the seven amino acids in virotoxin from the Destroying Angel toadstool[39] and the *cis-trans*-isomer is a component of a protein obtained from diatoms[39].



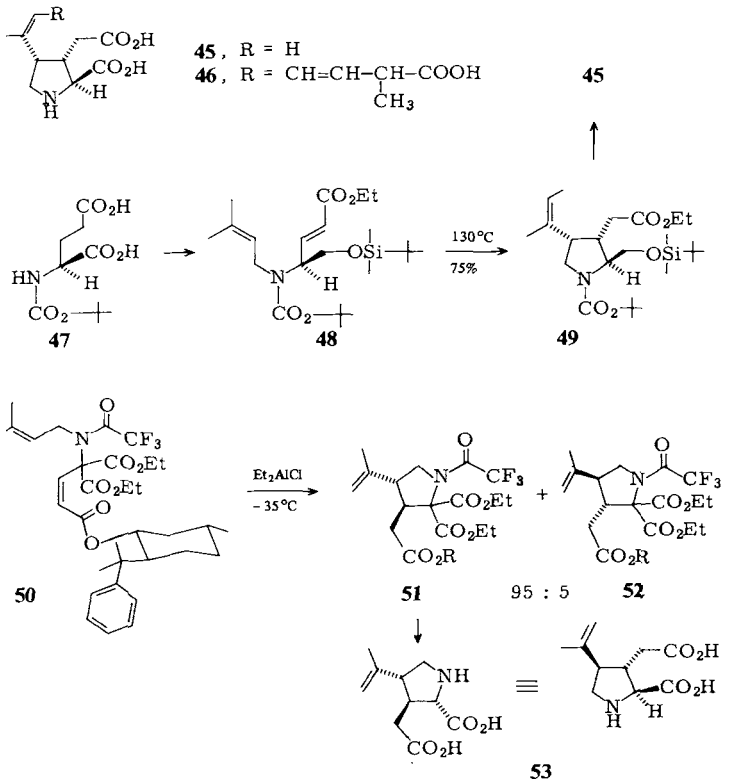
34 35 36 37 38 39 40 41

(2*S*,3*S*,4*S*)-3-Hydroxy-4-methylproline **44** is found in the antibiotic enchinocandin B[3i]. The kainic acid **45**[40], its C-4 epimer allokainic acid **53**[41] and the domoic acid **46**[42] have been isolated from the alga *Digenea simplex*. Because of interest in the neuron-stimulating activity of these compounds enantioselective syntheses have been developed.



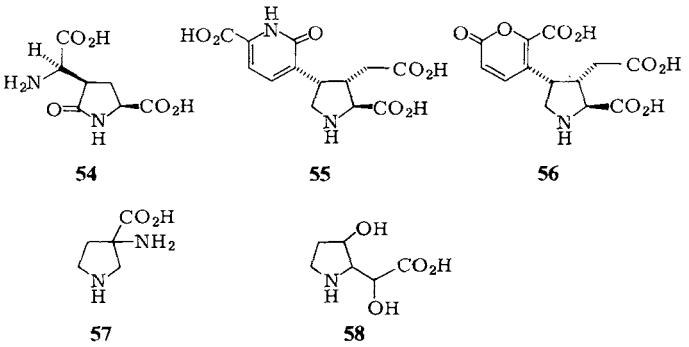
| | R | R' | R'' | R''' |
|---|---|---|---|---|
| **42** | OH | H | H | OH |
| **43** | H | OH | OH | H |
| **44** | OH | H | $CH_3$ | H |

(−)-α-Kainic acid **45** with the natural configuration was obtained from a glutamic acid derivative **47** by a thermal ene-reaction **48** → **49** with the induction of the (*S*,*S*)-configuration on the new chiral centers in **49** followed by removal of the silyl protecting group, oxidation, and ester hydrolysis[40]. The epimeric (+)-α-allokainic acid **53** is obtained by an analogous ene-reaction of the malonic ester **50**, in which the carboxy group attached to the *cis* double bond has been esterified with an optically active menthol derivative. Initiated by diethylaluminum chloride, **50** gives mainly the compound with the desired configuration **51** (95%) together with 5% of the unwanted stereoisomer **52**. When the starting material **50** contains a *trans* double bond the product ratio changes to 15 : 85[41].



**45**, R = H
**46**, R = CH=CH–CH(CH$_3$)–COOH

47 48 49 50 51 95 : 5 52 53



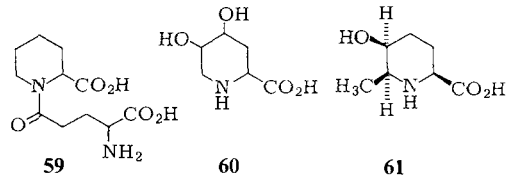
54 55 56 57 58

Other proline derivatives are a new amino acid **54** from *Pentaclethra macrophylla*[3h] and acromelic acids A **55** and B **56** which were isolated from the poisonous toadstool *Clitocybe acromelalga*[43]. *cis*-3-Amino-L-proline from *Morchella esculenta*[3b] and 4-carboxy-L-proline from *Chondria coerulesceus*[3j] should also be mentioned here. Cucurbitin **57**[44] obtained from the cucurbitaceae is no more a proline derivative than the pyrrolidineglycolic acid **58**, which was found to be a component of the depsipeptide detoxin-D[3e].

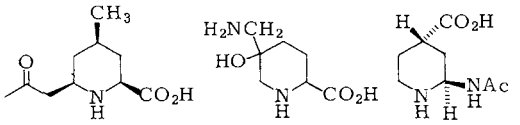
### 4.2. Piperidine, Pyridine, Quinoline, and Azepine Derivatives

Many new amino acids are derived from the long known pipecolic acid. The *N*-γ-L-glutamyl derivative **59** occurs in the seeds of *Gleditsia caspica*[2b]. The 3-hydroxy acid was found in halophytes[2a], the L-4-hydroxy acid in *Peganum harmala* and the 4,5-dihydroxypipecolic acid **60** in *Gymnocladus dioicus*[3j]. (2*S*,5*S*,6*S*)-5-Hydroxy-6-methylpipecolic acid **61** and its 5*R*-epimer are found free in *Fagus silvatica*[3i]. Trichoponamic acid **62** was isolated from *Trichoderma polysporum*[45].

5-Aminomethyl-5-hydroxypipecolic acid **63** could be identified in the hydrolyzate of *Pseudomanas* toxins[3l]; (2*R*,4*S*)-2-acetylamino-4-piperidinecarboxylic acid **64** is found in the leaves of *Calliandra haematocephala*[3e].

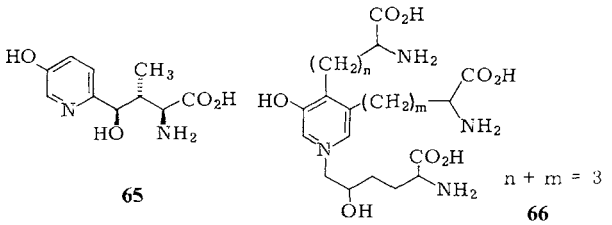


59 60 61



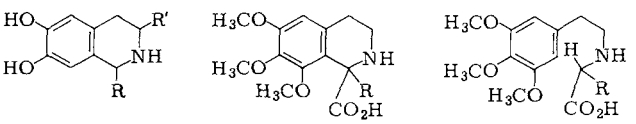
62 63 64

The pyridine derivative **65** is present as the *N*-terminal amino acid in the antibiotic nikkomycin[46,47], while the triamino acid **66** occurs in the bone collagen of cattle[3k].



65 66 (n + m = 3)

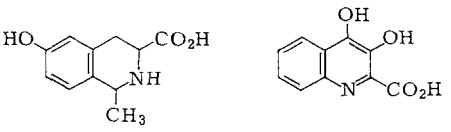
The tetrahydroisoquinolines **67** and **68** were isolated from the seeds of *Mucuna mutisiana* and *M. deeringiana*[2b]. Tris-*O*-methylpeyoxylic acid **69** and its methyl derivative **70** were found in extracts of the peyote cactus[2b], in which the possible precursor dihydro compounds mescaloxylic acid **71** and mescaloruvic acid **72** are also detected[2b]. The 6-hydroxy-1-methylcarboxylic acid **73** was isolated from *Euphorbia myrsinites*[3a] and 3,4-dihydroxy-2-quinolinecarboxylic acid **74** from the sponge *Aplysina aerophoba*[2a].



**67**, R = H, R' = $CO_2H$
**68**, R = $CH_3$, R' = H

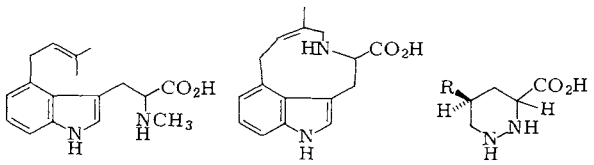
**69**, R = H
**70**, R = $CH_3$

**71**, R = H
**72**, R = $CH_3$



73 74

5-Hydroxy-L-tryptophan appears in several plants[2a], $N^{\alpha}$-methyl-4-(3-methyl-2-butenyl)-L-tryptophan **75** in *Lotus subglauca*[2a]; the cyclic clavipitic acid **76** from *Clavi-*

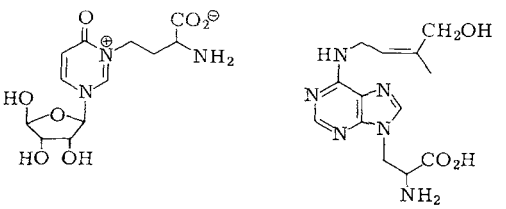


75 76

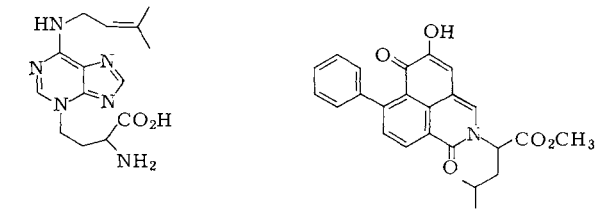
**77**, R = OH, L-
**78**, R = H, D-
**79**, R = Cl, D-

*ceps sp.* is possibly an intermediate in the biosynthesis of lysergic acid[3b].

The L-configuration of piperidazinecarboxylic acid **77** from monamycin has been correlated with that of L-ornithine; the configuration of the two D-amino-acids **78** and **79** from the same antibiotic was similarly established[3b].

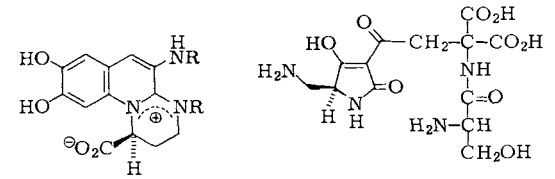


80 81



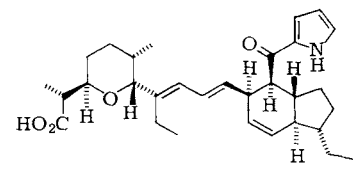
82 83

Transfer-RNA from *E. coli* contains the modified uridine **80**[3g]. Lupinic acid **81** from the seeds of *Lupinus angustifolius*[3h], and discadenin **82** from *Dictyostelium discoideum* as well as sinefungin from streptomyces griseolus[105] are purine derivatives with amino acid residues.



**84**, R, R = H, H
**85**, R, R = >C=O

86



87

Compounds such as the pigment of **83** from the blossom of *Lachanthus tinctoria*[3i], the alkaloids like **84**[48] from pseudobactin as well as compound **85**[3c] from the hydrolyzate of a fluorescent peptide produced by *Azotobacter vinelandii*, and antibiotics such as malonomycin **86**[49] or the ionophoric antibiotic X-14547A **87**[50] are formally amino acids or related compounds but have little in common with the amino acids dealt with here. The tetrahydropyridine and dihydroazepine derivatives which follow, however, are produced in ordinary amino acid metabolism.

The elucidation of the structures of the betalaine pigments[51,52] from higher plants, such as the betanins and vulgaxanthins from red beetroot *(Beta vulgaris)* or muscaaurins I and II from fly agaric *(Amanita muscaria)*, has revealed a number of new amino acids. Mild hydrolysis of

betanidin **88** gives cyclodopa **89** and betalamic acid **90**; similar treatment of muscaaurin I **91** gives ibotenic acid **92** and **90**, while muscaaurin II **93** gives, together with **90**, stizolobic acid **97**, which had been isolated shortly before from *Stizolobium hassio*. The origin of cyclodopa **89** from tyrosine **94** and dopa **95** is quite clear. For the formation of betalamic acid one must imagine an oxidative opening of the benzene ring adjacent to the hydroxy group in **95** at point 'a' and a recyclization of the intermediate A **96** by condensation between the amino group and the enolized α-keto acid. This biosynthetic route has been confirmed *in vivo* with $^{14}C$- and $^{3}H$-labeled tyrosine[53,54]. If the intermediate A **96** undergoes hemiacetal formation followed by oxidation to a lactone, stizolobic acid **97** is obtained. This pathway has also been confirmed with labeled precursors in the legume *Stizolobium hassio*.

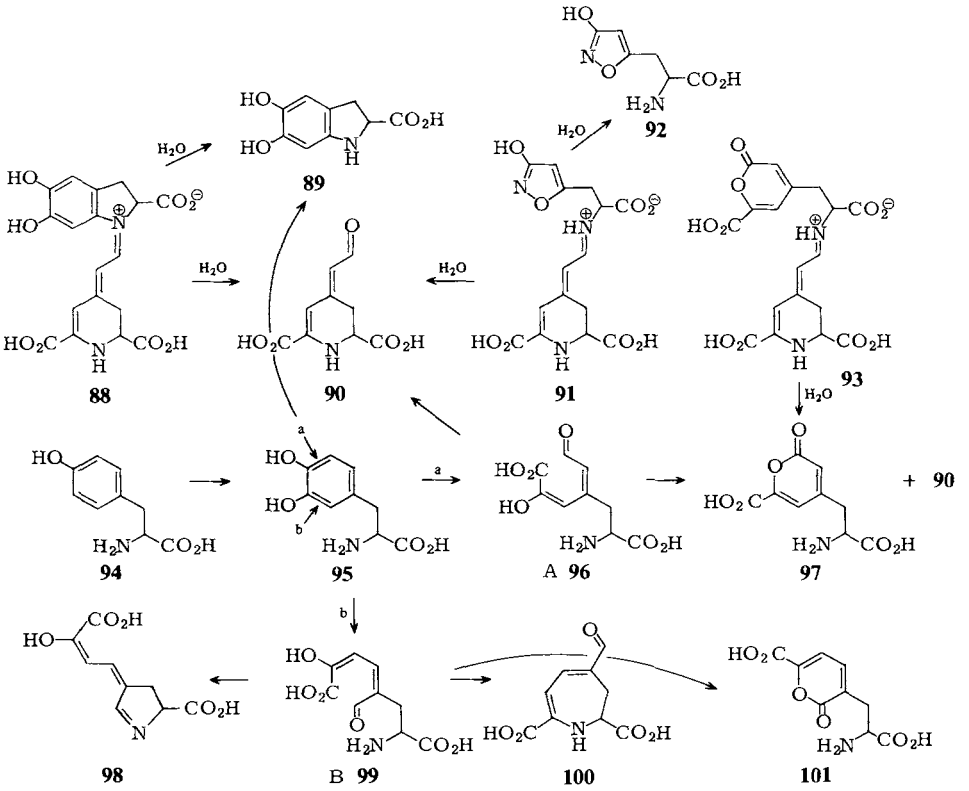
*ley*[56] has recently established the biosynthesis of the more or less unsaturated pyrrolidine moieties of the antibiotics anthramycin, tomaymycin, sibiromycin and lincomycin from tyrosine. To explain these results a cyclization of the same intermediate B **99** to compounds like **98** is required.

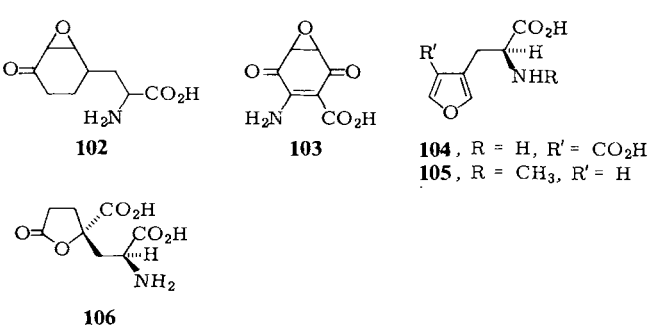
### 4.3. Oxygen Heterocycles

Related to the α-pyrones **97** and **101** are three epoxides and three furan derivatives. Anticapsin **102** is produced by *Streptomyces griseoplanus*[3d], the chloramphenicol antagonist **103** by *Streptococcus fulvoviolaceous*[3k], and (2*S*,9*S*)-2-amino-9,10-epoxy-8-oxodecanoic acid from chlamomycin a cyclic peptide with extreme cytostatic activity[106]. L-β-(4-Carboxy-3-furyl)alanine **104** occurs free in *Phyllotopsis nidulans* and the fruiting bodies of *Tricholomopsis rutilans*[3h]. *N*-Methyl-β-(3-furyl)alanine **105** is found in the cyclopeptide rhizonin A, a mycotoxin from *Rhizopus microsporus*[57]. Lycoperdic acid **106** was isolated from the fungus *Lycoperdon perlatum*[31].

A further yellow amino acid, muscaflavin, was isolated from fly agaric and identified as the dihydroazepine derivative **100**. This biosynthesis could be explained in terms of a cleavage of the benzene ring in dopa **95** at point 'b', followed by a cyclization of the intermediate B **99** analogous to that of A **96**. Oxidation of the hemiacetal of **99** yields stizolobinic acid **101** isomeric with **97**, which, together with **97**, occurs free in small amounts in beans and fungi. The unstable betalamic acid **90** has already been detected as the free amino acid.

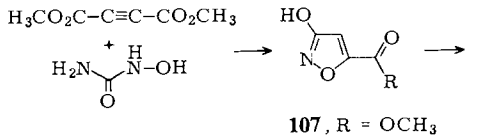
In the synthesis of muscaflavin **100** the formation of the intermediate B **99** by opening of a protected pyridine derivative was proposed. In fact the seven-membered ring in **100** is formed in this way, but first the preferred cyclization to a five-membered ring, a derivative of **98**, takes place[55]. This observation is of great interest, since *Hur-*



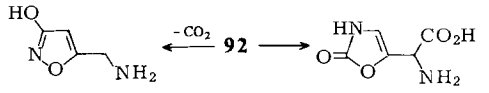



### 4.4. Isoxazoline Derivatives

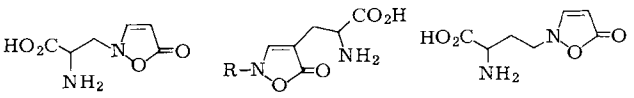
Ibotenic acid **92** from *Amanita muscaria* has already been mentioned; it occurs in this toadstool in quite large amounts and decarboxylates readily to muscimol **109** and rearranges photochemically to muscazone **110**[58]. Because of its alleged psychotropic activity improved syntheses of muscimol are repeatedly being developed[59]. In the most recent method[59c] *N*-hydroxyurea was added to dimethyl acetylenedicarboxylate to give **107**. The corresponding amide **108** was then reduced with borane-dimethyl sulfide, thus providing **109** in three steps in *ca.* 30% yield.



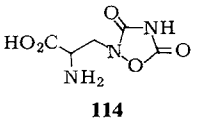
**107**, R = $OCH_3$
**108**, R = $NH_2$



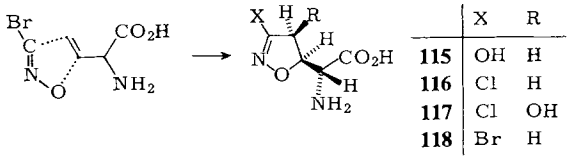
**109** **110**



**111** **112**, R = Glucosyl **113**



**114**

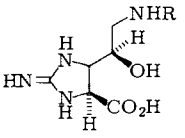


| | X | R |
|---|---|---|
| **115** | OH | H |
| **116** | Cl | H |
| **117** | Cl | OH |
| **118** | Br | H |

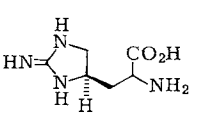
The two oxazolidines **111** and **112** were isolated from young pea seedlings and identified by spectroscopy and degradation. Treatment with weak base and subsequent acid hydrolysis gave α,β-diaminopropionic acid from **111** and D-glucose and glutamic acid from **112**. It was suggested that these highly UV-sensitive compounds take part in a photobiological process[3c]. They were also detected in other leguminosae, *e.g. Lathyrus odoratus*, in which 2-amino-4-(5-oxo-2-isoxazolyl)butyric acid **113** also occurs[3g]. The constitution of quisqualic acid **114** with the L-configuration from *Quisqualis fructus* could be proven by synthesis[3h]. Tricholomic acid **115** has been isolated from *Tricholoma*[60] and the chloroisoxazolidine derivatives **116** and **117**[3h], with antibacterial and antitumor activity, from cultures of *Streptomyces sviceus*. Here again synthetic routes were investigated[61], of which the 1,3-dipolar addition of bromonitrile oxide to vinylglycine to give **118** proved to be successful[61b].

### 4.5. Cyclic Guanidine Derivatives

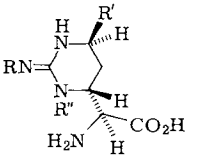
These compounds all occur as building units in the peptide antibiotics from microorganisms and are structurally and stereochemically related to arginine[3c]. The structure of the strongly basic amino acid streptolidin **119**, obtained from antibiotics such as streptolin, streptothricin and geo-



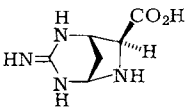
**119**, R = H
**120**, R = $CH_3$



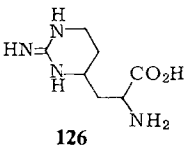
**121**



| | R | R′ | R″ |
|---|---|---|---|
| **122** | H | OH | H |
| **123** | H | H | H |
| **124** | $CH_3$ | H | $CH_3$ |



**125**

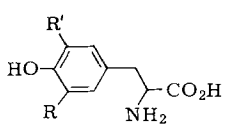


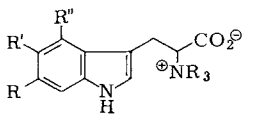
**126**

mycin by hydrolysis, which has been a subject of controversy was established by X-ray analysis and by synthesis from chiral sugar units[8b,62]. In the case of the *N*-methyl derivative **120**, similarly obtained from a streptothricin-type antibiotic, the configuration of the OH group is still obscure[3c]. The two α-epimers enduracididine and alloenduracididine **121** have been isolated from enduracidin[3b]. The two six-membered ring guanidine derivatives tuberactidine **122** and viomycidine **125**[3c] were obtained from the hydrolyzate of the highly antitubercular tuberactinomycin, and the capreomycidine **123** from the equally active capreomycin[63]. The relative and absolute configurations of stendomycidine **124** from the peptide antibiotic stendomycin have been established as L-*erythro*, mainly by ORD[3c]. Tetrahydrolathyrine **126** has been isolated from *Lanchocarpus costaricencis*[31].

## 5. Halogen-Containing and Other Aromatic Amino Acids

The chloro- and bromo-derivatives **127–131** of tyrosine were isolated from the hydrolyzates of the scleroproteins of molluscs. Halogenated tryptophane also occur in nature; the betaine 6-bromo-L-hypaphorine **132** in legumes



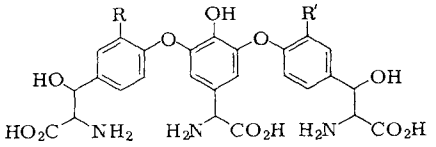


| | R | R′ |
|---|---|---|
| **127** | Cl | H |
| **128** | Cl | Br |
| **129** | Br | H |
| **130** | Cl | Cl |
| **131** | Br | Br |

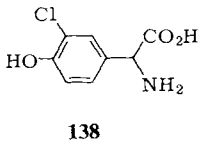
| | R | R′ | R″ | $R_3$ |
|---|---|---|---|---|
| **132** | Br | H | H | $(CH_3)_3$ |
| **133** | H | Cl | H | $H_3$ |
| **134** | H | H | Cl | 2H, $COCH_2CO_2C_2H_5$ |
| **135** | H | H | Cl | 2H, $COCH_2CO_2CH_3$ |

and sponges[64] and 5-chloro-D-tryptophan **133** as a component of the antibiotic longicatenamycin[65]. The positive Cotton effect indicates, as in the case of D-tryptophan, a D-configuration, which was confirmed by the ozonolysis of **133** to D-aspartic acid. The 4-chlorotryptophan derivatives **134** and **135** isolated from *Pisum sativum* also belong to the D-series[2a].

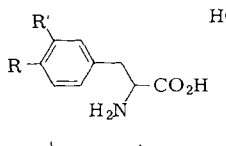
Antibiotics from the vancomycin group contain as a structural unit the unusual vancomycinic acid **136**, which itself contains 3-chloro-β-hydroxytyrosine units; the monochlorotricarboxylic acid **137** occurs in the glycopeptide antibiotic actinoidin and 3-chloro-4-hydroxyphenylglycine **138** is a component of the antibiotic LL-AV290[3g]. Two other chlorine-containing amino acids have already been mentioned with the unsaturated amino acids in Table 1[3g,3e] and the chloroisoxazolines **116** and **117** in Section 4.4.



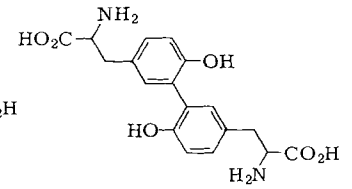
**136**, R = R' = Cl
**137**, R = H, R' = Cl



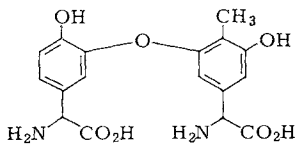
**138**



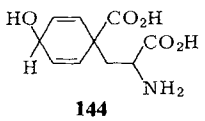
| | R | R' |
|---|---|---|
| **139** | H | $CH_2OH$ |
| **140** | OH | $CH_2OH$ |
| **141** | $NH_2$ | H |



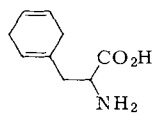
**142**



**143**



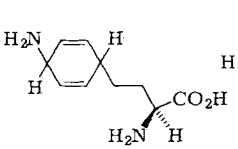
**144**



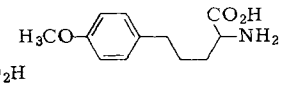
**145**

Before turning to sulfur-containing heterocycles, a few more phenylalanine derivatives from higher plants should be cited: the hydroxymethyl compounds **139** and **140** from *Caesalpinaia tinctoria* and the *p*-aminophenylalanine **141** from *Vigna vexillata*[2b].

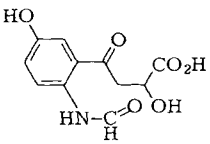
The dimeric tyrosine **142** was identified as a component of alkali-soluble connective tissue protein[2b] and may have been formed by phenol oxidation[66]. Whether the antibiotic ristocetin, which is reminiscent of **136** and **137**, or ristomycin A **143**[31] is formed analogously is an open question. Pretyrosine **144**, derived from prephenic acid in the blue-green alga *Pseudomonas aeruginosa*, is of biosynthetic interest, being enzymatically converted into phenylalanine or tyrosine **94**[67]. Acid degradation of **144** gave phenylalanine. Further dihydroarenes are: L-β-(1,4-cyclohexadienyl)alanine **145** from rats, *Leuconostoc destranicum* and streptomycetes[2a]; the amino acid antibiotic L-2-amino-4-(4-amino-2,5-cyclohexadienyl)butyric acid **146**[3g];



**146**



**147**



**148**

(+)-*trans*-2,3-dihydro-3-hydroxyanthranilic acid from *Str. aureofaciens S-652*[68]. L-β-(2,5-Dihydroxyphenyl)alanine from streptomycetes[2a] and *N*-carbamoyl-2-(4-hydroxyphenyl)glycine from the leaves of *Vicia faba*[2a], 3-carboxy-L-tyrosine from the seeds of *Reseda odorata*[69], 3-formylaminosalicylic acid from antimycin A3[70], alternamic acid **147**[71] from the toxin alternariolide in *Alternaria mali*, blespharismone **148** from *Blespharisma japonicum* and finally the oxime of the *p*-hydroxyphenylpyruvic acid[3h] from the sponge *Hymeniacidon sanguinea* are all new derivatives of aromatic amino acids.

## 6. Sulfur-, Selenium- and Phosphorus-Containing Amino Acids

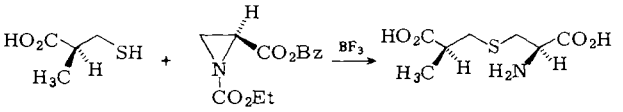
Many new sulfur-containing amino acids from the plant and animal kingdoms are derivatives or homologues of cysteine and methionine (Table 2).

Table 2. New sufur-containing amino acids.

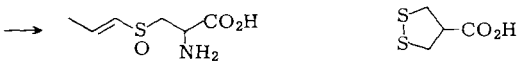
| Sulfur-containing amino acid | isolated from | Ref. |
|---|---|---|
| *N*-Formylmethionine | *Clostridium pasteurianum*, rubredoxin, the thorax of the honey bee | [2a] |
| *N*-Acetylmethionine | thorax of bees | [2a] |
| L-Homomethionine | cabbage | [2a] |
| *N*-Methylmethionine sulfoxide | red algae | [3h] |
| *S*-(2-Carboxy-2-hydroxyethyl)cysteine | human urine | [2a] |
| *S*-(Carboxymethyl)homocysteine | urine of cystathionuric and homocystinuric patients | [2a] |
| *S*-(3-Carboxy-3-hydroxypropyl)cysteine | | [2a] |
| *S*-(3-Carboxy-3-hydroxypropylthio)homocysteine | | [2a] |
| *S*-(2-Carboxy-2-hydroxyethylthio)homocysteine | | [2a] |
| *S*-(3-Carboxy-3-hydroxypropyl)homocysteine | | [2b] |
| *S*-(Carboxymethylthio)homocysteine | | [2b] |
| *S*-(2-Carboxy-2-hydroxyethylthiomethyl)-L-cysteine | *Acacia georginae* | [2b] |
| Cystathionine sulfoxide | urine of cystathionuric patients | [3h] |
| Perhydro-1,4-thiazepin-3,5-dicarboxylic acid | | [3h] |
| α-*S*-Cysteinylthymine | collagen from cattle bones | [3k] |

(−)-*S*-(2-Carboxypropyl)-L-cysteine **151**[12] is found in the glutathione-like tripeptide from onions and garlic and is converted into *trans*-*S*-1-propenyl-L-cysteine *S*-oxide **152**, the precursor of the lachrymatory principle of the onion[1]. Asparagusic acid **153**[73] found in asparagus, is also formed from **151**. The absolute configuration of **151** was established by the synthesis of both stereoisomers. Both enantiomers of 3-mercapto-2-methylpropionic acid ester **149** were reacted with the aziridinecarboxylic acid ester **150**, which is readily available from L-serine, in the presence of $BF_3$ to give **151**. After removal of the protecting group only **151** derived from (*S*)-**149** showed a negative optical rotation corresponding to the natural acid[12].

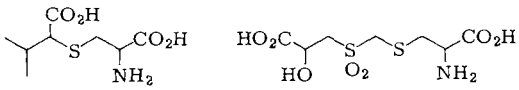
Further examples are the cysteine derivative isovalthine **154**[74], which was first isolated some time ago from the urine of people with an excessive cholesterol level, dichrostachinic acid **155**[75] from the seeds of *Dichrostachys glomerata*, L-1,4-thiazinane-3-carboxylic acid **156**[3k] from the alga *Heterochordaria abietina* and dopa with two cysteine residues **157**[3h] from the eyes of the alligator gar *Lepisosteus spatula*.



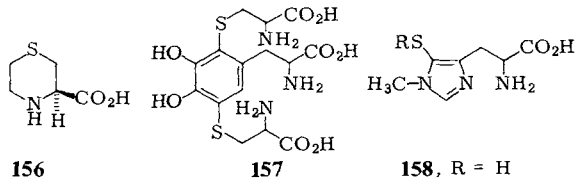
(*S*)-**149** **150** (*S*)-**151**



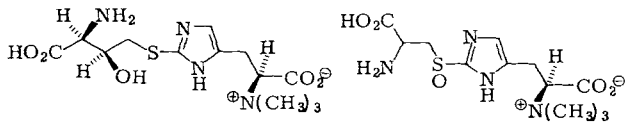
**152** **153**



**154** **155**



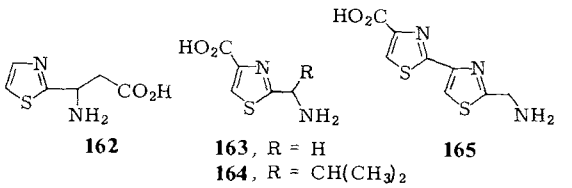
**156** **157** **158**, R = H
**159**, R = S–dimer



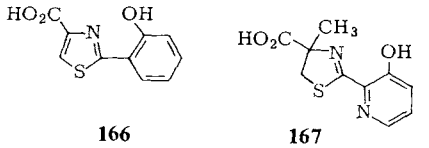
**160** **161**

5-Mercapto-1-methyl-L-histidine **158** can be separated from the hydrolyzate of the $Fe^{III}$-binding adenochrome of *Octopus vulgaris*. Recently **158** has been found in the eggs of sea urchins which also contain the corresponding disulfide **159**[76]. The mercaptohistidine derivatives clithioneine **160**[77] and *S*-(2-amino-2-carboxyethyl)ergothionine **161**[78] were isolated from the toadstool *Clitocybe acromelalga* and *Neurospora crassa*, respectively.

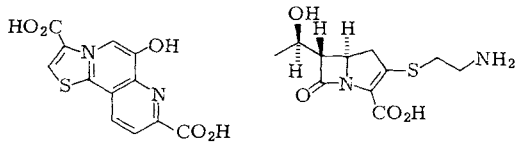
β-(2-Thiazolyl)-β-alanine[79] **162** from bottromycin and the other thiazole derivatives such as **163** which are com-



**162** **163**, R = H **165**
**164**, R = $CH(CH_3)_2$



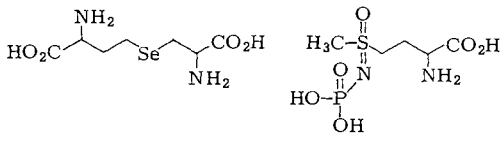
**166** **167**



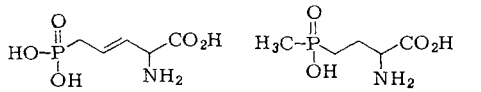
**168** **169**

ponents of a cyclic peptide from the sea hare *Dolabella auricularia*[80], **164**[81a] from ascidiacyclamide, the *sec*-butyl isomer of **164** from bacitracin[81b] and related compounds, the absolute configuration of which can be derived from degradation products obtained with singlet $O_2$[81c], the bithiazolylcarboxylic acid **165** as the *N*-terminal amino acid of the anticancer antibiotic bleomycin $A_2$[82], aeruginic acid **166**[83] from *Pseudomonas aeruginosa*, **167**[84] from *Streptomyces antibioticus*, berninamycinic acid **168** from the antibiotic berninamycin A[85] and the penicillin-like antibiotic thienamycin **169**[86] conclude the list of new sulfur-containing amino acids.

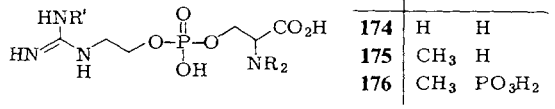
Several examples of selenium- and phosphorus-containing amino acids have been confirmed. Selenocysteine was identified as amino acid No. 35 in the peptide chain of the enzyme glutathione peroxidase from cattle erythrocytes[87], *Se*-methylselenocysteine[3b] was found in *Astragalus bisculatus*, selenomethionine[3f] in lima beans and selenocystathionine **170**[2a] in *Morinda reticulata*. The *N*-Phosphonosulfonimidoxyl derivative **171**[3f] was isolated from an unclassified *Streptomyces* as a metabolite.



**170** **171**



**172** **173**



| | R | R' |
|---|---|---|
| **174** | H | H |
| **175** | $CH_3$ | H |
| **176** | $CH_3$ | $PO_3H_2$ |

D-2-Amino-5-phospho-3-pentenoic acid **172**[3i] occurs in a tripeptide from *Streptomyces plumbeus*. The phosphate ester of 4-hydroxypipecolic acid[3k] was isolated from *Pel-*

*tophorum*. Phosphinothricin **173**[3g] is the *N*-terminal amino acid in a tripeptide, with two alanine residues, which is a component of an antibiotic. L-Lombricine **174** from *Lumbricus terrestris* is also found in smaller quantities in the marine worm *Thalassema neptuni*, from whose muscles the $N^{\alpha}$,$N^{\alpha}$-dimethyl derivative, L-thalassamin **175**, and *N*-phosphothalassamin **176** were isolated[3e,88].

## 7. Aliphatic Amino Acids

New amino acids whose constitutions differ only slightly from the regular protein amino acids have also been found in large numbers. Because of the rarity of the nitrile group in nature[89], β-cyanalanine from the embryos of *Vicia sativa* and *Acacia georginae*[2b] and L-2-amino-4-cyanobutyric acid from *Chromobacterium violaceum* cultures, which contain cyanide ion in the nutrient solution[3c], are mentioned first.

### 7.1. Neutral α-Amino Acids

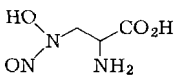
α-Amino acids with the "unnatural" D-configuration have been repeatedly found: D-alanine[2b] in the cell walls of bacteria and also in higher plants, D-valine in valinomycin, and D-isoleucine[3b] in monamycin as well as D-Ala, D-Phe, D-Asp and D-Glu in a toxic peptide lophyrotonin from larvae of a fly (*Laphyrotoma interrupta*), which in Australia can be fatal for cattle[107]. With the cyclic peptide or peptidolactono-antibiotics the interesting question arises as to whether the D-amino acids are incorporated as such or whether they are first built in as the L-amino acids and then epimerized. In the latter case D-isoleucine must be derived from L-alloisoleucine, which has not yet been found in nature, although *N*-methyl-γ-methyl-L-alloisoleucine is found in etamycin and triostin C[2a]. Furthermore, *N*-methylalloisoleucine[3c] was found in cycloheptamycin, 2-amino-4-oxopentanoic acid[2a] in *Clostridium stricklandii*, and isoleucine, acylated on the nitrogen by jasmonic and dihydrojasmonic acids, in the fungus *Giberella fujikuroi*[2a]. Glutathione derivatives of leucotrienes play an important role in the human body[90].

### 7.2. α-Branched Amino Acids

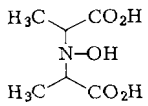
These compounds are of interest as antimetabolites and enzyme inhibitors, as for example α-methyldopa. They also occur naturally; like α-aminoisobutyric acid (α-methylalanine) and (−)-isovaline (2-aminovaleric acid, "β-ethylalanine") in peptide antibiotics. According to the X-ray crystallographic analysis of the *N*-chloroacetyl derivative, (−)-isovaline has the D-configuration[91], and is readily available through Schöllkopf's lactim-ether synthesis[92] with 93% enantioselectivity.

### 7.3. Hydroxy-α-Amino Acids

New hydroxy-α-amino acids are: *N*-(2-hydroxyethyl)-glycine and -alanine[2a] from the seaweed *Petalonia jascia* and from Rumen protozoa, *O*-ethyl-, *O*-*n*-propyl- and *O*-*n*-butyl-L-homoserine[3a] from *Corynebacterium ethanolaminophilum*, D-allothreonine from pseudobactin[48], *threo*-L-2-amino-3,4-dihydroxybutyric acid[2a] and L-β-hydroxynorvaline[2a] from microorganisms, (2*S*,4*S*)-(+)-γ-hydroxynorvaline and the (4*R*)-(−)-epimer[2b] from *Boletus satanus*, β-hydroxyvaline[2b] from an antibiotic, (2*S*,3*R*,4*R*)-γ-hydroxyisoleucine[2b] from the seeds of *Trigonella foenum-graecum*, γ,δ-dihydroxyisoleucine[2a] from *Amanita phalloides*, as well as alanosine **177**[93] from *Streptomyces alanosinicus*. Finally, we have the following four *N*-hydroxyamino acids: L-2-amino-5-(1-hydroxyguanidino)valeric acid ($N^5$-hydroxyarginine)[3f] from *Nanniizzia gypsea*, the D-enantiomer from the Fe(III) complex pseudobactin[48], $N^{\epsilon}$-hydroxylysine from aerobactin[94] and compound **178** from the fly agaric[95] which forms, *in situ*, the pale blue complex amavadin with vanadium.



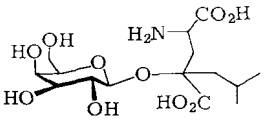
**177**



**178**

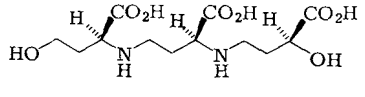
### 7.4. Acidic Amino Acids and Diaminodicarboxylic Acids

New amino acids in this group are: *threo*-β-hydroxy-L-aspartic acid[3h] from streptomyces and the compound with a D-configuration from the Fe(III) complex pseudobactin[48], *erythro*-β-hydroxy-L-aspartic acid[2a] from *Astralagus sinicus*, β-carboxyaspartic acid from the ribosomal protein of *E. coli*[96], *threo*-β-methyl-L-aspartic acid[2a] from the antibiotic amphomycin, *threo*-β-hydroxy-L-glutamic acid[2a] from streptomyces, (2*S*,4*R*)-4-methylglutamic acid[2b] from *Gleditsia caspica*, (2*S*,3*S*,4*R*)-3-hydroxy-4-methylglutamic acid[2b] from *Gleditsia caspica* and from *Gymnocladus dioicus*, as well as β-hydroxy-γ-methylglutamic acid[3i] from the seeds of the Kentucky coffee tree.

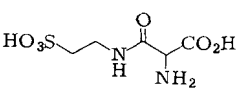


**179**

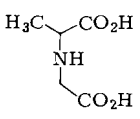
(2*S*,4*R*)-4-(β-D-Galactopyranosyloxy)-4-isobutylglutamic acid[3f] **179** from *Reseda odorata* is the first example, in the higher plants, of a glycoside in which the sugar is attached to the hydroxyl group of an aliphatic aminohydroxy acid. Further acidic amino acids are: 2-amino-4,5-hydroxyadipic acid from human urine[3k], 2-amino-4-methylpimelic acid[3h] from the fruiting body of *Lactarius quietus*, 2,6-



**180**



**181**

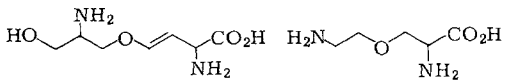


**182**

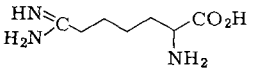
diamino-3-hydroxypimelic acid[2a] from the cell walls of microorganisms, 2,6-diamino-7-hydroxyazelaic acid[3c] from edeine A and B, avenic acid **180**[97] from oat roots (chelates with iron), arcamin **181**[98] from *Acra zebra* and strombin **182**[98] from *Strombus gigas*.

### 7.5. Basic Amino Acids

New basic amino acids to be mentioned are: β-acetamido-L-alanine[3a] from *Acacia armata*, β-(3-hydroxyureido)-L-alanine[3f] from streptomyces, L-2-amino-3-(oxalamino)propionic acid[2a] from *Lathyrus sativus*, 2-amino-3-(1-hydroxyureido)propionic acid[3f] from *Quisqualis fructus*, 4-guanidinobutyric acid together with 2,3-diaminopropionic acid from the seeds of *Trichosanthes cucumeroides*[99], 2,3-diaminobutyric acid from asparatocin (the L-*threo*- and D-*erythro* forms occur in amphomycin)[2a], 4-amino-2-(6-methyloctanoylamino)butyric acid[2a] from *Bacillus colistinus* as well as L-2-amino-4-(lactoylamino)butyric acid[2b] from *Beta vulgaris*. *O*-(2-amino-3-hydroxypropyl)homoserine, dihydrorhizobitoxin and the corresponding β,γ-unsaturated 2-amino-4-(2-amino-3-hydroxypropoxy)-*trans*-3-butenoic acid **183**[2b], known as rhizobitoxin, were isolated from *Rhizobium japonicum*. **183** deactivates β-cystathionase in bacteria and plants and prevents the formation of ethylene from methionine (see **6** and **7** in Section 3). δ-Amidinooxy-L-norvaline was isolated from a bacterial culture[3f]. Other new basic amino acids are: 2,4-diaminovaleric acid[2a] from *Clostridium stricklandii*, (2*S*,4*R*,5*R*)-4,5-dihydroxyornithine[3i] from the antibiotic



**183** **184**

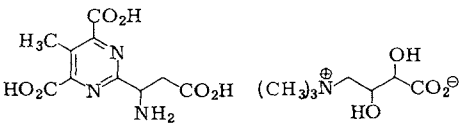


**185**

echinocandin B, $N^{\delta}$-(1-iminoethyl)-L-ornithine[2b] from streptomyces (acts like an arginine metabolite), 2-amino-5-(1-methylguanidino)valeric acid[2a] from rat-liver proteins, 2-amino-5-(3,3-dimethylguanidino)valeric acid and 2-amino-5-(2,3-dimethylguanidino)valeric acid[3c] from human urine, γ-hydroxyarginine[100] from sea cucumbers, γ-hydroxycitrullin[2a] from *Vicia fulgens* and related species, $N^{\varepsilon}$,$N^{\varepsilon}$-dimethyllysine[2a] from amoebae, $N^{\varepsilon}$,$N^{\varepsilon}$,$N^{\varepsilon}$-trimethyl- and $N^{\varepsilon}$-methyllysine[2a] from myosine, β-hydroxy-$N^{\varepsilon}$,$N^{\varepsilon}$,$N^{\varepsilon}$-trimethyllysine[3i] from *Neurospora crassa*, δ-hydroxy-$N^{\varepsilon}$,$N^{\varepsilon}$,$N^{\varepsilon}$-trimethyl-L-lysine[3c] and the corresponding *O*-phosphoric acid ester from the cell walls of diatoms, *threo*-γ-hydroxy-L-lysine[3h] from the antibiotics cerexin A and B, $N^{\varepsilon}$-acetyl-*allo* δ-hydroxy-L-lysine[3l] from *Beta vulgaris*, $N^{\alpha}$,$N^{\varepsilon}$-(2,3-dihydroxybenzoyl)-L-lysine[3c] from *Azotobacter vinelandii*, γ-oxa-L-lysine[2a] **184** from *E. coli* and streptomycetes, indospicine[2a] **185** from plants (should have heptatoxic and teratogenic activity), $N^{\varepsilon}$-(4-amino-2-hydroxybutyl)lysine[2a] from cattle brain, and $N^{\varepsilon}$-acetyl-$N^{\varepsilon}$-hydroxylysine as the α-amide of citric acid in the Fe(III) complex from *Aerobacter aerogenes*[94,101].

### 7.6. Non-α-Amino Acids

Most amino acids in which the amino group does not occur in the α-position were formerly isolated from peptide antibiotics and are themselves antibiotics such as **86** and **87** or have complex structures such as the pigment **83** or the alkaloids **84** and **85**. In addition the following β- and γ-amino acids belong to this group: isoserine and β-tyrosine[2a] from edeine A and B, 4-amino-2,3-dihydroxy-3-methylbutyric acid[2a] from carcinophilin, 5-amino-4-hydroxyvaleric acid[2a] from *Rhodospirillum rubrum*, puretanin (3-(4-aminobutylamino)propionic acid)[2a] from, *inter alia*, human brain and urine, 3-amino-3-phenylpropionic acid[3c] from *Rocella canariensis*, 4-amino-2-hydroxy-3-oxo-butyric acid[3k] from human urine, $N^{\beta}$-methyl-L-β-arginine[3k] from the antibiotic LL-BM 547 B, γ-hydroxy- and δ-hydroxy-β-lysine[2a,b] from tuberactinomycin A as well as 4-amino-3,6-dihydroxymethylhexanoic acid[2b] from pepstatin A and 4-amino-3-hydroxy-2-methylhexanoic acid[2b], also from pepstatin A. β-2-(Thiazolyl)-β-alanine **162**[79] has already been mentioned in Section 6.



**186** **187**

The heterocyclic-substituted alanine **186**[2b] was found in bleomycin. Anthopleurine **187**[102], the alarm substance in sea anemones, has the trimethylammonium group in the γ-position.

## 8. Outlook

It is to be expected that the number of new amino acids will continue to increase, although not at the same rate as in the last 30 years. Already the number is overwhelming and one can ask whether it is still justifiable to group them roughly according to their structural features. However, so long as so little is known about their biosynthetic relationships and their function in metabolism, the form of classification chosen here may be accepted on the grounds that it at least helps to identify new naturally occurring amino acids.

Many modern developments in the chemistry of natural amino acids deserve more attention, for example the recognition of new metabolic pathways for tyrosine as a precursor of pigments and antibiotics which can be used as supporting evidence for the evolutionary tree, or the psychotropic activity of isooxazole derivatives such as ibotenic acid. Nature makes use of the *N*-hydroxyamino acids as the building units of chelating agents for the accumulation of heavy metals from the environment[95], or for the transportation of iron[94,101]. Last, but not least, the determination of the age of bones from classical antiquity[103], or the checking of the age of the Dead Sea Scrolls by means of measurements of the racemization of amino acids such as aspartic acid from the collagen which the

samples contain[104] may be of general interest and useful for non-chemists[108].

Received: June 29, 1983 [A 472 IE]
German version: *Angew. Chem. 95* (1983) 827
Translated by Dr. *D. Maass*, Kronberg/Ts. (Germany)

[1] H. Musso, *Angew. Chem. 68* (1956) 313.
[2] a) *International Review of Science, Organic Chemistry Series One 6* (1973) 1; b) *Two 6* (1976) 1.
[3] a) *Amino Acids, Peptides and Proteins*, Specialist Periodical Reports, Chem. Soc., London *1* (1969) 1; b) *2* (1970) 1; c) **3** (1971) 1; d) *4* (1972) 1; e) *5* (1974) 1; f) *6* (1975) 1; g) *7* (1976) 1; h) *8* (1976) 1; i) *9* (1978) 1; j) *10* (1979) 1; k) *11* (1981) 1; l) *12* (1981) 1.
[4] W. R. Gray, B. S. Hartley, *Biochem. J. 89* (1963) 59.
[5] K. R. Woods, K. T. Wang, *Biochim. Biophys. Acta 133* (1967) 369.
[6] H. Laatsch, *Chromatogr. J. 173* (1979) 398.
[7] F. Weygand, R. Geiger, *Chem. Ber. 92* (1959) 2099; F. Weigand, G. Kippling, D. Palm, *ibid. 93* (1960) 2619; H. Döpp, S. Maurer, A. N. Sasaki, H. Musso, *Liebigs Ann. Chem. 1982*, 254.
[8] a) After its occurrence in geomycin previously also called geamin; H. Brockmann, H. Musso, *Chem. Ber. 88* (1955) 648; b) B. W. Bycroff, T. J. King, *J. Chem. Soc. Chem. Commun. 1972*, 652.
[9] B. Feibush, E. Gil-Av, *Tetrahedron 26* (1970) 1361; E. Gil-Av, P. E. Hare, A. Tishbee, *J. Am. Chem. Soc. 102* (1980) 5115; *J. Chromatogr. 112* (1975) 121.
[10] a) F. Kerek, G. Snatzke, *Angew. Chem. 87* (1975) 133; *Angew. Chem. Int. Ed. Engl. 14* (1975) 109; b) U. Nagai, M. Kawai, *Tetrahedron Lett. 22* (1981) 653.
[11] A. B. Mauger, O. A. Stuart, E. Katz, K. T. Mason, *J. Org. Chem. 42* (1977) 1000.
[12] R. J. Parry, M. V. Naidu, *Tetrahedron Lett. 24* (1983) 1133.
[13] R. Destro, A. Colombo, *J. Chem. Soc. Perkin Trans. 2 1979*, 896.
[14] J. F. Bagli, D. Kluepfel, M. St. Jacques, *J. Org. Chem. 38* (1973) 1253. Synthesis from D-fructose: L. Baufi, M. Gracia-Beretta, L. Colombo, C. Gennari, C. Scolastico, *J. Chem. Soc. Perkin Trans. 1 1983*, 1613.
[15] A. Holm, P. J. Scheuer, *Tetrahedron Lett. 21* (1980) 1125.
[16] B. B. Snider, J. V. Duncia, *J. Org. Chem. 46* (1981) 3223.
[17] M. Ahmed, M. Y. Jarrah, E. R. H. Jones, A. F. Magalhaes, M. G. Roberts, V. Thaller, *J. Chem. Res. 1981*, 262.
[18] T. Hiyama, M. Kai, *Tetrahedron Lett. 24* (1983) 2103.
[19] K. Lürssen, K. Naumann, R. Schröder, *Naturwissenschaften 66* (1979) 264.
[20] N. Amrhein, D. Seebeck, H. Skorujska, S. Tophof, J. Stöckigt, *Naturwissenschaften 68* (1981) 619.
[21] C. Gröger, H. Musso, I. Roßnagel, *Chem. Ber. 113* (1980) 3621.
[22] H. Musso, H. Nozaki: *IUPAC Current Trends in Organic Synthesis*, Pergamon Press, London 1983, p. 371.
[23] P. Lindberg, R. Bergmann, B. Wickberg, G. M. Hatfield, P. P. Schaumberg, *J. Chem. Soc. Chem. Commun. 1975*, 946; *J. Chem. Soc. Perkin Trans. 1 1977*, 684.
[24] A. Ishihara, K. Shiraishi, H. Sato, S. Sakamura, K. Nishiyama, R. Sakai, A. Furasaki, T. Matsumoto, *J. Am. Chem. Soc. 99* (1977) 636. New synthesis: M. Suzuki, E. E. Gooch, C. H. Stammer, *Tetrahedron Lett. 24* (1983) 3839.
[25] A. Jöhl, W. G. Stoll, *Helv. Chim. Acta 42* (1959) 156.
[26] E. A. Bell, M. Y. Qureshi, R. J. Pryce, D. H. Janzen, P. Lemke, J. Chardy, *J. Am. Chem. Soc. 102* (1980) 1409.
[27] M. C. Pirrung, *Tetrahedron Lett. 21* (1980) 4577.
[28] M. Budesinsky, Z. Prochazka, H. Budzikiewicz, A. Römer, H. Ripperger, K. Schreiber, G. Scholz, *Tetrahedron 37* (1981) 191.
[29] K. Nomoto, Y. Mino, T. Ishida, H. Yoshioka, N. Ota, M. Inoue, S. Takagi, T. Takemoto, *J. Chem. Soc. Chem. Commun. 1981*, 338.
[30] T. T. Howarth, A. G. Brown, T. J. King, *J. Chem. Soc. Chem. Commun. 1976*, 266.
[31] H. Wieland, B. Witkop, *Justus Liebigs Ann. Chem. 543* (1940) 171.
[32] J. C. Sheehan, H. G. Zachau, W. B. Lawson, *J. Am. Chem. Soc. 79* (1957) 3933.
[33] K. G. Untch, G. A. Gibbon, *Tetrahedron Lett. 1964*, 3259.
[34] M. Pailer, W. G. Kump, *Monatsh. Chem. 90* (1959) 396.
[35] J. W. W. Morgan, *Chem. Ind. (London) 1964*, 542.
[36] F. Irreverre, K. Morita, A. V. Robertson, B. Witkop, *J. Am. Chem. Soc. 85* (1963) 2824.
[37] J. D. Ogle, R. B. Arlinghaus, M. A. Logan, *J. Biol. Chem. 237* (1962) 3667.
[38] J. C. Sheehan, R. R. Kuhn, *J. Org. Chem. 29* (1964) 2008.
[39] J. U. Kahl, Th. Wieland, *Liebigs Ann. Chem. 1981*, 1445.
[40] W. Oppolzer, K. Thirring, *J. Am. Chem. Soc. 104* (1982) 4978.
[41] W. Oppolzer, C. Robbiani, K. Bättig, *Helv. Chim. Acta 63* (1980) 2015.
[42] T. Takemoto, K. Daigo, Y. Kondo, K. Kondo, *J. Pharm. Soc. Jpn. 1966*, 86, 874.
[43] K. Konno, H. Shirahama, T. Matsumoto, *Tetrahedron Lett. 24* (1983) 939.
[44] H. J. Monteiro, *J. Chem. Soc. Chem. Commun. 1973*, 2.
[45] T. Fujita, Y. Takaishi, A. Okamura, *J. Chem. Soc. Chem. Commun. 1981*, 585.
[46] W. A. König, K. P. Pfaff, H. H. Bartsch, H. Schmalle, H. Hagenmaier, *Liebigs Ann. Chem. 1980*, 1728.
[47] W. Hass, W. A. König, *Liebigs Ann. Chem. 1982*, 1615. Synthesis: B. J. Banks, A. G. M. Barrett, M. A. Russell, D. J. Williams, *J. Chem. Soc. Chem. Commun. 1983*, 873.
[48] M. Teintze, M. B. Hossain, C. L. Barnes, J. Leong, D. van der Helm, *Biochemistry 20* (1981) 6446.
[49] J. L. van der Baan, J. W. F. K. Barnick, F. Bickelhaupt, *Tetrahedron 34* (1978) 223.
[50] M. P. Edwards, S. V. Ley, S. G. Lister, B. D. Palmer, *J. Chem. Soc. Chem. Commun. 1983*, 630.
[51] H. Musso, *Tetrahedron 35* (1979) 2843.
[52] H. Reznik, *Ber. Dtsch. Bot. Ges. 88* (1975) 179.
[53] N. Fischer, A. S. Dreiding, *Helv. Chim. Acta 55* (1972) 649.
[54] G. Impellizzeri, M. Piattelli, *Phytochemistry 11* (1972) 2499.
[55] H. Barth, G. Burger, H. Döpp, M. Kobayashi, H. Musso, *Liebigs Ann. Chem. 1981*, 2164.
[56] L. H. Hurley, *Acc. Chem. Res. 13* (1980) 263.
[57] P. S. Steyn, A. A. Tuinman, F. R. van Herden, P. A. van Rooyen, P. L. Wessels, C. J. Rabie, *J. Chem. Soc. Chem. Commun. 1983*, 47.
[58] T. Takemoto, T. Nakajiama, R. Sakuma, *Yakugaku Zasshi 84* (1964) 1186, 1232, 1233; *Chem. Abstr. 62* (1965) 7050, 8121, 11901.
[59] a) P. Krogsgaard Larsen, S. B. Christensen, *Acta Chem. Scand. B 30* (1976) 281; b) B. E. McCarry, M. Savard, *Tetrahedron Lett. 22* (1981) 5153; c) V. Jäger, M. Frey, *Liebigs Ann. Chem. 1982*, 817.
[60] T. Takemoto, T. Nakajima, *Yakugaku Zasshi 84* (1964) 1183.
[61] a) J. E. Baldwin, C. Hoskins, L. Kruse, *J. Chem. Soc. Chem. Commun. 1976*, 795; b) A. A. Hagedorn III, B. J. Miller, J. O. Nagy, *Tetrahedron Lett. 21* (1980) 229.
[62] a) T. Goto, T. Ohgi, *Tetrahedron Lett. 1974*, 1413; b) S. Kusumoto, S. Tsuji, T. Shiba, *ibid. 1974*, 1417.
[63] T. Shiba, T. Ukita, K. Mizuno, T. Teshima, T. Wakamiya, *Tetrahedron Lett. 1977*, 2681.
[64] W. D. Raverty, R. H. Thomson, T. J. King, *J. Chem. Soc. Perkin Trans. 1 1977*, 1204.
[65] a) T. Shiba, Y. Mukunoki, H. Akiyama, *Tetrahedron Lett. 1974*, 3085; b) *Bull. Chem. Soc. Jpn. 48* (1975) 1902.
[66] H. Musso, *Angew. Chem. 75* (1963) 965; *Angew. Chem. Int. Ed. Engl. 2* (1963) 723.
[67] N. Patel, D. L. Pierson, R. A. Jensen, *J. Biol. Chem. 252* (1977) 5839.
[68] J. R. D. McCormick, J. Reichenthal, U. Hirsch, N. O. Sjolander, *J. Am. Chem. Soc. 84* (1962) 3711.
[69] P. O. Larsen, A. Kjaer, *Acta Chem. Scand. 16* (1962) 142.
[70] E. E. van Tamelen, J. P. Dickie, M. E. Loomans, R. S. Dewey, F. M. Strong, *J. Am. Chem. Soc. 83* (1961) 1639.
[71] T. Okuno, Y. Ishita, A. Sugawara, Y. Mori, K. Sawai, T. Matsumoto, *Tetrahedron Lett. 1975*, 335.
[72] M. Entzeroth, T. Kunczik, L. Jaenicke, *Liebigs Ann. Chem. 1983*, 226.
[73] R. J. Parry, A. E. Mizusawa, M. Ricciardone, *J. Am. Chem. Soc. 104* (1982) 1442.
[74] S. Oomori, S. Mizuhara, *Arch. Biochem. 96* (1962) 179.
[75] R. Gmelin, *Hoppe-Seyler's Z. Physiol. Chem. 327* (1962) 186.
[76] A. Palumbo, M. d'Ischia, G. Misuraca, G. Proto, *Tetrahedron Lett. 23* (1982) 3207.
[77] K. Konno, H. Shirahama, T. Matsumoto, *Tetrahedron Lett. 22* (1981) 1617.
[78] Y. Ishikawa, S. E. Israel, D. B. Melville, *J. Biol. Chem. 249* (1974) 4420.
[79] Y. Seto, K. Torii, K. Bori, K. Inabata, S. Kuwata, H. Watanabe, *Bull. Chem. Soc. Jpn. 47* (1974) 151.
[80] G. R. Pettit, Y. Kamano, P. Brown, D. Gust, M. Inoue, C. L. Herald, *J. Am. Chem. Soc. 104* (1982) 905.
[81] a) T. Hamamato, M. Endo, M. Nakagawa, T. Nakanishi, K. Mizukawa, *J. Chem. Soc. Chem. Commun. 1983*, 323; b) E. G. Seebauer, E. P. Duliba, D. A. Scogin, R. B. Gennis, R. L. Belford, *J. Am. Chem. Soc. 105* (1983) 4926; c) J. E. Biskupiak, C. M. Ireland, *J. Org. Chem. 48* (1983) 2302.
[82] Y. Aoyagi, K. Katano, H. Suguna, J. Primeau, L. H. Chang, S. M. Hecht, *J. Am. Chem. Soc. 104* (1982) 5537.
[83] Y. Yamada, N. Seki, T. Kitahara, M. Takahashi, M. Matsui, *Agric. Biol. Chem. 34* (1970) 780.
[84] H. U. Naegeli, H. Zähner, *Helv. Chim. Acta 63* (1980) 1400.
[85] J. M. Liesch, D. S. Millington, R. C. Pandey, K. L. Rinehart, Jr., *J. Am. Chem. Soc. 98* (1976) 8237; J. M. Liesch, J. A. McMillan, R. C. Pandey, I. C. Paul, K. L. Rinehart, *ibid. 98* (1976) 299.
[86] G. Albers-Schönberg, B. H. Arison, O. D. Hensens, J. Hirshfield, K. Hoogsteen, E. A. Kaczka, R. E. Rhodes, J. S. Kahan, F. M. Kahan, R.

W. Ratcliffe, E. Walton, L. J. Ruswinkle, R. B. Morin, B. G. Christensen, *J. Am. Chem. Soc. 100* (1978) 6491.
[87] R. Ladenstein, A. Wendel, *Eur. J. Biochem. 133* (1983) 51.
[88] N. van Thoai, Y. Robin, Y. Guillou, *Biochemistry 11* (1972) 3890.
[89] For example ricinine, indolylacetonitrile, diatretyn 2, latyrus factor, bursatellin; Y. Gopichand, F. J. Smitz, *J. Org. Chem. 45* (1980) 5383; cyanocyclin A, T. Hayashi, Y. Nawata, *J. Chem. Soc. Perkin Trans 2 1983*, 335.
[90] B. Samuelsson *Angew. Chem. 94* (1982) 881; *Angew. Chem. Int. Ed. Engl. 21* (1982) 902; *Science 220* (1983) 568; *Angew. Chem. 95* (1983) 854; *Angew. Chem. Int. Ed. Engl. 22* (1983) 805.
[91] R. Bosch, H. Brückner, G. Jung, W. Winter, *Tetrahedron 38* (1982) 3579.
[92] U. Schöllkopf, W. Hartwig, U. Groth, K. O. Westphalen, *Liebigs Ann. Chem. 1981*, 696.
[93] Y. Isoua, H. Kurita, M. Ohmori, M. Sato, *Bull. Chem. Soc. Jpn. 46* (1973) 1847.
[94] P. J. Maurer, M. J. Miller, *J. Am. Chem. Soc. 105* (1983) 240.
[95] H. Kneifel, E. Bayer, *Angew. Chem. 85* (1973) 542; *Angew. Chem. Int. Ed. Engl. 12* (1973) 508.
[96] M. R. Christy, T. H. Koch, *J. Am. Chem. Soc. 104* (1982) 1771.
[97] S. Fushiya, Y. Sato, S. Nozoe, K. Nomoto, T. Takemoto, *Tetrahedron Lett. 21* (1980) 3071.
[98] A. W. Sangsler, S. E. Thomas, *Tetrahedron 31* (1975) 1135.
[99] T. Mukakami, N. Mori, M. Nagasawa, *J. Pharm. Soc. Jpn. 88* (1968) 488.
[100] Y. Fujita, *Bull. Chem. Soc. Jpn. 33* (1960) 1379.
[101] W. R. Harris, C. J. Carrano, K. N. Raymond, *J. Am. Chem. Soc. 101* (1979) 2722.
[102] N. R. Howe, Y. M. Sheikh, *Science 189* (1975) 386.
[103] P. S. Zurer: „Archaeological Chemistry", *Chem. Eng. News 61* (1983) No. 8, p. 26.
[104] S. Weiner, Z. Kustanovich, E. Gil-Av, W. Traub, *Nature (London) 287* (1980) 820.
[105] J. W. Lyga, J. A. Secrist, *J. Org. Chem. 48* (1983) 1982
[106] Synthesis: U. Schmidt, Th. Beuttler, A. Lieberknecht, H. Griesser, *Tetrahedron Lett. 24* (1983) 3573.
[107] D. H. Williams, S. Santikarn, F. De Angelis, R. J. Smith, D. G. Reid, P. B. Oelrichs, J. K. McLead, *J. Chem. Soc. Perkin Trans. 1 1983*, 1869.
[108] *Note added in proof:* Synthesis of the peptide alkaloid zizyphin A containing a β-aminostyryl substituted proline moiety has recently been reported: U. Schmidt, A. Lieberknecht, H. Bökens, H. Griesser, *J. Org. Chem. 48* (1983) 2680. An interesting synthesis of tabtoxin from *Pseudomonas tobaci* has been reported. This bacterium causes wildfire disease on tobacco leafs: J. E. Baldwin, P. D. Bailey, G. Gallacher, K. A. Singleton, P. M. Wallace, *J. Chem. Soc. Chem. Commun. 1983*, 1049.

# Secologanin, a Biogenetic Key Compound— Synthesis and Biogenesis of the Iridoid and Secoiridoid Glycosides

**By Lutz-F. Tietze***

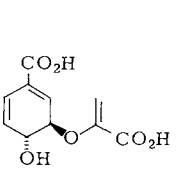
*Dedicated to Professor Hans Brockmann on the occasion of his 80th birthday*

The monoterpene glycoside secologanin is a key intermediate in the biosynthesis of most indole, cinchona, ipecacuanha, and pyrroloquinoline alkaloids, as well as of simple monoterpene alkaloids. More than a thousand alkaloids are formed from secologanin *in vivo*; this represents almost a quarter of this large group of natural products. It is also the parent compound of the secoiridoids. Many of the compounds derived from secologanin display a high degree of biological activity and are employed as pharmaceuticals, *e.g.*, the dimeric indole alkaloid leurocristine (vincristine) which is used very successfully in the treatment of acute leukemia. A knowledge of the biosynthesis and biological reactions of secologanin provides a sound basis for the biosynthesis-orientated classification of numerous natural products and the taxonomy of many plants. Secologanin and structurally related substances can be synthesized in a few steps by stereocontrolled photochemical and thermal cycloadditions. Its biomimetic reaction with amines and amino acids yields other natural products and compounds of pharmacological interest.

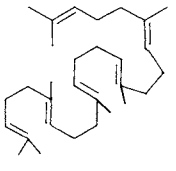
## 1. Introduction

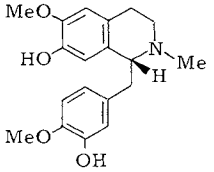
The biosynthesis of natural products proceeds according to simple general principles and only involves a few building blocks. The so-called biogenetic key compounds are especially important; they are generally polyfunctional molecules which occupy a central position in biosynthetic pathways and act as starting compounds for a multitude of other natural products.

An example of one such biogenetic key compound is chorismic acid **1**, which reacts *in vivo* to produce *o*- and *p*-hydroxybenzoic acids and *o*- and *p*-aminobenzoic acids. *p*-Hydroxybenzoic acid as well as *o*- *and p*-aminobenzoic acids undergo further biosynthetic reactions, *p*-hydroxybenzoic acid yielding the ubiquinones, *o*-aminobenzoic acid the amino acid tryptophan, and *p*-aminobenzoic acid, folic acid. Chorismic acid is also the precursor of prephenic acid, which can be converted into the amino acids tyrosine and phenylalanine. Other key compounds worthy of mention are squalene **2**, from which the triterpenes and



**1**


**2**



**3**

[*] Prof. Dr. L.-F. Tietze
Institut für Organische Chemie der Universität
Tammannstrasse 2, D-3400 Göttingen (Germany)

 © Verlag Chemie GmbH, 6940 Weinheim, 1983 0570-0833/83/1111-0828 $ 02.50/0 

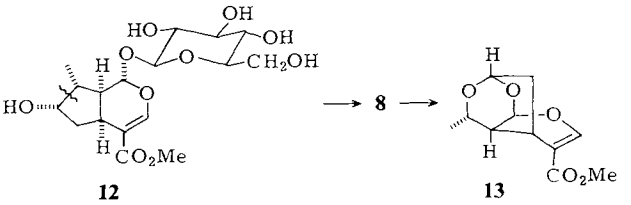
steroids are derived, and the benzyltetrahydroisoquinoline reticulin **3**, formed from the amino acid tyrosine[1], which functions as a precursor in the biosynthesis of the aporphine, morphine, and erythrina alkaloids. A knowledge of the key intermediates which act as common precursors in the biosynthesis of various natural products provides a basis for the biologically sound classification of these compounds and for a meaningful, chemically orientated plant taxonomy[2]. Furthermore, comparison of biogenetic key compounds with novel natural products can help to elucidate their structures; key compounds of this type can also serve as educts for the biomimetic synthesis of natural products[3].

The most important key compound for alkaloid biosynthesis which is not derived from an amino acid is the monoterpene glycoside secologanin **8**. The majority of the indole alkaloids[4,5], the ipecacuanha[6], cinchona[7] and pyrroloquinoline[8] alkaloids, and simple monoterpene alkaloids[9] are formed from secologanin.

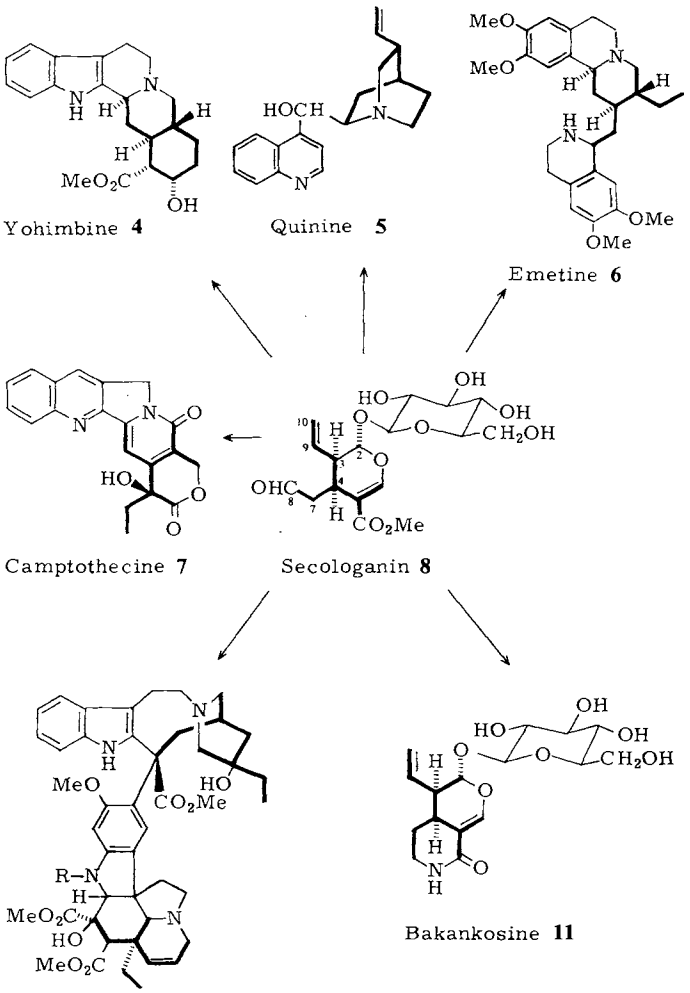
Examples are the indole alkaloid yohimbine **4**, which was isolated from various *Rauwolfia* and *Vinca* species and is used as an aphrodisiac in veterinary medicine[10], and the cinchona alkaloid quinine **5**, which is the oldest known antimalarial agent and has now regained importance for dealing with pathogenic agents which have become resistant to synthetic pharmaceuticals[12a]. Other alkaloids derived from secologanin **8** include the ipecacuanha alkaloid emetine **6**, which is effective in the treatment of amoebic dysentry[12], the pyrroloquinoline alkaloid camptothecin **7**[13], which once seemed to be a promising cytostatic agent[14], and the monoterpene alkaloid bakankosine **11**[15]. The dimeric indole alkaloids leurocristine (vincristine) **10** and vincaleukoblastine **9** are also formed from secologanin **8** *in vivo*, and these substances are used with great success to treat acute leukemia and Hodgkin's disease[16] (Scheme 1).

Furthermore, secologanin **8** is the parent compound of the secoiridoids[17]: sarracenin **13**[18] is an example of such a compound. It was isolated from *Sarracenia flava*, and the extract of these plants displays a strong cytostatic action[19].

This brief review article illustrates the importance of secologanin **8** as a biogenetic key compound: It is the precursor of more than a thousand alkaloids and other natural products. Biologically, secologanin **8** is closely related to the iridoid glycoside logonin **12**, from which it is derived by cleavage of the cyclopentane ring.



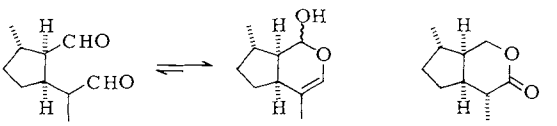
**12** **13**




Scheme 1. Secologanin **8** as a biogenetic key intermediate in the biosynthesis of alkaloids and secoiridoids. The secologanin moiety is shown in bold type.

## 2. Structure and Origin of the Iridoids and Secoiridoids

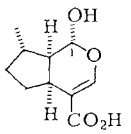
The iridoids and secoiridoids represent two widely distributed classes of natural products which are almost exclusively of plant origin[20]. However, the parent compound iridodial **14** and related substances such as the iridolactone **15** are found in the defensive secretions of some species of ants[21].



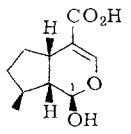
**14a** **14b** **15**

The iridoids are characterized by the presence of a *cis*-linked partially hydrogenated cyclopenta[c]pyran skeleton (iridene).

The formulas, nomenclature, and numbering of the iridoid skeleton used in the literature are inconsistent. Of the two formulas **A** and **B** usually employed, formula **A** is to be preferred as it is consistent with the usual way of representing both the methyl group in the biosynthetic precursors (*e.g.* geraniol) and the centers of chirality in the subsequent biosynthetic products (monoterpenoid indole alkaloids).



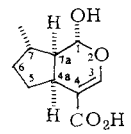
A



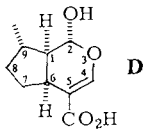
B

The iridoid skeleton can be named and numbered according to the nomenclature used for heterocycle **C** or bicycle **D**. Considerable simplification can be achieved by introducing the name "iridene" (saturated system: iridane = *cis*-2-oxabicyclo[4.3.0]nonane) for the basic iridoid skeleton (see **E**). This is, however, a nonsystematic name[28]. Here, we will adopt the numbering used in **E**.

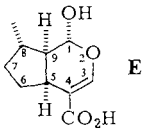
It should be noted that the designation of the absolute configuration at C-1 (formula **A**) may differ if the substituents at C-1 are changed. In the glycosides, C-1 has an (*S*)-configuration, whereas in the aglycones (formulas **C**—**E**) it has an (*R*)-configuration.—The traditional designation is used for secologanin **8** (see Scheme 1).



C



D



E

**C**: (1*R*,4a*S*,7*S*,7a*R*)-1-Hydroxy-7-methyl-1,4a,5,6,7,7a-hexahydrocyclopenta[*c*]pyran-4-carboxylic acid.

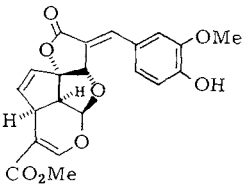
**D**: (1*R*,2*R*,6*S*,9*S*)-2-Hydroxy-9-methyl-3-oxobicyclo[4.3.0]non-4-ene-5-carboxylic acid.

**E**: (1*R*,5*S*,8*S*,9*R*)-1-Hydroxy-8-methyl-3-iridene-4-carboxylic acid.

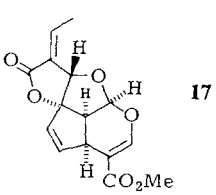
The majority of the iridoids are linked to D-glucose at C-1. There are also iridoids which are either bonded to glucose *via* glycosidic bonds at other positions[22], have other sugar residues[23], or only exist as aglycones[20a].

The carbon skeleton of the iridoids is generally composed of nine or ten C atoms. However, compounds belonging to this class of natural products are known which possess nineteen (*e.g.* oruwacin **16**[24]), fourteen (*e.g.* plumericin **17**[27]), thirteen (fulvoplumierin **18**[26]), or eight carbon atoms (*e.g.* unedoside **19**[27,28]). The constitution and absolute configuration of several iridoid glycosides have been determined by X-ray structure analysis[29].

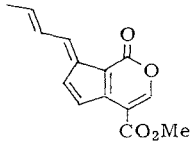
**16**



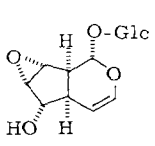
**17**



**18**



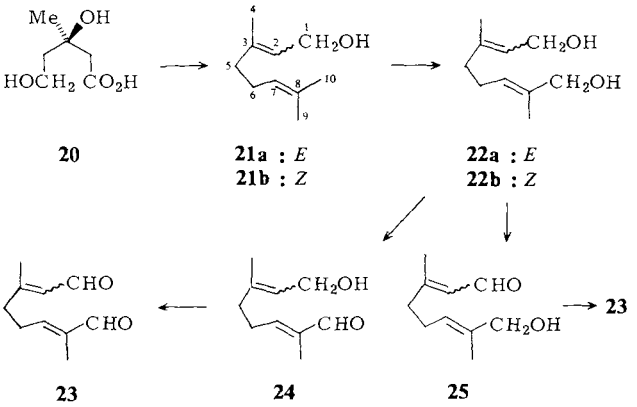
**19**



The secoiridoids are all derived from secologanin **8** and, apart from a few exceptions[30], all of these compounds contain ten C atoms; they may or may not be glycosidically bonded.

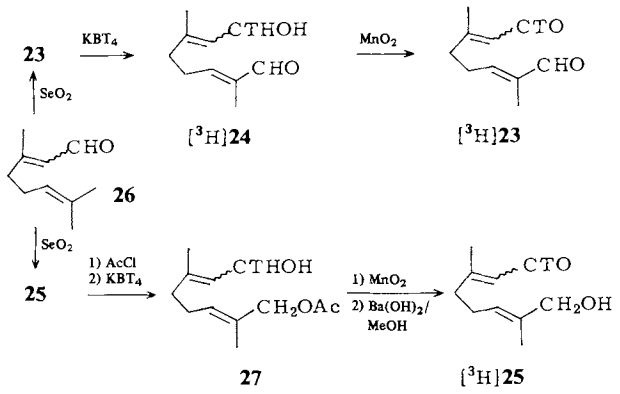
## 3. Biosynthesis of Loganin and Secologanin

The origin of the $C_9/C_{10}$ framework of the alkaloids shown in Scheme 1—which as we now know is derived from secologanin **8**—remained unclear for a long time and gave rise to much speculation. Dihydroxyphenylalanine[31] and shikimic acid[32] as well as acetyl CoA[33] were discussed as possible bioeducts. *Wenkert*[34] and *Thomas*[35] were the first to suggest that a cyclopentanoid monoterpene could be a precursor. *Battersby et al.*[36] and *Arigoni et al.*[37] were able to demonstrate that the iridoid glycoside loganin **12** is an intermediate in indole alkaloid biosynthesis; subsequently *Battersby et al.*[38] identified the secoiridoid secologanin **8** as the ultimate nitrogen-free precursor. In plants, loganin **12** and secologanin **8** are produced from geraniol **21a** or nerol **21b**, which are themselves synthesized from two molecules of mevalonic acid **20**[39]. To form the cyclopentane ring, C-6 in **21a** or **21b** must be transformed into an electrophilic center. This is achieved by specific oxidation with an oxygen-, NADPH-, and cytochrome $P_{450}$-dependent monooxygenase to give 10-hydroxygeraniol **22a** or 10-hydroxynerol **22b**[40,41], followed by the hydroxy aldehyde **24** and finally the dialdehyde **23**[42]. Alternatively, oxidation at C-1 could yield the aldehyde **25** and then the dialdehyde **23**. Experiments in which *Catharanthus roseus* G Don was fed with the labeled compounds [1-$^3H_1$]**24** and [1-$^3H_1$]**25** show, however, similar incorporation rates into loganin **12**, so that it is not possible in this experiment to decide between these two pathways[42].



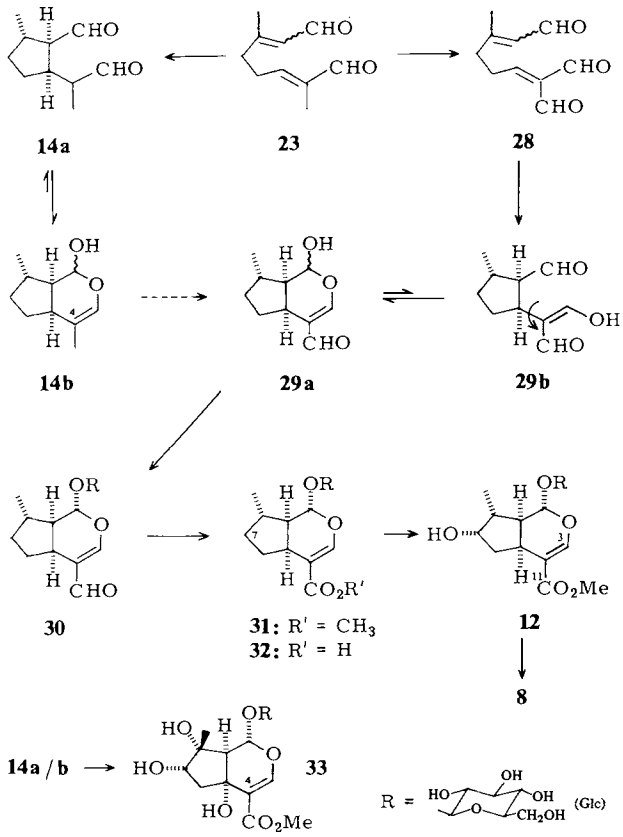

**20** **21a** : *E* **21b** : *Z* **22a** : *E* **22b** : *Z* **23** **24** **25**

The appropriately labeled compounds can be synthesized[42] by oxidizing citral **26** (a mixture of 64% geranial and 36% neral) with excess selenium dioxide to give the dialdehydes **23** or with less than the stoichiometric amount of selenium dioxide to give the hydroxy aldehydes **25**. Selective reduction of **23** with [$^3$H]potassium tetrahydridoborate produces the hydroxy aldehydes [$^3$H]**24** labeled at the C-1 position; these can be converted into the dialdehydes [$^3$H]**23** specifically labeled at C-1 by oxidation with manganese dioxide. The hydroxy aldehydes [$^3$H]**25** labeled at C-1 are synthesized by acetylation of the hydroxy aldehydes **25** and reduction with [$^3$H]potassium tetrahydridoborate to give **27**. Oxidation with manganese dioxide and subsequent solvolysis with barium hydroxide in methanol afford [$^3$H]**25**.



**26**, [$^3$H]**23**, [$^3$H]**25**: 64%*E* + 36%*Z*

The dialdehydes **23** can cyclize to give iridodial **14a/b** (Scheme 2). The careful studies of *Inouye*[39c] have shown that this compound is the precursor of numerous iridoids having a methyl group at C-4. The biosynthesis of loganin **12** and secologanin **8** in *Catharanthus roseus* G Don, however, does not proceed *via* iridodial[43] **14a/b** but presumably *via* the acyclic trialdehyde **28**[40a], iridotrial **29a/b**, its glycoside **30**, and deoxyloganin **31**[44]. Deoxyloganic acid **32** may be the actual precursor which is first hydroxylated at C-7 and is then converted into loganin **12** by formation of the methyl ester[44b]. Ester formation at the stage of loganin **12** and secologanin **8** seems to be reversible (this does not apply to **32**) since the corresponding acids of **8** and **12** have also been detected in plants. Unlike the synthesis of loganin **12** and secologanin **8**, other compounds with a methoxycarbonyl group at C-4, such as lamiide **33**,

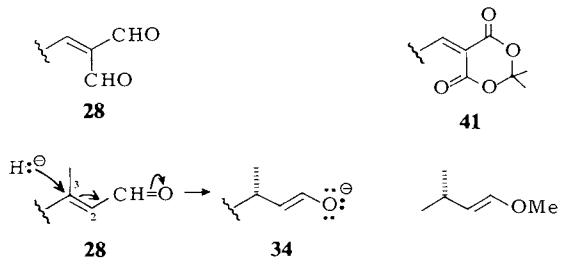


Scheme 2. Formation of the cyclopenta[c]pyran system (iridene skeleton) in the biosynthesis of the iridoids.

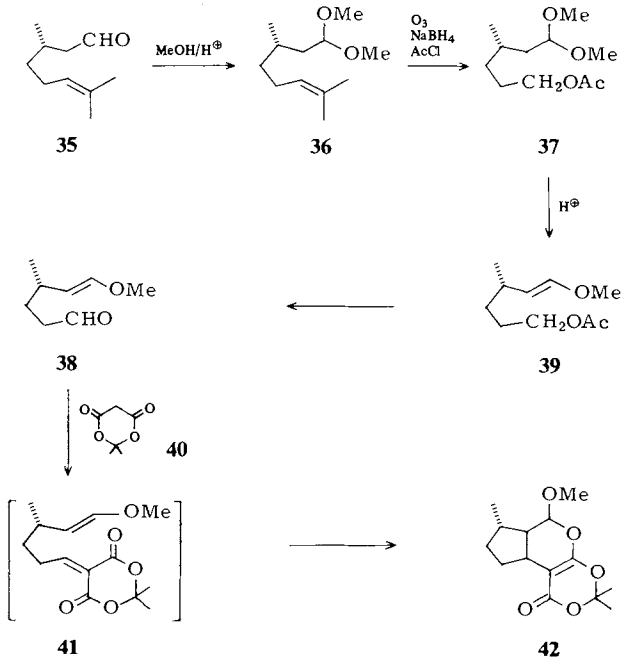
can be produced in certain plants (*e.g.* the deadnettle) from iridodial **14a/b** by an oxidative process[39a].

Since the C-3 and C-11 atoms of loganin **12** are equivalent at one stage in the *in vivo* reaction, it can be concluded that iridotrial **29a/b** is an intermediate in the biosynthesis of loganin **12** and secologanin **8**. Thus, after feeding geraniol **21a** specifically labeled at C-9, half of the radioactivity is located at position C-3 of loganin **12** and half at position C-11[39,44b].

A reductive Michael addition has been postulated for the cyclization of the trialdehyde **29**, which has not so far been used in feeding experiments. We have tried to achieve such a cyclization *in vitro* with the compound **41**[45]. An alkylidene derivative of Meldrum's acid was employed instead of the highly unstable alkylidenemalondialdehyde part structure in **29**. An enol ether functional group was used as an equivalent for the enolate **34** which is to be expected after hydride addition to the α,β-unsaturated aldehyde in **29**.



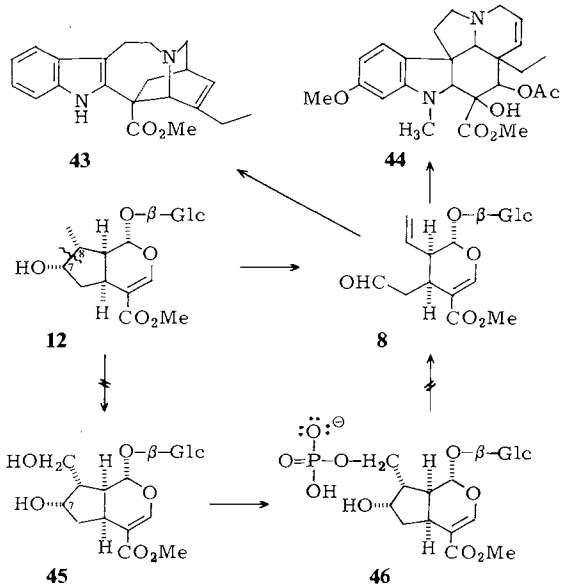
The aldehyde **38** required for the synthesis of **41**[45b] can be prepared in a few steps from enantiomerically pure (*S*)-citronellal **35**. Acetalization of **35** to **36** and subsequent ozonolysis, reductive work-up, and acetylation yield **37**. The acid-catalyzed elimination of **37** to give the enol ether **39** (an approximately 1:1 mixture of the *E/Z* isomers is obtained, which can be separated by distillation) with subsequent solvolysis of the ester functional group and oxidation of the primary hydroxy group affords the aldehyde



**38**. Condensation of **38** with Meldrum's acid **40** produces the alkylidene-1,3-dicarbonyl compound **41** within a few minutes; this cannot, however, be isolated since it cyclizes immediately in an intramolecular Diels-Alder reaction with inverse electron demand[46] to produce the iridoid derivative **42**.

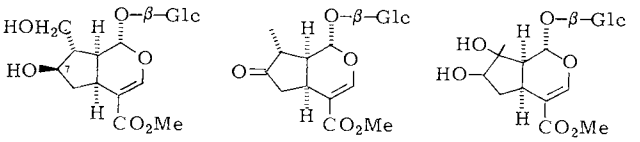
The reaction sequence described represents a novel approach to the synthesis of the iridoids and also verifies that it is possible to induce the *in vitro* cyclization of a tricarbonyl compound to afford a cyclopenta[*c*]pyran skeleton, as postulated by *Arigoni et al.*[40a].

When secologanin **8** is formed from loganin **12**, the methylcyclopentane ring is cleaved to give a δ,ε-unsaturated aldehyde. Neither the exact mechanism of this reaction nor the enzymes involved are yet known. *Battersby et al.*[47] suggested that hydroxyloganin **45** is an intermediate. As the monophosphate **46** this compound could be cleaved by heterolytic fragmentation to yield secologanin **8**. We were the first to accomplish the total synthesis of hydroxyloganin **45** and 7-epihydroxyloganin **47**[48]. However, administration of [$CO_2{}^{14}CH_3$,7-$^3$H]hydroxyloganin **45** and [$CO_2{}^{14}CH_3$]7-epihydroxyloganin **47** to *Catharanthus roseus* G Don results in very low absolute incorporation into the indole alkaloids catharanthine **43** (<0.02%) and vindoline **44** (<0.01%), which are synthesized *in vivo* from secologanin **8**; under the same conditions the incorporation of [$CO_2{}^{14}CH_3$]loganin **12** is more than 10 times greater[49]. It can thus be assumed that hydroxyloganin **44** and epihydroxyloganin **47** do not act as intermediates in the conversion of loganin **12** into secologanin **8**. The objection that hydroxyloganin **45** is not transported to the site of secologanin biosynthesis seems to be improbable since loganin **12**, which is chemically similar, can be metabolized by the plant. It is also highly unlikely that hydroxyloganin **45** is formed and cleaved in a multienzyme complex and, hence, plants cannot convert free **45** into secologanin **8**. In addition, hydroxyloganin **45** is presumably not a natural iridoid. Isolation experiments with *Menyanthes trifoliata*—a plant which contains numerous iridoids and secoridoids—show that **45** is present at less than the 0.0001% level (limit of detection)[49].

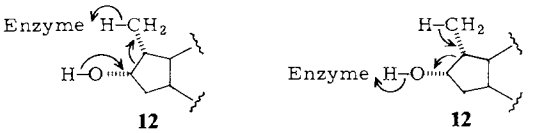



Similar results have been obtained by *Inouye et al.*[50], who has recently prepared hydroxyloganin **45** and epihydroxyloganin **47** from the iridoid geniposide and after labeling these compounds administered them to *Lonicera morrowii* and *Adina pululifera*.

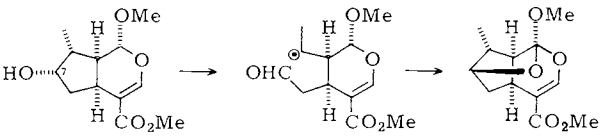
The results of feeding experiments performed with [$^3$H]loganin labeled at C-7 and C-8—the labeling pattern is retained during its conversion into secologanin **8**—preclude intermediates such as dehydrologanin **48**, the diol derivative **49**, and other loganin derivatives which are $sp^2$-hybridized or disubstituted at C-7 and/or C-8[39c].




It must, therefore, be concluded that cleavage of the cyclopentane ring in loganin **12** proceeds directly *via* an oxidative radical or ionic process.



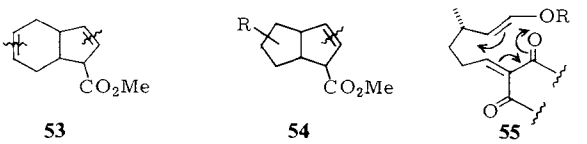

The reaction of loganinaglucone-*O*-methyl ether **50** with lead tetraacetate to form the tricyclic compound **52** may be regarded as a possible model reaction. Here, the open-chain radical **51** has been proposed as an intermediate since the configuration at C-7 is inverted during the oxidation[51].




## 4. Synthesis of Iridoids; Preparation of Hydroxyloganin and 7-Epihydroxyloganin

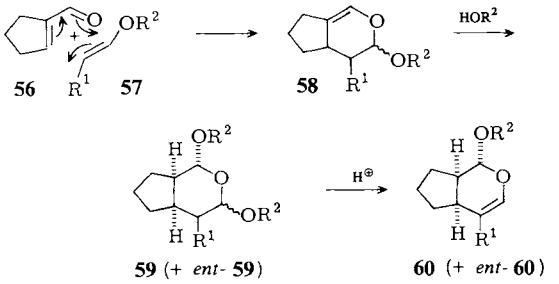
The cyclopenta[c]pyran ring (iridane skeleton) of the iridoids can be synthesized by several methods[52]. The most important of these are:

1) the double cleavage and cyclization of bicyclononadiene derivatives **53** first used by *Büchi et al.* for the synthesis of genipin[53],
2) the cleavage and cyclization of bicyclooctene derivatives **54**[54],

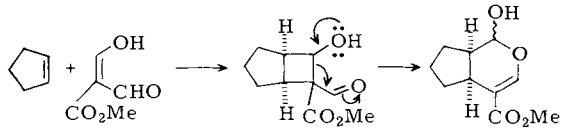


3) the intramolecular Diels-Alder reaction of compounds of type **55**[45],

4) the intermolecular Diels-Alder reaction of cyclopentenecarbaldehydes **56** and enol ethers **57** to **58**, and subsequent isomerization of the double bond by an addition-elimination sequence (**59** → **60**)[55],



**56** **57** **58** **59** (+ *ent*-**59**) **60** (+ *ent*-**60**)

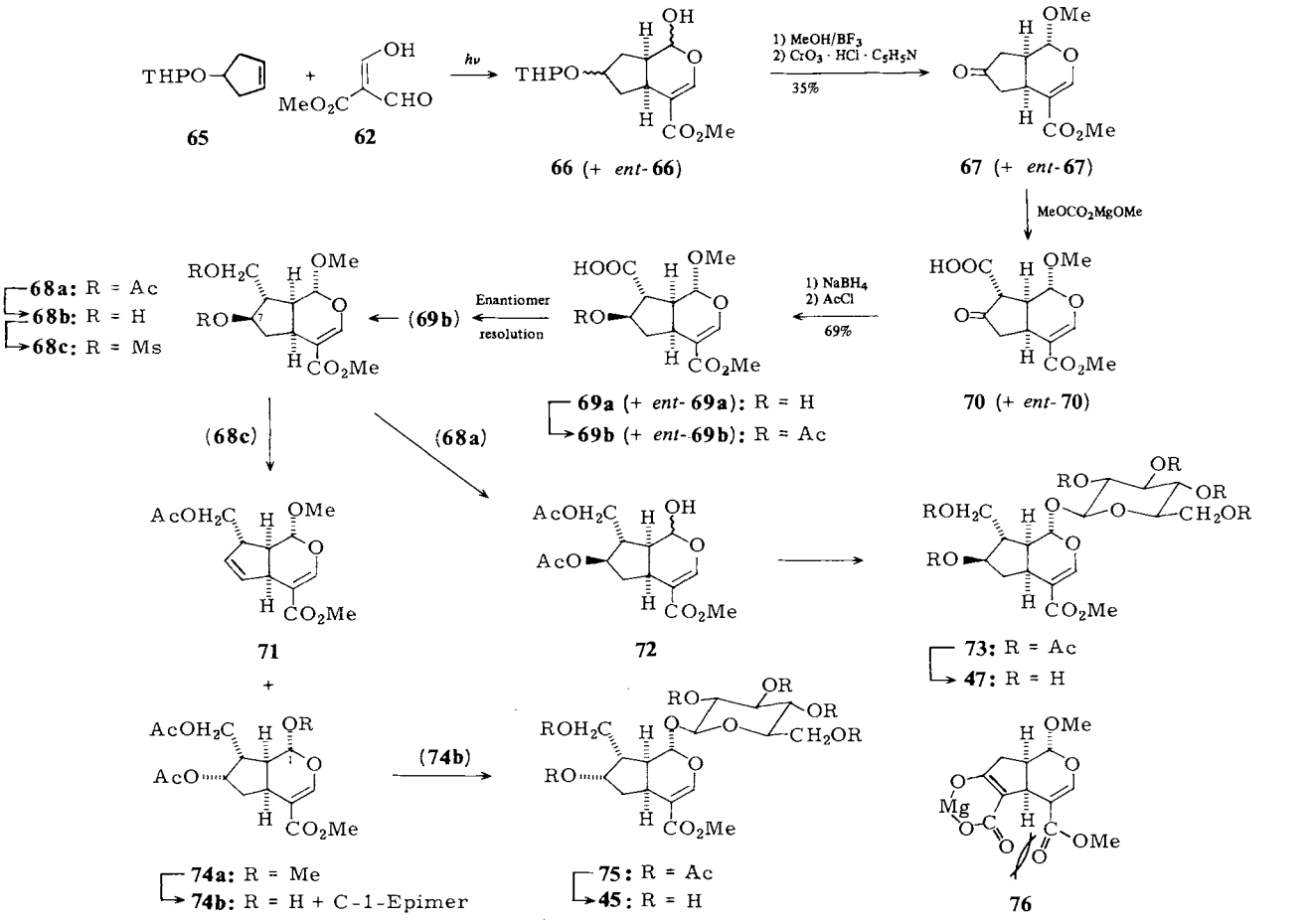


**61** **62** **63** (+ *ent*-**63**) **64** (+ *ent*-**64**)

5) the photochemical cycloaddition[56] of cyclopentene and a tricarbonyl compound **62**. A cyclobutane derivative **63** may act as an intermediate which is cleaved in a retroaldol reaction and then recyclized to the dihydropyran system **64**[57,48].

Hydroxyloganin **44**[48] and 7-epihydroxyloganin **47**[49] have been synthesized using photochemical cyclizations (Scheme 3). Irradiation of the tetrahydropyranyl ether **65** and methyl diformylacetate **62** affords the iridoid skeleton **66**. Reaction with methanol in the presence of boron trifluoride gives the acetal at C-1 and liberates the secondary hydroxy functionality. Subsequent oxidation yields the ketone **67**, which has also been utilized as an intermediate in the synthesis of loganin **12**[57a]. The missing $C_1$-unit is introduced as a carboxyl rather than as a hydroxymethyl group using methylmagnesium carbonate[58]. Thereby, resolution can be performed at a later stage in the synthesis to avoid formation of diastereomers in the subsequent glycosidation. The reaction proceeds regioselectively to yield exclusively the very sensitive keto acid **70**, which, without isolation, is reduced stereoselectively to the hydroxy acid **69a** with sodium tetrahydridoborate. Acetylation affords the acetoxycarboxylic acid **69b** as the sole product (69%, based on **67**); this compound can be resolved into its enantiomers simply and almost quantitatively using enantiomerically pure 1-phenylethylamines.

The high selectivity of the carboxylation **67** → **70**, which is presumably thermodynamically controlled, probably arises because the regioisomeric magnesium salt **76** is destabilized by steric interactions[59]. The possibility that "nonclassical" electronic interactions destabilize **76** or the $\Delta^6$-enolate primarily formed from **67** cannot, however, be excluded. The selectivity of the reduction step is a result of



Scheme 3. Synthesis of hydroxyloganin **45** and 7-epihydroxyloganin **47**. THP = tetrahydropyranyl. If in addition to the compound shown its enantiomer is also formed, the latter is designated by the prefix "*ent*-" before the formula number.

the folded shape of the molecule, which only allows the reducing agent to approach from the convex side. Neighboring group participation of the carboxy group would have the same effect.

Reduction of the carboxy group in (enantiomerically pure) **69b** with diborane and subsequent acetylation gives the diacetate **68a**, which can be converted into the hemiacetal **72** by acid-catalyzed reaction with acetic acid/perchloric acid/water. Glycosidation of **72** with 2,3,4,6-tetra-*O*-acetyl-β-D-glucose in the presence of boron trifluoride-ether affords a low yield of 7-epihydroxyloganin hexaacetate **73**, which undergoes solvolysis with barium hydroxide in methanol to give epihydroxyloganin **47**. For the problem of the glycosidation of the iridoid aglycones, see Section 9.

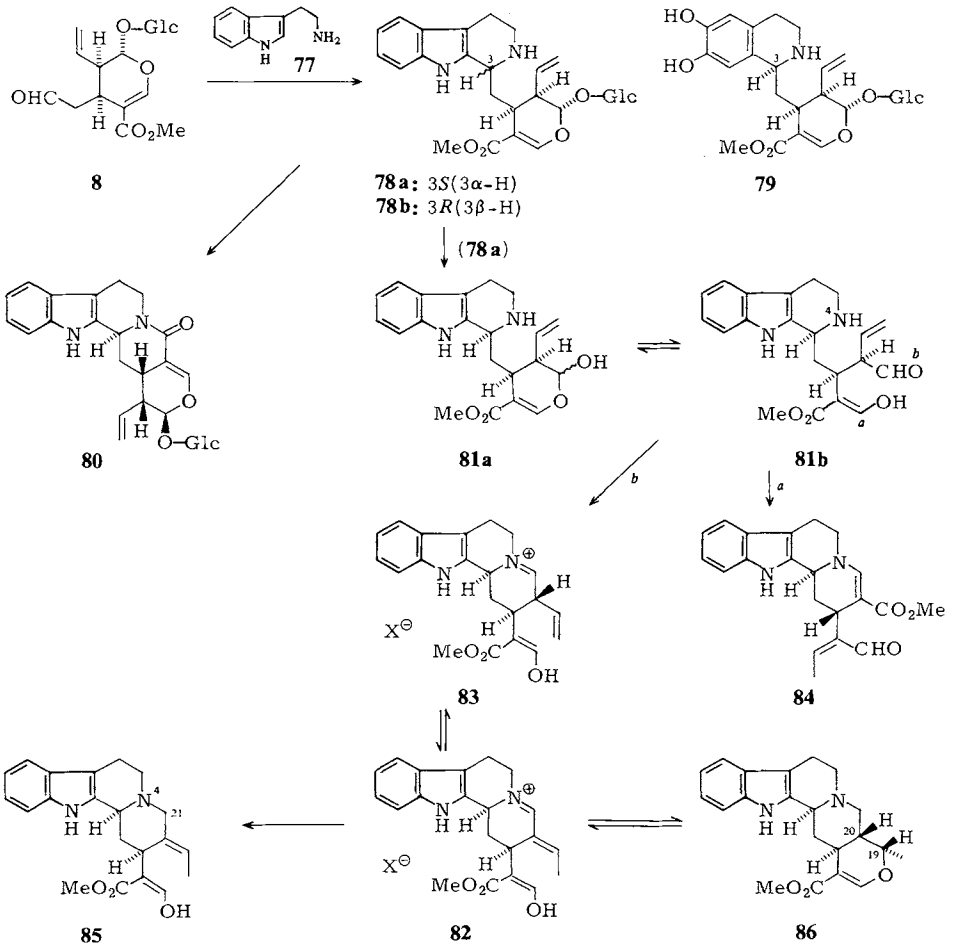
To synthesize hydroxyloganin **45** from **68a**, the C-7 center must be epimerized. This is accomplished by nucleophilic substitution with tetraethylammonium acetate *via* an $S_N2$ reaction of the bismethanesulfonate **68c** obtained from of the diol **68b.** The configuration at every center of chirality in the diacetate **74a** corresponds to that in loganin **12**. The olefin **71** is obtained as a by-product of the reaction. Cleavage of the acetal **74a** to afford **74b**, glycosidation of the latter to **75**, and solvolysis to give **45** can be performed in a manner analogous to that used in the synthesis of epihydroxyloganin **47**.

The introduction of the isotopic labels tritium and carbon-14 into **45** and **47**, respectively, follows by reduction of the keto acid **70** with [$^3$H]sodium tetrahydridoborate and esterification of the carboxylic acids obtained after hydrolysis of **45** and **47** with [$^{14}$C]diazomethane.

## 5. Biosynthesis of Monoterpenoid Indole Alkaloids

In the biosynthesis of the monoterpenoid indole alkaloids[4, 60], secologanin **8** condenses with tryptamine **77** to produce strictosidine **78a**, the first nitrogen-containing precursor of this class of compounds. Strictosidine **78a** also acts as an intermediate in the biosynthesis of the cinchona (*e.g.* quinine **5**) and pyrroloquinoline alkaloids (*e.g.* camptothecine **7**). The ipecacuanha alkaloids (*e.g.* emetine **6**) are, however, synthesized *via* desacetylisoipecoside **79**, which is formed from secologanin **8** and dopamine [4-(2-aminoethyl)pyrocatechol][61] (Scheme 4).

Strictosidine synthase has been isolated from cell cultures of *Catharanthus roseus* G Don and is the enzyme specific for the reaction of secologanin **8** with tryptamine **77** to give **78a** (this enzyme is unable to metabolize tryptophan)[62]. If **8** and **77** are allowed to react non-enzymatically, an almost 1:1 mixture of strictosidine **78a** and the epimeric compound vincoside **78b** is obtained; the latter is not a precursor of the monoterpenoid indole alkaloids.




Scheme 4. Biosynthesis of monoterpenoid indole alkaloids from secologanin **8**.

In the further course of the biosynthesis, enzymatic cleavage[63] of the glycosidic bond of **78a** may occur to form the aglycone **81a** which exists in equilibrium with the dialdehyde **81b**. It has not yet been possible to detect either of these compounds as intermediates since they immediately react further[64]. Condensation of either the enolized formyl group *a* with *N*-4 and subsequent isomerization of the double bond affords vallesiachotamine **84**, or the ammonium salt **83** is formed by reaction of the formyl group *b* with *N*-4 *via* an α-amino alcohol. Isomerization of the CC double bond leads to 4,21-dehydrogeissoschizine **82**, which undergoes hydrogenation of the iminium double bond to yield geissoschizine **85**. **82** can also be converted into ajmalicine **86** or its C-19, C-20 configurational isomers by intramolecular nucleophilic 1,4-addition of the enol functionality to the α,β-unsaturated heterodiene system and subsequent hydrogenation.

Strictosidine **78a** can, however, react in other ways: Thus, strictosidinelactam **80** can be formed prior to cleavage of the glycosidic bond; this compound is a precursor of the pyrroloquinoline alkaloids, *e.g.*, camptothecine **7**[8].

The multiplicity of possible reactions which can be undergone, therefore, accounts for the many different monoterpenoid indole alkaloids.

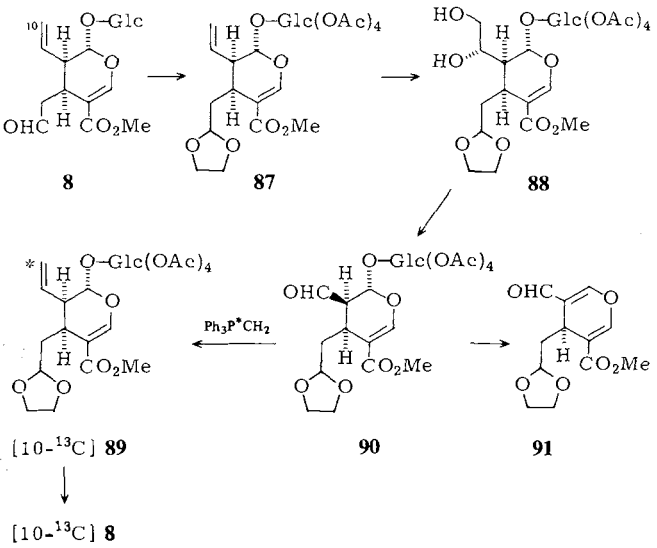
The key reaction steps in the biogenesis have been elucidated using cell cultures, cell-free enzyme systems, and isolated enzymes[65,60]. There is, however, no direct evidence for the existence of intermediates whose high reactivity precludes their isolation. It is also still uncertain whether some of the isolated substances involved in the enzymatic reactions function directly as intermediates or whether they are formed in secondary equilibria.

## 6. Synthesis of [10-$^{13}$C]Secologanin from Natural Secologanin

So far, studies on the biosynthesis have been performed almost solely using radioactively labeled precursors. This method has the chief disadvantage that it is impossible to follow the individual reaction steps directly. However, if $^{13}$C-labeled precursors are employed the successive sequence of reaction steps can be followed and evaluated kinetically with the aid of NMR spectroscopy. We have, therefore, synthesized a $^{13}$C-labeled secologanin **8**[66a] which can be utilized in biogenesis studies either directly or after conversion into $^{13}$C-labeled strictosidine **78a**. C-10 was selected as the labeling site since the hybridization and chemical environment of this C atom change during the enzymatic reaction, thus allowing identification of the intermediate products.

The label is introduced at C-10 by cleavage of the terminal double bond and a subsequent Wittig reaction (Scheme 5).

Secologanin **8**, isolated from *Symphoricarpus rivularis*[66b], was converted into the peracetylated acetal **87** by acetalization and subsequent acetylation. Oxidation of **87** with an equimolar amount of osmium tetraoxide proceeds stereoselectively to give the diol **88**. Tetraacetyl glucose (30%) can also be isolated. This indicates that oxidative degradation of the dihydropyran ring also occurs during this reaction[67].

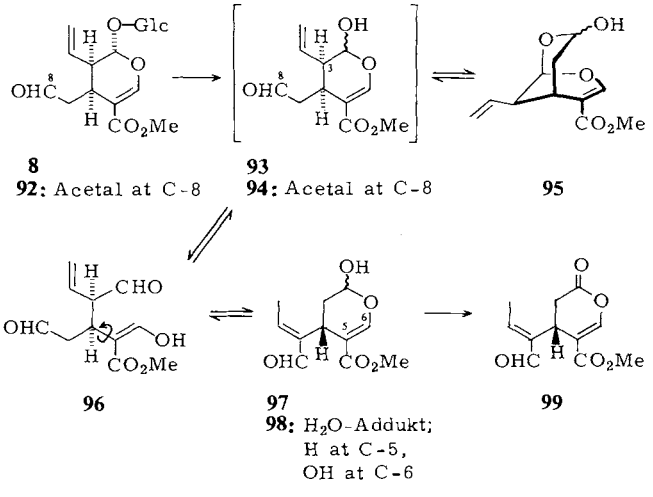



Scheme 5. Synthesis of [10-$^{13}$C]secologanin [10-$^{13}$C]**8**.

Oxidative cleavage of **88** with lead tetraacetate affords a very high yield of the aldehyde **90**, which readily forms the pyran **91** upon cleavage of tetraacetyl glucose. This elimination is also the reason why the $^{13}$C-labeled secologanin derivative [10-$^{13}$C]**89** can only be obtained in a yield of 25% in the Wittig reaction with a [$^{13}$C]methanide. Labeled secologanin [10-$^{13}$C]**8** is produced from **89** by solvolysis and cleavage of the acetal. At present, we are using NMR spectroscopy to investigate the enzymatic glycoside cleavage of [$^{13}$C]secologanin and [$^{13}$C]strictosidine.

## 7. Enzymatic Glycoside Cleavage of Secologanin and Biomimetic Synthesis of Elenolide

The products of the enzymatic glycolysis of secologanin **8** have previously been identified[68]. At pH 5.2, **8** reacts with β-glucosidase (from almonds, 1 weight equivalent) to give the bicyclic compound **95** within a few minutes. The expected aglycone **93** could not be detected. If, however, the secologanin derivative **92** undergoes glycosidic cleav-



age good yields of the aglycone **94** are obtained[69a]. Compounds of this type isomerize at C-3 very readily[69]; this has not been taken into sufficient consideration in many biomimetic reactions of secologanin and loganin.

Under the conditions required for glycoside cleavage, the bicyclic compound **95** formed from **8** is slowly converted into the epimeric hemiacetals **97**, and it can be assumed that the aglycone **93** and the open-chain aldehyde **96** function as intermediates in this reaction.

**95** reacts with silver perchlorate to afford **97** in good yield. The bishemiacetal **98** is also obtained and can be almost quantitatively dehydrated to give **97**[69a].

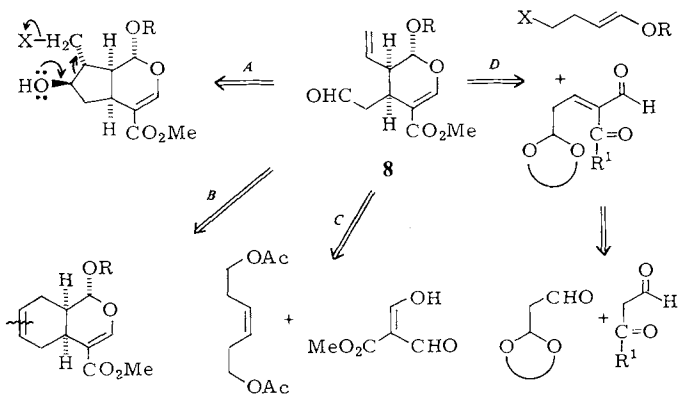
It seems likely that such reactions also occur in biological systems. Thus elenolide **99**, which has been isolated from *Olea europa* L, has a comparable structure[70].

This finding provided a simple, stereoselective, biomimetic synthesis for elenolide **99** in which both the relative and absolute configurations of this compound could be determined. Oxidation of **97** with pyridinium chlorochromate in the presence of sodium acetate gives **99** in 80% yield[71].

## 8. Total Synthesis of Secoiridoids: Secologanin and Sarracenin; Biomimetic Synthesis of Bakankosine

Secologanin **8** is of value not only because of its importance in biosynthesis but also as an educt for the synthesis of compounds of pharmacological interest. It can be isolated from the leaves and young shoots of *Lonicera tatarica* and *Lonicera morrowii* in *ca.* 1.5% yield (relative to the fresh weight). The berries of *Symphoricarpus rivularis* have also proved to be a good source of this compound since the extraction is easier and gives a purer product[66b]. However, due to the high water content of the berries the concentration of secologanin **8** in them is only 0.3% (relative to the fresh weight).

The isolation of **8** from plant material is, however, generally tedious, complicated to perform, and is not suitable for preparing large quantities. A total synthesis of secologanin **8** and especially of its derivatives is, therefore, desirable. These substances can then be allowed to react with amines and amino acids in biomimetic syntheses to yield compounds of pharmacological interest[72]. Possible retrosyntheses of secologanin **8** are given in Scheme 6.

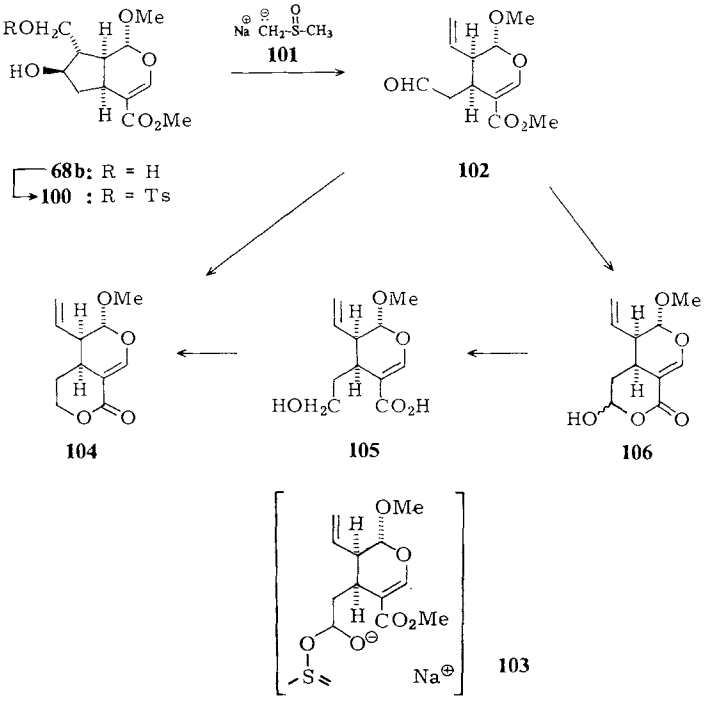


Scheme 6. Retrosynthetic analysis of secologanin **8**. *A-D* see text.

Secologanin **8** is a highly functionalized molecule with one free aldehyde group and two others which are blocked in the form of a glycosidic acetal and an enol ether. It also contains an ester functionality and a vinyl group. Synthesis of this molecule is made problematic by its polyfunctionality and especially by the thermodynamically less stable *cis*-arrangement of the alkyl side chains on the dihydropyran ring.

The first synthesis of the secologanin system[73] started, therefore, with a *cis*-linked cyclopenta[c]pyran ring system in analogy to the biosynthetic pathway (Scheme 9: A). The sensitive δ,ε-unsaturated aldehyde group of **8** was formed in the last step of the synthesis by heterolytic fragmentation[74].

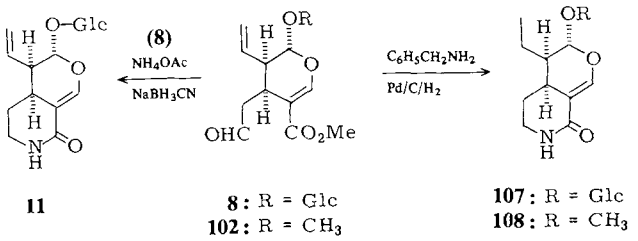
The diol **68b** (see Section 4) was converted into the monotosylate **100**, which can be cleaved within a few seconds by allowing it to react with the strong base sodium methylsulfinylmethanide **101** to give the secologanin derivative **102** in 67% yield. At longer reaction times and in the presence of excess **101**, the lactol **106** is also obtained; this



compound arises either by cleavage of the methyl ester by nucleophilic substitution or by formation of an intermediate of type **103**.

Reaction of **102** with sodium tetrahydridoborate affords sweroside aglycone-*O*-methyl ether **104**. Reduction of the lactol **106** yields primarily the corresponding hydroxycarboxylic acid **105**, which dehydrates to **104** on heating.

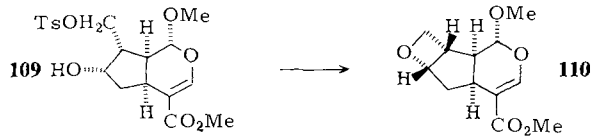
If **102** is reductively aminated with benzylamine (palladium/carbon, hydrogen), the bakankosine derivative **108** is obtained in a single step. In the same manner secologanin **8** can be transformed almost quantitatively into dihydrobakankosine **107**. The alkaloid bakankosine **11** can be synthesized with retention of the vinyl double bond by allowing **8** to react with sodium cyanotrihydridoborate in the presence of ammonium acetate; however, the yield is poor[74]. This permitted the relative and absolute configurations of **11** to be determined.



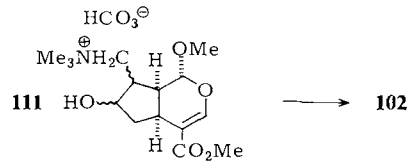

**11** **8**: R = Glc; **102**: R = $CH_3$ **107**: R = Glc; **108**: R = $CH_3$

The secologanin, sweroside, and bakankosine derivatives can be synthesized in both enantiomeric forms since the dihydroxy compound **68b** used as educt is also accessible as its enantiomer *ent*-**68b**.

Unlike **100**, the monotosylate **109**, which possesses the same relative configurations as loganin **12** at all its centers of chirality, does not react with strong bases to form a fragmentation product, but is converted quantitatively into the oxetane **110** by an intramolecular nucleophilic substitution[73]. The reaction of **109** can be interpreted as additional evidence against formation of hydroxyloganin **44** as an intermediate in the synthesis of secologanin **8** from loganin **12**. An explanation for the different reactivities of **100** and **109** is provided by the studies of *Hoffmann, Gleiter,* and *Stohrer*[76].



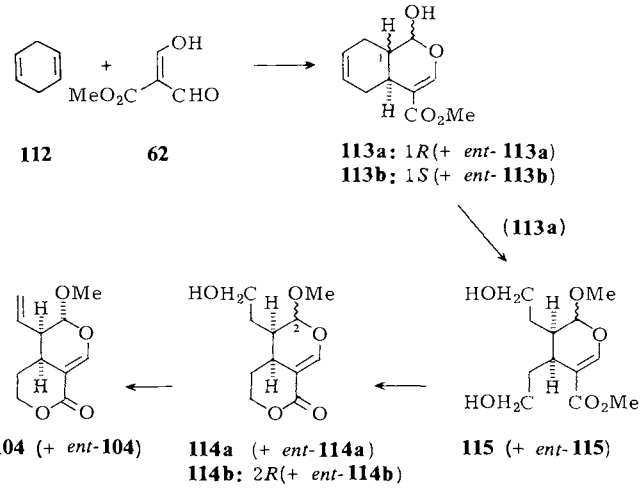
**109** **110**



**111** **102**

A novel fragmentation of the cyclopenta[c]pyran ring skeleton to give **102** can also be accomplished by flash pyrolysis of the γ-hydroxyammonium compound **111** at 350°C[77]. **111** can be synthesized from the ketone **67** *via* a Mannich reaction[78].

Preparation of **102** from the oxabicyclodecadiene system **113a** is based on a concept comparable to that used for the synthesis of **102** from **68b**, and has the advantage that the alkene **112** can be obtained more easily[79] (Scheme 6: B). **113a** can be prepared straightforwardly by photochemical cycloaddition of 1,3-cyclohexadiene **112** and methyl diformylacetate **62**. Whereas, however, formation of the cyclopenta[c]pyran skeleton in **68b** from cyclopentane derivatives and **62** results solely in *cis*-fused products, this reaction leads also to formation of the *trans*-isomer **113b** which can be separated. After acetalization of **113a** at C-1, the cyclohexene double bond is cleaved selectively by ozonolysis at −70°C to give the unstable dialdehyde (72%), which can be reduced to the diol **115** with sodium tetrahydridoborate The high selectivity of this reaction is remarkable, since selective ozonolysis of the vinyl group in secologanin **8** without destroying the dihydropyran ring can either not be achieved or only affords low yields. The cyclohexene system in **113a** can also be cleaved to afford **115**—albeit with poorer yields—by *cis*-hydroxylation with osmium tetraoxide and subsequent cleavage with periodate. Hydrolysis to the corresponding hydroxy acid and cyclization with loss of water yields the hydroxylactone **114a**. The racemic (2*R*)-lactone **114b**,

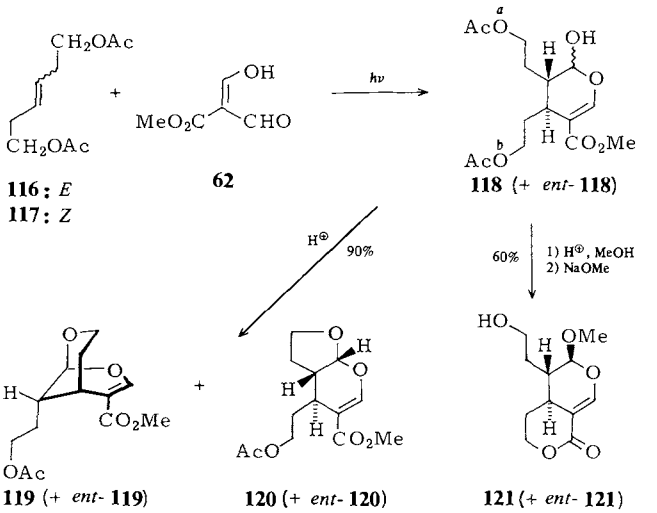



**112** **62** **113a**: 1*R*(+ *ent*-**113a**); **113b**: 1*S*(+ *ent*-**113b**)

**104** (+ *ent*-**104**) **114a** (+ *ent*-**114a**); **114b**: 2*R*(+ *ent*-**114b**) **115** (+ *ent*-**115**)

which is purified by chromatography, can be converted into the racemic sweroside aglycone-*O*-methyl ether **104** by transformation into an alkyl selenide and subsequent oxidative elimination. The secologanin derivative **102** can be obtained from **104** in a few steps.

Compounds of the secologanin type can also be readily synthesized on a larger scale by a further method: The photochemical cycloaddition of the readily accessible (*E*)- or (*Z*)-alkenes **116** or **117** with **62**, which proceeds in 70% yield (Scheme 6: *C*).




**116**: *E* **117**: *Z* **62** **118** (+ *ent*-**118**)

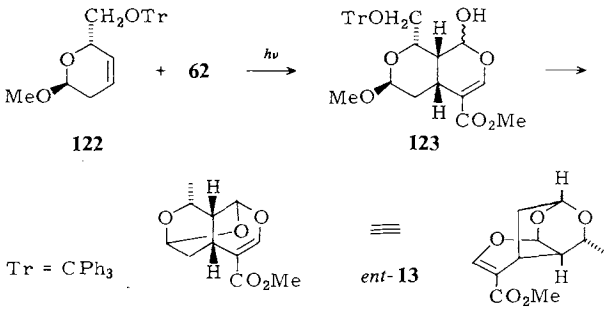
**119** (+ *ent*-**119**) **120** (+ *ent*-**120**) **121** (+ *ent*-**121**)

This method, however, only leads to the *trans*-substituted dihydropyran derivative **118**. Loss of stereochemical integrity in **117** indicates that biradical intermediates are formed, consistent with postulates made about photochemical cycloadditions of this type[56]. However, isomerization of a *cis*-substituted cycloadduct which may be formed primarily from **117** would also furnish the thermodynamically more stable *trans*-substituted dihydropyran **118**[69].

The two acetoxy groups in **118** can be differentiated in two ways: acid catalyzed reaction of **118** results in quantitative conversion into a 3:1 mixture of the bridged system **119** and the annelated compound **120**, which are in equilibrium with one another under the reaction conditions. Under conditions of acid catalysis, pure **119** and **120** form a 3:1 mixture of the constitutional isomers. In **119** the acetylated primary hydroxy group *b* of the cycloadduct **118** is protected by acetylation, and in **120** the group *a* is protected in the form of an acetal, whereas the second acetylated hydroxy groups in each of these two compounds can be selectively further reacted. Both compounds are valuable educts for the biomimetic synthesis of pharmacologically important compounds of the monoterpenoid indole alkaloid type.

The acetoxy groups in the cycloadduct **118** can also be differentiated by acid-catalyzed reaction with methanol and subsequent Zemplén saponification to afford the *trans*-sweroside derivative **121**; this compound can also be subjected to further reactions.

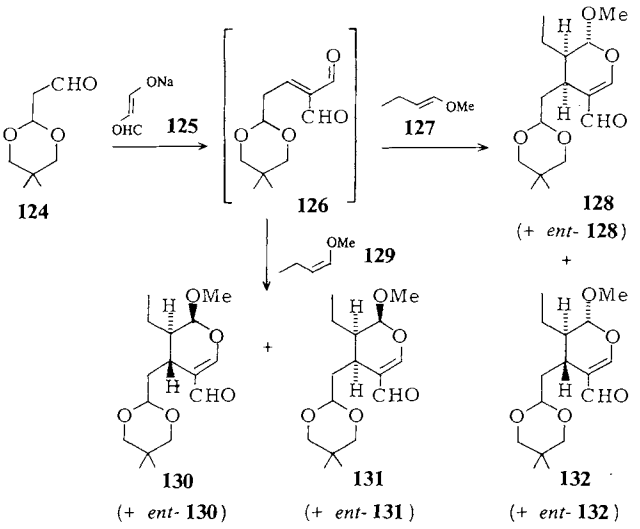
Photochemical cyclization is also a suitable method of preparing enantiomerically pure secoiridoids. Thus, it is possible to synthesize enantiomerically pure sarracenin **13** (which can be isolated from the carnivorous plant *Sarracenia flava*)[118]) and its unnatural isomer *ent*-**13** in a few steps from the galactose derivatives[81] *ent*-**122** and **122**, respectively, and methyl diformylacetate **62**. The main product of the photochemical cyclization of **122** and **62** is the bicyclic compound **123**[82,83].




Recently, we have developed a novel, surprisingly simple, flexible concept for synthesizing compounds of the secologanin type[84]. Here the $C_{10}$ skeleton of **8** is constructed from one $C_4$ and two $C_3$ units in a "one-pot" reaction (Scheme 6: *D*). The key step is a Diels-Alder reaction with inverse electron demand between the $C_4$ enol ether **127** and an alkylidene-1,3-dicarbonyl compound **126** which can be obtained *in situ* by condensation of the sodium salt of malondialdehyde **125** with the monoacetal of malondialdehyde **124**.

The cycloaddition gives the secologanin derivative **128** (48%); the relative configuration at each of its centers of chirality corresponds to that of secologanin **8**. The stereoisomer **132** is also obtained in 16% yield; however, this can be separated by chromatography. If the (*Z*)-enol ether **129** is used, an approximately 1:1 mixture of the two stereoisomers **130** and **131** is produced in 64% yield.

The Diels-Alder reaction of the alkylidene-1,3-dicarbonyl compound **126** (which cannot be isolated) is complete within a few minutes at 20°C. The markedly higher reactivity of the heterodiene unit in **126** compared to simple




α,β-unsaturated aldehydes can be explained through a decrease of the LUMO energy of the heterodiene by the electron acceptor functionality in the α-position[46].

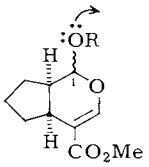
## 9. Synthesis of Iridoid Glycosides

Whereas considerable progress has been made in the last years regarding the isolation[20], structure determination[85], and the biogenesis of the iridoid and secoiridoid glycosides, as well as in the synthesis of the non-glycosidic compounds of this class of natural products, very few studies on the total synthesis of glycosidically bonded iridoids have been carried out. This is mainly because glycosidation of the corresponding iridoid aglycones is exceedingly difficult. Thus, in the glycosidation step in the synthesis of loganin **12**, which represents the first, and so far the only, total synthesis of a natural iridoid glycoside, the yield amounts only to 1.4%[57a]. Previously, *Schmid et al.*[85b] showed that the Koenigs-Knorr method was not suitable for the synthesis of iridoid glycosides.

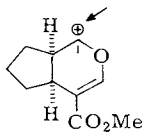
In principle, glycosidation of iridoid aglycones of type **133** can be achieved in two ways:

1) Nucleophilic attack of the hemiacetal hydroxy group of **133** at C-1 of a reactive glucose derivative such as acetobromoglucose **139**, 3,4,6-tri-*O*-acetyl-1,2-anhydroglucose triacetate **140**, or an orthoester[86].
2) Nucleophilic attack of the hemiacetal hydroxy group of tetraacetyl-β-D-glucose **141** or the trimethylsiloxy group of **142** at C-1 of the aglycone **133**. Here, it must be assumed that the carbenium ion **137** acts as an intermediate, since for steric reasons a $S_N2$-like transition state seems less probable and would lead to the "wrong" stereoisomer.

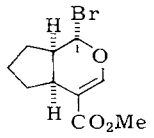
Reaction of **133** with acetobromoglucose **139** in the presence of silver carbonate, mercury cyanide/bromide, and mercury succinate using Koenigs-Knorr and related procedures[86] which give good yields of β-glucosides with alcohols and monosaccharides, fails completely. This is probably due to the low nucleophilicity of the hemiacetal



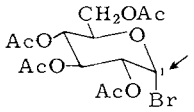
**133**: R = H
**134**: R = Me
**135**: R = Ac
**136**: NHAc instead of OR



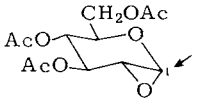
**137**



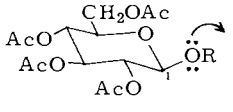
**138**



**139**



**140**

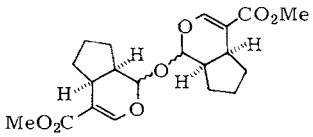


**141**: R = H
**142**: R = $SiMe_3$

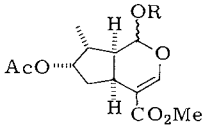
hydroxy group in **133**. If, however, silver perchlorate or silver trifluoromethanesulfonate is used as a heavy metal salt, a mixture of isomeric glycosides can be obtained from **133** in 28% yield; this mixture can be separated after solvolysis of the acetyl groups[87]. The dimeric aglycones **143** are also formed.

Loganin **12**, with a β-glycosidic bond, and the α-glycoside **147** can be obtained in 13% and 5% yield, respectively, from the 7-*O*-acetyl-loganin aglycone **144** after performing a complicated separation. Reaction of **133** with **140** in the presence of catalytic quantities of boron trifluoride-ether gives solely the α-glycoside; yields are moderate[88]. Small quantities of another glycoside were also detected in which the glucosyloxy group adopts the unfavorable *cis*-position with respect to the cyclopentane ring.

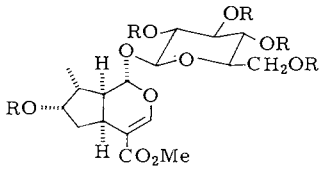
In the second glycosidation method the aglycone **133** or **144** must be transformed into a carbenium ion which can



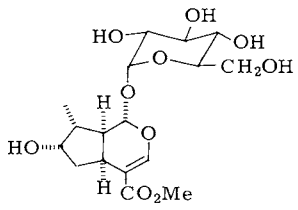
**143**



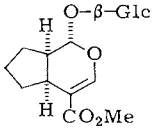
**144**: R = H
**145**: R = Ac



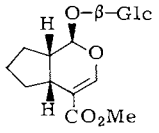
**12**: R = H
**146**: R = Ac



**147**



**148**



**149**

then react with **141** or **142** with retention of the configuration of the glucose derivative at C-1. The cation **137** can be synthesized from **133** either directly with boron trifluoride-ether or after conversion into the bromide **138** with silver perchlorate. However, glycosidation does not proceed stereoselectively since the sugar component isomerizes under the reaction conditions. Furthermore, the dimeric aglycones **143** are formed preferentially and, hence, the yield of the desired β-glycoside **148** only amounts to 10%.

The procedures described are totally unsatisfactory with regard to yield and selectivity. They have, however, provided new information about the mechanism of glycosidation and supplied a wealth of NMR spectroscopic[89] and chiroptic data[90] which facilitate determination of the relative and absolute configurations of isomeric iridoid glycosides.

A new method has been described recently which at last promises to solve the problem, and thus open up an approach to the synthesis of the iridoid glycosides[91].

The dimethyl acetals of aldehydes can be converted selectively into the previously almost inaccessible glycosides with a 1,1′-diacetal structure by allowing them to react with β-trimethylsilyl glycoside **147** in the presence of catalytic amounts of trimethylsilyl trifluoromethanesulfonate (TMS-triflate). At −70°C only the β-glycosides are produced with retention of configuration at C-1 of **142**[92]; at 20°C exclusively the α-glycosides are formed[93] since anomerization of the trimethylsilyl glycoside **142** happens before the reaction with the acetal[94].

The methyl acetal **134** reacts very slowly at −70°C; at −20°C partial anomerization of **142** occurs to give a mixture of the α- and β-glycosides. Nevertheless, reaction with the acetylated hemiacetal *rac*-**135** in acetonitrile as a solvent affords after saponification the β-glycosides **148** and **149** in 70% yield within 10 h at −30°C. α-Glycosides and C-1 epimers of the aglycone component were not detected (< 5%). A slight blemish in this reaction is the formation of the amide *rac*-**136** (9%) by addition of the cation *rac*-**137** to the solvent. If liquid sulfur dioxide is employed—this is not used very commonly as a solvent in organic chemistry but is very easy and clean to work with—the two β-glycosides **148** and **149** are obtained in 91% yield at −50°C. Solvolysis of the enantiomerically pure acetylated aglycone **135**, which can be prepared from **148** by glycosidic cleavage with emulsin and subsequent acetylation, provides the desired β-glycoside **148** in 87% yield (!); the iridoid glycoside has the correct absolute configuration at all its centers of chirality.

Similarly, penta-*O*-acetyl-loganin **146** can be synthesized in 75% yield from di-*O*-acetyl-loganol **145** and **142** in the presence of catalytic amounts of TMS triflate in liquid sulfur dioxide at −40°C. The amount of α-glycoside obtained (**147**, peracetylated) is less than 10%. Other products are not formed. **146** can easily be converted into the natural product loganin **12** by solvolysis.

## 10. Outlook

So far, the designed synthesis of pharmaceuticals according to the "Rational Drug Design" model has only

found restricted application[95] because information about the structure of the receptors in the control systems of the human and animal organisms is still very limited. For the development of new pharmaceuticals it is, at present, best to start with model structures whose biological activity and biological sites of attack are known. In this respect, compounds derived from secologanin are of great interest. The elegant, simple syntheses of secologanin derivatives which have been developed recently have provided potent educts for biomimetic reactions. Reaction of these substances with amines and amino acids should give a multitude of biologically active compounds.

It has not yet been possible to synthesize glycosidically bonded iridoids and secoiridoids. Development of a high-yield, stereoselective glycosidation method has finally opened up a route for total syntheses of this widely distributed class of natural products. It also allows specifically [$^{13}$C]-labeled compounds of this type to be prepared. The reaction of substances thus labeled in cell cultures, cell-free enzyme systems, or with isolated enzymes should prove highly useful in solving the problems remaining in the biosynthesis of this class of natural compounds and of the ipecacuanha and monoterpenoid indole alkaloids. One of the main centers of interest in the future will be the characterization of the enzymes involved in the individual biosynthetic reactions. Use of suitable derivatives as substrates should provide information about the selectivity and perhaps even the structure of the active centers of the enzymes concerned. Cooperation between chemists and biologists should produce the best results.

*I wish to thank my coworkers for their enthusiasm, dedication and skill in completing the research projects described here. I am particularly grateful to Prof. G. Büchi, Cambridge, USA, Prof. A. R. Battersby, Cambridge, England, Prof. G. Sheldrick, Göttingen, and Prof. C. R. Hutchinson, Madison, for fruitful discussions and excellent collaboration.*

*Support by the Deutsche Forschungsgemeinschaft, the Ministerium für Wissenschaft und Forschung des Landes Nordrhein-Westfalen, and the Fonds der Chemischen Industrie is greatfully acknowledged.*

Received: August 23, 1983 [A 473 IE]
German version: *Angew. Chem. 95* (1983) 840

[1] B. Franck, *Angew. Chem. 91* (1979) 453; *Angew. Chem. Int. Ed. Engl. 18* (1979) 429.
[2] P. M. Smith: *The Chemotaxonomy of Plants*, Edward Arnold, London 1976; D. Rast, *Chem. Unserer Zeit 5* (1971) 43.
[3] For example, W. S. Johnson, *Angew. Chem. 88* (1976) 33; *Angew. Chem. Int. Ed. Engl. 15* (1976) 9.
[4] J. D. Phillipson, M. H. Zenk: *Indole and Biogenetically Related Alkaloids*, Academic Press, London 1980; Atta-ur-Rahman, A. Basha: *Biosynthesis of Indole Alkaloids*, Clarendon Press, Oxford 1983; G. A. Cordell, *Lloydia 37* (1974) 219.
[5] The ergot alkaloids and compounds of the harman and physostigmine type are also indole alkaloids. They are not, however, synthesized from secologanin and thus do not contain the monoterpenoid $C_9$ or $C_{10}$ fragment.
[6] A. R. Battersby, R. J. Parry, *Chem. Commun. 1971*, 901; A. R. Battersby, B. Gregory, *ibid. 1968*, 134.
[7] A. R. Battersby, R. J. Parry, *Chem. Commun. 1971*, 30, 31; A. R. Battersby, E. S. Hall, *ibid. 1970*, 194.
[8] C. R. Hutchinson, A. H. Heckendorf, P. E. Daddona, E. Hagaman, E. Wenkert, *J. Am. Chem. Soc. 96* (1974) 5609; E. Winterfeldt, T. Korth, D. Pike, M. Boch, *Angew. Chem. 84* (1972) 265; *Angew. Chem. Int. Ed. Engl. 11* (1972) 289; M. Boch, T. Korth, J. M. Nelke, D. Pike, H. Radunz, E. Winterfeldt, *Chem. Ber. 105* (1972) 2126.
[9] D. Gross, *Fortschr. Chem. Org. Naturst. 28* (1970) 140; W. C. Wildman, J. Le Men, K. Wiesner in W. I. Taylor, A. R. Battersby: *Cyclopentanoid Terpene Derivatives*, Marcel Dekker, New York 1969.
[10] M. Hesse: *Alkaloidchemie*, Thieme, Stuttgart 1978.
[11] E. Mutschler: *Arzneimittelwirkungen*, Wissenschaftliche Verlagsgesellschaft, Stuttgart 1981.
[12] a) See [11], p. 576; b) see [11], p. 573.
[13] C. R. Hutchinson, *Tetrahedron 37* (1981) 1047.
[14] M. E. Wall, M. C. Wani, C. E. Cook, K. H. Palmer, A. T. McPhail, G. A. Sim, *J. Am. Chem. Soc. 88* (1966) 3888.
[15] E. Bourquelot, H. Heressey, *J. Pharm. Chem. 28* (1908) 433; E. W. Warnhoff in P. de Mayo: *Molecular Rearrangements*, Part *II*, Wiley, New York 1964, p. 947; *G. Büchi*, personal communication.
[16] D. Gröger, D. Erge, H. G. Floss, *Z. Naturforsch. B 21* (1966) 827; T. Fehr, W. Acklin, D. Arigoni, *Chem. Commun. 1966*, 801; G. H. Svoboda, *Lloydia 24* (1961) 173.
[17] H. Inouye, S. Ueda, Y. Takeda, *Heterocycles 4* (1976) 527.
[18] D. H. Miles, U. Kokpol, J. Bhattacharyya, I. L. Atwood, K. E. Stone, T. A. Bryson, C. Wilson, *J. Am. Chem. Soc. 98* (1976) 1569.
[19] D. H. Miles, U. Kokpol, L. H. Zalkow, S. J. Steindel, J. B. Narbors, *J. Pharm. Sci. 63* (1974) 613.
[20] a) L. J. El-Naggar, J. L. Beal, *J. Nat. Prod. 43* (1980) 649; b) J. M. Bobbitt, K.-P. Segebarth in W. I. Taylor, A. R. Battersby: *Cyclopentanoid Terpene Derivatives*, Marcel Dekker, New York 1969, p. 1; V. Plouvier, J. Favre-Bonvin, *Phytochemistry 10* (1971) 1697; O. Sticher, U. Junod-Busch, *Pharm. Acta Helv. 50* (1975) 127; S. R. Jensen, B. J. Nielsen, R. Dahlgreen, *Bot. Not. 128* (1975) 148; R. Hegenauer, P. Kooiman, *Planta Med. 33* (1978) 1.
[21] G. W. K. Cavill, D. L. Ford, *Aust. J. Chem. 13* (1960) 296; G. W. K. Cavill, D. L. Ford, H. D. Locksley, *ibid. 9* (1956) 288.
[22] For example, M. L. Scarpati, P. Esposito, *Gazz. Chim. Ital. 97* (1967) 1209.
[23] For example, H. Achenbach, R. Waibel, I. Addae-Mensah, *Tetrahedron Lett. 21* (1980) 3677.
[24] E. K. Adesogan, *Phytochemistry 18* (1979) 175.
[25] G. Albers-Schönberg, H. Schmid, *Helv. Chim. Acta 44* (1961) 1447.
[26] G. Albers-Schönberg, W. von Philipsborn, L. M. Jackman, H. Schmid, *Helv. Chim. Acta 45* (1962) 1406; G. Büchi, J. A. Carlson, *J. Am. Chem. Soc. 90* (1968) 5336; *91* (1969) 6470.
[27] T. A. Geissman, W. F. Knaack, Jr., J. O. Knight, *Tetrahedron Lett. 1966*, 1245; H. Rimpler, H. Pistor, *Z. Naturforsch. C 29* (1974) 368.
[28] K. Weinges, H. von der Eltz, G. Hartz, *Liebigs Ann. Chem. 1982*, 872.
[29] P. G. Jones, G. M. Sheldrick, K.-H. Glüsenkamp, L.-F. Tietze, *Acta Crystallogr. B 36* (1980) 481; P. J. Lentz, Jun., M. G. Rossmann, *Chem. Commun. 1969*, 1269; N. Masaki, M. Hirabayashi, K. Fuji, K. Osaki, H. Inouye, *Tetrahedron Lett. 1967*, 2367.
[30] H. Inouye, Y. Takeda, S. Uesato, K. Uobe, T. Hashimoto, *Tetrahedron Lett. 21* (1980) 1059.
[31] R. B. Woodward, *Angew. Chem. 68* (1956) 13.
[32] E. Wenkert, *Experientia 15* (1959) 165.
[33] E. Leete, S. Ghosal, *Tetrahedron Lett. 1962*, 1179.
[34] E. Wenkert, *J. Am. Chem. Soc. 84* (1962) 98.
[35] R. Thomas, *Tetrahedron Lett. 1961*, 544.
[36] A. R. Battersby, R. S. Kapil, J. A. Martin, L. Mo, *Chem. Commun. 1968*, 133.
[37] P. Loew, D. Arigoni, *Chem. Commun. 1968*, 137.
[38] A. R. Battersby, A. R. Burnett, P. G. Parsons, *Chem. Commun. 1968*, 1280.
[39] a) F. McCapra, T. Money, A. I. Scott, I. G. Wright, *Chem. Commun. 1965*, 537; b) H. Goeggel, D. Arigoni, *ibid. 1965*, 538; c) H. Inouye, *Planta Med. 33* (1978) 193.
[40] a) S. Escher, P. Loew, D. Arigoni, *Chem. Commun. 1970*, 823; b) A. R. Battersby, S. H. Brown, T. G. Payne, *ibid. 1970*, 827; c) K. M. Madyastha, T. D. Meehan, C. J. Coscia, *Biochemistry 15* (1976) 1097.
[41] *Arigoni* et al. [40a] found a higher incorporation rate for **22b** than for **22a**. In contrast, geraniol **21a** is oxidized in the allyl position somewhat more quickly by the relevant monooxygenase than neraol **22b**[40c]. Neryl and geranyl pyrophosphates, the latter of which have been shown to be a precursor of the iridoids, are not hydroxylated by the monooxygenase.
[42] A. R. Battersby, M. Thompson, K.-H. Glüsenkamp, L.-F. Tietze, *Chem. Ber. 114* (1981) 3430.
[43] R. M. Bowman, E. Leete, *Phytochemistry 8* (1969) 1003.
[44] a) H. Inouye, S. Ueda, Y. Aoki, Y. Takeda, *Tetrahedron Lett. 1969*, 2351; *Chem. Pharm. Bull. 20* (1972) 1287; A. R. Battersby, A. R. Burnett, P. G. Parsons, *Chem. Commun. 1970*, 826; b) but cf. K. M. Madyastha, C. J. Coscia, *Recent Adv. Phytochem. 13* (1979) 85.
[45] a) L.-F. Tietze, H. Denzer, unpublished results; b) L.-F. Tietze, T. Eicher: *Reaktionen und Synthesen im organisch-chemischen Praktikum*, Thieme, Stuttgart 1981, p. 364.

[46] L.-F. Tietze, G. von Kiedrowski, K. Harms, W. Clegg, G. Sheldrick, *Angew. Chem. 92* (1980) 130; *Angew. Chem. Int. Ed. Engl. 19* (1980) 134; L.-F. Tietze, G. von Kiedrowski, B. Berger, *ibid. 94* (1982) 222; *21* (1982) 221.
[47] A. R. Battersby, *Pure Appl. Chem. 14* (1967) 117.
[48] L.-F. Tietze, *Angew. Chem. 85* (1973) 763; *Angew. Chem. Int. Ed. Engl. 12* (1973) 757; *Chem. Ber. 107* (1974) 2499.
[49] A. R. Battersby, N. D. Westcott, K.-H. Glüsenkamp, L.-F. Tietze, *Chem. Ber. 114* (1981) 3439.
[50] K. Inoue, Y. Takeda, T. Tanahashi, H. Inouye, *Chem. Pharm. Bull. 29* (1981) 981.
[51] J. J. Partridge, N. K. Chadha, S. Faber, M. R. Uskoković, *Synth. Commun. 1* (1971) 233.
[52] O. P. Verma, S. Kumar, B. C. Jashi, *Herba Pol. 26* (1980) 195; K. Hisoi, *Annu. Rep. Tohoku College Pharm. 28* (1981) 27.
[53] a) G. Büchi, B. Gubler, R. S. Schneider, J. Wild, *J. Am. Chem. Soc. 89* (1967) 2776; b) cf. also M. Nakane, C. R. Hutchinson, *J. Org. Chem. 45* (1980) 4233.
[54] Boon-Wai Au-Yeung, I. Fleming, *J. Chem. Soc. Chem. Commun. 1977,* 81; K. Hiroi, H. Miura, K. Kotsuji, S. Sato, *Chem. Lett. 1981,* 559; M. Demuth, K. Schaffner, *Angew. Chem. 94* (1982) 809; *Angew. Chem. Int. Ed. Engl. 21* (1982) 820; K. Kon, S. Isoe, *Helv. Chim. Acta 66* (1983) 755; P. Callant, R. Ongena, M. Vandewalle, *Tetrahedron 37* (1981) 2085; P. Callant, H. D. Wilde, M. Vandewalle, *ibid. 37* (1981) 2079; K. Furuichi, T. Miwa, *Tetrahedron Lett. 1974,* 3689; T. Sakan, K. Abe, *ibid. 1968,* 2471.
[55] L.-F. Tietze, *Chem. Ber. 107* (1974) 2491.
[56] P. de Mayo, *Acc. Chem. Res. 4* (1971) 41.
[57] a) G. Büchi, J. A. Carlson, J. E. Powell, Jr., L.-F. Tietze, *J. Am. Chem. Soc. 92* (1970) 2165; *95* (1973) 540; b) J. J. Partridge, N. K. Chadha, M. R. Uskoković, *ibid. 95* (1973) 532.
[58] M. Stiles, *J. Am. Chem. Soc. 81* (1959) 2598.
[59] S. W. Pelletier, R. L. Chappell, P. C. Parthasarathy, N. Lewin, *J. Org. Chem. 31* (1966) 1747.
[60] a) N. Nagakura, M. Rüffer, M. H. Zenk, *J. Chem. Soc. Perkin Trans. 1 1979,* 2308; b) A. I. Scott, S.-L. Lee, M. G. Culver, W. Wan, T. Hirata, F. Guéritte, R. L. Baxter, H. Nordlöv, C. A. Dorschel, H. Mizukami, N. E. Mackenzie, *Heterocycles 15* (1981) 1257; c) J. Stöckigt in J. D. Phillipson, M. H. Zenk: *Indole and Biogenetically Related Alkaloids,* Academic Press, London 1980, p. 113; d) J. P. Kutney, L. S. L. Choi, T. Honda, N. G. Lewis, T. Sato, K. L. Stuart, B. R. Worth, *Helv. Chim. Acta 65* (1982) 2088.
[61] Desacetylisoipecoside **79** (3α-H) is a biological precursor of the ipecacuanha alkaloids, *e.g.,* emetine **6** with an 8α-H configuration, whereas desacetylipecoside (**79**, 3β-H instead of 3α-H) is a precursor of the corresponding compounds with an 8β-H configuration, *e.g.* alangiside. The biosynthesis of the indole alkaloids does not proceed *via* separate pathways of this type; strictosidine **78a** (3α-H) acts as a precursor for both stereochemical series. A. R. Battersby, N. G. Lewis, J. M. Tippett, *Tetrahedron Lett. 1978,* 4849; N. Nagakura, G. Höfle, D. Coggiola, M. H. Zenk, *Planta Med. 34* (1978) 381.
[62] U. Pfitzner, M. H. Zenk, *Planta Med. 46* (1982) 10.
[63] T. Hemscheidt, M. H. Zenk, *FEBS Lett. 110* (1980) 187.
[64] J. Stöckigt, M. Rueffer, M. H. Zenk, G.-A. Hoyer, *Planta Med. 33* (1978) 188.
[65] A. I. Scott, S.-L. Lee, *J. Am. Chem. Soc. 97* (1975) 6906; J. Stöckigt, J. Treimer, M. H. Zenk, *FEBS Lett. 70* (1976) 267.
[66] a) L.-F. Tietze, S. Henke, *Angew. Chem. 93* (1981) 1005; *Angew. Chem. Int. Ed. Engl. 20* (1981) 970; b) L.-F. Tietze, S. Henke, S. Brand, H. C. Uzar, unpublished results.
[67] See also G. N. Saunders, J. R. Purdy, S. McLean, *Can. J. Chem. 61* (1983) 276.
[68] G. Kinast, L.-F. Tietze, *Chem. Ber. 109* (1976) 3640; R. T. Brown, C. L. Chapple, *Tetrahedron Lett. 1976,* 787.
[69] a) H. C. Uzar, Dissertation, Universität Göttingen 1981; b) H. Meier, Diplomarbeit, Universität Göttingen 1982.
[70] L. Panizzi, M. L. Scarpati, G. Oriente, *Gazz. Chim. Ital. 90* (1960) 1449; H. C. Beyerman, L. A. van Dijck, J. Levisalles, A. Melera, W. L. C. Veer, *Bull. Soc. Chim. Fr. 1961,* 1812.
[71] L.-F. Tietze, H. C. Uzar, *Angew. Chem. 91* (1979) 574; *Angew. Chem. Int. Ed. Engl. 18* (1979) 539.
[72] a) R. T. Brown in J. D. Phillipson, M. H. Zenk: *Indole and Biogenetically Related Alkaloids,* Academic Press, London 1980; b) L.-F. Tietze, W. Schul, unpublished results.
[73] L.-F. Tietze, *J. Am. Chem. Soc. 96* (1974) 946; G. Kinast, L.-F. Tietze, *Chem. Ber. 109* (1976) 3626.
[74] C. A. Grob, P. W. Schiess, *Angew. Chem. 79* (1967) 1; *Angew. Chem. Int. Ed. Engl. 6* (1967) 1; C. A. Grob, *ibid. 81* (1969) 543 bzw. *8* (1969) 535.
[75] a) L.-F. Tietze, *Tetrahedron Lett. 1976,* 2535; b) H. Inouye, S. Tobita, M. Moriguchi, *Chem. Pharm. Bull. 24* (1976) 1406.
[76] R. Gleiter, *Angew. Chem. 86* (1974) 770; *Angew. Chem. Int. Ed. Engl. 13* (1974) 696; R. Gleiter, W.-D. Stohrer, R. Hoffmann, *Helv. Chim. Acta 55* (1972) 893.
[77] L.-F. Tietze, G. Kinast, H. C. Uzar, *Angew. Chem. 91* (1979) 576; *Angew. Chem. Int. Ed. Engl. 18* (1979) 541.
[78] G. Kinast, L.-F. Tietze, *Angew. Chem. 88* (1976) 261; *Angew. Chem. Int. Ed. Engl. 15* (1976) 239.
[79] C. R. Hutchinson, K. C. Mattes, M. Nakane, J. J. Patridge, M. R. Uskoković, *Helv. Chim. Acta 61* (1978) 1221.
[80] P. Marx, Dissertation, Universität Göttingen 1981.
[81] Natural (−)-**13** and unnatural (+)-sarracenin ent-**13** are obtained from L- and D-galactose, respectively.
[82] L.-F. Tietze, K.-H. Glüsenkamp, M. Nakane, C. R. Hutchinson, *Angew. Chem. 94* (1982) 81; *Angew. Chem. Int. Ed. Engl. 21* (1982) 70.
[83] Further synthesis of sarracenin: a) racemic: J. K. Whitesell, R. S. Matthews, A. M. Helbling, *J. Org. Chem. 43* (1978) 785; J. K. Whitesell, R. S. Matthews, M. A. Minton, A. M. Helbling, *J. Am. Chem. Soc. 103* (1981) 3468; b) enantiomerically pure: S. W. Baldwin, M. T. Grimmins, *ibid. 104* (1982) 1132; S. Takano, K. Morikawa, S. Hatakeyama, *Tetrahedron Lett. 24* (1983) 401.
[84] L.-F. Tietze, K.-H. Glüsenkamp, W. Holla, *Angew. Chem. 94* (1982) 793; *Angew. Chem. Int. Ed. Engl. 21* (1982) 787.
[85] Iridoids were already known as crystalline substances in the 19th century. Loganin **12** was, for example, first isolated from the fruits of *Strychnos nux vomica* L in 1884 by *Dunstan* and *Short:* a) W. R. Dunstan, F. W. Short, *Pharm. J. Trans. 14* (1884) 1025; b) The first correct structure determination of an iridoid was made by *Halpern* and *Schmid:* O. Halpern, H. Schmid, *Helv. Chim. Acta 41* (1958) 1109; c) More recent structure determinations: L. Jahodar, *Farm. Obz. 47* (1978) 353; H. Rimpler, *Planta Med. 33* (1978) 313; R. K. Chaudhuri, F. Ü. Afifi-Yazar, O. Sticher, T. Winkler, *Tetrahedron 36* (1980) 2317; A. Bianco, P. Passacantilli, *Gazz. Chim. Ital. 110* (1980) 547; S. Damtoft, S. R. Jensen, B. J. Nielsen, *Phytochemistry 20* (1981) 2717; F. Bellesia, U. M. Pagnoni, R. Trave, G. D. Andreeti, G. Bocelli, P. Sgarabotto, *J. Chem. Soc. Perkin Trans. 2 1979,* 1341.
[86] H. Paulsen, *Angew. Chem. 94* (1982) 184; *Angew. Chem. Int. Ed. Engl. 21* (1982) 155; G. Wulff, G. Röhle, *ibid. 86* (1974) 173 bzw. *13* (1974) 157.
[87] L.-F. Tietze, U. Niemeyer, P. Marx, *Tetrahedron Lett. 1977,* 3441; L.-F. Tietze, U. Niemeyer, *Chem. Ber. 111* (1978) 2423.
[88] L.-F. Tietze, P. Marx, *Chem. Ber. 111* (1978) 2442.
[89] L.-F. Tietze, U. Niemeyer, P. Marx, K.-H. Glüsenkamp, *Tetrahedron 36* (1980) 1231.
[90] L.-F. Tietze, U. Niemeyer, P. Marx, K.-H. Glüsenkamp, L. Schwenen, *Tetrahedron 36* (1980) 735.
[91] L.-F. Tietze, R. Fischer, *Angew. Chem. 95* (1983) 902; *Angew. Chem. Int. Ed. Engl. 22* (1983) 887.
[92] L.-F. Tietze, R. Fischer, *Angew. Chem. 93* (1981) 1002; *Angew. Chem. Int. Ed. Engl. 20* (1981) 969.
[93] L.-F. Tietze, R. Fischer, *Tetrahedron Lett. 22* (1981) 3239.
[94] L.-F. Tietze, R. Fischer, H.-J. Guder, *Synthesis 1982,* 946.
[95] K. H. Büchel, *Naturwissenschaften 66* (1979) 173; H. König, *Angew. Chem. 92* (1980) 802; *Angew. Chem. Int. Ed. Engl. 19* (1980) 749; G. Adam, *Z. Chem. 21* (1981) 273.

# Synthesis of Peptide Hormones using Recombinant DNA Techniques**

By Friedrich Wengenmayer*

Recombination of genetic material enables the creation of new bacterial strains which can synthesize specific proteins in large amounts. Such bacteria permit the production of previously inaccessible proteins. They can therefore be used as starting materials for the production of drugs which will open up new paths for therapy. Several proteins produced by bacteria after DNA recombination are presently undergoing clinical trials while others are already being produced on a large scale. Thus, in the area of recombinant DNA techniques the transition from the research laboratory to industrial exploitation has occurred much faster than was anticipated several years ago. The methods, possibilities and problems encountered in the synthesis of peptide hormones by bacteria after DNA recombination are outlined, using insulin, somatostatin, and growth hormone as examples. Great emphasis is placed on the molecular biological aspects of this approach.

## 1. Introduction

After the first successful attempts to transfer antibiotic resistance genes to bacteria[1], the field of molecular biology developed rapidly, not least because of the wide variety of practical applications offered by recombinant DNA techniques and DNA transfer.

It was expected that the stable integration of a particular human gene into bacteria would lead to strains which could be used to isolate clinically relevant proteins. The advantages are obvious: the simple culture media and the short generation time of bacteria make it possible to produce proteins which are otherwise difficult to obtain.

From the beginning, interest focused on the production of peptide hormones. There are several reasons for this:

- Most peptide hormones are species specific. Thus, peptides isolated from animal tissue cannot be used in humans since they are inactive due to differences in sequence and structure. This problem can be overcome by recombinant DNA techniques, which allow the production of human hormones in bacteria after the appropriate gene transfer.
- The isolation of some peptide hormones required enormous efforts. In order to obtain less than one milligram of thyrotropin releasing hormone the groups of *Schally* and *Guillemin* had to start their purification from the hypothalami of 80000 sheep[2] or 200000 pigs[3]. And it is anticipated that the future isolation of other therapeutically important peptides and proteins will meet with similar difficulties unless it becomes possible to use genetically engineered bacteria for their production.
- Furthermore, the long years of experience in the successful treatment of diabetes with insulin led to the expectation that other metabolic disorders could also be treated in a similar way once the appropriate hormones were available.

As a result of efforts by several groups, the first peptide hormones produced *via* recombinant DNA techniques are now in hand. Human insulin, synthesized in bacteria, is commercially available, human growth hormone, somatostatin and thymosin α-1 are undergoing clinical trials, and other peptide hormones like relaxin, glucagon and GRF (growth hormone releasing factor) are imminent.

## 2. Isolation of Peptide Hormones

Before discussing recombinant DNA techniques, I will briefly mention the conventional methods used in the production of peptide hormones.

The classical isolation from animal organs is the method of choice for longer polypeptides. The organs are usually obtained from slaughtered animals; for example, the insulin used in the treatment of diabetes is isolated from the pancreas of pig or cow, since these animal hormones are very similar to human insulin (cf. Section 6.3).

In Germany the requirement for insulin is approximately 250 kg per year, which means that pancreatic glands of 2.5 million animals have to be extracted. Worldwide, approximately 2000 kg insulin from about 20 million animal pancreatic glands is prepared. Considerable effort and time goes into the collection and transport of these organs, since they have to be frozen quickly in order to avoid degradation and changes in the structure.

Not only is animal tissue used to obtain clinically important peptides and proteins, but also, in special cases, human organs are the source of the desired material. For example, in the case of the treatment of children deficient in growth hormone, it is not possible to employ equivalent animal hormones since there are too many structural differences. Thus, for the treatment of *ca.* 800 children in England several thousand human pituitary glands are col-

[*] Dr. F. Wengenmayer
Pharma Forschung Biochemie H825
Hoechst Aktiengesellschaft
Postfach 800320, D-6230 Frankfurt am Main 80 (Germany)

[**] Based on a lecture delivered at the GDCh Symposium on Biotechnology and Drug Research in Schliersee on September 28, 1982.

 © Verlag Chemie GmbH, 6940 Weinheim, 1983 0570-0833/83/1111-0842 $ 02.50/0 

lected for the isolation of the required human growth hormone[4].

In general, the isolation of peptide hormones from tissue becomes impossible if the concentration of the desired hormone is extremely low or if the animal hormone is inactive in humans.

Chemicals synthesis of peptide hormones is a viable alternative to tissue isolation, especially in the case of smaller molecules. Examples of such peptides are the nonapeptide oxytocin and the decapeptide luteinizing hormone releasing hormone (LHRH), both of which are in clinical use.

In special cases where the quantities required lie in the order of one kg per year, industrial synthesis can be carried out up to a chain length of about 30 amino acids. This is the case of the gastrointestinal hormone secretin which contains 27 amino acids. In theory even larger proteins can be synthesized, as was demonstrated for insulin[5]. However, the costs for the synthesis and purification on an industrial scale are immense and therefore the synthetic approach cannot compete with the isolation from animal organs.

The amount of peptide produced by genetically engineered bacteria under ideal conditions is limited only by the size of the fermenter; furthermore, the length of the polypeptide chains should in principle create no problems. Recombinant DNA therefore opens up for the first time a route for the preparation of a variety of clinically important human proteins in sufficient quantities. Examples are polypeptide hormones, interferons and lymphokines.

As a first step in the production of a human protein in a bacterium, one has to develop a bacterial strain containing the corresponding gene stably integrated. In most cases further manipulations of the genetic material are necessary to insure a high yield of the protein.

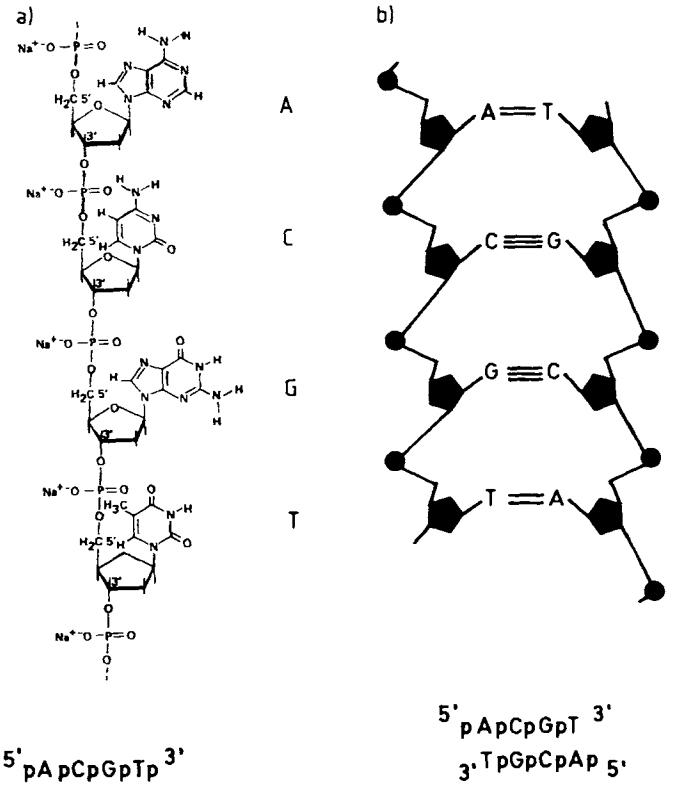



Fig. 1. Schematic representation of deoxyribonucleic acid (DNA). a) single stranded DNA; b) double stranded DNA. The two complementary strands of opposite directionality are held together by the interaction between the bases on each strand as indicated.

## 3. DNA Preparation

In human and animal cells the genetic material, deoxyribonucleic acid (DNA) is located in the nucleus. All the information concerning the amino acid sequence of every single protein synthesized by the organism is encoded in it. Furthermore, DNA also contains a variety of regions responsible for complex regulatory and control processes within the cell.

DNA consists of two anti-parallel 2-deoxyribose phosphate chains which carry at the 1′ position of each ribose one of the four bases adenine (A), thymine (T), cytosine (C) or guanine (G) (Fig. 1). Both chains are held together by hydrogen bonds between A and T and G and C respectively. Since A is always located opposite a T and G always opposite a C, the two chains are complementary but of opposite sense. Further details of the DNA structure are not the subject of discussion in this article.

The information for a particular amino acid sequence of a protein is encoded on a stretch of DNA in such a way that three consecutive bases determine the respective amino acid. Using the four available bases such a triplet code leads to 64 possible combinations (Table 1). Of these, three triplets are stop codons (TAA, TAG and TGA), one is a start codon (ATG) and the others encode amino acids with up to six different triplets coding for the same amino acid (*e.g.* leucine, serine, arginine).

Table 1. Coding of the amino acids by base triplets of mRNA. The first letter of the first base of the triplet is shown in the left-hand column, the first letter of the second base in the top row, and that of the last base in the extreme right-hand column. Usually the genetic code is represented as the RNA code. Since the mRNA strand is complementary to one of the two DNA strands, the sequence of the DNA strands can be deduced from the base-pairing rule. The examples mentioned in the text always refer to the DNA strand with the same base sequence as in mRNA.

| | U | C | A | G | |
|---|---|---|---|---|---|
| U | Phe | Ser | Tyr | Cys | U |
| | Phe | Ser | Tyr | Cys | C |
| | Leu | Ser | stop | stop | A |
| | Leu | Ser | stop | Trp | G |
| C | Leu | Pro | His | Arg | U |
| | Leu | Pro | His | Arg | C |
| | Leu | Pro | Glu | Arg | A |
| | Leu | Pro | Glu | Arg | G |
| A | Ile | Thr | Asn | Ser | U |
| | Ile | Thr | Asn | Ser | C |
| | Ile | Thr | Lys | Arg | A |
| | Met,start | Thr | Lys | Arg | G |
| G | Val | Ala | Asp | Gly | U |
| | Val | Ala | Asp | Gly | C |
| | Val | Ala | Glu | Gly | A |
| | Val | Ala | Glu | Gly | G |

Of crucial importance for the rapid development and propagation of recombinant DNA techniques was the discovery of restriction enzymes[6] and the possibility to covalently join DNA fragments with the enzyme DNA ligase[7].

Restriction enzymes recognize characteristic base sequences of the DNA, cutting the double strand either within the recognition sequence or in its neighborhood (Table 2). Up to date approximately 80 different recognition sequences for restriction enzymes from a wide variety of bacterial strains have been described[8]. To prevent restriction enzymes cutting the organism's own DNA, the recognition sequences of the DNA in the respective organisms are modified by specific methylases. Restriction enzymes therefore offer protection from foreign DNA which has invaded the organism and which is cut before a possible modification. Whether this is the only function of restriction enzymes in bacteria cannot yet be answered fully.

Table 2. Recognition sequences of some restriction enzymes. Cleavage sites on each strand are indicated by the arrows. The enzymes Hae III and Xmn I create blunt ends, Hha I cleavage results in 3′ protruding ends, and Eco RI as well as EcoR II produce 5′ protruding ends. N symbolizes T, C, G or A while N′ is the respective complementary base.

| Recognition sequence | Restriction enzyme |
|---|---|
| —5′G G C C 3′— <br> —3′C C G G 5′— | Hae III (from Haemophilus aegyptius) |
| —G A A T T C— <br> —C T T A A G— | Eco RI (from E.coli) |
| —N C C(A)G G N— <br> —N′G G(T)C C N′— | Eco RII (from E.coli) |
| —G C G C— <br> —C G C G— | Hha I (from Haemophilus haemolyticus) |
| —G A A N N N T T C— <br> —C T T N′N N′N′ N′A A G— | Xmn I (from Xanthomonas manihotis) |

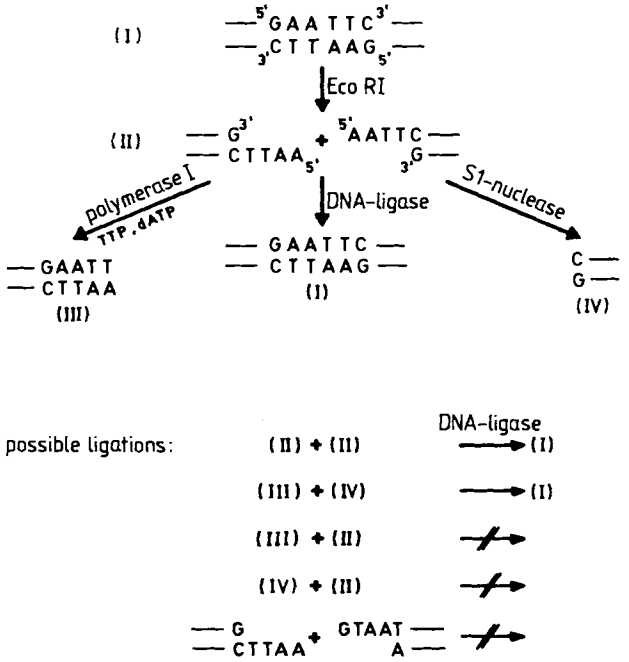






Fig. 2. Some enzymatic reactions of DNA *in vitro*. EcoR I cleavage results in fragments with 5′ overlapping ends which can be converted into blunt ends using S1 nuclease or polymerase I. Blunt ends are ligated by DNA ligase, staggered ends can only be joined if they have complementary sequences.

DNA fragments with blunt or staggered ends are obtained by the action of restriction enzymes. Staggered ends can be enzymatically converted into blunt ends (Fig. 2). This is achieved either with polymerase I which fills in the recessed end or with single strand specific nucleases (S1 nuclease, mung bean nuclease) which degrade the single stranded protruding end.

The enzyme DNA-ligase joins either DNA fragments with blunt ends or with staggered ends, provided that base pairing between the strands can occur. The term used for covalently joining DNA fragments is called "*in vitro* recombination of nucleic acids" and this area of research has recently been reviewed[9].

In order to obtain DNA coding for a human protein, several routes can be taken: a) chemical synthesis of DNA; b) isolation of a DNA fragment containing the gene; c) enzymatic synthesis using mRNA as a template.

### 3.1. Chemical Synthesis of DNA

The amino acid sequence of a human protein can be used to deduce the DNA sequence. Since in most cases one has a choice of several triplets (codons) for one amino acid, the synthesis can be varied according to different requirements. In most cases codons would be chosen in such a way as to yield appropriate restriction sites.

Looking for example at the peptide sequence -Glu-Phe- one has to combine one of the triplets coding for glutamic acid (GAA, GAG) with a codon for phenylalanine (TTT, TTC). Choosing -GAA-TTC- results in a restriction site for the enzyme Eco RI. Such a site consisting of six base pairs occurs statistically once in $4^6$, namely 4096 base pairs. Careful planning of such restriction sites in a chemical DNA synthesis will aid in joining or exchanging whole blocks of DNA.

Different organisms have different codon usage with respect to particular amino acids[14]. Table 3 clearly shows that in *Escherichia coli* the triplet CTG is commonly used for leucine whereas it finds no use at all in the yeast proteins studied so far. In yeast the predominant codon for leucine is clearly TTG. Similar differences are found for the other amino acids.

Table 3. Codon usage of the triplets coding for leucine, proline and glutamic acid in yeast and *E. coli*. Other amino acids show similar trends. Triplets of the mRNA are represented; base U instead of base T. The table is reproduced from *Ikemura et al.* [10].

| | | Yeast [%] | E.coli [%] |
|---|---|---|---|
| Leu | UUA | 6 | 5 |
| | UUG | 89 | 8 |
| | CUU | 2 | 8 |
| | CUC | 0 | 8 |
| | CUA | 3 | 2 |
| | CUG | 0 | 69 |
| Pro | CCU | 13 | 10 |
| | CCC | 0 | 6 |
| | CCA | 87 | 15 |
| | CCG | 0 | 69 |
| Glu | CAA | 98 | 22 |
| | CAG | 2 | 78 |

It is likely that DNA with codons not commonly used in *E. coli* will not yield large amounts of protein in this bacterium since the whole apparatus for protein synthesis is geared towards the normal *E. coli* conditions. Thus, it is advantageous to choose codons in such a way that they are closely matched to the organism in which the protein synthesis is going to take place.

Methods for DNA synthesis have undergone rapid development in recent years and a summary of the state of the art is described in [11]. In a well equipped and trained laboratory it is possible today to synthesize and purify several oligonucleotides of 20–30 base pairs in length within a few weeks. Several automated synthesizing machines are on the market which can be used continuously to synthesize any desired sequence. Genes for human interferons of over 500 base pairs in length[12] as well as DNA coding for both chains of insulin[13] have been successfully synthesized.

One cannot stress strongly enough the importance of chemical DNA synthesis for the production of biologically active substances in microorganisms. The synthesis of small 'linker' and 'adaptor' molecules carrying specific restriction sites is of special importance, since after joining them to DNA fragments they allow the insertion of such fragments into particular restriction sites.

### 3.2. Isolation of a Gene Fragment

In principle it is possible to isolate the desired DNA fragment from the respective genomic DNA. Human cells contain about 150000 different genes and approximately $5 \times 10^9$ base pairs[15]. The fact that it is nevertheless a realistic task to attempt the isolation of a gene[16] demonstrates the enormous power of modern molecular biological methods.

Genes for a variety of proteins have already been isolated and their nucleotide sequence completely determined[17]. The coding region for a protein in genes of higher organisms (*e.g.* cells which possess a nucleus, eukaryotic cells) is frequently interrupted by non-coding sequences. The function of these sequences (introns) is still unclear and they are removed from the precursors mRNA during the expression of the gene (Fig. 3). This event is called splicing[18]. Bacterial genes are organized in a simpler fashion and so far only one case of bacterial introns has been reported in an archaebacterium[123]. Therefore genes of higher organisms are not correctly processed in bacteria[19]. Introns are not recognized and cannot be removed from the precursor mRNA. Depending on the nucleotide sequence of the intron, this either leads to premature chain termination or to longer 'nonsense' proteins. Since the genes coding for most of the human hormones contain introns it is not possible to insert them directly into bacteria in order to produce the protein and alternative methods to obtain the appropriate DNA have to be employed. This does not, however, imply that it is impossible to use intron free parts of these genes which can then be complemented by synthetic DNA.

An exception worth mentioning are the genes for interferons from human leucocytes and fibroblasts. Interferons

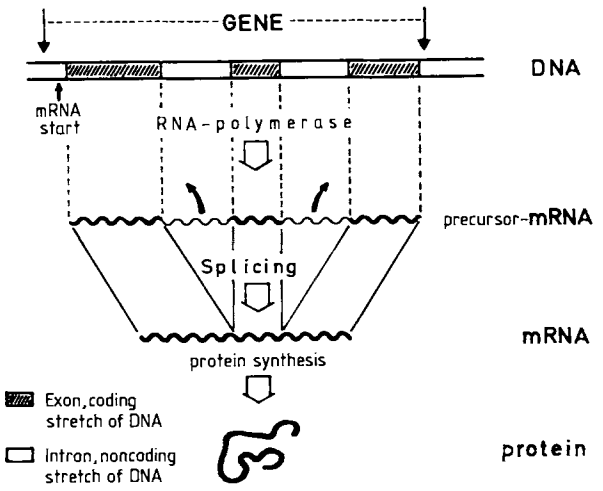



Fig. 3. Expression of a gene containing two introns. In the genes of higher organisms the coding sequences are frequently interrupted by non-coding DNA stretches. Expression of a gene is initiated by the synthesis of a precursor mRNA which is subsequently converted into mRNA *via* splicing. Mature mRNA is the template for protein synthesis.

are synthesized in eukaryotic cells in reaction to a virus infection. Furthermore, it is thought that interferons stimulate the immune system and therefore could play a role in the treatment of some types of cancer[20]. Since for a long time it was only possible to obtain interferons in minute amounts from human cell cultures, and because of the potential applications of these proteins, intensive research has been carried out in an effort to produce them in bacteria *via* recombinant DNA techniques.

Recently, several groups have succeeded in elucidating the sequences for different interferon genes[21]. It has been found that leucocyte interferon genes have no introns and thus can be used for production of the corresponding protein in bacteria. This opened the way for the rapid production of several interferons, some of which are already undergoing clinical trials[20]. Furthermore, hybrid interferons with a variety of interesting characteristics were created by joining parts from different genes *via* common restriction sites[22].

### 3.3. Enzymatic Synthesis of DNA from mRNA

As shown in Figure 3, protein synthesis in the cell starts with the synthesis of mRNA (or precursor mRNA). Using one DNA strand as a template, the enzyme RNA polymerase synthesizes a complementary strand of mRNA. This mRNA exhibits the same base sequence at the ribose phosphate chain as the non-transcribed DNA strand with the exception that thymine is substituted by uracil.

The mRNA contains through its base sequence signals for the binding to the ribosome as well as for start and stop of the protein synthesis.

Transcription of deoxyribonucleic acid (DNA) into messenger ribonucleic acid (mRNA) is not a unique event. In a cell specialized in the production of a particular hormone the respective DNA fragment is transcribed many times into mRNA, which results in mRNA concentrations up to several thousandfold the concentration of the gene.

It is possible to synthesize DNA enzymatically *in vitro* from isolated mRNA (Fig. 4)[23–26]. Therefore the isolation of mRNA is usually the first step in the production of a genetically engineered bacterial strain. In the purification of eukaryotic mRNA one exploits the fact that its 3′ end contains a poly A sequence which allows its separation by affinity chromatography on oligo-dT-cellulose[27].

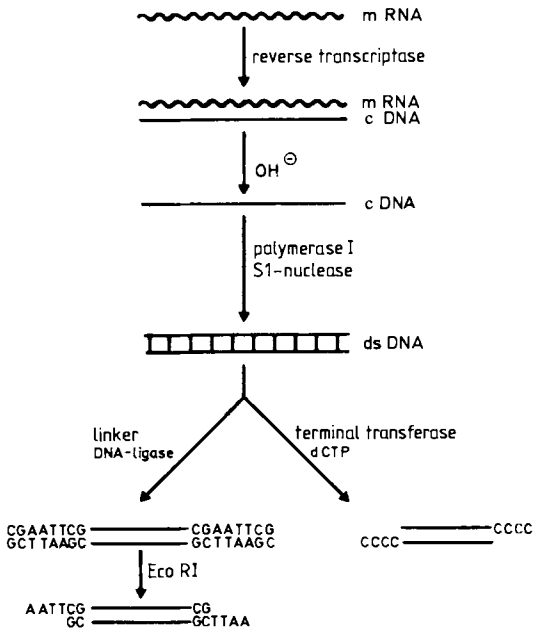



Fig. 4. *In vitro* synthesis of DNA from mRNA. The enzyme reverse transcriptase copies mRNA into single stranded DNA, termed cDNA (copy or complementary DNA). The mRNA is subsequently destroyed by hydrolysis with alkali. The DNA is converted into the double stranded form with polymerase I and blunt ends are created by S1 nuclease. In order to insert the DNA into a plasmid, synthetic oligonucleotides comprising appropriate restriction sites are jointed to the ends. Another method involves the ligation of homopolymers to the DNA ends.

The mRNA is transcribed into cDNA (copy or complimentary DNA) by the enzyme reverse transcriptase which requires a small oligonucleotide complementary to the 3′ end of the mRNA to start the synthesis. This oligonucleotide, called primer, is the 5′ end of the growing cDNA chain. Since the 3′ end of eukaryotic mRNA contains a poly A sequence, oligo $dT_{12-18}$ can be used as a non specific primer. This will lead to transcription of all mRNA molecules present in the preparation into cDNA (Fig. 5). It is however possible to employ selective conditions which will permit the transcription of only a single mRNA into cDNA. This involves the use of a synthetic primer of at least 12 nucleotides in length which is complementary to the 3′-end of the selected mRNA (Fig. 5)[28].

The sequence information necessary for the synthesis of the primer can be deduced from the amino acid sequence of the *C*-terminal region of the protein. In the most favorable case this end should contain amino acids which are encoded by a single triplet (tryptophan and methionine) in order to predict the nucleotide sequence unambiguously. In practice one chooses a sequence of five amino acids which show a very low multiplicity of the genetic code.

In order to assess which of the discussed methods is the most suitable to obtain DNA it is important to consider the length of the desired DNA fragment. To date cDNA preparation is preferred for DNA pieces of 150 nucleotides and longer; however, bearing in mind the rapid development of DNA synthesis this could well change in the near future.

## 4. Plasmids

DNA prepared by either of the above three routes (Section 3) is introduced into bacteria with the aid of plasmids. Plasmids are circular DNA molecules which are considerably smaller than the bacterial chromosome and can occur in bacterial cells (Fig. 6). Frequently plasmids carry resistance genes for antibiotics and are often responsible for the rapid spread of antibiotic resistance. Commonly used plasmids replicate independently of the bacterial chromosome; under favorable conditions, for example in the presence of chloramphenicol, there can be up to 500 plasmid copies per bacterial cell. Plasmid DNA can easily be separated from the chromosomal DNA of the bacterium[29]; purifica-

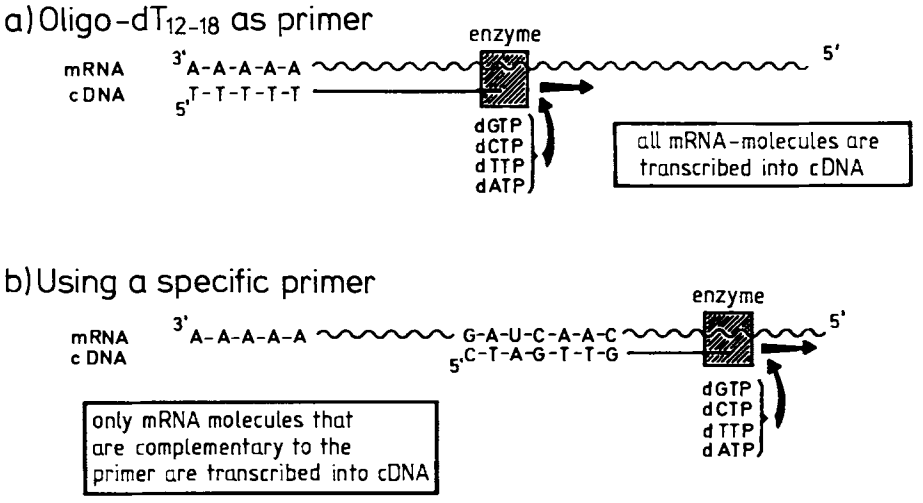



Fig. 5. Synthesis of cDNA from mRNA with reverse transcriptase: a) oligo $dT_{12-18}$ as primer; b) synthetic oligonucleotide as primer. (The length of the primer has been shortened for the sake of space; it should be at least 12 nucleotides long.)

tion is achieved by centrifugation in a CsCl gradient in the presence of the intercalating dye ethydium bromide. Due to their different structures chromosomal and plasmid DNA bind different amounts of this dye and hence exhibit different densities[26,39].

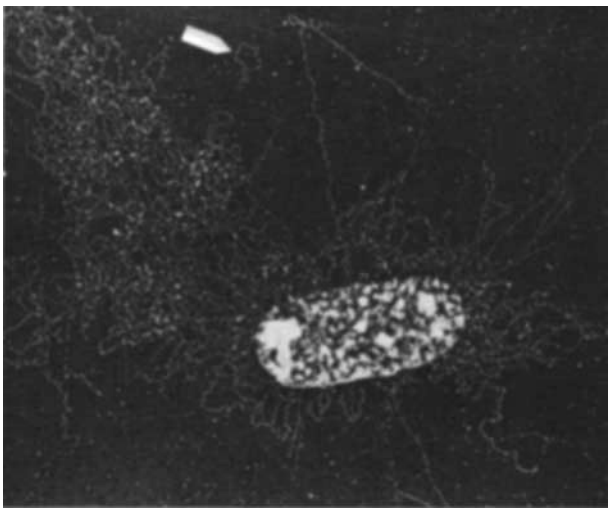


Fig. 6. Electronmicrograph [30] of an *E. coli* bacterium, whose cell wall has been made permeable. At the top of the picture a plasmid which was originally inside the cell is indicated by an arrow. The conglomerate of fibers represents the much larger bacterial chromosome.

In order to use plasmids as vectors transporting foreign DNA into bacteria, it is important that isolated and modified plasmids can easily be reintroduced under simple experimental conditions. This process is called transformation. In the presence of calcium chloride (*ca.* 50 mM) the cell wall and cell membrane of a variety of bacteria are changed in such a way that foreign DNA can penetrate into the cell.

From 1 μg of plasmid DNA about $10^6$ transformants are obtained. The transformants can easily be detected and selected *via* plasmid borne antibiotic resistances.

The multiplication of DNA *via* insertion in a plasmid and introduction into bacteria is frequently referred to as "molecular cloning" (Fig. 7). The underlying concept results in several practical consequences.

1. Any desired DNA fragment can be replicated with the help of plasmids and can subsequently be studied. This enables the investigation of processes which alter the genetic material. In the field of medicine this includes for example malignant transformations, viral infections and possibly conditions connected with aging. Needless to say, hereditary diseases can be studied as well. Preliminary important results concerning the initiation of tumors have already been reported[31]. The question, however, of whether the results of these investigations on DNA can soon be used for new possibilities in therapy, cannot be answered as yet.

2. Insertion of a DNA fragment coding for a protein into bacteria can yield an excellent source for the production of the protein.

Starting from naturally occurring plasmids a variety of specialized plasmids have been constructed (*e.g.* pUC 8[32] and pUR 250[33]). Figure 8 shows the most commonly used

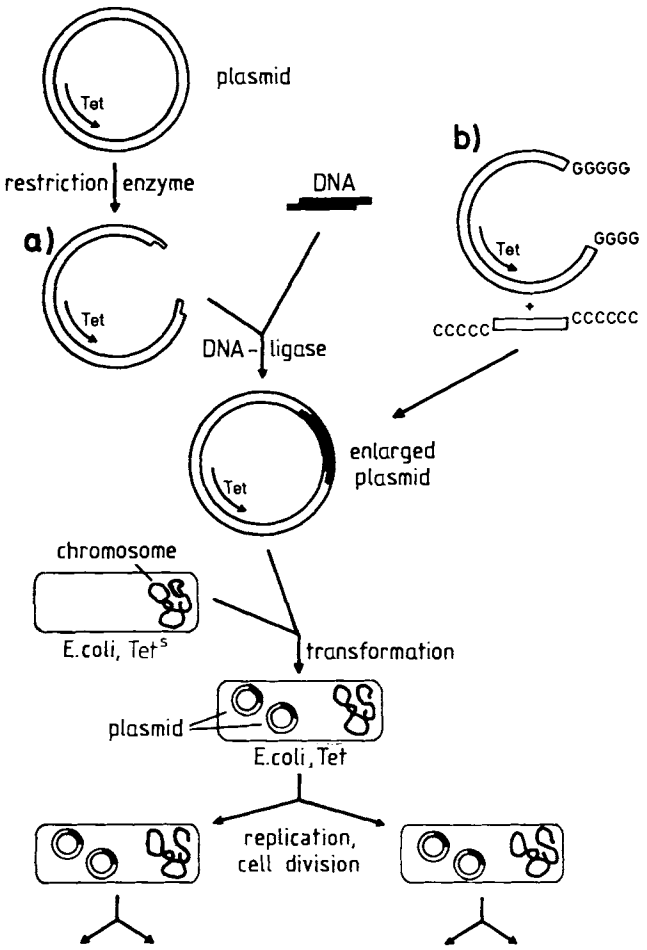



Fig. 7. DNA cloning *via* insertion into a plasmid and subsequent transformation. The circular plasmid is linearized by digestion with a restriction enzyme which has a single recognition site on the plasmid DNA.—a) Foreign DNA with suitable ends is introduced and the enlarged plasmid is used for transformation; b) insertion of DNA into the plasmid using complementary homopolymers [40]. The plasmid shown as an example carries the tetracycline (Tet) resistance gene, so that the plasmid-containing bacteria which were previously tetracycline-sensitive (Tet$^s$), can therefore easily be selected by adding the antibiotic to the medium.

plasmid at the present time, pBR 322[34]. Plasmids contain a region called origin (Or), where replication of the plasmid is initiated. Most of the plasmids used contain in addition several unique restriction sites as well as at least one antibiotic resistance gene in order to facilitate the selection.

After *in vitro* recombination and subsequent DNA replication it is necessary to use analytical methods to characterize the cloned DNA fragments. This is achieved by digesting the DNA with a variety of restriction enzymes and subsequent electrophoretic separation of the resulting fragments[41]. Such restriction analysis is useful for the sequencing procedure employed afterwards, which yields the final information about the DNA composition. Both sequencing methods, either that of *Maxam* and *Gilbert*[35] or of *Sanger et al.*[36], can be carried out quickly and give reliable results. Nowadays, in order to obtain a protein sequence, it is in many cases quicker to isolate the respective structural gene, sequence the DNA, and deduce the amino acid sequence from the nucleotide sequence. Indeed, in cases of certain large proteins the final amino acid se-

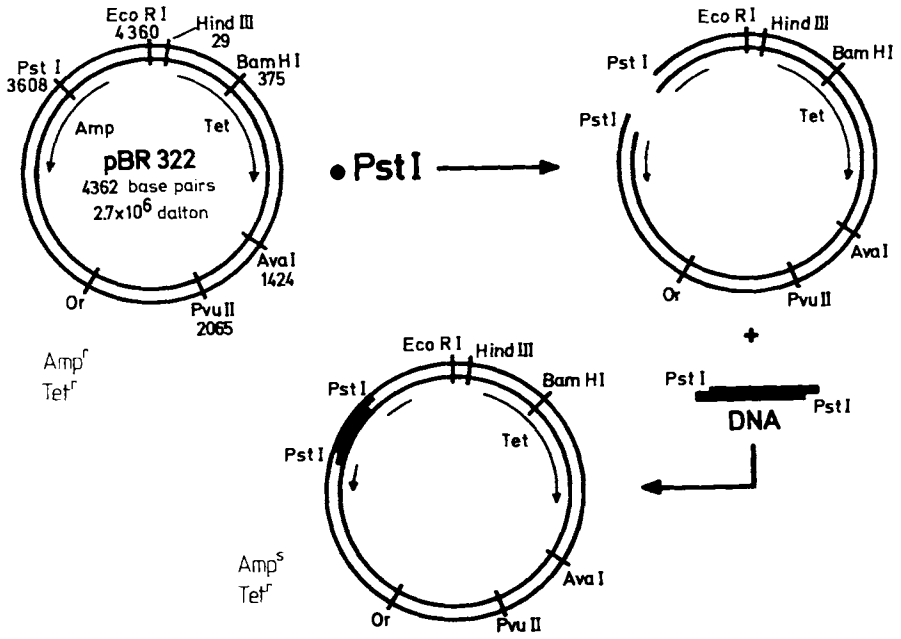



Fig. 8. Insertion of DNA into the Pst I restriction site of the plasmid pBR 322. The positions of several singular restriction sites are indicated. The plasmid contains resistant genes for ampicillin (Amp) and tetracycline (Tet), Or is the origin of replication. Insertion of DNA into the Pst I site abolishes ampicillin resistance. $Amp^s$ and $Tet^r$ bacteria can be recognized using replica plates containing ampicillin and tetracycline.

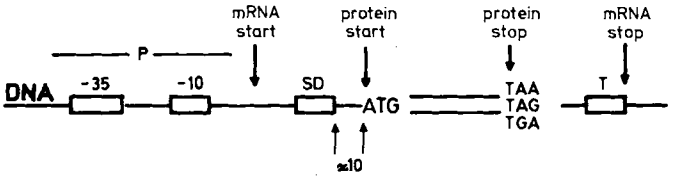
quence could only be completed using the DNA sequencing data in addition to partial amino acid sequence data of these proteins[37,38].

## 5. Gene Expression in *Escherichia coli*

Expression of a structural gene consists in the synthesis of the mRNA (transcription) and the synthesis of the protein (translation). In order to express a particular gene in *E. coli* it is not sufficient to stably integrate the DNA *via* a plasmid into the bacterium. In addition, the DNA has to contain important signal sequences[42,43] (Fig. 9).

From mRNA synthesis the enzyme RNA polymerase has to bind to a particular sequence on the DNA, the promotor. Depending on the amount of mRNA synthesized, promotors are termed weak or strong promotors. Comparison of a large number of promotor sequences led to the discovery of homologous sequences in the regions $-10$ and $-35$ in front of the mRNA start[44,45]. These are obviously sequences that are signals for the start of transcription. Figure 9 shows the consensus sequences derived from such comparisons which comprise the most frequent nucleotides for each position[45–47]. Nucleotide changes within the promotor lead to changes in transcription frequency, especially alterations in the 'constant' parts. Apart from the above mentioned promotor structure, more complex structures exist which regulate gene expression through several promotors[48].

In order to achieve high protein yields one needs in addition to a strong promotor an efficient protein synthesis machinery. Protein synthesis is carried out on the ribosomes with mRNA as a template[49]. It is therefore necessary to have a sequence on the mRNA which codes for the association and binding of the ribosome. Such sequences have been postulated after sequence analysis of the ribosome by *Shine* and *Dalgarno*[50] and later confirmed[51,52].




consensus sequences:

-35 : −TGTTGACA−TT−
-10 : −TGTTATAATG−

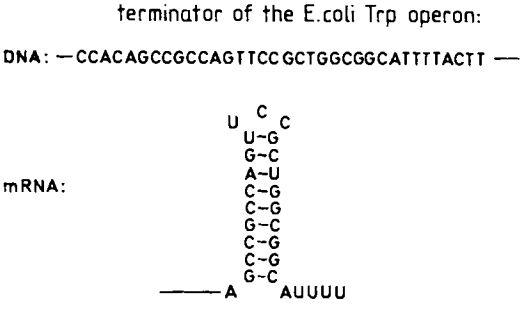



Fig. 9. Signal sequences for gene expression in prokaryotes. Regions approximately 35 and 10 nucleotides in front of the transcription start are labeled $-35$ and $-10$, respectively, P, promotor; SD, Shine-Dalgarno sequence; T, terminator. The indicated sequences [45] are located on the non-transcribed DNA strand (sequence equivalent to mRNA). The sequence of the terminator given [43] is representative of other terminator sequences which also contain complementary sequences.

The Shine-Dalgarno sequence (SD-sequence) is approximately 3—9 nucleotides long and is located 3—11 nucleotides in front of the start codon (AUG) for the protein synthesis. It is complementary to the 3′ end of the 16S RNA of the ribosome:

3′HO-AUUCCUCCACUA__

Further signal sequences are start and stop codons for protein synthesis. The start codon is AUG which also codes for the amino acid methionine. In most proteins the *N*-terminal methionine is removed by specific enzymes. One or several of the triplets UAA, UAG and UGA stop protein synthesis.

The SD sequence and signals for protein synthesis exert their function only on the mRNA. Since, however, mRNA is the copy of one of the DNA strands, these signals are also encoded in the DNA where the base uracil is substituted by thymine.

mRNA synthesis is terminated by special DNA structures, terminators, which are located in front of the last nucleotide of the mRNA[53]. Comparison of several such sequences have yielded no consensus sequence[45]. It was however noticed that they contain complementary sequences which can form hairpin loops (Fig. 9), from which it was concluded that termination is most probably caused by the structure of the mRNA itself rather than by the structure of the DNA[45].

For gene expression of a eukaryotic protein in bacteria it is desirable to have a fast rate of synthesis, which in addition should be subject to regulation. It is therefore useful to employ control sequences which are used in *E. coli* and which cause high concentrations of specific bacterial proteins.

Regulatory sequences combined with the appropriate structural genes are called operons. The following operons are frequently used to aid expression of eukaryotic DNA in *E. coli:* the lactose operon, the tryptophan operon, and promotors of the bacteriophage λ.

### 5.1. The Lactose Operon

In *E. coli* the enzymes β-galactosidase, permease and transacetylase are involved in the degradation of lactose. The structural genes for these enzymes as well as their regulatory sequences on the DNA are known as the *lac* operon.

Enzymes of the *lac* operon are only synthesized by the bacterium if lactose (or another inducer) is present in the medium. Investigations of this regulatory system are all based on the work of *Jacob* and *Monod*[54]. Figure 10 illustrates the structure and the regulatory mechanism of the *lac* operon.

With optimal induction it is possible to obtain β-galactosidase, a protein of molecular weight 500000 and composed of four subunits, in concentrations up to 30% of the total *E. coli* proteins. The possibility of switching on the synthesis of β-galactosidase at any given moment upon addition of appropriate substances into the medium (induci-

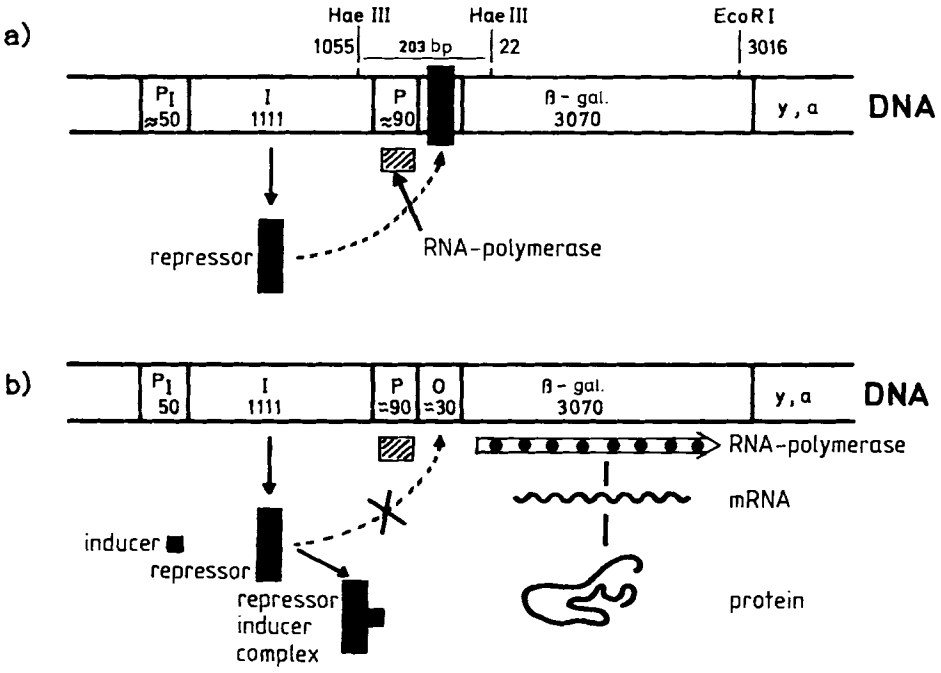



Fig. 10. Structure and regulation of the *lac* operon in *E. coli.*—a) The structural gene I with its promotor $P_I$ codes for a repressor protein, which binds to a site between the promotor P and the structural gene for β-galactosidase. This site on the DNA of the *lac* operon is called the operator (O). The repressor-operator complex blocks RNA polymerase; thus no mRNA is formed and no protein of the *lac* operon synthesized. y and a are the two other structural genes of the *lac* operon.—b) In the presence of the inducer lactose, an inducer-repressor complex is formed which no longer can bind to the operator. Therefore RNA polymerase is able to transcribe the DNA into mRNA and biosynthesis of β-galactosidase as well as the other proteins encoded by the *lac* operon proceeds. Numbers indicate fragment sizes in base pairs.

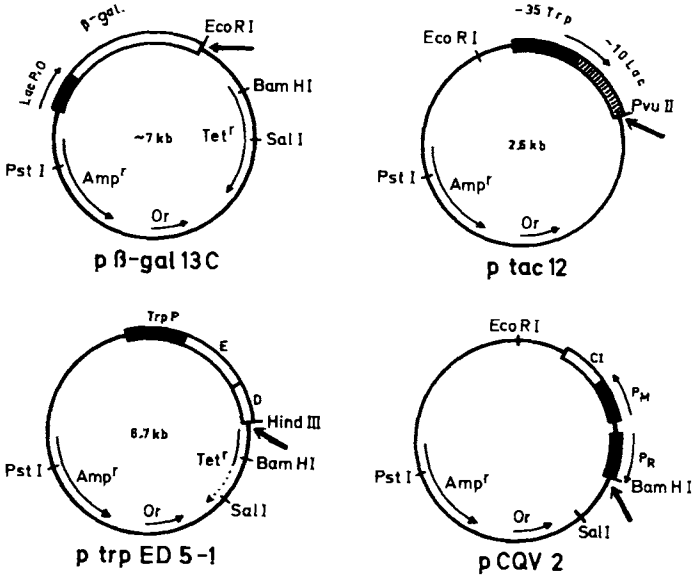



Fig. 11. Four vectors used for the expression of eukaryotic DNA. Insertion sites are indicated by arrows. - p β-gal 13C [60]: Insertion of DNA into the EcoR I restriction site results in synthesis of a chimeric protein containing 1005 amino acids of the β-galactosidase under control of the *lac* operon. - p tac 12 [65]: Expression of DNA inserted into the Pvu II site is achieved under control of a fusion promotor containing the −35 region of the *trp* promotor and the −10 region of the *lac* promotor. - p trp ED 5-1 [66]: Under control of the *trp* promotor the E protein of the tryptophan pathway is synthesized as well as a chimeric protein consisting of 92 amino acids of the D protein and the protein encoded by the inserted DNA. pCQV 2 [67]: DNA inserted into the Bam HI site is transcribed under the control of the $P_R$ promotor. $P_R$ is regulated *via* the thermolabile repressor CI.

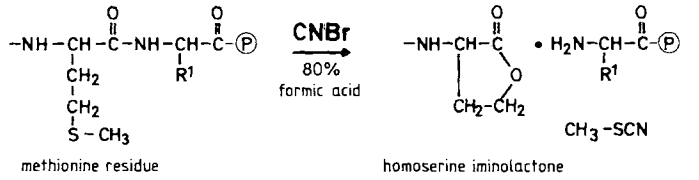



Fig. 12. BrCN cleavage of a peptide from a chimeric protein.

bility) as well as the high concentration of the enzyme in *E. coli* itself, renders the use of the regulatory units of the *lac* operon a tempting thought for the production of other proteins. Furthermore, one can use mutants which contain base changes in the promotor and show improved characteristics for high expression[55]. It is possible to isolate the regulatory region of the *lac* operon (promotor, operator and the coding sequence for the first seven amino acids of β-galactosidase) on a 203 base pair Hae III fragment[56]. Using synthetic linkers one can add suitable restriction sites to the ends of the fragment, and, after insertion into a plasmid, this fragment ensures expression of the attached structural gene[56–59].

One can also use the Eco RI site at position 3016 in the structural gene of β-galactosidase[37] for the insertion of foreign DNA. This leads to a chimeric protein comprising the first 1005 amino acids of β-galactosidase followed by the desired protein[58,60–63] (Fig. 11). In both cases the remainder of the β-galactosidase has to be cleaved off from the desired protein; this can be achieved either enzymatically or by chemical methods. The method of choice is determined by the amino acid composition of the desired protein and the cleavage site. For example, trypsin cleaves at the *C*-terminus of the amino acids lysine and arginine, and chymotrypsin cleaves at the aromatic residues and leucine. Of the chemical methods, cleavage with BrCN[65] (Fig. 12) at methionine is the most commonly used method at the present time.

The reading frame of the DNA should not be altered by the inserted DNA, as frame shifts lead to nonsense proteins or premature termination of the polypeptide chain.

### 5.2. The Tryptophan Operon

The biosynthetic pathway for tryptophan in bacteria branches at the chorismate stage from that of the aromatic amino acids (Fig. 13). The subsequent steps in the formation of tryptophan are catalyzed by enzymes, whose struc-

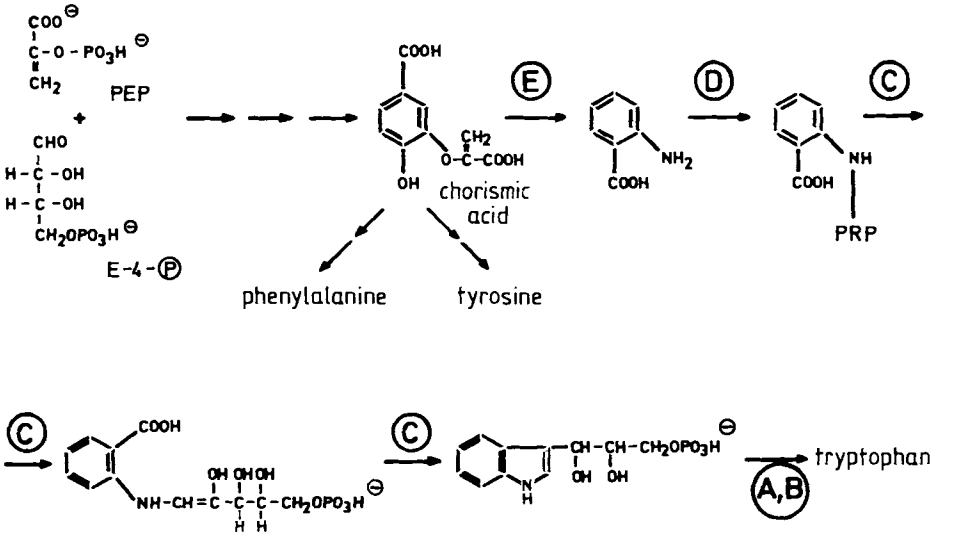



Fig. 13. Biosynthetic pathway of tryptophan. Abbreviations of enzymes are: Ⓔ anthranilate synthetase; Ⓓ anthranilate phosphoribosyltransferase; Ⓒ phosphoribosyl anthranilate isomerase and indole-3′-glycerol p-synthetase; Ⓑ and Ⓐ tryptophan synthetase, subunits α and β. PEP = phosphoenolpyruvate; E-4-Ⓟ = erythrose-4-phosphate; PRP = phosphoribosyl phosphate.

tural genes are sequentially encoded on the DNA and regulated simultaneously[68] (Fig. 14).

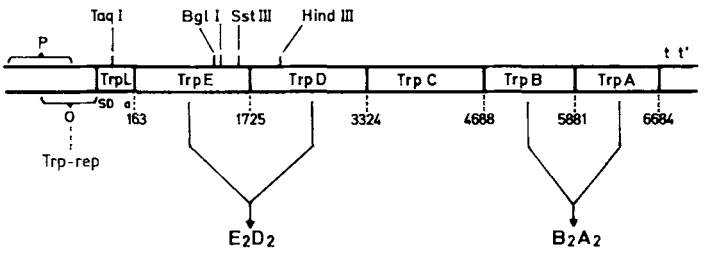



Fig. 14. Structure of the *trp* operon in *E. coli*. The structural genes E to A are regulated simultaneously; the mechanism of regulation is described in the text. Numbers indicate distances in base pairs beginning from the transcription start. Within L, E and D some restriction sites are indicated. Abbreviations used are: P = promotor; O = operator; L = leader peptide; a = attenuator; SD = Shine-Dalgarno sequence; t,t' = terminator sequences.

The *trp* repressor, which is encoded on another part of the DNA, can only bind to the operator after association with L-tryptophan (Trp)[69]. In the absence of tryptophan in the medium, RNA polymerase can interact with the promotor and transcription of the five structural genes takes place. This regulation is further modified by the so called attenuation. RNA polymerase starts transcription at sequences which encode a 14 amino acid long leader peptide. This peptide contains two tryptophan residues. Depending on the speed of translation, which is also dependent upon the concentration of tryptophan in the medium, the secondary structure of the mRNA is varied. If the movement of the ribosomes along the mRNA is fast (tryptophan in the medium), the mRNA forms structures for termination in the region of the attenuator and thus transcription is stopped. If the concentration of tryptophan in the medium is low, the slow movement of the ribosomes leads to alternative mRNA structures, so that RNA polymerase continues transcription of the subsequent five structural genes[70,71]. At the end of the *trp* operon transcription is stopped *via* two terminators.

The *trp* operon is therefore inducible by absence of tryptophan, resulting in high concentrations of the proteins E and D.

Restriction sites within the *trp* operon which can be used to insert foreign DNA are shown in Figure 14. A Taq I site is located between the SD sequence and the start codon for the leader peptide. Using this site it is possible to separate the regulatory units from the attenuation mechanism, since the latter is only exerted after synthesis of the leader peptide. Furthermore, one can avoid the formation of a chimeric protein by using the start codon of the gene coding for the protein to be expressed[72].

Chimeric proteins can be synthesized using proteins E and D since they are the first ones in the synthesis chain. The whole *trp* operon, up to the Hind III site in the D protein, has been inserted into a plasmid[66] (Fig. 11), and the conserved Hind III site used to insert the gene for human growth hormone which is subsequently expressed under control of the *trp* operon[73]. The E protein has also been used in the construction of proteins[74]. The regulatory region of the *trp* operon containing a DNA stretch coding for the first seven amino acids of the E protein has been inserted into the Hind III site of pBR 322. Thus, a set of plasmids has been constructed which allows the insertion of foreign DNA in all three reading frames[75]. Using these plasmids the expression of influenza antigens under control of the *trp* promotor has been achieved[76].

In addition, the construction of promotors containing parts of the *lac* and *trp* promotor has been successfully carried out[65,77] (Fig. 11). Using this *tac* promotor, in some cases higher expression rates were obtained than with the *lac* or *trp* promotors alone.

### 5.3. Bacteriophage λ Promotors

Infection of *E. coli* by the bacteriophage λ results either in phage multiplication and lysis of the bacterium or in integration of the phage DNA into the bacterial chromosome (Fig. 15).

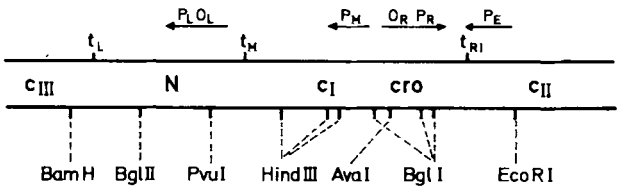



Fig. 15. Simplified genetic map of the bacteriophage λ in the region of 35000—40000 base pairs [78]. In the lytic cycle transcription starts at $P_R$ and $P_L$; the proteins N and cro are synthesized. Transcription stops at $t_L$ and partially at $t_{RI}$. The action of N allows transcription to proceed past $t_{RI}$ and $t_L$, cro takes part in the regulation of $P_R$ and $P_L$. In the lysogenic cycle only $c_I$ is expressed under control of $P_M$. $c_I$ is a repressor for multiple binding sites in the operators $O_R$ and $O_L$, thus the lytic cycle is blocked.

The early promotors of bacteriophages are designed to use the bacterial RNA polymerase to express their own genes, and thus weaken bacterial protein synthesis. They are probably highly suitable for stimulating synthesis of particular gene products in large amounts.

The $O_L$,$P_L$ regulatory unit has been introduced into plasmids in order to produce large amounts of certain proteins[79]. Induction is achieved using strains that contain a thermolabile $c_I$ repressor encoded on their DNA[80]. At temperatures around 30°C the repressor is active and the bacteria grow without the gene product regulated by the $P_L$ promotor. Raising the temperature to 43°C inactivates the $c_I$ repressor, and thus activates the $P_L$ promotor and synthesis of the subsequent structural gene products starts.

The $P_R$ promotor has also been used in the construction of an expression plasmid[67]; the structural gene for the thermolabile repressor has been introduced into the same plasmid (Fig. 11).

## 6. Examples of Peptide Hormones obtained by DNA Recombination

### 6.1. Somatostatin

The first peptide hormone which was shown to be present in bacterial extracts after DNA recombination was somatostatin[58]. It is a polypeptide, containing 14 amino acids (Fig. 16), which is found in several organs such as the pancreas, the hypothalamus and the stomach.

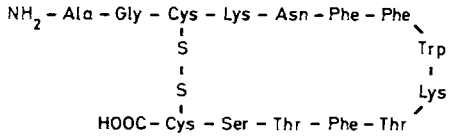



Fig. 16. Amino acid sequence of the human peptide hormone somatostatin.

Somatostatin inhibits the secretion of several other hormones; for example, growth hormone, insulin, glucagon and gastrin. It was chosen as a model to study peptide production *via* recombinant DNA techniques as its amino acid sequence was known, sensitive radioimmunoassays were available, and its size was compatible with methods for DNA synthesis. Using the known amino acid sequence, *Itakura et al.*[58] synthesized the appropriate DNA. Codons were selected according to the *E. coli* codon usage.

Two expression vectors were constructed in order to obtain somatostatin (Fig. 17 A and B). The first plasmid contains the promotor, the operator and the first 27 nucleotides (9 amino acids) of the *lac* operon followed by an ATG triplet and the DNA sequence coding for somatostatin. The presence of the promotor and operator ensure that protein synthesis of somatostatin can be regulated and is only carried out in the presence of an inducer (*e.g.* lactose). Two stop codons were attached to the end of the somatostatin DNA (symbolized by STP). After induction one expects the synthesis of a peptide with the following structure:

Met-(9 aa of β-galactosidase)-Met-somatostatin

The methionine in front of the somatostatin was introduced in order to obtain the free somatostatin after BrCN cleavage.

The second expression vector was constructed in a similar way; in this case, however, 3015 base pairs (corresponding to 1005 amino acids) of β-galactosidase were positioned in front of the somatostatin DNA. In this case too, an ATG triplet was introduced in order to have a methionine at the beginning of the somatostatin, thus enabling cleavage of the hybrid protein into the desired peptide hormone. Using the first plasmid no somatostatin was found in the bacterial extract; however, employing the second vector led to detectable amounts of somatostatin after cleavage of the hybrid protein with BrCN. In both cases the same regulatory system was used, and it is thus likely that transcription and translation occurred with the same frequencies. The explanation for the different results may lie in the rapid proteolytic degradation of the short peptide.

Proteins from other organisms are often recognized by bacteria as "foreign" and therefore rapidly degraded, although they have been synthesized by the bacterium itself after gene transfer. To avoid such degradation of peptide hormones synthesized in bacteria is still a major unsolved problem. In the case of the second expression vector, the synthesized somatostatin is protected from proteolytic attack by the large β-galactosidase residue. It should be mentioned that the procedure described above, involving the introduction of a methionine into the amino acid sequence in order to enable cleavage with BrCN, is only valid for peptide hormones which do not contain any further methionine residues in their sequence, since otherwise additional undesired cleavage would occur.

In the meantime the first clinical trials on somatostatin from *E. coli* have been carried out. It was hoped to use this hormone—now available in larger amounts—to treat particular cases of diabetes; however, as judged by the published data, such hopes have not been fulfilled as yet.

Recent molecular biological studies on the biosynthesis of somatostatin have revealed that the peptide is synthesized initially as a larger, inactive precursor-protein containing 116 amino acids[97,98]. The sequence of the active somatostatin is located at the *C*-terminal end of the pre-

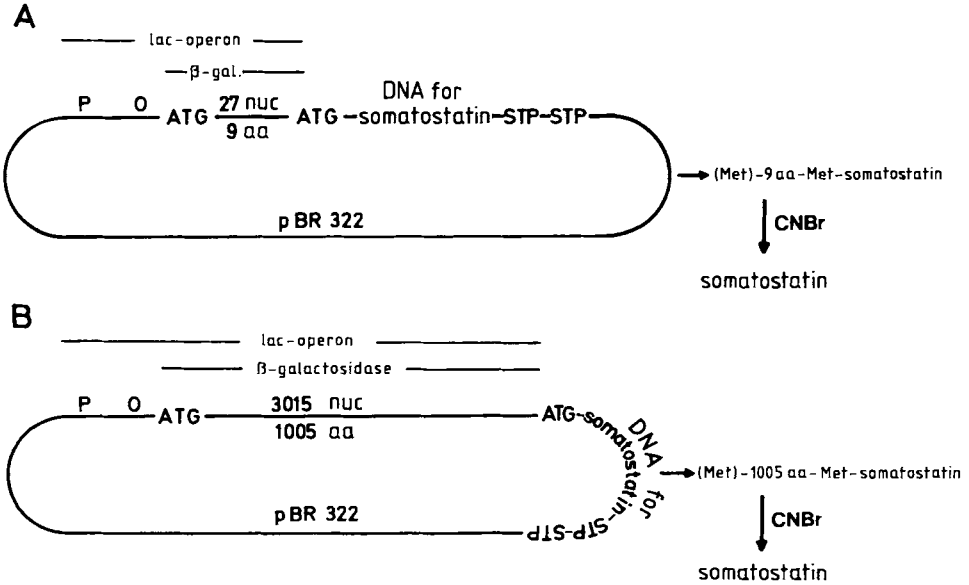



Fig. 17. Expression vectors used for synthesis of somatostatin in bacteria [58]. Both plasmids use the *lac* operon for expression and differ only in the location of the insertion site. Further particulars are given in the text.

somatostatin[*]; the mechanism of cleavage of the active portion has not yet been elucidated.

### 6.2. Human Growth Hormone

Human growth hormone (GH) is synthesized in the pituitary and consists of 191 amino acids. Pituitary hormones are crucially involved in growth and child development. Lack of one or several of these hormones can be overcome by using an appropriate substitution therapy. Children deficient in growth hormone are usually treated over a period of ten years with growth hormone extracted from human pituitary glands[81, 82]. *Tanner*[83] estimates the fraction of children who require to be treated with growth hormone to be approximately 1 : 7000. About 40% of dwarf children show normal concentrations of growth hormone (immunological assays); however, this hormone does not contain full biological activity[84, 85], probably due to variations in the amino acid required.

Apart from the treatment of dwarfism the use of growth hormone is being discussed for the following medical conditions: burns, stomach ulcers and ulcers of the colon, bone fractures and osteoporosis (deficiency of bone tissue)[84].

Growth hormones extracted from animals possess a different amino acid sequence compared to the human ones, and therefore human pituitary glands (from corpses) were the only source for these hormones.

The use of molecular biological methods led to the discovery of a whole gene family of human growth hormones and provided insight into the structure, expression and evolution of these genes[86].

The functional gene contains four introns with the boundaries of intron B occupying two alternative positions[87]. Different processing of the precursor mRNA leads to two distinct proteins containing 191 and 176 amino acids, respectively. 15% of the biological activity of growth hormone is attributed to the protein with the alternative amino acid sequence (176 aa)[88].

The mRNA for growth hormone encodes a pre-hormone which contains 26 additional amino acids at the *N*-terminal end. Such signal sequences are characteristic for proteins which are secreted from the cell and are probably cleaved off during transport through the cell membrane[89]. Combination of synthetic DNA coding for the 24 *N*-terminal amino acids and DNA transcribed from mRNA (550 bp) yielded a structural gene for human growth hormone. Expression in *E. coli* was achieved using a plasmid containing two *lac* promotors in tandem[90]. The reported yield was 2.4 mg/L; in the meantime however, this value may have been considerably increased. In the construction of the expression vector the structural gene for growth hormone was coupled directly behind the SD-sequence of the *lac* operon. The start signal for protein synthesis was introduced as the triplet ATG in the synthetic DNA fragment. Thus the growth hormone produced in bacteria contains an additional *N*-terminal methionine compared to the 191 amino acids of the naturally occurring protein. BrCN treatment to remove the methionine is not possible in this case, since growth hormone contains two further methionine residues and therefore would lead to cleavage of the protein. A practical way has not yet been found to remove this *N*-terminal methionine. Preliminary comparisons of the *in vivo* activity in rats of natural and bacterial growth hormone did not manifest any differences[91]. The first batch produced for human experiments, however, showed unpleasant side effects which were probably due to bacterial toxins[4]. Additional purification steps should easily overcome this problem.

The results of further clinical trials will have to be awaited in order to finally assess the possible uses of human growth hormone produced in bacteria.

### 6.3. Insulin

Insulin is produced in the β-cells of the pancreas and is critically involved in the regulation of glucose levels in the blood.

A large proportion of diabetics, comprising 1.5% of the total population, is dependent upon daily injections of insulin. For obvious reasons it is not possible to use human organs for extraction of the hormone, and therefore animal pancreatic glands are used which contain insulin with amino acid sequences closely related to the human one. Bovine insulin differs from human insulin in two amino acids in the A-chain and only one amino acid in the B-chain. In porcine insulin only the last amino acid of the B-chain is substituted (Thr for Ala).

Using trypsin under appropriate conditions the *C*-terminal alanine of the B-chain can be substituted for threonine, thus pig insulin can be converted into human insulin[92]. This procedure is now carried out on a commercial scale by several producers and the peptide hormone obtained in this manner is known as "semi-synthetic human insulin".

Like most other hormones, insulin is synthesized in the cell as a longer prehormone (Fig. 18)[93]. The preproinsulin contains an additional 24 amino acid long *N*-terminal peptide which is cleaved off during transport into the endoplasmic reticulum. It is probable that this peptide contains a signal sequence for the transport mechanism[89]. The conversion of proinsulin into insulin starts at the Golgi apparatus and continues during formation of the insulin granula in the β-cells.

The prospects of an increasing demand for insulin (the number of confirmed diabetics worldwide is increasing by approximately 3% per annum) and the possibility of producing human insulin have led almost automatically to attempts to prepare insulin from genetically engineered bacteria.

Enticed not least by the economic prospects of insulin production, a large number of groups began work on the isolation of the insulin gene and the determination of its structure[94] (Fig. 19).

Starting from mRNA the first cDNA to be cloned was that of rat insulin[95], and not much later a cDNA clone of human insulin was obtained[93, 96].

[*] Here a prehormone signifies an inactive precursor molecule which can be converted into the active hormone by cleavage of an *N*-terminal polypeptide. In contrast, by analogy to proinsulin, a prohormone should be a precursor molecule which is transformed into the active hormone by cleavage of a non-terminal polypeptide. Of course, in the latter case at least two cleavages are necessary.

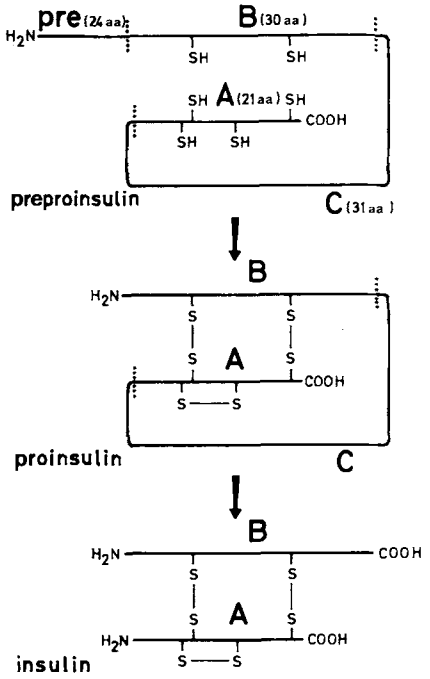



Fig. 18. Biosynthesis of insulin from preproinsulin. The chain segments Pre, B, C and A are marked with the numbers of amino acids they contain. The C-peptide is composed of 31 amino acids. Cleavage of proinsulin results in the release of the C-peptide and two additional dipeptides; thus, the A- and B-chain of human insulin are connected by a 35 amino acid long peptide. It is possible that the disulfide bridges are already formed at the stage of preproinsulin.

Active insulin consists of two separate polypeptide chains (A and B) which are connected *via* disulfide bridges. During biosynthesis, the three-dimensional structure of the proinsulin facilitates the formation of the correct disulfide bridges. Enzymes involved in the conversion of proinsulin into insulin have not yet been isolated[99]. Since it is not possible to encode the formation of disulfide bridges between different polypeptides on the DNA, one has to resort to other measures in order to produce insulin in genetically engineered bacteria.

Two alternative pathways can be followed to synthesize insulin in bacteria (Fig. 20 and Fig. 21). Using the procedure outlined in Figure 20 one initially obtains proinsulin, which subsequently has to be converted into insulin. The second possibility for insulin production is based on the separate synthesis of the A and B polypeptide chains which afterwards have to be oxidized to yield active insulin. Since oxidation results not only in the formation of the correct disulfide bridges, but leads also to a variety of inter- and intramolecular combinations, high losses are expected to occur at this stage.

The synthesis of proinsulin in bacteria has been described several times[101], and successful oxidation of the chains has also been reported[102].

With highly purified preparations of insulin rare cases of immunologically adverse reactions against these drugs occur. So far only minute differences in the immunogenic-

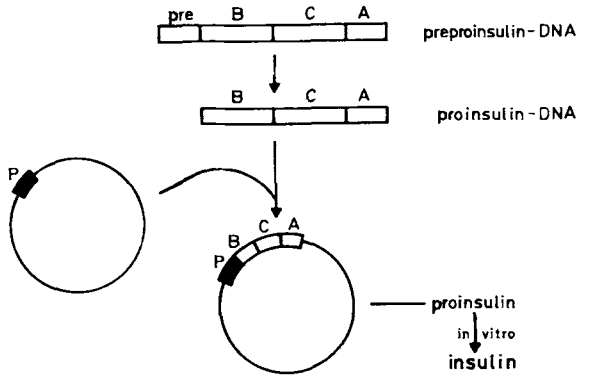



Fig. 20. Synthesis of human insulin by conversion of bacterial proinsulin. Reverse transcription of mRNA yields the DNA of preproinsulin. After removal of the pre-fragment, the DNA is integrated into an expression vector. The so produced proinsulin is enzymatically converted into active insulin [100].

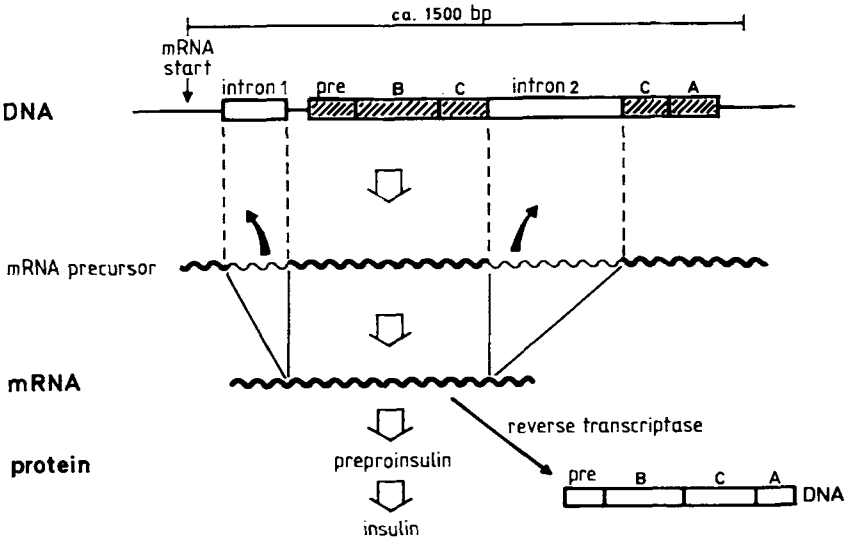



Fig. 19. Structure of the human insulin gene [18]. Two introns are excised from the precursor mRNA (the first one is located in front of the coding sequence for the pre-chain, the second is inside the coding sequence for the C-chain). Using reverse transcriptase and other enzymes (cf. Section 3.3) it is possible to transcribe the mRNA *in vitro* into DNA. This results in a structural gene without introns, since they were already removed by splicing.

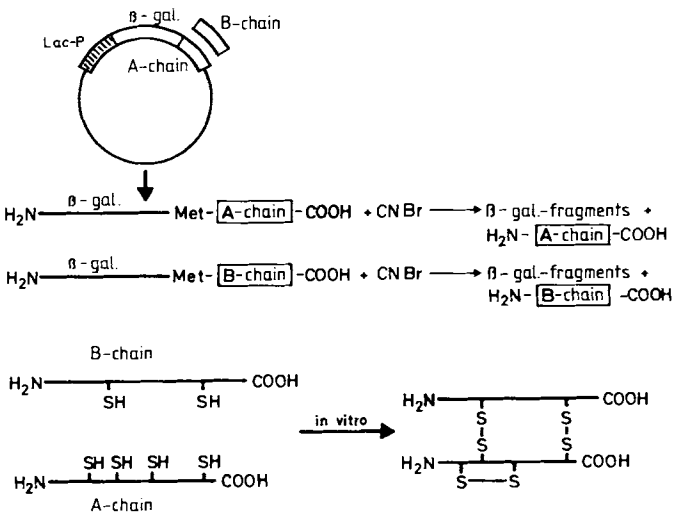



Fig. 21. Synthesis of human insulin in bacteria *via* oxidation of the separate chains. DNA coding for the A- and B-chains of insulin is chemically synthesized [13] and separately inserted into expression vectors. After isolation of the polypeptides [60] the disulfide bridges are formed in an additional step.

ity of highly purified pig and human insulin preparations have been observed[103].

### 6.4. Other Peptide Hormones

Relaxin has a similar structure to insulin; it also consists of two polypeptide chains linked by disulfide bridges. During biosynthesis preprorelaxin is initially formed, which, after cleavage of the pre-portion and removal of a C chain, is converted into active relaxin. There are surprising similarities in the length of the chains as well as in the arrangement of the disulfide bridges between insulin and relaxin.

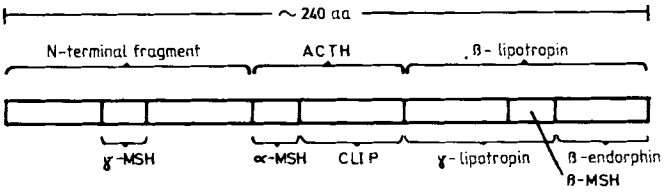
Relaxin is synthesized in the placenta and uterus during pregnancy and is released into the blood stream immediately before birth. It aids the birth process by loosening the connective tissue. The nucleotide sequence of the gene has been determined and later confirmed by the biological activity of a synthetic protein[104].

As described for insulin (Section 6.3), the DNA fragments coding for the A and B chains of relaxin have been synthesized and expressed in *E. coli* as chimeric proteins[105].

Apart from the examples discussed above, DNA coding for a variety of other peptide hormones from different organisms has been cloned and its nucleotide sequence determined. In many cases the structure of the genes has been characterized as well. The following represents some examples of the numerous publications which have appeared recently: thyrotropin[106], HPL—human placental lactogen[107], epidermal growth factor[108], the common α-subunit of the hormones HCG, LH, FSH and TSH (human chorionic gonadotropin, luteinizing hormone, follicle stimulating hormone and thyroid stimulating hormone)[109], parathormone[110], glucagon[111], and gastrin[112].

Expression of thymosin α-1 (in its deacetyl form) has been achieved as a hybrid protein after chemical synthesis of the gene[113].

The use of the cloning methods illustrated above has not only permitted determination of the structure and sequence of particular genes, but has also led to the discovery and investigation of new regulatory principles. Pro-opiomelanocortin (POMC) is a protein (molecular weight 29000 dalton) which yields a variety of peptide hormones after cleavage (Fig. 22). It is synthesized in different tissues: pituitary, hypothalamus, placenta and lung. It is interesting to note that POMC is cleaved differently in different tissues. In the anterior pituitary it is predominantly converted into ACTH and β-lipotropin, and in the median pituitary (in mice) it is rapidly converted into MSC, CLIP, β-endorphine and γ-lipotropin. The sequence analysis of the gene has been carried out and the molecular basis for the cleavage is being investigated at present[114].




ACTH = adrenocorticotrophic hormone
MSH = melanocyte stimulating hormone
CLIP = corticotropin-like intermediate lobe peptide

Fig. 22. Structure of the pro-opiomelanocortin precursor protein.

Another example for the synthesis of different gene products from the same gene, depending on the cell type, is the calcitonin gene. This hormone plays an important role in the regulation of calcium levels. It contains several introns and the coding sequences are combined in different ways in the thyroid and the hypothalamus, since the mRNA is processed differently. Calcitonin is synthesized in the thyroid, while the peptide predicted from the mRNA sequence in the hypothalamus has not yet been characterized in its function[115].

## 7. Outlook

The advantages of hormone production in genetically engineered bacteria in comparison with classical methods of extraction from organs have been repeatedly pointed out:

- the possibility of synthesizing a peptide with the human amino acid sequence;
- independence of animal or human organs;
- almost no limits with respect to quantity;
- the possibility of introducing variations in the amino acid sequence *via* deliberate changes in the DNA sequence, thus opening the way to detect new properties of peptide hormones.

How do the yields of a hormone produced in genetically engineered bacteria compare to the yields achieved by isolation from organs?

The proportion of the desired protein in a genetically manipulated bacterial strain can be estimated to be *ca.* 10%

of the total protein, the upper limit being approximately 500 mg peptide hormone per liter of bacterial culture. To my knowledge, however, this could not be maintained and values of *ca.* 100 mg/L are today regarded as good yields. In the pancreas, for example, one finds about 100 mg insulin per kg of tissue. In addition to this straight comparison of yield one has to take into account that proinsulin synthesized in bacteria has to undergo further processing in order to be converted into biologically active insulin. This superficial comparison does not take into account the different efforts involved in purifying the hormone either from pancreas or from a bacterial extract. For most other peptide hormones the comparison is easily decided in favor of DNA recombination since these hormones usually occur in considerably smaller quantities in the respective organs.

Apart from factors illustrated in Figure 23, the yield of a peptide hormone produced in bacteria is influenced to a large extent by the intracellular location of the hormone. Signal sequences[89] are used to transport the synthesized proteins into the periplasmatic space, where they have a much greater stability than in the cytoplasm of a bacterium[116]. Aggregation of these proteins in the bacterium is a possible way of protection from proteolytic degradation[117].

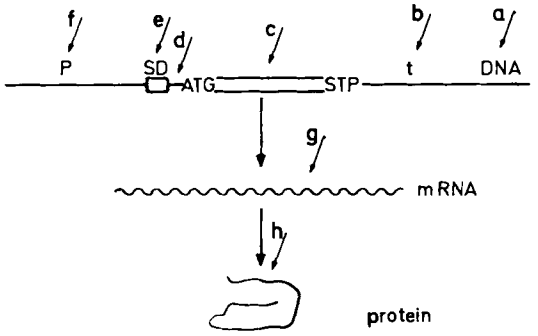



Fig. 23. Schematic representation of some factors which may influence the yield of a protein synthesized in bacteria after DNA-recombination. a) Stability of the plasmid, copy number of the plasmid in the bacterial cell; b) strength and structure of the terminator; c) codon usage for the different amino acids; d) distance between the Shine-Dalgarno sequence and the start signal for protein synthesis; e) nature of the Shine-Dalgarno sequence; f) strength and structure of the promotor and adjoining sequences, inducibility; g) mRNA stability; h) stability of the pre-hormone or hormone in bacteria.

The enzymes involved in proteolytic degradation of eukaryotic proteins synthesized in bacteria are still largely unknown. Recently, eight soluble proteolytic enzyme activities in *E. coli* have been reported[118]; it is, however, unclear if all or only a few of these initiate the proteolytic degradation. These factors do not therefore permit a clear prediction with respect to yield for any particular peptide hormone produced in bacteria after DNA recombination.

Molecular biology opens up the way to produce scarcely available peptide hormones in large quantities. Using somatostatin, growth hormone, and insulin as examples, some of the inherent problems have been illustrated. Most difficulties will probably be overcome in the near future. One can envisage several possible solutions: the use of protease-free bacterial strains in the production of peptide hormones; isolation of an enzyme which selectively removes *N*-terminal methionine; or the construction of hybrid peptides which ensure high yields. At the end of this decade the proportion of hormones produced *via* gene technology should well exceed 50% of the total.

Apart from *E. coli* other organisms will be used in the production of proteins in the near future; worth mentioning here are *Bacillus subtilis* and yeast.

*B. subtilis* allows the secretion of proteins into the medium. Up to now most of the plasmids used in *B. subtilis* were not stable and recombination with chromosomal DNA occurred, followed by deletion of the plasmid. Recently, however, major breakthroughs have been reported: proteins like α-amylase[119], hepatitis B antigen[120], and even proinsulin[121] have been obtained from *B. subtilis*.

Due to the eukaryotic nature of yeast it is envisaged that post-translational modifications occur in a similar fashion as in higher organisms. This is important for the production of proteins which have to be modified after synthesis (*e.g.* glycosylation, cleavage of a signal peptide) for biological activity.

Based on their DNA sequence, the existence of a variety of peptides and proteins has been predicted, although their physiological role is still unclear[114, 115, 122]. This aspect of recombinant DNA work, namely the discovery of new proteins and the elucidation of their biological function, may soon become of equal importance for medicine as the production of known substances.

*The help of Anique Fourmont, Petra Schmidt and Bernhard von Niessen in the preparation of this manuscript is gratefully acknowledged.*

Received: August 4, 1983 [A 474 IE]
German version: *Angew. Chem. 95* (1983) 874
Translated by Dr. *Angela M. Gronenborn*, London

[1] S. N. Cohen, A. C. Y. Chang, H. W. Boyer, R. B. Helling, *Proc. Natl. Acad. Sci. USA 70* (1973) 3240.
[2] R. G. Guillemin, E. Sakiz, D. N. Ward, *Proc. Soc. Exp. Biol. Med. 118* (1965) 1132.
[3] A. V. Schally, A. Arimura, C. Y. Bowers, A. J. Kastin, S. Sawano, T. W. Redding, *Recent Prog. Horm. Res. 24* (1968) 497.
[4] P. Newmark, *Nature (London) 294* (1981) 200.
[5] J. Maienhofer, E. Schnabel, H. Bremer, O. Brinkhoff, R. Zabel, W. Sroka, H. Klostermeyer, D. Brandenburg, T. Okuda, H. Zahn, *Z. Naturforsch. B 18* (1963) 1120; P. G. Katsoyannis, A. Tometsko, C. Zalut, *J Am. Chem. Soc. 88* (1966) 166.
[6] W. Arber, *Angew. Chem. 90* (1978) 79; *Angew. Chem. Int. Ed. Engl. 17* (1978) 73.
[7] L. Ferreti, V. Sgaramella, *Nucleic Acids Res. 9* (1981) 85, 3695.
[8] R. J. Roberts, *Nucleic Acids Res. 11* (1983) r135.
[9] J. E. Davies, H. G. Gassen, *Angew. Chem. 95* (1983) 26; *Angew. Chem. Int. Ed. Engl. 22* (1983) 13.
[10] J. Ikemura, *J. Mol. Biol. 158* (1982) 573.
[11] H. G. Gassen, A. Lang: *Chemical and Enzymatic Synthesis of Gene Fragments: A Laboratory Manual*, Verlag Chemie, Weinheim 1982.
[12] M. D. Edge, A. R. Greene, G. R. Heathcliffe, P. A. Meacock, W. Schuch, D. B. Scanlon, T. C. Atkinson, C. R. Newton, A. F. Markham, *Nature (London) 292* (1981) 756; S. Tanaka, T. Oshima, K. Ohsaye, T. Ono, A. Mitono, A. Ueno, H. Nakazoto, M. Tsujimoto, N. Higashi, T. Noguchi, *Nucleic Acids Res. 11* (1983) 1707.
[13] R. Crea, A. Kraszewski, T. Hirose, K. Itakura, *Proc. Natl. Acad. Sci. USA 75* (1978) 5765.
[14] M. Grouy, C. Gautier, *Nucleic Acids Res. 10* (1982) 7055; H. Grosjean, W. Fiers, *Gene 18* (1982) 209; W. Konigsberg, G. N. Godson, *Proc. Natl. Acad. Sci. USA 80* (1983) 687.
[15] A. L. Lehninger: *Biochemistry*, Worth, New York 1975.
[16] R. Knippers: *Molekulare Genetik*, Thieme, Stuttgart 1981.
[17] EMBL - Nucleotide Sequence Data Library, Postfach 102209, D-6900 Heidelberg 1.

[18] F. H. C. Crick, *Science 204* (1979) 264.
[19] O. Mercereau-Puijalon, P. Kourilsky, *Nature (London) 279* (1979) 647.
[20] K. Munk, H. Kirchner: *Interferon - Properties, Mode of Action, Production, Clinical Application*, Karger, Basel 1982; *Antiviral Research*, Abstr. 1, No. 2, Elsevier, Amsterdam 1983.
[21] S. Nagata, H. Taira, A. Hall, L. Johnsrud, M. Streuli, J. Ecsôdi, W. Boll, K. Cantell, C. Weissmann, *Nature (London) 284* (1980) 316; T. Taniguchi, L. Guarente, T. M. Roberts, D. Kimelman, J. Douhan III, M. Ptashne, *Proc. Natl. Acad. Sci. USA 77* (1980) 5230; R. Derynck, E. Remaut, E. Saman, P. Stanssens, E. DeClercq, J. Content, W. Fiers, *Nature (London) 287* (1980) 193; D. V. Goeddel, D. W. Leung, T. J. Dull, M. Gross, R. M. Lawn, R. McCandliss, P. H. Seeburg, A. Ullrich, E. Yelverton, P. W. Gray, *ibid. 290* (1981) 20.
[22] P. K. Weck, S. Apperson, N. Stebbing, P. W. Gray, D. W. Leung, H. M. Shepard, D. V. Goeddel, *Nucleic Acids Res. 9* (1981) 6153.
[23] A. Efstratiadis, F. C. Kafatos, A. M. Maxam, T. Maniatis, *Cell 7* (1976) 279.
[24] M. P. Wickens, G. N. Buell, R. T. Schimke, *J. Biol. Chem. 253* (1978) 2483; G. N. Buell, M. P. Wickens, F. Payvar, R. T. Schimke, *ibid. 253* (1978) 2471.
[25] H. Okayama, P. Berg, *Mol. Cell. Biol. 2* (1982) 161; H. Land, M. Grez, H. Hauser, W. Lindenmaier, G. Schütz, *Nucleic Acids Res. 9* (1981) 2251.
[26] T. Maniatis, E. F. Fritsch, J. Sambrook: *Molecular Cloning - A Laboratory Manual*, Cold Spring Harbor Laboratory Publications, Cold Spring Harbor 1982.
[27] H. Aviv, P. Leder, *Proc. Natl. Acad. Sci. USA 69* (1972) 1408.
[28] B. E. Noyes, M. Mevarech, R. Stein, K. L. Agarwal, *Proc. Natl. Acad. Sci. USA 76* (1979) 1770; K. L. Agarwal, J. Brunstedt, B. E. Noyes, *J. Biol. Chem. 256* (1981) 1023.
[29] H. C. Birnboim, J. Doly, *Nucleic Acids Res. 7* (1979) 1513; D. S. Holmes, M. Quigley, *Anal. Biochem. 114* (1981) 193.
[30] C. Grobstein in: *Recombinant DNA*, Scientific American Inc., New York 1978, p. 131.
[31] P. W. J. Rigby, *Nature (London) 297* (1982) 451; J. M. Bishop, *Cell 32* (1983) 1018.
[32] J. Vieira, J. Messing, *Gene 19* (1982) 259; J. Messing, J. Vieira, *ibid. 19* (1982) 269.
[33] U. Rüther, *Nucleic Acids Res. 10* (1982) 5765.
[34] F. Bolivar, R. L. Rodriguez, P. J. Greene, M. C. Betlach, H. L. Heyneker, H. W. Boyer, J. H. Crosa, S. Falkow, *Gene 2* (1977) 95.
[35] A. M. Maxam, W. Gilbert, *Methods Enzymol. 65* (1980) 499; W. Gilbert, *Angew. Chem. 93* (1981) 1037.
[36] F. Sanger, A. R. Coulson, *J. Mol. Biol. 94* (1975) 441; F. Sanger, *Angew. Chem. 93* (1981) 937; A. J. Smith, *Methods Enzymol. 65* (1980) 560.
[37] A. Kalnins, K. Otto, U. Rüther, B. Müller-Hill, *EMBO J. 2* (1983) 593; A. V. Fowler, I. Zabin, *ibid. 2* (1983) 597.
[38] P. J. Farabaugh, *Nature (London) 274* (1978) 765; K. Beyreuther, *ibid. 274* (1978) 767.
[39] R. Radloff, W. Bauer, J. Vinograd, *Proc. Natl. Acad. Sci. USA 57* (1967) 1514.
[40] A. M. Michelson, S. H. Orkin, *J. Biol. Chem. 257* (1982) 14773.
[41] H. O. Smith, M. L. Birnstiel, *Nucleic Acids Res. 3* (1976) 2387.
[42] H. Kössel, *Biol. Unserer Zeit 12* (1982) 39.
[43] A. M. Wu, T. Platt, *Proc. Natl. Acad. Sci. USA 75* (1978) 5442.
[44] D. Pribnow, *Proc. Natl. Acad. Sci. USA 72* (1975) 784.
[45] M. Rosenberg, D. Court, *Annu. Rev. Genet. 13* (1979) 319.
[46] H. Schaller, C. Gray, K. Herrmann, *Proc. Natl. Acad. Sci. USA 72* (1975) 737.
[47] W. Sibenlist, R. B. Simpson, W. Gilbert, *Cell 20* (1980) 269.
[48] M. H. Irani, L. Orosz, S. Adhya, *Cell 32* (1983) 783.
[49] H. G. Gassen, *Angew. Chem. 94* (1982) 15; *Angew. Chem. Int. Ed. Engl. 21* (1982) 23.
[50] J. Shine, L. Dalgarno, *Nature (London) 254* (1975) 34.
[51] J. A. Steitz, D. A. Steege, *J. Mol. Biol. 114* (1977) 545.
[52] G. F. E. Scherer, M. D. Walkinshaw, S. Arnott, D. J. Morré, *Nucleic Acids Res. 8* (1980) 3895.
[53] W. M. Holmes, T. Platt, M. Rosenberg, *Cell 32* (1983) 1029.
[54] F. Jacob, J. Monod, *J. Mol. Biol. 3* (1961) 318.
[55] A. E. Silverstone, R. R. Arditti, B. Magasanik, *Proc. Natl. Acad. Sci. USA 66* (1970) 773.
[56] K. Backmann, M. Ptashne, W. Gilbert, *Proc. Natl. Acad. Sci. USA 73* (1976) 4174.
[57] O. Mercereau-Puijalon, A. Royal, B. Cami, A. Garapin, A. Krust, F. Gannon, P. Kourilsky, *Nature (London) 275* (1978) 505.
[58] K. Itakura, T. Hirose, R. Crea, A. D. Riggs, H. L. Heyneker, F. Bolivar, H. W. Boyer, *Science 198* (1977) 1056.
[59] F. Fuller, *Gene 19* (1982) 43.
[60] D. V. Goeddel, D. G. Kleid, F. Bolivar, H. L. Heyneker, D. G. Yansura, R. Crea, T. Hirose, A. Kraszewski, K. Itakura, A. D. Riggs, *Proc. Natl. Acad. Sci. USA 76* (1979) 106.
[61] J. Shine, I. Fettes, N. C. Y. Lan, J. L. Roberts, J. D. Baxter, *Nature (London) 285* (1980) 456.
[62] P. Charnay, M. Gervais, A. Louise, F. Galibert, P. Tiollais, *Nature (London) 286* (1980) 893.
[63] A. R. Davis, D. P. Nayak, M. Ueda, A. L. Hiti, D. Dowbenko, D. G. Kleid, *Proc. Natl. Acad. Sci. USA 78* (1981) 5376.
[64] E. Gross, B. Witkop, *J. Am. Chem. Soc. 83* (1961) 1510.
[65] E. Amann, J. Brosius, M. Ptashne, *Nucleic Acids Res.*, in press.
[66] R. A. Hallewell, J. S. Emtage, *Gene 9* (1980) 27.
[67] C. Queen, *J. Mol. Appl. Genet. 2* (1983) 1.
[68] C. Yanofsky, T. Platt, I. P. Crawford, B. P. Nichols, G. E. Christie, H. Horowitz, M. van Cleemput, A. M. Wu, *Nucleic Acids Res. 9* (1981) 6647.
[69] I. P. Crawford, G. V. Stauffer, *Annu. Rev. Biochem. 49* (1980) 163.
[70] T. Platt, *Cell 24* (1981) 10.
[71] C. Yanofsky, *Nature (London) 289* (1981) 751; I. Stroynowski, C. Yanofsky, *ibid. 290* (1981) 34.
[72] J. C. Edman, R. A. Hallewell, P. Valenzuela, H. M. Goodman, W. J. Rutter, *Nature (London) 291* (1981) 503.
[73] J. A. Martial, R. A. Hallewell, J. D. Baxter, H. M. Goodman, *Science 205* (1979) 602.
[74] D. G. Kleid, D. Yansura, B. Small, D. Dowbenko, D. M. Moore, M. J. Grubman, P. D. McKercher, D. O. Morgan, B. H. Robertson, H. L. Bachrach, *Science 214* (1981) 1125.
[75] W. Tacon, N. Carey, S. Emtage, *Mol. Gen. Genet. 177* (1980) 427.
[76] J. S. Emtage, W. C. A. Tacon, G. H. Catlin, B. Jenkins, A. G. Porter, N. H. Carey, *Nature (London) 283* (1980) 171.
[77] H. A. de Boer, L. J. Comstock, M. Vasser, *Proc. Natl. Acad. Sci. USA 80* (1983) 21.
[78] S. E. Luria, J. E. Darnell Jr., D. Baltimore, A. Campbell: *General Virology*, 3rd Ed., Wiley, New York 1978, p. 211.
[79] H. Shimatake, M. Rosenberg, *Nature (London) 292* (1981) 128; R. R. Reed, *Cell 25* (1981) 713; C. M. Joyce, N. D. F. Grindley, *Proc. Natl. Acad. Sci. USA 80* (1983) 1834.
[80] H. U. Bernard, D. R. Helinski, *Methods Enzymol. 68* (1979) 482.
[81] A. Skottner, A. Forsman, K. Fhölenhag, A. Helleberg, E. Löfberg, L. Fryklund, B. Vangbo, B. Skoog in J. L. Gueriguian: *Insulins, Growth Hormones and Recombinant DNA Technology*, Raven Press, New York 1981, p. 109.
[82] S. D. Frasier, T. Aceto Jr., A. B. Hayles, V. G. Mikity, *J. Clin. Endocrinol. Metab. 44* (1977) 22.
[83] J. M. Tanner in J. L. Gueriguian: *Insulins, Growth Hormones and Recombinant DNA Technology*, Raven Press, New York 1981, p. 133.
[84] D. Rudman in J. L. Gueriguian: *Insulins, Growth Hormones and Recombinant DNA Technology*, Raven Press, New York 1981, p. 161.
[85] D. Rudman, M. H. Kutner, R. D. Blackston, R. A. Cushman, R. P. Bain, J. H. Patterson, *New Engl. J. Med. 305* (1981) 163.
[86] D. D. Moore, M. A. Conkling, H. M. Goodman, *Cell 29* (1982) 285; D. D. Moore, M. D. Walker, D. J. Diamond, M. A. Conkling, H. M. Goodman, *Recent Prog. Horm. Res. 38* (1982) 197.
[87] F. M. De Noto, D. D. Moore, H. M. Goodman, *Nucleic Acids Res. 9* (1981) 3719.
[88] V. J. Lewis, I. F. Bonewald, L. J. Lewis, *Biochem. Biophys. Res. Commun. 72* (1980) 511.
[89] G. Blobel, B. Dobberstein, *J. Cell Biol. 67* (1975) 835.
[90] D. V. Goeddel, H. L. Heyneker, T. Hozumi, R. Arentzen, K. Itakura, D. G. Yansura, M. J. Ross, G. Miozzari, R. Crea, P. H. Seeburg, *Nature (London) 281* (1979) 544.
[91] K. C. Olson, J. Fenno, N. Lin, R. N. Harkins, C. Snider, W. H. Kohr, M. J. Ross, D. Fodge, G. Prender, N. Stebbing, *Nature (London) 293* (1981) 408.
[92] R. Obermeier, R. Geiger, *Hoppe-Seyler's Z. Physiol. Chem. 357* (1976) 759.
[93] G. I. Bell, W. F. Swain, R. L. Pictet, B. Cordell, H. M. Goodman, W. J. Rutter, *Nature (London) 282* (1979) 525.
[94] G. I. Bell, R. L. Pictet, W. J. Rutter, B. Cordell, E. Tischer, H. M. Goodman, *Nature (London) 284* (1980) 26.
[95] A. Ullrich, J. Shine, J. Chirgwin, R. L. Pictet, E. Tischer, W. J. Rutter, H. M. Goodman, *Science 196* (1977) 1313.
[96] I. Sures, D. V. Goeddel, A. Gray, A. Ullrich, *Science 208* (1980) 59.
[97] T. G. Warren, D. Shields, *Proc. Natl. Acad. Sci. USA 79* (1982) 3729.
[98] L.-P. Shen, R. L. Pictet, W. J. Rutter, *Proc. Natl. Acad. Sci. USA 79* (1982) 4575.
[99] K. Docherty, R. J. Carroll, D. F. Steiner, *Proc. Natl. Acad. Sci. USA 79* (1982) 4613.
[100] W. Kemmler, J. D. Peterson, D. F. Steiner, *J. Biol. Chem. 246* (1971) 6786.
[101] L. Villa-Komaroff, A. Efstratiadis, S. Broome, P. Lomedico, R. Tizard, S. P. Naber, W. L. Chick, W. Gilbert, *Proc. Natl. Acad. Sci. USA 75* (1978) 3727; K. Talmadge, J. Kaufman, W. Gilbert, *ibid. 77* (1980) 3988; S. J. Chan, J. Weiss, M. Konrad, T. White, C. Bahl, S.-D. Yu, D. Marks, D. F. Steiner, *ibid. 78* (1981) 5401; S. P. Naber, L. Villa-Komaroff, S. Broome, A. Rossini, V. Lauris, W. L. Chick, *Gene 21* (1983) 95.

[102] R. E. Chance, E. P. Kroeff, J. A. Hoffmann in J. L. Gueriguian: *Insulins, Growth Hormones and Recombinant DNA Technology*, Raven Press, New York 1981, p. 71.
[103] G. E. Sonnenberg, M. Berger, *Dtsch. Med. Wochenschr. 108* (1983) 927.
[104] P. Hudson, J. Haley, M. John, M. Cronk, R. Crawford, J. Haralambidis, G. Tregear, J. Shine, H. Niall, *Nature (London) 301* (1983) 628.
[105] H. Richards, A. Stewart, J. Warwick, S. Roberts, L. Bell, J. Smith, *Acta Endocrinol. (Copenhagen) 103* (1983) 252.
[106] N. C. Vamvakopoulos, J. J. Monahan, I. A. Kourides, *Proc. Natl. Acad. Sci. USA 77* (1980) 3149.
[107] H. A. Barrera-Saldana, P. H. Seeburg, G. F. Saunders, *J. Biol. Chem. 258* (1983) 3787.
[108] A. Gray, T. J. Dull, A. Ullrich, *Nature (London) 303* (1983) 722.
[109] J. C. Fiddes, H. M. Goodman, *J. Mol. Appl. Genet. 1* (1981) 3.
[110] G. N. Hendy, H. M. Kronenberg, J. T. Potts, A. Rich, *Proc. Natl. Acad. Sci. USA 78* (1981) 7365.
[111] G. I. Bell, R. F. Santerre, G. T. Mullenbach, *Nature (London) 302* (1983) 716.
[112] E. Boel, J. Vuust, F. Norris, K. Norris, A. Wind, J. F. Rehfeld, K. A. Marcker, *Proc. Natl. Acad. Sci. USA 80* (1983) 2866.
[113] R. Wetzel, H. L. Heyneker, D. V. Goeddel, P. Jhurani, J. Shapiro, R. Crea, T. L. K. Low, J. E. McClure, G. B. Thurman, A. L. Goldstein, *Biochemistry 19* (1980) 6096.
[114] N. G. Seidah, M. Chrétien, *Proc. Natl. Acad. Sci. USA 78* (1981) 4236; A. C. Y. Chang, M. Cochet, S. N. Cohen, *ibid. 77* (1980) 4890; M. Cochet, A. C. Y. Chang, S. N. Cohen, *Nature (London) 297* (1982) 335.
[115] S. G. Amara, V. Jonas, M. G. Rosenfeld, E. S. Ong, R. M. Evans, *Nature (London) 298* (1982) 240.
[116] K. Talmadge, W. Gilbert, *Proc. Natl. Acad. Sci. USA 79* (1982) 1830.
[117] Y.-S. E. Cheng, D. Y. Kwoh, T. J. Kwoh, B. C. Soltvedt, D. Zipser, *Gene 14* (1981) 121.
[118] K. H. S. Swamy, A. L. Goldberg, *Nature (London) 292* (1981) 652.
[119] I. Palva, *Gene 19* (1982) 81.
[120] K. Hardy, S. Stahl, H. Kupper, *Nature (London) 293* (1981) 481.
[121] K. Mosbach, S. Birnbaum, K. Hardy, J. E. Davies, L. Bulow, *Nature (London) 302* (1983) 543.
[122] P. Newmark, *Nature (London) 303* (1983) 655.
[123] B. P. Kaine, R. Gupta, C. R. Woese, *Proc. Natl. Acad. Sci. USA 80* (1983) 3309.

# The Prostaglandins: From the Laboratory to the Clinic (Nobel Lecture)**

**By Sune Bergström***

The chemistry and biochemistry of the prostaglandins are now described in textbooks, and I have reviewed the early work in this area several times[1–4]. Here, I will instead discuss some of the early prostaglandin work carried out in Sweden and its background, together with some recent developments in the clinical fields that I have been associated with.

Now let me digress for a moment. My scientific work started in 1934 when I participated with Dr. *Erik Jorpes* in his early work on heparin. More than anyone, he is responsible for purifying heparin and introducing it as a drug into the clinic. At that time, Professor *Einar Hammarsten* was Director of the Chemistry Department of the Karolinska Institute, then one of the leading laboratories in the world in the field of nucleic acids and peptide hormones (*e.g.* secretin and cholecystokinin).

Dr. *Jorpes* always maintained that it was unfortunate that no work was being undertaken on lipids or steroids in Sweden. He financed my trip to England in 1938, where I spent a few months working on bile acids with Dr. *G. A. D. Haslewood* at Hammersmith Postgraduate Medical School. The following year I was awarded a fellowship from the British Council to work for a year at Dr. *Marrian*'s laboratory in Edinburgh. It was cancelled when the War broke out, but I was then lucky enough to get a Swedish American Fellowship, and worked for a year and a half at Columbia University and at the Squibb Institute with Dr. *Oskar Wintersteiner* on cholesterol autoxidation (1940–1942). After returning home, I started working on the autoxidation of linoleic acid and identified the structure of the main reaction products. It was established that conjugation of the double bonds took place and that oxygen was introduced as a hydroperoxy group at C-9 or C-13. I also found that the lipoxygenase enzyme of soybeans, which had just been described by Dr. *Sumner*, yielded the same products as the heavy metal-catalyzed autoxidation. At that time I was working in Dr. *Hugo Theorell*'s laboratory, and we started to cooperate on the purification of the soybean lipoxygenase enzyme.

My involvement with the prostaglandins started at the Meeting of the Physiological Society of the Karolinska Institute, October 19th, 1945, where I reported my work on the oxidation of linoleic acid. Dr. *Hugo Theorell* was chairman, Dr. *Yngve Zotterman* secretary, and Dr. *Ulf von Euler* signed the protocol.

After this meeting, *von Euler* asked me if I might be interested in studying his lipid extracts of sheep vesicular glands that he had stored since before the war. I agreed, and we began a most stimulating and pleasant cooperation.

The first observation that there were some biologically active compounds in human semen had been made in the Department of Obstetrics and Gynecology of Columbia University in New York. In 1930 *Kurzrok* and *Lieb*, with the technical cooperation of Dr. *Sara Ratner*[5], reported that when they were doing artificial inseminations in women they sometimes got violent contractions, sometimes relaxation of the uterus.

[*] Prof. Dr. S. Bergström
Karolinska Institutet
S-10405 Stockholm (Sweden)

[**] Copyright © The Nobel Foundation 1983.—The Nobel Foundation, Stockholm, is thanked for permission to print this article.

It is interesting to note that I met Dr. *Kurzrok* and worked in the same laboratory at Columbia University as Dr. *Sara Ratner* for a year, but never heard anything about prostaglandins.

In 1933, the British pharmacologist *Goldblatt*[6, 7] reported that human semen contained a factor that reduced blood pressure and stimulated smooth muscle.

At about the same time, Dr. *von Euler* was making a thorough study of the occurrence of compound P, a peptide he had discovered a few years earlier, in various organs. In semen and in extracts of "prostate" or vesicular glands of monkeys, sheep, and goats there is a strong blood-pressure decreasing factor that also stimulates smooth muscles. He showed that the factor involved was different from compound P, that it was lipid soluble, and he gave it the name prostaglandin. Dr. *Theorell* had shown that the substance behaved as an acid in his electrophoresis apparatus[8–10].

In the early work, we used the rabbit intestinal strip test to follow the activity. We mainly used counter-current extractions to purify *von Euler*'s crude extract.

I had just brought home one of Dr. *Lyman Craig*'s stainless steel counter-current extraction machines that proved ideal for working with these small amounts. We managed to purify the crude extract about 500 times. The most active fractions consisted of unsaturated hydroxy acids that were free of nitrogen[11].

The work was interrupted for a few years due to my appointment to the Chair of Physiological Chemistry at the University of Lund in 1948.

A practically empty institution had to be rebuilt, re-equipped, and staffed, but it was a very fortunate time (1948) for biomedical sciences in Sweden. The large build-up of resources for basic biomedical research in Swedish universities, initiated by the former Prime Minister *Tage Erlander*, had just started. The Swedish Medical Research Council had also just been founded. An additional advantage during the following decade was that the National Institutes of Health (NIH) in the USA started their unique international programme of supporting biomedical research.

We were fortunate to receive quite sizeable grants for our work in the field of steroid and bile acid metabolism from NIH over a number of years.

A group of able graduate students could then be trained in these fields—*Bengt Borgström, Jan Sjövall, Sven Lindstedt, Henry Danielsson, Bengt Samuelsson,* and *Rolf Blomstrand*. They all more or less directly contributed to the early development of prostaglandins that started up again in the fifties.

Collection of sheep glands was organized in Sweden and Norway. Using counter-current fractionations and partition chromatography, we were able to isolate small amounts of two crystalline compounds, prostaglandin $E_1$ and prostaglandin $F_{1\alpha}$[12–14] in 1957.

The correct empirical formulas were determined in cooperation with *Wolfgang Kirsten*, who had developed an ultramicro carbon-hydrogen determination in Dr. *Einar Stenhagen*'s laboratory in Uppsala. Together with the molecular weight, determined by Dr. *Ragnar Ryhage* in his mass spectrometer the formulas were found to be $C_{20}H_{34}O_5$ and $C_{20}H_{36}O_5$, respectively.

Collection of sheep glands was then extended to Sweden, Norway, Iceland, Greenland, and also to the USA through the Hormel Institute. These activities were generously supported by the Upjohn Co., USA.

In 1958–1959 the whole research group moved from Lund to the Department of Chemistry at the Karolinska Institute in Stockholm. What really played a decisive role in the prostaglandin work was the mass spectrometer development that Dr. *Ragnar Ryhage* was carrying out there. He had built the first functioning combined gas chromatograph-mass spectrometer. The structures of $PGE_1$ and $PGF_{1\alpha}$ were deduced largely from mass spectrometric identification of the products formed by oxidative degradation of these prostaglandins and the compounds formed from $PGE_1$ by treatment with weak acid or base (Fig. 1). The structure was then confirmed and the stereochemistry determined by Dr. *Sixten Abrahamsson* in Gothenburg on a derivative of $PGF_{1\alpha}$. It took him about a year with the technology available in those days. Today it would take less than three weeks. The absolute configuration was finally settled[25, 26].

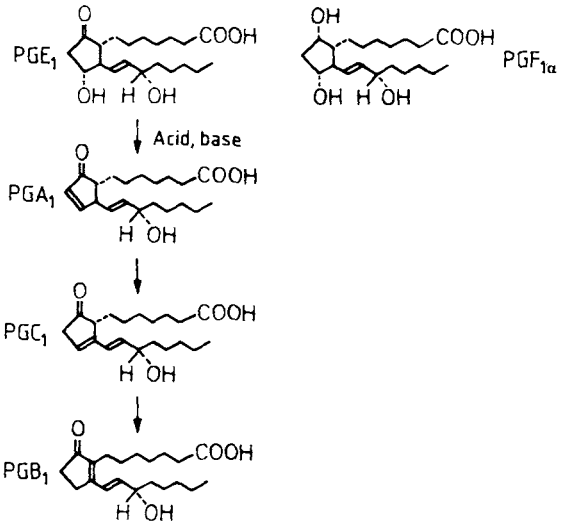



Fig. 1. The influence of weak acids and bases on the prostaglandins $PGE_1$ and $PGF_{1\alpha}$.

By 1962 the six prostaglandins listed in Figure 2 had been isolated and their structures determined[15–24]. It had also been found that these prostaglandins occur in many tissues other than the male reproductive organs.

These structures with 20 carbon atoms have *cis*-double bonds located in the same positions as in certain essential fatty acids, which made us suspect that these acids might be precursors.

I then telephoned Dr. *David van Dorp* at Unilever Research Laboratories in Holland, where these acids had previously been synthesized and isotopically labeled. When I asked him if he could supply isotopically labeled $C_{20}$ acids, it turned out that he was also planning to start investigating whether they were precursors, and that he had just prepared isotopically labeled dihomo-γ-linoleic acid for

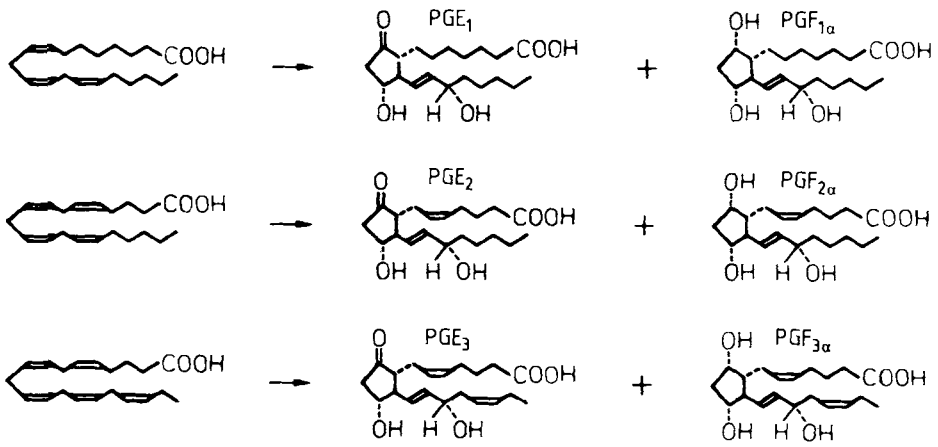



Fig. 2. Biosynthesis of prostaglandins from $C_{20}$ carboxylic acids with homogenates of sheep vesicular glands.

this purpose. He was most generous and sent us samples of the labeled acid. Simultaneously, we both started incubating the labeled acids with homogenates of sheep glands and could inform each other after two days that labeled prostaglandin $E_1$ and prostaglandin $F_{1\alpha}$ were indeed produced in good yields. We published our findings at the same time in 1964. This work was then followed up by studies using labeled tetraenoic arachidonic acid and the pentaenoic acid shown in Figure 2, which yielded prostaglandins of the 2 and 3 series, respectively[27-30].

As the yields could be up to 70%, these enzymatic methods were of great practical importance for obtaining material for further biochemical, physiological, and pharmacological work.

We prepared several grams of various prostaglandins, Unilever made considerably more, and the Upjohn Co. must have prepared hundreds of grams.

In spite of the efficiency of the enzymatic synthesis, supply became critical around 1970 when prostaglandins were needed for clinical investigations before large-scale total syntheses had been developed. An unexpected discovery was then made by *Weinheimer* and *Spraggins*[31], who had been studying the biochemistry of marine organisms in the Gulf of Mexico. They found that up to 1.5% of the dry weight of *Gorgonia* corals consisted of 15-epiprostaglandin $PGA_2$, which can easily be transformed into the common prostaglandins. For several years prostaglandins obtained from corals were used in clinical trials, but from about 1973 onwards the demand has been met by total syntheses.

After the structure of the prostaglandins was published, many projects were undertaken to prepare them by total synthesis.

Dr. *E. J. Corey,* who had collaborated with us in studies of the biosynthesis of bile acids using stereospecifically labeled cholesterol, was the first to succeed. In a series of classical papers in 1968—69[32-37], he described several elegant methods that still form the basis for most synthetic work in the prostaglandin field.

By that time many pharmaceutical companies had become interested in the field, and large synthetic programmes to synthesize prostaglandin analogues were started. These synthetic efforts were in part guided by the knowledge of metabolism of prostaglandins accumulated in Stockholm. More than 5000 prostaglandin analogues have now been prepared and tested in one way or another.

When the biosynthesis from the precursor acids was performed using lung homogenates, it was found that the prostaglandins formed were extensively further metabolized to inactive compounds[38-41] as indicated in Figure 3, *i.e.,* by reduction of the double bond between C-13 and C-14 and dehydrogenation at C-15. These reactions are so effective *in vivo* that prostaglandins are usually almost completely inactivated by one passage through the lungs. In later work it was found that these inactive compounds are further oxidized *in vivo* at the β- and γ-positions before excretion. A possible way to block the first reactions is to replace the C-15 hydrogen with a methyl group. The 15-methyl-prostaglandins prepared by *Bundy et al.* at the Upjohn Co.[42] turned out to be very useful for clinical work, and 15-methyl-$PGF_{2\alpha}$ is now a registered drug. Some of the different analogues that have been studied in clinical trials are listed in Figure 4. Efforts to obtain compounds with longer acting or more specific effects are continuing.

In the early sixties we had some difficulty convincing our colleagues to study the properties of prostaglandins in various pharmacological and physiological systems. This changed, especially after studies performed by Drs. *Dan Steinberg, Martha Vaughan,* and *Jack Orloff* at the NIH were published[43-47]. They were working with rat adipose tissue that releases glycerol and fatty acids due to increased lipolysis upon being stimulated with adrenaline, noradrenaline, glucagon or adenocorticotropin-releasing hormone (ACTH). It was found that $PGE_1$ and $PGE_2$ strongly inhibit the effects of all these compounds. $PGE_1$ and $PGE_2$ were also found to counteract both the lipolysis and the blood pressure effect of adrenaline *in vivo*. Later, it was found that these effects were mediated by a decrease in the level of cAMP in fat cells. In most other cell types, E-prostaglandins raise the level of cAMP. In some cases, the F-prostaglandins have been shown to influence the level of cGMP. I do not intend to discuss this field further here, but these findings explain why various prostaglan-

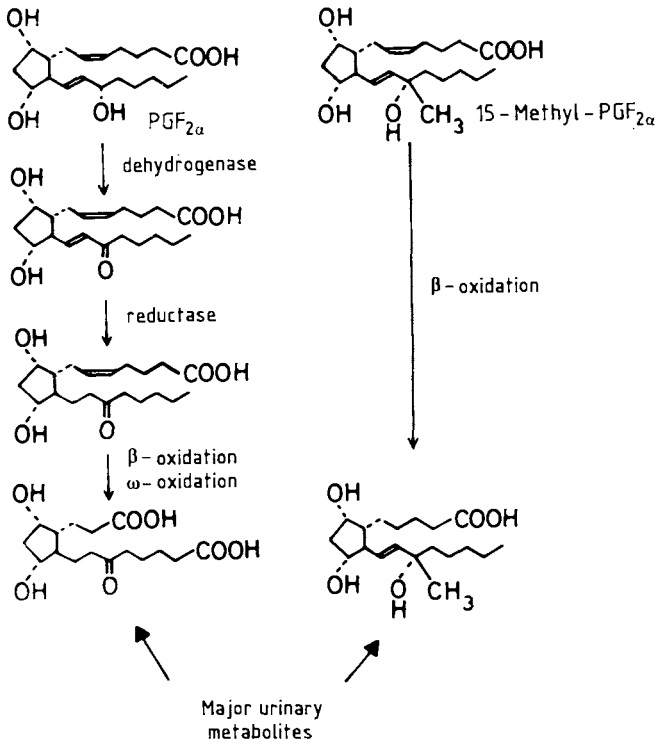



Fig. 3. Main metabolic pathway of $PGF_{2\alpha}$ and its inhibition by the methyl group at C-15.

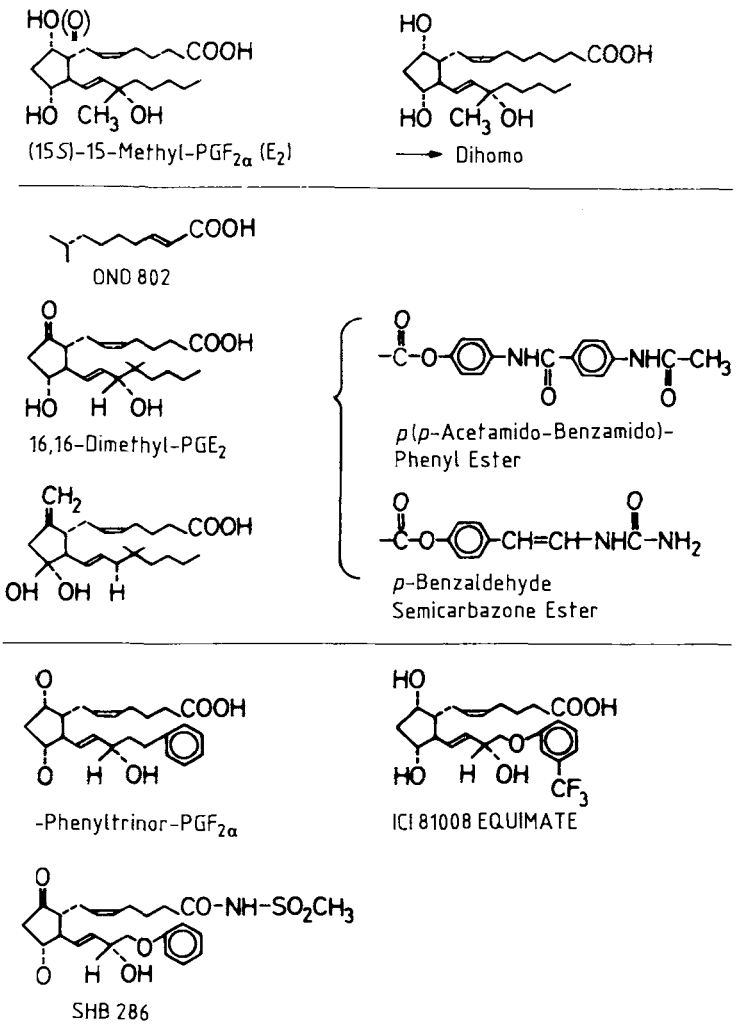



Fig. 4. Some prostaglandin analogues that have been studied in clinical trials.

dins can influence the metabolism of so many different cell types. A comprehensive summary of the early studies of the biological effects of prostaglandins was published in 1968[48].

It turned out that not only were there very large differences between the effects of different prostaglandins and their analogues, but also in their effects in different animal species. Clearly, one had to turn to clinical studies to explore the physiological role and therapeutic potential of these compounds.

The first study on the cardiovascular effects of pure prostaglandins in humans was carried out at the Karolinska Institute[49, 50]. In humans, $PGE_1$ lowers blood pressure and increases heart rate. My colleagues Drs. *Lars A. Carlson, Bengt Pernow,* and *Lennart Kaijser* and their respective coworkers performed much of the early, fundamental work on the effects of various analogues on the human cardiovascular system[51–54].

Dr. *Carlson* and his coworkers demonstrated that if it is administered intraarterially, 0.01 mg of $PGE_1$ can cause a tenfold increase in the flow of blood through an arm (Fig. 5). No change was observed in the flow of blood in the other arm since the compound is inactivated during passage through the lungs[55]. Together with Dr. *Anders Olsson,* he has developed this observation into a therapy for peripheral vascular diseases that in some cases has a dramatic effect.

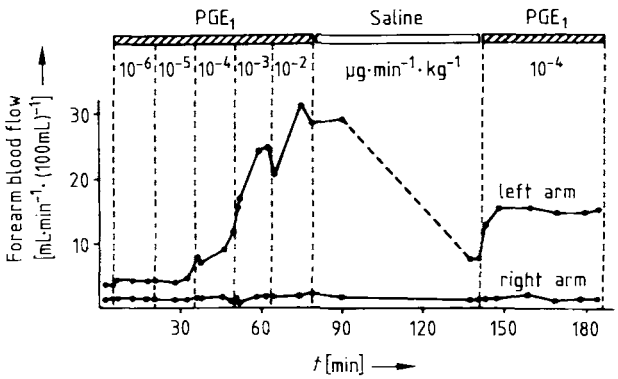



Fig. 5. The effect on forearm blood flow of continuous intra-arterial infusion of $PGE_1$ into the left brachial artery.

Another therapeutic application relates to the ductus arteriosus. It normally closes soon after birth. In certain congenital malformations, however, the E-prostaglandins have found clinical application to keep the ductus open for a few days to enable corrective surgery to be performed with less danger for the newborn baby. Furthermore, the open ductus can be closed by administration of cyclooxygenase inhibitors such as aspirin or indomethacin, *etc.* which inhibit the local synthesis of prostaglandins.

I will now turn to the effects of prostaglandins on the gastrointestinal tract, a field where Dr. *Robert* of the Upjohn Co. has been very active. In experiments on animals he found that gastric secretion could be inhibited by oral administration or by injecting prostaglandins of the E-type. The methyl analogues (15*S*)-15-methyl-$PGE_2$ and 16,16-dimethyl-$PGE_2$ were many times more active than $PGE_2$ itself[58]. Early clinical studies were performed in Stockholm by Dr. *Sven Andersson* and Dr. *B. Nylander*[57],

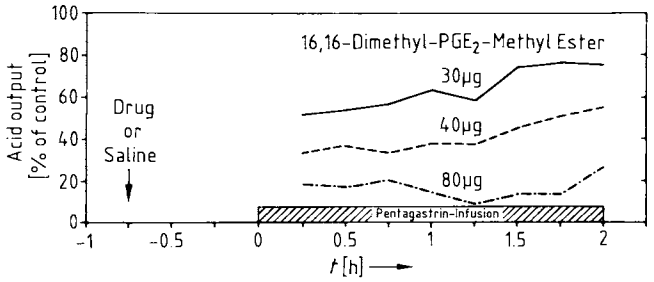



Fig. 6. The effect of the methyl ester of 16,16-dimethyl-$PGE_2$ on gastric secretion.

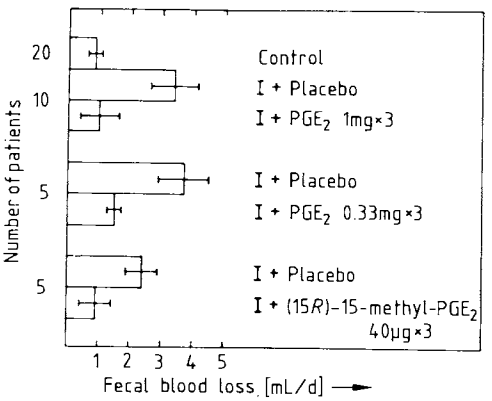



Fig. 7. The effect of prostaglandins on fecal blood loss upon administration of indomethacin. I = 3 × 50 mg indomethacin; duration of each experiment one week; in each case the data refer to the last three days of an experiment.

who found that an oral dose of only 80 µg of the methyl ester of 16,16-dimethyl-$PGE_2$ practically blocked the pentagastrin-stimulated gastric secretion in humans for several hours (Fig. 6). This work has been continued and expanded by Dr. *Catja Johansson* and her coworkers. Extensive clinical trials in many countries have been performed, and these indicate that several analogues have a healing effect on ulcers (for a recent summary see [58]).

Another important observation made by Dr. *Robert* was a phenomenon that he called "cytoprotection". If large doses of indomethacin or aspirin are administered to rats or if boiling water, strong acid, or base are given orally to anesthesized rats, extensive erosions and/or bleeding of the gastric mucosa occur, and the animals usually die within a few days. However, if less than 1 µg of 16,16-dimethyl-$PGE_2$ is administered orally 30 minutes beforehand, the mucusa is protected. An interesting observation made by *Robert et al.*[59] is that mild irritants like dilute ethanol can effect a certain protection, presumably by stimulating the mucosal cells to increase the biosynthesis of prostaglandins. Cytoprotection can be observed with prostaglandins at doses that do not inhibit acid secretion, and some prostaglandins stimulate secretion of mucus and bicarbonate. The mechanism of cytoprotection is not clear[58]. The effect is not limited to the gastrointestinal mucosa. Liver and kidney cells can also be protected to some extent from necrosis caused by carbon tetrachloride, *etc.* by administration of 16,16-dimethyl-$PGE_2$[60].

At this point we examined the effects of cytoprotective prostaglandins on some clinical side effects of indomethacin and aspirin. Normally, *ca.* 1 mL of blood is lost from the gut per day. The usual therapeutic dose of indomethacin increases this to 3 to 5 mL and in a few cases causes serious bleedings. It was shown at the Karolinska Institute for the first time that only 0.33 mg of $PGE_2$ or 40 µg of 15-methyl-$PGE_2$[61,62] three times a day completely protects the patient from this bleeding caused by indomethacin (Fig. 7). It is, however, still too early to evaluate the therapeutic value of administering prostaglandins to reduce the side effects of these drugs.

The last aspects that I shall discuss are related to fertility and the use of prostaglandins in obstetrics and gynecology. This is where the prostaglandins were discovered, and that is where they have found their greatest application so far.

Dr. *Marc Bygdeman* had just started his doctorate with Dr. *von Euler* when pure prostaglandins became available. He studied the effects of the different prostaglandins first *in vitro* and then *in vivo* in Dr. *Ulf Borell*'s department at the Karolinska Institute together with Dr. *Nils Wiquist*. They first demonstrated clinically that $PGE_1$ causes uterine contractions when injected in small amounts. This of course led to the expectation that it might be possible to induce labor or interrupt pregnancies by administering prostaglandins[63–65].

Dr. *Sultan Karim* was the first to report on the clinical use of prostaglandins to induce labor.

The first therapeutic abortion with $PGF_{2\alpha}$ was performed in May 1969 at the Karolinska Institute. During that summer Dr. *Karim* was in Stockholm and was informed about it. Back in Uganda, he confirmed and expanded this finding and showed that $PGE_2$ also could be used to induce pregnancy interruption. The results of both groups were published in the same issue of Lancet in January 1970[66,67].

An intense activity then started all over the world exploring these findings with normal prostaglandins, and later with some of the analogues shown in Figure 4. The early clinical data obtained in Stockholm are summarized in Figure 8[66–73].

First, the two natural prostaglandins $PGE_2$ and $PGF_{2\alpha}$ were studied extensively. When administered intravenously they caused very pronounced side effects. When administered intra- or extra-amniotically, the side effects were tolerable.

The (15*S*)-15-methyl-$PGF_{2\alpha}$ supplied by the Upjohn Co. was then studied and found to be much more active, but had considerably less side effects. It could also be injected intramuscularly, and we developed vaginal suppositories containing the methyl ester; it is now a registered drug in many countries.

16,16-Dimethyl-$PGE_2$ was even more active—sometimes being highly effective after oral administration of less than 1 mg. However, the side effects were more pronounced, and it was less stable. Recently, an analogue of 16,16-dimethyl-$PGE_2$ in which the carbonyl group at C-9 has been replaced by a methylene group has been extensively studied since it combines high activity with high stability and has only slight side effects[74].

| | $PGE_{2\alpha}$ | $PGE_2$ | (15S)-15-Methyl-$PGF_{2\alpha}$ | 16,16-Dimethyl-$PGE_2$ |
|---|---|---|---|---|
| Intravenous | ca. 100mg (50–100µg/min) | ca. 5mg 5µg/min | ca. 5mg 5µg/min | ca. 0.5mg 0.5µg/min |
| Intra-amniotic | 40–50mg (1×) | 5–10mg (1×) | 2.5mg (1×) | |
| Extra-amniotic | ca. 5mg (ca. 9×0.75mg) | 1–2mg (6×) | 1mg (1×) | |
| I. Vaginal suppositories | [250mg (5×50mg)] | 60–80mg (3–4×20mg) | ca. 3mg (Me-ester) (1×3mg) | ca. 4mg (4×1mg) |
| I. Muscular | — | — | 2mg (6×0.3) | — |
| Oral | — | — | — | 0.2–0.6mg (60% Success) |

Fig. 8. Summary of early clinical trials indicating approximate doses of prostaglandins for interruption of pregnancy.

At that time an important development was initiated by SIDA (Swedish International Development Authority). In the sixties they had become heavily involved in supporting family planning in many developing countries; however, they found that the methods available left much to be desired and, therefore, were considering how best to stimulate and support research and development in this field.

The Director, *Ernst Michanek,* and *Carl Wahren* had developed advanced plans to start an international research foundation at the Karolinska Institute for this purpose. However, for various reasons, it was decided to make a feasibility study of alternative possibilities in conjunction with the Ford Foundation and the World Health Organization (WHO); a study in which I had the honor to participate. This resulted in 1971–72 in the creation of the WHO's "Special Programme" for research on human reproduction. Attention was focused on the needs of developing countries. Voluntary contributions to the programme soon exceeded 10 million US dollars annually, of which more than half was provided by Swedish sources.

One of the "task forces" of the programme was devoted to exploring the potential of the prostaglandins to interrupt pregnancy. During the first five years I had the stimulating assignment of serving as chairman of this group of distinguished experts. The exploratory work carried out at the Karolinska Institute and by Dr. *Karim*'s group formed the basis for extensive internationally coordinated clinical trials with drugs supplied by the Upjohn Co. Figure 9 shows the locations of the clinics involved, and Figure 10 the number of cases completed. The task force has continued its activities under the chairmanship of Dr. *Bygdeman*.

The most important new development has been the interruption of pregnancy during the "postconceptional" pe-

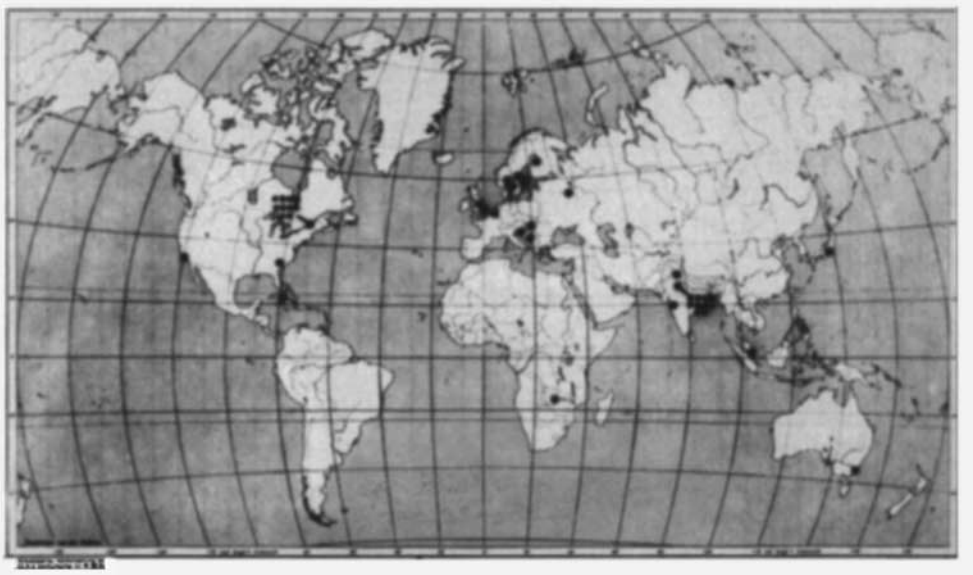


Fig. 9. Participating clinics in coordinated trials of the WHO Prostaglandin Task Force (1972–1977).

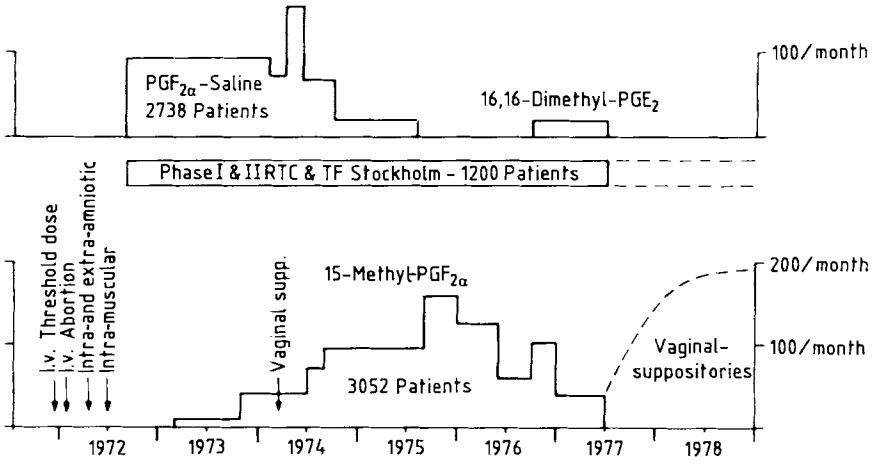



Fig. 10. Number of patients participating in coordinated trials of the WHO Prostaglandin Task Force.

riod, *i.e.* in the first three weeks after a missed menstrual period.

I have a very vivid memory of a late evening in Bombay when Dr. *Borell*, Dr. *Bygdeman*, and I were compiling results of abortions carried out at different stages of pregnancy in which we found a success rate of practically 100% complete abortions (see Fig. 11). This observation has been studied extensively, and Dr. *Bygdeman et al.* have just completed a successful trial with a 100 cases in Stockholm in which the patients self-administered the drug at home. This method obviously has a very great potential, especially in developing countries.

The therapeutic use of prostaglandins is, however, not limited to interruption of pregnancy. It is also used for induction of labor, treatment of serious bleeding after delivery, and for dilatation during diagnostic curettage.

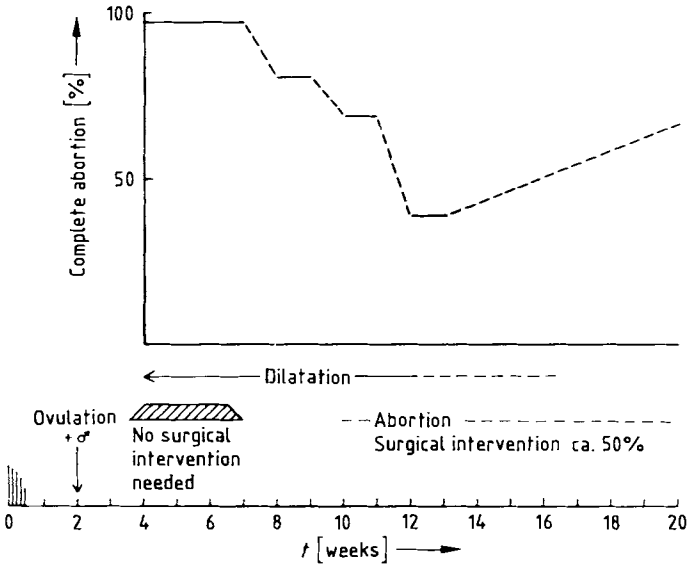



Fig. 11. Percentage of "complete" abortions after interruption of pregnancy with prostaglandins at various times.

Promising results have been reported of treating eclampsia with $PGA_1$.

A summary of the applications of prostaglandins in this area is given in Figure 12.

Prostaglandins have also found extensive use in animal husbandry, especially for "syncronization" of herds of cattle, *i.e.* injection of cows with 25 mg of $PGF_{2\alpha}$ at an appropriate time interrupts their cycles, and the whole herd can be inseminated three days later.

Prostaglandin precursors and the enzymatic systems appear to be present in practically every cell and can biosynthesize characteristic mixtures depending on cell type and conditions. Since the highest concentration is found in the lowest animal species, one can speculate that the ease of autoxidation of the percursor acids—a reaction that even has been reported to produce prostaglandins in minute amounts[75]—led to their utilization in metabolism at an early stage of evolution for many different functions.

Apparently, prostaglandins mainly play a role as local regulators—even if $PGF_{2\alpha}$ functions as a classical hormone in sheep, where it is produced in the uterus at the end of the cycle and transported in the blood to the ovary, causing luteolysis.

The complex pattern of arachidonic acid metabolism makes studies of the functions of prostaglandins in complex regulatory mechanisms in organs like the kidney, lung, *etc.* a difficult and challenging task.

Figure 13 illustrates how the field has developed from the early publications on the isolation, structure and biosynthesis to the present level of more than 5000 papers annually!

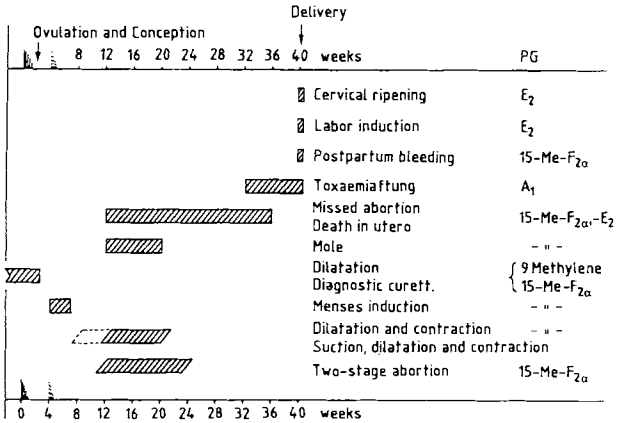



Fig. 12. Summary of therapeutic utility of prostaglandins in gynecology obstetrics.

Where did all these scientists get their prostaglandins? This is also answered in Figure 13. The Upjohn Company supplied something like 75000 samples during this period, and it can be seen that most of the samples gave rise to a publication, at least up to *ca.* 1970. At that point the prostaglandin-containing coral was found in the Gulf of Mexico. A number of pharmaceutical companies then collected corals, started synthetic programmes, and then also supplied samples to scientists.

Here it is appropriate to point out that the whole prostaglandin field would have been very much slower in developing without the outstanding research and development work initiated and organized at Upjohn by Dr. *David Weisblat.*

The prostaglandin story illustrates, once again, the importance of interaction between the pharmaceutical indus-

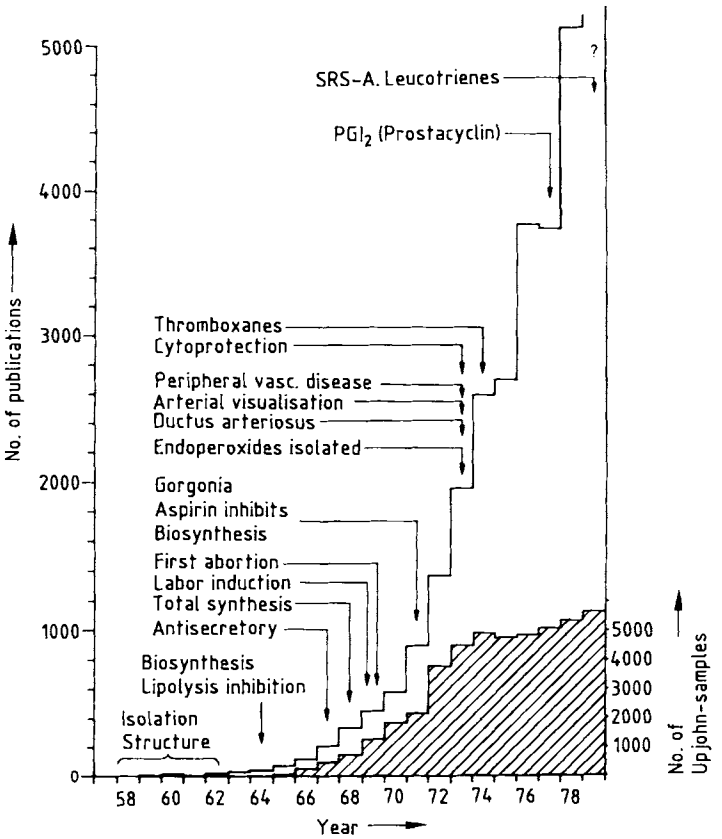



Fig. 13. Number of annual publications related to prostaglandins (left ordinate) and the number of free samples of prostaglandins distributed by Upjohn (right ordinate).

try and academic biomedical scientists. In this case, the World Health Organization's special programme for human reproduction has also greatly contributed to the speed of development and to the build up of research and development capabilities in this field in developing countries.

Received: August 1, 1983 [A 475 IE]
German version: *Angew. Chem. 95* (1983) 865

[1] S. Bergström: "The Prostaglandins". *Recent Prog. Horm. Res. 22* (1966) 153-175.
[2] S. Bergström: "Prostaglandins: Members of a New Hormonal System". *Science 157* (1967) 382-391.
[3] S. Bergström: "Isolation, Structure and Action of the Prostaglandins" in S. Bergström, B. Samuelsson: *Prostaglandins, Proc. 2nd Nobel Symp., Stockholm, June 1966.* Almqvist & Wiksell and Interscience, Stockholm and New York, resp., 1967, p. 21-30.
[4] S. Bergström, B. Samuelsson: "Prostaglandins". *Annu. Rev. Biochem. 34* (1965) 101-108.
[5] R. Kurzrok, C. C. Lieb: "Biochemical Studies of Human Semen. II. The Action of Semen on the Human Uterus". *Proc. Soc. Exp. Biol. Med. 28* (1930) 268-272.
[6] M. W. Goldblatt: "A Depressor Substance in Seminal Fluid". *J. Soc. Chem. Ind. London 52* (1933) 1056-1057.
[7] M. W. Goldblatt: "Properties of Human Seminal Plasma". *J. Physiol. London 81* (1935) 208-218.
[8] U. S. von Euler: "Zur Kenntnis der pharmakologischen Wirkungen von Nativsekreten und Extrakten männlicher accessorischer Geschlechtsdrüsen". *Arch. Exp. Pathol. Pharmakol. 175* (1934) 78-81.
[9] U. S. von Euler: "A Depressor Substance in the Vesicular Gland". *J. Physiol. London 84* (1935) 21P.
[10] U. S. von Euler: "On the Specific Vasodilating and Plain Muscle Stimulating Substances From Accessory Genital Glands in Man and Certain Animals (Prostaglandin and Vesiglandin)". *J. Physiol. London 88* (1937) 213-234.
[11] S. Bergström: "Prostaglandinets kemi". *Nord. Med. 42* (1949) 1465-1466.
[12] S. Bergström, J. Sjövall: "The Isolation of Prostaglandin". *Acta Chem. Scand. 11* (1957) 1086.
[13] S. Bergström, J. Sjövall: "The Isolation of Prostaglandin F from Sheep Prostate Glands". *Acta Chem. Scand. 14* (1960) 1693-1700.
[14] S. Bergström, J. Sjövall: "The Isolation of Prostaglandin E from Sheep Prostate Glands". *Acta Chem. Scand. 14* (1960) 1701-1705.
[15] S. Bergström, F. Dressler, L. Krabisch, R. Ryhage, J. Sjövall: "The Isolation and Structure of a Smooth Muscle Stimulating Factor in Normal Sheep and Pig Lungs". *Ark. Kemi 20* (1962) 63-66.
[16] S. Bergström, F. Dressler, R. Ryhage, B. Samuelsson, J. Sjövall: "The Isolation of two Further Prostaglandins from Sheep Prostate Glands". *Ark. Kemi 19* (1962) 563-567.
[17] S. Bergström, L. Krabisch, B. Samuelsson, J. Sjövall: "Preparation of Prostaglandin F from Prostaglandin E". *Acta Chem. Scand. 16* (1962) 969-974.
[18] S. Bergström, L. Krabisch, J. Sjövall: "Smooth Muscle Stimulating Factors in Ram Semen". *Acta Chem. Scand. 14* (1960) 1706-1710.
[19] S. Bergström, R. Ryhage, B. Samuelsson, J. Sjövall: "The Structure of Prostaglandin E, $F_1$ and $F_2$". *Acta Chem. Scand. 16* (1962) 501-502.
[20] S. Bergström, R. Ryhage, B. Samuelsson, J. Sjövall: "Degradation Studies on Prostaglandins". *Acta Chem. Scand. 17* (1963) 2271-2280.
[21] S. Bergström, R. Ryhage, B. Samuelsson, J. Sjövall: "The Structures of Prostaglandin $E_1$, $F_{1\alpha}$ and $F_{1\beta}$". *J. Biol. Chem. 238* (1963) 3555-3564.
[22] S. Bergström, B. Samuelsson: "Isolation of Prostaglandin $E_1$ from Human Seminal Plasma". *J. Biol. Chem. 237* (1962) PC3005-PC3006.
[23] B. Samuelsson: "The Structure of Prostaglandin $E_3$". *J. Am. Chem. Soc. 85* (1963) 1878-1879.
[24] B. Samuelsson: "Isolation and Identification of Prostaglandins from Human Seminal Plasma". *J. Biol. Chem. 238* (1963) 3229-3234.
[25] S. Abrahamsson, S. Bergström, B. Samuelsson: "The Absolute Configuration of Prostaglandin $F_{2\text{-}1}$". *Proc. Chem. Soc. 1962,* 332.
[26] D. H. Nugteren, D. A. van Dorp, S. Bergström, M. Hamberg, B. Samuelsson: "Absolute Configuration of the Prostaglandins". *Nature London 212* (1966) 38-39.
[27] S. Bergström, H. Danielsson, D. Klenberg, B. Samuelsson: "The Enzymatic Conversion of Essential Fatty Acids into Prostaglandins". *J. Biol. Chem. 239* (1964) PC4006-PC4008.
[28] S. Bergström, H. Danielsson, B. Samuelsson: "The Enzymatic Formation of Prostaglandin $E_1$ from Arachidonic Acid". *Biochim. Biophys. Acta 90* (1961) 207-210.
[29] D. A. van Dorp, R. K. Beerthuis, D. H. Nugteren, H. Vonkeman: "The Biosynthesis of Prostaglandins". *Biochim. Biophys. Acta 90* (1964) 204-207.
[30] D. A. van Dorp, R. K. Beerthuis, D. H. Nugteren, H. Vonkeman: "Enzymatic Conversion of all-*cis*-Polyunsaturated Fatty Acids into Prostaglandins". *Nature London 203* (1964) 839-941.
[31] A. J. Weinheimer, R. L. Spraggins: "The Occurrence of Two New Prostaglandin Derivatives in the Gorgonian *Plexora Homomalla.* Chemistry of Coelenterates. XV." *Tetrahedron Lett. 1969,* 5185-5188.
[32] E. J. Corey, I. Vlattas, N. H. Andersen, K. Harding: "A New Total Synthesis of Prostaglandins of the $E_1$ and $F_1$ Series Including 11-Epiprostaglandins". *J. Am. Chem. Soc. 90* (1968) 3247.
[33] E. J. Corey, N. H. Andersen, R. M. Carlson, J. Paust, E. Vedejs, I. Vlattas, R. E. K. Winter: "Total Synthesis of Prostaglandins. Synthesis of the Pure dl-$E_1$, -$F_{1\alpha}$, -$F_{1\beta}$, -$A_1$ and -$B_1$ Hormones". *J. Am. Chem. Soc. 90* (1968) 3245-3247.
[34] E. J. Corey, N. M. Weinshenker, T. K. Shaaf, W. Huber: "Stereo-controlled Synthesis of Prostaglandins $F_{1\alpha}$ and $E_2$ (dl)". *J. Am. Chem. Soc. 91* (1969) 5675-5677.

[35] E. J. Corey, I. Vlattas, K. Harding: "Total Synthesis of Natural *(levo)* and Enantiometric *(dextro)* Forms of Prostaglandin $E_1$". *J. Am. Chem. Soc. 91* (1969) 535–536.

[36] E. J. Corey, Z. Arnold, J. Hutton: "Total Synthesis of Prostaglandins $E_2$ and $F_{2\alpha}$ (dl) via a Tricarbocyclic Intermediate". *Tetrahedron Lett. 1970,* 307–310.

[37] E. J. Corey, R. Noyori, T. K. Schaaf: "Total Synthesis of Prostaglandins $F_{1\alpha}$, $E_1$, $F_{2\alpha}$, and $E_2$ (Natural Forms) from a Common Synthetic Intermediate". *J. Am. Chem. Soc. 92* (1970) 2586–2587.

[38] E. Änggård, K. Green, B. Samuelsson: "Synthesis of Tritium-labeled Prostaglandin $E_1$ and Studies on its Metabolism in Guinea Pig Lung". *J. Biol. Chem. 240* (1965) 1932–1940.

[39] E. Änggård, B. Samuelsson: "Biosynthesis of Prostaglandins from Arachidonic Acid in Guinea Pig Lung". *J. Biol. Chem. 240* (1965) 3518–3521.

[40] E. Änggård, B. Samuelsson: "The Metabolism of Prostaglandins in Lung Tissue" in S. Bergström, B. Samuelsson: *Prostaglandins, Proc. 2nd Nobel Symp., Stockholm, June 1966,* Almqvist & Wiksell and Interscience, Stockholm and New York, resp., 1967, p. 97–106.

[41] E. Änggård, B. Samuelsson: "Metabolism of Prostaglandin $E_1$ in Guinea Pig Lung: The Structure of Two Metabolites". *J. Biol. Chem. 239* (1964) 4097–4102.

[42] G. L. Bundy, F. H. Lincoln, N. A. Nelson, J. E. Pike, W. P. Schneider: "Novel Prostaglandin Syntheses". *Ann. N. Y. Acad. Sci., Prostaglandins 180* (1971) 76–79.

[43] D. Steinberg, M. Vaughan, P. Nestel, S. Bergström: "Effects of Prostaglandin E Opposing those of Catecholamines on Blood Pressure and on Triglyceride Breakdown in Adipose Tissue". *Biochem. Pharmacol. 12* (1963) 764–766.

[44] D. Steinberg, M. Vaughan, P. J. Nestel, O. Strand, S. Bergström: "Effects of the Prostaglandins on Hormone-induced Mobilization of Free Fatty Acids". *J. Clin. Invest. 43* (1964) 1533–1540.

[45] J. Orloff, J. S. Handler, S. Bergström: "Effect of Prostaglandin ($PGE_1$) on the Permeability Response of the Toad Bladder to Vasopressin, Theophylline and Adenosine 3′,5′-Monophosphate". *Nature London 205* (1965) 397–398.

[46] J. Orloff, J. Grantham: "The Effect of Prostaglandin ($PGE_1$) on the Permeability Response of Rabbit Collecting Tubules to Vasopressin" in S. Bergström, B. Samuelsson: *Prostaglandins, Proc. 2nd Nobel Symp., Stockholm, June 1966,* Almqvist & Wiksell and Interscience, Stockholm and New York, resp., 1967, p. 143–146.

[47] J. Orloff, J. Handler: "The Role of Adenosine 3′,5′-Phosphate in the Action of Antidiuretic Hormone". *Am. J. Med. 47* (1967) 757–768.

[48] S. Bergström, L. A. Carlson, J. R. Weeks: "The Prostaglandins: A Family of Biologically Active Lipids". *Pharmacol. Rev. 20* (1968) 1–48.

[49] S. Bergström, H. Dunér, U. S. von Euler, B. Pernow, J. Sjövall: "Observations on the Effects of Infusion of Prostaglandin E in Man". *Acta Physiol. Scand. 45* (1959) 145–151.

[50] S. Bergström, R. Eliasson, U. S. von Euler, J. Sjövall: "Some Biological Effects of Two Crystalline Prostaglandin Factors". *Acta Physiol. Scand. 45* (1959) 133–144.

[51] L. A. Carlson: "Metabolic and Cardio-vascular Effects in vivo of Prostaglandins" in S. Bergström, B. Samuelsson: *Prostaglandins, Proc. 2nd Nobel Symp., Stockholm, June 1966,* Almqvist & Wiksell and Interscience, Stockholm and New York, resp., 1967, p. 123–132.

[52] L. A. Carlson, L.-G. Ekelund, L. Orö: "Clinical and Metabolic Effects of Different Doses of Prostaglandin $E_1$ in Man". *Acta Med. Scand. 183* (1968) 423–430.

[53] L. A. Carlson, D. Hallberg: "Basal Lipolysis and Effects of Noradrenaline and Prostaglandin $E_1$ on Lipolysis in Human Subcutaneous and Omental Adipose Tissue". *J. Lab. Clin. Med. 71* (1968) 368–377.

[54] L. A. Carlson, E. Irion, L. Orö: "Effect of Infusion of Prostaglandin $E_1$ on the Aggregation of Blood Platelets in Man". *Life Sci. 7* (1968) 85–90.

[55] S. Bevegård, L. Orö: "Effect of Prostaglandin $E_1$ on Forearm Blood Flow". *Scand. J. Clin. Lab. Invest. 23* (1969) 347–353.

[56] A. Robert: "The Inhibitory Effects of Prostaglandins on Gastric Secretion" in G. B. J. Glass: *Prog. in Gastroenterol. 3* (1977) 777–801.

[57] B. Nylander, S. Andersson: "Gastric Secretory Inhibition Induced by Three Methyl Analogs of Prostaglandin $E_2$ Administered Intragastrically to Man". *Scand. J. Gastroenterol. 9* (1974) 751–758.

[58] C. Johansson, S. Bergström: "Prostaglandins and Protection of the Gastroduodenal Mucosa". *Scand. J. Gastroenterol. Suppl. 77* (1982) 21–46.

[59] A. Robert, C. Lancaster, A. J. Hanchar, J. E. Nezamis: "Mild Irritants Prevent Gastric Necrosis through Prostaglandin Formation: Histological Study". *Gastroenterology 74* (1978) 1086.

[60] M. J. Ruwart, B. D. Rush, N. M. Friedle, R. C. Piper, G. J. Kolaja: "Protective Effects of 16,16-Dimethyl $PGE_2$ on the Liver and Kidney". *Prostaglandins 21* (1981) 97–102.

[61] C. Johansson, B. Kollberg, R. Nordemar, B. Samuelsson, S. Bergström: "Protective Treatment with Prostaglandin $E_2$ in the Gastrointestinal Tract during Indomethacin Treatment of Rheumatic Patients". *Gastroenterology 76* (1980) 479–483.

[62] M. M. Cohen, G. Cheung, D. M. Lyster: "Prevention of Aspirin-Induced Faecal Blood Loss by Prostaglandin $E_2$". *Gut 21* (1980) 602–606.

[63] M. Bygdeman, R. Eliasson: "A Comparative Study on the Effect of Different Prostaglandin Compounds on the Motility of the Isolated Human Myometrium". *Med. Exp. 9* (1963) 409–415.

[64] M. Bygdeman: "The Effect of Different Prostaglandins on Human Myometrium in vitro". *Acta Physiol. Scand. 63, Suppl. 242* (1964) 1–78.

[65] M. Bygdeman, S. Kwon, N. Wiqvist: "The Effect of Prostaglandin $E_1$ on Human Pregnant Myometrium in vivo" in S. Bergström, B. Samuelsson: *Prostaglandins, Proc. 2nd Nobel Symp., Stockholm, June 1966.* Almqvist & Wiksell and Interscience, Stockholm and New York, resp., 1967, p. 93–96.

[66] U. Roth-Brandel, M. Bygdeman, N. Wiqvist, S. Bergström: "Prostaglandins for Induction of Therapeutic Abortion". *Lancet 1970 I,* 190–191.

[67] S. M. M. Karim, G. M. Filshie: "Therapeutic Abortion Using Prostaglandin $F_{2\alpha}$". *Lancet 1970 I,* 157.

[68] N. Wiqvist, M. Bygdeman: "Therapeutic Abortion by Local Administration of Prostaglandins". *Lancet 1970 II,* 716–717.

[69] M. Bygdeman, N. Beguin, M. Toppozada, M. Wiqvist, S. Bergström: "Intra-Uterine Administration of 15(*S*)-15 Methyl $PGF_{2\alpha}$ for Induction of Abortion". *Lancet 1972 I,* 13–36.

[70] M. Bygdeman, K. Green, M. Toppozada, N. Wiqvist, S. Bergström: "The Influence of Prostaglandin Metabolites on the Uterine Response to $PGF_{2\alpha}$. A Clinical and Pharmacokinetic Study". *Life Sci. 14* (1974) 521–531.

[71] M. Bygdeman, J. N. Martin, N. Wiqvist, K. Green, S. Bergström: "Reassessment of Systematic Administration of Prostaglandins for Induction of Midtrimester Abortion". *Prostaglandins 8* (1974) 157–169.

[72] M. Bygdeman, K. Gréen, V. Lundström, M. Ramadan, S. Fotiou, S. Bergström: "Induction of Abortion by Vaginal Administration of 15(*S*)15-methyl Prostaglandin $F_{2\alpha}$ Methyl Ester. A Comparison of Two Delivery Systems". *Prostaglandins 12* (1976) 27–51.

[73] M. Bygdeman, A. Ganguli, K. Kinoshita, V. Lundström: "Development of a Vaginal Suppository Suitable for Single Administration for Interruption of Second Trimester Pregnancy". *Contraception 15* (1977) 129–141.

[74] K. Gréen, O. Vesterqvist, M. Bygdeman, N. J. Christenssen, S. Bergström: "Plasma Levels of 9-Deoxo-16,16-dimethyl-9-methylene-$PGE_2$ in Connection with its Development as an Abortifacient". *Prostaglandins 24* (1982) 451–466.

[75] D. H. Nugteren, H. Vonkeman, D. A. van Dorp: "Non-Enzymatic Conversion of all-*cis* 8,11,14-Eicosatrienoic Acid into Prostaglandin $E_1$". *Recl. Trav. Chim. Pays-Bas 86* (1967) 1237–1245.

**When submitting manuscripts, authors of articles which are intended for publication as "Communications" are requested to conform to the guidelines reproduced at the beginning of each issue following the list of contents.**

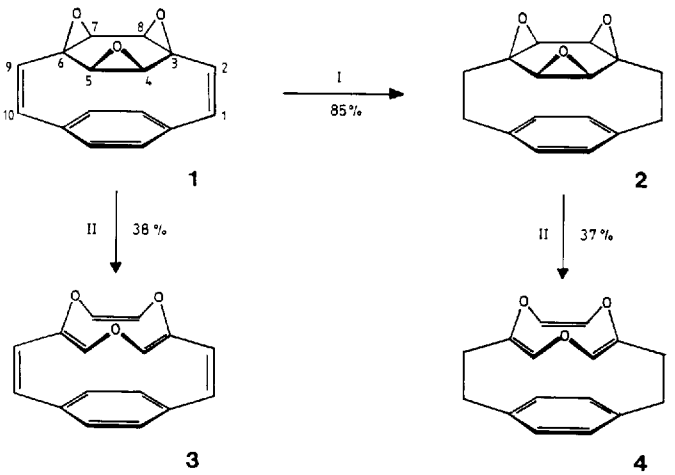
## Valence Isomerization of Phane-Bridged *cis*-Trioxatris-*o*-homobenzenes**

By *Michael Stöbbe, Ulrich Behrens, Gunadi Adiwidjaja, Peter Gölitz,* and *Armin de Meijere**

*Dedicated to Professor Hans Brockmann on the occasion of his 80th birthday*

*cis*-Benzene trioxide, with its almost planar cyclohexane ring, undergoes the $3\sigma \rightarrow 3\pi$ rearrangement characteristic of *cis*-tris-σ-homobenzenes to 1,4,7-trioxonin only above 200°C[1]. In view of the geometry-dependence of the [2+2+2]-cycloreversion observed in the carbocyclic tris-homobenzene system[2], it is of interest to know how much the deformation forced upon the trioxide six-membered ring in **1**[3] by phane-bridging influences its kinetic stability.

According to a crystal structure analysis, the epoxide rings in **1**, with a mean interplanar angle of 106.5° to the saturated six-membered ring, are oriented in almost the same fashion as those in the unbridged *cis*-benzene trioxide[1b], but the two substituted corners of the skeletal six-membered ring are bent at an angle of about 9.2° out of the plane of the other four C-atoms. Surprisingly, this saturated ring is thus less bent than the benzene ring in **1**, where the corresponding angle is 12.9°.




**1** **2** **3** **4**

I: $H_2/PtO_2$, EtOH, R.T., 10 h; II: 550°C, $10^{-3}$ torr.

[*] Prof. Dr. A. de Meijere, Dr. G. Adiwidjaja, Dr. U. Behrens, Dr. P. Gölitz, M. Stöbbe
Fachbereich Chemie der Universität
Martin-Luther-King-Platz 6, D-2000 Hamburg 13 (Germany)

[**] This work was supported by the Stiftung Volkswagenwerk and the Fonds der Chemischen Industrie.

In the [2.2]paracyclophane trioxide **2**, where the bridging bonds are longer, the bending of the trioxide six-membered ring might be correspondingly smaller. **2** cannot be obtained directly from [2.2]paracyclophane analogously to **1**[3] but only by catalytic hydrogenation of **1**. **2** is much more soluble than **1** in organic solvents, is stable at room temperature, and like **1** decomposes below its melting point (>260°C). In the $^1$H-NMR spectrum of **2** a remarkably large shift difference of 0.98 ppm is observed in each case for the signals of the two protons on C-2 and on C-9, which must be due to the diamagnetic anisotropy of the oxirane ring[5].

Both **1** and **2** could be sublimed at 170—180°C/$10^{-3}$ torr through a quartz tube heated to 550°C. The condensates obtained at −196°C contained, aside from the educts, the phane-bridged 1,4,7-trioxonins **3** and **4**, respectively, in almost the same relative amounts (21%). **3** and **4** were purified by chromatography ($SiO_2$, $CH_2Cl_2$/pentane 2:1 and $CHCl_3/Et_2O$ 1:1, respectively) and subsequent sublimation (70°C/$10^{-2}$ torr) and characterized by NMR spectroscopy. Both differ considerably from their precursors in their properties; for example, they even dissolve in pentane, are considerably more volatile, and have lower melting points (117—118 and 123—124°C, respectively).

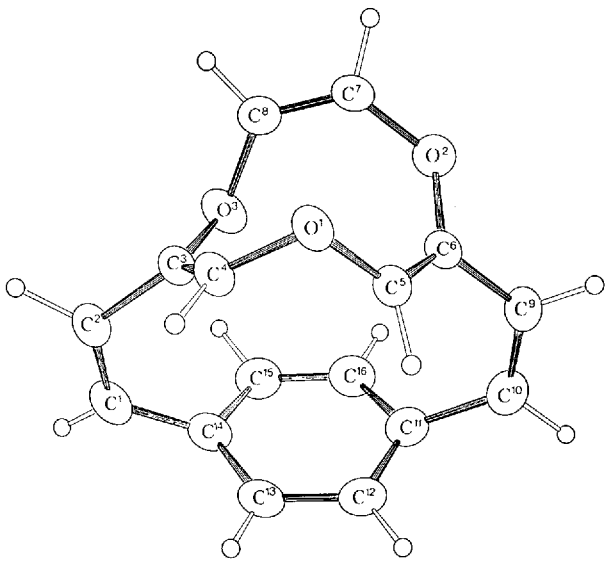



Fig. 2. ORTEP diagram and crystal structure parameters of the phane-bridged 1,4,7-trioxonin **3** (monoclinic crystals, $P2_1/c$, $Z=4$, $a=716.2(1)$, $b=2505.8(2)$, $c=758.8(1)$ pm, $\beta=114.18(1)°$, $\rho_{X\text{-ray}}=1.35$ g/cm$^3$; 2168 evaluated reflections, $\theta \leq 70°$, $Cu_{K\alpha}$; $R=5.0$, $R_w=5.0\%$). $C^1C^2$: 133.3; $C^2C^3$: 149.3; $C^3C^4$: 132.6; $C^5C^6$: 132.7; $C^7C^8$: 130.7; $C^6C^9$: 147.2; $C^9C^{10}$: 133.7; $C^{10}C^{11}$: 149.1; $C^{11}C^{12}$: 138.4; $C^{11}C^{16}$: 139.1; $C^{12}C^{13}$: 138.5; $C^{13}C^{14}$: 138.0; $C^{14}C^{15}$: 139.0; $C^{15}C^{16}$: 137.5; $C^4O^1$: 139.6; $C^5O^1$: 139.1; $C^6O^2$: 136.8; $C^7O^2$: 137.0; $C^3O^3$: 138.0; $C^8O^3$: 139.0 pm.

**3** is storable for prolonged periods at 0°C in the refrigerator, whereas **4** polymerizes within a few days, both in solution and in the solid state.

These findings for the rearrangement of **1** and **2** show, at least qualitatively, that the kinetic stability of the *cis*-benzene trioxide[1] is not significantly affected by phane-bridging such as in **1** and **2**. Contrary to expectation, even the conformation of the trioxonin ring in **3** is not notably

influenced by the bridging; the conformation preferred in the crystal (see Fig. 2) is not crown- but saddle-shaped, as in 1,4,7-troxonin[1b]. Since the change in conformation in all these cases[6] is not likely to require much extra energy, **3** and **4** may, like the parent system, be regarded as potential novel crown ether-like ligands for metal complexes.

Received: March 14, 1983;
revised: July 1, 1983 [Z 313 IE]
Publication delayed at authors' request
German version: *Angew. Chem. 95* (1983) 904
The complete version of this communication appears in:
*Angew. Chem. Suppl. 1983*, 1221–1227

CAS Registry number:
**1**, 77944-57-1; **2**, 87462-60-0; **3**, 87462-61-1; **4**, 87462-62-2.

[1] a) R. Schwesinger, H. Prinzbach, *Angew. Chem. 84* (1972) 990; *Angew. Chem. Int. Ed. Engl. 11* (1972) 942; b) R. Schwesinger, H. Fritz, H. Prinzbach, *Chem. Ber. 112* (1979) 3318; c) E. Vogel, H. J. Altenbach, C. D. Sommerfeld, *Angew. Chem. 84* (1972) 986; *Angew. Chem. Int. Ed. Engl. 11* (1972) 939.

[2] D. Kaufmann, H.-H. Fick, O. Schallner, W. Spielmann, L.-U. Meyer, P. Gölitz, A. de Meijere, *Chem. Ber. 116* (1983) 587.

[3] I. Erden, P. Gölitz, R. Näder, A. de Meijere, *Angew. Chem. 93* (1981) 605; *Angew. Chem. Int. Ed. Engl. 20* (1981) 583.

[5] a) K. Tori, K. Aono, K. Kitahonoki, R. Muneyuki, Y. Takano, H. Tanida, T. Tsuji, *Tetrahedron Lett. 1966*, 2921; b) T. Preuss, A. de Meijere, unpublished results; cf. T. Preuss, Dissertation, Universität Hamburg 1983.

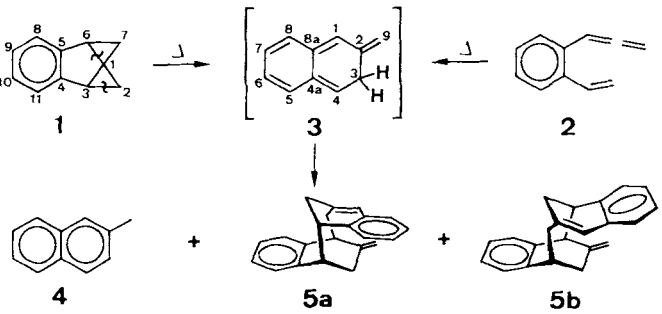
[6] We are indebted to a referee for bringing this point to our notice.

## Thermolysis and Reactions of 4,5-Benzotricyclo[4.1.0.0$^{1,3}$]hept-4-ene and *o*-(Propadienyl)styrene**

By *Udo H. Brinker**, *Gabriele Wilk*, and *Klaus Gomann*

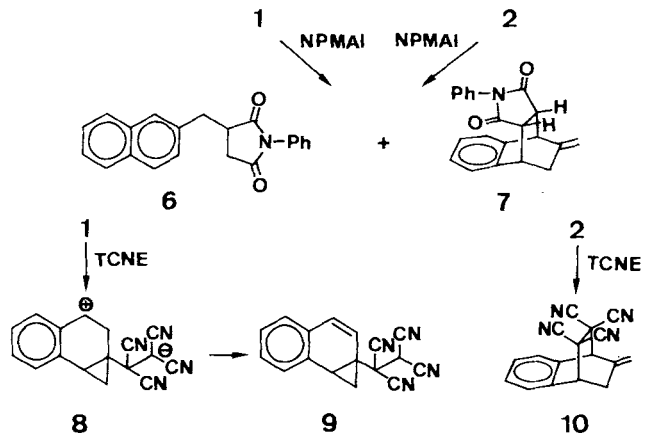
Investigations of the reaction behavior of strained[1a,b] and highly unsaturated hydrocarbons[1c] are especially suitable for revealing relationships between structure and reactivity[1d]. 4,5-Benzotricyclo[4.1.0.0$^{1,3}$]hept-4-ene **1**[2] and *o*-(propadienyl)styrene **2**[2] are thermolabile $C_{11}H_{10}$ compounds. **1** and **2** rearrange quantitatively at a measurable rate even at 30°C. In each case the product mixture consists of more than 90% of six dimers together with small amounts of 2-methylnaphthalene **4**. The position of the two halves of the molecule in both major dimers **5a** and **5b** was determined by NOE difference $^1$H-NMR experiments. Both **4** as well as **5a**, **b** are formed *via* the intermediate **3**, which contains an *o*-quinodimethane moiety. **4** can be formed from **3** by a catalytically induced 1,3-H shift. The formation of the dimers **5a** and **5b** can be regarded as $[4\pi+6\pi]$- and $[4\pi+10\pi]$-cycloadditions, respectively, of two molecules of **3**. Consistent with the Woodward-Hoffmann rules[4a], **5a** and **5b** are present as *exo*-adducts. They are each formed in about the same ratio irrespective of whether **3** results from the rearrangement of **1** (41 and 42%) or **2** (39 and 44%).

The thermolyses of **1** and **2** were monitored by measurement of the decrease in intensity of characteristic $^1$H-NMR signals compared to an internal standard[5a]. The decrease




| | **1**→**3** (46°C) | **3**←**2** (46°C) |
|---|---|---|
| log*A* | 13.97 ± 0.22[5b] $s^{-1}$ | 9.55 ± 0.36[5b] $s^{-1}$ |
| $E_a$ | 26.46 ± 0.31 kcal $mol^{-1}$ | 19.70 ± 0.56 kcal $mol^{-1}$ |
| $\Delta H^+$ | 25.82 ± 0.31 kcal $mol^{-1}$ | 19.06 ± 0.56 kcal $mol^{-1}$ |
| $\Delta S^+$ | 3.3 ± 1.0 cal $mol^{-1}$ $K^{-1}$ | −17.0 ± 1.80 cal $mol^{-1}$ $K^{-1}$ |

in concentration of **1** and **2** obeys the rate law for irreversible first-order reactions. The temperature-dependence of the reaction rates measured for **1** and **2**, respectively, between 30.25 and 60.95°C, and 30.25 and 61.4°C, at seven and six temperatures, respectively, can be described in terms of Arrhenius parameters. That the formation of the intermediate **3** in the reactions of **1** and **2** is the rate-determining step is shown by the reactions with different concentrations (1.2 and 4 M) of *N*-phenylmaleic acid imide (NPMAI) at 52.2°C. In each case the reaction rates are consistent with those of the reactions without NPMAI. The Diels-Alder adduct **7**, formed by addition of NPMAI to C-1 and C-4 of **3**, has the *endo*-conformation[4]. The ene reaction to give **6** competes with the formation of **7** (**7**:**6** = *ca.* 2:1 from **1** or **2**).




The allene **2** undergoes the diene synthesis with the more reactive dienophile tetracyanoethylene (TCNE) in THF at 60°C to give **10**. An ene adduct[6] corresponding to **10** could not be detected by $^1$H-NMR spectroscopy.

The reaction of the tricycle **1** with TCNE in THF proceeds completely differently. Spontaneous reaction ($t_{1/2}$ < 15 min) with formation of **9** takes place even at room temperature. Apparently, even before rearrangement to **3** can take place (**1**: $t_{1/2}$(25°C) ≈ 51 h), TCNE attacks the central C-atom in the strained spiropentane moiety. The zwitterion **8** is stabilized by transfer of a H-atom to give **9**.

The values of the activation parameters of the rearrangement of **2** would suggest a concerted electrocyclization to

[*] Priv.-Doz. Dr. U. H. Brinker, G. Wilk, K. Gomann
Abteilung für Chemie der Universität
Universitätsstrasse 150, D-4630 Bochum 1 (Germany)

[**] This work was supported by the Deutsche Forschungsgemeinschaft, the Fonds der Chemischen Industrie, and Degussa (gifts of chemicals). We thank Dr. *R. Siegfried* for help in solving the HPLC separation problems, Priv.-Doz. Dr. *H. Duddeck* and *M. Kaiser* for carrying out the NOE-difference $^1$H-NMR measurements, and Prof. Dr. *D. Hasselmann* for valuable discussions.

3. On the other hand, the rearrangement of the tricycle **1** could take place *via* retro-Diels-Alder reaction or *via* diradicals as intermediates. The conversion into **3** might be initiated by rupture of the C2–C3 and/or C1–C6 bonds.

Hydrogenation (Pt/C, pentane) of **1** affords 4- and 5-methyl-2,3-benzobicyclo[3.1.0]hex-2-ene in 55 and 25% yield, respectively, whereby the C1–C2 and C2–C3 bonds of one three-membered ring of the spiropentane moiety are broken.

Received: June 6, 1983;
revised: September 14, 1983 [Z 410 IE]
German version: *Angew. Chem. 95* (1983) 892
The complete version of this communication appears in:
*Angew. Chem. Suppl. 1983*, 1228–1240

CAS Registry numbers:
**1**, 74410-87-0; **2**, 74410-89-2; **4**, 91-57-6; **5a**, 87482-58-4; **5b**, 87482-59-5; **6**, 87482-60-8; **7**, 87482-61-9; **9**, 87482-62-0; **10**, 87482-63-1; NPMAI, 83-25-0; TCNE, 670-54-2.

[1] a) A. Greenberg, J. F. Liebman: *Strained Organic Molecules*, Academic Press, New York 1978; b) A. de Meijere, *Angew. Chem.* **91** (1979) 867; *Angew. Chem. Int. Ed. Engl. 18* (1979) 809; c) S. R. Landor, H. Hopf, T. L. Jacobs in S. R. Landor: *The Chemistry of Allenes*, Vol. 2, Academic Press, New York 1982; d) J. J. Gajewski: *Hydrocarbon Thermal Isomerizations*, Academic Press, New York 1981.

[2] U. H. Brinker, J. Streu, *Angew. Chem. 91* (1980) 641; *Angew. Chem. Int. Ed. Engl. 19* (1980) 631.

[4] a) R. B. Woodward, R. Hoffmann: *The Conservation of Orbital Symmetry*, Verlag Chemie, Weinheim 1970; b) I. Fleming: *Frontier Orbitals and Organic Chemical Reactions*, Wiley, London 1976.

[5] a) Thermolyses in sealed NMR tubes in a thermostat (±0.05°C), recording of the $^1$H-NMR spectra at *ca.* 0°C; b) standard deviations according to the least squares method.

[6] 5-Methylene-1,3-cyclohexadiene, a structural subunit in **3**, undergoes the ene reaction with TCNE at RT: D. Hasselmann, K. Loosen, *Angew. Chem. 90* (1978) 641; *Angew. Chem. Int. Ed. Engl. 17* (1978) 606.

## Tricyclo[4.1.0.0$^{1,3}$]hept-4-enes as Intermediates**

By *Udo H. Brinker**, *Klaus Gomann*, and *Ruth Zorn*

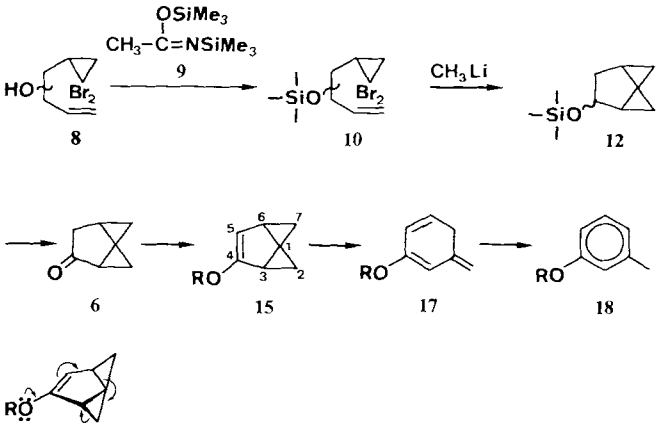
Of the isomers of toluene, tricyclo[4.1.0.0$^{1,3}$]hept-4-ene **1** claims special interest. The possible interaction between the spiropentane moiety and the double bond should be reflected, *inter alia*, in the thermal behavior of **1**. The reputedly more stable benzo-annelated analogue **2** rearranges irreversibly, even at 30°C[1].



1 2 3 4

**1** has been discussed as intermediate in the reaction of *cis*-(1,3-butadienyl)cyclopropylidene **3** to 5-methylene-1,3-cyclohexadiene **4**[2]. **1** could be formed by intramolecular addition to the terminal double bond in **3** and then be converted in a retro-Diels-Alder reaction or *via* diradicals as intermediates into **4**[2b]. Labeling experiments are not only consistent with this possibility, however, but also with a reaction *via* intermediary *cis*-1,2,4,6-heptatetraene[2b]. **4** aromatizes in a base-catalyzed reaction to toluene.

An alternative entry to **1** could be provided by the ketone **6** as educt, which already has the [4.1.0.0$^{1,3}$]-moiety



a: R = H; b: R = Li; c: R = SiMe$_3$

available. **6** can be prepared in a four-step reaction from 1,5-hexadien-3-ol. The mixture of the isomeric alcohols **8** has been obtained (yield 30%) by addition of dibromocarbene and has then been converted with *N*-(trimethylsilyl)acetamide acid trimethylsilyl ester **9** into the silyl ethers **10** (yield 86%). Reaction of **10** with methyllithium (−80 to −100°C) afforded a mixture of silyl ethers in 63% yield, 13% being the tricyclic silyl ether **12**. Also at the temperatures employed the cyclopropylidene(carbenoid)-allene rearrangement [8] to the allenyl silyl ethers dominated over the competing intramolecular addition to give **12**[8]. Cleavage of ether and oxidation to **6** were accomplished in one step with pyridinium chlorochromate (yield 64%). The low thermal stability of **6** [$t_{1/2}$(40°C in $CCl_4$) *ca.* 11 h] necessitates the conversion **6** → **1** being carried out below 25°C. Following the method of *Ireland et al.*[14a], **6** was allowed to react at −78°C with lithium diisopropylamide and then converted with chlorodiethyl phosphate into the phosphate; this (and/or an already rearranged product) was then reduced with lithium in ammonia. Apart from toluene, 1-methyl-1,4-cyclohexadiene, the product of a Birch reduction, was isolated. In which sequence substitution, rearrangement, reduction and aromatization take place remains open. Addition of water at −20°C to the enolate **15b**, or to the already rearranged **17b**, furnished *m*-cresol **18a**. By reaction of **6** with triethylamine at 0°C and addition of trifluoromethanesulfonic acid trimethylsilyl ether it was possible to detect the already rearranged silyl ether **17c** by $^1$H-NMR spectroscopy; concomitantly, the decrease in the amount of **17c** with time at the expense of the formation of **18c** by aromatization could be monitored. The formation of **18a** and **18c** is consistent with a retro-Diels-Alder reaction[19] of **15a** and **15c**, respectively, or with their decomposition *via* diradicals as intermediates with rupture of the C2–C3 and/or C1–C6 bonds. *p*-Cresol or *p*-cresol-trimethylsilyl ethers could not be detected. These compounds should be formed by rupture of the C1–C3 and/or C6–C7 bonds in **15a** or **15c** and subsequent aromatization.

The sole formation of **18a** and **18c**, respectively, can be due to interaction between the C2–C3 bond and the OR function. Likewise, **15** could rearrange in a retro-Diels-Alder reaction exclusively to the thermodynamically more stable **17**, from which **18** is formed.

Received: June 6, 1983; revised: September 14, 1983 [Z 411 IE]
German version: *Angew. Chem. 95* (1983) 893
The complete version of this communication appears in:
*Angew. Chem. Suppl. 1983*, 1241–1255

[*] Priv.-Doz. Dr. U. H. Brinker, K. Gomann, R. Zorn
Abteilung für Chemie der Universität
Universitätsstr. 150, D-4630 Bochum 1 (Germany)

[**] Carbene Rearrangements, Part 15. This work was supported by the Deutsche Forschungsgemeinschaft and the Fonds der Chemischen Industrie. We thank Dr. *F. Scheidt* for help in solving GC problems. – Part 14: [2b].

CAS Registry numbers:
**6**, 87462-29-1; **8** (isomer 1), 87462-24-6; **8** (isomer 2), 87462-25-7; **9**, 10416-59-8; **10** (isomer 1), 87462-26-8; **10** (isomer 2), 87462-27-9; **12** (isomer 1), 87462-28-0; **12** (isomer 2), 87507-92-4; **18c**, 17902-31-7; TFTMSE 27607-77-8; 1,5-hexadien-3-ol, 924-41-4; dibromocarbene, 4371-77-1; *m*-Cresol, 108-39-4; chlorodiethyl phosphate, 814-49-3.


[1] U. H. Brinker, G. Wilk, K. Gomann, *Angew. Chem. 95* (1983) 892; *Angew. Chem. Int. Ed. Engl. 22* (1983) 868; *Angew. Chem. Suppl. 1983*, 1228–1240.

[2] a) U. H. Brinker, I. Fleischhauer, *Angew. Chem. 91* (1979) 424; *Angew. Chem. Int. Ed. Engl. 18* (1979) 396; b) I. Fleischhauer, U. H. Brinker, *Tetrahedron Lett. 24* (1983) 3205.

[8] a) W. Kirmse: *Carbene Chemistry*, 2nd edit., Academic Press, New York 1971; b) W. M. Jones, U. H. Brinker in A. P. Marchand, R. E. Lehr: *Pericyclic Reactions*, Vol. I, Academic Press, New York 1977.

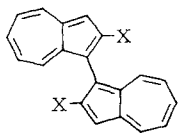
[14] a) R. E. Ireland, G. Pfister, *Tetrahedron Lett. 1969*, 2145.

[19] J. Sauer, R. Sustmann, *Angew. Chem. 92* (1980) 773; *Angew. Chem. Int. Ed. Engl. 19* (1980) 779.


## Resolution, Circular Dichroism, and Absolute Configuration of 1,1'-Biazulenes**


By *Akio Tajiri**, *Masahiko Fukuda*, *Masahiro Hatano*, *Tadayoshi Morita*, and *Kahei Takase*


*rac*-2,2'-Dimethyl-1,1-biazulene *rac*-**1a**[4] has been resolved directly with the aid of HPLC using a commercially available (+)-polytriphenyl-methyl methacrylate column[5] (RT, hexane/2-propanol 80:20). The fraction of **1a** that



**1** : X = H
**1a**: X = $CH_3$
**1b**: X = $OCH_3$

elutes first is levorotatory and exhibits a distinct negative CD couplet in the region 30000–40000 $cm^{-1}$ (Fig. 2), whereas the second fraction, which is dextrorotatory, gives a mirror image of the CD spectrum. Accordingly, *rac*-**1a** is considered to be completely resolved.

A given excited electronic state of azulene (Fig. 3a) gives rise in *rac*-1,1'-biazulene **1** to two electronic states A and B of point group symmetry $C_2$, of which the B state is energetically more stable (Fig. 3b). Both the A←A and B←A transitions of *rac*-**1** originate from an excitation of azulene in which the long axis polarization has a particular value of the dipole strength[6] and a non-zero rotational strength for all values of the dihedral angle $\alpha$ between the planes of the azulene groups except 0 and 180°. Provided the absolute configuration is *R* (see Fig. 3c), a chirality consideration[9] leads to the negative CD band associated with the B←A transition and to the positive band associated with the A←A transition (Fig. 3d). A similar consideration reverses the sign of CD bands for *S*-configuration; however, the B state is lower in energy than the A state.


[*] Dr. A. Tajiri, M. Fukuda, Prof. M. Hatano
Chemical Research Institute of Non-aqueous Solutions
Tohoku University, Sendai 980 (Japan)
Dr. T. Morita, Prof. K. Takase
Department of Chemistry, Faculty of Science
Tohoku University, Sendai 980 (Japan)



[**] This work was partly supported by a Grant-in-Aid for Scientific Research from the Ministry of Education, Science and Culture of Japan, and by a grant from the Nissan Science Foundation (*M. H.*).

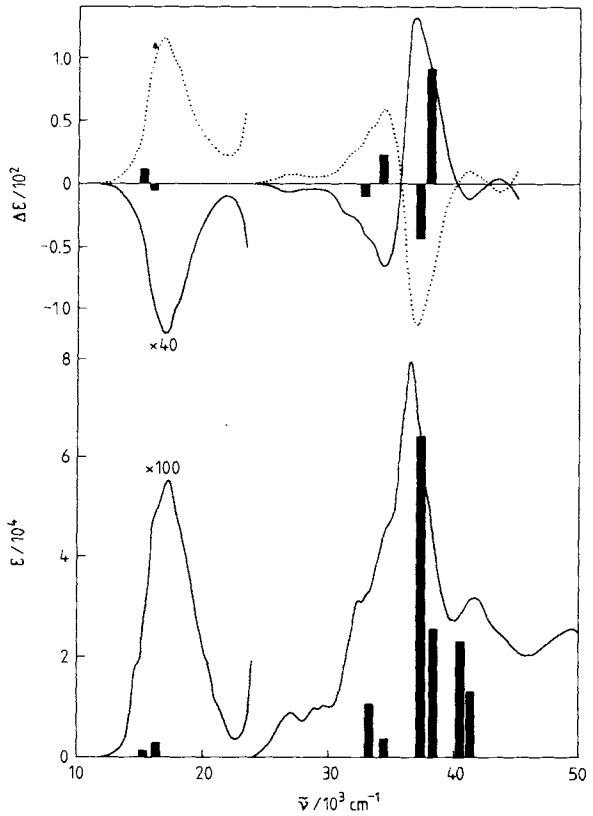




Fig. 2. Experimental (curves) and calculated (columns) absorption spectra (bottom) and CD spectra (top) of **1a** at room temperature (—— first fraction, ····· second fraction).

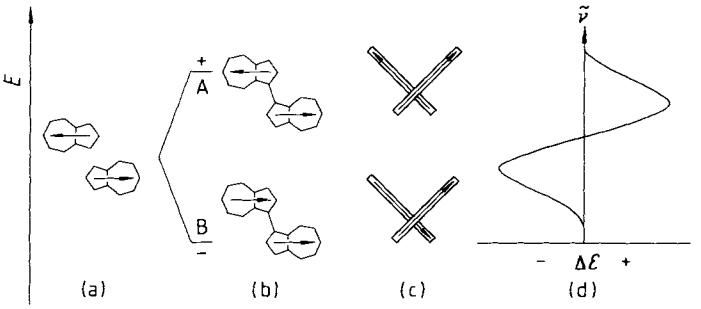



Fig. 3. The exciton chirality rule for (*R*)-1,1'-biazulene, (*R*)-**1**.

This was further confirmed by CNDO/S calculations assuming *R*-configuration and a dihedral angle of 130°, determined from the minimum of the potential energy curve calculated for **1** by the CNDO/2 method. The B←A transition predicted at 37300 $cm^{-1}$ is calculated to exhibit negative circular dichroism and is assigned to the observed negative CD band at 34400 $cm^{-1}$; the A←A transition at 37900 $cm^{-1}$ is predicted to show positive CD and is assigned to the observed positive CD band at 37200 $cm^{-1}$. We therefore conclude that the first fraction of *rac*-**1a** corresponds to 1,1'-biazulene with absolute configuration *R*(−) and that the second fraction is *S*(+).

In contrast to the remarkable stability of (*R*)- and (*S*)-**1a** in solution, the CD spectra of (*R*)- and (*S*)-2,2'-dimethoxy-1,1'-biazulene **1b** indicate that they are configurationally unstable and racemize rapidly at room temperature. From an Arrhenius plot, the energy of activation ($E_a$) and rate of

racemization ($k$) are determined to be *ca.* 71 kJ/mol and *ca.* $3.8 \times 10^{-3}$ $s^{-1}$ (39°C), respectively. The energy of racemization for (*R*)- and (*S*)-**1b** is comparable to those found for 1,1'-binaphthyl derivatives[12]. The steric hindrance caused by two substituents should be smaller in **1b** than in **1a**, since in **1b** the two methyl groups are further apart due to the presence of the oxygen atoms between the azulene skeleton and the two methyl groups.

Received: July 5, 1983;
revised: August 30, 1983 [Z 452 IE]
German version: *Angew. Chem. 95* (1983) 911
The complete manuscript of this communication appears in:
*Angew. Chem. Suppl. 1983*, 1283-1290

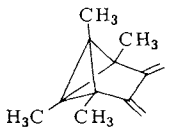
CAS Registry numbers:
(+)-**1**, 87507-85-5; (+)-**1a**, 87461-60-7; (*R*)-**1a**, 87507-86-6; (*S*)-**1a**, 87507-87-7; (+)-**1b**, 87461-61-8; (*R*)-**1b**, 87507-88-8; (*S*)-**1b**, 87507-89-9.

[4] T. Morita, K. Takase, *Bull. Chem. Soc. Jpn. 55* (1982) 1144.
[5] H. Yuki, Y. Okamoto, I. Okamoto, *J. Am. Chem. Soc. 102* (1980) 6356; M. Nakazaki, K. Yamamoto, M. Maeda, *J. Org. Chem. 46* (1981) 1985; Y. Okamoto, I. Okamoto, H. Yuki, *Chem. Lett. 1981*, 835; Y. Okamoto, S. Honda, I. Okamoto, H. Yuki, S. Murata, R. Noyori, H. Takaya, *J. Am. Chem. Soc. 103* (1981) 6971; Daicel Chemical Industries Ltd., Himeji 671-12 (Japan) are thanked for a gift of the column.
[6] R. Hagen, E. Heilbronner, P. A. Straub, *Helv. Chim. Acta 51* (1968) 45.
[9] N. Harada, K. Nakanishi: *Circular Dichroism Spectroscopy—Exciton Coupling in Organic Stereochemistry*, University Science Books, Mill Valley, CA 1983.
[12] A. S. Cooke, M. M. Harris, *J. Org. Chem. C 1967*, 988.

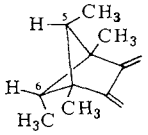
## 3,4-Bismethylenetricyclo[3.1.0.0$^{2,6}$]hexane—Synthesis and Diels-Alder Addition to Tetracyanoethylene**

By *Franz Lanzendörfer* and *Manfred Christl**

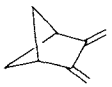
Addition of tetracyanoethylene (TCNE) to diene **1** proceeds $30.5 \times 10^6$ times as fast as that of TCNE to **2**[1]. *Hogeveen et al.*[1] suggested that this dramatic difference arises from orbital interactions between the strained σ-systems and the unsaturated bridges in **1** and **2** as well as in their TCNE adducts.



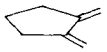
**1**



**2**



**3**

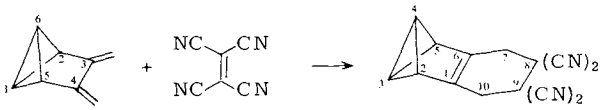


**4**

Recently, *Schwager* and *Vogel*[2] proposed an alternative explanation; they suggested that the *syn*-oriented methyl groups at C-5 and C-6 in **2** sterically hinder addition of TCNE since the rate of reaction of the methyl-group free hydrocarbon **3** is 850-fold that of **2** (Table 1). Even in **3** the cyclobutane ring retards the reaction for steric reasons, since the quasi-planar **4**, which has nearly the same HOMO energy, adds TCNE 1400 times as fast as **3**[3] (Table 1).

[*] Prof. Dr. M. Christl, F. Lanzendörfer
Institut für Organische Chemie der Universität Würzburg
Am Hubland, D-8700 Würzburg (Germany)

[**] This work was supported by the Fonds der Chemischen Industrie and by the Deutsche Forschungsgemeinschaft.



**5** **6**

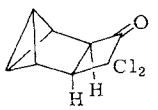
Table 1. HOMO energies (1st ionization potentials) of dienes **1**—**5** and relative rate constants for addition of **1**—**5** to TCNE.

| Diene | HOMO [eV] | Ref. | $k_2$ (rel., 20°C) | Ref. |
|---|---|---|---|---|
| **1** | 7.82 | [1] | 30500000 | [1] |
| **4** | 8.54 | [3] | 1190000 | [3] |
| **5** | 8.27 | [4] | 250000 | — |
| **3** | 8.50 | [4] | 850 | [2] |
| **2** | 8.22 | [1] | 1 | [1] |

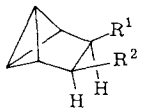
We have now synthesized the title compound **5** and studied its reaction with TCNE in benzene to afford **6** (70% isolated yield, m.p. = 164—166°C). Based on the second-order rate constants ($k_2 = 0.57$ and 0.25 $L \cdot mol^{-1} \cdot s^{-1}$ at 22 and 9°C, respectively), the relative reactivity of **5** is only 1/120th of that of the tetramethyl derivative **1** (Table 1). The four methyl groups of **1**, therefore, accelerate the addition of TCNE—probably by raising the energy of the HOMO (Table 1). A similar orbital effect may also operate on proceeding from **3** to **2**; however, the corresponding increase in reaction rate is more than compensated for by the steric hindrance of the *syn*-orientated methyl groups at C-5 and C-6 of **2**.

The factor of *ca.* 300 between the addition constants of **3** and **5** should also apply to **1** and **2** as an intrinsic effect of the systems; the five orders of magnitude difference between their addition constants are attributable to the influence of the methyl groups. However, the differences between the HOMO energies (0.23 eV) and steric demands of **3** and **5** are sufficient to account for this intrinsic effect of the systems, which makes a discussion of orbital effects in the products[1] unnecessary.

We synthesized **5** from the dichloroketene adduct **7**[5] of benzvalene, which was allowed to react with sodium methoxide to afford the ester **8** (70% yield). This was subsequently allowed to react with triphenyltin hydride to give the monochloro compound **9** (92%), which was reduced by $LiAlH_4$ to yield the (chloromethyl)(hydroxymethyl) derivative **10** (93%). After conversion into the mesylate **11** (94%), double elimination with potassium *tert*-butoxide in dimethyl sulfoxide led to **5** (28% after preparative GC).



**7**



**8**, $R^1 = CO_2CH_3$, $R^2 = CHCl_2$
**9**, $R^1 = CO_2CH_3$, $R^2 = CH_2Cl$
**10**, $R^1 = CH_2OH$, $R^2 = CH_2Cl$
**11**, $R^1 = CH_2O{-}SO_2{-}CH_3$, $R^2 = CH_2Cl$

Both analytical and spectroscopic data are consistent with the structures proposed for the novel compounds. Of note are the NMR spectra of **5** and **6**[6]: Whereas the chemical shifts of **5** deviate only slightly from the values expected for a normal bicyclo[1.1.0]butane system, **6** displays the anomalies exhibited by benzvalene[7] with the central bicyclo[1.1.0]butane CH groups (C-3,4; 3,4-H) absorbing at very low field, although in **5** *and* **6** the respec-

 © *Verlag Chemie GmbH, 6940 Weinheim, 1983* *0570-0833/83/1111-0871 $ 02.50/0* 

tive σ-systems are each bridged by two $sp^2$-hybridized C atoms. The reason for this is possibly the different symmetries of the π* orbitals[7a] in the diene and monoene bridge-moieties of **5** and **6**, respectively.

Received: July 6, 1983 [Z 453 IE]
German version: *Angew. Chem. 95* (1983) 896

CAS Registry numbers:
**5**, 55678-69-8; **6**, 87495-14-5; **7**, 54220-48-3; **8**, 87495-15-6; **9**, 87495-16-7; **10**, 87495-18-9; **11**, 87495-17-8; TCNE, 670-54-2.

[1] H. Hogeveen, W. F. J. Huurdeman, D. M. Kok, *J. Am. Chem. Soc. 100* (1978) 871.
[2] L. Schwager, P. Vogel, *Helv. Chim. Acta 63* (1980) 1176.
[3] R. Sustmann, M. Böhm, J. Sauer, *Chem. Ber. 112* (1979) 883.
[4] Prof. Dr. *R. Gleiter*, Universität Heidelberg, is thanked for this data.
[5] G. E. Gream, L. R. Smith, J. Meinwald, *J. Org. Chem. 39* (1974) 3461; L. R. Smith, G. E. Gream, J. Meinwald, *ibid. 42* (1977) 927.
[6] **5**: $^1$H-NMR ($CDCl_3$): $\delta = 2.48$ (t, $J_{1,2} = 1.8$ Hz, 1,6-H), 2.72 (t, 2,5-H), 4.90 and 5.10 (each br. s, $CH_2$). $^{13}$C-NMR ($C_6D_6$): $\delta = 11.7$ (d, 219.5 Hz, C-1,6), 39.2 (d, 172.3 Hz, C-2,5), 98.8 (t, 157.9 Hz, $CH_2$), 150.1 (s, C-3,4). — **6**: $^1$H-NMR ([$D_6$]acetone): $\delta = 3.48$ (s, 7,10-H), 2.24 (t, $J_{2,3} = 3.0$ Hz, 2,5-H), 4.06 (t, 3,4-H). $^{13}$C-NMR ([$D_6$]acetone): $\delta = 32.7$ (t, 139.7 Hz, C-7,10), 38.6 (d, 168.9 Hz, C-2,5), 40.2 (s, C-8,9), 46.3 (d, 211.2 Hz, C-3,4), 112.4 (s, CN), 135.3 (s, C-1,6).
[7] a) M. Christl, R. Herbert, *Org. Magn. Reson. 12* (1979) 150; b) M. Christl, *Angew. Chem. 93* (1981) 515; *Angew. Chem. Int. Ed. Engl. 20* (1981) 529.

## $SbF^{2+}$ as a Lewis Acid in $Na(SbF)PO_4 \cdot nH_2O$ (n = 2–4) and $NH_4(SbF)PO_4 \cdot H_2O$

By *Rainer Mattes** and *Klaus Holz*

$SbF_3$ forms adducts with numerous oxygen-containing compounds, and in this respect behaves as a Lewis acid; for example, the adducts with alkali metals or ammonium sulfates and ammonium nitrates have been studied. Recently, compounds with $SbF_2^+$ groups have been described; namely, $M^I(SbF_2)SO_4$ with $M^I$ = Rb, Cs[3], $K(SbF_2)HPO_4$[4], and $(SbF_3 \cdot SbF_5)_2$[5]. The novel compounds $Na(SbF)PO_4 \cdot nH_2O$ (n = 2–4) **1** and $NH_4(SbF)PO_4 \cdot H_2O$ **2** crystallize from 0.1–0.3 M solutions of $SbF_3$ and $NH_4H_2PO_4$ and $NaH_2PO_4$, respectively, after filtration from the immediately formed precipitate. They contain the previously unknown $SbF^{2+}$ group, which is coordinatively unsaturated and is, therefore, a strong Lewis acid.

X-ray structure analysis of **1** and **2** indicated that both compounds crystallize in highly symmetrical, almost identical layer structures. The four oxygen atoms of the $PO_4^{3-}$ anions are each bonded to different $SbF^{2+}$ groups. The antimony atoms are octahedrally coordinated if the stereochemically active 5s lone-pair is viewed as a sixth ligand. The Sb–F distance in **1** is 193.4(4) and in **2** 192.3(4) pm; the Sb–O distances vary from 216 to 220 pm. Because of the large spatial requirements of the lone-pair of electrons, all F–Sb–O angles are smaller than 79°. $PO_4$ tetrahedra and :$SbFO_4$ octahedra form layers with tetragonal symmetry, cross-linked *via* the oxygen atoms. In these layers, the fluorine atoms are orientated alternatingly upwards and downwards. $VOPO_4 \cdot 2H_2O$ and $NbOPO_4 \cdot 3H_2O$ are the first two further examples of the simple structure principle realized here (Fig. 1): the alternating linkage of tetrahedra and octahedra *via* four edges to planar layers. These compounds are interesting because of their intercalation behavior[6].

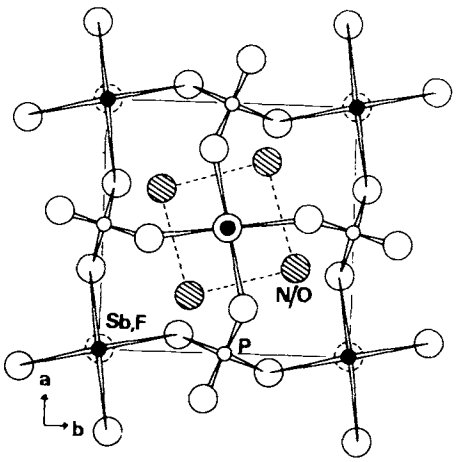



Fig. 1. Crystal structure of a layer of **2** (solid circles: Sb; F lies above or below Sb). Space group $I\bar{4}$, $a = 656.5(2)$, $c = 1439.8(5)$ pm, $Z = 4$; 646 reflections with $F > 3.92\sigma(F)$, 46 parameters, $R = 0.025$, $R_w = 0.035$. Further details on the crystal structure investigation can be obtained from the Fachinformationszentrum Energie Physik Mathematik, D-7514 Eggenstein-Leopoldshafen by quoting the depository number CSD 50609, the names of the authors, and the journal citation.

The layers in **1** and **2** are stacked differently. In **2**, the fluorine atoms and lone-pair of electrons of neighboring layers face each other in the body-centered unit cell. The distance between the layers (1/2 of the *c*-axis) is 714.9(3) pm. The $NH_4^+$ ions and the $H_2O$ molcules are located between the layers, statistically distributed over just one point position. These form circular groups $(NH_4{-}OH_2)_2^{2+}$ *via* N–H···O hydrogen bonds of 290.0(8) pm length; these groups are bonded *via* further hydrogen bonds to the oxygen atoms of the immediately over- and underlaying layers. The hydrogen-bond systems are of importance for stabilizing the overall structures: under the same reaction conditions but using $KH_2PO_4$ instead of $NH_4H_2PO_4$, the compound $K(SbF_2)HPO_4$ of different composition is formed[4].

With respect to the sequence of the layers, the structure of **1** is disordered. Reflection of an A layer in the plane perpendicular to the *b*-axis through the P-, Sb-, and F-atoms gives rise to the "enantiomeric" B layer. Layers A and B are stacked along the *c*-direction in statistical sequence with a distance of 867.9(17) pm. X-Ray structure studies indicate the space group $P2_1/m$ in which all four-fold point positions are half-occupied. The diffuse images of all the reflections in the [001] direction is also indicative of the disrupted periodicity.

The high symmetry of the compounds is also apparent in their relatively band-deficient vibrational spectra. The Raman spectrum exhibits two intense bands in the PO stretching frequency region: $\nu_s(PO_4)$ at 958 and 955 $cm^{-1}$, respectively, and $\nu_{as}(PO_4)$ at 1004 and 1008 $cm^{-1}$, respectively (for **1** and **2**, respectively); $\nu$(SbF), which is also intense, appears at 540 for **1**, but for **2** at 605 $cm^{-1}$ (here, the difference in the layer sequence is probably decisive). The $^{125}$Sb Mössbauer spectra (measured at 4 K with Ba $^{121m}SnO_3$ as source) of **1** and **2** display a broad absorption band having a shoulder at the lower velocity side of the source. The values of the isomeric shifts ($\delta = -5.76(1)$ and $-4.98(1)$ mm/s in **1** and **2**, respectively), which are smaller than in $SbF_3$[8], indicate a lower s-electron density at the antimony nucleus, *i.e.*, the s lone-pair of electrons is

[*] Prof. Dr. R. Mattes, K. Holz
Anorganisch-chemisches Institut der Universität
Corrensstrasse 36, D-4400 Münster (Germany)

more involved in bonding to the ligands than in $SbF_3$; the quadrupole coupling constants $\Delta E_Q$ of 14.4(1) and 18.0(1) mm/s, respectively, are smaller than in $SbF_3$ since the coordination polyhedron is less distorted.

Received: July 1, 1983 [Z 439 IE]
German version: *Angew. Chem. 95* (1983) 898
The complete manuscript of this communication appears in: *Angew. Chem. Suppl. 1983*, 1315-1322

CAS Registry numbers:
**1**, 87462-30-4; **2**, 87462-31-5; $SbF_3$, 7783-56-4.

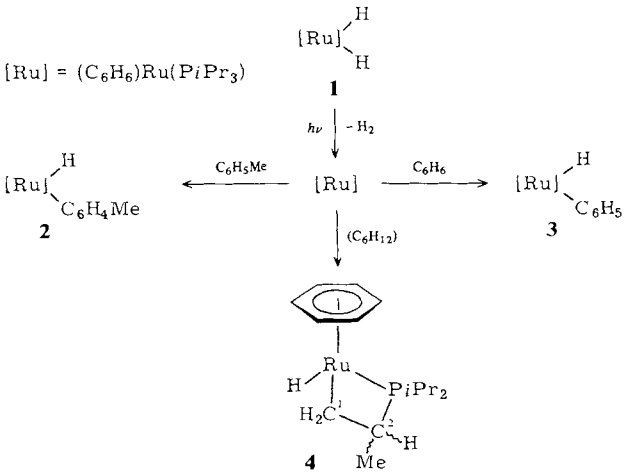
[3] R. Fourcade, M. Bourgault, B. Bonnet, B. Ducourant, *J. Solid State Chem. 43* (1982) 81.
[4] S. Hürter, R. Mattes, D. Rühl, *J. Solid State Chem. 46* (1983) 204.
[5] R. J. Gillespie, D. R. Slim, J. E. Vekris, *J. Chem. Soc. Dalton Trans. 1977*, 971.
[6] K. Beneke, G. Lagaly, *Inorg. Chem. 22* (1983) 1503; J. W. Johnson, A. J. Jacobson, *Angew. Chem. 95* (1983) 422; *Angew. Chem. Int. Ed. Engl. 22* (1983) 412.
[8] T. Birchall, B. Ducourant, R. Fourcade, G. Mascherpa, *J. Chem. Soc. Dalton Trans. 1982*, 2313.

## Aryl(hydrido)ruthenium Complexes by C–H Addition: Isolation of a Four-Membered Metallacycle as Intermediate**

By *Heidrun Kletzin* and *Helmut Werner**

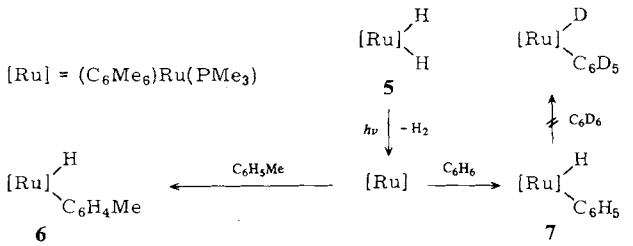
The problems surrounding the activation of C–H bonds by transition metals are currently attracting a great deal of interest[1a]. *Chatt* and *Davidson* first showed in 1965 that a coordinatively unsaturated metal complex of the type $RuL_4$ ($L_2 = C_2H_4(PMe_2)_2$) reacts with an aromatic hydrocarbon ($C_{10}H_8$) to give an aryl(hydrido)metal compound[1b]. Later, *Green et al.* found that the complex $W(C_5H_5)_2$ formed on thermolysis or photolysis of $(C_5H_5)_2WH_2$ behaves similarly, and in the presence of arenes forms compounds of the type $(C_5H_5)_2WH(R)$[1c]. It has recently been demonstrated that saturated, unsubstituted hydrocarbons (cyclohexane, neopentane) are also able to add oxidatively to 16-electron fragments such as $(C_5Me_5)Ir(PMe_3)$[2a] or $(C_5Me_5)Ir(CO)$[2b], which are formed on photolysis of $(C_5Me_5)IrH_2(PMe_3)$ and $(C_5Me_5)Ir(CO)_2$, respectively.

We have now found that the complexes $(C_6H_6)RuH_2(PiPr_3)$ **1**[3a] and $(C_6Me_6)RuH_2(PMe_3)$ **5**[3b], structurally related with $(C_5Me_5)IrH_2(PMe_3)$, also form aryl(hydrido)metal compounds on photolysis in arenes[4]. In cyclohexane, with **1** as educt, however, no reaction with the solvent is observed, but an intramolecular oxidative addition of a methyl C–H bond of the triisopropylphosphane ligand to the metal (Schemes 1 and 2). The irradiation time (Philips HPK 125 W) for formation of **2** or **3** is 2 h, of **4** 3 h, and of **6** or **7** 5 h at room temperature. Presumably in the photolysis of **1** or **5** the corresponding coordinatively unsaturated fragment $(C_6R_6)Ru(PR'_3)$([Ru]) is formed initially and then reacts with the arene or (in $C_6H_{12}$) with a C–H bond of the phosphane. The solvent



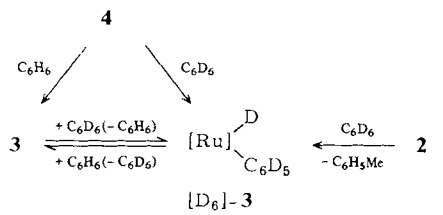

Scheme 1.

does not participate in the formation of **4** since the complex (with Ru–H bonding) is also formed in $C_6D_{12}$.




Scheme 2.

The metallaheterocycle **4** reacts with benzene at room temperature in *ca.* 5 min to give the hydrido(phenyl)-complex **3** and with $C_6D_6$, analogously, to give [$D_6$]-**3**. The 16-electron fragment $(C_6H_6)Ru(PiPr_3)$ ([Ru]) is presumably once again formed as intermediate. **3** and [$D_6$]-**3** are interconvertible at room temperature. These reactions are essentially slower than those of **4** with $C_6H_6$ or $C_6D_6$; completion of reaction is reached only after *ca.* 24 h. A Ru($\eta^2$-$C_6H_6$)- or Ru($\eta^2$-$C_6D_6$)-intermediate could be formed during conversion of **3** into [$D_6$]-**3** and *vice versa*, as has recently been assumed for similar rhodium compounds[5a]. The hydrido(tolyl)-complex **2** reacts with $C_6D_6$ at 40 °C in 6 h to give [$D_6$]-**3**; the identity of **2** is confirmed by independent synthesis from $(C_6H_6)Ru(C_6H_4Me)(PiPr_3)Br$ and $NaBH_4$ in ethanol.




That the postulated intermediate [Ru] in the reactions of **1** and **5** (Schemes 1 and 2), in contrast to $(C_5Me_5)Ir(PMe_3)$[2a] and $(C_5Me_5)Ir(CO)$[2b], does not react with cyclohexane to give a cyclohexyl(hydrido)-complex under the chosen conditions is presumably due to a greater lability of the RuH(R) group with respect to reductive

[*] Prof. Dr. H. Werner, H. Kletzin
Institut für Anorganische Chemie der Universität
Am Hubland, D-8700 Würzburg (Germany)

[**] Delivered in a lecture at the XIIth Sheffield-Leeds International Symposium on Organometallic, Inorganic and Catalytic Chemistry in Sheffield (England) on March 28, 1983. This work was supported by the Deutsche Forschungsgemeinschaft, the Fonds der Chemischen Industrie, and by gifts of chemicals from BASF AG, Ludwigshafen and DEGUSSA AG, Hanau. We thank Dr. *G. Lange* and Dr. *D. Scheutzow* for recording the mass spectra and 400 MHz NMR spectra.

elimination rather than to a lower reactivity of [Ru] towards an $sp^3$-C–H bond. 5d-Metals (such as, *e.g.*, iridium) form more stable M–H and M–C bonds than 4d-metals (such as, *e.g.*, ruthenium), another finding consistent with the results published recently by *Jones* and *Feher*[5b]. We assume that a higher charge density at the central atom caused by the ligand in addition to the greater number of electrons of the metal effects stabilization of the M–H and M–C bonds. This hypothesis is supported by the fact that the complex **7** (with the better donor $C_6Me_6$ compared to $C_6H_6$), unlike **3**, does not react with $C_6D_6$ to give $(C_6Me_6)RuD(C_6D_5)(PMe_3)$ even on prolonged heating at 50 °C.

Received: July 13, 1983 [Z 465 IE]
German version: *Angew. Chem.* 95 (1983) 916

CAS Registry numbers:
**1**, 85413-08-7; **2**, 87556-34-1; **3**, 87556-30-9; 4 (isomer 1), 87556-31-8; **4** (isomer 2), 87585-20-4; **5**, 82498-40-6; **6**, 87556-32-9; **7**, 87556-33-0.

[1] a) G. W. Parshall: *Homogeneous Catalysis*, Wiley-Interscience, New York 1980; b) J. Chatt, J. M. Davidson, *J. Chem. Soc. 1965*, 843; c) M. L. H. Green, P. J. Knowles, *J. Chem. Soc. Chem. Commun. 1970*, 1677; M. L. H. Green, G. Gianotti, *ibid. 1972*, 1114; M. Berry, K. Elmitt, M. L. H. Green, *J. Chem. Soc. Dalton Trans. 1979*, 1950.

[2] a) A. H. Janowicz, R. G. Bergman, *J. Am. Chem. Soc. 104* (1982) 352; *105* (1983) 3929; b) J. K. Hoyano, W. A. G. Graham, *ibid. 104* (1982) 3723.

[3] a) H. Werner, H. Kletzin, *J. Organomet. Chem. 243* (1983) C59; b) *ibid. 228* (1982) 289.

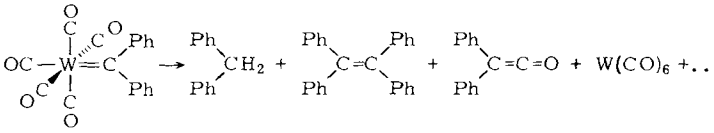
[4] All the compounds gave correct elemental analyses. NMR in $C_6D_6$ (4 in $C_6D_{12}$) at room temperature. **2**: yellow oil; $^1$H-NMR: $\delta(C_6H_4)=7.56$ (m), 6.78 (m), $\delta(C_6H_6)=5.00$ (m), $\delta(C_6H_4CH_3)=2.33$ (s), $\delta(PCHCH_3)=1.80$ (m), $\delta(PCHCH_3)=1.00$ and 0.97 (dd, $J_{PH}=12.8$, $J_{HH}=6.8$ Hz), $\delta(RuH)=-9.06$ (d, $J_{PH}=50.0$ Hz); $^{31}$P-NMR: $\delta=70.18$ (s). **3**: yellow oil; $^1$H-NMR: $\delta(C_6H_5)=7.81$ (m), 6.94 (m), $\delta(C_6H_6)=5.00$ (m), $\delta(PCHCH_3)=1.80$ (m), $\delta(PCHCH_3)=1.00$ and 0.96 (dd, $J_{PH}=12.2$, $J_{HH}=6.4$ Hz), $\delta(RuH)=-9.00$ (d, $J_{PH}=50.0$ Hz); $^{31}$P-NMR: $\delta=69.77$ (s). **4**: yellow oil (obtained as 70:30-mixture of two diastereomers); $^1$H-NMR: $\delta(C_6H_6)=4.98$ (m), $\delta(PCHCH_3)=1.69$ (m), $\delta(PCHCH_3)=1.15$ (m), $\delta(RuH)=-8.16$ and $-8.63$ (dd, $J_{PH}=43.0$, $J_{HH}=3.2$ Hz), signals of $C^1H_2$, $C^2H$ and $C^2CH_3$ masked by $PiPr_2$ signals; $^{13}$C-NMR (400 MHz, 10 °C): $\delta(C_6H_6)=82.88$ (s), 82.64 (s), $\delta(C^1)=-10.74$ (d, $J_{PC}=45.9$ Hz), $-7.16$ (d, $J_{PC}=42.3$ Hz), $\delta(C^2)=42.80$ (d, $J_{PC}=35.9$ Hz), 44.85 (d, $J_{PC}=32.6$ Hz). **6**: bright yellow crystals, decomp. > 78 °C; $^1$H-NMR: $\delta(C_6H_4)=6.95$ (m), $\delta(C_6H_4CH_3)=2.33$ (s), $\delta(C_6Me_6)=1.93$ (m), $\delta(PMe_3)=0.95$ (d, $J_{PH}=8.5$ Hz), $\delta(RuH)=-10.80$ (d, $J_{PH}=58.0$ Hz); $^{31}$P-NMR: $\delta=6.41$ (s). **7**: bright yellow crystals, decomp. > 52 °C; $^1$H-NMR: $\delta(C_6H_5)=7.33$ (m), $\delta(C_6Me_6)=1.93$ (m), $\delta(PMe_3)=0.95$ (d, $J_{PH}=8.5$ Hz), $\delta(RuH)=-10.80$ (d, $J_{PH}=58.0$ Hz); $^{31}$P-NMR: $\delta=6.58$ (s).

[5] a) W. D. Jones, F. J. Feher, *J. Am. Chem. Soc. 104* (1982) 4240; b) *Organometallics 2* (1983) 562.

## Intramolecular Carbene-Carbon Monoxide Coupling in Chromium and Tungsten Complexes**

By *Helmut Fischer**

Transition-metal induced CC bond-forming reactions between CO and $CR_2$ as well as between two $CR_2$ moieties have recently been proposed as possible steps in the Fischer-Tropsch synthesis. Bond formation between two $CR_2$ ligands giving the dimer is a reaction characteristic of the decomposition of carbene complexes: thermolysis of pentacarbonyl(diphenylcarbene)tungsten **1** in refluxing heptane gives diphenylmethane **2** (10%) and tetraphenylethylene **3** (35%)[1]. Among the organic products formed in the mild thermolysis (20 to 50 °C) of dilute solutions of **1** $5\times10^{-2}$ to $10^{-3}$ mol/L) in polar or nonpolar solvents (methylcyclohexane, toluene, dibutyl ether, 1,1,2-trichloroethane), in addition to **2** and **3** the product of CO-carbene coupling, diphenylketene **4** was detected in 20 to 70% yield.



**1** **2** **3** **4**

Diphenylketene was identified by comparison of its spectra and its gas chromatogram with those of an authentic sample. At 50 °C the half-life of **1** upon thermolysis in 1,1,2-trichloroethane is *ca.* 1400 s ($[\mathbf{1}]_0=0.008$ mol/L). With increasing concentration of the complex the reaction rate increases slightly, whereas the yield of **4** decreases. The thermolysis proceeds significantly slower in nonpolar solvents than in polar. The reaction rate is reduced by the presence of free CO in the solvent, particularly with nonpolar solvents. The chromium compound analogous to **1** reacts at least 50 times faster or under even milder conditions (half-life at 32 °C, *ca.* 150 s). **4** is also formed from the chromium complex by warming the solid substance *in vacuo* (32 °C, *ca.* 15 min). If the thermolysis of **1** under $^{13}$CO is interrupted after *ca.* 25% conversion and the resultant **4** subsequently converted by treatment with methanol into methyl diphenylacetate, mass spectroscopic analysis of this ester indicates that $^{13}$CO is *not* incorporated into **4**. The CO group in the diphenylketene therefore originates from the coordination sphere of the metal. Hexacarbonyltungsten, which is formed simultaneously, consists of a mixture of $(^{12}CO)_{6-n}(^{13}CO)_nW$ (n = 0 to 4).

These results together with the results of kinetic studies and the determination of the yield of **4** as a function of the concentration of complex indicate that bond formation between a CO and the $CPh_2$ ligand to give diphenylketene proceeds *intramolecularly* in a $(CO)_4W(CPh_2)$ complex fragment produced by elimination of CO. In contrast, the dimerization of the carbene ligand to tetraphenylethylene presumably proceeds *via* a dinuclear intermediate. Whether this intermediate dissociates directly, eliminating olefin **3**, or whether carbene transfer occurs to form a biscarbene complex from which **3** cleaves off cannot yet be clarified. A corresponding bimolecular mechanism involving formation of a biscarbene complex has been proposed for the thermolysis of pentacarbonyl(2-oxacyclopentylidene)chromium on the basis of kinetic studies[2]. Scheme 1 may, therefore, be the best description of the course of the thermolysis of **1**.

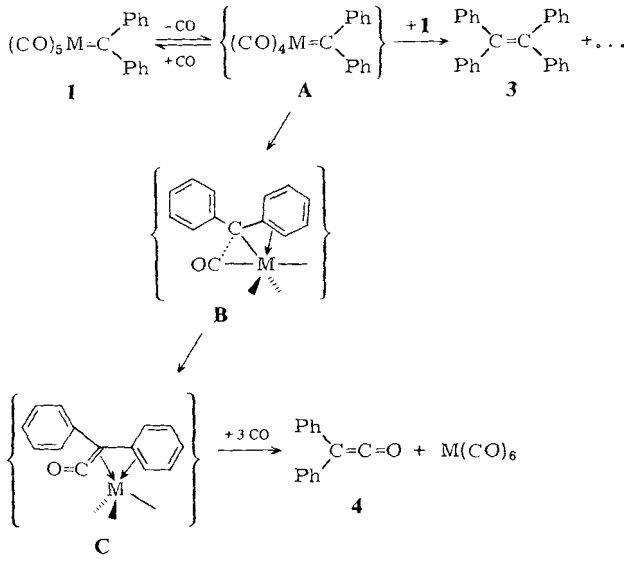
Tricarbonyl(vinylcarbene)iron complexes related to intermediate **B** are known. In the presence of CO at room temperature, they insert CO into the metal-carbene carbon bond[3].

Carbonylation of a diphenylcarbene- to afford a diphenylketene-ligand has previously been reported using manganese complexes; however, the reaction is slower and requires high pressure[4]. In contrast to these reactions, the coupling of coordinated CO and $CPh_2$ in **1** and the analogous chromium complex occurs spontaneously under very

[*] Dr. H. Fischer
Anorganisch-chemisches Institut der Technischen Universität München
Lichtenbergstrasse 4, D-8046 Garching (Germany)

[**] Kinetic and Mechanistic Studies of Reactions of Transition-Metal Complexes, Part 14. This work was supported by the Deutsche Forschungsgemeinschaft. Priv.-Doz. Dr. F. R. Kreissl is thanked for the mass spectra.—Part 13: H. Fischer, E. O. Fischer, R. Cai, D. Himmelreich, *Chem. Ber. 116* (1983) 1009.

 © *Verlag Chemie GmbH, 6940 Weinheim, 1983* *0570-0833/83/1111-0874 $ 02.50/0* 



Scheme 1.

mild conditions without having to be induced by external CO or other nucleophiles. These results corroborate the mechanism proposed by *Rüchardt* and *Schrauzer* for the formation of ketenes in the reaction of diazoalkanes with tetracarbonylnickel[5a]. The ready interconversion (carbene)carbonyl complex/ketene complex (corresponding to **A** ⇌ **C**) could be proved in an iron system by labeling experiments[5b], and corresponds to the predictions of MO calculations[5c].

For chromium and tungsten compounds, both types of C-C coupling reactions—carbene-carbene and CO-carbene—have now been shown to occur simultaneously and at the same complex.

Received: July 13, 1983;
revised: August 23, 1983 [Z 463 IE]
German version: *Angew. Chem. 95* (1983) 913

[1] C. P. Casey, T. J. Burkhardt, *J. Am. Chem. Soc. 95* (1973) 5833.
[2] C. P. Casey, R. L. Anderson, *J. Chem. Soc. Chem. Commun. 1975*, 895.
[3] T. Mitsudo, T. Sasaki, Y. Watanabe, Y. Takegami, S. Nishigaki, K. Nakatsu, *J. Chem. Soc. Chem. Commun. 1978*, 252; J. Klimes, E. Weiss, *Angew. Chem. 94* (1982) 207; *Angew. Chem. Int. Ed. Engl. 21* (1982) 205; *Angew. Chem. Suppl. 1982*, 477.
[4] W. A. Herrmann, J. Plank, *Angew. Chem. 90* (1978) 555; *Angew. Chem. Int. Ed. Engl. 17* (1978) 525.
[5] a) C. Rüchardt, G. N. Schrauzer, *Chem. Ber. 93* (1960) 1840; b) W. A. Herrmann, J. Gimeno, J. Weichmann, M. L. Ziegler, B. Balbach, *J. Organomet. Chem. 213* (1981) C26; c) P. Hofmann, L. A. Perez-Moya, unpublished results.

## Facile Synthesis of the (±)-6-Deoxycarminomycinone from Aloe-Emodin**

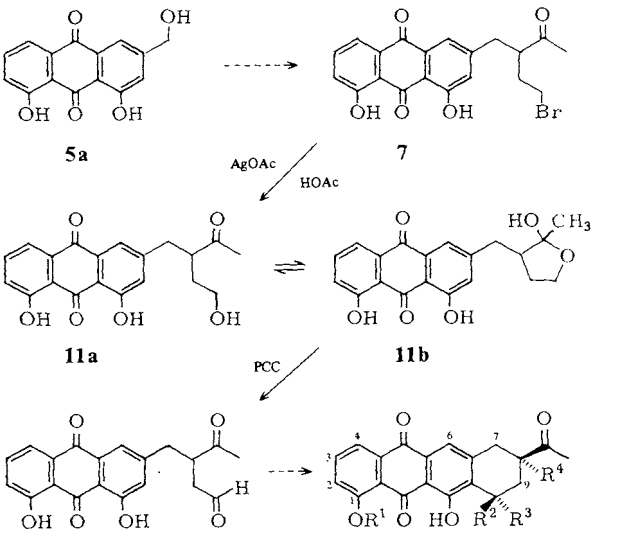
By *Karsten Krohn** and *Burkhard Sarstedt*

*Dedicated to Professor Hans Brockmann on the occasion of his 80th birthday*

The daunorubicin group of antitumour antibiotics[5] has recently been extended by the discovery of the possibly less toxic analogous 6-deoxy compounds (*e.g.* **2b**)[2]. We report here a seven-step synthesis of the racemic 6-deoxycarminomycinone **2a**[***] from the readily accessible aloe-emodin **5a**.

The acetal of the keto bromide **7**, which can be prepared in three stages from **5a** (70% yield)[18], surprisingly does not cyclize to the linearly condensed naphthacenequinone **3a** after reduction to the leuco form, but to a benzo[*a*]anthracene[18]. Since aldehydes always add to phenols at the *ortho*-position to the OH group, we synthesized the aldehyde **9** in order to study its cyclization.

Bromide **7** reacts with silver acetate in glacial acetic acid to afford a product (87%) which, according to the $^1$H-NMR spectrum ($CDCl_3$), is a mixture of the keto alcohol **11a** and the cyclic hemiacetal **11b**. The keto aldehyde **9** (55%) is formed by oxidation of **11a/11b**. Reduction of aldehyde **9** with alkaline dithionite to give leuco-anthraquinone is followed within a few minutes by the spontaneous cyclization to the 3 : 1 mixture of alcohols **12** and **13** (80%). The *cis*- and *trans*-compounds **12** and **13**, respectively, can be readily separated by chromatography. Because of the *trans*-diaxial interaction between 9(a)-H and 10-H the structure of **12** can be assigned straightforwardly from the $^1$H-NMR spectrum. The synthesis of **2a** is completed by hydroxylating C-8; for this purpose, the stereoisomers **12** and **13** need not be separated.



**2a**, $R^1 = R^2 = H$, $R^3 = R^4 = OH$
**2b**, $R^1 = CH_3$, $R^2 = H$, $R^3 = R^4 = OH$
**3a**, $R^1$–$R^4 = H$
**12**, $R^1 = R^3 = R^4 = H$, $R^2 = OH$
**13**, $R^1 = R^2 = R^4 = H$, $R^3 = OH$
**14**, $R^1 = R^3 = H$, $R^2 = R^4 = OH$

Oxygenation of the enolate obtained from **12/13** (dimethyl formamide, potassium *tert*-butoxide, −20°C) in the presence of triethyl phosphite leads to a mixture of (±)-6-deoxycarminomycinone **2a** (11%) and the epimer **14** (32%), which equilibrates upon addition of trifluoracetic acid (**2a** : **14** = 8 : 1)[3]. The spectroscopic data of racemic **2a** (m.p. = 215–216°C) are consistent with the literature values[8]. Chromatographically, (±)-**2a** behaves like optically active 6-deoxycarmonomycinone (m.p. = 176–177°C), which was obtained from naturally occurring 6-deoxydaunomycinone **2b**[2] by cleavage of the methyl ether ($AlCl_3$)[28].

Received: July 7, 1983 [Z 455 IE]
German version: *Angew. Chem. 95* (1983) 897
The complete manuscript of this communication appears in: *Angew. Chem. Suppl. 1983*, 1267–1282

[*] Prof. Dr. K. Krohn, Dr. B. Sarstedt
Institut für Organische Chemie der Technischen Universität
Schleinitzstrasse, D-3300 Braunschweig (Germany)

[**] Synthetic Anthracyclinones, Part 24. This work was supported by the Deutsche Forschungsgemeinschaft and the Fonds der Chemischen Industrie. Prof. *F. Arcamone* (Farmitalia, Milano) is thanked for a sample of 6-deoxydaunomycinone.—Part 23: K. Krohn, *Liebigs Ann. Chem.*, in press.

[***] The numbering follows IUPAC Nomenclature.

CAS Registry numbers:
(±)-**2a**, 77397-59-2; (±)-**2b**, 77172-23-7; (±)-**3a**, 83344-26-7; **(5b)**, 75694-01-8; (±)-**7**, 87393-66-6; (±)-**9**, 87393-67-7; (±)-**10**, 87393-68-8; (±)-**11a**, 87393-69-9; **11b**, 87393-70-2; (±)-**12**, 87393-71-3; (±)-**13**, 87393-72-4; (±)-**14**, 87421-48-5; allyl acetoacetate, 1118-84-9.


[2] F. Arcamone, G. Cassinelli, F. Di Matteo, S. Forenza, M. C. Ripamonti, G. Rivola, A. Vigevani, J. Clardy, T. McCabe, *J. Am. Chem. Soc. 102* (1980) 1462.

[3] H. Sekizaki, M. Jung, J. M. McNamara, Y. Kishi, *J. Am. Chem. Soc. 104* (1982) 7372.

[5] F. Arcamone: *Doxorubicin*, Academic Press, New York 1981.

[8] A. S. Kende, S. D. Boettger, *J. Org. Chem. 46* (1981) 2799.

[18] K. Krohn, W. Baltus, *Liebigs Ann. Chem. 1982*, 1579.

[28] Note added in proof: **2a** has also been isolated as a natural product: G. Cassinelli, G. Rivola, D. Ruggieri, F. Arcamone, A. Grein, F. Merli, C. Spalla, A. M. Casazza, A. Di Marco, G. Pratesi, *J. Antibiot. 35* (1982) 176.

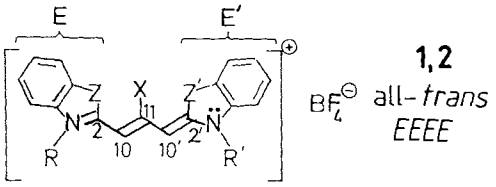

## First Proof of di-, tri-, and all-*cis*-Conformations in Sterically Hindered Trimethinecyanines (Carbocyanines) of the Indoline and Benzothiazole Series**


By *Rudolf Allmann, Hans-Joachim Anis, Reinhard Benn, Walter Grahn*, Stanislaw Olejnek,* and *Alicja Waśkowska*


We have undertaken a systematic investigation of the effects of structural variations on the charge distribution and stereochemistry in cyanines and other cationic polymethines. These properties are of importance for the chemical and physical properties of the dyes and for their applications in photography[3] and laser technology. In addition, cyanines are model compounds for the chromophore of (bacterio)rhodopsin[5].

To study the steric effects, we selected the readily accessible trimethinecyanines (carbocyanines) **1** and **2** for the following reasons:

1) Molecular models of **1** and **2** indicate that if their methine chains (C2–C10–C11–C10′–C2′) adopt the normal planar all-*trans*-conformation, marked steric interactions occur between the terminal groups E,E′ and bulky substituents X.
2) According to previously reported UV/VIS[6], $^1$H-NMR spectroscopic[7], and X-ray crystallographic[8] findings, these interactions are relieved by torsions about the nonrigidized methine chains and by changing from the all-*trans*- to the mono-*cis*-(*EZEE* and *EEZE*) conformations. Opposing substituent-induced shifts and changes in intensity of the absorption bands of **1a** and **2a** (see Table 2+4) suggest that the steric effects of X lead, in particular, to conversion of the all-*trans*-form into unknown conformations.




**1,2** all-*trans* *EEEE*

To determine these and to clarify the effects of substituents X on the light absorption of **1a** and **2a**, we have studied **1** and **2d** by $^1$H-NMR spectroscopy between *ca.* −100 and 35 °C. We interpret the temperature-dependent spectra of the methyl, ethyl, and phenyl derivatives **1b**, **1c**, and **1e** as arising from isomerization between the degenerate conformers tri-*cis*(*ZEZZ*) **3** and tri-*cis*′(*ZZEZ*) **3′**, which in **1b** is frozen at −98 °C ($\Delta G_c^{\ddagger} = 38.5$ kJ/mol). In contrast, in the *tert*-butyl compound **1d** the process, which is interpreted as isomerization between the degenerate conformers all-*cis* **4** and all-*cis*′ **4′**, is frozen at *ca.* 0 °C ($E_A = 48.43 \pm 1.09$ kJ/mol, $\Delta S^{\ddagger} = -11.5 \pm 1$ J K$^{-1}$ mol$^{-1}$). The previously unobserved[7] temperature dependence of the $^1$H-NMR spectrum of the *tert*-butyl compound **2d** with benzothiazole groups can be explained by isomerization

Table 2+4 (Extract). Longest wavelength absorption maxima and conformations of the trimethines **1** and **2** in methanol.

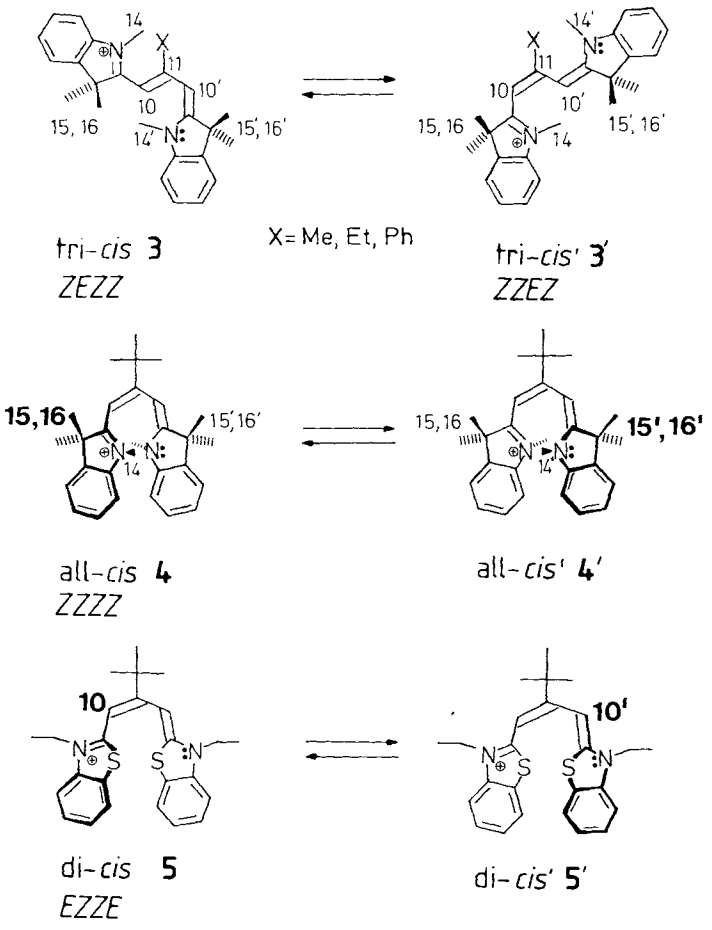
| | | **1**, Z=Z′=CMe$_2$, R=R′=Me Indoline Series | | | **2**, Z=Z′=S, R=R′=Et [a] Benzothiazole Series | | |
|---|---|---|---|---|---|---|---|
| | X | $\lambda_{max}$ [nm] | $\varepsilon \cdot 10^{-4}$ [L·mol$^{-1}$·cm$^{-1}$] | Conformation in solution | $\lambda_{max}$ [nm] | $\varepsilon \cdot 10^{-4}$ [L·mol$^{-1}$·cm$^{-1}$] | Conformation in solution |
| **a** | H | 544 | (13.1) | all-*trans*(*EEEE*) planar | 556.5 | (14.2) | all-*trans*(*EEEE*) planar [7] |
| **b** | Me | 551.5 | (6.74) | tri-*cis*(*ZEZZ* and *ZZEZ*) twisted cation cf. **3** and **3′** | 542 | (13.3) | mixture of mono-*cis*(*EEZE*) and *EZEE*, twisted; prevalent isomer) and all-*trans* [7] |
| **c** | Et | 553.5 | (5.29) | tri-*cis*(*ZEZZ* and *ZZEZ*) twisted cation cf. **3** and **3′** | 547.5 | (13.1) | mixture of mono-*cis*(*EEZE*) and *EZEE*, twisted; prevalent isomer) and all-*trans* [7] |
| **d** | *t*-Bu | 529 | (2.16) | all-*cis*(*ZZZZ*) helical cation cf. **4** and **4′** | 593 | (2.10) | di-*cis*(*EZZE*) helical cation cf. **5** and **5′** |
| **e** | Ph | 570.5 | (5.78) | tri-*cis*(*ZEZZ* and *ZZEZ*) twisted cation cf. **3** and **3′** | 560 | (19.7) | mixture of all-*trans*(prevalent isomer) and mono-*cis*(*EEZE* and *EZEE*, twisted) [7] |

[a] To facilitate comparison, we assign a higher priority to nitrogen than to sulfur.


[*] Priv.-Doz. Dr. W. Grahn, H.-J. Anis
Institut für Organische Chemie der Technischen Universität
Schleinitzstrasse, D-3300 Braunschweig (Germany)
Prof. Dr. R. Allmann, Dr. S. Olejnek, A. Waśkowska
Fachbereich Geowissenschaften der Universität Marburg (Germany)
Dr. R. Benn
Max-Planck-Institut für Kohlenforschung,
Mülheim a. d. Ruhr (Germany)



[**] Conformational Analysis of Polymethines, Part 1. This work was supported by the Deutsche Forschungsgemeinschaft and by the Fonds der Chemischen Industrie. We thank Dr. *T. Debaerdemaeker*, Universität Ulm, for the MULTAN calculations on the structures of **1b** and **1d**.




between the degenerate conformers di-*cis*(*EZZE*) **5** and di-*cis*'-(*EZZE*) **5'**, which is frozen at −96 °C.

The $^1$H-NMR spectroscopic findings were corroborated by X-ray structure analyses of **1b**, **1d**, and **2d**. In the crystal, the cations of the cyanines adopt the same conformations as in solution. The pronounced twisting of the methine chain in **1d**, for example, forces the N atoms separated by 298 pm to lie almost on top of each other (cf. **4** and **4'**).

In principle, the cations in **1** and **2** can assume ten conformations which form five classes: all-*trans*, mono-, di-, tri-, and all-*cis* (cf. **3**–**5**). Now, one example of each of these is known. A sixth conformation, the unsymmetrical di-*cis*(*ZZEE* and *EEZZ*)-form, was observed in the crystalline 10,10'-dimethyltrimethinecyanine of the indoline series[17].

The steric demands of the substituents X and the groups E,E' determine the respective conformation and the position of equilibrium between the conformers (Table 2+4). In accord with inspection of molecular models, the steric interactions between X and E,E' in the all-*trans*-form adopted by **1a** and **2a** thus cause the changes in conformation. The different effects of the alkyl and phenyl groups X on the light absorption of **1a** and **2a** (Table 2+4) arise from these conformational changes which, because of the different steric demands of the groups E and E', produce different effects in the two dye series. This becomes particularly noticeable with the *tert*-butyl group: in the indoline series **1** this leads to the hypsochromic shift of the longest wavelength absorption band and to a change in conformation from all-*trans* to all-*cis*; in contrast, in the benzothiazole series **2** it leads to a bathochromic shift of the longest wavelength absorption band and transformation of the all-*trans*- into the all-*cis*-form and not—as previously suggested[7]—into the mono-*cis*-form.

Received: February 22, 1982;
revised: September 6, 1983 [Z 990 IE]
German version: *Angew. Chem. 95* (1983) 900
The complete version of this manuscript appears in:
*Angew. Chem. Suppl. 1983*, 1147–1175

CAS Registry numbers:
**1a**, 87450-54-2; **1b**, 87450-58-6; **1c**, 87450-56-4; **1d**, 87450-60-0; **1e**, 87450-62-2; **2**, 87461-57-2.

[3] a) D. M. Sturmer, D. W. Heseltine: "Sensitizing and Desensitizing Dyes" in T. H. James: *The Theory of the Photographic Process*, 4th edit., Macmillan, New York 1977, p. 194ff; b) L. G. S. Brooker, F. L. White, D. W. Heseltine, G. H. Keyes, S. G. Dent Jr., E. J. van Lare, *J. Phot. Sci. 1* (1953) 173; *Chem. Abstr. 48* (1954) 3823d.

[5] a) F. Derguini, C. G. Caldwell, M. G. Motto, V. Balogh-Nair, K. Nakanishi, *J. Am. Chem. Soc. 105* (1983) 646; b) T. Kakitani, H. Kakitani, B. Honig, K. Nakanishi, *ibid. 105* (1983) 648.

[6] J. Fabian, H. Hartmann: *Light Absorption of Organic Colorants*, Springer, Berlin 1980, p. 183f.

[7] P. M. Henrichs, S. Gross, *J. Am. Chem. Soc. 98* (1976) 7169.

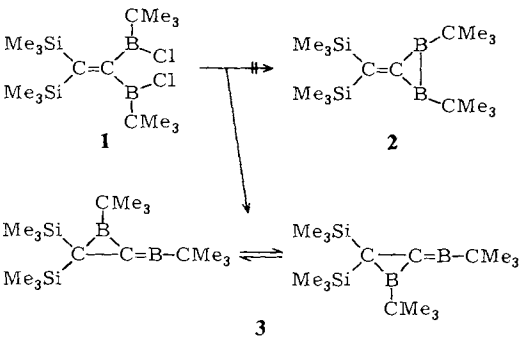
[8] a) S. Dähne, S. Kulpe: "Structural principles of unsaturated organic compounds. With special reference to X-ray analyses of coloured substances", *Abh. Akad. Wiss. DDR, Abt. Math., Naturwiss., Tech. 8N* (1977) 1; *Chem. Abstr. 88* (1978) 189321m; b) K. Nakatsu, H. Yoshioka, S. Nishigaki: "X-Ray Crystallographic Studies on Photographic Dyes", *Kwansei Gakuin University Annual Studies 29* (1980) 213.

[17] R. Allmann, D. Kucharczyk, *Z. Kristallogr., Kristallgeom., Kristallphys., Kristallchem. 162* (1983) 6.

## A Boron-Carbon Double Bond**

By *Hartmut Klusik* and *Armin Berndt**

2,4-Diboramethylenecyclopropane [borirane-2-ylideneborane(2)] **3** is the first compound containing a B=C double bond. It is formed on reaction of 1,1-bis(*tert*-butylchloroboryl)-2,2-bis(trimethylsilyl)ethene **1**[1] with K/Na alloy in boiling pentane (yield 60%).

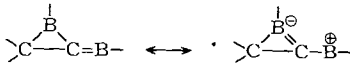



The structure of **3** follows from $^1$H-, $^{13}$C- and $^{11}$B-NMR spectra[2]. Signals for the two C-atoms of the $C_2B_2$ skeleton appear below −40 °C at $\delta = 115.2$ and 25.0 in the region for $sp^2$ and $sp^3$ C-atoms; both signals show line-broadening characteristic of a C-atom bound to boron. Hence the structure of a 2,3-diboramethylenecyclopropane[3] for **2** can be ruled out. Below −11 °C the B atoms give rise to

[*] Prof. Dr. A. Berndt, H. Klusik
Fachbereich Chemie der Universität
Hans-Meerwein-Strasse, D-3550 Marburg (Germany)

[**] This work was supported by the Fonds der Chemischen Industrie. We thank Dr. *P. H. M. Budzelaar* and Dr. *S. M. van der Kerk*, Utrecht, for the first hints on the structure of the compound **3**, and Prof. *K. Dehnicke*, Marburg, and Prof. *P. v. R. Schleyer*, Erlangen, for valuable discussions.

two signals at $\delta = 52$ and 18, which are shifted noticeably upfield compared to those of trialkylboranes ($\delta^{11}B \approx 80$). Upfield shifts are characteristic of sp-hybridized boron atoms: for iminoboranes, signals were found at $\delta = 2$–13[4]. We therefore assign the signal at $\delta = 18$ to the B-atom of the B=C bond; the upfield shift for the B-atom in the three-membered ring is presumably due to conjugation with the double bond.

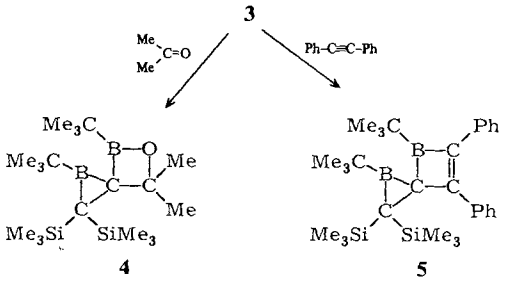


The *tert*-butyl groups also give rise to two signals in the intensity ratio 1:1 in the $^1$H-NMR spectrum below $-47$°C, and in the $^{13}$C-NMR spectrum below $-30$°C. Increasing the temperature leads *via* line-broadening to coalescence and line-narrowing, both in the case of these signals as well as the signals of the boron atoms. In contrast, only one sharp signal is observed for the two trimethylsilyl groups between $-100$ and $+25$°C in the $^1$H-, $^{13}$C- and $^{29}$Si-NMR spectra.

From the coalescence temperatures ($-47$, $-30$ and $-11$°C) for $^1$H, $^{13}$C and $^{11}$B and the accompanying shift differences there results an energy barrier of 11.4 kcal/mol, which we assign to the topomerization of **3** by diboramethylenecyclopropane rearrangement.

**3** shows two bands in the Raman spectrum at 1675 and 1715 cm$^{-1}$ in the intensity ratio 4:1, which we ascribe to the $^{11}$B=C and $^{10}$B=C stretching vibrations, respectively.

**3** is storable for months in the absence of oxygen and water and no change is observed on heating at 100°C for 1 h. The stability of the compound is probably due to steric shielding by the four bulky substituents. Even the derivative of **3** in which one trimethylsilyl is replaced by a methyl group undergoes dimerization. **3** reacts with acetone at $-60$°C to give the 1,2-oxaboretane **4**, and with tolane at $-30$°C to give the 2-boretene **5**.



The structures of **4** and **5** are consistent with the $^1$H- and $^{13}$C-NMR spectra[2]. The spatial proximity of a $Me_3Si$ group to a methyl- and phenyl group, respectively, in **4** and **5** manifests itself in **4** in restricted rotation of this trimethylsilyl group, in **5** in significant shielding of its protons ($\delta^1H = -0.23$ compared to $+0.2$ in the case of **4**). At room temperature, products are formed from **4** and **5** whose structures are under investigation.

Received: February 28, 1983; revised: September 22, 1983 [Z 292 IE]
German version: *Angew. Chem. 95* (1983) 895

[1] H. Klusik, C. Pues, A. Berndt, unpublished results.

[2] **3**: colorless liquid, b.p. = 65°C/$10^{-2}$ torr; $^1$H-NMR ($CDCl_3$): $\delta = 1.23$ (s, 18H, *t*Bu, RT), 1.26, 1.11 (s, each 9H, *t*Bu, $-55$°C), 0.02 (s, 18H, $SiMe_3$, RT); $^{13}$C-NMR ($CD_2Cl_2$): $\delta = 115.2$ (s, 1C, C=B; $-90$°C), 32.3 (q, 6C, Bu, RT), 31.6, 30.7 (q, each 3C, *t*Bu, $-90$°C), 23.2, 17.6 (s, each 1C, $BCMe_3$, $-90$°C), 25.0 (s, 1C, BCSi, $-90$°C), $-0.3$ (s, 6C, $SiMe_3$, RT); $^{11}$B-NMR ($CD_2Cl_2$): $\delta = 34$ (RT), 52, 18 (each 1B, $-30$°C); MS (intensities [%] in the molecular ion region *m/z* 304–309): exp. 4.07, 44.05, 100, 25.95, 11.83, 5.59; calc. 4.66, 41.82, 100, 29.43, 9.86, 1.75.—**4**: white solid, decomposition at RT, $\tau_{1/2} \approx 3$ d; $^1$H-NMR ($CDCl_3$, RT): $\delta = 1.56$, 1.42 (s, each 3H, $CH_3$), 1.20, 0.95 (s, each 9H, *t*Bu), 0.21, 0.19 (s, each 9H, $SiMe_3$); $^{13}$C-NMR ($CDCl_3$, $-40$°C): $\delta = 88.8$ (s, 1C, CO), 40.3, 26.0 (s, each 1C, BCB and BCSi), 30.4, 29.6 (q, each 1C, $CH_3$), 29.2, 28.2 (q, each 3C, *t*Bu), 23.0, 22.5 (s, each 1C, $BCMe_3$), 5.8, 5.6, 4.8 (q, each 1C, $SiMe_3$), 5.6 (q, 3C, $SiMe_3$, RT), 3.7 (q, 3C, $SiMe_3$); $^{11}$B-NMR ($CDCl_3$, RT): $\delta = 81$ (1B, $BC_3$), 57 (1B, BO).—**5**: $^1$H-NMR ($CD_2Cl_2$, $-30$°C): $\delta = 7.6$–7.2 (m, 10H, arom. H), 1.19, 0.91 (s, each 9H, *t*Bu), 0.14, $-0.23$ (s, each 9H, $SiMe_3$); $^{13}$C-NMR ($CD_2Cl_2$, $-30$°C): $\delta = 180.1$ (br, 1C, $sp^2$-C), 144.8, 137.4, 137.1 (s, each 1C, $sp^2$-C), 128.6–127.4 (10C, $sp^2$-CH), 56.2, 27.0 (s, each 1C, BCB and BCSi), 30.3, 28.8 (q, each 3C, *t*Bu), 24.1, 22.0 (s, each 1C, $BCMe_3$), 3.1 (q, 6C, $SiMe_3$); $\delta^{11}$B not determinable because of line widths of 2500 Hz.

[3] K. Krogh-Jespersen, D. Cremer, D. Poppinger, J. A. Pople, P. v. R. Schleyer, J. Chandrasekhar, *J. Am. Chem. Soc. 101* (1979) 4843.

[4] P. Paetzold, C. von Plotho, *Chem. Ber. 115* (1982) 2819; H. Nöth, S. Weber, B. Rasthofer, C. Narula, A. Konstantinov, *Pure Appl. Chem. 55* (1983) 1453.

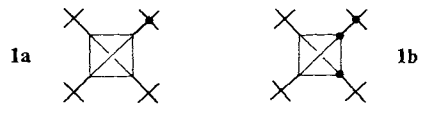
## Tetra-*tert*-butyltetrahedrane: $^{13}$C-$^{13}$C Coupling Constants and Hybridization

By *Thomas Loerzer, Reinhard Machinek, Wolfgang Lüttke*, Lothar Hermann Franz, Klaus-Dieter Malsch,* and *Günther Maier**

*Dedicated to Professor Hans Brockmann on the occasion of his 80th birthday*

NMR coupling constants $^1J$(C–C) represent a spectroscopic quantity with which the electron distribution in CC bonds can be characterized[1]. We therefore determined $^1J$(C–C) for the most highly strained hydrocarbon, tetra-*tert*-butyltetrahedrane **1**[2].

In the NMR investigation the problems associated with the limited sensitivity of measurement and the magnetic equivalence of the tetrahedrally arranged C atoms had to be overcome. According to model calculations the complete set of data should be obtainable from the tetrahedrane **1a** in which a *tert*-butyl group is labeled to 90 atom-% with $^{13}$C at one of the quaternary centers. Together with the $^{13}$C-atoms occurring in natural abundance at the corners of the tetrahedron one obtains, *inter alia*, the isotopomer **1b**; its ABM spin system enables determination of the coupling constant $^1J(C_r-C_r)$ between the ring carbon atoms. **1b** has a natural abundance of $2.7 \times 10^{-4}$ and is therefore just measurable with modern spectrometers.



•: $^{13}$C-Atom

**1a** was synthesized using [1-$^{13}$C]-1,1-dimethylethyllithium and 2-bromo-3,4,5-tri-*tert*-butylcyclopentadienone as starting materials[3]. Evaluation of the {$^1$H}-$^{13}$C-NMR spectrum of **1a** (330 mg **1a**, solvent [$D_{10}$]$Et_2O$, 50.4 MHz) gave the data listed in Table 1.

[*] Prof. Dr. W. Lüttke, Dr. T. Loerzer, R. Machinek
Organisch-chemisches Institut der Universität
Tammannstrasse 2, D-3400 Göttingen (Germany)
Prof. Dr. G. Maier, Dr. L. H. Franz, Dr. K.-D. Malsch
Institut für Organische Chemie der Universität
Heinrich-Buff-Ring 58, D-6300 Giessen (Germany)

 © Verlag Chemie GmbH, 6940 Weinheim, 1983 0570-0833/83/1111-0878 $ 02.50/0 

Table 1. $^{13}C$-$^{13}C$ coupling constants [Hz] of tetra-*tert*-butyltetrahedrane [a].

| $^1J(C_r-C_r)$ | $^1J(C_r-C_q)$ | $^2J(C_r-C_q)$ | $^1J(C_q-C_m)$ |
|---|---|---|---|
| 9.2 | 64.0 | −0.7 | 35.8 |

[a] $C_r$ = ring C-atom, $C_q$ = quaternary C-atom of a *tert*-butyl group, $C_m$ = methyl C-atom. Mean error: ±0.05 Hz.

The value of 9.2 Hz for $^1J(C_r-C_r)$ is almost as large as $^1J(C-C)$ for cyclopropane (12.4 Hz)[4a], thus indicating a similar s-character of the hybrid orbitals participating in the ring C–C bonds; for cyclopropane this can be determined very accurately from $^1J(CH)$ as 0.179[4a]. If it is assumed that the contribution of the non-contact terms to the overall coupling in these compounds is the same, then a somewhat smaller s-character of 0.161, corresponding to an $sp^{5.20}$-hybridization, is obtained with the previously reported relationship $^1J_{CC}=658\ s_1s_2-7.9$ for the hybrid orbitals of the tetrahedral C-atoms of **1** which participate in the ring CC bonding. Our SCPT-INDO calculations[4b], however, suggest that the contribution of the (here negative) non-contact terms in **1** is about 20% greater than in cyclopropane. If this is taken into consideration, then only a slightly greater s-character of *ca.* 0.170 results for **1** ($sp^{4.88}$; INDO[5a]: $sp^{4.99}$).

A further indicator for the hybridization of the C-atoms of the tetrahedrane skeleton can be obtained from the $^1J(C_r-C_q)$ coupling constant. Using the sum rule for hybrid orbitals[1a], it can be concluded that the hybrid orbital pointing from the $C_r$ to the $C_q$ atom is $sp^{1.04}$-hybridized (INDO[5a]: $sp^{1.21}$) and causes a correspondingly greater coupling constant. A comparison with the analogous couplings of various *tert*-butyl substituted hydrocarbons (Table 2) shows that the value for **1** (64.0 Hz) agrees well with that for *tert*-butylacetylene (66.1 Hz), whose acetylenic C-atoms unequivocally exhibit sp hybridization.

Table 2. $^{13}C$-$^{13}C$ coupling constants [Hz] [a] of *tert*-butyl compounds [4b].

| | $H_3C^x-C^q(CH_3)_3$ | $H_2C=C^xH-C^q(CH_3)_3$ | $HC\equiv C^x-C^q(CH_3)_3$ |
|---|---|---|---|
| $^1J(C_x-C_q)$ | 35.5 | 42.3 | 66.1 |
| $^1J(C_q-CH_3)$ | 35.5 | 35.5 | 35.4 |

[a] Mean error: ±0.1 Hz.

It follows from the hybridization of the C-atoms of the tetrahedrane skeleton that the axes of the "endocyclic" hybrid orbitals are in each case bent outwards from the edge of the ideal tetrahedron by about 28.4°. Thus, the "bent-bond" character is much more pronounced here than in the case of cyclopropane (21.3°)[4a].

The theoretical predictions[5] on the bonding properties of the tetrahedrane system are in agreement with these results.

Received: July 15, 1983 [Z 471 IE]
German version: *Angew. Chem.* 95 (1983) 914
CAS Registry number:
Tetra-*tert*-butyltetrahedrane, 66809-06-1.

[1] a) W. A. Bingel, W. Lüttke, *Angew. Chem. 93* (1981) 944; *Angew. Chem. Int. Ed. Engl. 20* (1981) 899; b) J. Kowalewski, *Prog. Nucl. Magn. Reson. Spectrosc. 12* (1977) 1.

[2] Review article on the tetrahedrane problem: N. S. Zefirov, A. S. Koz'min, A. V. Abramenkov, *Russ. Chem. Rev. 47* (1978) 163.

[3] G. Maier, S. Pfriem, U. Schäfer, K.-D. Malsch, R. Matusch, *Chem. Ber. 114* (1981) 3965.

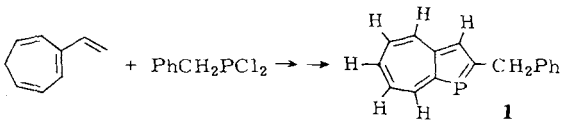
[4] a) J. Wardeiner, W. Lüttke, R. Bergholz, R. Machinek, *Angew. Chem. 94* (1982) 873; *Angew. Chem. Int. Ed. Engl. 21* (1982) 872; b) T. Loerzer, Dissertation, Universität Göttingen 1983.

[5] a) J. M. Schulman, T. J. Venanzi, *J. Am. Chem. Soc. 96* (1974) 4739; b) Z. Maksić, L. Klasinc, M. Randić, *Theor. Chim. Acta 4* (1966) 273; c) K. Kovačević, Z. B. Maksić, *J. Org. Chem. 39* (1974) 539; d) H. Kollmar, *J. Am. Chem. Soc. 102* (1980) 2617.

## 1-Methoxy-3-phenyl-2-phosphaazulene—the First Synthesis of 2-Phosphaazulenes

By *Gottfried Märkl**, *Ernst Seidl*, and *Irene Trötsch*

We recently described the synthesis of **1**, the first 1-phosphaazulene, in which the initial step is a McCormack cycloaddition of benzyldichlorophosphane to vinylcycloheptatriene[1b].

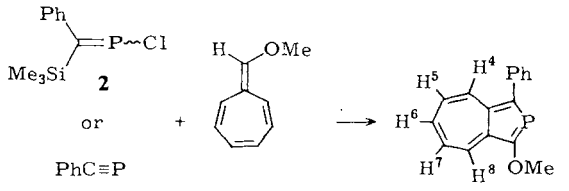



**1**

The synthesis of the first 2-phosphaazulene starts from the 1-chloro-2-phenyl-2-trimethylsilylphosphaethane **2**[1a] or the 2-phenyl-1-phosphaethyne **3** formed on elimination of chlorotrimethylsilane from **2**—whose dienophilic reactivity we recently demonstrated by [4+2]-cycloaddition with α-pyrones and cyclopentadienones to give $\lambda^3$-phosphorins[2].

According to *Daub et al.*[3], the electron-rich 8-methoxyheptafulvene **4** reacts regioselectively with reactive alkenes and alkynes, *e.g.* 1,1-dicyanoethenes, nitroethenes or diethyl acetylenecarboxylate, to give 3,8a-dihydroazulenes, which on suitable substitution can be converted into azulenes with 2,3-dichloro-5,6-dicyano-1,4-benzoquinone (DDQ) *via* dehydrogenation or with acid catalysts by elimination of methanol.

We have now found that **2** (or **3**, see ref.[2]) reacts with **4** in boiling xylene in the presence of KF/[18]crown-6 in 2 h in a regioselective [8+2]-cycloaddition to give the 1-methoxy-3-phenyl-2-phosphaazulene **5**. After chromatographic isolation and purification, **5** is obtained in the form of red platelets (yield 6%, m.p. 85—87 °C) which dissolve in $CHCl_3$ to give a green solution[4].

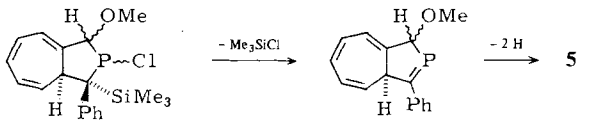



The $^1H$-NMR spectrum of **5**[5a] clearly demonstrates the regioselectivity of the cycloaddition; presence of the isomeric 1-phosphaazulene can be ruled out. As in the case of **1**, the downfield shift of the signals of the ring protons 4-H and 8-H, and to a lesser extent of 6-H, is consistent with the dipolar structure of the azulenes. The $^{31}P$-NMR chemical shift ($CDCl_3/CHCl_3$, $\delta=+177.9$) is characteristic for trivalent phosphorus with coordination number 2 in a resonance-stabilized system ($\delta$(**1**) = +168.3; $\delta$(2,4,6-triphe-

[*] Prof. Dr. G. Märkl, E. Seidl, I. Trötsch
Institut für Organische Chemie der Universität
Universitätsstraße 31, D-8400 Regensburg (Germany)

nyl-$\lambda^3$-phosphorin) = +178). The UV spectrum of **5** is likewise consistent with the azulene structure[5b], as is shown by a comparison with the longwave absorption maxima of 1-methoxyazulene[6] and 1-phenylazulene[7].

In the [8+2]-cycloaddition of **2** to **4**, the tetrahydroazulene **6**, or by primary formation of **3**, the dihydroazulene **7** must be formed initially. The aromatization of **6** or **7** to **5**




**6** **7**

must then proceed *via* a chlorotrimethylsilane elimination and a dehydrogenation (spontaneous dehydrogenations to azulenes are known[8]). The 1-phenyl-2-phosphaazulene to be expected in a primary acid-catalyzed elimination of methanol could not be observed.

Received: July 18, 1983 [Z 475 IE]
German version: *Angew. Chem. 95* (1983) 891

CAS Registry numbers:
**2**, 74483-17-3; **3**, 76684-21-4; **4**, 71133-64-7; **5**, 87509-02-2.

[1] R. Appel, W. Westerhaus, *Angew. Chem. 92* (1980) 578; *Angew. Chem. Int. Ed. Engl. 19* (1980) 556; b) G. Märkl, E. Seidl, *Angew. Chem. 95* (1983) 58; *Angew. Chem. Int. Ed. Engl. 22* (1983) 57; *Angew. Chem. Suppl. 1983*, 75.

[2] G. Märkl, G. Yu Jin, E. Silbereisen, *Angew. Chem. 94* (1982) 383; *Angew. Chem. Int. Ed. Engl. 21* (1982) 370.

[3] W. Pickl, W. Rieger, A. Bäumler, G. Hirmer, J. Daub, *Tetrahedron Lett.*, in press; K. M. Rapp, J. Daub, *ibid. 1976*, 2011; K. M. Rapp, T. Burgemeister, J. Daub, *ibid. 1978*, 2685; A. Hasenhündl, K. M. Rapp, J. Daub, *Chem. Lett. 1979*, 597; W. Bauer, I. Betz, J. Daub, L. Jakob, W. Pickl, K. M. Rapp, *Chem. Ber. 116* (1983) 1154; J. Bindl, J. Daub, A. Hasenhündl, M. Meiner, K. M. Rapp, *ibid. 116* (1983) 2408; see also K. Hafner, M. Römer, W. aus der Fünten, *Justus Liebigs Ann. Chem. 1967*, 376.

[4] Characteristic mass spectroscopic and correct elemental analysis data were obtained.

[5] a) $^1$H-NMR spectrum ($CDCl_3$, 250 MHz): $\delta = 8.33$ (d, with fine structure, $^3J_{7\text{-H}/8\text{-H}} = 10$ Hz, $^4J_{6\text{-H}/8\text{-H}} \approx 1.1$ Hz, $^4J_{P/H} \approx 1.5$ Hz, 8-H); 8.14 (d with fine structure, $^3J_{4\text{-H}/5\text{-H}} = 10.2$ Hz, $^4J_{4\text{-H}/6\text{-H}} \approx 1.0$ Hz, $^4J_{P/H} \approx 1.5$ Hz, 4-H); 7.01 (dd (pseudotriplet), $^3J_{5\text{-H}/6\text{-H}} = 10.0$ Hz; $^4J_{5\text{-H}/7\text{-H}} \approx 1.10$ Hz, $^5J_{P/H} \approx 1.20$ Hz, 5-H); 6.88 (dd, $^3J_{6H/7H} = 10.0$ Hz, $^5J_{P/H} = 1.20$ Hz, 7-H); 7.32–8.00 (m, 6-H probably at 7.44 (dd with fine structure) and phenyl-H); 4.26 (d, $^4J_{P/H} = 1.09$ Hz, OMe); b) UV spectrum (*n*-hexane): $\lambda_{max}$ [nm] ($\varepsilon$) = 860 sh (126), 768 (224), 726 sh (210), 398 sh (1370), 386 (1420), 331 (11460), 303 (10600), 291 (11420), 273 sh (9990).

[6] L. L. Replogle, *J. Org. Chem. 29* (1964) 2805.

[7] P. A. Plattner, A. Fürst, M. Gordon, K. Zimmermann, *Helv. Chim. Acta 33* (1950) 1910; E. P. Serebryakov, *Zh. Org. Khim. 9* (1973) 2389.

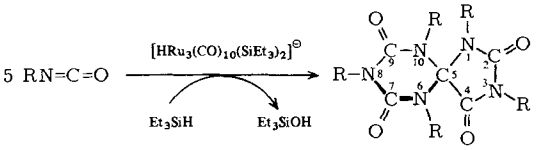
[8] W. Treibs, H. Froitzheim, *Justus Liebigs Ann. Chem. 465* (1949) 43; see also [1].

## Novel Catalytic Application of a Transition-Metal Cluster: Spirocyclization of Alkyl Isocyanates

By *Georg Süss-Fink*, Gerhard Hermann,* and *Ulf Thewalt*

Ever since transition-metal clusters were discussed as catalysts[1], a great variety of such compounds have been prepared and characterized[2]. However, novel catalytic applications of these complexes still remain to be discovered[3]. Herein we report a novel homogeneously catalyzed spirocyclization of alkyl isocyanates providing a surprisingly simple access to [4.5]-spiroheterocycles. The reaction proceeds in the presence of triethylsilane and the cluster anion $[HRu_3(CO)_{10}(SiEt_3)_2]^-$, discovered recently in catalytic silylation reactions[4], as the catalyst (precursor).

Reaction of MeNCO with $Et_3SiH$ and $[N(PPh_3)_2][HRu_3(CO)_{10}(SiEt_3)_2]$ (5000 : 1000 : 1) in tetrahydrofuran solution at 150 °C yields the spirocyclic compound **1**, which upon cooling crystallizes from the reaction solution. Triethylsilanol and its condensation product hexaethyldisilanol are formed as by-products. The oxygen atom of one of the five isocyanate molecules incorporated in **1** is apparently removed by triethylsilane. Other aliphatic isocyanates react analogously, but the spirocyclization products, because of their better solubility, are only isolable by chromatographic methods. Phenyl isocyanate does not react under these conditions. The cluster anion employed as the catalyst is actually altered under the reaction conditions, but the organometallic residue obtained from the solution remains catalytically active on further use.




| R | Me | Et | *n*Pr |
|---|---|---|---|
| | **1** | **2** | **3** |

The composition of the compounds **1**–**3** is confirmed by elemental analysis and (high resolution) mass spectrometry. The spectroscopic data (IR, $^1$H-NMR, $^{13}$C-NMR) are consistent with a spirocyclic system of NR- and CO-structural units. The structure of the methyl derivative **1** was determined by X-ray crystallography (Fig. 1).

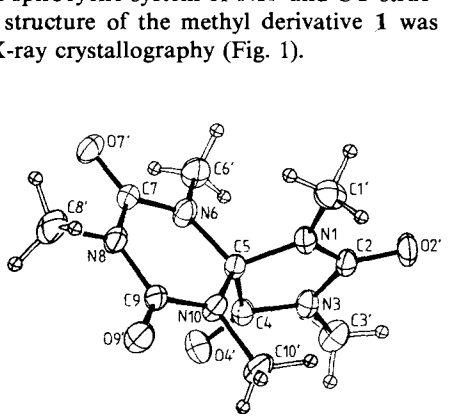



Fig. 1. Structure of the spiroheterocycle **1** in the crystal. Bond lengths [Å] in the rings: N1–C2 1.353(3), C2–N3 1.404(4), N3–C4 1.352(3), C4–C5 1.556(4), C5–N1 1.454(3), C5–N6 1.442(3), N6–C7 1.355(3), C7–N8 1.377(3), N8–C9 1.378(4), C9–N10 1.359(3), N10–C5 1.446(3). Further details of the crystal structure investigation are available on request from the Fachinformationszentrum Energie Physik Mathematik, 7514 Eggenstein-Leopoldshafen on quoting the depository number CSD 50537, the names of the authors, and full citation of the journal.

Both rings in the molecule of **1** are almost planar and are perpendicular with respect to each other (deviations of the ring atoms from each of the best planes < 0.04 Å; angle between planes 90.5°). Except for the CN bonds protruding from the spiro-atom C5, whose length suggests single

[*] Dr. G. Süss-Fink [**], G. Herrmann
Laboratorium für Anorganische Chemie der Universität
Universitätsstrasse 30, D-8580 Bayreuth (Germany)
Prof. Dr. U. Thewalt
Sektion für Röntgen- und Elektronenbeugung der Universität
Oberer Eselsberg, D-7900 Ulm (Germany)

[**] Present address: Laboratoire de Chimie de Coordination Organique, Université de Rennes, Campus de Beaulieu, F.35042 Rennes Cédex (France)

 © Verlag Chemie GmbH, 6940 Weinheim, 1983 0570-0833/83/1111-0880 $ 02.50/0 

bonding (mean value 1.447 Å), all the remaining ring CN bonds (1.352 to 1.404 Å) exhibit double bond character.

Received: July 19, 1983; revised: August 19, 1983 [Z 476 IE]
German version: *Angew. Chem. 95* (1983) 899
The complete version of this communication appears in:
*Angew. Chem. Suppl. 1983*, 1203–1208

CAS Registry numbers:
**1**, 87482-40-4; **2**, 87482-41-5; **3**, 87482-42-6; MeNCO, 624-83-9; $(N(PPh_3)_2][HRu_3(CO)_{10}(SiEt_3)_2]$, 80376-22-3; EtNCO, 109-90-0; PrNCO, 110-78-1

[1] B. F. G. Johnson, J. Lewis, *Pure Appl. Chem. 44* (1975) 43; E. L. Muetterties, *Bull. Soc. Chim. Belg. 84* (1975) 959; R. Ugo, *Catal. Rev. Sci. Eng. 11* (1975) 225.
[2] B. F. G. Johnson: *Transition Metal Clusters*, Wiley, New York 1980.
[3] E. L. Muetterties, M. J. Krause, *Angew. Chem. 95* (1983) 135; *Angew. Chem. Int. Ed. Engl. 22* (1983) 135.
[4] G. Süss-Fink, *Angew. Chem. 94* (1982) 72; *Angew. Chem. Int. Ed. Engl. 21* (1982) 73; *Angew. Chem. Suppl. 1982*, 71; G. Süss-Fink, J. Reiner, *J. Organomet. Chem. 221* (1981) C36.

## 1,2,4-Thiadiazole-3,5-dicarbonitrile by Reaction of Cyanogen with Sulfur**

By *Herbert W. Roesky**, *Klaus Keller*, and *Jan. W. Bats*

Cyanogen **1** reacts with sulfur trioxide in a criss-cross cycloaddition (molar ratio 1:2) to give a bicycle in which the CC bond of the cyanogen remains intact[1]. Reactions of **1** with elemental sulfur have so far never been described in the literature. As product of such a reaction in dimethylformamide at 120°C according to

$$1/8\,S_8 + 2(CN)_2 \longrightarrow (CN)_4S$$
$$\mathbf{1} \qquad\qquad \mathbf{2}$$

we have now isolated colorless crystals of the compound **2** (m.p. 67°C, yield 29%). It follows from the $^{13}$C-NMR spectrum that **2** contains four non-equivalent carbon atoms ($\delta = 161.5, 147.6, 111.7, 110.1$). No bands appear in the C≡N stretching vibration range in the IR spectrum, whereas the Raman spectrum shows three bands at 2248, 2256, and 2267 cm$^{-1}$. In the FI-mass spectrum of **2** the molecule appears at $m/z = 136$ and the fragment $(CN)_2S^+$ at $m/z = 84$.

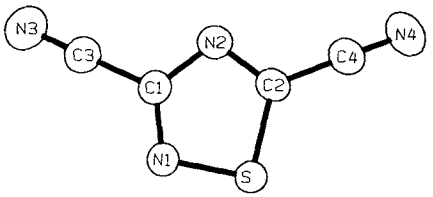



Fig. 1. Structure of 1,2,4-thiadiazole-3,5-dicarbonitrile **2** in the crystal. Bond lengths [Å] and angles [°]: N1–S 1.621(2), C2–S 1.697(2), C2–N2 1.301(3), C1–N2 1.357(3), C1–N1 1.300(3), C2–C4 1.428(3), C4–N4 1.139(3), C1–C3 1.438(3), C3–N3 1.129(3); N1–S–C2 92.1(1), C1–N1–S 107.9(2), N1–C1–N2 120.3(2), C1–N2–C2 106.7(2), N2–C2–S 113.1(2). Further details of the crystal structure investigation are available on request from the Fachinformationszentrum Energie Physik Mathematik, D-7514 Eggenstein-Leopoldshafen, on quoting the depository number CSD 50279, the names of the authors, and full citation of the journal.

[*] Prof. Dr. H. W. Roesky, K. Keller
Institut für Anorganische Chemie der Universität
Tammannstrasse 4, D-3400 Göttingen (Germany)
Dr. J. W. Bats
Institut für Kristallographie und Mineralogie der Universität
Senckenberganlage 30, D-6000 Frankfurt am Main 11 (Germany)

[**] This work was supported by the Deutsche Forschungsgemeinschaft and Hoechst AG.

According to a single crystal structure analysis the molecule is almost planar (Fig. 1). Only one carbonitrile group C3N3 slightly deviates from the plane of the thiadiazole ring[2]. The packing leads to a contact distance of 305.0(2) pm between S and N4′ of an adjacent molecule; this distance is substantially shorter than the sum of the van der Waals' radii (335 pm). All other intermolecular distances are too long for participation of bonding between molecules.

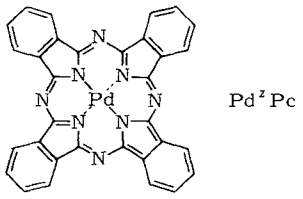
Received: October 14, 1982 [Z 174 IE]
Publication delayed at authors' request
German version: *Angew. Chem. 95* (1983) 904
The complete version of this communication appears in:
*Angew. Chem. Suppl. 1983*, 1323–1332

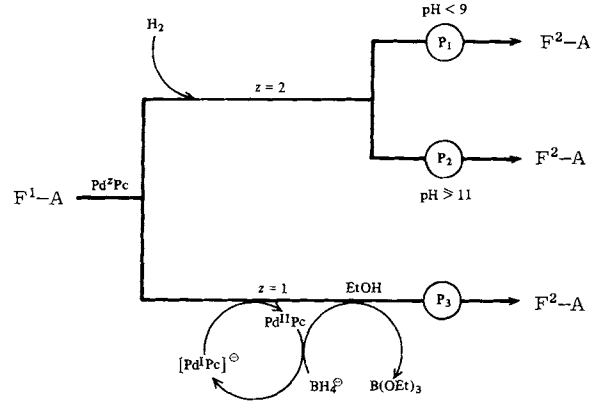
[1] H. W. Roesky, N. Amin, G. Remmers, A. Gieren, U. Riemann, B. Dederer, *Angew. Chem. 91* (1979) 243; *Angew. Chem. Int. Ed. Engl. 18* (1979) 223.
[2] Cf. F. Kurzer, *Adv. Heterocycl. Chem. 5* (1965) 119; J. Goerdeler, I. El Tom, *Chem. Ber. 98* (1965) 1544; J. Goerdeler, P. Mertens, *ibid. 103* (1970) 1805.

## Reaction Control by Catalysts with Variable Specificity: Stable Palladium-Phthalocyanine as Hydrogenation Catalyst with Three Catalytic Patterns**

By *Heiner Eckert**, *Gudrun Fabry*, *Yvonne Kiesel*, *Gabriele Raudaschl*, and *Christoph Seidel*

The directed control of the course of a reaction might be realized by means of a catalyst having variable specificity[1]. The specificity of a metal-complex catalyst is dependent upon internal and external parameters (respectively, the metal and its valence *z*, type of ligand field *etc.*[3], and carrier material, reaction medium, reaction conditions, res-




Scheme 1. Reaction control by directed variation of the specificity of the catalyst Pd$^z$Pc with the catalytic patterns $P_1$–$P_3$. F = functional group, A = alkyl or aryl residue (see also Table 1).

[*] Dr. H. Eckert, G. Fabry, G. Raudaschl, C. Seidel, Y. Kiesel
Organisch-chemisches Institut der Technischen Universität München
Lichtenbergstrasse 4, D-8046 Garching (Germany)

[**] Metal-Phthalocyanine Catalysts, Part 3. This work was supported by the Deutsche Forschungsgemeinschaft. – Part 2: [3a].

Table 1. Catalytic patterns $P_i$ of the catalyst $Pd^zPc$ in the conversion $A-F^1 \rightarrow A-F^2$ as a function of the valency $z$ and the pH value (see Scheme 1).

| $F^1$ | A | $z=2$ pH < 9 $P_1$ | $z=2$ pH > 11 $P_2$ | $z=1$ $P_3$ | $F^2$ |
|---|---|---|---|---|---|
| C=C, C≡N | Alkyl, Aryl | + | + | + | CH–CH, CH–NH |
| $NO_2$, CH=O | Aryl | + | + | + | $NH_2$, $CH_3$($P_3$ : $CH_2OH$) |
| $NO_2$, CH=O, Hal | Alkyl | – | – | + | $NH_2$, $CH_2OH$, H |
| Hal | Aryl | – | + | – | H |
| C=O, COCl, C≡N | Alkyl, Aryl | – | – | + | CHOH, $CH_2OH$, $CH_2NH_2$ |
| $CO_2-CH_2-Ph$ | Alkyl, Aryl | + | + | – | $CO_2H$ |
| $X-CH_2-Ph$ (X– = O–, N–, CON–), $CO_2R$, $CONR_2$ | Alkyl, Aryl | – | – | – | $F^1$ |

idence time, *etc.*) of the catalyst as well as the specific catalytic pattern $P_i$. The usual methods for achieving a certain specificity are either irreversible (*e.g.* modification of the catalyst by partial poisoning or special carrier materials) or lead to no significant catalytic pattern (*e.g.* kinetic control *via* the residence time)[2]; in both cases only a particular type of reaction can be catalyzed.

If, on the other hand, variation of the internal and external parameters is reversible *and* this variation causes specific catalytic patterns ($P_1$, $P_2$, $P_3 \ldots P_n$), then various reactions can be catalyzed with one catalyst, possibly even several successive steps of a multistep reaction.

In the case of thermally, chemically and photochemically stable palladium-phthalocyanine $Pd^zPc$, three patterns of catalysis can be regulated (Scheme 1 and Table 1).

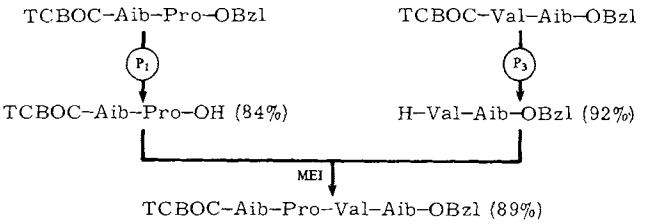
According to catalytic pattern $P_1$, CC and CN double bonds as well as aromatic aldehydes and nitro compounds can be hydrogenated with $H_2$ on blue $Pd^{II}Pc$ ($z=2$) at pH < 9; benzyl esters can also be cleaved by hydrogenation; at pH ≥ 11, hydrogenation can be carried out according to $P_2$; the same reactions are catalyzed as in the case of $P_1$, but in addition the selective dehalogenation of aryl halides can be carried out. Changing the valency to $z=1$ by addition of $NaBH_4$ effects catalysis on black $[Pd^IPc]^\ominus$ according to $P_3$[3a]. CC and CN double bonds (olefins, enamines, and azomethines), aliphatic and aromatic aldehydes, ketones, acyl chlorides, nitriles and nitro compounds as well as aliphatic halides can be reduced in good yields and *O*-β-haloalkyl groups reductively fragmented. Aryl halides remain intact and benzyl groups are not attacked reductively. The changes in the catalytic pattern are reversible: by oxidative acidolysis of the hydride and appropriate adjustment of the pH the catalytic pattern $P_1$ or $P_2$ is again possible.

If the variability of the specificity of the catalyst is expressed in terms of the specific catalytic patterns $P_i$, then the sum of the catalytic patterns $P_i$ can be defined as the *effective specificity S*.

$$S = \sum_{i=1}^{n} P_i ; \qquad i = 1, 2, 3 \ldots n$$

Consequently, in the case of $Pd^zPc$, $S=3$.

Catalyses on uncharged $Pd^{II}Pc$ necessitate a π-electron-rich system in the substrate. In contrast, the nucleophilic $[Pd^IPc]^\ominus$ anion catalyzes reactions at the electrophilic center of a substrate. As a consequence, the catalytic patterns $P_1-P_3$ are also inversely selective with respect to certain reactions. The possibilities for controlling reactions in multistep syntheses can be illustrated by the synthesis of the subsequence 13–16 TCBOC-Aib-Pro-Val-Aib-OBzl[7a] of the peptide antibiotic alamethicin[9] (see Scheme 2).




Scheme 2. Reaction control by the catalyst $Pd^zPc$ in the synthesis of the subsequence of alamethicin[7,9].

Reaction according to $P_1$ leads to selective cleavage of the benzyl residue with retainment of the TCBOC residue, whereas reaction according to $P_3$ leads to removal of TCBOC residue (inverse selectivity), with the benzyl residue remaining intact.

A self-initiation of the system $Pd^{II}Pc/H_2$/solvent in air could not be observed in any of the experiments. The catalyst $Pd^{II}Pc$ can be recovered quantitatively and used again without further treatment.

Received: December 23, 1982;
supplemented: September 7, 1983 [Z 230 IE]
German version: *Angew. Chem. 95* (1983) 894
The complete version of this communication appears in:
*Angew. Chem. Suppl. 1983,* 1291–1314

CAS Registry numbers:
$Pd^IPc^-$, 87566-95-8; $Pd^{II}Pc$, 20909-39-1.

[1] a) P. Heimbach, J. Kluth, H. Schenkluhn, *Kontakte 1982,* 3.
[2] a) J. Halpern, *Inorg. Chim. Acta 50* (1981) 11; b) L. Cerveny, V. Ruzicka, *Catal. Rev. Sci. Eng. 24* (1982) 503.
[3] a) H. Eckert, Y. Kiesel, *Angew. Chem. 93* (1981) 477; *Angew. Chem. Int. Ed. Engl. 20* (1981) 473; b) H. Eckert, Y. Kiesel, *Synthesis 1980,* 947; c) R. Scheffold, E. Amble, *Angew. Chem. 92* (1980) 643; *Angew. Chem. Int. Ed. Engl. 19* (1980) 629; e) A. Fischli, *Helv. Chim. Acta 65* (1982) 1167 and references cited therein; m) Y. Ohgo, S. Takeuchi, J. Yoshimura, *Bull. Chem. Soc. Jpn. 44* (1971) 283.
[7] a) TCBOC = 2,2,2-trichloro-*tert*-butyloxycarbonyl [7b]; Aib = 2-aminoisobutyric acid; Pro = proline; Val = valine; Bzl = benzyl; MEI = 2-morpholinoethyl isocyanide [7c]; b) H. Eckert, M. Listl, I. Ugi, *Angew. Chem. 90* (1978) 388; *Angew. Chem. Int. Ed. Engl. 17* (1978) 361; c) H. Aigner, G. Koch, D. Marquarding in W. Voelter, E. Wünsch, Y. Ovchinnikov: *Chem. Pept. Proteins, Proc. USSR-FRG Symp. 3rd, 1980,* de Gruyter, Berlin 1982, p. 209.
[9] a) H. Eckert, D. Marquarding, unpublished; b) G. D. Smith, V. Z. Pletnev, W. L. Duax, T. M. Balasubramanian, H. E. Bosshard, E. W. Czerwinski, N. E. Kendrick, F. S. Mathews, G. R. Marshall, *J. Am. Chem. Soc. 103* (1981) 1493.

 © Verlag Chemie GmbH, 6940 Weinheim, 1983 0570-0833/83/1111-0882 $ 02.50/0 

# Flip-Flop Hydrogen Bonds in β-Cyclodextrin—A Generally Valid Principle in Polysaccharides?**

By *Wolfram Saenger**, *Christian Betzel*, *Brian Hingerty*, and *George M. Brown*

*Dedicated to Professor Friedrich Cramer on the occasion of his 60th birthday*

In crystal structure analyses on cyclodextrins (CD)[1] the positions of all H atoms could be determined only in a few structures of α-CD but not in any of the larger β- and γ-forms, because of the large size of the unit cells and of the disorders frequently found in host molecules or molecules of water of hydration. But a knowledge of such positions is required in order to define the many H-bridges of type O–H···O. All H-atom positions in α-CD·6$H_2O$[4], and now even in β-CD·11$H_2O$, have been determined by neutron diffraction, revealing in the latter case an interesting scheme of hydrogen bonds.

In β-CD·11$H_2O$ the 11 water molecules in the β-CD cavity and between the cyclodextrin molecules are randomly distributed over 18 positions. The neutron diffraction investigation shows that this disorder is accompanied by a disorder of the H-bonds, leading to interactions of the type O–H···H–O, where the two H-atoms are only about 1 Å apart form each other, *i.e.* too near for both to be present at the same time. This is confirmed by the occupation parameters of the H atoms, which are on average 0.5 and, to a good approximation, add to give 1.0 for a hydrogen bond of this type. From this, it was concluded that an equilibrium O–H···O ⇌ O···H–O of normal H-bonds is established and that we "see" only the averaged state. Since in some cases these systems form longer chains,

$$\text{O–H···O–H···O–H···} \rightleftharpoons \text{H–O···H–O···H–O···}$$

and a flipping of the OH groups from one direction to the other must proceed cooperatively, we have called the O–H···H–O bridges flip-flop bonds[7].

Calorimetric measurements on β-CD·11$H_2O$ indicated an exothermic reaction at −46 °C[8], which we interpret as a flip-flop ordering process in one of the two possible directions. Recent neutron diffraction studies at −100 °C confirm this, and show that flip-flop bridges indeed behave dynamically and not only exist in static disorder.

Similar H-bridges of the type O–H···H–O have already been found in ice and ice-clathrates and effect the zero-point entropy in ice of 0.87 cal $mol^{-1}$ $K^{-1}$[10]. The disorder of the H-atoms in these systems is enforced by the high crystallographic symmetry, which fixes the positions of all the atoms. Since all O–H···H–O bridges in β-CD·11$H_2O$ are formed symmetry-independently, a *fundamentally* new situation is present here which probably has general validity for the hydration of complex molecular structures.

Several flip-flop arrangements are present in the crystal of β-CD·11$H_2O$, but only two characteristic ones will be discussed here. The first flip-flop chain winds itself around the $2_1$ screw axis and runs as an "infinite" spiral through the whole crystal structure. The chain is made up of water molecules W1 and hydroxy groups O(26), O(37), which belong to the same β-CD molecule.

···H–OW1–H···H–O(26)–H···H–O(37)–H···
H–OW1–H···H–O(26)–H···

Chains running through the entire lattice have already been observed in other structures, as also in α-CD·6$H_2O$; these chains, however, represent the normal type O–H···O–H···O–H, and all O–H···O bridges point in the same direction, indicating the influence of the cooperative effect[13].

The second characteristic flip-flop arrangement is limited to the β-CD molecule, in which *intra*molecular flip-flop bridges are formed between all O(2),O(3) hydroxy groups of adjacent glucose moieties (Fig. 2); the hydroxy H-atoms not participating in the flip-flop bonds do, however, participate in hydrogen bonding to "external" hydroxy groups (see also Fig. 1 in Supplement).

The formation of the flip-flop bridges between O(2) and O(3) is favored by an almost ideal O(2)···O(3) distance (mean value 2.85 Å), which is slightly greater than the

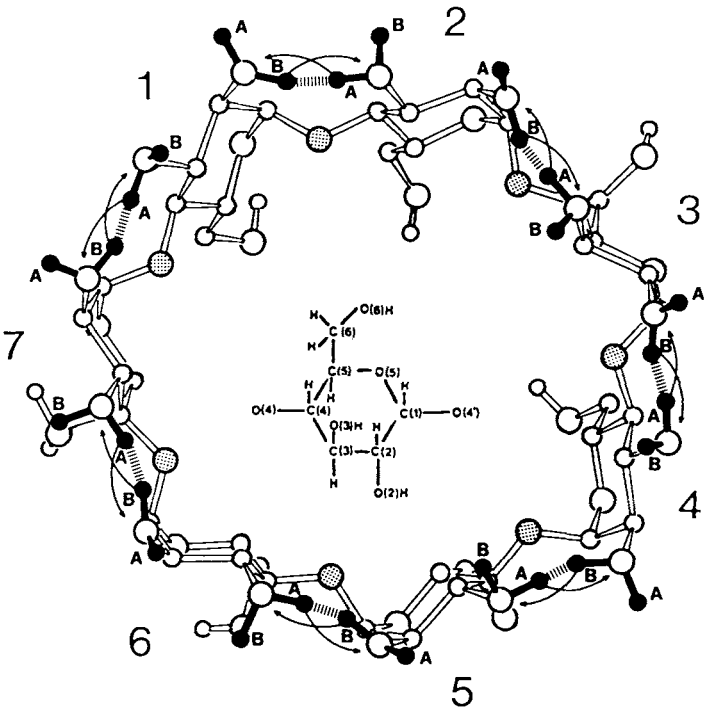



Fig. 2. Molecular structure of β-cyclodextrin in the crystal of β-CD·11$H_2O$. H-atoms on O(6) are shown as small open circles, on O(2),O(3) as small black circles, all other H-atoms have been omitted; O- and C-atoms are symbolized by large and medium sized circles, glucosidic O-atoms by dotted circles. The formula in the center illustrates the atomic designation. The ring-shaped structure of β-CD is stabilized by flip-flop hydrogen bridges of the type O–H···H–O between hydroxy groups O(2) and O(3) of neighboring glucose moieties. The corresponding H-atoms (A and B) cannot be present at the same time since the distances indicated by |||||||||| (≈1 Å) are too short. The H-atoms in each H-bridge are either only in position A or in position B (flip-flop). O–H···O Bridges between H-atoms (A, B) and O-atoms are indicated by bent arrows; they are in dynamic equilibrium. Between the positions A and B, which are adjacent to the glucosidic oxygen, and these oxygen atoms there are short distances of 2.23(5) to 2.58(2) Å, which are smaller than the sum of the van der Waals' radii (2.6 Å) and indicate weak attraction. Other distances in the H-bridges are: O(2)···O(3) 2.80(1) to 2.97(1) Å, O–H 0.87(2) to 0.98(2) Å, H···H 0.93(2) to 1.21(3) Å, O···H 1.83(2) to 2.12(3) Å.

[*] Prof. Dr. W. Saenger, C. Betzel
Institut für Kristallographie der Freien Universität
Takustrasse 6, D-1000 Berlin 33 (Germany)
Dr. B. Hingerty, Dr. G. M. Brown
Divisions of Biology and Chemistry, Oak Ridge National Laboratory
Oak Ridge, TN 37830 (USA)

[**] This work was supported by the Bundesministerium für Forschung und Technology and by the Fonds der Chemischen Industrie. *G. M. B.* and *B. H.* received support from the U. S. Department of Energy (Contract W-7405-ENG-26 with Union Carbide Corporation).

standard distance of 2.75—2.80 Å. In addition, closer contacts (2.23(5)—2.58(2) Å) exist between H-atoms in O(2),O(3) flip-flop bridges and the adjacent glucosidic O(4) atoms than correspond to the ideal van der Waals' H···O distance of 2.6 Å; this points to an attraction, which, however, is weaker than in normal O—H···O hydrogen bridges with significantly shorter H···O distances of *ca.* 1.8 Å.

The flip-flop bridges should be of general significance in systems in which, similarly as in β-CD, special steric conditions provide favorable prerequisites. To such systems belong, in particular, polysaccharides such as starch, which has a helical structure—irrespective of whether one considers the A-, B- or V-form—and always contains neighboring O(2),O(3), hydroxy groups. Flip-flop bridges are entropically favored over normal O—H···O bonds, because of two energetically almost equivalent states. The H/D exchange, which is markedly smaller for β-CD than for α-CD and starch, also suggests particularly strong intramolecular interactions for the bonding of the hydrogen atoms to O(2),O(3).

Received: April 22, 1983; revised: September 29, 1983 [Z 351 IE]
German version: *Angew. Chem. 95* (1983) 908
The complete version of this communication appears in:
*Angew. Chem. Suppl. 1983*, 1191—1202

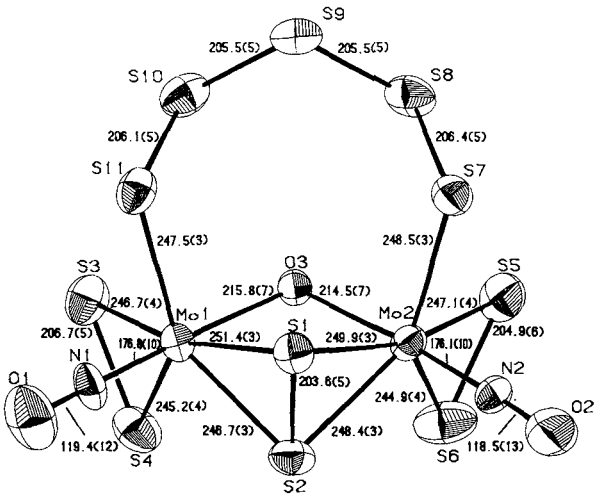
[1] J. Szejtli: *Cyclodextrins and their Inclusion Complexes*, Akadémiai Kiadó, Budapest 1982; W. Saenger, *Angew. Chem. 92* (1980) 343; *Angew. Chem. Int. Ed. Engl. 19* (1980) 344.
[4] B. Klar, B. Hingerty, W. Saenger, *Acta Crystallogr. B36* (1980) 1154.
[7] W. Saenger, C. Betzel, B. Hingerty, G. M. Brown, *Nature (London) 296* (1982) 581.
[8] T. Fujiwara, M. Yamazaki, Y. Tomizu, R. Tokuoka, K.-I. Tomita, T. Matsuo, H. Suga, W. Saenger, *Nippon Kagaku Kaishi 1983*, 181.
[10] L. Pauling, *J. Am. Chem. Soc. 57* (1936) 2680; F. Hollander, G. A. Jeffrey, *J. Chem. Phys. 66* (1977) 4699.
[13] G. A. Jeffrey, S. Takaji, *Acc. Chem. Res. 11* (1978) 264.

## $[Mo_2(NO)_2(S_2)_3(S_5)OH]^{3-}$, a Complex Containing a Bidentate $S_5^{2-}$-Bridging Ligand in a $\{S_5Mo_2(S_2)\}$-Heterocycle with Cyclooctasulfur Geometry

By *Achim Müller**, *Werner Eltzner*, *Hartmut Bögge*, and *Erich Krickemeyer*

The structural chemistry of sulfur-containing complexes with a central $\{MoNO\}^{3+}$ moiety is very interesting. Thus, in $[Mo_4(NO)_4(S_2)_6O]^{2-}$ **1**[1a] and $[Mo_4(NO)_4(S_2)_5(S)_3]^{4-}$ **2**[1b], which have almost the same stoichiometry, one finds four different types of coordinated $S_2^{2-}$ ligands. Salts of **1** and **2** can be obtained, under slightly different conditions, by reaction of $\{MoNO\}^{3+}$-complexes[2] with $S_x^{2-}$ or $H_2S$. We have now succeeded in isolating the novel diamagnetic complex $[Mo_2(NO)_2(S_2)_3(S_5)OH]^{3-}$ **3** (Fig. 1a) in crystals of the salts $K_{1.5}(NH_4)_{1.5}[Mo_2(NO)_2(S_2)_3(S_5)OH]\cdot 2H_2O$ **3a** and $(NH_4)_3[Mo_2(NO)_2(S_2)_3(S_5)OH]\cdot 2H_2O$ **3b** and in characterizing it by elemental analysis, ESCA, UV/VIS, IR[3] and Raman spectroscopy, magnetic measurements and by a complete X-ray structure analysis of **3b**[4].

In the binuclear complex **3**, the anions $OH^-$, $S_2^{2-}$ ("roof-shaped" coordinated) and $S_5^{2-}$ act as bridging ligands. A complex with a bridging $S_5^{2-}$ ligand has hitherto not been reported. The pentagonal bipyramidal coordination of the molybdenum atoms, which also occurs in **1** and **2**, is completed by a side-on bonded $S_2^{2-}$-ligand and an NO-ligand. The equatorial plane of the bipyramids is made up of sulfur atoms only.



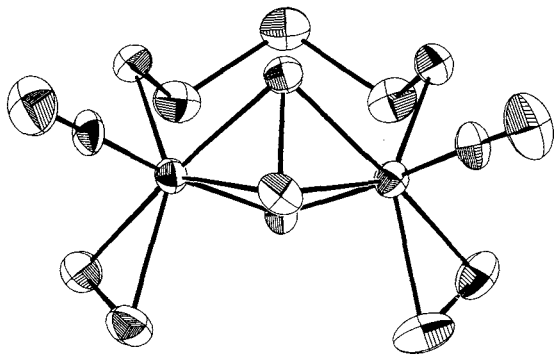



Fig. 1. Structure of the anionic complex **3** in crystals of **3b** in two different projections. Selected bond angles: S—S—S 108.2, S—S—Mo 108.1, S—Mo—S′ 111.6 (cf. text), Mo—S′—Mo 97.3, N—Mo—O3 173.4 (mean values), Mo—O—Mo 104.9(3)°. Further details of the crystal structure determination are available on request from the Fachinformationszentrum Energie Physik Mathematik, D-7514 Eggenstein-Leopoldshafen on quoting the depository number CSD 50 504, the names of the authors, and full citation of the journal.

One structural aspect is particularly interesting since the eight-membered heterocyclic moiety $\{S_5Mo_2(S_2)\}$ has practically the same geometry as that of cyclooctasulfur (cf. Fig. 1b); the eighth ring atom (S′) is hereby assumed to be at the center of the $S_2^{2-}$ group. (A systematic structural chemistry of $S_2^{2-}$-complexes could perhaps be developed on the basis of this concept!).

The formation of **3** appears to be favored primarily by the fact that the pentagonal-bipyramidal environment of the central atoms, which is frequently observed in the case of $\{MoNO\}^{3+}$ complexes, is retained, but probably also because a crown form of the $\{S_5Mo_2(S_2)\}$-heterocycle is achieved, as in $S_8$. We suspect that it will be possible to prepare further metal complexes with "units" which formally correspond to derivatives of cyclooctasulfur.

Remarkably, **3** (in contrast to **1** and **2**) is formed only after prolonged reaction, the oxidation of $S_2^{2-}$ to $S_5^{2-}$ by atmospheric oxygen possibly playing an essential role (cf. Procedure[5]).

Received: June 15, 1983 [Z 422 IE]
German version: *Angew. Chem. 95* (1983) 905

[*] Prof. Dr. A. Müller, W. Eltzner, Dr. H. Bögge, E. Krickemeyer
Fakultät für Chemie der Universität
Postfach 8640, D-4800 Bielefeld 1 (Germany)

[1] a) A. Müller, W. Eltzner, H. Bögge, S. Sarkar, *Angew. Chem. 94* (1982) 555; *Angew. Chem. Int. Ed. Engl. 21* (1982) 535; *Angew. Chem. Suppl. 1982*, 1167–1176; b) A. Müller, W. Eltzner, N. Mohan, *Angew. Chem. 91* (1979) 158; *Angew. Chem. Int. Ed. Engl. 18* (1979) 168; further experimental details in A. Müller, R. G. Bhattacharyya, W. Eltzner, N. Mohan, A. Neumann, S. Sarkar in H. F. Barry, P. C. H. Mitchell: *Proc. 3rd Int. Conf. Molybdenum*, Climax Molybdenum Comp., Ann Arbor 1979, p. 79.

[2] A. Müller, W. Eltzner, S. Sarkar, H. Bögge, P. J. Aymonino, N. Mohan, U. Seyer, P. Subramanian, *Z. Anorg. Allg. Chem. 503* (1983) 22.

[3] Main absorption bands in the IR spectrum (anion vibrations of **3b**; CsI pellet): ~3580 w ($\nu$(OH)), 1560 s ($\nu$(NO)), 810 m $\nu$(Mo(OH)Mo), 608 m ($\nu$(MoN): $\delta$(NO)), 521 m ($\nu(S_2)$), 474 w/425 m ($\nu(S_5)$), 341/315 m ($\nu$(MoS)) $cm^{-1}$.

[4] **3b** crystallizes in the space group $P2_1/n$, $a = 1114.8(4)$, $b = 1588.0(5)$, $c = 1206.7(4)$ pm, $\beta = 97.09(3)$, $Z = 4$; $R = 0.065$ for 2587 independent reflections (Syntex $P2_1$; $Mo_{K\alpha}$). The single crystal structure analysis of the isostructural complex **3a** leads to almost the same structure of the anion **3**.

[5] *Procedure:* A mixture of $(NH_4)_6Mo_7O_{24}\cdot 4H_2O$ (2.5 g), $NH_2OH$–HCl (2.1 g) and KSCN (15 g) or $NH_4SCN$ (15 g) (**3a** and **3b**, resp.) in water (20 mL) is heated with stirring for 1 h at 80 °C. To the solution, which contains $[Mo(NO)(NH_2O)(NCS)_4]^{2-}$ [2], 55 mL of ammonium polysulfide solution is added [obtained by passing $H_2S$ (*ca.* 1.5 H) into a suspension of 9 g sulfur in an aqueous $NH_3$ solution (200 mL 25% solution diluted with 300 mL $H_2O$)]—for **3a** in addition 2 g $KH_2PO_4$ and 4 g $Na_2HPO_4$ as buffer—and transferred to a 300 mL Erlenmeyer flask (in all operations covered with a watch glass). The mixture is heated to 50–55 °C for 1d and then allowed to cool to room temperature. **3a**: After 2 weeks the precipitated orange-red crystals obtained as sole reaction product (besides sulfur) are filtered off and washed with ethanol and $CS_2$. (Any precipitate produced after 1 week is filtered off). Yield 1.0 g—**3b**: procedure as for the isostructural compound **3a**. However, along with the orange-red, lance-shaped crystals **3b** (formed at the glass/air/solution contact) also sulfur (as a result of the high $NH_4^+$-content and the low pH value of the solution) and $NH_4^+$ the salt of **2** [1b] separate out at the bottom of the flask. Yield (separated mechanically) 0.1 g.

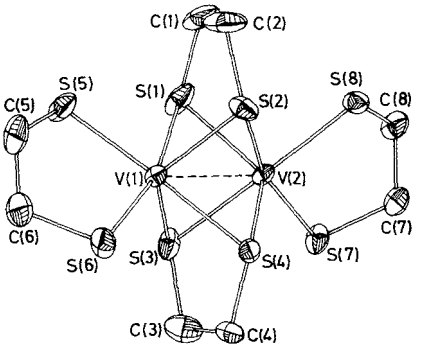



Fig. 1. Structure of the anionic complex **1** in crystals of the salt **2** with vibration ellipsoids (140 K, 50% probability, without H atoms). Selected distances [pm] ($\sigma$ 0.1 pm): V(1)···V(2) 257.5; V–(μ-S): V(1)–S(2) 236.8, V(1)–S(3) 239.3, V(1)–S(1) 248.5, V(1)–S(4) 249.3, V(2)–S(1) 237.5, V(2)–S(4) 238.5, V(2)–S(2) 248.0, V(2)–S(3) 249.2; V–($S_{term}$): V(1)–S(5) 238.4, V(1)–S(6) 238.0, V(2)–S(8) 237.0, V(2)–S(7) 236.6; Range of SVS angles [°] ($\sigma$ 0.05°): V(1) 70.59 to 161.39, V(2) 70.75 to 164.79. Further details of the crystal structure investigation are available on request from the Fachinformationszentrum Energie Physik Mathematik, D-7514 Eggenstein-Leopoldshafen on quoting the depository number CSD 50534, the names of the authors, and full citation of the journal.

## $[Ph_4P]_2[V_2(SC_2H_4S)_4]\cdot 4MeOH$: The First Polynuclear Vanadium-Sulfur Complex with Pure Sulfur Coordination**

By *Detlef Szeymies, Bernt Krebs,* and *Gerald Henkel**

Polynuclear vanadium complexes with complete sulfur coordination were hitherto unknown. We have now been able to prepare the binuclear complex $[V_2(SC_2H_4S)_4]^{2-}$ **1** (Fig. 1) as the first representative of this class of compounds by reaction of $VCl_3$ with 1,2-ethanedithiolate and to isolate the dianion in red-brown crystals of $[Ph_4P]_2[V_2(SC_2H_4S)_4]\cdot 4MeOH$ **2**.

The complex **1** is also the first vanadium-sulfur compound in which the ligands have "pure thiolate character", since special electronic conditions are associated with the ligands of the known dithiolene complexes[3].

**1** could serve as an entry to the chemistry of polynuclear thiolate or sulfide-thiolate complexes of vanadium, which is well developed in the case of iron or molybdenum as demonstrated by numerous examples.

The metal atoms in the dinuclear anion **1** are symmetrically bridged by the S atoms of two 1,2-ethanedithiolate ligands in such a way that an almost square arrangement of the sulfur atoms results (S···S 281.9(1) to 301.8(1) pm, S···S···S 89.15(4) to 90.37(4)°, mean deviation from the best plane *ca.* 10 pm). The coordination number for each $V^{III}$ atom is increased to 6 by a terminally bound 1,2-ethanedithiolate ligand. The resulting coordination polyhedron can be derived from an ideal trigonal prism by rotating the S(5)–S(6) edge twofold the around axis on which the vanadium atoms are sited. This is demonstrated in Figure 2, which shows a schematic projection along the V–V axis to the plane of the four bridging sulfur atoms. The S(5)–S(6) edge of the prism is twisted through an angle μ from ideal symmetry; for the distorted prisms of the two metal atoms this angle is *ca.* 30° ($\mu_{V(1)}$) and 36° ($\mu_{V(2)}$), respectively.

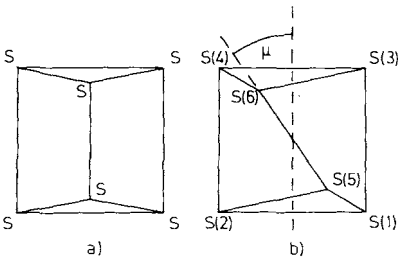



Fig. 2. Sulfur coordination about the metal atom V(1) (b), derived from an ideal trigonal prism (a).

The S···S distance within the terminal ligands, with an average value of 318.8 pm, is about 18 pm longer than the mean S···S distance within the bridging ligands (300.8 pm). This difference can be attributed to the *gauche* conformation of the terminal ligands, while the bridge ligands are in the eclipsed conformation. A particularly remarkable feature of the structure of **1** is the short distance between adjacent bridging S atoms which do not belong to the same dithiolate moiety. With an average value of 284.0 pm this distance is *ca.* 17 pm shorter than the S···S distance within the bridge ligands, and is thus indicative of a weakly bonding S···S interaction, as has also been discussed for the short S···S distance of *ca.* 307 pm in the mononuclear dithiolene complexes of vanadium, rhenium and molybdenum[3].

It has already been suggested that the structurally uncharacterized compounds $Cp_2V_2(SMe)_4$[18] and $Cp_2V_2(S_2C_2(CF_3)_2)_2$[19] contain a central $V_2S_4$ unit; the exis-

[*] Dr. G. Henkel, D. Szeymies, Prof. Dr. B. Krebs
Anorganisch-chemisches Institut der Universität
Corrensstrasse 36, D-4400 Münster (Germany)

[**] This work was supported by the Minister für Wissenschaft und Forschung des Landes Nordrhein-Westfalen and by the Fonds der Chemischen Industrie.

tence of a $V_2S_4$ core has now been demonstrated by a structural analysis in the case of **1**.

The distance between the vanadium atoms in the binuclear anion **1** is 257.5(1) pm. It thus lies between the values observed in $Cp_5V_5O_6$ (V···V 273.7(3) to 276.3(2) pm)[20] or $Cp_2V_2(CO)_5$ (V···V 246.2(2) pm), respectively, and $Cp_2V_2(CO)_4PPh_3$ (V···V 246.6(1) pm)[21], for which VV single and double bonds were discussed.

The UV/VIS spectrum of **1** shows two weak absorption bands at 615 and 540 nm and a shoulder at 470 nm. An intense band appears at 367 nm accompanied by a shoulder with about the same intensity at *ca.* 309 nm.

The IR spectrum exhibits a double absorption band below 400 $cm^{-1}$ at 365/354 $cm^{-1}$ (solid, CsI pellet); this could be caused by V–S stretching vibrations.

Received: July 8, 1983 [Z 458 IE]
German version: *Angew. Chem. 95* (1983) 903
The complete version of this communication appears in:
*Angew. Chem. Suppl. 1983*, 1176–1190

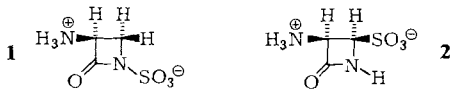
[3] R. Eisenberg, H. B. Gray, *Inorg. Chem. 6* (1967) 1844.
[18] R. H. Holm, R. B. King, F. G. A. Stone, *Inorg. Chem. 2* (1963) 219.
[19] R. B. King, *J. Am. Chem. Soc. 85* (1963) 1587.
[20] F. Bottomley, P. S. White, *J. Chem. Soc. Chem. Commun. 1981*, 28; F. Bottomley, D. E. Paez, P. S. White, *J. Am. Chem. Soc. 104* (1982) 5651.
[21] F. A. Cotton, B. A. Frenz, L. Kruczynski, *J. Am. Chem. Soc. 95* (1973) 951; J. C. Huffman, L. N. Lewis, K. G. Caulton, *Inorg. Chem. 19* (1980) 2755.

## Synthesis and Structure of (*Z*)-3-Amino-4-oxo-2-azetidinesulfonic Acids**

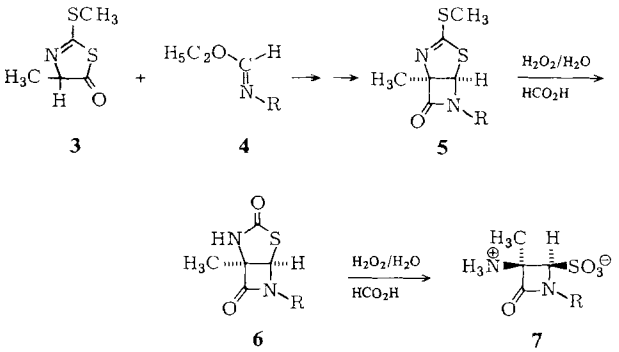
By *Dieter Hoppe**, *George M. Sheldrick**, *Ernst Egert*, and *Petra Kaars*

*Dedicated to Professor Hans Brockmann on the occasion of his 80th birthday*

Monobactams—*N*-acylated derivatives of the (*S*)-3-amino-2-oxo-1-azetidinesulfonic acid **1**—are naturally occurring β-lactam antibiotics[1]. Derivatives of the isomer **2** have so far never been described in the literature[2].



Herein we report a simple total synthesis of diastereomerically pure (racemic) (*Z*)-aminosulfonic acid **7** by oxidative-hydrolytic opening of the five-membered ring in the heterocycles **5**[3]; these dihydrothiazole-annelated azetidinones are obtained in only two steps from the thiazolone **3** and the formimidic acid esters **4**[3]. The conversion **5**→**7** was accomplished with aqueous $H_2O_2$ in formic acid—conditions under which we had previously obtained amines from open-chain imidothiocarbonates[4]. Reaction of with $H_2O_2$ in the molar ratio 1:6.5 in presence of *p*-toluene-**5**-sulfonic acid as catalyst afforded the crystalline, high-melting (m.p. > 260 °C) betaine **7** (Table 1); with a **5** : $H_2O_2$ ratio of 1 : 3, the 4-thia-2,6-diazabicyclo[3.2.0]heptane-3,7-diones **6** can be isolated. Thus, reaction is initiated by oxidation of the exocyclic sulfur atom in **5**; this is followed by hydrolysis and further oxidation steps.



| 4–7 | a | b | c |
|---|---|---|---|
| R | $C_6H_5$ | $H_3CO_2C$, $CH_3$, $CH_3$ | $C_6H_5CH_2O_2C$, $CH_3$, $CH_3$ |

Table 1. Yields of the reactions **5**→**6** and **5**→**7** [a].

| | Yield [%] | |
|---|---|---|
| | **6** [b, c] | **7** [d, e] |
| **a** | 76 | 89 |
| **b** | 68 | 75 |
| **c** | 65 | 70 |

[a] The products were obtained analytically pure. [b] Per mmol **5**: 3.0 mmol 30% aqueous $H_2O_2$ in 2.0 mL 98% $HCO_2H$ and 0.04 mmol *p*-TsOH; 8 h at −10 °C. [c] After purification by column chromatography; yields refer to **5**. [d] As described under [b], but with 6.5 mmol $H_2O_2$ and 4 h at 0 °C. [e] Yields refer to **5** after crystallization from methanol.

As was to be expected from the structure of the bicycles **5** and **6**, and has been confirmed by an X-ray structure analysis of **7b** (Fig. 1), the $NH_3^{\oplus}$ and the $SO_3^{\ominus}$ groups in **7** are *cis* oriented. The four-membered ring is almost planar. As in other monocyclic β-lactams[6] a planar amide grouping is favored: N(4) deviates by only about 6.4 pm from

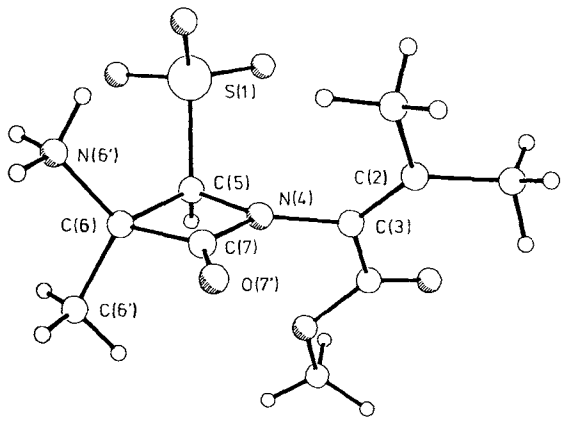



Fig. 1. Structure of **7b** in the crystal. Selected bond lengths [pm] and angles [°] (standard deviations 0.4 pm and 0.2°, respectively). C(3)–N(4) 142.3; N(4)–C(5) 146.5; N(4)–C(7) 137.1; C(5)–C(6) 156.3; C(6)–C(7) 154.6; C(7)–O(7') 120.0; C(5)–S(1) 178.2; C(6)–N(6') 147.9; C(6)–C(6') 151.9; C(5)–N(4)–C(7) 95.5; C(6)–C(5)–N(4) 87.6; C(7)–C(6)–C(5) 85.0; N(4)–C(7)–C(6) 91.6; N(4)–C(7)–O(7') 133.3.

[*] Prof. Dr. D. Hoppe, Dr. P. Kaars
Institut für Organische Chemie der Universität
Tammannstrasse 2, D-3400 Göttingen (Germany)
Prof. G. M. Sheldrick, Dr. E. Egert
Institut für Anorganische Chemie der Universität
Tammannstrasse 4, D-3400 Göttingen (Germany)

[**] Studies on the β-Lactam Synthesis Part 7. This work was support by the Deutsche Forschungsgemeinschaft and the Fonds der Chemischen Industrie (Liebig Fellowship for *E. E.*).—Part 6: D. Hoppe, M. Kloft, *Liebigs Ann. Chem. 1980*, 1527.

the plane of its three neighbors. In the crystal there are two hydrogen bonds between the ammonium group and the sulfonate moieties of their neighboring molecules; the third hydrogen atom of the $NH_3^{\oplus}$ group takes part in inter- as well as intramolecular bridging. The planes of the four-membered ring and the unsaturated side chain are twisted through an angle of about 62.9° with respect to each other; presumably the loss of an enamide resonance is a consequence of the dense crystal packing.

Received: July 11, 1983 [Z 460 IE]
German version: *Angew. Chem. 95* (1983) 912
The complete version of the communication appears in:
*Angew. Chem. Suppl. 1983*, 1333–1342

CAS Registry numbers:
(±)-**3**, 87586-83-2; (*E*)-**4b**, 87586-84-3; (*E*)-**4c**, 87586-85-4; (±)-**5a**, 87586-86-5; (±)-**5b**, 87586-87-6; (±)-**5c**, 87586-88-7; (±)-**6a**, 87586-89-8; (±)-**6b**, 87597-05-5; (±)-**6c**, 87586-90-1; (±)-**7a**, 87586-91-2; (±)-**7b**, 87586-92-3; (±)-7c, 87586-93-4.

[1] a) A. Imada, K. Kitano, K. Kintaka, M. Muroi, M. Asai, *Nature 289* (1981) 590; b) R. B. Sykes, C. M. Cimarusti, D. P. Bonner, K. Bush, D. M. Floyd, N. H. Georgopapadakou, W. H. Koster, W. C. Liu, W. L. Parker, P. A. Principe, M. L. Rathnum, W. A. Slusarchyk, W. H. Trejo, J. S. Wells, *ibid. 291* (1981) 489; c) D. M. Floyd, A. W. Fritz, J. Pluscec, E. R. Weaver, C. M. Cimarusti, *J. Org. Chem. 47* (1982) 5160.

[2] For the synthesis of (*E*)-3-acylamino-4-oxo-2-azetidinesulfinic acids from penicillin derivatives: C. M. Pant, J. Steele, R. J. Stoodley, *J. Chem. Soc. Perkin Trans. 1 1982*, 595.

[3] E. Raude, D. Hoppe, *Angew. Chem. 89* (1977) 553; *Angew. Chem. Int. Ed. Engl. 16* (1977) 544.

[4] a) D. Hoppe, L. Beckmann, *Liebigs Ann. Chem. 1979*, 2066; b) D. Hoppe, E. Raude, *ibid. 1979*, 2076.

[6] Structure analyses of monocyclic 2-azetidinones: a) J. L. Luche, H. B. Kagan, R. Parthasarathy, G. Tsoucaris, C. de Rango, C. Zelwer, *Tetrahedron 24* (1968) 1275; R. Parthasarathy, *Acta Crystallogr. B 26* (1970) 1283; b) E. F. Paulus, D. Kobelt, H. Jensen, *Angew. Chem. 81* (1969) 1048; *Angew. Chem. Int. Ed. Engl. 8* (1969) 990; c) G. Kartha, G. Ambady, *J. Chem. Soc. Perkin Trans. 2 1973*, 2042; d) H. Fujiwara, R. L. Varley, J. M. van der Veen, *J. Chem. Soc. Perkin Trans. 2 1977*, 547.

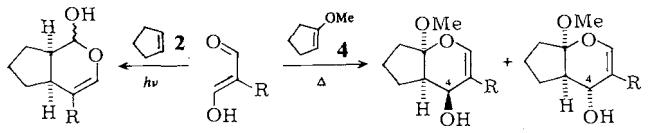
## Acceleration and Asymmetric Induction of Intermolecular Diels-Alder-Reactions of Triacyl Compounds**

By *Lutz-F. Tietze** and *Karl-Heinz Glüsenkamp*

*Dedicated to Professor Karl Winnacker on the occasion of his 80th birthday*

Triacyl compounds are readily accessible educts which have been used with considerable success in the synthesis of complex natural products by photochemical cycloaddition[1]. Thus, photochemical reaction of methyl diformylacetate **3a** with cyclopentene **2** affords, in a single step, the molecular framework of the iridoids **1a**, a widely distributed class of natural products[1a]. We have shown that triacyl compounds such as **3b** also undergo thermal cycloadditions with enol ethers such as **4** and with thioenol ethers[2]: the diastereomeric dihydropyran derivatives *rac*-**5b** and *rac*-**6b** are formed in the ratio 3 : 1 from **4** within a few hours at 20 °C.

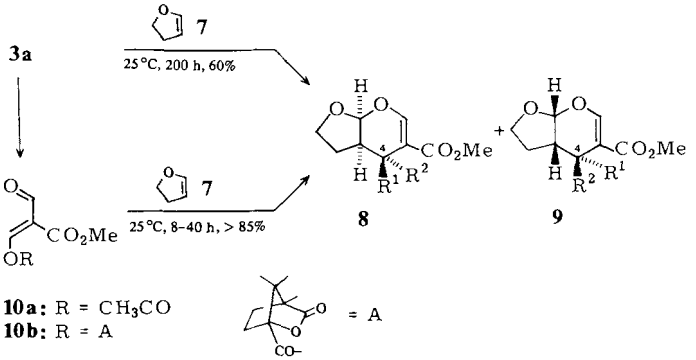
In contrast, less reactive triacyl compounds such as **3a** only form cycloadducts with exceedingly reactive enol ethers. After 200 h, reaction of **3a** with 1-methoxycyclopentene **4** (molar ratio: 1 : 3) at 20 °C leads to the diastereomers *rac*-**5a** and *rac*-**6a** (82%) in the ratio 3 : 1. With dihydrofuran **7** the cycloadducts **8a/9a** and **8b/9b** in the ratio 3 : 1 are obtained in 60% yield after 200 h, the reaction being incomplete; with dihydropyran practically no reaction occurs[4a]. However, if the sodium salt of **3a** is acylated to **10a** with acetyl chloride before the Diels-Alder reaction, the cycloaddition with **7** proceeds quantitatively in 8 h. The diastereomeric enantiomer-pairs **8c/9c** and **8d/9d** are formed in 85% yield. It is notable here that the diastereomeric ratio of 1 : 2 is almost inverted relative to the reaction with **3a**[4b].



**1** **3** **5** **6**

**a**: R = $CO_2Me$; **b**: R = CHO

Presumably the higher reactivity of the *O*-acyl compound **10a** in this Diels-Alder reaction with inverse electron demand[3] arises from a lowering of the energy of the LUMO of the diene component.



**10a**: R = $CH_3CO$
**10b**: R = A



| | $R^1$ | $R^2$ | |
|---|---|---|---|
| **8a** | OH | H | **9a** |
| **8b** | H | OH | **9b** |
| **8c** | OAc | H | **9c** |
| **8d** | H | OAc | **9d** |
| **8e** | O–A | H | **9e** |
| **8f** | H | O–A | **9f** |

**8a/9a, 8b/9b, 8c/9c,** and **8d/9d** are enantiomeric pairs.

Use of chiral acid chlorides for the *O*-acylation allows an asymmetric induction. Reaction of the sodium salt of **3a** with camphanoyl chloride in the presence of dihydrofuran **7** at 20 °C gives a mixture of diastereomers **8e** and **9e** as well as **8f** and **9f** (in **8e** and **9e** as well as **8f** and **9f** the dihydropyran systems exhibit enantiomeric properties) *via* **10b** after 40 h. The diastereomeric pairs **8e/9e** and **8f/9f**, which are formed in the ratio 1 : 2, can be separated by chromatography. The ratio of **8f** to **9f** is 1 : 3.2, corresponding to 52% *d.e.* Pure **9f** can be obtained in 41% yield by crystallization. The absolute configuration of **9f** was determined by X-ray structure analysis[5].

Received: July 15, 1983 [Z 468 IE]
German version: *Angew. Chem. 95* (1983) 901

[*] Prof. Dr. L.-F. Tietze, Dr. K.-H. Glüsenkamp
Institut für Organische Chemie der Universität
Tammannstrasse 2, D-3400 Göttingen (Germany)

[**] Intermolecular Hetero-Diels-Alder Reactions, Part 4. This work was supported by the Fonds der Chemischen Industrie.—Part 3: [3b].

[1] a) L.-F. Tietze, *Angew. Chem. 95* (1983) 840; *Angew. Chem. Int. Ed. Engl. 22* (1983) 828; G. Büchi, J. A. Carlson, J. E. Powell, Jr., L.-F. Tietze, *J.*

*Am. Chem. Soc. 92* (1970) 2165; *95* (1973) 540; J. J. Partridge, N. K. Chadha, M. R. Uskokovic, *ibid. 95* (1973) 532; L.-F. Tietze, U. Niemeyer, *Chem. Ber. 111* (1978) 2423; b) L.-F. Tietze, K.-H. Glüsenkamp, M. Nakane, C. R. Hutchinson, *Angew. Chem. 94* (1982) 81; *Angew. Chem. Int. Ed. Engl. 21* (1982) 70; *Angew. Chem. Suppl. 1982*, 126; S. W. Baldwin, M. T. Grimmins, *J. Am. Chem. Soc. 104* (1982) 1132; cf. also P. de Mayo, *Acc. Chem. Res. 4* (1971) 41.

[2] L.-F. Tietze, K.-H. Glüsenkamp, K. Harms, K. Remberg, G. M. Sheldrick, *Tetrahedron Lett. 23* (1982) 1147; cf. also R. R. Schmidt, M. Maier, *ibid. 23* (1982) 1789.

[3] a) G. Desimoni, G. Takoni, *Chem. Rev. 75* (1975) 651; R. Sustmann, *Pure Appl. Chem. 1979*, 569; b) L.-F. Tietze, K.-H. Glüsenkamp, W. Holla, *Angew. Chem. 94* (1982) 793; *Angew. Chem. Int. Ed. Engl. 21* (1982) 787.

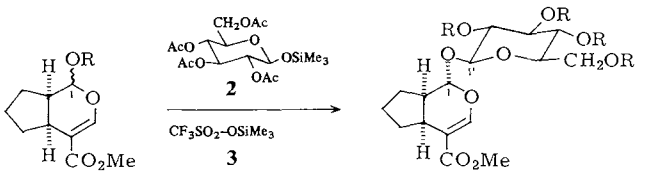
[4] a) **3a** (1.00 mmol) is suspended in 5 mL of oxygen-free toluene/dichloromethane (10 : 1), treated with 2—3 mmol of **4** or **7**, and stirred for 200 h at 20°C. After evaporation of the solvent, the residue is chromatographed on silica gel (ether). **5a**: 60% ($R_F$ = 0.48), **6a**: 22% ($R_F$ = 0.29), **8a**/**9a**: 45% ($R_F$ = 0.32). $^1$H-NMR ($CDCl_3$): 4-H: **5a**: $\delta$ = 4.74 (d, $J$ = 7.0 Hz); **6a**: $\delta$ = 4.34 (d, $J$ = 1.0 Hz, after H/D exchange); **8a**/**9a**: $\delta$ = 5.02 (d, $J$ = 7.0 Hz).—b) 1.00 mmol of the dried Na salt of **3a** (60°C, 40 h *in vacuo*) is suspended in 5 mL of anhydrous, oxygen-free toluene, treated with 2.00 mL of enol ether followed by 1.30 mmol of acetyl chloride; the mixture is then stirred for 8—40 h at 20°C. After evaporation of the solvent, the residue is chromatographed on silica gel at 5°C (**8c**/**9c** + **8d**/**9d**: ether; **8e**, **8f**, **9e**, **9f**: ether/petroleum ether 3 : 1). **8c**/**9c** and **9f** are purified by crystallization. **8c**/**9c**: m.p. = 107—109°C. $^1$H-NMR ($CDCl_3$): $\delta$ = 5.78 (d, $J$ = 2.0 Hz; 1H, 4-H). **9f**: m.p. = 170°C, $[\alpha]_{20}^{D}$ −90 ($c$ = 0.2 in $CHCl_3$). $^1$H-NMR ($CDCl_3$): $\delta$ = 5.95 (d, $J$ = 2.0 Hz; 1H, 4-H).

[5] L.-F. Tietze, K.-H. Glüsenkamp, K. Harms, G. M. Sheldrick, unpublished results.

## Stereoselective Synthesis of Iridoid Glycosides**

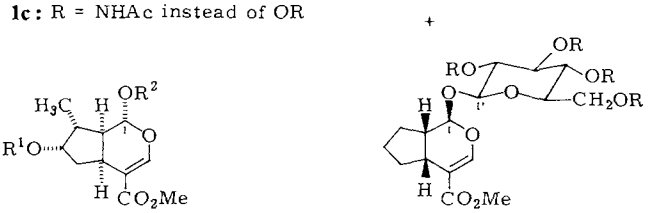
By *Lutz-F. Tietze** and *Roland Fischer*

The iridoid glycosides are a widely distributed class of natural products. As characteristic structure element they contain a partially hydrogenated cyclopenta[c]pyran which is linked β-glycosidically at C-1 to D-glucose[1]. Glycosidation of iridoid aglycones is associated with considerable difficulties[2]. Thus in the preparation of loganin **6c**, the first and, to date, only total synthesis of a naturally occurring iridoid glycoside, low yields were obtained in the formation of the glycosidic bond[3].




**1a**: R = Me
**1b**: R = Ac
**1c**: R = NHAc instead of OR

**4a**: R = Ac
**4b**: R = H




**6a**: $R^1$ = Ac, $R^2$ = Ac (C-1: *R* + *S*)
**6b**: $R^1$ = Ac, $R^2$ = β-D-Glc(OAc)$_4$
**6c**: $R^1$ = H, $R^2$ = β-D-Glc

**5a**: R = Ac
**5b**: R = H

[*] Prof. Dr. L.-F. Tietze, R. Fischer
Institut für Organische Chemie der Universität
Tammannstrasse 2, D-3400 Göttingen (Germany)

[**] Iridoids, Part 19. This work was supported by the Fonds der Chemischen Industrie.—Part 18: L.-F. Tietze, K. H. Glüsenkamp, W. Holla, *Angew. Chem. 94* (1982) 793; *Angew. Chem. Int. Ed. Engl. 21* (1982) 787.

We now describe an efficient and stereoselective synthesis of iridoid glycosides using trimethylsilyl trifluoromethanesulfonate **3** as catalyst. In the course of investigations on the synthesis of glycosides with 1,1′-diacetal part structures, we were able to show that acetals reacted with the trimethylsilyl-β-glucoside **2** in the presence of catalytic amounts of **3** to form selectively the α- and β-glycosides[4a]. However, the reaction of the racemic model compound iridoid aglycone-*O*-methyl ether *rac*-**1a** with **2** and catalytic amounts of **3** in acetonitrile at −30°C proceeds exceedingly slowly, leading to anomerization[4c] of **2** as a side reaction. In contrast, the reaction with *rac*-**1b** leads in 10 h at −30°C to a 1 : 1-mixture of the two diastereomeric β-glycosides **4a** and **5a**, which can be separated by column chromatography (silica gel, petroleum ether/ethyl acetate 3 : 1) and solvolyzed (NaOMe, MeOH, 20°C, 95% yield) to the free glycosides **4b** and **5b**. α-Glycosides and C-1 epimers were not detected (< 3%). Since the mixture of acetates *rac*-**1b**, which are epimeric at C-1[4b], is used in the reaction, it must be presumed that a carbocation occurs as intermediate at C-1. The exclusive formation of the stereoisomer with *trans*-orientation of the glucose moiety to the cyclopentane ring probably arises from steric effects. However, a disadvantage is the formation of the amide **1c**, which is obtained in 8% yield from **1b** and acetonitrile. This side reaction does not occur when dichloromethane, chloroform, or toluene is used as solvent; however, the glycosidation becomes slower, leading to partial anomerization of **2** and formation of α-glycosides. If, in contrast, the reaction of *rac*-**1b** with **2** and 30 mol-% **3** is conducted in liquid $SO_2$ at −50°C, the β-glycosides **4a** and **5a**[5] are obtained in 91% yield (α-glycosides < 5%). Reaction of enantiomerically pure **1b**, obtained from **4b** by glycosidic cleavage using emulsin and subsequent acetylation, leads to glycoside **4a** in 92% yield.

By analogy, reaction of loganol diacetate **6a** (30 mol-% **3**, −40°C, 60 h) results in its conversion into loganin pentaacetate **6b** in 75% yield (α-glucoside < 10%), which can be solvolyzed (NaOMe, MeOH, 20°C, 4 h, 93% yield) to the natural product loganin **6c**.

Received: July 15, 1983 [Z 469 IE]
German version: *Angew. Chem. 95* (1983) 902

[1] L.-F. Tietze, *Angew. Chem. 95* (1983) 840; *Angew. Chem. Int. Ed. Engl. 22* (1983) 828; L. J. El-Naggar, J. L. Beal, *J. Nat. Prod. (Lloydia) 43* (1980) 524.

[2] a) O. Halpern, H. Schmid, *Helv. Chim. Acta 41* (1958) 1109; b) L.-F. Tietze, U. Niemeyer, *Chem. Ber. 111* (1978) 2423; c) L.-F. Tietze, U. Niemeyer, P. Marx, K.-H. Glüsenkamp, *Tetrahedron 36* (1980) 1231; d) L.-F. Tietze, U. Niemeyer, P. Marx, K.-H. Glüsenkamp, L. Schwenen, *ibid. 36* (1980) 735.

[3] G. Büchi, J. A. Carlson, J. E. Powell, Jr., L.-F. Tietze, *J. Am. Chem. Soc. 92* (1970) 2165; *95* (1973) 540. The yield of the glycosidation was 1.4%. Using other methods this could be increased to 10% [2b].

[4] a) L.-F. Tietze, R. Fischer, *Tetrahedron Lett. 22* (1981) 3239; *Angew. Chem. 93* (1981) 1002; *Angew. Chem. Int. Ed. Engl. 20* (1981) 969; b) *rac*-**1a** signifies a 1 : 1 mixture of **1a** and its mirror image, *i.e.*—since **1a** is a mixture of the C-1 epimers—of four chemical species; c) L.-F. Tietze, R. Fischer, H. J. Guder, *Synthesis 1982*, 946.

[5] 0.5 mL $SO_2$ is condensed into *rac*-**1b** (24.0 mg, 0.10 mmol) and **2** (50.4 mg, 0.12 mmol) at *ca.* −190°C. Subsequently, the mixture is warmed to −50°C, treated with 5.1 mL **3** (30 mol-%), and stirred for *ca.* 50 h at −50°C (TLC monitoring, silica gel, hexane/ethyl acetate 3 : 1). After addition of 30 μL triethylamine and 20 μL saturated $NaHCO_3$ solution, the solvent is evaporated and the residue extracted with dichloromethane and chromatographed.—The spectroscopic data for the glycosides are consistent with the values in the literature [2c]. The absolute configuration of **4b** was determined from the chiroptic data [2d].—$^1$H- and $^{13}$C-NMR ([D$_6$]-acetone/D$_2$O, TMS int.):—$\delta$-values, $J$ in Hz (in parenthesis), 1-H: **4b**: 5.07 (6.5); **5b**: 5.19 (6.5); **6c**: 5.34 (4.0). 1′-H: **4b**: 4.69 (7.5); **5b**: 4.75 (7.5); **6c**: 4.74 (7.5). C-1: **4b**: 97.87; **5b**: 102.42; **6c**: 98.25. C-1′: **4b**: 99.75; **5b**: 104.21; **6c**: 100.32.

 © Verlag Chemie GmbH, 6940 Weinheim, 1983 0570-0833/83/1111-0888 $ 02.50/0 

## Formation of Alkyl Radicals by Thermal Bimolecular Reaction of Alkanes and Alkenes

By *Jürgen O. Metzger**

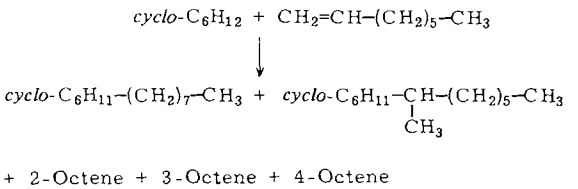
The symproportionation (a) of an alkane and an alkene to give two alkyl radicals is a thermodynamically feasible elementary reaction that has long been sought[1]. It is the reverse of the disproportionation of alkyl radicals. In contrast to the intensively investigated homolysis of single bonds (b)—the reversal of the recombination of alkyl radicals—the symproportionation has so far never been unequivocally demonstrated[2].

$$R^1H + CH_2{=}CH{-}R^2 \rightleftharpoons {}^{\circ}R^1 + CH_3{-}\overset{\oplus}{C}H{-}R^2 \quad (a)$$

$$R^1{-}R^2 \rightleftharpoons {}^{\circ}R^1 + {}^{\circ}R^2 \quad (b)$$

The activation enthalpy of the bimolecular reaction (a) is substantially lower than that of the monomolecular homolysis (b); it is equal to the negative reaction enthalpy of the radical disproportionation and is thus easy to evaluate by thermochemical methods[3]. In some special cases a knowledge of the symproportionation was considered essential for interpreting the course of a reaction: A classical example is the initiation reaction of the spontaneous polymerization of styrene. However, recent findings by *Pryor* would appear to contradict such an initiation reaction[1b].

We have already shown in earlier experiments that alkanes can be added to alkenes in a thermally initiated reaction[10]. Kinetic studies on the addition of cyclohexane to 1-octene clearly revealed that a radical chain reaction is involved.




Cyclohexane was allowed to react with 1-octene (molar ratio 100:1) at 360—450°C and 200 bar with total exclusion of oxygen until *ca.* 90% conversion. 1-Octene reacts in two parallel reactions with formation of the adducts 1-cyclohexyloctane and 2-cyclohexyloctane (total yield of adducts *ca.* 50% referred to 1-octene; ratio of the two regioisomers 94.9:5.1) as well as isomeric octenes. In addition, *n*-octane and cyclohexylcyclohexane are also detected in the product mixture. The kinetics of the initiation reaction can be described in terms of equation (c).

$$v_{start} = k_i[\text{1-octene}][\text{cyclohexane}] \quad (c)$$

$$cyclo\text{-}C_6H_{12} + CH_2{=}CH{-}(CH_2)_5{-}CH_3 \underset{k_t}{\overset{k_i}{\rightleftharpoons}} cyclo\text{-}C_6H_{11}^{\circ} + CH_3{-}\overset{\oplus}{C}H{-}(CH_2)_5{-}CH_3 \quad (d)$$

The experimentally determined value of $\lg(k_i/k_t)^{1/2} = -6.89$ yields the quasi steady-state radical concentration $[\text{cyclohexyl}]_{exp} = 5.82 \times 10^{-8}$ mol/L at 450°C and 200 bar. This value is in good agreement with the radical concentration of $[\text{cyclohexyl}]_{calc} = 5.83 \times 10^{-8}$ mol/L obtained on calculation of the equilibrium (d) from the thermochemical data.

The results of the kinetic investigation can only be satisfactorily explained in terms of the initiation reaction (d). Other initiation reactions such as homolysis of CC bonds of the alkane and of the alkene, bimolecular disproportionation of alkene, or intermediary formation of a 1,2-diradical combined with an H-abstraction from the alkane, lead to other rate equations, other activation energies, or completely different A factors.

A two-step reaction path *via* a 1,2-diradical can be confidently ruled out; it would be orders of magnitude slower than the observed reaction. This means that the thermal formation of radicals from alkane and alkene must proceed in one step as bimolecular metathesis, *i.e.* indeed as a reversal of the disproportionation of alkyl radicals with the same transition state[1a]. Thus, the kinetics and thermodynamics are consistent with an initiation reaction as depicted in equation (a). This can be used for the investigation of radical reactions over a wide range of temperatures and without the addition of special radical initiators. This type of reaction obviously plays an important role in cracking processes[26]; it must also proceed intramolecularly and is possibly of significance in thermal intramolecular reactions such as the retro-ene reaction.

Received: January 26, 1983;
revised: September 13, 1983 [Z 256 IE]
German version: *Angew. Chem. 95* (1983) 914
*The complete version of this communication appears in: Angew. Chem. Suppl. 1983*, 1256—1266

CAS Registry numbers:
*cyclo*-$C_6H_{12}$, 110-82-7; $CH_2{=}CH(CH_2)_5CH_3$, 111-66-0.

[*] Priv.-Doz. Dr. J. O. Metzger
Fachbereich Chemie der Universität
Postfach 2503, D-2900 Oldenburg (Germany)

[1] a) N. N. Semjonow: *Einige Probleme der chemischen Kinetik und Reaktionsfähigkeit*, Akademie-Verlag, Berlin 1961, p. 298; b) W. A. Pryor: *Organic Free Radicals, ACS Symp. Ser. 69* (1978) 33.
[2] M. L. Boyd, M. H. Back, *Can. J. Chem. 46* (1968) 2427.
[3] S. W. Benson: *Thermochemical Kinetics*, Wiley, New York 1976, p. 156.
[10] a) J. O. Metzger, J. Hartmanns, P. Köll, *Tetrahedron Lett. 22* (1981) 1891; b) J. O. Metzger, J. Hartmanns, D. Malwitz, P. Köll, "Thermal Organic Reactions in Supercritical Fluids", in M. E. Paulaitis, J. M. L. Penninger, R. D. Gray, H. W. P. Davidson: *Chemical Engineering at Supercritical Fluid Conditions*, Ann Arbor Science Publ., Ann Arbor 1983, p. 515.
[26] A. V. Gorokhovskii, A. D. Stepukhoviek, *Kinet. Katal. 22* (1979) 839.

## [2]-[Cyclohexatetraoctane][cyclooctacosane]catenane, the First Hydrocarbon Catenane**

By *Gottfried Schill**, *Norbert Schweickert*, *Hans Fritz*, and *Walter Vetter*

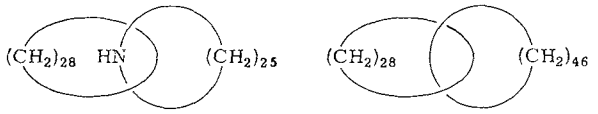
*Dedicated to Professor Karl Winnacker on the occasion of his 80th birthday*

We previously obtained catenanes from precatenanes by specific cleavage of particular bonds[1]. The [2]-catenanes thus obtained contain a quinoid nucleus in one macrocycle and a nitrogen atom in the other. The simplest previously isolated catenane **1a** was synthesized by chemically degrading this system[2]. We have now prepared and isolated

[*] Prof. Dr. G. Schill, N. Schweickert
Institut für Organische Chemie der Universität
Albertstrasse 21, D-7800 Freiburg (Germany)
Prof. Dr. H. Fritz
Ciba-Geigy AG, CH-4002 Basel (Switzerland)
Dr. W. Vetter
Hoffmann-La Roche AG, CH-4002 Basel (Switzerland)

[**] This work was supported by the Deutsche Forschungsgemeinschaft and by the Fonds der Chemischen Industrie.

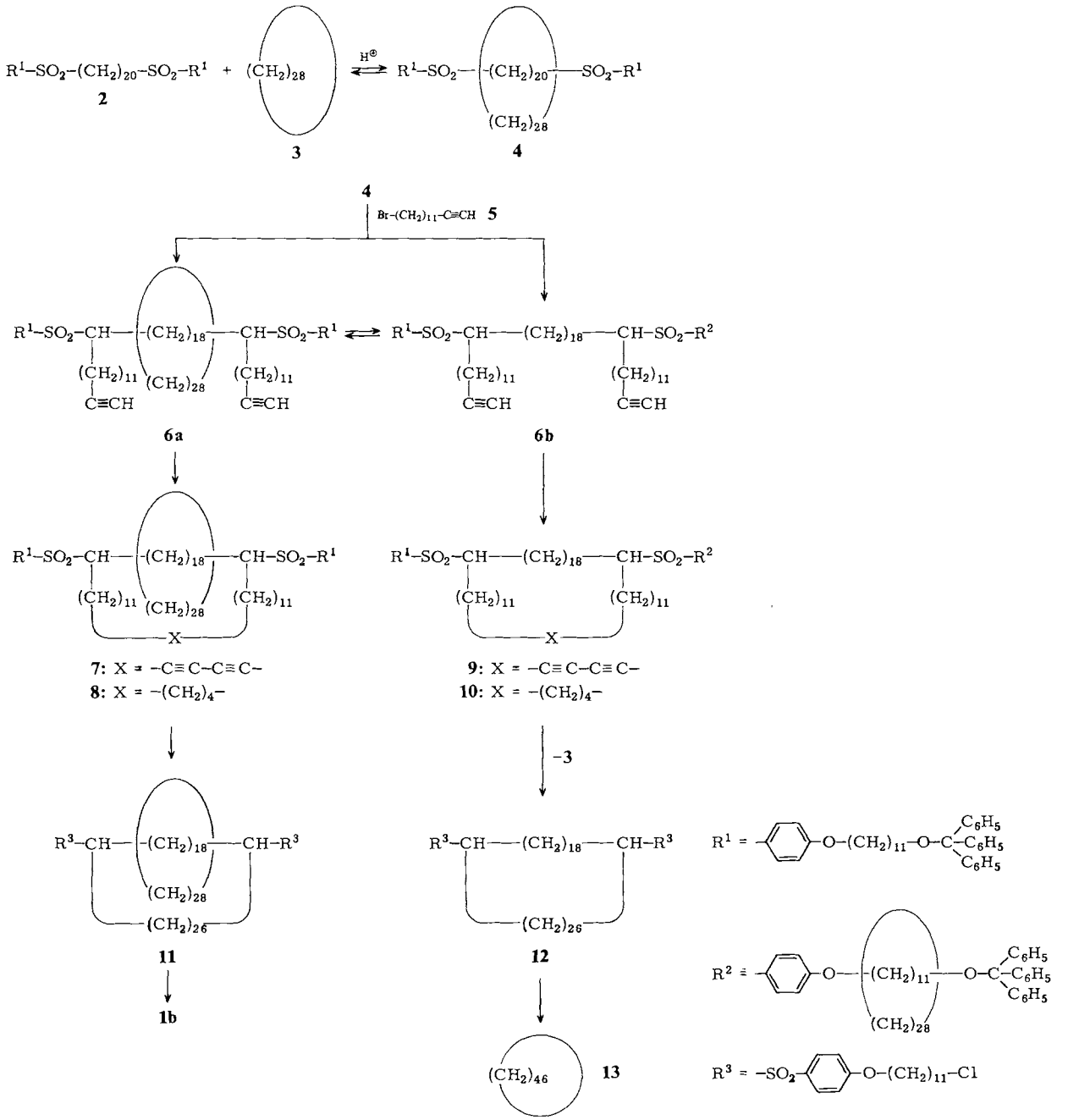
the catenane **1b** in pure form, the first hydrocarbon representative of this class of compounds[3,4].



**1a** **1b**

By analogy to *Harrison*'s synthesis of rotaxanes[5], the dumbbell shaped compound **2** was heated with cyclooctacosane **3** for 1 h at 100 °C in the presence of *p*-toluenesulfonic acid as catalyst. The rotaxane **4** is formed in an equilibrium reaction as a consequence of reversible cleavage of the trityl ether groups (10% yield, colorless oil). **4** was metalated twice with lithium diisopropylamide in tetrahydrofuran (THF)/hexamethylphosphoric triamide at −55 °C and alkylated with 13-bromo-1-tridecyne **5** to afford **6** (50%, colorless oil). Thin layer chromatography ($Al_2O_3$, petroleum ether/THF = 4 : 1) indicates that **6** consists of two compounds with similar $R_f$ values. The same spot pattern is again observed after storing the chromatogram for several hours and re-development in the second dimension. To explain this result, we propose that a mixture of translationally isomeric[6] rotaxanes **6a** and **6b** is present, the barrier to whose interconversion is just large enough at room temperature to permit their separation.

Glaser oxidation of the mixture of isomers **6a**, **b** in ether/pyridine in the presence of copper(II) acetate and subsequent catalytic hydrogenation of the products of cyclization **7** and **9** led to a mixture of the catenane **8** and the rotaxane **10**. To separate the two compounds, the triphenylmethyl groups were cleaved under acid-catalyzed conditions and the two dichlorides **11** and **12** prepared using triphenylphosphane/tetrachloromethane. Reductive cleavage of catenane **11** (colorless, viscous oil) with sodium amalgam in THF/ethanol and catalytic hydrogenation led to the catenane **1b** (90%, colorless crystals, from ethanol



 © Verlag Chemie GmbH, 6940 Weinheim, 1983 0570-0833/83/1111-0890 $ 02.50/0 

m.p. = 58–59.5 °C) (cyclooctacosane **3**: m.p. = 47–48 °C, cyclohexatetracontane **13**: m.p. = 81–83 °C).

In the $^{13}$C-NMR spectrum of **1b** (100.6 MHz, $CDCl_3$, 30 °C) the signals at $\delta = 29.65$ and 29.61 appear for the 28- and 46-membered ring, respectively. Compared to the two isolated macrocycles, the signals for the 28-membered ring and 46-membered ring are shifted to lower field by 0.52 ppm and 0.11 ppm, respectively. A similar shift has previously been observed for the 28-membered ring of another catenane[7]. These shifts to low field are most probably caused by van der Waals' interactions. This explanation is consistent with the smaller shift of the 46-membered ring, since in this case the interactions are distributed over more carbon atoms.

The electron impact (EI) mass spectrum (70 eV, 240 °C, direct inlet) displays the molecular ion of catenane **1b** as a low intensity peak (*m/z* 1036, 0.7% of the base peak at *m/z* 57). The two macrocyclic components of **1b** are represented by peaks of relatively high intensity at *m/z* 644 (13%) and *m/z* 392 (18%), respectively. H-Transfers between the two macrocycles, as frequently observed in catenanes[8], are indicated by the occurrence of $(M^{\oplus} - H)$ and $(M^{\oplus} - H_2)$ peaks for both macrocycles. By analogy to ion-molecule reactions of small alkanes[9, 10], it must be assumed that these ions are formed by loss of $H_2$ from intermediate, unstable, protonated macrocycles.

The CI mass spectrum with methane as reactant corroborates the results of the EI spectrum.

Received: July 4, 1983 [Z 442 IE]
German version: *Angew. Chem. 95* (1983) 909

CAS Registry numbers:
**1b**, 87494-55-1; **2**, 87494-56-2; **3**, 297-24-5; **4**, 87494-57-3; **5**, 87494-58-4; **6a**, 87508-92-7; **7**, 87494-60-8; **8**, 87494-62-0; **11**, 87494-64-2; **12**, 87494-63-1; **13**, 87494-54-0.

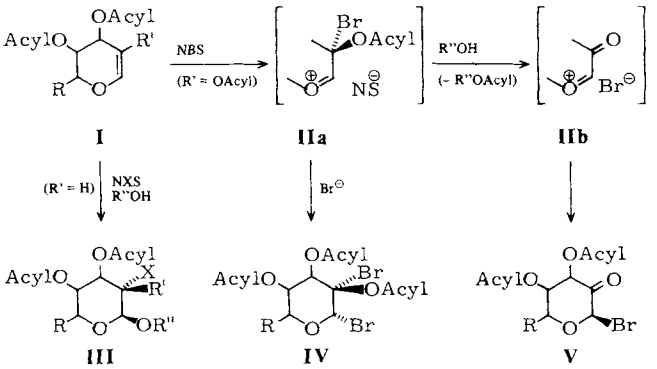
[1] G. Schill, *Chem. Ber. 100* (1967) 2021; E. Logemann, K. Rissler, G. Schill, H. Fritz, *ibid. 114* (1981) 2245.
[2] E. Logemann, G. Schill, W. Vetter, *Chem. Ber. 111* (1978) 2615.
[3] Hydrocarbon catenanes were detected mass spectroscopically among the higher molecular products formed by metathesis of cyclododecene: R. Wolovsky, *J. Am. Chem. Soc. 92* (1970) 2132; D. A. Ben-Efraim, C. Batich, E. Wasserman, *ibid. 92* (1970) 2133.
[4] A similar synthesis leading to mixtures of catenanes has been reported: G. Agam, A. Zilkha, *J. Am. Chem. Soc. 98* (1976) 5214.
[5] I. T. Harrison, *J. Chem. Soc. Perkin Trans. 1 1974*, 301.
[6] G. Schill, K. Rissler, H. Fritz, W. Vetter, *Angew. Chem. 93* (1981) 197; *Angew. Chem. Int. Ed. Engl. 20* (1981) 187.
[7] H. Fritz, E. Logemann, G. Schill, T. Winkler, *Chem. Ber. 109* (1977) 1258.
[8] W. Vetter, E. Logemann, G. Schill, *Org. Mass Spectrom. 12* (1977) 351.
[9] L. W. Sieck, S. Searles, P. Ausloos, *J. Chem. Phys. 54* (1971) 91.
[10] A. S. Blair, E. J. Heslin, A. G. Harrison, *J. Am. Chem. Soc. 94* (1972) 2935.

## A Facile, Efficient Synthesis of Acylated Glyculosyl Bromides from Hydroxyglycal Esters**

By *Frieder W. Lichtenthaler**, *Eckehard Cuny*, and *Sabine Weprek*

*Dedicated to Professor Friedrich Cramer on the occasion of his 60th birthday*

The reaction of glycal esters with *N*-bromo- or *N*-iodosuccinimide (NBS and NIS, respectively) in the presence of an alcohol leads stereoselectively to alkoxy halides (**I**→**III**, R′ = H) which have proved to be useful intermediates for the synthesis of 2-deoxy-α-glycosides[1]. With hydroxyglycal esters (**I**, R′ = OAcyl) this reaction (*e.g.* NBS/methanol in dichloromethane, 30 min) takes a different course: not 2-acyloxy-2-bromoglycosides (**III**, R′ = OAcyl) are formed as expected by analogy to the bromination **I**→**IIa**→**IV**[2], but the glyculosyl bromides **V** are elaborated smoothly and stereospecifically since the initially formed bromo adduct **IIa** is not attacked by the *O*-nucleophile (R″OH) at the anomeric carbon but at the 2-acyloxy group, leading to **V** via intermediate **IIb**.




X = Br, I; R = H, $CH_3$, $CH_2OAc$; Acyl = Acetyl(Ac), Benzoyl(Bz)

Contrasted with the previous three-step method of converting hydroxyglycal esters into α-glyculosyl bromides—involving hydroxylaminolysis[3a], deoximation[3b], and photobromination[3c]—the extended one-step process **I**→**IIa**→**IIb**→**V** proves to be an improved, general method (Table 1): not only monosaccharide derivatives (**1a**—**1d**) but also compounds derived from cellobiose and lactose afford the corresponding ulosyl bromides **2a**—**2f** in 80–90% yield. In this way, monosaccharide building blocks are made readily accessible that are as suitably functionalized for oligosaccharide synthesis as for the construction of non-carbohydrate natural products.

Among the versatile reactions undergone by ulosyl bromides of note is their ready reconversion back to the glycal stage by the Perkow reaction[4], whereby pyranoid enolphosphates such as **3b** and **3c** become accessible, as well as their β-selective alcoholysis. A silver carbonate-induced reaction leads smoothly to β-glycosiduloses, *e.g.*, **4a**, which is reduced uniformly by $BH_4^{\ominus}$ to isopropyl-β-D-mannopyranoside (79%)—a two step sequence that amply demonstrates the synthetic potential of the ulosyl bromides **2a**—**2f** for the construction of β-D-mannose-containing oligosaccharides. If the alcoholysis is followed by β-elimination, *e.g.* by stirring with bicarbonate in acetone, the β-D-enolone glycosides (**5a**—**5c**) are cleanly obtained, being of importance as versatile chiral building blocks. In the β-selective acidolysis of ulosyl bromides with sodium acetate or benzoate, elimination occurs under the reaction conditions; peracylated β-D-enolones such as **5d**—**5f** thus become satisfactorily accessible for the first time.

**5c** is a glycoside and **5f** is the dibenzoate of β-D-actinospectose, a 2,3-diketohexose which occurs in the antibiotic spectinomycin[6a] and in the arrow poison glycosides of the uscharin type[6b]. This emphasizes the synthetic potential of ulosyl bromides, and opens the possibility of synthesizing for the first time *Calotropa* cardenolides in which sugar and steroidal aglycones are linked as in structure **7**[6b],

[*] Prof. Dr. F. W. Lichtenthaler, Dr. E. Cuny, S. Weprek
Institut für Organische Chemie der Technischen Hochschule
Petersenstrasse 22, D-6100 Darmstadt (Germany)

[**] Sugar Enolones, Part 20. This work was supported by the Deutsche Forschungsgemeinschaft and the Fonds der Chemischen Industrie.—Part 19: [5].

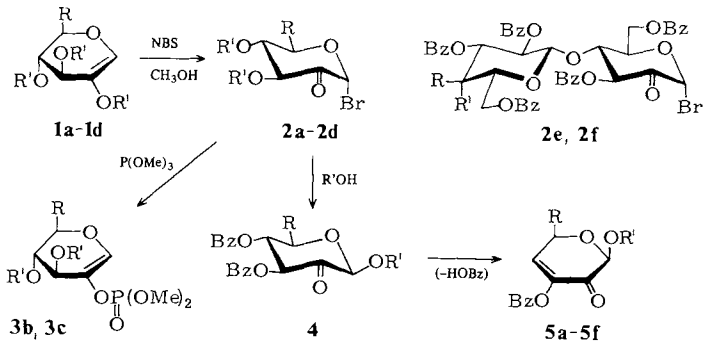
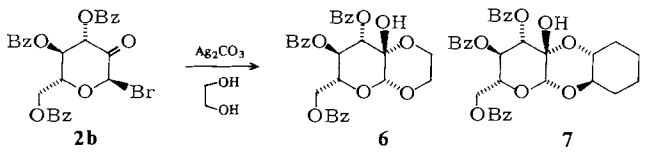



Table 1. NBS/Methanol-induced conversion of hydroxyglycal esters **1** into ulosyl bromides **2** and ensuing products: conditions [a], yields and physical data [b]. Ac = acetyl, Bz = benzoyl.

| Educt | Product | R | R' | Cond. [a] | Yield [%] | M.p. [°C] | $[\alpha]_D^{22}$ ($c$ = 1, $CHCl_3$) |
|---|---|---|---|---|---|---|---|
| **1a** | **2a** | $CH_2OAc$ | Ac | A | 92 | syrup | +233.7 |
| **1b** | **2b** | $CH_2OBz$ | Bz | A | 89 | 179–180 | +208.2 |
| **1c** | **2c** | Me | Bz | A | 83 | 125–126 | +191.4 |
| **1d** | **2d** | H | Bz | A | 78 | syrup | +100.6 |
| **1e** [c] | **2e** | — | — | A | 82 | amorph | + 80.3 |
| **1f** [c] | **2f** | — | — | A | 79 | amorph | +111.3 |
| **2b** | **3b** | $CH_2OBz$ | Bz | B | 93 | 106–107 | – 95.1 |
| **2c** | **3c** | Me | Bz | B | 85 | 115–116 | –185.7 |
| **2b** | **4b** | $CH_2OBz$ | $CHMe_2$ | C | 85 | 110–111 | – 52.5 |
| **2b** | **4b** | $CH_2OBz$ | $C_6H_{11}$ | C | 72 | 135–136 | – 46.6 |
| **2b** | **5a** | $CH_2OBz$ | $CHMe_2$ | D | 69 | 123–124 | –118.1 |
| **2b** | **5b** | $CH_2OBz$ | $C_6H_{11}$ | D | 74 | 137–138 | –116.0 |
| **2c** | **5c** | Me | $C_6H_{11}$ | D | 84 | 103–104 | – 95.0 |
| **2b** | **5d** | $CH_2OBz$ | Ac | E | 68 | 145–147 | – 70.8 |
| **2b** | **5e** | $CH_2OBz$ | Bz | E | 86 | 104–105 | – 74.6 |
| **2c** | **5f** | Me | Bz | E | 76 | 82–83 | – 89.0 |
| **2b** | **6** | — | — | F | 76 | 181–182 | – 7.7 |
| **2b** | **7** | — | — | F | 72 | amorph | – 8.9 |

[a] A: **1** in dichloromethane with methanol and NBS (1.2 mol equiv. each) 30 min, 25°C; work-up by washing with 10% $Na_2S_2O_3$ sol. and water.—B: $P(OMe)_3$, 10 min, 25°C.—C: $Ag_2CO_3$/isopropyl alcohol (1 mol equiv. each) in $CH_2Cl_2$, 1.5 h, 25°C.—D: stirred in $CH_2Cl_2$ under anhydrous conditions with $Ag_2CO_3$ and isopropyl alcohol (1.2 mol equiv. each) or cyclohexanol for 1.5 h at 25°C, followed by $NaHCO_3$/acetone, 10 h, 25°C.—E:anhydr. NaOAc or NaOBz in dimethoxyethane, 5 h, 25°C.—F: $Ag_2CO_3$/glycol or *trans*-1,2-cyclohexanediol in $CH_2Cl_2$, 5 h, 20°C.—[b] Combustion analysis data, molecular weights (FD/EI-MS) and NMR results are consistent with the structures assigned; typical $^1$H-NMR data (300 MHz in $CDCl_3$): **2b** [3d] and **2c** [5].—**3b**: 7.05 (1-H), 6.00 (3-H), 5.72 (4-H), 4.80 (5-H); $J_{3,4}$, $J_{4,5}$ = 3.6 Hz.—**4b**: 5.22 (1-H), 5.98 (3-H), 5.92 (4-H), 4.52 (5-H), $J_{3,4}$ = 10.0, $J_{4,5}$ = 8.0 Hz.—**5a**: 5.19 (1-H), 6.91 (4-H), 5.08 (5-H), $J_{4,5}$ = 3.5 Hz.—**5c**: [5].—**5e**: 6.66 (1-H), 7.03 (4-H), 5.23 (5-H), $J_{4,5}$ = 3.2 Hz.—**5f**: [5].—**6**: 4.85 (1-H), 5.22 (3-H), 5.86 (4-H), 4.10 (5-H), $J_{3,4} = J_{4,5} \approx 9.9$ Hz. [c] **1e**: hepta-*O*-benzoyl-hydroxycellobial [3a].—**1f**: hepta-*O*-benzoyl-hydroxylactal, m.p. = 93–96°C, $[\alpha]_D^{20}$ +52 ($c$ = 1, $CHCl_3$); preparation analogous to **1e**.

since alcoholysis with diols not only leads to the β-glycoside (*e.g.* **2b**→**6** and **2b**→**7**) but to the cyclohemiketal by formal annelation of a dioxane ring.



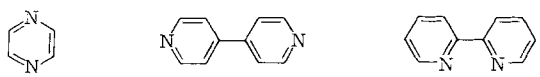

Received: July 15, 1983 [Z 470 IE]
German version: *Angew. Chem.* 95 (1983) 906

[1] K. Tatsuta, K. Fujimoto, M. Kinoshita, S. Umezawa, *Carbohydr. Res. 54* (1977) 85; J. Thiem, H. Karl, J. Schwentner, *Synthesis 1978*, 696.
[2] F. W. Lichtenthaler, T. Sakakibara, E. Oeser, *Carbohydr. Res. 59* (1977) 47; *Chem. Ber. 113* (1980) 471.
[3] a) F. W. Lichtenthaler, P. Jarglis, *Tetrahedron Lett. 21* (1980) 1425; b) F. W. Lichtenthaler, E. S. H. El Ashry, V. H. Göckel, *ibid. 21* (1980) 1429; c) F. W. Lichtenthaler, P. Jarglis, *Angew. Chem. 94* (1982) 643; *Angew. Chem. Int. Ed. Engl. 21* (1982) 625; *Angew. Chem. Suppl. 1982*, 1449; d) F. W. Lichtenthaler, P. Jarglis, W. Hempe, *Liebigs Ann. Chem. 1983*, in press.
[4] F. W. Lichtenthaler, *Chem. Rev. 61* (1961) 607; F. W. Lichtenthaler, F. Cramer, *Chem. Ber. 95* (1962) 1971.
[5] F. W. Lichtenthaler, A. Löhe, E. Cuny, *Liebigs Ann. Chem. 1983*, in press.
[6] a) W. Rosenbrook, Jr., *J. Antibiot. 32* (1979) S-211; and literature cited therein; b) H. T. A. Cheung, T. R. Watson, J. N. Seiber, C. Nelson, *J. Chem. Soc. Perkin Trans. 1 1980*, 2169; and literature cited therein.

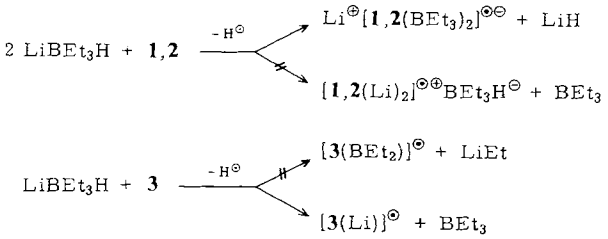
## Radical Products in Single Electron Transfer Reactions of Lithium Triethylhydridoborate Detected by ESR and Multinuclear ($^1$H, $^{10}$B, $^{11}$B, $^{14}$N)-ENDOR Spectroscopy

By *Wolfgang Kaim** and *Wolfgang Lubitz**

Lithium triethylhydridoborate, $LiBEt_3H$ ("Super-hydride"), is one of the most powerful known hydride reductants, exceeding even the reducing capabilities of lithium tetrahydridoaluminate, $LiAlH_4$[1]. Reactions of alkyl derivatives and hydrides of Li, Mg, Zn, and Al with electron-deficient substrates have recently been shown to involve radicals generated *via* single electron transfer (SET) processes[4]; however, the identity of these stable paramagnetic products as radical anion complexes of non-radical metal fragments has not always been properly defined[4a,c]. Since aromatic N-heterocycles such as pyrazine **1**[6], 4,4′-bipyridine **2**, and 2,2′-bipyridine **3** have proven to be highly suitable SET substrates[4], we studied the reactions of these compounds with $LiBEt_3H$ in tetrahydrofuran (THF).




Persistent radicals were formed, and their identity was established by comparison of their ESR spectra with those of species generated by conventional routes[8].




In addition, we have obtained ENDOR (electron nuclear double resonance) and TRIPLE (electron nuclear-nuclear triple resonance) spectra of solutions of the paramagnetic complexes $[\mathbf{1}(BEt_3)_2]^{\odot\ominus}$ and $[\mathbf{2}(BEt_3)_2]^{\odot\ominus}$. These show signals not only from $^1$H, $^{14}$N, but also from the boron isotopes $^{10}$B and $^{11}$B, which could be detected by these techniques for the first time (Fig. 2).

[*] Dr. W. Kaim
Institut für Anorganische Chemie der Universität
Niederurseler Hang, D-6000 Frankfurt am Main 50 (Germany)
Dr. W. Lubitz[+]
Institut für Organische Chemie der Freien Universität
Takustrasse 3, D-1000 Berlin 33 (Germany)
[+]Present address: Department of Physics
University of California, La Jolla, CA 92093 (USA)

 © Verlag Chemie GmbH, 6940 Weinheim, 1983 0570-0833/83/1111-0892 $ 02.50/0 

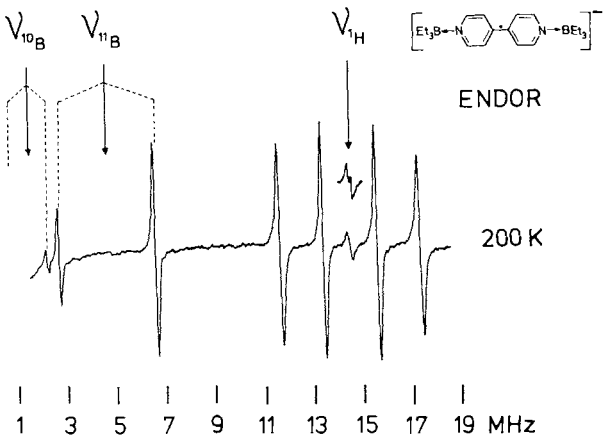
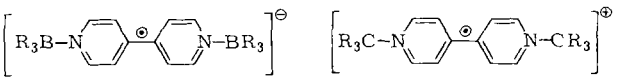



Fig. 2. Electron nuclear double resonance (ENDOR) spectrum of the radical complex $[2(BEt_3)_2]^{\odot\ominus}$ obtained from 4,4'-bipyridine **2** and $LiBEt_3H$ in THF. According to the ENDOR resonance condition $\nu_{ENDOR}=|\nu_n \pm a_n/2|$, line-pairs for three $^1H$ hyperfine couplings and one $^{11}B$ hyperfine coupling are detected centered around the respective free nuclear frequencies $\nu_n$ ($^1H$: $\nu_H=14.40$ MHz, nuclear spin $I=1/2$; $^{11}B$: 81.17% natural abundance, $\nu_{^{11}B}=4.62$ MHz, $I=3/2$). For $^{10}B$ (18.83%, $\nu_{^{10}B}=1.55$ MHz, $I=3$), the low-frequency line lies below 1 MHz and could not be detected. Signals from $^{14}N$ are only detectable at higher temperatures (cf. Supplement). Experimental conditions: 100 W rf power, 40 mW microwave power (X-band), frequency modulation 10 kHz, frequency modulation depth ±60 kHz, 1 scan (time constant 1.25 s).

The arrangement of the radical complex with the spin residing almost exclusively in the π-system of the heterocycle is very favorable for the ENDOR detection of heteronuclei such as boron coordinated to the heterocyclic nitrogen[12]. Complete analysis of the spectra yields the hyperfine coupling constants with their signs, as well as information on the relaxation behavior of the various nuclei.

The selectivity of formation of the radical products deserves special comment: In contrast to $LiAlH_4$, $LiBEt_3H$ reacts with **1** to form an anionic complex rather than the triple ion $[1(Li)_2]^{\odot\oplus}$[4b,6]. The formation of $[1(BEt_3)_2]^{\odot\ominus}$ may be due to the high Lewis acidity of triethylborane. The corresponding radical complex with 4,4'-bipyridine **2** is isoelectronic with the well-known viologen radical cations:



Conversely, 2,2'-bipyridine **3** yields the $Li^{\oplus}$ ion pair and not the diorganoboronium complex. Clearly, chelation of the small species $^{\oplus}BR_2$ by the 2,2'-bipyridine radical anion is not a highly favorable process[8c]. It thus seems that coordinative effects in hydride reductions not only determine the nature of the diamagnetic reduction products but also the radical species resulting from escape paths[6] in SET reactions. For identification of these radical species, the combination ENDOR/TRIPLE has proven to be the spectroscopic method of choice, in particular because heteronuclear studies are possible.

Received: July 6, 1983 [Z 454 IE]
German version: *Angew. Chem. 95* (1983) 915
The complete manuscript of this communication appears in: *Angew. Chem. Suppl. 1983*, 1209–1220

[1] H. C. Brown, S. Krishnamurthy, *J. Am. Chem. Soc. 95* (1973) 1669; *Tetrahedron 35* (1979) 567; H. C. Brown, S. C. Kim, S. Krishnamurthy, *J. Org. Chem. 45* (1980) 1.
[4] a) W. Kaim, *Angew. Chem. 94* (1982) 150; *Angew. Chem. Int. Ed. Engl. 21* (1982) 140; *Angew. Chem. Suppl. 1982*, 289; b) *ibid. 94* (1982) 150; *21* (1982) 141; *1982*, 298; c) *J. Am. Chem. Soc. 104* (1982) 3833; d) *Z. Naturforsch. B 37* (1982) 783.
[6] Cf. W. Kaim, *Angew. Chem. 95* (1983) 201; *Angew. Chem. Int. Ed. Engl. 22* (1983) 171.
[8] a) W. Kaim, *Z. Naturforsch. B 36* (1981) 677; the boron radical complex should be reformulated as $[1(BEt_3)_2]^{\odot\ominus}$; b) *J. Organomet. Chem. 241* (1983) 157; c) *Chem. Ber. 114* (1981) 3789.
[12] M. Plato, W. Lubitz, K. Möbius, *J. Phys. Chem. 85* (1981) 1202.

# BOOK REVIEWS

**Biotechnology, A Comprehensive Treatise in 8 Volumes.** Edited by *H.-J. Rehm* and *G. Reed*. Verlag Chemie, Weinheim. Vol. 1: **Microbial Fundamentals.** 1981, xii, 520 pp., bound, DM 425.00; Vol. 3: **Biomass, Microorganisms for Special Applications, Microbial Products I, Energy form Renewable Resources.** Edited by *H. Dellweg*. 1983, xix, 642 pp., bound, DM 425.00

At a time when over 200 companies worldwide have endeavors in biotechnology, a comprehensive treatment of the field in a series such as the one from Verlag Chemie is welcome indeed. It would be difficult for a series such as this to satisfy everyone, and this reviewer has his own points of contention. Still, if these two volumes are representative of the others to follow, the series should be an excellent reference source for anyone who seeks a starting point on a technical topic in biotechnology. Thus, students, instructors, and practitioners alike should find the series valuable. However, I do think the price could significantly limit the appeal.

The first two volumes of the series are intended for a discussion of the principles of biotechnology; the remaining six volumes are to deal with specific applications. Volumes 2 (Fundamentals of Biochemical Engineering) and 4 to 8 (Vol. 4: Microbial Products II; 5: Food and Feed Production with Microorganisms; 6a: Microbial Transformations; 6b: Special Microbial Processes; 7: Enzymes in Biotechnology; 8: Microbial Degradations) have not yet been released.

The cover titles on the applications volumes would appear somewhat redundant. It might have been better to or-

ganize the applications volumes according to industry, *e.g.* energy, food, pharmaceutical, waste utilization, *etc.* But perhaps such an approach was considered and found not to be practical.

Volume 1 starts with a review by *A. Kocková-Kratochvilová* of the taxonomy of animal, plant and microbial viruses as well as the prokaryotes and the eukaryotes. *C. L. Cooney* provides an overview of the methods of measurement of microbial growth and of how the nutritional and environmental factors might affect such growth. *H. W. Doelle* devotes nearly 100 pages to a presentation of the basic pathways through which the microorganisms derive energy for growth and maintenance. *J. F. Martin* and *P. Liras* extend this topic to the formation of secondary metabolites.

Volume 1 also contains well-presented contributions on the principles of genetics *(R. P. Elander, A. L. Demain)* and the techniques used in its practice: Mutation *(G. K. Jacobson)*, Hybridization *(K. Esser, U. Stahl)*, Genetic Engineering *(A. Pühler, W. Heumann)*. *K. Nakayama* and *A. Dietz* present complementary chapters on the sources and the maintenance of cultures in industry. *V. Vossius* introduces the topic of patent protection in this special sector. *A. Fiechter* reviews the batch and continuous culture of cells, appropriately including plant and animal cells. I agree with this author that plant and animal cell biotechnology will continue to gain in importance and I hope that one of the future volumes will devote more attention to this topic.

Volume 3 is the first of two volumes devoted to microbial products. The microbial cell mass as the product in itself is discussed in four chapters on "Biomass" and five chapters on "Special Applications."

*E. Oura* begins the subject by considering carbohydrates as the substrate (glucose, molasses, spent sulfite liquor, whey, starch). *A. Einsele* extends the discussion to higher alkanes as substrates. *U. Faust* and *P. Präve* deal with methane and methanol as substrates. The production of phototrophic microalgae is thoroughly analyzed by *A. Richmond*. There then follows an illustrated account of the cultivation of Edible mushrooms (fungi) by *F. Zaražil* and *K. Grabbe*.

The "special applications" considered in this volume are: Starter cultures for milk and meat processing *(R. K. Robinson)*, Microbes for the improvement of plant and soil health *(H.-J. Rehm, B. Novák)*, Nitrogen fixation and the production of legume inoculants *(H. Marečková)*, and The *in-vitro* and *in-vivo* production of microbial insecticides *(R. J. Quinlan, S. G. Lisansky)*. These chapters should be considered brief introductions to the topics. The remainder of volume 3 deals with products other than cell mass. Perhaps the most comprehensive chapter of these two volumes is the one on ethanol fermentations *(N. Kosaric, A. Wieczorek, G. P. Cosentino, R. J. Magee, J. E. Prenosil)*. An overview of acetic acid and citric acid as microbial products is presented by *H. Ebner* and *H. Follman* and by *M. Röhr, C. P. Kubicek*, and *J. Kominek*. The latter group of authors also briefly introduces the production of gluconic acid. Another brief presentation is on the production of lactic acid *(K. Buchta)*. This author introduces several other organic acids that could become of interest depending upon the trend in world oil prices, *e.g.* itaconic acid, malic acid, and oxogluconic acid.

The production of amino acids by microbes and by enzymatic synthesis is reviewed by *K. Soda, H. Tanaka*, and *N. Esaki. I. W. Sutherland* discusses strain development, production, product recovery, and the uses of extracellular polysaccharides. Microbial emulsifiers and de-emulsifiers are dealt with by *N. Kosaric, N. C. C. Gray*, and *W. L. Cairns*. *G. W. Barnard* and *D. O. Hall* conclude volume 3 with a discussion of the production of ethanol and methane from biomass.

In some of the chapters, the authors seem to have been forced to sacrifice depth of coverage in order to mention more of the microbes and the products reported in the literature. There is some redundance. For example, aspects of ethanol production, as well as a few points on microorganism growth, are covered in more than one chapter. It is incumbent upon the reader to integrate these. However, I do not see this as a major problem. In a diverse field such as biotechnology, a comprehensive but fully unified treatment would be an extremely difficult endeavor.

Since the series is intended to be a comprehensive treatise, the authors of future volumes may wish to include information on product uses, costs and production volumes. Not all the authors of volume 3 have done this. Comments on competing production schemes both inside and outside biotechnology would also help the reader gain a better perspective of the field.

The only other concern is that the very nature of a series such as this dictates that several years would pass before the entire series is published. This creates a time lag in the information presented and makes an integration of the topic more difficult. And, the detailed listing of the contents would not be known until much later. Despite all this, the editors and the publisher are to be sincerely commended for undertaking this formidable task.

Where might this series find a place among its possible surrogates such as Kirk and Othmer's *Encyclopedia of Chemical Technology* (Wiley Interscience), *Advances in Biochemical Engineering* (Springer), *Microbial Technology* and *Annual Reports on Fermentation Processes* (Academic Press), and *Topics in Enzyme and Fermentation Technology* (Wiley) *etc.* should become clearer after further volumes of this work are released. These two volumes suggest the place would be an honorable one.

*Bhavender P. Sharma* [NB 595 IE]
Corning Glass Works, Corning NY (USA)

**Advances in Chemical Physics, Vol. 50. Dynamics of the Excited State.** By *K. P. Lawley*. John Wiley & Sons, Chichester 1982. vii, 667 pp., bound, £ 35.90.

The purpose of the series "Advances in Chemical Physics" is to provide the reader with access to those areas of chemical physics in which he himself does not specialize but which are of interest to him. The rapid development taking place in many areas and the abundance of original publications create a great need for review articles from the pens of experts. The present volume fulfills this need in an exemplary manner, as does the series as a whole.

In the last few years laser spectroscopy has opened up new vistas in the experimental investigation of excited molecular states. Parallel to this, new theoretical models have been developed. The present volume contains nine reports concerning important areas which impressively cover the experimental and theoretical progress, in particular in the study of the excited states of small molecules and of the interaction of such molecules with each other and with the field of radiation.

*M. A. A. Clyne* and *I. S. McDermid* report on laser-induced fluorescence as a method of investigating the electronically excited states of small molecules. Much has been learned about the dynamic and spectroscopic properties of small molecules and radicals, which have been excited under precise, defined conditions, by means of tunable, narrow band dye lasers. The experimental technique is also comprehensively described. As much progress has also occurred in the area of multiphonon excitation with infrared quanta. *D. S. King* reports on chemical reactions influenced by such excitation, molecular dynamics, energy transport and distribution of excitation energy among the products following multiquantum infrared excitation.

The subject of the contribution by *A. M. F. Lau* is laser predissociation and autoionization by photons. *S. R. Leone* discusses the results of single photon ionization and dissociation of molecules. The distribution of the end-products, the dissociation time, the fluorescence polarization and the angular distribution of the products allow a detailed insight into the primary photochemical processes. Excited metal atoms can pass on their energy in collision with molecular gases. *W. H. Breckenridge* and *H. Umemoto* report on this area which is of such great importance for laser technology. *I. V. Hertel*'s contribution is concerned with the energy exchange between electronic and vibrational excitation. The measurement of effective cross sections, angular distributions and polarization are discussed.

Exclusively or mainly theoretical methods and results are discussed by *M. Quack* (The Reaction Dynamics and Statistical Mechanics of the Production of Highly Excited States by High Intensity Infrared Radiation), by *D. M. Hirst* (Calculation of the Potential Surfaces of Excited States) and *T. A. Brunner* and *D. Pritchard* (Fitting Laws for the Treatment of Rotation Inelastic Collisions).

Taken as a whole this book allows an insight into the basic concepts and into the latest results in some areas of molecular physics where—because of the advent of the laser—there have been especial advances in recent years. The individual contributions are well written, fit quickly and understandably into the general scheme, and include a tremendous number of literature references. Such books are of inestimable value to the molecular physicist and the physical chemist. The production is excellent, the price acceptable.

*H. C. Wolf* [NB 582 IE]
Physikalisches Institut
der Universität Stuttgart

**Electrical Properties of Polymers.** Edited by *D. A. Seanor.* Academic Press, New York 1982, xi, 379 pp., bound, $ 52.00.

The tendency of publishers to assemble a range of individual reports of varying quality and with only a slight connection with each other and to market them is unfortunately increasing. This book is an example of the abuse.

In the first chapter *D. A. Seanor* gives a cursory review of electrical phenomena, measuring techniques and the electrical properties of various material classes and states of aggregation of polymers, under the title "Electrical Conduction in Polymers". The polymers with metal-like conduction (*e.g.* the polyacetylenes), which are decisive in recent work, are only mentioned here, as in the rest of the book, in passing. The section on ionic conduction in polymers is interesting, although, here too, there is no mention of the PEO salt complexes which are relevant for electrochemical applications.

It is characteristic of the quality of the article and of the book in general that the problem of the connection between the electrical properties and morphology of partially crystalline polymers are discussed in terms of an outdated model proposed by *Flory* (not *Florey* as given in the legend to Fig. 10!) dating from the year 1953!

Under the ambitious title "Structure and Charge Generation in Organic Molecular Self Assemblies", *J. H. Perlstein* deals in Chapter 2 (30 pp.) solely with thiapyrylium salts dispersed in polycarbonate. It becomes clear that not even the structure of the interstitial complex has been unequivocally established.

The topic "Photophysical Processes, Energy Transfer and Photoconduction in Polymers" is treated by *R. F. Cozzens* in *ca.* 30 pages in Chapter 3. Without going into details there is a very elementary introduction, attended by a plethora of historical citations concerning the photoconductivity of polymers and its technical application.

Chapter 4 (80 pp.) by *V. Y. Merrit,* entitled "Photovoltaic Phenomena in Organic Solids", devotes all of 11 lines to the subject of polymers. The author's remark that polymers behave in a very complex manner is diverting in the context of this book.

The subject matter of the 5th chapter by *H. Carr* (20 pp.) has been treated several times recently in other monographs and progress reports. The same applies to the remaining chapters of the book; in some cases similar reviews have recently been published elsewhere by the same authors. An example is *G. M. Sessler*'s contribution "Polymeric Electrets" in Chapter 6 (40 pp.). The two remaining chapters deal with "Contact Electrification of Polymers" (*D. K. Davies,* 40 pp.) and with "Dielectric Breakdown Phenomena in Polymers" (*P. Fisher,* 45 pp.).

Whoever buys this book will at least enjoy its solid getup and the careful work of the bookbinder.

*Gerhard Wegner* [NB 591 IE]
Institut für Makromolekulare Chemie
der Universität Freiburg

**Anthracycline Antibiotics.** Edited by *H. S. El Khadem.* Academic Press, New York 1982. xii, 285 pp., bound, $ 25.00.

This volume is a compilation of the presentations at the Anthracycline Symposium held in New York in August 1981. The choice of topics takes account of the interdisciplinary character of anthracycline chemistry—ranging from pharmacology through microbiology to total synthesis.

In the first report *Narayanan et al.* present the National Cancer Institute's (NCI) screening programme for anthracycline derivatives. Besides an introduction to the evaluation of screening results a good summary is given of the range of substances (*ca.* 400) prepared to date by derivatization of daunorubicin. Scientists not working in the field will note that the NCI's screening results occasionally differ from those of other groups. Next *Arcamone et al.* report on the results of investigating doxorubicin (adriamycin). The group from Farmitalia has made important contributions, both in the area of structure effectivity relations and in the isolation and synthesis of new glycosides. It is sufficient here to mention the syntheses first reported of a furanoglycoside and of *enantio*-4-demethoxydaunorubicin which, as expected, is biologically inactive. *T. Oki* summarizes the work of the Sanraku Ocean group in his contribution. This Japanese company is to be thanked for the

isolation and structural characterization of dozens of new anthracyclines derived from aclavinone. The microbiological investigations of *Umezawa et al.* are included, which concern the microbiological glycosidation by particular Streptomyces mutants. A further report on industrial research (Upjohn) is given by *Wiley* in his review of nogalamycin chemistry. Even though nogalamycin derivatives originally did not belong to the favorites of the pharmacologists, the Upjohn workers have succeeded in synthesizing a derivative (7-*con*-*O*-methylnogarol) which has a comparatively low cardiac toxicity. Interestingly enough this derivative only interacts slightly with double-stranded DNA, which throws new light on the mode of action of anthracycline antibiotics. The systematic variation of the natural products, daunorubicin and doxorubicin, is the main theme of a report by *Acton et al.* The discussion of the chemical derivatization is closely linked with the biological action and with pharmacological considerations. Probably the most important result is that the *N*-alkylated derivatives of the natural products do not exhibit mutagenicity.

Mainly synthetic themes are treated in the second portion of the volume. Firstly, *Kende et al.* and *Swenton et al.* describe the results obtained by their groups in the area of aglycone synthesis. *Kende* concentrates on 11-deoxy-anthracyclines of the aclavinone type, while *Swenton* presents the daumomycinone synthesis *via* quinone acetals developed by his group. Although the work of other groups is naturally only mentioned in passing, both reports provide a deeper insight into the basic synthetic concepts. The great enthusiasm of both authors comes through to the reader. Finally, there are three presentations from *Horton, Monneret* and *El Khadem* concerned with glycoside syntheses. Although the problem of monoglycosidation seems to be basically solved (even for nitrogen-free sugars), the synthesis of the di- and the trisaccharides is only just beginning. The reviewer applauds the fact that the difficult chapter on oligosaccharide synthesis, partly with very rare sugars, is presented as a summary, even though some problems concerning yield and selectivity have not been completely solved.

The volume is very carefully edited and arranged; the reviewer could find only a few mistakes. The anthracycline chemist is stimulated by the results of well-known workers presented from their own personal viewpoints. In particular the summary of the work from the industrial laboratories facilitates literature studies. However, the book can be recommended not just to specialists. The clearly arranged presentation provides a rapid introduction to a fascinating chapter of interdisciplinary research.

*Karsten Krohn* [NB 587 IE]
Institut für Organische Chemie
der Technischen Universität Braunschweig

**Recent Books**

**The following books have been received by the editor. All the publications listed are available through W & P Buchversand für Wissenschaft und Praxis, Boschstrasse 12, D-6940 Weinheim (Federal Republic of Germany). Tel. (06201) 606-0, Telex 465516 vchwh d, Telefax (06201) 602328.**

**Phase Transfer Catalysis.** 2nd improved and supplemented edition. Edited by *E. Dehmlow* and *S. Dehmlow*. Verlag Chemie, Weinheim 1983. xiv, 386 pp., bound, DM 138.00.—ISBN 3-527-25897-3

**Sicherheit in chemischen und verwandten Laboratorien.** Edited by *F. Heske*. Verlag Chemie, Weinheim 1983. 128 pp., stitched, DM 46.00.—ISBN 3-527-26066-8

**Ellis Horwood Series in Chemical Science: Chemical Nomenclature Usage.** Edited by *R. Lees* and *A. F. Smith*. Ellis Horwood Ltd., Chichester 1983. 172 pp., bound, £ 19.50.—ISBN 0-85312-368-3

**Organic Chemistry Series. Vol. 1:** Stereoelectronic Effects in Organic Chemistry. By *P. Deslongchamps*. Pergamon Press, Oxford 1983. xi, 375 pp., Paperback, £ 15.25.—ISBN 0-08-029248-8

**Ettore Majorana International Science Series. Bioelectrochemistry I: Biological Redox Reactions.** Edited by *G. Milazzo* and *M. Blank*. Plenum Press, New York 1983. vi, 348 pp., bound, $ 52.50.—ISBN 0-306-41340-X

**Das Bergbau-Handbuch.** Fourth edition. Published by the Wirtschaftsvereinigung Bergbau e.V. in Bonn. Verlag Glückauf GmbH, Essen 1983. 312 pp., bound, DM 54.00.—ISBN 3-7739-0396-0

**Das große Werkbuch Elektronik.** 4th completely revised and improved edition. By *D. Nührmann*. Franzis-Verlag GmbH, München 1983. 1218 pp., bound, subscription price until 31. 12. 1983 DM 88.00, after 1. 1. 1984 DM 108.00.—ISBN 3-7723-6544-2

**Progress in Organic Chemistry. An Appreciation of Henry Taube. Vol. 30.** Edited by *S. J. Lippard*. John Wiley, Chichester 1983. xii, 528 pp., bound, £ 61.75.—ISBN 0-471-87022-6

*Registered names, trademarks, etc. used in this journal, even without specific indication thereof, are not to be considered unprotected by law.*

© Verlag Chemie GmbH, D-6940 Weinheim, 1983. - Printed in the Federal Republic of Germany by Zechnersche Buchdruckerei, Speyer/Rhein.

All rights reserved (including those of translation into foreign languages). No part of this issue may be be reproduced in any form - by photoprint, microfilm, or any other means - nor transmitted or translated into a machine language without written permission from the publishers. Only single copies of contributions, or parts thereof, may be reproduced for personal use. Copies reproduced and used other than for private purposes in an industrial or commercial undertaking are subject to copyright and, in such cases, a copyright fee must be paid to the VG WORT, Abteilung Wissenschaft, Goethestr. 49, 8000 München 2, from whom conditions of payment can be obtained on request.

**Valid for users in the USA:** The appearance of the code at the bottom of the first page of an article in this journal (serial) indicates the copyright owner's consent that copies of the article may be made for personal or internal use, or for the personal or internal use of specific clients. This consent is given on the condition, however, that the copier pay the stated per-copy fee through the Copyright Clearance Center, Inc., for copying beyond that permitted by Sections 107 or 108 of the U.S. Copyright Law. This consent does not extend to other kinds of copying, such as copying for general distribution, for advertising or promotional purposes, for creating new collective works, or for resale. For copying from back volumes of this journal see 'Permissions to Photo-Copy: Publisher's Fee List' of the CCC.

**Editorial office:** Pappelallee 3, D-6940 Weinheim, Federal Republic of Germany, Telephone (06201) 602315, Telex 465516 vchwh d, Telefax (06201) 602328.

**Editors:** *P. Gölitz, I. G. Neil, O. Smrekar, A. Stimson.*

**Publishers:** Verlag Chemie GmbH. (Managing Directors: *Prof. Dr. Helmut Grünewald* and *Hans Dirk Köhler*), Pappelallee 3, D-6940 Weinheim, Federal Republic of Germany.

Correspondence concerning advertisements should be addressed to Verlag Chemie GmbH. (Advertising Manager *R. J. Roth*), Boschstr. 12, P.O. Box 1260/1280, D-6940 Weinheim, Federal Republic of Germany, Telephone Weinheim (06201) 602-0, Telex 465516 vchwh d, Telefax (06201) 602328.

ANGEWANDTE CHEMIE
International Edition in English
Volume 22 · Number 12
December 1983
Pages 897–1012

# Rhodium Catalysts for Enantioselective Hydrosilylation— A New Concept in the Development of Asymmetric Catalysts

**By Henri Brunner***

*Dedicated to Professor Ernst Otto Fischer on the occasion of his 65th birthday*

Following a survey of the asymmetric hydrogenation of prochiral olefins with transition metal/phosphane catalysts, the problem of chirality transfer from the optically active ligands of the catalyst to the substrate is discussed. A new concept for this chirality transfer is introduced; the conformational analysis of model compounds as well as the development of catalysts for enantioselective hydrosilylation demonstrate the usefulness of this concept.

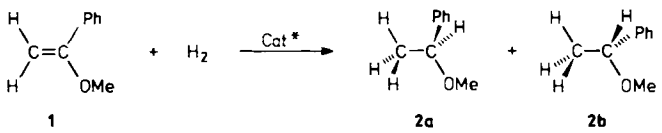
*For every reaction in which a new asymmetric center is created there exists a transition metal catalyst which—when added in small amounts—leads stereospecifically to one enantiomer. One only has to find it.*

## 1. Introductory Remarks

Enzymes catalyze the synthesis of optically active compounds from prochiral precursors. The reactions are usually stereospecific. Since an enzyme molecule converts its substrate 10000 to 1000000 times per minute[1], the optical activity contained in it is multiplied by this factor each minute. Enzyme reactions are thus prime examples for "asymmetric catalysis" in which large amounts of optically active products are formed from a small amount of "optically active information". However, enzyme reactions are often restricted to natural substrates, and reactivity as well as stereoselectivity rapidly decrease when the substrate is varied. This poses the following questions: How good are synthetic catalysts in asymmetric catalysis? Can they make a contribution to the increasing demand for enantiomerically pure optically active pharmaceuticals, foods, animal feeds, pesticides, organic chemicals, etc.?

## 2. Enantioselective Catalysis with Transition Metal/Phosphane Complexes

In 1968 *Horner et al.*[2] and *Knowles et al.*[3] independently discovered that prochiral olefins can be hydrogenated enantioselectively using rhodium complexes similar to Wilkinson's catalyst[4] but having optically active phosphane ligands. Scheme 1 shows this for one of the first asymmetric hydrogenations—the conversion of α-methoxystyrene **1** into α-methoxyethylbenzene **2a**, **b**.




**1** **2a** **2b**

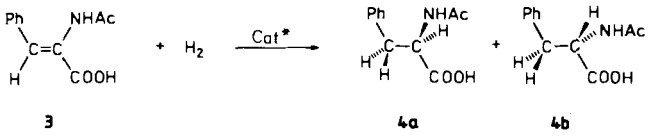
Scheme 1.

Using the catalyst [Rh(1,5-hexadiene)Cl]$_2$/(*S*)-(+)-PMePrPh[2] an optical yield of 4% *ee* for the (*R*)-product **2b** was achieved. The extraordinarily mild reaction conditions (room temperature, hydrogen at atmospheric pres-

[*] Prof. Dr. H. Brunner
Institut für Anorganische Chemie der Universität
Universitätsstrasse 31, D-8400 Regensburg (Germany)

 © Verlag Chemie GmbH, 6940 Weinheim, 1983 0570-0833/83/1212-0897 $ 02.50/0 

sure) and the possibility of converting dehydroamino acids into amino acids[5] soon resulted in world-wide attention for this area of research. Although the use of monodentate optically active phosphanes led to high optical inductions for some special substrates, it was only the switch to chelating phosphanes that brought decidedly better optical yields.

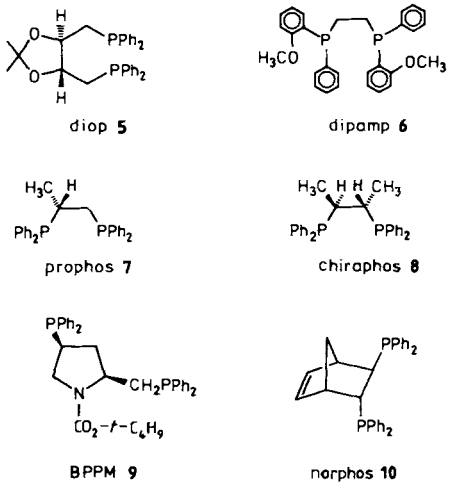



3 4a 4b

Scheme 2.

The synthesis of *N*-acetylphenylalanine **4a**, **b** from (*Z*)-α-(*N*-acetamido)cinnamic acid **3** according to Scheme 2 may be quoted as an example. The catalyst is formed *in situ* from the precatalyst $[Rh(cod)Cl]_2$ (cod = 1,5-cyclooctadiene) and the cocatalyst diop **5** (Scheme 3), and gives an optical induction of 81% *ee*. Thus (−)-diop, which is derived from naturally occurring tartaric acid, leads to *N*-acetylphenylalanine with an (*R*) : (*S*) ratio of 90.5 : 9.5[9]. These studies culminated several years ago in the development of an industrial process for the synthesis of L-Dopa, a drug used to treat Parkinson's disease[10–16]. Subsequently, hundreds of optically active phosphanes and prochiral substrates have been tested, not only for use in enantioselective hydrogenations, but also for transition-metal catalyzed enantioselective hydrosilylations, hydroformylations, and similar reactions[17–38].

Of the large number of optically active chelating phosphanes used in asymmetric catalysis, Scheme 3 depicts the six compounds **5**—**10** which have proved themselves in a multitude of catalytic reactions.




Scheme 3.

The tartaric acid derivative diop **5**[5] is the best known and most frequently used chelating phosphane. The ligand dipamp **6** is used in the Monsanto amino acid process for the synthesis of the L-Dopa. The asymmetric centers of prophos **7**[39] and chiraphos **8**[40,41] originate from lactic acid and tartaric acid, respectively. BPPM **9**[42] is a derivative of the amino acid proline, and norphos **10**[43,44] contains a norbornene skeleton. Both diop **5** and BPPM **9** form seven-membered chelate rings with metal atoms, whereas the other four ligands form five-membered rings. The acronyms in Scheme 3 have been accepted generally because the IUPAC names of ligands **5**—**10** occupy several lines.

The ligand dipamp is an exception in two respects, both in relation to the other five compounds in Scheme 3 as well as in relation to the majority of the other compounds tested so far. On the one hand, the chiral centers of dipamp are the phosphorus atoms themselves, whereas most other compounds contain the chiral center in the chelating bridge between the two P atoms; on the other hand, only one of the two rings on the doubly aryl-substituted P atoms is a phenyl ring, the other being an *o*-methoxyphenyl ring. In contrast, most of the commonly used chelating phosphanes are doubly phenyl-substituted at the P atoms. Despite these structural singularities of dipamp, the optical inductions achievable with this ligand do not differ significantly from those obtained with other chiral bisdiphenylphosphane ligands[17–22].

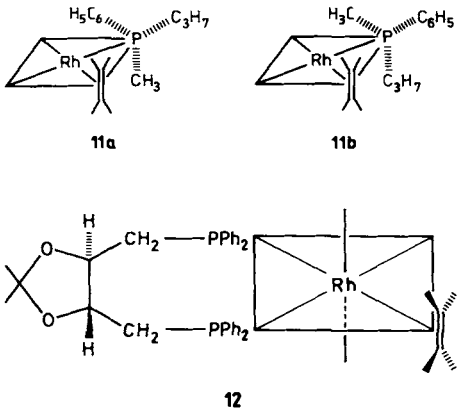
## 3. Increase in Stereoselectivity by Restriction of Conformational Variety

The development of models could not keep up with the rapid experimental progress, so that today asymmetric catalysis appears largely empirical. Progress was made more often by serendipitous discovery than by systematic planning. In the recent past, however, some guidelines have been developed which optically active phosphanes must fulfill to be suitable for use as ligands in catalysts. Some of the factors which favor high optical yields follow:

a) Use of monodentate rather than of bidentate ligands;
b) Formation of five-membered chelates;
c) Introduction of additional rigidity;
d) Aryl substitution of the P atoms of the chelating ligand.

A common feature of factors a)—c) is the restriction of the conformational variety available to the Rh/ligand system. This is especially evident in factor a). In complexes with monodentate ligands each rotamer with respect to the M—P bond, for example, **11a** and **11b** in Scheme 4 or other conformations, has to be viewed as a distinct catalyst with a certain *R* : *S* selectivity. The extreme dependence of stereoselectivity on small structural variations[9,24,45] usually results in low overall selectivity when this arises from different partial selectivities. With chelating ligands, however, free rotation around the M—P bond is removed, *e.g.* in **12** (Scheme 4). This difference finds its expression in the observation that a catalyst with the chelating ligand diop **5** leads to a significantly higher optical yield of 24.5% *ee*[46,47] in the hydrogenation of α-ethylstyrene to 2-phenylbutane than a catalyst with the monodentate ligand PMePrPh (7% *ee*)[2].

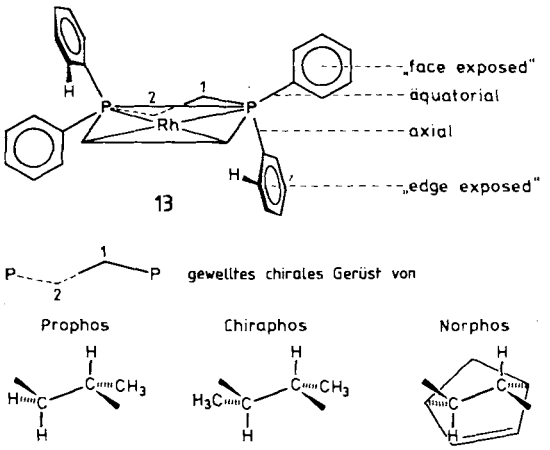
Point b) may be verified by a comparison of the complexes of diop **5** with those of propos 7, chiraphos **8**, and




Scheme 4.

norphos **10**. X-ray crystallographic studies of seven-membered chelate complexes of diop **5**, such as **12** (Scheme 4)[48–52], indicate that they adopt various ring geometries which can rapidly interconvert in solution. In contrast, the ligands prophos **7**, chiraphos **8**, and norphos **10** chelate metals to form puckered five-membered rings of a single type (**13**, Scheme 5). The preferred equatorial position of the methyl groups in prophos **7** and chiraphos **8**[40] or the rigid norbornene skeleton in norphos **10**[53] force the puckered five-membered ring into a δ- or λ-conformation. As shown in the lower part of Scheme 5, the (*S*)-configuration of the asymmetric centers in (2*S*)-prophos, (2*S*,3*S*)-chiraphos, and (2*S*,3*S*)-norphos leads to the δ-conformation of the five-membered chelate ring.

The δ/λ-conformation of the RhPC1C2P five-membered ring is defined here as in the corresponding structural element MNCCN in the numerous complexes of ethylenediamine[54]. The P–P connector (or the N–N connector in the en-complexes) and the C1–C2 bond form a pair of skew lines. Two such skew lines define a helix if one line is taken as the axis of the helix and the other as a tangent to it. For example, if the P–P connector in **13** (Scheme 5) is considered to be the axis and the C1–C2 bond a tangent to a helix, then a clockwise motion away from the observer is described by this helix. The chirality of the puckered RhPC1C2P-ring in **13** (Scheme 5) is, therefore, assigned the conformational symbol δ. Correspondingly its mirror image has the λ-conformation. This λ-conformation would be the result of an inversion of the five-membered ring in which C1 of **13** (Scheme 5) had moved down and C2 up. The asymmetric centers of (2*S*)-prophos and (2*S*,3*S*)-chiraphos would then have the H atoms in equatorial positions and the methyl groups axial. In ethylenediamine complexes[54–58] it is known that axial methyl groups suffer large steric interactions from other ligands. The λ-conformation of (2*S*)-prophos in the complex should thus be disfavored relative to the δ-conformation by *ca.* 2 kcal/mol, corresponding to only a few percent in the conformational equilibrium. For complexes of (2*S*,3*S*)-chiraphos, which contains two (*S*)-configurated carbon atoms, this tendency should be even more pronounced so that the fraction of λ-conformation may be vanishingly small. For (2*S*,3*S*)-norphos, participation of the λ-conformation is completely excluded because the bonds to the bridgehead atoms of the norbornene cannot reach the axial positions. The uniform ring conformation with five-membered rings as compared to seven-membered rings results in the high optical inductions of 90, 99, and 98% *ee* for prophos **7**, chiraphos **8**, and norphos **10**, respectively, compared to 81% *ee* for diop **5** in the model reaction in Scheme 2[9,39,40,44].




Scheme 5. Equatorial and axial positions of the face-exposed and edge-exposed phenyl moieties in the puckered chelate rings of the Rh complexes with ligands (2*S*)-prophos **7**, (2*S*,3*S*)-chiraphos **8**, and (2*S*,3*S*)-norphos **10**.

In a similar way, increasing the rigidity of the seven-membered ring in diop **5** (Scheme 3) by ketalization has a favorable effect on the optical induction[9]. The more flexible chelate ring with two OH-groups instead of the ketal ring in **5** results in significantly less selective catalysts than diop itself. Reduction of the conformational variety according to a)–c) and increase in optical yield can therefore be correlated.

## 4. Conformation of the Rhodium/Bisphosphane Chelate Rings

The increase in selectivity on aryl substitution at the P atoms—factor d) in Section 3—has different origins which are connected with the distance between the centers inducing chirality and the prochiral substrate. In **12** (Scheme 4) it can be seen that the chirality at the C atoms of the diop ligand, originally derived from tartaric acid, is separated by four bonds from the $sp^2$ centers of the substrate which become the new asymmetric centers, *i.e.* by *ca.* 6 Å. In those chelating phosphanes which form five-membered rings, the distance between the centers inducing chirality and the site where it is needed is one bond shorter. However, the distance is still so large that the question must be asked how the prochiral $sp^2$ centers in the coordinated substrate "feel" the chiral influence upon being converted to chiral $sp^3$ centers.

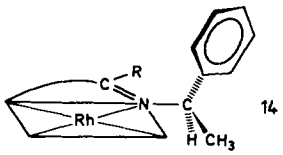
Certainly, the chiral information in the catalyst complex is also transmitted *via* the surrounding solvent cage. It appears, however, that the real transmitters are the phenyl rings at the P atoms. According to a proposal by *Knowles et al.*[50], and this has since been verified by numerous X-ray structure analyses[17,26,59,60], one has to envision this as depicted for the chelating phosphanes prophos **7**, chiraphos **8**, and norphos **10** in **13** (Scheme 5). C1 is located somewhat above the Rh-square and C2 somewhat below this plane. If the five membered-ring RhPC1C2P were planar,

the angles between all four P–C(phenyl) bonds and the Rh-plane would be equal and there would be no differentiation into axial and equatorial phenyl rings. However, since the bond from the right-hand P atom to C1 of the chelate ring points upward, the upper phenyl ring bound to this P atom occupies an equatorial position and the lower phenyl group is axial (see **13**). Correspondingly, the two phenyl groups at the left-hand P atom are equatorial and axial. These equatorial/axial positions of the phenyl rings in the $P(C_6H_5)_2$-groups arise because the chelate ring is puckered. Added to this is a second effect also shown in **13**. Frequently the two phenyl rings are nearly perpendicular to each other. While one of the phenyl rings is approximately parallel to the plane of the paper, the other is almost perpendicular to it. The two positions are distinguished as "face exposed" and "edge exposed". Thus each P atom of a diphenylphosphino group contains an equatorial phenyl ring in a "face exposed" position and an axial phenyl ring in a "edge exposed" position.

## 5. Chirality Transfer in the Catalyst from Optically Active Ligand to Substrate

Positioning the two phenyl rings at the P atom (axial/equatorial and face/edge exposed) causes chirality, which is determined by the puckering of the chelate ring and thus by the configuration of the asymmetric centers in the chelate skeleton. The chiral information is transmitted from the asymmetric center in the chelate framework through the $P(C_6H_5)_2$-groups to the catalytically active coordination sites at the metal atom. A substrate at the front right coordination site of the Rh-square encounters hardly any steric hindrance by the "face exposed" phenyl ring above the plane; however, below this plane strong steric interactions, especially with the *ortho*-hydrogen atom of the "edge exposed" phenyl ring, are to be expected. Even in those few chelating ligands in which the asymmetric P atoms bear the inducing chirality, the transfer of chirality to the substrate should proceed in a similar fashion. This is exemplified by dipamp **6** (Scheme 3), in whose complexes the *o*-methoxyphenyl group in the "face exposed" position is always equatorial[26, 50].

Although the chirality transfer through the two phenyl "ears" of the phosphorus is extraordinarily effective in numerous catalyses, for the following reasons it is not the optimal solution for asymmetric catalysis: The chelating phosphanes in Scheme 3 and the vast majority of optically active ligands used to date have different centers of chirality, *e.g.* the tartaric acid chirality in diop **5** and the proline chirality in BPPM **9**, *etc.* The transfer mechanism for all these specific chiralities, however, is the same. The $P(C_6H_5)_2$-transmitter can only react to the specific chiral information by positioning its phenyl rings more or less axial/equatorial and face/edge exposed. The prochiral substrate thus does not "see" the original chirality of the tartaric acid or proline *etc.*, but rather the phenyl "ears" of the transmitter only, whose positions do not differ substantially for the various specific inducing chiralities. Consequently, this transfer of chirality leads to a loss of information. One might therefore expect better results in asymmetric catalysis if the inducing center of chirality in the catalyst were located where the $P(C_6H_5)_2$-transmitter is situated. A loss of information due to transfer would then be avoided; the inducing chirality would interact directly with the substrate in the neighboring coordination site. This concept could be verified with the aid of a chelating ligand which is bound to rhodium *via* an N atom as shown in **14** (Scheme 6).




**14**

Scheme 6.

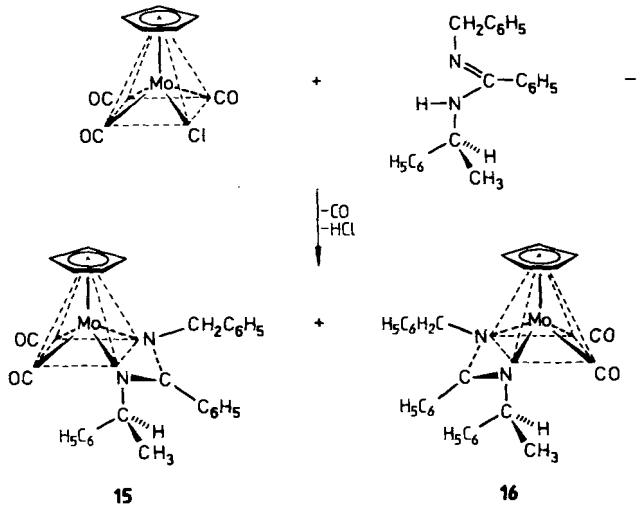
A chiral substituent at this N atom, *e.g.* the (R)–CHMePh-group, is then situated precisely where (Scheme 5) the phenyl groups transmitting the chirality were in the chelating phosphane complexes. If the chelating ring in **14** is planar and the nitrogen atom is $sp^2$-hybridized, the optically active group lies in the plane of the Rh atom. Schiff base condensation of carbonyl compounds with optically active primary amines should lead to imino ligands as in **14**, whose N atoms are also $\pi$-acceptors. With these Schiff base ligands the great potential of the known optically active primary amines[61] could be tapped. As discussed for mono-/bidentate phosphanes, the structural element =N–R* should form part of a chelating ring to eliminate rotation around the Rh–N bond and fix the optically active group R* in the desired position. Since the asymmetric center can rotate freely around the N–C* bond, one conformational problem remains: Can the optically active group assume several stable conformations or are some conformations clearly preferred? The latter would be the favorable case for asymmetric catalysis.

In the following, it will be shown using a model compound that the optically active group CHMePh can assume certain preferred conformations, depending on neighboring substituents R at the chelate ring and on other ligands at the metal atom. The application of this concept to asymmetric catalysis will then be described.

## 6. Diastereomeric $CpMo(CO)_2$amidinato Complexes with Labile Configuration at Mo

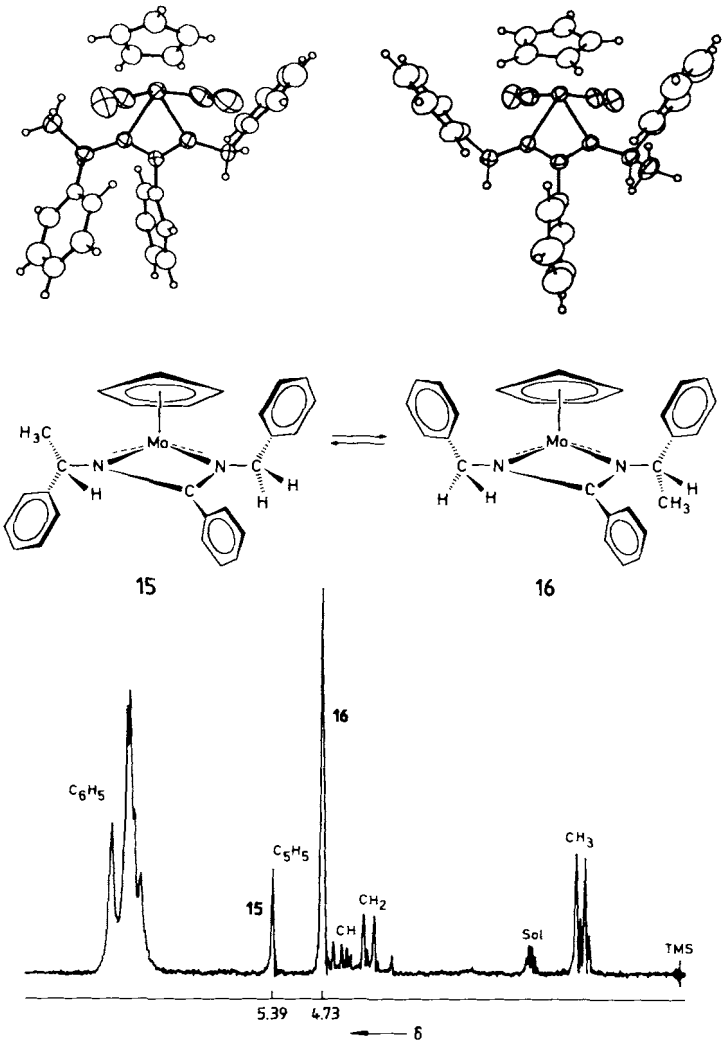
The synthesis of the model compounds starts from the square pyramidal $CpMo(CO)_3Cl$, in which the Cp-group occupies the apex of the pyramid, and an amidine derived from benzoic acid, in which one of the *N*-substituents is benzyl and the other (*S*)-1-phenylethyl, is shown in Scheme 7.

By elimination of CO and HCl two diastereomeric complexes, ($S_{Mo}S_C$)-**15** and ($R_{Mo}S_C$)-**16**, are formed in which the amidinate anion occupies the two vacant coordination sites of the basal square of the pyramid in two ways which only differ in the configuration about the Mo atom. The two isomers may be separated by fractional crystallization or by preparative liquid chromatography[62]. The separation can be monitored by $^1$H-NMR spectroscopy, since the chemical shifts of almost all resonances differ significantly




Scheme 7.

in both diastereomers (Scheme 8, bottom). This is especially true for the Cp-singlets, which are particularly suited for the determination of the diastereomeric purity.




Scheme 8. The diastereomers **15** and **16**: ORTEP representation of the structures (top) and $^1$H-NMR spectrum ([D$_6$]acetone) of the 20:80 equilibrium mixture (bottom).

Upon heating the separated diastereomers, *e.g.* in toluene, a change of configuration about Mo is observed[63-66]. The half-lives are approximately 30 min at 70°C. The course of this intramolecular isomerization can most simply be thought of as a rotation of the amidinate ligand by 180°[67], which transforms the ($S_{Mo}S_C$)-isomer **15** into the ($R_{Mo}S_C$)-isomer **16** and *vice versa*. After ten half-lives, an equilibrium mixture of diastereomers is produced, regardless of whether one started with **15** or **16**, or from a mixture of both. The lower part of Scheme 8 shows the spectrum of the equilibrium mixture **15** ⇄ **16**: integration indicates that this consists of 20% of **15** and 80% of **16**. The following formulas, which demonstrate the intramolecular interactions, are intended to indicate why isomer **16** is thermodynamically more stable.

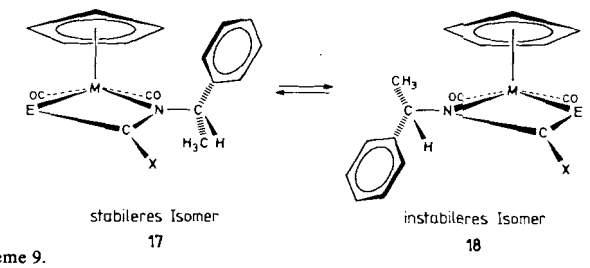
In these formulas the Cp-ring is oriented upward. The two carbonyl groups of the $CpMo(CO)_2$ fragment are located at the rear and are sketched lightly in Scheme 9 but omitted for clarity in the other formulas. X-ray structural analyses show that the chelate ring, which is tilted forward, is completely planar and that $C_{ipso}$ of the ring-bound phenyl group and the two extra-annular C atoms of the *N*-substituents also lie in this plane.

Despite their complicated structure, the model compounds **15** and **16** have only limited possibilities of changing the structure of the molecule by intramolecular rotations. Rotation around the metal-Cp axis or the metal-CO bonds have no stereochemical consequences. According to X-ray structure analyses, the phenyl ring connected to the chelate ring is almost always perpendicular to the ligand plane. Derivatives with a methyl group or hydrogen atom in place of this phenyl ring (see Section 8) do not pose any problem with respect to rotamers. The only intramolecular motions which change the geometry of molecules **15** and **16** are rotations of the *N*-substituents around the N–C bonds in connection with adjustment of their phenyl rings, the conformational problem to be discussed in the following section.

## 7. Conformational Analysis of the Diastereomers

The rules which emerged in the conformational analysis of these compounds with respect to the position of the *N*-substituents are listed in decreasing order of importance[62,68-71] (cf. Scheme 9):

1) C–H bond in the ligand plane
2) Ph/Cp attraction
3) Me/Cp repulsion




Scheme 9.

Decisive for the conformation is that the C–H bond of the asymmetric center always lies in the ligand plane pointing away from the molybdenum. This conformation

determining effect is a consequence of the steric hindrance of the substituents X (methyl or phenyl) with the substituents of the asymmetric C*-atom. Putting the methyl or phenyl substituents of C* close to the ligand plane would result in extremely short distances to X. The steric interaction with the neighboring methyl or phenyl substituent on the chelate ring is least for the small H-substituent.

Given the priority order[*] of the ligands Cp > NR* > E, the chiral center at the metal atom of **17** in Scheme 9 assumes the *R*-configuration[66,72-75]. With an (*S*)-configurated asymmetric C atom the phenyl ring in the ($R_{Mo}S_C$)-diastereomer **17** is directed upwards and approaches the Cp ring so closely that the distance between the midpoints of the Cp and phenyl rings is only *ca.* 5 Å, as in solid benzene. Similar to solid[76,77] and liquid[78] benzene, as well as to benzene dimers in the gas phase[79], the Cp and phenyl rings are mutually perpendicular and form a T-shaped arrangement. This interaction is energetically favored, and is designated the "β-phenyl effect" because of the β-position of the phenyl group relative to the metal atom[80-82].

Rotation of the E,N-chelating ligand in **17** by 180° with respect to the $CpMo(CO)_2$-fragment results in **18** (Scheme 9), the ($S_{Mo}S_C$)-isomer. Since according to rule 1 the C–H bond of the asymmetric center in the ligand plane is directed away from the metal, an (*S*)-configuration at the asymmetric carbon atom directs the methyl group upwards and the phenyl group downwards. The very weak interaction Me/Cp is energetically unfavorable, *i.e.* it has a repulsive effect. In the equilibrium the ($R_{Mo}S_C$)-isomer **17** dominates.

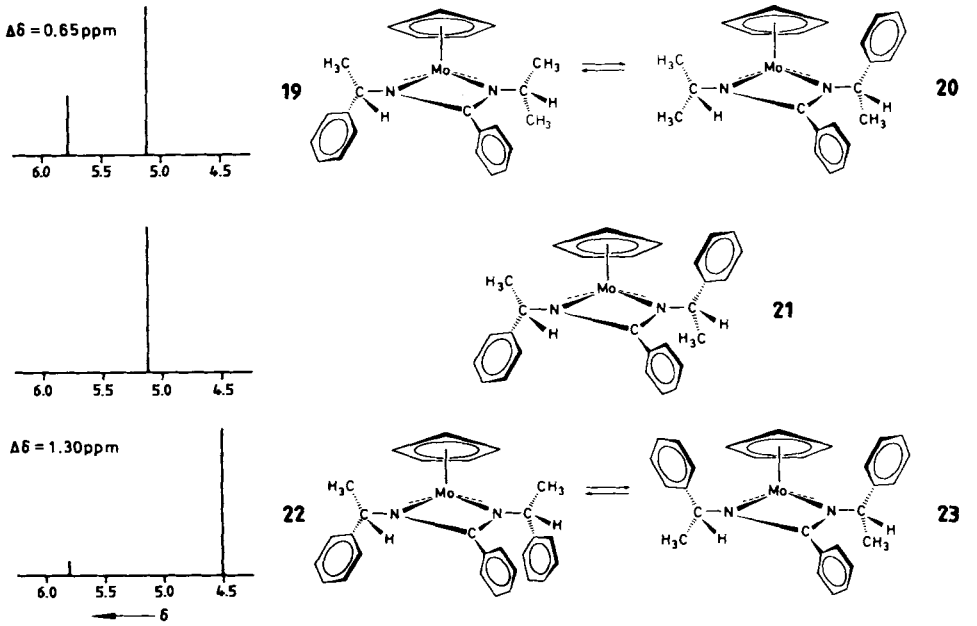
With $E = N-CH_2C_6H_5$ we return to example **15**/**16** in Scheme 8[62,68-71]. For this system it was possible to obtain single crystals for both the thermodynamically more stable ($R_{Mo}S_C$)-isomer **16** and the less stable ($S_{Mo}S_C$)-isomer **15** and to carry out X-ray structure analyses[68,69]. The ORTEP drawings shown above the formulas of **15** and **16** confirm that the orientations of both *N*-substituents, 1-phenylethyl and benzyl, adhere to the above-mentioned rules. In both diastereomers the C–H bonds of the *N*-substituents on both sides lie in the ligand plane. In the thermodynamically more stable isomer **16** the two phenyl rings are directed upwards. This "winner"-type exhibits two stabilizing Ph/Cp interactions. In the thermodynamically less stable isomer **15** the phenyl ring of the benzyl group points upwards, but the phenyl ring of the 1-phenylethyl group hangs downwards. This "mixed"-type thus experiences a stabilizing Ph/Cp interaction and a destabilizing Me/Cp interaction. That the Ph/Cp interaction in **15** and **16** is actually stabilizing results from the following consideration: The 1-phenylethyl group orients its only C*–H bond in the ligand plane in both **15** and **16**, but, in contrast, the benzyl group does so with two different C–H bonds. If the amidinato ligand were to remain rigid throughout the 180° rotation which converts the "winner"-type **16** into the "mixed"-type **15**, the same C–H bonds would lie in the ligand plane in **15** as in **16**. However, both phenyl rings in **15** would hang downwards. To exploit the Ph/Cp attraction, the benzyl group in "mixed"-type **15** therefore rotates by 120°, and hence in **15** and **16** different C–H bonds of the benzyl group lie in the ligand plane.

X-ray structures of a dozen similar compounds indicate that the C–H bond of the 1-phenylethyl group lies practically in the ligand plane[68,69,83,84]. Small deviations are confined to the thermodynamically less stable diastereomers and consistently show the C–H bond pointed slightly above the ligand plane[70]. The reason for this minor deviation from the conformational rules 1–3 appears to be the Me/Cp repulsion, which is attenuated by this torsion.

The results of the X-ray structure determinations imply that the intramolecular interactions are more important than packing effects in the crystal lattice. $^1$H-NMR evidence confirms that the conformations found in the solid state are also the preferred conformations in solution. In the equilibrium **15** ⇌ **16** the "winner"-type **16** outweighs the "mixed"-type **15** (80 : 20)[62]. The chemical shifts of the Cp signals exhibited by diastereomers **15** and **16** (Scheme 8, bottom) differ by *ca.* 0.5 ppm. This can be attributed to the fact that the Cp ring of the "winner"-type **16** is located in the inner anisotropic region of the two phenyl rings, whereas the Cp ring of the "mixed"-type **15** experiences only one such anisotropic region. The Cp signal of **16** is therefore shifted to higher field relative to that of **15**[62]. Correspondingly, in all the diastereomers examined to date the Cp signals of the thermodynamically more stable isomers lie at higher field[62-71].

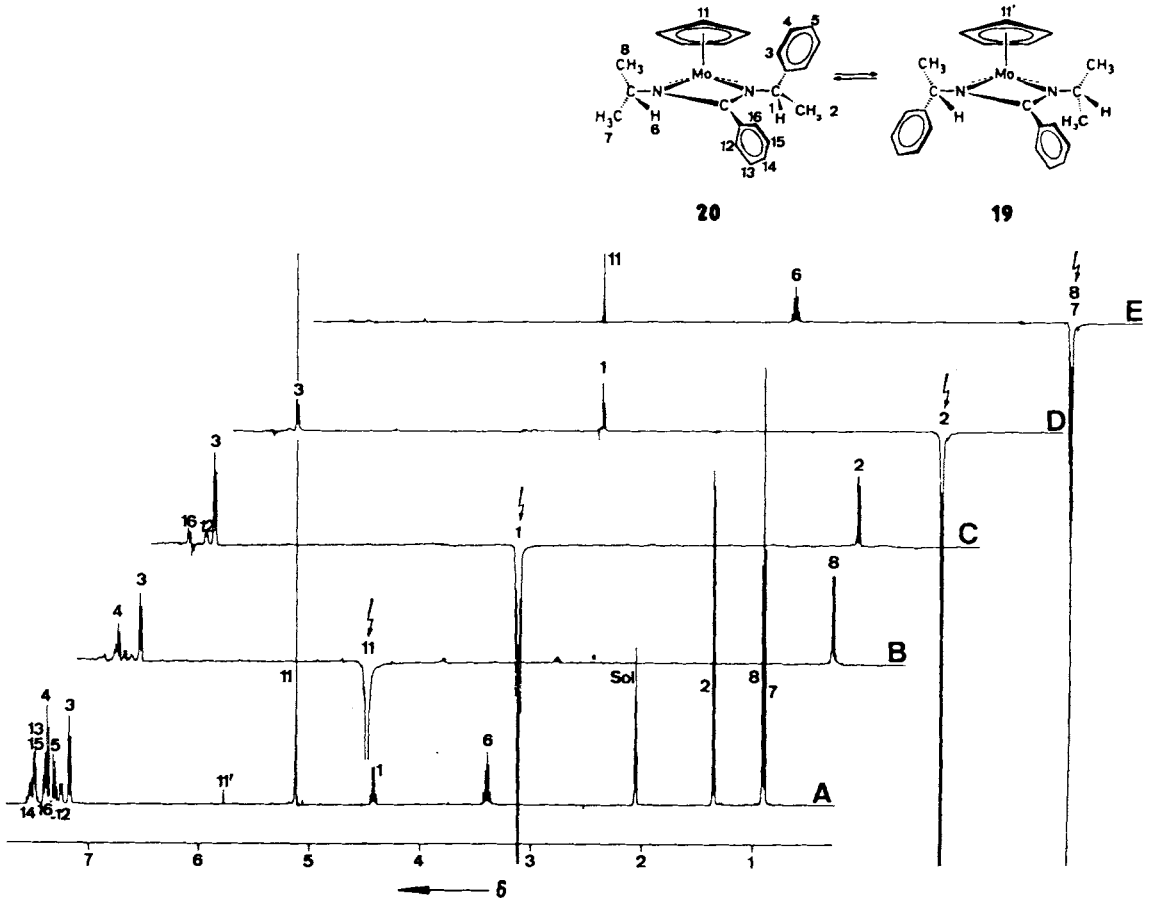
The three isomers **21**, **22**, and **23** (Scheme 10) demonstrate impressively the stabilization by Ph/Cp attraction and destabilization by Me/Cp repulsion. If the (*S*)-phenylethyl group is introduced at one N atom and the (*R*)-form at the other N atom of the amidinate complexes, two isomers are possible (Scheme 10, bottom). One is a "winner"-type **23**, with two Ph/Cp attractions, and the other a "loser"-type **22**, with two hanging phenyl groups and two Me/Cp repulsions. At equilibrium the diastereomers **22** and **23** are in the ratio 6 : 94: the Cp-signal of the "winner"-type is shifted by 1.3 ppm to higher field (two Ph/Cp interactions) with respect to the position of the "loser"-type[70]. If the same optically active (*S*)-1-phenylethyl group at both N atoms is used to synthesize the $CpMo(CO)_2$amidinate complex, isomer **21** is obtained (Scheme 10, center). Whereas "winner"-type **23** and "loser"-type **22** interconvert upon change of configuration at the Mo-atom, the "mixed"-type **21** transforms, so to speak, into itself in this metal-centered rearrangement. With the prerequisite that both C*–H bonds in **21** lie in the ligand plane, one Ph/Cp attraction and one Me/Cp repulsion result. Thus the anisotropic effect of only one phenyl ring is experienced by the Cp group so that the chemical shift of **21** lies exactly halfway between those of the isomeric compounds **22** and **23** (Scheme 10). The diastereomers **19** and **20**, substituted at the N atoms with (*S*)-1-phenylethyl and isopropyl groups, fit neatly into this picture with their diastereomeric ratio of 30 : 70 and their chemical shifts (Scheme 10, top)[62].

[*] The *R,S* system proposed by *Cahn, Ingold,* and *Prelog* [74] makes no provision for inclusion of π-bonded ligands in the sequence rule. *Tirouflet* [72] and *Baird* [73] have suggested that polyhapto ligands be considered as pseudoatoms with atomic number equal to the sum of the atomic numbers of the π-bonded atoms. Thus, for example, $\eta^6$-$C_6H_6$, $\eta^5$-$C_5H_5$, and $\eta^2$-$C_2H_4$ are classified as pseudoatoms having the atomic numbers 36, 30, and 12, respectively.




Scheme 10. $^1$H-NMR line spectra of the compounds **19**—**23**. The ring-current effect of the phenyl substituents influences the position of the Cp signals.

As shown for **20** in Scheme 11, nuclear Overhauser effect (NOE) difference spectroscopy provides direct proof that the conformations depicted in Schemes 8—12 are also those preferred in solution[71,85,86]. Spectrum A shows the 400 MHz $^1$H-NMR spectrum of **20** contaminated with 3% of diastereomer **19**. Upon saturation of the Cp-signal 11 of **20** (spectrum B) the signals of protons 3 and 4 of the 1-phenylethyl substituent and those of the methyl group 8 of the isopropyl substituent are enhanced, corresponding to their close proximity in space. In contrast, no enhance-



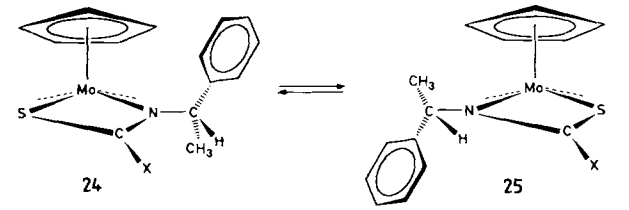

Scheme 11. A = 400 MHz $^1$H-NMR spectrum of **20/19** in [D$_6$]acetone. B to E = $^1$H-NMR-NOE difference spectra after saturating the signals indicated by the arrows (cf. also text).

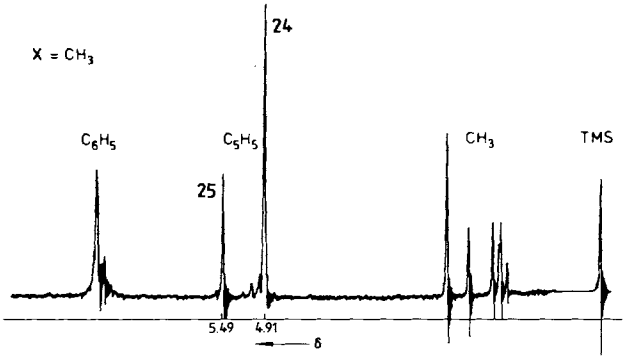
ment is found in the signals of protons 1 and 6 nor in those of methyl groups 2 and 7, which lie far removed from the Cp-ring. In spectra C and D the signals 1 and 2, respectively, are saturated. Enhancements are observed for the *ortho*-phenyl protons 3 as well as for the methyl group 2 and the proton 1, *i.e.* those substituents bonded to the same C atom.

Close proximity in space of the Cp-protons 11 with the protons 1 and 6 and with the methyl group 2, respectively, is precluded by spectra C and D. However, upon saturation of the methyl group 8 of the isopropyl substituent the resonances for both 6 and the neighboring Cp-ring 11 are enhanced (spectrum E)[71]. These NOE difference spectra thus confirm the preferred conformations deduced from the diastereomeric ratios and chemical shifts.

## 8. Equilibria of Diastereomeric CpMo(CO)$_2$thioamidato Complexes

The thioamidato complexes **24** and **25** in Scheme 12, which are similar to the amidinato complexes **15**—**23**, also contain a planar four-membered chelate ring[83,84].




| X | H | $CH_3$ | $C_6H_5$ | $C_{10}H_7$ |
|---|---|---|---|---|
| **24**:**25** | 50:50 | 69:31 | 77:23 | 87:13 |

Scheme 12. Equilibrium of diastereomers **24** ⇌ **25**. 60 MHz-$^1$H-NMR spectrum ([D$_8$]toluene, 40 °C) and dependence of the position of equilibrium on substituents X.

With these compounds, too, the two diastereomers interconvert *via* an intramolecular metal-centered rearrangement. The stability of diastereomers **24** and **25** is also determined by the interaction of the substituents at the asymmetric C atom with the other substituents. Under the assumption that the C*—H bond lies in the ligand plane, complexes with "large" substituents X = $C_{10}H_7$ (1-naphthyl), $C_6H_5$, and $CH_3$ are thermodynamically more stable in the form of diastereomer **24** due to the Ph/Cp attractive interaction than as diastereomer **25** with a Me/Cp repulsive interaction. For the system derived from acetic acid with X = $CH_3$, this results in a diastereomeric ratio of 69:31 (Scheme 12, bottom) and in a shift of the Cp-signal to high field in the favored isomer **24** (Scheme 12, middle). Similar high field shifts are exhibited by the complexes derived from benzoic acid and 1-naphthoic acid (X = $C_6H_5$ and 1-$C_{10}H_7$, resp.), whose diastereomer ratios are 77:23 and 87:13, respectively.

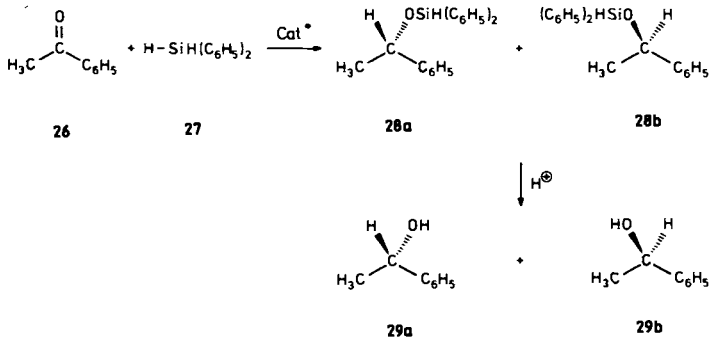
More than 50 different CpMo(CO)$_2$amidinato and -thioamidato complexes—more than a dozen of which have been studied by X-ray structure analysis—confirm this conformational concept without exception. It holds even for complexes with methyl substituted Cp-rings in which the rotation of the five-membered ring around the metal-ring axis and the associated repulsion of the methyl group and the neighboring phenyl group do not cancel out the Ph/Cp attraction[91]. However, difficulties are encountered with rules 1—3 (Section 7) if it is attempted to extend the conformational analysis to five-membered chelate rings. Apparently, additional interactions of the substituents of the expanded chelate ring with other groups in the molecule, *e.g.* the metal carbonyls, are introduced which are absent in CpMo(CO)$_2$-complexes with four-membered chelate rings[92–95].

Difficulties of an entirely different kind are encountered in the transition to CpMo(CO)$_2$thioamidato complexes derived from formic acid with X = H. Here, both diastereomers ($S_{Mo}S_C$)-**24** and ($R_{Mo}S_C$)-**25** are present in equal amounts in the equilibrium mixture (Scheme 12, below) and both exhibit approximately the same chemical shifts for the Cp-ring. This basic change when X = H results from the absence of steric hindrance between the chelate ring and the Me- and Ph-substituents of the asymmetric C atom. Thus rule 1 (Section 7), the basis of the conformational analysis, no longer holds.

The result of the conformational analyses of CpMo(CO)$_2$amidinato and -thioamidato complexes is, thus, that the substituents of an asymmetric center at the N-atom of a chelate ring assume certain preferred conformations, despite free rotation about the N—C* bond. These conformations are determined by Ph/Cp attractions, Me/Cp repulsions, and especially by the neighboring substituent X at the chelate ring.

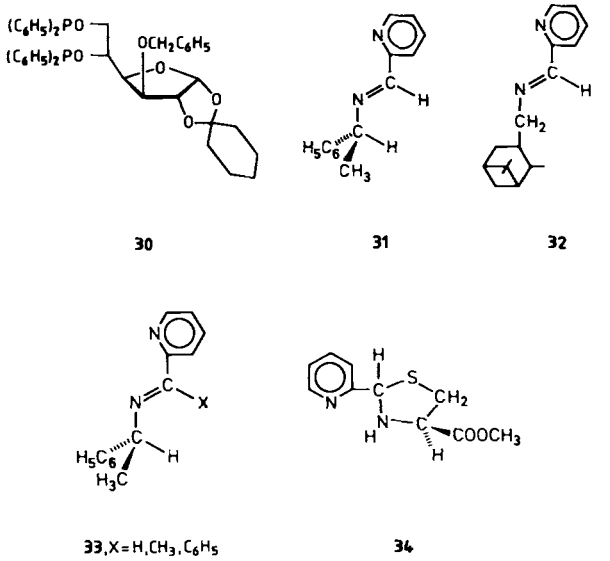
## 9. Asymmetric Hydrosilylation with Catalysts Containing Nitrogen Ligands

Asymmetric hydrosilylation of prochiral ketones with compounds containing SiH bonds is only moderately successful when those Rh/phosphane catalyst systems are used which are highly efficient for hydrogenations. For example, in the model reaction of acetophenone **26** with diphenylsilane **27**, which leads to the diphenylsilyl ethers **28a** and **28b** and to 1-phenylethanols **29a** and **29b** after hydrolysis[46,96,97] (Scheme 13), the precatalyst [Rh(cod)Cl]$_2$ with diop **5** as cocatalyst only results in 32% and with norphos **10** only in 16% optical induction[46,98,99]. Until recently, the best result achieved for the model reaction was 55% optical induction employing the system [Rh(cod)Cl]$_2$/glucophinite, where glucophinite **30** is a P-containing chelate ligand which is derived from D-glucose (Scheme 14)[100].



Scheme 13.

In comparison, chelating ligands with a lateral center of asymmetry based on model compound **14** were a distinct improvement. In the model reaction of Scheme 13 the precatalyst $[Rh(cod)Cl]_2$ with the pyridineimine **31**—a derivative of (−)-1-phenylethylamine—gives 57.3% *ee*[101] and with the pyridineimine **32**—a derivative of (−)-3-aminomethylpinane—even 78% *ee*[102] (Scheme 14). Similar stereoselectivities are observed in the asymmetric hydrosilylation of other prochiral ketones such as benzyl methyl ketone and *tert*-butyl methyl ketone[99]. Chelate complexes of the type **14** are thus not only catalytically active but their enantioselectivity also surpasses those catalyst which transfer chiral information as outlined in Scheme 5.



Scheme 14.

Catalysts with the ligands **31** and **32** demonstrate the superiority of the concept of direct interaction between the inducing chirality center and the coordination site at the metal where the prochiral substrates are converted into the optically active compounds, compared with the principle of using two phenyl rings to transfer the chiral information.

A connection between the conformation of $CpMo(CO)_2$-derivatives and the results of asymmetric hydrosilylation is also indicated. The conformational analysis of thioamidato complexes (Scheme 12) shows that the position of the substituents at the asymmetric C atom is principally determined by the substituents X. A corresponding variation of this substituent X from H to $CH_3$ and $C_6H_5$ (**33**, Scheme 14) also results in large variations in the optical induction of the asymmetric hydrosilylation from 57% *ee* (*S*) to 18% *ee* (*R*) and 9% *ee* (*S*)[101] in the catalyst system $[Rh(cod)Cl]_2$/**33**. A direct parallel between the model complex **24**/**25** and the system $[Rh(cod)Cl]_2$/**33** should not be expected, since the model exhibits interactions such as Ph/Cp attraction or Me/Cp repulsion, which are absent in the catalyst. However, the influence of the conformation of the chiral substituent at the chelate ring by the neighboring moiety X is apparent.

The restriction of rotational freedom around the metal-ligand bond, the use of five-membered chelate rings, and the introduction of additional rigidity are known to enhance induction with optically active chelating phosphanes. For ligands **31**—**34**, with their laterally bound centers of asymmetry, the first two points are taken into consideration by the structures favoring five-membered chelate rings. According to the results of the conformational analysis, the lateral asymmetric centers in complexes **31**, **32**, and **33** should assume certain preferred conformations, but a further restriction of conformational variety, *e.g.* by incorporation of the asymmetric center in a ring skeleton, should have a further positive effect on the optical induction. This concept is realized in **34**, in which the asymmetric center of cysteine is part of a thiazolidine ring. The added rigidity allows the optical induction achieved with the $[Rh(cod)Cl]_2$/**34** catalyst to be increased to 87.6% *ee*[102], the highest value obtained so far for the model reaction in Scheme 13.

## 10. Summary and Prospects

Complexes with the ligands **31**–**33** correspond to type **14** (Scheme 6). One end of the chelating ligand is an imino group with a chiral substituent and the other a pyridine nitrogen. If the Rh atom of the catalyst is assumed to be octahedrally coordinated, four additional coordination sites beyond the two for the chelate ligand have to be filled. Of these, three are *cis* to =N−R*; one in, one above, and one below the plane of the chelate ring. A further position is *trans* to =N−R* in the plane of the chelate ring (Scheme 6). These four positions are stereochemically different. The *cis*-positions are directly influenced by the chiral substituent; in contrast, the *trans*-position is far removed from the inducing chirality center. One might therefore attempt to introduce the same optically active R*-group at both N atoms of the chelating ligand. A ligand of that kind would have a $C_2$-axis. In an octahedral chelate complex all positions of the Rh-octahedron would be under the direct influence of the chiral groups. Furthermore, the four remaining coordination sites in such a chelate complex would become pairwise equivalent. This reduction of the number of possible binding sites for the substrate from four to two should facilitate a further increase in stereoselectivity.

The catalysts $[Rh(cod)Cl]_2$/**31**—**34** with their laterally bound centers of asymmetry are not catalytically active in the asymmetric hydrogenations described in Section 2. The success achieved in hydrosilylation suggests, however, that

systems of the type **14** should be used in asymmetric catalyses such as Grignard cross-coupling, hydroformylation, olefin oligomerization, olefin/diazoalkane cyclopropanation, Michael addition, *etc.* One could thus exploit the advantage of the new concept, *i.e.* of bringing a multitude of chiralities derived from optically active amines into direct contact with those positions at the central metal at which the conversion of the prochiral substrate into the optically active product takes place. It is to be hoped that these developments in the area of enantioselective catalysis constitute a step toward the goal stated in the thesis which precedes this review.

Received: May 20, 1983 [A 477 IE]
German version: *Angew. Chem. 95* (1983) 921
Translated by: *K. H. Theopold*, Ithaca, NY

[1] A. L. Lehninger: *Biochemistry*, 2nd edit., Worth, New York 1975, p. 208.
[2] L. Horner, H. Siegel, H. Büthe, *Angew. Chem. 80* (1968) 1034; *Angew. Chem. Int. Ed. Engl. 7* (1968) 942.
[3] W. S. Knowles, M. J. Sabacky, *Chem. Commun. 1968*, 1445.
[4] J. A. Osborn, F. H. Jardine, J. F. Young, G. Wilkinson, *J. Chem. Soc. A 1966*, 1711.
[5] H. B. Kagan, T. P. Dang, *J. Am. Chem. Soc. 94* (1972) 6429.
[6] J. D. Morrison, R. E. Burnett, A. M. Aguiar, C. J. Morrow, C. Philips, *J. Am. Chem. Soc. 93* (1971) 1301.
[7] W. S. Knowles, M. J. Sabacky, B. D. Vineyard, *J. Chem. Soc. Chem. Commun. 1972*, 10.
[8] J. D. Morrison, W. F. Masler, *J. Org. Chem. 39* (1974) 270.
[9] T. P. Dang, J. C. Poulin, H. B. Kagan, *J. Organomet. Chem. 91* (1975) 105.
[10] W. S. Knowles, M. J. Sabacky, B. D. Vineyard, *Ann. N. Y. Acad. Sci. 172* (1970) 232.
[11] W. S. Knowles, M. J. Sabacky, B. D. Vineyard, *Chem. Eng. News 48* (1970) No. 29, p. 41.
[12] W. S. Knowles, M. J. Sabacky, B. D. Vineyard, *Chem. Eng. News 50* (1972) No. 6, p. 4.
[13] W. S. Knowles, M. J. Sabacky, B. D. Vineyard, *CHEMTECH 2* (1972) 590.
[14] W. S. Knowles, M. J. Sabacky, B. D. Vineyard, *Ann. N. Y. Acad. Sci. 214* (1973) 119.
[15] W. S. Knowles, M. J. Sabacky, B. D. Vineyard, *Adv. Chem. Ser. 132* (1974) 274.
[16] W. S. Knowles, M. J. Sabacky, B. D. Vineyard, D. J. Weinkauff, *J. Am. Chem. Soc. 97* (1975) 2567.
[17] H. B. Kagan in G. Wilkinson, F. G. A. Stone, E. W. Abel: *Comprehensive Organometallic Chemistry, Vol. 8*, Pergamon Press, Oxford 1982, p. 463.
[18] L. Markó, J. Bakos, *Aspects Homogeneous Catal. 4* (1981) 145.
[19] B. Bosnich, M. D. Fryzuk, *Top. Stereochem. 12* (1981) 119.
[20] V. Caplar, G. Comisso, V. Sunjic, *Synthesis 1981*, 85.
[21] H. Brunner, *Kontakte 1981*, 3.
[22] H. B. Kagan, *Ann. N. Y. Acad. Sci. 333* (1980) 1.
[23] M. Kumada, *Pure Appl. Chem. 52* (1980) 669.
[24] H. Brunner, *Chem. Unserer Zeit 14* (1980) 177.
[25] B. R. James, *Adv. Organomet. Chem. 17* (1979) 319.
[26] W. S. Knowles, B. D. Vineyard, M. J. Sabacky, B. R. Stults in M. Tsutsui: *Fundam. Res. Homogeneous Catal., Vol. 3*, Plenum Press, New York 1979, p. 537.
[27] D. Valentine Jr., J. W. Scott, *Synthesis 1978*, 329.
[28] H. B. Kagan, J. C. Fiaud, *Top. Stereochem. 10* (1978) 175.
[29] R. Pearce, *Catalysis 2* (1978) 176.
[30] C. White, *Organomet. Chem. 7* (1978) 367.
[31] J. D. Morrison, W. F. Masler, M. K. Neubert, *Adv. Catal. 25* (1976) 81.
[32] J. D. Morrison, W. F. Masler, S. Hathaway, *Catal. Org. Synth. 1976*, 203.
[33] H. B. Kagan, *Pure Appl. Chem. 43* (1975) 401.
[34] I. Ojima, K. Yamamoto, M. Kumada, *Aspects Homogeneous Catal. 3* (1977) 185.
[35] I. Ojima in Y. Ishii, M. Tsutsui: *Fundam. Res. Homogeneous Catal., Vol. 2*, Plenum Press, New York 1978, p. 181.
[36] P. Pino, G. Consiglio in M. Tsutsui: *Fundam. Res. Homogeneous Catal., Vol. 3*, Plenum Press, New York 1979, p. 519.
[37] P. Pino, A. Stefani, G. Consiglio in B. Pullman: *Catalysis in Chemistry and Biochemistry, Vol. 12*, D. Reidel, Dordrecht 1979, p. 347
[38] G. Consiglio, P. Pino, *Top. Curr. Chem. 105* (1982) 77.
[39] M. D. Fryzuk, B. Bosnich, *J. Am. Chem. Soc. 100* (1978) 5491.
[40] M. D. Fryzuk, B. Bosnich, *J. Am. Chem. Soc. 99* (1977) 6262.
[41] J. Kötter, G. Greber, *Chem. Ber. 113* (1980) 2323.
[42] K. Achiwa, *J. Am. Chem. Soc. 98* (1976) 8265.
[43] H. Brunner, W. Pieronczyk, *Angew. Chem. 91* (1979) 655; *Angew. Chem. Int. Ed. Engl. 18* (1979) 620.
[44] H. Brunner, W. Pieronczyk, B. Schönhammer, K. Streng, I. Bernal, J. Korp, *Chem. Ber. 114* (1981) 1137.
[45] A. D. Calhoun, W. J. Kobos, T. A. Nile, C. A. Smith, *J. Organomet. Chem. 170* (1979) 175.
[46] W. Dumont, J. C. Poulin, H. B. Kagan, *J. Am. Chem. Soc. 95* (1973) 8295.
[47] T. Hayashi, M. Tanaka, I. Ogata, *Tetrahedron Lett. 1977*, 295.
[48] G. Balavoine, S. Brunie, H. B. Kagan, *J. Organomet. Chem. 187* (1980) 125.
[49] S. Brunie, J. Mazan, N. Langlois, H. B. Kagan, *J. Organomet. Chem. 114* (1976) 225.
[50] B. D. Vineyard, W. S. Knowles, M. J. Sabacky, G. L. Bachman, D. J. Weinkauff, *J. Am. Chem. Soc. 99* (1977) 5946.
[51] V. Gramlich, C. Salomon, *J. Organomet. Chem. 73* (1974) C61.
[52] V. Gramlich, G. Consiglio, *Helv. Chim. Acta 62* (1979) 1016.
[53] H. Brunner, A. F. M. M. Rahman, *J. Organomet. Chem. 214* (1981) 373.
[54] *Inorg. Chem. 9* (1970) 1.
[55] E. J. Corey, J. C. Bailar Jr., *J. Am. Chem. Soc. 81* (1959) 2620.
[56] C. J. Hawkins: *Absolute Configuration of Metal Complexes*, Wiley-Interscience, New York 1971.
[57] Y. Saito: *Inorganic Molecular Dissymmetry*, Springer, Heidelberg 1979.
[58] O. Samuel, R. Couffignal, M. Lauer, S. Y. Zhang, H. B. Kagan, *Nouv. J. Chim. 5* (1981) 15.
[59] D. A. Slack, I. Greveling, M. C. Baird, *Inorg. Chem. 18* (1979) 3125.
[60] K. E. Koenig, M. J. Sabacky, G. L. Bachman, W. C. Christopfel, H. D. Barnstoff, R. B. Friedman, W. S. Knowles, B. R. Stults, B. D. Vineyard, D. J. Weinkauff, *Ann. N. Y. Acad. Sci. 333* (1980) 16.
[61] P. Newman: *Optical Resolution Procedures for Chemical Compounds, Vol. 1: Amines and Related Compounds*, Optical Resolution Information Center, New York 1979.
[62] H. Brunner, J. Lukassek, G. Agrifoglio, *J. Organomet. Chem. 195* (1980) 63.
[63] H. Brunner, *Top. Curr. Chem. 56* (1975) 65.
[64] H. Brunner, *Chem. Unserer Zeit 11* (1977) 157.
[65] H. Brunner, *Acc. Chem. Res. 12* (1979) 250.
[66] H. Brunner, *Adv. Organomet. Chem. 18* (1980) 151.
[67] H. Brunner, W. A. Herrmann, *Chem. Ber. 106* (1973) 632.
[68] H. Brunner, G. Agrifoglio, I. Bernal, M. Creswick, *Angew. Chem. 92* (1980) 645; *Angew. Chem. Int. Ed. Engl. 19* (1980) 641.
[69] I. Bernal, M. Creswick, H. Brunner, G. Agrifoglio, *J. Organomet. Chem. 198* (1980) C4.
[70] H. Brunner, G. Agrifoglio, *J. Organomet. Chem. 202* (1980) C43.
[71] H. Brunner, G. Agrifoglio, R. Benn, A. Rufińska, *J. Organomet. Chem. 217* (1981) 365.
[72] C. Lecomte, Y. Dusausoy, J. Protas, J. Tirouflet, A. Dormond, *J. Organomet. Chem. 73* (1974) 67.
[73] K. Stanley, M. C. Baird, *J. Am. Chem. Soc. 97* (1975) 6598.
[74] R. S. Cahn, C. K. Ingold, V. Prelog, *Angew. Chem. 78* (1966) 413; *Angew. Chem. Int. Ed. Engl. 5* (1966) 385.
[75] V. Prelog, G. Helmchen, *Angew. Chem. 94* (1982) 614; *Angew. Chem. Int. Ed. Engl. 21* (1982) 567.
[76] G. E. Bacon, N. A. Curry, S. A. Wilson, *Proc. R. Soc. A 279* (1964) 98.
[77] E. G. Cox, D. W. J. Cruickshank, J. A. S. Smith, *Proc. R. Soc. A 247* (1958) 1.
[78] A. H. Narten, *J. Chem. Phys. 48* (1968) 1630.
[79] K. C. Janda, J. C. Hemminger, J. S. Winn, S. E. Novick, S. J. Harris, W. Klemperer, *J. Chem. Phys. 63* (1975) 1419.
[80] H. Brunner, R. Lukas, *Chem. Ber. 112* (1979) 2528.
[81] H. Brunner, I. Bauer, R. Lukas, *Z. Naturforsch. B 34* (1979) 1418.
[82] H. Brunner, D. K. Rastogi, *Inorg. Chem. 19* (1980) 891.
[83] M. G. Reisner, I. Bernal, H. Brunner, J. Wachter, *J. Organomet. Chem. 137* (1977) 329.
[84] G. M. Reisner, I. Bernal, *J. Organomet. Chem. 220* (1981) 55.
[85] R. Benn, J. Klein, A. Rufińska, G. Schroth, *Z. Naturforsch. B 36* (1981) 1595.
[86] R. Benn, A. Rufińska, G. Schroth, *J. Organomet. Chem. 217* (1981) 94.
[87] H. Brunner, W. A. Herrmann, J. Wachter, *J. Organomet. Chem. 107* (1976) C11.
[88] H. Brunner, J. Wachter, *Angew. Chem. 88* (1976) 342; *Angew. Chem. Int. Ed. Engl. 15* (1976) 316.
[89] H. Brunner, J. Wachter, *Chem. Ber. 110* (1977) 721.
[90] H. Brunner, E. Bauer, J. Wachter, *Chem. Ber. 111* (1978) 379.
[91] H. Brunner, B. Schönhammer, *Z. Naturforsch. B 38* (1983) 852.

[92] H. Brunner, D. K. Rastogi, *Bull. Soc. Chim. Belg. 89* (1980) 883.
[93] I. Bernal, W. H. Ries, H. Brunner, D. K. Rastogi, *Inorg. Chem.*, in press.
[94] D. K. Rastogi, S. Rastogi, *Polyhedron 1* (1982) 233.
[95] H. Brunner, G. Riepl, R. Benn, A. Rufińska, *J. Organomet. Chem. 253* (1983) 93.
[96] T. Hayashi, K. Yamamoto, M. Kumada, *Tetrahedron Lett. 1974*, 4405.
[97] N. C. Payne, D. W. Stephan, *Inorg. Chem. 21* (1982) 182.
[98] T. Hayashi, K. Yamamoto, K. Kasuga, H. Omizu, M. Kumada, *J. Organomet. Chem. 113* (1970) 127.
[99] H. Brunner, G. Riepl, *Chem. Ber.*, in press.
[100] T. H. Johnson, K. C. Klein, S. Thomen, *J. Mol. Catal. 12* (1981) 37.
[101] H. Brunner, G. Riepl, *Angew. Chem. 94* (1982) 369; *Angew. Chem. Int. Ed. Engl. 21* (1982) 377; *Angew. Chem. Suppl. 1982*, 769.
[102] H. Brunner, G. Riepl, H. Weitzer, *Angew. Chem. 95* (1983) 326; *Angew. Chem. Int. Ed. Engl. 22* (1983) 331; *Angew. Chem. Suppl. 1983*, 445.

# Phosphorus Ylides in the Coordination Sphere of Transition Metals: An Inventory

**By Hubert Schmidbaur***

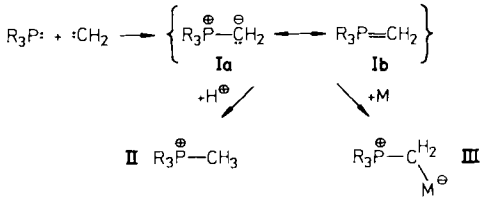
*Dedicated to Professor Ernst Otto Fischer on the occasion of his 65th birthday*

Phosphorus ylides are not only classical reagents in organic chemistry, but also play an increasingly important role as novel components in organometallic compounds. These metallic "ylide complexes" are either synthesized from "preformed ylides" and coordination compounds by addition or substitution, on the building block principle, or they are formed, in sometimes complicated reactions, from phosphanes, metal complexes, and $C_1$ substrates in the coordination sphere of the metals. The resulting metal-carbon bonds are greatly modified in their properties by the immediate presence of the phosphonium center and often belong to the most stable of M-C structural units. The metal can come from any group of the periodic table, including the lanthanoids and actinoids. Numerous preparative and structural studies are gradually enabling us to gain an overall picture of the scope of this area of research.

## 1. Introduction

Phosphorus ylides are remarkable compounds from many points of view. Too little emphasized, however, is the fact that they can be classified as phosphane-stabilized carbenes, and may thus constitute the oldest and best studied class of carbene complexes[1]. In contrast to such complexes with all the other elements these phosphorus-carbene complexes are very stable even in the absence of stabilizing substituents or salt components. This exceptional position vividly manifests itself on comparison with the carbene complexes of the homologous amines, arsanes or stibanes (nitrogen, arsenic and antimony ylides) or of sulfanes (sulfur ylides), which decompose very easily and act as carbene carriers. Therefore, phosphorus ylides are not only described as dipolar carbene complexes with the formula **Ia**, but also in the sense of a formal charge compensation as neutral molecules **Ib**[2,3]. Their reactions and most of their physical properties, however, give a clear indication that their actual bonding pattern is much closer to the 1,2-zwitterionic structure **Ia**. The functional effect of the two reactive centers—carbanion and phosphonium group—is, however, differently exhibited and the phosphonium unit remains very much in the background during the primary step of almost all the reactions.

The absolute dominance of the carbanion formed by polarization of the carbene function becomes obvious in ylides and particularly in "salt-free" ylides from an extraordinarily high *Brønsted basicity*, which is of importance in the secondary process known as "transylidation" in reactions with free ylides[4].




The exceptional donor character with respect to practically all metals M (formula **III**), which in many cases suffices to drive almost all other ligands out of the metal's coordination sphere, is even more striking[5]. There are alternatives, however, if an ylide attack is also possible at one of the ligands already present, whereupon the strong nucleophilicity of the ylide comes into play, which also constitutes the most important characteristic of ylide reactivity in organic chemistry[1].

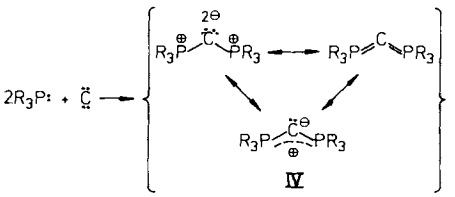
The three important characteristic features of the phosphorus ylides—basicity, donor activity, and nucleophilicity—are expressions of the excess charge on the ylide C atom, which is not adequately compensated by the $P^{\oplus}$ center and which expresses itself differently depending on the

[*] Prof. Dr. H. Schmidbaur
Anorganisch-chemisches Institut der Technischen Universität München
Lichtenbergstrasse 4, D-8046 Garching (Germany)

nature of the reaction partner. From this it will be clear that the enormous variety of oxidation levels, coordination numbers, and complex geometries that characterize metals, offers a plethora of interaction possibilities for ylides that are only now beginning to be understood.

It must be emphasized here that—as can be seen from formula **III**—ylide complexes of metals principally constitute organometallic compounds, whose novel metal-carbon bonds lie under the electronic and steric influence of the onium center. In contrast to syntheses with organometallic reagents (RLi, MNgX, *etc.*) the cation accompanying the anion (**Ia**!) stays in the product (**III**) which is formed after attachment to the metal, whereas otherwise the organic residue is separated from the $Li^{\oplus}$ or $Mg^{2\oplus}$ cations.

This rapidly expanding research area has received further impetus from new developments ranging from multifunctional ylides, on the one hand, to multinuclear metal compounds on the other. The symmetrical ylides of type **IV** bearing the trivial name "carbodiphosphoranes" play an important role among the multifunctional ylides and may be formulated as bisphosphane complexes of naked carbon.



**IV**

It should be noted that other similar element-carbon-element bridges $E{=}C{=}E$ or $\overset{\oplus}{E}{-}\overset{2\ominus}{\underset{\cdot\cdot}{C}}{-}\overset{\oplus}{E}$ are, as yet, almost completely unknown, which once again emphasizes the special position of the phosphorus double ylides.

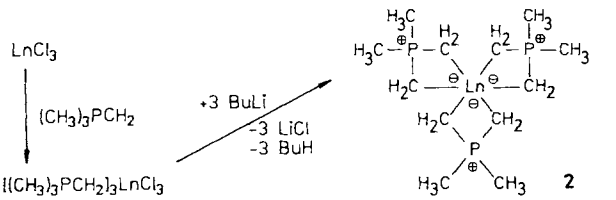
The stimulus for working with ylide complexes results from the real possibility of utilizing the compounds for metal-catalyzed reactions and for other purposes. The ever increasing use of tertiary phosphanes as additional ligands in stoichiometric or catalytic reactions at transition metal complexes makes it more likely that ylide complexes play a part as intermediates or products in such processes. In fact it has been known for a long time that phosphorus ylides can be formed in the coordination spheres of metals, and hence the directed introduction of preformed ylides is no longer the only preparative route to these complexes.

The literature concerning the formation and reactions of ylides at metal centers, which is rapidly becoming more difficult to survey, has been reviewed several times from various points of view[1, 5–7]. These valuable reviews will now be supplemented here, in that developments of recent years will be put into perspective with the basic discoveries of the past. The subject can best be systematized according to the *periodic table*, since the interested reader is usually seeking element-specific information, which is most easily made available to him *via* this approach. Newer results are treated in more detail than earlier ones, which have already received greater attention[1, 5–7]. The subject will deliberately be restricted in this article to *transition metal compounds*. The corresponding compounds of phosphorus ylides with main group metals will be described in a further paper. A review article on the complex chemistry of the *sulfur* ylides has been published recently[8].

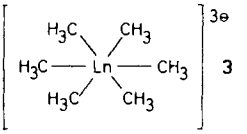
## 2. Complexes of Phosphorus Ylides with Scandium, Lanthanum, the Lanthanoids, and Actinoids

It is characteristic of the special position of ylide complexes amongst organometallic compounds that, even with the elements of Group 3A where the development of the chemistry of σ-bonded organometallic compounds had a late start, derivatives of methylenephosphoranes $R_3P{=}CH_2$ already play a significant role.

It was first shown in 1976[9] that the elements La, Pr, Nd, Sm, Gd, Ho, Er and Lu could form stable "homoleptic" ligand sheaths (**2**) with "difunctionalized $(CH_3)_3PCH_2$"[10, 11] that is with the corresponding anion $[(CH_3)_2P(CH_2)_2]^{\ominus}$. The "mixed" halide complexes **1** are reaction intermediates. Complexes of type **1** and **2** are exceedingly sensitive to oxidation and hydrolysis, but some are stable to 200°C under an inert gas. Compounds of type **2** were precursors for the hexamethylmetalate anions **3**, first described some five years later[12]:

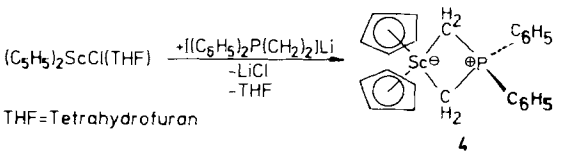


**1** **2** Ln=La,Pr,Nd,Sm,Gd,Ho,Er,Lu



**3**

It was also discovered in 1976[13] that the bis($\eta^5$-cyclopentadienyl)scandium residue could be combined with diphenylphosphoniobismethanide to form a stable organometallic compound: The pale yellow, crystalline complex **4** is formed from $(C_6H_5)_2P(CH_3)CH_2$[14] *via* the lithiated intermediate; like the diamagnetic members of the series **2**[12] it could be characterized NMR spectroscopically.

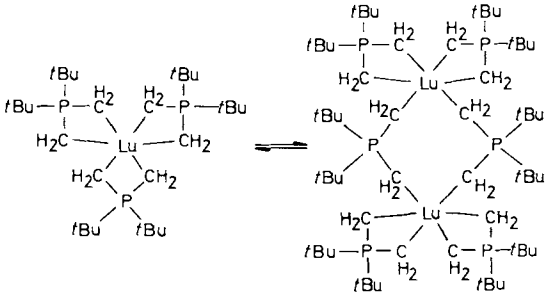


THF=Tetrahydrofuran

**4**

The sixfold *tert*-butyl-substituted homologue of **2**, Ln = Lu, that has recently been synthesized[15], has proven even more suitable for spectroscopic investigation, and it has been shown by means of temperature-dependent $^1H$-, $^{13}C$- and $^{31}P$-NMR spectra that there is an oligomer equilibrium **2a** ⇌ **2b** ⇌ ... in solution.

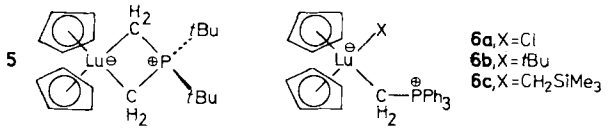
Consequently, these compounds behave like the homoleptic ylide complexes of nickel[16] or zirconium[17], in



2a 2b

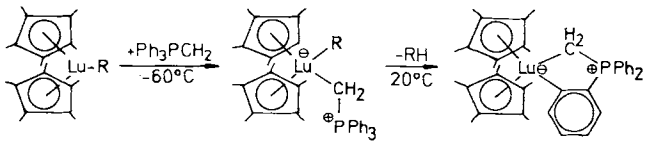
which the bidentate $[R_2P(CH_2)_2]^{\ominus}$ ligands can function both as bridge-builders as well as chelaters.

A lutetium analogue of **4** is, in contrast, strictly monomeric in benzene solution (**5**, decomp. 156°C)[15].



**6a**, X = Cl
**6b**, X = tBu
**6c**, X = $CH_2SiMe_3$

The mixed ylide/halide or ylide/alkyl complexes **6** formed from $(C_5H_5)_2LuCl$ or $(C_5H_5)_2LuR(THF)$ and $(C_6H_5)_3PCH_2$ in toluene are important examples of lanthanoid compounds with terminal monodentate-coordinated methylenephosphorane. Hydrolysis of **6a** leads to cleavage of Lu–C and formation of methyl(triphenyl)phosphonium chloride[18,19]. The alkyl compounds **6b** and **6c** can also be obtained from **6a** with alkylmetal reagents. $Me_3P{=}CHSiMe_3$ was used instead of $Ph_3P{=}CH_2$[19]. The hydride- and methyl-compounds **7a** and **7b**, until now only accessible with *pentamethyl*cyclopentadienyl ligands, can also yield 1:1 adducts (**8a** and **8b**, respectively) with $(C_6H_5)_3PCH_2$, but they undergo intramolecular metalation with expulsion of $H_2$ or $CH_4$ and formation of the cyclic ylide complex **9**, even at 20°C[20].

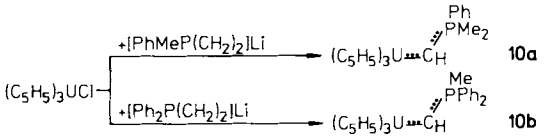


**7** **8** **9**

**a**, R = H, **b**, R = $CH_3$

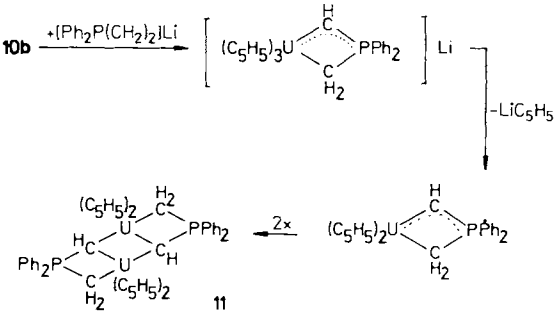
The reaction **8a**, **b** → **9** is not without precedent, since similar *ortho*-metalations also occur with platinum(0), which—in accord with the oxidation state of the metal—are classified as oxidative additions[21].

To date, the sole coordination partner for phosphorus ylides amongst the actinoids is uranium. Depending upon the stoichiometry of reaction, $(\eta^5\text{-}C_5H_5)_3UCl$ reacts with the lithiated ylides $C_6H_6(CH_3)_2P{=}CH_2$ and $CH_3(C_6H_5)_2P{=}CH_2$ to give a range of new organouranium compounds, some of which exhibit remarkable types of bonding. Thus, with a 1:1 ratio of reactants[22] the dark green complexes **10a** and **10b** are formed, of which the structure of **10a** has been established by X-ray diffraction[23]. According to the X-ray structure analysis this compound possesses the shortest U–C bond known to date (2.29(4) Å), suggesting the presence of multiple-bonding; the U=C=P angle is 142(1)°.



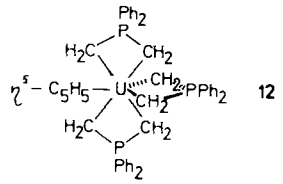
**10a**
**10b**

With molar ratios of 1:2, on the other hand, a red binuclear complex **11** is formed, presumably according to the mechanism outlined below; a monoclinic modification (containing 1/2 mol diethyl ether) and an orthorhombic modification (containing 1 mol *n*-pentane) have been elucidated by X-ray diffraction. The latter has been identified as (*M*)-[{(μ-*S*-CH)$P(C_6H_5)_2CH_2$}$U(C_5H_5)_2]_2$, taking into account the configuration at the chiral centers[24,25]. Both ylide ligands in the dimers are effective as bridging and as chelating agencies, whereby in each case one of the C atoms carries out both functions.



**11**

Finally, with a molar ratio of 1:3 a gold-colored, mononuclear organouranium compound **12** is obtained[22].



**12**

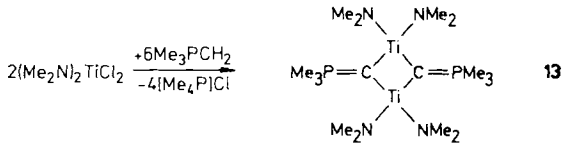
Aside from the remaining $\eta^5$-cyclopentadienyl ligand, **12** contains three diphenylphosphoniobismethanide ions as chelate forming ligands. The uranium atom is thus surrounded by eleven carbon atoms, of which six represent ylidic centers[22].

## 3. Complexes of Phosphorus Ylides with Titanium, Zirconium, and Hafnium

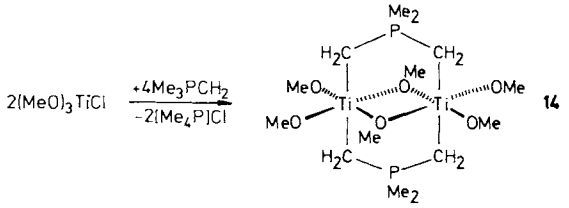
The first attempts at synthesizing organo-titanium and -zirconium compounds with ylidic ligands met with little success, since the simplest reactions, *e.g.* of $TiCl_4$ with $(CH_3)_3PCH_2$, only yield insoluble and hardly characterizable products[26]. Analytical data gave only rough indications of the stoichiometry.

However, novel prototypes of polynuclear ylide complexes were discovered on using dimethylamino- or methoxy-titanium halides as starting materials. Thus, reaction

of $[(CH_3)_2N]_2TiCl_2$ with $(CH_3)_3PCH_2$ affords the 1,3-dititanacyclobutane **13**[26], whereas reaction with $(CH_3O)_3TiCl$ yields the double octahedral species **14**[27]. In **14** the Ti atoms appear as substituents at the ylidic C atom—a situation which was previously only known in Si analogues[28]. The ylide braces of the coordination octahedron in **14** are unique. In both reactions the ylides are deprotonating in the sense of a transylidation, giving rise to the formation of $[(CH_3)_4P]Cl$ as a byproduct.

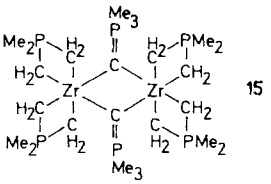


**13**



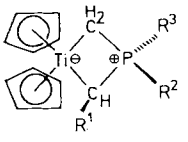
**14**

A stimulating analogy to the bonding observed in the titanium compound **13** has recently been discovered in the zirconium compound **15**, which is formed from $[(CH_3)_3CCH_2]_4Zr$ and $(CH_3)_3PCH_2$ as yellow, monoclinic crystals. The Zr–C bonds of the 1,3-dizirconiacyclobutane are extremely short, whereas the $PC_2Zr$ chelate rings correspond to the known models with other transition metals. The Zr–C bonds *trans* to the ylide bridges (equatorial) are, however, significantly longer than the apical Zr–C bonds.



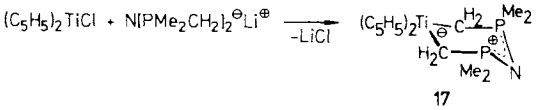
**15**

Derivatives which have a close relationship with their metal(III) analogues have been prepared by the reaction of bis($\eta^5$-cyclopentadienyl)metal halides of Group 4a with phosphorus ylides. According to magnetic and ESR studies the simplest type **16** is to be regarded as a genuine $Ti^{III}(d^1)$ complex[13].



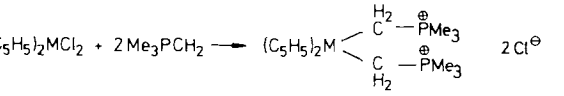
**16a**, $R^1$ = H, $R^2$ = $R^3$ = Ph; m.p. = 152–153 °C; purple
**16b**, $R^1$ = H, $R^2$ = Ph, $R^3$ = Me; m.p. = 147–150 °C; purple
**16c**, $R^1$ = H, $R^2$ = $R^3$ = Me; m.p. = 122–123 °C; black-green
**16d**, $R^1$ = Me, $R^2$ = $R^3$ = Et; m.p. = 61–63 °C; dark green

A related double ylide complex **17** exhibits similar properties[26].



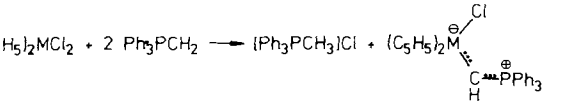
**17**

Without prelithiation of the ylides[26], the double onium salts **18** are formed,



**18a**, M = Ti
**18b**, M = Zr

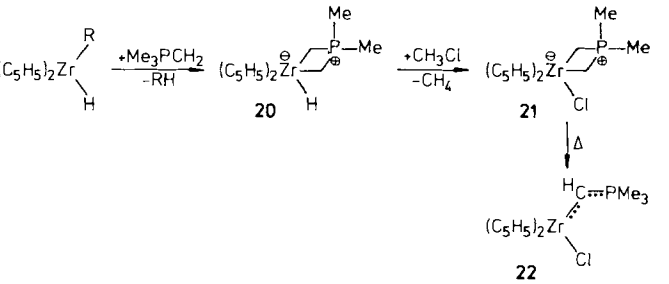
or, in the case of triphenylphosphoniomethanide when M = Zr or Hf, the transylidation product[27], **19**.



**19a**, M = Zr; m.p. = 199–210 °C; yellow
**19b**, M = Hf; m.p. = 120 °C (decomp.), yellow

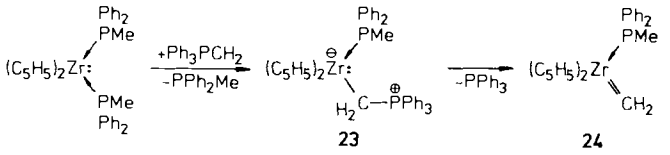
X-ray structure analysis of **19a** reveals that both of the bonds in the Zr–CH–P bridge possess substantial multiple bond character: Zr–C 2.152(8), P–C 1.708(6) Å, Zr–C–P 135.9(3)°. Thus, the bonding is similar to that in the uranium compound **10a**. Correspondingly, compounds **10a** and **19a** also behave similarly in their reactions, of which the important CO insertion has been studied in detail[23,28].

Yet another type of product is formed on reaction of alkylbis($\eta^5$-cyclopentadienyl)zirconium hydride with $(CH_3)_3PCH_2$: elimination of alkane takes place, resulting in formation of the green-colored ylide chelate **20**, which undergoes a hydride/chloride exchange with chloromethane to give the colorless derivative **21**[29].



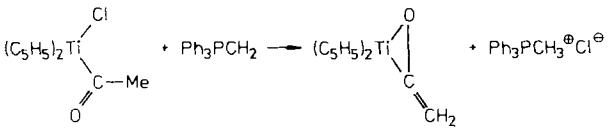
Thermal rearrangement of **21** at 65–70 °C leads to the yellow isomer **22**, which corresponds to the triphenylphosphonio compound **19a**. In the case of **19a**, isomerization to the ylide-chelate of type **21** is precluded, since no second alkyl group with an acid H atom is available at the P-atom[29].

An electron-rich bis($\eta^5$-cyclopentadienyl)zirconium(II) complex ($d^2$!) reacts with $(C_6H_5)_3PCH_2$ with transfer of methylene to the metal atom. The likely intermediate **23**, containing a $Zr–CH_2–P(C_6H_5)_3$ moiety, is converted by elimination of $P(C_6H_5)_3$ into the—albeit nonisolable—complex **24**[30,31].

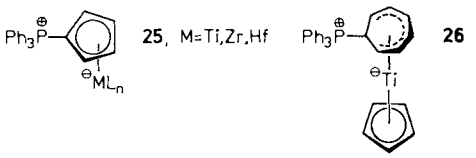


23 24

Reaction of an acetyl(chloro)titanium(IV) complex with $(C_6H_5)_3PCH_2$ does not lead to the formation of an ylide complex or to the product of a simple Wittig olefination, but to the formation of a metal ketene complex[32].



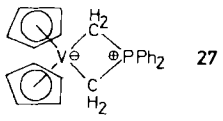
Phosphonio-cyclopentadienide and -cycloheptatrienide complexes of titanium, zirconium and hafnium (**25**, **26**) involve a special relationship between metal and ligand and will, therefore, not be considered here. None of the structures is as yet sufficiently well known[33,34].



25, M=Ti,Zr,Hf 26

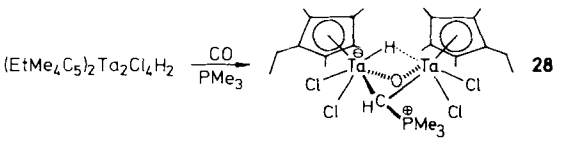
## 4. Complexes of Phosphorus Ylides with Vanadium and Tantalum

Vanadium and its homologues have as yet rarely been used as coordination centers for phosphorus ylides. True, the cation formulated as $[(C_6H_5)_3PCH_2]_4V^{2\oplus}$ constitutes one of the oldest examples of a transition metal-ylide complex[35], yet no other such vanadium compound has since been described, apart from the chelate **27**. The complex **27** can be synthesized according to the method given for **4** or **16a** and has been unequivocally identified as a $V^{III}(d^2)$ complex by ESR spectroscopy[13].



27

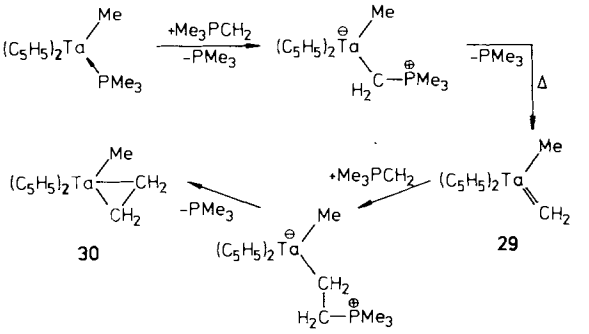
Surprisingly, a binuclear tantalum complex **28** was obtained on reaction of a dihydride precursor with CO followed by $P(CH_3)_3$[36].



28

The $[(CH_3)_3P^{\oplus}-CH]$ unit, which functions as a bridge ligand in **28**, is evidently formed in the course of this reaction from complexed CO, whereby oxygen is separated from the C atom and transformed into an oxo bridge. The overall process is one of the most remarkable findings yet in the field of ylide complexes. The molecular structure of **28** in the yellow, monoclinic crystal has been determined X-ray crystallographically. The P–C separation is 1.751(19) Å and, thus, can scarcely be classified as ylidic. The unequal Ta–C distances, on the other hand, are relatively short (2.187(17) and 2.354(17) Å)[37].

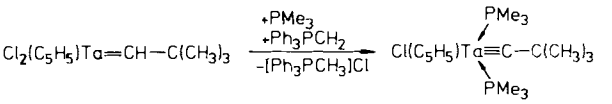
The nonisolable intermediate formed in the reaction of the electron-rich $Ta^{III}$ complex $(C_5H_5)_2TaCH_3[P(CH_3)_3]$ with $(CH_3)_3PCH_2$ should be formulated as an ylide adduct; elimination of phosphane, even under mild conditions, then furnishes the complex **29**, which reacts with further $(CH_3)_3PCH_2$ in a similar manner to yield the ethylene complex **30**[38].



30 29

Noteworthy here, is the ease of transfer of the carbene from the ylide to the metal, *i.e.* the ylide multiple bond (!) can be ruptured without difficulty. Closely related tungsten compounds exhibit similar behavior (cf. Section 5.3).

The reaction steps formulated above for $(CH_3)_3PCH_2$ can also be accomplished with $(CH_3)_3P{=}CHC_6H_5$, $(C_6H_5)_3P{=}CHC_6H_5$ and $(C_2H_5)_3P{=}CHCH_3$, but not with $(C_6H_5)_3P{=}CH{-}C(CH_3)_3$ and $(C_2H_5)_3P{=}CH{-}C(O)CH_3$, where limits are set by steric hindrance or reduction in nucleophilicity[38]. In contrast, in the reaction



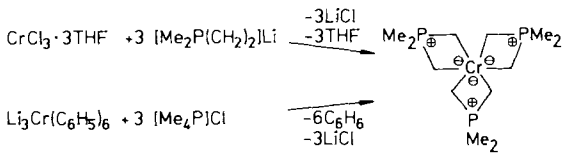
the ylide functions only as dehydrohalogenating base[39].

## 5. Complexes of Phosphorus Ylides with Chromium, Molybdenum, and Tungsten

### 5.1. Homoleptic Chromium- and Molybdenum-Ylide Complexes

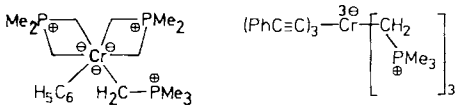
The homoleptic tris-chelate complex **31** was first isolated almost exactly ten years ago as a red, sublimable, crystalline substance. It represents the first phosphorus ylide derivative of trivalent chromium. The preparative methods used became models for the later synthesis of further analogous trivalent complexes of the earlier transition metals, which have already been mentioned.

Compound **31** is strongly paramagnetic ($\mu_{eff}=3.6\mu_B$), which is in good agreement with the $d^3$ state of the central atom, chromium(III)[40].



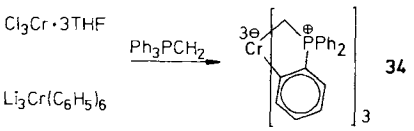
31

A red intermediate product **32**, in which the metal carries a further phenyl group, can also be isolated in the synthesis of **31** from $Li_3Cr(C_6H_5)_6$. The reaction of **31** with three equivalents of tolan[41] leads, with opening of the chelate rings, to formation of the yellow trisalkynyl complex **33**.



32 33

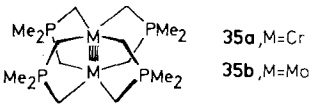
When the educts of the synthesis of **31** are allowed to react with ylides of the type $(C_6H_5)_3PCH_2$ rather than with metalated or metalatable alkyl-substituted ylides of the type $(CH_3)_3PCH_2$, then *ortho*-metalation of the phenyl rings occurs to give the ylide complex **34**[40]. Later, analogies for this mode of reaction were found, *inter alia*, for platinum and lutetium[20,21].



34

Chromium(II) and molybdenum(III) halides react with $(CH_3)_2P(CH_2)_2Li$ to yield binuclear complexes **35a** and **35b**, respectively, which have attracted continual attention[42,43]. X-ray diffraction studies[44,45] have revealed extremely short metal-metal distances (M≡M) in these diamagnetic compounds.

The particularly simple ylide ligands, whose coordinating $CH_2$ groups do not lead one to expect either back-bonding phenomena or other electronic or steric side effects, are almost ideal for further experimental investigation of the M≡M unit[46] and for its theoretical description[47].



**35a**, M=Cr
**35b**, M=Mo

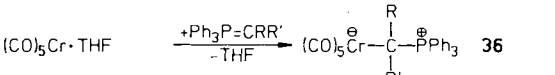
**35a, b** can be crudely described as having paddle-wheel structures, with a metal axis of 1.895(3) (Cr≡Cr) or 2.082(2) Å (Mo≡Mo). The metal carbon distances are 2.21—2.23 (Cr—C) and 2.30—2.32 Å (Mo—C). It is possible to distinguish long P–C methyl distances (1.81—1.90 Å) and short P–$CH_2$ distances (1.77—1.79 Å) at the quasi-tetrahedral P atom, thus indicating residual ylide character for the latter[44,45].

## 5.2. Carbonylmetal Complexes of Phosphorus Ylides

Carbonylmetal(0) complexes of phosphorus ylides count among the most investigated of the metallic ylide compounds. They are accessible *via* various, widely differing routes and have been the subject of intensive research for more than 20 years, not least because of their close relationship to the corresponding carbene complexes. The extensive findings are classified in this review article according to the methods of preparation.

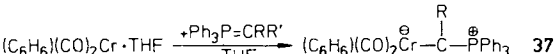
### 5.2.1. Direct Coordination of Ylide Ligands at the Metal

Whereas hexacarbonylchromium does not react with "salt-free" phosphorus ylides only by CO substitution, but rather by attack at the CO ligand, its tetrahydrofuran derivative $(CO)_5Cr\cdot THF$ is a suitably modified, selectively reacting starting compound for the introduction of ylides at the metal atom[48].



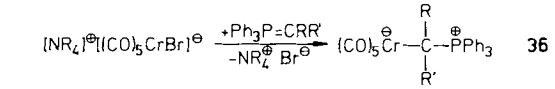
36

R=H,Me
R'=H,Ph,$PPh_2$,Me



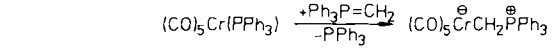
37

Benzene(dicarbonyl)chromium-tetrahydrofuran reacts analogously and yields complexes **37**, which have been described in seven different R,R'-combinations[50]. The halogen atoms of the complex salts $[(C_2H_5)_4N]^{\oplus}[(CO)_5CrBr]^{\ominus}$ are also good leaving groups, which facilitate the preparation of ylide complexes. Amongst the known examples (> 15), there are also some with phosphane ligands at the metal[51].

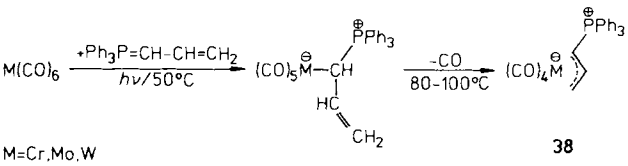


36

Ligand exchange also takes place in the triphenylphosphane derivative:



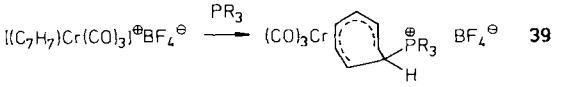
Reports that $Mo(CO)_6$ reacts with $(C_6H_5)_3P{=}CHCH_3$ to form a complex $(CO)_3Mo[(C_6H_5)_3P{=}CHCH_3]_3$ have not been confirmed[52]. The reaction of ylides with conjugated olefinic double bonds can lead to multiple CO exchange, whereupon π-allyl type complexes **38** can be formed[53–55]:



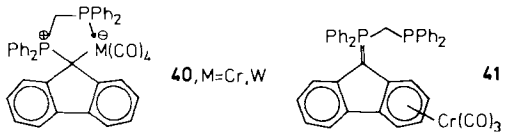
M=Cr,Mo,W 38

With phosphoniocyclopentadienide, $\eta^5$-$C_5H_4{=}PR_3$ coordination is achieved[56–59], which, because of the special constitution of the product (cf. also **25**) will not be dealt with here. $\lambda^5$-Phosphabenzene complexes are also not discussed[60]. A $(CO)_5W$ complex of $Ph_3P{=}C(SMe)_2$ was

found to be *S*-bonded[61]. On reaction of phosphanes with the tropylium(tricarbonyl)metal cation of chromium[62] (but not of molybdenum[63]), related $\eta^5$-organometallic compounds **39** with a phosphonium center in the side chain are formed.



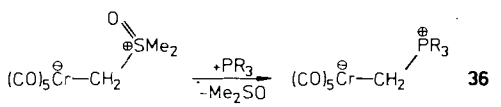
Fluorene ylides with additional phosphane function yield spirocyclic complexes **40**, but also, *e.g.*, the $\eta^6$-fluorene complex **41**[64].



### 5.2.2. Sulphane/Phosphane Exchange at Sulfur Ylide Complexes

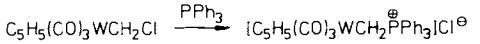
In the synthetic methods already discussed, an intact phosphorus ylide was coordinated to the metal atom. Important alternatives to this are the formation of the ylide within the coordination sphere of the metal, either from another ylide complex by onium-center exchange or (cf. Section 5.2.4) from a carbene complex by addition of a phosphane. The first method has been used to advantage on $(CO)_5Cr$ complexes of the dimethyl(oxo)sulfoniomethanide $(CH_3)_2S(O)CH_2$, whereby dimethyl sulfoxide proved to be an excellent leaving group. A particular advantage of this method is that unstable ylides can be fixed to the metal and stabilized[65].

Arsanes undergo similar reactions[66].



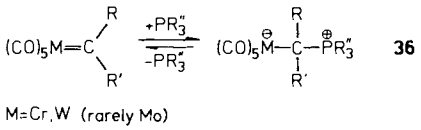
### 5.2.3. Ylide Complexes from Haloalkyltungsten Complexes

$(C_5H_5)(CO)_3WCH_2Cl$, a (chloromethyl)tungsten complex which is now readily accessible, can easily be converted into the corresponding ylide derivative by reaction with $P(C_6H_5)_3$ in boiling methanol[67]. Analogous substitution reactions have been demonstrated with Fe, Rh, Ru, *etc.* (cf. Sections 7 and 8).



### 5.2.4. Ylide Complexes from Stable Carbene Complexes and Phosphanes

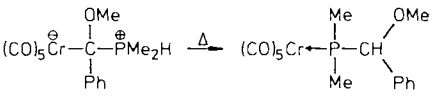
Although the first investigations had shown that the thermal reactions of $(CO)_5Cr$ carbene complexes with phosphanes and other nucleophiles finally lead to irreversible CO exchange[68,69], later studies showed that, under mild conditions, the reversible addition at the carbene carbon atom predominates[70-79]. This important reaction enables access to a series of ylide complexes, in as far as their substituent combinations at the carbene C atom are realizable. This applies in particular to phosphorus ylides with electron-rich substituents.



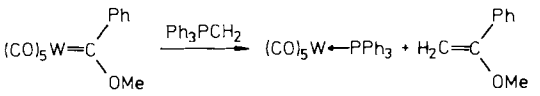
The reversibility of this equilibrium has been demonstrated kinetically[78]. Typical enthalpies of reaction lie in the range $-15$ to $-20$ kcal mol$^{-1}$. The rates of reaction are in the order Mo > W > Cr[79].

The reactions do not, however, always proceed according to the desired scheme. Apart from the CO exchange already mentioned, a strong substituent effect is also observed. Thus, $(CO)_5W{=}C(C_6H_5)_2$ reacts with $P(CH_3)_3$ in the expected manner[74], whereas reaction with $P(C_6H_5)_3$ leads to an unexpected cleavage of the ylide $(C_6H_5)_3P{=}C(C_6H_5)_2$ from the metal[76]. The last mentioned reaction is one of the few examples known where the intact ylide can be removed from the metal.

Ylides with P–H bonds can undergo rearrangement to phosphane complexes[71]:

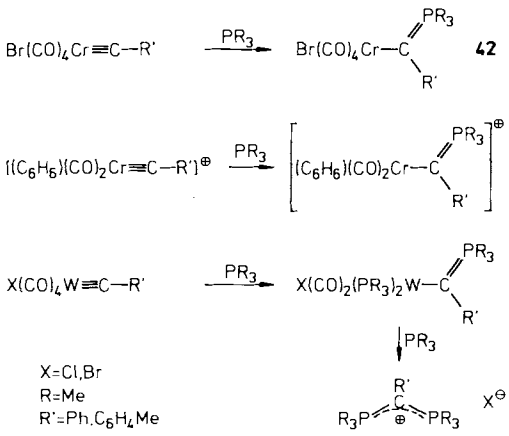


With ylides (instead of phosphanes), carbene complexes usually undergo Wittig olefination, whereby the $(CO)_5W$ fragment formally plays the role of the oxygen atom of the aldehyde or ketone (!)[80]:



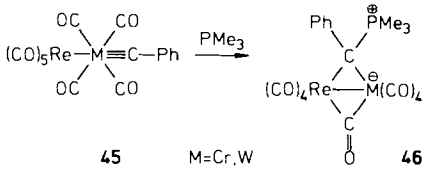
### 5.2.5. Reaction of Carbyne Complexes with Phosphanes

Phosphanes can add to metal carbynes analogously to their reaction with metal carbenes. Metal-substituted phosphorus ylides **42** are formed whose substituents depend on the reactants[81-86]. If the central atom is tungsten, an addi-



tional partial CO exchange takes place and, in certain circumstances, a cleavage of the metal carbon bond[87]; in this case semi-ylide salts **44** can be isolated.

The binuclear carbyne complexes **45** add $P(CH_3)_3$ to form an ylide-bridged product **46** whose constitution has been determined by X-ray diffraction analysis[85,86]. This reaction, which until now is without parallel, demonstrates that in suitable cases the bridging double coordination of an ylide to a metal is preferred over the terminal coordination (as in **42** or **43**).

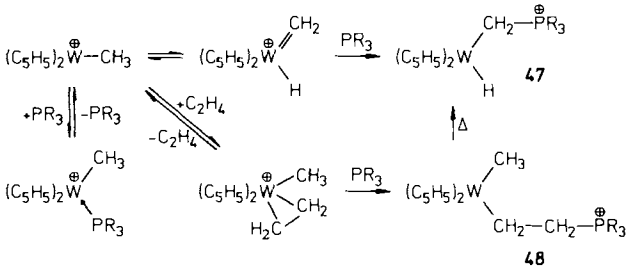


**45** M=Cr,W **46**

### 5.3. Ylide Complexes from Activated Alkyltungsten Compounds

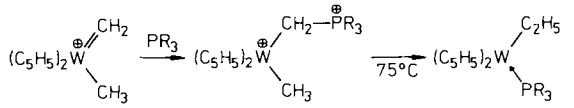
In the presence of donor molecules, alkyl compounds of bis(cyclopentadienyl)tungsten exhibit a complicated reaction behavior, the unraveling of which is of considerable interest for an understanding of the metal catalyzed reactions of olefins. Trapping the reactive intermediates with phosphanes to give ylide complexes has allowed great progress to be made in the study of this problem[88-90].

The ylide complexes **47** and **48** can be isolated with $P(CH_3)_3$ from the equilibria between metal hydride, alkylmetal compound, and metal-olefin complex, if suitable stoichiometric conditions are chosen:

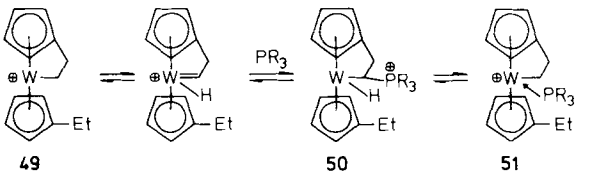


**47** **48**

Similar products are formed when carbene precursors are produced photochemically[91] or *via* radical sources and proton acceptors[92,93] from $(C_5H_5)_2W(CH_3)_2$ and $(C_5H_5)_2W(CH_3)C_2H_5$. The $PR_3$ components employed were $P(CH_3)_3$, $P(CH_3)_2C_6H_5$ and $P(C_6H_5)_2CH_3$. Both the kinetics and equilibrium of the reaction depend on the nature of the phosphane[94].

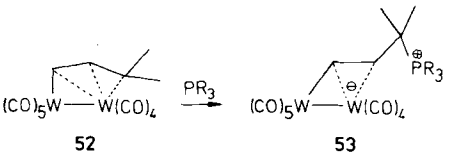


A similar equilibrium between the phosphanes $P(CH_3)_3$ and $P(CH_3)_2C_6H_5$ with the complex cation **49**, in which one of the cyclopentadienyl rings is additionally attached to the tungsten atom by a $C_2$ bridge, affords an ylide complex **50** which only slowly reacts to form the stable end product **51**[95].



**49** **50** **51**

The binuclear tungsten complex **52** with $\eta^1,\eta^2$-bonded 3,3-dimethylated allyl groups adds phosphanes at C-3 to give a product **53** with a $\sigma,\pi$-bonded bridge ligand[96].



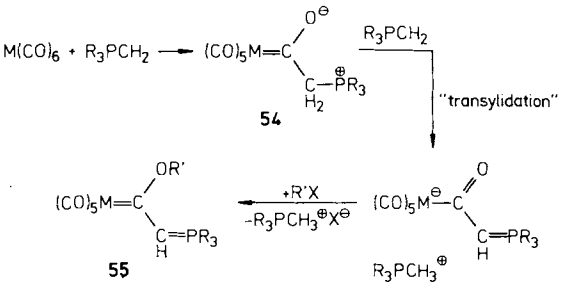
**52** **53**

The structure of one representative of the range of compounds formed from five different phosphanes was determined by X-ray diffraction. Because of its constitution, the bridge ligand in **53** can no longer be regarded as a phosphorus ylide[96].

Surprisingly, it has been found that a terminal ylide complex $[(Me_3P)_3(CO)ClWCH_2PMe_3]^{\oplus}$ is formed on reaction of the cationic carbene complex $[(Me_3P)_4ClW{=}CH_2]^{\oplus}$ with CO. The reaction has been interpreted as a W→C phosphane shift[97].

### 5.4. Ylide Reactions at the Ligands of Carbonyl Complexes

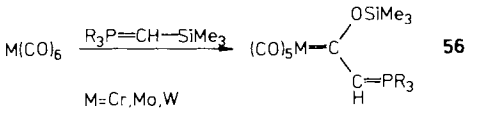
The finding that strongly nucleophilic phosphorus ylides attack the metal complexes $M(CO)_6$ at the CO ligand[98,99] could be explained step for step as a transylidation reaction[100]. The following scheme illustrates the reaction which has been confirmed for several cases (including also metals other than Cr, Mo, W):



**54** **55**

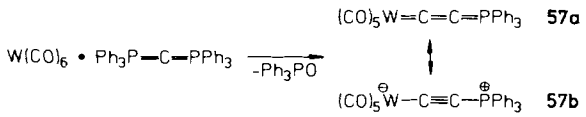
The zwitterionic carbene complex **54** is transformed with a second equivalent of ylide in a transylidation step into the corresponding anion, which can then be derivatized by *O*-alkylation to the neutral carbene complex **55** bearing ylide substituents[100]. Such a derivatization can also be accomplished with a powerful silylating agent ($RX = Me_3SiOSO_2CF_3$). An X-ray structure analysis has been performed on the product[101].

Related complexes can also be synthesized directly from the hexacarbonylmetal with silylated ylides[102]. An arsenic ylide corresponding to **56** is also known.



56

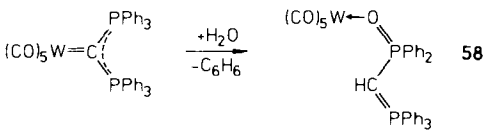
UV irradiation of $W(CO)_6$ and the double ylide $Ph_3P{=}C{=}PPh_3$ yields the acetylide **57**, which crystallizes as yellow needles (m.p. 140–142 °C)[99].



**57a** **57b**

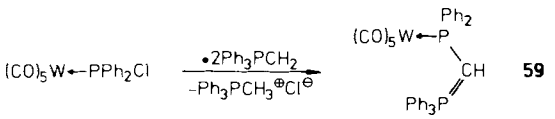
The reaction can be classified, on the basis of the mesomeric form **57a**, as a Wittig olefination of CO in the coordination sphere of the metal[99,100].

The simple $(CO)_5W$-adduct of hexaphenyl carbodiphosphorane obtainable from $(CO)_5W{\cdot}THF$ is easily hydrolyzed and, on reaction with water, yields adduct **58** with oxo-coordination; the structure of **58** has been confirmed by X-ray diffraction[103].



**58**

The reaction of a chloro(diphenyl)phosphane complex with ylides yields a related *P*-coordinated ylide complex **59**[104].



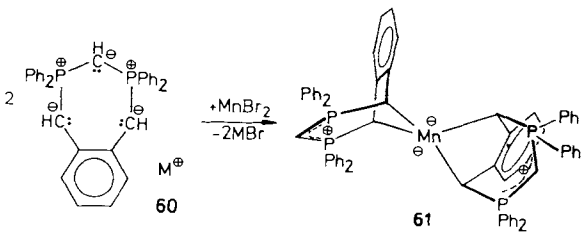
**59**

Metal complexes with arsane ligands, on the other hand, are cleaved by ylides at the M–As bond[105].

Reaction of $(C_6H_5)_3PCH_2$ with the binuclear complex $(C_5H_5)_2Mo_2(CO)_5$ yields a whole range of products, whose formation is still not completely clarified[106].

## 6. Complexes of Phosphorus Ylides with Manganese and Rhenium

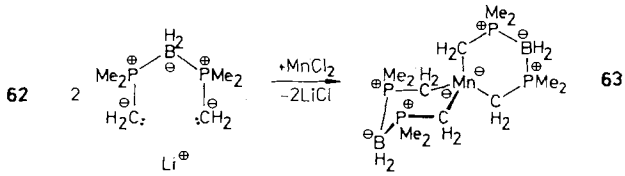
No simple coordination compounds of ylides with manganese have as yet been described. Only specific multiple ylides form homoleptic manganese complexes with phosphonium centers β to the metal atom. The best characterized of these are the bisbenzodiphosphepinyl complex **61** and the boron-containing bis-chelate **63**. The former is obtainable in good yields by the reaction of alkali-metal salts of the diphosphonio triple ylide **60** with the tetrahydrofuran adduct of $MnBr_2$[107].



**60** **61**

The metal atom of the paramagnetic, brilliant yellow product ($\mu_{eff.} = 5.9\,\mu_B$, $d^5$) is pseudotetrahedrally surrounded by four ylidic carbon atoms. Both the remaining carbanion centers (P–CH⊕–P) point away from the metal atom. The X-ray structure analysis was carried out on a bistetrahydrofuran adduct, whose solvate molecules are likewise not coordinated to the metal[107].

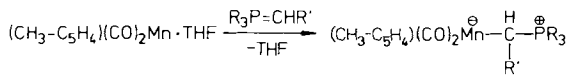
The manganese(II) complex **63** formed on reaction of the lithiated boranato-bisylide **62** with $MnCl_2{\cdot}THF$ also contains pseudotetrahedrally oriented ylidic C atoms. The yellow compound, which may be regarded as a simple tetraalkylmanganese, is paramagnetic ($\mu_{eff.} = 5.84\,\mu_B$, $d^5$). Crystal structure analysis revealed Mn–C distances of 2.214(4)–2.239(13) Å, which correspond to a carbon-manganese σ-bond. The P–$CH_2$ and P–$CH_3$ distances are *ca.* 1.75 and 1.82 Å, respectively, as are typical for other ylide complexes.



**62** **63**

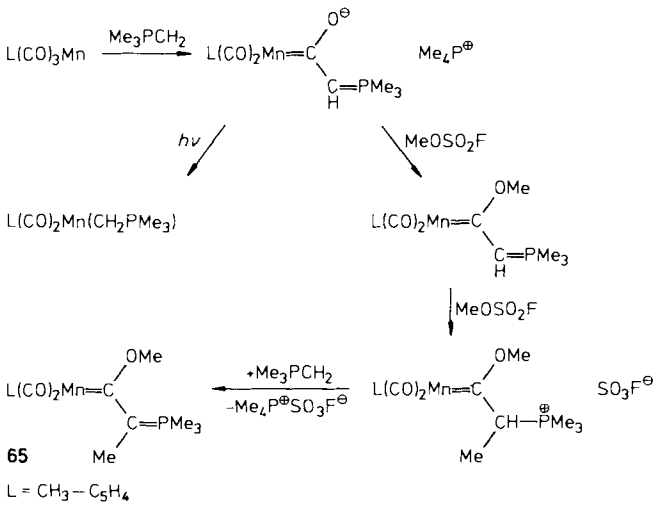
Both six-membered rings in **63** are in a chair conformation, the boron and phosphorus atoms have tetrahedral environments[108].

A wide variety of dicarbonyl(methylcyclopentadienyl)manganese complexes **64** are accessible from the THF precursor and free ylides (cf. also Section 5.2.1).



**64**: R′=H, $R_3$=$Ph_3$, $Ph_2Me$, $PhMe_2$, $Me_3$;
R′=Ph, $R_3$=$Ph_2Me$, $PhMe_2$, $Me_3$

The analogous tricarbonyl compounds, on the other hand, react with ylides at the CO ligands according to the scheme described for $Cr(CO)_6$ (cf. Section 5.4). The following scheme shows the reaction paths and products discovered up to now[109].

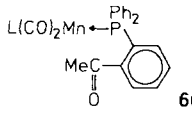


**65**

L = $CH_3-C_5H_4$

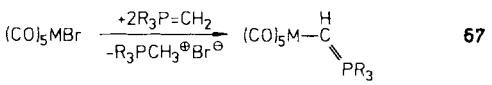
The structure of the end product **65** has been confirmed by X-ray diffraction[110].

Surprisingly, the course of the reaction with the ylide $(C_6H_5)_3P{=}CH_2$ is much more complicated. The complex **66** is one of the numerous compounds isolated from the product mixture[111].

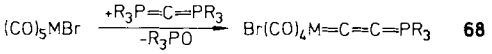


**66**

Bromo(pentacarbonyl)manganese and the analogous rhenium compound react with $(C_6H_5)_3P{=}CH_2$ (with transylidation, cf. Sections 2 and 3) to give the metal substituted ylide **67**[100]:



**67**

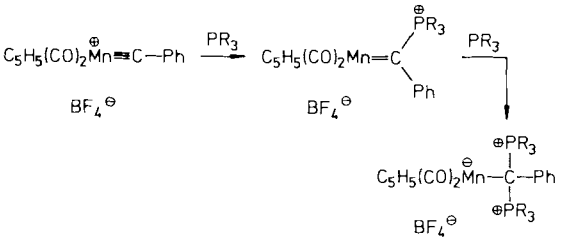


**68**

M=Mn, Re

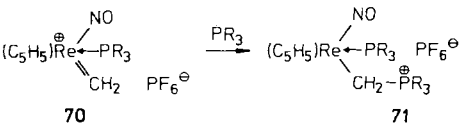
Pseudo-Wittig olefination and phosphane oxide cleavage occur once again with the double ylide and the same starting complexes[100] (cf. Section 5.4). The structure of the manganese compound **68**, which can also be formulated as an acetylide, has been confirmed by X-ray diffraction[111,112].

A carbyne complex of manganese also allows single and double addition of tertiary phosphane, according to the scheme described for the 6a-elements Cr, Mo, and W (Section 5.2.5). The product **69** then undergoes a cleavage of the Mn–C bond to yield $(R_3P)_2CR^{\oplus}X^{\ominus}$ salts[87].



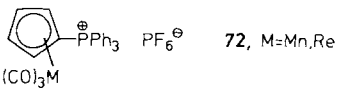
**69**

An ylide complex of rhenium **71** is obtainable by addition of phosphane to a cationic methylene complex **70**; the nitrosyl ligand is not attacked[113].



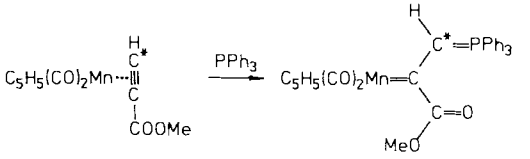
**70** **71**

Triphenylphosphoniocyclopentadienide can be readily incorporated as a ligand in the complex **72**[114].



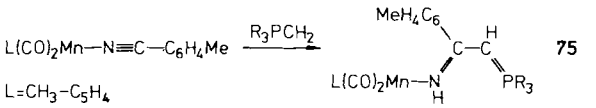
**72**, M=Mn,Re

Addition of $P(C_6H_5)_3$ to the alkyne complex **73** occurs at the *C atom, which in the product is no longer attached to the metal atom[115], so that the compound **74** contains an ylide function in the β-position. X-ray structure analysis confirms the P=C-bonding:



**73** **74**

The attachment of $C_6H_5(CH_3)_2P{=}CH_2$ to a nitrile complex leads to formation of the adduct **75**, whose structure was deduced from spectroscopic data alone[116].



**75**

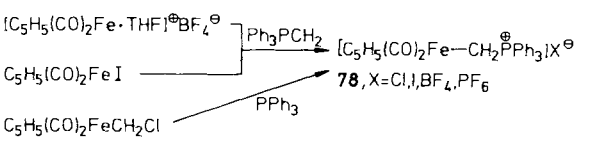
The ylide complexes **46** with Cr–Re and W–Re bonding have already been mentioned in Section 5.2.5[85,86].

## 7. Complexes of Phosphorus Ylides with Iron, Ruthenium, and Osmium

The elements of the eighth subgroup of the periodic system often reflect the synthetic principles and compound types already found with manganese and rhenium.

Homoleptic ylide complexes of iron only exist in the presence of complex ligands, such as have been described for the manganese complexes **61** and **63** (cf. Section 6). The $Fe^{II}$ analogues **76** and **77** are tetrahedral, high-spin complexes whose metal atoms coordinate exclusively aliphatic carbon atoms[107,108].

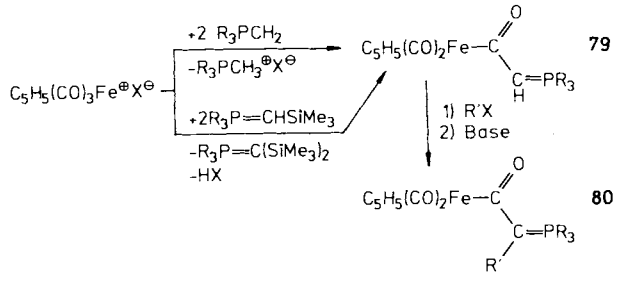
Ylide complexes which contain other ligands aside from the ylide are formed from reactive $C_5H_5(CO)_2FeL^{\oplus}$ precursors (L=tetrahydrofuran)[117] or the corresponding halides[118] by reaction with free ylides, or from the chloromethyl compounds with phosphane[67]. A range of structurally ill-defined adducts is formed on reaction of $(C_6H_5)_3P{=}C_5H_4$ with $FeCl_2$[119].



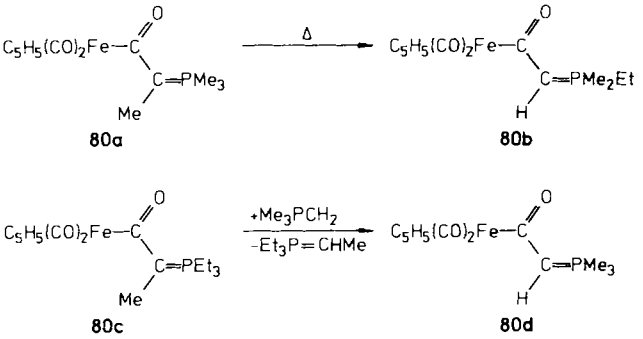
**78**, X=Cl,I,$BF_4$,$PF_6$

Unactivated $C_5H_5(CO)_3Fe^{\oplus}$, on the other hand, reacts (like $Fe(CO)_5$[98]), with ylides with attack at the CO ligands; transylidation yields the compounds **79** and **80**[120,121].

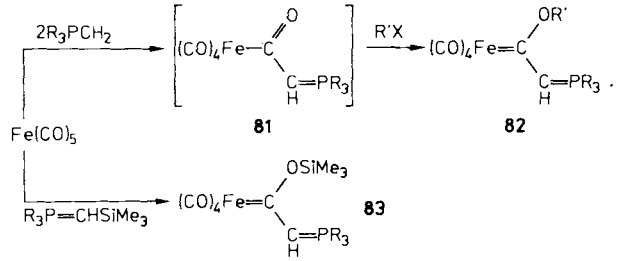
The complex **79** (R=$CH_3$) has been subjected to an X-ray structure analysis[121]. Of great interest are the novel



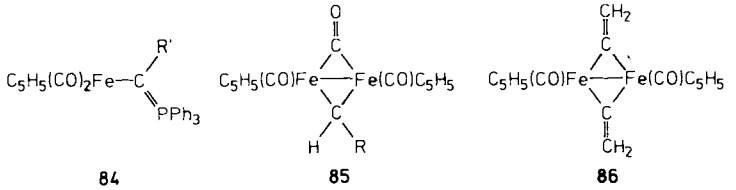
rearrangements **80a**→**80b** and the exchange of complete ylide units **80c**→**80d**. Plausible mechanisms have been suggested for both processes[122].



Ylides and $Fe(CO)_5$ yield a range of analogous products **81**—**83**[100, 102, 103].



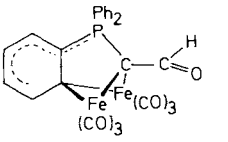
The binuclear complex $[C_5H_5Fe(CO)_2]_2$ reacts with $(C_6H_5)_3P{=}CHR'$ to give a mixture of products from which, *inter alia*, **84**—**86** have been isolated[111].



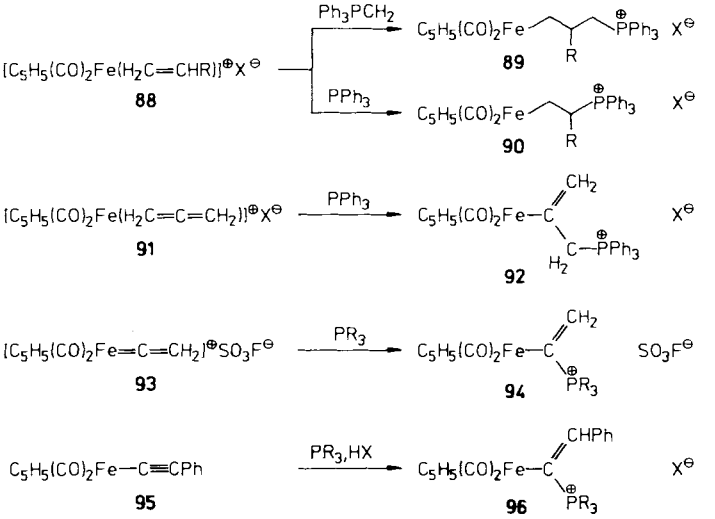
Reaction of $Fe_2(CO)_9$ with $Ph_3P{=}C{=}PPh_3$ is reported to lead to formation of $(CO)_3Fe(\mu\text{-}CO)[\mu\text{-}C(PPh_3)_2]Fe(CO)_3$, but its structure has not been confirmed[124].

The product **87**, which unexpectedly carries a formyl residue at a formally ylidic C-atom (confirmed by X-ray diffraction), is formed in the reaction of $Fe_3(CO)_{12}$ with $(C_6H_5)_3P{=}C(SnMe_3)_2$, a reaction which is extremely puzzling[125, 126].

The cationic ethylene complex **88** adds $Ph_3P{=}CH_2$ at one of the two olefinic C-atoms to form a γ-phosphonioalkylmetal compound **89**[117]. A series of alkyl derivatives **90**

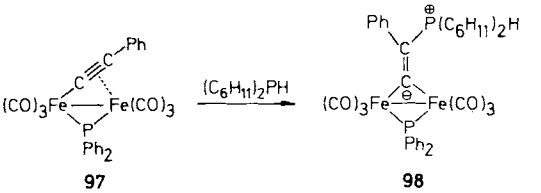


can also be obtained from olefin complexes **88** by nucleophilic attack of tertiary phosphanes at one of the two C atoms, which then carry the phosphonium center at the β-C atom[127]; they are stable when R = H, but very unstable when $R = C_6H_5$[128]. Derivatives of type **92** are obtainable from the related allene complexes **91**[128], while carbene complexes such as **93** yield "genuine" ylide (alkylidene) compounds **94**[129]. The latter are also accessible *via* the acetylides and phosphanes[130].



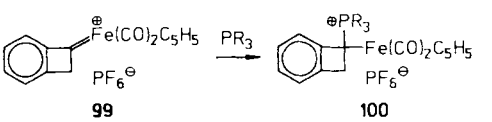
The structures of the compounds **94** and **96** have been determined by X-ray crystallography; the P—C distances are found to be 1.811 and 1.800 Å, respectively, and are thus not ylidic in nature[129, 130].

A comparable binuclear acetylide **97** yields a related complex **98** on reaction with dicyclohexylphosphane[131–133].



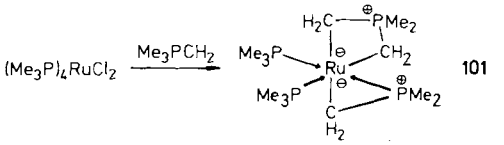
*Polyhapto*olefin-iron complexes react with phosphanes to give a range of phosphonium salts with π-bonded metal atoms which, on account of their difficultly defineable composition, are only mentioned in passing[134–137].

In the organoiron compound **100** the benzocyclobutyl residue is only $\eta^1$-bound; the precursor is the cationic carbene complex **99**[138].



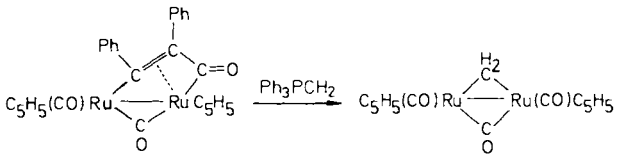
Reaction and transylidation of $(CO)_4Fe(PPh_2Cl)$ with $Ph_3P{=}CH_2$ yields the complex $(CO)_4Fe(PPh_2{-}CH{=}PPh_3)$ with *P*-coordinated ylide[104].

Ruthenium complexes of phosphorus ylides are so far limited to only a few examples. The complex **101**[139] contains the chelate-forming ligand $(CH_3)_2P(CH_2)_2^{\ominus}$.



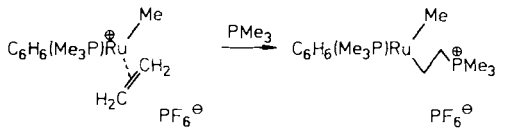
101

This octahedral complex additionally contains the $CH_2$-depleted fragment $(CH_3)_2PCH_2^{\ominus}$, which is formed by deprotonating a $P(CH_3)_3$ ligand. The reaction of $Ph_3P{=}CH_2$ with the binuclear ruthenium complex **102** surprisingly leads to a compound with a $CH_2$-bridge **103** and is thus reminiscent of the behavior of $[(C_5H_5)_2Fe(CO)_4]_2$[111]; the details of the reaction are still unclear[140].



102 103

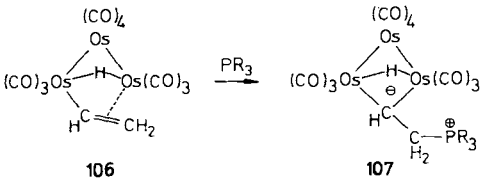
Cationic ethylene complexes such as **104** add tertiary alkylphosphanes to give γ-phosphonioalkylruthenium compounds **105**, which are related to the iron complexes **90** or **92**[141].



104 105

A $RuCl_3$ complex of $(C_6H_5)_3P{=}C(CH)_4$ of unknown structure requires further investigation[119].

Osmium complexes of phosphorus ylides in the strictest sense of the phrase are unknown. The products formed on reaction of tertiary phosphanes with trinuclear osmium clusters such as **106**, which contain phosphonium centers in the γ-position to the metal (**107**), are of peripheral interest[142, 143].



106 107

## 8. Complexes of Phosphorus Ylides with Cobalt, Rhodium, and Iridium

Homoleptic ylide complexes of cobalt (as in the case of Mn and Fe) are only obtainable with the triple ylide anions of **60** and **62**. These compounds, **108**[107] and **109**[108], correspond to the $Mn^{II}$ analogues **61** and **63**. The crystals of the paramagnetic $d^7$-compound **109** ($\mu_{eff.} = 4.2\mu_B$) are isomorphous with those of the manganese complex **63**. The molecules thus have $Co^{II}$-centers surrounded tetrahedrally by C atoms.

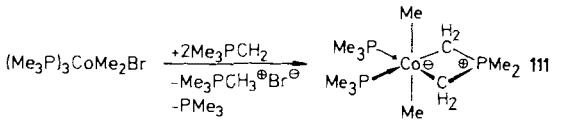
Terminal monodentate $(CH_3)_3P{=}CH_2$ is a component of the ligand sphere of a deep blue compound with the formula $[(CH_3)_3P{=}CH_2]_2CoCl_2$, **110**, whose exact structure, however, is not known. The substance, which is insoluble in all the usual solvents, is strongly paramagnetic and is formed in the course of the oxidative addition of $CH_2Cl_2$ to $(Me_3P)_4Co$, where intermediates with $Co{-}CH_2Cl$ units are probably formed[144–146]. An alternative synthetic possibility is the reaction of $(Me_3P)_3CoCl$ with $(CH_3)_3P{=}CH_2$[146].

$$3\,(Me_3P)_4Co + 2\,CH_2Cl_2 \longrightarrow (Me_3PCH_2)_2CoCl_2 + 2\,(Me_3P)_3CoCl + 4\,PMe_3$$

$$2\,(Me_3P)_3CoCl + 2\,Me_3P{=}CH_2 \longrightarrow (Me_3PCH_2)_2CoCl_2 + (Me_3P)_4Co + 2\,PMe_3$$

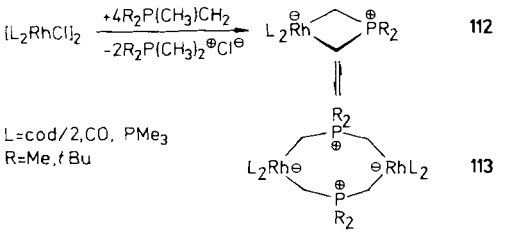
**110**

Chelate forming $(CH_3)_2P(CH_2)_2^{\ominus}$ units are realized in the diamagnetic $Co^{III}$-complex **111**, which is formed in a transylidation reaction[146]; its structure has been determined by X-ray diffraction[147].



111

Square planar rhodium(I) complexes contain the same chelate formers in various ligand combinations. Starting from 1,5-cyclooctadiene- or dicarbonyl-rhodium chloride the mononuclear complexes **112** are easily obtained *via* transylidation with free ylides and can dimerize to eight-membered metallocycles if the spatial requirements of the substituents allow it: **113**[148–150].



112

L=cod/2,CO, $PMe_3$
R=Me, *t*Bu

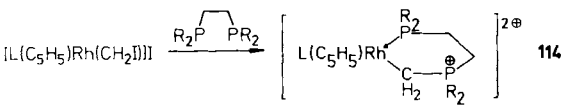
113

When L=CO and R=$CH_3$ the equilibrium (in toluene at 25 °C) lies on the side of the dimer with $\Delta H = -10.5$ kcal/mol[150]. Analogous complexes have been obtained with the cyclic ylides $(CH_2)_nP(CH_3){=}CH_2$ (n=4, 5) and the double ylide $(CH_3)_3P{=}N{-}P(CH_3)_2{=}CH_2$[149]. Some of the compounds are good hydrogenation catalysts[148]. The corresponding iridium compounds are known but unfavorable solubility behavior and difficulties in crystallizing them have, until now, hindered their satisfactory characterization[151].

Some mononuclear cationic rhodium(III) complexes with monodentate ylides are accessible *via* reaction of tertiary phosphanes with halomethyl precursors[152], *e.g.*

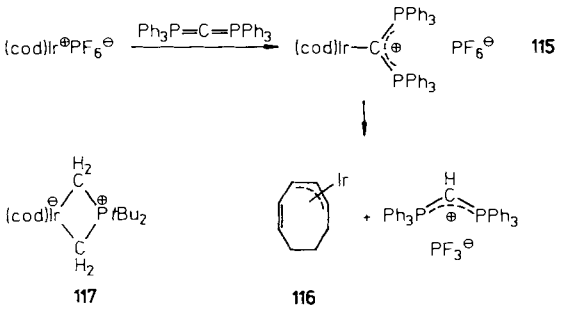
$$[C_5H_5(Me_3P)_2RhCH_2I]^{\oplus}I^{\ominus} \xrightarrow{PMe_3} [C_5H_5(Me_3P)_2RhCH_2PMe_3]^{2\oplus}2I^{\ominus}$$

The corresponding cyclic variants **114** are formed with bifunctional phosphanes[153–154].




**114**

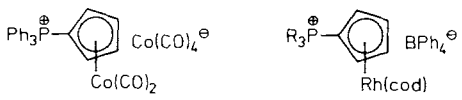
Hexaphenylcarbodiphosphorane reacts with $Co_2(CO)_8$ to give an ionic product $[(CO)_4Co{-}C(PPh_3)_2]^{\oplus}[Co(CO)_4]^{\ominus}$, but no details of the reaction have been quoted[100,124]. A similar coordination unit is found in the iridium complex **115**, which, however, decomposes in THF by intramolecular proton transfer and elimination to give the 1,8-cyclooctadienyl complex **116**[155].




**115** **117** **116**

Reaction of $[(cod)IrCl]_2$ with $(tert\text{-}Bu)_2MeP{=}CH_2$ leads *via* transylidation to formation of the mononuclear ylide complex **117**[156].

$Co_2(CO)_8$ likewise reacts with $Ph_3P{=}C(CH)_4$ with partial CO-exchange to give an ionic product **118a**, whose crystal structure has been determined[157].




**118a** **118b**

Triphenylphosphoniocyclopentadienide complexes of rhodium, such as **118b**, have a related structure[158]; instead of 1,5-cyclooctadiene (cod), they can also contain $C_7H_8$, $CO/PR_3$, $C_5Me_5$, *etc.*[159]. An ylide-adduct of $RhNO_3$ is also known[119].

## 9. Complexes of Phosphorus Ylides with Nickel, Palladium, and Platinum

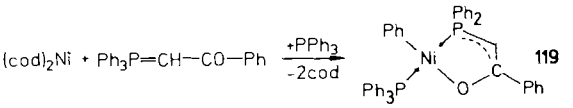
### 9.1. Homoleptic Ylide Complexes without Auxiliary Ligands

It was already found in 1972[160] that the coordination of monofunctional phosphorus ylides at nickel(0), for example by substitution of 1,5-cyclooctadiene, is accompanied by a rearrangement of the ylide in the sense of a Stevens rearrangement to give $Ni^0$ complexes of the isomeric tertiary phosphanes.

$$(cod)_2Ni + 4\,Ph_3P{=}CH_2 \xrightarrow[-2\,cod]{70^{\circ}C} (Ph_2PCH_2Ph)_4Ni$$

It was possible to develop this process into a catalytic ylide isomerization[160]. However, it has so far proven impossible to isolate a tetrakis(ylide)nickel(0) complex. Only in the presence of accessory ligands is it possible to fix monodentate ylides on $Ni^0$.

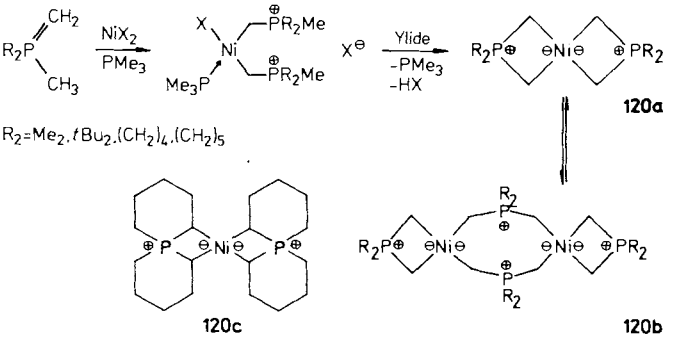
Reaction of $(cod)_2Ni^0$ with a *C*-benzoyl stabilized ylide in the presence of $PPh_3$ leads to oxidative addition of a phenyl group to the metal atom with formation of an arylnickel(II) complex **119**[161].



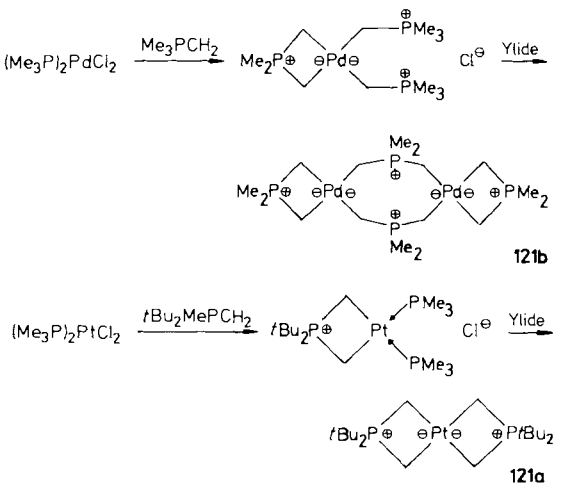

**119**

It has been postulated that **119** is one of the catalytically active species in the oligomerization of ethylene[162].

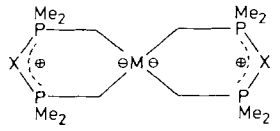
In contrast, it is possible to realize a homoleptic ligand sheath at the $Ni^{II}$ center with phosphonium bis-ylide anions. Reaction of nickel(II) halides with $Me_3P{=}CH_2$ or its homologues leads *via* intermediates with mixed ligands to transylidation and formation of the mono or binuclear ylide complexes **120a**, **b**[16,147,163].




Formation of **120a** is favored by bulky substituents R. A polycyclic variant **119c** is accessible after previous metalation of a spirophosphonium salt[164]. X-ray structure analyses have been carried out on **119b** and **119c**[147,164]. The corresponding $Pd^{II}$ and $Pt^{II}$ compounds were obtained by analogous reactions[163,165], *e.g.* according to



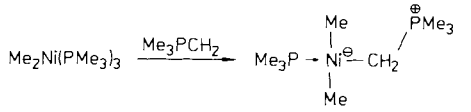
Both with $Ni^{II}$ as well as with $Pd^{II}$ and $Pt^{II}$, the nitrido-, methanido- and boronato-bis(phosphoniomethanide) anions $X(PMe_2CH_2)_2^{\ominus}$ yield isoelectronic, square planar complexes **127**, the structures of which have been determined by X-ray diffraction[108, 165–169].



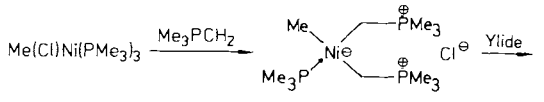
**122** M=Ni, Pd, Pt; X=N,CH,$BH_2$,$BMe_2$

## 9.2. Ylide Complexes of Alkylmetal Compounds and Metal-Phosphinomethanides

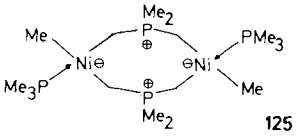
The $PMe_3$ complex of $(CH_3)_2Ni$ reacts with $Me_3P{=}CH_2$ with partial displacement of the tertiary phosphane to yield only the *trans*-configurated ylide complex **123**. Already in the case of $CH_3NiCl$, however, the reaction proceeds *via* the isolable intermediate **124** with transylidation to the binuclear ylide-bridged complex **125**, which resembles compounds of type **120b**[170].



**123**

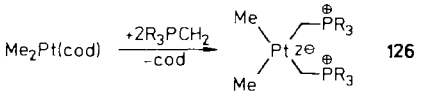


**124**



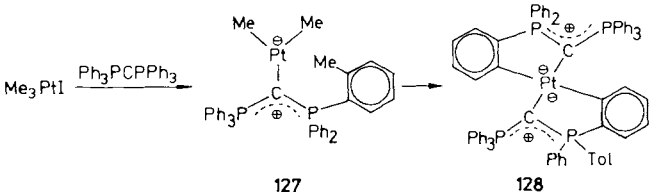
**125**

Reaction of the cod-complex of $(CH_3)_2Pt$ with ylides leads quantitatively to the *cis*-configurated complexes **126**[156].



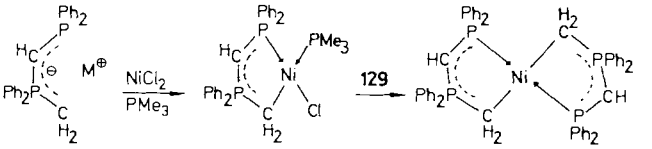
**126**

$(CH_3)_3PtI$ reacts with $Ph_3P{=}C{=}PPh_3$ in a complicated reaction to form the $Pt^{II}$ complex **128**, in which all the $CH_3$ groups have been cleaved from the metal[121]; **127** is postulated as an intermediate.



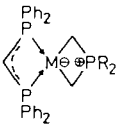
**127** **128**

The highly stable *trans* ylide complex **131** can be synthesized *via* the precursor **130** formed on reaction of the metalated ylide **129** with $PMe_3$-complexed $NiCl_2$; the structure of **131** has been determined X-ray crystallographically[171].



**129** **130** **131**

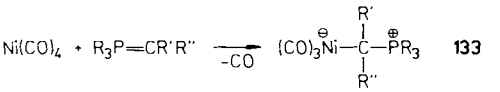
Bis(diphenylphosphano)methanide ligands and simple ylides form the similarly stable complexes **132**[172, 173]. X-ray data again reveal the environment of the metal to be square planar[172].



**132** M=Ni,Pd,Pt; R=Me,Et

## 9.3. Ylide Complexes of Carbonyl- and Cyclopentadienylnickel

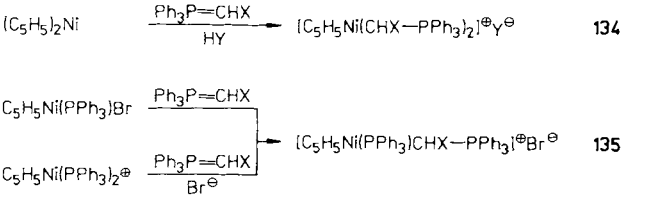
It was first demonstrated 15 years ago[174] that phosphorus ylides can displace at least one CO ligand from $Ni(CO)_4$. The tetrahedral $Ni^0$ complexes that result have since been synthesized in large numbers[102, 160] and one of them has been studied crystallographically[175].



**133**

The CO ligands are not attacked by silylated ylides (in spite of the higher affinity of silicon for oxygen)[102] and even the carbodiphosphorane $Ph_3P{=}C{=}PPh_3$ reacts with exclusive displacement of CO to give **133** ($R'R'' = PPh_3$)[100]; however just as little is known about the structure of the product as about that of the complex obtained on reaction of $(Ph_3P)_2Pt(C_2H_5)$ and $PH_3P{=}C{=}PPh_3$[98]).

Bis($\eta^5$-cyclopentadienyl)nickel reacts with $Ph_3P{=}CH_2$ with exchange of one of the two $C_5H_5$ rings to give the complex **134**, which is accessible in an analogous manner from $C_5H_5Ni(PR_3)_2^{\oplus}$. Appropriate stoichiometric reactions of the $C_5H_5Ni(PR_3)X$ precursors lead to the mixed cations **135**[176, 177].



**134**

**135**

X=Me,Et,*n*Pr,*n*Bu,Cl,OMe; "HX"=$Me_2$; Y=Br,$PF_6$

### 9.4. Formation of Ylide Complexes *via* Haloalkylmetal Precursors, from Olefin Complexes or by $CH_2$-Insertion

It was first reported in 1970[178] that $(R_3P)_4Pt^0$ complexes undergo oxidative addition with dihalomethanes, leading, *via* haloalkylmetal intermediates, to ylide complexes[179,180]. Under suitable reaction conditions it is possible to isolate the $ClCH_2Pt$ intermediate; hence, the second reaction step can be monitored separately[181,182].

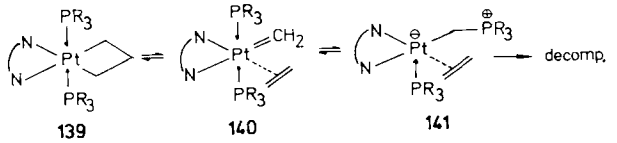
$$Pt(PPh_3)_4 \xrightarrow{CH_2ClI} cis\text{-}[(Ph_3P)_2Pt(Cl)CH_2PPh_3]^{\oplus}I^{\ominus} \quad \mathbf{136}$$

$$Pt(PEt_3)_4 \xrightarrow{CH_2I_2} trans\text{-}[(Et_3P)_2Pt(I)CH_2PEt_3]^{\oplus}I^{\ominus} \quad \mathbf{137}$$

$$(Ph_3P)_2Pt(CH_2Cl)Cl \xrightarrow{PPh_3} [(Ph_3P)_2Pt(Cl)CH_2PPh_3]^{\oplus}Cl^{\ominus} \quad \mathbf{138}$$

On changing the phosphane and in the presence of Lewis acid catalysts the compounds are inclined to isomerize (*cis/trans* or ligand isomerization). A typical structure has been elucidated X-ray crystallographically[179,180].

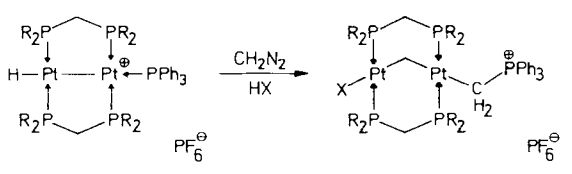
The six-fold coordinated platinacyclobutane compound **139** decomposes in the presence of tertiary phosphanes with formation of a series of hydrocarbons (such as cyclopropane, propylene, ethylene, and methane), whose formation is best interpreted in terms of an equilibrium, the position of which is influenced by the $PR_3$ components. It has not yet been possible to demonstrate directly the presence of the postulated ylide complex **141**[183].




**139** **140** **141**

Reaction of a 1,5-cyclooctadiene-$Pt^{II}$ complex $(R_2N_4)Pt(cod)$, R = 4-$C_6H_4NO_2$, with $PEt_3$ furnishes a σ,π-alkylmetal compound bearing a newly introduced onium center in position 2 of the ring. The structure has been elucidated by X-ray diffraction analysis[184].

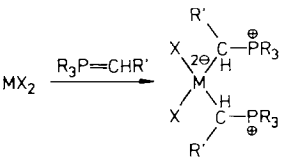
On treatment with diazomethane, the hydridodiplatinum complex **142** yields a μ-methylene-ylide complex **143** bearing a terminal $Ph_3PCH_2$ function. The mechanism of formation is unknown, but the structure has been confirmed by X-ray diffraction[185].




**142** **143** R=Ph

### 9.5. Ylide Complexes of Palladium(II) and Platinum(II) Halides

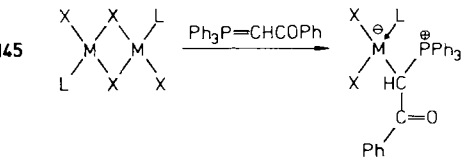
Complexes of $Pd^{II}$ and $Pt^{II}$ halides with phosphorus ylides, in which the ligand is bound to the central atom by a metal carbon bond, have been synthesized on a large scale and subjected to detailed studies. This is particularly true for the group of compounds with ylides which bear an additional donor function and can, thus, function as bidentate ligands. $PdX_2$ and $PtX_2$ react with phosphorus ylides in a molecular ratio of 1:2 to give products of the type **144**. The oldest examples are the adducts of $PdCl_2$ or $PtCl_2$ with $Ph_3P{=}CH{-}CO{-}Ph$[186].




**144**

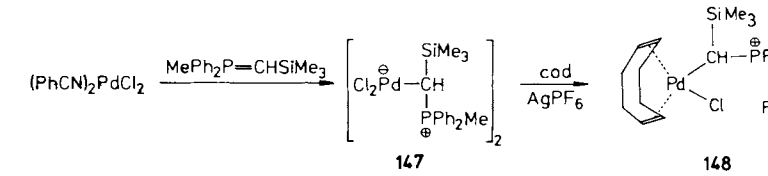
M = Pd, Pt; X = Cl; R = Ph; R' = COPh[186]
M = Pd; X = Cl; R = Ph; R' = COPh, COMe, COOMe[187]
M = Pd, Pt; X = Cl, SCN; R = Ph; R' = COPh, COMe, COOMe, COOEt, COCN[188]

The binuclear $M^{II}$ complexes **145** form the corresponding 1:1 compounds with an auxiliary ligand L[189]:



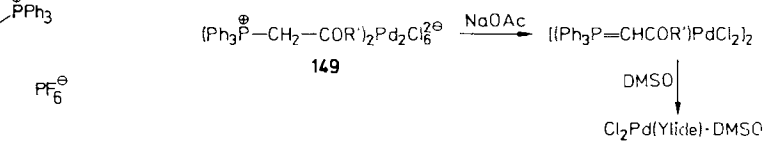

M = Pd; X = Cl; L = $PMe_3$, $PMe_2Ph$
M = Pt; X = Cl, Br, I; L = $PMe_3$, $PMe_2Ph$

Reaction of bisbenzonitrilepalladium(II) chloride with $MePh_2P{=}CHSiMe_3$ yields first the binuclear ylide complex **147**, which reacts further with diolefins and $AgPF_6$ to give a mononuclear cation complex **148**. The product has been identified by X-ray structure analysis[190,191].



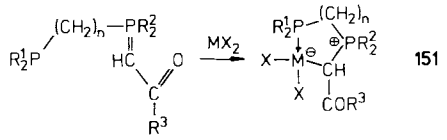

**147** **148**

With $Ph_3P{=}CHCOR'$ (R' = Me, Ph), the 1:2 complex $Cl_2Pd(ylide)_2$ is formed[192]. Complexes of the same ylide type can be obtained on starting with a salt precursor **149**, which yields the binuclear complex **150** even on treatment with the weak base sodium acetate. The binuclear complex **150** is cleaved to mononuclear species in donor solvents such as dimethyl sulfoxide (DMSO)[193]:




**149** **150**

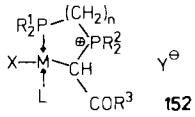
Ylides with a terminal phosphane function in the side chain are excellent chelaters of metal dihalides. The formation and structure of the products **151** have been studied in great detail.



**151**

n = 1; M = Pd, Pt; X = Cl; $R^1 = R^2 = R^3 = Ph$[194-197]; $R^1 = R^2 = Ph$, $R^3 = Me$, OMe[195]
n = 1; M = Pd, Pt; X = Cl, Br, I, SCN; $R^1 = R^2 = Ph$, $R^3 = Ph$, Me, OMe, OEt[198]
n = 0; M = Pd, Pt; X = Cl; $R^1 = R^2 = Ph$, $R^3 = Ph$, Me, OMe[198]
n = 1; M = Pd, Pt; X = Cl; $R^1 = R^2 = CH_2Ph$, $R^3 = Ph$[199]

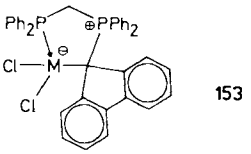
Ionic complexes **152** are formed with the same ylides from precursors of type **145**; again L has been varied within wide limits[200].



**152**

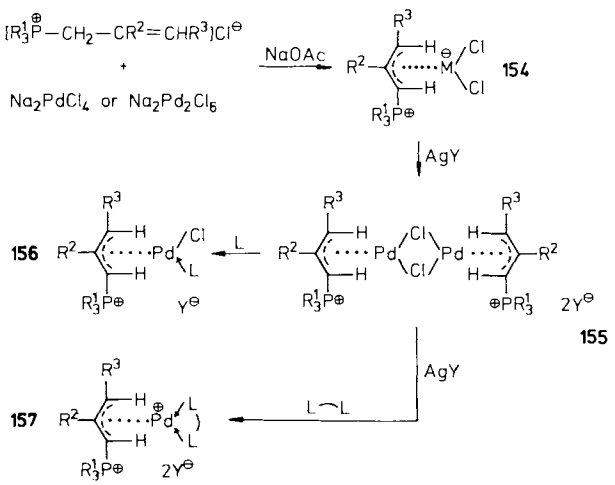
n = 0, 1; M = Pd, Pt; $R^1 = R^2 = R^3 = Ph$[201]; L = $PPh_3$, $P(C_6H_{11})_3$, $AsPh_3$, $PPh_2Me$, $P(OMe)_3$, SbPh, py, pyMe, pyrazole

The 1 : 1 complexes **153** of $PdCl_2$ and $PtCl_2$ with a fluorene ylide probably also have a similar five-membered ring structure as in **151**[64].



**153**

Allylphosphonium salts react with $Na_2Pd_2Cl_6$ or $Na_2PdCl_4$ in methanol in the presence of even weak bases (acetate) to give phosphonioalkylide complexes **154**. The stepwise removal of halogens with silver salts of poorly coordinating anions leads to binuclear dications **155** or, in the presence of donor molecules, to mononuclear complexes **156**[202-204].



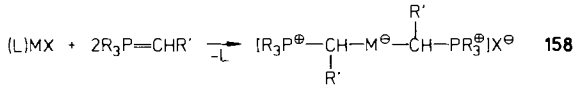
$R^1$ = Ph, Et; $R^2$ = H, Me; $R^3$ = H, Me; Y = $BF_4$, $PF_6$, $SO_3CF_3$; LL = cod, $Ph_3P{=}C(CH)_4$

Triphenylphosphoniocyclopentadienide, which has already been used in **156** as a donor, is also represented in a whole range of other $Pd^{II}$ and $Pt^{II}$ complexes[205, 206].

## 10. Complexes of Phosphorus Ylides with Copper, Silver, and Gold

The coinage metals form particularly simple complexes with ylides, which are distinguished by their stability towards oxidation and hydrolysis. They also belong to the most thermally stable organometallic compounds of these elements[207, 208].

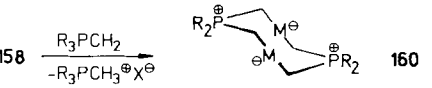
Homoleptic ylide complexes exist both with terminal monodentate ligands and with bridging bidentate ligands. The former are represented by the ionic compounds **158**, which are particularly common for M = Au with various residues R[209-217].



**158**

X = Cl (Br); M = Cu, Au; R = Me; R′ = H, $SiMe_3$
M = Cu, Ag, Au; R = Ph; R′ = H, Me, *i*Pr
M = Au; R = Et, *n*Bu; R′ = H;
M = Au; R = $NMe_2$; R′ = H
$[(Ph_3P{-}CHCOPh)_2Au]^{\oplus}AuCl_4^{\ominus}$[186]
$[\{Ph_3P{-}C(CH_2)_2\}_2Au]^{\oplus}Cl^{\ominus}$ **159**

Many of these complexes dissolve in water without decomposition and are easily characterized analytically and spectroscopically. The triphenylphosphoniocyclopropanide complex **159**[218] is a special case, which exhibits quite exceptional properties. In spite of the ring strain at the ylide C atom, the species nevertheless exhibits high stability. The most important reaction of these complexes, with their linear configuration and a coordination number of two for the central atom, is transylidation with excess ylides (as catalyst) to binuclear complexes **160**[219-228]:

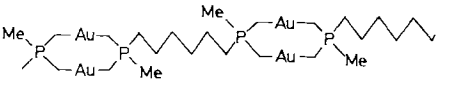


**160**

M = Cu, Ag, Au; R = Me, Et
M = Cu, Ag; R = Me, Ph
M = Au; $R^2 = (CH_2)_4$, $(CH_2)_5$, (*c*-$C_3H_5$)Me, (*c*-$C_5H_9$)Me

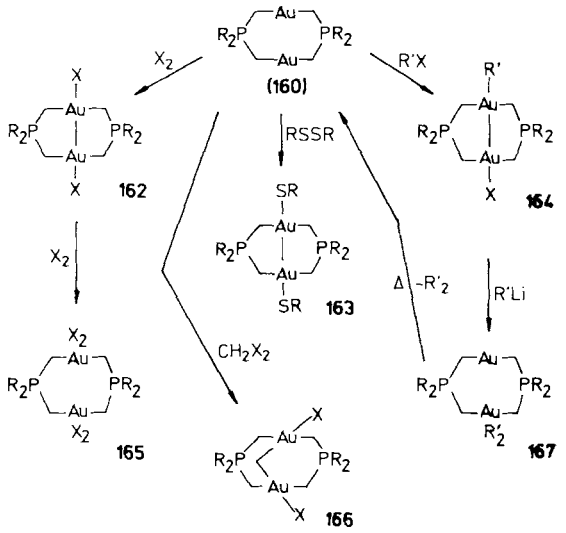
According to crystal structure data, these heterocycles, which without exception are stable and colorless, contain two almost parallel C–M–C axes of doubly coordinated metal atoms which are 2.843 (Cu)[224] or 3.023 Å (Au)[225, 226] apart. UV investigations[227] and theoretical calculations[228] indicate that the metal-metal interaction is very weak. The eight-membered ring of type **160** can also be incorporated in polymers[229], if α,ω-difunctional ylides are used (**161**):

Several complexes of types **158** and **160** have been tested for their pharmacological activity in polyarthritis. The effect is comparable with that observed with conventional preparations[215, 230].



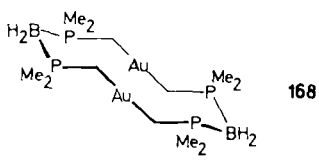
**161**

The auracycles **160** easily undergo oxidative addition on reaction with halogens[220,221], disulfides[231] and alkyl halides[232], whereby bicyclic gold(II) compounds **162** to **164** are first formed in which a transannular Au–Au bond has been confirmed by X-ray diffraction[221], by magnetic measurements and by Mössbauer[222,231] and Au-ESCA studies[222].




Further oxidation of **162** leads, with cleavage of the Au–Au bond, to the binuclear $Au^{III}$ complex **165**[220,222]. The $CH_3I$ adduct **164**, whose structure was originally deduced solely from NMR data[220], has recently been unequivocally confirmed by X-ray structural analysis[232]. On further alkylation it yields the unstable, unsymmetrical dialkyl derivative **167**, which easily undergoes thermal decomposition with elimination of ethane to give **160**.

Addition of dihalomethanes to **160** results in formation of a $CH_2$ bridge between the metal atoms, raising their coordination number from 2 (in **160**) to 4 (in **166**). Crystal structure analysis reveals a square planar ligand arrangement as is to be expected for $Au^{III}(d^8)$[233]. A gold(I) complex of the double anion **62** probably has the twelve-membered ring structure **168**[234].



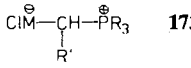

A large variety of ylide complexes of the coinage metals with additional ligands are also known and exist as cations or neutral molecules. Formulas **169** to **176** summarize the individual examples with monovalent central atoms:

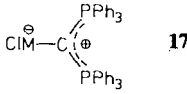
$Me_3SiCH_2CuCH_2PMe_2$ **169**[211]

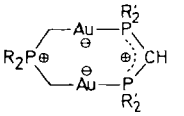
$[Me_3PCHCuCHPMe_3]^{\oplus}Cl^{\ominus}$ **170**, R′ = H, $SiMe_3$[211]

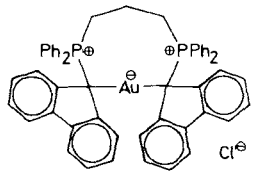
$RAuCHPMe_3$ **171**, R = Me, $CH_2SiMe_3$; R′ = H, $SiMe_3$

$[LAu{-}CR'_2{-}PR'_3]^{\oplus}X^{\ominus}$ **172**, X = Cl (Br);
L = $Me_3P$; R′ = H, H/$SiMe_3$, $SiMe_3$; R″ = Me[209,213]
L = $Ph_3P$; R′ = $SiMe_3$; R″ = Me[213]
L = $Ph_3P$; R′ = H, H/Me, W/*i*Pr; R″ = Ph[216]
X = $NO_3$;
L = $Ph_3P$; R′ = H/COPh; R″ = Ph[186]


**173**, M = Cu, Ag; R = Ph; R′ = H, Me, *i*Pr[236]

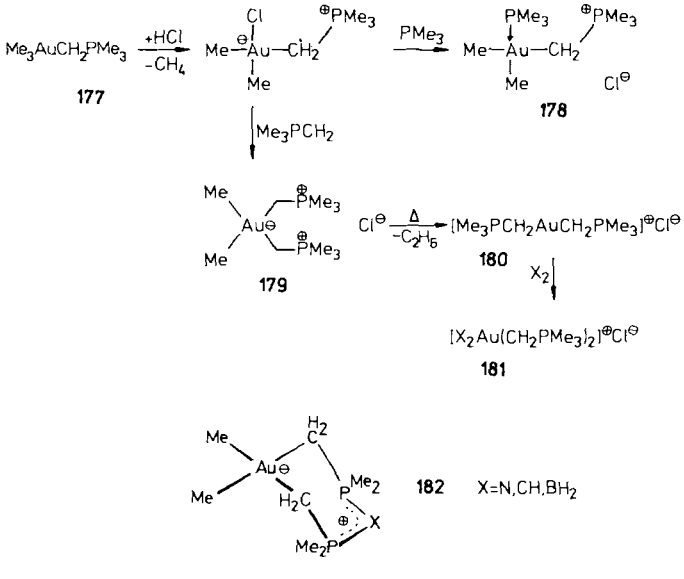

**174**, M = Cu, Ag, Au[237]


**175**, R = Me, Et, *t*Bu; R′ = Ph[173,235]


**176**[64]

In addition, some square planar complexes of trivalent gold with various alkyl-, halogen-, and ylide-ligand combinations have been described[213,214,236–238]. One example, **177**, has also been investigated by X-ray diffraction and by ESCA spectroscopy. The results show that the ylides are powerful donor ligands that have practically no back-bonding acceptor effect[238].

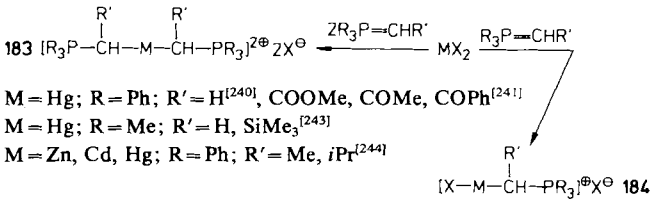
Three isoelectronic auracycles **182** are derived from $(CH_3)_2Au^{\oplus}$ and have been studied in detail, particularly by X-ray diffraction. The folding of the six-membered ring into the chair conformation depends on the nature of the bridge element X; the environment of the gold atom, however, remains practically constant[239,235].



## 11. Complexes of Phosphorus Ylides with the $d^{10}$-Metals Zinc, Cadmium, and Mercury

The guiding principle in the chemistry of the ylide complexes of the elements of the second subgroup is—similarly to that for the whole organometallic chemistry of these elements—strongly directional σ-bonding with small coordination numbers.

Homoleptic coordination compounds with monodentate ylide ligands are the cationic complexes **183**, which have been synthesized in large numbers and with a wide range of substituents[240–244].



**183** $[R_3P-\underset{\displaystyle R'}{\underset{|}{CH}}-M-\underset{\displaystyle R'}{\underset{|}{CH}}-PR_3]^{2\oplus}\,2X^{\ominus}$

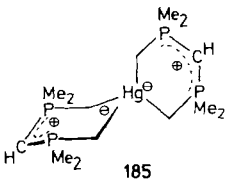
$M = Hg$; $R = Ph$; $R' = H$[240], COOMe, COMe, COPh[241]
$M = Hg$; $R = Me$; $R' = H$, $SiMe_3$[243]
$M = Zn$, Cd, Hg; $R = Ph$; $R' = Me$, $i$Pr[244]

**184** $[X-M-\underset{\displaystyle R'}{\underset{|}{CH}}-PR_3]^{\oplus}X^{\ominus}$

$M = Hg$; $X = Cl$; $R = Me$; $R' = H$[243]
$M = Hg$; $X = Cl$; $R = Ph$; $R' = COPh$[242]
$M = Hg$; $X = I$; $R = Me$; $R' = SiMe_3$[245]

If only small amounts of ylide are available the 1:1 complexes **184** are formed, alkyl metal analogues of which are also known $[R''-Hg-CHR'-PR_3]X$ ($R'' = Me$[243]).

The high donating power of the double ylides is demonstrated in the unusual chelate complex **185**, which is one of the few tetracoordinated organomercury compounds known[246].



**185**

Open chain and cyclic double ylides also yield complexes with the two lighter metals of the second subgroup, *i.e.* zinc and cadmium[247–249]. As is to be expected such complexes can be ascribed formulas of the type **63**, **76** and **109**[248]. In passing, the cadmium complexes of fluorinated phosphinatomethylide anions are worth mentioning. Their relationship to real ylide compounds is only of a formal nature[250].

Finally, however, the mercury complexes of triphenylphosphoniocyclopentadienide[251,119] are of greater interest. In the organometal compounds formed on reaction of this ylide with mercury(II) salts, the metal atom is $\eta^1$-coordinated to the C-3 atom of the $C_5H_4$ ring, as has been confirmed by an X-ray structural analysis of the adduct $[Ph_3P-C_5H_4 \cdot HgI_2]_2$. This unusual type of structure has otherwise never been observed amongst ylide complexes.

## 12. Outlook

The present review represents a snapshot glimpse at a field of chemistry that is in the process of rapid development. The trend in interest is unmistakably towards the intentional or accidental formation of ylides *in situ* at the metal atom, rather than the planned introduction of "preconstructed" ylides into a complex. The latter development seems temporarily complete now that the most important modes of formation and interactive mechanisms are known. However, these constitute but the preliminary studies necessary for an understanding of some of the complicated reactions in the system metal/phosphane/$C_1$ building block.

*Work in the author's laboratories was performed by a large number of co-workers, whose skill and enthusiasm are gratefully acknowledged. Thanks are also due to the Fonds der Chemischen Industrie, Deutsche Forschungsgemeinschaft, Hoechst AG, Degussa AG, and Proctor & Gamble Ltd. for generous and continued support.*

Received: July 25, 1983 [A 476 IE]
German version: *Angew. Chem. 95* (1983) 980
Translated by Dr. *F. Hampson*, Saarbrücken

[1] H. J. Bestmann, R. Zimmermann in Houben-Weyl-Müller: *Methoden der Organischen Chemie*, Vol. *E1*, p. 616, Thieme, Stuttgart 1982; and in G. M. Kosolapoff, L. Maier: *Organophosphorus Compounds*, Vol. *3*, p. 1, Wiley-Interscience, New York 1972.
[2] G. Wittig, *Angew. Chem. 92* (1980) 671.
[3] H. Schmidbaur, *Adv. Organomet. Chem. 14* (1976) 205.
[4] H. J. Bestmann, *Chem. Ber. 95* (1962) 58.
[5] H. Schmidbaur, *Acc. Chem. Res. 8* (1975) 62; *Pure Appl. Chem. 50* (1978) 19; *52* (1980) 1057.
[6] W. C. Kaska, *Coord. Chem. Rev. 48* (1983) 1.
[7] L. Weber in F. R. Hartley, S. Patai: *The Chemistry of the Metal-Carbon Bond*, Wiley, Chichester 1982, p. 91.
[8] L. Weber, *Angew. Chem. 95* (1983) 539; *Angew. Chem. Int. Ed. Engl. 22* (1983) 516.
[9] H. Schumann, S. Hohmann, *Chem. Ztg. 100* (1976) 336.
[10] G. Wittig, R. Polster, *Liebigs Ann. Chem. 599* (1976) 1.
[11] H. Schmidbaur, W. Tronich, *Chem. Ber. 101* (1968) 3556.
[12] H. Schumann, J. Pickardt, N. Bruncks, *Angew. Chem. 93* (1981) 127; *Angew. Chem. Int. Ed. Engl. 20* (1981) 120.
[13] L. E. Manzer, *Inorg. Chem. 15* (1976) 2567.
[14] H. Schmidbaur, M. Heimann, *Z. Naturforsch. B29* (1974) 485.
[15] H. Schumann, F. W. Reier, *J. Organomet. Chem. 235* (1982) 287.
[16] H. H. Karsch, H. Schmidbaur, *Chem. Ber. 107* (1974) 3684.
[17] G. W. Rice, G. B. Ansell, M. A. Modrick, S. Zentz, *Organometallics 2* (1983) 154.
[18] H. Schumann, F. W. Reier, *J. Organomet. Chem. 209* (1981) C10.
[19] H. Schumann, F. W. Reier, M. Dettlaff, *J. Organomet. Chem. 255* (1983) 305.
[20] P. L. Watson, *J. Chem. Soc. Chem. Commun. 1983*, 276.
[21] J. C. Baldwin, W. C. Kaska, *Inorg. Chem. 18* (1979) 687.
[22] R. E. Cramer, R. B. Maynard, J. W. Gilje, *Inorg. Chem. 20* (1981) 2466.
[23] R. E. Cramer, R. B. Maynard, J. C. Paw, J. W. Gilje, *J. Am. Chem. Soc. 103* (1981) 3589.
[24] R. E. Cramer, R. B. Maynard, J. W. Gilje, *J. Am. Chem. Soc. 100* (1978) 5562.
[25] R. E. Cramer, R. B. Maynard, J. W. Gilje, *Inorg. Chem. 19* (1980) 2564.
[26] H. Schmidbaur, W. Scharf, H.-J. Füller, *Z. Naturforsch. B32* (1977) 858.
[27] W. Scharf, D. Neugebauer, U. Schubert, H. Schmidbaur, *Angew. Chem. 90* (1978) 628; *Angew. Chem. Int. Ed. Engl. 17* (1978) 601.
[28] J. C. Baldwin, N. L. Keder, C. E. Strouse, W. C. Kaska, *Z. Naturforsch. B35* (1980) 1289.
[29] K. I. Gell, J. Schwartz, *Inorg. Chem. 19* (1980) 3207.
[30] J. Schwartz, K. I. Gell, *J. Organomet. Chem. 184* (1979) C1.
[31] J. Schwartz, *Pure Appl. Chem. 52* (1980) 733.
[32] D. A. Straus, R. H. Grubbs, *J. Am. Chem. Soc. 104* (1982) 5499.
[33] N. L. Holy, T. E. Nalesnik, L. T. Warfield, *Inorg. Nucl. Chem. Lett. 13* (1977) 569.
[34] B. Demerseman, P. H. Dixneuf, *J. Organomet. Chem. 210* (1981) C20.
[35] W. Hieber, E. Winter, E. Schubert, *Chem. Ber. 95* (1962) 3070.

[36] P. Belmonte, R. R. Schrock, M. R. Churchill, W. J. Youngs, *J. Am. Chem. Soc. 102* (1980) 2859.
[37] M. R. Churchill, W. J. Youngs, *Inorg. Chem. 20* (1981) 382.
[38] P. R. Sharp, R. R. Schrock, *J. Organomet. Chem. 171* (1979) 43.
[39] S. J. McLain, C. D. Wood, L. W. Messerle, R. R. Schrock, F. J. Hollander, W. J. Youngs, M. R. Churchill, *J. Am. Chem. Soc. 100* (1978) 5962.
[40] E. Kurras, U. Rosenthal, H. Mennenga, G. Oehme, *Angew. Chem. 85* (1973) 913; *Angew. Chem. Int. Ed. Engl. 12* (1973) 854.
[41] E. Kurras, U. Rosenthal, *J. Organomet. Chem. 160* (1978) 35.
[42] E. Kurras, U. Rosenthal, H. Mennenga, G. Oehme, G. Engelhardt, *Z. Chem. 14* (1974) 160.
[43] E. Kurras, U. Rosenthal, H. Mennenga, G. Oehme, *J. Organomet. Chem. 84* (1975) C13.
[44] F. A. Cotton, B. E. Hanson, W. H. Ilsley, G. W. Rice, *Inorg. Chem. 18* (1979) 2713.
[45] F. A. Cotton, B. E. Hanson, G. W. Rice, *Angew. Chem. 90* (1978) 1015; *Angew. Chem. Int. Ed. Engl. 17* (1978) 953.
[46] F. A. Cotton, P. E. Fanwick, private communication.
[47] A. Mitschler, B. Rees, R. Wiest, M. Benard, *J. Am. Chem. Soc. 104* (1982) 7501.
[48] L. Knoll, *J. Organomet. Chem. 148* (1978) C25.
[49] H. Berke, E. Lindner, *Angew. Chem. 85* (1973) 668; *Angew. Chem. Int. Ed. Engl. 12* (1973) 667.
[50] L. Knoll, *J. Organomet. Chem. 193* (1980) 47.
[51] L. Knoll, *J. Organomet. Chem. 182* (1979) 77.
[52] H. Bock, H. tom Dieck, *Z. Naturforsch. B 21* (1966) 739.
[53] K. A. O. Starzewski, H. tom Dieck, K. D. Franz, F. Hohmann, *J. Organomet. Chem. 42* (1972) C35.
[54] A. Greco, *J. Organomet. Chem. 43* (1972) 351.
[55] I. W. Bassi, R. Scordamaglia, *J. Organomet. Chem. 51* (1973) 273.
[56] E. W. Abel, A. Singh, G. Wilkinson, *Chem. Ind. (London) 1959,* 1067.
[57] J. C. Kotz, D. G. Pedrotti, *J. Organomet. Chem. 22* (1970) 425.
[58] D. Cashman, F. Lalor, *J. Organomet. Chem. 32* (1971) 351.
[59] V. N. Setkina, A. Zh. Zhakaeva, G. A. Panosyan, V. I. Zdanovitch, P. V. Petrovskii, D. N. Kursanov, *J. Organomet. Chem. 129* (1977) 361.
[60] M. Luckoff, K. Dimroth, *Angew. Chem. 88* (1976) 543; *Angew. Chem. Int. Ed. Engl. 15* (1976) 503; T. Debaerdemaeker, *ibid. 88* (1976) 544 and *15* (1976) 504.
[61] R. A. Pickering, R. A. Jacobsen, R. J. Angelici, *J. Am. Chem. Soc. 103* (1981) 817; R. A. Pickering, R. J. Angelici, *Inorg. Chem. 20* (1981) 2977.
[62] P. Hackett, G. Jaouen, *Inorg. Chim. Acta 12* (1975) L19.
[63] G. Deganello, T. Boschi, L. Toniolo, G. Albertin, *Inorg. Chim. Acta 10* (1974) L3.
[64] N. Holy, U. Deschler, H. Schmidbaur, *Chem. Ber. 115* (1982) 1379.
[65] L. Weber, *J. Organomet. Chem. 131* (1977) 49.
[66] L. Weber, R. Boese, W. Meyer, *Angew. Chem. 94* (1982) 938; *Angew. Chem. Int. Ed. Engl. 21* (1982) 926; *Angew. Chem. Suppl. 1982,* 1934.
[67] C. Botha, J. R. Moss, S. Pelling, *J. Organomet. Chem. 220* (1981) C21.
[68] E. O. Fischer, H. Fischer, H. Werner, *Angew. Chem. 84* (1972) 682; *Angew. Chem. Int. Ed. Engl. 11* (1972) 644.
[69] H. Werner, H. Rascher, *Helv. Chim. Acta 51* (1968) 1765; *Inorg. Chim. Acta 2* (1968) 181.
[70] F. R. Kreissl, C. G. Kreiter, E. O. Fischer, *Angew. Chem. 84* (1972) 679; *Angew. Chem. Int. Ed. Engl. 11* (1972) 643.
[71] F. R. Kreissl, E. O. Fischer, C. G. Kreiter, H. Fischer, *Chem. Ber. 106* (1973) 1262.
[72] H. Fischer, E. O. Fischer, C. G. Kreiter, H. Werner, *Chem. Ber. 107* (1974) 2459.
[73] E. O. Fischer, H. Fischer, *Chem. Ber. 107* (1974) 657.
[74] F. R. Kreissl, W. Held, *J. Organomet. Chem. 86* (1975) C10.
[75] F. R. Kreissl, W. Held, *Chem. Ber. 110* (1977) 799.
[76] C. P. Casey, T. J. Burkhardt, C. A. Bunnell, J. C. Calabrese, *J. Am. Chem. Soc. 99* (1977) 2127.
[77] H. G. Alt, J. A. Schwärzle, F. R. Kreissl, *J. Organomet. Chem. 152* (1978) C57.
[78] H. Fischer, *J. Organomet. Chem. 170* (1979) 309.
[79] H. S. Choi, D. A. Sweigart, *J. Organomet. Chem. 228* (1982) 249.
[80] C. P. Casey, T. J. Burkhardt, *J. Am. Chem. Soc. 94* (1972) 6543.
[81] F. R. Kreissl, *J. Organomet. Chem. 99* (1975) 305.
[82] F. R. Kreissl, P. Stückler, *J. Organomet. Chem. 110* (1976) C9.
[83] F. R. Kreissl, W. Uedelhoven, A. Ruhs, *J. Organomet. Chem. 113* (1976) C55.
[84] E. O. Fischer, A. Ruhs, F. R. Kreissl, *Chem. Ber. 110* (1977) 805.
[85] F. R. Kreissl, P. Friedrich, T. L. Lindner, G. Huttner, *Angew. Chem. 89* (1977) 325; *Angew. Chem. Int. Ed. Engl. 16* (1977) 314.
[86] W. Uedelhoven, D. Neugebauer, F. R. Kreissl, *J. Organomet. Chem. 217* (1981) 183.
[87] W. Uedelhoven, K. Eberl, W. Sieber, F. R. Kreissl, *J. Organomet. Chem. 236* (1982) 301.
[88] N. J. Cooper, M. L. H. Green, *J. Chem. Soc. Chem. Commun. 1974,* 761; *J. Chem. Soc. Dalton Trans. 1979,* 1121.
[89] M. L. H. Green, *Pure Appl. Chem. 50* (1978) 27.
[90] N. J. Cooper, M. L. H. Green, *J. Chem. Soc. Dalton Trans. 1979,* 1121.
[91] S. M. B. Costa, A. R. Dias, F. J. S. Pina, *J. Chem. Soc. Dalton Trans. 1981,* 314.
[92] J. C. Hayes, G. D. N. Pearson, N. J. Cooper, *J. Am. Chem. Soc. 103* (1981) 4648.
[93] J. C. Hayes, N. J. Cooper, *J. Am. Chem. Soc. 104* (1982) 5570.
[94] M. Canestrani, M. L. H. Green, *J. Chem. Soc. Chem. Commun. 1979,* 913.
[95] K. S. Chong, M. L. H. Green, *J. Chem. Soc. Chem. Commun. 1982,* 991.
[96] J. Levisalles, F. Rose-Munch, H. Rudler, J. C. Daran, Y. Dromzee, Y. Jeannin, *J. Chem. Soc. Chem. Commun. 1980,* 685.
[97] M. R. Churchill, H. J. Wasserman, *Inorg. Chem. 21* (1982) 3913.
[98] W. C. Kaska, D. K. Mitchell, R. F. Reichelderfer, *J. Organomet. Chem. 47* (1973) 391.
[99] C. Creaser, W. C. Kaska, *Transition Met. Chem. 3* (1978) 360.
[100] W. C. Kaska, D. K. Mitchell, R. F. Reichelderfer, W. D. Korte, *J. Am. Chem. Soc. 96* (1974) 2847.
[101] S. Voran, H. Blau, W. Malisch, U. Schubert, *J. Organomet. Chem. 232* (1982) C33.
[102] W. Malisch, H. Blau, S. Voran, *Angew. Chem. 90* (1978) 827; *Angew. Chem. Int. Ed. Engl. 17* (1978) 780.
[103] S. Z. Goldberg, K. N. Raymond, *Inorg. Chem. 12* (1973) 2923.
[104] L. Knoll, *Z. Naturforsch. B 33* (1978) 396.
[105] M. Luksza, K. Fiederling, U. Wanka, W. Malisch, *J. Organomet. Chem. 236* (1982) C1.
[106] K. Endrich, R. Korswagen, T. Zahn, M. L. Ziegler, *Angew. Chem. 94* (1982) 923; *Angew. Chem. Int. Ed. Engl. 21* (1982) 919; *Angew. Chem. Suppl. 1982,* 1906.
[107] H. Schmidbaur, T. Costa, B. Milewski-Mahrla, F. H. Köhler, Y.-H. Tsay, C. Krüger, J. Abart, F. E. Wagner, *Organometallics 1* (1982) 1266.
[108] G. Müller, D. Neugebauer, W. Geike, F. H. Köhler, J. Pebler, H. Schmidbaur, *Organometallics 2* (1983) 257.
[109] H. Blau, W. Malisch, *Angew. Chem. 92* (1980) 1063; *Angew. Chem. Int. Ed. Engl. 19* (1980) 1019.
[110] W. Malisch, H. Blau, U. Schubert, *Angew. Chem. 92* (1980) 1065; *Angew. Chem. Int. Ed. Engl. 19* (1980) 1020.
[111] R. Korswagen, R. Alt, D. Speth, M. L. Ziegler, *Angew. Chem. 93* (1981) 1073; *Angew. Chem. Int. Ed. Engl. 20* (1981) 1049.
[112] D. K. Mitchell, W. D. Korte, W. C. Kaska, *J. Chem. Soc. D 1970,* 1384.
[113] W. K. Wong, W. Tam, J. A. Gladysz, *J. Am. Chem. Soc. 101* (1979) 5440.
[114] A. N. Nesmeyanov, N. E. Kolobova, V. I. Zdanovitch, A. Zh. Zhakaeva, *J. Organomet. Chem. 107* (1976) 319; V. I. Zdanovitch, N. E. Kolobova, N. I. Vasyukova, Y. S. Nekrasov, G. A. Panosyan, P. V. Petrovskii, A. Zh. Zhakaeva, *ibid. 148* (1978) 63.
[115] N. E. Kolobova, L. L. Ivanov, O. S. Zhvanko, I. N. Chechulina, A. S. Batsanov, Y. T. Struchkov, *J. Organomet. Chem. 238* (1982) 223.
[116] L. Knoll, *J. Organomet. Chem. 186* (1980) C42.
[117] D. L. Reger, E. C. Culbertson, *J. Organomet. Chem. 131* (1977) 297.
[118] L. Knoll, *Z. Naturforsch. B 32* (1977) 1268.
[119] N. L. Holy, T. Nalesnik, L. Warfield, M. Mojesky, *J. Coord. Chem. 12* (1983) 157.
[120] L. Knoll, *J. Organomet. Chem. 152* (1978) 311.
[121] H. Blau, W. Malisch, S. Voran, K. Blank, C. Krüger, *J. Organomet. Chem. 202* (1980) C33; A. Stasunik, W. Malisch, *ibid. 247* (1983) C47.
[122] H. Blau, W. Malisch, *J. Organomet. Chem. 235* (1982) C1.
[123] L. Knoll, *Chem. Ber. 111* (1978) 814.
[124] W. C. Kaska, *loc. cit.* [6], p. 13.
[125] M. R. Churchill, F. J. Rotella, E. W. Abel, S. A. Mucklejohn, *J. Am. Chem. Soc. 99* (1977) 5820.
[126] M. R. Churchill, F. J. Rotella, *Inorg. Chem. 17* (1978) 2614.
[127] L. Cosslett, L. A. P. Kane-Maguire, *J. Organomet. Chem. 178* (1979) C17.
[128] P. Lennon, M. Malhavarao, A. Rosan, M. Rosenblum, *J. Organomet. Chem. 108* (1976) 93.
[129] B. E. Boland-Lussier, M. R. Churchill, R. P. Hughes, A. L. Rheingold, *Organometallics 1* (1982) 628, 635.
[130] N. E. Kolobova, V. V. Skripkin, G. G. Alexandrov, Y. T. Struchkov, *J. Organomet. Chem. 169* (1979) 293.
[131] A. J. Carty, G. N. Mott, N. J. Taylor, G. Ferguson, M. A. Khan, P. J. Roberts, *J. Organomet. Chem. 149* (1978) 345.
[132] A. J. Carty, G. N. Mott, N. J. Taylor, J. E. Yule, *J. Am. Chem. Soc. 100* (1978) 3051.
[133] Y. S. Wong, H. N. Paik, P. C. Chieh, A. J. Carty, *J. Chem. Soc. Chem. Commun. 1975,* 309.
[134] J. Evans, D. V. Howe, B. F. G. Johnson, J. Lewis, *J. Organomet. Chem. 61* (1973) C48.

[135] M. Gower, G. R. John, L. A. P. Kane-Maguire, T. I. Odiaka, A. Salzer, *J. Chem. Soc. Dalton Trans. 1979,* 2003.
[136] G. Schiavon, C. Paradisi, *J. Organomet. Chem. 243* (1983) 351.
[137] N. G. Connelly, R. M. Mills, M. W. Whiteley, P. Woodward, *J. Chem. Soc. Chem. Commun. 1981,* 17.
[138] A. Sanders, T. Bauch, C. V. Magatti, C. Lorenc, W. P. Giering, *J. Organomet. Chem. 107* (1976) 359.
[139] H. Schmidbaur, G. Blaschke, *Z. Naturforsch. B35* (1980) 584.
[140] D. L. Davies, A. F. Dyke, S. A. R. Knox, M. J. Morris, *J. Organomet. Chem. 215* (1981) C30.
[141] H. Werner, R. Werner, *J. Organomet. Chem. 174* (1979) C63.
[142] M. R. Churchill, B. G. DeBoer, J. R. Shapley, J. B. Keister, *J. Am. Chem. Soc. 98* (1976) 2357.
[143] M. R. Churchill, B. G. DeBoer, *Inorg. Chem. 16* (1977) 1141.
[144] H.-F. Klein, *Angew. Chem. 92* (1980) 362; *Angew. Chem. Int. Ed. Engl. 19* (1980) 362.
[145] H.-F. Klein, R. Hammer, *Angew. Chem. 88* (1976) 61; *Angew. Chem. Int. Ed. Engl. 15* (1976) 42.
[146] H. H. Karsch, H.-F. Klein, C. G. Kreiter, H. Schmidbaur, *Chem. Ber. 107* (1974) 3692.
[147] D. J. Brauer, C. Krüger, P. J. Roberts, Y.-H. Tsay, *Chem. Ber. 107* (1974) 3706.
[148] R. A. Grey, L. R. Anderson, *Inorg. Chem. 16* (1977) 3187.
[149] H. Schmidbaur, G. Blaschke, H. J. Füller, H. P. Scherm, *J. Organomet. Chem. 160* (1978) 41; T. Costa, H. Schmidbaur, *Chem. Ber. 115* (1982) 1367.
[150] R. L. Lapinski, H. Yue, R. A. Grey, *J. Organomet. Chem. 174* (1979) 213.
[151] T. E. Fraser, H. J. Füller, H. Schmidbaur, *Z. Naturforsch. B34* (1979) 1218.
[152] R. Feser, H. Werner, *Angew. Chem. 92* (1980) 960; *Angew. Chem. Int. Ed. Engl. 19* (1980) 940.
[153] H. Werner, R. Feser, W. Paul, L. Hofmann, *J. Organomet. Chem. 219* (1981) C29.
[154] H. Werner, L. Hofmann, W. Paul, *J. Organomet. Chem. 236* (1982) C65.
[155] W. C. Kaska, R. F. Reichelderfer, *J. Organomet. Chem. 78* (1974) C47.
[156] G. Blaschke, H. Schmidbaur, W. C. Kaska, *J. Organomet. Chem. 182* (1979) 251.
[157] N. L. Holy, N. C. Baenziger, R. M. Flynn, *Angew. Chem. 90* (1978) 732; *Angew. Chem. Int. Ed. Engl. 17* (1978) 686.
[158] G. Bombieri, G. Tresoldi, F. Faraone, G. Bruno, P. Caroli-Belluco, *Inorg. Chim. Acta 57* (1982) 1.
[159] G. Tresoldi, A. Recca, P. Finocchiaro, F. Faraone, *Inorg. Chem. 20* (1981) 3103.
[160] F. Heydenreich, A. Mollbach, G. Wilke, H. Dreeskamp, E. G. Hoffmann, G. Schroth, K. Seevogel, W. Stempfle, *Isr. J. Chem. 10* (1972) 293.
[161] W. Keim, F. H. Kowaldt, R. Goddard, C. Krüger, *Angew. Chem. 90* (1978) 493; *Angew. Chem. Int. Ed. Engl. 17* (1978) 466.
[162] W. Keim, R. F. Mason, P. Glockner, US-Pat. 3647914 (1972).
[163] H. Schmidbaur, G. Blaschke, H. P. Scherm, *Chem. Ber. 112* (1979) 3311.
[164] H. Schmidbaur, A. Mörtl, B. Zimmer-Gasser, *Chem. Ber. 114* (1981) 3161.
[165] H. Schmidbaur, H. P. Scherm, *Chem. Ber. 111* (1978) 797.
[166] H. Schmidbaur, H. J. Füller, V. Bejenke, A. Frank, G. Huttner, *Chem. Ber. 110* (1977) 3536.
[167] H. Schmidbaur, O. Gasser, C. Krüger, J. C. Sekutowski, *Chem. Ber. 110* (1977) 3517.
[168] H. Schmidbaur, G. Müller, *Angew. Chem. 90* (1978) 126; *Angew. Chem. Int. Ed. Engl. 17* (1978) 126.
[169] G. Müller, U. Schubert, H. Schmidbaur, *Chem. Ber. 112* (1979) 3302.
[170] H. H. Karsch, H.-F. Klein, H. Schmidbaur, *Chem. Ber. 107* (1974) 93.
[171] H. Schmidbaur, U. Deschler, B. Milewski-Mahrla, *Angew. Chem. 93* (1981) 598; *Angew. Chem. Int. Ed. Engl. 20* (1981) 586.
[172] J. M. Bassett, J. R. Mandl, H. Schmidbaur, *Chem. Ber. 113* (1980) 1145.
[173] H. Schmidbaur, J. R. Mandl, *Angew. Chem. 89* (1977) 679; *Angew. Chem. Int. Ed. Engl. 16* (1977) 640.
[174] K. F. Zinkgräf, Dissertation, Universität Heidelberg 1968.
[175] B. L. Barnett, C. Krüger, *J. Cryst. Mol. Struct. 2* (1972) 271.
[176] B. L. Booth, K. G. Smith, *J. Organomet. Chem. 178* (1979) 361.
[177] B. L. Booth, K. G. Smith, *J. Organomet. Chem. 220* (1981) 219.
[178] J. R. Moss, J. C. Spiers, *J. Organomet. Chem. 182* (1979) C20.
[179] N. J. Kermode, M. F. Lappert, B. W. Skelton, A. H. White, *J. Chem. Soc. Chem. Commun. 1981,* 698.
[180] N. J. Kermode, M. F. Lappert, B. W. Skelton, A. H. White, J. Holton, *J. Organomet. Chem. 228* (1982) C71.
[181] O. J. Scherer, H. Jungmann, *Z. Naturforsch. B36* (1981) 1663.
[182] O. J. Scherer, H. Jungmann, *J. Organomet. Chem. 228* (1982) C61.
[183] D. C. L. Perkins, R. J. Puddephatt, M. C. Rendle, C. F. H. Tipper, *J. Organomet. Chem. 195* (1980) 105.
[184] P. Overbusch, G. van Koten, D. M. Grove, A. L. Spek, A. J. M. Duisenberg, *Inorg. Chem. 21* (1982) 3254.
[185] R. J. Puddephatt, *J. Chem. Soc. Chem. Commun. 1982,* 614.
[186] P. A. Arnup, M. C. Baird, *Inorg. Nucl. Chem. Lett. 5* (1969) 65.
[187] G. Fronza, P. Bravo, C. Ticozzi, *J. Organomet. Chem. 157* (1978) 299.
[188] E. T. Wilewski, J. L. Silver, M. D. Jansson, J. L. Burmeister, *J. Organomet. Chem. 102* (1976) 365.
[189] H. Koezuka, G. E. Matsubayashi, T. Tanaka, *Inorg. Chem. 15* (1976) 417.
[190] K. Itoh, M. Fukui, Y. Ishii, *J. Organomet. Chem. 129* (1977) 259.
[191] R. M. Buchanan, C. G. Pierpont, *Inorg. Chem. 18* (1979) 3608.
[192] P. Bravo, G. Fronza, C. Ticozzi, *J. Organomet. Chem. 111* (1976) 361.
[193] H. Nishiyama, K. Itoh, Y. Ishii, *J. Organomet. Chem. 87* (1975) 129.
[194] Y. Oosawa, T. Miyamoto, T. Saito, Y. Sasaki, *Chem. Lett. 1975,* 33.
[195] Y. Oosawa, T. Saito, Y. Sasaki, *Chem. Lett. 1975,* 1259.
[196] H. Takahashi, Y. Oosawa, A. Kobayashi, T. Saito, Y. Sasaki, *Chem. Lett. 1976,* 15.
[197] H. Takahashi, Y. Oosawa, A. Kobayashi, T. Saito, Y. Sasaki, *Bull. Chem. Soc. Jpn. 50* (1977) 1771.
[198] Y. Oosawa, H. Urabe, T. Saito, Y. Sasaki, *J. Organomet. Chem. 122* (1976) 113.
[199] N. Sugita, T. Miyamoto, Y. Sasaki, *Chem. Lett. 1976,* 659.
[200] M. Kato, H. Urabe, Y. Oosawa, T. Saito, *Chem. Lett. 1976,* 51.
[201] M. Kato, H. Urabe, Y. Oosawa, T. Saito, Y. Sasaki, *J. Organomet. Chem. 121* (1976) 81.
[202] K. Itoh, H. Nishiyama, T. Ohnishi, Y. Ishii, *J. Organomet. Chem. 76* (1974) 401.
[203] M. F. Hirai, M. Miyasaka, K. Itoh, Y. Ishii, *J. Organomet. Chem. 160* (1978) 25.
[204] M. F. Hirai, M. Miyasaka, K. Itoh, Y. Ishii, *J. Organomet. Chem. 165* (1979) 391.
[205] M. F. Hirai, M. Miyasaka, K. Itoh, Y. Ishii, *J. Chem. Soc. Dalton Trans. 1979,* 1200.
[206] C. G. Pierpont, H. H. Downs, K. Itoh, H. Nishiyama, Y. Ishii, *J. Organomet. Chem. 124* (1977) 93.
[207] G. Tresoldi, F. Faraone, P. Piraino, F. A. Bottino, *J. Organomet. Chem. 231* (1982) 265.
[208] G. Wilkinson, F. G. A. Stone, E. W. Abel: *Comprehensive Organometallic Chemistry,* Vol. 2, Pergamon, Oxford 1982.
[209] H. Schmidbaur, R. Franke, *Angew. Chem. 85* (1973) 449; *Angew. Chem. Int. Ed. Engl. 12* (1973) 416.
[210] H. Schmidbaur, J. Adlkofer, W. Buchner, *Angew. Chem. 85* (1973) 448; *Angew. Chem. Int. Ed. Engl. 12* (1973) 415.
[211] H. Schmidbaur, J. Adlkofer, M. Heimann, *Chem. Ber. 107* (1974) 3697.
[212] Y. Yamamoto, H. Schmidbaur, *J. Organomet. Chem. 96* (1975) 133.
[213] H. Schmidbaur, R. Franke, *Chem. Ber. 108* (1975) 1321.
[214] H. Schmidbaur, R. Franke, *Inorg. Chim. Acta 13* (1975) 79.
[215] H. Schmidbaur, J. R. Mandl, A. Wohlleben-Hammer, A. Fügner, *Z. Naturforsch. B33* (1978) 1325.
[216] Y. Yamamoto, Z. Kanda, *Bull. Chem. Soc. Jpn. 52* (1979) 2560.
[217] Y. Yamamoto, *Chem. Lett. 1980,* 311.
[218] A. Schier, H. Schmidbaur, *Z. Naturforsch. B37* (1982) 1518.
[219] H. Schmidbaur, M. Heimann, *Z. Naturforsch. B29* (1974) 485.
[220] H. Schmidbaur, R. Franke, *Inorg. Chem. Acta 13* (1975) 84.
[221] H. Schmidbaur, J. R. Mandl, A. Frank, G. Huttner, *Chem. Ber. 109* (1976) 466.
[222] H. Schmidbaur, J. R. Mandl, F. E. Wagner, D. F. van de Vondel, G. P. van der Kelen, *J. Chem. Soc. Chem. Commun. 1976,* 170.
[223] H. Schmidbaur, H. P. Scherm, *Chem. Ber. 110* (1977) 1576.
[224] G. Nardin, L. Randaccio, E. Zangrando, *J. Organomet. Chem. 74* (1974) C23.
[225] H. Schmidbaur, J. R. Mandl, W. Richter, V. Bejenke, A. Frank, G. Huttner, *Chem. Ber. 110* (1977) 2236.
[226] H. Schmidbaur, H. P. Scherm, U. Schubert, *Chem. Ber. 111* (1978) 764.
[227] W. Ludwig, W. Meyer, *Helv. Chim. Acta 65* (1982) 934.
[228] P. K. Mehrotra, R. Hoffmann, *Inorg. Chem. 17* (1978) 2187.
[229] H. Schmidbaur, H. P. Scherm, *Z. Naturforsch. B34* (1979) 1347.
[230] K. C. Dash, H. Schmidbaur "Gold Complexes as Metallo-Drugs" in H. Sigel: *Metal Ions in Biological Systems,* Vol. *14,* p. 179, Marcel Dekker, New York 1982.
[231] H. Schmidbaur, J. R. Mandl, *Naturwissenschaften 63* (1976) 585.
[232] J. P. Fackler, J. D. Basil, *Organometallics 1* (1982) 871.
[233] P. Jandik, U. Schubert, H. Schmidbaur, *Angew. Chem. 94* (1982) 74; *Angew. Chem. Int. Ed. Engl. 21* (1982) 73; *Angew. Chem. Suppl. 1982,* 1.
[234] H. Schmidbaur, G. Müller, K. C. Dash, B. Milewski-Mahrla, *Chem. Ber. 114* (1981) 441.
[235] H. Schmidbaur, J. R. Mandl, J. M. Bassett, G. Blaschke, B. Zimmer-Gasser, *Chem. Ber. 114* (1981) 4333.
[236] Y. Yamamoto, H. Schmidbaur, *J. Organomet. Chem. 97* (1975) 479.

[237] H. Schmidbaur, C. E. Zybill, G. Müller, C. Krüger, *Angew. Chem. 95* (1983) 753; *Angew. Chem. Int. Ed. Engl. 22* (1983) 729.
[238] J. Stein, J. P. Fackler, C. Paparizos, H. W. Chen, *J. Am. Chem. Soc. 103* (1981) 2192.
[239] C. Krüger, J. C. Sekutowski, H. J. Füller, O. Gasser, H. Schmidbaur, *Isr. J. Chem. 15* (1976/77) 149.
[240] D. Seyferth, S. O. Grim, *J. Am. Chem. Soc. 83* (1961) 1610.
[241] N. A. Nesmeyanov, V. M. Novikov, O. A. Reutov, *Izv. Akad. Nauk SSSR Otd. Khim. Nauk 1964*, 722.
[242] N. A. Nesmeyanov, V. M. Novikov, O. A. Reutov, *J. Organomet. Chem. 4* (1965) 202.
[243] H. Schmidbaur, K. H. Räthlein, *Chem. Ber. 107* (1974) 102.
[244] Y. Yamamoto, H. Sugimoto, *Bull. Chem. Soc. Jpn. 53* (1980) 3176.
[245] D. R. Mathiason, N. E. Miller, *Inorg. Chem. 7* (1968) 709.
[246] H. Schmidbaur, O. Gasser, T. E. Fraser, E. A. V. Ebsworth, *J. Chem. Soc. Chem. Commun. 1977*, 334.
[247] H. Schmidbaur, T. Costa, *Chem. Ber. 114* (1981) 3063.
[248] H. Schmidbaur, G. Müller, *Monatsh. Chem. 111* (1980) 1233.
[249] H. Schmidbaur, W. Wolf, *Chem. Ber. 108* (1975) 2851.
[250] D. J. Burton, R. Takei, S. Shin-ya, *J. Fluorine Chem. 18* (1981) 197.
[251] N. C. Baenziger, R. M. Flynn, D. C. Swenson, N. L. Holy, *Acta Crystallogr. B34* (1978) 2300.

# Electron-Rich Half-Sandwich Complexes—Metal Bases *par excellence*

**By Helmut Werner***

*Dedicated to Professor Ernst Otto Fischer on the occasion of his 65th birthday*

Electron-rich, half-sandwich complexes of the type $C_nR_nML_2$ or $C_nR_nMLL'$ are built up of an aromatic five- or six-membered ring, a $d^8$-metal, and either a pair of two-electron donors or an equivalent chelating ligand. Such complexes behave like Lewis bases and react with a wide variety of electrophiles, El or ElX, to form products with a new metal-element bond. According to their reactivity they are comparable to the Vaska-type compounds. Certain of the products obtained after addition of the electrophile undergo interesting subsequent reactions in which, for example, metal complexes containing molecules that are unstable in the free state, such as CS, CSe, $CH_2S$, $CH_2Se$, $CH_2Te$, $CH_3CHS$, $CH_3CHSe$, $CH_2{=}C{=}S$, $CH_2{=}C{=}Se$, and $CH_2{=}C{=}Te$ are formed. Moreover, cycloadditions as well as reactions with coordinatively unsaturated transition-metal compounds which result in formation of heterometal binuclear complexes demonstrate that the metal bases $C_nR_nML_2$ and $C_nR_nMLL'$ are valuable synthetic building blocks. Furthermore, very recent investigations have indicated links between metal basicity and the problem of C—H activation.

## 1. Introduction

Half-sandwich complexes are almost as old as ferrocene—the progenitor of all sandwich compounds. Shortly after the structure of dicyclopentadienyliron had been accurately determined and analogous metallocenes had been synthesized, *Fischer* und *Hafner*[1] reported the synthesis of tetracarbonyl(cyclopentadienyl)vanadium, $C_5H_5V(CO)_4$. Later work—involving highly competitive research efforts in Munich and Harvard—produced the homologous manganese and cobalt complexes $C_5H_5Mn(CO)_3$ and $C_5H_5Co(CO)_2$[2,3]. Because the metal atom in these compounds is enclosed on only *one* side by a $C_nH_n$-disk (as in the metallocenes) but is bonded to conventional ligands on the other side, the structure resembles a "half-sandwich". This term was later applied to similar compounds: instead of CO, ligands such as NO, halogenides, isocyanides, phosphanes, and olefins were now coordinated to the metal, and instead of $C_5H_5$ other ring systems such as $C_4H_4$, $C_6H_6$, $C_7H_7$ or $C_8H_8$ were employed[4].

There was no indication in early publications[2,3] that half-sandwich complexes can behave as *metal bases, i.e.* that they react with electrophiles, El or ElX, to form new metal-element bonds[5]. Such behavior was hardly to be expected since both the carbonyl(cyclopentadienyl)metals mentioned above and most of the analogous compounds with the general formula $C_mH_mML_n$ are 18-electron complexes. At least in a formal sense these possess no lone pair of electrons capable of forming a covalent bond with a Lewis acid. Vaska-type compounds *trans*-$[MX(CO)L_2]$ (M = Rh, Ir; X = Cl, Br, I, $N_3$; L = $PR_3$, $P(OR)_3$, $AsR_3$ *etc.*) do possess such a lone pair of electrons and react not only with known electrophiles, *e.g.* HCl, $CH_3I$, $CH_3COCl$, $BX_3$, $SO_2$, *etc.* but also with $H_2$ or $R_3SiH$ by oxidative addition[6]. The Vaska-type compounds are thus typical metal bases, and it is not only thanks to their chemistry that the concept of *metal basicity* has become increasingly known since the beginning of the seventies[5].

The central atom in the *trans*-$[MX(CO)L_2]$ complexes is a *$d^8$-system*, as is the case in the dicarbonyl(cyclopentadienyl)metal compounds $C_5H_5M(CO)_2$ (M = Co, Rh, Ir). In an article which indicated the great significance of the nucleophilicity of transition-metal atoms in complexes having full valence shells, *Wilkinson et al.*[7] mentioned that

[*] Prof. Dr. H. Werner
Institut für Anorganische Chemie der Universität
Am Hubland, D-8700 Würzburg (Germany)

$C_5H_5Co(CO)_2$ is rapidly decomposed in strong acids, such as $H_2SO_4$ or $BF_3 \cdot H_2O$, whereas in weakly acid media, such as $CF_3CO_2H$, it is stable for at least 10 minutes. It did not prove possible using NMR spectroscopy to confirm the proposal that a cation $[C_5H_5CoH(CO)_2]^+$ was formed in the process.

The first evidence for such an interaction between the central atom in $C_5H_5Co(CO)_2$ and an electrophile was provided by *Kemmitt et al.*[8]. They isolated 1:1 adducts from the reaction of the half-sandwich complex with $HgX_2$ (X = Cl, Br, I), which they then compared with known compounds such as $C_4H_8S \cdot HgCl_2$, and whose formation they interpreted as a Lewis acid/Lewis base reaction. This suggestion was confirmed shortly thereafter[9] by X-ray crystallographic studies on $[C_5H_5Co(CO)_2HgCl_2]$. Similarly, with $HgCl_2$ and $HgBr_2$, $C_5H_5Rh(CO)_2$ forms 1:1 adducts whose IR data indicate the presence of a direct metal-metal bond[10].

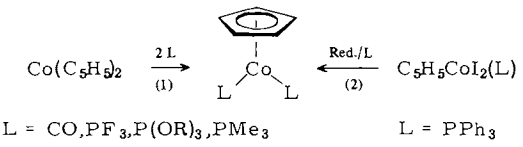
Further development of this field was stimulated by the work of *Graham et al.* which appeared in 1970/71[11]. They were the first to show that the compound $C_5H_5Rh(CO)(PMe_2Ph)$, *i.e.* a derivative of $C_5H_5Rh(CO)_2$, reacts with $Cl_2$, $Br_2$, $CH_3COBr$, and $CF_3COCl$ at low temperatures to form ionic compounds $[C_5H_5RhR(CO)PMe_2Ph]X$ (R = Cl, Br, $COCH_3$, $COCF_3$; X = halogen) which can be isolated as stable salts after exchanging $X^\ominus$ for $BPh_4^\ominus$[11a]. The iridium complex $C_5H_5Ir(CO)PPh_3$ not only behaves similarly but is also capable of forming a hydridometal cation with HBr in $CH_2Cl_2$ at −70 °C. This cation, $[C_5H_5IrH(CO)PPh_3]^+$, can again be isolated as the $BPh_4$ salt[11b]. Kinetic data for the compounds $C_5H_5M(CO)PPh_3$ indicate that the metal basicity increases along the sequence Co ≲ Rh < Ir (*i.e.* within the group from top to bottom) and that there is also an increase in basicity along the sequence $C_5H_5Co(CO)PPh_3$ < $C_5H_5Co(CO)PMePh_2$ < $C_5H_5Co(CO)PMe_2Ph$[11c]. It thus became evident that a better donor ligand would increase not only the electron density but also the nucleophilicity of the metal—an observation which has since been confirmed in many different ways in our own investigations.

## 2. Metal Bases having Five-Membered Ring Ligands

### 2.1. Synthetic Methods

Both ligand exchange reactions and redox reactions have been used for the preparation of metal bases having five-membered ring ligands. Thus, the dicarbonyl complex $C_5H_5Co(CO)_2$ mentioned in the introduction was synthesized from cobaltocene and CO by displacing one of the cyclopentadienyl ligands by two CO groups[2,3]. In this case, the ligand exchange is associated with reduction of cobalt(II) to cobalt(I). In the same way, the compounds $C_5H_5Co(PF_3)_2$[12] and $C_5H_5Co[P(OR)_3]_2$ (R = Me, Et, Ph)[13] are also accessible. Analogously, $C_5H_5Co(PMe_3)_2$ may be prepared according to reaction (1)[14], although this method is hardly recommended because of the amount of trimethylphosphane required.

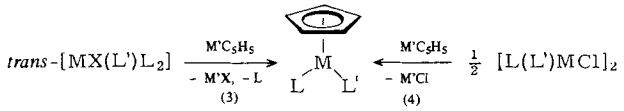
A reductive method starting from a cobalt(III) compound is given in reaction (2)[15]. The reducing agent is




*i*PrMgBr. The bis(triphenylphosphane)cobalt(I) complex $C_5H_5Co(PPh_3)_2$ is formed without having to add $PPh_3$ to the reaction mixture, although in low yield. The rhodium compound $C_5H_5Rh(PPh_3)_2$ is obtainable analogously[15]. In addition, starting from $[C_5Me_5RhCl_2]_2$ and L (molar ratio 1:4; L = $PMe_3$, $PMe_2H$, $PMe_2Ph$, $P(OMe)_3$) and using Na/Hg as the reducing agent, some of the half-sandwiches can be prepared almost quantitatively[16]. The reduction of $[C_5H_5Rh(C_2F_4Br)(PPh_3)Br]$ with Zn is highly unusual in that it yields the tetrafluoroethylene complex $C_5H_5Rh(C_2F_4)PPh_3$[11d]—an analogue of the compounds $C_5H_5Rh(C_2H_3R')PR_3$ obtained in reactions (4) and (7).

The most direct route to metal bases having five-membered ring ligands is offered by the exchange of coordinated halides for $C_5H_5$, $C_5H_4R$, $C_5Me_5$, or $C_9H_7$. Thus, for example, the cobalt complexes $C_5H_5CoL_2$ (L = $PMe_2Ph$, $PMePh_2$[17], $PPh_3$[18], $PEt_3$[19], and $PMe_3$[20]) may be prepared by allowing the appropriate paramagnetic cobalt(I) compound $ClCo(PR_3)_3$ to react with $M'C_5H_5$ (M' = Na, Tl) or $LiC_5Me_5$. $C_5H_5Co(PPh_3)_2$ can also be obtained from $CoH(N_2)(PPh_3)_3$ and $C_5H_6$[21].

Both Vaska-type compounds and binuclear complexes $[L_2MCl]_2$ and $[L(L')MCl]_2$ (M = Rh, Ir) are suitable educts for the preparation of the complexes $C_5H_5ML_2$ and $C_5H_5MLL'$ (M = Rh, Ir), respectivley, by substitution of a halide- by a cyclopentadienyl-ligand. Several examples of such syntheses are collected together in reactions (3) and (4).




M = Rh; L = L' = $PPh_3$[22]
M = Rh; L = $PPh_3$, L' = $C_2H_4$[11b]
M = Rh, Ir; L = $PPh_3$, L' = CO[11b]
M = Rh, Ir; L = $PPh_3$, L' = CS[23]
M = Rh, Ir; L = P(*i*Pr)$_3$, L' = $C_2R_2$[24,25]
M = Rh; L = L' = $P(OR)_3$[26]
M = Rh; L = $PR_3$, L' = $P(OR')_3$[27]
M = Rh; L = $PMe_3$, L' = $C_2H_3R'$[28]
M = Rh; L = P(*i*Pr)$_3$, L' = $C_2H_4$[28]
M = Ir; L = P(*i*Pr)$_3$, L' = $C_8H_{14}$[25]

According to reaction (3), the preparation of $C_5H_5Rh(PPh_3)_2$ involves a reaction type related to that used for the synthesis of $C_5H_5Rh(PMe_3)_2$[29,30] and $C_9H_7Rh(PMe_3)_2$[31] from $[Rh(PMe_3)_4]Cl$; in the cation of this salt the rhodium atom is square-planar coordinated[32]. Similarly, the compounds $(C_5H_4R)Rh(PMe_3)_2$ (R = *i*Pr, *t*Bu)[33] and $C_5Me_5Rh(PMe_3)_2$[16], which are analogous to $C_5H_5Rh(PMe_3)_2$, are obtained by allowing $[(PMe_3)_2RhCl]_2$ to react with $TlC_5H_4R$ or $NaC_5Me_5$.

Half-sandwich complexes of the type $C_5R_5M(CO)L$ and $C_5R_5M(C_2H_4)L$ (M = Co, Rh; R = H, Me) are also frequently prepared by ligand displacements, as in reactions (5) and (7). Replacement of CO by a phosphane or phosphite generally takes place under milder conditions than the displacement of ethylene. Kinetic studies by *Schuster-*

*Woldan* and *Basolo*[34] confirmed an A- or $S_N2$-type mechanism for the formation of $C_5H_5Rh(CO)L$ from $C_5H_5Rh(CO)_2$ and L [see reaction (5)]. Disubstitution as shown in reactions (6) and (8) has been observed only in a few instances up till now. Since the π-acceptor ligand CO or $C_2H_4$ is bonded much more firmly in the compounds $C_5H_5M(CO)L$ and $C_5H_5M(C_2H_4)L$ than in the educts, it is evident that reactions (6) and (8) involve a very high activation energy.

$$C_5R_5M(CO)_2 \xrightarrow[-CO]{+L} C_5R_5M(CO)L \xrightarrow[-CO]{+L} C_5R_5ML_2 \quad (5)\ (6)$$

$$C_5R_5M(C_2H_4)_2 \xrightarrow[-C_2H_4]{+L} C_5R_5M(C_2H_4)L \xrightarrow[-C_2H_4]{+L} C_5R_5ML_2 \quad (7)\ (8)$$

*Reaction (5):*

R=H; M=Co; L=$PPh_3$[34], $PMePh_2$, $PMe_2Ph$, $P(C_6H_{11})_3$[11c], $PMe_3$[35,36]

R=H; M=Rh; L=$PPh_3$, $P(nBu)_3$, $P(OMe)_3$[34], $PMe_2Ph$[11a], $PMe_3$[37]

R=Me; M=Co; L=$PMe_3$[20]

R=Me; M=Rh; L=$PMe_3$, $P_2Me_4$[38]

*Reaction (6):*

R=H; M=Rh; L=$P(OMe)_3$[34]

*Reaction (7):*

R=H; M=Co; L=$PMe_3$, $P(OMe)_3$[39]

R=H; M=Rh; L=$PMe_3$*, $P(nBu)_3$*[40]

R=Me; M=Rh; L=$PMe_3$, $P_2Me_4$[16]

*Reaction (8):*

R=H; M=Rh; L=$PMe_3$*, $PEt_3$*, $P(OEt)_3$*, $P(OC_6H_4Me)_3$*[40]

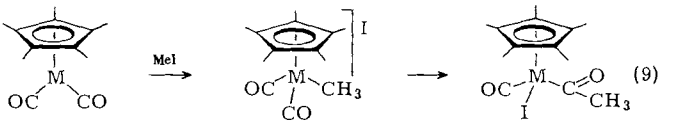
* not isolated, characterized by NMR spectroscopy.

The displacement of a phosphane ligand in $C_5H_5Co(PMe_3)_2$ by CO[41] or CNR (R=Me, *t*Bu, Ph)[42] is also possible. Interestingly, the corresponding reaction of $C_5Me_5Co(PMe_3)_2$ with CO yields the monocarbonyl compound, while with CNMe the bis(isocyanide) complex $C_5Me_5Co(CNMe)_2$ is formed[20].

## 2.2. Complexes of the Type $C_5R_5ML_2$

### 2.2.1. Dicarbonyl- and Bis(olefin)metal Complexes

$C_5H_5Co(CO)_2$ is not stable in acids[7], and nothing is known about the reactions of $C_5H_5Rh(CO)_2$ with HX to form $[C_5H_5RhH(CO)_2]X$. Dicarbonyl(cyclopentadienyl)metal compounds are thought to be inert toward methyl iodide[43], which is also to be expected in view of the good acceptor properties of CO and the resulting relatively low electron density at the metal. However, if $C_5H_5$ is replaced by $C_5Me_5$ and the central atom thus becomes more *electron-rich*, both $C_5Me_5Rh(CO)_2$ and $C_5Me_5Ir(CO)_2$ react with MeI [reaction (9)][44]. Whereas for M=Ir the reaction does not go beyond the stage of the salt-like complex **3**, the corresponding rhodium compound cannot be isolated and very rapidly yields the product **4** with CO insertion (or $CH_3$ migration[45a]). More recently, evidence has been presented that protonation of $C_5Me_5Ir(CO)_2$ gives the corresponding hydridometal cation[45b].




(9)

**1**,**2** **3** **4**

**1**,**4**: M = Rh; **2**,**3**: M = Ir

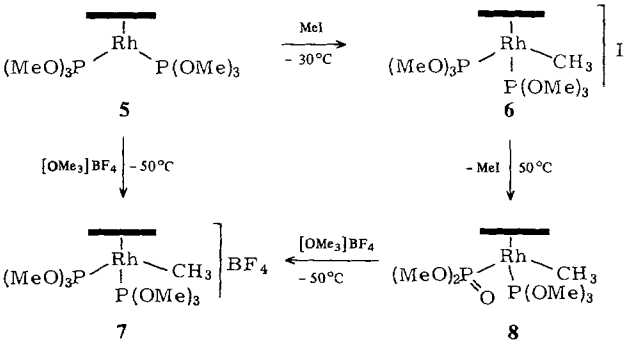
With HCl the compound $C_5H_5Rh(C_2H_4)_2$ forms the ethylrhodium(III) compound $C_5H_5RhC_2H_5(C_2H_4)Cl$[46]. A conjectured intermediate hydrido(olefin)metal cation could not be detected either here or in the reactions of mixed bis(olefin) complexes of the type $C_5H_5Rh(C_2H_4)(C_2H_3X)$ (X=F, CN, $CO_2Me$) with HCl[47]. That the rate of the reaction of $C_5H_5Rh(C_2H_3X)_2$ with HCl increases along the sequence $X=CN<CO_2Me<CH_3$[47], supports the postulated protonation at the metal. Since the donor character of the olefin increases along the same sequence, the resulting increase in electron density at the metal should favor electrophilic addition.

### 2.2.2. Bis(phosphite)metal Complexes

In addition to the carbonyl(phosphane) derivatives, the bis(phosphite) compounds have also played a major role in establishing the metal basicity of cyclopentadienylmetal complexes of the type $C_5R_5ML_2$ or $C_5R_5MLL'$. Although the first representative of this group, the complex $C_5H_5Rh[P(OMe)_3]_2$ had already been described in 1966[34], its reactivity was not investigated in detail at that time.

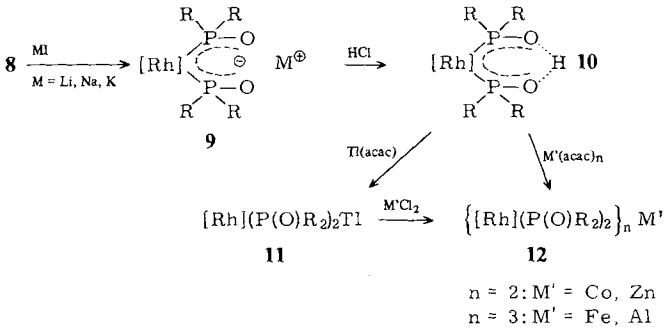
We were closely associated with compounds of this type in our endeavors to find new synthetic routes to trinuclear complexes of the "super-sandwich" type[48], $[C_5H_5Co(\mu\text{-}P(OR)_2O)_3Co(\mu\text{-}P(OR)_2O)_3CoC_5H_5]$. These compounds were initially prepared by pyrolysis of $C_5H_5Co[P(OR)_3]_2$ (R=Me, Et)[49], although—as *Kläui* and *Dehnicke*[50], and more recently *Brill et al.*[51] have demonstrated—they are more readily produced starting from cobalt(III)-trialkylphosphite or cobalt(III)-dialkylphosphonate complexes.

Attempts to obtain analogous trinuclear rhodium complexes starting from $C_5H_5Rh[P(OR)_3]_2$ proved to be unsuccessful[52,53]. We discovered from these studies, however, that the bis(phosphite) compounds $C_5H_5Rh[P(OR)_3]_2$ are good nucleophiles and that they react (at least for R=Me) even under very mild conditions with Brønsted acids, methyl iodide, or *Meerwein*'s reagent, $[OMe_3]BF_4$, to form the corresponding rhodium(III) complexes[54,55]. For the methylation reaction the sequence given in Scheme 1 has been confirmed[54].



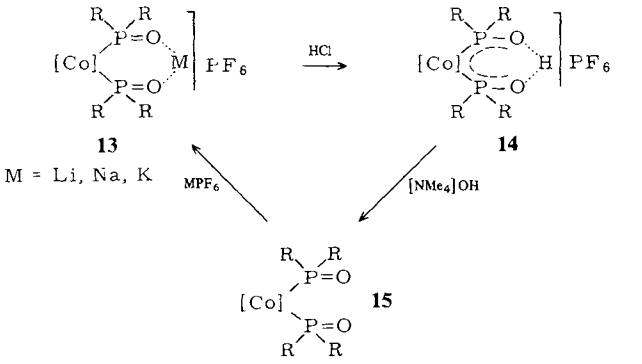

Scheme 1. The bar symbolizes a cyclopentadienyl ligand.

The iodide salt **6** obtained by electrophilic addition at −30°C in acetone eliminates methyl iodide when heated to form the phosphonate compound **8**, which is an isomer of the starting complex **5**. Evidently, the rupture of an O–$CH_3$ bond is highly favored kinetically compared to that of a Rh–$CH_3$ bond, an observation in accord with the high metal basicity of **5**. The conversion of **5** into **8** illustrates that trialkylphosphite complexes frequently behave like the intermediate moiety $[R'P(OR)_3]^+$ (R = alkyl) in the Michaelis-Arbuzov reaction and thereby offer a convenient route to metal phosphonate compounds.




Scheme 2. [Rh] = $C_5H_5RhCH_3$; R = OMe.

Proof of this is also to be seen in the subsequent reactions undergone by some of the products obtained from the metal bases $C_5H_5M[P(OMe)_3]_2$. Thus, **8** reacts with alkali metal iodides, for example, to yield rhodium(phosphonate) complexes **9**, which react with HCl to give **10**; the latter presumably contains a six-membered ring having a symmetric OHO bridge[56]. Starting from **10** or **11**, it is possible to prepare polynuclear complexes **12** (see Scheme 2) which are similar to the "super-sandwich" compounds[56,57]. The marked ability of metallabis(phosphonates) to complex alkali metal ions is also illustrated by the fact that the compounds **15** prepared from $(C_5H_4R)Co(CH_3)_2PR'_3$ (see Section 3.2) act as strong complexing agents toward $Li^+$, $Na^+$, and $K^+$. The complexes formed release the alkali metal ion $M^+$ from the coordination sphere only when HCl is added, but not on addition of water (see Scheme 3)[58].



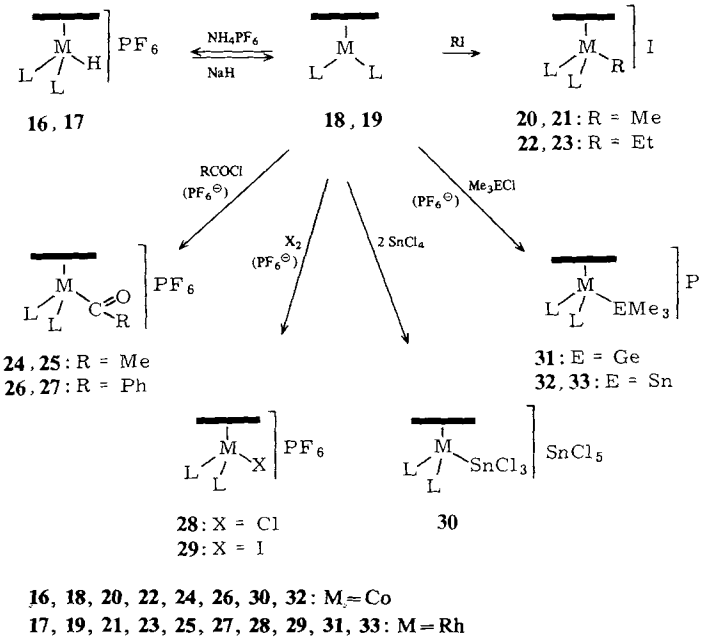

Scheme 3. [Co] = $(C_5H_4R')CoPMe_3$; R' = H, *i*Pr, *t*Bu; R = OMe.

The type of coordination of the $M^+$ cations by the oxygen atoms of the phosphonate groups was established by X-ray analysis of the complex $C_6H_6OsI[P(O)(OMe)_2]_2Na$, which is related to **9** and to the cation of **13**, and which crystallizes with one equivalent of NaI[59]. In this salt there exist intermolecular interactions between the sodium ions and a *pair* of $C_6H_6OsI[P(O)(OMe)_2]_2^-$ anions, with the result that the O=P–Os–P=O unit is no longer planar and the O···O distance relative to that in $C_6H_6OsI[P(O)(OMe)_2]_2H$ (a compound readily comparable with **10**) is substantially increased.

### 2.2.3. *Bis(phosphane)metal Complexes*

Since phosphanes are better donor ligands than phosphites, the $C_5H_5M(PR_3)_2$ complexes should also be stronger metal bases than their phosphite analogues $C_5H_5M[P(OR)_3]_2$. This prediction proved to be true, in particular when $PMe_3$ was used as a phosphane ligand. Whereas the compounds $C_5H_5M[P(OMe)_3]_2$ (M = Co, Rh), for example, can be protonated only with strong acids such as $CF_3CO_2H$ or $HBF_4$[55], the conversion of the phosphane complexes **18** and **19** into **16** and **17**, respectively, can be carried out using $NH_4PF_6$[17,29]. The high basicity of **18** is evidenced very clearly by the fact that the compound reacts slowly even with methanol to form the hydridometal cation $[C_5H_5CoH(PMe_3)_2]^+$[41].

Some typical examples illustrating the reactivity of the complexes **18** and **19** with electrophiles are summarized in Scheme 4[17,29,60]. In addition to the Lewis acids $SnCl_4$, $Me_3SnCl$, and $Me_3GeCl$ also $ZnCl_2$, $HgCl_2$, and CuCl (as a $PMe_3$ adduct) were allowed to react with **18** and compounds having Co–Zn, Co–Hg and Co–Cu bonds isolated[60]. Adducts of boron halides $BX_3$ (X = F, Cl, Br) with **14** are similarly accessible[61].

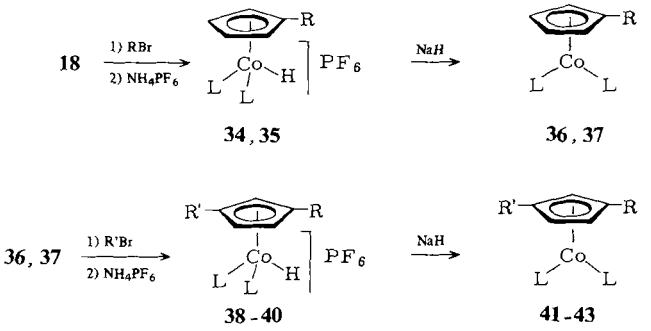



**16**, **18**, **20**, **22**, **24**, **26**, **30**, **32**: M = Co
**17**, **19**, **21**, **23**, **25**, **27**, **28**, **29**, **31**, **33**: M = Rh

Scheme 4. L = $PMe_3$.

The differing behavior of methyl and ethyl iodides, on the one hand, and isopropyl and *tert*-butyl halides, on the other, toward bis(trimethylphosphane) compounds of the type $C_5H_5M(PMe_3)_2$ is quite remarkable. Under the same conditions that **18** reacts with MeI and EtI to form **20** and

**22**, respectively (see Scheme 4), it forms the alkylcyclopentadienyl(hydrido)metal complexes $[(C_5H_4R)CoH(PMe_3)_2]Br$ with *i*PrBr and *t*BuBr[19,62]. The corresponding hexafluorophosphates **34** and **35** (Scheme 5) can readily be converted by NaH into the neutral compounds **36** and **37** which, after further reaction with *i*PrBr or *t*BuBr, afford the *doubly* ring-substituted products **38**, **39**, or **40**. Subsequent deprotonation with NaH yields the complexes **41**—**43**. These also react very rapidly with methyl iodide, *i.e.* an electrophilic addition involving the formation of a $Co-CH_3$ bond is possible even when two bulky substituents are present on the ring. The introduction of a third alkyl group to the cyclopentadienyl ligand, however, is not possible; **41**—**43** are inert toward *i*PrBr and *t*BuBr[19].




**34**, **36**: R = *i*Pr **38**, **41**: R = R' = *i*Pr
**35**, **37**: R = *t*Bu **39**, **42**: R = *i*Pr, R' = *t*Bu
**40**, **43**: R = R' = *t*Bu

Scheme 5. L = $PMe_3$.

It is surprising that in **40** and **43** (R = R' = *t*Bu) rotation about the metal-ring bond is so strongly hindered that *rigid conformers* are present in solution up to a temperature of *ca.* 100°C. It is likely here that the size of the phosphane ligands is an important factor. Even for **42** a frozen conformation can be detected below −10°C. The fact that the rotational barrier is lower than in **43**, and that for **41** there is absolutely no spectroscopic evidence of any hindrance to free rotation can be explained by means of a model based on a "gear wheel mechanism"[19,62]. For a 1,3-$(t\text{Bu})_2C_5H_3$ ring it is clearly not possible for the *tert*-butyl groups to pass the $PMe_3$ ligand as they rotate about the ring-metal axis (despite free rotation about the C-*t*Bu bond). However, if in the *t*Bu groups a $CH_3$ group replaces an H atom, *i.e.* *t*Bu is substituted for *i*Pr, the two ring substituents can probably arrange themselves in such a way that at the moment of passing a phosphane the H atom of the isopropyl group is directed "inwards" and—like the teeth on a gear wheel—fits in-between the methyl groups on the phosphorus (Fig. 1).

MO calculations[63] indicate that the barrier to rotation about the ring-metal bond in half-sandwich complexes of the type $C_5H_5ML_2$ and $C_5H_5ML_3$ is extremely low. Thus, for purely electronic reasons the formation of preferred conformers is not to be expected. Steric effects should thus play the determining role. Recently, using NMR spectroscopy *Pomeroy* and *Harrison*[64] succeeded in demonstrating rotational hindrance in a similar compound $[C_6H_4(t\text{Bu})_2]Ru(CO)(SiCl_3)_2$.

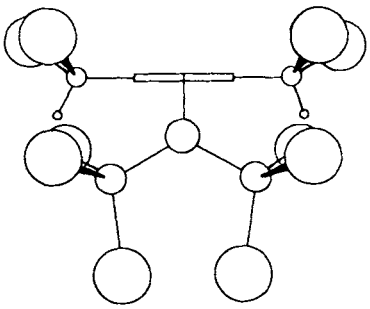
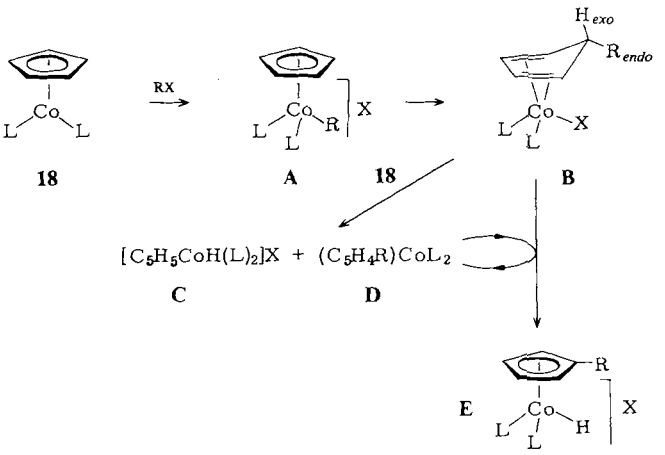


Fig. 1. Proposal based on a model of the space-filling capacity of 1,3-$(i\text{Pr})_2C_5H_3Co(PMe_3)_2$ **41** [62].

A proposal for the mechanism of the highly unusual ring substitution of **18** is shown in Scheme 6[19]. It draws on concepts which help to understand the aromatic nature of cyclopentadienylmetal complexes such as $Fe(C_5H_5)_2$ or $C_5H_5Mn(CO)_3$[4]. We assume that in the initial step—completely analogously to that for the reactions of **18** with methyl and ethyl iodides—an electrophilic addition takes place and the ionic compound **A** is formed; intermediate **B** is produced from **A** by intramolecular rearrangement. Reaction of **B** with the metal base **D**, which acts autocatalytically as indicated in Scheme 6, leads to **E** (**34** and **35** in Scheme 5), which after completing the exchange can be isolated (along with small amounts of $[C_5H_5CoH(L)_2]X$) in more than 90% yield.

Evidence that the hydride hydrogen atom in **E** originates from the cyclopentadienyl ring in **18** (and not from the alkyl halide) is provided by the reaction of $C_5D_5Co(PMe_3)_2$ with *t*BuBr which leads to $[(C_5D_4R)CoD(PMe_3)_2]Br$[19]. Low-temperature NMR data[19] also support the formation of the postulated intermediate **B** as do our recently published results on a rapid H/D exchange between the cations $[C_5Me_5Co(PMe_3)(CNR)_2]^{2+}$ and $CD_3NO_2$ in the presence of traces of $NEt_3$. In this case it is assumed[20] that the intermediate formation of a cobalt(I) complex with an ($\eta^4$-$C_5Me_5$-*exo*-$CD_2NO_2$) ligand occurs.




Scheme 6. L = $PMe_3$; R = *i*Pr, *t*Bu.

The alternative to the proposal outlined in Scheme 6 would be a radical reaction. A one-electron transfer from **18** to the electrophile RX would then initially occur to

form a "contact radical pair", similar to that postulated for the intermediate in the reaction of carbonylmetalate ions $[M(CO)_5]^-$ (M = Mn, Re) with the corresponding halo complexes[65]. Co–R or $C_5H_5$–R bond formation could then occur from the radical pair $\{C_5H_5CoL_2^{\oplus\odot}, RX^{\ominus\odot}\}$.

One reason we believe this alternative is possible, although for RX = MeI, EtI unlikely, is the result of the reaction of **19** with *i*PrBr or *t*BuBr which produces a mixture of $[C_5H_5RhBr(PMe_3)_2]Br$, $[(C_5H_4R)RhBr(PMe_3)_2]Br$ and other compounds which have not yet been identified[33]. We assume that the cations involved are formed *via* free radicals, whose appearance as intermediates seems probable on the basis of CIDNP measurements[33]. A radical cation, $[C_5H_5Rh(PPh_3)_2]^{\oplus\odot}$, is also allegedly produced as an intermediate in the formation of $[(\eta^{10}\text{-}C_{10}H_8)Rh_2(PPh_3)_4](BF_4)_2$ from $C_5H_5Rh(PPh_3)_2$ and $AgBF_4$[66a]. *McKinney*[66b] was also able to synthesize the $BF_4$ salts of the corresponding cobalt complexes, $[C_5H_5CoL_2]^+$ (L = $PPh_3$, $PEt_3$, $PEtPh_2$, $P(OiPr)_3$), both by oxidizing $C_5H_5CoL_2$ and by reaction of $C_5H_5CoXL$ with $TlBF_4$ in the presence of L. Finally, the observation that $C_5Me_5Co(PMe_3)_2$ reacts with methyl iodide to form $[C_5Me_5CoI(PMe_3)_2]I$ and not $[C_5Me_5CoCH_3(PMe_3)_2]I$ fits well into the overall picture of conceivable radical reactions involving electron-rich half-sandwich compounds[20].

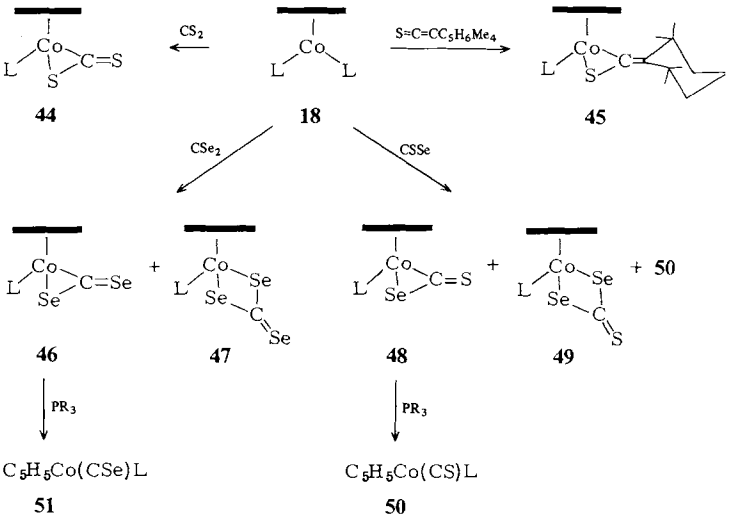
### 2.2.4. $CO_2$ Homologues as Electrophiles

Carbon dioxide, a well-known electrophile, has recently been allowed to react with electron-rich metal compounds, especially in connection with attempts to "activate" $CO_2$ by transition metals. However, there are very few notable results of such attempts[67]; $CO_2$ is evidently too inert toward "soft" bases, among which are the half-sandwich compounds discussed here.

Rather more reactive than $CO_2$ itself are its homologues (often designated as heteroallenes), some of which react very readily with metal bases. The pioneering work in this field was carried out by *Baird* and *Wilkinson*[68], who, as far back as 1966, studied the reactivity of the compounds $RhCl(PPh_3)_3$, $Pd(PPh_3)_4$, and $Pt(PPh_3)_3$ toward $CS_2$. Among others, they isolated the first thiocarbonylmetal complex, *trans*-$[RhCl(CS)(PPh_3)_2]$[69].

That *half-sandwich* compounds behave in a similar way was primarily established by *Yamazaki et al.*[15,22]. By allowing $C_5H_5M(PPh_3)_2$ (M = Co, Rh) to react with $CS_2$ they obtained—albeit in modest yields—the complexes $C_5H_5M(\eta^2\text{-}CS_2)PPh_3$ in which, as in **44**, the carbon disulfide is probably bonded to the metal *via* the C atom and one S atom[70].

Because $C_5H_5Co(PMe_3)_2$ **18** and $C_5H_5Rh(PMe_3)_2$ **19** are stronger metal bases than the analogous triphenylphosphane derivatives, they react significantly faster with $CS_2$ and other $CO_2$ homologues and yield—as shown in Scheme 7 using **18** as example[71–73]—a whole series of novel metal(I) and metal(III) complexes. The initial step in these reactions involves attack of the nucleophilic metal center at the electrophilic C atom of the heteroallene. The subsequent elimination of a phosphane ligand will probably be favored because $PMe_3$ forms—at least with $CS_2$ and $CSe_2$—zwitterionic 1:1 adducts which are rather insoluble in organic solvents and thus precipitate. The heteroallene complexes **46** and **48** react with free trimethyl- or triphenylphosphane to give the corresponding thio- or selenocarbonylcobalt compounds **50** or **51**[71–73]. Brief mention will also be made of the reactivity of **50** and **51** toward electrophilic substrates in Section 2.3.1.

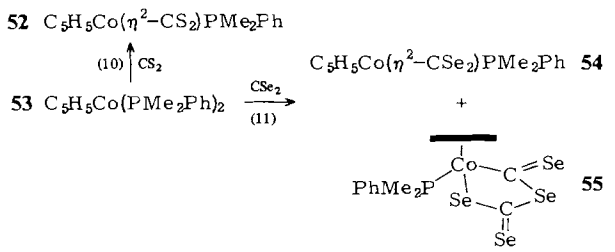



**44** **18** **45** **46** **47** **48** **49** **51** **50**

Scheme 7. L = $PMe_3$.

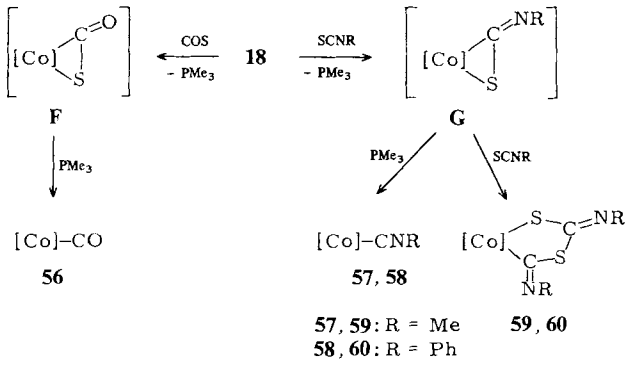
X-ray structural analyses have been carried out on **44** and **45**[70,72]. These have revealed very similar distances for the three-membered CoCS ring and also an almost identical SCX bond angle (X = S or C) for the no longer linear $CS_2$ or thioketene molecules in the complex. It thus appears that both heteroallenes possess rather comparable ligand characteristics. An X-ray analysis of **48** is now underway, and we are very optimistic that the result will confirm the structural proposal presented in Scheme 7. Recently, we were able to confirm for the palladium compound $[1,2\text{-}C_6H_4(CH_2PPh_2)_2]Pd(\eta^2\text{-}CSSe)$ that the thiocarbonyl selenide is indeed coordinated to the metal *via* C and Se and not *via* C and S[74].

$C_5H_5Co(PMe_2Ph)_2$ **53** behaves quite similarly to **18** towards $CO_2$ homologues[73]. Using $CS_2$, compound **52**, *i.e.* the analogue of **44**, is formed practically quantitatively, while with $CSe_2$ the five-membered ring complex **55** is obtained in addition to **54** (and small amounts of $C_5H_5Co(PMe_2Ph)CSe_3$). The formation of **55** can be interpreted according to a 1,3-dipolar cycloaddition of **54** to a second $CSe_2$ molecule. A compound having the composition $C_5H_5Rh(PMe_3)C_2S_4$, which is structurally very closely related to **55**[75], is formed in the reaction of $C_5H_5Rh(PMe_3)C_2H_4$ with $CS_2$. As confirmed in this particular instance by X-ray analysis, the atoms of the metallaheterocycle are roughly coplanar. Moreover, the C–S distances in the ring and to the exocyclic sulfur atoms are almost identical, which suggests the presence of a highly delocalized $\pi$-electron system[75]. The reaction of **53** with CSSe yields compounds analogous to **49** and **50**[73]. It is possible here also that an $\eta^2$-CSSe complex is initially formed which immediately reacts with $PMe_2Ph$ or CSSe to give the products indicated.



The results summarized in Scheme 7 and in equations (9) and (10) generally support that—in contrast to the reactions of the half-sandwich complexes **18** and **53** with $CS_2$—use of the more reactive heteroallenes CSSe and $CSe_2$ yields *via* the initially formed $C_5H_5Co(\eta^2\text{-}CSSe)PR_3$ or $C_5H_5Co(\eta^2\text{-}CSe_2)PR_3$ compounds further, secondary products, some of which are structurally novel. Presumably both the lower dissociation energy of the C–Se bond (as compared to the C–S bond) and the greater reactivity of the CoCSe three-membered ring in the *dihapto*-bonded CSSe and $CSe_2$ complexes are responsible for their formation.

The CoCS three-membered ring in the compounds **F** and **G** postulated as the primary intermediate in the reactions of **18** with COS and SCNR is probably even more labile. These intermediates react very rapidly with the $PMe_3$ released in the primary step by $SPMe_3$ elimination to form the carbonyl or isocyanide complexes **56** or **57**, and **58** which—as shown below—are themselves metal bases (see Section 2.3.2). The course of the reaction of **18** with SCNR outlined in Scheme 8 is supported by the fact that under certain conditions (especially with excess isothiocyanate) the metallaheterocycles **59** and **60** are isolated in addition to **57** and **58**. These heterocycles structurally resemble the compounds **55** and $C_5H_5Rh(PMe_3)C_2S_4$[42].



Scheme 8. [Co] = $C_5H_5CoPMe_3$.

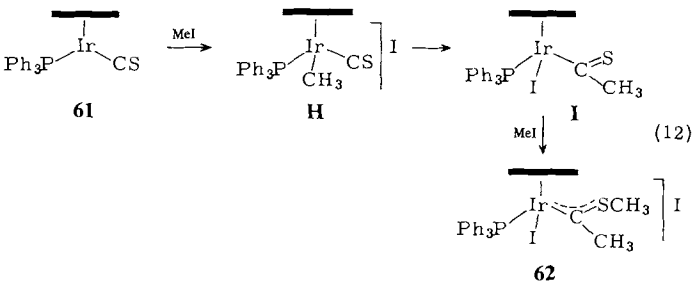
## 2.3. Complexes of the Type $C_5R_5MLL'$

### 2.3.1. *Carbonyl(phosphane)- and Thiocarbonyl(phosphane)metal Complexes*

In terms of their nucleophilicity, the $C_5R_5M(CO)PR'_3$ (R = H, Me; M = Co, Rh, Ir; R' = alkyl, aryl) half-sandwich complexes—numerous examples of which are known—occupy an intermediate position between the bis(phosphane)- and dicarbonylmetal compounds. As *Graham et al.* have shown for $C_5H_5Co(CO)PR'_3$ ($PR'_3 = PPh_3$, $PMePh_2$, $PMe_2Ph$), $C_5H_5Rh(CO)PPh_3$, $C_5H_5Ir(CO)PPh_3$, *etc.*[11], they react with alkyl halides (especially with methyl iodide) to form the acyl complexes.

Protonation to afford the hydridometal cations $[C_5R_5MH(CO)PR'_3]^+$ has proved to be successful in only a few cases so far. Starting from the carbonyl(tri*phenyl*phosphane) compounds $C_5H_5M(CO)PPh_3$ only the iridium derivative forms a stable cation of this type[11b], which merely confirms the tendency to increasing basicity according to the scheme 3d- < 4d- < 5d-element (in the same triad) put forward by *Shriver*[5]. When we turn to the carbonyl(tri*methyl*phosphane) complexes $C_5H_5M(CO)PMe_3$ a stable salt, $[C_5H_5RhH(CO)PMe_3]X$ (X = $BF_4$, $CF_3SO_3$), can be isolated for M = Rh[37]. The corresponding $C_5Me_5Rh$ compound can be prepared similarly[38].

Only very little is known about the reactivity of phosphane(thiocarbonyl) complexes, $C_5H_5M(CS)PR'_3$, towards electrophiles. *Faraone et al.*[23] have studied the reaction of $C_5H_5Ir(CS)PPh_3$ **61** with excess methyl iodide and isolated the thiocarbene compound **62**. The reaction pathway postulated in reaction (12) is based on the plausible assumption that **61** behaves similarly to $C_5H_5Ir(CO)PPh_3$[11b], and that the intermediate **H** is produced primarily by oxidative addition of a methylcarbenium ion to the metal. It is quite possible that there is a further intermediate between **H** and **I** involving a *dihapto*-bonded thioacyl group, as indicated by *Roper et al.* for the corresponding osmium complexes[76].

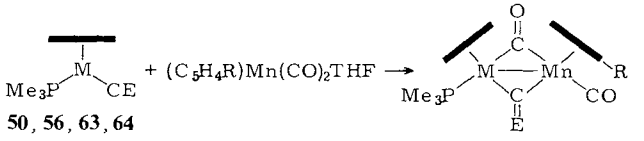


(12)

In reacting with methyl iodide, the trimethylphosphane compounds **50** and **64** yield—in contrast to **61**—no products analogous to **H**, **I**, or **62**. Even electrophilic addition at the sulfur atom with formation of a methylthiocarbyne complex (which occurs in the reaction of [W(CS)(CO)(diphos)$_2$] with $CF_3SO_3Me$[77]), cannot be proven[73]. **50** reacts with $CH_2I_2$ to give a mixed product containing both $[C_5H_5CoI(PMe_3)_2]I$ and, rather surprisingly, the binuclear compound $C_5H_5Co(\mu\text{-}CS)_2Co(PMe_3)C_5H_5$, whose structure, with unsymmetric CS bridges as a characteristic feature, has been established by X-ray analysis[78].

The carbonyl- and thiocarbonyl(trimethylphosphane) complexes **56** and **63**, and **50** and **64** behave very similarly toward the 16-electron species $[(C_5H_4R)Mn(CO)_2]$ (R = H, Me). The latter are typical electrophiles[79], and accordingly react with the half-sandwich metal bases to give the binuclear compounds **65**–**68** [reaction (13)] in high yield[14,73,80,81]. We assume that an interaction initially takes place between the nucleophilic metal center in **50**, **56**, **63**, or **64** and the electronically and coordinatively unsaturated manganese atom, followed by stabilization re-

sulting from the formation of the CO or CS bridges. X-ray crystallographic studies of **65**[82] and **66**[83] indicate that a *cis*-arrangement of the cyclopentadienyl ligands is preferred in each case. The CS group in **66** and **68** is exclusively bridging (and is not in a terminal site), a fact which emerges particularly from the IR data[73]. In the synthesis of **66** and **68** a second product is also formed containing a $C_5H_5Mn(CO)_2$ group as the ligand on the sulfur atom[81]. The yields obtained vary according to the amount of $C_5H_5Mn(CO)_2THF$ used.



**50**, **56**, **63**, **64**

**56**, **65**: M = Co; E = O
**50**, **66**: M = Co; E = S
**63**, **67**: M = Rh; E = O
**64**, **68**: M = Rh; E = S

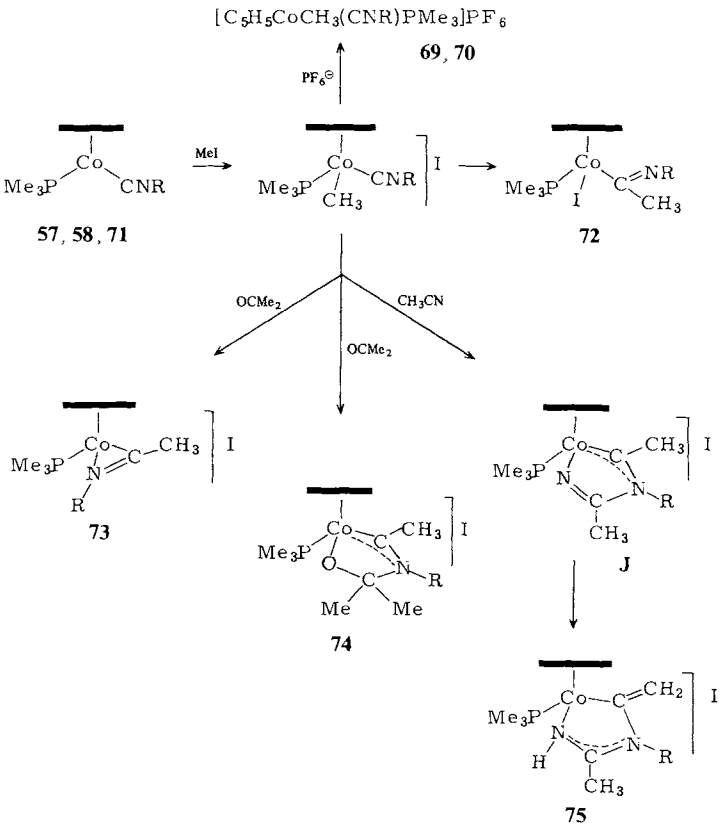
**65**, **67**: R = Me
**66**, **68**: R = H (13)

### 2.3.2. *Isocyanide(phosphane)metal Complexes*

The isocyanide complexes $C_5H_5M(CNR)PMe_3$ (M = Co, Rh) behave as nucleophiles toward both methyl iodide and heteroallenes. Interestingly, the course of the reactions of the cobalt compounds **57**, **58** and **71** (Scheme 9) with MeI is utterly dependent upon the group R of the isocyanide ligand. With R = Me and *t*Bu, in pentane as solvent the $[C_5H_5CoCH_3(CNR)PMe_3]^+$ cations are obtained which can be characterized readily as the $PF_6$ salts **69**, **70**. With R = Ph, the corresponding cationic complex is rather unstable and rapidly rearranges to form the neutral imidoylcobalt(III) compound **72** when the attempt is made to dissolve and recrystallize it from acetone/ether[42]. This subsequent reaction is to be expected in view of the similar ligand characteristics of CO and CNR and the comparable metal basicity of $C_5H_5Co(CO)PMe_3$ **56** and $C_5H_5Co(CNR)PMe_3$ (**57**, **58**, **71**).

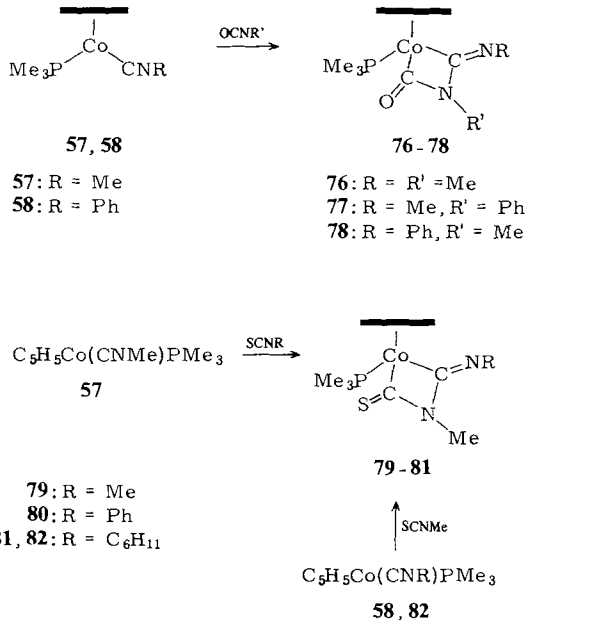
However, if the methyl isocyanide and *tert*-butyl isocyanide complexes $[C_5H_5CoCH_3(CNR)PMe_3]I$ are dissolved in acetone, no product analogous to **72** is formed. When R = *t*Bu another cation (**73** with iodide as the anion) having a *dihapto*-bonded imidoyl group is obtained after migration of the $CH_3$ group from the metal to the isocyanide carbon[42]. It is conceivable that an intermediate analogous to **72** or **73** is also formed when $[C_5H_5CoCH_3(CNMe)PMe_3]I$ is dissolved in acetone; however, this is extremely labile and thus reacts with the solvent *via* a [3+2]-cycloaddition to form the metallaheterocycle **74** (Scheme 9)[84]. This product has been characterized by X-ray structure analysis[85]. The reaction of $[C_5H_5CoCH_3(CNMe)PMe_3]I$ with acetonitrile gives **75**, a five-membered ring compound containing Co; this is probably formed *via* intermediate **J**. The structure of **75** has also been established by X-ray analysis[84].

The reaction of **57** with methyl and phenyl isocyanates and of **58** with methyl isocyanate probably proceeds *via* attack of the nucleophilic cobalt atom at the electrophilic center of the heteroallene to yield the four-membered ring compounds **76**—**78** (Scheme 10)[86]. Methyl isothiocyanate reacts analogously with **57**, **58**, and **82**. Surprisingly, the



Scheme 9. **57**, **69**, **74**, **75**: R = Me; **70**, **71**, **73**: R = *t*Bu; **58**, **72**: R = Ph.

metallaheterocycles **79**—**81** prepared in this way are also formed from $C_5H_5Co(CNMe)PMe_3$ and SCNR, which suggests the intermediate formation of a four-membered ring containing a sulfur atom. Cleavage of a C—S bond and renewed ring closure leads to the thermodynamically stable product bearing a methyl group on the ring nitrogen atom. As indicated by X-ray crystallographic studies of the complexes **79** and **80**, planar CoCNC four-membered



**57**, **58**

**57**: R = Me
**58**: R = Ph

**76**-**78**

**76**: R = R' = Me
**77**: R = Me, R' = Ph
**78**: R = Ph, R' = Me

**79**: R = Me
**80**: R = Ph
**81**, **82**: R = $C_6H_{11}$

**79**-**81**

$C_5H_5Co(CNR)PMe_3$

**58**, **82**

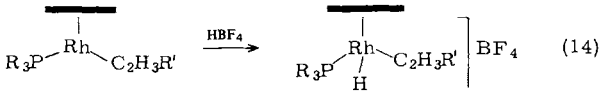
Scheme 10.

rings are present whose C and N atoms are, as expected, coordinated in a strictly trigonal-planar manner[86]. Protonation and methylation of the heterocycles **76—81** lead to formation of cyclic aminocarbenecobalt compounds, which also opens up a route to metallaindole derivatives[87].

In connection with the preparation of **80** from **57** it should also be mentioned that the isocyanide compound $C_5H_5Co(CO)CNMe$ is formed when the complex $C_5H_5Co(CO)PMe_3$ **56**—which is comparable with **57**—reacts with SCNPh[80]. In contrast, the reaction of $C_5H_5Co(CO)PPh_3$ with SCNPh leads to $C_5H_5Co(\eta^2$-SCNPh)$PPh_3$, among others, and not to a four-membered ring species related to **80**[88].

### 2.3.3. *Olefin(phosphane)metal Complexes*

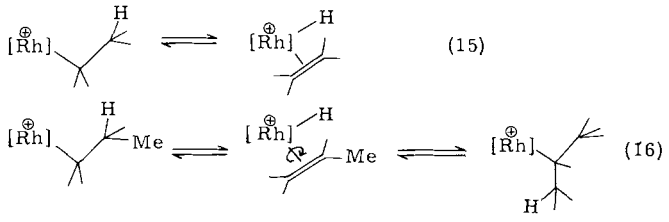
The lack of evidence of attack by a proton at the metal in the reaction of bis(olefin)rhodium complexes with HCl is certainly not mirrored by the mixed olefin(phosphane) compounds **83—85**. Using $HBF_4$ in ether, one obtains the $BF_4$ salts **86—88**, which are also relatively stable in solution (*e.g.* $CH_3NO_2$)[28]. The temperature dependence of the NMR spectra and deuteration experiments indicate that in solution a rapid proton exchange takes place involving the olefinic protons and the hydridic proton. The positions of the equilibria in reactions (15) and (16) are certainly shifted to the side of the hydrido(olefin) complexes, since it has proved impossible either by $^1H$- or $^{13}C$-NMR spectroscopy to establish the presence of an alkylrhodium cation[28].




(14)

**83-85** **86-88**

**83**, **86**: R = Me, R' = H
**84**, **87**: R = R' = Me
**85**, **88**: R = *i*Pr, R' = H



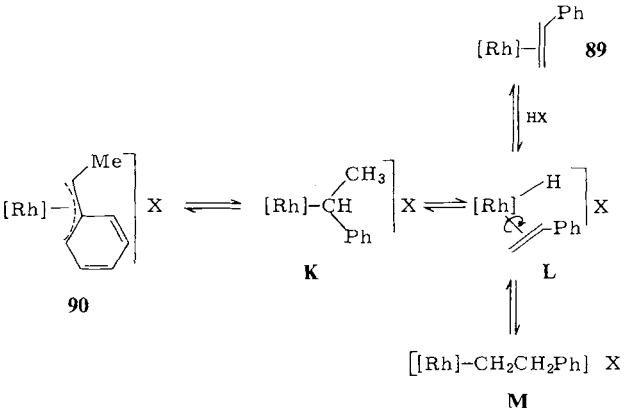
(15)

(16)

[Rh] = $C_5H_5RhPMe_3$

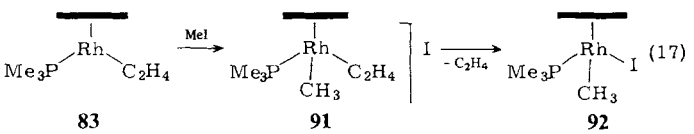
It is interesting to note that protonation of the propene-rhodium compound **84** yields the two diastereomeric pairs of **87**, not in equal amounts but roughly in the ratio 70:30, *i.e.* an *asymmetric induction* occurs[89]. Since the configuration at the two chiral centers (the metal and the methyl-substituted carbon atom of propene) is constantly changing as a result of equilibrium (16), one diastereomer is rapidly transformed into another. This is evidenced in the NMR spectra by the line broadening of the signals from the ring and phosphane protons or carbons atoms[28].

The reaction of the styrene complex **89** with $HBF_4$ or $CF_3CO_2H/NH_4PF_6$ leads to a product corresponding analytically to a hydrido(olefin) compound analogous to **86—88**. The IR and NMR spectra of this product, however, show no evidence of an Rh—H bond. As proved by X-ray structure analysis (X = $PF_6$), in the crystal exclusively **90** is present, *i.e.* the methylbenzyl group formed from the proton and the styrene is linked to the metal *via* a $\pi$-allyl type bond[28]. The formation of **90** probably takes place *via* the intermediates **K** and **L** which—as demonstrated by labeling experiments—are in equilibrium with **M** and **90** (Scheme 11). The fact that the complex **90**—in contrast to other $\eta^3$-methylbenzyl metal compounds—possesses a rigid rather than a fluctuating structure in solution may arise because the rhodium(III) has the preferred octahedral coordination[28].




Scheme 11. [Rh] = $C_5H_5RhPMe_3$; X = $BF_4$, $PF_6$.

The methylation of the rhodium atom in **83** takes place similarly [reaction (17)]. The ethylene(methyl) complex formed, **91**, is stable at room temperature and reacts only upon warming in tetrahydrofuran (THF) to eliminate $C_2H_4$ and yield **92**. The analogous compound obtained by allowing **89** to react with MeI ($PhCHCH_2$ instead of $C_2H_4$) is much more labile than **91** and rearranges to **92** when dissolved in $CH_3NO_2$[28]. It would appear that in cations of composition $[C_5R_5RhCH_3(C_2H_3R')PR_3]^+$ the positive charge is stabilized by increasing donor character in the ligands. It is thus easy to understand why the compound $[C_5H_5RhCH_3(C_2H_4)PPh_3]I$ described by *Graham et al.*[11d] rapidly eliminates ethylene even at room temperature, whereas **91** does not. However, what does not fit into this picture is the fact that the cations $[C_5Me_5RhCH_3(C_2H_4)L]^+$ (L = $PMe_3$, $P_2Me_4$) formed by methylating $C_5Me_5Rh(C_2H_4)L$ are very labile, and in solution in the presence of iodide they are spontaneously converted into the neutral complexes $C_5Me_5RhCH_3(L)I$[16].

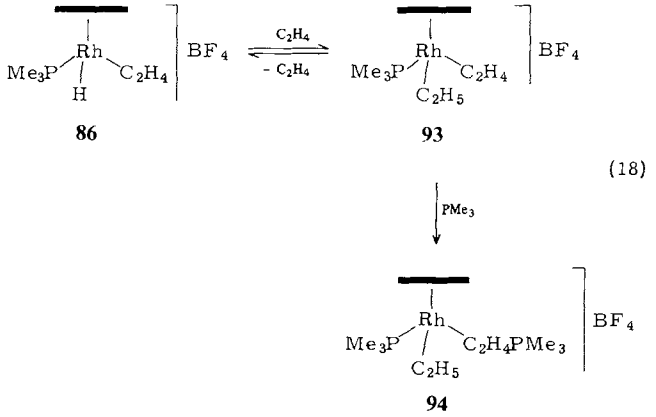



(17)

**83** **91** **92**

A number of subsequent reactions involving the ethylene(hydrido) cation **86** should also be mentioned. With $Cl^-$, $Br^-$ and $I^-$ as reagents, even at room temperature in-

sertion of the olefin into the Rh–H bond occurs to form the ethyl(halo) complexes $C_5H_5RhC_2H_5(PMe_3)X$ (X = Cl, Br, I)[37]. In the reaction of **86** with ethylene an insertion also occurs, although the product formed, **93**, is stable only under a $C_2H_4$ atmosphere and transforms into **86** when any attempt at isolation is made. However, $PMe_3$ undergoes nucleophilic addition to the ethylene to yield the β-phosphonioethyl compound **94**[37]. Insertion of $C_2H_4$ into the Rh–$C_2H_5$ bond in **93** could not be detected, even with ethylene under pressure.



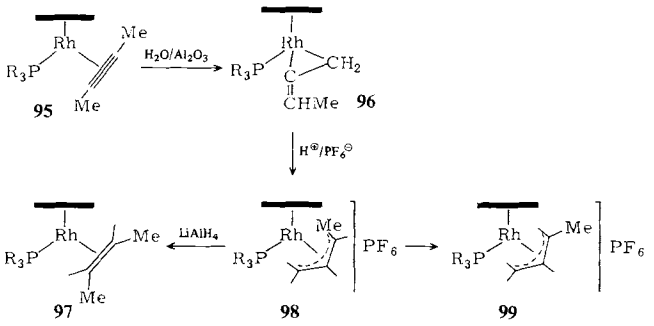

Displacement of olefin occurs when **86** reacts with $P(iPr)_3$ and the $BF_4$ salt of the cation $[C_5H_5RhH(PMe_3)P(iPr)_3]^+$ is obtained. This can readily be deprotonated, providing access to the mixed bis(phosphane) complex $C_5H_5Rh(PMe_3)P(iPr)_3$[37].

### 2.3.4. *Alkyne(phosphane)- and Vinylidene(phosphane)metal Complexes*

The reversibility of olefin insertion into the metal-hydride bond in hydrido(olefin)metal complexes is well documented[90], as is evident, for example, in reactions (15) and (16) and in Scheme 11. On the other hand, there is no proof of a corresponding equilibrium between alkyne(hydrido)- and vinylmetal compounds. All presently known syntheses of vinyl complexes from alkynes have been carried out by allowing a metal hydride to react with $C_2R_2$ or $RC_2H$, *i.e.* the M–CR=CHR– (or M–CH=CHR– and M–CR=$CH_2$–) linkages have not been produced by reactions between alkynemetal compounds and acids HX[91].

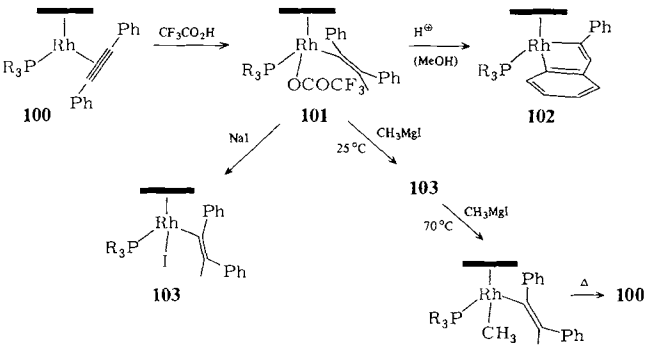
The compounds **95** and **100** recently prepared by us, which are analogues of the olefin complexes **83**—**85**, react with $CF_3CO_2H$ or $HBF_4$ even at room temperature[24]. After addition of $PF_6^-$, **95** forms the *syn*-1-methylallyl complex **98**, which is slowly converted into the thermodynamically more stable *anti*-isomer **99**[91]. Investigation of the reaction pathway indicates that in the presence of a weak acid such as $H_2O$ (on $Al_2O_3$) an initial rearrangement of **95** to the isomeric methylallene compound **96** is followed by protonation to yield the allyl complex. The *syn*-configuration of the 1-$MeC_3H_4$ group in **98** has been confirmed by NMR data and by the formation of the *cis*-2-butene compound **97** upon addition of a hydride ion.

The reaction of **100** with $CF_3CO_2H$ yields the complex **101**, which is known from X-ray analysis to contain a vinyl



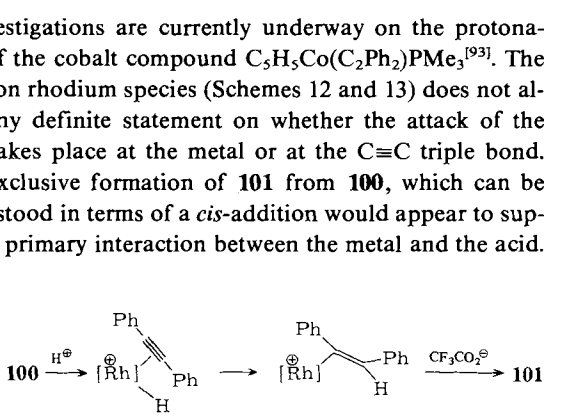

Scheme 12. R = *i*Pr.

ligand with phenyl substituents in *cis*-positions[92]. Among the subsequent reactions of this compound, special mention must be made of the rearrangement to the metallaheterocycle **102**, which is isomeric with **100**. This rearrangement takes place in methanol upon addition of $NH_4PF_6$ or traces of $CF_3CO_2H$. We assume that the trifluoroacetate group of **101** is initially displaced by the solvent, and that the cationic intermediate formed reacts by *ortho*-metallation. The lability of the Rh–$OCOCF_3$ bond in **101** is evident from the smooth reaction with NaI or $CH_3MgI$ to form **103**[24]. The five-membered metallacycle in **102** possesses an approximate chair-like conformation which, together with the varying C–C bond distances, suggests that there is no delocalized π-electron system present[24].



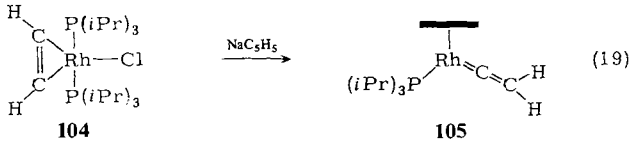

Scheme 13. R = *i*Pr.

Investigations are currently underway on the protonation of the cobalt compound $C_5H_5Co(C_2Ph_2)PMe_3$[93]. The work on rhodium species (Schemes 12 and 13) does not allow any definite statement on whether the attack of the acid takes place at the metal or at the C≡C triple bond. The exclusive formation of **101** from **100**, which can be understood in terms of a *cis*-addition would appear to support a primary interaction between the metal and the acid.



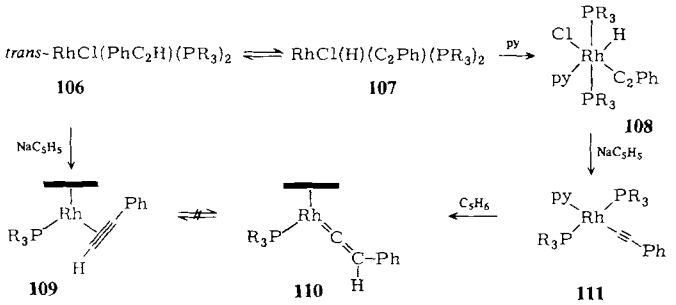

However, in view of results on the stereochemical course of reactions of metal hydride complexes with alkynes[91], caution seems to be indicated here.

An attempt to obtain the acetylenerhodium compound $C_5H_5Rh(C_2H_2)PiPr_3$ analogous to **95** or **100** by allowing **104** to react with $NaC_5H_5$ led rather surprisingly to almost quantitative formation of the vinylidene complex **105**[94].




**104** **105** (19)

Depending on the reaction conditions, the phenylacetylene compound **106** reacts with $NaC_5H_5$ to form either the alkyne complex **109** or the vinylidene complex **110**[95]. A conversion of this type of a 1-alkyne to a vinylidene ligand in the coordination sphere of a transition metal has already been observed in related cyclopentadienylmanganese, cyclopentadienyliron, and cyclopentadienylruthenium compounds. In general, it has been explained by assuming the formation of an alkynyl(hydrido) intermediate[96]. Such an intermediate was first isolated during the reaction of **106** to form **110**[95]. The equilibrium between **106** and **107** in ether or toluene can be shifted completely to the right by addition of pyridine to yield the chiral octahedral complex **108**. The latter reacts with $NaC_5H_5$ in THF at room temperature to give the phenylvinylidene compound **110**. If, however, a solution of **108** in THF is very rapidly treated at 0°C with an equimolar amount of $NaC_5H_5$ and worked-up in the cold, the square-planar complex **111** is isolated[95]. This complex reacts with cyclopentadiene virtually quantitatively to give **110**; when $C_5D_6$ is used, $C_5D_5Rh(=C=CDPh)PiPr_3$ is formed[97].

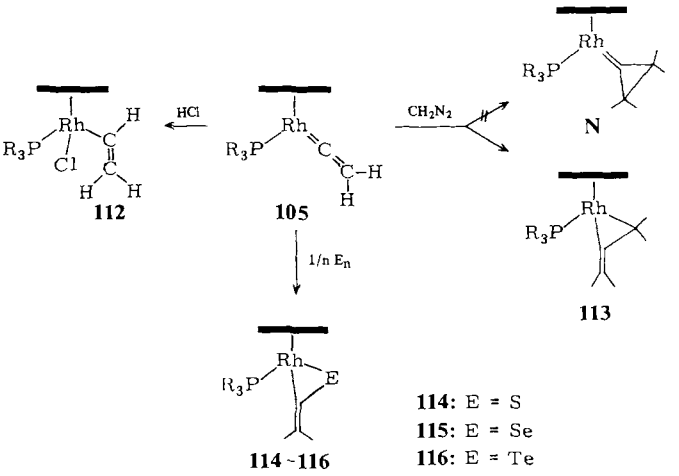



Scheme 14. R = *i*Pr.

The reaction sequence shown in Scheme 14 illustrates that although the conversion of a 1-alkyne into a vinylidene ligand actually involves an alkynyl(hydrido) intermediate there is no intramolecular hydride shift from the metal to the carbon as originally supposed[96]. In fact, a two-step elimination/addition is responsible for the final isomerization which occurs. Rearrangement of **109** into **110** (or *vice versa*) is not observed either on irradiation or on after leaving the compound to stand for a considerable time in solution[95].

As established by X-ray structure analysis, there is a fairly short bond in complex **110** between the metal and the α-C atom of the phenylvinylidene which is some 15–20 pm shorter than in carbenerhodium compounds[95]. This distance points to considerable overlap of the orbitals involved in the Rh–C-π bond, which indicates that there should be a high electron density at the metal center. Accordingly, the vinylidenerhodium complexes should also behave as metal bases.

The first tentative steps in this direction seem to support this suggestion. Thus, **105** reacts with HCl (1:1) in benzene to yield the chloro(vinyl)rhodium compound **112**, whose formation may take place *via* a hydrido(vinylidene)rhodium cation[97]. Using $CH_2N_2$ in the presence of $Cu^{2+}$ leads to the allene complex **113** but not to the isomeric carbene compound **N** which should result from $CH_2$ addition to the vinylidene C=C double bond. The electrophile $CH_2$ thus clearly prefers the more electron-rich Rh=C instead of the C=C bond in adding to the "metallaallene" moiety $C_5H_5(L)Rh=C=CH_2$. It thereby provides a new synthetic route to allenemetal complexes[97].

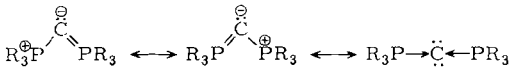



Scheme 15. R = *i*Pr.

Recently, by making use of the electrophilic addition of a sulfur, selenium, or tellurium atom to the Rh=C bond in **105**, it became possible for the first time to prepare transition-metal compounds with thio-, seleno- and telluroketenes, $CH_2=C=E$, *i.e.* with molecules which are very short-lived (E = S, Se) or unknown (E = Te) in the free state (Scheme 15)[94]. The complexes **114** and **115** are remarkably stable both in the solid state and in solution, whereas the telluroketene compound **116** reacts slowly in solution to form **105** and metallic tellurium. X-ray analysis of **114** has shown that in the crystal *both* enantiomers are present[94]. Overall, there is a close analogy between the structural data of **114** and those of complex **45** obtained from the half-sandwich complex **18** (see Scheme 7). This complex, **45**, contains the thioketene 1,1,3,3-tetramethyl-2-thiocarbonylcyclohexane as ligand, which in contrast to $CH_2=C=S$ is stable in the free form. *Behrens et al.*[98] have isolated from this compound and, more recently, from di-*t*-butylthioketene, mono- and binuclear thioketene complexes by reaction with various carbonylmetal compounds. In these thioketene complexes the appropriate thioketene is coordinated either *via* the sulfur (*i.e. monohapto*) or as a bridge between two metal atoms. Some iridium(I) and platinum(0) complexes with $\eta^2$-bonded bis(trifluoromethyl)thioketene described in 1970 by *Stone et al.*[99] are structurally related to **114** (and **45**); they were synthesized, however, not from $(CF_3)_2C=C=S$ but rather from heterocyclic, $CF_3$-substituted sulfur compounds.

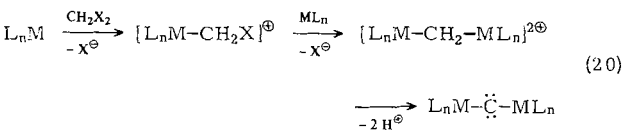
### 2.4. Reactions of $C_5R_5ML_2$ and $C_5R_5MLL'$ with Dihalogeno- and Trihalogenomethanes

In a brief review on the chemistry of carbodiphosphoranes which appeared in 1979, *Schmidbaur*[100] advanced the provocative suggestion that the bonding patterns in $C(PR_3)_2$ molecules could be described not only in terms of the resonance structures **a** and **b** but also as an extreme case in terms of **c**.



**a** **b** **c**

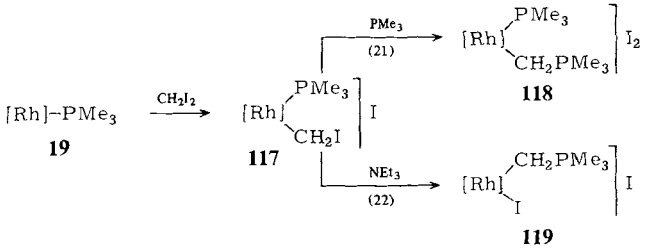
We took this as a challenge and attempted to prepare binuclear metal complexes according to reaction (20). In such complexes both of the metal atoms would be linked only by a carbido bridge. The metal base, $ML_n$, would then act as a donor toward the "naked" C atom, just as the phosphane group in the above-mentioned formula **c** for carbodiphosphoranes.



(20)

As a test molecule we first selected the bis(trimethylphosphane)rhodium complex **19**, which reacts with $CH_2I_2$ under exactly the same conditions as it does with methyl iodide to form the iodomethylrhodium(III) compound **117** in 62% yield[101]. The latter is stable for several days in nitromethane, although in dimethyl sulfoxide it rapidly loses "$CH_2$" to form $[C_5H_5RhI(PMe_3)_2]I$.

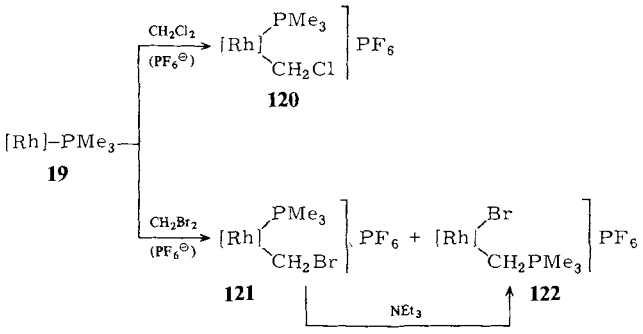
The presence of a reactive C–I bond in the cation of **117** is evidenced by its reaction with $PMe_3$, which leads quantitatively to **118**. With $NEt_3$, no nitrogen-ylide complex analogous to **118** is formed from **117**, which rather surprisingly isomerizes to **119**[101]. The anion clearly is not involved in this rearrangement since the $BF_4$ salt also reacts analogously to **117**.



[Rh] = $C_5H_5RhPMe_3$

The conversion of **117** to **119** is catalyzed not only by $NEt_3$ but also by NaOMe and—disappointingly in view of our stated objective—by the complex **19**. Even after changing the reaction conditions and replacing **19** by the more reactive half-sandwich compounds $C_5H_5Rh(CNMe)_2$, $C_5H_5Fe(CO)_2^-$, and $C_5H_5Mo(CO)_3^-$[39,109] it is not possible to isolate a binuclear complex having a $CH_2$ bridge *without* a metal-metal bond.

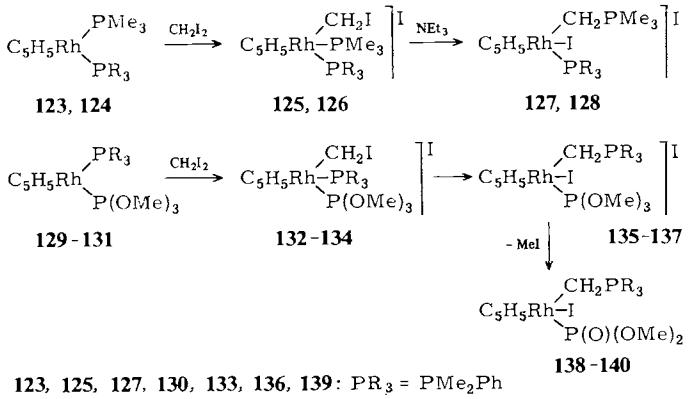
To determine what factors influence the conversion of a halogenmethyl(phosphane) complex into a halogen(methylenephosphorane) complex, we changed both the dihalomethane and the metal base. **19** also reacts smoothly with $CH_2Cl_2$ (though somewhat less rapidly than with $CH_2I_2$) to form the cation $[C_5H_5RhCH_2Cl(PMe_3)_2]^+$, whose $PF_6$ salt **120** is exceptionally stable[109]. When **19** reacts with $CH_2Br_2$ a mixed product is formed from which after dissolving and reprecipitating with $NH_4PF_6$ the bromomethyl complex **121** and the isomeric methylenephosphorane **122** can be isolated; the latter is obtained quantitatively after addition of $NEt_3$. Isomerization of **120** could not be observed even after it was allowed to stand for some considerable time in the presence of triethylamine[39].



Scheme 16. [Rh] = $C_5H_5RhPMe_3$.

The products obtained by starting from the mixed bis(phosphane) complexes **123**, **124** and the phosphane(phosphite) compounds **129**–**131** are summarized in Scheme 17[27,102]. Two striking points are that in the rearrangement it is always the better donor ligand which migrates and that in the case of **132**–**134** the isomerization takes place even *without* adding $NEt_3$ or another base. Kinetic measurements[39] reveal that the rate of the reaction of **132** to **135** is—after an induction period—practically independent of the concentration of the educt and increases with increasing polarity of the solvent. Since addition of iodide ions has no effect on the rate, the mechanism might be compared to that of some anionotropic rearrangements of organic compounds in which a concerted pathway is very probable on the basis of labeling experiments[103]. The observation that the rate of isomerization of **132** to **135** is significantly increased by addition of $NEt_3$ and the fact that the complex $[C_5H_5RhCH_2Br(PMe_3)P(OMe)_3]PF_6$ does not rearrange are consistent with a non-stepwise 1,2-shift of the iodide and phosphane. Such a mechanism could also apply to the reactions of other phosphanemetal compounds, *e.g.* $Co(PMe_3)_4$, $Pt(PPh_3)_4$, or $Pt(PEt_3)_3$ with dihalomethanes, which lead to methylenephosphorane complexes[104–106].

Similarly to **19** (Scheme 16), **123** and **124**, the chelate complexes **141** and **142** also react with $CH_2I_2$ by oxidative addition to yield the iodomethyl compounds **143** and **144**[27]. Although **144** is inert and does not isomerize even in the presence of NaOH, the reaction of **143** with $NEt_3$, involving insertion of $CH_2$ into one of the Rh–P bonds, leads to the quantitative formation of the metallaheterocycle **145** (Scheme 18). The Rh–I bond in the latter is fairly labile and thus at room temperature in the presence of



123, 124 125, 126 127, 128

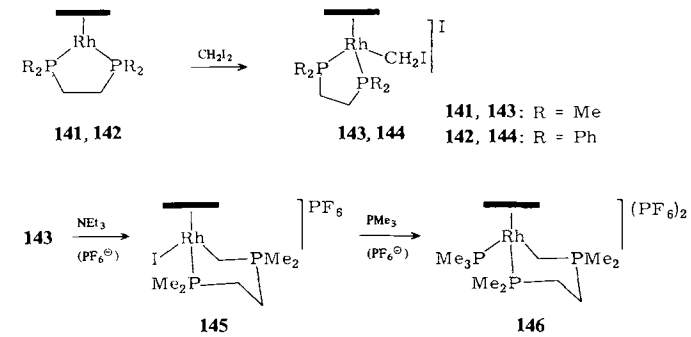
129-131 132-134 135-137

138-140

123, 125, 127, 130, 133, 136, 139: $PR_3 = PMe_2Ph$
124, 126, 128, 131, 134, 137, 140: $PR_3 = PMePh_2$
129, 132, 135, 138: $PR_3 = PMe_3$

Scheme 17.

$PMe_3$ (and subsequent addition of $NH_4PF_6$) the complex **146** is formed. The relatively broad $^1$H-NMR signals indicate that in solution a rapid interconversion of the two possible chair conformations probably takes place[27]. An alternative method of preparing **146** from **147** and $C_2H_4(PMe_2)_2$ proved not to be successful.



141, 142 143, 144

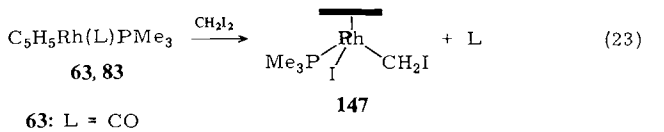
141, 143: R = Me
142, 144: R = Ph

145 146

Scheme 18.

The reactions of the cobalt compounds analogous to **19**, **129**, and **141** with $CH_2Cl_2$, $CH_2ClI$, and $CH_2I_2$ proceed very rapidly even at $-78$ °C, although they give no products containing a Co–$CH_2Cl$ or Co–$CH_2I$ bond. In addition to paramagnetic species, all that can be isolated from the reaction mixture are the halometal complexes $[C_5H_5CoXL_2]X$ (X = Cl, I)[102]. Investigations of the reactivity of $C_5H_5Co(CO)PMe_3$ with dihalomethanes have proven that this result is not due to the instability of methylenephosphoranecobalt(III) compounds.

The metal bases $C_5H_5Rh(CO)PMe_3$ **63** and $C_5H_5Rh(C_2H_4)PMe_3$ **83**, which are weaker nucleophiles than the bis(phosphane) compounds $C_5H_5Rh(PMe_3)PR_3$ **19**, **123**, and **124**, also react under very mild conditions with $CH_2I_2$[107]. In this case the neutral complex **147** is formed. The unique course of the reaction of the carbonyl compound **63** is remarkable insofar as an acyl complex, $C_5H_5RhCOCH_2I(PMe_3)I$, analogous to



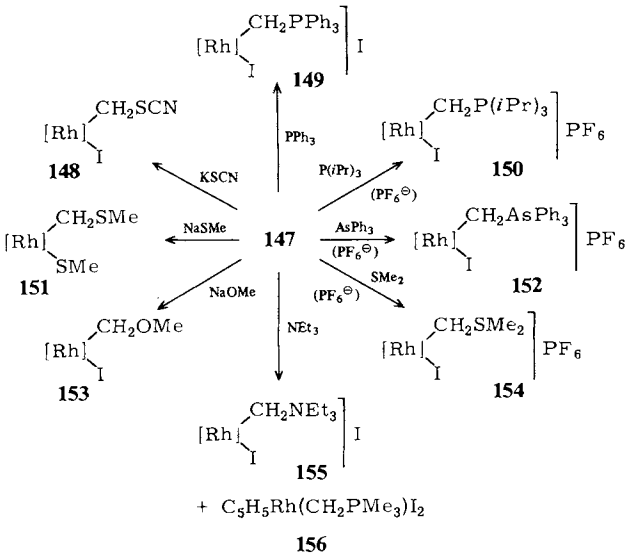
(23)

63, 83 147

63: L = CO
83: L = $C_2H_4$

$C_5H_5RhCOCH_3(PMe_3)I$, cannot be observed[108]. The course of the reaction of **83** with $CH_2I_2$ depends on the solvent used. Whereas in ether only **147** is formed, in methanol mainly the compound $C_5H_5RhI_2(PMe_3)$ is produced *via* elimination of $CH_2$[107].

The reactivity of the C–I bond towards nucleophiles renders the complex **147** (rather like **117**) a very suitable starting material for the synthesis of numerous novel organorhodium compounds (see Scheme 19). In particular, formation of the complexes **152**, **154**, and **155** should be mentioned in which the ylides $Ph_3AsCH_2$, $Me_2SCH_2$ and $Et_3NCH_2$, which are unstable in the free state, are fixed at the metal[107].



149 148 150 151 147 152 153 154 155

+ $C_5H_5Rh(CH_2PMe_3)I_2$

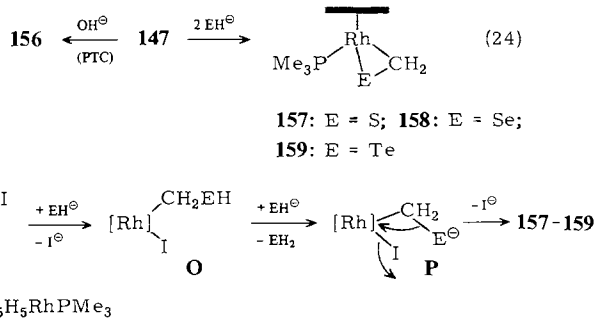
156

Scheme 19. [Rh] = $C_5H_5RhPMe_3$.

The isomer **156**, obtained together with **155** in the reaction of **147** with $NEt_3$, is formed quantitatively when **147** reacts with NaOH in a two-phase benzene/water system in the presence of triethylbenzylammonium chloride acting as phase transfer catalyst (PTC)[109]. The expected formation of the hydroxymethyl compound $C_5H_5RhCH_2OH(PMe_3)I$ — by analogy to the synthesis of **153** from **147** and NaOMe — does not occur, although the former could be a suitable starting material for the preparation of Rh=$CH_2$ complexes.

In contrast to $OH^-$, the weaker bases $SH^-$, $SeH^-$ and $TeH^-$ effect a substitution of the C–I bond in **147** and thereby open up a simple route to thio-, seleno- and telluroformaldehyderhodium compounds[110]. The structure of **158** has been confirmed by X-ray structure analysis[111]. The synthetic pathway adopted may involve proton abstraction from the initially formed intermediate **O** by $EH^\ominus$ (which is present in excess) and a subsequent substitution of iodide by the more nucleophilic chalcogen atom in **P** to form the three-membered ring of the product.

Independently, but at the same time as us, *Roper et al.*[112] obtained the chalcogenoformaldehydeosmium complexes $Os(\eta^2\text{-}CH_2E)(CO)_2(PPh_3)_2$ (E = S, Te) from osmiumhalomethyl or osmiumformaldehyde precursors. Moreover, *Herberhold et al.*[113] and *Herrmann et al.*[114] recently succeeded in preparing binuclear manganese compounds



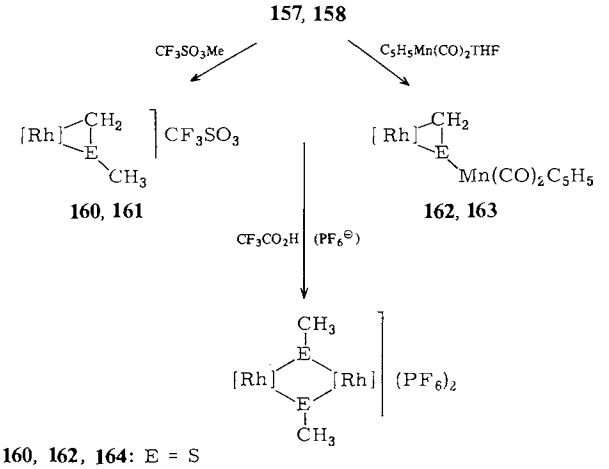
157: E = S; 158: E = Se;
159: E = Te

[Rh] = $C_5H_5RhPMe_3$

Scheme 21. [Rh] = $C_5H_5RhPMe_3$.

with $CH_2S$, $CH_2Se$, or $CH_2Te$ as the bridging ligand by allowing $[C_5R_5Mn(CO)_2]_2E_n$ (E = S, Se; R = H, Me; n = 1 or 2) or $[C_5H_5Mn(CO)_2]_3Te$ to react with $CH_2N_2$.

Several results pertaining to the reactivity of complexes **157** and **158** toward Lewis acid substrates are summarized in Scheme 20. Accordingly, it is clear that electrophilic addition occurs directly at the chalcogen atom in the reactions with $CF_3SO_3Me$ and $C_5H_5Mn(CO)_2THF$. However, in the reaction with $CF_3CO_2H/NH_4PF_6$ it is possible that the metal is initially protonated and that this is followed by a hydrogen shift to the $CH_2E$ carbon atom. **162** and **163** are the first examples of binuclear compounds in which a thioformaldehyde or selenoformaldehyde ligand links two *different* metal centers[115].



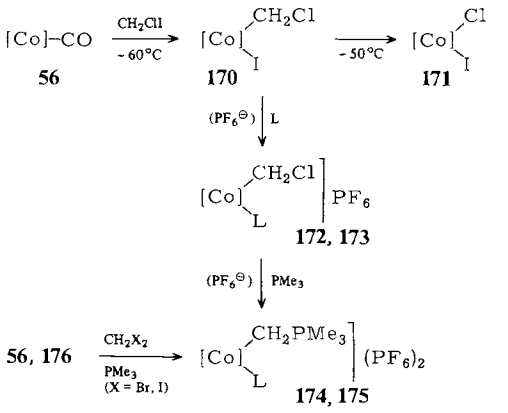
160, 162, 164: E = S
161, 163, 165: E = Se

Scheme 20. [Rh] = $C_5H_5RhPMe_3$.

The ethylene(phosphane) complex **83** reacts not only with $CH_2I_2$ [see reaction (23)] but also with other di- and trihalomethanes[116]. The reaction with $CH_2ClI$ proceeds at almost the same rate as with $CH_2I_2$, which is plausible since in both cases the cleavage of a C–I bond occurs. In the case of $CH_2Br_2$ only a very slow reaction takes place, which (in ether/pentane) affords **167** after two days at room temperature or after 15 h at 45 °C (Scheme 21). $CH_2Cl_2$ does not react at all under similar conditions. The observed difference in the reaction rate reflects very clearly the C–X bonding energy differences; in going from C–I to C–Cl there is an increase of *ca.* 105 kJ/mol.

The compounds **168** and **169** obtained using $CHBr_3$ and $CHI_3$, respectively, can readily be handled in the solid state, although they are labile in solution. In nitromethane, for example, they form, among other products, $C_5H_5RhBr_2(PMe_3)$ or $C_5H_5RhI_2(PMe_3)$. The complexes $C_5Me_5RhCHX_2(CO)X$, which correspond to **168** and **169** insofar as their properties are concerned, are formed from $C_5Me_5Rh(CO)_2$ and $CHX_3$ (X = Br, I)[116]. **169** and its $C_5Me_5$ analogue represent the first isolated diiodomethyl transition-metal compounds whose reactivity is of interest on the basis of the results presented in Scheme 19 and reaction (24).

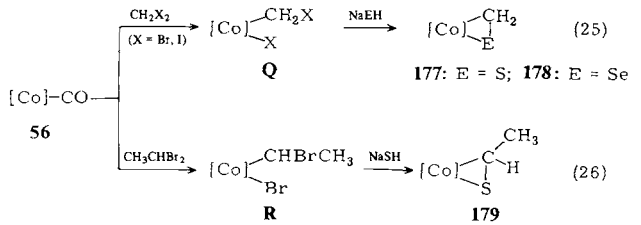
The carbonyl(phosphane)cobalt complex **56** is considerably more reactive toward dihalomethanes than its rhodium analogue **63**. At −60 °C with $CH_2ClI$ the compound **170**, which has been characterized by NMR spectroscopy, is obtained; even at −50 °C in acetone, this eliminates $CH_2$ to form **171**. Addition of an equimolar amount of $PMe_3$ or $P(OMe)_3$ to **170** results in formation of the cationic chloromethylcobalt complexes **172** and **173**, which react at room temperature with trimethylphosphane to give **174** and **175**, respectively. These compounds can also be prepared from **56** or **176** and $CH_2X_2/PMe_3$ simply by mixing the reactands (molar ratio 1 : 1); $C_5H_5Co(CO)_2$ is also formed. In this case it can be assumed that an intermediate analogous to **170** is formed in which the cobalt-halogen bonds are evidently so labile that a very rapid subsequent reaction with the phosphane takes place. Astonishingly, the formation of **174** and **175** is independent of the polarity of the solvent; in toluene, ether, or acetone no difference is observed either in the reaction rate or in the composition of the products (Scheme 22)[117].



172, 174: L = $PMe_3$
173, 175: L = $P(OMe)_3$
176: $C_5H_5Co(CO)P(OMe)_3$

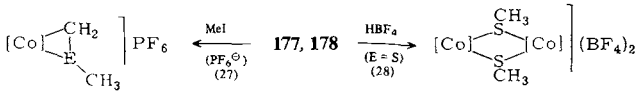
Scheme 22. [Co] = $C_5H_5CoPMe_3$.

Preparation of the thioformaldehyde- and selenoformaldehyde cobalt complexes **177** and **178**, respectively, is possible *via* the conjectured intermediate **Q** formed from **56** and $CH_2X_2$. At least as important as this result is the isolation of the first *dihapto*-bonded thioacetaldehydemetal compound, which is formed—in addition to small amounts of $C_5H_5CoBr_2(PMe_3)$—according to reaction (26)[117]. Like the chalcogenoformaldehydes, $CH_2E$, thioacetaldehyde is also unstable in the monomeric form and has previously not been fixed in a complex, despite ligand characteristics which are comparable to those of $CH_2S$. In this context it should be mentioned that *Herrmann et al.*[114] were able to generate not only $CH_2Se$ and $CH_2Te$ but also the dimethylseleno ketone $Me_2CSe$—which is also unstable in the free state—as bridging ligand between two Mn atoms.




[Co] = $C_5H_5CoPMe_3$

The reactivity of the complexes **177** and **178** corresponds to that of the rhodium compounds **157** and **158**. Methylation can be achieved even with methyl iodide, a fact which confirms the great nucleophilicity of the sulfur and selenium atoms in CoCE three-membered rings[117].




**180**: E = S; **181**: E = Se

**182**

[Co] = $C_5H_5CoPMe_3$

## 3. Metal Bases with Six-Membered Ring Ligands

### 3.1. $d^8$-Systems

From the structural and bonding point of view, the aromatic metal compounds $C_6R_6ML_2$ and $C_6R_6MLL'$ (M = Fe, Ru, Os) are comparable to the cyclopentadienylmetal complexes, $C_5R_5ML_2$ and $C_5R_5MLL'$ (M = Co, Rh, Ir). The metal atom now is in the oxidation state zero and, like $Co^I$, $Rh^I$ and $Ir^I$, thus represents a $d^8$ system. In contrast to the cyclopentadienyl complexes $C_5R_5ML_2$, until recently principally only compounds of the type $C_6R_6ML_2$ were known with $L_2$ = diolefin (*e.g.* $C_4H_6$, 1,3-$C_6H_8$, 1,3-$C_7H_{10}$, and 1,5-$C_8H_{12}$). Most of these were prepared by the "Grignard method"[118]. Before 1978 (*i.e.* when we began our studies[119]), only a few iron complexes with *monodentate* ligands L existed, namely with $L = PF_3$[120] and CO[121]. Because of the pronounced π-acceptor properties of trifluorophosphane or carbon monoxide, these complexes are probably only weak metal bases.

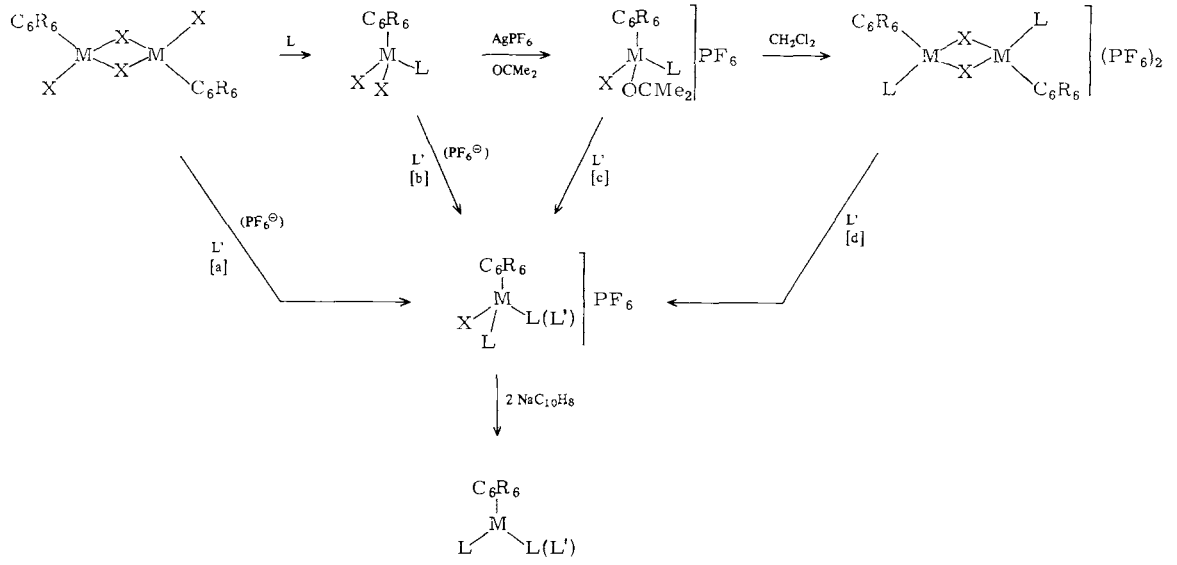
#### *3.1.1. Synthetic Methods*

The synthesis of the bis(trifluorophosphane) complexes $(C_6H_5Me)Fe(PF_3)_2$ and $C_6H_6Fe(PF_3)_2$ has been carried out using metal atom vaporization techniques[120]. By this means, the corresponding phosphite compounds $C_6R_6Fe[P(OMe)_3]_2$ ($C_6R_6 = C_6H_6$, $C_6H_5Me$, 1,4-$C_6H_4Me_2$, 1,3,5-$C_6H_3Me_3$), and $(C_6H_5Me)Fe[P(OEt)_3]_2$, as well as the phosphane complex $(C_6H_5Me)Fe(PMe_3)_2$ are also accessible[122]. In the cocondensation of iron atoms with arenes it seems likely that molecules such as $Fe(C_6R_6)$ or $Fe(C_6R_6)_2$ are formed initially and that these then react with the phosphite or phosphane. The preparation of $C_6Me_6Fe(CO)_2$ proceeds *via* the complex $Fe(C_6Me_6)_2$, which can be isolated as a solid. In the reaction, an $\eta^4$-bonded six-membered ring is probably substituted by the CO groups[121].

For the synthesis of the ruthenium and osmium compounds $C_6R_6ML_2$ ($L = PR_3$, $P(OR)_3$) and $C_6R_6MLL'$ ($L = PR_3$; $L' = P(OR)_3$, CO, CNR, $C_2H_3R$), a reductive procedure employing $NaC_{10}H_8$ as the reducing agent has proved to be useful[123]. The starting materials for the procedure are the salts of the cations $[C_6R_6MXL_2]^+$ or $[C_6R_6MXLL']^+$, which can be obtained from the halide-bridged compounds $[C_6R_6MX_2]_2$ by one of the routes indicated in Scheme 23[124, 131, 134]. It depends primarily upon the ligands L and L' which is the best preliminary step for the preparation of the salts. The acetone complexes can be isolated only for M = Ru (R = H[124], Me[125]; X = Cl; $L = PMe_3$, $PMe_2Ph$, $PMePh_2$, $PPh_3$); for M = Os only the binuclear dications $[(C_6H_6OsL)_2(\mu\text{-}X)_2]^{2+}$ are stable. The synthesis of the ruthenium compounds $[C_6H_6RuCl(PR_3)_2]PF_6$ ($PR_3 = PMe_2Ph$, $PMePh_2$, $PPh_3$) has also been carried out by allowing $[(C_6H_6Ru)_2(\mu\text{-}Cl)_3]PF_6$ to react with the appropriate phosphane[126].

Apart from $NaC_{10}H_8$, experiments were also performed using Na, Na/Hg, NaH, $NaNH_2$, $Li_2CH_2$, $Li_2C_8H_8$, Mg, $Co(C_5H_5)_2$, and diphenylketyl Na as reducing agents although no satisfactory result could be achieved. The successful synthesis of the metal(0) complexes $C_6R_6ML_2$ and $C_6R_6MLL'$ using $NaC_{10}H_8$ has the disadvantage that it is not at all easy to completely separate the naphthalene formed during the reduction from the highly volatile and very soluble products. In the case of thermally relatively stable compounds (*e.g.* M = Os, $L = PMe_3$, $L' = C_2H_4$, $C_3H_6$), this is possible *via* the hydridometal cations and their deprotonation with NaH[127].

Unexpectedly, the complex $C_6H_6Os(PMe_3)_2$ could not be obtained by reducing $[C_6H_6OsI(PMe_3)_2]PF_6$ with $NaC_{10}H_8$. Even the attempt to exchange the olefinic ligand in **183** and **184** by trimethylphosphane did not succeed. Rather the hydrido(phenyl)osmium(II) compound **186** forms by oxidative addition of an $(sp^2)C-H$ bond to the electron-rich metal center. When R = H it is possible to isolate the intermediate **185**. The conversion of the $C_6H_6Os$ into the $OsH(C_6H_5)$ moiety occurs strictly *intra*molecularly, as may be seen from the quantitative formation of **186** in $C_6D_6$ as solvent[128]. It may be that in the initial step after attack of the trimethylphosphane at the metal a reorientation of the benzene from an $\eta^6$- to an $\eta^4$-mode of coordination occurs. This has been postulated by *Muetter-*



Scheme 23. Possible routes to the salts $[C_6R_6MXLL']PF_6$.

[a] $C_6R_6 = C_6H_6$, 1,4-$C_6H_4(Me)iPr$, $C_6Me_6$; M = Ru; X = Cl; L' = $PMe_3$
$C_6R_6 = C_6H_6$; M = Ru; X = Br, I; L' = $PMe_3$
$C_6R_6 = C_6H_6$; M = Ru; X = Cl; L' = $PMe_2Ph$, $PMePh_2$, $PPh_3$
$C_6R_6 = C_6H_6$; M = Os; X = I; L' = $PMe_3$

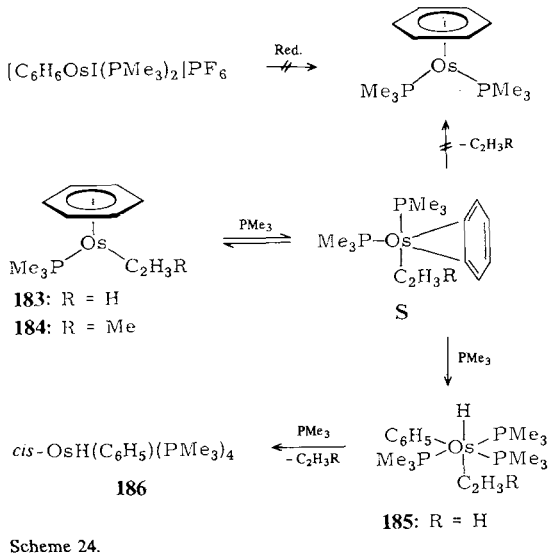
[b] $C_6R_6 = C_6H_6$; M = Ru; X = Cl; L = $PMe_2Ph$, $PPh_3$, $P(OMe)_3$; L' = $PMe_3$
$C_6R_6 = C_6H_6$; M = Ru; X = Cl; L = $PPh_3$; L' = $PMe_2Ph$, $PMePh_2$
$C_6R_6$ = 1,4-$C_6H_4(Me)iPr$, $C_6Me_6$; M = Ru; X = Cl; L = CO; L' = $PMe_3$
$C_6R_6 = C_6H_6$; M = Os; X = I; L = $PPh_3$, $P(OMe)_3$, CNR (R = Me, *t*Bu, *p*-Tolyl, Ph); L' = $PMe_3$

$C_6R_6 = C_6H_6$; M = Os; X = I; L = $PMe_3$; L' = $PMe_2Ph$
$C_6R_6 = C_6H_6$; M = Os; X = I; L = $PMe_3$, $PPh_3$; L' = CO

[c] $C_6R_6 = C_6H_6$; M = Ru; X = Cl; L = $PMe_3$; L' = $PMe_2Ph$, $PPh_3$, $P(OMe)_3$
$C_6R_6 = C_6H_6$; M = Ru; X = Cl; L = $PPh_3$; L' = $PMe_2Ph$, $PMePh_2$, $P(OMe)_3$, $P(OPh)_3$

[d] $C_6R_6 = C_6H_6$; M = Ru; X = I; L = $PMe_3$; L' = CO
$C_6R_6 = C_6H_6$; M = Os; X = I; L = $PPh_3$; L' = $PMe_3$, $PPh_3$
$C_6R_6 = C_6H_6$; M = Os; X = I; L = $P(OMe)_3$; L' = $PMe_3$, $P(OMe)_3$

*ties et al.*, for example, in the catalytic hydrogenation process based on areneruthenium complexes[129]. Kinetic measurements are consistent with the conjectured reaction sequence in Scheme 24[130].



**183**: R = H
**184**: R = Me

Scheme 24.

### 3.1.2. Reactions with Electrophiles

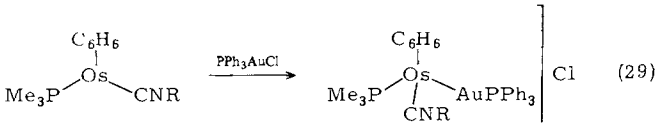
As might be expected, the complexes $C_6R_6ML_2$ and $C_6R_6MLL'$ react with Brønsted acids and with methyl iodide or $[OMe_3]BF_4$ to form salts of the cations $[C_6R_6ML_2]^+$ and $[C_6R_6MLL']^+$, respectively. These are considerably more stable (thermally and towards oxidizing agents) than the metal(0) compounds. Here, too, the metal basicity depends quite significantly on the donor strengths of the ligands L and L'. Whereas, for example, the bis(trimethylphosphane) complexes $C_6R_6Ru(PMe_3)_2$ ($C_6R_6 = C_6H_6$, 1,4-$C_6H_4(Me)iPr$, $C_6Me_6$) react even at −78 °C with $NH_4PF_6$ in methanol to form the compounds $[C_6R_6RuH(PMe_3)_2]PF_6$, the formation of $PMePh_2$ and $PPh_3$ analogues occurs only at room temperature[123]. Moreover, for the synthesis of $[C_6Me_6RuH(PMe_3)CO]PF_6$, $[C_6H_6RuH(PMe_3)C_2H_4]BF_4$, and $[(C_6H_5Me)FeH(P(OMe)_3)_2]BF_4$ it is necessary to use acids stronger than $NH_4^+$, such as $CF_3CO_2H$ or $HBF_4$[122a, 123, 127].

It is generally found that 1) the presence of a good π-acceptor ligand such as CO or $C_2H_4$ weakens the metal basicity and 2) the osmium(0) compounds are more reactive than the homologous iron and ruthenium complexes.

Methylation proceeds just as smoothly as protonation. Here, the reaction rate here also depends characteristically on the metal and on the nature of the ligands. Thus, for example, $C_6H_6Os[P(OMe)_3]_2$ reacts with methyl iodide to form $[C_6H_6OsCH_3(P(OMe)_3)_2]I$[123], whereas $[OMe_3]BF_4$ is necessary for the formation of the corresponding cationic iron complex[122a]. In the case of bis(phosphane)ruthenium compounds of the type $C_6R_6Ru(PR_3)_2$, there is a decrease in the rate of methylation along the sequence $PMe_3$ > $PMe_2Ph$ > $PMePh_2$ > $PPh_3$ (for $C_6R_6 = C_6H_6$) and $C_6H_6$ > 1,4-$C_6H_4(Me)iPr$ > $C_6Me_6$ (for $PR_3 = PMe_3$)[123]. This indicates that, in addition to electronic effects, steric effects also play a role in determining the ease of attack of the electrophile at the metal atom in $C_6R_6ML_2$ complexes.

Only $C_6H_6Ru(PMe_3)_2$ **191** reacts smoothly with ethyl iodide to give the corresponding ethyl compound $[C_6H_6RuC_2H_5(PMe_3)_2]^+$ (which is isolated as the $PF_6$ salt **192**[123]). When **191** is allowed to react with *n*-propyl and *n*-butyl bromides or iodides, in addition to the expected products $[C_6H_6RuR(PMe_3)_2]X$, the corresponding metal halide complexes $[C_6H_6RuX(PMe_3)_2]X$ are also formed. As for the analogous reactions of the cyclopentadienyl compounds, $C_5R_5M(PMe_3)_2$ (see Section 2.2.3), this result suggests the formation of radical intermediates. Of the Lewis acidic trimethylelement halides $Me_3ECl$ (E = Si, Ge, Sn), only the tin compound affords a product having the composition $[C_6H_6RuEMe_3(PMe_3)_2]X$ upon reaction with $C_6H_6Ru(PMe_3)_2$[123]. Under the same conditions, $Me_3SiCl$ and $Me_3GeCl$ form mixtures of products in which only the hydridoruthenium cation $[C_6H_6RuH(PMe_3)_2]^+$ can be unequivocally detected.

Recently, two complexes containing an osmium-gold bond have been prepared by oxidative addition of $PPh_3AuCl$ to $C_6H_6Os(PMe_3)CNR$ (**187**, **188**)[131]. According to the IR data of **189** and **190**, the possibility of the isocyanide forming a bridge between the two metal atoms can be excluded. The $PPh_3Au^+$ cation thus behaves completely analogously to a proton towards the compounds **187** and **188**, which is certainly to be expected from their isolobal relationship[132].




(29)

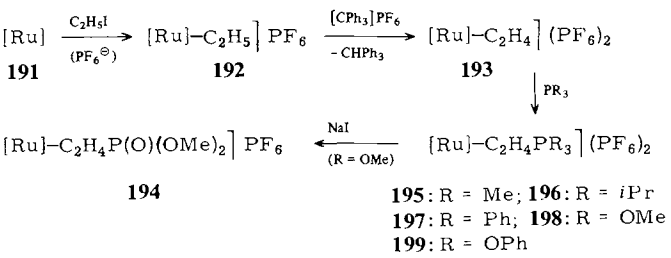
**187**, **188** **189**, **190**

**187**, **189**: R = Me
**188**, **190**: R = *p*-Tolyl

Overall, the metal basicity of the arenemetal complexes $C_6R_6ML_2$ would even appear to exceed that of the cyclopentadienylmetal compounds $C_5R_5ML_2$. While the $PF_6$ salts of the cations $[C_5H_5MH(PMe_3)_2]^+$ **16** and **17** readily react with NaH to form the neutral complexes $C_5H_5M(PMe_3)_2$ **18** and **19**, respectively, deprotonation of the analogous benzeneruthenium and benzeneosmium compounds $[C_6H_6RuH(PMe_3)_2]^+$ and $[C_6H_6OsH(PPh_3)_2]^+$ does not occur under the same conditions[123]. These cations react very slowly even with MeLi or *t*BuLi to form **191** and $C_6H_6Os(PPh_3)_2$, respectively. Measurements (MS and PES) currently being made to determine the ionization potentials should provide information on how these values differ for typical derivatives of the two complex series $C_5R_5ML_2$ and $C_6R_6ML_2$, and how this may be correlated with the difference in metal basicity.

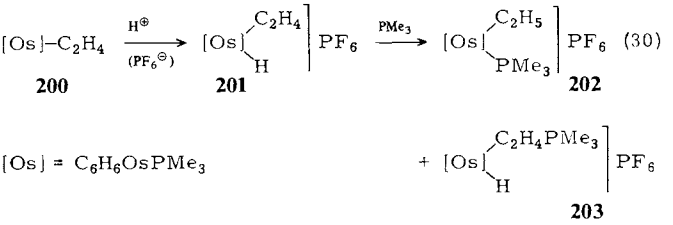
### *3.1.3. Subsequent Reactions of the Primary Products*

The ethyl compound $[C_6H_6RuC_2H_5(PMe_3)_2]^+$ formed from **191** reacts with $[CPh_3]PF_6$ to give the dication $[C_6H_6Ru(PMe_3)_2C_2H_4]^{2+}$, which behaves as an electrophile and reacts with phosphanes or phosphites even at room temperature. The process, which involves the conversion of the Ru–$C_2H_4$ π-bond into an Ru–$C_2H_4PR_3$ σ-bond, yields the complexes **195**–**199** (Scheme 25)[133]. It has not been possible to eliminate a hydride ion from the methyl compound $[C_6H_6RuCH_3(PMe_3)_2]^+$. Reaction of the hydrido complex $[C_6H_6RuH(PMe_3)_2]PF_6$ with $[CPh_3]PF_6$ in acetone leads to the $PF_6$ salt of the dication $[C_6H_6Ru(PMe_3)_2(OCMe_2)]^{2+}$. This salt contains an unusually inert Ru–$OCMe_2$ bond, and is therefore not a suitable starting material for the preparation of octahedral ruthenium(II) complexes of general type $[C_6H_6Ru(PMe_3)_2L]^{2+}$ (L = $PR_3$, $P(OR)_3$, CO, *etc.*)[134].




Scheme 25. [Rh] = $C_6H_6Ru(PMe_3)_2$.

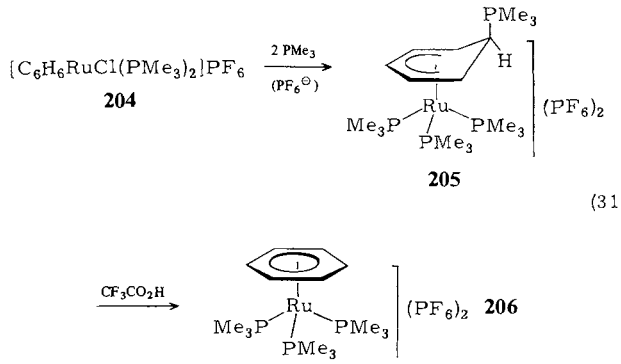
Nucleophilic addition of a phosphane to coordinated ethylene has also been observed in the reactions of $[C_6H_6MCH_3(PMe_3)C_2H_4]PF_6$ (M = Ru, Os) and **201** with $PMe_3$[127]. In the latter case, according to reaction (30) a mixture of **202** and **203** is obtained which contains the two isomers in a ratio of 3:2. The ruthenium complex analogous to **201** yields exclusively the ethyl compound **192** with trimethylphosphane. The variable mobility of the ligands in the $[C_6H_6RuH(PMe_3)C_2H_4]^+$ and $[C_6H_6OsH(PMe_3)C_2H_4]^+$ cations is, in general, reflected in the NMR spectra, of which only that for the ruthenium complex shows a temperature dependence consistent with an equilibrium between the ethylene(hydrido) and ethyl tautomers[127].




(30)

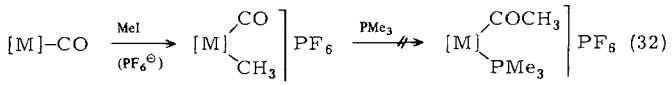
In addition to the $[C_6H_6MR(PMe_3)C_2H_4]^+$ cations obtained from $C_6H_6Ru(PMe_3)C_2H_4$ and **200**, the structurally related $[C_6H_6RuCl(PR_3)PR'_3]^+$ complexes are also capable of adding a phosphane. According to reaction (31), in the reaction of **204** and $PMe_3$, for example, the ($\eta^5$-6-phosphoniocyclohexadienyl)ruthenium(II) compound **205** is obtained. In this process, addition of phosphane to the ring occurs initially and is followed by substitution of the chloride[135]. At low temperatures, rotation about the metal-ring bond in the cations $[(6\text{-}C_6H_6PMe_3)Ru(PMe_3)_2PR_3]^{2+}$ with R = Ph or $NMe_2$ is so strongly hindered that rigid rotamers can be observed. The C–$PMe_3$ bond in **205** can easily be cleaved by trifluoroacetic acid and thus opens up a route to half-sandwich complexes of the type $[C_6H_6Ru(PR_3)(PR'_3)L]^{2+}$ (*e.g.* **206**) which are not accessible by any other method[135].

Surprisingly, the carbonyl(methyl) complexes **209** and **210**, prepared according to reaction (32), are highly inert



(31)

and react neither with $PMe_3$ nor with iodide ions by CO insertion (or by methyl group migration) to form the acetyl compounds $[C_6R_6MCOCH_3(PMe_3)_2]PF_6$ and $C_6R_6MCOCH_3(PMe_3)I$, respectively[123,136]. For adjacent CO and $CH_3$ groups such immobility is very unusual and is paralleled only in the behavior of $OsCH_3(CO)_2(PPh_3)_2I$[137]. The acetylruthenium cation of composition $[C_6H_6RuCOCH_3(PMe_3)_2]^+$ also cannot be obtained by reacting **191** with $CH_3COCl$; in this instance only decomposition (even at −78 °C) is observed[123].

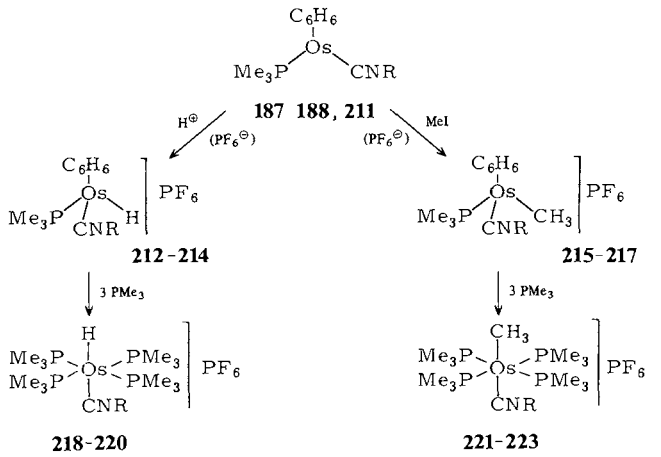


(32)

**207, 208** **209, 210**

**207, 209**: [M] = $C_6Me_6RuPMe_3$; **208, 210**: M = $C_6H_6OsPMe_3$

The related isocyanide(methyl) compounds **215—217** are similarly as inert as **209** and **210**. In contrast to the cobalt complexes $[C_5H_5CoCH_3(PMe_3)CNR]X$ (see Scheme 9), the cations of **215—217** do not rearrange either in acetone or in acetonitrile—not even in the presence of a large excess of iodide ions—to form acetimidoyl compounds; nor do they react to form metallaheterocycles[131a]. With trimethylphosphane in acetone, the complexes **221—223** having the $CH_3$ and CNR ligands in the *trans* position are formed by displacing the six-membered ring (Scheme 26);



**187, 212, 215, 218, 221**: R = Me
**188, 213, 216, 219, 222**: R = *p*-Tolyl
**211, 214, 217, 220, 223**: R = *t*Bu

Scheme 26.

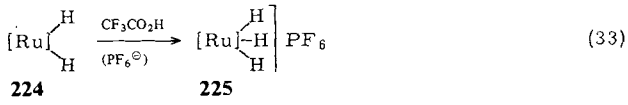
the hydrido(isocyanide) compounds **212—214** react analogously[131b]. The stability of the Os—$CH_3$ bond in **221—223** and of the Os—H bond in **218—220** evidently prevents migration of a methyl or hydride ligand to the isocyanide group. Accordingly, even in the presence of an excess of $PMe_3$ (or CNR), the formation of corresponding cationic imidoylosmium complexes cannot be observed.

### 3.2. $d^6$-Systems

In contrast to the cyclopentadienylmetal compounds $C_5H_5Co(CO)_2$ and $C_5H_5Rh(CO)_2$ which—as mentioned in the introduction—are rapidly decomposed in $H_2SO_4$ or $BF_3 \cdot H_2O$, the arenechromium tricarbonyls $C_6R_6Cr(CO)_3$ are transiently stable in strongly acidic media (*e.g.* $HSO_3F$ in $SO_2$[138] or $CF_3CO_2H/BF_3 \cdot H_2O = 1/1$[139]) and form hydridometal cations $[C_6R_6CrH(CO)_3]^+$ which can be detected by IR and NMR spectroscopy. Substitution of a CO group in $C_6R_6Cr(CO)_3$ by a phosphane such as $PPh_3$ increases the electron density at the metal, and thus protonation, even with $CF_3CO_2H$ in toluene (ratio 1 : 10), becomes possible[140]. If the compounds $C_6R_6M(CO)_2PMe_2Ph$ (M = Cr, Mo, W) are used as starting materials, the formation of two isomers of $[C_6R_6MH(CO)_2PMe_2Ph]^+$ (with H and $PMe_2Ph$ in the *cis* and *trans* positions respectively) as well as their rearrangement have been detected by NMR spectroscopy[141]. To isolate stable salts of the type $[C_6R_6MHL_3]X$, it is necessary to start out from the appropriate tris(phosphane) complexes, such as $C_6H_6Mo(PMePh_2)_3$ or $C_6H_6Mo(PMe_2Ph)_3$, which react with $CF_3CO_2H$ or HCl in ethanol to yield the corresponding hydridomolybdenum cations[142]. The manganese compounds $C_5H_5Mn(PR_3)_3$ (R = Me, OMe, OEt)[143], which are structurally related to $C_6H_6Mo(PR_3)_3$, rapidly decompose when dissolved in acidic media. Accordingly, it is not yet possible to make any statement about the existence of the hydrido complexes $[C_5H_5MnH(PR_3)_3]^+$.

Of the presently known areneruthenium and areneosmium compounds having a $d^6$-electron configuration, the dihydrido complexes $C_6H_6RuH_2[PiPr_3]$, $C_6Me_6RuH_2(PR_3)$ (R = Me, Ph), and $C_6H_6OsH_2[PiPr_3]$ are metal bases[144]. They react even at −78 °C with $CF_3CO_2H/NH_4PF_6$ or $HBF_4$ in ether to form $[C_6R_6MH_3(PR_3)]^+$ cations which possess a fluxional structure in solution at room temperature. This behavior corresponds to that of the $[MH_3(PMe_3)_4]^+$ cations in which the metal is similarly in the oxidation state +4 and which are formed from the compounds $MH_2(PMe_3)_4$ (M = Ru, Os) and $NH_4PF_6$[145]. It is especially noteworthy that the complex **226**, which is closely related to **224**, yields a binuclear cation upon protonation[146]. The low tendency of rhodium to form compounds having the oxidation state +5 (as would be the case in a cation of the type $[C_5H_5RhH_3(PR_3)]^+$) obviously prevents formation of a mononuclear product.

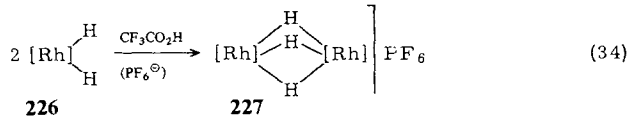
As well as the dihydrido complexes, the analogous dimethylruthenium(II) complexes also react with Brønsted acids. The reactions carried out using **229** are summarized in Scheme 27[144b,147]. Since the ligands $H^-$ and $CH_3^-$ are comparable in their ability to act as σ-donors, it may also



(33)

224 225

[Ru] = $C_6H_6RuP(iPr)_3$

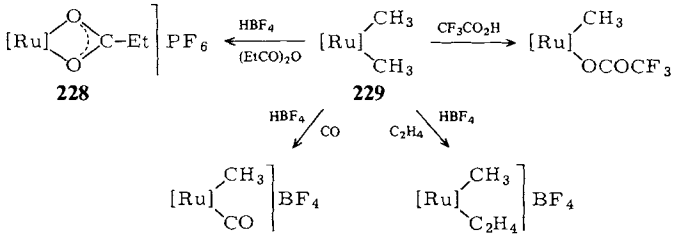


(34)

226 227

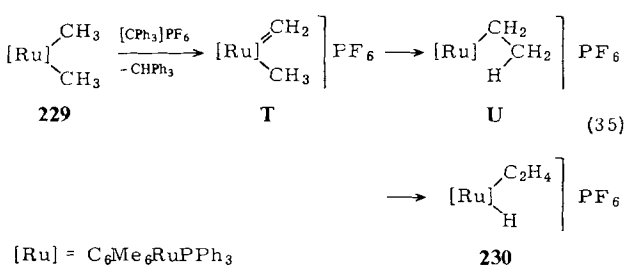
[Rh] = $C_5H_5RhP(iPr)_3$

be assumed that in the reactions of **229** an initial protonation at the metal takes place followed by a reductive elimination of methane. The dimethylcobalt compounds $(C_5H_4R')Co(CH_3)_2PMe_3$ (R′=H, *i*Pr, *t*Bu) behave analogously[148]. The bis(trifluoroacetato) complexes $(C_5H_4R')Co(OCOCF_3)_2PMe_3$, formed from the dimethylcobalt complexes in the presence of excess trifluoroacetic acid, yield with $P(OMe)_3$ in a sequence of reaction steps the phosphonate compounds mentioned in Scheme 3 (see Section 2.2.2). The circle is thereby completed to the starting point of our own studies on electron-rich half sandwich complexes.



Scheme 27. [Ru] = $C_6Me_6RuPPh_3$.

The compound **229** reacts very readily not only with $HBF_4$ or $CF_3CO_2H$ but also with Lewis acids such as $[CPh_3]^+$. Thereby, the ethylene(hydrido) complex **230**, whose structure has been determined by X-ray analysis, is obtained in high yield[149]. As established by labeling experiments the solvent does not participate in this reaction. The mechanism of the CC bond formation presumably involves primary attack of the trityl cation on a C–H bond of one of the Ru–$CH_3$ groups to eliminate a hydride ion, and subsequent formation of the coordinatively unsaturated ethyl compound **U** from the intermediate **T** by intramolecular rearrangement. The compound **U** stabilizes itself by a β-H migration to form the ethylene(hydrido) complex.



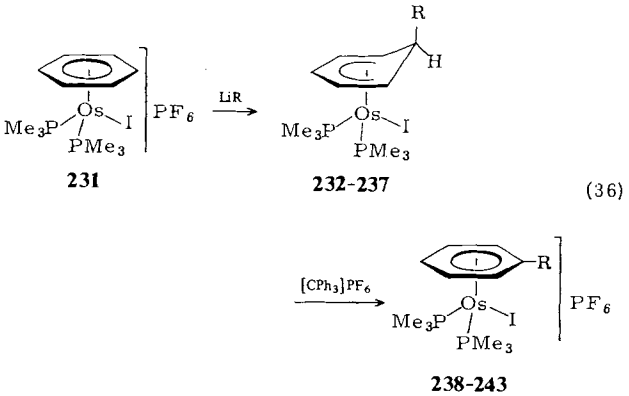
(35)

229 T U 230

[Ru] = $C_6Me_6RuPPh_3$

*Cooper et al.* have discovered a completely analogous conversion of an $M(CH_3)_2$ moiety into an $MH(C_2H_4)^+$ group for $M=(C_5H_5)_2W$[150]. In this case it was possible to show that in the primary step an electron transfer takes place from the dimethyl compound to the trityl cation and that the trityl radical reacts with the paramagnetic moiety $[(C_5H_5)_2W(CH_3)_2]^+$. There are no indications of similar radical processes in the formation of **230** (nor in the formation of the homologous osmium complex[144b]). The CC bond formed during the conversion of **T** into **U** [see reaction (35)] represents, in addition, a model reaction for an elementary step in the heterogeneous Fischer-Tropsch synthetic process. The most generally accepted mechanism for this is that $CH_2$ and $CH_3$ groups are formed on the surface of the catalyst and that the chain is built up by successive insertion of methylene units into metal-alkyl bonds[151]. After β-H elimination (analogous to that in the conversion of **U** into **230** according to reaction (35)), α-olefins are formed which are, of course, known to be primary products of the Fischer-Tropsch synthesis.

Finally, a $d^6$-metal system should be mentioned which can be protonated and was discovered during our attempts to synthesize the metal base $C_6H_6Os(PMe_3)_2$. The compound $[C_6H_6OsI(PMe_3)_2]PF_6$ **231**, which—as indicated in Scheme 24—cannot be reduced by $NaC_{10}H_8$ to form $C_6H_6Os(PMe_3)_2$, reacts with lithiumorganyls, LiR, by *exo*-addition of the carbanion to the arene ring to produce the cyclohexadienyl complexes **232—237**[152]. The latter react with $[CPh_3]PF_6$ to yield the corresponding ring-substituted areneosmium(II) compounds **238—243** together with $CHPh_3$. This result is surprising insofar as there are only a few examples currently known where cyclohexadienylmetal complexes $(\eta^5\text{-}C_6H_6R)ML_n$ in which the group R is in the *exo*-position react with trityl salts by hydride elimination[153].



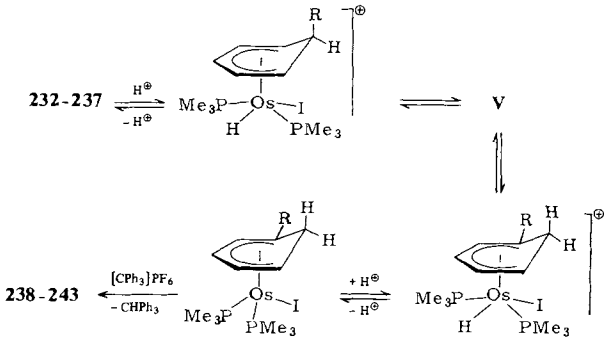
(36)

231 232-237 238-243

**232**, **238**: R = Me **235**, **241**: R = *n*Bu
**233**, **239**: R = Et **236**, **242**: R = *t*Bu
**234**, **240**: R = *n*Pr **237**, **243**: R = Ph

Mechanistic investigations on the conversion of **232—237** into **238—243** indicate that the hydride abstraction does not take place directly but occurs only in the presence of protons (formed, for example, from $[CPh_3]^+$ in acetone)[154]. In the primary step a hydridoosmium(IV) cation is formed which for R = *t*Bu can be isolated as the $PF_6$ salt. However, with the other R groups it rearranges intramolecularly to afford an isomer in which R is found in the olefinic part of the ring. In the intermediate **V** either a cyclo-

hexadiene ligand (formed by hydride migration from the metal to the $C^1$ carbon atom) or an OsCH three-center bond could be present—as in similar manganese complexes[155]. Deprotonation of the hydrido cation formed from **V** (which for R = Me and *n*Bu was isolated as the $PF_6$ salt) yields a cyclohexadienyl compound with a $CH_2$ group in the ring which then reacts with $[CPh_3]^+$ by hydride elimination.




Scheme 28.

The reaction sequence shown in Scheme 28 demonstrates that even the complexes **232—237** function as metal bases. Because of the coordination of two trimethylphosphane ligands, the metal clearly has a relatively high electron density and accordingly is able to react by proton addition. The cyclopentadienylruthenium and cyclopentadienylosmium(II) compounds, $C_5H_5MX(PMe_3)_2$ (M = Ru, X = Cl; M = Os, X = Br) recently synthesized by *Bruce et al.*, also form stable hydridometal cations with $HPF_6$ and behave completely analogously to **232—237**[156]. This, together with results obtained using $[C_6H_6OsI(PMe_3)_2]$, increases the number of examples known which show that not only half-sandwich complexes having a $d^8$ configuration at the metal but also those with a $d^6$ metal center are capable of oxidative additions.

## 4. Conclusions

Following in the footsteps of the square-planar Vaska-type compounds (including Wilkinson's catalyst), the half-sandwich complexes $C_5R_5ML_2$ and $C_6R_6ML_2$ have established themselves in coordination chemistry over the past decade—primarily due to the contributions discussed in this review—as an additional group of *metal bases* having a $d^8$-metal system. Their nucleophilicity is determined primarily—as has been documented in many instances—by the donor properties of the ligands $C_nR_n$ and L. As the donor strength increases electron density increases at the metal and hence facilitates the attack of any electrophile. As far as is known there are only minor differences between the cyclopentadienyl- and arenemetal complexes. This can be understood qualitatively from MO calculations carried out by *Hoffmann* and *Albright*[157] which show that half-sandwich complexes $C_nR_nML_2$ (n = 5 or 6) possess an energetically relatively high-lying occupied molecular orbital which has non-bonding character with respect to the metal-ligand bonds present. Its electron density distribution can be described as shown in Figure 2.

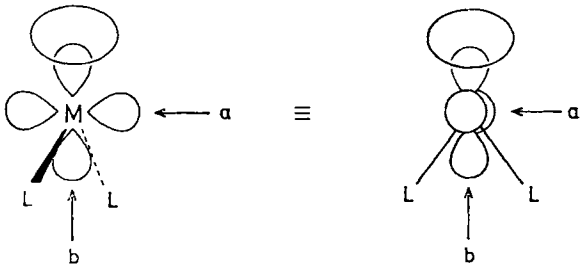


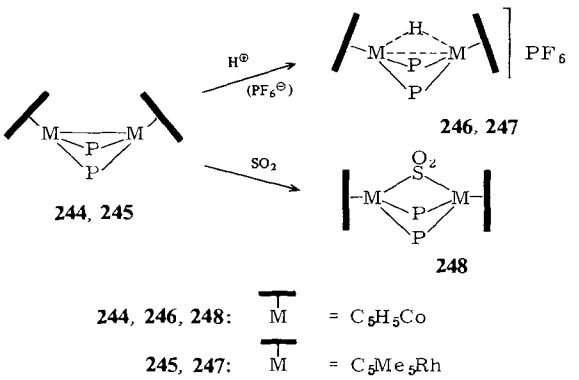

Fig. 2. Electron density distribution in an occupied MO of $C_5R_5ML_2$ or $C_6R_6ML_2$ [157].

Such an MO (whose "shape" very closely resembles the $d_{z^2}$ orbital of the metal in a planar $d^8$ system) represents, according to *Roald Hoffmann*[158], "the spearhead of nucleophilic activity of the compounds $C_nR_nML_2$". This "spearhead" clearly exceeds even the nucleophilicity of the phosphorus atom in a phosphane, as is evidenced by the reaction of $C_5Me_5Rh(CO)PMe_2PMe_2$ with methyl iodide (which leads *via* the cation $[C_5Me_5RhCH_3(CO)PMe_2PMe_2]^+$ to the compound $C_5Me_5RhCOCH_3(PMe_2PMe_2)I$)[38]. Kinetic measurements by *Pearson* and *Figdore*[159] support the conclusion that the rate of methylation of the $C_5H_5M(CO)PPh_3$ (M = Co, Rh, Ir) complexes at room temperature is 10—100 times that for uncoordinated $PPh_3$.

In addition to the electronic factors determining the metal-base character of the half-sandwich compounds $C_5R_5ML_2$ and $C_6R_6ML_2$, steric factors cannot be entirely neglected when considering the reactivity. Results obtained to date suggest that a substantial number of electrophiles are capable of addition to a metal to form a metal-element bond. Such results also indicate that when bulky (space-filling) Lewis acids are used radical reactions frequently occur which are in most cases associated with decomposition. This behavior can be understood by recalling that the metal in the five- and six-membered ring $ML_2$ complexes is relatively well shielded by the ligands, as should be apparent from Figure 2. A fairly large electrophile thus has difficulty in interacting with the nucleophilic center. In several cases the reactivity is directly paralleled by the space-filling capacity of L (*e.g.* expressed in terms of the Tolman cone angle[160]). Thus, for instance, the rate of the reaction of $C_5H_5CoL_2$ with methyl iodide decreases with increasing bulkiness of the ligand L (according to the sequence: $PMe_3 < PMe_2Ph < PEt_3 < PMePh_2 < PPh_3$)[161].

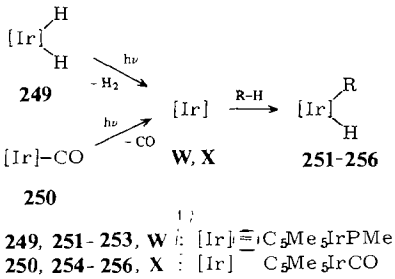
Interestingly enough, the metal basicity of cyclopentadienylcobalt and rhodium compounds is not confined to species having only *one* metal center. The binuclear complexes **244**[162] and **245**[163], in which the two metal atoms are coordinated in a *formally* similar way to those in the compounds $C_5R_5M(PMe_3)_2$, react for example with Brønsted acids and $SO_2$ by electrophilic addition to the metal-metal bond[162-164]. The hydrido bridge formed upon protonation can be opened by Lewis bases thus allowing formation of binuclear cobalt(III) and rhodium(III) hydrido complexes. These may be viewed as potential reducing agents and are capable, for example, of intramolecularly converting an isocyanide- into a formimidoyl-ligand and an alkyne- into a vinyl-group[165]. From these observa-

tions it seems that bridge building could be a means of increasing the reactivity of metal clusters (and perhaps also of metal surfaces).




Scheme 29. P = $PMe_2$.

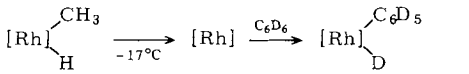
What are the trends for the future? An extremely relevant topic—which is connected at least indirectly with the chemistry of metal bases $C_nR_nML_2$—is the "activation" (or, more precisely, the facile cleavage) of C–H bonds by transition metals[166]. Although there is still no concrete evidence that compounds of the type $C_5R_5ML_2$ or $C_6R_6ML_2$ react *directly* with aliphatics or arenes, the corresponding moieties $[C_5R_5ML]$ and $[C_6R_6ML]$ are definitely able to do so. Thus, *Janowicz* and *Bergman*[167] and, independently, *Hoyano* and *Graham*[168] have recently found (see Scheme 30) that UV irradiation of solutions of both **249** and **250** in benzene, cyclohexane or neopentane leads to oxidative addition with formation of the corresponding aryl(hydrido) or alkyl(hydrido) iridium complexes $C_5Me_5IrH(R)L$ (R = Ph, $C_6H_{11}$, $CH_2CMe_3$). The authors assume that in these reactions a 16-electron moiety $[C_5Me_5IrL]$ (**W**, **X**) is initially formed which then reacts with a C–H bond in the hydrocarbon.




249, 251-253, W: [Ir] = $C_5Me_5IrPMe_3$
250, 254-256, X: [Ir] = $C_5Me_5IrCO$

Scheme 30.

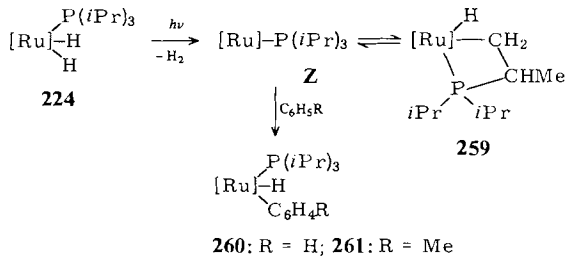
Results obtained over the last few months provide evidence that not only iridium but also analogous rhodium and ruthenium compounds can effect such a C–H bond cleavage. Low temperature photolysis of $C_5Me_5RhH_2(PMe_3)$ in pure propane yields the spectroscopically characterized complex $C_5Me_5RhH(nPr)PMe_3$. This complex reacts at −15 °C by reductive elimination of $C_3H_8$, but upon addition of $CHBr_3$ it can be converted into the stable product $C_5Me_5Rh(nPr)(PMe_3)Br$[169]. The hydrido(methyl) compound **257** prepared from $C_5Me_5RhCH_3(PMe_3)Cl$ is also extremely labile and very rapidly forms the complex **258** in $C_6D_6$[169].




[Rh] = $C_5Me_5RhPMe_3$

(37)

With other phosphane ligands it is possible to stabilize an intermediate such as **W** or **Y** [see Scheme 30 and reaction (37)] even by means of *intramolecular* C–H addition. Thus for example, photolysis of $C_6H_6RuH_2[P(iPr)_3]$ **224** at room temperature in $C_6H_{12}$ or $C_6D_{12}$ and leads to isolation of **259**, which can be characterized by elemental analysis and NMR spectroscopy. By dissolving **259** in benzene or toluene and allowing the reaction to take place in the *dark*, the corresponding aryl(hydrido) complex **260** or **261** is obtained. It seems probable that the moiety actually reacting is the intermediate **Z**. This C–H bond cleavage *without any simultaneous irradiation* may offer a possibility to make other, more sensitive hydrocarbons react with transition metals and thereby bring a new stimulus to the problem of "C–H activation".




Scheme 31. [Ru] = $C_6H_6Ru$.

In an article which appeared in 1970 and made the concept of *metal basicity* popular, *Shriver*[5] wrote that "It can be anticipated that metal basicity will become an increasingly important concept because current vigorous activity in the synthesis of new low oxidation-state complexes will lead to new metal bases and because available spectroscopic tools allow convenient recognition of metal-base interaction with Lewis acids". This expectation has been more than fulfilled, not least in investigations of the behavior of electron-rich half sandwich complexes. It may well be conceivable that $d^8$ systems of the type $C_nR_nML_2$ or $C_nR_nMLL'$, where M is $Fe^0$, $Ru^0$ and $Os^0$, as well as $Co^I$, $Rh^I$ and $Ir^I$, will soon find counterparts in other systems having $Ni^{II}$, $Pd^{II}$, and $Pt^{II}$ as the central atom. This again would represent an extension of the palette of nucleophilic transition-metal compounds, which nowadays are relatively common and are no longer curiosities.

*I should like first and foremost to thank my co-workers in this field whose names appear in the literature citations. Without their involvement and enthusiasm it would not have been possible to reach our goals. Thanks are also due to colleagues who by carrying out numerous X-ray analyses have contributed to the success of these investigations: Dr. C. Burschka, Dr. G. Evrard, Prof. C. Krüger, Prof. U. Schubert, Prof. M. L. Ziegler and their co-workers. Finally, our*

*success is due in large measure to support by the Deutsche Forschungsgemeinschaft, the Fonds der Chemischen Industrie and the companies BASF, Bayer and Degussa, all of which I heartily thank. Last but not least, I extend cordial thanks to Professor Sir Jack Lewis, Cambridge (U. K.), whose kind invitation made it possible for me to prepare this article in the stimulating atmosphere of the Chemical Laboratory in Lensfield Road and in Robinson College.*

Received: July 7, 1983 [A 478 IE]
German version: *Angew. Chem. 95* (1983) 932

[1] E. O. Fischer, W. Hafner, *Z. Naturforsch. B 9* (1954) 503.
[2] E. O. Fischer, H. P. Fritz, *Adv. Inorg. Chem. Radiochem. 1* (1959) 56.
[3] G. Wilkinson, F. A. Cotton, *Prog. Inorg. Chem. 1* (1959) 1.
[4] G. E. Coates, M. L. H. Green, K. Wade: *Organometallic Compounds, Vol. II*, Chapman and Hall, London 1968.
[5] D. F. Shriver, *Acc. Chem. Res. 3* (1970) 231.
[6] a) L. Vaska, *Acc. Chem. Res. 1* (1968) 335; b) J. P. Collman, W. R. Roper, *Adv. Organomet. Chem. 7* (1968) 53; c) J. Halpern, *Acc. Chem. Res. 3* (1970) 386.
[7] A. Davison, W. McFarlane, L. Pratt, G. Wilkinson, *J. Chem. Soc. 1962*, 3653.
[8] D. J. Cook, J. L. Dawes, R. D. W. Kemmitt, *J. Chem. Soc. A 1967*, 1547.
[9] I. N. Nowell, D. R. Russell, *Chem. Commun. 1967*, 817.
[10] J. L. Dawes, R. D. W. Kemmitt, *J. Chem. Soc. A 1968*, 1072.
[11] a) A. J. Oliver, W. A. G. Graham, *Inorg. Chem. 9* (1970) 243; b) A. J. Oliver, W. A. G. Graham, *ibid. 9* (1970) 2653; c) A. J. Hart-Davis, W. A. G. Graham, *ibid. 9* (1970) 2658; d) A. J. Oliver, W. A. G. Graham, *ibid. 10* (1971) 1165; e) A. J. Hart-Davis, W. A. G. Graham, *ibid. 10* (1971) 1653.
[12] T. Kruck, W. Hieber, W. Lang, *Angew. Chem. 78* (1966) 208; *Angew. Chem. Int. Ed. Engl. 5* (1966) 247.
[13] V. Harder, J. Müller, H. Werner, *Helv. Chim. Acta 54* (1971) 1.
[14] B. Juthani, Dissertation, Universität Würzburg 1980.
[15] H. Yamazaki, N. Hagihara, *Bull. Chem. Soc. Jpn. 44* (1971) 2260.
[16] B. Klingert, H. Werner, *Chem. Ber. 116* (1983) 1450.
[17] H. Werner, W. Hofmann, *Chem. Ber. 110* (1977) 3481.
[18] H. Yamazaki, Y. Wakatsuki, *J. Organomet. Chem. 139* (1977) 157.
[19] H. Werner, W. Hofmann, *Chem. Ber. 114* (1981) 2681.
[20] H. Werner, B. Heiser, B. Klingert, R. Dölfel, *J. Organomet. Chem. 240* (1982) 179.
[21] P. V. Rinze, J. Lorberth, H. Nöth, B. Stutte, *J. Organomet. Chem. 19* (1969) 399.
[22] Y. Wakatsuki, H. Yamazaki, *J. Organomet. Chem. 64* (1974) 393.
[23] F. Faraone, G. Tresoldi, G. A. Loprete, *J. Chem. Soc. Dalton Trans. 1979*, 933.
[24] H. Werner, J. Wolf, U. Schubert, K. Ackermann, *J. Organomet. Chem. 243* (1983) C63.
[25] H. Werner, A. Höhn, unpublished results; see A. Höhn, Diplomarbeit, Universität Würzburg 1983.
[26] H. Neukomm, H. Werner, *Helv. Chim. Acta 57* (1974) 1067.
[27] H. Werner, L. Hofmann, W. Paul, *J. Organomet. Chem. 236* (1982) C65.
[28] H. Werner, R. Feser, *J. Organomet. Chem. 232* (1982) 351.
[29] H. Werner, R. Feser, W. Buchner, *Chem. Ber. 112* (1979) 834.
[30] R. A. Jones, F. M. Real, G. Wilkinson, A. M. R. Galas, M. B. Hursthouse, *J. Chem. Soc. Dalton Trans. 1981*, 126.
[31] H. Werner, R. Feser, *Z. Naturforsch. B 35* (1980) 689.
[32] R. A. Jones, F. M. Real, G. Wilkinson, A. M. R. Galas, M. B. Hursthouse, K. M. Abdul Malik, *J. Chem. Soc. Dalton Trans. 1980*, 511.
[33] R. Feser, Dissertation, Universität Würzburg 1981; R. Feser, L. Hofmann, H. Werner, unpublished results.
[34] H. G. Schuster-Woldan, F. Basolo, *J. Am. Chem. Soc. 88* (1966) 1657.
[35] A. Spencer, H. Werner, *J. Organomet. Chem. 171* (1979) 219.
[36] T. Aviles, M. L. H. Green, *J. Chem. Soc. Dalton Trans. 1979*, 1116.
[37] R. Feser, H. Werner, *J. Organomet. Chem. 233* (1982) 193.
[38] H. Werner, B. Klingert, *J. Organomet. Chem. 218* (1981) 395.
[39] L. Hofmann, H. Werner, unpublished results.
[40] R. Cramer, L. P. Seiwell, *J. Organomet. Chem. 92* (1975) 245.
[41] W. Hofmann, Dissertation, Universität Würzburg 1980.
[42] H. Werner, S. Lotz, B. Heiser, *J. Organomet. Chem. 209* (1981) 197.
[43] P. M. Maitlis, *Chem. Soc. Rev. 10* (1981) 1.
[44] J. W. Kang, P. M. Maitlis, *J. Organomet. Chem. 26* (1971) 393.
[45] a) F. Calderazzo, *Angew. Chem. 89* (1977) 305; *Angew. Chem. Int. Ed. Engl. 16* (1977) 299; b) J. Plank, D. Riedel, W. A. Herrmann, *ibid. 92* (1980) 961; *19* (1980) 937.
[46] R. D. Cramer, *J. Am. Chem. Soc. 87* (1965) 4717.
[47] L. P. Seiwell, *Inorg. Chem. 15* (1976) 2560.
[48] H. Werner, *Angew. Chem. 89* (1977) 1; *Angew. Chem. Int. Ed. Engl. 16* (1977) 1.
[49] V. Harder, E. Dubler, H. Werner, *J. Organomet. Chem. 71* (1974) 427.
[50] W. Kläui, K. Dehnicke, *Chem. Ber. 111* (1978) 451.
[51] D. K. Towle, S. J. Landon, T. B. Brill, T. H. Tulip, *Organometallics 1* (1982) 295.
[52] H. Neukomm, Dissertation, Universität Zürich 1976.
[53] For the recently described synthesis of trinuclear complexes of composition $[C_5Me_5Rh(\mu\text{-}P(OMe)_2O)_3M(\mu\text{-}OP(OMe)_2)_3RhC_5Me_5]$ see: W. Kläui, H. Otto, W. Eberspach, E. Buchholz, *Chem. Ber. 115* (1982) 1922.
[54] H. Neukomm, H. Werner, *J. Organomet. Chem. 108* (1976) C26.
[55] H. Werner, H. Neukomm, W. Kläui, *Helv. Chim. Acta 60* (1977) 326.
[56] H. Werner, R. Feser, *Z. Anorg. Allg. Chem. 458* (1979) 301.
[57] H. Werner, Tri Ngo-Khac, R. Feser, unpublished results; see also: H. Werner, Tri Ngo-Khac, D. Friebel, P. Köhler, D. Reinen, *Z. Naturforsch. B 36* (1981) 322.
[58] H. Werner, W. Hofmann, *Chem. Ber. 115* (1982) 127.
[59] U. Schubert, R. Werner, L. Zinner, H. Werner, *J. Organomet. Chem. 253* (1983) 363.
[60] K. Dey, H. Werner, *J. Organomet. Chem. 137* (1977) C28; *Chem. Ber. 112* (1979) 823.
[61] K. Dey, unpublished results.
[62] W. Hofmann, W. Buchner, H. Werner, *Angew. Chem. 89* (1977) 836; *Angew. Chem. Int. Ed. Engl. 16* (1977) 795.
[63] T. A. Albright, R. Hoffmann, *Chem. Ber. 111* (1978) 1578.
[64] R. K. Pomeroy, D. J. Harrison, *J. Chem. Soc. Chem. Commun. 1980*, 661.
[65] D. L. Morse, M. S. Wrighton, *J. Organomet. Chem. 125* (1977) 71.
[66] a) R. J. McKinney, *J. Chem. Soc. Chem. Commun. 1980*, 603; b) *Inorg. Chem. 21* (1982) 2051.
[67] R. Eisenberg, D. E. Hendriksen, *Adv. Catal. 28* (1979) 119.
[68] M. C. Baird, G. Wilkinson, *Chem. Commun. 1966*, 514; *J. Chem. Soc. A 1967*, 865.
[69] M. C. Baird, G. Wilkinson, *Chem. Commun. 1966*, 267.
[70] H. Werner, K. Leonhard, C. Burschka, *J. Organomet. Chem. 160*, 291 (1978).
[71] H. Werner, O. Kolb, *Angew. Chem. 91* (1979) 930; *Angew. Chem. Int. Ed. Engl. 18* (1979) 865.
[72] H. Werner, O. Kolb, U. Schubert, K. Ackermann, *Angew. Chem. 93* (1981) 583; *Angew. Chem. Int. Ed. Engl. 20* (1981) 593.
[73] O. Kolb, Dissertation, Universität Würzburg 1983.
[74] H. Werner, M. Ebner, W. Bertleff, U. Schubert, *Organometallics 2* (1983) 891.
[75] H. Werner, O. Kolb, R. Feser, U. Schubert, *J. Organomet. Chem. 191* (1980) 283.
[76] G. R. Clark, T. J. Collins, K. Marsden, W. R. Roper, *J. Organomet. Chem. 157* (1978) C23.
[77] B. D. Dombeck, R. J. Angelici, *Inorg. Chem. 15* (1976) 2397.
[78] H. Werner, O. Kolb, U. Schubert, K. Ackermann, *J. Organomet. Chem. 240* (1982) 421.
[79] a) W. Strohmeier, *Angew. Chem. 76* (1964) 873; *Angew. Chem. Int. Ed. Engl. 3* (1964) 730; b) E. O. Fischer, M. Herberhold: *Essays in Coordination Chemistry, Exper. Suppl. IX*, Birkhäuser, Basel 1964, p. 259.
[80] H. Werner, B. Juthani, *J. Organomet. Chem. 209* (1981) 211.
[81] O. Kolb, H. Werner, *Angew. Chem. 94* (1982) 207; *Angew. Chem. Int. Ed. Engl. 21* (1982) 202.
[82] G. Evrard, unpublished results.
[83] H. Werner, O. Kolb, U. Schubert, unpublished results.
[84] H. Werner, B. Heiser, A. Kühn, *Angew. Chem. 93* (1981) 305; *Angew. Chem. Int. Ed. Engl. 20* (1981) 301.
[85] H. Werner, B. Heiser, U. Schubert, unpublished results; see: B. Heiser, Dissertation, Universität Würzburg 1983.
[86] H. Werner, B. Heiser, C. Burschka, *Chem. Ber. 115* (1982) 3069.
[87] B. Heiser, H. Werner, M. L. Ziegler, unpublished results.
[88] a) J. Fortune, A. R. Manning, *J. Organomet. Chem. 190* (1980) C95; b) A. R. Manning, personal communication.
[89] a) K. Stanley, M. C. Baird, *J. Am. Chem. Soc. 97* (1975) 6598; b) H. Brunner, *Adv. Organomet. Chem. 18* (1980) 186.
[90] For further work in this connection, see a) J. W. Byrne, H. V. Blaser, J. A. Osborn, *J. Am. Chem. Soc. 97* (1975) 3871; b) J. W. Byrne, J. R. Kress, J. A. Osborn, L. Picard, R. E. Weiss, *J. Chem. Soc. Chem. Commun. 1977*, 662; c) H. F. Klein, R. Hammer, J. Groß, U. Schubert, *Angew. Chem. 92* (1980) 835; *Angew. Chem. Int. Ed. Engl. 19* (1980) 809; d) R. B. A. Pardy, M. J. Taylor, E. C. Constable, J. D. Mersh, J. M. K. Sanders, *J. Organomet. Chem. 231* (1982) C25.
[91] S. Otsuka, A. Nakamura, *Adv. Organomet. Chem. 14* (1976) 245.
[92] U. Schubert, P. Erk, unpublished results.
[93] K. Leonhard, H. Werner, *Angew. Chem. 89* (1977) 656; *Angew. Chem. Int. Ed. Engl. 16* (1977) 649.
[94] H. Werner, J. Wolf, R. Zolk, U. Schubert, *Angew. Chem. 95* (1983) 1022; *Angew. Chem. Int. Ed. Engl. 22* (1983) 981.

[95] J. Wolf, H. Werner, O. Serhadli, M. L. Ziegler, *Angew. Chem. 95* (1983) 428; *Angew. Chem. Int. Ed. Engl. 22* (1983) 414.
[96] a) A. B. Antonova, N. E. Kolobova, P. V. Petrovsky, B. V. Lokshin, N. S. Obezyuk, *J. Organomet. Chem. 137* (1977) 55; b) M. I. Bruce, R. C. Wallis, *Aust. J. Chem. 32* (1979) 1471; c) A. Davison, J. P. Selegue, *J. Am. Chem. Soc. 102* (1980) 2455.
[97] J. Wolf, unpublished results.
[98] a) U. Behrens, F. Edelmann, *J. Organomet. Chem. 118* (1976) C41; b) D. Wormsbächer, F. Edelmann, U. Behrens, *Chem. Ber. 114* (1981) 153; *115* (1982) 1332.
[99] M. Green, R. B. L. Osborn, F. G. A. Stone, *J. Chem. Soc. A 1970,* 944.
[100] H. Schmidbaur, *Nachr. Chem. Tech. Lab. 27* (1979) 620.
[101] R. Feser, H. Werner, *Angew. Chem. 92* (1980) 960; *Angew. Chem. Int. Ed. Engl. 19* (1980) 940.
[102] L. Hofmann, Diplomarbeit, Universität Würzburg 1981.
[103] H. R. Christen: *Grundlagen der organischen Chemie,* Verlag Sauerländer-Diesterweg-Salle, Aarau-Frankfurt/Main 1970, chapt. 18.
[104] H. F. Klein, R. Hammer, *Angew. Chem. 88* (1976) 61; *Angew. Chem. Int. Ed. Engl. 15* (1976) 42.
[105] J. R. Moss, J. C. Spiers, *J. Organomet. Chem. 182* (1979) C20.
[106] N. J. Kermode, M. F. Lappert, B. W. Skelton, A. H. White, J. Holton, *J. Chem. Soc. Chem. Commun. 1981,* 698.
[107] H. Werner, R. Feser, W. Paul, L. Hofmann, *J. Organomet. Chem. 219* (1981) C29.
[108] B. Heiser, Diplomarbeit, Universität Würzburg 1980.
[109] W. Paul, Diplomarbeit, Universität Würzburg 1981.
[110] W. Paul, H. Werner, *Angew. Chem. 95* (1983) 333; *Angew. Chem. Int. Ed. Engl. 22* (1983) 316; *Angew. Chem. Suppl. 1983,* 396.
[111] G. Müller, C. Krüger, unpublished results.
[112] a) T. J. Collins, W. R. Roper, *J. Chem. Soc. Chem. Commun. 1977,* 901; b) C. E. L. Headford, W. R. Roper, *J. Organomet. Chem. 244* (1983) C53.
[113] M. Herberhold, W. Ehrenreich, W. Bühlmeyer, *Angew. Chem. 95* (1983) 332; *Angew. Chem. Int. Ed. Engl. 22* (1983) 315.
[114] W. A. Herrmann, J. Weichmann, R. Serrano, K. Blechschmitt, H. Pfisterer, M. L. Ziegler, *Angew. Chem. 95* (1983) 331; *Angew. Chem. Int. Ed. Engl. 22* (1983) 314; *Angew. Chem. Suppl. 1983,* 363.
[115] H. Werner, W. Paul, G. Müller, C. Krüger, unpublished results.
[116] H. Werner, W. Paul, *J. Organomet. Chem. 236* (1982) C71.
[117] L. Hofmann, H. Werner, unpublished results.
[118] a) E. O. Fischer, H. Werner: *Metal π-Complexes, Vol. 1* (Complexes with Di- and Oligo-olefinic Ligands), Elsevier, Amsterdam 1966; b) J. Müller, C. G. Kreiter, B. Mertschenk, S. Schmitt, *Chem. Ber. 108* (1975) 273; c) P. Pertici, G. Vitulli, M. Paci, L. Porri, *J. Chem. Soc. Dalton Trans. 1980,* 1961, and literature cited therein.
[119] H. Werner, R. Werner, *Angew. Chem. 90* (1978) 721; *Angew. Chem. Int. Ed. Engl. 17* (1978) 683.
[120] a) D. L. William-Smith, L. R. Wolf, P. S. Skell, *J. Am. Chem. Soc. 94* (1972) 4042; b) R. Middleton, J. R. Hull, S. R. Simpson, C. H. Tomlinson, P. L. Timms, *J. Chem. Soc. Dalton Trans. 1973,* 120.
[121] S. R. Weber, H. H. Brintzinger, *J. Organomet. Chem. 127* (1977) 45.
[122] a) S. D. Ittel, C. A. Tolman, *J. Organomet. Chem. 172* (1979) C47; b) S. D. Ittel, F. A. Van-Catledge, J. P. Jesson, *J. Am. Chem. Soc. 101* (1979) 3874; c) S. D. Ittel, C. A. Tolman, *Organometallics 1* (1982) 1432.
[123] R. Werner, H. Werner, *Chem. Ber. 115* (1982) 3781.
[124] H. Werner, R. Werner, *Chem. Ber. 115* (1982) 3766.
[125] H. Kletzin, Diplomarbeit, Universität Würzburg 1981.
[126] D. R. Robertson, T. A. Stephenson, T. Arthur, *J. Organomet. Chem. 162* (1978) 121.
[127] R. Werner, H. Werner, *Chem. Ber. 116* (1983) 2074.
[128] R. Werner, H. Werner, *Angew. Chem. 93* (1981) 826; *Angew. Chem. Int. Ed. Engl. 20* (1981) 793.
[129] E. L. Muetterties, J. R. Bleeke, A. C. Sievert, *J. Organomet. Chem. 178* (1979) 197.
[130] K. Zenkert, H. Werner, unpublished results.
[131] a) R. Weinand, Diplomarbeit, Universität Würzburg 1982; b) H. Werner, R. Weinand, *Z. Naturforsch. B38* (1983), in press.
[132] R. Hoffmann, *Angew. Chem. 94* (1982) 725; *Angew. Chem. Int. Ed. Engl. 21* (1982) 711.
[133] H. Werner, R. Feser, R. Werner, *J. Organomet. Chem. 181* (1979) C7.
[134] R. Werner, Dissertation, Universität Würzburg 1982.
[135] a) R. Werner, H. Werner, *J. Organomet. Chem. 210* (1981) C11; b) H. Werner, R. Werner, *Chem. Ber. 116* (1983), in press.
[136] H. Werner, R. Werner, *J. Organomet. Chem. 174* (1979) C67.
[137] K. R. Grundy, W. R. Roper, *J. Organomet. Chem. 216* (1981) 255.
[138] C. P. Lillya, R. A. Sahatjian, *Inorg. Chem. 11* (1972) 889.
[139] B. V. Lokshin, V. I. Zdanovich, N. K. Baranetskaya, V. N. Setkina, D. N. Kursanov, *J. Organomet. Chem. 37* (1972) 331, 339.
[140] L. A. Fedorov, P. V. Petrovskii, E. I. Fedin, N. K. Baranetskaya, V. I. Zdanovich, V. N. Setkina, D. N. Kursanov, *J. Organomet. Chem. 99* (1975) 297.
[141] T. C. Flood, E. Rosenberg, A. Sarhangi, *J. Am. Chem. Soc. 99* (1977) 4334.
[142] M. L. H. Green, L. C. Mitchard, W. E. Silverthorn, *J. Chem. Soc. A 1971,* 2929.
[143] H. Werner, B. Juthani, *J. Organomet. Chem. 129* (1977) C39.
[144] a) H. Werner, H. Kletzin, *J. Organomet. Chem. 243* (1983) C59; b) H. Kletzin, unpublished results; see H. Kletzin, Dissertation, Universität Würzburg, in preparation.
[145] a) H. Werner, J. Gotzig, *Organometallics 2* (1983) 547; b) J. Gotzig, unpublished results.
[146] H. Werner, J. Wolf, *Angew. Chem. 94* (1982) 309; *Angew. Chem. Int. Ed. Engl. 21* (1982) 296.
[147] H. Werner, H. Kletzin, *J. Organomet. Chem. 228* (1982) 289.
[148] W. Hofmann, H. Werner, *Chem. Ber. 115* (1982) 119.
[149] H. Kletzin, H. Werner, O. Serhadli, M. L. Ziegler, *Angew. Chem. 95* (1983) 49; *Angew. Chem. Int. Ed. Engl. 21* (1983) 46.
[150] J. C. Hayes, N. J. Cooper, *J. Am. Chem. Soc. 104* (1982) 5570.
[151] W. A. Herrmann, *Angew. Chem. 94* (1982) 118; *Angew. Chem. Int. Ed. Engl. 21* (1982) 117.
[152] H. Werner, R. Werner, C. Burschka, *Chem. Ber. 116* (1983), in press.
[153] a) I. U. Khand, P. L. Pauson, W. E. Watts, *J. Chem. Soc. C 1969,* 2024; b) A. N. Nesmeyanov, N. A. Volkenau, L. S. Shilovtseva, V. A. Petrakova, *J. Organomet. Chem. 85* (1975) 365.
[154] R. Werner, H. Werner, *Chem. Ber. 116* (1983), in press.
[155] M. Brookhart, W. Lamanna, W. R. Pinhas, *Organometallics 2* (1983) 638.
[156] M. I. Bruce, I. B. Tomkins, F. S. Wong, B. W. Skelton, A. H. White, *J. Chem. Soc. Dalton Trans. 1982,* 687.
[157] T. A. Albright, R. Hoffmann, unpublished results; see also: P. Hofmann, *Angew. Chem. 89* (1977) 551; *Angew. Chem. Int. Ed. Engl. 16* (1977) 536.
[158] R. Hoffmann, personal communication (7. June 1976).
[159] R. G. Pearson, P. E. Figdore, *J. Am. Chem. Soc. 102* (1980) 1541.
[160] C. A. Tolman, *Chem. Rev. 77* (1977) 313.
[161] W. Hofmann, Dissertation, Universität Würzburg 1980.
[162] a) H. Werner, W. Hofmann, *Angew. Chem. 91* (1979) 172; *Angew. Chem. Int. Ed. Engl. 18* (1979) 158; b) H. Werner, W. Hofmann, R. Zolk, L. F. Dahl, J. Kocal, A. Kühn, *Organometallics,* in press.
[163] B. Klingert, H. Werner, *J. Organomet. Chem. 252* (1983) C47.
[164] W. Hofmann, H. Werner, *Angew. Chem. 93* (1981) 1088; *Angew. Chem. Int. Ed. Engl. 20* (1981) 1014.
[165] a) R. Zolk, H. Werner, *J. Organomet. Chem. 252* (1983) C53; b) H. Werner, B. Klingert, R. Zolk, unpublished results.
[166] a) G. W. Parshall: *Homogeneous Catalysis,* Wiley-Interscience, New York 1980; b) F. A. Cotton, G. Wilkinson; *Advanced Inorganic Chemistry,* 4th edit., Wiley, New York 1980.
[167] A. H. Janowicz, R. G. Bergman, *J. Am. Chem. Soc. 104* (1982) 352.
[168] J. K. Hoyano, W. A. G. Graham, *J. Am. Chem. Soc. 104* (1982) 3723.
[169] W. D. Jones, F. J. Feher, *Organometallics 2* (1983) 562.
[170] a) H. Werner, Plenary lecture XII. Sheffield-Leeds International Symposium on Organometallic, Inorganic and Catalytic Chemistry, Sheffield 28th March 1983; b) H. Kletzin, H. Werner, *Angew. Chem. 95* (1983) 916; *Angew. Chem. Int. Ed. Engl. 22* (1983) 873.

# The Electrochemistry of Black Carbons

**By Jürgen O. Besenhard* and Heinz P. Fritz**

*Dedicated to Professor Ernst Otto Fischer on the occasion of his 65th birthday*

"Modifications" of carbon—as long as they predominantly have the layered graphite structure—exhibit the following properties: 1) electrical conductance, 2) the ability to accomodate ions or molecules between the layers of the lattice, and 3) the ability to react *via* functional groups at their surfaces (largely at the layer edges). The first of these properties has led to carbon being used as an "inert" electrode material; this aspect will not be considered in this article. The combination of the first and second properties leads to the possibility of electrochemical intercalation. This aspect of black carbon's properties will be described, using both literature data and our own results, in terms of both the basic information and the methodology associated with its uses. In addition to the formation of graphite salts the origin of graphite oxide and the various methods which have been used to analyze these materials will be reviewed. The functional groups [(cf. 3) above] can also be reacted electrochemically. Here, particular emphasis will be placed on detailed results obtained from chemically modified carbon electrodes and also from surface oxides and fluorides. Reference will be made to the technological uses of surface oxidized carbon fibers in composite materials and also generally to possible future uses of graphite based compounds.

## 1. Introduction

The term "black carbons" may sound rather alchemistic for those chemists more used to reading about compounds with well defined names. However, this trivial, phenomenological description is the smallest common denominator for the many, and indeed varied, forms of elementary carbon which at least have a predominantly graphite-like *layered structure* and therefore also exhibit electrical conductance. Carbon is alone among the elements in that it exists, in its elementary form, in almost every possible structural order and morphology, from well defined three-dimensionally ordered graphite to X-ray amorphous glassy carbon[1–4].

The aim of this article is to describe the chemistry *of* carbon electrodes; not the chemistry *at* such electrodes. Thus, reactions which take place at the surface of "inert" carbon electrodes will not be discussed.

The chemistry and the electrochemistry of black carbon can be described in terms of one of two types of reaction: Intercalation (or insertion) reactions and surface reactions. In the *intercalation reactions* cations or anions, and often also solvating neutral molecules, come between the graphite-like ordered carbon layers and, thus, the distance between these layers is increased. Since the intercalated ions are generally held between two carbon layers directly facing each other (AαA stacking) and, preferentially, tend to locate themselves at the midpoint between the carbon-carbon hexagons one is led to make the analogy with the metallocenes or the arene-metal complexes. However, this analogy should be made only with reservation because, despite considerable efforts[5–10], some with the aid of electrochemical methods[11,12], it has proven impossible to produce conclusively intercalation compounds of graphite with the transition elements which are typical of metallocene chemistry.

There are several, in part very up to date and specialized, review articles on the subject of graphite intercalation (cf. Table 1). However, the electrochemistry associated with this topic, an area which has grown particularly rapidly in the last few years, has generally been either ignored or, at best, only superficially treated. The aim of this article

Table 1. Review articles and readily available conference proceedings on "Graphite Intercalation".

| Year | Major Topic | Ref. |
|---|---|---|
| 1959 | Chemistry, properties | [25] |
| 1959 | Chemistry, properties | [26] |
| 1960 | Chemistry, properties | [27] |
| 1960 | Chemistry, properties | [28] |
| 1965 | Chemistry, properties | [29] |
| 1976 | Chemistry, properties | [30] |
| 1977 | Reaction mechanisms | [31] |
| 1978 | Electrical conductivity | [32] |
| 1979 | Electrical conductivity | [33] |
| 1979 | Physical properties | [34] |
| 1979 | Chemistry, properties | [35] |
| 1979 | Structure | [36] |
| 1979 | Optical spectroscopy | [37] |
| 1980 | Chemistry | [38] |
| 1981 | Properties | [39] |
| 1981 | Preparation, structure, optical spectroscopy, electrical conductivity. | [40] |
| 1982 | Electrochemical applications | [41] |
| 1982 | Optical spectroscopy | [42] |
| 1982 | Structure | [43] |
| 1982 | Chemistry, fluorine compounds | [44] |
| 1983 | Chemistry, properties | [45] |
| 1977 | Intercalation Compounds of Graphite | [46] |
| 1979 | Layered Materials and Intercalates | [47] |
| 1980 | Intercalation Compounds of Graphite | [48] |
| 1980 | Physics and Chemistry of Layered Materials | [49] |
| 1982 | Intercalated Graphite | [50] |
| 1983 | Intercalation Compounds of Graphite | [51] |

[*] Priv.-Doz. Dr. J. O. Besenhard, Prof. Dr. H. P. Fritz
Anorganisch-chemisches Institut der Technischen Universität München
Lichtenbergstrasse 4, D-8046 Garching (Germany)

 © Verlag Chemie GmbH, 6940 Weinheim, 1983 0570-0833/83/1212-0950 $ 02.50/0 

is to fill this gap. Other areas, such as the applications of graphite compounds as "molecularly wrapped reagents"[13-17] and also as heterogeneous catalysts[18-22] (especially for the stereospecific anionic polymerization by alkali metal-graphite[23,24]) have already been reviewed in detail.

The *surface reactions* of black carbon are generally reactions of C atoms at the edges of the layers or at other lattice defects, or reactions of other functional groups which are bound to such C atoms. Large effects from surface reactions are thus only to be expected from microcrystalline carbon materials. At the basal planes, on the other hand, essentially only physical adsorption is observed[52]. This physical adsorption is of interest in its own right because of its regularity (cf. *e.g.* [53-57]).

The classical chemistry of the functional groups attached to the carbon lattice has already been reviewed under a variety of headings[58-61]. Some of the more recent articles describe the functionalization of carbon fibers for composite materials[62-69]. Naturally, there are also numerous articles which discuss the properties, production and applications of charcoals and carbon blacks.

Electrochemical studies on the surface reactivity have also been reviewed up to about 1975[70,71] and some developments in the area of "chemically modified" carbon electrodes have been described[72-74].

Therefore, only the newest results from the areas "chemically modified electrodes" and "electrochemical surface oxidation of carbon fibers" will be discussed in this article.

## 2. Historical

Carbon as an electrode material has interested electrochemists for a very long time. Of course, the object of this interest has not always been the development of intercalation and surface compounds. In the first instance, carbon has long been of interest—in view of its thermodynamic characteristics—as a surprisingly "inert" electrode material which has proven especially useful as an anode in corrosive environments (*e.g.* in the production of $Cl_2$, $ClO_3^-$ and in electrolyses of molten alkali and alkaline earth halides). It is, therefore, also not surprising to note that the authors of the initial, preliminary reports about the reactions of carbon anodes to yield inclusion compounds (*e.g.* in $HClO_4$[75] or $HNO_2$[76]), or to form surface compounds (*e.g.* in $HF \cdot KF$[77]), complained about these unwanted side reactions.

Moreover, electrochemists have felt themselves under pressure, for more than 100 years, to develop an electrochemical cell in which, in conjunction with an $O_2$-cathode, carbon or simply coal could be used as a fuel. The efforts to build such fuel cells, based on the initial investigations by *A. C. Becquerel* (1855)[78], *Ostwald* (1894)[79] and others (cf. [80]), in particular on alkaline electrolytes at high temperature, have repeatedly failed. More recently, therefore, the efforts have been directed towards developing a process in which $H_2$ and CO, obtained by gasification of coal, are oxidized in conventional fuel cells[80,81].

Electroorganic syntheses in which the carbon electrodes function as a reactant also have a very long history. Examples of such processes are the production of urea (C-anodes in aqueous $NH_3$ and $(NH_4)_2CO_3$[82,83]) or that of mellitic acid (C-anodes in alkaline solution[84]). $O_2$, CO and $CO_2$, were recognized at a very early date as the major by-products formed during electrolyses at carbon anodes in acid, alkaline and aqueous solution[85,86], whereas larger molecules (*e.g.* $H_2CO$ or $CH_2(OCH_3)_2$[87]) were found to occur at most in only trace amounts. On electrolyzing aqueous suspensions of brown coal, the coal is reductively converted into soluble compounds, but the yields are variable and depend on the precise conditions used[88]; a variety of aromatic compounds are produced such as, *e.g.*, benzoic acid and pyrocatechol, as well as low molecular weight organic acids such as succinic, malonic and oxalic acids. The glow-discharge electrolysis of aqueous graphite suspensions (20—25 g graphite/100 mL) in 1 M LiOH yielded mainly $H_2$, together with CO, $CO_2$ and $CH_3$ as by-products[89].

## 3. Electrochemical Intercalation

### 3.1. Background

Electrochemical intercalation reactions are confined to electron/ion transfer reactions[90-96]. *Guest ions (cations* $M^+$ or anions $X^-$) penetrate (during the cathodic reduction of the anodic oxidation of carbon electrodes) into the van der Waals gaps between the carbon layers and enlarge the inter-layer distance. The corresponding (negative or positive) charges are accepted into the carbon host lattice.

$$C_n + M^{\oplus} + e^{\ominus} \underset{\text{cathodic reduction}}{\rightleftharpoons} M^{\oplus}C_n^{\ominus} \quad (1a)$$

$$C_n + X^{\ominus} - e^{\ominus} \underset{\text{anodic oxidation}}{\rightleftharpoons} C_n^{\oplus}X^{\ominus} \quad (1b)$$

For such a reaction mechanism it is necessary that electrons can be conducted by $C_n$ and that "mixed conduction" (*i.e.* electron and $M^+$ or $X^-$ conduction) occurs in $M^+C_n^-$ or in $C_n^+X^-$.

Furthermore, the host lattice must be capable of accepting, not only sterically but also electronically, the guest ions; *i.e.* a suitable energy band structure must be available. The band structure of graphite compounds has been discussed in a large number of both theoretical and experimental papers (*e.g.*[32,40,97-105]). Qualitatively, the available levels which accept or give up electrons are very high or low and the corresponding $M^+C_n^-$ or $C_n^+X^-$ phases are thus strong reducing or oxidizing agents, respectively. As a consequence, such structures are only possible for cations $M^+$ which are stable to reduction (*e.g.* alkali and alkaline earth metal ions) or with anions which are stable to oxidation (*e.g.* $ClO_4^-$, tetrafluoro anions, and hexafluoro anions).

Intercalation reactions of the types (1a) and (1b) are, ideally, reversible and "topotactic"; *i.e.* the reaction leads to a different inter-layer distance but the carbon atom arrangement within the layers remains, essentially, unchanged. Only in exceptional cases does electrochemical intercalation give rise to binary phases $M^+C_n^-$ or $C_n^+X^-$.

Examples of such cases are the electrochemical intercalation of cations from solid[106], polymeric[107], or molten[108,109] electrolytes. More generally, ternary phases $M^+(solv)_yC_n^-$ or $C_n^+(solv)_yX^-$ are produced because the solvent from the electrolyte is also accepted into the carbon lattice.

$$C_n + M^{\oplus} + e^{\ominus} + y\,solv \underset{\text{anodic oxidation}}{\overset{\text{cathodic reduction}}{\rightleftharpoons}} M^{\oplus}(solv)_yC_n^{\ominus} \quad (2a)$$

$$C_n + X^{\ominus} - e^{\ominus} + y\,solv \underset{\text{anodic oxidation}}{\overset{\text{cathodic reduction}}{\rightleftharpoons}} C_n^{\oplus}(solv)_yX^{\ominus} \quad (2b)$$

From the degree of solvation it is possible to distinguish between two-dimensional and three-dimensional solvated phases (cf. Fig. 1).

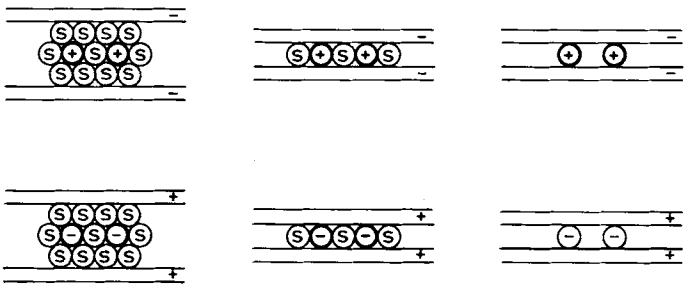


Fig. 1. Schematic diagram showing the three-dimensional and two-dimensional solvated and unsolvated cationic and anionic intercalation compounds; S = Solvent.

In the two-dimensional solvates the distance between the carbon layers is determined either by the size of the solvent molecule (*e.g.* in $K(THF)_1C_{24}$ (THF = tetrahydrofuran)[110] or in $Na(DME)_yC_{32}$ and $K(DME)_yC_{32}$ (DME = 1,2-dimethoxyethane)[111]) or by the size of the ions. The latter is true, for example, for $C_n(NM)_2PF_6$ or $C_n(NM)_2AsF_6$ (NM = nitromethane)[112,113], where the distances between the carbon atom layers for the solvated and the unsolvated phases $C_nPF_6$ and $C_nAsF_6$ are practically identical (cf. Section 3.5). Occasionally, other forms of solvation have also been discussed (*e.g.* "one-sided" solvation, as in the benzene solvated phases $K(Bz)_yC_n$) in which the included ions are separated only from one of the two carbon layers by a solvent molecule[114–117]. However, the mobility of the ions and the solvent molecules in ternary phases is normally so great, even at room temperature, that the model of a "melted intercalation layer" generally applies.

Of course, all the various types of graphite compounds described above can be synthesized not only by cathodic reduction or anodic oxidation but also with the aid of chemical reducing or oxidizing agents. However, the electrochemical method has important advantages[118]:

- —the products are free from impurities arising from the reducing or oxidizing agent,
- —the degree of oxidation or reduction can be controlled,
- —the rate of reaction can be controlled[*],
- —the thermodynamics of the intercalation processes can be followed by the electrochemical potential,
- —from the relationships between current, potential, and time it is possible, at least qualitatively, to study the kinetics of the process.

In contrast to the above advantages, the electrochemical intercalation reaction is difficult to "scale up" due to the necessity for electrical contact between the large number of small particles. Nevertheless, making contact between a large number of small particles is possible using, for example, high pressures[119], fluid-bed reactors[120], or "stirred electrodes" (a suspension of the particles to be reacted is stirred onto net-like electrodes).

A special feature of the intercalation of graphite is the formation of a *regular* array of unoccupied layer gaps (= stage formation) when only a low concentration of the guest species is present. In compounds of stage s the guest containing layers are separated by s carbon layers; non-integer values of s (*e.g.* 1.5) are used to describe alternating layer sequences (*e.g.* guest-C-guest-C-C-...). Stages from s = I to *ca.* s = VII can be confidently determined *via* X-ray techniques, but even considerably higher s values have also been postulated. More recently it has been suggested ([122], see Fig. 2) that where s > I all the layers contain some guest species but that the guest species form "islands", stagewise, within the otherwise empty interlayer gaps.

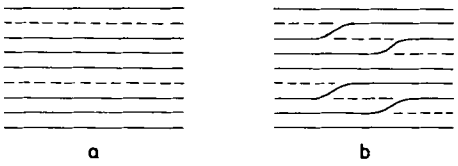



Fig. 2. Classical (a) and more recent (b) model of a stage III; ——— carbon layer, ------- guest layer (according to Ref. [122]).

Carbon which has only a slight degree of structural order cannot be used to produce intercalation compounds with higher stages s.

The distribution of the guest species among the interlayer spaces can be described as either "commensurable" or "incommensurable". In commensurable structures the guests are ordered according to the "raster" of the carbon layers, *i.e.* they form superstructures. Commensurable structures are frequently found in binary compounds $M^+C_n^-$ in which the metal atoms take up an ordered structure and are positioned above the mid-point of particular carbon-carbon hexagons.

As the temperature of such compounds is raised, order/disorder transitions leading to incommensurable structures can be observed.

Finally, it should be noted that the notation $M^+C_n^-$, $M^+(solv)_yC_n^-$, $C_n^+X^-$ and $C_n^+(solv)_yX^-$ need not necessarily reflect a full charge transfer, that is an ionicity $f = 1$. In particular, there is some doubt about the degree of ionicity in unsolvated and two-dimensionally solvated phases. Unfortunately, despite the fact that $f$ can be measured by a variety of physical methods[123–125] its determination remains a problem. Thus, the literature contains very erratic data not only for $C_n^+$ (= acceptor) com-

[*] The crystallinity of the intercalation compound (not only for carbon lattices) can be decisively influenced by the rate of reaction. This has been demonstrated in a transition temperature study of superconducting phases of $K_x(H_2O)_yTaS_2$ prepared by different methods [121].

pounds (compare for example: [126] with [127] and also [128,129]) but also for the $C_{\overline{n}}$ (=donor) compounds (compare for example the lower values in [130–132] with the higher values in [133,134]). Generally, it is found that the ionicity increases with increasing dilution.

### 3.2. Standard Electrochemical Methods and Their Application to Intercalation Reactions

Electrochemistry—where the emphasis is on the chemistry—has expanded rapidly in the last few years, mainly because of the availability of relatively cheap commercial equipment for the easy control of both current and potential.

For studying the processes involved in intercalation reactions two methods have proved particularly useful, namely cathodic or anodic intercalation

- —with constant current and continuous plotting of the electrochemical potential of the product in comparison with a reference electrode and
- —with continuously changing potential controlled by a potentiostat and, under this forced potential, plotting the resulting current.

These methods can also be used for the controlled preparation of intercalation compounds.

#### *3.2.1. Controlled Current (= Galvanostatic) Reactions*

In the simplest case a constant current $I$ is allowed to flow between the desired substance (working electrode W) and a counter electrode C in a divided cell (Fig. 3). The potential difference between the working electrode and a reference electrode R is then measured *via* a chart recorder with a high input resistance (Fig. 4).

The experimental parameter $E'$, measured by such experiments, is not the equilibrium potential since it also contains a term due to the overpotential. Of the various types of overpotential (cf. textbooks on electrochemical kinetics, *e.g.* [135,136] and [137–140]), those due to diffusion controlled concentration gradients in solids and, in particular for porous electrodes, those due to the concentration gradients in the electrolyte phase ($\eta_{d(solid)}$, $\eta_{d(liquid)}$) are the most relevant for intercalation reactions. In comparison,

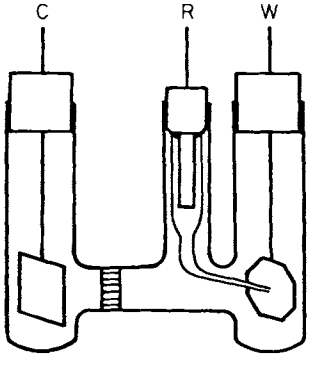



Fig. 3. Partitioned electrolysis cell with working electrode W, reference electrode R and counter electrode C.

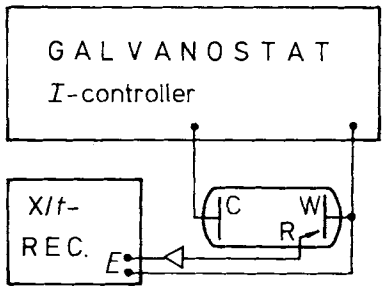



Fig. 4. Principle of a galvanostatic reaction technique with an electrolysis cell, galvanostat and an X/$t$ chart recorder equipped with an impedance transformer.

the charge-transfer overpotential $\eta_{CT}$ is, generally, negligible.

Using Ohm's relationship for the potential drop $I \cdot R$ ($R$ is given by the electrical resistance between the working and the reference electrodes) one can write:

$$E' = E + \eta_{d(solid)} + \eta_{d(liquid)} + \eta_{CT} + \cdots + I \cdot R \qquad (3)$$

A complete separation of the various overpotential terms is only partly realizable and in any case requires very complicated experimental techniques (cf. Section 3.7). When the current density is small enough[*] equation (3) can be simplified to $E' \approx E$. Qualitatively, this assumption is easily verified; *e.g.* using a pulsed current (when $E'_{\text{under load}}$ should be negligibly different from $E'_{\text{open cell}}$).

Figure 5 (left-hand side) shows a constructed potential-charge curve for the anodic intercalation of graphite (with the condition that the packing density of the anions in the interlayer spaces remains constant).

The plateaus on the potential curve indicate 2-phase regions (mixtures of two neighboring stages)—pure stages form infinitesimal limits due to the imposed, strict stoichiometry. The higher the stage s the smaller the difference between the potentials $E_{(s+1)/s}$ and $E_{s/(s-1)}$ for the coexisting stages s and s+1.

Thus, from the characteristic potential *vs* charge curves a phase analysis can be made and—assuming that the current yield is 100%—one can determine the stoichiometric factor n for the individual stages $C_nX$. The current yield and/or the reversibility of the intercalation reaction can be checked by current reversal, *i.e.* by removal or "deintercalation". Ideally, current reversal should yield a mirror image of the characteristic intercalation curve. Obtaining a plot for $E$ or $E'$ is almost a prerequisite for the preparation of a particular stage or stoichiometry of intercalation product.

#### *3.2.2. Controlled Potential (= Potentiostatic) Reactions*

Potentiostatic experiments are normally begun at the equilibrium potential of the working electrode, *i.e.*, at $I=0$; the potential is then varied at a constant rate $\Delta E/\Delta t$

[*] Because of the relatively rapid diffusion within highly oriented graphite, the crystallites with a basal plane area of several mm² can easily "cope with" prism current densities, that is with current densities referred to the areas of the sides of the prism, in the order of 1 mA·cm$^{-2}$.

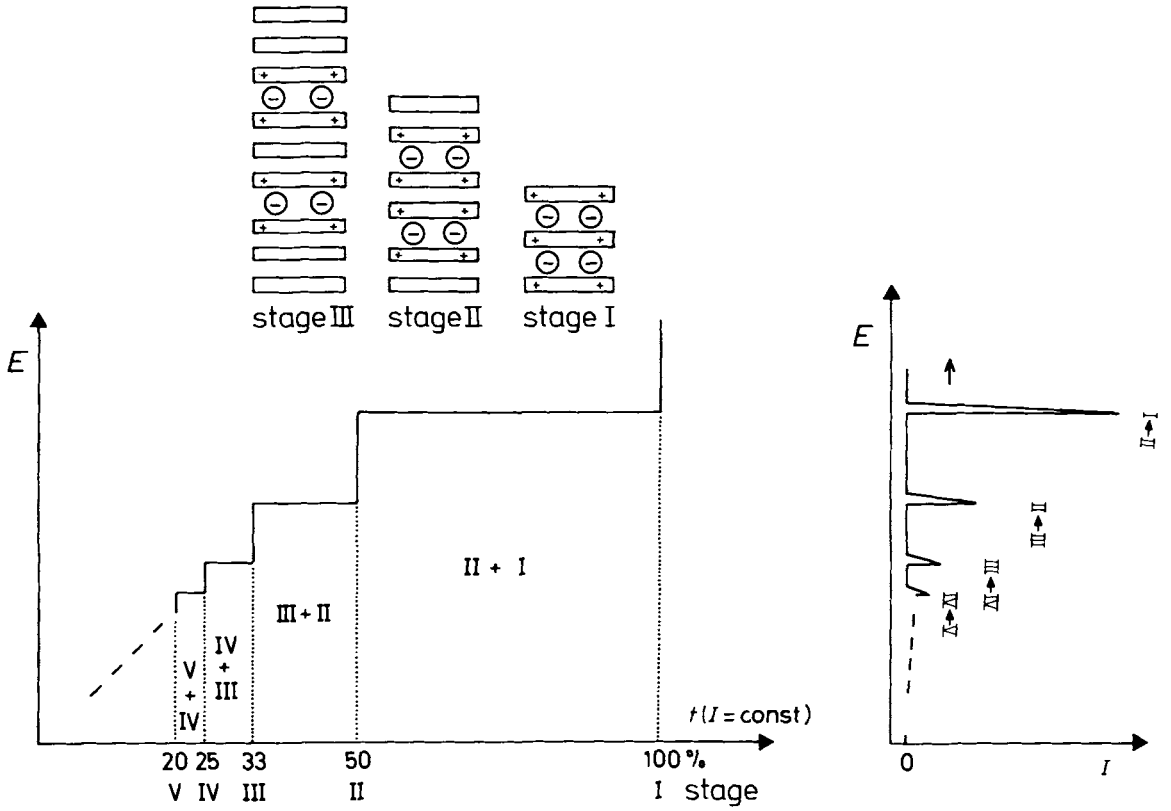



Fig. 5. Electrochemical intercalation with stage formation; bottom left: constructed $E$/charge curve, bottom right: constructed $I/E$ curve for $\Delta E/\Delta T$ = constant.

and the resulting current is plotted. An electronic potentiostat is used to bring the potential of the working electrode (measured against a reference electrode, the latter being connected to a high impedance input of the potentiostat) to a particular value by adjusting $I$. This method, which is called linear sweep voltammetry, is similar to the method used in polarography (Fig. 6).

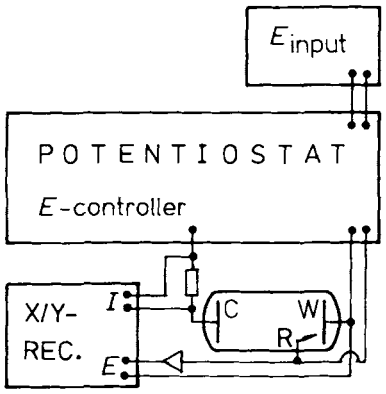



Fig. 6. Principle of the potentiostatic reaction technique with electrolysis cell, potentiostat, desired voltage source (generally a triangular voltage generator) and an X/Y chart recorder.

Figure 5 (right-hand side) shows the current curve to be expected during the formation of an intercalation compound of various stages: the potential plateaus of the galvanostatic technique are transformed into current peaks. No current flows during the sweeps of the potential areas between these plateaus.

Subsequent reversal of the direction of potential change (= cyclic voltammetry) leads to a mirror image plot about the axis $I=0$ for reversible reactions and for reactions where conditions are close to equilibrium, *i.e.* when the rate of change of the potential $v$ is slow enough[*].

The various types of overpotential which have been described above each lead to a characteristic peak broadening during cyclic voltammetry. For simple reactions, and in particular for reactions in solution, the kinetic parameters can be derived from such peak broadening effects[141–144]. A similar, in depth analysis has also been attempted for intercalation reactions and for reactions involving mixed conductors[145–147]. However, the large number of experimental variables and the difficulties associated with the control of these variables make such analyses difficult. This is particularly true for reactions involving polycrystalline electrodes where parameters such as the orientation and size of the crystallites and pores and the ionic and electronic intercrystalline orientation are difficult to estimate.

### 3.3. Galvanostatic and Potentiostatic Anodic Intercalation of Graphite in $H_2SO_4$—a Model Reaction

The anodic oxidation of graphite to $C_n(H_2SO_4)_y(HSO_4)$ and the corresponding back reaction were originally described by *Rüdorff* and *Hofmann*[148], who also observed the stepwise changes in $E$. X-ray and other analytical data

[*] Good peak resolution from crystallites of highly oriented graphite with a basal plane area of several mm$^2$ is only achieved when $v < ca.$ 0.1 Vh$^{-1}$.

were used to corroborate the stoichiometry of the stage I as $C_{24}(H_2SO_4)_2(HSO_4)$[148,149] and the corresponding commensurable $C_8X$ structure. The oxidation of graphite in $H_2SO_4$ has since been followed potentiometrically by many other authors[150–154]. A sharp potential break has generally been observed corresponding to a stoichiometry $C_{48}^+$; this has led to the suggestion that there is a correlation between the stoichiometry and the stage s of $C_{24\times s}^+$.

However, more recent potentiometric results[120,155–159] using a very low current density—*i.e.* "close to equilibrium" conditions—on highly oriented pyrolytic graphite (HOPG) indicate a rather more complicated relationship between stoichiometry and stage. These experiments on the graphite/$H_2SO_4$ system have a model character in as much as the results obtained can be usefully generalized not only with respect to other graphite compounds but also for the intercalation of other layered host lattices.

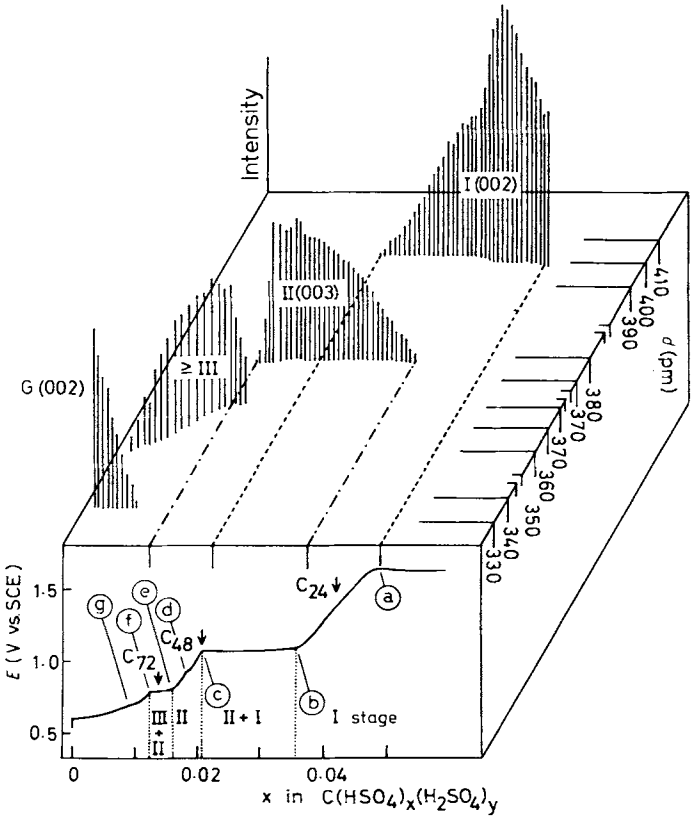



Fig. 7. Galvanostatic oxidation of HOPG (highly oriented pyrographite) close to equilibrium in 96% $H_2SO_4$ (Sample *ca.* 4×4×0.03 mm; $I=15$ μA); top: inter-layer distances and the corresponding intensities of the strongest 00l-reflections from each stage; bottom: *E*/charge curve (for details of the points a–g see text), SCE = saturated calomel electrode.

The potential change during the slow, galvanostatic oxidation of HOPG in $H_2SO_4$ is shown in Figure 7[*]. There are significant differences between the trace in Figure 7 and the constructed plot in Figure 5 (bottom left); in particular in the "inclined" potential areas which are characteristic of 1-phase preparations. In 1-phase graphite compounds the packing density of the intercalated ions is variable although the stage remains constant, thus leading to nonstoichiometric and incommensurable structures. The dependence of the variable electrochemical potential on the ion density is qualitatively analogous to the EMF of amalgam chains, which is determined by the concentration term $\ln c1/c2$. A quantitative appraisal taking into account the receptivity of the host lattice for the ions and the electrons necessary for compensating the charge of the ions or defect electrons can be found in [145,160].

The characterization of compounds as 1- or 2-phase according to the potential curves obtained can be corroborated by X-ray analysis. In Figure 7 the strongest 001-reflections[*], their positions, and their intensities are given for each stage. The diffraction pattern was taken *in situ* with an electrolysis cell mounted on a two-circle diffractometer (Fig. 8). Similar assignments have also been used by other workers (*e.g.* [161–163]).

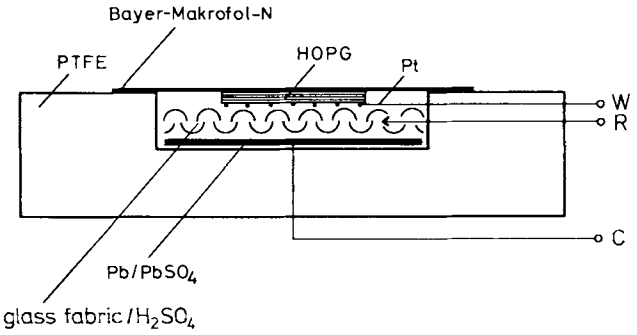



Fig. 8. Electrolysis cell for the 2-circle diffractometer. PTFE = polytetrafluoroethylene.

It is easily seen in Figure 7 that in the 1-phase region of stage I (b–a) no parts of stage II are present and that in the 2-phase region of stages II + I (c–b) both stages are always present *etc.* The expected sequence of the n-values (24, 48, 72...) according to the model $n=24\times s$ is, however, certainly not observed; only the potential break at $C_{48}$ fits with this sequence. The observed potential breaks (marks a–g) correspond to the following n-values (determined from several measurements): a) 21—20/b) 29—27/c) 48/d) 56—54/e) *ca.* 60/f) 84—81/g) *ca.* 110.

Two points particularly worthy of note from Figure 7 are the "additional" potential break in the apparent 1-phase region of stage II (d) and the increasing anion density with decreasing distance between the layers in the 1-phase region of stage I.

For confirming results, and as an aid to explaining such small but important effects for the understanding of the intercalation process, *in situ* dilatometry has proved very useful. With this method the macroscopic swelling of the graphite crystal[**] can be measured.

The bottom half of Figure 9 shows a cyclic voltammogram of HOPG in $H_2SO_4$ in its, perhaps unusual, "unfolded" form. The relationship between the graphs in the lower parts of Figures 7 and 9 can easily be followed by comparing the points a–f.

[*] In order to linearize the abscissa the $C_n(H_2SO_4)_y(HSO_4)$ phases are represented as $C(HSO_4)_x(H_2SO_4)_y$.

[*] The lattice plane spacings along the crystallographic c-axis, *i.e.*, perpendicular to the layers.

[**] Such studies do not necessarily require single crystals; HOPG, which is a polycrystalline material [39], albeit with a very regular crystallite order, is quite adequate.

Carrying out the reaction potentiostatically with a linear change in potential is particularly advantageous for an *in situ* structural analysis since the 2-phase "information branches" with their greater current density are quickly recorded and, thus, the resolution in the 1-phase region is better.

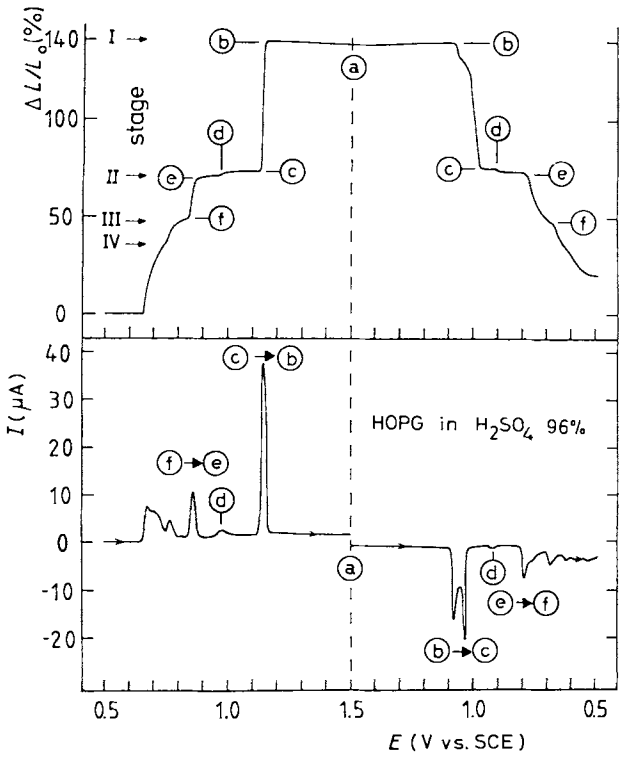



Fig. 9. Oxidation/reduction of HOPG in 96% $H_2SO_4$ (slow cyclic voltammetry, $v = 1.4$ mV min$^{-1}$); top: relative expansion of the crystal along the c-axis, bottom: current/potential curve (for details of the points a—f see text).

In the plot of the relative expansion in the c-direction $\Delta L/L_0$ (shown in the top half of Fig. 9) the 1-phase regions appear as plateaus, whereas the 2-phase regions appear as almost vertical jumps. In the 1-phase region of stage I it is again clear that as the anion density increases the interlayer separation decreases due to Coulombic attraction; during the back reaction this process is reversed and the inter-layer distance expands.

From the expanded plot the "additional" potential break d can be unambiguously ascribed to a slight change in the interlayer gaps in a "pseudo-1-phase" region of stage II. There are clearly two second stages, IIa and IIb, which can be differentiated on the basis of their anion packing densities[*]. From the back reaction it can be seen that the transition IIa/IIb is reversible.

In contrast, the "split" peak b→c during the back reaction suggests that this part of the reaction is irreversible. Since this splitting has not been observed in 99% $H_2SO_4$[**] it can be ascribed to a hydration or hydrolysis of the primary, electrochemically formed product (EC-mechanism, *i.e.* a secondary chemical reaction following a primary electrochemical reaction).

Even after complete back reaction the original value in the dilatometer is only sometimes reached[155]; due to particular experimental difficulties (*e.g.* the ingress of electrolyte into the capillary space) the original value is not always achievable. X-ray measurements have shown that, without doubt, the end product of the reverse reaction is graphite.

Figure 10 shows the design of the high resolution dilatometer. The sample displaces the ferrite core of a coil which is part of an oscillatory circuit whose resonance frequency can be calibrated in units of length[155].

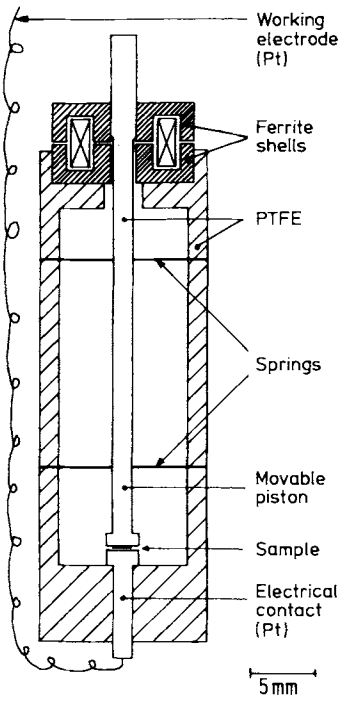



Fig. 10. Dilatometer for electrochemical experiments.

Potential/stoichiometry or current/potential curves with clear profiles (such as those shown in Fig. 7 and Fig. 9) can only be obtained using good crystalline graphite samples. Poor crystal material (where the C-atom sites and, as a consequence, those of the guest ions and molecules are non-equivalent and additionally where the diffusion of the guests into the layer gaps is significantly hindered) can be identified by the "smeared" curves which they produce. This is exemplified in Figure 11, which shows the change

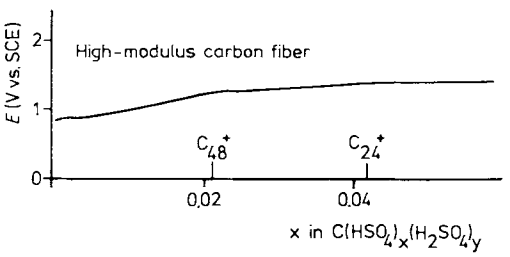



Fig. 11. Galvanostatic oxidation of highly oriented carbon fibers (Celion GY 70, Celanese USA) close to equilibrium in 96% $H_2SO_4$; the potentials were measured pointwise 2 min after each current break.

[*] Very recent X-ray experiments have shown that the stacking sequence of the carbon layers also changes at the transition from stage IIa to IIb [159].

[**] At even greater concentrations an exclusively electrochemical reaction is no longer possible due to partial self-oxidation.

in potential during a "near to equilibrium" oxidation of carbon fibers[*] (checked by a pulsed reaction).

Further possibilities for characterizing carbon materials by electrochemical measurements are described in Section 3.8.

### 3.4. Anodic Intercalation of Graphite in Other Acid Electrolytes

The $H_2SO_4$ system, described in detail in Section 3.3, can be seen as a model for many other Brønsted acid systems containing little or no water. However, as the water concentration in the system increases, side reactions, such as the production of $O_2$ or $CO_2$ and CO, become dominant and, in addition, a partial hydrolysis of the "acid graphite salt" $C_n(HX)_yX$ to "graphite oxide" takes place (cf. Section 3.7). The acid HX, of course, must be sufficiently stable towards oxidation; the redox potentials of acid graphite salts of stage I are approximately +1 V relative to the $H_2$ electrode.

#### *3.4.1. Concentrated Acids Containing Little Water*

The stoichiometries of most of the acid graphite salts of stage I which have been described in the literature closely approach the "ideal" of $C_{24}(HX)_2X$. However, it must be emphasized that the sequence of 1- and 2-phase regions shown by the $H_2SO_4$ example, and the appearance of incommensurable structures which are a result of this sequence, is only *qualitatively* applicable to the complete class of compounds.

Thus, it is not surprising that analytical results often yield "uneven" stoichiometries, and, in particular, that the number of neutral molecules HX often deviates significantly from 2, with a dependence on the size of X.

Typical results for y in $C_n(HX)_yX$ of stage I are: $H_2SO_4$ ($y=2$[148], $y=2.5$[166], $y=2.42$[167]); $H_2F_2$ ($y=2$[168]); $HClO_4$ ($y=2$[166,169]); $HSO_3F$ ($y=2.5$[170,171]); $HNO_3$ ($y=3$[172]); $HSO_3CF_3$ ($y=1.63$[167]).

Well characterized phases $C_n(HX)_yX$ of stage I have been obtained, for example, by the anodic oxidation of graphite in the following acid media: $H_2SO_4$[148,150–159], $HClO_4$[150,151], $HNO_3$[151], $H_2F_2$[168], $HSO_3F$[173], $HSO_3Cl$[151,174] and $HSO_3CF_3$[167,175]. Graphite has also been anodically intercalated in $H_2SeO_4$, $HIO_4$, $H_3AsO_4$[151], $CF_3COOH$[176] and also in fluoride-containing acids such as $HBF_4$ and $HPF_6$. However, the products of these latter reactions remain almost uncharacterized; indeed, complications may be expected due to loss of HF during the reactions. Surprisingly, no intercalation takes place in $H_3PO_4$. The compounds formed when $HX=HSO_3Cl$ remain controversial: it has been assumed that predominantly $SO_3$ and $H_2SO_4$ or $H_2S_2O_7$ are accepted into the lattice[177].

The anodic oxidation of graphite in $CF_3COOK/CF_3COONa$ melts leads essentially to fluorocarbons and $CO_2$[178]. There are also indications that where $HX=H_2SO_4$ iso-polyacids occur in the interlayer gaps[179,180]. Furthermore, simple acid anhydrides (*e.g.* $SO_3$[181] and $Cl_2O_7$[182] have been intercalated in graphite. In the latter case the compounds are not "molecular" intercalation compounds but rather partially ionic compounds such as $C_n^{2+}(SO_3)_ySO_4^{2-}$, "two-dimensionally solvated" by acid anhydrides[181]. That there is a stoichiometric "upper limit" of $C_{12}^+$ for salt-like compounds in the system graphite/$H_2SO_4$ has also been occasionally discussed[154,183].

Very similar relationships exist for the metal halide-graphite compounds (*e.g.* "$AlCl_3$-graphite", "$AsF_5$-graphite"); these compounds are also partially ionic (*e.g.* $C_n^+(AlCl_3)_yAlCl_4^-$). As is to be expected on the basis of such structures "$AlCl_3$-graphite" can only be prepared from $AlCl_3$ and graphite in the presence of oxidizing reagents such as $Cl_2$. Such reactions have been thoroughly discussed in several reviews on graphite compounds (cf. [30,38,45]). "$AlCl_3$-graphite" can be prepared electrochemically *via* the anodic oxidation of graphite in molten $LiCl/AlCl_3$; in this process the partial pressure of $Cl_2$ which is required for the chemical intercalation process can be correlated with the electrochemical potential[184]. In a similar way, $BiCl_3$[185] and $BF_3\cdot O(C_2H_5)_2$[179,186] have also been intercalated by partial anodic oxidation.

#### *3.4.2. Dilute Acids*

With increasing water content of the acid medium, only the higher stages of the acid graphite salts become accessible. For example: in 10 M $H_2SO_4$ stage II can be prepared, whereas in 6 M $H_2SO_4$ the lowest stage that can be prepared is stage IV, and in 1 M $H_2SO_4$ stage XX[187,188]. The variation in potential during the galvanostatic anodic oxidation of HOPG in 70–100% $H_2SO_4$ is qualitatively the same as that shown in Figure 7, *i.e.*, $H_2O$ has almost no influence on the phase sequence until the maximum anion packing density is reached. Beyond this limit, further oxidation leads to the release of $O_2$, $CO_2$ and CO and the formation of "graphite oxide" (GO), a compound made up of C, H and O with covalent C–O bonds. These products result from the hydrolysis of acid salts which are no longer stable in the presence of water. This is particularly true for the salts of stage I:

$$C_n^{\oplus}(HX)_yX^{\ominus} + H_2O \longrightarrow \text{"}C_nOH\text{"} + (y+1)\,HX \qquad (4)$$

In very dilute acids the development of gases predominates[189] whereas, for example, in 70% $HClO_4$ or 80% $H_2SO_4$, GO is formed with a current yield of practically 100%[190].

Obviously, during intercalation in dilute acids $H_2O$ also diffuses into the interlayer spaces. For any one stage the distance between the layers shows a clear dependence on $H_2O$ content and, indeed, it has been shown that the interlayer distance decreases with increasing $H_2O$ content[187].

Very soon after such compounds were first prepared, the idea of using graphite salts $C_n(HX)_yX$ as positive, active electrode materials in rechargeable batteries was put forward[148]. However, since the time-honored, negative electrodes (especially Pb, Zn and Cd) could not be used in concentrated acids it is only reasonable that attempts have been made using dilute acids as electrolytes. *Fujii* has studied, for example, such a rechargeable cell with $H_2$(Pd) as

[*] The interlayer distance in these fibers is *ca.* 340 pm and is thus typical of a turbostratic ordering of the C-planes. The "layer packets" are relatively thin (< 10 nm [164, 165]) and corrugated.

the negative electrode in 12 M $H_2SO_4$[191] and with Cu as the negative electrode in 15 M $H_2SO_4$; he has reported high cycle numbers (up to 6500 charge/discharge cycles)[192].

In more recent studies, *Beck et al.* have used $HBF_4$, $H_2F_2$, and $HClO_4$ instead of $H_2SO_4$[193–201]. In these studies the acid concentration was generally between 20—80% by weight. Under these conditions Cu, Pb, Zn, and Fe are all suitable anode materials, and as cathode a mechanically stable, hot-pressed composite from 80% natural graphite and 20% polypropylene was preferentially used. However, because of the high water content of the acids, the graphite salts of stage II determine the upper charge limit for the graphite cathode, and consequently the energy density of such accumulators is very low. For the cell $C_{48}(H_2F_2)_2HF_2$/50% $H_2F_2$/Zn with a discharge voltage of 2.2 V[198] a theoretical energy density of 70 Wh $kg^{-1}$ can be calculated. For the "heavy" acids and more noble metal anodes the values are considerably less favorable; for comparison, the theoretical energy density of a lead acid accumulator is 161 Wh $kg^{-1}$ (cf., *e.g.*, [202,203]).

### 3.5. The Anodic Intercalation of Graphite in Neutral Electrolytes

In neutral, aqueous solutions it is either not possible to prepare ionic graphite compounds or they are not stable[*].

Only the development of $O_2$ at the graphite anode or the oxidation of the graphite to covalent carbon compounds has been observed in such solutions (see Section 3.4). In contrast, in many nonaqueous solutions compounds of the general formula $C_n^{+}(solv)_yX^{-}$ are easily prepared by the anodic oxidation of graphite. However, these compounds generally decompose within a few days because, in order to prepare the electrolyte solutions, very polar solvents have to be used and these are not stable to oxidation[**]. Nevertheless, there are a large number of solvents which are *kinetically* stable enough (*i.e.* that oxidize slowly enough), so the compounds $C_n(solv)_yX$ can at least be prepared.

The possibility of anodically oxidizing graphite in nonaqueous solution has proved interesting, in particular, in connection with efforts to develop a rechargeable lithium battery along the lines of equation (5)[175,204–217] (cf. also Section 5.1):

$$Li + C_n^{\oplus}(solv)_yX^{\ominus} \underset{\text{Charge}}{\overset{\text{Discharge}}{\rightleftharpoons}} LiX + C_n + y\,solv \qquad (5)$$

Despite the high voltage of such cells (up to *ca.* 5.2 V), the energy density, taking solvation into account, is only moderate ($E_{theor.}$ is of the order of 200 Wh·$kg^{-1}$). Furthermore, up to now no suitably stable solvent has been found. The cyclic voltammogram in Figure 12 demonstrates that such graphite electrodes are reversible.

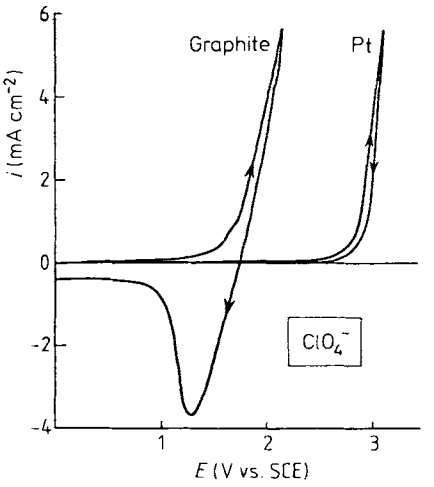



Fig. 12. Oxidation/reduction curve of graphite foil (a fine crystalline and well textured material with *ca.* 50% pore volume [1]) in 1 M $LiClO_4$/propylene carbonate, $v = 5$ mV $s^{-1}$; for comparison: an inert electrode under identical conditions.

The stoichiometry of the $C_n(solv)_yX$ phases has been determined from potential measurements made during galvanostatic oxidations. For stage I n is generally *ca.* 24 (1-phase region ± about 15%, as for $C_n(H_2SO_4)_y(HSO_4)$) and for stage II n is *ca.* 48[175,209,211,218–221]. The progress of the *E*/charge curve is usually very similar to that for the anodic oxidation of graphite in $H_2SO_4$; even such details as the "break" in the "pseudo-1-phase" region of stage II (corresponding to d in Fig. 1) are frequently observed during the anodic oxidation of graphite in nonaqueous electrolyte solutions. The degree of solvation y depends on the nature of the solvent: In two-dimensionally solvated phases (*e.g.* where solv = nitromethane) y is *ca.* 2[221] and in three-dimensionally solvated phases it is usually greater. For the $PF_6^-$ compounds solvated with propylene carbonate (PC) a value of y = 4 has been reported[218,219]. In the latter compounds the inter-layer distance (stage I: 1410 pm[219]) and, in particular the calculated structure factors[220] fit with the assumed tetrahedral coordination of $PF_6^-$ by PC. On the basis of polarity considerations, the carbonyl groups must be directed towards the carbon planes[219].

Table 2 is an up to date list of the anions ($X^-$) and the solvents (solv) which are known to form $C_n(solv)_yX$ phases. The "blank spaces" in Table 2 are completely accidental and do not have any fundamental significance. For solv = NM (nitromethane) the self-decomposition is the slowest. The anodic intercalation of doubly charged anions generally fails because of the insolubility of the corresponding salts in the commonly used solvents; normally, only 1:1 salts with large anions are suitably soluble.

In addition, there are also a number of products from the self-decomposition or "over-oxidation" of $C_n(solv)_yX$ which have, as yet, not been fully explained. Since these products often still show "redox activity" they have frequently been suggested as possible candidates for the active material in battery electrodes[224,232]. With the exception of NM-solvated phases, which can also be prepared *via* the reaction of $NO^+X^-$[225,226,228,230] and $NO_2^+X^-$[225–227,229,231] with graphite in nitromethane, the electrochemical method provides the sole route to this

[*] Thus, the trend already seen in aqueous acid solutions is seen to be continued: As the solution becomes more dilute the electrochemical potential of the graphite salts increases and the potential at which $O_2$ starts to be released decreases.

[**] The standard potential of the phases $C_n(solv)_yX$ of stage I is *ca.* +2 V.

Table 2. $C_n^+(solv)_yX^-$ phases known to date [a].

| solv \ $X^-$ | $F^-$ | $BF_4^-$ | $AlCl_4^-$ | $PF_6^-$ | $AsF_6^-$ | $SbF_6^-$ | $CF_3SO_3^-$ | $ClO_4^-$ | $HSO_4^-$ |
|---|---|---|---|---|---|---|---|---|---|
| AA | | | | [175] | | | | | |
| AN | | | | [175, 209] | | | | [175, 211] | |
| CFME | | | | | | | | [175] | |
| DMSA | | | | | | | | [175] | |
| DMSI | | | | | | | [204, 212] | [175, 208, 224] | |
| EC | | [175] | | | | | | | |
| ES | | | | | | | | [175] | |
| MSL | | [206] | | [206] | | | | | |
| NM | [222] | [225, 226, 229] | [228] | [112, 225, 226, 231] | [113, 221, 227] | [225, 226, 229, 230] | | [175, 211] | |
| OFTEE | | | | | | | | [175] | |
| PC | | [175, 211] | [175, 223] | [175, 209, 211, 219, 220] | [175, 211, 220] | [175, 220] | | [175, 209, 211, 213, 219] | [175] |
| SL | | [206] | | [206] | | | | [175] | |

[a] AA = acetic anhydride, AN = acetonitrile, CFME = chloroformic acid methyl ester, DMSA = dimethyl sulfate, DMSI = dimethyl sulfite, EC = ethylene carbonate, ES = ethylen sulfite, MSL = 3-methylsulfolane, NM = nitromethane, OFTEE = orthoformic acid triethyl ester, PC = propylene carbonate, SL = sulfolane.

class of materials[233,234]. If an acid, as well as the organic solvent, is present in the electrolyte solution, it is possible to produce $C_n^+(HX)_x(solv)_yX^-$ phases, *e.g.* $C_{48}^+(HBF_4)_{1.4}(ET_2O)_{0.9}BF_4^-$[235].

Unsolvated $C_n^+X^-$ phases can be prepared from ternary, solvated phases, especially those containing very volatile solvents, simply by pumping off the solvent *in vacuo*[175,211]. It is also possible that the anodic oxidation of graphite in $SO_2ClF$ solution (*e.g.* of $Bu_4N^+$ salts) leads directly to unsolvated phases[118]. It is at least clear that $SO_2ClF$ is a very weak solvating agent, since in such solutions, for example of $PF_6^-$ or $AsF_6^-$ graphite salts, the stoichiometry approaches $C_{12\times s}^+$, *i.e.* the anion packing density is doubled. The salts of stage I are not very stable and thus, as for other graphite compounds containing fluoro-anions[236–238], partial covalent fluorination of the carbon planes is the major side reaction.

The products obtained *via* electrolysis in $SO_2ClF$ have a composition $C_nX$ at room temperature and under normal pressure. Nevertheless, because of the highly volatile nature of $SO_2ClF$ (b.p. +7.1 °C) it cannot be excluded that a desolvation has already occurred under these conditions. Figure 13 shows the potential changes observed during a galvanostatic oxidation of graphite foil in saturated $Bu_4NAsF_6/SO_2ClF$.

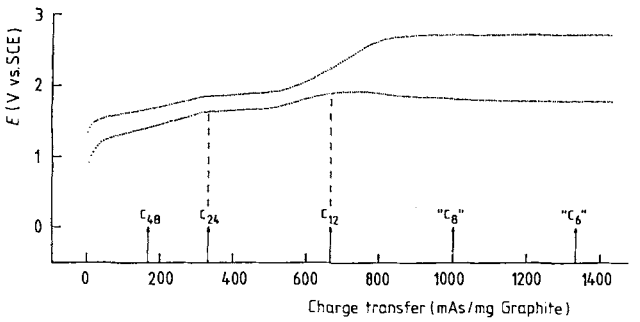



Fig. 13. Pulsed galvanostatic oxidation of a graphite foil in saturated $Bu_4NAsF_6/SO_2ClF$ (Sample *ca.* 7 × 7 × 0.2 mm; $I = 200\ \mu A$); top: current circuit open (in each case for 66 s); bottom: current circuit closed (in each case for 78 s).

The potential breaks close to $C_{24}^+$ (stage II, d = 1137 pm) and $C_{12}^+$ (stage I, d = 800 pm) corresponding to a stage sequence $C_{12\times s}$[240] can be seen; the irreversible oxidation beyond the point corresponding to $C_{12}^+$ leads to the formation of covalent C–F bonds. In this case, when no current is flowing, the potential decreases slightly as the degree of fluorination increases. This behavior is typical of covalent graphite fluorides $C_nF$[145,241].

*Bartlett et al.* have described the preparation of a "graphite salt" $C_8^+AsF_6^-$ *via* an oxidation of graphite with $O_2^+AsF_6^-$ in $SO_2ClF$[126,242,243]; however, the stoichiometry of $C_8^+$ does not agree with the potential curve shown in Figure 13. Hence, we believe that the products which have an analytical composition $C_8AsF_6$ also contain some non-ionic groups $C_nF \cdot AsF_5$ (cf. also [244]) and thus can be represented by the formula $C_{24}^{2+}F(AsF_5)(AsF_6^-)_2$.

Other $C_8^+$ compounds have also been postulated (*e.g.* in[126,245]) but the completely ionized state of these compounds has been questioned since the carbon atom can avoid a high "charge-transfer" (electrochemically it has a standard potential higher than +2 V) by forming covalent bonds. In contrast, the reaction of $AsF_5 + F_2$ with graphite has been shown to yield a stage sequence $C_{12\times s}$ similar to that produced during anodic oxidation[246]. $C_{12}^+$ salts have also been formulated with $CF_3SO_3^-$[247] and with a range of other anions[245,248,249].

The electrochemically prepared $C_nPF_6$ and $C_nAsF_6$ phases generally have relatively good degrees of crystallinity and thus well defined and reproducible inter-layer distances. On the other hand, the inter-layer distances reported for the compounds prepared from $O_2^+AsF_6^-$ or $AsF_5 + F_2$ are very variable (for stage I compounds: 810 pm for "$C_8AsF_6$"[242]; 786 pm for "$C_{8.1}AsF_6$"[245]; 804 pm for $C_{13.1}AsF_6$[245]).

### 3.6. Cathodic Intercalation of Graphite in Aprotic Electrolyte Solutions

The cathodic reduction of graphite in electrolyte solutions which are suitably stable against reduction[*] (*e.g.* alkali metal, $NR_4^+$- and $SR_3^+$-salts in ethers, esters, amides, sulfoxides *etc.*) always leads to solvated $M^+(solv)_yC_n^-$

[*] The standard potential of $A^+(solv)_yC_n^-$ phases of stage I is *ca.* −2 V and is thus about 1 V more positive than that of the alkali metals A.

phases. The unsolvated phases can, when desired, be obtained by removing the solvent *in vacuo*[250]. Analogous products containing doubly charged cations also exist (*e.g.* $Mg(HMPT)_{2.1}C_{130}$[251]; where HMPT = hexamethylphosphoric triamide). However, due to the limited solubility of most $M^{2+}$ salts in organic solvents it is only possible in a restricted number of cases to prepare these salts *via* cathodic intercalation.

The early work on the cathodic reduction of graphite in solutions of $NR_4^+$ and $K^+$ salts in liq. $NH_3$ demonstrated the formation only of the very unstable $NR_4^+(NH_3)_yC_n^-$[252,253] and $K^+(NH_3)_yC_n^-$[254] phases. In contrast, the DMSO-solvated phases $A^+(DMSO)_yC_n^-$ (where $A = Li^+$, $Na^+$, $K^+$, $Rb^+$ or $Cs^+$) and $NMe_4^+(DMSO)_yC_n^-$ (DMSO = dimethyl sulfoxide)[255-257] are considerably more stable. The relationship stoichiometry/stage for these phases has been determined from their *E*/charge curves. When $A^+ = K^+$, $Rb^+$ and $Cs^+$ and also for $NMe_4^+$ the limiting stoichiometry for stage I is around $C_{24}^-$ (1-phase region ± *ca.* 15%) and that for stage II at *ca.* $C_{48}^-$. When $A^+ = Li^+$ or $Na^+$ it is possible that the anion packing density is even greater[256]. In solvents which are poorer solvating agents than DMSO higher packing densities have been achieved (*e.g.* $Li^+(DME)_yC_{18}^-$ from the reduction of a graphite foil in $LiClO_4$/DME (DME = 1,2-dimethoxyethane[256]).

The reversibility of the electrochemical reduction of graphite in an $NMe_4^+$-electrolyte is corroborated by the evidence presented in Figure 14; on an inert electrode such as Pt the $NMe^+$ cation will be irreversibly reduced.

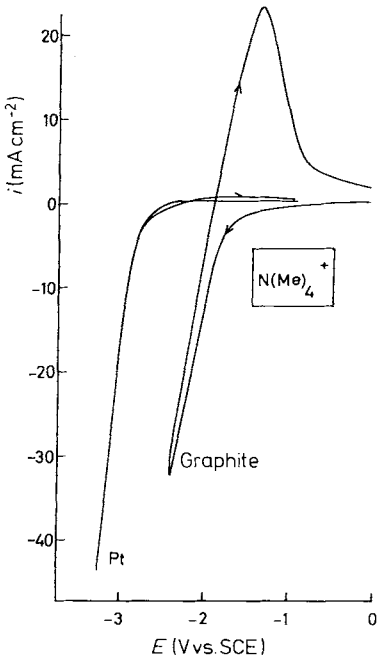



Fig. 14. Reduction/oxidation of graphite foil in saturated $NMe_4Cl$/DMSO, $v = 50$ mV $s^{-1}$; for comparison: an inert electrode under identical conditions.

Naturally, by varying the nature of $A^+$, $NR_4^+$ and/or the solvent a great variety of $M^+(solv)_yC_n^-$ phases can be electrochemically produced. The stability of these phases is in most cases questionable since, as is also the case for the $C_n^+(solv)_yX_n^-$ phases, the necessarily, strongly polar organic solvents are only *kinetically* stable relative to their reduction by the graphite compounds. The apparent stability of the "free" alkali metals in many of these solvents is simply due to a "passivating" surface layer (see *e.g.* [258-262]).

The stability of $M^+(solv)_yC_n^-$ phases can easily be checked by an electrochemical "back titration". Figure 15 shows the principle of this technique using the back oxidation of $K^+(DMSO)_yC_{24}^-$ and $Li^+(DME)_yC_{18}^-$ as examples. Here it can be seen that $K^+(DMSO)_yC_{24}^-$ can be back-oxidized with a charge yield of some 90% at *ca.* −2 V *vs.* SCE (*i.e.* reversible, close to the potential of formation), whereas the charge yield for $Li^+(DME)_yC_{18}^-$ is only about 60%, and at a potential of *ca.* +1 V *vs.* SCE the oxidation of decomposition products from the starting materials begins to take place. The phases $A^+(PC)_yC_n^-$ are extremely unstable[175,255,263].

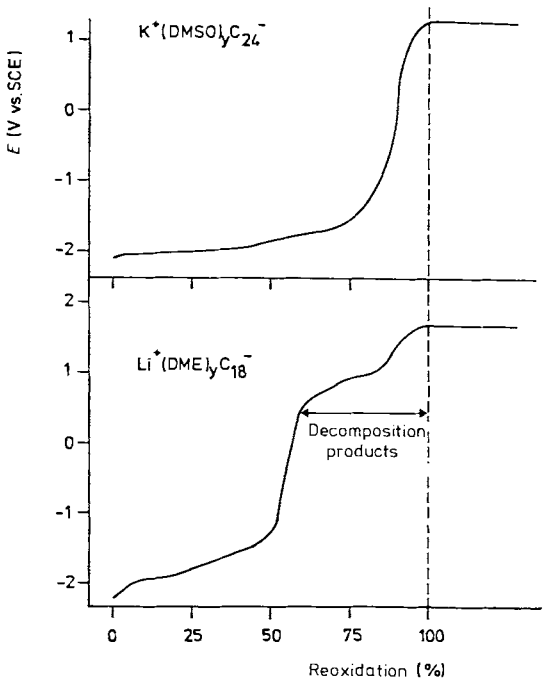



Fig. 15. Galvanostatic back oxidation of $K^+(DMSO)_yC_{24}^-$ and $Li^+(DME)_yC_{18}^-$, $I = 250$ μA·cm$^{-2}$; time scale: 100% back oxidation corresponds to 300 min, time required for sample preparation is also 300 min.

An alternative method for the preparation of solvated alkali metal-graphite compounds is by secondary solvation[264,265] of binary compounds prepared from the elements at higher temperature (*e.g.* [25,26,38,266,267]) or by A-transfer in unpolar media[268-270]. An additional alternative is the reduction of graphite in ethers in the presence of alkali metal salts of organic radical anions such as sodium dihydronaphthylide (*e.g.* [271,272], cf. also [256] and references therein) or in solutions of alkali metals in "electron solvating" solvents such as HMPT[273,274] or liq. $NH_3$ (*e.g.* [25-27, 266]). The chemical reduction of graphite in solution leads (depending on the solvent used) to formation of the corresponding ether-, HMPT-, or $NH_3$-solvated alkali metal-graphite.

Until now DMSO-solvated phases and $NR_4^+(solv)_yC_n^-$ phases have only been prepared electrochemically.

The DMSO-containing phases are three-dimensionally solvated and have especially large inter-layer distances; *e.g.* 1582 pm for stage I of $NMe_4^+(DMSO)_yC_n^-$ or 1493 pm for stage I of $K^+(DMSO)_yC_n^-$[257]. These inter-layer distances and an estimated volume (*i.e.*, the volume of the inter-layer gaps less the volume of the unsolvated cations ($NMe_4^+$ or $K^+$), where the remaining volume was assumed to be filled with DMSO whose density was taken to be equal to $DMSO_{liq}$) indicated, in each case, an approximately sixfold, octahedral coordination of the cations by DMSO[219]. However, this result is not in accordance with the findings of *Okuyama et al.*[275], who, on the basis of gravimetric experiments, report a degree of solvation of $y=3$ for $K^+(DMSO)_yC_n^-$. It is possible that various degrees of solvation exist for such phases, as also is the case for $K^+(THF)_yC_{24}^-$[264,276,277].

The electrochemical potential of $A^+(solv)_yC_n^-$ in terms of the alkali metal A are very dependent on the nature of the solvent; as the donicity[257] of the solvent decreases the electrochemical potential of $A^+(solv)_yC_n^-$ approaches that of the free alkali metal. The ionic character of solvated alkali metal-graphites is considerably better developed than that of the binary phases $AC_n$, as can be seen from their surprisingly high electrical conductivity. Furthermore, little $H_2$ is produced when such compounds react with water. The latter reaction has been used by *Bergbreiter* and *Killough*[278,279] as an ionicity indicator in accordance with equation (6a) or (6b).

$$A^{\oplus}C_n^{\ominus} + H_2O \longrightarrow AOH + H^{\oplus}C_n^{\ominus} \quad (6a)$$

$$AC_n + H_2O \longrightarrow AOH + C + 1/2\,H_2 \quad (6b)$$

### 3.7. Electrochemical Preparation and Analysis of Graphite Oxide

Graphite oxide (GO) is a rather nebulous term for C,H and O-containing compounds with a layer structure derived from their graphite precursor and *covalent* C–O bonds, which are formed by "overoxidation" of acidic graphite salts in the presence of water.

Overoxidation is taken to mean exceeding the maximum possible (ionic) charge transfer to the conjugated π-system; thus, overoxidation can then only lead to covalent oxidation products. The electrochemical potential at which overoxidation begins depends on the nature of the partner (nucleophile) available for the covalent bond. Thus, for example, the maximum possible (ionic) charge transfer to the carbon planes decreases with increasing water content for overoxidation in aqueous Brønsted acids[280]. The classical method for synthesizing GO is by the oxidation of graphite with strong oxidizing agents in Brønsted acids containing water; for example, in fuming $HNO_3 + KClO_3$[281,282], in $H_2SO_4 + HNO_3 + KClO_3$[282–284], or in $H_2SO_4 + NaNO_3 + KMnO_4$[282,285]. The mechanism of the reaction involves acid graphite salts as intermediates[286].

All the above methods yield a graphite oxide as end product which is no longer electrically conducting and has a high degree of oxidation. In the following discussion the degree of oxidation will be quoted in terms of oxidation equivalents per C atom.

Thus, graphite oxide with the idealized stoichiometry $C_8O_2(OH)$[287] has a degree of oxidation of 0.75. The dominating functional groups in GO are $>C=O$ and $\geqslant C-OH$[288]. Furthermore, it can be assumed that the C–C layers in GO are partially puckered ($sp^3$ hybridized carbon[289,290]) despite the fact that if keto-enol tautomerism is considered then it is possible to envisage a considerable degree of (covalent) oxidation without the formation of puckered structures[287,291].

To date very little is known about *electrochemically* produced GO (EGO) obtained from the anodic overoxidation of graphite in aqueous acids. The maximum degree of oxidation x of EGO is considerably lower than that obtainable for conventional GO ($x = \max.$ *ca.* 0.5)[41,190]. Further electrochemical oxidation is not possible due to the drastically reduced electrical conductivity. The formation of EGO from aqueous salt solutions[292] has also been reported. In many respects, the properties of EGO are very similar to those of GO; *e.g.* the interlayer distance *d* of washed and vacuum-dried preparations is *ca.* 650 pm (empirical formula: "$C_{4.6}O \cdot 0.75\,H_2O$", x *ca.* 0.43[293], starting material: graphite foil, oxidized in 70% $HClO_4$) as compared with $d = 590$–$670$ pm for conventional, chemically prepared samples[287]. In addition, both GO and EGO swell in similar ways in polar media. During intercrystalline swelling the inter-layer distances of EGO often expand more than 100%[41,294–296] (*e.g.* from 650 pm to 1000 pm in $H_2O$, to *ca.* 1150 pm in nitrobenzene, to *ca.* 1430 pm in PC and to *ca.* 1640 pm in pyridine).

On the basis of these similarities it seems reasonable to assume that EGO and GO differ essentially only in their degrees of oxidation. However, it is worth noting that in the region where EGO formation begins (the plateau marked by a in the lower part of Fig. 7 and by A in Fig. 16a), formation of acid salts $C_n(HX)_yX$ containing peroxysulfates has also been discussed[154,248,249].

A remarkable property of EGO is its ability to undergo back reduction to graphite with current and material yields of practically 100%. However, it should be noted that after such an oxidation/reduction cycle the graphite structure is considerably altered, whereas a similar cycle going only as far as the acid salt leads to little change in the original lattice. Nevertheless, the reversibility of the formation of EGO is interesting for energy storage. The formation of EGO is not, however, reversible in a thermodynamic sense, because the reduction of EGO occurs at a much more negative potential than the back oxidation (in 70% $HClO_4$ *ca.* +0.8 and +1.6 V *vs.* SCE, respectively), owing to considerable reaction overpotential. The gap between the "discharging" and "charging" processes widens with increasing dilution of the acid medium. In alkali media the reduction is irreversible[297]. The oxidation and reduction of a graphite foil is shown in Figures 16a and b. The oxidation up to the mark A in Figure 16a corresponds to an oxidation to the acid salt $C_n(HClO_4)_y(ClO_4)$ of stage I. The further oxidation, from A to B, corresponds to the formation of EGO[*]. Beyond B, $O_2$ development dominates.

[*] The properties of EGO still emersed in the acid medium in which it has been produced are, of course, not identical with those of washed and vacuum-dried material. Thus, for example, the inter-layer distance of EGO in acid media is almost the same as that in the acid salts of stage I.

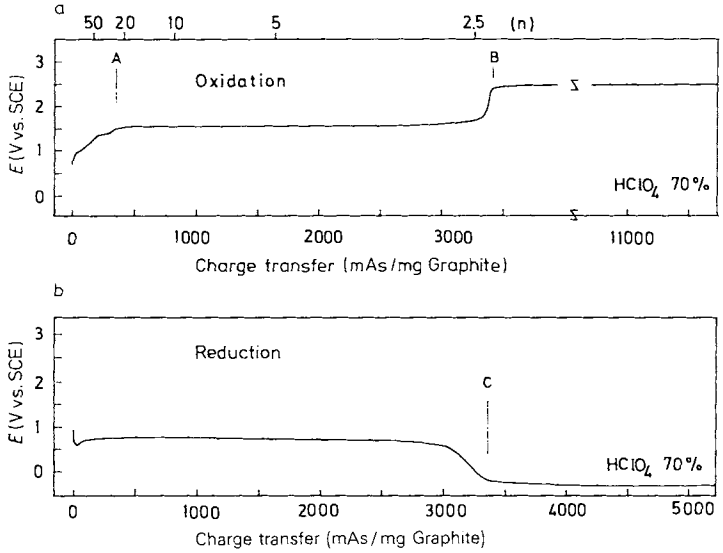



Fig. 16. Galvanostatic oxidation (a) and reduction (b) of graphite foil in 70% $HClO_4$, $I = 1$ mA cm$^{-2}$.

During the back reaction almost 100% of the charge equivalents used can be measured up to the point when $H_2$ starts to develop (mark C). This type of oxidation/reduction cycle is repeatable but the number of lattice defects accumulates and the conductance of the material continually decreases. In comparison to the intercalation of ions in graphite the formation of EGO is a relatively slow, *i.e.* kinetically unfavorable, electrode reaction. This can be qualitatively demonstrated in that the length of the plateau regions in Figures 16a and b decreases rapidly as the current density $i$ increases, whereas the "intercalation region" (start: A) is much less influenced by $i$[158].

Quantitative information on the kinetics of electrochemical reactions requires, in the first instance, a separation of the total polarization into its various components (cf. Section 3.2). The most effective method for this task is "impedance spectroscopy", in which the real and imaginary parts of the complex alternating current resistance of the working electrode is measured over as wide a range of frequencies as possible (*e.g.* [298–304]). Provided the situation is not too complicated, analysis of the data obtained permits an equivalent circuit diagram to be constructed in which the major components are: the electrolyte resistance $R_{EL}$, the "charge transfer resistance" $R_{CT}$, the double-layer capacity $C_{DL}$ and the "Warburg-impedance" $W$[*]. The essential parts of an equivalent circuit diagram which has often been used for describing electrode processes is given in Figure 17.

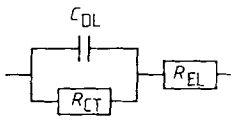



Fig. 17. A simplified equivalent circuit for the phase boundary electrode/electrolyte without diffusion effects being taken into account; $C_{DL}$ = capacity of the double layer, $R_{CT}$ = charge-transfer resistance, $R_{EL}$ = resistance of the electrolyte.

[*] $W$ is a difficult component to handle in terms of electronic calculations since it describes a complex resistance related to diffusion controlled reactions. In the following examples the experimental parameters have been so chosen as to make $W$ negligible.

The alternating current can flow across the working electrode/electrolyte phase boundary *via* a Faradayic reaction and/or *via* the double layer capacity $C_{DL}$. This arrangement corresponds to $C_{DL}$ and $R_{CT}$ being connected in the circuit in parallel. Furthermore, since the resistance of the electrolyte $R_{EL}$ (between the working and reference electrodes) cannot be eliminated experimentally it has to be included as a resistance in series. Since the double layer becomes "blocked" on measuring the resistance with an alternating current or voltage of the frequency $f \rightarrow 0$, the sum of the resistances $R_{EL} + R_{CT}$ can be obtained. For $f \rightarrow \infty$ the capacitive resistance $R_C = 1/\omega C \rightarrow 0$ and thus only $R_{EL}$ is measured. By varying the frequency $0 < f < \infty$ and plotting $R_{real}$ against $R_{imaginary}$ (= frequency response locus of the electrode impedance) a semicircle is obtained in Figure 17 for the equivalent circuit diagram, the diameter of which is equal to $R_{CT}$ (cf. Fig. 18).

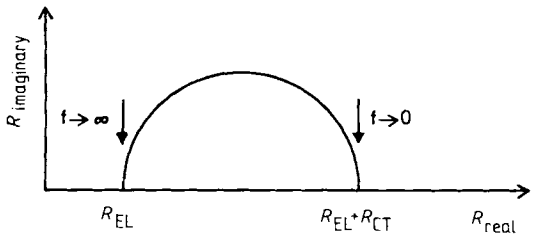



Fig. 18. Frequency response locus for the electrical impedance of the equivalent circuit in Figure 17.

Using impedance spectroscopy to monitor the anodic oxidation of graphite in aqueous acids the occasionally drastic changes in the resistance of the charge transfer reaction which coincide with the transition from simple intercalation to the formation of EGO and finally to the development of $O_2$ can be followed. For example, during the oxidation of HOPG in 96% $H_2SO_4$ (shown in Figure 19) it can be seen that towards the end of the period in which EGO is formed the value of $R_{CT}$ rapidly increases and finally achieves a very high value during the period when $O_2$ is produced.

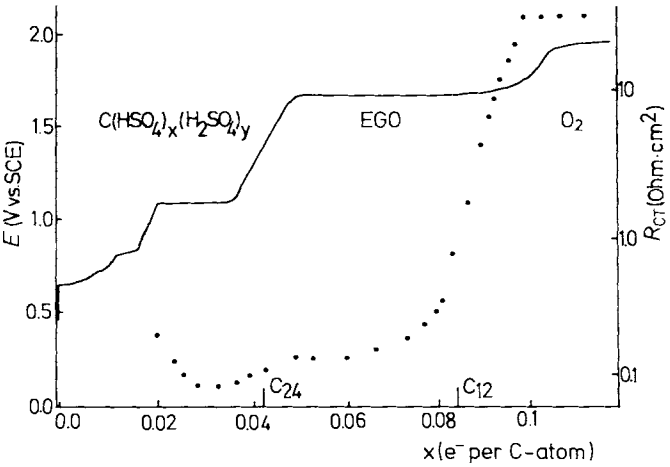



Fig. 19. Galvanostatic oxidation of HOPG in 96% $H_2SO_4$ (sample *ca.* 5 × 5 × 0.07 mm; $I = 100$ μA) with simultaneous measurement of the charge-transfer resistance $R_{CT}$ (frequency range 2.5 Hz–50 kHz; superimposed alternating current in the range 5–50 μA); the values of $R_{CT}$ are given solely on the basis of the prismatic areas.

In contrast the value of $R_{CT}$ is surprisingly low for the intercalation region. The values of about 0.1 Ohm·cm$^2$ calculated from $R_{CT}$ and the prismatic area of the HOPG electrode suggest that the electrochemical step of the intercalation reaction proceeds essentially uninhibited. The exchange current densities $i_0$ are, according to $i_0 = R \cdot T/n \cdot F \cdot R_{CT}$[139,305], in the region of 100 mA·cm$^{-2}$ (for comparison: $H_2$ on Pt in 1 N acid yields a value of $i_0 = 1$ mA·cm$^{-2}$ and Ag in $10^{-3}$ M $Ag^+$ yields a value of $i_0 = 150$ mA·cm$^{-2}$[139]).

The lack of any considerable barrier to the progress of the intercalation reaction is particularly remarkable in view of the considerable *deformation* of the carbon atom planes associated with the process. The transition zone from original to a more than 100% expanded inter-layer distance apparently travels as a "wave" through the lattice without requiring any significant activation energy. The limit to the intercalation reaction rate controlled by the diffusion of the guest species into the host lattice was not measured in these experiments. This limit is particularly noticeable in low frequency measurements and also when high current densities and long diffusion paths are involved. The diffusion coefficients $D$ of guest ions and molecules in laminar graphite compounds have been measured by a variety of different techniques. Although the absolute values recorded have a considerable spread, a value at room temperature of between $10^{-6}$ and $10^{-8}$ cm$^2$·s$^{-1}$ may be taken as standard (*e.g.* "$HNO_3$" in HOPG: $3.38 \times 10^{-6}$ cm$^2$ s$^{-1}$[306]; "$Br_2$" in HOPG: $2.45 \times 10^{-8}$ cm$^2$ s$^{-1}$[306]; $H_2SO_4^-$ in pyrolytic graphite: $9.75-13.6 \times 10^{-6}$ cm$^2$ s$^{-1}$[192]; anions in acid graphite salts: $10^{-7}-10^{-8}$ cm$^2$ s$^{-1}$[195,196,198,199]. The almost perfect semicircle produced from the measurements (Fig. 20) confirm that in this case the relatively simple equivalent circuit diagram without a diffusion related component is perfectly adequate.

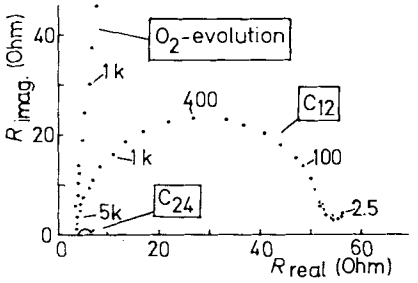



Fig. 20. Characteristic frequency response locus of the electrical impedance during the oxidation of HOPG in 96% $H_2SO_4$; the curves correspond to the three points in Figure 19 (at a stoichiometry of "$C_{24}$", "$C_{12}$" and during the development of $O_2$).

The experimental arrangement derived from the galvanostatic circuit (Fig. 4) used for such experiments is shown in Figure 21. In this arrangement the constant direct current is modulated with an alternating current of variable frequency. The resulting modulation of $E$ can then be analyzed in terms of both phase and amplitude (for a "frequency response analyzer" cf. [307,308]).

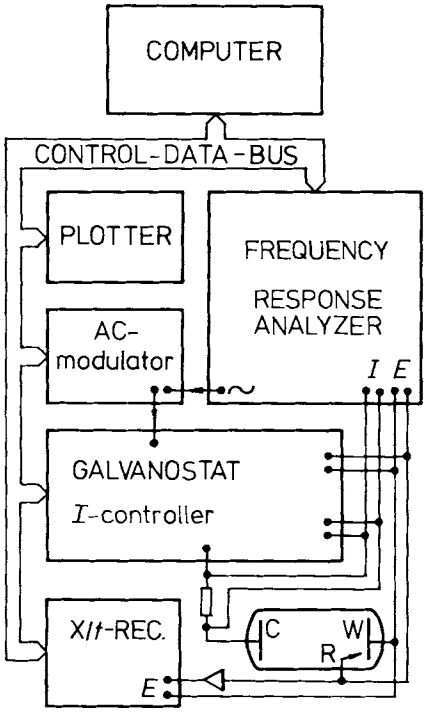



Fig. 21. Schematic diagram showing the experimental arrangement for impedance spectroscopy under galvanostatic conditions.

### 3.8. Electrochemical Intercalation as an Aid for the Characterization of Carbon Materials

The kinetics of intercalation reactions are partly dependent on the degree of order in the host lattice. At high concentrations of defects in the host lattice an influence on the thermodynamics of the process becomes noticeable. Thus, electrochemical measurements can be used as a method of *characterizing* the host lattice materials[153,309-311]. In the following discussion of the characterization of carbon fibers with varying degrees of crystallinity the example of "oxidation/reduction in $H_2SO_4$" will be used. Such fibers are, for example, produced from the graphitization of polyacrylonitrile or cellulose fibers and have proved particularly useful as reinforcing elements in composite materials[68,312]. It has already been shown (see Fig. 11) that the $E$/charge curves for carbon fibers have virtually no profile in comparison to those for HOPG. Naturally, this lack of profile also affects the cyclic voltammogram (cf. Fig. 22). Furthermore, the difference between the first and the second sweep is particularly remarkable.

When carbon with a low degree of order is intercalated for the *first time* a relatively high "additional" voltage is necessary[34,68,311,313-317]. This additional voltage is required, for example, in order to break up cross-links between the carbon planes. Thus, this "overvoltage" is thermodynamically and not kinetically controlled. Intercalation of graphite from the gas phase for the first time requires a corresponding "threshold" vapor pressure[318,319]. The second intercalation process for such materials takes place at essentially the same potential as for highly ordered materials (the arrows in Figure 23 mark the positions of the peaks corresponding to stages IV—I of an HOPG electrode under the same experimental conditions). It is in-

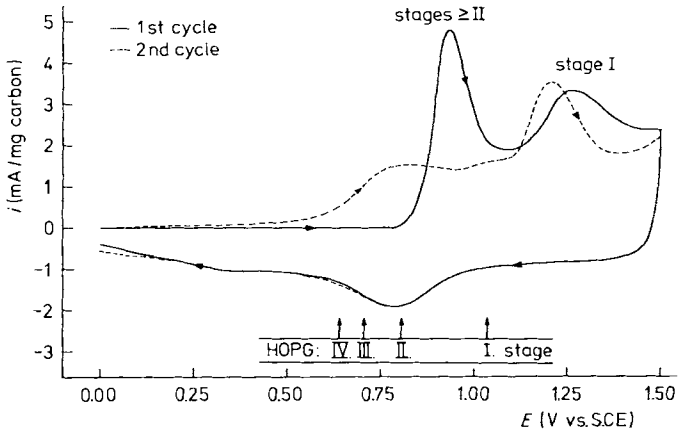



Fig. 22. Cyclic voltammogram (1st and 2nd cycles) of a highly orientated carbon fiber (Thornel 100, Union Carbide) in 96% $H_2SO_4$, $v = 5$ mV·s$^{-1}$.

teresting to note that the formation of higher stage $C_n(H_2SO_4)_yHSO_4$ phases is not observed during the first intercalation process: for example, with the carbon fiber Celion GY 70 only stages I and II were obtained. In contrast, after one complete intercalation/deintercalation cycle the higher stages can be synthesized. For the preparation of fiber-based intercalation compounds with either oxidation sensitive anions or reduction sensitive cations a "precycle" using more stable ions is often very useful[118]. The additional voltage necessary for the "first time" intercalation of carbon fibers can be used as a "crystallinity indicator". With decreasing crystallinity the additional voltage increases (cf. Fig. 23) until finally no intercalation takes place at all.

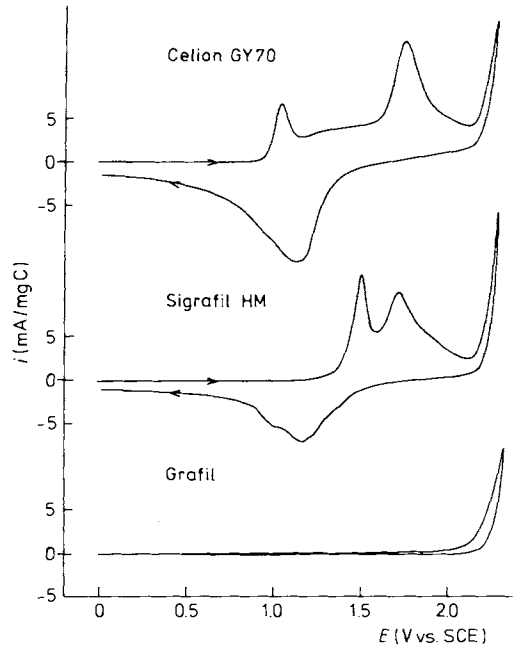



Fig. 23. Cyclic voltammograms (in each case the 1st cycle) of carbon fibers having different degrees of crystallinity (characterized for example by *Franklin*'s *p*-value [320], *Young*'s modulus $E$ [N m$^{-2}$] and 001-linewidth $b$ [degree $2\theta$]); in 96% $H_2SO_4$, $v = 5$ mV·s$^{-1}$:
Celion GY 70: $p = 0.731$, $b = 0.70$, $E = 5.2 \times 10^{11}$;
Sigrafil HM: $p = 0.940$, $b = 1.55$, $E = 3.5 \times 10^{11}$;
Grafil: $p = (1.886)$, $b = (3.50)$, $E = 2.4 \times 10^{11}$.

In contrast, the potential required for the preparation of EGO is practically independent of the nature of the graphite starting material since the breaking of any cross-links present has already occurred during the formation of the acid salts. Other electrochemical parameters can also be used for the characterization of carbon materials; *e.g.* the completeness of the galvanostatic deintercalation (HOPG, in contrast to less ordered materials, can be almost quantitatively deintercalated). Of course, these "electrochemical parameters", which in some cases are very easy to measure, can be correlated with structural parameters such as the mean inter-layer distance, the 001 line width, *Franklin*'s p-values *etc.*[320], as well as the modulus of elasticity and the electrical conductance[311].

## 4. Surface Electrochemistry of Black Carbons

### 4.1. Basic Information

The anisotropic character of carbon having a layered structure makes itself particularly noticeable in terms of the electrochemical properties of the material. Thus, the double layer capacities $C_{DL}$ of the basal planes are around 3 μF·cm$^{-2}$, although those of the prismatic planes are generally >50 μF·cm$^{-2}$[70]. However, it must be remembered that the plane edges do not end at the prismatic planes with "dangling bonds" but rather that they are saturated with heteroatoms—in aqueous solutions generally with oxygen containing species. These "surface oxides" have already been thoroughly reviewed[58-61,70]. In aqueous electrolyte solutions only the "acid surface oxides" are important; essentially these are composed of carboxyl groups, alcoholic and phenolic hydroxyl groups, and quinones. Additionally, keto-enol tautomerism and the formation of lactones must also be considered[59,60,321-323].

Electrochemical methods such as the polarography of carbon suspensions (*e.g.* [71,324-327]) and, in particular, the cyclic voltammetry of carbon electrodes can also be used for studying the surface oxides. However, electrochemical analysis has proved useful almost solely for the identification of quinonoid groups in various environments. In contrast, monitoring the reduction of the other (difficultly reducible) groups is a difficult task—at least in aqueous solution. This difficulty is due partly to the production of $H_2$ which occurs as a side reaction and partly to the slow kinetics associated with these reactions. The latter lead, for example, to the peak potential of the cyclic voltammograms being very dependent on the scan rate $v$.

Finally, it should be noted that there is a difference between the surface oxides and GO or EGO: GO and EGO have their O functionalities between the carbon planes, whereas in the surface oxides they are only found at plane edges or in lattice defects on the basal planes. Electrochemically, GO and EGO have very different reduction behavior to that of the surface oxides: whereas the reduction of EGO in strongly acid media is close to its formation potential (*e.g.* according to the upper and middle curves in Fig. 23, in 96% $H_2SO_4$ *ca.* +1.25 V *vs* SCE or +1.5 V *vs* $H_2$ and thus corresponding to a very strong oxidizing agent) and is thus *quasireversible*, the surface oxides, except for a relatively small number of quinonoid groups,

are reduced *irreversibily*, close to the potential at which $H_2$ starts to be produced. Thus, the reduction of the surface oxides is similar to that of other organic molecules with the same functional groups.

The surface oxides are of decisive importance in many technical applications of carbon, and particularly of active charcoal[333] or carbon black[334], for example in absorbents, fillers for rubber and other polymeric materials[334–336], and printing inks *etc.* More recently, surface oxides have received considerable attention from electrochemists who have employed them as "anchor groups" for the irreversible coating of electrode surfaces with specific reactive compounds. In contrast, basal planes can only be coated *via* adsorption and thus by reversible processes. Since electrode reactions are heterogeneous processes their rates and also the product ratios produced can be dramatically changed by using such "chemically modified" electrodes.

### 4.2. Chemically Modified Carbon Electrodes

The term modification of electrode surfaces means the intentional coating of such surfaces with foreign molecules[337]. *Miller et al.*[338] were the first to attach optically active amino acids to the surface of a graphite electrode. Somewhat later it became obvious that the basal plane and the layer edge surfaces of pyrolytically prepared graphite have very different reactivities with respect to modification.

The formation of covalent linkages occurs preferentially at the layer edges[339,340] whereas physical adsorption occurs on both basal and prismatic planes, although smaller background currents have been observed for the basal planes[341].

Since this general topic has already been covered by several comprehensive articles[71–73,342] only a discussion of the more recent literature and a brief description of the experimental techniques will be given here. The production of modified electrodes or the immobilizing of foreign molecules on the surface of electrodes takes place in several stages. Particularly important is the preparation of the carbon surface. If the modification is to occur *via* an adsorption then the oxygen-containing species must generally be removed as completely as possible. Where the modification involves the formation of covalent bonds the first stage is generally an oxidation or reduction process and a bridging group is then attached to the surface before the desired substrate is finally attached to the bridging groups.

Cleaning of the graphite surface is commonly carried out by polishing the surface or in an argon plasma[343]; a suitable apparatus has recently been described[344]. The reduction of the carbon surface is either achieved chemically with, for example, $LiAlH_4$ (the carboxyl groups are converted into hydroxyl groups by such a process) or electrochemically[345] (whereby subsequent reaction with nucleophiles is made possible). Oxidation of the carbon surface can be achieved chemically (*e.g.* with $KMnO_4$[346], NaOCl[58] or $O_2$ at high temperature[338]), electrochemically (*e.g.* by anodic oxidation in $H_2SO_4$ or $HNO_3$[347]), or physically (*i.e.* in an RF-oxygen plasma[348,349]). The plasma process allows the production of a larger number of functional groups on the surface and thus of more "anchoring sites" than can be achieved by conventional electrochemical processes[349]. The oxidized or reduced electrode surfaces are generally coated with an "anchoring group" before the actual effective material is applied. Typical anchoring groups are provided for example by the reaction of thionyl chloride[338,347] and acetyl chloride[350] with the HOOC-groups on the electrode surface. Other examples are the often used reaction of cyanuric chloride with the surface HO-groups[349,351–355], the reaction of phenolic groups with iminodiacetic acid[346], or the silanization technique, which is commonly used for metal electrodes and has been applied to carbon electrodes by *Murray et al.*[356]. Where necessary, a pre-reduction can be carried out to convert the HOOC- surface-groups into $HO-CH_2$-groups, which can then be coupled with the desired reagent. Where no achoring group is used, the transition between covalent bonding and chemical or physical adsorption becomes more difficult to define. An early paper which deserves explicit mention is one which describes the coupling of olefins to an "oxide-free" carbon surface[357]. In the reviews already published[71–73,342] there are many references to the utility of this principle.

Closely related to this technique is the adsorption of polymeric material onto electrode surfaces. Vinyl compounds such as 4-vinylpyridine[71] or vinylferrocene (*e.g.* [358]) have often been used to produce such polymeric materials. Further examples of polymers which have been utilized for electrode coating are polyacrylic acid[359], quinonoid polymers[360] and poly(xyleneviologen)[361]. More and more commonly, papers are published in which the polymers are used simply as an embedding medium for redox systems. In addition to the information given in [71–73,342], the coordination of Ru(III)(edta) in or on layers of poly(4-vinylpyridine) on transparent graphite electrodes (prepared by depositing carbon onto a quartz support from the gas phase[362]) and the compounds formed from cyano complexes of Mo, W and Fe[363,364] or of $(Ru(bipy)_3)^{2+}$[365] on polymers are worth mentioning. In the latter example the graphite electrode so coated is described as part of a photogalvanic cell.

A possible application for graphite electrodes coated with redox polymers is for the deionization of water[366,367]. In water softening processes multiply charged cations are cathodically preferentially deposited.

To regenerate these preparations the polarity of the "cationic and anionic absorbants" are simply reversed. A glass-carbon-electrode coated with Berlin Blue has been used spectroelectrochemically[368]. Iron-porphyrin, also coated onto a glass-carbon electrode, has been used for the reduction of $O_2$; it is interesting to note that effective reduction is only observed when the Fe-porphyrin units are orientated flat on the electrode surfaces and not when they are perpendicular to the surface[369]. Electrocatalytic effects have been observed with graphite electrodes coated with metal phthalocyanines of Fe, Co, Ni and Cu[370,371]; in the case of the iron compound such electrodes have also been used for studying adsorbed species *via* Mössbauer spectroscopy[372]. An example of a biochemical application of these electrodes is that of the immobilization of flavoen-

zymes on the surface of a cyanuric chloride modified graphite electrode[334]; the reduction of FAD demonstrated that a direct electron transfer between the enzyme and the electrode had taken place.

Although modified carbon electrodes have been shown to have many uses with respect to both electroanalytical and kinetic studies, this is not the case regarding electrosynthetic applications.

In the first report of a modified graphite electrode *Miller*[338] used a "chiral" electrode for synthesizing an optically active alcohol *via* a cathodic reduction of a ketone. The results are, however, in disagreement with the analogous experiments of *Horner* and *Brich*[347]. More recently, an assymmetric reduction of prochiral active olefins at a poly-l-valine coated electrode has been described for the first time. Yields of optically active materials of 23 and 43% were obtained[373]. It is possible that the lack of examples regarding the use of coated electrodes for electrosynthesis is due to the unsatisfactory stability of such coatings. In the case of the polymer coated electrodes in particular, swelling in the electrolyte solution is observed and, in the adsorbed species, even a leaching of some of the redox reagents is found to take place. Thus, it is important that developments on modified carbon electrodes concentrate not only on surface modifications but also on modifications within the electrode material itself.

### 4.3. Surface Oxides and Three-Dimensionally Distributed "Defect Oxides"

The classical techniques already described in Section 4.2 for the surface oxidation of carbon and the anodic oxidation in dilute, aqueous electrolyte solutions cannot be employed for attack at intact basal planes of graphitic carbon[374]. Extending the length of the oxidation reaction time or making the conditions more drastic (*e.g.* $H_3PO_4$ at 135 °C[375] or hydrogen sulfate in the molten state at 180–320 °C[376]) only lead to a complete disintegration of the starting material (mainly to $CO_2$), which begins at the layer edges. In an attempt to hinder the disintegration of the electrode material industrial carbon anodes have been impregnated for example with oil or pitch (*e.g.* [377] and extensive patent literature); this seals off the pores, which, because of their poor accessibility have little effect on the desired electrode reaction, but present a large surface area for corrosive attack.

Since it is generally the basal planes which are most exposed on a carbon electrode it is important, for example, that the basal planes are also functionalized for efficient surface modification. Such basal plane modification is possible to a limited extent by a two stage process in which EGO is synthesized (cf. Section 3.7) and then reduced back to "graphite".

The "graphite" obtained from the reduction of EGO is characterized by a high concentration of lattice defects. C–C bonds which are broken during the formation of EGO are only partially re-formed during the reduction process. The number of these "irreversible" defects can be greatly increased by successive formation and reduction of EGO[378].

The electrochemical introduction of lattice defects is relatively easy, and because of the characteristic reaction potentials of the defects the process can even be followed almost quantitatively. This is exemplified in Figure 24, which shows the fifth cycle (−0.7 to +2.1 V *vs* SCE) of the oxidation/reduction of a highly orientated carbon fiber (Celion GY 70) in 96% $H_2SO_4$; a first cycle under essentially the same experimental conditions is shown in the top part of Figure 23.

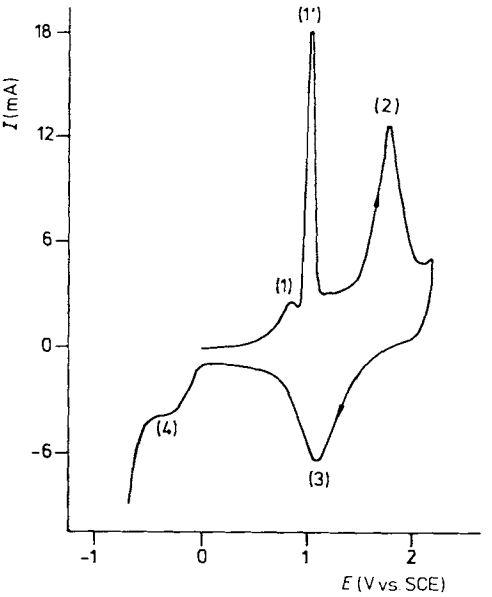



Fig. 24. Cyclic voltammogram (5th cycle) of carbon fibers (Celion GY 70) in 96% $H_2SO_4$, $v = 2.5$ mV·s$^{-1}$, $F$(geom) = *ca.* 0.7 cm$^2$ (for an explanation of the points 1–4 see text).

The peaks (1), (2) and (3) correspond, similarly[*] to the peaks in the first cycle, to the formation of acid salts $C_n(H_2SO_4)_yHSO_4$, EGO and the back reduction of this product to "graphite", respectively. The 3rd peak is only poorly resolved in this fifth cycle. The (1′) peak which was not yet visible in the first oxidation half-cycle corresponds to the oxidation at defect sites left over from the reduction of EGO. "Peak" (4) correlates with peak (1′) and represents the kinetically very slow reduction of the oxidation products arising during the progress of peak (1′). The areas of peaks (1′) and (4) grow rapidly as the number of completed cycles increases, whereas those of peaks (2) and (3) grow only slowly. However, after five completed cycles the electrical conductivity and the mechanical stability of the fiber electrode are rapidly lost. If this "cyclic treatment" is constrained within the potentials −0.7 and +1.2 V, thus avoiding any renewed formation and back reduction of EGO, then the areas and shapes of peaks (1′) and (4) remain constant.

Assuming that one-electron processes are involved, it can be calculated from the areas of peaks (1′) and (4) that *ca.* 15% of the C atoms are in the form of reactive defects and are thus functionalized or functionalizable. Such a high percentage of active sites excludes the possibility of their interpretation as "surface oxides at the layer edges".

[*] Compared with the first cycle, the formation of $C_n(H_2SO_4)_yHSO_4$ begins in the fifth cycle at less positive potentials (cf. Fig. 23).

Nevertheless, the potential range of the reduction "peaks" (4) lies in exactly the same place at which surface oxides are typically, at least in part, reduced (cf. Section 4.4). Thus, it can be assumed that at least the functional groups involved are very similar to those of the surface oxides[*]. Certainly, in these very disturbed carbon lattices it is not only the layer edges which are oxidizable but rather the lattice defects generally, so that analogous to the "surface oxides" it is better to call these products "defect oxides". A variety of technical applications for the defect oxides of black carbon can be envisaged (cf. Section 5). They are relatively good electrical conductors[**], and at the same time they are highly functionalized on the basal planes, on the plane edges, and within the material itself. Similar reactions can be carried out on defect oxides as on surface oxides; they can be "chemically modified" in the same way as for −C−OH groups with, for example, Cl−$SiMe_3$[379]. In this way a higher grade of modification can be obtained than can be produced from conventional surface oxide starting materials. This has been demonstrated using the example of the reduction of *o*-nitrophenol adsorbed onto a trimethylsilylated carbon fiber electrode. For the conventional fibers (*i.e.* having only the surface oxides at the layer edges) the silylable proportion of the total surface area and thus the amount of adsorbed *o*-nitrophenol was low, whereas the electrodes based on defect oxide fibers adsorbed so much *o*-nitrophenol that it must be assumed that not only the basal plane but also defects within the electrode had undergone silylation[379].

### 4.4. Surface Fluorides

The electrochemical surface oxidation of carbon is not restricted to the synthesis of surface oxides. Carbon anodes in fluoride melts have been, for example, considerably fluorinated; in this process "graphite fluorides" develop[30,38,45,241,380,381] which form poorly conducting surface layers. This phenomenon ("anode effect"[382–385], which is a considerable technical problem (for example in the production of Al), as well as the general behavior of carbon anodes in fluoride melts have been widely studied (cf. the review[386] and also, *e.g.* [387–391]). The fluorination of electrodes has also been used as a means of protecting the electrodes against corrosion[392]. An electrochemical synthesis of graphite fluorides $(CF_x)_n$ analogous to the formation of graphite salts (Eq. 1b) is not possible; because of its covalent character, $(CF_x)_n$ is not a mixed conductor. The only report of such a process is that of an indirect electrochemical production of $(CF_x)_n$ *via* the attack of $F^-$ on $C_n^+(solv)_yX^-$ in accordance with the following equation[145]:

$$C_n^{\oplus}(solv)_yX^{\ominus} + F^{\ominus} \longrightarrow C_nF + y\,solv + X^{\ominus} \quad (7)$$

[*] ESCA measurements (C 1s and O 1s) of *R. Schlögl* (Universität München) on carbon fibers which were removed from the electrolyte solution and washed with water after a single oxidation/reduction cycle at 0 V *vs* SCE (*i.e.* before the reduction (4)) showed the presence of many ≥C−O− groups and only a few >C=O groups.

[**] Due to considerable perturbation of the structure of the carbon planes a drastic drop in the electrical conductivity is to be expected. This effect is compensated, and sometimes overcompensated, by an increase in the electrical conductance following an increase in the concentration of the defect electrons in the valence band as a consequence of the oxidation. The resulting conductivity of defect oxides is generally some 100% more than that of the starting material [41, 118].

### 4.5. Electrochemical Surface Oxidation of Carbon Fibers

Because of their excellent mechanical properties in relation to weight, carbon fibers[1–3,393–395] are finding increasing application in high grade fiber/polymer composites. The quality of composite materials is often limited by the unsatisfactory anchorage of the fibers to the polymerizate, *i.e.* the strength of the fibers cannot be fully utilized. The anchoring of the fibers within the polymer matrix is to some extent purely mechanical (determined by surface roughness[396–398]), but by and large it is of a chemical nature: surface groups (generally surface oxides) *react* during the polymerization for example with an epoxide phenol or an amine component[62–64,66,399–401]. Thus, an improvement in the anchorage of fibers to the polymer matrix has the prerequisite that the surface functionality of the fiber is optimal. The surface oxidation of carbon fibers can also be carried out both in the gas phase (*e.g.* $O_2$[62–66,68], $O_3$[396,402]) and in solution (*e.g.* with $Ce^{4+}$, $HNO_3$[62–66,68]) as well as anodically[403–406].

The type of surface oxide produced generally depends on the method of oxidation[407]. Thus, for example, the oxidation with $HNO_3$ yields more carbonyl groups than does the oxidation with air[408–410]. Furthermore, the −COOH group is well suited as an anchorage site, whereas the surface oxides obtained from the oxidation with $O_3$ are, for example, not so good[396]. Following the electrochemical surface oxidation of carbon fibers ESCA measurements have demonstrated the presence of −COOH, >C=O, and ≥COH groups[406]. Electrochemical surface oxidation is a process which can be carried out quite easily (similarly to the surface oxidation of glassy carbon[322,411]) on fibers with low degrees of crystallinity and consequently a high concentration of lattice defects which are *not possible* to intercalate (cf. Fig. 23, lower part). In principle, the yield of surface oxides can be determined electrochemically (cf. Fig. 25); however, the carboxyl groups, in particular, would probably be very difficult to reduce since $HNO_3$-oxidized and, consequently, carboxyl-rich fibers exhibit only a small amount of cathodically reducible surface oxides, despite the fact that thermogravimetric analysis indicates a considerable degree of surface oxidation[412–414].

The "roughening" of the surface by oxidation can be measured not only by the BET method but also by measuring the capacity of the double layer[415–417]. In the case of "Grafil" fibers (for data see Fig. 23) an increase by a factor of 15 or 250 (measured at the potential at which $H_2$ develops) has been observed[414] after electrochemical preoxidation (corresponding to Fig. 25, 1 or 10 min, respectively, with 10 mA/mg fiber in 0.5 M $H_2SO_4$) and subsequent reduction (10 min at the $H_2$ potential)[*]. Comparable values can only be obtained in refluxing 65% $HNO_3$ after very long reaction times (a factor 30 after 34 h or a factor 150 after 72 h). Furthermore, the fibers lose much of their mechanical strength after 72 h of $HNO_3$-treatment, whereas

[*] The considerable increase in the capacity of the double layer cannot simply be attributed to an increase in the surface area, since it is probable that the capacity of the double layers at basal and prismatic planes are very different and, thus, lattice defects in the basal planes greatly increase their double layer capacities. SEM photographs (magnification × 10000) show a surprisingly low degree of "roughening" of the fiber surface after oxidation.

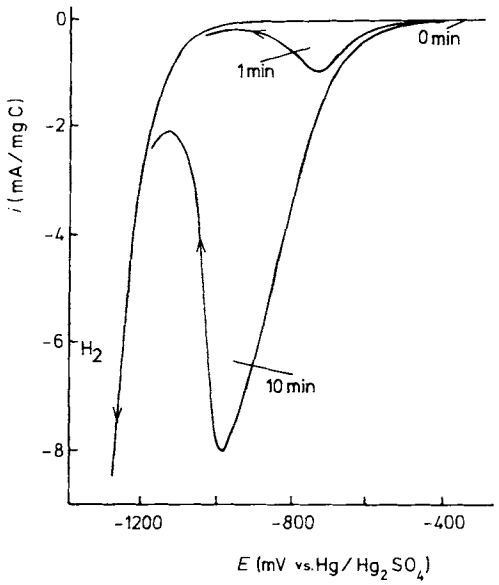



Fig. 25. $I \cdot R$-corrected voltammogram of the reduction of surface oxides on Grafil fibers (for data see Fig. 23) in 0.5 M $H_2SO_4$ ($O_2$ free), $v \approx 5$ mV·s$^{-1}$; the minutes given refer to the duration of the previous oxidation in 0.5 M $H_2SO_4$ at 10 mA/mg fiber.—$I \cdot R$ correction: The resistance $R$ between the reference and working electrodes leads, when current flows, to a voltage drop $I \cdot R$, which in turn leads to a corresponding error in the potential curve. With small currents and when $R$ is constant such errors could be accepted but due to disintegration of the covering layer $R$ is expected to vary so that a correction for $R$ is necessary. This is possible by simultaneously measuring the impedance at high frequencies (in this case 20 Hz) which essentially measures only the electrolytic resistance and that of the covering layer (cf. Fig. 17 and 18). The resulting value of $R$ is multiplied by $I$ and the voltage drop $I \cdot R$ automatically added to the desired voltage signal.

on anodic oxidation the mechanical strength of the material remains essentially intact[414].

In contrast to fibers of low crystallinity, those of *highly oriented,* graphitic carbon are very difficult to surface oxidize, both by chemical and electrochemical techniques. This is because the number of C-atoms along the layer edges and the number of lattice defects are much lower in the latter; this can be demonstrated, for example, by BET surface area measurements or by titration or electrochemical reduction of the surface oxides. In addition, the highly orientated fibers, and particularly those derived from PAN (PAN = polyacrylonitrile), have an "onion skin" morphology at their surfaces, *i.e.* mainly basal planes are exposed[66,418]. Because of the problems associated with intercalation, such as loss of mechanical strength, the more drastic oxidation techniques (roughly speaking those which lead to graphite oxide formation) cannot be used. Thus, the technique described in Section 4.3 for the functionalization of basal planes cannot be used since it involves a considerable degree of intercalation into the fibers with a corresponding deterioration in their physical properties.

An alternative technique commonly employed, at least on a laboratory scale, is an electrochemical surface treatment analogous to that described in Section 4.3 for the preparation of 3-dimensionally distributed defect oxides by cycling, for example in 96% $H_2SO_4$, between $-0.7$ and $+2.1$ V *vs* SCE (cf. Fig. 24). However, since highly orientated carbon fibers with a typical diameter of 5—10 μm are almost quantitatively intercalated within a few seconds[118] it is obvious that potentials close to $+2.1$ V can only be applied for a very short time. The best results are obtained using a "cycling frequency" of about 50 Hz, since with much higher frequencies the major effect of an alternating current is a continuous reversal of the charge at the double layer, and with lower frequencies the risk of intercalation within the fibers increases. "Cyclization" of Celion GY 70 fibers in 96% $H_2SO_4$ (20 s of cycling treatment, 50 Hz, $-1.4$ to $+2.1$ V *vs* SCE) produced *ca.* 2.5 mAs/mg of electrochemically reducible oxides without any noticeable intercalation as measured by X-ray analysis and electrical conductance[414].

Nevertheless, the high oxide coverage of fibers with a low degree of crystallinity (the "10 min" curve in Figure 25 corresponds to *ca.* 400 mAs/mg) cannot be achieved for the highly orientated material.

Particularly worthy of note is that very little surface oxidation takes place when graphite fibers are cyclically treated at 50 Hz in electrolyte solutions in which no intercalation is possible (for example in dilute acids or $H_3PO_4$), suggesting a mechanism which involves primary intercalation (cf. also [419]).

## 5. Possible Applications

Electrochemical reactions involving black carbon materials often produce electron conducting materials with very unusual properties. Thus, considerable attention has been paid to the possible industrial applications of such materials. Indeed, there are a great number of ideas for applications but, apart from a few exceptions, these ideas have not been realized.

The subject of general applications[41] and of specific applications with special reference to electrochemical energy sources[420] have been reviewed recently, so this Section will be limited to a brief discussion of the major points.

### 5.1. Electrochemical Energy Sources

"Graphite fluoride" $(CF_x)_n$ with a degree of fluorination $x < 1$ has been used as the positive electrode in lithium batteries with organic electrolytes (*e.g.* [41,241,420–427]). The working voltage of these batteries is close to 2.8 V and the theoretical energy content is about 2190 Wh·kg$^{-1}$[427]; the practical energy content of commercial cells (Matsushita National-Panasonic) is about 300 Wh·kg$^{-1}$. The discharging reaction does not yield simply $LiF + C_n$, but rather a ternary compound $Li^+[(CF_x)_n]^-$[241,426,428–430]. Teflon[431], chlorinated C-polymers[432], chlorinated graphite[433], and chlorinated amorphous carbon[434] have all been suggested as positive electrode materials for Li-batteries.

Graphite oxide (GO) attracted attention at a very early date as potential substitute for $MnO_2$ in Leclanché cells; for this application *Brown* and *Storey* used a material prepared by electrochemical oxidation in dilute $HNO_3$[435,436]. Like $(CF_x)_n$, GO and EGO can also be reduced in organic Li-containing electrolytes[41,420,437–439] but, as in the case of polar electrolyte solutions, the swelling of the electrodes creates some problems[41].

Many other graphite compounds such as the metal halide-graphites, *e.g.* "$FeCl_3$-graphite", have also been discussed as positive electrode materials for Li-batteries[433,440-445] without any clear advantages becoming obvious. Because of the sensitivity of the electrolyte solutions to oxidation, rechargeable batteries on the basis of Eq. (5) in Section 3.5 are almost unrealizable. $LiC_n$ in combination with a polymeric electrolyte has been suggested as a material for negative electrodes[107]. An interesting thermogalvanic cell has been put forward by *Lalancette*[446], and improved versions were later reported by *Endo et al.*[447] and other workers[448,449]. This cell is composed of two electrodes of unequal concentrations, made, for example, from "$Br_2$-graphite" or "$HNO_3$-graphite". Such cells can be continually or discontinually regenerated by applying a temperature gradient.

*Flandrois* has suggested nickel-cadmium accumulators with modified Ni-electrodes; these yield very finely distributed $Ni(OH)_2$ or NiOOH and graphite as products from the "$NiCl_2$-graphite" starting material[420,450,451].

### 5.2. Electron Conducting Ion Exchangers

Graphite oxide[41,287,290,452] and also "defect oxides" (cf. Section 4.3) have a notable cation-exchange capacity which remains after the reduction of the quasireversibly reducible portion[41]. This exchange property, on an *electrically conducting* support, allows them to be used for example, for the production of highly dispersed noble metal coatings on carbon materials (an exchange of the noble metals is achieved by subsequent chemical or electrochemical reduction[41,453,454]). Accumulators[455] with electrodes composed of ion-exchanging carbon felt have also been suggested.

### 5.3. Roughening of Carbon Electrodes

Carbon electrodes can be roughened by electrochemical oxidation. This effect has already been discussed for the surface oxidation of carbon fibers and is of particular importance for electrochemical analysis *at* carbon electrodes[456], mainly because polarization effects are thus reduced (the electrodes in this context are mostly composed of glassy carbon[1-4]). There are many examples in the literature for such roughening procedures and for the uses of the electrodes produced (*e.g.* [457-459]). Recently, a material with comparable surface roughness ("reticulated vitreous carbon") has become commercially available[460].

### 5.4. Graphite Compounds as Intermediates in Electrochemical Syntheses

Lamellar graphite compounds formed in accordance with equations (1a, b) or (2a, b) are strong reducing or oxidizing agents, respectively, which can undergo a secondary reaction with a component of the electrolyte solution to yield "graphite" (EC-mechanism; an *e*lectrochemical reaction proceeds a *c*hemical reaction). Since electrochemical intercalation reactions are generally "fast" and, for example, the conversion of many organic compounds at the electrode surface are kinetically slow, the electrochemical reductions or oxidations occur considerably faster *via* a graphite intermediate than by the direct process at inert electrodes.

Although not very useful, an example of such a process is the reduction of propylene carbonate (PC) to propene with, for example, $LiClO_4$ as supporting electrolyte: at the inert electrode, Li metal is essentially the sole product, whereas at the graphite electrode, propene is formed with a current yield of almost 100%[263,461]. The primary electrochemical product in the process is $Li^+(PC)_yC_n^-$[255,263]. The instability of solvated graphite compounds with respect to self decomposition suggest that this reaction pathway is of general importance.

The secondary reactions of the phases $NR_4^+(solv)_yC_n^-$, $PR_4^+(solv)C_n^-$, $SR_3^+(solv)_yC_n^-$ have been studied on numerous occasions[345,462-465]. In these reactions it is possible to obtain surface modified carbon electrodes (*e.g.* polycarboxylated or polybutylated[345]) *via* a complex reaction with electrophiles.

### 5.5. Other Applications

In addition to the more general areas of application which have been described above several more specific areas of application for electrochemical reactions of black carbon have been proposed. Thus, for example, electrochromic displays have been described[466,467] using the reversible color change associated with the formation of $A^+(DMSO)_yC_n^-$.

A new modification of carbon, which presumably involves an sp-hybridized C-chain, can be produced by the electrochemical reduction of polytetrafluoroethylene (PTFE) in, for example, $NBu_4BF_4$/dimethyl formamide[468]. The chemical reduction of PTFE (for example, with Na in $NH_{3(liq)}$ or with Li-amalgam[469-473]) yields identical products and, indeed, an electrochemical mechanism has been demonstrated for the reduction using $Li_xHg$[469,474,475]. At the "dry" contact, $Li_xHg$/PTFE, a local element is formed, and the necessary charge transport is achieved by $Li^+$ ions in the solid phase.

PTFE has been widely used as the hydrophobic component in gas diffusion electrodes (for fuel cells) (*e.g.* [81,476]); more recent experiments suggest that graphite fluoride is particularly suitable for this purpose[477].

For studying the electrical conductivity of ionic graphite compounds[*] an electrochemical preparation has proved especially suitable[148, 150, 154, 215, 248, 257, 479-481] because the "chemical charge-transfer" (*not* the ionicity) can be easily varied. The measurement of the conductivity of intercalated carbon fibers can even be carried out *in situ, i.e.* in the electrolyte solution, since the "electrolytic short circuit" can be negligible in comparison to the high electrical conductivity. The bottom half of Figure 26 shows such a conductivity trace that was measured concomitantly with a cyclic voltammogram[118,439].

[*] Graphite is an intrinsic semiconductor whose valence and conduction bands approximately overlap (*e.g.* [27, 71]. The reduction or oxidation of graphite leads to a considerable increase in the number of electrons in the conduction band or the number of defect electrons in the valence band, respectively, and thus to the formation of "synthetic metals" [478].

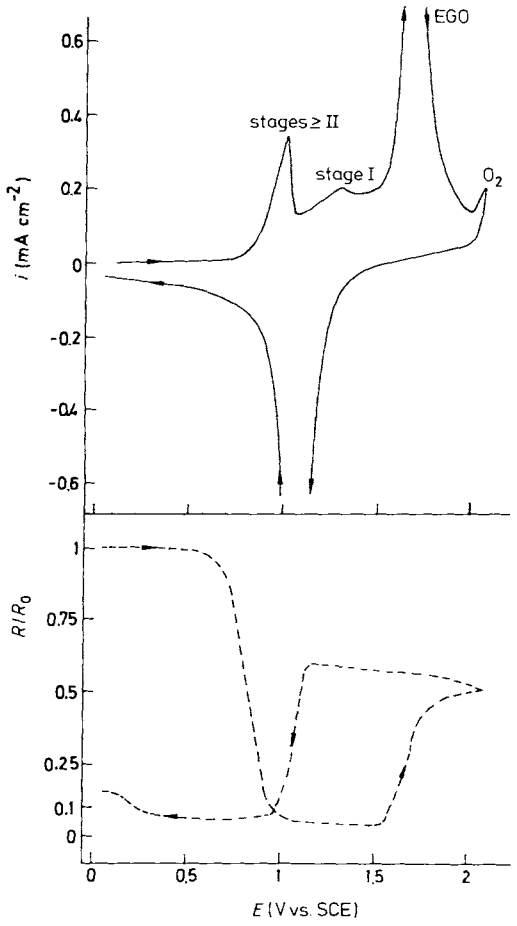



Fig. 26. Cyclic voltammetry on a Celion GY 70 single fiber in 96% $H_2SO_4$ (cf. Fig. 23), $v = 10$ mV·s$^{-1}$; top: current/potential curve, bottom: simultaneous resistance measurement (actual resistance $R$/starting value $R_0$).

Particularly worth noting are: the sharp decrease in $R/R_0$ at the start of the intercalation process, the increase in $R/R_0$ during the formation of EGO and its subsequent decrease during the back reduction of EGO, and, lastly, the relatively small resistance of the "residual compound" between the end of the reduction and 0 V *vs* SCE. After the deintercalation of graphite compounds, "residual compounds" generally remain in which the guest molecules and ions are bound within lattice defects[26, 30, 31, 34, 38, 318, 482]. Thus, the residual compound which remains, even at 0 V *vs* SCE, retains an ionic character ($C_n^+$) and a consequently higher conductivity. Such "residual compounds", and especially those derived from relatively defect-rich graphite materials (such as carbon fibers), are stable for a surprisingly long time[483].

Finally, there are two other properties of surface oxides and graphite oxides which are important electrochemically. The electrochemical potential of surface oxides is notably pH dependent[456, 484–487]: the electrode potential varies by approximately 20 mV/pH. Thus, glassy carbon can be utilized as indicator electrode for potentiometric acid/base titrations[485, 486]. It has been known for a long time that graphite oxide catalyzes the decomposition of $H_2O_2$ (*e.g.* [488, 489]). In this context the exceptional activity of GO as a catalyst for the electrochemical reduction of $O_2$[471, 487, 490] is worth noting since this reduction is known to occur *via* $H_2O_2$ as an intermediate (*e.g.* [492–494]).

A completely new area of interest should develop for fabrics made from *activated* carbon fibers whose properties are very similar to those of activated charcoal; for example the specific surface area ($N_2$ BET) is between 900 and 1400 m$^2$/g[495]. The electrochemical potential of such cloths can, in contrast to active charcoal, be easily adjusted. In this way the adsorption/desorption processes of neutral molecules can be controlled since these processes are extremely dependent on the electrochemical potential[496].

## 6. Outlook

The electrochemistry of black carbons can, to a large extent, be generalized as the "electrochemistry of polymers with conjugated π-systems". In the last few years many of the "old" reactions of graphite have been "extended", in particular, to polyacetylenes and poly(*p*-phenylenes) and also to polymers containing heteroatoms such as polyphenylene sulfides and polythiazenes. This is true for the non-electrochemical processes such as, for example, reduction (="n-doping") with alkali metals (in particular with sodium/naphthalene in ether), oxidation (="p-doping") with halogens, and also the reactions with Lewis acids and metal halide oxidizing agents such as $AsF_5$, $FeCl_3$, *etc.* The flood of pertinent publications exceeds those concerned with carbon generally by an order of magnitude so that only a few reviews, books, and conference proceedings can be referred to here[497–500]. The great interest in this class of compounds is due to the fact that the n- and p-doped polyenes, like the $C_n^-$ and $C_n^+$ graphite compounds, respectively, have a very much larger electrical conductivity than the starting materials.

The electrochemistry of such "polyenes" is also very similar to that of their corresponding graphite compound analogues. In particular the electrochemical reduction and oxidation in organic electrolyte solutions and the associated possibility of constructing rechargeable batteries (Eq. 5, where for polyacetylene "C" is replaced by "CH") has fascinated many research groups[501, 502].

The problems associated with Li batteries using $(CH)_n$ cathodes are similar to those which have hindered the de-

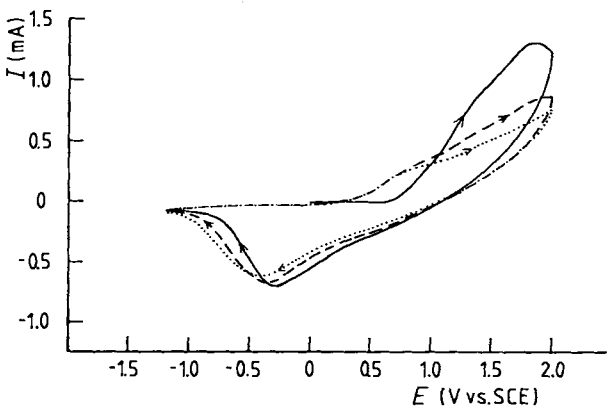



Fig. 27. Cyclic voltammogram of *cis*-polyacetylene (*ca.* 5 × 5 mm film, weight 0.54 mg) in 0.25 M $LiClO_4$/PC, $v = 10$ mV·s$^{-1}$, oxidation in the 1st cycle to "$(CH)^{+}_{25}ClO_4^-$"; —— 1st cycle, –– 2nd cycle, ..... 3rd cycle.—The authors wish to thank Dr. *K. Menke*, Max-Planck-Institut für Festkörperforschung, Stuttgart, for donating the polyacetylene film.

velopment of their graphite analogues: insufficient long term stability of the electrolyte solutions, a tendency to solvate, and, lastly, a low energy density. The theoretical energy density for a $Li/(CH)_n^+ClO_4^-$ cell, n = 14.3, is 255 Wh $kg^{-1}$ without taking solvation into account[502], whereas that for some more conventional rechargeable Li batteries is approximately 1000 Wh $kg^{-1}$[503–506]. In addition, the incomparable stability of the graphite matrix has not been achieved using "polyenes"; irreversible deterioration have in some cases been observed after only a few oxidation/reduction cycles[507] (cf. Fig. 27).

The electrochemistry of "polyenes" in concentrated or aqueous acids is also very similar to that of graphite (*e.g.* [507–509]).

The well established electrochemistry of "black carbon" can thus furnish a fund of information which can be relatively easily applied to many other polymer systems with conjugated π-systems.

*The authors are indebted to many coworkers and in particular to H. Möhwald and also Dr. E. Theodoridou, R. Sauter and E. Wudy for their work in conjunction with our own research which is quoted here. The authors also wish to thank the many collegues and especially W. Biberacher, Dr. W. Foag and Dr. A. Lerf for their intensive cooperation which enabled the solving of some of the problems discussed here which are of a particularly interdisciplinary nature. The authors also wish to acknowledge the liberal support of SIGRI Elektrographit GmbH, Meitingen who supplied a wide range of carbon samples and the Deutsche Forschungsgemeinschaft and the Fonds der Chemischen Industrie without whose financial help many of the problems could not have been investigated.*

Received: August 29, 1983 [A 479 IE]
German version: *Angew. Chem. 95* (1983) 954
Translated by *Stephen D. Pask*, München

[1] O. Vohler, P. L. Reiser, R. Martina, D. Overhoff, *Angew. Chem. 82* (1970) 401; *Angew. Chem. Int. Ed. Engl. 9* (1970) 414.
[2] O. Vohler, E. Bäder, H. V. Kienle, P. Kleinschmit, H. Linke, M. Voll in: *Ullmanns Encyklopädie der technischen Chemie*, Vol. 14, Verlag Chemie, Weinheim 1977, pp. 595–651.
[3] Kirk-Othmer: *Encyclopedia of Chemical Technology*, Vol. 4, Wiley, New York 1978, pp. 556–666, 689–709.
[4] 1982 Annual Book of ASTM Standards, Part 17, American Society for Testing and Materials, Philadelphia 1982.
[5] H. Klotz, A. Schneider, *Naturwissenschaften 49* (1962) 448.
[6] A. Knappwost, W. Metz, *Z. Phys. Chem. Frankfurt am Main 64* (1969) 178.
[7] Y. N. Novikov, M. E. Kazakov, A. V. Zvarikina, I. S. Astakhova, M. E. Vol'pin, *Zh. Strukt. Khim. 12* (1971) 486; *J. Struct. Chem. 12* (1971) 446.
[8] M. E. Vol'pin, Y. N. Novikov, N. D. Lapkina, V. 1. Kasatochin, Y. T. Struchkov, M. E. Kazakov, R. A. Stukan, V. A. Povitskij, Y. S. Karimov, A. V. Zvarikina, *J. Am. Chem. Soc. 97* (1975) 3366.
[9] G. Bewer, N. Wichmann, H. P. Boehm, *Mater. Sci. Eng. 31* (1977) 73.
[10] R. Schlögl, H. P. Boehm, 15th Biennal Conf. on Carbon, Philadelphia 1981, Ext. Abstr. p. 373.
[11] P. Touzain, A. Chamberod, A. Briggs, *Mater. Sci. Eng. 31* (1977) 77.
[12] A. Métrot, R. Vangelisti, P. Willmann, A. Hérold, *Electrochim. Acta 24* (1979) 685.
[13] J. M. Lalancette et al., *Can. J. Chem. 50* (1972) 3058; *52* (1974) 589; *54* (1976) 2110, 2505.
[14] H. B. Kagan, *Chemtech. 6* (1976) 510.
[15] H. B. Kagan, *Pure Appl. Chem. 46* (1976) 177.
[16] R. Setton, *Mater. Sci. Eng. 31* (1977) 303.
[17] L. B. Ebert, L. Matty, *Synth. Met. 4* (1982) 345.
[18] K. Herrmann, *Nachr. Chem. Tech. Lab. 25* (1977) 662.
[19] R. Setton, F. Beguin, S. Piroelle, *Synth. Met. 4* (1982) 299.
[20] J.-C. Volta, *Synth. Met. 4* (1982) 319.
[21] M. E. Vol'pin, Y. N. Novikov, V. M. Kopylov, L. M. Kananashvili, T. B. Kakuliya, *Synth. Met. 4* (1982) 331.
[22] H.-F. Klein, Kontakte *1982*, 3.
[23] M. A. M. Boersma, *Catal. Rev.-Sci. Eng. 10* (1974) 243.
[24] J. Gole, G. Merle, J. P. Pascault, *Synth. Met. 4* (1982) 269.
[25] W. Rüdorff, *Adv. Inorg. Chem. Radiochem. 1* (1959) 224.
[26] G. R. Hennig, *Prog. Inorg. Chem. 1* (1959) 125.
[27] A. R. Ubbelohde, F. A. Lewis: *Graphite and Its Crystal Compounds*, Oxford University Press, Oxford 1960.
[28] R. C. Croft, *Q. Rev. Chem. Soc. 14* (1960) 19.
[29] A. Hérold, R. Setton, N. Platzer in A. Pacault: *Les Carbones*, Vol. 2, Masson, Paris 1965, p. 462.
[30] L. B. Ebert, *Annu. Rev. Mater. Sci. 6* (1976) 181.
[31] J. G. Hooley in R. M. A. Lieth: *Physics and Chemistry of Materials with Layered Structures*, Vol. 1, Reidel, Doredrecht 1977, p. 1.
[32] J. E. Fischer, T. E. Thompson, *Phys. Today 31* (1978) 36.
[33] J. E. Fischer in F. Lévy: *Physics and Chemistry of Materials with Layered Structures*, Vol. 6, Reidel, Dordrecht 1979, p. 481.
[34] A. R. Ubbelohde in [33], p. 1.
[35] M. S. Whittingham, L. B. Ebert in [33], p. 533.
[36] A. Hérold in [33], p. 321.
[37] M. S. Dresselhaus, G. Dresselhaus in [33], p. 423.
[38] H. Selig, L. B. Ebert, *Adv. Inorg. Chem. Radiochem. 23* (1980) 281.
[39] A. W. Moore, *Chem. Phys. Carbon 17* (1981) 233.
[40] M. S. Dresselhaus, G. Dresselhaus, *Adv. Phys. 30* (1981) 139.
[41] J. O. Besenhard, E. Theodoridou, H. Möhwald, J. J. Nickl, *Synth. Met. 4* (1982) 211.
[42] M. S. Dresselhaus, G. Dresselhaus, *Top. Appl. Phys. 51* (1982) 3.
[43] S. A. Solin, *Adv. Chem. Phys. 49* (1982) 455.
[44] N. Bartlett, B. W. McQuillan in M. S. Whittingham, A. J. Jacobson: *Intercalation Chemistry*, Academic Press, New York 1982, p. 19.
[45] W. C. Forsman, T. Dziemianowicz, K. Leong, D. Carl, *Synth. Met. 5* (1983) 77.
[46] Franco-American Conf. on Intercalation Compounds of Graphite, La Napoule 1977; *Mater. Sci. Eng. 31* (1977) 1–355.
[47] Int. Conf. on Layered Materials and Intercalates, Nijmegen 1979, *Physica B+C 99* (1980) 1–555.
[48] 2nd Int. Conf. on Intercalation Compounds of Graphite, Provincetown 1980, *Synth. Met. 2* (1980) 1–372; *3* (1981) 1–302.
[49] Yamada Conf. IV on Physics and Chemistry of Layered Materials, Sendai 1980, *Physica B+C 105* (1981) 1–509.
[50] M. S. Dresselhaus, G. Dresselhaus, J. E. Fischer, M. J. Moran, Intercalated Graphite, Boston 1982; North-Holland, New York 1983.
[51] 3rd Int. Conf. on Intercalation Compounds of Graphite, Pont-à-Mousson 1983; *Synth. Met.*, in press.
[52] N. N. Argul, A. V. Kiselev, *Chem. Phys. Carbon 6* (1970) 1.
[53] M. W. Cole, D. R. Frankl, D. L. Goodstein, *Rev. Mod. Phys. 53* (1981) 199.
[54] K. Carneiro, L. Passell, W. Thomlinson, H. Taub, *Physica B+C 107* (1981) 237.
[55] S. Ramesh, J. D. Maynard, *Phys. Rev. Lett. 49* (1982) 47.
[56] E. F. Wassermann, *Surf. Sci. 117* (1982) 267.
[57] C. Bouldin, E. A. Stern, *Phys. Rev. B 25* (1982) 3462.
[58] H. P. Boehm, E. Diehl, W. Heck, R. Sappock, *Angew. Chem. 76* (1964) 742; *Angew. Chem. Int. Ed. Engl. 3* (1964) 669.
[59] H. P. Boehm, *Angew. Chem. 78* (1966) 617; *Angew. Chem. Int. Ed. Engl. 5* (1966) 533; *Adv. Catal. 16* (1966) 179; H. P. Boehm, H. Knözinger in J. R. Anderson, M. Boudart: *Catalysis - Science and Technology*, Vol. 4, Springer, Berlin 1983, p. 40.
[60] J. B. Donnet, *Carbon 6* (1968) 161.
[61] B. R. Puri, *Chem. Phys. Carbon 6* (1970) 191.
[62] D. W. McKee, V. J. Mimeault, *Chem. Phys. Carbon 9* (1973) 151.
[63] J. B. Donnet, P. Ehrburger, *Carbon 15* (1977) 143.
[64] E. Fitzer, K.-H. Geigl, W. Hüttner, R. Weiss, *Carbon 18* (1979) 389.
[65] L. T. Drzal in R. L. Patrick: *Treatise Adhesion and Adhesives*, Vol. 5, Marcel Dekker, New York 1981, p. 21.
[66] E. Fitzer, R. Weiss in Verein Deutscher Ingenieure, VDI-Ges. Kunststofftechnik: *Processes and Uses of Carbon Fibre Reinforced Plastics*, VDI-Verlag, Düsseldorf 1981, p. 45.
[67] P. G. Rose in [66], p. 5.
[68] G. Gynn, R. N. King, S. F. Chappel, M. L. Deviney, *U. S. Rep.* AFWAL-TR-81-4096, NTIS No. AD-A108233 (1981).
[69] K. Wolf, R. E. Fornes, J. D. Memory, R. D. Gilbert, *Chem. Phys. Carbon 18* (1982) 93.
[70] R. E. Panzer, P. J. Elving, *Electrochim. Acta 20* (1975) 635.
[71] J.-P. Randin in A. J. Bard: *Encyclopedia of Electrochemistry of the Elements*, Vol. 7, Marcel Dekker, New York 1976, p. 1.
[72] K. D. Snell, A. G. Keenan, *Chem. Soc. Rev. 8* (1979) 259.
[73] R. M. Murray, *Acc. Chem. 13* (1980) 135.
[74] N. Oyama, H. Matsuda, *Denki Kagaku 49* (1981) 396.
[75] L. Sprösser, *Z. Elektrochem. Angew. Phys. Chem. 7* (1901) 1083.
[76] H. J. M. Creighton, W. H. Ogden, *Trans. Am. Electrochem. Soc. 48* (1925) 9.

[77] O. Ruff, *Ber. Dtsch. Chem. Ges. A 69* (1936) 181.
[78] A. C. Becquerel, reference to *Gmelins Handbuch der anorganischen Chemie*, Vol. 14, Part B2, Verlag Chemie, Weinheim 1968, p. 753.
[79] W. Ostwald, *Z. Elektrochem. Angew. Phys. Chem. 1* (1894) 122.
[80] R. W. Coughlin, G. Kreysa, *Chem.-Ing.-Tech. 55* (1983) 8.
[81] W. Vielstich, *Brennstoffelemente*, Verlag Chemie, Weinheim 1965.
[82] A. Millot, *C. R. Acad. Sci. 101* (1885) 432.
[83] F. Fichter, *Z. Elektrochem. Angew. Phys. Chem. 16* (1910) 612.
[84] A. Bartoli, G. Papasogli, *Gazz. Chim. Ital. 11* (1881) 468; *12* (1882) 113.
[85] M. Faraday, *Poggendorfs Ann. 33* (1834) 301, 433, 481; reference to *Chem. Zbl. 2* (1836) 276.
[86] V. Sihvonen, L. Tuura, *Acta Chem. Fenn. B6* (1933) 56.
[87] V. Sihvonen, *Z. Elektrochem. Angew. Phys. Chem. 44* (1938) 659.
[88] W. Fuchs, I. Schmidt, O. Veiser, *Erdöl Kohle 7* (1959) 542.
[89] H. P. Fritz, R. Huber, *Z. Naturforsch. B32* (1977) 1.
[90] M. S. Whittingham, *J. Electrochem. Soc. 124* (1977) 1387.
[91] M. S. Whittingham, *Prog. Solid State Chem. 12* (1978) 41.
[92] R. Schöllhorn, *Physica B+C 99* (1980) 89.
[93] R. Schöllhorn, *Angew. Chem. 92* (1980) 1015; *Angew. Chem. Int. Ed. Engl. 19* (1980) 983.
[94] M. S. Whittingham, R. R. Chianelli, *J. Chem. Educ. 57* (1980) 569.
[95] R. Schöllhorn in L. Pietronero, E. Tesatti: *Physics of Intercalation Compounds*, Springer, Berlin 1981, p. 33.
[96] M. S. Whittingham, *J. Electroanal. Chem. 118* (1981) 229.
[97] I. L. Spain, D. J. Nagel, *Mater. Sci. Eng. 31* (1977) 183.
[98] N. A. W. Holzwarth, S. Tabii, *Mater. Sci. Eng. 39* (1977) 195.
[99] J. E. Fischer, *Mater. Sci. Eng. 31* (1977) 211.
[100] H. Kamimura, K. Nakao, T. Ohno, T. Inoshita, *Physica B+C 99* (1980) 401.
[101] D. P. Divincenco, N. A. W. Holzwarth, S. Rabii, *Physica B+C 99* (1980) 407.
[102] J. Blinowski, C. Rigaux, *Synth. Met. 2* (1980) 297.
[103] G. Dresselhaus, S. Y. Leung, M. Shayegan, T. C. Chien, *Synth. Met. 2* (1980) 321.
[104] F. Batallan, I. Rosenmann, C. Simon, *Synth. Met. 2* (1980) 353.
[105] N. A. W. Holzwarth, S. G. Louie, S. Rabii in [50], p. 107.
[106] P. Pfluger, V. Geiser, S. Stolz, H.-J. Güntherodt, *Synth. Met. 3* (1981) 27.
[107] R. Yazami, P. Touzain, Int. Meeting on Lithium Batteries, Rome 1982, Ext. Abstr. p. 63; R. Yazami, P. Touzain, *J. Power Sources 9* (1983) 365.
[108] A. Hérold, *Bull. Soc. Chim. Fr. 1955*, 999.
[109] Y. N. Novikov, M. E. Vol'pin, *Russ. Chem. Rev. 40* (1971) 733.
[110] J. Amiell, P. Delhaes, F. Beguin, R. Setton, *Mater. Sci. Eng. 31* (1977) 243.
[111] O. Ginderow, *Ann. Chim. 6* (1971) 5.
[112] D. Billaud, A. Pron, F. L. Vogel, *Synth. Met. 2* (1980) 177.
[113] A. Chenite, D. Billaud, *Carbon 20* (1982) 120.
[114] I. Rashkov, I. M. Panayotov, N. N. Tyutyulkow, *Bull. Soc. Chim. Fr. 1975*, 1271.
[115] G. Merle, I. Rashkov, C. Mai, J. Gole, *Mater. Sci. Eng. 31* (1977) 35.
[116] G. Merle, C. Mai, J. Golé, I. Rashkov, *Carbon 15* (1977) 243.
[117] L. Bonnetain, P. Touzain, A. Hamwi, *Mater. Sci. Eng. 31* (1977) 45.
[118] J. O. Besenhard, H. Möhwald, J. J. Nickl, *Synth. Met. 3* (1981) 187.
[119] S. Watanake, T. Kondo, J. Ishigaro, *Jpn. Kokai* 81909 89, reference to *Chem. Abstr. 95* (1981) 117759s.
[120] A. Inioui, A. Métrot, A. Storck, *Electrochim. Acta 27* (1982) 1247.
[121] W. Biberacher, A. Lerf, J. O. Besenhard, H. Möhwald, T. Butz, 5th Int. Conf. on Ternary and Multinary Compounds, Cagliari 1982.
[122] N. Daumas, A. Hérold, *C. R. Acad. Sci. C268* (1969) 373.
[123] I. L. Spain, K. J. Volin in [50], p. 173.
[124] L. Pietronero, S. Strässler in [95], p. 23.
[125] L. Pietronero, S. Strässler, *Rev. Chim. Miner. 19* (1982) 545.
[126] N. Bartlett, R. N. Biagoni, B. W. McQuillan, A. S. Robertson, A. C. Thompson, *J. Chem. Soc. Chem. Commun. 1978*, 200.
[127] J. E. Fischer, *J. Chem. Soc. Chem. Commun. 1978*, 544.
[128] L. B. Ebert, D. R. Mills, J. C. Scanlon, H. Selig, *Mater. Res. Bull. 16* (1981) 831.
[129] R. S. Markiewicz, J. S. Kasper, H. R. Hart, Jr., L. V. Interrante in [95], p. 132.
[130] P. Delhaes, J. C. Rouillon, J. P. Manceau, D. Guérard, A. Hérold, *J. Phys. Paris Lett. 37L* (1976) 127.
[131] P. Delhaes, *Mater. Sci. Eng. 31* (1977) 225.
[132] L. Pietronero, S. Strässler, *Phys. Rev. Lett. 47* (1981) 593.
[133] L. R. Hanlon, E. R. Falardeau, J. E. Fischer, *Solid State Commun. 24* (1977) 377.
[134] B. R. Weinberger, J. Kaufer, A. J. Heeger, J. E. Fischer, M. J. Moran, N. A. W. Holzwarth, *Phys. Rev. Lett. 41* (1978) 1417.
[135] K. J. Vetter: *Elektrochemische Kinetik*, Springer, Berlin 1961.
[136] W. Vielstich, W. Schmickler: *Elektrochemie II, Kinetik elektrochemischer Systeme*, Steinkopff, Darmstadt 1976.
[137] G. Kortüm: *Lehrbuch der Elektrochemie*, Verlag Chemie, Weinheim 1966.
[138] G. Milazzo: *Elektrochemie I*, Birkhäuser, Basle 1980.
[139] C. H. Hamann, W. Vielstich: *Elektrochemie*, Vol. I and II, Verlag Chemie, Weinheim 1975 and 1981.
[140] J. O'M. Bockris, A. K. N. Reddy, *Modern Electrochemistry*, Vol. I and II, Plenum Press, New York 1970.
[141] R. N. Adams: *Electrochemistry at Solid Electrodes*, Marcel Dekker, New York 1969.
[142] E. R. Brown, R. F. Large in A. Weissberger, B. W. Rossiter: *Techniques of Chemistry*, Vol. I, Part IIA, Wiley-Interscience, New York 1971, p. 423.
[143] S. Piekarski, R. N. Adams in [142], p. 531.
[144] R. S. Nichelson, I. Shain, *Anal. Chem. 36* (1964) 706; *37* (1965) 178, 190.
[145] M. Armand, Habilitationsschrift, Universität Grenoble 1978.
[146] J. R. Dahn, R. R. Haering in [95], p. 61; J. R. Dahn, R. R. Haering, *Solid State Ionics 2* (1981) 19.
[147] L. Heyne, *Top. Appl. Phys. 21* (1977) 169.
[148] W. Rüdorff, U. Hofmann, *Z. Anorg. Allg. Chem. 238* (1938) 1.
[149] W. Rüdorff, *Z. Phys. Chem. B45* (1940) 42.
[150] L. C. F. Blackman, J. F. Mathews, A. R. Ubbelohde, *Proc. R. Soc. A258* (1960) 329.
[151] M. J. Bottomley, G. S. Parry, A. R. Ubbelohde, D. A. Young, *J. Chem. Soc. 1963*, 5674.
[152] S. Aronson, C. Frishberg, G. Frankl, *Carbon 9* (1971) 715.
[153] D. Horn, H. P. Boehm, *Z. Anorg. Allg. Chem. 456* (1979) 117.
[154] A. Métrot, J. E. Fischer, *Synth. Met. 3* (1981) 201.
[155] W. Biberacher, A. Lerf, J. O. Besenhard, H. Möhwald, T. Butz, *Mater. Res. Bull. 17* (1982) 1383.
[156] C. H. Olk, V. Yeh, F. J. Holler, P. C. Eklund in [50], p. 259.
[157] A. Métrot in [51], Abstr. p. 7; *Synth. Met.*, in press.
[158] J. O. Besenhard, W. Biberacher, W. Foag, H. Möhwald, E. Wudy in [51], Abstr. p. 8; *Synth. Met.*, in press.
[159] B. Bouayad, H. Fuzellier, M. Lelaurain, A. Métrot, F. Rousseaus in [51], Abstr. p. 50; *Synth. Met.*, in press.
[160] M. B. Armand in D. W. Murphy, J. Broadhead, B. C. B. Steele: *Materials for Advanced Batteries*, Plenum Press, New York 1980, p. 145.
[161] J. R. Dahn, M. A. Py, R. R. Haering, *Can. J. Phys. 60* (1982) 307.
[162] R. R. Chianelli, J. C. Scanlon, B. M. L. Rao, *J. Electrochem. Soc. 125* (1978) 1563.
[163] R. R. Chianelli, J. C. Scanlon, B. M. L. Rao, *J. Solid State Chem. 29* (1979) 323.
[164] Z. Mencik, H. K. Plummer, Jr., L. Bartosiewicz, *Carbon 13* (1975) 417.
[165] A. Fourdeux, C. Herinckx, R. Perret, W. Ruland, *C. R. Acad. Sci. C 269* (1969) 1597.
[166] S. Aronson, S. Lemont, J. Weiner, *Inorg. Chem. 10* (1971) 1296.
[167] D. Horn, H. P. Boehm, *Mater. Sci. Eng. 31* (1977) 87.
[168] W. Rüdorff, *Z. Anorg. Allg. Chem. 254* (1947) 319.
[169] H. Fuzzellier, A. Hérold, *C. R. Acad. Sci. C276* (1973) 1887.
[170] A. Métrot, P. Willmann, A. Hérold, 5th London Carbon and Graphite Conf. 1978, Abstr. p. 685.
[171] R. Vasse, G. Furdin, J. Melin, *Rev. Chim. Miner. 18* (1981) 312.
[172] D. E. Nixon, G. S. Parry, A. R. Ubbelohde, *Proc. R. Soc. A 291* (1966) 324.
[173] P. Touzain, E. Buscarlet, L. Connetain, *Carbon 16* (1978) 403.
[174] A. R. Ubbelohde, *Carbon 10* (1972) 201.
[175] J. O. Besenhard, Dissertation, Technische Universität München 1973; available from NTIS (USA), N74-30505.
[176] W. Rüdorff, W.-F. Sieke, *Chem. Ber. 91* (1958) 1348.
[177] A. Yaddaden, B. Iskander, P. Vast, *Ann. Chim. Fr. 6* (1981) 351.
[178] O. John, P. Tissot, *J. Appl. Electrochem. 10* (1980) 593.
[179] B. Iskander, P. Vast, *J. Raman Spectrosc. 11* (1981) 247.
[180] M. Ladjadj, A. Yaddaden, P. Vast in [51], Abstr. p. 67; *Synth. Met.*, in press.
[181] A. Yaddaden, M. Ladjadj, P. Vast, *Rev. Chim. Miner. 19* (1982) 602.
[182] H. P. Boehm, J. N. Meussdoerffer, *Carbon 9* (1971) 521.
[183] R. Fujii, K. Matsuo, *Tanso 73* (1973) 44.
[184] M. Fouletier, M. Armand, *Carbon 17* (1979) 927.
[185] E. Stumpp, K. Wloka, *Synth. Met. 3* (1981) 209.
[186] A. Métrot, P. Willmann, A. Hérold, *Mater. Sci. Eng. 31* (1977) 83.
[187] H. Fuzellier, A. Métrot, B. Bouayad, A. Hérold, 15th Biennial Conf. on Carbon, Philadelphia 1981, Ext. Abstr. p. 391.
[188] R. Fujii, *Nippon Kagaku Kaishi 1975*, 1888; reference to *Chem. Abstr. 84* (1976) 51404b.
[189] E. G. Vlasov, I. L. Mor'yasin, M. N. Fokin, *Issled. Zashch. Met. Korroz. Khim. Prom. 6* (1978) 62; reference to *Chem. Abstr. 91* (1979) 201125x.
[190] J. O. Besenhard, H. P. Fritz, *Z. Anorg. Allg. Chem. 416* (1975) 106.
[191] R. Fujii, *Denki Kagaku 41* (1973) 52.
[192] R. Fujii, *Rep. Governm. Ind. Res. Inst., Osaka 353* (1978) 1.
[193] R. Wurmb, F. Beck, K. Boehlke, DOS 2532512 (1975).
[194] F. Beck, H. Krohn, H. Junge, *Ber. Bunsenges. Phys. Chem. 84* (1980) 1023.
[195] F. Beck, H. Junge, H. Krohn, *Electrochim. Acta 26* (1981) 759.

[196] F. Beck, H. Junge, H. Krohn, *Power Sources 8* (1981) 245.
[197] F. Beck, H. Krohn, *DECHEMA Monographie*, Vol. 92, Verlag Chemie, Weinheim 1982, p. 57.
[198] F. Beck, W. Kaiser, H. Krohn, *Angew. Chem. 94* (1982) 83; *Angew. Chem. Int. Ed. Engl. 21* (1982) 69; *Angew. Chem. Suppl. 1982*, 57.
[199] F. Beck, H. Krohn, W. Kaiser, *J. Appl. Electrochem. 12* (1982) 505.
[200] H. Krohn, F. Beck, H. Junge, *Ber. Bunsenges. Phys. Chem. 86* (1982) 704.
[201] H. Krohn, F. Beck, R. Herrmann, *Chem.-Ing.-Tech. 54* (1982) 530.
[202] F. von Sturm: *Elektrochemische Stromerzeugung*, Verlag Chemie, Weinheim 1969.
[203] K. Wiesener, J. Garche, W. Schneider: *Elektrochemische Stromquellen*, Akademie-Verlag, Berlin 1981.
[204] D. N. Bennion, *U. S. Rep.* NTIS No. AD 701411 (1969).
[205] D. N. Bennion, J. S. Dunning, *U. S. Rep.* NTIS No. AD 722384 (1970).
[206] A. Brenner, *J. Electrochem. Soc. 118* (1971) 461.
[207] W. H. Tiedemann, D. N. Bennion, Meeting of the Electrochemical Society, Cleveland 1971, Paper 44.
[208] J. S. Dunning, W. H. Tiedemann, L. Hsueh, D. N. Bennion, *J. Electrochem. Soc. 118* (1971) 1886.
[209] J. O. Besenhard, H. P. Fritz, *Z. Naturforsch. B 26* (1971) 1125.
[210] H. P. Fritz, J. O. Besenhard, DBP 2139714 (1971).
[211] J. O. Besenhard, H. P. Fritz, *Z. Naturforsch. B 27* (1972) 1294.
[212] J. S. Dunning, W. H. Tiedemann, L. Hsueh, US-Pat. 3844837 (1972).
[213] T. Ohzuku, Z. Takehara, S. Yoshizawa, *Denki Kagaku 46* (1978) 438.
[214] Y. Takada, R. Fujii, K. Matsuo, Int. Symp. on Carbon – New Processes and New Applications, Toyohashi 1982, Ext. Abstr. p. 470.
[215] T. Nogami, M. Nawa, H. Mikawa, *J. Chem. Soc. Chem. Commun. 1982*, 1158.
[216] R. MacCallum, J. S. McKechni, C. A. Vincent, *Mater. Res. Bull. 18* (1983) 743.
[217] D. Billaud, A. Chenite, A. Métrot, *Power Sources 9* (1983), in press.
[218] D. Billaud, A. Métrot, P. Willmann, A. Hérold, Carbon '80, Baden-Baden 1980, Prepr. p. 140.
[219] J. O. Besenhard, H. P. Fritz, H. Möhwald, J. J. Nickl, Carbon '80, Baden-Baden 1980, Prepr. p. 147.
[220] A. Jobert, P. Touzain, L. Bonnetain, *Carbon 19* (1981) 193.
[221] D. Billaud, A. Chenite, A. Métrot, *Carbon 20* (1982) 493.
[222] A. Chenite, A. Métrot, D. Billaud, A. Hérold in [51], Abstr. p. P26.
[223] P. Touzain, A. Jobert, *Electrochim. Acta 26* (1981) 1133.
[224] J. O. Besenhard, H. P. Fritz, *J. Electrochem. Soc. 119* (1972) 1697.
[225] D. Billaud, A. Pron, F. L. Vogel, A. Hérold, *Mat. Res. Bull. 15* (1980) 1627.
[226] D. Billaud, A. Pron, F. L. Vogel, *Synth. Met. 2* (1980) 177.
[227] A. Chenite, D. Billaud, *Carbon 20* (1982) 120.
[228] K. Leong, W. C. Forsman, F. L. Vogel, 15. Biennial Conf. on Carbon, Philadelphia 1981, Ext. Abstr. p. 398.
[229] W. C. Forsman, H. E. Mertwoy, *Synth. Met. 2* (1980) 171.
[230] W. C. Forsman, H. E. Mertwoy, *Carbon 20* (1982) 255.
[231] G. R. Miller, H. Resing, F. L. Vogel, A. Pron, T. C. Wu, D. Billaud, *J. Phys. Chem. 84* (1980) 3333.
[232] S. L. Deshpande, D. N. Bennion, *J. Electrochem. Soc. 125* (1978) 687.
[233] D. N. Bennion, S. L. Deshpande, *U. S. Gov. Rep.*, NTIS No. AD-A035409 (1976).
[234] S.-C. S. Wang, D. N. Bennion, *J. Electrochem. Soc. 128* (1981) 1827.
[235] A. Métrot, P. Willmann, A. Hérold, *Carbon 19* (1981) 119.
[236] H. Selig, M. J. Vasile, F. A. Stevie, W. A. Sunder, *J. Fluorine Chem. 10* (1977) 299.
[237] L. Streifinger, H. P. Boehm, R. Schlögl, R. Pentenrieder, *Carbon 17* (1979) 195.
[238] R. Pentenrieder, H. P. Boehm, *Rev. Chim. Miner. 19* (1982) 371.
[239] H. Selig, P. K. Gallagher, L. B. Ebert, *Inorg. Nucl. Chem. Lett. 13* (1977) 427.
[240] J. O. Besenhard, H. Möhwald, J. J. Nickl, unpublished.
[241] N. Watanabe, *Solid State Ionics 1* (1980) 87.
[242] N. Bartlett, B. McQuillan, A. S. Robertson, *Mater. Res. Bull. 13* (1978) 1259.
[243] N. Bartlett, R. N. Biagoni, E. M. McCarron, B. W. McQuillan, F. L. Tanzella in W. E. Hatfield: *Molecular Metals*, Plenum Press, New York 1979, p. 293.
[244] L. B. Ebert, R. A. Huggins, J. I. Brauman, *Mater. Res. Bull. 11* (1976) 615.
[245] N. Bartlett, E. M. McCarron, B. W. McQuillan, T. E. Thompson, *Synth. Met. 1* (1979/80) 211.
[246] E. M. McCarron, N. Bartlett, *J. Chem. Soc. Chem. Commun. 1980*, 404.
[247] S. Karunanthy, F. Aubke, *Carbon 20* (1982) 237.
[248] J. E. Fischer, A. Métrot, P. J. Flanders, W. R. Salaneck, C. R. Brucker, *Phys. Rev. B 23* (1981) 5576.
[249] W. R. Salaneck, C. F. Brucker, J. E. Fischer, A. Métrot, *Phys. Rev. B 24* (1981) 5037.
[250] M. Nominé, L. Bonnetain, *C. R. Acad. Sci. C 264* (1967) 2084.
[251] J.-P. Pascault, M. Prost, C. Stein, J. Golé, *Bull. Soc. Chim. Fr. 1971*, 1167.
[252] H. H. Sick, Dissertation, Universität Tübingen 1959.
[253] O. Rubisch, Dissertation, Universität Tübingen 1957.
[254] W. F. K. Wynne-Jones, *Proc. Symp. Colston Res. Soc. 10* (1958) 35; reference to *Chem. Abstr. 53* (1969) 21046d.
[255] J. O. Besenhard, H. P. Fritz, *J. Electroanal. Chem. 53* (1974) 329.
[256] J. O. Besenhard, *Carbon 14* (1976) 111.
[257] J. O. Besenhard, H. Möhwald, J. J. Nickl, *Carbon 18* (1980) 399.
[258] F. P. Dousek, J. Jansta, J. Riha, *J. Electroanal. Chem. 46* (1973) 281.
[259] R. Jasinski, *Adv. Electrochem. Electrochem. Eng. 8* (1971) 253.
[260] A. N. Dey, *Thin Solid Films 43* (1977) 131.
[261] A. N. Dey, *Electrochim. Acta 21* (1976) 377.
[262] R. V. Moshtev, Y. Geronov, B. Puresheva, *J. Electrochem. Soc. 128* (1981) 1851.
[263] G. Eichinger, *J. Electroanal. Chem. 74* (1976) 183.
[264] F. Béguin, R. Setton, A. Hamwi, P. Touzain, *Mater. Sci. Eng. 40* (1979) 167.
[265] R. Setton, F. Béguin, J. Jegoudez, C. Mazières, *Rev. Chim. Miner. 19* (1982) 360.
[266] W. Rüdorff, *Chimia 19* (1965) 489.
[267] A. Hérold, *C. R. Acad. Sci. C 275* (1972) 571.
[268] H.-J. Klein, J. Gross, J. O. Besenhard, *Angew. Chem. 92* (1980) 480; *Angew. Chem. Int. Ed. Engl. 19* (1980) 491.
[269] J. O. Besenhard, H.-F. Klein, J. Gross, H. Möhwald, J. J. Nickl, *Synth. Met. 4* (1981) 51.
[270] J. O. Besenhard, I. Kain, H.-F. Klein, H. Möhwald, H. Witty in [50], p. 221.
[271] M. Nominé, L. Bonnetain, *J. Chim. Phys. 66* (1969) 1731.
[272] I. B. Rashkov, I. M. Panayotov, V. C. Shishkova, *Carbon 17* (1979) 103.
[273] D. Ginderow, R. Setton, *Carbon 6* (1968) 81.
[274] R. Setton, Int. Symp. on Carbon – New Processes and New Applications, Toyohashi 1982, Ext. Abstr. p. 427.
[275] N. Okuyama, T. Takahashi, S. Kanayama, H. Yasunaga, *Physica B 105* (1981) 298.
[276] J. Amiell, P. Delhaes, F. Béguin, R. Setton, *Mater. Sci. Eng. 31* (1977) 243.
[277] J. Jegoudez, C. Mazières, R. Setton in [51], Abstr. p. 39; *Synth. Met.*, in press.
[278] D. E. Bergbreiter, J. M. Killough, *J. Chem. Soc. Chem. Commun. 1976*, 913.
[279] D. E. Bergbreiter, J. M. Killough, *J. Am. Chem. Soc. 100* (1978) 2126.
[280] J. O. Besenhard, M. Bindl, H. Möhwald, unpublished.
[281] B. C. Brodie, *Justus Liebigs Ann. Chem. 114* (1860) 6.
[282] H. P. Boehm, W. Scholz, *Justus Liebigs Ann. Chem. 691* (1965) 1.
[283] L. Staudenmaier, *Ber. Dtsch. Chem. Ges. 31* (1898) 1481.
[284] V. Kohlschütter, P. Haenni, *Z. Anorg. Allg. Chem. 105* (1919) 121.
[285] W. S. Hummers, R. E. Offeman, *J. Am. Chem. Soc. 80* (1958) 1339.
[286] H. P. Boehm, M. Eckel, W. Scholz, *Z. Anorg. Allg. Chem. 353* (1967) 236.
[287] W. Scholz, H. P. Boehm, *Z. Anorg. Allg. Chem. 369* (1969) 327.
[288] F. Rodriguez-Reinoso, A. Martin Pozuelo, J. de D. Lopez-Gonzalez, A. Martin Rodriguez, *An. Quim. 75* (1979) 448.
[289] G. Ruess, *Monatsh. Chem. 76* (1947) 381.
[290] A. Clauss, R. Plass, H. P. Boehm, U. Hofmann, *Z. Anorg. Allg. Chem. 291* (1957) 205.
[291] K. E. Carr, *Carbon 8* (1970) 245.
[292] S. I. Rempel, B. N. Driker, T. N. Prisekina, L. V. Yur'eva, N. N. Skornyakov, *Tr. Ural. Lesotekh. Inst. 28* (1972) 157; reference to *Chem. Abstr. 79* (1973) 60750k.
[293] J. O. Besenhard, *Z. Naturforsch. B 32* (1977) 1210.
[294] U. Twittmann, Staatsexamensarbeit (R. Schöllhorn), Universität Münster 1976.
[295] A. Ramirez Garcia, J. Cano Ruiz, D. M. S. MacEwan, *Nature London 203* (1964) 1063.
[296] A. Angoso Catalina, R. J. Ruano Casero, J. B. Vericad Raga, *An. Quim. 73* (1977) 512.
[297] A. G. Voloshin, I. P. Kolesnikov, *Elektrokhimiya 16* (1980) 270; *Sov. Electrochem. 16* (1980) 236.
[298] J. H. Sluyters, *Rec. Trav. Chim. Pays-Bas 79* (1960) 1092.
[299] J. H. Sluyters, J. J. C. Oomen, *Rec. Trav. Chim. Pays-Bas 79* (1960) 1101.
[300] M. Sluyters-Rehbach, J. H. Sluyters in A. J. Bard: *Electroanalytical Chemistry*, Vol. 4, Marcel Dekker, New York 1970, p. 3.
[301] I. Epelboin, M. Keddam, *J. Electrochem. Soc. 117* (1970) 1052.
[302] R. D. Armstrong, M. F. Bell, A. A. Metcalfe, *J. Electroanal. Chem. 77* (1977) 287.
[303] R. D. Armstrong, M. F. Bell, A. A. Metcalfe in H. R. Thirsk, *Electrochemistry*, Vol. 6, Chem. Soc., London 1967, p. 98.
[304] K. Hladky, L. M. Callow, J. L. Dawson, *Br. Corros. J. 15* (1980) 20.
[305] A. S. Baranski, W. R. Fawcett, *J. Electrochem. Soc. 129* (1982) 901.
[306] M. B. Dowell, D. S. Badorrek, *Carbon 16* (1978) 241.
[307] L. Zwengel, H. Schmeisser, *Versuchs-Forsch.-Ing. 4* (1979) p. 127.

[308] C. Gabrielli, *Identification of Electrochemical Processes by Frequency Response Analysis*, Solartron-Schlumberger Internal Report, Farnborough (1980).
[309] D. Horn, H. P. Boehm, Carbon '76, Baden-Baden 1976, Prepr. p. 159.
[310] A. V. Yuzhania, D. V. Kokoulina, L. A. Mashkovich, L. A. Dronseiko, A. F. Kuteinikov, *Electrokhimiya 15* (1979) 308; *Soviet Electrochem. 15* (1979) 259.
[311] J. O. Besenhard, H. Möhwald, J. J. Nickl, *Rev. Chim. Miner. 19* (1982) 588.
[312] Verein Deutscher Ingenieure, VDI-Ges. Kunststofftechnik: *Processes and Uses of Carbon Fiber Reinforced Plastics*, VDI-Verlag, Düsseldorf 1981.
[313] A. R. Ubbelohde, *Nature London 223* (1969) 495.
[314] A. R. Ubbelohde, *J. Chim. Phys., Special Volume 1969*, 64.
[315] A. R. Ubbelohde, *Carbon 7* (1969) 523.
[316] A. R. Ubbelohde, *Carbon 10* (1972) 201.
[317] R. Fujii, *Denki Kagaku 44* (1976) 481.
[318] J. G. Hooley, *Chem. Phys. Carbon 5* (1969) 321.
[319] J. G. Hooley, *Carbon 18* (1980) 83.
[320] R. E. Franklin, *Acta Crystallogr. 4* (1951) 1253.
[321] V. A. Garten, D. E. Weiss, J. B. Willis, *Aust. J. Chem. 10* (1957) 295.
[322] J. S. Mattson, H. B. Mark, Jr., *J. Colloid Interface Sci. 31* (1969) 131.
[323] S. S. Barton, B. H. Harrison, *Carbon 13* (1975) 283.
[324] J. V. Hallum, H. V. Drushel, *J. Phys. Chem. 62* (1958) 110.
[325] J. B. Donnet, G. Henrich, *Bull. Soc. Chim. Fr. 1960*, 1609.
[326] I. F. Jones, R. C. Kaye, *J. Electroanal. Chem. 20* (1969) 213.
[327] P. H. Given, L. W. Hill, *Carbon 7* (1969) 649.
[328] B. D. Epstein, E. Dalle-Molle, J. S. Mattson, *Carbon 9* (1971) 609.
[329] K. Kinoshita, J. A. S. Bett, *Carbon 11* (1973) 403.
[330] K. F. Blurton, *Electrochim. Acta 18* (1973) 860.
[331] J. P. Randin, E. Yeager, *J. Electroanal. Chem. 58* (1975) 313.
[332] A. Z. Zaidenberg, A. M. Skundin, E. F. Dyukkiev, Y. K. Kalnin, *Elektrokhimiya 19* (1983) 174.
[333] J. S. Mattson, H. B. Mark, Jr.: *Activated Carbon*, Marcel Dekker, New York 1971.
[334] J.-B. Donnet, A. Voet: *Carbon Black*, Marcel Dekker, New York 1976.
[335] A. Voet, *Macromol. Rev. 15* (1980) 327.
[336] E. K. Sichel: *Carbon Black – Polymer Composites*, Marcel Dekker, New York 1982.
[337] P. R. Moses, L. Wier, R. W. Murray, *Anal. Chem. 47* (1975) 1882.
[338] B. F. Watkins, J. R. Behling, E. Kariv, L. L. Miller, *J. Am. Chem. Soc. 97* (1975) 3549.
[339] C. A. Koval, F. C. Anson, *Anal. Chem. 50* (1978) 223.
[340] B. E. Firth, L. L. Miller, M. Mitani, T. Rogers, J. Lennox, R. W. Murray, *J. Am. Chem. Soc. 98* (1976) 8271.
[341] N. Oyama, F. C. Anson, *J. Am. Chem. Soc. 101* (1979) 739.
[342] A, Merz, *Nachr. Chem. Tech. Lab. 30* (1982) 16.
[343] N. Oyama, A. P. Brown, F. C. Anson, *J. Electroanal. Chem. 87* (1978) 435.
[344] P. Janda, *Chem. Listy 77* (1983) 200.
[345] G. Bernard, J. Simonet, *J. Electroanal. Chem. 112* (1980) 117.
[346] M. Karayama, S. Suzuki, Nippon Kagaku Kaishi 1982, 66; *Chem. Abstr. 96* (1982) 114994q.
[347] L. Horner, W. Brich, *Justus Liebigs Ann. Chem. 1977*, 1354.
[348] J. Evans, T. Kuwana, *Anal. Chem. 49* (1978) 1632; *51* (1979) 358.
[349] R. D. Rocklin, R. W. Murray, *J. Electroanal. Chem. 100* (1979) 271.
[350] D. C. S. Tse, T. Kuwana, G. P. Royer, *J. Electroanal. Chem. 98* (1979) 345.
[351] A. M. Yacynych, T. Kuwana, *Anal. Chem. 50* (1978) 640.
[352] M. F. Dautartes, J. F. Evans, T. Kuwana, *Anal. Chem. 51* (1979) 104.
[353] R. M. Ianiello, T. J. Lindsay, A. M. Yacynych, *Anal. Chem. 54* (1982) 1098.
[354] R. M. Ianiello, T. J. Lindsay, A. M. Yacynych, *Anal. Chim. Acta 141* (1982) 23.
[355] H. J. Wieck, R. M. Iannello, J. A. Osborn, A. M. Yacynych, *Anal. Chim. Acta 140* (1982) 19.
[356] D. F. Untereker, J. C. Lennox, L. M. Wier, P. R. Moses, R. W. Murray, *J. Electroanal. Chem. 81* (1977) 309.
[357] S. Mazur, T. Matusinovic, K. Cammann, *J. Am. Chem. Soc. 99* (1977) 3888.
[358] S. M. F. Dautartes, J. F. Evans, *J. Electroanal. Chem. 109* (1980) 301.
[359] G. H. Heider, Jr., M. B. Gelbert, A. M. Yacynych, *Anal. Chem. 54* (1982) 322.
[360] M. Fukui, A. Kitani, C. Degrand, L. L. Miller, *J. Am. Chem. Soc. 104* (1982) 28.
[361] P. Martigny, F. C. Anson, *J. Electroanal. Chem. 139* (1982) 383.
[362] N. S. Scott, N. Oyama, F. C. Anson, *J. Electroanal. Chem. 110* (1980) 303.
[363] N. Oyama, S. Yamaguchi, Y. Nishiki, K. Tokuda, H. Matsuda, *J. Electroanal. Chem. 139* (1982) 371.
[364] R. J. Mortimer, F. C. Anson, *J. Electroanal. Chem. 138* (1982) 325.
[365] N. Oyama, S. Yamaguchi, M. Kaneko, A. Yamada, *J. Electroanal. Chem. 139* (1982) 215; M. Kaneko, A. Yamada, N. Oyama, S. Yamaguchi, *Makromol. Chem. Rapid Commun. 3* (1982) 769.
[366] B. B. Arnold, G. W. Murphy, *J. Phys. Chem. 65* (1961) 135.
[367] A. Factor, T. O. Rouse, *J. Electrochem. Soc. 127* (1980) 1313.
[368] K. Itaya, H. Akahoshi, S. Toshima, *J. Electrochem. Soc.* **129** (1982) 1498.
[369] N. Kobayashi, M. Fujihira, T. Osa, S. Dong, *Chem. Lett. 1982*, 575.
[370] M. E. Munoz, M. S. Ureta, J. H. Zagal, *Bol. Soc. Chil. Quim. 27* (1982) 121; *Chem. Abstr. 97* (1982) 13886w.
[371] R. A. Bull, F.-R. Fan, A. J. Bard, *J. Electrochem. Soc. 130* (1983) 1636.
[372] D. Scherson, S. B. Yao, E. B. Yeager, J. Eldridge, M. E. Kordesch, R. W. Hoffman, *Appl. Surf. Sci. 10* (1982) 325; *Chem. Abstr. 97* (1982) 135597y.
[373] S. Abe, T. Tonaka, T. Fuchigami, *J. Am. Chem. Soc. 105* (1983) 3630.
[374] G. R. Henning, Proc. of the 5th Int. Conf. on Carbon 1961, Vol. 1, p. 143.
[375] K. Kinoshita, J. Bett, *Carbon 11* (1973) 237.
[376] A. J. Arvia, W. E. Triaca, H. A. Videla, *Electrochim. Acta 15* (1970) 9.
[377] M. A. Rabah, A. A. Abdul Azim, A. Ismail, *J. Appl. Electrochem. 11* (1981) 49.
[378] E. Theodoridou, J. O. Besenhard, H. P. Fritz, *J. Electroanal. Chem. 122* (1981) 67.
[379] E. Theodoridou, J. O. Besenhard, H. P. Fritz, *J. Electroanal. Chem. 124* (1981) 87.
[380] Y. Kita, N. Watanabe, Y. Fujii, *J. Am. Chem. Soc. 101* (1979) 3832.
[381] N. Watanabe, *Physica B 105* (1981) 17.
[382] N. Watanabe, T. Asaue, *Denki Kagaku 39* (1971) 123.
[383] A. J. Calandra, C. M. Ferro, C. E. Castellano, M. Fernandez, *Acta Cient. Venez. 31* (1980) 526.
[384] Y. Kanaya, N. Watanabe, *Denki Kagaku 40* (1972) 417.
[385] N. Watanabe, M. Ishii, S. Yoshizawa, *Denki Kagaku 29* (1961) E179.
[386] *Gmelins Handbuch der Anorganischen Chemie*, Vol. 14, Part B-2, Verlag Chemie, Weinheim 1968, p. 783.
[387] N. Watanabe, M. Ishii, S. Yoshizawa, *Denki Kagaku 30* (1962) 171; N. Watanabe, M. Inoue, S. Yoshizawa, *ibid. 31* (1963) 168.
[388] H. Imoto, T. Nakajima, N. Watanabe, *Bull. Chem. Soc. Jpn. 48* (1975) 1633.
[389] N. Watanabe, S. Koyama, H. Imoto, *Bull. Chem. Soc. Jpn. 53* (1980) 273, 3093, 3103.
[390] D. Dumas, J. Brenet, *C. R. Acad. Sci. C265* (1967) 1395.
[391] N. Watanabe, *J. Fluorine Chem. 22* (1983) 205.
[392] R. Jasinski, G. Brilmyer, L. Helland, *J. Electrochem. Soc. 130* (1983) 1634.
[393] E. Fitzer, A. K. Fiedler, D. J. Müller, *Chem.-Ing.-Tech. 43* (1971) 923.
[394] R. J. Diefendorf, E. Fitzer, M. Heym, *Chem.-Ing.-Tech. 48* (1976) 765.
[395] E. Fitzer, *Angew. Chem. 92* (1980) 375; *Angew. Chem. Int. Ed. Engl. 19* (1980) 375.
[396] J. C. Goan, S. P. Prosen: *Interfaces in Composites*, ASTM STP, American Society for Testing and Materials, Philadelphia 1969, p. 3.
[397] R. L. Crane, V. J. Krukonis, *Ceramics Bull. 54* (1974) 184.
[398] S. Brelant, *Carbon 19* (1981) 329.
[399] R. J. Dauksys, *J. Adhes. 5* (1973) 211.
[400] L. T. Drzal, *Carbon 15* (1977) 129.
[401] L. T. Drzal, J. A. Mescher, D. L. Hall, *Carbon 17* (1979) 375.
[402] G. I. Emel'yanora, L. F. Atyaksheva, T. I. Treylazova, *Mater.-Vses. Mezhvuz. Konf. Ozonu 1977*, 12; reference to *Chem. Abstr. 89* (1978) 165586w.
[403] US-Pat. 3657082 (1968); Br. Pat. 1297946 (1969); 1326736 (1969); 2204156 (1971); DBP 2163071 (1971); Br. Pat. 1433712 (1974).
[404] N. L. Weinberg, T. B. Reddy, *J. Appl. Electrochem. 3* (1973) 73.
[405] G. Gynn, R. N. King, S. F. Chappell, M. L. Deviney, *U. S. Rep.* NTIS No. AD-A 108233 (1981).
[406] A. Proctor, P. M. A. Sherwood, *Carbon 21* (1983) 53.
[407] G. Mamantov, D. B. Freeman, F. J. Miller, H. E. Zittel, *J. Electroanal. Chem. 9* (1965) 305.
[408] F. M. Lang, M. de Noblet, J. B. Donnet, J. Lahage, E. Papirer, *Carbon 5* (1967) 47.
[409] J. B. Donnet, F. Hueber, C. Reitzer, J. Oddoux, G. Riess, *Bull. Soc. Chim. Fr. 1962*, 1727.
[410] J. B. Donnet, F. Hueber, N. Perol, J. Jaeger, *J. Chim. Phys. 60* (1963) 426.
[411] D. Laser, M. Ariel, *J. Electroanal. Chem. 52* (1974) 291.
[412] H. P. Böhm, G. Bewer, 4th Int. Carbon and Graphite Conf., London 1974, Prepr. p. 102.
[413] E. Fitzer, K.-H. Geigl, L. M. Manocha, 5th Int. Carbon and Graphite Conf., London 1978, p. 405.
[414] J. O. Besenhard, R. Sauter, unpublished.
[415] R. Dietz, M. E. Peover, *J. Mater. Sci. 6* (1971) 1441.
[416] I. L. Kalnin, Carbon '76, Bad Honnef 1976, Prep. p. 94.
[417] I. L. Kalnin, 14th Biennial Conf. on Carbon, Pennsylvania 1979, Ext. Abstr. p. 218.
[418] P. Kwizera, M. S. Dresselhaus, J. S. Perkins, C. R. Desper, 15th Biennial Conf. on Carbon, Philadelphia 1981, Ext. Abstr. p. 102; P. Kwizera, M. S. Dresselhaus, D. R. Uhlmann, J. S. Perkins, C. R. Desper, *Carbon 20* (1982) 387.

[419] M. A. Rabah, A. A. Abdul Azim, A. Ismail, *J. Appl. Electrochem. 11* (1981) 41.
[420] S. Flandrois, *Synth. Met. 4* (1982) 255.
[421] G. Eichinger, J. O. Besenhard, *J. Electroanal. Chem. 72* (1976) 1.
[422] H. P. Fritz, J. O. Besenhard in: *Elektrochemische Energietechnik, Entwicklungsstand und Aussichten*, Der Bundesminister für Forschung und Technologie, Bonn 1981, p. 44.
[423] N. Watanabe, *Prog. Batteries Sol. Cells 4* (1982) 14.
[424] M. L. Kronenberg, G. E. Blomgren in J. O'M. Bockris, D. E. Conway, E. Yeager, R. E. White: *Comprehensive Treatise of Electrochemistry*, Vol. 3, Plenum Press, New York 1981, p. 247.
[425] N. S. Bubyreva, B. K. Marenko, Y. P. Pavlov, I. M. Perederii, N. D. Rozenblyum, O. A. Tomin, *Elektrokhimiya 18* (1982) 1105.
[426] K. Ueno, N. Watanabe, T. Nakajima, *J. Fluorine Chem. 19* (1982) 323.
[427] a) A. Morita, T. Iijima, T. Fuji, H. Agawa, *J. Power Sources 5* (1980) 111; b) M. Fukuda, T. Iijima in J.-P. Gabano: *Lithium Batteries*, Academic Press, London 1983, p. 211.
[428] M. Fukuda, T. Iijima, *Power Sources 5* (1975) 713.
[429] M. S. Whittingham, *J. Electrochem. Soc. 122* (1975) 526.
[430] N. Watanabe, M. Endo, K. Ueno, *Solid State Ionics 1* (1980) 501.
[431] V. Dechenaux, F. Drouet, J. P. Gabano, Y. Jumel, DOS 2210370 (1972).
[432] M. Armand, Fr. Pat. 2326047 (1975).
[433] S. Maximovitch, M. Levart, M. Fouletier, N. Nguyen, G. Bronoël, *J. Power Sources 3* (1978) 215.
[434] N. Yokota, N. Watanabe, S. Tokuda, Y. Kanaya, H. Shimizu, DOS 2264057 (1973).
[435] B. K. Brown, *Trans. Am. Electrochem. Soc. 53* (1928) 113; B. K. Brown, O. W. Storey, *ibid. 53* (1928) 129.
[436] Burgess Battery Company, DRP 527695 (1926).
[437] H. F. Hunger, G. J. Heymach, *J. Electrochem. Soc. 120* (1973) 1161.
[438] H. F. Hunger, G. J. Heymach, *U. S. Rep.*, NTIS No. AD 755159 and AD/A 037855.
[439] J. O. Besenhard, Habilitationsschrift, Technische Universität München 1979.
[440] M. Armand, P. Touzain, *Mater. Sci. Eng. 31* (1977) 319.
[441] Ming-hui Li, Rui-min Yang, Yuan-chun Quin, Int. Meeting on Lithium Batteries, Rome 1982.
[442] R. Yazami, P. Touzain, L. Bonnetain in [51], Abstr. p. 6; *Synth. Met.*, in press.
[443] K. Kinoshita, *Carbon 12* (1974) 686.
[444] P. Touzain, M. Armand, Carbon '76, Bad Honnef 1976, Prepr. p. 154.
[445] W. K. Behl, D. D. Beals, G. R. Frysinger, *J. Electrochem. Soc. Jpn. 37* (1969) 215.
[446] J. M. Lalancette, R. Roussel, *Can. J. Chem. 54* (1976) 3541.
[447] M. Endo, M. Inagaki in [51], Abstr. p. 20; *Synth. Met.*, in press.
[448] M. Inagaki, H. Kitamura, Y. Maeda in [51], Abstr. p. 59; *Synth. Met.*, in press.
[449] M. Inagaki, A. Matsumoto, M. Sakai, Y. Maeda, Int. Symp. on Carbon, New Processing and New Applications, Toyohashi 1982, Ext. Abstr. p. 474; M. Inagaki, A. Matsumoto, M. Sakai, Y. Maeda; reference to *Chem. Abstr. 98* (1983) 115703x.
[450] S. Flandrois, J. M. Masson, J. C. Rouillon, *Synth. Met. 3* (1981) 195.
[451] S. Flandrois, F. Baron in [50], p. 237.
[452] H. Janakowska, S. Neffe, A. Swiatkowski, *Electrochim. Acta 20* (1981) 1861.
[453] P. A. Attwood, R. J. Bird, B. D. McNicol, R. T. Short, *J. Chem. Soc. Faraday Trans. 1 75* (1979) 2312.
[454] B. D. McNicol, P. Attwood, R. T. Short, *J. Chem. Soc. Faraday Trans. 1 77* (1981) 2017.
[455] S. Otani, *Chem. Lett. 1973*, 1115.
[456] L. Dunsch, *Z. Chem. 14* (1974) 463.
[457] L. Bjelica, R. Parsons, R. M. Reeves in S. Bruckenstein, J. D. E. McIntyre, B. Miller, E. Yeager: *Proc. 3rd Symp. on Electrode Processes, Electrochem. Soc. 1980*, p. 190.
[458] F. G. Gonon, C. M. Fombarlet, M. J. Buda, J. F. Pujol, *Anal. Chem. 53* (1981) 1386.
[459] L. Falat, H.-Y. Cheng, *Anal. Chem. 54* (1982) 2111.
[460] J. Wang, *Electrochim. Acta 26* (1981) 1721.
[461] A. N. Dey, B. P. Sullivan, *J. Electrochem. Soc. 117* (1970) 222.
[462] J. Simonet, H. Lund, *J. Electroanal. Chem. 75* (1977) 719.
[463] G. Bernard, J. Simonet, H. Lund, *J. Electroanal. Chem. 96* (1979) 249.
[464] L. Hall, J. Simonet, H. Lund, *J. Electroanal. Chem. 100* (1979) 197.
[465] G. Bernard, M. A. Martre, J. Simonet, *Electrochim. Acta 25* (1980) 805.
[466] P. Pfluger, H. U. Künzi, H.-J. Güntherodt, *Appl. Phys. Lett. 35* (1979) 771.
[467] P. Pfluger, P. Oelhafen, H. U. Künzi, R. Jeker, E. Hauser, K. P. Ackermann, M. Müller, H.-J. Güntherodt, *Physica B 99* (1980) 395.
[468] D. J. Barker, D. M. Brewis, R. H. Dahm, L. R. J. Hoy, *Electrochim. Acta 23* (1978) 1107.
[469] J. Jansta, F. P. Dousek, V. Patzelova, *Carbon 13* (1975) 377.
[470] Z. Pelzbauer, J. Baldrian, J. Jansta, F. P. Dousek, *Carbon 17* (1979) 317.
[471] F. P. Dousek, J. Jansta, J. Baldrian, *Carbon 18* (1980) 13.
[472] J. Jansta, F. P. Dousek, *Carbon 18* (1980) 433.
[473] L. Cervinka, F. P. Dousek, J. Jansta, H. G. Neumann, H. Steil, *Carbon 19* (1981) 413.
[474] F. P. Dousek, J. Jansta, *Electrochim. Acta 20* (1975) 1.
[475] J. Jansta, F. P. Dousek, *Electrochim. Acta 26* (1981) 233.
[476] E. Y. Weissman, *J. Electrochem. Soc. 144* (1967) 658.
[477] K. Horita, G. Kano, N. Watanabe, *Denki Kagaku 50* (1982) 334.
[478] A. R. Ubbelohde, *Nature London 232* (1971) 43.
[479] L. C. F. Blackman, J. F. Mathews, A. R. Ubbelohde, *Proc. R. Soc. A 256* (1960) 15.
[480] A. Métrot, P. Willmann, T. McRae, A. Herold, *Carbon 17* (1979) 182.
[481] E. McRae, A. Métrot, P. Willmann, A. Herold, *Physica B 99* (1980) 541.
[482] I. B. Rashkov, I. M. Panayotov, V. C. Shishkova, *Carbon 17* (1979) 103, 479.
[483] E. Samcovà, K. Štulic, J. Doležal, *Collect. Czech. Chem. Commun. 37* (1972) 60.
[484] H. E. Zittel, J. F. Miller, *Anal. Chem. 37* (1965) 200.
[485] J. Doležal, K. Štulik, *J. Electroanal. Chem. 17* (1968) 87.
[486] V. Majer, J. Vesely, K. Štulik, *J. Electroanal. Chem. 45* (1973) 113.
[487] A. G. Voloshin, I. P. Kolesnikova, *Zh. Prikl. Khim. 51* (1978) 1570.
[488] I. P. Kolesnikova, A. G. Voloshin, *Kinet. Katal. Engl. Transl. 16* (1975) 700.
[489] I. I. Vasilenko, *Khim. Kinet. Katal. 1979*, 201; reference to *Chem. Abstr. 91* (1979) 182070g.
[490] W. G. Berl, *Trans. Faraday Soc. 83* (1943) 253.
[491] A. G. Voloshin, I. P. Kolesnikova, *Electrokhimiya 11* (1975) 1903; *Soviet. Electrochem. 11* (1975) 1776.
[492] E. Berl, *Trans. Electrochem. Soc. 76* (1939) 359.
[493] M. O. Davies, M. Clark, E. Yeager, F. Hovorka, *J. Electrochem. Soc. 106* (1959) 56.
[494] J. P. Randin in [424], Vol. 4, Plenum Press, New York 1981, p. 473.
[495] Chemical Defence Establishment, Porton Down, Salisbury, Wiltshire (U. K.), Data Sheet.
[496] H. Jehring: *Elektrosorptionsanalyse mit der Wechselstrompolarographie*, Akademie Verlag, Berlin 1974.
[497] C. I. Simionescu, V. Percec, *Prog. Polym. Sci. 8* (1982) 133.
[498] S. Flandrois in [195], p. 15.
[499] R. B. Seymour: *Conductive Polymers*, Plenum Press, New York 1981.
[500] Conference Internationale sur la Physique et la Chimie des Polymer Conducteurs, Les Arcs-Bourg Saint Maurice 1982.
[501] P. J. Nigrey, D. MacInnes Jr., D. P. Nairns, A. G. MacDiarmid, A. Heeger, *J. Electrochem. Soc. 128* (1981) 1651.
[502] K. Kaneto, M. Maxfield, D. P. Nairns, A. G. MacDiarmid, *J. Chem. Soc. Faraday Trans. 1 78* (1982) 3417.
[503] K. M. Abraham, *J. Power Sources 7* (1981/82) 1.
[504] K. M. Abraham, S. B. Brummer in [427b], p. 371.
[505] J. O. Besenhard, R. Schöllhorn, *J. Electrochem. Soc. 124* (1977) 968.
[506] J. O. Besenhard, J. Heydecke, H. P. Fritz, *Solid State Ionics 6* (1982) 215.
[507] H. Möhwald, Dissertation, Universität München, in preparation.
[508] F. Beck, H. Krohn in [51], Abstr. p. 9; *Synth. Met.*, in press.
[509] S. C. Gau, J. Milliken, A. Pron, A. G. MacDiarmid, A. J. Heeger, *J. Chem. Soc. Chem. Commun. 1979*, 662.

**When submitting manuscripts, authors of articles which are intended for publication as "Communications" are requested to conform to the guidelines reproduced at the beginning of each issue following the list of contents.**

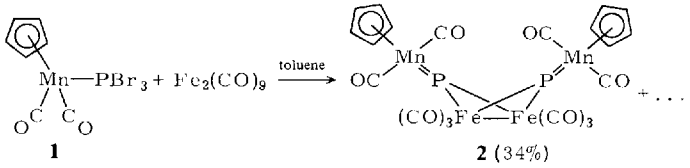
## Naked Phosphorus Atoms as Trigonally Planar Coordinated Bridge Ligands**

By *Heinrich Lang, Laszlo Zsolnai,* and *Gottfried Huttner** 

*Dedicated to Professor Ernst Otto Fischer on the occasion of his 65th birthday*

Compounds in which a phosphorus atom is $\mu_3$-bonded to three transition-metal centers in a trigonal planar coordination have so far never been described. Since it was found that complexes with planar threefold bridging arsenic atoms are accessible by reaction of haloarsanediyl complexes with organometallic nucleophiles[1], we attempted the synthesis of trigonally planar coordinated $\mu_3$-phosphorus in a similar way.

Indeed, the complex **2** could be obtained as the first compound containing this structural element by reductive dehalogenation of $(\eta^5\text{-}C_5H_5)Mn(CO)_2PBr_3$ **1** with $Fe_2(CO)_9$.




**1** **2** (34%)

**2** dissolves in *n*-pentane or toluene, yielding wine-red solutions. Crystals of **2** exhibit the metallic luster characteristic of the chromophoric system of metal complexes containing trigonally planar coordinated elements of the fifth main group[2]. The composition of **2** is confirmed by elemental analysis and by the mass spectrum. IR and $^1$H-NMR spectra are consistent with a hindered rotation about the P–Mn axes. The $^{31}$P-NMR spectrum indicates an unconventional structure; it shows a singlet at $\delta = 977$, *i.e.* with the largest downfield shift known so far. Only "phosphinidene" complexes exhibit similarly extreme signal positions $[(\eta^5\text{-}C_5H_5)Mn(CO)_2]_2P\text{–}C_6H_5$: $\delta = 884$)[9]. A bonding system in which the P atom is involved in phosphorus-p$\pi$/metal-d$\pi$ interactions—with its low-lying LUMOs[7, 10], due to the "weak" $\pi$-bonding—apparently increases the paramagnetic contribution to the chemical shift to a considerable extent. The trigonal-planar environment of the phosphorus atoms in **2**, indicated by the $\delta(^{31}P)$ value, was proven by an X-ray structure analysis (Fig. 1).

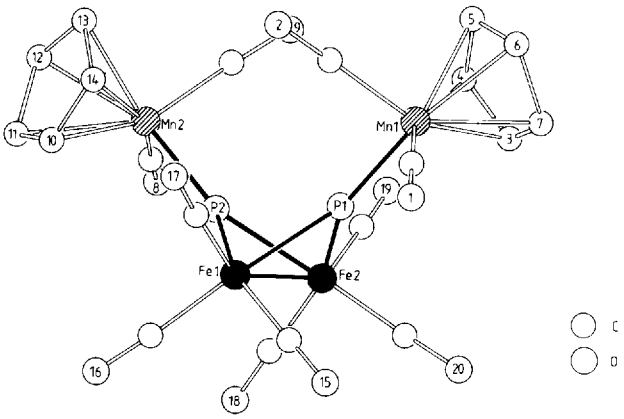



Fig. 1. Molecular structure of the complex **2**, a compound with trigonally planar coordinated phosphorus atoms. Further details of the crystal structure investigation are available on request from the Fachinformationszentrum Energie Physik Mathematik, D-7514 Eggenstein-Leopoldshafen, on quoting the depository number CSD 50601, the names of the authors, and full citation of the journal.

The tetranuclear complex **2** has almost $C_2$-symmetry. The two P atoms each lie in a plane with their three nearest neighbor atoms (maximum deviation 5.0 pm); the interplanar angle for Fe1–P1–Fe2 and Fe1–P2–Fe2 is 94.1°. The vacant p-orbital of the phosphorus is predominantly filled by back-bonding from manganese donor orbitals: the manganese-phosphorus bond, with a length of 210 pm, is even shorter than the corresponding bonds in phosphinidene complexes, which are similarly shortened by manganese-d$\pi$–phosphorus-p$\pi$ interactions[4].

Received: July 5, 1983 [Z 444 IE]
German version: *Angew. Chem. 95* (1983) 1016
The complete version of this communication appears in: *Angew. Chem. Suppl. 1983,* 1451–1462

[1] G. Huttner, B. Sigwarth, J. von Seyerl, L. Zsolnai, *Chem. Ber. 115* (1982) 2035.
[2] B. Sigwarth, L. Zsolnai, O. Scheidsteger, G. Huttner, *J. Organomet. Chem. 235* (1982) 43; and references cited therein.
[4] G. Huttner, H.-D. Müller, A. Frank, H. Lorenz, *Angew. Chem. 87* (1975) 714; *Angew. Chem. Int. Ed. Engl. 14* (1975) 705.
[7] N. M. Kostić, R. F. Fenske, *J. Organomet. Chem. 233* (1982) 337.
[9] H. Lang, G. Huttner, unpublished.
[10] G. Huttner, J. von Seyerl, M. Marsili, H.-G. Schmid, *Angew. Chem. 87* (1975) 455; *Angew. Chem. Int. Ed. Engl. 14* (1975) 572.

[*] Prof. Dr. G. Huttner, H. Lang, L. Zsolnai
Lehrstuhl für Synthetische Anorganische Chemie der Universität
Postfach 5560, D-7750 Konstanz (Germany)

[**] This work was supported by the Deutsche Forschungsgemeinschaft and the Fonds der Chemischen Industrie.—We thank Prof. Dr. *Marianne Baudler* and Dr. *J. Hahn,* Universität Köln, for the $^{31}$P-NMR measurements.

## Diphosphorus, :P≡P:, as Eight-Electron Ligand**

By *Heinrich Lang, Laszlo Zsolnai,* and *Gottfried Huttner** 

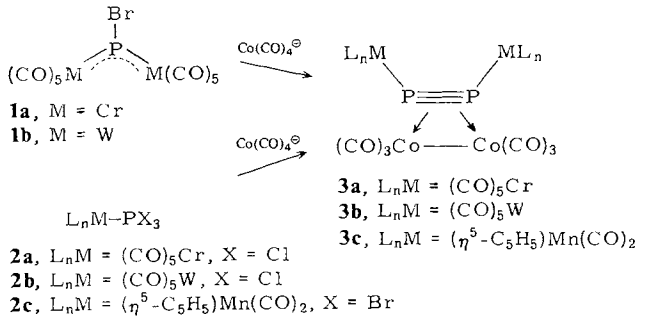
*Dedicated to Professor Ernst Otto Fischer on the occasion of his 65th birthday*

It was already demonstrated some time ago that the $P_2$ and $As_2$ molecular homologues of dinitrogen can be stabilized as side-on bonded 4$\pi$-donor ligands in carbonylcobalt complexes $Co_2(CO)_6E_2$ (E = P, As). We have now found

[*] Prof. Dr. G. Huttner, H. Lang, L. Zsolnai
Lehrstuhl für Synthetische Anorganische Chemie der Universität
Postfach 5560, D-7750 Konstanz (Germany)

[**] This work was supported by the Deutsche Forschungsgemeinschaft and the Fonds der Chemischen Industrie.

that the phosphorus lone pairs of the diphosphorus coordinated in $Co_2(CO)_6P_2$ allow additional coordination of a 16-electron complex fragment at each of the two phosphorus atoms with formation of the compounds **3**. Synthesis of **3** was accomplished by reaction of halophosphanediyl- ("phosphinidene") complexes **1** or halophosphane complexes **2** with tetracarbonylcobaltate.




**1a**, M = Cr
**1b**, M = W

**3a**, $L_nM = (CO)_5Cr$
**3b**, $L_nM = (CO)_5W$
**3c**, $L_nM = (\eta^5\text{-}C_5H_5)Mn(CO)_2$

**2a**, $L_nM = (CO)_5Cr$, X = Cl
**2b**, $L_nM = (CO)_5W$, X = Cl
**2c**, $L_nM = (\eta^5\text{-}C_5H_5)Mn(CO)_2$, X = Br

The $P_2$-unit in the new complexes **3** functions as an 8-electron ligand, whose side-on bonding in the cluster corresponds to that known for other E≡E ligands, particularly that in $Co_2(CO)_6P_2$[3]. The X-ray structure analysis of **3a** (Fig. 1) shows that the PP bond (206 pm) is only slightly lengthened compared to that in the parent compound $Co_2(CO)_5P(C_6H_5)_3P_2$[3b] (201.9 pm) by the additional coordination *via* the lone pairs of electrons. The Co–P distances in **3a** (mean value 224.7 pm) are likewise scarcely different from those in the $\mu_2$-parent compound (mean value 226.4 pm).

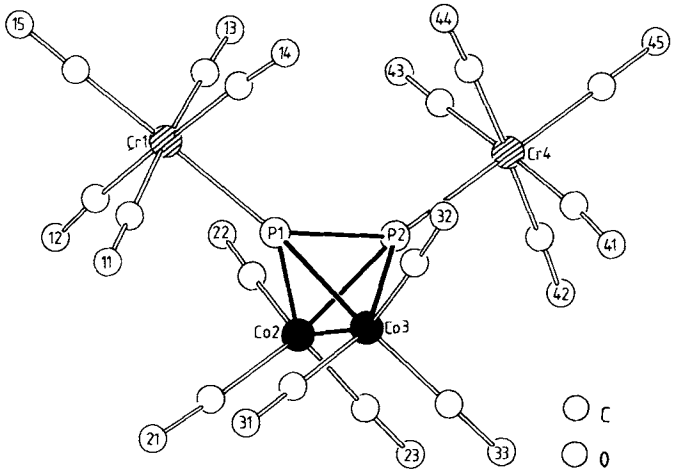
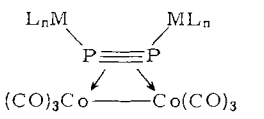



Fig. 1. Molecular structure of the tetranuclear complex **3a** in the crystal. Further details of the crystal structure investigation are available on request from the Fachinformationszentrum Energie Physik Mathematik, D-7514 Eggenstein-Leopoldshafen, on quoting the depository number CSD 50603, the names of the authors, and full citation of the journal.

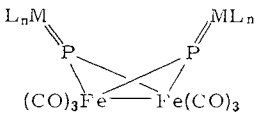
Compounds **3** form deep red (**3b**) and green-blue (**3c**) crystals, which are readily soluble in apolar solvents. The EI mass spectra give clear patterns which reveal the successive cleavage of all carbonyl groups. The $^{31}$P-NMR spectra show $\delta$-values between 44 (**3b**) and 197 (**3c**) for the $P_2$ ligands.

Compound **3c** has formally the same composition as $[\eta^5\text{-}(C_5H_5)Mn(CO)_2]_2(\mu_3\text{-}P)_2Fe_2(CO)_6$, **4**[13]. In order to obtain closed shell electron configurations, the phosphorus atoms of **4** have to donate two additional electrons in comparison with **3c**.




**3c**

$L_nM = (\eta^5\text{-}C_5H_5)Mn(CO)_2$




**4**

This difference in electron demand leads in the case of **4** to complete cleavage of the PP bond and to formation of $\mu_3$-phosphorus bridges in which all five valence electrons of the trigonally planar coordinated phosphorus atoms participate in the metal-phosphorus bonding. It remains to be shown whether the transition $\mu_4\text{-}P_2 \rightleftharpoons 2\,\mu_3\text{-}P$ may be realized as a redox reaction in one and the same system.


Received: July 28, 1983 [Z 490 IE]
German version: *Angew. Chem. 95* (1983) 1017
The complete version of this communication appears in: *Angew. Chem. Suppl. 1983*, 1463–1476

CAS Registry numbers:
**1a**, 87869-44-1; **1b**, 87869-45-2; **2a**, 18461-41-1; **2b**, 21223-85-8; **2c**, 32841-54-6; **3a**, 87869-46-3; **3b**, 87869-47-4; **3c**, 87869-48-5; $Na_2[Cr_2(CO)_{10}]$, 15616-67-8; $Na_2[W_2(CO)_{10}]$, 15616-70-3; $PBr_3$, 7789-60-8; $NaCo(CO)_4$, 14878-28-5.



[3] a) A. S. Foust, C. F. Campana, J. D. Sinclair, L. F. Dahl, *Inorg. Chem. 18* (1979) 3047; b) C. F. Campana, A. Vizi-Orosz, G. Pályi, L. Markó, L. F. Dahl, *ibid. 18* (1979) 3054; c) G. Váradi, A. Vizi-Orosz, S. Vastag, G. Pályi, *J. Organomet. Chem. 108* (1976) 225; d) A. Vizi-Orosz, G. Pályi, L. Markó, *ibid. 60* (1973) C25; e) A. S. Foust, M. S. Foster, L. F. Dahl, *J. Am. Chem. Soc. 91* (1969) 5633.

[13] H. Lang, L. Zsolnai, G. Huttner, *Angew. Chem. 95* (1983) 1016; *Angew. Chem. Int. Ed. Engl. 22* (1983) 976; *Angew. Chem. Suppl. 1983*, 1451–1462.

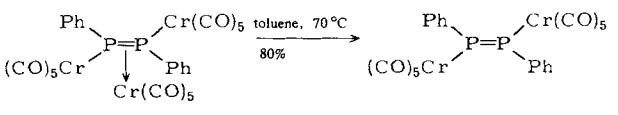

## $(C_6H_5)_2P_2[Cr(CO)_5]_2$, a Diphosphene Complex with Free Phosphorus–Phosphorus Double Bond**


By *Jutta Borm, Laszlo Zsolnai,* and *Gottfried Huttner**


*Dedicated to Professor Ernst Otto Fischer on the occasion of his 65th birthday*

As homologues of the azo compounds {R–Ë=Ë–R} (E = P, As, Sb), some diphosphenes (R = 2,4,6-$t$Bu$_3$C$_6$H$_2$, $(Me_3Si)_3C$, $(Me_3Si)_2CH$[1a], $(Me_3Si)_2N$[1b]) which are stable in the free state have only recently been reported in the literature. The existence of such species as side-on coordinated ligands with E = P, As[2, 3], and Sb[3] had already been demonstrated earlier. In all previously characterized complexes the reactive E=E double bond is stabilized by interaction with a metal center[2, 15]; in addition, the two lone pairs can be coordinatively active[3]. The binuclear complex **2** is the first stable derivative of an unstable diphosphene, in which only the n-electron pairs are complexed, while the P=P double bond remains free.

The novel complex **2** is formed on heating the trinuclear compound **1**, which—as analogue of other $R_2E_2[M(CO)_5]_3$ complexes[3]—is readily accessible from $Na_2Cr_2(CO)_{10}$ and $(CO)_5Cr(PPhCl_2)$.




**1** **2**


[*] Prof. Dr. G. Huttner, J. Borm, L. Zsolnai
Lehrstuhl für Synthetische Anorganische Chemie der Universität
Postfach 5560, D-7750 Konstanz (Germany)



[**] This work was supported by the Deutsche Forschungsgemeinschaft and the Fonds der Chemischen Industrie.

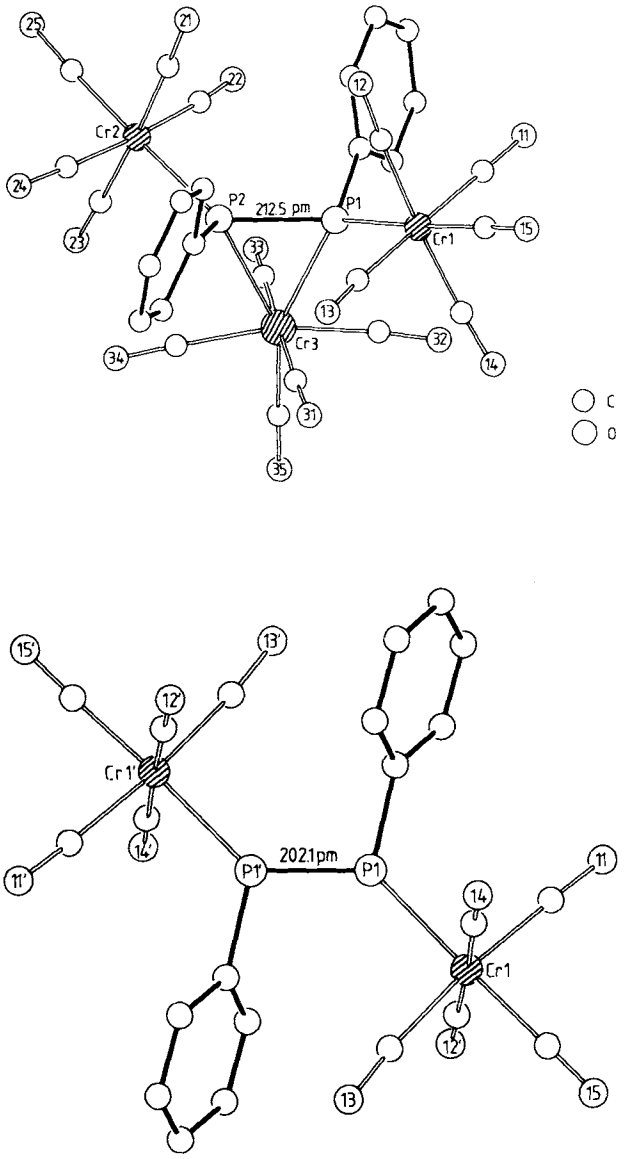



Fig. 1. The molecular structure of the $Ph_2P_2$-complexes **1** (top) and **2** (bottom) in the crystal. Further details of the crystal structure investigation are available on request from the Fachinformationszentrum Energie Physik Mathematik, D-7514 Eggenstein-Leopoldshafen, on quoting the depository number CSD 50604, the names of the authors, and the full citation of the journal.

In **1**, diphenyldiphosphene is bound both *via* the lone electron pairs as well as *via* the central double bond (cf. Fig. 1).

As a result of the side-on coordination, the P=P bond in **1** is lengthened from 203 to 212.5 pm compared to that in free diphosphenes[1]. Thermal cleavage of the side-on bonded $Cr(CO)_5$-group leads to the centrosymmetric complex **2**, whose P=P bond length in a planar framework geometry (maximum deviation 3 pm) corresponds to a diphosphene P=P double bond. This means that the end-on bonded $Cr(CO)_5$-groups in **2** have no influence on the PP bond order, even though they shield the reactive double bond to such an extent that the system is stable even without protection by bulky organic substituents[1, 15].

The stabilization of a reactive multiple bond by blocking of the lone pairs, as found in **2**, has its analogy in the stability of diazene complexes homologous to **2**[8].

The electronic influence of the pentacarbonylchromium groups is obvious from the $^{31}$P-NMR spectrum: whereas free diphosphenes show signals in the range $\delta = 470-600$[1], the signal of **2** appears at $\delta = 927$.

Received: August 1, 1983 [Z 501 IE]
German version: *Angew. Chem. 95* (1983) 1018
The complete version of this communication appears in: *Angew. Chem. Suppl. 1983*, 1477–1492

[1] a) M. Yoshifuji, I. Shima, N. Inamoto, *J. Am. Chem. Soc. 103* (1981) 4587; *104* (1982) 6167; G. Bertrand, C. Couret, J. Escudié, S. Majid, J.-P. Majoral, *Tetrahedron Lett. 23* (1982) 3567; C. Couret, J. Escudié, J. Satgé, *ibid. 23* (1982) 4941; A. H. Cowley, J. E. Kilduff, S. K. Mehrotra, N. C. Norman, M. Pakulski, *J. Chem. Soc. Chem. Commun. 1983*, 528; b) E. Niecke, R. Rüger, *Angew. Chem. 95* (1983) 154; *Angew. Chem. Int. Ed. Engl. 22* (1983) 155; E. Niecke, R. Rüger, M. Lysek, S. Pohl, W. Schoeller, *ibid. 95* (1983) 495 and *22* (1983) 486; *Angew. Chem. Suppl. 1983*, 639.

[2] P. S. Elmes, P. Leverett, B. O. West, *J. Chem. Soc. Chem. Commun. 1971*, 747; J. C. Green, M. L. H. Green, G. E. Morris, *ibid. 1974*, 212; P. S. Elmes, M. L. Scudder, B. O. West, *J. Organomet. Chem. 122* (1976) 281; E. Camillo, A. Coda, K. Prout, J. C. Daran, *Acta Crystallogr. B 33* (1977) 2608; J. M. Jacob, E. Weiss, *J. Organomet. Chem. 153* (1978) 31; H. Schäfer, *Z. Naturforsch. B 34* (1979) 1358; B. Deppisch, H. Schäfer, *Z. Anorg. Allg. Chem. 490* (1982) 129; H. Vahrenkamp, D. Wolters, *Angew. Chem. 95* (1983) 152; *Angew. Chem. Int. Ed. Engl. 22* (1983) 154; P. J. Sullivan, A. L. Rheingold, *Organometallics 1982*, 1547; J. Chatt, P. B. Hitchcock, A. Pidcock, C. P. Warrens, K. R. Dixon, *J. Chem. Soc. Chem. Commun. 1982*, 932.

[3] G. Huttner, H.-G. Schmid, A. Frank, O. Orama, *Angew. Chem. 88* (1976) 255; *Angew. Chem. Int. Ed. Engl. 15* (1976) 234; G. Huttner, U. Weber, B. Sigwarth, O. Scheidsteger, *ibid. 94* (1982) 210 and *21* (1982) 215; *Angew. Chem. Suppl. 1982*, 411.

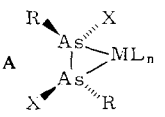
[8] D. Sellmann, *Angew. Chem. 86* (1974) 692; *Angew. Chem. Int. Ed. Engl. 13* (1974) 639; G. Huttner, W. Gartzke, A. Allinger, *J. Organomet. Chem. 91* (1975) 47.

[15] *Note added in proof:* See, however: K. M. Flynn, M. M. Olmstead, Ph. P. Power, *J. Am. Chem. Soc. 105* (1983) 2085. The $^{31}$P-NMR shift of 384.55 ppm for a diphosphene complex given in this paper is, however, improbable.

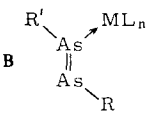
## Synthesis and Structure of a Diarsenechromium Complex with an Unsupported Arsenic-Arsenic Double Bond**

By *Alan H. Cowley**, *Jon G. Lasch*, *Nicholas C. Norman*, and *Marek Pakulski*

Previously described diarsene (RAs=AsR) complexes are of the $\eta^2$-type **A** and involve arsenic-arsenic bond orders of *ca.* 1.5[1–3]. We now report the synthesis and X-ray crystal structure of a new type of diarsene complex **B** which features an unsupported AsAs double bond.



**A** R = $C_6H_5$, X = $Cr(CO)_5$; $ML_n$ = $Cr(CO)_5$[1]
R = $C_6F_5$, X = :; $ML_n$ = $Fe(CO)_4$[2], $Pt(PPh_3)_2$[3]



**B** **1**, R = 2,4,6-($t$Bu)$_3C_6H_2$; $ML_n$ = $Cr(CO)_5$; R′ = $CH(SiMe_3)_2$

The diarsene complex **1** was prepared by the reaction of the uncoordinated diarsene[4] with $Cr(CO)_5THF$ in tetrahydrofuran (THF) solution and purified by chromatography (silica gel/*n*-hexane). Orange crystals of **1** (m.p. = 138–139 °C) formed from *n*-hexane solutions held at −20 °C.

[*] Prof. Dr. A. H. Cowley, J. G. Lasch, Dr. N. C. Norman, Dr. M. Pakulski
Department of Chemistry, University of Texas at Austin
Austin, TX 78712 (USA)

[**] This work was supported by the U. S. National Science Foundation and the Robert A. Welch Foundation.

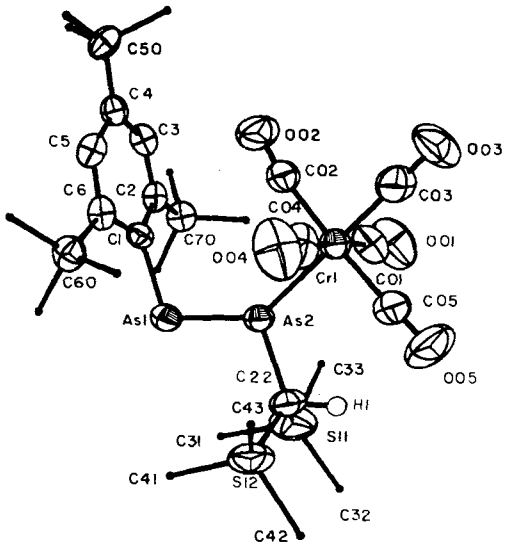
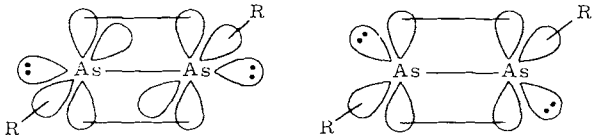



Fig. 1. Structure of **1** in the crystal. Selected bond lengths [Å] and angles [°]: As1–As2 2.246(1), As1–C1 1.964(5), As2–C22 1.989(5), As2–Cr1 2.454(1); As2–As1–C1 104.0(1), As1–As2–C22 105.2(2), As1–As2–Cr1 138.48(3), Cr1–As2–C22 116.3(2).

The X-ray structure analysis of **1** (Fig. 1) reveals that the $Cr(CO)_5$ group is attached to only one As atom. The AsAs bond length of 2.246(1) Å in **1** is considerably shorter than the range of 2.43–2.46 Å observed for AsAs single bonds[5], and the values of 2.388(7)[2] and 2.371[1] Å reported for $\eta^2$-diarsene complexes of type **A**. Moreover, within experimental error, the $C_2As_2Cr$ framework is planar. These facts suggest the presence of a double bond between the As atoms. This is supported by the UV/VIS spectrum of **1** which exhibits peaks expected for the As=As chromophore [$\lambda_{max}$ = 240 ($\varepsilon$ = 36700), 293 (16750), 345 (3800), and 470 nm (7800)].




All the skeletal bond lengths in **1** are longer than those of the uncoordinated diarsene due to the steric demands of the $Cr(CO)_5$ group. However, the largest increase occurs at the AsAs double bond (*ca.* 0.02 Å). Interestingly, *both* CAsAs angles increase upon coordination. The bond angle increase at As2 is not ascribable to steric effects and is presumably due to rehybridization of arsenic from approximately sp (**I**) to $sp^2$ (**II**).

Received: September 20, 1983 [Z 558 IE]
German version: *Angew. Chem. 95* (1983) 1019
The complete manuscript of this communication appears in: *Angew. Chem. Suppl. 1983*, 1493–1502

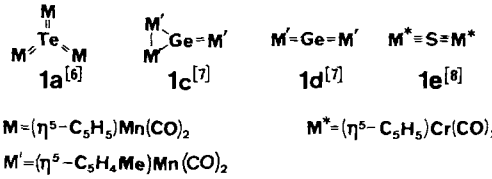
[1] G. Huttner, H.-G. Schmid, A. Frank, O. Orama, *Angew. Chem. 88* (1976) 255; *Angew. Chem. Int. Ed. Engl. 15* (1976) 234.
[2] P. S. Elmes, P. Leverett, B. O. West, *J. Chem. Soc. Chem. Commun. 1971*, 747.
[3] P. S. Elmes, M. L. Scudder, B. O. West, *J. Organomet. Chem. 122* (1976) 281.
[4] A. H. Cowley, J. G. Lasch, N. C. Norman, M. Pakulski, *J. Am. Chem. Soc. 105* (1983) 5506.
[5] a) L. K. Maxwell, S. B. Hendricks, V. M. Mosely, *J. Chem. Phys. 3* (1935) 699; b) J. H. Burns, J. Waser, *J. Am. Chem. Soc. 79* (1957) 859; c) K. Hedberg, E. W. Hughes, J. Waser, *Acta Crystallogr. 14* (1961) 369; d) A. L. Rheingold, P. J. Sullivan, *Organometallics 2* (1983) 327.

## Addition of Methylene to Multiple Bonds between Ligand-Free, Main-Group Elements and Transition Metals—A General Reaction[1]

By *Wolfgang A. Herrmann**, *Josef Weichmann*, *Ulrich Küsthardt*, *Adolf Schäfer*, *Rolf Hörlein*, *Christian Hecht*, *Erdmuthe Voss*, and *Ricardo Serrano*

*Dedicated to Professor Ernst Otto Fischer on the occasion of his 65th birthday*

Multiple bonds between transition metals are centers of high reactivity unless bulky ligands prevent approach of the reactands. Sterically exposed metal-metal multiple bonds are thus not inferior to active metal surfaces with regard to metal-centered addition, fragmentation, and coupling reactions of saturated or unsaturated hydrocarbons—examples of potential applications in catalysis[2]. Only recently have some complexes **1** been prepared containing multiple bonds between "naked" main-group elements and transition metals[6–8]. According to *Kostić* and *Fenske*[9], multiple bond character is required for theoretical reasons in the germanium compound **1d**.




The particular advantages of type **1** complexes are that they not only are preparatively readily accessible and, nevertheless, very reactive, but also that they contain distinctly different types of reaction centers (cf. Mn and Ge); they are, therefore, ideal candidates for model studies in catalysis. After conversion of the $\mu_3$-tellurium complex **1a** into a $\mu_2,\eta^2$-telluroformaldehyde derivative[10] (**2a** in Scheme 1), we recognized the generality of the method used and, as an example, now report the synthesis and unusual properties of a novel type of metallaspiro compound **2b**.

The germanium-manganese complex **1b** can be prepared more straightforwardly and in higher yield (40–60%) using our synthetic method, *i.e.* reaction of the solvent-stabilized complex fragment $(\eta^5\text{-}C_5H_5)Mn(CO)_2$ with gaseous germane in the presence of acid (cf. Scheme 1 and Supplement). By way of contrast, the two-step germylpotassium route[7] gives only small yields (1%) of **1c**[7].

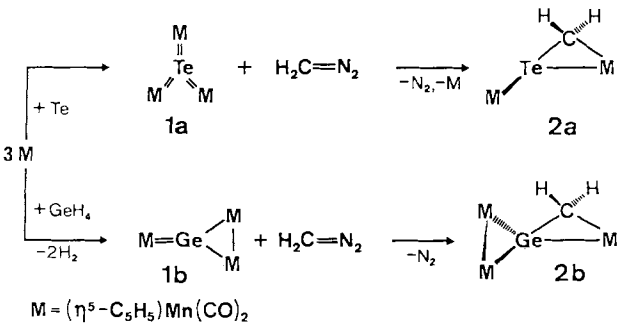
$GeH_4$ reacts with $(\eta^5\text{-}C_5Me_5)Mn(CO)_2$ in the presence of traces of sulfuric acid to afford exclusively the orange complex $(\mu_2\text{-}Ge)[(\eta^5\text{-}C_5Me_5)Mn(CO)_2]_2$ having a strictly linear Mn–Ge–Mn skeleton known for compound **1d**)[**]; here, the bulky $C_5Me_5$ ligands prevent formation of the trinuclear compound analogous to **1b**, **c**. We observed the same effect in the synthesis of the tellurium complex $(\mu_2\text{-}Te)[(\eta^5\text{-}C_5Me_5)Mn(CO)_2]_2$ (**1f**, cf. Supplement).

Solutions of **1b** in tetrahydrofuran (THF) react with diazomethane over the temperature range −20 to 0°C with evolution of dinitrogen. According to elemental analysis and spectroscopic data (FD-MS, IR, NMR), the product

[*] Prof. Dr. W. A. Herrmann, Dr. J. Weichmann, U. Küsthardt, A. Schäfer, R. Hörlein, C. Hecht, E. Voss, Dr. R. Serrano
Institut für Anorganische Chemie der Universität
Niederurseler Hang, D-6000 Frankfurt am Main 50 (Germany)

[**] Note added in proof: The linear geometry of this compound has been confirmed by X-ray structure analysis, according to which the Mn–Ge distances are *ca.* 218 pm, and are thus a little shorter than in the methylcyclopentadienyl derivative **1d** [7] (*I. Bernal, J. D. Korp*, unpublished results).

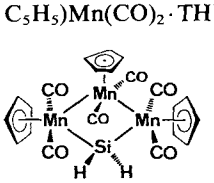
**2b** (air-stable, brown crystals; m.p. 112°C), isolated in 85–95% yield, has the structure of a previously unknown $\mu_3,\eta^2$-methylenegermanediyl complex and results from addition of $CH_2$ to the Mn=Ge multiple bond of **1b**; the seemingly much less reactive Mn–Ge single bonds are not affected by diazomethane.




Scheme 1.

Although in the two typical cases addition of methylene to **1a**[10] and **1b** proceeds quite uniformly (Scheme 1), the products **2a** and **2b** exhibit completely different properties: The $CH_2Te$ complex has a rigid structure with a pyramidally configurated Te atom; in contrast, the $CH_2Ge$ complex has a fluxional structure ($^1$H-NMR, $CD_2Cl_2$): Below −50°C, three well resolved $C_5H_5$ signals appear, two of which broaden upon increasing the temperature and collapse into a single line at *ca.* 20°C; simultaneously, a very broad $CH_2$-signal appears. This observation can be assigned either to an opposing rotation of the two three-membered rings at the spiro-Ge atom in **2b** or to a *cis/trans*-isomerization within the binuclear fragment $(\eta^5\text{-}C_5H_5)_2Mn_2(CO)_4$. Of greater chemical significance is the different thermolysis behavior of compounds **2a** and **2b**. Although the $CH_2Te$ complex decomposes rapidly at 180°C, the tellurium-carbon bond remains intact. In contrast, the $CH_2Ge$ complex **2b** decomposes *slowly* above *ca.* 50°C and *immediately* upon melting (112°C) to form both ethylene *quantitatively* (GC) and the *intact* precursor **1b** (MS, IR, NMR); the latter species can add again to methylene. In the presence of hydrogen (1 atm) this thermolysis affords significant amounts of methane. In accord with NMR data ($\delta(CH_2) \approx 1.9$), the reversible elimination of methylene classifies **2b**, in contrast to **2a**, as a thermolabile metallaspiro compound in which, for the first time, a methylene group bridges a substituent-free main group element and a transition metal. **2b** reacts with $[D_2]$diazomethane (THF/$Et_2O$, 25°C) with $CH_2/CD_2$ exchange.

Because of the greater strength of the Si–H bond compared to a Ge–H bond, the route developed for the synthesis of **1b** was expected to be less successful for the synthesis of the homologous silicon compound. The major product (≈70%) of the reaction of $(\eta^5\text{-}C_5H_5)Mn(CO)_2\cdot THF$ with $SiH_4$ was the novel silanediyl



**3**

complex **3** (elemental analysis, MS, IR, NMR); the colorless derivative $(\mu\text{-}SiH_2)_2[(\eta^5\text{-}C_5H_5)Mn(CO)_2]_2$ as well as the red silicon compound $(\eta^5\text{-}C_5H_5)_3Mn_3(CO)_6Si$ are formed as by-products (in each case *ca.* 5%). With $(\eta^5\text{-}C_5Me_5)Mn(CO)_2\cdot THF$, pure monosilane gives the hydrido(silylene) complex of composition $(\mu\text{-}SiH_2)[(\eta^5\text{-}C_5Me_5)Mn(CO)_2H]_2$ (Me=$CH_3$).

Received: May 30, 1983; revised: October 7, 1983 [Z 401 IE]
German version: *Angew. Chem. 95* (1983) 1019
The complete manuscript of this communication appears in: *Angew. Chem. Suppl. 1983*, 1543–1557

[1] Transition Metal Methylene Complexes, Part 50. This work was supported by the Deutsche Forschungsgemeinschaft and the Fonds der Chemischen Industrie, Hoechst AG, VARTA AG, and Messer-Griesheim.—Part 49: W. A. Herrmann, C. Bauer, J. M. Huggins, H. Pfisterer, M. L. Ziegler, *J. Organomet. Chem.*, in press.
[2] Reviews: a) W. A. Herrmann, *Adv. Organomet. Chem. 20* (1982) 159; b) W. A. Herrmann in B. L. Shapiro: Organometallic Compounds, Texas A & M University Press, College Station 1983, pp. 383–405.
[6] M. Herberhold, D. Reiner, D. Neugebauer, *Angew. Chem. 95* (1983) 46; *Angew. Chem. Int. Ed. Engl. 22* (1983) 59; *Angew. Chem. Suppl. 1983*, 10–22.
[7] W. Gäde, E. Weiss, *J. Organomet. Chem. 213* (1981) 451; J. Schiemann, P. Hübener, E. Weiss, *Angew. Chem. 95* (1983) 1021; *Angew. Chem. Int. Ed. Engl. 22* (1983) 980.
[8] T. J. Greenhough, B. W. S. Kolthammer, P. Legzdins, J. Trotter, *Inorg. Chem. 18* (1979) 3543.
[9] N. M. Kostić, R. F. Fenske, *J. Organomet. Chem. 233* (1982) 337.
[10] W. A. Herrmann, J. Weichmann, R. Serrano, K. Blechschmitt, H. Pfisterer, M. L. Ziegler, *Angew. Chem. 95* (1983) 331; *Angew. Chem. Int. Ed. Engl. 22* (1983) 314; *Angew. Chem. Suppl. 1983*, 363–395.

## $\mu_2$-E[V(CO)$_3$diphos]$_2$ (E = S, Se, Te): Complexes with Linear VEV Multiple-Bond Systems

By *Jan Schiemann, Peter Hübener,* and *Erwin Weiss**

*Dedicated to Professor Ernst Otto Fischer on the occasion of his 65th birthday*

Novel transition metal-main group element compounds containing multiple bonds have attracted a great deal of interest in recent years. Typical examples are the cyclopentadienyl or methylcyclopentadienyl complexes $[(\eta^5\text{-}C_5H_5)Cr(CO)_2]_2S$[1a], $[(\eta^5\text{-}C_5H_4Me)Mn(CO)_2]_2Ge$[1b], $[(\eta^5\text{-}C_5H_4Me)Mn(CO)_2]_3Ge$[1c], and $[(\eta^5\text{-}C_5H_5)Mn(CO)_2]_3Te$[1c]. The synthesis of vanadium-chalcogen compounds with multiple bonds in linear VEV groups (E = S, Se, Te) has now also been accomplished.

We obtained the binuclear sulfur compound **1** *via* routes (a) and (b)[2] (diphos = ethylenebis(diphenylphosphane)).

$$Na[V(CO)_4diphos] \xrightarrow[20°C,\ H_2O]{Na_2SO_3/H^+} [V(CO)_3diphos]_2S\ \mathbf{1}\ (ca.\ 25\%) \quad (a)$$

$$Na[V(CO)_4diphos] \xrightarrow[20°C,\ H_2O]{Na_2S/H^+} \mathbf{1}\ (ca.\ 50\%) \quad (b)$$

For the preparation of the selenium and tellurium compounds **2** and **3** we have so far only used route (a), with appropriate modification.

$$Na[V(CO)_4diphos] \xrightarrow{Na_2SeO_3/H^+} [V(CO)_3diphos]_2Se\ \mathbf{2}\ (ca.\ 25\%)$$
$$\xrightarrow{Na_2TeO_3/H^+} [V(CO)_3diphos]_2Te\ \mathbf{3}\ (ca.\ 25\%)$$

In all cases, the mechanism of the reaction is still unclear.

An X-ray structure analysis of the red, diamagnetic complex **1** reveals a centrosymmetric molecule (Fig. 1) with very short V–S distances (217.2 pm). Values for comparison are not available, since **1** is the first carbonylvanadium compound containing sulfido ligands. In other S-contain-

[*] Prof. Dr. E. Weiss, Dr. J. Schiemann, Dr. P. Hübener
Institut für Anorganische und Angewandte Chemie der Universität
Martin-Luther-King-Platz 6, D-2000 Hamburg 13 (Germany)

ing compounds the V–S distances are always greater than 230 pm.

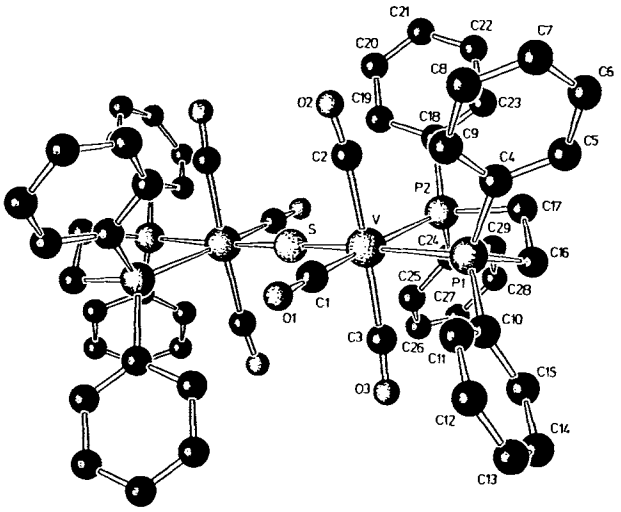
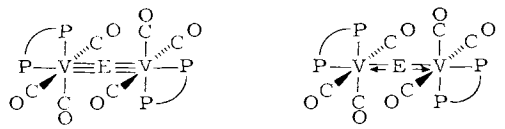


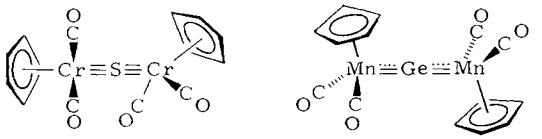

Fig. 1. Molecular structure of **1** in the crystal([V(CO)$_3$diphos]$_2$S·3C$_6$H$_5$CH$_3$). Triclinic, P$\bar{1}$, $a=1214.9(4)$, $b=1259.1(7)$, $c=1388.8(7)$ pm, $\alpha=77.60(4)$, $\beta=73.02(3)$, $\gamma=63.77(3)°$, $Z=1$; $Mo_{K\alpha}$ radiation, Patterson and direct methods (SHEL-X), $R=6\%$ for 2789 reflections (H positions calculated). Bond lengths [pm]: V–S 217.2(1), V–P1 248.9(2), V–P2 248.7(4), V–C1 194.1(3), V–C2 199.9(9), V–C3 198.7(9); angles [°]: V–S–V 180.0, P1–V–P2 79.9. Further details of the crystal structure investigation are available on request from the Fachinformationszentrum Energie Physik Mathematik, D-7514 Eggenstein-Leopoldhsafen on quoting the depository number CSD 50456, the names of the authors, and the full citation of the journal.

According to their composition and spectroscopic data the complexes **2** and **3** undoubtly have a structure analogous to that of **1**. In principle, three $\nu$(CO) absorption bands are to be expected for the fragment V(CO)$_3$, the same as for the whole molecules **1**–**3** when they have a center of symmetry. The four bands observed for **1** and **2**[4] indicates loss of the symmetry center in the dissolved state. Probably there is extensive rotation about the VEV axis in solution, resulting in formation of a mixture of various rotamers.

On the basis of the electron balance rule the complexes **1**–**3** are formulated with double and triple bonds (**B** and **A**, respectively).



**A** E = S, Se, Te **B**



**4** **5**

The actual bond order could lie between double and triple, as in the case of the cyclopentadienyl complexes **4**[1a] and **5**[1b]. The partial triple bonding reported by *Kostić* and *Fenske*[5] to be present in **5** and thus the easier internal rotation are consistent both with the centrosymmetric molecular structure in the crystal as well as with the occurrence of rotamers without a center of symmetry in solution.

Received: September 22, 1983;
revised: October 18, 1983 [Z 566 IE]
German version: *Angew. Chem. 95* (1983) 1021

[1] a) T. J. Greenhough, B. W. S. Kolthammer, P. Legzdins, J. Trotter, *Inorg. Chem. 18* (1979) 3543; b) W. Gäde, E. Weiss, *J. Organomet. Chem. 213* (1981) 451; c) M. Herberhold, D. Reiner, D. Neugebauer, *Angew. Chem. 95* (1983) 46; *Angew. Chem. Int. Ed. Engl. 22* (1983) 59; *Angew. Chem. Suppl. 1983*, 10–22.

[2] Compound **1** is also formed in the reaction of Na[V(CO)$_4$diphos] with $S_3N_3Cl_3$ in tetrahydrofuran at −78 °C (yield *ca.* 1%).

[3] Procedure: For the synthesis of **1** (route (b)) an aqueous suspension (200 mL) of Na[V(CO)$_4$diphos] (1.17 g, 2.0 mmol) and $Na_2S\cdot 9H_2O$ (0.7 g, 3.0 mmol) is acidified dropwise with 2 N $H_2SO_4$ and then stirred for 12 h. The resulting precipitate is filtered off (G3 frit), washed twice with water, and dried. The product, which is still hydrous, is dissolved in ether (20 mL) on the frit. After separation of the aqueous phase the etheral solution is filtered, the solvent removed, and the residue recrystallized from toluene/hexane (1:1) (cooling to *ca.* −30 °C). Yield 0.54 g (49%).—For the synthesis of **1**, **2**, or **3** (according to route (a)) an aqueous solution (200 mL) of Na[V(CO)$_4$diphos] (2.0 mmol) and $Na_2EO_3$ (2.0 mmol) is acidified dropwise with 1 M $H_3PO_4$ and then stirred for *ca.* 12 h. In each case the resulting precipitate is worked-up as described above. Yields *ca.* 25%.

[4] IR ($CH_2Cl_2$): $\nu$(CO) in cm$^{-1}$ for **1**: 1983 m, 1920 s, 1885 vs, 1850 s; for **2**: 1980 m, 1930 s, 1885 vs, 1852 vs; for **3**: 1970 m, 1925 s, 1880 vs.

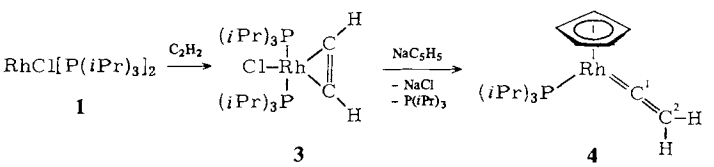
[5] N. M. Kostić, R. F. Fenske, *J. Organomet. Chem. 233* (1982) 337.

## Synthesis and Structure of [($\eta^5$-C$_5$H$_5$)RhP(*i*Pr)$_3$($\eta^2$-EC=CH$_2$)] with E = S, Se, Te: Generation and Stabilization of Thioketene, Selenoketene, and Telluroketene at a Transition Metal**

By *Helmut Werner**, *Justin Wolf*, *Ralf Zolk*, and *Ulrich Schubert*

Whereas thioketene CH$_2$=C=S and selenoketene CH$_2$=C=Se are extremely reactive molecules and are only detectable in the gas phase, telluroketene is unknown[1]. We have now succeeded in generating these species, CH$_2$=C=E (E = S, Se, Te), in a straightforward way as ligands in the coordination sphere of a transition metal.

Recently, we showed that the reaction of RhCl[P(*i*Pr)$_3$]$_2$ **1** with PhC$_2$H and NaC$_5$H$_5$ leads to the phenylvinylidene complex C$_5$H$_5$Rh(=C=CHPh)P(*i*Pr)$_3$ **2** *via* alkyne-, alkynyl(hydrido)-, and alkynylrhodium intermediates[2]. Using similar conditions, **1** also reacts with acetylene. In pentane as solvent the yellow, air-sensitive complex **3** is obtained, which according to its IR spectrum probably has a metallacyclopropene structure[3]. The *trans*-orientation of the triisopropylphosphane ligands can be deduced from the $^1$H-NMR data. A similar structure has been proposed for RhCl(C$_2$H$_2$)[P(C$_6$H$_{11}$)$_3$]$_2$[4].




**1** **3** **4**

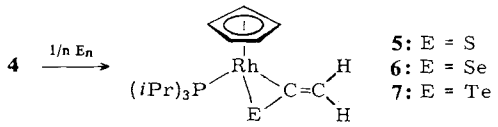
Reaction of **3** with NaC$_5$H$_5$ (tetrahydrofuran, 25 °C, 1 h) yields the vinylidene complex **4** (yield 35%)[3]. In addition

[*] Prof. Dr. H. Werner, J. Wolf, R. Zolk, Prof. Dr. U. Schubert
Institut für Anorganische Chemie der Universität
Am Hubland, D-8700 Würzburg (Germany)

[**] This work was supported by the Deutsche Forschungsgemeinschaft, the Fonds der Chemischen Industrie, and by gifts of chemicals from BASF AG, Ludwigshafen, and DEGUSSA AG, Hanau. We are grateful to Drs. *G. Lange*, *W. Buchner*, and *D. Scheutzow* for the MS and NMR spectra.

to the IR data structural proof is provided principally by the $^{13}$C-NMR spectrum (in $C_6D_6$) which, apart from signals of the phosphane- and cyclopentadienyl-carbon atoms, contains two doublets of doublets at $\delta = 311.41$ and 94.14; these are assigned, respectively, to $C^1$ and $C^2$ of the vinylidene ligand. In the case of the phenylvinylidene compound **2**[3] the corresponding signals are observed at $\delta = 316.99$ and 116.31, respectively.

Complex **4** reacts with sulfur (in hexane), selenium, and tellurium (in benzene) to afford the intensely colored chalcogenoketenerhodium compounds **5**—**7** in good yield (E = S: 45%, E = Se and E = Te: 70%)[3]. The reactivity of the chalcogenes decreases markedly from sulfur *via* selenium to tellurium; red selenium is considerably more reactive than the gray allotrope. Whereas **5** (red) and **6** (red-brown) are air-stable, **7** (green) is readily oxidized. Solutions of **7** (*e.g.* in $C_6H_6$) slowly decompose to yield **4** and tellurium; additional products cannot be detected.




**5**: E = S
**6**: E = Se
**7**: E = Te

The NMR spectra of **5**—**7**[3] support the proposed structure. Since the compounds are chiral, two signals for the diastereotopic methyl groups of the $P(iPr)_3$ ligand are observed in the $^1$H-NMR spectra of **5** and **6**; in **7** the diastereotopic shift is too small to be resolved. For E = S, the $CH_2$ protons of the chalcogenoketenes give rise to an AX-, for E = Se an $A_2$-, and for E = Te an AB-pattern; for E = S and Se additional PH coupling arises.

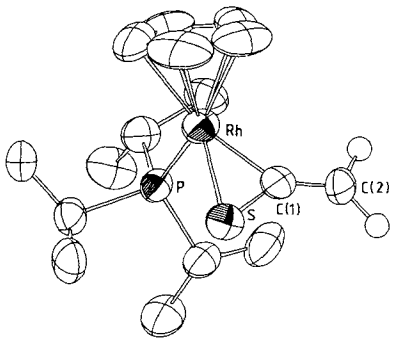



Fig. 1. Crystal structure of **5**. The disorder of the thioketene ligand is not indicated. Selected bond lengths [pm] and angles [°]: Rh—P 228.6(2), Rh—S 238.0(3), Rh—C(1) 196(2), S—C(1) 169(3), C(1)—C(2) 131(3); S—Rh—P 92.7(1), S—Rh—C(1) 44.7(6), P—Rh—C(1) 95.1(6), Rh—S—C(1) 54.3(7), Rh—C(1)—C(2) 140.5(18), S—C(1)—C(2) 138.1(18).

Figure 1 shows the result of the crystal structure analysis of **5**[5]. In the crystal **5** is disordered in such a way that each site is occupied by both enantiomers in the ratio of *ca.* 87:13. The plane through Rh, P, and the centroid of the five-membered ring exactly bisects the C(1)-S bond; the planes $C_5$(middle)-Rh-P and Rh-S-C(1) enclose an angle of 86.7°. C(2) lies only 8(2) pm outside the Rh-S-C(1) plane. The angle S-C(1)-C(2) is almost the same as the angle S-C-S in $C_5H_5(PMe_3)Co(\eta^2\text{-}CS_2)$ **8**[6a] and the angle S-C-C in $C_5H_5(PMe_3)Co(\eta^2\text{-}SC{=}CCMe_2(CH_2)_3CMe_2)$ **9**[6b].

To our knowledge **5**—**7** are the first metal complexes of unsubstituted thio-, seleno-, and telluroketene. Both we[6b] and *Behrens et al.*[7a] have already synthesized mono- and binuclear metal compounds with *substituted* thioketenes; of these, **9** is similar in structure to **5**. *Stone et al.*[7b] obtained iridium(I) and platinum (0) complexes with $\eta^2$-bonded bis(trifluoromethyl)thioketene, however, not starting from (the still unknown) $(CF_3)_2C{=}C{=}S$ but from $CF_3$-substituted heterocyclic sulfur compounds.

Received: July 22, 1983 [Z 484 IE]
German version: *Angew. Chem. 95* (1983) 1022

[1] a) H. Bock, B. Solouki, G. Bert, P. Rosmus, *J. Am. Chem. Soc. 99* (1977) 1663; H. Bock, S. Aygen, P. Rosmus, B. Solouki, *Chem. Ber. 113* (1980) 3187, and literature cited therein; b) D. R. Hogg, J. K. Lundquist, A. Ohno, *Org. Comp. Sulphur, Selenium, Tellurium 6* (1981) 131.

[2] J. Wolf, H. Werner, O. Serhadli, M. L. Ziegler, *Angew. Chem. 95* (1983) 428; *Angew. Chem. Int. Ed. Engl. 22* (1983) 414.

[3] All compounds gave correct elemental analyses, and correct molecular mass determination were obtained for **4**—**7**: IR in KBr, for **4** in hexane. $^1$H- and $^{13}$C-NMR at 25 °C in $C_6D_6$, int. TMS.—**3** yellow crystals, m.p. = 153 °C; IR: $\nu$(C=C) = 1712 cm$^{-1}$; $^1$H-NMR (60 MHz): $\delta(C_2H_2) = 3.54$ (dt, $J_{RhH} = 2.5$, $J_{PH} = 0.3$ Hz), $\delta(PCHCH_3) = 2.50$ (m), $\delta(PCHCH_3) = 1.47$ (dvt, $J_{HH} = 6.0$, $N = 12.0$ Hz).—**4**: brown crystals, m.p. = 66 °C; IR: $\nu$(C=C) = 1622 cm$^{-1}$; $^1$H-NMR (60 MHz): $\delta(C_5H_5) = 5.47$ (m), $\delta(CCH_2) = 2.95$ (dd, $J_{PH} = 4.6$, $J_{RhH} = 1.5$ Hz), $\delta(PCHCH_3) = 2.30$ (m), $\delta(PCHCH_3) = 1.34$ (dd, $J_{PH} = 13.4$, $J_{HH} = 7.6$ Hz); $^{13}$C-NMR (400 MHz): $\delta(CCH_2) = 311.41$ (dd, $J_{RhC} = 66.1$, $J_{PC} = 27.6$ Hz), $\delta(CCH_2) = 94.14$ (dd, $J_{RhC} = 17.0$, $J_{PC} = 3.7$ Hz), $\delta(C_5H_5) = 85.93$ (s), $\delta(PCHCH_3) = 24.43$ (d, $J_{PC} = 22.9$ Hz), $\delta(PCHCH_3) = 19.87$ (s).—**5**: red crystals, m.p. = 161 °C; IR: $\nu$(C=C) = 1618 cm$^{-1}$; $^1$H-NMR (100 MHz): $\delta(CH_2) = 5.81$ (dd, $J_{HH} = 2.7$, $J_{PH} = 1.0$ Hz) and 5.55 (dd, $J_{HH} = 2.7$, $J_{PH} = 1.1$ Hz), $\delta(C_5H_5) = 5.10$ (dd, $J_{PH} = 1.4$, $J_{RhH} = 0.6$ Hz), $\delta(PCHCH_3) = 1.92$ (m), $\delta(PCHCH_3) = 1.04$ (dd, $J_{PH} = 13.4$, $J_{HH} = 7.0$ Hz) and 1.00 (dd, $J_{PH} = 13.3$, $J_{HH} = 7.0$ Hz).—**6**: red-brown crystals, m.p. = 169 °C; IR: $\nu$(C=C) = 1615 cm$^{-1}$; $^1$H-NMR (100 MHz): $\delta(CH_2) = 5.79$ (d, $J_{PH} = 1.1$ Hz), $\delta(C_5H_5) = 5.09$ (dd, $J_{PH} = 1.5$, $J_{RhH} = 0.6$ Hz), $\delta(PCHCH_3) = 2.02$ (m), $\delta(PCHCH_3) = 1.05$ and 1.04 (dd, $J_{PH} = 13.4$, $J_{HH} = 7.1$ Hz).—**7**: green crystals, m.p. = 102 °C; IR: $\nu$(C=C) = 1572 cm$^{-1}$ $^1$H-NMR (100 MHz): $\delta(CH_2) = 5.68$ (dd, $J_{HH} = 4.4$, $J_{RhH} = 1.2$ Hz) and 5.51 (d, $J_{HH} = 4.4$ Hz), $\delta(C_5H_5) = 5.12$ (dd, $J_{PH} = 1.5$, $J_{RhH} = 0.6$ Hz), $\delta(PCHCH_3) = 2.12$ (m), $\delta(PCHCH_3) = 1.03$ (dd, $J_{PH} = 13.3$, $J_{HH} = 7.1$ Hz).

[4] H. L. M. van Gaal, J. P. J. Verlaan, *J. Organomet. Chem. 133* (1977) 93.

[5] Monoclinic (from pentane), space group $P2_1/n$, $Z = 4$; $a = 887.7(5)$, $b = 1644.2(8)$, $c = 1213.9(6)$ pm, $\beta = 91.98(4)°$, $V = 1770.7 \times 10^6$ pm$^3$; $\varrho$(calc.) = 1.45 g/cm$^3$; $3° \leq 2\theta \leq 48°$ ($Mo_{K\alpha}$, $\lambda = 71.069$ pm); 2783 independent reflections, empirical absorption correction, location of the hydrogen atoms predominantly from difference Fourier syntheses, in part calculated from the ideal geometry; $R_1 = 0.074$, $R_2 = 0.078$ for 2269 structure factors ($F_0 \geq 3.92$). Further details of the crystal structure analysis can be obtained from the Fachinformationszentrum Energie Physik Mathematik, D-7514 Eggenstein-Leopoldshafen, by quoting the depository number CSD 50533, the names of the authors, and the journal citation.

[6] a) H. Werner, K. Leonhard, C. Burschka, *J. Organomet. Chem. 160* (1978) 291; b) H. Werner, O. Kolb, U. Schubert, K. Ackermann, *Angew. Chem. 93* (1981) 583; *Angew. Chem. Int. Ed. Engl. 20* (1981) 593.

[7] a) D. Wormsbächer, F. Edelmann, U. Behrens, *Chem. Ber. 114* (1981) 153; *115* (1982) 1332; b) M. Green, R. B. L. Osborn, F. G. A. Stone, *J. Chem. Soc. A 1970*, 944.

## Synthesis and Structure of $[CuMo(CH_3CO_2)_2(L)(CO)_2(\eta^5\text{-}C_5H_5)]$: Monomeric Copper(II) Diacetate as Building Block of a Heterometallic Binuclear Complex**

By *Helmut Werner**, *Joachim Roll*, *Klaus Linse*, and *Manfred L. Ziegler*

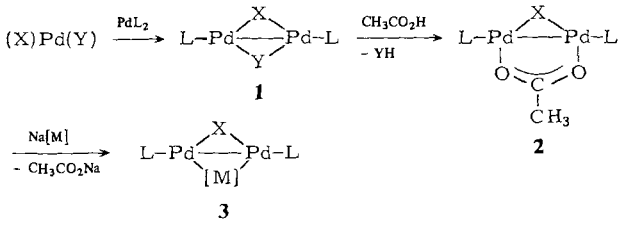
Metal complexes with heteronuclear metal-metal bonds are currently enjoying considerable interest in connection

[*] Prof. Dr. H. Werner, J. Roll
Institut für Anorganische Chemie der Universität
Am Hubland, D-8700 Würzburg (Germany)
Prof. Dr. M. L. Ziegler, K. Linse
Anorganisch-chemisches Institut der Universität Heidelberg (Germany)

[**] This work was supported by the Deutsche Forschungsgemeinschaft and the Fonds der Chemischen Industrie. We thank Dr. *D. Scheutzow* for the 400 MHz NMR spectra and Prof. Dr. *U. Schubert* for valuable discussions.

with the preparation of selective, heterogeneous catalysts[1]. Above all, the most promising goal is the synthesis of compounds containing an electron-deficient and an electron-rich transition metal, which exert a synergistic interaction on each other.

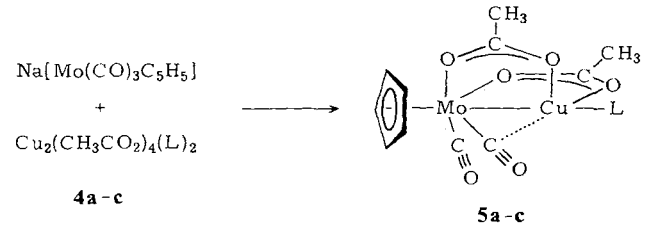
We have already shown that heterometallic trinuclear metal clusters, *e.g.* **3**, can be synthesized stepwise from mononuclear metal starting materials[2].



X = 2-$MeC_3H_4$; Y = $C_5H_5$; L = $P(iPr)_3$; [M] = $Mo(CO)_3C_5H_5$[2b]

In the compounds **1–3**, palladium is present in the oxidation state +1. Since both $Cu^{II}$ and $Pd^{I}$ are $d^9$-systems, and numerous binuclear complexes of $Cu^{II}$ with carboxylate bridges are known, we also attempted to achieve a ligand exchange between $CH_3CO_2$ and [M] (as in the reaction **2**→**3**) in the pyridine adducts of dimeric copper(II) acetate.

The reaction of $Na[Mo(CO)_3C_5H_5]$ (≡Na [M]) with **4a–c** ($C_6H_6$, 25 °C, **2d**) affords the pale red, air-sensitive solids **5a–c**, which can be separated by column chromatography from $[C_5H_5Mo(CO)_3]_2$[7] formed as a by-product. **5a–c** are diamagnetic and contain Cu and Mo in the ratio 1:1. From the intensities of the $^1$H-NMR signals it follows that there are one pyridine and two acetate ligands present per cyclopentadienyl ring[3].



**4a-c** **5a-c**

**a**: L = $C_5H_5N$; **b**: L = 4-$CH_3C_5H_4N$; **c**: L = 4-$tC_4H_9C_5H_4N$

In addition to the signals for the $C_5H_5$, $RC_5H_4N$, and $CH_3CO_2$ carbon atoms, the $^{13}$C-NMR spectra of **5a–c** each exhibit a signal at *ca.* 252 ppm[3] which corresponds to the CO groups. According to the chemical shift, these should be in a bridging position[4]. However, as proved by the crystal structural analysis[5] of **5b** only weakly bridging CO groups are found in the crystal. Whereas the carbonyl group C(2)–O(2) has largely terminal character, C(1)–O(1) is to be considered as "semibridging"[6]. Of note is the distance Cu–Mo, which is significantly shorter than that in the Cu–Mo compounds with μ–S bridges thoroughly studied by *Müller et al.*[8]. The five-membered rings MoOCOCu are planar and form an angle of 84.29° with each other.

As indicated by ongoing studies, heterometallic binuclear complexes are also probably formed in the reactions of **4a–c** with $Na[W(CO)_3C_5H_5]$. In addition to those and $[C_5H_5W(CO)_3]_2$[7], the compound $C_5H_5W(CO)_3(OCOCH_3)$ is also obtained, which is not accessible from $C_5H_5W(CO)_3CH_3$ and $CH_3CO_2H$ and which has been characterized by a crystal structure analysis[9].

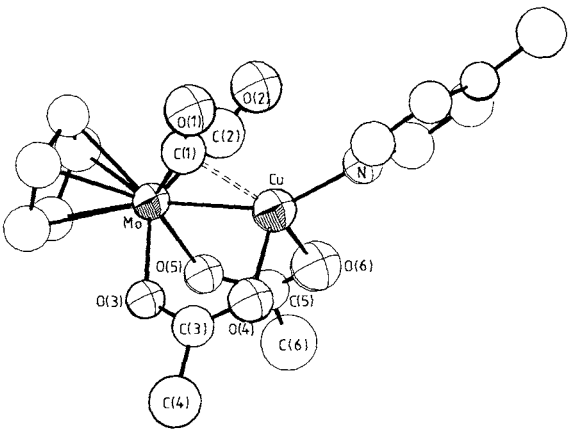



Fig. 1. Selected distances [pm] and angles [°]: Cu–Mo 255.8(1), Mo–C(1) 196.6(9), Mo–C(2) 195.3(9), Cu···C(1) 213.7(9), Cu···C(2) 246.0(8), Mo–O(3) 216.9(6), Mo–O(5) 216.5(5), Cu–O(4) 211.6(6), Cu–O(6) 210.7(5), Cu–N 199.5(6), C(1)–O(1) 120.6(11), C(2)–O(2) 118.4(11), C(3)–O(3) 126.8(9), C(3)–O(4) 123.4(9), C(5)–O(5) 127.7(8), C(5)–O(6) 122.3(9), Mo–C(1)–O(1) 164.5(6), Mo–C(2)–O(2) 172.6(7), C(1)–Mo–C(2) 76.9(4), Mo–Cu–N 150.4(2), O(3)–Mo–O(5) 77.1(2), O(4)–Cu–O(6) 94.4(2), O(5)–Mo–Cu 77.3(1), O(3)–Mo–Cu 79.6(1), O(6)–Cu–Mo 94.1(1), O(4)–Cu–Mo 93.7(1), O(4)–Cu–N 100.5(2), O(6)–Cu–N 110.4(2).

Received: July 22, 1983 [Z 485 IE]
German version: *Angew. Chem. 95* (1983) 1023

[1] P. Braunstein, R. Bender, J. Kervennal, *Organometallics 1* (1982) 1236; and literature cited therein.
[2] a) H. Werner, H.-J. Kraus, P. Thometzek, *Chem. Ber. 115* (1982) 2914; b) H. Werner, P. Thometzek, *Angew. Chem. 94* (1982) 707; *Angew. Chem. Int. Ed. Engl. 21* (1982) 692; c) P. Thometzek, H. Werner, *J. Organomet. Chem. 252* (1983) C29.
[3] 60 Mz $^1$H-NMR and 400 MHz $^{13}$C-NMR at 25 °C in $C_6H_6$ and $C_6D_6$, respectively, int. TMS. IR in KBr.—**5a**: $^1$H-NMR: δ($C_5H_5$) 5.30 (s), δ($CH_3CO_2$) 2.25 (s); $^{13}$C-NMR: δ(CO) 252.36 (s), δ($CH_3CO_2$) 177.04 (s), δ($C_5H_5$) 98.01 (s), δ($CH_3CO_2$) 22.72 (s); IR: ν(CO) 1955 (sh), 1905, 1795 cm$^{-1}$.—**5b**: $^1$H-NMR: δ($C_5H_5$) 5.30 (s), δ($CH_3CO_2$) 2.25 (s), δ($CH_3C_5H_4N$) 1.72 (s); $^{13}$C-NMR: δ(CO) 252.49 (s), δ($CH_3CO_2$) 177.09 (s), δ($C_5H_5$) 98.05 (s), δ($CH_3CO_2$) 22.78 (s); IR: ν(CO) 1955 (sh), 1905, 1800 cm$^{-1}$.—**5c**: $^1$H-NMR: δ($C_5H_5$) 5.30 (s), δ($CH_3CO_2$) 2.25 (s), δ($tC_4H_9C_5H_4N$) 1.00 (s); $^{13}$C-NMR: δ(CO) 252.40 (s), δ($CH_3CO_2$) 176.95 (s), δ($C_5H_5$) 98.00 (s), δ($CH_3CO_2$) 22.74 (s); IR: ν(CO) 1960 (sh), 1905, 1805 cm$^{-1}$.
[4] M. H. Chisholm, *Prog. Inorg. Chem. 20* (1976) 299.
[5] Red crystals (from toluene/pentane), triclinic, space group $P\bar{1}$, $Z=4$; $a=812.8(2)$, $b=1534.9(8)$, $c=1608.6(5)$ pm, $\alpha=106.61(4)$, $\beta=98.11(3)$, $\gamma=90.25(3)°$, $V=1901.75\cdot10^6$ pm$^3$; $\rho$(calc.) 1.72 g/cm$^3$, $\rho$(exp.) 1.77 g/cm$^3$; $2°\leq2\theta\leq55°$ ($Mo_{K\alpha}$, $\lambda=71.069$ pm); 3195 independent reflections with $I<3.0\sigma(I)$; $R_{iso}=0.076$, $R_{aniso}=0.053$, $R_w=0.036$. Further details of the crystal structure analysis can be obtained from the Fachinformationszentrum Energie Physik Mathematik, D-7514 Eggenstein-Leopoldshafen, by quoting the depository number CSD 50532, the names of the authors, and the journal citation.
[6] F. A. Cotton, *Prog. Inorg. Chem. 21* (1976) 1.
[7] R. D. Adams, D. M. Collins, F. A. Cotton, *Inorg. Chem. 13* (1974) 1086.
[8] A. Müller, E. Diemann, R. Jostes, H. Bögge, *Angew. Chem. 93* (1981) 957; *Angew. Chem. Int. Ed. Engl. 20* (1981) 934; and literature cited therein.
[9] H. Werner, J. Roll, P. Thometzek, R. Zolk, unpublished results; see J. Roll, Diplomarbeit, Universität Würzburg 1983.

## Small Heterocycles containing Phosphorus and Tellurium**

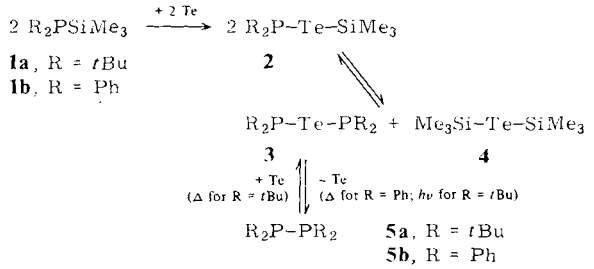
By *Wolf-Walther du Mont*, Tevfik Severengiz,* and *Bernd Meyer*

Tellurium differs markedly from the other chalcogens in its reactivity towards phosphanes; most characteristic is

[*] Prof. Dr. W.-W. du Mont, T. Severengiz, Dr. B. Meyer
Fachbereich Chemie der Universität Oldenburg
Postfach 2503, D-2900 Oldenburg (Germany)

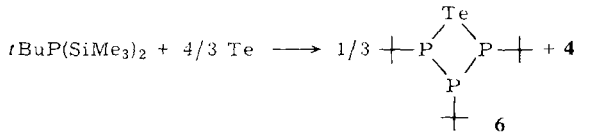
[**] This work was supported by the Deutsche Forschungsgemeinschaft.

the lability of $P^V-Te^{II}$ compounds (tellurium atom transfer between phosphanes)[1]. Thus, we have recently shown that tellurium can be inserted into the P–Si bond of di-*tert*-butyl(trimethylsilyl)phosphane **1a**, but is incapable of inducing a further oxidation of the tellurophosphinite **2a**[2a]. The insertion product merely equilibrates with the symmetrically substituted tellurium compounds **3** and **4**. We have now found that when a less bulky silylphosphane is used as starting material, a novel P–P coupling by detelluration (**3**→**5**) follows the reaction steps **1**→**2** and **2**→**3**+**4**: diphenyl(trimethylsilyl)phosphane **1b** reacts smoothly with tellurium to give tetraphenyldiphosphane **5b** and bis(trimethylsilyl) telluride **4**.

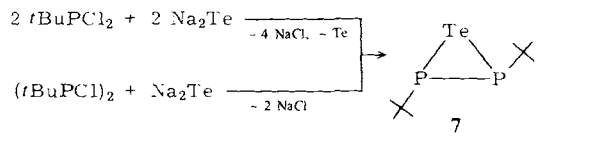



A tellurophosphinous anhydride **3b** is apparently unstable and decomposes with formation of the diphosphane **5b**, though conversely the bulkier diphosphane **5a** reacts thermally with elemental tellurium to give **3a**[2b].

All three types of reaction: Te-insertion, dismutation, and P–P coupling detelluration can be drawn on to explain the unexpected formation of a telluratriphosphetane **6** from *tert*-butylbis(trimethylsilyl)phosphane and tellurium.




The four-membered heterocycle **6** is formed in almost quantitative crude yield ($^{31}$P-NMR) when the silylphosphane is stirred with tellurium powder in excess at room temperature for about 14 d. After removal of **4** under reduced pressure, **6** remains as a red liquid[3]. If the reaction temperature is increased, cyclophosphanes $(tBuP)_n$ (n = 3, 4) and the telluradiphosphirane **7** are formed as well as **6**. The three-membered heterocycle **7** is formed as main product when sodium telluride is allowed to react with *tert*-butyldichlorophosphane or with 1,2-di-*tert*-butyl-1,2-dichlorodiphosphane.




The structures proposed by us for **6** and **7** have been confirmed by EI and FI-MS data as well as by $^{31}$P- and $^{125}$Te-NMR coupling patterns[3]. The highly resolved $^{125}$Te-NMR signal of **6** appears as a doublet split into a triplet (Fig. 1). The contribution of the coupling between tellurium and the adjacent phosphorus nuclei characteristically differs from $P^V=Te^{II}$ couplings (1600–2300 Hz) and is even smaller than $^2J$(TeP). The telluradiphosphirane **7**—the first molecule with tellurium in a three-membered ring[2a,3]—can be regarded as an epitelluride of di-*tert*-butyldiphosphene. The NMR data of **7** allow its unequivocal placement in the series of thia- and selenadiphosphiranes described by *Baudler et al.*[4]. The tendency of **7** to release tellurium has hitherto precluded its isolation in the pure state; however, we are attempting to preparatively exploit the detelluration of **7**.

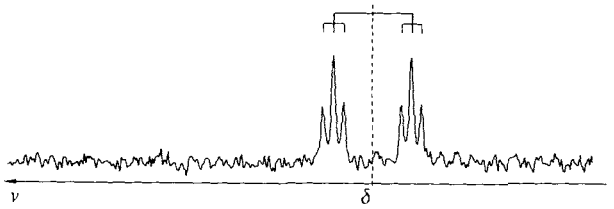



Fig. 1. $^{125}$Te-NMR spectrum of the telluratriphosphetane **6**. Bruker WP 80 FT-NMR spectrometer, 25.271 MHz for $^{125}$Te, $\delta$ = 2994.568 Hz (–118 ppm rel. ditolyl ditelluride as standard), $J$ = 84 Hz (d), 10.7 Hz (t).

Received: July 26, 1983 [Z 449 IE]
German version: *Angew. Chem. 95* (1983) 1025

CAS Registry numbers:
**6**, 87869-43-0; *t*-BuP(SiMe$_3$)$_2$, 42491-33-8; Te, 13494-80-9.

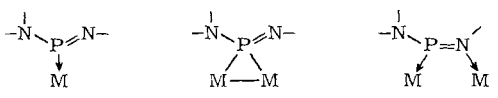
[1] W.-W. du Mont, H.-J. Kroth, *J. Organomet. Chem. 113* (1976) C35.
[2] a) W.-W. du Mont, *Angew. Chem. 92* (1980) 562; *Angew. Chem. Int. Ed. Engl. 19* (1980) 554; b) *Abstr. 3rd Int. Symp. Inorg. Ring Systems, Graz 1981.*
[3] The composition of **6** is confirmed by elemental analysis. We thank Prof. Dr. *J. Müller*, Technische Universität Berlin, for the FI-MS spectra of **6** ($M^+$ at $m/z$ 394) and **7** ($M^+$ at $m/z$ 306). $^{31}$P-NMR data: **6**: $\delta = -4$, $-60.2$ ($AM_2$, $J$(PP) = ±172.6 Hz); **7**: $\delta = -69$ (s, $J(^{125}Te^{31}P) = \pm 229.3$ Hz.—Procedure for the preparation of **6**: A mixture of *tert*-butylbis(trimethylsilyl)phosphane (22.4 g, 95.6 mmol) [5] and tellurium powder (16.9 g, 132.4 mmol) is stirred in the dark for 14 d at room temperature. After removal of excess tellurium by decantation, **4** is drawn off in a $N_2$-cooled trap. The residue is diluted with 40 mL pentane, filtered, and once again evaporated to dryness at 0.1 mbar. There remains 22.2 g (57%) of **6** as a red liquid.
[4] M. Baudler, H. Suchomel, G. Fürstenberg, U. Schings, *Angew. Chem. 93* (1981) 1087; *Angew. Chem. Int. Ed. Engl. 20* (1981) 1044.
[5] H. Schumann, L. Rösch, *Chem. Ber. 107* (1974) 854.

## N,P-Coordination of an Amino(imino)phosphane**

By *Otto J. Scherer*, Jürgen Kerth, Ralf Anselmann,* and *William S. Sheldrick*

*Dedicated to Professor Ernst Otto Fischer on the occasion of his 65th birthday*

Of the conceivable possibilities of coordination of the amino(imino)phosphanes >N–P=N– only those of type **A**[1a,b] and type **B**[1c] have hitherto been verified.

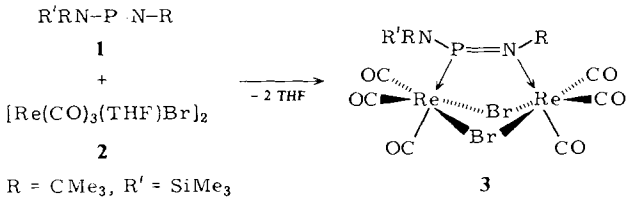



**A** **B** **C**

[*] Prof. Dr. O. J. Scherer, J. Kerth, R. Anselmann,
Prof. Dr. W. S. Sheldrick
Fachbereich Chemie der Universität
Erwin-Schrödinger-Strasse, D-6750 Kaiserslautern (Germany)

[**] This work was supported by the Fonds der Chemischen Industrie through a grant to *J. K.*

Using **1** and **2** as starting compounds, we have now been able to prepare **3**, a compound of type **C** in which the amino(imino)phosphane **1** is coordinatively bridged as four-electron donor to two rhenium atoms *via* the imino-N atom and the P atom.




**3**[4] forms yellow-orange crystals which are sensitive to hydrolysis, readily soluble in benzene, moderately soluble in ether, and sparingly soluble in pentane.

The crystal structure analysis[5] shows (Fig. 1) that *trans*-**1** isomerizes to *cis*-**1** through the $\mu$-$\eta^1$,$\eta^1$-coordination of the P=N moiety of the molecule. In the process the NPN angle widens from 104.9°[2] to 122.6°, while the PN bond lengths remain almost unchanged.

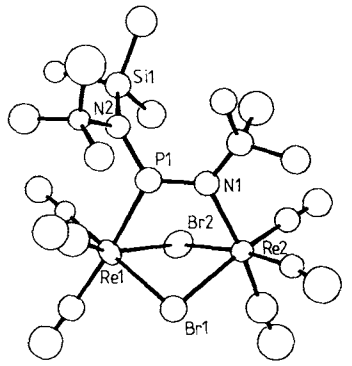



Fig. 1. Structure of **3** in the crystal. Selected bond lengths [Å] and angles [°]: P1–N1 1.56(2), P1–N2 1.66(2), P1–Re1 2.481(6), Re1–Br1 2.626(2), Re1–Br2 2.578(3), Re2–Br1 2.625(2), Re2–Br2 2.631(2), N1–Re2 2.21(2), Re1...Re2 3.603(1), N1–P1–Re1 111.9(7), N1–P1–N2 122.6(9), P1–N1–Re2 119.7(9), P1–N1–C11 121(1), Br1–Re1–Br2 83.74(9), Br1–Re2–Br2 82.75(9), Re1–Br1–Re2 86.67(5), Re1–Br2–Re2 87.53(7). Dihedral angle between the faces Re1Br1Br2 and Re2Br1Br2 134.4; sum of angles at P1: 356.0, N1: 359.7, N2: 359.1.

**3** is the first representative of the class of substances $Re_2(\mu\text{-}Br)_2(CO)_6(\mu\text{-}Ph_nE\text{–}EPh_n)$, E = P, n = 2[3a]; E = S, Se or Te, n = 1[3b], in which the ligand with E–E bridge is replaced by one with a four-electron donor double-bond system (–P=N–). The shortening of the bond length (2.308(6) → 1.56(2) Å) on going from the P–P[3a] to the P–N bridge is so drastic that the molecule compensates for this by the $Re(\mu\text{-}Br)_2Re$ fragment folding itself stronger about the Br–Br axis (angle between the normals to the $ReBr_2$ planes = 45.6° in the case of **3** and 23.4° in the P–P derivative[3a]; the Re...Re distance becomes shorter (**3**: 3.603(1), P–P derivative: 3.890(1) Å[3a]) and the two edge-sharing coupled distorted octahedra are oriented markedly more towards face-sharing coupling (Re...Re distance in the case of the Br face-sharing $[(OC)_3Re(\mu\text{-}Br)_3Re(CO)_3]^-$: 3.46 Å[3c]).

The $^{31}P\{^1H\}$-NMR signal[4b] (200 MHz, $CD_2Cl_2$, $H_3PO_4$ ext.) of **3** (with the *cis*-**1** ligand), with $\delta = 303.4$ is shifted only slightly upfield compared to that of the free ligand *trans*-**1** (327.4[4a]).

Received: July 8, 1983; revised: August 10, 1983 [Z 456 IE]
German version: *Angew. Chem. 95* (1983) 1003

[1] a) S. Pohl, *J. Organomet. Chem. 142* (1977) 185, 195; b) O. J. Scherer, R. Konrad, C. Krüger, Y.-H. Tsay, *Chem. Ber. 115* (1982) 414; c) O. J. Scherer, R. Konrad, E. Guggolz, M. L. Ziegler, *Angew. Chem. 94* (1982) 309; *Angew. Chem. Int. Ed. Engl. 21* (1982) 297; *Angew. Chem. Suppl. 1982*, 730.

[2] S. Pohl, *Angew. Chem. 88* (1976) 723; *Angew. Chem. Int. Ed. Engl. 15* (1976) 687; S. Pohl, *Chem. Ber. 112* (1979) 3159.

[3] a) J. L. Atwood, J. K. Newell, W. E. Hunter, I. Bernal, F. Calderazzo, I. P. Mavani, D. Vitali, *J. Chem. Soc. Dalton Trans. 1978*, 1189; b) F. Calderazzo, D. Vitali, R. Poli, J. L. Atwood, R. D. Rogers, J. M. Cummings, I. Bernal, *ibid. 1981*, 1004; c) R. L. Davis, N. C. Baenziger, *Inorg. Nucl. Chem. Lett. 13* (1977) 475.

[4] **3**: a) **1** (0.3 mL, 1.06 mmol) [O. J. Scherer, N. Kuhn, *Angew. Chem. 86* (1974) 899; *Angew. Chem. Int. Ed. Engl. 13* (1974) 811] is added to a suspension of **2** (600 mg, 0.71 mmol) in $CH_2Cl_2$ (10 mL) at 0°C under argon, stirred for a further 1 h at 0°C (orange solution), and the solvent removed in a vacuum. The residue is taken up in ether (15 mL), filtered over filter-flocks and allowed to crystallize out at *ca.* –90°. Yield 400 mg (60%).—b) $^1$H-NMR (90 MHz, $CH_2Cl_2$, TMS int.): $\delta = 0.34$ (s, 9H, $SiCH_3$), 1.39 (s, 9H, $CCH_3$), 1.74 (s, 9H, $CCH_3$); $^{13}C\{^1H\}$-NMR (200 MHz, $CDCl_2$, TMS int., 253 K): $\delta$(CO on Re(N)): 192.1 (s), 191.8 (s) (2CO); $\delta$(CO on Re(P)): 189.9 (d), *cis*-$^2J_{PC} = 8.5$ Hz; 188.5 (d), *cis*-$^2J_{PC} = 9.1$ Hz; 188.2 (d), *trans*-$^2J_{PC} = 115.7$ Hz; IR (pentane): $\nu$(CO) = 2060 (m), 2035 (s), 2020 (sh), 1980 (m), 1945 (m), 1930 (s), 1920 (s), 1900 (w).

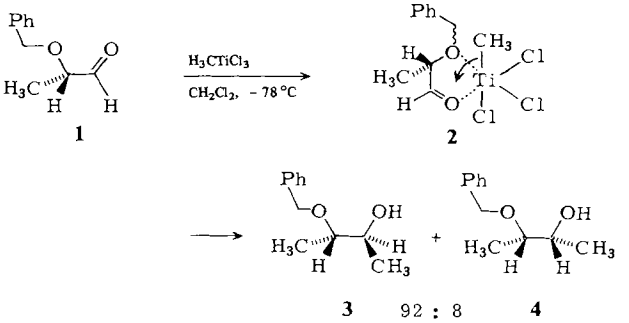
[5] Monoclinic, space group $P2_1$, $Z = 2$; $a = 8.944(2)$, $b = 16.246(3)$, $c = 10.280(3)$ Å, $\beta = 115.86(3)°$; 1846 independent reflections; $R = 0.066$, $R_w = 0.075$. Further details of the crystal structure investigation are available on request from the Fachinformationszentrum Energie Physik Mathematik, D-7514 Eggenstein-Leopoldshafen, on quoting the depository number CSD 50517, the names of the authors, and full citation of the journal.

## Chelation or Non-Chelation Control in Stereoselective Reactions of Titanium Reagents with Chiral Alkoxycarbonyl Compounds**

By *Manfred T. Reetz**, *Kurt Kesseler*, *Susi Schmidtberger*, *Bernd Wenderoth*, and *Rainer Steinbach*

Following the pioneering work of *Cram* on chelation control in Grignard additions involving alkoxycarbonyl compounds[1], a number of publications on this topic have appeared[2]. We wish to report that chelation-controlled 1,2- and 1,4-asymmetric inductions are possible using Lewis acidic titanium reagents, and that diastereoselectivity can be *reversed* by changing the ligands at titanium[3] (non-chelation control). This extends our previous work on 1,3-asymmetric induction involving β-alkoxy aldehydes[10].

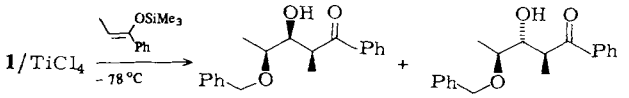
The reaction of the Lewis acidic $H_3CTiCl_3$[3] with aldehyde **1** leads *via* chelate **2** to the adducts **3** and **4** (92 : 8). Chelation mediated 1,2-asymmetric inductions of 90–96% are also observed if **1** is first chelated with $TiCl_4$ and subsequently treated with dialkylzinc, allylsilanes, or silyl enol ethers.




[*] Prof. Dr. M. T. Reetz, K. Kesseler, S. Schmidtberger, Dr. B. Wenderoth, Dr. R. Steinbach
Fachbereich Chemie der Universität
Hans-Meerwein-Strasse, D-3550 Marburg (Germany)

[**] This work was supported by the Deutsche Forschungsgemeinschaft and the Fonds der Chemischen Industrie.

Reaction of the *Z*-configurated trimethylsilyl enol ether of propiophenone with **1**/$TiCl_4$ leads to formation of practically only one (**9**) of the four possible diastereomers; this product, formed *via* chelation control, has *syn*-stereochemistry at the two new chiral centers. Since the *Mukaiyama* aldol addition normally affords mixtures of *syn*/*anti*-adducts[7], an unusual phenomenon is operating. $SnCl_4$ gives the same result.

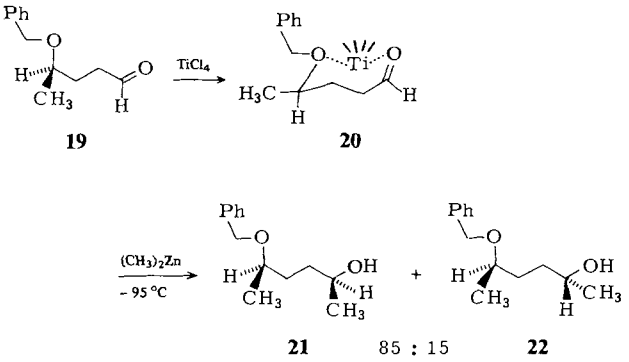



**9** 97 : 3 **10**

With titanium reagents which contain alkoxy- instead of chloro-ligands, *the 1,2-asymmetric induction can be reversed: e.g.*, the weak Lewis acid $H_3CTi(O\text{-}iPr)_3$ **13**[3] reacts with **1** to give **3** and **4** in the ratio 8 : 92. The observed stereoselectivity, which can be accounted for by *Anh*'s model[14], has not been observed previously using any other methylmetal reagents.

**13** allows for this type of control even in complicated cases, *e.g.*, in the reaction with a protected furanose. Reversal of diastereoselectivity is also observed in the addition of the tris(isopropoxy)titanium enolate derived from propiophenone (**9** : **10** = 13 : 87).

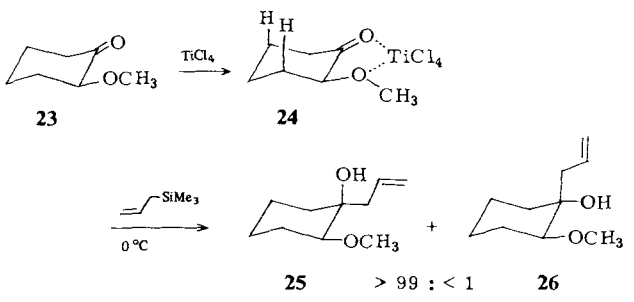
Unusually high 1,4-asymmetric induction is achieved by chelating the γ-benzyloxy aldehyde **19** with $TiCl_4$.




**19** **20**

**21** 85 : 15 **22**

Finally, chelation control is also feasible with the chiral ketone **23**. Presumably, **24** is the intermediate, since allyltrimethylsilane adds to **23** in the presence of $TiCl_4$ to afford practically only **25**. Weakly Lewis acidic reagents such as allylmagnesium chloride or allyltitanium tris(diethylamide) afford only 3 : 1 mixtures of **25** and **26**. Previously, the role played by chelation has only been deduced indirectly from stereochemical information[1,2]. $^1H$- and $^{13}C$-NMR spectroscopic studies of **23** in the presence of $TiCl_4$ suggest formation of the chelate **24** before stereoselective introduction of the allyl moiety.




**23** **24**

**25** > 99 : < 1 **26**

Received: July 27, 1983;
revised: September 5, 1983 [Z 488 IE]
German version: *Angew. Chem. 95* (1983) 1007
The complete version of this communication appears in:
*Angew. Chem. Suppl. 1983*, 1511–1526

[1] D. J. Cram, K. R. Kopecky, *J. Am. Chem. Soc. 81* (1959) 2748; review on stereoselectivity in acyclic systems: P. A. Bartlett, *Tetrahedron 36* (1980) 3.
[2] W. C. Still, J. H. McDonald, *Tetrahedron Lett. 21* (1980) 1031; W. C. Still, J. A. Schneider, *ibid. 21* (1980) 1035, and literature cited therein.
[3] General review on this principle: M. T. Reetz, *Top. Curr. Chem. 106* (1982) 1; see also B. Weidmann, D. Seebach, *Angew. Chem. 95* (1983) 13; *Angew. Chem. Int. Ed. Engl. 22* (1983) 31.
[7] T. Mukaiyama, K. B. Banno, K. Narasaka, *J. Am. Chem. Soc. 96* (1974) 7503; for chelation control in the addition of diketene to a chiral aldehyde see: T. Izawa, T. Mukaiyama, *Chem. Lett. 1978*, 409.
[10] M. T. Reetz, A. Jung, *J. Am. Chem. Soc. 105* (1983) 4833.
[14] N. T. Anh, *Top. Curr. Chem. 88* (1980) 40; other recent examples of Felkin-Anh products: Y. Yamamoto, K. Maruyama, *Heterocycles 18* (1982) 357; W. R. Roush, D. J. Harris, B. M. Lesur, *Tetrahedron Lett. 24* (1983) 2227.

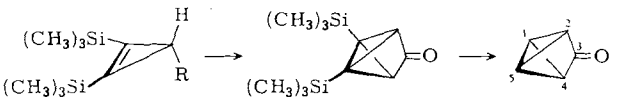
## Tricyclo[2.1.0.$0^{2,5}$]pentan-3-one**

By *Günther Maier**, *Manfred Hoppe*, and *Hans Peter Reisenauer*

*Dedicated to Professor Karl Winnacker on the occasion of his 80th birthday*

The long-sought[1a] title compound **3** is interesting for a number of reasons: Is there, by analogy to the tetra-*tert*-butyl derivative[2], a route from **3** to the unsubstituted tetrahedrane **4**, or does the photoelimination of CO in an argon matrix lead directly to cyclobutadiene **5**? If the latter occurs, can free cyclobutadiene or a CO complex of **5** be detected?

Preparation of **3**: Hydrolysis of methyl 2,3-bis(trimethylsilyl)-2-cyclopropene-1-carboxylate[3a] with chlorotrimethylsilane/sodium iodide yields the carboxylic acid **1a**. Treatment of **1a** with oxalyl bromide leads to formation of the acid bromide **1b**, which—without further purification—can be converted into the diazoketone **1c**. Heating




**1** **2** **3**

**1a**, R = $CO_2H$; **1b**, R = COBr; **1c**, R = $COCHN_2$

**1c** with CuBr gives 1,5-bis(trimethylsilyl)tricyclo[2.1.0.$0^{2,5}$]pentan-3-one **2**. Desilylation of **2** occurs using KF/dibenzo[18]crown-6. Subsequent gas chromatographic separation (OV 101, 100 °C), which is associated with considerable losses, leads to a colorless oil. The spectroscopic data of this product (Table 1), which is stable at room temperature, are consistent with assignment to structure **3**. Here, the $^{13}C$-H coupling constant of C-1/C-5 of

[*] Prof. Dr. G. Maier, M. Hoppe, Dr. H. P. Reisenauer
Institut für Organische Chemie der Universität
Heinrich-Buff-Ring 58, D-6300 Giessen (Germany)

[**] Small Rings. Part 49. This work was supported by the Deutsche Forschungsgemeinschaft.—Part 48: T. Loerzer, R. Machinek, W. Lüttke, L. H. Franz, K.-D. Malsch, G. Maier, *Angew. Chem. 95* (1983) 914; *Angew. Chem. Int. Ed. Engl. 22* (1983) 878.

 © Verlag Chemie GmbH, 6940 Weinheim, 1983 0570-0833/83/1212-0990 $ 02.50/0 

Table 1. **1a—c**, **2**, and **3**: Reaction conditions, yields, and physical and spectroscopic properties: IR [$cm^{-1}$], NMR ($CDCl_3$; $\delta$-values rel. TMS).

**1a**: $CH_3CN$, 20 h, 80°C; 67%; colorless crystals, m.p. = 86—88°C.—IR ($CCl_4$): 1770 (C=C), 1685 (C=O).—$^1$H-NMR: 0.29 (s, 18H), 1.87 (s, 1H); $^{13}$C-NMR: −1.8, 18.1, 124.4, 176.2

**1b**: 30 min, 60°C; colorless oil.—IR (film): 1790, 1750 (C=O).—$^1$H-NMR: 0.30 (s, 18H), 2.34 (s, 1H); $^{13}$C-NMR: −1.7, 33.2, 126.7, 178.0

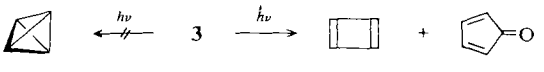
**1c**: Ether, 15 h, −20°C; 32% (rel. to **1a**); yellow oil.—IR (film): 2100 ($CN_2$), 1745 (C=C), 1620 (C=O).—$^1$H-NMR: 0.22 (s, 18H), 2.04 (s, 1H), 4.76 (s, 1H); $^{13}$C-NMR: −1.6, 28.7, 50.6, 127.2, 201.1

**2**: $CHCl_3$, 2 h, 60°C; colorless oil.—IR (film): 1780 (C=O).—$^1$H-NMR: 0.21 (s, 18H), 1.92 (s, 2H); $^{13}$C-NMR: −0.8 ($CH_3$), 0.6 (C-1, C-5), 42.1 (C-2, C-4), 182.7 (C=O).—MS ($C_9H_{17}Si_2$, M−CO−$CH_3$): 181.0868 (calc.), 181.0867 (found)

**3**: $CH_3CN$, 2 h, 25°C; ≈10%; colorless oil.—IR ($CD_3CN$): 1775 (C=O).—$^1$H-NMR: 2.08 (t, 2H, $J$ = 1 Hz), 4.01 (t, 2H, $J$ = 1 Hz); $^{13}$C-NMR: −1.0 (C-1, C-5, $J(^{13}C\text{-}H)$ = 247.4 Hz), 36.6 (C-2, C-4, $J(^{13}C\text{-}H)$ = 189.3 Hz), 184.0 (C=O).—MS($C_4H_4$, M−CO): 52.0317 (calc.), 52.0315 (found)

247.4 Hz, the highest value reported to date, provides particularly significant evidence; this high value arises from the considerable ring strain in **3**[4] and the associated acetylenic character of the C—H bonds involved.

Matrix irradiation of **3**: Photolysis (monochromatic, 240 nm) of **3** in argon at 10 K proceeds slowly. After 16 h, the carbonyl bands typical of **3** [1878 (m), 1853 (w), 1829 (m), 1810 (vs), 1792 (m), 1729 (m), 1779 (s) $cm^{-1}$] disappear to 70%. Instead, absorptions for CO [2138 (s) $cm^{-1}$], cyclobutadiene **5** [1241 (m), 721 (vw), 571 (s) $cm^{-1}$], cyclopentadienone[3b] **6** [1727, 1724, 1332, 1136, 822 $cm^{-1}$], and acetylene [secondary product from **5**: 3270, 730—750 $cm^{-1}$] are observed.




**4** **5** **6**

Conclusion: Irradiation of tricyclopentanone **3** gives no evidence[5] to suggest formation of tetrahedrane **4**: cyclobutadiene **5** is formed as the major product. Since the CO band occurs at the frequency expected, the presence of a complex[3c] of cyclobutadiene with CO—which would be consistent with theoretical considerations[1b]—is precluded.

Received: July 28, 1983 [Z 494 IE]
German version: *Angew. Chem.* 95 (1983) 1009

CAS Registry number:
**1a**, 87883-31-6; **1b**, 87883-32-7; **1c**, 87883-33-8; **2**, 87883-34-9; **3**, 31519-30-9; **5**, 1120-53-2; **6**, 13177-38-3; methyl 2,3-bis(trimethylsilyl)-2-cyclopropene-1-carboxylate, 26208-99-1; acetylene, 74-86-2.

[1] a) W.-D. Stohrer, R. Hoffmann, *J. Am. Chem. Soc.* 94 (1972) 1661; b) A. Schweig, W. Thiel, *Tetrahedron Lett. 1978*, 1841; *J. Comput. Chem. 1* (1980) 129; K. B. Lipkowitz, *J. Am. Chem. Soc. 100* (1978) 7535.

[2] G. Maier, S. Pfriem, U. Schäfer, K.-D. Malsch, R. Matusch, *Chem. Ber. 114* (1981) 3965.

[3] a) G. Maier, M. Hoppe, H. P. Reisenauer, C. Krüger, *Angew. Chem. 94* (1982) 445; *Angew. Chem. Int. Ed. Engl. 21* (1982) 437; *Angew. Chem. Suppl. 1982*, 1061; b) H. W. Lage, H. P. Reisenauer, G. Maier, *Tetrahedron Lett. 23* (1982) 3893; c) G. Maier, U. Schäfer, W. Sauer, H. Hartan, J. F. M. Oth, *ibid. 1978*, 1837.

[4] a) M. Christl, *Chem. Ber. 108* (1975) 2781; b) M. Christl, H.-J. Lüddeke, A. Nagyrevi-Neppel, G. Freitag, *ibid. 110* (1977) 3745; c) M. Christl, R. Herbert, *ibid. 112* (1979) 2022; d) in tricyclo[2.1.0.0$^{2,5}$]pentane [G. D. Andrews, J. E. Baldwin, *J. Am. Chem. Soc. 99* (1977) 4851] the $^{13}$C-H coupling constant of C-1/C-3 of 210 Hz certainly corresponds to the expectation value but not the chemical shift of this C-atom ($\delta$ = 20.8), which in comparison to **3** and the numerous bicyclobutane derivatives investigated by *Christl* appears at extremely low field.

[5] A weak band at 927 $cm^{-1}$ cannot be assigned to any of the products mentioned. It is curious that tetrahedrane **4** should exhibit its only intense IR absorption in this region (940 $cm^{-1}$): J. M. Schulman, J. Venanzi, *J. Am. Chem. Soc. 96* (1974) 4739.

## Synthesis and Structure of $[Na(tmeda)_2]^{\oplus}[HNi_2(C_2H)_4]^{\ominus}$**

By *Klaus Richard Pörschke*, Wolfgang Kleimann, Günther Wilke, Karl Heinz Claus,* and *Carl Krüger*

Tris(ethene)nickel(0) **1**[2] reacts below −70°C with alkali metal trialkyl(hydrido)aluminates and -gallates in diethyl ether/tetrahydrofuran (THF) or ether/amine mixtures as solvent to afford the yellow, crystalline, thermally labile compounds $[M_A(n\text{-donor})_n]^{\oplus}[R_3M'\text{—}H\text{—}Ni(C_2H_4)_2]^{\ominus}$ **2** ($M_A$ = Li, Na; M' = Al, Ga; R = Me, Et, *i*Bu)[1]. Above −70°C in ether/*N,N,N',N'*-tetramethylethylenediamine (tmeda), the alkali metal-μ-hydridotetrakis(ethene)diniccolate(0) complexes **3** and **4** are formed by release of the $R_3M'$-solvate complexes.

$$2\ Ni(C_2H_4)_3 + M_AHAlR_3 \xrightarrow[-40\,°C]{\text{Ether/tmeda}} [M_A(tmeda)_2]^{\oplus}[HNi_2(C_2H_4)_4]^{\ominus} + 2\ C_2H_4 + AlR_3\cdot Solv$$

**1**

**3**, $M_A$ = Li
**4**, $M_A$ = Na

R = Me, Et, *i*Bu

The lithium compound **3** was obtained as a sparingly soluble, yellow precipitate from ether, and the sodium compound **4** could be isolated as yellow-brown crystals. Both salts were characterized by elemental analysis, NMR spectra, and by their reactions, and the structure of **4** was determined by X-ray structure analysis. The compounds are particularly interesting since the nickel atoms are only coordinated by ethene and a hydride ion[3].

Both in solution and in the solid state the ion pairs **3** and **4** are stable only below −20°C. NMR spectra indicate that tmeda is released from the complex cations upon its dissolution in THF. Reaction with alcohols leads to hydrogenation of the ethene to afford ethane, without formation of free hydrogen. The presence of the hydride hydrogen is confirmed by the formation of methane from methylating agents such as methyl iodide or dimethyl sulfate.

In **3** and **4** the ethene is relatively strongly bonded. It cannot be displaced by norbornene, and no exchange with free ethene is observed by $^1$H-NMR spectroscopy. However, with cyclooctatetraene the ethene is liberated quantitatively. **3** reacts with CO in ether at −70°C to give yellow $[Li(tmeda)_2]^{\oplus}[HNi_2(CO)_6]^{\ominus}$ **5**. Compounds with the same complex anion are known[1,4], and its existence has previously been proved by X-ray crystallography[4]. In contrast to the binuclear niccolates **3** and **4**, the fragment $[(C_2H_4)_2NiH]^{\ominus}$—in accord with theoretical considerations[8]—readily adds ethene.

The low temperature 400 MHz $^1$H-NMR and 100.6 MHz $^{13}$C-NMR spectra are consistent with a trigonal-planar coordination of the nickel atoms by two ethene ligands

[*] Dr. K. R. Pörschke, Dr. W. Kleimann, Prof. Dr. G. Wilke, K. H. Claus, Prof. Dr. C. Krüger
Max-Planck-Institut für Kohlenforschung
Postfach 01 13 25, D-4330 Mülheim a. d. Ruhr 1 (Germany)

[**] The Lewis Acidity of Nickel(0), Part 5.—Part 4: [1].

and a hydride ligand, with the ethene C atoms in the coordination plane. The strong shielding of the ethene C and H atoms of **4**, the chemical shifts of which are similar to the values found for $[Li(tmeda)_2]^{\oplus}[CH_3Ni(C_2H_4)_2]^{\ominus}$ **9**[6,9] in $[D_8]$THF, indicates that the extent of charge transfer from the hydride H atom to the bis(ethene)nickel(0) groups is greater than that from the hydridoaluminate group in **2**.

The crystal structure analysis of **4** indicates that the individual ions of the ion pair are present as separate entities. In the anion, two precisely trigonal-planar bis(ethene)nickel(0) moieties are linked *via* a hydride bridge. The angle between the coordination planes is 95.1°. The average values of the lengths of the Ni–C bonds (1.986(9) Å) and the complexed C=C bonds (1.412(8) Å) correspond to the values expected. The hydride H atom can be localized unequivocally and its parameters refined. The Ni–H–Ni unit is not linear, and a Ni–Ni distance of 2.596(1) Å is found; the electron deformation density indicates the presence of a metal-metal interaction.

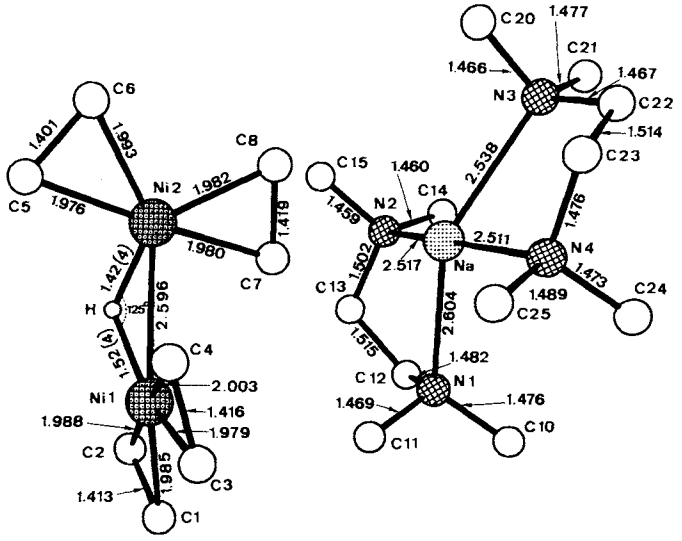



Fig. 1. Crystal structure of the ion pair **4**. Space group $P2_1/c$, $a=9.021(2)$, $b=16.949(6)$, $c=17.559(2)$ Å, $\beta=103.43(2)°$, $Z=4$. 11332 of the diffractometer data (4103 unobserved, $2\sigma$) collected at 100 K were used to solve the structure ($R=0.050$, $R_w=0.054$). This data set is the basis for a detailed investigation of the electron density distribution in **4** in combination with theoretical considerations. Further details on the crystal structure analysis can be obtained from the Fachinformationszentrum Energie Physik Mathematik, D-7514 Eggenstein-Leopoldshafen, by quoting the depository number CSD 50622, the names of the authors, and the journal citation.

The geometry of the Ni–H–Ni three-centered bond system corresponds both to that of the carbonyl complex $[(Ph_3P)_2N]^{\oplus}[HNi_2(CO)_6]^{\ominus}$ (Ni–Ni 2.864(3) Å)[4] and to that of the isoelectronic, doubly H-bridged phosphane complex $[\{(C_6H_{11})_2P(CH_2)_3P(C_6H_{11})_2\}NiH]_2$ (Ni–Ni 2.441(1) Å).

Received: September 12, 1983 [Z 545 IE]
German version: *Angew. Chem. 95* (1983) 1032
The complete version of this communication appears in: *Angew. Chem. Suppl. 1983*, 1527–1536

[1] W. Kleimann, K. R. Pörschke, G. Wilke, *Chem. Ber.*, in press.
[2] K. Fischer, K. Jonas, G. Wilke, *Angew. Chem. 85* (1973) 620; *Angew. Chem. Int. Ed. Engl. 12* (1973) 565.
[3] Compounds **3** and **4** have already been discussed in a review article: K. Jonas, C. Krüger, *Angew. Chem. 92* (1980) 513; *Angew. Chem. Int. Ed. Engl. 19* (1980) 520.
[4] G. Longoni, M. Manassero, M. Sansoni, *J. Organomet. Chem. 174* (1979) C41.
[6] K. Jonas, K. R. Pörschke, C. Krüger, Y.-H. Tsay, *Angew. Chem. 88* (1976) 682; *Angew. Chem. Int. Ed. Engl. 15* (1976) 621.
[9] K. R. Pörschke, K. Jonas, G. Wilke, R. Benn, R. Mynott, R. Goddard, C. Krüger, *Chem. Ber.*, in press.

## Activity of Coordinated 1,4-Diaza-1,3-dienes (dad) in C-C Bond Forming Reactions: 1,5-Dihydropyrrol-2-ones from (dad)$Fe(CO)_3$ and Dimethyl Acetylenedicarboxylate**

By *Hans-Werner Frühauf*, Frank Seils, Maria J. Romao,* and *Richard J. Goddard*

Reactions of 1,4-diaza-1,3-dienes (dad) coordinated to transition metals in which C-C bonds are formed have hitherto only been observed for binuclear complexes $(dad)M_2(CO)_6$ of, *e.g.*, molybdenum and particularly of ruthenium[4]. In the latter, the authors[4] claim that the unsymmetrical 6e-coordination mode of the dad system in these complexes, which we first described for the corresponding iron complexes[2], is crucial for the activation of dad for C-C bond formation.

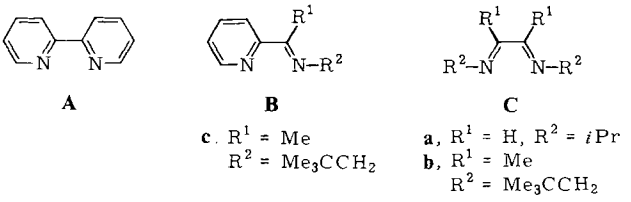



Fig. 1. 1,4-Diaza-1,3-diene (dad) ligand types and examples of substituents.

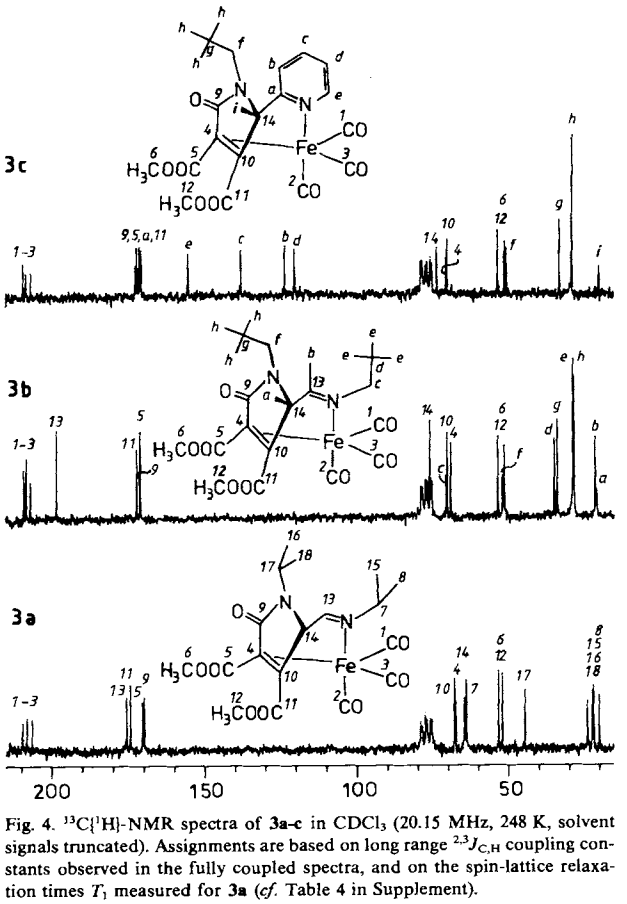
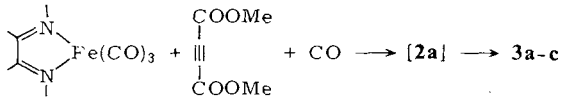



Fig. 4. $^{13}C\{^1H\}$-NMR spectra of **3a-c** in $CDCl_3$ (20.15 MHz, 248 K, solvent signals truncated). Assignments are based on long range $^{2,3}J_{C,H}$ coupling constants observed in the fully coupled spectra, and on the spin-lattice relaxation times $T_1$ measured for **3a** (*cf.* Table 4 in Supplement).

[*] Prof. Dr. H.-W. Frühauf, F. Seils
FB 6, Fachgebiet Organische Chemie der Universität—Gesamthochschule
Bismarckstrasse 90, D-4100 Duisburg 1 (Germany)
M. J. Romao [+], Dr. R. J. Goddard [+]
Max-Planck-Institut für Kohlenforschung
Lembkestrasse 5, D-4330 Mülheim a. d. Ruhr (Germany)
[+] X-Ray structure analysis

[**] This work was supported by the Fonds der Chemischen Industrie.

Treatment of compounds **1a-c** of dad-type B or C (cf. Fig. 1) with dimethyl acetylenedicarboxylate under CO gives 1,5-dihydropyrrol-2-ones as their $Fe(CO)_3$-complexes **3a-c**. At elevated temperatures the synthetically interesting heterocycles can, *e.g.* from **3a**, be displaced by adding dad and regenerating the starting tricarbonyl **1a** (see Fig. 4 for formulas **3a-c**).



**1a-c**

(dad)$Fe(CO)_3$

The reaction clearly demonstrates that C-C bond formation is also feasible for dad coordinated to a transition metal solely through the nitrogen lone pairs; the above mentioned 6e-coordination mode, which involves the π-electrons of one C=N moiety, is not a necessary prerequisite.

The structure of **3a** was solved by single crystal X-ray analysis. According to their spectroscopic (cf. Fig. 4 and Table 5) and other properties, the structures of **3b** and **3c** resemble that of **3a**. Despite this, there are marked differences in the product forming reactions. Whereas **3b** and **3c**

Table 5. IR bands $\nu$ (C≡O) stretches for **3a-c**: in $CHCl_3$.

| Compd. | $\nu$ (C≡O) [$cm^{-1}$] [a] |
|---|---|
| **3a** | 2064, 2003, 1981 |
| **3b** | 2060, 1998, 1980 |
| **3c** | 2063, 2002, 1983 |

[a] Wavenumber calibration by DCl gas; precision better ±0.5 $cm^{-1}$.

are formed without observable intermediates, **3a** results from rearrangement of an isomeric precursor **2a**, which could be isolated in pure crystalline form below 0°C and characterized spectroscopically and by elemental analysis.

Received: September 9, 1983 [Z 544 IE]
German version: *Angew. Chem. 95* (1983) 1014
The complete manuscript of this communication appears in:
*Angew. Chem. Suppl. 1983*, 1435-1450

[2] H.-W. Frühauf, A. Landers, R. Goddard, C. Krüger, *Angew. Chem. 90* (1978) 56; *Angew. Chem. Int. Ed. Engl. 17* (1978) 64.
[4] G. van Koten, K. Vrieze, *Adv. Organomet. Chem. 21* (1982) 151.

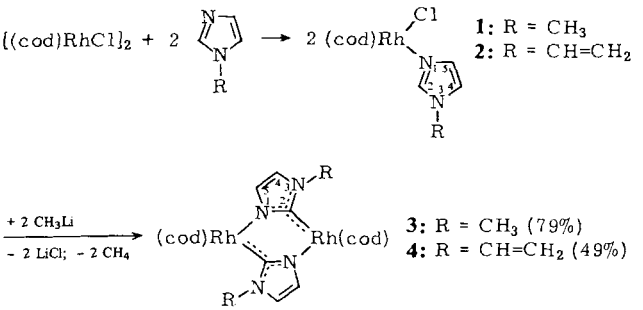
## Conversion of Imidazole into μ-2,3-Dihydro-1*H*-imidazole-1,2,2-triyl Ligands**

By *Jörn Müller** and *Rainer Stock*

*Dedicated to Professor Ernst Otto Fischer on the occasion of his 65th birthday*

Binuclear bis($\eta^4$-cyclodiene-μ-chlororhodium) complexes can be cleaved by suitable P and N donor ligands L into mononuclear species ($\eta^4$-cyclodiene)Rh(L)Cl. Thus, reaction of $[(cod)RhCl]_2$[1] (cod = 1,5-cyclooctadiene) with $P(CH_3)_3$ affords the compound $(cod)Rh[P(CH_3)_3]Cl$, which can readily be converted into $(cod)Rh[P(CH_3)_3]CH_3$ with methyllithium[2].

By analogy, the reactions of $[(cod)RhCl]_2$ with 1-methyl- or 1-vinylimidazole (molar ratio 1:2) in tetrahydrofuran (THF) give the complexes **1** and **2** (**1** has already been described[3] but incompletely characterized). Surprisingly, the action of $CH_3Li$ on **1** and **2** in *n*-hexane does not lead to isolation of the expected $(cod)Rh(L)CH_3$ species; rather, they eliminate methane to form the binuclear complexes **3** and **4**, in which, for the first time, μ-2,3-dihydro-1*H*-imidazole-1,2,2-triyl ligands occur *via* orthometalation of the 2-position of the imidazole rings.



**1**: R = $CH_3$
**2**: R = $CH=CH_2$

**3**: R = $CH_3$ (79%)
**4**: R = $CH=CH_2$ (49%)

The orange-red compounds **3** and **4** decompose without melting only at temperatures above 200°C. Whereas **1** and **2** decompose in the reverse way to their mode of formation when it is attempted to volatilize them in the mass spectrometer, high intensity peaks of the molecular ions of **3** and **4** appear under EI conditions (70 eV) (**3**: *m/z* 584; **4**: *m/z* 608).

The $^1H$- and $^{13}C$-NMR spectra of **3** and **4** are consistent with a $C_i$ symmetry for the complexes, *i.e.* the ligand spheres of the two Rh atoms are not coplanar ($C_{2h}$ symmetry). If the ligand configuration expected for four-coordinated rhodium(I) is assumed, the observed $C_i$ symmetry suggests a pyramidal geometry, at least for the $N^1$ atoms of the bridging ligands; a planar RhCNRhCN six-membered ring with slightly tilted cod ligands would be a conceivable structural alternative.

The signals for $H^2$ ($\delta$ *ca.* 8.3) in **1** and **2** are absent in **3** and **4**. The carbene character of $C^2$ in **3** and **4** expresses itself in a large shift of the $^{13}C$-NMR signal by *ca.* 40 ppm to low field relative to the signal of $C^2$ in **1** and **2** ($\delta$ values in [$D_8$]THF): **3** 180.8; **4** 184.0 ppm); at the same time, in **3** and **4** a large $^{103}Rh$-$C^2$ coupling of *ca.* 51 Hz is found. In contrast to **3** and **4**, in solution **1** and **2** exhibit dynamic behavior, which results in a marked broadening and coalescence, respectively, of the olefinic cod-NMR signals.

In **3** and **4** the valence shells of the Rh atoms have only 16 electrons. The mode of formation of the compounds *via* an orthometalation is related to the thermolysis of 1,3-dimethylimidazolium pentacarbonylhydridochromate(1−), which *via* elimination of $H_2$ led to the first metal complex of 1,3-dimethyl-2,3-dihydro-1*H*-imidazole-2-ylidene[4].

Received: March 9, 1983 [Z 309 IE]
Publication delayed at the authors' request
German version: *Angew. Chem. 95* (1983) 1000
The complete manuscript of this communication appears in:
*Angew. Chem. Suppl. 1983*, 1537–1542

[*] Prof. Dr. J. Müller, R. Stock
Institut für Anorganische und Analytische Chemie
der Technischen Universität
Strasse des 17. Juni 135, D-1000 Berlin 12 (Germany)

[**] This work was supported by the Fonds der Chemischen Industrie.

[1] J. Chatt, L. M. Venanzi, *J. Chem. Soc. 1957*, 4735.
[2] J. Müller, R. Stock, unpublished results.
[3] G. Zassinovich, G. Mestroni, A. Camus, *J. Organomet. Chem. 91* (1975) 379.
[4] K. Öfele, *J. Organomet. Chem. 12* (1968) P42.

## Lithium Complexes with *pentahapto*-Bonded Cyclopentadienyl Ligands

By *Peter Jutzi**, *Ewald Schlüter*, *Carl Krüger*, and *Siegfried Pohl*

*Dedicated to Professor Ernst Otto Fischer on the occasion of his 65th birthday*

According to MO calculations, cyclopentadienyllithium $C_5H_5Li$ has a pentagonal-pyramidal structure[1], and is thus the simplest metallocene[1a]. Experimentally there is spectroscopic evidence for a structural element of this type for solutions of $C_5H_5Li$ in donor solvents[2], but the isolation and unequivocal characterization of such species have not yet been described[3]. Addition of the mono-, di-, and tridentate nitrogeneous bases quinuclidine, tetramethylethylenediamine (tmeda), and pentamethyldiethylenetriamine (pmdeta), respectively, to a solution of tris(trimethylsilyl)cyclopentadienyllithium **1**[4] in hexane leads to isolation of the air-sensitive, crystalline 1:1 adducts **2a—c**. These compounds are also readily soluble in hexane and, according to molecular weight determinations using cryoscopic methods, exist as monomers in benzene[5a].

| | | Base | M.p. [°C] |
|---|---|---|---|
| $(Me_3Si)_3C_5H_2Li \cdot$base | **2a** | quinuclidine | 86 |
| | **2b** | tmeda | 124 |
| | **2c** | pmdeta | 79 |

The X-ray crystal structure analyses of **2b** and **2c**[5b] indicate that in each case the cyclopentadienyl ring is $\eta^5$-coordinated to the alkali metal atom[6]. The structures of the complexes **2b** and **2c** are very similar since in the latter only two nitrogen atoms of the potentially tridentate base pmdeta are coordinated to the lithium atom (Fig. 1).

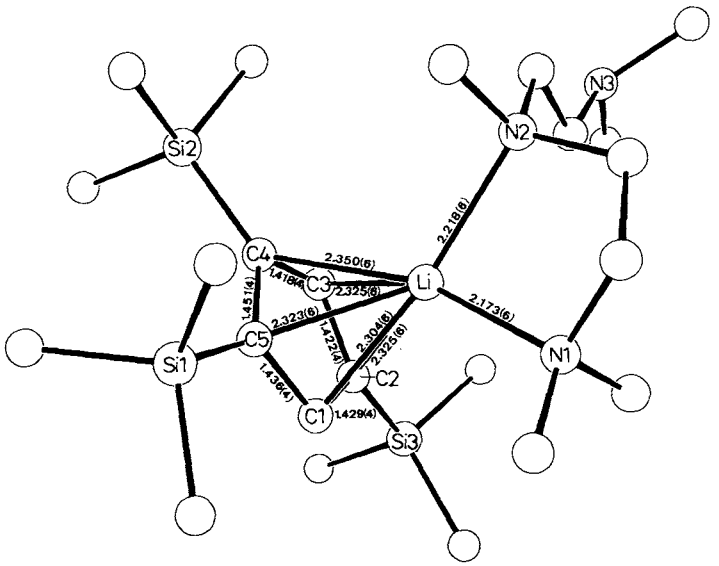



Fig. 1. Crystal structure of the lithium compound **2c**.

[*] Prof. Dr. P. Jutzi, E. Schlüter, Priv. Doz. Dr. S. Pohl
Fakultät für Chemie der Universität
Postfach 8640, D-4800 Bielefeld 1 (Germany)
Prof. Dr. C. Krüger
Max-Planck-Institut für Kohlenforschung
Postfach 011325, D-4330 Mülheim a. d. Ruhr 1 (Germany)

So far, the base-free compound **1** has only been obtained in X-ray amorphous form. Mass spectroscopic studies indicate that in the gas phase **1** is monomeric.

Received: September 10, 1983 [Z 557 IE]
German version: *Angew. Chem. 95* (1983) 1015

CAS Registry numbers:
**2a**, 87870-96-0; **2b**, 87870-97-1; **2c**, 87870-98-2.

[1] a) S. Alexandratos, A. Streitwieser Jr., H. F. Schaefer III, *J. Am. Chem. Soc. 98* (1976) 7959; b) E. D. Jemmis, P. von R. Schleyer, *ibid. 104* (1982) 4781.

[2] R. H. Cox, H. W. Terry Jr., L. W. Harrison, *J. Am. Chem. Soc. 93* (1971) 3297; P. Fischer, J. Stadelhofer, J. Weidlein, *J. Organomet. Chem. 116* (1976) 65.

[3] G. Stucky, *Adv. Chem. Ser. 130* (1974) 85.

[4] P. Jutzi, R. Sauer, *J. Organomet. Chem. 50* (1973) C29.

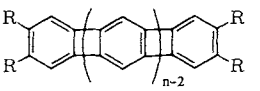
[5] a) $^1$H-NMR spectra ($C_6D_6$): **2a**: $\delta(SiCH_3)=0.38$ (s, 9H) and 0.48 (s, 18H), $\delta(CH_{quinuclidine})=0.9-2.2$ (m, 13H), $\delta(C_5H_2)=6.88$ (s, 2H); **2b**: $\delta(SiCH_3)=0.37$ (s, 9H) and 0.51 (s, 18H), $\delta(NCH_2)=1.44$ (s, 4H), $\delta(NCH_3)=1.75$ (s, 12H), $\delta(C_5H_2)=6.8$ (s, 2H); **2c**: $\delta(SiCH_3)=0.40$ (s, 9H) and 0.53 (s, 18H), $\delta(NCH_2, NCH_3)=1.91-2.19$ (m, 23H), $\delta(C_5H_2)=6.89$ (s, 2H).—b) Crystal data: **2b**: $P2_1/c$, $a=13.952(4)$, $b=32.755(9)$, $c=12.317(4)$ Å, $\beta=101.08°$, $V=5523.9$ Å$^3$, $\rho_{calc}=0.97$ g·cm$^{-3}$, $Z=8$, 8047 reflections, 4333 of which are observed ($I>2\sigma(I)$, refined parameters: 459, $R=0.108$, $R_w=0.109$; **2c**: $P2_1/n$, $a=12.3897(8)$, $b=17.235(1)$, $c=14.7806(5)$ Å, $\beta=92.58(9)°$, $V=3152.95$ Å$^3$, $\rho_{calc}=0.9708$ g·cm$^{-3}$, $Z=4$, $\mu=14.73$ cm$^{-1}$ (absorption correction, $\lambda_{Cu}=1.54179$ Å), 6552 reflections, 3996 of which are observed ($I>2\sigma(I)$), refined parameters: 475, $R=0.0542$, $R_w=0.0635$. Further details on the crystal structure analysis can be obtained from the Fachinformationszentrum Energie Physik Mathematik, D-7514 Eggenstein-Leopoldshafen by quoting the depository number CSD 50638, the names of the authors, and the journal citation.

[6] The compound $Me_3SiC_5H_4Li \cdot$tmeda has a structure similar to that of **2b** and **2c**: M. F. Lappert, A. Singh, A. H. White, personal communication.

## The Structure and Reactivity of 2,3,7,8-Tetrakis(trimethylsilyl)terphenylene***, a Novel Linear Multiphenylene**

By *George H. Hovakeemian* and *K. Peter C. Vollhardt**

We recently reported[1] an iterative approach to the synthesis of the theoretically interesting linear multiphenylenes **1** and **2**[2] using a synthetic sequence involving both palladium and cobalt as catalysts.




**1**, R = H, n = 3
**2**, R = $(CH_3)_3Si$, n = 3

The central benzene ring in **1** and **2** is extraordinarily reactive, undergoing complete and all-*cis* hydrogenation, in the case of R = H faster than cycloheptene[1]. We now report further unusual transformations of **2** together with its X-ray structure.

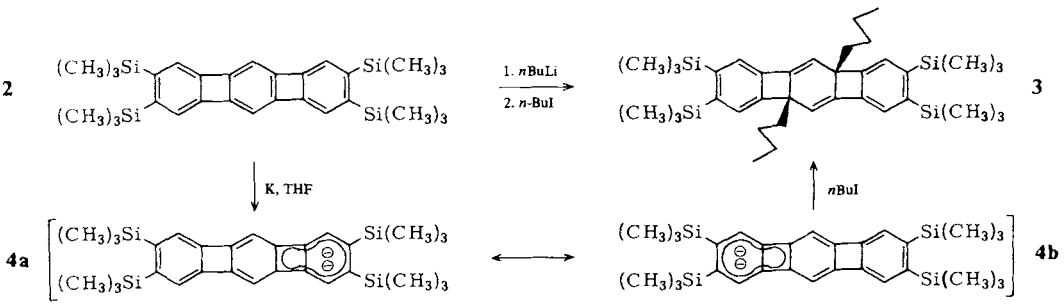
In order to pinpoint the acidity[3] of the H atoms of the central benzene ring, **2** was treated with *n*-butyllithium in tetrahydrofuran (THF) at −78 °C. A blue solution ensued

[*] Prof. Dr. K. P. C. Vollhardt, Dr. G. H. Hovakeemian
Department of Chemistry, University of California, Berkeley
and the Materials and Molecular Research Division,
Lawrence Berkeley Laboratory
Berkeley, CA 94720 (USA)

[**] This work was supported by the National Institutes of Health (CA 20713). *K. P. C. V.* is a Camille and Henry Dreyfus Teacher-Scholar (1978—1983). *G. H. H.* is on sabbatical leave from the University of Kuwait. The X-ray structural analyses were carried out by Dr. *F. J. Hollander*, staff crystallographer.

[***] According to IUPAC rules the title compound would be 2,3,7,8-tetrakis(trimethylsilyl)cyclobutabenzo[1,2-*b*]biphenylene.

 © *Verlag Chemie GmbH, 6940 Weinheim, 1983* *0570-0833/83/1212-0994 $ 02.50/0* 




which when quenched with *n*-butyl iodide gave the very strained *cis*-dibutyl adduct **3** in 81% yield (m.p. 165.5–166°C), whose structure was ascertained by X-ray crystallography. Other combinations of alkyllithium and alkylating reagents effected similar double additions.

Remarkable also was the reduction of **2** to the dianion **4**, a transformation which converts a neutral $[4n+2]\pi$-system into a [4n] polycyclic dianion. Exposure of the orange-red starting material to a potassium mirror in $[D_8]$THF instantly produced an emerald green solution of the presumed radical anion, which turned red-brown on further reduction to **4**. Despite the $[4n]\pi$-system and the addition of two negative charges, the chemical shift of the central benzene protons increased (from $\delta=6.34$ to $\delta=6.52$), whereas that on the outside ring decreased only slightly (from $\delta=6.75$ to $\delta=6.23$). An explanation for this astonishing behavior might be found within the framework of other results concerned with the problem of aromaticity in polycyclic ions[4], which indicate that such systems tend to maximize the development of aromatic circuits at the expense of those involving only the periphery. Thus, resonance structures such as **4a** and **4b** might be strong contributors to the ground state of the molecule, diamagnetic ring currents offsetting the charge effect. Protonation of **4** ($CH_3OH$, $H_2O$) gave a white solid, which on exposure to air instantly reformed **2**, indicating a considerable driving force for re-aromatization. On the other hand, butylation gave **3**.

Because of its unusual reactivity, an X-ray structural analysis of **2** was undertaken (Fig. 1)[5]. The molecule contains a crystallographic inversion center in the middle of the central ring. Although basically flat, it deviates significantly from planarity. The $Me_3Si$ group at C2 is bent by 0.27 Å out of the plane defined by C3C2C1C6. Relevant bond lengths and angles are compiled in Table 1.

In comparison with the structures of 1,2-dihydro-4,5-bis(trimethylsilyl)cyclobutabenzene[6a] and biphenylene[6b], several features are unusual. First, the unreactive outer benzene rings exhibit considerably more pronounced bond fixation than the model compounds, and are in the order of that found in the antiaromatic 1,2-di-*tert*-butyl-3,4,5,6-tetramethylcyclobutabenzene[6a]. Second, the bonds of the fused four-membered ring are remarkably short, particularly compared to those in biphenylene, and are very similar in length to those found in benzene itself. Third, the reactive central six-membered ring shows very little bond alternation, being best described as two strongly interacting allyl units.

The structure-activity relationships described here suggest that multiphenylenes are not simply extended biphenylenes, but indeed novel $\pi$-systems with unusual properties.

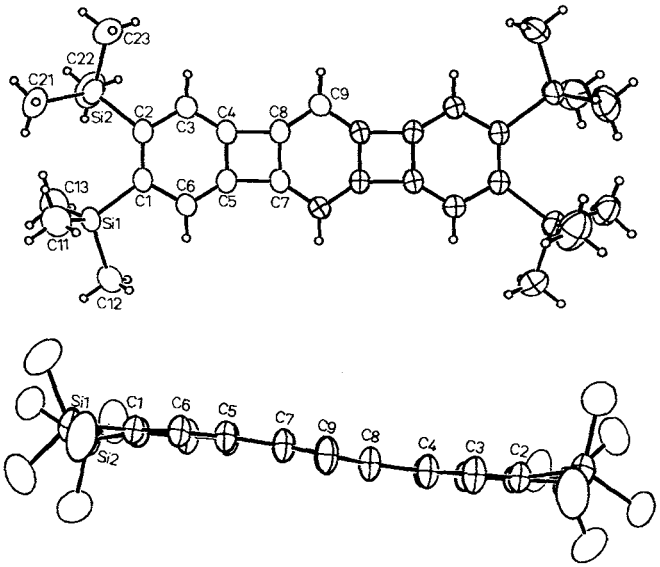



Fig. 1. Crystal structure of **2**. Top: frontal view; bottom: side-view. The numbering does not follow IUPAC rules but the requirements of the X-ray structure analysis.

Table 1. Selected bond lengths and bond angles for **2**. Estimated standard deviations are shown in parenthesis.

| Bond lengths [Å] | | Bond angles [°] | |
|---|---|---|---|
| Si1C1 | 1.891(1) | Si1C1C2 | 127.73(9) |
| Si1C11 | 1.855(2) | Si1C1C6 | 112.52(9) |
| Si1C12 | 1.868(2) | Si2C2C1 | 128.46(9) |
| Si1C13 | 1.861(2) | Si2C2C3 | 111.06(9) |
| Si2C2 | 1.907(1) | C2C1C6 | 119.75(11) |
| Si2C21 | 1.859(2) | C1C2C3 | 120.05(11) |
| Si2C22 | 1.865(2) | C2C3C4 | 118.07(12) |
| Si2C23 | 1.864(2) | C1C6C5 | 118.32(11) |
| C1C2 | 1.397(2) | C3C4C5 | 122.01(11) |
| C2C3 | 1.436(2) | C4C5C6 | 121.74(11) |
| C1C6 | 1.441(2) | C5C4C8 | 90.22(10) |
| C3C4 | 1.359(2) | C4C5C7 | 90.14(10) |
| C5C6 | 1.356(2) | C5C7C8 | 89.89(10) |
| C4C5 | 1.397(2) | C4C8C7 | 89.72(10) |
| C4C8 | 1.513(2) | C7C8C9 | 124.02(12) |
| C5C7 | 1.512(2) | C8C7C9 | 124.04(11) |
| C7C8 | 1.407(2) | C8C9C7 | 111.94(12) |
| C8C9 | 1.385(2) | C3C4C8 | 147.58(13) |
| C7C9 | 1.385(2) | C6C5C7 | 147.91(12) |
| | | C4C8C9 | 146.10(12) |
| | | C5C7C9 | 145.96(12) |

Received: May 18, 1983;
revised: September 19, 1983 [Z 390 IE]
German version: *Angew. Chem.* 95 (1983) 1001

CAS Registry numbers:
**2**, 87710-30-3; **3**, 87884-51-3.

[1] B. C. Beris, G. H. Hovakeemian, K. P. C. Vollhardt, *J. Chem. Soc. Chem. Commun. 1983*, 502.
[2] J. W. Barton, D. J. Rowe, *Tetrahedron Lett. 24* (1983) 299.
[3] K. P. C. Vollhardt, *Pure Appl. Chem. 52* (1980) 1645; R. P. Thummel, *Isr. J. Chem. 22* (1982) 11.
[4] M. Rabinovitz, I. Willner, A. Minsky, *Acc. Chem. Res. 16* (1983) 298.
[5] Monoclinic, $P2_1/c$, $a=6.6856(9)$, $b=9.5412(9)$, $c=25.1327(29)$ Å, $\beta=96.446(10)°$, $V=1593.0(6)$ Å$^3$ at 25°C, $Z=2$, $\rho_{calc}=1.074$ g cm$^{-3}$, $\mu_{calc}=1.96$ cm$^{-1}$; $Mo_{K\alpha}$ radiation: (graphite monochromator); scan range $=3° \le 2\theta \le 55°$; reflections collected $=4169$; 3650 unique with $F^2 > 3\sigma(F^2)$, $R=3.87$, $R_w=5.62$. Further details of the crystal structure investigation can be obtained on request from the Fachinformationszentrum Energie Physik Mathematik, D-7514 Eggenstein-Leopoldshafen, by quoting the depository number CSD 50611, the names of the authors, and the journal citation.
[6] a) K. P. Moder, E. N. Duesler, N. J. Leonard, *Acta Crystallogr. B36* (1981) 289; b) A. Yokozeki, C. F. Wilcox, Jr., S. H. Bauer, *J. Am. Chem. Soc. 96* (1974) 1026; c) W. Winter, T. Butters, *Acta Crystallogr. B37* (1981) 1524.

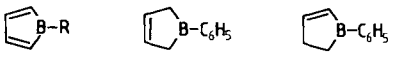
## A Novel and General Route to ($\eta^5$-Borole)metal Complexes: Compounds of Manganese, Ruthenium, and Rhodium**

By *Gerhard E. Herberich*, Bernd Hessner, Wilfried Boveleth, Herbert Lüthe, Roland Saive,* and *Ljerka Zelenka*

*Dedicated to Professor Ernst Otto Fischer on the occasion of his 65th birthday*

As four-electron ligands, boroles **1** are able to form transition metal complexes with *closo*- and *nido*-structures[3]. Such complexes are sparsely documented and have hitherto only been accessible *via* specific synthetic routes.

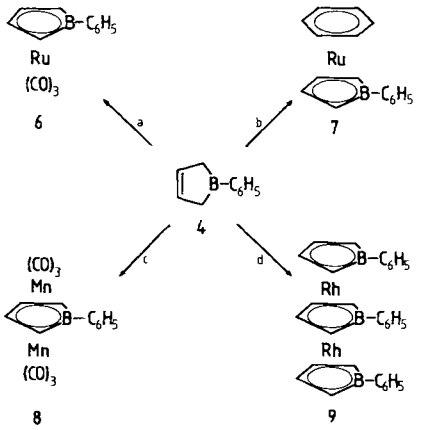
Herein we wish to report a general synthetic approach, which, for the first time, enables a systematic and versatile access to (borole)metal complexes. Reaction of 1-phenyl-2,5-dihydroborole **4**[7] with a wide variety of transition-metal complexes leads to catalytic isomerization to 1-phenyl-2,3-dihydroborole **5**[8] and dehydrogenating complexation with formation of ($\eta^5$-borole)metal complexes.




1 4 5

Thus, **4** reacts with $Ru_3(CO)_{12}$ on heating to give the (borole)tricarbonylruthenium complex **6** in 35% yield. Reaction with $Ru(C_6H_6)(C_6H_8)$ in liquid benzene at 160°C leads to formation of the complex **7** (22%) as main product. Reaction with $Mn_2(CO)_{10}$ in boiling mesitylene affords the triple-decked complex **8** (15%). Dehydrogenating complexation with the catalytically highly active $[(C_2H_4)_2RhCl]_2$ proceeds exceptionally smoothly, slowly furnishing the triple-decked complex **9** (80–95%), even at room temperature.

Each of the new complexes **6–9** contains *pentahapto*-bonded borole rings. This has already been demonstrated by an X-ray structural analysis in the case of the 2-ethyl derivative of **8**[4], and, in all cases, has been established from $^{11}$B-NMR data[1,3]. In the case of the triple-decked




a: $Ru_3(CO)_{12}$, toluene, 90°C, 6 d; b: $Ru(C_6H_6)(C_6H_8)$, benzene, 160°C, 3 d; c: $Mn_2(CO)_{10}$, mesitylene, 155–160°C, 3 d; d: $[(C_2H_4)_2RhCl]_2$, tetrahydrofuran, 20°C, 16 h (thereafter 65°C, 4 h).

complex **9** the $^{11}$B signal of the central ligand appears, consistent with a general rule, at higher field than the signal of the outer ligands and is less broadened by nuclear quadruple relaxation because of the higher coordination number at the B atom.

Our synthetic approach permits other groups at the B atom, *e.g.* alkyl, amino, and, in certain cases, halogen groups. Introduction of organic substituents at the ring C atoms is also possible. Depending on the system, the hydrogen eliminated from the dihydroborole during the dehydrogenating complexation is liberated as $H_2$ or HCl, or is consumed by olefin hydrogenation ($C_2H_4 \rightarrow C_2H_6$).

Received: June 24, 1983 [Z 427 IE]
German version: *Angew. Chem. 95* (1983) 1024
The complete version of this communication appears in: *Angew. Chem. Suppl. 1983*, 1503–1510

[1] G. E. Herberich, B. Buller, B. Hessner, W. Oschmann, *J. Organomet. Chem. 195* (1980) 253.
[3] G. E. Herberich in G. Wilkinson, F. G. A. Stone, E. W. Abel: *Comprehensive Organometallic Chemistry*, Vol. *1*, p. 381, Pergamon Press, Oxford 1982.
[4] G. E. Herberich, J. Hengesbach, U. Kölle, G. Huttner, A. Frank, *Angew. Chem. 88* (1976) 450; *Angew. Chem. Int. Ed. Engl. 15* (1976) 433; G. E. Herberich, J. Hengesbach, G. Huttner, A. Frank, U. Schubert, *J. Organomet. Chem. 246* (1983) 141.
[7] G. E. Herberich, B. Hessner, D. Söhnen, *J. Organomet. Chem. 233* (1982) C35.
[8] G. E. Herberich, B. Hessner, D. Söhnen, unpublished.

## Metal-Induced C-C Coupling by Reductive Dimerization of Thioaroyl Groups**

By *Ekkehard Lindner*, Ingobert P. Butz, Wolfgang Hiller, Riad Fawzi,* and *Sigurd Hoehne*

*Dedicated to Professor Ernst Otto Fischer on the occasion of his 65th birthday*

Metal-induced C-C coupling reactions are of considerable value for the synthesis of important organic interme-

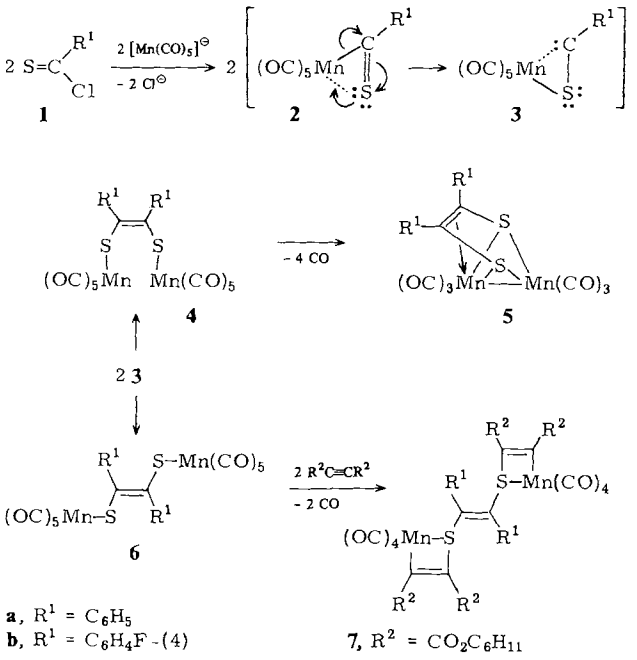
[*] Prof. Dr. G. E. Herberich, Dr. B. Hessner, W. Boveleth, H. Lüthe, R. Saive, L. Zelenka
Institut für Anorganische Chemie der Technischen Hochschule
Professor-Pirlet-Strasse 1, D-5100 Aachen (Germany)

[**] Derivatives of Boroles, Part 3.—Part 2: see [1].

[*] Prof. Dr. E. Lindner, I. P. Butz, Dr. W. Hiller, R. Fawzi, Dr. S. Hoehne
Institut für Anorganische Chemie der Universität
Auf der Morgenstelle 18, D-7400 Tübingen 1 (Germany)

[**] Preparation and Properties of and Reactions with Metal-Containing Heterocycles, Part 34. This work was supported by the Deutsche Forschungsgemeinschaft and the Fonds der Chemischen Industrie.—Part 33: E. Lindner, G. A. Weiss, W. Hiller, R. Fawzi, *J. Organomet. Chem.*, **255** (1983) 245.

diates and final products[1]. In the course of investigations of suitable model reactions, we succeeded in performing such a C-C coupling by means of the reaction between $[Mn(CO)_5]^-$ and thioaroyl chloride **1** in tetrahydrofuran at −78 °C. The first step possibly involves nucleophilic attack of the Lewis base $[Mn(CO)_5]^-$ at the thioaroyl carbon atom. The thioaroyl derivatives **2**, which presumably form as intermediates, rearrange to the carbenoids **3** which dimerize to give **4** and **6**. The *cis*-compounds **4** are stabilized by the favorable arrangement of the metal atoms leading to complex **5** *via* coordination of the lone-pairs of electrons of the sulfur atoms and displacement of CO.




**a**, $R^1 = C_6H_5$
**b**, $R^1 = C_6H_4F$-(4)

The *trans*-species **6**, which are unstable in solution, can be trapped by electrophilic alkynes in a [2+2]-cycloaddition to afford the compounds **7**, which are thermally stable and also stable towards atmospheric oxidation. The complexes **5a**, **b**, **6a**, **b**, and **7a**, **b**, which can be isolated in crystalline form, were characterized by complete elemental analysis and by mass-, IR-, Raman- and $^{13}C\{^1H\}$-NMR spectroscopy; moreover, **5a**[10], **6b**, and **7b** were also characterized by X-ray structure analysis[11] (Fig. 1).

Notable structural features of **6b** and **7b** are the sterically bulky $(OC)_5MnS$ and thiamanganacyclobutene moieties, respectively, which are linked *via* a 1,2-ethenediyl group. In **6b** the Mn–C(5) distance of 180 pm for the CO ligand lying opposite the S atom is considerably shorter than the average value of the other Mn–CO bonds (187 pm). The Mn–S distances in **6b** and **7b** (240.5 and 243.4 pm, respectively) lie in the upper expectation range. As a result of the strain in the four-membered ring caused by the C(5)=C(7) bond (131.1 pm), the Mn–S bond length in **7b** is increased. Nevertheless, the fact that **7b** is more stable than **6b** can be attributed to the coordinative saturation of the sulfur. In **6b**, apart from S–Mn–C(2), the S–Mn–C angles of the S atom *cis* to the CO ligands are up to 5° smaller than those of octahedrally coordinated Mn; the CO ligands are therefore displaced towards the Mn–S bond. The opposing deviation of C(2)–O(2) results from the steric repulsion between this CO ligand and the 4-fluorophenyl group bonded to C(6'). In contrast, the coordination octahedra of the metal in **7b** is markedly distorted.

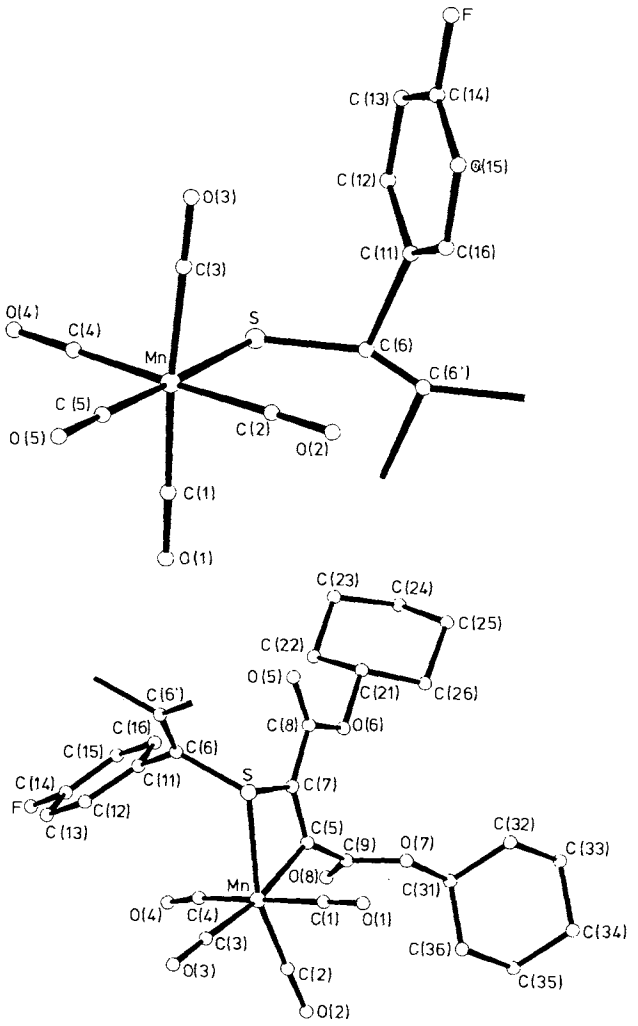



Fig. 1. Structures of **6b** (above) and **7b** (below). Since both compounds have centers of inversion, only one half of the respective molecules is shown.

Received: July 12, 1983; revised: August 24, 1983 [Z 462 IE]
German version: *Angew. Chem. 95* (1983) 1004
The complete version of this communication appears in: *Angew. Chem. Suppl. 1983*, 1388–1398

[1] W. A. Herrmann, *Angew. Chem. 94* (1982) 118; *Angew. Chem. Int. Ed. Engl. 21* (1982) 117.
[10] E. Lindner, I. P. Butz, S. Hoehne, W. Hiller, R. Fawzi, *J. Organomet. Chem.*, in press.
[11] Monoclinic crystals of **6b** from *n*-hexane (500 bar CO pressure), $P2_1/n$, $a = 1072.2(3)$, $b = 1175.7(2)$, $c = 1123.6(3)$ pm, $\beta = 111.16(3)°$, $Z = 2$, $\rho_{calc} = 1.680$ g·cm$^{-3}$. Structure solved by Patterson method. $R = 0.049$ (1034 reflections with $I \geq 3\sigma(I)$, $\theta = 3–22°$). Triclinic crystals of **7b** from $CCl_4$/*n*-hexane (1:4), $P\bar{1}$, $a = 1112.4(2)$, $b = 1131.6(3)$, $c = 1237.4(2)$ pm, $\alpha = 88.48(2)$, $\beta = 66.69(2)$, $\gamma = 80.31(2)°$, $Z = 1$, $\rho_{calc} = 1.346$ g·cm$^{-3}$. Structure solved using MULTAN. $R = 0.069$ (3871 reflections with $I \geq 3\sigma(I)$, $\theta = 3–34°$). Further details of the crystal structure analysis can be obtained from the Fachinformationszentrum Energie Physik Mathematik, D-7514 Eggenstein-Leopoldshafen, by quoting the depository number CSD 50499, the names of the authors, and the journal citation.

## $Rb_7NaGe_8$ and $K_7NaGe_8$, Zintl Compounds with $Na(Ge_4)_2$ Units

By *Jaime Llanos, Reinhard Nesper,* and *Hans Georg von Schnering*

*Dedicated to Professor Ernst Otto Fischer on the occasion of his 65th birthday*

The binary Zintl compounds ME (M, M′ = Na, K, Rb, Cs; E, E′ = Si, Ge) are characterized by the tetrahedral anions $E_4^{4-}$[1]. In an attempt to define the stability ranges of the various structures, we have synthesized the ternary compounds $ME_xE'_{1-x}$ and $M_xM'_{1-x}E$, respectively. Crystals of these ternary compounds are prepared from the elements and are black with a metallic luster. Like the binary germanides, these materials are extremely reactive, spontaneously igniting in the presence of moisture.

The $ME_xE'_{1-x}$ compound $Na_4Ge_2Si_2$ has the NaSi structure, containing tetrahedra which are composed of mixed anions $(E_xE'_{4-x})^{4-}$[2]. The $M_xM'_{1-x}E$ compounds $Rb_7NaGe_8$ and $K_7NaGe_8$ on the other hand, possess a novel cubic structure. To date, only the Rb compound has been studied in detail[3].

The novel cubic structure also contains the tetrahedral anions $Ge_4^{4-}$, which are surrounded by the cations in a similar way as in the binary phases NaGe, KGe and RbGe. The metal atoms act as $\mu_3$-ligands, coordinating the faces of the tetrahedra. In this way, distorted cubane-like species $M_4Ge_4$ are formed as primary structural units; their variable packing leads to the above-mentioned structure types[4]. The different sizes of the cations in $Rb_7NaGe_8$ modify this structural principle in a surprising way, which also explains the remarkable composition of this compound. Each Na atom links two $Ge_4$ tetrahedra *via* $2\times3$ equivalent Na–Ge bonds to form the quasi-linear $[Na(Ge_4)_2]$ unit (Fig. 1). The average distances $\bar{d}$(Ge–Ge) = 257.2 pm in the $Ge_4$ tetrahedron are as large as in the binary phases, but the individual distances are considerably different (253–262 pm). In particular, the face of the tetrahedron coordinated by the Na atom is enlarged. Six of the large cations are located above the vacant triangular faces of the tetrahedra and are also in contact with neighboring anions. The bond lengths (Na–Ge 298.1, Rb–Ge 361.8) are in the usual range. The structure of the unit consisting of Na, 6 M, and 8 Ge corresponds to two condensed cubanes with a shared apex (Na atom). According to the reaction $2\,Me_4Ge_4 = M_7Ge_8 + M$, one eighth of the M atoms is eliminated and can no longer participate in coordination to $Ge_4^{4-}$. Double cubanes of this type pack optimally and simply in the space group Pa3, forming one cavity per double cubane group[4]. The seventh large cation of $Rb_7NaGe_8$ is located in this large cavity, surrounded at relatively large distances by six Ge atoms (Rb–Ge = 406.6 pm) and, in addition, by six cations at a distance of 438.9 pm. The structure type is thus characterized by the formula $Rb\{Rb_6[Na(Ge_4)_2]\}$, which indicates that the aristotype is represented by a quarternary compound (*e.g.* "$CsK_6NaGe_8$"). Consequently, this compound was recently obtained. The expected distribution of cations for that structure is exactly fulfilled[6].

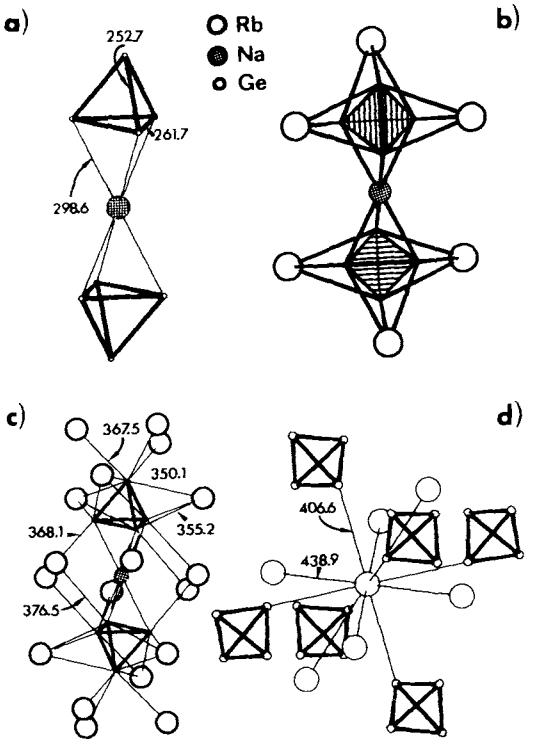



Fig. 1. Structural elements of $Rb_7NaGe_8$: a) Quasi-linear unit $[Na(Ge_4)_2]$ with markedly increased tetrahedral faces in the direction of coordination to the Na atom. b) Condensed double cubane $Rb_7NaGe_8$ with highly distorted tetrahedral star [5]. c) Enlarged coordination of the double cubane. d) Environment around Rb2: octahedral coordination by six tetrahedron apices Ge2 without direct contact to a cubane moiety. The neighboring atoms of type Rb1 give an impression of the size of the cavity in which Rb2 lies. All distances in pm.

[*] Prof. Dr. H. G. von Schnering, J. Llanos, Dr. R. Nesper
Max-Planck-Institut für Festkörperforschung
Heisenbergstrasse 1, D-7000 Stuttgart 80 (Germany)

Received: July 18, 1983 [Z 474 IE]
German version: *Angew. Chem. 95* (1983) 1026

CAS Registry numbers:
$Rb_7NaGe_8$, 87803-53-0; $K_7NaGe_8$, 87803-54-1.

[1] E. Busmann, *Z. Anorg. Allg. Chem. 313* (1961) 90; J. Witte, H. G. von Schnering, *ibid. 327* (1964) 260.
[2] J. Llanos, R. Nesper, H. G. von Schnering, *Z. Naturforsch. B*, in press.
[3] Synthesis of $Rb_7NaGe_8$: The elements (Na : Rb : Ge) are melted in welded Nb ampules in the ratio 1 : 1.5 : 1.5 at 1170 K; the mixture is then allowed to cool over 12 h and the excess metal removed *in vacuo* (550 K, $10^{-2}$ mbar, 6 h).—*Crystal structure analysis* of $Rb_7NaGe_8$: Pa3, $a = 13.165(4)$ Å, $Z = 4$, 1047 *hkl*, $R = 0.042$. $K_7NaGe_8$: Pa3, $a = 12.684(1)$ Å, isotypic according to powder photographs. Further details of the crystal structure investigation can be obtained from the Fachinformationszentrum Energie Physik Mathematik, D-7514 Eggenstein-Leopoldshafen, by quoting the depository number CSD 50550, the names of the authors, and the journal citation.
[4] H. G. von Schnering, R. Nesper, *Z. Kristallogr.*, in press.
[5] K. Schubert: *Kristallstrukturen zweikomponentiger Phasen*, Springer, Berlin 1964.
[6] J. Llanos, Dissertation, Universität Stuttgart 1983.

## Conformational Inversion of Tetraisopropylethylene: No Cog-Wheel Mechanism!

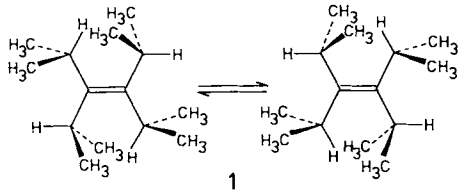
By *Otto Ermer**

*Dedicated to Professor Shneior Lifson on the occasion of his 70th birthday*

The most favorable minimum energy conformation $M_1$ of tetraisopropylethylene **1** has $C_{2h}$ symmetry and a planar double bond, as predicted computationally[1a] in 1974 and

[*] Priv.-Doz. Dr. O. Ermer
Abteilung für Chemie der Universität
Postfach 102148, D-4630 Bochum 1 (Germany)

confirmed crystallographically[1b] in 1980. The authors who described the first synthesis of **1**[2] in 1975 considered a "cog-wheel" ("gearing") mechanism for the conformational inversion of **1**, implying a single-step interconversion with synchronous rotation (by 180°) of the isopropyl groups about the $C(sp^2)-C(sp^3)$ bonds.



**1**

An inversion barrier of 17 kcal $mol^{-1}$ ($\Delta G^{+}$) was derived from NMR data[2b]. We report here empirical calculations with the aid of our consistent force field[3a,b], which show that the inversion of **1** does not follow a cog-wheel pathway, but proceeds stepwise such that the four isopropyl groups rotate consecutively *via* three intermediate minima.

For the inversion of **1** seven minima ($M_1-M_7$) are relevant, which may be characterized by the orientation of the methine C–H bonds with respect to the double bond (*syn-* or *antiperiplanar*). Some calculated energetical and structural data as well as the symmetries are collected in Figure 1 (Newton-Raphson optimizations). The seven minima may be linked by eight non-equivalent interconversion paths, since the number of different paths emanating from a minimum must be equal to the number of its non-equivalent isopropyl groups (Fig. 2).

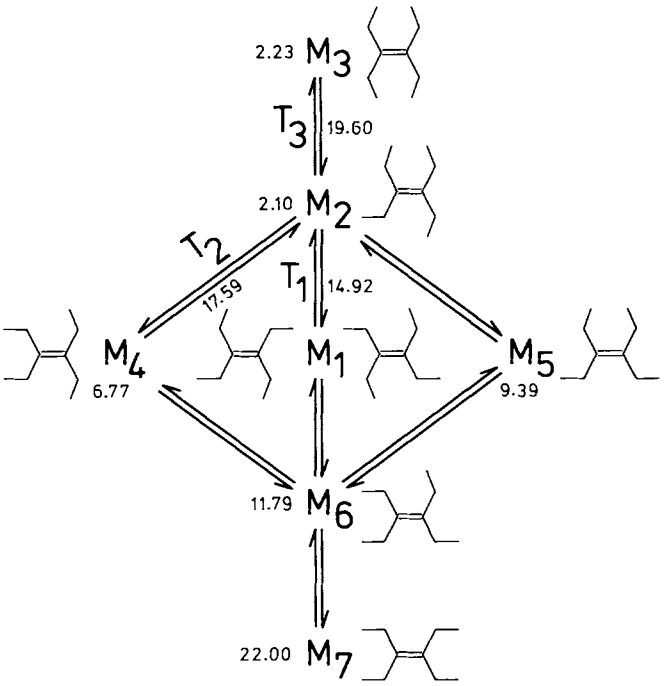



Fig. 2. Chart of the non-equivalent partial inversion paths of **1** (with relative potential energies in kcal $mol^{-1}$). Only the methine C–H bonds are drawn to indicate the orientation of the isopropyl groups in the minima.

As a consequence of the numerous, rather weakly restricted torsional degrees of freedom in **1**, the localization of the transition states for the partial inversions of the chart of Fig. 2 was difficult and time-consuming. To sim-

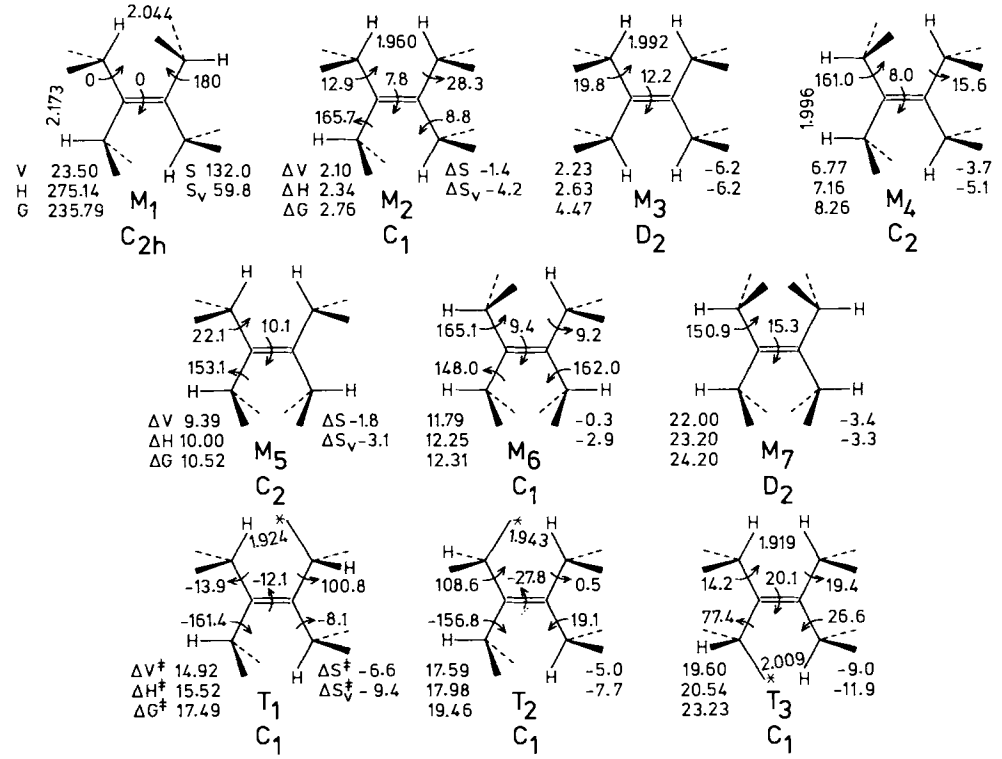



Fig. 1. Calculated minima (M) and transition states (T) of **1** relevant for the inversion process. Structural data: H–C–C=C torsion angles, double bond twist angles [°], short H···H contacts [Å]. Except for $M_1$, the energies [kcal $mol^{-1}$] and entropies [cal $mol^{-1}$ $K^{-1}$] given are relative quantities referring to $M_1$ (standard symbols; *V* optimum potential energies, $S_v$ harmonic vibrational entropies). The congested methyl groups of the rotating isopropyl groups in the transition states are indicated by an asterisk.

plify the calculation, interconversions involving $M_5$, $M_6$, and $M_7$ were not considered. These minima have 1,2-*cis*-configurated isopropyl groups with four methyl groups in close proximity which, according to model considerations, is particularly unfavorable. With this assumption, only the three interconversions involving $M_1$—$M_4$ had to be considered in the detailed analysis. The associated transition states could be located with appropriate eigenvector methods[3b,c]. Some important energetical and structural properties of the most favorable transition states for these three partial inversions are also included in Figure 1. As expected, they are characterized by particularly short nonbonded H···H distances which are the origin of the present conformational barriers. The energetically cheapest inversion process calculated for **1** proceeds in four steps (partial inversions involving the hindered rotation of a single isopropyl group) from $M_1$ *via* $M_2$ to $M_4$, and from there along equivalent paths *via* $M_2'$ to the inverted $C_{2h}$ minimum $M_1'$. The second (third) step of the inversion is rate-determining (transition state $T_2$) with a calculated free energy of activation $\Delta G^{\neq}$ of 19.46 kcal mol$^{-1}$. The moderate computational overestimation of the inversion barrier (experimental value 17 kcal mol$^{-1}$[2b]) is probably due to the excessive hardness of our nonbonded H···H potential at short distances[4]. The activation entropies of all three calculated partial inversions are markedly negative. This appears to arise from a vibrational effect since the stronger H···H repulsions in the transition states as compared to the minima lead to frequency increases and thus to entropy decreases for the saddle points (Fig. 1).

Our calculations thus support a distinctly stepwise inversion mechanism of **1**. The consecutive rotations of the four isopropyl groups proceed *via* deep intermediate minima, which shows that a synchronous cog-wheel mechanism is energetically considerably less favorable than the stepwise partial inversions. This is due to the fact that more short H···H contacts occur simultaneously if the isopropyl groups rotate synchronously than with consecutive single rotations.

The example presented here leads to the more general conclusion that despite the conceptually appealing mechanical model, cog-wheel mechanisms are by no means the rule for conformational interconversions in overcrowded molecules. In fact, rather the opposite seems true: Unequivocally proven cog-wheel processes are scarce; probably the most convincing evidence in favor of such a process has been put forward for bis(9-triptycyl)methane and related compounds[5].

Received: August 8, 1983; revised: October 11, 1983 [Z 510 IE]
German version: *Angew. Chem. 95* (1983) 1010
The complete version of this communication appears in:
*Angew. Chem. Suppl. 1983*, 1353—1363

[1] a) O. Ermer, S. Lifson, *Tetrahedron 30* (1974) 2425; b) G. Casalone, T. Pilati, M. Simonetta, *Tetrahedron Lett. 21* (1980) 2345.
[2] a) R. F. Langler, T. T. Tidwell, *Tetrahedron Lett. 1975*, 777; b) D. S. Bomse, T. H. Morton, *ibid. 1975*, 781.
[3] a) O. Ermer, S. Lifson, *J. Am. Chem. Soc. 95* (1973) 4121; b) O. Ermer: *Aspekte von Kraftfeldrechnungen*, Wolfgang Baur Verlag, München 1981; c) O. Ermer, *Tetrahedron 31* (1975) 1849; *J. Am. Chem. Soc. 98* (1976) 3964.
[4] O. Ermer, S. A. Mason, *J. Chem. Soc. Chem. Commun. 1983*, 53.
[5] W. D. Hounshell, C. A. Johnson, A. Guenzi, F. Cozzi, K. Mislow, *Proc. Natl. Acad. Sci. USA 77* (1980) 6961; F. Cozzi, A. Guenzi, C. A. Johnson, K. Mislow, W. D. Hounshell, J. F. Blount, *J. Am. Chem. Soc. 103* (1981) 957; H.-B. Bürgi, W. D. Hounshell, R. B. Nachbar, K. Mislow, *J. Am. Chem. Soc. 105* (1983) 1427; Y. Kawada, H. Iwamura, *J. Org. Chem. 45* (1980) 2547; *J. Am. Chem. Soc. 103* (1981) 958.

## Disulfur and Diselenium as Strong Acceptor Ligands in $(\eta^5\text{-}C_5H_5)Re(CO)_2S_2$ and $[\eta^5\text{-}C_5(CH_3)_5]Mn(CO)_2Se_2$**

By *Max Herberhold*, Dietmar Reiner,* and *Ulf Thewalt*

*Dedicated to Professor Ernst Otto Fischer on the occasion of his 65th birthday*

Disulfur complexes of transition metals are distinguished by the exceptionally wide variation in their structures and types of bonding[1]. Nevertheless, it would seem that the pronounced acceptor properties of the $S_2$ ligand have so far never been documented. These have now been established from the IR and NMR spectra of the novel disulfur complex $CpRe(CO)_2S_2$ **2** (Cp = $\eta^5$-cyclopentadienyl). According to an X-ray structure analysis (Fig. 1), **2** contains an $\eta^2$-coordinated $S_2$ ligand which occupies the place of a CO group in the half-sandwich complex $CpRe(CO)_3$ **1**.

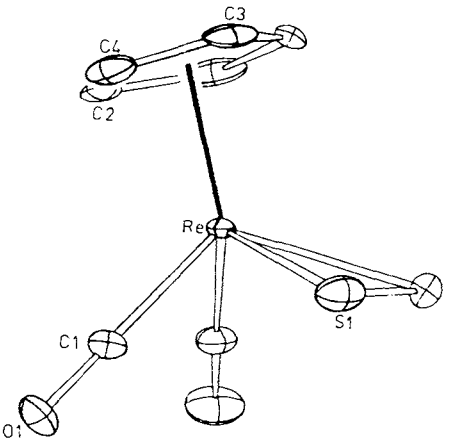
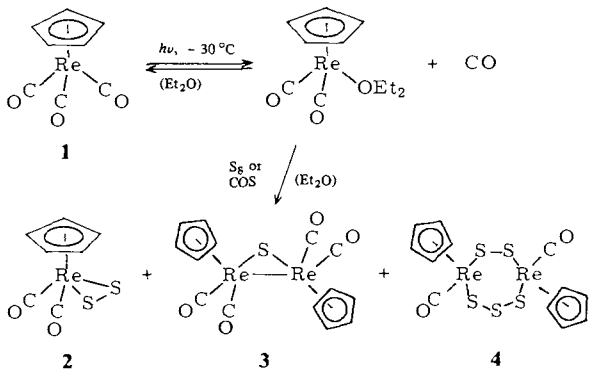



Fig. 1. Molecular structure of the disulfur-rhenium complex **2** in the crystal. Important bond lengths [Å] and angles [°]: Re-S1 2.410, S1-S1' 1.996; S1-Re-S1' 48.9, C1-Re-C1' 77.9, Re-C1-O1 179.4. The molecule has crystallographic mirror image symmetry. Further details of the crystal structure investigation are available on request from the Fachinformationszentrum Energie Physik Mathematik on quoting the depository number CSD 50557, the names of the authors, and full citation of the journal.

Photolysis of **1** in diethyl ether leads primarily to cleavage of CO with formation of the solvent-stabilized complex $CpRe(CO)_2(OEt_2)$. Further reaction with either sulfur




[*] Prof. Dr. M. Herberhold, Dr. D. Reiner
Laboratorium für Anorganische Chemie der Universität
Universitätsstrasse 30, D-8580 Bayreuth (Germany)
Prof. Dr. U. Thewalt
Sektion für Röntgen- und Elektronenbeugung der Universität
Oberer Eselsberg, D-7900 Ulm (Germany)

[**] This work was supported by the Deutsche Forschungsgemeinschaft and the Fonds der Chemischen Industrie.

or carbon oxide sulfide yields a complex mixture of products containing, *inter alia*, the diamagnetic complexes **2**—**4**. The structures of **2**—**4** were determined by X-ray crystallography[4].

In the IR spectrum of the red-brown mononuclear disulfur complex **2**, the pattern of the CO stretching absorptions (baricenter 1979.5 $cm^{-1}$) appears at higher wavelengths than in the spectrum of the parent compound **1** (baricenter 1965.3 $cm^{-1}$). A corresponding increase is also observed in the (approximate) force constants $k$(CO), which were calculated from the $\nu$(CO) frequencies. The $k$(CO) values are better suited for a comparison of complexes of differing symmetry than the experimentally observed CO valence absorptions. Both in the $^1$H- and in the $^{13}$C-NMR spectrum, the singlet of the Cp ring in **2** is shifted downfield compared to that in **1**. All these data (Table 1) are consistent with the novel $S_2$ ligand removing more charge from the [$CpRe(CO)_2$] fragment than the original CO group. Accordingly, $S_2$ is a better acceptor ligand than CO—as are other sulfur-containing two-electron ligands (*e.g.* $CS_2$ and CS[6]).

A corresponding comparison of $Cp^*Mn(CO)_3$ **5** ($Cp^* = \eta^5$-pentamethylcyclopentadienyl) with the diselenium complex $Cp^*Mn(CO)_2Se_2$ **6** formed therefrom infers that $Se_2$ also surpasses the CO ligand in acceptor ability (Table 1).

The molecular structures of the dichalcogen complexes **2** and **6** are consistent with the spectroscopically derived transfer of charge from the metal to a side-on bonded $E_2$ ligand (E = S and Se, resp.). The S—S' distance (1.996(5)Å) in **2** lies between the values for single bonding and double bonding (cf. S=S 1.89 Å, $S_8$ 2.06 Å[7]); it is short compared to the lengths observed in other complexes with $\eta^2$-coordinated $S_2$ ligands (1.99—2.09 Å[1]). The Re—S distance (2.410(2) Å) is shorter than the sum of the covalent (single bond) radii, which can be taken to be 2.55 Å using $Re_2(CO)_{10}$ (1.52 Å)[8] and $S_8$ (1.03 Å)[7] as reference compounds. According to a preliminary X-ray structure analysis of **6**, the Se—Se (2.263(8) Å) and Mn—Se (2.463(4) Å) distances are likewise unusually short when compared with those in suitable reference compounds (Se=Se 2.19 Å and $Se_8$ 2.34 Å[7]; $Mn_2(CO)_{10}$, Mn—Mn 2.90 Å[8]).

In view of the short $E_2$ bond lengths, the ligands $S_2$ and $Se_2$ in **2** and **6**, respectively, can be regarded as the coordination-stabilized form of the (unstable) heteroolefins S=S and Se=Se, whose double bonds are lengthened by $\pi$-complex formation. In contrast to the formulation of anionic $S_2^{\ominus}$ or $S_2^{2\ominus}$ ligands, frequently proposed in recent studies (cf.[1]) and even more strongly emphasizing the acceptor character of the dichalcogen ligands, the model used here with $S_2$ and $Se_2$ as uncharged two-electron ligands also reveals the analogy to the complexes $CpM(CO)_2L$ (M = Mn, Re) containing other neutral acceptor ligands (L = CO, CS, $CS_2$[6]).

Received: August 1, 1983 [Z 497 IE]
German version: *Angew. Chem. 95* (1983) 1028
The complete version of this communication appears in: *Angew. Chem. Suppl. 1983*, 1343—1352

[1] Review: A. Müller, W. Jaegermann, J. H. Enemark, *Coord. Chem. Rev. 46* (1982) 245.
[4] The binuclear complexes **3** and **4** will be reported on separately: M. Herberhold, D. Reiner, T. Debaerdemaeker, K. Ackermann, U. Thewalt, unpublished.
[6] M. Herberhold, M. Süß-Fink, *Angew. Chem. 89* (1977) 192; *Angew. Chem. Int. Ed. Engl. 16* (1977) 194; *Chem. Ber. 111* (1978) 2273.
[7] A. F. Wells: *Structural Inorganic Chemistry*, 4th Ed., pp. 571—573. Clarendon Press, Oxford 1975.
[8] M. R. Churchill, K. N. Amoh, H. J. Wasserman, *Inorg. Chem. 20* (1981) 1609.

Table 1. Spectroscopic data of the complexes **1**, **2**, **5** and **6**.

| Complex | $CpRe(CO)_3$ **1** | $CpRe(CO)_2S_2$ **2** | $Cp^*Mn(CO)_3$ **5** | $Cp^*Mn(CO)_2Se_2$ **6** |
|---|---|---|---|---|
| IR: | | | | |
| $\nu$(CO) [$cm^{-1}$] | 2024(s) [a] | 2014(s) [a] | 2002(s) [b] | 1987(vs) [b] |
| | 1936(vs) | 1945(s) | 1917(vs) | 1941(s) |
| $k$(CO) [$N \cdot cm^{-1}$] | 15.60 | 15.82 | 15.28 | 15.58 |
| $^1$H-NMR: | | | | |
| $\delta(C_5H_5)$ | 5.39 [c] | 5.78 [c, e] | | |
| $\delta(CH_3)$ | | | 1.90 [d] | 1.91 [d] |
| $^{13}$C-NMR (0 °C): | | | | |
| $\delta$(Ring) | 84.4 [c] | 90.2 [c] | 96.8 [d] | 102.6 [d] |
| $\delta(CH_3)$ | | | 10.3 | 10.3 |

[a] In $Et_2O$; [b] in THF; [c] in $CDCl_3$; [d] in [$D_6$]acetone; [e] −20 °C.

## An Arsanylketene by Elimination from an Oxaarsatungstacyclopentene Complex**

By *Fritz Roland Kreissl*, Mathias Wolfgruber*, and *Werner Sieber*

*Dedicated to Professor Ernst Otto Fischer on the occasion of his 65th birthday*

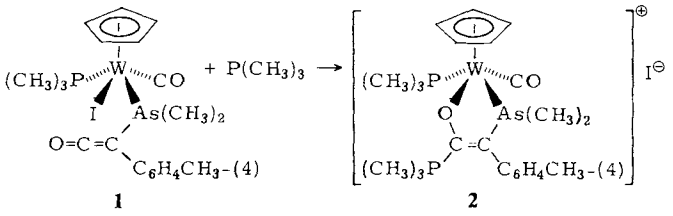
Arsenic- and phosphorus-substituted ketenes could hitherto not be obtained by organochemical methods[2], even though their preparation in the coordination sphere of tungsten has already been achieved on numerous occasions[3]. The dissolution and isolation of the intact ketene ligands thus presented a stimulating challenge.

The arsanylketene ligand could be cleaved from **1** with carbon monoxide (100 °C/60 bar) with formation of $\eta^5$-$C_5H_5(CO)_2[P(CH_3)_3]WHal$, but could not be detected without sign of decomposition. In contrast, all attempts to displace phosphanyl- and arsanylketene ligands with trimethylphosphane initially led *via* attack of the phosphane at the central ketene carbon to cationic phospha- and arsatungstaheterocycles[4] of type **2**; mass spectroscopic findings (FD), however, pointed to the possibility of thermal liberation of the original ketene ligands. In the case of the

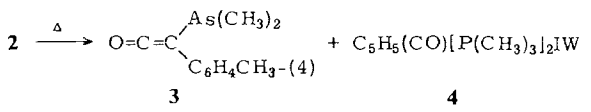
[*] Priv.-Doz. Dr. F. R. Kreissl, M. Wolfgruber, W. Sieber
Anorganisch-chemisches Institut der
Technischen Universität München
Lichtenbergstrasse 4, D-8046 Garching (Germany)

[**] Transition-Metal-Ketene Compounds, Part 16. This work was supported by the Deutsche Forschungsgemeinschaft and the Fonds der Chemischen Instustrie.—Part 15: [1].

arsenic compound **2** this reaction could be reproduced for the first time on a preparative scale. When carried out in boiling toluene the novel arsanylketene **3** was formed in almost quantitative yield together with nearly quantitative amounts of tungsten complex **4**[5].



**1** **2**



**3** **4**

The surprisingly stable ketene **3** is a yellow, "cacodyl-like" smelling oil, which was characterized IR, $^1$H-NMR, $^{13}$C-NMR, and mass spectroscopically. The spectroscopic data for the free ketene and the complexed ketene moiety differ only slightly (Table 1). The expected high-field shift of all NMR signals of **3** compared to those of **1** is naturally greatest in the case of the $As(CH_3)_2$ group.

Table 1. IR-, $^1$H-NMR, and $^{13}$C-NMR spectroscopic data for **1** and **3**.

| | | **1** | **3** |
|---|---|---|---|
| IR (in $CH_2Cl_2$) [$cm^{-1}$] | $\nu$(C=C=O) | 2095 vs | 2074 vs |
| $^1$H-NMR (in $CD_2Cl_2$, $\delta$-value rel. $CDHCl_2 = 5.4$) | $C_6H_4$ | 7.30 s, 4H | 7.17 s, 4H |
| | $AsCH_3$ | 1.89 d, 6H $J = 3.0$ OHz | 1.26 s, 6H |
| | $CH_3$ | 2.47 s, 3H | 2.38 s, 3H |
| $^{13}$C{$^1$H}-NMR (in $CD_2Cl_2$, $\delta$-value rel. $CD_2Cl_2 = 54.2$) | CO-ketene | 182.90 | 183.77 |
| | C-ketene | 31.26 | 28.80 |
| | $C_6H_4$ | 137.91–125.56 | 134.88–127.41 |
| | $CH_3$ | 21.44 | 21.45 |
| | $AsCH_3$ | 15.51 | 11.08 |

The mass spectrum of **3** (EI, 70 eV), whose signals were already contained in spectra of **1** and **2**, shows the molecular ion as base peak, the fragmentation of which triggered off with the successive cleavage of a methyl radical and a carbon monoxide molecule.

Received: May 18, 1983 [Z 389 IE]
German version: *Angew. Chem. 95* (1983) 1002

[1] F. R. Kreissl, M. Wolfgruber, W. Sieber, K. Ackermann, *J. Organomet. Chem., 252* (1983) 239.
[2] S. Patai: *The Chemistry of Ketenes, Allenes and Related Compounds, Part 1 and 2*, Wiley, Chichester 1980.
[3] F. R. Kreissl, M. Wolfgruber, W. Sieber, H. G. Alt, *Angew. Chem. 95* (1983) 159; *Angew. Chem. Int. Ed. Engl. 22* (1983) 149; *Angew. Chem. Suppl. 1983*, 148; M. Wolfgruber, W. Sieber, F. R. Kreissl, *Chem. Ber.*, in press.
[4] F. R. Kreissl, M. Wolfgruber, W. Sieber, *Organometallics, 2* (1983) 1266.
[5] A suspension of **2** (1.7 g, 2.16 mmol) in toluene (40 mL) is heated under reflux until complete dissolution. After removal of solvent the ketene **3** is extracted with pentane. Yellow oil, yield 0.43 g (86%). Molecular weight: calc. 236.018, obs. 236.019 (MS, $^{12}$C, $^1$H, $^{16}$O). The complex **4** present in the residue can be purified by chromatography on silica gel ($CH_2Cl_2$). Reddish-brown powder, yield 0.97 g (82%).

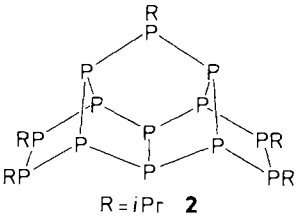
## $P_{12}iPr_4$ and $P_{13}iPr_5$, Two Novel Polycyclic Organophosphanes**

By *Marianne Baudler*, Yusuf Aktalay, Volker Arndt, Karl-Friedrich Tebbe,* and *Magda Fehér*

*Dedicated to Professor Ernst Otto Fischer on the occasion of his 65th birthday*

We recently found that dehalogenation of dichloro(organo)phosphanes with magnesium in the presence of white phosphorus, as well as thermolysis of bi- and tricyclic organophosphanes, in particular $P_7R_5$ and $P_9R_5$, open up a preparative route to polycyclic organophosphanes $P_nR_m$ ($m < n$) with $n \geq 8$[1]. In each case, mixtures of several compounds are formed, which with small alkyl groups R are largely insoluble and, therefore, cannot be separated. However, the solubility increases with the number of C atoms in the substituents and, hence, isolation of individual species becomes possible[1a].

Using the "thermolysis route", we have now prepared the tetraisopropyldodecaphosphane(4) **1** and the pentaisopropyltridecaphosphane(5) **2**[5] and have clarified the structures of the pentacyclic $P_{12}$(4)- and $P_{13}$(5)-frameworks.



R = *i*Pr **2**

**1** and **2** form light yellow platelets and needle-shaped crystals, respectively, which do not change up to 250 °C and which are stable under an inert gas atmosphere. They are readily soluble in arenes and tetrahydrofuran (THF), moderately soluble in cyclohexane, but, in contrast, sparingly soluble in aliphatic hydrocarbons. The compounds, which in the solid state are only slightly sensitive to atmospheric oxygen, are rapidly oxidized in solution. The compositions of **1** and **2** are corroborated by correct elemental analysis and molecular weight determinations (MS: **1**: *m/z* 544; **2**: *m/z* 618).

The $^{31}$P{$^1$H}-NMR spectra of **1** and **2** exhibit a series of substructured signal groups in the region $\delta = +85$ to $-30$, which is characteristic for condensed phosphorus five- and six-membered rings[1c]. The quasi-triplet structure of the respective high-field groups at $\delta \simeq -30$ indicates the presence of a two-atom bridge as component of a norbornane-analogous part structure[1c]. Consistent with this, the X-ray structure analysis of **1**[2] yielded the molecular geometry shown in Figure 1; **1** is accordingly a 3,4,9,10-tetraisopropylpentacyclo[6.4.0.0$^{2,6}$0.$^{5,12}$.O$^{7,11}$]dodecaphosphane. The bond lengths and angles of the $P_{12}$(4)-framework (approximate $C_{2v}$ symmetry) exhibit considerable differences; above all, the zero-bridges of the central $P_8$(4)-moiety are markedly lengthened. The needles of **2** were too thin for

[*] Prof. Dr. M. Baudler, Dr. Y. Aktalay, Dr. V. Arndt, Prof. Dr. K.-F. Tebbe, Dr. M. Fehér
Institut für Anorganische Chemie der Universität
Greinstrasse 6, D-5000 Köln 41 (Germany)

[**] Contributions to the Chemistry of Phosphorus, Part 137. This work was supported by the Minister für Wissenschaft und Forschung des Landes Nordrhein-Westfalen and by the Fonds der Chemischen Industrie.—Part 136: M. Baudler, J. Hellmann, *Z. Anorg. Allg. Chem.*, in press.

 © *Verlag Chemie GmbH, 6940 Weinheim, 1983* *0570-0833/83/1212-1002 $ 02.50/0* 

an X-ray structure analysis. Because of the common mode of formation with **1** and $P_{11}iPr_5$[1c] as well as of the analogy of the $^{31}P\{^1H\}$-NMR spectrum with that of **1** and $P_{11}Et_5$[1c], it is highly probable that **2** is a 3,4,7,10,11-pentaisopropylpentacyclo[7.4.0.0$^{2,6}$.0$^{5,13}$.0$^{8,12}$]tridecaphosphane.

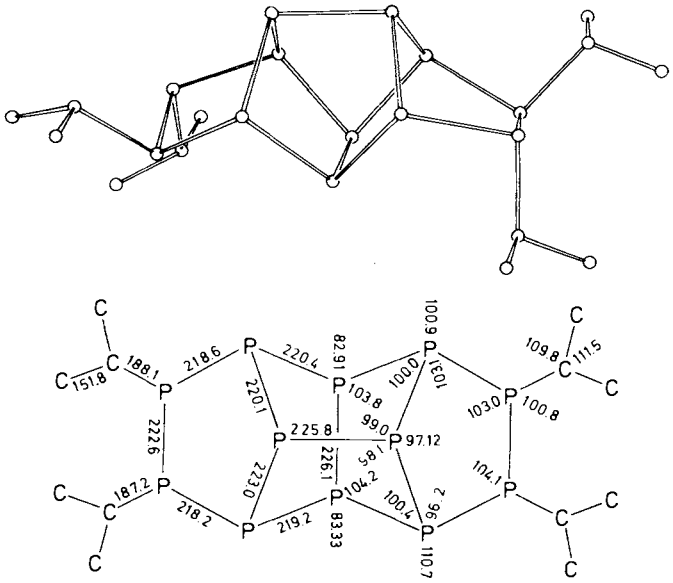



Fig. 1. Molecular structure of **1** in the crystal [2]; top: ORTEP representation; bottom: projection of the molecule parallel to the $C_2$ axis with average bond lengths in pm ($\sigma \leq 0.7$ pm) and selected average angles in degrees ($\sigma \leq 0.6°$; exceptions: $110.7 \pm 1.2°$ and $96.2 \pm 1.4°$).

Some time ago we were able[3] to detect mass spectroscopically the phosphorus hydrides $P_{12}H_4$ and $P_{13}H_5$, respectively, among the products of hydrolysis of calcium phosphide and in the products of thermolysis of diphosphane; however, their structures were not yet amenable to experimental investigations. Since in **1** and **2** significant steric influences of the substituents on the constitution of the phosphorus frameworks can be ruled out[1b], the hydrides can be considered to be the parent compounds of **1** and **2**, respectively.

The polycycloalkane $C_{12}H_{16}$ corresponding to **1** is known[3c], but not the **2**-analogue $C_{13}H_{18}$.

The $P_{12}$(4)- and $P_{13}$(5)-frameworks are essential structural units of Hittorf's phosphorus, in which they are linked alternatingly *via* the two-atom bridges as common zero-bridges to form five-cornered cylinders[4]. In **1** and **2** unaltered, P-rich part structures of the element occur for the first time as discrete molecules.

Received: July 25, 1983 [Z 486 IE]
German version: *Angew. Chem. 95* (1983) 1005

[1] a) M. Baudler, V. Arndt, *Z. Naturforsch.*, in press; b) M. Baudler, *Angew. Chem. 94* (1982) 520; *Angew. Chem. Int. Ed. Engl. 21* (1982) 492; c) M. Baudler, V. Arndt, *Z. Anorg. Allg. Chem.*, in press.

[2] Triclinic, $P\bar{1}$, $a = 879.8(3)$, $b = 1088.5(2)$, $c = 1414.1(3)$ pm, $\alpha = 93.01(2)$, $\beta = 107.61(2)$, $\gamma = 92.92(2)°$, $Z = 2$, 4516 reflections, 3549 of which with $|F| \geq 4\sigma(F)$, $R = 0.026$, $R_w = 0.029$ (P and C anisotropic, freely refined H sites with common isotropic temperature coefficients). For further details on the crystal structure analysis, see: M. Fehér, K.-F. Tebbe, *Z. Naturforsch. B*, in press.

[3] a) M. Baudler, H. Ständeke, M. Borgardt, H. Strabel, J. Dobbers, *Naturwissenschaften 53* (1966) 106; b) M. Baudler, *Pure Appl. Chem. 52* (1980) 755; c) D. McNeil, B. R. Vogt, J. J. Sudol, S. Theodoropulos, E. Hedaya, *J. Am. Chem. Soc. 96* (1974) 4673.

[4] H. Thurn, H. Krebs, *Angew. Chem. 78* (1966) 1101; *Angew. Chem. Int. Ed. Engl. 5* (1966) 1047.

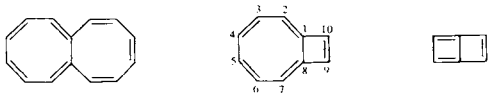
[5] Procedure: A mixture (45 g) consisting of approximately 60% $P_9iPr_5$, 20% $P_7iPr_5$, 5% $P_7iPr_3$, as well as further isopropylphosphanes (obtained by reaction of $iPrPCl_2$ and $PCl_3$ (5:4) with magnesium in boiling THF) is thermolyzed for 7 h at 230 °C. The yellow-brown, highly viscous product is taken up in 30 mL cyclohexane and chromatographed portionwise on $Al_2O_3$ (dried by heating *in vacuo*) using *n*-hexane and cyclohexane; the chromatographic process is monitored using $^{31}P$-NMR and mass spectroscopy. The fractions having the highest amount of **2** are combined, the solvent is evaporated off, and the more soluble portions are removed from the residue by extraction with *n*-pentane ($3 \times 5$ mL). Several recrystallizations from THF/pentane (3:1) yields 0.18 g pure **2** (not optimized); pure **1** is obtained from the mothor liquor.

## Octalene—Bicyclo[6.2.0]decapentaene Conversion Mediated by Transition-Metal Complexes

By *Dieter Kawka, Peter Mues,* and *Emanuel Vogel**

*Dedicated to Professor Ernst Otto Fischer on the occasion of his 65th birthday*

The naphthalene- and azulene-isomer bicyclo[6.2.0]decapentaene is a molecule of current interest, both from the synthetic[1] and theoretical[2] point of view, due to the question of whether the *fusion* of two antiaromatic [4n]annulenes leads to an aromatic bicycle with a peripheral $(4n+2)\pi$-electron system. After *Schröder et al.*[1b,d,g] had succeeded in opening an entry to substituted bicyclo[6.2.0]decapentaenes, *Oda et al.*[1i] were able in 1980 to prepare the parent compound **2** for the first time starting from bicyclo[4.2.0]octa-3,7-diene-2,5-dione.



**1** **2** **3**

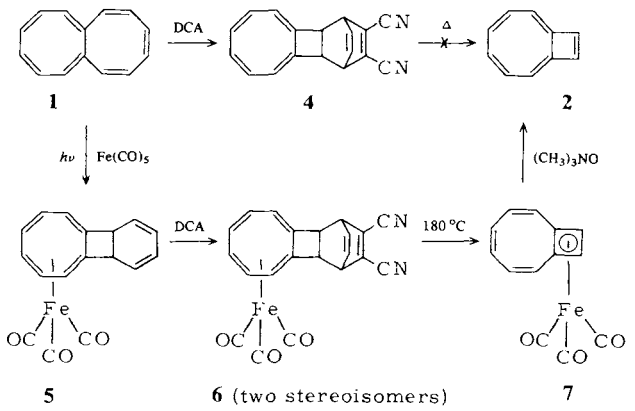
Parallel to *Oda*'s studies we attempted the synthesis of **2** from the olefinic octalene **1**[3] by the classical sequence of Diels-Alder reaction with an acetylenic dienophile and Alder-Rickert cleavage. In combination with transition-metal complex chemistry this concept now enabled an alternative access to **2**.

Reaction of octalene with dienophiles such as maleic anhydride[3c] or dicyanoacetylene (DCA) afforded sterically uniform 1:1 adducts, which—as suggested by the structure of the corresponding Diels-Alder adducts of cyclooctatetraene—derive from the tricyclic octalene valence isomer with a central four-membered ring, whereas reaction with 4-phenyl-1,2,4-triazole-3,5-dione yields an adduct with the carbon skeleton unchanged [(8+2)-cycloaddition][3a]. The octalene-dicyanoacetylene adduct **4** of interest here is obtained on heating a mixture of **1** and dicyanoacetylene (50% excess) in acetone (40–50 °C; 18 h); m.p. 163–164 °C (yield 34%). Contrary to our expectation the Alder-Rickert cleavage of **4** presented problems. Under analytical conditions [injection of a solution of **4** in dichloromethane into the injector of a gas chromatograph at 240 °C] the adduct **4** did in fact thermolyze in the expected way to give **2** and phthalic dinitrile, but on attempted translation of the reaction to the preparative scale a complex mixture of products was always formed, from which **2** could be isolated only with difficulty.

A way out of this impasse was opened by the observation that irradiation of a mixture of **1** and pentacarbonyl-

[*] Prof. Dr. E. Vogel, D. Kawka, Dr. P. Mues
Institut für Organische Chemie der Universität
Greinstrasse 4, D-5000 Köln 41 (Germany)

 © *Verlag Chemie GmbH, 6940 Weinheim, 1983* *0570-0833/83/1212-1003 $ 02.50/0* 




iron in pentane furnished the 1:1 complex **5** (together with 1:2 complexes), which, like the adduct **4**, derives from the octalene valence isomer with a central four-membered ring; red crystals, m.p. 112–113 °C (yield 22%). According to an X-ray structure analysis, the tricarbonyliron group and the six-membered ring in **5** are located on opposite sides of the eight-membered/four-membered ring system. As anticipated, **5** readily undergoes Diels-Alder reactions at the diene system of the six-membered ring, which is easily accessible from both sides. The addition of dicyanoacetylene leads to the chromatographically readily separable stereoisomeric adducts **6a** and **6b**, whose configurations still await assignment; **6a**: m.p. 143–144 °C (yield 56%), **6b**: m.p. 159–161 °C (yield 28%). In view of the tendency of tricarbonyl(1–4-η-9,10-dimethylbicyclo[6.2.0]decapentaene)iron to isomerize to thermodynamically stable tricarbonyl(1,8–10-η-9,10-dimethylbicyclo[6.2.0]decapentaene)iron at 90 °C[1g], it would appear that the thermal conversion of **6a/6b** into the cyclobutadiene complex **7** (and phthalic dinitrile) is predestined. When a mixture of solid **6a/6b** is heated to 180 °C the complex **7** is in fact formed in a smooth reaction [violet crystals, m.p. 74–75 °C (yield 62%)], without any trace of the assumed intermediate 1–4-η-bicyclo[6.2.0]decapentaene(tricarbonyl)iron being detectable[5]. The oxidative liberation of **2** from **7** with trimethylamine *N*-oxide dihydrate in acetone (20 h, room temperature) presented no difficulties; with diammonium hexanitratocerate(IV), however, only indefinable products were obtained. The bicyclo[6.2.0]decapentaene **2**, purified by chromatography on silica gel, precipitates from concentrated pentane solution at −78 °C as orange-red crystals (needles); these were dried *in vacuo* at the same temperature; m.p. < −30 °C (yield 70%).

The spectra of **2**[1i,2e], which have now been supplemented by the $^{13}$C-NMR spectrum [(75.4 MHz, $CD_2Cl_2$): $\delta = 143.90$ (C-9,10), 140.80 (C-1,8), 122.86, 122.60 (C-3,4,5,6), 109.90 (C-2,7)], do not as yet allow conclusions to be drawn about the π-electronic structure. In the case of the $^1$H-NMR spectrum [(90 MHz; $C_6D_6$): $\delta = 6.35$ (s, H-2,3,4,5,6,7), 7.47 (s, H-9,10)] it is still unclear why the chemical shifts of the four-membered and eight-membered ring protons differ by no less than 1.1 ppm. Consistent with the theoretical arguments put forward by *Aihara*[2d], it is obvious that application of the ring-current criterium for aromaticity to annelated ring systems such as **2** is inadmissible. On the basis of the structure analysis of 9,10-diphenylbicyclo[6.2.0]decapentaene[1h], it can be safely assumed that **2** is virtually planar and that the non-cyclobutadienoid resonance structure (as in Formula **2**) is most plausible. Interestingly, force field calculations predict an almost planar carbon skeleton even for an olefinic **2** parameterized to 1,3-butadiene. It thus appears attractive to determine by measurement of the heat of hydrogenation whether **2** profits energetically through delocalization of the peripheral 10π-electron system.

The possibility that **2** can—in analogy to its formation from **1**—be converted by the agency of transition-metal complexes into the butalene **3** hitherto not isolated in substance[9] [complex intermediates: **7**, dicyanoacetylene adduct of **7**, and butalene(tricarbonyl)iron] is presently under investigation.

Received: July 26, 1983;
revised: September 26, 1983 [Z 487 IE]
German version: *Angew. Chem. 95* (1983) 1006
The complete version of this communication appears in:
*Angew. Chem. Suppl. 1983*, 1371–1378

[1] a) P. J. Garratt, R. H. Mitchell, *Chem. Commun. 1968*, 719; b) G. Schröder, H. Röttele, *Angew. Chem. 80* (1968) 665; *Angew. Chem. Int. Ed. Engl. 7* (1968) 635; c) P. J. Garratt, K. P. C. Vollhardt, R. H. Mitchell, *J. Chem. Soc. C 1970*, 2137; d) G. Schröder, S. R. Ramadas, P. Nikoloff, *Chem. Ber. 105* (1972) 1072; e) F. A. Kaplan, B. W. Roberts, *J. Am. Chem. Soc. 99* (1977) 513, 518; f) M. Oda, H. Oikawa, N. Fukazawa, Y. Kitahara, *Tetrahedron Lett. 1977*, 4409; g) M. Magon, G. Schröder, *Liebigs Ann. Chem. 1978*, 1379; h) C. Kabuto, M. Oda, *Tetrahedron Lett. 21* (1980) 103; i) M. Oda, H. Oikawa, *ibid. 21* (1980) 107; j) B. C. Berris, K. P. C. Vollhardt, *Tetrahedron 38* (1982) 2911.

[2] a) R. Breslow, *Acc. Chem. Res. 6* (1973) 393; b) A. Rosowsky, H. Fleischer, S. T. Young, R. Partch, W. H. Saunders, Jr., V. Boekelheide, *Tetrahedron 11* (1960) 121; c) M. Randić, *J. Am. Chem. Soc. 99* (1977) 444; d) J. Aihara, *ibid. 103* (1981) 5704; e) A. Tajiri, M. Hatano, M. Oda, *Chem. Phys. Lett. 78* (1981) 112; f) T. C. W. Mak, W.-K. Li, *J. Mol. Struct. 89* (1982) 281; g) N. L. Allinger, Y. H. Yuh, *Pure Appl. Chem. 55* (1983) 191.

[3] a) E. Vogel, H.-V. Runzheimer, F. Hogrefe, B. Baasner, J. Lex, *Angew. Chem. 89* (1977) 909; *Angew. Chem. Int. Ed. Engl. 16* (1977) 871; b) J. F. M. Oth, K. Müllen, H.-V. Runzheimer, P. Mues, E. Vogel, *ibid. 89* (1977) 910 and *16* (1977) 872; c) P. Mues, Dissertation, Universität Köln 1980.

[5] For an interpretation of the thermal 1–4-η-bicyclo[6.2.0]decapentaene(tricarbonyl)iron—1,8–10-η-bicyclo[6.2.0]decapentaene(tricarbonyl)iron isomerization in terms of a "partially allowed" haptotropic rearrangement see: T. A. Albright, P. Hofmann, R. Hoffmann, C. P. Lillya, P. A. Dobosh, *J. Am. Chem. Soc. 105* (1983) 3396.

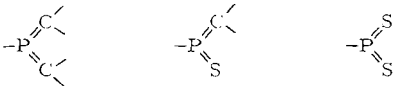
[9] On the detection of butalene as short-lived intermediate see: R. Breslow, J. Napierski, T. C. Clarke, *J. Am. Chem. Soc. 97* (1975) 6275.

## The First Organodithioxophosphorane**

By *Rolf Appel**, *Falk Knoch*, and *Holger Kunze*

*Dedicated to Professor Ernst Otto Fischer on the occasion of his 65th birthday*

Until now, the last member of the triply coordinated planar phosphoranes **1**[1], **2**[2], and **3** was missing; its existence had previously only been speculated about[3].



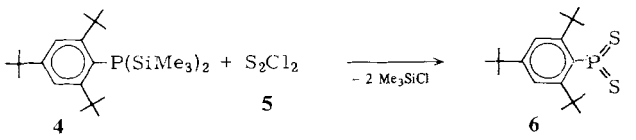

**1** **2** **3**

We have now been able to synthesize the first compound of this type. Dithioxo(tri-*tert*-butylphenyl)phosphorane **6** was obtained by reaction of bis(trimethylsilyl)(tri-*tert*-butylphenyl)phosphane **4**[4] with disulfur dichloride **5**.

This result is surprising in that phenylbis(trimethylsilyl)phosphane reacts with $S_2Cl_2$ and phenyldichlorophos-

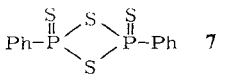
[*] Prof. Dr. R. Appel, F. Knoch, H. Kunze
Anorganisch-chemisches Institut der Universität
Gerhard-Domagk-Strasse 1, D-5300 Bonn 1 (Germany)

[**] Low-Coordinated Phosphorus Compounds. Part 24.—Part 23: R. Appel, W. Paulen, *Angew Chem. 95* (1983) 807; *Angew. Chem. Int. Ed. Engl. 22* (1983) 785.




4 5 6

phane with disulfane to afford the dimeric compound **7**[5].



**7**

**6** forms as a yellow, amorphous powder; when recrystallized from toluene/acetontrile it is orange. Its composition is consistent with the results of elemental analysis, cryoscopic molecular weight determination and mass spectroscopy; its structure is established by $^{31}P\{^1H\}$-NMR spectroscopy and X-ray diffraction analysis (Fig. 1)[6].

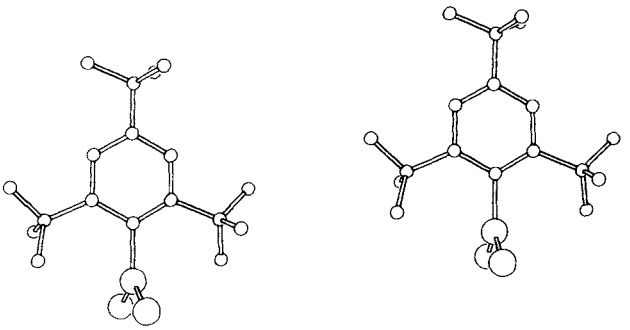


Fig. 1. Stereoscopic projection of the molecular structure of **6** (without H atoms) in the crystal (monoclinic, $P2_1/n$, $a=1021.7(4)$, $b=1032.4(3)$, $c=1910.2(8)$ pm, $\beta=98.4(3)°$, $V=1993.3\cdot10^6$ pm$^3$, $\varrho_{calc}=1.13$ g/cm$^3$, $Z=4$). The structure was solved by direct methods (SHELXTL) from 3129 single-crystal diffractometer data and refined to $R=6.5\%$ ($R_w=5.6\%$). Geometry: $CPS_2$ moiety planar, torsion angle of the aryl group to the $PS_2$ plane *ca.* 80°; angles (*CPS*) *ca.* 117° (*SPS*) 126°; distances (PS) 190 pm, (SS) 338 pm.—Further details on the crystal structure determination can be obtained from the Fachinformationszentrum Energie Physik Mathematik, D-7514 Eggenstein-Leopoldshafen, by quoting the depository number CSD 50568, the names of the authors, and the journal citation.

Both the monomeric compound **6** and the dimer **7** react with alcohols ROH to form the dithiophosphonic acid *O*-monoester aryl-P(S)(SH)(OR).

*Procedure:* A solution of **5** (1.35 g, 10 mmol) in 25 mL *n*-pentane is slowly added dropwise into a solution of **4** (4.23 g, 10 mmol) in 50 mL *n*-pentane cooled with methanol/dry-ice. When the addition is complete, the reaction mixture is allowed to warm up, the amorphous precipitate filtered off, and the solvent removed *in vacuo*. The residue is taken up in a little toluene and the resultant solution treated with acetonitrile until it becomes turbid. At the onset of crystallization the solution is stored in the refrigerator at *ca.* −3 °C until this is complete. Yield of **6**: 2.45 g (72%), m.p. = 148 °C.

Received: July 28, 1983; revised: August 31, 1983 [Z 492 IE]
German version: *Angew. Chem.* *95* (1983) 1008

[1] a) R. Appel, J. Peters, A. Westerhaus, Angew. Chem. *94* (1982) 76; *Angew. Chem. Int. Ed. Engl. 21* (1982) 80; b) R. Appel, A. Westerhaus, *Tetrahedron Lett. 23* (1982) 2017.
[2] E. Niecke, D. A. Wildbredt, *J. Chem. Soc. Chem. Commun. 1981*, 72.
[3] S. O. Lawesson, lecture presented at the International Conference on Phosphorus Chemistry, Durham 1981.
[4] W. Paulen, Dissertation, Universität Bonn 1983.
[5] M. Baudler, H. W. Valpertz, *Z. Naturforsch. B 22* (1967) 222.
[6] $^{31}P\{^1H\}$-NMR ($C_6D_6$; 32.203 MHz, $H_3PO_4$ ext.): $\delta=295.3$ s.

## A Novel Stable Silaethene**

By *Nils Wiberg** and *Gerhard Wagner*

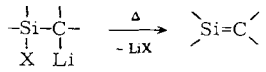
*Dedicated to Professor Ernst Otto Fischer on the occasion of his 65th birthday*

Recently, *Brook et al.* were able to isolate the "silaenol ether" **1** (R = 1-adamantyl), the first silaethene stable at room temperature, and characterize it spectroscopically and by X-ray structure analysis[1]. As a second example, we now wish to describe "silaene" **2**.

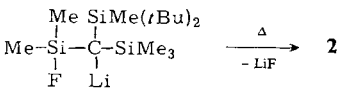


**1** **2**

As described for other silaethenes[2], **2** can be obtained by "thermal salt elimination" (X = electronegative moiety):




In this respect, a tetrahydrofuran adduct of compound **3**, which loses LiF above *ca.* 100 °C, serves as a silaethene precursor[3].

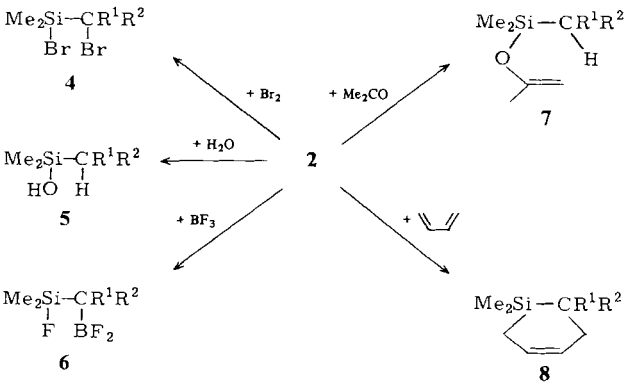



**3**

At room temperature in the presence of chloro(trimethyl)silane, **3** is rapidly transformed into **2**, which can be obtained in crystalline form by slow crystallization from diethyl ether at −78 °C[4].

The silaethene **2** exhibits the expected mass spectrum (molecular ion at *m/z* 300) and $^1$H-NMR spectrum (90 MHz, THF, 30 °C: $\delta=0.446$ ($Me_2$Si), 0.082 (Si*Me*($t$Bu)$_2$), 0.049 (Si*Me*$_3$), 0.969 (SiMe($t$Bu)$_2$).

Compound **2** decomposes within a few days at room temperature (at 100 °C, very rapidly) to afford secondary products which, from mass spectroscopic studies, contain dimers of **2**. **2** reacts vigorously with oxidizing reagents such as atmospheric oxygen or bromine, in the latter case




$R^1$ = $SiMe_3$; $R^2$ = $SiMe(tBu)_2$

[*] Prof. Dr. N. Wiberg, G. Wagner
Institut für Anorganische Chemie der Universität
Meiserstrasse 1, D-8000 München 2 (Germany)

[**] Compounds of Silicon, Part 55. This work was supported by the Deutsche Forschungsgemeinschaft.—Part 54: See [2].

to form the dibromoadduct **4**. With water, **2** affords the silanol **5**, and with boron trifluoride, the compound **6**. Reaction with acetone leads, as expected, to **7**, the product of an ene reaction; with 1,3-butadiene, the Diels-Alder adduct **8** is formed.

The relatively high thermal stability of **2** with respect to dimerization can be attributed to the bulky *tert*-butyl groups (even at −78 °C, $Me_2Si{=}C(SiMe_3)_2$ dimerizes very rapidly[2]). In contrast to **1**, **2** lies at the limits of isolability under normal conditions and exhibits the high reactivity observed for non-isolable silaethenes.

Received: July 28, 1983; revised: September 8, 1983 [Z 493 IE]
German version: *Angew. Chem. 95* (1983) 1027

[1] A. G. Brook, S. C. Nyburg, F. Abdesaken, B. Gutekunst, G. Gutekunst, R. Krishna, M. R. Kallury, Y. C. Poon, Y.-M. Chang, W. Wong-Ng, *J. Am. Chem. Soc. 104* (1982) 5667.

[2] N. Wiberg, G. Preiner, O. Schieda, G. Fischer, *Chem. Ber. 114* (1981) 2087, 3505, 3518.

[3] Preparation of **3**: Reaction of $tBu_2SiHF$ with $LiCH(SiMe_3)_2$ at 130 °C leads to $tBu_2SiH{-}CH(SiMe_3)_2$, which, *via* $tBu_2SiBr{-}CH(SiMe_3)_2$ (reaction with $Br_2$ in $CCl_4$ at room temperature) and $tBu_2SiF{-}CH(SiMe_3)_2$ (reaction with KF in $C_6H_6$ in the presence of [18]crown-6 for 1 week) is converted into $tBu_2SiF{-}CLi(SiMe_3)_2$ (reaction with LiMe in tetrahydrofuran for 1 week at room temperature). A solution of $tBu_2SiF{-}CLi(SiMe_3)_2$ in diethyl ether rearranges over a period of a few weeks to afford **3**. The necessary $tBu_2SiHF$ is obtainable by fluoridation of $tBu_2SiHCl$ (from $HSiCl_3 + 2\,LitBu$ in pentane at room temperature) with $ZnF_2$ at 90 °C, and the necessary $LiCH(SiMe_3)_2$ by analogy to $LiCBr(SiMe_3)_2$ (cf. [2]) by the action of LiBu and $Me_3SiCl$ on $HCBr_3$.

[4] The crystals contain tetrahydrofuran, which according to X-ray structure analysis, is loosely bound to the unsaturated Si atom of **2**. Thermolysis of the diethyl ether adduct of **3** leads to solvent-free **2**, which to date could not be obtained in crystalline form suitable for X-ray structure analysis.

## Synthesis and Structure of a Macrocycle with a Skeletal Framework of Arsenic, Carbon, Oxygen, and Nitrogen Atoms**

By *Herbert W. Roesky*, Habibollah Djarrah, Joachim Lucas, Mathias Noltemeyer,* and *George M. Sheldrick*

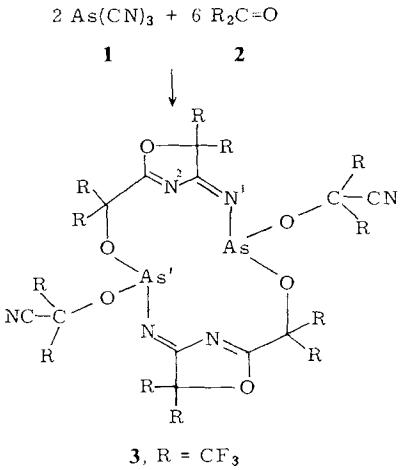
*Dedicated to Professor Karl Winnacker on the occasion of his 80th birthday*

Macrocyclic compounds containing members capable of coordination have been the subject of intensive studies in recent years, because they can be used as complexing agents and for the fixation of smaller guest molecules[1,2].

We have now found that the reaction of arsenic(III) cyanide **1** with hexafluoroacetone **2** in the molar ratio 1 : 3 unexpectedly leads[3] to formation of a fourteen-membered heterocycle **3**.

Depending on the solvent, **3** crystallizes as a colorless adduct containing two molecules of dichloromethane or acetonitrile, which can easily be removed by heating to 80 °C and 100–110 °C, respectively, in an oil pump vacuum. An X-ray structure analysis of a single crystal showed that two arsenic atoms in **3** are coupled *via* two identical bridges of the sequence $N^1{-}C{-}N^2{-}C{-}C{-}O$; each bridge also contains a dihydrooxazole ring (with $N^2$).

The planes of the two halves of the molecule are folded at an angle of 90° to each other by coordinative As–$N^2$ interaction (mean atomic distance 265 pm). Thus, one side of the molecule is completely shielded by $CF_3$ groups, whereas on the other side a solvent molecule (acetonitrile) is taken up in each of the coordination spheres of the arsenic atoms (As–$NCCH_3$ 301 pm). A penetration of these ligands into the macrocycle is however impossible because of the short As···As distance (437 pm).




The structure of **3** (cf. Supplement) clearly demonstrates that during its formation all the As–C bonds in **1** are ruptured. Two CN groups are needed for the construction of the fourteen-membered ring, the third migrates to the carbonyl-C atom of an exocyclically bonded hexafluoroacetone molecule.

Received: August 4, 1983 [Z 505 IE]
German version: *Angew. Chem. 95* (1983) 1029
The complete version of this communication appears in: *Angew. Chem. Suppl. 1983,* 1424–1434

[1] D. J. Cram, *Science 219* (1983) 1177.

[2] J.-M. Lehn, *Struct. Bonding (Berlin) 16* (1973) 1.

[3] *Procedure:* 4.0 g (24.09 mmol) of **2** is passed into a solution of **1** (2.3 g, 15.03 mmol) in $CH_3CN$ (60 mL) at 0 °C. Unreacted **2** is immediately refluxed back into the reaction mixture by means of a condenser (dry ice). The mixture is stirred for 3 h and then allowed to warm to room temperature. After filtration and cooling of the filtrate to 60 °C a colorless crystalline solid precipitates out. Yield 1.5 g (14%); m.p. 171 °C. The solvent molecules in the adduct $3 \cdot 2\,NCCH_3$ are detectable by $^1$H-NMR spectroscopy: $\delta(CH_3CN) = 2.0$. $^{19}$F-NMR ($CH_3CN$): $\delta = 84.2, 48.6, 85.9$.

## $[Ni(S_4)_2]^{2\ominus}$, a Homoleptic Tetrasulfido-Nickel(II) Complex

By *Achim Müller*, Erich Krickemeyer, Hartmut Bögge, William Clegg,* and *George M. Sheldrick*

*Dedicated to Professor Ernst Otto Fischer on the occasion of his 65th birthday*

The existence of numerous binary and tertiary metal sulfide minerals with three-dimensional network structures would suggest that it ought to be possible, under selective conditions, to obtain pure, discrete sulfido-complexes and -clusters, too (cf. in this respect, *e.g.*, the preparation of

[*] Prof. Dr. H. W. Roesky, H. Djarrah, J. Lucas, Dr. M. Noltemeyer, Prof. G. M. Sheldrick
Institut für Anorganische Chemie der Universität
Tammannstrasse 4, D-3400 Göttingen (Germany)

[**] This work was supported by the Deutsche Forschungsgemeinschaft and by Hoechst AG.

[*] Prof. Dr. A. Müller, E. Krickemeyer, Dr. H. Bögge
Fakultät für Chemie der Universität
Postfach 8640, D-4800 Bielefeld 1 (Germany)
Prof. G. M. Sheldrick, Dr. W. Clegg
Institut für Anorganische Chemie der Universität
Tammannstrasse 4, D-3400 Göttingen (Germany)

$[Mo_2(S_2)_6]^{2\ominus}$[1], or $[Cu_3(S_6)_3]^{3\ominus}$[2]). Potential ligands for this purpose are, aside from $S^{2\ominus}$, the polysulfide ions $S_n^{2\ominus}$.

We have now been able to isolate $[Ni(S_4)_2]^{2\ominus}$ **1**—the first "binary nickel-sulfur" complex and the first complex containing only $S_4^{2-}$ ligands—as the reddish-black, diamagnetic $[(C_2H_5)_4N]^+$-salt **1a**[3], and to characterize it by elemental analysis, IR, Raman, UV/VIS/NIR spectroscopy, magnetic measurements, and a complete X-ray structure analysis (Fig. 1).

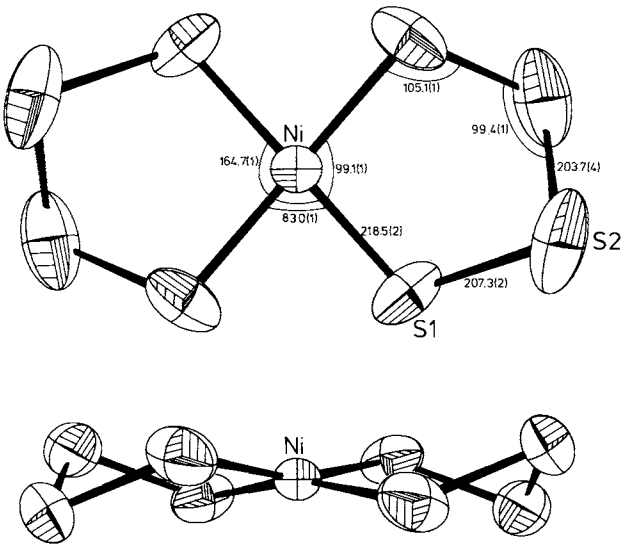



Fig. 1. Structure of the anionic complex **1** (two projections) in the tetraethylammonium salt **1a** (tetragonal crystals, space group $P\bar{4}n2$, $a = 1044.8(2)$, $c = 1276.2(3)$ pm, $Z = 2$; $R = 0.038$ for 1238 independent reflections ($F_0 > 4.0\sigma(F_0)$), $Mo_{K\alpha}$ radiation). Atomic distances in [pm], bond angles in [°]. Further details of the crystal structure investigation are available on request from the Fachinformationszentrum Energie Physik Mathematik, D-7514 Eggenstein-Leopoldshafen, on quoting the depository number CSD 50553, the names of the authors, and full citation of the journal.

The anion **1** with point symmetry $D_2$ exists as a spirobicycle in which the central Ni is surrounded by an approximately square-planar array of four S-atoms.

In the vibrational spectra of **1a** characteristic bands [IR(solid/CsI pellet) and Raman (solid, $\lambda_e = 647.1$ nm)] are found at 480, 430, 375 ($\nu(S_4)$), 280($\nu_{as}(NiS_4)$) and 480 ($\nu_s(S_4)$), 293 ($\nu_s(NiS_4)$), 153 $cm^{-1}$, respectively. The solid state electronic spectrum [reflection; substance distributed on cellulose] shows the characteristic d→d transitions of a $NiS_4$ chromophore ($d^8$Ni): 14.9 ($^1A_{1g} \rightarrow {}^1A_{2g}$), 21.3 ($^1A_{1g} \rightarrow {}^1B_{1g}$)[4]; further bands are observed at 27.4 and 33.3 $10^3$ $cm^{-1}$.

The new complex **1** extends the series of the transition-metal complexes containing only polysulfido ligands, namely $S_2^{2\ominus}$-($[Mo_2(S_2)_6]^{2\ominus}$[1]), $S_4^{2\ominus}$- (**1**), $S_5^{2\ominus}$ ($[Pt(S_5)_3]^{2\ominus}$[1b]) and $S_6^{2\ominus}$ ligands ($[Cu_3(S_6)_3]^{3\ominus}$[2]). It is our aim to find conditions[5] under which pure discrete metal-sulfur aggregates, but also the corresponding mononuclear complexes, can be prepared (the first such species have only recently been described); of particular interest are structures which represent sections from crystal lattices of sulfide minerals.

Received: August 10, 1983 [Z 514 IE]
German version: *Angew. Chem. 95* (183) 1030

[1] a) A. Müller, W. Jaegermann, J. H. Enemark, *Coord. Chem. Rev. 46* (1982) 245; experimental details: A. Müller, R. G. Bhattacharyya, B. Pfefferkorn, *Chem. Ber. 112* (1979) 778; A. Müller, R. G. Bhattacharyya, W. Eltzner, N. Mohan, A. Neumann, S. Sarkar in H. F. Barry, P. C. H. Mitchell: *Proc. 3rd Int. Conf. Molybdenum*, Climax Molybdenum Comp., Ann Arbor 1979, p. 59; b) F. A. Cotton, G. Wilkinson: *Advanced Inorganic Chemistry*, 4th Ed., Wiley-Interscience, New York 1980, p. 851.

[2] A. Müller, U. Schimanski, *Inorg. Chim. Acta Lett., 77* (1983) 187.

[3] *Procedure:* 4 g of $[(C_2H_5)_4N]Br$ is dissolved with stirring in 50 mL of methanolic ammonium polysulfide (100-mL Erlenmeyer flask). After stepwise addition of 2 g $Ni(CH_3COO)_2 \cdot 4H_2O$, the mixture is heated to 45 °C, quickly filtered, and the dark brown filtrate stored in a closed flask at room temperature. After 1 h the precipitated shiny black crystals of **1a** are filtered off and washed with isopropanol (analytically pure) and $CS_2$; yield 0.9 g.—For the preparation of the methanolic ammonium polysulfide solution a stream of $NH_3$ is passed into 1L of absolute methanol for 1 h. After addition of 100 g sulfur ($S_8$), $H_2S$ is passed through the solution for 1 h. The sulfur is almost completely dissolved during the reaction. Any undissolved material is removed by filtration.

[4] For the assignment cf. A. B. P. Lever: *Inorganic Electronic Spectroscopy*, Elsevier, Amsterdam 1968.

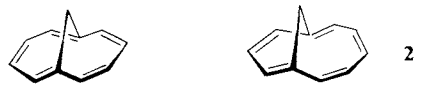
[5] Slight differences in the preparative cconditions (*e.g.* different polysulfide concentrations) can lead to different products. Thus, *e.g.*, from the same solution, $[Mo_3S(S_2)_6]^{2\ominus}$ is obtained on heating and $[Mo_2(S_2)_6]^{2\ominus}$ at room temperature[1b]. *Note added in proof:* The corresponding Pd complex ($[(C_2H_5)_4N]_2[Pd(S_4)_2]$, shiny black crystals) could also be obtained and characterized by an X-ray structure analysis.

## Resonance Energy of Bridged [10]Annulenes**

By *Wolfgang R. Roth*, Manfred Böhm, Hans-Werner Lennartz,* and *Emanuel Vogel*

*Dedicated to Professor W. von E. Doering on the occasion of his 65th birthday*

The numerous experiments carried out to test the Hückel rule, which culminated in the discovery (or rediscovery) of the tropylium ion by *Doering* some 30 years ago, have enriched organic chemistry with a plethora of aromatic and nonaromatic cyclically-conjugated ring systems (annulenes and ionic species derived therefrom). Although many of these ring systems have been the subject of detailed investigation from the chemical, spectroscopic, and structural point of view, their thermodynamical behavior has so far been studied only in isolated cases. We have now analyzed the effect of conjugation on the bridged [10]annulenes **1**[1] and **2**[2] by measurement of the heats of hydrogenation.




We have used the resonance energy as a measure of the stabilization. This is not an observable quantity, but the difference between the experimentally determined enthalpy of formation and that of a hypothetical model built up additively from localized two-center bonds. To calculate this value we have adopted the method proposed by *Dewar*, who defined 1,3-butadiene as a "normal" polyene and designated deviations compared to the bonding of this reference compound as resonance[6a].

As a rule the enthalpy of formation of the model is either estimated from bond increments or determined by quantum mechanical calculations. Both methods are unsatisfactory. The inadequacies can be avoided if the heat of formation of the model is derived from force field calcula-

[*] Prof. Dr. W. R. Roth, M. Böhm, H.-W. Lennartz
Abteilung für Chemie der Universität
Postfach 102148, D-4630 Bochum (Germany)
Prof. Dr. E. Vogel
Institut für Organische Chemie der Universität Köln (Germany)

[**] Heats of Hydrogenation, Part 5. This work was supported by the Deutsche Forschungsgemeinschaft and the Fonds der Chemischen Industrie.—Part 4: [7].

tions. If the force field is adjusted to 1,3-butadiene then a comparison of the experimentally determined enthalpy of formation with the calculated value directly affords the resonance energy normalized to 1,3-butadiene. We found by such a comparison for a large number of polyenes that there is good agreement (0.5 kcal/mol) between experimental and calculated enthalpies of formation in acyclic systems, *i.e.* there is no greater resonance stabilization than in 1,3-butadiene[7]. On the other hand, for "cyclohexatriene" an additional stabilization of 26.1 kcal/mol is obtained, which is in good agreement with the resonance energy (23.3 kcal/mol[6b]) derived from quantum mechanical calculations.

The calculated resonance energies of the bridged [10]annulenes **1** and **2** are listed together with the values of naphthalene **4** and azulene **5** for comparison in Table 1. In the case of **1**, **2**, and **5** the experimental enthalpies of formation were ascertained by measurements of heats of hydrogenation. Since the enthalpies of formation of the products of reduction of **1** and **2** are not known, these values were taken from force field calculations, so that the enthalpies of formation have a "pseudo-experimental" character. However, in view of the high reliability of the method in the case of saturated hydrocarbons, the errors might very well be small.

Table 1. Enthalpies of formation and resonance energies of some cyclic polyenes.

| Cpd. | | $H_f^0$(g) exp. [kcal/mol] | $H_f^0$(g) calc. [a] [kcal/mol] | Resonance energy [kcal/mol] |
|---|---|---|---|---|
| 3 |  | 19.81 | 45.88 | 26.1 |
| 4 |  | 36.05 | 76.70 | 40.7 |
| 1 |  | 77.1 [7]<br>75.2 | 94.33 | 17.2 |
| 5 |  | 73.5 | 89.60 | 16.1 |
| 2 |  | 95.5 | 102.03 | 6.5 |
| 6 |  | 62.3 [7] | 68.36 | 6.1 |
| 7 |  | 35.0 [7] | 39.69 | 4.7 |
| 8 |  | 44.6 | 48.54 | 3.9 |

[a] Modified MM2 force field [7].

The resonance energies determined for the bridged [10]annulenes **1** and **2** and for **4** and **5** revealingly reflect the different chemical reactivity of these compounds: **1** and **5** are markedly more reactive than naphthalene **4**, yet share with it the ability to form substitution products on reaction with electrophilic agents[1]. The annulene **2**—in striking contrast to **1**—even polymerizes in air and no longer shows any tendency to form substitution products with electrophiles[2].

The noticeably different resonance energies of **1** and **2**, together with the different degree of deviation of the $C_{10}$ perimeter from planarity, may be caused mainly by the transannular interaction (homoconjugation *via* C1—C6), which is only possible in **1**. This interpretation is supported, not only by the observed increase in resonance energy (bracket effect) in the transition from **8** to **7** and **6**, but is also indicated by the short C1—C6 distance in **1** (2.235 Å), by the absorption and emission spectra[14], and by the circular dichroism[15] of **1**. In the light of the C1—C6 interaction in **1** derived from the resonance energy and the spectra it appears justified to regard 1,6-methano[10]annulene as 9,10-homonaphthalene.

Received: August 15, 1983 [Z 516 IE]
German version: *Angew. Chem. 95* (1983) 1011
The complete version of this communication appears in: *Angew. Chem. Suppl. 1983*, 1379—1387

[1] E. Vogel, H. D. Roth, *Angew. Chem. 76* (1964) 145; *Angew. Chem. Int. Ed. Engl. 3* (1964) 228; E. Vogel, *Chem. Soc. Spec. Publ. No. 21* (1967) 113.
[2] a) S. Masamune, D. W. Brooks, K. Morio, R. L. Sobczak, *J. Am. Chem. Soc. 98* (1976) 8277; b) L. T. Scott, W. R. Brunsvold, *ibid. 100* (1978) 4320; L. T. Scott, W. R. Brunsvold, M. A. Kirms, I. Erden, *ibid. 103* (1981) 5216.
[6] a) M. J. S. Dewar: *The Molecular Orbital Theory of Organic Chemistry*, McGraw-Hill, New York 1969; b) H. Kollmar, *J. Am. Chem. Soc. 101* (1979) 4832, and references cited therein.
[7] W. R. Roth, F.-G. Klärner, G. Siepert, H.-W. Lennartz, *Chem. Ber.*, in press.
[14] H. J. Dewey, H. Deger, W. Frölich, B. Dick, K. A. Klingensmith, G. Hohlneicher, E. Vogel, J. Michl, *J. Am. Chem. Soc. 102* (1980) 6412.
[15] K. A. Klingensmith, W. Püttmann, E. Vogel, J. Michl, *J. Am. Chem. Soc. 105* (1983) 3375.

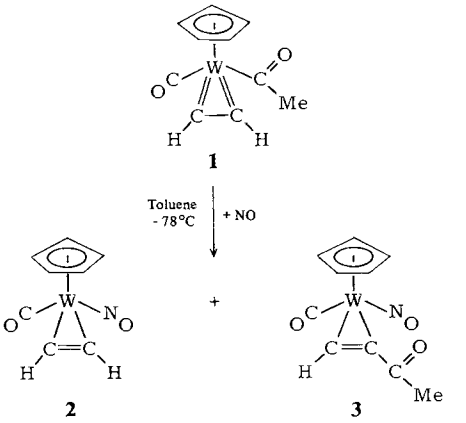
## The Transformation of Acetylene from a Four- to a Two-Electron Ligand: Acetylene(carbonyl)nitrosyl Complexes of Tungsten**

By *Helmut G. Alt** and *Heidi I. Hayen*

*Dedicated to Professor Ernst Otto Fischer on the occasion of his 65th birthday*

[CpW(CO)($C_2H_2$)COMe] **1** is a highly reactive, easily accessible alkyne complex in which $C_2H_2$ behaves formally as a four-electron ligand. We have now found that solutions of **1** in toluene at −78 °C react instantaneously with gaseous nitric oxide to form the two monomeric nitrosyl(alkyne) complexes **2** (51%) and **3** (9%) which can be separated by column chromatography.

[**2**, IR (THF): $\nu$(CO) = 1985, $\nu$(NO) = 1605,

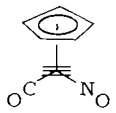



**1** **2** **3**

[*] Priv.-Doz. Dr. H. G. Alt, H. I. Hayen
Laboratorium für Anorganische Chemie der Universität
Universitätsstrasse 30, D-8580 Bayreuth (Germany)

[**] This work was supported by the Deutsche Forschungsgemeinschaft and the Fonds der Chemischen Industrie.

$\nu$(C≡C) = 1723 cm$^{-1}$; $^1$H-NMR, $^{13}$C-NMR; MS: *m/z* 333 ($M^+$) relative to $^{184}$W; m.p. = 142–146 °C.—**3**, IR (THF): $\nu$(CO) = 2008, $\nu$(NO) = 1602, $\nu$(C≡C) = 1700, $\nu$(C=O) = 1650 cm$^{-1}$; $^1$H-NMR, $^{13}$C-NMR; MS: *m/z* 375 ($M^+$) relative to $^{184}$W; at room temperature greasy.] Compared to those of **1**, the $^1$H- and $^{13}$C-NMR signals of the acetylene ligands in **2** and **3** are shifted to high field ($\Delta\delta \approx 4$ and 80 ppm, respectively), which can be expected as the result of a transformation from a four- to a two-electron ligand. This assumption is also corroborated by the increase in the coupling constants $^1J$(C,H) ($\approx$220 Hz) and $^2J$(C,H) ($\approx$22 Hz) in **2** and **3** relative to **1** or [CpW(CO)($C_2H_2$)Me][2]. In accord with this, the $\nu$(C≡C) band is shifted markedly to higher wavenumbers, whereas the $\nu$(NO) band is located in the region typical for terminal three-electron nitrosyl ligands. In **2** and **3**, astonishingly high barriers for rotation of the $C_2H_2$ ligand around the tungsten-alkyne bond axis are found: in contrast to the analogous chromium complex [CpCr(CO)($C_2H_2$)NO] ($\Delta G^+ = 55.9$ kJ/mol in [D$_8$]toluene[4]), temperature-dependent $^1$H-NMR measurements of **2** and **3** indicate $\Delta G^+ > 90$ kJ/mol. We therefore assume the involvement of metallacyclopropene mesomeric structures in **2** and **3**, as postulated for [Cp$_2$Ta(alkyne)H] (alkyne = substituted acetylene) for the same reasons[5]. The formation of metallacyclopropene derivatives is also corroborated by the observation of $^2J$(W,H) couplings (7.3, 9.2, and 6.1 Hz, resp.) in the $^1$H-NMR as well as $^1J$(W,C) couplings (51, 32 and 48 and 15 Hz, resp.) and $^1J$(C,H) couplings ($\approx$228 Hz) in the $^{13}$C-NMR spectrum, which indicate a significant contribution from a metal-carbon σ bond. Consequently, $\Delta G^+$ is not the only criterion for classifying an alkyne formally as a two- or four-electron ligand. Our spectroscopic findings were confirmed by the results of calculations using the EHMO method[9]: for the acetylene ligand in [CpMo(CO)($C_2H_2$)NO] the rotation barrier around the metal-alkyne bond axis was determined to be 146 kJ/mol. For the lowest energy conformation an orientation of the alkyne ligand is predicted in which the –C≡C– axis and the



metal-CO axis are no longer coplanar but are twisted by 20°[10]. This probably arises from the better π-acceptor behavior of the NO ligand compared to CO. The synthesis of **2** and **3** described here is also remarkable from a preparative point of view. Previously, it had not proved possible to convert the parent compound [CpW(CO)$_2$NO] into derivatives of the type [CpW(CO)(L)NO] (L = alkene, alkyne) by photo-induced exchange of a CO ligand.

Received: August 18, 1983; revised: October 5, 1983 [Z 520 IE]
German version: *Angew. Chem. 95* (1983) 1030
The complete version of this communication appears in:
*Angew. Chem. Suppl. 1983*, 1364–1370

[2] C. G. Kreiter, K. Nist, H. G. Alt, *Chem. Ber. 114* (1981) 1845.
[4] M. Herberhold, H. Alt, C. G. Kreiter, *J. Organomet. Chem. 42* (1972) 413.
[5] J. A. Labinger, J. Schwartz, J. M. Townsend, *J. Am. Chem. Soc. 96* (1974) 4009.
[9] B. E. R. Schilling, R. Hoffmann, J. W. Faller, *J. Am. Chem. Soc. 101* (1979) 592.
[10] In contrast, the X-ray structure analysis of [(C$_5$Me$_5$)W(CO)($C_2H_2$)Me] indicates that the C≡C axis of the alkyne ligand and the W–CO axis are almost parallel and coplanar H. G. Alt, U. Thewalt, unpublished results.

## Structural Relationship of [($C_6H_5$)$_4$As]NdCl$_4$·8 H$_2$O and NdCl$_3$·6 H$_2$O: Transition from a Three-Dimensional to a Layer Structure

By *Werner Urland** and *Ulrich Schwanitz-Schüller*

The hydrates of the lanthanoid chlorides MCl$_3$·6 H$_2$O (M = Nd–Lu) contain the complex cation [M(H$_2$O)$_6$Cl$_2$]$^{\oplus}$[1]. Reaction of NdCl$_3$·6 H$_2$O with aqueous ($C_6H_5$)$_4$AsCl in CH$_3$CN/C$_2$H$_5$OH leads to formation of the novel compound [($C_6H_5$)$_4$As]NdCl$_4$·8 H$_2$O[6]. The structure of this compound (Fig. 1) is likewise determined by the cation [Nd(H$_2$O)$_6$Cl$_2$]$^{\oplus}$. The arrangement of the complex cations corresponds to a two-dimensional section of the NdCl$_3$·6 H$_2$O structure, but now with H$_2$O molecules as well as Cl$^{\ominus}$ ions bridging the cations. These layers are separated by intercalated ($C_6H_5$)$_4$As$^{\oplus}$ ions; the original structure of NdCl$_3$·6 H$_2$O is formally dissected. The bridging Cl$^{\ominus}$ ion (Cl(2) in Fig. 1) can be regarded as the site of incision, which now exhibits a remarkably unilateral instead of distorted octahedral coordination. The Cl(2)-anion lies outside of a distorted tetrahedron of water molecules, its "free side" faces the ($C_6H_5$)$_4$As$^{\oplus}$ layer. The transition from a spatial network to a layer structure necessitates a change in composition. The number of bridging Cl$^{\ominus}$ ions per [Nd(H$_2$O)$_6$Cl$_2$]$^{\oplus}$ moiety is doubled. At the same time cavities are created in the layer, and these are occupied by water molecules. The water molecules apparently stabilize the unilaterally coordinated bridging Cl(2). The orientation of the H$_2$O molecules points to strong hydrogen bonding and to interactions with the Cl$^{\ominus}$ ions. Such a cross-linking to layers is structure-determining and concomitantly enforces the layer-like arrangement of the ($C_6H_5$)$_4$As$^{\oplus}$ counterions. This is unusual, since columnar

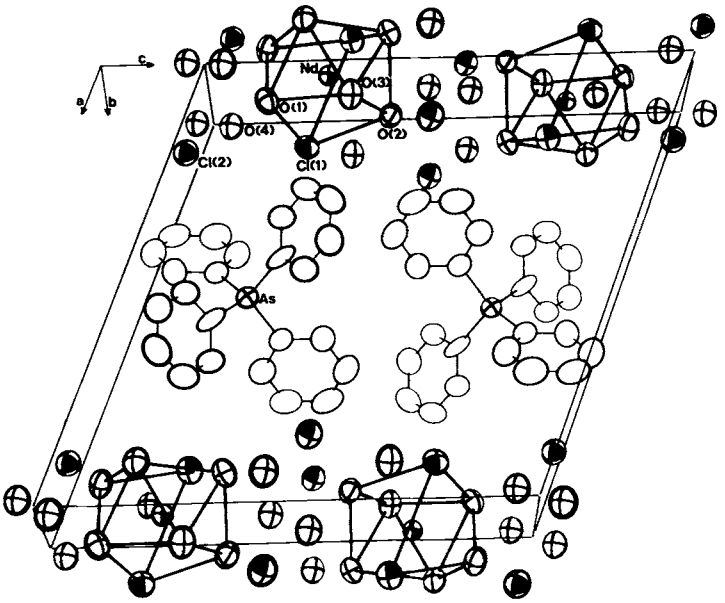



Fig. 1. Structure of [($C_6H_5$)$_4$As]NdCl$_4$·8 H$_2$O (ORTEP diagram, thermal vibration ellipsoids with 75% probability). Monoclinic crystals, P2/c, $a$ = 1576.0(2), $b$ = 664.7(1), $c$ = 1593.2(2) pm, $\beta$ = 110.86(1)°, $Z$ = 2, $R$ = 0.018, $R_w$ = 0.021. Selected distances [pm]: Nd–O(1) 248.6(2), Nd–O(2) 246.3(1), Nd–O(3) 246.3(1), Nd–Cl(1) 279.68(6) [5].

[*] Priv.-Doz. Dr. W. Urland, U. Schwanitz-Schüller
Max-Planck-Institut für Festkörperforschung
Heisenbergstrasse 1, D-7000 Stuttgart 80 (Germany)

stacking of the $(C_6H_5)_4As^{\oplus}$ ions has mainly been observed hitherto in compounds of similar composition[2].

Received: August 19, 1983; revised: October 5, 1983 [Z 521 IE]
German version: *Angew. Chem. 95* (1983) 1031
The complete version of this communication appears in:
*Angew. Chem. Suppl. 1983*, 1399–1408

[1] *Gmelin Handbuch der Anorganischen Chemie C4a*, Springer, Berlin 1982.
[2] U. Müller, *Acta Crystallogr. B36* (1980) 1075.
[5] Further details of the crystallographic investigation are available on request from the Fachinformationszentrum Energie Physik Mathematik, D-7514 Eggenstein-Leopoldshafen, on quoting the depository number CSD 50547, the names of the authors, and full citation of the journal.
[6] According to thermogravimetric investigations the compound loses its water of crystallization in the temperature range of about 70–140°C. At the same time, the color changes from lilac to dove-blue.

## Alkyne Complexes of Tungsten(IV)**

By *Klaus H. Theopold, Steven J. Holmes,* and *Richard R. Schrock**

Alkyne ligands can be regarded as dianions[1]. Our interest in the chemistry of alkyl, alkylidene, and alkylidyne complexes of tungsten(*VI*)[3] therefore urged us to attempt the preparation of simple alkyne complexes of tungsten(IV), for we hoped that these compounds would behave like tungsten(VI) complexes in their reactions with alkylating agents. This in fact turned out to be the case, and we now report on the first mild protonation of an alkyne ligand with formation of a vinyl-$W^{VI}$ derivative. The synthesis of $W(C_2R_2)Br_4$ and $Mo(C_2R_2)Cl_4$ (R = Me, Ph) was actually described[4] some ten years ago, while $[Mo(C_2Ph_2)Cl_4]_x$ has recently been the subject of further study, together with the new compounds $[W(C_2Ph_2)Cl_4]_x$, $[Nb(C_2Ph_2)Cl_3]_4$, and $Re(C_2Ph_2)Cl_5$[5].

Tungsten tetrachloride reacts with alkynes in diethyl ether at room temperature to give $W(C_2R_2)Cl_4 \cdot Et_2O$ (R = Me, Et, Ph). Ether-free $W(C_2Ph_2)Cl_4$ is formed on reaction of $WCl_6$ with diphenylacetylene in $CH_2Cl_2$; in the presence of ether it is readily converted into $W(C_2Ph_2)Cl_4 \cdot Et_2O$. The IR spectra of these complexes show a band at 1700–1750 $cm^{-1}$ characteristic of a strongly bound alkyne ("metallacyclopropene"). The chemical shifts of the alkyne C-atoms in the NMR spectra (cf. Supplement) with $(^{13}C) \approx 270$ are, to the best of our knowledge, greater than all previously reported values.

In view of the formation of the ether adduct it is not surprising that $W(C_2R_2)Cl_4$ also adds chloride ions.

$$W(C_2R_2)Cl_4 + [NEt_4]Cl \xrightarrow{CH_2Cl_2} [NEt_4]^{\oplus}[W(C_2R_2)Cl_5]^{\ominus}$$

The anionic alkyne complexes thus formed are especially suitable for alkylations with dialkylzinc, whereby compounds of the type $W(C_2R_2)R'_3Cl$ are obtained in good yields (60–80%).

$$[NEt_4]^{\oplus}[W(C_2R_2)Cl_5]^{\ominus} \xrightarrow[0.5\ NEt_4Cl]{1.5\ ZnR'_2} W(C_2R_2)R'_3Cl$$

$CH_2Cl_2$ R = Et, R' = Me; R = Me, R' = $CH_2SiMe_3$

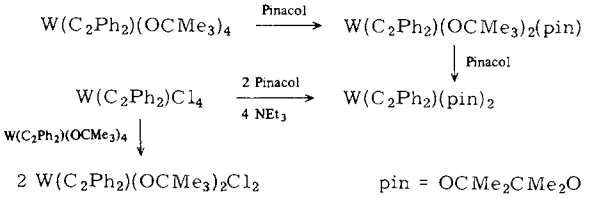
Attempts to prepare $W(C_2Et_2)(CH_2CMe_3)_3Cl$ resulted in the formation of a mixture of products, from which $W(C_2Et_2)(CHCMe_3)(CH_2CMe_3)_2$ could be isolated as a distillable yellow oil in poor yield.

All of the chemistry concerning the formation of alkyl (and alkylidene) complexes is remarkably similar to that recently reported for phenylimido complexes[3b]. We therefore propose to extend the concept of alkyne-metal interaction: alkyne ligands are not only doubly charged anions, but also *good π-donors*, analogous to the imido and oxo ligands.

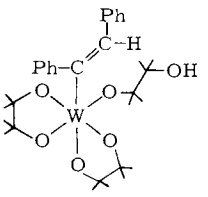



$d^2$-Metal-C(alkyne) bond distances are usually quite short (*ca.* 205 ppm) so that especially for third row metals the overlap of metal d orbitals with the ligand π-system is likely to be substantial. In certain situations, therefore, the alkyne functions as a strongly π-bonded dianionic auxiliary ligand which stabilizes the $d^0$ oxidation state of the metal center.

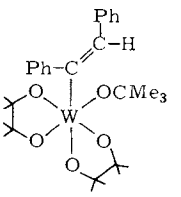
$W(C_2Ph_2)Cl_4$ reacts smoothly with $LiOCMe_3$ to give yellow crystalline $W(C_2Ph_2)(OCMe_3)_4$ in high yield. Several related complexes can be prepared in a similar fashion.




Consistent with our description of the alkyne ligand, $W(C_2Ph_2)(pin)_2$ reacts with pinacol to produce $W(pin)_3$ and *cis*-stilbene in high yield. As expected, the $^1$H-NMR spectrum of $W(pin)_3$ shows two singlets. In the presence of (+)-1-(9-anthryl)-2,2,2-trifluoroethanol one of these signals splits into a doublet, demonstrating the presence of a racemic mixture of both enantiomers of the chiral complex. On monitoring the course of the reaction $^1$H-NMR spectroscopically we found evidence for the existence of an intermediary vinyl complex **A**.




**A**




**B**

The reaction of $W(C_2Ph_2)(pin)_2$ with *tert*-butyl alcohol leads to the analogous vinyl complex **B**, which could be isolated and characterized.

Received: August 19, 1983 [Z 522 IE]
German version: *Angew. Chem. 95* (1983) 1012
The complete version of this communication appears in:
*Angew. Chem. Suppl. 1983*, 1409–1423

[*] Prof. Dr. R. R. Schrock, Dr. K. H. Theopold, Dr. S. J. Holmes
Department of Chemistry, Massachusetts Institute of Technology
Cambridge, MA 02139 (USA)

[**] This research was supported by the National Science Foundation (CHE 81-21282) and, in part, by the National Institutes of Health (GM 31978).

[1] S. Otsuka, A. Nakamura, *Adv. Organomet. Chem. 14* (1976) 245, and references cited therein.
[3] a) R. R. Schrock, *Science 219* (1983) 13; b) S. F. Pedersen, R. R. Schrock, *J. Am. Chem. Soc. 104* (1982) 7483.
[4] A. Greco, F. Pirinoli, G. Dall'asta, *J. Organomet. Chem. 60* (1973) 115.
[5] E. Hey, F. Weller, K. Dehnicke, *Naturwissenschaften 70* (1983) 41.

# Structure Analysis of a $CaF_2$ Single Crystal with an Edge Length of only 6 μm: An Experiment using Synchrotron Radiation

By *Rolf Bachmann, Heinz Kohler, Heinz Schulz*, Hans-Peter Weber, Vladimir Kupčik, Michael Wendschuh-Josties, Andreas Wolf,* and *Reinhard Wulf*

Until now the high intensity and low divergence of the X-ray radiation from an electron synchrotron has been used in structural analysis 1) to reduce the measuring time (*e.g.* to minimize radiation damage of protein crystals); 2) to enable selection of the optimal wavelength for the experiment (*e.g.* for determination of the phases using anomalous dispersion); and 3) to increase the spatial resolution (*e.g.* in powder spectra to achieve separation of previously unresolved peaks)[1].

Furthermore, the high brightness of the radiation and its natural collimation lead to a considerable increase in the signal/noise ratio of the Bragg reflections. We have used this property to answer the question to what extent accurate reflection intensities can also be measured on extremely small crystals. The work was carried out at the synchrotron radiation laboratory "Hasylab" at DESY (Hamburg). For this purpose, a five-circle diffractometer was used[2] which is equipped with a germanium (111) double monochromator. Its angular resolution of 1/1000° permits the measurements of reflections having a width at half-height $< 1/100°$ (Fig. 1). Single crystals of $CaF_2$ of various sizes were investigated with synchrotron radiation (storage ring DORIS II, 3.5 GeV, 60—25 mA). The results were compared with those from a conventional molybdenum X-ray source (2 kW). $CaF_2$ was chosen as standard substance since it consists only of light elements with small atom scattering factors. The smallest crystal which could be measured using a conventional X-ray tube had a volume of 2000 $\mu m^3$. Using synchrotron radiation, a data set ($(\sin\vartheta/\lambda)_{max} = 0.73$ Å$^{-1}$) was recorded on a crystal with a volume of only 200 $\mu m^3$ (Fig. 2). Previously, measurements were only made on similarly small crystals, but which exhibited a 30-fold larger crystal scattering power[3].

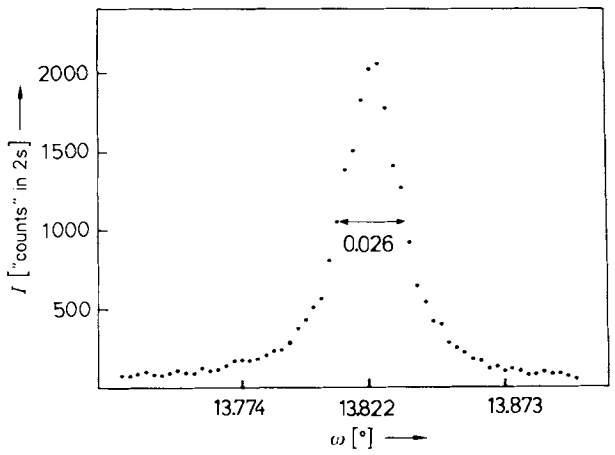



Fig. 1. ω-Scan ("rocking curve") of the (220) reflection.

[*] Prof. Dr. H. Schulz, Dr. R. Bachmann, H. Kohler, Dr. H. P. Weber
Max-Planck-Institut für Festkörperforschung
Postfach 800665, D-7000 Stuttgart 80 (Germany)
Prof. Dr. V. Kupčik, M. Wendschuh-Josties, A. Wolf, R. Wulf
Mineralogisch-kristallographisches Institut der Universität
D-3400 Göttingen (Germany)

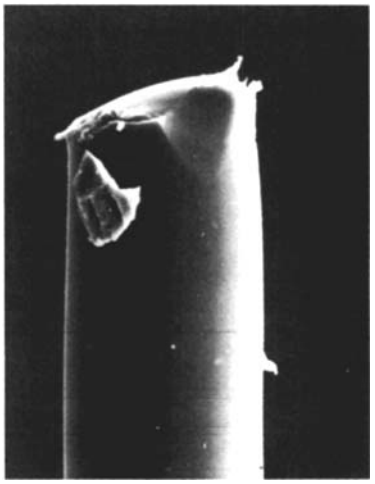


Fig. 2. 1000-fold magnification of the calcium fluoride crystal mounted on a glass pin. The width of the photograph corresponds to the diameter of a human hair; the bar at the bottom edge corresponds to 10 μm.

Table 1. Crystal scattering power [a]: comparison of the measured $CaF_2$ crystal with a crystal of similar size.

| | $\rho = \frac{\Sigma e}{v}$ [$10^{24}$ cm$^{-3}$] | $V_{cryst.}$ [$10^{-12}$ cm$^3$] | $\lambda$ [$10^{-8}$ cm] | $S$ [$10^{12}$] |
|---|---|---|---|---|
| $CaF_2$ | 0.929 | 200 | 0.9101 | 130.1 |
| $Re_2P$ [3] | 7.317 | 200 | 0.7107 | 3840 |

[a] The crystal scattering power $S$ is defined as $I^2 \cdot V_{cryst.} \cdot \lambda^3$, where $\Sigma e$ is the number of electrons per unit cell of volume $v$, $V_{cryst.}$ is the volume of the crystal, and $\lambda$ is the wavelength.

Our experiment showed that single crystal diffraction measurements can also be performed on crystallites having a crystal scattering power of *ca.* $10^{14}$ (Table 1). Until now, many substances from which larger crystals could not be grown could only be studied with powder techniques, which provide less information. In the future it is expected that the structures of numerous interesting groups of substances from different areas of solid-state chemistry (*e.g.*, ion-conducting crystals such as NASICON, and catalysts such as zeolites), mineralogy (*e.g.* lamella of zone-structured crystals) and biochemistry (*e.g.* protein crystals) will be solved. Moreover, the use of small crystals leads to a considerable reduction of systematic error such as absorption and extinction, which are both dependent on the crystal size. In the present case, the influence of the absorption can be neglected. A preliminary crystal structure refinement makes it very probable that the 24 measured reflections are not influenced by extinction. For this purpose, the known temperature factors of $CaF_2$ were used[4]. In contrast, in the standard crystal project of a $CaF_2$ sphere of 440 μm radius of the American Crystallographic Association, 85% of the reflections are extinction attenuated by more than 10%[4b]. Preliminary refinement of our data gave an unweighted $R$-value of 4%. It follows that a signal/noise ratio is achieved which corresponds to that obtained using conventional diffractometer measurements, despite the extremely small size of the crystal.

By preparing the crystals using a micromanipulator and by increasing the radiation intensity with a "wiggler"[5], it should even be possible in the near future to make measurements on single crystals whose crystal scattering power is at least one order of magnitude less.

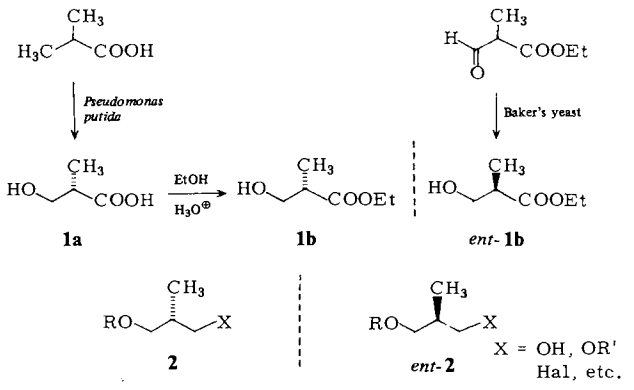
Received: August 29, 1983 [Z 553 IE]
German version: *Angew. Chem.* 95 (1983) 1013

[1] J. C. Phillips, A. Wlodawer, M. Yevitz, K. O. Hodgson, *Proc. Natl. Acad. Sci. USA 73* (1976) 128; J. C. Phillips, A. Wlodawer, J. M. Goodfellow, K. D. Watenpaugh, L. C. Sieker, L. H. Jensen, K. O. Hodgson, *Acta Crystallogr. A 33* (1977) 445; D. E. Cox, J. B. Hastings, W. Thomlinson, C. T. Prewitt, *Nucl. Instrum. Methods 208* (1983) 573.
[2] V. Kupčik, R. Wulf, M. Wendschuh, A. Wolf, A. Paehler, *Nucl. Instrum. Methods 208* (1983) 519.
[3] W. Jeitschko, personal communication (1983); see also R. Rühl, W. Jeitschko, *Abstr. 8th Eur. Crystallogr. Meet. Liège 1983*, 216.
[4] a) W. H. Zachariasen, *Acra Crystallogr. A 24* (1968) 425; b) M. J. Cooper, *ibid. A 26* (1970) 208; c) M. J. Cooper, K. D. Rouse, *ibid. A 27* (1971) 622.
[5] P. Guertler, A. Jackson, *Nucl. Instrum. Methods 208* (1983) 163.

## Preparation of Ethyl (*R*)-(−)-3-Hydroxy-2-methylpropanoate by Yeast Reduction of Ethyl α-Formylpropanoate

By *Max F. Züger, Fabio Giovannini,* and *Dieter Seebach**

Derivatives of 3-hydroxy-2-methylpropanoic acid **1a** are useful chiral building blocks. This is mainly due to the fact that "interconversion" of the functionalized C atoms of **1** provides both enantiomeric building blocks **2** and *ent*-**2**[1a]. The (*S*)-(+)-acid **1a** is formed by hydroxylation of the (*Re*)-methyl group of isobutyric acid with *Pseudomonas putida*[1b], a microorganism which is not easy to grow in the routine organic chemistry laboratory. Furthermore, the free acid is labile, its isolation from the fermentation broth is not easy, and the interconversion of the "enantiotopic branches" requires several steps[1].




**3a**, R = $C_2H_5$ ($[\alpha]_D^{20}$ +1.2, 50% *ee*)
**3b**, R = $CH(CH_3)_2$ ($[\alpha]_D^{20}$ −2.5, 60% *ee*)
**3c**, R = $CH_2C_6H_5$ ($[\alpha]_D^{20}$ +17.3, 46% *ee*)
**3d**, R = $C_6H_5$ ($[\alpha]_D^{20}$ +38.9, 83% *ee*)

[*] Prof. Dr. D. Seebach, F. Giovannini, M. F. Züger
Laboratorium für Organische Chemie
der Eidgenössischen Technischen Hochschule, ETH-Zentrum
Universitätstrasse 16, CH-8092 Zürich (Switzerland)

We have now found that simple yeast reduction[2] of ethyl α-formylpropanoate[3] (*ca.* 12 g/L water) produces the (*R*)-(−)-ester *ent*-**1b** in 60—65% *ee* (70—80% yield). Enantiomerically pure ester *ent*-**1b** ($[\alpha]_D^{20}$ −21.6° (*c* = 4, $CH_3OH$; ref. [1b] 19.9°) is prepared *via* the crystalline 3,5-dinitrobenzoate in an overall yield of 25% (calculated from the formyl ester)[4]. Optimization of the reaction with other microorganisms has already led to appreciable increases of the *ee*-values.

Asymmetric reductions of other formyl esters with fermenting yeast are also possible. Thus we obtained the optically active hydroxy esters **3a,b,c** of unknown absolute configuration in 50–70% yield as well as ethyl (*R*)-tropate **3d**[5].

Received: April 11, 1983 [Z 337 IE]
witheld for publication at the authors' request
German version: *Angew. Chem. 95* (1983) 1024

CAS Registry numbers:
**1b**, 87884-36-4; **1b** 3,5-dinitrobenzoate, 87884-37-5; **3a**, 87884-38-6; **3b**, 87884-39-7; **3c**, 87884-40-0; **3d**, 33173-46-5; ethyl α-formylpropionate, 27772-62-9; 3,5-dinitrobenzoyl chloride, 99-33-2; ethyl 2-formylbutanoate, 36873-42-4; ethyl 2-formyl-3-methylbutanoate, 21474-92-0; ethyl β-formylbenzenepropanoate, 2016-00-4; ethyl α-formylbenzeneacetate, 17838-69-6.

[1] a) Review: A. Fischli in R. Scheffold: *Modern Synthetic Methods*, Salle + Sauerländer, Aarau 1980, p. 269. Most recent examples: P. R. McGuirk, D. B. Collum, *J. Am. Chem. Soc. 104* (1982) 4496; S. Masamune, B. Imperiali, D. S. Garvey, *ibid. 104* (1982) 5528.—b) C. T. Goodhue, J. R. Schaeffer, *Biotechnol. Bioeng. 13* (1971) 203.
[2] Sucrose (375 g), baker's yeast (250 g), 2 L water, 30°C; 4 g formyl ester added at beginning and 21 g over 16 h; usual work-up after 1.5 d. Cf. procedure in: B. Seuring, D. Seebach, *Helv. Chim. Acta 60* (1977) 1175; E. Hungerbühler, D. Seebach, D. Wasmuth, *ibid. 64* (1981) 1467; D. Seebach, M. F. Züger, *ibid. 65* (1982) 495.—Cf. the yeast reductions of α-alkyl-β-keto esters: G. Fráter, *ibid. 63* (1980) 1383; R. W. Hoffmann, W. Helbig, W. Ladner, *Tetrahedron Lett. 23* (1982) 3479.
[3] From ethyl propanoate and ethyl formate with NaH in ether, cf. Houben-Weyl, *Methoden der Organischen Chemie, Vol. VII*, 1, Thieme, Stuttgart 1954, p. 48.
[4] From **1b**, 3,5-dinitrobenzoylchloride, $Et_3N$ in ether, the benzoate (m.p. 50—54°C) is obtained in 95% yield; it is dissolved in boiling ether and precipitated with vigorous stirring by addition of *ca.* half the volume of pentane (20°C→0°C). After 3, 4, 5, and 6 recrystallizations the *ee* is 85, 91, 97, and 100%, respectively. M.p. of enantiomerically pure benzoate (40% yield): 61.5—62.5°C, $[\alpha]_D^{20}$ −12.25 (c = 2, $CH_2Cl_2$). Hydrolysis to **1b**: 1.2 equiv. KOH in THF, 1 h, 0°C (88% yield).
[5] All $[\alpha]_D$-values at *c* = 4 in MeOH; % *ee* of **3a** and **3b** with *Mosher*'s reagent, of **3c** by crystallization of the 3,5-dinitrobenzoate to constant $[\alpha]_D$ and m.p., and of **3d** by comparison with literature data.

*Registered names, trademarks, etc. used in this journal, even without specific indication thereof, are not to be considered unprotected by law.*

© Verlag Chemie GmbH, D-6940 Weinheim, 1983. - Printed in the Federal Republic of Germany by Zechnersche Buchdruckerei, Speyer/Rhein.

All rights reserved (including those of translation into foreign languages). No part of this issue may be be reproduced in any form - by photoprint, microfilm, or any other means - nor transmitted or translated into a machine language without written permission from the publishers. Only single copies of contributions, or parts thereof, may be reproduced for personal use. Copies reproduced and used other than for private purposes in an industrial or commercial undertaking are subject to copyright and, in such cases, a copyright fee must be paid to the VG WORT, Abteilung Wissenschaft, Goethestr. 49, 8000 München 2, from whom conditions of payment can be obtained on request.

**Valid for users in the USA:** The appearance of the code at the bottom of the first page of an article in this journal (serial) indicates the copyright owner's consent that copies of the article may be made for personal or internal use, or for the personal or internal use of specific clients. This consent is given on the condition, however, that the copier pay the stated per-copy fee through the Copyright Clearance Center, Inc., for copying beyond that permitted by Sections 107 or 108 of the U.S. Copyright Law. This consent does not extend to other kinds of copying, such as copying for general distribution, for advertising or promotional purposes, for creating new collective works, or for resale. For copying from back volumes of this journal see 'Permissions to Photo-Copy: Publisher's Fee List' of the CCC.

**Editorial office:** Pappelallee 3, D-6940 Weinheim, Federal Republic of Germany, Telephone (06201) 602315, Telex 465516 vchwh d, Telefax (06201) 602328.

**Editors:** *P. Gölitz, I. G. Neil, O. Smrekar, A. Stimson.*

**Publishers:** Verlag Chemie GmbH. (Managing Directors: *Prof. Dr. Helmut Grünewald* and *Hans Dirk Köhler*), Pappelallee 3, D-6940 Weinheim, Federal Republic of Germany.

Correspondence concerning advertisements should be addressed to Verlag Chemie GmbH. (Advertising Manager *R. J. Roth*), Boschstr. 12. P.O. Box 1260/1280, D-6940 Weinheim, Federal Republic of Germany, Telephone Weinheim (06201) 602-0, Telex 465516 vchwh d, Telefax (06201) 602328.

# AUTHOR INDEX [*Angew. Chem. Int. Ed. Engl. 22* (1983)]

GE = Reference to Volume *95* (1983) of the German Edition of Angewandte Chemie. S = Reference to the Supplement Edition of Angewandte Chemie [*Angew. Chem. Suppl. 1983*].—"GE" reference for a Book Review can be found in the Author Index of the German Edition.


ABEL, E. W. 797
Abramovitch, R. A. 420
Ackermann, K. 411 [GE 419; S 488]
Adam, W. 529, 546 [GE 525, 566]
Adiwidjaja, G. 867 [GE 904; S 1221]
Akkerman, O. S. 248 [GE 242; S 234]
Aktalay, Y. 1002 [GE 1005]
Allmann, R. 876 [GE 900; S 1147]
Alt, H. G. 149, 544, 1002 [GE 159, 569, 1030; S 148, 803, 1364]
Altenbach, H.-J. 410 [GE 424; S 571]
Anders, E. 619 [GE 635]
Andersson, K. 495 [GE 507; S 609]
Andersson, S. 69 [GE 67]
Ando, K. 418 [GE 416]
Angelici, R. J. 163 [GE 160; S 184]
Anis, H.-J. 876 [GE 900; S 1147]
Anselmann, R. 984 [GE 1003]
Appel, R. 61, 785, 1004 [GE 63, 807, 1008]
Arigoni, D. 737 [GE 746]
Arndt, V. 1002 [GE 1005]
Arvanaghi, M. 712 [GE 726]
Atwood, J. L. 494 [GE 506; S 678]

BACHMANN, R. 1011 [GE 1013]
Bader, J. 322 [GE 325; S 463]
Baker, M. D. 166, 791 [GE 157, 813; S 92, 1075]
Barnes, C. L. 501 [GE 498; S 668]
Barthels, R. 783 [GE 799]
Bartholomé, E. 564
Basosi, R. 49 [GE 55; S 57]
Bats, J. W. 881 [GE 904; S 1323]
Battersby, A. R. 734 [GE 742]
Baudler, M. 632, 775, 1002 [GE 632, 803, 1005]
Bauer, Hans 548 [GE 565]
Bauer, Heinz 730 [GE 740]
Bauer, Helmut 334 [GE 330]
Becker, B. C. 241 [GE 238; S 282]
Becker, G. 413 [GE 417; S 501]
Becker, H.-D. 495 [GE 507; S 609]
Behnken, P. E. 722 [GE 738; S 929]
Behr, A. 503 [GE 505; S 655]
Behrens, G. 500 [GE 511]
Behrens, U. 153, 867 [GE 148, 904; S 156, 1221]
Bender, W. 617 [GE 634; S 818]
Benn, R. 390, 774, 779, 876 [GE 381, 814, 808, 900; S —, —, —, 1147]
Berger, S. 321 [GE 321]
Bergström, S. 858 [GE 865]
Berkulin, W. 246 [GE 248]
Berndt, A. 877 [GE 895]
Bernheim, M. 53 [GE 48; S 34]
Bertani, R. 246 [GE 241; S 228]
Besenhard, J. O. 950 [GE 954]
Bestmann, H. J. 167, 780, 782 [GE 154, 810, 812]
Betzel, C. 883 [GE 908; S 1191]
Bibber, J. W. 501 [GE 498; S 668]
Bickelhaupt, F. 248 [GE 242; S 234]
Biekert, E. 564
Bieri, J. H. 713 [GE 736]
Binger, P. 774 [GE 814]
Blachnik, R. 317 [GE 313; S 405]
Blechschmitt, K. 314 [GE 331; S 363]
Blum, W. 51 [GE 59]
Boag, N. M. 249 [GE 243; S 198]
Boche, G. 53 [GE 48; S 34]
Bock, H. 787 [GE 817; S 1088]
Bock, R. 67
Boersma, J. 329 [GE 335]
Boese, R. 498 [GE 510; S 620]
Bogdanović, B. 728 [GE 749]
Bögge, H. 561, 884, 1006 [GE 574, 905, 1030; S 747, —, —]
Böhm, M. 1007 [GE 1011; S 1379]
Böhm, M. C. 329 [GE 334]
Bonet, J.-J. 711 [GE 757; S 1025]
Bönnemann, H. 728 [GE 749]
Borm, J. 977 [GE 1018; S 1477]
Bossek, U. 328 [GE 320]
Boucher, E. A. 256
Boukouvalas, J. 618 [GE 646; S 860]
Boveleth, W. 996 [GE 1024; S 1503]
Braslavsky, S. E. 656 [GE 670]
Bräuchle, C. 582 [GE 612]
Braun, A. M. 792 [GE 816]
Braun, M. 788 [GE 802]
Breitschaft, W. 717 [GE 727]
Briaire, J. 334 [GE 330]
Brinker, U. H. 868, 869 [GE 892, 893; S 1228, 1241]
Brinkmann, R. 728 [GE 749]
Broadhurst, M. J. 47 [GE 57; S 1]
Brockmann, H. Jr. 551 [GE 563; S 778]
Brown, G. M. 883 [GE 908; S 1191]
Brown, J. M. 47 [GE 57; S 1]
Brunner, H. 164, 331, 549, 897 [GE 162, 326, 567, 921; S 84, 445, —, —]
Büch, H. M. 774 [GE 814]
Buddrus, J. 548 [GE 565]
Budzelaar, P. H. M. 48, 329 [GE 61, 335]
Bühlmeyer, W. 315 [GE 332]
Burkard, U. 65 [GE 50]
Burland, D. M. 582 [GE 612]
Buschmann, J. 410 [GE 423; S 537]
Butz, I. P. 996 [GE 1004; S 1388]

CÁNOVAS, A. 721 [GE 747; S 1053]
Carturan, G. 246 [GE 241; S 228]
Casnati, G. 563 [GE 562; S 794]
Catalan, J. 323 [GE 323; S 411]
Caubère, P. 599 [GE 597]
Ceccon, A. 559 [GE 572; S 734]
Cecconi, F. 554 [GE 554; S 718]
Cederbaum, L. S. 210 [GE 221]
Cherdron, H. 764 [GE 763]
Chevrier, B. 247 [GE 252]
Christl, M. 871 [GE 896]
Ciani, G. 333 [GE 322]
Cilento, G. 529 [GE 525]
Claus, K. H. 991 [GE 1032; S 1527]
Clegg, W. 621, 1006 [GE 630, 1030; S 874, —]
Colin, J. 247 [GE 252]
Conrad, H. 404 [GE 427]
Consiglio, G. 333 [GE 322]
Cornelisse, J. 718 [GE 752; S 994]
Cotton, F. A. 563
Coudert, G. 64 [GE 50]
Cowley, A. H. 978 [GE 1019; S 1493]
Cretton, A. 405 [GE 426; S 551]
Cuny, E. 891 [GE 906]

DARTMANN, M. 552 [GE 570]
Dauplaise, D. L. 560 [GE 573]
Davies, J. E. 13 [GE 26]
Davis, P. D. 419 [GE 422; S 564]
De Cian, A. 247 [GE 252]
Deffense, E. 716 [GE 729; S 1005]
Delcanale, M. 563 [GE 562; S 794]
Dellweg, H. 893
de Meijere, A. 867 [GE 904; S 1221]
Demuth, M. 721 [GE 747; S 1053]
Dent, W. 625 [GE 647]
Depke, G. 786 [GE 806]
Devant, R. 788 [GE 802]
Dick, K. 715 [GE 730; S 957]
Diederich, F. 715 [GE 730; S 957]
Diener, E. 631 [GE 641]
Diercks, R. 778 [GE 801; S 1138]
Dingwall, J. G. 498 [GE 504]
Djarrah, H. 1006 [GE 1029; S 1424]
Dobrowolski, D. C. 720 [GE 729]
Domcke, W. 210 [GE 221]
Dorf, U. 777 [GE 800; S 1120]
Dossena, A. 563 [GE 562; S 794]
Dötz, K. H. 732 [GE 750; S 1045]
du Mont, W.-W. 983 [GE 1025]
Dupuis, J. 622 [GE 633]
Dürr, H. 332 [GE 321; S 347]

ECKERT, H. 881 [GE 894; S 1291]
Eckstein, F. 423 [GE 431]
Edelmann, F. 153 [GE 148; S 156]
Effenberger, F. 65 [GE 50]
Egert, E. 886 [GE 912; S 1333]
Ehrenreich, W. 315 [GE 332]
Elguero, J. 323 [GE 323; S 411]
El Khadem, H. S. 895
Elschenbroich, C. 330 [GE 319]
El-Tamany, S. 633 [GE 631]
Eltzner, W. 884 [GE 905]
Engel, K. 494 [GE 506; S 678]
Engels, R. 492 [GE 502; S 691]
Ennen, B. 244 [GE 237; S 222]
Erker, G. 494, 777 [GE 506, 800; S 678, 1120]
Ermer, O. 251, 402, 998 [GE 251, 414, 1010; S —, —, 1353]
Eschenmoser, A. 630, 631, 735, 736 [GE 639, 641, 743, 744]

FABRY, G. 881 [GE 894; S 1291]
Fawzi, R. 996 [GE 1004, S 1388]
Fehér, M. 775, 1002 [GE 803, 1005]
Fenske, D. 407 [GE 420]
Fischer, E. O. 411 [GE 419; S 488]
Fischer, H. 874 [GE 913]
Fischer, Klaus 326 [GE 324; S 419]
Fischer, Konrad 724 [GE 741; S 1017]
Fischer, R. 888 [GE 902]
Flack, H. D. 405 [GE 426; S 551]
Flammang, R. 323, 542 [GE 323, 551; S 411, —]
Foote, C. S. 720 [GE 729]
Frank, C. 322 [GE 325; S 463]
Franz, L. H. 878 [GE 914]
Fresenius, W. 67
Freyberger, G. 49 [GE 62]
Frieden, C. 168
Fritz, G. 730 [GE 740]
Fritz, H. 889 [GE 909]
Fritz, H. P. 950 [GE 954]
Frühauf, H.-W. 992 [GE 1014; S 1435]

Fügedi, P. 255 [GE 245; S 254]
Fukuda, C. 417 [GE 412; S 480]
Fukuda, M. 870 [GE 911; S 1283]
Fyfe, C. A. 259 [GE 257]

GAMBARO, A. 559 [GE 572; S 734]
Gano, J. E. 165 [GE 155; S 193]
Garegg, P. J. 793 [GE 809]
Gassen, H. G. 13, 505 [GE 26, —]
Gassmann, E. 792 [GE 816]
Gassner, T. 619 [GE 635]
Gebert, W. 328, 727 [GE 320, 739]
Gerson, F. 556 [GE 571]
Geuder, W. 489 [GE 501]
Ghilardi, C. A. 554, 790 [GE 554, 800; S 718, 1066]
Giese, B. 622, 753 [GE 633, 771]
Gilardi, R. D. 254 [GE 237; S 271]
Giovannini, F. 1012 [GE 1024]
Gleiter, R. 329, 588 [GE 334, 500; S —, 661]
Glüsenkamp, K.-H. 887 [GE 901]
Gobbi, G. C. 259 [GE 257]
Godber, J. 624 [GE 645; S 898]
Goddard, R. J. 992 [GE 1014; S 1435]
Gokel, G. W. 257
Golding, B. T. 618 [GE 646; S 860]
Gölitz, P. 867 [GE 904; S 1221]
Gollnick, K. 726 [GE 751]
Gomann, K. 868, 869 [GE 892, 893; S 1228, 1241]
Gómez, J. 711 [GE 757; S 1025]
Gompper, R. 543, 717 [GE 553, 727; S 812, —]
Gotthardt, H. 548 [GE 565]
Gould, I. R. 625 [GE 647]
Graalmann, O. 621 [GE 630; S 874]
Graefe, J. 625 [GE 634]
Graf, H. 487 [GE 497]
Grahn, W. 876 [GE 900; S 1147]
Grathwohl, M. 634
Greißinger, D. 60 [GE 56; S 47]
Griesbeck, A. 726 [GE 751]
Grim, S. O. 254 [GE 237; S 271]
Grimme, W. 617 [GE 636]
Gross, G. 542, 543 [GE 551, 552]
Gruehn, R. 82 [GE 80]
Grundler, G. 776 [GE 805]
Guillaumet, G. 64 [GE 50]
Günther, Harald 350, 499 [GE 381, 509]
Günther, Helmut 322 [GE 325; S 463]
Günzler, H. 67

HAASE, M. 621 [GE 630; S 874]
Habermann, D. 716 [GE 729; S 1005]
Häbich, D. 711 [GE 755; S 1035]
Hafner, A. 713 [GE 736]
Hafner, K. 490 [GE 496]
Hahn, M. 491 [GE 499; S 583]
Hall, H. K. Jr. 440 [GE 448]
Hanack, M. 724, 784, 786 [GE 741, 804, 806; S 1017, —, —]
Harada, J. 502 [GE 504; S 599]
Hartmann, G. 723 [GE 753; S 945]
Hatano, M. 870 [GE 911; S 1283]
Haushalter, R. C. 558 [GE 560; S 766]
Havinga, E. 718 [GE 752; S 994]
Hawthorne, M. F. 722 [GE 738; S 929]
Hayen, H. I. 1008 [GE 1030; S 1364]
He, D.-W. 728 [GE 749]
Hecht, C. 979 [GE 1019; S 1543]
Heck, J. 330 [GE 319]
Heckendorn, R. 556 [GE 571]
Heilbronner, E. 402 [GE 414]
Hellmann, H. 564
Henkel, G. 318, 319, 885 [GE 314, 317, 903; S 307, 323, 1176]
Hensen, K. 725 [GE 739; S 973]
Herberhold, M. 59, 315, 1000 [GE 46, 315, 1028; S 10, —, 1343]
Herberich, G. E. 996 [GE 1024; S 1503]
Herrmann, G. 880 [GE 899; S 1203]
Herrmann, W. A. 314, 413, 979 [GE 331, 417, 1019; S 363, 501, 1543]
Hesse, M. 621 [GE 630; S 874]
Hessner, B. 996 [GE 1024; S 1503]
Hierholzer, B. 787 [GE 817; S 1088]
Higuchi, T. 418 [GE 416]
Hiller, W. 996 [GE 1004; S 1388]
Himmel, S. 416 [GE 418]
Hingerty, B. 883 [GE 908; S 1191]
Hirashima, T. 52 [GE 61; S 70]
Hirotsu, K. 418 [GE 416]
Hlavatsch, J. 154 [GE 153]
Hoehne, S. 996 [GE 1004; S 1388]
Hoell, D. 243 [GE 240; S 299]
Hoffmann, H. M. R. 719, 795, 796 [GE 737, 795, 796; S 985, —, —]
Hoffmann, M. 406 [GE 417; S 543]
Holmes, S. J. 1010 [GE 1012; S 1409]
Holz, H. 872 [GE 898; S 1315]
Holzwarth, A. R. 656 [GE 670]
Hong, C. Y. 562 [GE 568]
Hopf, H. 633 [GE 631]
Hoppe, D. 54, 886 [GE 64, 912; S —, 1333]
Hoppe, M. 990 [GE 1009]
Hoppe, W. 456 [GE 465]
Hörlein, R. 979 [GE 1019; S 1543]
Hovakeemian, G. H. 994 [GE 1001]
Hrovat, D. A. 625 [GE 647]
Hübener, P. 980 [GE 1021]
Huber, W. 67
Huber, Walter 242 [GE 239; S 288]
Hufnagel, A. 325 [GE 327]
Hugues, F. 624 [GE 645; S 898]
Hümmer, W. 786 [GE 806]
Hünerbein, J. 61 [GE 63]
Hünig, S. 489 [GE 501]
Hunter, W. E. 494 [GE 506; S 678]
Husain, A. 50 [GE 51]
Huttner, G. 976, 976, 977 [GE 1016, 1017, 1018; S 1451, 1463, 1477]

IMOTO, T. 253, 417, 417 [GE 244, 412, 412; S 243, 471, 480]
Inamoto, N. 418 [GE 416]
Inoue, T. 253 [GE 244; S 243]
Irngartinger, H. 403 [GE 415]
Ismail, Z. M. 719 [GE 737; S 985]
Ito, S. 502 [GE 504; S 599]

JACOBS, H. J. C. 718 [GE 752; S 994]
Jacobson, A. J. 412 [GE 422]
Jacobson, R. H. 165 [GE 155; S 193]
Jähne, G. 488 [GE 500; S 661]
Janssen, E. 779 [GE 808]
Jenny, T. A. 792 [GE 816]
John, R. A. 47 [GE 57; S 1]
Johnson, J. W. 412 [GE 422]
Jonas, K. 620, 716 [GE 637, 729; S 920, 1005]
Jones, K. 734 [GE 742]
Jostes, R. 561 [GE 574; S 747]
Jung, R. 548 [GE 565]
Jutzi, P. 56, 250, 994 [GE 55, 244, 1015]

KAARS, P. 886 [GE 912; S 1333]
Kadenbach, B. 275 [GE 273]
Kaesz, H. D. 249 [GE 243; S 198]
Kaim, W. 171, 892 [GE 201, 915; S —, 1209]
Kalcher, W. 413 [GE 417; S 501]
Kaliba, C. 252 [GE 247; S 264]
Kappert, M. 63 [GE 60; S 23]
Kato, H. 253, 417, 417 [GE 244, 412, 412; S 243, 471, 480]
Kauermann, H. 549 [GE 567]
Kauffmann, T. 244 [GE 237; S 222]
Kaul, H.-A. 60 [GE 56; S 47]
Kawka, D. 1003 [GE 1006; S 1371]
Keim, W. 503 [GE 505; S 655]
Keller, H.-L. 324 [GE 318; S 427]
Keller, K. 881 [GE 904; S 1323]
Kennedy, J. P. 505
Kerth, J. 503, 984 [GE 510, 1003]
Kesseler, K. 989 [GE 1007; S 1511]
Kiesel, Y. 881 [GE 894; S 1291]
Kiesele, H. 254 [GE 253; S 210]
Kim, S. 562 [GE 568]
Kinoshita, T. 502 [GE 504; S 599]
Kirste, B. 150 [GE 149; S 128]
Klauck, G. 332 [GE 321; S 347]
Klebe, G. 725 [GE 739; S 973]
Kleimann, W. 991 [GE 1032; S 1527]
Klein, H. 49 [GE 62]
Klein, H.-P. 60 [GE 56; S 47]
Klessinger, M. 335
Kletzin, H. 46, 873 [GE 49, 916]
Klingebiel, U. 621 [GE 630; S 874]
Klinowski, J. 259, 614 [GE 257, 643]
Klug, A. 565 [GE 579]
Klusik, H. 877 [GE 895]
Knobler, C. B. 249, 722 [GE 243, 738; S 198, 929]
Knoch, F. 61, 1004 [GE 63, 1008]
Koch, E. 225 [GE 185]
Koepe, G. 620 [GE 637; S 920]
Kohl, F. 56 [GE 55]
Kohler, H. 1011 [GE 1013]
Koltzenburg, G. 500 [GE 511]
Korzeniowski, S. H. 257
Köppel, H. 210 [GE 221]
Kos, A. J. 733 [GE 755]
Kraus, H.-J. 250 [GE 244]
Krause, M. J. 135 [GE 135]
Kräutler, B. 736 [GE 744]
Krebs, B. 113, 318, 319, 552, 885 [GE 113, 314, 317, 570, 903; S —, 307, 323, —, 1176]
Kreissl, F. R. 149, 493, 1001 [GE 159, 503, 1002; S 148, 631, —]
Kreuzer, M. 627 [GE 638; S 851]
Krickemeyer, E. 984, 1006 [GE 905, 1030]
Kriechbaum, G. W. 413 [GE 417; S 501]
Krieger, C. 731 [GE 748]
Krimmer, H.-P. 490 [GE 496]
Krohn, K. 875 [GE 897; S 1267]
Krüger, C. 250, 503, 547, 620, 721, 729, 774, 779, 994, 991 [GE 244, 505, 564, 637, 747, 753, 814, 808, 1015, 1032; S —, 655, 786, 920, 1053, —, —, —, —, 1527]
Kubota, F. 629 [GE 639; S 835]
Kuhn, W. 732 [GE 750; S 1045]
Kumar, K. 167 [GE 154]
Kunz, H. 62, 62, 783 [GE 47, 64, 799; S —, 39, —]
Kunze, H. 1004 [GE 1008]
Künzer, H. 321 [GE 321]
Kupčik, V. 1011 [GE 1013]
Kupfer, R. 252 [GE 247; S 264]
Kurreck, H. 51, 150, 787 [GE 59, 149, 817; S —, 128, 1088]
Küsthardt, U. 979 [GE 1019; S 1543]

LAMMER, O. 623 [GE 629; S 887]
Lang, A. 504
Lang, H. 976, 976 [GE 1016, 1017; S 1451, 1463]
Lanzendörfer, F. 871 [GE 896]
Lasch, J. G. 978 [GE 1019; S 1493]
Lauer, U. 561 [GE 574; S 747]
Laurent, H. 406 [GE 413]
Lawley, K. P. 894
Lawrence, J. F. 66
Lehmkuhl, H. 779 [GE 808]
Lennartz, H.-W. 1007 [GE 1011; S 1379]
Lentes, K.-U. 773 [GE 794]

Leonhardt, W. 632 [GE 632]
Levy, J. 53 [GE 45]
Lewis, N. J. 735, 736 [GE 743, 744]
Ley, H. † 564
Lichtenthaler, F. W. 891 [GE 906]
Lieberknecht, A. 550 [GE 575]
Limbäcker, B. 503 [GE 505; S 655]
Lindberg, B. 793 [GE 809]
Lindner, E. 996 [GE 1004; S 1388]
Linse, K. 982 [GE 1023]
Lipták, A. 255 [GE 245; S 254]
Liu, C. 158 [GE 156]
Llanos, J. 998 [GE 1026]
Lochschmidt, S. 545 [GE 561; S 710]
Loerzer, T. 878 [GE 914]
Löhr, H.-G. 409 [GE 425; S 527]
Loubinoux, B. 64 [GE 50]
Lubitz, W. 787, 892 [GE 817, 915; S 1088, 1209]
Lucas, J. 1006 [GE 1029; 1424]
Luger, P. 410 [GE 423; S 537]
Luksza, M. 416 [GE 418]
Lupón, P. 711 [GE 757; S 1025]
Lüthe, H. 996 [GE 1024; S 1503]
Lüttke, W. 878 [GE 914]
Lysek, M. 486 [GE 495; S 639]

MACHINEK, R. 878 [GE 914]
Maercker, A. 246, 733 [GE 248, 755]
Maessen, P. A. 718 [GE 752; S 994]
Mahmoud, K. A. 544 [GE 569; S 803]
Maier, G. 878, 990 [GE 914, 1009]
Malisch, W. 60, 151, 416 [GE 56, 151, 418; S 47, 114, —]
Malsch, K.-D. 878 [GE 914]
Mangia, A. 563 [GE 562; S 794]
Maquestiau, A. 323, 542 [GE 323, 551; S 411, —]
Marchelli, R. 563 [GE 562; S 794]
Maréchal, E. 505
Margaretha, P. 505
Märkl, G. 57, 879 [GE 58, 891; S 75, —]
Martin, H.-D. 283 [GE 281]
Massa, W. 330 [GE 319]
Matsuura, T. 629 [GE 639; S 835]
Mattes, R. 245, 872 [GE 246, 898; S—, 1315]
Mayer, B. 283 [GE 281]
Mayr, H. 49 [GE 62]
McCabe, R. W. 618 [GE 646; S 860]
McGarrity, J. F. 405 [GE 426; S 551]
McIntosh, D. F. 166 [GE 157; S 92]
Meier, G. P. 56 [GE 53]
Meier, H. 627 [GE 638; S 851]
Metzger, J. O. 889 [GE 914; S 1256]
Mews, R. 158, 723 [GE 156, 753; S —, 945]
Meyer, A. Y. 45 [GE 45]
Meyer, B. 983 [GE 1025]
Midollini, S. 554, 790 [GE 554, 800; S 718, 1066]
Miehling, W. 164 [GE 162; S 84]
Minsky, A. 45 [GE 45]
Mitchell, S. A. 166, 674 [GE 157, 706; S 92, —]
Miyamoto, I. 253, 417, 417 [GE 244, 412, 412; S 243, 471, 480]
Morandini, F. 333 [GE 322]
Morita, T. 870 [GE 911; S 1283]
Mues, P. 1003 [GE 1006; S 1371]
Muetterties, E. L. 135 [GE 135]
Müllen, K. 241, 242, 243 [GE 238, 239, 240; S 282, 288, 299]
Müller, A. 561, 884, 1006 [GE 574, 905, 1030; S 747, —, —]
Müller, G. 729 [GE 753]
Müller, J. 993 [GE 1000; S 1537]
Murrell, J. N. 256
Musso, H. 1, 816 [GE 1, 827]
Mynott, R. 620 [GE 637; S 920]

NAZAR, L. F. 624 [GE 645; S 898]
Nesper, R. 998 [GE 1026]
Neugebauer, D. 59, 156 [GE 46, 161; S 10, 169]
Neugebauer, F. A. 320 [GE 329; S 457]
Neumann, G. 241 [GE 238; S 282]
Newkome, G. R. 739
Nichol, L. W. 168
Niecke, E. 155, 486, 552 [GE 154, 495, 570; S —, 639, —]
Niessner, M. 53 [GE 48; S 34]
Nishiguchi, I. 52 [GE 61; S 70]
Nixdorf, M. 403 [GE 415]
Noltemeyer, M. 1006 [GE 1029; S 1424]
Norman, N. C. 978 [GE 1019; S 1493]
Nussbaumer, C. 737 [GE 746]
Nussberger, R. 736 [GE 744]

OGAWA, H. 253, 417, 417 [GE 244, 412, 412; S 243, 471, 480]
Ohnishi, R. 162 [GE 158; S 140]
Olah, G. A. 50, 390, 712 [GE 51, 356, 726]
Olejnek, S. 876 [GE 900; S 1147]
Orlandini, A. 554, 790 [GE 554, 800; S 718, 1066]
Osawa, E. 1 [GE 1]
Ossowski, P. 793 [GE 809]
Ozin, G. A. 166, 624, 674, 791 [GE 157, 645, 6706 813; S 92, 898, —, 1075]

PADWA, A. 625 [GE 647]
Pahl, C. 413 [GE 417; S 501]
Pakulski, M. 978 [GE 1019; S 1493]
Panzer, H. P. 560 [GE 573]
Parnis, J. M. 791 [GE 813; S 1075]
Paszyc, S. 623 [GE 642]
Paudler, W. W. 739
Paul, W. 316 [GE 333; S 396]
Paulen, W. 785 [GE 807]
Peter, M. G. 773 [GE 794]
Peters, E.-M. 546 [GE 566]
Peters, K. 332, 546 [GE 321, 566; S 347, —]
Petzoldt, K. 406 [GE 413]
Pfaltz, A. 735 [GE 743]
Pfisterer, H. 314 [GE 331; S 363]
Philipsborn, W. von 713 [GE 736]
Pickel, P. 725 [GE 739; S 973]
Pille, W. 327 [GE 327]
Pilotti, Å. 793 [GE 809]
Pinkerton, A. A. 405 [GE 426; S 551]
Pletcher, D. 421
Pohl, K. 727 [GE 739]
Pohl, S. 486, 994 [GE 495, 1015; S 639, —]
Pontzen, T. 775 [GE 803]
Pörschke, K. R. 547, 991 [GE 564, 1032; S 786, 1527]
Prakash, G. K. S. 50, 390, 712 [GE 51, 356, 726]
Prewo, R. 713 [GE 736]
Puff, H. 409 [GE 425; S 527]

QUINKERT, G. 637 [GE 651]

RABE, J. 795, 796 [GE 795, 796]
Rabek, J. F. 802
Rabinovitz, M. 45, 53 [GE 45, 45]
Rancourt, D. 624 [GE 645; S 898]
Ratz, R. 550 [GE 552]
Rau, H. 550 [GE 552]
Raudaschl, G. 881 [GE 894; S 1291]
Raulfs, F.-W. 633 [GE 631]
Rawdah, T. N. 390 [GE 356]
Reed, G. 893
Reetz, M. T. 989 [GE 1007; S 1511]
Regitz, M. 553 [GE 564; S 726]
Rehm, H.-J. 893
Reiner, D. 59, 1000 [GE 46, 1028; S 10, 1343]
Reinhardt, G. 617 [GE 636]
Reisenauer, H. P. 990 [GE 1009]
Reitmeier, R. 411 [GE 419; S 488]
Rest, A. J. 544 [GE 569; S 803]
Richter, W. J. 51 [GE 59]
Riemenschneider, C. 54 [GE 64]
Rienäcker, R. 625 [GE 634]
Riepl, G. 331 [GE 326; S 445]
Röder, T. 782 [GE 812]
Roesky, H. W. 881, 1006 [GE 904, 1029; S 1323; 1424]
Roland, E. 326 [GE 324; S 419]
Roll, J. 982 [GE 1023]
Romanin, A. 559 [GE 572; S 734]
Romao, M. J. 992 [GE 1014; S 1435]
Rösch, L. 557 [GE 572]
Rosenthal, R. J. 625 [GE 647]
Rossi, C. 49 [GE 55; S 57]
Rost, W. 321 [GE 328; S 451]
Roth, W. R. 1007 [GE 1011; S 1379]
Rothenberg, A. S. 560 [GE 573]
Roy, R. 614 [GE 643]
Rufińska, A. 774, 779 [GE 814, 808]
Rüger, R. 155, 486, 552 [GE 154, 495, 570; S —, 639, —]
Rühter, G. 55 [GE 52; S 63]

SAALFRANK, R. W. 321 [GE 328; S 451]
Sadakari, N. 417 [GE 412; S 471]
Saenger, W. 883 [GE 908; S 1191]
Saito, I. 629 [GE 639; S 835]
Saive, R. 996 [GE 1024; S 1503]
Salem, L. 635
Salzer, A. 713 [GE 736]
Samuelsson, B. 805 [GE 854]
Sander, J. 244 [GE 237; S 222]
Sandros, K. 495 [GE 507; S 609]
Sangokoya, S. A. 254 [GE 237; S 271]
Sapunov, V. N. 739
Sarkar, S. 561 [GE 574; S 747]
Sarstedt, B. 875 [GE 897; S 1267]
Sasaki, K. 502 [GE 504; S 599]
Saupe, T. 731 [GE 748]
Schäfer, A. 979 [GE 1019; S 1543]
Schaffner, K. 656 [GE 670]
Schanbacher, U. 152 [GE 150]
Schaper, W. 167 [GE 154]
Schat, G. 248 [GE 242; S 234]
Schaumann, E. 55 [GE 52; S 63]
Scherer, O. J. 404, 503, 984 [GE 427, 510, 1003]
Schieferstein, L. 620 [GE 637; S 920]
Schiemann, J. 980 [GE 1021]
Schiess, P. 246 [GE 248]
Schildknecht, H. 617, 695 [GE 634, 689; S 818, —]
Schill, G. 889 [GE 909]
Schings, U. 775 [GE 803]
Schleyer, P. von R. 48, 733 [GE 61, 755]
Schlüter, E. 994 [GE 1015]
Schmickler, H. 241 [GE 238; S 282]
Schmid, R. 739
Schmidbaur, H. 156, 729, 907 [GE 161, 753, 980; S 169, —, —]
Schmidpeter, A. 545 [GE 561; S 710]
Schmidt, E. 546 [GE 566]
Schmidt, R. 330 [GE 319]
Schmidt, R. R. 406, 776 [GE 417, 805; S 543, —]
Schmidt, U. 152, 550 [GE 150, 575]
Schmidtberger, S. 989 [GE 1007; S 1511]
Schmitt, P. 499 [GE 509]
Schneider, G. 58 [GE 54]
Schneider, O. 784 [GE 804]
Schnering, H. G. von 332, 407, 408, 546, 998 [GE 321, 420, 421, 566, 1026; S 347, —, —, —, —]
Schnieders, C. 243 [GE 240; S 299]

Schobert, R. 780 [GE 810]
Schoeller, W. 486 [GE 495; S 639]
Scholand, H. 245 [GE 246]
Schöllhorn, R. 555 [GE 555]
Schomburg, D. 65 [GE 52]
Schrock, R. R. 1010 [GE 1012; S 1409]
Schubert, B. 496 [GE 499; S 703]
Schubert, H. 553 [GE 564; S 726]
Schubert, K. 150 [GE 149; S 128]
Schubert, U. 981 [GE 1022]
Schuetz, H.-J. 322 [GE 325; S 463]
Schuh, W. 409 [GE 425; S 527]
Schulte-Frohlinde, D. 500 [GE 511]
Schultheiß-Reimann, P. 62 [GE 64; S 39]
Schulz, H. 1011 [GE 1013]
Schurig, V. 327, 772, 772 [GE 327, 797, 798; S —, 1130, —]
Schwanitz-Schüller, U. 1009 [GE 1031; S 1399]
Schwarz, H. 51, 786 [GE 59, 806]
Schwarzenbach, D. 405 [GE 426; S 551]
Schwarzenbach, R. 380 [GE 345]
Schwarzensteiner, M.-L. 543 [GE 553; S 812]
Schweickert, N. 889 [GE 909]
Schweizer, H. J. 82 [GE 80]
Scrivanti, A. 246 [GE 241; S 228]
Seanor, D. A. 895
Seebach, D. 31, 1012 [GE 12, 1024]
Seetz, J. W. F. L. 248 [GE 242; S 234]
Seidel, C. 881 [GE 894; S 1291]
Seidl, E. 57, 879 [GE 58, 891; S 75, —]
Seils, F. 992 [GE 1014; S 1435]
Selig, H. 53 [GE 45]
Seppelt, K. 789 [GE 813; S 1106]
Serhadli, O. 46, 414 [GE 49, 428]
Serrano, R. 341, 979 [GE 331, 1019; S 363, 1543]
Severengiz, T. 983 [GE 1025]
Shaik, S. S. 210 [GE 221]
Shallenberger, R. S. 803
Shea, K. J. 419 [GE 422; S 564]
Sheldrick, G. M. 621, 723, 886, 1006, 1006 [GE 630, 753, 912, 1029, 1030; S 874, 945, 1333, 1424, —]
Sheldrick, W. S. 984 [GE 1003]
Shibayama, K. 418 [GE 416]
Shimozono, K. 629 [GE 639; S 835]
Sieber, W. 149, 493, 1001 [GE 159, 503, 1002; S 148, 631, —]
Siegel, R. 320 [GE 329; S 457]
Sigg, L. 380 [GE 345]
Simon, A. 95 [GE 94]
Simon, H. 322 [GE 325; S 463]
Singh, M. M. 163 [GE 160; S 184]
Siray, M. 785 [GE 807]
Sironi, A. 333 [GE 322]
Skalski, B. 623 [GE 642]
Slaich, P. K. 618 [GE 646; S 860]
Smit, C. J. 492 [GE 502; S 691]
Snow, R. J. 734 [GE 742]
Specker, H. 325 [GE 327]
Spliethoff, B. 728 [GE 749]
Staab, H. A. 334, 731 [GE 330, 748]
Stahl, E. 507 [GE 515]
Stark, H. 637 [GE 651]
Starke, U. 557 [GE 572]
Steckhan, E. 497 [GE 508]
Steffen, R. 555 [GE 555]
Steinbach, R. 989 [GE 1007; S 1511]
Stella, L. 337 [GE 368]
Stöbbe, M. 867 [GE 904; S 1221]
Stock, R. 993 [GE 1000; S 1537]
Stohrer, W.-D. 613 [GE 642]
Stone, F. G. A. 797
Stowasser, B. 490 [GE 496]
Stumm, W. 380 [GE 345]
Stupp, H.-P. 773 [GE 794]
Suchy, A. 489 [GE 501]
Süss-Fink, G. 880 [GE 899; S 1203]
Swiridoff, W. 491 [GE 499; S 583]
Szeymies, D. 885 [GE 903; S 1176]
Szilágyi, G. 157 [GE 156; S 120]

TAJIRI, A. 870 [GE 911; S 1283]
Takase, K. 870 [GE 911; S 1283]
Taniguchi, Y. 253, 417, 417 [GE 244, 412, 412; S 243, 471, 480]
Tebbe, K.-F. 775, 1002 [GE 803, 1005]
Theis, M. 733 [GE 755]
Theopold, K. H. 1010 [GE 1012; S 1409]
Thewalt, U. 60, 880, 1000 [GE 56, 899, 1028; S 47, 1203, 1343]
Thiem, J. 58 [GE 54]
Thies, H. 51 [GE 59]
Thomas, J. M. 259, 614 [GE 257, 643]
Thrasher, J. S. 789 [GE 813; S 1106]
Tietze, L.-F. 828, 887, 888 [GE 840, 901, 902]
Tiezzi, E. 49 [GE 55; S 57]
Tölg, G. 67
tom Dieck, H. 778 [GE 801; S 1138]
Trautwein, A. 561 [GE 574; S 747]
Tremel, W. 318, 319 [GE 314, 317; S 307, 323]
Trötsch, I. 879 [GE 891]
Tsay, Y.-H. 620, 721 [GE 637, 747; S 920, 1053]
Tuck, B. 498 [GE 504]
Turro, N. J. 625 [GE 647]

ULLRICH, V. 487 [GE 497]
Umland, H. 152 [GE 148; S 156]
Unterberg, H. 242 [GE 239; S 288]
Urland, W. 1009 [GE 1031; S 1399]

VAHRENKAMP, H. 154, 326 [GE 152, 324; S —, 419]
Valensin, G. 49 [GE 55; S 57]
van der Helm, D. 501 [GE 498; S 668]
van der Kerk, G. J. M. 48, 329 [GE 61, 335]
van der Kerk, S. M. 48 [GE 61]
van der Kerk-van Hoof, A. 48 [GE 61]
Van de Sande, C. C. 191 [GE 165]
Vane, J. R. 741 [GE 782]
van Tilborg, W. J. M. 492 [GE 502; S 691]
Vedejs, E. 56 [GE 53]
Venzo, A. 559 [GE 572; S 734]
Vetter, W. 889 [GE 909]
Vogel, E. 410, 1003, 1007 [GE 410, 1006, 1011; S 571, 1371, 1379]
Vogler, A. 154 [GE 153]
Vögtle, F. 409 [GE 425; S 527]
Vollhardt, K. P. C. 994 [GE 1001]
Voran, S. 151 [GE 151; S 114]
Voss, B. 410 [GE 424; S 571]
Voss, E. 979 [GE 1019; S 1543]
Vu, D. 408 [GE 421]

WACHTER, J. 549 [GE 567]
Waditschatka, R. 630, 631 [GE 639, 641]
Wagner, C. T. 413 [GE 417; S 501]
Wagner, G. 1005 [GE 1027]
Wagner, I. 816 [GE 827]
Wagner, K. 555 [GE 555]
Waldmann, H. 62 [GE 47]
Walton, F. R. 563
Wamhoff, H. 157 [GE 156; S 120]
Waśkowska, A. 876 [GE 900; S 1147]
Weber, E. 616 [GE 632; S 840]
Weber, H.-P. 1011 [GE 1013]
Weber, L. 498, 516 [GE 510, 539; S 620, —]
Weber, R. 772 [GE 797; S 1130]
Weichmann, J. 314, 979 [GE 331, 1019; S 363, 1543]
Weidmann, B. 31 [GE 12]
Weigert, W. M. † 564
Weigt, E. 721 [GE 747; S 1053]
Weise, E. 564
Weiss, E. 496, 980 [GE 499, 1021; S 703, —]
Weiss, J. 491 [GE 499; S 583]
Weiss, R. 247 [GE 252]
Weissberger, A. 421
Weissermel, K. 764 [GE 763]
Weitzer, H. 331 [GE 326; S 445]
Wenderoth, B. 989 [GE 1007; S 1511]
Wendschuh-Josties, M. 1011 [GE 1013]
Wengenmayer, F. 842 [GE 874]
Wenska, G. 623 [GE 642]
Wentrup, C. 542, 543 [GE 551, 552]
Weprek, S. 891 [GE 906]
Werner, H. 46, 316, 414, 873, 927, 981, 982 [GE 49, 333, 428, 916, 932, 1022, 1023; S —, 396, —, —, —, —, —]
Wettach, R. H. 165 [GE 155; S 193]
Wiberg, N. 1005 [GE 1027]
Wickel, U. 317 [GE 313; S 405]
Wiechert, R. 406 [GE 413]
Wieghardt, K. 328, 491, 727 [GE 320, 499, 739; S —, 583, —]
Wienkamp, R. 497 [GE 508]
Wieschollek, R. 244 [GE 237; S 222]
Wilk, G. 868 [GE 892; 1228]
Wilke, G. 547, 991 [GE 564, 1032; S 786, 1527]
Wilkinson, G. 797
Willfahrt, J. 65 [GE 50]
Willhalm, A. 545 [GE 561; S 710]
Wippermann, T. 250 [GE 244]
Wistuba, D. 772 [GE 798]
Witthohn, K. 551 [GE 563; S 778]
Wolf, A. 1011 [GE 1013]
Wolf, J. 414, 981 [GE 428, 1022]
Wolfgruber, M. 149, 493, 1001 [GE 159, 503, 1002; S 148, 631, —]
Wolmershäuser, G. 404 [GE 427]
Wolters, D. 154 [GE 152]
Wormsbächer, D. 153 [GE 148; S 156]
Wriede, U. 55 [GE 52; S 63]
Wright, P. A. 614 [GE 643]
Wulf, R. 1011 [GE 1013]
Würthwein, E.-U. 252 [GE 247; S 264]

YAMAGISHI, A. 162 [GE 158; S 140]
Yang, S. 562 [GE 568]
Yoshifuji, M. 418 [GE 416]

ZELENKA, L. 996 [GE 1024; S 1503]
Zengerly, T. 725 [GE 739; S 973]
Ziegler, M. L. 46, 314, 413, 414, 503, 982 [GE 49, 331, 417, 428, 510, 1023; S —, 363, 501, —, —, —]
Zolk, R. 981 [GE 1022]
Zorn, R. 869 [GE 893; S 1241]
Zountsas, J. 627 [GE 638; S 851]
Zsolnai, L. 976, 976, 977 [GE 1016, 1017, 1018; S 1451, 1463, 1477]
Zuckerman, J. J. 501 [GE 498; S 668]
Züger, M. F. 1012 [GE 1024]
Zybill, C. E. 156, 729 [GE 161, 753; S 169, —]

# SUBJECT INDEX

(R) = Review Article (C) = Short Communication (B) = Book Review


ACARNIDINE, Synthesis of acylpolyamines: acetylspermidines and $C_{12:0}$-acarnidine (C) 618

Acceptor ligands, Disulfur and diselenium as strong acceptor ligands in $(\eta^5\text{-}C_5H_5)Re(CO)_2S_2$ and $[\eta^5\text{-}C_5(CH_3)_5]Mn(CO)_2Se_2$ (C) 1000

Aceheptylenide ion, Direct synthesis of a [13]annulenide ion (C) 241

Acetylene(carbonyl)nitrosyl complexes, The transformation of acetylene from a four- to a two-electron ligand: acetylene(carbonyl)nitrosyl complexes of tungsten (C) 1008

Acetylenes, Novel synthesis of acetylenes (C) 167

Acrylic esters, Preparation of 2-(1-hydroxyalkyl)acrylic esters; simple three-step synthesis of mikanecic acid (C) 795
A new, efficient and stereocontrolled synthesis of trisubstituted alkenes *via* functionalized acrylic esters (C) 796

Addition, Bond-forming initiation in spontaneous addition and polymerization reactions of alkenes (R) 440
Formation of CC bonds by addition of free radicals to alkenes (R) 753
Kinetic and thermodynamic control in the reaction of $(Ph_3P)_2PtO_2$ with (*E*)-2-butenal (C) 47
The zirconocene-induced coupling of butadiene with carbonyl compounds (C) 494
of alkanethiols to diketene—a correction (C) 498
Base-induced isomerization of cycloalkenynes in competition with addition reactions (C) 627
Aryl(hydrido)ruthenium complexes by C—H addition: isolation of a four-membered metallacycle as intermediate (C) 873

Adducts, $[Me_3Si(py)]^{\oplus}X^{\ominus}$ (X = Br, I): X-ray structural analysis of the 1:1-adducts of bromo- or iodotrimethylsilane and pyridine (C) 725

Aldol reaction, Stereoselective aldol reaction with (*R*)-*N*-acetyl-α-phenylglycinol (C) 788

Aldosterone-antagonist, A novel synthetic route to the aldosterone-antagonist spirorenone (C) 406

Alkadienylcarbamates, Regio- and diastereoselective synthesis of (4-hydroxy-3-methyl-1,2-alkadienyl)carbamates from α-titanated 2-butynylcarbamates and aldehydes (C) 54

Alkanethiols, Addition of alkanethiols to diketene—a correction (C) 498

Alkenes, A new, efficient and stereocontrolled synthesis of trisubstituted alkenes *via* functionalized acrylic esters (C) 796

Alkylbenzenes, $\eta^6$-Bonded alkylbenzenes as novel bridging ligands in dinuclear complexes of iron and cobalt (C) 620

Alkyl radicals, Formation of alkyl radicals by thermal bimolecular reaction of alkanes and alkenes (C) 889

Alkyne complexes, The transformation of acetylene from a four- to a two-electron ligand: acetylene(carbonyl)nitrosyl complexes of tungsten (C) 1008
of tungsten(IV) (C) 1010

Alkyne ligand, Synthesis of $[C_5H_5Rh(PhC{\equiv}CH)P(iPr)_3]$ and $[C_5H_5Rh(={=}C{=}CHPh)P(iPr)_3]$: mechanism of the conversion of an alkyne ligand into a vinylidene ligand (C) 414

Alkynes, Novel synthesis of acetylenes (C) 167

Alkynylamines, 1-Alkynylamines by electrophilic amination (C) 53

Allyl cations, [2+2]-Cycloadditions of allyl cations (C) 49

Aloe-Emodin, Facile synthesis of the (±)-6-deoxycarminomycinone from aloe-emodin (C) 875

Aluminum atoms, Probing the environment of Al atoms in noncrystalline solids: $Al_2O_3$—$SiO_2$ gels, soda glass, and mullite precursors (C) 614

Amino acids, New naturally occurring amino acids (R) 816

Amino acid synthesis, Trifluoromethanesulfonates of α-hydroxycarboxylates—educts for the racemization-free synthesis of *N*-substituted α-amino acids (C) 65

Amino(imino)phosphane, N,P-coordination of an amino(imino)phosphane (C) 984

Aminopenicillanic acid, Synthesis of the chiral synthetic building block (1*R*,5*S*)-3-phenyl-4-oxa-2,6-diazabicyclo[3.2.0]hept-2-en-7-one from 6-aminopenicillanic acid (C) 711

Amino protecting group, The 2-(2-pyridyl)ethoxycarbonyl-(Pyoc) residue—an acid- and base-stable, hydrophilic protecting group for the amino function in peptide synthesis (C) 783

Analytical chemistry, Organic trace analysis by liquid chromatography (B) 66
Analytiker-Taschenbuch (B) 67

Analytical methods, Holographic methods for the investigation of photochemical and photophysical properties of molecules (R) 582

Annulene, A novel planar antiaromatic dibenzo[8]annulene (C) 332
2D-NMR spectroscopy in annulene chemistry: complete assignment of the $^{13}C$-NMR spectrum of 9,11-bisdehydrobenzo[18]annulene by $^1H,^{13}C$ shift correlation (C) 499
Resonance energy of bridged [10]annulenes (C) 1007

Annulene dioxide, Synthesis of an [18]annulene dioxide: an oxygen-bridged [18]annulene possessing equivalent Kekulé structures (C) 417
Synthesis of hetero[17]annulene dioxides and a [16]annulene dioxide using furan building blocks (C) 417

Annulenide ion, Direct synthesis of a [13]annulenide ion (C) 241

Annulenone, Straightforward preparation and stabilization of 2-*trans*-4,7:10,13-diepoxy[15]annulenone (C) 253

Anthracycline antibiotics (B) 895

Antiaromaticity, Unusual NMR phenomena of anthracene and phenanthrene dianions—thermal stimulation of triplet states in antiaromatic systems (C) 45
A novel planar antiaromatic dibenzo[8]annulene (C) 332

Antibiotics, Anthracycline antibiotics (B) 895

Antimony compounds, Synthesis and structure of metallocene cations of the Vb elements arsenic and antimony (C) 250
Synthesis and structure of a bicyclic SbNP compound with intramolecular donor-acceptor bonding (C) 404
$SbF^{2+}$ as a Lewis acid in $Na(SbF)PO_4 \cdot nH_2O$ (n = 2–4) and $NH_4(SbF)PO_4 \cdot H_2O$ (C) 872

Aromaticity, Quenching of the aromaticity of the 5-dibenzo[*a,d*]cycloheptenylium ion by complexing with $(CO)_3Cr$ (C) 559

Arsanylketenes, Generation and stabilization of phosphanyl- and arsanylketenes within the coordination sphere of tungsten (C) 149
An arsanylketene by elimination from an oxaarsatungstacyclopentene complex (C) 1001

Arsenic-arsenic double bond, Synthesis and structure of a diarsenechromium complex with an unsupported arsenic-arsenic double bond (C) 978

Arsenic compounds, Synthesis and structure of metallocene cations of the Vb elements arsenic and antimony (C) 250
Dicarbonyl($\eta^5$-cyclopentadienyl)(di-*tert*-butyl-$\lambda^4$-arsanediyl)molybdenum and -tungsten—the first complexes with a metal-arsenic double bond (C) 416

Arsenic phosphorus sulfide, Equilibria in the formation of $A_4B_3$ molecules (C) 317

Arylindenes, Can radicals participate in pericyclic reactions? Model reactions for electron-transfer induced valence isomerization of 1-arylindenes (C) 254

Asarone, Olefins from β-hydroxycarboxylic acids—synthesis of isomerically pure α- and β-asarone (C) 628

Asymmetrically sensitized photoreaction, Asymmetry of emission quenching and product formation in an asymmetrically sensitized photoreaction (C) 550

Asymmetric catalysts, Rhodium catalysts for enantioselective hydrosilylation—a new concept in the development of asymmetric catalysts (R) 897

Asymmetric induction, Acceleration and asymmetric induction of intermolecular Diels-Alder reactions of triacyl compounds (C) 887

Asymmetric reduction, Preparation of ethyl (*R*)-(−)-3-hydroxy-2-methylpropanoate by yeast reduction of ethyl α-formylpropanoate (C) 1012

*"Atmungsferment"*, Structure and evolution of the *"Atmungsferment"* cytochrome c oxidase (R) 275

Atomic radii, Intermetallic compounds and the use of atomic radii in their description (R) 95

Azaallenium salts, Reactions of *N*-methylenecarboxamides with electrophiles: 1-alkoxy-2-azaallenium salts and *N*-acyl(methylene)ammonium salts (C) 252

Azatriphosphetidines as cyclotrimers of an iminophosphane—synthesis and crystal structure (C) 552

Azetidinesulfonic acids, Synthesis and structure of (*Z*)-3-amino-4-oxo-2-azetidinesulfonic acids (C) 886

Azetones, Thietones, oxetones, and azetones (C) 543

Azirines, Kinetics of the reaction of electron deficient olefins with nitrile ylides generated by laser flash photolysis of substituted azirines (C) 625

BASICITIES, The relative basicities of imidazole and benzimidazole (C) 323

Benzene, Aerial oxidation of benzene in the presence of electrochemically generated $Cu^+$ ions (C) 502
*p*-(*o,p*)-*o*-Tribenzene and *p*-(*o,p*)-(*o,o*)-*p*-tetrabenzene, Diels-Alder oligomers of benzene (C) 617

Benzene dioxide, *syn*-Benzene dioxide/1,4-dioxocin systems *via* a Diels-Alder route (C) 410
Benzimidazole, The relative basicities of imidazole and benzimidazole (C) 323
Benzocyclobutenes, Unexpected ring-opening of benzocyclobutenes upon reaction with lithium in tetrahydrofuran (C) 246
Benzodioxepin, 2*H*-1,5-Benzodioxepin and 3-halo derivatives (C) 64
Benzyl(triethyl)ammonium permanganate, Detonation of benzyl(triethyl)ammonium permanganate (C) 625
Benzynes, 1,2-Benzynes from 6-halopentafulvenes (C) 490
Biazulenes, Resolution, circular dichroism, and absolute configuration of 1,1'-biazulenes (C) 870
Bicyclo[6.2.0]decapentaene, Octalene-bicyclo[6.2.0]decapentaene conversion mediated by transition-metal complexes (C) 1003
Bile pigments, Solution conformations, photophysics, and photochemistry of bile pigments; bilirubin and biliverdin dimethyl esters and related linear tetrapyrroles (R) 656
Bimetallic complex, $[Cl_2FeS_2MoO(S_2)]^{2-}$, a novel bimetallic complex with unusual electronic structure and a substituted tetrachalcogenometalate as "ligand" (C) 561
Bioassay, Adventures and excursions in bioassay: the stepping stones to prostacyclin (Nobel lecture) (R) 741
Biomimetic synthesis of primary enamides by decarboxylation of α,β-dehydroamino acids (C) 550
Bioorganic chemistry, Four-membered ring peroxides as excited state equivalents: a new dimension in bioorganic chemistry (R) 529
Biotechnology, a comprehensive treatise in 8 volumes (B) 893
Bipyridinium compounds, Phanes with two 4,4'-bipyridinium moieties—a new class of compounds (C) 489
Bisdehydrobenzo[18]annulene, 2D-NMR spectroscopy in annulene chemistry: complete assignment of the $^{13}C$-NMR spectrum of 9,11-bisdehydrobenzo[18]annulene by $^1H,^{13}C$ shift correlation (C) 499
Bis(dimethylamino)fluorene, 4,5-Bis(dimethylamino)fluorene, a new "proton sponge" (C) 731
Bisdioxetane, Crystal structure of 2,4,5,7,9,10-hexaoxa-1,3,6,8-tetraphenyltricyclo[6.2.0.0$^{3,6}$]decane: an authentic bisdioxetane (C) 546
Bisnorcobester, 5,15-Bisnorcobester: an unexpected mode of formation (C) 736
A simple route to 5-nor-, 15-nor-, and 5,15-bisnorcobesters (C) 737
Bis(tetramethylethylenedioxy)silane, Strong distortion of the tetrahedral geometry in a spirosilicate: molecular structure of bis(tetramethylethylenedioxy)silane (C) 65
Bond formation, Bond forming initiation in spontaneous addition and polymerization reactions of alkenes (R) 440
Formation of CC bonds by addition of free radicals to alkenes (R) 753
Reversal of the regioselectivity in the zirconocene-induced coupling of a ketone with isoprene (C) 777
Activity of coordinated 1,4-diaza-1,3-dienes (dad) in C-C bond forming reactions: 1,5-dihydropyrrol-2-ones from (dad)Fe(CO)$_3$ and dimethyl acetylenedicarboxylate (C) 992
Metal-induced C-C coupling by reductive dimerization of thioaroyl groups (C) 996
Bonding electron density distribution in tetra-*tert*-butylcyclobutadiene—a molecule with an obviously non-square four-membered ring (C) 403
Borirenes, Synthesis of borirenes and diboretenes—a novel class of 2π-aromatic compounds (C) 48
Borolemetal complexes, A novel and general route to ($\eta^5$-borole)metal complexes: compounds of manganese, ruthenium, and rhodium (C) 996
Boron-carbon double bond, A boron-carbon double bond (C) 877
$\mu_3$-Bridging, Capping of metal atom triangles in clusters by $R_3PAu$ moieties (C) 326
Bridging ligands, Seleno- and telluroformaldehyde as bridging ligands in organometallic complexes (C) 314
$\eta^6$-Bonded alkylbenzenes as novel bridging ligands in dinuclear complexes of iron and cobalt (C) 620
Naked phosphorus atoms as trigonally planar coordinated bridge ligands (C) 976
Butadiene, The zirconocene-induced coupling of butadiene with carbonyl compounds (C) 494
Butadienyltriazoles, 1-(1,3-Butadienyl)triazoles from 1-vinyltriazoles and electron-rich alkynes—cleavage to "push-pull" 1,3-butadienes (C) 553
Butenal, Kinetic and thermodynamic control in the reaction of $(Ph_3P)_2PtO_2$ with (*E*)-2-butenal (C) 47
Butyl cation, C-Scrambling in the *tert*-butyl cation (C) 50
Butynylcarbamates, Regio- and diastereoselective synthesis of (4-hydroxy-3-methyl-1,2-alkadienyl)carbamates from α-titanated 2-butynylcarbamates and aldehydes (C) 54

CAGE MOLECULE, Unprecedented oxidative addition of the $P_4S_3$ cage molecule with phosphorus-phosphorus bond cleavage; synthesis and molecular structure of $[Ir(\mu\text{-}P_4S_3)(PPh_3)Cl(CO)]_2$ (C) 790
Carbanions, Successive electron transfers in molecules with two electrophoric groups: novel singlet, doublet, and triplet states (C) 242
The structure of tris(diphenylthiophosphinoyl)methanide, a mesomerically stabilized carbanion (C) 254
Carbene-carbon monoxide coupling, Intramolecular carbene-carbon monoxide coupling in chromium and tungsten complexes (C) 874
Carbene complex, Synthesis and structure of $(CO)_4\overline{W[C(NEt_2)PMePh]}$, a novel cyclic carbene complex (C) 411
A carbene-complex route to vitamin E (C) 732
Carbenes, Expansion of three-membered heterocycles to five-membered cyclic carbenes—novel reactions of aziridine, oxirane, and thiirane with CO and CS ligands in iron, ruthenium, and manganese complexes (C) 163
Carbocyanines, First proof of di-, tri-, and all-*cis*-conformations in sterically hindered trimethinecyanines (carbocyanines) of the indoline and benzothiazole series (C) 876
Carbodications, Stable carbodications (R) 390
The *endo*-3,10-dimethyltricyclo[5.2.1.0$^{2,6}$]deca-4,8-dien-3,10-diyl dication, a novel bishomoaromatic/allylic dication and its rearrangement to the symmetrical *cis-anti-cis*-3,10-dimethyltricyclo[5.3.0.0$^{2,6}$]deca-4,8-dien-3,10-diyl dication (C) 712
Carbodiphosphorane, Coinage metal complexes of hexaphenylcarbodiphosphorane—organometallic compounds with coordination number 2 (C) 729
Carbon, The electrochemistry of black carbons (R) 950
Carbonylation, Metal-induced carbonylation of a phosphane-stabilized "carbyne ligand": conversion of a phosphorus ylide-carbonylmetal adduct into an $\eta^1$-ketenyl complex (C) 151
Carbonyl olefinations with organomolybdenum compounds (C) 244
Carborane, Synthesis and structure determination of $[(PEt_3)RhC_2B_9H_{10}]_2$—a binuclear rhodacarborane containing four bonds between two icosahedra (C) 722
Carbyne ligand, Metal-induced carbonylation of a phosphane-stabilized "carbyne ligand": conversion of a phosphorus ylide-carbonylmetal adduct into an $\eta^1$-ketenyl complex (C) 151
Carminomycinone, Facile synthesis of the (±)-6-deoxycarminomycinone from aloeemodin (C) 875
Caronaldehyde acid methyl ester, Diastereo- and enantioselective synthesis of (1*R*,3*R*)-caronaldehyde acid methyl ester and (1*R*,3*R*)-chrysanthemic acid methyl ester from (*R*)-glycerinaldehyde acetonide (C) 63
Catalysis by molecular metal clusters (R) 135
Allyl(hydrido)platinum(II)-catalyzed partial hydrogenation of dienes (C) 246
Catalysts, Novel nickel-oligomerization catalysts with arsenic-oxygen chelate ligands (C) 503
Solution-phase metal atom preparation of catalytically active zeolite-encapsulated metal clusters; characterization and application to the selective reduction of CO to butene (C) 624
"Organically solvated" magnesium for the synthesis of transition-metal complexes and catalysts (C) 728
Reaction control by catalysts with variable specificity: stable palladium-phthalocyanine as hydrogenation catalyst with three catalytic patterns (C) 881
Catenane, [2]-[Cyclohexatetraoctane][cyclooctacosane]catenane, the first hydrocarbon catenane (C) 889
Cercosporin, a singlet oxygen generator (C) 720
Chain-forming step, A model reaction of an elementary step in the Fischer-Tropsch synthesis: $[C_6Me_6RuH(C_2H_4)PR_3]^+$ from $C_6Me_6Ru(CH_3)_2PR_3$ (C) 46
Charge-transfer absorption, Cation-induced charge-transfer absorption of intramolecular quinhydrones with oligooxaparacyclophane structure (C) 334
Chelating ligands, The structure of tris(diphenylthiophosphinoyl)methanide, a mesomerically stabilized carbanion (C) 254
Novel nickel-oligomerization catalysts with arsenic-oxygen chelate ligands (C) 503
Chelation control, Chelation or non-chelation control in stereoselective reactions of titanium reagents with chiral alkoxycarbonyl compounds (C) 989
Chemical technology, Ullmanns Encyklopädie der technischen Chemie (B) 564
Chemical transport, Preparation of solid-state compounds by chemical transport—interpretation and control using the cooperative transport model (R) 82
Chiral synthetic building block, Synthesis of the chiral synthetic building block (1*R*,5*S*)-3-phenyl-4-oxa-2,6-diazabicyclo-[3.2.0]hept-2-en-7-one from 6-aminopenicillanic acid (C) 711
Chromatography, A quarter century of thin-layer chromatography—an interim report (R) 507
Chromatographic resolution of cyclic organic compounds on a Λ-Tris(1,10-phenanthroline)ruthenium(II) montmorillonite column (C) 162
Isotope effects in the low-pressure, high-pressure, and thin-layer chromatography of the lanthanoids (C) 325
Chromium compounds, $\mu_2$-($\eta^5$:$\eta^5$-Cyclooctatetraene)-bis($\eta^5$-cyclopentadienylchromium): a "siamese twin" of two half-open sandwich moieties (C) 330

Chrysanthemic acid methyl ester, Diastereo- and enantioselective synthesis of (1*R*,3*R*)-caronaldehyde acid methyl ester and (1*R*,3*R*)-chrysanthemic acid methyl ester from (*R*)-glycerinaldehyde acetonide (C) 63
Circular dichroism, Resolution, circular dichroism, and absolute configuration of 1,1'-biazulenes (C) 870
Clathrands, A novel type of ionic clathrands for numerous inclusion compounds (C) 409
Clusters, Catalysis by molecular metal clusters (R) 135
Exchange of the apical tin atom in the *nido*-cluster $(CH_3)_5C_5Sn^+$ (C) 56
Reversible opening of a thioketene-iron cluster containing a $\mu_2$-$C_2$,$\mu_2$-*S*-thiocarbonyl group (C) 153
FT-FIR spectroscopy of ligand-free metal clusters; matrix effects on the molecular geometry of trichromium, $Cr_3$ (C) 166
Synthesis and structure of $[AsPh_4][Ru_6H(\mu\text{-}O{=}CNMe_2)_2(\mu\text{-}CO)_4(CO)_{14}]\cdot Me_2C{=}O$; a cyclic hydrido-hexametallic anion (C) 249
$[Co_3\{\mu_3\text{-}S\}\{o\text{-}(SCH_2)_2C_6H_4\}_3]^{2-}$: the first trinuclear cobalt cluster with tetrahedral $CoS_4$-coordination (C) 318
Capping of metal atom triangles in clusters by $R_3PAu$ moieties (C) 326
Synthesis of a tetranuclear manganese(IV) cluster with adamantane skeleton: $[(C_6H_{15}N_3)_4Mn_4O_6]^{4+}$ (C) 328
$(C_5H_5)_6Ni_2Zn_4$—the first zinc-containing mixed-metal cluster (C) 329
Synthesis and structure of $[\{[CH_3C(CH_2PPh_2)_3]IrP_3\}_3Cu_5Br_4]CuBr_2$—a 21 atom Ir/Cu/P/Br cluster (C) 554
Cobalt cluster, $[Co_3\{\mu_3\text{-}S\}\{o\text{-}(SCH_2)_2C_6H_4\}_3]^{2-}$: the first trinuclear cobalt cluster with tetrahedral $CoS_4$-coordination (C) 318
Cobester, 5,15-Bisnorcobester: an unexpected mode of formation (C) 736
A simple route to 5-nor-, 15-nor-, and 5,15-bisnorcobesters (C) 737
Cog-wheel mechanism, Conformational inversion of tetraisopropylethylene: no cog-wheel mechanism (C) 998
Color photography, Dye diffusion systems in color photography (R) 191
Columnar structure, Construction of an alternating (Rh, Rh, Ir, Ir)$_\infty$-columnar structure *via* a quasiracemate (C) 327
Complexation gas chromatography, Derivatization-free enantiomer resolution of chiral alcohols and ketones by high-resolution complexation gas chromatography (C) 772
Quantitative separation of deuterated tetrahydrofurans $C_4H_{4(\beta)}H_{4-n(\alpha)}D_{n(\alpha)}O$ by complexation gas chromatography on a cobalt(II) complex (C) 772
Complexing, Quenching of the aromaticity of the 5-dibenzo[*a*,*d*]cycloheptenylium ion by complexing with $(CO)_3Cr$ (C) 559
Complexing agents, Synthesis and structure of a macrocycle with a skeletal framework of arsenic, carbon, oxygen, and nitrogen atoms (C) 1006
Complex ion pair, Synthesis and structure of $[Na(tmeda)_2]^{\oplus}[HNi_2(C_2H_4)_4]^{\ominus}$ (C) 991
Conformations, Solution conformations, photophysics, and photochemistry of bile pigments; bilirubin and biliverdin dimethyl esters and related linear tetrapyrroles (R) 656
First proof of di-, tri-, and all-*cis*-conformations in sterically hindered trimethinecyanines (carbocyanines) of the indoline and benzothiazole series (C) 876
Conformational inversion of tetraisopropylethylene: no cog-wheel mechanism (C) 998
Coordination, Phosphorus ylides in the coordination sphere of transition metals. An inventory (R) 907
Tellurium as six-electron donor—synthesis and structure of $\mu_3$-Te[$Mn(CO)_2(\eta^5\text{-}C_5H_5)]_3$ (C) 59
$[Co_3\{\mu_3\text{-}S\}\{o\text{-}(SCH_2)_2C_6H_4\}_3]^{2-}$: the first trinuclear cobalt cluster with tetrahedral $CoS_4$-coordination (C) 318
$[Fe_2\{o\text{-}(SCH_2)_2C_6H_4\}_2\{SC_6H_5\}_2]^{2-}$ and $[Fe_2\{o\text{-}(SCH_2)_2C_6H_4\}_3]^{2-}$: binuclear thiolatoiron(II) anions with tetrahedral $FeS_4$-coordination (C) 319
Coinage metal complexes of hexaphenylcarbodiphosphorane—organometallic compounds with coordination number 2 (C) 729
$^{27}$Al-NMR spectroscopy: a probe for three-, four-, five-, and sixfold coordinated Al atoms in organoaluminum compounds (C) 779
$SbF^{2+}$ as a Lewis acid in $Na(SbF)PO_4\cdot nH_2O$ (n = 2–4) and $NH_4(SbF)PO_4\cdot H_2O$ (C) 872
N,P-coordination of an amino(imino)phosphane (C) 984
Lithium complexes with *pentahapto*-bonded cyclopentadienyl ligands (C) 994
Cope-rearrangement, Ring-opening by [3,3]-diphospha Cope-rearrangement (C) 61
Copper compounds, Are the previously described $[ClF_6][CuF_4]$ and $[Cu(H_2O)_4][SiF_6]$ identical? (C) 408
Copper(II) diacetate, Synthesis and structure of $[CuMo(CH_3CO_2)_2(L)(CO)_2(\eta^5\text{-}C_5H_5)]$: monomeric copper(II) diacetate as building block of a heterometallic binuclear complex (C) 982
Coriolin, Synthesis and structure of a linearly *anti*-annelated tetracycloundecane. A potential precursor for a coriolin synthesis (C) 721
Corrins, Novel methods for demetalating tetrapyrrolic metallo-macrocycles (C) 734
Acid-catalyzed demetalation of nickel-hydrocorphin and cobalt-corrin complexes with 1,3-propanedithiol (C) 735
Coupling constants, Tetra-*tert*-butyltetrahedrane: $^{13}C$-$^{13}C$ coupling constants and hybridization (C) 878
Crown ethers, Cation-induced charge-transfer absorption of intramolecular quinhydrones with oligooxaparacyclophane structure (C) 334
Surfactants with novel structural characteristics (C) 616
Macrocyclic polyether syntheses (B) 257
Crystallographic disorder, Cautionary example of incorrect structural assignment due to crystallographic disorder (C) 251
Crystal structure, Structural relationship of $[(C_6H_5)_4As]NdCl_4\cdot 8H_2O$ and $NdCl_3\cdot 6H_2O$: transition from a three-dimensional to a layer structure (C) 1009
Crystal structure investigation, Are the previously described $[ClF_6][CuF_4]$ and $[Cu(H_2O)_4][SiF_6]$ identical? (C) 408
Cubane type, A general method for the synthesis of heterometal clusters of the $M_2Fe_2S_4$-cubane type (M = Cr, Mo) (C) 549
Cyanoformyl chloride (C) 785
Cyanouracil, Photocycloaddition of 6-cyanouracil to ketene diethyl acetal: synthesis of a uracil derivative possessing a cyclobutenone framework (C) 629
Cyclic reaction, Straightforward preparation and stabilization of 2-*trans*-4,7:10,13-diepoxy[15]annulenone (C) 253
Cyclizations, Homolytic cyclizations of *N*-chloroalkenylamines (R) 337
Cycloadditions, [2+2]-Cycloadditions of allyl cations (C) 49
Photocycloaddition of 6-oxopurines and thymine to products with cyclobutane part structures (C) 623
Photocycloaddition of 6-cyanouracil to ketene diethyl acetal: synthesis of a uracil derivative possessing a cyclobutenone framework (C) 629
[4+2]-Cycloaddition of singlet oxygen to 2,5-dimethylfuran: isolation and reactions of the monomeric and dimeric endoperoxides (C) 726
Cycloalkenynes, Base-induced isomerization of cycloalkenynes in competition with addition reactions (C) 627
Cyclobutabenzene, Unexpected ring-opening of benzocyclobutenes upon reaction with lithium in tetrahydrofuran (C) 246
Cyclobutadiene, Three arguments supporting a rectangular structure for tetra-*tert*-butylcyclobutadiene (C) 402
Bonding electron density distribution in tetra-*tert*-butylcyclobutadiene—a molecule with an obviously non-square four-membered ring (C) 403
Tricyclo[2.1.0.$0^{2,5}$]pentan-3-one (C) 990
Cyclodextrin, Flip-flop hydrogen bonds in β-cyclodextrin—a generally valid principle in polysaccharides? (C) 883
Cyclohexadiene, 1,2-Cyclohexadiene (C) 542
Cyclopentadienylbis(ethene)cobalt, Synthesis and reactions of $\eta^5$-cyclopentadienylbis(ethene)cobalt (C) 716
Cyclopentadienyl ligands, Lithium complexes with *pentahapto*-bonded cyclopentadienyl ligands (C) 994
Cyclopentanecarboxylates, Novel one-step synthesis of oxocyclopentanecarboxylates by electrochemical reduction of cinnamic acid esters (C) 52
Cyclophanes, Cation-induced charge-transfer absorption of intramolecular quinhydrones with oligooxaparacyclophane structure (C) 334
New link between cyclophane and ferrocene chemistry (C) 633
Cyclopropane derivatives, 1-Lithio-1-phenylcyclopropanes—structure and dynamics (C) 243
Cytochrome c oxidase, Structure and evolution of the *"Atmungsferment"* cytochrome c oxidase (R) 275
Cytochrome P450 enzyme, Prostacyclin synthase, a cytochrome P450 enzyme (C) 487

DAILY RHYTHMS, Turgorins, hormones of the endogeneous daily rhythms of higher organized plants—detection, isolation, structure, synthesis, and activity (R) 695
Defect tetrahedral structure, GaGeTe, a novel defect tetrahedral structure (C) 407
Dehalogenation, Selective reductive dehalogenation of tertiary and benzylic halides with $Zn(BH_4)_2$ in diethyl ether (C) 562
Dehydrobenzene, 1,2-Benzynes from 6-halopentafulvenes (C) 490
Demetalation, Novel methods for demetalating tetrapyrrolic metallo-macrocycles (C) 734
Acid-catalyzed demetalation of nickel-hydrocorphin and cobalt-corrin complexes with 1,3-propanedithiol (C) 735
Deoxycarminomycinone, Facile synthesis of the (±)-6-deoxycarminomycinone from aloe-emodin (C) 875
Description of structure, On the description of complex inorganic crystal structures (R) 69
Intermetallic compounds and the use of atomic radii in their description (R) 95
Detonation of benzyl(triethyl)ammonium permanganate (C) 625
Deuteriofurans, Quantitative separation of deuterated tetrahydrofurans $C_4H_{4(\beta)}H_{4-n(\alpha)}D_{n(\alpha)}O$ by complexation gas chromatography on a cobalt(II) complex (C) 772
Deuteroporphyrin-IX dimethyl ester: assignment of the $^1$H-NMR spectrum by NOE measurements in presence of a diamagnetic shift reagent (C) 551
Dialkoxytrimethylene, 1,1-Dialkoxytrimethylene radical cations (C) 500
Diaminodiphosphene, Tetrakis(trimethylsilyl)diaminodiphosphene (C) 155

Diaminodiphosphenes—synthesis, crystal structure and bonding properties (C) 486
Dianions, Unusual NMR phenomena of anthracene and phenanthrene dianions—thermal stimulation of triplet states in antiaromatic systems (C) 45
Di(9-anthryl)ethylene, *cis*-1,2-Di(9-anthryl)ethylene: photochemical isomerization by intramolecular Diels-Alder reaction (C) 495
Diarsenechromium complex, Synthesis and structure of a diarsenechromium complex with an unsupported arsenic-arsenic double bond (C) 978
Diastereoselective syntheses of *C*-glycopyranosides (C) 622
Diazadienes, Diels-Alder reactions of dienes with alkynes catalyzed by diazadieneiron (C) 778
Activity of coordinated 1,4-diaza-1,3-dienes (dad) in C-C bond forming reactions: 1,5-dihydropyrrol-2-ones from (dad)$Fe(CO)_3$ and dimethyl acetylenedicarboxylate (C) 992
Diazaquinodimethanes, donor-substituted pyrazines, and dihydropyrazines (C) 717
Diazasilacyclopentenes, The one-electron oxidation of diazasilacyclopentenes (C) 621
Diazenidomolybdenum complex, $[Mo\{N_2C(S)SC_2H_5\}\{NH_2NC(S)SC_2H_5\}\{(CH_3)_2NCS_2\}_2]$—a sulfur-rich heptacoordinated diazenidohydrazido(1−)molybdenum complex (C) 245
Diazines, The versatile chemistry of 1,4-diazines: organic, inorganic and biochemical aspects (R) 171
Dibenzo[8]annulene, A novel planar antiaromatic dibenzo[8]annulene (C) 332
Dibenzo[*a*,*d*]cycloheptenylium ion, Quenching of the aromaticity of the 5-dibenzo[*a*,*d*]cycloheptenylium ion by complexing with $(CO)_3Cr$ (C) 559
Diboretenes, Synthesis of borirenes and diboretenes—a novel class of 2π-aromatic compounds (C) 48
Dicyanoketene: flash vacuum thermolysis of alkyl dicyanoacetates (C) 165
Diels-Alder oligomers, *p*-(*o*,*p*)-*o*-Tribenzene and *p*-(*o*,*p*)-(*o*,*o*)-*p*-tetrabenzene, Diels-Alder oligomers of benzene (C) 617
Diels-Alder reaction, *syn*-Benzene dioxide/1,4-dioxocin systems *via* a Diels-Alder route (C) 410
*cis*-1,2-Di(9-anthryl)ethylene: photochemical isomerization by intramolecular Diels-Alder reaction (C) 495
of dienes with alkynes catalyzed by diazadieneiron (C) 778
3,4-Bismethylenetricyclo[3.1.0.0$^{2,6}$]hexane—synthesis and Diels-Alder addition to tetracyanoethylene (C) 871
Acceleration and asymmetric induction of intermolecular Diels-Alder reactions of triacyl compounds (C) 887
Diepoxy[15]annulenone, Straightforward preparation and stabilization of 2-*trans*-4,7:10,13-diepoxy[15]annulenone (C) 253
Difluoroantimony cation, $SbF^{2+}$ as a Lewis acid in $Na(SbF)PO_4 \cdot nH_2O$ (n = 2–4) and **$NH_4(SbF)PO_4 \cdot H_2O$ (C) 872**
Difluoromethylene group, $(FMe_2Si)_2CF_2$: synthesis and reactions (C) 730
Diketene, Addition of alkanethiols to diketene—a correction (C) 498
Dilithioethane, 1,1-Dilithioethane (C) 733
Dimerization, Phosphane-induced, stepwise rearrangement of an octadienediyl palladium complex to seven- and nine-membered metallacycles (C) 774
Metal-induced C-C coupling by reductive dimerization of thioaroyl groups (C) 996
Dinuclear complexes, $\eta^6$-Bonded alkylbenzenes as novel bridging ligands in dinuclear complexes of iron and cobalt (C) 620
Dioxocin, *syn*-Benzene dioxide/1,4-dioxocin systems *via* a Diels-Alder route (C) 410
Diphospha Cope-rearrangement, Ring-opening by [3,3]-diphospha Cope-rearrangement (C) 61
Diphosphene, A diphosphene as tetrahedrane building block: synthesis of $[Fe_2(CO)_6(P_2tBu_2)]$ (C) 154
Tetrakis(trimethylsilyl)diaminodiphosphene (C) 155
Diaminodiphosphenes—synthesis, crystal structure and bonding properties (C) 486
Diphosphene complex, $(C_6H_5)_2P_2[Cr(CO)_5]_2$, a diphosphene complex with free phosphorus-phosphorus double bond (C) 977
Diphosphorus, :P≡P:, as eight-electron ligand (C) 976
Disaccharide synthesis, Synthesis and structure of the disaccharide fragment B-A of mithramycin (C) 58
Diselenium, Disulfur and diselenium as strong acceptor ligands in $(\eta^5\text{-}C_5H_5)Re(CO)_2S_2$ and $[\eta^5\text{-}C_5(CH_3)_5]Mn(CO)_2Se_2$ (C) 1000
Disorder, Cautionary example of incorrect structural assignment due to crystallographic disorder (C) 251
Disulfur and diselenium as strong acceptor ligands in $(\eta^5\text{-}C_5H_5)Re(CO)_2S_2$ and $[\eta^5\text{-}C_5(CH_3)_5]Mn(CO)_2Se_2$ (C) 1000
Dithian-2-yl methyl ester, 1,3-Dithian-2-yl methyl ester as two-step protecting group for the carboxy function in peptide synthesis (C) 62
Dithioxophosphorane, The first organodithioxophosphorane (C) 1004
DNA, Synthesis of peptide hormones using recombinant DNA techniques (R) 842
DNA synthesis, Chemical and enzymatic synthesis of gene fragments. A laboratory manual (B) 504
Dodecapentaenebis(tricarbonyliron), Organometallic variants of the Wittig reaction: synthesis and structure of *trans*-μ-(2-5; 8-11-η-dodecapentaene)bis(tricarbonyliron) (C) 713
Donor-acceptor bonding, Synthesis and structure of a bicyclic SbNP compound with intramolecular donor-acceptor bonding (C) 404
Dye diffusion systems in color photography (R) 191

ECOTOXICOLOGY, From environmental analytical chemistry to ecotoxicology—a plea for more concepts and less monitoring and testing (R) 380
Eight-Electron ligand, Diphosphorus, :P≡P:, as eight-electron ligand (C) 976
Electrical conductivity, Preparation and properties of tetrabenzoporphyrinatoiron(II) and its isocyanide complexes (C) 724
Polymeric electrically conductive phthalocyaninato(μ-s-tetrazine)iron (C) 784
Electrical properties of polymers (B) 895
Electrochemical reduction, Novel one-step synthesis of oxocyclopentanecarboxylates by electrochemical reduction of cinnamic acid esters (C) 52
Reactions at the counter electrode in electroreductions under aprotic conditions in one-compartment cells (C) 492
Electrochemistry, The electrochemistry of black carbons (R) 950
Aerial oxidation of benzene in the presence of electrochemically generated $Cu^+$ ions (C) 502
Industrial electrochemistry (B) 421
Electromicrobial reduction using yeasts (C) 322
Electron diffraction with the transmission electron microscope as a phase-determining diffractometer—from spatial frequency filtering to the three-dimensional structure analysis of ribosomes (R) 456
Electronic theory of chemical reactions, Electrons in chemical reactions; first principles (B) 635
Electron microscopy, From macromolecules to biological assemblies (Nobel lecture) (R) 565
E(lectron)N(uclear)DO(uble)R(esonance), $^{29}$Si-E(lectron)N(uclear)DO(uble)R(esonance) (C) 787
Electron transfer, Successive electron transfers in molecules with two electrophoric groups: novel singlet, doublet, and triplet states (C) 242
Electrophilic alkylation, Reactions of *N*-methylenecarboxamides with electrophiles: 1-alkoxy-2-azaallenium salts and *N*-acyl(methylene)ammonium salts (C) 252
Elimination, An arsanylketene by elimination from on oxaarsatungstacyclopentene complex (C) 1001
Enamides, Biomimetic synthesis of primary enamides by decarboxylation of α,β-dehydroamino acids (C) 550
Enantiomer resolution, Derivatization-free enantiomer resolution of chiral alcohols and ketones by high-resolution complexation gas chromatography (C) 772
Enantioselective hydrosilylation, Rhodium catalysts for enantioselective hydrosilylation—a new concept in the development of asymmetric catalysts (R) 897
of acetophenone with rhodium/thiazolidine catalysts (C) 331
Enantioselectivity, Reversal of the enantioselectivity in the enzymatic hydrolysis of juvenile hormone as a consequence of a protein fractionation (C) 773
Endoperoxides, [4+2]-Cycloaddition of singlet oxygen to 2,5-dimethylfuran: isolation and reactions of the monomeric and dimeric endoperoxides (C) 726
ENDOR-Spectroscopy, The first $^{13}$C-ENDOR investigation of an organic triradical in the quartet state; synthesis of a triply $^{13}$C-labeled trisgalvinol (C) 150
$^{29}$Si-E(lectron)N(uclear)DO(uble)R(esonance) (C) 787
Radical products in single electron transfer reactions of lithium triethylhydridoborate detected by ESR and multinuclear ($^1$H, $^{10}$B, $^{11}$B, $^{14}$N)-ENDOR spectroscopy (C) 892
Energy, Raw materials and energy: a challenge for polymer research (R) 764
Enol, (*Z*)-2-Methoxy-1,2-diphenylvinyl alcohol, a remarkably stable enol (C) 405
Environmental analytical chemistry, From environmental analytical chemistry to ecotoxicology—a plea for more concepts and less monitoring and testing (R) 380
Enzyme reaction, Reversal of the enantioselectivity in the enzymatic hydrolysis of juvenile hormone as a consequence of a protein fractionation (C) 773
Estrogens, The photooxygenation of estrogens: a new synthesis of 19-norsteroids (C) 711
Estrone, Stereoselective synthesis of enantiomerically pure natural products—estrone as example (R) 637
Ethanedithiol, Novel methods for demetalating tetrapyrrolic metallo-macrocycles (C) 734
Ethyl α-formylpropanoate, Preparation of ethyl (*R*)-(−)-3-hydroxy-2-methylpropanoate by yeast reduction of ethyl α-formylpropanoate (C) 1012
Excited state, Four-membered ring peroxides as excited state equivalents: a new dimension in bioorganic chemistry (R) 529
Advances in chemical physics, Vol. 50. Dynamics of the excited state (B) 894
Explosion, Detonation of benzyl(triethyl)ammonium permanganate (C) 625
Extraction, Highly selective extraction of uranyl ions by acyclic ligands containing L-phenylalanine moieties (C) 563

FERRIOSTIBANE-TRIMETHYLPHOSPHANE COMPLEXES, Transition-metal substituted stibanes as acceptors: $Cp(CO)(L)Fe—SbBr_2 \cdot PMe_3$ (L = CO,

$Me_3P$, MeNC) —1:1-ferriostibane-trimethylphosphane complexes (C) 60
Ferrocene, New link between cyclophane and ferrocene chemistry (C) 633
Fischer-Tropsch synthesis, A model reaction of an elementary step in the Fischer-Tropsch synthesis: $[C_6Me_6RuH(C_2H_4)PR_3]^+$ from $C_6Me_6Ru(CH_3)_2PR_3$ (C) 46
Solution-phase metal atom preparation of catalytically active zeolite-encapsulated metal clusters; characterization and application to the selective reduction of CO to butene (C) 624
Intramolecular carbene-carbon monoxide coupling in chromium and tungsten complexes (C) 874
Flash photolysis, Kinetics of the reaction of electron deficient olefins with nitrile ylides generated by laser flash photolysis of substituted azirines (C) 625
Flash vacuum thermolysis, Dicyanoketene: flash vacuum thermolysis of alkyl dicyanoacetates (C) 165
Flip-flop hydrogen bonds in β-cyclodextrin—a generally valid principle in polysaccharides? (C) 883
Force field calculations, Molecular mechanics calculations in organic chemistry: examples of the usefulness of a simple nonquantum mechanical model (R) 1
Formylpropanoate, Preparation of ethyl (*R*)-(−)-3-hydroxy-2-methylpropanoate by yeast reduction of ethyl α-formylpropanoate (C) 1012
Four-electron ligands, A novel and general route to ($\eta^5$-borole)metal complexes: compounds of manganese, ruthenium, and rhodium (C) 996
Four-electron redox reaction, Photochemical four-electron redox reaction of hexaazidoplatinate(IV) (C) 154
Fourier transform far-infrared spectroscopy, FT-FIR spectroscopy of ligand-free metal clusters; matrix effects on the molecular geometry of trichromium, $Cr_3$ (C) 166
of silver atoms and silver clusters entrapped in zeolite NaY (C) 791
Fourier transform methods, Modern pulse methods in high-resolution NMR spectroscopy (R) 350
Free radical reactions, Formation of CC bonds by addition of free radicals to alkenes (R) 753
Friedel-Crafts alkylation, Regiocontrolled prenylations and alkylations of furans: preparation of rosefuran and novel analogues (C) 719

GAS CHROMATOGRAPHY, Derivatization-free enantiomer resolution of chiral alcohols and ketones by high-resolution complexation gas chromatography (C) 772
Quantitative separation of deuterated tetrahydrofurans $C_4H_{4(\beta)}H_{4-n(\alpha)}D_{n(\alpha)}O$ by complexation gas chromatography on a cobalt(II) complex (C) 772
Genetic engineering, Synthetic gene fragments in genetic engineering—the renaissance of chemistry in molecular biology (R) 13
Germanium compounds, $Rb_7NaGe_8$ and $K_7NaGe_8$, Zintl compounds with $Na(Ge_4)_2$ units (C) 998
Glucopyranosyl derivatives, Synthesis of C-α- and C-β-D-glucopyranosyl derivatives from *O*-(α-D-glucopyranosyl) trichloroacetimidate (C) 406
Glycopeptide synthesis, *O*-Glycopeptide synthesis using 9-fluorenylmethoxycarbonyl (Fmoc)-protected synthetic units (C) 62
Glycoproteins, Synthesis of a tetrasaccharide of the core region of *O*-glycoproteins (C) 776
Glycopyranosides, Diastereoselective syntheses of *C*-glycopyranosides (C) 622
Glyculosyl bromides, A facile, efficient synthesis of acylated glyculosyl bromides from hydroxyglycal esters (C) 891
Gold compounds, Capping of metal atom triangles in clusters by $R_3PAu$ moieties (C) 326
Graphite, Incorporation of mercury into graphite *via* K/Hg intercalation compounds (C) 53

HAFNIUM COMPOUNDS, Zircona- and hafnacyclobutenes—a new route to metallacyclobutanes (C) 248
Half-sandwich complexes, Electron-rich half-sandwich complexes—metal bases par excellence (R) 927
Heavy atom effect in the photoelectron spectra of transition metal complexes (C) 329
Hetero[17]annulene dioxides, Synthesis of hetero[17]annulene dioxides and a [16]annulene dioxide using furan building blocks (C) 417
Heterocycles, Homolytic cyclizations of *N*-chloroalkenylamines (R) 337
Expansion of three-membered heterocycles to five-membered cyclic carbenes—novel reactions of aziridine, oxirane, and thiirane with CO and CS ligands in iron, ruthenium, and manganese complexes (C) 163
Heterocyclic chemistry, Contemporary heterocyclic chemistry: syntheses, reactions and applications (B) 739
Heteromacrocycle, Synthesis and structure of a macrocycle with a skeletal framework of arsenic, carbon, oxygen, and nitrogen atoms (C) 1006
Heterometal clusters, A general method for the synthesis of heterometal clusters of the $M_2Fe_2S_4$-cubane type (M = Cr, Mo) (C) 549
Synthesis and structure of $[\{[CH_3C(CH_2PPh_2)_3]IrP_3\}_3Cu_5Br_4]CuBr_2$—a 21 atom Ir/Cu/P/Br cluster (C) 554
$[Cl_2FeS_2MoO(S_2)]^{2-}$, a novel bimetallic complex with unusual electronic structure and a substituted tetrachalcogenometalate as "ligand" (C) 561
Heterometallic binuclear complex, Synthesis and structure of $[CuMo(CH_3CO_2)_2(L)(CO)_2(\eta^5\text{-}C_5H_5)]$: monomeric copper(II) diacetate as building block of a heterometallic binuclear complex (C) 982
Hexaphenylcarbodiphosphorane, Coinage metal complexes of hexaphenylcarbodiphosphorane—organometallic compounds with coordination number 2 (C) 729
Hexopyranoside acetophenone acetals, Formation, structure, and synthetic use of gluco- and galactopyranoside acetophenone acetals with 1,3-dioxane rings (C) 255
Holographic methods for the investigation of photochemical and photophysical properties of molecules (R) 582
Hydrazidinyl radicals, 1,5-Dimethylverdazyls, hydrazidinyl radicals with pyramidal 1,5-nitrogen atoms (C) 320
Hydrazido(1−)molybdenum complex, $[Mo\{N_2C(S)SC_2H_5\}\{NH_2NC(S)SC_2H_5\}\{(CH_3)_2NCS_2\}_2]$—a sulfur-rich heptacoordinated diazenidohydrazido(1−)molybdenum complex (C) 245
Hydride addition, Novel $\eta^3,\sigma$-sulfur double ylide chromium complexes by *endo*-hydride addition to cationic ($\lambda^6$-thiabenzene 1-oxide)chromium complexes (C) 498
Hydrido complexes, Photolysis of the cyclopentadienyl(hydrido) complexes $C_5H_5M(CO)_3H$ (M = Cr, Mo, W) in matrices and in solution: characterization of $[C_5H_5W(CO)_2H]_2$ and $[C_5Me_5W(CO)_2H]_2$ (C) 544
Hydrido-hexametallic anion, Synthesis and structure of $[AsPh_4][Ru_6H(\mu\text{-}O{=}CNMe_2)_2(\mu\text{-}CO)_4(CO)_{14}]\cdot Me_2C{=}O$; a cyclic hydrido-hexametallic anion (C) 249
Hydrogenation, Allyl(hydrido)platinum(II)-catalyzed partial hydrogenation of dienes (C) 246
Hydrogenation catalysts, Reaction control by catalysts with variable specificity: stable palladium-phthalocyanine as hydrogenation catalyst with three catalytic patterns (C) 881
Hydrogen bonds, Flip-flop hydrogen bonds in β-cyclodextrin—a generally valid principle in polysaccharides? (C) 883
Hydrosilylation, Rhodium catalysts for enantioselective hydrosilylation—a new concept in the development of asymmetric catalysts (R) 897
Enantioselective hydrosilylation of acetophenone with rhodium/thiazolidine catalysts (C) 331
Hydroxyglycal esters, A facile, efficient synthesis of acylated glyculosyl bromides from hydroxyglycal esters (C) 891
Hydroxy-2-methylpropanoate, Preparation of ethyl (*R*)-(−)-3-hydroxy-2-methylpropanoate by yeast reduction of ethyl α-formylpropanoate (C) 1012

IMIDAZOLE, The relative basicities of imidazole and benzimidazole (C) 323
Conversion of imidazole into μ-2,3-dihydro-1*H*-imidazole-1,2,2-triyl ligands (C) 993
INADEQUATE Pulse sequence, Structure determination by $^{13}C$-NMR spectroscopy using an INADEQUATE pulse sequence: differentiation of heteroatom-substituted organic constitutional isomers by means of $^{13}C$-$^{13}C$ coupling constants (C) 548
Inclusion complexes between a macrocyclic host molecule and aromatic hydrocarbons in aqueous solution (C) 715
Inclusion compounds, A novel type of ionic clathrands for numerous inclusion compounds (C) 409
Initiation, Bond-forming initiation in spontaneous addition and polymerization reactions of alkenes (R) 440
Inorganic oligomers, Thio- and seleno-compounds of main group elements—novel inorganic oligomers and polymers (R) 113
Interactions, Proximity effects in organic chemistry—The photoelectron spectroscopic investigation of non-bonding and transannular interactions (R) 283
Intercalation compounds, Incorporation of mercury into graphite *via* K/Hg intercalation compounds (C) 53
Intercalation reactions, Redox intercalation reactions of $VOPO_4\cdot 2H_2O$ (C) 412
Intermediates, Reactive intermediates (B) 420
Intermetallic compounds and the use of atomic radii in their description (R) 95
Intramolecular donor-acceptor bonding, Synthesis and structure of a bicyclic SbNP compound with intramolecular donor-acceptor bonding (C) 404
Inversion, Conformational inversion of tetraisopropylethylene: no cog-wheel mechanism (C) 998
Iridium-rhodium compounds, Construction of an alternating (Rh, Rh, Ir, Ir)$_\infty$-columnar structure *via* a quasiracemate (C) 327
Iridoid glycosides, Secologanin, a biogenetic key compound—synthesis and biogenesis of the iridoid and secoiridoid glycosides (R) 828
Stereoselective synthesis of iridoid glycosides (C) 888
Iron compounds, Optically active iron complexes with tetrahedral structure (C) 164
Iron sulfur anions, $[Fe_2\{o\text{-}(SCH_2)_2C_6H_4\}_2\{SC_6H_5\}_2]^{2-}$ and $[Fe_2\{o\text{-}(SCH_2)_2C_6H_4\}_3]^{2-}$: binuclear thiolatoiron(II) anions with tetrahedral $FeS_4$-coordination (C) 319
Isomerization, The cation di-μ-oxo-*trans*-dioxobis[(1,4,7-triazacyclononane)molyb-

denum(V)] (*Mo—Mo*) and its acid-catalyzed *cis*-isomerization (C) 491
Base-induced isomerization of cycloalkenynes in competition with addition reactions (C) 627
Octalene-bicyclo[6.2.0]decapentaene conversion mediated by transition-metal complexes (C) 1003
Isotope effects, Extremely long-range $^2H$ isotope effects on the chemical shifts in the $^{13}C$-NMR spectra of compounds with conjugated double bonds (C) 321
in the low-pressure, high-pressure, and thin-layer chromatography of the lanthanoids (C) 325

JUVENILE HORMONE, Reversal of the enantioselectivity in the enzymatic hydrolysis of juvenile hormone as a consequence of a protein fractionation (C) 773

KETENE, An arsanylketene by elimination from an oxaarsatungstacyclopentene complex (C) 1001
Ketene-alkyne conversion using Lewis acids (C) 493
Ketones, A method for the synthesis of ketones from phosphorus ylides and olefins *via* "mixed" diorganoborinates (C) 782
Kinetics, Linear control of temperature with time—a new approach to reaction kinetics (R) 225
Equilibria in the formation of $A_4B_3$ molecules (C) 317
Non-formal kinetics (B) 739

LACTAM ANTIBIOTICS, Synthesis and structure of (*Z*)-3-amino-4-oxo-2-azetidinesulfonic acids (C) 886
Lactones, A novel synthesis of macrocyclic lactones (C) 780
Lanthanoids, Isotope effects in the low-pressure, high-pressure, and thin-layer chromatography of the lanthanoids (C) 325
Lasers, Techniques of chemistry. Applications of lasers to chemical problems (B) 421
Lead-oxygen structural group, A novel lead-oxygen structural group: $Pb_8O_4^{8+}$ (C) 324
Leukotrienes, From studies of biochemical mechanism to novel biological mediators: prostaglandin endoperoxides, thromboxanes, and leukotrienes (Nobel lecture) (R) 805
Lewis acid, $SbF^{2+}$ as a Lewis acid in $Na(SbF)PO_4 \cdot nH_2O$ (n=2–4) and $NH_4(SbF)PO_4 \cdot H_2O$ (C) 872
Ligand-free metal clusters (R) 674
Solution-phase metal atom preparation of catalytically active zeolite-encapsulated metal clusters; characterization and application to the selective reduction of CO to butene (C) 624
Ligands, $[Mo\{N_2C(S)SC_2H_5\}\{NH_2NC(S)SC_2H_5\}\{(CH_3)_2NCS_2\}_2]$—a sulfur-rich heptacoordinated diazenidohydrazido(1−)-molybdenum complex (C) 245
$[Cl_2FeS_2MoO(S_2)]^{2-}$, a novel bimetallic complex with unusual electronic structure and a substituted tetrachalcogenometalate as "ligand" (C) 561
Pentacarbonylrhenium complexes with thiazylamide ligands (C) 723
Unprecedented oxidative addition of the $P_4S_3$ cage molecule with phosphorus-phosphorus bond cleavage; synthesis and molecular structure of $[Ir(\mu\text{-}P_4S_3)(PPh_3)Cl(CO)]_2$ (C) 790
$[Mo_2(NO)_2(S_2)_3(S_5)OH]^{3-}$, a complex containing a bidentate $S_5^{2-}$-bridging ligand in a $\{S_5Mo_2(S_2)\}$-heterocycle with cyclooctasulfur geometry (C) 884
Conversion of imidazole into μ-2,3-dihydro-1*H*-imidazole-1,2,2-triyl ligands (C) 993
Liquids, Properties of liquids and solutions (B) 256
Lithio-1-phenylcyclopropanes, 1-Lithio-1-phenylcyclopropanes—structure and dynamics (C) 243
Lithiumcarbamoyl-bis(ethene)nickel(0) (C) 547
Lithium-carbon structural units, $(PhC{\equiv}CLi)_4(tmhda)_2$, a polymeric organolithium compound with cubic $Li_4C_4$ structural units (C) 496
Lithium complexes with *pentahapto*-bonded cyclopentadienyl ligands (C) 994

MACROCYCLES, Inclusion complexes between a macrocyclic host molecule and aromatic hydrocarbons in aqueous solution (C) 715
A novel synthesis of macrocyclic lactones (C) 780
Magic-angle-spinning NMR (MAS-NMR) spectroscopy and the structure of zeolites (R) 259
Magnesium, "Organically solvated" magnesium for the synthesis of transition-metal complexes and catalysts (C) 728
Main group element-chalcogen compounds, Thio- and seleno-compounds of main group elements—novel inorganic oligomers and polymers (R) 113
Malonic ester dianion, Tetraethoxyallene: equivalent of the fictive malonic ester dianion—a versatile synthetic building block (C) 321
Manganese(IV) cluster, Synthesis of a tetranuclear manganese(IV) cluster with adamantane skeleton: $[(C_6H_{15}N_3)_4Mn_4O_6]^{4+}$ (C) 328
Mass spectroscopy, Generation of the phenyl cation by dissociative ionization of a dienynyl bromide in the gas phase (C) 786
Mercury, Incorporation of mercury into graphite *via* K/Hg intercalation compounds (C) 53
Mesomerism, The structure of tris(diphenylthiophosphinoyl)methanide, a mesomerically stabilized carbanion (C) 254
Metal-arsenic double bond, Dicarbonyl($\eta^5$-cyclopentadienyl)(di-*tert*-butyl-$\lambda^4$-arsanediyl)molybdenum and -tungsten—the first complexes with a metal-arsenic double bond (C) 416
Metal bases, Electron-rich half-sandwich complexes—metal bases par excellence (R) 927
Metal clusters, Catalysis by molecular metal clusters (R) 135
Ligand-free metal clusters (R) 674
Solution-phase metal atom preparation of catalytically active zeolite-encapsulated metal clusters; characterization and application to the selective reduction of CO to butene (C) 624
Metal-induced C-C bond formation, Activity of coordinated 1,4-diaza-1,3-dienes (dad) in C-C bond forming reactions: 1,5-dihydropyrrol-2-ones from (dad)$Fe(CO)_3$ and dimethyl acetylenedicarboxylate (C) 992
Metal-induced C-C coupling by reductive dimerization of thioaroyl groups (C) 996
Metallacycle, Aryl(hydrido)ruthenium complexes by C—H addition: isolation of a four-membered metallacycle as intermediate (C) 873
Metallacyclobutanes, Zircona- and hafnacyclobutenes—a new route to metallacyclobutanes (C) 248
Metallocene cations, Synthesis and structure of metallocene cations of the Vb elements arsenic and antimony (C) 250
Metal-metal bonds, Synthesis and structure of $[CuMo(CH_3CO_2)_2(L)(CO)_2(\eta^5\text{-}C_5H_5)]$: monomeric copper(II) diacetate as building block of a heterometallic binuclear complex (C) 982
Metal-metal multiple bonds, Addition of a phosphaalkyne to metal-metal multiple bonds (C) 413
Addition of methylene to multiple bonds between ligand-free main-group elements and transition metals—a general reaction (C) 979
Multiple bonds between metal atoms (B) 563
Metaphosphate derivatives, $P(NSiMe_3)_3^{\ominus}$—a derivative of the monomeric metaphosphate ion as building block for a tricyclic rhenium complex (C) 503
Metazidohemerythrin, $[\{(C_6H_{15}N_3)Fe\}_2(\mu\text{-}O)(\mu\text{-}CH_3CO_2)_2]^{2+}$, a dinuclear iron(III) complex with a metazidohemerythrin-type structure (C) 727
Methylation, The chemistry of pyrrocorphins: *C*-methylation of pyrrocorphinates at the ligand periphery (C) 631
Methylene addition, Addition of methylene to multiple bonds between ligand-free main-group elements and transition metals—a general reaction (C) 979
(Methylene)ammonium salts, Reactions of *N*-methylenecarboxamides with electrophiles: 1-alkoxy-2-azaallenium salts and *N*-acyl(methylene)ammonium salts (C) 252
Mikanecic acid, Preparation of 2-(1-hydroxyalkyl)acrylic esters; simple three-step synthesis of mikanecic acid (C) 795
Mimosa, A new phytohormone from *Mimosa pudica L.* (C) 617
Mithramycin, Synthesis and structure of the disaccharide fragment B-A of mithramycin (C) 58
Mixed crystals, Equilibria in the formation of $A_4B_3$ molecules (C) 317
Molecular biology, Synthetic gene fragments in genetic engineering—the renaissance of chemistry in molecular biology (R) 13
From macromolecules to biological assemblies (Nobel lecture) (R) 565
Molecular mechanics calculations in organic chemistry: examples of the usefulness of a simple non-quantum mechanical model (R) 1
Molybdenum compounds, Carbonyl olefinations with organomolybdenum compounds (C) 244
Synthesis and structure of $\mu_2$-oxobis[chloro(tetra-*p*-tolylporphyrinato)molybdenum(IV)]: a complex with central $Mo^{IV}$—O—$Mo^{IV}$ unit (C) 247
The cation di-μ-oxo-*trans*-dioxobis[(1,4,7-triazacyclononane)molybdenum(V)]-(*Mo—Mo*) and its acid-catalyzed *cis*-isomerization (C) 491
Molybdenum-sulfur compounds, $[Mo_2(NO)_2(S_2)_3(S_5)OH]^{3-}$, a complex containing a bidentate $S_5^{2-}$-bridging ligand in a $\{S_5Mo_2(S_2)\}$-heterocycle with cyclooctasulfur geometry (C) 884
Mucronin B, Total synthesis of mucronin B (C) 152
Multiphenylene, The structure and reactivity of 2,3,7,8-tetrakis(trimethylsilyl)terphenylene, a novel linear multiphenylene (C) 994
Multiple bonds, Addition of a phosphaalkyne to metal-metal multiple bonds (C) 413
Addition of methylene to multiple bonds between ligand-free main-group elements and transition metals—a general reaction (C) 979
$\mu_2$-E[V(CO)$_3$diphos]$_2$ (E=S, Se, Te): complexes with linear VEV multiple-bond systems (C) 980
between metal atoms (B) 563

NADH, Selective generation of NADH by visible light (C) 497
Natural products, Homolytic cyclizations of *N*-chloroalkenylamines (R) 337
Stereoselective synthesis of enantiomerically pure natural products—estrone as example (R) 637

Turgorins, hormones of the endogeneous daily rhythms of higher organized plants—detection, isolation, structure, synthesis, and activity (R) 695
Neodymium compounds, Structural relationship of $[(C_6H_5)_4As]NdCl_4 \cdot 8H_2O$ and $NdCl_3 \cdot 6H_2O$: transition from a three-dimensional to a layer structure (C) 1009
Nickel complexes, Synthesis and structure of $[Na(tmeda)_2]^{\oplus}[HNi_2(C_2H_4)_4]^{\ominus}$ (C) 991
Nickel(0) complexes, Lithiumcarbamoylbis(ethene)nickel(0) (C) 547
Nickel(II) complexes, $[Ni(S_4)_2]^{2\ominus}$, a homoleptic tetrasulfido-nickel(II) complex (C) 1006
Nickel-oligomerization catalysts, Novel nickel-oligomerization catalysts with arsenic-oxygen chelate ligands (C) 503
Nitrile ylides, Kinetics of the reaction of electron deficient olefins with nitrile ylides generated by laser flash photolysis of substituted azirines (C) 625
NMR Spectroscopy, Modern pulse methods in high-resolution NMR spectroscopy (R) 350
Unusual NMR phenomena of anthracene and phenanthrene dianions—thermal stimulation of triplet states in antiaromatic systems (C) 45
Extremely long-range $^2H$ isotope effects on the chemical shifts in the $^{13}C$-NMR spectra of compounds with conjugated double bonds (C) 321
2D-NMR spectroscopy in annulene chemistry: complete assignment of the $^{13}C$-NMR spectrum of 9,11-bisdehydrobenzo[18]annulene by $^1H,^{13}C$ shift correlation (C) 499
Structure determination by $^{13}C$-NMR spectroscopy using an INADEQUATE pulse sequence: differentiation of heteroatom-substituted organic constitutional isomers by means of $^{13}C$-$^{13}C$ coupling constants (C) 548
Deuteroporphyrin-IX dimethyl ester: assignment of the $^1H$-NMR spectrum by NOE measurements in presence of a diamagnetic shift reagent (C) 551
Probing the environment of Al atoms in noncrystalline solids: $Al_2O_3$—$SiO_2$ gels, soda glass, and mullite precursors (C) 614
$^{27}Al$-NMR spectroscopy: a probe for three-, four-, five-, and sixfold coordinated Al atoms in organoaluminum compounds (C) 779
NMR Studies of yeasts grown on substrates at "zero" level radioactivity (C) 49
Nobel lecture, From macromolecules to biological assemblies (Nobel lecture) (R) 565
Adventures and excursions in bioassay: the stepping stones to prostacyclin (Nobel lecture) (R) 741
From studies of biochemical mechanism to novel biological mediators: prostaglandin endoperoxides, thromboxanes, and leukotrienes (Nobel lecture) (R) 805
The prostaglandins: from the laboratory to the clinic (Nobel lecture) (R) 858
Non-Born-Oppenheimer effects, Symmetry breaking and non-Born-Oppenheimer effects in radical cations (R) 210
Noncrystalline solids, Probing the environment of Al atoms in noncrystalline solids: $Al_2O_3$—$SiO_2$ gels, soda glass, and mullite precursors (C) 614
Norcobester, A simple route to 5-nor-, 15-nor-, and 5,15-bisnorcobesters (C) 737
Norsteroids, The photooxygenation of estrogens: a new synthesis of 19-norsteroids (C) 711
Nucleophilic reagents, Organometallic compounds of titanium and zirconium as selective nucleophilic reagents in organic synthesis (R) 31
Nucleophilic substitution, On the stereochemistry of the $S_N2'$ reaction (C) 613
Nucleotide analogues, Phosphorothioate analogues of nucleotides—tools for the investigation of biochemical processes (R) 423

OCTADIENEDIYL PALLADIUM COMPLEX, Phosphane-induced, stepwise rearrangement of an octadienediyl palladium complex to seven- and nine-membered metallacycles (C) 774
Octalene-bicyclo[6.2.0]decapentaene conversion mediated by transition-metal complexes (C) 1003
Olefins, Kinetics of the reaction of electron deficient olefins with nitrile ylides generated by laser flash photolysis of substituted azirines (C) 625
Olefin synthesis, Olefins from β-hydroxycarboxylic acids—synthesis of isomerically pure α- and β-asarone (C) 628
Oligosaccharides, Syntheses of a branched hepta- and an octasaccharide with phytoalexin-elicitor activity (C) 793
One-electron oxidation, The one-electron oxidation of diazasilacyclopentenes (C) 621
Optical activity, Optically active iron complexes with tetrahedral structure (C) 164
Organoborinates, A method for the synthesis of ketones from phosphorus ylides and olefins *via* "mixed" diorganoborinates (C) 782
Organodithioxophosphorane, The first organodithioxophosphorane (C) 1004
Organometallic chemistry, Comprehensive organometallic chemistry (B) 797
Organomolybdenum compounds, Carbonyl olefinations with organomolybdenum compounds (C) 244
Organosilicon compounds, $(FMe_2Si)_2CF_2$: synthesis and reactions (C) 730
Orthosilicic acid ester, Strong distortion of the tetrahedral geometry in a spirosilicate: molecular structure of bis(tetramethylethylenedioxy)silane (C) 65
The crystal and molecular structure of bis(1,8-naphthalenedioxy)silane—a contribution to the controversy over planar, four-coordinated silicon in orthosilicic acid esters (C) 501
Oxetones, Thietones, oxetones, and azetones (C) 543
Oxidation, Aerial oxidation of benzene in the presence of electrochemically generated $Cu^+$ ions (C) 502
Oxidative coupling of the selenolate functions in $(C_6H_5)_3PC(Se)P(C_6H_5)_3$: crystal structure of $\{[(C_6H_5)_3P]_2CSe\}_2^{2\oplus} \cdot Fe_2OCl_6^{2\ominus} \cdot 4CH_2Cl_2$ containing a linear Fe—O—Fe axis (C) 156
Oxidoylide reactions, Some cautions in the interpretation of oxidoylide reactions based on $^{31}P$-NMR data (C) 56
Oxo-hexachlorodiferrate(III), Oxidative coupling of the selenolate functions in $(C_6H_5)_3PC(Se)P(C_6H_5)_3$: crystal structure of $\{[(C_6H_5)_3P]_2CSe\}_2^{2\oplus}Fe_2OCl_6^{2\ominus} \cdot 4CH_2Cl_2$ containing a linear Fe—O—Fe axis (C) 156

PALLADIUM-PHTHALOCYANINE, Reaction control by catalysts with variable specificity: stable palladium-phthalocyanine as hydrogenation catalyst with three catalytic patterns (C) 881
Peptide alkaloids, Total synthesis of mucronin B (C) 152
Peptide hormones, Synthesis of peptide hormones using recombinant DNA techniques (R) 842
Peptide synthesis, 1,3-Dithian-2-yl methyl ester as two-step protecting group for the carboxy function in peptide synthesis (C) 62
Permanganate, Detonation of benzyl(triethyl)ammonium permanganate (C) 625
Peroxides, Four-membered ring peroxides as excited state equivalents: a new dimension in bioorganic chemistry (R) 529
PE spectroscopy, Proximity effects in organic chemistry—the photoelectron spectroscopic investigation of non-bonding and transannular interactions (R) 283
Heavy atom effect in the photoelectron spectra of transition metal complexes (C) 329
Phanes with two 4,4'-bipyridinium moieties—a new class of compounds (C) 489
Valence isomerization of phane-bridged *cis*-trioxatris-*o*-homobenzenes (C) 867
Phenol, Aerial oxidation of benzene in the presence of electrochemically generated $Cu^+$ ions (C) 502
Phenyl cation, Generation of the phenyl cation by dissociative ionization of a dienynyl bromide in the gas phase (C) 786
Phosphaalkyne, Addition of a phosphaalkyne to metal-metal multiple bonds (C) 413
Phosphaallyl cations, 2-Phosphaallyl cations by formal insertion of $P^{\oplus}$ into the C=C double bond (C) 545
Phosphaazulene, 2-Benzyl-1-phosphaazulene (C) 57
1-Methoxy-3-phenyl-2-phosphaazulene—the first synthesis of 2-phosphaazulenes (C) 879
Phosphaketene, The first stable phosphaketene (C) 785
Phosphanes, N,P-coordination of an amino(imino)phosphane (C) 984
$P_{12}iPr_4$ and $P_{13}iPr_5$, two novel polycyclic organophosphanes (C) 1002
Phosphanylketenes, Generation and stabilization of phosphanyl- and arsanylketenes within the coordination sphere of tungsten (C) 149
Phosphiranes, The first X-ray structure analysis of a thiadiphosphirane (C) 418
Phosphoranes, Dephosphorylating "ylide diketone"-rearrangement of the arylcarbonyloxyalkylidenephosphoranes (C) 619
The first organodithioxophosphorane (C) 1004
Phosphorothioates, Phosphorothioate analogues of nucleotides—tools for the investigation of biochemical processes (R) 423
Phosphorus atoms, Naked phosphorus atoms as trigonally planar coordinated bridge ligands (C) 976
Phosphorus heterocycles, $(tBuP)_2C(tBuP)_2$—the first tetraphosphaspiro[2.2]pentane (C) 632
Small heterocycles containing phosphorus and tellurium atoms (C) 983
Phosphorus-nitrogen compounds, $P(NSiMe_3)_3^{\ominus}$—a derivative of the monomeric metaphosphate ion as building block for a tricyclic rhenium complex (C) 503
Phosphorus-phosphorus double bond, $(C_6H_5)_2P_2[Cr(CO)_5]_2$, a diphosphene complex with free phosphorus-phosphorus double bond (C) 977
Phosphorus polycycles, $P_{12}iPr_4$ and $P_{13}iPr_5$, two novel polycyclic organophosphanes (C) 1002
Phosphorus selenide sulfide, Equilibria in the formation of $A_4B_3$ molecules (C) 317
Phosphorus-silicon compounds, $(tBuP)_8Si_2$—a novel dispirocyclic silaphosphane (C) 775
Phosphorus-sulfur compounds, Unprecedented oxidative addition of the $P_4S_3$ cage molecule with phosphorus-phosphorus bond cleavage; synthesis and molecular structure of $[Ir(\mu\text{-}P_4S_3)(PPh_3)Cl(CO)]_2$ (C) 790
Phosphorus ylides in the coordination sphere of transition metals. An inventory (R) 907
Some cautions in the interpretation of oxidoylide reactions based on $^{31}P$-NMR data (C) 56
Metal-induced carbonylation of a phosphane-stabilized "carbyne ligand": conversion of a phosphorus ylide-carbonylmetal adduct into an $\eta^1$-ketenyl complex (C) 151

A method for the synthesis of ketones from phosphorus ylides and olefins *via* "mixed" diorganoborinates (C) 782
Photochemistry, Holographic methods for the investigation of photochemical and photophysical properties of molecules (R) 582
Photochemical four-electron redox reaction of hexaazidoplatinate(IV) (C) 154
Selective generation of NADH by visible light (C) 497
of previtamin $D_3$ at 92 K: formation of an unstable tachysterol$_3$ rotamer (C) 718
Topics in current chemistry 103: preparative organic photochemistry (B) 505
Experimental methods in photochemistry and photophysics (B) 802
Photocycloaddition, Some substituent effects in the photocycloaddition of dihalomaleiimides to uracils (C) 161
of 6-oxopurines and thymine to products with cyclobutane part structures (C) 623
of 6-cyanouracil to ketene diethyl acetal: synthesis of a uracil derivative possessing a cyclobutenone framework (C) 629
Photography, Dye diffusion systems in color photography (R) 191
Photoisomerization, *cis*-1,2-Di(9-anthryl)-ethylene: photochemical isomerization by intramolecular Diels-Alder reaction (C) 495
Photolysis of the cyclopentadienyl(hydrido) complexes $C_5H_5M(CO)_3H$ (M = Cr, Mo, W) in matrices and in solution: characterization of $[C_5H_5W(CO)_2H]_2$ and $[C_5Me_5W(CO)_2H]_2$ (C) 544
Photooxygenation, The photooxygenation of estrogens: a new synthesis of 19-norsteroids (C) 711
Photophysics, Experimental methods in photochemistry and photophysics (B) 802
Photoreaction, Asymmetry of emission quenching and product formation in an asymmetrically sensitized photoreaction (C) 550
Phthalocyaninato(μ-s-tetrazine)iron, Polymeric electrically conductive phthalocyaninato(μ-s-tetrazine)iron (C) 784
Phytoalexin-elicitor activity, Syntheses of a branched hepta- and an octasaccharide with phytoalexin-elicitor activity (C) 793
Phytohormones, Turgorins, hormones of the endogeneous daily rhythms of higher organized plants—detection, isolation, structure, synthesis, and activity (R) 695
A new phytohormone from *Mimosa pudica L.* (C) 617
Platinum compounds, Kinetic and thermodynamic control in the reaction of $(Ph_3P)_2PtO_2$ with (*E*)-2-butenal (C) 47
Polymerization, Bond-forming initiation in spontaneous addition and polymerization reactions of alkenes (R) 440
Carbocationic polymerization (B) 505
Polymer research, Raw materials and energy: a challenge for polymer research (R) 764
Polymers, Electrical properties of polymers (B) 895
Porphyrinatomolybdenum complexes, Synthesis and structure of $\mu_2$-oxobis-[chloro(tetra-*p*-tolylporphyrinato)molybdenum(IV)]: a complex with central $Mo^{IV}$—O—$Mo^{IV}$ unit (C) 247
Porphyrinogen, The chemistry of pyrrocorphins: stereoselectivity in the porphyrinogen→pyrrocorphin tautomerization (C) 630
Porphyrins, Novel methods for demetalating tetrapyrrolic metallo-macrocycles (C) 734
Previtamin $D_3$, Photochemistry of previtamin $D_3$ at 92 K: formation of an unstable tachysterol$_3$ rotamer (C) 718
Propanedithiol, Acid-catalyzed demetalation of nickel-hydrocorphin and cobaltcorrin complexes with 1,3-propanedithiol (C) 735
Prostacyclin, Adventures and excursions in bioassay: the stepping stones to prostacyclin (Nobel lecture) (R) 741
Prostacyclin synthase, a cytochrome P450 enzyme (C) 487
Prostaglandin endoperoxides, From studies of biochemical mechanism to novel biological mediators: prostaglandin endoperoxides, thromboxanes, and leukotrienes (Nobel lecture) (R) 805
Prostaglandins, The prostaglandins: from the laboratory to the clinic (Nobel lecture) (R) 858
Protecting group, 1,3-Dithian-2-yl methyl ester as two-step protecting group for the carboxy function in peptide synthesis (C) 62
*O*-Glycopeptide synthesis using 9-fluorenylmethoxycarbonyl (Fmoc)-protected synthetic units (C) 62
The 2-(2-pyridyl)ethoxycarbonyl-(Pyoc) residue—an acid- and base-stable, hydrophilic protecting group for the amino function in peptide synthesis (C) 783
Protein-protein-interactions (B) 168
Proton sponge, 4,5-Bis(dimethylamino)-fluorene, a new "proton sponge" (C) 731
Proximity effects in organic chemistry—The photoelectron spectroscopic investigation of non-bonding and transannular interactions (R) 283
Pulse methods, Modern pulse methods in high-resolution NMR spectroscopy (R) 350
Purines, Photocycloaddition of 6-oxopurines and thymine to products with cyclobutane part structures (C) 623
Push-pull 1,3-butadienes, 1-(1,3-Butadienyl)triazoles from 1-vinyltriazoles and electron-rich alkynes—cleavage to "push-pull" 1,3-butadienes (C) 553
Pyrazine, The versatile chemistry of 1,4-diazines: organic, inorganic and biochemical aspects (R) 171
Diazaquinodimethanes, donor-substituted pyrazines, and dihydropyrazines (C) 717
Pyridine, $[Me_3Si(py)]^{\oplus}X^{\ominus}$ (X = Br, I): X-ray structural analysis of the 1:1-adducts of bromo- or iodotrimethylsilane and pyridine (C) 725
Pyrrocorphin, The chemistry of pyrrocorphins: stereoselectivity in the porphyrinogen→pyrrocorphin tautomerization (C) 630
The chemistry of pyrrocorphins: *C*-methylation of pyrrocorphinates at the ligand periphery (C) 631

QUANTUM CHEMISTRY, Elektronenstruktur organischer Moleküle. Grundbegriffe quantenchemischer Betrachtungsweisen (B) 335
Quartet state, The first $^{13}$C-ENDOR investigation of an organic triradical in the quartet state; synthesis of a triply $^{13}$C-labeled trisgalvinol (C) 150
Quasi (III—V)-phases, GaGeTe, a novel defect tetrahedral structure (C) 407
Quasiracemate, Construction of an alternating (Rh, Rh, Ir, Ir)$_\infty$-columnar structure *via* a quasiracemate (C) 327
Quenching, Efficiency of the physical quenching of singlet oxygen with benzoquinone derivatives (C) 792
Quinhydrones, Cation-induced charge-transfer absorption of intramolecular quinhydrones with oligooxaparacyclophane structure (C) 334

RADICAL ANIONS, Successive electron transfers in molecules with two electrophoric groups: novel singlet, doublet, and triplet states (C) 242
Efficient method for generation of radical anions from benzene derivatives of low electron affinity (C) 556
Radical cations, Symmetry breaking and non-Born-Oppenheimer effects in radical cations (R) 210
Generation of the tetraphenylcyclobutadiene radical cation by ionizing gas-phase decarbonylation (C) 51
1,1-Dialkoxytrimethylene radical cations (C) 500
Radical products in single electron transfer reactions of lithium triethylhydridoborate detected by ESR and multinuclear ($^1$H, $^{10}$B, $^{11}$B, $^{14}$N)-ENDOR spectroscopy (C) 892
Radicals, The first $^{13}$C-ENDOR investigation of an organic triradical in the quartet state; synthesis of a triply $^{13}$C-labeled trisgalvinol (C) 150
Radioactivity, NMR Studies of yeasts grown on substrates at "zero" level radioactivity (C) 49
Raw materials and energy: a challenge for polymer research (R) 764
Reaction kinetics, Linear control of temperature with time—a new approach to reaction kinetics (R) 225
Reaction mechanism, Can radicals participate in pericyclic reactions? Model reactions for electron-transfer induced valence isomerization of 1-arylindenes (C) 254
Chelation or non-chelation control in stereoselective reactions of titanium reagents with chiral alkoxycarbonyl compounds (C) 989
Rearrangement, Dephosphorylating "ylide diketone"-rearrangement of the arylcarbonyloxyalkylidenephosphoranes (C) 619
Phosphane-induced, stepwise rearrangement of an octadienediyl palladium complex to seven- and nine-membered metallacycles (C) 774
Recombinant DNA techniques, Synthesis of peptide hormones using recombinant DNA techniques (R) 842
Redox intercalation reactions of $VOPO_4 \cdot 2H_2O$ (C) 412
Redox reaction, Photochemical four-electron redox reaction of hexaazidoplatinate(IV) (C) 154
Reducing agents, Complex reducing agents (CRA's)—versatile, novel ways of using sodium hydride in organic synthesis (R) 599
Regioselectivity, Reversal of the regioselectivity in the zirconocene-induced coupling of a ketone with isoprene (C) 777
Resolution, Chromatographic resolution of cyclic organic compounds on a Λ-Tris(1,10-phenanthroline)ruthenium(II) montmorillonite column (C) 162
circular dichroism, and absolute configuration of 1,1'-biazulenes (C) 870
Resonance energy of bridged [10]annulenes (C) 1007
Rhenium compounds, $P(NSiMe_3)_3^{\ominus}$—a derivative of the monomeric metaphosphate ion as building block for a tricyclic rhenium complex (C) 503
Rhodacarborane, Synthesis and structure determination of $[(PEt_3)RhC_2B_9H_{10}]_2$—a binuclear rhodacarborane containing four bonds between two icosahedra (C) 722
Rhodium catalysts for enantioselective hydrosilylation—a new concept in the development of asymmetric catalysts (R) 897
Ribosomes, Electron diffraction with the transmission electron microscope as a phase-determining diffractometer—from spatial frequency filtering to the three-dimensional structure analysis of ribosomes (R) 456
Ring expansion, Expansion of three-membered heterocycles to five-membered cyclic carbenes—novel reactions of aziridine, oxirane, and thiirane with CO and CS ligands in iron, ruthenium, and manganese complexes (C) 163
Ring-opening by [3,3]-diphospha Cope-rearrangement (C) 61
Unexpected ring-opening of benzocyclobutenes upon reaction with lithium in tetrahydrofuran (C) 246

Ring strain, Through-bond interaction *via* strained σ-bonds—the synthesis and PE spectrum of 1,5-dimethyltetracyclo-[3.3.0.0$^{2,8}$.0$^{4,6}$]octane-3,7-dione (C) 488
Thermolysis and reaction of 4,5-Benzotricyclo[4.1.0.0$^{1,3}$]hept-4-ene and *o*-(Propadienyl)styrene (C) 868
Tricyclo[4.1.0.0$^{1,3}$]hept-4-enes as intermediates (C) 869
Rosefuran, Regiocontrolled prenylations and alkylations of furans: preparation of rosefuran and novel analogues (C) 719
Ruthenium compounds, Synthesis and structure of [$AsPh_4$][$Ru_6H(\mu$-O=CNMe$_2$)$_2$($\mu$-CO)$_4$(CO)$_{14}$]·Me$_2$C=O; a cyclic hydrido-hexametallic anion (C) 249
Stereospecific reactions of chiral chlororuthenium(II) complexes with Grignard reagents (C) 333
Aryl(hydrido)ruthenium complexes by C—H addition: isolation of a four-membered metallacycle as intermediate (C) 873
Ruthenium(III) halides, Topotactic redox and exchange reactions of ruthenium(III) halides (C) 555

SANDWICH COMPLEXES, $\mu_2$-($\eta^5$:$\eta^5$-Cyclooctatetraene)-bis($\eta^5$-cyclopentadienylchromium): a "siamese twin" of two half-open sandwich moieties (C) 330
Scrambling, C-Scrambling in the *tert*-butyl cation (C) 50
Secododecahedrene, Cautionary example of incorrect structural assignment due to crystallographic disorder (C) 251
Secoiridoid glycosides, Secologanin, a biogenetic key compound—synthesis and biogenesis of the iridoid and secoiridoid glycosides (R) 828
Secologanin, a biogenetic key compound—synthesis and biogenesis of the iridoid and secoiridoid glycosides (R) 828
Selectivity, Organometallic compounds of titanium and zirconium as selective nucleophilic reagents in organic synthesis (R) 31
Selenoformaldehyde bridge, Seleno- and telluroformaldehyde as bridging ligands in organometallic complexes (C) 314
Selenoformaldehyde ligand, Synthesis of [($\eta^5$-$C_5H_5$)Rh($PMe_3$)($\eta^2$-$CH_2$E)] with E=S, Se, Te: thio-, seleno-, and telluroformaldehyde as ligands in mononuclear rhodium complexes (C) 316
Selenoketene, Synthesis and structure of [($\eta^5$-$C_5H_5$)Rh$P(i$Pr$)_3$($\eta^2$-EC=$CH_2$)] with E=S, Se, Te: generation and stabilization of thioketene, selenoketene, and telluroketene at a transition metal (C) 981
Selenolate/diselenide pair, Oxidative coupling of the selenolate functions in ($C_6H_5$)$_3$PC(Se)P($C_6H_5$)$_3$: crystal structure of {[($C_6H_5$)$_3$P]$_2$CSe}$_2^{2\oplus}$$Fe_2OCl_6^{2\ominus}$·4$CH_2Cl_2$ containing a linear Fe—O—Fe axis (C) 156
$^1$H,$^{13}$C Shift correlation, 2D-NMR spectroscopy in annulene chemistry: complete assignment of the $^{13}$C-NMR spectrum of 9,11-bisdehydrobenzo[18]annulene by $^1$H,$^{13}$C shift correlation (C) 499
Silaethene, A new stable silaethene (C) 1005
Silaphosphane, ($t$BuP)$_8$$Si_2$—a novel dispirocyclic silaphosphane (C) 775
Silicon-lead bonding, Tetrakis(trimethylsilyl)plumbane, the first organosilicon-lead compound (C) 557
Silver clusters, Fourier transform far-infrared spectroscopy of silver atoms and silver clusters entrapped in zeolite NaY (C) 791
Single electron transfer, Radical products in single electron transfer reactions of lithium triethylhydridoborate detected by ESR and multinuclear ($^1$H, $^{10}$B, $^{11}$B, $^{14}$N)-ENDOR spectroscopy (C) 892
Singlet oxygen, Cercosporin, a singlet oxygen generator (C) 720
[4+2]-Cycloaddition of singlet oxygen to 2,5-dimethylfuran: isolation and reactions of the monomeric and dimeric endoperoxides (C) 726
Efficiency of the physical quenching of singlet oxygen with benzoquinone derivatives (C) 792
$S_N2'$ Reaction, On the stereochemistry of the $S_N2'$ reaction (C) 613
Sodium hydride, Complex reducing agents (CRA's)—versatile, novel ways of using sodium hydride in organic synthesis (R) 599
Solids, Probing the environment of Al atoms in noncrystalline solids: $Al_2O_3$—$SiO_2$ gels, soda glass, and mullite precursors (C) 614
Solid-state chemistry, Preparation of solid-state compounds by chemical transport—interpretation and control using the cooperative transport model (R) 82
Thio- and seleno-compounds of main group elements—novel inorganic oligomers and polymers (R) 113
Topotactic redox and exchange reactions of ruthenium(III) halides (C) 555
Novel surface-modified solids by topochemical oxidation of Zintl anions (C) 558
Solid-state NMR spectroscopy, Magic-angle-spinning NMR (MAS-NMR) spectroscopy and the structure of zeolites (R) 259
Solutions, Properties of liquids and solutions (B) 256
Spermidines, Synthesis of acylpolyamines: acetylspermidines and $C_{12:0}$-acarnidine (C) 618
Spirocyclization, Novel catalytic application of a transition-metal cluster: spirocyclization of alkyl isocyanates (C) 880
Spirorenone, A novel synthetic route to the aldosterone-antagonist spirorenone (C) 406
Spirosilicate, Strong distortion of the tetrahedral geometry in a spirosilicate: molecular structure of bis(tetramethylethylenedioxy)silane (C) 65
The crystal and molecular structure of bis(1,8-naphthalenedioxy)silane—a contribution to the controversy over planar, four-coordinated silicon in orthosilicic acid esters (C) 501
Stereochemistry, On the stereochemistry of the $S_N2'$ reaction (C) 613
Stereocontrolled synthesis, A new, efficient and stereocontrolled synthesis of trisubstituted alkenes *via* functionalized acrylic esters (C) 796
Stereoselective aldol reaction with (*R*)-*N*-acetyl-α-phenylglycinol (C) 788
Stereoselective reactions, Chelation or nonchelation control in stereoselective reactions of titanium reagents with chiral alkoxycarbonyl compounds (C) 989
Stereoselective synthesis of enantiomerically pure natural products—estrone as example (R) 637
Stereoselective synthesis of iridoid glycosides (C) 888
Stereospecific alkylation, Stereospecific reactions of chiral chlororuthenium(II) complexes with Grignard reagents (C) 333
Stibanes, Transition-metal substituted stibanes as acceptors: Cp(CO)(L)-Fe—$SbBr_2$·$PMe_3$ (L=CO, $Me_3P$, MeNC)—1:1-ferriostibane-trimethylphosphane complexes (C) 60
Structure analysis, Electron diffraction with the transmission electron microscope as a phase-determining diffractometer—from spatial frequency filtering to the three-dimensional structure analysis of ribosomes (R) 456
Cautionary example of incorrect structural assignment due to crystallographic disorder (C) 251
of a $CaF_2$ single crystal with an edge length of only 6 μm: an experiment using synchrotron radiation (C) 1011
Substituent effects, Some substituent effects in the photocycloaddition of dihalomaleiimides to uracils (C) 161
Sugar chemistry, Advanced sugar chemistry. Principles of sugar stereochemistry (B) 803
Sulfur bridges, [$Mo_2(NO)_2(S_2)_3(S_5)OH]^{3-}$, a complex containing a bidentate $S_5^{2-}$-bridging ligand in a {$S_5Mo_2(S_2)$}-heterocycle with cyclooctasulfur geometry (C) 884
Sulfur coordination, [$Ph_4P]_2$[$V_2(SC_2H_4S)_4$]·4MeOH: the first polynuclear vanadium-sulfur complex with pure sulfur coordination (C) 885
Sulfur double-ylide chromium complexes, Novel $\eta^3$,σ-sulfur double-ylide chromium complexes by *endo*-hydride addition to cationic ($\lambda^6$-thiabenzene 1-oxide)chromium complexes (C) 498
Sulfur ylides, Metal complexes of sulfur ylides: coordination chemistry, preparative organic chemistry, and biochemistry (R) 516
Surface modification, Novel surface-modified solids by topochemical oxidation of Zintl anions (C) 558
Surfactants with novel structural characteristics (C) 616
Symmetry breaking and non-Born-Oppenheimer effects in radical cations (R) 210
Symmetry operations, On the description of complex inorganic crystal structures (R) 69
Symproportionation, Formation of alkyl radicals by thermal bimolecular reaction of alkanes and alkenes (C) 889
Synchrotron radiation, Structure analysis of a $CaF_2$ single crystal with an edge length of only 6 μm: an experiment using synchrotron radiation (C) 1011
Synthetic methods, Organometallic compounds of titanium and zirconium as selective nucleophilic reagents in organic synthesis (R) 31
Homolytic cyclizations of *N*-chloroalkenylamines (R) 337
Complex reducing agents (CRA's)—versatile, novel ways of using sodium hydride in organic synthesis (R) 599

TACHYSTEROL$_3$ ROTAMER, Photochemistry of previtamin $D_3$ at 92 K: formation of an unstable tachysterol$_3$ rotamer (C) 718
Taxane, The tricyclo[9.3.1.0$^{3,8}$]pentadecane system—a short synthesis of a C-aromatic taxane skeleton (C) 419
Tellurium compounds, Tellurium as six-electron donor—synthesis and structure of $\mu_3$-Te[Mn(CO)$_2$($\eta^5$-$C_5H_5$)]$_3$ (C) 59
Tellurium heterocycles, Small heterocycles containing phosphorus and tellurium atoms (C) 983
Tellurium-nitrogen compounds, A new route to tellurium-nitrogen compounds (C) 789
Telluroformaldehyde bridge, Seleno- and telluroformaldehyde as bridging ligands in organometallic complexes (C) 314
Telluroformaldehyde ligand, Synthesis of [($\eta^5$-$C_5H_5$)Rh($PMe_3$)($\eta^2$-$CH_2$E)] with E=S, Se, Te: thio-, seleno-, and telluroformaldehyde as ligands in mononuclear rhodium complexes (C) 316
Telluroketene, Synthesis and structure of [($\eta^5$-$C_5H_5$)Rh$P(i$Pr$)_3$($\eta^2$-EC=$CH_2$)] with E=S, Se, Te: generation and stabilization of thioketene, selenoketene, and telluroketene at a transition metal (C) 981
Terphenylene, The structure and reactivity of 2,3,7,8-tetrakis(trimethylsilyl)terpheny-

lene, a novel linear multiphenylene (C) 994
Tetrabenzene, *p*-(*o*,*p*)-*o*-Tribenzene and *p*-(*o*,*p*)-(*o*,*o*)-*p*-tetrabenzene, Diels-Alder oligomers of benzene (C) 617
Tetrabenzoporphyrinatoiron(II), Preparation and properties of tetrabenzoporphyrinatoiron(II) and its isocyanide complexes (C) 724
Tetra-*tert*-butylcyclobutadiene, Three arguments supporting a rectangular structure for tetra-*tert*-butylcyclobutadiene (C) 402
Bonding electron density distribution in tetra-*tert*-butylcyclobutadiene—a molecule with an obviously non-square four-membered ring (C) 403
Tetra-*tert*-butyltetrahedrane: $^{13}C$-$^{13}C$ coupling constants and hybridization (C) 878
Tetracyclo[3.3.0.0$^{2,8}$.0$^{4,6}$]octane-3,7-dione, Through-bond interaction *via* strained σ-bonds—the synthesis and PE spectrum of 1,5-dimethyltetracyclo[3.3.0.0$^{2,8}$.0$^{4,6}$]octane-3,7-dione (C) 488
Tetracycloundecane, Synthesis and structure of a linearly *anti*-annelated tetracycloundecane. A potential precursor for a coriolin synthesis (C) 721
Tetraethoxyallene: Equivalent of the fictive malonic ester dianion—a versatile synthetic building block (C) 321
Tetrahedral geometry, Strong distortion of the tetrahedral geometry in a spirosilicate: molecular structure of bis(tetramethylethylenedioxy)silane (C) 65
The crystal and molecular structure of bis(1,8-naphthalenedioxy)silane—a contribution to the controversy over planar, four-coordinated silicon in orthosilicic acid esters (C) 501
Tetrahedral structure, Optically active iron complexes with tetrahedral structure (C) 164
GaGeTe, a novel defect tetrahedral structure (C) 407
Tetrahedrane, A diphosphene as tetrahedrane building block: synthesis of [Fe$_2$(CO)$_6$(P$_2$*t*Bu$_2$)] (C) 154
Tetra-*tert*-butyltetrahedrane: $^{13}C$-$^{13}C$ coupling constants and hybridization (C) 878
Tricyclo[2.1.0.0$^{2,5}$]pentan-3-one (C) 990
Tetrahydrofuran, Twist conformation of tetrahydrofuran in the crystal (C) 410
Tetraphenylcyclobutadiene radical cation, Generation of the tetraphenylcyclobutadiene radical cation by ionizing gas-phase decarbonylation (C) 51
Tetraphosphaspiro[2.2]pentane, (*t*BuP)$_2$C(*t*BuP)$_2$—the first tetraphosphaspiro[2.2]pentane (C) 632
Tetrasaccharide, Synthesis of a tetrasaccharide of the core region of *O*-glycoproteins (C) 776
Tetrasulfido-nickel(II) complex, [Ni(S$_4$)$_2$]$^{2\ominus}$, a homoleptic tetrasulfido-nickel(II) complex (C) 1006
Tetrazocines, 1,3,5,7-Tetrazocines (C) 543
Theoretical methods, Molecular mechanics calculations in organic chemistry: examples of the usefulness of a simple nonquantum mechanical model (R) 1
Thiabenzene 1-oxide, Novel η$^3$,σ-sulfur double-ylide chromium complexes by *endo*-hydride addition to cationic (λ$^6$-thiabenzene 1-oxide)chromium complexes (C) 498
Thiadiazole-3,5-dicarbonitrile, 1,2,4-Thiadiazole-3,5-dicarbonitrile by reaction of cyanogen with sulfur (C) 881
Thiadiphosphirane, The first X-ray structure analysis of a thiadiphosphirane (C) 418
Thiazylamide, Pentacarbonylrhenium complexes with thiazylamide ligands (C) 723
Thiazylfluoride complexes, Synthesis of the thionitrosylrhenium dication [Re(CO)$_5$(NS)]$^{2+}$; reactions and structure of the thiazylfluoride complex [Re(CO)$_5$(NSF)]$^+$ (C) 162
Thietones, oxetones, and azetones (C) 543
Thin-layer chromatography, A quarter century of thin-layer chromatography—an interim report (R) 507
Thiocarbonyl compounds, A novel route to thiocarbonyl compounds (C) 55
Thioformaldehyde bridge, A binuclear complex with a thioformaldehyde bridge (C) 315
Thioformaldehyde ligand, Synthesis of [(η$^5$-C$_5$H$_5$)Rh(PMe$_3$)(η$^2$-CH$_2$E)] with E = S, Se, Te: thio-, seleno-, and telluroformaldehyde as ligands in mononuclear rhodium complexes (C) 316
Thioketene, Synthesis and structure of [(η$^5$-C$_5$H$_5$)RhP(*i*Pr)$_3$(η$^2$-EC=CH$_2$)] with E = S, Se, Te: generation and stabilization of thioketene, selenoketene, and telluroketene at a transition metal (C) 981
Thioketene-iron cluster, Reversible opening of a thioketene-iron cluster containing a μ$_2$-*C*$_2$,μ$_2$-*S*-thiocarbonyl group (C) 153
Thionitrosylrhenium dication, Synthesis of the thionitrosylrhenium dication [Re(CO)$_5$(NS)]$^{2+}$; reactions and structure of the thiazylfluoride complex [Re(CO)$_5$(NSF)]$^+$ (C) 162
Three-dimensional structure analysis, Electron diffraction with the transmission electron microscope as a phase-determining diffractometer—from spatial frequency filtering to the three-dimensional structure analysis of ribosomes (R) 456
Thromboxanes, From studies of biochemical mechanism to novel biological mediators: prostaglandin endoperoxides, thromboxanes, and leukotrienes (Nobel lecture) (R) 805
Through-bond interaction *via* strained σ-bonds—the synthesis and PE spectrum of 1,5-dimethyltetracyclo[3.3.0.0$^{2,8}$.0$^{4,6}$]octane-3,7-dione (C) 488
Thymine, Photocycloaddition of 6-oxopurines and thymine to products with cyclobutane part structures (C) 623
Tin-boron exchange, Exchange of the apical tin atom in the *nido*-cluster (CH$_3$)$_5$C$_5$Sn$^+$ (C) 56
Titanium compounds, Organometallic compounds of titanium and zirconium as selective nucleophilic reagents in organic synthesis (R) 31
Regio- and diastereoselective synthesis of (4-hydroxy-3-methyl-1,2-alkadienyl)carbamates from α-titanated 2-butynylcarbamates and aldehydes (C) 54
Titanium reagents, Chelation or non-chelation control in stereoselective reactions of titanium reagents with chiral alkoxycarbonyl compounds (C) 989
Tobacco mosaic virus, From macromolecules to biological assemblies (Nobel lecture) (R) 565
Topochemical oxidation, Novel surface-modified solids by topochemical oxidation of Zintl anions (C) 558
Topotactic reactions, Topotactic redox and exchange reactions of ruthenium(III) halides (C) 555
Trace analysis, Organic trace analysis by liquid chromatography (B) 66
Transition-metal cluster, Novel catalytic application of a transition-metal cluster: Spirocyclization of alkyl isocyanates (C) 880
Transition metals, Phosphorus ylides in the coordination sphere of transition metals. An inventory (R) 907
Transmission electron microscope, Electron diffraction with the transmission electron microscope as a phase-determining diffractometer—from spatial frequency filtering to the three-dimensional structure analysis of ribosomes (R) 456
Transport model, Preparation of solid-state compounds by chemical transport—interpretation and control using the cooperative transport model (R) 82
Tribenzene, *p*-(*o*,*p*)-*o*-Tribenzene and *p*-(*o*,*p*)-(*o*,*o*)-*p*-tetrabenzene, Diels-Alder oligomers of benzene (C) 617
Trichromium, FT-FIR spectroscopy of ligand-free metal clusters; matrix effects on the molecular geometry of trichromium, Cr$_3$ (C) 166
Tricyclo[5.2.1.0$^{2,6}$]deca-4,8-dien-3,10-diyl, The *endo*-3,10-dimethyltricyclo[5.2.1.0$^{2,6}$]-deca-4,8-dien-3,10-diyl dication, a novel bishomoaromatic/allylic dication and its rearrangement to the symmetrical *cis-anti-cis*-3,10-dimethyltricyclo[5.3.0.0$^{2,6}$]deca-4,8-dien-3,10-diyl dication (C) 712
Tricyclo[6.2.0.0$^{3,6}$]decane, Crystal structure of 2,4,5,7,9,10-hexaoxa-1,3,6,8-tetraphenyltricyclo[6.2.0.0$^{3,6}$]decane: an authentic bisdioxetane (C) 546
Tricyclo[4.1.0.0$^{1,3}$]hept-4-enes, Thermolysis and reaction of 4,5-Benzotricyclo-[4.1.0.0$^{1,3}$]hept-4-ene and *o*-(Propadienyl)-styrene (C) 868
as intermediates (C) 869
Tricyclo[3.1.0.0$^{2,6}$]hexanes, 3,4-Bismethylenetricyclo[3.1.0.0$^{2,6}$]hexane—synthesis and Diels-Alder addition to tetracyanoethylene (C) 871
Tricyclo[9.3.1.0$^{3,8}$]pentadecane, The tricyclo[9.3.1.0$^{3,8}$]pentadecane system—a short synthesis of a C-aromatic taxane skeleton (C) 419
Tricyclo[2.1.0.0$^{2,5}$]pentan-3-one (C) 990
Trimethinecyanines, First proof of di-, tri-, and all-*cis*-conformations in sterically hindered trimethinecyanines (carbocyanines) of the indoline and benzothiazole series (C) 876
Trioxatris-*o*-homobenzenes, Valence isomerization of phane-bridged *cis*-trioxatris-*o*-homobenzenes (C) 867
Triphosphetidines, Azatriphosphetidines as cyclotrimers of an iminophosphane—synthesis and crystal structure (C) 552
Tris(diphenylthiophosphinoyl)methanide, The structure of tris(diphenylthiophosphinoyl)methanide, a mesomerically stabilized carbanion (C) 254
Tungsten complexes, The transformation of acetylene from a four- to a two-electron ligand: acetylene(carbonyl)nitrosyl complexes of tungsten (C) 1008
Alkyne complexes of tungsten(IV) (C) 1010
Turgorins, hormones of the endogeneous daily rhythms of higher organized plants—detection, isolation, structure, synthesis, and activity (R) 695
Twist conformation of tetrahydrofuran in the crystal (C) 410

ULLMANNS Encyklopädie der technischen Chemie (B) 564
Uracil, Some substituent effects in the photocycloaddition of dihalomaleiimides to uracils (C) 161
Photocycloaddition of 6-cyanouracil to ketene diethyl acetal: synthesis of a uracil derivative possessing a cyclobutenone framework (C) 629
Uranyl ions, Highly selective extraction of uranyl ions by acyclic ligands containing L-phenylalanine moieties (C) 563

VALENCE ISOMERIZATION, Can radicals participate in pericyclic reactions? Model reactions for electron-transfer induced valence isomerization of 1-arylindenes (C) 254
Vanadium compounds, Redox intercalation reactions of VOPO$_4$·2H$_2$O (C) 412
μ$_2$-E[V(CO)$_3$diphos]$_2$ (E = S, Se, Te): complexes with linear VEV multiple-bond systems (C) 980
Vanadium-sulfur complex, [Ph$_4$P]$_2$[V$_2$(SC$_2$H$_4$S)$_4$]·4MeOH: the first polynuclear vanadium-sulfur complex with pure sulfur coordination (C) 885

Verdazyl, 1,5-Dimethylverdazyls, hydrazidinyl radicals with pyramidal 1,5-nitrogen atoms (C) 320
Vinyl alcohol, (*Z*)-2-Methoxy-1,2-diphenylvinyl alcohol, a remarkably stable enol (C) 405
Vinylidene ligand, Synthesis of $[C_5H_5Rh(PhC{=}CH)P(iPr)_3]$ and $[C_5H_5Rh(=C{=}CHPh)P(iPr)_3]$: mechanism of the conversion of an alkyne ligand into a vinylidene ligand (C) 414
Vinylimidazoles, A simple route to 2-vinylimidazoles (C) 560
Vitamin $B_{12}$, 5,15-Bisnorcobester: an unexpected mode of formation (C) 736
A simple route to 5-nor-, 15-nor-, and 5,15-bisnorcobesters (C) 737
Vitamin E, A carbene-complex route to vitamin E (C) 732

WITTIG REACTION, Some cautions in the interpretation of oxidoylide reactions based on $^{31}$P-NMR data (C) 56
Organometallic variants of the Wittig reaction: synthesis and structure of *trans*-μ-(2-5; 8-11-η-dodecapentaene)bis(tricarbonyliron) (C) 713
World energy supply: resources, technologies, perspectives (B) 634

YEASTS, NMR Studies of yeasts grown on substrates at "zero" level radioactivity (C) 49
Electromicrobial reduction using yeasts (C) 322
Preparation of ethyl (*R*)-(−)-3-hydroxy-2-methylpropanoate by yeast reduction of ethyl α-formylpropanoate (C) 1012
Ylide complexes, Novel $\eta^3,\sigma$-sulfur double-ylide chromium complexes by *endo*-hydride addition to cationic ($\lambda^6$-thiabenzene 1-oxide)chromium complexes (C) 498
Ylide diketone-rearrangement, Dephosphorylating "ylide diketone"-rearrangement of the arylcarbonyloxyalkylidenephosphoranes (C) 619
Ylides, Metal complexes of sulfur ylides: coordination chemistry, preparative organic chemistry, and biochemistry (R) 516
Phosphorus ylides in the coordination sphere of transition metals. An inventory (R) 907

ZEOLITES, Magic-angle-spinning NMR (MAS-NMR) spectroscopy and the structure of zeolites (R) 259
Solution-phase metal atom preparation of catalytically active zeolite-encapsulated metal clusters; characterization and application to the selective reduction of CO to butene (C) 624
Fourier transform far-infrared spectroscopy of silver atoms and silver clusters entrapped in zeolite NaY (C) 791
Zinc cluster, $(C_5H_5)_6Ni_2Zn_4$—the first zinc-containing mixed-metal cluster (C) 329
Zintl anions, Novel surface-modified solids by topochemical oxidation of Zintl anions (C) 558
Zintl compounds, $Rb_7NaGe_8$ and $K_7NaGe_8$, Zintl compounds with $Na(Ge_4)_2$ units (C) 998
Zirconium compounds, Organometallic compounds of titanium and zirconium as selective nucleophilic reagents in organic synthesis (R) 31
Zircona- and hafnacyclobutenes—a new route to metallacyclobutanes (C) 248
Zirconocene, The zirconocene-induced coupling of butadiene with carbonyl compounds (C) 494
Reversal of the regioselectivity in the zirconocene-induced coupling of a ketone with isoprene (C) 777